A11100 987927

NAT'L INST OF STANDARDS & TECH R.I.C.

A11100987927
/Catalog of National Bureau of Standards
QC100 .U57 NO.535 1978 V.1;PT. C.1 NBS-P

SPECIAL PUBLICATION 535
Volume 1, Part 2

National Bureau of Standards
Library, E-01 Admin. Bldg.
OCT 1 1981
191072
QC
100
.U57

# Catalog of National Bureau of Standards Publications 1966-1976

## Citations and Abstracts

U.S. Department of Commerce

# NATIONAL BUREAU OF STANDARDS

The National Bureau of Standards[1] was established by an act of Congress March 3, 1901. The Bureau's overall goal is to strengthen and advance the Nation's science and technology and facilitate their effective application for public benefit. To this end, the Bureau conducts research and provides: (1) a basis for the Nation's physical measurement system, (2) scientific and technological services for industry and government, (3) a technical basis for equity in trade, and (4) technical services to promote public safety. The Bureau's technical work is performed by the National Measurement Laboratory, the National Engineering Laboratory, and the Institute for Computer Sciences and Technology.

**THE NATIONAL MEASUREMENT LABORATORY** provides the national system of physical and chemical and materials measurement; coordinates the system with measurement systems of other nations and furnishes essential services leading to accurate and uniform physical and chemical measurement throughout the Nation's scientific community, industry, and commerce; conducts materials research leading to improved methods of measurement, standards, and data on the properties of materials needed by industry, commerce, educational institutions, and Government; provides advisory and research services to other Government Agencies; develops, produces, and distributes Standard Reference Materials; and provides calibration services. The Laboratory consists of the following centers:

Absolute Physical Quantities[2] — Radiation Research — Thermodynamics and Molecular Science — Analytical Chemistry — Materials Science.

**THE NATIONAL ENGINEERING LABORATORY** provides technology and technical services to users in the public and private sectors to address national needs and to solve national problems in the public interest; conducts research in engineering and applied science in support of objectives in these efforts; builds and maintains competence in the necessary disciplines required to carry out this research and technical service; develops engineering data and measurement capabilities; provides engineering measurement traceability services; develops test methods and proposes engineering standards and code changes; develops and proposes new engineering practices; and develops and improves mechanisms to transfer results of its research to the utlimate user. The Laboratory consists of the following centers:

Applied Mathematics — Electronics and Electrical Engineering[2] — Mechanical Engineering and Process Technology[2] — Building Technology — Fire Research — Consumer Product Technology — Field Methods.

**THE INSTITUTE FOR COMPUTER SCIENCES AND TECHNOLOGY** conducts research and provides scientific and technical services to aid Federal Agencies in the selection, acquisition, application, and use of computer technology to improve effectiveness and economy in Government operations in accordance with Public Law 89-306 (40 U.S.C. 759), relevant Executive Orders, and other directives; carries out this mission by managing the Federal Information Processing Standards Program, developing Federal ADP standards guidelines, and managing Federal participation in ADP voluntary standardization activities; provides scientific and technological advisory services and assistance to Federal Agencies; and provides the technical foundation for computer-related policies of the Federal Government. The Institute consists of the following divisions:

Systems and Software — Computer Systems Engineering — Information Technology.

[1] Headquarters and Laboratories at Gaithersburg, Maryland, unless otherwise noted; mailing address Washington,D.C. 20234.

[2] Some divisions within the center are located at Boulder, Colorado, 80303.

**The National Bureau of Standards was reorganized, effective April 9, 1978.**

ational Bureau of Standards
JUN 19 1979
not Acc-Circ
QC100
U57
no. 535
1978
c.2

## Volume 1, Part 2: Citations and Abstracts

# Catalog of National Bureau of Standards Publications, 1966-1976

Consolidated reprint of citations and abstracts from
NBS SP305, and its Supplements 1-8

Betty L. Burris and Rebecca J. Morehouse, Editors

Technical Information and Publications Division
National Bureau of Standards
Washington, DC 20234

U.S. DEPARTMENT OF COMMERCE
Juanita M. Kreps, Secretary

Dr. Sidney Harman, Under Secretary
Jordan J. Baruch, Assistant Secretary
for Science and Technology

NATIONAL BUREAU OF STANDARDS
Ernest Ambler, Director

U.S.
Special publ. 535

Issued 1978

**Library of Congress Catalog Number: 78-600145**

National Bureau of Standards Special Publication
535, Volume 1, Part 2

Consolidated reprint of citations and abstracts from
NBS SP305, and its Supplements 1-8, 1966-1976

Nat. Bur. Stand. (U.S.) Spec. Publ. 535, Vol. 1,
Pt. 2, 1112 pages (1978)

CODEN: XNBSAV

Issued 1978

**U.S. Government Printing Office**
**Washington: 1978**

---

For sale by the Superintendent of Documents, U.S. Government
Printing Office, Washington, DC 20402. (Order by SD Stock No.
003-003-02010-9). Price $23.75 per 2 part set; sold in sets only. (Add 25
percent additional for other than U.S. mailing.)

# PREFACE

Throughout the history of the National Bureau of Standards, publications have served as the single most effective means for conveying results of Bureau research to the Bureau's diverse audiences. Much of this research has lasting value, and publications reporting Bureau work of many years ago are still consulted by current researchers. Because of these facts, NBS is issuing this catalog of Bureau publications from 1966 through 1976. Each of the two volumes may be used separately, or they may be used to complement each other. Volume 1 consists of abstracts and a full bibliographic citation for each paper. It is an accumulation of the complete citations originally appearing in the NBS annual publications catalogs: NBS SP305 and its Supplements 1 through 8. It also contains availability information not only for currently in-print papers but also for NBS publications series which are no longer in print. Volume 2 consists of a permuted key word index for all papers. See the "Guide to Users of This Publication" for more details on how to most effectively use each volume.

The NBS publications series (presently consisting of 11 non-periodicals and 3 periodicals) provides a matrix which makes it possible to issue each NBS paper in a medium best calculated to reach its most interested specific audience. Throughout the years, this matrix has evolved to reflect changing emphases in Bureau work. Some former publications series have been eliminated; some have been modified; new ones have been created. The "Miscellaneous Publications" series, for example, was superseded by "Special Publications" in 1970. The NBS Journal of Research evolved into three publications, each reporting work in a different discipline, and now has further evolved to the present single volume which reports work in all NBS technical areas. NBS publications series, past and present, are listed and described. (Currently active NBS publications series are described more briefly on the inside back cover of this catalog's two volumes.)

One final note, as the years pass we have constantly attempted to expand the usefulness and comprehensiveness of our *annual* publications catalog. To this end, we have utilized new computer technology as it became available—for composition as well as for cataloging purposes. In earlier years we were only able to include the overall abstract for a conference or symposium Proceedings. For the past several years we have been able to include, in addition, abstracts for the individual papers presented. Also, for the past several years we have been able to include information on Patents, Grant/Contract Reports, and other items which we had not been able to cover previously—all this toward the end of increasing the catalog's usefulness in communicating NBS work to the public.

We hope this summary of former NBS effort will facilitate the work of those who use it. This two-volume catalog of NBS publications covering calendar years 1966 through 1976 will be updated by the annual catalog supplements. The 1977 supplement is currently available as NBS SP305, Supplement 9. (See Section 2.2.)

W. R. Tilley, Chief
Technical Information and
Publications Division

# CONTENTS

## FOR VOL. 1, PART 1 AND PART 2, VOL. 2

Page

Preface ........ III

A Guide to Users of This Publication ........ V

1. NBS Publication Program ........ IX
   - 1.1. Introduction ........ IX
   - 1.2. Periodicals ........ IX
   - 1.2.1. Journal of Research ........ IX
   - 1.2.2. DIMENSIONS/NBS ........ IX
   - 1.2.3. Journal of Physical and Chemical Reference Data (JPCRD) ........ IX
   - 1.3. Nonperiodicals ........ IX
   - 1.4. NBS Interagency Reports ........ XI
   - 1.5. Grantee/Contractor Reports and Patents ........ XI
   - 1.6. NBS Bibliographic Subscription Services ........ XI
   - 1.7. Papers Published by Others ........ XI
2. Purchase Procedures and Document Availability ........ XI
   - 2.1. Purchase Procedures ........ XI
   - 2.2. Announcement of NBS Publications ........ XII
   - 2.3. Catalogs of NBS Publications ........ XIII
   - 2.4. Functions of Depository Libraries in the United States ........ XIII
   - 2.5. Functions of U.S. Department of Commerce District Offices ........ XIV
   - 2.6. Availability of NBS Publications ........ XIV
     - A. Periodical Subscription Rates ........ XIV
     - B. Superseded NBS Reference Publications ........ XIV
     - C. Status of Publications Cited in This Document ........ XVII

## FOR VOL. 1, PART 1 ONLY

3. Titles and Abstracts of NBS Publications, 1966 Through 1976 ........ 1
   - 3.1. Journal of Research, Section A (July 1966 Through December 1976) ........ 1
   - 3.2. Journal of Research, Section B (July 1966 Through December 1976) ........ 88
   - 3.3. Journal of Research, Section C (July 1966 Through June 1972) ........ 124
   - 3.4. Journal of Physical and Chemical Reference Data ........ 145
   - 3.5. DIMENSIONS/NBS, article titles only ........ 162
   - 3.6. Monographs ........ 174
   - 3.7. Handbooks ........ 188
   - 3.8. Miscellaneous Publications ........ 192
   - 3.9. Special Publications ........ 195
   - 3.10. Applied Mathematics Series ........ 497
   - 3.11. National Standard Reference Data Series ........ 498
   - 3.12. Building Science Series ........ 507
   - 3.13. Federal Information Processing Standards Publications ........ 531
   - 3.14. Commercial Standards ........ 537
   - 3.15. Simplified Practice Recommendations ........ 537
   - 3.16. Voluntary Product Standards ........ 537
   - 3.17. Technical Notes ........ 545
   - 3.18. Consumer Information Series ........ 645
   - 3.19. NBS Interagency Reports ........ 646
   - 3.20. Grantee/Contractor Reports and Patents ........ 735

## FOR VOL. 1, PART 2 ONLY

4. Titles and Abstracts of Papers Published in Non-NBS Media, 1966 through 1976 ........ 754

## FOR VOL. 2 ONLY

5. Key Word Index

   - A Through L ........ 1
   - M Through Z ........ 793

# A GUIDE TO USERS OF THIS PUBLICATION

This 11-year record of NBS publications is available in two volumes, each of which may be used independently.

Volume 1, issued in two parts because of its ength, consists of abstracts for publications ssued by NBS from 1966 through 1976. It also contains general availability information for current and out-of-print NBS publications and a general overview of the NBS publications program. Frequently, the full abstract will satisfy the user's need for information and preclude the need for further research or for acquiring the full paper. Volume 1 reports papers by NBS publications series, as shown in its Table of Contents. If the user does know the NBS publications series involved but does not know the year of publication, this format will be especially useful.

Volume 2, also issued in two parts, consists of a permuted key word index. The key words for each publication or paper are arranged by shifting each group of key words so that each key word, in turn, appears alphabetically followed by the other key words in that group. Volume 2, which also contains the availability and overview information for current and out-of-print NBS publications, may be used in three ways:

(a) as a reference to the abstract given in Volume 1 of this catalog (for papers reported in the annual catalogs, SP305 and Supplements 1 through 8);

(b) as a reference to the abstract in the appropriate annual NBS publications catalog (if available to the reader; see list in Section 2.3);

(c) as a reference to the paper itself, available in a regional depository library, from the National Technical Information Service, or from the original publisher or publication medium, if the paper is still in print. (See availability information in Section 2.).

If the reader does not know the NBS publications series or title of the paper, or is interested in a specific subject matter area, the key word format of Volume 2 will prove useful.

Tables of the abbreviations used to identify various NBS publications series are given below. The tables include the Volume 1 page numbers on which the series listings begin.

## SYMBOLS FOR NBS PUBLICATIONS

### A. Symbols for the Periodicals

| NBS Journal of Research | Index Symbol | | | Issue Date | Volume 1 Page |
|---|---|---|---|---|---|
| | Vol. | Sec. | No. | | |
| Section A | J. Res. 70 through 80 | A | 1 through 6 | July 1966 through December 1976 | 1 |
| Section B | J. Res. 70 through 80 | B | 1 through 4 | July 1966 through December 1976 | 88 |
| Section C | J. Res. 70 through 76 | C | 1 through 4 | July 1966 through June 1972 | 124 |

| Journal of Physical and Chemical Reference Data | Index Symbol | | Issue Date | Page |
|---|---|---|---|---|
| | Vol. | No. | | |
| | JPCRD 1 through 5 | 1 through 4 | January 1972 through December 1976 | 145 |

| DIMENSIONS/NBS | Index Symbol | | Issue Date | Page |
|---|---|---|---|---|
| | Vol. | No. | | |
| | DIM/NBS 57 through 60 | 1 through 12 | January 1973 through December 1976 | 162 |

## B. Symbols for the Nonperiodicals

| NBS Nonperiodical Series | Index Symbol | Page |
|---|---|---|
| Monographs | Monogr. | 174 |
| Handbooks | H | 188 |
| Miscellaneous Publications | MP | 192 |
| Special Publications | SP | 195 |
| Applied Mathematics Series | AMS | 497 |
| National Standard Reference Data Series | NSRDS | 498 |
| Building Science Series | BSS | 507 |
| Federal Information Processing Standards | FIPS PUBS | 531 |
| Commercial Standards | CS | 537 |
| Simplified Practice Recommendations | SPR | 537 |
| Voluntary Product Standards | PS | 537 |
| Technical Notes | TN | 545 |
| Consumer Information Series | CIS | 645 |
| NBS Interagency Reports | NBSIR | 646 |
| Grantee/Contractor Reports and Patents | GCR and/or U.S. Patent | 735 |

## C. Symbols for the Papers Published in Non-NBS Media (1966–1976)

| NBS Papers Published in Non-NBS Media | Index Symbol | Volume 1, Page |
|---|---|---|
| Professional Journals, Books, Book Chapters, Proceedings, etc. | Arabic numbers: 9150 through 16658 | 754 |

SAMPLE
ENTRIES
FROM
VOLUMES
1 AND 2
FOLLOW

# CATALOG ENTRIES: HOW TO READ THEM

## A. Sample Entries from Volume 1

title

author(s)

NBS publication series and series number (also the index symbol)

bibliographic citation: publisher, publication medium, no. of pages, date of publication

Monogr. 138. **MeV total neutron cross sections,** R. B. Schwartz, R. A. Schrack, and H. T. Heaton II, Nat. Bur. Stand. (U.S.), Monogr. 138, 160 pages (Jan. 1974) SD Catalog No. C13.44:138.

key words (as indexed in Volume 2)

SD/GPO catalog or stock number or NTIS number*

Key words: MeV neutrons; neutron time-of-flight; neutron total cross sections.

This report is a compilation of the MeV neutron total cross section data measured at the National Bureau of Standards over the past several years. The measurements generally span the energy interval from 0.5 to 15 or 20 MeV; data are presented in graphical form for twelve normally occuring elements plus the separated isotopes $^{235}$U, $^{238}$U, and $^{239}$Pu. An appendix is included which gives complete details of the experimental technique.

abstract

---

*Verify this number in Status List (pages XVIII to XLIII)

Example of NBS published paper. (See Section 2 for status and availability.)

author(s)

title

arabic number index symbol

bibliographic citation: publisher or place of publication, Vol./no/pages, date of publication

**14434.** Lovas, F. J., Tiemann, E., Johnson, D. R., **Spectroscopic studies of the $SO_2$ discharge system. II. Microwave spectrum of the SO dimer,** *J. Chem. Phys.* **60,** No. 12, 5005-5010 (June 15, 1974).

key words (as indexed in Volume 2)

Key words: centrifugal distortion; dipole moment; microwave spectrum; molecular structure; sulfur monoxide dimer; rotational spectrum.

Microwave spectra assignable to a dimer of SO have been detected in an electric discharge of $SO_2$. A centrifugal distortion analysis has been carried out on the spectra from the ground state and the lowest excited vibrational state of $^{16}O^{32}S^{32}S^{16}O$ and the ground vibrational state of $^{16}O^{32}S^{34}S^{16}O$. The molecule was found to have a planar *cis* configuration with the following geometry: $r(SO) = 1.458(2)$ Å, $r_s(SS) = 2.0245(6)$ Å, and $\angle SSO = 112.7(5)°$. The observed dipole moment of OSSO is $\mu = 3.17(10)$ D.

abstract

Example of NBS paper published in non-NBS medium

## B. Sample Entries from Volume 2.

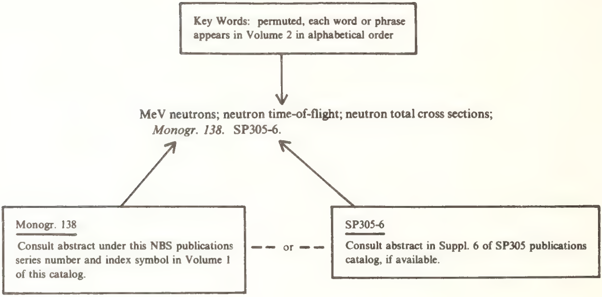

Key Words: permuted, each word or phrase appears in Volume 2 in alphabetical order

MeV neutrons; neutron time-of-flight; neutron total cross sections; *Monogr. 138.* SP305-6.

Monogr. 138

Consult abstract under this NBS publications series number and index symbol in Volume 1 of this catalog.

— — or — —

SP305-6

Consult abstract in Suppl. 6 of SP305 publications catalog, if available.

Example of NBS published paper. (See Section 2 for status and availability.)

---

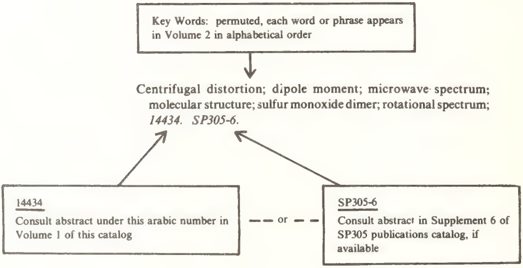

Key Words: permuted, each word or phrase appears in Volume 2 in alphabetical order

Centrifugal distortion; dipole moment; microwave spectrum; molecular structure; sulfur monoxide dimer; rotational spectrum; *14434. SP305-6.*

14434

Consult abstract under this arabic number in Volume 1 of this catalog

— — or — —

SP305-6

Consult abstract in Supplement 6 of SP305 publications catalog, if available

Example of NBS paper published in non-NBS medium

# 1. NBS PUBLICATION PROGRAM

## 1.1. INTRODUCTION

The formal publications of the National Bureau of Standards provide the primary means of communicating the results of NBS programs to its varied technical audiences as well as to the general public. Publications thus constitute a major end product of the Bureau's efforts. These take the form of the Bureau's periodicals, its nonperiodical series, interagency reports, and articles in the journals of professional organizations and technological associations.

The various media in which the results of NBS programs appear are as follows:

## 1.2. PERIODICALS

### 1.2.1. JOURNAL OF RESEARCH

Since July 1977, the Journal of Research has been published on a single-volume, bi-monthly basis. See the inside back cover for a description of the present Journal which reports NBS research and development in those disciplines of the physical and engineering sciences in which the Bureau is active.

Annual subscription: domestic $17.00; foreign, $21.25. Single copy, $3.00 domestic; $3.75 foreign.

The Journal was formerly published in three sections: Section A "Physics and Chemistry," Section B "Mathematical Sciences," and Section C "Engineering and Instrumentation." Papers published in these former versions of the Journal are reported in this catalog. Each section's coverage is briefly described below:

**A. Physics and Chemistry (July 1966 through December 1976)**

Contained papers of interest primarily to scientists working in these fields.

**B. Mathematical Sciences (July 1966 through December 1976)**

Presented studies and compilations designed mainly for the mathematician and the theoretical physicist.

**C. Engineering and Instrumentation (July 1966 through June 1972)**

Reported research and development results of interest chiefly to the engineer and to the applied scientist.

### 1.2.2. DIMENSIONS/NBS

This magazine is published to inform both the technical expert and the interested layman of the latest advances in science and technology, with primary emphasis on the work at NBS. The magazine highlights and reviews such issues as energy research, fire protection, building technology, metric conversion, pollution abatement, health and safety, and consumer product performance. In addition, it reports the results of Bureau programs in measurement standards and techniques, properties of matter and materials, engineering standards and services, instrumentation, and automatic data processing. Formerly issued monthly. The tables of contents for each issue of DIMENSIONS/NBS (formerly Technical News Bulletin) for the years 1973 through 1976 are listed in Section 3.5.

### 1.2.3. JOURNAL OF PHYSICAL AND CHEMICAL REFERENCE DATA (JPCRD)

This Journal is published quarterly by the American Chemical Society and the American Institute of Physics for the National Bureau of Standards. The objective of the Journal is to provide critically evaluated physical and chemical property data, fully documented as to the original sources and the criteria used for evaluation. Critical reviews of measurement techniques, whose aim is to assess the accuracy of available data in a given technical area, are also included. The principal source for the Journal is the National Standard Reference Data System (NSRDS). The Journal is not intended as a publication outlet for original experimental measurements such as are normally reported in the primary research literature, nor for review articles of a descriptive or primarily theoretical nature. (See also Section 1.3. National Standard Reference Data Series.)

## 1.3. NONPERIODICALS

Several categories of nonperiodical publications, described as follows, are listed in this catalog:

MONOGRAPHS—major contributions to the technical literature on various subjects related to the Bureau's scientific and technical activities.

HANDBOOKS—recommended codes of engineering and industrial practice (including safety codes) developed in cooperation with interested industries, professional organizations, and regulatory bodies.

MISCELLANEOUS PUBLICATIONS. The name of this series was changed to Special Publications in 1970.

SPECIAL PUBLICATIONS—include proceedings of conferences sponsored by NBS, NBS annual reports, and other special publications appropriate to this grouping such as wall charts, pocket cards, and bibliographies.

Special subject-matter subseries include Semiconductor Measurement Technology (SP400– ), Standard Reference Materials (SP260– ), and Precision Measurement and Calibration (SP300– ).

APPLIED MATHEMATICS SERIES—mathematical tables, manuals, and studies of special interest to physicists, engineers, chemists, biologists, mathematicians, computer programmers, and others engaged in scientific and technical work.

NATIONAL STANDARD REFERENCE DATA SERIES—provides quantitative data on the physical and chemical properties of materials, compiled from the world's literature and critically evaluated. Developed under a worldwide program coordinated by NBS, under authority of National Standard Data Act (Public Law 90-396). This series supplements the JPCRD, see also Section 3.4.

BUILDING SCIENCE SERIES—disseminates technical information developed at the Bureau on building materials, components, systems, and whole structures. The series presents research results, test methods, and performance criteria related to the structural and environmental functions and the durability and safety characteristics of building elements and systems.

TECHNICAL NOTES—studies or reports which are complete in themselves but restrictive in their treatment of a subject. Analogous to monographs but not so comprehensive in scope or definitive in treatment of the subject area. Often serve as a vehicle for final reports of work performed at NBS under the sponsorship of other government agencies.

Special subject-matter subseries include Optical Radiation Measurements (TN594– ) and Self Calibrations Manual for Optical Radiation (TN910– ).

COMMERCIAL STANDARDS AND SIMPLIFIED PRACTICE RECOMMENDATIONS. See Voluntary Product Standards below.

VOLUNTARY PRODUCT STANDARDS—developed under procedures published by the Department of Commerce in Part 10, Title 15, of the Code of Federal Regulations. The purpose of the standards is to establish nationally recognized requirements for products, and to provide all concerned interests with a basis for common understanding of the characteristics of the products. The National Bureau of Standards administers the Voluntary Product Standards program as a supplement to the activities of the private sector standardizing organizations.

FEDERAL INFORMATION PROCESSING STANDARDS PUBLICATIONS (FIPS PUBS)—publications in this series collectively constitute the Federal Information Processing Standards Register. Register serves as the official source of information in the Federal Government regarding standards issued by NBS pursuant to the Federal Property and Administrative Services Act of 1949 as amended, Public Law 89-306 (79 Stat. 1127), and as implemented by Executive Order 11717 (38 FR 12315, dated May 11, 1973) and Part 6 of Title 15 CFR (Code of Federal Regulations).

Public distribution of FIPS PUBS is by purchase from the National Technical Information Service, Springfield, VA 22161.

CONSUMER INFORMATION SERIES—practical information, based on NBS research and experience, covering areas of interest to the consumer. Easily understandable language and illustrations provide useful background knowledge for shopping in today's technological marketplace.

### 1.4. NBS INTERAGENCY REPORTS

A special series of interim or final reports on work performed by NBS for outside sponsors (both government and non-government). In general, initial distribution is handled by the sponsor; public distribution is by the National Technical Information Service (Springfield, VA 22161) in paper copy or microfiche form. (See pages XVIII to XLIII.)

### 1.5. GRANTEE/CONTRACTOR REPORTS AND PATENTS

Grantee/contractor reports are prepared by non-NBS persons or organizations working under grant or contract from the National Bureau of Standards. Those contract reports not incorporated into the formal NBS publication series are available directly from the National Technical Information Service (NTIS), Springfield, VA 22161, in paper copy or microfiche form unless otherwise stated. When ordering a report from NTIS you must order it by the "COM, PB, AD, or N" number as indicated.

Patents are obtained on NBS inventions of high commercial potential, in order to establish Government ownership of the patent rights. The patents are then made available for the grant of nonexclusive licenses to all qualified applicants. A limited exclusive license may be granted under a particular patent, however, if it appears that some period of exclusivity is necessary as an incentive for the investment of risk capital. For information on licensing any of the NBS held patents, write to the Office of the Legal Adviser, National Bureau of Standards, Washington, DC 20234. Copies of patents may be obtained from the U.S. Patent and Trademark Office, Washington, DC 20231 for 50 cents each.

### 1.6. NBS BIBLIOGRAPHIC SUBSCRIPTION SERVICES

The Cryogenic Data Center of the National Bureau of Standards, Boulder, CO has developed specialized bibliographic issuances designed to provide interested audiences with information on latest developments in certain specialized fields. These issuances, together with subscription information, are listed below:

**CRYOGENIC DATA CENTER CURRENT AWARENESS SERVICE** (Publications and Reports of Interest in Cryogenics). A literature survey issued weekly. Annual subscription: Domestic, $25.00; Foreign, $30.00.

**LIQUEFIED NATURAL GAS.** A literature survey issued quarterly. Annual subscription: $20.00.

**SUPERCONDUCTING DEVICES AND MATERIALS.** A literature survey issued quarterly. Annual subscription: $30.00.

Send subscription orders and remittances for the preceding bibliographic services to the National Bureau of Standards, Cryogenic Data Center (736.00), Boulder, CO 80303.

### 1.7. PAPERS PUBLISHED BY OTHERS

Many significant contributions by NBS authors are published in other journals. Up-to-date listings of these articles are carried regularly in the Journal of Research and the annual publications catalog (NBS SP305), along with abstracts, key words, and author/subject indexes. Except for the author index, the complete citations for years 1966–1976 have been reprinted in this two-volume catalog.

## 2. PURCHASE PROCEDURES AND DOCUMENT AVAILABILITY

### 2.1. PURCHASE PROCEDURES

Many recent publications of the Bureau are available from the Superintendent of Documents, U.S. Government Printing Office, Washington, DC 20402, at the prices listed in this publication. However prices are subject to change without notice. You may also order through the U.S. Department of Commerce Field Office nearest you. Microfiche copies of all recent NBS publications, and paper copies of many non-periodicals, may be ordered through the National Technical Information Service, U.S. Department of Commerce, Springfield, VA 22161. Note that three of the non-periodical series are available only from NTIS; these are FIPS PUBS., NBS Interagency Reports (NBSIR's), and Grantee/Contractor Reports (GCR's). This section includes current price lists of available publications, plus instructions on how to acquire reprints of articles by NBS authors, and how to get out-of-print material.

**How To Make Remittances.** Remittances for publications for which individual sales or subscription prices are shown should be mailed to Superintendent of Documents, U.S. Government Printing Office, Washington, DC 20402, by postal money order, express money order, or check. Postage stamps will not be accepted. Publications cannot be mailed before remittances are received. *Foreign remittances should be made either by international money order, draft on an American bank or UNESCO coupons.*

The letter symbol, publication number, full title of the publication, SD catalog or SD stock number MUST be given when ordering. The Superintendent of Documents allows a discount of 25 percent on orders of 100 or more copies of one publication.

Persons who make frequent purchases from the Superintendent of Documents may find a deposit account convenient. Deposits of $50 or more are accepted against which orders may be placed without making individual remittances or first obtaining quotations. Order blanks are furnished for this purpose. After the order has been processed, the order itself is returned, showing the publications supplied, explanations regarding those not sent, the amount of charge, and the balance on deposit.

No charge is made for postage on documents sent to points in the United States and its possessions. In computing foreign postage, the charge is approximately one-fourth of the current selling price of the publication. The charge is to cover the special handling required to comply with the customs and international mailing regulations.

**How To Make Remittances to NTIS.** Orders for publications purchased from the National Technical Information Service (NTIS) must be accompanied by postal money order, express money order, or check made out to the NTIS and covering total cost of the publications order. All inquiries or orders should be addressed to: National Technical Information Service, Springfield, VA 22161.

## 2.2. ANNOUNCEMENT OF NBS PUBLICATIONS

The National Bureau of Standards and the agencies mentioned below regularly issue the following official announcements dealing with NBS publications.

**DIMENSIONS/NBS.** Issued monthly by the National Bureau of Standards. In addition to publishing technical news of the Bureau, this periodical announces selected new publications in an NBS series. Available from the Superintendent of Documents, U.S. Government Printing Office, Washington, DC 20402. Annual subscription, $11.00; $13.75 foreign. Single copies, $1.10 domestic; $1.40 foreign each.

**NBS JOURNAL OF RESEARCH.** The Journal carries a listing of all NBS publications as issued. See Section 2.6 for subscription information.

*Monthly Catalog of United States Government Publications.* Issued monthly by the Superintendent of Documents, U.S. Government Printing Office, Washington, DC 20402. Annual subscription, with consolidated annual index, $45.00; $56.00 foreign.

*Selected List of U.S. Government Publications.* Issued monthly by the Superintendent of Documents. Each list is arranged by subject, with annotations, prices, and order form. May be obtained free from the U.S. Government Printing Office, Superintendent of Documents, Mail List Section, Stop SSOM, Washington, DC 20402.

*Business Service Check List.* Bi-weekly announcement of publications of the Department of Commerce. Lists titles and prices of National Bureau of Standards publications, as well as those of other offices of the Department of Commerce. Available from the Superintendent of Documents, U.S. Government Printing Office, Washington, DC 20402. Annual subscription, $9.00; $11.25 foreign.

*NBS Publications Newsletter.* This newsletter is issued approximately six times a year.

It presents full citations, including abstracts and availability information, for NBS papers announced during the report period. Its primary audience includes librarians, documentalists and science information specialists. However, other NBS audiences also find it useful as a guide to new NBS publications.

Contact: Editor, NBS Publications Newsletter, Technical Information and Publications Division, National Bureau of Standards, Washington, DC 20234.

## 2.3. CATALOGS OF NBS PUBLICATIONS

The following constitute a complete list of the titles of the Bureau's publications through December 31, 1977. The catalogs are available from the Superintendent of Documents, U.S. Government Printing Office, Washington, DC 20402, unless otherwise stated, or may be consulted in a library which maintains sets of National Bureau of Standards publications. Note that all citations in NBS SP305 and its Supplements 1 through 8 are accumulated into this two-volume catalog.

| | |
|---|---|
| Circular 460: Publications of the National Bureau of Standards 1901 to June 30, 1947. 375 pages including subject and author indexes. Brief abstracts are included for the period January 1, 1941 to June 30, 1947 | * |
| Supplement to Circular 460: Publications of the National Bureau of Standards, July 1, 1947 to June 30, 1957. 373 pages, including subject and author indexes | * |
| Miscellaneous Publication 240: Publications of the National Bureau of Standards, July 1, 1957 to June 30, 1960. First NBS Catalog to include Titles of Papers Published in Outside Journals 1950 to 1959. 391 pages, including subject and author indexes | * |
| Supplement to Miscellaneous Publication 240: Publications of the National Bureau of Standards published by NBS, July 1960 through June 1966; published by others, 1960 through 1965. 740 pages, including subject and author indexes | * |
| Special Publication 305: Publications of the National Bureau of Standards, published by NBS, July 1966 through December 1967; published by others, 1966–1967. 223 pages, a citation of titles and abstracts, with key words and author indexes | * |
| Supplement 1 to Special Publication 305: Publications of the National Bureau of Standards, 1968 through 1969. 497 pages, a citation of titles and abstracts, with key words and author indexes | * |
| Supplement 2 to Special Publication 305: Publications of the National Bureau of Standards, 1970. 378 pages, a citation of titles and abstracts, with key words and author indexes | * |
| Supplement 3 to Special Publication 305: Publications of the National Bureau of Standards, 1971. 342 pages, a citation of titles and abstracts, with key words and author indexes | * |
| Supplement 4 to Special Publication 305: Publications of the National Bureau of Standards, 1972. 449 pages, a citation of titles and abstracts, with key words and author indexes | $4.20 |
| Supplement 5 to Special Publication 305: Publications of the National Bureau of Standards, 1973. 349 pages, a citation of titles and abstracts, with key words and author indexes | $4.15 |
| Supplement 6 to Special Publication 305: Publications of the National Bureau of Standards, 1974. 523 pages, a citation of titles and abstracts, with key words and author indexes | $6.80 |
| Supplement 7 to Special Publication 305: Publications of the National Bureau of Standards, 1975. 595 pages, a citation of titles and abstracts, with key words and author indexes | $7.55 |
| Supplement 8 to Special Publication 305: Publications of the National Bureau of Standards, 1976. 728 pages, a citation of titles and abstracts, with key words and author indexes | $8.25 |
| Supplement 9 to Special Publication 305: Publications of the National Bureau of Standards, 1977. 601 pages, a citation of titles and abstracts, with key words and author indexes | $8.00 |

---

* Available by purchase from the National Technical Information Service, Springfield, VA 22161.

## 2.4. FUNCTIONS OF DEPOSITORY LIBRARIES IN THE UNITED STATES

The Superintendent of Documents, United States Government Printing Office, is authorized by law to furnish Government publications to designated depository libraries.

Under provisions of Title 44 of the United States Code, certain libraries are designated depositories for Government publications. Through them, Federal Government documents are made available to residents of every State, District of Columbia, Guam, Puerto Rico, and the Virgin Islands. Distribution to the libraries is made by the Office of the Superintendent of Documents.

It is sometimes impossible to obtain desired publications by purchase from the Superintendent of Documents. Stocks may have been exhausted or the document may be permanently out of print. In these instances the depositories render an invaluable service by keeping such publications permanently available. Every Government publication cannot be consulted at all depository libraries. Designated Regional Depositories are required to receive and retain one copy of all Government publications made available to depository libraries either in printed or microfacsimile form. All other libraries are allowed to select the classes of publications best suited to the interest of their particular clientele.

These libraries are now receiving selected publication series of the National Bureau of Standards for general reference use. Whether a given library has a copy of a particular publication can be determined by inquiring at the library.

## 2.5. FUNCTIONS OF U.S. DEPARTMENT OF COMMERCE DISTRICT OFFICES

Department of Commerce District Offices provide ready access, at the local level, to the services of the Department of Commerce as well as to its reports, publications, statistical statements, and surveys. Each District Office serves as an official sales agent of the Superintendent of Documents, U.S. Government Printing Office, making available for purchase locally a wide range of Government publications. The reference library maintained by each District Office contains many Government and private publications, periodicals, directories, reports, and other reference materials.

## 2.6. AVAILABILITY OF NBS PUBLICATIONS

### A. PERIODICAL SUBSCRIPTION RATES

| Periodical | Domestic [1] | Foreign [2] |
|---|---|---|
| Journal of Research of the National Bureau of Standards: Effective July 1977 issued bimonthly as single section. Separate Sections A and B discontinued with the June 1977 issues. Paper covers.... | $17.00 | $21.25 |
| Bound volume (1 volume per year), blue buckram ........... | (3) | (3) |
| DIMENSIONS/NBS, issued 10 times per year ................. | $11.00 | $13.75 |

NOTE—Send order, with remittance, to Superintendent of Documents, U.S. Government Printing Office, Washington, D.C. 20402.

[1] United States and its possssions.

[2] Foreign price incudes the cost of the publication and postage.

(3) Prices of the bound volumes vary. The Superintendent of Documents will furnish prices on request.

### B. SUPERSEDED NBS REFERENCE PUBLICATIONS

Those NBS publications not listed in the Price Lists are out of print and are not available from the Superintendent of Documents. Many can be consulted at libraries. Also, in many cases, photoduplicated copies can be purchased from the Library of Congress. For full information concerning this service, write to the Photoduplication Service, Library of Congress, Washington, DC 20540.

Certain NBS publications are out of print because they have been replaced, or partially replaced, by material issued by other organizations. In this connection NBS is able to offer the following information:

*Circular 410, National Standard Petroleum Oil Tables.* Information in this Circular has been incorporated in the ASTM–IP Petroleum Measurement Tables issued as D1250 by the American Society for Testing and Materials, 1916 Race Street, Philadelphia, PA 19103. Available at $12.75, 20% off to ASTM members. Tables 5 and 7 of the ASTM–IP Tables may also be purchased from the ASTM in separate reprint form at $2.25 and $2.00 per copy respectively.
*Circular 438, Static Electricity.* The National Fire Protection Association, 60 Batterymarch Street, Boston, MA 02110, has issued a publication by the same title, available from them as NFPA Publication 77, at $3.00.

*Circular 499, Nuclear Data.* Replaced by Atomic and Nuclear Data Tables, published by Academic Press, 111 Fifth Avenue, New York, NY 10003. Available by subscription for $108.00 per year.

*Circular 564, Tables of Thermal Properties of Gases.* A reprinted edition is available from University Microfilms, Inc., Ann Arbor, MI 48106. Order as OP 12,192 for $56.80. Microfiche of this Circular is available from Cryogenic Data Center, National Bureau of Standards, Boulder, CO 80302.

*Circular 576, Automotive Antifreezes.* For information on this subject consult American National Standards Institute, 1430 Broadway, New York, NY 10018.

*Circular 577 and Supplement, Energy Loss and Range of Electrons and Positrons.* These have been superseded by NASA Special Publication

3012, available from the National Technical Information Service, Springfield, VA 22161, at $6.75 hardcopy and $3.00 microfiche number N65–12506.

*Miscellaneous Publication 179, American Standard Building Code Requirements for Minimum Design Loads in Buildings and Other Structures.* The American National Standards Institute, 1430 Broadway, New York, NY 10018, has issued a publication on this subject. Available from them as A58.1–1969–1972, at $7.50.

*Miscellaneous Publication 187, Directory of Commercial and College Laboratories.* A new Directory of Testing Laboratories issued as 333D is published by the American Society for Testing and Materials, 1916 Race Street, Philadelphia, PA 19103, at $3.75.

*Miscellaneous Publication 211, American Standards Building Code Requirements for Masonry.* The American National Standards Institute, 1430 Broadway, New York, NY 10018, has issued a publication on this subject. Available from them as A41.1–1953–R1970, at $4.50.

*NBS Handbook 28, Part 1, 2, and 3, Screw Thread Standards.* Responsibility for screw thread standards for Federal Government has been transferred to General Services Administration (GSA). Standards will be promulgated as Federal Standard 28 by GSA. Technical Questions should be addressed to Mr. John McGlone, Directorate of Engineering and Standardization, Defense Logistics Agency (DISC), 700 Robbins Ave., Philadelphia, PA 19111, telephone (215) 697–4349. Questions regarding administration of the program should be addressed to Mr. Grant Beattie, Standards Control and Support Division, General Services Administration (Federal Supply Service), attn: FMHS, Washington, DC 20406, telephone (703) 557–0506.

*Handbook 30, National Electrical Safety Code (also H81 and its Supplements and H110–1).* All NBS publications on this subject have been superseded by National Electrical Safety Code, 1977 Edition, issued by the American National Standards Institute, 1430 Broadway, New York, NY 10018. Available from them as ANSI C2, at $6.50.

*Handbook 46, Code for Protection Against Lightning.* A United States of America Standards Institute Code for Protection Against Lightning (NFPA–78–1969) is available from the American National Standards Institute, 1430 Broadway, New York, NY 10018, at $4.25, as C5.1–1969–1975.

*Handbook 48, Control and Removal of Radioactive Contamination in Laboratories.* Reprints of this Handbook can be purchased as NCRP Report at $3.00 from NCRP Publications, Post Office Box 30175, Washington, DC 20014.

*Handbook 49, Recommendations for Waste Disposal of Phosphorus–32 and Iodine–131 for Medical Users.* Reprints of this Handbook can be purchased as NCRP Report 9 at $3.00 from NCRP Publications, Post Office Box 30175, Washington, DC 20014.

*Handbook 53, Recommendations for the Disposal of Carbon–14 Wastes.* Reprints of this Handbook can be purchased as NCRP Report 12 at $3.00 from NCRP Publications, Post Office Box 30175, Washington, DC 20014.

*Handbook 55, Protection Against Betatron-Synchrotron Radiations up to 100 Million Electron Volts.* February 26, 1954 has been combined with NBS Handbook 97. Available as NCRP Report 51, Radiation Protection Design Guidelines for 0.1–100 MeV Particle Accelerator Facilities from NCRP Publications, Post Office Box 30175, Washington, DC 20014 at $6.00.

*Handbook 58, Radioactive Waste Disposal in the Ocean.* Reprints of this Handbook can be purchased as NCRP Report 16 at $3.00 from NCRP Publications, Post Office Box 30175, Washington, DC 20014.

*Handbook 59, Permissible Dose from External Sources of Ionizing Radiations.* Reprints of this Handbook can be purchased as NCRP Report 39 at $5.00 per copy from NCRP Publications, Post Office Box 30175, Washington, DC 20014.

*Handbook 63, Protection Against Neutron Radiation up to 30 MeV.* Reprints of this Handbook can be purchased as NCRP Report 38 at $6.00 per copy from NCRP Publications, Post Office Box 30175, Washington, DC 20014.

*Handbook 65, Safe Handling of Bodies Containing Radioactive Isotopes.* Reprints of this Handbook can be purchased as NCRP Report 37 at $4.00 per copy from NCRP Publications, Post Office Box 30175, Washington, DC 20014.

*Handbook 69, Maximum Permissible Body Burdens and Maximum Permissible Concentrations of Radionuclides in Air and in Water for Occupational Exposure.* Reprints of this Handbook can be purchased at $3.00 per copy from NCRP Publications, Post Office Box 30175, Washington, DC 20014.

*Handbook 71, Specifications for Dry Cells and Batteries.* Available as C18.1–1972 from the American National Standards Institute, 1430 Broadway, New York, NY 10018, at $6.25.

*Handbook 73, Protection Against Radiations from Sealed Gamma Sources* (Supersedes H54). Reprints of this Handbook can be purchased as NCRP Report 40 at $5.00 per copy from NCRP Publications, Post Office Box 30175, Washington, DC 20014.

*Handbook 74, Building Code Requirements for Reinforced Masonry.* The American National Standards Institute, 1430 Broadway, New York, NY 10018 has issued a publication on this subject. Available from them as A41.2–1960 (R1970), at $3.25.

*Handbook 75, Measurement of Absorbed Dose of Neutrons and of Mixtures of Neutrons and Gamma Rays.* Reprints of this Handbook can be purchased as NCRP Report 25 at $3.00 per copy from NCRP Publications, Post Office Box 30175, Washington, DC 20014.

*Handbook 76, Medical X-ray Protection Up to Three Million Volts.* Now available as NCRP 33. Purchase from NCRP Publications, Post Office Box 30175, Washington, DC 20014 at $4.00.

*Handbook 80, A Manual of Radioactivity Procedures.* Reprints of this Handbook will be available as NCRP Report 58 (in press). For more information write to NCRP Publications, Post Office Box 30175, Washington, DC 20014.

*Handbook 81 and Its Supplements, Safety Rules for the Installation and Maintenance of Electric Supply and Communication Lines* (also H30 and H110–1). All NBS publications on this subject have been superseded by National Electrical Safety Code, 1977 Edition, issued by the American National Standards Institute, 1430 Broadway, New York, NY 10018. Available from them as ANSI C2, at $6.50.

*Handbook 84, Radiation Quantities and Units.* Reprints of this Handbook can be purchased as ICRU Report 19 at $5.00 per copy from ICRU Publications, Post Office Box 30165, Washington, DC 20014.

*Handbook 89, Methods of Evaluating Radiological Equipment and Materials.* Reprints of this Handbook can be purchased as ICRU Report 10F at $2.50 per copy from ICRU Publications, Post Office Box 30165, Washington, DC 20014.

*Handbook 96, Inspection of Processed Photographic Record Films for Aging Blemishes.* Reprints of this Handbook can be purchased as PH 1.28–1973 at $4.00 per copy from the American National Standards Institute, 1430 Broadway, New York, NY 10018.

*Handbook 97, Shielding for High-Energy Electron Accelerator Installations.* July 1, 1964 has been combined with NBS Handbook 55. Available as NCRP Report 51, Radiation Protection Design Guidelines for 0.1–100 MeV Particle Accelerator Facilities from NCRP Publications, Post Office Box 30175, Washington, DC 20014 at $6.00.

*Handbook 102, ASTM Metric Practice Guide.* Available as Z 210.1–1976 from the American National Standards Institute, 1430 Broadway, New York, NY 10018 at $4.00.

*Handbook 110–1, National Electrical Safety Code.* Part 1. Rules for Installation and Maintenance of Electric Supply and Communication Lines (also H30 and H81 and its Supplements). All NBS publications on this subject have been superseded by National Electrical Safety Code, 1977 Edition, issued by the American National Standards Institute, 1430 Broadway, New York, NY 10018. Available from them as ANSI C2, at $6.50.

*Technical Note 938, Recommended Practice for the Use of Metric (SI) Units in Building Design and Construction,* has been superseded by ASTM E 621–78, Standard Practice of the Use of Metric (SI) Units in Building Design and Construction. It is available from the American Society for Testing and Materials, 1916 Race Street, Philadelphia, PA 19103. Price $5.00.

## C. STATUS OF PUBLICATIONS CITED IN THIS DOCUMENT

The following list provides the current status of NBS-issued publications cited in this 11-year compilation, including those that have been superseded and those that are still in print at the Government Printing Office (GPO) or the National Technical Information Service (NTIS). NBS publications still available from the Superintendent of Documents, GPO, carry prices effective as of the date of this publication; but these prices are subject to change without notice. Publications shown as available from NTIS are represented by the NTIS price schedule in effect at the time of purchase. NTIS prices as of this date are given below. Again, prices are subject to change.

Publications not listed are out of print; the abstracts have been included in this catalog for information purposes. Your nearest regional depository library may still have copies of these items. (See Section 2.4.)

### NTIS PRICE SCHEDULE

**Customers in Canada, U.S., and Mexico please use this price schedule; other addressees write for Folder PR-360-4.**

| | | | | | |
|---|---|---|---|---|---|
| A01 | $3.00 | E01 | $3.25 | T01 | $110.00 |
| A02 | 4.00 | E02 | 4.75 | T02 | 125.00 |
| A03 | 4.50 | E03 | 6.25 | T03 | 175.00 |
| A04 | 5.25 | E04 | 7.50 | T04 | 250.00 |
| A05 | 6.00 | E05 | 9.00 | T05 | 300.00 |
| A06 | 6.50 | E06 | 10.50 | T06 | 350.00 |
| A07 | 7.25 | E07 | 12.50 | T07 | 400.00 |
| A08 | 8.00 | E08 | 15.00 | T08 | 450.00 |
| A09 | 9.00 | E09 | 17.50 | T09 | 500.00 |
| A10 | 9.25 | E10 | 20.00 | T10 | 550.00 |
| A11 | 9.50 | E11 | 22.50 | T11 | 600.00 |
| A12 | 10.75 | E12 | 25.00 | T12 | 650.00 |
| A13 | 11.00 | E13 | 28.00 | T13 | 675.00 |
| A14 | 11.75 | E14 | 31.00 | T14 | 750.00 |
| A15 | 12.00 | E15 | 34.00 | T15 | 800.00 |
| A16 | 12.50 | E16 | 37.00 | T16 | 850.00 |
| A17 | 13.00 | E17 | 40.00 | T17 | 900.00 |
| A18 | 13.25 | E18 | 45.00 | T18 | 950.00 |
| A19 | 14.00 | E19 | 50.00 | T19 | 1,000.00 |
| A20 | 14.50 | E20 | 60.00 | T99 | * |
| A21 | 15.00 | E99 | * | | |
| A22 | 15.25 | | | | |
| A23 | 15.50 | N01 | 28.00 | | |
| A24 | 16.25 | N02 | 50.00 | | |
| A25 | 16.50 | | | | |
| A99 | * | | | | |

*Contact NTIS for price quote

## MONOGRAPHS

| No. | Price |
|---|---|
| 2 (PB187-752) | * |
| 3 Vol. 1 | * |
| (COM71-01000-1) | * |
| 3 Vol. 2 | * |
| (COM71-01000-2) | * |
| 4 (PB-174-987) | * |
| 7 (COM73-10503) | * |
| 8 (PB186-237) | * |
| 10 (COM75-10235) | * |
| 13 (PB172-156) | * |
| 15 (PB192-874) | * |
| 20 (PB195-221) | * |
| 23 (PB183-992) | * |
| 25 Sec. 1 (PB178-429) | * |
| 25 Sec. 2 (PB178-430) | * |
| 25 Sec. 3 (PB178-431) | * |
| 25 Sec. 4 | * |
| 25 Sec. 5 | * |
| 25 Sec. 6 | * |
| 25 Sec. 7 | * |
| 25 Sec. 8 (PB194-872) | * |
| 25 Sec. 9 (COM72-50002) | * |
| 25 Sec. 10 (COM72-51079 | * |
| 25 Sec. 11 (COM74-50183) | * |
| 25 Sec. 12 (SN003-003-01376-5) | 1.50 |
| **25 Sec. 13 (SN003-003-01629-2)** | **1.80** |
| 27 & Suppls. See SP373 (COM72-51036) | * |
| 30 (PB193-908) | * |
| 31 (COM75-10045) | * |
| 34 Vol. 1 (COM71-00631) | * |
| 34 Vol. 2 | * |
| 36 (COM75-10175) | * |
| 39 (COM74-10933) | * |
| 40 (COM71-00693) | * |
| 41 (PB191-728) | * |
| 42 (COM72-10377) | * |
| 43 Vol. 1 (COM73-10636 | * |
| 43 Vol. 2 (COM73-10637) | * |
| 45 (PB186-433) | * |
| 46 (PB176-590) | * |
| 47 (COM71-00691) | * |
| 48 (PB246-865) | * |
| 49 (COM72-10380) | * |
| 52 (COM73-10500) | * |
| 54 (PB265-333) | * |
| 56 (COM75-10244) | * |
| 58 (PB193-909) | * |
| 60 (COM75-10053) | * |
| 63 (COM74-10737) | * |
| 66 (COM75-10245) | * |
| 67 (PB186-426) | * |
| 68 (COM71-00692) | * |
| 70 Vol. 1 (PB168-072) | * |
| 70 Vol. 2 (PB189-714) | * |
| 70 Vol. 3 (COM74-10794) | * |
| 70 Vol 4 (COM74-10795) | * |
| 70 Vol. 5 (COM74-10796) | * |
| 72 (PB186-427) | * |
| 73 (PB186-432) | * |
| 74 (PB195-213) | * |
| 75 | * |
| 76 (COM73-10502) | * |
| 77 (PB180-646) | * |
| 80 (PB257-342) | * |
| 82 (PB189-659) | * |
| 83 (COM75-10246) | * |
| 84 (COM72-10513) | * |
| 85 (COM72-10379) | * |
| 86 (COM75-10046) | * |
| 88 (SN003-003-00354-9) | 1.05 |
| 89 (AD700-466) | * |
| 91 (PB266-262) | * |
| 92 | * |
| 93 (COM73-10008) | * |
| 94 (N65-32001) | * |
| 96 | * |
| 98 | * |
| 99 | * |
| 100 | * |
| 101 | * |
| 102 | * |
| 103 | * |
| 104 | * |
| 105 | * |
| 106 | * |
| 107 | * |
| 109 (AD681-912) | * |
| 111 | * |
| 112 | * |
| 113 Vol. 1 (PB191-276) | * |
| 113 Vol. 2 (SN003-003-00304-2) | 1.65 |
| 113 Vol. 3 (PB192-746) | * |
| 116 | * |
| 117 (SN003-003-00751-0) | .55 |
| 118 (PB194-751) | * |
| 119 (COM71-50201) | * |
| 120 (SN003-003-00749-8) | .85 |
| 121 (COM75-10169) | * |
| 124 (COM74-11728 | * |
| 125 (SN003-003-01177-1) | 4.55 |
| 125 Sup. 1 (SN003-003-01391-9) | 1.05 |
| 126 (SN003-003-01052-9) | 2.10 |
| 127 (COM72-50359) | * |
| 128 (COM72-50903) | * |
| 129 (COM73-50098) | * |
| 130 (SN003-003-01120-7) | 1.10 |
| 131 (SN003-003-01076-6) | 10.70 |
| 132 (SN003-003-01082-1) | 15.80 |
| 133 (COM74-50309) | * |
| 134 (COM73-50582) | * |
| 135 (SN003-003-01157-6) | .85 |
| 136 (SN003-003-01160-6) | .50 |
| 137 (COM73-50960) | * |
| 138 (COM74-50459) | * |
| 139 (SN003-003-01317-0) | 1.35 |
| 140 (SN003-003-01202-5) | 9.20 |
| 141 (SN003-003-01289-1) | 5.50 |
| 142 (SN003-003-01290-4) | 5.45 |
| 143 (SN003-003-01373-1) | 1.10 |
| 144 (SN003-003-01416-8) | 5.05 |
| 145 Pt. 1 (SN003-003-01337-4) | 8.55 |
| 145 Pt. 2 (SN003-003-01338-2) | 6.80 |
| 146 (COM75-50997) | * |
| 147 (SN003-003-01412-5) | 2.15 |
| **147 Sup. 1 (SN003-003-01754-0)** | **1.10** |

## MONOGRAPHS (Continued)

| No. | Price | No. | Price | No. | Price |
|---|---|---|---|---|---|
| 48 (SN003-003-01370-6) | 1.15 | 153 (SN003-003-01651-9) | 1.35 | | |
| 49 (SN003-003-01390-1) | 1.35 | 154 (SN003-003-01612-8 | 1.70 | | |
| 50 (SN003-003-02187-3) | 1.40 | 157 (SN003-003-01681-1) | 4.55 | | |
| 51 (SN003-003-01621-7) | 4.50 | | | | |
| 52 (SN003-003-01552-1) | .85 | | | | |

*Available from The National Technical Information Service; use "PB", "AD", "COM", or NBS publication identification if no specific NTIS number is assigned. Available in Microfiche for $3.00; consult NTIS for paper copy price.

## MISCELLANEOUS PUBLICATIONS

| No. | Price | No. | Price | No. | Price |
|---|---|---|---|---|---|
| 179 | * | 260-11 | ** | 286 | *** |
| 187 | * | 260-12 | ** | 287 | ** |
| 211 (COM73-10871) | ** | 260-13 | ** | 291 | ** |
| 240 | ** | 260-14 | ** | 292 | ** |
| 240 Suppl | ** | 262-1 (PB261-051) | ** | 294 | ** |
| 256 (PB285-882) | ** | 262-2 (AD647-371) | ** | This series name was changed to Special Publications beginning with SP295 | |
| 260-1 (COM74-11061) | ** | 265 (COM74-10927) | ** | | |
| 260-2 (COM74-11063) | ** | 266 (PB168-063) | ** | | |
| 260-3 (COM74-11060) | ** | 269 (PB258-618) | ** | | |
| 260-4 (COM74-11059) | ** | 273 (COM75-11102) | ** | | |
| 260-5 (PB168-068) | ** | 274 | ** | | |
| 260-6 (COM74-11068) | ** | 275 (SN003-003-01266-1) | 8.50 | | |
| 260-7 (COM74-11067) | ** | 281 | ** | | |
| 260-8 (COM74-11066) | ** | 284 | ** | | |
| 260-9 (COM74-11065) | ** | | | | |
| 260-10 (COM74-11064) | ** | | | | |

*See page XVIII for additional information.

**Available from The National Technical Information Service; use "AD", "PB", "COM", or NBS publication identification if no specific NTIS number is assigned. Available in Microfiche for $3.00; consult NTIS for paper copy price.

***Superseded by NBS LC1071, free upon request from the Technical Information and Publications Division, National Bureau of Standards, Washington, DC 20234.

## SPECIAL PUBLICATIONS

| No. | Price |
|---|---|
| 250, 1978 Ed. (SN003-003-01916-0) | 3.00 |
| 260 (SN003-003-01445-1) | 1.50 |
| 260-16 (COM74-11062) | * |
| 260-18 | * |
| 260-19 (PB190-071) | * |
| 260-21 (COM74-11359) | * |
| 260-22 (COM74-11357) | * |
| 260-23 (COM71-00157) | * |
| 260-24 (COM72-50058) | * |
| 260-25 (COM74-11356) | * |
| 260-26 (SN003-003-00786-2) | .85 |
| 260-27 (COM74-11358) | * |
| 260-28 (COM71-50365) | * |
| 260-29 (COM71-50282) | * |
| 260-30 (COM71-50283) | * |
| 260-30 (COM71-50563) | * |
| 260-32 (SN003-003-01213-1 | .55 |
| 260-33 (COM72-50526) | * |
| 260-34 (COM72-50371) | * |
| 260-35 (COM72-50368) | * |
| 260-36 (COM72-50527) | * |
| 260-37 (COM72-50092) | * |
| 260-38 (COM72-50528) | * |
| 260-39 (COM72-50529) | * |
| 260-40 (COM72-50776) | * |
| 260-41 (COM72-50775) | * |
| 260-42 (COM72-50944) | * |
| 260-43 (COM73-50760) | * |
| 260-44 (COM73-50037) | * |
| 260-45 (COM73-50226) | * |
| 260-46 (SN003-003-01385-4) | 1.00 |
| 260-47 (COM74-50176) | * |
| 260-48 (SN003-003-01278-5) | .60 |
| 260-49 (SN003-003-01344-7) | .75 |
| 260-50 (SN003-003-01425-7) | 1.00 |
| 260-51 (SN003-003-01481-8) | 1.90 |
| 260-52 (SN003-003-01464-8) | 1.05 |
| 260-53 (SN003-003-01551-2) | 1.05 |
| 295 | * |
| 296 | * |
| 299 | * |
| 300 Vol. 1 (SN003-003-00072-8) | 9.00 |
| 300 Vol. 2 | * |
| 300 Vol. 3 (SN003-003-00074-4) | 8.05 |
| 300 Vol. 4 (SN003-003-00778-1) | 7.65 |
| 300 Vol. 5 (SN003-003-00916-4) | 8.65 |
| 300 Vol. 6 (SN003-003-00696-3) | 7.10 |
| 300 Vol. 7 (SN003-003-00887-7) | 9.65 |
| 300 Vol. 8 (SN003-003-00923-7) | 8.75 |
| 300 Vol. 9 (SN003-003-00917-2) | 7.65 |
| 300 Vol. 10 (SN003-003-01179-7) | 11.80 |
| 301 | * |
| 302 | * |
| 303 | * |
| 304 (SN003-003-01072-3) | .65 |
| 304A (SN003-003-01713-2) | .50 |
| 305 | * |
| 305 Sup. 1 (PB259-274) | * |
| 305 Sup. 2 (COM71-50354) | * |
| 305 Sup. 3 (COM72-50690) | * |
| 305 Sup. 4 (SN003-003-01081-2) | 4.20 |
| 305 Sup. 5 (SN003-003-01240-8) | 4.15 |
| 305 Sup. 6 (SN003-003-01361-7) | 6.80 |
| **305 Sup. 7 (SN003-003-01647-1)** | 7.55 |
| 306 | * |
| 306-2 | * |
| 306-3 (PB264-245) | * |
| 306-4 (COM73-10870) | * |
| 307 | * |
| 309 Vol. 2 | * |
| 310 | * |
| 312 (Vol. 1&2 (COM73-11439) | * |
| 313 | * |
| 314 (SN003-003-00091-4) | 6.45 |
| 317 Vol. 1 (COM71-50268-01) | * |
| 317 Vol. 2 (COM71-50268-02) | * |
| 319 (COM71-00066) | * |
| 320 (AD701-614) | * |
| 320 Sup. 1 (AD730-356) | * |
| 320 Sup. 2 (COM74-50034) | * |
| 321 (PB194-963) | * |
| 323 (COM72-50351) | * |
| 324 (COM71-50070) | * |
| 326 (COM71-50189) | * |
| 327 (PB193-564) | * |
| 329 (COM71-50172) | * |
| 329 Sup. 1 (COM73-50679) | * |
| 329 Sup. 2 (SN003-003-01362-5) | 9.35 |
| 330 **1977 Ed.** (SN003-003-01784-1) | 1.70 |
| 331 | * |
| 332 (PB194-959) | * |
| 333 (PB194-585) | * |
| 334 (COM74-11482) | * |
| 335 (COM75-10051) | * |
| 336 (SN003-003-00688-2) | 9.70 |
| 337 (COM71-00182) | * |
| 338 (COM74-10736) | * |
| 339 (COM71-50080) | * |
| 343 (COM71-50398) | * |
| 344 See SP398 | .25 |
| 345 (SN003-003-00884-2) | 2.70 |
| 345-1 (SN003-003-00731-5) | 1.70 |
| 345-2 (SN003-003-00824-9) | 3.20 |
| 345-3 (SN003-003-00859-1) | 1.75 |

*Available from The National Technical Information Service, use "AD", "PB", "COM", or NBS publication identification if no specific NTIS number is assigned. Available in Microfiche for $3.00; consult NTIS for paper copy price.

## SPECIAL PUBLICATIONS (Continued)

| No. | Price |
|---|---|
| 345-4 (SN003-003-00825-7) | 3.20 |
| 345-5 (SN003-003-00898-2) | 2.15 |
| 345-6 (SN003-003-00858-3) | 2.30 |
| 345-7 (SN003-003-00864-8) | 1.75 |
| 345-8 (SN003-003-00895-8) | 2.10 |
| 345-9 (COM71-50305) | * |
| 345-10 (SN003-003-00879-6) | 3.05 |
| 345-11 (SN003-003-00835-4) | 2.70 |
| 345-12 (SN003-003-00865-6) | 2.00 |
| 346 (COM71-50147) | * |
| 347 (COM71-50202) | * |
| 348 (SN003-003-00893-1) | 7.45 |
| 349 (COM72-50807) | * |
| 350 (COM71-50276) | * |
| 351 (SN003-003-01027-8) | 6.45 |
| 352 (COM75-10291) | * |
| 353 (COM71-50364) | * |
| 354 (COM72-50808) | * |
| 355 (COM71-50385) | * |
| 356 (SN003-003-00934-2) | 2.05 |
| 357 (SN003-003-00928-8) | 5.40 |
| 359 (COM72-50057) | * |
| 361 Vol. 1 (COM72-10309) | * |
| 361 Vol. 2 (COM72-50850) | * |
| 362 (SN003-003-01000-6) | 1.15 |
| 363 (SN003-003-00962-8) | 1.45 |
| 364 (COM72-50746) | * |
| 365 (SN003-003-01068-5) | .50 |
| 366 (SN003-003-01044-8) | 2.80 |
| 366-1 (COM74-50063) | * |

| No. | Price |
|---|---|
| 366-2 (SN003-003-01544-0) | 1.35 |
| 368 Rev. 1976 (SN003-003-01665-9) | .35 ea<br>4.65 (per 100 cps.) |
| 369 (SN003-003-01124-8) | 1.85 |
| 370 (SN003-003-01057-0) | .55 |
| 371 (COM73-50245) | * |
| 371-1 (SN003-003-01422-2) | 1.45 |
| 372 (SN003-003-01059-6) | 2.35 |
| 373 (COM72-51036) | * |
| 374 (SN003-003-01061-8) | 5.20 |
| 375 (COM73-50839) | * |
| 376 (SN003-003-01080-4) | .60 |
| 377 (SN003-003-01107-0) | .85 |
| 378 (COM73-50585) | * |
| 380 (SN003-003-01109-6) | 2.10 |
| 381 (COM73-50932) | * |
| 382 (SN003-003-01176-2) | 3.30 |
| 383 (SN003-003-01171-1) | 2.10 |
| **384 Rev. 1976 (SN003-003-01670-5)** | **2.45** |
| 385 (COM74-50307) | * |
| **386 (SN003-003-01593-8)** | **1.90** |
| 387 | * |
| 388 (COM74-50543) | * |
| 389 Superseded by LC1070 | ** |
| 390 (COM74-50352) | * |
| 391 (SN003-003-01260-2) | 2.50 |
| 392 (SN003-003-01272-6) | 1.30 |
| 393 (COM74-50350) | * |
| 394 (COM74-50523) | * |
| 395 (SN003-003-01300-5) | 4.25 |
| 396-1 (SN003-003-01274-2) | 1.25 |

| No. | Price |
|---|---|
| 396-2 (SN003-003-01457-5) | 1.10 |
| 396-3 (PB250-844) | * |
| **396-4 (SN003-003-01572-5)** | **1.55** |
| 398 (SN003-003-01331-5) | .35 |
| 399-1 (SN003-003-01339-1) | 2.35 |
| 399-2 (SN003-003-01333-1) | 2.85 |
| 399-3 (SN003-003-01334-0) | 2.90 |
| 400-1 (COM74-50305) | * |
| 400-2 (SN003-003-01226-2) | 1.50 |
| 400-3 (SN003-003-01236-0) | .60 |
| 400-4 (SN003-003-01354-4 | 1.70 |
| 400-5 (SN003-003-01372-2) | 1.10 |
| 400-6 (SN003-003-01313-7) | .60 |
| **400-7 (SN003-003-01635-7)** | **.75** |
| 400-8 (SN003-003-01374-9) | 1.30 |
| 400-9 (SN003-003-01357-9) | 1.00 |
| 400-10 (SN003-003-01358-7) | 3.55 |
| 400-11 (SN003-003-01428-1) | 1.00 |
| 400-12 (AD-A011121) | * |
| 400-13 SN003-003-01382-0) | .75 |
| 400-15 (SN003-003-01566-1) | 1.25 |
| 400-17 (SN003-003-01480-0) | 1.40 |
| **400-18 (SN003-003-01577-6)** | **1.25** |
| **400-19 (SN003-003-01606-3)** | **2.10** |
| 400-20 (SN003-003-01473-7) | 1.00 |
| **400-21 (SN003-003-01565-2)** | **1.30** |

*Available from The National Technical Information Service, use "AD", "PB", "COM", or NBS publication identification if no specific NTIS number is assigned. Available in Microfiche for $3.00; consult NTIS for paper copy price.

**Superseded by NBS LC1071, free upon request from the Technical Information and Publications Division, National Bureau of Standards, Washington, DC 20234.

## SPECIAL PUBLICATIONS (Continued)

| No | Price |
|---|---|
| 400-22 (SN003-003-01623-3) | 1.45 |
| 400-23 (SN003-003-01604-7) | 3.70 |
| 400-25 (SN003-003-01678-1) | 1.45 |
| 400-26 (SN003-003-01600-4) | .55 |
| 400-27 (SN003-003-01569-5) | 1.20 |
| 400-28 (SN003-003-01628-4) | 1.25 |
| 400-34 (SN003-003-01707-8) | 1.45 |
| 401 (COM74-50931) | * |
| 403 (SN003-003-01638-1) | 3.30 |
| 404 (SN003-003-01319-6) | 1.45 |
| 405 (SN003-003-01346-3) | 1.05 |
| 406 (SN003-003-01393-5) | 2.45 |
| 407 (SN003-003-01379-0) | 3.75 |
| 408 (SN003-003-01389-7) | 12.60 |
| 409 (SN003-003-01359-5) | 3.90 |
| 410 1977 Ed. (SN003-003-01736-1) | 2.00 |
| 411 (SN003-003-01356-1) | 3.10 |
| 412 (SN003-003-01341-2) | 2.65 |
| 413 1976 Ed. (SN003-003-01601-2) | 1.35 |
| 414 (ADA012377) | * |
| 415 (SN003-003-01363-3) | 1.75 |
| 417 (SN003-003-01395-1) | 6.75 |
| 418 (SN003-003-01398-6) | 1.00 |
| 419 (SN003-003-01410-9) | 2.80 |
| 420 (SN003-003-01408-7) | 3.00 |
| 421 (SN003-003-01418-4) | 1.65 |
| 422 1 & 2 (SN003-003-01458-3) set | 20.00 |
| 423 (SN003-003-01451-6) | 6.10 |
| 424 (SN003-003-01599-7) | 2.90 |
| 425 (SN003-003-01461-3) | 19.45 |
| 426 (SN003-003-01465-6) | 3.30 |
| 427 (SN003-003-01472-9 | 3.00 |
| 428 (SN003-003-01541-5) | 28.50 |
| 429 (SN003-003-01463-0). | 1.95 |
| 430 (SN003-003-01542-3) | .35 |
| 431 (SN003-003-01608-0) | 11.00 |
| 432 (SN003-003-01587-3) | .60 |
| 433 (SN003-003-01639-0) | 3.50 |
| 434 (SN003-003-01624-1) | .55 |
| 435 (SN003-003-01603-9) | 5.60 |
| 436 (SN003-003-01556-3) | 4.25 |
| 437 (SN003-003-01557-1) | 1.05 |
| 438 (SN003-003-01581-4) | 2.40 |
| 439 (SN003-003-01575-0) | .95 |
| 441 (SN003-003-01568-7) | 2.30 |
| 442 (SN003-003-01614-4) | 3.30 |
| 443 (SN003-003-01633-1) | 4.15 |
| 444 (SN003-003-01588-1) | 5.80 |
| 445-1 (SN003-003-01632-2) | 1.20 |
| 446 (SN003-003-01641-1) | 2.05 |
| 447 (SN003-003-01654-3) | 1.00 |
| 448 (SN003-003-01663-2) | 1.90 |
| 449 (SN003-003-01677-2) | 2.00 |
| 451 (SN003-003-01662-4) | 3.00 |
| 452 (SN003-003-01664-1) | 2.65 |
| 453 (SN003-003-01700-1) | 3.55 |
| 454 (SN003-003-01666-7) | 1.65 |
| 455 (SN003-003-01699-3) | 4.45 |
| 456 (PB262-111). | * |
| 457 (SN003-003-01685-3) | 1.80 |
| 459 (SN003-003-01686-1) | 3.40 |
| 460 (SN003-003-01737-0) | 2.35 |
| 462 (SN003-003-01729-9) | 4.60 |

*Available from The National Technical Information Service, use "AD", "PB", or "COM" number when ordering. Available in Microfiche for $3.00; consult NTIS for paper copy price.

## HANDBOOKS

| No. | Price |
|---|---|
| 28 1969(Pt.1) | * |
| 28 1957(Pt.2) | * |
| 28 1957(Pt.3) | * |
| 44 4th Ed. (SN003-003-00894-0) | 7.90 |
| 46 | * |
| 48 | * |
| 49 | * |
| 51 (SN003-003-00115-5) | .60 |
| 53 | * |
| 55 | * |
| 57 (PB248-218) | * |
| 58 | * |
| 59 | * |
| 63 | * |
| 64 (COM73-10872) | ** |
| 65 | * |
| 69 | * |
| 71 | * |
| 72 (SN003-003-00123-6) | 1.30 |
| 73 | * |
| 74 | * |
| 75 | * |
| 76 | * |
| 80 | * |
| 81 # | * |
| 81 Suppl. 2 | * |
| 84 | * |
| 85 (SN003-003-00131-7) | 2.20 |
| 86 (SN003-003-00132-5) | 1.30 |
| 87 (SN003-003-00133-3) | 2.10 |
| 88 (SN003-003-00134-1) | 1.05 |
| 89 | * |
| 90 (PB188-654) | ** |
| 91 (SN003-003-00135-0) | 11.00 |
| 92 (SN003-003-00136-8) | 2.10 |
| 94 (COM73-10635) | ** |
| 96 | * |
| 97 | * |
| 98 (COM72-10619) | ** |
| 99 | ** |
| 100 | ** |
| 101 | ** |
| 102 | * |
| 105-1 (COM72-50707) | * |
| 105-2 (COM71-50065) | * |
| 107 (PB191-898) | ** |
| 109 (COM72-50183) | ** |
| 110-1 | * |
| 111 (COM72-50698) | ** |
| 112 (COM73-50836) | ** |
| 113 (SN003-003-01274-6) | 2.15 |
| 114 (SN003-003-01377-3) | .90 |
| 115 (SN003-003-01323-4) | 2.90 |
| 115 Sup. 1 (SN003-003-01582-2) | 2.25 |
| 116 (SN003-003-01456-7) | 1.10 |
| 117 (SN003-003-01563-6) | .75 |
| 118 (SN003-003-01567-9) | 2.70 |
| **119 (SN003-003-01646-2)** | **5.10** |
| **120 (SN003-003-01667-5)** | **.70** |

#81 amends in part: Part 2, Definitions and the Grounding Rules of these Handbooks.

*See page XVIII for additional information.

**Available from The National Technical Information Service, use "PB", "COM", or NBS publication identification if no specific NTIS number is assigned.

Available in Microfiche for $3.00; consult NTIS for paper copy price.

## NATIONAL STANDARD REFERENCE DATA SERIES

| No. | Price | No. | Price | No. | Price |
|---|---|---|---|---|---|
| 1 (SN003-003-00627-1) | .55 | 22 (Vol. 2) (AD696-884) | * | 43 Suppl. (SN003-003-01429-0) | 1.10 |
| 2 | * | 23 | * | 44 (COM74-50175) | * |
| 3 Sec. 1 | * | 24 | * | 45 (SN003-003-01165-7) | .75 |
| 3 Sec. 2 | * | 25 | * | 46 (COM73-50623) | * |
| 3 Sec. 3 (COM72-50056) | * | 26 | ** | 47 (SN003-003-01125-8) | 2.25 |
| 3 Sec. 4 (COM71-50346) | * | 27 (SN003-003-00637-8) | 1.80 | 48 (SN003-003-01166-5) | .80 |
| 3 Sec. 5 (SN003-003-01444-3) | 1.80 | 28 | * | 49 (SN003-003-01190-8) | 1.70 |
| 3 Sec. 6 (SN003-003-00998-9) | 1.15 | 29 | * | 50 (AD771-200) | * |
| **3 Sec. 7 (SN003-003-01558-0)** | **.85** | 31 (PB189-028) | * | 51 (SN003-003-01414-1) | 1.20 |
| 4 (SN003-003-00646-7) | 6.45 | 32 (SN003-003-00729-3) | 1.15 | 52 (SN003-003-01262-9) | 1.15 |
| 5 | * | 33 (PB192-183) | * | 53 (SN003-003-01426-5) | 1.15 |
| 8 (PB189-698) | * | 34 (SN003-003-00770-6) | 1.65 | 54 (SN003-003-01406-1) | .85 |
| 9 | * | 35 Vol. 1 (SN003-003-00949-1) | 9.25 | 55 (SN003-003-01431-1) | .85 |
| 10 | * | 35 Vol. 2 (SN003-003-00935-1) | 7.95 | 56 (SN003-003-01396—0) | .85 |
| 12 | * | 35 Vol. 3 (SN003-003-00950-4) | 8.30 | **57 (SN003-003-01609-8)** | **.55** |
| 13 (SN003-003-00622-0) | 3.00 | 36 (COM71-50203) | * | **58 (SN003-003-01627-6)** | **.70** |
| 14 | * | 37 (SN003-003-00872-9) | 15.60 | | |
| 15 | * | 38 (COM71-50351) | * | | |
| 16 | * | 39 (SN003-003-00845-1) | 5.10 | | |
| 18 (SN003-003-00628-9) | 1.15 | 40 (COM72-50439) | * | | |
| 19 (SN003-003-00629-7) | .65 | 41 (COM72-50849) | * | | |
| 20 | * | 42 (COM72-50886) | * | | |
| 21 (PB191-956) | * | 43 (SN003-003-01083-9) | 1.05 | | |

*Available from The National Technical Information Service, use "AD", "PB", "COM", or NBS publication identification if no specific NTIS number is assigned. Available in Microfiche for $3.00; consult NTIS for paper copy price.

**Superseded by the Journal of Physical and Chemical Reference Data, Vol. 6, Supp. 1; available from the American Chemical Society, 1155 16th St., N. W., Washington, DC 20036.

## BUILDING SCIENCE SERIES

| No. | Price |
|---|---|
| 0 (COM71-00046) | * |
| 1 (PB189-713) | * |
| 2 Pt. 1 (COM72-10542) | * |
| 3 | * |
| 4 | * |
| 5 Pt. 2 | * |
| 6 | * |
| 7 | * |
| 8 (COM73-10487) | * |
| 9 (PB193-907) | * |
| 10 | * |
| 11 | * |
| 12 | * |
| 13 | * |
| 14 | * |
| 15 | * |
| 16 | * |
| 17 | * |
| 18 (PB193-736) | * |
| 19 | * |
| 20 (PB189-639) | * |
| 21 (PB189-459) | * |
| 22 (PB189-456) | * |
| 23 | * |
| 24 | * |
| 25 (PB188-789) | * |
| 26 | * |
| 27 (PB191-304) | * |
| 28 (PB193-924) | * |
| 29 (PB190-603) | * |
| 30 (COM71-00141) | * |
| 31 (PB193-601) | * |
| 32 (COM71-50078 | * |
| 33 (COM71-00159) | * |
| 34 (COM75-10286) | * |
| 35 (COM71-50591) | * |
| 36 (SN003-003-00850-8) | 1.55 |
| 37 (SN003-003-00857-5) | 1.25 |
| 38 (COM71-50345) | * |
| 39 (COM72-50068) | * |
| 40 (SN003-003-00940-7) | 3.95 |
| 41 (COM72-50533) | * |
| 42 (COM72-50675) | * |
| 43 (COM75-10173) | * |
| 44 (SN003-003-01071-5) | .65 |
| 45 (COM73-50725) | * |
| 46 (COM73-50188) | * |
| 47 (COM73-50975) | * |
| 48 (SN003-003-01212-2) | 4.85 |
| 49 (COM74-50353) | * |
| 50 (SN003-003-01282-3) | .55 |
| 51 (SN003-003-01267-0) | .90 |
| 52 (COM74-50537) | * |
| 53 (SN003-003-01284-0) | .85 |
| 54 (SN003-003-01307-2) | 1.25 |
| 55 (COM74-51188 | * |
| 56 (SN003-003-01335-8) | 2.35 |
| 57 (SN003-003-01364-1) | 1.20 |
| 58 (SN003-003-01349-8) | 2.00 |
| 59 (SN003-003-01392-7) | 1.30 |
| 60 (SN003-003-01352-8) | 1.05 |
| 61 (COM75-10473) | * |
| 62 (SN003-003-01738-8) | 1.90 |
| 63 (SN003-003-01407-9) | .70 |
| 64 (SN003-003-01360-9) | 1.35 |
| 65 (SN003-003-01394-3) | 1.00 |
| 66 (SN003-003-01417-6) | 2.10 |
| 67 (SN003-003-01468-1) | 1.20 |
| 68 (SN003-003-01419-2) | 1.25 |
| 69 (SN003-003-01622-5) | 4.60 |
| 70 (SN003-003-01437-1) | 1.55 |
| 71 (SN003-003-01459-1) | 2.25 |
| 72 (SN003-003-01474-5) | 1.80 |
| 73 (SN003-003-01479-6) | 1.25 |
| 74 (SN003-003-01477-0) | 1.55 |
| 75 | * |
| 76 (SN003-003-01644-6) | 1.45 |
| 77 (SN003-003-01539-3) | 2.35 |
| 78 (SN003-003-01537-7) | 1.25 |
| 79 (SN003-003-01546-6) | 1.15 |
| 80 (SN003-003-02183-1) | 1.15 |
| 81 (SN003-003-01591-1) | .45 |
| 82 (SN003-003-02185-7) | .50 |
| 83 (SN003-003-01592-0 | .55 |
| 85 (SN003-003-01619-5) | 2.25 |
| 86 (SN003-003-01637-3) | 1.05 |
| 87 (SN003-003-01642-0) | 4.40 |
| 88 (SN003-003-01693-4) | .65 |
| 89 (SN003-003-01706-0) | .75 |
| 90 (PB257-581) | * |
| 91 (SN003-003-01690-0) | 1.40 |
| 92 (SN003-003-01692-6) | .70 |

*Available from the National Technical Information Service; use “PB”, “COM” or NBS Publication identification if no specific NTIS number is assigned. Available in Microfiche for $3.00; consult NTIS for paper copy price.

## VOLUNTARY PRODUCT STANDARDS

| No. | Price | No. | Price | No. | Price |
|---|---|---|---|---|---|
| 1-74 (SN003-003-01387-1) | .85 | 48-71 (SN003-003-00925-3) | .35 | 60-73 (SN003-003-01248-3) | .40 |
| 15-69 (SN003-003-00188-1) | .40 | 50-71 (SN003-003-00877-0) | .35 | 61-74 (SN003-003-01421-4) | .45 |
| 20-70 (SN003-003-00192-9) | .40 | 51-71 (SN003-003-00963-6) | .35 | 62-74 (SN003-003-01375-7) | .55 |
| 38-70 (SN003-003-00842-7) | .45 | 52-71 (SN003-003-00990-3) | .35 | 63-75 (SN003-003-01415-0) | .50 |
| 39-70 (SN003-003-00840-1) | .65 | 57-73 (SN003-003-01182-7) | .40 | **64-75 (SN003-003-01583-1)** | **.35** |
| 42-70 (SN003-003-00901-6) | .65 | 58-73 (SN003-003-01295-5) | .40 | **65-75 (SN003-003-01585-7)** | **.35** |
| 46-71 (SN003-003-00936-9) | .35 | 59-73 (SN003-003-01255-6) | .45 | | |

## FEDERAL INFORMATION PROCESSING STANDARDS SERIES

| No. | Price | No. | Price | No. | Price |
|---|---|---|---|---|---|
| 0 | 3.50 | **17-1** | **4.00** | 34 | 3.50 |
| 1 | 3.50 | **18-1** | **4.00** | 35 | 4.00 |
| 2 | 3.50 | 19 | 3.50 | 36 | 3.50 |
| 3-1 | 3.50 | 20 | 3.50 | 37 | 3.50 |
| 4 | 3.50 | 21-1 | 13.50 | 38 | 4.50 |
| 5-1 | 3.50 | **22-1** | **4.00** | 39 | 3.50 |
| 6-2 | 4.00 | 23 | 3.50 | 40 | 4.50 |
| 7 | 3.50 | 24 | 4.00 | 41 | 3.50 |
| 8-4 | 3.50 | 25 | 3.50 | 42-1 | 3.50 |
| 9 | 3.50 | 26 | 3.50 | 43 | 4.50 |
| **10-2** | **4.00** | 27 | 3.50 | 44 | 3.50 |
| **11-1** | **4.00** | 28 | 3.50 | 45 | 4.00 |
| 12-2 | 7.50 | 29 | 3.50 | | |
| 13 | 3.50 | 30 | 3.50 | | |
| 14 | 3.50 | 31 | 5.00 | | |
| 15 | 3.50 | 32 | 5.00 | | |
| **16-1** | **4.00** | 33 | 4.00 | | |

Available only from the National Teachnical Information Service.

## APPLIED MATHEMATICS SERIES

| o. | Price | No. | Price | No. | Price |
|---|---|---|---|---|---|
| 1 See AMS25 | * | 23 (PB175-967) | * | 45 (COM74-10639) | * |
| 2 (PB194-385) | * | 24 (PB175-816) | * | 46 (PB186-429) | * |
| 3 (PB251-959) | * | 25 | * | 47 (PB251-902) | * |
| 4 (PB251-962) | * | 26 (PB178-415) | * | 48 (PB176-119) | * |
| 5 (COM73-10501) | * | 27 (AD694-116) | * | 49 (PB251-903) | * |
| 6 (PB251-862) | * | 28 (AD695-952) | * | 50 (PB176-520) | * |
| 7 (PB251-863) | * | 29 (AD695-953) | * | 51 (PB248-467) | * |
| 8 (PB251-864) | * | 30 (PB175-817) | * | 52 (PB251-904) | * |
| 9 (COM73-10498) | * | 31 (COM74-11112) | * | 53 (PB186-430) | * |
| 10 (PB251-960) | * | 32 (COM73-10499) | * | 54 (COM73-11111) | * |
| 11 (AD702-411) | * | 33 (PB175-818) | * | 55 (SN003-003-00279-8 | 12.65 |
| 12 (PB184-887) | * | 34 (SN003-003-00272-1) | 4.70 | 56 (PB190-608) | * |
| 13 (PB251-865) | * | 35 (PB251-103) | * | 57 (PB266-263) | * |
| 14 (SN003-003-00270-4) | 11.70 | 36 (PB251-871) | * | 58 (AD700-470) | * |
| 15 (PB251-866) | * | 37 (PB251-872) | * | 59 (SN003-003-00282-8) | 6.80 |
| 16 (PB251-867) | * | 38 (PB251-900) | * | 60 (SN003-003-00283-6) | 1.45 |
| 17 (PB251-868) | * | 39 (PB251-901) | * | 61 (PB188-790) | * |
| 18 (PB175-819) | * | 40 (PB186-428) | * | 62 (SN003-003-00993-8) | 1.20 |
| 19 (PB175-815) | * | 41 (PB176-521) | * | 63 (SN003-003-00988-1) | 3.45 |
| 20 (PB251-870) | * | 42 (PB175-819) | * | | |
| 21 (PB178-392) | * | 43 (PB176-127) | * | | |
| 22 (PB192-337) | * | 44 (AD698-954) | * | | |

*Available from The National Technical Information Service; use "PB", "AD", "COM", or NBS publication identification if no specific NTIS number is assigned. Available in Microfiche for $3.00; consult NTIS for paper copy price.

## CONSUMER INFORMATION SERIES

| No. | Price | No. | Price | No. | Price |
|---|---|---|---|---|---|
| 1 (SN003-003-00680-7) | .90 | 4 (SN003-003-00920-2) | 1.10 | 7 (SN003-003-01688-8) | .35 |
| 3 (SN003-003-00682-3) | .60 | 5 (SN003-003-00941-5) | .70 | 8 (SN003-003-01446-0) | .70 |
| | | 6 (SN003-003-01536-9) | 1.70 | | |

## TECHNICAL NOTES

| No. | Price | No. | Price | No. | Price |
|---|---|---|---|---|---|
| 1 (PB151-360) | * | 18-19 (PB195-218) | * | 40-9 (PB189-933) | * |
| 2 (PB151-361) | * | 18-20 (PB168-044) | * | 40-10 (PB189-934) | * |
| 2-2 (PB151-361-2) | * | 18-21 (PB195-219) | * | 40-11 (PB189-935) | * |
| 3 (PB151-362) | * | 18-22 (N661-3994) | * | 40-12 (PB189-936) | * |
| 4 (PB151-363) | * | 18-23 (COM74-10437) | * | 40-13 (PB151-399-13) | * |
| 5 (PB151-364) | * | 18-24 (COM74-10438) | * | 41 (PB151-400) | * |
| 6 (PB151-365) | * | 18-25 (COM74-10473) | * | 42 (PB151-401) | * |
| 7 (PB151-366) | * | 18-26 (COM74-10439) | * | 43 (PB151-402) | * |
| 8 (PB151-367) | * | 19 (PB151-378) | * | 44 (PB151-403) | * |
| 9 (PB151-368) | * | 20 (PB151-379) | * | 45 (PB151-404) | * |
| 10 (PB151-369) | * | 21 (PB151-380) | * | 46 (PB151-405) | * |
| 11 (PB151-370) | * | 22 (PB151-382) | * | 47 (PB151-406) | * |
| 12 (PB151-371) | * | 23 (PB151-382) | * | 48 (PB151-407) | * |
| 13 (PB151-372) | * | 24 (PB151-383) | * | 49 (PB151-408) | * |
| 14 (PB151-373) | * | 25 (PB151-384) | * | 50 (PB151-409) | * |
| 15 (PB151-374) | * | 26 (PB151-385) | * | 51 (PB161-552) | * |
| 16 (PB151-375) | * | 27 (PB151-386) | * | 52 (PB161-553) | * |
| 18 (PB151-377) | * | 28 (PB151-388) | * | 53 (PB161-554) | * |
| 18-2 (PB151-377-2) | * | 29 (PB151-388) | * | 54 (PB161-555) | * |
| 18-3 (PB151-377-3) | * | 30 (PB151-389) | * | 55 (PB161-556) | * |
| 18-4 (PB151-377-4) | * | 31 (PB151-390) | * | 56 (PB161-557) | * |
| 18-5 (PB151-377-5) | * | 33 (PB151-392) | * | 57 (PB161-558) | * |
| 18-6 (PB151-377-6) | * | 34 (PB151-393) | * | 58 (PB161-559) | * |
| 18-7 (PB151-377-7) | * | 35 (PB151-394) | * | 59 (PB161-560) | * |
| 18-8 (PB151-377-8) | * | 37 (PB151-396) | * | 60 (PB161-561) | * |
| 18-9 (PB151-377-9) | * | 38 (PB151-397) | * | 61 (PB161-562) | * |
| 18-10 (PB151-377-10) | * | 39 (PB151-398) | * | 62 (PB161-563) | * |
| 18-11 (PB151-377-11) | * | 40-1 (PB151-399-1) | * | 63 (PB161-564) | * |
| 18-12 (PB151-377-12) | * | 40-2 (PB151-399-2) | * | 64 (PB161-565) | * |
| 18-13 (PB151-377-13) | * | 40-3 (PB151-399-3) | * | 66 (PB161-567) | * |
| 18-14 (PB195-273) | * | 40-4 (PB151-399-4) | * | 67 (PB161-568) | * |
| 18-15 (PB195-215) | * | 40-5 (PB151-399-5) | * | 68 (PB161-569) | * |
| 18-16 (PB195-216) | * | 40-6 (PB151-399-6) | * | 69 (PB161-570) | * |
| 18-17 (PB195-217) | * | 40-7 (PB151-399-7) | * | 70 (PB161-571) | * |
| 18-18 (PB168-058) | * | 40-8 (PB189-932) | * | 71 (PB161-572) | * |

*Available from the National Technical Information Service; use "PB", "AD", "N", "COM", or NBS publication number when ordering. Available in Microfiche for $3.00; consult NTIS for paper copy price.

## TECHNICAL NOTES (Continued)

| o. | Price |
|---|---|
| 2 (PB161-573) | * |
| 3 (PB161-574) | * |
| 4 (PB161-575) | * |
| 5 (PB161-576) | * |
| 6 (PB161-577) | * |
| 7 (PB161-578) | * |
| 8 (PB161-579) | * |
| 9 (PB161-580) | * |
| 0 (PB161-581) | * |
| 1 (PB161-582) | * |
| 2 (PB161-583) | * |
| 3 (PB161-584) | * |
| 4 (PB161-585) | * |
| 5 (PB161-586) | * |
| 6 (PB161-587) | * |
| 7 (PB161-588) | * |
| 8 (PB161-589) | * |
| 9 (PB161-590) | * |
| 0 (PB161-591) | * |
| 1 (PB161-592) | * |
| 2 (PB161-593) | * |
| 3 (PB161-594) | * |
| 4 (PB161-595) | * |
| 5 (PB151-596) | * |
| 6 (PB161-597) | * |
| 7 (PB161-598) | * |
| 8 (PB186-280) | * |
| 9 (PB186-431) | * |
| 0 (COM74-10393) | * |
| 0-A | * |
| 1-1 (AD687-820) | * |
| 1-2 (AD687-821) | * |
| 2 (PB161-603) | * |
| 6 (PB161-607) | * |
| 7 (PB161-608) | * |
| 8 (PB161-609) | * |
| 9 (PB161-610) | * |
| 0 (PB161-611) | * |
| 1 (PB161-612) | * |
| 2 (PB161-613) | * |
| 3 (PB161-614) | * |
| 4 (PB161-615) | * |
| 5 (PB161-616) | * |
| 6 (PB161-617) | * |
| 7 (PB161-618) | * |
| 8 (PB161-619) | * |
| 9 (PB161-620) | * |
| 0 (PB161-621) | * |

| No. | Price |
|---|---|
| 120A (PB190-611) | * |
| 121 (PB161-622) | * |
| 122 (PB161-623) | * |
| 123 (PB161-624) | * |
| 124 (PB161-625) | * |
| 125 (PB161-626) | * |
| 128 (PB161-629) | * |
| 129 (PB161-630) | * |
| 129A | * |
| 130 (PB161-631) | * |
| 131 (PB161-632) | * |
| 132 (PB161-633) | * |
| 133 (PB161-634) | * |
| 134 (PB161-635) | * |
| 135 (PB161-636) | * |
| 136 (PB161-637) | * |
| 137 (PB161-638) | * |
| 138 (PB161-639) | * |
| 139 (PB161-640) | * |
| 140 (PB161-641) | * |
| 141 (PB161-729) | * |
| 142 (PB161-643) | * |
| 143 (PB161-644) | * |
| 146 (PB161-647) | * |
| 147 (PB161-648) | * |
| 148 (PB161-649) | * |
| 151 (PB191-730) | * |
| 154 (PB172-217) | * |
| 154A (PB182-435) | * |
| 160 | * |
| 163 (COM71-01002) | * |
| 164 (N-6314864) | * |
| 165 (AD401-044) | * |
| 166 (PB181-454) | * |
| 171 | * |
| 172 (PB193-915) | * |
| 173 (COM75-10523) | * |
| 174 (COM72-10376) | * |
| 177 (COM72-10514) | * |
| 178 (PB190-917) | * |
| 179 (PB190-610) | * |
| 180 (COM75-10083) | * |
| 182 (COM75-10283) | * |
| 183 (COM75-10052) | * |
| 187 (PB188-807) | * |
| 191 (PB182-538) | * |
| 194 See NSRDS1 | .55 |
| 195 (COM73-10418) | * |

| No. | Price |
|---|---|
| 196 (COM73-10483) | * |
| 197 (AD419-866) | * |
| 199 (AD683-408) | * |
| 200 (N64-14272) | * |
| 201 (PB182-539) | * |
| 202 | * |
| 204 (PB184-118) | * |
| 205 (COM73-10634) | * |
| 206-1 (COM73-10684) | * |
| 206-2 (COM73-10685) | * |
| 206-3 (COM73-10686) | * |
| 206-4 (COM73-10687) | * |
| 206-5 (COM73-10688) | * |
| 207 (COM73-10689) | * |
| 209 (PB168-043) | * |
| 210 (PB189-930) | * |
| 211 | * |
| 214 (PB189-931) | * |
| 215 (PB188-808) | * |
| 217 (PB189-103) | * |
| 218 (PB188-809) | * |
| 219 (PB186-279) | * |
| 220 (COM74-11077) | * |
| 221 (COM71-00690) | * |
| 223 (PB168-051) | * |
| 224 (PB184-119) | * |
| 225 (AD614-056) | * |
| 226 (PB168-042) | * |
| 227 (PB184-473) | * |
| 228 (PB191-731) | * |
| 229 (PB188-805) | * |
| 231 (COM72-10587) | * |
| 233 (COM75-10054) | * |
| 234 (COM73-10485) | * |
| 235 (COM73-10481) | * |
| 236 (AD437-308) | * |
| 237 (COM75-10166) | * |
| 245 (PB184-177) | * |
| 249 (PB168-046) | * |
| 252 (AD612-812) | * |
| 253 (PB184-176) | * |
| 255 (AD614-257) | * |
| 260 (PB168-041) | * |
| 262-A (COM73-10486) | * |
| 263 (COM75-10486) | * |
| 266 (PB195-214) | * |
| 267 (AD628-586) | * |

---

*Available from the National Technical Information Service, use "PB", "AD", "COM", "N", or NBS blication identification if no specific NTIS number is assigned. Available in Microfiche for .00; consult NTIS for paper copy price.

## TECHNICAL NOTES (Continued)

| No. | Price |
|---|---|
| 268 | * |
| 270-1 See TN270-3 | 3.25 |
| 270-2 See TN270-3 | 3.25 |
| 270-3 (SN003-003-00406-5) | 3.25 |
| 270-4 (SN003-003-00407-3) | 2.10 |
| 270-5 (COM71-50171) | * |
| 270-6 (SN003-003-00932-6) | 1.90 |
| 270-7 (COM73-50435) | * |
| 273 (PB248-534) | * |
| 275 (COM73-10484) | * |
| 277 | * |
| 278 | * |
| 279 (COM75-10375) | * |
| 280 (COM72-10590) | * |
| 285 (AD633-354) | * |
| 287 (PB182-436) | * |
| 288 | * |
| 291 | * |
| 292 (COM75-10335) | * |
| 293 (AD642-236) | * |
| 294 (PB176-289) | * |
| 295 | * |
| 297 (PB188-657) | * |
| 298 (PB186-238) | * |
| 300 (PB168-048) | * |
| 303 (AD611-400) | * |
| 304 (AD615-936) | * |
| 307 (PB168-040) | * |
| 309 (N-65-24999) | * |
| 310 (AD615-937) | * |
| 318 (COM75-10374) | * |
| 319 | * |
| 321 (COM75-10238) | * |
| 322 (COM75-10236) | * |
| 323 (COM75-10237) | * |
| 324 (AD654-887) | * |
| 331 | * |
| 332 | * |
| 334 (PB173-291) | * |
| 341 | * |
| 343 | * |
| 345 | * |
| 346 (PB194-282) | * |

| No. | Price |
|---|---|
| 347 | * |
| 349 | * |
| 355 | * |
| 360 (PB190-125) | * |
| 361 (COM73-50052) | * |
| 361 (SN003-003-01321-8) (Metric Version) | 1.25 |
| 362 (COM74-10482) | * |
| 363 | * |
| 364 | * |
| 365 | * |
| 365-1 (COM71-00048) | * |
| 366 | * |
| 367 | * |
| 368 | * |
| 370 (AD688-697) | * |
| 372 | * |
| 373 | * |
| 374 | * |
| 375 | * |
| 377 | * |
| 378 | * |
| 379 (SN003-003-00834-6) | .65 |
| 381 | * |
| 382 | * |
| 383 | * |
| 384 (COM75-10174) | * |
| 385 (PB190-548) | * |
| 386 (PB191-638) | * |
| 387 (COM74-50059) | * |
| 388 (COM71-50077) | * |
| 389 | * |
| 390 (PB191-639) | * |
| 391 | * |
| 392 (COM74-50057) | * |
| 393 (COM75-10043) | * |
| 397 (COM71-50060) | * |
| 398 (SN003-003-00814-1) | .40 |
| 399 (COM71-50294) | * |
| 400 | * |
| 403 | * |
| 406 | * |
| 409 | * |
| 410 | * |
| 411 | * |
| 412 | * |

| No. | Price |
|---|---|
| 414 (PB176-109) | * |
| 416 | * |
| 417 | * |
| 419 (PB179-432) | * |
| 420 | * |
| 421 | * |
| 423 | * |
| 425 | * |
| 426 | * |
| 428 | * |
| 431 | * |
| 432 | * |
| 434 | * |
| 435 | * |
| 436 | * |
| 437 | * |
| 438 (AD665-245) | * |
| 439 | * |
| 440 | * |
| 444 | * |
| 445 | * |
| 461 | * |
| 464 | * |
| 465 | * |
| 467 (COM72-50871) | * |
| 469 | * |
| 470 | * |
| 472 (AD681-330) | * |
| 473 | * |
| 474 (AD681-351) | * |
| 475 (AD683-808) | * |
| 476 | * |
| 477 | * |
| 478 (PB190-609) | * |
| 479 | * |
| 480 | * |
| 483 | * |
| 484 (AD692-231) | * |
| 485 | * |
| 486 | * |
| 487 | * |
| 488 (AD692-232) | * |
| 490 | * |
| 491 | * |
| 495 (AD695-820) | * |
| 496 (PB284-674) | * |

---

*Available from the National Technical Information Service, use "PB", "AD", "COM", "N", or NBS publication identification if no specific NTIS number is assigned. Available in Microfiche for $3.00; consult NTIS for paper copy price.

## TECHNICAL NOTES (Continued)

| D. | Price |
|---|---|
| 7 (AD695-821) | * |
| 8 (SN003-003-00590-8) | .65 |
| 8-1 (SN003-003-00774-9) | .60 |
| 8-2 (SN003-003-00686-6) | .70 |
| 0 (PB191-352) | * |
| 3 | * |
| 0 | * |
| 1 | * |
| 3 (AD702-871) | * |
| 5 (SN003-003-00606-8) | .65 |
| 7 | * |
| 9 (PB190-760) | * |
| 0 (AD702-833) | * |
| 2 (PB191-024) | * |
| 3 (PB191-057) | * |
| 4 (PB191-277) | * |
| 5 | 1.10 |
| 7 (AD710-906) | * |
| 8 (PB191-305) | * |
| 9 (PB192-153) | * |
| 0 (COM71-00047) | * |
| 2 (SN003-003-00776-5) | .75 |
| 3 (PB192-875) | * |
| 4 (PB192-877) | * |
| 5 (PB193-794) | * |
| 6 (PB192-953) | * |
| 3 (COM71-00081) | * |
| 4 (PB194-960) | * |
| 7 (COM71-00082) | * |
| 0 (COM71-00068) | * |
| 1 (COM71-50076) | * |
| 2 (SN003-003-00918-1) | 3.25 |
| 4 (PB194-750) | * |
| 5 (AD718-534) | * |
| 7 (COM74-10405) | * |
| 8 (COM71-50072) | * |
| 0 (AD719-976) | * |
| 2 (COM71-00128) | * |
| 3 (COM71-50341) | * |
| 6 (COM71-50062) | * |
| 8 (AD728-642) | * |

| No. | Price |
|---|---|
| 569 (COM74-10436) | * |
| 570 (COM71-50075) | * |
| 572 (COM71-50150) | * |
| 573 (COM71-50227) | * |
| 575 (COM75-10280) | * |
| 577 (COM71-50264) | * |
| 578 (COM75-10185) | * |
| 579 (COM75-10184) | * |
| 584 (COM71-50635) | * |
| 585 (COM72-50066) | * |
| 589 (COM72-50061) | * |
| 590 (COM71-50292) | * |
| 591 (COM75-10168) | * |
| 592 (SN003-003-00892-3) | 1.15 |
| 593 (COM72-50031) | * |
| 594-1 (COM72-50674) | * |
| 594-2 (COM72-51003) | * |
| 594-3 (COM75-10183) | * |
| 594-4 (COM73-50224) | * |
| 594-5 (SN003-003-00159-7) | .55 |
| 594-6 (SN003-003-01253-0) | .95 |
| 594-7 (SN003-003-01244-1) | .75 |
| 594-8 (COM74-50536) | * |
| 594-9 (SN003-003-01342-1 | 1.10 |
| 594-10 (SN003-003-01453-2) | .85 |
| 594-11 (SN003-003-01675-6) | 1.15 |
| 594-12 (SN003-003-01676-4) | .75 |
| **594-13 (SN003-003-01709-4)** | **1.40** |
| 595 (COM71-50362) | * |
| 596 (SN003-003-00904-1) | 1.05 |
| 597 (COM75-10176) | * |
| 598 (AD732-553) | * |
| 599 (COM71-50399) | * |
| 600 (COM71-50297) | * |
| 602 (SN003-003-00880-0) | .55 |

| No. | Price |
|---|---|
| 604 (SN003-003-00861-3) | .65 |
| 605 (COM71-50332) | * |
| 606 (COM71-50325) | * |
| 607 (AD734-035) | * |
| 609 (AD730-357) | * |
| 610 (COM72-50059) | * |
| 612 (COM72-50205) | * |
| 613 (COM72-50020) | * |
| 614 (COM72-50523) | * |
| 615 (COM72-50524) | * |
| 616 2nd Rev. (SN003-003-01798-1) | 1.30 |
| 618 (COM72-50695) | * |
| 619 (COM72-50955) | * |
| 620 (COM73-50584) | * |
| 621 (SN003-003-01055-3) | 1.10 |
| 622 (COM72-51039) | * |
| 623 (COM72-51040) | * |
| 624 (COM72-51041) | * |
| 625 (COM72-51081) | * |
| 626 (COM73-50038) | * |
| 627 (SN003-003-01108-8) | 1.00 |
| 628 (COM73-50263) | * |
| 629 (COM73-50100) | * |
| 631 (COM75-10334) | * |
| 632 (COM73-50238) | * |
| 633 (COM73-50239) | * |
| 634 (COM73-50339) | * |
| 635 (COM75-10177) | * |
| 637 (COM75-10082) | * |
| 638 (COM73-50727) | * |
| 640 (COM73-50805) | * |
| 641 (COM75-10281) | * |
| 642 (COM73-50973) | * |
| 643 (COM73-50885) | * |
| 644 (COM73-50972) | * |
| 645 (COM74-50133) | * |
| 646 (COM74-50842) | * |
| 648 (SN003-003-01246-7) | 1.25 |
| 649 (COM74-50308) | * |

---

*Available from the National Technical Information Service, use "PB", "AD", "COM", "N", or NBS ublication identification if no specific NTIS number is assigned. Available in Microfiche for 3.00; consult NTIS for paper copy price.

## TECHNICAL NOTES (Continued)

| No. | Price |
|---|---|
| 650 (COM74-50430) | * |
| 651 (SN003-003-01280-7) | .50 |
| 652 (SN003-003-01299-8) | .50 |
| 653 (COM74-50637) | * |
| 654 (COM74-50698) | * |
| 655 (COM74-51542) | * |
| 657 (COM75-50069) | * |
| 658 (COM75-50161) | * |
| 659 (SN003-003-01442-7) | .85 |
| 660 (SN003-003-01383-8) | 1.00 |
| 661 (SN003-003-01350-1) | .80 |
| 662 (SN003-003-01413-3) | .70 |
| 663 (SN003-003-01405-2) | 1.10 |
| 664 (COM75-10289) | * |
| 665 (SN003-003-01403-6) | 1.00 |
| 666 (COM75-10288) | * |
| 667 (SN003-003-01560-1) | 1.85 |
| 668 (SN003-003-01449-4) | 1.05 |
| 669 (COM75-10918) | * |
| 670 (SN003-003-01586-2) | 1.60 |
| 672 (SN003-003-01550-4) | 2.40 |
| 673 (PB246-934) | * |
| 674 (SN003-003-01559-8) | 1.50 |
| 675 (SN003-003-01596-2) | 1.30 |
| 677 (SN003-003-01597-1) | 1.20 |
| 680 (SN003-003-01616-1) | .50 |
| 681 (SN003-003-01652-7) | 1.05 |
| 682 (SN003-003-01653-5) | .80 |
| 683 (SN003-003-01657-8) | 1.00 |
| 684 (SN003-003-01732-9) | 3.85 |
| **685 (SN003-003-01789-2)** | **.65** |
| 686 (PB260-666) | * |
| 687 (SN003-003-01714-1) | .75 |
| 688 (SN003-003-01715-9) | .65 |
| 689 (PB263-104) | * |
| 690 (PB262-551) | * |
| 691 (PB263-103) | * |
| **692 (SN003-003-01734-5)** | **.55** |
| **693 (SN003-003-01710-8)** | **1.20** |
| **695 (SN003-003-01781-7)** | **2.80** |
| **696 Rev. 1977 (SN003-003-01850-3)** | **1.50** |
| **697 (SN003-003-01862-7)** | **2.20** |
| **698 (SN003-003-01864-3)** | **1.30** |
| **699 (SN003-003-01865-1)** | **2.75** |
| 700 (COM73-50015) | * |
| 702 (AD734-427) | * |
| 703 (COM71-50607) | * |
| 706 (COM72-50892) | * |
| 707 (COM72-50054) | * |
| 708 (COM72-50062) | * |
| 710-1 (COM72-50276) | * |
| 710-2 (COM72-50346) | * |
| 710-3 (COM72-50520) | * |
| 710-4 (COM72-50521) | * |
| 710-5 (COM72-50694) | * |
| 710-6 (SN003-003-01087-1) | 1.00 |
| 710-7 (COM73-50483) | * |
| 711 (COM72-50064) | * |
| 713 (COM72-50204) | * |
| 714 (SN003-003-00974-1) | 1.50 |
| 716 (COM72-50361) | * |
| 717 (AD740-674) | * |
| 718 (COM73-50206) | * |
| 720 (SN003-003-00989-0) | .6 |
| 721 (COM72-50467) | * |
| 723 (COM72-50535) | * |
| 724 See TN983 | |
| 725 (SN003-003-01003-1 | .7 |
| 726 (AD748-788) | * |
| 727 (COM72-50538) | * |
| 728 (COM72-50666) | * |
| 729 (COM72-50667) | * |
| 731 (SN003-003-01023-5) | .9 |
| 732 (SN003-003-01029-4) | .7 |
| 733 (COM72-50812) | * |
| 734 (COM72-50732) | * |
| 735 (COM72-50873) | * |
| 736 (COM72-50924) | * |
| 737 (COM75-10170) | * |
| 738 (COM72-50810) | * |
| 747 (SN003-003-01065-1) | 1.25 |
| 748 (COM73-50209) | * |
| 749 (COM73-50103) | * |
| 750 (COM72-51080) | * |
| 751 (SN003-003-01093-6) | .85 |
| 752 (COM73-50624) | * |
| 753 (SN003-003-01097-9) | 1.10 |
| 754 (COM73-50225) | * |
| 755 (SN003-003-01094-4) | .70 |
| 756 (COM73-50257) | * |
| 757 (SN003-003-01092-8) | .45 |
| 758 (SN003-003-01115-1) | 2.10 |
| 759 (SN003-003-01102-9) | .65 |
| 760 (SN003-003-01112-6) | .90 |
| 761 (SN003-003-01132-1) | 1.15 |

*Available from the National Technical Information Service, use "PB", "AD", "COM", "N", or NBS publication identification if no specific NTIS number is assigned. Available in Microfiche for $3.00; consult NTIS for paper copy price.

## TECHNICAL NOTES (Continued)

| o. | Price | No. | Price | No. | Price |
|---|---|---|---|---|---|
| 3 (SN003-003-01114-2) | .65 | 797 (SN003-003-01192-4) | .50 | 829 (SN003-003-01301-3) | 1.10 |
| 4 (SN003-003-01131-2) | .65 | 798 (COM73-50930) | * | 830 (COM74-50532) | * |
| 5 (SN003-003-01135-5) | .60 | 799 (COM74-50135) | * | 831 (SN003-003-01291-2) | .95 |
| 6 (COM73-50374) | * | 800 (COM74-50141) | * | 832 (SN003-003-01327-7) | .70 |
| 7 (AD758-981) | * | 801 (SN003-003-01292-1) | .60 | 833 (SN003-003-01302-1) | 1.20 |
| 8 (COM73-50379) | * | 802 (SN003-003-01217-3) | .60 | 834 (SN003-003-01294-7) | .55 |
| 9 (COM73-50677) | * | 803 (COM75-10279) | * | 835 (SN003-003-01353-6) | 1.95 |
| 0 (SN003-003-01136-3) | 1.40 | 804 (SN003-003-01229-7) | 2.00 | 836 (COM74-50567) | * |
| 1 (SN003-003-01137-1) | .95 | 805 (SN003-003-01231-9) | 1.20 | 837 (COM74-50636 | * |
| 2 (SN003-003-01140-1) | 1.25 | 806 (COM73-50928) | * | 838 (COM74-50841) | * |
| 3 (COM73-50534) | * | 807 (COM73-50971) | * | 839 (SN003-003-01303-0) | 1.85 |
| 4 (COM73-50535) | * | 808 (COM74-50085) | * | 840 (SN003-003-01315-3) | .55 |
| 5 (SN003-003-01141-0) | .50 | 809 (COM74-50174) | * | 841 (SN003-003-01312-9) | .60 |
| 6 (AD760-676) | * | 810 (SN003-003-01211-4) | .50 | 842 (SN003-003-01310-2) | 1.25 |
| 7 (COM73-50792) | * | 811 (SN003-003-01245-9) | 1.00 | 843 (COM74-50839) | * |
| 8 (COM73-50523) | * | 812 (SN003-003-01247-5) | .65 | 844 (SN003-003-01316-1) | .70 |
| 9 (COM73-50571) | * | 814 (SN003-003-01235-1) | 1.10 | 845 (COM74-50926) | * |
| 0 (SN003-003-01158-4) | .55 | 815 (SN003-003-01232-7) | .60 | 847 (SN003-003-01340-4) | .80 |
| 1 (COM73-50536) | * | 816 (COM74-50181) | * | 848 (COM74-50943) | * |
| 2 (SN003-003-01286-6) | .90 | 817 (SN003-003-01265-3) | .60 | 849 (COM74-50998) | * |
| 5 (COM73-50682) | * | 818 (SN003-003-01238-6) | .80 | 850 (SN003-003-01366-8) | .85 |
| 6 (SN003-003-01194-1) | .50 | 819 (COM74-50279) | * | 851 (COM74-51065) | * |
| 7 (SN003-003-01161-4) | .90 | 820 (COM74-50140) | * | 852 (COM74-51085) | * |
| 8 (COM73-50683) | * | 821 (SN003-003-01257-2) | .60 | 853 (SN003-003-01330-7) | .85 |
| 9 (SN003-003-01163-1) | 2.35 | 822 (COM74-50340) | * | 854 (SN003-003-01381-1) | 2.00 |
| 9-1 (SN003-003-01439-7) | .80 | 823 (SN003-003-01264-5) | .60 | 855 (SN003-003-01367-6) | 1.05 |
| 0 (COM73-50678) | * | 824 (SN003-003 01258-1) | .65 | 856 (SN003-003-01371-4) | .65 |
| 1 (COM73-50665) | * | 825 See TN983 |  | 857 (SN003-003-01423-1) | 1.05 |
| 2 (SN003-003-01183-5) | .80 | 826 (COM74-50346) | * | 858 (SN003-003-01433-8) | 3.75 |
| 3 (COM73-50831) | * | 827 (COM74-50457) | * |  |  |
| 4 (COM73-50927) | * | 828 (SN003-003-01287-4) | 2.05 |  |  |
| 6 (COM73-50876) | * |  |  |  |  |

---

*Available from the National Technical Information Service, use "PB", "AD", "COM", "N", or NBS blication identification if no specific NTIS number is assigned. Available in Microfiche for .00; consult NTIS for paper copy price.

## TECHNICAL NOTES—(Continued)

| No. | Price | No. | Price | No. | Pric |
|---|---|---|---|---|---|
| 859 (SN003-03-01543-1) | 4.15 | 884 (SN003-003-01471-1) | .45 | 910-1 (SN003-003-01590-3) | 2.1 |
| 860 (SN003-003-01401-0) | 2.05 | 885 (SN003-003-01476-1) | 1.45 | **910-3 (SN003-003-01785-0)** | **2.1** |
| 861 (SN003-003-01380-3) | .80 | 886 (SN003-003-01470-2) | .65 | 912 (SN003-003-01613-6) | 2.0 |
| 862 (SN003-003-01402-8 | .80 | 887 (SN003-003-01545-8 | 1.45 | 913 (SN003-003-01645-4) | 1.0 |
| 863 (SN003-003-01404-4) | 1.15 | 888 (SN003-003-01482-6 | 1.65 | 914 (SN003-003-01636-5) | .8 |
| 864 (SN003-003-01400-1) | 1.20 | 889 (SN003-003-01574-1) | 1.80 | 915 (SN003-003-01631-4) | .7 |
| 865 (SN003-003-01411-7) | 1.35 | 890 (SN003-003-01548-2) | 1.10 | 916 (SN003-003-01626-8) | 2.8 |
| 866 (SN003-003-01441-9) | 1.85 | 891 (SN003-003-02186-5) | 1.10 | 917 (SN003-003-01640-3) | .8 |
| 867 (SN003-003-01427-3) | 1.25 | 892 (SN003-003-01549-1) | 1.70 | 918 (SN003-003-01661-6) | 1.1 |
| 868 (SN003-003-01430-3) | 1.50 | 893 (SN003-003-01561-0) | 1.30 | 919 (SN003-003-01658-6) | 1.2 |
| 869 (SN003-003-01424-9) | .80 | 894 (SN003-003-01570-9) | 1.45 | 920 (SN003-003-01648-9) | 1.1 |
| 870 (SN003-003-01434-6) | 1.05 | 895 (SN003-003-01564-4) | 2.30 | 921 (SN003-003-01660-8) | 2.2 |
| 871 (SN003-003-01435-4) | .140 | 896 (SN003-003-01562-8) | 2.15 | 922 (SN003-003-01668-3) | 1.7 |
| 872 (SN003-003-01436-2) | 2.10 | 897 (SN003-003-01589-0) | 1.15 | 923 (SN003-003-01679-9) | .7 |
| 873 (SN003-003-01555-5) | .75 | 898 (SN003-003-01584-9) | .55 | 924 (SN003-003-01671-3) | 1.0 |
| 874 (SN003-003-01438-9) | 1.00 | 899 (SN003-003-01579-2) | 4.00 | 925 (SN003-003-01680-2) | 1.7 |
| 875 (SN003-003-01448-6) | .65 | 900 (SN003-003-01611-0) | .75 | 927 (SN003-003-01683-7) | 1.1 |
| 876 (COM75-11113) | * | 901 (SN003-003-01607-1) | 1.15 | 928 (SN003-003-01711-6 | 1.1 |
| 877 (SN003-003-01455-9) | .80 | 902 (SN003-003-01598-9) | 2.70 | 929 (SN003-003-01694-2) | .8 |
| 878 (SN003-003-01440-1) | .65 | 903 (SN003-003-01578-4) | .85 | 930 (SN003-003-01672-1) | .5 |
| 879 (SN003-003-01432-0) | 1.10 | 904 (SN003-003-01617-9) | .75 | 931 (SN003-003-01689-6) | 1.8 |
| 880 (SN003-003-01447-8) | .85 | 905 (SN003-003-01610-1) | 1.10 | 932 (SN003-003-01703-5) | 1.3 |
| 881 (SN003-003-01469-9) | 1.10 | 906 (SN003-003-01630-6) | 1.35 | | |
| 882 (SN003-003-01462-1) | .85 | 908 (SN003-003-01643-8) | 1.55 | | |
| 883 (SN003-003-01475-3) | 1.45 | 909 (SN003-003-01615-2) | 1.05 | | |

*Available from the National Technical Information Service; use "AD", or "COM" number whe ordering. Available in Microfiche for $3.00; consult NTIS for paper copy price.

## NBS INTERAGENCY REPORTS

These reports are available by purchase from he National Technical Information Service, pringfield, VA 22161. Those items in boldface enote the publications cited in this supplement. he prices are those in effect as of the date this ublication went to press. When ordering, use the "AD", "PB", "N" or "COM" number. The prices quoted are for paper copy domestic, add $2.25 additional for foreign mailing. Microfiche are available for $2.25 per set. Prices are subject to change without notice.

| o. | Price |
|---|---|
| **3-101 (COM73-10867)** | A05 |
| **3-102 (COM73-10856)** | A04 |
| **3-105 (COM73-10858)** | A03 |
| **3-110 (COM73-11191)** | A07 |
| **3-112 (COM74-10702-03)** | A04 |
| **3-113 (COM74-10702-01)** | A13 |
| **3-114 (COM74-10702-02)** | A13 |
| 3-116 (COM73-10859) | A04 |
| **3-119 (AD757789)** | A04 |
| **3-121 (COM73-10860)** | A06 |
| **3-125 (COM73-11189)** | A04 |
| **3-126 (COM73-10854)** | A06 |
| **3-127 (COM73-10857)** | A05 |
| **3-128 (AD760150)** | A04 |
| **3-129 (COM73-10853)** | A05 |
| **3-131 (COM73-10863)** | A04 |
| **3-132 (PB222300)** | A07 |
| **3-135 (COM73-10840)** | A03 |
| **3-138 (COM73-10868)** | A03 |
| **3-140 (COM73-10842)** | A02 |
| **3-141 (COM73-10841)** | A03 |
| **3-144 (PB220-849)** | A07 |
| **3-145 (COM75-10541)** | A03 |
| **3-146 (COM73-10989)** | A04 |
| 3-148 (COM73-10855) | A05 |
| **3-151 (COM73-10866)** | A02 |
| **3-152 (AD914258)** | A07 |
| **3-154 (COM73-10865)** | A02 |
| **3-156 (COM73-11286)** | A04 |
| **3-157 (COM74-10394)** | A03 |
| **3-159 (COM73-11174)** | A02 |
| **3-161 (PB225310)** | A04 |
| **3-163 (COM74-10542)** | A06 |
| **3-164 (COM73-10834)** | A03 |
| **3-165 (COM73-10837)** | A02 |
| **3-166 (COM73-10835)** | A02 |
| **3-167 (COM73-10836)** | A02 |
| **3-168 (COM73-10838)** | A03 |
| **3-169 (COM73-10839)** | A02 |
| **3-170 (COM73-10843)** | A03 |
| **3-172 (COM73-11175)** | A05 |
| **73-173 (COM73-10844)** | A03 |
| **73-175 (COM74-10395)** | A04 |
| **73-177 (COM75-10336)** | A03 |
| **73-180 (COM74-10130)** | A03 |
| **73-182 (COM73-11284)** | A05 |
| **73-183 (COM73-11177)** | A04 |
| **73-184 (COM73-11110)** | A05 |
| **73-185 (COM73-11287)** | A03 |
| **73-187 (PB221-188)** | A04 |
| **73-188 (PB221-183)** | A05 |
| **73-189 (COM73-11173)** | A03 |
| **73-190 (COM73-10831)** | A02 |
| **73-191 (PB221-695)** | A02 |
| **73-192 (COM73-10832)** | A02 |
| **73-197 (COM74-10468)** | A04 |
| **73-198 (COM74-11289)** | A02 |
| **73-199 (COM74-10129)** | A06 |
| **73-200 (COM74-10478)** | A03 |
| **73-201 (COM73-11221)** | A05 |
| **73-202 (COM74-10479)** | A03 |
| **73-203 (See NBSIR 74-430 COM74-10724)** | A06 |
| **73-206 (COM73-11262)** | A06 |
| **73-207 (AD769-266)** | A07 |
| **73-208 (COM74-10127)** | A03 |
| **73-209 (COM74-10469)** | A11 |
| **73-210 (COM74-11767)** | A10 |
| **73-211 (COM74-10950)** | A08 |
| **73-212 (COM74-11009)** | A07 |
| **73-213 (COM74-11771)** | A07 |
| **73-214 (COM74-11239)** | A06 |
| **73-215 (COM74-11010)** | A06 |
| **73-216 (COM74-11011)** | A07 |
| 73-217 (COM74-10470) | A03 |
| 73-218 (COM75-10144) | A03 |
| **73-220 (PB222-437)** | A02 |
| **73-221 (COM73-11113)** | A05 |
| **73-223 (COM73-11220)** | A05 |
| **73-228 (PB222-425)** | A02 |
| **73-231 (PB224-645)** | A03 |
| **73-233 (COM74-11770)** | A04 |
| **73-234 (COM74-10128)** | A03 |
| 73-240 (COM74-10986) | A03 |
| 73-242 (PB224-654) | A03 |

| No. | Price |
|---|---|
| 73-244 (AD-A003-900) | A04 |
| 73-246 (COM74-10989) | A02 |
| 73-248 (COM74-10474) | A05 |
| 73-251 (PB224-688) | A03 |
| 73-252 (AD775-082) | A12 |
| 73-254 (COM74-10987) | A02 |
| 73-256 (COM75-11443) | A02 |
| 73-257 (COM75-11444) | A02 |
| 73-258 (COM75-11445) | A02 |
| 73-259 (COM75-11446) | A02 |
| 73-260 (COM75-11440) | A02 |
| 73-261 (COM75-11441) | A02 |
| 73-262 (COM75-10370) | A04 |
| 73-263 (PB225-284) | A04 |
| 73-264 (PB243-541) | A02 |
| 73-265 (COM73-11453) | A04 |
| 73-266 (PB225-286) | A03 |
| 73-267 (COM73-11955) | A04 |
| 73-268 (AD768-303) | A03 |
| 73-275 (COM74-10126) | A04 |
| 73-277 (PB225-278) | A04 |
| 73-280 (AD782-094) | A06 |
| 73-281 (AD782-028) | A06 |
| 73-287 (COM73-11928) | A02 |
| 73-288 (COM73-11861) | A04 |
| 73-289 (COM74-10475) | A03 |
| 73-290 (COM74-10974) | A02 |
| 73-294 (AD787-327) | A04 |
| 73-295 (COM74-10471) | A02 |
| 73-297 (AD772-066) | A02 |
| 73-299 (PB243-543) | A03 |
| 73-301 (COM73-10762) | A03 |
| 73-302 (COM73-10869) | A05 |
| 73-303 (AD759-374) | A04 |
| 73-304 (COM74-10281) | A05 |
| 73-308 (COM73-10761) | A03 |
| 73-309 (COM73-11981) | A05 |
| 73-316 (COM73-11954) | A05 |
| 73-318 (N73-27390) | A09 |
| 73-320 (COM73-11971) | A02 |
| 73-322 (COM73-11464) | A03 |
| 73-326 (COM73-11465) | A02 |
| 73-329 (COM74-10608) | A05 |
| 73-330 (COM74-10609) | A04 |
| 73-331 (COM74-10238) | A05 |
| 73-335 (COM74-11051) | A05 |
| 73-338 (COM73-11660) | A03 |
| 73-339 (COM73-11985) | A13 |
| 73-341 (COM74-10885) | A03 |
| 73-342 (COM73-11978) | A13 |
| 73-343 (COM75-10282) | A05 |

| No. | Price |
|---|---|
| 73-344 (COM74-10749) | A03 |
| 73-345 (COM74-10239) | A04 |
| 73-346 (COM74-10240) | A03 |
| 73-347 (COM74-10674) | A04 |
| 73-348 (COM74-10241) | A03 |
| 73-349 (COM74-11374) | A04 |
| 73-351 (COM74-10784) | A04 |
| 73-402 (COM74-10472) | A07 |
| 73-403 (COM74-10016) | A07 |
| 73-404 (PB230-952) | A03 |
| 73-405 (COM74-10131) | A02 |
| 73-406 (COM74-11352) | A02 |
| 73-407 (COM74-11078) | A05 |
| 73-412 (COM74-10512) | A03 |
| 73-413 (COM74-10750) | A04 |
| 73-414 (COM74-10866) | A03 |
| 73-415 (COM75-11448) | A09 |
| 73-416 (COM74-10511) | A04 |
| 73-417 (COM74-10477) | A03 |
| 73-418 (COM74-11783) | A07 |
| 73-420 (COM74-11092) | A04 |
| 73-421 (COM74-11224) | A03 |
| 73-422 (COM74-11240) | A04 |
| 73-423 (COM74-11722) | A08 |
| 73-424 (COM74-10867) | A02 |
| 74-355 (N74-30195) | A04 |
| 74-357 (COM74-10551) | A04 |
| 74-359 (AD780-596) | A24 |
| 74-361 (COM74-11222) | A04 |
| 74-363 (COM74-11053) | A07 |
| 74-364 (COM74-11208) | A05 |
| 74-365 (COM74-11375) | A03 |
| 74-366 (COM74-11076) | A05 |
| 74-369 (COM74-11688) | A03 |
| 74-371 (COM74-11567) | A04 |
| 74-372 (ADA006-037) | A05 |
| 74-375 (COM74-11657) | A04 |
| 74-377 (COM74-11449) | A03 |
| 74-378 (COM74-11450) | A04 |
| 74-379 (PB247-658) | A03 |
| 74-380 (COM74-11686) | A06 |
| 74-381 (COM75-10522) | A04 |
| 74-382 (AD783-433) | A10 |
| 74-387 (COM74-11643 | A03 |
| 74-388 (COM74-11687) | A07 |
| 74-389 (COM74-11717) | A08 |
| 74-390 (COM74-11718) | A06 |
| 74-391 (COM74-10258) | A03 |
| 74-393 (COM75-10768) | A13 |
| 74-394 (COM75-10126) | A03 |
| 74-395 (COM75-10161) | A03 |

## NBS INTERAGENCY REPORTS (Continued)

| o. | Price |
|---|---|
| -396 (COM74-11766) | A03 |
| -398 (COM75-10130) | A15 |
| -426 (COM74-11074) | A06 |
| -430 (COM74-10724) | A06 |
| -432 (COM74-10751) | A04 |
| -434 (COM74-11079) | A02 |
| -438 (COM74-10980) | A03 |
| -439 (COM74-10985) | A02 |
| -442 (AD787-743) | A03 |
| -443 (COM74-11003) | A02 |
| -444 (COM74-10548) | A03 |
| -449 (COM75-10049) | A03 |
| **-452 (PB204-486)** | A06 |
| -454 (COM74-10988) | A02 |
| -455 (COM74-10865) | A03 |
| -456 (COM74-11793) | A02 |
| -457 (COM74-11792) | A05 |
| -458 (AD776-337) | A02 |
| -461 (PB246-623) | A03 |
| -464 (COM74-10785) | A05 |
| -465 (COM75-10417) | A04 |
| -466 (COM74-10700) | A21 |
| -467 (COM74-11754) | A04 |
| -470 (PB232-629) | A05 |
| -471 (COM74-10981) | A02 |
| -473 (COM74-11719) | A04 |
| -474 (AD778-340) | A03 |
| -477 (COM74-11784) | A03 |
| -479 (PB239-420) | A07 |
| -481 (COM74-11794) | A04 |
| -482 (COM75-10147) | A10 |
| -485 (AD780-704) | A02 |
| -486 (AD780-705) | A04 |
| -487 (COM74-10886) | A23 |
| -488 (COM75-10088) | A06 |
| -495 (COM74-11575) | A05 |
| -496 (COM74-11576) | A05 |
| -497 (COM74-11269) | A02 |
| -499 (COM74-11378) | A03 |
| -501 (COM75-10131) | A02 |
| -506 (COM74-11632) | A05 |
| **-507 (AD/A0001343)** | A03 |
| -509 (COM74-11377) | A02 |
| -510 (AD782-793) | A03 |
| -511 (COM74-11448) | A02 |

| No. | Price |
|---|---|
| 74-514 (COM75-10102) | A04 |
| 74-515 (COM74-11498) | A09 |
| 74-516 (COM74-11384) | A04 |
| 74-518 (PB239-633) | A05 |
| 74-519 (PB238-284) | A03 |
| 74-520 (COM74-11480) | A07 |
| 74-521 (COM75-10187) | A04 |
| 74-522 (COM75-10080) | A02 |
| 74-523 (COM75-11126) | A02 |
| 74-524 (COM74-11568) | A03 |
| 74-525 (AD782-564) | A02 |
| 74-526 (COM75-10087) | A04 |
| 74-527 (COM74-11720) | A04 |
| 74-529 (COM74-11495) | A04 |
| 74-530 (COM75-10041) | A03 |
| 74-533 (PB238-573) | A06 |
| 74-535 (COM74-11659) | A05 |
| 74-537 (COM74-11577) | A02 |
| 74-539 (COM74-11574) | A05 |
| 74-541 (COM75-10618) | A03 |
| 74-542 (COM75-10081) | A03 |
| 74-543 (COM74-11772) | A07 |
| 74-544 (COM74-11525) | A03 |
| 74-545 (COM74-11656) | A04 |
| 74-550 (COM74-11721) | A05 |
| 74-551 (COM74-11658) | A06 |
| 74-552 (COM74-11644) | A05 |
| 74-553 (COM75-10058) | A04 |
| 74-554 (COM74-10703) | A03 |
| 74-555 (COM74-10704) | A03 |
| 74-556 (COM74-10703) | A05 |
| 74-557 (COM75-11439) | A03 |
| 74-561 (COM75-10413) | A03 |
| 74-564 (COM74-11726) | A04 |
| 74-567 (COM74-11631) | A13 |
| 74-568 (COM74-11578) | A04 |
| 74-572 (COM74-11791) | A04 |
| 74-577-1 (COM74-11723) | A09 |
| 74-577-2 (COM74-11724) | A14 |
| 74-578 (COM74-11765) | A02 |
| 74-580 (PB248-465) | A02 |
| 74-581 (COM75-10127) | A03 |
| 74-582 (COM74-11645) | A03 |
| 74-583 (AD/A003-900) | A05 |
| 74-586 (COM75-10525) | A02 |
| 74-588 (COM75-10040) | A03 |
| 74-590 (COM75-11434) | A02 |

## NBS INTERAGENCY REPORTS (Continued)

| No. | Price |
|---|---|
| 74-591 (COM75-10101) | A02 |
| 74-595 (COM75-10057) | A02 |
| 74-596 (COM75-10209) | A03 |
| 74-597 (COM75-11069) | A03 |
| 74-600 (AD/A008-935) | A09 |
| 74-602 (COM75-10048 | A03 |
| 74-605 (COM75-10464) | A03 |
| 74-606 (COM75-10340) | A05 |
| 74-608 (COM75-10056) | A02 |
| 74-610 (COM75-10073) | A03 |
| 74-612 (COM75-10414) | A02 |
| 74-613 (COM75-10059) | A03 |
| 74-614 (COM75-11013) | A03 |
| 74-618 (COM75-11014) | A02 |
| 74-619 (COM75-10047) | A02 |
| 74-620 (PB246-622) | A02 |
| 74-621 (COM75-10422) | A03 |
| 74-623 (COM75-10210) | A05 |
| 74-624 (COM75-10412) | A03 |
| **74-625 (PB243-547)** | A03 |
| 74-626 (COM75-10411) | A02 |
| 74-627 (COM75-10134) | A02 |
| 74-628 (COM75-10514) | A02 |
| 74-629 (COM75-11281) | A03 |
| 74-631 (COM75-10208) | A02 |
| 74-632 (PB246-554) | A05 |
| 74-633 (COM75-10691) | A04 |
| 74-634 (COM75-10685) | A03 |
| 74-635 (COM75-10276) | A04 |
| 75-637 (COM75-10055) | A02 |
| 75-639 (AD/A005-410) | A02 |
| 75-641 (COM75-11209) | A05 |
| 75-647 (COM75-10418) | A03 |
| 75-649 (PB241-237) | A02 |
| 75-651 (COM75-11211) | A05 |
| 75-652 (COM75-11399) | A05 |
| 75-653 (PB248-097) | A03 |
| 75-654 (COM75-10367) | A02 |
| 75-658 (AD/A007-445) | A03 |
| 75-659 (AD/A008-538) | A03 |
| 75-660 (COM75-10669) | A03 |
| 75-661 (COM75-10763) | A03 |
| 75-662 (COM75-10420) | A02 |
| 75-664 (AD/A007-447) | A03 |
| 75-665 (COM75-10421) | A03 |
| 75-666 (COM75-11381) | A03 |
| **75-667 (PB241-267)** | A03 |
| 75-672 (COM75-10338) | A03 |
| 75-673 (COM75-10921) | A03 |
| 75-675 (COM75-10686) | A03 |
| 75-677 (COM75-10516) | A04 |
| **75-678 (PB248-687)** | A04 |
| 75-679 (COM75-10419) | A03 |
| 75-680 (COM75-10423) | A06 |
| 75-682 (COM75-10524) | A02 |
| 75-685 (COM75-10690) | A05 |
| 75-687 (COM75-11137) | A07 |
| 75-688 (COM75-11222) | A06 |
| 75-689 (COM75-11190) | A04 |
| 75-690 (COM75-11207) | A05 |
| 75-691 (COM75-11015) | A05 |
| 75-692 (PB250-385) | A06 |
| 75-693 (COM75-11194) | A02 |
| 75-696 (COM75-10527) | A05 |
| 75-697 (COM75-10920) | A04 |
| 75-699 (COM75-11016) | A03 |
| 75-700 (COM75-11280) | A04 |
| 75-701 (COM75-11282) | A02 |
| 75-702 (COM75-11433) | A03 |
| 75-703 (COM75-11278) | A03 |
| 75-705 (COM75-11277) | A03 |
| 75-706 (PB248-640) | A02 |
| 75-707 (COM75-11017) | A03 |
| 75-708 (COM75-10817) | A02 |
| 75-710 (COM75-11030) | A02 |
| 75-711 (COM75-10689) | A04 |
| 75-712 (COM75-11070) | A03 |
| 75-713 (COM75-11134) | A04 |
| 75-715 (COM75-11208) | A02 |
| 75-716 (COM75-11210) | A08 |
| 75-718 (COM75-10750) | A03 |
| **75-719 (PB251-410)** | A03 |
| 75-721 (PB246-864) | A03 |
| **75-722 (PB248-641)** | A03 |
| 75-723 (COM75-10753) | A04 |
| 75-729 (PB246-858) | A03 |
| 75-730 (AD/A018451) | A03 |
| 75-731 (COM75-11071) | A03 |
| 75-732 (COM75-11022) | A02 |
| 75-733 (COM75-11139) | A02 |
| 75-734 (COM75-11212) | A03 |
| **75-735 (PB256-295)** | A07 |
| 75-736 (COM75-11018) | A02 |
| 75-737 (COM75-11472) | A03 |
| 75-738 (COM75-11279) | A03 |
| 75-739 (COM75-11189) | A02 |
| 75-740 (COM75-11127) | A03 |
| 75-741 (COM75-11136) | A03 |
| **75-742 (PB248-744)** | A04 |

| No. | Price |
|---|---|
| 5-744 (COM75-11072) | A02 |
| 5-745 (PB347-657) | A03 |
| 5-746 (COM75-11432) | A04 |
| 5-747 (COM75-11131) | A03 |
| 5-748 (COM75-11031) | A05 |
| **5-750 (PB249-934)** | A03 |
| 5-751 (AD-A017-626) | A03 |
| **5-755 (PB248-642)** | A03 |
| **5-757 (PB248-914)** | A03 |
| 5-760 (AD/A016-843) | A10 |
| 5-761 (COM75-11377) | A06 |
| 5-763 (COM75-11276) | A10 |
| 5-766 (COM75-11376) | A04 |
| 5-767 (PB246-879) | A03 |
| **75-768 (PB247-943)** | A03 |
| 75-769 (PB246-978) | A11 |
| 75-770 (COM75-11370) | A03 |
| 75-772 (PB246-861) | A04 |
| 75-774 (COM75-11364) | A04 |
| **75-775 (PB248-864)** | A04 |
| 75-778 (PB246-435) | A04 |
| 75-779 (PB249-935) | A06 |
| 75-781 (AD/A015630) | A02 |
| **75-782 (PB248-643)** | A03 |
| 75-784 (PB246-862) | A04 |
| 75-785 (PB246-345) | A03 |
| **75-786 (PB251-411)** | A04 |
| 75-787 (AD/A016-844) | A04 |
| **75-788 (PB250-843)** | A03 |
| **75-790 (PB250-848)** | A16 |
| **75-791 (PB253-229)** | A04 |
| 75-793 (PB247-538) | A04 |
| 75-794 (PB247-203) | A03 |
| 75-795 (PB246-866) | A04 |
| 75-796 (PB247-656) | A02 |
| 75-797 (COM75-11465) | A02 |
| **75-801 (PB252-044)** | A08 |
| 75-804 (COM75-10395) | A03 |
| **75-805 (PB252-971)** | A03 |
| 75-806 (COM75-10368) | A04 |
| 75-807 (COM75-10396) | A05 |
| 75-809 (COM75-10989) | A03 |
| 75-810 (COM75-10919) | A06 |
| 75-812 (AD/A012889) | A03 |
| 75-814 (COM75-11132) | A04 |
| 75-816 (AD/A001250) | A04 |
| 75-818 (PB245439) | A03 |
| **75-819 (PB258554)** | A06 |
| 75-820 (PB246436) | A04 |
| 75-822 (PB246933) | A03 |
| 75-823 (PB246658) | A05 |
| **75-825 (PB258-913)** | A04 |
| **75-827 (PB247-938)** | A02 |
| **75-828 (PB249-041)** | A09 |
| 75-829 (PB248-855) | A03 |
| 76-844 (PB264-300) | A04 |
| **75-900 (PB250-859)** | A03 |
| 75-901 (PB246-860) | A03 |
| **75-902 (PB249-539)** | A03 |
| 75-903 (PB246859) | A03 |
| 75-908 (PB247-270) | A02 |
| 75-909 (PB246-863) | A02 |
| **75-910 (PB248-646)** | A06 |
| **75-913 (PB248-911)** | A03 |
| **75-915 (PB249-775)** | A02 |
| **75-916 (AD/A019648)** | A05 |
| 75-917 (PB247-655) | A02 |
| **75-918 (PB251-412)** | A05 |
| **75-920 (PB248-913)** | A03 |
| **75-923 (PB250-767)** | A02 |
| 75-924 (PB248-686) | A05 |
| **75-926 (PB257-467)** | A06 |
| **75-927 (PB255-809)** | A04 |
| **75-929 (PB261-498)** | A03 |
| **75-930 (PB258-250)** | A04 |
| **75-931 (PB261-030)** | A03 |
| **75-932 (PB257-425)** | A04 |
| **75-933 (PB248-983)** | A04 |
| **75-937 (PB265-614)** | A02 |
| 75-942 (PB256-644) | A04 |
| **75-943 (PB258-914)** | A05 |
| **75-944 (PB258-372)** | A03 |
| **75-947 (PB258-323)** | A04 |
| **75-950 (PB250-664)** | A03 |
| **75-951 (PB249-094)** | A03 |
| **75-952 (PB248-910)** | A03 |
| **75-953 (PB256-219)** | A03 |
| **75-954 (PB253-242)** | A03 |
| **75-955 (PB248-685)** | A08 |
| 75-956 (PB247-654) | A02 |
| **75-957 (PB250-769)** | A02 |
| **75-958 (PB248-743)** | A02 |
| **75-960 (PB249-774)** | A04 |
| **75-961 (PB257-466)** | A11 |

## NBS INTERAGENCY REPORTS (Continued)

| No. | Price |
|---|---|
| 75-962 (PB247-639) | A02 |
| 75-966 (PB250-768) | A02 |
| 75-967 (PB251-413) | A02 |
| 75-968 (PB250-845) | A03 |
| 75-971 (PB249-776) | A03 |
| 75-972 (PB259-630) | A05 |
| 75-973 (PB249-255) | A04 |
| 75-974 (PB249-777) | A06 |
| 75-975 (PB253-113) | A03 |
| 75-976 (PB248-986) | A03 |
| 75-977 (PB251-220) | A03 |
| 76-833 (PB250-846) | A03 |
| 76-834 (PB250-666) | A03 |
| 76-836 (PB254-459) | A03 |
| 76-837 (PB261-709) | A07 |
| 76-839 (PB252-013) | A08 |
| 76-840 (PB258-324) | A03 |
| 76-841 (PB256-319) | A03 |
| 76-842 (PB258-331) | A02 |
| 76-846 (PB258-327) | A03 |
| 76-848 (PB261-996) | A14 |
| 76-979 (PB248-992) | A02 |
| 76-980 (PB250-849) | A10 |
| 76-982 (PB248-699) | A15 |
| 76-983 (PB251-213) | A03 |
| 76-984 (PB262-020) | A07 |
| 76-985 (PB250-755) | A04 |
| 76-986 (PB250-858) | A04 |
| 76-987 (PB250-857) | A03 |
| 76-988 (PB254-469) | A05 |
| 76-990 (PB251-769) | A02 |
| 76-991 (AD/A021255) | A02 |
| 76-992 (AD/A021295) | A04 |
| 76-993 (PB253-227) | A03 |
| 76-996 (PB251-998) | A03 |
| 76-997 (PB254-298) | A05 |
| 76-998 (PB253-228) | A03 |
| 76-1000 (PB251-219) | A04 |
| 76-1002 (PB257-469) | A04 |
| 76-1003 (PB251-211) | A02 |
| 76-1007 (PB252-021) | A04 |
| 76-1008 (PB251-218) | A03 |
| 76-1010 (PB250-654) | A03 |

| No. | Price |
|---|---|
| 76-1011 (PB259-641) | A03 |
| 76-1012 (PB257-197) | A04 |
| 76-1013 (PB256-130) | A03 |
| 76-1014 (PB251-414) | A02 |
| 76-1015 (PB249-530) | A13 |
| 76-1016 (PB254-177) | A04 |
| 76-1017 (PB251-917) | A03 |
| 76-1018 (PB257-779) | A04 |
| 76-1019 (PB251-944) | A02 |
| 76-1020 (PB258-256) | A03 |
| 76-1021 (PB257-101) | A04 |
| 76-1022 (PB259-628) | A02 |
| 76-1023 (PB256-191) | A02 |
| 76-1024 (PB255-876) | A04 |
| 76-1025 (PB251-753) | A05 |
| 76-1027 (PB253-243) | A03 |
| 76-1028 (PB251-415) | A02 |
| 76-1029 (PB261-199) | A03 |
| 76-1031 (PB253-932) | A02 |
| 76-1034 (PB254-460) | A05 |
| 76-1037 (PB253-933) | A03 |
| 76-1038 (PB251-918) | A02 |
| 76-1039 (PB254-047) | A03 |
| 76-1040 (PB254-178) | A02 |
| 76-1041 (PB257-086) | A04 |
| 76-1043 (PB254-347) | A06 |
| 76-1046 (PB256-476) | A06 |
| 76-1049 (PB256-600) | A04 |
| 76-1050 (PB253-111) | A04 |
| 76-1052 (PB258-118) | A05 |
| 76-1054 (PB253-110) | A06 |
| 76-1056 (PB254-179) | A03 |
| 76-1058 (PB262-097) | A07 |
| 76-1059 (PB257-086) | A08 |
| 76-1060 (PB253-934) | A03 |
| 76-1061 (PB256-328) | A04 |
| 76-1063 (PB257-102) | A03 |
| 76-1064 (PB257-102) | A04 |
| 76-1066 (PB254-473) | A02 |
| 76-1067 (PB257-195) | A03 |
| 76-1069 (PB256-296) | A03 |
| 76-1070 (PB260-913) | A07 |
| 76-1072 (PB255-446) | A04 |
| 76-1074 (PB261-497) | A03 |
| 76-1076 (PB254-180) | A03 |

| No. | Price |
|---|---|
| 6-1081 (PB256-329) | A05 |
| 6-1082 (PB258-235) | A08 |
| 6-1083 (PB255-803) | A06 |
| 6-1084 (PB257-180) | A03 |
| 6-1087 (PB257-202) | A03 |
| 6-1089 (PB254-475) | A10 |
| 6-1090 (PB255-505) | A03 |
| 6-1091 (PB257-768) | A03 |
| 6-1093 (PB256-318) | A02 |
| 6-1095 (PB255-808) | A05 |
| 6-1096 (PB257-076) | A04 |
| 6-1097 (PB257-141) | A03 |
| 6-1098 (PB259-523) | A03 |
| 6-1099 (PB258-612) | A06 |
| 6-1100 (PB258-371) | A04 |
| 6-1102 (PB257-729) | A08 |
| 6-1107 (PB258-322) | A04 |
| 6-1109 (PB257-194) | A04 |
| 6-1110 (PB257-073) | A03 |
| 6-1112 (PB259-636) | A03 |
| 6-1115 (PB257-196) | A02 |
| 6-1120 (PB257-837) | A02 |
| 6-1124 (PB261-846) | A05 |
| 6-1126 (PB260-878) | A04 |
| 6-1130 (PB257-347) | A09 |
| 6-1131 (PB259-242) | A03 |
| 6-1132 (PB260-363) | A05 |
| 6-1133 (PB261-228) | A08 |
| 6-1136 (PB261-965) | A04 |
| 6-1137 (PB257-770) | A05 |
| 6-1138 (PB259-522) | A04 |
| 6-1140 (PB259-626) | A19 |
| 6-1141 (AD/A031530) | A03 |
| 6-1142 (PB263-099) | A02 |
| 6-1143 (PB257-769) | A03 |
| 6-1144 (PB259-243) | A02 |
| 6-1147 (PB259-637) | A03 |
| 76-1153 (PB259-638) | A02 |
| 76-1154 (PB260-400) Vol. 1 | A09 |
| 76-1154 (PB260-401) Vol. 2 | A07 |
| 76-1159 (PB261-994) | A03 |
| 76-1162 (PB260-879) | A04 |
| 76-1172 (PB261-217) | A03 |
| 76-1176 (PB261-995) | A03 |
| 76-1178 (PB262-114) | A06 |

## GRANTEE/CONTRACTOR REPORTS

| No. | Price |
|---|---|
| 73-1 (PB192-365) | A03 |
| 73-2 (PB194-614) | A05 |
| 73-3 (COM71-00605) | A10 |
| 73-4 (COM73-10323) | A04 |
| 73-5 (COM73-10951) | A08 |
| 73-6 (COM73-10959) | A04 |
| 73-7 (COM73-10958) | A04 |
| 73-8 (COM73-10954) | A10 |
| 73-9 (COM73-10953) | A03 |
| 73-10 (COM73-10952) | A08 |
| 73-11 (PB242-597) | A12 |
| 73-12 (COM73-10955) | A06 |
| 73-13 (COM73-10957) | A05 |
| 73-14 (COM73-10950) | A04 |
| 73-15 (PB242-582) | A15 |
| 73-16 (COM73-11265) | A04 |
| 73-17 (COM74-10932) | A07 |
| 73-18 (COM73-11783) | A03 |
| 73-19 (COM74-10481) | A04 |
| 73-21 (COM74-10722) | A07 |
| 74-22 (COM74-10934) | A16 |
| 74-23 (COM74-10929) | A02 |
| 74-24 (COM74-10983) | A05 |
| 74-25 (COM74-11075) | A07 |
| 74-26 (COM74-11633) | A06 |
| 74-27 (COM75-10143) | A06 |
| 74-28 (PB176-912) | A12 |
| 74-29 (PB176-913) | A04 |
| 74-30 (COM74-11732) | A03 |
| 74-31 (COM74-11733) | A02 |
| 74-32 (COM75-10039) | A04 |
| 75-33 (COM75-10133) | A11 |
| 75-34 (COM75-10128) | A04 |
| 73-35 (COM75-10341) | A05 |
| 75-36 (PB261-144) | A16 |
| 75-37 (PB261-145) | A06 |
| 75-38 (PB261-021) | A05 |
| 75-40 (COM75-10696) | A03 |
| 75-42 (COM75-10805) | A24 |
| 75-43 (AD-16782) | A06 |
| 75-44 (COM75-10991) | A10 |
| 75-45 (PB257-835) | A02 |
| 75-46 (PB247-235) | A09 |
| 75-47 (PB247-236) | A17 |
| 75-48 (PB248-781) | A09 |
| 75-50 (PB247-939) | A07 |
| 75-51 (PB247-483) | A15 |
| 76-54 (PB251-682) | A05 |
| 76-55 (PB250-571) | A04 |
| 76-56 (PB250-572) | A04 |
| 76-57 (PB250-573) | A06 |
| 76-58 (PB256-291) | A07 |
| 76-59 (PB256-639) | A10 |
| 76-60 (PB253-588) | A05 |
| 76-61 (PB253-553) | A05 |
| 76-63 (PB256-440) | A06 |
| 76-64 (PB255-445) | A05 |
| 76-69 (PB254-276) | A06 |
| 76-70 (PB254-748) | A04 |
| 76-71 (PB254-751) | A04 |
| 76-72 (PB256-190) | A06 |
| 76-73 (PB257-424) | A08 |
| 76-74 (PB256-771) | A03 |
| 76-75 (PB261-201) | A03 |
| 76-76 (PB261-200) | A06 |
| 76-79 (PB259-127) | A03 |

# EXPERIMENTAL TECHNOLOGY INCENTIVES PROGRAM REPORTS

| No. | Price |
|---|---|
| 73-01 (COM73-11373) | A12 |
| 73-02 (COM73-11375) | A08 |
| 73-03 (COM73-11374) | A06 |
| 73-04 (COM74-10256) | A02 |
| 73-05 (COM74-10257) | A04 |
| 73-06 (COM74-10258) | A03 |
| 73-07 (COM74-10939) Vol. 1 | A05 |
| 73-07 (COM74-10940) Vol. 2 | A14 |
| 75-01 (COM75-11369) | A07 |
| 76-03 (PB251-266) | A04 |
| 76-04 (PB251-683) | A15 |
| 76-05 (PB253-108) | A03 |
| 76-06 (PB253-918) | A09 |
| 76-08 (PB254-078) | A03 |
| 76-09 (PB252-488) | A03 |
| 76-10 (PB253-260) | A03 |
| 76-11 (PB253-115) | A06 |
| 76-12 (PB254-996) | A19 |
| 76-13 (PB253-475) | A03 |
| 76-14 (PB253-476) | A03 |
| 76-15 (PB253-477) | A03 |
| 76-16 (PB256-129) | A11 |
| 76-17 (PB254-233) | A10 |
| 76-18 (PB256-642) | A03 |
| 76-19 (PB256-643) | A03 |
| 76-22 (PB257-884) | A20 |
| 76-23 (PB258-991) | A03 |
| **76-24 (PB258-093)** | A11 |

# 4. TITLES AND ABSTRACTS OF PAPERS PUBLISHED IN NON-NBS MEDIA, 1977

Reprints from the journals listed in this Section may often be obtained directly from the authors. See Section 5.2 on page 109 for additional information.

9150. **A comparison between a switched and a correlation radiometer for cryogenic noise source measurements,** D. F. Wait and C. L. Trembach, (*ISA 20th Annual Conference and Exhibit, Los Angeles, Calif., Oct. 4-7, 1965*), *ISA Preprint* **14.4**-3-65 (Oct. 1965).

Key words: Cryogenic noise source measurements; microwave; noise source measurements; radiometer.

A microwave sum-and-difference-correlation (S-D-C) radiometer is compared theoretically and experimentally with a microwave switching (Dicke) radiometer. Particular emphasis is given to the precision with which each radiometer can compare cryogenic noise sources.

9151. **A miniature helium turbo-expander for cryogenic refrigeration systems,** M. T. Norton, (*Proc. XI Intern. Congress Refrigeration, Munich, Germany, Aug. 1963*), Book, *Progress in Refrigeration Science and Technology* **I**, 131-135 (Pergamon Press Inc., New York, N. Y., 1965).

Key words: Design; expansion turbine; gas bearings; helium refrigeration; performance; 9800 RPS; 200 Watts (30 °K).

The Cryogenic Engineering Laboratory is investigating the use of small turbo-expanders, supported by gas bearings, which produce small amounts of refrigeration at 4.2 °K and 30 °K. The turbine and externally pressurized gas bearings used with the 4.2 °K system have previously been reported.

This paper describes a helium turbine expander designed for use in a closed cycle system. The turbine was designed to extract about 200 Watts at 30 °K from the helium flow. The turbine is 7.9 mm in diameter, rotates at 9800 revolutions per second, and was designed for an inlet pressure of 4 atmospheres and 4:1 pressure ratio. Tests covering pressure ratios from 4:1 to 6.4:1 indicate a peak efficiency at 65 percent. The turbine design philosophy and performance data of this turbine are given.

9152. **A precision pulse-operated electronic phase shifter and frequency translator,** J. A. Barnes and A. Wainwright, *Proc. IEEE* **53,** No. 12, 2143-2144 (Dec. 1965).

Key words: Frequency translator; phase shifter; universal time.

A reference signal is processed through a voltage variable delay line and a narrow band filter. After a voltage pulse of proper amplitude and shape is applied to the voltage variable delay line, the output signal from the narrow band filter has exactly one cycle of phase less (or more depending upon pulse shape) than the reference signal. By suitable processing, it is possible to generate precise submultiples of the one cycle (360 °) of phase and thus realize precise and stable phase shifts.

This system has great utility in the generation of small but precise frequency offsets such as are used in the generation of the coordinated universal time scales. To this end a rather compact unit has been constructed to offset the frequency of a 100 KHz signal from 0 to -500 parts in $10^{10}$ in steps of 50 parts in $10^{10}$.

9153. **A survey of the thermodynamic data on heavier elements and their compounds: high-temperature enthalpy and vaporization equilibria,** T. B. Douglas, *Proc. 3d Meeting Interagency Chemical Rocket Propulsion Group, Working Group on Thermochemistry, El Segundo, Calif.*, Mar. 17-18, 1965, **I,** No. 82U, 5-16 (Chemical Propulsion Information Agency, Silver Spring, Md., July 1965).

Key words: Enthalpy; heavier elements; literature survey; refractory compounds; thermodynamic; vaporization.

A comprehensive, though not all-inclusive, survey of the published literature was undertaken for the purpose of determining where high-temperature enthalpy and vaporization-equilibrium data appear to be lacking or inadequate for Ti, Zr, W, Pb, Hg, I, Hf, Th, U, and their light-element compounds considered to be of possible importance in chemical propulsion and refractory applications. The results of this survey are summarized, and several examples are presented of the effects of uncertainties in the standard thermodynamic properties on calculated equilibria at high temperatures. It is pointed out that the first ionization potential of a molecule containing one alkali atom can be expected to exceed that of the free alkali atom by approximately the dissociation energy of the neutral molecule; and this relation is verified, within experimental uncertainty, for several examples.

9154. **Activation-analysis program and facilities at the National Bureau of Standards,** J. R. DeVoe and G. W. Smith, *Proc. 1965 Intern. Conf. Modern Trends in Activation Analysis, Texas A&M University, College Station, Texas,* pp. 225-229 (Apr. 1965).

Key words: Clean room; computers; counting rooms; feedback analysis; optimization of variables 10 MW nuclear reactor; pneumatic tubes; radiochemical laboratories; 14 MeV neutron generator; 100 MeV-40 KW LINAC.

The National Bureau of Standards' Radiochemical Analysis Section is now developing a capability in activation analysis to complement other analytical techniques using radioisotopes in analysis.

Activation analysis can be likened to spectrometric methods in which the re-emitted radiation from excited states (e.g. radioisotopes) which are often long (e.g. milliseconds to years) are measured and related to the kind and amount of element which interacted with the primary radiation. The analyst learns to discriminate from unwanted excitation processes by varying the type and energy of incident radiation, the length of time of the excitation, and the type of detector that measures the re-emitted or secondary radiation.

To be most effective for our applications of activation analysis a computer is best used in a regenerative feed-back loop which consists of selecting, in sequence; the proper nuclear reaction, time of irradiation, complexity of radiochemical separation, appropriate detector, stripping of time dependent radiation spectra, and judgment of the analyst. It should be emphasized that a selective combination of the above variables does not place too large a burden on any one of the variables. Plans for the development of facilities to carry out these concepts are discussed.

9155. **Additional observations on the electronic spectrum of copper (II) acetate monohydrate,** C. W. Reimann, G. F. Kokoszka, and G. Gordon, *J. Inorg. Chem.* **4,** No. 7, 1082-1084 (July 1965).

Key words: Bi-nuclear complex; copper (II) acetate monohydrate; polarized electronic absorption spectrum; tentative assignment based on selection rules.

The polarization properties of a previously undiscovered band in single crystals of copper (II) acetate monohydrate are reported. The absorption spectrum of copper (II) acetate monohydrate in the region 8000 cm$^{-1}$ to 30,000 cm$^{-1}$ is considered in terms of the requirements of the $C_{4v}$, $C_{2v}$, and $C_2$ symmetry groups.

9156. **Anniversaries in 1965 of interest to statisticians,** C. Eisenhart, *Am. Stat.* **19,** No. 5, 21-29 (Dec. 1965).

Key words: Anniversaries; history; probability; statistics; Pierre de Fermat; Gregor Mendel; Isaac Todhunter.

Patterned on the annual articles in the American Journal of Physics on "Anniversaries . . . of Interest to Physicists", this invited paper aims to initiate a similar series of articles in the American Statistician on "Anniversaries . . . of Interest to Statisticians".

The year 1965 marks the tercentennial of the death of Pierre de Fermat, co-founder, with Blaise Pascal, of the mathematical theory of probability; the centennial of the publication of Isaac Todhunter's *History of the Mathematical Theory of Probability . . .*; and the centennial of Gregor Mendel's oral presentation of the statistical laws of inheritance that today bear his name to the Brunn society for the Study of Natural Science. The lives and principal accomplishments of Fermat, Todhunter, and Mendel are reviewed from the viewpoint of their contributions to, and influence on, statistical theory and practice.

9157. **Applications of sulfur coating to integrating spheres,** S. T. Dunn, *Appl. Opt.* **4,** 877 (July 1965).

Key words: Coatings; infrared integrating sphere coatings; integrating spheres; sphere; sulfur coatings.

This letter describes several methods of preparing infrared integrating sphere coatings.

9158. **Atmospheric research and electromagnetic telecommunication,** H. G. Booker and C. G. Little, Part I, *IEEE Spectrum* **2,** No. 8, 44-52 (Aug. 1965); Part II, *IEEE Spectrum* **2,** No. 9, 98-103 (Sept. 1965).

Key words: Atmospheric research; electromagnetic; telecommunication; United States.

Part I--The broad subject of electromagnetic telecommunication in the United States is examined, with the stress on the importance of atmospheric research to this growing field.

Part II--The concluding portion of this two-part article presents an analysis of telecommunication-oriented atmospheric research in the United States for the fiscal year 1964.

9159. Unassigned.

9160. **Bond with reinforcing steel,** D. Watstein, *Am. Soc. Testing Mater. Spec. Tech. Publ.* **169A,** *Significance of Tests of Concrete Making Materials*, pp. 239-245 (July 1965).

Key words: Bond in pullouts and beams; bond strength; deformed reinforcement; review of bond literature.

A review is presented of the significance of various tests of bond between reinforcing steel and concrete. The effect of the more important parameters such as bar diameter, strength of concrete, and spacing of bars as determined in some recent researches is appraised, and the appropriate provisions of the standards for reinforced concrete construction are discussed. A brief discussion of the significance of bond and bond tests for prestressed concrete is also included.

9161. Unassigned.

9162. **Color,** D. B. Judd, *Encyclopedia of Physics*, pp. 113-116 (Reinhold Publ. Corp., New York, N. Y., 1965).

Key words: Chromatic adaptation; color; colorblindness; colorimetry; theories of color.

This three-page article gives the conditions for a color match by observers having normal vision and those having one or another of the six most common forms of abnormal vision. It gives the mathematical basis for color measurement, both visual and photoelectric, for automatic production of pictures in color, and for prediction of the influence of chromatic adaptation on color perception, and it indicates the chief property of four of the most respected theories of color.

9163. **Comments on the mechanism of the 337-micron CN laser,** H. P. Broida, K. M. Evenson, and T. T. Kiluchi, *J. Appl. Phys.* **36,** No. 10, 3355 (Oct. 1965).

Key words: Laser; radiation; rotational level; vibrational state; 337-micron CN laser.

Very intense laser radiation at 337 $\mu$ has been observed by Gebbie et al., when a pulsed electrical discharge is passed through various organic compounds such as HCN, $CH_3CN$ and $C_2H_5CN$. Chantry et al., suggest a laser transition in the vibrational state $v=2$ of the ground electronic state $X^2\Sigma$ of CN from the rotational level $K=8$ to $K=7$.

If the proposed explanation is correct, then a number of other transitions should occur, some with considerably higher probability than the observed emission.

9164. **Congruence subgroups of positive genus of the modular group,** M. Newman and M. Knopp, *Illinois J. Math.* **9,** No. 4, 577-583 (Nov. 1965).

Key words: Congruence groups; genus; modular group.

Let $\Gamma(n)$ be the principal congruence subgroup of $\Gamma$ of level $n$, $\Gamma_n$ the subgroup of $^{\Gamma}$ generated by $^{\Gamma}{}_{(n)}$ and $S=\begin{pmatrix} 1 & 1 \\ 0 & 1 \end{pmatrix}$, and $^{\Gamma}{}_0(n)$ the subgroup of $^{\Gamma}$ consisting of all elements $\begin{pmatrix} a & b \\ c & d \end{pmatrix}$ of $^{\Gamma}$ such that $c \equiv 0 \pmod{n}$. Then it is proved that if $G$ is a subgroup of $^{\Gamma}$ containing $^{\Gamma}{}_n$, then either $G={}^{\Gamma}$ or $G \subset {}^{\Gamma}{}_0(d)$, $d|n$, $d>1$. This is used to prove that a free congruence subgroup of $^{\Gamma}$ of level $n$ (i.e., a free subgroup of $^{\Gamma}$ containing $^{\Gamma}(n)$) is of positive genus, provided that $(n, 2.3.5.7.13)=1$.

9165. Unassigned.

9166. **Decays of positive-parity baryon resonances in a broken U(12),** H. Harari, D. Horn, M. Kugler, H. J. Lipkin, and S. Meshkov, *Phys. Rev.* **140,** No. 4B, B1003 (Nov. 1965).

Key words: Baryon; branching ratio; decay; decay width; meson; resonances; spurious; symmetry breaking; U(12) theory.

The positive parity baryonic resonances are classified and their decay widths calculated in a broken U(12).

9167. **Density and specific gravity,** J. K. Taylor, *Encyclopedia of Industrial Analysis* **1,** 546-560 (Interscience Publ. Inc., New York, N.Y., 1965).

Key words: Gravity; specific density.

Density is an important and significant property of matter. For pure materials, density values may serve as one means of identification. For binary mixtures, such measurements frequently provide convenient methods for analytical determination of composition. Density values also may be combined with other physical properties such as viscosity or refractive index for analytical or structural determinations. In solid-state chemistry, precise density data on pure materials may provide information of the number of dislocations present in a given specimen.

An extensive literature exists both on methods for measurement of density and on tabulations of measured values for a wide variety of materials. An exhaustive review of this literature is outside the scope of this chapter. In fact, the reader is urged to consult original sources, especially for details of precision methods. Instead, general considerations will be presented here, especially those that might be useful to the practicing analytical chemist.

9168. **Determination of trace amounts of cadmium and silver by substoichiometric radioisotopic dilution analysis,** A. R. Landgrebe, L. T. McClendon, and J. R. DeVoe, *Trans. Am. Nucl. Soc.* **8,** No. 2, 315-316 (1965).

Key words: Cadmium; dithizone; silver; sub-stoichiometric radioisotopic dilution analysis; trace amounts.

A new method, using a substoichiometric amount of the complexing reagent dithizone in radioisotope dilution analysis, was developed for the determination of trace amounts of silver and cadmium. Silver was determined in an acidic solution at pH 4.75, using a low concentration of dithizone, $10^{-8}$ g/ml. Cadmium was determined using ammonia-ammonium chloride buffer at the $\mu$g/ml level. The sensitivity of the method is limited by 1) there is a limit to which the organic reagent can be diluted and still retain the effect of substoichiometry, 2) the specific activity of the radioisotope, 3) impurities at low concentration, that may act with the substoichiometric reagent, 4) hydrolysis of the complexing reagent and analyzed elements, and 5) adsorption on glassware.

Two major advantages of the direct substoichiometric radioisotopic dilution analysis are 1) it is possible to determine a number of elements in the same sample by using agents, varying the pH, etc., 2) after adding the radioisotope to the solution being analyzed losses of the element being determined do not influence the results of the analysis.

9169. **Determination of trace amounts of tellurium in standard reference materials by neutron-activation analysis,** D. A. Becker and G. W. Smith, *Proc. 1965 Intern. Conf. Modern Trends in Activation Analysis, Texas A&M University, College Station, Texas*, pp. 230-235 (Apr. 1965).

Key words: Chemical separation; distillation; neutron-activation; tellurium.

For the first time, neutron activation was used for elemental analysis of NBS Standard Reference Materials at the National Bureau of Standards. The reference materials were of two general types, cartridge brass and white cast iron, and were analyzed for their tellurium content. Utilizing the nuclear reaction $Te^{130}$ $(n,\gamma)Te^{131}$ $\beta-I^{131}$, the samples were irradiated and the $I^{131}$ separated by $\vec{a}$ destructive distillation and solvent extraction technique. Chemical yields were obtained through the use of $I^{125}$ tracer. Tellurium concentrations of 2 to 800 ppm were determined, and the results compared to the results on identical samples obtained by polarography and emission spectroscopy.

9170. **Dissociation constant of acetic acid in deuterium oxide from 5 to 50 °. Reference points for a pD scale,** R. Gary, R. G. Bates, and R. A. Robinson, *J. Phys. Chem.* **69,** No. 8, 2750-2753 (1965).

Key words: Acetic acid; acidity in deuterium oxide; deuterium oxide; dissociation constant; heavy water; pD scale.

Electromotive force measurements of a cell without liquid junction have been used to determine the dissociation constant of acetic acid in deuterium oxide from 5 to 50 °. The enthalpy, entropy, and heat capacity changes on dissociation of acetic acid have been calculated. Values of - log $(a_{D+}\ \gamma_{Cl-})$ and the conventional $pa_D$ values for the equimolal (0.05 m) acetic acid-sodium acetate buffer solutions have been determined. These provide a second fixed point for standardizing the pD scale, supplementing the equimolal mixture of $KD_2PO_4$ and $Na_2DPO_4$ established in an earlier investigation.

9171. **Dissociation of $H_2^+$ by electron impact,** G. H. Dunn, B. Van Zyl, and R. N. Zare, *Phys. Rev. Letters* **15,** No. 15, 610 (Oct. 11, 1965).

Key words: Dissociation; $H_2^+$; electron.

The cross section for dissociation of $H_2^+$ by electron impact has been measured over the electron energy range 25 $eV^2$ to 600 eV. Results are found to agree well with available theory when the Franck-Condon factors are assumed to describe the vibrational state population of $H_2^+$.

9172. **Effects of thermal shrinkage on built-up roofing,** W. C. Cullen, *J. Bldg. Res. Instr.* **2,** No. 4, 23 (July-Aug. 1965).

Key words: Deterioration; insulation; radiative cooling; roofing, built-up.

The effects of thermal movement of bituminous built-up roof membranes are related to some common failures of built-up roofing observed in field exposures. A procedure for determining the amount of thermal movement of built-up membranes is described. Data are given for the thermal movement of various bitumens and reinforcing felts used in the construction of built-up roofs and for the composite membranes over a temperature range of +30 to -30 °F. The data obtained are related to field experiences and suggestions are presented which will prove beneficial in reducing the incidence of built-up failure due to thermal movement.

9173. **Elastic constants of single crystal $UO_2$ at 25 °C,** J. B. Wachtman, Jr., M. L. Wheat, H. J. Anderson, and J. L. Bates, *J. Nucl. Mater.* **16,** 39-41 (1965).

Key words: Compressibility; elastic constants; elastic compliances; single crystal; velocity of sound; uranium dioxide.

The elastic constants of single crystal $UO_2$ at 25 °C were determined to be $c_{11}=3.95 \pm (0.018)$, $c_{12}=1.21 \pm (0.019)$, and $c_{44}=0.641 \pm (0.0017)$ in units of $10^{12}d/cm^2$. The numbers in parentheses are computed standard errors of the corresponding constants based on about 16 measurements of each transit time equired in four independent determinations of the set of three elastic constants.

9174. **Electrical testing in chemical technology,** A. H. Scott, *Encyclopedia of Chemical Technology*, 2d ed., **7,** 716-726 (1965).

Key words: Electrical testing; conductance; dielectric conductance; conductivity; volume conductivity; insulation conductance; resistance; dielectric resistance; resistivity; dielectric constant; permittivity; dissipation factor; loss index; dielectric strength; arc resistance; tracking; measurements.

Electrical testing of one sort or another is being used today to (a) determine the electrical properties of materials for design purposes, (b) determine the purity of the materials, (c) check the uniformity of manufacture or the maunfacturing process, (d) aid in developing an understanding of the molecular structure of materials, (e) characterize materials, and (f) indicate the influence of environment on the properties of materials. The purpose of this article is to briefly describe such electrical measurements and to indicate their usefulness and limitations.

9175. **Electron spin resonance studies of the reaction of water-soluble polymers with hydroxyl radicals,** F. Sicilio, M. Dousset, R. E. Florin, and L. A. Wall, (*Proc. 150th American Chemical Society Meeting, Atlantic City, N.J., Sept. 12-17, 1965*), *Polymer Preprint* **6,** No. 2, 958-964 (Sept. 1965).

Key words: Free radicals; polyvinyl alcohol; polyethylene oxide; tetrahydrofuran; hydroxyl radicals; electron spin resonance.

Free radicals were generated from polyvinyl alcohol, ethylene glycol, polyethylene oxide, dimethyl ether, tetrahydrofuran and dioxane, by the action of hydroxyl radicals from $TiCl_3 + H_2O_2$ on the substrates in an aqueous flow system, and were observed by electron spin resonance. The radical $\cdot CH_2OCH_3$ from dimethyl ether had a concentration of 7.9 x $10^{-7}$ M .02 sec after mixing at 2 to 7 °C, and a rate constant for disappearance of 0.4 x $10^8$ liter/mole sec which is considerably greater than that for hydroxyl. The radical from polyvinyl alcohol is explainable either by abstraction from the $CH_2$ group, or by scission following abstraction from CHOH or $CH_2$. Tetrahydrofuran gives a very complicated spectrum attributed to the two cyclic radicals formed by abstraction in the 1 and 2 positions. The radical from polyethylene oxide appears to have four precisely equivalent protons with a splitting of 9.2 gauss, plus minor splittings, and is attributed to a positive ion radical, $\sim CH^{+\cdot}{}_2OCH_2\sim$ or $\sim OCH^{+\cdot}{}_2\text{-}CH_2O\sim$.

9176. **Fire test methods for paints,** A. F. Robertson, *Bldg. Res.*, pp. 48-52 (July-Aug. 1965).

Key words: Combustibility; endurance; fire; flammability tests; paints.

A discussion is presented of the applicability of various fire test methods to the evaluation of paint coatings from the fire safety viewpoint. Sixteen flammability test methods are briefly described and a limited amount of data are presented to show the type of correlation which exists between six of the test methods. It is emphasized that few, if any, of the paints currently available provide any but the most minor influence in delaying fire penetration through structures as measured by the fire endurance test ASTM Procedure E-119. Manufacturers are encouraged to attempt development of paints which show better performance by this method.

9177. **Floor coverings,** T. H. Boone, *Building Construction Handbook*, 2d Edition, Ed. F. S. Merritt, Section 13, pp. 13-1--13-8 (McGraw-Hill Book Co., Inc., New York, N. Y., 1965).

Key words: Adhesive industrial; characteristics; conductive; flooring; installation; standards.

Since every floor is a system comprising many parts, complete satisfaction with a flooring installation is experienced only when all parts perform well. Dissatisfaction can arise from failure to take into consideration during the earliest stages of building design the importance of each part, the type of environment, and traffic conditions to be encountered in the finished building.

This section summarizes the characteristics of nontextile floor coverings with the intent to be helpful in the selection of floor covering, adhesive, and in the preparation of the subfloor. Methods for properly installing these materials are described. Specifications, standards and floor trade associations are also listed.

9178. **Formation of crystallites of benzophenone in hydrocarbon glass,** R. Keller and D. Breen, *J. Chem. Phys.* **43,** No. 7, 2562-2563 (Oct. 1965).

Key words: Crystals; phosphorescence; triplet states.

Small, invisible crystallites of benzophenone are formed in dry hydrocarbon glass at 77 °K when the concentration exceeds $10^{-3}$ molar. The emission from these suspended crystallites is greatly reduced because of annihilation interactions between triplet excitons. The decay of phosphorescence of concentrated solutions following flash excitation was shown to result from a sum of the decay of phosphorescence of dissolved molecules plus the phosphorescent decay of benzophenone crystals. Additions of butyl alcohol to the dry hydrocarbon glass prevents the formation of these crystallites.

9179. Unassigned.

9180. **Gas-phase radiolysis and photolysis of neopentane,** S. G. Lias and P. Ausloos, *J. Chem. Phys.* **43,** No. 8, 2748-2759 (Oct. 1965).

Key words: Free radicals; ion-molecules reactions; neopentane; photolysis; radiolysis.

The photolysis of neo-$C_5H_{12}$-neo-$C_5D_{12}$ mixtures has been investigated at 1470 and 1236A. From the products formed in the absence and presence of NO or $H_2S$, the occurrence of the following fragmentation processes could be derived:

$$\begin{aligned} \text{neo-}C_5H_{12}^{*} \rightarrow\ & CH_4 + \text{iso-}C_4H_8 && (1)\\ & CH_3 + \text{iso-}C_4H_8 && (2)\\ & CH_3 + CH_3 + C_3H_6 && (3) \end{aligned}$$

These modes of decomposition also prevail when neopentane is excited by collision with electrons accelerated by an electrical field applied during radiolysis. At 1236Å, the relative probabilities of occurrence of processes 1, 2, and 3 are approximately 1.0, 4.5, and 1.1.

From the isotopic analysis of the products formed in the direct and inert gas sensitized radiolysis of neo-$C_5H_{12}$-neo-$C_5B_{12}$ mixtures in the presence of NO, $O_2$ or $I_2$ as free radical scavengers, it could be derived that the fragment ions $C_2H^+{}_3$, $C_2H^+{}_5$, $C_3H^+{}_5$, and $C_3H^+{}_7$ are formed.

9181. **Geomagnetic and solar data,** J. V. Lincoln, *J. Geophys. Res.* **70,** No. 13, 3227-3228 (July 1965); **70,** No. 15, 3761-3763 (Aug. 1965); **70,** No. 17, 4383-4384 (Sept. 1965); and **70,** No. 19, 4963-4964 (Oct. 1965).

Key words: Data, geomagnetic and solar; geomagnetic solar data; solar data, geomagnetic.

9182. **Growth of large sodium chloride crystals from solution for color-center studies,** P. M. Gruzensky, *J. Chem. Phys.* **43,** No. 11, 3807-3810 (Dec. 1, 1965).

Key words: Alkali halides; aqueous; chloride; color centers; conductivity; crystal growth; sodium.

Sodium chloride single crystals with edge dimensions as large as 2.5 cm were grown from aqueous solutions. Solutions were purified by chemical precipitation of trace contaminants and filtration through membrane filters. Crystal defects were apparent in the initial stages of growth, but the outer portions of crystals were free of dislocations. F-band coloration by x-rays at room temperature was not linear and the "first stage" was either absent or nearly so. Transition from extrinsic to intrinsic dc conductivity occurred at 350 °C with the extrinsic conductivity two orders of magnitude lower than for "pure" melt-grown crystals.

9183. **High-resolution infrared spectra of cyanogen and cyanogen $^{15}N_2$,** A. G. Maki, *J. Chem. Phys.* **43,** No. 9, 3193-3199 (Nov. 1965).

Key words: Bond distances; cyanogen; infrared; molecular structure; spectra.

The infrared absorption of $^{12}C_2{}^{14}N_2$ and $^{12}C_2{}^{15}N_2$ has been studied with a resolution of 0.08 to 0.04 $cm^{-1}$. The vibration-rotation band constants were determined for eight vibrational transitions of $^{12}C_2{}^{14}N_2$ and three vibrational transitions of $^{12}C_2{}^{15}N_2$. Many unresolved hot band Q-branches were also measured. The values for many vibrational and rotational constants are given. The bond distances determined from the rotational analysis and their three-standard-deviation error limits, are $r_0$ (C-C)$=1.38_9\pm0.030$Å and $r_0$ (C$\equiv$N)$=1.15_4\pm0.017$ Å. The N-N distance and corresponding error limits are $3.69_7\pm0.010$Å.

9184. **Human engineering in the design of a console for the comparison of volt boxes,** P. H. Lowrie, Jr., *ISA J.*, pp. 67-71 (July 1965).

Key words: Calibration console; console; high measurement accuracies; human engineering; volt boxes.

Too often the human element is not given adequate consideration in the design of precise measuring equipment. The dependence upon the operator for the attainment of high measurement accuracies cannot be denied. This paper describes a calibration console in which the human engineering factors were given the same consideration as the technical requirements. In this system the operator is considered to be a decision maker, and those functions not requiring judgment are handled automatically by the console. Most of the calculations are performed automatically by internal circuits, and the results are displayed digitally upon command. The console is an illustration in point that the principles of human engineering are as applicable to the precise measurements found in the standards laboratory as they are to the production line. The paper discusses the features of the console and points out some of the pitfalls that may be encountered in a design of this type.

9185. Unassigned.

9186. **Infrasonic waves from aurorae,** K. Maeda and J. M. Young, *Nature* **207,** No. 4994, 279-281 (July 1965).

Key words: Atmospheric resonances; auroral infrasound; infrasonic waves; thermal structure.

The effects of atmospheric thermal structure on the free-field propagation of auroral infrasound are discussed. Experimental data illustrating dispersion and near-sinusoidal oscillations near the Brunt frequency are shown. The effects of the large positive lapse rate layers, especially the one in the thermosphere, on atmospheric resonances are given particular attention.

9187. Unassigned.

9188. **International intercomparison of standards for microwave power measurement,** G. F. Engen, *IEEE Trans. Microwave Theory Tech.* **MTT-13,** No. 5, 713-715 (Sept. 1965).

Key words: International intercomparison; microwave; microwave power measurement.

In compliance with a recommendation of the International Scientific Radio Union (URSI) intercomparisons of microwave power standards have been made between Japan, the United Kingdom, and the United States.

Initially, there was a rather large difference in the Japan/United States comparisons; but, after several improvements in the design of the bolometer mounts employed as a transfer standard, consistently good agreement of the order of a few tenths of a percent has been realized.

In intercomparisons between the United Kingdom and either Japan or the United States, there was a small but rather consistent difference in the initial results. Again, the agreement has improved with more recent comparisons.

The microcalorimetric and impedance methods were employed by Japan and by the United States to evaluate the bolometer mount efficiency, whereas in the United Kingdom a combination of calorimetric, force-operated, and bolometric methods were used. The close agreement achieved is thus particularly significant because of the wide differences in the basic principles of the techniques employed.

As a result of this program, the accuracy limits of the different methods may now be stated with greater confidence. In addition, the interchange of ideas has yielded improved instrumentation.

9189. **International URSIGRAM and world days service "report on activities 1964",** A. H. Shapley, *URSI Info. Bull.* **150,** 43-55 (May 1965).

Key words: Radio science; world days service.

9190. **Interspecimen comparison of the refractive index of fused silica,** I. H. Malitson, *J. Opt. Soc. Am.* **55,** No. 10, 1205 (Oct. 1965).

Key words: Dispersion; fused silica; infrared materials; optical materials; refractive index.

The index of refraction of optical quality fused silica ($SiO_2$) was determined for 60 wavelengths from 0.21 to 3.71 microns at 20 °C. The dispersion equation

$$n^2-1=\frac{0.6961663\lambda^2}{\lambda^2-(0.0684043)^2}+\frac{0.4079426\lambda^2}{\lambda^2-(0.1162414)^2}+\frac{0.8974794\lambda^2}{\lambda^2-(9.896161)^2}$$

where $\lambda$ is expressed in microns was found to yield an absolute residual of $10.5\times10^{-6}$. The variation in index between 12 specimens was determined. Dispersive properties of the material and thermal coefficient of index are graphically presented. A comparison with previous NBS index data is discussed.

9191. **Intrinsic and lattice-induced distortion of the tetrachlorocuprate ion,** M. Sharnoff and C. W. Reimann, *J. Chem. Phys.* **43,** No. 9, 2993-2996 (Nov. 1965).

Key words: Copper doped tetrachlorozincate; e.p.r. analysis; Jahn-Teller effect; polarized ultraviolet spectrum; tetrachlorocuprate ion.

In an effort to determine how much of the distortion of the tetrahedral complex, $CuCl_4^=$, may be ascribed to the Jahn-Teller effect, we have studied the changes in the optical and EPR spectra which occur when this ion is embedded in several different lattices. Although the corresponding lattice constants of the isostructural crystals, $Cs_2CuCl_4$ and $Cs_2ZnCl_4$, differ by only about 3%, gross differences exist between the g-tensors of $CuCl_4^=$ suspended in these lattices. These findings are corroborated by a comparison of the optical spectra of the two complexes. The effects are discussed in terms of an LCAO-MO analysis of the primarily 3d(Cu) wave functions of the complex, and it is shown that the change in ionic distortion is connected almost exclusively with a small but significant change in the amount of 4p(Cu) character in the $t_2$ primarily 3d(Cu) orbitals. The analysis points towards the conclusion that the low symmetry (point group $C_s$) of the ion is an intrinsic property and that the dominant mechanism of the distortion of the ionic symmetry from $T_d$ is the Jahn-Teller effect.

9192. **Investigation of polymer pyrolysis with thermogravimetry,** J. H. Flynn and L. A. Wall, *(Proc. 150th American Chemical Society Meeting, Atlantic City, N.J., Sept. 12-17, 1965), Polymer Preprint* **6,** No. 2, 945-955 (Sept. 1965).

Key words: Calculation of kinetic parameters; determination of activation energies; preexponential factor; stability of polymers; thermogravimetric analysis; variation of the activation energy.

A detailed theoretical analysis of thermogravimetry as applied to polymer decomposition investigations, particularly in regard to elucidating kinetic and mechanistic details, has been made and pertinent mathematical relations presented. Cases considered are realistic ones based on isothermal pyrolytic studies and include: 1) where the rate is dependent upon the conversion raised to a simple power, 2) where the rate proceeds through a maximum with conversion and 3) composite situations.

The changes in the shape of the thermogravimetric curves resulting from the variation of the activation energy, preexponential factor, and heating rate for the various cases are compared and discussed. The effect of a linear temperature dependence in the preexponential factor on the character of the curves is also examined.

From these general considerations, it appears that, although thermogravimetric analysis may be sufficient for the approximate determination of activation energies and overall relative stability of polymers, in most cases, complementary isothermal studies are necessary for the unambiguous interpretation of the kinetics and the calculation of kinetic parameters.

9193. **Ionospheric effects of particles,** G. C. Reid, *Proc. COSPAR Polar Cap Panel Symp., Alpach, Austria, 1964*, pp. 221-231 (Academic Press Inc., New York, N. Y., 1965).

Key words: Auroral absorption; auroral radar; ionospheric disturbances; polar cap absorption; solar protons; sporadic-E.

This paper is a summary of a review paper presented at the COSPAR Polar-Cap Panel Symposium. Current knowledge concerning energetic-particle effects in the ionosphere is briefly discussed, and outstanding problems are emphasized.

9194. **Ion-pair process in $CH_3Cl$ photoionization,** V. H. Dibeler and J. A. Walker, *J. Chem. Phys.*, **43,** No. 5, 1842-1843 (Sept. 1965).

Key words: Ionization energy; ion pair process; photoionization.

A brief report on the first direct observation of both positive and negative members of an ion pair process by photoionization.

9195. **Line broadening,** W. L. Wiese, Book, *Plasma Diagnostic Techniques*, Ed. R. H. Huddleston and S. L. Leonard, **21,** 265-317, (Academic Press, Inc., New York, N. Y., 1965).

Key words: Dense plasma; line broadening; plasma diagnostic techniques; Stark effect.

Line broadening due to interatomic Stark effect, the most important type of line broadening in dense plasmas, has been recently the subject of extensive calculations by Griem, Kolb, Baranger, Shen and others. Subsequent experiments have borne out good agreement with the theoretical results and confirmed the theoretically estimated error limits. Consequently, the measurement of Stark half-widths has emerged as one of the most reliable and convenient methods for the determination of electron densities. Whenever possible, the strong, broad Balmer line *H* should be employed, if necessary by admixing a trace of hydrogen to the plasma. The experimental comparison studies indicate that precise half-width measurements of this line may give electron densities to within 7%. For other hydrogen lines and for isolated lines of heavier elements--if for the latter the results from several lines are averaged--uncertainties not greater than 10 to 15% may be expected. Measurements of Stark shifts of isolated lines should only be used if the shifts are not much smaller than the (half) half-widths. Again, as in the case of the widths, the average value over several lines should be used in order to achieve an accuracy comparable to that mentioned for the widths. Since not many cases of large shifts are known, shift measurements, though appealing in their simplicity, may be only occasionally applied.

An important advantage of the Stark width and shift measurements over other spectroscopic methods is that only relative intensities are required. Moreover, the electron densities from Stark broadening will be reliable even in cases where the existence of LTE is doubtful, while other methods which depend on equilibrium equations are not. The useful range of electron densities extends from $10^{15}$ cm$^{-3}$ upward, but for the higher hydrogen lines it may be extended about one order of magnitude toward lower densities.

The present situation with regard to Stark broadening is, however, still not satisfactory in some respects: More experimental checks of *H* are desirable to further improve the accuracy of this most important line. Secondly, the Stark parameter calculations should be extended to more elements. Furthermore, to reduce the amount of diagnostic work, it would be desirable to improve the accuracy for a few strong and characteristic lines per element. This is best done experimentally, and the results of the few available studies should be used from this point of view.

9196. **Magnetic core permeability measurement techniques,** R. D. Harrington and A. L. Rasmussen, *Proc. Magnetic Core Conf.* **7,** 11-24 (1965).

Key words: Frequency range; magnetic core; permeability techniques.

Techniques for measuring the initial complex permeability of magnetic cores in the frequency range from 1 kHz to 50 MHz are briefly discussed. Emphasis is directed toward studies recently carried out at the National Bureau of Standards.

At frequencies below 100 kHz, either a demountable coil or a specially designed Maxwell bridge is used for obtaining core data. The frequency range from 100 kHz to about 50 MHz is most conveniently covered through the use of the radio frequency permeameter. A brief survey of the development of the permeameter with a description of some recent measurements indicating that this method may be used to frequencies even greater than 50 MHz is given.

It has been found that toroidal coils are preferable to the permeameter for obtaining accurate measurements of the temperature coefficient of permeability. A brief description is given of a method for evaluating the inductance and resistance changes of such coils using a bridge as a null indicating device. The technique is capable of measuring temperature coefficients of permeability of the order of $10^{-6}$ per degree centigrade.

9197. **Magnetoacoustic absorption and the Fermi surface in potassium,** H. J. Foster, P. H. Meijer, and E. V. Mielczarek, *Phys. Rev.* **139,** No. 6A, A1849-A1857, (Sept. 1965).

Key words: Fermi surface; magnetoacoustic absorption; potassium; single crystals; zone refining.

Magnetoacoustic measurements in zone refined and oriented single crystals of potassium have yielded detailed information on the relative attenuation, the Fermi surface, and the phase factors in this metal for magnetic field directions lying along the $\langle 100 \rangle$, $\langle 110 \rangle$, and $\langle 112 \rangle$ axes, and within a few degrees on either side of these, perpendicular to a fixed direction of propagation of the longitudinal ultrasonic wave, i.e., $q\langle 110 \rangle$. The data show that the Fermi surface in potassium is only slightly distorted relative to its free electron value, bulging by about 0.3% in the $\langle 110 \rangle$ direction and pushed in by about 0.4% and 0.5%, respectively, in the $\langle 100 \rangle$ and $\langle \pm 111 \rangle$ directions within the Brillouin zone (BZ). The distortion in $k_f$ for potassium is therefore found to be less than 1% on the average: $k_f = (7.44 \pm 0.06^{*}) \times 10^{7}$ cm$^{-1}$. The average value of the phase factor for potassium is found to lie rather close to the free electron value of 0.375. (* Estimated limit to experimental error.)

9198. **Measurement of DC dielectric conductance (reciprocal resistance) at elevated temperatures,** A. H. Scott, *Proc. 6th Electrical Insulation Conf.*, Sept. 13-16, 1965, pp. 252-254 (1965).

Key words: Conductance; conductivity; dielectric; measurements; resistance; resistivity.

The new term adopted by Committee D-9 ASTM (DC Dielectric Conductance) for the conductance observed in electrical insulating materials differentiates this type of conductance from that in metals or other conducting materials. Measurements at elevated temperatures require special precautions and special emphasis on some of the usual precautions of measurement. Special cells or holders are required for these measurements.

9199. **Measurement of the 633-nm wavelength of helium-neon lasers,** K. D. Mielenz, R. B. Stephens, K. E. Gillilland, K. F. Nefflen, and R. B. Zipin, *Appl. Phys. Letters*, **7,** No. 10, 277-279 (Nov. 1965).

Key words: Isotopic laser wavelengths; non-isotopic laser wavelengths.

The wavelength of the $3s_2$-$2p_4$ transition of neon was measured by comparison of helium-neon lasers with the Krypton standard of length.

9200. **Measurements of ion-optical properties of a high resolution spectrometer for electron scattering,** S. Penner and J. W. Lightbody, *Proc. Intern. Symp. Magnetic Technologies, Stanford Linear Accelerator Center, Stanford Univ., Calif., Sept. 8-10, 1965*, pp. 154-163 (Oct. 1965).

Key words: Electron scattering; magnetic spectrometer; magneto-optics.

A double focusing magnetic spectrometer for electron scattering work is described. The spectrometer has been ray traced using positive ions from a 400 keV Van de Graaff accelerator. A large number of rays are traced and fitted to a second order transfer matrix by a least squares technique. Selected third order effects are also included. A comparison of measured matrix elements with theoretical predictions is presented. Agreement with theory is good. The intrinsic resolution of the instrument (for a point source) is approximately 1 part in $10^4$ FWHM using the maximum solid angle allowed by the vacuum chamber.

9201. **Measurements of the viscosity of parahydrogen,** D. E. Diller, (*Proc. IX Intern. Conf. Low Temperature Physics, Columbus, Ohio, Aug. 31-Sept. 4, 1964*), Book, *Low Temperature Physics*, **LT9,** Part B, 1227-1229 (Plenum Press Inc., New York, N. Y., 1965).

Key words: Liquid normal hydrogen; parahydrogen; shear viscosity; temperature dependence; viscosity of parahydrogen.

The coefficient of shear viscosity $\eta$ of parahydrogen has been measured by the torsional crystal method at temperatures from 14° to 100 °K and at pressures up to 345 atm. Twenty compressed fluid isotherms encompass the density range 0.003-0.087 g/cm³ and include the critical region. The precision and accuracy of the measurements is about 0.5%. The temperature dependence of $\eta$ changes sign at a density approximately twice the critical density. The viscosity at the critical point is estimated to be $35.5\pm5\times10^{-6}$ g/cm·sec. The viscosity of saturated liquid normal hydrogen is up to 5% greater than that of parahydrogen at the same temperature. Data of this report have been represented within experimental error by an empirical equation of the form $\eta=\eta_0(T) + A(\rho)\exp B(\rho)/T$, where $\eta_0(T)$ is the viscosity in the low-density limit and $A(\rho)$ and $B(\rho)$ are density-dependent coefficients.

9202. **Measuring the coordinates of a number of points in a complex, laboratory-scale model,** F. D. Ordway, *Rev. Sci. Instr.* **36,** No. 8, 1156-1159 (Aug. 1965).

Key words: Calibration points; complex laboratory-scale model; computer; coordinate systems; digital computer; number of points.

Points on the model, together with an array of marked calibration points, are measured with theodolites from two different locations. Distances between a number of pairs of calibration points are measured precisely, and estimates of the distances from the calibration points to the measuring locations are adjusted for the best fit to these precisely measured distances. After adjustment, the distances from calibration points to measuring locations are used to obtain the best estimate of the rotation matrix and translation vector relating the coordinate systems of the two theodolites. The resulting rotation-translation matrix is used with the two sets of angle measurements on each point of the model to obtain the Cartesian coordinates of the point. The Gram-Schmidt orthonormalization procedure is carried out at each step, with a digital computer.

9203. **Metrology essential to the space age,** A. G. McNish, *George Washington Univ. Mag.* **1,** No. 4, 10-14 (1965).

Key words: Modern technology; science comprehension; space age; what is metrology.

Understanding the physical world and the progress of civilization depends upon measurement.

9204. **Microwave spectrum of perchlorylfluoride,** D. R. Lide, *J. Chem. Phys.* **44,** No. 10, 3767-3768 (Nov. 1965).

Key words: Dipole moment; microwave; perchlorylfluoride; quadrupole coupling constant structure.

The microwave spectrum of perchlorylfluoride has been measured and analyzed. Digital averaging techniques were used to improve the signal-to-noise ratio of the very weak lines. The molecular constants determined for $Cl^{35}O_3F$ are $B_0=5258.682$, $D_J=0.0014$, $D_{JK}=0.0018$, and $eqQ=-19.2$ Mc/s. The OC10 angle is found to be in the range 114 °-116 °.

9205. **Morphological classification in the National Bureau of Standards mechanical translation system,** L. F. Meyers, *J. Assoc. Compt. Mach.* **12,** No. 4, 437-472 (Oct. 1965).

Key words: Linguistic work; mechanical translation system; morphological classification; translation system.

In linguistic work, morphology is the study of the rules by which words undergo changes in form. Morphological classification is the systematic organization of these rules. A detailed account of the morphological classification for Russian is given as used in the National Bureau of Standards project on the mechanical translation of Russian into English. The account includes the heuristic reasoning from which the classification system evolved, as well as complete classification tables, a description of the method of their construction, and some examples of their use.

9206. **Mossbauer line broadening in $SnO_2$,** R. H. Herber and J. Spijkerman, *J. Chem. Phys.*, **42,** No. 12, 4312-4314 (June 15, 1965).

Key words: High pressure; line broadening; Mossbauer spectroscopy; quadrupole splitting; stannic oxide.

Since stannic oxide, $SnO_2$ has been widely used in tin Mossbauer spectroscopy, and has been tentatively adopted as a secondary differential chemical shift standard (Gordon Conference, 1964) a careful study of this compound and its crystal structure has been made. Although published literature describes a single broad resonant absorbtion line, fine structure was observed. The broadening has been interpreted as an unresolved doublet, due to quadrupole splitting, arising from twinning in the (031) plane.

A table of comparison experiments of $SnO_2$ source or absorber for various tin compounds is included.

9207. **NBS offers method to prevent built-up roof splitting failure,** W. C. Cullen, *Roofing Siding Insulation Mag.* **40,** No. 4, 28-30 (Apr. 1965).

Key words: Built-up roof membrane; innovation; preventive measures; splitting failures; thermal shock.

Innovations in roof design and roofing construction procedures are described. The implementation of one or more of these procedures should reduce premature failures in built-up roofing membranes which are due to thermal contraction in cold climates.

9208. **Newly observed structure in the photoionization continua of Kr and Xe below 160Å,** K. Codling and R. P. Madden, *Appl. Opt.* **4,** 1431-1434 (Nov. 1965).

Key words: Atomic spectra; krypton; photoionization; vacuum ultraviolet; xenon.

The absorption spectra of Kr and Xe have been photographed in the 70-200Å region, revealing many weak, previously unobserved, resonances in the photoionization continua of these gases. The new structures occurring in the 110-115Å region for Kr and 145-160Å for Xe are due to two-electron excitation states involving an inner-shell *d* electron and an outer-shell *p* electron. The resulting configurations are characteristic of the neutral atom, although they lie, in energy, well above the 3rd ionization limits for these atoms. Additional resonances in Xe, photographed in the 90Å region, are due to the excitation of an inner-shell 4*p* electron. An improved value has been obtained for the $N_{III}$ edge of Xe, namely 145.6 (±0.5) eV. These spectra were obtained using the pure continuum radiated by the NBS 180 MeV electron synchrotron as a background source.

9209. **Progress in nuclear instrumentation, 1965 meeting of IEC committee TC45,** L. Costrell, *Mag. Std.* p. 9 (Jan. 1966).

Key words: Modules; nuclear instruments; progress; standards; state-of-the-art.

At the conclusion of World War II nuclear instrumentation was to a great extent concerned with detectors that required essentially unsophisticated electronics. The advent of the scintillation counter in the late 1940's called for an order of magnitude improvement in the associated instrumentation. Introduction of the semiconductor radiation detectors with their tremendous energy resolution capabilities stimulated additional sophistication of nuclear electronics.

9210. **Observatory reports, spectroscopy,** C. E. Moore, *Astron. J.* **70,** No. 9, 637-639 (Nov. 1965).

Key words: Atomic spectra; multiplet tables; rare-earth spectra; spectra, far ultraviolet; transition probabilities.

An annual report from the NBS in Washington on spectroscopic research of astrophysical interest, is presented. Analysis of rare-earth atomic spectra and of spectra observed in the far ultraviolet with synchrotron radiation as the source of excitation are discussed. Other topics reviewed briefly are: wavelength standards, transition probabilities, the revised solar table and new multiplet tables. A current bibliography is included.

9211. Unassigned.

9212. **Phase rule considerations and the solubility of tooth enamel,** W. E. Brown and B. M. Wallace, *Ann. N.Y. Acad. Sci.* **131,** Art. 2, 690-693 (Sept. 30, 1965).

Key words: Calcium; hydroxyapatite; phosphate; solubility isotherm.

The phase diagram is a particularly useful means of displaying solubility information because it makes it easier to take into account several variables at one time. The use of the phase diagram is illustrated in connection with the possible reactions hat can take place when NaF - $H_3PO_4$ solutions are used to treat enamel. A critical quantity proves to be the concentration of $Na^+$ ion in the treatment solution.

Calcium and phosphorus ions may not diffuse through enamel at the same rates. A situation in which calcium diffuses faster than phosphate would lead to increased concentrations of calcium, phosphate and hydrogen ions within the enamel. This in turn would lead to increased rates of diffusion and dissolution, thus helping to account for subsurface dissolution of enamel.

9213. Unassigned.

9214. **Photon absorption cross section of spherical nuclei,** M. G. Huber, H. J. Weber, M. Danos, and W. Greiner, *Phys. Rev. Letters* **15,** No. 12, 529-531 (Sept. 1965).

Key words: Nuclear physics; photonuclear absorption cross sections; spherical nuclei; theoretical physics.

The Dynamic Collective Theory is extended to vibrational nuclei. The results of the theory are compared with recent photonuclear measurements. Agreement obtains within the accuracy of both the theoretical treatment and the experimental uncertainties. It is concluded that the collective description of the giant resonance is valid in spherical nuclei.

9215. **Photoneutron production by $Li^6$, $Li^7$, $B^{10}$, $B^{11}$, and $O^{16}$,** E. Hayward and T. Stovall, *Nucl. Phys.* **69,** pp. 241-252 (July 1965).

Key words: Activation curve; cross-section; photoneutron.

The neutron emission cross sections have been measured from targets of $Li^6$, $Li^7$, $B^{10}$, $B^{11}$ and $O^{16}$ when they were irradiated with X-rays in the energy range from 7 to almost 30 MeV. The integrated cross sections are 0.40±0.03, 0.49±0.04, 0.46±0.03, 0.43±0.03 and 0.27±0.02 MeV mb respectively. The average cross sections for the lithium and boron targets appear to be essentially constant in the energy range 25-30 MeV. The data also suggest that the boron cross sections contain a great deal of structure up to the highest energies studied.

9216. **Photonuclear reactions,** M. Danos and E. G. Fuller, *Ann. Rev. Nucl. Sci.* **15,** 29-66 (1965).

Key words: Photon cross-sections; photon scattering; photonuclear absorption; photonuclear reaction.

The development of Photonuclear Physics since the last Annual Reviews report is described. The photon absorption process is treated both in the framework of the shell model and he collective model. The modern computational methods are described from an elementary point of view. The available calculations and experiments are described. Their agreement and their internal consistency is analyzed. The giant resonance region in heavy deformed nuclei seems to be already quite well understood, both experimentally and theoretically. The spherical non-closed shell heavy nuclei have not yet been investigated well enough. For light nuclei, experimental data of reasonable quality exist; the theoretical treatment is, however, not yet adequate. The energy region above the giant resonance is still terra incognita to a large extent.

9217. Unassigned.

9218. **Polymerization and pyrolysis of poly-1,2-dihydronaphthalene,** L. A. Wall, L. J. Fetters, and S. Straus, (*Proc. 150th American Chemical Society Meeting, Atlantic City, N. J., Sept. 12-17, 1965), Polymer Preprint* **6,** No. 2, 930-939 (Sept. 1965); *J. Polymer Sci.* Part B; *Polymer Letters* **5,** No. 8, 721-733 (Aug. 1967).

Key words: Degradation; polymerization; pyrolysis; thermal decomposition; thermal volatilization; 1,2-dihydronaphthalene.

Polymerization of 1,2-dihydronaphthalene, using anionic catalysts, gave intractable white powders insoluble in all solvents studied, with the exception of bis(phenoxyphenyl)ether at 290 °C. When dissolved, no appreciable viscosity increments could be detected suggesting either low molecular weights or degradation. In thermal volatilization studies, the polymer yields about 35% monomer and vaporizes at rates near those for polystyrene. Single compacted pellets volatilized faster, however. Unlike the initial powders, pellets had detectable electron spins which could be enhanced by partial pyrolysis. It is concluded that compacting the polymer enhances an exothermic decomposition mechanism.

9219. **Possible nuclear contribution to thermal expansion,** E. C. Hirschkoff and N. M. Wolcott, *Proc. Phys. Soc.* **86,** No. 6, 1372 (1965).

Key words: Ferromagnetism; hyperfine field; NMR; nuclear interaction; nuclear quadrupole resonance; thermal expansion.

A significant contribution to the thermal expansion of a ferromagnetic material at low temperatures due to nuclear interaction with the static hyperfine field is predicted. Some numerical examples are given for cobalt and rare earth metals.

9220. Unassigned.

9221. Unassigned.

9222. **Progress report on a test for cleanability,** M. D. Burdick, *Proc. Porcelain Enamel Inst. Forum,* **26,** 41-48 (1965).

Key words: Cleanability, porcelain enamel surfaces; fluorescent soils; porcelain enamel; soil, residual.

The possible use of fluorescent soils for evaluating the aesthetic cleanability of porcelain enamel surfaces is being explored by the Research Associates. The method being investigated consists of applying a soil containing a small amount of a fluorescent compound to a specimen surface, subjecting the surface to a standard cleaning treatment, and then evaluating the soil remaining on the surface by extracting the residual fluorescent material with toluene and measuring the fluorescence of the resulting solution with a fluorometer. Preliminary results showed that the method was capable of detecting as little as one part per billion of residual soil on a surface. Further work on the method is needed, however, to determine its reproducibility and the degree of correlation of the test data with actual service.

9223. **Progress report on the development of a standardized test for continuity of porcelain enamel coatings,** M. A. Rushmer, *Proc. Porcelain Enamel Inst. Forum,* **27,** 49-56 (1965).

Key words: Bubble structure; continuity of coating; corrosion resistance; high-voltage testing; porcelain enamel; porcelain enamel defects.

Both chemical and electrical methods were investigated for detecting coating discontinuities in porcelain enamels. Chemical methods were found to be time consuming; also, they were incapable of detecting subsurface flaws of a type that can lead to early corrosion of the metal. For these reasons, emphasis was placed on the use of a high-voltage discharge tester. Preliminary work with the tester showed that architectural enamels that rusted in service could be separated from those that did not rust by probing the enamel surface at 1.5 kV. A higher voltage, however, was required to obtain a separation of satisfactory and unsatisfactory hot-water tank enamels. Although these results have been promising, additional work is indicated.

9224. Unassigned.

9225. **Radiation of sound by earthquakes,** R. K. Cook, *$5^e$ Cong. Intern. Acoustique, Liege, Belgium,* 1965, **1b,** K19 (1965).

Key words: Earthquakes, radiation sound; ionospheric motions; radiation sound; sound waves.

Earthquakes cause large motions of the earth's surface which in turn radiate sound waves at infrasonic frequencies into the atmosphere. An analysis of the generation and propagation of sound waves into the upper atmosphere show that substantial ionospheric motions can occur. Such effects occurred during the Alaskan earthquake of March 1964.

9226. **Radiation-induced polymerization at high pressure of 3,3,3-trifluoropropene; 4,4,4,3,3-pentafluorobutene-1; and 5,5,5,4,4,3,3-heptafluoropentene-1,** D. W. Brown (*Proc. 150th American Chemical Society Meeting, Atlantic City, N.J., Sept. 12-17, 1965), Polymer Preprint* **6,** No. 2, 965-976 (Sept. 1965).

Key words: Gamma radiation; polymerization; pressure; poly-5,5,5,4,4,3,3-heptafluoropentene-1; poly-4,4,4,3,3-pentafluorobutene-1; poly-3,3,3-trifluoropropene.

The kinetics of the gamma-ray-induced polymerization of 3,3,3-trifluoropropene; 4,4,4,3,3-pentafluorobutene-1; and 5,5,5,4,4,3,3-heptafluoropentene-1 were investigated within the overall pressure range 1,800-15,000 atm and temperature range 21-161 °C. The polymerizations are free radical in character. Their activation enthalpies, volumes, and entropies increase in the order: propene, butene, pentene. The maximum polymerization rates observed exceeded 10%/hr. for each monomer at a dose rate of 1,500 rad/hr. The maximum intrinsic viscosities were 5.2 dl/g for polytrifluoropropene, 0.67 dl/g for polypentafluorobutene, and 0.12 dl/g for polyheptafluoropentene. The monomer transfer constant of 3,3,3-trifluoropropene was determined. Values range from $10^{-6}$ to $4 \times 10^{-3}$, increasing with temperature increases at constant pressure and with pressure decreases at constant temperature. Transfer effectively determines the molecular weight of polytrifluoropropene at temperatures above 70 °C; the molecular weights of the other polymers are probably determined largely by transfer under all the experimental conditions studied.

9227. **Relation of strength of thermally tempered glass to fracture mirror size,** M. K. Kerper and T. G. Scuderi, *Am. Ceram. Soc. Bull.* **44,** No. 12, 953-955 (Dec. 1965).

Key words: Fracture mirror size; modulus rupture; thermally tempered glass.

The typical fracture of glass broken in flexure has a smooth area which includes the fracture origin. The size of this smooth area or "mirror" is dependent upon the stress introduced in the glass by the thermal tempering process as well as that resulting from flexure during testing of the specimens. The sizes of the mirror in fractures originating on the surface of annealed, semi-tempered or tempered specimens shows a relationship to the modulus of rupture of each type of specimen. This is also true for fractures originating at the edge of annealed glass. For fractures originating at the edge of semi-tempered and tempered glass there is no consistent relationship between mirror size and modulus of rupture.

9228. **Scattering properties of concentric soot-water spheres for visible and infrared light,** R. W. Fenn and H. Oser, *J. Appl. Opt.* **4,** 1504-1509 (Nov. 1965).

Key words: Cloud physics; infrared light; light scattering; Mie Theory; scattering functions.

Based on the theory by Aden and Kerker, computations of the scattering and absorption properties for concentric spherical water-and-particles have been performed for visible and infrared wave lengths. Computations were performed for size parameter values up to 250. Results indicate that, for compound particles with a nucleus smaller than about one-tenth of the total diameter of the particle, the optical properties are almost completely determined by the outer shell. Some results of the computations are presented in graphical form for the scattering and absorption efficiency factors and the angular scattering functions.

The frequency dependence of the complex dielectric constant is not taken into account in the actual computations: absorption, scattering and total extinction are given for constant index of refraction. The theory does allow to take this dependence into account, however, if one wishes to do so.

9229. **Silicon-fluorine chemistry. II. Silicon-boron fluorides,** P. L. Timms, T. C. Ehlert, J. L. Margrave, F. E. Brinckman, T. C. Farrar, and T. D. Coyle, *J. Am. Chem. Soc.* **87,** No. 17, 3819-3823 (Sept. 1965).

Key words: Boron; fluorine; NMR; polysilanes; silicon; sub-halides.

Silicon difluoride reacts with boron trifluoride, producing a series of compounds with silicon-boron bonds. Nuclear magnetic resonance studies of the compounds $Si_2BF_7$ and $Si_3BF_9$ indicate that these are to be formulated as perfluorodisilanylboron difluoride and perfluorotrisilanylboron difluoride respectively. Physical and chemical studies of these new materials are reported.

9230. **Solid-vapor equilibrium in the system helium-methane,** M. J. Hiza and A. J. Kidnay, (*Proc. 1964 Cryogenic Engineering Conf., University of Pennsylvania, Philadelphia, Pa., Aug. 18-24, 1964*), Book, *Advances in Cryogenic Engineering* **11,** 338-348 (Plenum Press, Inc., New York, N. Y., 1966).

Key words: Experimental; helium-methane; low temperature; phase-equilibrium; solid-vapor.

Gas phase compositions in the solid-vapor region for the helium-methane system have been measured at seven integral temperatures from 55.00° to 87.00 °K up to 140 atmospheres pressure. Measurements were also made in the liquid-vapor region at 91.00 °K to provide a direct comparison with the only other gas phase data for this system available in the literature. A flow system was used in which methane was evaporated into a pure helium gas stream. The gas phase leaving the equilibrium cell was analyzed continuously with a hydrogen flame-ionization detector. The data obtained are presented in both tabular and graphical form. Comparison of 91.00 °K data from the present investigation with the data from the literature at 91.1 °K shows a disagreement between the two sets by as much as a factor of four.

9231. **Some applications of the wave front shearing interferometer,** J. B. Saunders, *Japanese J. Appl. Phys. Suppl.* **I, 4,** 99-105 (1965).

Key words: Interferometer; lens aberrations; prism interferometer; testing of lenses.

This paper gives the results of several applications of the wave front shearing prism interferometer. The instrument is very compact and easy to apply. It is applied to the testing of chromatic aberration of simple and compound lenses; and to the testing of wave forms that characterize the monochromatic aberrations (spherical, coma and astigmatism). Results are shown for several different type lenses. This interferometer is equally applicable to the testing of small lenses and large telescope objectives.

9232. **Some statistical properties of pulses from photomultipliers,** M. Gadsden, *Appl. Opt.* **4,** No. 11, 1446-1452 (Nov. 1965).

Key words: Noise, signal; photomultipliers; signal noise ratio; statistical properties; time intervals.

An examination of the integrated counts from 9502S and 9558A photomultipliers suggests that the statistical distribution is closely Poissonian. An examination of the time intervals between consecutive pulses has shown an interesting effect: with a 9502S tube, a highly significant, although small, number of intervals are much longer than expected on a random hypothesis. This effect is explicable in terms of a loss of electrons between cathode and anode. Data on the variation of the signal:noise ratio with differing discriminator bias levels are also presented.

9233. **SPACEWARN--An international mechanism for rapid distribution of information on satellites and space probes,** A. H. Shapley, *COSPAR Info. Bull.* **24,** 30-55 (July 1965).

Key words: Radio service; satellites and space probes; space and satellites.

9234. **Specification for dry cells and batteries,** W. J. Hamer, *ASA* **C18.1,** pp. 31 (1965).

Key words: Batteries; battery classification; battery performance; battery terminals; battery tests; battery types.

This standard for dry cells and batteries includes nomenclature, sizes, tests, and performance data on (1) Leclanche cylindrical cells, (2) Leclanche flat cells, (3) mercury cells, (4) silver oxide button cells, (5) alkaline manganese dioxide cells, (6) sealed nickel-cadmium cells, and on various types of batteries made with the above types of cells. The types of batteries covered include (1) lighting batteries, (2) safety-flasher batteries, (3) transistor hearing-aid batteries, (4) general transistor batteries, and (5) high- and low-voltage batteries. The tests are designed to evaluate the performance of the cells and batteries under simulated service conditions. Descriptions and drawings of various classes of terminals are given.

9235. **Spectrochemical analysis of high-temperature alloys by spark excitation in argon and nitrogen,** H. C. Dilworth, *Am. Soc. Testing Mater. Spec. Tech. Publ.* **376** (1965).

Key words: Alloys, high-temperature; ambient air; argon; atmospheres of argon; high-temperature alloys; nitrogen; nitrogen and ambient air; spark excitation.

Spark excitation of high-temperature alloys in atmospheres of argon, nitrogen, and ambient air were investigated. Compared to air, argon or nitrogen provide the following advantages: (1) Volatilization rates are more constant in time. (2) Background intensities are constant and independent of alloy composition. (3) Effects of metallurgical history on specimen excitation are minimized. Also, self-absorption is markedly reduced in argon. Because of these characteristics, calibration is simplified, and it is possible to analyze many different types of alloys with the same set of analytical curves. This results in a marked reduction in the number of primary standards needed for initial calibration. An effective device for shielding the spark excitation column and specimen surface with a stream of gas is described. Data are presented showing application of the method of excitation in argon and nitrogen to the analysis of a variety of high-temperature alloys.

9236. **Spin-lattice relaxation of rare earth ions in LaCl$_3$,** B. W. Mangum and R. P. Hudson, *Bull. Am. Phys. Soc. Series II*, **10,** No. 8, 1109 (Oct. 1965).

Key words: Rare-earth; spin-lattice relaxation.

Studies of spin-lattice relaxation of the ions Ce$^{3+}$, Nd$^{3+}$, Sm$^{3+}$, Ho$^{3+}$, and Er$^{3+}$ present in low concentrations (0.2 to 2 per cent) in the host lattice of LaCl$_3$ have been made in the liquid helium region by the pulsed-microwave method. The variation of the relaxation time, $\tau$, with temperature permits separation of the contributions to the relaxation from the two-phonon (resonant and non-resonant) and single phonon processes.

The substances studied are not "well-behaved"; features such as non-exponential decays and variability of the derived values for the splitting between the ground and first excited levels are discussed. Some of the ions exhibit a significant variation of $\tau$ with concentration and Nd$^{3+}$ shows an interestingly large anisotropy of $\tau$ in the Raman process.

9237. **Standard frequency and time services of the National Bureau of Standards,** D. H. Andrews, *Frequency* **3,** No. 6, 30-35 (Nov.-Dec. 1965).

Key words: Broadcast of standard frequencies; high frequency; low frequency; standard frequencies; time signals; very low frequency.

Detailed descriptions are given of eight technical services provided by the National Bureau of Standards radio stations WWV, WWVH, WWVB, and WWVL. These services are: 1. Standard radio frequencies; 2. Standard audio frequencies; 3. Standard musical pitch; 4. Standard time intervals; 5. Time signals; 6. UT2 corrections; 7. Radio propagation forecasts; and 8. Geophysical alerts.

9238. **Standardization of the differential chemical shift for Fe$^{57}$,** J. J. Spijkerman, F. C. Ruegg, and J. R. DeVoe, (*Proc. New England Nuclear Mossbauer Symp., New York, N.Y., Jan. 1964*), Book, *Mossbauer Effect Methodology*, pp. 115-120 (Plenum Press, Inc., New York, N. Y., 1965).

Key words: Crystal structure; differential chemical shift; Mossbauer spectroscopy; quadrupole splitting; sodium nitroprusside; standardization.

To provide Mossbauer data for Fe$^{57}$ on a uniform basis, to eliminate recalculation of data from various laboratories, and to provide tables of Mossbauer spectra, the National Bureau of Standards has included disodium pentacyanonitrosylferrate dihydrate, Na$_2$[Fe(CN)$_5$NO]$\cdot$2H$_2$O, in the Standard Reference Materials Program. Single crystals of sodium nitroprusside will be available by April 5, 1965 for this standardization. The crystals are supplied by a commercial manufacturer, and calibrated by NBS on a Mossbauer spectrometer, using an optical fringe counting technique.

The Mossbauer spectrum of a single crystal absorber, cut along the bc plane, is a well resolved, symmetric doublet. The center of this doublet is defined as the zero reference point for the differential chemical shift, with the containing absorber at 25.0 °C. The absorber crystals supplied will be 1cm x 1cm, with 25.0 mg/cm$^2$ of natural iron.

9239. **The ultrasonic velocity in fluid parahydrogen,** B. A. Younglove, (*Proc. IX Intern. Conf. Low Temperature Physics, Columbus, Ohio, Aug. 31-Sept. 4, 1965*), Book, *Low Temperature Physics* **LT9,** Part B, 1223-1226 (Plenum Press, Inc., New York, N. Y., 1965).

Key words: Adiabatic compressibility; hydrogen; sonic velocity.

The ultrasonic velocity in fluid parahydrogen has been measured in the temperature range 15° to 100 °K and in the density range 0.015 to 0.085 gm/cm$^3$. Also the ultrasonic velocity in normal and parahydrogen of the saturated liquid has been measured between 14.5 ° and 32.2 °K. The measurements in the compressed liquid were made either on isochores or isotherms as desired. The density at each point was calculated from the thermodynamic data of Goodwin, et al.

Ten megacycle crystals were used to generate and receive the sound by the pulsed method of Greenspan and Tschiegg in their measurements on water. In system tests using water good agreement was obtained. Standing wave measurements that were taken on the saturated liquid also agree well with the pulsed method. The results are compared with the velocity calculated from PVT and C$_v$ measurements of this laboratory and with measured values from the laboratory of A. Van Itterbeek.

9240. **Superconducting behavior of indium-lead alloys,** S. Gygax, J. L. Olsen, and R. H. Kropschot, (*Proc. IX Intern. Conf. Low Temperature Physics, Columbus, Ohio, Aug. 31-Sept. 4, 1964*), Book, *Low Temperature Physics* **LT9,** Part A, 587-590 (Plenum Press, Inc., New York, N. Y., 1965).

Key words: Ginzburg Landau theory; indium lead alloys; superconductivity.

In a recent publication Saint-James and de Gennes have pointed out that thin superconducting regions can exist close to the surface of a superconductor in a magnetic field H$_{c3}$ which is higher than the upper critical field H$_{c2}$ given by the Ginzburg Landau theory. They find H$_{c3}$=1.691 H$_{c2}$.

We have measured the temperature dependence and concentration dependence of H$_{c1}$, H$_c$, H$_{c2}$, and H$_{c3}$ on polycrystalline indium lead alloys in the $\alpha$ phase region. The experimental value found for H$_{c3}$ is within 10% of the theoretical value and the experimental values of K agree very well with the Ginzburg Landau theory.

9241. **Suppression of 60 c/s pickup when using sensitive DC amplifiers,** R. L. Nutall and D. C. Ginnings, *Electron. Design* **12,** No. 26, 34-35 (Dec. 20, 1965).

Key words: DC-amplifiers; filter; pickup.

Measurements with two commercial low-level DC amplifiers have shown that the use of simple one-stage series-resonant input filter (RLC) enables them to be used with 60 c/s pickup signals as large as volts, contrasted with tolerances of millivolts without the filter. The use of the filter also permits the amplifiers to be used in the presence of 60 c/s pickup with relatively high DC signal source impedances.

9242. **Tables of dielectric constants, dipole moments and dielectric relaxation times,** F. I. Mopsik, (*1964 Digest of Literature on Dielectric Conf. Electrical Insulation*), Natl. Acad. Sci.-Natl. Res. Council Publ. No. **1342,** 28, (Natl. Acad. Sci.-Natl. Res. Council, Washington, D. C., 1965).

Key words: Dielectric constants; dielectric relaxation times; dipole moments.

Dielectric constant and dipole moment data have been compiled from the 1964 literature. Much of the work continues in the regions of interest of the previous years. The most noteworthy measurement appears to be the detection of a dipole moment in deuterated acetylene due to isotopic substitution.

9243. **Tapered inlets for pipe culverts, discussion and author's closure,** J. L. French, *J. Hydraulics, Div. Am. Soc. Civil Eng.*, 286 (May 1965).

Key words: Culverts; hydraulics; inlets; model tests.

The original paper by the writer appeared in the March 1964 issue of the Journal of the Hydraulics Division, ASCE.

Discussions of the paper appeared in the November issue of the Journal, and the writer's closing discussion will appear in the March or May 1965 issue. The present digest of the paper is for Transactions, ASCE.

9244. **The ADI auxiliary publications program,** R. W. Zimmerer, *IEEE Trans. Microwave Theory Tech.* MTT-13, No. 6, 883-884 (Nov. 1965).

Key words: Documentation; information retrieval; publication.

A short Letter to the Editor of IEEE-MTT concerning The American Documentation Institute's Auxiliary Publications Program at the Library of Congress where the editor of any recognized journal can deposit documents with the Photoduplication Service. This letter recommends that the IEEE-MTT Journal start using this service.

9245. **The calibration of permanent magnet standards,** I. L. Cooter, (*ISA 20th Annual Conference and Exhibit, Los Angeles, Calif., Oct. 4-7, 1965*), *ISA Preprint* **14.**1-3-65 (1965).

Key words: Calibration, permanent magnet standards; magnet standards; permanent magnet standards; reference magnets.

The increased demand for the calibration of permanent magnets used as reference standards has required a new magnet calibration facility at the National Bureau of Standards, Washington, D. C. The method procedure and apparatus used in the calibration of reference magnets are described.

9246. **The correlation of experimental pressure-density-temperature and specific heat data for parahydrogen,** H. M. Roder, L. A. Weber, and R. D. Goodwin, (*Proc. XI Intern. Congress Refrigeration, Munich, Germany, Aug. 1963*), Book, *Progress in Refrigeration Science and Technology* **1,** 187-191 (Pergamon Press Inc., New York, N. Y., 1965).

Key words: Density; heat of vaporization; hydrogen; parahydrogen; specific heat; thermodynamic function.

The use of hydrogen in space vehicles and in nuclear devices demands precise knowledge of its mechanical and thermal properties.

The mechanical properties for parahydrogen are defined by nearly 1200 closely spaced experimental P-$\rho$-T points. The boundaries in temperature are 14° and 100 °K, while the experimental pressure ranges from 2 to 350 atm. The P-$\rho$-T surface was approximated by a large number of polynomials coupled with appropriate interpolation schemes. Use of the virial expansion allows extrapolation to pressures below 2 atm.

Thermal properties may be obtained after relating the experiment above to a second one in which the heat capacity at constant volume was determined for a variety of experimental conditions. At temperatures below critical these heat capacities are used as primary data, while at temperatures above critical they serve as check on the correlation between the statistically calculated specific heats and the P-$\rho$-T data. Further tests of the correlation arise when calculating thermodynamic functions.

As a result of this correlation it is now possible to compute as function of pressure and temperature such quantities as specific volume, enthalpy, entropy, specific heat at constant volume, specific heat at constant pressure, sonic velocity, the Joule-Thompson inversion, and the heats of vaporization.

9247. **The design of a federal statistical data center,** E. Glaser, D. Rosenblatt, and M. K. Wood, *Statistical Evaluation Report* No. **6,** Office of Statistical Standards, Bureau of the Budget, Appendix C, pp.1-19 (Office of the President, Washington, D. C., Dec. 1965).

Key words: Automatic data processing equipment; confidentiality audits; disaggregation; disclosure criteria; Federal statistical system; inherent computability; matching; probability master samples; propagation of error computations; statistical standards.

This paper treats the principles underlying the design of a Federal Statistical Data Center intended to provide a better integrated information network for use by Government, industry, and the research community in an age of large-scale computers.

9248. **The dielectric polarizability of fluid parahydrogen,** J. W. Stewart, (*Proc. IX Intern. Conf. Low Temperature Physics, Columbus, Ohio, Aug. 31-Sept. 4, 1965*), Book, *Low Temperature Physics* **LT9,** Part B, 1230-1232 (Plenum Press Inc., New York, N. Y., 1965).

Key words: Dielectric polarizability; dipole moment; fluid parahydrogen; macroscopic polarizability.

In the case of nonpolar substances such as hydrogen the macroscopic polarizability (induced dipole moment per unit mass per unit electric field) $P$ is related to the dielectric constant $\epsilon$ and the density $\rho$ through the Clausius-Mossotti equation:

$$P=\frac{\epsilon-1}{\epsilon+2}\cdot\frac{1}{\rho}$$

Elementary theory predicts that the righthand side of the equation, often called the Clausius-Mossotti function, should be a constant independent of density. Detailed verification of this requires accurate measurements of both $\epsilon$ and $\rho$ over as wide a range of conditions as possible. Sufficiently accurate measurements of $\rho$ have previously been available for *normal* hydrogen, but a really meaningful investigation of the constancy of $P$ for fluid parahydrogen over a wide range of density in both the gaseous and liquid states has been made possible only recently by the high-precision density measurements in this laboratory by Goodwin and his co-workers. Their values of $\rho$ are estimated to have an absolute precision of better than 0.1%. They are internally consistent to 0.02%. For corresponding precision in the calculated values of $P$, the dielectric constant must be determined to considerably higher accuracy.

9249. **The effect of insulation on the weathering of smooth-surfaced built-up roofs exposed to solar heating,** W. C. Cullen and W. H. Appleton, *Coal Tar Asphalts Related Mater.* **3,** 122-124 (Mar. 1965).

Key words: Built-up roofing; deterioration insulation; radiative cooling; solar heating.

The effects of solar heating on the weathering characteristics of smooth-surfaced, built-up roofings applied over insulation are discussed. Data are presented giving the temperatures attained at the underside of smooth-surfaced, built-up roofings placed either over insulation or directly on a concrete deck. Photographs are given showing the differences in the weathering between the insulated and non-insulated roofings observed in the laboratory and in the field. The data show that roofings placed over insulation are subjected to much higher maximum temperatures, more rapid temperature changes, and greater sub-cooling on clear nights than similar roofings placed directly on concrete decks.

9250. **The interaction of radiation with charged particles. I,** W. R. Chappell, W. E. Brittin, and S. J. Glass, *Il Nuovo Cimento* **38,** No. 3, 1186-1191 (Aug. 1965).

Key words: Charged particles; electrons and photons; interaction of radiation; radiation, charged particles.

We employ the Bogoliubov-Tyablikov transformation and an equation of motion method, utilizing part of the Hamiltonian for a system of interacting electrons and photons, to obtain the familiar dispersion relation, $\omega^2 = k^2c + \omega p^2$, for a system of quasi-photons. The equation of motion method can be used to obtain an extended dispersion relation when more terms of the Hamiltonian are taken into account.

9251. Unassigned.

9252. **The important atmospheric processes in the D region,** G. C. Reid, *Proc. COSPAR Polar Cap Panel Symp., Alpach, Austria, 1964*, pp. 15-19 (Academic Press Inc., New York, N. Y., 1965).

Key words: D region; ionosphere; negative ions; photodetachment; recombination.

This is a summary of a review paper delivered at the Symposium on High-Latitude Particles and their Effects on the Polar Ionosphere. Current knowledge of D-region reactions is reviewed and outstanding problems are discussed.

9253. **The microwave spectrum of dinitrogen trioxide,** R. L. Kuczkowski, *J. Am. Chem. Soc.* **87**, 5259-5260 (1965).

Key words: Dinitrogen trioxide; equilibrium; microwave spectrum; structure.

The microwave spectrum of four isotopic species of dinitrogen trioxide is reported which support the planar $ON\text{-}NO_2$ model with $C_s$ symmetry and from which the N-N bond is determined to be 1.85 with an estimated uncertainty of $\pm 0.03$Å.

9254. **The monomer-polymer equilibrium of $\alpha$-trideuteromethyl-$\beta,\beta$-dideuterostyrene,** L. J. Fetters and L. A. Wall, (*Proc. 150th American Chemical Society Meeting, Atlantic City, N. J., Sept. 12-17, 1965*), *Polymer Preprint* **6**, No. 2, 899-903 (Sept. 1965).

Key words: Equilibria; equilibrium concentration of monomer; $\alpha$-trideuteromethyl-$\beta,\beta$-dideuterostyrene; lowering of steric repulsions; polymeric anion; $\Delta H$; $\Delta S$.

The equilibria between $\alpha$-trideutero-methyl-$\beta,\beta$-dideuterostyrene and its polymeric anion in tetrahydrofuran has been investigated between 262 and 308 °K. The heat and entropy changes were both increased significantly by the deuteration. Qualitatively the effect observed appears best explained by the premise that a lowering of steric repulsions occurs with deuterium; and hence the effective volume for deuterium is less than that for hydrogen.

9255. **The NBS cryogenic data center,** V. J. Johnson, (*Proc. XI Intern. Conf. Refrigeration, Munich, Germany, 1963*), Book, *Progress in Refrigeration Science and Technology*, **1**, 110-114 (Pergamon Press, Oxford, England, 1965).

Key words: Cryogenic data center; cryogenic fluids; low temperature properties of materials; NBS cryogenic data center; thermodynamic and transport properties.

A brief description is given of the two principal activities of the Cryogenic Data Center, namely: the evaluation and compilation of data on low temperature properties of materials; and the acquisition, handling and dissemination of technical literature. A program for thorough evaluation and the compilation of thermodynamic and transport properties of cryogenic fluids and selected solids is mentioned. Four functions of the literature service are outlined and typical pictures of the operation included.

9256. **The NBS instrumentation for use in the measurement of spectral irradiances of solar simulators,** R. Stair and W. E. Schneider, *Proc. Intern. Symp. Solar Radiation Simulation, Los Angeles, Calif.*, Jan. 18-20, 1965, pp. 75-94 (Inst. Environmental Sciences and Am. Soc. Testing and Materials, 1965).

Key words: Integrating sphere; solar simulator; spectroradiometer; standard of spectral irradiance.

Three methods are described for the measurement of the spectral irradiances of solar simulators at the National Bureau of Standards. The design of acceptable equipment is significantly affected by large variations in sensitivity of photoelectric and thermoelectric detectors with the wavelength and over their surfaces. The first instrumentation consists of a conventional spectroradiometer in which the source flux is collected in an integrating sphere which insures accurate evaluation of the solar simulator flux in terms of that from a 1000-watt lamp standard of spectral irradiance. A MgO-coated sphere is used for the ultraviolet, visible and near infrared to 1.6 microns.

9257. **The radiation induced polymerization of hexafluoropropylene at high temperature and pressure,** R. E. Lowry, D. W. Brown, and L. A. Wall, (*Proc. 150th American Chemical Society Meeting, Atlantic City, N. J., Sept. 12-17, 1965*), *Polymer Preprint* **6**, No. 2, 977-984 (Sept. 1965), *J. Polymer Sci.* **4**, Part A-1, No. 9, 2229-2240 (Sept. 1966).

Key words: Activation enthalpy; hexafluoropropylene; high pressure; intrinsic viscosity; radiation induced polymerization; radiation intensity.

The radiation-induced polymerization of hexafluoropropylene was studied in the pressure and temperature range 4,500-15,000 atm and 100-230 °C, respectively. Retardation was a serious problem; data thought to apply to the unretarded polymerization are summarized below. At 1,500 rad/hr the polymerization rate was 15%/hr at 230 °C and 15,000 atm. The activation enthalpy and volume are 9.5 kcal/mol and -10 cc/mol respectively. The rate varies as the square root of the radiation intensity. The largest intrinsic viscosity of the polymer is 2.0 dl/g; values increase with temperature and pressure. At 130 °C and 10,000 atm the intrinsic viscosity was the same at two radiation intensities.

9258. **The response of flush diaphragm pressure transducers to thermal gradients,** L. Horn, (*20th Annual ISA Conference and Exhibit, Los Angeles, Calif., Oct. 4-7, 1965*), *Preprint No.* **13.3-4-65** (1965).

Key words: Flush diaphragm; pressure gage; temperature; temperature gradient; transducers.

The zero signal output of pressure transducers may alter during field use in the presence of thermal gradients. The changes can be large enough to cause serious questioning of the validity of test data taken without corrections for the zero shift.

Variations of up to 100% FS (full scale) have been found using transducers that indicated less than a 6% shift in the standard steady state temperature tests.

A simple method of dynamic testing is described and experimental results are given for a number of tests.

9259. **The theory of the chromospheric spectrum,** J. T. Jefferies, Book, *The Solar Spectrum*, Ed. C. DeJager, 131-150 (D. Reidel Publ. Co., Dordrecht, The Netherlands, 1965).

Key words: Chromospheric flash spectrum; chromospheric spectrum; solar disk; spectrum.

The article reviews the problems of interpretation of (a) weak lines in the chromospheric flash spectrum and (b) strong lines whose profiles are measured from center to limb on the solar disk. Typical methods for these interpretations are considered and new ones put forward. Outstanding problems are delineated.

9260. Unassigned.

9261. Unassigned.

9262. Unassigned.

9263. **Thermodynamics of the rigid-rotor at high temperature,** J. E. Kilpatrick, Y. Fukuda, and S. Y. Larsen, *J. Chem. Phys.* **43,** No. 2, 430-432 (July 1965).

Key words: Rigid-rotor, high temperatures; thermodynamic properties; thermodynamics, rigid-rotor.

It is shown that $Q_e$, the partition function for a rigid-rotor summed over even levels and $Q_0$, summed over odd levels, have exactly the same asymptotic (power series in $\sigma=h^2/2IkT$) expansion. No information as to differences in thermodynamic properties due to spin and statistics can be obtained from this expansion. The exchange partition function, $Q_e$-$Q_0$, is calculated directly and used to give simple expressions for the differences in thermodynamic properties between the *para, ortho*, and equilibrium cases.

9264. **Thermolytic chain scission of linear polyethylene and an ethylene-propylene copolymer,** H. Yu and L. A. Wall, (*Proc. 150th American Chemical Society Meeting, Atlantic City, N. J., Sept. 12-17, 1965*), *Polymer Preprint* **6,** No. 2, 940-944 (Sept. 1965).

Key words: Copolymer; ethylene-propylene; linear polyethylene; stress relaxation; thermolytic chain scission.

Thermolytic chain scission of a linear polyethylene and (70:30) ethylene-propylene copolymer was studied with the stress relaxation in vacuo at 260 ~ 320 °C. The mode of thermolytic chain scission is random along the backbone carbon-carbon bonds. The activation energy for the ethylene-propylene copolymer is found to be 42 kcal/mol; 73 kcal/mol for linear polyethylene. The results for the polyethylene are in agreement with those obtained by the study of rate of volatilization at 400 ~ 420 °C.

9265. Unassigned.

9266. **Voltmeter calibration to 1 GHz,** M. C. Selby, W. J. Blank, and R. P. Chariton, (1965 Wescon Conference, San Francisco, Calif., August 1965), *IEEE WESCON Tech. Papers* **9,** Part 6, No. 8.8, 1-12 (1965).

Key words: Calibration, high-frequency voltages; measurement, microwave voltages; voltage, high-frequency, calibration; voltage measurements; Voltage Tee.

A novel Voltage Tee to calibrate meters to 1 GHz is described. It eliminates errors caused by standing waves over an extremely wide range of voltmeter input impedances. It considerably reduces the RF calibration power required, as compared with conventional matched Tees.

9267. **Winter anomaly in ionospheric absorption and stratospheric warnings,** A. H. Shapley and W. J. G. Beynon, *Nature* **206,** 1242-1243 (June 1965).

Key words: Absorption, ionospheric; ionospheric absorption; stratospheric warnings; winter anomaly.

9268. **Methods of determining Coriolis zeta constants,** S. Abramowitz and I. W. Levin, *J. Mol. Spectry.* **19,** No. 4, 461-462 (Apr. 1966).

Key words: Band contours; $BF_3$; Coriolis force; force fields; high resolution; infrared; $\nu_3$; vibration-rotation; $\zeta_3$; $\zeta_4$.

The recently observed high resolution spectrum of the $\nu_3$ fundamental of $BF_3$ has been interpreted to yield a Coriolis $\zeta$ constant in agreement with that found from an investigation of the unresolved band contour.

9269. **Magnetization and critical fields of superconducting $SrTiO_3$,** E. Ambler, J. H. Colwell, W. R. Hosler, and J. F. Schooley, *Phys. Rev.* **148,** No. 1, 280-286 (Aug. 5, 1966).

Key words: Critical fields; heat capacity; magnetization curves; semiconducting $SrTiO_3$; superconducting $SrTiO_3$.

Magnetization curves from T=0.15 °K to $T_c$ have been measured for two specimens of semiconducting $SrTiO_3$ of electron density about $10^{20}$ $cm^{-3}$. Magnetic hysteresis was observed in each case. The temperature dependences of the first and second critical fields have been measured. The heat capacity has been measured down to 0.3 °K for one specimen, yielding $\gamma$, the coefficient of the linear term, and an independent value of $T_c$ at the upper part of the specific heat anomaly. Values of $H_c$ (0) derived on the basis of the heat capacity data are higher than the values of $H_c(0)$ obtained from the magnetization data. The Ginzburg-Landau k is shown to vary inversely with the electronic mobility, as expected.

9270. **The determination of heats of formation of refractory compounds,** G. T. Armstrong and E. S. Domalski, *Proc. 4th Meeting Interagency Chemical Rocket Propulsion Group, Working Group on Thermochemistry, Kennedy Space Flight Center, Florida*, March 16-18, 1966, **I,** No. 108, 15 (Chemistry Propulsion Information Agency, Silver Spring, Md., June 1966).

Key words: Aluminum borides; boron; boron carbide; carbon; fluorine; heat of combustion; polytetrafluoroethylene (Teflon); refractory compounds.

Refractory compounds have an application in propellants as possible ingredients of air breathing engines. In a study carried out for the Air Force Aero Propulsion Laboratory, Wright Patterson Air Force Base, the heats of combustion of several boron compounds in fluorine were studied with a view to determining their heats of formation from the elements. To determine auxiliary data for calculating the heats of formation of the compounds, the heats of combustion of fluorine of polytetrafluoroethylene (Teflon), graphite, and boron were determined also. Analysis of the compounds becomes a major problem in deriving heats of formation from the observed calorimetric data. The effects of analysis in the interpretation of the data are discussed. The presentation is in the nature of a summary. Details will be presented in projected publications.

9271. **What environment--for whom?** G. E. Auman, *Civil Service J.* **7,** No. 1, 6-11 (July-Sept. 1966).

Key words: Environment; personnel; professional environment; professional personnel; scientists and engineers; standing committee; technical personnel.

Since the early 1960's the Standing Committee of the Federal Council for Science and Technology has been studying, analyzing and making recommendations designed to improve the environment for Federal scientists and engineers. During 1965 the Committee queried 1,025 scientists and engineers in 17 Federal laboratories concerning the importance of 51 carefully selected environmental features and their satisfaction with provision of these features in the Federal service. The survey revealed extreme variations in the attitudes of respondents with regard to virtually every item. However, some clearly defined patterns and relationships among subgroups were identified when respondents were subclassified by discipline, education, grade level, type of work performed, employing laboratory, etc.

Overall the features ranking highest in importance were those concerned with professional values, appropriate and equitable pay, and adequate on-the-job support. Some items of generally low importance were patent rights, separate classification titles for scientists and engineers, security controls and sabbatical leave. In view of the wide disparity in satisfaction expressed by persons in individual laboratories and subgroups, it is suggested that agencies and laboratory directors might profitably undertake similar surveys and specific improvement programs for their installations.

9272. **Photoionization of *n*-butane at 1067-1048 Å, Decomposition of the parent ion and superexcited molecule,** P. Ausloos and S. G. Lias, *J. Chem. Phys.* **45,** No. 2, 524-535 (July 15, 1966).

Key words: Butane; ionization efficiency; ion-molecule reactions; ion-pair yields; photoionization; superexcited molecule.

*n*-$C_4D_{10}$, *n*-$C_4D_{10}$, $CD_3CH_2CH_2CD_3$, and $C_4D_{10}$ - $C_3D_6$ mixtures have been irradiated in the presence of oxygen with the argon resonance lines at 1067 Å and 1048 Å. On the basis of saturation ion current measurements, the ionization efficiency ratios $\eta_{C4D10}/\eta_{NO}$ and $\eta_{NO}\eta_{C4H10}/\eta_{NO}$ were estimated to be 0.48 $\pm 0.003$ and $0.465 \pm 0.003$, respectively. It is demonstrated that at the argon resonance lines the $C_4H_{10}^+$ ion undergoes fragmentation according to the following two processes:

$$\begin{aligned} C_4H_{10}^+ &\rightarrow C_3H_7^+ + CH_3 \\ &\rightarrow C_3H_6^+ + CH_4 \end{aligned}$$

The isotopic analysis of the propane fraction formed in the irradiation of *n*-$C_4H_{10}$-*n*-$C_4D_{10}$-$O_2$ mixtures indicates that the propyl ion which reacts with *n*-butane to form propane by a $H^-$ or $D^-$ ion transfer has the *sec*-propyl ion structure. It is further shown that, in agreement with recent studies on ion-molecule reactions, the $C_3H_6^+$ ion also reacts with $C_4H_{10}$ to form $C_3H_8$ ($H_2^-$-transfer). The yield of the parent ion was estimated by making use of the recently established $H_2$-transfer reaction: $C_4H_{10}^+ + C_3D_6 \rightarrow CD_3CDHCD_2H + C_4H_8^+$.

The fragmentation of the butane parent ion is strongly quenched by an increase in the pressure of butane, or upon addition of an inert gas. The following approximate relative efficiencies for the quenching of the fragmentation of the excited $C_4D_{10}^+$ ion are obtained: He - 1, N - 5, $C_4D_{10}$ - 35. It is also noted that the fragmentation of the $C_4D_{10}^+$ ion is more readily quenched by collision with He than that of the $C_4H_{10}^+$ ion by about a factor of 5.

The fragmentation of the neutral excited molecule has been examined briefly on the basis of the isotopic analysis of products formed in the photolysis of $CD_3CH_2CH_2CD_3$ - $O_2$ mixtures at 1470 Å, 1236 Å, and 1067 Å-1048 Å, and of those formed in the photolysis of $C_4D_{10}$ - $H_2S$ mixtures at 1236 Å. It is concluded that the modes of decomposition of the superexcited molecule are essentially identical to those observed for molecules excited at photon energies below the ionization energy, although the elimination of an $H_2$ molecule or an alkane may be of lesser importance at the shorter wavelength.

9273. **Ion-molecule reaction in the liquid and solid phase radiolysis of hydrocarbon mixtures,** P. Ausloos, A. A. Scala, and S. G. Lias, *J. Am. Chem. Soc.* **88,** 1583-1584 (1966).

Key words: Hydrocarbons; ion-molecule reactions; radiolysis.

Experimental results are presented which for the first time demonstrate that ion-molecule reactions occur in the liquid and solid phase radiolysis of hydrocarbons and that they can be investigated in a systematic manner.

9274. **The National Bureau of Standards and its contributions to geophysics,** D. Baker, *Trans. Am. Geophys. Union* **17,** No. 4, 563-568 (Dec. 1966).

Key words: Geophysics; gravity; ionosphere; seismology.

Almost from its inception the National Bureau of Standards has made contributions to the field of geophysics. Major contributions are reviewed, including gravity measurements, IGY participation, seismology, and atmospheric and ionospheric investigations.

9275. **Sodium-electron spin-exchange collisions,** L. C. Balling, *Phys. Rev.* **151,** No. 1, 1-6 (Nov. 4, 1966).

Key words: Electron; optical pumping; sodium; spin-exchange.

A spin-exchange optical pumping experiment to study collisions between sodium atoms and free electrons is reported. In this experiment, electrons in a weak magnetic field were polarized by spin-exchange collisions with optically pumped sodium atoms. The sodium-electron collisions were the principal source of the electron resonance linewidth, and they also produced a shift in the electron resonance frequency. The magnitudes of the linewidth and the frequency shift depend upon the scattering amplitude for sodium-electron collisions, the sodium polarization and the sodium atom density. The ratio of the frequency shift to the linewidth was 0.03. The sodium polarization was approximately 30%. The electron resonance frequency was lower when the sodium polarization was positive. The measurements of the electron linewidth and the frequency shift agree with theoretical values of the linewidth and frequency shift obtained from the sodium-electron scattering phase shifts which have been recently calculated by Garrett.

9276. **The absorption spectrum of RbD. Vibrational numbering of the $A^1\Sigma$ state of RbH,** I. R. Bartky, *J. Mol. Spectry.* **21,** No. 1, 1-3 (Sept. 1966).

Key words: Absorption spectroscopy; alkali metal hydrides; hydrides; isotope relations; molecular constants.

RbD has been observed in absorption from 5200-5400 Å. Of the several bands observed in this region, two have been analyzed in detail. The RbD spectrum correlates with the RbH spectrum only if the vibrational numbering of the $A^1\Sigma$ state of RbH is increased by 3. Revised molecular constants for RbH are given.

9277. **The absorption spectrum of cesium deuteride. The $A^1\Sigma$ state of CsH,** I. R. Bartky, *J. Mol. Spectry.* **21,** No. 1, 25-28 (Sept. 1966).

Key words: Absorption spectroscopy; alkali metal hydrides; hydrides; isotope relations; molecular constants.

An analysis of the visible absorption spectrum of CsD has shown that the vibrational numbering of the $A^1\Sigma$ state of CsH must be increased by 3. From this and previous reassignments of the $A^1\Sigma$ states of KH and RbH, it is now possible to exhibit the trends of the vibrational and rotational constants for the alkali metal hydrides.

9278. **The $A^1\Sigma$ - $X^1\Sigma$ transition of $^{39}$KH and $^{39}$KD. Vibration numbering and molecular constants,** I. R. Bartky, *J. Mol. Spectry.* **20,** No. 4, 299-311 (Aug. 1966).

Key words: Absorption spectroscopy; alkali metal hydrides; hydrides; isotope relations; molecular constants.

The absorption spectrum of KD has been observed in the 5100-5200 Å region. An analysis of the spectrum in this region has shown that the previous assignments of the KD and KH spectra are in error. The v′-numbering of KD must be increased by 3, and the J-numbering of the P and R branches must be decreased by 1; the v′-numbering of KH must be increased by 2. Re-analysis of the existing data on KH and KD has given a consistent set of vibrational and rotational constants for the states of these molecules.

9279. **An improved design for vacuum ultraviolet resonance lamps,** A. M. Bass, *Appl. Opt.* **5,** No. 12, 1967 (Dec. 1966).

Key words: Electric discharge; resonance lamp; vacuum ultraviolet; window seal.

A method is described for sealing lithium fluoride windows to resonance lamp discharge tubes so as to avoid damage to the seal by action of the discharge.

9280. **Message from outgoing editor,** R. W. Beatty, *IEEE Trans. Microwave Theory Tech.* **MTT-14,** No. 4, 170 (Apr. 1966).

Key words: Abstracts; editing; journals; publishing; redacting.

The outgoing editor notes the growth of the Transactions and the addition of the microwave abstracts. He calls attention to the formation of a panel of editors and their activities. He observes the intricate process of publishing a Transactions and notes that although it does not reach the readers promptly, steps are being considered which will speed up the process.

Recognition is given to the contributions of others in getting out the Transactions and confidence is expressed in the new editor and in the future of the Transactions.

9281. **Mass-spectrometric study of photoionization IV. Ethylene and 1,2-dideuteroethylene,** R. Botter, V. H. Dibeler, J. A. Walker, and H. M. Rosenstock, *J. Chem. Phys.* **45,** No. 4, 1298-1301 (Aug. 15, 1966).

Key words: Autoionization; 1,2-dideuteroethylene; ethylene; mass spectra; photoionization; Rydberg; threshold energies.

Photoionization efficiency curves for ions of the molecule and of selected fragments of $C_2H_4$ and CHDCHD are reported for the wavelength region from onset of ionization to 600Å. The minimum threshold of ionization is 10.50 eV for both molecules. In addition, certain features of the ion yield curves are discussed and identified as resulting from vibrationally excited states or from autoionization from Rydberg levels leading to electronically excited states. Threshold measurements of the acetylene ions permit calculation of heats of dissociation and indicate that the $C_2H_2^+$ ion is formed without excess activation energy. Of the vinyl ions, the threshold for the $C_2H_3^+$ ion is the most clearly defined and leads to a $C_2H_3$-H bond dissociation energy of 100 kcal/mol (418 kJ/mol).

9282. **Exchange and direct second virial coefficients for hard spheres,** M. E. Boyd, S. Y. Larsen, and J. E. Kilpatrick, *J. Chem. Phys.* **45,** No. 2, 499-508 (July 15, 1966).

Key words: Hard spheres; quantum statistics; quantum virial coefficient; second virial coefficient.

We have separated the quantum mechanical second virial coefficient for hard spheres, B, into two terms. The first represents the contribution of a Boltzmann gas, and the second is an exchange term embodying the effects of quantum statistics. Numerical computation of B to a high precision then allows us to analyze the temperature dependence of the exchange term - which is found to decrease exponentially with temperature - and to determine the asymptotic expansion of the Boltzmann term at high temperatures.

9283. **The National Standard Reference Data System,** E. L. Brady, *J. Chem. Doc.* **7,** No. 1, 6-9 (Feb. 1967).

Key words: Future plans; National Standard Reference Data System; objectives; operation; status.

The National Standard Reference Data System is a government-wide effort to give to the technical community of the United States optimum access to quantitative data on the physical and chemical properties of substances and their interactions, critically evaluated and compiled for convenience. The general functions of the System are to coordinate and integrate existing data evaluation and compilation activities into a systematic, comprehensive program, supplementing and expanding technical coverage when necessary, establishing and maintaining standards for the output of the participating groups, and providing mechanisms for the dissemination of the output as required. This program was established as a Federal policy in 1963 upon the recommendation of the Federal Council for Science and Technology. The National Bureau of Standards of the Department of Commerce has accepted responsibility for administering the effort. The plan of operation and the general status of activities initiated by the National Bureau of Standards will be described.

9284. Unassigned.

9285. **Photodetachment cross section, electron affinity, and structure of the negative hydroxyl ion,** L. M. Branscomb, *Phys. Rev.* **148,** No. 1, 11-18 (Aug. 5, 1966).

Key words: Cross section; electron affinity; molecular structure; negative hydroxyl ion; $OD^-$ ions; $OH^-$ ions; photodetachment.

Experimental data on the cross section for photodetachment of $OH^-$ and $OD^-$ ions are given and used to argue that $r_e(OH^-) = r_e(OH) \pm 0.0002$Å, that $\omega_e(OH^-) = 3700 \pm 560$ cm$^{-1}$ and that the OH electron affinity E. A. (OH) $= 1.83 \pm 0.04$ eV. Thus, the structure of $OH^-$ and OH are remarkably similar, which is consistent with the theoretical predictions of Cade.

9286. **Flash photolysis of methane in the vacuum ultraviolet. I. End-product analysis,** W. Braun, K. H. Welge, and J. R. McNesby, *J. Chem. Phys.* **45,** No. 7, 2650-2656 (Oct. 1, 1966).

Key words: Acetylene; combination; ethane; ethylene; flash photolysis; gas phase; hydrogen; hydrogen deuteride; insertion; methane; methyne; rate; vacuum ultraviolet.

Methane and mixtures of methane and methane-$d_4$ have been subjected to flash photolysis in the vacuum ultraviolet. Ethylene is the major hydrocarbon product. Isotopic distributions of the hydrogen, ethane and ethylene fractions as well as complete product analysis suggest that CH plays a dominant role in the photolysis. The CH is formed either by direct dissociation of excited methane or secondary flash photolysis of $CH_2$ in the flash. On the basis that acetylene is formed with unit efficiency by association of CH, and ethylene is formed by reaction of CH with methane, the collision yield of the latter reaction is about 1/82.

9287. **A vacuum ultraviolet flash photolysis apparatus,** W. Braun, A. M. Bass, and A. E. Ledford, Jr., *Appl. Opt.* **6,** No. 1, 47-49 (Jan. 1967).

Key words: Apparatus description; flash photolysis; vacuum ultraviolet.

An improved apparatus for performing vacuum ultraviolet flash photolysis-kinetic spectroscopy has been constructed. The device consists of a compact coaxial arrangement of six capacitors and six electrode pairs, symmetrically placed about a hexagonal reaction vessel of large aperture. The reaction vessel contains LiF windows to transmit far ultraviolet radiation. The six pairs of electrodes and six capacitors are connected separately and are synchronously fired, uniformly illuminating the reaction cell. The photolytic light pulse duration is about 5 $\mu$ sec. More than $10^{18}$ quanta enter the reaction vessel in the spectral region between 1050 Å and 1600 Å. The essential operating features of the apparatus are described.

9288. **Chemiluminescence of CH in the $O+C_2H_2$ reaction: Rotational relaxation and quenching,** W. Brennen and T. Carrington, *J. Chem. Phys.* **46,** No. 1, 7-18 (Jan. 1, 1967).

Key words: Acetylene; CH; chemiluminescence; cross section; emission spectrum; energy transfer; experimental; gas; oxygen atom; oxidation; population distribution; rotation.

Rotational distributions of $CH(A^2\Delta, v=0)$ were measured at pressures from 0.1 to 8.5 torr in the $O+C_2H_2$ reaction in the presence of large excess of $N_2$, Ar, or He. The reaction $N+NO \rightarrow N_2+O$ was used to produce O without $O_2$. Under all conditions the distributions are found to be a superposition of two Boltzmann distributions, one at 1200-1400 °K characteristic of the process leading to the formation of excited $CH(A^2\Delta)$, and one which stays close to the temperature of the reactor. Interpreting the fraction of molecules in this low temperature distribution as a measure of the extent of relaxation of the initial rotational distribution of excited CH, average relaxation rate constants are derived. With the collision partners mentioned above, 10 to 30 collisions are required for relaxation. A 14-level phenomenological model including only transitions between neighboring rotational levels ($K \rightarrow K \pm 1$) fits the experimental distributions well at all pressures studied if the downward rate constants, $k_{K-1,K}$ are approximately proportional to exp $(-2BK/kT)$, where $B=14.6\ cm^{-1}$ is the rotational constant for $CH(A^2\Delta, v=0)$ and $T=360$ °K. Other models are discussed. Rotational and vibrational distributions for $CD(A^2\Delta)$ are also described. Quenching of the $CH(A \rightarrow X)$emission by added oxygen was studied quantitatively and the results are consistent with a mechanism in which not $CH(A^2\Delta)$ but a precursor to its formation is removed by $O_2$. In the absence of $O_2$ the lifetime of the precursor is determined primarily by the atomic oxygen concentration.

When an electrical discharge through $O_2$ is used as the source of oxygen atoms for reaction with acetylene, the rotational distribution of $CH(A^2\Delta)$ and its pressure dependence is quite different from that described above. When acetylene reacts with the products of a discharge through $CO_2$ with excess $CO_2$ as heat bath, the rotational distribution of $CH(A^2\Delta)$ has a Boltzmann form at all pressures, with only the rotational temperature depending on pressure and approaching the gas kinetic temperature at high pressure.

9289. **Spin-relaxation effects on the EPR spectrum of gaseous *s*-state atoms,** R. L. Brown and W. Brennen, *J. Chem. Phys.* **46,** No. 1, 385-386 (Jan. 1, 1967).

Key words: Electron paramagnetic resonance; flow system kinetics; hydrogen atoms; nitrogen atoms; spin exchange cross sections; spin relaxation time.

Experimental evidence has been obtained which indicates that N atoms produced in a flow system by a microwave discharge through purified $N_2$ had a "spin-lattice" relaxation time of the order of 25 milliseconds. The residence time of the atoms in the EPR magnet was comparable to this. As a result, the atoms (which were generated outside of the magnet) arrived at the microwave cavity before reaching their equilibrium magnetization. The EPR absorption intensity was abnormally small since the population difference between the Zeeman levels was smaller than at equilibrium.

9290. Unassigned.

9291. **Influence of paramagnetic resonance on the static susceptibility. The lattice-bath relaxation time of neodymium ethylsulfate,** G. A. Candela and R. E. Mundy, *J. Chem. Phys.* **46,** No. 1, 47-54 (Jan. 1, 1967).

Key words: Electron static susceptibility; lattice-bath; neodymium ethylsulfate; relaxation time; spin saturation.

The spin-lattice-bath relaxation process of neodymium ethylsulfate was investigated by measuring simultaneously the change in the static susceptibility and the microwave power absorbed at electron spin resonance. This technique can be used at constant temperature to distinguish the spin-lattice process from the lattice-bath process. The relaxation time of neodymium ethylsulfate was studied at a microwave frequency of 14.5 G Hz as a function of temperature, helium exchange gas pressure, microwave power absorbed, two crystal orientations, and crystal size. At this microwave frequency the energy transfer from the lattice to the bath appears to be the rate determining process. The dominant lattice-bath relaxation time, $\tau_p$, is inversely proportional to the square of the bath temperature $\tau_p T^2=0.20$ sec $°K^2$ but is apparently independent of the crystal size, the helium exchange gas pressure, and crystal orientation. The experimental data are in essential agreement with the data obtained by other researchers using different methods.

9292. **Studies of some exploding wire light sources,** E. C. Cassidy and S. Abramowitz, *J. Soc. Motion Picture Television Eng.* **75,** No. 8, 735-737 (Aug. 1966).

Key words: Aluminum; AlH; AlO; atomic spectra; electrical discharges; exploding wires; light sources; time-resolved spectroscopy; titanium; TiO.

Continuous and time-resolved measurements of the spectral distribution of light emitted by various exploding wire systems have been obtained by use of a high-speed drum camera and a rotating shutter, respectively. Results from experiments with several systems show the effects of environment, pressure, energy, and wire material on the spectrum. Various intermediate species, produced by the explosion, are determined spectroscopically.

9293. **Interference in the photoionization of molecules,** H. D. Cohen and U. Fano, *Phys. Rev.* **150,** No. 1, 30-33 (Oct. 7, 1966).

Key words: Diatomic molecule; interference; photoionization; ultraviolet.

Atoms of a molecule exposed to far-ultraviolet light may be treated approximately as separate sources of photoelectrons. Interference from these sources modulates the spectrum of photoabsorption in accordance with Samson's observations on $N_2$ and $O_2$. A Born approximation calculation for $H_2^+$ displays details of this effect.

9294. **Vibrational spectrum of $ClNF_2$,** J. J. Comeford, *J. Chem. Phys.* **45,** No. 9, 3463-3465 (Nov. 1, 1966).

Key words: Chlorodifluoramine; infrared spectra; matrix-isolation; spectra; vibrational assignment; vibrational fundamentals.

The infrared spectrum of chlorodifluoramine has been examined for the region of the fundamentals in both the gas-phase and in an argon matrix at 20 °K. The previously unassigned fundamental, $\nu_6$, has been observed, completing the vibrational assignment.

9295. **Classification of the $Y_1^*(1765)$ and $Y_0^*(1520)$ resonances in the 1134 representation of SU(6),** J. J. Coyne, S. Meshkov, and G. B. Yodh, *Phys. Rev. Letters* **17,** No. 12, 666-668 (Sept. 19, 1966).

Key words: Baryon resonances; classification; decay widths; higher symmetry; SU(3); $SU(6)_W$.

The $Y_1^*(1765)$ $5/2^-$ resonance exhibits ratios of meson-baryon $(8 \times 8)$ decay widths to meson-baryon resonance $(8 \times 10)$ decay widths such as to indicate that it can be classified in the 1134 product representation of SU(6). A comparison of the decay modes of the $Y_0^*(1520)$ with those of the $Y_1^*(1765)$ shows that it, too, may be classified in the 1134.

9296. **Static theory of the giant quadrupole resonance in deformed nuclei,** M. Danos, W. Greiner, and B. C. Kohr, *Phys. Rev.* **151,** No. 3, 761-772 (Nov. 18, 1966).

Key words: Deformed nuclei; giant resonance; nuclear hydrodynamics; octupole deformation; photon absorption; quadrupole resonance.

The modes and frequencies of the giant quadrupole resonance of heavy deformed nuclei have been calculated. The quadrupole operator is computed and the absorption cross section is derived. The quadrupole sum rule is discussed and the relevant oscillator strengths have been evaluated for various orientations of the nucleus. The giant quadrupole resonances have energies between 20 and 25 MeV. The total absorption cross section is about 20% of the giant dipole absorption cross section. Of particular interest is the occurrence of the quadrupole mode in a direction of approximately $\theta = 1/4\pi$ from the symmetry axis. This may give information on the details of the nuclear shape.

9297. **Electrodynamic vibration standard with a ceramic moving element,** T. Dimoff, *J. Acoust. Soc. Am.* **40,** No. 3, 671-676 (Sept. 1966).

Key words: Air bearing; ceramic moving element; electrodynamic shaker; piezoelectric accelerometers; reciprocity; secondary standard; vibration standard.

This report describes a new rectilinear vibration exciter specifically developed for accurate calibration of piezoelectric accelerometers. It is an electrodynamic shaker using a permanent magnet with a ceramic moving element guided by an air bearing system. The moving element has a simple cross section and the driving coil is wound directly onto it. Its first axial resonance is near 25,000 Hz. The working range of the shaker extends from 5000 Hz to less than 5 Hz.

The moving element includes a means of mounting an internal accelerometer which can be used as a secondary standard. Alternatively, the moving element - accelerometer assembly can be calibrated by a reciprocity method and used as an absolute standard.

The results of measurements of transverse motion and harmonic distortion are presented as well as an example of pickup calibration.

9298. **A scattering chamber for use with cooled large area lithium-compensated silicon radiation detectors,** W. R. Dodge, J. A. Coleman, and S. R. Domen, *Nucl. Instr. Methods* **42,** No. 2, 181-187 (July 1966).

Key words: Detector telescope; large area detectors; photonuclear physics apparatus; scattering chamber; semiconductor detectors.

A scattering chamber designed to be used with large area lithium-compensated silicon radiation detectors has been constructed. The chamber has provision for cooling a circular array of detectors to 77 °K to achieve short charge collection times and good resolution. The apparatus was designed to be used with the NBS 180-MeV synchrotron in photoproton experiments in the 2 to 35 MeV proton energy interval.

9299. **Measurement of the mean energy required to create an electron-hole pair in silicon between 6 and 77 °K,** W. R. Dodge, S. R. Domen, T. F. Leedy, and D. M. Skopik, *Phys. Rev. Letters* **17,** No. 12, 653-655 (Sept. 19, 1966).

Key words: Energy, required to create an electron-hole pair; low temperature; recombination; Shockley theory of $\epsilon$; silicon radiation detectors; trapping.

Relative values of the mean energy required to create an electron-hole pair with $^{207}$Bi conversion electrons between 6 and 77 °K have been measured. The data show that $\epsilon$ exhibits no first order variation with temperature from 6 to 77 °K. Previous measurements had yielded values as high as 5.22±.02 eV/ electron-hole pair at 20 °K.

9300. **Calculated heats of dilute solid solution among the alkali halides other than cesium salts,** T. B. Douglas, *J. Chem Phys.* **45,** No. 12, 4571-4585 (Dec. 15, 1966).

Key words: Alkali halides; heats of solution; ion substitution; lattice relaxation; polarization energy; shell calculations; solid solutions.

Limiting high-temperature heats (energies) of dilute solid solution are calculated for all 96 cases of one NaCl-type alkali halide (except Cs salts) dissolving in another having a common ion. The direct-summation shell treatment used is based on a slightly modified Born-Mayer potential function and on the polarization energy up to terms square in the ion polarizabilities. Preliminary general expansion of the energy in positive powers (up to cubic) of the lattice-relaxation (ion-displacement) parameters of the first eight shells (98 neighbors) facilitated application to specific cases. In the linear solution for the minimum-potential lattice relaxation, one or two iterations for the first two shells sufficed. The convergence of the energy expansions and the sensitivity of the calculated energies to arbitrary variations in the semi-empirical parameters were extensively investigated. Comparison is made with calorimetric heats of solution in 16 cases, the agreement (averaging ±10 percent) lying within the experimental and computative errors.

9301. **Status of light-element heat-capacity calorimetry at the National Bureau of Standards: A review of the high-temperature thermodynamics of the BeO-H$_2$O system,** T. B. Douglas, *Proc. 4th Meeting Interagency Chemical Rocket Propulsion Group, Working Group on Thermochemistry, Kennedy Space Flight Center, Florida,* Mar. 16-17, 1966, **I,** No. 108, 27 (Chemistry Propulsion Information Agency, Silver Spring, Md., June 1966).

Key words: Beryllium oxide; calorimetry; chemical propulsion; equilibrium; estimates; thermodynamics.

Heat-capacity calorimetry recently completed and in progress at the National Bureau of Standards is reviewed briefly. After a critical review of the thermodynamic properties of the BeO-H$_2$O system, it is concluded that the product of the reaction between BeO(c) and H$_2$O(g) below 1850 °K is probably largely Be(OH)$_2$(g), but that higher hydrates may be sufficiently stable to hold considerable amounts of BeO in the gas phase at much higher temperatures.

9302. **Erratum: Statistical model for the beta zirconium hydrides,** T. B. Douglas, *J. Chem. Phys.* **45,** No. 3, 1080 (Aug. 1, 1966).

Key words: Beta zirconium hydrides; statistical model; zirconium hydrides.

An inadvertent error in sign is corrected in an equation in an article of the author's published earlier in the Journal of Chemical Physics. Only the correct equation, it is added, was used in the computations in the article.

9303. **Survey of infrared measurement techniques and computational methods in radiant heat transfer,** S. T. Dunn, J. C. Richmond, and J. F. Parmer, *J. Spacecraft Rockets* **3,** No. 7, 961-975 (July 1966).

Key words: Computational methods; emissivity; emittance measurements; radiant heat transfer; reflectance measurements; thermal radiation.

This paper is an analysis of 133 replies to a questionnaire sent to all known workers in the field of thermal radiation property measurements and radiant heat transfer computations. The questions were designed to obtain information on the current state of the art in these fields. In addition, the authors have supplemented the information obtained from the questionnaire to give a broad over all picture of the current status and future needs in each area covered. A brief summary of Russian literature in the field of thermal radiation property measurements is also included.

9304. Unassigned.

9305. **A method for calibrating volt boxes, with analysis of volt-box self-heating characteristics,** R. F. Dziuba and T. M. Souders, *IEEE Intern. Conv. Record*, **Part 10,** p. 17 (Mar. 21-25, 1966).

Key words: Calibration; errors; heating; voltage divider; volt-box.

A modification of the Julie ratiometric method for calibrating volt boxes has been under study at NBS to evaluate its performance as a useful calibration technique. The modification features speed of operation, high accuracy and rated voltage measurements. Evaluation of the method accelerated an investigation of self-heating errors of volt boxes that was in progress. The results of this study together with an analysis of self-heating curves are included.

9306. **Additional thoughts on precision calibration of accelerometers,** S. Edelman, *Test Engineering and Management* **XVI,** No. 5, p. 17 (Nov. 1966).

Key words: Accelerometer; calibration; comparison calibration; frequency range; shaker; vibration.

This consists of a number of comments on an article by W. P. Kistler. It shows why reliable calibration of vibration measuring instruments requires careful measurements over the entire frequency range of interest.

9307. **Anniversaries in 1966-67 of interest to statisticians Part I: Introduction and summary,** C. Eisenhart, *Am. Stat.* **21,** No. 2, 32-34 (Apr. 1967).

Key words: Anniversaries; statisticians, 1966, 1967.

Brief descriptions, with minimal documentation, of twenty-six anniversaries in 1966 and 1967 of potential interest to statisticians.

9308. **A study of the angular and energy distributions of radiation at small distances from a point source of gamma rays or neutrons,** C. Eisenhauer, *Nucl. Sci. Eng.* **27,** No. 2, 240-251 (Feb. 1967).

Key words: Air-scatter; angular distribution; energy spectrum; gamma rays; neutrons; point source; shielding; single scatter.

The theoretical expression for the singly scattered angular and energy flux of radiation from a point source is studied in the limit of very small source-detector separation distances, $(\mu_o r \ll 1)$. It is shown that both the angular and energy distributions are related in a simple way to the scattering kernel. Examples are given for gamma and neutron point sources in air. The applicability of the distributions at separation distances of the order of a mean free path $(\mu_o r \approx 1)$ is discussed.

9309. **Effects of errors in the chemical literature on the compilation of critically evaluated data,** W. H. Evans, *J. Chem. Doc.* **6,** No. 3, 135-136 (Aug. 1966).

Key words: Chemical literature; critical data; data evaluation; errors.

The various types of errors in data presented in the chemical literature and their effects on the critical evolution of the data are discussed. The relatively unsatisfactory state of errata is mentioned from the point of bringing the correction and the original publication together.

9310. **Some approximations to the Planck function in the intermediate region with applications in optical pyrometry,** D. E. Erminy, *Appl. Opt.* **6,** No. 1, 107-117 (Jan. 1967).

Key words: Brightness temperature; color temperature; effective wavelength; infrared and far infrared optical pyrometry; Planck equation; Rayleigh-Jeans equation; spectral radiance; Wien equation.

For many applications, a simple approximate equation for blackbody radiation can be more useful than is the Planck blackbody equation. An intermediate region exists where both the Rayleigh-Jeans equation and the Wien equation for blackbody radiation are inaccurate approximations to the Planck equation. Several approximate equations of simple mathematical form have been obtained which are more accurate in this intermediate region. These equations are applied to optical pyrometry to obtain formulae for brightness temperature and color temperature that can be used in the intermediate region.

9311. **Radiation absorption between the ultraviolet and x-ray bands,** U. Fano, *Science* **153,** No. 3735, 522-525 (July 29, 1966).

Key words: Absorption; radiation; spectroscopy; ultraviolet; x-rays.

A brief report is presented concerning the recent initial exploration of photoabsorption in a previously unmapped portion of the spectrum.

9312. **Approximate normal emissivity spectra in the infrared at elevated temperatures of single-crystal and polycrystalline calcium fluoride,** W. B. Fussell and J. C. Geist, *Appl. Opt.* **6,** No. 1, 119-124 (Jan. 1967).

Key words: Calcium fluoride; elevated-temperature emissivity; infrared absorption coefficients; infrared emissivity; polycrystalline $CaF_2$; single-crystal $CaF_2$.

A single-beam infrared spectroradiometric system has been used to measure the normal spectral emissivity of specimens of single-crystal and polycrystalline calcium fluoride in the infrared at elevated temperatures. The wavelength range was 2 to 12 microns and data were taken at sample temperatures of 500 and 600 °C. Room temperature data on the index of refraction of single-crystal calcium fluoride, and its rate of change with temperature, were extrapolated to 500 and 600 °C, and the normal spectral reflectivities were computed from the extrapolated indices at these temperatures. The computed reflectivities were then used to extract normal spectral absorption coefficients from the emissivity data. It was possible to compute absorption coefficients with reasonable accuracy at wavelengths of 6, 8, and 10 microns; the smallest estimated error was about 2% at 8 microns. The absorption coefficients increased markedly with temperature at these three wavelengths. The absorption coefficients of the polycrystalline material were consistently higher than the corresponding values for the single-crystal calcium fluoride. It was found that the spectral absorption coefficients at 8 and 10 microns varied approximately as the 2.1 and 1.6 power of the absolute temperature, respectively, between room temperature and 600 °C. These exponents lie within the range predicted by theory.

9313. **Definition of temperature in the kinetic theory of dense gases,** L. S. Garcia-Colin and M. S. Green, *Phys. Rev.* **150,** No. 1, 153-158 (Oct. 7, 1966).

Key words: Bulk viscosity; macroscopic equations of motion; macroscopic variable; non-equilibrium kinetic energy; temperature; total energy.

The question of the appropriate definition of temperature in the kinetic theory of dense gases is discussed. An apparent contradiction in the value of the bulk viscosity between two methods of making the transition from the kinetic to the hydrodynamic stage is resolved. It is shown that the definitions of temperature through the kinetic energy and through the total energy are equivalent. The general question of the appropriate choice of macroscopic variables in non-equilibrium statistical mechanics is discussed.

9314. **New method and problems in combinatorial optimization,** A. J. Goldman, *Washington Oper. Res. Council Newsletter* **5**, No. 8, 4-8 (Apr. 1966).

Key words: Algorithms; combinatorics; mathematics; matroids; networks; operations research; optimization.

This paper describes recent progress at the National Bureau of Standards in the field of combinatorial optimization.

9315. **A new contribution – NBS and engineering standards,** G. S. Gordon, *Safety Standards* **XVI,** No. 1, 3-4 (Jan.-Feb. 1967).

Key words: Engineering standards; international and national standards activities; OESLA; standards-making bodies.

The need for greater participation by NBS in helping to strengthen the nation's standards program was called for in the recent report of the LaQue Committee. The Office of Engineering Standards Liaison and Analysis *(OESLA)* has been established as the focal point at NBS for making available the technical resources of Bureau personnel *to assist* the federal, state and local governments, private engineering *standards-making bodies* and manufacturers in developing adequate representation of industrial, consumer and general public interests *in national and international standards activities.*

9316. **Air bath thermostat for use with absorption spectrophotometer,** J. H. Gould, *Rev. Sci. Instr.* **37,** No. 9, 1229-1231 (Sept. 1966).

Key words: Spectrophotometry; thermostat; ultraviolet-visible; $-150$ to $+60$ °C.

An automatically controlled absorption cell thermostat with a useful range of from $-150$ to $+60$ °C is described and has been successfully used with a commercial spectrophotometer. This apparatus accepts ordinary cylindrical absorption cells to 5 cm in length.

9317. **Note on normal subgroups of the modular group,** L. Greenberg, *Proc. Am. Math. Soc.* **17,** No. 5, 1195-1198 (Oct. 1966).

Key words: Factor set; group extension; level; modular group; parabolic class number; quotient surface; split extension.

Let $N$ be a normal subgroup of the modular group $\Gamma$, of index $\mu$ and parabolic class number $t$. It is shown that $\mu \leq 6t^4$. It follows immediately from this that there are only a finite number of normal subgroups with given parabolic class number. This is in sharp contrast to the case of non-normal subgroups. For it is known that for any integer $t \geq 1$, there are infinitely many subgroups of finite index with $t$ parabolic classes. It is also shown that if $p$ is a prime such that $p \equiv -1 \pmod 3$, then there are no normal subgroups with $p$ parabolic classes.

9318. **A new near-zone electric field-strength meter,** F. M. Greene, (Proc. 8th IEEE Symp., Electromagnetic Compatibility, San Francisco, Calif., July 11-13, 1966), *Symposium Digest, New Ideas for Electromagnetic Compatibility, 1966.*

Key words: Device; field; hazards; line; meter; telemetry.

The National Bureau of Standards has recently completed the development of prototype instrumentation for measuring the electric-field components of complex, high-level, near-zone electromagnetic fields from 0.1 to 1000 volts per meter, at frequencies from 150 kHz to 30 MHz with a present uncertainty of less than ±2 dB. The successful design of the NBS meters is based on the use of a novel form of telemetry, employing a completely non-metallic electrical transmission line, which apparently has not been fully exploited heretofore. This avoids the perturbing effects on the field being measured, usually caused by field-strength meters employing metallic RF transmission lines.

9319. **Baffled piston radiator: expansion of potential in far, paraxial field,** M. Greenspan, *J. Acoust. Soc. Am.* **40,** No. 1, 251-252 (July 1966).

Key words: Acoustics; diffraction, potential; piston radiator; potential diffraction; radiator, piston; sound.

The potential of a circular source, having radially symmetrical but otherwise arbitrary distribution, $v(r_o)$ of velocity over its face, is expanded as $\phi = z^{-1}e^{-ikz}(a_o + a_1 a^{-1} + . \; . \; .)$[Cylindrical coordinates $(r, \theta, z)$; center of source at $r = z = 0$]. We find $a_o$ to depend only on the total volume velocity at the source. If $v(r_o)$ is known, all $a_n$ can be calculated; if it is unknown, limits on $a_n$ can be set.

9320. **Growth of calcite crystals,** P. M. Gruzensky, (Proc. Intern. Conf. Crystal Growth, Boston, Mass., June 20-24, 1966), *Crystal Growth, a Suppl. to J. Phys. Chem. Solids* **D3,** 365-367 (Pergamon Press Inc., New York, N.Y., 1967).

Key words: Calcite; crystal growth; crystals; vapor phase diffusion.

Renewed interest in the growth of synthetic calcite crystals has been stimulated by the possible use of calcite as a host crystal for maser materials. A crystal growth method is described in which $(NH_4)_2CO_3$, by vapor phase diffusion, is slowly brought into contact with a solution containing 2 wt percent $CaCl_2$ and 20 wt percent $NH_4Cl$. Transparent rhombs are obtained with edge dimensions of 3-4 mm, which are verified to be calcite by x-ray diffraction measurements.

9321. **A modified Monte-Carlo quadrature,** S. Haber, *Math. Compt.* **20,** No. 95, 361-368 (July 1966).

Key words: Analysis; integration; mathematics; Monte-Carlo; multiple integration; numerical analysis; numerical integration; quadrature.

A modification of Simple Monte-Carlo quadrature is proposed, which uses very simple forms of stratified sampling and of the "method of antithetic variates." The new procedure is fully automatic, requiring no preliminary analysis of the integrand, and converges somewhat faster than Simple Monte-Carlo. Results of experimental calculations are presented.

9322. **Abstraction of hydrogen atoms from isobutane-$d_9$ by methylene,** M. L. Halberstadt and J. R. McNesby, *J. Chem. Phys.* **45,** No. 5, 1666-1669 (Sept. 1, 1966).

Key words: Abstraction; isobutane-$d_9$; ketene; methylene; photolysis.

The photolysis of ketene at 3130 Å in the presence of isobutane-$d_9$ was carried out at 320 °C in order to determine the mechanism of methyl radical formation. The two possibilities considered are:

Mechanism I – insertion followed by internal relaxation and finally expulsion of a methyl radical.
Mechanism II – direct abstraction.

Mechanism II was found to be the only detectable mode of methyl radical formation. The effect of pressure on the isotopic methane distribution was studied and an attempt is made to explain the effect in terms of a DeMore-Benson process.

9323. **Two quantum photoionization of Cs and $I^-$,** J. L. Hall, *J. Quantum Electron* **QE-2,** No. 4, xxi (April 1966); *IEEE J. Quantum Electron* **QE-2,** No. 9, 361-363 (Sept. 1966).

Key words: Atomic calculations; nonlinear optical phenomenon; two-photon ionization.

Brief review of a recent experiment which measured the photodetachment probability for $I^-$ ions due to simultaneous absorption of two ruby quanta.

9324. **Unassigned.**

9325. **A nonmagnetic laboratory for the National Bureau of Standards,** F. K. Harris, *IEEE Spectrum* **3,** No. 11, 85-87 (Nov. 1966).

Key words: Absolute ampere determination; calculable inductor; current balance; national electrical units; nonmagnetic facility; Pellat dynamometer; proton precession frequency.

Plans are discussed for a nonmagnetic laboratory to be built on the Gaithersburg campus of the National Bureau of Standards for absolute electrical measurements and other purposes. The operation of the NBS current balances and the proton gyromagnetic ratio apparatus is briefly reviewed, and a short history of the national electrical units since the creation of the Bureau is included.

9326. **Spectral radiance of a low current graphite arc,** A. T. Hattenburg, *Appl. Opt.* **6,** No. 1, 95-100 (Jan. 1967).

Key words: Arc; blackbody; graphite; spectral radiance; spectroradiometer; temperature.

The spectral radiance of the anode of a low-current graphite arc has been determined throughout most of the 850 to 210 nm region, utilizing a recently developed high-accuracy spectroradiometer. The estimated standard deviation uncertainty varies from about 1.5% at the longer wavelengths to about 5% at the shorter. Results are given at twenty wavelength points in the region, and also as a continuous function of wavelength throughout most of the region, excluding some areas of high molecular band radiation originating in the arc stream.

9327. **The "volt standard" moves to Gaithersburg, Maryland,** W. J. Hamer, *J. Wash. Acad. Sci.* **56,** 101-108 (May 1966).

Key words: Electromotive force; standard cell facilities; standard cell transfer; standard cells; volt standard.

A description is given of the transfer of the nation's "volt standard" from its present location in Washington, D.C., to its new location on a site near Gaithersburg, Md. Factors involved in transfer are discussed and a brief description is given of new standard cell facilities in the new laboratory at Gaithersburg.

9328. **Mass-spectrometric study of the rate of the reaction CO + OH,** J. T. Herron, *J. Chem. Phys.* **45,** No. 5, 1854-1855 (Sept. 1, 1966).

Key words: Activation-energy; atom-transfer reaction; carbon dioxide; carbon monoxide; gas phase; hydrogen atom; hydroxyl-radical; rate constant.

The rate constant of the reaction $CO+OH \rightarrow CO_2+H$ has been directly measured at 300 °K to be 5.4±2.0 (estimated uncertainty) x $10^{10}$ $cm^3$ $mole^{-1}$ $sec^{-1}$. This value combined with published high temperature rate data leads to k=9.2 x $10^{11}$ exp (−1000/RT).

9329. **Mass spectrometric study of the rates of the reactions of nitrogen atoms with olefins,** J. T. Herron, *J. Phys. Chem.* **70,** No. 9, 2803-2807 (Sept. 1966).

Key words: Atoms; mass; mechanisms; nitrogen; olefins; rates; spectrometry.

A mass spectrometric study has been made of the rates of the reactions of nitrogen atoms with a series of olefins. At 340 °K the rates are: $C_2H_4$, k~1.0±0.5; $C_3H_6$, k=1.9±0.6; $C_4H_8-1$, k=2.0±0.4; t−$C_4H_8-2$; k=1.7±0.4; iso−$C_4H_8$, k=4.2±1.0; $C_2(CH_3)_4$, k=2.4±0.6; $C_4H_6-1,3$, k=3.5±1.0; all x $10^{10}$ $cm^3$ $mol^{-1}$ $sec^{-1}$.

9330. **The forbidden $I^1\Sigma^- - X^1\Sigma^+$ absorption bands of carbon monoxide,** G. Herzberg, J. D. Simmons, A. M. Bass, and S. G. Tilford, *Can. J. Phys.* **44,** 3039-3045 (1966).

Key words: Absorption; carbon monoxide; forbidden transition; high resolution; spectrum; vacuum ultraviolet.

The forbidden $I^1\Sigma^- - X^1\Sigma^+$ transition of CO has been observed at high resolution in the vacuum ultraviolet region. Eight bands have been analyzed to determine rotational and vibrational constants for the $I^1\Sigma^-$ state. The bands consist of a single Q-branch which gains intensity through a rotational mixing of the $I^1\Sigma^-$ and $A^1\Pi$ states. The local perturbations between the I and A states are summarized and discussed. Also an apparent "vibrational" perturbation in the v=4 and 5 energy levels of the I state is described. Indirect evidence suggests the perturbing state is a $^3\Pi$.

9331. **An ultrasonic pressure gage,** P. L. M. Heydemann, (Proc. ASME Winter Meeting, New York, N.Y., Nov. 27-Dec. 1, 1966), *Am. Soc. Mech. Eng. Publ.* No. 66-WA/PT-5 (1967); *J. Basic Eng.* **89,** No. 3, 551-553 (Sept. 1967).

Key words: Delay line; frequency stability; gage; high pressure; self-excited pulse repetition; temperature compensation; ultrasonics; velocity of sound.

The transit time of short ultrasonic pulses in solid rods is used to measure pressures throughout the fluid range. Self-excited regenerating circuits are used. Measurements to 3500 bar with an uncertainty of .3 bar and to 20 kbar with an uncertainty of 2 bar are reported. Further improvements, temperature compensation and stability are discussed.

9332. **Higher symmetries and the $2^+$ mesons,** D. Horn, J. J. Coyne, S. Meshkov, and J. C. Carter, *Phys. Rev.* **147,** No. 4, 980-984 (July 29, 1966).

Key words: Higher symmetry scheme; λ quark content; nonet of $2^{++}$ mesons; Schwinger mass formula; $SU(6)_W$; 405 representation.

The two-body decays of the recently completed nonet of $J^{PC}=2^{++}$ mesons offer the tempting possibility of delineating in which bigger multiplet of some particular higher symmetry scheme they might be embedded. In this paper, these decays are calculated according to $SU(6)_W$. In such an approach the mesons may be accommodated in either the 189 or 405 representations of SU(6). We show that using only the two-body decay modes of the nonet of spin 2 mesons, one cannot in principle determine whether thay belong in a 189 or 405 representation. This impasse may be broken by ordering states by their λ quark content in which case 189 is eliminated from consideration. In the process, we find that the Schwinger mass formula, which is not satisfied by the experimental masses, should not properly be used for the 405, but should be replaced by a similar relation which is extremely well satisfied.

9333. **A high directivity, broadband coaxial coupler,** P. A. Hudson, *IEEE Trans. Microwave Theory Tech.* **MTT-14,** No. 6, 293-294 (June 1966).

Key words: Coaxial; coupler; directional; reflectometer; RF power.

A new 4-port coaxial directional coupler having high directivity ($>50$ dB) over relatively broad frequency bands has been designed and constructed. The coupler is the $\lambda/4$ type cut for 1150 MHz and is useful in the frequency bands 700 to 1500 MHz and 3000 to 4000 MHz. Precision connectors (14 mm) are used on all ports and the VSWR of both primary and secondary lines is less than 1.01.

A brief description is given of the performance characteristics of the coupler when used as the equivalent of a matched generator in intercomparing RF power meters.

9334. **Cerous magnesium nitrate: a magnetic temperature scale 0.002-2 °K,** R. P. Hudson and R. S. Kaeser, *Physics* **3,** No. 2, 95-113 (Feb. 1967).

Key words: Cerous magnesium nitrate; low temperature scale; magnetic thermometer.

Isentropic demagnetizations from known starting conditions yielded a determination of the entropy-magnetic susceptibility, or S-$\chi$, relation for single-crystal spheroids of the paramagnetic salt cerous magnesium nitrate, CMN. Enthalpy differences, $\Delta Q$, between the low temperature end-points thus reached and a (arbitrary) reference temperature near 1 °K [determined by gamma ray heating] yielded a corresponding Q-S curve, whence one obtained S-T and $\chi$-T, T being the thermodynamic temperature. The salt exhibits a broad maximum in $\chi$ centered on $S/R=0.32$, for which region the absolute temperature is determined to be $0.001_5$ °K. Our results disagree significantly with those of other workers (even S-$\chi$, which is not subject to large experimental error) save for the observation that CMN obeys the Curie law at least down to 0.006 °K.

At high temperatures ($T>0.006$ °K), all specimens show a heat capacity $C/R=bT^{-2}$ with $b=5.76 \times 10^{-6}$. Superimposed upon this is a small "anomaly" first appearing at approximately 0.015 °K and reaching a maximum near 0.025 °K. The attribution of such an effect to small concentrations of magnetic impurities cannot be reconciled with the results of chemical analysis. Other evidence, moreover, supports the idea of a nonmagnetic origin for this anomaly.

9335. **Production and reaction of atomic fluorine in solids. Vibrational and electronic spectra of the free radical HNF,** M. E. Jacox and D. E. Milligan, *J. Chem. Phys.* **46,** No. 1, 184-191 (Jan. 1, 1967).

Key words: F atom reactions; force constants; HNF; $HNF_2$; infrared spectrum; matrix isolation; NF; $NF_2$; thermodynamic properties; visible-ultraviolet spectrum.

The species $H^{14}NF$, $H^{15}NF$, and $D^{14}NF$ have been produced in an argon matrix at 14 °K by the reaction of photolytically produced atomic fluorine with NH. Sufficient concentrations of these species have been obtained for direct detection of two vibrational fundamentals, appearing at 1000 and 1432 cm$^{-1}$ for $H^{14}NF$, as well as of an electronic transition between 3900 and 5000 Å involving a progression in the upper state bending frequency. Force constants and thermodynamic properties have been derived for HNF. Other species observed in these experiments include NF, $NF_2$, and $HNF_2$. Evidence is presented indicating that the hydrogen atom can be abstracted from $HN_3$ by atomic fluorine.

9336. **Physiological optics at the National Bureau of Standards,** D. B. Judd, *Appl. Opt.* **6,** No. 1, 13-26 (Jan. 1967).

Key words: Color; gloss; light; perception of color; photometry; physiological optics; psychophysics; scaling of color.

Published work in physiological optics at the National Bureau of Standards is summarized under the headings: evaluation of light-dark patterns, light measurement, color measurement, color differences, and color perception. The bearing of this work on standard methods of the American Society of Testing and Materials, of the Illuminating Engineering Society, and of the American Standards Association, and on recommendations of the International Commission on Illumination is indicated. The purposes and methods of current work are briefly described.

9337. **Vacuum ultraviolet spectrum of neutral silicon,** V. Kaufman, L. J. Radziemski, Jr., and K. L. Andrew, *J. Opt. Soc. Am.* **56,** No. 7, 911-915 (July 1966).

Key words: Atomic spectrum of silicon; carbon spectra; electrodeless discharge; germanium spectra; nitrogen spectra; silicon I; silicon spectra; vacuum ultraviolet standards.

Measurements have been made on about 200 Si I lines in the region 1548 to 2100 Å excited by a low pressure source, resulting in wavelength values with uncertainties, in general, of less than 0.0015 Å. Some of the vacuum ultraviolet wavelengths had been calculated by Radziemski and Andrew (*J. Opt. Soc. Am.* **55,** 474 (1965), and a comparison of 75 measured and calculated values shows that they agree on the average to 0.0007 Å. A plot of the differences shows the scatter to be much greater than any systematic difference. This indicates that the calculated wavelengths are compatible with the set of Ge I lines used as standards in measuring the Si I lines. The new data have also led to an extension and slight revision of the odd level analysis. New measurements on other Ge I lines and strong lines in the spectra of Ge II, Si II, N I, and C I are also reported. These lines should be useful as auxiliary standards in this spectral region. All of the spectrograms were taken in the first order of a 10.7-meter Eagle vacuum spectrograph with a reciprocal dispersion of 0.78 Å/mm. The source was an electrodeless discharge lamp containing $SiCl_4$ and $GeCl_4$ vapor with argon or helium carrier gas at a total pressure no greater than 0.5 torr.

9338. **Measurement and calculation of Cu II, Ge II, Si II, and C I vacuum-ultraviolet lines,** V. Kaufman and J. F. Ward, *J. Opt. Soc. Am.* **56,** No. 11, 1591-1597 (Nov. 1966).

Key words: Carbon; copper; germanium; Ritz; silicon; spectrum; standards; ultraviolet; vacuum; wavelengths.

The discharge in a water-cooled copper hollow-cathode containing germanium and silicon was photographed with the NBS 10.6-meter Eagle vacuum spectrograph to investigate a portion of the vacuum ultraviolet spectrum of singly ionized copper in first, second, and third orders. 32 of the 33 Cu II lines of the 4p-6s transition for which Ritz calculations have been made were investigated as to their suitability as standards. 104 other lines of Cu II in the interval 861-1623 Å were observed and measured in the second and/or third orders with estimated wavelength uncertainties of 0.0006 Å. Included in this group are two previously unobserved lines of the 4p-6s transition, four members of the calculable 4s-5p transition, and the three ground state transitions (a $^1S_0$-4p $^1P_1$, $^3P_1$, $^3D_1$). This latter group of three lines allows the calculation of shorter wavelength lines.

Some vacuum ultraviolet multiplets of C I, Si II, and Ge II in the wavelength range 1492-1602 Å, were also measured in second order. These lead to an extension, modification or confirmation of the present lists of calculated wavelengths of these spectra. A precise measurement of the Lyman Beta line of hydrogen in third order is an added confirmation of the presence of the Lamb shift of the 1 $^2S$ state of hydrogen.

9339. **Newly measured and calculated wavelengths in the vacuum ultraviolet spectrum of neutral nitrogen,** V. Kaufman and J. F. Ward, *Appl. Opt.* **6,** No. 1, 43-46 (Jan. 1967).

Key words: Atomic spectrum; calculated wavelengths; nitrogen; spectrum; vacuum ultraviolet.

The NBS 10.7-meter vacuum spectrograph was used in second order to obtain precision measurements on seven N I lines at 1492/4 ($2p^3\,{}^2D^\circ-2p^23s\,{}^2P$) and 1742/5 Å ($2p^3\,{}^2P^\circ-2p^23s\,{}^2P$). Combining these values with other available information on the energy levels of the neutral nitrogen atom, 78 calculated wavelengths of N I from 908 to 1745 Å are given with uncertainties of ±0.001 Å or better.

9340. **Nitrogen on rhenium observed with the field emission microscope,** R. Klein and J. W. Little, *Surface Sci.* **6,** No. 2, 193-207 (Feb. 1967).

Key words: Chemisorption; field emission; nitrogen; rhenium.

The adsorption of nitrogen on rhenium was observed with a field emission microscope. Nitrogen decreases the work function of rhenium but also decreases the pre-exponential term of the Fowler-Nordheim expression. The result is a small decrease in emission with nitrogen adsorption. Surface migration could not be directly observed because desorption precedes it. There are two chemisorbed binding states associated with nitrogen on rhenium. The first is little stronger than physisorbed but accounts for most of the nitrogen in a saturated layer at 50 °K. The second is inferred from small pattern changes above 750 °K. The weakly bound state probably consists of a number of states with a distribution of desorption energies.

9341. **A zero-range treatment of the three-body photodisintegration cross section of $^3$H and $^3$He,** J. M. Knight, J. S. O'Connell, and F. Prats, *Phys. Letters* **22,** No. 3, 322-325 (Aug. 15, 1966).

Key words: Cross section; differential cross section; $^3$H; $^3$He; photodisintegration; zero-range.

Zero-range theory is used to construct bound and continuum state wave functions. The total and differential electric dipole photodisintegration cross sections for three-body breakup of $^3$He and $^3$H are calculated using these wave functions.

9342. **New standard for the calibration of microphones,** W. Koidan, *Mag. Std.* **37,** No. 5, 141-144 (May 1966).

Key words: Calibration; microphones; standard.

This article discusses the background, contents and use of a new American Standard, Calibration of Microphones, S1.10-1966, published by the American Standards Association, Incorporated.

9343. **Lack of uniqueness in the International Practical Temperature Scale above the gold point,** H. J. Kostkowski, *Metrologia* **3,** No. 1, 28-29 (Jan. 1967).

Key words: Infrared pyrometer; International Practical Temperature Scale; optical pyrometer; radiation thermometry; standards; temperature.

The International Practical Temperature Scale (IPTS) above the gold point is shown to vary with wavelength. Although the extent of this variation is barely significant relative to the present uncertainty of realizing the scale, the IPTS should be unique; and to achieve this a wavelength must be specified in the definition.

9344. **A new radiometric equation and its application,** H. J. Kostkowski, *Appl. Opt.* **5,** No. 12, 1559 (Dec. 1966).

Key words: Blackbodies; non-blackbody emission; optical radiation; radiometry; sources; spectral radiance.

A simple equation has been found which gives, at any wavelength, the ratio of the spectral radiances of two arbitrary sources when their spectral radiances at some particular wavelength are equal. The main advantages of the equation are its simplicity and the fact that it does not involve temperature explicitly; a limitation is that Wien's radiation equation is required. The new equation is derived and various applications are given.

9345. **Optical constants of germanium,** R. E. LaVilla and H. Mendlowitz, *Appl. Opt.* **6,** No. 1, 61-68 (Jan. 1967).

Key words: Characteristic electron energy loss; far ultraviolet; germanium; Kronig-Kramers dispersion relations; optical properties; sum rules.

We have attempted to assess the disagreement of various investigators on the optical properties of germanium in the far uv. The analysis subjected the reported data, out to about 25 eV to the following tests: 1. An internal consistency check when possible by applying the Kronig-Kramers dispersion relations to the optical constants. 2. An evaluation of the optical oscillator strength distribution for the spectrum under study. 3. Correlation of the values of Im $1/\epsilon^*$ from the optical data with the characteristic electron energy loss spectrum for the material. 4. Evaluation of the oscillator strength sum for the electron energy loss distribution. A set of optical constants derived from the characteristic electron energy loss data are presented and discussed. Also, an estimate of source of the errors incurred in the application of the Kronig-Kramers dispersion relations are given and discussed in terms of optical data.

9346. **Radiance temperature at 6500 Å of the graphite arc,** R. D. Lee and E. Lewis, *Appl. Opt.* **5,** No. 11, 1858 (Nov. 1966).

Key words: Graphite arc; pyrometry; standard; temperature.

The radiance temperatures of over twenty positive electrodes in a graphite arc were measured with the NBS photoelectric pyrometer and were found to range from 3786 °K to 3808 °K. The radiance temperatures were measured to an accuracy of 2 deg K (standard deviation uncertainty) with a pyrometer sensitivity of 0.2 deg K.

9347. **The NBS photoelectric pyrometer and its use in realizing the International Practical Temperature Scale above 1063 °C,** R. D. Lee, *Metrologia* **2,** No. 4, 150-162 (Oct. 1966).

Key words: Blackbody; International Practical Temperature Scale; optical; photoelectric pyrometer; radiance sources; standards; temperature.

A photoelectric pyrometer has been developed with which the International Practical Temperature Scale (IPTS) above the gold point, 1063 °C, is realized about 5 times more accurately than the prevalently used disappearing filament visual pyrometer. Estimated uncertainties, at a 95% confidence level, of realizing the IPTS with the photoelectric instrument are 0.12 deg C at 1063 °C, 0.24 deg C at 1256 °C, and 3 deg C at 3525 °C. The design, evaluation, and calibration to realize the IPTS are discussed.

9348. **Real two-dimensional representations of the free product of two finite cyclic groups,** J. Lehner and M. Newman, *Proc. Camb. Phil. Soc.* **62,** 135-141 (1966).

Key words: Free products; groups; representations.

All real discrete representations of the free product of two finite cyclic groups by a group of linear fractional transformations are determined.

9349. **Coriolis zeta constants and force field for osmium tetraoxide,** I. W. Levin and S. Abramowitz, *Inorg. Chem.* **5,** 2024-2026 (1966).

Key words: Coriolis constant; force field; infrared; osmium tetraoxide; vibration-rotation.

The infrared spectrum of osmium tetraoxide in the region of its infrared active fundamental absorption bands. Coriolis zeta constants have been determined from the unresolved vibration-rotation band contours. These constants have then been utilized as constraints in the determination of the general force field for osmium tetraoxide.

9350. **Government, industry and engineering. NBS in a new setting,** S. Lichtenstein, *Automotive Ind.* **135,** No. 10, 119-124 (Nov. 15, 1966).

Key words: Basic and applied research; calibration; instrumentation; interchangeability of parts; mass production; standardization; testing.

Sixty-five years of industrial progress—exemplified by the rapid development of the modern, mass-production automotive industry—are discussed in relation to the National Bureau of Standards' 65-year history as the Bureau prepares dedication observances for its new facilities in Gaithersburg. Typical NBS contributions to automotive progress are cited, and they are linked with activities of units devoted to metrology, mechanics, weights and measures, mandatory standards, organic standards, materials evaluation, and product standards.

9351. **The battle against corrosion,** S. Lichtenstein, *Compressed Air Mag.* **71,** No. 12, 12-13 (Dec. 1966).

Key words: Basic and applied research; economics of corrosion; industrial design; materials protection; structural failure.

Corrosion is discussed as a technological and economic "disease" eating away at metals and materials, depleting natural resources, and causing injury and death where accidents and explosions result from weakening of structures. Dollar estimates of costs to the Nation and the Federal Government are given. Anti-corrosion work of the National Bureau of Standards' Institute for Materials Research is described and highlights of a half-century of achievement are noted. Corrosion control is linked to progress in nuclear power, oceanography, water desalination, military operations, space and supersonic transport, health, safety and conservation.

9352. **Nuclear giant quadrupole resonance,** R. Ligensa, W. Greiner, and M. Danos, *Phys. Rev. Letters* **16,** No. 9, 364-367 (Feb. 28, 1966).

Key words: Absorption; collective model; cross section; deformed nuclei; giant quadrupole resonances; photons.

The description of the giant quadrupole resonance of deformed nuclei is extended to include the coupling between the different collective modes. The interaction with the odd particle is also included. The results are compared with recent experimental photon absorption cross sections.

9353. **Current algebras and matrix elements of the axial-vector current,** H. J. Lipkin, H. R. Rubinstein, and S. Meshkov, *Phys. Rev.* **148,** No. 4, 1405-1407 (Aug. 26, 1966).

Key words: Axial-vector current; chiral; $G_A$; $G^*$; representation-mixing; sum-rules; vector current.

The assumption that the space integrals of the time components of the vector and axial-vector currents satisfy the commutation rules of the Lie Algebra U(3) x U(3) has led to a number of interesting results. The following experimentally measurable quantities are calculated directly from the algebra without writing down the sum rules: $G_A$—the strength of the axial-vector coupling constant in $\beta$-decays; $G^*$—the strength of the axial-vector transition between the nucleon and the N*(1238), and the d/f ratio for the axial-vector current of the baryon octet.

9354. **Determination of the effective force constants between a substitutional impurity and its nearest neighbors in an alkali halide crystal,** R. A. MacDonald, *Phys. Rev.* **150,** No. 2, 597-602 (Oct. 14, 1966).

Key words: Alkali halide crystal; Born-Mayer potential; deformation dipole model; effective force constants; isotopic impurities; local mode frequencies; nearest-neighbor interaction; substitutional impurity; U-centers.

The forces between a substitutional impurity and its nearest neighbors in an alkali halide crystal with rocksalt structure are determined in the harmonic approximation. The deformation dipole model is used for the lattice dynamics of the perfect crystal. Two independent force constants are involved in the problem which is treated in two ways. First, the two force constants are obtained from the equation of motion for the local mode of vibration using experimental values of the local mode frequencies due to $H^-$ and $D^-$ impurities in Na*Cl* and K*Cl*, and assuming that the force constants are the same for different isotopes of the impurity. This method yields no real solutions for the force constants for U-centers in K*Cl*. The second method assumes that the force constants for the impurity (say $H^-$) are the same as those in an alkali hydride crystal having the same lattice spacing as the alkali halide crystal. A Born-Mayer interatomic potential is used for this calculation. The first method gives 45% softening of the force constants for U-centers in Na*Cl*, the second method gives 70% softening. The results are compared with those of previous theories and with experimental results on the KBr:$Li^+$ system.

9355. **Instrumental aspects of synchrotron XUV spectroscopy,** R. P. Madden, D. L. Ederer, and K. Codling, *Appl. Opt.* **6,** No. 1, 31-38 (Jan. 1967).

Key words: Grazing-incidence; 3-meter; monochromator alignment; 0.06 Å resolution; spectrograph; synchrotron light.

Electron synchrotrons are becoming increasingly important as sources of extreme uv radiation for physical experiments. The NBS 180 MeV machine has been utilized for gas absorption studies over a 4-year period, during which a 3-meter grazing incidence spectrograph and monochromator have been designed, constructed, and put into operation. The instruments are extremely stable to vibration and temperature variation, and are operating with a slit limited resolution of the order of 0.06 Å. The design principles and features of these instruments are described, and a highly-successful prealignment procedure for grazing-incidence spectrometers is outlined. The effect of the unusual characteristics of this light source on the illumination and performance of the spectroscopic instruments is discussed.

9356. **Possible observation of $In^{115}$ nuclear electric hexadecapole transitions,** R. J. Mahler, L. W. James, and W. H. Tantilla, *Phys. Rev. Letters* **16,** No. 7, 259-261 (Feb. 14, 1966).

Key words: Hexadecapole; induced; nuclear; transition; ultrasonically.

This letter reports the observation of ultrasonically induced $\Delta m = \pm 3$, $In^{115}$ nuclear spin transition in InAs single crystal.

9357. **Nuclear hexadecapole interactions,** R. J. Mahler, *Phys. Rev.* **152,** No. 1, 325-330 (Dec. 2, 1966).

Key words: Angular dependence; hexadecapole; hexadecapole transitions; phonon interactions; saturation factor; 4-3m symmetry.

The nuclear hexadecapole matrix elements for the static and the one phonon-nuclear interactions are developed and are evaluated for $\Delta m=\pm 3$ and $\Delta m=\pm 4$ nuclear transitions involving a spin 9/2 nucleus in a crystal with 4-3m symmetry. An expression for the saturation factor for a general interaction which gives rise to nuclear spin transitions involving the change in the z-component of the spin by any amount $\Delta m=\pm n$ is developed and is used to derive the angular variation of the one-phonon, $\Delta m=\pm 3$ and $\Delta m=\pm 4$ nuclear hexadecapole interaction. Finally a method to end the speculation about the observation of the hexadecapole interaction is presented.

9358. **Effects of space radiation on refractive properties of optical glass,** I. H. Malitson, M. J. Dodge, and M. E. Gonshery, *Proc. Annual Conf. Photography, Science and Engineering, San Francisco, Calif., May 9-13, 1966,* p. 75 (1966).

Key words: Optical glasses; radiation effects; refractive index.

A report is given of the effects of gamma and electron radiations on the refractive properties of certain normal and cerium-protected optical glasses that may be used for lens components of high-resolution cameras and television systems. Refractive index changes as large as $2 \times 10^{-4}$ for unprotected glass and $6 \times 10^{-5}$ for non-darkening glasses were observed after irradiation. Data are given showing that radiation-induced index and dispersion changes can last for periods of weeks and fluctuate with time. High purity fused silica was found to be radiation resistant.

9359. **Infrared spectra of HCl, DCl, HBr, and DBr in solid rare-gas matrices,** D. E. Mann, N. Acquista, and D. White, *J. Chem. Phys.* **44,** No. 9, 3453-3467 (May 1966).

Key words: Hydrogen bromide; hydrogen chloride; infrared; rare gas matrix; spectrum.

The infrared absorption spectra of HCl, DCl, HBr, and DBr, trapped in solid rare-gas matrices at liquid hydrogen and liquid helium temperatures, are reported. In the region of their fundamentals, the spectra of all these diatomic molecules consist of a number of bands; some which exhibit reversible changes in intensity and line width with temperature and others which are temperature independent.

The temperature dependent features have been identified as rotation-vibration bands of the matrix isolated diatomic molecule. The spacings of these bands are appreciably less than the separations of corresponding bands in the free molecule spectrum indicating a hindrance to rotation due to lattice-molecule interactions. Two different types of lattice-molecule couplings are examined in the interpretation of the results.

It is shown that the temperature independent bands, identified as vibrational transitions owe their existence to the presence of trace nitrogen impurities in the solidified rare-gas matrices, or concentration effects.

9360. **A pycnometer for small volumes of liquids,** S. Marantz and G. T. Armstrong, *Chem.-Anal.* **55,** 114-115 (Oct. 1966).

Key words: Density; liquids; pycnometer.

The design, calibration, and performance of a small volume (0.1 cm$^3$) pycnometer is described. The instrument can be used to measure liquid densities to a 0.1 percent accuracy.

9361. **Excitation and ionization in arc and spark spectroscopic sources,** M. Margoshes, *Appl. Spectry.* **21,** No. 2, 92-99 (1967).

Key words: Arc; Boltzmann equilibrium; excitation; ionization; line intensity; Saha equilibrium; spark; spectrochemical analysis; spectroscopic source.

A description is given of the mathematical theories which are applicable to the excitation and ionization of atoms in plasmas at thermal equilibrium. These processes are controlled by the temperature and electron density in the plasma; some methods of determining these parameters are given. It is shown that, even with the limited data available, the theories can be applied to practical problems which arise in spectrochemical analysis.

9362. **Effect of nuclear alignment on the 14 MeV total neutron cross section of $^{165}$Ho,** H. Marshak, A. C. B. Richardson, and T. Tamura, *Phys. Rev.* **150,** No. 3, 996-1010 (Oct. 21, 1966).

Key words: Black nucleus model; cryogenic target; coupled-channel calculation; nuclear alignment; nuclear deformation; optical model; Van de Graaff; 14 MeV neutrons; $^{165}$Ho.

The effect of nuclear alignment on the total cross section of the highly deformed $^{165}$Ho nucleus has been measured using 14 MeV neutrons. The aligned $^{165}$Ho target was obtained by cooling a metal single crystal to 0.33 °K. A finely collimated beam of 14 MeV neutrons was produced by careful collimation of the alpha particle produced in the $^3$H(d,n)$^4$He reaction and by detecting it in fast coincidence with its associated neutron. The measured total cross section is $(5.29\pm 0.10)$ b. The fractional change in the total cross section, for our value of nuclear alignment $(f_2=0.31)$, is $+(3.52\pm 0.75)$ %, where the positive sign indicates a larger cross section for nuclei aligned perpendicular to the incident beam than for randomly oriented nuclei. These results are in excellent agreement with the predictions of the optical model using an adiabatic coupled-channel calculation. The optical-model parameters used are in good agreement with those obtained from other measurements, and in particular the value of the deformation parameter $\beta=+0.30$ is the same as that used in our earlier work. It was also found that 14 MeV is not yet a sufficiently high energy to use the black nucleus model to interpret our results.

9363. **X-ray fiber optics,** L. Marton, *Appl. Phys. Letters* **9,** No. 5, 194-195 (Sept. 1, 1966).

Key words: Fiber optics; x rays.

The possibility of the creation of fiber optics for x rays is investigated. While the aims in the creation of such fiber optics are similar to those in light optics, the technical means for achieving it are quite different.

9364. **A nomogram for determining azimuth and horizontal trace velocity from tripartite measurements,** H. Matheson, *Earthquake Notes* **XXXVII,** No. 1, 33-37 (Mar. 1966).

Key words: Nomogram; tripartite nomogram.

The direction normal to a traveling plane wave front and the wave's horizontal trace velocity at the earth's surface, are easily determined by observing the wave at three noncollinear points. Reduction of the data involves the solution of several trigonometric equations. This note describes a nomogram which reduces this task to 30 seconds with ruler and pencil.

9365. **Resonances in inelastic electron scattering from $H_2$,** M. G. Menendez and H. K. Holt, *J. Chem. Phys.* **45,** No. 8, 2743-2744 (Oct. 15, 1966).

Key words: Electron scattering; $H_2$, $H_2^-$; resonances; vibrational excitation.

Resonance structure in the electron scattering from $H_2$ has been observed in two inelastic channels corresponding to excitation to the first and second vibration levels of $H_2(X^1\Sigma_g^+)$ An overlapping of resonances due to at least two $H_2^-$ states lying between 11 and 13 eV is apparent. The structure in the inelastic channels is compared to the observed resonance structure in the transmission channel. The resonances are found to effect the inelastic channels more strongly than the transmission channel The excitation function for direct vibrational excitation to the v=1 level was measured near threshold and found to increase approximately linearly in this region.

9366. **Time-dependent behavior of activated molecules. High-pressure unimolecular rate constant and mass spectra,** F. H. Mies and M. Krauss, *J. Chem. Phys.* **45,** No. 12, 4455-4468 (Dec. 15, 1966).

Key words: Activated complex; activated molecules; activated state; decay; dissociation; high pressure rate constant; kinetics; lifetime; mass spectra; metastable molecules; predissociation; quantum mechanics; resonance scattering; theoretical; unimolecular dissociation.

A quantum mechanical theory of the unimolecular decay of metastable, or activated molecules is developed using Fano's treatment of resonance scattering. A resonance state is synonymous with the so-called activated molecule in unimolecular kinetics, and a set of widths are associated with each state which is a measure of the coupling to the various dissociation continuum channels (each channel designates an "activated complex"). If the widths are small compared to the spacings between those neighboring states which are coupled to the same continua, then an ensemble of molecules prepared in a given activated state will decay exponentially in time, as does a radiating or autoionizing excited atomic state. However, unimolecular decay is fundamentally a problem in "overlapping" resonances widths, and is best considered using Fano's theory, which incorporated proper treatment of the overlap. This paper is particularly concerned with the implications of overlapping widths on the high pressure rate constant, and on mass spectra.

There are two effects of overlapping which are most striking. First, the time decay of a metastable molecule is no longer a pure exponential, but for the special cases considered is represented by a sum of exponential, oscillatory, and/or linear terms, which certainly affects the interpretation of mass spectra. Second, the high pressure rate constant is related to the initial rate of decay of a canonical ensemble of activated molecules, and proper consideration of overlap imposes an upper bound on the rate of dissociation without any artificially imposed restrictions on the widths. This bound yields the "universal rate constant" kT/h times a transmission coefficient which is a function of the widths and *spacings* of the activated molecules, and has an upper limit of one.

9367. **Bandlike structure from continuum-continuum emission: the $He_2$ 600-Å bands,** F. H. Mies and A. L. Smith, *J. Chem. Phys.* **45,** No. 3, 994-1000 (Aug. 1, 1966).

Key words: Atomic; collisions; continuous; deexcitation; He; $He_2$; metastable; radiative; spectra; theory; vacuum-ultraviolet.

The continuous spectrum produced by the radiative deexcitation of metastable atoms by atom impact is an example of molecular continuum-continuum transitions. It is shown that if the upper molecular state has a deep attractive well and the lower state is repulsive, the continuous spectrum will show banded structure similar to that obtained in bound-continuum transitions from high vibrational states. The analysis is applied to the radiative deexcitation of $He(2^1S)$ by He, which gives rise to the "600 Å bands." The structure and temperature dependence of these bands are well explained as banded continuum-continuum emission. Structured continua observed in other rare gases are discussed in terms of the molecular states involved.

9368. **Infrared spectrum of the free radical $CF_3$ isolated in inert matrices,** D. E. Milligan, M. E. Jacox, and J. J. Comeford, *J. Chem. Phys.* **44,** No. 10, 4058-4059 (May 1966).

Key words: $CF_2$ reactions; $CF_3$ free radical; $CF_3Br$ photolysis; F atom reactions; $HCF_3$ photolysis; infrared spectrum; matrix isolation technique.

The free radical $CF_3$ has been stabilized in inert gas and nitrogen matrices at cryogenic temperatures following (1) the reaction of photolytically produced $CF_2$ and F atoms, (2) the vacuum ultraviolet photolysis of $HCF_3$ and of $CF_3Br$, and (3) the reaction of photolytically produced C and F atoms. The concentration of $CF_3$ obtained in these studies has been sufficient for direct infrared observation of three of its vibrational fundamentals, at 703, 1084, and 1248 $cm^{-1}$. It is concluded that $CF_3$, unlike $CH_3$, is nonplanar in its ground state.

9369. **Matrix-isolation study of the photolysis of cyanogen azide. II. The symmetric stretching fundamental of the free radical NCN,** D. E. Milligan and M. E. Jacox, *J. Chem. Phys.* **45,** No. 5, 1387-1391 (Sept. 1, 1966).

Key words: Carbon atom production; carbon atom reactions; cyanogen azide; force constants; infrared spectrum; NCN free radical; thermodynamic properties; ultraviolet photolysis.

The photolysis of $Ar:N_3CN$ samples at 14 °K with the full light of a cadmium arc has been found to permit complete conversion of the cyanogen azide to the free radical NCN, plus molecular nitrogen. At the high concentration of NCN thus achieved a weak absorption appears at 2672 $cm^{-1}$. The photolytic behavior of this feature and its shifts upon isotopic substitution support its assignment as the combination band $(\nu_1+\nu_3)$ of NCN, permitting deduction of a value of 1197 $cm^{-1}$ for $\nu_1$ of this species. The thermodynamic properties of NCN have been revised in accord with this assignment. The carbon-nitrogen stretching force constant approaches a value characteristic of a doubly bonded species, and the stretching interaction constant is relatively large and positive. Cyanogen azide photolyzes in both its 2750 and its 2200 Å absorption regions to produce $NCN+N_2$. However, NCN itself photolyzes when subjected to radiation near 2500 Å, producing carbon atoms in the $^3P$ state, which, in turn, may react with $N_2$ to form the free radical CNN.

9370. **Unassigned.**

9371. **Recombination of $He^+$ and $He^{++}$ in the afterglow of a helium discharge,** E. R. Mosburg, Jr., *Phys. Rev.* **152,** No. 1, 166-176 (Dec. 2, 1966).

Key words: Brush-cathode plasma; collisional-radiative recombination; helium afterglow; recombination coefficient.

Studies of the time dependence of atomic and molecular light intensities, electron density, atomic metastable densities and electron temperature have allowed the determination of the $He^+$ – electron recombination coefficient as a function of electron density and temperature. The results are in reasonable agreement with the theory of collisional-radiative recombination. The mechanisms controlling metastable densities and heating of the electron gas are discussed. In particular, the disappearance of the $2^3S$ metastable atom seems best explained in terms of collisonal de-excitation by electrons.

9372. **A new guide for photographers,** C. S. McCamy, *Mag. Stds.* **37,** No. 8, 223-224 (Aug. 1966).

Key words: Exposure; photography; standards.

The new "American Standard Photographic Exposure Guide" presents and relates data which provide means of calculating camera settings for daylight and moonlight exposure of black-and-white and color films. The appendix gives guidance for photographing sunsets, clouds, the moon, artificial satellites, rainbows, cities at night, fireworks, lightning, aurora, stars, and eclipses. The standard is based on extensive picture tests.

9373. **Concepts, terminology, and notation for optical modulation,** C. S. McCamy, *Photo. Sci. Eng.* **10,** No. 6, 314-325 (Nov.-Dec. 1966).

Key words: Absorptance; contrast; modulation; notation; optical density; propagance; reflectance; reflectance factor; symbols; transmittance; transmittance factor.

Reflectance, transmittance, and optical density are regarded as kinds of flux modulation factors. Transmittance is defined as the ratio of transmitted flux to the incident flux, while transmittance factor is here defined for an optical system as the ratio of the emergent flux with the sample in the system to the emergent flux with the sample removed. Transmission density is defined as the negative logarithm of transmittance factor. This is essentially a new definition to accord with an old practice. Reflection, transmission, and fluorescence are considered generically as propagation and generalized modulation terms are proposed. A coordinate system and functional notation are adopted to systematize the description of optical systems which use or measure modulation. Simplified notation of the form D(g;S:g′;S′) describes most cases. Terms, symbols, and notation are proposed for standardization.

9374. **Mass-spectrometric investigation of the nickel-fluorine surface reaction,** J. D. McKinley, *J. Chem. Phys.* 45, No. 5, 1690-1693 (Sept. 1, 1966).

Key words: Fluorine; high temperature; kinetics; mass spectrometry; nickel; surface reaction.

Mass spectrometric measurements have been made of the reaction of polycrystalline nickel at temperatures between 900 and 1600 °K with fluorine at pressures between $10^{-7}$ and $10^{-4}$ torr. Gaseous NiF, $NiF_2$ and F are the major products, and are formed rapidly on the surface at rates linear with fluorine pressure. NiF is present on the surface over the entire temperature range and desorbs above 1100 °C; the desorption step involves rupture of a Ni(substrate)–NiF bond and has an activation energy of 28 kcal $mol^{-1}$. $NiF_2$ formation and desorption are important between 900 and 1600 °K with a maximum rate at 1250-1300 °K. The rate limiting step in the formation of $NiF_2$ has an activation energy of 39 kcal $mol^{-1}$ and is probably dissociation of fluorine on the surface.

9375. **Classification of normal subgroups of the modular group,** M. Newman, *Trans. Am. Math. Soc.* **126,** No. 2, 267-277 (Feb. 1967).

Key words: Congruence groups; modular group; normal subgroups; parabolic classes.

The normal subgroups of the classical modular group are studied, and theorems such as the following are proved:

(1) There are no normal subgroups of index 12q, where q is a prime $> 11$.

(2) There are exactly $1+(q/3)$ normal subgroups of index 6q, where q is a prime $> 3$ and $(q/3)$ is the Legendre symbol.

(3) If there is no normal subgroup of index $\mu$ and q is a prime $>\mu$, then there is no normal subgroup of index $q^k\mu$ for all $k \geqq 0$.

9376. **Momentum autocorrelation function for systems with finite spatial boundaries,** R. Nossal, *J. Chem. Phys.* **45,** No. 4, 1097-1100 (Aug. 15, 1966).

Key words: Diffusion coefficients; momentum correlation function; statistical mechanics.

An exact analytical expression is obtained for the momentum autocorrelation function of a particle moving in a one dimensional box and slowed by dynamical friction. Comparison is made with the results of Rahman's computer experiment for liquid Argon.

9377. **Equilibrium pressures of oxygen over $Ag_2O$–Ag at various temperatures,** E. M. Otto, *J. Electrochem. Soc.* **113,** No. 7, 643-645 (July 1966).

Key words: Dissociation by heat; entropy; equilibrium; heat of reaction; oxygen pressures; silver oxide.

Although earlier investigators showed the dissociation of $Ag_2O$ to be reversible and equilibrium points had been obtained there was a range from 191 to 302 °C that had not been studied. This region has now been studied. From all the data available and heat capacity data $\Delta H°_{298}$ and $\Delta S°_{298}$ have been calculated to be 14.690 kcal/mol $O_2$ and 31.916 cal/deg, respectively. (1 calorie=4.1840 joules.)

9378. **Conformation of polyesters adsorbed on solid surfaces,** P. Peyser, D. J. Tutas, and R. R. Stromberg, *J. Polymer Sci.* **5,** Pt. A-1, 651-663 (1967); *Book, Fundamental Aspects of Fiber Reinforced Plastic Composites,* Ed. R. T. Schwartz and H. S. Schwartz, pp. 163-176 (Interscience Publ., New York, N.Y., 1968).

Key words: Adsorption; configuration of adsorbed polymer; conformation of adsorbed polymer; ellipsometry; infrared; polymer adsorption; polyester.

The conformation of a polyester, poly(ethylene *o*-phthalate), of relatively low molecular weight was studied after adsorption. The extension of the adsorbed molecule in a poor solvent on several planar metal surfaces was studied by ellipsometry and the fraction, *p*, of attached groups on colloidal silica particles in a good solvent was determined by the shift in the infrared absorption frequency between free and adsorbed carbonyl groups. In contrast to previously reported results for polystyrene, the extension normal to the surface remained constant (~70 Å) while the concentration of polymer in the adsorbed film increased during the adsorption period. The value of *p*(0.34 for MW=5400) is relatively high and was independent of surface population for the range of solution concentrations measured. Differences between these results and those for polystyrene are interpreted as resulting from differences in interaction energy and chain stiffness.

9379. **Acoustical thermometer and the National Bureau of Standards provisional temperature scale 2-20 (1965),** H. Plumb and G. Cataland, *Metrologia* **2,** No. 4, 127-139 (Oct. 1966).

Key words: Acoustical thermometry; isotherms below 20 °K; low temperature thermometry; primary thermometry; speed of sound; ultrasonic interferometer.

An acoustical thermometer has been developed at the National Bureau of Standards to determine values of temperature that approximate the Thermodynamic Temperature Scale. The instrument, called an ultrasonic interferometer in acoustical literature, has been used to determine isotherms of the speed of sound in helium gas as a function of pressure. Each isotherm has been extrapolated to zero pressure to approximate the condition of an ideal gas; from the resulting intercepts, values of temperature were calculated.

The instrument and its operation are described and the data for isotherms, which have been determined at approximately every degree from 2-20 °K, are listed. The isotherm data have been treated both graphically and by electronic computer analysis (by the method of least squares) to yield values of temperature that are the basis for a new temperature scale–NBS Provisional Scale 2-20 (1965). When the scale is compared with other existing scales, $T_{58}$ and NBS (1955), in regions of overlap, the agreement with NBS (1955) is excellent but noticeable departures from $T_{58}$–the helium-4 vapor pressure scale are indicated.

9380. **Microwave spectrum of $CF_2$,** F. X. Powell and D. R. Lide, Jr., *J. Chem. Phys.* **45,** No. 3, 1067-1068 (Aug. 1, 1966).

Key words: $CF_2$; dipole moment; free radical; microwave spectrum; structure.

The microwave spectrum of the transient species $CF_2$ has been detected and analyzed. Eight rotational transitions have been assigned and the rigid-rotor constants determined. The CF distance is found to be 1.30 Å and the FCF angle is 104.9°.

9381. **The RF connector,** R. C. Powell, *Microwave J.* **10,** No. 3, 69 (Feb. 1967).

Key words: Coaxial techniques; precision coaxial measurements; RF connector.

This paper describes the need for and the process of development of precision coaxial techniques. It is intended as an introductory article to an issue devoted to precision coaxial measurements.

9382. **Comparison of Langmuir probe and spectrometric electron temperature measurements,** R. S. Powers, Jr., *J. Appl. Phys.* **37,** No. 10, 3821-3826 (Sept. 1966).

Key words: Electron temperature; Langmuir probe; plasma; spectrometric.

Langmuir probes are often used for temperature measurements in plasmas, due to their convenience and to their ability to give time-resolved measurements. Since probe results are subject to several suspicions, we compare probe and spectrometric electron temperature measurements in a particular low-temperature plasma in which this is possible. We find probe temperatures to be high by amounts between 40 and 4% over an electron temperature range between 410 and 920 °K.

9383. **Low temperature speed of sound in single crystal ice,** T. M. Proctor, Jr., *J. Acoust. Soc. Am.* **39,** No. 5, 972-977 (May 1966).

Key words: Elastic constants; lattice dynamics; lattice parameter changes; single crystal ice; speed of sound; thermodynamic properties.

Only one of the previous measurements of the elastic constants and speed of sound in single-crystal ice-I had been extended below −30 °C. All of the five independent elastic constants have now been measured down to 65 °K. Elastic constant data have been fitted to second-degree polynomials. From these polynomials a 0 °K value for the $c_{ij}$'s is extracted and a Debye characteristic temperature of 225 °K is calculated. This Debye temperature compares favorably with that previously computed from heat capacity data. No sudden changes in the pseudo-elastic anisotropic factor $c_{33}/c_{11}$ are found to take place at 190 °K as had been previously reported.

9384. **Ionization energies of the neutral rare earths,** J. Reader and J. Sugar, *J. Opt. Soc. Am.* **56,** No. 9, 1189-1194 (Sept. 1966).

Key words: Calculation; ionization; neutral; rare earths; series.

The ionization energies of the neutral rare earths have been derived by means of interpolated values for the differences between the $4f^N6s^2$, $4f^N6s7s$, and $4f^N6s8s$ configurations and the difference in the effective quantum numbers of the $4f^N6s7s$ and the $4f^N6s8s$ configurations. In Ce I the $4f5d^2ns$ series was used. The results in eV are:

| | | |
|---|---|---|
| Ce I 5.65 | Sm I 5.63 | Er I 6.10 |
| Pr I 5.42 | Eu I 5.68 | Tm I 6.18 |
| Nd I 5.49 | Dy I 5.93 | Yb I 6.25 |
| Pm I 5.55 | Ho I 6.02 | |

The uncertainty is estimated to be ±0.02 eV in all cases but Ce I for which the estimated uncertainty is ±0.06 eV. Values for La I, Gd I, and Lu I obtained spectroscopically by other workers are also tabulated. The present results are compared with those obtained by means of surface ionization. The calculated result for Tb I was inconclusive because of the lack of sufficient knowledge of the energy level structure.

9385. **Comparison of direct and sensitized photolysis of 3-methylpentanal in vapor phase,** R. E. Rebbert and P. J. Ausloos, *J. Am. Chem. Soc.* **89,** No. 7, 1573-1579 (Mar. 29, 1967).

Key words: Aldehyde; energy transfer; photolysis; triplet state; vapor phase.

The direct and the benzene- and acetone-sensitized photolysis of 3-methylpentanal produces butene-1, *trans*-butane-2, and *cis*-butene-2 by an intramolecular rearrangement process in which a hydrogen atom is transferred to the carbonyl group from a γ-carbon atom. In the direct photolysis an increase in temperature or a decrease in wavelength of the incident light results in an increase in the percentage yield of butene-1 and in the ratio *cis*/*trans*-butene-2. The distribution of the butenes depends upon the amount of energy given to the aldehyde whether by the direct or sensitized photolysis. The benzene- and acetone-sensitized experiments give additional evidence that the intramolecular rearrangement which involves the photo-elimination of olefins can proceed through a triplet excited state. The following additional information was obtained in the course of this study: (1) The aldehyde undergoes both triplet-triplet and singlet-singlet energy transfer with benzene. (2) In the acetone-aldehyde systems only triplet-triplet energy transfer occurs. (3) A comparison of the distribution of butenes which was obtained in the acetone-sensitized experiments with the butene distribution in the direct photolysis at the same temperature indicates that $<81$ kcal are transferred to the aldehyde by acetone in a triplet-triplet energy transfer reaction.

9386. **Molecular thermodynamics of simple liquids, pure components,** H. Renon, C. A. Eckert, and J. M. Prausnitz, *I& EC Fundamentals* **6,** No. 1, 52-58 (Feb. 1967).

Key words: Argon; molecular complexity; molecular thermodynamics; Prigogine's cell theory; thermodynamic properties; three-parameter theorem.

Thermodynamic properties of simple liquids are calculated from an analytical partition function which is based on a modification of Prigogine's cell theory and on a three-parameter theorem of corresponding states. The partition function gives an excellent representation of the configurational properties of fifteen liquids ranging in molecular complexity from argon to neopentane. Three characteristic molecular parameters are sufficient to calculate the configurational energy and entropy, the volume, coefficient of expansion and compressibility. These parameters are a molecular size, a pair-potential energy, and a term which is closely related to non-central intermolecular forces; this last parameter is a nearly linear function of Pitzer's acentric factor. The main application of this statistical thermodynamic treatment follows from its straightforward extension to liquid mixtures as discussed in Part II.

9387. **Atomic standards of frequency and time,** J. M. Richardson and J. F. Brockman, *Phys. Teacher* **4,** No. 6, 247-256 (Sept. 1966).

Key words: Atomic frequency standards; atomic time; cesium atomic beam; frequency and time standards; standards; standard time scales.

The national standard of time is provided by an atomic device at the National Bureau of Standards. Thus, for the first time in our civilization, the basis of our measurement of time is atomic instead of astronomical. The major reasons for this change are that modern science can measure the resonance of an atom more accurately than it can measure the motions of stars and planets, all of the factors affecting atoms are better understood, and the atomic resonance appears to be more stable than planetary motions. This change has improved our accuracy of measurement by three orders of magnitude.

Presently, the best atomic clocks are based on atomic cesium beams such as the three at NBS. Further research, however, may reveal a better choice of atom or method. NBS is presently using four radio stations to distribute time (and its reciprocal, frequency) to the nation and over much of the globe but, again, research is being conducted on newer techniques which offer higher accuracies.

The change from astronomical to atomic time will have little effect on our daily living habits, but it will permit our technology to accomplish things we couldn't do before and to do the same things more economically.

9388. **Measurements of relative oscillator strengths of some C II multiplets,** J. R. Roberts and K. L. Eckerle, *Phys. Rev.* **153,** No. 1, 87-90 (Jan. 1, 1967).

Key words: Carbon II; coulomb approximation; electron density; electron temperature; equivalent electrons; local thermal equilibrium; oscillator strength (f-value); optical depth; oxygen II; plasma; T-tube.

An electric shock tube (T-tube) filled with a mixture of 95% He and 5% $CO_2$ at 0.5 torr initial pressure was the source for spectroscopic measurements of some C II oscillator strengths. The absorption oscillator strengths of the C II 2512 Å, 2837 Å, 3920 Å, and 3876 Å multiplets were measured relative to the 4267 Å C II multiplet. The plasma electron temperature was determined by the relative line intensities of the 4254 Å and 4642 Å O II lines.

9389. **The momentum autocorrelation function in a Bernoulli chain,** R. J. Rubin and P. Ullersma, *J. Math. Phys.* **7,** No. 10, 1877-1885 (Oct. 1966).

Key words: Coupled harmonic oscillators; momentum autocorrelation function; statistical dynamics; statistical mechanics.

This paper is devoted to the study of the statistical dynamics of the small amplitude coplanar vibrations of a compound pendulum consisting of $N+1$ particles suspended in series by weightless strings in a gravitational field. All particles have the same mass m, except for the top particle whose mass is $m(1+2)$; and all strings are of equal length. The behavior of this system in the limit in which $N \rightarrow \infty$ is of particular interest because the maximum normal mode frequency is proportional to $N^{1/2}$. In the limit $N \rightarrow \infty$, asymptotic formulas with error estimates arc obtained for the time-dependence of the momentum autocorrelation function of: (1) the top particle when $2=0$; (2) the bottom particle when $2=0$; and (3) the top particle when $N \gg 2 \gg 1$.

9390. **An examination of the effects of heat transfer and compressible flow on the performance of laminar flowmeters,** F. W. Ruegg and H. H. Allion, *Proc. Flow Measurement Conf., Am. Soc. Mech. Eng. Fluid Meters Golden Anniversary, Pittsburgh, Pa., Sept. 26-28, 1966,* pp. 253-273 (1966).

Key words: Compressible flow; flowmeter; gas meter; heat transfer; laminar flow; meter calibration.

Laminar meters are now widely used for measurement of gas flow, and high accuracy can be achieved with proper calibration and use. It has been found necessary to modify Poiseuille's law for laminar flow to explain the performance of meters over the wide range of flow conditions encountered. A one-dimensional flow analysis is used to derive the effects of meter shape, heat transfer, and compressibility of the gas on meter performance. A relationship between the meter flow coefficient and the similarity parameters of Reynolds number, Prandtl number, Mach number, and Knudsen number is given in a form that is convenient for both the calibrator and user of the meter. The small but significant effects predicted are compared with experimental results.

9391. **Gas-phase photolysis of isopentane at photon energies below and above the ionization energy,** A. A. Scala and P. Ausloos, *J. Chem. Phys.* **45,** No. 3, 847-854 (Aug. 1, 1966).

Key words: Hydrocarbons; ion-molecule reaction; isopentane; photoionization; photolysis.

The photolysis of $(CH_3)_2CDCH_2CH_3$, $(CH_3)_2CHCH_2CD_3$ and of equimolar $(CH_3)_2CHCH_2CH_3$-$(CD_3)_2CDCD_2CD_3$ mixtures has been investigated in the presence of NO at 1470 Å (8.4 eV), 1236 Å (10 eV) and at 1048 Å-1067 Å (11.54 – 11.72 eV). Furthermore, in order to obtain quantitative information concerning the free radicals produced in the fragmentation processes, $(CD_3)_2CDCD_2CD_3$ has been photolyzed at 1236 Å in the presence of various concentrations of $H_2S$.

Fragmentation of the excited isopentane molecule produced at 8.4 or 10 eV, as well as of the superexcited molecule formed at 11.54-11.72 eV, yields mainly olefinic products and the following radicals, in order of decreasing yield: $H \cong CH_3 \cong C_2H_5 \cong C_3H_7$. In addition, on the basis of the various isotopically labeled products, it is concluded that methane, ethane, and propane are split off from the excited isopentane molecule by formation of (a) the corresponding carbene (1,2-elimination), or (b) the corresponding olefin (1,3-elimination). When the energy of the photon is increased from 8.4 to 10.0 eV, the 1,2-elimination processes become more important relative to the 1,3-elimination processes in all cases. At 11.54-11.72 eV, the parent ion decomposes to form methane and ethane mainly by a 1,3-elimination mechanism. It is derived from the results that, in addition to the $C_4H_8^+$ and $C_3H_6^+$ ions formed by the latter fragmentation processes, the ions $C_4H_9^+$ and $C_3H_7^+$ are produced with ion pair yields (M/N) of 0.15 and 0.06, respectively. The ion pair yield of the parent ion is estimated to be 0.35. In contrast to observations derived from an earlier investigation of photoionization of n-butane at 11.54-11.72 eV, an increase in pressure from 0.15 to 15 torr has only a minor effect on the fragmentation of the parent ion.

9392. **Ion-molecule reactions in the condensed phase radiolysis of hydrocarbon mixtures. I. 2-methylbutane and 3-methylpentane,** A. A. Scala, S. G. Lias, and P. Ausloos, *J. Am. Chem. Soc.* **88,** No. 24, 5701-5707 (Dec. 20, 1966).

Key words: Ion-molecule reaction; liquid phase photolysis; liquid phase radiolysis; 2-methylbutane; 3-methylpentane.

In the condensed phase, parent ions of 2-methylbutane and 3-methylpentane transfer an $H_2$-molecule to cyclopropane as well as to smaller unsaturated hydrocarbons according to the reaction: $C_nH_{2n+2}^+ + C_{m'}H_{m''} \rightarrow C_n^+ + C_{m'}H_{m''+2}$. The relative probabilities for the transfer of an $H_2$-molecule from $C_5H_{12}^+$ to cyclopropane, ethylene, propylene, 1-butene, acetylene, and 2-butene are, respectively, 2.4, 1.4, 1.0, 0.9, 0.77, and <0.1. When cyclopropane-$d_6$ is added to iso-$C_5H_{12}$, $CD_2HCD_2CD_2H$ is formed as a product with a yield which increases as the square root of the cyclopropane-$d_6$ concentration from a G-value of 0.117 at 0.03 mole percent additive to 1.53 at 20 mole percent additive, while all lower perprotonated hydrocarbon products diminish proportionately. Similarly, addition of electron scavengers such as $CCl_4$ to an i-$C_5H_{12}$-$(CD_2)_3$ (1:0.03) mixture increases $G(CD_2HCD_2CD_2H)$ to a value as high as 2.85 while the G-value of products such as $C_2H_6$, $C_2H_4$, or $C_3H_8$ drop by factor of five. The importance of the $H_2$-transfer reaction to our understanding of the condensed phase radiolysis of alkanes is discussed.

9393. **Electron affinity of tungsten determined by its positive and negative self-surface ionization,** M. D. Scheer and J. Fine, *Phys. Rev. Letters* **17,** No. 6, 283-284 (Aug. 8, 1966).

Key words: Electron affinity; positive and negative self-surface ionization; tungsten.

It has been shown that negative as well as positive ions are evaporated from an incandescent tungsten surface thereby establishing that the tungsten atom has a positive electron affinity. When equilibrium is assumed between the metal surface and the evaporating ions, a quantitative estimate of the electron affinity can be obtained from a measurement of the positive to negative ion emission ratio at some known surface temperature. Measurements in the 2260 to 2350 °K temperature range yield a value of 0.5 eV for the electron affinity of tungsten.

9394. **The adsorption kinetics of nitrogen on rhenium,** M. D. Scheer and J. D. McKinley, *Surface Sci.* **5**, No. 3, 332-344 (Nov. 1966).

Key words: Adsorption kinetics; nitrogen; rhenium; sticking coefficient; surface coverage.

The adsorption of room temperature nitrogen on atomically clean polycrystalline rhenium has been studied. The sticking coefficients at zero coverage were found to be 0.060, 0.009, and 0.007 at rhenium surface temperatures of 205, 300, and 373 °K respectively. These values are between one and two orders of magnitude smaller than those in the nitrogen-tungsten system. The dependence of the sticking coefficient upon surface coverage and temperature could be accounted for by assuming an intermediate state weakly bound to an adsorption site. These sites were assumed to be uniformly distributed over the surface. Their concentration was found to be less than 1/10 of the number of substrate rhenium atoms/cm$^2$. The binding energies of the intermediate state and the permanently adsorbed state were in the ratio of about 1/20 for both the nitrogen-rhenium and nitrogen-tungsten systems. In view of this similarity, it is difficult to account for the large difference in sticking probabilities unless one assumes that tungsten absorbs energy from the intermediate binding state much more efficiently than does the rhenium.

9395. **Ferrimagnetic resonance low-field effects in rod samples,** L. B. Schmidt, R. D. Harrington, and W. E. Case, *Proc. IEEE* **55**, No. 1, 120-121 (Jan. 1967).

Key words: External tensor permeability; ferrimagnetic resonance; ferrites; garnet; low magnetic field effects; permeability; spin waves; tensor permeability; YIG.

A previously unreported absorption which is indicated in the curve of the imaginary part of the external permeability of rod-shaped samples is reported. This curve was transformed from intrinsic permeability data obtained from measurements on polycrystalline garnet samples of different densities. This energy absorption revealed in the loss curve of the external permeability occurs in the vicinity of the dc field at which the intrinsic tensor permeability resonates and appears to be affected by the porosity of the material. The phenomenon is more noticeable at L-band frequencies than at S-band frequencies.

9396. **Flash photolysis of matrix-isolated cyanogen azide in solid nitrogen,** L. J. Schoen, *J. Chem. Phys.* **45**, No. 8, 2773-2776 (Oct. 15, 1966).

Key words: Decay; flash photolysis; lifetime; matrix isolation; primary process.

Flash photolysis combined with matrix isolation spectroscopy has been employed to investigate the decomposition of a cyanogen azide-nitrogen solid at 20.4 °K. Two primary processes have been observed leading to the formation of NCN radicals either in an electronically excited $^1\Delta_g$ level or in the $^3\Sigma_g^-$ ground state. The first order decay of NCN ($^1\Delta_g$) has been studied and the mean lifetime in the solid found to be approximately 500 microseconds.

9397. **Superconductivity in semiconducting SrTiO$_3$,** J. F. Schooley and W. R. Thurber, (Proc. Intern. Conf. Physics of Semiconductors, Kyoto, Japan, Sept. 8-11, 1966), *J. Phys. Soc. Japan* **21**, Paper XVI-2, 639-642 (Suppl. 1966).

Key words: Semiconductors; strontium titanate; superconductivity.

Superconductivity that occurs in a substance which is semiconducting at higher temperatures possesses features which are different from ordinary metallic superconductivity. The occurrence of superconductivity in a material of relatively low charge carrier concentration $n_c$ is due largely to an unusually high density of states at the Fermi surface N(O); heat capacity and superconducting critical field experiments, among others, show the presence of the large N(O). The variability in $n_c$ within an essentially constant electronic energy band structure leads to a corresponding variation in the superconducting transition temperature $T_c$. The presence of anisotropic Fermi surfaces in multi-valley semiconductors can result in unusually large and anisotropic pressure effects. The relatively low carrier concentrations in semiconductors leads to unusually deep penetration of static magnetic fields in the superconducting state. Finally, the static dielectric constant, which can be quite large in semiconductors, can be varied by combining similar semiconductors into mixed crystals; to the extent that the superconducting properties depend upon the dielectric properties, variation in $T_c$ results.

9398. **The dispersion of distributions derived from folding simple distributions,** R. A. Schrack, *Nucl. Instr. Methods* **45**, No. 2, 319-321 (Dec. 1966).

Key words: Dispersion; distributions; folding; gaussian; square; trapezoidal; triangular.

A graph is presented for obtaining the dispersion (full width at half maximum) of distributions, obtained by folding pairs of simple symmetric distributions. The gaussian, triangular, trapezoidal, and square distributions are considered.

9399. **Divergence in the density expansion of the transport coefficients of a two-dimensional gas,** J. V. Sengers, *Phys. Fluids* **9**, No. 9, 1685-1696 (Sept. 1966).

Key words: Dense gases; rigid disks; rigid spheres; thermal conductivity; transport coefficients; triple collisions; viscosity.

An analysis is presented of the first density correction to the viscosity and thermal conductivity coefficient of a two-dimensional gas of rigid disks. The existence of a divergence in the density expansion is established explicitly. For a two-dimensional gas the triple collision contribution to the transport coefficients diverges logarithmically with the time between collisions. In particular, for rigid disks, the coefficient of the logarithmic singularity in the viscosity and thermal conductivity is evaluated in the first Enskog approximation. The possibility that as a consequence the transport coefficients depend logarithmically on the density is discussed.

9400. **Triple collision contribution to the transport coefficients of a rigid sphere gas,** J. V. Sengers, *Phys. Fluids* **9**, No. 7, 1333-1347 (July 1966).

Key words: Dense gases; rigid spheres; thermal conductivity; transport properties; triple collisions; viscosity.

An analysis is made of the triple collision integrals which appear in the expression for the first density correction to the thermal conductivity and the viscosity of a gas of rigid spheres. It is shown that these triple collision integrals can be written as a sum of integrals associated with six triple collision events, each of which consists of a certain sequence of correlated successive binary collisions. A number of integrations are carried out and the originally 15-fold triple collision integrals are reduced to seven-fold integrals in a form suitable for numerical analysis. The results are compared with the approximate predictions given by the Enskog theory for a dense gas of rigid spheres.

9401. **Correcting for astigmatism in the Czerny-Turner spectrometer and spectrograph,** A. B. Shafer, *Appl. Opt.* **6,** No. 1, 159-160 (Jan. 1967).

Key words: Astigmatism; Czerny-Turner; spectrograph; spectrometer.

It is shown that the Czerny-Turner spectrometer and spectrograph can be made approximately stigmatic by using torroidal mirrors.

9402. **Exactly solvable nonlinear relaxation processes. Systems of coupled harmonic oscillators,** K. E. Shuler and G. H. Weiss, *J. Chem. Phys.* **45,** No. 4, 1105-1110 (Aug. 15, 1966).

Key words: Harmonic oscillators; master equation; nonequilibrium processes; nonlinear relaxation; relaxation processes; stochastic processes.

A class of nonlinear relaxation processes is discussed which involves the interaction of two finite systems characterized by special forms of the transition probabilities. For the particular set of transition probabilities it is possible to reduce the initial set of coupled nonlinear kinetic equations to a set of linear equations with time dependent coefficients which are amenable to exact analytical solutions. This reduction is effected through the use of summational invariants expressed in terms of the appropriate combinations of the moments of the distribution functions of the two systems. The vibrational-vibrational relaxation of two interacting systems of harmonic oscillators A and B has been worked out as a specific example. For the type of relaxation processes discussed here it is found that the relaxation of system A is independent of the form of the initial distribution of system B (and thus of its time history) and vice versa.

9403. **Observation of the $D^1\Delta \leftarrow X^1\Sigma^+$ transition of CO in the vacuum-ultraviolet region,** J. D. Simmons and S. G. Tilford, *J. Chem. Phys.* **45,** No. 8, 2965-2968 (Oct. 15, 1966).

Key words: Absorption spectrum; CO; diatomic spectrum; electronic transition; rotational analysis; vacuum-ultraviolet region.

A weak new band in the vacuum-ultraviolet absorption spectrum of CO has been observed and analyzed as the $D^1\Delta \leftarrow X^1\Sigma^+(1\text{-}0)$ band for both $C^{12}O^{16}$ and $C^{13}O^{16}$. The observed rotational intensity distribution indicates this transition arises through mixing of the $D^1\Delta$ state with neighboring states, principally the $A^1\Pi$ state of the strong electric-dipole-allowed fourth-positive system. A brief correlation of observed electronic states with those arising from various electronic configurations is given.

9404. **Angle and channel dependence of resonance in e-He scattering near 60 eV,** J. A. Simpson, M. G. Menendez, and S. R. Mielczarek, *Phys. Rev.* **150,** No. 1, 76-78 (Oct. 7, 1966).

Key words: Angular difference; He, $He^-$; inelastic scattering; resonances; scattering.

The $He^-$ resonances at 57.1 and 58.2 eV in the electron scattering from He were studied as a function of angle in three inelastic channels corresponding to excitation of the $(1s2s)^3S$, $(1s2s)^1S$, and $(1s2p)^1P$ states of He. The line shapes of the resonances are found to vary with angle. The use of the Fano-Cooper formula, developed for the case of photon absorption, to resonances in inelastic electron scattering is discussed along with a simple procedure for determining the line profile indices. The angular dependence of the $^1S$, $^3S$, and $^1P$ excitations at 56.5 eV was also measured out to about 60°.

9405. **Anomalous energy spreads in electron beams,** J. A. Simpson and C. E. Kuyatt, *J. Appl. Phys.* **37,** No. 10, 3805-3809 (Sept. 1966).

Key words: Electron beams; energy distribution.

Energy distributions of 2 to 10 eV electron beams were measured in a deflection analyzer. The performance of the analyzer was monitored by use of a second one in tandem. In agreement with earlier measurements in higher energy beams the energy distribution varied with current. At low currents the energy distribution was Maxwellian at a temperature corresponding to the cathode temperature. As the current increased toward the space charge limit the energy width increased. The excess energy width could be fitted to a curve linear in maximum current density and varying inversely with beam energy to the three-halves power. No shift in most probable energy was found. The results are not in quantitative agreement with the higher energy low space charge measurements.

9406. **The new tungsten-filament lamp standards of total irradiance,** R. Stair, W. E. Schneider, and W. B. Fussell, *Appl. Opt.* **6,** No. 1, 101-105 (Jan. 1967).

Key words: Blackbody; lamp standard; total irradiance.

The NBS standard of total irradiance as presently issued in the form of a 50-watt carbon filament lamp was originally calibrated more than 50 years ago. Recently, needs for higher accuracy and wider ranges of total irradiance have necessitated the setting up of three sizes (100-, 500-, and 1000-watt) of tungsten-filament lamp standards of total irradiance. These standards operate at a higher temperature than was possible with the carbon-filament lamps, and are shielded, except for a narrow area of the bulb in front of the filament, so that the reception of long-wavelength flux from the lamps is reduced to a minimum. The new lamps were calibrated by the use of a blackbody at a known temperature together with a quartz plate whose spectral transmittance was accurately determined. The quartz plate limits the flux received from the blackbody to the spectral region below about 4.5 microns and thus reduces errors resulting from water vapor absorption at 6 microns and longer wavelengths. Comparisons show the new standards to be in close agreement with the carbon-filament lamp standard.

9407. **Resolving power predictions from lens design data,** O. N. Stavroudis, *Appl. Opt.* **6,** No. 1, 129-135 (Jan. 1967).

Key words: Correlation; lens design; resolving power.

A relationship between longitudinal spherical and longitudinal chromatic aberration and resolving power is discussed and an experiment using this relationship to predict resolving power from design data is described. The results show a high degree of correlation between resolving power predicted by this method and that obtained by measurement on real lenses.

9408. **Glass-molten salt interactions,** K. H. Stern, *Chem. Rev.* **66,** No. 4, 355-372 (July 25, 1966).

Key words: Conductance; diffusion; electrodes; electrolysis; glass; molten salts.

Phenomena involved in the interactions between glass and molten salts are described and discussed. These include diffusion and electrochemical phenomena occurring at the glass-molten salt interface. Their application to the design of glass membrane reference electrodes for use in molten salts is discussed. The electrical properties of glass at elevated temperatures are considered from a mechanistic point of view.

9409. **Observation of the superconducting energy gap in a semiconductor (GeTe),** P. J. Stiles, L. Esaki, and J. F. Schooley, *Phys. Letters* **23,** No. 3, 206-207 (Oct. 17, 1966).

Key words: GeTe; semiconductor; superconducting energy gap; tunnel junction.

A report of the first observation of the superconducting energy gap in a semiconductor, GeTe, is given. The gap was observed in a tunnel junction of Al-$Al_2O_3$-GeTe.

9410. **Lightness change of grays induced by change in reflectance of gray background,** H. Takasaki, *J. Opt. Soc. Am.* **56,** No. 4, 504-509 (Apr. 1966).

Key words: Contrast; crispening; lightness; Munsell value; reflectance.

A relatively small gray sample looks lighter (darker) when it is placed on darker (lighter) background. This phenomenon is an example of the well-known contrast effect. The purpose of this paper is to make a quantitative determination of the effect, and to derive a formula for it.

For any given gray sample and gray surround on the left side, the observer was instructed to choose, for the different gray surround on the right, a different gray sample appearing equally light as that on the left. It was found that lightness of a sample changes rapidly with regard to its reflectance when this reflectance is close to that of background. This effect was named the "crispening effect"

Several models (Von Kries coefficient law, Hurvich-Jameson induction) were tried, but none of them reproduced the experimentally discovered crispening effect. A fairly successful empirical formula was developed by adding to the formula for the induction theory a term for the crispening effect.

9411. **Chromatic changes induced by changes in chromaticity of background of constant lightness,** H. Takasaki, *J. Opt. Soc. Am.* **57,** No. 1, 93-96 (Jan. 1967).

Key words: Chromatic induction; color; contrast; crispening; opponent color theory; surround color; three components color theory.

A relatively small gray sample looks reddish (greenish) when it is placed on a green (red) background, and yellowish (bluish) when it is placed on a blue (yellow) background. This phenomenon is an example of the well-known contrast effect. The purpose of this paper is to make a quantitative determination of the effect, and to check whether the empirical formula previously derived for lightness contrast applies also to chromatic contrast. Two series of color samples were prepared so that in the dominator-modulator system proposed by Judd, only one of the three fundamental responses varied. For a given member of one of these two series viewed on a surround of any member of the same series on the left side, the observer was instructed to choose, for a surround of a different member of the series on the right, the member of the series producing most nearly the same color appearance. The crispening effect which was found in lightness was also found in each of the chromatic responses, green and violet; and the empirical formula derived for lightness contrast was found to apply with fair success to the observations of each of the five observers, each with a different set of constants.

9412. **Zeeman effect and magnetic hyperfine structure in the low frequency transitions of $H_2CO$,** H. Takuma, K. M. Evenson, and T. Shigenari, *J. Phys. Soc.* **21,** 1622-1623 (1966).

Key words: $H_2CO$; magnetic hyperfine structure; RF transition; Zeeman effect.

The Zeeman structure and the center frequencies of the $4_{31}\rightarrow 4_{32}$ and the $5_{32}\rightarrow 5_{33}$ transition of $H_2CO$ were measured. The spectra agreed with theory using recently redetermined molecular constants.

9413. **Micrometer U-tube manometers for medium-vacuum measurements,** A. M. Thomas and J. L. Cross, *J. Vacuum Sci. Technol.* **4,** No. 1, 1-5 (Jan.-Feb. 1967).

Key words: Manometers; mercury; micrometer; oil; U-tube; vacuum measurement; water.

A family of U-tube manometers, suitable for use as standard instruments, has been designed and constructed at the National Bureau of Standards to cover the range of pressures from 100 to $1 \times 10^{-2}$ torr. In these instruments the levels of the two liquid surfaces are measured by adjusting micrometers with conical points ground on the ends of the spindles. One hundred mm and fifty mm range mercury manometers, with spindles approaching the liquid surface from above, are used for differential or absolute pressure measurements up to 100 torr. Pressures less than 3.5 torr are measured with oil manometers, in which the micrometer spindles approach the surfaces from below. Measurements made with the mercury manometer have an uncertainty of about $4 \times 10^{-3}$ torr plus eight parts in one hundred thousand of the reading. Measurements made with the oil manometer have an uncertainty of about $4 \times 10^{-4}$ torr plus two parts in ten thousand of the reading.

9414. **Intramolecular insertion of isobutylidene in the vacuum ultraviolet photolysis of isobutane,** E. Tschuikow-Roux and J. R. McNesby, *Trans. Farady Soc.* **62,** No. 524, 2158-2163 (Aug. 1966).

Key words: Insertion; isobutane; isobutylidene; photolysis; vacuum ultraviolet.

The direct photolysis of isobutane was carried out at the Xe resonance line (1470 Å) at 25 °C over the pressure range 5.3 to 410 torr (1 torr = 1/760 atmos = 133.32 $N/m^2$) with and without added nitrogen. Specifically, evidence for the intramolecular insertion of isobutylidene resulting from the carbene elimination of $H_2$ was sought and found. From the $C_4$ product distribution at the highest pressure it was deduced that the ratio of isomerization of isobutylidene to intramolecular cyclization is 19:1.

9415. **Reactions of ethylidene in the vacuum ultraviolet photolysis of ethylene,** E. Tschuikow-Roux, J. R. McNesby, W. M. Jackson, and J. L. Faris, *J. Phys. Chem.* **71,** No. 5, 1531-1533 (April 1967).

Key words: Carbene; ethylene; ethylidene; gas phase; photolysis; solid phase; vacuum ultraviolet.

Ethylene was photolyzed at the 1470 Å Xe resonance line both in the gas and solid phase (36 °K). The gas phase photolysis gave no products characteristic of bimolecular reactions of ethylidene. However, in the condensed phase, photolysis gives methylcyclopropane and much larger amounts of cyclopropene and methylcyclopropene. The mechanisms of production of these products are discussed as well as the relationship of ethylene photolysis to the photolysis of other sources of ethylidene.

9416. **Electronically excited NO by photodissociation of $NO_2$ and NOCl,** K. H. Welge, *J. Chem. Phys.* **45,** No. 4, 1113-1117 (Aug. 15, 1966).

Key words: Fluorescence; nitric oxide; nitrogen dioxide; nitrosyl chloride; vacuum ultraviolet.

The photodissociations of $NO_2$ and NOCl yielding electronically excited NO are observed by the fluorescence of NO($\gamma$) and NO($\beta$) bands:

$$NO_2 \xrightarrow{h\nu} NO(A^2\Sigma^+, v=0)+O(^3P)$$

$$NO_2 \xrightarrow{h\nu} NO(B^2\Pi, v=0, 1, 2, 3)+O(^3P)$$

$$NOCl \xrightarrow{h\nu} NO(A^2\Sigma^+, v=0, 1, 2)+Cl(^2P^0)$$

Dissociation of $NO_2$ is observed at wavelengths 1165, 1236, and 1295 Å but not at 1470 Å and longer wavelengths. Dissociation of NOCl is found at wavelengths from 1165 Å up to about 1600 Å. The $NO(A^2\Sigma^+)$ and $NO(B^2\Pi)$ molecules from $NO_2$ and NOCl are strongly rotationally excited.

9417. **Formation of $NH(c^1\Pi)$ and $NH(A^3\Pi_i)$ in the vacuum-uv photolysis of $HN_3$,** K. H. Welge, *J. Chem. Phys.* **45,** No. 11, 4373-4374 (Dec. 1, 1966).

Key words: Fluorescence; hydrazoic acid; NH; photolysis; vacuum ultraviolet.

The fluorescence of $NH(c^1\Pi, v{=}0,1)$ and $NH(A^3\Pi_i, v{=}0,1)$ is obtained when $HN_3$ is photolyzed in a flow system at wavelengths from 1236 Å up to about 1750 Å. Rotational levels of the $c^1\Pi$, v=0 state are observed up to $K \simeq 20$.

The formation of $NH(c^1\Pi)$ is attributed to the photodissociation of $HN_3$ into $N_2(X^1\Sigma_g^+)+NH(c^1\Pi)$ and that of $NH(A^3\Pi_i)$ to some not identified secondary reactions. This explanation is based on the finding that the $NH(c^1\Pi)$ emission is not affected by the flow rate whereas the $NH(A^3\Pi_i)$ emission decreased with increasing flow rate.

9418. **Formation of $N_2(A^3\Sigma^+)$ and $N(^2D,^2P)$ by photodissociation of $HN_3$ and $N_2O$ and their reactions with NO and $N_2O$,** K. H. Welge, *J. Chem. Phys.* **45,** No. 1, 166-170 (July 1, 1966).

Key words: Energy transfer; fluorescence; hydrazoic acid; nitrous oxide; photolysis.

The formation of $NO(A^2\Sigma^+)$ and $NO(B^2\Pi)$ in the photolysis of $N_2O$ at 1236 Å and 1470 Å was investigated by observing the fluorescence of the γ and β bands. The β band fluorescence is obtained when pure $N_2O$ is photolyzed at 1236 Å and 1470 Å in a flow system. The β bands are observed with vibrational excitation up to V′=3. The β bands disappear with the addition of small amounts of NO whereas the emission of rotationally hot γ bands is obtained. The γ bands are observed with vibrational excitation up to v′=2. According to the energetics, $NO(A^2\Sigma^+)$ and $NO(B^2\Pi)$ are formed at 1470 Å as well as at 1236 Å not by direct photodissociation of $N_2O$ but by secondary reactions. No fluorescence is obtained when $N_2O$ or $N_2O/NO$ mixtures are irradiated at wavelengths ≧ 1600 Å, i.e., within the long wavelength absorption band of $N_2O$.

The γ and β band fluorescence is explained by the following mechanism: photodissociation of $N_2O$ At 1236 Å and 1470 Å,

$$N_2(A^3\Sigma_u^+)+O(^3P)$$

$$N_2O$$

$$N(^2D \text{ and/or } ^2P)+NO(X^2\Pi),$$

followed by the reaction

$$N(^2D \text{ and/or } ^2P)+N_2O \rightarrow NO(B^2\Pi)+N_2$$

$$NO(B^2\Pi) \rightarrow NO(X^2\Pi)+\beta \text{ bands.}$$

This reaction is intercepted effectively by NO, possibly through

$$N(^2D \text{ and/or } ^2P)+NO \rightarrow N_2+O$$

thus causing the disappearance of the β band emission with the addition of NO. At sufficiently high concentration, NO reacts with $N_2(A^3\Sigma_u^+)$ via

$$N_2(A^3\Sigma_u^+)+NO(X^2\Pi) \rightarrow N_2(X^1\Sigma_g^+)+NO(A^2\Sigma^+)$$

$$NO(A^2\Sigma^+) \rightarrow NO(X^2\Pi)+\gamma \text{ bands.}$$

The emission of γ bands is also obtained in the photolysis of $HN_3/NO$ mixtures at 1470 Å and 1236 Å. This observation is explained by the photodissociation

$$HN_3 \rightarrow N_2(A^3\Sigma_n^+) \rightarrow NH(X^3\Sigma^-)$$

followed by the above reaction between $N_2(A^3\Sigma_u^+)$ and NO, yielding $NO(A^2\Sigma^+)$. The other possibility, that O atoms which are formed by photodissociation of NO react with $HN_3$ to form excited NO – as in the $O/N_2H_4$ atomic flame – is excluded.

9419. **EPR in single crystals of $NiBr_2$,** J. S. Wells and D. R. Winder, *J. Chem. Phys.* **45,** No. 1, 410-411 (July 1, 1966).

Key words: Antiferromagnetic; EPR; g value; K-band spectrometer; $NiBr_2$; single crystal.

Previously reported EPR measurements on $NiBr_2$ gave a single g value and linewidth for the resonance in a powdered sample. We have made measurements with a K-band spectrometer on a single crystal of this material as work preliminary to measuring the internal fields in the antiferromagnetic state. The spectra have been examined at 300 and 76 °K. At 300 °K, $g_\perp'=2.21\pm0.02$, $g_\parallel=2.19\pm0.02$, $\Delta H_\perp=800$ gauss and $\Delta H_\parallel=1000$ gauss. At 76 °K, $g_\perp=2.23\pm0.01$, $g_\parallel=2.16\pm0.01$, $\Delta H_\perp=400$ gauss and $\Delta H_\parallel=600$ gauss. At 4 °K, the resonance was not observed within the range of our spectrometer.

9420. **Matrix elements of general potentials in the harmonic-oscillator representation,** R. M. Wilcox, *J. Chem. Phys.* **45,** No. 9, 3312-3316 (Nov. 1, 1966).

Key words: Fourier transform; function V(q); harmonic oscillator; matrix elements.

The m, n matrix element of an arbitrary potential function V(q) in the one-dimensional harmonic oscillator representation is shown to be given by

$$\langle m|V(q)|n\rangle = \sum_{r=0}^{m} \frac{\alpha[m!n!]^{1/2}}{r!(m-r)!(n-r)!} \int_{-\infty}^{\infty} dy g(\alpha y) e^{-1/2y2}(iy)^{m+n-2r},$$

where $\alpha \equiv (2\omega/\hbar)^{1/2}$, and g (αy) is the Fourier transform of V(g). This formula is specialized to the cases where V(g) is given by $q^j e^{-1/2}\gamma q^2$, $e^i \alpha^{uq}$, and $q^{-1} \sin(\alpha\lambda q)$, where j is a non-negative integer and γ, u, and λ are real parameters. Results are compared, where possible, with previous work.

9421. **Chemisorption of nitric oxide on tungsten,** J. T. Yates, Jr. and T. E. Madey, *J. Chem. Phys.* **45,** No. 5, 1623-1634 (Sept. 1, 1966).

Key words: Adsorption; chemisorption; desorption; dissociation; field emission microscopy; kinetic; nitric oxide; surface; surface diffusion; tungsten; work function.

The chemisorption of NO on polycrystalline W has been investigated using a combination of ultrahigh vacuum techniques: flash desorption mass spectroscopy and field emission microscopy. It has been found that NO chemisorbs non-dissociatively on W at room temperature. Dissociation occurs at elevated temperature with an activation energy of about 47 kcal/mole (197 kJ/mole). Kinetic evidence indicates that dissociation involves the interaction of an adsorbed NO molecule with a neighbor empty site. At high NO coverage, dissociation is rate controlling for the liberation of ω-mode nitrogen near 1000 °K. Heating of an NO-shadowed W field emission tip above ~700 °K results in the formation of a *receding* boundary which remains sharp during the entire course of its backward motion over the initially covered region. This behavior is consistent with a model involving dissociation of NO at the boundary where empty sites are available. For monolayer NO (1.4 x $10^{15}$ molecules $cm^{-2}$) on polycrystalline W, $\Delta\phi=+1.85\pm0.10$ eV; this corresponds to an average surface dipole moment of 0.35 debye per chemisorbed NO molecule at full coverage.

9422. **The effect of other metallic ions on the electrocrystallization of silver from nitrate solutions,** J. P. Young, *Plating* **54,** No. 3, 272-274 (Mar. 1967).

Key words: Crystal growth; dendrite; electrocrystallization; electrodeposited crystals; electrodeposited dendrites; silver.

Silver dendrites of various configuration and forms were grown electrolytically on small cathode surfaces in silver nitrate solutions to which small amounts of other metal ions had been added to alter the characteristics of the non-epitaxial silver formations.

9423. **Effect of surface patch fields on field-emission work-function determinations,** R. D. Young and H. E. Clark, *Phys. Rev. Letters* **17,** No. 7, 351-353 (Aug. 15, 1966).

Key words: Energy distribution; field emission; patch fields; single crystal planes; work function.

Laplace's equation is used to show that substantial electrostatic patch fields exist on field emission tips due to work function differences over the various single-crystal planes. The implications of these previously neglected fields are discussed in regard to their effect on measurements of work function. A derivation is given for a new energy distribution method of determining work functions, and a method is suggested for obtaining values of work function which are independent of both the patch fields and the applied field.

9424. **Anomalous work function of the tungsten (110) plane,** R. D. Young and H. E. Clark, *Appl. Phys. Letters* **9,** No. 7, 265-268 (Oct. 1, 1966).

Key words: Energy distribution; field emission; patch fields; tungsten; work function; (110) plane.

Work function measurements have been carried out on the densely packed (110) plane of tungsten. Field ion microscope techniques have been used to obtain atomically perfect single crystal (110) planes. Field electron emission energy distributions have been combined with Fowler-Nordheim measurements to give work function values at 77 °K. The electrostatic patch fields which exist at the measured surface result in corrections which tend to increase the work function value. The measurements reported here are not corrected for patch fields and range in value from 7.1 eV to 8.7 eV for the (110) plane. Future measurements will employ a newly discovered technique involving a family of energy distribution plots which eliminates the correction for patch fields.

9425. **Translational diffusion in polymer solutions,** R. Zwanzig, *J. Chem. Phys.* **45,** No. 5, 1858-1859 (Sept. 1, 1966).

Key words: Diffusion coefficient; polymer; solution; theory.

Kirkwood's theory of the translational diffusion coefficient of a polymer molecule in solution is criticized. It is shown to give incorrect results, by a factor of 11/12, for a rigid ring-shaped polymer.

9426. **Ground state of bis(acetylacetonato) copper (II),** H. C. Allen, Jr., *J. Chem. Phys.* **45,** No. 2, 553-555 (July 15, 1966).

Key words: Bis(acetylacetonato) copper (II); bis(3-phenyl-2,4-pentanedionato copper (II); crystal spectrum; polarized spectrum.

Existing data on the polarized crystal spectrum of bis(acetylacetonato) copper (II) are interpreted. Through the use of a lower molecular symmetry than had previously been used, it is possible to present an interpretation consistent with that for the spectra of other bis copper (II) chelates.

9427. **A network-simulation approach to the railroad freight train scheduling and car sorting problem,** W. P. Allman, *Proc. 4th Intern. Conf. Operational Research, Boston, Mass., Aug. 29-Sept. 2, 1966,* (Arthur D. Little Inc., Cambridge, Mass., 1966).

Key words: Freight operations; GPSS; railroads; scheduling; SIMSCRIPT; simulation; sorting.

These interdependent questions must be answered simultaneously, and in accordance with overall operating objectives of the railroad interprise. Policies must be revised periodically when significant changes in demand traffic patterns occur.

The paper describes a simulation model which permits experimentation with various alternative railroads freight operating policies at a total-network level. The model has been constructed with the SIMSCRIPT simulation programming language. Model inputs include time-dependent freight car origin-destination demand data, train routes and schedules, yard sorting and operation policies, and assignments of cars to trains for hauling. Freight cars are sorted at yards, and picked up and dropped off by trains which haul them thru the network. Model outputs include several railroad operation performance measures such as origin-destination transit times, activity volumes, train lengths, delays incurred by cars at yard operations, and operating costs.

9428. **Mass flowmeters in cryogenic service,** W. J. Alspach, C. E. Miller, and T. M. Flynn, (Proc. ASME Flow Measurement Conf., Pittsburgh, Pa., Sept. 26-28, 1966), *Book, Flow Measurement Symposium,* pp. 34-56 (American Society of Mechanical Engineers, Pittsburgh, Pa., Sept. 1966); *Mech. Eng.* **89,** No. 5, 105-113 (May 1967).

Key words: Accuracy; calibration; commodity transfer; cryogenic; cryogenic processes; density; flowmeters; mass flow; mass flowmeters; performance results; propellant management; substitute fluid; volume flow.

This paper concerns cryogenic fluid mass flow measurement by a variety of techniques, including those that are available and those that are being developed. Attention is given to the principle of operation, performance results, and operational and design characteristics.

The problem of cryogenic fluid flowmeter calibration is examined and discussed with reference to available facilities, techniques, limitations, and accuracy. The problem of calibration for special cryogenic applications, such as slush hydrogen and cold gasses, where no calibration facilities are available is also examined. Inferred calibration from a substitute fluid calibration or design practices is also reviewed.

To improve the mass flow measurement of cryogenic fluids, discussions are directed towards measurement technique selection, density measurements for inferential mass systems, improvements in volumetric flow measurements, improvements in direct measuring mass flowmeters, and improvements in calibration.

9429. **Cryogenic coil for megajoule energy storage,** V. Arp, *Proc. Intern. Symp. Magnet Technology,* Ed. H. Brechna and H. S. Gordon, pp. 625-629, (U.S. Atomic Energy Commission, 1965).

Key words: Aluminum; cryogenic magnet; energy storage; induction coil; liquid hydrogen.

A liquid hydrogen cooled induction coil is being constructed for short time energy storage of $10^6$ joules. The coil is made of very pure aluminum having an electrical resistivity of about $3 \times 10^{-9}$ ohm cm at 20 °K. The coil parameters are dictated by its proposed use for the Army Missile Command, and are as follows: inductance of $50\mu$ henries, charging time of 10 seconds or less from zero to peak current of 200,000 amperes, and maximum terminal voltage during discharge of 12,000 volts. The coil will be housed in a non-metallic dewar, and powered from batteries. Details of the coil and cryostat design and electrical circuits will be discussed. The basic design is capable of being pushed to higher energy storage without major difficulty.

9430. **Electron microscopy and diffraction of synthetic corundum crystals. II. Dislocations and grain boundaries in impurity-doped aluminium oxide,** D. J. Barber and N. J. Tighe, *Phil. Mag.* **14,** No. 129, 531-544 (Sept. 1966).

Key words: Aluminium oxide; dislocations; electron microscopy; grain boundaries; impurities; sapphire.

Boules of aluminium oxide containing various impurities, grown by the Verneuil technique, have been examined by transmission electron microscopy. Most of the samples have dislocation densities ~6 x $10^5$ $cm^{-2}$, excluding grain boundaries. This is two orders of magnitude higher than that for comparable undoped crystals. There is a higher incidence of low angle boundaries and the characteristics of these are described. The samples rarely contain internal precipitates; furthermore, precipitates in sapphire do not normally create significant numbers of dislocations.

The interactions of a singularity with a basal network of dislocations with 1/3 $\langle 11\bar{2}0\rangle$ Burgers vectors are analyzed. The configuration is not consistent with the singularity being a $\langle 10\bar{1}0\rangle$ dislocation, but it can be explained by assigning the singularity a 1/3 $\langle 10\bar{1}1\rangle$ vector.

9431. **The determination of mercury in latex paints and paint films containing mercury fungicides,** H. W. Berger, *J. Paint Technol.* **38,** No. 498, 371-376 (July 1966).

Key words: Analysis; colorimetric; dithizone; paint film; fungicide; latex; mercury; paint.

A new method has been developed for the spectrophotometric analysis of mercury in latex paints. The method, based on the complexing of Hg(II) with diphenylthiocarbazone, can be used to assay the mercury in the whole paint, the dry film, and in commercial fungicides, as well as other industrial and agricultural materials. The procedure is rapid, requires only simple techniques, and is capable of an average accuracy of 1%. Inorganic pigments, and other components usually found in latex paints, do not interfere with the analysis.

9432. **Roofing research,** T. H. Boone, *Military Engr.* **58,** No. 385, 344-345 (Sept.-Oct. 1966).

Key words: Liquid-applied coatings; membrane movements; prefabricated sheets; radiative cooling; roofing research; solar heating.

The Building Research Division of the National Bureau of Standards has for many years studied roof systems, constituent materials and components. Highlights of the roofing research in the last five years and a brief resume of the results of this research are given. Description of some of the newly-developed roofing systems and the present status of roofing research are also discussed.

9433. **Adhesive bonding of various materials to hard tooth tissues. VI. Forces developing in direct-filling materials during hardening,** R. L. Bowen, *J. Am. Dental Assoc.* **74,** No. 3, 439-445 (Feb. 1967).

Key words: Adhesion; bonding; dental; filling materials; hardening; shrinkage; strain; stress; tensile.

Tensile forces will develop when dental filling materials shrink as they harden within a cavity, if there is bonding to the cavity walls. A test method was devised by which these forces could be measured. This was done by observing the loading required to maintain constant distance between two opposing walls (having known area) of an artificial cavity. If several broad assumptions are made, it can be estimated that a tensile stress of at least 49 kg/$cm^2$ (700 psi) at the walls of a cavity may develop during the hardening of a direct filling resin. The corresponding stress for a silicate cement would be about 35 kg/$cm^2$ (500 psi). Other direct filling materials were also investigated. The magnitude of the stress depended on the exact test method, the material, and other factors.

The strength of adhesive bonding between a direct filling material and the cavity walls of a tooth must exceed the tensile stresses that develop during the hardening of the filling material, if the bonding is to remain intact.

9434. **Dielectric constants of $PbMoO_4$ and $CaMoO_4$,** W. S. Brower and P. H. Fang, *Phys. Rev.* **149,** No. 2, 646 (Sept. 16, 1966).

Key words: Calcium molybdate; dielectric constant; lead molybdate; single crystal.

The dielectric constants $\epsilon'$ of $PbMoO_4$ and $CaMoO_4$ were measured at 24.5 °C in air. Two specimens of each orientation were measured. The average values and the deviations for the measured dielectric constants are as follows: $PbMoO_4$:$\epsilon' \| a$, 34.0±0.4; $\epsilon' \| c$, 40.6±0.2; $CaMoO_4$:$\epsilon' \| a$, 24.0±0.2; $\epsilon' \| c$, 20.0±0.2.

9435. **Measurement of thermal neutron flux,** R. S. Carter, C. O. Muehlhause, and V. W. Meyers, *IEEE Trans. Nucl. Sci.* **NS-14,** No. 1, 414-415 (Feb. 1967).

Key words: Absolute gamma ray source strength; black glass beads; thermal neutron flux.

A new technique has been developed for the measurement of thermal neutron flux. Small glass beads (~1 mm radius) are made black to thermal neutrons by the inclusion of $B^{10}$. In addition, a 1/v activator such as cobalt, dysprosium, or indium is incorporated in the glass to measure the fluence ($nvt$). Following activation over a measured time interval, the absolute source strength of a Co bead is determined by $\gamma$-$\gamma$ coincidence. The flux is directly proportional to the gamma ray source strength. The Dy and In beads are calibrated relative to a Co bead.

9436. **Collagen aggregation phenomena,** J. M. Cassel, *Biopolymers* **4,** 989-997 (1966).

Key words: Collagen; end-to-end bonding; hydrophobic bonding; lateral aggregation; native aggregation; temperature coefficient.

Three processes by which tropocollagen units associate to yield highly specific aggregates have been examined. From the temperature coefficients of the amounts aggregated it is concluded that the complex "native" aggregation is endothermic whereas both end-to-end and lateral aggregation are exothermic. These results combined with additional information lead to the conclusion that "native" aggregation is an entropy driven process in which hydrophobic bonding plays the dominant role. In contrast the reactions producing the lateral aggregate and the aggregate in which end-to-end bonding is dominant are electrostatically governed.

9437. **Glass research at the National Bureau of Standards,** G. W. Cleek, *Glass Ind.* **47,** No. 12, 663-669 (Dec. 1966).

Key words: Glass research; glass technology; properties of glass.

A general account of the research and development in glass technology at the National Bureau of Standards is presented. A brief history of the Bureau's interest in glass is given, followed by a description of the present effort on specific projects in the Inorganic Glass Section of the Inorganic Materials Division.

9438. **Effective charge carrier lifetime in silicon p-i-n junction detectors,** J. A. Coleman and L. J. Swartzendruber, (Proc. 10th

Scintillation and Semiconductor Counter Symp., Washington, D.C., Mar. 23-24, 1966), *IEEE Trans. Nucl. Sci.* **NS-13,** No. 3, 240-244 (June 1966).

Key words: Charge carrier lifetime; lithium-compensated silicon; semiconductor nuclear radiation detectors.

An estimate of the effective charge carrier lifetime can be obtained from a determination of the collection efficiency as a function of the transit time for charge carriers produced by incident short-range radiation in a p-i-n junction detector. The results of this method have the advantage of being independent of both the charge carrier mobility and the depletion depth of the detector. Effective lifetimes as low as a few microseconds ($\tau_e$) for electrons produced by natural alpha particles have been observed in several 2 mm thick lithium-compensated silicon detectors operating at room temperature. No significant bias dependent windows which might cause misleading interpretation of the results were observed. Window effects were investigated by measuring the changes in pulse height of detector output signals initiated by natural alpha particles incident on the detectors at angles up to 45 degrees. The electron lifetimes were observed to decrease when the detector was operated at liquid nitrogen temperature. The short effective lifetimes that can occur in lithium-compensated silicon set a lower limit on the field strengths that must be maintained for efficient charge collection in thick p-i-n junction detectors. Effective hole lifetimes can also be obtained using this technique but with the present geometry of lithium-compensated silicon detectors this measurement is more difficult if short-range particles are used. The effects of charge carrier lifetime and amplifier pulse rise and fall times on the observed radiation-induced pulse shapes are discussed.

9439. **Interface kinetics and the stability of the shape of a solid sphere growing from the melt,** S. R. Coriell and R. L. Parker, (Proc. Intern. Conf. Crystal Growth, Boston, Mass., June 20-24, 1966), *Crystal Growth, a Suppl. to J. Phys. Chem. Solids* **J3,** 703-708 (Pergamon Press Inc., New York, N.Y., 1967).

Key words: Crystal growth; diffusion; heat flow; interface; kinetics; morphology; sphere; stability.

The effects of linear interface kinetics and of square law interface kinetics on the stability of the shape of a sphere growing in a diffusion field are investigated theoretically. Slow interface kinetics can greatly enhance the stability, by several orders of magnitude in certain cases. The sphere can be stable even if its surface energy is zero. Numerical estimates are made for salol and for tin.

9440. **The ionization constant of deuterium oxide from 5 to 50°,** A. K. Covington, R. A. Robinson, and R. G. Bates, *J. Phys. Chem.* **70,** 3820-3824 (1966).

Key words: Deuterium oxide; heavy water; ionization constant; isotope effects.

Electromotive force measurements of a cell without liquid junction have been used to determine the ionization constant of deuterium oxide from 5 to 50°. The value found for p*K* at 25° is 14.955 (molality scale), 14.869 (molarity scale), and 16.653 (mole fraction scale). Enthalpy, entropy, and heat capacity changes for the dissociation process have been evaluated.

9441. **Mechanical relaxation in polychlorotrifluoroethylene,** J. M. Crissman and E. Passaglia, *J. Polymer Sci.* Pt. C, No. 14, 237-245 (1966).

Key words: Apparatus; isothermally crystallized sample; loss compliance; loss modulus; mechanical relaxation; polychlorotrifluoroethylene; quenched sample; storage modulus; tan δ; torsion pendulum; varying crystallinities.

Measurements of the viscoelastic functions $\Delta$, $G'$, $G''$, $J'$, and $J''$ as functions of temperature from −180 to +180 °C have been obtained, using a torsion pendulum apparatus, for several samples of polychlorotrifluoroethylene having widely different crystallinities as determined by density. The low crystallinity samples show two relaxations: a very broad one ($\gamma$) centered at about −35 °C which appears to be split into two processes, and one ($\beta$) at 84 °C. In the higher crystallinity samples, a third process ($\alpha$) appears at about 137 °C, and the high temperature side of the $\gamma$ relaxation peak is lower in magnitude as compared to the lower crystallinity specimens. For the $\beta$ peak, which is assumed to be associated with the glass transition, the peak value for $G''$ is essentially independent of crystallinity, while both $\Delta$ and $J''$ show decreases in magnitude with increasing crystallinity. The relationship between the magnitude of the relaxation peak and crystallinity, and dependence of this relationship upon the viscoelastic function chosen to characterize the relaxation are discussed.

9442. **Soft X-ray spectrum of Ni and comparison with photoemission and ion neutralization results,** J. R. Cuthill, A. J. McAlister, and M. L. Williams, *Phys. Rev. Letters* **16,** No. 22, 993-995 (May 30, 1966).

Key words: Ag; Cu; double electron photoexcitation; Ni; photoemission; soft X-ray spectrum.

The soft X-ray $M_{2,3}$ spectrum of Ni has been observed, and new features found. The spectrum agrees well with ion neutralization results on Ni, but disagrees sharply with the density of states deduced from the photoemission spectrum of Ni. A double electron photoexcitation process which removes this discrepancy is suggested and shown to fit the available photoemission data on Ni and Cu and Ag as well.

9443. **Molecular emission spectra in the soft x-ray region,** R. D. Deslattes and R. E. LaVilla, *Appl. Opt.* **6,** No. 1, 39-42 (Jan. 25, 1967).

Key words: Molecular energy levels; molecules; x-ray spectra.

Spectra from several chlorine-containing hydrocarbon molecules excited to x-ray fluorescence have been recorded by a double crystal spectrometer with high resolving power. This study focuses on the region near the occurrence of the transition $\rightarrow\beta_{1,3}(1s^{-1}\kappa 3p^{-1})$ in chlorine. Whereas the free atom spectrum (from a single vacancy process) consists of an unresolved spin-orbit doublet, e.g., in argon, the molecular spectra often contain several lines. In free atom spectra and in molecular spectra also, there are extra lines or unresolved multiplets (satellites) due to multiple vacancy processes. In this report, these satellite lines are experimentally sorted out of the spectra and the remaining emission peaks associated with possible final state configuration containing a vacancy, i.e., the electronic terms of the molecule.

9444. **Mossbauer spectrometry,** J. R. DeVoe and J. J. Spijkerman, *Anal. Chem.* **38,** 382R-393R (1966).

Key words: Chemical structure analysis; Mossbauer spectroscopy.

A review of the applications of Mossbauer spectroscopy to chemical analysis, and a bibliography of publications on these applications in 1965 are presented. The principle of the spectrometer as well as a discussion of errors associated with its use are described. Current theoretical interpretation of some aspects of the Mossbauer spectrum are discussed. Chemical structure analysis is the most prevalent application to date, and other applications, such as metallurgy and quantitative analysis appear to be promising.

9445. **Some relations for straight dislocation,** R. deWit, *Phys. Stat. Sol.* **20,** 567-573 (1967).

Key words: Continuum; crystal; defect; dislocation; displacement; interaction; isotropic; strain; stress.

Expressions are presented for the stress, strain, dilatation, and displacement due to a straight dislocation, as well as the force per unit length and the total force on a straight dislocation due to another straight dislocation. They differ from previous expressions in the literature in that they are given completely in tensor or vector notation. They are limited to the case of a *linear, isotropic, infinite* continuum.

9446. **The self-energy of dislocation configurations made up of straight segments,** R. deWit, *Phys. Stat. Sol.* **20,** 575-580 (Mar. 1967).

Key words: Continuum; crystal; defect; dislocation; energy; interaction; isotropic; straight.

Three general expressions are presented: the first is the interaction energy between two non-parallel straight dislocation segments, the second is the interaction energy between two parallel straight segments, and the third is the self-energy of a straight segment. These can be used to determine the total energy of any dislocation configuration made up of piecewise straight segments. They differ from previous expressions in the literature primarily in that they are given completely in vector notation and in that self-energy includes a core traction term. The expressions are limited to the case of a *linear, isotropic, infinite* continuum. As an example, the formulas are applied to the case of a stacking-fault tetrahedron.

9447. **Anomaly in Young's modulus and internal friction of $5SrTiO_3 \cdot 3La_{2/3}TiO_3$ below 100 °C,** R. W. Dickson, *J. Am. Ceram. Soc.* **49,** No. 11, 628 (Nov. 1966).

Key words: Internal friction; lanthanum titanate; phase change; resonance; strontium titanate; vacancies; Young's modulus.

A rapid decrease in Young's modulus with decreasing temperature suggests that some type of phase change may occur in $5SrTiO_3 \cdot 3La_{2/3}TiO_3$ near 80 °C despite the lack of evidence in x-ray patterns.

9448. **Effects of packing pressures on the properties of spherical alloy amalgams,** G. T. Eden and R. M. Waterstrat, *J. Am. Dental Assoc.* **74,** No. 5, 1024-1029 (Apr. 1967).

Key words: Adaptability; amalgams; dental amalgam; dentistry; mercury-silver alloys; packing pressure; particle size; silver-tin alloys; spherical alloy; spherical-alloy amalgam.

The properties of dental amalgams prepared from spherical-alloy particles are compared with the properties of amalgams prepared from irregularly shaped conventional alloy particles. The spherical-alloy amalgams were found to be as strong or stronger than the conventional amalgams and in addition the spherical alloy amalgams possess a superior property of "adapting" their shape to that of the cavity walls particularly when they are condensed under low packing pressure. The spherical alloy amalgams also are capable of retaining a greater fraction of their strength at low packing pressures where the conventional amalgams lose their strengths rapidly.

The use of spherical-alloy amalgams offers the dentist superior "adaptability" and better control over such variables as rate-of-hardening, setting expansion strength, carvability, mercury content, etc., through a more effective control of alloy particle size and shape.

9449. **A broad-line proton magnetic resonance study of cobalt tetracarbonyl hydride,** T. C. Farrar, F. E. Brinckman, T. D. Coyle, A. Davison, and J. W. Faller, *Inorg. Chem.* **6,** No. 1, 161-163 (Jan. 1967).

Key words: Bond length; broad-line; carbonyl; cobalt; cobalt tetracarbonyl hydride; hydride; nuclear magnetic resonance; proton.

The broad-line proton magnetic resonance spectrum of cobalt tetracarbonyl hydride, $HCo(CO)_4$, has been measured. The Co-H bond distance is determined to be 1.2 Å with an estimated overall uncertainty of ±0.1 Å. The use of the n.m.r. method for structural investigation of polycrystalline solids is discussed.

9450. **Proton broad-line n.m.r. study of $[^2H_6]$ dimethoxy$[^{11}B]$-borane,** T. C. Farrar, J. Cooper, and T. D. Coyle, *Chem. Commun.* **17,** 610-611 (1966).

Key words: Bond lengths; boron; broad-line; dimethoxyborane; hydride; nuclear magnetic resonance; proton.

The broad-line proton magnetic resonance spectrum of polycrystalline $H^{11}B(OCD_3)_2$ has been measured at 29.95 MHz from the melting point to −180 °C. The spectrum shows well-resolved fine structure arising from intramolecular dipolar coupling of the hydridic hydrogen with the $^{11}B$ nucleus. The boron-hydrogen distance is determined to be 1.25 Å with a standard deviation of 0.05 Å.

9451. **Initial kinetic parameters from thermogravimetric rate and conversion data,** J. H. Flynn and L. A. Wall, *J. Polymer Sci. Letters* **5B,** No. 2, 191-196 (Feb. 1967).

Key words: Energy of activation; initial kinetic parameters; non-isothermal kinetics; polyethylene; polymer degradation; stability of polymers; thermogravimetry.

A new method for determining the initial activation energy for a volatilization process is developed from the limiting characteristics of rate versus conversion plots and a few simple variants thereof. At low conversion, the energy of activation of linear polyethylene was $E(0.003<C<0.025;\ 630\ °K<T<680\ °K) \cong 36$ kcal/mol, while a sample preheated at 200 °C in a vacuum for an hour gave $E(0.003<C<0.04;\ 640\ °K<T<685\ °K) \cong 60$ kcal/mol.

9452. **Development of performance standards,** B. E. Foster, *Military Engr.* **58,** No. 385, 335-336 (Sept.-Oct. 1966).

Key words: Accelerated tests; bathtubs; external wall units; innovation; long-time behavior; performance standards.

The performance concept in building has been the subject of a great deal of discussion and study during the past several years. When applied to materials and components, difficulties arise in devising performance-type tests which will predict the probable life expectancy in a particular environment or application. A brief discussion of two projects undertaken by the Building Research Division of the National Bureau of Standards, one on external wall units and the other on bathtubs, in which important performance elements were identified, and performance-type tests recommended for all properties except those of anticipated long-time behavior illustrates the problem. The general present lack of satisfactory accelerated test procedures will require that for some time to come performance-type tests must be supplemented by technical judgement rendered by experts experienced in the properties of materials and their probable interactions.

9453. **Magnetic susceptibility of insulating and semiconducting strontium titanate,** H. P. R. Frederikse and G. A. Candela, *Phys. Rev.* **147,** No. 2, 583-584 (July 15, 1966).

Key words: Bandstructure; insulator; magnetic susceptibility; Pauli paramagnetism; semiconductor; strontium titanate.

The magnetic susceptibility of strontium titanate with and without charge carriers has been measured at 300, 78, and 4.2 °K. Insulating $SrTiO_3$ shows a magnetic moment, which is partly diamagnetic and partly (Van Vleck) paramagnetic. The free-carrier contribution is mainly paramagnetic because of the high density of states. As the concentration of carriers is increased the temperature dependence disappears. At the highest concentration (~6 x $10^{20}$/cc), pure Pauli paramagnetism is observed. The density-of-states effective mass at the bottom of the conduction band deduced from these measurements is $5m_0$, in good agreement with values from transport experiments.

9454. **Nucleation in polymers,** F. Gornick and J. D. Hoffman, *Ind. Engr. Chem.* **58,** No. 2, 41-53 (Feb. 1966).

Key words: Chain folding; crystal growth; crystallization kinetics; homogeneous nucleation; interfacial energy; nucleation; polychlorotrifluoroethylene; polyethylene; polymers; surface free energy.

This article is a review of current theories and experimental data on homogeneous nucleation and crystal growth with chain folding in linear polymers.

9455. **Determination of glycerol in paper,** E. L. Graminski and B. W. Forshee, *Tappi* **49,** No. 7, 324-326 (July 1966).

Key words: Animal glue; glucose; glycerol; mannitol; melamine resin; paper; sucrose.

Glycerol in paper can be determined by extraction with water and oxidation with sodium periodate in a slightly acidic medium. The formic acid produced during the oxidation is a measure of the glycerol present. Polyhydroxy alcohols and sugars having three or more adjacent hydroxy groups also produce formic acid when oxidized with periodate. The presence of these materials can be ascertained by determining the molar ratio of periodate consumed to the formic acid produced. If the molar ratio is less than 2:1 or the formic acid produced after a 60-minute oxidation is significantly higher than that produced after five minutes, interfering material is present. Information concerning the chemical nature of the interfering material may be obtained from the change in periodate/formic acid ratio between 5- and 60-minute oxidations.

9456. **Inversion temperatures and pressures for cryogenic gases and their mixtures,** R. D. Gunn, P. L. Chueh, and J. M. Prausnitz, *Cryogenics* **6,** No. 6, 324-329 (Dec. 1966).

Key words: Corresponding states; cryogenic gases; generalized inversion curve; Joule-Thomson coefficient; mixtures.

A generalized Joule-Thomson inversion curve has been obtained from volumetric data for gases with acentric factors less than 0.10. The curve is plotted in coordinates of reduced pressure and reduced temperature and a deviation function is provided for gases which, because of quantum effects, do not conform to classical corresponding states behavior. Semi-empirical mixing rules are recommended for calculating the inversion curve of gas mixtures. For two binary systems (hydrogen-methane and helium-nitrogen) it was found that at constant temperature, a plot of inversion pressure versus mole fraction goes through a strong maximum. Calculated results for mixtures compare favorably with the very limited experimental data now available.

9457. **The nucleation of Hg on W as observed by field-emission microscopy,** S. C. Hardy, (Proc. Intern. Conf. Crystal Growth, Boston, Mass., June 20-24, 1966), *Crystal Growth, a Suppl. to J. Phys. Chem. Solids* **C13,** 287-293 (Pergamon Press Inc., New York, N.Y., 1967).

Key words: Electron field emission; Hg on W; nucleation.

The nucleation of Hg from the vapor onto W has been studied under ultra-high-vacuum conditions in a field-emission microscope. A critical supersaturation for formation of nuclei is measured from 184 °K to 240 °K. Below 210 °K, the temperature dependence of the critical supersaturation data is found to fit the model of disc-shaped critical nuclei with no entropy of mixing contribution to their free energy of formation. At higher temperatures, the data indicate that nucleation occurs by the impingement of subcritical clusters.

9458. **Avalanche radiation from the bulk of long, thin, forward-biased $p^+$-$p$-$n^+$ silicon diodes,** G. G. Harman, *Appl. Phys. Letters* **9,** No. 5, 207-209 (Sept. 1, 1966).

Key words: Hot electrons; silicon diodes; visible radiation.

Avalanche radiation has been observed from the bulk of long, thin, forward-biased $p^+$-$p$-$n^+$ silicon diodes with applied field strengths as low as 1000 V/cm. At higher fields, surface arc erosion streaks occurred and these followed crystallographic plane directions rather than the applied field orientation. Possible explanations are given for the several effects that contribute to the observed phenomena.

9459. **Estimate of extrinsic stacking-fault energies from dislocation configurations,** W. F. Hartl, R. deWit, and R. E. Howard, *J. Appl. Phys.* **38,** No. 1, 1-4 (Jan. 1967).

Key words: Dislocations; extrinsic faults; silver-tin alloy; stacking fault energy.

In this paper we use straight-line models of observed extrinsic nodes to estimate extrinsic stacking-fault energies. Using isotropic elasticity theory and neglecting interactions, we find simple expressions for the energy in terms of the inscribed radii of the nodes. We apply the results to observed extended nodes in silver-8 at.% tin alloy and find a ratio of extrinsic to intrinsic stacking-fault energy of about 3.

9460. **Dissociation constant of morpholinium ion and related thermodynamic quantities from 0 to 50°,** H. B. Hetzer, R. G. Bates, and R. A. Robinson, *J. Phys. Chem.* **70,** No. 9, 2869-2872 (Sept. 1966).

Key words: Bases; dissociation constant; emf measurements; morpholine; morpholinium ion; thermodynamic quantities.

The thermodynamic dissociation constant of morpholinium ion ($MH^+$) at 11 temperatures from 0 to 50° has been determined from emf measurements of hydrogen-silver chloride cells without liquid junction. The dissociation constant ($K_a$) for the process $MH^+ + H_2O \rightleftharpoons M + H_3O^+$ is given as a function of $T$(°K) by the equation $-\log K_a = 1663.29/T + 4.1724 - 0.0042239T$. At 25°, $-\log K_a$ is 8.492, $\Delta H°$ is 39,030 joules mole$^{-1}$, $\Delta S°$ is $-31.7$ joules deg$^{-1}$ mole$^{-1}$, and $\Delta C_p°$ is 48 joules deg$^{-1}$ mole$^{-1}$.

9461. **Solid-vapor equilibrium in the system neon-methane,** M. J. Hiza and A. J. Kidnay, *Cryogenics* **6,** No. 6, 348-354 (Dec. 1966).

Key words: Low-temperature phase-equilibrium; methane; minimum gas phase equilibrium concentration; neon; neon-methane binary system; solid-vapor equilibrium.

Gas phase compositions in the solid-vapor region for the neon-methane system were measured at eight integral temperatures from 50 to 87 °K up to 100 atmospheres pressure. A flow system was used in which methane was evaporated into a stream of pure neon gas. The equilibrium methane content of the gas phase leaving the equilibrium cell was analyzed continuously with a hydrogen flame-ionization detector. A comparison of these data at 76 °K with data for the hydrogen-methane and helium-methane systems is made to show the relative non-ideality of the neon system. Theoretical calculations of the concentration minima for this system are in poor agreement with experimental values.

9462. **Analysis of the $\alpha$, $\beta$, and $\gamma$ relaxations in polychlorotrifluoroethylene and polyethylene: dielectric and**

**mechanical properties,** J. D. Hoffman, G. Williams, and E. Passaglia, *J. Polymer Sci.* Pt. C, No. 14, 173-235 (1966).

Key words: Annealing; chain fold; chain rotation; chain twisting; defect; dielectric relaxation; mechanical relaxation; polychlorotrifluoroethylene; polyethylene; polymer; semicrystalline; vacancy.

Theoretical models for the $\alpha_c$ and $\gamma_c$ relaxation effects found in chain-folded polymer crystals (single crystal mats and bulk) are presented, and compared with the available dielectric and mechanical loss data for polyethylene and polychlorotrifluoroethylene. Details of morphology and crystal structure that can be varied by crystallization and annealing procedures, e.g., roughness of chain-folded surfaces, number of intercrystalline links and cilia, number of chain-end defects and dislocations, and the existence of the extended-chain phase, are brought into the discussion. The $\alpha_c$ process, which consists of two overlapping mechanisms, is a result of motions of chain folds, and reorientation (with translation) of chains in the interior. (Chain twisting also occurs for long chains. The theory connects the data on the *n*-paraffins and their polar derivatives (n-ketones, esters, ethers) with the results on polymers: the common feature is the chain reorientation and twisting process. A new theory of chain twisting is introduced. The $\gamma_c$ relaxation is a result of reorientation of chains in a "loose" chain-end induced defect (a vacancy row) in the polymer crystal. When the effect of chain twisting is included, the theory successfully predicts the unusually broad and asymmetric loss curve found in the polymer, and is consistent with experimental activation energies.

The $\beta$ relaxation arising in the amorphous component of PCTFE is analyzed, and its upward shift in temperature with increasing crystallinity discussed in terms of the Adam-Gibbs theory of relaxation in the glassy state. The $\gamma_a$ amorphous relaxation, and the δ relaxation which is found at cryogenic temperatures, are also discussed.

9463. **Condensation of dry air on a liquid hydrogen cooled surface in the pressure range $10^{-3}$ to 10 torr (Knudsen number of $10^{-4}$ to 1),** J. Hord, *Cryogenics* **6,** No. 5, 285-293 (Oct. 1966).

Key words: Air collector; air condensation; air sampling; air solidification at 20 °K; cryodeposit; cryodeposit surface temperature; cryopumping; cryopumping air at 20 °K in the transition pressure regime; geysering; heat transfer to air condensing at 20 °K.

The rate of condensation of dry air on a liquid hydrogen cooled surface has been determined experimentally and compared with analytical predictions. Free molecule flow theory appears adequate for high conductance systems at bulk air pressures up to $10^{-1}$ torr. At higher pressures this formulation predicts condensation rates which are too large. Continuum bulk flow theory and free molecule flow theory agree fairly well throughout the pressure range investigated; however, bulk theory is more compatible with experiment. Theoretical and experimental condensation rates are presented as a function of air bulk pressure and cryodeposit (solid air frost) surface temperature. Surging (slug flow) of static liquid hydrogen refrigerant inside small bore tubes was experimentally observed and is presented as a function of heat flux. The liquid hydrogen was vented to the atmosphere from a tube designed to provide 0.33 g acceleration along the tube axis.

9464. **Kinetics of solute-enhanced diffusion in dilute face-centered-cubic alloys,** R. E. Howard and J. R. Manning, *Phys. Rev.* **154,** No. 3, 561-568 (Feb. 1967).

Key words: Correlation factors; diffusion; dilute alloys; impurities; jump frequencies; solute atoms; vacancies.

A theory of the effect of solutes on solvent self-diffusion in dilute f.c.c. alloys is given based on the model of nearest-neighbor interactions between solute impurities and vacancies. The parameters of the theory are the four vacancy jump frequencies in the neighborhood of an impurity and the vacancy jump frequency in the pure crystal. No assumptions are made about the relative magnitudes of these frequencies. This distinguishes the present theory from previous theories based on the same model. The theory is used to deduce for each of nine dilute Ag-based alloys sets of jump frequency ratios (and corresponding impurity correlation factors) that are consistent with measured values of the solute enhancement coefficient and of the impurity diffusion coefficient. The desirability of isotope effect measurements to determine the impurity correlation factors is emphasized.

9465. **Moisture permeation of leather and plastics used in shoes,** J. R. Kanagy, *J. Am. Leather Chemists' Assoc. Tech. Note* **LXII,** No. 2, 115-122 (Feb. 1967).

Key words: Absorption, water; adsorption, water vapor; leather; permeation; water vapor permeability.

Data are given on moisture permeation of leather and plastics exposed both to water and water vapor. The rate of moisture permeation of some plastics is equivalent to that of some leather now used. The permeation of moisture through leather depends upon the tannage, and by adopting the proper tannage could be greatly increased. However, leathers that are highly permeable to water are not practical for use in shoes, and in this respect man-made materials will undoubtedly be able to compete with leather. Other properties, such as insulation and ability to mold to the feet, are characteristics which will continue to make leather a preferred material for shoes.

9466. **Note on the variation of the results of the Mullen burst test over the area of a hide,** J. R. Kanagy, *J. Am. Leather Chemists' Assoc. Tech. Note* **LXII,** No. 1, 63-67 (Jan. 1967).

Key words: Burst of leather; extension; grain-crack; Mullen test.

Variation of the Mullen test results was determined over hide by cutting the entire area into 3 by 3 inch pieces and testing each of the specimens. Percentage stretch with increase in load was determined, and the point at which grain-crack occurred was noted. Grain-crack is prevalent in specimens from locations on the butt of the hide. In this position stretch increases rapidly with load because of the physical structure of the fibers. Ninety percent of the specimens which cracked were from the small area of the butt which constituted three to four square feet. The other areas of a full-grown cattle hide were almost entirely free of grain-crack when subjected to 600 pounds in the Mullen tester.

9467. **Optical power increase in GaAs laser diodes coated with reflecting aluminum silicone mixture,** H. K. Kessler, *Proc. IEEE Letter* **55,** No. 1, 99-100 (Jan. 1967).

Key words: Aluminum-silicone compound; GaAs lasers; heat sink; optical power.

GaAs laser output power has been increased by using the reflectance of an aluminum-silicone mixture coated on a laser diode. After such application, the light output increased from one side by 50 percent, and better heat dissipation from the diode was observed.

9468. **Surface aspects of the thermal degradation of GaAs *p-n* junction lasers and tunnel diodes,** H. Kessler and N. N. Winogradoff, *IEEE Trans. Electron. Devices* **Ed-13,** No. 10, 688-691 (Oct. 1966).

Key words: Degradation; gallium arsenide; lasers; light emission; surface effects; tunnel diodes.

Owing to the similarity of the junction widths and doping levels in epitaxially formed GaAs lasers and conventional tunnel diodes, the gradual degradation of the latter under use might be expected to be intensified in the case of lasers operating under high duty cycle or CW conditions.

It was found that the current-voltage characteristics of both the lasers and tunnel diodes underwent considerable thermal degradation even when no bias was applied, and that the degradation was limited to *surface* or "junction edge" effects.

The degradation of the current-voltage characteristic was correlated with degradation in the light output under forward bias. It was concluded that degradation under forward bias was also a surface effect induced by heating rather than by deterioration of the junction in the bulk, as commonly believed. Methods of controlling the degradations are discussed.

9469. **Ellipsometric-potentiostatic studies of iron passivity. I. Anodic film growth in slightly basic solutions,** J. Kruger and J. P. Calvert, *J. Electrochem. Soc.* **114,** No. 1, 43-49 (Jan. 1967).

Key words: Anodic oxidation; ellipsometry; iron; iron oxide films; kinetics; passivity; potentiostat.

Cathodically reduced iron was anodically oxidized at potentials in the passive region of the anodic polarization curve in slightly basic sodium borate-boric acid solutions by means of a potentiostat. The kinetics of film growth were studied using an ellipsometer coupled with a fast recording technique, which enabled a determination of the rate of film formation for times less than 1 sec. This study of the kinetics of film growth using a nonelectrochemical technique agreed with kinetic results based on total charge measurements. Three stages of growth were detected: (1) First stage – growth limited by a diffusion process in the solution; (2) Second stage – start of limitation of growth by the film involving the combination of several processes difficult to characterize by any rate law; (3) Third stage – growth obeying either a logarithmic or inverse logarithmic rate law. The latter was found to imply that the passive film consisted of an outer layer poorly conductive for electrons.

9470. **Pyroelectric effect in bone and tendon,** S. B. Lang, *Nature* **212,** No. 5063, 704-705 (Nov. 12, 1966).

Key words: Bone; collagen; hydroxyapatite; piezoelectricity; pyroelectricity; tendon.

The pyroelectric coefficients (at constant stress) of one of the phalanges, the femur, and the hoof tendon of a cow were measured. The coefficients, which ranged from 2.5 to $4.1 \times 10^{-13}$ coulomb $cm^{-2}$ $°C^{-1}$ over the temperature span, −35 to 60 °C, were the smallest yet measured in any material. The results indicate that the collagen of bone and tendon is responsible for both the piezoelectric and pyroelectric effects. The pyroelectric effect in bone and tendon is probably too small to be of physiological significance.

9471. **Remote positioner for rotary switches,** S. B. Lang and A. M. Gray, *Rev. Sci. Instr.* **37,** No. 6, 799-801 (June 1966).

Key words: Remote positioner; rotary switches; vibrating-reed electrometer.

A remote positioner for rotary switches was designed for use on a vibrating-reed electrometer to provide automatic range switching between two preselected levels. The positioner consisted of a bi-directional rotary solenoid motor, driven by a capacitor pulse-counter circuit (diode pump), and was controlled by three rotary switch decks. The positioner was mounted external to the electrometer. The positioner can be used for automatic range switching on many types of electronic apparatus.

9472. **Kinetics of growth of multicomponent chains,** J. I. Lauritzen, Jr., E. A. DiMarzio, and E. Passaglia, *J. Chem. Phys.* **45,** No. 12, 4444-4454 (Dec. 15, 1966).

Key words: Composition; growth rate; kinetics; multicomponent; steady-state.

A theory is presented by which the rate of growth and composition (including all pair and higher distributions) of a chain growing in a multicomponent system may be calculated. Each position in the chain may be occupied by any of the components of the system. Only nearest-neighbor interactions are assumed and the rate constants $\alpha^{ij}$ for addition of Species *j* to a chain ending in Species *i*, and $\beta^{ij}$, for the removal of Species *j* from a chain ending in *i,j* are assumed known and independent of chain length, except for those referring to the first step of the chain, which are distinct. The full kinetic equations for the growth of such chains are formulated and a solution obtained for steady-state conditions. It is shown that when the matrix of $\alpha^{ij}/\beta^{ij}$ is indecomposable and primitive a solution of the equations which is independent of chain length always exists for sufficiently long chains and computational methods for obtaining this solution for a relatively large number of components (of the order of 10) are presented. In addition, the relationship of $\alpha^{ij}/\beta^{ij}$ to the energetics of the system is derived.

9473. **Chlorine K$\beta$ x-ray emission spectra from several chlorinated hydrocarbon and fluorocarbon molecular gases,** R. E. LaVilla and R. D. Deslattes, *J. Chem. Phys.* **45,** No. 9, 3446-3448 (Nov. 1, 1966).

Key words: Chlorinated molecular gases; chlorine; K$\beta$ x-ray emission.

Emission profiles have been obtained in x-ray fluorescence for the four chlorinated derivatives of methane ($CH_3Cl$, $CH_2Cl_2$, $CHCl_3$, $CCl_4$), and five chlorinated fluoromethanes ($CF_3Cl$, $CF_2Cl_2$, $CFCl_3$, $CHFCl_2$, $CHF_2Cl$) in the gas phase. The chloromethanes contain two prominent lines whereas the chlorofluoromethanes have multiplet structures up to four lines. These structures are interpreted in terms of the molecular orbital determined final state hole energies.

9474. **Electronic data processing in urban tranportation planning,** B. M. Levin and R. E. Schoefer, (Proc. Second Annual Conference on Applications of E.D.P. Systems for State and Local Government, Apr. 1-2, 1966, New York, N.Y.), *Book, The Large-Scale Public E.D.P. System: Its Problems and Prospects,* pp. 169-177 (University of New York, N.Y., 1966).

Key words: Data processing; systems analysis; transportation planning; urban transportation.

The goal of urban transportation planning is to develop a plan for an efficient, balanced transportation system for an urban area – one which will promote a desirable pattern of human activities. While the process has been standardized to some extent, each study must nevertheless acquire and manage a massive amount of information about the particular region with which it is concerned. From this information, models which can be used to predict future land use patterns, travel demands, and the workings of the transportation system are developed and calibrated. Using computerized versions of these models, transportation planners have the capability to propose and test a large variety of future transportation systems, so that one which is well-suited to the future needs of the urban area can be found.

9475. **Structural interpretation of immiscibility in oxide systems. IV. Occurrence, extent, and temperature of the monotectic,** E. M. Levin, *J. Am. Ceram. Soc.* **50,** No. 1, 29-38 (Jan. 1967).

Key words: Borates; glassformers; immiscibility; liquid immiscibility; modifiers, network; oxide systems; silicates.

Liquid immiscibility data in known binary oxide systems are analyzed in relation to three fundamental aspects. Occurrence of immiscibility in glassforming systems is related to differences in ionic field strengths or electrostatic bond strengths between the network cation with oxygen and the modifier cation with oxygen. If this difference is either too small or too large, immiscibility will not be present. Analysis also indicates that immiscibility is not to be expected in binary phosphate and vanadia systems. Factors governing the extent of immiscibility are essentially unrelated to its occurrence; and in borate and silicate systems, immiscibility is inversely correlated with the number of oxygens per modifier cation in the modifier rich liquid. Temperature of the monotectic almost always lies between the melting point of the glassformer and the first compound beyond the immiscibility gap. Properties of the monotectic, such as, the primary phase under the two liquids and location of the eutectic, are fixed according to whether the monotectic temperature is above or below the m. pt. of the glassformer. Principles of immiscibility are summarized.

9476. **The system $Sc_2O_3$-$B_2O_3$,** E. M. Levin, *J. Am. Ceram. Soc.* **50,** No. 1, 53-54 (Jan. 1967).

Key words: Boric oxide; liquid immiscibility; oxide systems; phase diagram; scandium oxide.

The phase diagram of the system $Sc_2O_3$-$B_2O_3$ has been determined experimentally, by the "quenching" technique. The system is characterized by a single binary compound, $ScBO_3$, melting congruently at 1610 °C and by a region of liquid immiscibility extending at 1526 °C from almost pure $B_2O_3$ to 34.0 mol.% $Sc_2O_3$. Immiscibility from qualitative and quantitative standpoints is consistent with the previously elucidated structural interpretation of immiscibility.

9477. **Analysis of lanolin in soap,** F. J. Linnig, *Soap Chem. Specialties* XVLL, No. 7, 55-57 (July 1966).

Key words: Borax; ion-exchange resin; lanolin, soap.

A new method has been developed for the determination of lanolin in lanolin-borax-soap mixtures. A mixed cation-anion exchange resin is used to remove the soap and borax from an aqueous solution of the whole sample. The resin is separated by filtration and washed with an organic solvent to remove lanolin. The solvents are evaporated, and the residue weighed as lanolin. This procedure is simpler and more rapid than the present method, and should be more accurate.

9478. **Embrittlement of high strength AISI 4340 steel in boiling NaCl solution,** H. L. Logan and J. M. Wehrung, *Corrosion* **22,** No. 9, 265-269 (Sept. 1966).

Key words: Boiling sodium chloride solution; delayed failure; high strength steel; hydrogen diffusion; hydrogen embrittlement; internal initiation; stress corrosion.

The resistance of high strength AISI 4340 steel tubing, quenched in oil and tempered to 425 °F, to corrosive media has been investigated. The exterior surface of the specimen was exposed to boiling NaCl, the interior cavity was evacuated, and the specimen was subjected to a tensile stress. Specimens failed, with little evidence that cracking was developing, after several hours exposure and after hydrogen had penetrated through the specimen wall. The appearance of the initial fracture and its mode of development indicate that it originated within the specimen wall. The data indicate that failure resulted from hydrogen embrittlement.

9479. **Stress-corrosion cracking of cold-reduced austenitic stainless steels,** H. L. Logan and M. J. McBee, *Mater. Res. Std.* 7, No. 4, 137-145 (Apr. 1967).

Key words: Atmospheric corrosion tests; chemical attack; cold working; corrosion; cracking; stainless steels; steels; stress corrosion.

The effects of specimen orientation with respect to the direction of rolling or prior rolling on the susceptibility to stress-corrosion cracking in a boiling $MgCl_2$ solution were determined for both annealed and cold-reduced types 301, 304, 310, and 321 stainless steels. Threshold stresses for the most susceptible orientations were determined in a boiling 0.5 *N* NaCl, 0.1 *N* $NaNO_2$ solution to be 60 to 110 percent of the yield strengths of the materials. None of the steels cracked in a marine atmosphere during 15 months' exposure stressed at 90 percent of their yield strengths. The effects on the threshold stresses of varying amounts of cold work differed from steel to steel and are reported. The effects of internal stress patterns and welding were also investigated for some of these steels and are described.

9480. **Phase relations between $Cr_2O_3$ and $IrO_2$ in air,** C. L. McDaniel and S. J. Schneider, *J. Am. Ceram. Soc.* **49,** No. 5, 285-286 (May 1966).

Key words: $Cr_2O_3$-$IrO_2$ system; dissociation; phase relations; platinum metal oxides; solid solution.

A study has been made by X-ray diffraction analysis of the reactions that occur in an air environment between $Cr_2O_3$ and Ir or $IrO_2$. In air Ir oxidizes at low temperatures to form $IrO_2$ which in turn dissociates at 1020 °C. The pseudobinary system $Cr_2O_3$-$IrO_2$ contains a quasi-solid solution region existing from 100 mole % $IrO_2$ to approximately 21 mole % $Cr_2O_3$ with a maximum dissociation temperature at 1040 °C. Up to at least 2100 °C no reaction occurred between $Cr_2O_3$ and Ir.

9481. **Emission spectrometry,** M. Margoshes and B. F. Scribner, *Anal. Chem.* **38,** No. 5, 297R-310R (Apr. 1966).

Key words: Atomic absorption spectrometry; atomic emission spectrometry; atomic fluorescence spectrometry; flame photometry; spectroscopy.

The literature of analytical interest in atomic emission spectrometry, flame photometry, and atomic absorption spectrometry is reviewed for the years 1964-65. The topics included are books and reviews, spectral descriptions and classifications, instrumentation, excitation, standards, calibration, and analytical applications. Literature citations total 351.

9482. **Chemical substructure searching with linear notations,** B. A. Marron, G. R. Boltosky, and S. J. Tauber, *J. Chem. Doc.* **6,** 92-95 (May 1966).

Key words: Chemical; computers; Hayward notation; information retrieval; linear notation; structures; substructure searches.

An experimental computer system was developed that performs chemical structure and substructure searches directly on linear notations.

9483. **Comments on "Nature of the critical nucleus in heterogeneous vapor-solid nucleation",** A. J. Melmed and S. C. Hardy, *Surface Sci.* **6,** No. 4, 481-482 (April 1967).

Key words: Critical nucleus; field-electron emission microscopy; heterogeneous nucleation; vapor deposition.

It is shown that a recent field-electron-emission microscope experiment was significantly misinterpreted and that, therefore, the conclusions cannot be considered meaningful.

9484. **The structure of field-evaporated hexagonal close-packed metal surfaces: rhenium and ruthenium,** A. J. Melmed, *Surface Sci.* **5,** No. 3, 359-379 (Nov. 1966).

Key words: Field evaporation; field ion microscopy; hcp metals; surface structure.

Field-ion micrographs of field-evaporated ruthenium are analyzed and compared with similar micrographs of rhenium.

Certain surface topological features appearing in Ru at 21 °K and 77 °K do not appear in Re at these same temperatures, although the metals are both hcp. The Ru field-evaporated surface clearly develops an exposed A,B,A,B,... sequence, giving half the number of distinguishable net plane edges, in the same crystallographic regions. The difference is discussed in terms of geometric and electronic factors which influence the field evaporation process.

9485. **Determination of the composition of complexes and their instability constant by calorimetry. II. The complex in fused potassium chloride and cadmium chloride,** W. H. Metzger, Jr., A. Brenner, and H. I. Salmon, *J. Electrochem. Soc.* **114,** No. 2, 131-138 (Feb. 1967).

> Key words: Calorimeter; calorimetry; complex ion; enthalpy determination; KCl-$CdCl_2$ system; molten salts.

A new method of determining the composition of complexes in solution and their equilibrium constant has been developed which is based on the determination of the partial molal heat effect developed when a small increment of each salt is added in turn to a series of mixtures covering the whole range of composition. The method was applied to the molten KCl-$CdCl_2$ system which was shown to contain the 1:1 complex with an instability constant of 0.32 at a temperature of 600 °C and 780 °C. A calorimeter was developed which permitted the addition of the increments of salt to the molten mixture while the latter was continually stirred.

9486. **Analyzing liquid $H_2$ with NMR,** C. E. Miller, W. J. Alspach, and T. M. Flynn, *Cryogenic Engr. News* **1,** No. 8, 66 (June 1966).

> Key words: Analyzer; cryogenics; hydrogen; instrument; instrumentation; liquefier; liquid hydrogen; measurement; nuclear spin relaxation time; ortho-para; relaxation time; $T_1$.

The nuclear spin relaxation time ($T_1$) of liquid hydrogen is shown as a function of the ortho-para composition of the fluid. A scheme is suggested whereby an ortho-para analyzer might be made which depends upon this fact. Such an instrument would have fast response, not depend on a reference gas, and be useful under flowing (dynamic) conditions.

9487. **Fracture topography of brittle polymers,** S. B. Newman, *Polymer Engr. Sci.* **5,** No. 3, 159-165 (July 1965).

> Key words: Brittle polymers; fracture topography; kinetics; polymeric solids; primary fracture front; topography.

Fracture surfaces record the kinetics of failure at two levels in the structure of polymeric solids. The first is evidenced by the formation of geometric markings resulting from the interaction of the primary fracture front with secondary fractures developing radially just ahead of the primary fracture. These markings are often visible to the unaided eye and have minimal dimensions in the micron range. The second fracture phenomenon appears to involve the orientation of molecular chains or bundles. Such orientation manifests itself in the interference-color producing film found on the fracture surfaces of poly(methylmethacrylate) and polystyrene. It is also apparent in the free or adherent film found on the surfaces of large fractured crazes. Some evidence is presented for the existence in these films of chain bundles 30A or less in diameter. Similar mechanisms are apparently operating in the production of "craze matter" and of fracture surface films.

9488. **Reflection of soft x-rays by organic fibers,** S. B. Newman, *J. Appl. Polymer Sci.* **10,** No. 12, 1929-1935 (1966).

> Key words: Fibers; microfocus tubes; microradiography; nylon; polyacrylonitrile; polyamides; reflection of x-rays; soft x-rays; x-rays.

An artifact observed in point projection microradiographs of polymeric fibers and filaments obtained with 8 A x-rays is recorded and described. The phenomenon has been related to fiber-beam geometry and the high reflection efficiency of soft x-rays for these materials.

9489. **Kinetics and statistics of structural changes in polyacrylonitrile,** K. Noh and H. Yu, *J. Polymer Sci. Letters* **4B,** No. 10, 721-726 (Oct. 1966).

> Key words: Cyanide groups; initiation; isolation; naphthylidiene ring; polyacrylonitrile; propagation.

The structural changes attending the heat treatment of polyacrylonitrile at 170 °C~220 °C were analyzed on the basis of the naphthylidiene type ring formation. The kinetics of the ring formation was found to be first order with respect to cyanide groups along the polymer chain. About 20% of the cyanide groups remain unreacted irrespective of the heating temperature. The observed first order kinetics is consistent with the statistical analysis of the ring formation mechanism which is well established in the literature.

9490. **Galvanic pitting in metallic coatings,** F. Ogburn and M. Schlissel, *Plating* **54,** No. 1, 54-62 (Jan. 1967).

> Key words: Corrosion; corrosion currents; electroplating; galvanic corrosion; pitting; pitting corrosion.

An electrolytic cell is described which simulates a corrosion pit extending through a metal coating and permits measurement of the cell currents. Such cells were used to investigate the galvanic currents between coatings of chromium, copper, and nickel and substrates of zinc, iron, nickel, and copper. The investigation included outdoor salt spray and corrodkote exposures; and determinations of the effects of anode size, depth of electrolyte, and proximity of a second anode on cell currents. An equation for the cell current as a function of the cell parameters is discussed and compared with experiments.

9491. **Flow properties of aqueous suspensions containing kaolins of varying degrees of crystallinity,** W. C. Ormsby and J. H. Marcus, *J. Am. Ceram. Soc.* **50,** No. 4, 190-195 (Apr. 1967).

> Key words: Cation exchange capacity; cone-plate viscometer; crystallinity; flow properties; kaolins; surface area.

A study was made of the influence which varying degrees of crystal perfection of several Georgia kaolins had on the flow properties of aqueous systems containing these clays. The fractionated clay samples were characterized with respect to clay mineral composition, crystallinity, surface area, and cation exchange capacity. A recording Ferranti cone-plate viscometer equipped with truncated cones was used to examine the clay-water mixtures under a variety of experimental conditions. Emphasis was placed on high shear-rate measurements of systems of intermediate water content.

A comparison of results for bulk samples and fine particle-size fractions of different clays showed a general qualitative correlation between viscosity (or consistency) and degree of crystallinity. In these samples, which were usually pseudoplastic, the viscosity tended to increase with decrease in crystallinity. Coarse particle-size fractions of the various clays exhibited essentially Newtonian behavior while samples of intermediate particle size and relatively good crystallinity exhibited dilatancy. The extent of dilatancy was usually a function of the degree of crystallinity.

The viscosity of the fine particle-size fractions of a single, well-crystallized clay, which exhibited an apparent increase in crystallinity with decrease in particle size, increased as the particle size decreased. This correlation between viscosity and particle size was also noted for the fine fractions of a poorly crystallized clay in which the crystallinity was essentially independent of the particle size.

In general, results indicated that dilatant and associated properties were controlled by the degree of crystal perfection whereas the viscous and plastic properties, at a given water content, were generally dependent upon the particle size.

9492. **Dissociation of acetic acid-$d_4$ in deuterium oxide from 5 to 50° and related isotope effects,** M. Paabo, R. G. Bates, and R. A. Robinson, *J. Phys. Chem.* **70,** 2073-2077 (1966).

Key words: Acetic acid-$d_4$; acid-base; deuterium oxide; dissociation constants; emf; ionization; isotope effects; thermodynamics; weak electrolytes.

The dissociation constant of acetic acid-$d_4$ ($CD_3COOD$) in deuterium oxide ($D_2O$) has been determined by the emf method at ten temperatures from 5 to 50°. From the variation of the dissociation constant with temperature, the changes of enthalpy, entropy, and heat capacity have been derived. The four dissociation processes, namely those for ordinary acetic acid in ordinary water, for deuterioacetic acid in ordinary water, and for these two acids in deuterium oxide, are compared.

9493. **Dissociation of 4-aminopyridinium ion in 50 weight percent methanol – water and related acidity functions from 10° to 40 °C,** M. Paabo, R. A. Robinson, and R. G. Bates, *Anal. Chem.* **38,** No. 11, 1573-1575 (Oct. 1966).

Key words: Acid-base equilibria; aminopyridine; dissociation constant; electrolytic dissociation; methanol-water solvents; thermodynamics.

The dissociation constant of 4-aminopyridinium ion in 50 wt.% methanol-water has been determined by the electromotive force method from 10° to 40 °C. The pK value at 25 °C is 8.520 compared with 9.114 in water. The changes in free energy, enthalpy, and entropy in the dissociation process have been calculated. Values of $p(a_H\gamma_{Cl})$ and $pa_H{}^*$ are given for buffer solutions containing equimolal amounts of 4-aminopyridine and its hydrochloride.

9494. **Bonding porcelain teeth to acrylic resin denture bases,** G. C. Paffenbarger, W. T. Sweeney, and R. L. Bowen, *J. Am. Dental Assoc.* **74,** 1018-1023 (Apr. 1967).

Key words: Bonding; coupling agent; denture; plastic; porcelain adhesion; resin; silane; teeth.

The chemical bonding of porcelain teeth to both cold- and heat-curing denture bases of acrylic resins was accomplished by the use of a silane coupling agent, gamma-methacryloxypropyltrimethoxysilane. In tension the procelain-resin interface did not rupture – invariably the teeth did. Untreated teeth showed no measurable bonding to the resin. Because of a lack of adhesion between porcelain teeth and acrylic resins the design of most current porcelain teeth provide for mechanical locking using metal pins or undercut wells and canals (diatoric form). These designs weaken the teeth unduly and can be eliminated by the use of a solid tooth which has been treated with an appropriate silane. The bonding strengthens the denture since it makes the effective cross-sectional area greater and prevents seepage between the tooth and the plastic and so aids oral hygiene and esthetics.

9495. **Recent advances in U.S.A. research on dental amalgams and possible applications,** G. C. Paffenbarger, *Intern. Dental J.* **16,** No. 4, 450-465 (Dec. 1966).

Key words: Amalgam; dental; research.

Current research on dental amalgam in the United States is developing information regarding the extrusion of amalgam restorations from cavities; the desirability of low mercury-to-alloy ratios; the design of universal technics for mixing and compacting; the effect of residual mercury content; the relation among compressive, tensile and transverse strengths; the phases present in the hardened amalgam; corrosion; and the advantages of amalgam made from spherical alloy powder.

9496. **Growth of calcium molybdate crystals by a temperature-gradient zone-melting technique,** H. S. Parker and W. S. Brower, (Proc. Intern. Conf. Crystal Growth, Boston, Mass., June 20-24, 1966), *Crystal Growth, a Suppl. to J. Phys. Chem. Solids* **E-12,** 489-491 (Pergamon Press Inc., New York, N.Y., 1967).

Key words: Calcium molybdate; crystal growth; lithium sulfate; single crystals; temperature gradient zone melting; traveling solvent.

Calcium molybdate crystals were grown using the temperature gradient zone melting technique. Lithium sulfate was used as flux and growth temperatures were in the 830-960 °C temperature range. Initial zone thicknesses ranged from about $1.3 \times 10^{-3}$ cm to $7.0 \times 10^{-2}$ cm, and regrowths of from 0.4 to 1.2 mm were obtained during heatings of 48-96 hours.

9497. **Galvanic corrosion of metals in cementing materials,** J. W. Pitts, *Military Engr.* **59,** No. 387, 40-41 (Jan.-Feb. 1967).

Key words: Aluminum conduit; calcium chloride; concrete; corrosion in concrete; corrosion in plaster; dissimilar metals; galvanic corrosion; gypsum plaster.

A brief discussion is presented of some corrosion problems that have developed in recent years resulting from the use of dissimilar metals embedded in portland cement concrete and gypsum plaster. It is shown how dissimilar metals embedded in such cementing materials can form short-circuited galvanic cells and how corrosion of the anodes has led to failures of both steel-reinforced concrete containing aluminum conduit and of gypsum plaster-metal lath systems in which copper tubing was embedded. Examples of failures are cited. Some of the variables that affect the degree of corrosion are discussed and some general precautionary measures are recommended.

9498. **Thermal insulation in buildings,** F. J. Powell, *Military Engr.* **58,** No. 38, 275-276 (July-Aug. 1966).

Key words: Indoor thermal environment; insulated construction; insulation research; thermal building design; thermal insulation; thermal performance standards.

The role of thermal insulation in the design of a building is presented from the viewpoint of the engineer. Presently used design procedures and other limitations, environmental and applications factors that influence the performance of a thermal design and some current research problems that involve insulated constructions are discussed. The benefits from the use of thermal insulation and their importance to a nation are given.

9499. **The crystal and molecular structure of dichloro(1,10-phenanthroline)zinc,** C. W. Reimann, S. Block, and A. Perloff, *Inorg. Chem.* **5,** No. 7, 1185-1189 (July 1966).

Key words: Crystal structure; dichloro(1,10-phenanthroline) zinc; molecular structure; tetrahedral.

Crystals of dichloro(1,10-phenanthroline)zinc are monoclinic with four molecules in a unit cell of dimension $a = 9.73$, $b = 15.67$, $c = 7.97$ Å, $\beta = 101° 5'$, space group $P2_1/n$. Three-dimensional data were used, and the structure was solved as a heavy-atom problem. The coordination about the zinc atom is distorted tetrahedral. The 1,10-phenanthroline molecule itself is essentially planar, and the zinc atom departs 0.13 Å from this plane. The chlorine atoms are nearly equidistant from the zinc atom. The plane of the zinc and two chlorine atoms makes an angle of 79° with the plane of the 1,10-phenanthroline molecule.

9500. **Study suggests value of shared computers,** A. E. Rikli, S. I. Allen, and S. N. Alexander, *Mod. Hosp.* **106,** No. 5, 100-108 (May 1966).

Key words: Administration; hospital data communications; laboratory; nursing station; pharmacy; real-time hospital information system; remote data input.

A survey of real-time hospital information systems in advanced stages of development has been made and is reported briefly here. By definition, such a system is one that is in direct communication with portions of the hospital environment by receiving data, processing transactions, and returning results with sufficient responsiveness to affect patient care and administrative decisions near the time of occurrence of medical or hospital events. Eight hospitals qualified under the definition, and the general conclusion to be drawn is that more design studies and experimentation with equipment and techniques are essential to solving the special communications and information problems of hospitals.

9501. **Dislocation node determinations of the stacking-fault energy in silver-tin alloys,** A. W. Ruff, Jr. and L. K. Ives, *Acta. Met.* **15,** 189-198 (Feb. 1967).

Key words: Dislocations; electron microscopy; silver-tin alloy; stacking-fault energy.

Direct measurements by transmission electron microscopy on extended dislocation nodes in alloys of tin in silver have led to values for the intrinsic stacking-fault energy. The values decreased smoothly from 23 erg/cm$^2$ for pure silver to 4.5 erg/cm$^2$ for 7.8 at.% tin, near the f.c.c. phase limit. The results are compared with previous determinations in other silver-base alloys, and sources of systematic error are discussed. A comparison of different theoretical analyses is included.

9502. **The stacking-fault energy in $\alpha$-silver-tin alloys,** A. W. Ruff, Jr. and L. K. Ives, *Canadian J. Phys.* **45,** 787-795 (1967).

Key words: Dislocation nodes; dislocations; electron microscopy; silver-tin alloys; stacking-fault energy; stacking faults.

Direct measurements by transmission electron microscopy on extended dislocation nodes in alloys of tin in silver have led to values for the intrinsic stacking-fault energy. The values decreased smoothly from 23 erg/cm$^2$ for pure silver to 4.2 erg/cm$^2$ for 7.8 at.% tin. The results are compared with previous determinations in other silver-base alloys.

9503. **Low-frequency motions and barrier to rotation in phosphonium iodide,** J. J. Rush, *J. Chem. Phys.* **44,** No. 4, 1722-1723 (Feb. 15, 1966).

Key words: Barrier to rotation; electrostatic model; inelastic neutron scattering; phosphonium iodide ($PH_4I$).

The vibrational spectrum of $PH_4I$ has been investigated by the energy-gain scattering of cold neutrons ($E_n \leq 5$ meV). Three distinct inelastic-scattering maxima are observed at energy gains corresponding to 110, 335, and 614 cm$^{-1}$. The 335 and 614 cm$^{-1}$ peaks are attributed to the torsional oscillations of the $PH_4^+$ ion and the 110 cm$^{-1}$ peak to the translational optic vibrations. The barrier to rotation for the torsional mode of 335 cm$^{-1}$ was computed to be 7.1±0.5 kcal/mole based on the observed energy of the peak. This agrees well with the value of 7.5 kcal/mole derived from an electrostatic model.

9504. **Motions of water molecules in potassium ferrocyanide trihydrate, water, and ice: a neutron scattering study,** J. J. Rush, P. S. Leung, and T. I. Taylor, *J. Chem. Phys.* **45,** No. 4, 1312-1317 (Aug. 15, 1966).

Key words: Ferroelectrics; $H_2O$; ice; inelastic scattering; $K_4Fe(CN)_6 \cdot 3H_2O$; librations; low-frequency modes; neutron cross-sections; neutron spectra; phase transition.

The motions of $H_2O$ molecules in ferroelectric potassium ferrocyanide trihydrate, water, and ice have been investigated by total cross section and differential inelastic scattering measurements with cold neutrons. The results show no significant change in the average rotational or translational freedom of the water molecules in KFCT at or near its ferroelectric transition. The inelastic neutron spectra for KFCT exhibit broad peaks at about 425 and 160 cm$^{-1}$, both above and below the transition, which are assigned primarily to the librational and optic translational modes of the $H_2O$ molecules, respectively. Moreover, both the total cross section and inelastic scattering results indicate a greater freedom of motion of the $H_2O$ molecules in the KFCT lattice than in either water or ice. In addition, a decrease in the total cross section of $H_2O$, and in its variation with neutron wavelength is observed at the water-ice transition, indicating a significant change in the frequency distribution. The neutron results are compared with the results of NMR and infrared measurements.

9505. **Neutron-scattering study of the motions of water molecules in hydrated salts of transition metals,** J. J. Rush, J. R. Ferraro, and A. Walker, *Inorg. Chem.* **6,** No. 2, 346-351 (Feb. 1967).

Key words: Cold neutrons; coordination; hydrated salts; hydrates; hydrogen-bonding; neutron scattering; vibration spectra; water librations.

The low-frequency motions of water molecules in a series of hydrated transition metal salts have been investigated by the energy-gain scattering of cold neutrons. The compounds studied include $CuSO_4 \cdot H_2O$, $CuSO_4 \cdot 5H_2O$, $Co(NO_3)_2 \cdot 2H_2O$, $Co(NO_3)_2 \cdot 6H_2O$, $Cu(NO_3)_2 \cdot 3H_2O$, and $UO_2(NO_3)_2 \cdot 6H_2O$. Broad bands observed in the spectra at neutron energy gains of 500-800 cm$^{-1}$ are assigned to the wagging and rocking modes of the coordinated and hydrogen-bonded water molecules. Bands around 400-500 cm$^{-1}$ are attributed both to $M\text{-}OH_2$ stretching modes and to the $H_2O$ torsional vibrations around the bisectrix. Maxima are also observed at energy transfers below 300 cm$^{-1}$, which are tentatively assigned to hydrogen-bond stretching vibrations and possibly to $H_2O\text{-}M\text{-}OH_2$ deformation modes. Comparison of the various spectra appears to indicate that the average strength of binding of the water molecules does not change significantly in proceeding from the higher to the lower hydrates. The neutron results are compared in detail to previous infrared and structure results.

9506. **Vibration spectra of yttrium and uranium hydrides by the inelastic scattering of cold neutrons,** J. J. Rush, H. E. Flotow, D. W. Connor, and C. L. Thaper, *J. Chem. Phys.* **45,** No. 10, 3817-3825 (Nov. 15, 1966).

Key words: Cold neutrons; frequency; inelastic scattering; metal hydrides; neutron scattering; optical vibration; vibration spectrum.

The vibration spectra of the hydrides and deuterides of yttrium and uranium have been investigated by the energy-gain scattering of cold neutrons. The measured spectra are all split into two bands, one at higher energies, due to the optical hydrogen vibrations, and another at lower energies due to metal-atom vibrations. Values have been obtained for the peaks and widths of the single optical hydrogen bands in $YH_2$, $YD_2$, $UH_3$, and $UD_3$ by the calculation of approximate frequency distributions from the observed neutron time-of-flight spectra. The derived peak frequencies in cm$^{-1}$ are: $YH_2$, 1025±60; $YD_2$, 725±40; $UH_3$, 970±60; $UD_3$, 710±40. The relative width at half-maximum for the hydrogen band in $UH_3$ is about double that for $YH_2$. The distribution of hydrogen vibrations in hexagonal $YH_3$ and $YD_3$ is considerably broader, and exhibits several maxima, due to hydrogens at different sites in the lattice. The hydrogen modes in all the compounds can be correlated reasonably well with the known crystal structures. The results are in satisfactory agreement with hydrogen frequencies calculated previously from heat-capacity data.

9507. **Unassigned.**

9508. **On the solution of the stefan problem for whisker growth,** J. A. Simmons, H. Oser, and S. R. Coriell, (Proc. Intern. Conf. Crystal Growth, Boston, Mass., June 20-24, 1966), *Crystal Growth, a Suppl. to J. Phys. Chem. Solids* **C8,** 255-264 (Pergamon Press Inc., New York, N.Y., 1967).

Key words: Curtis approximation; Dittmar-Neumann approximation; mean stay time; stefan problem; surface concentration; surface self-diffusion; whisker growth.

An integral equation which describes whisker length as a function of time is derived from the implicit exact solution of Simmons, Howard, and Parker using a conservation principle. A convergent iterative method is employed to obtain numerically the exact growth curves and concentration profiles. Utilizing a dimensionless formulation, growth curves are shown to comprise (except for a short transient period) a one-parameter family dependent only on a dimensionless evaporation parameter. The Dittmar-Neumann and Curtis approximations are compared with the exact solution and are found to deviate significantly in some parts of the growth range; however, in those parts of the growth range where physical limits on the surface concentration are satisfied, both approximations are in good agreement with the exact solution. Methods and limitations are discussed for calculating the coefficient of surface self-diffusion and mean stay time from whisker growth data.

9509. **Measurement of optical constants: optical constants of liquid mercury at 5461 Å,** L. E. Smith and R. R. Stromberg, *J. Opt. Soc. Am.* **56,** No. 11, 1539-1542 (Nov. 1966).

Key words: Complex refractive index; ellipsometry; mercury; optical constants; refractive index; surface films.

The optical constants of liquid mercury have been measured by ellipsometry at a wavelength of 5461 Å. Discrepancies among values from the literature are discussed and the magnitude of the important sources of error are evaluated. The effects on the measured index of several different types of surface films between the mercury and several contact media have been calculated and compared. Errors in alignment are shown to cause large changes in the measured refractive index as well as an apparent dependence upon the angle of incidence.

9510. **Relation between refractive index and density of glasses resulting from annealing compared with corresponding relation resulting from compression,** S. Spinner and R. M. Waxler, *Appl. Opt.* **5,** No. 12, 1887-1889 (Dec. 1966).

Key words: Annealing; density; glass; hydrostatic compression; polarizability; refractive index.

The change in refractive index and associated change in density of glasses on annealing has been determined by Tool, Tilton and Saunders. The corresponding changes for the same glasses, produced by hydrostatic compression, are presented here and compared with those of Tool, Tilton and Saunders. It is found that for a given increase in density on annealing the increase in index is greater than for the same measured increase in density on compression.

The results are interpreted in terms of equations developed by Lorentz-Lorenz, Pockels, and Mueller to show first, that in all cases, whether from annealing or compression, there is a decrease in polarizability on increase in density (these results are in agreement with those of previous investigators); and second, that the decrease in polarizability for a given increase in density is greater on compression than on annealing.

9511. **Elastic properties of NiTi as a function of temperature,** S. Spinner and A. G. Rozner, *J. Acoust. Soc. Am.* **40,** No. 5, 1009-1015 (Nov. 1966).

Key words: Annealed specimens; cold-worked specimens; elastic moduli; internal friction; nickel-titanium alloy; temperature dependence.

Young's modulus, shear modulus, and internal friction of the intermetallic compound NiTi have been measured as a function of temperature from about −180° to 600 °C, in the kilocycle-per-second range. Annealed and cold-worked specimens were used All the specimens showed the same general pattern, with a minimum in elastic moduli occurring about 70°-140 °C, depending upon the particular specimen, and a maximum in internal friction occurring some 50 °C below the minimum in elastic modulus. Young's modulus was the same for all the specimens (694 kbar) within experimental error, but the shear modulus of the cold-worked specimens was more than 10% higher than that for the annealed specimens.

9512. **Interactions in aqueous nonelectrolyte solutions. I. Solute-solvent equilibria,** R. H. Stokes and R. A. Robinson, *J. Phys. Chem.* **70,** 2126-2131 (1966).

Key words: Hydration; mixed solutions; nonelectrolytes; solvation; sucrose solutions.

Solutes which interact with the solvent by a series of solvation equilibria to form species which mix according to the ideal solution law are considered. General expressions relating the solvent activity to the molality and the equilibrium constants are given. Sucrose solutions can be described with considerable accuracy by the assumption of a number of possible solvation sites equal to the number of oxygen atoms in the solute molecule, with a single equilibrium constant given the same value for each site.

Mixed solutions of several solutes conforming to this model are shown to obey very simple equations relating the molalities at isopiestic equilibrium between solutions of the separate and mixed solutes. A similar relation between the activity coefficients is given. Examples of systems which conform to these mixture relations are given, and it is suggested that cases of large departures from the relations may be taken as evidence of specific solute-solute interactions.

9513. **Thermal correction and crystal growth in horizontal boats, flow pattern, velocity measurement, and solute distribution,** H. P. Utech, W. S. Brower, and J. G. Early, (Proc. Intern. Conf. Crystal Growth, Boston, Mass., June 20-24, 1966), *Crystal Growth, a Suppl. to J. Phys. Chem. Solids* **B29,** 201-205 (Pergamon Press Inc., New York, N.Y., 1967).

Key words: Crystal growth; fused salts; magnetic fields; molten metals; solute distribution; thermal convection.

The characteristics of thermal convection in open horizontal boats containing molten metals or fused salts subject to a horizontal temperature gradient are shown in a motion picture. A technique for determining flow direction and mean flow velocity in systems whose convective flow is characterized by erratic temperature fluctuations (e.g. metals and salts) was developed and checked by comparing velocities measured by this technique with those observed directly in the molten salt.

The effectiveness of a magnetic field in suppressing convective flow is illustrated by comparing the distribution of solute in a specimen solidified unidirectionally in the presence of a field with the distribution in a sample grown normally, i.e. without any field.

9514. **Monte Carlo studies of lattice-model polymer chains. II. End-to-end length,** P. H. Verdier, *J. Chem. Phys.* **45,** No. 6, 2122-2128 (Sept. 15, 1966).

Key words: Distribution; end-to-end length; lattice model; Monte Carlo; polymer chain dynamics; relaxation; simulation.

The relaxation and the equilibrium behavior of lattice-model polymer chains are studied by simulation on a digital computer. Results are presented for the behavior of the square of end-to-end length $l^2$ for chains of 8, 16, 32, and 64 beads, with and without excluded volume restrictions. It is found that the relaxation of the lattice-model chains without excluded volume is remarkably similar to that of statistical-bead models. The introduction of excluded volume restrictions causes drastic qualitative changes in the relaxation behavior of the longer chains, and lengthens the time required for their relaxation by factors of up to 15. While the distribution in $l^2$ for the longer chains with excluded volume departs noticeably from Gaussian form at quite small and quite large values of $l^2$, it appears close to Gaussian in a range from one-third to three times the mean-square value of $l^2$.

9515. **Monte Carlo studies of lattice-model polymer chains. I. Correlation functions in the statistical-bead model,** P. H. Verdier, *J. Chem. Phys.* **45,** No. 6, 2118-2121 (Sept. 15, 1966).

Key words: Autocorrelation; correlation; end-to-end length; Fokker-Planck equation; polymer chain dynamics; radius of gyration; relaxation; statistical-bead model.

A method is presented for obtaining correlation functions in the free-draining statistical-bead model (Rouse model) of a polymer chain. Autocorrelation functions for the squares of end-to-end length and radius of gyration are given as functions of the number of statistical segments in the chain.

9516. **Unassigned.**

9517. **Nonstoichiometric A15-type phases in the systems Cr-Pt and Cr-Os,** R. M. Waterstrat and E. C. van Reuth, *Trans. Met. Soc. AIME* **236,** No. 8, 1232-1233 (Aug. 1966).

Key words: Alloy phases; atomic ordering; A15-type phases; chromium alloys; electron compounds; intermediate phases; nonstoichiometric phases; osmium alloys; platinum alloys; transition elements.

The composition ranges of stability for binary A15-type phases in the systems Cr-Pt and Cr-Os have been determined. These do not include the "ideal" $A_3B$ stoichiometric composition at 1200 °C and 1400 °C respectively. X-ray diffraction studies reveal that long-range atomic ordering is incomplete in these phases with an unusually low degree of order occurring in the Cr-Os phase. Density measurements on the Cr-Os phase lead to the conclusion that there are insufficient vacant lattice sites in this phase to account for the apparent low degree of atomic ordering.

A composition shift is observed for the A15-type phases in the systems Cr-Pt, Cr-Ir, and Cr-Os which parallels a similar composition shift previously observed in binary sigma phases. This suggests that "electronic factors" may influence the stability of both the A15-type phases and the sigma phases.

9518. **Fermi controlled recombination as a junction design factor in GaAs laser diodes,** N. N. Winogradoff and H. K. Kessler, *Int. J. Electronics* **21,** No. 4, 329-335 (1966).

Key words: Compensated GaAs; epitaxial GaAs lasers; Fermi levels; radiative recombination.

Since our first observation of the enhancement of radiative recombination rates in GaAs p-n junctions produced by the incorporation of shallow donors in the p-type side of the junction, the effect has been found to be quite general and has also been observed in GaP. Although several models for the radiative process have been proposed they do not provide a satisfactory explanation of the role of compensation. A new model based on Shockley and Read's statistics of recombination through an impurity center is described. It provides agreement with the experimentally observed differences in the light output of diffused, graded, and narrow, abrupt p-n junctions with and without compensation in the p-type side, and with the difference in the time delay between the leading edge of the current pulse and the commencement of lasing in diffused and epitaxial GaAs lasers at room temperature.

9519. **Radiative recombination within a space-charge region in a semiconductor,** N. N. Winogradoff, *J. Appl. Phys.* **37,** No. 10, 3916-3917 (Sept. 1966).

Key words: Gallium arsenide; germanium; p-n junctions; radiative recombination; silicon; space charge regions.

Since light emission from forward biased junctions is usually due to radiative recombination through a recombination center, the minima in the light output observed when cathode rays or a narrow beam of light traversed a p-n junction can be explained in terms of the recombination statistics of the centers in the space charge region rather than in terms of the separation of the free carriers by the junction field as is commonly believed. Furthermore, it is shown that under certain conditions of excitation, the luminescence in the space charge region can be a maximum.

9520. **Specific heat of natural rubber and other elastomers above the glass transition temperature,** L. A. Wood and N. Bekkedahl, *J. Polymer Sci. Letters* **5,** 169-175 (1967).

Key words: Butadiene-acrylonitrile copolymer; butadiene-styrene copolymers; crystallization of rubber; elastomers; polybutadiene; polyethylene; polyisobutylene; rubber; specific heat.

A survey is given of literature values of the specific heat $C_p$ as a function of temperature (above the glass transition temperature) for the elastomers, including natural rubber, polyisobutylene, polybutadiene, several butadiene-styrene copolymers, and a butadiene-acrylonitrile copolymer. The values of $dC_p/dt$ (where t is the temperature) found for natural rubber were abnormally low in the range −68 to +2 °C and abnormally high in the range 17° to 47 °C. The most probable explanation is that crystallization of the unvulcanized rubber was predominating in the first range, and melting of these crystals was predominating in the second range.

9521. **Effect of sample thickness and operating voltage on the contrast of Kossel transmission photographs,** H. Yakowitz, *J. Appl. Phys.* **37,** No. 12, 4455-4458 (Nov. 1966).

Key words: Divergent x-ray beams; Kossel; Kossel sample preparation; photographic contrast; transmission of x rays; x-ray diffraction.

The photographic contrast of transmission Kossel patterns is examined in terms of the voltage and thickness variables since other parameters in the contrast equation generally cannot be controlled by the investigator; they are fixed functions of the material. It is shown that there is no single thickness yielding maximum contrast. However, manipulation of the contrast equation yields an approximation to the thickness and operating voltage relationship giving Kossel transmission photographs of nearly optimum contrast. Methods for calculating this relationship for any crystal-radiation combination are described. It is assumed throughout that the crystal is not completely free of imperfections; however, neither is the crystal assumed to be completely mosaic.

9522. **Ellipsometric errors due to multiple reflections in mica quarter-wave plates,** H. T. Yolken, R. M. Waxler, and J. Kruger, *J. Opt. Soc. Am.* **57,** No. 2, 283-284 (Feb. 1967).

> Key words: Ellipsometer; multiple reflections; quarter-wave plate.

Experiments performed to determine the source of the large differences in polarizer readings between the ellipsometric zones found that the origin of these polarizer reading differences lay in multiple reflections occurring in the quarter-wave plate. Coating the quarter-wave plate with anti-reflective layers markedly reduced the zone differences.

9523. **Analysis and computer simulation of the production and distribution systems of a tufted carpet mill,** J. A. Yurow, *J. Ind. Eng.* **XVIII,** No. 1, 135-140 (Jan. 1967).

> Key words: Industrial dynamics; simulation; tufted carpet mill.

The problem of simulating a multi-line tufted carpet mill by means of a continuous flow simulation language is translated into the problem of simulating a mill producing only four lines. Simulation of the planning and allocation of production time for each line under yarn availability constraints is studied in detail.

9524. **Simultaneous diffraction with the three-circle diffractometer,** M. Zocchi and A. Santoro, *Acta Cryst.* **22,** Pt. 3, 331-334 (Mar. 1967).

> Key words: Diffraction; diffractometer; neutrons; simultaneous; three-circle; x ray.

The geometrical conditions of simultaneous diffraction with a three-circle diffractometer have been derived for all the crystal-systems and for any crystal orientation. It is shown that $\lambda$-independent simultaneous diffraction takes place among reciprocal lattice points located on the same vertical net, that multiplicity is generally odd, and that it obeys special conditions in all cases in the cubic system and, for particular orientations and classes of reflection, in the hexagonal and tetragonal systems. Finally, procedures are suggested for avoiding taking intensity measurements under conditions of simultaneous diffraction.

9525. **Spectral distribution of solar radiation at the earth's surface,** D. M. Gates, *Science* **151,** No. 3710, 523-529 (Feb. 1966).

> Key words: Aerosol; air mass; ozone; solar radiation; spectral distribution; water vapor concentration; wavelength; wavenumber.

The spectral distribution of direct sunlight at the earth's surface at sea level is calculated as a function of the air mass and of aerosol, ozone, and water vapor concentration. A solar constant of 2.0 cal $cm^{-2}$ $min^{-1}$ is used for these calculations. The spectral distribution of sunlight is presented on a wavelength basis and also on a wavenumber basis. For sea level the spectral distributions of skylight and of global radiation incident on a horizontal surface are given. Finally, the variation with altitude of the spectral distribution of direct sunlight incident on a surface perpendicular to the sun's rays is presented.

9526. **Electrical feedthrough for pressures to 10 kbar,** P. L. M. Heydemann, *Rev. Sci. Instr. Laboratory Notes* **38,** No. 4, 558-559 (Apr. 1967).

> Key words: Electrical connector; feedthrough; high pressure; resistance gage; ultrasonics.

For ultrasonic experiments at high pressure and for measurements with manganin resistance gages an electrical feedthrough was developed which is both easily fabricated and convenient to use. The electrical feedthrough (EFT) described here is designed for low current applications at frequencies ranging from d.c. to over 50 MHz. EFTs with one, two and four leads have been made. The insulation resistance between leads and between a lead and the shield is typically above 1000 MΩ. The EFT can therefore be used in connection with very sensitive bridge circuits. The EFT is made from parts that are easily available. It is readily attached to and removed from various kinds of high pressure equipment by means of a standard type fitting.

9527. **Relaxation of moments derived from a master equation,** K. E. Shuler and G. H. Weiss, *J. Chem. Phys.* **45,** No. 4, 1110-1112 (Aug. 15, 1966).

> Key words: Exponential relaxation; master equation; moments; probability distributions; relaxation; transition probabilities.

Previous work on the relaxation of moments derived from a master equation [J. Math. Phys. **3,** 550 (1962)] has been extended to master equations for joint probability distributions and to nonlinear master equations involving product probability distributions. Necessary and sufficient conditions on the transition probabilities are given to obtain *closed* moment equations. The special case of simple, one-term, exponential relaxation of the moments is also discussed.

**9528.** Abramowitz, S., Levin, I. W., **Force fields for some Group VI hexafluorides,** *J. Chem. Phys.* **44,** No. 9, 3353-3356 (May 1, 1966).

Key words: Band contours; force fields; gas phase; infrared; sulphur hexafluoride; tellurium hexafluoride; vibration-rotation.

The Coriolis zeta constants were determined for the infrared active $F_{1u}$ modes of $SF_6$ and $TeF_6$ from gas phase band contour measurements. These Coriolis data were applied toward determining the general force fields for these Group VI hexafluorides.

**9529.** Abramowitz, S., Levin, I. W., **Vibrational analysis of $SeF_6$ and $WF_6$,** *Inorg. Chem.* **6,** 538-541 (1967).

Key words: Coriolis constants; force field; infrared; $SeF_6$; vibration-rotation; $WF_6$.

The gas phase infrared vibration-rotation spectra of $SeF_6$ and $WF_6$ have been observed in the region of their infrared active fundamental absorption bands. Coriolis coupling constants, evaluated from the observed contours, are used as constraints for the general force fields for these molecules.

**9530.** Achenbach, P. R., **Performance criteria for building components and systems,** *Proc. Porcelain Enamel Institute Forum, University of Illinois, Urbana, Ill., Sept. 28-30, 1966,* **28,** 176-195 (1966).

Key words: Building components; codes; laboratory procedures; performance characteristics; performance criteria; specifications; standards.

The Building Research Division of the National Bureau of Standards has conducted a number of technical investigations which led to the development of new test procedures for evaluating the significant performance requirements of building components and systems. These investigations have typically produced performance data which could be used by appropriate organizations in establishing criteria of acceptability. Laboratory studies of this type have been completed on underground heat distribution systems, ducts for heating and air conditioning systems, and sanitary plumbing fixtures and a similar study is in progress on exterior wall systems for residential buildings. In each of these studies the Building Research Division has collaborated with multi-discipline task groups of the Building Research Advisory Board of the National Academy of Sciences-National Research Council in developing the list of important performance characteristics in qualitative language. The work done on these projects is used to illustrate the sequence of activities required in developing performance criteria, the importance of collaboration among representatives of industry, professional societies, codes and standards organizations, and government bodies in selecting acceptable performance levels, the problems involved in devising adequate laboratory test procedures for building components made of widely-differing materials, and the incomplete state of administrative procedures for implementation of performance criteria on a national scale.

**9531.** Achenbach, P. R., Phillips, C. W., Penney, R. W., **A testing and rating method for refrigerated trucks with respect to cooling load,** *Annex to Proc. Intern. Inst. Refrigeration, Comm. VII,* pp. 29-35 (London, England, Sept. 1966).

Key words: Air leakage; cooling load; refrigerated trucks; solar heating; testing and rating methods.

A testing and rating method for refrigerated delivery trucks has been developed under the sponsorship of the U.S. Department of Agriculture and the Truck Body and Equipment Association. The method is applicable to insulated vehicles used for short-haul delivery of frozen food at a low temperature or fresh produce at a medium temperature. It involves a measurement of the steady-state transmission of heat from ambient air to cargo space under selected conditions of test and the use of a correction factor for the effect of solar radiation on a stationary vehicle. The essentials of the testing and rating procedure and of the laboratory studies carried out to develop the procedure are described.

**9532.** Achenbach, P. R., **Air-to-air heat pumps for military housing,** *Military Eng.* **384,** 270 (July-Aug. 1966).

Key words: Air-to-air heat pumps; annual energy cost; energy usage; residential air conditioning.

The National Bureau of Standards has performed laboratory and field studies of electric air-to-air heat pumps as a part of the technical investigations sponsored by the three agencies of the Department of Defense. These studies have developed information on the coefficient of performance and heating and cooling capacities of typical systems used for residential applications, design data useful for estimating energy usage and maximum power demand for similar installations, some information relative to the unexpectedly high rate of motor-compressor failure, and comparisons of the annual cost of year-around air conditioning using heat pumps and gas heating systems combined with conventional air conditioners for cooling. The annual cost of heating and cooling these military houses with air-to-air heat pumps averaged about $100 for a unit electric energy cost of 0.8¢/kWh.

**9533.** Alexander, S. N., **Computer languages and their use,** *Am. Mgmt. Assoc. Mgmt. Bull.* **79,** 8-12 (1966).

Key words: Documentation of software; economics of software; man/machine interface problems; problem-oriented languages; software usage.

Three levels of computer programming languages are discussed in terms of their effectiveness as tools for solving the man/machine interface problem. In this respect, the least effective of the three is the assembly level language which in general is used only when maximum system performance is required. At the next level of effectiveness are the procedure-oriented languages such as FORTRAN, COBOL, and ALGOL. In general, these are at a level of abstraction considerably above that of machine commands, but are still not at the working level of the average application analyst. The third level, problem-oriented languages, are generally much closer to the specific mode of expression used by the analyst in describing the solution to a given problem. Several examples of this type of language are given including some that make use of ordered or graphical arrangements of inputs to facilitate the external mode of expression. The paper concludes with brief discussions of software documentation and the economic aspects of software development and utilization.

**9534.** Allan, D. W., **Statistics of atomic frequency standards,** *Proc. IEEE* **54,** No. 2, 221-230 (Feb. 1966).

Key words: Atomic frequency standards; power spectral density; short- and long-term frequency stability.

A theoretical development is presented which results in a relationship between the expectation value of the standard deviation of the frequency fluctuations for any finite number of data samples and the infinite time average value of the standard deviation, which provides an invariant measure of an important quality factor of a frequency standard. A practical and straightforward method of determining the power spectral density of the frequency fluctuations from the variance of the frequency fluctuations, the sampling time, the number of samples taken, and the dependence on system bandwidth is also developed. Additional insight is also given into some of the problems that arise from the presence of "flicker noise" (spectrum proportional to $|\omega|^{-1}$) modulation of the frequency of an oscillator.

The theory is applied in classifying the types of noise on the signals of frequency standards made available at NBS, Boulder Laboratories, such as: masers (both H and $N^{15}H_3$), the cesium beam frequency standard employed as the U.S. Frequency Standard, and rubidium gas cells.

"Flicker noise" frequency modulation was not observed on the signals of masers for sampling times ranging from 0.1 second to 4 hours. In a comparison between the NBS hydrogen maser and the NBS III cesium beam, uncorrelated random noise was observed on the frequency fluctuations for sampling times extending to 4 hours; the fractional standard deviations of the frequency fluctuations were as low as 5 parts in $10^{14}$.

**9535.** Allion, H. H., **Calibration and use of laminar flowmeters,** (Proc. 25th Annual Gas Measurement Short Course, Aug. 25, 1965), *West Virginia Univ. Tech. Bull.* **77,** 34-43 (1965).

Key words: Accuracy; calibration; compressible flow; differential meter and effects; fluid meter; incompressible flow; laminar flow; Mach number; Reynolds number; viscous flow; volumetric flow.

The laminar meters discussed are made of one or more uniform passages each having a depth or diameter small in relation to its length. Resistance to flow is largely viscous and may be analyzed in a fairly simple fashion in the incompressible case. For gas flow in these meters, treatment of the effects of deviations from incompressible theory is quite complex; however, errors resulting from ignoring these deviations when predicting meter response at other than calibration conditions are apparently less than the measurement errors over a fairly wide range of conditions. In some applications linear response and independence from pressure level may be approximated closely.

**9536.** Allred, C. M., Lawton, R. A., **A precision current comparator,** (Annual ISA Conf., New York, N.Y., Oct. 1966), *ISA Preprint,* No. 12.8-2-66 (1966).

Key words: Antenna; attenuation; comparator; current; phase; precision.

A technique capable of precise comparison of currents in different parts of a network or between currents in different networks is discussed. With proper conditions, this comparison can be done with negligible perturbation of the networks under measurement. Experiments on a coaxial system at 30 MHz are discussed.

**9537.** Andrews, D. H., **Of time and frequency,** *Book, How to Listen to the World,* pp. 3-7 (World Publ., Hellerup, Denmark, Jan. 1967).

Key words: Atomic time; frequency and time; International Time Bureau; standard audio frequencies; standard radio frequencies; time and frequency; worldwide radio stations.

Following a short historical background of timekeeping, the author proceeds to describe Universal Time and how it is approximated by Atomic Time with corrections prescribed by the International Time Bureau. The use of radio broadcasts by various nations to disseminate time signals, standard radio frequencies and standard audio frequencies is described. Other services are also noted. The article includes an extensive listing of worldwide radio stations broadcasting standard frequencies and/or time signals. This tabulation is divided into two parts; Table I listing stations using frequencies above 1 megahertz, and Table II listing stations using frequencies below 1 megahertz.

**9538.** Arenhovel, H., Danos, M., Greiner, W., **Photonuclear effect in heavy deformed nuclei,** *Phys. Rev.* **157,** No. 4, 1109-1125 (May 20, 1967).

Key words: Collective model; nuclear Raman effect; nuclear structure; photon absorption cross sections; photon scattering; photonuclear effect.

The theory of Raman scattering is extended to include electric quadrupole radiation. The results obtained are used to compute the elastic and Raman scattering cross sections of heavy deformed nuclei. The dipole and quadrupole resonances are described by a previously developed theory which includes surface vibrations and rotations. The computed cross sections are compared with experimental data for all those nuclei where both absorption and scattering cross sections are available. Some discrepancies still exist in certain details; however, the overall agreement between theory and experiment is very good.

**9539.** Armstrong, G. R., **Calorimetry,** *1967 McGraw-Hill Yearbook of Science and Technology,* pp. 124-127 (1967).

Key words: Calorimetry, biological; calorimetry, international; calorimetry, new developments; calorimetry, review; fuel calorimetry.

The present status of calorimetry is reviewed. Several new and promising instruments for accurate calorimetry and the development of new or improved techniques for calorimetric processes are discussed. The relationship of calorimetry to the U.S. fuel technology, to the rocket propellant program, and to molecular biophysics is briefly discussed.

**9540.** Arni, H. T., **Resistance to weathering,** Significance of Tests of Concrete and Concrete Making Materials, *Am. Soc. Testing Mater. Spec. Tech. Publ.* **169A,** 261-274 (1966).

Key words: Concrete; de-icing scaling; durability; freezing-and-thawing; weathering.

Deterioration due to physical processes produced by exposure to natural weathering is discussed. The most recent theories on the mechanisms of freezing-and-thawing damage are presented, and freezing-and-thawing tests now specified and proposed are discussed. The effects of de-icing chemicals and of weathering processes other than freezing and thawing are also considered.

**9541.** Arp, V. D., Collier, R. S., Kamper, R. A., Meissner, H., **One-dimensional solutions of the Ginzburg-Landau equations for thin superconducting films,** *Phys. Rev.* **145,** No. 1, 231-236 (May 6, 1966).

Key words: Ginzburg-Landau theory; magnetic field; superconductor; thin film.

Solutions to the Ginzburg-Landau equations have been obtained for plane films in a longitudinal magnetic field. Only symmetrical one-dimensional solutions were generated, but without restrictive assumptions on $\kappa$ or $\psi$. The critical field has been calculated from these solutions as a function of $\kappa$ and $d/\lambda$. Curves are given to show how the behavior of films at the critical field depends on the various parameters involved.

The computer solutions join smoothly onto those derived in the limit $\psi \to 0$. The limit of validity of these solutions in the face of the vortex solutions of Abrikosov and the asymmetrical solutions of Saint-James and deGennes is determined, and a "phase diagram" in the $\kappa$, $d$ plane for all types of solutions is suggested.

**9542.** Ashley, A., Douglas, C. A., **Can infrared improve visibility through fog?,** *Illum. Eng.* **61,** No. 4, 243-250 (Apr. 1966).

Key words: Atmospheric optics; aviation lighting; infrared; visual range.

The fundamental system parameters-atmospheric attenuation, detector sensitivity, radiant intensity of source, and effects of background are examined to determine whether or not the use of infrared sources and detectors, instead of visible sources and the eye, for marking airport runways and taxiways offer, sufficient potential to warrant further consideration of their use as airport marker "lights". The evaluation is based on theory and previous experimental work. At present there are no advantages in the use of infrared sources and detectors as a replacement for the current visible sources and further consideration is not warranted at this time.

**9543.** Ausloos, P., **Radiation and photochemistry,** *Ann. Rev. Phys. Chem.* **17,** 205-236 (1966).

Key words: Photochemistry; radiation chemistry.

A critical review of major publications on Photochemistry and Radiation Chemistry published in 1965.

**9544.** Ausloos, P., Lias, S. G., **$H_2S$ as a free-radical interceptor in the gas-phase radiolysis and photolysis of propane,** *J. Chem. Phys.* **44,** No. 2, 521-529 (Jan. 1966).

Key words: Free radicals; $H_2S$; ion-molecule reactions; photolysis; propane; radical scavenger; radiolysis.

The gas-phase photolysis (1236 Å) and the $\gamma$-ray radiolysis of $C_3D_8$ has been investigated in the presence of varying concentrations of $H_2S$. When 10% or more $H_2S$ is added to $C_3D_8$, the majority of the D, $CD_3$, $C_2D_3$, and $C_2D_5$ radicals abstract an H atom from $H_2S$ to form HD, $CD_3H$, $C_2D_3H$, and $C_2D_5H$, respectively. The fully deuterated molecules formed in these mixtures result from the unimolecular elimination of a stable molecule from $C_3D_8$ or $C_3D_8^+$ and from fast bimolecular processes such as ion-molecule reactions or $CD_2$ insertions.

The mechanisms of the radiolysis and the photolysis proposed in earlier studies have been re-examined in the light of the information derived from the $C_3D_8-H_2S$ experiments and of some additional photolysis experiments on $CD_3CH_2CD_3-NO$ mixtures. The results indicate that the modes of decomposition of the neutral excited propane molecule are as follows:

$$\begin{aligned} C_3D_8 &\rightarrow C_2D_6+CD_2, \\ &\rightarrow CD_4+C_2D_4, \\ &\rightarrow D_2+C_3D_6, \\ &\rightarrow CD_3+C_2D_5, \\ &\rightarrow D+C_3D_7. \end{aligned}$$

The internally excited $C_2D_4$, $C_2D_5$, $C_3D_6$, and $C_3D_7$ species formed in these primary processes decompose to form D, $CD_3$, $C_2D_2$, $C_2D_3$, and $C_2D_4$ unless they are collisionally stabilized.

In the radiolysis of $C_3D_8-H_2S$ mixtures, yields of the free radicals can be adequately accounted for by taking into account the modes of fragmentation of the parent ion and of the excited propane. The $C_2D_5^+$ ions are shown to react with $H_2S$ in part by the deuteron-transfer reaction

$$C_2D_5^+ + H_2S \rightarrow C_2D_4 + DH_2S^+.$$

The effect of pressure and the effectiveness of HI as a free-radical interceptor in the radiolysis have been examined.

**9545.** Ausloos, P., Lias, S. G., Scala, A. A., **Investigating ion-molecule reactions by analyzing neutral products formed in the radiolysis and photoionization of hydrocarbons,** *Adv. Chem. Ser.* **58,** 264-277 (1966).

Key words: Analysis of neutral products; ion-molecule reactions; neutral products; photoionization of hydrocarbons; radiolysis and photoionization of hydrocarbons.

The analysis of neutral products from the radiolysis and photoionization of suitable deuterium labeled hydrocarbons or hydrocarbon mixtures provides information concerning (a) the relative rates of $H^+$, $H^-$, $H_2^-$, and $H_2$ transfer reactions, and (b) the structure of the reacting ion or reaction complex. The reaction cross-section of a given ion with various alkanes generally increases with increasing polarizability of the neutral molecule. The actual increase in rate is, however, faster than that of the collision cross-section given by: $2\pi e(\alpha/\mu)^{1/2}$. Good quantitative and qualitative agreement exists between the information on reactions of parent ions obtained from gas phase radiolysis studies and that derived from photoionization experiments carried out at wavelengths slightly above the ionization energy of the molecule.

**9546.** Baird, R. C., **RF measurements of the speed of light,** *Proc. IEEE* **55,** No. 6, 1032-1039 (June 1967).

Key words: Methods and limitations; recent results; review; speed of light.

Modern RF measurements of the speed of light are reviewed, with emphasis on those methods capable of attaining an accuracy of 1.0 km/s or better. The geodimeter and microwave interferometer methods are discussed in some detail because of the significant role they have played in arriving at our present value for *c*. Serious limitations of the microwave resonant cavity method are pointed out and brief mention is made of the electrical units and band spectrum methods. A recent measurement by Karolus and Helmberger, who obtained the value 299 792.1±0.2 km/s, is mentioned. Some experimental factors that should be considered in planning future speed-of-light measurements are presented, and an experiment involving lasers, now in progress at NBS, is described briefly. The conclusion is that the presently accepted value of 299 792.5±0.3 km/s is still valid. Only two or three measurements have been completed since its adoption nearly ten years ago and they are not of sufficient accuracy to warrant re-evaluation of *c*.

**9547. Unassigned.**

**9548.** Barber, D. J., **Electron microscopy of irradiation-induced defect clusters in magnesium fluoride,** *Phys. Stat. Solids* **16,** 531-547 (1966).

Key words: Dislocation loops; electron microscopy; magnesium fluoride; point defects; precipitation; radiation damage.

The passage of electrons through thin crystals of magnesium fluoride produces point defects. These defects are mobile at temperatures normally attained under the electron beam, and they can give rise both to dislocation loops and to precipitate platelets. The aggregation of these radiation-induced defects can be controlled by using a cooled specimen stage in the electron microscope. This allows the growth and characteristics of the defect clusters to be studied. Dislocation loops lie on $\{011\}$ planes and they sometimes show stacking fault contrast; their Burgers vectors are $1/2\langle 01\bar{1}\rangle$ and $\langle 01\bar{1}\rangle$. Prolonged irradiation can produce precipitates on and within the loops. Higher beam intensities produce precipitates directly. The nature of the loops and precipitates is discussed in relation to the production of point defects by ionization mechanisms and irradiation-stimulated migration.

**9549.** Barbrow, L. E., **Photometry,** *Encyclopedia of Physics,* pp. 516-519 (Reinhold Publ. Corp., New York, N.Y., 1966).

Key words: Luminance; luminous flux; luminous intensity; photometric brightness; photometry; reflectance; transmittance.

The photometric quantities luminous density and flux, illuminance and luminance, and luminous reflectance, transmittance, directional reflectance factor, and directional transmittance factor are defined, the methods of measuring them are briefly described, and the factors which affect the accuracy of the measurements are discussed. Included is a table of the currently internationally agreed-upon symbols for the photometric and related radiometric quantities and units.

**9550.** Barger, R. L., **Rare-gas collision broadening in the lowest $^3P_1$ level of Cd,** *Phys. Rev.* **154,** No. 1, 94-97 (Feb. 5, 1967).

Key words: Cadmium; cross sections; double resonance; level crossing.

Alignment depolarization collision cross sections have been measured for the lowest $^3P_1$ level of cadmium broadened by the rare gases. Cross sections obtained with the Hanle effect (zero-field level crossing) and the method of modulated-light double resonance are the same within approximately 5%. They agree with theoretical predictions except in the case of helium, for which the measured cross section is nearly twice as large as the theoretical value. Average experimental values (units of $10^{-16}$ cm$^2$) for He, Ne, Ar, Kr, and Xe, respectively, are 51, 52, 81, 118, and 165.

**9551.** Barghausen, A. F., **Medium-frequency sky wave propagation in middle and low latitudes,** *IEEE Trans. Broadcasting* **BC-12,** No. 1, 1-14 (June 1966).

Key words: Absorption; antennas; broadcasting; ground waves; ionosphere; medium frequency; polarization; propagation; radio; reflection coefficients; sky waves.

A comparison is presented between empirically derived medium frequency sky wave propagation curves for the United States and Europe. Substantial differences are noted when the respective curves are applied to other geographical areas than those intended at the time of their derivation. Using the same data and recent measurements of the reflection coefficients at vertical incidence, a set of semi-empirical curves are derived which are believed to be applicable to both areas.

Finally, it is shown that none of these propagation curves are pertinent to the low latitudes where very large polarization coupling losses are observed. A short sample of measurements is presented with a brief explanation using simplified magnetoionic theory to account for these losses.

**9552.** Barnes, J. A., **Atomic timekeeping and the statistics of precision signal generators,** *Proc. IEEE* **54,** No. 2, 207-220 (Feb. 1966).

Key words: Atomic frequency standards; atomic time; stability; statistics.

Since most systems that generate atomic time employ quartz crystal oscillators to improve reliability, it is essential to determine the effect on the precision of time measurements that these oscillators introduce. A detailed analysis of the calibration procedure shows that the third finite difference of the phase is closely related to the clock errors. It was also found, in agreement with others, that quartz crystal oscillators exhibit a "flicker" or $|\omega|^{-1}$ type of noise modulating the frequency of the oscillator.

The method of finite differences of the phase is shown to be a powerful means of classifying the statistical fluctuations of the phase and frequency for signal generators in general. By employing finite differences it is possible to avoid divergences normally associated with flicker noise spectra. Analysis of several cesium beam frequency standards have shown a complete lack of the $|\omega|^{-1}$ type of noise modulation but an unexplained noise with a spectral variation proportional to $|\omega|^{-1/3}$ for frequency fluctuations was observed for $|\omega|$ less than $10^{-3}$ to $10^{-4}$ sec.$^{-1}$ depending on the particular standard.

**9553.** Barnes, J. A., Allan, D. W., **A statistical model of flicker noise,** *Proc. IEEE* **54,** No. 2, 176-178 (Feb. 1966).

Key words: Flicker; model; noise; statistical.

By the method of fractional order of integration it is shown that it is possible to derive the characteristics of flicker noise from those of "white," band limited noise. A formal expression for the relation of flicker noise to white noise is given. An approximate method, amenable to the use of digital computers, is also given for the generation of flicker noise modulated numbers from random, independent numbers.

**9554.** Barnes, J. A., **The development of an international atomic time scale,** *Proc. IEEE* **55,** No. 6, 822-826 (June 1967).

Key words: Atomic frequency standards; atomic time; coordination.

The paper reviews briefly the methods of generating atomic time and the errors inherent in the resulting scales. An atomic clock consists of an atomic frequency standard and an "integrator" to accumulate the phase of the signal. Because of noise perturbing the instantaneous frequency, an ensemble of identical atomic clocks will show a distribution of (epoch) times which is unbounded as the system evolves in time. The recognition of this problem has important consequences in national and international coordination of time scales and the construction of average atomic time scales.

Also of significance is the not completely resolved question of weighting of individual standards in the construction of average time scales. In spite of these difficulties it is pointed out that through coordination and proper data handling, most of the advantages of astronomical time scales can be realized by atomic time scales. A statement of some of the problems facing any attempts at coordination is presented without any suggested solutions.

**9555.** Bates, A. A., **Building code viewpoints,** (Building Research Institute Fall Conf., Codes Session, Washington, D.C., Nov. 16, 1966), *J. Bldg. Res. Inst.* **4,** No. 1, 48-49 (Jan.-Feb. 1967).

Key words: Building code; climate; control; coordinate; economics; geography; political; technical; technology; zoning.

The advancing technology of building as well as the steep continuing rise in costs, particularly of home-building, both make it inevitable that building will become an essentially industrialized activity. The unification of building codes is equally inevitable under the inescapable pressure for widened and simplified industrial markets. This is a world-wide trend already far advanced in all other developed countries. Rather than trying to obstruct the unification of building codes the industries and interests concerned would do well to organize their efforts toward an effective community of action which will make it possible to utilize modern technologies in the rebuilding of our cities. Ultimately in the United States as in every other advanced nation where precisely the same impersonal technological and economic forces are operative this will eventuate in a nation-wide building code. The problem is how to bring this about at a rate and in a manner which will best serve the interests of all concerned.

**9556.** Bates, R. G., **Acidity functions for amphiprotic media,** *Book, Chemistry of Nonaqueous Solvents* **1,** Chapt. III, 97-128 (Academic Press, Inc., New York, N.Y., 1966).

Key words: Acid-base behavior; acidity functions; nonaqueous media; pH.

The nature of acid-base interaction processes in solvents of varied characters is discussed and the usefulness of various units for measuring acidity in these media is examined. Both electrometric and indicator acidity functions are considered.

**9557.** Bates, R. G., **Acids, bases, and buffers,** (Proc. Symp. Current Concepts of Acid-Base Measurements, New York Academy of Sciences, New York, N.Y., Nov. 23, 1964), *Ann. N.Y. Acad. Sci.* **133,** Art. 1, 25-33 (1966).

Key words: Acids; bases; buffer capacity; pH scale.

The Arrhenius, Bronsted, and Lewis concepts of acidity are reviewed and expressions for the properties of buffer solutions are derived.

**9558.** Bates, R. G., **Electrometric methods of pH determination,** *Book, Standard Methods of Chemical Analysis, 6th Edition, IIIA. Instrumental Analysis,* Ed. F. J. Welcher, Chapt. 26, pp. 521-532 (D. VanNostrand Co., Inc., Princeton, N.J., 1966).

Key words: Glass electrodes; hydrogen electrodes; pH measurement.

This chapter discusses the nature of the definition of pH and the operational pH scale, describes the most useful pH-responsive electrodes and the most common reference electrodes and salt bridges, and sets forth the characteristics of modern pH instrumentation. Careful instructions for standardization of pH assemblies and for the measurement of the pH of unknown or test solutions are given, the limitations of experimental pH numbers are described, and the mode of interpretation of the measured pH is outlined.

**9559.** Bates, R. G., **Hydrogen-ion concentration,** *Encyclopedia of Chemical Technology, 2nd Edition* **11,** 380-390 (John Wiley and Sons, Inc., New York, N.Y., 1966).

Key words: Acidity; hydrogen ions; pH.

The definitions of acidity scales and methods for determining pH are reviewed.

**9560.** Bates, R. G., **pH determination,** *Encyclopedia of Industrial Chemical Analysis* **3,** 146-161 (John Wiley and Sons, Inc., New York, N.Y., 1966).

Key words: Glass electrodes; industrial analysis; pH determination; pH instrumentation; reference electrodes; temperature effects.

Procedures for the determination of pH by both electrometric and indicator methods are set forth. The NBS reference standard solutions are described. Other topics discussed include the limitations of measured pH values, glass electrodes and reference electrodes, pH instrumentation, temperature effects, and the special requirements of industrial pH control.

**9561.** Bates, R. G., **Proposal for the practical measurement of pH in amphiprotic and mixed solvents,** *Intern. Union Pure Appl. Chem. Info. Bull.* No. 26, 50-54 (Aug. 1966).

Key words: Amphiprotic and mixed solvent media; deuterium oxide; pH scale.

Procedures analogous to those on which a practical pH scale has been based can be used profitably to establish operational acidity scales in certain other amphiprotic and mixed solvent media. A universal pH scale relating proton activity uniformly to the aqueous standard reference state is not yet a practical possibility, but separate scales for each medium can be achieved and will fulfill most of the requirements. The best choice of unit appears to be $\mathrm{pa}_H^*$ or $-\log (m_{H} \cdot {}_s\gamma_H)$, where ${}_s\gamma_H$ is referred to the standard state in each particular medium $s$. Data for reference solutions in 50 wt. percent methanol and in deuterium oxide are given.

**9562.** Bates, R. G., **The Acheson medalist, Warren G. Vosburg, his life and career,** *J. Electrochem. Soc.* **113,** 309C (1966).

Key words: Acheson medal; electrochemistry; Vosburg, W. C.

Reflections on the personal life and professional career of the medalist.

**9563.** Bates, R. G., Robinson, R. A., **Acid-base behavior in methanol-water solvents,** (Proc. Intern. Symp. Electrochemical Society, Toronto, Canada, May 4-6, 1964), *Book, Chemical Physics of Ionic Solutions,* Chapt. 12, pp. 211-235 (John Wiley and Sons, Inc., New York, N.Y., 1966).

Key words: Acidity; acids; bases; medium effects; methanol-water solvents.

Data for (a) the standard potential of the cell Pt; $H_2$ (g., 1 atm), HX (in methanol-water solvents), AgX;Ag (where X = Cl, Br, or I); (b) the activity coefficients and relative partial molal heat content of HX in methanol-water media; and (c) the $pK$ and related thermodynamic quantities for the dissociation of weak acids in these solvents have been collected and critically examined. When the observed solvent effects on $pK$ for acids of different charge types are corrected for changes in the electrostatic energy of dissociation, one obtains a fairly uniform solvent parameter. The change of this parameter as methanol is added to the solvent confirms the view that enrichment with methanol produces a more basic mixture up to a composition of about 80 wt. % methanol, after which the total basicity declines as the water concentration becomes low. A standard activity scale for methanol-water solvents, based on the unit $p\mathrm{H}^*$, is proposed.

**9564.** Beatty, R. W., **Impedance measurements and standards for uniconductor waveguide,** *Proc. IEEE* **55,** No. 6, 933-941 (June 1967).

Key words: Impedance standard; reflection coefficient; reflectometers; standing-wave ratio; waveguide impedance.

A tutorial review is presented of the measurement of impedance and reflection coefficient in uniconductor waveguide. Impedance in a waveguide operating in a particular mode is defined and related to measured quantities such as the reflection coefficient and the VSWR.

Emphasis is given to the rectangular waveguide operating in its dominant mode and to the tuned reflectometer as an instrument for achieving the most accurate results. The evolution of the tuned reflectometer at NBS is outlined and recent techniques are discussed. Different types of standards of reflection coefficient are described and the advantages and limitations of each are mentioned.

**9565.** Beatty, R. W., **Microwave standards and measurements in the U.S.A., 1963-1966,** (Proc. XV General Assembly of URSI, Munich, Germany, Sept. 5-15, 1966), *Book, Progress in Radio Science 1963-1966,* Pt. 1, pp. 194-260 (International Scientific Radio Union, Munich, Germany, 1966).

Key words: Antenna gain; attenuation; field strength; impedance; measurement; microwave; noise; phase shift; power; progress; reflection coefficient; review; standards; survey.

A report is given on progress within the U.S.A. in the development of microwave standards and measurement methods at frequencies from 1 to 300 GHz. The period covered is the three years 1963-1966. The following topics are included within the scope of this report: power; noise; reflection coefficient and impedance; phase shift; attenuation and loss; and field strength and antenna gain.

**9566.** Beatty, R. W., **The system of electromagnetic quantities at frequencies above 1 GHz,** *Metrologia* **2,** No. 1, 46-54 (Jan. 1966).

Key words: Coaxial connectors; electromagnetic quantities; international comparisons of standards; microwave measurements; microwave standards.

The system of electromagnetic quantities at frequencies above $10^9$ cycles per second is briefly described, giving emphasis to those techniques and standards which have been most thoroughly evaluated and tested. The quantities included are power, noise temperature, reflection coefficient and impedance, phase shift, attenuation, and field strength. The measurement of frequency and wavelength, and of the microwave properties of materials is not within the scope of this paper.

In addition to a brief review, some of the problems involved in obtaining a higher order of accuracy are discussed. Comparisons of standards of different nations are mentioned and the benefits to be derived from such comparisons are described. Areas needing further research, as well as those which would benefit from international cooperation are designated.

Although a highly detailed and technical presentation is avoided, numerous references are given. In addition, a selected list of definitions is appended.

**9567.** Beatty, R. W., Weinschel, B. O., **Scanning the issue,** *Proc. IEEE* **55,** No. 6, 737-740 (June 1967).

Key words: Lasers; radiation; radio frequencies; radio frequency measurements; radio metrology; visible radiation.

This is the first special issue of the Proceedings of the IEEE to be devoted exclusively to the extensive subject of RF (radio frequency) measurements. Because it attempts to cover the entire field, the issue is rather large.

It consists entirely of invited papers which are grouped in two main sections; the first containing ten editorial and general articles, and the second containing 31 papers on specific technical subjects.

For the purpose of this issue, radio frequencies are considered to begin at approximately 30 kHz (30,000 cycles per second) and go upwards. The upper limit is not as yet clearly defined, but includes frequencies of coherent sources of visible radiation, such as lasers.

Because of the demanding requirements of military and space applications, many important improvements have recently been made in the science and art of RF measurements. Many are not yet covered in today's textbooks and are available here for the first time in one volume. This collection of techniques is designed to bring the engineer and scientist up to date and to serve as a reference issue on the present state-of-the-art of accurate RF measurements.

**9568.** Beehler, R. E., Glaze, D. J., **Evaluation of a thallium atomic beam frequency standard at the National Bureau of Standards,** *IEEE Trans. Instr. Meas.* **IM-15,** No. 1 & 2, 55 (Mar.-June 1966).

Key words: Cesium standard; frequency standard; thallium standard.

The original NBS cesium standard (NBS. I) has been converted to a thallium standard and was operated for 1 1/2 years with a typical precision of 2 x $10^{-12}$ and an accuracy of 1 x $10^{-11}$. Experiments are described which were performed to establish these precision and accuracy estimates. These results, which are comparable to those obtained with longer cesium standards, are considered sufficiently encouraging to justify the conversion of a longer cesium standard to thallium for a more thorough evaluation.

**9569.** Beehler, R. E., Glaze, D. J., **The performance and capability of cesium beam frequency standards at the National Bureau of Standards,** *IEEE Trans. Instr. Meas.* **IM-15,** No. 1 & 2, 48 (Mar.-June 1966).

Key words: Atomic beam; cesium; frequency standard; U.S. frequency standard.

NBS. II, the older of the two cesium atomic beam frequency standards which are used alternatively as the United States Frequency Standard, has been operating for more than five years. The contribution to inaccuracy produced by uncertainties in the C field has been reduced by a factor of 30 to ±2 x $10^{-13}$. The average precision of measurement (standard deviation of the mean) has been demonstrated to be 1 x $10^{-12}$ for averaging times of 1 hour and x $10^{-13}$ for 12 hours. The overall accuracy is considered to be ±8 x $10^{-12}$. A new cesium standard, NBS. III, with an interaction length of 3.66 meters is in operation and has demonstrated an improved average precision of 5 x $10^{-13}$ over 1 hour and an accuracy of ±5 x $10^{-12}$. The C field contributions to inaccuracy in this machine have been reduced to ±1 x $10^{-13}$. Considerable effort has been devoted to the detection and elimination of small frequency shifts produced by various electronic components of the excitation systems. In spite of the various improvements effected, a small unexplained difference in frequency of 1 x $10^{-12}$ continues to exist between the standards. The extremely high stability of the difference frequency, however, suggests that resolution of the difficulties should result in an accuracy capability of perhaps ±1 x $10^{-12}$.

**9570.** Beehler, R. E., Halford, D., Harrach, R., Allan, D., Glaze, D., Snider, C., Barnes, J., Vessot, R., Peters, H., Vanier, J., **An intercomparison of atomic standards,** *Proc. IEEE* **54,** No. 2, 301-302 (Feb. 1966).

Key words: Cesium; hydrogen maser; frequency comparison.

A group of two cesium beam frequency standards and three hydrogen masers were brought together for extensive intercomparisons at the National Bureau of Standards. After thorough evaluation of each of the two types of frequency standards a preliminary value of the free-space frequency for the transition $F=1 \leftrightarrow F=0$ of the ground electronic state in hydrogen has been obtained. This preliminary value is 1420,405,751.7860±0.0043 Hz. The uncertainty of 0.0043 Hz corresponds to an uncertainty of 3.2 parts in $10^{12}$.

**9571.** Beers, Y., Russell, T. W., **Evaluation of a Stark voltmeter,** *IEEE Trans. Instr. Meas.* **IM-15,** No. 4, 380-388 (Dec. 1966).

Key words: $CH_3CN$ (Acetonitrile); dipole moment; Fabry-Perot interferometer; Stark effect.

An absorption Stark voltmeter using a Fabry-Perot absorption cell with a rotational transition of $CH_3CN$ at 36 GHz has been built and evaluated. The rotational constant and dipole moment of this molecule have been redetermined and found to have the values 9198.56±0.10 GHz and 3.9185±0.0020 Debye, respectively. The short term precision of the device as used as a standard cell was better than one part in $10^5$, but there were unexplained drifts of 2 parts in $10^4$ per day. The accuracy of the device as a means of measuring voltage in terms of atomic and molecular constants, is 5 parts in $10^4$. The principal errors are due to the measurement of the plate spacing (which could be reduced by using an optical interferometer to measure spacing), pulling the interferometer resonance by the external circuit, and the effects of field nonuniformities due to the coupling holes.

**9572.** Beers, Y., **WWV moves to Colorado,** Part I, **QST 51,** No. 1, 11-14 (Jan. 1967); Part II, **QST 51,** No. 2, 30-55 (Feb. 1967).

Key words: Frequency broadcasts; history of broadcasts; standards of time and frequency; time and frequency.

This is a semi-popular account of the move of WWV from Greenbelt to Fort Collins, written at the request of the Editor of the leading amateur radio magazine "QST". It describes the role of NBS in providing standards of time and frequency, the history of the broadcasts, the usage of the broadcasts, and the new station.

**9573.** Bell, G. D., Paquette, D. R., Wiese, W. L., **Relative transition probabilities for prominent Ni I and Ni II lines in the near-ultraviolet,** *Astrophys. J.* **143,** No. 2, 559-572 (Feb. 1966).

Key words: Line strength; nickel-carbonyl; Ni I and Ni II; oscillator strength; relative measurements; transition probabilities; wall-stabilized arc.

Relative transition probabilities of 16 Ni I lines and 53 Ni II lines in the wavelength range from 2000-3600 Å have been measured with a wall-stabilized arc. The arc was operated at 10 amps in argon with a small admixture (.01%) of nickel-carbonyl. The spectrum was photoelectrically observed through the hollow electrodes. The relative intensity calibrations were performed with calibrated tungsten strip lamps or by utilizing the continuous emission of a hydrogen arc operated at known plasma conditions. The axis temperature of the argon nickel-carbonyl arc was determined from intensity measurements of argon lines of known transition probabilities and the application of the arc plasma equations. For the great majority of the relative f-values the experimental and theoretical uncertainties are 8 percent or better, but for a few weak lines the uncertainties go as high as 30 percent. Comparisons with other experimental and theoretical results are undertaken and fair agreement is obtained.

**9574.** Bender, P. L., **Polarization of cosmic OH 18-cm radiation;** *Phys. Rev. Letters* **18,** No. 14, 562-564 (Apr. 3, 1967).

Key words: OH radiation; polarization; saturation effect.

The mechanism suggested by Heer for producing polarization of OH stimulated emission has been investigated. It does not appear to be applicable to cosmic OH sources.

**9575.** Bennett, L. H., **Influence of an external magnetic field on nuclear resonance in ferromagnetic materials,** *J. Appl. Phys.* **37,** No. 3, 1242-1243 (Mar. 1, 1966).

Key words: Critical field; field dependence; nickel pellets; nickel powder; nuclear resonance; permeability.

The reduction in the amplitude of the nuclear magnetic resonance signal, as well as a change in line shape, upon the application of an external steady magnetic field has been measured for pure nickel at room temperature. Both the transverse and longitudinal configurations (steady field and rf field perpendicular and parallel, respectively) were measured for a sample of nickel powder and for bulk nickel. The signal amplitude drops faster in the longitudinal configuration than in the transverse for each specimen. The reduction in amplitude is considerably less for the pellets than for the powder. There is no sign of a critical field as previously reported. A comparison of the resonance results with the apparent permeabilities is presented.

**9576.** Bennett, L. H., Swartzendruber, L. J., **Ferromagnetic iron alloys lacking a hyperfine field at the iron site,** *Physics Letters* **24A,** No. 7, 359-360 (Mar. 27, 1967).

Key words: Alloys; cobalt; ferromagnetism; hyperfine fields; iron; moments; Mossbauer effect; superconductivity; titanium.

Although ferromagnetism has been reported for $TiFe_xCo_{1-x}$ when $0.3 \leqq x \leqq 0.7$, the Mossbauer effect shows no evidence for the existence of a localized moment at the iron site. Thus the magnetization is most likely due to a diffuse moment associated with the Ti atoms, implying itinerant ferromagnetism.

**9577.** Ben-Reuven, A., **Impact broadening of microwave spectra,** *Phys. Rev.* **145,** No. 1, 7-22 (May 1966).

Key words: Absorption; dielectric loss; gases; impact; line shape; microwave; permeability; permittivity; pressure broadening; relaxation; spectra.

A unified treatment of pressure-broadening phenomena in the microwave spectra of gases is worked out by adaptation of the theories of Baranger and Fano, in which the effects of inelastic collisions are properly taken into account. The rate of relaxation in non-resonant spectra (Debye relaxation) is expressed in terms of collision cross sections. Small deviations from the Debye shape are related to a second moment of the relaxation matrix. Damping in resonance lines is studied, taking into account the coupling of the positive and negative resonance transitions by collisions. A general expression of the line shape as a function of frequency and pressure is given in the impact approximation. The ammonia inversion spectrum serves to demonstrate its applicability.

**9578.** Ben-Reuven, A., **Symmetry considerations in pressure-broadening theory,** *Phys. Rev.* **141,** No. 1, 34-40 (Jan. 1966).

Key words: Collisions; gases; molecules; pressure broadening; radiation; relaxation; spectra; symmetry.

Symmetry properties of the Zwanzig-Fano relaxation matrix are studied. Its invariance under rotations and inversion is proven for isotropic gases, to all orders in the gas density. Each multipole radiation operator is confined to a distinct invariant subspace in the Liouville space of operators. These invariant subspaces form the basis for the reduction of the relaxation matrix; therefore, the various multipole spectra are broadened independently. Properties of the relaxation matrix under Liouville conjugation are studied, and expressions are given relating matrix elements in which Liouville-conjugate pairs of vectors are involved.

**9579.** Berkeley, J. F., Brenner, A., Reid, W. E., Jr., **Vapor deposition of tungsten by hydrogen reduction hexafluoride process variables and properties of the deposit,** *J. Electrochem. Soc.* **114,** No. 6, 561-568 (June 1967).

Key words: Deposition of tungsten; hydrogen reduction; investigation of variables; tungsten hexafluoride; vapor deposition.

An investigation of the variables involved in the deposition of tungsten from a mixture of tungsten hexafluoride and hydrogen has shown that the fastest rate of deposition (about 5 mils thickness in 2 min) was obtained at atmospheric pressure with a hydrogen/tungsten hexafluoride ratio of 1.5 (by volume) at a temperature of 800-850 °C. The presence of hydrogen fluoride or chloride in the reacting gases diminished the rate of deposition. The deposits had about the same hardness, electrical conductivity, and density as commercial wrought tungsten. The tensile strength of the deposits was about 30,000 lb/in.$^2$. The internal stress within the deposits was also about 30,000 lb/in.$^2$. Codeposition of carbon, from carbon monoxide, greatly increased the hardness of the deposits.

**9580.** Berger, M. J., Seltzer, S. M., **Additional stopping power and range tables for protons, mesons and electrons,** *NASA-SP* **3036** (1966).

Key words: Bremsstrahlung efficiency; electrons; mesons; protons; range; stopping power.

This report is a supplement to earlier tabulations in NAS-NRC Publication 1133 (also contained in NASA Reports SP-3012 and SP-3013). Data are given for liquid $H_2$, LiF, Si, Ge, propane and freon. In addition, earlier tables for electrons in muscle and bone are corrected.

**9581.** Berger, H. W., **The estimation of molecular weights of vinyl acetate copolymers in latex paints,** *J. Paint Technol.* **39,** No. 508, 310-315 (May 1967).

> Key words: Copolymer; intrinsic viscosity; latex; Mark-Houwink; molecular weight; polymer; polyvinyl acetate.

A viscometric technique has been used for the estimation of the molecular weights of vinyl acetate copolymers used in manufacturing latex paints. The whole paint is diluted with boiling acetone and the dissolved polymer is separated from pigments by centrifuging. The intrinsic viscosity, $[\eta]$, of the polymer in acetone at 25 °C is obtained and used to calculate a quantity related to the molecular weight. The various values for a and K, the constants in the Mark-Houwink Equation, that have been reported in the literature for PVA in acetone are used empirically to derive the equation, $\log \bar{M} = 1.45 \log [\eta] + 5.521$. This equation is used as the basis for the estimation of the molecular weights of PVA copolymers in experimental latex emulsions, experimental paints formulated with those latexes, and proprietary paints.

**9582.** Berman, H. A., West, E. D., **Density and vapor pressure of nitromethane 26° to 200 °C,** *J. Chem. Eng. Data* **12,** No. 2, 197-199 (Apr. 1967).

> Key words: Density and vapor pressure; nitromethane density; nitromethane vapor pressure; vapor and density pressure.

The density of nitromethane between 25 and 200 °C and its vapor pressure between 130 and 200 °C have been determined experimentally. Within these limits, the density is represented by the equation

$$d = 1.1615 - 1.1952 \times 10^{-3}\, t - 1.553 \times 10^{-6}\, t^2$$

and the vapor pressure by the equation

$$\log_e P = 10.8210 - 3905.39/(t+260)$$

where $d$ is in g/cm$^3$, $P$ in atm, and $t$ in °C.

**9583.** Bernstein, B., **Time-dependent behavior of an incompressible elastic fluid. Some homogeneous deformation histories,** *Acta Mechanica* **II,** No. 4, 329-354 (1966).

> Key words: BKZ theory; biaxial strain; constant rate of strain; creep; elastic fluid; elastic strain energy function; finite strain; non-linear behavior; non-Newtonian fluids; normal stresses; pure shear; simple extension; simple shear; stress relaxation; time effects; uniaxial strain; viscoelasticity.

The theory of the incompressible elastic fluid is designed to describe viscoelastic behavior under finite strain. In terms of this theory it is shown how to calculate the stress response to any strain history. The calculations are carried out and the results displayed for a number of homogeneous strain histories. A knowledge of the response to single step stress relaxation in a given geometry allows one to calculate easily response to any other history in the same geometry. Furthermore, from biaxial stress relaxation data one may calculate the time dependent stress response in any geometry in a manner which resembles the method for predicting the equilibrium response in an isotropic elastic material. An important class of histories comprises the motions following the rest history. To calculate the stress response for such a motion over a given time interval it suffices to have stress relaxation data over the same time interval. Stress response is also calculated for some uniaxial strain histories as well as steady simple shear.

**9584.** Billick, I. H., Dishon, M., Shulz, M., Weiss, G. H., Yphantis, D. A., **The effects of rotor deceleration on equilibrium sedimentation experiments,** *Proc. Natl. Acad. Sci.-Natl. Res. Council* **56,** No. 2, 399 (Aug. 1966).

> Key words: Centrifuge; equilibrium sedimentation; Lamm equation; rotor deceleration; sedimentation.

It is the purpose of this note to present some results of a combined numerical and theoretical analysis of rotor deceleration, applicable to equilibrium sedimentation experiments. These results indicate the magnitude of errors in the data from sedimentation experiments where rotor slowing occurs. Of possibly greater interest is the conclusion that artificially induced rotor slowing can be used to substantially speed up equilibrium sedimentation experiments. We have developed the theory for the rectangular approximation to the Lamm equation, and concurrently solved the Lamm equation numerically by a method already described. Detailed accounts of both the theoretical analysis and the numerical results will be presented elsewhere.

**9585.** Blair, B. E., Crow, E. L., Morgan, A. H., **Five years of VLF worldwide comparison of atomic frequency standards,** *Radio Sci.* **2,** No. 6, 627-636 (June 1967).

> Key words: Analysis of variance; atomic frequency standard errors; portable clock; VLF propagation.

The VLF radio broadcasts of GBR(16.0 kHz), NBA(18.0 or 24.0 kHz), and NSS(21.4 kHz) have enabled worldwide comparisons of atomic frequency standards to parts in $10^{10}$ or better when received over varied paths and at distances up to 9000 or more kilometers. This paper summarizes a statistical analysis of such comparison data from laboratories in England, France, Switzerland, Sweden, Russia, Japan, Canada, and the United States during the 5-year period 1961-1965. The basic data are differences in 24-hour average frequencies between the local atomic standard and the received VLF radio signal expressed as parts in $10^{10}$. The analysis of the more recent data finds the receiving laboratory standard deviations, $\alpha_i$, and the transmission standard deviation $\tau$, to be parts in $10^{11}$. Averaging standard frequencies over an increasing number of days has the effect of reducing $\alpha_i$ and $\tau$ to some extent. The variation of the $\alpha_i$ with propagation distance is studied. The VLF-LF long-term mean differences between standards are compared with the recent portable clock tests, and there is agreement to parts in $10^{11}$ or better. To separate further the sources of variation, including propagation and receiving laboratory systems, in future VLF comparisons of widely separated atomic frequency standards, we propose long-term, round-robin experiments with portable atomic standards.

**9586.** Blunt, R. F., **Optical absorption of cobalt in manganese fluoride,** *J. Chem. Phys.* **44,** No. 6, 2317-2320 (Mar. 1966).

> Key words: Cobalt in manganese fluoride; crystal spectra; manganese fluoride; optical absorption; polarized crystal spectra.

The polarized crystal spectra of cobalt-doped $MnF_2$ have been measured down to near 4.2 °K. Three broad, anisotropic bands near 7200, 14,000, and 20,000 cm$^{-1}$ are seen that are presumably due to the spin-allowed ${}^4T_{1g}(F) \rightarrow {}^4T_{2g}(F)$, ${}^4A_{2g}(F)$, and ${}^4T_{1g}(P)$ transitions of substitutional Co$^{2+}$, $3d^7$ ions. The $D_{2h}$ symmetry provided by the rutile structure of the $MnF_2$ lattice produced marked orthorhombic splitting of about 3000 cm$^{-1}$ in the ${}^4T_{1g}(P)$ band. Several weak spin-forbidden bands are also seen. The observed anisotropy indicates that the ${}^4T_{2g}(F)$ band is largely magnetic dipole while the other two are electric dipole. These latter parity-forbidden transitions are aided by coupling with odd lattice vibrations. Application of the appropriate selection rules allows tentative identification of several of the states involved.

**9587.** Blunt, R. F., Cohen, M. I., **Irradiation-induced color centers in magnesium fluoride,** *Phys. Rev.* **153,** 1031-1038 (Jan. 1967).

Key words: Color centers; magnesium fluoride; radiation damage.

Color centers, produced by 50-kV x rays, have been studied in the rutile-structured $MgF_2$, largely at room temperature. An initial; slightly anisotropic, absorption band near 260 nm is tentatively identified as due to *F* centers. Subsequent optical bleaching results in the formation of a strong band at 370 nm and several weak bands, including one at 320 nm. Both of these appear only for $E \perp c$ and are believed to be due to *M* centers. This choice of models is suggested, in part, by the observation of typical trapped-electron ESR spectra in irradiated samples. Bleaching studies show that the 320-nm band arises from centers lying along the $\langle 110 \rangle$ directions, while the 370-nm band seems to be cylindrically symmetric about the *c* axis. Furthermore, the 320-nm band is reversibly convertible into the 370-nm band. Selection rules have been derived for $(ls)^2 \rightarrow (ls2p)$ transitions in each of the four possible *M*-center configurations permitted in the rutile structure. It is found that of the two types having F-F bonds in the (001) plane, one identifies rather well with the 370-nm band and the other with the 320-nm band.

**9588.** Boden, N., Gutowsky, H. S., Hansen, J. R., Farrar, T. C., **Nuclear magnetic relaxation studies of $(CD_3O)_2{}^{11}BH$,** *J. Chem. Phys.* **46,** 2849 (1967).

Key words: Boron-11; $H^{11}B(OCD_3)_2$; hydride; hydrogen; liquid; proton; quadrupole coupling constant; spin-spin coupling constant.

The relaxation of quadrupolar nuclei in liquids lends itself in favorable cases to the approximate determination of quadrupole coupling constants which are not readily accessible by other means. In the present Note we report such an estimate of the $^{11}B$ quadrupole coupling constant $e^2qQ_{^{11}B}/h$ in dimethoxy($d_6$)borane($^{11}B$), $(CD_3O)_2{}^{11}BH$. The result is 2.6 MHz. Also, an activation energy of approximately 1.2 kcal $mole^{-1}$ was found for molecular reorientations in the liquid. The temperature-independent magnitude of the scalar internuclear coupling constant $J_{^{11}BH}$ was found to be 162.0 Hz, with an estimated uncertainty of ±1.0 Hz.

**9589.** Botter, R., Dibeler, V. H., Walker, J. A., Rosenstock, H. M., **Experimental and theoretical studies of photoionization-efficiency curves for $C_2H_2$ and $C_2D_2$,** *J. Chem. Phys.* **44,** No. 3, 1271-1278 (Feb. 1966).

Key words: $C_2D_2$; $C_2H_2{}^+$; $C_2D_2{}^+$; $C_2H^+$; $C_2D^+$; mass spectrometer; monochromator; photoionization.

Photoionization-efficiency curves for $C_2H_2$ and $C_2D_2$ have been remeasured in the wavelength region from onset of ionization to 600 Å, using a gold-coated grating and the Hopfield continuum as a photon source. The curve shapes of the molecule ions near threshold are compared with calculations of the Franck-Condon factors. Nearly exact agreement between experiment and calculation is obtained when taking into account hot bands. A general discussion is given for the shape of the molecule ion curve and for that of the fragment ions, $C_2H^+$ and $C_2D^+$. The observed onsets of ionization for the latter ions are $17.2_2$ eV and $17.3_4$ eV, respectively.

**9590.** Bowman, R. R., **Field strength: High accuracy measurements above 1 GHz,** *Proc. IEEE* **55,** No. 6, 981-990 (June 1967).

Key words: Antenna range design; field strength; gain corrections; high accuracy gain measurements; horn antennas; multi-path interference; two-antenna method.

To calibrate antennas for state-of-the-art field strength measurements, standard horns are needed with gain uncertainties well within ±0.1 dB. To attain this degree of accuracy for absolute gain measurements, the two-antenna method is recommended. This method is considered to be essentially an insertion loss measurement (with many additional problems and sources of error), and a working formula is derived that is suitable for gain measurements of high accuracy. The problems that appear to be most limiting in gain measurements, insufficient antenna separation and multi-path interference, are chosen for detailed discussion. (The discussion concerning multi-path interference has application to anechoic chamber evaluations and radar cross-section measurements as well as to gain measurements). It is concluded that error estimates of less than ±0.1 dB for horn gain measurements have been somewhat optimistic. Several ambiguities and sources of error have been overlooked or inadequately discussed, and additional discussion is presented to provide a more complete basis for horn gain measurements of high accuracy.

**9591.** Bozman, W. R., **Computer aided typesetting,** *Book, Advances in Computers* **7,** Chapt. 4, 195-207 (Academic Press, Inc., New York, N.Y., 1966).

Key words: Automation; computers; photocomposition; printing; publication; typesetting.

Several examples are given of typesetting prepared by a computer.

**9592.** Bradley, W. F., Graf, D. L., Roth, R. S., **The vaterite-type $ABO_3$ rare-earth borates,** *Acta. Cryst.* **20,** Pt. 2, 283-287 (Feb. 1966).

Key words: Borates; rare-earth; vaterite.

Approximate models for both the room temperature and high temperature modifications of the vaterite-type rare earth borate structure are deduced from X-ray powder diffraction data. A study of structure sensitive information, including optical properties and infrared absorption characteristics, leads to the conclusion that the low temperature form contains borate tetrahedra whereas the high temperature modification probably contains triangular borate ions inclined to the *c*-axis.

**9593.** Brady, G. W., McIntyre, D., Myers, M. E., Jr., Wims, A. M., **Critical scattering of the perfluoroheptane-iso-octane system,** *J. Chem. Phys.* **44,** No. 5, 2197-2198 (Mar. 1, 1966).

Key words: Correlation function; critical phenomena; critical scattering; scattered intensity; small angle x-ray scattering.

The critical opalescence of mixtures of perfluoroheptane-iso-octane near and at the critical concentration has been examined by x-ray scattering measurements over a large angular range.

The measurements are discussed and shown to agree well with the assumed correlation function proportional to $e^{-Kr} \cdot r^{-1.1}$ near the critical temperature.

**9594.** Brauer, G. M., **Dental applications of polymers: A review,** *J. Am. Dental Assoc.* **72,** 1151-1158 (May 1966).

Key words: Acrylic; dental resins; denture base materials; methacrylates.

The properties of acrylic polymers make them especially useful for denture base materials and plastic teeth. Plastic fillings have not been too successful due to their high coefficient of thermal expansion and lack of bonding to tooth structure. A cavity liner impervious to the mouth fluids that bonds to tooth structure is needed. If such a liner were available, the need for a filling material that matches the thermal expansion of the tooth would be less critical.

For taking impressions, silicones and polysulfides have been employed successfully. The possible application of other plastics such as epoxy, aziridino, polycarbonates and semi-organic polymers is reviewed.

**9595.** Brauer, G. M., **Measurement of the surface area and the heats of wetting of dentin powders,** (Proc. Second Workshop on Adhesive Restorative Materials, Charlottesville, Va., December 1965), *Book, Adhesive Restorative Dental Materials* **II,** 203-223 (Department of Health, Education, and Welfare, Public Health Service, Washington, D.C., 1966).

Key words: Dentin; heats of wetting; organic content of dentin; surface area.

This progress report describes the measurement of the "apparent heats of immersion" of powdered dentin which was characterized by surface area measurements and determination of organic matter. The specific surface of ground dentin which is nearly independent of particle size was found to be around 10 $m^2/g$. The percentage of volatile matter amounted to 30.0%. The measurement of the apparent heat of wetting of dentin gave a mean value from 5 runs of 0.894 $cal/m^2$, with a computed standard error of 0.040 $cal/m^2$ (or $7.96 \pm 0.35$ cal/g). From the magnitude of this value it appears that there may be some chemical interaction between water and the surface of the dentin. (1 cal = 4.1840 joules.)

The difference in the "apparent heat of immersion" by aqueous solutions containing ionic species or organic functional groups and the heat of wetting of dentin by pure water is indicative of any reaction of the added species with components of the tooth surface. Measurements of these heats of reaction should assist in developing methods for modifying tooth surface and in determining those groups that will bond effectively to tooth structure in an aqueous environment.

**9596.** Brauer, G. M., **The relationship between laboratory tests on solubility of zinc oxide-eugenol type cements and their behavior in the mouth,** *N.Y. J. Dentistry* **37,** No. 4, 146-149 (Apr. 1967).

Key words: Filling material: *o*-ethoxybenzoic acid; solubility and disintegration; zinc oxide-eugenol cement.

The solubility and disintegration in water and dilute acids of zinc oxide-eugenol (ZOE) and especially modified cements of improved physical properties containing *o*-ethoxybenzoic acid (EBA) is considerably lower than that of other dental cements. Contrary to these laboratory findings EBA fillings fail rapidly under oral conditions. Thus, a low solubility value may be useful in comparing the relative solubility of products of similar composition, but is not necessarily an indication of the success of such restorations in the mouth. Development of a reliable test that accurately predicts length of clinical service will require more basic knowledge of the material and of the many parameters encountered in the oral cavity.

**9597.** Braun, W., McNesby, J. R., Bass, A. M., **Flash photolysis of methane in the vacuum ultraviolet. II. Absolute rate constants for reactions of CH with methane, hydrogen, and nitrogen,** *J. Chem. Phys.* **46,** No. 6, 2071-2080 (Mar. 15, 1967).

Key words: CH; flash photolysis; hydrogen; kinetic spectroscopy; methane; nitrogen; rate constant; vacuum ultraviolet.

By means of kinetic spectroscopy, the concentration of CH has been measured in the flash photolysis of methane. Measurements were made by following the attenuation of $C^2\Sigma^+ \leftarrow X^2\Pi$ Q branch at 3143 Å where the disappearance of CH is of the first order in CH. Experiments were conducted with pure methane, methane+$H_2$, and methane+$N_2$. The reactions and the corresponding rate constants in $mole^{-1}cm^3sec^{-1}$ are

| | |
|---|---|
| $CH+CH_4 \rightarrow C_2H_5+H$ | $k=2.0 \times 10^{12}$ |
| $CH+H_2 \rightarrow CH_3$ | $k=6.2 \times 10^{11}$ |
| $CH+N_2 \rightarrow$ products | $k \simeq 4.3 \times 10^{10}$ |
| $CH+CH \rightarrow C_2H_2$ | $k \simeq 1.6 \times 10^{14}$ |

**9598.** Brenner, A., **Electrolysis of nonaqueous systems,** *Book, Advances in Electrochemistry and Electrochemical Engineering,* Ed. C. W. Tobias **5,** 205-248 (John Wiley and Sons, Inc., New York, N.Y., 1967).

Key words: Aluminum; beryllium; electrolysis; liquid ammonia; lithium; magnesium; nonaqueous systems, electrolysis of; potassium; sodium.

A survey is presented of the electrodeposition from organic solutions of lithium, sodium, potassium, beryllium, magnesium, and aluminum. The attempts to electrodeposit the rare earth metals are discussed. Also treated are the electrodeposition of metals from liquid ammonia and the electrolysis of essentially pure liquids, both organic and inorganic.

**9599.** Brenner, F. C., **The mechanics of durable press,** *J. Apparel Res. Found.* **1,** No. 2, 5-9 (Mar. 1966).

Key words: Durable press; fiber; uncured resin cellulose fabric; wash and wear performance.

Garments produced by the "durable press" processes exhibit superior "wash and wear" performance. The unique feature of the process is that the garment is made from an uncured resin treated cellulose fabric and the curing operation is carried out on the finished garment.

The treatment achieves its effect by reducing stresses built into the fabric and garment during manufacture. Stress is reduced by cutting the cellulose chains. The resin also coats the fibers with a lubricant and protects the fiber from penetration by water.

**9600.** Broberg, J. B. **Modular hardware for on-line handling of nuclear data,** *IEEE Trans. Nuclear Sci. NS*-**13,** No. 1, 192-198 (Feb. 1966).

Key words: Computer; data handling; instrumentation; nuclear; on-line.

At the National Bureau of Standards a flexible data handling system for use with the NBS Linac has been built. In developing this system the need for ease of modifications, ease of coding, and flexibility were carefully considered.

The NBS system is designed around a building block concept. Certain of these building blocks represent the necessary interface between the specialized input-output devices and the computer while the remainder of the blocks represent specific devices such as analog-to-digital converters, scalers, and other devices to facilitate man-machine communication at both local and remote stations.

The modular concept of both hardware and software development has allowed for great flexibility in the devices connected to the computer at any time and in the programs required for use with these devices. New hardware building blocks have been added to the system with no difficulty and with no change in existing programs.

The general building-block approach to the NBS system together with examples of specific units will be described.

**9601.** Brower, W. S., Fang, P. H., **Dielectric constants of $PbWO_4$ and $CaWO_4$,** *J. Appl. Phys.* **38,** No. 5, 2391 (Apr. 1967).

Key words: Calcium tungstate; dielectric constant; lead tungstate; single crystal.

The dielectric constants ($\epsilon'$) $PbWO_4$ and $CaWO_4$ were measured at 24.5 °C in air. Two specimens of each orientation were measured. The averages and deviations therefrom of the two measured values of the reflective dielectric constants are as follows:

$$PbWO_4 \epsilon' \| a 23.6 \pm 0.3; \ \epsilon' \| c 31.0 \pm 0.4;$$

$$CaWO_4 \epsilon' \| a 11.7 \pm 0.1; \ \epsilon' \| c 9.5 \pm 0.2.$$

**9602.** Brown, D. W., Wall, L. A., **The radiation-induced copolymerization of tetrafluoroethylene and 3,3,3-trifluoropropene at high pressure,** (Proc. Symp. Compilations of Data on Chemical and Physical Properties of Substances, 152nd National Meeting, Am. Chem. Soc., New York, N.Y., Sept. 13, 1966), *Polymer Preprint* **7,** No. 2, 1116-1132 (Sept. 1966).

Key words: Copolymerization; pressure; radiation and reactivity ratios; tetrafluoroethylene; trifluoropropene.

A study was made of the gamma-ray induced copolymerization of tetrafluoroethylene (TFE) and 3,3,3-trifluoropropene (TFP). Copolymerizations were carried out at 100 °C and 5000 atm pressure and at 21 °C and various pressures up to 8000 atm. The reactivity ratios calculated from the composition data indicate that the propagation rate constants favor addition of TFP by a factor of three to seven; individual values depended little on the polymerization pressure and temperature. Polymerization rates changed little with monomer composition between zero and 75% TFE; between 75 and 95% TFE they increased by a factor of ten. As many as 850,000 (molecules) were polymerized per 100 electron volts absorbed.

The copolymers are soluble in hexafluorobenzene at 29.6 °C if they contain less than 70% TFE. Intrinsic viscosities range from 0.1 to about 10 dl/g. From various considerations it appears likely that the degree of polymerization is about equal to the kinetic chain length in high pressure polymerizations at 21 °C; at autogenous pressure or at 5000 atm and 100 °C monomer transfer reduces the value considerably.

**9603.** Brown, E. H., **On the complex structure of the universe,** *J. Math. Phys.* **7,** No. 3, 417-425 (Mar. 1966).

Key words: Complex structure; electromagnetic fields; physical axioms; universe-complex structure.

A complex space-time is constructed from physical axioms. Both gravitational and electromagnetic fields are approximations to parts of a geometric object defined on this complex space, while other parts may represent strong and weak interactions. The intersections of the singularities of the three independent geometric invariants are identified as elementary particles. This identification leads to geometric definitions of mass and momentum and suggests the geometric significance of internal quantum numbers.

**9604.** Brown, P. J., **The role of NBS in motor vehicle safety research,** (Proc. Regional Meeting Society of Automotive Engineers, Gaithersburg, Md., Apr. 18, 1967), *SAE* No. 670204, p. 3 (June 1967).

Key words: Braking system; occupant restraint system research; research information exchange; role of NBS motor vehicle safety; tire system research.

The relationship of the National Traffic Safety Agency and NBS and an outline of the research programs in tire systems, occupant restraint systems, and braking systems. The immediate goals and objectives as well as the long-range objectives will be stipulated.

**9605.** Brown, R. L., **EPR spectrum of gas phase sulfur atoms,** *J. Chem. Phys.* **44,** No. 7, 2827-2828 (Apr. 1, 1966).

Key words: Atomic $g$ factors; atomic hydrogen; atomic reactions; electron paramagnetic resonance; sulfur atoms.

Ground-state S atoms have been detected by means of their paramagnetic resonance spectrum among the products of a reaction of $H_2S$ with discharged wet $H_2$. Atomic $g$ factors were determined for the $^3P$, and $^3P_2$ multiplet levels. The values were $g(^3P_1) = 1.501029 \pm 0.000042$ and $g(^3P_2) = 1.500541 \pm 0.000024$.

**9606.** Brown, R. L., Radford, H. E., **L-uncoupling effects on the electron-paramagnetic-resonance spectra of $N^{14}O^{16}$,** *Phys. Rev.* **147,** No. 1, 6-12 (July 8, 1966).

Key words: Electron-paramagnetic-resonance spectra; high resolution; L-uncoupling effects; microwave frequencies; S-band microwave frequencies; X-band.

High resolution paramagnetic resonance spectra have been obtained for the molecules $N^{14}O^{16}$ and $N^{15}O^{16}$ in the $J = 3/2$ and $J = 5/2$ rotational levels of the $^2\Pi_{3/2}$ ground state at X-band and S-band microwave frequencies. The results are: $g_J(N^{14}O^{16}; J = 3/2) = 0.777246 \pm 0.000018$, $g_J(N^{15}O^{16}; J = 3/2) = 0.778072 \pm 0.000020$; $g_J(N^{14}O^{16}; J = 5/2) = 0.316648 \pm 0.000045$; and $g_J(N^{15}O^{16}; J = 5/2) = 0.317617 \pm 0.000040$ for the molecular $g$ factors. The indicated uncertainties are estimated limits of error. The measured $g$ factors were compared with those calculated from the theory of magnetic effects on $\Lambda$-type doubling previously developed by Radford. Somewhat improved values for the $\Lambda$-type doubling frequencies and nuclear hyperfine structure coupling constants were also obtained.

**9607.** Brown, W. E., **Crystal chemistry of calcium phosphates,** *Proc. 1964 Technical Session on Cane Sugar Refining Research, New Orleans, La., Nov. 9-10, 1964,* pp. 26-34 (Agriculture Research Service, New Orleans, La., Mar. 1966).

Key words: Calcium phosphates; chemistry of calcium phosphates; crystal chemistry; thermodynamic and kinetic factors.

The capacity of the precipitate in the defecation step to remove impurities and its filterability are dependent on the physical and chemical nature of the crystallites. Depending on thermodynamic and kinetic factors prevailing at the time of precipitation, one or more of the salts hydroxyapatite, octacalcium phosphate, and anhydrous dicalcium phosphate, may form; variability in the process should be sought in the identity of the precipitate. The properties of the precipitate are thought to be especially dependent on the structural relationship between hydroxyapatite and octacalcium phosphate. Octacalcium phosphate may play a vital role in the growth of the crystallites even though it is metastable in the sugar solution.

Hydroxyapatite is the prototype for the principal crystalline phase in bone char. Two other calcium orthophosphates, beta-tricalcium phosphate and tetracalcium phosphate, can be stable under the conditions used to revivify bone char and may contribute to its chemical behavior.

**9608.** Brown, W. E., **Crystal growth of bone mineral,** *Book, Clinical Orthopaedics* **44,** 205-220 (J. B. Lippincott Co., Philadelphia, Pa., 1966).

Key words: Bone mineral; crystal growth; hydroxyapatite; octacalcium phosphate.

Formation of hydroxyapatite *in vitro* occurs either (1) through direct precipitation, or (2) by the initial formation of octacalcium phosphate followed by hydrolysis *in situ* to hydroxyapatite. The two processes lead to crystals with distinctive morphologies. A third process for the formation of hydroxyapatite (alternate precipitation of octacalcium phosphate and hydrolysis to hydroxyapatite on the unit-cell level) could lead to crystals with either morphology. Octacalcium phosphate plays a vital, albeit transitory, role in two of these processes and allows the interpretation of properties of apatitic materials without assumptions regarding the existence of arbitrary and ill-defined crystalline species. The effects of fluoride ions, in particular, on the properties of apatitic materials become understandable in terms of octacalcium phosphate as an intermediary in the crystallization of hydroxyapatite.

The role of octacalcium phosphate in the formation of tooth and bone is likely to be equally as great as that *in vitro*. Some of these possibilities are discussed for the first time.

**9609.** Brualdi, R., Newman, M., **Inequalities for the permanental minors of non-negative matrices,** *Can. J. Math.* **18,** 608-615 (1966).

Key words: Minors; non-negative matrices; permanents; stochastic matrices.

It is shown that if $A$ is an $n \times n$ non-negative substochastic matrix then the $r^{th}$ permanental compound of $A$ is also substochastic. If in addition $A$ is doubly stochastic, then it is shown that the sum of all principal permanental minors of order $r$ does not exceed $(n-1/r)+(n-1/r-1)$ per (A), with equality if and only if $A$ is the identity matrix.

**9610.** Burke, R. W., Menis, O., **Extraction-spectrophotometric determination of antimony as a ternary complex,** *Anal. Chem.* **38,** 1719 (Nov. 1966).

Key words: Antimony; brilliant green; dye impurity; extraction-spectrophotometric; ferrous and non-ferrous alloys; mechanism; sealed tube dissolution.

A critical examination is presented of the many parameters associated with the extraction-spectrophotometric determination of $Sb^{+5}$ as the ternary chloro complex of brilliant green, a triphenylmethane dye. The basic problem of dissolving the sample without residue problems and without volatilization of antimony is also discussed. A sealed tube dissolution procedure yields only $Sb^{+3}$, the requisite form. The step-wise reactions that may preclude the formation of the colored complex are discussed in terms of the interaction of the following variables: Oxidation and hydrolysis mechanism, spectral dependency on final choice of oxidant, role of $H^+$ and $Cl^-$ in the oxidation-extraction steps, the side reaction due to impurities in the dye, and the extraction characteristics of the ternary complex. The method has been applied to the analysis of both ferrous and non-ferrous standard reference materials with good success. The coefficient of variation is 2%.

9611. Bussey, H. E., **Measurement of RF properties of materials—a survey,** *Proc. IEEE* **55,** No. 6, 1046-1053 (June 1967).

Key words: Dielectric constant; dielectric loss; ferromagnetic resonance; permeability; radio materials measurement; review of radio materials.

Methods for radio and microwave measurements of dielectric and magnetic properties of materials are categorized, referenced, and placed in perspective. The reference period extends to mid-1966. Measurement errors are analyzed for appropriate cases where possible.

**9612.** Bussey, H. E., **Progress in measurement of electromagnetic properties of material, 1963 to mid-1966,** (Proc. XV General Assembly of URSI, Munich, Germany, Sept. 5-15, 1966), *Book, Progress in Radio Science 1963-1966,* Pt. 1, pp. 265-289 (International Scientific Radio Union, Munich Germany, 1966).

Key words: Bibliography; dielectric constant; ferromagnetic resonance; permeability; permittivity; review.

Progress on radio and microwave measurements of dielectric and magnetic properties of materials is reviewed mainly for the period 1963 to mid-1966. Important materials properties, theoretical analysis of circuits containing materials, and representative measurement methods are reviewed. In addition, some earlier basic work is referenced.

**9613.** Butler, T. W., Bloss, R. L., **A device for use in applying strain gages to cylindrical specimens,** *Exp. Mech.* **6,** No. 10, 528 (Oct. 1966).

Key words: Adhesive; application; curing; cylinder; installation; strain gage.

A simple device is described which applies a uniform pressure to the exterior of a cylindrical specimen. This device has been used in connection with a regulated air supply to apply pressure while curing strain gage installations.

**9614.** Calfee, R. F., Gates, D. M., **Calculated slant path absorption and distribution of stratospheric water vapor,** *Appl. Opt.* **5,** No. 2, 287-292 (Feb. 1966).

Key words: Atmospheric water vapor; calculated slant path; ratio model; water vapor.

A procedure is described for determining the amount and distribution of water vapor along a slant path through the atmosphere above 13.7 km. A multilayer analysis is used in which the transmittance of each layer is calculated and the accumulative effect obtained at the altitude of observation. The method depends upon the contribution of each line to the absorptance in a finite spectral region. From the analysis of recorded spectra a constant mixing ratio model is found to give a good fit.

**9615.** Calvert, W., **Observations of ionospheric irregularities and plasma resonances by the fixed-frequency topside sounder satellite,** (Proc. NATA Advanced Study Institute, Finse, Norway, April 1965), *Book, Electron Density Profiles in Ionosphere and Exosphere,* Ed. J. Frihagen, pp. 281-298 (North Holland Publ. Co., Amsterdam, The Netherlands, 1966).

Key words: Aurora; electrostatic wave; ionosphere; ionospheric ducting; ionospheric irregularity; ionospheric scattering; plasma resonance; radio sounding; satellite; topside.

The Explorer XX topside sounder is producing unique observations of ionospheric irregularities in electron density and of plasma-wave electrostatic resonances. The echoes from the irregularities are consistent with elongation along the earth's field and arise by two mechanisms: scattering and ducting. Scatter irregularities are invariably observed in sheets at high latitudes and are probably intimately associated with aurora. Duct irregularities, observed also at lower latitudes, are continuous between hemispheres and permit radio echoes from the conjugate reflection level. As the result of varying antenna attitude, the pattern of the resonance response is very complicated. While the patterns depend on gross changes in the conditions of observation, they are repeatable from day to day and give some insight into the excitation mechanism.

**9616.** Campbell, P. G., Wright, J. R., **Oxidation products in an oxygen-blown Kuwait asphalt,** *Ind. Eng. Chem. Product Res. Develop.* **5,** No. 4, 319-323 (Dec. 1966).

Key words: Additives; asphalt-Kuwait; flux; hardening; infrared spectroscopy; oxygen.

A Kuwait asphalt flux, which is ordinarily very difficult to harden, was treated with oxygen to prepare a coating-grade asphalt. Oxidative changes were measured by increase in softening point and by infrared spectroscopy. The infrared spectra of the coating-grade asphalt to which model organic compounds were added were compared with the spectrum of the original asphalt. The principal oxygen-containing products formed during hardening (oxidation), as assigned by infrared analysis, confirmed previous findings with asphalts from other geographical sources.

**9617.** Cannon, E. W., **Digital computers,** *Book, Encyclopedia of Physics,* Ed. R. M. Besancon, pp. 124-125 (Reinhold Publ. Corp., New York, N.Y., 1966).

Key words: Analog and digital computers; computers, digital; digital computers.

A general description of analog and digital computers is provided.

**9618.** Capps, W., Macedo, P. B., O'Meara, B., Litovitz, T. A., **Temperature dependence of the high-frequency moduli of vitreous $B_2O_3$,** *J. Chem. Phys.* **45,** No. 9, 3431-3438 (Nov. 1, 1966).

Key words: $B_2O_3$; high-frequency moduli; ultrasonic velocity.

Measurements of ultrasonic velocity allowed the calculation of the high-frequency shear and bulk moduli of $B_2O_3$ from 80 °C below to 300 °C above the glass transition. The temperature dependences of these moduli were found to be consistent with a semi-empirical extension of the theory of Zwanzig and Mountain.

**9619.** Case, W. E., Harrington, R. D., **Magnetization of iron for magnetometer calibrations,** *Proc. IEEE* **54,** No. 12, 2004-2005 (Dec. 1966).

Key words: Ferromagnetism; magnetization of pure iron; magnetometer calibration; measurement of magnetization.

It is shown that ultra pure iron spheres allow a simple and accurate calibration of vibrating sample magnetometers over a field range from 600 to 5000 oersteds using only one voltage and field reading. The same spheres may also be used to calibrate other types of magnetometers in this field range by simply assuming the magnetization M is related to the field $H_0$ by $M=(3)/(4\pi)H_0$.

**9620.** Casella, R. C., **Optical properties of $SrTiO_3$ under applied stress and electric field,** *Phys. Rev.* **154,** No. 3, 743-749 (Feb. 15, 1967).

Key words: Electro-optical effects; energy bands; selection rules; stress-optical effects; strontium titanate.

Motivated by recent experiments on the effects of uniaxial stress on the superconducting transition and normal-state transport properties of $SrTiO_3$, we have carried out a symmetry analysis, obtaining the perturbed band structure and optical selection rules for the cases of uniaxial stress along the (111) and (001) axes and of static electric field along (001). A comparison of the last case with $BaTiO_3$ in the $C_{4v}$ ferroelectric phase suggests a model with a reversal in the order of the valence bands in $SrTiO_3$ relative to that proposed earlier. Selection rules for polarized light are obtained for both models and criteria for deciding experimentally which is correct are stated. An example is given of how the sign of the relative energy shift of the conduction valleys with stress may be determined optically.

**9621.** Casella, R. C., **Comparison of three spin alegebras employed in SU(6) theories,** *Phys. Rev.* **147,** No. 4, 962-964 (July 1966).

Key words: Hadrons; little group; spin algebras; SU(6); W spin.

The Lipkin-Meshkov (LM) W spin, Foldy-Wouthuysen (FW) mean spin, and an algebra constructed from the four generators of the Wigner little group provide SU(2) algebras which can be imbedded in an SU(6) description of moving hadrons. It is shown that when acting on particle states obeying the Dirac equation, all three are identical. Differences occur with regard to behavior under charge conjugation. In particular, the FW spin acts on particles and antiparticles alike and, in the quark model does not lead to the LM spin flip between the vector and pseudoscalar mesons.

**9622.** Cassel, J. M., Christensen, R. G., **Volume change on formation of native collagen aggregate,** *Biopolymers* **5,** 431-437 (1967).

Key words: Collagen; dilatometry; hydrophobic bonding; "native" aggregation; volume change.

The volume change which occurs in dilute tropocollagen solution as a result of the phase transition producing the "native" form of collagen aggregate has been measured dilatometrically. A volume increase of 0.8 x $10^{-3}$ml/g. collagen in phosphate buffer (pH 7-7.5) was determined. The volume expansion is attributed to a reduction in the organization of water molecules around nonpolar surfaces of the individual tropocollagen units. This volume expansion is consistent with a previous hypothesis that hydrophobic bonding is the driving force in this collagen aggregation.

**9623.** Cassidy, E. C., Neumann, K. K., **Photographic and spectroscopic studies of exploding wires in a sealed vessel,** (Proc. 7th Intern. Cong. High-Speed Photography, Zurich, Switzerland, Sept. 12-18, 1965), *Book, Kurzzeitphotographie,* Ed. O. Helwich, pp. 178-185 (Verlag Dr. Othmar Helwich, Darmstadt, West Germany, 1967).

Key words: Electrical discharge; exploding wires; high-speed; photographic; spectrographic; time-resolved.

Investigations of the mixing process between exploding wires and a confined air environment are described. The various high-speed framing camera, combined framing camera and drum camera, drum camera, periodic still, and ultraviolet photographic techniques employed for time resolution of the explosion are described and illustrated. The photographic results are correlated with time-resolved (by photographic and photoelectric techniques) spectroscopic observations. Results have suggested a method and suitable intervals (during the explosion) for estimating the average temperature of the exploding vapor column. A phenomenon apparently due to reflecting shock waves was observed in a later stage of the explosion.

**9624.** Cassidy, E. C., Zimmerman, S. W., Neumann, K. K., **A method for time-resolved electrical measurements in high-current discharge experiments,** *Rev. Sci. Instr.* **37,** No. 2, 210-214 (Feb. 1966).

Key words: Circuit; electrical measurements; high-current circuit; high-current discharge; high-voltage circuit; resistive component; time-resolved electrical measurements; voltage.

A method for measurement of the resistive component of the instantaneous voltage across a sample installed in a high-voltage, high-current circuit is described. Simultaneous measurement of the current permitted time-resolved determination of electrical energy dissipation, power, and resistance of the sample. The system was calibrated calorimetrically, and measurements were made with exploding wire samples.

**9625.** Caswell, R. S., **Deposition of energy by neutrons in spherical cavities,** *Radiation Res.* **27,** No. 1, 92-107 (Jan. 1966).

Key words: Cavity chamber; energy deposition; linear energy transfer; neutrons; proportional counter.

A theoretical description of the interaction of neutrons with a spherical cavity has been developed in terms of four types of recoil particle interactions with the cavity called for convenience insiders, starters, stoppers, and crossers. Energy loss distributions are calculated for polyethylene-ethylene and tissue cavities and are found to agree with experimental measurements within the probable uncertainty of those measurements. Conditions for optimum use of proportional counter cavity dosimeters and the interpretation of measurements made with these instruments are discussed.

**9626.** Cataland, G., Plumb, H., **Calibration of germanium thermometers from 2°-20 °K,** (Proc. Intern. Inst. Refrigeration, Comm. 1, Boulder, Colorado, 1966, Annexe 1966-5), *Suppl. Bull. Inst. Intern. Froid,* pp. 153-163 (Louvain, Belgium, 1966).

Key words: Calibration at low temperature; germanium resistors; low temperature thermometry.

The National Bureau of Standards Provisional Temperature Scale 2-20 (1965) has been established for calibrating thermometers between 2° and 20 °K. The scale is the result of measurements with the National Bureau of Standards Acoustical Thermometer which determined isotherms of the speed of sound in helium-4 gas as a function of pressure. The isotherms were extrapolated to zero pressure, to approximate an "ideal gas", and from the intercepts values of temperature on the Thermodynamic Temperature Scale have been calculated. A group of reproducible germanium thermometers, calibrated at the isotherm temperatures, maintain the scale [NBS P 2-20 (1965)] against which submitted thermometers are calibrated.

To perform calibrations of submitted thermometers, a comparator was constructed. The temperature of the comparator can be maintained constant within 0.0005 °K for extended periods of time at any desired temperature within the calibration range. Calibrations of submitted thermometers consist of resistance determinations at approximately each degree from 2° to 20 °K. We attempt to fit a polynomial of the form

$$\log_{10}R = \sum_{n=0}^{m} A_n(\log_{10}T)^n,$$

– where the upper limit of $m$ is varied in individual functional fittings from 3 to 8 – to the individual resistor's calibration. For some types of resistors reasonable fittings (±.005 °K) of the calibration data are achieved.

**9627.** Catanzaro, E. J., **Correlation of some Precambrian rocks and metamorphic events in parts of Wyoming and Montana,** *Mt. Geol.* **4,** No. 1, 9-21 (1967).

Key words: Correlation; geochronology; geology; Montana; Precambrian; Wyoming.

A survey of the geology and geochronology of six areas in Wyoming and Montana, including the Beartooth, Bighorn, Wind River, Little Belt and Medicine Bow Mountains, and southwestern Montana suggests the presence of only three dateable pre-Belt Precambrian events: (1) >3100 m.y. The formation of the detrital zircon material now found in the Beartooth Mountains rocks; (2) 2700 m.y. A metamorphic event in all six areas; (3) 1900 m.y. A metamorphic event in the Little Belt and Medicine Bow Mountains and southwestern Montana. The age results suggest the possibility of stratigraphic correlation of metasedimentary rock formations in all six areas.

**9628.** Catanzaro, E. J., **Triple-filament method for solid-sample lead isotope analysis,** *J. Geophys. Res.* **72,** No. 4, 1325-1327 (Feb. 15, 1967).

Key words: Isotopes; lead; mass spectrometry; triple-filament.

A triple-filament method for lead isotope analysis has been devised. The source consists of rhenium-ribbon sample filaments and a platinum ribbon ionizing filament. Samples may be mounted as $PbCl_2$, $Pb(NO_3)_2$, or $Pb(OH)_2$; the $Pb(OH)_2$ appears to have the best qualities. Stable lead ion signals of $6 \times 10^{-11}$ amps are consistently obtained with 500 $\mu$g lead samples, while 20 $\mu$g samples give stable signals of $4 \times 10^{-13}$ amps. The triple-filament method does not have the ionization efficiency of the single-filament PbS or $PbC_2O_4$ methods, but it has much greater precision. Ten analyses of a reference sample gave 95% confidence limits (per analysis) of $Pb^{204}/Pb^{206} = 0.054\%$, $Pb^{207}/Pb^{206} = 0.023\%$, and $Pb^{208}/Pb^{206} = 0.071\%$.

**9629.** Catanzaro, E. J., Murphy, T. J., **Magnesium isotope ratios in natural samples,** *J. Geophys. Res.* **71,** No. 4, 1271-1274 (Feb. 15, 1966).

Key words: Isotope ratios; magnesium; natural; relative; survey.

Magnesium isotope ratios of 60 natural samples, including carbonate, evaporite, silicate, oxide, sea water, brine, meteorite, and biological samples, were measured by thermal emission mass spectrometry. Statistical analysis of the data reveals no evidence of variations among the natural samples or between any of the natural samples and a reference sample of magnesium metal. The 95% confidence limits are ±0.11% and ±0.22% for the $Mg^{24}/Mg^{25}$ and $Mg^{24}/Mg^{26}$ ratios, respectively.

**9630.** Chamberlain, G. E., **Multichannel resonances in the inelastic scattering of electrons by helium,** *Phys. Rev.* **155,** No. 1, 46-51 (Mar. 5, 1967).

Key words: Cross section; electron; excitation threshold; helium; inelastic scattering; negative ion; resonance.

Resonance structure due to intermediate negative-ion states has been observed in the differential cross section for inelastic scattering of electrons at zero angle in helium. Resonances were observed in all four of the $1s \rightarrow 2s$, $2p$ channels within the incident-energy range of 19.5 to 24 eV.

**9631.** Chang, S. S., Bestul, A. B., Horman, J. A., **Critical configurational entropy at glass transformation,** *Proc. VII Intern. Cong. Glass, Brussels, Belgium, 1965,* pp. 26.1-26.15 (Gordon and Breach, New York, N.Y., 1966).

Key words: Configurational entropy; critical configurational entropy; glass transformations; molecular configurational relaxation.

When an equilibrium supercooled liquid transforms to a glass, the amount of configurational entropy which it possesses at the glass transformation is trapped into the glass. By two different methods, and a distinguishable variation of one of them, it is shown experimentally that the value of this configurational entropy at glass transformation for most glasses for which data exist to evaluate it is near 0.7 cal deg$^{-1}$ per "bead" as defined by Wunderlich. These beads are equivalent to molecular chain links for polymers. The above stated result is obtained first by evaluating configurational entropy from experimental data on molecular configurational relaxation times, using a reinterpretation of the Williams-Landel-Ferry equation, for the temperature dependence of such relaxation times, in terms of configurational entropy rather then free volume. Secondly, the configurational entropy at glass formation is evaluated independently as the calorimetrically determined residual entropy of the glass at absolute zero temperature. In addition the above results imply a fixed value for the ratio of the glass transformation temperature to the reference temperature at which configurational entropy would vanish for an equilibrium supercooled liquid. This implication would provide a third method of evaluating configurational entropy at the glass transformation if the necessary reference temperature could be determined experimentally by a non-calorimetric method. The implications of the configurational entropy reinterpretation of the Williams-Landel-Ferry equation are examined.

**9632.** Chang, T. T., **Paramagnetic resonance spectrum of $W^{5+}$ in rutile ($TiO_2$),** *Phys. Rev.* **147,** No. 1, 264-267 (July 8, 1966).

Key words: Paramagnetic resonance spectrum; resonance; rutile; tungsten.

The paramagnetic resonance spectrum of $W^{5+}$ substitutional in $TiO_2$ was measured and analyzed. Both hyperfine lines and superhyperfine lines are observed. In the superhyperfine spectrum there is one group of relatively weak lines that is probably due to "forbidden" transitions. The g-factors are: $g_c = 1.4431$, $g_{110} = 1.5944$, $g_{110} = 1.4725$. The hyperfine coupling constants are $A_c = 63.7 \text{ x } 10^{-4} \text{ cm}^{-1}$, $A_{1\bar{1}0} = 92.5 \text{ x } 10^{-4} \text{ cm}^{-1}$, $A_{110} = 40.8 \text{ x } 10^{-4} \text{ cm}^{-1}$.

**9633.** Chivers, H. J. A., Hargreaves, J. K., **Slow fluctuations between conjugate points in the auroral absorption of cosmic noise,** *J. Atmos. Terrest. Phys.* **28,** 337-342 (1966).

Key words: Auroral absorption; conjugate points; cosmic noise; ionospheric absorption; slow fluctuations.

Ionospheric absorption is being measured with riometers at three pairs of conjugate points. When the ratio of absorption at a northern site to that at its southern conjugate is calculated for selected periods, it is found that the absorption ratio often exhibits slow fluctuations, which sometimes assume a quasi-sinusoidal appearance. Some properties of the fluctuations are described. Evidence is presented which indicates that the phenomenon is inter-hemispheric.

**9634.** Christ, W. W., Smith, G. V., **Comparison of the Hall-Petch parameters of zone-refined iron determined by the grain size and extrapolation methods,** *Acta Met.* **15,** 809-816 (May 1967).

Key words: Extrapolation methods; grain size; Hall-Petch parameters; iron, zone-refined; zone-refined, iron.

The dependence of the lower yield strength of zone-refined iron containing 0.0020 wt.% (carbon plus nitrogen) on grain size has been investigated at room temperature. In spite of the rather limited grain size variation possible with such pure metal, a meaningful determination of the Hall-Petch parameters has been made by the grain size method: friction stress $-2.5$ kg/mm$^2$, Petch slope $-2.4$ kg.mm$^{3/2}$. It is shown that tensile data obtained where the grain diameter is comparable to the minimum specimen dimension should not be included in the grain size method of analysis.

Analysis of tensile data by the extrapolation method produces Hall-Petch parameters which (1) are internally inconsistent, and (2) compare unfavorably with results of the grain size method. It is concluded that the extrapolation method in its present form is not an adequate substitute for the grain size method of evaluating the Hall-Petch parameters of iron.

**9635.** Cleek, G. W., **The optical constants of some oxide glasses in the strong absorption region,** *Appl. Opt.* **5,** No. 5, 771-775 (May 1966).

Key words: Fused silica; infrared absorption; infrared reflection; optical constants; oxide glasses; phosphate glass; silicate glasses.

The optical constants, $n$ and $k$, have been calculated for fused silica, three silicate glasses and a phosphate glass from reflectance measurements made in the strong absorption region, from about 7 to 13 $\mu$m. Plots of the $2nkv$ product, which corresponds to the conductivity, as a function of frequency are used to determine the location of the resonance frequencies in the infrared.

**9636.** Codling, K., **Structure in the photoionization continuum of $N_2$ near 500 Å,** *Astrophys. J.* **143,** No. 2, 552-557 (Feb. 1966).

Key words: Absorption spectrum; extreme ultraviolet; photoionization; Rydberg series.

The absorption spectrum of neutral $N_2$ has been studied in the 100-600 Å region, utilizing the pure continuum radiated by the 180 MeV electron synchrotron as a background source. A 3-meter grazing incidence spectrograph of 0.06 Å resolution was used to photograph the spectrum. Discrete structure was observed only in the 470-570 Å region. This previously unobserved structure appears to correspond basically to a single state of neutral $N_2$ having vibrational spacings very similar to those of the known $C^2\Sigma_u^+$ state of $N_2^+$. There are signs of a second state; the two states appear to form a Rydberg series converging to a limit at 23.6 eV. The structure involves transitions to autoionizing electronic states lying at higher energies than any previously reported for neutral $N_2$.

**9637.** Codling, K., **Structure in the photoionization continuum of $SF_6$ below 630 Å,** *J. Chem. Phys.* **44,** No. 12, 4401-4402 (June 15, 1966).

Key words: Absorption spectrum; Rydberg series; $SF_6$; spectral region 80 Å to 630 Å; vibrational band.

The absorption spectrum of neutral $SF_6$ has been studied in the far ultraviolet spectral region (80 Å to 630 Å) using the pure continuum radiated by the NBS 180 MeV electron synchrotron as a background source. A well-developed vibrational band was observed in the 550-600 Å region. A Rydberg series of neutral $SF_6$ was observed in the 450-500 Å region, converging to a limit at 26.83 (±0.04) eV. Additional absorption features were evident with peaks at 435 Å and 350 Å. Absolute absorption cross-section measurements were made at 539, 584, and 704 Å. The values obtained were 170Mb, 70Mb, and 100Mb, respectively; the error in these measurements is thought to be no more than 25%.

**9638.** Codling, K., Madden, R. P., Ederer, D. L., **Resonances in the photoionization continuum of Ne I (20-150 eV),** *Appl. Phys. Rev.* **155,** No. 1, 26-37 (Mar. 5, 1967).

Key words: Absorption spectrum; analysis; Ne I; resonances; synchrotron light; 20-150 eV.

The absorption spectrum of neon in the region 20-150 eV has been studied photographically and photoelectrically, using synchrotron light as a background source. Discrete structure has been observed in three distinct energy ranges. The first is between the $^2P_{1/2,\ 3/2}$ limit near 22 eV, involving resonances analogous to those observed by Beutler in Ar, Kr, and Xe; the second is the region between 44 and 60 eV, the structure here being classified as due to two types of excitation: (i) the excitation of a subshell $s$ electron, (ii) the simultaneous excitation of two outer $p$ electrons; the third region is near 80 eV, where two weak resonances are observed, due presumably to the simultaneous excitation of a subshell $s$ and an outer $p$ electron. The resonance profiles of the states $2s2p^6np\ ^1P^\circ_1$, where $n = 3,4$, and 5, and the two-electron excitation state $2p^4(^3P)3s3p\ ^1P^\circ_1$ have been studied quantitatively and values of $q, \Gamma$ and $\rho$ determined for each.

**9639.** Codling, K., Madden, R. P., Hunter, W. R., Angel, D. W., **Transmittance of tin films in the far ultraviolet,** *J. Opt. Soc. Am.* **56,** No. 2, 189-192 (Feb. 1966).

Key words: Absorption; films; spectra; tin; transmittance; ultraviolet; x-rays.

The transmission spectra of tin films ranging in thickness from 680 to 1690 Å have been studied in detail in the spectral range 1000-80 A, utilizing both photoelectric and photographic detection. The photoelectric results, using a multiline source, give measured values of transmittance, while the photographic results, using the pure continuum radiated by the NBS 180 MeV electron synchrotron, show the behavior of the transmittance curves between measured data points. These new measurements, giving continuous and extended information, allow an interpretation of the transmission characteristics of tin in terms of atomic and solid state parameters. In particular, the photographic data locate the $N_{IV,V}$ x-ray edges with increased accuracy [$N_V = 23.8$ ($\pm 0.1$) eV; $N_{IV} = 24.9$ ($\pm 0.1$) eV]. Of practical importance, a film of thickness 680 Å has a transmittance of over 20% from 700 to 525 Å. Of theoretical significance is a broad absorption feature centered near 190 Å, due to the high oscillator strength for transition of the 4*d* electron to continuum states of *f* symmetry.

**9640.** Collier, R. S., Kamper, R. A., **Energy gap of superconducting tin films in a magnetic field,** *Phys. Rev.* **143,** No. 1, 323-328 (Mar. 1966).

Key words: Electron tunneling; Ginzburg-Landau theory; magnetic field; superconduction; thin film; tin; vortex model.

We have observed the behavior of clean superconducting thin films of tin in both parallel and perpendicular magnetic fields. The results are quantitatively consistent with an interpretation based on the Ginzburg-Landau theory. For the parallel field we have generated one-dimensional numerical solutions of their equations, while for the perpendicular field we have used a refinement of a vortex model proposed by Tinkham which is based on their expression for free energy.

**9641.** Colson, J. P., Eby, R. K., **Melting temperatures of copolymers,** *J. Appl. Phys.* **37,** No. 9, 3511-3514 (Aug. 1966).

Key words: Comonomer concentration; comonomer defect; copolymers; defect energy; equilibrium melting temperature; lamella thickness; melting temperature; surface energy; tetrafluoroethylene-hexafluoropropylene.

The melting temperatures (532 to 580 °K) of copolymers of tetrafluoroethylene and hexafluoropropylene have been measured on a microscope hot stage. The copolymers had concentrations of perfluoromethyl groups between 0.0275 and 0.075 groups per carbon atom and lamella thicknesses which varied from 340 to 500 Å independently of comonomer concentration. An equation based on the concept of inclusion of the groups within the lamellar crystals as defects has been fitted to the data. The constants of fitting yield the equilibrium melting temperature, $616.6 \pm 4.9$ °K, the surface energy, $4.5 \times 10^{-13} \pm 1.6 \times 10^{-13}$ erg/fold, and the perfluoromethyl defect energy, $0.047 \pm 0.003$ eV/defect. Within the limits of error, these values are shown to be satisfactory by the possible comparisons with previously reported values or with values deduced from physical models. Neglecting the effect of lamella thickness yields a significantly poorer fit of the data.

**9642.** Cooper, J. W., Ormonde, S., Humphreys, C. H., Burke, P. G., **Autoionizing D states in He below the $n = 2$ level of $He^+$,** *Proc. Phys. Soc.* **91, 285-287 (1967).**

Key words: Autoionizing series; calculation; close coupling; level width; resonance.

Positions and widths of the autoionizing $^1D$ and $^3D$ levels lying below the $n = 2$ level of $He^+$ are calculated by close coupling methods and compared with experiment and previous calculations.

**9643.** Coriell, S. R., Parker, R. L., **Role of surface diffusion in stabilizing the surface of a solid growing from solution to vapor,** *J. Appl. Phys.* **37,**No. 4, 1548-1550 (Mar. 15, 1966).

Key words: Cylindrical and spherical shapes; solution or vapor; spherical shapes; vapor.

The effect of surface diffusion on the stability of shape of a solid growing by diffusion in a supersaturated solution of vapor is considered. Cylindrical and spherical shapes are treated. It is found that under some conditions surface diffusion can provide a significant enhancement of the stability.

**9644.** Cornog, J. R., Bryan, H. L., Jr., **Search methods with transistor patent applications,** *IEEE Spectrum* **3,** No. 2, 116-121 (Feb. 1966).

Key words: EDP system; patent; patent information retrieval; patent search; transistor.

As the world has become more technically oriented, the number of patent applications has been increasing also too rapidly for the Patent Office to assimilate them comfortably with current techniques. When an application for a patent is received, it must be evaluated as to novelty by a specialist who searches the prior art for similar patents. Previously, all such searches were done manually, which meant that the examiner had to rely entirely on his knowledge and experience. In an effort to remedy the situation the Office has instituted mechanized search methods. In order to ascertain the differences in patterns of thinking associated with manual and mechanized searches, a study was carried out in which a patent application in the transistor art was searched both manually and by a mechanized method. The mechanized search in this case permitted more patents to be analyzed more quickly but, being completely literal, it does not allow for hunches or browsing.

**9645.** Corruccini, R. J., **Properties of liquid hydrogen,** (Proc. Intern. Inst. Refrigeration, June 9-11, 1965), Chapter in *Liquid Hydrogen,* pp. 65-106 (Paris, France, 1965).

Key words: Cryogenic; hydrogen; liquid; low-temperature; properties.

A review is presented of the physics of liquid hydrogen, and extensive extracts are provided of the available data on those of its physical properties that are important in technology.

**9646.** Costrell, L., **Progress in nuclear electronics,** Chapter in *Radioisotopes for Aerospace, Part 1: Advances and Techniques,* pp. 1-13 (Plenum Press, New York, N.Y., 1966).

Key words: Modules; nuclear instruments; progress; standards; state-of-the-art.

At the conclusion of World War II nuclear instrumentation was to a great extent concerned with detectors that required essentially unsophisticated electronics. The advent of the scintillation counter in the late 1940's called for an order of magnitude improvement in the associated instrumentation. Introduction of the semiconductor radiation detectors with their tremendous energy resolution capabilities stimulated additional sophistication of nuclear electronics.

**9647.** Cox, A. P., Kuczkowski, R. L., **The microwave spectrum, structure, dipole moment, and quadrupole coupling of trans-nitrous acid,** *J. Am. Chem. Soc.* **88,** No. 22, 5071-5074 (Nov. 1966).

Key words: Dipole moment; microwave spectra; nitrous acid; quadrupole coupling constants; structure.

Mixtures of NO, $NO_2$ and $H_2O$ in a waveguide cell have produced pressures of nitrous acid sufficient for the assignment of the trans-isomer by microwave spectroscopy. Accurate values of the B and C ground-state rotational constants have been determined for the normal, deuterated and nitrogen-15 species of trans-nitrous acid.

The data are consistent with the expected planar configuration and on this basis the following structure has been calculated for trans-nitrous acid:

$$N-O(H)=1.433,\ N-O=1.177,\ \text{and}\ O-H=0.954\ \text{Å}$$

$$\angle ONO=110°39'\ \text{and}\ \angle NOH=102°3'.$$

Quadrupole coupling constants for the nitrogen-14 nucleus in the normal and deuterated species have been determined; the values for trans-$HNO_2$ are:

$$\chi_{aa}=1.91,\ \chi_{bb}=-5.39\ \text{and}\ \chi_{cc}=3.48\ \text{Mc/s}.$$

The components of the dipole moment in the nitrogen-15 molecule have been determined to be $\mu_a = 1.387 \pm 0.01$ D, $\mu_b = 1.223 \pm 0.06$ D and yield a value for the total dipole moment = $1.85 \pm 0.06$ D inclined at an angle of $41°24' \pm 24'$ to the a principal axis.

The structure of trans-nitrous acid is discussed on the basis of this data.

**9648.** Coyle, T. D., Johannesen, R. B., Brinckman, F. E., Farrar, T. C., **Nuclear magnetic resonance studies of inorganic fluorides. II. Solvent effects on J($^{29}$Si–$^{19}$F) in silicon tetrafluoride,** *J. Phys. Chem.* **70,** No. 5, 1682-1684 (May 1966).

Key words: Fluorine; fluorosilanes; nuclear magnetic resonance; $SiF_4$; silicon; solvent; spin coupling constants.

Solvent dependence of the $^{29}$Si–$^{19}$F nuclear spin coupling constant has been observed for $SiF_4$ in solutions in a range of 24 solvents. Similar effects are noted in related molecules.

**9649.** Crawford, M. L., Hudson, P. A., **A dual-load flow calorimeter for RF power measurement to 4 GHz,** (Annual ISA Conf. New York, N.Y., Oct. 1966), *ISA Preprint* No. 12.8-3-66 (Oct. 1966).

Key words: Coaxial; flow calorimeter; radio frequency power.

A new dual-load flow coaxial calorimeter power meter has been constructed at the National Bureau of Standards, Boulder Laboratories. Designed for use as a reference standard, the frequency range of the calorimeter extends up to 4 GHz and beyond. The power range extends from 2 W to 100 W with an error limit of 0.38 percent.

Design details, error analysis, and results of intercomparison with other standards are given.

**9650.** Crow, E. L., **Optimum allocation of calibration errors,** *Ind. Quality Control* **23,** No. 5, 215-219 (Nov. 1966).

Key words: Calibration of errors; national standards; optimum allocation; secondary standards.

Answers are given to two questions, with emphasis on the second. (a) How do the errors accumulate from echelon to echelon in a hierarchy of calibrations? (b) If a certain accuracy is required at the final echelon of a hierarchy, what is the best way to achieve that accuracy, or, more specifically, what is the optimum allocation of errors among the echelons? The criterion for optimization is taken to be the minimization of the total cost of achieving a given accuracy.

**9651.** Cullen, W. C., Boone, T. H., **Progress in the development of a thermal-shock resistance factor for bituminous built-up roofing membranes,** *Am. Soc. Testing Mater. Spec. Tech. Publ.* **409,** 151-161 (Apr. 1967).

Key words: Development; roofing membrane; strength properties; thermally induced forces; Thermal-Shock Resistance Factor.

The resistance of bituminous built-up roofing membranes to thermally induced forces is considered in terms of their strength properties such as breaking load in tension, modulus of elongation and apparent linear thermal expansion coefficient. The development of a Thermal-Shock Resistance Factor is described and values are given for three bituminous built-up membranes at temperatures of −30 °F (−34.4 °C), 0 °F (−17.8 °C) and 73 °F (22.8 °C). The apparent relation between the values obtained in the laboratory and the observed performance of roofing membranes in service is considered. The utilization of the Thermal-Shock Resistance Factor in the reduction of potential failures of bituminous built-up roofing membranes in service from thermally induced forces is also discussed.

**9652.** Currie, L. A., **Systematic errors in "recovery" and "detection" efficiency as related to radiochemical analysis,** Proc. 11th Annual Bio-Assay and Analytical Chemistry Meeting, Albuquerque, New Mexico, Oct. 7-8, 1965, *AEC* No. 651008, pp. 35 (Clearinghouse for Federal Scientific and Technical Information, Springfield, Va., 1967).

Key words: Bio-assay; carbon-14; detection efficiency; isotope dilution; "over-all" yield; radiochemical analysis; random errors; systematic errors; thorium chemical yield.

Evidence of systematic error in the assay of thorium arose when the chemical yield from a biological sample seemed to depend upon the detection method. When $\alpha$-counting and spectrophotometry were applied to different aliquots of the same sample, following chemical purification, the discordant chemical yields pointed to variations in detection efficiency. The difficulty arises because determination of the chemical yield is based upon the known disintegration rate of a "spike" which has been chemically processed, and upon the detection efficiency, which is generally determined by means of a standard which may not have been chemically processed. Thus, if the nature of the original sample or the resultant material in any way influences the final detection efficiency, the calculated recovery and its relative variance must be incorrect.

Systematic errors in recovery and detection efficiency may be eliminated in one of two ways: (1) direct measurement of the "over-all" yield—the product of chemical yield and detection efficiency, (2) accurate determination of both the chemical yield and the detection efficiency by such methods as isotope dilution and internal (efficiency) monitoring, respectively. Experimental illustrations are given for analyses of thorium and of carbon-14.

**9653.** Cutkosky, R. D., Lee, L. H., **An improved transportable ten picofarad capacitor,** *Proc. 11$^e$ Session, Comite Con. d'Electricite, May 10-12, 1965,* pp. 65-66 (Gauthier-Villars, Paris, France, 1965).

Key words: Capacitance standards; fused silica dielectric; picofarad capacitor; shock sensitivity; stability of value; ten picofarad capacitor; transportable ten picofarad capacitor; unit of capacitance; volume dependence.

By design modifications improvements have been achieved in the performance of 10-pF capacitance standards with fused silica dielectric as regards voltage dependence, shock sensitivity, and stability of value. It is suggested that standards of the new design are suitable for interlaboratory comparisons of the unit of capacitance.

**9654.** Danielson, B. L., **An optical power limiter,** *Appl. Opt.* **6,** No. 1, 158-159 (Jan. 1967).

Key words: Fluorescence; light flux; optical power limiter; photomultiplier tube; saturation.

A power limiting detector is described which is suitable for use in monitoring laser or other high intensity radiation in the 2900 to 3400 Å region. This device employs the saturable single crystal phosphor $CaF_2$(Ce, Mn) in connection with a photomultiplier tube which is sensitive to the sensitized Stokes-shifted $Mn^{2+}$ fluorescence. The maximum fluorescent intensity of this crystal can be controlled by appropriate choice of impurity concentrations. Limiting the light flux in this way minimizes fatigue effects and possible damage due to inadvertent overloading of the photomultiplier tube.

**9655.** Danielson, B. L., **Saturation effects in the sensitized fluorescence of $CaF_2$ (Ce, Mn),** *Phys. Rev.* **142,** No. 1, 228-230 (Feb. 4, 1966).

Key words: Fluorescence; quantum efficiencies; resonant energies; sensitized fluorescence.

The visible fluorescence of $Ce^{3+}$ and $Mn^{2+}$ impurities in crystals of $CaF_2$ has been investigated under conditions of intense uv irradiation. A change in the fluorescent quantum efficiencies for both impurities is observed at high intensities. In particular, the resonant energy transfer from a $Ce^{3+}$ sensitizer to a neighboring $Mn^{2+}$ begins to saturate. A simple model is postulated to explain this effect. From this model an estimate can be made of the number of sensitizable sites surrounding the $Ce^{3+}$ The rather large numbers obtained, about 150, may be due to some pairing of the $Ce^{3+}$ and $Mn^{2+}$ ions.

**9656.** Danos, M., Gillet, V., **Stretch scheme, a microscopic description of rotations in nuclei,** *Phys. Rev. Letters* **17,** No. 13, 703-705 (Sept. 26, 1966).

Key words: Nuclear levels; nuclear rotation; nuclear spectroscopy; nuclear structure; quantum mechanical precession; rotational states.

A good angular momentum wave function containing the maximum possible intrinsic angular momenta leads to rotational spectra. The rotational excitation energies arise from the residual two-body force.

**9657.** Danos, M., Greiner, W., **Treatment of nuclear reactions above the two-particle threshold,** *Z. Phys.* **202,** 125-149 (1967).

Key words: Configuration interaction; continuum states; nuclear reactions; nuclear structure; sequential decays; two-particle reactions.

In principle, an exact formalism for describing nuclear reactions above the two-particle emission threshold is developed. The eigenchannels, i.e., the eigenstates of the S-matrix, are computed directly from the shell model. No artificial assumptions have to be made about the properties of the rescattering of the two final state particles; the final state interactions are completely taken into account. Detailed prescriptions are given on how to reduce the exact description to a form amenable to numerical computations. Finally, long lived intermediate states leading to the so-called sequential decays can, if so desired, be singled out and treated separately. This again involves no specific assumptions. The treatment is applicable also above the three- or more-particle threshold.

**9658.** Danos, M., Greiner, W., **Eigenchannel theory of nuclear reactions,** *Phys. Rev.* **146,** No. 3, 708-712 (June 1966).

Key words: Nuclear continuum states; nuclear reactions; nuclear scattering; scattering matrix; shell model; S-matrix eigenstates.

A method is proposed by which the eigenstates and the eigenvalues of the S-matrix, i.e., the eigenchannels, can be directly computed from the nuclear problem, for example from the shell model. The calculation of all cross sections, viz. partial and total cross sections, is then exceedingly simple. The characteristics of the eigenchannels are described and the relation with other reaction theories is briefly discussed.

**9659.** Davis, J. C., **Technical committee 1.2 activities in psychrometry,** *ASHRAE J.* **8,** No. 4, 64 (Apr. 1966).

Key words: Instrumentation-measurement; metric psychrometric charts; psychrometric charts; psychrometric formula; temperature for moist air and enthalpy; thermodynamic watt bulb temperature.

**9660.** Davis, M. M., Hetzer, H. B., **Titrimetric and equilibrium studies using indicators related to Nile Blue A,** *Anal. Chem.* **38,** 451-461 (Mar. 1966).

Key words: Acid-base indicators; acidity in nonaqueous solvents; aprotic solvents; Methyl Yellow; Nile Blue A and derivatives; Nile Blue oxazone; nonaqueous acid-base spectrophotometry; nonaqueous acid-base titrations; phenyl diethyl Nile Blue; *p*-tolyl di-*n*-propyl Nile Blue base; relative strengths of indicator dyes; solvatochromism.

The behavior of Nile Blue A and several closely related dyes in nonaqueous spectrophotometry and titrimetry was explored. Nile Blue A was used as the salt, the anhydro-base, and the oxazone. The other dyes were the chloride or anhydro-base having an alkyl, aralkyl, or aryl group attached to the 5-amino nitrogen in place of hydrogen. The arylamino derivatives, though less basic than Nile Blue A, are much stronger than Methyl Yellow and are useful reference bases in aprotic solvents. Their applicability in determining stoichiometry and the relative strengths of strong and moderately strong acids is discussed. The strengths of the indicators relative to sulfonephthaleins and other common acid-base indicators are different in aqueous and non-aqueous solvents, pointing to a useful role in non-aqueous differentiating titrations.

**9661.** Davis, M. M., Paabo, M., **Comparative strengths of aliphatic acids and some other carboxylic acids in benzene at 25°,** *J. Org. Chem.* **31,** 1804-1810 (1966).

Key words: Absorbance data; acid-base association constants; acid dimerization constants; acidic strengths in benzene; aliphatic acids; benzene; bromophthalein magenta E; carboxylic acids; comparative strengths; diphenylguanidine; tetrabromophenolphthalein ethyl ester.

In continuation of earlier measurements (M. M. Davis and H. B. Hetzer, *J. Res. Natl. Bur. Std.* **60,** 569 (1958)), the strengths of the following acids (HA) in benzene have been determined: all of the straight-chain aliphatic acids containing from 2 to 20 carbon atoms except the 15- and 19-carbon acids; isobutyric acid and trimethylacetic (pivalic) acids; and *o*-benzoylbenzoic, *trans*-cinnamic, 2,4- and 2,5-dimethylbenzoic, 2-furoic, and 1- and 2-naphthoic acids. The relative strengths in benzene are expressed as equilibrium constants ($K_{BHA}$) for 1:1 association of HA with 1,3-diphenylguanidine (B) in the presence of the indicator acid (3′,3″,5′,5″-tetrabromophenolphthalein ethyl ester, "bromophthalein magenta E"). Dimerization constants ($K_{1,2}$) for some of the carboxylic acids have also been deduced from the absorbance data; the values compare favorably with those available from other measuring procedures. The new results conform to linear relationships between log $K_{BHA}$ (benzene, B = DPG) and p$K_a$ (water) derived previously for *meta*- and *ortho*-substituted acids. The significance of the results and other theoretical and experimental aspects of the work are discussed.

**9662.** Dean, J. W., Flynn, T. M., **Temperature effects on pressure transducers,** *ISA Trans.* **5,** No. 3, 223-232 (July 1966).

Key words: Cryogenic; flame; nuclear radiation; pressure transducers; temperature effects.

Temperature effects on pressure transducers have been determined both analytically and experimentally. Although the experimental work was performed at low temperatures, the analysis indicates that similar effects will result from cryogenic, flame, or nuclear radiation environments. These effects are classified as zero shifts, sensitive shifts, and thermal gradients. The prime causes of these effects are changes in material properties as a function of temperature and mismatching of material properties due to temperature gradients. Recommendations as to pressure-transducer mountings are made for the purpose of reducing the possibility of large, temperature-induced errors.

**9663.** De Simone, D. V., **Technological innovation: Its environment and management,** *U.S. Department of Commerce* **Cl.2:T22** (Supt. Docs., Government Printing Office, Washington, D.C., Jan. 1967).

Key words: Innovation; invention; social invention; technology transfer.

A report of the Panel on Invention and Innovation of the Secretary of Commerce which gives seventeen key recommendations for improving the environment for invention and innovation. Three main factors were examined as they affect invention and innovation: taxation, finance, and competition. No major changes in the laws governing these factors were deemed necessary.

**9664.** De Simone, D. V., **The innovator,** *Engineer* **8,** No. 1, 8-9 (Jan.-Feb. 1967).

Key words: Innovation; invention; inventors; technical application.

The inventor is essential to the advance of new ideas in technology—the innovator, the key to the application of technology. The innate independence of both causes problems in the institutionalized development system. The advantages and disadvantages of corporate environment on inventiveness are discussed.

**9665.** Deslattes, R. D., **A two-crystal, vacuum monochromator,** *Rev. Sci. Instr.* **38,** No. 5, 616-620 (May 1967).

Key words: Double crystal instrument: vacuum instrument; x-ray spectrometer.

Design and construction of a vacuum two-crystal instrument for high resolution spectroscopy at long wavelengths is reported. The instrument provides for coordinated rotations of both crystals, source, and detector. The usable scan range is 8° in Bragg angle and is limited only by the characteristics of the tangent drive system.

**9666.** Deslattes, R. D., **Single axis, two-crystal x-ray instrument,** *Rev. Sci. Instr.* **38,** No. 6, 815-820 (June 1967).

Key words: Crystal x-ray instrument; single axis; two-crystal x-ray instrument; x-ray instrument.

Design features of a two-crystal instrument capable of measurements of diffraction angles to an accuracy of the order of 0.1″ are presented. The instrument is of simple geometry, employs a stable and massive chassis, and derives its precision from components of general availability. Diffraction angles are generated in 1° increments by a precise indexing mechanism and interpolated by means of a sine arm driven by a micrometer.

**9667.** Deslattes, R. D., Peiser, H. S., Bearden, J. A., Thomsen, J. S., **Potential applications of the x-ray/density method for the comparison of atomic-weight values,** *Metrologia* **2,** No. 3, 103-111 (July 1966).

Key words: Atomic weights; crystal densities; crystal perfection; experimental methods; lattice parameters.

Without presenting experimental details, this report outlines and reappraises the principles involved in measurement of crystal lattice parameters and density for the determinations of atomic-weight values.

Attention is drawn to the advantages to be derived from a comparison of densities and lattice spacings with those of a crystal of mononuclidic elements, rather than from absolute measurements of x-ray spacings and density.

Errors arising from physical and chemical imperfections are discussed as are the general techniques of adequate precision for density and lattice spacings measurements.

Recent literature data is used by way of illustration to derive the effective atomic weight of calcium appertaining to a group of calcite samples from that of a group of silicon crystals (really an unsuitable "standard"). The calcium value obtained is 40.0795±0.0019 (probable error); it compares with IUPAC's adopted 40.08 and a "physical value" of 40.078 from nuclidic masses and isotopic abundance measurements. There are several elements for which the x-ray/density method is judged to be potentially the most promising for atomic-weight re-determinations in the foreseeable future.

**9668.** Deslattes, R. D., Simson, B. G., **Demountable high power source for soft x-ray region,** *Rev. Sci. Instr.* **37,** No. 6, 753-754 (June 1966).

Key words: Continuum source; secondary excitation; x-rays.

A demountable x-ray source capable of operation up to three kilowatts is described. Construction is largely of stainless steel using elastomer seals. The source is of use in exciting secondary spectra and producing bremmstrahlung for absorption studies.

**9669.** Deslattes, R. D., Simson, B. G., LaVilla, R. E., **Gas density stabilizer for flow proportional counters,** *Rev. Sci. Instr.* **37,** No. 5, 596-599 (May 1966).

Key words: Flow gas counters; gas density stabilizer; gas gain.

A controller for gas density (pycnostat) is described with particular view to gain stabilization in flow proportional counters. The device is capable of operation at small flow rates and at pressures both above and below atmospheric. Constructional details and performance measurements are reported.

**9670.** Deslattes, R. D., Torgesen, J. L., Paretzkin, B., Horton, A. T., **Observations of dislocations in ammonium dihydrogen phosphate: Production of dislocation-free crystals,** *J. Appl. Phys.* **37,** No. 2, 541-548 (Feb. 1966).

Key words: Crystal perfection; diffraction topography; single crystals; solution growth.

The results of etch pit and diffraction topographic studies on ammonium dihydrogen phosphate (ADP) are reported. These studies were carried out on specimens sectioned by abrasive wheel and string-saw from large single crystals grown from aqueous solution. The two characterization methods are shown to be in approximate one-to-one correspondence in the case of sections produced by abrasive sawing.

Absence of both etch pits and topographic images in sections made by string-sawing of material well removed from the seed region is taken to indicate that this material is dislocation free. Preliminary results on the plasticity of ADP are reported. The mechanical results are consistent with dominant slip along the equivalent pair of tetragonal axes and minor, although significant, slip along the unique tetragonal axis. Diffraction contrast profiles calculated on the basis of these slip assignments by means of the schematic theory of contrast due to Bonse are in disagreement with the shape and parity of the observed images.

**9671.** Deutch, J. M., Zwanzig, R., **Anomalous specific heat and viscosity of binary van der Waals mixtures,** *J. Chem. Phys.* **46,** No. 5, 1612-1620 (Mar. 1, 1967).

Key words: Heat capacity; solution critical point; van der Waals mixtures; viscosity.

This article investigates the behavior of several properties of a model binary van der Waals mixture near the solution critical point. The behavior of the heat capacity is determined from an exact analysis of the partition function. For the shear and bulk viscosity, the time dependence of the currents appearing in the time correlation function formulas is determined from linearized hydrodynamic equations. For the heat capacity and the shear viscosity the results of this model are identical to those originally obtained by Fixman by a different procedure. Comparison is also made with the results obtained by Zwanzig and Mountain for these quantities in a one component van der Waals system near the liquid-vapor critical point. One finds, in qualitative agreement with available experiments, that the shear viscosity of a binary mixture diverges at the critical point while the shear viscosity of the one component system is well behaved. This is a consequence of the increasing lifetime of concentration fluctuations compared to density fluctuations as the critical point is approached.

**9672.** DeVoe, J. R., Spijkerman, J. J., **Mössbauer spectroscopy: Applications to aerospace,** Chapter in *Radioisotopes for Aerospace, Part 2, Systems and Applications,* pp. 254-269 (Plenum Press, Inc., New York, N.Y., 1966).

Key words: Aerospace; applications; materials structure analysis; Mössbauer Effect; spectrometer; standards.

The principle of the Mössbauer Effect will be discussed. A few possible applications of the technique with respect to physics and engineering in aerospace will be outlined. Of greater interest are the possible applications of the technique for determining chemical structure and solid state properties of materials. Solid phase transitions of materials subjected to severe conditions similar to that existing in space can be measured by Mössbauer Effect.

The National Bureau of Standards' Mössbauer spectrometer will be discussed and some data taken on a number of materials (such as tecktites, steels, glasses, and metal alloys) will be presented.

**9673.** deWit, R., Howard, R. E., **On the definition of the stacking-fault energy in binary alloys,** *Acta Met.* **14,** No. 3, 431-433 (1966).

Key words: Stacking-fault energy in binary alloys; thermodynamic treatments of the segregation of solute atoms in stacking faults.

We wish to discuss the relation between two recent thermodynamic treatments of the segregation of solute atoms at stacking faults in binary alloys. In one of these treatments, the equation relating the concentration of segregated solute to the stacking-fault energy is derived by means of an application of the Gibbs adsorption equation, while in the other treatment, the segregation equation is obtained by minimizing an expression for the free energy of the crystal, including the faulted region. The latter method of obtaining the segregation equation was used earlier by Suzuki. The segregation equations obtained by the two methods are different in form. We wish to point out, however, that this difference is only apparent and is due in part to a disguised difference in the way the stacking-fault energy is defined in the two treatments. We shall show that the possibility of such an ambiguity in the definition of stacking-fault energy arises in the case of an alloy but not in a pure metal.

**9674.** deWit, R., Ruff, A. W., Jr., **The elastic energies of non-regular hexagonal dislocation loops,** *Phil. Mag.* **15,** No. 137, 1065-1069 (May 1967).

Key words: Dislocation; elastic energy; loops; stacking fault.

The elastic energies of dislocation loops have been calculated as a continuous function of shape from equilateral triangle to hexagon. A smooth decrease in energy is found in this sequence; a relatively rapid change is associated with truncation of the triangle corners. The results compared with previous calculations for other geometric shapes. The effect of a stacking fault in the loop plane is also considered.

**9675.** Diamond, J. J., Dragoo, A. L., **Studies of molten alumina in the arc-image furnace,** *Rev. Hautes Temper. et Refract.* **3,** 272-279 (1966).

Key words: Alumina; arc-image furnace; heat of vaporization; molten alumina; temperature measurement; vaporization; vapor pressure; water in alumina; water vapor.

Aluminum oxide was melted in vacuum and in atmospheres of $H_2$, He, $O_2$, $N_2$, Ar, air, and water vapor with an arc-image furnace. Water vapor was found to dissolve rapidly in molten alumina and to boil out vigorously when it was made supersaturated in a water vapor atmosphere. In spite of this solubility water vapor does not appreciably enhance the vaporization of molten alumina. The rate of vaporization of molten alumina in vacuum was determined in the temperature range 2493 to 2606 °K and the mean third law heat of vaporization found to be 729.0 kcal $mol^{-1}$, with a standard error in the mean of 0.9 kcal $mol^{-1}$. Some problems associated with the measurement of the temperature of molten alumina were studied and are discussed.

**9676.** Dibeler, V. H., Reese, R. M., Krauss, M. D., **Mass spectrometric study of the photoionization of small molecules,** (Proc. 3rd Intern. Conf. Mass Spectrometry, Paris, France, Sept. 1964), *Book, Advances in Mass Spectrometry* **3,** 471-488 (Institute of Petroleum, London, England, 1966).

Key words: Mass spectrometer; mass spectrometric study; photoionization of small molecules; small molecules; ultraviolet monochromator; windowless vacuum.

A windowless vacuum ultraviolet monochromator and mass spectrometer are combined for the study of photoionization processes in the energy range 2000 to 600 Å (6 to 21 eV). The apparatus and techniques of measurement are described briefly and photoionization curves are given for the molecules: argon, krypton, xenon, hydrogen, deuterium, acetylene, acetylene-$d_2$, benzene and benzene-$d_6$. The ionization energies of the $^2P_{3/2}$ and $^2P_{1/2}$ states of the rare gases are measured and autoionized levels are observed between the doublets of krypton and xenon. The first ionization energies of $H_2$ and $D_2$ are measured and autoionization ascribed to the D and D′, $'\pi_u$ state is observed. First ionization energies of $C_2H_2$, $C_2D_2$, $C_6H_6$ and $C_6D_6$ are measured and vibrational levels of the ground state of the ions are detected. No electronically excited state is observed in acetylene at energies below 14 eV. In benzene, autoionized Rydbergs are observed leading to a second onset of ionization about 2.2 eV above the first ionization threshold. The shape of the curve above the first onset suggests similar energies for the lowest bonding $\pi$ and $\sigma$ orbitals.

**9677.** Dise, J. R., **The role of the CCRL,** *Construct. Specifier* **20,** 54-60 (June 1967).

Key words: Cement and concrete testing laboratories; concrete and cement testing laboratories; inspection of cement and concrete testing laboratories.

The history and methods of operation of the Cement and Concrete Reference Laboratory are described together with the benefits which can be derived from the inspection of cement and concrete testing laboratories.

**9678.** Dodge, W. R., Coleman, J. A., Domen, S. R., Whittaker, J. K., **Lithium compensated silicon focal plane detectors for electron scattering spectrometers,** *Rev. Sci. Instr.* **37,** No. 9, 1151-1159 (Sept. 1966).

> Key words: Electron scattering spectrometer; focal plane detectors; lithium-compensated silicon; low temperature radiation detectors; photonuclear physics apparatus; rectangular counters.

In order to utilize the inherent resolving power of a double focusing, 169.8°, 76.2 cm radius-of-curvature magnetic spectrometer being constructed at the National Bureau of Standards for elastic- and inelastic-electron nuclear scattering studies, focal plane counters were needed whose dimension along the direction of momentum dispersion was 1 mm. This paper describes the fabrication techniques and performance of lithium compensated silicon 1 x 1 x 60-mm radiation detectors which seem well suited for use as focal plane detectors for the above spectrometer. Differential and integral pulse height distributions for 10-40 MeV electrons incident on the counters are presented as a function of the temperature and bias voltage. Effects due to the finite width of the counters are discussed. A tunnel diode discriminator which provides the desired binary information to the NBS data processing system is described.

**9679.** Doepker, R. D., Ausloos, P., **Gas-phase radiolysis of cyclopentane. Relative rates of $H_2^-$-transfer reactions from various hydrocarbons to $C_3H_6^+$,** *J. Chem. Phys.* **44,** No. 5, 1951-1958 (Mar. 1966).

> Key words: Cyclopentane; gas-phase radiolysis; hydrocarbons; radiolysis.

The radiolysis of cyclo-$C_5D_{10}$ has been investigated in the presence of various saturated and unsaturated perprotonated hydrocarbons. On the basis of the isotopic analysis of the propanes formed in these mixtures and several other experimental observations it is concluded that the $C_3D_6^+$ ion, which is the major ion produced in the fragmentation of $C_5D_{10}^+$, reacts with various saturated hydrocarbons ($AH_2$) as follows:

$$C_3D_6^+ + AH_2 \rightarrow CD_3CDHCD_2H + A^+. \qquad \text{(a)}$$

Rates of this process relative to that of the reference reaction

$$C_3D_6^+ + \text{cyclo-}C_5D_{10} \rightarrow C_3D_8 + C_5D_8^+ \qquad \text{(b)}$$

have been measured with an accuracy of better than 2%. It is suggested that the saturated hydrocarbons also transfer an $H^-$ ion to $C_3D_6^+$ according to to the following reaction:

$$C_3D_6^+ + AH_2 \rightarrow C_3D_6H + AH^+. \qquad \text{(c)}$$

Although in agreement with theory the total rate of reaction of $C_3D_6^+$ with $AH_2$ is generally seen to increase with an increase in molecular weight of $AH_2$, there are appreciable variations in the rates of the $H_2^-$-transfer reaction (a) versus that of the $H^-$-transfer reaction (c) with a change in structure of the hydrocarbon molecule. Reaction (c) is usually favored when $AH_2$ is a branched hydrocarbon, except for neopentane which is entirely unreactive toward $C_3D_6^+$. Unsaturated hydrocarbons do not transfer an $H_2^-$ ion to $C_3D_6^+$ but probably undergo a condensation-type process. The radiolysis of cylopentane has also been investigated in the presence of $O_2$, NO, and $(CH_3)_3N$. It is demonstrated that the $C_3H_6^+$ and $C_5H_{10}^+$ ions transfer their charge to NO, or $(CH_3)_3N$ and that at a pressure of 20 torr approximately 20% of the parent ions undergo ring opening prior to the charge-transfer process.

**9680.** Doepker, R. D., Ausloos, P., **Gas-phase radiolysis of cyclobutane,** *J. Chem. Phys.* **44,** No. 4, 1641-1647 (Feb. 1966).

> Key words: Cycloalkanes; ion-molecule reactions; ion-pair yields; radiolysis; unimolecular decomposition.

The gas-phase radiolysis of cyclo-$C_4H_8$ and cyclo-$C_4D_8$ has been investigated in the presence of $O_2$, NO, $H_2S$, $NH_3$, and several organic compounds. From the products formed, it could be inferred that the following fragmentation processes occur:

$$C_4H_8^+ \rightarrow C_3H_5^+ + CH_3$$

$$C_4H_8^+ \rightarrow C_2H_4^+ + C_2H_4$$

$$C_4H_8^+ \rightarrow C_2H_5^+ + C_2H_3$$

$$C_4H_8^+ \rightarrow C_3H_4^+ + CH_4$$

At 20 torr, the ion-pair yields which can be ascribed to some of these processes are lower than the corresponding ion-pair yields observed in the mass spectrometer at a pressure of $10^{-5}$ torr.

When compounds such as NO(I.P. = 9.25 eV) or $(CH_3)_3N$(I.P. = 7.8 eV) are added to cyclobutane, butene (I.P. = 9.13 − 9.58 eV) is a major product. On the other hand, when organic or inorganic compounds whose ionization energy is higher than that of butene are added to cyclobutane, the yield of butene is, in most cases, negligibly small. The formation of butene can be tentatively accounted for by a ring opening of the parent ion followed by charge transfer. On the basis of this mechanism, a minimum value of 0.42±0.02 can be ascribed to $M(C_4H_8^+)/N$.

When an electrical field is applied in the saturation current region, during radiolysis of cyclobutane-NO mixtures, the yields of methane, ethane and butene which have the parent ion or fragments thereof as precursors, remain unchanged. On the other hand, the yields of products such as ethylene, allene, acetylene, and 1,3-butadiene whose formation is, in part, attributed to the decomposition of neutral excited molecules, are seen to increase due to increased excitation by electron impact. In the absence of an electrical field, the number of neutral excited molecule decompositions per ion pair is estimated to be ≦0.65±0.05.

**9681.** Doepker, R. D., Lias, S. G., Ausloos, P., **Photolysis of cyclopentane at 1470, 1236, and 1048-1067 Å,** *J. Chem. Phys.* **46,** No. 11, 4340-4346 (June 1, 1967).

> Key words: Cycloalkanes; cyclopentane; free radical reactions; ion molecule reactions; photoionization; photolysis.

The photolysis of cyclopentane has been investigated at 1470, 1236 and 1048-1067 Å. The primary process, cyclo-$C_5H_{10} + h\nu \rightarrow C_5H_8 + H_2$ is of major importance at 1470 Å, but its quantum yield diminishes at shorter wavelengths where processes involving C-C cleavage become more predominant. The products formed in the gas-phase photolysis of cyclo-$C_5D_{10} - H_2S$ mixtures and in the solid-phase photolysis of cyclo-$C_5H_{10}$ indicate that the excited cyclopentane molecule undergoes ring opening to form a 1-pentene molecule. In the gas phase, the internally excited 1-pentene decomposes entirely to form methyl and ethyl radicals. Evidence is also obtained for the occurrence of the dissociative process: $C_5H_{10} \rightarrow C_2H_4 + C_3H_6$ where $C_3H_6$ consists of cyclopropane and propylene. At 1048-1067 Å (11.6 − 11.8 eV), ionization is extensive (ionization potential of cyclo-$C_5H_{10}$ = 10.5 V). Saturation current measurements yielded a value of 0.64 for $\eta_{C5H10}/\eta_{NO}$. On the basis of an isotopic analysis of the propane formed in the photoionization of $C_5D_{10} - C_5H_{10} - O_2$ mixtures it is shown that the parent ion dissociates as follows: $C_5H_{10}^+ \rightarrow C_3H_6^+ + C_2H_4$ and that the $C_3H_6^+$ ions participate in an $H_2^-$ transfer reaction: $C_3H_6^+ + C_5H_{10} \rightarrow C_3H_8 + C_5H_8^+$. Fragmentation of the parent ion diminishes with an increase in pressure. The collisional deactivation process is more pronounced for the perdeuterated than for the perprotonated cyclopentane ion. The data also indicate that a fraction of the parent ions undergoes ring opening to form *cis*- or *trans*-2-pentene as a final product.

9682. Douglas, C. A., **Review of elementary theory of the photometry of projection apparatus,** *Illum. Eng.* **62,** No. 4, 246-253 (Apr. 1967).

Key words: Critical distance; illumination; light projectors; photometric distance; photometry; signal lighting.

Equations based upon simple geometric relations are developed for the illuminance produced by a projector such as a searchlight, beacon, or floodlight at a distance from the projector. When the beam is rotationally symmetrical but not collimated and the image, virtual or real, subtends a smaller angle at the point of observation than does the objective of the projector, illuminance varies inversely as the square of the distance to the image. If the angle subtended by the image is larger than that subtended by the objective, the illuminance varies inversely as the square of the distance to the objective. The distance at which the two angles are equal is defined as the critical distance. Equations relating critical distance to the radius of the source, the radius of the objective, and the magnification of the system are developed. Approximations for use when the beam of the projector is asymmetric are developed. Very good agreement was found between the computed variation of illuminance with distance and the measured variation of illuminance with distance for a projector forming a virtual image 150 feet behind the objective.

9683. Dibeler, V. H., Walker, J. A., **Photoionization efficiency curve for $SF_6$ in the wavelength region 1050 to 600 Å,** *J. Chem. Phys.* **44,** No. 12, 4405-4406 (June 15, 1966).

Key words: Electronically excited state; mass spectrometer; photoionization; Rydberg levels; sulfurhexafluoride; threshold energy.

The threshold energy of $SF_5^+$ at 811 Å (15.29 eV) has been determined by photoionization. An electronically excited state with a threshold at 750 Å (16.53 eV) resulting from partially resolved autoionizing Rydberg levels in the region of 775 Å has been observed also.

9684. Dunn, G. H., **Franck-Condon factors for ionization of $H_2$ and $D_2$,** *J. Chem. Phys.* **44,** No. 7, 2592-2594 (Apr. 1966).

Key words: Franck-Condon factors $H_2(^1\Sigma_g^+)$; ionization $D_2(^1\Sigma_g^+)$; vibrational eigenenergies $D_2^+$.

Franck-Condon factors for ionization of $H_2(^1\Sigma_g^+)$ and $D_2(^1\Sigma_g^+)$ are presented for 19 levels in $H_2^+(^2\Sigma_g^+)$ and 27 levels in $D_2^+(^2\Sigma_g^+)$. Comparisons are made with calculations, using less accurate potential functions for the molecular ion. Vibrational eigenenergies are given for $D_2^+$.

9685. Dunn, G. H., Van Zyl, B., **Electron impact dissociation of $H_2^+$,** *Phys. Rev.* **154,** No. 1, 40-51 (Feb. 1967).

Key words: Crossed beam technique; dissociation; electron impact; $H_2^+$.

The absolute cross section for dissociation of $H_2^+$ by electron impact has been measured for electron energies between 10 eV and 1500 eV using a crossed beam technique which is described in some detail. The measured cross section can be represented by the function $\sigma = 217/E \log_{10} E - 184$, where the cross section $\sigma$ is in units of $\pi a_0^2$ and the electron energy E is in electron volts. Comparison is made with relevant theory, and the agreement in magnitude of the cross section between experiment and theory is found to be surprisingly (and possibly fortuitously) good. The shape of the cross section as described by the above expression does not agree well with theory.

9686. Eberhard, J. P., **Forces shaping the role of the architect,** *Proc. Second Architectural Center Conf., Boston, Mass., May 13-14, 1966,* p. 12 (Boston Architectural Center, Boston, Mass., May 1966).

Key words: Architectural design; design systems; technological design.

A panel discussion of the use of systems concept as applied to architectural design problems in the building process. The role of the architect as a designer in the larger complex of the city is discussed.

9687. Eberhard, J. P., **Technology for the city,** *Intern. Sci. Technol.* **57,** 18-29 (Sept. 1966).

Key words: City design; city systems; systems technology; technological planning.

The ability to build better cities lies in the technological base from which we work. Only when the "systems" characteristics of the city are recognized can technological resources be coupled to solving urban problems. When cities are seen as "continuous urban systems" unrestricted by political or geographical boundaries, we can create high-technology, systems-oriented companies with the capability to design and build better future cities.

9688. Eberhard, J. P., **The city as a system,** *Proc. Mid-American Conf. Urban Design, Kansas City, Mo., Mar. 30-31, 1966,* p. 2530 (Midwest Research Institute, Kansas City, Mo., 1966).

Key words: City design; city systems; city technology; systems technology.

A panel review of city problems analyzed in terms of the systems and subsystems operating in the city complex. Suggests that knowledge of the systems characteristics of the city offers ways to evaluate urban problems by planners. Systems approach is only logical way to apply modern technology to urban problems.

9689. Eby, R. K., Colson, J. P., **Relaxations in polyethylene: Orientation of the lamellar crystals,** *J. Accoust. Soc. Am.* **39,** No. 3, 506-510 (Mar. 19, 1966).

Key words: *a, c* face of cell; compliance; crystallization-oriented; lamella thickness; logarithmic-decrement; modulus; polyethylene; relaxations; shear; temperature; torsion pendulum.

A torsion pendulum has been used to make mechanical measurements on linear polyethylene between −175° and +110 °C at about one Hz. Samples which had been oriented by crystallization in a temperature gradient were measured together with unoriented but otherwise equivalent samples. The data are analyzed to show that the $\alpha$ relaxation in polyethylene is sensitive to the orientation of the deformation with respect to structural symmetry. For shearing in the *a, c* face of the unit cell and associated lamella boundaries the average overall direction is different from the average for shearing in all possible planes in the cell and boundaries. The $\gamma$ relaxation does not exhibit this difference. The data show a lack of correlation between lamella thickness and various viscoelastic parameters such as the real part of the modulus and the magnitude of the relaxations. The results show a need for further mechanical measurements on samples that are more nearly perfectly oriented and more fully characterized with respect to structural details and imperfections.

9690. Eckerle, K. L., McWhirter, R. W. P., **Departures from the local thermal equilibrium in a magnetically-driven shock wave,** *Phys. Fluids* **9,** No. 1, 81-89 (Jan. 1966).

Key words: Electromagnetic T-tube; local thermal equilibrium; population density of atomic energy levels.

An experimental study is reported of the time-resolved spectrum of the plasma produced by the magnetically driven shock wave in a T-tube. It is shown that the population densities of the excited levels of helium ions in the plasma depart from the values they would have in Local Thermal Equilibrium. On the other hand, if LTE is assumed and the electron temperature estimated for the intensity ratio of He II (4686 Å) to He I (5876 Å), then in the conditions of the experiment an error of a factor of two in the electron temperature arises. The reason for the departure from LTE was shown to be the rapid rate of change of the plasma conditions (especially the electron temperature). This is so great that the ionization and recombination rates, being slower, cause the population densities to lag behind the electron density and electron temperature. These rates were found to be consistent with the rates calculated by Bates et al., in their collisional-radiative model for the ionization and recombination of hydrogen-like ions.

**9691.** Eckert, C. A., Renon, H., Prausnitz, J. M., **Molecular thermodynamics of simple liquids—mixtures,** *I & EC Fundamentals* **6,** No. 1, 58-67 (Feb. 1967).

Key words: Analytical partition function; molecular parameters; molecular size; simple liquids; thermodynamic properties.

Thermodynamic properties of simple liquids are calculated from an analytical partition function which is based on a modification of Prigogine's cell theory and on a three-parameter theorem of corresponding states. The partition function gives an excellent representation of the configurational properties of fifteen liquids ranging in molecular complexity from argon to neopentane. Three characteristic molecular parameters are sufficient to calculate the configurational energy and entropy, the volume, coefficient of expansion and compressibility. These parameters are a molecular size, a pair-potential energy, and a term which is closely related to non-central intermolecular forces; this last parameter is a nearly linear function of Pitzer's acentric factor. The main application of this statistical thermodynamic treatment follows from its straightforward extension to liquid mixtures as discussed in Part II.

**9692.** Edmiston, C., Krauss, M., **Pseudonatural orbitals as a basis for the superposition of configurations. I. $He_2^+$,** *J. Chem. Phys.* **45,** No. 5, 1833-1839 (Sept. 1, 1966).

Key words: Electronic energy; $He_2^+$; molecular quantum mechanics; pseudonatural orbitals.

The use of pseudonatural orbitals (PNO) is proposed to improve the rate of convergence in the superposition of configurations (SOC). Natural orbitals are determined for selected electron pairs in the Hartree-Fock field of the $n$-2 electron core and are then used as the basis for the total SOC calculation. Since these natural orbitals are not natural for the $n$-electron system they are considered false or pseudonatural orbitals when used in the $n$-electron problem.

The PNO basis has been applied to $He_2^+$ and $H_3$ to test the convergence. Complete results are reported here only for $He_2^+$. The PNOs are quite successful in speeding up the convergence of the SOC and rendering the calculation of correlation energy quite practical in general. Gaussian type orbitals (GTO) are used throughout and were not a serious impediment to obtaining quantitative accuracy. In fact, the large number of unoccupied Hartree-Fock orbitals consequent upon the use of a GTO basis permit a straightforward determination of the PNO orbitals.

**9693.** Edmonds, D. K., Smith, R. V., **Comparison of mass-limiting two-phase flow in a straight tube and in a nozzle,** *Proc. Symp. Two-Phase Flow, University of Exeter, Devon, England, June 21-23, 1965,* pp. 401-414 (University of Exeter, Devon, England, 1966).

Key words: Mass-limiting two-phase flow; nozzle; tube.

This paper reports the experimental data obtained at mass-limiting and near-mass-limiting conditions for a straight tube and two nozzle test sections. The experimental system was a Refrigerant 11 flow loop. Fluid qualities entering the test sections were 0.042, 0.116, and 0.156.

It was noted that as the pressure differential between the exit-plane and the receiver was increased the exit-plane pressure approached a constant value for all test sections. The mass flow also approached a constant value for the straight tube, but for the nozzles the mass flow continued to increase with increasing differential pressure but at a lower rate of increase. The deviations from the straight tube behavior were greater for the nozzle with the largest angle of convergence.

Predicted mass-limiting flow rates from the Fauske and a metastable model were compared with the experimental data. The models adequately predicted the flow rate for data where the exit-plane pressure was almost constant (within ±30%).

**9694.** Eicke, W. G., Jr., Ellis, H. H., **On long-term stability of Zener reference diodes,** *Proc. 11$^e$ Session, Comite Con. d'Electricite, May 10-12, 1965,* pp. 73-77 (Gauthier-Villars, Paris, France, 1965).

Key words: Diodes, reference; long-term stability; reference diodes; Zener reference diodes.

This paper gives a summary of a three-year study of the stability of Zener diodes when operated intermittently or continuously. The diodes that were studied under intermittent use were in use for periods of 5 to 10 minutes with periods of two to four weeks between measurements. The diodes studied had normal voltage ranging from 8.1 to 9.2. The studies were conducted at 25.00± °C. The studies indicated that the Zener voltage gave stable output voltage to within 3 to 10 ppm over a three-year period.

**9695.** Eisenhart, C., Birnbaum, A., **Anniversaries in 1966-67 of interest to statisticians. Part II. Tercentennials of Arbuthnot and De Moivre,** *Am. Stat.* **21,** No. 3, 22-29 (June 1967).

Key words: Abraham De Moivre; *Annuities upon Lives*; "Argument for Divine Providence"; *Arithmetica Memorativa*; Bernoulli's theorem; *Doctrine of Chances*; generating functions; John Wallis; *Laws of Chance*; Martin Scriblerus; normal approximation; Poisson distributions; Scriblerus Club; statistical test; William Buckley.

Brief recognition is given to the quadricentennial of the publication of *Arithmetica Memorativa* (1567) of William Buckley (?-1550) and to the 350th anniversary of the birth of John Wallis (1616-1703), whose *Algebra* (1685) contained the earliest treatment of permutations and combinations in the English language. Much fuller recognition is accorded the tercentennials of the birth of John Arbuthnot (1667-1735), deviser of the earliest statistical test of significance; and of the birth of Abraham De Moivre (1667-1754), who made the most extensive, and the most important contributions to the purely mathematical theory of probability before Laplace (1749-1827), many of whose results he anticipated.

**9696.** Eisenhauer, C., **Development of the engineering method and some simplified methods of structure shielding analysis,** (Lecture Notes, OCD Summer Inst., Kansas State University, Manhattan, Kansas, 1962-1963, 1965), *TR-40, Radiation Shielding&Analysis and Design Principles as Applied to Nuclear Defense Planning,* **V-1—V-IV** (Supt. Docs., Government Printing Office, Washington, D.C., Nov. 1966).

Key words: Fallout protection in structures; radiation shielding; structures.

These lecture notes describe the technical basis for the procedures currently being used by the Office of Civil Defense to evaluate fallout protection in structures. The notes describe in detail how the equations and charts used in these procedures were derived from fundamental calculations of radiation shielding. Examples are given for simple structures.

**9697.** Ellerbruch, D. A., **UHF and microwave phase-shift measurements,** *Proc. IEEE* **55,** No. 6, 960-969 (June 1967).

Key words: Measurements; microwave; phase shift; standards; UHF; uncertainties.

A phase-shift standard, a measurement system, and the techniques for determining the corresponding limit of uncertainty are all required for obtaining the phase-shift characteristics of UHF and microwave components. Differential phase-shift standards, measurement techniques, and measurement uncertainties are all discussed in a general sense and a comprehensive bibliography is included to supplement the general discussion.

**9698.** Estin, A. J., Anderson, M. M., **Time-resolved microwave interferometry as a diagnostic tool for decaying plasma afterglows,** *Rev. Sci. Instr.* **37,** No. 4, 468-470 (Apr. 1966).

Key words: Density; diagnostic; electron; interferometry; microwave; plasma; time resolution.

Two laboratory techniques are described for making time-resolved microwave interferometry measurements of electron density in a decaying plasma afterglow. The time resolution is of the order of 10 microseconds and thus permits at least several hundred sampling periods in the decay of a typical helium afterglow. A simple criterion is given for the error introduced in phase on account of the time-varying medium.

**9699.** Evenson, K. M., Broida, H. P., **Measurements of collisional energy transfer between rotational energy levels in CN,** *J. Chem. Phys.* **44,** No. 4, 1637-1641 (Feb. 15, 1966).

Key words: Chemical bonds; cyanogen, molecular energy levels; electron transition; microwave spectroscopy; nuclear spins.

A microwave-optical technique which selectively populates a single rotational level of CN and permits the observation of the redistribution of this population was utilized to measure the rates of collisional energy transfer between rotational energy levels of the B doublet-sigma state of CN. CN was formed in the A doublet-Pi state by the addition of CH2C12 to the afterglow of a nitrogen discharge. The near coincidence of the K = 4, v = 0 level of the A doublet-Pi state with the K = 4, v = 0 level of the B doublet-sigma state permits microwave transitions near 10 GHz from the more populated Pi level to the sigma level. The increased population in the rotational levels neighboring the K = 4 level of the B doublet-sigma state was detected by measuring the increased optical emission due to the B doublet-sigma-A doublet-sigma transition near 3875 Å. Collisional energy transfer was measured over a pressure range from 0.1 to 5 torr for changes in rotational quantum number ranging from one to ten. It is shown that rotational transitions having changes in rotational quantum number greater than unity take place with high probability, contrary to the optical selection rule delta-K = plus or minus 1, and that approximately every gas kinetic collision produces a rotational transition. The relaxation time for the fourth rotational level was found to be 0.00000012 (plus or minus 30%) sec at a pressure of 1 torr.

**9700.** Farley, D. T., Jr., **Observations of the equatorial ionosphere using incoherent backscatter,** (Proc. NATA Advanced Study Institute, Finse, Norway, Apr. 1965), *Book, Electron Density Profiles in the Ionosphere and Exosphere,* Ed. J. Frihagen, pp. 446-469 (North-Holland Publ. Co., Amsterdam, The Netherlands, 1966).

Key words: Backscatter; electron and ion temperature; electron density; equatorial ionosphere; incoherent backscatter; ionic composition.

Measurements of electron density, electron and ion temperature, and ionic composition have been made in Peru using the incoherent backscatter technique. The paper reports some of the more recent results, particularly those of 1-3 February, 1965. In the latter period, continuous measurements of electron density were obtained up to altitudes above 4000 km. Between 3000 and 5000 km, the densities varied by about a factor of two throughout the day. At lower heights there was, at times, strong evidence of rapid vertical motion. During the day, temperature equilibrium between the ions and electrons prevailed above about 400 km, but $T_e/T_i$ reached values approaching three at lower heights. Equilibrium appeared to exist at all heights at night. A limited number of measurements of the ionic composition show no evidence of $He^+$ ions during the day, and the $O^+$ and $H^+$ densities become equal at about 900 km. During the night, however, $He^+$ does appear to be present in significant amounts, and the relative concentration of $O^+$ drops to 50% at about 700 km.

**9701.** Farrar, T. C., **Electron paramagnetic resonance and nuclear magnetic resonance as analytical tools,** (Conf. Purification of Materials, New York Academy of Sciences), *Ann. N.Y. Acad. Sci.* **137,** 323-334 (Jan. 1966).

Key words: Analytical tools; electron paramagnetic resonance; nuclear magnetic resonance; paramagnetic resonance; spectroscopy; tools, analytical.

Nuclear magnetic resonance (NMR) spectroscopy is becoming an increasingly important and useful analytical tool. The advantages (such as rapid, non-destructive analysis), disadvantages (such as large sample requirement and low sensitivity), and limitations of high-resolution, broad-line and pulsed NMR techniques as applied to analytical problems are pointed out. Recent developments in instrumentation which have significantly increased the stability and sensitivity of NMR techniques are discussed.

Examples of the use of high-resolution NMR to determine the structure and the purity of samples of the recently-synthesized molecules $HBF_2$, $Si_3BF_2$, and $Si_3BF_2$ are given. The results of a broad-line NMR study to determine the number and the position(s) of the hydrogen atoms in the molecule $Re_3(CO)_{12}H_x$ are presented.

Although paramagnetic species can be detected in concentrations as low as $10^{-11}$ M, electron paramagnetic resonance (e.p.r.) has been used for quantitative analysis only in a few cases. It is somewhat more useful for qualitative analysis. At this time its prospects for developing into a useful analytical tool seem limited. The reasons for this are briefly discussed.

**9702.** Farrar, T. C., Ryan, W., Davison, A., Faller, J. W., **Manganese-hydrogen bond distance in $HMn(CO)_5$,** *J. Am. Chem. Soc.* **88,** No. 1, 184 (Jan. 5, 1966).

Key words: Bond distance; broad-line second moment; carbonyl; hydride; hydrogen; manganese; nuclear magnetic resonance; proton.

The second moment of the proton NMR absorption spectrum of a sample of $HMn(CO)_5$ was determined; its value is 26.6±0.6 $G^2$. This value corresponds to a value of 1.28±0.01 Å for the Mn–H bond distance.

**9703.** Fatiadi, A. J., **Effects of temperature and of ultraviolet radiation on pyrene adsorbed on garden soil,** *Environ. Sci. Technol.* **1,** No. 7, 570-572 (July 1967).

Key words: Aromatic; hydrocarbons; particulates; photochemical; photooxidation; polycyclic; pyrene; reaction; 1,1′-bipyrene; 1,6- and 1,8-pyrenediones.

The chemical and photochemical changes of pyrene adsorbed on soil have been studied. It was found that pyrene adsorbed on soil and subjected to either heat or ultraviolet radiation underwent self-coupling to 1,1′-bipyrene, apparently by free-radical mechanisms; this product was not found from pyrene adsorbed on a number of other particulates. Also formed in the pyrene—soil reaction were 1,6- and 1,8-pyrenediones, probably by a different reaction-path.

**9704.** Fatiadi, A. J., **Novel aromatization of inositols in dimethyl sulfoxide—acetic anhydride,** *Chem. Commun.* **9,** 441 (May 10, 1967).

Key words: Acetic anhydride; aromatization; inositol; methyl sulfoxide.

A novel method has been discovered for the aromatization of inositols. The procedure involves treatment of inositols with a mixture of methyl sulfoxide and acetic anhydride.

**9705.** Fatiadi, A. J., **Preparation of inososes from their phenylhydrazones by use of a cation-exchange resin; separation of certain phenylhydrazones from phenylosazones,** *Carbohydrate Res.* **1,** No. 6, 489-491 (1966).

Key words: Cation-exchange resin; inosose phenylhydrazones; inosose phenylosazones; preparation of inososes from phenylhydrazones; removal of phenylhydrazine residue from phenylosazones.

Cation-exchange resin of the sulfonic-acid type conveniently removes the phenylhydrazine residue from inosose phenylhydrazones. The liberated phenylhydrazone combines with the resin, obviating an extraction process. The yields of inosose are about the same as those obtained by the benzaldehyde exchange reaction.

Inosose phenylosazones are unaffected by the resin, and consequently can be separated from inosose phenylhydrazones.

**9706.** Fearn, J. E., Brown, D. W., Wall, L. A., **Polymers and telomers of perfluoro-1,4-pentadiene,** *J. Polymer Sci.* **4,** Pt. A-1, 131-140 (Jan. 1966).

Key words: Dechlorination; gamma ray initiation; pentadiene; polymerized; pressure; 3,5,6-trichloro-octafluorohexanoic.

Perfluoro-1,4-pentadiene was prepared from 3,5,6-trichlorooctafluorohexanoic acid by pyrolysis and subsequent dechlorination with zinc in a high-boiling ether. This process also yielded three isomers of chloroheptafluoro-1,4-pentadiene. Polymerization studies showed that the monomer yielded rubbery samples, powdery samples, oils, and at least four dimers. There was also strong evidence that the 1,4-diene is converted into the 1,3-diene under conditions of polymerization.

**9707.** Fehsenfeld, F. C., Schmeltekopf, A. L., Goldan, P. D., Schiff, H. I., Ferguson, E. E., **Thermal energy ion-neutral reaction rates. I. Some reactions of helium ions,** *J. Chem. Phys.* **44,** No. 11, 4087-4094 (June 1, 1966).

Key words: Helium ions; ion-neutral; ions, helium; reaction rates; thermal energy.

A flowing, steady-state afterglow system has been utilized to measure room-temperature ion-neutral reaction rates. A description of the apparatus and technique is given. Measured rate constants for $He^+$ reactions with $O_2$, $N_2$, CO, NO, and $CO_2$ are reported, as well as upper limits for the reactions of $He^+$ with $H_2$, Ne, and Ar, and an estimate for the reaction of $He_2^+$ with Ne and $N_2$.

The reactions of $He^+$ with $O_2$, $N_2$, CO, NO, and $CO_2$ are all rapid, the rate constants all being $\approx 10^{-9}$ cm$^3$ sec$^{-1}$, implying essentially a reaction per collision.

**9708.** Feldman, A., **Piezo-optical effects in solids by sample rotation,** *Physics Letters* **23,** No. 11, 627-628 (Dec. 1966).

Key words: Modulation technique; optical; piezo-optical; semiconductor; silicon; strontium titanate.

The differential absorption and reflection coefficients of uniaxially stressed Si and $SrTiO_3$ were determined by rotating the samples in a linearly polarized light beam.

**9709.** Fetters, L. J., Pummer, W. J., Wall, L. A., **Monomer-polymer equilibria of deuterated $\alpha$-methylstyrenes,** *J. Polymer Sci.* Pt. A-1, **4,** No. 12, 3003-3011 (Dec. 1966).

Key words: Anionic polymerization; heats and entropies of the polymerizations of deuterated $\alpha$-methylstyrenes.

The equilibria between $\alpha$-trideuteromethyl-$\beta$,$\beta$-dideuterostyrene, $\alpha$-methyl-2,3,4,5,6-pentadeuterostyrene, and perdeutero-$\alpha$-methylstyrene and their respective polymeric anions in tetrahydrofuran have been investigated between 253 and 308 °K. The heat and entropy changes were both increased by deuteration of the alkyl group. Qualitatively the effect observed appears best explained by the premise that a lowering of steric repulsions occurs with deuterium and hence the effective volume for deuterium is less than that for hydrogen.

**9710.** Fey, L., Barnes, J. A., Allan, D. W., **An analysis of low information rate time control unit,** *Proc. 20th Annual Symp. Frequency Control, Atlantic City, New Jersey, April 19-21, 1966,* pp. 629-635 (1966).

Key words: Flicker noise; meteor burst; multi-loop servo; oscillator correction; time synchronization; VLF propagation.

Computer simulation has been used to study the feasibility of producing a synchronized time station requiring minimum attention to operate.

The device simulated consists of a multiloop servo system to correct the output phase of a quartz crystal and to simultaneously compensate for the linear frequency drift common to these oscillators. Upon the occurrence of occasional phase comparison, such as propagated from VLF transmission during the time of day when propagation conditions are most stable, the servo incorporates a resulting phase correction and establishes a new linear frequency drift compensation rate based on the past history of the oscillator—allowing extrapolation of the phase of the reference signal until the next phase comparison occurs. This in effect results in a remote, phase locked system operating automatically with an intermittant reference.

The effect on such a system of flicker noise modulation, the characteristic type of noise associated with quartz crystal oscillators in the domain of interest is treated, along with servo system time constant considerations.

The use of such a system is discussed in relation to applications such as unmanned standard time and frequency stations, meteor burst synchronization, and the operation of atomic time scales with intermittant frequency calibrations. From available data, one anticipates a synchronization precision of 1 microsecond at stations as remote as 1,500 kilometers using the meteor burst technique. The system would be both low in initial cost and in operation.

**9711.** Fey, L., Looney, C. H., **A dual frequency VLF timing system,** *IEEE Trans. Instr. Meas.* **IM-15,** No. 4, 190-195 (Dec. 1966).

Key words: Multiple VLF transmissions; portable clock; standard time broadcasts; VLF propagation; worldwide clock synchronization.

The use of high precision portable clocks and radio signals is discussed in relation to synchronization of remotely located clocks. The demonstrated inherent phase stability, approximately two $\mu$s rms, of very low frequency (VLF) propagation and its low attenuation rate with distance, have led to various approaches to exploit these virtues in timing applications. The system considered here employs two carrier frequencies with timing information contained in their difference frequency to permit indentification of a specific cycle of one of the carrier frequencies. Such a system makes stringent demands on phase stabilities of the transmitted signals and of the receiving system as well as that of the propagation medium itself.

The present system, whose development has been supported jointly by NBS and NASA, makes use of NBS radio station WWVL at Fort Collins, Colorado. Receivers are of the standard VLF phase tracking servo type. A special signal generator is used in conjunction with the local clock to simulate the transmitted signal in order to relate the local time scale to that at the transmitter.

One of the carrier frequencies is maintained at 20 kHz. With a second frequency (500 Hz removed from this frequency), carrier cycle identification was achieved on about 90 percent of the days for over a month on the path from Fort Collins, Colorado, to Greenbelt, Maryland. Since January 4, 1966, the difference frequency has been 100 Hz, with somewhat more fluctuation in results. However, lower precision is required for the initial synchronization. The results of averaging to improve this performance will be discussed.

9712. Fitzgerrell, R. G., **Swept-frequency antenna gain measurements,** *IEEE Trans. Ant. Prop.* **AP-14,** No. 2, 173-178 (Mar. 1966).

Key words: Antenna gain; frequency measurement; standard antenna; swept-frequency.

This paper presents a method of making a swept-frequency antenna gain measurement which yields a result based upon the known frequency of a standard antenna. This antenna consists of a 295-mm length of X-band waveguide with a cover flange on one end. It is an inexpensive and very satisfactory gain standard. The error analysis, which gives the accuracy of the resulting gain figure, consists of evaluating the conjugate mismatch losses at the antenna feed point or junction. This method of measuring gain is shown to yield useful gain data from an antenna test range that is not free of reflections. Gain vs. frequency curves are given for the standard gain antenna and a test antenna, having estimated accuracies of at least 0.27 dB and 1.00 dB, respectively.

9713. Flynn, J. H., Wall, L. A., **A quick direct method for the determination of activation energy from thermogravimetric data,** *Polymer Letters* **4B,** No. 5, 323-328 (May 1966).

Key words: Activation energy; applied kinetic analysis; determination of kinetic parameters; non-isothermal kinetics; thermogravimetric variation of heating rates.

A quick simple method for determining energy of activation from thermogravimetric weight-loss vs. temperature data at two or more constant heating rates is presented. The activation energy is accurately obtained from the slope of a logarithm heating rate vs. reciprocal absolute temperature plot at constant degree of conversion. The independence of activation energy from degree of conversion and temperature may be tested by determining it at various values of constant weight loss.

9714. Flynn, T. M., **Liquid hydrogen engineering instrumentation,** (Proc. Intern. Inst. Refrigeration, June 9-11, 1965), *Book, Liquid Hydrogen,* pp. 295-338 (Paris, France 1965).

Key words: Cryogenic liquid; engineering and instrumentation; hydrogen; liquid hydrogen; liquid level; measurement of pressure.

Prudent liquid hydrogen engineering requires the measurement of both extensive and intensive properties of the cryogenic liquid. Transducers are required for liquid level (quantity), both point and continuous systems, and mass rate systems. In addition, there must be transducers of pressure, temperature, density, and occasionally, quality. This paper discusses some of the devices and practices currently used for the measurement of pressure, temperature, flow rate, and liquid level in liquid hydrogen systems.

9715. Flynn, T. M., Timmerhaus, K. D., **Superconducting devices,** (Proc. Inst. Refrigeration, Comm 1, Boulder, Colo., June 15-17, 1966, Annexe 1966-5), *Book, Liquid Helium Technology,* pp. 23-29 (Paris, France 1967).

Key words: Bearings; bolometer; electron microscope; helium; hydrogen; level gauging; liquid level; magnet; motor; pump; rectifier; solenoid; superconductivity; switch; temperature; thermometer.

Superconductors may be treated as engineering materials having three unusual properties: (1) a transition occurs between two different states which depends upon external parameters, (2) zero resistivity is exhibited in one state, and (3) perfect diamagnetism is exhibited.

This paper views superconductors in this way, as engineering materials, and examines applications of these properties. Examples include applications of superconductors to thermometry, bolometry, level gauging, rectifiers, magnets (briefly), bearings, motors, electron microscope lenses, and a helium pump.

9716. Forman, R. A., **Nuclear magnetic resonance of nitrogen-14 in potassium azide,** *J. Chem. Phys.* **45,** No. 4, 1118-1123 (Aug. 1966).

Key words: Azides; nitrogen; nuclear magnetic resonance; nuclear quadrupole.

The nuclear magnetic resonance of $^{14}$N split by large quadrupole interactions has been observed in single crystals of potassium azide ($KN_3$). The observed spectrum at arbitrary orientation consists of eight resonance lines, which can be decomposed into two groups of four lines each. The resonances in each group are of the same apparent intensity, and one group is twice as intense as the other. The quadrupole coupling constants and asymmetry parameters of the two inequivalent nitrogens have been obtained from a rotation study. For the end nitrogen $e^2qQ/h = 1.79\pm0.03$ MHz with $\eta = 0.04\pm0.02$. For the central nitrogen $e^2qQ/h = 1.028\pm0.03$ MHz with $\eta = 0.03\pm0.02$. Unsuccessful attempts were also made to observe the pure quadrupole resonance of the end nitrogens.

9717. Forman, R. A., Kahn, A. H., **Line shapes due to anisotropic interactions in magnetic resonance experiments,** *J. Chem. Phys.* **45,** No. 12, 4586-4588 (Dec. 1966).

Key words: Anisotropic interactions; computer calculations; line shapes; magnetic resonance.

Magnetic resonance line shapes resulting from anisotropic interactions of the form $a_p(3\cos^2\theta - 1)$ have been calculated. Typical shapes are displayed. Of particular importance is the presence of a reasonably strong resonance peak occurring in the absorption derivative at the position of the step ($\theta = 0°$) in the absorption curve.

9718. Forman, R. A., McKneely, T., **A cooling system for a laboratory magnet,** *Appl. Spectry.* **20,** 189 (May-June 1966).

Key words: Closed water system; magnetic field stability; NMR; temperature fluctuation.

The cooling system is described for use with a 5 kW magnet system which enables one to obtain high electrical and thermal stability.

**9719.** Foster, D. E., **Chemical admixtures,** *Am. Soc. Testing Mater. Spec. Tech. Publ.* **169A,** Significance of Tests of Concrete and Concrete Making Materials, 356-564 (1966).

Key words: Accelerating concrete admixtures; concrete admixtures; set-retarding; water-retarding.

A description of the water-reducing, set-retarding, and accelerating concrete admixtures commonly used in the United States is given, together with their effects on freshly mixed and hardened concrete. The problems encountered in writing specifications for these products are discussed from the standpoint of the tests required, and the statistical problems involved in comparing treated with untreated concrete.

**9720.** Fowler, B. O., Moreno, E. C., Brown, W. E., **Infrared spectra of hydroxyapatite, octacalcium phosphate and pyrolyzed octacalcium phosphate,** *Arch. Oral Biol.* **11,** 477-492 (May 1966).

Key words: Infrared spectra of calcium phosphate; pyrolyzed octacalcium phosphate.

Infrared spectra of hydroxyapatite, octacalcium phosphate, and pyrolyzed octacalcium phosphate were studied in the range 4,000 to 400 cm$^{-1}$, and probable band assignments are given. Unreported bands were found for both octacalcium phosphate (13 bands) and hydroxyapatite (5 bands); the hydroxyapatite band at 631 cm$^{-1}$ was reassigned to the librational mode of the hydroxyl group.

The pyrolysis reactions of octacalcium phosphate were studied by IR absorption, weight loss, and pyrophosphate analysis. The major products between 325 and 600 °C were hydroxyapatite and $\beta-Ca_2P_2O_7$ and $\beta-Ca_3(PO_4)_2$. Simple dehydration was continuous from 50 to about 400 °C. Formation of $\beta-Ca_2P_2O_7$, instead of $\gamma-Ca_2P_2O_7$, was detected at a lower temperature (325 °C) than has been reported. The maximum amount of pyrophosphate formed, about 40% at 500 °C, was intermediate between the amounts predicted by reactions postulated in other studies. From 700 to 900 °C, the pyrophosphate content approximated the expected values.

**9721.** Fowler, H. A., Erginsoy, C., **Is proton channeling a diffraction process?** *Physics Letters* **24A,** No. 7, 390-391 (Mar. 27, 1967).

Key words: Channeling; diffraction; energy loss; protons; stopping power.

Some stopping-power limitations are suggested on a dynamical-diffraction model of proton channeling at 1-5 MeV.

**9722.** Fowler, H. A., Marton, L. L., **Widths of Kikuchi lines in germanium,** *J. Appl. Phys.* **38,** No. 4, 1735-1738 (Mar. 15, 1967).

Key words: Cross-section; electron diffraction; electron scattering; germanium; Kikuchi lines.

Transmission Kikuchi patterns at 80 keV from wedges of germanium have been measured with high angular resolution. Linewidths are compared with the Fourier potential calculated from a simple coherent-elastic-amplitude model. Germanium shows a higher experimental curve of scattering amplitude per unit cell volume than silicon, as may be expected from its greater atomic scattering potential. Suppressed contrast is found for the (111) reflection; this is interpreted as an overlap between the halves of the line-pair or band.

**9723.** Frederikse, H. P. R., Hosler, W. R., Thurber, W. R., **Experimental evidence concerning the conduction band of SrTiO$_3$,** (Proc. Intern. Conf. Physics of Semiconductors, Kyoto, Japan, Sept. 8-13, 1966), *J. Phys. Soc. Japan* **Suppl. 21,** 32-36 (1966).

Key words: Band structure; effective mass; electronic transport properties; semiconductor; strontium titanate.

Experimental information about the conduction band of semiconducting SrTiO$_3$ is compared with the calculated band structure. Measurements of transport properties, magnetic susceptibility and plasma frequency yield rather high average effective masses. Low-field magnetoresistance as well as piezoresistance experiments have been performed on SrTiO$_3$. Although some disagreement remains, the weight of the evidence is in favor of a many-valley structure of the lowest conduction band as predicted by theory.

**9724.** Frederikse, H. P. R., Hosler, W. R., Thurber, W. R., **Magnetoresistance of semiconducting SrTiO$_3$,** *Phys. Rev.* **143,** No. 2, 648-651 (Mar. 1966).

Key words: Energy band structure; magnetoresistance; semiconductor; strontium titanate.

The magnetoresistance of reduced and doped SrTiO$_3$ was measured at 4.2 °K in fields up to 8000 Oe. The effect was studied for directions of primary current and magnetic field along the major crystalline axes. Results are in agreement with the theoretical prediction of 3 (or 6) energy minima on the $\langle 100 \rangle$ axes. Assuming an isotropic collision time, the effective-mass ratio is either 4.0 or 0.34.

**9725.** Frederikse, H. P. R., Hosler, W. R., Thurber, W. R., Babiskin, J., Siebenmann, P. G., **Shubnikov – de Haas effect in SrTiO$_3$,** *Phys. Rev.* **158,** No. 3, 775-778 (June 15, 1967).

Key words: Band structure; high magnetic field; oscillatory magnetoresistance; Shubnikov – de Haas effect; strontium titanate.

The magnetoresistance of semiconducting SrTiO$_3$ has been investigated in high magnetic fields (up to 150 kOe). In the temperature range 1.4 to 2.1 °K, for fields or more than 50 kOe, well-developed Shubnikov – de Haas-type oscillations have been observed. The data support a conduction band consisting of spheroids along the $\langle 100 \rangle$ crystalline axes, having 3 minima at the points $X_3$. The periods of oscillation as well as the temperature dependence of the amplitude and the magnetic field saturation lead to the following values for the transverse and longitudinal effective masses: $m_t = 1.5m_0 \pm 15\%$; $m_l = 6.0m_0 \pm 30\%$.

**9726.** Frederikse, H. P. R., Schooley, J. F., Thurber, W. R., Pfeiffer, E., Hosler, W. R., **Superconductivity in ceramic, mixed titanates,** *Phys. Rev. Letters* **16,** No. 13, 579-581 (Mar. 28, 1966).

Key words: Ceramic; ferroelectric; mixed compounds; semiconductors; superconductivity; titanates.

Superconductivity has been observed in slightly reduced, ceramic samples of $(Ba_xSr_{1-x})TiO_3$ and $(Ca_ySr_{1-y})TiO_3$ for $x \leqq 0.10$ and $y \leqq 0.3$. Some of the insulating compounds are ferroelectrics; reduced specimens are semiconductors. The superconducting transition temperatures reach higher values (0.55 °K) than that of reduced SrTiO$_3$. A connection with the high static dielectric constants of the (unreduced) titanates is suggested.

**9727.** French, J. L., **Discussion of the paper "Flow in culverts and related design philosophies,"** *J. Hydraulics Div. Am. Soc. Civil Eng.* **93,** No. Hy 1, 85-91 (Jan. 1967).

Key words: Culverts; hood inlets; hydraulics; tapered inlets.

An evaluation is made of certain conclusions advanced in a paper by Fred W. Blaisdell. The paper, entitled "Flow In Culverts And Related Design Philosophies" appeared in the Journal of the Hydraulics Division, American Society of Civil Engineers, March 1966. The present paper will form a discussion of Mr. Blaisdell's paper and will appear in a subsequent issue of the same publication.

The present discussion of Mr. Blaisdell's paper illustrates the use of tapered inlets in the design of culverts. The use of a minimum performance curve in the design of culverts is concluded to be acceptable, notwithstanding certain reservations advanced by Mr. Blaisdell. The concept of "balanced design" as applied to culverts is discussed in terms of the assessment of the risks of hydraulic overloading to the various component parts of the structure and it is concluded that the design rate of flow for the culvert and a structure or channel immediately downstream of the culvert need not be identical. And finally it was suggested that the experimental data so far presented have not demonstrated beyond reasonable question that the performance assigned to the hood inlet is applicable at prototype size as well as at model size.

**9728.** Frenkel, L., Kryder, S. J., Maryott, A. A., **Debye relaxation in symmetric-top-foreign-gas mixtures; temperature dependence of collision cross sections,** *J. Chem. Phys.* **44,** No. 7, 2610-2619 (Apr. 1, 1966).

Key words: Collision cross sections; Debye relaxation; foreign-gas mixtures; gas mixtures; relaxation-rate parameters.

The Debye relaxation spectra of three symmetric-top gases $CH_3Cl$, $CHF_3$, and $SO_2F_2$, in the pure state and in dilute mixtures with the foreign gases, He, $H_2$, $D_2$, Ar, $N_2$, $CH_4$, $CO_2$, and $C_3F_8$, were obtained over the temperature range $-20°$ to 145 °C at a frequency of 1220 MHz. Relaxation-rate parameters and the corresponding collision cross sections are derived. The cross sections vary with the absolute temperature as $T^{-m}$, where the value of $m$ ranges from 0.3 to 0.9 for the different systems. The cross sections are considered from a classical kinetic viewpoint and an empirical relation is obtained which accurately relates the dielectric cross section to the effective viscosity cross section (or the corresponding Lennard-Jones parameters), the internal-to-orbital-angular-momentum ratio, and one additional parameter related in some way to the shape (prolateness or oblateness) of the top. Deviations in the shape of these spectra from the simple Debye form, which are attributable to a distribution of relaxation rates, are examined in some detail and correlated with the effective collision number.

**9729.** Frenkiel, F. N., Klebanoff, P. S., **Higher-order correlations in a turbulent field,** *Phys. Fluids* **10,** No. 3, 507-520 (Mar. 1967).

Key words: Acoustic noise; air or water flow; atmospheric and oceanographic turbulence; boundary layer turbulence; higher-order correlations; physical origin; random processes of physical origin; turbulent field.

Higher-order time-correlations and the associated skewnesses and flatnesses were measured in a turbulent field downstream of a grid using high-speed computing techniques. The results were obtained using samples of 160 020 digitized data recorded at time intervals of 1/12 800 sec during time periods of approximately 12.5 sec. Comparison is made between the measured correlations and the higher-order correlation curves corresponding to a Gaussian probability density distribution of turbulent velocities. The departures from Gaussianity are shown, and non-Gaussian probability distributions are proposed which correspond considerably better to experimental reality. Several relations between correlation coefficients of different orders are obtained for the non-Gaussian probability distributions and confirmed by comparison with the measured correlations, skewnesses, and flatnesses.

**9730.** Frenkiel, F. N., Klebanoff, P. S., **Space-time correlations in turbulence,** (Proc. Symp. Dynamics of Fluids and Plasma, University of Maryland, College Park, Md., Oct. 7-9, 1965), *Book, Dynamics of Fluids and Plasma,* Ed. S. Pai et al., pp. 257-274 (Academic Press Inc., New York, N.Y., 1966).

Key words: Computer; correlations: even-order, odd-order, space-time; hot-wire anemometer; Taylor's approximation; turbulence; wind tunnel.

Space-time correlations of the component of turbulent velocities along the direction of mean velocity were measured in a turbulent field downstream of a grid using high-speed computing techniques. These results provide new information in that the space-time evaluation is carried out to much higher orders than had previously been measured. Space-time correlations of even order up to the eighth, and of odd order up to the fifth are presented. The applicability of Taylor's space-time approximation, i.e. the concept of a frozen pattern of turbulence moving with the mean velocity, to these higher order correlations is examined. The higher even-order correlations are compared with the results obtained from the second-order correlations assuming a Gaussian distribution for the turbulent velocities, and the different behavior of the various odd-order correlations is demonstrated.

**9731.** Fuller, E. G., **Photoneutron reactions,** (Proc. Intern. Conf. Study of Nuclear Structure with Neutrons, Antwerp, Belgium, July 14-23, 1965), *Book, Nuclear Structure Study with Neutrons,* Ed. M. Neve de Mevergnies, P. VanAssche, and J. Vervier, pp. 359-375 (North Holland Publ. Co., Amsterdam, The Netherlands, 1966).

Key words: Cross sections; photoneutron angular distributions; photoneutrons; photoneutron spectra.

The papers on Photoneutron Reactions submitted to the International Conference on the Study of Nuclear Structure with Neutrons are discussed in the context of a general review of this field.

**9732.** Garfinkel, S. B., Baerg, A. P., Zigman, P. E., **Certificates of radioactivity standards,** Report of the Subcommittee on the Use of Radioactivity Standards, *Natl. Acad. Sci.-Natl. Res. Council,* pp. 1-11 (Washington, D.C., Dec. 1966).

Key words: Certificates; combination of errors; commercial standards; measurements; precision; radioactivity standards; standards accuracy.

Recommendations for certificates of standards of radioactivity are presented. It is hoped that commercial producers of such standards in the United States of America will use these recommendations in the preparation of certificates which they supply with their standards.

**9733.** Garfinkel, S. B., Hutchinson, J. M. R., **The standardization of Co$^{57}$,** *Intern. J. Appl. Radiation Isotopes* **17,** No. 10, 587-593 (Oct. 1966).

Key words: Cobalt-57; coincidence counting; radioactivity standardization.

A new method is described for standardizing radioactive cobalt-57 for total disintegration rate. Systematic errors due to maximum uncertainties in the decay scheme are estimated to be less than 0.6%.

**9734.** Garvin, D., Rosenstock, H. M., **Two National Bureau of Standards data centers—chemical kinetics and mass spectrometry,** *J. Chem. Doc.* **7,** No. 1, 31-34 (Feb. 1967).

Key words: Chemical kinetics; information retrieval; mass spectrometry.

Two current information retrieval centers, one for chemical kinetics, the other for mass spectrometry are described. The methods and philosophies of operation of these programs are compared. The role of specialized information systems in promoting data evaluation, the evaluation of their usefulness as sources for reference material, the choice of techniques, and possibilities for intercenter coordination are discussed.

9735. Geil, G. W., **Some effects of notch geometry on tensile behavior of annealed type 310 stainless steel,** *J. Mater.* **1,** No. 3, 583-608 (Sept. 1966).

Key words: Fracture; initial cracking; multiaxial stresses; notch geometry; 310 stainless steel; stress concentrations; tensile deformation; workhardening.

A study was made of the influence of notch geometry (angle, depth and root radius) on the tensile deformation and fracture characteristics of circumferentially notched cylindrical tensile specimens of annealed 310 stainless steel at ambient temperatures. Specimens with a root radius of 0.05 inch or less and theoretical stress concentration factors of 1.6 or greater, regardless of notch angle or depth, exhibited cracking at small plastic strains. These strains were generally much smaller than the strains at maximum load. The cracking slowly increased in depth in a discontinuous manner with increase in applied stress and extension of the specimen until a condition of plastic instability was reached, resulting in a final rapid fracture of the specimen. Notched specimens with a root radius of 0.10 inch or greater, and theoretical stress concentration factors less than 1.6 did not exhibit any cracking at the root of the notch prior to the final rapid fracture.

9736. Geist, J., Kneissl, G. J., Weidner, V. R., **High purity powdered CsI as a high reflectance infrared diffuser,** *Appl. Opt.* **6,** No. 7, 1280-1281 (July 1967).

Key words: Body scatterer; cesium diode; diffuse reflector; powdered iodide; sulfur.

The spectral reflectance of powdered CsI is compared with that of flowers of sulfur between 2.5$\mu$m and 20$\mu$m. The experimental procedure is described and room temperature data are presented. The reflectance of ultra pure powdered CsI was found to be appreciably higher than that of the flowers of sulfur beyond 7$\mu$m.

9737. Geltman, S., Takayanagai, K., **Excitation of molecular rotation by slow electrons II,** *Phys. Rev.* **143,** No. 1, 25-30 (Mar. 1966).

Key words: Electrons; electron spin; modular rotation; nonvanishing electron spin; rotational excitation; slow electrons.

A previous study is here extended to consider the effects on rotational excitation of the nonvanishing electronic spin of $O_2$ and the short range static fields of the $H_2$, $N_2$, and $O_2$ molecules. The spin effect is found to be negligible, while the effect of short range interactions can be quite large in certain energy regions. This permits a qualitative explanation of the heretofore unexplained ratio of the observed electron relaxation rates in oxygen and nitrogen.

9738. Goebel, D. G., **Generalized integrating-sphere theory,** *Appl. Opt.* **6,** No. 1, 125-128 (Jan. 1967).

Key words: Absolute reflectance techniques; general equation; hemispherical reflectance measurements; integrating-sphere theory.

A general equation is developed for the efficiency of an integrating sphere with a nonuniform coating. The only assumptions are that the interior is a perfect sphere and that all areas reflect perfectly diffusely. Three special cases of the general equation are examined for the basic applications of integrating spheres as mixing mechanisms in hemispherical reflectance measurements and in absolute reflectance techniques.

9739. Gerstenberg, H., O'Connell, J. S., **Three-body photodisintegration of He$^3$,** *Phys. Rev.* **144,** No. 3, 834-838 (Apr. 22, 1966).

Key words: Bremsstrahlung; cross section; cryostat; helium-3; helium-4; neutrons; photodisintegration.

The $He^3(\gamma,n)2p$ cross section has been measured in 1-MeV steps from threshold to 30 MeV using the National Bureau of Standards betatron and a He$^4$ cryostat to produce a 40-cm$^3$ liquid-He$^3$ target. The measured cross section shows a broad peak between 14 and 20 MeV with a maximum cross section at about 0.90 mb. The cross section and bremsstrahlung-weighted cross section integrated up to 28 MeV give 12.1±10% MeV mb and 0.68±10% mb, respectively. Theoretical calculations of the three-body photodisintegration cross section overestimate the experimental cross section by factors of 3 to 10.

9740. Giarratano, P. J., Smith, R. V., **Comparative study of forced convection boiling heat transfer correlations for cryogenic fluids,** (Proc. 1965 Cryogenic Engineering Conf., Rice University, Houston, Texas, Aug. 23-25, 1965), *Book, Advances in Cryogenic Engineering* **11,** 492-506 (Plenum Press Inc., New York, N.Y., 1966).

Key words: Boiling; cryogenic; film; forced convection; hydrogen; nitrogen; nucleate.

This study compares predictive reliability of several common forced convection boiling heat transfer correlations using available cryogenic experimental data. A statistical method is used to compare the correlations and results indicate that none of the proposed predictive methods fall in a very respectable range of reliability and, furthermore, for design purposes, the simpler correlations seem to compare favorably with the more complex approaches.

9741. Gillilland, K. E., Cook, H. D., Mielenz, K. D., Stephens, R. B., **Use of a laser for length measurement by fringe counting,** *Metrologia* **2,** No. 3, 95-98 (July 1966).

Key words: Automatic fringe counting interferometer; fringe counting; interferometer; laser for length measurement; length measurement.

The use of a 633-nm He-Ne laser of normal neon isotopic abundance as a light source for an automatic fringe counting interferometer was found to improve the counting precision and extend the usefulness of the interferometer to the full one meter limit of its carriage travel.

A 91-mm length was measured in terms of Hg$^{198}$ and laser fringes. From the fringe counts obtained and the wavelength of the Hg$^{198}$ line, the laser vacuum wavelength was measured to be 632.991 46 nm with a standard error of 1.1 x $10^{-7}$. With the laser wavelength so determined, each decimeter interval of a one meter line standard was measured by counting laser fringes. All measured decimeter interval lengths agreed with the assigned values within the mutual limits of uncertainty, the largest discrepancy being less than 0.5 um.

The result obtained for the total length of the line standard agreed with the assigned length of the line standard to 7 parts in $10^8$, which is well within the mutual limits of uncertainty.

This method is being applied to routine calibration of line standards using a stabilized isotopic He-Ne laser.

9742. Glaser, E., Rosenblatt, D., Wood, M. K., **The design of a Federal statistical data center,** *Am. Stat.* **21,** No. 1, 12-20 (Feb. 1967).

Key words: Automatic data processing equipment; disaggregation; Federal statistical system; inherent computability; matching; probability master samples; propagation of error computations; statistical standards.

This paper treats the principle underlying the design of a Federal statistical data center intended to provide a better integrated information network for use by Government, industry, and the research community in an age of large-scale computers.

**9743.** Glass, S. J., Chappell, W. R., **The interaction of radiation with charged particles. II. Dispersion relation for transverse modes,** *Il Nuovo Cimento* **38,** No. 1, 79-88 (Mar. 1966).

Key words: Charged particles; dispersion relation; equation of motion; radiation; transverse excitation.

Quasiphotons are introduced and an equation of motion method is used to obtain a dispersion relation for transverse excitations for a system of electrons interacting with radiation.

**9744.** Goebel, D. G., Caldwell, B. P., Hammond, H. K. III, **Use of an auxiliary sphere with a spectrophotometer to obtain absolute reflectance,** *J. Opt. Soc. Am.* **56,** No. 6, 783-788 (June 1966).

Key words: Absolute; reflectance; spectral.

Reflectance measurements that are made on a scale that is not relative to an arbitrary standard are often called "absolute" measurements. The method presented here uses an auxiliary sphere with a double-beam integrating-sphere spectrophotometer to make measurements on an absolute basis. The basic requirements are: (1) The auxiliary sphere must be uniformly coated with a highly-reflecting, highly-diffusing material. (2) A flat plate must be coated in an identical manner to provide a measure of the coating reflectance. (3) The interior-surface area of the sphere and the area of the entrance port must be measured.

The theory of the method is discussed and an error analysis is made. Reflectance data are reported for specimens of smoked MgO and pressed powders of MgO and $BaSO_4$.

The precision of repeatability has been evaluated from measurements of a Vitrolite-reference standard. More than a dozen measurements at each of eight wavelengths made over a 3-year period exhibited a standard deviation of 0.003 for the spectral reflectance.

**9745.** Goldberg, K., **Hadamard matrices of order cube plus one,** *Proc. Am. Math. Soc.* **17,** No. 3, 744-746 (June 1966).

Key words: Block designs; Hadamard matrices; incidence matrices.

If $H$ is an Hadamard matrix of order $h$, with the property that $H+H^T = 2I$, then there exists an Hadamard matrix of order $(h-1)^3+1$ with the same property.

**9746.** Goldman, D. T., **Reactor physics in the resonance and thermal regions,** *J. Franklin Inst.* **283,** No. 5, 437-438 (May 1967).

Key words: Absorption; neutron; reactor; resonance; thermalization.

A review of papers presented at a topic conference of the American Nuclear Society.

**9747.** Goldman, D. T., **The calculation of nuclear cross-sections by the optical model,** (Proc. Intern. Atomic Energy Agency Conf. Nuclear Data for Reactors, Vienna, Austria, 1966), *Book, Nuclear Data for Reactors* **1,** 339-364 (1967).

Key words: Calculations; cross-section; neutron; nuclear cross-sections; nucleus; optical model scattering.

It is well recognized that there will always be limitations to the amount and certainty of microscopic nuclear cross-section data which are available for direct input into reactor design calculations. Therefore, scattering models for the interaction between incident nucleons and the target nucleus have been proposed and used to obtain appropriated values of necessary cross-sections, both where experimental data are lacking and to differentiate between conflicting data. The generic term for such computations is conveniently "optical model calculations" wherein the two-body internucleon potential is replaced by effective nuclear potential.

This paper presents a systematic derivation of nuclear cross-sections beginning with the interaction between an incident particle and the target nucleons. The replacement of the exact potential by an effective potential results, to first order, in the ordinary time-independent Schrödinger equation. This equation, including a complex and spin-orbit potential is solved for the resultant wave function. By writing the wave function in its scattering solution form, it is possible to compute the shape elastic cross-section and the polarization directly in Legendre moment expansions. The compound nucleus cross-section, as given originally by the statistical model of Hauser and Feshbach, arises naturally by examining the total wave function. By using the entire solution, including the complete interaction potential, it is possible to generalize these calculations to include the effect of non-spherical potentials and to derive the distorted wave Born approximation. The equations derived in this manner have been used in writing ABACUS-1 and OPTIC, two widely utilized optical model programmes developed by colleagues and the author at Knolls Atomic Power Laboratory. The results obtained from calculations with suitably adjusted potential parameters, have provided confidence for further use of these optical model techniques in providing cross-section information.

**9748.** Gorden, R., Jr., Ausloos, P., **Gas-phase photolysis and radiolysis of methane. Formation of hydrogen and ethylene,** *J. Chem. Phys.* **46,** No. 12, 4823-4834 (June 15, 1967).

Key words: Free radical reactions; ion-molecule reactions; photolysis; radiolysis.

The photolysis of $CH_4$ and of $CH_4-CD_4$ mixtures has been investigated at 1236 Å (10.0 eV) and at 1048-67 Å (11.6-11.8 eV). The excited methane molecule dissociates to form $H_2$, H, $CH_3$, $CH_2$, CH, and probably also C. The CH and $CH_2$ radicals insert into methane to form internally excited $C_2H_5$ and $C_2H_6$ species, respectively. Below one atmosphere, all $C_2H_5$ radicals decompose to form $C_2H_4$, while the ethane molecules are partially stabilized. The relative quantum yield of CH increases about threefold when the wavelength is reduced from 1236 Å to 1048-67 Å. On the basis of an isotopic analysis of the hydrogen produced in the photolysis of $CD_4-H_2S$ mixtures, it is concluded that at 1236 Å, D-atoms constitute at least 65% of the "molecular" deuterium yield.

In the radiolysis, ethylene is largely, although not exclusively formed by the insertion of CH into methane. It is demonstrated that addition of small concentrations of an unsaturated hydrocarbon to methane profoundly affects the ion-molecule reaction mechanism and, therefore, does not lead to a dependable value of the "initial" ethylene yield as suggested in earlier studies. Upon application of an electrical field, the production of CH and $CH_2$ is augmented in the saturation current region. The importance of the latter two radicals in the direct and rare-gas-sensitized radiolysis is examined briefly. The formation of hydrogen in the radiolysis will be discussed on the basis of new information derived from $CD_4-H_2S$ experiments. The production of hydrogen in the radiolysis of $Xe-CH_4-CD_4-NO$ mixtures has also been reexamined in view of a recent study in which it was asserted that all of the hydrogen in such a mixture is due to the unimolecular decomposition process

$$CH_4 \rightarrow CH_2 + H_2.$$

Our data disagree with this view and actually demonstrate that CH and $CH_2$ play a minor role in the xenon-sensitized radiolysis of methane.

**9749.** Gorden, R., Jr., Doepker, R., Ausloos, P., **Photoionization of propylene at 1236 Å reactions of $C_3D_6^+$ with added alkanes,** *J. Chem. Phys.* **44,** No. 10, 3733-3740 (May 1966).

Key words: $H_2^-$-transfer reactions; hydrocarbons; ion-molecule reaction; photoionization; photolysis; propylene.

$C_3H_6-C_3D_6-O_2$ mixtures have been irradiated at 1236 Å (10 eV) in the presence and absence of an applied electrical field with the purpose of obtaining information about the ion-molecule reaction mechanism. On the basis of a number of observations, it was calculated that the product, propane, can be ascribed to the reaction $C_{3m}H_{6m}^+ + C_3H_6 \rightarrow C_{3m}H_{6m-2}^+ + C_3H_8$, $(m>2)$. When alkanes ($RH_2$) whose ionization energy is less than 10 eV are added to $C_3D_6-O_2$ mixtures, the following $H_2^-$-transfer reaction occurs: $C_3D_6^+ + RH_2 \rightarrow CD_3CDHCD_2H + R^+$. Relative rates of the reaction of $C_3D_6^+$ with various alkanes have been determined and compare favorably with values obtained in a recent radiolytic study in which cyclopentane-$d_1$ was used as a source of $C_3D_6^+$ ions.

The optimum experimental conditions, under which meaningful saturation ion currents can be obtained in the photoionization apparatus, are described. On the basis of measurements of the saturation ion current in NO and propylene at 1236 Å, values of 0.197 and 0.208 were obtained for the photoionization efficiencies of $C_3H_6$ and $C_3D_6$, respectively. The latter measurements made it possible to express the products in the number of molecules formed per ion pair as well as in the number of molecules formed per quantum absorbed.

**9750.** Gordon, G. S., **A new service by NBS. An aid in making the Bureau's technical resources available to private standards organizations, manufacturers, and government agencies,** *Proc. 15th Annual Meeting Standards Engineering Society, Atlantic City, N.J., Sept. 14, 1966,* pp. 73-75 (1966).

Key words: Focal point; OESLA established at NBS; standards-making bodies.

The Office of Engineering Standards Liaison and Analysis was established as a focal point for assistance to standards-making bodies. Its functions will be to catalyze, strengthen existing institutions, identify new areas of technical activity in the standards field, assist the internal technical engineering standards activities at NBS in reaching maximum effectiveness, and build bridges of communication between NBS and both government and non-government groups in national and international standardization. The LaQue Committee in 1965 recognized the need for developing a national standards effort by tying together the efforts of several hundred standards-making organizations and developing the concept of the USA Standards Institute, and recommended expansion of the Bureau's cooperation with industry and USASI in making technical experts available to serve on committees and as delegates to international ISO, IEC, and COPANT meetings.

**9751.** Gordy, L. H., Harman, G., **The use of semiconductors for the study of boiling heat transfer to low temperature liquids,** *Cryogenics* **7,** 89-92 (Apr. 1, 1967).

Key words: Cryogenic heat transfer; measurements; semiconductors.

It is shown that semiconductors, such as silicon and germanium, can be advantageously used to study boiling heat transfer from solids to low temperature liquids. Measurements can be made quickly and automatically. Widely different types of resistance vs. temperature characteristics can be obtained from these materials and such characteristics can influence the nature of the nucleate to film-boiling transition. Because these materials have large positive temperature coefficients of resistance, the transitions are thermally self-regulating. All heat flux data obtained from such samples lie within normal experimental values.

**9752.** Gornick, F., Ross, G. S., Frolen, L. J., **Crystal nucleation in polyethylene: The droplet experiment,** *J. Polymer Sci.* Pt. C, **18,** 79-91 (1967).

Key words: Crystallization; homogeneous nucleation; kinetics; microscopy; polyethylene; surface free energy.

The droplet technique was utilized to obtain estimates of the isothermal rate of homogeneous crystal nucleation in highly supercooled melts of unfractionated linear polyethylene. In a typical experiment a cell containing a suspension of several hundred micron-size spherical droplets of the polymer was placed on a microscope hot stage and quenched from a temperature well above the melting point of polyethylene to the desired crystallization temperature. When viewed between crossed polarizers, the droplets were initially invisible but, upon freezing, they appeared as visible birefringent spheres. The time dependence of the process was followed by time-lapse photography. Half times ($\tau 1/2$) for the freezing of those droplets remaining unfrozen by the time the crystallization temperature was attained were thus obtained at a series of undercoolings and related to the desired nucleation rate constant I(nuclei-cm$^{-3}$-sec$^{-1}$) by the equation $I = ln2/\tau 1/2v$, where v is the droplet volume.

The temperature dependence of I, as obtained by the above procedure, was analyzed in accord with current theories of homogeneous nucleation of chain-folded polymer crystals. From this analysis, an estimate, 14,960 ergs$^3$ cm$^{-6}$ was made of the quantity ($\sigma^2\sigma_e$), where $\sigma$ and $\sigma_e$ are respectively the lateral and end-surface free energies of the crystal.

**9753.** Grabner, L. H., **Oscillatory photoconductivity and luminescence in $SrTiO_3$,** (Proc. Cairo Solid Sate Conf. American University, Cairo, Egypt, Sept. 3-8, 1966), *Book, Interaction of Radiation with Solids,* Ed. A. Bishay, pp. 155-160 (Plenum Press Inc., New York, N.Y., 1967).

Key words: Electric field quenching; luminescence; negative resistivity; photoconductivity; strontium titanate.

Photocurrents and luminescence in $SrTiO_3$ oscillate at low temperatures (~4 °K) at a threshold of about 100 volts/cm. Voltage-current curves show negative differential resistance in the region of oscillation. We suggest that these effects are due to the field ionization, into the valence band, of a hole trapped 1 eV from the valence band. The hole is ionized by the local field ($\sim 10^6$ V/cm) which differs from the externally applied field of $10^2$ V/cm because of the high dielectric constant of $SrTiO_3$ ($\sim 10^4$) at low temperatures.

**9754.** Gray, J. E., Bussey, H. E., **Instrumentation and measurements,** *Book, 1965 Digest of Literature on Dielectrics* **29,** Chapt. I, pp. 1-25 (Publ. 1461, Nat. Acad. Sci.-Natl. Res. Council, Washington, D.C., 1967).

Key words: Dielectric breakdown; dielectric constant; dielectric standards; electrical insulation; instrumentation; measurement; permittivity.

A classified bibliography of abstracts from the literature of instrumentation and measurement applicable to the study of dielectric materials has been prepared for publication as the first chapter of the Digest of Literature on Dielectrics for 1965.

**9755.** Green, M. S., **Lectures on critical phenomena,** (Proc. Summer School of Theoretical Physics, Cargese, Corsica, Summer 1964), *Book, Cargese Lectures in Theoretical Physics & Statistical Mechanics,* Ed. B. Jancovici, pp. 59-88 (Gordon and Breach Publ., New York, N.Y., 1964).

Key words: Critical phenomena in liquid vapor systems; liquid vapor systems; statistical mechanics; thermodynamics of phase changes.

Some speculative ideas on the theory of critical phenomena in liquid vapor systems are presented. As a background for these fundamental maximum principles of statistical mechanics, thermodynamics of phase changes in the activity temperature plane and sequence of Legendre transformations are discussed. It is suggested that critical phenomena will be simpler when expressed in term distribution functions rather than the potentials and that the critical points correspond to the existence of the zero eigenvalue of the derivative matrix of the transport from potentials of average force to potentials.

**9756.** Green, M. S., Garcia-Colin, L. S., Chaos, F., **The Chapman-Enskog solution of the generalized Boltzmann equation,** *Physica* **32,** 450 (1966).

Key words: BBGKY hierarchy; Bogolyubov's functional assumption; Chapman-Enskog method; dense gases; transport properties.

The generalization of the Chapman-Enskog method is applied to systems of equations which are obtained when Bogolyubov's functional assumption is introduced into the BBGKY hierarchy. A system of inhomogeneous equations is derived from the solution of which the transport coefficients may be determined.

The kernel of these equations is shown to have different left and right eigenfunctions with zero eigenvalues. The method, while dependent on the Bogolyubov assumption, is independent of the assumption of a power series expansion for the transport coefficients.

**9757.** Green, M. S., Vincentini-Missoni, M., Sengers, J. M. H. L., **Scaling-law equation of state for gases in the critical region,** *Phys. Rev. Letters* **18,** No. 25, 1113-1117 (June 19, 1967).

Key words: Compressibility; critical exponents; critical isotherm; critical region; density gradients; equation of state; gases; gravity effect; scaling law.

The Widom-Kadanoff scaling-law equation of state has been confirmed for a variety of gases in a range of ±50% of the critical density and within a few percent above and below the critical temperature. Using a new procedure motivated by the scaling law the exponent $\delta$ describing the shape of the critical isotherm was found to be close to 5 while the compressiblity exponents $\gamma$ and $\gamma'$ were found to be both equal to about 1.4.

**9758.** Greenberg, L., **On a theory of Ahlfors and conjugate subgroups of Kleinian groups,** *Am. J. Math.* **LXXXIX,** No. 1, 56-68 (Jan. 1967).

Key words: Conjugate subgroups; Fuchsian group; Hilbert nullstallensatz; Kleinian group; parabolic triangle group; prime ideal; region of discontinuity.

A gap in a theorem of L. Ahlfors is filled and a generalization of the problem is studied.

**9759.** Greenberg, L., **Fundamental polyhedra for Kleinian groups,** *Ann. Math.* **84,** No. 3, 433-441 (Nov. 1966).

Key words: Euler characteristic; fundamental polyhedron; hyperbolic space; Kleinian group; limit set; region of discontinuity.

The following theorem is proved: Let $\Gamma$ be a Kleinian group whose limit set contains at least two points. If $\Gamma$ has a fundamental polyhedron (in hyperbolic 3-space) with a finite number of sides, then the region of discontinuity in the complex plane cannot be connected and simply connected. From this, it follows that there exist finitely generated Kleinian groups which have no finite-sided fundamental polyhedron. This is in surprising contrast to the case of Fuchsian groups.

**9760.** Greenberg, L., **Fundamental polygons for Fuchsian groups,** *J. Anal. Math.* **18,** 99-105 (1967).

Key words: F-regular region; Fuchsian group; fundamental polygon; horocyclic region; hypercyclic region; simple fundamental polygon.

It is proved that a certain class of fundamental polygons for finitely generated Fuchsian groups are finite-sided. This is already known for convex polygons. However, this paper gives a much shorter proof for a wider class of polygons.

**9761.** Greene, F. M., **Field-strength standards and measurements (30 Hz to 1000 MHz),** *Proc. IEEE* **55,** No. 6, 970-981 (June 1967).

Key words: Calibration of field-strength meters; electric-field-strength standards; magnetic-field-strength standards; near-zone electric-field-strength standards; standard-antenna calibration method; standard-field calibration method.

A description is given of the various CW field-strength standards and associated measurement instrumentation and techniques developed over the past twenty-five or thirty years at the National Bureau of Standards. These are used for the calibration of both commercial and military field-strength meters in various frequency bands of the overall range from 30 Hz to 1000 MHz. The techniques used are applicable only for evaluating the strength of steady-state, ac fields varying sinusoidally in time, and are not intended for use in broadband applications of any kind.

Two principal types of field-strength standards and a prototype near-zone field-strength meter are described. These are as follows:

(a) *Magnetic-Field-Strength Standards* used over the frequency range 30 Hz to 30 MHz for the calibration of CW field-strength meters employing small-loop receiving antennas;

(b) *Electric-Field-Strength Standards* used over the frequency range 30 to 1000 MHz for the calibration of CW field-strength meters employing half-wavelength self-resonant dipole receiving antennas; and

(c) *Near-Zone Electric-Field-Strength Meter and Interim Field-Strength Standards* used over the frequency range 150 kHz to 30 MHz for the evaluation of hazards of high-level electromagnetic radiation to ordnance devices and other uses.

**9762.** Haber, S., **A functional inequality,** *Proc. Am. Math. Soc.* **73,** No. 10, 1103-1104 (Dec. 1966).

Key words: Functional equations; inequalities; inverse functions; real functions.

It is shown that if $f$ is a continuous increasing function then $f(x) \cdot f^{-1}(x) > (1-\epsilon)x^2$, for some sets of values of $x$.

**9763.** Haigh, P. J., Forman, R. A., Frisch, R. C., **Nuclear magnetic resonance of $^7$Li and $^1$H in solid lithium imide, lithium amide, and lithium nitride,** *J. Chem. Phys.* **45,** No. 3, 812-816 (1966).

Key words: Ammonia analogues; hydrogen; lithium; nuclear magnetic resonance; resonance.

Nuclear magnetic resonance lines of $^7$Li nuclei have been observed in solid, polycrystalline samples of $LiNH_2$, $Li_2NH$, and $Li_3N$. Proton resonance lines have also been observed in the first two samples. In $LiNH_2$ there is a splitting of the resonance line due to first order quadrupole effects which indicates a coupling constant of 119±2 kHz (estimated limit to maximum error) at room temperature. In $Li_2NH$ no quadrupole effects are seen which is in agreement with the fact that the lithium nuclei in this compound are situated in sites of cubic symmetry. In $Li_3N$ both first and second order quadrupole effects have been observed simultaneously. From these data coupling constants for $Li_3N$

have been found to be 296±4 kHz and 200±10 kHz at room temperature. An unexplained line was also observed at low magnetic fields for this compound. These effects were found to vary with temperature and with the purity of the sample.

9764. Hall, J. L., Morey, W. W., **Optical heterodyne measurement of neon laser's millimeter wave difference frequency,** *Appl. Phys. Letters* **10,** No. 5 152-155 (Mar. 1, 1967).

> Key words: Frequency-millimeter wave difference; heterodyne measurement; millimeter wave difference frequency; neon laser's millimeter wave difference frequency; optical heterodyne measurement.

We report detection and measurement of the millimeter wave difference frequency between two near laser lines at 1.152 $\mu$. The two spectral transitions, separated by 2.26 Å, oscillate in pure neon in a single laser device, producing about 150 $\mu$W total power in several longitudinal modes. The many resulting 51.3-kmc beat frequencies have been studied by optical heterodyne techniques. A type of diode has been found which has enough microwave sensitivity *and* enough optical sensitivity to combine the optical detector and the microwave heterodyne functions in a single element. The preliminary value for the difference in frequency between the $2S_2|\to|2P_4$ and $2S_4\to 2P_7$ transitions in neon at 150 mtorr is (51,360±150) Mc. This value is not in agreement with the value calculated from NBS Circular 467, Vol. I of Sitterly's *Atomic Energy Levels*.

9765. Hall, M. B., Larsen, N. T., Little, W. E., **Combination RF radiation and fluid pressure seal,** *Proc. IEEE* **54,** No. 11, 1585-1586 (Nov. 1966).

> Key words: Electrical measurements; fluid pressure seal; pressed woven metal; radiofrequency; waveguide joints; woven metal.

Radiation leakage by extraneous paths from sources to detectors frequently limits the dynamic range of precision electrical measurements in the radio-frequency range. Elimination of leakage paths becomes more difficult with increasing frequency. Correct use of gaskets made of pressed woven metal eliminates measurable leakage but does not insure a low, stable reflection from waveguide joints. Furthermore, commercially available woven-metal gaskets require special grooved flanges. Lead washers suppress leakage sufficiently for many purposes when freshly inserted between waveguide flanges, but their effectiveness decreases with time, particularly if they are removed and reinserted. A commercial (recent) gasket material consisting of silver powder embedded in vinyl polymer has proved to be very effective, at least when fresh. A recent publication describes RF leakage tests on a number of gaskets of different designs and materials.

A new type of microwave gasket for use, for example, between waveguide flanges has been developed at the NBS Boulder Laboratories. It is convenient, requiring only moderate pressure, and may be reused. The new gasket can be made thin, and hence, ight. It provides simultaneously a microwave radiation and a fluid pressure seal, and the reflection it introduces can be made small. It is expected that variations of the materials of construction will provide for various other combinations of desirable properties.

9766. Hamer, W. J., **Electrochemistry,** *Encyclopedia of Physics,* Ed. R. M. Besancon, pp. 200-203 (Reinhold Publ. Corp., New York, N.Y., 1966).

> Key words: Batteries; conductivity; electrolysis; electrophoretic separation; Faraday; ionization.

This article deals with the scientific discipline known as electrochemistry and the development of the field from the time of Alessandro Volta to the present. *Topics covered include:* Voltaic couples, electromotive series of the elements, electrolysis, electrolytic and electronic conductors, electrolytic solutions, ionization, the Debye-Hückel theory of interionic attraction, Faraday's laws of electrolysis and the Farady constant, and electrochemical thermodynamics. The article concludes with a listing of the applications of electrochemistry. These include electrochemical analysis; electrochemical synthesis of dyestuffs, fertilizers, plastics, insecticides; electrophoretic separation of proteins in biology and medicine, in corrosion, and in the development of storage batteries and dry cells.

9767. Hanley, H. J. M., **Comparison of the Lennard-Jones, exp-6, and Kihara potential functions from viscosity data of dilute argon,** *J. Chem. Phys.* **44,** No. 11, 4219-4222 (June 1966).

> Key words: Argon; kinetic theory; phase studies; potential functions; special functions; thermodynamics; transport properties.

Experimental viscosity coefficients of argon are used to illustrate how the variation of the parameters of the Lennard-Jones, exp-6, and Kihara functions effect the correlation of the Chapman-Enskog transport theory with experimental data. By rationalizing the choice of the parameters, better correlations are possible than obtained by previous workers and it is shown that the Kihara function gave the best results.

9768. Harari, H., Horn, D., Kugler, M., Lipkin, H. J., Meshkov, S., **W spin for any spin,** *Phys. Rev.* **146,** No. 4, 1052-1057 (June 1966).

> Key words: Arbitrary spin state; basic spin; linear combinations; ordinary spin states; spin states; W spin.

The general "W spin" properties of an arbitrary spin state constructed from any number of basic spin 1/2-objects are discussed in detail. Explicit formulae for expressing the eigenstates of $W^{-2}$ as linear combinations of ordinary spin states are given and some properties of the transformation matrices are discussed.

9769. Harrach, R. J., **Radiation-field-dependent frequency shifts of atomic beam resonances,** *J. Appl. Phys.* **38,** No. 4, 1808-1819 (Mar. 15, 1967).

> Key words: Atomic beam; cesium beam; frequency shifts; frequency standards; radiation field.

Radiation-field-dependent frequency shifts arising in atomic beam spectroscopy are treated theoretically and experimentally. Shifts due to fundamental and unavoidable interactions between the radiation field and the atoms comprising the beam are distinguished from those due to various "apparatus effects." Precise measurements of frequency shifts are made for a cesium beam experiencing Ramsey-type excitation. For the magnetic field-sensitive transitions $(F,M_F)=(4,\pm 1)\leftrightarrow(3,\pm 1)$, the magnitude of the shifts is about 1 part in $10^{10}$ of the resonance frequency value, per milliwatt variation of input power to the radiation field. The shifts vary with input intensity in a nonmonotonic fashion and are shown to result from nonuniformity in the static magnetic *c*-field of the apparatus. Much smaller shifts of about 5 parts in $10^{13}$ per milliwatt are observed for the magnetic-field-insensitive transition $(F,M_F)=(4,0)\leftrightarrow(3,0)$. The major features of these shifts are shown to arise from spectral impurities in the radiation exciting the transition and a small phase difference between the pair of separated radiation fields. The bearing these results have on evaluating the accuracy an atomic beam frequency standard is discussed.

9770. Harrach, R. J., **Some accuracy limiting effects in an atomic beam frequency standard,** *Proc. 20th Annual Symp. Frequency Control, Atlantic City, N.J., Apr. 19-21, 1966,* pp. 424-435 (1966).

Key words: Accuracy; cesium beam; frequency shifts; frequency standard.

The accurate resonance frequency of the transition $(F,M_F) = (4,0) \leftrightarrow (3,0)$ in the ground state of cesium-133 is expressed in the form of an operational equation for an atomic beam spectrometer. Emphasized are the terms in this equation which correct for the beam direction dependence and radiation field dependence of measured resonance frequencies: $1/2[\nu_{res_i}(P_l) + \nu_{res_j}(P_l)] - 1/2(S_i + S_j)P_l$, where i and j refer to opposite beam directions through the apparatus, $P_l$ is the microwave power exciting the transition, and $S_i$ and $S_j$ are rates of linear frequency shift. The results of a detailed theoretical analysis are given which specify the contributions to these terms by various apparatus and fundamental shift-inducing effects.

This approach to accuracy specification is applied to the United States frequency standard, a National Bureau of Standards atomic beam machine designated NBS III, through a set of experiments using an atomic hydrogen maser as a highly stable reference frequency source. The corrections determined are $-3.2 \times 10^{-12}$ for beam direction dependence, $-2.2 \times 10^{-12}$ for power dependence and $+0.4 \times 10^{-12}$ for second-order Doppler shift. The uncertainties in these corrections and contributions from other sources give a present $1\sigma$ estimate of accuracy capability of $\pm 1.1 \times 10^{-12}$ for NBS III. This figure should be reducible by one order of magnitude through efforts to eliminate systematic errors in the measurements of $\nu_{res_i}$ and $\nu_{res_j}$.

**9771.** Harris, F. K., Cooter, I. L., Dunfee, B. L., Harris, W. P., Hermach, F. L., Peterson, C., **Electrical standards and measurements,** *Electro. Technol.* **97,** 53-70 (Jan. 1967).

Key words: Absolute measurements; electrical reference standards; electrical units; precise electrical measurements.

The basis of the electrical units and their derivation for the mechanical units is briefly reviewed. Methods used by the Electricity Division of the National Bureau of Standards for the establishment of measurement reference standards are discussed together with the techniques employed in extending the range of measurement from the reference standard to higher and lower values.

**9772.** Harris, W. P., **A new ultra-low frequency bridge for dielectric measurements,** *1966 Annual Report Conf. Electrical Insulation and Dielectric Phenomena, National Academy of Sciences-National Research Council, Mt. Pocono, Pa., 1966,* pp. 72-74 (1967).

Key words: Bridge; dielectric measurements; dielectrics; electrical measurements; low frequency; measurements, dielectric; measurements, electrical; ultra-low frequency.

**9773.** Harris, W. P., **Apparent negative impedances and their effect on three-terminal dielectric loss measurements,** *(1965 Annual Report Conf. Electrical Insulation), Natl. Acad. Sci.-Natl. Res. Council Publ. 1356,* pp. 83-86 (Natl. Acad. Sci.-Natl. Res. Council, Washington, D.C., 1966).

Key words: Dielectric losses; dielectric materials; dielectric measurements; errors; low-loss; negative impedances; negative losses.

Tee networks consisting of "stray" impedances can cause "errors" in the conductance and capacitance of three-terminal capacitance measurements. In particular, a tee with two capacitive arms and a resistance leg to ground can introduce a negative component of conductance. Therefore, a three-terminal capacitor can appear to have zero or negative losses. A measurement of the dielectric loss of a material can indicate a negative loss unless steps are taken to eliminate by careful cell design this source of error.

A component of negative loss can arise from the coaxial cables connecting the cell or capacitor to the bridge. This error can be reduced by the use of coaxial chokes or by a feedback circuit.

**9774.** Hayward, E., **Some aspects of the photodisintegration of light nuclei,** *Proc. Intern. School of Physics "Enrico Fermi", Course* **XXXVI,** Ed. C. Bloch, July-Aug. 1965, Monastero, Italy, pp. 559-565 (Academic Press, Inc., London, England, 1966).

Key words: Intermediate structure; isotopic spin; photodisintegration.

The photonuclear giant resonance is discussed from the point of view of isotopic spin mixing and intermediate structure.

**9775.** Heidemann, H. G. M., Kuyatt, C. E., Chamberlain, G. E., **Inelastic electron scattering from $H_2$,** *J. Chem. Phys.* **44,** No. 2, 440-441 (Jan. 1966).

Key words: Electrons; energy-loss spectra; inelastic electron scattering.

Energy-loss spectra have been measured for 13.7- to 50.7-eV electrons in $H_2$. For incident energies below about 16 eV, energy-loss peaks are observed due to either or both of the $a\ {}^3\Sigma_g{}^+$ and $c\ {}^3\Pi_u$ states of $H_2$. The excitation cross section of the $v = 0$ and $v = 1$ vibrational levels to the $\beta\ {}^1\Sigma_u{}^+$ state show sharp and large resonances, corresponding in energy with resonances in the total scattering. The absolute electron energy scale in $H_2$ was recalibrated to an estimated accuracy of 0.1 eV.

**9776.** Heidemann, H. G. M., Kuyatt, C. E., Chamberlain, G. E., **Resonances in the elastic and inelastic electron scattering from $N_2$,** *J. Chem. Phys.* **44,** No. 1, 355-358 (Jan. 1, 1966).

Key words: Doppler broadening; electronic excitation; low energy elastic electron scattering; low energy inelastic electron scattering; Lyman-Birge-Hopfield bands; metastable states; molecular nitrogen; negative ions; nitrogen window; resonances; vibrational excitation.

A sharp and isolated resonance of the "helium window" type has been discovered in electron transmission measurements in $N_2$ at 11.48±0.05 eV (believed accurate to within 0.05 eV). Additional resonance structure is observed at 11.75 and 11.87 eV. The E ${}^3\Sigma_g{}^+$ state is coincident in energy with the 11.87 eV structure and is found to exhibit an excitation probability sharply peaked near threshold. The series of resonances previously known to exist between 1.8 and 3.5 eV as a consequence of an $N_2{}^-$ state with vibrational structure, has been studied with improved resolution and by different procedures.

**9777.** Heinrich, K. F. J., **Electron probe microanalysis,** *Book, Experimental Methods of Materials Research. Advances in Materials Research,* pp. 145-162 (John Wiley and Sons Inc., New York, N.Y., 1967).

Key words: Characteristics of probe analysis; electron microanalysis; electron probe microanalysis; microanalysis, electron probe; probe.

This paper introduces the reader into the principles and techniques of electron probe microanalysis. After a brief description of the instrument, the characteristics of probe analysis, such as range of elements, spatial resolution, sensitivity, and conditions necessary for the specimen, are discussed. The corrections to be applied in quantitative analysis are enumerated and explained. Several signal evaluation systems, particularly for scanning microprobe analysis, are described, including the use of signals other than x-rays. The fields of application are briefly indicated.

9778. Heinrich, K. F. J., **Identification to inclusions with the electron probe microanalyzer,** *Am. Soc. Testing Mater. Spec. Tech. Publ.* **393** (Jan. 1966).

Key words: Electron probe microanalysis; microanalyzer; particle size.

Direct identification of the components of inclusions and precipitates can be performed with the aid of the electron probe microanalyzer. Although the method is restrictive as to minimum particle size, range of detectable elements, and attainable accuracy, satisfactory characterization of the inclusions is generally possible. Special techniques applicable to inclusions and precipitates and recent applications are discussed.

9779. Henderson, M. B., **Introductory remarks at the symposium on problems of small information groups,** (Div. Chem. Lit. Symp., Problems of Small Information Groups, 151st National Meeting Am. Chem. Soc., Pittsburgh, Pa., Mar. 25, 1966), *J. Chem. Doc.* **6,** 143 (Aug. 1966).

Key words: Chemical literature; documentation services; remarks; small information groups.

The Symposium on Problems of Small Information Groups, presented before the Division of Chemical Literature, ACS, on March 25, 1966, addressed itself to the problems of information groups with three or fewer professionals on the staff. Possible solutions to some of the problems of such groups were presented, as for example, problems of physical storage, distribution, and evaluation of information systems, and cooperation in the establishment and operation of information networks.

9780. Henig, S., **A proposal for a supplement to the patent system,** *Design News* **21,** No. 1, 84-89 (Jan. 5, 1966).

Key words: Anti-trust violations; better products; copiers; developer-producer's; dormant patents; higher productivity; improvements; industrial stimulus; industrial trade associations; "limit right"; material/product/process improvements; non-inventions; quasi-property; right to royalties; supplementary system; traditional property-rights; unrestricted copying; useful service.

It is postulated that the patent system is inadequate as an industrial stimulus toward both higher productivity and better products. The need is indicated for a supplementary system applicable to improvements which may be non-inventions. A proposal, using a quasi-property concept termed "limit right", describes a system which specifies: a developer-producer's right to royalties from copiers of material/product/process improvements when the latter are put into useful service; unrestricted copying of such improvements so as to exclude other traditional property rights; a means of encouraging the use of industrial trade associations to collect, distribute, and adjudicate royalties. A projection of practice under the system shows that it would be largely self-regulating through each industry's trade association. Contrasted with the patent system, the proposal is shown to be *directly* inductive toward the end of bringing benefits of improved manufacture and produce to the marketplace, and non-inductive to anti-trust violations. An optional measure of superseding property-rights in the area of dormant patents is directed at hastening development effort for these.

9781. Henry, R. J. W., Lipsky, L., **Multichannel photoionization of atomic systems,** *Phys. Rev.* **153,** No. 1, 51-56 (Jan. 1967).

Key words: Close-coupling; core relaxation; multi-channel; neon; photoionization; standing waves; 2p shell.

Expressions for multi-channel photoionization are obtained with the dipole approximation assuming LS coupling, which, while including the effects of coupling between channels, give separate contributions for each channel. The explicit form of the cross sections for atomic systems with configurations $1s^22s^22p^4$ is obtained assuming superpositions of determinantal wave functions (Hartree-Fock) for initial and final states. The effects of core relaxation are considered. The formalism is applied to the photoionization of neon with the result that coupling between channels and core relation have a larger effect on the individual channel cross sections than on the total cross section. Both effects tend to bring the dipole velocity and length forms of the cross section into closer agreement with each other, but improvement is appreciable only near threshold.

9782. Hermach, F. L., Williams, E. S., **Thermal converters for audio-frequency voltage measurements of high accuracy,** *IEEE Trans. Instr. Meas.* **IM-15,** No. 4, 260-268 (Dec. 1966).

Key words: Audio-frequency; comparator; standards; thermal convectors; thermoelements; transfer standards; voltage comparator; voltage measurements.

The ac-dc differences of a reference group of thermoelements have been evaluated at audio frequencies to a few ppm at currents from 5 to 20 mA. A technique for comparing the ac-dc differences of two thermoelements with an uncertainty of about 2 ppm has been developed. Two 5 mA thermoelements are used with a plug-in set of resistors of computable reactances to form thermal voltage converters for voltage measurements. With this same technique adjacent ranges of these converters can be compared to step up from 0.5 to 500 V to better than 10 ppm.

9783. Hermach, F. L., **Thermal converters used as transfer standards for the measurement of alternating current and voltage,** *Proc. 11^e Session Comite Con. d'Electricite, May 10-12, 1965,* pp. 83-88 (Gauthier-Villars, Paris, France, 1965).

Key words: ac-dc transfer standards; alternating current and voltage; thermal converters; transfer standards.

This report to the Advisory Committee outlines recent progress at NBS in the development of ac-dc transfer standards (comparators) for measurements of alternating current and voltage with 20 ppm accuracy or better at audio frequencies. Electrothermic transfer standards of the thermocouple type offer good prospects of meeting this goal. Their ac-dc differences appear to be very stable. The standards can be read with high precision and are rugged and portable. Furthermore, they can readily be intercompared for ac-dc difference, to step up and down the current and voltage scale with a precision of a few ppm. They are thus worthy of consideration for international comparisons of the accuracy of alternating current and voltage measurements.

9784. Herron, J. T., **Mass spectrometric study of the reactions of O atoms with NO and $NO_2$,** *Erratum, J. Chem. Phys.* **44,** No. 9, 3645 (May 1966).

Key words: Atoms; mass spectrometer; O atoms; spectrometric study.

9785. Heydemann, P. L. M., **The Bi I-II transition pressure measured with a dead weight piston gage,** *J. Appl. Phys.* **38,** No. 6, 2640-2644 (May 1967).

Key words: Bismuth; free piston gage; high pressure; polymorphic phase transition; transition pressure; volume change.

A dead weight piston gage was used to determine the Bismuth I-II transition pressure and the volume change at the transition. The transition pressure for one sample, believed to contain less than .001% impurities, was found to be 25,306±60 (estimated uncertainty) bars. With another sample, of substantially less purity and of larger grain size, a transition pressure of 25,500±60 bars was measured. The average relative volume change was .035.

**9786.** Hoeve, C. A. J., **Adsorption isotherms for polymer chains adsorbed from $\Theta$ solvents,** *J. Chem. Phys.* **44,** No. 4, 1505-1509 (Feb. 15, 1966).

Key words: Adsorption; chain; concentration; interface; isotherm; polymer; polystyrene; segment; $\Theta$ solvent.

In the case of interacting polymer chains near the interface, the first layer at the interface corresponding to the thickness of segments, is treated as a polymer solution to which the Flory-Huggins theory is applied. Interaction in other layers is assumed to be absent for $\Theta$ solvents. On minimizing the free energy, adsorption isotherms are calculated. The amount of adsorbed polymer increases without limit and the fraction of segments in the first layer decreases to zero with increase in molecular weight and solution concentration. The root-mean-square distance of segments from the interface is also calculated and is found to vary approximately proportional to the square root of the molecular weight, in good agreement with experiment.

**9787.** Hoffman, J. D., **Dielectric relaxation in molecular crystals: Multiple site models,** *Book, Molecular Relaxation Processes, Chemical Society Spec. Publ. No.* **20,** pp. 47-60 (The Chemical Society and Academic Press, Inc., New York, N.Y., 1966).

Key words: Dielectric relaxation; long chain molecule; molecular crystals; multiple site model; potential barrier to rotation; relaxation times.

The multiple site model of dielectric relaxation in molecular crystals is reviewed. In this model, a dipolar molecule, which is incorporated in a crystal lattice, may orient into one of several equilibrium positions upon rotation about a single axis in an anisotropic crystalline field. The equilibrium sites are mapped out by a 360° rotation of the dipolar molecule in the crystalline lattice assuming that the interaction of the dipole with its neighbors is a Lennard-Jones potential or a volume overlap potential. From this calculation it is seen that each accessible equilibrium site is separated from its neighboring site by a potential barrier to rotation. Differential equations, which describe the rate at which dipoles leave and enter a site as a function of the elementary transition probabilities over the potential barrier, are set up. The solutions to these equations give decay functions $\psi_\beta = \exp[-f_\beta(\alpha)t]$ where $f_\beta(\alpha)$ is the reciprocal of the relaxation time of the $\beta$ mode and is a general function of the transition probabilities of all neighboring pairs of sites. If there are five equilibrium sites then there will be five modes or relaxation times of which one will be trivial (equilibrium).

The model is used to describe the dielectric relaxation of long chain ketone molecules in a urea lattice and relaxation in other long chain paraffin-like crystalline substances.

**9788.** Hornbeck, G. A., **Optical methods of temperature measurement,** *Appl. Opt. Lead Article* **5,** No. 2, 179 (Feb. 1966).

Key words: Boltzmann; Draper; Jeans; Kirchoff; optical; Planck; pyrometry; radiance; Rayleigh; Stefan; temperature; Wien.

The history of the laws of thermal radiation is briefly reviewed, and the theoretical relations basic to some of the optical methods of temperature measurement are given. Comments on a number of optical methods are presented, as well as a selected reference with each method where more detail is available. In conclusion, several problems, in areas of uncertainty in the field optical methods of temperature measurement, are suggested in the belief that a solution to these problems will greatly enhance the technical value of this field.

**9789.** Howard, R. E., **Random-walk method for calculating correlation factors: Tracer diffusion by di-vacancy and impurity-vacancy pairs in cubic crystals,** *Phys. Rev.* **144,** No. 2, 650-651 (Apr. 15, 1966).

Key words: Calculations; correlation factors; di-vacancy and impurity-vacancy pairs; random walk; tracer diffusion.

The random-walk technique is extended in a way that allows correlation factors to be calculated in all cases where principle axes for diffusion can be found. The results are applicable both to tracer and to impurity diffusion. Explicit calculations are given of correlation factors for the diffusion of tracers by bound impurity-vacancy pairs in fcc metals and NaCl-type ionic crystals, and by bound di-vacancy pairs in NaCl-type ionic crystals, CsCl-type ionic crystals, and fcc metals. Appropriate modifications for the "isotope effect" are made for the case of impurity-vacancy pairs.

**9790.** Huber, M. G., Danos, M., Weber, H. J., Greiner, W., **Collective treatment of the giant resonances in spherical nuclei,** *Phys. Rev.* **155,** No. 4, 1073-1084 (Mar. 1967).

Key words: Cross section; dipole-quadrupole interaction; giant resonances.

In a collective treatment the energies of the giant resonances are given by the boundary conditions at the nuclear surface which is subject to vibration in spherical nuclei. Therefore, a coupling between these two collective motions is consistently present. Its general form is given by angular momentum and parity conservation, the coupling constants being completely determined within the hydrodynamical model.

In the present treatment the influence of the surface vibrations on the total photon absorption cross section has been calculated. It turned out that in most of the spherical nuclei this interaction leads to a pronounced structure in the cross section. The agreement with the experiments in medium heavy nuclei is striking; many of the experimental characteristics are reproduced by the present calculations. In some nuclei, however, there are indications of single particle excitations which are not yet contained in this work.

**9791.** Hudson, G. E., **Some characteristics of commonly used time scales,** *Proc. IEEE* **55,** No. 6, 815-821 (June 1967).

Key words: Broadcast time signals; standard frequency and time signals; time; time and frequency standards; time scales.

Various examples of ideally defined time scales are given. Realizations of these scales occur with the construction and maintenance of various clocks, and in the broadcast dissemination of the scale information. Atomic and universal time scales disseminated via standard frequency and time-signal broadcasts are compared. There is a discussion of some studies of the associated problems suggested by the International Radio Consultative Committee (CCIR).

**9792.** Hudson, P. A., **Measurement of RF and baseband pulse quantities,** *Proc. IEEE* **55,** No. 6, 851-855 (June 1967).

Key words: Measurement; peak pulse power; pulse modulation; RF power.

This paper is a survey of the principal methods developed during the past twenty years for the measurement of RF peak pulse power. The basic principles involved for each method are described together with accuracies attainable under normal operating conditions. General techniques for pulse power measurement and precautions to be observed are also given.

**9793.** Hughes, A. N., Scheer, M. D., Klein, R., **The reaction between O($^3$P) and condensed olefins below 100 °K,** *J. Phys. Chem.* **70,** No. 3, 798-805 (Mar. 1966).

Key words: Low temperature chemistry; olefins; oxidation; oxygen atom.

The addition of oxygen atoms to condensed simple olefins has been studied in the 77 to 90 °K temperature range. The ground state O($^3$P) atoms were generated in the gas by dissociation of $O_2$ on rhenium or tungsten surfaces heated to 2300 °K.

At 90 °K and oxygen pressures below 40 millitorr, the major products were found to be the unfragmented epoxides and carbonyls. Above 50 millitorr ozonides and oxygenated products characteristic of rupture at the double bond were observed. Above 100 millitorr only the ozonides and its fragments were produced. At 77 °K, the ozonolysis reaction occurred at much lower oxygen pressures. Comparison of these results with those obtained in the gas phase at 300 °K indicates that the low temperature environment efficiently removes the excess energy from the excited biradical formed in the primary act of O atom addition to the double bond. In all cases studied, fragmentation was less extensive than in the comparable gas phase process.

9794. Hunt, C. M., **Nitrogen sorption measurements and surface areas of hardened cement pastes,** (Highway Research Board Symp. Structure of Portland Cement Paste, Washington, D.C., Jan. 1965), *Highway Research Board Special Report* **90,** 112-122 (1966).

Key words: Cement pastes; nitrogen sorption; pastes; water cement.

Surface area by nitrogen adsorption and also nonevaporable water were determined on hardened cement pastes of four water cement ratios, ranging from 0.251 to 0.501, and four ages, ranging from 1 day to 180 days.

Water-cement ratio made very little difference in the surface area of hardened pastes at 1-day but with pastes at later ages, evidence suggests that surface area may reach a limiting value which is a function of the original water-cement ratio. The ratio of surface area by nitrogen adsorption to nonevaporable water was not constant but increased with increasing hydration in paste of water-cement ratio 0.501 and changed very little or even decreased slightly in paste of water-cement ratio 0.251.

The degree of subdivision of the paste during drying exerted a significant effect on the measured surface area except for specimens of high water-cement ratio measured early in the hydration process. In most cases pastes which were dried as cylinders, 1/2-inch in diameter and 1/2-inch long, had lower surface areas than specimens of the same pastes which were crushed to smaller particle sizes below 1 mm before drying. The sorption isotherm and calculated pore size distribution of a paste after different drying treatment were also determined.

9795. Huntley, L. E., Jones, R. N., **Impedance of lumped circuits,** *Proc. IEEE* **55,** No. 6, 900-911 (June 1967).

Key words: Capacitance; inductance; impedance and admittance; measurement; radio frequency; resistance; standards; state of the art.

This paper is a tutorial presentation dealing with two and three terminal lumped parameter impedance measurements at radio frequencies. Included is a very brief historical discussion with particular emphasis upon more important recent developments such as precision coaxial connectors and coaxial air line standards. The relationship of impedance standards to standards of length and time is shown together with a discussion of instruments and measurement techniques in current use. Special attention is given to particular areas of measurement difficulty. Also included is a presentation of the state of the art wherein commercial instrumentation is compared with best practices from the standpoint of accuracy. The paper concludes with comments and recommendations for improving measurement and measurement agreement.

9796. Huntoon, R. D., **Status of the National Standards for physical measurement,** *Science* **150,** No. 3693, 169-178 (Oct. 8, 1965).

Key words: Ampere; candela; current; degree Kelvin; International System of Units; kilogram; length; luminous intensity; mass; meter; metric system; second; standards for physical measurement; temperature; time.

This article outlines various stages of sophistication in the development of a measurement system, from a "unit-standard" system to a consistent system in which standards are tied to atomic and molecular properties in an independently reproducible way. The present stage of development of our measurement system is discussed in this context, and predictions are made regarding its future development.

9797. Huntoon, R. D., **The basis of our measurement system,** *Phys. Teacher* **4,** No. 3, 113-120 (Mar. 1966).

Key words: Degree Kelvin; kilogram; measurement system; meter; physical constant; second; standard; unit.

This article outlines various stages of sophistication in the development of a measurement system, from a "unit-standard" system to a consistent system in which standards are tied to atomic and molecular properties in an independently reproducible way. The present stage of development of our measurement system is discussed in this context, and predictions are made regarding its future development.

9798. Hust, J. G., Stewart, R. B., **Thermodynamic property computations for systems analysis,** *ASHRAE J.* **8,** No. 2, 64-68 (Feb. 1966).

Key words: Calculated properties; entropy of gases, saturated fluids, and liquids; equations of state; systems analysis; thermodynamic property computations.

Methods for calculating thermodynamic properties from equations of state and zero pressure properties are reviewed. The calculation of entropy of gases, saturated fluids, and liquids is considered in detail. Particular attention is given to the determination of the two phase boundary and thermodynamic consistency of the calculated properties.

A method of iterative solution for implicit variables and its application to thermodynamic calculations are discussed. In addition methods of least squares are considered. Normal equations resulting from the usual minimization procedure are compared with corresponding equations of the constrained least squares problem. Discussion is also included on a technique for fitting related thermodynamic data simultaneously.

9799. Hutchinson, J. M. R., **Alpha-gamma angular correlations in three heavy odd-*A* nuclides,** *Phys. Rev.* **157,** No. 4, 1093-1098 (May 1967).

Key words: Alpha particles; americium-243; angular correlations; neptunium-237; partial wave branching; uranium-233.

Angular correlations between alpha particles and gamma rays have been measured in liquid sources of three separate nuclides, americium-243, uranium-233, and neptunium-237. The angular-correlation functions were experimentally determined for five transitions, and the relative angular-momentum mixing ratios for these transitions were deduced. The mixing ratios of $L = 2$ and 0 agree with theory, but the $L = 4$ and 2 mixing ratios are somewhat higher than predicted. Upper limits of the half-lives of 99-keV and 45-keV states in $Th^{229}$ were measured, respectively, as $0.8 \times 10^{-9}$ and $1.2 \times 10^{-9}$ sec. From a comparison of the attenuated angular correlation in $Am^{243}$, and a previously measured angular correlation in $Am^{241}$, it is deduced that an extranuclear interaction occurs whose time duration is less than $1.2 \times 10^{-9}$ sec.

**9800.** Hutchinson, J. M. R., Walker, D. H., **A simple and accurate method of calibration by photopeak efficiencies,** *Intern. J. Appl. Radiation Isotopes* **18,** No. 1, 86-89 (Jan. 1967).

Key words: Accurate method of calibration; gamma-ray photopeak efficiency; photopeak efficiency curve.

The gamma-ray photopeak efficiency curve for a 3″ x 3″ NaI(Tl) crystal is presented assuming the peak distribution to be a gaussian shape. A simple and accurate method for determining gamma-ray emission rate is discussed. A small, but systematic discrepancy, between present and past photopeak efficiency curves, is noted. Using this method, the number of 0.908 MeV gamma rays per disintegration of yttrium-88 was found to be 0.936±0.013.

**9801.** Hyman, A., Perloff, A., Mauer, F., Block, S., **The crystal structure of sodium tetraborate,** *Acta. Cryst.* **22,** No. 6, 815-821 (June 1967).

Key words: Crystal structure; sodium tetraborate; symbolic addition; x-ray.

Single crystals of sodium tetraborate, $Na_2O.4B_2O_3$, have been synthesized and studied. The structure has been determined using the method of symbolic addition. The space group is $P2_1/a$ with unit cell dimensions: $a = 6.507 \pm 0.001$ (estimated uncertainty), $b = 17.796 \pm 0.002$, $c = 8.377 \pm 0.001$, and $\beta = 96°34' \pm 2'$; $Z = 4$. The structure consists of two infinite, independent, and interlinking boron-oxygen networks, each containing alternating single and double rings. The sodium atoms serve to hold the networks together through coordination with oxygen atoms.

**9802.** Inscoe, M. N., **Losses due to adsorption during filtration of aqueous solutions of polycyclic, aromatic hydrocarbons,** *Nature* **211,** No. 5053, 1083-1085 (Sept. 3, 1966).

Key words: Aqueous solutions; filter media; filtration phenanthrene; hydrocarbons; polycyclic aromatic hydrocarbons.

During filtration, phenanthrene and other hydrocarbons are adsorbed from aqueous solutions by various filter media. Losses are particularly pronounced when membrane filters are used.

**9803.** Isbell, H. S., Fatiadi, A. J., **Phenylhydrazono-phenylazo tautomerism. Part I.** ***xylo*-4,5,6-trihydroxy-2-oxo-1,3-bis(phenylhydrazono)cyclohexane and 4-oxo-1-phenyl-5-phenylazo-2-pyridazine derivatives,** *Carbohydrate Res.* **2,** No. 2, 204-215 (June 1966).

Key words: Absorption spectra of pyridazine derivatives; cyclic polyhydroxy ketones; inositol, triketo-; nuclear magnetic resonance of pyridazine derivatives; phenylhydrazono-phenylazo tautomerism; pyridazine derivatives; *xylo*-trihydroxycyclohexenediolic acid preparation of bis-phenylhydrazon of-; *xylo*-4,5,6-trihydroxy-2-oxo-1,3-bis(phenylhydrazono)cyclohexane.

The positions of the phenylhydrazono groups in xylo-4,5,6-trihydroxy-oxo-1,3-bis(phenylhydrazono)cyclohexane were established by degradation of the compound with sodium metaperiodate and identification of the reaction product. The dialdehyde initially formed by periodate oxidation (but not isolated) cyclized to 4-oxo-1-phenyl-5-phenylazo-3-pyridazinecarboxaldehyde, which gave a crystalline methyl hemiacetal, an oxime, a semicarbazone, and, by oxidation, the corresponding monocarboxylic acid and sodium salt. Upon treatment with phenylhydrazine at 50°, the carboxaldehyde gave a red crystalline phenylhydrazone which, with phenylhydrazine at 130° gave a product that appears to be 4-oxo-1-phenyl-5-(phenylhydrazo)-3-pyridazine-carboxaldehyde phenylhydrazone.

The reactions provide a route to a series of new pyridazine derivatives which may prove valuable for the synthesis of unusual compounds for biological and medical research.

**9804.** Ives, L. K., Ruff, A. W., Jr., **Extended dislocation nodes i a silver-tin alloy,** *J. Appl. Phys.* **37,** No. 4, 1831-1837 (Mar. 15 1967).

Key words: Alloys; dislocation; dislocation nodes; stackin faults; transmission electron microscopy.

A study of dislocation nodes formed in silver-tin solid solutio alloys has been conducted using the technique of transmissio electron microscopy. In alloys of 6 and 8 at. % Sn, both extrinsi and intrinsic stacking faults were observed at three-fold dislocation nodes. Burgers vector data obtained from diffraction contrast studies were in agreement with predictions based o geometric considerations. From a qualitative comparison of th node extensions, the extrinsic fault energy was found to be a least twice the intrinsic fault energy. Both fault energies were observed to decrease with increasing solute concentration. A many of the nodes containing extrinsic faults, the dislocation curvature was small or negative; at the intrinsically faulted node positive curvatures were always observed. It is believed that th dislocation constrictions or cross-linking dislocations required a the extrinsically faulted nodes were responsible for this difference. Motion under stress of the extrinsically faulted node was observed, consistent with the coplanar Burgers vecto geometry. The general occurrence of both types of faults in lo stacking fault energy FCC materials is predicted.

**9805.** James, T. C., **Exact vibrational matrix elements for molecular hydrogen and the intensity of the quadrupole rotation-v bration spectrum,** *Astrophys. J.* **146,** No. 2, 572-580 (No 1966).

Key words: Hydrogen; intensity; quadropole spectrum rotation-vibration interaction; vibrational matrix element

Accurate vibrational overlap integrals and matrix elements o $\xi = (r\&re)/re$, $\xi^2$, and $\xi^3$ have been calculated for lines in th $1-0$, $2-0$, $3-0$, and $4-0$ rotation-vibration bands of molecula hydrogen. The affect of rotation-vibration interaction has bee considered and values are given for Q, S, and some O branc lines. The calculations were carried out using a computer pro gram written by R. N. Zare. These results are used to analyz the intensity measurements in the quadrupole rotation-vibratio spectrum which have been made by Rank and his associate The possibility of predicting the intensity of the $4-0$ band, an of using the $2-0$, and the $3-0$ bands for rotational temperatu measurements is discussed.

**9806.** Jennings, D. A., **Calorimetric measurement of pulsed lase output energy,** *IEEE Trans. Instr. Meas.* **IM-15,** No. 4, 161 164 (Dec. 1966).

Key words: Calorimetric measurement; laser, pulsed; ou put energy; pulsed laser.

There are several methods by which one may measure th energy output of the pulsed laser. However, the technique whic seems to be most promising as far as accuracy and precision a concerned is the calorimetric method. We have designed, buil and calibrated calorimeters for measuring the output energy the pulsed ruby laser (6943 Å). The heart of the calorimeter is small absorption cell containing an aqueous solution of CuSO The temperature of the absorption cell, as measured by a the mocouple, indicates the energy absorbed by the calorimeter. T calorimeter was calibrated in two different ways: 1) the know heat capacity of the absorption cell and thermocouple sensitivi calibration gives a calorimeter calibration, which agrees with 0.3 percent of 2) an electrical energy substitution calibratio which is obtained via a heater wire contained in the absorptio cell solution. A method has been devised by which two calorim ters may be intercompared. Calorimeters which we have bui and calibrated agree with each other to about 0.7 percent. Th specific calorimeter has been designed to measure energies up 30 J and will take peak powers of up to 200 $MW/cm^2$. .

**9807.** Jensen, M. W., **Quantity control—a tool of industry, and arm of government,** *Proc. Annual Conf. Soc. Advancement of Food Service Research, Washington, D.C., Apr. 18, 1966.*

Key words: Measures; product quality; standards; weights.

Weights and Measures regulatory control in the United States is discussed; the role of the National Bureau of Standards and of the States is explored. The program of NBS in voluntary product standardization also is briefly discussed.

**9808.** Jensen, M. W., **Thoughts on weights and measures,** *Soap and Chemical Specialties* **VLII,** No. 4, 99 (Apr. 1966).

Key words: NBS authority; package control; State authority; weights and measures.

The regulatory control of weighing and measuring in commerce is a function of the States and their political subdivisions and is carried on under the universally acknowledged "police powers" of the States. The National Bureau of Standards is the principal technical resource for the States in this field. Specifically, the Bureau provides assistance to the States and to affected segments of industry and business in the areas of physical standards, testing equipment, test methods, administrative procedures, and technical training.

Operating through the National Conference on Weights and Measures, and directly with the individual states, the Office of Weights and Measures of the Bureau is the prime mover toward nationwide uniformity in weights and measures laws, regulations, and control methods.

Recently, concentration in the weights and measures field has been on package labeling and on package net content. Model laws, model regulations and control procedures have been developed and are widely utilized.

**9809.** Jesch, R. L., Jickiling, R. M., **Impedance measurements in coaxial waveguide systems,** *Proc. IEEE* **55,** No. 6, 912-923 (June 1967).

Key words: Air lines; coaxial; impedance; measurements; standards; transmission line; waveguide.

This article is a tutorial review of impedance measurements and standards in coaxial waveguide systems propagating a TEM wave. It describes the development of coaxial air lines as impedance standards, reviews representative measurement methods, and discusses the errors and measurement techniques of the slotted line in detail. A list of selected references to pertinent literature is included.

**9810.** Johannesen, R. B., Farrar, T. C., Brinckman, F. E., Coyle, T. D., **Nuclear magnetic resonance studies of inorganic fluorides. I. High-resolution $^{19}$F spectra of $Si_2F_6$ and $(SiF_3)_2O$,** *J. Chem. Phys.* **44,** No. 3, 962-964 (Feb. 1, 1966).

Key words: Chemical shifts; fluorine; fluorsilanes; nuclear magnetic resonance; silicon; spin coupling constants.

Fluorine nmr spectra of hexafluorodisilane and hexafluorodisiloxane have been recorded and analyzed. The $^{19}F-^{19}F$ and $^{29}Si-^{19}F$ spin coupling constants were obtained from the satellite spectra arising from the $^{29}$Si-substituted molecules present in natural abundance. The "near" and "far" $^{29}Si-^{19}F$ coupling constants in $Si_2F_6$ were found to be of opposite sign.

**9811.** Johnson, D. P., Hutton, U. O., **Discussion of ASME paper 60-WA-333, November 30, 1960,** Chapter in *High Pressure Measurement,* A. A. Giardini and E. C. Lloyd, eds., pp. 350-351 (Butterworth, Inc., London, England, 1963).

Key words: Calibration; fixed point; freezing pressure; manganin gage; mercury; pressure standards.

The various determinations of the freezing pressure of mercury at 0 °C and the use of this manometric fixed point in the calibration of manganin wire pressure gages is reviewed. After Bridgman's measurements, published in 1912, of the freezing pressure of mercury (7640 kg/cm² at 0 °C) no determinations were made for 40 years. Five determinations have been made in the decade between 1952 and 1962. These fall in the range between 7714 and 7723 kg/cm² or 7565 to 7574 bars.

**9812.** Johnston, R. G., Canfield, L. R., Madden, R. P., **Reflective scattering from substrates and evaporated films in the far ultraviolet,** *Appl. Opt.* **6,** 715 (Apr. 1967).

Key words: Far ultraviolet; optical polishing; scattering; substrates; surface roughness; thin films.

Measurements of radiation reflectively scattered from mirror surfaces have been made at the wavelengths 1216 Å and 584 Å. Several glass and fused silica substrates with differing degrees of surface roughness have been studied, as well as evaporated films of aluminum and gold as a function of film thickness. A relatively small area detector was scanned in angle about the sample, and the detected energy integrated over the scattering angle. The results indicate that fused silica can be polished to a smoother surface than glass, that a smooth substrate surface is significantly advantageous in obtaining evaporated films having surfaces with low scatter, and that gold films are considerably smoother than aluminum films of equal thickness.

**9813.** Jones, E., Lee, D., Edelman, S., **Improved transfer standard for vibration pickups,** *J. Acoust. Soc. Am.* **41,** No. 2, 354-357 (Feb. 1967).

Key words: Accelerometer; axial motion; ceramic; comparison calibration; transfer standard; transverse motion; vibration pickups.

This paper describes a vibration transfer standard designed to provide comparison calibrations of pickups with minimum degradation. Features of the design are the use of a ceramic housing of a stiff, light, glossy material, provision of a means for evaluating the quality of the motion by the use of three integral accelerometers oriented parallel to the nominal direction of motion, and design of the geometry to minimize differences in motion between the pickup being calibrated and the standard. The useful frequency range is 10 to 10,000 Hz.

**9814.** Jones, M. C., Nagamoto, T. T., Brennan, J. A., **Heat transfer to a subliming solid-vapor mixture of hydrogen below its triple point,** *AIChE J.* **12,** No. 4, 790-795 (July 1966).

Key words: Cryogenics; dimensional analysis; heat transfer; hydrogen; low pressure; solid-vapor; tube; two-phase flow.

Heat transfer coefficients have been measured over a range of Reynolds numbers for a solid-vapor mixture of parahydrogen discharging through a heated brass tube below the triple point pressure. A simple empirical correlation is given which is shown by dimensional analysis to account for most of the system variables.

**9815.** Jones, R. N., Huntley, L. E., **Precision coaxial connectors in lumped parameter immittance measurement,** *IEEE Trans. Instr. Meas.* **15,** No. 4, 375-380 (Dec. 1966).

Key words: Coaxial; connectors; immittance; lumped-parameter; measurement; precision; radio frequency.

Amid the concern surrounding the design and application of precision coaxial connectors for use in precise electrical measurements there is one area which has received very little attention. This has to do with the application of such connectors to measurements in the lumped-parameter region. This paper points out the significant sources of error in lumped-parameter measurements which are attributable to connector uncertainties and shows how they can be greatly reduced through the application of precision coaxial connectors. Where these connectors are utilized in lumped-parameter immittance measurements, extensions of frequency, magnitude and accuracy are realized. Specific examples are discussed.

**9816.** Jordan, J. E., Amdur, I., **Almost "head-on" collisions in the scattering of fast argon atoms by hydrogen isotopes,** *J. Chem. Phys.* **46,** No. 10, 4145-4146 (May 1967).

Key words: Hydrogen; intermolecular potential; molecular beam.

A significant difference between the measured elastic cross sections for argon atoms scattered by $H_2$ from those of argon scattered by $D_2$ is reported. Measurements in the same apparatus of helium beams scattered by $H_2$ and $D_2$ show that there is no significant difference in the interaction potential for $H_2$ and $D_2$. The measured difference is a verification of a theoretical prediction that scattering at small impact parameters can reduce the measured cross section when the mass of the beam atom is much larger than the target atom. The difference in cross sections for $Ar-D_2$ and $Ar-H_2$ can be used to obtain potential energies involved in collisions at very small interaction distances.

**9817.** Judd, D. B., **Color appearance,** *Proc. Intern. Color Comm., Lucerne, Switzerland, 1965,* **1,** 27-51 (Mar. 1966).

Key words: Ambient-light color; color; color appearance; color-matching; normal and abnormal vision.

Summaries of the researches that have formed the basis of predicting color appearance are given as follows: color-matching functions for normal and abnormal vision, simultaneous and successive contrast, von Kries coefficient law of chromatic adaptation, and perceptual separation of object color and ambient-light color. In addition, prediction of the color appearance of non-flat objects is discussed; and the approach to empirical formulas for hue, lightness, and saturation of objection-color perceptions developed in 1940 is described and the shortcomings of the formulas are discussed. Finally, the evidence for the "crispening' effect in lightness perception discovered by Takasaki is presented and discussed.

**9818.** Judd, D. B., **Color designation and specification,** *Encyclopedia of Industrial Analysis* **1,** 315 (1966).

Key words: Color; colorimetry; vision.

Tristimulus colorimetry is summarized from basic assumptions to the 1931 CIE standard observer and the 1964 CIE supplementary observer and coordinate system for large-field colorimetry. Three types of tristimulus colorimetry (visual, photoelectric, spectrophotometric) are described including operating procedures, methods of reducing the data, and a summary of applications. A similar treatment is given of approximate colorimetry by systematic collections of color standards (Munsell, Ostwald, Maerz & Paul dictionary) including determination of the ISCC-NBS color designation. Definitions of radiometric, photometric, and colorimetric terms used are given in the form of a glossary.

**9819.** Judd, D. B., **Fundamental studies of color vision from 1860 to 1960,** *Proc. Natl. Acad. Sci.* **55,** No. 6, 1313-1330 (June 1966).

Key words: Chromatic adaptation; color blindness; color-matching functions; color vision; deuteranopia; opponent-colors theory; protanopia; three-components theory of color vision; tritanopia.

The color-matching functions determined since Maxwell's time (1860) have been reduced to the primaries previously (1807) proposed by Young, and the modern determinations are shown to be in good agreement. The principal theories of color vision are summarized under the headings: three-components (Young, Helmholtz, Konig), opponent-colors (Hering), two-stage theories (von Kries-Schrodinger, and Hurvich-Jameson), and three-stage theories (Muller, Adams). The results of quantifying these theories by appeal to modern determinations of color-matching functions is shown. For example, by the Young theory, predictions of the spectral absorptance of three retinal photo-pigments are derived, and from the Helmholtz-Konig theories, the responses of three types of retinal receptors responsible for color vision are derived. The various experimentally determined relations between the three principal forms of partial color-blindness and normal color vision are inter-compared and checked against the various theories, and a brief review of the results of studies of chromatic adaptation (von Kries coefficient law; Stiles two-color increment thresholds) and their theoretical implications is given.

**9820.** Judd, D. B., **Interval scales, ratio scales, and additive scales for the sizes of differences perceived between members of a geodesic series of colors,** *J. Opt. Soc. Am.* **57,** No. 3, 380-386 (Mar. 1967).

Key words: Additive scales; color geodesics; color scales; geodesics; interval scales; ratio scales; scales; scaling.

From larger-smaller judgments of color differences, compared visually two at a time, the perceived sizes may be evaluated on an interval scale. Given numbers B so evaluated, and such that B is linearly connected to some power *p*, less than one, of the physical measure D (such as distance on any chromaticity diagram) of the differences, the additive constant $K_{br}$ such that the numbers $B+K_{br}$ are expressed on a ratio scale, may be found from judgments of ratios of sizes of pairs of color differences. To evaluate *p*, it is sufficient to observe the three differences, 12, 23, and 13 among three colors forming a geodesic series, and chosen so that $B_{12}$ is not much different from $B_{23}$. The scale formed by the numbers $(B+K_{br})^{1/p}$ is additive if the D-scale is additive. A close approximation may be found without determining $K_{br}$ or *p*. This approximation is based on the empirical discovery that the additivity condition:

$$(B_{12}+K_{bd})^{1/p}+(B_{23}+K_{bd})^{1/p}=(B_{13}+K_{bd})^{1/p},$$

though it implies that $K_{bd}$ depends strongly on *p*, is satisfied about equally well by any choice of *p*. It is sufficient, therefore to derive the additive scale by setting $p=1$, and computing $K_{b}$ as $B_{13}-B_{12}-B_{23}$.

**9821.** Judd, D. B., **Progress report for OSA committee on uniform color scales,** *Proc. Intern. Color Comm., Lucerne, Switzerland 1965,* **1,** 399-407 (Mar. 1966).

Key words: Color chips; color scales; painted color chips rhombohedral lattice-sampling method; uniform colo scales.

This committee, organized in 1947, has been engaged sinc 1955 in experiments intended to result in the production o several hundreds of painted color chips that would sample th paint gamut as uniformly as possible by the regular rhombohedral lattice-sampling method. The first experiment (1956 determined a locus of chromaticity points on the CIE (x,y)-diagram for colors of Munsell value 6/ perceived as having the sam saturation (departure from gray). The second experiment (1957 determined 40 chromaticity points on this locus equally space in hue. The third experiment (1961) determined chromaticnes spacing near grays of Munsell 3/, 6/, and 8/. The latest exper ment is a preparation of 43 chips intended to give a uniform triangular sampling at Munsell 6/, and a check of the spacin uniformity by 70 observers each making judgments of "larger or "smaller" for 142 of the pairs of differences among the 4 chips. Some tentative conclusions are presented.

**9822.** Judd, D. B., **Reflectance spectrophotometry,** *Encyclopedia of Industrial Chemical Analysis* **3,** 376-392 (John Wiley and Sons, Inc., New York, N.Y., 1966).

Key words: Color; color matches; light-diffusing specimens; reflectance spectrophotometry; spectrophotometry.

Five commercially available spectrophotometers adapted to the measurement of light-diffusing specimens are described. The use of these instruments for qualitative and quantitative analysis of such specimens by means of the Kubelka-Munk model is presented together with the methods for formulating colorants required to produce both nonmetameric and metameric color matches.

**9823.** Judd, D. B., **Terms, definitions, and symbols in reflectometry,** *J. Opt. Soc. Am.* **57,** No. 4, 445-452 (Apr. 1967).

Key words: Definitions in reflectometry; photometry; radiometry; reflectance; symbols in reflectometry; terms in reflectometry.

Angular conditions of incidence are described as hemispherical, conical, or directional; the same adjectives are used to describe the angular conditions of collection. This classification of angular conditions leads to nine kinds of reflectance; symbols for them are proposed in which $2\pi$, $g$, and $\theta_0$, $\phi_0$ refer to hemispherical, conical, and directional incidence, $2\pi$, $g'$, and $\theta_r$, $\phi_r$ refer to the corresponding kinds of collection. Use of the perfectly reflecting mirror and of the perfectly reflecting diffuser as reference standards in reflectometry is discussed. Three of the nine reflectance ratios, specimen to perfect diffuser, in which the collection is directional have already been named radiance [luminance] factor. It is proposed to differentiate them by angular condition of incidence. It is also proposed to name the other six ratios: reflectance factor qualified by the same adjectives identifying the type of incidence and collection as are used for reflectance. The interrelationships of these 18 concepts are shown both by formulas for computing one from another and by diagrams indicating the process (integration, summation, averaging, equality, reflectance of perfect diffuser, and reciprocity) by which values of one concept may be computed from those of another.

**9824.** Judd, D. B., **Progress report for OSA committee on uniform color scales,** *Die Farbe* **14,** 287-295 (1965).

Key words: Color chips; color scales; painted color chips; uniform color scales.

This committee, organized in 1947, has been engaged since 1955 in experiments intended to result in the production of several hundreds of painted color chips that would sample the paint gamut as uniformly as possible by the regular rhombohedral lattice-sampling method. The first experiment (1956) determined a locus of chromaticity points on the CIE (x,y)-diagram for colors of Munsell value 6/ perceived as having the same saturation (departure from gray). The second experiment (1957) determined 40 chromaticity points on this locus equally spaced in hue. The third experiment (1961) determined chromaticness spacing near grays of Munsell 3/, 6/, and 8/. The latest experiment is a preparation of 43 chips intended to give a uniform triangular sampling at Munsell 6/, and a check of the spacing uniformity by 70 observers each making judgments of "larger" or "smaller" for 142 of the pairs of differences among the 43 chips. Some tentative conclusions are presented.

**9825.** Kaeser, R. S., Ambler, E., Schooley, J. F., **Vibrating coil magnetometer for use at very low temperatures,** (Proc. 1965 Cryogenic Engineering Conf., Rice University, Houston, Texas, Aug. 23-25, 1965), Chapter in *Advances in Cryogenic Engineering* **11,** 694-698 (Plenum Press, Inc., New York, N.Y., 1966); *Rev. Sci. Instr.* **37,** No. 2, 173-175 (Feb. 1966).

Key words: Cryogenic; demagnetization; instrumentation; magnetic moment; magnetization; magnetometer; vibrating coil.

A vibrating coil type magnetometer is described for measuring magnetization curves of small specimens in the magnetic cooling range of temperature. For a 3 mm diameter sphere the sensitivity of magnetic moment measurements is $10^{-6}$ emu. At this sensitivity the amplitude of vibration is 0.5 mm, and at 0.3 °K the extra heat influx into the sample thereby introduced is less than 10 erg/min. Examples of magnetization curves are shown.

**9826.** Kamas, G., Morgan, A. H., Jespersen, J. L., **Preliminary results of some new measurements of phase velocity at VLF,** *Radio Science* **1,** No. 12, 1409-1410 (Dec. 1966).

Key words: Ionosphere; phase velocity; VLF.

A new measurement of the phase velocity of VLF radio waves is described. The measured value of the phase velocity at 18.6 kc/s, for distances greater than 2400 kilometers from the transmitter, was $-0.0021\pm0.0006$ in the form $v_p/c-1$. For both 18.6 and 20.0 kc/s, at distances less than 2400 kilometers, the phase velocity varied with distance from the transmitter.

**9827.** Kanagy, J. R., **Physical and performance properties of leather,** Chapter 64 in *The Chemistry and Technology of Leather* 4, 369-416 (Reinhold Publ. Corp., New York, N.Y., 1965).

Key words: Fiber structure; hide; insulator leather; mechanical properties; physical properties; stability.

This Chapter gives an outline of the properties of leather including both strength and mechanical properties such as compressibility and flexing. In addition its value as an insulator and its stability to temperature and atmospheric conditions are discussed. The nature of the hide is described with regard to fiber structure and chemical composition in order to give a better understanding of its properties and indicate how it might be modified. The information should be useful in developing further uses for leather and to stimulate further research in the study of its properties.

**9828.** Kasuya, T., Lide, D. R., Jr., **Measurements on the molecular nitrogen pulsed laser,** *Appl. Opt.* **6,** No. 1, 69-80 (Jan. 1967).

Key words: Accurate wavelength measurements; laser; molecular nitrogen pulsed laser; nitrogen molecule; nitrogen pulsed laser; pulsed laser emission; rotational band spectrum.

Accurate wavelength measurements of the pulsed laser emission from the nitrogen molecule have been made. About one hundred new stimulated emission lines which belong to the first and second positive systems were obtained and identified as to rotational quantum number. The relative intensities of the laser lines in the rotational band spectrum are analyzed. Some characeristics of the oscillations, including the recovery time after the laser pulse, are discussed.

**9829.** Keegan, H. J., Weidner, V., **Infrared reflectance of frost,** *J. Opt. Soc. Am. Letter* **56,** No. 4, 523-524 (Apr. 1966).

Key words: Carbon dioxide; frost; infrared; spectral reflectance; water.

The infrared reflectance spectra of water frost and of two forms of solid carbon dioxide ("frost" and crushed commercial "dry ice"), were obtained over the spectral range 4000 to 450 $cm^{-1}$ on a high-resolution spectrophotometer with a reflectance attachment.

**9830.** Keenan, R. G., Marcus, J. M., DeVoe, J. R., **Simultaneous determination of copper and zinc in human lung tissue by**

**neutron activation analysis,** *Am. Ind. Hygiene Assoc. J.* **27,** 128-134 (Mar.-Apr. 1966).

Key words: Biosyntheses; catalysis in biosyntheses; copper; human lung tissue; lung tissue; neutron-activation analysis.

Certain trace elements including copper and zinc are constituents of numerous enzymes and function as essential catalysts in biosyntheses. The expanded interest in these substances has supplied a demand for microanalytical techniques of increased sensitivity, accuracy and precision if meaningful conclusions are to be derived from the analytical data. This paper shows that good precision may be realized in the activation analysis of complex biological specimens with only a few one-step chemical separations.

The nuclear reactions $Cu^{63}$ (n,γ) $Cu^{64}$ (12.8h) and $Zn^{68}$ (n,γ) $Zn^{69m}$ (13.8h) were used for the analysis. The samples were irradiated in a thermal neutron flux of $10^{13}$ n/cm²/sec. The copper was extracted as the acetylacetonate into chloroform from an acetate system buffered at a pH of 4.75. The remaining aqueous phase was extracted with chloroform to remove most of the acetylacetone dissolved in the aqueous phase. The zinc was extracted as the dithizonate into chloroform and was back-extracted into 1% HCl for counting. Careful internal standardization was used for correction of results for variation in chemical yields.

Applications of the method to the simultaneous determination of copper and zinc in lung samples provided values of the same order of magnitude as those reported by Tipton and Cook for U.S. adults using emission-spectrographic procedures which were between 7 and 10 ppm for copper and 40 and 70 ppm for zinc. Comparison of the precision of this method with that of emission spectroscopy indicates that this activation technique has at least three times better precision.

**9831.** Keffer, C., Migheil, A., Mauer, F., Swanson, H., Block, S., **The crystal structure of twinned low-temperature lithium phosphate,** *Inorg. Chem.* **6,** No. 1, 119-125 (June 1967).

Key words: Crystal structure; differential thermal analysis, lithium; lithium phosphate; twinning.

It is shown that lithium phosphate ($Li_3PO_4$) prepared by precipitation from an aqueous solution differs from the form that has been described in the literature. When heated it transforms irreversibly at 502±5° to the familiar form. The low-temperature orm crystallizes in space group $Pmn2_1$ with $a_0 = 6.1150 \pm 0.0010$ Å, $b_0 = 5.2394 \pm 0.0011$ Å, and $c_0 = 4.8554 \pm 0.0010$ Å; $Z = 2$. It exhibits merohedral twinning with the twin plane normal to the $z$ axis. The multiplicity of the predominant image is 0.75. All atoms are tetrahedrally coordinated. The final reliability index is 0.054.

**9832.** Keller, R. A., Dolby, L. J., **Rate constants and the mechanism for the transfer of triplet excitation energy,** *J. Am. Chem. Soc.* **89,** 2768-2770 (May 1967).

Key words: Energy transfer; fluorescence; phosphorescence; triplet states.

The intramolecular transfer of triplet excitation between chromophors held approximately 15 Å apart by rigid steroid bridge was measured for the two molecules shown below. The acceptor in both cases is the naphthalene chromophor. The rate constant for transfer is 25 sec.$^{-1}$ for I and 0.04 sec.$^{-1}$ for II. The 1000 fold difference in these rate constants is paralleled by the 1000 fold difference in the triplet state lifetime for the two donor chromophors. The transfer mechanism indicated by these results involves spin-orbital coupling to the singlet system in the donor chromophor combined with dipole-dipole coupling between the singlet systems of the two chromophors and spin-orbital coupling back to the triplet system in the acceptor chromophor. In both cases the transfer of singlet excitation energy was more complete than the transfer of triplet excitation energy.

**9833.** Kelly, F. J., **An equation for the local thermal emissivity at the vertex of a diffuse conical or V-groove cavity,** *Appl. Opt.* **5,** 925-927 (June 1966).

Key words: Diffuse conical or V-groove cavity; emissivity, vertex of a diffuse conical or V-groove cavity; equation, apparent local emissivity; vertex of a diffuse conical or V-groove cavity; V-groove cavity.

An exact, closed-form expression is derived for the apparent local emissivity at the vertex of a diffuse conical or V-groove cavity. This expression is obtained by a substitution into an approximate equation for the apparent local emissivity of a point within a cavity of any shape. The exact expression depends only on the emissivity of the cavity wall material and the angle factor between the point at the cavity vertex and the cavity opening. Agreement is very good between the values predicted by the expression and those obtained from a numerical solution of the integral equation characteristic of a diffuse conical cavity.

**9834.** Kerns, D. M., Grandy, W. T., **Perturbation theorems for waveguide junction, with applications,** *IEEE Trans. Microwave Theory Tech.* **MIT-14,** No. 12, 85-92 (Feb. 1966).

Key words: Compensation theorems; immittance-matrix elements; perturbation theorems; waveguide junctions.

Perturbation or "compensation" theorems are derived for waveguide junctions. These express changes in immittance-matrix elements, due to changes in the junction, in terms of integrals over products of changed and unchanged basis-fields associated with the junction and its adjoint. Media involved are required only to be linear.

Applications are made to half-round obstacles in rectangular waveguide, to finite conductivity in the obstacle problem, and to the junction of rectangular with filleted waveguide. It is observed that the common expedient of approximating perturbed fields by unperturbed ones does not always lead to correct lowest-order results.

**9835.** Kerper, M. J., Scuderi, T. G., **Mechanical properties of chemically strengthened glasses at high temperatures,** *J. Am Ceram. Soc.* **49,** No. 11, 613-618 (Nov. 1966).

Key words: Chemically strengthened glass; elevated temperature; glass; strength; Young's modulus.

Young's modulus, shear modulus, and modulus of rupture o two chemically strengthened glasses were determined a elevated temperatures. The results showed that the Young' modulus and shear modulus decrease with increasing temperature with a sharp inflection present slightly above room temperature.

The modulus of rupture is not affected by short exposure t temperatures up to 260 °C, but drops appreciably when expose to temperatures above 204 °C for 200 hours or more.

Measurement of deflection at room temperature showed th two chemically strengthened glasses to exhibit about five time as much delayed elasticity as did thermally tempered soda-lime silica glass.

**9836.** Kerper, M. J., Scuderi, T. G., **Modulus of rupture of glas below room temperature,** *Am. Ceram. Soc. Bull.* **45,** No. 9 782-783 (Sept. 1966).

Key words: Glass; low temperature; strength.

The modulus of rupture of seven different commercial glasse was determined at 0 °F (−17.8 °C) and −50 °F (−45.6 °C). Th results showed that for all glasses and for all conditions of temper the modulus of rupture increased as the temperature decreased.

9837. Kerper, M. J., Scuderi, T. G., **Relation of fracture stress to the fracture pattern for glass rods of various diameters,** *Am. Ceram. Soc. Bull.* **45,** No. 12, 1065-1066 (Dec. 7, 1966).

Key words: Fracture; fracture pattern; glass; mirror-size; strength.

Five different size glass rods ranging in diameter from 0.16 inch to 1.5 inch were broken and the relationship between the fracture stress and fracture pattern determined. The results showed that the size of the rod affected the fracture stress but did not affect the relationship between the size of the smooth, or "mirror" part of the fracture face and fracture stress.

9838. Kessler, H. K., **Cooler for semiconductor light emitters, laser and photodetectors,** *Rev. Sci. Instr.* **37,** 517-518 (Apr. 1966).

Key words: Cryogenic cooler; light emitters; mode switching; photo detectors; semiconductor lasers.

A device for cooling lasers and radiation detectors by means of a jet of gas permits control of the temperature of the laser or detector over a wide range of temperatures not normally accessible by cryogenic cooling techniques.

9839. Kessler, K. G., **Some experiments with Zeeman shifted levels,** (Proc. Zeeman Centennial Conf., Amsterdam, The Netherlands, Sept. 9-11, 1965), *Physica* **33,** 29-46 (1967).

Key words: Atomic beams; double resonance; isotope shifts; Lande *g*-factor; mercury hyperfine structure; Zeeman filter.

A review of some applications of the Zeeman effect to studies of the resonance line of mercury. Techniques discussed include Zeeman scanning of an atomic beam, double resonance, level crossing and the Zeeman filter. Examples are drawn in large part from the work of Dr. Bitter's group at MIT and of the author and his colleagues at NBS. Fundamental data obtained in these studies include the hyperfine structure, isotope shifts and Zeeman splitting, in both naturally occurring and short-lived isotopes, the Lande *g*-factor and the lifetime of the $^3P_1{}^0$ states.

9840. Kidnay, A. J., Hiza, M. J., **High pressure adsorption isotherms of neon, hydrogen, and helium at 76 °K,** (Proc. 1966 Conf., Boulder, Colo., June 13-15, 1966), Chapter in *Advances in Cryogenic Engineering* **12,** 730-740 (Plenum Press, Inc., New York, N.Y., 1967).

Key words: Adsorption potential; charcoal; helium; high-pressure physical adsorption; hydrogen; low temperature; neon; zeolite.

A desorption technique was used to measure the physical adsorption isotherms of hydrogen and helium on a synthetic zeolite and of hydrogen, helium, and neon on an activated cocoanut shell charcoal at 76 °K in the pressure range of 1 to 95 atmospheres.

The Polanyi adsorption potential theory, as modified by Dubinin, was used in an attempt to obtain a general correlation of these isotherms. The results, while not completely general, should allow the prediction of the high pressure isotherms of neon, hydrogen, and helium at any temperature with an accuracy sufficient for most engineering calculations.

9841. Kidnay, A. J., Hiza, M. J., **The low temperature removal of small quantities of nitrogen or methane from hydrogen gas by physical adsorption on a synthetic zeolite,** *AIChE J.* **12,** No. 1, 58-63 (Jan. 1966).

Key words: Hydrogen gas; low temperature; methane; nitrogen; physical adsorption; synthetic zeolite; zeolite.

A flow system was used to measure the physical adsorption isotherms of two mixtures of nitrogen and hydrogen and two mixtures of methane and hydrogen on a synthetic zeolite. The measurements were made at liquid nitrogen temperature and at pressures of 4 to 85 atm. Static systems were used to measure the pure component isotherms of nitrogen, methane, and hydrogen at the same temperature and over the appropriate pressure ranges.

Although many different methods have been proposed for using pure component adsorption isotherms to predict the mixture isotherm, the only method giving quantitative agreement with the data of this study is the empirical "adsorption enhancement factor."

In addition to the adsorption isotherms, the concentration-time or break-through curves of the mixtures were measured at flow rates ranging from 40 to 300 lb.(hr.)-ft.$^{-2}$. The method proposed by Eagleton and Bliss was used to correlate these curves.

9842. Kidnay, A. J., Meyers, A. L., **A simplified method for the prediction of multicomponent adsorption equilibria from single gas isotherms,** *AIChE J.* **12,** No. 5, 981-986 (Sept. 1966).

Key words: Adsorption; adsorption azeotropes; ideal adsorbed solution; multicomponent adsorption equilibria; spreading pressure.

The ideal adsorbed solution theory of Myers and Prausnitz provides an accurate and thermodynamically consistent method for predicting multicomponent adsorption equilibria. The major difficulty in the application of this theory lies in the calculation of the spreading pressure curves for the pure adsorbates. The purpose of this article is to show that in many cases of practical interest, the spreading pressure calculations may be greatly simplified or altogether eliminated with little or no loss in the accuracy of the calculations. The problem of adsorption azeotropy is also briefly discussed.

9843. Kieffer, L. J., Dunn, G. H., **Electron impact ionization cross section data for atoms, atomic ions, and diatomic molecules: I. Experimental data,** *Rev. Mod. Phys.* **38,** No. 1, 1-33 (Jan. 1966).

Key words: Absolute cross sections; critical review; electron impact; multiply charged ions; relative cross sections.

This review includes a compilation and critical evaluation of absolute cross sections for ionization of atoms and diatomic molecules by electron impact. Experimental techniques used for ionization are surveyed. Selected relative cross sections for production of multiply charged ions and a brief discussion of relative cross section data near threshold are presented. Absolute limits are not set on the size of probable systematic errors in the various experiments.

9844. Kieffer, L. J., Van Brunt, R. J., **Energetic ions from $N_2$ produced by electron impact,** *J. Chem. Phys.* **46,** No. 7, 2728-2734 (Apr. 1967).

Key words: Angular distributions; appearance potentials; electron impact; energetic ions; energy distributions; $N_2$.

Energy distributions, appearance potentials, and angular distributions of $N^+$ ions produced by electron impact on $N_2$ have een observed. The energy distribution and appearance potential of the $N^{++}$ ions from electron impact on $N_2$ were also observed. The data are interpreted to give the abundance of the "zero energy" $N^+$ and the $N^{++}$ ions. The appearance potential data for the "zero energy" $N^+$ ions disagree with previous measurements, and a possible interpretation indicates that the conclusion of previous investigators that no excited ions are produced may not be valid.

**9845.** King, R. C., Armstrong, G. T., **A study of the heat of formation of oxygen difluoride,** Proc. 5th Meeting of ICRPG, Working Group on Thermochemistry 1, 69, *CPIA Publ.* **146** (May 1967).

Key words: Calorimetry, fluorine flame; fluorine, reaction with hydrogen; hydrofluoric acid, heat of formation; hydrogen, reactions with fluorine, oxygen difluoride and oxygen; oxygen, reaction with hydrogen; oxygen difluoride, heat of formation; oxygen difluoride, reaction with hydrogen.

The enthalpies of the reactions below $\Delta H^\circ_{303}$ were determined in a flow calorimeter operated at one atm. pressure, to be respectively, in kcal $mol^{-1}$, $-227.52$ (0.16), $-153.38$ (0.06), and $-68.28$ (0.03). The numbers in parentheses are the standard deviations of the means for 13, 5, and 6 experiments, respectively. The enthalpy of formation of $OF_2(g)$, $\Delta H^\circ_{f298}$,

$$OF_2(g) + 2H_2(g) + 99H_2O(l) = 2[HF \cdot 50H_2O](l)$$

$$F_2(g) + H_2(g) + 100H_2O(l) = 2[HF \cdot 50H_2O](l)$$

$$1/2\ O_2(g) + H_2(g) = H_2O(l)$$

$$F_2(g) + 1/2\ O_2(g) = OF_2(g)$$

was calculated from the measured enthalpy changes to be $+5.86$ kcal $mol^{-1}$. The average bond energy $E(O-F)$ in the gaseous molecule of $OF_2$ was calculated to be 45.72 kcal $mol^{-1}$. The results of the second reaction are compared with other recently derived data on HF(aq).

**9846.** Kirchoff, W. H., **The microwave spectrum and dipole moment of pyrazole,** *J. Am. Chem. Soc.* **89,** No. 6, 1312-1316 (Mar. 1967).

Key words: Dipole moment; gas phase pyrazole; microwave spectrum; pyrazole; rotational constants.

The microwave spectrum of pyrazole in the region 8000 Mc/s to 35000 Mc/s has been assigned. The rotational constants are A = 9618.92±0.14 Mc/s, B = 9412.59±0.13 Mc/s and C = 4755.88±0.11 Mc/s. The dipole moment $\mu = 2.214 \pm 0.015$ D was calculated from the Stark effect of the $0_{0,0} \rightarrow 1_{0,1}$ and $0_{0,0} \rightarrow 1_{1,1}$ transitions but only after the perturbation treatment had been extended to fourth order. The indicated uncertainties are three times the standard errors obtained from the least squares fit. The interpretation of the data shows that in the gas phase pyrazole is a planar molecule with no in-plane symmetry axis.

**9847.** Klebanoff, P. S., **The effect of a two-dimensional roughness element on boundary layer transition,** (Proc. Eleventh Intern. Congress Applied Mechanics, Munich, Germany, 1964), Chapter in *Applied Mechanics,* H. Gortler, ed., pp. 803-805 (Springer-Verlag, Berlin, Germany, 1966).

Key words: Hot-wire anemometry; instability; laminar boundary layer; roughness; transition.

This paper is in the nature of a summary of the results obtained from an experimental investigation of the effect of a two-dimensional roughness element on boundary layer transition. The method of investigation and the main results obtained are described. It is revealed that the basic mechanism by which a two-dimensional roughness element induces earlier transition from laminar to turbulent flow in boundary layers is by the destablizing influence of the distorted flow in the immediate downstream vicinity of the roughness.

**9848.** Klein, F. S., Herron, J. T., **Erratum: Mass spectrometric study of the reactions of O atoms with NO and $NO_2$,** *J. Chem. Phys.* **44,** No. 9, 3645-3646 (May 1, 1966).

Key words: Kinetics; nitric oxide; nitrogen dioxide; oxygen; oxygen atoms; rate constants.

In an earlier paper (*J. Chem. Phys.*) the reactions of O atoms with $O_2$, NO, and $NO_2$ were discussed in terms of the general mechanism

$$\begin{aligned} O + XO \underset{B}{\overset{A}{\rightleftharpoons}} [OXO]^* + M &\xrightarrow{C} XO_2 + M \\ &\xrightarrow{D} X + O_2 \\ &\xrightarrow{E} XO_2 + h\nu \end{aligned}$$

In derived rate constants $k_B$ and $k_D$ for the $NO_2$ reaction were anomalously low due to an arithmetic error on our part and the use of a misquoted rate constant from the literature. The values have now been corrected.

**9849.** Klose, J. Z., **Atomic lifetimes in neon I,** *Phys. Rev.* **141,** No. 1, 181-186 (Jan. 1966).

Key words: Delayed coincidence; lifetimes, atomic; neon; spectra, atomic.

Mean lives of a number of electronically excited atomic levels in Ne I have been determined using a method of delayed coincidence. Following a detailed description of the experimental procedure, the measured values of the mean lives of the $2p_1$ through $2p_9$, $3p_1$, $3p_{10}$, and $4d'_1$ (Paschen notation) levels in neutral neon are given. These lifetimes, determined from transitions with associated wavelengths extending from ≈ 3400 Å to ≈ 6400 Å, ranged in value from ≈ 14 nsec ($10^{-9}$ sec) to ≈ 500 nsec. The lifetimes were estimated to contain possible systematic errors varying from 5 to 20 percent and are presented in comparison with corresponding results of other workers.

**9850.** Klose, J. Z., **Mean lives of atomic levels excited by electron impulse,** *Proc. Intern. Conf. Electronic Excitation of an Atomic Vapor--Applicable to Spectroscopy, Grenoble, France, May 23-26, 1966* (Centre Natl. de la Recherche Scientifique, Paris, France, 1967).

Key words: Atomic levels; electron impulse; mean lives; slow electrons.

The life-time of the atomic levels of rare gases is measured by the recording of the de-excitation of levels reached by the impulses of slow electrons, by means of the technique of delayed coincidence. The order of length of the life-times measured is 15 to 30 ns. (He, Ne, Ar).

**9851.** Knight, B. L., Timmerhaus, K. D., Flynn, T. M., **A superconducting liquid-level sensor for slush hydrogen use,** (Proc. 1965 Cryogenic Engineering Conf., Rice University, Houston, Texas, Aug. 23-25, 1965), Chapter in *Advances in Cryogenic Engineering* **11,** 218-222 (Plenum Press, Inc., New York, N.Y., 1966).

Key words: Liquefied gases, liquid level gages; liquid level gages, hydrogen; liquid rocket propellants; performance (engineering); sensors; superconductors.

A system of three superconducting niobium stannide liquid-level sensors was constructed and tested in triple-point liquid hydrogen. Tests indicated that the sensors were capable of detecting, in a linear fashion, the liquid level of the system over a range of about 60% of the total sensor length. One of the sensors was shown to be capable of detecting a liquid-level change on the order of 0.2 mm. Sensitivity of the sensors was investigated and was shown to be a function of the current applied to the sensors as well as a function of several physical characteristics of the sensors themselves. A heat balance was used to obtain an approximation to the measurement error of the sensors.

**9852.** Koch, H. W., **Electron beams: National Bureau of Standards and the new technology,** *Science* **156,** No. 3773, 321-328 (Apr. 1967).

Key words: Electrons; nuclear physics; particle accelerators; radiation measurement standards; radiation power; radiation processing; x rays.

High-energy electron beams can now be generated with radiation powers of hundreds of kilowatts and can be measured with energy resolutions of several parts in $10^4$. The importance of this new technology to science, industry, and the public is related to the measurement research and services of the National Bureau of Standards.

**9853.** Koch, H. W., Eisenhower, E. H., **Radioactivity criteria for radiation processing of foods,** Chapter 7 in *Radiation Preservation of Foods,* pp. 87-108 (Advances in Chemistry Series **65,** Am. Chem. Soc., Washington, D.C., 1967).

Key words: Detection; induced radioactivity; maximum permissible concentrations; photonuclear reactions; processing; radiation; threshold energies.

The high-dose-level processing of foods by high-energy electrons and x rays can induce measurable radioactivity in foods. Such radioactivity might, but fortunately need not, present a food wholesomeness problem. The amount of induced radioactivity can be controlled and limited so as to be non-measurable by limiting the maximum energy of the radiation to 10 MeV. Therefore, non-measurability is one useful criterion. Another criterion may be developed from considerations of the maximum permissible concentration of radioactivity in foods and of the deliberate or chance nature of the occurrence of the activity. The bases of the various criteria and of possible future developments are detailed by a consideration of the characteristics of photonuclear radioactivities, the detection methods and capabilities, the influence of production parameters, and the maximum permissible concentrations.

**9854.** Kokoszka, G. F., Allen, H. C., Jr., Gordon, G., **Magnetic and optical spectra of two dimeric copper-chloride pyridine-*n*-oxide complexes,** *J. Chem. Phys.* **46,** 3013 (Apr. 1967).

Key words: Copper chloride-pyridine-*n*-oxide; exchange coupled; magnetic spectra; optical spectra; triplet state.

The electron paramagnetic resonance spectra and the optical absorption spectra of dichlorobispyridine-*n*-oxide copper(II) $[(C_5H_5NO)_2CuCl_3]$ and dichloromonoaquopyridine-*n*-oxide copper(II) $[C_5H_5NOCuCl \cdot H_2O]$ have been observed at room temperature. The magnetic resonance studies were carried out at both X-band and K-band frequencies. The observed spectra could be fit to an $S = 1$ spin Hamiltonian. The direction of the maximum zero field splitting did not correspond to the principal $z$ axis of the $g$ tensor. For the $(C_5H_5NO)_2CuCl_2$ the angle between these two directions was about 23° and for the $C_5H_5NOCuCl \cdot H_2O$ the angle was about 27°. A study of the intensity of the E.P.R. signal as a function of temperature indicated that the triplet state was about 550 cm$^{-1}$ above the single ground state for the $(C_5H_5NO)_2CuCl_2$ and about 885 cm$^{-1}$ above the singlet state for the other complex. The optical spectra for both examples revealed two bands in the 8000- to 15,000-cm$^{-1}$ region and a higher energy transition at about 22,000 cm$^{-1}$.

**9855.** Kokoszka, G. F., Allen, H. C., Jr., Gordon, G., **The electron paramagnetic resonance spectrum of tetrakis-t-butoxyvanadium (IV),** *Inorg. Chem.* **5,** No. 1, 91-93 (Jan. 1966).

Key words: Electron paramagnetic spectrum; paramagnetic resonance spectrum; tetrakis-t-butoxyvanadium.

The electron paramagnetic resonance spectrum of tetrakis-t-butoxyvanadium (IV), $[V(OR)_4]$, has been measured in the temperature range of 30° to −196 °C. The measurements were made on pure $V(OR)_4$, 1-2% $V(OR)_4$ in $Ti(OR_4)$ and 1-2% $V(OR)_4$ in $CS_2$. The spectrum was essentially the same in all the samples. At 30 °C $\langle g \rangle = 1.964$ and $\langle a \rangle = 0.0064$ cm$^{-1}$ while at −196 °C in the solid the magnetic parameters are $g\| = 1.940$, $gN = 1.984$, $A\| = 0.0125$ cm$^{-1}$ and $A = 0.0086$ cm$^{-1}$. These parameters are interpreted in terms of the molecular orbital-theory and the model due to Murao is used to account for the low value of the effective spin-orbit coupling constant, 156 cm$^{-1}$.

**9856.** Kokoszka, G. F., Reimann, C. W., Allen, H. C., Jr., **The optical and magnetic spectra of copper-doped dichloro(1,10-phenanthroline) zinc,** *J. Phys. Chem.* **71,** No. 1, 121-126 (Jan. 1967).

Key words: Dichloro(1,10-phenanthroline) copper; dichloro(1,10-phenanthroline) zinc; d-d transition; electron spin resonance spectrum; polarized optical spectrum.

The optical and magnetic spectra of copper-doped dichloro(1,10-phenanthroline) zinc have been observed. In this complex the cupric ion is a distorted tetrahedral environment which is not common for this ion. Two d-d transitions were observed at 11,630 and 13,800 cm$^{-1}$. The parameters in the spin Hamiltonian are found to be $g_z = 2.297 \pm 0.002$, $g_x = 2.058 \pm 0.002$, $g_y = 2.062 \pm 0.002$, $A_z = 4 \times 10^{-4}$ cm$^{-1}$, $A_x = 9 \pm 4 \times 10^{-4}$ cm$^{-1}$ and $A_y = 9 \pm 4 \times 10^{-4}$ cm$^{-1}$. From the ligand superhyperfine structure it is found that hybridization on the nitrogen is sp$^2$ and that the bonding orbital on the chlorine is essentially pure p. From the copper hyperfine structure it is found that there is very little admixture of the 4p functions in the ground state. The indicated uncertainties are due to the uncertainty of the alignment of the crystal in the applied magnetic field and are maximum estimated values.

**9857.** Kostkowski, H. J., **Optical, pyrometry,** *Encyclopedia of Physics,* R. Besaucon, ed., pp. 563-564 (Reinhold Publ. Corp., New York, N.Y., Jan. 1966).

Key words: Optical pyrometry; pyrometry; radiation thermometry; temperature measurement.

A typical visual optical pyrometer, a method of calibrating it from basic principles and the estimated accuracy of such a calibration are outlined. Spectral emissivity and brightness temperature are defined, and other type radiation pyrometers are briefly discussed.

**9858.** Kopec, C. S., **Measurement of gears,** Chapter 15 in *Handbook of Industrial Metrology,* pp. 424-450 (Prentice-Hall, Inc., Englewood Cliffs, N.J., 1967).

Key words: Analytical inspection; composite inspection; gears; index; involute; lead; metrology; process control.

This chapter contains 26 pages of information on gear measuring methods, practices and basic definitions. The data presented cover only those practices and inspection methods which are recognized and accepted throughout the gear industry as being reliable. The methods described provide measurements which are accurate and repeatable to a degree compatible with the specified quality. Experienced personnel, using calibrated instruments in a suitable environment, are required.

Process control is the method by which gear accuracy is maintained through control of manufacturing equipment, methods, and processes. When analytical inspection of gear elements is required, methods are described for measuring the following tooth elements: runout, pitch, profile, lead, backlash, tooth thickness, and composite method of gear inspection.

**9859.** Krasnansky, V. J., Parker, M. S., Florin, R. E., **The effect of gamma irradiation on a polyamide,** *J. Phys. Chem.* **70,** No. 1, 40-46 (Jan. 1966).

Key words: Diffusion-controlled reaction; electron spin resonance; irradiation; kinetics of intermediates; polyamide; radical.

Electron spin resonance and optical spectroscopy were used to study the kinetics of intermediates produced by the irradiation of a polyamide MXD-6. This polymer derived from meta xylylene diamine and adipic acid showed remarkable stability to irradiation in previous studies. Experienced personnel, using calibrated instruments in a suitable environment, are required. It is concluded that the colored intermediate is a radical species, whose molar extinction coefficient is $\sim 10^5$ at 3000 Å.

At temperatures above 85 °C the decay of the active species measured by both methods tends to become second order after an initial rapid decay. This complex decay rate during the initial period was attributed to radicals having a very high decay rate or a diffusion controlled bimolecular reaction of pairs. The derived activation energy for diffusion was 19 to 29 kcal/mole.

**9860.** Kruger, J., **Use of ellipsometry in the study of corrosion,** *Corrosion* **22,** No. 4, 88-97 (Apr. 1966).

Key words: Corrosion; ellipsometry; film thickness; surface measurement techniques.

Ellipsometry by determining the change in the state of polarization (ellipticity) of polarized light reflected from a metal surface bearing a thin film enables one to measure the thickness of this film and its optical properties. Because corrosion processes are strongly affected by the presence of thin films, ellipsometry is an especially valuable tool in corrosion research because it allows one to observe film formation, dissolution, or property changes while these phenomena are actually occurring on a metal surface immersed in any transparent environment. Experimentally the use of ellipsometry mainly requires an experimental cell that allows one to reflect light from the corroding or passive metal surface under study. Thus it does not interfere with other techniques, such as, for example ultra-high vacuum surface preparation or potentiostatic studies, allowing them to be carried out simultaneously along with ellipsometric measurements.

Some of the experimental complications that must be considered in applying ellipsometry to corrosion studies are surface roughening, changes in the optical properties of the solution, non-uniformity of films, effect of light on the corrosion process, and phase changes in the corrosion product films.

The following specific examples serve as a small sampling of the many ways in which ellipsometry may be applied to corrosion studies: (1) The determination of the nature and rate of growth of passive films on iron in inorganic inhibitor solutions. (2) The separation of the different stages in the early growth process of films formed by potentiostatic anodic polarization on iron in neutral solutions. (3) The determination of the point in the corrosion of copper when a new phase begins to form in the corrosion product film.

**9861.** Ku, H. H., **Statistical concepts in metrology,** Chapter 2 in *Handbook of Industrial Metrology,* pp. 20-54 (Prentice-Hall, Inc., Englewood Cliffs, N.J., 1967).

Key words: Industrial metrology, measurement process; statistical analysis; statistical concepts.

These two sections of the chapter, statistical concepts of a measurement process and statistical analysis of measurement data, are part of the text book *Handbook of Industrial Metrology* sponsored by the American Society of Tool and Manufacturing Engineers.

Beginning with the differentiation between arithmetic and measurement numbers, the properties of the latter are developed and described, leading to a discussion of precision and accuracy at the end of the first section.

A basic kit of tools for the comparison and manipulation of means and variances are given in the second section, including a collection of propagation of error formulas. The use of control chart techniques for monitoring stability is emphasized. Examples are given using actual calibration data of NBS.

Selected references are given for topics introduced but not treated in detail.

**9862.** Kuczkowski, R. L., Lide, D. R., Jr., **Microwave spectrum, structure, dipole moment, and barrier to internal rotation of phosphorus trifluoride-borane,** *J. Chem. Phys.* **46,** No. 1, 357-365 (Jan. 1967).

Key words: Barrier; coriolis; dipole moment; microwave spectrum; phosphorus trifluoride-borane; structure.

The microwave spectrum of several isotopic species of phosphorus trifluoride-borane ($F_3P^{11}BH_3$) has been measured and the following structural parameters determined: d(BH) = $1.207\pm0.006$ Å; d(FF) = $1.538\pm0.008$ Å; d(FB) = $1.836\pm0.012$ Å; angle HBH = $115°04'\pm1°$; angle FPF = $99°50'\pm1°$. The dipole moment 0 was evaluated from Stark splitting as $1.06 \pm 0.02$ D.

The vibrational satellite spectrum associated with the excited $\nu_{12}$ (E) and $\nu_6$ ($A_2$) states for $F_3P^{11}BH_3$ was found to be strongly perturbed and was fitted to the theory for a first order coriolis interaction. The analysis of this perturbation and the measurement of the $\nu_{12}$ fundamental in the infrared spectrum permitted the inactive torsional fundamental $\nu_6$ to be determined as $197\pm5$ cm$^{-1}$. This leads to a potential barrier to internal rotation of $3240\pm150$ cal/mol.

The enthalpy of dissociation for the reaction $2F_3HBH_3 \geqslant 2PF_3 + B_2H_6$ (298°) was determined as 10.99 kcal/mol. The experimental results are compared to those found for other related compounds. The indicated uncertainties represent maximum error believed to be possible.

**9863.** Kuczkowski, R. L., Lide, D. R., Jr., Krisher, L. C., **Microwave spectra of alkali hydroxides: Evidence for linearity of CsOH and KOH,** *J. Chem. Phys.* **44,** No. 8, 3131-3132 (Apr. 15, 1966).

Key words: Alkali hydroxides; CsOH; KOH; microwave spectra.

The microwave spectra of CsOH and KOH have been observed. Both molecules show a spectrum characteristic of a linear molecule.The K–O and Cs–O distances are found to be 2.18 and 2.40 Å, respectively.

**9864.** Kuehner, E. C., Leslie, R. T., **Sublimation,** *Encyclopedia of Industrial Chemical Analysis* **3,** 572-584 (John Wiley & Sons, New York, N.Y., 1966).

Key words: Analogous to distillation; analysis-sublimation; condensation temperatures; solid substance; sublimation; sublimators.

Sublimation is considered analogous to distillation and their advantages are compared. Methods of sublimation and types of sublimators are discussed. A section on sublimation analysis is included in which characteristics of a solid substance, such as condensation temperatures, are applied to the identification and quantitative analysis of material.

**9865.** Kulin, G., **Wind effect on pre-existing waves,** Chapter 16 in *Proc. 1965 ASCE Conf. Coastal Engineering, Santa Barbara, Calif., Oct. 1965,* pp. 369-389 (Am. Soc. Civil Engrs., 1966).

Key words: Water waves; wave damping; waves, wind stress on; wind setup; wind-wave interaction; wind waves.

Wind action on pre-existing waves is examined experimentally in a wind-wave channel, in which the pre-existing waves are generated mechanically by a paddle at the windward end of the channel. Air is blown over these waves, in the direction of wave travel, at velocities up to about 30 feet per second, with the formation of wind-generated waves essentially suppressed by addition of a wetting agent to the water. Wind shear forces on these regular wavy surfaces are deduced for a variety of wave geometries.

**9866.** Kupiec, C.,Muehlhause, C. O., **NBSR converter tube,** *Trans. Am. Nucl. Soc.* **9,** No. 2, 582-583 (Nov. 1966).

Key words: Converter tube; fast neutron; NBSR; pile reactivity; radiation effects; radioactive; Research Reactor; thermal neutron.

There are plans to incorporate a high-power-density fast-neutron converter tube in the National Bureau of Standards 10-MW Research Reactor, the NBSR. The purpose of such a facility would be for radiation effects studies where the flux is free from a thermal-neutron component. A converter of this type would allow the experimenter to irradiate relatively large samples without allowing them to become excessively radioactive or appreciably perturb pile reactivity.

**9867.** Kurss, H., **Analysis of multimode experimental data,** *IEEE Trans. Ant. Prop.* **AP-14,** No. 3, 401-402 (May 1966).

Key words: Analysis; determinants; experimental data; multimode; nonlinear parameters; rms error.

An approach for minimizing the rms error in approximating a given function by prescribed sum involving variable parameters is solved as follows: First the nonlinear parameters are determined so as to minimize a certain ratio of two determinants. Then the linear parameters are determined as the solution of a system of linear equations.

**9868.** Kusuda, T., Achenbach, P. R., **Coincident summer weather characteristics of six selected cities in the United States,** (Proc. Symp. Weather, Toronto, Canada, June 27-29, 1966), *ASHRAE J.* **8,** No. 11, 34-42 (1966).

Key words: Coincident summer weather characteristics; fallout shelter; thermal environment; ventilation requirements.

Survival criteria rather than comfort criteria are often used for designing the ventilation and air-conditioning equipment for fallout shelters for economic reasons. Consequently, the choice of design weather conditions assumes unusual importance. Coincident diurnal values of dry-bulb temperature, dewpoint temperature, and solar radiation were obtained from U.S. Weather Bureau records for the hottest day, hottest week, most humid day, and most humid week each year for a 10-year period for six cities. It was shown that the diurnal pattern of coincident dry-bulb and wet-bulb temperatures during extremely hot and humid periods could not be derived directly from the currently available handbook data reporting percentile levels of temperature for total summer hours. A harmonic analysis of these data was made so that coincident cyclic values of several parameters could be introduced into digital or analog computer studies of the thermal environment of a shelter. Three different sets of design psychrometric data for the ventilating air were used to study the effect of coincident climatic data in repetitive diurnal cycles on the environment of two sizes of fallout shelters.

**9869.** Kusuda, T., Achenbach, P. R., **Outdoor air psychrometric criteria for summer ventilation of protective shelters,** *ASHRAE Trans.* **71,** Pt. 1, 76-87 (Jan. 25-28, 1965).

Key words: Coincident dry- and wet-bulb temperature; fallout shelter ventilation; thermal environment.

A forced ventilation system using outdoor air, powered either manually or by emergency power sources, often provides six cities. the best combination of reliability and economy for protective shelters where outdoor conditions and occupancy characteristics are not extreme. In above-ground shelters, an assumption that the ventilating air must remove all of the sensible and latent heat released inside the shelter is a reasonably good design criterion in most cases. This report analyzes the relation between ventilation rate, heat release inside the shelter, and outdoor and shelter psychrometric conditions based on this assumption. The ventilation rates required to maintain an effective temperature of 85 in the shelter for various selected outdoor design criteria are calculated for the cities of Houston, Phoenix, and Minneapolis. It is shown that none of the published non-coincident dry-bulb and wet-bulb temperature criteria expressed on a percentile basis are adequate for calculating ventilation rates on an equal-risk basis for various climates. A method for calculating ventilation adequacy factors that is applicable to any city for which suitable outdoor coincident dry-bulb and wet-bulb temperature data are available is described and illustrated.

**9870.** Kusuda, T., Achenbach, P. R., **Earth temperature and thermal diffusivity at selected stations in the United States,** *ASHRAE Trans.* **71,** Pt. 1, 61-75 (Jan. 25-2 8 1965).

Key words: Amplitude; earth temperature; earth temperature phase shift; thermal diffusivity; underground installations.

To provide information related to the heat transfer in underground installations, 63 sets of data showing annual variations of monthly average earth temperatures at various depths throughout the 48 contiguous states of the United States of America have been compiled and analyzed for the Office of Civil Defense. These data have been used to compute the annual average amplitude and phase angle of the earth temperature by a least-squares method. Thermal diffusivities of earth computed from the observed temperature data by both the amplitude method and phase lag method were compared for selected earth temperature stations. The earth temperature characteristics were also compared with those of air and ground water temperatures.

**9871.** Kuyatt, C. E., Simpson, J. A., **Electron monochromator design,** *Rev. Sci. Instr.* **38,** No. 1, 103-111 (Jan. 1967).

Key words: Anomalous energy spreads; electron beams; electron optical limitations; high-resolution electron monochromator; space charge; spherical deflectors.

A study has been made of all the known factors which limit the performance of high-resolution (0.07 to 0.01 eV FWHM) monochromators. These limiting factors have been incorporated into design equations for the optimum (maximum current ouput) monochromator. The conclusions are tested by performance measurements on a prototype instrument. The results require the introduction into the design equation of a new limiting factor, an anomalous energy spread in dense electron beams, which is empirically determined.

**9872.** Kuyatt, C. E., Simpson, J. A., Mielczarek, S. R., **Resonances in electron scattering from $H_2$, HD, and $D_2$,** *J. Chem. Phys.* **44,** No. 2, 437-439 (Jan. 15, 1966).

Key words: Absolute electron energy scale; $D_2$, $D_2^-$; electron scattering resonances; HD, $HD^-$; $H_2$, $H_2^-$; vibrational constants of $H_2^-$.

Resonances in the transmission of electrons through $H_2$, HD, and $D_2$ have been studied for electrons of energy 11 to 13 eV. In $H_2$ and HD pairs of resonances were observed, indicating that there exist two electronic states of $H_2^-$ and $HD^-$, each with well developed vibrational structure. In $D_2$ only one series of resonances is observed. The single series is attributed to the overlap of two states of $D_2^-$ because of a smaller vibrational separation. The absolute energy scale for the resonances has been recalibrated to an estimated accuracy of 0.1 eV.

**9873.** Lafferty, W. J., Lide, D. R., Jr., **Microwave spectrum of excited vibrational states of FCN,** *J. Mol. Spectry.* **23,** No. 1, 94-96 (May 1967).

Key words: Fermi resonance; infrared spectrum; microwave spectrum; rotational constants; unperturbed vibrational frequencies; vibrational spectrum.

The microwave and infrared spectra of FCN are reported. The band centers of $\nu_2^1$ and $\nu_1$ have been obtained from resolved infrared bands. The band center for $2\nu_2^0$ has been obtained from both a "hot band" Q branch and, less accurately, by direct observation of the unresolved band. The rotational constants of all $\Sigma$ vibrational states up to *ca.* 2100 $\text{cm}^{-1}$, and several $\pi$ and $\Delta$ states have been obtained from the microwave spectrum. Combination of the microwave and infrared work permits correction for the Fermi resonance between $\nu_1$ and $2\nu_2^0$. Unperturbed vibrational frequencies for $2\nu_2^0$ and $\nu_1$ are reported. The value of the Fermi resonance matrix element is $35.2_8 \pm 0.4\ \text{cm}^{-1}$.

**9874.** Lance, H. W., **The national measurement systems of various countries,** *IEEE Trans. Instr. Meas.* **IM-15,** No. 4, 397-403 (Dec. 1966).

Key words: Measurement system; national standards laboratories; precision electromagnetic measurements; standards laboratories.

This paper is a summary of an informal panel discussion which formed one session of the 1966 Conference on Precision Electromagnetic Measurements. In contrast to the other sessions, this one was concerned primarily with broad management problems rather than with detailed technical matters. The members of the panel, from nine different countries, had been asked to consider the measurement system of their country, their national standards laboratory (or its equivalent), and the scientific and technical program of the laboratory. Although time limitations prevented a thorough discussion, many worthwhile facts and opinions emerged.

**9875.** Landgrebe, A. R., Gills, T. E., DeVoe, J. R., **Application of radiometric techniques to quantitative paper chromatography of iron, copper, manganese, and cobalt,** *Anal. Chem.* **38,** No. 9, 1265-1266 (Aug. 1966).

Key words: Analysis; Co; Cu; Fe; Mn; NBS Standard Reference Material 671; nickel oxide; paper chromatography; radiometric methods.

A radioactive reagent was used for the quantitative determination of iron, copper, manganese, and cobalt after separating them by paper chromatography. The method has been applied to the analysis of a sample of nickel oxide (NBS Standard Reference Material No. 671). With this method which is operable at the $\mu$g/ml level, values of 0.37, 0.19, 0.14, and 0.32 percent for Fe, Cu, Mn, and Co respectively were found and the relative standard deviation of a single determination for Fe, Cu, Mn, and Co were 7.1, 6.8, 3.8, and 4.1 percent. Comparison of these results with those of other analytical techniques were made.

**9876.** Landgrebe, A. R., McClendon, L. DeVoe, J. R., **A determination of trace amounts of iron and cobalt in the same sample by substoichiometric radioisotopic dilution analysis,** (Proc. 1964 Winter Meeting American Nuclear Society, San Francisco, Calif., Nov. 30-Dec. 3, 1964), *Trans. Am. Nucl. Soc.* **7,** No. 2, 337-338 (1964).

Key words: Analysis; cobalt; Dowex 50-X8; EDTA; iron; nickel oxide; radioisotopic dilution; standard reference material.

A method of analysis for iron and cobalt was developed for the concentration range of $10^{-3}$ to $10^{-8}$ M. The method involves using a limiting amount of EDTA to complex iron or cobalt. The noncomplexed ions were removed from solution with a cationic exchanger (Dowex 50-X8) leaving a constant amount of cobalt or iron EDTA complex in solution. Trace amounts of naturally occurring cobalt and iron were determined with good sensitivity as long as radioisotopes of high specific activity were used. NBS standard reference material (671, 672, and 673) of nickel oxide were also analyzed for iron and cobalt.

**9877.** Larsen, S. Y., Witte, K., Kilpatrick, J. E., **On the quantum mechanical pair-correlation function of $^4$He gas at low temperatures,** *J. Chem. Phys.* **44,** No. 1, 213-220 (Jan. 1, 1966).

Key words: Loww temperature; pair-correlation; quantum-mechanical.

The density independent part of the direct and exchange correlation functions for $He^4$, using the deBoer and Michels Lennard Jones potential, have been calculated at 2°, 1°, .1 °K. The necessary wave functions were obtained by numerical integration of the Schrodinger equation. The peak of the direct correlation function is much less than its classical value and occurs at a slightly larger radius. The tail (large *r*) agrees very well with the form given by the Wigner-Kirkwood expansion. The exchange correlationn function which represents the entire effect of the spin and statistics of the system vanishes very rapidly with increasing temperatures.

**9878.** Laufer, A. H., McNesby, J. R., **The chain decomposition of propane initiated by vacuum ultraviolet photolysis,** *J. Phys. Chem.* **70,** 4094-4096 (1966).

Key words: Photolysis; propane chain decomposition; vacuum ultraviolet.

Mixtures of propane and propane-$d_8$ were photolyzed at 1470 Å from 25-320 °C. Isotopic compositions of the hydrogen and methane products were determined. While the methane is predominantly $CH_4$ and $CD_4$ at room temperature, the chain decomposition of *n*-propyl with the consequent formation of isotopically mixed methanes became increasingly important as the temperature was raised. The chain length was found to vary from 0.07 at room temperature to a lower limit of 7.9 at 320 °C.

**9879.** LaVilla, R. E., Deslattes, R. D., **K-absorption fine structure of sulfur in gaseous $SF_6$,** *J. Chem. Phys.* **44,** No. 12, 4399-4400 (June 15, 1966).

Key words: Absorption; fine structure; K-edge; molecular gas; $SF_6$, sulfur; x-ray.

Measurements are reported on the K-absorption fine structure of sulfur in gaseous $SF_6$. The results differ qualitatively from previous measurements on molecular gases of lower coordination. Comparison is also made with preliminary results on $H_2S$.

**9880.** Layer, H. P., Deslattes, R. D., **A simple nonscanning camera for x-ray diffraction contrast topography,** *J. Appl. Phys.* **37,** No. 9, 3631-3632 (Sept. 1966).

Key words: Camera; diffraction; dislocation; topography; x-ray.

A new x-ray topographical camera has been developed that is applicable to both Laue and Bragg geometrics for normal and anomalous transmission, that results in a significant reduction of experimental complexity along with quite acceptable exposure times.

**9881.** Leaderman, H., **Viscoelastic behavior,** *Encyclopedic Dictionary of Physics* **7,** 633-634 (Pergamon Press, Inc., London, England, 1962).

Key words: Linear viscoelastic behavior; relaxation times; retardation times.

A brief summary of the mathematical description of mechanical properties of materials which show linear viscoelastic behavior.

**9882.** Lee, R. D., **Calibration of the NBS photoelectric pyrometer of 1961,** *Proc. Comite Consultatif de Thermometrie, 7th Session, Paris, France, Sept. 24-25, 1964,* pp. 74-78 (July 10, 1966).

Key words: Calibration, NBS photoelectric pyrometer of 1961; International Practical Temperature Scale; NBS photoelectric pyrometer; photoelectric pyrometer, NBS; pyrometer, photoelectric, NBS.

Factors affecting the reproducibility of the NBS Photoelectric Pyrometer are listed, and progress in reducing these factors are described. A calibration to realize the International Practical Temperature Scale (IPTS) above 1063 °C to 1256 °C is described. At present, the estimated uncertainty in realizing the IPTS is about 0.1 °C at 1063 °C, 0.2 °C at 1256 °C, and is predicted to be 0.8 °C at 2400 °C.

**9883.** Lehner, J., **Representations of discrete groups,** *Proc. Symp. Pure Mathematics, California Institute of Technology, Pasadena, Calif., Nov. 21-22, 1963, Chapter VIII, Theory of Numbers,* pp. 203-208 (Am. Math. Soc., Providence, R.I., 1965).

Key words: Abstract groups; discrete groups; discrete matrix subgroup; F-groups; matrix subgroup.

It is shown that certain properties of a class of finitely generated abstract groups known as F-groups are preserved when the F-group is imbedded in SL(2, reals) as a discrete matrix subgroup. Thus the abstract structure of the F-group determines to a certain extent the topological properties of the matrix group.

**9884.** Leslie, R. T., **Distillation as a tool for purification of research quantities of material,** *Ann. N.Y. Acad. Sci.* **137,** 19-29 (Jan. 20, 1966).

Key words: Distillation; material; purification of research quantities of materials; research quantities.

Distillation can increase the purity of nearly any "real" vaporizable mixture if sufficient effort is made. The method is invaluable for purifying relatively small quantities of material for research purposes.

The selection of the proper still column for a particular problem can be based on a knowledge of the characteristics of a few basic types of columns. Some operating procedures which favor good results can be outlined in a general way, but testing of stills by the operator using mixtures whose behaviors can be predicted under various conditions is recommended.

Some possibilities for the improvement of still columns are suggested.

**9885.** Leslie, R. T., Kuehner, E. C., **Distillation analysis,** *Encyclopedia of Chemistry,* p. 344 (Reinhold Publ. Corp., New York, N.Y., 1966).

Key words: Analysis; concentration; distillation; separation.

Mixtures of volatile materials, either liquid or solid, can be analyzed by information obtained by vaporization at constant pressure or at constant temperature. Miniature and micromethods can be used when necessary. Distillation under carefully prescribed conditions is often useful for control purposes. Gas-liquid chromatography has some advantage for precise analysis. Preseparation or preconcentration of trace constituents by distillation, combined with other methods of analysis, is often useful.

**9886.** Lester, W., Krauss, M., **Some aspects of the coulomb hole of the ground state of $H_3^+$,** *J. Chem. Phys.* **44,** No. 1, 207-212 (Jan. 1966).

Key words: Electronic structure; $H_3^+$; molecular quantum mechanics.

The Coulomb hole for the linear and equilateral configurations of the ground state of $H_3^+$ is calculated using a Gaussian basis set. A modification of the method of Coulson and Neilson which determines the distribution function, $f(r_{12})$, instead of the distribution function of the interelectronic distance $f(r_{12})$ was used. Curves of $f(r_{12})$ and the Coulomb hole function are plotted for selected orientations of the electron-pair to the nuclear arrangements. The method allows a graphic presentation of the dependence of the size of the Coulomb hole on the nuclear geometry of the polyatomic system.

**9887.** Levin, E. M., **Liquid immiscibility in the rare earth oxide-boric oxide systems,** *Phys. Chem. Glasses* **7,** No. 3, 90-93 (June 1966).

Key words: Boric oxide; liquid immiscibility; phase equilibria; rare earth oxides.

Three experimental methods were used to determine the composition of the modifier-rich liquids in the following binary sytems with $B_2O_3$: $La_2O_3$, $Nd_2O_3$, $Sm_2O_3$, $Eu_2O_3$, $Gd_2O_3$, $Dy_2O_3$, $Y_2O_3$, $Ho_2O_3$, $Er_2O_3$, $Tm_2O_3$, $Yb_2O_3$, $Lu_2O_3$, $Sc_2O_3$. With decreasing ionic radius (increasing atomic number), the extent of immiscibility increased from 21.5% for the $La_2O_3$ system to 34.0 mol% for the $Sc_2O_3$ system. With the exception of the $La_2O_3$ and the $Nd_2O_3$ systems temperatures of the monotectics increased monotonically from 1136° for $Sm_2O_3$ to 1526 °C for $Sc_2O_3$. Index of refraction of the quenched modifier-rich liquid was a maximum (1.732) for $Eu_2O_3$. Competing ionic field strengths between the glass-forming and modifier cations with oxygen govern the existence of immiscibility. Structural considerations governing the number of oxygens associated per modifier cation determine the extent of immiscibility.

**9888.** Levin, I. W., Abramowitz, S., **Force fields for group IV tetrafluorides and group V trifluorides,** *J. Chem. Phys.* **44,** No. 7, 2562-2567 (Apr. 1, 1966).

Key words: Coriolis constants; force fields; Group IV tetrafluorides; Group V trifluorides; vibration-rotation band contours.

The Coriolis zeta constants of the degenerate modes of $SiF_4$, $GeF_4$, $NF_3$, $PF_3$, and $AsF_3$ were obtained from infrared band contour measurements. These Coriolis coupling data provided the necessary constraints for determining unique force fields for the $F_2$ and E symmetry species of the $XF_4$ and $XF_3$ molecules, respectively. In an attempt to limit the force field for the $A_1$ species of the $XF_3$ molecules, the rotational distortion constants, $D_J$ and $D_{JK}$, were calculated for a range of values of $F_{12}$, with the E species force constants in this calculation remaining fixed from the zeta constant data.

**9889.** Lichtenstein, S., **Corrosion's many faces,** *Southern Eng.* **85,** No. 1, 44-47 (Jan. 1967).

Key words: Basic and applied research; economics of corrosion; industrial design; materials protection; structural failure.

Corrosion is discussed as a technological and economic "disease" eating away at metals and materials, depleting natural resources, and causing injury and death where accidents and explosions result from weakening of structures. Dollar estimates of costs to the nation and the Federal Government are given. Anticorrosion work of the National Bureau of Standards' Institute for Materials Research is described and highlights of a half-century of achievement are noted. Corrosion control is linked to progress in nuclear power, oceanography, water desalination, military operations, space and supersonic transport, health, safety, and conservation.

**9890.** Lichtenstein, S., **NBS hunts for better ways to control corrosion,** *Mater. Eng.* **65,** No. 5, 21-23 (May 1967).

Key words: Corrosion; ellipsometry; field-electron emission microscopy; low-energy diffraction; NBS corrosion section; passivity; ultra-high vacua.

NBS contributions to a mosaic of evidence on the nature of corrosion processes are described, including thin-film and passivity studies under ultra-clean conditions, underground studies, polarization and cathodic protection, galvanic effects, and stress and atmospheric corrosion in marine environments.

**9891.** Lide, D. R., Jr., **Correction of some erroneous calculations of the Einstein A coefficient for the 18 cm transition of OH,** *Nature* **213,** No. 5077, 694-695 (Feb. 18, 1967).

Key words: Einstein A coefficient; hydroxyl; radical; transition probability.

The Einstein A coefficient for the 18 cm A doublet transition of OH is calculated to be $8.53.10^{-11}\text{sec}^{-1}$. It is shown that previous values of A are incorrect.

**9892.** Lide, D. R., Jr., **Interpretation of the far infrared laser oscillation in ammonia,** *Physics Letters* **24A,** No. 11, 599-600 (May 1967).

Key words: Ammonia; infrared; inversion; laser; molecular; spectrum.

The interpretation of the laser emission spectrum of ammonia in the far infrared is considered. The P branch of the $v_2 = 3'' - 2''$ transition is shown to coincide closely with the observed laser spectrum. However, only the low K transitions are observed. Possible reasons for the absence of the expected strong $K = 3$ lines are discussed.

**9893.** Lide, D. R., Jr., **Microwave spectroscopy,** *Encyclopedia of Industrial Chemical Analysis* **2,** 600-611 (John Wiley & Sons, Inc., New York, N.Y., 1966).

Key words: Chemical analysis; microwave spectroscopy; microwave studies; molecular structure; rotational spectra; spectra, rotational; spectroscopy, microwave.

The experimental techniques used in microwave spectroscopy are described. A brief outline of the theory of rotational spectra is given. The information on molecular structure which can be obtained from microwave studies is discussed. Some comments are made on the use of microwave spectroscopy in chemical analysis.

**9894.** Lide, D. R., Jr., **Microwave studies of rotational isomerism,** *Trans. Am. Crystallographic Assn.* **2,** 106-116 (1966).

Key words: Butadiene; isomerism; microwave spectroscopy; propionaldehyde; rotational; structure.

The application of microwave spectroscopy to the study of rotational isomerism is reviewed. Molecules of the butadiene type are found to exist predominantly in the planar *trans* form; no spectra from other isomers have been detected. Normal propyl compounds show both *trans* and *gauche* isomers at room temperature. Two isomers are also found in propionaldehyde and related compounds. Conclusions regarding structure and stability of rotational isomers are discussed.

**9895.** Lide, D. R., Jr., Kuczkowski, R. L., **Structure of the alkali hydroxides. I. Microwave spectrum of gaseous CsOH,** *J. Chem. Phys.* **46,** No. 12, 4768-4774 (June 1967).

Key words: Cesium hydroxide; dipole moment; high temperature; microwave; molecular structure; spectrum; vibration.

The microwave spectra of gaseous CsOH and CsOD have been studied in a high-temperature spectrometer. The spectrum indicates a linear or near-linear molecule with a large-amplitude, low-frequency bending vibration. A large number of excited states involving the bending mode and the Cs—O stretching mode have been identified. The rotational constant $B_v$ shows an unusual variation as the bending mode is excited; the cause is not yet understood. The Cs—O bond length is found to be 2.40 ± 0.01 Å and the O—H distance is probably about 0.97 Å. The electric dipole moment is 7.1 ± 0.5 D. Relative intensity measurements indicate a Cs—O stretching frequency of about 400 $\text{cm}^{-1}$ and a bending frequency in the neighborhood of 300 $\text{cm}^{-1}$. All of the evidence supports a highly ionic cesium—oxygen bond.

**9896.** Linnig, F. J., Parks, E. J., Stiehler, R. D., **Effect of certain crystalline substances on physical properties of elastomers. I. Stress-strain behavior,** *Rubber Chem. Technol.* **39,** No. 4, Pt. 1, 1041-1052 (Sept. 1966).

Key words: Anisotropic; β-naphthyl group; glass transition temperature; phenyl β-naphthylamine; physical forces; reinforcement; reversible; rubber vulcanizates; stiffening.

Some crystalline organic compounds containing a β-naphthyl group have been found under certain conditions to produce a pronounced stiffening of rubber vulcanizates. When these materials are removed by extraction, the reinforcing effect vanishes. Reinforcement by the most effective of the materials examined, phenyl β-naphthylamine, is obtained with vulcanizates made from various elastomers and vulcanizing agents, and is essentially independent of the state of cure. In some instances about 5 percent PBNA produces the same stiffness as 30-40% carbon black but the stiffness is markedly reduced by flexing. Less than 3 percent crystalline PBNA may produce an isotropic Young's modulus of about 20 $\text{kg/cm}^2$ at room temperature. At higher concentrations of PBNA, anisotropic effects are observed. The temperature coefficient of Young's modulus is negative analogous to that for vulcanizates containing carbon black. The addition of PBNA to a rubber vulcanizate does not affect significantly the glass-transition temperature.

The reversible nature of reinforcement with PBNA indicates a physical mechanism. However, the effect is not in accord with existing physical theories of reinforcement. This work strongly suggests that profound reinforcement can result from physical forces alone.

**9897.** Lipkin, H. J., Meshkov, S., **Spin independence, W-spin, parity and SU(6) symmetry,** *Phys. Rev.* **143,** No. 4, 1269-1274 (Mar. 25, 1966).

Key words: Collinearity; lorentz invariance; W-spin.

The assumption of strict spin independence of strong interactions between elementary particles forbids all three meson and meson-baryon-baryon couplings, such as $\rho\pi\pi$, $NN\pi$, and $N^*N\pi$. It is shown that these catastrophies may be avoided, even in the nonrelativistic limit, by adopting a modified definition of spin-independence, i.e., W-spin independence. A nonrelativistic definition of W-spin is obtained which requires only a trivial change to yield the relativistic description. The consequences of the assumption of W-spin independence are explored.

**9898.** Lipkin, L. E., Watt, W. C., Kirsch, R. A., **The analysis, synthesis and description of biological images,** *Ann. N.Y. Acad. Sci.* **128,** No. 3, 984-1012 (Jan. 31, 1966).

Key words: Biological images; cell analysis; image display; pattern recognition; syntax.

There may be distinguished two approaches to characterizing the properties of biological images: the statistical approach traditionally used for mechanized image-processing, and the articular approach generally used among biologists. We discuss both approaches, but focus attention on the second, for we hold that an articular approach allows the expression of much that is effectively impossible to express in the form of numerical measurements; and we know of no inherent reason why a computer cannot deal with information of a nonquantitative nature.

The articulation of biological images necessarily takes place on two fronts: the imposition of an articular structure on the image itself; and the expression of this construal in English sentences. We will study both kinds of articulation, and we will suggest how they may be brought together, in the form of linked pictorial and linguistic *grammars*. The computer system which this paper envisions will be able to analyze a presented image with respect to a pictorial grammar, and to formulate and accept descriptions of that image, in English sentences, with respect to a linguistic grammar. It will be able to present pictorial instances of English descriptions, and in other ways to respond to English directives.

**9899.** Loebenstein, W. V., **Surface studies of natural and synthetic bone mineral and teeth,** (Proc. 2d Workshop, Adhesive Restorative Dental Materials, Univ. of Virginia, Charlottesville, Va., Dec. 8-9, 1965), Chapter IV in *Adhesive Restorative Dental Materials, Surface measurements--synthesis and evaluation of dental adhesives,* pp. 213-223 (Dept. of Health, Education, and Welfare, Washington, D.C., 1966).

Key words: Adsorption; anorganic bone mineral and dentin; bone; calcium phosphate; hydroxyapatite; octacalcium phosphate; pore size distribution; pore volume; surface area; surface chemistry; teeth.

Low temperature nitrogen adsorption measurements have been performed using dentin and bone as well as synthetic calcium phosphate preparations. Surface areas ranging from about 1-1/2 to nearly 150 $m^2 \cdot g^{-1}$ have been found. Pore size distribution calculated from the isotherm data shows promise of being a valuable and sensitive tool for aiding in the comparison of crystallographic forms and for detection of subtle changes in structure not measurable by other means presently in use. The pore structure of bone mineral in the range 20-30 Å appears to be entirely independent of the collagen matrix.

**9900.** Loftus, T. P., Weaver, J. T., Petree, B., **Effect of humidity on ionization measurements using cavity and free-air chambers,** *Radiology* **86,** No. 1, 149 (Jan. 1966).

Key words: Cavity and free-air chambers; free-air chambers; humidity on ionization measurements; ionization measurements.

Measurements are described that show the effect of humidity on the measurement of gamma radiation with cavity ionization chambers. It is found that the chamber current does not vary by more than 0.06 percent as the relative humidity is changed by more than 50 percent. A calculation, based on the assumption that the air and its moisture produce ionization independently, predicts a decrease of about 0.4 percent for the measurement in moist air. The discrepancy is believed to be connected with the value used for the average energy required to produce an ion pair in moist air.

Similar results were obtained with free-air chamber exposed to 60 kVcp x rays. A current increase of only 0.03 percent was observed when the relative humidity was changed from 48 to 13 percent, although the calculated increase is 0.3 percent.

**9901.** Logan, H. L., McBee, M. J., Bechtoldt, C. J., Sanderson, B. T., Ugiansky, G. M., **Chemical and physical mechanism of salt stress-corrosion cracking in the titanium 8-1-1 alloy,** (Proc. Stress Corrosion Cracking Symp., Seattle, Wash., Nov. 1965), *Am. Soc. Testing Mater. Spec. Tech. Publ.* **397,** pp. 215-229 (1966).

Key words: Corrosion products; high temperature corrosion; preoxidation; salt stress corrosion; solid state reactions; stress-corrosion cracking; titanium 8-1-1 alloy.

The mechanism of salt stress-corrosion cracking of the Ti-8-1-1 alloy was investigated. Specially designed specimens coated with NaCl or $NaCl + MgCl_2 \cdot 6H_2O$ and stressed to 75 percent of their yield strength at 750 °F failed in as short a time as 18 hours. Gaseous oxygen and NaCl or oxidation at 750 °F prior to coating the specimen with NaCl were required to produce cracking. X-ray diffraction studies indicated that anatase, rutile and unidentified corrosion products were formed as a result of the reaction of NaCl and oxygen with the alloy.

**9902.** Logan, H. L., **The stress corrosion of metals,** *Book,* 306 pp. (John Wiley & Sons, Inc., New York, N.Y., Nov. 1966).

Key words: Aluminum alloys; copper alloys; magnesium alloys; nickel alloys; steels; stress corrosion; stress corrosion failures; testing techniques.

This is the first volume in English in which a single author has brought together previously published material on this subject. In 306 pages, the work covers a broad study of stress corrosion phenomena in alloy systems and correlates the information with today's theories on the mechanism of stress corrosion cracking.

Separate chapters deal with stress corrosion cracking in low carbon steels, high strength steels for aerospace, various stainless steels, and copper, aluminum, nickel, magnesium titanium, and miscellaneous precious metal alloys. In each chapter, techniques are discussed for eliminating stress corrosion. Methods of identifying failures as well as analyzing the failures are set forth in an additional chapter. The final feature of the book provides methods of evaluating the resistance of metals to stress corrosion.

**9903.** Logan, H. L., Yolken, H. T., **The role of hydrogen in the stress-corrosion cracking of low carbon steel in a nitrate solution,** *Proc. 2d Intern. Congress Metallic Corrosion, New York, N.Y., Mar. 1963,* p. 109 (Natl. Assoc. Corrosion Engr., Houston, Texas, 1966).

Key words: Corrosion; embrittlement; hydrogen; steel; stress-corrosion cracking.

The relative susceptibilities of four low carbon steels (0.20 percent carbon) to failure by hydrogen embrittlement and nitrate stress corrosion were compared (notched specimens being used in each case). The susceptibilities to failure, paths of attack, and rates of crack propagation were different in the two processes. Failure, once cracking was initiated, was much more rapid by hydrogen embrittlement than in nitrate stress corrosion cracking but was slow compared to brittle fracture. Diffusion of hydrogen into the steel was at least 50 times greater in hydrogen embrittlement than in nitrate stress cracking.

**9904.** Lonie, M., **Voluntary product standards—what they mean to the consumer,** *J. Home Econ.* **58,** No. 1, 22 (Jan. 1966).

Key words: Procedure; products; quality; standards.

The principal purpose of the talk is to emphasize the character of the contribution made by the National Bureau of Standards in the development of commercial standards and simplified practice recommendations, technically and editorially, and how this benefits the consumer.

It emphasizes how the widened exposure to the standards both in and out of the Bureau tends to raise the quality level of commodities covered. It cites examples to show that the "consumer" is not always the "ultimate" consumer. It stresses the point that standards developed according to the procedures of the Bureau are better standards than they would otherwise be.

**9905.** Lovell, W. S., **Molecular and ionic interactions in dielectrics,** Chapter III in *1965 Digest of Literature on Dielectrics* **29,** 81-198 (National Academy of Sciences—National Research Council, Washington, D.C., 1966).

Key words: Dielectric constant; dielectric polarization and refraction; dielectric relaxation; dipole moments; electrical conductance of liquids and solutions; internal rotation; molecular interactions; pressure broadening.

A survey is given of the 1965 literature treating molecular interactions, pressure broadening, dielectric polarization and refraction, dielectric constant, dipole moments, dielectric relaxation, internal rotation, and electrical conductance of liquids and solutions.

**9906.** Lyon, H. W., Waterstrat, R. M., Paffenbarger, G. C., **Soft tissue response to implants of gallium alloys and silver amalgam alloys,** *J. Am. Dental Assoc.* **72,** No. 3, 659-664 (Mar. 1966).

Key words: Amalgam alloys; gallium alloys; gold-gallium alloys; silver-amalgam control specimens; soft tissue.

Twenty implants of gold-gallium alloys and 20 silver-amalgam controls were placed subcutaneously in ten NMRI-D strain rats for six months. Silver amalgam control specimens elicited a mild, innocuous response. In contrast, gold-gallium alloy implants not only caused a severe foreign body response (fibrosis) from the host tissues but also fragmented and partially disintegrated. These results were exactly similar to those obtained in a previous experiment wherein palladium-gallium alloy implants were subjected to identical procedures. Disintegration of the experimental alloys was probably due to corrosion of the $AuGa_2$ phase rather than an electrolytic reaction between this phase and the gold.

**9907.** McCamy, C. S., **Photographic standardization and research at the National Bureau of Standards,** *Appl. Opt.* **6,** No. 1, 27-30 (Jan. 1967).

Key words: Densitometry, NBS; photography; standardization.

The Photographic Research Section of NBS provides physical standards of measurement and calibration services, cooperates with national and international standardizing organizations, and conducts research related directly to the utilization of photographic materials and processes. Standardization and research in sensitometry, standard light sources, emulsion making, preservation of photographs, precise densitometry, and image evaluation have spanned a half century.

**9908.** McClintock, M., Jennings, O. A., Mizushima, M., **Light scattering from time-dependent molecular orientations at Raman frequencies in liquids,** *Bull. Am. Phys. Soc., Series II,* **12,** No. 5, 711 (May 1967).

Key words: Benzene; carbon tetrachloride; Raman scattering.

The profiles of several Raman lines arising from nontotally symmetric molecular vibrations in liquid benzene and carbon tetrachloride have been measured using 4880 Å radiation from an argon ion laser as a source of illumination. These profiles have been analyzed on the assumption that scattering occurs from time-dependent molecular reorientations of small angle in the liquid, analogous to those producing depolarized scattering at the Rayleigh line. On this basis, the half width at half maximum of the 606 $cm^{-1}$ Raman line in benzene was found to be 3.3 $cm^{-1}$, and the half width of the "orientation" line underlying this Raman line was found to be 24.3 $cm^{-1}$. The rotational relaxation time calculated for the $\nu_{18}$ vibrationally excited molecule is therefore $1.38 \times 10^{-12}$ seconds. This is short compared with a period of rotation and supports the assumption of rotational Brownian motion. It is also shorter than the rotational relaxation time for the molecule in the ground vibrational state, and indicates that there is weaker rotational coupling between molecules in the ground state than between vibrationally excited molecules and those in the ground state. The depolarization ratios of the Raman and the orientation components of the 606 $cm^{-1}$ line for linearly polarized incident light were found to be 0.748 and 0.749 respectively, in agreement with the theoretically predicted 0.750.

**9909.** McLaughlin, W. L., **Microscopic visualization of dose distributions,** *Intern. J. Appl. Radiation Isotopes* **17,** 85-96 (1966).

Key words: Dose distribution; dyes; electron beams; energy transfer; films; gamma radiation; high resolution; molecular excitations; radiation chemistry; radiation processing.

Colorless cyanides of triphenylmethane dyes when suitably activated can be made into films that become deeply colored upon irradiation with short-wave ultraviolet and ionizing radiations, but are not sensitive to near ultraviolet radiation or visible light. The response range for x rays, $\gamma$-rays, and electrons is approximately $10^5$ to $10^8$ rads. Experiments show that, because of their stability, low energy dependence, and high spatial resolution, these solid systems have excellent potential for visual inspection off high-level dose distributions on a microscopic scale. Since molecular excitations due to low-energy secondaries are most important to the over-all radiation effects, the relatively large sensitivity of such dye systems expected in the intermediate and far ultraviolet may represent an advantage in dosimetry.

**9910.** McNesby, J. R., **Vacuum-ultraviolet photolysis of parafin hydrocarbons,** Chapter 2 in *Chemical and Biological Actions of Radiation,* **IX,** 39-67 (Masson and Co., Editors and Publ., Paris, France, 1966).

Key words: Carbenes; hydrocarbons; photochemistry; ultraviolet.

The vacuum ultraviolet photolysis of some simple hydrocarbons is reviewed in detail with regard to its relationship to the chemistry of excited carbenes. Various sources of carbenes are reviewed and the relationships between the observed chemistry for the various sources are examined and generalized.

**9911.** McNish, A. G., **The international system of units,** *Am. Soc. Quality Control Annual 1965 Tech. Conf. Trans. Industrial Quality Control* **22,** No. 9, 465-469 (Mar. 1966).

Key words: Customary units for length; engineering calculations; International System of units; length; system of units; units of length.

The International System of units is advantageous in engineering calculations because of its completeness and simplicity. No difficulty is experienced in its application in the United States, although it is inconsistent with our customary units for length, mass, and temperature.

**9912.** McNish, A. G., **The nature of measurement,** Chapter 1 in *Handbook of Industrial Metrology,* pp. 2-12 (Prentice-Hall, Inc., Englewood Cliffs, N.J., 1967).

Key words: Accuracy; measurement principles; precision.

General principles for measurement. Accuracy and precision are discussed.

**9913.** McNish, A. G., **Reply by A. G. McNish,** *Phys. Today* **19,** No. 4, 15-16 (Apr. 1966).

Key words: Metric system; physical constants; SI; units.

In response to a criticism of units used in a previous article "New Values for the Physical Constants," it is pointed out that dimensional procedures are highly arbitrary and require only that they be consistent.

**9914.** Macedo, P. B., Capps, W., Litovitz, T. A., **Two-state model for the free volume of vitreous $B_2O_3$,** *J. Chem. Phys.* **44,** No. 9, 3357-3364 (May 1, 1966).

Key words: Free volume; structure of $B_2O_3$; two-state model.

New data on the density of $B_2O_3$ from 25 °C to 320 °C are given. A two-state equation of state for the volume is presented which fits the volume data from 350 °C to 1400 °C. A specific structure for the two states is suggested and shown to be consistent with Raman data. Below 350 °C and at high pressures the data indicated that the two-state expressions for free volume still hold but the volume of the close-packed structure becomes temperature and pressure dependent.

The viscosity of $B_2O_3$ from the glass transition up to 1400 °C and at high pressure is consistent with the equation of state and the Hybrid equation of Macedo and Litovitz. The viscosity values above 1400 °C indicate a break-up of the two-state structures and the beginning of multi-state behavior which results in a temperature dependent activation energy. The onset of this effect causes the "apparent" activation energy to increase above 1400 °C.

**9915.** Madden, R. P., Codling, K., **Autoionization spectra of the noble gases,** (Proc. Symp. Atomic Interactions and Space Physics, Goddard Space Flight Center, Greenbelt, Md., Aug. 10-11, 1966), Chapter in *Autoionization Astrophysical Theoretical and Laboratory Experimental Aspects,* pp. 129-151 (Mono Book Corp., Baltimore, Md., 1966).

Key words: Autoionization; far ultraviolet absorption spectra; He through Xe; one and two electron excitation; resonance profiles; synchrotron light source; 20-180 eV.

The absorption spectra of the noble gases He through Xe have been studied extensively in the region 20-180 eV (600-70 Å), utilizing as a background source the pure continuum radiated by the orbiting electrons in the NBS 180 MeV electron synchrotron. Discrete structures, or resonances, have been observed in the photoionization continua of each of these gases. These resonances are due to the existence of autoionizing states of the neutral atoms lying at energies, in general, well above their first ionization limits. The structures have been classified into two types of transitions; on the one hand, one-electron excitation involving either an outer-shell, sub-shell or inner-shell electron, on the other, involving the excitation of any two electrons simultaneously, such that the energy required was appropriate for the present region of observation.

**9916.** Madey, T. E., Yates, J. T., Jr., **Kinetics of desorption of the beta-nitrogen states chemisorbed on tungsten,** *J. Chem. Phys.* **44,** No. 4, 1675-1684 (Feb. 15, 1966).

Key words: Adsorption; binding states; chemisorption; desorption; kinetics; nitrogen; tungsten.

The kinetics of desorption of the strongly chemisorbed $\beta_1$ and $\beta_2$ nitrogen states on tungsten have been studied. Independent techniques of isotopic mixing and flash-filament desorption have been employed. The rate of production of $^{14}N^{15}N(g)$ from $^{14}N_2(g)$ and $^{15}N_2(g)$ in a steady state flow experiment is completely accounted for by the kinetically determined rate of desorption from the chemisorbed layer. $\beta_1$-nitrogen appears to desorb by first order kinetics. $\beta_2$-nitrogen desorbs in a complex manner with higher order kinetics. The apparent $\beta_2$ desorption order decreases markedly as temperature increases. A superposition of two or more unresolved substates in the $\beta_2$ state is postulated. The temperature variation of desorption order can be accounted for by a lack of achievement of equilibrium between the spatially-separate $\beta_2$ substates during desorption at scan rates of 12.5 °K/sec or greater.

Above 1500 °K, where the steady state coverage of nitrogen is very low, a sticking coefficient of less than 0.02 has been measured. The sticking coefficient is nearly constant in the range 1500-1700 °K and over a 25-fold pressure range.

**9917.** Mahler, R. J., **Angular dependence of the one-phonon-nuclear quadrupole interactions,** *J. Phys. Chem. Solids* **27,** 871-879 (1966).

Key words: Angular dependence; phonon-nuclear quadrupole interaction.

The angular dependence of the $\Delta m = \pm 1$ and $\Delta m = \pm 2$ nuclear quadrupole interactions is developed in a crystal with $T_d$ symmetry assuming a lattice potential $V = f(r)$ and that the phonons have a definite wave number and polarization. The results can be used to explain experiments involving the interaction of a nuclear spin system with externally added phonons.

**9918.** Mahler, R. J., Daniel, A. C., Parrish, P. T., **Observation of two intrinsic nuclear relaxation rates in antiferromagnetic $KMnF_3$,** *Phys. Rev. Letters* **19,** No. 2, 85-87 (July 10, 1967).

Key words: Antiferromagnetism; magnon-Raman process; nuclear magnetic resonance; relaxation time; spin echo technique; temperature dependence.

$F^{19}$ nuclear spin-lattice relaxation ($T_1$) measurements are reported in two samples of $KMnF_3$ over the temperature range 1.35 °K to 22 °K and with zero external magnetic field. The high temperature relaxation rate ($1/T_1$) exhibits a $T^7$ temperature dependence in one sample and a $T^5$ in the other. At the low temperatures both samples are characterized by an approximate $\exp(\alpha/T)$ dependence.

**9919.** Maki, A. G., **Measurement of the direct $\iota$-doublet transitions in carbonyl sulfide,** *J. Mol. Spectry.* **23,** No. 1, 110-111 (May 1967).

Key words: Carbonyl sulfide; energy levels; $\iota$-doublet transitions; microwave spectra; molecular structure; OCS; spectra; spectroscopy.

Microwave measurements are given for the $\Delta J = 0$, $\iota$-doublet transitions in $^{16}O^{12}C^{32}S$. Accurate values of the $\iota$-doubling constants are given and compared with previous, less accurate values.

**9920.** Maki, A. G., Forneris, R., **Infrared and Raman spectra of some trihalide ions: $ICl_2^-$, $IBr_2^-$, $I_3^-$, $I_2Br^-$, and $BrCl^-$,** *Spectrochim. Acta* **23A,** 867-880 (1967).

Key words: Force constants; infrared spectrum; Raman spectrum; trihalide ions.

The Raman spectrum and infrared absorption spectrum have been studied for a number of trihalide compounds. All three fundamental vibrations were located for each trihalide ion and the force constants are given. Differences in the spectra as the cation is changed are attributed to differences in the anion structures and/or differences in the crystal lattice which result in differing selection rules and force constants. The force constants are interpreted as indicating that the bottom of the potential well for the central atom of the trihalide ions is unusually flat. In agreement with previous observations the stretching force constants were found to have a value about half that of the corresponding halogen or interhalogen molecules.

**9921.** Mandel, J., Lashof, T. W., **Processing of numerical test data,** Chapter 2 in *Testing of Polymers,* J. V. Schmitz, ed., **2,** 33-82 (Interscience Publ., New York, N.Y., 1966).

Key words: Data processing; design of experiments; performance tests; polymers, analysis of test data in statistical analysis; test data, analysis; test methods, comparison of; homogeneity, tests of.

After a general introduction in which basic statistical concepts are discussed, the chapter proceeds with a brief treatment of statistical methods of experiment design for performance tests, for tests of homogeneity of materials, and for interlaboratory studies of test methods. Statistical methods of data analysis are also discussed. The chapter ends with a section on the presentation of data and a bibliography.

**9922.** Mandel, J., Kanagy, J. R., **Sampling of leather for physical and chemical examination,** Chapter 50 in *The Chemistry and Technology of Leather* **4,** 223-242 (Reinhold Publ. Corp., New York, N.Y., 1965).

Key words: Acceptance sampling; letter; quality control; sampling; statistics; test variability.

A presentation of some general principles of sampling, with application to the sampling of leather.

The topics discussed in this chapter include: (1) General statistical principles of sampling: effect of sample size and of lot size; (2) Formulas for the determination of sample size; (3) The selection of a sampling location on a leather side; (4) Tables of the variability of physical and chemical tests between locations and between hides; (5) Acceptance sampling; and (6) A survey of the literature.

**9923.** Mangum, B. W., Colwell, J. H., **Low-temperature heat capacity of $NdCl_3$ and $PrCl_3$,** *J. Appl. Phys.* **38,** No. 3, 1468-1469 (Mar. 1, 1967).

Key words: Heat capacity; magnetic entropy; magnetic susceptibility; $NdCl_3$ (neodymium trichloride); $PrCl_3$ (praeseodymium trichloride); temperature measurement.

Heat capacities of $PrCl_3$ and $NdCl_3$ have been measured between 0.3 °K and 4 °K. The dominant feature of the heat capacity curves is a broad anomaly indicating a region of extensive short-range magnetic ordering. The anomaly in $NdCl_3$ has a maximum at 0.47 °K and fits closely that of a linear Ising chain model. In addition, two small peaks appear at the same temperatures as the sharp spikes found in the magnetic susceptibility. $PrCl_3$ has a sharp peak in the heat capacity at 0.4 °K which is presumably associated with long-range ordering. The broad anomaly in $PrCl_3$ has a maximum at 0.8 °K. The magnetic entropy change for the temperature region of the measurements is approximately 80% of R $\log_e 2$ for both salts.

**9924.** Mangum, B. W., Hudson, R. P. **Spin-lattice relaxation in some rare-earth trichlorides,** *J. Chem. Phys.* **44,** No. 2, 704-713 (Jan. 15, 1966).

Key words: $Ce^{3+}$, $Nd^{3+}$, $Sm^{3+}$, $Ho^{3+}$, and $Er^{3+}$; electron-lattice interaction; $LaCl_3$; pulsed microwave; rare-earth; relaxation; spin-lattice; trichlorides.

Studies of *spin-lattice relaxation* of the ions $Ce^{3+}$, $Nd^{3+}$, $Sm^{3+}$, $Ho^{3+}$, and $Er^{3+}$ present in low concentrations (0.2 to 2 percent) in the host lattice of $LaCl_3$ have been made in the liquid helium region by the pulsed-microwave method. The variation of the relaxation time, $\tau$, with temperature permits separation of the contributions to the relaxation from the two-phonon (resonant and non-resonant) and single phonon processes.

The substances studied are not "well-behaved;" features such as non-exponential decays and variability of the derived values for the splitting between the ground and first excited levels are discussed. Some of the ions exhibit a significant variation of $\tau$ with concentration and $Nd^{3+}$ shows an interestingly large anisotropy of $\tau$ in the Raman process.

**9925.** Mann, D. B., Ludtke, P. R., Sindt, C. F., Chelton, D. B., **Liquid-solid mixtures of hydrogen near the triple points,** (Proc. 1965 Cryogenic Engineering Conf., Rice University, Houston, Texas, Aug. 23-25, 1965), Chapter in *Advances in Cryogenic Engineering* **11,** 207-217 (Plenum Press, Inc., New York, N.Y., 1966).

Key words: Cryogenic; crystallization; freezing; growth; hydrogen; liquid-solid phase; melting; nucleation; particle size; production; rate.

Properties and characteristics of liquid-solid mixtures of hydrogen are discussed, including production methods, solid particle size distribution, aging effects, and terminal velocities of the solid particles in the liquid melts. The equipment and techniques for observation and measurements are described.

The equipment developed and the results described are part of an effort to determine techniques and parameters pertinent to the study of production, storage and pipe line transport of this upgraded fuel.

**9926.** Mann, D. B., Sindt, C. F., Ludtke, P. R., Chelton, D. B., **Slush hydrogen characteristics,** *Proc. Conf. Long-Term Cryo-Propellant Storage in Space, National Aeronautics and Space Administration, Huntsville, Ala., Oct. 12-13, 1966.*

Key words: Cryogenic; fluid transport; freezing; hydrogen-liquid solid; production.

The utilization of slush hydrogen as an upgraded fuel is dependent upon knowledge of its physical and transport properties and characteristics. A NASA-sponsored program designed to acquire this information is in progress.

Experimental measurements of solid particle size distribution, aging effects and terminal velocities of the solid particles in the liquid melt have been completed. Transport characteristics have been predicted using these measured parameters. These predictions are currently being submitted to experimental verification.

Two 100 gallon dewars connected by 75 feet of vacuum-insulated transfer line comprise the experimental flow loop. Pressure sensing transducers and visual observation through glass ports allow acquisition of transport data over a broad range of flow rates.

Handling and investigative techniques such as dewar-to-dewar transfer, straining of the solids through wire mesh screen, and vertical temperature profiles of the settled mixture are presented in the context of a continuing experimental and analytical research program.

**9927.** Mann, D. E., Calder, G. V., Seshadri, K. S., White, D., Linevsky, M. J., **Geometry and vibrational spectra of the alkaline-earth dihalides. I. $MgF_2$,** *J. Chem. Phys.* **46,** No. 3, 1138-1143 (Feb. 1967).

Key words: Assignment; frequency; geometry; infrared; matrix; MgF, $Mg^{24}F_2$, $Mg^{26}F_2$.

The infrared spectra of vaporized $MgF_2$ isolated at liquid hydrogen temperatures in both argon and krypton matrices are reported. Six major regions of absorption have been found vis. 240, 450, 477, 483, 740 and 840 cm$^{-1}$. On the basis of corresponding matrix spectra of $Mg^nF_2$, $Mg^{26}F_2$ and a 1:1 mixture of $Mg^nF_2 - Mg^{26}F_2$, it is possible to demonstrate unequivocally that the 240, 477, 740 and 840 cm$^{-1}$ absorptions are due to molecular species containing one magnesium atom. The 450 and 483 cm$^{-1}$ features are clearly attributable to polymeric species. From the magnitude of the measured isotope shifts the 740 cm$^{-1}$ and 477, 240 and 840 cm$^{-1}$ absorptions have been assigned to MgF and $\nu_1$, $\nu_2$, $\nu_3$ of $MgF_2$ respectively. The observation of $\nu_1$ shows that $MgF_2$ is bent. The higher resolution and precise frequency measurement employed in this work have been used to calculate the apex angle. This lies in the range 145 to 160° the most probable value being 150°.

**9928.** Manning, J. R., **Diffusion and the Kirkendall shift in binary alloys,** *Acta Met.* **15,** 817-826 (May 1967).

Key words: Binary alloys; diffusion; diffusion coefficients; Kirkendall shift; thermodynamic equations for diffusion; vacancies.

In alloys, the directions of successive vacancy jumps are correlated to one another. This tends to reduce the net vacancy flux in a Kirkendall shift experiment. The magnitude of the vacancy flux, including correlation effects, is calculated assuming that vacancies are not bound to any particular atoms and that fluctuations in average local composition can be ignored. New equations for the intrinsic diffusion coefficients, Kirkendall shift, and interdiffusion coefficient in binary alloys are obtained. The Kirkendall shift and interdiffusion coefficient given by these equations are larger than those predicted by Darken, but smaller than those obtained when vacancy correlations are neglected. The appearance of cross terms and additional diagonal terms in the general thermodynamic equations is discussed.

**9929.** Margoshes, M., **Recent advances in excitation of atomic spectra,** *Proc. XII Intern. Spectroscopy Colloquium, Exeter, England,* pp. 26-42 (Hilger and Watts, London, England, 1965).

Key words: Atomic properties; atomic spectra; chemical analysis; chemiluminescent and fuel-rich flames; controlled atmospheres; plasma jet.

Some recent developments are reviewed in methods of exciting atomic spectra for chemical analysis and the measurement of atomic properties. Among the subjects included are the plasma jet, arc and spark discharges in controlled atmospheres, chemiluminescent and fuel-rich flames, and wall-stabilized arcs. The present knowledge of the characteristics of excitation sources is briefly considered, and a summary is given of calculations of detection limits by flame photometry and atomic absorption spectrometry.

**9930.** Marshak, H., Richardson, A. C. B., Tamura, T., **Total cross section for 14-MeV neutrons using aligned $^{165}$Ho nuclei,** *Phys. Rev. Letters* **16,** No. 5, 194-197 (Jan. 31, 1966).

Key words: Deformed nucleus; $^{165}$Ho; neutron cross section; nuclear orientation.

The effect of nuclear deformation on the total cross section of $^{165}$Ho has been measured using 14-MeV neutrons and an aligned target. The aligned $^{165}$Ho target was obtained by cooling a metal single crystal to 0.33 °K using the NBS $^3$He refrigerator. A finely collimated beam of 14-MeV neutrons was obtained by careful collimation of the alpha particle produced in the reaction $^3H(d,T)^4He$ and by detecting it in coincidence with its associated neutron. The NBS 2 MV Van de Graaff was used to provide a 1 $\mu$Å, 300 keV deuteron beam. The results were successfully explained using an adiabatic coupled-channel calculation and the Optical Model potential. The data do not agree with the predictions of the Black Nucleus Model as we would expect since the wave length of a 14-MeV neutron is only equal to the radius of the holmium nucleus.

**9931.** Marton, L., **Correction of spherical aberration of axially symmetrical magnetic lenses,** *Rev. Sci. Instr.* **38,** No. 1, 130-131 (Jan. 1967).

Key words Diamagnetic corrective element; electron lens; spherical aberration.

It is pointed out that in a magnetic lens of rotational symmetry, correction of the spherical aberration is possible by abandoning paraxial image formation and introducing a diamagnetic corrective element on the axis.

**9932.** Marton, L., **Progress in electron physics during the last 20 years,** *Proc. Third Czechoslovak Conf. Electronics and Vacuum Physics, Prague, Czechoslovakia, Sept. 23, 1965,* pp. 17-25 (Czechoslovak Academy of Sciences, Prague, Czechoslovakia, 1967).

Key words: Electron physics; history.

Review of progress in electron physics with a short introduction covering pre-war period. Emphasis is laid on the developments of the post-war years with the conclusion that although the greatest accomplishments of electron physics were in the pre-war years, the last 20 years have seen very notable progress in the understanding of the nature and of the interactions of the electron.

**9933.** Maryott, A. A., Kryder, S. J., **Microwave line shape and the inversion spectrum of $ND_3$ and $ND_3$-argon mixtures,** *J. Chem. Phys.* **46,** No. 7, 2856-2857 (Apr. 1967).

Key words: Argon mixtures; inversion spectrum; line shape; microwave absorption; $ND_3$; pressure broadening.

The microwave loss index associated with the inversion spectrum of $ND_3$ has been measured at 1600 MHz for pure $ND_3$ over the pressure range 0.02 to 3 atmos. and for dilute mixtures of $ND_3$ in argon up to 25 atmos. These results confirm in detail Ben-Reuven's line shape relation.

**9934.** Marzetta, L. A., **Simple contact type temperature controller,** *Rev. Sci. Instr.* **37,** No. 6, 789 (June 1966).

Key words: Mercury-toluene thermometer; temperature controller.

A simple, low cost temperature controller is described. The circuit has two independent current paths: one provides an On-Off control current, and the other a preselected current for the background heat. With the stated components, 250 watts of heater power can be controlled. For applications such as laboratory liquid baths, 1/1000 °C stability is possible.

**9935.** Mather, J., **Invariance of the homology of a lattice,** *Proc. Am. Math. Soc.* **17,** No. 5, 1120-1124 (Oct. 1966).

Key words: Combinatorics; homology; lattice.

Rota, Kan, Peterson, and Whitehead have developed a homology theory for finite lattices which *a priori* depends upon the choice of a cross-cut of the lattice. It is shown here that the different cross-cuts of a lattice lead to simplicial complexes which have the same homotopy type and are therefore homology equivalent.

**9936.** Melmed, A. J., Klein, R., **Field-ion microscopy of ruthenium at 77 °K,** *J. Less-Common Metals* **10,** 225-228 (1966).

Key words: Atomic resolution; electropolishing of ruthenium; field evaporation; field-ion microscopy; heat of sublimation; ruthenium; surface structure.

Ruthenium, recently available in wire form, has been used to obtain a field-ion micrograph. A pattern with good image stability using helium as the imaging gas, has been obtained with the tip at 77 °K. From this, the most recent value of 6.79 eV for the heat of sublimation of ruthenium, rather than the previously used value of 5.52 eV is supported as being correct.

**9937.** Mendlowitz, H., **Calculated line strengths for the transition array for $d^2s$-$d^2p$: Application to Ni II,** *Astrophys. J.* **143,** No. 2, 573-590 (Feb. 1966).

Key words: $d^2s+d^2p$; intermediate coupling; *LS* coupling; Ni II; relative line strengths.

Transition arrays for the square root of the strengths of the transitions relative to a radial integral parameter are presented for $d^2s \rightarrow d^2p$ ($d^8s \rightarrow d^8p$) in *LS* coupling. The relative strengths in Ni II for the transitions between the configurations $3d^84s \rightarrow 3d^84p$ are calculated in intermediate coupling and are compared with earlier calculations by Gruzdev (1962) and with experiments of Bell, Paquette, and Wise (1965).

**9938.** Meshkov, S., **$SU_3$ reaction predictions and symmetry breaking,** Elementary Particles Conf., Institute for Theoretical Physics, University of Colorado, Summer 1964, *Lectures Theoret. Phys.* **VII B,** 36-50 (1965).

Key words: Octet symmetry breaking; Q plots; reaction cross section; strong interactions; sum rules; superresonance; U-spin equalities.

An information and useful way to examine the role of unitary symmetry in strong interactions is to consider the predictions that can be made about reaction cross sections and to correlate them with experiment. When compared at the same Q value, the sum rules seem to fit the data without symmetry breaking. However, we find that predictions of pure $SU_3$ invariance are badly violated for "U-spin equalities." The inclusion of octet symmetry breaking is sufficient to explain this violation. In addition, the Q plots of the reactions involved suggest the possibility of super-resonances.

**9939.** Meshkov, S., Yodh, G. B., **SU(3) reaction inequalities at high energies,** *Phys. Rev. Letters* **18,** No. 12, 474-481 (Mar. 1967).

Key words: High energy differences; Q-plot inequalities; SU(3) reactions.

SU(3) reaction inequalities which had been thought to be violated are re-examined and found to agree with experiment at high energy. The comparison is made for both integrated and forward amplitudes. The apparent validity of SU(3) puts limits on the high energy behavior of the amplitude differences $|M(K^-p \rightarrow K^-p) - M(\pi^-p \rightarrow \pi^-p)|$ and $|M(K^+p \rightarrow K^+p) - M(\pi^+p \rightarrow \pi^+p)|$.

**9940.** Mielenz, K. D., **On the diffraction profiles of spectrograph slits of finite width,** *Optik* **25,** No. 3, 138-139 (May 17, 1967).

Key words: Diffraction; partial coherence; spectrograph slit.

In an earlier paper, the author presented a measured curve of line intensity vs. slit width, for the case of partially coherent spectrograph slit illumination. The result of a theroretical calculation is now presented which supports the experimental curve.

**9941.** Mielenz, K. D., **Spectroscope slit images in partially coherent light,** *J. Opt. Soc. Am.* **57,** No. 1, 66-74 (Jan. 1967).

Key words: Diffraction; luminosity; optimal performance; partial coherence slit illumination; resolution; spectroscopic slit.

The apparatus function of prism or grating spectroscopes with finite slits is derived for the general case of partially coherent illumination of the slit. Numerical results are presented for the border cases of coherent and incoherent slit illumination, as well as for full and partial illumination of the spectroscope aperture.

The dependence of line intensity and line width on slit width, as well as the optimum slit width, are determined for each of these cases. It is shown that the performance of the spectroscope reaches an optimum when the aperture is at least fully illuminated.

**9942.** Mielenz, K. D., Stephens, R. B., Gillilland, K. E., Nefflen, K. F., **Measurement of absolute wavelength stability of lasers,** *J. Opt. Soc. Am.* **56,** No. 2, 156-162 (Feb. 1966).

Key words: Fringe; interferometer; laser; optical; photoelectric; precision; scanning; stability; standard; wavelength.

A technique was devised to measure the absolute wavelength stability of a gas laser by direct interferometric comparison with a mercury 198 standard lamp. The apparatus used is described; its limits of precision are discussed.

The wavelength fluctuations of a free-running, unstabilized helium-neon laser were measured and found to be of the magnitude (several parts in $10^7$) due to thermal and mechanical instabilities of the laser cavity.

Manual control of the laser was seen to yield a wavelength constancy (a few parts of $10^8$) comparable to the limits of accuracy of interferometric standard sources.

**9943.** Mighell, A. D., Perloff, A., Block, S., **The crystal structure of the high temperature form of barium borate, $BaO \cdot B_2O_3$,** *Acta Cryst.* **20,** Part 6, 819-823 (June 1966).

Key words: $BaO \cdot B_2O_3$; barium borate; borate; crystal; structure; x-ray.

The crystal structure of the high temperature form of $BaO \cdot B_2O_3$ (M.P. = 1095 ± 5 °C) was determined by conventional three-dimensional Patterson and electron-density syntheses. The heavy atom was used to establish the initial phases. $BaO \cdot B_2O_3$ crystallizes in the rhombohedral space group R3c with 18 formula units per hexagonal cell. Unit-cell dimensions, referred to hexagonal axes, are a = b = 7.2351, c = 39.192 Å. Least-squares refinement with 498 independent reflections yielded a reliability index of 5.7%, based on the observed data only. The anion in the structure is nearly planar $(B_3O_6)^{-3}$ group constructed of three $BO_3$-triangles each of which shares two of the three corners. The structure contains two crystallographically distinct barium atoms located in positions having point symmetry 32 and 3. About the barium in the 32 symmetry position the oxygens are arranged in a trigonal prism. About the barium which lies in the 3 symmetry position the oxygen coordination is 9-fold.

**9944.** Miller, C. E., Flynn, T. M., **On the problem of measuring transient temperature in cryogenic fluids,** *ISA Trans.* **6,** No. 2, 133-138 (Apr.-May-June 1967).

Key words: Cryogenic; instrumentation; measurement; metrology; response time; sensor; temperature; thermometer; time constant.

The complex and frequently unpredictable energy exchange mechanisms that govern the dynamic behavior of cryogenic sensors makes the measurement of transient temperatures extremely difficult. Without suitable models by which to predict and evaluate sensor performance, considerable measurement errors can and do occur. The intent of this paper is simply to delineate in detail those factors which give rise to this situation. The validity of using notions based on the performance of the "ideal" thermometer for characterizing the cryogenic case is also discussed.

**9945.** Miller, C. E., Flynn, T. M., Grady, T. K., Waugh, J. S., **Nuclear spin relaxation in liquid hydrogen,** *Physica* **32,** No. 2, 244-251 (Feb. 1966).

> Key words: Cryogenic; liquid hydrogen; nuclear magnetic resonance; nuclear relaxation.

The proton longitudinal relaxation time, $T_1$, has been measured in dilute liquid solutions of *ortho*hydrogen in *para*hydrogen over a range of temperature and compostion.

Below 1.75% orthohydrogen the temperature dependence of $T_1$ observed at higher concentration is reversed. This fact is interpreted in terms of an anisotropic intermolecular force which is of longer range for *ortho-ortho* than for *ortho-para* pairs, in keeping with previous interpretations of $T_1$ in the gaseous state.

**9946.** Miller, C. K. S., Daywitt, W. C., Arthur, M. G., **Noise standards, measurements, and receiver noise definitions,** *Proc. IEEE* **55,** No. 6, 865-875 (June 1967).

> Key words: Error analysis; noise factor; noise source; noise temperature; radiometer.

This paper covers four topics; (1) basic principles of noise measurement, (2) the switching radiometer, (3) a survey of noise sources, and (4) concepts of noise factor and noise temperature. The first section presents basic formulas used in analyzing radiometers. The second discusses the switching radiometer briefly tracing its development and useage in the standards field. The third section surveys the development of hot and cold thermal noise sources, noise diodes, and gas-discharge noise generators. The last section presents and discusses the basic definitions of receiver noise performance.

**9947.** Milligan, D. E., Jacox, M. E., **Matrix isolation study of the infrared and ultraviolet spectra of the free radical CNN,** *J. Chem. Phys.* **44,** No. 8, 2850-2856 (Apr. 15, 1966).

> Key words: Carbon suboxide photolysis; C atom reactions; C atom sources; CNN free radical; cyanogen azide photolysis; force constants; infrared spectrum; matrix isolation; NCN free radical; thermodynamic properties; ultraviolet spectrum.

Features appearing at 393, 1241, and 2847 $cm^{-1}$ after photolysis of matrix-isolated cyanogen azide with 2100-2800 Å radiation are shown to exhibit parallel behavior. Isotopic data are consistent with the assignment of these three features as fundamentals of the free radical CNN, produced by the reaction of carbon atoms with molecular nitrogen. Ultraviolet absorptions at 4189 and 3964 Å can also be assigned to CNN. The force constants and thermodynamic properties of CNN have been derived. The carbon-nitrogen bond is found to have approximately triple bond character, and the nitrogen-nitrogen bond approximately double bond character.

**9948.** Moore, C. E., **A report on the International Conference on Spectroscopy, Bombay, India, Jan. 9-18, 1967,** *Appl. Opt.* **6,** No. 5, 836, 849, 850.

> Key words: Indian Conference on Spectroscopy; International Conference on Spectroscopy; molecular spectroscopy.

The First International Conference on Spectroscopy was held in Bombay, India, January 9-18, 1967. Three International Unions, Astronomy, Physics, and Chemistry, supported the Organizing Committee in arranging for the Conference. Some 200 scientists from 13 countries attended. There were 30 invited papers and more than 100 contributed papers in all. Most of them dealt with molecular spectroscopy, but a few touched on interstellar spectra, solar spectroscopy in the x-ray region and laser spectroscopy.

**9949.** Moore, C. E., **Annual report on spectroscopy,** *Astron J.* **71,** No. 9, 796-797 (Nov. 1966).

> Key words: Atomic spectra; rare-earth spectra; solar spectrum; transition probabilities.

This report is furnished annually to the Astronomical Journal in order to present to astrophysicists the spectroscopic work that they are particularly interested in. It is published with the Observatory Reports and provides a brief summary of activity at the National Bureau of Standards.

**9950.** Moore, C. E., **Future spectroscopy for late-type stars,** Chapter in *Proc. Colloquium on Late-Type Stars, June 13-17, 1966, Trieste, Italy,* Margherita Hack, ed., pp. 15-24 (Observatorio Astronomico di Trieste, Italy).

> Key words: Atomic spectra; molecular spectra; rare-earth spectra; reference data programs; solar spectra; spectra of late-type stars; sun-spot spectra.

The subject is reviewed with the idea of the application of spectroscopy to work on abundances. Two main topics are discussed: the general characteristics of the observed stellar spectra and the available data on laboratory spectra needed to identify the stellar lines. The impact of the developments in space technology has greatly expanded the observed range of stellar spectra. This is handled by regions, the ultraviolet, the visible, and the infrared. More laboratory programs are needed to meet present needs for data on both atomic and molecular spectra. The existing programs are discussed. Encouraging progress on the analyses of selected rare-earth spectra is reported. These promise to be of great astrophysical interest.

**9951.** Moore, C. E., **Transactions of the triple commission for spectroscopy, Subcommittee D,** *J. Opt. Soc. Am.* **55,** No. 6, 745 (1965).

> Key words: Atomic spectra; rare-earth spectra; transition probabilities; triple commission for spectroscopy; ultraviolet atomic spectra.

The present report has been prepared with the idea of emphasizing the astrophysical needs for data on atomic spectra. It is to be given at a meeting of the Triple Commission for Spectroscopy, being held in Copenhagen on August 19, 1965. The meeting is arranged in connection with the 8th European Congress on Molecular Spectroscopy, Aug. 14-20, 1965. The author is one of two members representing the International Astronomical Union on the Triple Commission, which in turn encompasses representatives from the IAU, IUPAP, and IUPAC.

**9952.** Moore-Sitterly, C. E., **Commission on fundamental spectroscopic data,** (Proc. 12th General Assembly of the I.A.U., Hamburg, Germany, Aug. 26, 1964), *Trans. Intern. Astron. Union* **XIIB,** 173-185 (1966).

> Key words: Standard wavelengths; transition probabilities of spectral lines; wavelength standards.

The proceedings of the meeting of Commission 14 are discussed. Current progress in the work on standards of wavelengths and transition probabilities are discussed. Also discussed are the future needs in spectroscopy.

**9953.** Moore-Sitterly, C. E., **Molecules in the sun,** Chapter in *Proc. Symp. Sun Spots Honoring Galileo, Florence, Italy, Sept. 9-12, 1964,* G. Richini, ed., pp. 181-185 (G. Barbera, ed., Florence, Italy, 1966).

Key words: Molecules; spectroscopy; sun-molecules.

Molecules in the sun presented at a symposium, September 9-12, 1964 in Florence, Italy, honoring Galileo.

**9954.** Morgan, A. H., **Distribution of standard frequency and time signals,** *Proc. IEEE* **55,** No. 6, 827-836 (June 1967).

Key words: Portable clocks; satellite timing; standard frequency; standard frequency broadcasts; time signals.

This paper reviews the present methods of distributing standard frequency and time signals (SFTS), which include the use of high frequency, low frequency, and very low frequency radio signals, portable clocks, satellites, and RF cables and lines. The range of accuracies attained with most of these systems are included along with an indication of the sources of error. Information is also included on the accuracy of signals generated by frequency dividers and multipliers.

Details regarding the techniques, the propagation media, and the equipment used in the distribution systems described are not included. Also, the generation of the signals is not discussed.

**9955.** Morris, E. E., Spencer, L. V., **The small-angle limit for twice-scattered rays from a point-isotropic source,** *Nucl. Sci. Eng.* **27,** No. 2, 485-488 (Feb. 1967).

Key words: Angular distribution; gamma radiation; logarithmic divergences; point isotropic; small-angle limit; twice-scattered.

The small-angle limit of the twice-scattered flux from a point-isotropic, monoenergetic source of gamma radiation is calculated. Importance is attached to this limit because of a logarithmic divergence of the angular distribution of the twice-scattered flux. Comments intended to facilitate the application to neutrons are given at the end.

**9956.** Mosburg, E. R., Jr., **Nonlinear diffusion with recombination in an electron beam excited plasma,** *Phys. Fluids* **9,** No. 4, 824-826 (Apr. 1966).

Key words: Collisional-radiative recombination; electron beam; electron density; light density; nonlinear diffusion; plasma; radial distribution; recombination mechanisms.

The radial distributions of electron density and light intensity are calculated from the nonlinear diffusion equations with a recombination term added. Two-body and three-body recombination mechanisms are considered in addition to the intermediate case of collisional-radiative recombination.

**9957.** Mountain, R. D., **A note on thermal expansion coefficients of rare gas solids,** *J. Phys. Chem. Solids* **28,** 1071-1073 (Dec. 29, 1966).

Key words: Corresponding states; lattice vibration spectrum; solid argon; solid krypton; solid xenon; thermal expansion coefficient.

Recent measurements of the thermal expansion coefficient of solid argon, krypton and xenon are shown to violate the law of corresponding states. The failure of the law of corresponding states is related to the different ways the lattice vibration spectra of these crystals change as pressure is applied to the lattice.

**9958.** Mountain, R. D., **Interpretation of Brillouin spectra,** *J. Chem. Phys.* **44,** No. 2, 832-833 (Jan. 15, 1966).

Key words: Brillouin scattering; carbon disulfide-light scattering; intensity of scattered light; light scattering liquids; thermal relaxation density fluctuations in liquids.

When a fluid consists of molecules having internal degrees of freedom weakly coupled to the translational degrees of freedom of the fluid (phonons), it is not correct to refer to the phonons as isotropic fluctuations in the density. This is relevant to the interpretation of Brillouin scattered light in terms of the properties of the scattering fluid. law of corresponding states. An approximate expression for the ratio of the intensity of the unshifted component to that of the Brillouin components is presented and applied to $CS_2$.

**9959.** Mountain, R. D., **Spectral distribution of scattered light in a simple fluid,** *Rev. Mod. Phys.* **38,** No. 1, 205-214 (Jan. 1966).

Key words: Brillouin scattering; carbon dioxide-light scattering; critical point; density fluctuations in fluids; Landau-Placzek intensity ratio; negative dispersion; non-local hydrodynamics; thermal diffusivity.

The spectral distribution of light scattered by density fluctuations in a dense, monoatomic, one-component fluid is calculated from the time dependence of the density fluctuations predicted by the linearized, hydrodynamic equations of irreversible thermodynamics.

The results of Landau and Placzek are verified and a procedure for deriving correction terms is discussed with the dispersion in the velocity of thermal sound waves obtained as an illustration. Particular attention is paid to the critical region. The properties of carbon dioxide are used to estimate the spectral distribution of critical opalescence. A comparison is made between light-scattering and sound-propagation experiments. Space dispersion near the cirtical point in the pressure and thermal conductivity is examined briefly. Finally, some of the experimental problems involved in measuring the spectral distribution of the scattered light are discussed.

**9960.** Mountain, R. D., Zwanzig, R., **Shear relaxation times of simple fluids,** *J. Chem. Phys.* **44,** No. 7, 277-279 (Apr. 1966).

Key words: Argon; bulk viscosity; shear relaxation time; shear viscosity; simple fluid; time correlation function.

This article presents a calculation of shear relaxation times of monatomic fluids covering both the liquid and dense gas phases. The times, which are not experimentally accessible at present, are calculated using low frequency viscosity data and theoretical estimates of the high frequency elastic moduli which were produced earlier by the authors. Numerical values of the relaxation times at various temperatures and densities are presented graphically. Except at very low densities, the times are on the order of $10^{-13}$ sec.

**9961.** Myers, V., **Scattering of cold neutrons in ammonium carbonate, ammonium citrate, and ammonium acetate,** *J. Chem. Phys.* **46,** No. 10, 4034-4035 (May 1967).

Key words: Ammonium compounds; cold neutron scattering; torsional and translational vibrations.

Neutron energy gain spectra have been measured in $(NH_4)_2CO_3$, $(NH_4)_2HC_6H_5O_7$, and $NH_4C_2H_3O_2$ at 20 °C using the Brookhaven slow chopper facility. Each spectrum exhibits two peaks that are characteristic of optical modes. The spectra of ammonium carbonate and ammonium citrate are similar to those of the body centered cubic lattice phase of the ammonium halides in which the ammonium ion has torsional and translational optical vibrations.

**9962.** Nahman, N. S., **The measurement of baseband pulse risetimes of less than $10^{-9}$ seconds,** *Proc. IEEE* **55,** No. 6, 855-864 (June 1967).

Key words: Baseband pulse rise-times; basic instrumentation system; fractional nanosecond pulse rise-times; oscillographic systems; pulse comparison techniques; pulse rise-times.

This is a review paper dealing with the measurement of fractional nanosecond pulse rise time in which the following subjects are discussed: oscillographic systems, pulse comparison techniques, a basic instrumentation system, and the distortion of pulses by transmission lines. Extensive references are provided. Included in the discussion is a delineation of equivalent time oscillographic sampling systems and a classification into three sampling categories: sequential, random, and multiple. Also considered are single transient oscillographic systems employing either traveling wave deflection structure cathode ray tubes or multiple sampling methods. In order to clearly present the rise time limitations caused by TEM transmission lines, attention is given to the distortion incurred by pulses upon passing through such lines. Some suggestions and predictions relating to future work are presented.

**9963.** Newton, C. J., Ruff, A. W., **X-ray diffraction measurement of stacking faults in alpha silver-tin alloys,** *J. Appl. Phys.* **37,** No. 10, 3860-3868 (Sept. 1966).

Key words: Dislocations; electron microscopy; silver-tin alloys; stacking faults; x-ray diffraction.

Stacking fault probabilities and dislocation densities were studied by means of x-ray diffraction and transmission electron microscopy in both filed and compressed bulk specimens from a series of dilute silver alloys. In the filed samples the observed stacking fault probabilities increased smoothly from $3 \times 10^{-3}$ for pure silver to $66 \times 10^{-3}$ for 10.3 at.% tin. The compressed bulk specimens led to values of $6 \times 10^{-3}$ and $95 \times 10^{-3}$ respectively. Direct determinations of the dislocation densities were made in the bulk specimens (1 to $5 \times 10^{11}$ cm$^{-2}$) leading to computed values for the stacking fault energy in the range 2 to 6 ergs/cm$^{-2}$, with a slight dip for pure silver. Values for the dislocation density in the filed samples were also calculated. The effect of directed residual stresses measured on the bulk specimens was shown to be negligible with respect to the low angle diffraction line shifts attributed to faulting.

**9964.** Nimeroff, I., **Comparison of uncertainty ellipses calculated from two spectrophotometric colorimetry methods by an automatic-computer program,** *J. Opt. Soc. Am.* **56,** No. 2, 230-237 (Feb. 1966).

Key words: Automatic-computer program; colorimetry; computer program; ellipses; photometric colorimetry; spectrometric colorimetry.

The parameters and equations for calculating uncertainty of chromaticity coordinates in spectrophotometric tristimulus colorimetry have already been derived for the 10°-field standard-observer system. From the variability data for eleven optical filters obtained from two methods of spectrophotometric tristimulus colorimetry, standard-observer-system method and actual-observer method, two sets of chromaticity uncertainty ellipses are derived and intercompared. The similarity between corresponding ellipses of these two sets of ellipses leads to the conclusion that the system-derived uncertainty ellipses, based on the variances and covariances of the spectral tristimulus values of the large-field standard-observer system, can be used to estimate observer-derived chromaticity-uncertainty ellipses.

The equations which are the basis of the automatic-computer program and with which to compute uncertainty ellipses are given to aid anyone who wishes to arrange such a program in his laboratory. The fixed combinations of the spectral tristimulus values and of their variances and covariances can be readily prepared by researchers who may wish to use desk calculators to compute uncertainty ellipses for actual-observer data or for standard-observer data, respectively.

**9965.** Nimeroff, I., **The variability of color measurement,** *Color Eng.* **5,** No. 2, 24-29 (Mar.-Apr. 1966).

Key words: Colorimetry; propagation of errors; uncertainty in chromaticity coordinates; uncertainty in spectral tristimulus values; uncertainty in spectrophotometric data; uncertainty in spectroradiometric data; uniform chromaticity spacing; variability.

Because all the components in the equations for computing chromaticity coordinates in spectrophotometric colorimetry are measured, these components are subject to measurement uncertainty. The problem of determining the chromaticity uncertainty can be treated most simply by the application of the theory of propagation of errors in a computed result. The ellipse is chosen as the most convenient closed plane curve by which to represent the area of uncertainty in the chromaticity diagram with which the true chromaticity point can be expected to lie a specified fraction of the time. The theory has been applied to determining chromaticity uncertainty resulting separately from uncertainties in spectral irradiance of a source, spectral emittance of objects and spectral response of normal human observers. In actual practice the effects of these uncertainties should be computed coincidently. On the basis of experience it is suggested that a complete standard observer system, consisting of means, variances, and covariances of the spectral tristimulus values, in xyz and uvw coordinates, be recommended by Commission Internationale de l'Eclairage (CIE) for use in color measurement.

**9966.** Ninham, B. W., Powell, C. J., Swanson, N., **Plasmon damping metals,** *Phys. Rev.* **145,** No. 1, 209-217 (May 6, 1966).

Key words: Aluminum; characteristic electron energy loss half-width; corrected theory; metals; plasmon damping.

A report is given of a theoretical and experimental investigation into the degree of plasmon damping in metals as a function of momentum transfer. A previous theoretical result by DuBois is corrected and extended by taking into account polarization effects. Measurements are reported of the change in half-width $\Delta E_{1/2}$ of the dispersed $\approx$ 15 eV aluminum plasmon energy loss peak, excited by 20 keV electrons, as a function of electron scattering angle $\theta$. The results can be expressed in the form $\Delta E_{1/2} = A + B\,\theta^2 + C\theta^4$, and there is good agreement between the values of B and C obtained from the revised theory and those found experimentally.

**9967.** Nossal, R. J., **Validity of the convolution approximation for the Van Hove G(r,t) function,** *Phys. Rev.* **143,** No. 1, 74-77 (Mar. 4, 1966).

Key words: Convolution approximation; Van Hove G(r,t).

The validity of the convolution approximation is examined by expanding the spatial Fourier transform of both the true and approximate G(r,t) in powers of the density. By comparing the expansions it is seen that, for small and intermediate k values, terms which are retained in the approximation are comparable to terms which are neglected. Also, since for large k an ideal gas calculation of G(r,t) is sufficient, it is concluded that there is no value of k for which an unmodified convolution approximation can be meaningfully applied.

**9968.** Nossal, R. J., Zwanzig, R., **Approximate eigenvalues of the Liouville operator in classical variables,** *Phys. Rev.* **157,** No. 1, 120-126 (May 5, 1967).

Key words: Eigenfunctions; hydrodynamic variables; irreversible processes; Liouville operator; many-body systems.

A variational solution of the Liouville Equation is used to obtain collective coordinates for simple classical fluids. Comparison is made with macroscopic analogs determined from relevant hydrodynamic equations. Approximate eigenfunctions of the Liouville operator, when constructed from linear combinations of the spatial fourier transforms (fluctuations) of the mass, momentum, and energy density operators for the fluid, are found appropriate to low frequency disturbances. When time derivatives of fluctuations are included among trial functions the variational procedure provides fluid state counterparts of usual solid state phonons.

9969. Ohashi, M., Paffenbarger, G. C., **Melting, flow and thermal expansion characteristics of some dental and commercial waxes,** *J. Am. Dental Assoc.* **72,** No. 5, 1141-1150 (May 1966).

Key words: Flow; melting; thermal expansion; waxes.

The literature on pertinent properties of waxes that may be suitable in dental impression materials is meager. To provide more data, the melting point and range (ASTM D 87-57), some flow characteristics (ADA Specification No. 4), and the linear thermal expansion (ADA Specification No. 4) were determined on 66 dental and commercial waxes. Instead of plotting the time-temperature curve the more sensitive temperature-rate cooling curve was employed. These curves were useful in identifying waxes and variations among lots or batches. The arrests in the curves were as high as 141 °C and as low as 41 °C. Supercooling was observed in six instances. The flow of wax cylinders (6 mm high) under a 2,000-gram load at 30, 37, 40, and 45 °C had a variable relationship with melting points. The coefficients of linear thermal expansion ranged from $1{,}000 \times 10^{-6}/°C$ (25-30 °C) to as low as $110 \times 10^{-6}/°C$ (25-30 °C).

9970. Ohashi, M., Woelfel, J. B., Paffenbarger, G. C., **Pressures exerted on complete dentures during swallowing,** *J. Am. Dental Assoc.* **73,** No. 3, 625-630 (Sept. 1966).

Key words: Brinell indentation used to measure force; clinical; measuring area dentures; swallowing pressure on dentures; variation in pressure.

The projected areas of the tissue-bearing surfaces of dentures were determined by making tracings on tared pieces of cellulose acetate sheets. The upper dentures of 21 patients had projected areas ranging from 22.8 to 36.6 $cm^2$ (3.5 to 5.7 $in^2$), the lower dentures from 14.5 to 24.4 $cm^2$ (2.2 to 3.8 $in^2$). The areas of the upper dentures were from 1.2 to 1.9 times the area of the lower dentures. The forces exerted on complete dentures during swallowing were measured by a Brinell indentation method employed in a modified "Coble Intra-Oral Balancer." Forces ranged on the average from 1.5 to 15.8 kg (3.3 to 34.8 lb). The pressure on the upper dentures ranged on the average from 0.06 to 0.56 $kg/cm^2$ (0.85 to 8.0 $lb/in^2$; for the lower dentures, 0.09 to 0.80 $kg/cm^2$ (1.3 to 11.4 $lb/in^2$).

9971. Okabe, H., **Photochemical studies by means of a field ion mass spectrometer,** *Z. Naturforsch.* **21a,** 135 (1966).

Key words: Field low mass spectrometry; hydrazine; photodissociation; propene; 1-butene.

A mass spectrometric investigation was carried out on the direct photolyses of propene, 1-butene, and hydrazine at 1849 Å with a field ion source in a flow system. Comparisons were made with Pt tip and wire emitters. It was found that, without illumination, mass spectra obtained with the wire were accompanied by a number of fragment peaks amounting to almost 1 percent. Since these peaks interfere with those produced photochemically, the tip emitter was used mostly for the photochemical studies although it gave 100 times less current and was less stable. The photochemical products formed at a gas pressure of 10 $\mu$ by a low-pressure mercury lamp were detected after approximately 10 m sec. The three main peaks observed in the propene photolysis were at masses 27, 28, and 56, indicating the processes:

$$C_3H_6 + hv \rightarrow C_2H_3 + CH_3,\ C_3H_6 + hv \rightarrow C_2H_4 + CH_2,\ CH_2 + C_3H_6 + C_4H_8.$$

The photolysis of 1-butene gave four main peaks at masses 40, 41, 42, and 70, suggesting steps, $C_4H_8 + hv \rightarrow C_3H_4 + (H + CH_3)$ or $CH_4$, $C_4H_8 + hv \rightarrow C_3H_5 + CH_3$, $C_4H_8 + hv \rightarrow C_3H_6 + CH_2$, $CH_2 + C_4H_8 \rightarrow C_5H_{10}$.

The only peak found with the photolysis of hydrazine was at mass 17, indicating the step, $N_2H_4 + hv \rightarrow NH_3 + NH$.

The possibility of forming these products by secondary processes is discussed.

9972. Ondrejka, A. R., **Peak pulse voltage measurement (baseband pulses),** *Proc.* IEEE **55,** No. 6, 882-885 (June 1967).

Key words: Oscilloscope; peak voltage; pulse; sampling; slideback; standard.

Several methods are presently being used for the measurement of pulse voltage. Oscilloscopes are particularly useful because they provide information concerning the shape of the pulse, besides a measure of the peak voltage. Besides the oscilloscope, several peak voltmeter circuits are mentioned. These include pulse stretching, sampling, and the slideback method. A standard pulse generator is described which provides a calibrated pulse voltage suitable for voltmeter calibration and other uses.

9973. Ormsby, W. C., Bolz, L. A., **Microtexture and composition of reaction products in the system kaolin-lime-water,** *J. Am. Ceram. Soc.* **49,** No. 7, 364-365 (July 1966).

Key words: Calcium silicate hydrates; composition; electron diffraction; electron microscopy; kaolin-lime-water; micro- texture.

Textural and compositional features of reaction products in the kaolin-lime-water system were examined by electron microscopy and electron diffraction. Electron micrographs of replicas of fracture surfaces of compacted mixtures and transmission electron micrographs of powdered compacts showed considerable attack of kaolinite particles by hydrated lime and indicated the formation of significant amounts of calcium silicate hydrate phases. Electron diffraction of reaction products confirmed the presence of calcium silicate hydrates. The presence of these hydrates is undoubtedly responsible for the stabilizing effects of lime which have previously been reported in the literature.

9974. Oser, H. J., Editor and Translator, **Functional analysis and numerical mathematics,** *Book by L. Collatz,* Academic Press Inc., New York, N.Y. 1966.

Key words: Approximation theories; functional analysis; Hilbert and Banach spaces; iterative methods; numerical analysis; operators.

This book was written primarily for graduate students in mathematics and physics, this book highlights the dramatic changes which have occurred in numerical mathematics during the past twenty years. The increased use of electronic computers and the tendency to develop more abstract methods are the primary factors in these rapid advances.

The text is mainly concerned with those parts of functional analysis which have proven useful for numerical applications including Hilbert space theory, Banach spaces, metric spaces and pseudometric spaces, the theory of Frechet derivatives, and topological fixed-point theorems. Problems concerning iterative methods, differential and integral equations, and approximation theory are used to illustrate the applications.

9975. Otto, E. M., **Equilibrium pressures of oxygen over oxides of lead at various temperatures,** *J. Electrochem. Soc.* **113,** No. 6, 525-527 (June 1966).

Key words: Dissociation; entropy; equilibrium; heat of reaction; intermediate oxides; irreversibility; lead oxides; oxygen pressures; thermogravimetry.

PbO$_2$ apparently requires four stages of decomposition to each PbO. Based on thermogravimetric studies the intermediate products appear to be 5PbO$_2$ · 4PbO, 4PbO$_2$ · 5PbO and Pb$_3$O$_4$. Though the first three stages seem irreversible, they too come to steady state in decomposition, but no recombination takes lace. $\Delta H°$ and $\Delta S°$ values have been calculated for the four tages.

**976.** Paabo, M., Bates, R. G., Robinson, R. A., **Dissociation of acetic acid-d$_3$ in aqueous solution and related isotope effects from 0 to 50°,** *J. Phys. Chem.* **70,** 540-543 (1966).

Key words: Acetic acid-d$_3$; dissociation constant; isotope effects; thermodynamics of dissociation; weak acids.

The dissociation constant of acetic acid-d$_3$ CD$_3$COOH) in ordinary water (H$_2$O) has been determined by e.m.f. methods at 11 emperatures from 0 to 50 °C. From the variation of the dissociaion constant with temperature the changes of enthalpy, entropy, nd heat capacity for the dissociation process have also been lerived and compared with similar data for ordinary proto-acetic cid in aqueous solution. The pK of the deuterioacetic acid is rom 0.012 to 0.016 unit greater than that of the protoacid, and he temperature (22.9 °C) at which the dissociation constant asses through a maximum is only slightly higher than the coresponding temperature (22.4 °C) found earlier for the protoacid. Moreover, the changes of enthalpy, entropy, and heat capacity accompanying the dissociation of the two acids at room temperaure do not appear to differ by an amount significantly greater han the combined errors of the two determinations.

**977.** Paabo, M., Bates, R. G., Robinson, R. A., **Dissociation of ammonium ion in methanol-water solvents,** *J. Phys. Chem.* **70,** No. 1, 247-251 (1966).

Key words: Acid-base; ammonia; ammonium; buffer solutions; dissociation constant; electrolytes; ionization; methanol; nonaqueous; solvent effects.

The acidic dissociation constant of ammonium ion in five nethanol-water solvents at 25 °C has been determined from neasurements of the electromotive force of cells with hydrogen nd silver-silver chloride electrodes. The solvents studied conained 10, 20, 33.4, 50, and 70% methanol by weight. The p$K_a$ of mmonium ion follows the same general course as that of other ation acids studied previously, decreasing initially as methanol s added to the aqueous solvent and passing initially through a ninimum at a solvent composition in the vicinity of 70 wt. % nethanol. The results are interpreted in terms of combined electrostatic effects and a solvent "basicity effect." Values of pa$*_H$ for equimolal ammonia-ammonium chloride buffer soluions in the methanol-water solvents are given.

**978.** Paffenbarger, G. C., Stanford, J. W., Kumpula, M. P., Sweeney, W. T., **Guide to dental materials, 1966-1967,** *Am. Dental Assoc.* **3d ed.,** 188 pages (Chicago, Ill., 1966).

Key words: American Dental Association; casting; ceramic materials; certified products; dental; instruments; materials; metals; polymers; specifications standards.

The seventh edition of this booklet covers all changes made in he *Guide to Dental Materials* since the sixth edition which was published in March 1964. Also included are changes in the List of Certified Dental Materials and the bibliography of dental research at the National Bureau of Standards since the sixth ediion.

**979.** Page, C. H., **The mathematical representation of physical entities,** *IEEE Trans. Educ.* **E10,** No. 2, 70-74 (June 1967).

Key words: Abstract unit; angle; dimensional analysis; measurement unit; numeric; quantity calculus; quantity equation.

Mathematics comprises abstract operations upon abstract elements. For the application of mathematics to the sciences, we must not only know the rules for manipulating symbols, but must also define the correspondences between the mathematical abstractions and the concepts to which application is made.

Certain basic postulates about physical observables yield the structure of their mathematical representation. An understanding of this structure yields an understanding of measure equations, quantity equations, measurement units, abstract units, and the mathematical nature of dimensional analysis. Writing equations in a dimensionally homogeneous form is often convenient, but not necessary; sometimes an inhomogeneous formulation is more useful.

**9980.** Parker, K., Goldman, D. T., Wallin, L., **Neutron cross section evaluations—past, present, and future,** (Proc. Intern. Atomic Energy Conf., Reactors, Vienna, Austria, 1966), Chapter in *Nuclear Data for Reactors* **II,** 293 (1967).

Key words: Compilation; cross section; evaluation; neutron; nuclear reactions.

A listing in computer output of all known neutron cross sections evaluations performed throughout the world is given.

**9981.** Parker, R. L., **Report on International Conference on Crystal Growth (ICCG),** (Proc. Intern. Conf. Crystal Growth, Boston, Mass., Dec. 1966), *Phys. Today* **19,** No. 12, 109-111 (Dec. 1966).

Key words: Crystal; crystal growth; ICCG, Report 1966; International Conference (ICCG).

An International Conference on Crystal Growth (ICCG) took place June 20-24, 1966 in Boston. The purpose of the Conference was to further the science and art of crystal growth by providing a forum for reporting and discussing recent original research in this field. The present report gives a brief summary of certain of the technical subjects dealt with at the Conference.

**9982.** Parrish, P. T., Daniel, A. C., Mahler, R. J., **$F^{19}$ relaxation in AFM KMnF$_3$,** *Bull. Am. Phys. Soc. Series II,* **12,** No. 3, 284 (Mar. 1967).

Key words: Antiferromagnetism; low temperature; magnon Raman process; spin lattice relaxation time.

The $T_1$ of $F^{19}$ nuclei located at one of the two possible sites in antiferromagnetic KMnF$_3$ has been measured as a function of temperature through the range of 22° to 1.3 °K in zero external magnetic field. In the 22° to 12 °K range, the relaxation rate followed a $T^7$ dependence corresponding to a relaxation time of 1.8 msec at 22 °K and 60 msec at 12 °K. This temperature variation of the relaxation rate is characteristic of a magnon Raman-process with a non-exponential magnon density variation due to phonon-magnon interactions. The preliminary data indicates a distinct, much slower fall off of $T_1$ below 12 °K, with the minimum value of $T_1$ being 510 msec at 1.3 °K. The corresponding temperature dependence of the relaxation rate is an apparent exponential which is slower than that expected for a two or three-magnon process below $T_{AE}$.

**9983.** Payne, B., F., **Absolute calibration of vibration generators with time-sharing computer as integral part of system,** *Shock Vibration Bull.* **36,** Part 6, 183-194 (Feb. 1967).

Key words: Accelerometers; calibration; shakers; time-shared computers; vibration standard.

Improved shakers with a simplified ceramic moving element and a reference accelerometer now permit reciprocity calibration over a wider frequency range from 10 Hz to 5000 Hz. This paper describes present NBS shaker calibration procedure, using a time-sharing computer, in which magnitude and phase lag measurements are made. Calibrations to 10 kHz are planned.

A teletypewriter gives access to a central commercial computer which can accept commands and data from punched paper tape or from the keyboard. The data may be recorded from digital measuring instruments by a special coupling system. Data reduction is rapid and permits errors to be corrected quickly. The combined use of the computer and the digital data recording system cuts the calibration time to about one-fourth the time required by previous methods. Monitoring the quality of motion of the shaker through the use of the computer makes possible improved accuracy of the calibration process. As an example, a calibration of one of the improved shakers is presented.

**9984.** Perloff, A., Block, S., **The crystal structure of the strontium and lead tetraborates, $SrO \cdot 2B_2O_3$ and $PbO \cdot 2B_2O_3$,** *Acta Cryst.* **20,** Part 2, 274-279 (Feb. 1966).

Key words: Borate; crystal structure; strontium and lead tetraborates.

$SrO \cdot 2B_2O_3$ and $PbO \cdot 2B_2O_3$ are isostructural. These compounds crystallize in the orthorhombic system, $P2_1nm$, with two formula units in a cell of dimensions $a = 4.237$, $b = 4.431$, $c = 10.706$ Å for $SrO \cdot 2B_2O_3$ and $a = 4.244$, $b = 4.457$, $c = 10.840$ Å for $PbO \cdot 2B_2O_3$. A detailed structure analysis was carried out for the Sr compound only.

The structure was solved by conventional Patterson and electron density syntheses utilizing the heavy atom to establish the initial phases. Least squares refinement on three-dimensional data yielded a final R-factor of 7.1 percent.

The results reveal an unusual type of borate framework. All boron atoms are tetrahedrally coordinated. The unusual feature is the occurrence of an oxygen atom common to three tetrahedra.

Although the tetrahedra form a three-dimensional network by corner sharing the borate network gives the appearance of a layer-like structure because there are comparatively few links in the $c$ direction. The layers can be described in terms of chains (parallel to $a$) of six membered rings having B – O edges in common. These chains are joined by non-ring oxygens to form layers which are parallel to the $a$ $b$ plane.

The Sr coordination is not clearly defined. There are nine nearest neighbor oxygens at distances ranging from 2.52-2.84 Å. There are six more oxygens at 3.04-3.20 Å which could conceivably be considered as part of the Sr coordination sphere.

**9985.** Persson, K. B., Uhlenbrock, D. A., Johnson, E. G., **Cyclotron harmonic emission from the abnormal negative glow plasma,** *Bull. Am. Phys. Soc., Series II,* **12,** No. 5, 756 (May 1967).

Key words: Cyclotron harmonic radiation; electron beam; magnetic field; plasma.

Experimental evidence indicates that our observed cyclotron harmonic radiation is strong parallel with the magnetic field and that it is directly or indirectly associated with the plasma maintaining electron beam. The search for mechanisms accounting for these facts lead to the following model. The secondary electron generated in an ionization process produces a helical space charge wave packet in the dense back ground plasma. When this packet is generated in a uniform back ground plasma it can be shown that the electron cyclotron harmonics radiate essentially only perpendicular to the magnetic field. Strong radiation parallel with the magnetic field at the harmonic frequencies is generated when the packet is produced in a spatially non-uniform plasma with the dimensions of the non-uniformity comparable to the relevant cyclotron radius. The spatial non-uniformities are produced by the beam electrons forming "density tracks" in the plasma and/or by cathode non-uniformities.

**9986.** Peterson, R. L., **Short-range order in the Weiss molecular field approximation,** *Bull. Am. Phys. Soc., Series II,* **12,** No. 4, 502 (Apr. 1967).

Key words: Magnetism; molecular field theory; short-range order.

The Weiss molecular field theory (WMFT) of ferromagnetism, as commonly used, has the well-known defect that the short-range order and heat capacity vanish in zero applied field and temperatures above Curie's point. We here point out that the same use of the WMFT also gives an isentropic susceptibility equal to zero at all fields and temperatures, and two different results for the isothermal susceptibility, depending upon which of two direct methods of calculation are used. These difficulties are all traced to the use of the assumption that different spins are uncorrelated. We argue that this assumption is not consistent within the framework of the WMFT, and show that the molecular field assumption by itself provides a measure of the spin correlations. The assumption that only nearest neighbor spins are correlated is shown to be consistent at high temperature and to yield the correct high-temperature expression for the short-range order and heat capacity. Thus we argue that when correctly used, the WMFT does not possess the gross defects usually attributed to it. The discussion applies also to antiferromagnetism.

**9987.** Peterson, R. L., **Formal theory of nonlinear response,** *Rev. Mod. Phys.* **39,** No. 1, 69-77 (Jan. 1967).

Key words: Isothermal susceptibility; nonlinear response theory; nonlinear transport theory; response functions; transport coefficients.

This paper presents the derivation of formal, exact expressions for "generalized response coefficients," quantities which characterize the response of a system to conservative forces of arbitrary strength and time dependence. The development avoids all expansions of the response in powers of the driving forces. The generalized response coefficients thus provide the basis for calculations of nonlinear effects in those situations for which expansions in powers of the forces are not suitable. It is shown how the linear and higher order response functions obtained first by Kubo can be obtained in a relatively more simple way. The expressions corresponding to static forces are considered in some detail. Generalized response coefficients are also derived for systems in equilibrium; the lowest order of these is just the isothermal susceptibility, as usually defined.

**9988.** Peyser, P. Stromberg, R. R., **Conformation of adsorbed polystyrene measured by attenuated total reflection in the ultraviolet region,** *J. Phys. Chem.* **71,** No. 7, 2066-2074 (June 1967).

Key words: Adsorption of polymers; attenuated total reflection; conformation of adsorbed polymer molecules; frustrated total reflection; index of refraction in ultraviolet region; polymer adsorption; refractive index in ultraviolet region; total reflection; ultraviolet spectrophotometry.

Attenuated total reflection (ATR) in the ultraviolet region was used to measure the extension and concentration of an adsorbed layer of polystyrene. The polystyrene was adsorbed on a quartz surface from cyclohexane solution at the theta temperature. The ATR prism, which allowed 15 to 16 reflections, was constructed from synthetic crystalline quartz. It was designed to be placed in a spectrophotometer without the need of additional optical components. The measured adsorbed polymer "extension" agreed reasonably well with similar ellipsometric measurements on nearly the same system. The study reported here was restricted to the use of an adsorbed layer that could be treated as a homogeneous film. The possible use of the method to determine the concentration distribution of adsorbed segments normal to the surface is discussed. Measurements in the ultraviolet region of the refractive indices of the polymer solutions and of the benzene-methanol and toluene-methanol solutions that were used to test the method are also described.

**9989.** Piccirelli, R. A., **Some properties of the long-time values of the probability densities for moderately dense gases,** *J. Math. Phys.* **7,** 922 (1966).

Key words: Long-time values; moderately dense gases; probability densities.

It has been argued that for sufficiently large times the $n$-particle probability densities of a moderately dense, simple gas become time-independent functionals of the one-particle probability densities. Proofs are given for several properties of the power series representation of these functionals. In particular, it is shown that the equilibrium value of the $n$-particle functional is identical to the usual equilibrium probability density term by term and that the corresponding generalized Boltzmann collision integral vanishes as it should. The two forms of the functional, one due to Bogoliubov and one due to Green and Cohen, are shown to be formally identical. It is argued that the higher terms of these two series probably diverge *together*.

In the course of the discussion several new properties of the coefficient operators of the power series for the functional are derived. Moreover, an integral equation for the $n$-particle functional is derived which may have solutions not representable as functional power series in the one-particle probability density.

**9990.** Pitts, J. W., Moore, D. G., **Apparatus for studying the effects of atmospheric pollution and cyclic dew formation on the deterioration of materials,** *Mater. Res. Std.* **6,** No. 7, 328-333 (July 1966).

Key words: Accelerated corrosion; atmospheric corrosion; corrosion mechanisms; humidity cabinet; laboratory corrosion apparatus; photomicrography; reflectometry; sulfur dioxide; thermoelectric heat pump; water vapor condensation.

An apparatus and procedure for simulating atmospheric corrosion are described. The apparatus was used to study qualitatively the kinetics of moisture condensation and evaporation, and the resulting corrosion of a metal surface. The effect of varying time of exposure and amount of contaminant ($SO_2$) in the atmosphere on the corrosion rate of polished iron is illustrated with photomicrographs. A quantitative rating of the apparent progress of corrosion was made with reflectance measurments.

**9991.** Placious, R. C., **Dependence of 50 and 100 keV bremsstrahlung on target thickness, atomic number, and geometric factors,** *J. Appl. Phys.* **38,** No. 5, 2030-2038 (Apr. 1967).

Key words: Efficiencies; low energy; Monte Carlo predictions; photon emission angles; thick target bremsstrahlung.

Experimental data have been obtained for the bremsstrahlung spectra produced with 50 and 100 keV electrons incident on different targets. The spectrum per unit solid angle per incident electron is measured for photon emission angles of 30, 70, and 110 degrees, for normal and oblique incidence of the electrons on the targets having atomic numbers of 13, 50, and 79, and for four target thicknesses equal to different fractions of the electron range in the given material. Also, results are given for the bremsstrahlung production efficiencies per unit solid angle at a given emission angle. The experimental results show good agreement with the theoretical predictions of Berger and Seltzer, which are based on thin target bremsstrahlung cross sections and which employ Monte Carlo calculations to account for multiple scattering and energy loss effects.

**9992.** Pollack, G. L., **Effect of normal-fluid motion on third sound in liquid-helium films,** *Phys. Rev.* **143,** No. 1, 103-109 (Mar. 1966).

Key words: Energy attenuation; helium film; liquid helium; normal fluid viscosity; third sound.

Some theoretical consequences are derived of a proposed viscous force on the normal-fluid component of the He II film. Compared to earlier calculations, in which the normal fluid was assumed to be immobile, this new assumption allows large energy attenuations such as have recently been observed in third sound in He II films and in a wave mode of He II partially clamped in narrow channels. Atkins' three equations describing third sound are modified to take account of energy and entropy transfer associated with normal-fluid motion, and wave modes are obtained which simultaneously satisfy these equations and the normal-fluid equation of motion with a viscous force $-\mathrm{Rv}_n$. The four wave variables are: T and T′, respectively, the local fluctuations in film thickness and temperature, $v_s$, and $v_n$. Attenuation and velocity of the wave mode corresponding to third sound are calculated at temperatures from 1.2 °K through $T\lambda$ for all values of the dimensionless viscosity coefficient $(R/\omega\rho)$. The maximum calculated attenuation varies from 0.47 cm$^{-1}$ at 12 °K to 17.3 cm$^{-1}$ at 2.1 °K; at the lower temperature the observed attenuation is about 2 cm$^{-1}$. However, the anomalously rapid decrease in velocity of third sound observed by Everitt et al. could not be explained in this manner. Evidence for normal-fluid motion in the film is presented and some feasible experiments for detecting it are described.

**9993.** Post, M. A., **The determination of bound styrene in insoluble emulsion polymerized styrene-butadiene copolymers,** *J. Appl. Chem.* **17,** No. 7, 203-208 (July 1967).

Key words: Absorbance ratio method; bound styrene; infrared; insoluble styrene-butadiene copolymers; masonry paints.

Bound styrene is determined in insoluble emulsion polymerized styrene-butadiene copolymers by measurement of the $10.3\mu\mathrm{m}/13.2\mu\mathrm{m}$ absorbance ratio using the baseline method. This ratio is obtained from the infrared spectrogram of the copolymer and the styrene content is determined from a standard curve. The standard curve is constructed from absorbance ratios of $10.3\mu\mathrm{m}/13.2\mu\mathrm{m}$ derived from the infrared spectrograms of cast films of styrene-butadiene latexes over a range of percentage compositions. Bound sytrene is determined in these latexes by nitration of the isolated and extracted copolymers. Styrene content based on nitration is determined from standard curves relating styrene concentration to spectrophotometric absorbance measurements at wavelengths of 285.0 nm, 273.8 nm, and 265.0 nm. The source of the styrene for these curves is NBS standard rubber No. 1500.

**9994.** Post, M. A., **The determination of bound styrene in soluble high styrene-butadiene resins,** *J. Paint Technol. Eng. Official Digest* **38,** No. 497, 335-342 (June 1966).

Key words: Absorbance ratio method; bound styrene; infrared; masonry paints; styrene-butadiene resins.

Bound styrene is determined in high styrene-butadiene resins by measurement of the $10.3\mu/3.25\mu$ absorbance ratio, using the baseline method. This ratio is obtained from the infrared spectrogram of the purified copolymer, and the percent styrene is read from a standard curve. The standard curve is constructed from absorbance ratios of $10.3\mu/3.25\mu$ derived from the infrared spectrograms of accurately weighed mixtures of purified polystyrene and purified polybutadiene. These polymers are isolated from their respective latexes. It is shown that this method is useful for analyzing crude resins as well as purified copolymers.

**9995.** Powell, R. L., **Thermophysical properties of metals at cryogenic temperatures,** *Am. Soc. Testing Mater. Spec. Tech. Publ.* **387,** *Behavior of Materials at Cryogenic Temperatures,* pp. 134-148 (1966).

Key words: Cryogenic temperature; metals; thermophysical properties.

The low temperature thermophysical properties of metals can only be fully understood by utilizing the fundamental concepts of electrons, lattice vibrations, and their interactions. After the introduction, the properties of specific heat and thermal conductivity are each discussed with the emphasis on understanding the various contributions to the total observed effect. Based on the above discussions, temperature dependencies for each property are given for various representative metals and alloys. The importance of inter-relations between the various themophysical properties is also noted. With an understanding of basic concepts, inter-relations, and effects of different contributions, one can often make reasonable estimates for the values of the thermophysical properties of new materials or of known materials with different chemical impurities or mechanical or metallurgical treatments. References are given to several good books, review articles, and compilations of numerical values. Information is also given on sources of specialized or up-to-date bibliographie and data collections.

**9996.** Power, E. A., **A suggested experiment to measure part of the transverse electromagnetic mass of the electron,** *Proc. Roy. Soc. (London)* **292,** No. 1430, 424-432 (May 31, 1966).

Key words: Atomic beam; electromagnetic; electron; hyperfine; mass; measurement; self-energy.

The changes in self energy of a non-relativistic charged particle are calculated where such changes are due to confinement of the charge within conducting plates. This confinement will alter the mode structure of the virtual photons involved in the transverse self energy calculation: it will lead to a reduction in the number of modes at the *long* wavelength limit and, where the modes have a wavelength comparable to the distance, L, between the plates, the normal integrals over virtual momenta are replaced by sums over the integers describing the modes. It is found that mass changes of 1 part in $10^{10}$ can be induced by plate separations of the order of a millimeter. It is suggested that such relative mass shifts could be measured by the use of high precision atomic beam techniques, such as those used in "atomic clocks". The atomic beam would be directed between two closely spaced parallel conducting plates (or through long cylindrical tubes) located between the oscillating fields used to excite a transition between the hyperfine-structure levels. The mass change will be reflected in frequency shifts of the hfs separation of the same order as the mass change. With a high precision cesium beam apparatus, such as those at NBS, it should be possible to demonstrate not only that changes do indeed occur but also obtain a quantitative estimate of such effects as a function of the plate separation, L. It is predicted that the frequency shifts should be inversely proportional to L.

**9997.** Power, E. A., **Zero-point energy and the Lamb shift,** *Am. J. Phys.* **34,** No. 6, 516-518 (June 1966).

Key words: Electron; hydrogen; Lamb shift; self energy.

A suggestion by Feynman that the Lamb shift energy can be obtained from the changes in zero-point energy due to the presence of the atoms involved is work through in detail for the Bethe non-relativistic contribution to the energy shift. The self energy of a free electron is obtained in the same way and is equivalent to the state independent shift due to the $e^2A^2/2mc^2$ term in the normal perturbation methods.

**9998.** Pruitt, J. S., **Secondary electron trajectories in a Faraday cup magnetic field,** *Nucl. Instr. Methods* **39,** 329 (Feb. 1966).

Key words: Electrons; escape; Faraday; magnetic; orbits; solenoidal.

Orbits of electrons with energies between 10 eV and 1 MeV have been studied in inhomogeneous magnetic fields to choose a deflecting magnet for the capture of secondary electrons generated in the mouth of a Faraday cup. The results show that a solenoidal field abets their escape, but the field of two repelling bar magnets completely stops electrons with energies less than about 1 keV. Additional information relevant to Faraday Cup design is also presented.

**9999.** Pummer, W. J., Antonucci, J. M., **Aromatic fluorocarbon polymers,** (Proc. 152nd American Chemical Society Meeting, New York, N.Y., Sept. 13, 1966), *Polymer Preprint* **7,** No. 2, 1071-1076 (Sept. 1966).

Key words: Fluorinated styrenes; fluoroaryl polymers; para and meta linked polymers; pendant pentafluorophenyl ring; polyperfluorophenylene ethers; polyperfluorophenylenes; sulfides; vinyl ethers.

Recent synthetic work has led to the preparation of a variety of fluoroaryl polymers. Most of the polymers synthesized are similar in structure to the hydrocarbon analogs except for the fluorine atoms. On this basis, the fluorinated polymers, presented in this paper, will be classified and discussed according to structural features. The first class of polymers contains the polyperfluorophenylenes which will include both the para and meta linked polymers. In the second class, the polymers contain an atom or group of atoms between the fluorinated rings, such as oxygen, sulfur and oxydifluoromethylene groups. Some polymers in this category are the polyperfluorophenylene ethers and sulfides. The final group of polymers contains a pendant pentafluorophenyl ring attached to the main polymer chain such as the various fluorinated styrenes and vinyl ethers.

In all cases, the method of polymerization, physical properties and thermal stability of the polymers will be discussed and whenever possible, comparisons will be made between the fluorinated and hydrocarbon polymers.

**10000.** Radford, H. E., **Free radical microwave absorption meter,** *Rev. Sci. Instr.* **37,** No. 6, 790-792 (June 1966).

Key words: Free radical; microwave absorption.

This note describes a simple microwave spectrometer which can be used to measure absolute concentrations of free radicals at any point in a conventional gas flow reaction system. The spectrometer displays true absorption line profiles and is sensitive to microwave line depths (peak absorption coefficient X path length) as small as $10^{-5}$. The instrument may be assembled from commercially available components, at a cost comparable with that of a good optical monochromator.

**10001.** Radziemski, L. J., Jr., Andrew, K. L., Kaufman, V., Litzen, U., **Vacuum ultraviolet wavelength standards and improved energy levels in the first spectrum of silicon,** *J. Opt. Soc. Am.* **57,** No. 3, 336-340 (Mar. 1967).

Key words: Energy levels; silicon; spectroscopy; standards; vacuum ultraviolet; wavelength.

Vacuum ultraviolet Si I wavelengths have been recalculated using all available low-pressure-source data. One hundred calculated and forty-one measured wavelengths, all with uncertainties of less than 0.002 Å should be useful as wavelength standards in the region 1560 to 2000 Å. Seventy-seven of the proposed standards were originally calculated by Radziemski and Andrew (*J. Opt. Soc. Am.* **55,** 474 (1965)) and although the two sets of wavelength values agree to within their uncertainties, the new set is more internally consistent. Included also is a complete list of low-pressure-source levels for Si I, which contains new values for 30 odd levels previously determined exclusively from relatively high-pressure (450-740 torr) arc data.

**10002.** Ramaley, D., Shafer, J. F., **Direct ratio readings from a universal ratio set,** *Instr. Control Systems* **39,** 73-74 (Jan. 1966).

Key words: Direct-reading ratio sets; ratio sets; universal ratio sets.

A method for modifying commercially available universal ratio sets to permit their use as direct-reading ratio sets has been developed. This modification is the outgrowth of a series of seminars held at the National Bureau of Standards, Radio Standards Laboratory, Boulder, Colorado, at which some of the participants were from standards laboratories equipped with universal ratio sets but not with direct-reading ratio sets. A simple scheme was devised whereby a few minor connections to the circuit of a universal ratio set, terminated in external binding posts, make the instrument suitable for use also as a direct-reading ratio set, thus providing the equivalent of two separate instruments in a single set. The direct-reading ratio set is especially well adapted to intercompare resistors closely adjusted to nominal values with a minimum of required computation.

**10003.** Rasberry, S. D., Scribner, B. F., Margoshes, M., **Characteristics of the laser probe for spectrochemical analysis (a summary),** *Proc. XII Intern. Spectroscopy Colloquium, Exeter, England, 1965,* pp. 336-339 (Hilger & Watts, London, England, 1966).

Key words: Laser probe; spectrochemical analysis.

An extended summary is given of a paper presented at the XII International Spectroscopy Colloquium, Exeter, England, July 12-16, 1965. The paper discusses some practical aspects of the use of the laser probe for spectrochemical analysis of minute samples.

**10004.** Rasberry, S. D., Scribner, B. F., Margoshes, M., **Laser probe excitation in spectrochemical analysis. I. Characteristics of the source,** *Appl. Opt.* **6,** No. 1, 81-86 (Jan. 1967).

Key words: Analysis; emission; emission spectra; high energy; high power; illuminating system; laser probe; laser vaporization; Q-switched ruby laser; qualitative; spark excitation; spectrochemical.

A laser probe for spectrochemical analysis is described. A high energy laser beam is focused onto a specimen to vaporize a sample from a small area, and the vapor thus formed is further excited by a spark discharge. The characteristics of emission spectra with and without auxiliary spark excitation are compared. Spectrograph illuminating systems for qualitative and quantitative analysis were investigated. Some difficulties were encountered with the laser probe, and modifications were made to the instrument to alleviate some of these problems. Some typical analytical applications are discussed.

**10005.** Rasberry, S. D., Scribner, B. F., Margoshes, M., **Laser probe excitation in spectrochemical analysis. II. Investigation of quantitative aspects,** *Appl. Opt.* **6,** No. 1, 87-94 (Jan. 1967).

Key words: High energy; high power; laser probe; laser vaporization; photographic emulsion; pit volume; Q-switched ruby laser; quantitative; spark excitation; spectral intensity; spectrochemical analysis.

A study has been made of quantitative analysis by a laser probe with spark excitation of the sample vapor. Random errors come largely from variations in laser energy and from photometric errors. The parameters of the spark circuit affect the line intensities; however, these factors are well controlled. Correlations have been established between the energy of the laser beam, the size of the pit formed, and spectral intensities. Single-spike laser operation has been found to be preferable for most purposes to multiple-spike operation. At present, the coefficients of variation for analysis are 15 to 40 percent.

**10006.** Reader, J., **Nuclear moments of $Pm^{147}$,** *Phys. Rev.* **141,** No. 3, 1123-1128 (Jan. 1966).

Key words: Electronic structure; energy levels; hollow cathode; hyperfine structure; interferrometer; nuclear moments; optical; promethium 147.

The nuclear magnetic dipole and electric quadrupole moments of $Pm^{147}$ have been derived from an analysis of the optical hyperfine structure of singly ionized $Pm^{147}$. The hyperfine constants for the $[4f^5\ {}^6H_{5/2}, 6s]_2$ ground state are $A = -\ 10.24 \pm 0.20$ mK; $B = -\ 10.6 \pm 2.6$ mK. By using the known atomic beams data for the $[4f^5 6s^2\ {}^6H_{7/2}]$ state of neutral Pm to subtract out the contribution of the $[4f^5\ {}^6H_{5/2}]$ core to the observed magnetic splitting factor, the splitting factor of the $6s$ electron was found to be $a_{6s}=+214.2 \pm 4.9$ mK. The nuclear moments deduced from the hyperfine constants are $\mu_I(Pm^{147}) = +2.58 + 0.07$ nm and $Q(Pm^{147}) = +0.74 \pm 0.20$ b.

**10007.** Rebbert, R. E., Ausloos, P., **Vacuum-ultraviolet photolysis of solid propane at 20° and 77 °K,** *J. Chem. Phys.* **46,** No. 11, 4333-4340 (June 1, 1967).

Key words: Free radicals; photolysis; primary dissociations; propane; solid phase.

The photolysis of $CD_3CH_2CD_3$, $CH_3CD_2CH_3$, and $C_3H_8 - C_3D_8$ mixtures has been investigated at 1470 Å (8.4 eV), 1236 Å (10 eV) and 1048-1067 Å (11.6-11.8 eV) both at 20° and 77 °K. On the basis of the isotopic analysis of the products it is concluded that the following primary fragmentation processes occur:

$$
\begin{aligned}
C_3H_8 + h\nu \rightarrow\ & C_3H_7 + H \\
\rightarrow\ & + C_3H_6 + H_2 \\
\rightarrow\ & + C_2H_6 + CH_2 \\
\rightarrow\ & + C_2H_5 + CH_3 \\
\rightarrow\ & + C_2H_4 + CH_4
\end{aligned}
$$

Hydrogen, methane, and ethane are mainly formed by elimination processes from a single carbon atom which results in the simultaneous formation of a carbene in each case. In this respect the primary processes occurring in the solid phase are the same as those reported to occur in the gas phase. The elucidation of the primary processes in the condensed phase is facilitated because of the inhibition of secondary decomposition of the internally excited fragments formed in the processes above. On the other hand, the occurrence of geminate disproportionation and combination leads to difficulties in determining the relative quantum yields of the primary processes of the first and fourth listed above. It is noted that the C-H and C-C cleavage reactions in one and four increase in importance when the energy of the incident photon is augmented.

Although propane ions, which have an ionization energy of 11.07 eV in the gas phase must be produced at 1048-1067 Å, no concrete information could be obtained as to the fate of these ions in the solid phase. The data, however, show that decomposition of the superexcited molecules is of major importance at these wavelengths.

**10008.** Reed, R. P., **The plate-like martensite transformation in Fe-Ni alloys,** *Acta Met.* **15,** No. 8, 1287-1296 (Aug. 1967).

Key words: Fe-Ni alloys; low temperatures; martensite.

The martensite morphological and crystallographic characteristics in Fe, 29-35 w/o Ni alloys have been investigated. Optical microscopy results indicate that as the nickel content increases the martensite plates become less fragmented, internal twinning increases, and the pole normal to the midrib plane swings toward the $(011)\gamma$-$(111)\gamma$ line. Two types of internal twinning have been found in high Ni martensites. The $M_s$ temperatures were determined for this series of alloys and are generally about 20 °C higher than previously thought. Results for the midrib variation with temperature and prestrain are also reported.

**10009.** Reed, R. P., **Deformation twinning in Ni and fcc Fe-Ni alloys,** *Phil. Mag.* **15,** No. 137, 1051-1055 (May 1967).

Key words: Deformation twinning; Fe-Ni alloys; low temperature; nickel.

Using electron and optical microscopy techniques, deformation twinning has been found in Ni and fcc Fe–Ni alloys at low temperatures (76-4 °K).

**10010.** Reed, R. P., Breedis, J. F., **Low-temperature phase transformations,** *Am. Soc. Testing Mater. Spec. Tech. Publ.* **387,** Behavior of Materials at Cryogenic Temperatures, pp. 60-132 (1966).

Key words: Cryogenics; crystal structure; martensite; metals; phase transformations.

Changes in crystallographic structures can occur solely at low temperatures by a diffusionless, shear-type of transformation to a product structure termed martensite. This paper presents a review of martensitic transformations which occur in ferrous and nonferrous alloys. Specifically, kinetic, structure, and the theoretical approaches to describing diffusionless transformations are treated.

The kinetic characteristics pertinent to this class of transformations include dependence upon temperature, time, applied stress, and chemical composition. The structural aspects of martensitic transformations include their morphology and crystallography. Four general types of martensite transformation morphology have been observed in steels and in nonferrous alloys. With particular reference to steels, the product structures may be morphologically described as either: (1) plates, (2) sheets comprised of martensite crystals or laths, (3) homogeneous sheets, or (4) surface martensite. Theories pertaining to martensitic transformations relate either to the initiation or to the subsequent growth of a product. Theories employing thermodynamic analyses or dislocation models generally are concerned with nucleation, while crystallographic theories attempt to predict the mode of growth and the final orientations of the product. Both approaches are discussed.

Approximately 650 references appear in the extended bibliography which lists almost all articles published in English after 1940, in addition to major articles published in other languages. Tables which attempt to classify articles are also included to simplify research of martensite literature.

**10011.** Reese, R. M., Rosenstock, H. M., **Photoionization mass spectrometry of NO,** *J. Chem. Phys.* **44,** No. 5, 2007-2009 (Mar. 1, 1966).

Key words: Autoionization; mass spectrometry; nitric oxide; photoionization; Rydberg series.

The photoionization of NO has been studied in the 1360-600 Å range with mass analysis. All autoionization peaks found here below 900 Å have been assigned to diffuse lines observed in absorption by Huber. In the 1130-900 Å range, several new vibrational progressions are deduced.

**10012.** Reid, G. C., **Physics of the D region at high latitudes,** (Proc. NATO Advanced Study Institute, Finse, Norway, April 1965), Chapter in *Electron Density Profiles in Ionosphere and Exosphere,* J. Frihagen, ed., pp. 17-26 (North Holland Publ. Co., Amsterdam, The Netherlands, 1966).

Key words: D region; electron density profiles; free electrons; high latitudes; photochemical reaction rates.

It is shown that the assumption that collisional detachment of negative ions plays an important part in determining nighttime electron density profiles at high latitudes leads to major contradictions. Multiple-frequency data obtained at twilight during a polar-cap absorption event suggest a quite different view of the nighttime D regions, which is consistent with an almost complete disappearance of free electrons below about 75 km, and an almost complete maintenance of the daytime profile above this level. The lack of change of the upper region between daytime and nighttime conditions can be understood if the negative ions there suffer associative detachment reactions with atomic oxygen, and if the atomic oxygen height distribution is governed by dynamical processes (transport and turbulent mixing) rather than simply by photochemical reaction rates. It is shown that other evidence is consistent with this picture of the nighttime D region at high latitudes.

**10013.** Richardson, J. M., editor, **U.S.A. National Committee Report, Fifteenth General Assembly, Munich, September 1966: Commission 1, Radio Measurement Methods and Standards, Progress in Radio Measurement Methods and Standards,** *Radio Science* **1,** No. 11, 1333-1342 (Nov. 1966).

Key words: Coaxial connectors; electromagnetic properties of materials; frequency standards; lasers; microwaves; radio measurement methods; radio measurement standards; time standards.

Progress in radio measurement methods and standards within the United States during the Triennium 1963 through 1965 is reviewed for inclusion in the report of the U.S. National Committee of URSI to the 1966 General Assembly. Topics surveyed are high precision atomic frequency standards, high precision quartz frequency standards, scientific aspects of Universal and/or Atomic time and frequency transmissions, standards and measurements at 30 kc/s to 1 Gc/s, standards and measurements at 1 to 300 G c/s, precision coaxial connectors, swept-frequency techniques, measurements of electromagnetic properties of materials, and laser standards and measurements. The topics are treated within the length limitation imposed by USNC/URSI.

**10014.** Richardson, J. M., **Introduction,** (Proc. 1966 Conf. Precision Electromagnetic Measurements, Boulder, Colo., June 21-23, 1966), *IEEE Trans. Instr. Meas.* **IM-15,** No. 4, 138 (Dec. 1966).

Key words: Electromagnetic measurements; functional elements; physical measurements.

It is appropriate, at each biennial Conference on Precision Electromagnetic Measurements, to examine the importance of this series in the scheme of things. Recently we have come to recognize that the field of physical measurements has functional elements and complicated interactions characteristic of a vast system. We may call this complex the system of physical measurement. There is a comparatively small group of people who work at the limits of attainable accuracy in order to keep the system valid and current. There is also a huge number of people who use the system as a means to the ends of science, engineering, manufacturing, trade, and everyday life. This conference exists so that the keepers of the system can communicate their work to each other and also to users of the system. No other conference addresses itself exclusively to the dynamically changing techniques of precision electromagnetic measurement and to how they can be put to use.

**10015.** Richardson, J. M., **Progress in the distribution of standard time and frequency, 1963 through 1965,** (Proc. XV General Assembly of URSI, Munich, Germany, Sept. 5-15, 1966), Chapter in *Progress in Radio Science 1963-1966,* **Part 1,** pp. 40-62 (International Scientific Radio Union, Munich, Germany, 1966).

Key words: Frequency; portable clocks; standard frequency broadcasts; time; time signals; VLF propagation.

Progress in accurate long distance distribution of standard time and frequency, as reported in the literature from 1963 through 1965, is summarized. Techniques are by VLF, LF, and HF radio propagation, by satellite relay, and by portable clocks. Effects on standard frequency transmissions of variations in VLF propagation with geophysical phenomena are quantitatively understood. VLF and LF transmissions have provided careful, long-term, statistical comparison of remotely located atomic frequency standards. Precision of at least 2 parts in $10^{11}$ for a 24-hour observation period is possible. The phase of some standard frequency transmitters is routinely steered by VLF from distances up to 5300 km. Global distribution of standard time by VLF to microsecond resolution has been shown feasible. The null beat between two neighboring VLF carriers propagates stably enough to mark a particular VLF cycle, and the beat period can be long enough to enable ordinary time signals to mark a particular null beat. Intercontinental time synchronization by microwave pulses has been accomplished via Telstar and Relay II satellites. Accuracy is set at several microseconds. Portable cesium clocks have served as global transfer standards with degradation of timing accuracy of only about a microsecond per trip. Results by all the above methods are consistent with each other and with stated accuracies of atomic standards involved.

**10016.** Richmond, J. C., **Effect of surface roughness on emittance of nonmetals,** Chapter in *Thermophysics and Temperature Control of Spacecraft and Entry Vehicles* **18,** 167-172 (Academic Press Inc., New York, N.Y., 1966); *J. Opt. Soc. Am.* **56,** No. 2, 253-254 (Feb. 1966).

Key words: Absorptance; alumina; ceramic; emissivity; emittance; optical; reflectance; roughness; scattering theory.

It has been observed experimentally, both at NBS and elsewhere, that the emittance of polished metals can be markedly increased by roughening the surface, by as much as a factor of 2 or 3. For non-metals and particularly white ceramic materials, on the other hand, the emittance appears to be essentially independent of surface roughness, at least for wavelengths below 7 or 8 microns. This apparent anomaly is explained on the basis of the differences in the optical properties of the two types of materials.

**10017.** Richmond, J. C., Kneissl, G. J., Kelley, D. L., Kelly, F. J., **Procedures for precise determination of thermal radiation properties,** *Tech. Rept.* **ARML-TR-66-302** (Air Force Materials Laboratory, Air Force Systems Command, Wright-Patterson Air Force Base, Ohio, Aug. 1966).

Key words: Emissivity; emittance; high temperature reflectance; infrared reflectance; radiation properties; reflectance; spectral emittance; spectral reflectance; thermal radiation; total emittance.

An error analysis of the shallow cavity technique for measuring total normal emittance of ceramic materials at very high temperatures showed that there was an error due to the translucency of the specimens that was as much as $+60$ percent for alumina, and a second error due to thermal gradients in the specimen that was on the order of $-10$ percent. Two new techniques were devised in the hope of greatly reducing the translucency error. Progress was made in developing codes to compute and correct for the thermal gradients present in the specimen. The laser-source integrating sphere reflectometer for measuring reflectance of specimens at very high temperatures was extensively redesigned to eliminate errors due to flux reaching the detector on the first reflection, and to convert the reflectometer from the substitution to the comparison mode. A literature search was made of techniques for measuring thermal radiation properties of solids at temperatures above 2500 °K (4000 °F).

**10018.** Risley, A. S., Bussey, H. E., **Interpretation of ferromagnetic resonance measurement made in a nonresonant system,** *IEEE Trans. Instr. Meas.* **IM-5,** No. 4, 393-396 (Dec. 1966).

Key words: Cavity resonator model; ferromagnetic resonance measurement; nonresonant system; short circuited waveguide.

The loaded line width, $\Delta H_m$ (loaded by the coupling), and the resonator coupling coefficient, $\beta$, assuming a cavity resonator model, were measured on ferrimagnetic resonant YIG spheres in a (nonresonant) short circuited waveguide. The coupling was varied over a wide range by changing the angle $\phi$ between the dc and driving rf magnetic fields. The results showed that the unloaded line width, $\Delta H = \Delta H_m/(1+\beta)$, was essentially constant during changes in coupling. It is therefore tentatively concluded that the cavity resonator model furnishes an accurate model for separating unloaded from loaded line width. Other methods for obtaining ΔH, namely using a matched waveguide, or a pick-up loop, or the usual cavity perturbation method were less satisfactory.

The coupling coefficient was 1.06 times theoretical for widely different sample sizes and all reasonable angles $\phi$. It follows that line width can be determined very simply from a simple reflection measurement without measuring the width.

**10019.** Risley, A. S., Johnson, E. G., Jr., Bussey, H. E., **Polycrystalline spin wave theory of ferromagnetic resonance compared with tilting experiment,** *J. Appl. Phys.* **37,** No. 2, 656-668 (Feb. 1966).

Key words: Ferromagnetic resonance; polycrystalline spin wave; spin wave.

Schlömann's spin wave theory of polycrystalline ferromagnetic resonance has been tested in detail using the tilting method reported earlier. Among the quantities measured were the linewidth $\Delta H$, and the maximum value of the imaginary part of the effective susceptibility $(\chi_m'')^{eff}$. The measurement method is equivalent to measuring asymmetric ($N_x \neq N_y$) ellipsoids and thus, introduces another shape dependence in addition to that due to spin waves. Direct comparison with the symmetric ($N_x = N_y$) form of the theory is inaccurate. A proper comparison can be made in two ways: (1) generalizing the theory to include the $N_x \neq N_y$ case and then using the data directly, (2) transforming the data and then comparing with the $N_x = N_y$ theory. Both comparisons are reported and their equivalence is demonstrated.

It is concluded that Schlömann's theory does not fit the data within the spin wave (SW) manifold. It is suggested that the theory of Sparks may provide a better fit. The difference between coupling models seems to be the basic difference between the two theories. Experimentally and theoretically, $\Delta H$ and $(\chi_m'')^{eff}$ are different quantities. The dispersive effects of spin wave coupling are shown to be the cause of the difference between the theoretical $\Delta H$ and $(\chi_m'')^{eff}$.

**10020.** Risley, A. S., Johnson, E. G., Jr., Bussey, H. E., **Erratum: Polycrystalline spin-wave theory of ferromagnetic resonance compared with the tilting experiment,** *J. Appl. Phys.* **37,** No. 9, 3646 (Aug. 1966).

Key words: Dipolar narrowing; ferrites; ferromagnetic resonance relaxation; polycrystals; porosity; spin wave.

A more complete test of Schlömann's spin wave, SW, theory of polycrystalline ferromagnetic resonance, FMR, has been made. This theory is compared with measurements made by the tilting method reported earlier. Among the quantities measured were the line width, ΔH, and the maximum value of the imaginary part of the effective susceptibility, $s''_{max}$. The measurement method is equivalent to measuring asymmetric ($N_x \neq N_y$) ellipsoids, which introduces another shape dependence in addition to that due to SW's. Direct comparison with the symmetric ($N_x = N_y$) form of the theory is inaccurate. A proper comparison can be made in two ways: (1) generalizing the theory to include the $N_x \neq N_y$ case and then using the data directly, (2) transforming the data and then comparing with the $N_x = N_y$ theory. Both comparisons are reported and their equivalence is demonstrated.

It is concluded that Schlömann's theory does not fit the data within the SW manifold. It is suggested that the theory of Sparks may provide a better fit. The difference between coupling models seems to be the basic difference between the two theories.

Experimentally and theoretically, ΔH and $s''_{max}$ are different quantities. The dispersive effects of SW coupling are shown to be the cause of the difference between the theoretical ΔH and $s''_{max}$. ΔH does not provide an adequate description of the FMR; $s''_{max}$ is a necessary additional parameter.

**10021.** Ritter, J. J., Coyle, T. D., **Convenient safety cutoff device for water cooled equipment,** *Rev. Sci. Instr.* **37,** No. 4, 523 (Apr. 1966).

Key words: Cutoff; electric; flow-sensitive switch; safety.

This note describes a device to detect interruptions in the flow of cooling water through laboratory apparatus. A control circuit is provided to deactivate equipment and to shut off water supply to prevent flooding.

**10022.** Robertson, A. F., **Report on the conference on burns and flame retardant fabrics (Dec. 1966), New York, N.Y.,** *Fire Res. Abstr. Rev.* **9,** No. 2, 119-122 (1967).

Key words: Accidents, clothing fires; clothing, flame resistance; burn injuries, fire-retardant clothing; flame resistance, clothing; retardant treated fabrics.

A summary is presented of subject meeting which was held on 2 and 3 December 1966.

**10023.** Rosberry, F. W., **The measurement of homogeneity of optical materials in the visible and near infrared,** *Appl. Opt.* **5,** No. 6, 961-966 (June 1966).

Key words: Homogeneity; index gradient; infrared; interferometer; laser; measurement; optical; refractive index; shadowgraph.

A procedure is described for determining the inhomogeneities of a sample of optical material in terms of small changes in index of refraction at discrete points over the measured surface. The method is used in the visible and near infrared regions of the spectrum. A He-Ne gas laser source was used for the infrared measurements. The variation in index was mapped with contour lines enclosing areas of similar index variations. The largest index change in one cm distance was noted and recorded as the maximum gradient per cm. Over 25 different samples of six different materials were examined. The results are presented in a chart indicating the range of maximum index gradients of the samples observed. Data are shown to illustrate the possibility of determining index values to higher precision than the material justifies.

**10024.** Rosenberg, S. J., **Metals for use in orthopedics, Chapter in** *Orthotics Etcetra,* S. Licht, ed., **9,** 77-94 (E. Licht Publ., New Haven, Conn., 1966).

Key words: Alloys, aluminum; aluminum alloys; magnesium alloys; orthopedics, metals; titanium alloys.

**10025.** Rosenblatt, D. R., **Aggregation in matrix models of resource flows II. Boolean relation matrix methods,** *Am. Stat.* **21,** No. 3, 32-37 (June 1967).

Key words: Aggregation; automatic theory; Boolean matrices; consolidation; DeMorgan-Pierce-Schroder relation algebra; input-output models; indecomposability; Markov chains; mathematical economics; mathematical logic; primitivity and automatic theory; relation, calculus.

A Boolean relation matrix approach is taken to issues of aggregation in matrix models of resource flows involving substochastic matrices A,B. The following results are shown: (i) an aggregation matrix is many-one and onto: (ii) if B is a consolidation of A with weight matrix regular, then if A is indecomposable (primitive), B is indecomposable (primitive): but, if the weight matrix is singular the preceding conclusions fail; if B is a consolidation of A. $(I-B)^{-1}$ exists if, and only if, for every indecomposable stochastic submatrix $A_k$ of A, the image under the consolidation of every row index of $A_k$ is connected in the associated graph of B to the image of a "nonstochastic row" index of A.

**10026.** Rosenblatt, J. R., **Comments on presentation by Albert A. Anctil,** (Proc. 11th Conf. Design of Experiments in Army Research Development and Testing, Dover, N.J., Oct. 20-22, 1965), *U.S. Army ARO-D Report* **66-2,** pp. 509-510 (U.S. Army Research Office, Durham, N.C., May 1966).

Key words: Curve-fitting; statistics.

Discussion of a paper entitled "Statistical analysis of tensile strength-hardness relationships in thermochemically treated steels," including remarks on the interpretation of a goodness-of-fit measure for the relationships.

**10027.** Rosenstock, H. M., **Franck-Condon factors and the mass spectra of small molecules,** (Proc. Intern. Mass Spectrometry Conf., ASTM E-14, The Hydrocarbon Research Group and GAMS, Paris, France, Sept. 1964). *Adv. Mass Spectrometry* **3,** 435-439 (1966).

Key words: Acetylene probability; Franck-Condon factors; photoionization; transition; vibrational.

This paper is not a review paper but is rather a status report of the theory relating to the mass spectra of small molecules and includes, in outline, some recent work carried out at the National Bureau of Standards.

**10028.** Rossmassler, S. A., **The National Standard Reference Data System program in atomic and molecular properties** (Proc. Symp. Compilations of Data on Chemical and Physical Properties of Substances, 152d National Meeting, Am. Chem. Soc., New York, N.Y., Sept. 12, 1966), *J. Chem. Doc.* **7,** No. 1, 15-18 (Feb. 1967).

Key words: Atomic; compilation; data; data center; molecular; properties.

In general, Atomic and Molecular properties are taken to mean properties primarily characteristic of the individual atoms or molecules rather than of any system or state of aggregation. For operational convenience, the area includes also certain general and fundamental physical constants.

An Advisory Panel listed sixty-three specific properties and gave high priority to twenty-eight of these. The Office of Standard Reference Data is supporting or monitoring sixteen projects which are concerned with fourteen of these high priority topics. Most of the projects are continuing ones. Five of the activities perform data center or information center functions.

In several cases, joint support or cooperative programs have been developed, and we are seeking to extend this type of activity.

To provide reasonable current coverage of the general area, the number of projects should be doubled (high priority topics only) or trebled (high priority plus related moderate priority topics) as rapidly as possible. Projects being initiated in other countries (cf. next paper by R. M. S. Hall) are already assuming some of this burden.

Ten compilations of data and a similar number of bibliographies and secondary publications will have appeared by the end of calendar year 1966.

**10029.** Row, R. V., **Evidence of long-period acoustic-gravity waves launched into the F region by the Alaskan earthquake of March 28, 1964,** *J. Geophys. Res. Letter* **71,** 343-345 (Jan. 1966).

Key words: Acoustic-gravity waves; Alaskan earthquake; Doppler sounder; F region; ionograms; ionospheric disturbances.

Evidence of disturbances to the ionosphere caused by the Alaskan earthquake of (03:36 U.T.) March 28, 1964 have been published recently by Leonard and Barnes (1965) and Baker and Davies (1965). The data presented by both pairs of authors are shown to be mutually compatible. It is suggested that the large long period disturbance seen on Doppler records at Boulder and vertical sounder ionograms at Boulder and other locations are a manifestation of long period ducted acoustic-gravity waves launched into the ionosphere near the epicenter.

**10030.** Rubin, R. J., **Brownian motion models,** (Summer Institute on Spectral Theory and Statistical Mechanics, Brookhaven National Laboratory, Upton, L.I., N.Y., July-Aug. 1965), *Brookhaven Natl. Lab. Publ.* **PNL993 (T422),** (Clearinghouse for Federal Scientific and Technical Information, Springfield, Va. 22151, 1966).

Key words: Brownian motion; momentum autocorrelation function; statistical mechanics.

Two recent investigations of the ensemble average motion of a particle in a harmonically coupled system of particles are outlined and reviewed, namely the investigations of Rubin and Ford, Kac and Mazur.

**10031.** Rubin, R. J., **Random-walk model of adsorption of a chain-polymer molecule on a long rigid-rod molecule,** *J. Chem. Phys.* **44,** No. 5, 2130-2138 (Mar. 1966).

Key words: Adsorption; chain polymer; critical energy; generating function; lattice model; partition function; random walk.

A lattice model of adsorption of a flexible chain molecule on a rod-like molecule is investigated. The rod-like molecule is represented by the lattice sites on the z-axis of a simple cubic lattice. The sites which are nearest neighbors to the z-axis are adsorbing sites. The dimensionless adsorption energy per momomer unit is $\Theta = \epsilon/kT$. The problem of enumerating polymer chain configurations taking into account the increased probability of occupying adsorbing sites and the zero probability of occupying z-axis sites is formulated and solved as a random walk problem. The average fraction of monomer units in adsorbing sites $f_R(\Theta)$ is computed in the limit in which the number of monomer units in the polymer chain approaches infinity. There is a critical value of the adsorption energy $\Theta c = \ln(6/5)$ such that for $\Theta < \Theta_c$, $f_R(\Theta) = 0$. For $\Theta > \Theta_c$, $f_R(\Theta)$ is an increasing function of $\Theta$ with all derivatives equal to zero at $\Theta_c = \ln(6/5)$. In the analogous simple cubic model of adsorption of a polymer chain molecule at a plane solution surface, the same value of the critical energy has been obtained. For $\Theta < \ln(6/5)$ the average fraction of monomer units in adsorbing surface sites is zero, i.e., $f_S(\Theta) = 0$. For $\Theta > \ln(6/5)$, $f_S(\Theta)$ is an increasing function of $\Theta$ whose right-hand slope is 25 at $\Theta = \ln(6/5)$.

**10032.** Rubin, R. J., **Random walk with an excluded origin,** *J. Math. Phys.* **8,** No. 3, 576-581 (Mar. 1967).

Key words: Excluded origin; restricted random walk.

The mean square end-to-end distance $R_N^2$ is calculated for the subset of all random walk configurations of a D-dimensional simple cubic lattice which do not return to the starting point. Explicit results are obtained in the limit $N \gg 1$ for the one-, two-, and three-dimensional lattices. The values of the first two terms in the asymptotic series for $R_N^2$ are, respectively, $N + N$, $N + N/\log N$, and $N + .435/N^{-1/2}$.

An unexpected relation is obtained between $R_N^2$ and $S_N$, the average number of different lattice sites visited in an N-step random walk on a perfect lattice. It is $R_N^2 = S_N(S_{N+1} - S_N)^1$.

**10033.** Rubin, S. **Standards for galvanomagnetic devices,** *Solid-State Electron.* **9,** No. 5, 559-566 (May 1966).

Key words: Flux sensitive resistors; galvanomagnetic devices; Hall effect; magneto resistors; photoresistors; standard terminology.

A review is given of the Military Standard and the IEC standard for Hall effect devices. Points of outstanding interest such as linearity definitions are detailed. A review of a proposed standard for magnetoresistive devices is given. Similarities between the two standards are noted as are some of the similarities with standards for other flux sensitive resistors such as thermistors and photoresistors.

**10034.** Rubin, S., **Standards for galvanomagnetic devices,** (Proc. Committee on Hall Effect Applications, Cambridge, Mass., Nov. 8-9, 1965), Chapter in *Solid State Electronics* **9,** No. 65, 559-566 (Pergamon Press, Inc., New York, N.Y., 1966).

Key words: Galvanomagnetic device; Hall effect device; Hall element; magnetoresistive device; magnetoresistor; standard terminology.

A summary is given of existing and "in-process" standards for Galvanomagnetic devices. Controversial items in the IEC standard for Hall effect devices, 47(Secretariat)196, May 1965, are reviewed, and note is made of USA and Japanese comments on his document. Items in the USA document, 47(USA), September 1965, commenting on 47(Secretariat)196, are reviewed, and particular emphasis is given to items relating to linearity error, particularly as a percent of reading, to residual voltages, and to sensitivity indices.

A summary of items in an "in-process" document for "Standard Definitions and Terminology for Magnetoresistive Devices," is given. The concept of compatibility between definitions for flux and temperature sensitive resistors (i.e., magnetoresistors, thermistors, and photoresistors) is introduced. Some overlapping areas of application are noted. The linear input-output characteristics obtainable from a device which has a square law characteristic is noted and appropriate definitions for both characteristics are introduced.

Copies of four documents dealing with standard terminology and definitions for Hall Effect Devices are included as appendices.

**10035.** Rubin, S., **Transistorized UHF marginal oscillator and its application for the measurement of the magnetic flux density,** *Proc. IEEE Letter* **53,** No. 9, 1249-1250 (Sept. 1965).

Key words: Density, magnetic flux; flux density; magnetic flux density; marginal oscillator; oscillator, marginal; UHF marginal oscillator.

A transistorized marginal oscillator operating in the UHF region has been used to measure flux density in a Helmholtz coil at 17.5 mT, with an accuracy of better than a part in $10^3$. The instrument uses plug-in oscillator modules to simplify frequency changing. The results achieved indicate the feasibility of such a device for measurement of magnetic flux density in the 1 to 50 mT range in industrial environments and with accuracies approaching a part in $10^4$.

**10036.** Ruegg, F. W., Dorsey, W. W., **The flow field of a body-stabilized two-dimensional V-flame,** *Combust. Flame* **10,** No. 1, 1-10 (Dec. 1966).

Key words: Flame field; flame holder calculation; flame simulation; flame speed; flame vorticity; V-flame.

A two-dimensional, V-shaped flame is simulated by a combination of source and sink sheets of fluid in a general stream. Complex variable theory is used to determine the flow field of the simulated flame. Adjustment of the strength of the sink sheet on the interior symmetry flame axis yields a flame speed that is constant within about one percent along the front. Two 22-degree half-angle flames are calculated. In both cases a portion of the flame front near the apex of the flame and the sink are found to be enclosed within a body shaped as a flameholder. Actual flames in the calculated approach fields would generate appreciable vorticity in the flame gas, but the calculated field downstream from the simulated flame is irrotational.

**10037.** Ruff, A. W., Ives, L. K., **Quench defects formed in a low-stacking fault-energy silver tin alloy,** *J. Appl. Phys.* **37,** No. 8, 3073-3079 (July 1966).

Key words: Dislocation loops; dislocations; electron microscopy; quenching; silver-tin alloy; stacking fault tetrahedra.

A transmission electron microscopy study of defects was conducted in quenched and plastically deformed samples of a silver–8 at. percent tin alloy. After quenching from 750 °C and aging at 200-300 °C, dislocation loops and small faulted defects were found distributed randomly in low numbers. Many examples of aligned rows of clustered defects were observed together with stacking fault growth on existing screw-oriented dislocations. Helical dislocations with visibly extended segments were found which are believed to indicate the process of tetrahedron formation in ⟨110⟩ rows. A specific mechanism is proposed to explain the observations. Extensive plastic deformation is also observed to produce such features.

**10038.** Rumfelt, A. Y., Elwell, L. B., **Radio frequency power measurements,** *Proc. IEEE* **55,** No. 6, 837-850 (June 1967).

Key words: Bolometer mount efficiency; mismatch error; power measurement; power meter; substitution error.

The need for improved accuracy in and understanding of all kinds of measurements has come with the recent rapid advances in modern technology. RF power measurement, the subject of this paper, is no exception to this requirement. The basic principles of bolometric, calorimetric, and certain other types of power meters are reviewed. The methods for making accurate RF power measurements are discussed in detail. Emphasis is given to the techniques for eliminating or accounting for the errors due to mismatch, dc or LF substitution, and bolometer mount efficiency.

**10039.** Rush, J. J., **Cold-neutron study of hindered rotations in solids and liquid methyl chloroform, neopentane and ethane,** *J. Chem. Phys.* **46,** No. 6, 2285-2291 (Mar. 1967).

Key words: Barrier to rotation; cosine potential; globular molecules; hindered rotation; methyl group; molecular reorientation; neutron scattering; neutron spectra; phase transitions; torsional vibrations.

The low-frequency modes of methylchloroform, neopentane, and ethane in their solid and liquid phases have been investigated by the scattering of cold neutrons. The energy-gain spectra for these compounds in their low-temperature solid phases exhibit broad bands peaked at about 52, 50 and 82 cm$^{-1}$ for $CH_3CCl_3$, $C(CH_3)_4$, and $C_2H_6$, respectively, which are attributed to whole-molecule librations and translations in the lattice. In the high-temperature phases of the "globular" compounds $CH_3CCl_3$ and $C(CH_3)_4$, these spectral bands are no longer peaked, but are quite diffuse and blend into a considerably broadened elastic peak. These results show that the phase transitions below the melting points are associated with a change from strongly hindered to quasi-free rotation, in agreement with the results of previous experiments. The barrier to molecular reorientation is estimated to be approximately $< 1$ kcal/mole in the high-temperature phase of each compound.

Bands are also observed in the $CH_3CCl_3$ and $C(CH_3)_4$ spectra peaked at about 300 and 286 cm$^{-1}$, respectively, which are assigned primarily to the torsional oscillations of the methyl groups. These peak positions show no significant change in proceeding from the liquid to the solid phases, indicating little intermolecular contribution to the forces hindering methyl-group reorientation. One of the liquid ethane spectra exhibits a shoulder around 260 cm$^{-1}$, which is possibly due to torsional vibrations. Assuming three-fold cosine potentials, with no interaction between methyl groups "average" barriers to rotation of 5.8 and 5.2 kcal/mole are calculated from the torsional peaks for $CH_3CCl_3$ and $C(CH_3)_4$. The $CH_3CCl_3$ barrier is considerably higher than the value derived from thermodynamic results for $CH_3CCl_3$ (and ethane) gas.

**10040.** Rush, J. J., Ferraro, J. R., **Neutron and infrared spectra of $HCrO_2$ and $DCrO_2$,** *J. Chem. Phys.* **44,** No. 6, 2496-2498 (Mar. 15, 1966).

Key words: Chromous acid; $DCrO_2$; $HCrO_2$; hydrogen bond; infrared spectra; isotope effect; lattice modes; neutron spectra; vibration spectra.

The vibrational spectra of $HCrO_2$ and $DCrO_2$ have been investigated by the energy-gain scattering of cold-neutrons, and by infrared absorption spectra from 4000-30 cm$^{-1}$. The infrared measurements are in agreement with previous results above 400 cm$^{-1}$. In addition, no absorptions are observed between 400 and 30 cm$^{-1}$, a region not covered in previous measurements. These results appear to support previous evidence for asymmetric hydrogen bonds at $DCrO_2$ and essentially symmetric bonds in $HCrO_2$. The neutron spectra exhibit a number of maxima, including a band peaked at about 225 cm$^{-1}$ in $HCrO_2$ (and a less intense peak around 180 cm$^{-1}$ in $DCrO_2$), probably due to low-frequency optic lattice modes. A comparison of the neutron and infrared results appears to raise some uncertainty concerning the assumption of symmetric hydrogen bonds in $HCrO_2$.

**10041.** Rush, J. J., Hamilton, W., **Free rotation of methyl groups in dimethyltin difluoride,** *Inorg. Chem.* **5,** No. 12, 2238-2239 (Dec. 1966).

Key words: Barrier to rotation; cross-section slope; free rotation; methyl group; neutron wavelength; total neutron cross section.

Total cross sections for long-wavelength neutrons have been measured for polycrystalline $(CH_3)_2SnF_2$. The variation of the scattering cross section per hydrogen atom with neutron wavelength was determined to be $12.0 \pm 0.5$ barns/Å-H. Comparison of this value with previous results on methyl-substituted compounds and with theoretical calculations leads to the conclusion that the methyl groups in $(CH_3)_2SnF_2$ are rotating almost freely, with a barrier to reorientation of approximately $< 0.3$ kcal/mole.

**10042.** Rush, J. J., Connor, D., Carter, R., **Study of $D_2O$ ice as a cold-neutron source,** *Nucl. Sci. Engr.* **25,** No. 4, 383-389 (1966).

Key words: Cold neutrons; $D_2O$(ice); (leakage) spectra; neutron; (neutron) flux; (neutron) moderation; (neutron) spectra; neutron temperature; (neutron) thermalization; transport (effects).

The leakage flux from a large cylinder (18 × 18 in.) of $D_2O$ with a beam of pile neutrons incident at its center has been studied at $D_2O$ temperatures from 22° to 293 °K. Intensities through beryllium and graphite filters, as well as indium foil transmissions, have been measured to determine cold-neutron fractions and neutron temperatures for the emerging spectra. The results of these measurements show that large volumes of $D_2O$ ice can be useful as low-temperature moderators in reactors. The percentage of leakage neutrons with $\lambda_n \geqslant 3.95$A is 21 percent at 22 °K, a 20-fold increase over the fraction at 293 °K, and about twice the value at 100 °K. The neutron temperature of the leakage spectrum, calculated from the transmission data assuming a Maxwellian distribution, decreases with moderator temperature, reaching a value of about 75° for $D_2O$ at 22 °K. An abrupt increase in the fraction of cold neutrons is observed at the $D_2O$ freezing point, which is shown to be primarily due to a change in the transport rather than the moderating properties of the $D_2O$. This result clearly illustrates the fact that any moderator acts as a neutron filter as well as a thermalizing medium, so that the emerging energy distribution is dependent on the variation of the neutron with cross section energy.

**10043.** Rush, J. J., Taylor, T. I., **Study of low-frequency motions in several ferroelectric salts by the inelastic scattering of cold neutrons,** *Proc. 3d Symp. Inelastic Scattering of Neutrons, Bombay, India, 1965,* **II,** 333 (1965).

Key words: Ammonium salt; barrier to rotation; ferroelectric; neutron scattering; phase transition; torsional vibrations; vibration spectra.

For $K_4Fe(CN)_6 \cdot 3H_2O$ ($T_c = 249$ °K) scattered spectra were obtained at 121, 175 and 296 °K. The results were quite similar in both the high temperature and ferroelectric phases. A broad band centered at an energy gain $435 \pm 40$ cm$^{-1}$ ($54 \pm 5$ MeV) is observed at all three temperatures and assigned to the librations of the water molecules. A second broad peak around 165 cm$^{-1}$ is possibly due to the translational motions of the water molecules in the lattice.

The room-temperature spectra for $NH_4HSO_4$ ($T_c$ at 154 and 270 °K) and $(NH_4)_2SO_4$ ($T_c = 224$ °K) show broad bands peaked at about 260 cm$^{-1}$ and 300 cm$^{-1}$, respectively, which are primarily due to the torsional motions of the ammonium ions. The $NH_4HSO_4$ spectrum at 177 °K shows an indication of splitting, with little shift in the center of the band. At 125 °K the spectrum is clearly split, with peaks at $290 \pm 25$ and $190 \pm 16$ cm$^{-1}$. The $(NH_4)_2SO_4$ results at 172 °K also exhibit a split band, with peaks centered at $335 \pm 25$ and $200 \pm 16$ cm$^{-1}$. In both cases the higher-energy peaks are assigned to torsional vibrations. The $(NH_4)_2BeF_4$ spectra also show broad "torsional" bands with several indicated maxima in the 175-290 cm$^{-1}$ range. No great differences were observed in the spectra above and below the ferroelectric transitions for any of the ammonium salts.

The results for all of the compounds studied indicate that the ferroelectric transitions are not related to any large change in the average rotational freedom of the ammonium ions and water molecules. In addition the measurements show that the average barriers to reorientation are relatively small ($V_o$ is approximately $< 4$ kcal/mole) in every case. The results are compared with total cross-section data and with data obtained by other techniques.

**10044.** Russell, D. H., Larson, W., **R.F. attenuation,** *Proc. IEEE* **55,** No. 6, 942-959 (June 1967).

Key words: Attenuation; coaxial; measurements; standards; waveguide.

A tutorial review of r-f attenuation measurement methods and standards is presented.

Accepted and proposed definitions and attenuator models are discussed. Commonly used standards operating from d-c through most waveguide bands are compared with the "ideal" interlaboratory standard. Characteristics of fixed resistive, waveguide below-cutoff and rotary-vane standards are included.

Measurement methods are classified and described including comments concerning convenience and accuracy of various methods, and references are given which cover most of the basic and important research in the field.

**10045.** Santoro, A., Zocchi, M., **Absorption correction in the Weissenberg methods,** *Acta Cryst.* **22,** 918-919 (June 1967).

Key words: Absorption correction; Weissenberg methods; x ray.

A procedure is described for calculating the direction cosines of the incident and diffracted beams in a reference system attached to the crystal for the general case of the Weissenberg method.

**10046.** Santoro, A., Zocchi, M., **Multiple diffraction in the Weissenberg methods,** *Acta Cryst.* **21,** No. 3, 293-297 (Sept. 1966).

Key words: Crystal structure; diffraction; multiple diffraction; Weissenberg method.

The conditions for multiple diffraction due to symmetry have been derived for the Weissenberg geometry, for the various crystal systems and for the most commonly used rotation axes.

It is shown that the equal-cone method is the most appropriate in intensity measurements.

**10047.** Saylor, C. P., **Accurate microscopical determination of optical properties on one small crystal,** Chapter in *Advance in Optical and Electron Microscopy,* R. Barer and V. E. Cosslett, eds., **1,** 41-76 (Academic Press, Inc., New York, N.Y., 1966).

Key words: Crystal; microscopical determination; optical properties; wavelength.

By rotating a crystal about one axis and using phase, double diaphragm, or interference contrast, refractive indices of a typical crystal can be microscopically determined for any wavelength with an error that is not greater than 0.00002. For such accuracy, the diameter of the crystal must be about 20$\mu$ or larger. Precautions involve careful orientation, precise matching of index with that of immersion fluid, and correct determination of the refractive index of the fluid.

**10048.** Schafft, H. A., French, J. C., **A survey of second breakdown,** *IEEE Trans. Electron. Devices* **ED-13,** No. 8-9, 613-618 (Aug.-Sept. 1966).

Key words: Breakdown; diodes; reliability; second breakdown; thermal instability; transistors.

The existence of a "new high current mode of transistor operation" now generally known as second breakdown, was first reported by Thornton and Simmons in 1958 and was used to explain the mysterious failures that were observed to occur under certain operating conditions. Since then, with the production of higher power and higher frequency transistors, the problems resulting from the existence of second breakdown have proliferated. Interest in the phenomenon has grown concurrently and many papers about second breakdown can be found in the literature. These papers cover a range of interest that extends from theoretical studies of the basic mechanisms involved to interpretations of specifications for transistor operation free of second breakdown. A complete understanding of second breakdown has not yet been achieved and several concepts of second breakdown prevail. The purpose of this paper is to review historically the work that has been reported in order to present a coherent and comprehensive picture of the present status of second breakdown.

**10049.** Scala, A., Ausloos, P., **Gas phase radiolysis and vacuum ultraviolet photolysis of 2- and 3-pentanone,** *J. Phys. Chem.* **70,** No. 1, 260-269 (Jan. 1966).

Key words: Ion-molecule reactions; ion pair yields; pentanone; photolysis; primary processes; radiolysis.

In the photolysis of 3-pentanone and 2-pentanone at 1470 Å and 1236 Å, the major modes of fragmentation of the electronically excited ketones are as follows:

$$C_2H_5COC_2H_5{*} \rightarrow C_2H_5+CO+C_2H_4+H \qquad (1)$$

$$\rightarrow CH_3+CH_2COC_2H_5 \text{ (or } CH_2CO + C_2H_5\text{)} \qquad (2)$$

$$CH_3COCH_2CH_2CH_3{*} \rightarrow CH_3CO \text{ (or } CH_3+CO\text{)}+C_2H_4 + CH_3 \qquad (3)$$

$$\rightarrow CH_3CO \text{ (or } CH_3+CO\text{)}+C_3H_6 + H \qquad (4)$$

On the basis of experiments carried out with $C_2H_5COC_2H_5$ – $C_2D_5COC_2D_5$ mixtures it can be concluded that "molecular" elimination of methane does also occur to a minor extent. Isotopic analysis of the products formed in the photolysis of $CD_3COCD_2$ – $CH_2CH_3$ further indicates that the elimination process

$$CD_3COCD_2CH_2CH_3{*} \rightarrow CD_3COCD_2H+C_2H_4 \qquad (5)$$

does take place, but to a lesser extent than at 2537 and 3130 Å.

In the radiolysis neutral excited molecules and ions are produced. When an electrical field is applied during the radiolysis, increased excitation by electron impact occurs. At low field strengths molecules are mainly excited to the first upper singlet and/or triplet state, and decompose in much the same way as reported in the earlier near-ultraviolet photolysis studies. When the field strength is increased the ketone is excited to a higher singlet state and decomposes according to process 1 to 4. Products which are not affected by the application of an electrical field such as $C_3H_4$ and 1-$C_4H_8$ can be ascribed to ion molecule reactions. It is proposed that in the radiolysis, transfer of a proton from various fragment ions to the pentanone molecule does occur, and that this is followed by neutralization of the protonated pentanone to yield hydrogen as a product.

**10050.** Schafft, H. A., French, J. C., **Second breakdown and current distributions in transistors,** *Solid-State Electron.* **9,** No. 7, 681-688 (July 1966).

Key words: Diodes; failure mechanisms; internal current distributions; second breakdown; semiconductors; temperature sensitive phosphors; transistors.

A study of second breakdown in transistors, which included the use of temperature-sensitive phosphors to reveal current distributions, has emphasized how intimately the susceptibility of the transistor to second breakdown is linked to the internal distribution of current or of energy dissipation. The effect of such factors as the base drive and internal structural irregularities on the internal current distribution is described. A better understanding of the role of the base drive in second breakdown was achieved and led to a test which was used to distinguish second breakdown from other low voltage modes that have been recently reported to be different levels of second breakdown.

**10051.** Schafft, H. A., Schwuttke, G. E., Ruggles, R. L., Jr., **Second breakdown and crystallographic defects in transistors,** *IEEE Trans. Electron. Devices* **ED-13,** No. 11, 738-742 (Nov. 1966).

Key words: Dislocations; failure mechanisms; second breakdown; semiconductors; transistors; x-ray diffraction microscopy.

A study was conducted to determine the effect, on second breakdown in transistors, of some of the crystallographic defects that can develop during handling and fabricating procedures. X-ray diffraction microscopy was used to detect these defects. The susceptibility to second breakdown of about 1500 epitaxial planar silicon transistors diffused on two wafers was measured and the site of the current constriction of second breakdown was registered on most of these transistors. These data were then compared with the x-ray topographs. Any effect of the gross dislocations seen, was masked by other factors, such as surface induced effects, that were not discernible in the x-ray topographs. Evidence was found, however, to indicate that a faulted emitter structure that has been correlated with the emitter diffusion step may be of importance. The heating in the transistor at the second breakdown current constriction site to temperatures above 600 °C and recrystallized laser-induced melt regions smaller than about 30$\mu$m in diameter produced no crystallographic changes nor any frozen in strain fields detectable in the x-ray topographs.

**10052.** Scharf, K., **Exposure rate measurements of x and gamma rays with silicon radiation detectors,** *Health Phys.* **13,** No. 6, 575-586 (June 1967).

Key words: Dosimetry; exposure rate measurements; gamma rays; radiation detection devices; radiation detectors; radiation monitoring; semiconducting devices; silicon; x rays.

The steady-state d.c. current and voltage signals produced by x or gamma rays in silicon radiation detectors used either as photovoltaic cells or photodiodes are shown to be dependent on such circuit parameters as load resistance and bias voltage used in the respective exposure rate measurement. Non-linear exposure rate dependence of radiation-produced signals may result from choosing unsuitable circuit parameters and no singular value of sensitivity or signal per unit exposure rate can be ascribed to an individual detector without specifying the circuit parameters used. Measurements are reported with silicon detectors of the diffused p-n junction type illustrating these performance features, and a measuring method is suggested which makes it possible to measure with high precision the generated photocurrent at zero voltage applied at the detector which is independent of circuit parameters and proportional to exposure rate over a wide range. Measurements using this method are reported of exposure rates ranging up to $10^5$ R/hr of 30-kV x rays of 0.09 mm Al HVL, and from approximately 1 R/hr to 30 R/hr of $^{60}$Co gamma rays.

**10053.** Schlemper, E. O., Hamilton, W. C., Rush, J. J., **Structure of cubic ammonium fluosilicate: neutron-diffraction and neutron**

**inelastic scattering studies,** *J. Chem. Phys.* **44,** No. 6, 2499-2505 (Mar. 15, 1966).

Key words: Ammonium ions; barriers to rotation; crystal structure; disorder; inelastic scattering; neutron diffraction; neutron scattering; $(NH_4)SiF_6$; torsional vibrations.

The motion of the ammonium ion in the cubic phase of $(NH_4)_2SiF_6$ has been investigated by the inelastic scattering of slow neutrons. The prominent feature of the neutron energy gain spectrum is a moderately broad band peaked at $168 \pm 8$ cm$^{-1}$ with a shoulder at $305 \pm 25$ cm$^{-1}$ (estimated uncertainties). These are assigned to the 1-0 and 2-0 transitions of a rotational motion of the ammonium ion. A precision refinement of single crystal neutron diffraction data has also been completed. There is a well-defined disorder of the ammonium groups. Although a model with a static three-fold disorder, with each 1/3 hydrogen atom undergoing harmonic vibration gives a very satisfactory fit to the data, such a model is probably unrealistic in view of the fact that the disordered positions are only 0.75 A apart. A more realistic model is one involving an ordered hydrogen atom undergoing thermal motion in a very anharmonic potential well. We propose a model in which the hydrogen atom is relatively free to move over a region of about 1 A$^2$ by small rotations of the ammonium ion but with a very high barrier toward a reorientation which involves an interchange of two hydrogen atoms. Such a model is an agreement with both the neutron diffraction and the inelastic scattering data.

**10054.** Schneider, S. J., McDaniel, C. L., **The melting point of $Al_2O_3$ in vacuum,** *Rev. Hautes Témper. Réfract.* **3,** 351-361 (1966).

Key words: Alumina; dissociation; melting point; vacuum environment.

The National Bureau of Standards has initiated a program to determine, under a variety and proportional to exposure rate over a wide range. of environmental conditions, the melting points of a number of the more refractory metal oxides. The present paper, the first in a series, reports results obtained in an investigation of the melting point of $Al_2O_3$ (corundum) in vacuum. Equipment has been constructed which will permit the heating of small samples under blackbody conditions to 3000 °C in vacuum or inert atmosphere. The furnace essentially consisted of two concentric covered tungsten crucibles supported by three tungsten rods in the center of a water-cooled, copper, load concentrator. The outer crucible served as the susceptor for induction heating. The inner crucible acted as both the specimen container and the blackbody enclosure for temperature measurements. Theoretical calculations as well as experimental testing indicated that the blackbody-container had an effective emittance of 0.999 at 2000 °C. Temperatures were continuously monitored with a recording photoelectric spectral pyrometer which has a sensitivity of ± 0.2° at 1063 °C and ± 1° at 2000 °C. Experiments were conducted on specimens obtained from three different sources of $Al_2O_3$, each having a purity in excess of 99.9%. The data indicated that the melting point of $Al_2O_3$ in vacuum ($\sim 6.5 \times 10^{-5}$ torr) is 2051 °C (IPTS). The overall maximum uncertainty of the melting point was estimated to be no greater than ± 4 °C. Precision of the measurements was within ± 1.5 °C.

**10055.** Schwerdtfeger, W. J., **Cathodic protection of copper in a severely corrosive soil,** *IEEE Trans. Ind. Gen. Appl. IGA-***3,** No. 1, 66-69 (Jan.-Feb. 1967).

Key words: Cathodic protection; copper; corrosion current; corrosion rate; polarization; potential; soil corrosion.

This paper describes a laboratory procedure used in developing electrical requirements pertinent to the cathodic protection of copper for a given situation. The work was prompted by severe corrosion of copper tubing used underground at a housing development. The soil environment was reported as having a low resistivity (about 200 ohm-cm) and a high concentration of sulfate ion.

Specimens of the same type of copper tubing, one arranged to corrode freely (control) and the other under cathodic protection (cathode), were exposed in the laboratory to a sample of the soil for a period of 130 days.

Polarization data obtained on the control were used to evaluate the cathodic protection simultaneously applied to the cathode. After 130 days, the specimens were removed from the soil and cleaned. The cathode was well protected, the metal loss being less than 3 percent of that on the control which was almost perforated in a few places.

**10056.** Scott, A. H., **Anomalous conductance behavior in polymers,** (1965 Annual Report Conf. Electrical Insulation), *Natl. Acad. Sci.-Natl. Res. Council Publ.* **1356,** pp. 98-102 (Natl. Acad. Sci.-Natl. Res. Council, Washington, D.C., 1966).

Key words: Anomalous d-c conductance; conductive rubber electrodes; epoxy; polycarbonate; polystyrene; polyvinylbutyl; polyvinylchloride; tinfoil electrodes.

Conductance measurements on polymer materials are found to be affected by discharge currents even though the specimen has not had a voltage applied to it. It is necessary to fully discharge a specimen (sometimes for several days) before a repeatable conductance measurement is obtained. The discharge currents are amplified by the use of conductive rubber electrodes rather than tinfoil electrodes. Conductivities that were obtained with conductive rubber electrodes were lower in all cases than those obtained with tinfoil electrodes.

**10057.** Scott, A. H., Harris, W. P., **Long-time effects of humidity change on the dielectric properties of certain polymers,** (Proc. 1962 Annual Rept. Conf. Electrical Insulation, Hershey, Pa., Oct. 15-17, 1962), *Natl. Acad. Sci.-Natl. Res. Council Publ.* **1080,** pp. 41-44 (1963).

Key words: Dielectric properties of certain polymers; humidity change; polycarbonate; polyethylene; polystyrene; properties of certain polymers; polymers.

The results of a study of the long-time effects of humidity change on the dielectric properties are given for three materials: polyethylene, polystyrene, and polycarbonate. The polyethyiene and polystyrene specimens were disks about 4 cm in diameter with gold electrodes. Measurements on polycarbonate specimens were made using the air-gap method without contact electrodes. The electrical properties of some specimens were still changing at the end of three years. The results are given in the form of graphs.

**10058.** Scott, W. W., Jr., Frederick, N. V., **The measurement of current at radio frequencies,** *Proc. IEEE* **55,** No. 6, 886-891 (June 1967).

Key words: Ammeter; calibration; current; electrodynamic; measurement; radio-frequency; standards; thermocouple.

The state of the art of radio-frequency current measurements is reviewed with emphasis on what the authors consider are the most useful current standards. In particular, thermocouple and electrodynamic ammeters are discussed in detail. Reference is made to photoammeters, air thermometer ammeters, and other types of current measuring apparatus, some of which deserve additional development. Extensive referencing is included for the convenience of investigators interested in an intensive review of radio-frequency current measurements.

**10059.** Selby, M. C., **Voltage measurement at high and microwave frequencies in coaxial systems,** *Proc. IEEE* **55,** No. 6, 877-882 (June 1967).

Key words: High frequency voltages; microwave voltages; standards of rf voltage; voltage measurement.

The progress and up-to-date state of the art in measuring voltages at frequencies to 10 GHz and higher at three accuracy echelons is briefly described. The trend towards higher frequencies in voltmeter design is indicated. Justifications for this trend are listed. Advantages of voltage measurements and standards over computation of voltages from power and impedance measurements are briefly discussed. Some pending development problems are indicated and major steps are proposed to improve the application of voltmeters at frequencies above 30 MHz.

**10060.** Selby, M. C., **Brief report of the XV URSI General Assembly, Com. I, on the status of international intercomparisons of high frequency and microwave electrical quantities,** (Proc. XV General Assembly of URSI, Munich, Germany, Sept. 5-15, 1966), Chapter in *Progress in Radio Science 1963-1966,* **Pt. 1,** pp. 113-116 (International Scientific Radio Union, Munich, Germany, Sept. 1966).

Key words: International intercomparisons; radio measurements.

A report is given on the intercomparisons completed, in progress, and planned under the auspices of URSI and the CIPM.

**10061.** Selby, M. C., **International comparison of high frequency electromagnetic quantities,** *Proc. IEEE* **55,** No. 6, 745-747 (June 1967).

Key words: Electrical quantities at high frequencies, measurement of; high frequency electrical measurements; international agreement on electromagnetic measurements.

Activities to establish international agreement on measurements of high frequency electrical quantities have been in progress since 1957 at the initiative of the URSI (International Radio Scientific Union) and the International Committee of Weights and Measures (CIPM). Results accomplished and the overall up-to-date status are presented.

**10062.** Selby, M. C., **International comparison of measurements at high frequencies,** *IEEE Spectrum* **3,** No. 1, 89-98 (Jan. 1966).

Key words: Electrical quantities; high frequencies; international comparison of measurements; measurements at high frequencies.

The status of international agreement in measuring electrical quantities at frequencies above approximately 30 kHz, as of 1965, is analyzed. An attempt is made to tell (1) why it is necessary to agree internationally on measurements of high frequency electrical quantities, (2) for what specific quantities and related ranges ("measurands") agreement is desirable at present, (3) what has been done in the past towards that end, and (4) what is being planned for the future. Aims and relative responsibilities and authorities of the International Electrotechnical Commission (IEC), of the International Radio Scientific Union (URSI), and of the International Bureau of Weights & Measures (BIPM) are briefly indicated.

**10063.** Selby, M. C., **Remarks for XV URSI General Assembly Session on progress at $f \leq 1$ GHz,** (Proc. XV General Assembly of URSI, Munich, Germany, Sept. 5-15, 1966), Chapter in *Progress in Radio Science 1963-1966,* **Pt. 1,** pp. 157-162 (International Scientific Radio Union, Munich, Germany, Sept. 1966).

Key words: Measurement of field strength; measurement of pulsed voltage; measurement of rf voltage; measurement of thermal noise.

Several recent NBS contributions in the area of electromagnetic measurement are briefly described, namely, a miniaturized near-zone electric-field probe, a thermal noise comparator, a pulse-peak voltmeter and a special Tee for rf voltage calibrations.

**10064.** Selby, M. C., **The system of electromagnetic quantities at 30 kHz to 1 GHz,** *Metrologia* **2,** No. 1, 37-45 (Jan. 1966).

Key words: Electromagnetic quantities; frequencies; standards; units.

The system of electromagnetic quantities, units, and standards at frequencies of 30 kHz to approximately 1 GHz is briefly described. Its application at the National Bureau of Standards is used as an example. The system with some likely modifications seems in operation in several technically developed countries and is tentatively suggested for newly developing countries. Basic and derived physical quantities, and conceptual bases of standards and methods of measurement are described. Ranges of accuracies are given and suggestions for extensions of the system and for establishing validity via international comparison are pointed out.

**10065.** Sengers, J. M. H. L., **Compressibility, gas,** *Encyclopedia of Physics,* R. Besaucon, ed., pp. 118-120 (Reinhold Publ. Corp., New York, N.Y., Jan. 1966).

Key words: Compressibility; compressibility factor; gases; radial distribution function; speed-of-sound.

A definition of compressibility is given. Also a brief discussion is given of experimental methods for determining this quantity, its experimental behavior and an explanation of this behavior in terms of molecular theory. Some references to recent reviews of experimental and theoretical effort are added.

**10066.** Shafer, A. B., **Hamilton's mixed and angle characteristic functions and diffraction aberration theory,** *J. Opt. Soc. Am.* **57,** No. 5, 630-639 (May 1967).

Key words: Aberration; diffraction; Hamilton's characteristic functions.

The use of Hamilton's mixed and angle characteristic functions in wave and diffraction aberration calculations is theoretically examined. The relation of Hamilton's mixed and angle characteristic functions to the wave aberration function is shown. From this relation a wave aberration function is derived. The mixed and angle characteristic functions as utilized in diffraction theory via the Luneberg-Debye integrals are examined. The mathematical and physical approximations are discussed. The use of the Luneberg-Debye diffraction integrals for image evaluation is examined and some difficulties are pointed out. It is concluded that the above methods are poor approximations to more rigorous methods.

**10067.** Shapiro, S. L., McClintock, M., Jennings, D. A., **Brillouin scattering in liquids at 4880Å,** *IEEE Quantum Electron.* ***QE-2,*** No. 5, 89-93 (May 1966).

Key words: Argon ion laser; Brillouin scattering; hypersonic velocity; organic liquids; Rayleigh wings.

An argon ion laser has been used as a source of 4880Å radiation to study Brillouin scattering in liquids. Hypersonic velocities were measured in benzene, carbon disulfide, carbon tetrachloride chloroform, methylene chloride, methylene iodide, toluene, and water at a scattering angle of 89° 45′. The width of the Brillouin line was found to be 0.042 $cm^{-1}$ in toluene and 0.040 $cm^{-1}$ in methylene chloride. Depolarization factors of the

Brillouin lines were measured in carbon disulfide, benzene, and toluene. The structure of the Rayleigh lines and depolarization of the Rayleigh wings were also measured in benzene, carbon disulfide, and toluene. Widths of the Rayleigh wings were approximately 6.8 cm$^{-1}$ in benzene, 7.6 cm$^{-1}$ in carbon disulfide, and 8.5 cm$^{-1}$ in toluene. From measurements of Brillouin scattering intensity, approximate values of the electrostrictive coupling constants of the other seven liquids were calculated relative to those of carbon disulfide.

**10068.** Sharnoff, M., Reimann, C. W., **Charge-transfer spectrum of the tetrachlorocuprate ion,** *J. Chem. Phys.* **46,** No. 7, 2634-2640 (Apr. 1, 1967).

Key words: Band assignments; charge transfer spectra; $Cs_2CuCl_4$; $Cs_2ZnCl_4(Cu)$; tetrachlorocuprate ion; single crystals.

The polarized ultraviolet absorption spectra of the tetrahedral $CuCl_4^{=}$ ion oriented in single crystals of $Cs_2CuCl_4$ or $Cs_2ZnCl_4$ have been observed. The spectral bands are identified by means of an analysis which takes into account the observed variations with lattice of the band intensities and positions and which allows for the effects upon the spectra of terms of rhombic symmetry known to be present in the ionic Hamiltonian. The resulting band assignments are significantly different from those of Ferguson. Salient differences between the $Cs_2CuCl_4$ observed spectra and those reported by Ferguson are noted and tentatively explained.

**10069.** Shields, W. R., **The evolution of the accuracy of isotopic analysis by thermal ionization from 2% to 0.2%,** (Proc. Symp. Nuclear Materials Management, IAEA, Vienna, Austria, Aug. 30-Sept. 3, 1965), Chapter in *Nuclear Materials Management,* pp. 737-746 (Intern. Atomic Energy Agency, Vienna, Austria, Feb. 1966).

Key words: Isotopes; precise analysis; thermal ionization; uranium.

A detailed study of the parameters that affect the precision, both internal and external, of an isotopic analysis has been made. The magnitude of the effects of some of these parameters on the analysis of transuranic elements is shown.

The product of this research is a table of the best estimates of the isotopic compositions of sixteen uranium isotope standards distributed by the National Bureau of Standards. The current level of analytical proof of these values is given along with a discussion of the work (in progress) that is necessary to change the analytical precision statements to accuracy statements.

**10070.** Shoub, H., Gross, D., **Doors as barriers to fire and smoke,** *Proc. Symp. Fire Testing, Lancaster, Pa., June 24-25, 1965,* pp. I-1—I-10 (Armstrong Cork Co., Lancaster, Pa., 1965).

Key words: Doors, dwelling; dwelling unit entrance doors; fire and smoke barriers, dwelling unit entrance doors.

A study was made of means for improving dwelling unit entrance doors as fire and smoke barriers. Existing combustible doors and frames could be modified to enhance their fire resistance, but it did not appear practical to raise them to the level of rated commercial fire door assemblies. Fire retardant paints, except those consisting of heavy, reinforced, intumescent-type coatings, provided little or no increase in fire resistance.

Several modifications of existing doors were not effective in preventing the transmission of smoke. However, controlling the pressure levels on both sides of a door, as by suitable venting, appeared to offer a means of reducing smoke penetration into an area.

It is recommended that current methods of fire tests of doors, and criteria relating to their fire and smoke transmission be improved.

**10071.** Shumaker, J. B., Jr., Popenoe, C. H., **Experimental transition probabilities for the ArI 4s-4p array,** *J. Opt. Soc. Am.* **57,** No. 1, 8-10 (Jan. 1967).

Key words: Argon; plasma; spectroscopy; transition probability.

Thermal arc measurements of transition probabilities are reported for the entire 4s-4p transition array of argon I. Except for a few very weak lines the experimental values agree closely with the recent intermediate coupling calculations of Garstang and Van Blerkom.

**10072.** Sicilio, F., Florin, R. E., Wall, L. A., **Kinetics of the hydroxyl radical in aqueous solution,** *J. Phys. Chem.* **70,** No. 1, 47-52 (Jan. 1966).

Key words: Aqueous solutions; electron spin resonance; hydroxyl radicals; kinetics; resonance spectra.

The electron spin resonance spectrum of hydroxyl radical, generated from titanous ion and hydrogen peroxide in a flow system, was studied as a function of flow rate, temperature, and variations in composition of mixture. Two peaks occur, a principal peak at $g = 2.0128$ and a usually minor peak at $g = 2.0114$. The intensity of the minor peak is increased by large concentrations of titanous chloride or sulfate, increased slightly by large concentrations of titanic salts, and lowered by excess sulfuric acid. The minor peak is thought to be the spectrum of hydroxyl associated with titanic ion.

At 20 °C and 28 °C the concentration of hydroxyl shows a maximum as flow rate is varied, while the concentration increases monotonically with increasing flow rate at 58 °C. At low flow rates (time after mixing 0.5 to 4 sec) there appears to be an approach to second-order disappearance with $k = 4.5 \times 10^5$ $\ell$/mole sec at 28 °C and an activation energy of 11 kcal. 11 kcal/mole(46kJ/mole).

**10073.** Simpson, J. A., **The production and use of monoenergetic electron beams,** *Proc. 8th Annual Electron & Laser Beam Symp., Ann Arbor, Mich.,* G. I. Haddad, ed., pp. 437-447 (Apr. 1966).

Key words: Electrons; electron beam; electron energy distributions; space charge.

The generation of dense electron beams of energy half-width below 0.1 eV presents special problems. Among these are generation of tightly collimated beams of very low energy space charge effects in deflectors and anomalous energy spreads. A discussion of one successful attack on these problems will be given together with examples of the uses of such beams in electron optics.

**10074.** Simpson, J. A., Kuyatt, C. E., Mielczarek, S. R., **Absorption spectrum of $SF_6$ in the far ultraviolet by electron impact,** *J. Chem. Phys.* **44,** No. 12, 4403-4404 (June 15, 1966).

Key words: Forward inelastic electron scattering; oscillator strength; sulfur hexafluoride; ultraviolet absorption cross section.

Measurements of forward inelastic scattering of 400 eV electrons from $SF_6$ were made and used to derive relative ultraviolet absorption cross sections. The relative values were normalized to an ultraviolet absorption measurement at 23.00 eV. Agreement with additional u-v measurements at 21.2 and 17.6 eV was excellent. Oscillator strengths for three absorption bands between 10 and 15 eV, as derived from the electron scattering measurements, are in fair agreement with the corresponding values measured by u-v absorption. The total oscillator strength for excitations up to 32 eV is found to be 15.3.

**10075.** Simson, B. G., Deslattes, R. D., **Kinematic locator for crystal alignment,** *Rev. Sci. Instr.* **37,** No. 3, 300-301 (Mar. 1966).

Key words: Crystal alignment; crystal polishing; kinematic locator; spectrometer alignment.

A kinematic locator with one rotational degree of freedom is described. This device makes possible the transfer of aligned crystals within 2 seconds of arc.

**10076.** Sligh, J. L., Brenner, A., **Galvanostalametry: A technique for chemical analysis,** *J. Electrochem. Soc.* **114,** No. 5, 461-465 (May 1967).

Key words: Chemical analysis; electrolyte discharge; electro-reducible or -oxidizable; galvanostalametry; hydrogen; oxygen.

A method utilizing a novel technique to designate the endpoint of a diffusion controlled electro-reducible or -oxidizable reaction has shown promising analytical capability. The apparatus consists of a J-shaped, evacuated glass tube in which a column of electrolyte is suspended under tensile stress in the longer limb. One electrode is sealed into the top of the J and the other into the short limb. The formation of a minute amount of gas at the upper electrode by electrolytic discharge of hydrogen or oxygen causes the column of electrolyte to suddenly drop. It has been found that, in the constant-current electrolysis of a suitable supporting electrolyte containing an electroreactive ion, the transition time required for the column to drop is a function of the concentration of the ion. The use of this method as an analytical tool and its relationship to chronopotentiometry are discussed.

**10077.** Smith, E. L., Bowman, H. S., Weissler, P. G., Cook, R. K., **Bone-air cancellation,** *Bull. Lab. Electroacoustique* **9,** 45-50 (Apr. 1966).

Key words: Air-conduction; audiometry; bone-air cancellation; bone-conduction; hearing; masking; psychoacoustics; threshold.

An experimental study using bone-air cancellation to correlate the sensation levels of the air and bone signals and the occlusion effect of audiometric earphones has been made. Attempts were also made to use cancellation in lieu of masking in bone-conduction threshold determinations.

**10078.** Smith, G. W., Becker, D. A., Lutz, G. J., Currie, L. A., DeVoe, J. R., **Determination of trace elements in standard reference materials by neutron activation analysis,** *Anal. Chim. Acta* **38,** 333-340 (1967).

Key words: Accuracy; activation; analysis; decay curve resolution; gamma-ray attenuation; geometrical location; neutron; neutron self-shielding; precision; similar gamma-ray energy; Standard Reference Materials; trace.

Neutron activation analysis with its high sensitivity and accuracy in trace analysis, is being used at the NBS for analysis of Standard Reference Materials. Problems affecting precision and accuracy have been encountered and solutions to four problems are discussed. First, the positive bias introduced by induced radioactivity of similar gamma-ray energy was found in the determination of interstitial argon in ultra-pure silicon. A decay curve resolution technique was used to compensate for the error. Secondly, errors due to differences in geometrical location between sample and standard during irradiation were observed. Flux gradients were determined by copper foil flux monitoring to give necessary means of correction. Thirdly, errors are caused by differences in neutron self-shielding between sample and standard during irradiation. An empirical correction method was used and computer program written for calculation. Examples are given. Finally, the problem of gamma-ray attenuation during counting of sample and standard has been explored. A theoretical and experimental study gives the necessary corrections. It is concluded that careful study is vital to assure accurate analyses by neutron activation analysis on trace elements in complex matrices such as many Standard Reference Materials.

**10079.** Smith, J. C., **Wave propagation in a three-element linear spring and dashpot model filament,** *J. Appl. Phys.* **37,** No. 4, 1697-1704 (Mar. 15, 1966).

Key words: Dashpot model filament; filaments; linear model; model filament; wave propagation.

Mathematical expressions are derived for the particle velocity, stress, and strain distributions in the wave that results when a semi-infinite viscoelastic filament is subjected at one end to constant velocity tensile impact. The equations governing the stress-strain-time behavior of the filament are assumed to be those for a linear model consisting of a spring coupled in parallel with a spring and dashpot in series. These equations are so formulated that by changing a single parameter either the spring branch or spring and dashpot branch can be made to dominate. The general solution, and special solutions describing the behavior at the wave front and at the point of impact are derived. Approximate solutions for rough calculations are also given. The application of these solutions in the interpretation of experimental data is discussed.

**10080.** Smith, W. W., Gallagher, A. C., **Radiation lifetime of the first $^2P_{3/2}$ state of ionized calcium and magnesium by the Hanle effect,** *Phys. Rev.* **145,** No. 1, 26-35 (May 6, 1966).

Key words: $Ca^+4^2P_{3/2}$ state; collisional depolarization; Hanle effect; $Mg^+3^2P_{3/2}$ state; radiative lifetime.

The lifetimes of the $Ca^+4^2P_{3/2}$ state and $Mg^+3^2P_{3/2}$ state have been measured by the Hanle-effect method with optical excitation from the ground states of the ions. The lifetimes are, respectively, $6.72 \pm 0.20 \times 10^{-9}$ sec. and $3.67 \pm 0.18 \times 10^{-9}$ sec. The ions were produced by introducing traces of calcium or magnesium into an argon discharge. Alignment depolarization cross sections, $\sigma$, were obtained for the collisional depolarization of the following states of calcium and magnesium due to collisions with argon.

$$\sigma(Ca4^1P_1 \text{ state}) = 1.9 \pm 0.3 \times 10^{-14} \text{ cm}^2$$

$$\sigma(Mg3^1P_1 \text{ state}) = 1.9 \pm 0.3 \times 10^{-14} \text{ cm}^2$$

$$\sigma(Ca^+4^2P_{3/2} \text{ state}) = 1.4 \pm 0.2 \times 10^{-14} \text{ cm}^2$$

$$\sigma(Mg^+3^2P_{3/2} \text{ state}) = 1.3 \pm 0.25 \times 10^{-14} \text{ cm}^2.$$

**10081.** Spangenberg, W. G., Rowland, W. R., Mease, N. E., **Measurements in a turbulent boundary layer maintained in a nearly separating condition,** (Proc. Symp. Fluid Mechanics of Internal Flow, General Motors Research Labs., Warren, Mich., 1965), Chapter in *Fluid Mechanics of Internal Flow,* Gino Sovarn, ed., pp. 110-151 (Elsevier Publ. Co., Amsterdam, The Netherlands, 1967).

Key words: Adverse pressure; boundary layer; near-separating flow; skin friction near-zero; turbulence; turbulent boundary layer.

A turbulent boundary layer on a smooth, flat wall was investigated where the pressure was increasing with increasing distance downstream such as to maintain the boundary layer in the condition of near separation. The investigation was conducted with air flowing in a channel having the boundary-layer wall as the bottom. The width was sufficient to permit realization of two-dimensional boundary-layer flow. Venting and sloping incorporated in the upper wall provided the control of pressure gradient by progressively decreasing the velocity within the duct with increasing distance downstream. The maximum free-stream velocity was always about 84 ft per sec. The depth was sufficient to realize a free stream above the boundary layer except at the farther downstream positions where the boundary-layer flow itself reached the upper wall and escaped through the vents. Measurements of turbulence as well as of mean flow are made in order to reveal more of the mechanics of such flows than hitherto known. Measurements of turbulence were made with hot-wire instrumentation, and these comprised turbulence intensity, transverse integral scale, and turbulent shearing stress. Mean velocities were measured both with the hot-wire anemometer and total-head tube. Skin friction was estimated from mean-velocity profiles. Results were obtained for two slightly different pressure distributions, one yielding a closer approach to separation and vanishing skin friction than the other.

**10082.** Sparks, L. L., Powell, R. L. **Cryogenic thermocouple thermometry,** *Meas. Data* **1,** No. 2, 82-90 (Mar.-Apr. 1967).

Key words: Cryogenics; thermocouples; thermometry.

Commercially available low-temperature thermocouple wire from all major U.S. manufacturers has been exhaustively tested to determine the inhomogeneity and interchangeability characteristics of the wire. Spot calibrations between liquid-helium and liquid-nitrogen temperatures, and between liquid-nitrogen and ice temperatures, show that the NBS interim low-temperature tables are sufficient for most engineering and scientific requirements. Preliminary work on several gold-iron alloys indicates that these alloys will allow more accurate thermoelectric temperature measurement in the liquid/helium-hydrogen temperature range. Research, now well underway, will lead to establishment of standard thermocouple tables for temperatures from liquid helium up to 0 °C for all of the cryogenically useful commercial thermocouple alloys.

**10083.** Spector, N., **Analysis of the spectrum of neutral erbium (Er I),** *J. Opt. Soc. Am.* **56,** No. 3, 341-349 (Mar. 1966).

Key words: Absorption lines of erbium (Er I); energy levels of erbium (Er I); erbium (Er I), spectrum analyzed.

First results of a continuing analysis of Er I are given: 30 low levels belonging to the odd configurations $4f^{11}5d6s^2$ and $4f^{11}5d6s$, as well as 138 high levels of even parity are assigned *J*-values. More than 300 absorption lines are classified. The connection of the odd levels to the $4f^{12}6s^2$ configuration is established, using transitions in the infrared. The energy matrices in intermediate coupling for the subconfiguration $f^{11}(^4\mathrm{I})d$ have been calculated and are given. The theoretical formulas were adjusted by a least-squares fit to 19 observed levels designated as $4f^{11}\ (^4\mathrm{I}_{7\ 1/2}{}^{6}{}_{1/2})\ 5d6s^2$ resulting in new values for 6 electrostatic and 2 spin-orbit interaction parameters. The rms error was 186 cm$^{-1}$. Calculated percentage compositions in various coupling schemes show the $J_1 = j$ type to be the best for these levels.

**10084.** Spijkerman, J. J., Ruegg, F. C., DeVoe, J. R., **A standard reference material for Mössbauer spectrometry of iron and its compounds,** *Technical Reports Series* **50,** Applications of the Mössbauer Effect in Chemistry and Solid-State Physics, pp. 254-259 (International Atomic Energy Agency, Vienna, Austria, 1966).

Key words: Iron and its compounds; Mössbauer spectrometry; spectrometry-Mössbauer; standard reference materials.

The rapid development of the Mössbauer effect has resulted in a new spectrometric method for chemical structure analysis. The various sources used in Mössbauer spectroscopy requires a reference material to provide Mössbauer data on a uniform basis. A series of standard reference materials for Mössbauer spectroscopy will be made available from the National Bureau of Standards, U.S.A. The first in this series is a single crystal of disodium pentacyanonitrosylferrate dihydrate, $Na_2[Fe(CN)_5NO]\cdot 2H_2O$. The crystals are supplied by a commercial manufacturer, and calibrated by NBS on a Mössbauer spectrometer, using an optical fringe counting technique. The Mössbauer spectrum of a single crystal absorber, cut along the bc plane, is a well resolved, symmetric doublet. The center of this doublet is defined as the zero reference point for the differential chemical shift, with the containing absorber at 25.0 °C. The absorber crystals supplied will be 1cm × 1cm, with 25.0 mg/cm$^2$ of natural iron.

**10085.** Stabler, T. M., **State standards and laboratories,** *Scale J.* **53,** No. 1, 3 (Oct. 1966).

Key words: Calibration and measurement; instruments; length; mass; state measurement centers; state standards.

The program of the Federal Government to supply new standards of mass, length, volume, and instruments to each State is now underway. Ten States have been chosen to receive them beginning January 1966. These States have had to provide suitable laboratories and qualified personnel to perform the calibrations and to promote measurement. The National Bureau of Standards will assist the States in the establishment of the laboratories and in the training of the technologists. The final goal is to have established the State Measurement Center in all 50 States.

**10086.** Stabler, T. M., **The role of the National Bureau of Standards in the establishment of measurement capability at the state level,** 1966 ISA Conference Proceedings (21st Conf., Oct. 24-27, 1966, New York, N.Y.), *Instr. Soc. Am. Preprint* **16.**1-3-66, pp. 1-3 (Oct. 1966).

Key words: Laboratory; measure; standards; States; training; weights.

The program of the Federal Government to supply new standards and instruments to each State is now underway. Ten States have been chosen to receive certain standards as of this winter. These States have had to provide suitable laboratories and qualified personnel to perform the calibrations and to promote measurement. The National Bureau of Standards will assist the States in the establishment of the laboratories and in the training of the technologists. The final goal is to establish a well-equipped State Measurement Center in each of the 50 States.

**10087.** Stair, R., **The measurement of solar radiation, with principal emphasis on the ultraviolet component,** *Air Water Pollut. Intern. J.* **10,** 665-688 (1966).

Key words: Solar radiation; stratospheric ozone; ultraviolet solar radiation.

A review is presented covering much of the scientific work of the past half century relating to the measurement of the spectral distribution of radiant energy (in particular in the ultraviolet region) from the sun. Mention is made of those special solar disturbances that are expected to result in large variations of the ultraviolet solar emission as well as the absorbing medium, ozone, which through its turbulence and distribution further affects greatly the spectral distribution of the solar radiation reaching the earth's surface at any locality. Various instrumentations and the standards employed by the different laboratories are discussed in some detail with emphasis placed upon some of their shortcomings and the great lack of accurate solar spectral data, in particular within the ultraviolet region. Finally, new instrumentation offering promise of considerable usefulness in obtaining rapidly more accurate data in this area is described.

**10088.** Stavroudis, O. N., **Two-mirror systems with spherical reflecting surfaces,** *J. Opt. Soc. Am.* **57,** No. 6, 741-748 (June 1967).

Key words: Cassegrainian systems; collimators; cubic equations; optical design; reflecting systems; third order spherical aberration.

An analysis is made of two-mirror systems consisting of spherical refracting surfaces. Solutions are found for those systems having zero third order spherical aberration. It is shown that no practical solution exists for the configuration resembling the Gregorian telescope. For the configuration resembling the Cassegrainian telescope three one-parameter families of solutions obtain. These are given by

$$c_1 = (q - 1)/2\, t_o \quad t_1 = (t_o - f)/q \quad c_2 = q/2f$$

$$t_o = f\, 27f/32 \sec^2\theta \quad q = -3[1 + 4 \cos 2/3\, (\theta + \pi r)]^{-1}$$

where $c_1$ and $c_2$ are the two curvatures; $t_1$, the axial separation of the two reflecting surfaces; $t_o$, the distance from a focus to the corresponding surface; and f, the focal length. The free parameter is $\theta$ and $r = 0, 1, -1$.

**10089.** Stearns, C. O., **Computed performance of moderate size, super-gain, end-fire arrays,** *IEEE Trans. Ant. Prop.* ***AP*-14,** No. 2, 241-242 (Mar. 1966).

Key words: Antenna arrays; computed performance; end-free antenna arrays; radiation patterns; super-gain antennas.

Using an approach developed by Block, Medhurst, and Pool, numerical calculations were carried out of gains, currents, and radiation patterns, for a series of moderate-size super-gain antennas. These were linear end-fire arrays of equally spaced, parallel, side-by-side, infinitesimal, half-wave dipoles with element spacings of 0.05, 0.10, 0.15, 0.20, 0.25, and 0.30 wavelength for 2 to 17 elements.

A rapid increase in the required precision in current values with an increase in the number of elements sets an upper limit on the number of elements for a given element spacing. For 0.05-wavelength element spacing, the largest number of elements which could be computed using eight-figure precision was 5; while for 0.30-wavelength spacing the performance of a 17-element antenna could be computed. However, these computations can be verified far beyond the practicability of a real antenna.

**10090.** Stephens, R. E., **Experimental verification of superachromatism,** *J. Opt. Soc. Am.* **56,** No. 2, 213-214 (Feb. 1966).

Key words: Achromatism; superachromatism.

To experimentally verify superachromatism a five-element prism, to deviate a beam of light approximately 30 degrees without dispersion or distortion, has been designed and constructed from three types of Schott glass. When tested on a spectrometer, viewing a narrow slit with a telescope magnification of approximately 30 times, no dispersion could be seen. Pointings on 7 isolated spectrum lines separated by a monochromator show a maximum dispersion of 3 seconds, 1 part in 36,000.

**10091.** Stokesberry, D. P., **A large signal IGFET dc source follower,** *Proc. IEEE* **54,** No. 1, 66 (Jan. 1966).

Key words: Constant gain; dc source follower; field-effect transistor.

The low transconductance and small dynamic range of an insulated-gate field effect transistor limit its usefulness in dc source follower circuits. This limitation is removed by a modified circuit, which exhibits source follower action while maintaining a constant drain-to-source voltage.

**10092.** Straus, S., Brown, D. W., **The thermal decomposition of poly-3,3,3-trifluoropropene made at high pressure,** (Proc. 152nd American Chemical Society Meeting, New York, N.Y., Sept. 13, 1966), *Polymer Preprint* **7,** No. 2, 1128-1132 (Sept. 1966).

Key words: High pressure; initiation rate; poly-3,3,3-trifluoropropene; pyrolysis; random component; thermal decomposition; volatilization.

Poly-3,3,3-trifluoropropene prepared by irradiating the monomer at various temperatures and pressure has been pyrolyzed in vacuo in the temperature range 397-432 °C. At 402 °C the pyrolysis rates at 20 percent volatilization vary by a factor of 20 depending on the polymerization conditions. The rate of volatilization decreases smoothly with the fraction volatilized except with the most stable polymer, with which the rate is constant over a considerable portion of the pyrolysis. Molecular weight drops are extremely rapid and the monomer yield is only about 0.3 percent. Dimer and trimer are thought to be formed in yields of 5 and 15 percent respectively. The overall behavior probably results from a mechanism with a large random component but with an initiation rate that depends on the polymerization conditions and the extent of pyrolysis.

**10093.** Streever, R. L., Uriano, G. A., **Nuclear-resonance spin-echo study of $^{61}$Ni hyperfine fields in ferromagnetic Ni-Al, Ni-V, and Ni-Cr systems,** *Phys. Rev.* **149,** No. 1, 295-301 (Sept. 9, 1966).

Key words: Hyperfine-field and atomic-moment; Ni-Al; Ni-Cr; Ni-V; nuclear magnetic resonance.

The nuclear-magnetic-resonance line shapes of $^{61}$Ni have been studied in ferromagnetic Ni rich Ni-Al, Ni-V and Ni-Cr powders by plotting the spin-echo amplitude as a function of frequency across the inhomogeneously broadened resonance lines. The measurements were made at 4.2 °K in alloys containing concentrations of up to 12.3 at.% Al, 5.5% V and 5.3% Cr. In all three systems, the average hyperfine fields decreased approximately linearly with increasing solute concentration. A general discussion of the relationship between the average hyperfine field and the atomic moments is presented. The major contribution to the hyperfine field is believed due to the moment on the parent atom with a smaller contribution from moments on neighboring atoms via conduction electron polarization. The detailed structure of the resonance spectra is analyzed. It is found that the magnetic disturbances are spatially more widespread in the Ni-Al and Ni-V systems than in the Ni-Cr system. The Ni-Cr system in turn has a more delocalized behavior than the Ni-Co system previously studied. The results in the Ni-V and Ni-Cr system are consistent with results obtained by Collins and Low using neutron scattering techniques.

**10094.** Strobridge, T. R., Chelton, D. B., **Size and power requirements of 4.2 °K refrigerators,** (Proc. 1966 Conf., Boulder, Colo., June 13-15, 1966), Chapter in *Advances in Cryogenic Engineering* **12,** 576-584 (Plenum Press, Inc., New York, N.Y., 1967).

Key words: Cyclic refrigerators; physical characteristics; refrigerators.

A survey to determine the physical characteristics of 4.2 °K cyclic refrigerators is presented. Although the data acquired through the survey show considerable scatter, the expected trends can be detected and attempts have been made to establish guides by which the weight, volume, and power requirements for various capacity refrigerators may be estimated. No attempt is made to assess the reliability, the interval of maintenance free operation, or the capital costs.

**10095.** Stromberg, R. R., **Adsorption of polymers,** Chapter 3 in *Treatise of Adhesives and Adhesion,* **Vol. 1** *Theory,* pp. 68-118 (Marcel Dekkers, Inc., New York, N.Y. 1967).

Key words: Adsorption of polymers; adsorption of polymers review; interface studies; polymer adsorption; polymer adsorption review; review of polymer adsorption; surface studies.

The adsorption of polymers from solution onto solid surfaces is comprehensively reviewed. The theoretical treatments that are described, compared, and evaluated include the diffusion equation approach, a thermodynamic approach, and a direct combinational evaluation of the partition-function approach. This last treatment, together with certain modifications, apparently is the most correct treatment. Much of the experimental effort in polymer adsorption has been directed toward a determination of the extension of the adsorbed molecule normal to the surface. The measurement of this extension by means of ellipsometry, viscosity, and other techniques, is discussed in some detail, with emphasis given to the configuration of the adsorbed molecule. Measurement of the number of attachments to a surface are also included. Other subjects discussed are rates of adsorption and parameters influencing the adsorption isotherm such as molecular weight, solvent, and temperature dependence.

**10096.** Swanson, N., Powell, C. J., **Inelastic scattering cross sections for 20-keV electrons in Al, Be and polystyrene,** *Phys. Rev.* **145,** No. 1, 195-208 (May 6, 1966).

Key words: Al; Be; cross-sections; electrons; inelastic scattering; polystyrene.

Measurements are reported of the inelastic scattering cross sections associated with the characteristic energy losses of 20-keV electrons transmitted through thin films of Al, Be and polystyrene. These measurements have been made using two techniques which overcome several sources of systematic error in previous measurements.

For materials which have narrow characteristic loss lines (such as Al), it is possible to establish the form of the differential cross section and the generalized oscillator strength for the $\approx 15$ eV Al plasmon energy loss for scattering angles between zero and 20 mrad, the cutoff angle. The differential cross section has been used in repeated two-dimensional folding calculations to correct the intensity measurements of the multiple plasmon losses at the larger scattering angles where unambiguous intensity measurements could not be made. For materials which have broad characteristic loss peaks, such as polystyrene, it is not possible to establish the variation of generalized oscillator strength $f(q)$ with momentum transfer $q$. If it can be assumed that $f(q) \approx f(0)$ for small $q$, a cross section for a given loss can be obtained from an energy loss spectrum measured at one scattering angle. The cross-section measurement accuracy is improved by a comparison of two energy loss spectra, that of a standard (such as Al) and that of a material of unknown loss cross sections, which have been obtained at zero angle under the same measurement conditions.

**10097.** Takasaki, H., **An automatic ellipsometer. Automatic polarimetry by means of an ADP polarization modulator III,** *Appl. Opt.* **5,** No. 5, 759-764 (May 1966).

Key words: ADP modulator; automatic ellipsometer; ellipsometer; optics; polarimetry; thin film.

An analytical and experimental study of an automatic ellipsometer is reported. The polarized beam is modulated simultaneously by two ADP cells and the corresponding two signals are separated and are used to adjust polarizer and analyzer settings in any of the four zones. The reproducibility of the setting has been demonstrated to be of the order of .01 degree.

**10098.** Taylor, J. K., **Measurement of density and specific gravity,** Chapter 81 in *Treatise on Analytical Chemistry, Part 1, Theory and Practice* **7,** I. M. Kolthoff, P. J. Elving, and E. B. Sandell, eds., 4561-4610 (Interscience Publ., New York, N.Y. 1967).

Key words: Density; dilatometry; gases, density measurements; liquids, density measurements; solids, density measurements; specific gravity.

Density is an important and significant property of matter. For pure materials, density values may serve as one means of identification. For binary mixtures, such measurements frequently provide convenient methods for analytical determination of composition. Density values also may be combined with other physical properties such as viscosity or refractive index for analytical or structural determinations. In solid-state chemistry, precise density data on pure materials may provide information of the number of dislocations present in a given specimen.

An extensive literature exists both on methods for measurement of density and on tabulations of measured values for a wide variety of materials. An exhaustive review of this literature is outside the scope of this chapter. In fact, the reader is urged to consult original sources, especially for details of precision methods. Instead, general considerations will be presented here, especially those that might be useful to the practicing analytical chemist.

**10099.** Thomas, L., Norton, R. B., **Possible importance of internal excitation in ion-molecule reactions in the F region,** *J. Geophys. Res.* **71,** No. 1, 227-230 (Jan. 1, 1966).

Key words: Electron loss rate; electron temperature; F region; internal excitation; ion molecule; ionosphere; magnetic disturbance and aurorae.

The apparent electron loss rate in the *F* region is determined by ion-molecule reactions involving $O^+$ ions and $O_2$ or $N_2$ molecules. The present paper considers whether a dependence of the rate coefficients on internal excitation of the reactants could be important in the ionosphere and examines briefly the excitation and deactivation processes involved. Particular attention is paid to vibrational excitation of $N_2$ molecules and it is suggested that excitation by electron impact may be important especially during conditions of high electron temperature as might be expected during magnetic disturbances and aurorae.

**10100.** Tilford, S. G., Simmons, J. D., **Electric quadrupole transition in the $A\ ^1\Pi \leftarrow X\ ^1\Sigma^+$ system of CO,** *J. Chem. Phys.* **44,** No. 11, 4145-4147 (June 1, 1966).

Key words: Diatomic molecule; electric dipole; electric quadrupole; heteronuclear diatomic molecule.

In the fourth positive system, $A\ ^1\Pi \leftarrow X\ ^1\Sigma^+$, of CO, electric quadrupole transitions ($\Delta J = 2$) have been observed for the first time in bands of an electric dipole *allowed* transition. This system also represent the first example of an electric quadrupole transition to be observed in a heteronuclear diatomic molecule. The quadrupole transition probability has been determined to be $\approx 1.1 \times 10^3\ \text{sec}^{-1}$. This value compares well with the value of $\approx 2.0 \times 10^3\ \text{sec}^{-1}$ determined for the quadrupole transition probability of the electric dipole *forbidden* $a\ ^1\Pi_g \leftarrow X\ ^1\Sigma_g^+$ transition in the isoelectronic $N_2$ molecule.

**10101.** Tisone, G. C., Branscomb, L. M., **Detachment of electrons from $H^-$ by electron impact,** *Phys. Rev. Letters* **17,** No. 5, 236-238 (Aug. 1, 1966).

Key words: Cross section; electron beam; electron detachment; electron impact; ionization; negative ion.

**10102.** Torgesen, J. L., **Purification of single-crystal growth,** *Ann. N.Y. Acad. Sci.* **137,** 30-43 (1966).

Key words: Crystal growth; crystallization; single-crystal growth.

Full exploitation of crystallization's efficiency to purify is realized only as (1) surface-to-volume ratio is minimized; (2) trapping of impurities at intergrain boundaries is avoided; and (3) the process is conducted near equilibrium. These criteria are most nearly satisfied when crystallization is conducted to favor single-crystal growth. Phenomena which limit the attainment of complete purification are (1) formation of solid solutions, substitutional and interstitial; (2) occlusion of impurities at physical lattice defects; and (3) adsorption of impurities with subsequent occlusion through the morphology and kinetics of growth processes.

The distribution coefficient, a measure of purification efficiency, is the ratio of impurity concentration in the crystalline phase to that in the mother phase. It is dependent on diffusion, material transport, and adsorption. Theoretical and experimental evidence point to the conclusion that as crystallization occurs nearer equilibrium, as homogeneity in the fluid phase is more closely approached, the distribution coefficient approaches a limiting value, usually less than 1.

Techniques are described for the growth of single crystals from vapor, from melt (excluding zone refining) and from solution. Examples of attained purities are given. Solution growth is emphasized for advantages gained from lower temperature conditions.

**10103.** Tryon, M., Horowitz, E., **Rubber and rubber products,** Chapter 59 in *Standard Methods of Chemical Analysis, 6th Edition, IIIB. Instrumental Analysis,* F. J. Welcher, ed., pp. 1664-1763 (D. VanNostrand Co., Inc., Princeton, N.J., 1966).

Key words: Instrumental analysis of rubber; rubber, instrumental analysis.

A compilation of selected methods for analysis of rubber and rubber products by instrumental techniques.

**10104.** Tsai, D. H., Beckett, C. W., **Shock wave propagation in cubic lattices,** *J. Geophys. Res.* **71,** No. 10, 2601-2608 (May 15, 1966).

Key words: Crystal; cubic lattice; Hooke's law forces; lattice dynamics; Morse potential function; numerical computation; shock compression; shock propogation; shock wave.

We have studied from a lattice dynamics viewpoint the propagation of a strong one-dimensional shock wave in a semi-infinite cubic lattice. Our model included the simple cubic, face-centered and body-centered cubic configurations. The interactions between various neighbors, and different types of interactions, ranging from Hooke's law forces to forces corresponding to Morse type potential functions, were considered. The equations of motion were solved approximately by a numerical method. Our results showed that the computed shock velocity increased with particle velocity approximately in a linear manner, in good qualitative agreement with experimental data. However, the computed stress profile of the shock wave was not steady in time, and this unsteadiness raises some questions on the interpretation of the pressure-volume relationship of the shock compressed lattice.

**10105.** Tsang, W., **Thermal decomposition of 4,4-dimethylpentene-1 in a single pulse shock tube,** *J. Chem. Phys.* **46,** No. 7, 2817-2822 (Apr. 1, 1967).

Key words: Allyl radicals; allylic resonance energy; single pulse shock tube; t-butyl radicals; thermal decomposition; 1-butene; 1,5 hexadiene; 4-methylpentene-1; 4,4-dimethylpentene-1.

4,4-dimethylpentene-1 has been pyrolyzed in a single pulse shock tube. The initial process is apparently the breaking of the allylic carbon-carbon bond. The rate expression for the reaction,

$$C_4H_9-C_3H_5 \xrightarrow{k} t-C_4H_9\cdot + C_3H_5\cdot$$

has been found to be

$$k = 10^{15.8} \exp(-65{,}500/RT)\mathrm{sec}^{-1}.$$

Assuming no activation energy for the recombination process this leads to a value of 12 kcal for the allylic resonance energy.

**10106.** Tsang, W., **Thermal decomposition of hexamethylethane, 2,2,3-trimethylbutane and neopentane in a single pulse shock tube,** *J. Chem. Phys.* **44,** No. 11, 4283-4295 (June 1, 1966).

Key words: Bond energies; decomposition; hexamethylethane; isopropyl radical; methyl radicals; neopentane; pyrolysis; shock tubes; *t*-butyl radicals; 2,2,3-trimethylbutane.

Hexamethylethane, 2,2,3-trimethylbutane and neopentane have been pyrolyzed in a single pulse shock tube. The initial steps of the main reactions involve the breaking of carbon-carbon bonds. The rate parameters of the following reactions

$$C_4H_9-C_4H_9 \rightarrow 2\,t-C_4H_9\cdot,$$

$$C_4H_9-C_3H_7 \xrightarrow{k_{II}} t-C_4H_9\cdot + i-C_3H_7\cdot$$

and

$$C_4H_9-CH_3 \xrightarrow{k_{III}} t-C_4H_9\cdot + CH_3\cdot$$

have been found to be

$$k_I = 10^{16.3} \exp(-68{,}500/RT)\ \mathrm{sec}^{-1},$$

$$k_{II} = 10^{16.2} \exp(-73{,}000/RT)\ \mathrm{sec}^{-1}\ (1100\ ^\circ\mathrm{K}\ \text{and}\ 4\ \mathrm{atm.})$$

and

$$k_{III} = 10^{16.1} \exp(-78{,}200/RT)\ \mathrm{sec}^{-1}.$$

**10107.** Turgel, R. S., **A comparator for thermal AC-DC transfer standards,** ( *ISA Proceedings, Proc. 21st Annual ISA Conference and Exhibit, New York, N.Y., Oct. 24-27, 1966*) (ISA Preprint No. 12.3-1-66, Oct. 1966).

Key words: AC; calibration; DC; intercomparison; thermoelement; transfer standard.

Thermal transfer standards play an important role in precision a-c measurements. They are calibrated by intercomparison with standards of known ac-dc difference. A comparator is described that simplifies such routine calibrations. A sequence of null balances in the measuring circuit operates a simple analog computer which indicates the result of the intercomparison directly in parts per million of ac-dc difference.

**10108.** Vessot, R., Peters, H., Vanier, J., Beehler, R., Halford, D., Harrach, R., Allan, D., Glaze, D., Snider, C., Barnes, J., Cutler, L., Bodily, L., **An intercomparison of hydrogen and cesium frequency standards,** *IEEE Trans. Instr. Meas.* **IM-15,** No. 4, 165-176 (Dec. 1966).

Key words: Atomic clocks; cesium beam; clocks; frequency fluctuations; frequency standards; hydrogen maser; hyperfine separation; maser; noise; standards; time standards; wall shift.

Intercomparisons of average frequency and of frequency stability were made among one Hewlett-Packard 5060A cesium beam, two Varian Associates H-10 atomic hydrogen masers, and the National Bureau of Standards NBS III cesium beam designated as the United States Frequency Standard. Each of the standards displayed a white noise frequency fluctuation behavior with a transition into an approximate flicker of frequency fluctuation behavior for longer time intervals. The rms fractional frequency fluctuation between adjacent samples, $\sigma(\tau,N=2)$, was $6 \times 10^{-11}\tau^{-1/2}$ down to a flicker level of about $3 \times 10^{-13}$ for the hp 5060A cesium beam ($10^2 \leqslant \tau \leqslant 10^4$s), $1 \times 10^{-11}\tau^{-1/2}$ down to a flicker level of less than $1 \times 10^{-13}$ for NBS III cesium beam ($10^2 \leqslant \tau \leqslant 10^4$s), and $5 \times 10^{-13}\tau^{-1/2}$ down to a flicker level of about $1 \times 10^{-14}$ for the H-10 hydrogen masers ($10^{\circ} \leqslant \tau \leqslant 10^4$s). The accuracy capabilities of NBS III and H-10 No. 4 are now $1.1 \times 10^{-12}$ and $0.47 \times 10^{-12}$, respectively ($1\sigma$ estimate).

A discrepancy of only 1.1 parts in $10^{12}$ was observed between the average frequencies of the hp 5060A cesium beam and the NBS III cesium beam, with the former being higher in frequency.

In terms of the frequency of the $Cs^{133}$ hyperfine transition ($F=4$, $m_F=0$) ↔ ($F=3$, $m_F=0$), defined as 9192 631 770.0000 Hertz, the measured frequency of the $H^1$ hyperfine transition ($F=1$, $m_F=0$) ↔ ($F=0$, $m_F=0$) was $\nu_H = 1420\ 405\ 751.7864 \pm 0.0017$ Hertz. This is believed to be the most accurate and precise measurement of any physical quantity.

**10109.** Vieth, D. L., Yakowitz, H., **Design considerations for a Kossel microdiffraction camera,** *Rev. Sci. Instr.* **37,** No. 2, 206-209 (Feb. 1966).

Key words: Camera design concepts for electron probe microanalyzer; electron probe microanalyzer; Kossel microdiffraction technique.

A Kossel microdiffraction camera has been adapted to the National Bureau of Standards electron probe microanalyzer. Complete design concepts for any Kossel camera are discussed and evaluated. The details of their conversion to the National Bureau of Standards Kossel microdiffraction camera are given. The major concepts adopted were: (1) Transmission camera, (2) Inclusion of microgoniometric capabilities, (3) Film cassette in air rather than vacuum, (4) Variable source to film distance of 6 to 11 cm. Transmission pseudo-Kossel patterns of an aluminum crystal employing Cu radiation are shown to illustrate the capabilities of the camera.

**10110.** Vinti, J. P., **Effects of a constant force on a Keplerian orbit,** *Proc. Astronomical Union Symp. No. 25, Athens, Greece, Aug. 15-Sept. 3, 1964,* pp. 355-362 (1966).

Key words: Constant force; elliptic orbit; Keplerian orbit.

This paper applies the von Zeipel method to the perturbations by a constant force of a satellite in an elliptic orbit. As expected, the method fails in spherical coordinates but works in parabolic coordinates. The results account for the short-periodic and the first-order secular terms and go far enough to indicate that the long-periodic and the second-order secular terms can be calculated in physically achievable cases. The calculation of the latter effects depends on the resolution into constant and long-periodic terms of the Hamiltonian resulting after short-periodic terms have been eliminated. In contradistinction to the case where the perturbing potential is a zonal harmonic, this resolution requires an infinite Fourier series rather than a trigonometric polynomial. It is feasible whenever the applied force does not lie in the plane of the orbit. When the force is coplanar, however, the orbit eventually intersects the earth, so that there is less interest in following the orbit over a long interval of time.

**10111.** Vinti, J. P., **The spheroidal method in the theory of the orbit of an artificial satellite,** *Proc. Symp. Celestial Mechanics, Mathematische Forschungsinstitut, Oberwolfach, Germany, Mar. 1964,* pp. 97-111 (1964).

Key words: Artificial satellite; gravitational potential; oblate planet; satellite spherical method.

This paper developed the physical foundations for the formulation of a gravitational potential, in oblate spheroidal coordinates, appropriate for an oblate planet. As applied to the Earth, the adequacy of the model follows from the minuteness of the deviations of the resulting geoid from the true sea-level figure of the Earth. For the motion of an artificial satellite, the potential leads to a solution in quadratures, which is found. Inversion then leads to expressions for the coordinates as functions of time. Finally, von Zeipel's theory gives the perturbations produced by the small effects not represented by the model.

**10112.** Voth, R. O., Norton, M. T., Wilson, W. A., **A cold moderator refrigerator incorporating a high-speed turbine expander,** (Proc. 1965 Cryogenic Engineering Conf., Rice University, Houston, Texas, Aug. 23-25, 1965), Chapter in *Advances in Cryogenic Engineering* **11,** 126-138 (Plenum Press, Inc., New York, N.Y., 1966).

Key words: Brayton cycle; cold neutron moderator; cryogenic refrigerator; gas bearings; turbine expander.

The thermal cycle and high speed gas bearing supported turbine expander chosen for a 1000 watt refrigerator used in a nuclear research program is described. Results of the refrigerator tests under operational conditions are presented. A bearing analysis extends previous work to include the effect of end leakage on the performance of Sixsmith type gas bearings.

**10113.** Wachtman, J. B., Jr., Peiser, H. S., **Symmetry conditions on jump rates occurring in relaxation times associated with point defect motion,** *J. Phys. Chem. Solids* **27,** 975 (1966).

Key words: Crystallographic point group; jump rates; point defects; relaxation times; space group; symmetry condition.

Relaxation times for mechanical or dielectric relaxation processes associated with atomic jump frequencies which are all symmetrically equivalent may differ for algebraic reasons but are usually of the same order of magnitude. If two or more symmetrically inequivalent jump rates are necessary for the relaxation process, the relaxation times may differ by orders of magnitude. Symmetry considerations can give the maximum and the minimum number of symmetrically inequivalent jump rates required. The results have been tabulated for the most general type of point defect neighboring a fixed trapping center for the case of complete removal of degeneracy.

**10114.** Wachtman, J. B., Jr., Spinner, S., Brower, W. S., Fridinger, T., Dickson, R.W., **Internal friction in rutile containing Ni or Cr,** *Phys. Rev.* **148,** No. 2, 811-816 (Aug. 1966).

Key words: Activation energy; internal friction; point defect; reduction; rutile; symmetry conditions.

Rutile containing Ni gives an internal friction peak centered near 50 °C at 2 kHz characterized by $H = 15.3 \pm 2.4$ kcal/mole and $\tau_0 = 3 \times 10^{-15 \pm 1.7}$ sec; this peak occurs for tensile stress along [100] or [110]. A peak centered near 200 °C with $H = 21.4 \pm 2.1$ kcal/mole and $\tau_0 = 8 \times 10^{-15 \pm 1.0}$ sec occurs for stress along [100] but not for stress along [110]. Rutile containing Cr gives similar peaks characterized by $H = 13.5 \pm 2.4$ kcal/mole and $\tau_o = 2 \times 10^{-14 \pm 1.6}$ sec and by $H = 22.2 \pm 1.5$ kcal/mole and $\tau_o = 4 \times 10^{-15 \pm 0.9}$ sec. Light reduction in vacuum decreases the amplitude of the low temperature peak and enhances the high temperature peak in both cases. Heavy reduction of rutile containing Cr removes both peaks but they reappear upon subsequent reoxidation. The evidence suggests that the motion of interstitial cations is involved and that reduction causes the formation of a compound defect. A tentative interpretation is given in terms of unpaired $Ni^{3+}$ interstitials for the low temperature peak and of interstitial pairs composed of $Ni^{3+} - Ti^{3+}$ for the high temperature peak in Ni-doped specimens; the corresponding peaks in Cr-doped rutile are tentatively interpreted in terms of $Ti^{4+}$ interstitials and of interstitial pairs consisting of $Ti^{4+} - Ti^{3+}$. It is possible to have two charge-compensating $Cr^{3+}$ on adjacent substitutional sites and preserve the last two models.

**10115.** Waclawski, B. J., Hughey, L. R., Madden, R. P., **Effect of oxygen on the photoelectron yield from tungsten in the vacuum ultraviolet,** *Appl. Phys. Letters* **10,** 305 (1967).

Key words: Oxygen adsorption; photoelectric effect; tungsten; vacuum ultraviolet.

The effect of adsorbed oxygen on the photoelectron yield of bulk polycrystalline tungsten was studied at photon energies of 7.7, 10.2, 11.8, 16.9, and 21.2 eV. Use of ultra-high vacua $\sim 3 \times 10^{-10}$ torr ensured sample cleanliness prior to oxygen exposure. The photoelectron yield decreases with oxygen exposure because of the increase in the electronic work function of the tungsten photocathode. However, at $h\nu = 21.2$ eV, an increase in photoelectron yield with oxygen exposure also appears and is believed to be due to photoelectron emission from the adsorbed oxygen atoms.

**10116.** Walker, R. F., **Temperature measurement in high temperature chemistry: 1000–3000 °C,** *Rev. Hautes Témper, et Réfract,* **3,** 301-308 (1966).

Key words: High temperature chemistry; international temperature scale; melting points; pyrometry; secondary reference points; temperature measurement.

The uncertainty of temperature measurements is one of the principal causes of error in the measurement of the thermodynamic and kinetic properties of substances above the gold point. In terms of international standards, the ultimate accuracy of temperature measurements depends on the consistency of the International Practical Temperature Scale (IPTS) with the thermodynamic temperature scale. The accuracy achieved in measuring other properties depends on the accuracy of calibration of the temperature measuring instruments in accordance with the IPTS, and on the ability to use the instruments under prescribed physical and chemical conditions. The higher the temperatures, the more difficult it becomes to meet these prescribed conditions.

The present status of the IPTS is reviewed briefly. A summary is given of the precision and accuracy achievable with common temperature measuring instruments. The potential advantages and limitations of newer instruments, such as photoelectric pyrometers, are also indicated. It is concluded that in the field of high temperature chemistry the principal limitation is the inability to use the instruments under ideal conditions. Higher precision and accuracy would be achievable if additional internal checks, such as internationally recognized secondary reference points, were available to the experimentalist. Severe problems of both a chemical and physical nature are, however, attendant on the provision of such reference points, and these are briefly discussed.

**10117.** Wall, A. C., **The photometry of colored light,** *Illum. Engr.* **62,** No. 4, 239-242 (Apr. 1967).

Key words: Filters; photocells; photometers; photometry; phototubes; spectral correction of phototubes.

The photosensitor of a photometer must be corrected to have a spectral sensitivity as close as possible to the CIE photopic luminous efficiency function. A correction-by-filter technique is described, applicable to photosensitors which are used in the measurement of "colored light," which, in this paper, designates light which has a spectral distribution different from that of the light with which the photometer is calibrated. Three types of photosensitors with their associated auxiliary filters were investigated, as well as one type of barrier-layer cell with an integral filter. The photosensitors were first calibrated by exposing them to illumination from a lamp operating at 2854 °K. Then, to test the adequacy of the spectral correction-by-filter technique, twenty-two 2-by-2-inch squares of colored glass whose luminous transmittance was computed from spectrophotometric data were placed in turn in the light beam and readings proportional to the irradiance incident on each photosensitor were taken. If the spectral correction were perfect, the ratio of the reading obtained with the filtered light to the reading with the unfiltered light would be equal to $\tau_s$, the luminous transmittance of the filter obtained from the spectrophotometric measurements. Factors were calculated to convert the ratios obtained to $\tau_s$ for the color-corrected photosensitors and for five types of non-color-corrected photosensitors.

**10118.** Wall, L. A., **Polymerization of fluoroolefins and related monomers,** (Proc. 152nd American Chemical Society Meeting, New York, N.Y., Sept. 13, 1966), *Polymer Preprint* **7,** No. 2, 1112-1115 (Sept. 1966).

Key words: Fluorine-containing monomers; fluorodienes; fluoroolefins; fluoro monomers; fluoropropylenes; fluorovinyl; free radical; gamma rays; high pressures; ionic catalysts; monomers; perfluorostyrene; phenyl ethers; polymerizations.

Although some fluorine-containing monomers polymerize readily, there are many which have not as yet been polymerized either by free radical or ionic catalysts. In order to investigate the reasons for the somewhat general tendency of these monomers to resist polymerization, we have initiated a systematic study using high pressures and γ-rays to induce polymer formation.

The technique has been successful for many fluoro monomers, fluoropropylenes, fluorodienes, perfluorostyrene and some fluorovinyl phenyl ethers. In a general way, the results suggest in many cases that slow propagation steps, easy transfer processes with monomer or impurities, and in some cases a tendency to thermally dimerize, interfere with the formation of high polymer.

**10119.** Wall, L. A., Straus, S., Florin, R. E., **Pyrolysis of vinyl and vinylidene fluoride polymers: influence of prior gamma irradiation,** *J. Polymer Sci.* **4A,** No. 2, 349-365 (Feb. 1966).

Key words: Fluoride polymers; gamma irradiation; irradiation, gamma; polymers; quantitative comparisons; vinyl and vinylidene.

Quantitative comparisons were made between the rates of thermal volatilization of several fluoropolymers before and after exposure to γ-radiation. The effects of γ-irradiation on poly(vinyl fluoride) and poly(vinylidene fluoride) were also investigated by swelling and sol-gel ratios. With both polymers as well as with polytrifluoroethylene, crosslinks occur predominantly, though there is an appreciable number of scissions. The rates of volatilization and char formation were enhanced by γ-radiation, whereas the previously studied polytrifluoroethylene did not produce more char upon irradiation, although radiation did accelerate its volatilization. It is believed that in polytrifluoroethylene the enhanced rates of volatilization occur by a different mechanism than in the case of the vinyl and vinylidene fluoride polymers.

**10120.** Wall, L. A., Straus, S., Flynn, J. H., McIntyre, D., Simha, R., **The thermal degradation mechanism of polystyrene,** *J. Phys. Chem.* **70,** No. 1, 53-62 (Jan. 1966).

Key words: Computer calculation; intermolecular transfer; molecular weights; polystyrene; pyrolysis; theory of free radical degradation.

New and extensive measurements of (1) the rates of volatilization and (2) the molecular weights as a function of the extent of pyrolysis are reported for various polystyrene samples, in particular, fractions spanning a broad range of molecular weights. The experimental observations are shown to be described quite well by the results of computer calculations based on the theory of free radical degradation and a mechanism involving four elementary reactions—initiation, depropagation, intermolecular transfer, and termination by disproportionation.

**10121.** Washer, F. E., **Effect of chromatic aberration on the resolving power of photographic objectives,** *J. Opt. Soc. Am.* **57,** No. 5, 625-629 (May 1967).

Key words: Chromatic aberration; critical aperture; relative contrast; resolving power.

An empirical method for the estimation of the probable resolving power of a lens affected by longitudinal chromatic aberration is discussed. Values of the resolving power at a series of values of the f-number are calculated for selected values of longitudinal chromatic aberration, $d_c$. The variation of resolving power with f-number is presented graphically for selected values of longitudinal chromatic aberration and relative contrast. Indication is given of a critical aperture for which the resolving power is a maximum for a given set of values of chromatic aberration and relative contrast. The variation of relative contrast with resolving power is presented graphically for several values of the f-number for a lens having selected amounts of longitudinal chromatic aberration. A method for predicting the resolving power of a given lens-film combination is also indicated.

**10122.** Washer, F. E., **Resolving power related to aberration,** *Photogrammetric Eng.* **XXXII,** No. 2, 213-226 (Mar. 1966).

Key words: Aberration, optical; lens resolving power; resolution, optical; resolving power.

An heuristic method which accounts for the discrepancy between measured and theoretical values of resolving power of lenses is presented. The analysis also accounts for the sharp decline in contrast with increasing values of resolving power expressed in lines per mm in the image plane. Analyses are given of the probable effects on resolution and contrast of the fraction of the lens area transmitting image-forming light, longitudinal chromatic aberration, and longitudinal spherical aberration. An example is given that demonstrates change in focus with change in resolving power and shows how it is readily explained on the basis of simple diffraction theory.

**10123.** Weisman, H. M., **Needs of American Chemical Society members for property data,** *J. Chem. Doc.* **7,** No. 1, 10-14 (Feb. 1967).

Key words: American Chemical Society; chemical and physical properties; compilation; data; NSRDS; Office of Standard Reference Data; questionnaire; survey; users.

In August of 1965 the American Chemical Society, on behalf of the NBS Office of Standard Reference Data, sent a questionnaire to its membership asking for information on their needs for compilations of critically evaluated data. Through this questionnaire, the Office of Standard Reference Data obtained information on the preferences and needs of the chemical profession for data compilations, and equally importantly, located a substantial number of compilation activities of which it was not aware. Further, the Office of Standard Reference Data identified dozens of individuals who are both interested and competent to undertake additional projects. Approximately 16,000 replies were received. Overwhelmingly, response was that present compilations of data satisfy poorly or at best only moderately the requirements of the membership of ACS. The survey identified the properties which ACS workers most often sought in the literature as well as those data compilations most often consulted by respondents. Many worthwhile comments and suggestions were contributed as to approaches taken, compilation priorities and techniques of format and presentation.

**10124.** White, J. A., **Theory of the magnetic torque anisotropy of the samarium iron garnet,** *Proc. Phys. Soc. (Great Britain)* **90,** 1095-1109 (1967).

Key words: Anisotropy of samarium iron garnet; iron garnet; magnetic torque anisotropy; samarium iron garnet.

It is observed that the anisotropy measured by Pearson above 80 °K varies nearly as $T^{-3}$. This is the temperature dependence to be expected if the samarium ions in the garnet are subjected to an isotropic exchange field and a crystal Stark field of predominantly cubic symmetry. The magnitude of the anisotropy corresponds to an exchange field $\beta H_{ex}/k = 29$ °K. This is considerably less than the 55 °K which, for an isolated cubic quartet, produces the splittings in $Sm^{3+}$ observed calorimetrically. It is suggested that the exceptionally large exchange splittings at $T = 0$ and apparently large exchange field can be understood as the result of an exchange field of 29 °K combined with (1) partial decoupling of the spin and orbital angular moments by the Stark and exchange fields, (2) restoration by the exchange field of some of the angular momentum quenched by the crystal field, and (3) rhombic anisotropy of the exchange field and crystal field.

**10125.** Whittaker, J. K., **A zero-crossing discriminator with picosecond time slewing,** *IEEE Trans. Nucl. Sci.* **NS-13,** No. 1, 399-405 (Feb. 1966).

Key words: Discriminator; picosecond; resolution; time-invariant; wide-range; zero-crossing.

A zero-crossing type of discriminator with a very wide dynamic range and a short dead-time is described. When used with a 56 AVP photomultiplier with a linear dynode resistor chain, a light amplitude variation of at least 125:1 may be accommodated. The relative time shift of the output discriminator pulse is then only 200 p.s.

**10126.** Whittaker, J. K., **A 100 Mc/s 2 out of 3 gate,** *Nucl. Instr. Methods* **45,** No. 1, 138-140 (Nov. 1966).

Key words: Coincidence; direct-coupled; gate; nanosecond; time-of-flight; 2 out of 3; 100 Mc/s.

A direct-coupled gate to determine when any two out of three inputs are present is described. The gate will function up to at least 100 megapulses per second and employs negative logic signals of nominal amplitude—1 volt.

**10127.** Whittaker, J. K., **A simple current generator,** *Nucl. Instr. Methods* **39,** No 1, 183-184 (Jan. 1966).

Key words: Current; generator; magnetic; stable; transistor; variable.

This letter describes two versions of a simple current generator which may be used to drive low impedance magnetic deflection systems. For this application a high resolution control with good stability is essential and it is necessary to be able to control the current in both directions about zero without switching. The circuits to be described have satisfied these conditions and the two versions have respective output currents of ± 40 mA and ± 400 mA.

**10128.** Wiederhorn, S. M., **Effects of environment on the fracture of glass,** *Proc. RIAS Conf., Baltimore, Md., June 7-8, 1965,* pp. 293-317 (Gordon and Breach, New York, N.Y., 1966).

Key words: Cleavage; corrosion; crack propagation; fracture; glass; static fatigue.

This paper briefly reviews previous work on the topic of delayed fracture of glass, and then presents the results of a new experimental approach to the subject. Using the double-cantilever cleavage technique, it was possible to observe crack motion and to accurately measure crack velocities in glass. The temperature and stress dependence of the crack velocity indicates that the observed fracture is an activated process with an activation energy of 19,500 calories/mole. The existence of a static fatigue limit is inferred from the experimental data. Experimental results will be discussed with reference to current theories of static fatigue.

**10129.** Weiderhorn, S. M., **Fracture surface energy of soda-lime glass,** (Proc. Conf. Role of Grain Boundaries and Surface in Ceramics, North Carolina State University, Raleigh, N.C., Nov. 16-18, 1964), Chapter in *Materials Science Research* **3,** 503-528 (Plenum Press, Inc., New York, N.Y., 1966).

Key words: Crack propagation; fracture surface energy; glass; soda-lime glass; static fatigue; stress corrosion; surface energy.

The fracture energy of soda-lime glass was measured at temperatures of 77 °K, 195 °K, and 300 °K in various media using the double-cantilever cleavage technique. Values obtained for the fracture energy were 3.20 joules/meter$^2$ in $N_2(l)$, 3.10 joules/meter$^2$ in toluene $(l)-CO_2(s)$ and 2.83 joules/meter$^2$ in dry $N_2(g)$.

During the experiment slow crack motion was always observed prior to catastrophic failure of the specimens. The crack motion was complex, depending on the stress at the crack tip and the concentration of water in the medium surrounding the crack. Experimental results will be discussed with respect to several different mechanisms of crack growth.

**10130.** Wilcox, R. M., **Exponential operators and parameter differentiation in quantum physics,** *J. Math. Phys.* **8,** No. 4, 962-982 (Apr. 1967).

Key words: Baker-Campbell-Hausdorff formula; density matrix; differential equations; expansions; exponential operators; harmonic oscillator; Lie algebra; normal ordering of operators; operator identities; parameter differentiation; quantum statistics; similarity transformations; Weyl prescription.

Elementary parameter-differentiation techniques are developed to systematically derive a wide variety of operator identities, expansions, and solutions to differential equations of interest to quantum physics. The treatment is largely centered around a general closed formula for the derivative of an exponential operator with respect to a parameter. Derivations are given of the Baker-Campbell-Hausdorff formula and its dual, the Zassenhaus formula. The continuous analogs of these formulas which solve the differential equation $dY(t)/dt = A(t)Y(t)$, the solutions of Magnus and Fer, respectively, are similarly derived in a recursive manner which manifestly displays the general repeated-commutator nature of these expansions and which is quite suitable for computer programming. An expansion recently obtained by Kumar and another new expansion are shown to be derivable from the Fer and Magnus solutions, respectively, in the same way. Useful similarity transformations involving linear combinations of elements of a Lie algebra are obtained. Some cases where the product $e^Ae^B$ can be written as a closed-form single-exponential are considered which generalize results of Sack and of Weiss and Maradudin. Closed-form single-exponential solutions to the differential equation $dY(t)/dt = A(t)Y(t)$ are obtained for two cases and compared with the corresponding multiple-exponential solutions of Wei and Norman. Normal ordering of operators is also treated and derivations, corollaries, or generalization of a number of known results are efficiently obtained. Higher derivatives of exponential and general operators are discussed by means of a formula due to Poincare which is the operator analog of the Cauchy integral formula of complex variable theory. It is shown how results obtained by Aizu for matrix elements and traces of derivatives may be readily derived from the Poincare formula.

Some applications of the results of this paper to quantum statistics and to the Weyl prescription for converting a classical function to a quantum operator are given. A corollary to a theorem of Bloch is obtained which permits one to obtain harmonic-oscillator canonical-ensemble averages of general operators defined by the Weyl prescription. Solutions of the density-matrix equation are also discussed. It is shown that an initially canonical ensemble behaves as though its temperature remains constant with a "canonical distribution" determined by a certain fictitious Hamiltonian.

**10131.** Wilson, W. K., **NBS to dedicate Gaithersburg facility,** *J. Wash. Acad. Sci.* **56,** No. 7, 165-167 (Oct. 1966).

Key words: National Bureau of Standards, dedication; National Bureau of Standards History; National Bureau of Standards Mission.

General discussion of the plans of the National Bureau of Standards for the dedication of its Gaithersburg, Maryland laboratory complex on November 15, 1966.

**10132.** Winogradoff, N., Kessler, H. K., **Compensation and band tailing effects in high power room temperature GaAs lasers,** *Solid-State Communications* **5,** 155-158 (Pergamon Press, Ltd., London, England, Jan. 1967).

Key words: Compensation with donors; epitaxial gallium arsenide lasers; laser characteristics.

A reduction in the density of states of a two level system would facilitate the production of an inverted electron population. Such a low density of states system can be produced by the incorporation of shallow donors into p-type material in such concentrations that mergence of the impurity bands with the intrinsic bands result in the formation of "tails" of states at the bottom and top of the intrinsic conduction and valence bands respectively.

The low density of states in these tails results in (1) low room temperature thresholds; (2) negligible time delays between the leading edge of the current pulse and the onset of lasing; and (3) high peak power outputs.

The behaviour of a series of vapour phase epitaxially formed p-n junctions with and without compensation will be discussed and recent achievements in high power outputs with compensated lasers will be described and correlated with field effect experiments the results of which show that the enhanced light output in compensated material is not due to radiative transitions between acceptor and donor impurity centers.

**10133.** Winogradoff, N. N., Kessler, H. K., **Radiative recombination lifetimes in laser excited silicon,** *Appl. Phys. Letters* **8,** No. 4, 99 (Feb. 1966).

Key words: GaAs laser; laser pulse shapes; lifetime; optical pumping; radiative recombination; ruby laser; silicon; stimulated emission.

At high excitation intensities, the decay lifetime for radiative recombination in a wide range of "long lifetime" silicon samples was found to be $<2 \times 10^{-8}$ seconds. The emission occurred at $1.10\mu$ at room temperature.

Correlation of the non-linear emission with excess photoconductivity suggests stimulated radiative transistions to the light hole band.

The fast decay provides a passive, non-critical attenuator for observing pulse shapes of intense laser flashes.

**10134.** Wolfe, W. C., **Bonding adhesives and paints to treated concrete,** *CSI Mono.* **9MI,** Construction Specifier, pp. 1-8 (Aug. 1966).

Key words: Asphaltic tile adhesives; cement water-based paints; concrete surfaces; paints; water-based paints.

The object of this investigation was to determine the effect of surface treatment of concrete on the adhesion of paints or asphaltic adhesives for asphalt or vinyl asbestos tile. Qualitative and quantitative tests were performed on treated and untreated concrete specimens. The results of the tests indicated that concrete curing and parting agents, oils, and waxes are more compatible with asphalt cutback than with asphalt emulsion adhesive. The tests did not show any oozing of adhesive between tiles or curling of tiles at the corners.

Cement-water paints adhered poorly to concrete treated with curing agents. Organic coatings adhered well to concrete treated with curing agents based on butadiene-styrene copolymer or chlorinated rubber. Likewise, paints formulated with butadiene-styrene copolymer or chlorinated rubber in hydrocarbon solvents adhered to most curing agents. Paints made up in hydrocarbon solvents were more compatible with curing agents, oils, and waxes than were water-based paints.

**10135.** Wolfe, W. C., **Testing scouring powder abrasion,** *Detergent Age* **2,** No. 10, 22 (Mar. 1966).

Key words: Abrasives; bathtubs; cleansers; detergents; particle; plastic; plumbing; porcelain; sieve; silica; sinks.

Five leading brands of household scouring powders were examined in order to establish a formulation for testing the abrasion or wear resistance of sanitary plumbing fixtures. A test abrasive of known composition and representative of commercial products was desired.

The products examined all contained sodium dodecylbenzenesulfonate as the detergent, usually chlorine bleach, sometimes bactericide, and about 90 percent by weight of abrasive. The abrasive, in each case, was fine quartz powder, mostly less than 44 microns particle size, but containing some particles between 149 and 250 microns in diameter, which might scratch porcelain enamel or plastic.

**10136.** Wood, L. A., **Physical constants of different rubbers,** *Polymer Handbook,* J. Brandrup and E. H. Immergut, ed., pp. VI-57 – VI-68 (Interscience Publ., Inc., New York, N.Y., 1966).

Key words: Butyl rubber; constants; natural rubber; neoprene; physical constants; polymers; properties; rubbers; styrene-butadiene rubber.

Selected values from the literature are tabulated for about 25 physical constants for natural rubber, styrene-butadiene rubber (SBR), Butyl rubber (IIR), and polychloroprene rubber (CR or Neoprene). This is a requested revision of the table published in the Smithsonian Physical Tables, 9th Edition, 1954.

**10137.** Wright, J. R., Gray, V. E., **Measurement of photochemical degradation in rigid poly(vinyl chloride) by color reactions with N,N-dimethyl-p-phenylenediamine,** (Proc. Conf. Plastics in Building Structures, London, England, June 14-16, 1965), *Plastics Inst. Trans. J. Suppl.* **1,** 113-118 (June 14, 1966).

Key words: Color reactions; opaque pigments; photodegradation; poly(vinyl chloride); rigid plastic; ultraviolet absorbers.

Rigid poly(vinyl chloride) materials which had been exposed to sunlight and to carbon-arc and xenon-arc radiation were subjected to physical and chemical testing to measure the effects of photodegradation. Opaque pigments and ultraviolet absorbers were found to protect the plastic from photodegradation but heat stabilizers varied greatly in their photostability. The color changes and physical strength changes produced during exposure were not directly related.

**10138.** Wyckoff, J. M., **Modular software for on-line handling of nuclear data,** *IEEE Trans. Nucl. Sci.* **NS-13,** No. 1, 199 (Feb. 1966).

Key words: Digital computer; experiment; modular; nuclear data; on-line; programs; SDS 920.

Modular programming for the handling of nuclear data on-line with a general purpose digital computer considerably simplifies the programming task. A system called ROMEO implementing this concept has been developed. More than 150 relocatable, self-contained programs of some 30 types have been prepared and used in a nuclear physics experiment using an SDS 920 computer. These programs, falling into the housekeeping, data accumulate, data manipulate and data output categories, are described briefly and their use in the experiment is discussed. About 30 of these programs are loaded concurrently with loading and deleting possible during the experiment.

**10139.** Yakowitz, H., **Precision of cubic lattice parameter measurements by the Kossel technique,** *Trans. Symp. Electron Probe Analysis, Oct. 12-15, 1964, Washington, D.C., 1964,* pp. 417-438 (John Wiley & Sons, Inc., New York, N.Y., 1966).

Key words: Cubic lattice measurements, precision; Kossel technique for cubic lattice measurements.

The major factors affecting the precision of cubic lattice parameter measurement by means of the Kossel technique are considered. It is shown that three special cases can be solved rigorously for projection distortion effects and that obtaining these cases is not difficult. The fact that a lens ratio method should be employed to reduce measured lengths on the film to lattice parameter values is emphasized. General formulae for the lattice parameter and the geometric sensitivity are presented. Correction and minimization of errors resulting from refractive index effects and temperature variations is indicated to be possible. An example of the determination of the lattice parameter of LiF is given. The sensitivity of the method, expressed the relative standard error of the mean lattice parameter of LiF, is given by

$$\Delta a/a_{LiF} = 2.5_4 \times 10^{-6}.$$

**10140.** Yee, K. W., Deslattes, R. D., **Transistorized current stabilizer for x-ray tubes with directly heated cathodes,** *Rev. Sci. Instr.* **38,** No. 5, 637-638 (May 1967).

Key words: Controlled impedance; current; emission; regulator; stabilizer; x-ray tube.

An instrument is described which stabilizes the emission current in x-ray tubes with directly heated cathodes. Transistors are used in the amplifier and loading circuits. Emission currents from 20 mA to 1A are maintained constant to within 0.1 percent for periods of about a half-hour.

**10141.** Young, R. D., **Field emission ultramicrometer,** *Rev. Sci. Instr.* **37,** No. 3, 275-278 (Mar. 1966).

Key words: Contour; displacement; distance; distance-measurement; field emission; instrument; measurement; micrometer; precise; sensitive.

A simple, contact free, ultrasensitive distance and displacement measuring instrument has been investigated. Experiments demonstrate that the instrument is capable of operating at spacings as small as a few hundred angstroms. Calculations indicate that distances of $10^{-3}$ to $10^{-6}$ cm and less can be reproduced to within about one part in $10^5$. With suitable calibration, distance measurements in the $10^{-3}$ to $10^{-6}$ cm range can be expected to have accuracies limited only by available calibration techniques. The instrument would be most useful as a null or differential distance measuring device. It has the unusual property that resolution improves over several orders of magnitude as the null or measurement point is approached. Since the instrument contains no optical or mechanical lever systems, or delicately balanced bridges, it has inherent long term stability. Proposed applications include: (1) measurement of ball and hole diameters (contact free), (2) differential thermal expansion cell, (3) mechanical vibration sensor, (4) surface profile delineator (contact free), and (5) surface contour delineator (contact free).

**10142.** Yu, H., **The unperturbed dimension temperature coefficients of some fluorine-containing polymers,** (Proc. 152nd American Chemical Society Meeting, New York, N.Y., Sept. 13, 1966), *Polymer Preprint* **7,** No. 2, 1143-1145 (Sept. 1966).

Key words: Energy component; fluorine-containing polymers; hydrocarbon chain backbone; unperturbed dimension temperature coefficients.

Thermoelastic measurements on amorphous networks of some fluorine-containing polymers were performed.

**10143.** Yu, H., Bur, A. J., Fetters, L. J., **Rodlike behavior of poly(n-butyl)isocyanate from dielectric measurements,** *J. Chem. Phys.* **44,** No. 7, 2568-2576 (Apr. 1, 1966).

Key words: Dielectric measurements; dilute benzene solution; polybutylisocyanate; rotary diffusion.

The rotary diffusion of poly(n-butyl)-isocyanate was studied by dielectric dispersion in dilute benzene solution. The correlation between the observed dielectric relaxation time and the molecular weight is interpreted on the basis of a hydrodynamic rod of very large axial ratio.

**10144.** Zapas, L. J., Craft, T., **Correlation of large longitudinal deformations with different strain histories,** *Rubber Chem. Technol.* **40,** No. 2, 506-516 (Mar. 1967).

Key words: BKZ theory; constant rate of strain; creep; elastic fluid; nonlinear behavior; polyisobutylene; polyvinylchloride; recovery; stress relaxation.

It is shown that the BKZ incompressible elastic fluid theory is in excellent agreement with experimental results obtained in simple extension. From single step stress-relaxation data, the stress-strain response for a number of other simple extension histories are calculated from the theory and are compared with experiments.

**10145.** Zwanzig, R., **Approximate eigenfunctions of the Liouville operator in classical many-body systems,** *Phys. Rev.* **144.** No. 1, 170-177 (Apr. 1966).

Key words: Classical; collective variables; eigenfunctions; eigenvalues; many-body; spectrum; variational; Vlasov.

A variational criterion is used to find approximate eigenfunctions and eigenvalues of the Liouville operator in classical many-body systems. The trial functions are taken to be sums over molecules of functions depending on the position and momentum of a single molecule. In a harmonic lattice, this approach leads to exact eigenfunctions and eigenvalues. In a fluid, the eigenvalue spectrum is continuous, and the eigenfunctions are related to those found by Van Kampen in his study of the linearized Vlasov equation for a plasma. The time dependence of the fluid current density is found by means of these eigenfunctions and eigenvalues. The results show persistent free particle propagation and damped sound wave propagation, with relative importance depending on the magnitude of the sound velocity.

**10146.** Zwanzig, R., **Probability and entropy of macroscopic fluctuations,** *Math. Phys.* **7,** No. 8, 1552-1556 (Aug. 1966).

Key words: Entropy; macroscopic fluctuations; thermodynamic force.

A macroscopic fluctuation is a fluctuation of order N in an N particle system. This article contains a calculation of the probability of a macroscopic fluctuation, and its associated entropy, which is asymptotically correct in the limit of large N. Sufficiently small macroscopic fluctuations are shown to obey the same Gaussian distribution law as spontaneous microscopic fluctuations (of order $N^{1/2}$). The modifications necessary to describe large macroscopic fluctuations are found. The entropy of a macroscopic non-equilibrium state is expressed by means of various moments calculated at equilibrium. The non-linear thermodynamic force for a non-equilibrium state far from equilibrium is found. The calculation is based on a cumulant expansion of the characteristic function of the probability distribution, and a stationary phase estimate of its Fourier transform.

**10147.** Richardson, J. M., **Time standards,** *Encyclopaedic Dictionary of Physics, Supplementary* **1,** 351-355 (Pergamon Press, Inc., New York, N.Y., 1966).

Key words: Time standards; unit of measurement; unit of time.

A unit of measurement for any quantity is usually an abstraction which specifies the idealized concept underlying the realization of the unit. A standard on the other hand is a physical embodiment of the unit. Thus standards may occur at any level of use and accuracy. This paper concerns time standards at the highest level of accuracy and at the most inclusive level of use; namely, at the level at national and international standardization.

**10148.** Young, T. R., **Linear measurements,** Chapter 3 in *Handbook of Industrial Metrology,* pp. 55-81 (Prentice-Hall, Inc., Englewood Cliffs, N.J., 1967).

Key words: Contours; datum deformation; irregular areas; length; linear measurement; process evaluation; shape.

General principles involved in the measurement of length, size and shape are discussed. The importance of definition and evaluation of the measurement process is shown. Deformation of datum defining size or shape are indicated and engineering concepts useful in determining magnitudes of deformation are reviewed; examples of deformations frequently encountered in linear metrology are shown.

**10149.** Astin, A. V., **International standardization and expanded world trade,** *Mag. Std.* **37,** No. 7, 191-194 (July 1966).

Key words: International Organization for Standardization; international standards; technology transfer; world trade.

The lack of adequate international standards for goods and services is a significant deterrent to expanded world trade. The echnical committees, subcommittees, and working groups of the nternational standards-making bodies are the heart of the standards-making process. Greater participation by the United States in these activities would be to its advantage. Better communication of information about national and international standards is needed. International standards facilitate the transfer of technology from the most advanced nations to the less advanced.

**10149A.** Beaty, E. C., Browne, J. C., Dalgarno, A., **Ion mobilities in helium,** *Phys. Rev. Letters* **16,** No. 17, 723-724 (Apr. 1966).

Key words: Helium; ion mobilities; mass analysis; metastable.

**0150.** Allman, W. P., **A computer simulation model of railroad freight transportation systems,** *Intern. Railway Cong. Assoc. Monthly Bull. Cybernetics and Electronics* **4,** No. 2, 45-57 (Feb. 1967).

Key words: Computer simulation model; network-simulation; railroad freight transportation systems; transportation systems:

A railroad may be viewed as a network of nodes (yards) and inks (railroad lines), with time-dependent demands for the movement of freight cars imposed upon it. Incident to car movement are the following key operating policy questions of railroad freight operations: (a) When and where should regularly-scheduled trains run? (b) For each yard, what should the car classification (sorting) policy be? (c) Over each line of a train's route, what cars should be assigned to the train for hauling?

These interdependent questions must be answered simultaneously, and in accordance with overall operating objectives of the railroad enterprise. Policies must be revised periodically when significant changes in demand traffic patterns occur.

The paper describes a simulation model which permits experimentation with various alternative railroads freight operating policies at a total-network level. The model has been constructed with the SIMSCRIPT simulation programming language. Model nputs include time-dependent freight car origin-destination demand data, train routes and schedules, yard sorting and operation policies, and assignments of cars to trains for hauling. Freight cars are sorted at yards, and picked up and dropped off by trains which haul them thru the network. Model outputs include several railroad operation performance measures such as origin-destination transit times, activity volumes, train lengths, delays incurred by cars at yard operations, and operating costs.

**10151.** Bean, B. L., **A method of producing sturdy specimens of pressed powders for use in x-ray spectrochemical analysis,** *Appl. Spectry.* **20,** No. 3, 191-193 (May-June 1966).

Key words: Powders, compacted or pressed; spectrochemical analysis; x-ray spectrochemical analysis.

Sturdy specimens of compacted or pressed powders may be produced for x-ray spectrochemical analysis as follows: A sleeve with sides about 0.16 cm (1/16 inch) thick and diameter 0.02 cm less than the inside diameter of the mold is placed in the mold. The powder is spread on the lower plunger of the mold. The sleeve is then removed and boric acid poured in the formed peripheral trench and on top of the powder. The specimen is then pressed. A specimen with strong edges and backing is prepared that may be reused many times because the boric acid edges support the pressure of the sample holder instead of the pressed sample powder.

**10152.** Haber, S., **A modified Monte-Carlo quadrature. II,** *Math. Compt.* **21,** No. 99, 388-397 (July 1967).

Key words: Analysis; integration; mathematics; Monte-Carlo; multiple integration; numerical analysis; numerical integration; quadrature.

A modification of Simple Monte-Carlo quadrature is proposed, which uses very simple forms of stratified sampling and of the "method of antithetic variates." The new procedure is fully automatic, requiring no preliminary analysis of the integrand, and converges somewhat faster than Simple Monte-Carlo. Results of experimental calculations are presented.

**10153.** Arthur, M. G., Allred, C. M., Cannon, M. K., **A precision noise power comparator,** *IEEE Trans. Instr. Meas.* **IM-4,** 301-305 (Dec. 1964).

Key words: Noise power comparator; power comparator; prototype noise power comparator; radiometers; spectral densities.

This paper describes a prototype noise power comparator based upon a theory given by Allred. Operating at 3 MHz, it is a null-type instrument, the principal components of which are a reference CW voltage generator, a hybrid four-port, a dual-channel amplifier and bandpass filter, and an analog multiplier. Unlike other radiometers, no rapid switching of the noise power or reference voltage is performed.

The instrument can compare noise powers having effective noise temperatures in the range from below liquid nitrogen temperature to greater than 30,000 °K. Two noise generators having known spectral densities are used to calibrate the comparator. The accuracy of comparison is 1 percent at 77 °K and increases to 0.2 percent at 29,000 °K.

**10154.** Schafer, G. E., **A systems concept of electromagnetic measurements in the U.S.A.,** *Proc. IEEE* **55,** No. 6, 775-778 (June 1967).

Key words: Electromagnetic measurement; National Measurement System; radio standards.

A brief description of a systems concept of the National Measurement System proposed by Dr. R. D. Huntoon, Director, Institute for Basic Standards, is given first. Activities of the Radio Standards Laboratory as a functional element of this system are then described. Some benefits of looking at RSL as an element of this system are given.

**10155.** Simmons, J. A., Coriell, S. R., Ogburn, F., **Calculation of currents of local galvanic cells,** *J. Electrochem. Soc.* **114,** No. 8, 782-787 (Aug. 1967).

Key words: Corrosion currents; galvanic cells; galvanic currents; Laplace's equation; pitting corrosion.

The current flow for a local electrolyte cell with rectangular anode and cathode is calculated as a function of polarization parameter, electrolyte thickness and conductivity, anode and cathode size, and zero current potential difference. The total current is obtained from the numerical computation (with error analysis) of a series solution of Laplace's equation assuming a linear polarization relation at the electrode-electrolyte interface. For high values of the polarization parameter and sufficiently thick electrolytes an asymptotic formula obtains for the current approximately proportional to the anodic fraction, as was found by Waber et al. However, in general the cell geometry greatly influences the amount of current given by Allred. flow, especially for anode shapes near to linear rather than square. This effect can be greater than an order of magnitude. The calculated results are compared with experimental data obtained by Ogburn and Schlissel and are shown to be in good agreement. Corrosion currents in randomly pitted surfaces may be estimated from the above results.

**10156.** Stromberg, R. R., Smith, L. E., **Conformation of polystyrene adsorbed on liquid mercury,** *J. Phys. Chem.* **71,** No. 8, 2470-2474 (July 1967).

> Key words: Adsorption; adsorption of polymers; conformation of adsorbed polymers; ellipsometry; mercury; polymer adsorption; polystyrene.

Measurement of the extension of polystyrene adsorbed in liquid mercury from cyclohexane near the theta temperature indicates that the molecule is attached at a relatively large number of sites and that the conformation remains constant during most of the adsorption period. In addition, the extension is approximately independent of molecular weight for the range studied (537,000 to 3,300,000). These results are in contrast to previous measurements on polycrystalline metallic surfaces. The behavior may be attributed in part to the large value of the contribution of the London dispersion forces to the surface free energy of mercury as compared to other metals. Other possibilities are also discussed.

**10157.** Bekkedahl, N., **Crystallization of natural rubber,** *Rubber Chem. Technol.* **40,** No. 3., xxv-xxvii (June 1967).

> Key words: Chain folding; contractility; crystallization; dilatometry; heat engine; melting; polymers; rubber; stark rubber.

This review article presents a resume of the research work that has been done at the National Bureau of Standards during the past thirty-five years in the field of crystallization of polymeric materials, with special emphasis on natural rubber. It contains only information on results of research work that has already been published.

**10158.** Brooke, R. L., Cruz, J. E., **Current distribution and impedance of lossless conductor systems,** *IEEE Trans. Microwave Theory Tech.* **MTT-15,** No. 6, 358-364 (June 1967).

> Key words: Characteristic impedance; current distribution; general method; matrix solution; rectangular transmission line; time-domain reflectometer; variable impedance.

A general method for determining the characteristic impedance of lossless, uniform, go and return systems is developed. The current distribution within the system is determined by means of a matrix equation programmed for computer solution. Knowing the current distribution, the inductance per unit length and characteristic impedance are obtained. The results obtained by applying this method to several rectangular coaxial systems are compared with the predictions of an approximate analytic expression. The reflection coefficient of a variable characteristic impedance coaxial line is measured on a "Time Domain Reflectometer" (TDR) and the results are compared with both the matrix method and the approximate analytic expression.

**10159.** Johnson, D. P., Heydemann, P. L. M., **Dead weight piston gauge for pressures to 26 kilobars,** *Rev. Sci. Instr.* **38,** No. 9, 1294-1300 (Sept. 1967).

> Key words: High pressure; piston gauge; pressure measurement; transition pressure.

The design and operation of a dead weight piston gauge for pressures to 26 kilobars is described. The gauge is of the controlled clearance type. The diameter of the gauge piston is 0.2 cm. It is loaded directly with up to 840 kg of weights. A volume of about 1 cm³ is provided inside the gauge for the material under test. The use of this gauge for transition pressure determinations is briefly discussed.

**10160.** Post, M. A., **Determination of bound styrene in insoluble emulsion polymerised styrene-butadiene copolymers,** *J. Appl. Chem.* **17,** 203-208 (July 1967).

> Key words: Absorbence ratio method; bound styrene; infrared; insoluble styrene-butadiene copolymers; masonry paints.

Bound styrene is determined in insoluble emulsion polymerised styrene-butadiene copolymers by measurement of the 10·3 $\mu$m/13·2 $\mu$m absorbence ratio using the baseline method. This ratio is obtained from the infra-red spectrogram of the copolymer. The styrene content is then determined from a standard curve. The standard curve is constructed from absorbence ratios of 10·3 $\mu$m/13·2 $\mu$m derived from the infra-red spectrograms of cast films of styrene-butadiene latices over a range of compositions in which the bound styrene has been determined by nitration of the isolated and extracted copolymers. Styrene content based on nitration is determined from standard curves relating styrene concentration to spectrophotometric absorbence measurements at wavelengths of 285·0 nm, 273·8 nm and 265·0 nm. The source of the styrene for these curves is NBS standard rubber No. 1500.

**10161.** Kieffer, L. J., Dunn, G. H., **Dissociative ionization of $H_2$ and $D_2$,** *Phys. Rev.* **158,** No. 1, 61-65 (June 5, 1967).

> Key words: Dissociative ionization; energy distributions; Franck-Condon principle; $D_2$; $H_2$.

Energy distributions of $H^+$ ($D^+$) from dissociative ionization of $H_2$ ($D_2$) are reported. Evidence of the $2p\sigma u$ states being the major source of energetic ions is presented. Calculated and measured energy distributions do not agree well. Possible explanations are suggested.

**10162.** Brown, R. L., **Effects of impurities on the production of oxygen atoms by a microwave discharge,** *J. Phys. Chem.* **71,** No. 8, 2492-2495 (1967).

> Key words: Atomic oxygen; catalysis; flow system reactions; kinetic EPR spectroscopy; microwave discharges; reactions of oxygen atoms.

The catalytic effects of impurities on the production of O-atoms in microwave discharges have been studied in a flow system by measuring with EPR methods the concentrations of $O_2(^3\Sigma_g^-)$, $O_2(^1\Delta_g)$, O, and H-atoms as a function of the amounts of $H_2O$, $D_2O$, and $N_2$ added to the $O_2$ upstream from the discharge. The effects of varying the microwave power to the discharge, the $O_2$ flow rate, and the total pressure were also examined.

**10163.** Gniewek, J. J., Moulder, J. C., Kropschot, R. H., **Electrical conductivity of high purity copper,** *Proc. Tenth Intern. Conf. Low Temperature Physics, Moscow, USSR, Aug. 31-Sept. 9, 1966,* pp. 366-370 (Viniti, Moscow, USSR, 1967).

> Key words: Copper; electrical conductivity; low temperature; size effect.

The low temperature electrical conductivity of copper single crystals ($R_{273}/R_4 > 30,000$) and polycrystalline wire ($R_{273}/R_4 > 10,000$) has been measured between 4 °K and 77 °K.

Between 14 and 30 °K the resistance is proportional to $T^n$ where $n = 4.8 \pm 0.1$. Size effects are observed using both eddy current and direct current techniques in samples as large as 2 mm in diameter. Assuming diffuse reflection of the electrons from the surface, direct current size effect measurements give a $\rho_b \ell_b = 0.53 \times 10^{-11} \Omega \mathrm{cm}^2$ which is less than the free electron value of $0.66 \times 10^{-11} \Omega \mathrm{cm}^2$.

**10164.** Schofer, R. E., Goodyear, F. F., **Electronic computer applications in urban transportation planning,** (Proc. 22nd Natl. Conf. Association for Computing Machinery, Washington, D.C., Aug. 29-31, 1967), *A.C.M. Publ.* **P-67,** pp. 247-253 (Thompson Book Co., Washington, D.C., July 1967).

Key words: Data processing; systems analysis; transportation planning; urban transportation.

The goal of urban transportation planning is to develop a plan for an efficient, balanced transportation system for an urban area; one which will promote a desirable pattern of human activities. While the process has been standardized to some extent, each study must nevertheless acquire and manage a massive amount of information about the specific region with which it is concerned. This information, together with computer representations of transportation networks and travel patterns, is used to produce estimates of future travel demand and utilization of facilities. Thus, computers play an important role in providing transportation planners with the capability for evaluating a variety of proposed transportation systems in order to recommend allocation of government resources and to guide transportation policy. This paper describes specific computer applications to the process of transportation planning.

**10165.** Melmed, A. J., **Epitaxial growth of iron on tungsten field emission points,** *Surface Sci.* **7,** No. 3, 478-481 (July 1967).

Key words: Crystal growth; epitaxy; Fe-W alloying; field emission microscopy; vapor deposition.

Iron crystals can be grown from the vapor phase on tungsten field emission points. The crystals tend to nucleate at edges of W (011) planes and grow in the same orientation as the substrate, sometimes with an apparent small parallel displacement. Interdiffusion of W into the growing Fe crystals can occur and evidence for this is presented.

**10166.** Gruzensky, P. M., **Growth of large sodium chloride crystals from solution for color center studies,** *J. Chem. Phys.* **43,** No. 11, 3807 (Dec. 1, 1965).

Key words: Alkali halides; aqueous; chloride; color centers; conductivity; crystal growth; sodium.

Sodium chloride single crystals with edge dimensions as large as 2.5 cm were grown from aqueous solutions. Solutions were purified by chemical precipitation of trace contaminants and filtration through membrane filters. Crystal defects were apparent in the initial stages of growth, but the outer portions of crystals were free of dislocations. F-band coloration by x rays at room temperature was not linear and the "first stage" was either absent or nearly so. Transition from extrinsic to intrinsic dc conductivity occurred at 350 C with the extrinsic conductivity two orders of magnitude lower than for "pure" melt-grown crystals.

**10167.** Melmed, A. J., **Helium field-ion microscopy of hexagonal close-packed metals,** (Proc. Symp. The Structure of Surfaces, Durham, N.C., Nov. 1966), *Surface Sci.* **8,** No. 12, 191-205 (July-Aug. 1967).

Key words: Field evaporation; field-ion microscopy; hexagonal close-packed metals; surface structure.

The atomic structure of curved hexagonal close-packed metal surfaces is complicated compared to curved surfaces of body-centered cubic metals. He field-ion microscopy of Ru and Re field-evaporated surfaces discloses apparent differences in the surface structures developed under similar experimental conditions. The effect of temperature and field strength on the structure developed by field-evaporation is analyzed, and the structures of the (100) and (001) plane regions in particular are discussed in relation to their respective field-ion images.

**10168.** Hamer, W. J., **History of the National Standard of electromotive force,** (Proc. 22nd ISA Conf. and Exhibit, Chicago, Ill., Sept. 11-14, 1967), *ISA Preprint* No. M2-1-MESTIND-67, pp. 1-10 (1967).

Key words: Absolute volt; Gibbs' phase rule; history of volt; legal volt; volt standards.

The history of the National Standard of electromotive force is traced from the meeting of the International Electrical Congress in Chicago in 1893 to the present time. Included are discussions of the transfer of the "volt standard" from its old location in Washington, D.C. to its new location near Gaithersburg, Maryland, of the stability of standard cells, of the application of Gibbs' Phase Rule to standard cells, and the relation between the legal and absolute volts.

**10169.** Newman, S. B., Young, R. W., **Indentation hardness of the fingernail,** *J. Invest. Dermatol.* **49,** No. 1, 103-105 (Mar. 17, 1967).

Key words: Fingernail; hardness; Knoop indenter.

Indentation hardness using the Knoop indenter has been used as a quantitative criterion in physiological studies of the human nail plate. Data were collected and are presented to show that values reported in the literature are in serious error. A number of parameters affecting Knoop numbers are examined in an effort to determine the source of error.

**10170.** Halberstadt, M. L., McNesby, J. R., **Insertion of methylene into alkanes,** *J. Am. Chem. Soc.* **89,** No. 14, 3417-3420 (1967).

Key words: I-butane; insertion; ketene; methane; methylene; n-butane; photolysis; propane.

Ketene was photolyzed in the presence of mixtures of pairs of hydrocarbons with NO added to scavenge alkyl radicals. The relative rates of insertion for methane:primary propane:secondary propane are 0.43:1.0:0.43 and for ethane:primary n-butane:secondary n-butane they are 1.0:1.0:0.88. In the case of isobutane, the relative rates of insertion into primary and tertiary bonds are 1.0:0.13. When effects of recombination of alkyl radicals formed by abstraction of H by $CH_2$ are eliminated by the NO scavenger, insertion is seen to be essentially indiscriminate. It is suggested that the singlet $CH_2$ lies not more than about 2.5 kcal above the ground state triplet.

**10171.** Utech, H. P., **Interpretation of de Grinberg's experiments on lateral surface fringes in sodium chloride,** *Phys. Stat. Sol.* **20,** K41-K43 (1967).

Key words: Bands; crystals; Czochralski; fringes; sodium chloride.

Results of a recent experiment by de Grinberg on lateral surface fringes in sodium chloride are questioned in the light of two alternative theories which the author had apparently overlooked. It is suggested that further experiments be conducted to distinguish between the three possible mechanisms.

**10172.** Bender, P. L., **Laser measurements of long distances,** *Proc. IEEE* **55,** No. 6, 1039-1045 (June 1967).

Key words: Interferometric measurements; laser measurements; modulated laser beams; radio frequency techniques; range measurements.

The extension of radio frequency techniques to the optical region of the spectrum has made possible many types of measurements which were not feasible before. One area in which important scientific contributions can be expected during the next few years is the use of lasers to measure long distances with high accuracy. Three types of distance measurements which have been discussed in the literature and which are now being investigated actively are: (a) interferometric measurements over distances of up to hundreds of meters through evacuated or sealed-off tubes; (b) measurements with modulated laser beams over distances of perhaps one to fifty kilometers with corrections made for the atmospheric index of refraction along the path; and (c) range measurements to artificial satellites and to the moon using laser radar. Some of the possible geophysical and geodetic applications of such measurements will also be discussed.

**10173.** Young, T. R., **Linear measurements,** Chapter 3 in *Handbook of Industrial Metrology,* pp. 55-81 (Prentice-Hall, Inc., Englewood Cliffs, N.J., 1967).

Key words: Contours; datum deformation; irregular areas; length; linear measurement; process evaluation; shape.

General principles involved in the measurement of length, size and shape are discussed. The importance of definition and evaluation of the measurement process is shown. Deformation of datum defining size or shape are indicated and engineering concepts useful in determining magnitudes of deformation are reviewed; examples of deformations frequently encountered in linear metrology are shown.

**10174.** Heck, C. K., Hiza, M. J., **Liquid-vapor equilibrium in the system helium-methane,** *AIChE. J.* **13,** No. 3, 593-599 (May 1967).

Key words: Helium; helium-methane binary system; liquid-vapor equilibrium; low-temperature; methane; phase-equilibrium; solubility of helium in liquid methane.

Liquid and gas phase compositions for the system helium-methane have been measured at 15° intervals from 95° to 185 °K up to 200 atmospheres pressure. Data for these seven isotherms were taken in a gas phase recirculation apparatus using chromatographic analysis. In most regions the phase compositions obtained are thought to be within ±3 percent of the mole fraction of the minor component. The maximum deviation from the enhancement factor curve at the lowest concentration levels was 16 percent. These data are in excellent agreement with most of the very recent data but are in poor agreement with the older data for this system.

**10175.** Reed, R. P., Mikesell, R., **Low temperature (295-4 °K) mechanical properties of selected copper alloys,** *J. Materials* **2,** No. 2, 370-392 (June 1967).

Key words: Copper; copper alloys; low temperatures; mechanical properties.

Fifteen copper alloys, including brasses, bronzes, and commercially pure coppers were tested to determine their tensile, notch tensile, Youngs modulus, and impact properties. Tests were performed at 295, 195, 76, 20, and 4 °K. It was found that copper alloys, in general, have improved room low temperature properties as compared to room temperature properties. The exception to this result is a cast Ni-Al bronze alloy, which is brittle at low temperatures. In 9 alloys the yield and tensile strengths at 4 °K were less than at 20 °K. A discussion of this strength reduction at low temperatures is presented.

**10176.** McNish, A. G., **Metrology, essential of space age,** *George Washington University Mag.* **1,** No. 4, 10-14 (1965).

Key words: Education; metrology; standards; units.

Understanding the physical world and the progress of civilization depends upon measurement.

**10177.** Fry, B. M., **Microprinting fills the bill,** *Business Graphics,* pp. 21-25 (Jan. 1967).

Key words: Clearinghouse for Federal Scientific and Technical Information; microphoto; microprinting; printing; systems.

The Clearinghouse for Federal Scientific and Technical Information, part of NBS, is a focal point for the collection, announcement and sale of copies of unclassified U.S. Government R&D reports released for public sale by the sponsoring Federal agencies. Approximately 50,000 new reports and Government-sponsored translations of foreign technical material are received each year. The article describes Clearinghouse reproduction services as part of the system to meet the demand for over 2,000,000 copies of documents in microfiche and paper copy each year. The Clearinghouse reproduction plant makes use of the latest technology in microphotography, electrostatic copying and offset printing. The article highlights the role of the reproduction plant as a laboratory in testing new equipment and ideas to improve service to customers.

**10178.** Mosburg, E. R., Jr., Lojko, M. S., **Non-linear diffusion with recombination in electron beam excited plasma,** *Phys. Fluid Res. Notes* **9,** No. 4, 824-826 (Apr. 1966).

Key words: Diffusion; radial distribution; recombination-electron ion and plasma.

The non-linear diffusion equations for an isothermal plasma with a recombination term added are treated for the case of cylindrical geometry and no magnetic field. The radial electron density and light intensity distributions are given for various values of the ratio of the recombination loss rate to diffusion loss rate. The light intensities are computed on the basis of two-body and three-body recombination as well as the intermediate case of collisional-radiative recombination.

**10179.** Newman, M., **Note on partitions modulo 5,** *Math. Compt.* **21,** No. 99, 481-482 (July 1967).

Key words: Density; partitions; Ramanujan congruences.

It is shown that the density of the integers n such that p(n) is divisible by 5, is strictly greater than 1/5.

**10180.** Marton, L., Toots, J., **Optical properties of germanium in the far ultraviolet,** *Phys. Rev.* **160,** No. 3, 602-606 (Aug. 15, 1967).

Key words: Characteristic electron energy loss; dielectric constant; far ultraviolet; germanium; optical constants; reflectance.

Reflectance measurements for Ge films evaporated *in situ* are reported for 16 wavelengths between 490 and 1610 Å, corresponding to photon energies of 25.2 and 7.7 eV. Measurements were taken after 3-min exposures to ambient pressures of $5\times10^{-7}$ torr. Reflectance values at a number of angles of incidence were used to compute the optical constants: the refraction index $n$, the extinction coefficient $k$, and the real and imaginary parts of the frequency-dependent dielectric constant $\epsilon(\omega) = \epsilon_1 + e\ i\epsilon_2$. Values are also presented for the characteristic electron energy-loss functions, i.e., the volume loss, $-\text{Im}\epsilon^{-1}$, and the surface loss, $-\text{Im}(\epsilon+1)^{-1}$. The quantity $-\text{Im}\epsilon^{-1}$ peaked at 16.1 eV and had a half-width of 3.9 eV. Electron oscillator strengths, summed between 8 and 25 eV, gave a $\hbar\omega_p$ value of 13.7 eV. The present data are in better agreement with the accepted plasma theory than are previous data. Some changes of optical characteristics caused by exposure to ambient pressures and air are presented.

**10181.** Scheer, M. D., Fine, J., **Positive and negative self-surface ionization of tungsten and rhenium,** *J. Chem. Phys.* **46,** No. 10, 3998-4003 (May 15, 1967).

Key words: Electron affinity; ion sublimation energy; mass spectrometry; positive and negative atomic ions; rhenium; self-surface ionization; tungsten.

The self-surface ionization of tungsten and rhenium has been nvestigated with a specially designed mass spectrometer. It has been found that both positive and negative singly charged atomic ons sublime from these metal surfaces in the 1900-2600 °K temperature range. The assumption that these processes can be described by a generalized Saha-Langmuir equation has been shown to be valid. The energies required for positive ion sublimation were found to be 12.1 ± 0.2 and 10.7 ± 0.1 eV for tungsten and rhenium, respectively. The negative ion sublimation energy for rhenium was determined as 12.6 ± 0.2 eV and that for ungsten is given by approximately the same value. At 2300 °K, he ratio of positive to negative ions evaporating from these surfaces was found to be about 40 for tungsten and about 20,000 for rhenium. These results are consistent with the following estimates for the electron affinities: A(W) = 0.5 ± 0.3 eV and A(Re) = 0.3 ± 0.2 eV.

**10182.** Selby, M. C., **Progress in the U.S. on electromagnetic standards and measurements at 30 kHz to 1 GHz, 1963 through 1965,** *IEEE Trans. Instr. Meas.* **IM-16,** No. 2, 172-178 (June 1967).

Key words: Attenuation measurements; field strength measurements; high frequency measurements; impedance measurements; phase measurements; progress in radio measurements; thermal noise measurements; voltage measurements.

A digest of highlights is presented on the most significant U.S. contributions to the measurement of attenuation, impedance, voltage, current, field strength, thermal noise, and phase at 30 kHz to 1 GHz. A total of approximately 30 contributions are digested in this section of the report. The following accomplishments are among them: a super-sensitive detector for a complex-insertion-ratio measurement system having accuracies of about 0.0005 dB/10 dB at 30 MHz; exact equations for mutual and self-inductance of various combinations of filaments, tapes, and bars; a modified Twin-T-Bridge for measuring resistances of 100 to 10,000 ohms to 15 MHz; a set of Q-factor standards for frequencies to 45 MHz based on accumulated data and experience over 5 years; a unique adjustable characteristic-impedance coaxial line measurement of Q's greater than 100,000 of cryogenic circuits at frequencies to 300 MHz; a novel Tee-junction to enable calibrations of voltmeters of any practicable input impedances with VSWR's ranging from 1 to 200, to 1 GHz and higher; a miniaturized dipole-antenna field strength meter, employing a semiconducting plastic transmission line, to measure complex near-zone fields of 0.1 to 1000 volts per meter, from 150 kHz to 30 MHz; a prototype 3-MHz model of precision thermal noise-power comparators for an equivalent noise-temperature range of 75 to 30,000 °K at accuracies of 0.2 to 1 percent.

**10183.** McCamy, C. S., **Proposed recommended practice for description and selection of conditions for photographing specimens,** *Photo. Sci. Eng.* **10,** No. 4, 185-191 (July-Aug. 1966).

Key words: Appearance; camera description; lighting description; specimen photography.

A "Proposed Recommended Practice for Description and Selection of Conditions for Photographing Specimens" has been prepared for the American Society for Testing and Materials so that the photographic method of recording appearance can be made more reproducible from one laboratory to another, for various specimens, and for a given specimen at different times. The proposal defines terms and symbols and provides a systematic method of describing the arrangement of lights, camera, and subject; the characteristics of the illumination; the nature of the photographic process, and the viewing system. Conditions for photographing certain common forms of specimens are recommended. Conventions for exhibiting and publishing photographs of specimens include an orientation mark and a coordinate system for pictures.

**10184.** Reed, R. P., **Reply to "Comments on Reed Letter, by H. M. Otte,"** *Acta Met.* **15,** No. 6, 1082-1083 (June 1967).

Key words: Low temperatures; martensite; stacking faults.

This brief reply answers the assertion raised by Otte regarding previously published identification of deformation faulting in Fe-Ni alloys. It asserts that the published results quoted by Otte are not faults, but surface martensite.

**10185.** Young, D., **Scheduling a vehicle between an origin and a destination to maximize traveler satisfaction,** (Proc. 22nd Natl. Conf. Association for Computing Machinery, Washington, D.C., Aug. 29-31, 1967), *A. C. M. Publ.* **P-67,** pp. 233-245 (Thompson Book Co., Washington, D.C., July 1967).

Key words: Computer algorithm; iterative equation; optimal scheduling; parametric analysis; transportation vehicle; utility functions.

This paper presents an algorithm for scheduling a transportation vehicle on a single-link (origin to destination) network, so as to achieve a high degree of passenger satisfaction. The paper includes an explanation of traveler utility functions, a description of the iterative equation upon which the scheduling calculation is based, and a section on numerical results obtained using the algorithm. The latter section illustrates the role of the computer in performing the parametric analyses important for comprehensive evaluation of alternative transportation facilities.

The paper is extracted from research being done at the Technical Analysis Division of the National Bureau of Standards for the Northeast Corridor Transportation Project. Its contents should not be interpreted as representing policies of the Northeast Corridor Project.

**10186.** Melmed, A. J., **Surface self-diffusion of nickel and platinum,** *J. Appl. Phys.* **38,** No. 4, 1885-1892 (Mar. 1967).

Key words: Activation energy; field emission microscopy; nickel; platinum; surface-diffusion; surface properties.

The surface rearrangement of nickel and platinum due to (1) an electric field (build-up) and (2) surface tension (annealing) as the net driving force, has been studied by field-electron emission microscopy over the temperature range 510°–750 °K for Ni and 550°–850 °K for Pt. An Arrhenius-type relationship between temperature and time was found in both cases, so that an activation energy could be associated with each process. It is assumed that this is an average activation energy for surface diffusion.

The results of the field build-up experiments gave an activation energy of $Q_f = 19.1 \pm 1.9$ kcal/mole for Ni over the negative field range $(28-38) \times 10^6$ V/cm, and $Q_f = 26.3 \pm 2.6$ kcal/mole for Pt over the negative field range $(27-39) \times 10^6$ V/cm. It was possible to measure the effect of the electric field using a method devised earlier by Bettler and Charbonnier. This gave calculated zero-field activation energies of 20.6 ± 2.1 kcal/mole for Ni and 29.7 ± 3.0 kcal/mole for Pt. The results of the annealing experiments (no electric field) gave an activation energy of $Q_0 = 21.4 \pm 2.1$ kcal/mole for Ni and 29.5 ± 3.0 kcal/mole for Pt. (The foregoing indicated uncertainties are estimated over-all limits of error.) It is concluded from the agreement between the results of the two different types of measurement that either type of measurement (for fcc metals) may be used to determine the same quantity within a 10 percent uncertainty.

**10187.** McNish, A. G., **The aurora,** *Proc. NATO Advanced Study Institute, Bad Homburg, Germany, July 22-Aug. 2, 1963,* D. S. Bleil, ed., pp. 77-93 (Plenum Press Inc., New York, N.Y., 1964).

Key words: Corpuscular; ionization; magnetosphere; particle flux.

The present state of knowledge regarding the aurora is reviewed.

**10188.** Altschuler, H. M., **The conference on precision electromagnetic measurements,** *Proc. IEEE* **55,** No. 6, 782 (June 1967).

Key words: Conference; Conference on Precision Electromagnetic Measurements; electromagnetic measurements; measurements; precision measurements.

The character of the biennial Conference on Precision Electromagnetic Measurements (CPEM) is described. The scope of the Conference is compared with that of the special issue of the Proceedings of the IEEE on Measurements. Some of CPEM's history is recounted and its increasing international coverage is noted. It is concluded that the challenge to CPEM grows with the expansion of the fields it covers.

**10189.** Altschuler, H. M., **The role of the NBS Radio Standards Laboratory,** *Proc. IEEE* **55,** No. 6, 778-781 (June 1967).

Key words: High frequency; measurements; microwave; physical properties; physical quantities; physics; standards; standards laboratory; time and frequency.

This paper describes three major roles played by the NBS Radio Standards Laboratory in the field of electromagnetic measurements. It highlights the primary technical areas of the Laboratory with specific examples of the work involved, and mentions the various services which the Laboratory provides to the nation. It also describes the dynamic character and wide range of research in radio metrology at a national standards laboratory.

**10190.** Levin, E. M., **The system $Y_2O_3$-$V_2O_5$,** *J. Am. Ceram. Soc.* **50,** No. 7, 381-382 (July 1967).

Key words: Phase diagram; $V_2O_5$; $Y_2O_3$; yttrium vanadate.

The phase diagram of the system $Y_2O_3$-$V_2O_5$ has been determined experimentally, by the "quenching" method. The subsystem $YVO_4$-$V_2O_5$ is a simple eutectic one, with a solidus temperature of 672 ± 3 °C. Yttrium vanadate, of industrial importance, melts congruently at 1810 ± 25 °C. The subsystem $YVO_4$-$Y_2O_3$ is probably pseudobinary because of oxygen losses from the phases of composition $4Y_2O_3{:}V_2O_5$ and $5Y_2O_3{:}V_2O_5$. The composition $4Y_2O_3{:}V_2O_5$ exists in at least three different phases.

**10191.** Robertson, A. F., **U.S. Department of Commerce and the flammability of clothing fabric,** *Bull. N.Y. Acad. Med. Second Series* **43,** No. 8, 706-710 (Aug. 1967).

Key words: Clothing; clothing fire accidents; fabric flammability; fabrics; fire casualties.

The National Bureau of Standards has conducted studies of existing and modified test methods for measurement of flammable hazards associated with clothing fabrics. Recently, a cooperative program has been initiated with the Public Health Service to secure burn accident experience records which should yield information on the type of fabrics currently associated with clothing burn injuries. This program is just starting and it will be some years before valid information of the national picture becomes available. To date, however, there appears to be no technical evidence to show that a significant modification of the burn accident experience can be achieved without major changes in the flammable behavior of clothing fabrics. Thus, we hope industry will continue research on and development of permanently-retardant-treated fabrics which will be economically, esthetically, and usefully acceptable to the public. It appears, in spite of the lack of direct evidence, that such fabrics will significantly reduce, but not eliminate, clothing fire injuries.

**10192.** Chilton, C. J., Conner, J. P., Steele, F. K., **A comparison between solar x-ray emission and VLF sudden phase anomalies,** *Proc. IEEE* **53,** No. 12, 2018-2026 (Dec. 1965).

Key words: VELA satellite; VLF sudden phase anomalies measurements; solar x-ray emission measurements.

Original VLF sudden phase anomaly data obtained during October 1963 are presented for comparison with solar x-ray emission measurements made by VELA satellites during the same period.

**10193.** Meyer-Arendt, J. R., **A note on the evaluation of interference photographs,** *Acta Histochem.* **22,** 58-61 (1965).

Key words: Interference photographs; photographs; wavefront deformation.

Interference patterns should be evaluated with respect to two parameters, namely the spatial displacement and the contrast of the fringes. The contrast permits the deduction of the degree of wavefront deformation in one of the two bundles brought to interference. A series of representative figures are shown in a plot.

**10194.** Fatiadi, A. J., **A novel, facile preparation of 1,1′-bipyrene,** *J. Org. Chem.* **32,** 2903 (Sept. 1967).

Key words: Periodate oxidation of pyrene; synthesis of 1,1′-bipyrene.

An improved procedure is described for the synthesis of 1,1′-bipyrene.

**10195.** Saunders, J. B., **A simple, inexpensive wavefront shearing interferometer,** *Appl. Opt.* **6,** No. 9, 1581-1583 (Sept. 1967).

Key words: Interferometer; prism interferometer; wavefront shearing interferometer.

An efficient wavefront shearing interferometer is easy to produce from two small right-angle prisms. A cube beam divider becomes such an interferometer when two of its faces are aluminized. Any chosen angle of shear is obtained by a simple rotation of one prism relative to the other. Chromatic compensation is achieved by sliding one prism relative to the other along their common face.

**10196.** Klemperer, W. K., **Angular scattering law for the moon at 6 meter wavelength,** *J. Geophys. Res. Letter* **70,** No. 15, 3798-3800 (Aug. 1965).

Key words: Angular scattering law; meter wavelength; radar echoes; short-pulse.

Short-pulse (100 $\mu$sec) radar echoes have been obtained from the moon using the NBS-Instituto Geofisico del Peru 50 Mc/s facility near Lima, Peru. The results of an analysis of the data in terms of the angular scattering law $P(\theta)$ are compared with a recent theory of P. Beckmann (1965). The physical significance of the absence of any marked departure from the smooth $P(\theta)$ curve is pointed out.

**10197.** Ma, M. T., **Another method of synthesizing nonuniformly spaced antenna arrays,** *Trans. IEEE Ant. Prop.* **AP-13,** No. 5, 833-834 (Sept. 1965).

Key words: Amplitude excitations; antenna arrays; element spacings; nonuniformly spaced antenna arrays; synthesizing nonuniformly spaced antenna arrays.

A formulation for synthesizing an optimum nonuniformly paced but symmetrical array by adjusting both the amplitude excitations and element spacings is given. This is accomplished by applying Haar's theorem which is known in a branch of nathematics. It is shown that the solution obtained according to he method proposed here is optimum in the senses that, with espect to a chosen set of element spacings, (1) the maximum deviation between the synthesized and desired patterns is ninimized, (2) the side lobes can be made equal and their level ninimum for a specified beamwidth, (3) the side lobe level and beamwidth are not mutually constrained so that a solution better han the Dolph-Chebyshev array is possible, (4) a minimum number of elements required to synthesize a desired pattern can be determined, and (5) the solution is unique.

**10198.** Cottony, H. V., **Antennas,** *Encyclopedia of Physics,* R. M. Besancon, ed., pp. 25-28 (Reinhold Publ. Co., New York, N.Y., 1966).

Key words: Antennas; circuits; contiguous electronic circuit; electronic circuit; information energy; terminal impedance.

The functions and properties of antennas are outlined in a 1500 word article for use in an encyclopedia. The presentation s presented from a viewpoint that an antenna is a network designed to facilitate the transfer of information energy from circuits to space and reverse.

The relationship between an antenna and the contiguous elecronic circuit is determined and fully described by the terminal mpedances of the circuit and antenna. Because of the three-dimensional nature of propagating medium and the nature of electromagnetic wave, the performance of an antenna as a radiator is more complex. For full description, it requires the specifications of its radiation pattern in space, and the polarization of the radiated electromagnetic wave.

Six illustrations of different types of antennas are presented.

**10199.** Macek, J. H., **Application of the Fock expansion to doubly excited states of the helium atom,** *Phys. Rev.* **160,** No. 1, 170-174 (Aug. 5, 1967).

Key words: Applications; generalizations; helium; hyperspherical coordinates; power series; Schrödinger equation; solution.

A method of integrating the Schrödinger equation developed by Fock for S states of the helium atom is extended to all angular momentum states. The method makes use of an expansion in powers of R and log R, where $R=(r_1^2+r_2^2)$. Some applications and generalizations are explored. The convergence of the series is investigated.

**10200.** Powell, C. J., **Characteristic energy losses of 8 keV electrons in liquid In-Al and In-Bi alloys,** *Advan. Phys.* **16,** No. 62, 203 (Apr. 1967).

Key words: Characteristic-electron-energy-losses; electronic excitations; In-Al alloys; In-Bi alloys; liquid alloys.

Measurements have been made of the characteristic energy losses of 8 keV electrons in a series of liquid In-Al and In-Bi alloys in order to avoid the confusing effects of phase mixtures present in most similar studies of solid alloy systems. Loss spectra were measured in a reflection-type scattering geometry with total electron scattering angles of 15° and 70°. Two principal energy loss peaks, identified as being due to surface plasmon and to volume plasmon excitation, were found to vary as a function of alloy composition in each system. Deviations from the variaion expected from a simple free-electron model could be interpreted in some cases in terms of an interband electronic nsition occurring near the measured volume and surface energy-loss peaks. For bismuth-rich In-Bi alloys and for indium-rich In-Al alloys the transition energy and oscillator strength could be estimated and shown as a function of composition.

**10201.** Kerns, D. M., **Coping with multiple reflections in precise measurement of the speed of light with a microwave Michelson interferometer,** (Proc. URSI Symp. Electromagnetic Wave Theory, Delft, The Netherlands, September 1965), Chapter in *Electromagnetic Wave Theory,* pp. 245-249 (Pergamon Press Inc., New York, N.Y., 1967).

Key words: Interferometer; microwave; multiple reflections; speed of light; waveguide junction.

A microwave version of the Michelson interferometer is currently being used for a precise determination of the speed of light. In preliminary experiments, multiple reflections between the antenna and the movable mirror of the system have been found to produce apparent variations in c, which, if uncorrected, would be an order of magnitude greater than tolerable. This paper establishes a theorem that should enable substantial elimination of errors due to multiple reflections. It is also shown that the four-arm junction in the arrangement—usually visualized as an ideal magic T—need have no special properties and in particular need have none of the ideal properties that distinguish an ideal magic T.

**10202.** Zare, R. N., Bender, P. L., **Cross section for Na($^2P_{1/2}$, $^2P_{3/2}$) intramultiplet transactions induced by collisions with hydrogen atoms,** *Proc. Am. Phys. Soc. Meeting, Los Angeles* **10,** 1183 (American Physical Society, New York, N.Y., 1965).

Key words: Atom wavefront; hydrogen atoms; inelastic collisions.

The cross sections for the transfer of excitation between the $3^2P_{1/2}$ and $3^2P_{3/2}$ states of sodium induced by inelastic collisions with hydrogen atoms have been calculated using the impact parameter approximation. When two atoms approach each other a quasi-molecule is formed which may be characterized by its spin and projection of its total angular momentum on the molecular axis. For the Na*-H system the electronic wavefunctions are taken to be the antisymmetrized products of the separated atom wavefunctions, from which the $^1\Sigma$, $^3\Sigma$, $^1\Pi$ and $^3\Pi$ energy splittings are determined as a function of internuclear distance. The transition probability for each velocity and impact parameter is found by integrating along the collision trajectory the coupled differential equations arising from the time-dependent Schrödinger equation. Upon averaging overall impact parameters and the distribution in velocities we obtain for the total cross section $\sigma$ (Na $^2P_{1/2} \rightarrow$ Na $^2P_{3/2}$) 61.8, 58.0 and 55.2 $\pi a_0^2$ at $T = 5000$, 7500 and 10,000 °K. Corrections to these values still have to be made for deviations from straight-line paths and for the neglect of van der Waals forces, although these are anticipated to be small.

**10203.** Cushen, W. E., **C. S. Peirce on benefit-cost analysis of scientific activity,** *Operations Res.* **15,** No. 4, 641 (July-Aug. 1967).

Key words: Benefit-cost; history; Peirce; philosophy; pragmatism; research priorities; weights and measures.

A very early paper on benefit-cost analysis of research projects was published in the Appendix to the Coast Survey's Annual Report 1876. A special issue of *Operations Research,* devoted to applications, is reprinting the original article, authored by Charles Sanders Peirce, who is better known as the father of pragmatism in American philosophical circles. The paper by Cushen serves to introduce the reprint and to paint a brief scene for its use and interpretation.

**10204.** Kerns, D. M., **Definitions of v, i, Z, Y, a, b, Γ, and S,** *Proc. IEEE* **55,** No. 6, 892-900 (June 1967).

Key words: Admittance matrix; impedance concepts; impedance matrix; scattering matrix; waveguide junction; waveguide n-port.

Concepts and conditions underlying the establishment and use of the immittance- and scattering-matrix description of waveguide n-ports are discussed. The discussion is intended to be critical and intensive rather than general. Needed results of electromagnetic (and waveguide) theory are assumed. Emphasis is placed on defining basic quantities needed in the matrix scheme. These include: generalized voltage and current, v and i, for waveguide modes; modal impedance; modal characteristic mpedance; the immittance matrices, Z and Y; traveling-wave amplitudes, a and b; the scattering matrix, S; and reflection coefficient, Γ. Theoretical properties of Z, Y, and S are not discussed; applications are indicated but not discussed.

**10205.** Bowen, R. L., **Development of an adhesive restorative material,** (Proc. 2nd Workshop, Adhesive Restorative Dental Materials, University of Virginia, Charlottesville, Va., Dec. 8-9, 1965), Chapter 4 in *Adhesive Restorative Dental Materials,* No. 2, p. 225 (U.S.) Public Health Service Publ. 1494, Supt. Doc. U.S. Government Printing Office, Washington, D.C., $1.00, 1966).

Key words: Adhesive; bonding; dental material bonding; resin; restorative.

Recent findings, primarily from the literature, are reviewed on the subject of adhesive, restorative, dental materials. One mode of attack on the problem is described. In this, an inorganic-organic composite is used as the restorative material. The inorganic reinforcing fillers serve primarily to reduce the material's thermal expansion. A coupling agent improves the bonding between the phases. Bonding between the organic resin phase and the tooth surface is also improved by a coupling agent (surface-active comonomer).

**10206.** Robertson, B., **Equations of motion in nonequilibrium statistical mechanics. II. Energy transport,** *Phys. Rev.* **160,** No. 1, 175-183 (Aug. 5, 1967).

Key words: Energy transport; equations of motion; exact flux operator; heat conductivity; heat wave equation; nonequilibrium statistical mechanics.

The exact equations of motion for the space- and time-dependent coordinates of an arbitrary many-body system have been derived previously. These equations are integrodifferential equations whose kernels are generalizations of correlation functions and therefore are related to Green functions. In this paper an exact general expression for a flux operator is used to rewrite the equations. Then they become memory-retaining nonlocal generalizations of the diffusion equation. The formalism is applied to energy transport, and the usual expression for heat conductivity is derived without making the usual assumptions. Finally, a simple function is assumed for the kernel, and the equation then reduces to a well known heat conduction and wave equation.

**10207.** Weinstock, J., **Equivalence between two formalisms of plasma fluctuations,** *Phys. Fluids* **9,** No. 3, 621-622 (Mar. 1966).

Key words: Auto-correlation function; distribution function; kinetic theory; plasma fluctuation.

It is pointed out that the expression for auto-correlation functions which is given in terms of the two-time distribution function is related by a trivial identity to the expression for auto-correlation functions which is given in terms of the usual distribution function.

**10208.** Okabe, H., **Excited species and their contribution to NO ($\beta$,$\gamma$) fluorescence in the photodissociation of $N_2O$,** *J. Chem. Phys.* **47,** No. 1, 101-109 (July 1, 1967).

Key words: Energy transfer; excited species; fluorescence; gas phase; $N_2O$; photolysis; vacuum ultraviolet;

The fluorescence intensity and the yield of the NO $\beta$ bands, originating from photodissociation of $N_2O$, was measured as a function of wavelength of incident light in the vacuum ultraviolet region. Photon energies required for the occurrence of the fluorescence are far less than the threshold energy to produce $NO(A^2\Sigma^+, B^2\Pi_r)$ directly from $N_2O$, indicating that the emission is due to secondary processes. The fluorescence intensity curve follows closely the absorption curve of $N_2O$ indicating that excited species responsible for the emission are produced from dissociation of electronically excited $N_2O$ rather than from the direct dissociation to these species. A mechanism of fluorescence is discussed on the basis of the threshold energy above which a specific photochemical process is possible. Reactions responsible for the $\beta$ emission in the absorption region 1400 to 1550 Å of $N_2O$ are production of $N(^2D)$ and $O(^1S)$ followed by $N(^2D) + N_2O \rightarrow N_2 + NO(B^2\Pi_r)$ and $O(^1S) + N_2O \rightarrow NO + NO(B^2\Pi_r)$. In the region below 1440 Å, $N(^2P)$ and $N_2(B^3\Pi^g, B'^3\Sigma_u^-)$ also can contribute to the emission. When NO was added to $N_2O$, the fluorescence intensity increased considerably and the emission changed from $\beta$ to $\gamma$ bands. Reactions which produce the emission in the absorption region 1400 to 1550 Å are

$$N_2O \xrightarrow{h\nu} N_2(A^3\Sigma_u^+) + O(^3P)$$

followed by $N_2(A^3\Sigma_u^+) + NO \rightarrow N_2 + NO(A^2\Sigma^+)$. Below 1350 Å additional excited molecules $N_2(B^3\Pi_g, B'^3\Sigma_u^-)$ can contribute to the emission in similar reactions.

**10209.** Bridges, J. M., Wiese, W. L., **Experimental determination of transition probabilities and Stark widths of S I and S II lines,** *Phys. Rev.* **159,** No. 1, 31-38 (July 5, 1967).

Key words: Arc; atomic spectroscopy; plasma; Stark broadening; sulfur; transition probability.

Absolute transition probabilities and Stark widths for some prominent multiplets of S I and S II have been determined experimentally. A well-stabilized arc was operated in $SO_2$ with a small hydrogen admixture. The spectroscopic measurements were performed photoelectrically. Side-on observations were transformed via the Abel inversion to give the radial dependence of the measured quantities. Measurements of the absolute intensity of O I lines and the width of $H_\beta$ served for the plasma analysis; the results of these measurements together with the application of equilibrium and conservation relations for arc plasmas enabled the determination of the temperature and various particle densities. Mass separation effects are taken into account. The measured Stark widths generally agree well with values calculated from Stark broadening theory; in the case of S II lines the agreement with very recently calculated values is substantially better than that with earlier theoretical data.

**10210.** Frederikse, H. P. R., Hosler, W. R., **Hall mobility in $SrTiO_3$,** *Phys. Rev.* **161,** No. 3, 822-827 (Sept. 15, 1967).

Key words: Electron mobility; ionized impurity scattering; optical mode scattering; strontium titanate; temperature dependence of mobility.

Electron mobilities in reduced and doped $SrTiO_3$ have been deduced from measurements of conductivity and Hall coefficient between 1 and 1000 °K. Above room temperature scattering by e highest two longitudinal optical modes determines the mobili- . Expressions based on intermediate electron-phonon coupling ield good agreement. Below 10 °K ionized impurity scattering the dominant collision process. Using a screened Coulomb otential, one obtains mobility values of the right order of mag- ude.

0211. Wallace, M. R., Milliken, L. T., Toner, S. D., **Identification of dyes in paper by extraction and chromatographic analysis,** *TAPPI* **50,** No. 9, 121A-124A (Sept. 1967).

Key words: Chemical analysis; chemical tests; chromatography; dyes.

A chromatographic procedure is described for the determina- on of a range of direct and acid dyes in dyed paper. It can be sed for the identification of individual dyes in complex mixtures n unknown samples, and is simple and inexpensive enough to se in routine quality control and testing of dyes and dyed paper. $R_f$ values and visual appearances serve immediately to identify ost of the paper dyes studied. Comparisons with known eferences give good estimates of the quantities of each dye resent. Individual basic dyes could not be identified by this rocedure, but the presence of a basic dye could be detected by appearance in the solvent front. In a mixed furnish containing oth acidic and basic dyes the acidic dyes could be determined ithout interference by the basic dyes. $R_f$ values for the principle haracteristic bands of 26 dyes are listed.

0212. Fehsenfeld, F. C., Megill, L. R., Droppleman, L. K., **Interpretation of cyclotron resonance line shapes in slightly ionized gases,** *J. Chem. Phys.* **43,** No. 10, 3618-3624 (Nov. 1965).

Key words: Cyclotron resonance line shapes; ionized gases; line shapes; resonance line shapes.

The dependence of cyclotron resonance line shape on the elocity dependence of the collision frequency for three different istribution functions is calculated. Several sets of data for vari- us collision frequency dependency upon energy are calculated. hese include, in addition to simple one term power laws, results or four gases using measured collision frequencies. Because the ne shape is strongly influenced by the energy dependency of the ollision frequency, the calculation of collision frequencies from ne width data requires an accurate knowledge of the variation f collision frequency with energy. Moreover, with previously sed analyses, large errors in the deduced collision frequency ay be caused, for some gases, by the presence of small admix- ures of other gases, or ions. The examples which are given to il- strate the above statements indicate that extreme care must be xercised if reliable experimental data are to be obtained.

0213. VanZandt, T. E., **Ionosphere,** *Encyclopedia of Physics,* R. M. Besancon, ed., pp. 348-349 (Reinhold Publ. Co., New York, N.Y., 1966).

Key words: Electron concentration; height range; ionic composition; ionosphere; ionospheric regions.

214. Klose, J. Z., **Lifetimes of some 4p levels in argon I,** *J. Opt. Soc. Am.* **57,** No. 10, 1242-1244 (Oct. 1967).

Key words: Argon; delayed coincidence; lifetimes, atomic; spectra, atomic.

Mean lives of four electronically excited atomic levels in Ar I ave been determined using a method of delayed coincidence. he measured values of the mean lives of the $2p_1$ through $2p_4$ Paschen notation) levels in neutral argon determined from ransitions with associated wavelengths extending from 6677 to 147 Å are as follows: $2p_1$, 21 ± 2 nanoseconds; $2p_2$, 25 ± 1 nsec; $2p_3$, 26 ± 1 nsec; and $2p_4$, 31 ± 2 nsec. The lifetimes were estimated to contain systematic errors varying from 5 to 15 percent and are presented in comparison with corresponding results of other workers.

10215. Arms, R. J., Hama, F. R., **Localized-induction concept on a curved vortex and motion of an elliptic vortex ring,** *Phys. Fluids* **8,** No. 4, 553-559 (Apr. 1965).

Key words: Curved vortex; elliptic vortex ring; localized-induction; motion of vortex ring; vortex; vortex motion.

The localized-induction concept for the induction effect of a smooth curved vortex on itself is derived. This concept is applicable to the limiting case of a vortex filament of infinitesimal core size and of negligible long-distance effect, and was already successfully utilized in the investigations of the motion and deformation of a curved vortex filament given various initial configurations. Two theorems obtained under this concept are that the arc length of a vortex filament and the projected area of a closed vortex filament are both invariant with respect to time. These theoretical predictions are examined by a numerical analysis of the motion of an initially plane elliptic vortex ring of various eccentricities.

10216. Costrell, L., **Lou Costrell of NBS speaks out on the revolution in instrument packaging,** *IEEE Trans. Nucl. Sci.* **15,** No. 8, 78-84 (Aug. 1967).

Key words: Instrument; interchangeability; modules; nuclear; standard.

The interchangeability problem posed by the advent of modular instrumentation has been alleviated by the development of a Standard Nuclear Module (NIM) system by the AEC Committee on Nuclear Instrument Modules. The Committee held its first meeting in March 1964. The completed specifications were issued in July 1964 and laboratory utilization and industry exhibit of the NIM system began in November 1964. Acceptance by the laboratories and by the nuclear instrument industry has been so rapid and so overwhelming that by September 1966 more than 70 percent of the total modular nuclear instruments produced in the U.S. were in the NIM system. The percentage today is even higher and the impact is world wide. Since all necessary components are available, other fields and other industries can readily adopt the system.

10217. Hermach, F. L., **Low-frequency electrical calibrations at the National Bureau of Standards,** (Proc. 22nd Annual ISA Conf. and Exhibit, Chicago, Ill., Sept. 11-14, 1967), **ISA Preprint** No. M5-1-MESTIND-67 (1967).

Key words: Electrical calibrations; electrical standards; low-frequency calibrations; low-frequency standards.

Charts are presented to show the present range and accuracy of NBS calibrations of standards of resistance, capacitance, inductance, voltage, and current, from direct current through 50 kHz. The chains of measurements by which these and other calibrations are related to the basic NBS standards of voltage and resistance are also shown.

10218. Milligan, D. E., Jacox, M. E., **Matrix-isolation study of the reaction of carbon atoms with chlorine. The electronic and vibrational spectra of the free radical $CCl_2$,** *J. Chem. Phys.* **47,** No. 2, 703-707 (July 15, 1967).

Key words: Carbon atoms; $CCl_2$ radical; $CF_2$ radical; chlorine; cyanogen azide; electronic spectrum; infrared spectrum; matrix isolation.

Studies of the photolysis of $N_3CN$ in the presence of $Cl_2$ in Ar and $N_2$ matrices at 14 °K provide evidence for the formation of the free radical $CCl_2$ by the reaction of photolytically produced

C atoms with $Cl_2$. The two stretching fundamentals of $CCl_2$ appear at 721 and 748 $cm^{-1}$. The corresponding fundamentals of $^{13}CCl_2$ have also been observed. When the sample is warmed above about 30 °K, these features disappear, and $CCl_4$ features grow in intensity, indicating the $CCl_2$ can react with $Cl_2$ with little or no activation energy. The valence angle of $CCl_2$ probably lies between 90° and 110°. A weak band system appearing between 4400 and 5600 Å, with an average band separation of 305 $cm^{-1}$, may also be attributed to $CCl_2$. Analogy with the electronic absorption spectrum of $CF_2$ suggests that $CCl_2$ possesses a ground singlet state and that this band system arises from a transition between the ground state electronic configuration and the first excited electronic configuration of $CCl_2$, involving an extensive progression in the upper state bending vibration.

**10219.** McNish, A. G., **Measurement standards,** *IEEE Student J.* **4,** No. 2, 24-31 (Mar. 1966).

Key words: Length; mass; temperature; time; units of measurement.

All *units of measurement*, including the ampere of current and candela of light intensity – two base units included in the new International System of Units, are ultimately derived from four original prototype units – the meter of *length*, kilogram of *mass*, degree Kelvin of *temperature*, and second of *time*. To make all measurement units more effective tools, the standards that physically embody or define three of the prototypes – length, time, and temperature – have been changed in recent years.

**10220.** Roberts, J. R., Eckerle, K. L., **Measurements of Stark profiles of C II and Ca II lines,** *Phys. Rev.* **159,** No. 1, 104-107 (July 5, 1967).

Key words: C II; Ca II; experimental; monochromator; profile scans; Stark profiles; T-tube.

An electromagnetic *T* tube was the source of a plasma used to measure line profiles of singly ionized atoms. The profiles of C II lines emitted by a plasma composed of He and $Co_2$ in the ratio 95:5 were scanned with a monochromator. The profile scans were accomplished by repeated firings of the T tube while advancing the monochromator in wavelength steps. Also measured was the profile of the 3934 Å Ca II resonance line emitted by a plasma composed of He, $H_2$, and $CO_2$ in the ratio 20:10:70 with Ca as an impurity. The profile of the 3889 Å He I line was also measured and its halfwidth was used to determine the plasma electron density in the case of the C II lines. Likewise $H_\alpha$ was used to determine the electron density in the case of the Ca II line. The experimental C II and Ca II Stark-profile half-widths were compared with the theoretically calculated values.

**10221.** Corliss, E. L. R., **Mechanistic aspects of hearing,** *J. Acoust. Soc. Am.* **41,** No. 6, 1500-1516 (June 1967).

Key words: Auditory analysis; auditory perception; communication theory; ear behavior; hearing; mechanistic model of hearing; resolving power of the ear.

The results of a number of apparently diverse experiments on human hearing can be summarized via a simple model. Two mechanisms are required: One element emits unit responses whose number is proportional to the instantaneous amplitude of a sound. The other is a selector mechanism, analogous to a resonant circuit, that integrates the responses. Correspondingly, just two parameters are involved: the threshold of hearing and the "Q" of the selector mechanism. The system of equations representing the model makes it possible to derive the necessary parameters from the results of a number of different types of experiments. The theory of the selector mechanism is based upon a recent study of the limits of performance of a system capable of storing oscillatory energy reversibly, but the remainder of the theoretical description makes use of ordinary communication theory.

The discrimination ability of the normal ear is shown to be proportional to the one-fourth power of the level above threshold, and to relate closely to the sensation of loudness. Many features of the behavior of normal and impaired ears can be predicted by application of familiar network theory to the parameters derived from the model. The properties of the model may be used as criteria in the choice of experiments to develop explicit data on the way the ear performs its function.

**10222.** Durst, R. A., Taylor, J. K., **Modification of the fluoride activity electrode for microchemical analysis,** *Anal. Chem.* **39,** No. 12, 1483-1485 (Oct. 1967).

Key words: Electrochemical analysis; fluoride, analysis for; fluoride electrode; microchemical analysis; potentiometry; specific ion electrode.

A fluoride activity electrode has been modified for operation in the inverted position by converting the inner reference solution to a gel. Operation in this position makes possible the use of the single-crystal fluoride-sensitive membrane as the sample "container" and permits the measurement of sample volumes as small as one drop (50 $\mu$l). A calibration curve is obtained for solutions containing $10^{-1}$ *M* to $10^{-6}$ *M* NaF in 0.1 *M* $KNO_3$. The precision to which the fluoride concentration can be read from this calibration curve is calculated from the slope of the curve at the various concentrations and the standard deviation of the e.m.f. measurements. In the concentration range from $10^{-1}$ *M* to $10^{-3}$ *M* NaF, the calculated error is about 2 percent. At the $10^{-5}$ *M* NaF level, 10 nanograms of fluoride can be determined with an error of approximately 0.7 nanogram. For sample volumes of 50 $\mu$l, the modified fluoride electrode was found to exhibit a usable response in the range from $10^{-1}$ *M* to $5 \times 10^{-6}$ *M* fluoride.

**10223.** Durst, R. A., Taylor, J. K., **Modified linear null-point potentiometry,** *Anal. Chem.* **39,** No. 12, 1374-1379 (Oct. 1967).

Key words: Electroanalysis; linear potentiometry; microtitration; null-point potentiometry; potentiometry; silver.

A modification of the technique of precision null-point potentiometry has been developed in which a linear titration curve is obtained when the logarithm of the amount of coulometrically generated titrant is plotted against the concentration cell potential. The equivalence point is evaluated graphically and by computer techniques. The analyses of standard 0.1 ml samples containing 0 to 13 $\mu$g of silver are discussed in detail. This technique was found to be applicable down to one nanoequivalent (0.1 $\mu$g) of silver with an error of less than 5 percent. Below this value, a positive deviation occurs due to the spontaneous dissolution of the silver indicator electrodes. The interference effects of several cations are also discussed.

**10224.** Ruffa, A. R., **Nature of ionic deformations in crystals; application to an analysis of the magnetic properties of the alkali-halide and alkaline-earth oxide crystals,** *Phys. Rev.* **159,** No. 3, 742-754 (July 15, 1967).

Key words: Alkali earth oxides; alkali halides; deformation; diamagnetism; ionic; ionic sizes; kinetic energy; paramagnetism; polarizabilities.

Absolute diamagnetic susceptibilities for the alkali-halide crystals are obtained theoretically and compared with the observed magnetic susceptibilities of these crystals in order to determine the crystalline paramagnetic susceptibilities. The paramagnetic susceptibilities obtained in this way are found to bey the linear relationship $\chi_{para} = 0.11\chi_{dia}$. Theoretical analysis onfirms this relationship for the alkali halides and indicates, in ddition, that (1) Virtually all of the increased kinetic energy hich the ions acquire in the process of crystallization takes the orm of rotational kinetic energy; (2) the angular deformations of he ions in all the alkali halides are the same in that the average igenvalues of the square of the angular momentum operator per lectronic orbital is constant for all these crystals; and (3) the eneral relationship between $\chi_{dia}$ and $\chi_{para}$ for an ionic crystal is f the form $\chi_{para} = C\chi_{dia}$, where $C$ is very nearly proportional to he average cohesive energy per ion of the crystal. The last conlusion is confirmed in the alkaline-earth oxides where $C \approx 0.5$, accord with the fact that the cohesive energies of these rystals are about five times those of the alkali halides. Furthernore, this analysis indicates that an ionic crystal with a large nough cohesive energy is paramagnetic, in agreement with obervation.

**0225.** Mebs, R. W., Bennett, L. H., Leibowitz, J. R., **Nuclear magnetic acoustic resonance in KTaO$_3$**, *Physics Letters* **24A,** No. 12, 665-666 (June 5, 1967).

> Key words: Dislocation damping of acoustic waves; nuclear magnetic acoustic resonance; nuclear magnetic resonance; nuclear quadrupole coupling; potassium tantalate.

Direct acoustic excitation of the $^{181}$Ta nuclear spin is observed t room temperature in KTaO$_3$.

**0226.** Lide, D. R., Jr., Maki, A. G., **On the explanation of the so-called CN laser,** *Appl. Phys. Letters* **11,** No. 2, 62-64 (July 15, 1967).

> Key words: CN; emission; far infrared; HCN; laser; spectra.

It is shown that the major features of the far infrared "CN aser" are due to the HCN molecule. The intense line at 337 nicrons and other near-by lines are explained as transitions inolving the $11^{1}0$ and $04^{0}0$ vibrational states, which are mixed by Coriolis perturbation. The mechanism of the laser is discussed.

**0227.** Mighell, A. D., Reimann, C. W., **On the structure of pyrazole,** *J. Phys. Chem.* **71,** No. 7, 2375-2376 (June 1967).

> Key words: Betaine form; pyrazole; structure; x-ray.

The structure of pyrazole has been reexamined based upon an nalysis of the complete crystal and molecular structure of ichlorotetra(pyrazole)nickel (II), Ni(C$_3$H$_4$N$_2$)$_4$Cl$_2$. This analyis shows that a relocation of a hydrogen atom in the previously eported structure of pyrazole is required to bring the two formutions of pyrazole into agreement. The relocation of the ydrogen atom, however, alters the previous conclusions regardng the relative contribution of the betaine form to the resonance ybrid.

**0228.** Kokoszka, G. F., Reimann, C. W., Allen, H. C., Jr., Gordon, G., **Optical and magnetic measurements on single crystals of copper(II)-doped tris(phenanthroline)zinc(II)nitrate dihydrate,** *Inorg. Chem.* **6,** No. 9, 1657-1661 (1967).

> Key words: D-d transitions; EPR spectrum; Jahn-Teller effect; polarized optical spectrum; trisphenanthroline copper(II) nitrate dihydrate; trisphenanthroline zinc(II) nitrate dihydrate.

The electron paramagnetic resonance spectrum in single rystals of copper(II)-doped tris(phenanthroline)zinc(II) nitrate ihydrate has been observed between 4 and 350 °K. The results ave been interpreted in terms of a Jahn-Teller effect for the opper(II) ion. At 350 °K the spectrum is nearly isotropic with $= 2.13$ and no observed hyperfine splitting. At 77 °K nisotropy of the $g$ tensor is observed with $g_{\|}=2.273$, $g_{\perp}=2.064$, $A = 160 \times 10^{-4}$ cm$^{-1}$, $B < 7 \times 10^{-4}$ cm$^{-1}$, $A' = 12.5 \times 10^{-4}$ cm$^{-1}$, and $B' = 10.5 \times 10^{-4}$ cm$^{-1}$. No significant change in the spectrum was observed at temperatures below 77 °K. The optical d-d transitions and their polarization properties are reported. Two bands are observed at 7000 and 14,900 cm$^{-1}$. The 14,900-cm$^{-1}$ band is split at 77 °K into components at 14,700 and 15,200 cm$^{-1}$. The optical axes do not coincide with the principal magnetic axes.

**10229.** Crow, E. L., Siddiqui, M. M., **Robust estimation of location,** *J. Am. Stat. Assoc.* **62,** No. 318, 353-389 (June 1967).

> Key words: Asymptotic theory; efficiency; median; order statistics; probability distributions; robust estimators; statistical estimation; weighted means; wild observations.

The problem of estimating a location parameter from a random sample when the form of distribution is unknown or there is contamination of the target distribution is attacked by deriving estimators which are efficient over a class of two or more forms ("pencils") of continuous symmetric unimodal distributions. The pencils considered are the normal, double exponential, Cauchy, parabolic, triangular, and rectangular (a limiting case). The estimators considered are special symmetrical linear combinations of order statistics: trimmed means, Winsorized means, "linearly weighted" means, and a combination of the median and two other order statistics. These are also compared asymptotically with a Hodges-Lehmann estimator. Efficiencies are tabulated for sample sizes of 4 or 5, 8 or 9, 16 or 17, and ∞. The theory required for deriving asymptotic variances is presented. Efficiencies of at least 0.82 relative to the best estimator for any single pencil are achieved by using the best trimmed mean or linearly weighted mean over a range of pencils of distributions from the normal to the Cauchy. However, the combination of the median and two other order statistics is almost as efficient (0.80) over the same range and is more efficient than the other estimators if the range is extended through the rectangular pencil.

**10230.** Schafft, H. A., **Second breakdown—A comprehensive review,** *Proc. IEEE* **55,** No. 8, 1272-1288 (Aug. 1967).

> Key words: Circuit reliability; diodes; failure mechanisms; failure modes; review; second breakdown; semiconductor devices; thermal breakdown; transistor reliability; transistors.

This paper is a comprehensive review of the published literature dealing with the phenomenon of second breakdown in semiconductor devices and the problems it creates in the design, fabrication, testing, and application of transistors.

**10231.** Robinson, E. J., Geltman, S., **Single- and double-quantum photodetachment of negative ions,** *Phys. Rev.* **153,** No. 1, 4-8 (Jan. 1967).

> Key words: Double-quantum; elastic scattering; negative ions; photodetachment; single-quantum.

The recent measurement of the transition probability for the double-quantum detachment of an electron from I$^-$ has prompted a new theoretical study of this problem. A central field model for bound and free states is used, in which a parameter is adjusted in the potential to yield the observed binding energies of the negative ions. An implicit sum method, requiring the solution of inhomogeneous radial equations, is used to evaluate the sums over intermediate states. The results for I$^-$ lie within the experimental uncertainty. The single-quantum photodetachment and electron elastic scattering (from the neutral atom) cross sections are also given for the ions studied: C$^-$, O$^-$, F$^-$, Si$^-$, S$^-$, Cl$^-$, Br$^-$, I$^-$.

**10232.** Bean, B. R., Warner, B. D., **Some radio-physical considerations in studies of the fine scale structure of the at-**

**mosphere,** *Proc. Intern. Conf. Fine Scale Structure of the Atmosphere, Moscow, USSR, June 1965*, pp. 215-224 (1965).

Key words: Angular scatter; atmospheric fine structure; dot angels; radar returns; radio path-length variations; refractive index; water vapor density.

Radar returns from the clear air have been extensively utilized as a method of studying the fine structure of the atmosphere. These studies have heretofore utilized a single radar. Presented here are the first tentative results of a two-radar study of the angular "scattering" pattern of clear air returns. These preliminary results for warm, turbulent, summer days indicate that the "dot angels" returns are more in agreement with a scatter mechanism rather than with specular reflection. It is also demonstrated that the electrical path length may be used to determine the average water vapor content of the radio path.

**10233.** Milligan, D. E., Jacox, M. E., **Spectroscopic study of the vacuum-ultraviolet photolysis of matrix-isolated HCN and halogen cyanides. Infrared spectra of the species CN and XNC,** *J. Chem. Phys.* **47,** No. 1, 278-285 (July 1, 1967).

Key words: CN free radical; cyanogen; cyanogen bromide; cyanogen chloride; cyanogen fluoride; halogen isocyanides; hydrogen cyanide; hydrogen isocyanide; infrared spectrum; matrix isolation technique; ultraviolet spectrum; vacuum ultraviolet photolysis.

Vacuum-ultraviolet photolysis of HCN isolated in Ar and $N_2$ matrices at 14 °K is found to lead to the production of HNC in concentration sufficient for direct infrared observation of all three vibrational fundamentals. The spectrum of this species is found to be appreciably perturbed by the presence of $N_2$. The force constants and thermodynamic properties of HNC have been revised to the values appropriate to this species in an environment free of perturbation by an adjacent $N_2$ molecule. The free radical CN is also produced in these systems in concentration sufficient for direct observation not only of the $B(^2\Sigma^+) - X(^2\Sigma^+)$ transition but also of the ground-state vibrational fundamental. Isotopic data supporting this identification are presented. Upon vacuum-ultraviolet photolysis of matrix-isolated FCN, two infrared absorptions appear which can be identified with the stretching fundamentals of the species FNC. In analogous experiments on the species ClCN and BrCN, infrared absorptions tentatively assigned to ClNC and BrNC have been observed.

**10234.** Smith, E. K., **Sporadic-E ionization,** *Annual Supplement Encyclopedic Dictionary of Physics,* J. Therolis, ed., **Suppl. I,** 329-331 (Pergamon Press Inc., New York, N.Y., 1966).

Key words: Auroral types of sporadic E; equatorial; ionization; sporadic-E.

A brief review is presented on the structure of the sporadic-E layer, its temporal characteristics, and finally of the current thinking of the cause of equatorial, temporate and auroral types of sporadic E.

**10235.** Schooley, J. F., Frederikse, H. P. R., Hosler, W. R., Pfeiffer, E. R., **Superconductive properties of ceramic mixed titanates,** *Phys. Rev.* **159,** No. 2, 301-305 (July 10, 1967).

Key words: $BaSrTiO_3$; $CaSrTiO_3$; ceramics; magnetization; mixed titanates; semiconductors; $SrTiO_3$; superconductivity.

The superconducting transition temperature of a series of mixed barium-strontium and calcium-strontium titanate ceramic specimens have been determined. For several of these samples the low-field magnetization has also been investigated. The results are compared with those obtained from single-crystal $SrTiO_3$.

**10236.** Peterson, R. L., **Suppressed and accelerated spin-lattice relaxation,** *Phys. Rev.* **159,** No. 2, 227-233 (July 10, 1967).

Key words: Inelastic phonon-boundary scattering; phonon avalanche; phonon bottleneck; spin-lattice relaxation; spin-phonon interactions.

The transient magnetic behavior of a paramagnetic substance, after an initial disturbance, is considered theoretically for a variety of situations in which the lattice temperature rises as a result of energy flow from the magnetic (electron spin) system. The direct and $T^9$ Raman spin-phonon processes are considered. Coupling between phonon modes, and leakage of energy into a bath are taken into account. Graphs of the resultant behavior are presented. Effects such as suppressed and accelerated spin relaxation, and rapid decay (phonon avalanche) after spin inversion, are discussed. It is pointed out that experiments performed without the usual helium bath may provide reliable measurements of inelastic phonon-boundary scattering.

**10237.** Ochs, G. R., **Synchrotron radiation measurements near the magnetic equator,** Chapter in *Radiation Trapped in the Earth's Magnetic Field,* B. McCormac, ed., pp. 703-713 (D. Riedel Publ. Co., Dordrecht, The Netherlands, 1966).

Key words: Decay; intensity; magnetic equator; observations; radio frequencies; starfish; synchrotron radiation.

The radiation produced in the radio spectrum by relativistic electrons injected into trapped orbits in the earth's magnetic field at the time of the Starfish nuclear explosion of July 9, 1962, has been monitored near Lima, Peru, for one year at 30 Mc/s and almost three years at 50 Mc/s. After an initial brief transient increase of 4.5 × $10^4$ °K, the excess antenna temperature at 50 Mc/s rapidly decreased to 1 × $10^4$ °K. Later, the temperature $T_{50}$ at a time t days after the explosion approximately followed the law,

$$T_{50} = 6600e^{-(t/270)},$$

for $t > 90$ days. At 30 Mc/s, the initial transient increase was not observed, but the subsequent behavior was similar. The decay was more rapid and the early signal was of greater intensity, however. After the first three months, the temperature $T_{30}$ approximately followed the law,

$$T_{30} = 16000e^{-(t/180)}.$$

**10238.** Utton, D. B., **Temperature dependence of the nuclear quadrupole resonance frequency of $^{35}$Cl in $KClO_3$ between 12 ° and 90 °K,** *J. Chem. Phys.* **47,** No. 2, 371-373 (July 15, 1967).

Key words: Bayer-Kushida theory; chlorine; nuclear quadrupole resonance; potassium chlorate; temperature variation; 12 °K – 90 °K.

A precise measurement of the temperature dependence of the N.Q.R. frequency of $Cl^{35}$ in $KClO_3$ has been made at constant pressure in the range 12 °K – 90 °K. Analysis using the Bayer-Kushida theory predicts lattice modes at 60 $cm^{-1}$ and 126 $cm^{-1}$ A comparison is made with the Raman spectrum.

**10239.** Shimazaki, T., **The application of the partial correlation analyses to the study of the occurrence probability of spread-F** (Proc. AGARD Conf. Spread F and Its Effects Upon Radiowave Propagation and Communication, Copenhagen Denmark, Aug. 1964), *AGARDograph* **95,** pp. 167-188 (W and J. Mackay, London, England, 1966).

Key words: Charged particles; extra-terrestrial origins; higher solar activity; hydromagnetic waves; solar activity spread-F.

It is well known that the spread-F occurrence probability is inversely correlated to solar activity during the solar cycle at mos stations except at very high latitudes. This is strange because extra-terrestrial origins of spread-F, such as impinging charged particles or hydromagnetic waves, may develop more strongly and more extensively during higher solar activity. The cause of this apparent inverse correlation may be sought in the ionospheric and upper atmospheric conditions.

In past studies, several ionospheric parameters have been considered as the possible factors which control the occurrence of spread-F, and the correlation coefficients between each parameter and the occurrence probability of spread-F have been examined. However, each of these correlations has ignored the effect of other parameters. Before examining the correlation between each parameter and the spread-F occurrence probability, the effect of other factors should be eliminated systematically. The technique of partial correlation is useful for this purpose.

In this study, the partial correlation coefficients between various ionospheric, solar and geomagnetic parameters and the spread-F occurrence probability are studied for Washington and Wakkanai. The result shows that the partial correlation analyses give better and more reasonable results than the simple one in many respects.

**10240.** Reimann, C. W., Mighell, A. D., Mauer, F. A., **The crystal and molecular structure of tetrakis-pyrazole-nickel chloride, $Ni(C_3H_4N_2)_4Cl_2$,** *Acta Cryst.* **23,** Part 1, 135-141 (July 1967).

Key words: Octahedral complex; single crystal; structure; tetrakis-pyrazole-nickel chloride; x-ray.

The crystal and molecular structure of tetrakis-pyrazole-nickel chloride $Ni(C_3H_4N_2)_4Cl_2$ was determined by single crystal x-ray diffraction techniques. $Ni(C_3H_4N_2)_4Cl_2$ crystallizes in the monoclinic system with $a = 13.876 \pm 0.001$, $b = 9.263 \pm 0.006$, $c = 14.451 \pm 0.003$ Å, $\beta = 116.83 \pm 0.01°$, space group C2/c, $\rho_o = 1.61$ gm cm$^{-3}$ and $Z = 4$. Three-dimensional data (2401 reflections) were used and the structure solved by an analysis of the Patterson. The $Ni(C_3H_4N_2)_4Cl_2$ molecule is centric with the nickel atom at the center of an octahedron formed by two chlorine atoms and a nitrogen atom from each of the four pyrazole molecules. One pair of coordinated nitrogen atoms lies 2.097 Å and the other pair 2.087 Å from the nickel atom. The nickel-chlorine vector makes an angle of 0.4° with the normal to the plane of the coordinating nitrogen atoms and the chlorine atom lies 2.507 Å from the nickel atom. The pyrazole rings were found to be planar within experimental error. Final refinement by a three-dimensional anisotropic least-squares analysis resulted in an R value of 5.4 percent.

**10241.** Davies, K., Barghausen, A. F., **The effect of spread F on the propagation of radiowaves near the equator,** (Proc. AGARD Conf. Spread F and Its Effects Upon Radiowave Propagation and Communication, Copenhagen, Denmark, Aug. 1964), *AGARDograph* **95,** pp. 437-466 (W. and J. Mackay, London, England, 1966).

Key words: Frequency measuring technique; high frequency; ionosonde technique; propagation studies; radio waves; spread F.

A phenomonological description is given of certain aspects of high-frequency radio propagation studies, via the ionosphere, in Africa. Using the ionosonde technique with oblique propagation and a frequency measuring technique the following phenomena were studied, primarily from an engineering viewpoint: (1) F scatter, (2) flutter fading, (3) accuracy of MUF calculations. The measurements were carried out at two epochs of the sunspot cycle. The main features of the data are: (1) F scatter is more prevalent on magnetically quiet days at high solar activity but is nearly absent at low solar activity. (2) The duration of flutter fading is roughly proportional to the change of layer height (or phase path) near sunset. (3) The rate of amplitude fading appears to decrease with increase of frequency during the evening disturbance. (4) On the whole, there is relatively good agreement between maximum observed frequencies (MOFs) and those calculated from midpoint data. Predicted values, however, show discrepancies being too small for paths to the north of the dip equator and too large near the dip equator.

**10242.** Kieffer, L. J., Van Brunt, R. J., **The energies of $N^+$ from the dissociative ionization of $N_2$,** (Proc. 18th Annual Gaseous Electronics Conf., Minneapolis, Minn., Oct 21, 1965), *Bull. Am. Phys. Soc.* **11,** No. 4, 499 (1966).

Key words: Angular distribution; dissociative ionization; electron impact.

Using an apparatus previously described in the literature, the energy distribution and angular distribution of energetic $N^+$ ions from the dissociative ionization of $N_2$ by electron impact have been observed. The data are not consistent with the measurements of Tate and Lozier. Ions were observed with energies from 1.0 eV to 17.0 eV. One interesting feature of these data is that there are two well defined groups of ions. The angular distribution data does not indicate any significant anistropy as observed previously for $H_2$.

**10243.** Richardson, J. M., **The functions of Commission I of the International Scientific Radio Union,** *Proc. IEEE* **55,** No. 6, 743-745 (June 1967).

Key words: International Scientific Radio Union (URSI); measurements; radio; standards.

The distinctive task of Commission I of the International Scientific Radio Union (URSI) is to extend the ability of all radio scientists to make valid measurements as a necessary means for the international exchange of scientific and engineering results. The Commission concentrates on: improved measurement methods applicable either to new phenomena or to closer tolerances for familiar phenomena, the highest national and international levels of accuracy, and progress for the long term. The Commission functions by surveying both progress and deficiencies in radio measurements and standards, by evaluating new results for their lasting contribution to the measurement structure of radio, by recommending the general adoption of proven advances and the pursuit of further research to remove deficiencies, and by giving its recommendations force and effect through the efforts of its members. A sketch of the international and national URSI organizations and operations is given. The functions are performed mainly by organizing technical meetings devoted to measurement and instrumentation, by encouraging pertinent publications, and by committee interactions with other international organizations having related interests. The organization has exerted significant impact on time and frequency standards, on international uniformity of radio standards, and on precision coaxial connectors as an aid to more accurate radio techniques.

**10244.** Winogradoff, N. N., Owen, K., Curnutt, R. M., **The radiative band pinch effect and temperature dependence of radiative recombination in GaAs,** *Int. J. Electronics* **22,** No. 3, 229-233 (Mar. 29, 1967).

Key words: GaAs; quantum efficiency; radiative recombination; ruby laser; temperature dependence.

Localized heating of GaAs by intense ruby laser flashes cause a reduction or "pinching" of the band gap in the illuminated region. The increase in wavelength of the recombination radiation from this region permits the study of the temperature dependence of the internal quantum efficiency without absorption in the colder, wide band gap regions.

The results show that the internal quantum efficiency decrease with an increase in temperature.

**10245.** Chivers, H. J. A., Hargreaves, J. K., **The use of multiple antennas in studies of absorption at conjugate points,** *Proc. Symp. High Latitude Particles and the Ionosphere, Alpbach, Austria, 1964,* pp. 257-264 (Academic Press Inc., New York, N.Y., 1965).

Key words: Absorption measurement; antennas-multiple; magnetically conjugate regions; multiple antenna.

As part of a program of absorption measurements in magnetically conjugate regions, a multiple antenna based on the corner reflector has been constructed. The use of this antenna is described and some preliminary results are mentioned.

**10246.** Milligan, D. E., Jacox, M. E., Abouaf-Marguin, L., **Vacuum-ultraviolet photolysis of acetylene in inert matrices. Spectroscopic study of the species $C_2$,** *J. Chem. Phys.* **46,** No. 12, 4562-4570 (June 15, 1967).

Key words: Acetylene; $C_2$; $HC_2$; infrared spectrum; Mulliken bands of $C_2$; Swan bands of $C_2$; ultraviolet spectrum; vacuum ultraviolet photolysis.

The vacuum ultraviolet photolysis of acetylene isolated in Ar, Ne, and $N_2$ matrices at 4° and at 14 °K is shown to lead to the appearance of a number of visible-ultraviolet absorption bands which may be assigned to the species $C_2$, as well as to an 1848 $cm^{-1}$ infrared absorption assigned, with the aid of isotopic substitution studies, to the free radical $HC_2$. The (O,O) band of the Mulliken system of $C_2$ is observed with great intensity at 2382 Å (Ar matrix) or at 2323 Å (Ne matrix), indicating that the $x^1\sigma^+{}_g$ state of $C_2$ is the ground state of this species not only in the gas phase but also in the matrix. Features assigned by previous workers to the Swan transition of triplet $C_2$ appear at 5206 and 4725 Å. A third member of the progression, not previously observed, appears at 4334 Å. Experiments utilizing $C_2D_2$ and $C_2H_2$ (58% $^{13}C$) support the assignment of these features to $C_2$. The 5206 Å band system decreases in intensity and finally disappears when the sample is subjected to radiation of wavelength near 2500 Å. Problems associated with the assignment of these features are discussed, and a possible mechanism for their photolytic destruction is suggested.

**10247.** Geltman, S., Holøein, E., **Variational calculations for quartet states of three-electron atomic systems,** *Phys. Rev.* **153,** No. 1, 81 (1967).

Key words: Basis functions; $He^-$; $Li^+$; Rayleigh-Ritz variational method.

The conventional Rayleigh-Ritz variational method in which one uses pure Slater-type orbitals and correlated factors $r^2_{u\nu}$ in the basis functions has been applied to obtain the eigenvalues of the five lowest lying states with symmetries $^4P^o$, $^4P^e$ and $^4S^e$ for three-electron atomic systems. To find the absolute minimum which is attainable for each eigenvalue, the nonlinear parameters (exponential parameters) have been varied freely in submatrices up to order 30 with 20 noncorrelated and 10 correlated basis functions. This variation has been carried through separately to find the five lowest eigenvalues of each symmetry in Li and for only the lowest one in $He^-$. For the other members of the isoelectronic sequence up to $Z = 10$, the absolute minima of the three lowest lying eigenvalues are found approximately by using the correlated subset of order 30 with common fixed exponential parameters for each symmetry and by freely varying the scale parameter.

The lowest $^4P^o$ state is found to be bound in $He^-$ with a binding energy $\geqslant .033$ eV. No sign of binding is indicated for the lowest $^4S^e$ state, but the lowest $^4P^e$ state is also found to be bound by $\geqslant .20$ eV.

The results for Li indicate as certain that the transitions $^4S^e(1) - {}^4P^o(1)$ and $^4P^e(1) - {}^4P^o(1)$ are responsible for the two observed multiplets present at 2934 Å and 3714 Å, respectively, in the optical spectrum. These lines cannot be classified in the normal singly-excited spectrum of the atom or ion.

The results for Li are compared in detail with those obtained by recent electron impact experiments and by other theoretical calculations.

**10248.** Florin, R. E., **Comment on "Paramagnetic resonance of alkyl nitroxides,"** *J. Chem. Phys.* **47,** No. 1, 345-346 (July 1, 1967).

Key words: Diethylamine; diethyl nitroxide; dimethylamine; dimethyl nitroxide; electron spin resonance; free radicals; oxidation.

Intense ESR spectra of dimethyl nitroxide and diethyl nitroxide were obtained by mixing an amine carbonate solution of pH about 8, containing hydrogen peroxide, with ceric ammonium sulfate in a rapid flow mixer. In water at 25 °C, the spectral parameters are: $(CH_3)_2NO$, $a^N = 17.1$ G, $a_\beta{}^H = 14.6$ G, $g = 2.0055$; $(C_2H_5)_2NO$, $a^N = 16.8$ G, $a_\beta{}^H = 11.6$ G, $g = 2.0054$. The splittings are 10-20 percent larger than those reported in chloroform.

**10249.** Wait, J. R., **Characteristics of a slotted-sphere antenna immersed in a compressible plasma,** (Proc. Conf. Microwave Behaviour of Ferrimagnetics and Plasmas), *Conf. Publ.* No. 13, pp. 1-4 (Inst. Electrical Engineers, London, England, 1965).

Key words: Antenna; compressible plasma; plasma; slotted-sphere antenna.

Radiation from a spherical antenna in a compressible plasma is considered. The model is a perfectly conducting rigid sphere which is excited by an annular slot. The configuration is such that Maxwell's equations, when combined with a (single fluid) continuum theory of fluid dynamics, are separable.

In general, it is found that the electromagnetic component $G_e$ of the radiation conductance is only slightly modified from that expected in a cold plasma. On the other hand, the electroacoustic component $G_p$ of the radiation conductance has an appreciable magnitude for the warm plasma.

Numerical results indicate that $G_p$ may become very large for certain values of the parameters. These are interpreted as resonances of the azimuthal surface waves which propagate along the rigid metal-plasma boundary.

**10250.** Vinti, J. P., **The spheroidal method in satellite astronomy,** Chapter in *Space Mathematics* **5,** Part 1, 119-129 (American Mathematical Society, Providence, Rhode Island, 1966).

Key words: Astronomy; dynamical astronomy; oblate planet; satellite astronomy; spheroidal method.

To calculate the drag-free orbit of an artificial satellite of an oblate planet, the author has devised a very accurate approximation for its gravitational potential, leading to separability of the problem in oblate spheroidal coordinates. The present paper sketches the procedures for finding this potential and for calculating the corresponding orbit. It then discusses the remaining perturbing potential and a method for accounting for its effect on the orbit.

**10251.** Niesen, E., **Protection circuit insulated for high voltage,** *Rev. Sci. Instr.* **38,** No. 5, 689 (May 1967).

Key words: Circuit; high voltage; microamperes; millivolts; optical meter relay.

A circuit using standard components for floating an optical meter relay at high voltage is presented. By plugging in available optical meter relays, sensitivities in microamperes to amperes, millivolts to kilovolts can be controlled for a high or low limit.

0252. Brualdi, R. A., Newman, M., **Proof of a permanental inequality,** *Quart. J. Math.* **17,** No. 67, 234-238 (Sept. 1966).

Key words: Non-negative row-stochastic matrix; permanental inequality; row-stochastic matrix.

The principal result of this note is that if A is a non-negative ow-stochastic matrix then per(I-A) $\geqslant$ 0 where per(A) denotes he permanent of A. The case of equality is discussed.

0253. Kerns, D. M., Grandy, W. T., Jr., **Perturbation theorems for waveguide junctions, with applications,** *IEEE Trans. Microwave Theory Tech.* **MTT-14,** No. 2, 85-92 (Feb. 1966).

Key words: Matrix elements; perturbation approach; waveguide junctions.

Perturbation theorems are derived in the context of a theory of aveguide junctions. These theorems express changes in imedance or admittance matrix elements, due to changes in a aveguide junction, in terms of integrals over products of perurbed and unperturbed basis fields associated with the junction nd with its adjoint. Media involved are required only to be near.

Concepts of first-order perturbation theory are discussed riefly, and the term "correct to the lowest order" is precisely efined. The need of explicit theorems telling when one may exect results actually correct to the lowest order is noted.

Two problems are solved approximately by the perturbation pproach: (1) reflection at the junction of rectangular waveguide vith filleted waveguide of the same main dimensions; and (2) the ffect of finite conductivity of both obstacle and waveguide wall or half-round inductive obstacles in rectangular waveguide.

0254. Larson, W., **Analysis of rotationally misaligned stators in the rotary-vane attenuator,** *IEEE Trans. Instr. Meas.* **IM-16,** No. 3, 225-231 (Sept. 1967).

Key words: Attenuator; attenuation difference; attenuation error; misaligned stator; rotary-vane attenuator.

Two types of errors are caused by misaligned stators in the roary-vane attenuator. For each type of error the actual attenuaion will differ from the indicated attenuation values throughout nost of the usable range of the attenuator.

This analysis illustrates that these two types of errors are reated to the technique of alignment used in establishing the zero eference of the rotating vane to the stator vanes. Equations peraining to these errors are discussed and are solved with the aid of tables of attenuation error as a function of vane angle error for otary-vane attenuators. Graphs of both types of errors are resented determining the parameters needed to establish limits of machining tolerances for each waveguide size.

10255. Moore, G. A., **Application of computers to quantitative analysis of microstructures,** Chapter in *Proc. Second Intern. Congress for Stereology, Chicago, Ill., Apr. 8-13, 1967,* H. Elias, ed., pp. 281-284 (Springer-Verlag, New York, N.Y., 1967).

Key words: Automatic scanning (of micrographs); computer processing (of micrographs); logical modification of pictures; precision scanning (of micrographs); quantitative microscopy; stereological analysis.

Stereological projections from any micrograph require evaluaion of particle size and shape, thus observation on a dense raster imited only by the resolution of the microscope and observing system. The required large number of observations dictate automatic scanning and computer processing of the image. Results are limited by statistical inefficiency and precision of observaion. Using high precision scanning equipment, the inaccuracies of measurement remain comparable to the limits imposed by statistics. Presently attainable precision is, however, an order of magnitude better than can normally be obtained by manual methods.

The presence or absence of a specific phase can be represented by a two-dimensional binary array which can be rapidly processed to yield the required measurements. Logical modification by the computer is frequently necessary to substitute for some of the logical discriminations normally made by the human analyst and to facilitate the desired measurements. Logical processes can reveal stereological relationships, construct morphological models, and dissect and describe the individual particles.

**10256.** Franklin, A. D., **Born-model calculation of point-defect formation energies in alkaline-earth fluorides,** (Proc. 2nd Meeting Point Defects in Non-metallic Solids, University of Sussex, Brighton, England, Sept. 26-28, 1966) *Proc. British Ceram. Soc.* **9,** 15-24 (July 1967).

Key words: Alkaline earth fluorides; Born model; energies of formation; ionic crystals; point defects.

A Born-model calculation of the lattice energy required to form anion and cation vacancies and interstitials has been performed for $SrF_2$ and $BaF_2$, following techniques used earlier for $CaF_2$. Anion Frenkel pairs are the favored intrinsic defects for $SrF_2$ and $BaF_2$ as well as for $CaF_2$, the formation energy decreasing somewhat from $CaF_2$ to $BaF_2$. In the presence of substitutional trivalent cation impurities, the tendency to form anion interstitials as the charge-compensating defect should be strongest in $BaF_2$, least in $CaF_2$, with $SrF_2$ again intermediate.

**10257.** McCrackin, F. L., **Configuration of isolated polymer molecules adsorbed on solid surfaces studied by Monte-Carlo computer simulation,** *J. Chem. Phys.* **47,** No. 6, 1980-1986 (Sept. 15, 1967).

Key words: Adsorption; configurations; four-choice cubic lattice; Monte Carlo; polymers.

The configurations of adsorbed polymer molecules with excluded volume were simulated on a four-choice simple cubic lattice using a computer. The average values of the fraction of segments on the surface, loops off the surface, normal distance of the end of the molecule from the surface, root mean square of the normal distance, maximum normal distance from the surface, and root-mean-square end-to-end distance were calculated for various lengths of the molecules and various attractive energies between segments and the surface. When these averages over the configurations are compared with previous results which do not account for the excluded-volume effect, important differences are found.

**10258.** Silver, A. H., Zimmerman, J. E., Kamper, R. A., **Contribution of thermal noise to the line-width of Josephson radiation from superconducting point contacts,** *Appl. Phys. Letters* **11,** No. 6, 209-211 (Sept. 15, 1967).

Key words: Josephson radiation; line-width; point contacts; superconductivity; thermal noise.

The line-width of the Josephson oscillations of a voltage-biased superconducting point contact has been measured between 1.4 °K and 8 °K, with bias resistors $R$ between $1.7 \times 10^{-10}\ \Omega$ and $2.6 \times 10^{-5}\ \Omega$. Within the experimental accuracy the line-width is proportional to $RT$, and is consistent with the estimated theoretical value $8kTR/\Phi_0^2$, where $k$ is Boltzmann's constant and $\Phi_0$ is the flux quantum. Line-widths below 0.1 Hz have been observed at 4.2 °K for $R = 1.7 \times 10^{-10}\ \Omega$, providing an experimental upper limit to other noise sources and indicating that this is useful as a voltmeter and thermometer below $10^{-16}$ V and $10^{-4}$ °K.

**10259.** Hust, J. G., McCarty, R. D., **Curve-fitting techniques and applications to thermodynamics,** *Cryogenics* **7,** No. 4, 200-206 (Aug. 1967).

Key words: Constraints; curve fitting; least squares; nonlinear; thermodynamics; weighting.

The general problem of least squares fitting is considered. For completeness, derivations of well-known relations are included along with the developments of new techniques for imposing constraints on the unknown parameters, and of fitting data for several different properties simultaneously for both linear and non-linear equations. Several thermodynamic applications are included to illustrate the techniques developed.

**10260.** Phillips, C. W., Penny, R. W., **Development of a method for testing and rating refrigerated truck bodies,** *USDA Tech. Bull.* No. 1376 (Superintendent of Documents, U.S. Government Printing Office, Washington, D.C. 20402, Sept. 1967, 15 cents).

Key words: Air leakage; cooling loads; rating and testing; refrigerated truck bodies; simulated solar heating; weight gain.

A recommended standard method is presented for testing and rating the cooling load due to heat transmission and air and moisture leakage into refrigerated truck bodies used for stop and go delivery of perishable chilled or frozen food. Results of laboratory tests of five typical vehicles, with and without simulated solar heating, were used as a basis for determining criteria for the testing and rating procedure. A steady-state test procedure, with appropriate multipliers to account for solar heating is recommended. Rating conditions of 0 °F and 35 °F interior temperature and 100 °F and 50 percent ambient temperature and relative humidity are suggested. Means for calculating air leakage rate from observed weight gain rate under standard test conditions are incorporated. Measurement of service cooling loads caused by warm cargo or by air exchange through opening and closing of doors is not included in the recommended procedure. However, such service loads must be considered in determining the capacity of an adequate refrigeration system.

**10261.** Bowen, R. L., Argentar, H., **Diminishing discoloration in methacrylate accelerator systems,** *J. Am. Dental Assoc.* **75,** No. 4, 918-923 (Oct. 1967).

Key words: Accelerators; color formation; discoloration; methacrylate; N,N - dimethyl - 3,5 - dimethylaniline; polymerization.

A method was devised for accentuating the formation of discoloration products that may form during the free radical polymerization of methacrylates at room temperature. Various accelerators and stabilizers were compared on an equimolar basis. The selection of the materials was based on literature information regarding current theories of free radical polymerization and the absorption of visible light by organic compounds. The use of the sterically hindered phenol, butylated hydroxytoluene, did not produce discoloration whereas, the use of hydroquinone or the monomethylether of hydroquinone had a darkening effect. A compound (N,N-dimethyl-3,5-dimethylaniline) was synthesized which was an effective accelerator and which produced less discoloration than N,N-dimethyl-p-toluidene.

**10262.** Schweitzer, W. G., Jr., Birky, M. M., White, J. A., **Ears on the line profile of decay transitions in a gas laser,** *J. Opt. Soc. Am.* **57,** No. 10, 1226-1230 (Oct. 1967).

Key words: Laser; lifetime; line profile; neon.

In a gas laser a spectrum line, whose upper state is the lower state of the laser transition, may contain a structure due to the laser action. We have observed this structure, which we refer to as ears, on the 6096-Å neon line emitted spontaneously in a 1.15 $\mu$ He-Ne laser. The width of the ear was measured interferometrically and compared with the width predicted from the phenomenological width $\gamma_{ab}/\pi$ in the laser transition.

**10263.** Foley, C. L., Kruger, J., Bechtoldt, C. J., **Electron diffraction studies of active, passive, and transpassive oxide films formed on iron,** *J. Electrochem. Soc.* **114,** No. 10, 994-1001 (Oct. 1967).

Key words: Electron diffraction; gamma-$Fe_2O_3$; iron; passivation.

Iron foil specimens were anodically polarized by means of a potentiostat in 1N $H_2SO_4$, 0.1N NaOH and a sodium borate boric acid solution (pH, 8.5). Both passive, active and transpassive regions of the polarization curve were studied for each solution. The oxide films were examined while still in contact with the iron foil by selected area transmission electron diffraction. Five iron planes were studied: {100}, {110}, {111}, {210} and {211}, and the epitaxial relationship of the oxide to the iron substrate determined. Evidence was found indicating that in all of the electrolytes used the passive film contained $\gamma$-$Fe_2O_3$, while the non-passive films did not.

**10264.** Peverley, J. R., Meijer, P. H. E., **Entropy and susceptibility of a pure dipole-dipole substance,** *Phys. Stat. Sol.* **23,** No. 1, 353-360 (1967).

Key words: Cerous magnesium nitrate; Curie-Weiss constant; dipole-dipole interaction (pure); entropy; lattice sums; magnetic susceptibility; transition temperature.

Recalculation of the lattice sums for a pure dipole-dipole interaction show that the Curie-Weiss constant, for fields perpendicular to the *c*-axis is equal to 0.273 mdeg for cerous magnesium nitrate. A *g*-value of 1.82 was used. The temperature dependence of the entropy was determined and is compared with the experimental values of Hudson and Kaeser. All lattice sums have been determined as a function of slight changes in the lattice constants. The *z*-component of the dipolar lattice sum is determined by means of a new procedure to improve the slow convergence of this series.

**10265.** Mullen, L. O., Hiza, M. J., **Experimental apparatus and procedures for evaluating parameters affecting the pumping efficiency of a cryogenically cooled plane,** *J. Vacuum Sci. Technol.* **4,** No. 5, 219-229 (Sept.-Oct. 1967).

Key words: Capture coefficient; cryocondensation; cryogenically cooled surfaces; cryopump; partial pressure measurements; pressure calibration with vapor pressures; pressure anisotropy; pumping efficiency; pumping speed; speed factor measurements; sticking coefficient; vacuum techniques.

The collection efficiency of a plane acting as a pump in a vacuum system can be determined by measuring the rate at which molecules of a given species strike and the rate at which they return from that plane. This paper discusses an experimental vacuum system incorporating a moveable partial pressure analyzer capable of making such measurements. The experimental procedure discussed here provides a means for evaluating parameters affecting the pumping efficiency. Efficiency values obtained by the present approach are compared with values obtained from kinetic theory and from speed factor measurements The experimental data show that much of the deviation of reported pumping efficiencies can be explained by fragmentation of the test gas molecules and by a pressure anisotropy in the tes dome. A means of calibrating the analyzer with vapor pressure data is also discussed.

**10266.** Brombacher, W. G., **40 years of precise measurement** *Instr. Control Systems* **40,** No. 9, 87-92 (Sept. 1967).

Key words: Pressure gages; pressure measurement; vacuum measurement.

Progress in pressure measurement during the past 40 years is described. Most types of pressure-sensitive elements now available were already in use then. The advances made have consisted mainly of (a) increasing measurement range (b) increasing sensitivity, accuracy, and dependability, and (c) increasing use of gages to automate industrial processes.

**10267.** Rebbert, R. E., Ausloos, P., **Gas-phase photolysis of ethyl iodide at 2537 and 2288 Å. Reactions of hot ethyl radicals with added hydrocarbons,** *J. Chem. Phys.* **47,** No. 8, 2849-2855 (Oct. 15, 1967).

Key words: Alkyl radicals; deactivation; ethyl iodide; "hot" radicals; hydrogen abstraction; photolysis.

The photolysis of $C_2H_5I$ and $C_2D_5I$ have been investigated at 2537 Å and 2288 Å in the presence of thermal alkyl radical scavengers such as $O_2$ and $I_2$. The ethane (quantum yields at 2537 Å: $\Phi_{C_2H_6}=0.82\times10^{-3}$, $\Phi_{C_2O_6}=0.29\times10^{-3}$) formed in such mixtures can be entirely ascribed to abstraction of a H (or D) atom by a "hot" ethyl radical formed in the primary dissociation of ethyl iodide. When $C_2D_5I$ or $C_2H_5I$ is photolyzed in the presence of a cyclo-$C_6H_{12}$ − cyclo-$C_6D_{12}$ − $O_2$ mixture (1:1:0.1), or of a cyclohexane-1,1,2,2,3,3-$d_6$ − $O_2$ mixture, the relative probability for abstraction of an H atom versus that for abstraction of a D atom ($\pi_H/\pi_D$) is equal to $1.5\pm0.1$. Added gases do reduce the probability of the abstraction process. The relative quenching probability of the "hot" $C_2D_5^*$ radical by different additives is as follows: He − 0.50; Ne − 0.62; $N_2$ − 1.00; and $CO_2$ − 1.51.

When $C_2H_5I$ is photolyzed at 2537 Å in the presence of $CD_3CH_2CD_3$, $CH_3CD_2CH_3$ or $CD_3CH_2CH_2CD_3$ the relative probability per atom for the abstraction of a primary compared to a secondary H-atom in a hydrocarbon molecule by a hot ethyl radical is 1:4.5. Moreover, the quantum yield for ethane formation at 2537 Å per secondary hydrogen atom for a series of cycloalkanes and normal alkanes is $0.32\pm0.07\times10^{-3}$.

**10268.** Marinenko, G., Taylor, J. K., **High-precision coulometric iodimetry,** *Anal. Chem.* **39,** No. 13, 1568-1571 (Nov. 1967).

Key words: Arsenious oxide; constant-current coulometry; current efficiency; high-precision analysis; iodimetry.

On the basis of measurement of the potential of the working platinum anode as a function of current density and concentration of KI in solution, conditions were established for 100.0000 percent efficient generation of iodine. NBS Standard Reference Material arsenious oxide was analyzed utilizing optimum conditions for generation of iodine and for the stoichiometric reaction of arsenious acid with iodine. The precision of the method for titration of 0.5g samples of $As_2O_3$ is about 0.003 percent. Analysis of data for the assay of samples ranging in size from 100mg to 1g indicates no bias in the method. Coulometric assay of SRM 83c is 99.986 ± 0.003 percent, which is in close agreement with the titrimetric comparison of 83c to iodine, purified by sublimation. This fact serves as additional evidence of the accuracy of the developed method.

**10269.** Lloyd, E. C., **Improving pressure and vacuum measurement standards,** *Instr. Control Systems* **40,** No. 9, 105-109 (Sept. 1967).

Key words: Accuracy; calibration; measurement; pressure; standards; vacuum.

Results of NBS developments are outlined in a number of projects relating to standards for improved measurement of pressures throughout the range from vacuum to very-high pressures. In the vacuum range this includes techniques for generation of stable reference pressures, and improved absolute instruments for force per unit area measurement down to $10^{-9}$ torr. In the range from a few millibars to hundreds of kilobars the use of fixed points, and the performance of improved piston gages and interpolation instruments, are described. Problems presently limiting accuracy of calibration and NBS investigations of possible solutions are mentioned. Two new "accuracy charts" are presented showing present and possible future NBS capabilities.

**10270.** Powell, C. J., **Inelastic scattering of kilovolt electrons by solids and liquids: determination of energy losses, cross sections, and correlations with optical data,** *Health Phys.* **13,** No. 12, 1265-1275 (1967).

Key words: Characteristic energy losses; comparison with optical data; cross sections; inelastic scattering; kilovolt electrons; liquids; solids.

Some recent measurements of the inelastic scattering of kilovolt electrons by solids and liquids are described. The determination of energy losses and cross sections is discussed as well as factors influencing the accuracy of measurement. The degree of correlation between optical and electron energy loss experiments also is described.

**10271.** McIntyre, D., Wims, A. M., **Light scattering phenomena near the critical point,** (Proc. 2nd Interdisciplinary Conf. Electromagnetic Scattering ICES-11, University of Massachusetts, Amherst, Mass., June 28-30, 1965), Chapter in *Electromagnetic Scattering,* R. L. Rowell and R. Stein, eds., pp. 457-484 (Gordon and Breach, Inc., New York, N.Y., 1967).

Key words: Binary mixtures; coexistence curves; critical mixtures; critical opalescence; light scattering; phase separations.

The scattering from liquids and liquid mixtures near their critical points has been extensively studied in recent years. The existing experimental data are discussed with respect to their usefulness and limitations in sorting out the various statistical mechanical descriptions of critical phenomena. Scattering measurements on polystyrene-cyclohexane, cyclohexane-aniline, perfluoroheptane-isooctane, nitroethane-3-methylpentane are reported and discussed.

**10272.** Matsushita, S., **Lunar tides in the ionosphere,** *Encyclopedia of Physics* **XLIX/2,** 547-602 (Springer-Verlag, Berlin, Germany, 1967).

Key words: Ionosphere; lunar tides; lunar variations; surface atmosphere.

All previous work on lunar tidal variations in the ionospheric F2, F1, E, Es, and D layers by various researchers are thoroughly reviewed and are compared with recent results of lunar tides obtained from ionospheric electron density profile data and also with radio observations of lunar tidal winds in the ionosphere. A world-wide behavior of the lunar tides in different ionospheric layers is then obtained.

After reviewing lunar tidal variations in the surface atmosphere, geomagnetic lunar variations at several places are examined, and a new lunar current system at about 100 Km altitude is suggested. Based on this current system the lunar tides in the ionosphere are discussed theoretically, taking into consideration both hydro and electro dynamical motions.

**10273.** Wegstein, J. H., Rafferty, J. F., **Machine oriented fingerprint classification system,** Proc. First Natl. Symp. Law Enforcement Science and Technology, Chicago, Illinois, Mar. 7-9, 1967, Chapter V in *Information Storage and Retrieval,* S. A. Yefsky, ed., **1,** 495-465 (Academic Press Inc., New York, N.Y., 1967).

Key words: Automated; bifurcations; classification; descriptor; endings; fingerprint; Henry system; identification; minutia; ridge; system.

The current state-of-the-art leads one to believe that computers and their associated high-speed mass stores can be utilized in handling large fingerprint files. Toward this end, a single-print classification system is explored. Requirements and objectives are listed. Needed measurements and statistical analyses of variations in details of fingerprints are identified.

**10274.** Dibeler, V. H., Walker, J. A., **Mass-spectrometric study of photoionization. VI. $O_2$, $CO_2$, COS, and $CS_2$,** *J. Opt. Soc. Am.* **57,** No. 8, 1007-1012 (Aug. 1967).

Key words: Autoionization; $CO_2$; COS; $CS_2$; electronic; excited states; heats of formation; ionization thresholds; ions; mass spectrometry; $O_2$; photoionization; radicals; Rydberg series; vaccum ultraviolet.

Photoionization efficiency curves are obtained for the molecule and fragment ions of the subject molecules in the wavelength region extending from onset of ionization to 600 Å. The initial onset of $O_2^+$ is observed at 12.072 eV. Autoionization in the continuum is correlated with various progressions of Rydberg series. Curves for both $O^+$ and $O^-$ ions formed by the ion-pair process from $O_2$ are obtained and 1.48 eV is derived for the electron affinity of oxygen atoms. The shape of the $CO_2^+$ curve including structure ascribed to autoionization is discussed. The unresolved $^2\Pi_g$ doublet threshold is observed at 13.77 eV with the first vibrational level at 13.93 eV. The onset of the $O^+$ fragment ion indicates about 0.04 eV excess energy in the dissociation process. It is suggested that dissociative ionization occurs from the autoionizing Rydberg level just above the calculated threshold value. Partially resolved doublet components of $COS^+$ are observed at 11.18 and 11.22 eV, respectively. Intense autoionization is observed. Various thermochemical values are calculated from the fragment ion thresholds. The doublet components of the ion ground state of $CS_2^+$ are observed at 10.059 and 10.12 eV, respectively. Intense autoionization is observed at wavelengths which are in excellent agreement with known Rydberg levels for the molecule. Although the $S^+$ ion is formed with excess energy, the $CS^+$ ion gives a value of 11.71 eV for the ionization energy of the CS radical. This is in agreement with, but more precise than, a directly measured electron impact value.

**10275.** Jacox, M. E., Milligan, D. E., **Matrix-isolation study of the reaction of carbon atoms with HCl. The infrared spectrum of the free radical HCCl,** *J. Chem. Phys.* **47,** No. 5, 1626-1633 (Sept. 1, 1967).

Key words: C atom reactions; cyanogen azide; electronic spectrum; force constants; HCCl free radical; HCl reaction; infrared spectrum; matrix isolation; monochlorocarbodiimide; monochlorocyanamide; NCN reactions; photolysis; thermodynamic properties.

The infrared spectrum of samples of cyanogen azide plus hydrogen chloride isolated in an argon or a nitrogen matrix at 14 °K and subjected to photolyzing radiation under conditions previously shown to lead to the production of carbon atoms includes features at 815 and 1201 $cm^{-1}$ which may be assigned to the free radical HCCl. $^{13}C$- and D-substitution experiments are consistent with this identification. A band system extending between about 7500 and 5600 Å corresponds to the band system previously reported for HCCl in the gas phase. These observations confirm the production of HCCl in the present experiments and indicate that the lower state of the transition observed for HCCl in the gas phase studies is the ground state. The force constants and thermodynamic properties of HCCl have been estimated. Evidence is presented for the reaction of NCN, a photolytic intermediate in the production of carbon atoms from cyanogen azide, with HCl to produce an incompletely characterized species, probably either monochlorocyanamide or monochlorocarbodiimide. HCCl reacts with HCl with little or no activation energy, leading to the stabilization of $CH_2Cl_2$.

**10276.** Horowitz, E., **Metallo-organic polymers,** *Mod. Plastics* **45,** No. 3, 146-148 (Nov. 1967).

Key words: Metallo-organic polymers; role of metal and ligand; synthesis; thermal stability.

Certain organic molecules containing electron-donating groups such as derivatives of bis(8-hydroxyquinoline) can be reacted with metal ions to yield metallo-organic polymers in which the metal atoms are linked in the backbone. Both linear and cross-linked polymers have been prepared and their thermal stabilities have been investigated. It has been shown that the thermal stability of these polymers is related to the properties of the metal and the composition of the organic component.

**10277.** Mountain, R. D., Litovitz, T. A., **Negative dispersion and Brillouin scattering,** *J. Acoust. Soc. Am.* **42,** No. 2, 516-517 (Aug. 1967).

Key words: Brillouin scattering; elastic modulus; liquid; negative dispersion relaxation of viscosity; temporal absorption.

The fluctuations in density observed in Brillouin scattering may be represented as temporally absorbed waves. Negative dispersion occurs for these waves although it may be masked by positive dispersion due to relaxation processes. Numerical estimates of velocity and of negative dispersion are made for $CCl_4$ at 20 °C. The importance of measuring both the position and the width of the Brillouin peaks in order to obtain the elastic modulus of the liquid is stressed.

**10278.** Johannesen, R. B., **NMR studies of inorganic fluorides. III. $Si_3F_8$,** *J. Chem. Phys.* **47,** No. 3, 955-960 (Aug. 1, 1967).

Key words: Chemical shift; double resonance; fluorine; fluorosilanes; nuclear magnetic resonance; octafluorotrisilane; silicon; spin coupling constants.

A high-resolution NMR study of octafluorotrisilane, $Si_3F_8$, is reported. The chemical shifts of $^{19}F$ and $^{29}Si$, relative to $SiF_4$ as a reference, are given. Coupling constants, including in every case the relative sign, are given for isotopic species containing not more than one $^{29}Si$ atom. The results are compared with the corresponding values for $SiF_4$ and $Si_2F_6$.

**10279.** Dibeler, V. H., **$N_2O$ bond dissociation energy by photon impact,** *J. Chem. Phys.* **47,** No. 6, 2191-2192 (Sept. 15, 1967).

Key words: Bond-dissociation energy; $N_2O$, $N_2^+$, photoionization.

A brief report is made of the dissociative ionization of $N_2O$ to give the $N_2^+$ ion from ordinary and from $^{15}N$-labeled material. The latter is employed to avoid the effects of nitrogen impurity. The resulting experimental value of $D(N_2\text{-}O) = 39.0$ kcal $mol^{-1}$ is in good agreement with the value calculated from heats of formation.

**10280.** Bennett, L. H., **Nuclear magnetic resonance in sodium thallide,** *Acta Met.* **14,** No. 8, 997-999 (1966).

Key words: Alloys; compounds; intermetallic; Knight shift nuclear magnetic resonance; sodium; thallium; x-ray diffraction.

The nuclear magnetic resonance signal for $Tl^{203,205}$ is observed in sodium thallide alloys. It is determined that the previously reported negative Knight shift value of one percent for NaTl wa essentially correct, and the more recently reported negative value of one-half percent was in fact for $NaTl_2$. A crystal structure is proposed for $NaTl_2$.

**10281.** Bennett, L. H., **Nuclear magnetic resonance in zintl intermediate phases LiCd and LiZn,** *Phys. Rev.* **150,** No. 2, 418-420 (Oct. 1966).

Key words: B-32 structure; Knight shifts; LiCd; linewidths; LiZn; nuclear magnetic resonance; zintl phase.

The nuclear magnetic resonances have been observed for $Li^7$ and $Cd^{113}$ in LiCd and for $Li^7$ and $Zn^{67}$ in LiZn. The Knight shift for $LiCd^{113}$ is 0.39 percent for $LiZn^{67}$ 0.20 percent, for LiCd or LiZn less than 0.01 percent. An energy band scheme is proposed.

**10282.** Utton, D. B., **Nuclear quadrupole resonance thermometry,** *Metrologia* **3,** No. 4, 98-105 (Oct. 1967).

Key words: Instrumentation; nuclear quadrupole resonance thermometry 12 °K – 297 °K; potassium chlorate.

The nuclear quadrupole resonance frequency of $^{35}Cl$ in $KClO_3$ has been studied in the temperature range 12 °K – 297 °K. The combined uncertainties in the frequency and temperature measurements correspond to ±.001 °K in the range 50 °K – 297 °K, deteriorating to ±.004 °K at 30 °K and ±.010 °K at 20 °K. Both the nuclear resonance spectrometer and the temperature control apparatus are described. The experimental data are fitted to a theoretical expression in the temperature range 12 °K – 90 °K; at higher temperatures the data are fitted to empirical polynomials.

**10283.** Smith, A. L., **Observing the effect of a change in mass on deBroglie wavelength: the 600-Å bands of $^3He_2$,** *J. Chem. Phys.* **47,** No. 4, 1561-1562 (Aug. 15, 1967).

Key words: Band strengths; continuum emission; deBroglie wavelength; diatomic molecule; $He_2$; helium isotopes; radiative deexcitation; ultraviolet spectra; quantum mechanics.

The band-like continuum emitted in the radiative deexcitation of singlet metastable $^3He$ by $^3He$ has been observed. This spectrum and the corresponding continuum in $^4He$ are interpreted as reflecting the structure of a standing deBroglie wave over an attractive potential well. The $^3He$ continuum contains one less maximum than does the $^4He$ continuum in the range $602\ \text{Å} < \lambda < 666\ \text{Å}$; i.e., for two particles of different mass moving with the same energy over the same attractive well, the lighter particle has the longer deBroglie wavelength. The shifts in peak positions are accounted for quantitatively by calculating the continuum-continuum band strengths of the $A^1\Sigma_u^+ \rightarrow X^1\Sigma_g^+$ transition of $He_2$ for both isotopes.

**0284.** Mork, K. J., **Pair production by photons on electrons,** *Phys. Rev.* **160,** No. 5, 1065-1071 (Aug. 1967).

Key words: Cross sections; electron pairs; exchange; numerical integration; photons.

The cross section for production of electron pairs by unpolarized photons in the field of an electron is calculated. The total cross section is obtained by numerical integration. The contributions to the total cross section from different diagrams (exchange and $\gamma$-$e$ terms) are calculated separately, and it is shown that Borsellino's result for the cross section is valid for photon energies above about 8 MeV, the deviation from the correct cross section being of order 1 percent at this energy. Votruba's results for the total cross section are confirmed for energies very close to threshold (within about 10 keV of threshold). The results of Kopylov *et al.* appear to be in error by a factor of 2. Dividing their results by this factor, we find agreement with ours within limits of error. The recoil momentum distribution is computed numerically for some energies and it is found to agree with the results of Borsellino. At high energies it is also in agreement with the results of Suh and Bethe. The momentum distribution for pair production in the field of a very heavy particle is also calculated for some energies from the formulas of Borsellino and Jost *et al.* From a comparison of the recoil distributions for pair production on electrons with that on very heavy particles, an estimate of the error in the Wheeler-Lamb results can be made. Comparison with some experiments is given.

**10285.** Fatiadi, A. J., **Periodic acid, a novel oxidant of polycyclic aromatic hydrocarbons,** *Chem. Commun.* **21,** 1087-1088 (1967).

Key words: Aprotic solvent; paraperiodic acid; polycyclic aromatic hydrocarbons; reaction mechanism; sodium periodate.

Certain polycyclic, aromatic hydrocarbons can be oxidized in good yield to quinones with paraperiodic acid in aprotic solvents containing a small proportion of water. No reaction was observed when oxidation was attempted with sodium periodate, instead of periodic acid. A possible reaction path for the oxidation has been suggested.

**10286.** Fatiadi, A. J., Isbell, H. S., **Phenylhydrazono-phenylazo tautomerism. Part II. Structures of 2-oxo-1,3-bis(phenylhydrazono) compounds and related compounds,** *Carbohydr. Res.* **5,** 302-319 (1967).

Key words: Diphenylformazans; enolic phenylhydrazono-phenylazo structure; infrared spectra; molecular structure; nuclear magnetic resonance; oxo-bis (phenylhydrazono) compounds; phenylhydrazono-phenylazo tautomerism; phenylosazones; tautomerism; ultraviolet spectra.

The structures of xylo-4,5,6-trihydroxy-2-oxo-1,3-bis(phenylhydrazono) cyclohexane (*1*), 2-oxo-1,3-bis(phenylhydrazono) cyclohexane (*2*), 2-oxo-1,3-bis(phenylhydrazono)cyclopentane (*3*), 3-oxo-2,4-bis(phenylhydrazono)cyclohexanecarboxylic acid (*4*), 2-oxo-1,3-bis(phenylhydrazono)indane (*5*), and 2-oxo-1,3-bis(phenylhydrazono)propane (*6*), were studied by comparison of their n.m.r., u.v., visible and i.r. spectra with the spectra of reference compounds of known structures. The results show the compounds exist in two forms. The red forms have an enolic (chelated) phenylhydrazono – phenylazo structure.

A similarity of the compounds to the diphenylformazans is noted and substantiated by a comparison of absorption spectra. Compound 2 crystallizes from aqueous ethyl alcohol in the form of a yellow hydrate shown to have a phenylhydrazono structure. On dehydration, the yellow hydrate yields the red enolic form. The structures of the 1,2,3-tris(phenylhydrazono) derivatives of cyclohexane, cyclopentane and cyclohexanecarboxylic acid were also studied.

**10287.** Coriell, S. R., Jackson, J. L., **Probability distribution of the radius of gyration of a flexible polymer,** *J. Math. Phys.* **8,** No. 6, 1276-1284 (June 1967).

Key words: Brownian chain; distribution; Gaussian; polymer; radius of gyration; Tchebichef Polynomial.

Various aspects of the mathematics of the probability distribution $P_N(S_x)$ of one component of the square of the radius of gyration of an ideal Brownian chain with N units are presented. A rigorous expression for $P_N(S_x)$ in the form of a contour integral is obtained. The resulting integral is written in terms of Tchebichef Polynomials. Various rigorous and approximate results are obtained for both the limiting distribution (N infinite) and for finite N.

**10288.** Hord, J., **Response of pneumatic pressure-measurement systems to a step input in the free molecule, transition, and continuum flow regimes,** *ISA Trans.* **6,** No. 3, 252-260 (July 1967).

Key words: Response of pneumatic pressure-measurement systems in the free molecule, transition, and continuum flow regimes; response of pneumatic pressure-sensing tubulation; response of pneumatic transmission lines; time constants of pneumatic pressure lines; time lag and delay in pneumatic pressure-sensing lines; time response of pneumatic pressure-sensing systems to step inputs.

A simplified analysis of the response of pressure-sensing devices and their interconnecting tubing is presented. The results are conveniently presented in the form of time equations, with a fraction of the applied step (usually 63.2%) attained at the sensor as the variable. A single algebraic equation adequately predicts the response of pressure-measuring systems in the free molecule, transition, and continuum flow regimes. Two very simple algebraic equations may be used to predict time response in the free molecule and continuum flow regimes. The formulas are limited where viscous flow occurs, and they are not restricted for free molecule flow. All of the formulas are suitable for field engineering applications. The literature is synthesized by comparing the results from selected references with those of the analysis. Factors influencing transient pressure measurements are reviewed.

**10289.** Lane, N. F., Geltman, S., **Rotational excitation of diatomic molecules by slow electrons: application to $H_2$,** *Phys. Rev.* **160,** No. 1, 53-67 (Aug. 5, 1967).

Key words: Diatomic molecules; electron scattering; $H_2$; rigid rotator; rotational excitation.

The theory of electron scattering from a rigid rotator is applied to the case of low-energy scattering of electrons from hydrogen molecules in ground electronic and vibrational states. The coupled equations are solved numerically and the resulting $S$ matrix is used to calculate elastic, rotational excitation, and rotational de-excitation cross sections. The electron-molecule interaction potential is based on the approximate charge distribution of $H_2$ and includes the effects of polarization, which are shown to be important. Cross sections are given for several rotational states, and it is pointed out that while the elastic and inelastic cross sections are found to depend on the initial rotational angular momentum $j$ of the molecule, their variation in $j$ is such that the total cross section remains independent of $j$. The effects of "back coupling" and coupling with higher rotational states are illustrated by comparing the results of the close-coupling calculation with those of the Born and distorted-wave methods; the distorted-wave and close-coupling results for rotational excitation are found to agree within 20 percent for all energies.

**10290.** Schoen, L. J., **Sapphire window mountings for low temperature spectroscopy,** *Rev. Sci. Instr.* **38,** No. 10, 1531-1532 (Oct. 1967).

Key words: Cryostat; deposit; thermal conductivity; thermal contact; window holder.

Two newly designed sapphire window mountings suitable for use at cryogenic temperatures are described. These should prove valuable in maintaining efficient, reproducible and trouble free thermal contact with conventional refrigerants.

**10291.** Oppenheim, I., Shuler, K. E., Weiss, G. H., **Stochastic theory of multistate relaxation processes,** *Adv. Mol. Relaxation Processes* **1,** No. 1, 13-68 (Nov. 1967).

Key words: First passage times; Fokker-Planck equation; Markov processes; master equation; relaxation processes; stochastic processes.

The stochastic theory of multistate relaxation processes is discussed with special reference to Markov Processes, the derivation and properties of the Master Equation, the derivation and properties of the Fokker-Planck Equation and First Passage Time problems. The theory developed is then applied to a number of examples.

**10292.** Danos, M., Gillet, V., **Stretch scheme, a shell-model description of deformed nuclei,** *Phys. Rev.* **161,** No. 4, 1034-1044 (Sept. 20, 1967).

Key words: Deformed nuclei; nuclear moments of inertia; nuclear rotation; nuclear shell model; nuclear spectra; nuclear structure.

A good angular momentum wave function containing the maximum possible intrinsic angular momenta leads to a microscopic description of the nuclear rotational spectra in terms of spherical shell model states. The rotational excitation energies arise from the residual two-body force. In the actual model calculations the only approximation was a partial violation of the exclusion principle. The computed departures from the I(I + 1) law are consistent with the experiment. Reasons are given for the preference of positive over negative intrinsic deformations.

**10293.** Coyle, T. D., Ritter, J. J., **Structure, isomerization, and cleavage of 1,2-bis(dichloroboryl)ethylene,** *J. Am. Chem. Soc.* **89,** 5739-5740 (1967).

Key words: Acetylene; organoboron compounds; proton magnetic resonance; protonolysis; stereochemistry; tetrachlorodiborane(4); 1,2-bis(dichloroboryl)ethylene.

The product of the reaction of tetrachloroborane(4) with excess acetylene has been shown to be the *cis* isomer of 1,2 bis(dichloroboryl)-ethylene. This compound can be converted to the corresponding *trans* isomer by ultraviolet irradiation Cleavage of the isomerically pure, deuterated organoboron compounds with ammoniacal silver oxide produces isomerically pure dideuteroethylenes. Acetic acid cleavage is not stereospecific.

**10294.** Weiss, A. W., **Superposition of configurations and atomic oscillator strengths—carbon I and II,** *Phys. Rev.* **162,** No. 1, 71 80 (Oct. 5, 1967).

Key words: Atomic energy levels; oscillator strengths; superposition of configurations; wavefunctions.

Variational wavefunctions are computed for the ground state and a number of excited states of carbon I and II by the method of superposition of configurations. To accelerate convergence the virtual orbitals are obtained from a pseudo-natural orbital transformation on a single electron-pair, out of all those possible within a given quantum shell. Expansions of up to 50 configurations are generated and used to study the effects of correlation on the oscillator strengths. The method appears to be fairly successful in correcting for most of the correlation error in both the energy and "correlation sensitive" oscillator strengths. Term value are substantially improved over the Hartree-Fock, and generally, although not always, f-values appear to be obtainabl with an accuracy of about 25 percent.

**10295.** Barbrow, L. E., **The metric system in Illuminating Engineering,** *Illum. Engr.* **LXII,** No. 11, 638-640 (Nov. 1967).

Key words: Exitance; illumination; luminance; lux; metric units; nit; SI units in illuminating engineering.

The most commonly used unit of illumination in the USA the footcandle. There are two commonly used units of luminance, the footlambert and the candela per square inch. The growing international adoption of SI units makes it advisable fo illuminating engineers to introduce the use of these units in the publications in the immediate future and to understand the impl cations of the use of the SI units. The SI unit of illumination the lux (one lumen per square meter). The SI unit of luminance is one candela per square meter (sometimes named the nit). Or of the basic principles and advantages of SI is that there can be only one unit for each quantity; thus there cannot be an SI unit similar to footlambert which is expressed in terms of lumens per unit area. Council of the Illuminating Engineering Society has been officially requested to (1) approve the policy of having SI units given primary use in its publications, and (2) promote the deprecation of "lumens per unit area" as a unit of luminance and sponsor its use solely as a unit of luminous exitance (formerly emittance).

**10296.** Meshkov, S., Yodh, G. B., **SU(3), meson-baryon scattering, and asymptotic limits,** *Phys. Rev. Letters* **19,** No. 10, 603-608 (Sept. 4, 1967).

Key words: Asymptotic; baryons; mesons; reaction; scattering; SU(3).

The meson-baryon total cross sections and elastic-scattering data in the forward direction are fitted using SU(3)-invariant $t$-channel amplitudes. The analysis implies that (1) $0 \leq \sigma_{tot}(s \rightarrow \infty) \leq 15.5$ mb, and (2) $-0.11 \leq \mathrm{Re}T(s,t=0)/\mathrm{Im}T(s,t=0) \leq 0$ as $s \rightarrow \infty$.

**10297.** Tomezsko, E. S. J., Furukawa, G. T., **Thermal titration of platinum black and the initial heat of adsorption for hydrogen,** *J. Catalysis* **8,** No. 4, 386-388 (Aug. 1967).

Key words: Adsorption of hydrogen on platinum black; heat of adsorption of hydrogen; platinum black; thermal titration.

The heat of adsorption of hydrogen on platinum black was investigated by means of an automatically controlled adiabatic calorimeter. When the platinum black was carefully freed of adsorbed oxygen, no rapid decrease was observed in the heats of adsorption with increasing coverage of hydrogen. The heat of adsorption of hydrogen on clean platinum surface was found to be 17.5 (73.2 kJ/mole) kcal/mole of hydrogen, with an estimated uncertainty of ±0.2 kcal/mole (±0.8 kJ/mole).

**10298.** Dragoo, A L., Diamond, J. J., **Transitions in vapor-deposited alumina from 300° to 1200°C,** *J. Am. Ceramic Soc.* **50,** No. 11, 568-574 (Nov. 1967).

Key words: Alpha alumina; alumina; amorphous alumina; delta alumina; gamma alumina; intermediate aluminas; metastable aluminas; phase transitions; theta alumina.

The transition of amorphous alumina to $\alpha$-alumina was studied by x-ray diffraction, electron diffraction, DTA, TGA, and microscopic observation. The amorphous alumina was prepared by condensing vapor from evaporating molten alumina in vacuo onto the glass envelope of the vacuum chamber. The amorphous alumina was transformed to a poorly crystalline material by heating for 16 hr between 570° and 670 °C. Between 670° and 1200 °C, the poorly crystalline alumina was converted to $\alpha$-alumina via two parallel series of transition aluminas. The principal series was $\gamma$-alumina to $\delta$-alumina to $\alpha$-alumina. A minor amount of $\theta$-alumina developed from the initial crystallization and persisted throughout the duration of the principal series as a parallel path. Some conversion of $\delta$- to $\theta$-alumina was detected above 900 °C. DTA produced an unexplained exothermic peak at 320 °C and a second exothermic peak at 860 °C which corresponded to formation of metastable aluminas.

**10299.** Urbach, P. F., **User reaction as a system design tool at CFSTI,** *Proc. Fourth Annual National Colloquium on Information Retrieval, May 3-4, 1967,* A. B. Tonik, ed., pp. 7-18 (International Information, Inc., Philadelphia, Pa., 1967).

Key words: Announcement journals; demand; document dissemination; important dissemination; system design; unit price; users chargers and costs; users study; users survey.

User reaction to the operation of document announcement and dissemination systems at CFSTI was measured by a number of user studies ranging from questionnaires covering the gamut of CFSTI services to experiments in which user interaction with the system was monitored. In one experiment, user reaction was monitored to compare the relative impact of a free and paid announcement service upon document sales. On the basis of the results, the free announcement service was discontinued. In another experiment, the sales prices of documents were modified and resulting sales monitored to establish the relationship between sales price and document demand. The knowledge of this relationship was used together with cost estimates to set a near optimum document price. Document sales are used as a criterion for measuring the effectiveness of announcement media and experiments to determine cost benefit relationships for various announcement media have been developed.

**10300.** Christensen, R. G., Cassel, J. M., **Volume changes accompanying collagen denaturation,** *Biopolymers* **5,** 685-689 (1967).

Key words: Collagen; denaturation; dilatometry; hydration; partial specific volume; solvation.

A dilatometric technique is employed to measure the volume changes occurring on denaturation of collagen solutions and tendons. Partial specific volumes of tropocollagen are calculated to be 0.686 ml/g in water and 0.689 ml/g in 0.1M citrate buffer. From data on non-aqueous solutions, it is estimated that most of the volume change arises from changes in polymer configuration rather than from changes in solvation.

**10301.** Allan, D. W., Fey, L., Machlan, H. E., Barnes, J. A., **An ultra-precise time synchronization system designed by computer simulation,** *Frequency* **6,** No. 1, 11-14 (Jan. 1968).

Key words: Computer simulation; flicker noise; frequency drift; optimum prediction; third order feedback system; time scales; time synchronization.

Any two independent time scales will exhibit time departure due to two main causes, i.e., systematic differences in the frequency standards and inherent random noise processes. For time synchronization, some theoretical considerations indicate the plausibility of a third-order feedback system which will automatically remove the systematic difficulties of typical frequency standards used in time scale work. Because of the random nature of the second difficulty, the whole system is simulated with a computer to determine the systems feasibility and operating parameters. Two basic assumptions are that time comparisons for synchronization would be intermittent and that the model for the frequency standard is represented by a systematic linear frequency drift with a random flicker noise spectrum ($1/|\omega|$) of the frequency fluctuations.

On the basis of the computer results an electromechanical system was designed and built. When the input to the system is the frequency from a high quality quartz crystal oscillator, the output frequency has no frequency drift. If synchronization is performed every 12 hours, the rms time error predicted by the system at the time of the next synchronization is 70 nanoseconds, which is near optimum.

**10302.** Arenhovel, H., Hayward, E., **Scattering of plane-polarized photons by the giant resonances of nuclei,** *Phys. Rev.* **165,** No. 4, 1170-1174 (Jan. 20, 1968).

Key words: Giant resonance; photon scattering; polarized photons; sum rule.

The cross sections for the electric dipole scattering of plane polarized photons are expressed in terms of the angular momentum transferred to the nucleus in the two-step scattering process. These scattering cross sections have been evaluated in the dynamic collective model for a number of vibrational nuclei at 15.1 MeV and for a number of deformed nuclei at 11.4 and 15.1 MeV. A sum rule is derived that relates the total scattering cross section for an odd-A nucleus to that of its even-even neighbor.

**10303.** Astin, A. V., **A time for action in international standardization,** *Mater. Res. Std.* **8,** No. 5, 18-24 (May 1968).

Key words: Consumers; evaluation; purchasing; standards.

Technology and economics find a common challenge in the field of international standardization. How well or poorly America faces this challenge will have a great influence on the stature of the United States in the world markets. Since the resources for standards used in U.S. trade are in the private sector, it behooves private industry and groups such as ASTM in the private sector to fulfill the urgent need for sound standards.

**10304.** Ausloos, P., **Chemical changes induced by high energy radiation. The present state of our knowledge,** *Scientia* **CII,** 1-14 (Sept.-Oct. 1967).

Key words: Chemical changes; free radical reactions; high-energy radiation; ion-molecule reactions.

The chemical changes in matter brought about by absorption of low energy radiation such as visible and ultraviolet light have been intensively investigated for several decades. On the other hand, the chemical transformations induced by high energy radiation (X, gamma, $\beta$, $\alpha$-rays) were long considered to be of such complexity that the task of unravelling them was considered insurmountably difficult. However, during the last decade, impressive advances have been made towards achieving an understanding of the fundamental chemical processes induced by high energy radiation. Many experimental techniques, some of which are new and some of which have been used in other areas of physics or physical chemistry, have now been brought to bear on the problem. Through these various approaches definitive information has been obtained concerning the existence and reactions of the various highly reactive intermediate species (radicals, ions, excited molecules produced by high energy radiation. The understanding of such systems has now reached a degree of sophistication such that high energy radiation can be used to obtain accurate information about various well defined chemical and physical processes which are of general scientific interest.

**10305.** Ausloos, P., Lias, S. G., **Gas-phase photolysis of hydrocarbons in the photoionization region,** *Radiation Res. Rev.* **1,** No. 1, 75-107 (Mar. 1967).

Key words: Absorption; excitation; hydrocarbons; ionization; gas phase photolysis.

When a molecule is irradiated with photons whose energy is higher than the threshold for ionization, not only ions but also neutral excited molecules, similar in lifetime and behaviour to those formed at lower energies, will be produced. Until very recently, most studies of molecules irradiated in the photoionization region have been concerned only with ionization phenomena. Such studies ranged from simple measurements of ion currents during photolysis to actual identification and quantitative measurement of the ions formed, by means of a light source linked with a mass spectrometer. In these studies, which have been reviewed recently, the fate of the excited molecules was generally not considered since the light sources used were of such low intensity that the steady state concentration of neutral intermediates was necessarily well below the limits of detection for uncharged species.

The study of the behaviour of neutral excited molecules is of concern to the photochemist and radiation chemist who usually deduce information about primary and secondary processes from a chemical analysis of the final products formed when a compound is irradiated in a closed vessel. The recent development of high intensity monochromatic light sources in the vacuum ultraviolet wavelength range made possible the use of traditional photochemical methods in the investigation of events following absorption of radiation in the photoionization region. This review is primarily concerned with presenting information derived from such studies; the emphasis will be on information obtained from analysis of end products formed upon photolysis in a closed system. Information from studies concerned with physical measurement of ionization phenomena will be presented here whenever pertinent, but a complete survey of these studies is not within the scope of this review.

It is evident that, in addition to permitting the study of the excitation events which accompany photoionization phenomena, the use of a closed system also allows the investigator a certain flexibility in the design of his experiments denied him by the nature of the instrumentation in alternate approaches such as mass spectrometry. For example, pressure and temperature can easily be varied over wide ranges permitting him to determine the effect of these parameters on ionic and neutral fragmentation mechanisms.

**10306.** Ausloos, P., Lias, S. G., **Gas-phase radiolysis of hydrocarbons,** Chapter in *Actions Chimique et Biologiques des Radiations,* M. Haissinsky, ed., **10,** 1 (Masson and Company, Paris, France, 1967).

Key words: Free radicals; hydrocarbon; ion molecule reactions; neutral excited molecules; radiolysis.

This manuscript is a critical review of the gas phase radiolysis of hydrocarbons covering the literature up to September 1, 1966.

**10307.** Ausloos, P., Lias, S. G., **Photoionization of cycloalkanes in the gas phase. A study of charge transfer-processes,** Chapter in *The Chemistry of Ionization and Excitation,* G. Johnson and G. Schales, eds., pp. 77-89 (Taylor and Francis, Ltd., London, England, 1967).

Key words: Charge transfer; cycloalkanes; photochemistry.

The photoionization of cyclopentane (I.P. 10·5 eV), cyclohexane (I.P. 9·9 eV) and cycloheptane (I.P. 10 eV) has been investigated at 11·6 – 11·8 eV using an argon resonance lamp as light source. It is shown that because of the limited degree of fragmentation of the parent cycloalkane ion at these energies, the importance of charge transfer between the different cycloalkanes can be evaluated. The yield of the parent cycloalkane ion is estimated by measuring the products $CD_3CDHCD_2H$ and $C_3D_8$ formed by the $H_2$ and $D_2$-transfer reactions:

$$C_nH_{2n}^+ + C_3D_6 \rightarrow C_nH_{2n-2}^+ + CD_3CDHCD_2H,$$

$$C_nD_{2n}^+ + C_3D_6 \rightarrow C_nD_{2n-2}^+ + C_3D_8.$$

On the basis of these reactions, charge transfer can readily be established in mixtures such as $C_6H_{12} + C_6D_{12}$, $C_6D_{12} + C_5H_{10}$, $C_5D_{10} + C_7H_{14}$, and $C_6D_{12} + C_7H_{14}$ to which small amounts of propylene-$d_6$ has been added. It is, for instance, noted that charge transfer occurs from $C_6D_{12}^+$ to $C_6H_{12}$ as well as from $C_6H_{12}^+$ to $C_6D_{12}$. In addition, the cyclohexane parent ions can transfer their charge to propylene. Taking this process into account, a value of 0·38 is obtained for the equilibrium ratio $C_6D_{12}^+/C_6H_{12}^+$ independent of the composition of the mixture. In the mixtures of cycloalkanes of different chemical identity, charge transfer from the parent ion with the higher ionization potential to that with the lower ionization potential occurs efficiently. It is shown that charge transfer occurs in all cases with a rate which is comparable to that of the $H_2$ and $D_2$-transfer reactions, whose rate is probably close to the collision rate.

**10308.** Ausloos, P., Scala, A. A., Lias, S. G., **Ion-molecule reactions in the condensed-phase radiolysis of hydrocarbon mixtures. II. Cyclopentane and cyclohexane,** *J. Am. Chem. Soc.* **89,** 3677-3683 (1967).

Key words: Cyclohexane; cyclopentane; free radical; $H_2$-transfer reactions; ion-molecule reactions.

The radiolysis of $c$-$C_5H_{10}$ and $c$-$C_5H_{12}$, as well as of equimolar $c$-$C_5H_{10}-c$-$C_5D_{10}$ and $c$-$C_5H_{12}-c$-$C_6D_{12}$ mixtures, has been investigated in the presence of 0.5 to 5 mole percent $(CD_2)_3$, $C_2D_2$, $C_2D_4$, or $CD_3CDCD_2$. Isotopic analysis of the products formed in the radiolysis of cycloalkane$-(CD_2)_3$ mixtures points to the occurrence of the following ion-molecule reactions: (a) $C_nH_{2n}^+ + (CD_2)_3 \rightarrow C_nH_{2n-2}^+ + CD_2HCD_2CD_2H$ and (b) $C_nH_{2n}^+ + (CD_2)_3 \rightarrow C_nH_{2n-1}^+ + CD_2HCD_2CD_2$. The formation of $n$-propyl radicals in reaction b is confirmed by the production of $CD_3CD_2CD_2H$ as a major species in the radiolysis of $C_nD_{2n}-(CD_2)_3-H_2S$ mixtures. The ion-molecule character of the reactions is further confirmed by the facts that addition of a known parent ion interceptor such as $H_2S$ reduces $G$(propane), while addition of an electron scavenger such as $CCl_4$ raises $G$(propane). When cyclopentane is the solvent, the $H_2$-transfer reaction (a) is of major importance. The most efficient $H_2$-acceptor molecule for the cyclopentane parent ion is $C_2D_4$, and the least efficient is $C_2D_2$. When $c$-$C_5H_{10}-c$-$C_5D_{10}$ (1:1) mixtures are irradiated in the presence of deuterated $H_2$-acceptor molecules such as $C_2D_4$ or $C_2D_2$, the ratio of products of reaction a, $C_2D_4H_2/C_2D_6$ or $C_2D_2H_2/C_2D_4$, is greater than unity, indicating the occurrence of charge-transfer processes favoring the formation of $c$-$C_5H_{10}^+$: (c) $c$-$C_5D_{10}^+ + c$-$C_5H_{10} \rightarrow c$-$C_5H_{10}^+ + c$-$C_5D_{10}$. A decrease in the mole percent of the $C_2D_4$ or $C_2D_2$ from 6 to 2 percent raises $C_2D_4H_2/C_2D_6$ or $C_2D_2H_2/C_2D_4$ from 1.7 to 2.6, demonstrating that relatively high concentrations of $H_2$-acceptor molecules can interfere with the charge-transfer mechanism. When cyclohexane is the solvent, reaction b predominates over reaction a. A plot of the square root of the $(CD_2)_3$ concentration *vs.* $G$(propane) yields a straight line which goes through the origin, demonstrating the difficulty of obtaining chemical evidence for the presence of free ions.

**10309.** Balling, L. C., $g_I/g_J$ **ratios of Rb$^{85}$ and Rb$^{87}$**, *Phys. Rev.* **163,** No. 1, 114-118 (Nov. 5, 1967).

Key words: G-factor; nuclear moment; optical pumping; rubidium.

An optical-pumping experiment has been performed to measure $g_I/g_J$(Rb$^{85}$) and $g_I/g_J$(Rb$^{87}$). The measurements were made in a magnetic field of 40 G. The field was produced by a precision-wound solenoid surrounded by three coaxial magnetic shields. The magnetic field varied by three parts in $10^6$ over the volume of the optical pumping cells. The optical-pumping cells were filled with various pressures of helium and neon buffer gases. The measured ratios did not depend upon the nature or pressure of the buffer gas. The results of the measurements were $g_I/g_J(\mathrm{Rb}^{85}) = -1.46648(8) \times 10^{-4}$; $g_I/gJ,(\mathrm{Rb}^{87}) = -4.96997(9) \times 10^{-4}$.

**10310.** Barnes, J. A., Allan, D. W., **An approach to the prediction of coordinated universal time,** *Frequency* **5,** No. 6, 15-20 (Nov.-Dec. 1967)..

Key words: Coordinated Universal Time; offset frequency; prediction; rotation of the earth.

By computing the root mean square of the third differences of the fluctuations of Universal Time for various sample times, a spectral classification of the fluctuations is made. For periods from 0.02 years to 20 years, the data indicates a power spectral density for the fluctuations given by $|\omega|^{-\alpha}$ where $\alpha$ lies in the range $3 \leqslant \alpha \leqslant 5$.

Based on the spectral classification, some simple and practical methods of predicting frequency offsets for coordinated Universal Time are compared to theoretically optimum (linear) prediction. Three methods are considered and are applied to past UT 2 data for comparison. A conclusion from the paper is that the frequency offset for the coordinated time scales may be predicted such that no resets of epoch are required for roughly 60 percent of the years for which the prediction is made.

**10311.** Bates, R. G., Covington, A. K., **Behavior of the glass electrode and other pH-responsive electrodes in biological media,** *Ann. N.Y. Acad. Sci.* **148,** 67-80 (Feb. 1, 1968).

Key words: Antimony electrode; bioelectrodes; biological systems; electrodes; glass electrode; membrane electrodes; pH measurement; quinhydrone electrode.

The theory and experimental techniques underlying the use of hydrogen-ion-responsive electrodes in biological systems are reviewed. Particular attention is given to the development of special forms of electrodes for bio-medical purposes and to applications reported during the past 15 years.

**10312.** Bender, P. L., **Radio reflection by free radicals in earth's atmosphere,** *Science* **158,** No. 3807, 1487-1488 (Dec. 15, 1967).

Key words: Alouette II satellite; earth's atmosphere; free radicals; magnetic dipole radiation.

The suggestion by Barry, Coleman, Libby, and Libby that some of the signals observed by the Alouette II satellite were due to stimulated emission of magnetic dipole radiation from free radicals is shown to be incorrect.

**10313.** Bennett, L. H.,, Swartzendruber, L. J., Watson, R. E., **Hyperfine fields and electronic structure of CsCl-type ternary alloys of the first transition series,** *Phys. Rev.* **165,** No. 2, 500-505 (Jan. 10, 1968).

Key words: Alloys; electronic specific heat; electronic structure; Fe Co; hyperfine fields; isomer shift; Knight shift; s-admixture; Ti.

The $^{59}$Co Knight shift $K$ and the $^{57}$Fe isomer shift have been measured in $TiFe_{1-x}Co_x$ alloys over most of the composition range $0 \leqslant x \leqslant 1$. The experimental results are discussed in terms of correlations with electron concentration and $s$ admixture in the $d$ bands. At room temperature, $K$ varies from a maximum of $(3.2 \pm 0.2)$ percent at $x \approx 0.8$, and roughly follows the electronic specific heat as the composition is vation, from $-0.15 \pm 0.01$ (mm/sec relative to pure Fe) at TiFe to $-0.19 \pm 0.02$ at TiCo, is similar to that of Fe in Cr-Mn The $^{47,49}$Ti Knight shift in TiFe $(0.26 \pm 0.04)$ percent at room and at liquid-nitrogen temperatures.

**10314.** Berger, M. J., **Energy deposition in water by photons from point isotropic sources,** *J. Nucl. Med. Suppl.* **1,** 15-25 (Feb. 1968).

Key words: Absorbed fraction; buildup factor; energy absorption; gamma rays; photons; point-isotropic source.

This pamphlet contains tabulations of energy absorption buildup factors for point isotropic gamma ray sources for use in nineteen source energies between 3 MeV and 15 keV. An analytical representation of the buildup factors in the form of a polynomial in the source-detector distance is also given.

**10315.** Berman, H. A., West, E. D., Rozner, A. G., **Anomalous heat capacity of TiNi,** *J. Appl. Phys.* **38,** No. 11, 4473-4476 (Oct. 1967).

Key words: Titanium-nickel heat capacity; titanium-nickel phase transition.

Calorimetric measurements on a sample of TiNi (50 atomic percent Ti) show that the heat-capacity maximum at approximately 87 °C represents a higher-order transition. The transition was shifted to lower temperatures each time the material was heated through the transition from slightly above room temperature to about 150-200 °C. The transition enthalpy decreased in three such cycles from 4150 to 3375 J/mole TiNi.

**10316.** Blandford, J. M., **A progress report on the NBS-ARF apparel materials evaluation project,** *First Annual Conf. Apparel Research Foundation, Washington, D.C., Nov. 29-Dec. 1, 1967,* (Apparel Research Foundation, Washington, D.C. 20036, 1967).

Key words: Apparel materials; quality control; test methods.

A project on the evaluation of apparel materials, to be conducted in collaboration with the Apparel Research Foundation (ARF), was initiated in the Materials Evaluation Division of the Institute for Applied Technology (IAT) in July 1967. Its objective is to aid the small manufacturers of apparel in evaluating the essential properties of materials purchased and products fabricated. This report summarizes a survey made by visits with experts in representative apparel companies and supplier firms of the operations and problems which relate to quality control and testing; current evaluation and testing procedures; value to the industry of the project; and development of the project.

**10317.** Bowman, R. R., **Remarks on the paper "Field strength above 1 GHz: Measurement procedures for standard antennas,"** *Proc. IEEE* **56,** No. 2, 216 (Feb. 1968).

Key words: Electromagnetic horns; error analysis; gain corrections; gain measurements.

Some comments concerning error analysis and the measurement of standard gain horns are made in reply to a correspondence item by E. V. Jull.

**10318.** Brady, E. L., Wallenstein, M. B., **The national standard reference data system,** *Science* **156,** No. 3776, 754-762 (May 12, 1967).

Key words: Critical evaluation; information centers; information services; NSRDS; physical properties; standard reference data.

The National Standard Reference Data System is a government-wide effort to give to the technical community of the United States optimum access to the quantitative data of physical science, critically evaluated and compiled for convenience. This program was established in 1963 through action of the President's Office of Science and Technology and the Federal Council for Science and Technology, acting upon the recommendation of FCST's Committee on Scientific and Technical Information. The National Bureau of Standards has been assigned responsibility for administering the effort. The general objective of the System is to coordinate and integrate existing data evaluation and compilation activities into a systematic, comprehensive program, supplementing and expanding technical coverage when necessary, establishing and maintaining standards for the output of the participating groups, and providing mechanisms for the dissemination of the output as required.

**10319.** Brauer, G. M., **New developments in zinc oxide-eugenol cement,** *Ann. Dentistry* **26,** No. 2, 44-50 (1967).

Key words: Dental cements; dental materials; EBA cements; new developments in dental materials; zinc oxide-eugenol cements.

During the last few years considerable interest has been generated in improving zinc oxide-eugenol materials. A better understanding of the setting mechanism of these cements has become available which has lead to the development of modified ZOE cements usually containing *o*-ethoxy-benzoic acid (EBA). These materials show reactions to the tissues including the dental pulp similar to ZOE cements. Physical properties of the EBA containing cements approach those of the biologically less desirable zinc phosphate cements.

**10320.** Brehm, B., Gusinow, M. A., Hall, J. L., **Electron affinity of helium via laser photodetachment of its negative ion,** *Phys. Rev. Letters* **19,** No. 13, 737-741 (Sept. 25, 1967).

Key words: Electron affinity; electrons; energy analysis; helium; laser photodetachment; monochromatic (laser) light; negative ions.

We have measured the electron affinity of helium ($2^3S$) using the technique of energy analysis of electrons photodetached from a beam of negative ions by monochromatic (laser) light. Uncertainties in the contact potentials are eliminated by comparison with an ion of known affinity ($H^-$). The $4P_{5=2}$ state of $He^-$ is found to be bound with respect to the $2^3S$ state of neutral helium by 80.0 millivolts, with a probable error of 2 millivolts.

**10321.** Brown, R. L., Dittmann, S., **Vibrational relaxation and quenching in the yellow nitrogen afterglow,** *Chem. Commun.* **21,** 1144-1146 (Nov. 8, 1967).

Key words: Active nitrogen; afterglow; atom recombination; nitrogen atoms; quenching; vibrational relaxation.

The vibrational distribution in the $B^3H_g$ state of molecular nitrogen populated by recombination of nitrogen atoms has been found to depend on pressure and on the nitrogen atom concentration. These effects can be explained by a mechanism involving quenching of the $B^3H_g$ state by nitrogen atoms and by carrier gas molecules and collision induced vibrational relaxation.

**10322.** Burley, G., **The "memory effect" in silver iodide,** *Acta Cryst.* **23,** Part 1, 1-5 (July 1967).

Key words: Alpha-phase; crystallography; silver iodide; site-occupation; structure; structure memory.

Radial distribution and least squares site occupation analyses were performed on powder diffraction patterns of the high temperature phase of silver iodide taken at 155 °C and 250 °C. A preferential occupation of certain sites by the silver atoms occurs near the transition temperature at 147 °C, involving those silver atom positions nearest to those in the low-temperature wurtzite- and sphalerite-type structures, respectively. The regeneration of a particular derivative low-temperature structure is thus facilitated, and a crystallographic explanation can be given for the observed "memory effect."

**10323.** Cassidy, E. C., Abramowitz, S., **Time-resolved spectroscopic studies of exploding wires in controlled atmospheres,** *Appl. Spectry.* **21,** No. 6, 360-364 (Nov.-Dec. 1967).

Key words: Electrical discharges; exploding wires; high-speed measurement techniques; high-speed photography; time-resolved spectroscopy.

Electrically exploded wires in various controlled atmospheres were employed for excitation of atomic and molecular species. The spectrographic time histories of the various constituents (stable and unstable) of the explosion mixture were studied with the use of a rotating drum camera, focussed on the exit slit plane of a spectrograph. A rotating high-speed shutter was then utilized to study the spectrum of selected intermediate species. Results obtained with aluminum wires in various atmospheres are presented, in order to illustrate the experimental techniques involved. Several considerations found to be important in the design of the explosion chamber are discussed.

**10324.** Chamberlain, G. E., Simpson, J. A., Mielczarek, S. R., Kuyatt, C. E., **Effect of double scattering on cross-section measurements at large momentum transfer,** *J. Chem. Phys.* **47,** No. 10, 4266-4267 (Nov. 15, 1967).

Key words: Cross section; differential; electron; experimental; helium; inelastic; pressure dependence.

Experimental evidence from measurements of inelastic electron scattering in helium is given to show that for large momentum transfer double scattering causes apparent cross section values to be too large. These errors occur at pressures usually thought to be sufficiently low to observe only single scattering.

**10325.** Chappell, S. E., Sparrow, J. H., **The average energy required to produce an ion pair in argon, nitrogen, and air for 1- to 5-MeV alpha particles,** *Radiation Res.* **32,** No. 3, 383-403 (Nov. 1967).

> Key words: Air; alpha particles; argon; average energy; ion pair; measurement; nitrogen.

The absolute value of W, the average energy required to produce an ion pair, has been measured in argon, nitrogen and air for alpha particles with initial energies between 1 and 5 MeV. Six alpha-particle sources having different energies were fabricated by placing various thicknesses of mylar film over a collimated polonium-210 (5.3 MeV) alpha-particle source. For each source the total ionization produced in each gas by a determined number of alpha particles was measured in a parallel plate ionization chamber. Then the mean energy of each source was evaluated by using a time-of-flight apparatus. From these combined results, W was calculated. It was found to be constant within experimental error for argon but exhibited an increase in value of approximately 1 percent for nitrogen and air over the specified energy range. These results for nitrogen and air disagree with the energy dependence for W found by other investigators.

**10326.** Christ, B. W., Giles, P. M., **Metallurgical uses of the Fe$^{57}$ Mössbauer effect in metallic iron and plain carbon steels,** Chapter in *Advances in Mössbauer Methodology* 3, 37-65 (Plenum Press, Inc., New York, N.Y., Jan. 1967).

> Key words: Carbon steels; Fe$^{57}$ iron; retained austenite hyperfine interactions; tempering.

Literature describing the Fe$^{57}$ Mössbauer effect in metallic iron, steels and ferrous compounds occurring in steels is reviewed and compared with new, computer-analyzed data obtained in 298 °K measurements on metallic iron and carbon steels. Characteristics of Mössbauer patterns are sensitive to carbon content and thermomechanical history. Relative to standard sodium nitroprusside, the average effective magnetic field (EMF) for three grades of recrystallized iron is 339 ± 3 kilo-oersteds.

Patterns reveal several superimposed hyperfine interactions between 0.02 and 1 w/o C. The most intense magnetic hyperfine pattern (MHP) is attributable to iron atoms remote from interstitials. The EMF of this pattern increases with increasing C in solution, e.g., 355 ± 3 kilo-oersteds at 1 w/o C. In quenched 0.3, 0.7 and 1 w/o C alloys, irregularities in peak shape arise from sets of iron atoms with various C near-neighbor configurations. A weak, resolvable MHP exhibiting a small quadrupole effect and an EMF 20 percent smaller than that of the intense pattern originates at iron atoms with one carbon nearest neighbor.

Phases identifiable by their patterns include ferrite, martensite, austenite, cementite, and ϵ-carbide. Dislocations produce no detectable effect. Application of Mössbauer spectroscopy to the study of martensite tempering and quantitative analysis for retained austenite is discussed.

**10327.** Christ, B. W., Smith, G. V., **Strengthening of polycrystalline iron by nitrogen,** *Trans. ASM* **60,** 732-734 (1967).

> Key words: Carbide strengthening; hydrogen-purified iron; nitride strengthening; nitrogen ferrite; polycrystalline; solid solution strengthening; tensile tests.

The strengthening of polycrystalline iron by an interstitial impurity has been measured in tensile tests on 0.050-inch diameter wire. Nitrogen was introduced into hydrogen-purified iron by equilibration with an ammonia-hydrogen mixture. The distribution of nitrogen was changed by varying the rate of cooling from the solution temperature. Nitrogen in solid solution is not as effective a strengthener as carbon in solid solution. Nitride precipitation occurring during air cooling results in strengthening comparable to that due to carbide precipitation during quench aging. The observed linear variation of flow strength with nitrogen concentration supports the Schoeck-Seeger or Mott-Nabarro models of solution strengthening.

**10328.** Christ, B. W., Smith, G. V., **Yield and flow stress increase in pure polycrystalline iron during 600 °C treatment after wet hydrogen purification,** *Scripta Met.* **1,** No. 3, 123-130 (1967).

> Key words: Hydrogen-purified iron; Luder's strain; polycrystalline iron; tensile properties; ultimate tensile stress; yield stress.

The tensile properties of polycrystalline iron (0.060 mm grain size) have been measured at 298 and 163 °K. Wet hydrogen treatment of rolled and drawn zone-refined iron for 7 hours at 750 °C decreased the average yield stress and ultimate tensile stress at 298 °K from 16,500 and 30,600 psi to 7,600 and 27,600 psi, respectively. The wet-hydrogen purified iron displayed practically no Luder's extension at room temperature but exhibited 6-7 percent Luder's extension at 163 °K. Annealing at 600 °C for 20 and 40 hours in both dry hydrogen and sealed vycor capsules ($10^{-5}$ torr) caused an upward shift in the stress-elongation curve at 163 °K. These results are discussed in terms of the influence of possible structural modifications during 600 °C annealing on the athermal and thermal components of stress.

**10329.** Chueh, P. L., Prausnitz, J. M., **Third virial coefficients of nonpolar gases and their mixtures,** *AIChE J.* **13,** No. 5, 896-902 (Sept. 1967).

> Key words: Nonpolar gases; quantum gases; third virial coefficients; virial equation.

While much attention has been given to second virial coefficients of nonpolar gases, experimental and theoretical studies on third virial coefficients are scarce. This work presents a correlation of third virial coefficients within the framework of the corresponding-states principle. The correlation is useful for estimating third virial coefficients of pure and mixed nonpolar gases, including the quantum gases helium, hydrogen and neon. The importance of third virial cross-coefficients in phase equilibrium predictions is illustrated with calculations for the solid-gas, methane-hydrogen system at 76 °K.

Brief attention is given to the pressure-series form of the virial equation. Because of fortuitous cancellations, it is shown that, for reduced temperatures above 1.4, the pressure-series, truncated after the second term, is applicable to a wider range of density than the density series truncated after the second term. However, when both series are truncated after the third term, the density series appears to be superior regardless of reduced temperature.

**10330.** Colwell, J. H., **The heat capacity of a mixed titanate superconductor,** *Physics Letters* **25A,** No. 8, 623-624 (Oct. 1967).

> Key words: Electronic band structure; heat capacity; mixed titanate; phase transition; semiconductor; $SrTiO_3$; superconductor.

The heat capacity of semiconducting $Sr_{0.925}Ba_{0.075}TiO_3$ has been measured in the temperature region 0.3 to 4 °K. This material becomes superconducting with a transition temperature, $T_c$, of about 0.53 °K. The heat capacity increases gradually with decreasing temperature below $T_c$ and has a broad maximum at 0.45 °K. There is an unusual heat capacity anomaly just above $T_c$ which is described as a gradual decrease in the electronic heat capacity coefficient, $\gamma$, between 0.8 and 2.0 °K. The change in $\gamma$ is interpreted as a phase transition causing a change in the number of occupied valleys in the conduction band. In the phase existing at the superconducting transition the conduction band has the same number of valleys and a comparable density of states at the Fermi surface as that in semiconducting $SrTiO_3$.

**10331.** Corliss, C. H., **Revision of the NBS tables of spectral-line intensities below 2450 Å,** *Spectrochim. Acta* **23B,** 117–127 (1967).

Key words: Atomic spectra; intensities; spectral-line intensities; ultraviolet intensities.

A calibration is applied to the intensity measurements of the 1400 lines below 2500 Å in the NBS Tables of Spectral-Line Intensities. Tables of the new values are presented with the lines arranged by element and by wavelength.

**10332.** Cullen, W. C., Boone, T. H., **A thermal-shock resistance factor for bituminous built-up roofing membranes,** Part 1, *Roofing Siding Insulation Mag.* **44,** No. 11, 30-35 (Nov. 1967); Part 2, *Roofing Siding Insulation Mag.* **44,** No. 12, 35-39 (Dec. 1967).

Key words: Development; roofing membrane; strength properties; thermally induced forces; thermal-shock resistance factor.

The resistance of bituminous built-up roofing membranes to thermally induced forces is considered in terms of their strength properties such as breaking load in tension, modulus of elongation and apparent linear thermal expansion coefficient. The development of a Thermal-Shock Resistance Factor is described and values are given for three bituminous built-up membranes at temperatures of −30 °F (−34.4 °C), 0 °F (−17.8 °C), 30°F (−1.1 °C) and 73 °F (22.8 °C). The apparent relation between the values obtained in the laboratory and the observed performance of roofing membranes in service is considered. The utilization of the Thermal-Shock Resistance Factor in the reduction of potential failures of bituminous built-up roofing membranes in service from thermally induced forces is also discussed.

**10333.** Currie, L. A., **Limits for qualitative detection and quantitative determination, application to radiochemistry,** *Anal. Chem.* **40,** No. 3, 586-593 (Mar. 1968).

Key words: Activation analysis; analytical chemistry; decision level; detection limit; determination limit; hypothesis testing; interference; Poisson distribution; radioactivity.

The occurrence in the literature of numerous, inconsistent and limited definitions of a detection limit has led to a re-examination of the questions of signal detection and signal extraction in analytical chemistry and nuclear chemistry. Three limiting levels have been defined: $L_C$—the net signal level (instrument response) above which an *observed* signal may be reliably recognized as "detected"; $L_D$—the "true" net signal level which may be *a priori* expected to lead to detection; and $L_Q$—the level at which the measurement precision will be satisfactory for quantitative determination. Exact defining equations as well as series of working formulae are presented both for the general analytical case and for radioactivity. The latter, assumed to be governed by the Poisson distribution, is treated in such a manner that accurate limits may be derived for both short- and long-lived radionuclides either in the presence or absence of interference. The principles are illustrated by simple examples of spectrophotometry and radioactivity, and by a more complicated example of activation analysis in which a choice must be made between alternative nuclear reactions.

**10334.** Cuthill, J. R., McAlister, A. J., Williams, M. L., Watson, R. E., **Density of states of Ni: Soft-x-ray spectrum and comparison with photoemission and ion neutralization studies,** *Phys. Rev.* **164,** No. 3, 1006-1007 (Dec. 15, 1967).

Key words: Density of states; emission spectrum; linear detection; nickel; oxide free; paramagnetic; soft x-ray; transition probability.

Soft x-ray studies have been made on paramagnetic Ni and interpreted in terms of the single-particle density of states. In particular, the $M_{2,3}$ emission spectrum has been investigated, using improved experimental techniques. Measurements were made at 960 °C, at an average pressure of $5 \times 10^{-8}$ Torr, using an oxide-free surface. Fine structure was observed in the spectrum. Although first-principles correction of self-absorption effects and satellite and subband overlap is not yet possible, careful consideration is given them, with the result that the $M_3$ band can be resolved from the accompanying structure in a plausible way. Most of its features can be taken with reasonable confidence to be characteristic of the true $M_3$ emission band. Comparison is made with earlier soft x-ray results, with band calculations for paramagnetic Ni, and with ion neutralization and photoemission measurements on ferromagnetic Ni. Systematic variations in transition matrix elements and lifetime broadening appear important when relating any experiment with theory, and an aspect of each of these problems has been considered quantitatively. The variation obtained is more severe for the photoemission than for the soft-x-ray analysis. The ion-neutralization and soft-x-ray results appear closer to the single-particle density of states.

**10335.** Damburg, R. J., Geltman, S., **Excitation of n = 2 states in hydrogen by electron impact,** *Phys. Rev. Letters* **20,** No. 10, 485-487 (Mar. 4, 1968).

Key words: Close-coupling; electron impact; excitation; hydrogen; Lyman $\alpha$; polarization.

A possible source of incompleteness in the most recent close coupling calculations for the excitation cross sections of the n = 2 levels in hydrogen, some of the results of which disagree with experiment, is pointed out. We present a method which removes this difficulty by the implicit inclusion of all important effective polarization potential terms of order $\alpha/r^4$.

**10336.** Daney, D. E., Mann, D. B., **Quality determination of liquid-solid hydrogen mixtures,** *Cryogenics* **7,** No. 5, 280-285 (Oct. 1967).

Key words: Liquid-solid hydrogen mixtures; quality determination; rocket propellant; slush hydrogen.

A theoretical and experimental investigation of the feasibility of predicting the quality of liquid-solid hydrogen mixtures from the mass fraction of vapor pumped off in the freeze-thaw process is presented. Three independent methods of experimental quality determination were used to check the correctness of the qualities predicted from the measured mass fraction pumped off in forming liquid-solid mixtures. In all cases only freshly made mixtures were used.

It is suggested that an independent means of determining the edge of the triple-point region, such as measurement of the vapor pressure, be used. With this modification, measurement of the mass fraction pumped off during the freeze-thaw process provides a simple, non-destructive and accurate method of bulk quality determination. The method is not appropriate for cases in which a partial transfer from the dewar is made and it requires accurate knowledge of the heat leak if long storage times are to be used. Low accuracy in large volume gas flowmeters also places a restriction on the method.

**10337.** deWit, R., **Thermodynamic force on a dislocation,** *J. Appl. Phys.* **39,** No. 1, 137-141 (Jan. 1968).

Key words: Concentration; crystal; defect; dislocation; energy; equilibrium; force; hydrostatic; pressure; vacancy.

The thermodynamic force on a dislocation is defined as the negative gradient of the Gibbs free energy of the crystal with respect to dislocation motion. This is shown to lead to a consistent force expression which contains two terms: the Peach-Koehler force due to the stress and the Bardeen-Herring force due to the vacancy concentration. The precise definition of these two terms is arbitrary, though their sum is unique. Various forms of the force expression are derived in terms of different reference vacancy concentrations, including the original forms of Weertman and Lothè and Hirth.

**10338.** Dibeler, V. H., Liston, S. K., **Mass-spectrometric study of photoionization. VIII. Dicyanogen and the cyanogen halides,** *J. Chem. Phys.* **47,** No. 11, 4548-4555 (Dec. 1, 1967).

Key words: Autoionization; BrCN; $C_2N_2$; ClCN; FCN; heats of formation; ICN; mass spectrometer; photoionization; Rydberg levels; vacuum uv monochromator.

Photoionization-yield curves are obtained for the molecule and selected radical ions of $C_2N_2$, FCN, ClCN, BrCN, and ICN from threshold to 600 Å. Vibrationally excited states of ions and autoionization of Rydberg levels in the molecules are observed and discussed briefly. The $X^+$ ion thresholds in the heavier cyanogen halides are used to obtain: $\Delta Hf_0°(\mathrm{CN}) = 101.5$ kcal mole$^{-1}$, $\Delta Hf_0°(\mathrm{CN}^+) = 430.0$ kcal mole$^{-1}$, and $I(\mathrm{CN}) = 14.2$ eV. These are applied to compute $\Delta Hf_0°(\mathrm{FCN}) = 5.6$ kcal mole$^{-1}$, $D(\mathrm{F-CN}) = 5.0$ eV, $I(C_2) = 12.15$ eV, and other thermodynamic properties. The formation of $\mathrm{CN}^+$ from dicyanogen apparently includes about 0.6 eV excess energy near the threshold.

**10339.** Dickson, G., Oglesby, P. L., **Elastic constants of dental amalgam,** *J. Dental Res.* **46,** No. 6, Part 2, 1475 (Nov.-Dec. 1967).

Key words: Bulk modulus; dental amalgam; elastic constants; Poisson's ratio; pulse-echo technic; shear modulus; Young's modulus.

Elastic constants of dental amalgam were determined by an ultrasonic pulse-echo technic. Longitudinal and transverse wave velocities of a 5.5 MHz pulse were determined in cylindrical amalgam specimens 8mm in diameter by 6 to 15 mm in length. Values of $9.1 \times 10^6$ psi for Young's modulus, $3.4 \times 10^6$ psi for shear modulus, $9.1 \times 10^6$ psi for bulk modulus and 0.33 for Poisson's ratio were obtained for amalgams containing 49 percent mercury. Values for all of these constants increased as the mercury content of specimens was reduced to 35 percent.

**10340.** DiMarzio, E. A., **Some contributions to the kinetics of growth of multicomponent chains with application to the problems of ciliation and fractionation in polymer crystallization,** *J. Chem. Phys.* **47,** No. 9, 3451-3469 (Nov. 1, 1967).

Key words: Crystallization; kinetics; multicomponent chains; polymer crystallization.

The problem of the growth rate and purity of crystals formed by the sequential deposition of molecules in a mixed system is solved. The solution is given in terms of the fundamental rates $a_\nu^{ij}(\beta_{\nu+1}^{ij})$ for laying down (taking off) species $j$ at the $(\nu + 1)$th position of the growing crystal given that species $i$ occupies the $(\nu)$th position. The fundamental rates are thus dependent on nearest-neighbor interaction but not on neighbors further removed. The method used complements a previously used method and additionally solves the problem for $\nu$-dependent $\alpha_\nu^{ij}$ and $\beta_\nu^{ij}$. The $\nu$ dependence of the $\alpha$'s and $\beta$'s allows for the stochastic-like distribution of the various species in the substrate upon which we are growing our linear chain of molecules. It is shown that there exists one unique flux-determined steady-state solution for a wide variety of initial conditions. Several diagrams descriptive of various physical processes are displayed. The one describing ciliation (the growth process which results in the ends of polymer chains dangling out of the crystal lamella) is treated in some detail. It is found that there are two classes of $\alpha$'s and $\beta$'s. One class gives large growth rates and very little ciliation. The second class gives growth rates which are orders of magnitudes smaller and results in much ciliation. It is concluded that when chain-folded crystallization occurs the amount of material dangling out of the crystal is less than 50 percent of the total amount of material participating. The problem of fractionation in polymers is treated. Formulas are given for the purity of polymer crystals which are formed by high molecular weight material crystallizing concomitantly with polymeric material of lower molecular weight and/or of different kind. Fractionation can be substantial even when the molecular weights of the mixed system are all large. Simple formulas are derived. More complicated diagrams that allow for more than nearest-neighbor interaction can be reduced to the nearest-neighbor case but with a larger number of components.

**10341.** Eberhard, J. P., **Systems and design—an extrapolation to 2000 A.D.,** *Mater. Res. Std.* **8,** No. 5, 12-17 (May 1968).

Key words: City planning; human factors; standards; systems engineering.

Systems analysis is necessary for a thorough re-thinking of major hardware problems of the city. One of the problems concerns itself with performance standards in this context and their need to include an understanding of how they interact with man. A need for an ideal model of the highest concept of civilization must be defined in order to build a practical approach to urban systems design and construction. It is hoped that new mass production techniques may provide practical solutions to the problem of low cost urban living units that will be both attractive as well as providing inspiration. This paper was originally presented at the Third Annual Meeting of the National Academy of Engineering, 20-24 September, 1967, University of Michigan, Ann Arbor, Mich.

**10342.** Eberhard, J. P., Schofer, R. E., **The role of technology in developing future transportation systems,** *Proc. Analysis and Control of Traffic Flow Symp., Detroit, Michigan, Jan. 9-10, 1968,* pp. 1-4 (Society of Automotive Engineers, Inc., New York, N.Y., 1968).

Key words: Future transportation; regional transportation; technology; transportation; transportation technology; urban transportation.

As we approach the twenty-first century it is becoming increasingly apparent that, as megalopolitan areas increase in size and number throughout the country, we must search for new transportation technologies. In this paper, the authors set forth some of the areas where more and better coordinated research needs to be done.

There are three basic types of transportation technologies. The planning technology entails the obtaining of enough information in advance to develop sound transportation systems to meet future requirements. More research is needed to determine the impact on transportation requirements made by a changing city form. Secondly, research directed at improved operating strategies for existing systems will provide information needed for the development of future systems. Finally, more work is needed in the area of transportation hardware technology. No proposal should go without careful evaluation; latent technologies must be explored in the search for better systems.

Governments can encourage technological innovation by defining areas of needed research, sponsoring research, disseminating information on research activities, and by coordinating research efforts.

To preserve the vitality of transportation in the United States, the Federal Government must assume the overall responsibility for encouraging development of new transportation technologies.

**10343.** Eick, J. D., Caul, H. J., Smith, D. L., Rasberry, S. D., **Analysis of gold and platinum group alloys by x-ray emission with corrections for interelement effects,** *Appl. Spectry.* **21,** No. 5, 324-328 (Sept.-Oct. 1967).

Key words: Gold and platinum group alloys; noble metal alloys; x-ray emission.

The x-ray emission analysis of noble metal alloys was investigated critically to determine optimum conditions for accurate analysis. The analytical curves for the elements Cu, Pd, Pt, and Zn were found to be linear with a deviation of less than ±0.2 percent. However, a nonlinear relationship existed for gold and for silver. These discrepancies could not be eliminated by variation in sample preparation. An interelement effect due to x-ray absorption and enhancement was found and was corrected to an accuracy of 0.2 percent by means of a mathematical treatment suggested by Lucas-Tooth and Price. The analysis by x-ray emission can be accomplished in approximately one-tenth of the time necessary for conventional wet chemical methods.

**10344.** Fatiadi, A. J., **Acetic anhydride phosphoric acid as an acetylating agent,** *Carbohydrate Res.* **6,** 237-240 (1968).

Key words: Acetic anhydride; acetylation; anhydrous phosphoric acid; esterification.

Anhydrous phosphoric acid in acetic anhydride can be recommended as an efficient agent for the acetylation of carbohydrates, enediols, enols, inositols, and sterically hindered phenols. A mixture of anhydrous phosphoric acid with higher fatty acid anhydrides (isobutyric, butyric, or propionic) has been used successfully for the esterification of inositols.

**10345.** Fatiadi, A. J., **Stable radicals obtained by treatment of azulene with periodic acid and other oxidants,** *Chem. Commun.* **8,** 456-458 (Apr. 24, 1968).

Key words: Azulene; periodic acid; polymeric product; stable free radical.

Treatment of the non-benzenoid, aromatic hydrocarbon azulene with periodic acid gives a free radical which is extremely stable to air and heat; the product has been found to be polymeric. Treatment of azulene with iodic acid of antimony pentachloride also gives stable free radicals. for conventional wet chemical methods.

**10346.** Faust, J. W., Jr., Ogburn, F., Kahan, D., Ruff, A. W., Jr., **Twin configurations in FCC dendrites,** *J. Electrochem. Soc.: Solid State Science* **114,** No. 12, 1211-1212 (Dec. 1967).

Key words: Dendrites; electrodeposition; growth twins; silver.

The authors discuss possible configurations of intersections of twin planes which might be present in dendrites of diamond-type materials and fcc metals. They show that for dendrites growing in a [110] direction there will be a mismatch boundary wherever two or more twin planes intersect.

Experimental evidence is given for the existence of a configuration of two crossing twin lamellas with two mismatch boundaries in a silver dendrite.

**10347.** Fine, J., Scheer, M. D., **Positive and negative self-surface ionization of molybdenum,** *J. Chem. Phys.* **47,** No. 10, 4267-4268 (Nov. 15, 1967).

Key words: Electron affinity; ion sublimation energy; mass spectrometry; molybdenum; positive and negative ions; self-surface ionization.

The positive and negative self surface ionization of molybdenum has been observed in the 1800-2100 °K temperature range. The positive and negative ion sublimation energies were found to be 9.5 and 10 eV respectively. The electron affinity was determined as 1.0±0.2 eV. (estimated uncertainty)

**10348.** Franklin, A. D., **Born model calculation of enthalpies of solution in CaF$_2$,** *J. Am. Ceram. Soc.* **50,** No. 12, 648-652 (Dec. 1967).

Key words: Born model of ionic solids; CaF$_2$; enthalpy of solution; ionic solids; lattice expansion.

The Born model of ionic solids was used to calculate the lattice energy, as an estimate of the enthalpy of solution, needed to dissolve NaF and YF$_3$ in CaF$_2$, in the limit of infinite dilution. For NaF sufficient experimental data are available to provide resonable estimates for the parameters describing the repulsive interactions between Na$^+$ and surrounding ions, and the calculated enthalpy of solution is in good agreement with the available experimental value, 1.4 ± 0.3 eV for NaF. For YF$_3$ the experimental data are not available and the estimated enthalpy of solution of about zero is subject to a large uncertainty. The results for NaF are consistent with the model normally assumed, in which each substitutional Na$^+$ ion is accompanied by an F$^-$ vacancy; however, they do not rule out charge compensation by interstitial Na$^+$ ions. The calculations also yield an estimate for the lattice expansion.

**10349.** Frenkiel, F. N., Klebanoff, P. S., **Correlation measurement in a turbulent flow using high-speed computing methods,** *Phys. Fluids* **10,** No. 8, 1737-1747 (Aug. 1967).

Key words: Correlations; even-order; grid; hot-wire anemometer; isotropy; nonlinear response; odd-order; turbulence.

Third-order time-correlations downstream of a grid were measured with a hot-wire anemometer using high-speed computing methods. The nonlinear response of the hot-wire to the fluctuations of velocities is taken into account as well as the effect of transverse velocities. It is found that the third-order correlations are substantially different from previous results and demonstrate that the assumption of isotropy is not adequate for these correlations downstream of a grid. The nonlinear response does not significantly affect the difference $u_1^2u_2 - u_1u_2^2$. Since previous conclusions concerning the nature of third-order correlations were based on the measurements of such differences they masked the effects of nonlinearity on the individual correlations. Correlations of fifth-order are also presented and their relations to the third-order correlation are discussed. Although the nonlinear corrections are quite important for odd-order correlations they are negligible for correlations of even-order.

**10350.** Goldstein, J. I., Majeske, F. J., Yakowitz, H., **Preparation of electron probe microanalyzer standards using a rapid quench method,** *Advan. X-ray Anal.* **10,** 431-446 (1967).

Key words: Al-Mg; Au-Si; electron probe standards; quantitative microanalysis; splat cooling; standard preparation.

Standards for microprobe anlysis can be made to serve two purposes: (1) Proposed correction models can be tested with them, and (2) Analysis can be performed more accurately in the system which includes the standard. Few microprobe standards are presently available because they must be homogeneous on the micron scale and their composition must be known accurately. A modified Duwez splat cooling method is described which enables the investigator to prepare suitable standards in most cases. The apparatus which is relatively simple and inexpensive is described in detail. The systems Au-Si and Al-Mg were chosen as test cases. Suitable standards were prepared at different concentrations in each system. The analytical results for all compositions in Al-Mg are presented and discussed.

**10351.** Gorden, R., Jr., Ausloos, P., **Photolysis of ethylene at 1048-1067 Å. Reactions of $C_2H_4^+$ and fragmentation of the superexcited ethylene molecule,** *J. Chem. Phys.* **47,** No. 5, 1799-1806 (Sept. 1, 1967).

Key words: Cis-2-butene; ethylene; hydrocarbons; photoionization; trans-2-butene.

$C_2H_4 - NO$, $C_2H_4 - O_2$ and $C_2H_4 - (CH_3)_2NH - O_2$ mixtures have been irradiated with an argon resonance lamp emitting only the 1048 and 1067 Å lines. The ionization efficiency ratios: $\eta_{C_2D_4}/\eta_{NO}$, $\eta_{C_2H_4}/\eta_{NO}$, $\eta_{C_2D_4}/\eta_{C_2H_4}$ were determined to be 0.30 ± 0.003, 0.27 ± 0.003 and 1.12 respectively. Trans-2-buene and cis-2-butene are major products when NO (I. P. = 9.25 eV) or $(CH_3)_3NH$ (I. P. = 8.24 eV) are added to $C_2H_4$. Radiation of pure $C_2H_4$ or of $C_2H_4 - O_2$ mixtures yielded only minor races of $2-C_4H_8$. In accord with earlier radiolysis studies we ascribe the formation of $2-C_4H_8$ to the charge transfer process:

$$C_4H_8^+ + NO \text{ (or } (CH_3)_2NH \rightarrow C_4H_8 + NO^+ \text{ (or } (CH_3)_2NH^+)$$

where $C_4H_8^+$ may possess some excess internal energy carried over from the exothermic condensation reaction $(C_2H_4^*)^+ + C_2H_4 \rightarrow (C_4H_8^*)^+$. For a constant $C_2H_4 - NO$ mixture $M(C_4H_8)/N$ increases drastically with an increase of the pressure of $C_2H_4$ from 0.1 to 6 torr. Also, in pure $C_2H_4$, $M(CH_3)/N$ which s close to unity at 0.5 torr is seen to diminish to 0.2 when the pressure is raised to 29.8 torr. These effects are largely ascribed to a competition between decomposition and stabilization of the $[C_4H_8^*]^+$ product ion.

A rate constant of $10^7$ sec$^{-1}$ is derived for the unimolecular decomposition of $(C_4H_8^*)^+$ assuming that stabilization occurs at every collision with $C_2H_4$. It is shown that Ne is about 100 times less efficient than $C_2H_4$ in stabilizing $(C_4H_8^*)^+$.

The superexcited $C_2H_4^*$ dissociates as follows, $C_2H_4^* \rightarrow C_2H_2 + H_2$ and $C_2H_4^* \rightarrow C_2H_2 + 2H$. Isotopic analysis of the hydrogen formed in the photoionization of $CH_2CD_2$ shows that the relative probabilities for the elimination of $H_2$, HD and $D_2$ from $CH_2CD_2^*$ are the same for the superexcited molecule as for the excited molecule formed by absorption of 8.4 to 10 eV photons.

**10352.** Grosch, H. R. J., **The National Bureau of Standards program in computer sciences and technology,** *Statist. Reptr.* **68-3,** 37-41 (Superintendent of Documents, U.S. Government Printing Office, Washington, D.C. 20402, Sept. 1967, 20 cents).

Key words: Brooks Bill; computer standards; computer technology; data processing; government.

The NBS Center for Computer Sciences and Technology was established in 1965 to perform the Bureau's work in the field of computer technology—a broad program of standardization activities, applied research, and services to Federal agencies. Work on standards includes that on USASCII (for use in Federal procurement, under the terms of the Brooks Bill of October 1, 1965) and on optical character recognition. Services to other branches of government include providing data processing services, computational assistance, and consultation. The activities of the center's Technical Information Exchange and the continued experimentation with computers will have industry-wide benefits.

**10353.** Gross, D., Loftus, J. J., Robertson, A. F., **Method for measuring smoke from burning materials,** *Am. Soc. Testing Mater. Spec. Tech. Publ.* **422,** 166-204 (1967).

Key words: Aerosol; combustion; fire hazard; pyrolysis; smoke; smoke density; visual obscuration.

Based on a study of possible smoke-measuring methods, a laboratory test has been developed for the photometric measurement of smoke from burning materials. The method assumes the applicability of Bouguer's law to the attenuation of light by smoke, and smoke quantity is therefore reported in terms of optical density rather than light absorptance or transmittance. Optical density is the single measurement most characteristic of a "quantity of smoke" with regard to visual obscuration.

Experiments have been performed on a variety of building finish materials under both flaming and nonflaming (smoldering) conditions, and the results are reported in terms of (a) maximum smoke accumulation, (b) maximum rate of smoke accumulation, and (c) the time period to reach an arbitrary "critical" smoke level.

**10354.** Haber, S., **A theorem on arbitrary functions,** *Am. Math. Monthly* **74,** No. 8, 973-975 (Oct. 1967).

Key words: Arbitrary functions; continuity; maxima; real variable.

It is shown that if $a_i$ and $b_i$, $i = 1, \ldots, n$ are arbitrary real functions of a real variable, then the function $f(x,y) = a_1(x)b_1(y) + \ldots + a_n(x)b_n(y)$ has a certain partial continuity property.

**10355.** Haber, S., **Midpoint quadrature formulas,** *Math. Compt.* **21,** No. 100, 719-721 (Oct. 1967).

Key words: Computing; integration; numerical analysis; quadrature.

A family of quadrature formulas for the interval (0,1) can be defined by partitioning the interval into subintervals and taking as nodes the midpoints of these intervals, with the lengths of the intervals serving as coefficients. The errors of these formulas are determined.

**10356.** Hafner, H., Simpson, J. A., Kuyatt, C. E., **Comparison of the spherical deflector and the cylindrical mirror analyzers,** *Rev. Sci. Instr.* **39,** No. 1, 33-35 (Jan. 1968).

Key words: Cylindrical mirror; electron energy analyzer; electron optics; spherical deflector.

The calculated performance of the cylindrical mirror deflection energy analyzer for charged particles is compared with that of the spherical analyzer. It is shown that through terms in $\sim^3$ the cylindrical device is significantly superior.

**10357.** Haller, W., **Correlation between chromatographic and diffusional behaviour of substances in beds of pore controlled glass. Contribution to the mechanism of steric chromatography,** *J. Chromatog.* **32,** 676-684 (1968).

Key words: Chromatography; diffusion; gel chromatography; gel filtration; gel-permeation chromatography; glass chromatography; GPC; pore-controlled glass; restricted diffusion; steric-exclusion chromatography.

Chromatography and diffusion experiments were performed with columns and suspensions of grains of pore-controlled glass of 620 Å pore diameter. The elution positions of tobacco mosaic virus and of benzyl alcohol coincide with the actual void volume and the total fluid volume of the column. A spherical virus (MS2) of 260 Å diameter eluted at a normalized elution volume of $k_e = 0.44$, and its peak position shifted only very slightly over a wide range of elution rates.

The diffusional uptake of virus (MS2) by the porous glass grains from a well stirred suspension indicated that the total pore volume of the glass was accessible to the virus. It took approximately 30 seconds for one half of the ultimate amount of virus to penetrate the glass. In the light of these results it is very unlikely that a volume exclusion mechanism determines the elution position of the virus. Since porous glass columns of uniform and controlled pore size display elution spectra similar to those of gel columns, it is also unlikely that volume exclusion governs the elution spectrum in steric chromatography on gels.

**10358.** Haller, W., **Virus isolation with glass of controlled pore size: MS2 bacteriophage and Kilham virus,** *Virology* **33,** No. 4, 740-743 (Dec. 1967).

Key words: Chromatography; glass; Kilham rat virus; MS2 virus; porous glass; virus.

MS2 bacteriophage and tritiated Kilham Rat virus have been isolated from natural lysates by restricted-diffusion chromatography on pore-controlled glass. Measurements of infectivity and hemagglutinating activity, as well as radioactivity and UV absorption, were used to determine recovery and purity of isolated viruses. The recoveries proved to be nearly 100 percent and the viruses were essentially host protein free.

**10359.** Hamer, W. J., **A Joule centennial,** *J. Chem. Educ.* **45,** No. 2, 123-125 (Feb. 1968).

Key words: B.A. resistance unit; equivalent; Joule; Joule centennial; mechanical equivalent of heat.

The centennial of Joule's determination of the mechanical equivalent of heat by electric means is noted. His results are compared with those he had obtained eighteen years earlier by mechanical means, namely, by the agitation of water. The cause for the difference Joule found in the results obtained by the two methods is discussed. The main cause of the difference rested with the assignment of a value for the B.A. (British Association for the Advancement of Science) unit of resistance in cgs units. It is pointed out that this factor played a part in the establishment of the international electric units by the Chicago International Electrical Congress of 1893.

**10360.** Hamer, W. J., **Evaluation procedures and annual performance data for Leclanché cells,** *Electrochem. Technol.* **5,** No. 11-12, 490-498 (Nov.-Dec. 1967).

Key words: Advances in dry cells; battery nomenclature; dry cell specifications; dry cell standards; dry cell tests; international dry cell standards.

This paper deals with the development over the past 48 years of so-called "standardized tests" for the evaluation of Leclanché cells and batteries. Data covering this time period or a part of this time period are given for (1) general-purpose flashlight cells, (2) industrial flashlight cells, (3) railroad lantern batteries, (4) photoflash cells, (5) No. 6 cells for various end uses, (6) radio "A" batteries, (7) radio "B" batteries, (8) hearing-aid "A" batteries, (9) hearing-aid "B" batteries, and (10) transistor hearing-aid batteries. The presently used standard tests, 27 in number, are described. A history of the development of dry cells of the Leclanché type is also included.

**10361.** Hanley, H. J. M., Childs, G. E., **Discrepancies between viscosity data for simple gases,** *Science* **159,** No. 3819, 1114-1117 (Mar. 8, 1968).

Key words: Argon; correlation; dilute gas; discrepancies; high temperature viscosity; potential function.

It has been known for some time that Kestin and his co-workers have reported dilute gas viscosity coefficients which differ from the usually accepted values. Recent work supplements Kestin's results. We show that there is no evidence for not accepting this different data. We feel that the whole subject of dilute gas viscosity measurements above room temperature should be reexamined both from the experimenter's and correlater's viewpoint. There is evidence that published tables may be incorrect by as much as 10 percent above about 600 °K.

**10362.** Hanley, H. J. M., **Thermodynamics of transport phenomena in membrane systems,** *J. Chem. Educ.* **44,** No. 12, 717-719 (Dec. 1967).

Key words: Continuous systems; diffusion flow; discontinuous systems; membranes; nonequilibrium thermodynamics; porous media; thermal transpiration; transport phenomena; viscous flow.

This article shows how the theory of nonequilibrium thermodynamics, developed for continuous systems, can be applied to systems with a membrane. The idea being to develop a straightforward pedagogical thermodynamic approach to transport processes in this type of system which will encourage a reader to dig deeper. Some points on the "continuous" versus "discontinuous" approach to nonequilibrium thermodynamics are also mentioned. The development is based on a discussion of nonisothermal diffusion flow in a porous medium.

**10363.** Hayward, H. W., Tauber, S. J., **The HAYSTAQ experiment,** Chapter 26 in *Proc. ICIREPAT Fifth Annual Meeting, London, England, Aug. 31-Sept. 10, 1965*, pp. 337-350 (Thompson Book Co., Washington, D.C., 1967).

Key words: Chemistry; compounds; computer; file organization; HAYSTAQ; Hayward; information retrieval; linear notation; Markush; mixtures; reactions; representations; screens; structures; topological codes.

The background of the Haystaq system is recapitulated. Shortcomings of an earlier chemical structure representation are reviewed; the scope and some advantages of the Hayward notation are stated. Suggestions are made for representing mixtures and classes of compounds. The scope is stated of notations for classes of reactions. The organization of files of chemical information and patterns of retrieval are discussed. Capabilities, limitations, and future implications of the techniques evolved are pointed out.

**10364.** Hetzer, H. B., Robinson, R. A., Bates, R. G., **Conventional $pa_H$ values for buffer solutions of piperazine phosphate from 0° to 50 °C,** *Anal. Chem.* **40,** 634-636 (Mar. 1968).

Key words: Buffer solutions; pH; piperazine phosphate.

Piperazine phosphate, a salt of the composition $PzH_3PO_4$ — where $Pz = C_4H_{10}N_2$ — has a pH value of 6.26 at 25 °C in the 0.05*m* aqueous solution (*1*). Its solutions, therefore, contain both the $PzH_2^{2+}$ and $PzH^+$ cations and both the primary and secondary phosphate anions $H_2PO_4^-$ and $HPO_4^{2-}$. The salt is available commercially and is readily crystallizable from water. Its buffer capacity and stability are high, and the salt is a useful buffer substance. We have now made emf measurements of the $pa_H$ values of 0.02*m* and 0.05*m* solutions of piperazine phosphate from 0° to 50 °C.

**10365.** Hollstein, M. G., DeVoe, J. R., **Determination of medium-weight elements by gamma-excited x-ray fluorescence,** (Proc. Second Symp. on Low Energy X- and Gamma Sources and Applications, University of Texas, Austin, Texas, Mar. 27-29, 1967), *Oak Ridge National Laboratory-IIC*-**10,** pp. 483-502 (1967).

Key words: Gamma-excitation; medium-weight elements; molybdenum; quantitative analysis; tin; x-ray fluorescence.

The application of gamma-excited x-ray fluorescence in the determination of medium weight elements has been studied. The pertinent components of the spectrometer are an $^{241}$Am source and a solid state detector, with a low-noise preamplifier and multi-channel analyzer. The resolution of the system is between 1.2 and 1.3 keV (FWHM) for 8 to 45 keV photons. Three different techniques of sample mounting were investigated. For single elements in the range from Cu to Dy the estimated detection limits are 10-100 $\mu$g and 0.01-1 mg/ml, depending upon the sample mounting procedure. The corresponding $K_\alpha$-peak intensities are $2 \times 10^4 - 3 \times 10^3$ cpm per mg and $4 \times 10^4 - 6 \times 10^2$ cpm per mg/ml, respectively. For testing the application of the method two series of NBS Standard Reference Materials were analyzed for Sn and Mo as minor constituents within a concentration range from about 0.04 to 9 percent. The best results were obtained by direct counting of the solid samples. Using this technique, a non-destructive analysis for Mo and Sn can be performed in a relatively short time with a precision of a few percent, a detection limit of about 100 ppm and a sensitivity of $6 \times 10^3$ to $1.4 \times 10^4$ cpm per percent concentration.

**10366.** Holt, H. K, **Frequency-correlation effects in cascade transitions involving stimulated emission,** *Phys. Rev. Letters* **19,** No. 22, 1275-1277 (Nov. 27, 1967).

Key words: Laser; line profile; neon.

The effect of the frequency correlation of photons emitted in an atomic cascade transition on the frequency profile of the light emitted in the second transition when the first transition is participating in laser action is examined.

**10367.** Holt, H. K., **Observation of the effect of frequency correlations on a cascade transition,** *Phys. Rev. Letters* **20,** No. 9, 410-412 (Feb. 26, 1968).

Key words: Laser; line profile; neon.

The effect of frequency correlations on a cascade transition has been observed.

**10368.** Hudson, R. P., **Generation of matrix elements of angular-momentum operators,** *J. Opt. Soc. Am. Letters to Editor* **57,** No. 12, 1552-1553 (Dec. 1967).

Key words: Angular momentum operators; matrix elements.

A simple numerical array is shown to give the matrix elements of certain important angular momentum operators.

**10369.** Hummer, D. G., **Non-coherent scattering-III. The effect of continuous absorption on the formation of spectral lines,** *Monthly Notices Roy. Astron. Soc.* **138,** No. 1, 73-108 (Jan. 1968).

Key words: Continuous absorption; non-coherent scattering; Planck function; source function; spectral lines.

The formation of spectral lines by completely redistributed non-coherent scattering is systematically investigated for situations in which photo-ionization or extinction by dust grains occurs at the line frequencies. Particular attention is given to cases for which the source function associated with the continuous opacity differs from the Planck function at the local electron temperature. Very large effects are found to occur, even when the ratio of continuous opacity to line opacity is very small. Extensive numerical results are presented, and the relevant scaling laws and the generalized thermalization length are discussed.

**10370.** Ito, J., **A new yttrium magnesium silicate garnet, $Y_6Mg_5Si_5O_{24}$ and its rare earth and nickel analogues,** *Mater. Res. Bull* **2,** 1093-1098 (1967).

Key words: Crystal chemistry; hydrothermal synthesis; rare-earth garnet; x-ray powder analysis.

A new magnesium yttrium silicate garnet and its rare-earth analogues with 4 and 6 coordinated magnesium and nickel ions have been synthesized hydrothermically. Its solid solubility with yttrium aluminum garnet was investigated.

**10371.** Jensen, M. W., **Milk meters, farm milk tank testing, and plastic containers for milk,** *Proc. 31st Annual Meeting International Association of Milk Control Agencies, Biloxi, Mississippi, Oct. 23-25, 1967,* pp. 26-31 (1968).

Key words: Farm milk tanks; milk handling; milk meters; plastic milk containers.

The role of the National Bureau of Standards in weights and measures administration was discussed, as were current technical developments in mechanical metering of milk, gauging and testing of farm milk tanks, and acceptance for measuring and packaging purposes of plastic containers for milk.

**10372.** Jespersen, J. L., Kamas, G., Morgan, A. H., **A proposed ranging system with application to VLF timing,** *IEEE Trans. Instr. Meas.* **IM-16,** No. 4, 282-285 (Dec. 1967).

Key words: Dispersion; range; time; VLF.

In general, without a clock it is not possible to determine the range between a radio transmitting and receiving site by making only passive observations at the receiving site. However, if the medium is dispersive, signals transmitted simultaneously from the same site, at different carrier frequencies, will not arrive simultaneously at some distant point. Thus, the difference in arrival time is related to the observer's distance from the transmitter. This effect is considered in conjunction with the VLF two-frequency timing system.

**10373.** Johannesen, R. B., **NMR studies of inorganic fluorides. IV. Relative signs of coupling constants in $CH_3SiF_3$, $HSiF_3$, and $HPF_2$,** *J. Chem. Phys.* **47,** No. 8, 3088-3089 (Oct. 15, 1967).

Key words: Double resonance; fluorine; fluorosilanes; hydrogen; nuclear magnetic resonance; phosphorus; relative signs; silicon; spin coupling constants.

The high-resolution n.m.r. spectra of $CH_3SiF_3$, $HSiF_3$, and $HPF_2$ have been recorded, and all of the coupling constants, including the relative signs, are reported (except for $J_{^{13}C-^{29}Si}$).

**10374.** Johannesen, R. B., Brinckman, F. E., Coyle, T. D., **Nuclear magnetic resonance studies of inorganic fluorides. V. Fluorosilanes,** *J. Phys. Chem.* **72,** 660-667 (1968).

Key words: Chemical shift; coupling constant; double resonance; fluorine; fluorosilanes; nuclear magnetic resonance; silicon; spin-coupling; solvent effects.

Nuclear magnetic resonance (nmr) chemical shifts of $^{19}$F nuclei and $^{29}Si-^{19}F$ coupling constants have been measured for a number of compounds containing silicon–fluorine bonds. For most of these, $^{29}$Si chemical shifts were also determined by (heteronuclear) ($^{19}F-\{^{29}Si\}$) double resonance. With few exceptions, $^{19}$F and $^{29}$Si resonances in substituted fluorosilanes are on the low-field side of the corresponding resonances in $SiF_4$. The $^{29}$Si shift in the $SiF_6^{2-}$ ion is about 75 ppm to high field of $SiF_4$ and is well outside the range of previously reported silicon shift values. Magnitudes of $^{29}Si-^{19}F$ coupling constants range from 167.6 Hz in $Si_2OF_6$ to 384.9 Hz in $Si_2Cl_5F$. The variation of these parameters with the nature and extent of substitution on silicon is discussed. A significant solvent dependence of the chemical shifts in $SiF_4$ and similar compounds has been observed.

**10375.** Judd, D. B., **A flattery index for artificial illuminants,** *Illum. Eng.* **62,** No. 10, 593-598 (Oct. 1967).

Key words: Color; flattery; illuminants; preference; rendition of color.

Artificial illuminants are used for (1) light-dark discrimination of objects, (2) critical appraisal of colored objects, and (3) appreciative viewing of colored objects. A light source that renders object colors in accord with their preferred colors may be said to flatter those objects. A flattery index has been derived for light sources used for appreciative viewing of colored objects to measure the degree to which such sources render object colors as we would like to see them. This index is based solely on spectral distribution and is modeled after the index of color rendition recently recommended by the CIE. It uses 10 of the 14 test samples established for appraisal of color rendition, and it uses the same definition of reference illuminants. It is scaled so that the reference illuminant receives a flattery index of 90, and a test illuminant rendering object colors precisely in accord with the preferred colors of the test samples receives a flattery index of 100. The test sample representative of the human complexion receives about one-third of the total weight; the two test samples representative of food colors, about one-third; the seven other test samples the remainder.

**10376.** Kamper, R. A., **Millidegree noise thermometry,** *Proc. Symp. Physics of Superconducting Devices, University of Virginia, Charlottesville, Va., Apr. 28-29, 1967,* pp. M-1 – M-5 (Office of Naval Research, Washington, D.C., 1968).

Key words: Josephson effect; linewidth; millidegree; noise; superconductivity; thermometry.

Assuming that the linewidth of the A. C. Josephson radiation is caused entirely by thermal fluctuations in the bias voltage, we show that it can be used with quite simple instrumentation to measure absolute temperatures down to one millidegree or lower.

**10377.** Klein, R., Scheer, M. D., **Mechanism of $O(^3P)$ addition to condensed films. II. Propene, 1-butene, and their mixtures,** *J. Phys. Chem.* **72,** No. 2, 616-622 (Feb. 1968).

Key words: Low temperature chemistry; olefins; oxidation; oxygen atom; propylene; 1-butene.

The kinetics of $O(^3P)$ addition to condensed films of propene and 1-butene has been investigated at 90 °K. The reaction rate was found to be independent of olefin concentration for both propene and 1-butene using propane as an inert dilutent. Films containing mixtures of propene and 1-butene yielded mostly $C_3$ products at high olefin concentration and approached a limiting value of about 1.6 for the $C_3/C_4$ product ratio at infinite dilution in propane. When $C_3D_6$ films were used, the ratio of carbonyl to epoxide was measurably less than that obtained with $C_3H_6$. The results are interpreted in terms of a model which depicts the olefin film to be a nearly perfect sink for $O(^3P)$ atoms. The primary process is assumed to be the formation of a triplet adduct which undergoes either ring closure to form the epoxide or an intramolecular migration of a hydrogen atom to produce a carbonyl compound. The latter exhibits the expected isotope effect when D is substituted for H in the olefin reactant. The behavior of propene-1-butene mixtures can be accounted for qualitatively by assuming that propene not only reacts more rapidly but diffuses more easily than does the 1-butene.

**10378.** Knight, J. M., O'Connell, J. S., Prats, F., **Two- and three-body photodisintegration cross sections of $^3$H and $^3$He,** *Phys. Rev.* **164,** No. 4, 1354-1359 (Dec. 20, 1967).

Key words: Cross sections; dipole; final state interactions; helium 3; photodisintegration; tritium.

Electric dipole photodisintegration cross sections of $^3$H, $^3$He into deuteron plus nucleon and into three nucleons are calculated using simple zero range forms for the initial and final state wave functions. Final state interaction between nucleon pairs in s-states are taken into account. Shape fits to the experimental data are obtained, but the required normalization of the ground state wave function is found to differ between two- and three-body breakup.

**10379.** Kolbenstvedt, H., **Energy transfer in the collision of electron beams,** *Phys. Rev.* **163,** No. 1, 112-114 (Nov. 5, 1967).

Key words: Average; cross-section; distribution; electrons; energy; isotropic; motion; scattering.

The cross section for electron-electron scattering differential in energy transfer, is derived for the case that both electrons are in motion in the laboratory system. The result is valid for all electron energies much higher than the Rydberg energy.

For the case in which both electrons are nonrelativistic and one of the electrons has an isotropic velocity-distribution, the cross section is averaged over the directions of motion of this electron.

**10380.** Kolbenstvedt, H., **Simple theory for K-ionization by relativistic electrons,** *J. Appl. Phys.* **38,** No. 12, 4785-4787 (Nov. 1967).

Key words: Collision; cross section; electrons; energy; ionization; photons; silver; tin.

The total cross section for ionization of K-electrons by electrons has been derived using the method of virtual photons combined with the photoelectric cross section for distant collisions and the Møller cross section for close collisions. Good agreement with experiments is obtained for the elements silver ($Z = 47$) and tin ($Z = 50$) when the electron energy is much higher than the ionization energy.

**10381.** Koonce, C. S., Cohen, M. L., Schooley, J. F., Hosler, W. R., Pfeiffer, E. R., **Superconducting transition temperatures of semiconducting $SrTiO_3$,** *Phys. Rev.* **163,** No. 2, 380-390 (Nov. 10, 1967).

Key words: Semiconductors; $SrTiO_3$; superconductivity; transition temperatures.

The superconducting transition temperature $T_c$ of $SrTiO_3$ has been measured for specimens having electron carrier concentrations $n_c$ from $6.9 \times 10^{18}$ cm$^{-3}$ to $5.5 \times 10^{20}$ cm$^{-3}$. The curve exhibits a maximum in $T_c$ for $n_c$ near $9 \times 10^{19}$ cm$^{-3}$. The transition temperature has also been calculated using one adjustable parameter $\xi$, the intervalley deformation potential, in addition to the known normal-state properties of $SrTiO_3$. A good fit to the experimental curve is obtained.

**10382.** Krause, R. E., Jr., Douglas, T. B., **The vapor pressure, vapor dimerization, and heat of sublimation of aluminum fluoride, using the entrainment method,** *J. Phys. Chem.* **72,** No. 2, 475-481 (Feb. 1968).

Key words: Aluminum fluoride; entrainment method; heat of sublimation; temperature; vapor dimerization; vapor pressure.

The vapor pressure $P$ of anhydrous aluminum fluoride was measured at eight temperatures between 1194 and 1258 °K by an entrainment method. The standard deviation of $P$ from a least-square fit was 0.15 percent, and possible systematic errors of 0.5 percent in $P$ and 1° in $T$ were estimated. Smoothed values of $P$ and $dP/dT$ at 1225 °K were determined. Considering $P$ as the sum of the ideal monomeric and twice the dimeric vapor pressure, the other two thermodynamic properties necessary to define (1) $AlF_3() \rightleftharpoons AlF_3(g)$ and (2) $2AlF_3(g) \rightleftharpoons Al_2F_6(g)$ were taken as (a) $\Delta S°(1)$, derived from published spectroscopic and crystalline heat capacity data, and (b) $2\Delta H°(1) + \Delta H°(2)$, reported in a recent mass spectrometric study. The derived results at 1225 °K along with their estimated uncertainties were $\Delta H°(1) = 67.0 \pm 0.4$ kcal, $\Delta S°(1) = 43.0 \pm 0.4$ eu, and $\Delta G°(2) = -7 \pm 1$ kcal.

0383. Kuriyama, M., **Distortion correction in anomalous absorption coefficients,** *Phys. Stat. Sol.* **24,** 743-748 (1967).

> Key words: Anomalous transmission; atomic displacement; Debye-Waller factor; distorted crystal; Laue case; photon Green's function; theory; x-ray diffraction.

Based on the theory of x-ray diffraction by a distorted crystal which has recently been completed by the present author, the emperature-and distortion-correction in anomalous absorption oefficients has been studied in the case of a single symmetrical Bragg reflection (a symmetrical Laue case).

If the distribution of atomic displacements is given, then the nomalous absorption coefficient has the distortion correction of he same form, in terms of the second moment of the distribution, s the Debye-Waller factor. If the displacement of atoms in a istorted crystal is replaced by a proper time-average value of he thermal motion of atoms, then the temperature correction in he absorption coefficient is given by the Debye-Waller factor multiplied by the structure factor.

0384. Kuriyama, M., **Theory of X-ray diffraction by a distorted crystal,** *J. Phys. Soc. Japan* **23,** No. 6, 1369-1379 (Dec. 1967).

> Key words: Atom; Bragg condition; displacement; distorted crystal; electron overlap; Green's function; lattice; photon; theory; x-ray diffraction.

Based on the quantum theory of X-ray diffraction by a perfect crystal (M. Ashkin and M. Kuriyama, *J. Phys. Soc. Japan* **21** 1966), 1549), a diffraction theory for a distorted crystal has been developed. The scattering amplitude for the case of a single Bragg reflection has been obtained in terms of a lattice sum including the displacement of each atom. A basic assumption for his formulation is that there is no overlap of the electron wave unctions of the displaced atoms. The existing basic assumption n the dynamical theory for a distorted crystal, that the local distortion in the crystal must change very slowly so that the local wave field can be described by the dynamical theory for a perfect crystal, has been successfully ruled out in the present formulaion. A criticism has also been made to the so-called "Fourier" expansion of polarizability or electron distribution in the distorted crystal, which has been important for the dynamical heory.

10385. Lafferty, W. J., **Direct *l*-type doubling transitions in some axially symmetric molecules,** *J. Mol. Spectry.* **25,** No. 8, 359-364 (Mar. 1968).

> Key words: Cyanocetylene; direct *l*-type doubling transitions; fluorocyanogen; *l*-type doubling constants; *l*-type resonance; methyl cyanide; microwave spectroscopy.

Direct *l*-type doubling transitions have been observed in the states $\nu_2{}^1$ in FCN, $\nu_7{}^1$ and $3\nu_7{}^1$ in cyanoacetylene and $\nu_8(E)$ in methyl cyanide. Precise values for q and the higher order term $\mu$ have been obtained for each of these vibrations. The effect of the *l*-type resonance between the $\pi$ and $\Phi$ levels of $3\nu_7$ of cyanoacetylene is discussed.

10386. Landgrebe, A. R., McSharry, W. O., Cefola, M., **The radiometric titration of trace amounts of zinc,** *Intern. J. Appl. Radiation Isotopes* **19,** 1, 23-26 (1968).

> Key words: Batch; column; cationic exchanger; EDTA; radiometric; titrations; zinc.

A method of radiometric titration for the determination of trace amounts of metals has been developed. The EDTA complex of the metal to be determined is formed, and the excess, uncomplexed metal ions are removed by means of a cationic exchanger. A titration curve is then constructed by plotting the activity of the liquid phase, versus the amount of EDTA added. Both the batch and column method were tried in this laboratory, and it is our opinion that the batch method is easier from a manipulative point of view. A new method of determining the end point was developed. If both the resin and solution are counted, this is a simple way of determining the half equivalent point. Methods are underway to maximize the sensitivity for zinc by chelating radiometric titration.

10387. Landgrebe, A. R., Rodriguez-Pasques, R. H., Schima, F. J., **The rapid radiochemical separation of radioactive praseodymium from radioactive cerium,** *Intern. J. Appl. Radiation Isotopes* **19,** No. 2, 147-149 (1968).

> Key words: Cerium; linac; praseodymium; precipitation; radioactive; rapid separation; solvent extraction.

A method of rapid radiochemical separation was developed to separate the cerium and praseodymium radioactivities produced after a praseodymium target was irradiated at the NBS Linac. The praseodymium metal is dissolved in nitric acid and the solution is divided into at least two portions. One fraction is used to precipitate cerium (IV) iodate, giving an aqueous phase free of cerium radioactivity. A second fraction is extracted with hydrogen di-(2 ethylhexyl) orthophosphoric acid (HDEHP). The organic phase is free from any praseodymium radioactivities.

10388. LeLevier, R. E., Branscomb, L. M., **Ion chemistry governing mesospheric electron concentrations,** *J. Geophys. Res., Space Physics* **73,** No. 1, 27-41 (Jan. 1, 1968).

> Key words: Ion chemistry; mesospheric electron concentrations; microscopic chemical reactions; negative ions.

A theory and methodology for investigating the ion chemistry governing mesospheric electron concentrations is presented. In this theory, macroscopic reaction coefficients are defined in terms of the microscopic chemical reactions that take place between positive ions, electrons, and negative ions. The role of minor constituents of the atmosphere, O, $O_3$, $CO_2$, NO, and $NO_2$, is discussed using reaction rates measured in the laboratory. One reaction, the associative detachment of $O_2^-$ by atomic oxygen, is so fast that mechanisms for inhibiting or suppressing this reaction are required. The need for such mechanisms is dictated by field data on riometer absorption induced by the nuclear explosions of the 1962 Christmas Island air drops. The importance of terminating negative ions, i.e., negative ions that withstand the attack of atomic oxygen, is emphasized. Also emphasized is the influence of the ion-ion mutual neutralization coefficient of terminating negative ions. Four illustrative models of the ion chemistry are presented ranging from the simplest $O_2^-$ model which is certainly unrealistic, to a more complex model involving six species of negative ions. This model, which is suggested by recent measurements of reaction rates in the laboratory, does not include the effect of water vapor in the reaction scheme since little laboratory data exist on the reaction of negative ions with water.

10389. Little, W. E., Ellerbruch, D. A., Engen, G. F., **An analysis of the "quarter-wave" technique of reducing the errors in UHF and microwave impedance measurement,** *IEEE Trans. Microwave Theory Tech.* **MTT-15,** No. 9, 504-507 (Sept. 1967).

> Key words: Impedance measurement; microwave; quarter wave; reflection coefficient measurement; standing wave machine; UHF.

An analysis is given of the "quarter-wave" impedance measurement technique. This technique, which finds its widest potential application in conjunction with standing wave machines, permits the approximate elimination of the error due to residual reflection or VSWR. If the other sources of error are small, the potential reduction in error is in the ratio $|t_{11}| / 2|S_{11}|$, where $S_{11}$ and $t_{11}$ are the residual reflection coefficients of the standing wave machine and quarter wavelength section respectively.

**10390.** Logan, H. L., **Some techniques used in the study of stress corrosion cracking,** *Am Soc. Testing Mater. Spec. Tech. Publ. Stress Corrosion Testing* **425,** 127-144 (1967).

Key words: Experimental techniques for stress corrosion testing; high strength steels; hydrogen embrittlement; low carbon steels; stainless steels; stress-corrosion; titanium alloys.

Techniques used at the National Bureau of Standards in the study of stress-corrosion cracking of metals are described together with precautions taken in these investigations. Especially designed specimen of low carbon and stainless steels and a titanium alloy and supplementary techniques for obtaining data as to the mechanism of the stress-corrosion process are also described. A specimen and technique recently used to determine whether hydrogen plays a part in the delayed failures of high strength steels in chloride solutions is described.

**10391.** Lovell, W. S., Anderson, M. M., Seiller, F. E., **Laser harmonics useful for frequency translation,** *Appl. Opt.* **6,** No. 8, 1430-1432 (Aug. 1967).

Key words: Accidental coincidences; frequency locking; frequency translation; laser harmonics.

Accidental coincidences betweeen laser fundamental and harmonic frequencies usable (in principle) for frequency translation are tabulated.

**10392.** Madey, T. E., Yates, J. T., Jr., **Work function studies: Chemisorption of diatomic molecules on single-crystal tungsten,** *Nuovo Cimento, Suppl. Series I,* **5,** No. 1, 483-505 (1967).

Key words: Adsorption; carbon monoxide; chemisorption; desorption; electron reflection; nitrogen; oxygen; single crystal; sticking coefficient; thermionic emission; work function.

The work function changes accompanying the chemisorption of diatomic molecules on single crystal (100) and (110) tungsten have been studied using a modification of Shelton's retarding potential method. Each crystal wafer was cut and polished to the desired orientation on both sides, suspended by fine W wires, and heated by electron bombardment. This mode of suspension and heating allowed measurements of surface coverage to be made with a minimum of error due to edge effects and desorption from support loads. The work function difference $\phi(110)-\phi(100)=0.65$ eV was found to be independent of which crystal was used as emitter. The changes in work function and electron reflection upon chemisorption, as well as measurements of surface coverage and sticking coefficients have been made, where possible, for $N_2$, $O_2$, and CO on these two crystals.

**10393.** Maki, A. G., Jr., Lide, D. R., Jr., **Microwave and infrared measurements on HCN and DCN: observations on *l*-type resonance doublets,** *J. Chem. Phys.* **47,** No. 9, 3206-3210 (Nov. 1, 1967).

Key words: Deuterium cyanide; hydrogen cyanide; infrared spectra; microwave spectra; molecular constants; molecular structure; spectra.

Microwave measurements have been made on the direct doublet splittings ($\Delta J=0$ transitions) of the $01^10$, $02^20$, $03^10$, and $03^30$ levels of DCN and the $01^10$ and $02^20$ levels of HCN. The sensitivity of the Δ and Φ level splittings to certain vibrational and rotational constants enables us to obtain new values for those constants. New infrared measurements are given for $\nu_1$, $3\nu_2{}^1$, $4\nu_2{}^0-\nu_2{}^1$ and $4\nu_2{}^2-\nu_2{}^1$ of HCN.

**10394.** Mann, R. H., Maryott, A. A., **Dipole moment of $CO(CO)_3NO$ from the nonresonant microwave absorption of the vapor,** *J. Chem. Phys.* **47,** No. 10, 4275-4276 (Nov. 15, 1967).

Key words: Cobalt tricarbonyl nitrosyl; dipole moment; gas phase; nonresonant; microwave absorption.

The electric dipole moment of cobalt tricarbonyl nitrosyl $(CO(CO_3)NO)$ in the vapor phase was determined by the method of nonresonant microwave absorption in dilute mixtures with $CO_2$ and $SF_6$. The dipole moment is found to be 0.363 D with an estimated uncertainty of about 3 percent.

**10395.** Manson, S. T., Cooper, J. W., **Photoionization in the soft x-ray range: Z dependence in a central-potential model,** *Phys. Rev.* **165,** No. 1, 126-138 (Jan. 5, 1968).

Key words: Central potential model; photoabsorption cross section; photoionization cross section; soft x-rays.

Using one electron model with a realistic central potential, photoionization calculations have been performed which emphasize the soft x-ray spectral range (~ 100 eV to ~ 2 keV). The $M_{II,III}$(3p) subshell was studied in Ar, Cu and Ge, as well as the $M_{IV,V}$(3d) and $M_{II,III}$ in Kr, Rh, Xe, Eu, Au and Fm in an effort to explain the combined Z and energy dependence of the photoionization cross sections for these subshells. In addition, calculations have been performed for 3s, 4s, 5s, 4p, 5p, 4d, 5d and 4f subshells in certain elements. The results, which are considerably different from the predictions of the hydrogen-like model, show certain regularities which are explained in terms of the potentials. Comparisons with experiment show that the model correctly predicts the gross spectral shape of photoionization cross sections but the results are somewhat numerically inaccurate in the vicinity of large absorption peaks. This calculation is considered to be a first approximation which can be improved by taking exchange into account more exactly and by including electron-electron correlation.

**10396.** Marantz, S., Armstrong, G. T., **Heats of combustion of *trans*-stilbene and *trans*-2,2.,4,4′,6,6′-hexanitrostilbene (HNS),** *J. Chem. Eng. Data* **13,** No. 1, 118-121 (Jan. 1968).

Key words: Bond energy, (C=C) bond; hexanitrostilbene, heat of combustion; stilbene, heat of combustion.

The standard heats of combustion, $\Delta H^\circ_{c298}$, of *trans*-stilbene(c) and *trans*-2,2′,4,4′,6,6′-hexanitrostilbene(c) were measured in an oxygen bomb calorimeter and were $-1759.28$ and $-1535.54$ kcal. mole$^{-1}$, respectively. Estimated uncertainties of these results, respectively, were 0.93 and 1.08 kcal. moles$^{-1}$ including contribution of errors from both random and systematic sources. With these results, the standard heats of formation, $\Delta H^\circ_{f298}$, of *trans*-stilbene(c) and *trans*-2,2′,4,4′,6,6′-hexanitrostilbene(c) were $-32.68$ and $-13.89$ kcal. mole$^{-1}$, respectively. The standard heats of formation of the gas phases were $-12.0$ and $+29.2$ kcal. mole$^{-1}$, respectively. In the light of these results, and analogous data for toluene(g) and trinitrotoluene(g), the addition of six nitro groups to *trans*-stilbene may be interpreted as weakening the central C=C bond by 34.1 kcal. mole$^{-1}$.

**10397.** Margoshes, M., **What's in that microgram? You can be sure . . . to 10 ppm,** *Sci. Res.* **3,** No. 5, 40-42 (Mar. 4, 1968).

Key words: Electron microprobe; emission spectrometry laser; mass spectrometry; microanalysis; spark; x-ray spectrometry.

Spectrometric methods of microanalysis are briefly reviewed and compared. The techniques considered include emission spectrometry with the laser probe and microspark, mass spectrometry with laser, spark, and sputtering vaporization; and x-ray spectrometry with the milliprobe and electron microprobe.

**10398.** Marshak, H., Langsford, A., Wong, C. Y., Tamura, T., **Total neutron cross section of oriented $^{165}$Ho from 2 to 135 MeV,** *Phys. Rev. Letters* **20,** No. 11, 554-558 (Mar. 11, 1968).

Key words: Black nucleus; coupled-channel calculations; nuclear deformation effect; nuclear orientation; nuclear Ramsauer effect; $^{165}$Ho nucleus; optical model; total neutron cross section.

The effect of nuclear orientation on the total neutron cross section of the highly deformed $^{165}$Ho nucleus has been measured from 2 to 135 MeV. The data are successfully fitted by adiabatic coupled-channel calculations. The origin of this effect can also be understood by a semi-empirical model which makes use of both the black-nucleus model and the nuclear Ramsauer effect.

**10399.** Marzetta, L. A., **Incorrect usage of exact closed-loop voltage gain formula in operational amplifiers,** *Analog Dialogue Letter* **2,** No. 1, 6 (Mar. 1968).

Key words: Closed-loop gain; operational amplifiers; voltage gain.

Much of the literature currently available on operational amplifiers has been found to contain an incorrectly applied gain formula. The publications in question offer an expression for calculating exact closed-loop voltage gain in amplifiers. In their neglect of the phasor nature of one of the factors, the formula can lead to serious errors when applied to operational type amplifiers.

**10400.** Maximon, L. C., Tzara, C., **Influence of the radiative background on muon and electron scattering from nuclei,** *Physics Letters* **26B,** No. 4, 201-203 (Jan. 22, 1968).

Key words: Electron scattering; inelastic scattering; muon scattering; radiative corrections; radiative tail.

The influence of radiative tails and radiative corrections to inelastic scattering on nuclei at low excitation is compared for muons and electrons. It is found that only for low momentum transfers $Q \leq 50$ MeV/c is the radiative background substantially less for muons than for electrons.

**10401.** May, L., Snediker, D. K., **Criteria for selection of absorber mounting materials in Mössbauer spectroscopy,** *Nucl. Instr. Methods* **55,** 183-188 (1967).

Key words: Absorber mounting devices; absorption coefficients; gamma-rays and x-rays; half-thickness; Mössbauer spectroscopy; 14.4 keV.

The criteria for the selection of materials for mounting absorbers include their mechanical and chemical properties and their attenuation of the $\gamma$-rays and x-rays emitted from the Mössbauer source. Attenuation of the 14.4-keV $\gamma$-ray and 6.3-keV x-ray associated with $^{57}$Fe was measured for nine commercial materials including plastics and metals. The linear absorption coefficients and half-thicknesses for each material were measured. The usefulness and limitations of each material are discussed, along with three different absorber mounting techniques.

**10402.** May, L., Spijkerman, J. J., **Mössbauer spectroscopy,** *Chemistry* **40,** 14-17 (Dec. 1967).

Key words: Chemistry; Mössbauer spectroscopy.

A review of Mössbauer spectroscopy is presented for the high school senior and college freshman chemistry students. The fundamental concepts of nuclear resonance fluorescence are described in particular for its application to chemistry. Specific examples are given of how Mössbauer spectroscopy solved analytical and structural problems. A list of selected references are included for further study by the readers.

**10403.** Mielenz, K. D., Nefflen, K. F., Rowley, W. R. C., Wilson, D. C., Engelhard, E., **Reproducibility of helium-neon laser wavelengths at 633 nm,** *Appl. Opt.* **7,** No. 2, 289-293 (Feb. 1968).

Key words: Frequency-stabilized; helium-neon; krypton 86 lamp; Lamb dip; laser; wavelength.

Measurements on helium-neon lasers stabilized on the Lamb dip, performed at NBS, NPL, and PTB, have shown that the wavelengths of such lasers are reproducible within approximately 1 part in $10^7$.

Beyond this limit, different lasers were found to emit different wavelengths. In addition, the wavelength of a given laser may vary during the life of its discharge tube. Pressure shifts appear to be a major cause of such variations.

**10404.** Milligan, D. E., Jacox, M. E., **Infrared and ultraviolet spectroscopic study of the products of the vacuum-ultraviolet photolysis of methane in Ar and $N_2$ matrices. The infrared spectrum of the free radical $CH_3$,** *J. Chem. Phys.* **47,** No. 12, 5146-5156 (Dec. 15, 1967).

Key words: Free radical; infrared; matrix isolation; methyl; methylene; photolysis; rotation; spectrum; ultraviolet; vacuum ultraviolet.

The vacuum ultraviolet photolysis of methane in an argon or a nitrogen matrix at 14 °K leads to the formation of a sufficient concentration of the methyl radical for observation both of its 1500 Å electronic transitions and of its out-of-plane deformation fundamental, which appears at 611 cm$^{-1}$ for $CH_3$ trapped in a nitrogen matrix. The value observed for this fundamental of $CD_3$ is in reasonable agreement with the value previously derived from analysis of the 2160 Å band system. Isotopic substitution studies support the assignment of the 611 cm$^{-1}$ feature to $\nu_2$ of $CH_3$. Data are consistent with the previous report of a planar structure. Evidence is presented suggesting that $CH_3$ may rotate in an argon matrix. Although $CH_2$ has not been directly observed, an appreciable concentration of $CH_2N_2$ appears in the $N_2$ matrix experiments. Three electronic transitions of CH are observed in the argon matrix experiments, and there is evidence for the production of a small concentration of C atoms.

**10405.** Milligan, D. E., Jacox, M. E., **Matrix-isolation study of the infrared and ultraviolet spectra of the free radical NCO,** *J. Chem. Phys.* **47,** No. 12, 5157-5168 (Dec. 15, 1967).

Key words: C atom reaction; CN reaction; $HN_3$ photolysis; infrared spectrum; matrix isolation; NCO free radical; NO reaction; $O^3$ atom reaction; ultraviolet spectrum; vacuum ultraviolet photolysis.

The free radical NCO is stabilized in sufficient concentration for direct infrared and ultraviolet spectroscopic identification upon vacuum ultraviolet photolysis of HNCO suspended in various matrix materials at 4° and 14 °K. Observations on the $B(^2\Pi)-X(^2\Pi)$ electronic transition of NCO have been extended to shorter wavelengths than those previously reported. Isotopically substituted NCO has been prepared in supplementary experiments involving the vacuum ultraviolet photolysis of $CO{:}HN_3$ and $Ar{:}HCN{:}N_2O$ samples, as well as by the mercury arc photolysis of matrix-isolated samples of $NO + N_3CN$. The three vibrational fundamentals of ground-state NCO appear at 487, 1275, 1922 cm$^{-1}$ in an Ar matrix. The values obtained for the stretching force constants suggest that the carbon-oxygen bond may be somewhat stronger than the carbon-nitrogen bond. There is an appreciable positive stretching-interaction force constant. NCO is found to photolyze when subjected to radiation of wavelength near 2537 Å, leading to the production of N + CO. Reactions occurring in the various systems investigated are discussed.

**10406.** Moore-Sitterly, C. E., **Annual report on spectroscopy,** *Astron. J.* **72,** No. 9, 1117-1118 (Nov. 1967).

Key words: Atomic spectra; lanthanon spectra; molecular spectra; rare earth spectra; transition probabilities; ultraviolet spectra.

Astrophysicists are keenly interested in the spectroscopic programs at this Bureau. The present type of report is furnished annually to the Astronomical Journal to be published with the Observatory Reports. It provides a brief summary of our progress in fields of astrophysical interest.

**10407.** Moore-Sitterly, C. E., **Necrology: Carl C. Kiess,** *J. Opt. Soc. Am.* **58,** No. 2, 292-293 (Feb. 1968).

Key words: Kiess, Carl C.; obituary.

**10408.** Myers, V. W., **Inelastic scattering of cold neutrons in polycrystalline gray tin,** *J. Phys. Chem. Solids* **28,** 2207-2210 (Feb. 1967).

Key words: Cold neutron scattering; force constants; gray tin; phonon energies.

The inelastic scattering of cold neutrons by polycrystalline gray tin (diamond structure) at 0 °C has been investigated using the Brookhaven cold neutron facility. It is possible to obtain information on the phonon critical points. There is a narrow peak centered at about 7 meV phonon energy which is attributed to the transverse acoustic modes. A broad band centered around 23 meV is probably due to a combination of the longitudinal optic and acoustic modes. The results are consistent with single crystal dispersion measurements in Si and Ge when the frequencies are scaled inversely as the square root of the mass. This indicates that the force constants in Si, Ge, and Sn are of the same strength.

**10409.** O'Connell, J. S., Prats, F., **Photodisintegration of the trinucleon system in a separable potential model,** *Physics Letters* **26B,** No. 4, 197-200 (Jan. 22, 1968).

Key words: Cross sections; electric dipole; helium-3; photodisintegration; separable potential; tritium.

Two- and three-body photodisintegration cross sections of $^3$H and $^3$He are calculated. The ground state wave function used is an exact solution of the three-body Schrödinger equation with separable potentials of the Yamaguchi type. The final states contain the interactions between nucleon pairs. Results are shown both for the Yamaguchi-Sitenko-Kharchenko set and for the Tabakin set of interaction parameters.

**10410.** Ohashi, M., Stanford, J. W., Paffenbarger, G. C., **Pertinent data on some physical properties of different investments used in the casting of gold alloys,** *J. Nihon Univ. Sch. Dent.* **9,** No. 3, 121-126 (Sept. 1967).

Key words: Alloy castings; gold alloys; hygroscopic inlay; thermal inlay; thermal partial denture.

Fineness, time of setting, compressive strength, linear thermal expansion, normal setting expansion, and surface defects of alloy castings were determined using casting investments of three types thermal inlay, hygroscopic inlay, and thermal partial denture. The use of the normal setting expansion combined with either the hygroscopic or thermal expansion to compensate for the shrinkage of casting gold alloys is discussed.

**10411.** Okabe, H., Lenzi, M., **Photodissociation of $NH_3$ in the vacuum ultraviolet,** *J. Chem. Phys.* **47,** No. 12, 5241-5246 (Dec. 15, 1967).

Key words: Adsorption; excited NH; excited $NH_2$; fluorescence; $NH_3$; photodissociation; vacuum ultraviolet.

Two photodissociation processes of $NH_3$ producing electronically excited radicals have been studied in the vacuum ultraviolet. $NH_3 \rightarrow NH_2 A^2A_1 + H$ (1) – $NH_3 \rightarrow NH\ c^1\Pi + H_2$ (2). The intensity of the fluorescence from these radicals, lying in the spectral regions 4000 Å to 6000 Å and at 3240 Å respectively, has been measured as a function of wavelength of incident light with a resolution of 7 Å. The fluorescence curves thus obtained were compared with the absorption spectrum of $NH_3$. It is shown that the process (1) may be correlated with the $^1E''$ (1665 Å bands), $^1A_2''$ (1434 Å bands), $^1A_2''$ (1330 Å bands), 1286 Å bands and the continuum (1250 to 1600 Å). On the other hand, the process (2) may be associated with the continua (1250 Å to 1600 Å and below 1250 Å). The threshold wavelength of process (2) is $1325 \pm 7$ Å. The electronic energy 'a' of the first singlet state NH $a^1\Delta$ with respect to the ground triplet state $X^3 =^-$ is $a \leqslant 1.6 + 0.1$ eV which is obtained from the threshold wavelength together with the heat of reaction ($3.9 \pm 0.1$ eV) $NH_2 \rightarrow NH\ X^3\Sigma^- + H_2$ and the electronic energy of the NH $c^1$ II (3.813 eV) with respect to the $a^1\Delta$. Various other primary processes are discussed in conjunction with the absorption spectrum. For incident light of wavelength below 1200 Å the ionization process $NH_3 \rightarrow NH_3^+ + e$ (3) and the process (2) both of which may arise from the continuum become predominant. Dissociation processes appear to be dictated by the spin conservation rule.

**10412.** Pella, P. A., Landgrebe, A. R., DeVoe, J. R., Purdy, W. C., **Differential controlled-potential coulometry utilizing substoichiometric radioisotope dilution,** *Anal. Chem.* **39,** 1781-1785 (Dec. 1967).

Key words: Cadmium; coulometry; electrolysis; radioactive tracers; radioisotope dilution; substoichiometric; trace analysis; zinc spelter.

A controlled-potential coulometric procedure is described which permits the utilization of the principle of substoichiometric radioisotope dilution. This technique employs two identical cells connected in series. Under prescribed conditions, the same amount of the element to be analyzed is deposited in each cell. The procedure involves the addition of a known amount of the element to the control cell, which is held at a constant potential, and an unknown amount to the sample cell. An equal, known amount of a radioisotope of that element is then added to each cell. The difference in the amount is determined by measuring the radioactivity remaining in each of the cells after a finite electrolysis time. This method was applied to the determination of cadmium in an NBS Standard Reference Material, zinc spelter, with a result of 0.0928 percent with a standard deviation of the mean of 0.0005 percent.

**10413.** Pfeiffer, E. R., Schooley, J. F., **Effect of stress on the superconductive transition temperature of strontium titanate,** *Phys. Rev. Letters* **19,** No. 14, 783-785 (Oct. 2, 1967).

Key words: Anisotropic uniaxial stress effect; hydrostatic pressure; reduced strontium titanate; single crystal; stresses; superconductive transition temperatures; uniaxial stresses.

The superconductive transition temperatures $T_c$ of single crystal specimens of reduced strontium titanate have been measured as functions of hydrostatic and uniaxial compressional stresses up to 1.5 kbar. The prominent features of the experimental results are a large non-linear hydrostatic pressure effect and an anisotropic uniaxial stress effect. The relative decrease of transition temperature with pressure $d \ln T_c / d\,p$ is about an order of magnitude larger than that seen in metallic superconductors.

**10414.** Pierce, E. T., Price, O. W., Edelman, S. E., Jones, E., **Accelerometer resonances affect vibration measurement,** *J. Environ. Sci.* **10,** No. 6, 17-21 (Dec. 1967).

Key words: Accelerometer; calibration; pickup; resonance; vibration.

Errors in vibration measurement can be caused by unintended lative motion in the pickup. Near the resonant frequency of ich relative motion, the pickup can affect the motion of surface which it is attached. The paper gives details of two cases of sonances of this kind; resonances which are unexpected on e basis of the usual mass-spring theory.

**415.** Post, M. A., **Qualitative and quantitative determination of emulsion-polymerised binders in latex paints,** *J. Appl. Chem.* **17,** 315-320 (Nov. 1967).

Key words: Acrylic; identification; infrared spectroscopy; latex paints; polyvinyl acetate; separation; styrene-butadiene; vinyl-acrylic.

Methods for the separation and identification by infrared abrption spectroscopy of styrene-butadiene, acrylic, vinyl-acryl- and polyvinyl acetate homopolymer and dibutyl maleate polymer in emulsion paints based on these materials are esented. Detailed procedures for their quantitative determinaon are discussed.

**416.** Preston, G. T., Chapman, T. W., Prausnitz, J. M., **Transport properties of cryogenic liquids and their mixtures,** *Cryogenics* **7,** No. 5, 274-279 (Oct. 1967).

Key words: Corresponding-states principle correlation; cryogenic liquids and liquid mixtures; mutual-diffusivity; self-diffusivity; thermal conductivity.

Based on the corresponding-states principle, a correlation is esented for the viscosities, thermal conductivities and self-difsivities of nine cryogenic liquids from the triple-point temperaıres to temperatures close to the critical. Experimental data are duced with two molecular parameters for each liquid: a characristic energy and a characteristic size. The correlations are usel for predicting transport properties of pure liquids at temperaıres where experimental data are not available; in addition, sing reasonable mixing rules, the correlations may be used to stimate transport properties of liquid mixtures.

**0417.** Prince, E., Rush, J. J., **Many disciplines unite to study solid structure and dynamics,** *Phys. Today* **21,** No. 2, 95-99 (Feb. 1968).

Key words: Crystal dynamics; crystallography; crystal structure; inorganic; molecular solid; organic; polymers; rotation; spectroscopy.

A review is presented of the Second Materials Research Symosium, "Molecular Dynamics and Structure of Solids," sponored by the NBS Institute for Materials Research and held at BS on October 16-19, 1967.

**0418.** Pytte, E., Bennett, H. S., **Ultrasonic attenuation in the Heisenberg paramagnet. II. Antiferromagnets,** *Phys. Rev.* **164,** No. 2, 712-715 (Dec. 10, 1967).

Key words: Antiferromagnetic insulators; correlation function; ferromagnetic insulators; Heisenberg; Néel point; ultrasonic attenuation.

The propagation of sound waves in antiferromagnetic insulars is studied within the framework of two models which escribe the interaction between the spin system and the lattice. n particular, expressions for the ultrasonic attenuation coefficient near the Néel point are obtained in terms of time dependent orrelation functions. The attenuation coefficient is found to be roportional to the square of the phonon frequency, to increase apidly in the vicinity of the Néel point, and to be less singular an the attenuation coefficient for ferromagnetic insulators.

**10419.** Rasberry, S. D., Caul, H. J., Yezer, A., **X-ray fluorescence analysis of silver dental alloys with correction for a line interference,** *Spectrochim. Acta* **23B,** 345-351 (Mar. 1968).

Key words: Analysis; line interference correction; silver dental alloys; specimen preparation; spectrometry; x-ray fluorescence.

An x-ray fluorescence spectrometric method has been developed for the rapid analysis of granular silver dental amalgam alloys having the nominal composition, in percent, of silver 69, tin 26, copper 4, and zinc 1. Several methods of specimen preparation were investigated; a method employing briquettes pressed at 1400 kg/cm² without binder was the most satisfactory. Analytical curves relating intensitites of $K_\alpha$ lines to concentration of silver, copper, and zinc were linear but no calibration curve could be obtained for the tin $K_\alpha$ line due to line interference from the silver $K_\beta$ emission. To correct for this interference, the ratio of intensities (Sn $K_\alpha$ + Ag $K_\beta$)/Ag $K_\alpha$ was plotted versus the ratio of concentrations Sn/Ag, producing a linear analytical curve. Observed typical coefficients of variation for the method were Ag 0.4 percent, Sn 0.8 percent, Cu 3 percent, and Zn 0.6 percent.

**10420.** Risley, A. S., **Parallel pump susceptibility of YIG under cw drive conditions,** *Physics Letters* **25A,** No. 6, 471-472 (Sept. 25, 1967).

Key words: Parallel pump susceptibility; sample heating; saturation.

The parallel pump susceptibility $\chi''$, has been measured versus the level and time duration of applied rf power. Unlike previously reported data taken by the pulse technique, $\chi''$ increases at the higher drive levels.

**10421.** Rodriguez-Pasques, R. H., Mullen, P. A., George, G. A., Harding, J. E., **Transmission through aluminum of beta-particles emitted by infinitely-thick sources,** *Intern. J. Appl. Radiation Isotopes* **18,** No. 12, 835-847 (1967).

Key words: Beta absorption; beta-particle energy; beta-particle transmission; half-thickness; infinitely-thick sources; low-level; synthetic beta sources; transmission curves.

The problem of determining the energy of beta particles emitted from sources containing low concentrations of radioactive substances is examined. Transmission curves of beta particles emitted by "infinitely-thick" disc-shaped sources were obtained with two different detectors and compared to the curves similarly obtained for beta particles coming from very thin "weightless" deposits on similar solid discs. Different matrix materials and beta-particle energies were used. The curves were studied for shape, secondary radiations and half-thickness. A series of curves were also obtained from four different potassium-salt thick sources, in order to investigate possible influences from variations of effective atomic number.

No substantial difference was found between the curves corresponding to the three types of sources, in connection with half-thickness-maximum-energy relationship.

Guiding rules are proposed for the determination of maximum beta-ray energies by means of absorption studies and half-thickness determination.

**10422.** Ronn, A. M., Lide, D. R., Jr., **Infrared-microwave double resonance using a $CO_2$ laser,** *J. Chem. Phys.* **47,** No. 9, 3669-3670 (Nov. 1, 1967).

Key words: Double resonance; infrared; laser; methyl bromide; microwave; pumping; saturation.

A double resonance experiment is described in which a vibrational transition is pumped with a carbon dioxide laser and the effect of the pumping is detected through a rotational transition in the microwave region. Positive results have been found with methyl bromide. The interpretation of the results are discussed.

**10423.** Ruegg, F. C., **Multiplex for dual-spectrum Mössbauer spectrometry,** (Proc. Second Symp. on Low Energy X- and Gamma Sources and Applications, University of Texas, Austin Texas, Mar. 27-29, 1967), *Oak Ridge National Laboratory-IIC*-**10,** pp. 157-175 (1967).

Key words: Dual spectra; Mössbauer; multiplex; spectroscopy.

It is often desirable to have the capability of accumulating two Mössbauer spectra simultaneously with both spectra having exactly the same Doppler velocity dependence. This is possible with a multiplexing system which allows accumulation of two spectra simultaneously and storing of each spectrum in a 200 channel subgroup of a multichannel analyzer. The memory of the analyzer which is operated in the time mode is used on a demand basis by the two detector systems, and the counts are routed to the proper subgroup in complimentary channel locations, i.e., the channel location in the second subgroup is the channel number in the first subgroup plus 200. The logic, circuitry and performance are described.

**10424.** Rush, J. J., **Neutron-scattering study of hindered rotations in methylbenzenes,** *J. Chem. Phys.* **47,** No. 10, 3936-3941 (Nov. 15, 1967).

Key words: Barrier to rotation; cosine potential; frequency spectra; hindered rotation; internal rotation; methylbenzenes; methyl groups; neutron scattering; torsional modes.

The low-frequency modes of a number of methylbenzenes in their solid and liquid phases have been investigated by the energy-gain scattering of cold neutrons. The compounds studied include benzene, o-xylene (1,2), hemimellitene (1,2,3), mesitylene (1,3,5), durene (1,2,4;5), prehnitene (1,2,3,4), and hexamethylbenzene. The neutron spectra for molecules with adjacent methyl groups (e.g. o-xylene) exhibit bands peaked near 170 $cm^{-1}$, which are assigned primarily to the $1 \rightarrow 0$ transitions of the torsional oscillations of the methyl groups. The hemimellitene and prehnitene spectra appear to show a second broad maximum in the region of 100 $cm^{-1}$, which is attributed to torsional modes due to methyl groups centered between two adjacent groups. Previous results on hexamethylbenzene show torsional bands peaked at 120 and 137 $cm^{-1}$, respectively, above and below the λ-transition near 115 °K. The mesitylene spectra indicate less hindrance to rotation of the methyl groups in this compound, with torsional frequencies less than 100 $cm^{-1}$. In addition, the results for all the compounds in their solid phases show broad bands below 90 $cm^{-1}$, which are assigned to whole-molecule librations and translations.

If simple threefold cosine potentials are assumed for all the methyl groups, "average" barriers to rotation 2 and $\sim$ 0.7 kcal/mol are calculated from the average torsional peak frequencies of 170 and $\sim$ 95 $cm^{-1}$, respectively. A comparison of these results indicates that methyl groups surrounded by two adjacent groups on the benzene ring experience a considerably different potential (and possibly a significantly lower barrier) than that experienced by methyl groups with one neighboring group. The neutron results are compared in detail with nmr and thermodynamic data.

**10425.** Rush, J. J., **Neutron-scattering study of low-frequency modes in urea and ferroelectric thiourea,** *J. Chem. Phys.* **47,** No. 10, 4278-4279 (Nov. 15, 1967).

Key words: Ferroelectric; libration; molecular vibrations; neutron spectra; phase transitions; potential barrier; rotation; thiourea; urea.

The low frequency modes in crystalline urea and three phases of thiourea have been investigated by the inelastic scattering of cold neutrons. The neutron spectra for thiourea in phases I, III and V exhibit bands peaked around 490, 110 and 46 $cm^{-1}$ which are attributed, respectively, to $NH_2$ librations and whole-molecule librational and translational modes. The fact that there is little change in these spectra in passing from phases I to V suggests little correlation between molecular motions and the ferroelectric transitions in this compound. The spectrum for urea at 295 °K shows bands peaked around 550, 168, 138 and 74 $cm^{-1}$, whose assignments are similar to those for thiourea. A comparison of the results for the two compounds suggests that hydrogen bonds in thiourea, if they exist, are much weaker than in urea and have little effect on the transition mechanisms.

Assuming twofold cosine potentials for the $NH_2$ groups, rotational barriers of 22 and 17.5 kcal/mol are calculated from the librational peaks in urea and thiourea.

**10426.** Scala, A. A., Ausloos, P., **Condensed-phase photolysis and radiolysis of 2-methylbutane,** *J. Chem. Phys.* **47,** No. 12, 5129-5139 (Dec. 15, 1967).

Key words: Condensed phase radiolysis; ionization; photolysis; 2-methylbutane.

The condensed phase photolysis of $i\text{-}C_5H_{12}-i\text{-}C_5D_{12}$ mixtures, and of $CH_3CD(CH_3)CH_2CH_3$ has been investigated at photon energies above and below the ionization energy of 2-methylbutane (10.32 eV), that is, at 1470 Å (8.4 eV), 1236 Å (10.0 eV) and 1048-67 Å (11.6-11.8 eV). The electronically excited 2-methylbutane molecule undergoes essentially the same decomposition processes in the condensed phase as in the gas phase. The internally excited fragments formed in primary processes are entirely deactivated. In the krypton and argon sensitized radiolysis at 77° and 20 °K, respectively, energy transfer from the rare gas matrix to 2-methylbutane occurs with high efficiency. In these experiments, all products can be accounted for by decomposition of neutral excited 2-methylbutane, formed by excitation transfer and/or neutralization of ions formed in charge transfer reactions with rare gas ions.

In the radiolysis of pure 2-methylbutane in the presence of oxygen at 77 °K or at 195 °K, ethane and propane are almost entirely formed through molecular elimination and geminate radical disproportionation processes. Addition of an electron scavenger such as $CCl_4$ lowers the yields of these products, as well as those of the corresponding olefins (e.g. $C_8H_6$ and $C_2H_4$ indicating that in the pure alkane, these products are mainly formed as a result of neutralization of the parent ion. Apparently fragmentation of the parent ion is unimportant. The product butane ($G \sim 0.1$) can however, with some degree of certainty be related to the reaction of the fragment $C_4H_8^+$ ion. The modes of formation of other products, such as the pentenes and the hydrogen remain unexplained.

**10427.** Schima, F. J., Hutchinson, J. M. R., **Energy of the isomeric transition in $^{109}$Ag,** *Nucl. Phys.* **A102,** 667-672 (1967).

Key words: Measured $E_\gamma$; radioactivity; $^{109}$Cd.

The energy of the isomeric transition in $^{109}$Ag, from the decay of $^{109}$Cd, has been measured by intercomparison with x rays of well-known energies. Using a Ge(Li) detector with 1.45 keV resolution, the gamma-ray energy was found to be 88.041 keV with an uncertainty believed to be less than .087 keV.

**10428.** Schneider, W. E., Stair, R., Jackson, J. K., **Spectral irradiances as determined through the use of prism and filter spectroradiometric techniques,** *Appl. Opt.* **6,** No. 9, 1479-148 (Sept. 1967).

Key words: Filter-spectroradiometer; measurement techniques; prism-spectroradiometer; radiometry; sources spectral irradiance.

Two spectroradiometers, one based on a conventional prism onochromator and the other on a system employing narrow and-pass interference filters, have been set up and indepenently used in the determination of the spectral irradiances of a umber of sources over the wavelength range 0.25 $\mu$m to 2.5 $\mu$m. asically, the method of calibration for each system consists of omparing the spectral irradiance of the source under investigaon to that of an NBS standard of spectral irradiance. The esults obtained with each system on a number of "continuous" ources agree to about one percent whereas the differences in the pectral irradiances obtained with the two set-ups on a number of ne sources range up to several percent.

429. Schofer, R. E., Levin, B. M., **The urban transportation planning process,** *Socio-Econ. Plan. Sci.* **1,** 185-197 (Pergamon Press Ltd., London, England, 1967).

Key words: Modal choice; systems analysis; transportation planning; travel forecasting; urban transportation.

The goal of urban transportation planning is to develop a plan r efficient, balanced transportation system for an urban ea—one which will promote a desirable pattern of human acvities. While the process has been standardized to some extent, ach study must nevertheless acquire and manage a massive nount of information about the specific region with which it is oncerned. This information, together with computer representaons of transportation networks and travel patterns, is used to roduce estimates of future travel demand and utilization of acilities. Thus computers play an important role in providing ansportation planners with the capability for evaluating a ariety of proposed transportation systems in order to recomnend allocation of government resources and to guide transporation policy. This paper describes specific computer applicaons to the process of urban transportation planning.

0430. Shirley, J. H., **Effect of a sinusoidal excitation amplitude on the performance of an atomic-beam spectrometer,** *Phys. Rev.* **160,,** No. 1, 95-99 (Aug. 5, 1967).

Key words: Atomic beam; frequency shift; Rabi spectrometer; Schrödinger equation; transition probability; velocity average.

A theoretical analysis has been made of the transition probailities for a Rabi-type atomic beam spectrometer in which the xciting field amplitude seen by the atoms has a sinusoidal rather an a rectangular envelope. The time-dependent Schrödinger quation was integrated numerically and a velocity average of e transition probabilities performed. The results indicate that e line width increases as the fourth root of the excitation power nd that frequency shifts due to coupling of the exciting field ith other atomic states can be reduced by an order of magitude.

0431. Simpson, J. A., **Electron guns,** Chapter in *Methods of Experimental Physics,* Sources of Atomic Particles, **Volume 4,** Atomic and Electron Physics, pp. 84-95 (Academic Press Inc., New York, N.Y., 1967).

Key words: Atomic source; electron gun; electron physics.

The physical limitations on electron beams are discussed. esign procedures for electron guns of optimum performance re given and illustrated by examples from the literature.

0432. Simpson, J. A., **Special sources of monoenergetic electrons,** Chapter in *Methods of Experimental Physics,* Sources of Atomic Particles, **Volume 4,** Atomic and Electron Physics, pp. 124-135 (Academic Press Inc., New York, N.Y., 1967).

Key words: Atomic source; electron source; monoenergetic electron.

10433. Smith, J. C., Fenstermaker, C. A., **Strain-wave propagation in strips of natural rubber subjected to high-velocity transverse impact,** *J. Appl. Phys.* **38,** No. 11, 4218-4224 (Oct. 1967).

Key words: High-speed photography; impact testing; natural rubber; strain waves; viscoelasticity.

If a flexible filament, marked at intervals along its length is struck transversely by a flying projectile, high speed photography reveals a shifting of the marks caused by passage of a strain wave, and analysis of these shifts provides data on the strain and average strain velocity in the wave. Tests were performed on strips of lightly vulcanized natural rubber at transverse impact velocities up to 65 m/s, and the resulting strain-velocity distributions analyzed for viscoelastic effects. The analysis showed that although creep effects were small in the observation time interval of 1 msec to 8 msec after impact, significant creep must have occurred at the point of impact within the first millisecond, and additional significant creep occurs at times greater than 8 msec. The strain wave front velocity calculated from the quasi-static stress-strain curve was 35.2 m/s, but a value of approximately 60 m/s was observed in the tests. The strain at the wave front, however, tended to attenuate as the wave propagated causing a progressive decrease in the observed value of the strain wave front velocity.

10434. Sparks, L. L., Powell, R. L., **Metals characterization by low-temperature thermoelectric methods,** *Meas. Data* **1,** No. 5, 89-96 (Sept.-Oct. 1967).

Key words: Cryogenic tests; impurity characterization; metals; thermoelectric.

The thermoelectric properties of wire specimens provide a means of determining the effective electronic purity or homogeneity of metals and alloys. This characterization method is described in detail and examples are given of tests on commercial copper and high-purity platinum. The method involves use of a cryogenic liquid, usually liquid nitrogen or helium.

10435. Spijkerman, J. J., **Application of Mössbauer spectroscopy to structure analysis,** (Proc. Second Symp. on Low Energy X- and Gamma Sources and Applications, University of Texas, Austin, Texas, Mar. 27-29, 1967), *Oak Ridge National Laboratory-IIC*-**10,** pp. 85-100 (1967).

Key words: Chemical shift; magnetic hyperfine splitting; Mössbauer spectroscopy; Mössbauer spectrum parameters; quadrupole splitting; structural analysis.

A unique characteristic of the Mössbauer effect is its wide applicability to many scientific disciplines such as physics, chemistry, molecular biology and metallurgy. As a result of this versatility, Mössbauer spectroscopy becomes a very useful tool for structural analysis.

Furthermore it complements many of the physico-chemical methods available by obtaining microscopic information, where macroscopic measurements have been made before.

The Mössbauer spectrum parameters of chemical shift, quadrupole splitting, magnetic hyperfine splitting, and their temperature dependence uniquely characterize the material. The interpretation of these parameters in terms of structural analyses and their relation to other spectroscopic techniques is discussed. A specific example is the determination of austenite and martensite in steel, with particular emphasis on the dynamic equilibrium exhibited by these carbon impurity states.

10436. Spijkerman, J. J., **The Mössbauer chemical shift in tin chemistry,** *Advan. Chem. Ser.* **68,** 105-112 (1968).

Key words: Chemical shift; Mössbauer spectroscopy; tin chemistry.

The Mössbauer spectra of a large number of organic and inorganic tin compounds have been published. From these spectra, the oxidation state of tin in most compounds can be determined.

To interpret the Mössbauer spectra properly, the relationship between the chemical shift and the electron density at the Sn nucleus must be established. This requires that the magnitude and sign of $\Delta R/R$ (a factor that relates the change in the effective charge radius of the tin nucleus on passing from the excited to the ground state) must be known; in most instances, this factor can be determined from nuclear shell model calculation, but, for tin, it must be evaluated experimentally. The discussion includes the results of the various experiments that were designed to obtain this factor so that the chemical shift observed for tin compounds could be interpreted correctly.

**10437.** Stern, K. H., **Glass-membrane potentials in mixed anion melts,** *J. Electrochem. Soc. Tech. Note* **114,** No. 12, 1257-1258 (Dec. 1967).

> Key words: Galvanic cells; membrane potentials; molten salts.

The emf of the four-ion concentration cell with membrane

$$Ag|Ag^+, Na^+, Cl^-, Br^-|glass|Ag^+, Na^+, Cl^-, Br^-|Ag$$

is derived for the case $X_{Na+} \ll X_{Ag+}$ by assuming that the cationic chemical potentials are additive functions in the mole fractions of the thermodynamic components, e.g., $\mu_{Ag+} = X_{AgCl}\ \mu_{AgCl} + X_{AgBr}\ \mu_{AgBr}$. For solutions very dilute in sodium, corrections for non-ideality are negligible. Experimental results agree satisfactorily with calculated ones.

**10438.** Stromberg, R. R., Peyser, P., Tutas, D. J., **Conformation of polyesters adsorbed on solid surfaces,** Chapter in *Fundamental Aspects of Fiber Reinforced Plastic Composites,* R. T. Schwartz and H. S. Schwartz, eds., pp. 163-176 (Interscience Publ., New York, N.Y., 1968).

> Key words: Adsorption; configuration of adsorbed polymer; conformation of adsorbed polymer; ellipsometry; infrared; polyester; polymer adsorption.

The conformation of a polyester, poly(ethylene *o*-phthalate), of relatively low molecular weight was studied after adsorption. The extension of the adsorbed molecule in a poor solvent on several planar metal surfaces was studied by ellipsometry and the fraction, *p*, of attached groups on colloidal silica particles in a good solvent was determined by the shift in the infrared absorption frequency between free and adsorbed carbonyl groups. In contrast to previously reported results for polystyrene, the extension normal to the surface remained constant ($\sim 70$ Å) while the concentration of polymer in the adsorbed film increased during the adsorption period. The value of $p$ (0.34 for $MW = 5400$) is relatively high and was independent of surface population for the range of solution concentrations measured. Differences between these results and those for polystyrene are interpreted as resulting from differences in interaction energy and chain stiffness.

**10439.** Swanson, N., **Characteristic energy-loss spectra and $-\mathrm{Im}(1/\epsilon)$ for amorphous and polycrystalline $Al_2O_3$,** *Phys. Rev.* **165,** No. 3, 1067-1070 (Jan. 15, 1968).

> Key words: Aluminum oxide; characteristic energy loss; cross section; dielectric constant; oscillator strength; plasmon.

Characteristic energy loss spectra of 20 keV electrons in amorphous and polycrystalline $Al_2O_3$ have been measured in transmission at zero scattering angle. The dominant loss peak, due to plasmon excitation, occurred at $22.6 \pm 0.2$ eV and $24.3 \pm 0.2$ eV for the amorphous and polycrystalline films, respectively. Lower lying weaker losses were observed at about 8.7 eV and 13.5 eV in both films, with an additional loss at 17.7 eV in the polycrystalline film. Using a previously developed technique, values of $-\mathrm{Im}\ \epsilon^{-1}$ and electron energy loss oscillator strength were derived from the loss spectra. The results for anodized $Al_2O_3$ are in excellent agreement with existing optical measurements.

**10440.** Swartzendruber, L. J., Bennett, L. H., **The effect of Fe on the corrosion rate of copper rich Cu-Ni alloys,** *Scripta Met.* **2,** 93-98 (1968).

> Key words Copper; corrosion; d-electron; iron; magnetic moment; Mössbauer effect; nickel.

The occurrence of a minimum in the reduction of the corrosion rate in hot sea water upon the addition of small quantities of Fe to copper rich Cu-Ni alloys is studied in relation to the Mössbauer spectra of $^{57}Fe$ in these alloys. It is proposed that as long as Fe remains in solid solution it reduces the corrosion rate due to the formation of local magnetic moments, but when Fe rich precipitates are formed the corrosion rate increases.

**10441.** Taylor, L. S., **Responsibilities of the physician in his use of radiation,** *Rev. Mex. Radiol.* **XVIII,** No. 69, 22-31 (Jan.-Feb. 1964).

> Key words: Radiation exposure; radiation hazards.

After comparing various sources of radiation exposure to which the public is subjected, suggestions are given with regard to the responsibility of the medical profession in the protection of patients during medical procedures.

Attention is directed to the substantial difference in practice between the radiologist and the general practitioner. Practically all of the conditions under which the general practitioner has to operate militate against maximizing the protection of the patient as well as the staff.

Public concern over radiation hazards in medical procedures has reached such proportions that better doctor-patient relationships in the administration of radiation are clearly called for.

**10442.** Tauber, S. J., Bolotsky, G. R., Fraction, G. F., Kirby, C L., Reed, G. R., **Algorithms for utilizing Hayward chemica structure notations,** Chapter 27 in *Proc. ICIREPAT Fifth Annual Meeting, London, England, Aug. 31-Sept. 10, 1965,* pp 351-377 (Thompson Book Co., Washington, D.C., 1967).

> Key words: Chemical structures; computer; connection tables; Hayward notation; matrices; molecular formulae.

Computer techniques are described for obtaining connectior tables representing chemical structures from Hayward linea notations and binary structure matrices from connection tables The general approach and some of the detail are described fo obtaining Hayward notations from connection tables. Severa types of data derivable from Hayward notations are mentioned and a computer technique is described for calculating molecula formulae. Data formats and restrictions are described, and logical flow charts are presented.

**10443.** Van Blerkom, D., Hummer, D. G., **The ionization structure of planetary nebulae-VI. The Lyman continuum problen** *Monthly Notices Roy. Astron. Soc.* **137,** No. 3, 353-374 (Nov 1967).

> Key words: Ionization structure; Lyman continuur problem; planetary nebulae; radiation.

Because of the recent evidence that a planetary nebula doe not completely absorb Lyman continuum radiation for a substar tial part of its life, we have used a generalized discrete-ordinat method to obtain accurate numerical solutions to the ionizatio balance problem in pure hydrogen, plane-parallel model nebula of various optical thicknesses. The effects of incomplete absorption, interior boundary conditions and non-Planckian stellar fluxes are examined.

We find that the density of neutral hydrogen in the nebula increases by less than a factor of two as the optical thickness varies from 0.5 to $\infty$, and is insensitive to large deviations in the stellar flux from the Planckian distribution, if the total number of Lyman photons is constant. The radius of the Strömgren sphere differs by about 5 percent for the two boundary conditions considered.

The accuracy of two simple approximations are assessed, and conditions for their validity are obtained.

**10444.** Van Zyl, B., Dunn, G. H., **Dissociation of $N_2^+$ and $O_2^+$ by electron impact,** *Phys. Rev.* **163,** No. 1, 43-45 (Nov. 5, 1967).

Key words: Dissociation; electron impact; interaction energies; $N_2^-$; $O_2^-$.

Cross sections for dissociation of $N_2^+$ and $O_2^+$ by electron impact were measured for interaction energies between 10 eV and 500 eV and between 15 eV and 500 eV respectively. The cross section versus interaction-energy curves exhibit maxima in the vicinity of 75 eV and decrease monotonically at higher energies with an A/E log BE dependence. Maximum cross section values are 4.3 $\pi a_0^2$ for $N_2^+$ and 4.1 $\pi a_0^2$ for $O_2^+$. The curves are remarkably similar at the higher interaction energies. The ion targets are typical of those formed by bombardment of gas by electrons of 150 eV and greater, and some may be in excited electronic states.

**10445.** Vriens, L., Simpson, J. A., Mielczarek, S. R., **Tests of Born approximations: differential and total $2^3S$, $2^1P$, and $2^1S$ cross sections for excitation of He by 100- to 400-eV electrons,** *Phys. Rev.* **165,** No. 1, 7-15 (Jan. 5, 1968).

Key words: Born approximation; cross sections; electrons; excitation cross sections; helium; Ochkur approximation.

The angular dependence of $2^3S$, $2^1P$ and $2^1S$ excitation of He for incident electron energies from 100 to 225 eV ($2^3S$) and 400 eV ($2^1P$ and $2^1S$) has been measured. Apparent generalized oscillator strengths f(K) and differential cross sections for the transition $1^1S \rightarrow 2^1P$ are obtained by normalizing on the optical oscillator strength of Schiff and Pekeris. From the experimental intensity ratios $2^3S/2^1P$ and $2^1S/2^1P$ we then calculate differential $1^1S \rightarrow 2^3S$ and $1^1S \rightarrow 2^1S$ cross sections. The differential cross sections are integrated to get total cross sections. The f(K) found here for $2^1P$ and $2^1S$ excitation decrease faster with increasing K than in earlier studies. Departures from the Born approximation appear only below 200 eV for $2^1P$ excitation, but occur at higher energy for $2^1S$ excitation and are larger for large momentum transfers. The angular dependence found for $2^3S$ excitation disagrees strongly with the Ochkur approximation. Our total $2^3S$ cross sections are much lower than all other existing theoretical and experimental data.

**10446.** Weiss, A. W., **Theoretical electron affinities for some of the alkali and alkaline-earth elements,** *Phys. Rev.* **166,** No. 1, 70-74 (Feb. 5, 1968).

Key words: Atomic wavefunction; correlation energy; electron affinity; superposition of configurations.

The $(ns)^2$ correlation energies for the negative ions, $Li^-$, $Na^-$ and $K^-$, have been calculated by the method of superposition of configurations. Comparisons with Hartree-Fock calculations of the neutral species yield electron affinities of .62, .54, and .47 eV respectively. A study of the computed ionization potentials of the neighboring isoelectronic atoms and ions suggests a maximum uncertainty of .1 eV. Similar calculations on the $ns(np)^2\,{}^4P$ states of $Be^-$ and $Mg^-$ indicate they are metastable with electron affinities, relative to the nsnp $^3P$ of the neutral, of .24 and .32 eV respectively.

**10447.** Weiss, A. W., **Theoretical multiplet strengths for Mg I, Al II, and Si III,** *J. Chem. Phys.* **47,** No. 9, 3573-3578 (Nov. 1, 1967).

Key words: Multiplet strengths; superposition of configurations; wavefunctions.

Superposition of configurations wavefunctions have been computed for the ground state and some lower excited states of the first three members of the magnesium isoelectronic sequence. The excited states are all those with configurations involving the low-lying orbitals, 3s, 3p, 3d and 4s. Multiplet strengths were also computed for all the allowed electric dipole transitions among these states. Only excitations of the outer two valence electrons were included in the multi-configuration expansion, with the virtual orbitals being derived from a pseudonatural orbital transformation. Comparisons are made with predictions of the Z-expansion method.

**10448.** Wells, J. S., Matarrese, L. M., and Sukle, D. J., **Electron spin resonance in single crystals of anhydrous copper sulfate,** *J. Chem. Phys.* **47,** No. 7, 2259-2262 (Oct. 1, 1967).

Key words: Anhydrous copper sulfate; antiferromagnetic resonance; electron spin resonance.

The magnetic resonance of synthetic anhydrous copper sulfate has been investigated at 23.3 GHz at temperatures between 77 °K and 4.1 °K. In the paramagnetic region, the observed resonance consists of two lines. One of these is relatively narrow and remains essentially fixed even down to 4.1 °K. The second line is unusually broad and its behavior indicates that it is due to the copper ions in the anhydrous crystal. The g values and corresponding line-widths have been measured for the broad line at 77 °K. As the temperature drops to the Neel point, this broad line increases in width, shifts, and disappears rather rapidly, indicating that it is associated with the antiferromagnetic phase.

**10449.** Whittaker, J. K., **Instability and decoupling in nuclear electronics,** *Nucl. Instr. Methods* **57,** No. 1, 156 (Dec. 1967).

Key words: Decoupling; $f_T$; high frequency; instability; low frequency; NIM System.

The instabilities which can occur in semiconductor electronics and the necessary decoupling to remove these instabilities and their effects are discussed, with particular reference to the present concept of modular electronic systems.

**10450.** Wilcox, R. M., **Some thoughts on Fitzgerald's particle waves,** *J. Acoust. Soc. Am.* **42,** No. 3, 678-679 (Sept. 1967).

Key words: Deformation phenomena; Fitzgerald, E. R.; particle-waves; phonon.

The particle-wave theory recently put forth by E. R. Fitzgerald to explain various deformation phenomena in crystalline solids is criticized. The theory is shown to be based upon a misconception regarding the nature of phonons.

**10451.** Williams, G., Lauritzen, J. I., Jr., Hoffman, J. D., **Effect of chain twisting on the effective barrier to reorientation for a hindered rotator,** *J. Appl. Phys.* **38,** No. 11, 4203-4208 (Oct. 1967).

Key words: Activation energy; chain twisting; hindered rotator; parabolic potential model; sinusoidal potential model; two-site model.

The effective barrier to reorientation is calculated for a chain which may occupy two equivalent energy states, 180° apart for the case where the chain is allowed to twist during the reorientation process. Results are obtained for (I) a "parabola-anti-parabola" and (II) a cosine form for the intermolecular energy. The results for (I) and (II) are similar, but differ both in form and magnitude from that obtained earlier using a cusplike barrier. Both (I) and (II) lead to the conclusion that a chain will behave as a rigid rod up to a critical chain length, and then exhibit twisting for all lengths exceeding this critical value.

**10452.** Yakowitz, H., Heinrich, K. F. J., **Quantitative electron probe microanalysis: Absorption correction uncertainty**, *Mikrochim. Acta* **1**, 182-200 (1968).

Key words: Absorption of x-rays; Al-Mg analysis; electron microprobe; errors in microanalysis; microprobe absorption correction comparisons; microprobe experimental conditions; quantitative microanalysis.

The accuracy of the x-ray absorption correction for quantitative microprobe analysis is affected by errors in the input parameters (mass attenuation coefficients, x-ray emergence angle, and operating voltage), as well as by inaccuracies in the proposed absorption correction models. If the mass attenuation coefficient is known within 5 percent, then to keep the error of this correction below 1 percent, the absorption function, $f(\chi)$, must be equal to or higher than 0.8. Experimental conditions leading to small absorption corrections are discussed, and the advantages of high x-ray emergence angles are demonstrated. As an illustration, the analysis (theoretical and experimental) of aluminum-magnesium alloys is discussed.

**10453.** Yates, J. T., Jr., Madey, T. E., Payn, J. K., **Desorption by electron impact: Carbon monoxide, nitric oxide and oxygen on tungsten,** *Nuovo Cimento Suppl. Series I,* **5,** No. 2, 558-581 (1967).

Key words: Binding states; carbon monoxide; chemisorption; cross section; electronic desorption; electron impact; ion energy distribution; nitric oxide; oxygen; threshold voltage; tungsten.

The interaction of low energy electrons with chemisorbed species has been employed as a tool for the characterization of various binding states for CO, NO, and Oxygen on a polycrystalline tungsten ribbon. The apparatus employed is similar to that of Redhead.

Cross sections as a function of coverage for positive ion desorption, and average cross sections for neutral desorption have been measured. Threshold energies for ion production and ion energy distributions are compared for these three oxygen-bearing adsorbates. The electronic desorption phenomenon is shown to be useful for observing details of thermal interconversion and desorption from various binding states in the chemisorbed layer.

**10454.** Armstrong, R. W., **NBS dynamic seat belt tester,** *Proc. 10th Stapp Car Crash Conf., 6571st Aeromedical Research Laboratory, Alamogordo, New Mex., Nov. 8-9, 1966,* pp. 38-45 (Society of Automotive Engineers, New York, N.Y., 1966).

Key words: Acceleration; anthropomorphic dummy; automobile crash simulator; dynamic tests; flywheel; seat belts.

The NBS Dynamic Seat Belt Tester provides relatively inexpensive laboratory equipment capable of simulating an automobile crash. The machine is economical to operate with reproducible output. The sled of the test machine carries a seat and belted dummy or other equipment and is given an acceleration simulating the deceleration experienced by the passenger compartment of an automobile in a 30 mile per hour crash. The acceleration is produced by a rotating flywheel through a tow tape attached to the sled. The ratio of the combined momentum of the flywheel and the sled to that of the dummy is about that of an automobile to a passenger. The test machine has an overall length of 35 feet and is adequately powered by a 10 horsepower motor.

**10455.** Astin, A. V., **Welcoming remarks,** (Proc. Fifth Transducer Workshop, National Bureau of Standards, Gaithersburg, Md., Oct. 3-4, 1967), *Telemetry Working Group Document* **112-68,** pp. 3-4 (Secretariat, Range Commanders Council, White Sands Missile Range, New Mexico, 1968).

Key words: NBS; transducer workshop.

Welcoming remarks addressed to attendees of the Fifth Transducer Workshop (Oct. 3-4, 1967, National Bureau of Standards, Gaithersburg, Md.) describe NBS' responsibilities as a scientific and technical service agency. NBS activities are generally in two major program areas—physical measurement system and transfer of technology. Mentioned as being instrumental in carrying out these responsibilities are such Bureau efforts as the data program, materials research program, assistance to standards-writing groups, and a number of specialized information services.

Further remarks call attention to the new NBS facilities, particularly those available for conference activities.

**10456.** Beckett, C. W., **Status of properties research in the kilodegree range,** Chapter 1 in *The Characterization of High-Temperature Vapors,* J. L. Margrave, ed., pp. 3-15 (John Wiley and Sons, Inc., New York, N.Y., 1967).

Key words: High temperature chemistry; high temperatures; kilodegree range; thermodynamic properties; vapors.

This paper is an informal discussion of the status of thermodynamic and other properties at high temperatures in relation to current technical needs. It contains comment on a few noteworthy achievements, some unexplored areas, and on the lag between basic research on properties and well-known technical needs. It is to be included in the transactions of an ACS symposium on high temperature chemistry at the request of the publisher.

**10457.** Berendt, R. D., Winzer, G. E., Burroughs, C. B., **A guid to airborne, impact, and structure-borne noise control in multifamily dwellings,** U.S. Dept. Housing and Urban Development, *FT/TS*-**24** (Superintendent of Documents, Governmen Printing Office, Washington, D.C., Jan. 1968, $2.50).

Key words: Airborne; multifamily; noise control; structure borne noise control.

The guide analyzes the basic causes of the airborne, impac and structure-borne noise problems in multifamily dwellings an recommends corrective measures, building structures and construction techniques to alleviate and control such problems.

Airborne and impact sound insulation criteria for three grade of multifamily dwellings are presented and recommended for us by the FHA in its Minimum Property Standards. Sound insulation data, fire ratings, descriptions and architectural illustration are presented for 137 wall constructions and 111 ceiling-floo structures. The guide is illustrated with 345 detailed architectural drawings which show the proper construction and installation of wall and floor assemblies, building equipment, appliance heating, air-conditioning, plumbing and electrical systems, services or utilities required for adequate sound insulation, nois control and privacy in multifamily dwellings.

In addition, the guide summarizes the sound insulation criteri of various foreign countries and contains three appendices whic discuss fire ratings, the relationship between laboratory and fiel measurements of sound insulation and common noise sources.

Highly technical and mathematical discussions were purposely avoided in the writing of this guide, so that it could be widel used and readily understood by architects, builders, craftsme ymen and others engaged in the design and construction of ultifamily residences.

**458.** Bloss, R. L., **The measurement of strain,** (Proc. 22nd Annual ISA Conf., Chicago, Ill., Sept. 11-14, 1967), *ISA Preprint* No. PI-1-PHYMMID-67 (1967).

Key words: Extensometer; historical; measurement; state of the art; strain; strain gage.

This paper presents a brief overview of the field of strain mea- rement, including some discussion of philosophy, history and urrent "state of the art" of the field. There is some discussion of enefits that have resulted from the technical advances in the eld of strain measurement, and a few predictions of future evelopments.

**459.** Bowman, H. A., Gallagher, W., Schoonover, R. M., **The development of a working density standard,** (Proc. 20th Annual ISA Conf., Oct. 4-7, 1965, Los Angeles, Calif.), *ISA Preprint* No. 14.8-4-65 (1965).

Key words: Density; density standard; hydrostatic weighing; volume; volumetric measurement.

Inasmuch as density is the ratio between two well stan- rdized quantities, any working standard of density must be onsistent with them. The establishment of fixed reference oints on the density scale presents several unique problems hich demand techniques and apparatus of interest to instru- entation scientists. NBS has gone far down the road toward a orking standard. Progress to date and goals believed achievable the present state of the art will be discussed.

**460.** Bozman, W. R., **The application of computers in printing scientific manuscripts,** Chapter 13 in *New Techniques in Office Operations*, pp. 120-124 (The Business Press, Elmhurst, Ill., Mar. 1968).

Key words: Computer typesetting; data processing; photocomposing; phototypesetting.

A description is given of the use of computers to help prepare file of information on 30,000 organic and inorganic crystals. ome of the problems of input keyboarding, and data corrections e discussed, as well as cross-checking the data for internal con- stency and preparation of the final output magnetic tape for peration of a phototypesetting machine.

**461.** Brady, G., McIntyre, D., Myers, M. E., Jr., Wims, A. M., **Critical scattering of perfluoroheptane-isooctane system,** (Proc. Conf. Small-Angle X-Ray Scattering, Syracuse University, Syracuse, N.Y., June 1965), Chapter in *Small-Angle X-Ray Scattering*, H. Brumberger, ed., pp. 425-448 (Gordon and Breach, Science Publ. Inc., New York, N.Y., 1967).

Key words: Correlation function; critical opalescence; critical phenomena; isooctane; low angle x-ray scattering; perfluoroheptane.

The critical opalescence of mixtures of perfluoroheptane- ooctane near and at the critical concentration has been ex- mined by x-ray scattering measurements over a large angular ange.

The measurementss are discussed and shown to agree well ith the assumed correlation function proportional to $e^{-kr/r^{1.1}}$ ear the critical temperature. The evidence for the persistence of rge molecular clusters away from the critical point is reviewed.

**0462.** Braun, W., Lenzi, M., **Resonance fluorescence method for kinetics of atomic reactions. Reactions of atomic hydrogen with olefins,** *Discussions Faraday Soc.* **44,** 252-262 (1967).

Key words: Absolute rate constants; apparatus; flash photolysis-emission spectroscopy; hydrogen atom reactions; Lyman-$\alpha$ fluorescence; olefins.

Using the technique of flash photolysis, absorption of Lyman-$\alpha$ radiation by H atoms and measurement of the subsequent Lyman alpha emission, the absolute rate constants for the reaction of hydrogen atoms with several olefins have been measured at room temperature. The method distinguishes hydrogen from deuterium atoms and can be used to measure either.

The absolute limiting high pressure rate constants at room temperature for the reactions H + $C_2H_4$, $C_2D_4$, and trans-2-butene, have been found to be approximately the same, $k = 1.0 \pm (15\%) \times 10^{-12}$ cc molecule$^{-1}$ sec$^{-1}$. The absolute rate constant for the reaction H + isobutene was found to be $k = 3.8 \pm (15\%) \times 10^{-12}$ cc molecule$^{-1}$ sec$^{-1}$. For the reaction H + $C_2H_4$ a pressure effect on the bimolecular rate constant has been observed and this effect on the bimolecular rate constant has been observed and this effect is discussed. The experimental method is described in detail since it appears to be the first of its kind and in principle generally applicable to the study of reactions of atoms other than hydrogen or deuterium.

**10463.** Bridges, J. M., Wiese, W. L., **Comparison of the Stark widths of the Balmer lines $H_\beta$ and $H_\alpha$,** *Proc. Seventh Intern. Conf. Phenomena in Ionized Gases*, B. Perovic and D. Tosic, eds., **III**, pp. 165-167 (Gradevinska Knjiga Publ. Co., Beograd, Yugoslavia, 1966).

Key words: Balmer lines $H_\alpha$ and $H_\beta$; half-widths; line profiles; Stark broadening; wall-stabilized arc.

The Stark broadened profiles of the Balmer lines $H_\alpha$ and $H_\beta$ were studied photoelectrically in a wall-stabilized arc. The arc was operated in argon to which small amounts of hydrogen were added. These relatively low hydrogen concentrations were required to avoid self-absorption of $H_\alpha$. Repeated measurements of the half-widths were undertaken for currents from 15 to 50 amps and compared with recent Stark broadening calculations. Normalizing theory and experiment for the case of $H_\beta$, for which refined calculations are available, one consistently observes that the theoretical half-widths for $H_\alpha$ are about 20 percent too small for the range of electron densities from $2\text{-}6 \times 10^{-16}$cm$^{-3}$.

**10464.** Brown, W. E., **A mechanism for growth of apotitic crystals,** (Proc. Intern. Symp. Composition, Properties and Fundamental Structure of Tooth Enamel, London, England, Apr. 1964), Chapter in *Tooth Enamel*, pp. 11-14 (John Wright and Sons, Ltd., Bristol, England, 1965).

Key words: Apotitic crystals; crystals; enamel; tooth enamel.

**10465.** Bullis, W. M., Coleman, J. A., **Characterization of germanium and silicon for nuclear radiation detectors,** Chapter in *Nucleonics In Aerospace*, P. Polishuk, ed., pp. 166-175 (Plenum Press Inc., New York, N.Y., 1968).

Key words: Carrier drift mobility; carrier trapping; charge collection efficiency; energy resolution; gamma ray detectors; Hall mobility; infrared absorption; lithium drift mobility; lithium precipitation; oxygen; photoconductive decay lifetime; reverse recovery time.

Semiconductor detectors have been extensively used for about eight years. Uncontrolled variations in the quality of germanium and silicon intended for this application have occurred during this period for reasons which, even now, are not well understood. Crystals are presently selected on the basis of room temperature resistivity, photoconductive decay lifetime and etch pit density. Use of these parameters does not always enable one to discriminate between material suitable for detector fabrication and material which is not. This paper describes a research program now in progress at the National Bureau of Standards which has the objective of identifying those parameters which will be the most useful in specifying detector-grade material. Because of the immediacy of the problem, study of results of this program should also be applicable in the characterization of detector-grade silicon.

**10466.** Bur, A. J., Roberts, D. E., **High polymeric materials,** *1964 Digest of Literature on Dielectrics* **28,** 231-260 (National Academy of Sciences – National Research Council, Washington, D.C., 1964).

> Key words: Biopolymers; dipole moments; effects of radiation; relaxation phenomena; semiconducting polymers; technology.

The literature on polymer dielectrics published in 1964 is reviewed. The following subjects are covered: theory; relaxation phenomena; dipole moments; semiconducting polymers; biopolymers; effects of radiation; and technology. (229 references).

**10467.** Butterfield, M. A., **Care and preservation of the new media-equipment needs,** *Proc. A Pioneer Presentation of a National Symposium on the Impact of Automation on Documentation, Denver, Colo., Apr. 27-29, 1967,* pp. 60-64 (1968).

> Key words: Analog library storage; archival storage and retrieval; automated archival equipment; automated archives; automated library equipment; automated library storage; digital library storage; library storage and retrieval.

Automated storage systems are postulated for librarians and archivists of the future. Equipment requirements are discussed for accessing, storing, and retrieving information on magnetic tape media. Problem areas are presented for both analog and digital recording methods.

**10468.** Campbell, P. G., Wright, J. R., **Asphalt hardening by gaseous oxidants: the relationship between softening point and chemical change as measured by infrared spectroscopy,** *J. Mater.* **2,** No. 3, 581-596 (Sept. 1967).

> Key words: Asphalt flux; carbonyl absorbance; coating-grade asphalt; infrared analysis; nitrogen oxides; oxidation; softening point; sulfur dioxide.

The use of oxidized asphalts has been increasing steadily and much work had been reported on the process of blowing asphalt fluxes to produce a coating grade asphalt. Previous work was reviewed in which asphalt fluxes were treated with various oxidants (oxygen, ozone, air, nitrogen oxides) at relatively mild temperatures and the complex changes taking place during the hardening process were studied by infrared spectroscopy. This work was extended to include other gaseous mixtures (sulfur dioxide, sulfur dioxide-air, nitrogen dioxide-air).

The study of the effects of the gaseous oxidants on the softening points of the asphalt fluxes with time of blowing indicated that, in every case, the rate of softening point increase was greater than that obtained when air alone was used to harden the flux. Infrared spectral analysis, in which changes in functionality are detected, was found to be a convenient method to follow the asphalt hardening process.

**10469.** Canfield, L. R., Johnson, R. G., Codling, K., Madden, R. P., **Comparison of an ionization chamber and a thermopile as absolute detectors in the extreme ultraviolet,** *Appl. Opt.* **6,** No. 11, 1886-1888 (Nov. 1967).

> Key words: Absolute radiometry; detectors; extreme ultraviolet; ionization chamber; monochromator; thermopile.

A comparison has been made between a calibrated thermopile and an argon ionization chamber as absolute detectors of radiant flux of wavelengths 584 and 735 Å. Corrections were applied to the data to account for the absorption due to gases in the monochromator, the energy carried away from the thermopile by photoejected electrons, non-uniformity of response across the surface of the thermopile and uneven illumination of the thermopile by the flux from the monochromator. The two detectors were found to agree within the 3 percent estimated probable error in the measurements.

**10470.** Cassidy, E. C., **Time-resolved studies of spectra produced by electrically exploded wires,** *Naturwissenschaften* **55,** No. 3 125-128 (1968).

> Key words: AlO; atomic spectra; electrical discharge exploding wire; molecular spectra; time-resolved spectroscopy.

Time-resolved spectroscopic studies of electrically exploded wires are described. The spectral distribution of the radiation emitted by aluminum and titanium wires exploded in various controlled atmospheres are given. Atomic and molecula species produced by the explosion are identified. The effects o environment, pressure, and electrical energy input on the explosion spectrum are discussed, and conditions which were found to be conducive to the production of several selected spectral features by the exploding wire method are indicated. This pape summarizes the results of spectroscopic exploding wire studies at the U.S. National Bureau of Standards over the past few years.

**10471.** Catanzaro, E. J., **Absolute isotopic abundance ratios o three common lead reference samples,** *Earth and Planetary Sci Letters* **3,** No. 4, 343-346 (1968).

> Key words: Absolute ratios; isotopic abundances; lead reference samples.

The absolute isotopic abundance ratios have been determined for three common lead reference samples, using solid-sample mass spectrometry. Samples of known isotopic composition prepared from nearly pure separated $^{206}$Pb and $^{208}$Pb isotopes were used to calibrate the mass spectrometers. The resulting absolute values are as follows. GS 4: $^{204}$Pb/$^{206}$Pb = 0.061888 ± 0.000065, $^{207}$Pb/$^{206}$Pb = 0.95342 ± 0.00036, $^{208}$Pb/$^{206}$Pb = 2.218 ± 0.0010; NBS 200: $^{204}$Pb/$^{206}$Pb = 0.068353 ±s 0.000072 $^{207}$Pb/$^{206}$Pb = 1.00538 ± 0.00038, $^{208}$Pb/$^{206}$Pb = 2.3675 ± 0.0011 C.I.T. Pb Std.: $^{204}$Pb/$^{206}$Pb = 0.060151 ± 0.000063, $^{207}$Pb/$^{206}$P = 0.93081 ± 0.00035, $^{208}$Pb/$^{206}$Pb = 2.1835 ± 0.0010. The indicated uncertainties are overall limits of error based on 95 percent confidence limits for the mean and allowances for effects o known sources of possible systematic error.

**10472.** Clark, J. E., Harrison, C. W., **Accelerated weathering o polymers: radiation,** *Appl. Polymer Symp.* **4,** 97-110 (Sep 1967).

> Key words: Carbon arc; degradation; irradiance; photo degradation; plastics; polymers; radiation; radiometry sun; weathering; xenon arc.

The objective of this work was to study the radiation characteristics in three artificial weathering devices and to do a prelim nary survey of the effects of high-intensity irradiation on plastic

An absolute radiometer was used to measure radiation characteristics in the xenon arc and sunshine carbon and enclosed carbon arc Weather-Ometers. The irradiance from the xenon ar was stable over one hour, but the irradiance from the carbon arc fluctuated. Irradiance received in one hour at the sample dru for sunshine and enclosed carbon arcs ranged from 315 to 102 W/m² and 297 to 679 W/m², respectively, while the xenon ar showed a relatively constant irradiance of 910 W/m². All thre devices had a maximum irradiance near the center of the samp drum with intensities at top and bottom being 15-40 percent les

Seven plastic films were exposed to a xenon arc over a 20 fold intensity range by decreasing the arc-to-sample distance.

At up to 6.1 times earth-level sunlight, no significant changes resulted within 100 hours. At 81 times earth-level sunlight, white-pigmented film decomposed within 30 hours and clear films showed changes in ultraviolet and infrared spectra within 59 hours. At 379 times earth-level sunlight, five clear plastics decomposed within 12 hours or less.

**10473.** Coleman, J. A., **Germanium for gamma-ray detectors. A review of current problems,** (Proc. IAEA, Vienna, Austria, June 6-7, 1966), Chapter in *Lithium-Drifted Germanium Detectors, STI/Publ./***132,** pp. 37-41 (International Atomic Energy Agency, Vienna, Austria, 1966).

Key words: Gamma ray detectors; germanium; semiconductor detectors.

The performance of germanium gamma radiation detectors depends, to a large extent, on the quality of the germanium used to produce the devices. Presently, the demand for better resolution, faster response times, and larger volume detectors imposes severe requirements on the germanium for detectors in terms of crystal purity and perfection. The specifications commonly used to describe germanium for detectors, such as resistivity, carrier lifetime, and etch pit density, were originally derived from those used by the semiconductor device industry. The relevance of these specifications for material to produce a detector with good performance, including long-term stability, is not well-understood. A semiconductor detector requires extreme perfection throughout a large volume single crystal. Common transistors and diodes have much smaller volumes and often operate at much higher currents and noise levels than a radiation detector; therefore, material requirements are usually not as stringent as those for detectors.

The Electron Devices Section of the NBS is engaged in studies of the correlations between the properties of semiconductor materials and the performance of semiconductor devices fabricated from such material. Presently, the effects of carrier lifetimes and mobility and impurities such as oxygen, copper and gold in germanium, on the performance and stability of gamma ray detectors are being investigated. The use of germanium gamma ray detectors at NBS for such applications as activation analysis, photonuclear reaction studies, decay scheme investigations and Mössbauer spectroscopy is limited at the present time, but it is expected to be greatly expanded in the very near future.

**10474.** Coleman, J. A., Love, D. P., Trainor, J. H., Williams, D. J., **Low-energy proton damage effects in silicon surface-barrier detectors,** *IEEE Trans. Nucl. Sci.* **NS-15,** No. 1, 482-490 (Feb. 1968).

Key words: Detector; proton; radiation effect; semiconductor; silicon.

In order to predict the useful lifetime of semiconductor detectors which operate in the Earth's trapped radiation belts, the effects of damage by 50 keV, 200 keV, 600 keV and 1 MeV protons on silicon, surface-barrier, transmission detectors have been studied for fluences from $10^{10}$ to $10^{14}$ protons/cm$^2$. Detector current, noise and capacitance increased with fluence, with significant increases occurring after $10^{13}$ protons/cm$^2$. Bias-voltage-dependent multiple peaking was observed with Am-241 alpha particles. The effect of damage by protons with these low energies is significantly reduced in transmission detectors if the protons enter the rear, aluminum contact rather than the front, gold contact.

**10475.** Cook, R. L., Kirchhoff, W. H., **Further investigations on the microwave spectrum of NSF: evaluation of the molecular force field, centrifugal distortion constants, and the dipole moment,** *J. Chem. Phys.* **47,** No. 11, 4521-4527 (Dec. 1, 1967).

Key words: Dipole moment; microwave spectrum; pyrazole; Stark effect; structure; tautomerism.

The measurements of the microwave spectrum of NSF has been extended to include transitions involving J as high as 40 and the centrifugal distortion effects have been accounted for. By combining the analysis of the vibrational and rotational spectra, the molecular force field for NSF has been calculated and the following quadratic potential constants, in mdynes/Å, were obtained: $f_1 = 10.703$, $f_2 = 2.872$, $F_\alpha/d^2 = 0.411$ and $f_{2\alpha}/d = 0.014$. Here 1 refers to the SN bond, 2 to the SF bond, $\alpha$ to the NSF bond angle and d is the geometric mean of the SN and SF bond distances. It was found that the data were too insensitive to calculate $f_{1\alpha}$ and $f_{12}$ and these constants were assumed to be zero.

The dipole moment was calculated from the Stark effect of the $5_{1,4} - 4_{2,3}$ transition and was found to be $1.902 \pm 0.012$ D, where the uncertainty represents the spread in the value of the dipole moment obtained from different methods of treating the data.

**10476.** Covington, A. K., Paabo, M., Robinson, R. A., Bates, R. G., **Use of the glass electrode in deuterium oxide and the relation between the standardized pD ($pa_D$) scale and the operational pH in heavy water,** *Anal. Chem.* **40,** No. 4, 700-706 (Apr. 1968).

Key words: Acidity; deuterium electrode; deuterium oxide; glass electrode; heavy water; pD measurement.

Commercial glass electrodes have been compared both directly and indirectly with the deuterium gas electrode at 25 °C in buffered solutions of pD from 1 to 13. It is confirmed that the glass electrode functions as well in heavy water as in ordinary water. The relation between the operational pH of a buffer solution in heavy water (obtained with a glass electrode standardized in an ordinary light buffer solution) and its pD or $pa_D$ value obtained from measurements on cells without liquid junction has been examined and correction factors determined for both glass and gas electrodes. The operational pH of buffer solutions in heavy water at 25 °C, measured with the glass electrode, can be converted into a pD value by adding 0.41 (molar scale) or 0.45 (molal scale) for $2 < pD < 9$.

**10477.** Deslattes, R. D., **Photoionization of the M shell of xenon,** *Phys. Rev. Letters* **20,** No. 10, 483-484 (Mar. 4, 1968).

Key words: M-shell; photoionization; xenon.

New measurements of the continuum photoionization cross sections of xenon in the region 670-800 eV are reported. These reveal, in the region of the $M_N$ and $M_I$ edges, extreme non-hydrogenic behavior previously observed only at longer wavelengths.

**10478.** Deslattes, R. D., **X-ray monochromators and resonators from single crystals,** *Appl. Phys. Letters* **12,** No. 4, 133-135 (Feb. 15, 1968).

Key words: Monochromators; single crystals; x-ray resonators.

Single crystal specimens shaped so as to permit successive x-ray diffraction by two non-parallel atomic planes are fixed wavelength monochromators. It is shown that certain plane pairs in Si and Ge pass wavelengths sufficiently close to strong characteristic lines to allow production of intense highly monochromatic beams. For interplanar angles of $2\pi/n$, resonators and retroreflectors may be obtained.

**10479.** Domsitz, M. G., **Transducer activities at NBS,** (Proc. Fifth Transducer Workshop, National Bureau of Standards, Gaithersburg, Md., Oct. 3-4, 1967), *Telemetry Working Group Document* **112-68,** pp. 11-12 (Secretariat, Range Commanders Council, White Sands Missile Range, New Mexico, 1968).

Key words: Transducer activities; transducer instrumentation; transducers.

**10480.** Foster, B. E., **Attenuation of x-rays and gamma rays in concrete,** *Mater. Res. Std.* **8,** No. 3, 19-24 (Mar. 1968).

Key words: Concrete shields; gamma-ray attenuation; x-ray attenuation.

Concrete is widely used as a shielding material against x-ray and gamma-ray sources. The purpose of the paper is to furnish a brief elementary background for the concrete technologist on the physics of x-ray shielding. A brief description is given of the characteristics of x-ray and gamma rays. This is followed by a short discussion of attenuation by the photoelectric, pair-production, and Compton effect mechanisms, as a function of x-ray or gamma-ray energy, and barrier material. Performances of various shielding materials in various energy ranges are compared, and the problems in shield design brought about by the scattering processes are discussed.

**10481.** Goldman, D. T., **Suggested procedures for utilizing MUFT resonance parameters to include Doppler broadening,** *Nucl. Sci. Engr.* **31,** No. 2, 346-349 (Feb. 1968).

Key words: Doppler broadening; neutron; resonances; slowing down.

Keeping within the MUFT framework a method is proposed for including the effect of Doppler (temperature) broadening of resonances on the calculation of resonance integrals. This method is seen to be simple in its application. Some attempt has been made to determine its range of validity especially in comparison with the technique presently in use in MUFT. Finally, an additional proposal is made to replace the Narrow Resonance Infinite Mass approximation presently in use in MUFT with the Narrow Resonance approximation for all nuclei.

**10482.** Hall, J. L., Siegel, M. W., **Angular dependence of the laser photodetachment of the negative ions of carbon, oxygen, and hydrogen,** *J. Chem. Phys.* **48,** No. 2, 943-945 (Jan. 15, 1968).

Key words: Angular distribution; $C^-$; $H^-$; negative ion; $O^-$; photodetachment; photoelectron spectroscopy.

The angular distribution of electrons photodetached by polarized (laser) light from (a beam of) negative ions is dependent on the type of initial and final angular momentum states available. In $O^-$ and $C^-$, a p-type electron is photodetached into either s-wave or d-wave continuum states. The experimental angular distributions are consistent with the predicted strong destructive interference between the s-wave and d-wave channels.

For $H^-$, only s-p transitions are expected, which is consistent with the experimental observation of pure $\cos^2\theta$ behavior in this case.

**10483.** Hilten, J. S., **The National Bureau of Standards inter-agency transducer project—a progress report,** (Proc. Fifth Transducer Workshop, National Bureau of Standards, Gaithersburg, Md.. Oct. 3-4, 1967), *Telemetry Working Group Document* **112-68,** pp. 17-36 (Secretariat, Range Commanders Council, White Sands Missile Range, New Mexico, 1968).

Key words: Acceleration; calibrator; dual centrifuge; dynamic; Inter-agency Transducer Project; life-cycling; pressure; shock tube; thermal transient; transducer.

This paper describes some of the techniques and apparatus used for the evaluation of pressure and acceleration transducers. Both static and dynamic tests are covered. Included are earth's field static calibrator, dual centrifuge, earth's field dynamic calibrator, shock tube, quick opening valve pressure calibrators, thermal transient test, temperature storage and cycling test, and life-cycling test.

**10484.** Hughes, E. E., **A simple technique for the absolute determination of atmospheric oxygen,** *Environ. Sci. Technol.* **2,** No. 3, 201-203 (Mar. 1968).

Key words: Atmospheric composition; gas analysis; oxygen analysis.

A method is presented for the absolute determination of oxygen at concentrations near atmospheric. The oxygen in a sample is determined gravimetrically after reaction with either white phosphorus or a sodium-potassium alloy. The method requires little time and simple laboratory equipment. and is capable of yielding values for oxygen concentrations having an overall uncertainty of ± 0.1 mole percent.

**10485.** Hughes, E. E., Dorko, W. D., **Accurate mass spectrometric determination of low concentrations of carbon dioxide in nitrogen,** *Anal. Chem.* **40,** No. 4, 750-755 (Apr. 1968).

Key words: Air analysis; carbon dioxide; gas analysis; mass spectrometric analysis.

A method for the rapid and accurate determination of low concentrations of carbon dioxide in nitrogen has been developed. The method is based on high-pressure mass spectrometry in which the mass 44 to mass 28 ratio is compared to the same ratio in a carefully calibrated standard. Concentrations from 180 to 380 parts per million were determined with an accuracy of better than 1 percent.

**10486.** Kasuya, T., Lafferty, W. J., Lide, D. R., Jr., **Microwave spectrum, structure, boron quadrupole coupling constants, and dipole moment of difluoroborane,** *J. Chem. Phys.* **48,** No. 1, 1-4 (Jan. 1, 1968).

Key words: Difluoroborane; dipole moment; microwave spectra; molecular structure; quadrupole coupling constants; rotational constants.

The microwave spectra of $HB^{10}F_2$, $HB^{11}F_2$, $DB^{10}F_2$, and $DB^{11}F_2$ have been assigned. Rotational constants are 74494.82, 10496.74, and 9181.67 MHz for $HB^{11}F_2$; 77244.25, 10495.35, and 9221.49 MHz for $HB^{10}F_2$; 52896.09, 10498.29, and 8740.56 MHz for $DB^{11}F_2$; and 54081.82, 10496.89, and 8771.57 MHz for $DB^{10}F_2$. The structural parameters obtained from these constants and their estimated uncertainties are $r_{BF} = 1.311 \pm 0.005$ Å, $r_{BH} = 1.189 \pm .010$ Å and $\angle FBF = 118.3° \pm 1°$. The quadrupole coupling constants have been obtained. The dipole moment is $0.971 \pm 0.010$ D.

**10487.** Kushner, L. M., **The role of the Institute for Applied Technology,** (Proc. Fifth Transducer Workshop, National Bureau of Standards, Gaithersburg, Md., Oct. 3-4, 1967), *Telemetry Working Group Document* **112-68,** pp. 5-10 (Secretariat, Range Commanders Council, White Sands Missile Range, New Mexico, 1968).

Key words: Technological measurements; transfer of technology.

Welcoming address describing the major programs of the Institute for Applied Technology at the National Bureau of Standards.

**10488.** Lias, S. G., Ausloos, P., **Gas-phase photolysis and radiolysis of isobutane,** *J. Chem. Phys.* **48,** No. 1, 392-400 (Jan. 1, 1968).

Key words: Free radical reactions; ion-molecule reactions; isobutane; photoionization; photolysis; primary processes.

The photolysis of $(CH_3)_3CH$, $(CH_3)_3CD$, and of $(CH_3)_3CH-(CD_3CD$ and $(CD_3)_3CD-H_2S$ mixtures has been investigated at 1470 Å (8.4 eV), 1236 Å (10.0 eV), and 1048-67 Å (11.6-11.8 eV). Since the irradiating photons in these experi-ents have energies both higher and lower than the ionization ergy of isobutane (10.6 eV), the modes of decomposition of e "superexcited" molecule can be compared with those of the olecule excited to states below the ionization potential. On the sis of isotopic analyses of the major products, it was deter- ned that the following primary modes of decomposition of the cited isobutane molecule occur in the photolysis at all three ergies: $i\text{-}C_4H_{10}^* \rightarrow CH_4 + C_3H_6$; $i\text{-}C_4H_{10}^* \rightarrow C_3H_8 + CH_2$; i- $H_{10}^* \rightarrow CH_3 + sec\text{-}C_3H_7$; $C_4H_{10}^* \rightarrow H_2 + i\text{-}C_4H_8$. Most of the opyl radicals decompose further: $C_3H_7$ - H + $C_3H_6$; $C_3H_7$ - $H_3 + C_2H_4$. An increase in photon energy increases the rela- e importance of C–C cleavage processes. The parent ions rmed in the photolysis with 11.6-11.8 eV photons decompose form $C_3H_6^+$ and sec-$C_3H_7^+$. The $C_3H_6^+$ ions react with isobu- ne to form sec-$C_3H_7$ radicals or propane: $C_3H_6^+ + i\text{-}C_4H_{10} \rightarrow$ $H_3CHCH_3 + C_4H_9^+$; $C_3H_6^+ + i\text{-}C_4H_{10} \rightarrow C_3H_8 + c\ C_4H_8^+$. he probability of the former reaction is 1.5 times that of the tter, in agreement with a value for this ratio derived from the diolysis of $C_4D_{10} - H_2S$ and $C_4H_{10} - C_4D_{10}$ mixtures. The le of superexcited molecules in the radiolysis is discussed and is estimated that the number of dissociating neutral excited olecules per ion pair is no greater than 0.46.

**489.** McKinley, J. D., **Effects of the reaction with bromine on nickel surface morphology,** *Surface Sci.* **10,** No. 2, 287-290 (May 1968).

> Key words: Bromine; electron micrograph; nickel; single crystal; surface morphology; surface reaction.

Electron micrographs of single crystal nickel specimens show at exposure of nickel to bromine at 800 °K produces etch pits ounded by {100} crystallographic planes. The surface reaction oduct is volatile $NiBr_2$; reaction proceeds by recession of the 00} planes into the metal.

**490.** Maienthal, E. J., Taylor, J. K., **Polarographic methods in determination of trace inorganics in water,** Chapter 10 in *Trace Inorganics in Water, Advances in Chemistry Series* **73,** 172-182 (American Chemical Society, Washington, D.C., Apr. 1968).

> Key words: Polarographic analysis; trace analysis; water analysis.

Polarography is a particularly suitable method for the deter- ination of trace inorganic material in water. Owing to the selec- vity of electrode processes, interferences and hence prior hemical separations are minimized. Often several elements may e determined concurrently in the same supporting electrolyte. nodic stripping and linear sweep voltammetry give an in- eased sensitivity which permits determinations in the ppb nge to be made. Polarographic methodology is reviewed. A rvey of the literature concerned with determination of trace in- rganic material in water is given. Procedures used in this labora- ry for the determination of such elements as aluminum, ar- enic, cadmium, copper, indium, iodine, iron, lead, tellurium, and inc are discussed. The matrices include laboratory distilled ater, river water, and reactor cooling water. In addition a com- arative technique is described whereby precisions of better than percent can be obtained at the 0.1 ppm level.

**0491.** Maki, A. G., **Assignment of some DCN and HCN laser lines,** *Appl. Phys. Letters* **12,** No. 4, 122-124 (Feb. 15, 1968).

> Key words: DCN; emission; far infrared; HCN; lasers: spectra.

The far infrared laser lines in DCN are explained as being due o transitions involving the $22^{0}0$ and $09^{1c}0$ levels which are nixed by a Coriolis resonance at J = 21. The HCN laser lines ear 130 microns are explained by a Coriolis resonance which ffects the $12^{0}0$, $12^{2}0$, and $05^{1}0$ levels. New laser transitions are redicted for these systems.

**10492.** Mies, F. H., **Quantum oscillations in the shape of pressure-broadened atomic lines,** *J. Chem. Phys.* **48,** No. 1, 482-494 (Jan. 1, 1968).

> Key words: Atomic lines; band strengths; broadening; continuum-continuum transitions; diatomic molecules; emission absorption; interaction potential; pressure broadening; quantum mechanics; wavefunctions; W.K.B.

Oscillatory or bandlike structure is predicted to occur in the wings of pressure broadened atomic lines when the interaction potential between the emitting atom M* and the perturbing atom A is deeply attractive compared to kT and the interaction in the final state is repulsive. The oscillations in intensity arise from quantum effects and are associated with the nodal structure of the continuum wavefunction which describes the dissociated state of the diatomic molecule (A + M*). The number of maxima in the line shape is a measure of the number of bound states which can be supported in the potential while the amplitude and resolution of the oscillations depends on the long range behavior of the potential. The bandlike structure, which may extend over thousands of $cm^{-1}$ on the long wavelength side of the atomic emission line, is resolvable as long as $kT <$ approximately 1/10 the vibrational quantum $\hbar\omega_e$ of the AM* molecule. This is a generalization of similar bandlike structure which has been calculated *and observed* to occur in the collision induced radiation of helium metastable atoms and which is merely a special case of pressure broadening involving forbidden lines. Specific calculations are presented for the broadening of the hydrogen Lyman $\alpha$ line by H(1s), and the visible absorption spectra of H(1s) in the presence of free protons.

The quantum theory of line shape which is employed here was first developed by Jablonski but then neglected due to difficulties involved in evaluating essentially the bandstrength for continuum-continuum transitions of diatomic molecules. Jablonski introduced the W.K.B. and other approximations into his theory which reduced it to the classical statistical theory. These approximations are compared to exact quantum mechanical calculations. The W.K.B. approximation is shown to be quite valid in the special case of attractive-repulsive transitions, but Jablonski then improperly averaged over these very quantum oscillations of interest here. This structure offers a unique and extremely sensitive method of studying interaction potentials involving excited states of atoms.

**10493.** Miller, K. J., Krauss, M., **Born inelastic differential cross sections in $H_2$,** *J. Chem. Phys.* **47,** No. 10, 3754-3762 (Nov. 15, 1967).

> Key words: Born cross-sections; differential cross-sections; Hartree-Fock; hydrogen; Rydberg states.

First Born differential cross-sections are calculated for inelastic electron scattering of 300 eV electrons from the ground electronic-vibrational state of $H_2$ into the vibrational levels of the B, B′, C, D, and D′ Rydberg states. The initial and final state electronic wavefunctions were approximated by Hartree-Fock functions. In order to facilitate the calculation, the molecular orbitals were expanded in a linear combination of Gaussian-type atomic orbitals.

The variation of the electronic scattering amplitude was examined as a function of the molecular orientation, internuclear separation, and scattering angle (or electron momentum transfer). Use of the Franck-Condon factors to determine relative intensities for scattering into different vibrational levels yields errors less than 20 percent, and hence these factors are a good approximation to the relative intensities.

The theoretical differential cross-section for zero-angle scattering is in good agreement with the most recent experimental data. However, it is shown that transition moments extracted from electron scattering data are overestimated and in poor agreement with the theoretical values.

**10494.** Motz, J. W., Sparrow, J. H., **A simple device for the energy and current measurement of an accelerator electron beam,** *Record of the IEEE 9th Ann. Symp. Electron, Ion, and Laser Beam Technology, Berkeley, Calif., May 9-11, 1967,* pp. 34-41 (San Francisco Press, Inc., San Francisco, Calif., May 1967).

Key words: Electron beam; energy current; Møller scattering; Mott scattering; secondary electron; thin foils.

A simple apparatus has been developed which permits the simultaneous measurement of the electron energy and current of an accelerator electron beam. This measurement is accomplished with negligible interference of the beam during the continuous operation of the accelerator and applies to electron energies greater than approximately 50 keV. The apparatus consists of a thin aluminum foil which intercepts the beam with a negligible energy loss (less than one kilovolt), and two cylindrical aluminum electrodes which are positioned respectively on the incident and exit sides of the foil with axes normal to the foil surface and coincident with the beam direction. With a suitable distribution of electric potentials in this system, the incident electrode current, $I_i$, is inversely proportional to the square of the electron velocity and the exit electrode current, $I_e$, is inversely proportional to the square of the product of the electron velocity and momentum. Therefore, when an electron beam passes through this system, the electron energy can be determined from the current ratio, $I_i/I_e$, and the incident electron current can be determined from the current, $I_i$, as shown in previous measurements with secondary emission monitors. The energy dependences described above for each electrode has been confirmed over a wide range of electron velocities by measurements carried out with a constant potential electron accelerator in the energy region from 50 to 500 keV.

**10495.** Rebbert, R. E., Ausloos, P., **Photolysis of methyl iodide in matrices of organic compounds at 20° and 77 °K. Reactions of hot methyl radicals,** *J. Chem. Phys.* **48,** No. 1, 306-311 (Jan. 1, 1968).

Key words: D-atom; H-atom; hot methyl radicals; methyl iodide; photolysis.

Methyl iodide—hydrocarbon and methyl iodide—alcohol matrices have been photolyzed with 2537 Å radiation both at 20 and 77 °K. The probability of abstraction of an H atom by the hot $CH_3$ radical formed upon photodissociation $CH_3I$ is at least a factor of 10 larger in the solid phase than in the gas phase. However, the relative probabilities of abstracting an H-atom from various organic compounds are about the same in both phases. Also hot $CH_3$ radicals are more reactive than $CD_3$ radicals in both phases.

Photolysis of $CH_3I$ or $CD_3I$ in the presence of (a) equimolar mixtures of perprotonated and perdeuterated hydrocarbons and (b) partially deuterium labelled hydrocarbons, shows that the hot methyl radicals abstracts an H-atom and D-atom with equal probability. The hot methyl radical does, however, exhibit a certain selectivity as to the position in the molecule from where it abstracts an H-atom. For instance, an H-atom is abstracted more readily when attached to a secondary carbon atom than to a primary carbon atom. This non-statistical behaviour is, however, less accentuated in the solid phase than in the gas phase. When the matrix consist of an unsaturated hydrocarbon, the hot methyl radical can add to the double bond as well as abstract an H-atom. It is shown that hot methyl radicals add to ethylene to form $nC_3H_7$ radicals which subsequently react with the I-atom with which they are in juxtaposition. At 20 °K about one fourth of the hot methyl radicals add to $C_2H_4$.

**10496.** Stern, J., **Activities of the Basic Instrumentation Section,** (Proc. Fifth Transducer Workshop, National Bureau of Standards, Gaithersburg, Md., Oct. 3-4, 1967), *Telemetry Working Group Document* **112-68,** pp. 13-15 (Secretariat, Range Commanders Council, White Sands Missile Range, New Mexico, 1968).

Key words: High temperatures; information services; instrumentation; transducer.

The activities of the Basic Instrumentation Section at the National Bureau of Standards are described. Major emphasis in the work of the Section is placed on the fundamentals of instrumentation, among them transducer problems in many areas including measurement of high temperatures. In addition considerable effort is devoted to the development of information services for the field of instrumentation and the necessary methodology for this.

**10497.** Tauke, J., Litovitz, T. A., Macedo, P. B., **Viscous relaxation and non-Arrhenius behavior in $B_2O_3$,** *J. Am. Ceramic Soc* **51,** No. 3, 158-163 (Mar. 1968).

Key words: $B_2O_3$; shear spectra of relaxation times; ultrasonic relaxation; viscous relaxation.

Ultrasonic shear and longitudinal relaxation measurement were made in $B_2O_3$ over a large temperature range (650°—1000 °C). From these data both the shear and volume relaxation time spectra were determined. Both spectra had the same temperature dependence, although the volume spectrum was always broade than the shear spectrum. The shear relaxation process can b represented by a single relaxation time above 800 °C in the region where the shear viscosity is Arrhenius. Both processes exhibit an increasingly broad distribution of relaxation times in th non-Arrhenius region. The temperature dependence of the shea spectrum was analyzed in terms of a distribution of activatio energies. A surprising conclusion of this study is that activatio energies smaller than the activation energy present in the Ar henius region appear at low temperatures.

**10498.** van Reuth, E. C., Waterstrat, R. M., **Atomic ordering i binary A15-type phases,** *Acta Cryst.* **B24,** Part 2, 186-196 (Feb 1968).

Key words: A15-type phase; atomic packing; beta-tungste phase; electronic structure; order-disorder transformation ordering of atoms; phase stability; sigma phases; transitio metals.

The degree of long-range order has been determined for 18 b nary A15-type phases containing only transition elements. tendency toward a lower degree of order was noted as the com ponent elements were chosen successively from columns in th periodic table approaching the Mn column. A comparison of th ordering in the A15-type phases with the ordering previously re ported for various binary sigma phases suggests that the re markable stability of these phases may result from an interdepen dence between the electronic structure and the ability of th atoms to undergo deformations in conforming to geometric packing requirements.

**10499.** Woelfel, J. B., Paffenbarger, G. C., **Evaluation of comple dentures lined with resilient silicone rubber,** *J. Am. Den Assoc.* **76,** 582-590 (Mar. 1968).

Key words: Candida albicans; dentures; dimension changes in dentures; oral tissues; resilient reliners; rete tion; silicone rubber; stability.

Twenty four complete dentures, which had been in use for least seven years, were lined with a soft resilient silicone rubbe The dentures did not warp or change dimensions significant during or after the lining. The liner was tasteless, odorless, w well tolerated by the tissues, did not bond well to the periphery of the hard denture base, could not be easily removed for the relief of inflamed mucosa, nor were the stability and retention of the dentures improved over that expected from rebasing or relining a denture with a hard resin. On half of the lined dentures colonies of Candida albicans developed on the silicone rubber. Many of the colonies could not be brushed or scraped off and attacked the lining. The liner is not a cure all for denture problems as has been reported in the literature and its routine use is not recommended, but it has some limited applications in special cases.

**10500.** Acquista, N., Schoen, L. J., Lide, D. R., Jr., **Infrared spectrum of the matrix-isolated OH radical,** *J. Chem. Phys.* **48,** No. 4, 1534-1536 (Feb. 15, 1968).

> Key words: Doublet; infrared; isotope; matrix; photolysis; radical.

Infrared absorption in the region of 3450 cm$^{-1}$ has been observed in water-rare gas matrices subjected to vacuum ultraviolet photolysis at 20.4 and 4.2 °K. The splittings and isotope frequency ratios obtained from $H_2O^{16}$-$D_2O^{16}$, $H_2O^{16}$-$H_2O^{18}$ and $D_2O^{16}$-$D_2O^{18}$ mixtures lead to the assignment of these spectra to trapped OH radicals. No evidence for rotational motion of OH is found in these experiments.

**10501.** Adams, J. W., Desch, R. F., **Experimental confirmation of barretter substitution error,** *IEEE Trans. Microwave Theory Tech.* **MTT-16,** No. 3, 201-202 (Mar.. 1968).

> Key words: Bolometer substitution error; microwave power measurement.

Agreement of measured values of substitution error in barretters with calculated values based on a theoretical analysis by Carlin and Sucher substantiates both the measured and calculated values. The confirmed theory has interesting possible applications such as confirmation of accuracy of existing measurement techniques and extension to millimeter wave power measurement.

**10502.** Alley, C. O., Bender, P. L., **Information obtainable from laser range measurements to a lunar corner reflector,** Chapter in *IAU-IUGG Symposium No. 32 on Continental Drift, Secular Motion of the Pole and the Rotation of the Earth* **32,** 86-90 (Reidel Publ. Co., Dordrecht, The Netherlands, 1968).

> Key words: Laser; lunar distance; surveyor.

It has been proposed to the U.S. National Aeronautics and Space Administration that optical retro-reflector packages be placed on the lunar surface under either the Surveyor or Apollo Programs. Methods for measuring the range to the reflectors with an expected accuracy of 15 cm have been presented. The new technique is briefly discussed, and an analysis of the determination of geocentric longitude is given, indicating a potential uncertainty of $0.25 \times 10^{-3}$ seconds of time.

**10503.** Ambrose, J. R., Kruger, J., **The stress-corrosion of Ti and Ti-8Al-1Mo-1V in methanol vapor,** *Corrosion Sci.* **8,** 119-124 (1968).

> Key words: Methanol; stress corrosion; titanium; titanium 8-1-1; vapor phase failure.

An investigation into the stress corrosion cracking of titanium and titanium 8Al-1V-1Mo in methanol has shown that failure will occur in the methanol vapor phase with times to failure being at least an order of magnitude shorter than previously reported. Those effects which significantly altered time to failure were system volume, metal surface condition, and environment composition.

**10504.** Astin, A. V., **Standards of measurement,** *Sci. Am.* **218,** No. 6, 50-62 (June 1968).

> Key words: Measurement accuracy; physical measurement; physical standards; standards for science.

Virtually all measurements made in science and technology depend upon the four independent standards for length, mass, time, and temperature. This article traces the development of standards for these four quantities, with emphasis on recent advances that make possible greater measurement accuracy in science and industry. The possibilities for achieving even greater accuracy in measuring the four basic quantities are discussed.

**10505.** Astin, A. V., **Voluntary standardization and the government (fifty years of cooperation),** *Mag. Stds.* **39,** No. 6, 167-172 (June 1968).

> Key words: Government/non-government cooperation; performance standards; safety codes; simplified practice recommendations; standards of quality; voluntary standardization.

A half-century of progress in cooperative development of voluntary national standards for science and technology is reviewed. Beginning with the 1919 reorganization of the American Engineering Standards Committee and Secretary of Commerce Herbert Hoover's "crusade for standardization," the article traces the growth of government and non-government agency teamwork to the present era in which some 500 national organizations collaborate in standardization on the basis of consensus and continuing review and modernization.

**10506.** Bates, R. G., **Standardization of acidity measurements. Extension of the pH concept to mixed solvents and heavy water,** *Anal. Chem.* **40,** 28A-38A (May 1968).

> Key words: Acidity scales; deuterium oxide; nonaqueous media; pD; pH; pH*; pH concept; standards for acidity.

The modern concept of the operational pH value is examined in detail. Procedures by which the NBS pH scale (based on conventional hydrogen ion activity) was established are reviewed, and it is shown how these same methods and concepts can be extended to set up useful scales for acidity in nonaqueous and mixed solvent systems (using the unit pH*) and in heavy water (using the unit pD). The availability, in the form of standard reference materials, of two new pH standards and three new pD standards is announced.

**10507.** Bennett, J. A., **To avoid fatigue failures, pay attention to details,** *Current Engr. Pract.* **9,** 12-16 (Sept. 1966).

> Key words: Crack initiation; fatigue; residual stress; service failures; stress concentration; surface hardening.

Several examples are cited to illustrate how apparently minor factors can cause fatigue fractures in engineering components. Failures such as these emphasize the fact that the development of fatigue cracks depends on the stress and strength conditions in small critical areas, not on the average stress in the cross section. Consequently the reliability of structures and machines subjected to fluctuating loads can be improved by eliminating sources of stress concentration, by improving the residual stress distribution, and by increasing the strength of the material at the surface.

**10508.** Billick, I. H., Dishon, M., Weiss, G. H., Yphantis, D. A., **Numerical solutions of the Lamm equation. IV. Rotor slowing experiments,** *Biopolymers* **5,** 1021-1028 (1967).

> Key words: Lamm equation; molecular weight; numerical solutions; rotor slowing; sedimentation equilibrium; ultracentrifugation.

This paper presents the results of a numerical solution of the Lamm equation for rotor slowing specified by $\omega^2 = \omega_0^2 \exp(-\lambda\tau)$, for parameters relevant for equilibrium experiments. It is shown that in the two component system it is theoretically possible to deduce s/D from measurements of the difference of concentration across the cell with rotor slowing, provided that the time at which the difference reaches a maximum is known.

**10509.** Billick, I. H., Schulz, M., Weiss, G. H., **Quasi-equilibrium sedimentation experiments with rotor deceleration,** *J. Phys. Chem.* **71,** No. 8, 2496-2502 (July 1967).

Key words: Equilibrium sedimentation; Lamm equation; rotor deceleration; ultracentrifugation.

This paper presents an analysis of the rectangular approximation to the Lamm equation suitable for analyzing experiments with variable rotor speeds. The theory is applied to the case specified by deceleration described by $\omega^2 = \omega_0^2 \exp(-\lambda\tau)$. It is shown that s/D for a two component system can be determined experimentally by a measurement of concentration difference across the cell at a specified time after the beginning of the experiment. The resulting experiment offers the possibility of considerable savings in time over conventional sedimentation equilibrium experiments. Another experiment, involving a quasi-equilibrium state is analyzed. It is found that the rate of approach to the quasi-equilibrium state is slower than the rate of approach to equilibrium for conventional sedimentation equilibrium experiments under comparable conditions.

**10510.** Bleicher, M. N., Knopp, M. I., **Lattice points in a sphere,** *Acta Arith.* **X,** 369-376 (1965).

Key words: Geometry of numbers; lattice points; sphere.

Let $R_3(x)$ be the remainder in the classical lattice point problem for a 3-sphere of radius $\sqrt{x}$ and center (0,0,0). We prove that as $x \to +\infty$,

$$R_3(x) = 0(x^{3/4} \log x)$$

and

$$R_{3(x)} = \Omega(x^{1/2} \log \log x).$$

**10511.** Bollacasa, D., Goldman, D. T., **Importance of upscattering in the calculation of neutron spectra,** *Proc. Intern. Atomic Energy Agency Symp. Neutron Thermalization and Reactor Spectra, Ann Arbor, Michigan, July 17-21, 1967,* **1,** 537-554 (International Atomic Energy Agency, Vienna, Austria, Jan. 1968).

Key words: Cross sections; epithermal energy; group averaging; neutron; reactor spectrum; scattering; slowing down density.

A study has been made of the effect of raising the thermal energy cutoff higher than .625 eV. In most neutron thermalization calculations, the assumption is made that there is no upscattering above .625 eV. This may be a poor assumption especially for moderator models with chemically bound hydrogen even at room temperature. In the study, a thermal cutoff energy of 3.06 eV was chosen. This was done because the upscattering above this energy is small and this energy corresponds to that of a group in a slowing down program used in the calculations. Neutron spectra and group averaged cross sections were computed and the inadequacy of a thermal cutoff of .625 eV was manifested by comparisons between calculations at these energy cutoffs. A discontinuity can be observed in joining the thermal and epithermal fluxes at .625 eV, while the joining is smooth at 3.06 eV. This provides the possibility of directly normalizing the thermal neutron source to the slowing down density from the epithermal energy region. Thus, neutron spectra in the thermal and epithermal energy regions can be calculated in one process. Comparisons were made in group constants with no upscattering included between .625 eV and 3.06 and with upscattering included up to 3.06 eV. Differences up to 9 percent were observed. These effects could become significant in the calculation of criticality factors if large resonances were present or if systems with large metal-to-water ratios were considered. A spectrum calculation for a SHA (a homogenous assembly) fuel element was compared to a measurement made of its asymptotic spectrum. Even though the agreement between calculation and experiment was not exact, the calculated spectrum closely matched the measured spectrum above .625 eV.

**10512.** Branscomb, L. M., **The role of atomic collision processes in astrophysics,** Chapter in *The Physics of Electronic and Atomic Collisions: Invited papers from the Fifth International Conference, Leningrad, U.S.S.R., July 17-23, 1967,* L. M. Branscomb, ed., pp. 12-31 (Joint Institute for Laboratory Astrophysics, University of Colorado, Boulder, Colorado, 1968).

Key words: Atomic collision processes in astrophysics, review; review, atomic collision processes in astrophysics.

This paper is the manuscript of a lecture in which the importance of atomic collision processes in the field of astronomy is summarized. The paper deals primarily with the formation of stellar spectra, particularly from the sun, as well as problems of low density astrophysics such as the interstellar medium and planetary nebulae.

**10513.** Branscomb, L. M., **Twenty years of physics: atoms, molecules and electrons,** *Phys. Today* **21,** No. 5, 36-39 (May 1968).

Key words: Atomic and molecular physics; *historical* review of electron.

This is a review of the field of electron atomic and molecular physics.

**10514.** Breen, D. R., Keller, R. A., **Intramolecular energ transfer between triplet states of weakly interactin chromophores. I. Compounds in which the chromophores ar separated by a series of methylene groups,** *J. Am. Chem. Soc* **90,** No. 8, 1935-1940 (Apr. 10, 1968).

Key words: Energy transfer; fluorescence; phosphorescence; triplet states.

The intramolecular transfer of triplet excitation energy fro the donor chromophor (phthalimide and carbazole) to the acceptor chromophor (naphthalene) was studied when th chromophors were separated by methylene groups. In all cases complete transfer of triplet excitation energy occurred. New absorption and emission bands not characteristic of eithe chromophor were observed and were attributed to charg transfer absorption and emission.

**10515.** Brenner, A., Metzger, W. H., Jr., **Determination of th composition of complexes and their instability constants b calorimetry III. The complex in fused sodium molybdate an molybdenum trioxide,** *J. Electrochem. Soc.* **115,** No. 3, 25 261 (Mar. 1968).

Key words: Calorimetry; complex salts; composition complex salts, determination of; fused salts; partial mol heat effect; sodium molybdate-molybdenum trioxi system.

A method of determining the composition of complexes solution and their instability constants, which is based on t measurement of the partial molal heat effect developed when small increment of each salt is added in turn to a series of mi tures covering the range of composition from 0 to 100 perce has been applied to the molten $Na_2MoO_4 - MoO_3$ system at 800 °C. The data show that one complex is formed consisting of one molecule of $Na_2MoO_4$ and two molecules of $MoO_3$. The instability constant was approximately unity and the complex was between 50 percent and 75 percent dissociated.

**10516.** Brown, R. L., Brennen, W., **Spin-relaxation effects on the EPR spectrum of gaseous nitrogen atoms,** *J. Chem. Phys.* **47,** No. 11, 4697-4705 (Dec. 1, 1967).

Key words: Electron paramagnetic resonance; flow system kinetics; nitrogen atoms; spin exchange cross sections; spin relaxation time.

Experimental evidence is presented which indicates that N atoms produced in a flow system by a microwave discharge through purified $N_2$ have a "spin-lattice" relaxation time $T_1$ of the order of 25 msec. In a fast flow system, the residence time of the atoms in the EPR magnet can easily be shorter than this. As a result, atoms which are generated outside of the magnet may arrive at the microwave cavity before they have had time to reach their equilibrium magnetization. Addition to the discharged gas of as little as 10 p.p.m. $O_2$ (which did not affect the N atom concentration) decreased the spin relaxation time, and led to increases as great as 7-fold in the N atom EPR signal. Because of the long relaxation time it was necessary to work at the low microwave power level of 0.006 $\mu$W to avoid saturation effects. Power saturation was governed primarily by the rate at which unsaturated atoms entered the cavity and not by collision relaxation processes. Interpretation of the effects of $O_2$ addition in terms of a two level spin model allowed us to estimate a value of $\sim 1.5 \times 10^{-15}$ cm$^2$ for the spin exchange cross section for N-$O_2$ collisions. Several qualitative observations regarding the nitrogen pink afterglow, electron production, and the effects of NO addition are also reported.

**10517.** Butterfield, M. A., **Optical character recognition as an archival tool,** *Proc. A Pioneer Presentation of a National Symposium on the Impact of Automation and Documentation, Denver, Colo., Apr. 27-29, 1967,* pp. 101-118 (1968).

Key words: OCR applications; OCR as an archival tool; OCR bibliography; OCR history and growth; OCR as a library tool; optical character recognition.

The exponential growth of technology and records in our Third Industrial Revolution will require librarians and archivists to adopt mechanized and automated techniques to overcome problems of volume. A suggest input mechanization technique is Optical Character Recognition (OCR). The history and growth of OCR is presented along with current status and specific uses. Typical user experiences are described. Bibliography.

**10518.** Caldwell, B. P., **Kubelka-Munk coefficients from transmittance,** *J. Opt. Soc. Am.* **58,** No. 6, 755-758 (June 1968).

Key words: Absorption; Kubelka-Munk coefficients; optical constants; scattering.

A simplified method is described for the exact computation of Kubelka-Munk coefficients from internal transmittance measurements of two specimens of the same material where one specimen is twice as thick as the other. Equations are derived for determining the scattering coefficient $S$, the absorption coefficient $K$, the Kubelka parameters $a$ and $b$, the internal transmittance $\tau_i$, the reflectance of an infinitely thick specimen $\rho\infty$, and the reflectance of a specimen with an ideal black background $\rho_0$. Graphs are given to estimate the range of error in $\rho\infty$, $S$, and $K$ as a function of estimated measurement errors in transmittance.

**10519.** Chang, S. S., Bestul, A. B., **Heat capacities for atactic polystyrene of narrow molecular weight distribution to 360 °K,** *J. Polymer Sci.* **6,** Part A-2, 849-860 (1968).

Key words: Annealed sample; atactic polystyrene; enthalpy increment; entropy increment; glass; glass transformation; heat capacity calorimetry; literature values; narrow molecular weight distribution; precise heat capacities.

Precise heat capacity values are reported over the temperature range from 10° to 360 °K for a narrow molecular weight distribution atactic polystyrene sample taken from the same stock from which National Bureau of Standards Standard Sample 705, Narrow Molecular Weight Distribution Polystyrene, was established. Data are reported for the sample as received and after an annealing procedure. At temperatures below about 60 °K a systematic difference comparable with the limits of experimental precision appears between the values obtained for the present sample as received, and after the annealing, although at higher temperatures the values for the two did not show any systematic difference beyond the limits of precision of the measurements. At temperatures above 100 °K, previously published values for atactic polystyrene samples of various molecular weight distributions and for isotactic polystyrene agree within about 0.5 percent of the values from this investigation. At temperatures below 100 °K significant heat capacity differences appear, especially between values for the atactic and the isotactic isomers, and even between atactic samples of different molecular weight distribution.

**10520.** Childs, G. E., Hanley, H. J. M., **Applicability of dilute gas transport property tables to real gases,** *Cryogenics* **8,** No. 2, 94-97 (Apr. 1968).

Key words: Dilute gas; dilute limit; low pressure; mean-free-path; transport properties; validity range; viscosity.

The pressure range for which published "dilute" or "low pressure" transport property tables may be used is experimentally defined. The method is based on the fact that, in a well defined temperature range, transport properties can be computed from kinetic theory expressions. The method is general but specific examples are given for neon, argon, krypton, xenon, oxygen and nitrogen.

**10521.** Cohen, M. I., Blunt, R. F., **Optical properties of $SrTiO_3$ in the region of the absorption edge,** *Phys. Rev.* **168,** No. 3, 929-933 (Apr. 15, 1968).

Key words: Absorption coefficient; band structure; electroreflectance; optical properties; perovskite; reflectivity; strontium titanate.

The absorption coefficient, reflectivity, and electroreflectance of $SrTiO_3$ in the neighborhood of the fundamental absorption edge are reported. The absorption coefficient shows an exponential rise with incident energy (Urbach rule) over five orders of magnitude its logarithm has a slope of 1/kT. The data indicate that the band gap of $SrTiO_3$ is about 3.4 eV. Additional results for reduced $SrTiO_3$ show that Redfield's model for an exponential edge is not applicable to this material. The reflectivity indicates structure in the region of 3.4 eV and the electroreflectance shows appreciable signal from 2.5 to 5.0 eV with some structure near 3.4 eV. The electroreflectance signal appears to be due to some process other than the Franz-Keldysh effect. It could be due to a shift or splitting in the major oscillator (4.4 eV), responsible for the refractive index, with induced lattice polarization.

**10522.** Cooper, M. J., **Comments on the scaling-law equation of state,** *Phys. Rev.* **168,** No. 1, 183-184 (Apr. 5, 1968).

Key words: Critical indices; equation of state; scaling-laws.

A generalization of Kadanoff's scaling arguments is shown to provide a functional equation whose solution is a two-parameter power-law form for the equation of state.

**10523.** Cooper, M. J., Mountain, R. D., **Interpretation of relaxation times in the "electric-field effect on critical opalescence,"** *J. Chem. Phys.* **48,** No. 3, 1064-1066 (Feb. 1, 1968).

Key words: Binary mixture; concentration fluctuations; critical opalescence; electric field effect and light scattering; relaxation time.

The relaxation time characterizing the response of concentration fluctuations in a binary mixture to the application of an electric field is related to the free relaxation of concentration fluctuations. Examination of light scattered by such systems in the vicinity of the critical mixing point indicates that the change in the turbidity of the fluid with time can*not* be related to the diffusion coefficient as simply as is the change in the intensity with time of the light scattered through a given angle which is related to the diffusion coefficient $D$ and change in the wavevector k by a factor $\exp(-2Dk^{2}t)$.

**10524.** Corliss, E. L. R., Burnett, E. D., Kobal, M. T., Bassin, M. A., **The relative importance of frequency distortion and changes in time constants in the intelligibility of speech,** *IEEE Trans. Audio Electroacoustics* **AU-16,** No. 1, 36-39 (Mar. 1968).

Key words: Measures of speech quality; perception of speech; sound reproduction; speech communication; speech intelligibility; telephony.

A recording technique developed by E. D. Burnett permitted changes to be made in the relative proportions of intermodulation and harmonic distortion introduced by squaring the input signal. This process was achieved by sending equal parts of the signal through a squaring device, and through a 90-degree phase dividing network followed by a squaring device, and combining the squared outputs. Coupling this procedure with the time-changing features inherent in the sound recording process, we were able to set up a sequence of intelligibility tests whose scores provided solutions to sets of simultaneous equations involving the variables of frequency doubling, frequency halving, and doubling and halving transition times. It was possible to set up an over-specified series of tests, so that more than one solution could be derived from the experiments.

Lowering of the characteristic frequency proved to have the most serious effect upon intelligibility. The next most serious was stretching the transition times. Doubling the frequency by second-harmonic distortion was considerably less damaging, though still significant. Reducing the transition times to half their initial values proved relatively trivial.

This work has been part of a program sponsored by Veterans Administration.

**10525.** Corliss, E. L. R., Burnett, E. D., Stimson, H. F., **Polyacusis, a hearing anomaly,** *J. Acoust. Soc. Am.* **43,** No. 6, 1231-1236 (June 1968).

Key words: Diplacusis; hearing; hearing loss; masking; physiology of hearing; pitch perception; theories of hearing.

A previously unrecognized anomaly of pitch was discovered by Dr. H. F. Stimson while testing his hearing. Signals above 3500 Hz did not produce the same pitch in each ear; the right ear's sensation was that of a sound at a lower frequency, for which he also had normal pitch perception. Between 3700 Hz and 5200 Hz the pitch perceived in the right ear was independent of the frequency of the stimulus. As intensity was raised, additional pitches appeared, and for an intense sound a chord was heard whose constituents were not harmonically related. Stimson can match these anomalous pitches with sinusoidal stimuli of the appropriate lower frequency within about 2 percent; part of this variation is a change of pitch with intensity. Tones in his normal pitch range having a pronounced overtone structure are perceived as multiple. Overtones falling in the anomalous range give rise to the anomalous pitch. This would indicate a Fourier type of analysis before pitch recognition. Beats are not excited by interference between the pitches evoked by signals in the anomalous range and those heard normally. Loudness studies show signal powers to be additive. Tone masking and loudness summation experiments yield data suggesting that the pitch recognition mechanism lies in that part of the auditory system in which loudness is perceived, i.e., beyond the cochlea.

**10526.** Cornell, R. G., Speckman, J. A., **Estimation for a simple exponential model,** *Biometrics* **23,** No. 4, 717-737 (Dec. 1967).

Key words: Biometrics; exponential model; non-linear estimation; statistics; statistical estimation.

In many public health situations an estimate is required of the parameter $\rho$ in the statistical model $Y = 1 - \exp(-\rho t)$, where $Y$ represents the expected value of an observed proportion $y$ at time (or dosage) $t$. Ten methods of estimating $\rho$ are discussed and illustrated: graphical, maximum likelihood, least squares weighted least squares, moments, partial totals, Fisher, Spearman and two finite differences methods. Comparisons are made on the basis of ease of computation and large and small sample properties.

The maximum likelihood estimate has desirable large sample properties and a limited Monte Carlo study indicates that it has favorable small sample properties. However, it is difficult to compute. If the $t$'s are equally spaced and small samples are used, the partial totals estimate has similar statistical properties and is much easier to compute. If the $t$'s are exponentially spaced, either Fisher's or Spearman's estimate, both of which are easy to compute, is recommended as an alternative to the maximum likelihood estimate.

**10527.** Cornog, J. R., Bryan, H. L., Jr., **Manual and machine assisted search methods used in examining patent application in the transistor art,** *Proc. Natl. Electronics Conf., Chicago Ill., Oct. 25-27, 1965,* **XXI,** 672-677 (1965).

Key words: Information retrieval; information storage mechanized; methodology; optical-coincidence; patents references; search; systems; thinking.

The thinking patterns of a U.S. patent examiner as he searched for prior art manually and by mechanized methods are contrasted in this paper. The specific analysis presented is for a search of the U.S. Patent Office references in the transistor art but generalizations in the Summary are based both on thi protocol and several from similar searches in the organometallics files. Some advantages and limitations of mechanized reference retrieval systems are given.

**10528.** Costrell, L., **Standard nuclear instrument module** (Adopted by AEC Committee on Nuclear Instrumen Modules, January 1968), *AEC Report* **TID-20893** (Rev. 2 (Superintendent of Documents, U.S. Government Printin Office, Washington, D.C., 1968, 25 cents.)

Key words: Instrument; interchangeability; module nuclear; standard.

The interchangeability problem posed by the advent of modular instrumentation has been alleviated by the development of Standard Nuclear Instrument Module (NIM) system by th AEC Committee on Nuclear Instrument Modules. The Committee held its first meeting on March 17, 1964. The complete specifications were issued in July 1964 and laboratory utilizatio and industry exhibit of the NIM system began in Novemb 1964. Acceptance by the laboratories and by the nuclear instr ment industry has been so rapid and so overwhelming that it estimated that NIM instruments constituted over two-thirds the total modular nuclear instrument production in the U.S.

1966 and between 85 percent and 95 percent in 1967. Since all necessary components are available, other fields and other industries can readily adopt the system.

**10529.** Coyle, T. D., Cooper, J., Ritter, J. J., **Preparation and some reactions of difluoroborane,** *Inorg. Chem.* **7,** No. 5, 1014-1020 (May 1968).

> Key words: Boron; difluoroborane; fluoride; hydride; hydroboration; isotope exchange; organoboron compounds.

Difluoroborane is produced by the direct interaction of boron trifluoride with diborane in the gas phase at 100 °C or above. Pyrolysis of $BF_3-B_2H_6$ mixtures at 250 °C for periods of 30 min to 1 hr, followed by rapid quenching, yields $HBF_2-BF_3$ mixtures free of $B_2H_6$. An alternative, synthetically useful route is the reaction of $HB(OCH_3)_2$ with excess $BF_3$. Difluoroborane undergoes rapid H−F exchange with boron trifluoride and H−D exchange with deuterated diborane, but does not exchange boron with diborane. Addition of difluoroborane to propene and isobutene yields *n*-propyldifluoroborane and isobutyldifluoroborane, respectively. Reactions with fluoroethylenes give boron trifluoride, ethylfluoroboranes, and less highly fluorinated olefins.

**10530.** Coyle, T. D., Ritter, J. J., **Reactions of diboron tetrahalides with some unsaturated organometallic compounds,** *J. Organometallic Chem.* **12,** 269-280 (1968).

> Key words: Addition reactions; boron; boron subhalides; organometallic compounds; tetrachlorodiborane(4); tetrafluorodiborane(4).

Tetrachloro- and tetrafluorodiborane(4) add to the double bond in a number of vinyl derivatives of boron, carbon, silicon, germanium, and tin to form 1,2-bis(dihaloboryl)ethyl derivatives. Most of the compounds are stable *in vacuo* at temperatures in excess of 150 °C. Tetrachlorodiborane(4) undergoes addition considerably more readily than does tetrafluorodiborane(4). Relative rates of addition have been determined and shown to be markedly dependent on the nature of the substituent on the vinyl group.

**10531.** Crumlish, J. D., Wirth, G. F., **A preliminary study of engineering seismology benefits,** *Environmental Science Services Administration, Coast and Geodetic Survey* (Superintendent of Documents, U.S. Government Printing Office, Washington, D.C., 20402, Aug. 1967, 35 cents).

> Key words: Benefit-costs; cost-effectiveness; economic benefits studies; engineering seismology; program evaluation and analysis; programming, planning, budgeting studies.

To examine the economic benefits of engineering seismology, a number of avenues were followed in this study. The main approach was a comparison of school earthquake damage records by pre-1933 and post-1933 construction categories. (In 1933, California began requiring strict earthquake-resistant design for public school facilities.)

This comparison revealed average damage of less than one percent for post-1933 schools compared to average damage as high as 78 percent for pre-1933 schools. School damage data for the Seattle (1965) earthquake and for the Alaska (1964) earthquake were also investigated.

**10532.** Cushen, W. E., **Systems engineering—Where did it come from . . . where will it go?,** *Consulting Engr.* **30,** No. 3, 130-134 (Mar. 1968).

> Key words: Decisions; gaming; government; management; operations research; systems engineering.

Systems engineering is entering a totally new applications area. This area broadly covers such service functions as transportation, pollution control, urban and rural development, crime control, and education. This introductory article describes some of the implicit modifications that will need to be made to the customary procedures of systems engineering if the tremendous potential of its use is to be realized. A "flashback" into the history of operations research, systems analysis, and the multidisciplinary problem-solving approach of the Defense and industrial establishments of the nation is provided for perspective.

**10533.** Cuthill, J. R., McAlister, A. J., Williams, M. L., **Soft x-ray spectroscopy of alloys: TiNi and the Ni-Al system,** *J. Appl. Phys.* **39,** No. 5, 2204-2208 (Apr. 1968).

> Key words: Absorption correction; density of states; lifetime broadening; nickel; overlapping spectra; soft x-ray spectra of alloys; temperature broadening; Ti-Al system; TiNi.

Meaningful comparisons can now be made between the soft x-ray spectra of pure metals and theoretical densities of states distributions. The comparison of the Ni-M spectrum with theoretical results is shown as an example. Also, useful information can now be obtained from alloy spectra although the analysis of alloy spectra involves all of the problems inherent in the interpretation of pure metal spectra plus additional problems. Overlapping spectra and more complex absorption corrections are two additional problems discussed. In fact, the soft x-ray spectroscopy technique should provide a crucial test of theoretical results on alloy systems.

Spectra from a series of Al-Ni compositions and the Ni-M spectrum from TiNi are discussed.

**10534.** Dehl, R. E., **Broadline NMR study of $H_2O$ and $D_2O$ in oriented rayon fibers,** *J. Chem. Phys.* **48,** No. 2, 831-835 (Jan. 15, 1968).

> Key words: Broadline NMR; $D_2O$; dipole-dipole interaction; $H_2O$; oriented water; quadrupole-field gradient interaction; rayon fibers.

The broadline NMR spectra of $H_2O$ and $D_2O$ absorbed in parallel fibers of highly crystalline rayon have been found to consist of two lines, whose separation depends upon the angle between the fiber axis and the magnetic field. The $D_2O$ splitting, resulting from quadrupole perturbation of the nuclear Zeeman levels, was about ten times greater than the $H_2O$ splitting, produced by direct nuclear dipole-dipole interaction. Two models for the partial orientation of water molecules are discussed, (I) in which the molecules rotate about a fixed axis, and (II) in which the molecules reorient rapidly about all possible axes, but maintain a small resultant projection, along the fiber axis. Model I is shown to be incorrect for the rayon fibers, on the basis of the combined $H_2O$ and $D_2O$ results; Model II, however, appears to be applicable not only to rayon but to other examples of partially oriented water as well.

**10535.** deMain, P. A. D., Marron, B. A., **The SOLID SYSTEM. I. A method for organizing and searching files,** (Proc. Third Annual Colloquium on Information Retrieval, Philadelphia, Pa., May 12-13, 1966). Chapter in *Information Retrieval, A Critical View,* G. Schecter, ed., pp. 243-282 (Thompson Book Co., Washington, D.C., 1967).

> Key words: Chemical structures; compressions; computer; files; information; storage and retrieval.

Here are described the *principles* of the SOLID SYSTEM, a *Self-Organizing, Large, Information Dissemination System.* In the SOLID SYSTEM, fully automatic compressors reduce both fast and slow (external) memory requirements to a minimum and provide item by item decoding by the system as the information is required. The computer constructs an INFORMATION REPRESENTATION (LABEL) and its BIT-MAPS for each document or query and then uses this information to locate or store information. With BIT-MAPS, storage requirements for LABEL are kept to a minimum. Together LABEL and its BIT-MAPS can preserve the hierarchic characteristics of the query or document to any depth. Override features permit any degree of uncertainty in both storage and retrieval. Unique non-algebraic transformation rules, easily executed by a computer, permit recanonicalization of LABEL and its BIT-MAPS to emphasize any kernel, class or group characteristic of the information when the system demands it.

The SOLID SYSTEM can be implemented with successively higher degrees of automation as usage, funds and "computer power" increase, without compromising either its early implementation or the later development of new techniques for entering the system.

Here chemical structural information is used to demonstrate the SOLID SYSTEM.

**10536.** DeSimone, D. V., **Education for innovation,** *IEEE Spectrum* **5,** No. 1, 83-90 (Jan. 1968).

Key words: Creative engineering; engineering education; innovation; invention; technological change.

Engineering education should encourage students to strive for a mastery of fundamentals and the cultivation of excellence – but this is not enough. Engineering education must be kept alive and relevant; and, to encourage creativity, it must stimulate the imaginations of students. The typical educational yardstick of a student's performance, however, is the accuracy with which he can repeat, by rote, information obtained from a lecture or text. Original or unconventional approaches to problems are discouraged, and their proponents often penalized, thus discouraging and depressing the student. Must inventiveness be sacrificed to education?

**10537.** DeVoe, J. R., Spijkerman, J. J., **Mössbauer spectrometry,** *Anal. Chem.* **40,** No. 5, 472R-489R (Apr. 1968).

Key words: Chemical applications; literature; Mössbauer spectroscopy; review.

A review of the literature on chemical applications of Mössbauer spectroscopy for 1966 and 1967 is presented. This is done primarily with a table of pertinent information on compounds and techniques. New developments in the field are also presented.

**10538.** Dibeler, V. H., Walker, J. A., **Mass spectrometric study of the photoionization of small polyatomic molecules,** (Proc. Conf. on Mass Spectrometry, Berlin, Germany, Sept. 1967), Chapter in *Advances in Mass Spectrometry* **4,** 767-780 (The Institute of Petroleum, London, England, 1968).

Key words: Bond dissociation; heats of formation; ionization energies; vacuum ultraviolet.

Photo-ionization measurements, absorption spectra, photoelectron spectra, and electron impact studies of $CO_2$, COS, $CS_2$, $NO_2$, and $N_2O$ have been reported by various authors. There remains considerable uncertainty and disagreement regarding thresholds of ionization, particularly for dissociative ionization. In some cases, the bond energies derived from the latter are of considerable interest. The present report describes results obtained as part of a continuing programme of study of the photo-ionization of polyatomic molecules. In this study, mass analysis is employed to identify and to select ionic species produced by radiation from photon sources over the wavelength region 1500 to 600 Å and with band-widths of 1 Å.

**10539.** Dick, C. E., Marella, A. B., Miller, W. C., **A simple beam positioning system for low energy electrons,** *Nucl. Instr. Methods* **60,** 346-348 (1968).

Key words: Beam positioning system; low energy electrons.

A servo system utilizing fabricated steering coils has been devised to hold the electron beam from a 4 MeV Van de Graaff accelerator on the entrance slit of a magnet system used for high momentum resolution. It performs extremely well.

**10540.** Dickson, P. F., Jones, M. C., **Infrared spectral reflectances of metals at low temperatures,** *Cryogenics* **8,** No. 1, 24-29 (Feb. 1968).

Key words: Compilation; cryogenic; infrared; metals; reflectance.

Experimental results of infrared spectral reflectances of ten pure metals and one alloy system at low temperatures are reviewed. Reflectances are in many cases calculated from published optical constants or obtained from absorptance measurements. Comparisons with room temperature measurements are made where possible and some observations regarding the effect of sample preparation technique and surface oxidation are made.

**10541.** Dickson, R. W., Anderson, R. C., **Temperature dependence of the elastic moduli of $91Y_2O_3 + 9ThO_2$ from 25° to 1100 °C,** *J. Am. Ceram. Soc.* **51,** No. 4, 233 (Apr. 1968).

Key words: Elastic moduli; Poisson's ratio; porosity; shear modulus; Young's modulus; yttria.

Young's modulus and the shear modulus of pore-free, transparent yttria sintered with thoria (90 $Y_2O_3 + 10$ $ThO_2$) were determined from 25 °C to 1100 °C. Poisson's ratio was calculated and shows a slight increase with increasing temperature.

**10542.** Durst, R. A., **Fluoride microanalysis by linear null-point potentiometry,** *Anal. Chem.* **40,** No. 6, 931-935 (May 1968).

Key words: Fluoride activity electrode; fluoride analysis; linear null-point potentiometry; microanalysis; microcell design; potentiometry.

The modified fluoride activity electrode is used as the sample electrode in the technique of linear null-point potentiometry for the determination of fluoride at subnanogram levels in sample volumes of 10 $\mu\ell$. The emf vs. titrant concentration data are plotted semilogarithmically, and the equivalence point is obtained by a linear interpolation to the null-point potential. Data analysis is also accomplished by computer techniques whereby the equivalence point is obtained from the intercept of a linear least squares fit of the data. Fluoride solutions $10^{-3}$ to $2 \times 10^{-6}M$ (containing 190 to 0.38 nanograms of fluoride in 10 $\mu\ell$) were determined with an accuracy of approximately 1 percent over the entire range and a relative standard deviation of the mean of about 0.5 percent for 5 determinations. At the lowest concentration level, $2 \times 10^{-6}M$ fluoride, the error in determining 380 picograms of fluoride was approximately 2 picograms.

**10543.** Durst, R. A., May, E. L., Taylor, J. K., **Improved technique for the microdetermination of silver by linear null-point potentiometry,** *Anal. Chem.* **40,** No. 6, 977-978 (May 1968).

Key words: Linear null-point potentiometry; microdetermination of silver; potentiometry; silver.

The determination of submicrogram amounts of silver by linear null-point potentiometry has been significantly improved through the use of several modifications of the technique Greater linearity of the titration curves, shorter analysis time and improved accuracy are achieved by pregeneration of the standard solutions and the establishment of an equilibrium null point potential. In this study, 54 nanograms of silver in a volume of 0.1 ml were determined with an error of less than 2 ng, while at concentrations above 10 $\mu M$, errors of less than 1 percent are easily obtained using the improvements discussed.

**10544.** Eisenhart, C., **Expression of uncertainties of final results,** *Science* **160,** No. 3833, 1201-1204 (June 14, 1968).

Key words: Accuracy; calibrations; expression of uncertainty; measurements; precision; standard error; systematic error; uncertainty.

The terms used to describe the precision and accuracy of measurements are defined and discussed. Specific rules are recommended for expressing the uncertainty of a reported value for four cases distinguished according to the relative magnitudes of the imprecision and the likely systematic error of the measurement process employed. Examples of recommended forms of uncertainty statements are given.

**10545.** Eisenhart, C., **Biography on Carl Friedrich Gauss,** *International Encyclopedia of the Social Sciences* **6,** 74-81 (The Macmillan Co. and The Free Press, New York, N.Y., 1968).

Key words: Gauss, Carl Friedrich; Method of Least Squares.

A biography of Gauss with particular attention to his role in the development of the Method of Least Squares.

**10546.** Eisenhauer, C., **Gamma radiation fluxes near a ground-air interface using an image source technique,** *Nucl. Sci. Engr.* **32,** 166-177 (1968).

Key words: Air-scatter; buildup factor; gamma rays; image source; interface; shielding; single scatter.

Calculations are made of the radiation flux of gamma rays which have originated from a point isotropic source and have been singly-scattered in the air lying beyond a plane interface. Calculations are made in the limit that the source-detector separation distance is small compared to a mean free path in air. These results are interpreted in terms of an image source. The results, combined with earlier calculations of the radiation flux reflected from a condensed medium, such as ground, predict the effect of the ground-air interface on radiation fluxes in air near the interface. The results are extrapolated to source-detector separation of the order of a mean free path by using infinite medium buildup factors. Comparisons with experiment show that the model produces results which are in qualitative agreement with experiment.

**10547.** Fatiadi, A. J., **Formation of arylazocyclohexene derivatives on acylation of certain inosose phenylhydrazones,** *Carbohydrate Res.* **7,** 89-94 (1968).

Key words: Acylation; arylazoethylenes; inosose phenylhydrazones.

It has been found that acetylation of *myo*-inosose-2 phenylhydrazone with acetic anhydride in the presence of pyridine at room temperature produces 1-phenylazo-1-cyclohexene-DL-*ido*-3,4,5,6-tetrol tetraacetate ($\beta$-elimination product) instead of the phenylhydrazone derivative reported. In contrast, acylation with propionyl anhydride and pyridine gives the phenylhydrazone pentapropionate. However, acylations of DL-*epi*-inosose-2 phenylhydrazone at 0 to 5 °C with acetic or propionic anhydrides give the corresponding pentaacylated phenylhydrazones.

**10548.** Fell, H., Mather, J., **Barely faithful algebras,** *Math. Monthly* **72,** No. 9, 1001-1003 (Nov. 1965).

Key words: Algebras; nontrivial linear associative algebras; nonzero element.

It is shown that nontrivial linear associative algebras, which are "barely faithful" in the sense that each nonzero element is a two-sided zero-divisor but neither a right nor a left annihilator, exist in all dimensions $\geqslant 4$ but not in lower dimensions.

**10549.** Flynn, D. R., O'Hagan, M. E., **Measurements of the thermal conductivity and electrical resistivity of platinum from 100 °C to 900 °C,** *Engelhard Ind. Tech. Bull.* **VIII,** No. 4, 117-147 (Mar. 1968).

Key words: Conductivity; electrical conductivity; electrical resistivity; heat conductivity; Lorenz function; platinum; reference material; resistivity; standard; thermal conductivity.

Measurements have been made of the thermal conductivity and the electrical resistivity of commercial grade platinum (99.98 percent pure) in the temperature range 100 to 900 °C. The measurements have been made with a view to providing accurate data on the thermal conductivity of platinum to serve as a basis for establishing platinum as a thermal conductivity standard reference material. Two methods of measuring the thermal conductivity have been employed, one an electrical method and the other a non-electrical method. In the electrical method, a direct current passed through a necked-down portion of the specimen and the thermal conductivity was determined in terms of the temperature and electrical potential distribution in the necked-down region. The second method was of the absolute guarded longitudinal heat flow type. The experiment was designed to permit measurements by both methods in the same apparatus and on the same specimen thereby providing as direct a comparison as possible between the methods. The data given by the two methods agree within experimental error and show the thermal conductivity of platinum to be a smoothly increasing function of temperature in the measured range. Additional measurements on samples of differing purities are necessary before platinum could be adopted as a thermal conductivity reference material.

**10550.** Fraction, G. F., Tauber, S. J., Walker, J. C., **Connection tables from Wiswesser line notation: A partial algorithm,** Proc. Wiswesser Line Notation Meeting of the Army Chemical Information and Data Systems Program, Edgewood Arsenal, Watertown, N.J., Oct. 6-7, 1966, *Edgewood Arsenal Spec. Publ.* **EASP-400-8,** pp. 139-197 (Jan. 1968).

Key words: Acyclic; benzene; chemical structure notations; connection tables; contractions; ring system; syntax analysis; transformation algorithm; Wiswesser.

An algorithm has been developed for transforming certain types of Wiswesser organic structure notations into connection tables. Acyclic and benzene structures are treated, and provision has been made for all of the types of contractions used by the Wiswesser notation system. A separate algorithm is presented for treating linearly fused ring aggregates. A syntax has been developed to describe those portions of Wiswesser notations which refer to non-benzene ring systems.

**10551.** Franklin, A. D., **Born model calculation of defect energies in $CaF_2$,** *J. Phys. Chem. Solids* **29,** 823-841 (1968).

Key words: Born model calculation; calcium fluoride; energies of formation; Frenkel pairs; interstitials; ionic crystals; point defects; Schottky pairs; vacancies.

A general formulation of the Born model as applied to the calculation of the energies to form point defects in ionic crystals is given, and then specialized to vacancies and interstitials of both kinds in $CaF_2$. After examination of the effects produced by several factors in the calculation, "best values" are chosen for the formation energies. These are used to compute the energies to form anion Frenkel pairs ($2.7 \pm 0.4$ eV/pair), cation Frenkel pairs ($7.5 \pm 0.8$ eV/pair), and Schottky trios ($5.1 \pm 0.7$ eV/trio). The results are in reasonable agreement with Ure's experimental results, which indicate that anion Frenkel pairs are the equilibrium defects in $CaF_2$, with a formation energy of 2.8 eV.

**10552.** Goldman, A. J., Nemhauser, G. L., **A transport improvement problem transformable to a best-path problem,** *Transportation Sci.* **1,** No. 4, 295-307 (Nov. 1967).

Key words: Algorithm; graph; network; optimization; shortest-path; transportation.

For each arc (i,j) of a transport network, suppose given an initial traversal disutility d(i,j) and a function f(i,j,r) describing the reduced disutility which would result from applying *r* units of resources to "improve" the arc. For each origin-destination pair, there arises the problem of how a limited resource budget should be allocated among the arcs so as to optimize a best path from origin to destination in the improved network. It is shown here that this problem is transformable to a best-path problem in an enlarged network. The allowable investment levels in individual arcs can be constrained as desired.

**10553.** Goldman, D. T., Muehlhause, C. O., **Neutron Physics,** Chapter 7 in *Handbook of Physics, Second Ed., Part 9, Nuclear Physics,* E. U. Condon and H. Odishaw, eds., pp. 9-195–9-211 (McGraw-Hill Book Co., New York, N.Y., 1967).

Key words: Diffraction; inelastic; interaction; materials; neutron; properties; reaction; scattering; structure; transport.

The enclosed paper is a review article written for the second edition of the "Handbook of Physics" edited by E. U. Condon and H. Odishaw. As such it is a revision of one of the authors' (C. O. Muehlhause) original articles. The paper deals with the general features of the physical properties of the neutrons, containing initially the fundamental properties of the neutrons, their mass, charge, moments and certain basic interactions. The history of a neutron is then traced from its generation in, e.g., a reactor spectrum, including a discussion of the interactions of the neutron with atomic nuclei. The theory of the transport of neutrons is then outlined. The next section deals with the utilization of thermal energy neutrons as a probe for the determination of the detailed characteristics of solids and liquids and suggests other techniques which have been used. Finally, effective range theory is introduced to interpret low energy neutron-proton scattering.

**10554.** Gray, V. E., Cadoff, B. C., **Survey of techniques for evaluating effects of weathering on plastics,** *Appl. Polymer Symp.* **4,** 85-95 (Sept. 1967).

Key words: Color and gloss measurements; colorimetric analysis; infrared analysis; oxidation; plastics; ultraviolet analysis; weathering.

This paper surveys those physical and chemical test methods that could be applied in the prediction of the performance of plastics under outdoor exposure.

Techniques to measure appearance, strength, and flexibility are reviewed. Color changes alone, although widely used, are shown to be an insufficient measure of weathering.

The more sensitive spectroscopic and chemical test methods that have been found to measure oxidation and hydrolysis products in polymeric materials are examined for usefulness in quantitatively measuring plastic degradation. The methods reviewed are used to determine carbonyl, carboxyl, peroxidic, and hydroxyl groups.

**10555.** Halford, D., **A general mechanical model for $|f|^\alpha$ spectral density random noise with special reference to flicker noise $1/|f|$,** *Proc. IEEE* **56,** No. 3, 251-258 (Mar. 1968).

Key words: Flicker noise; low frequency noise; mechanical model; modulation noise; noise; noise model; noise simulation; precision measurements; random noise; reasonable perturbations; spectral density; $1/f$ noise.

Any class of reasonable time-dependent perturbations occurring at random, under certain internal constraints, generates random noise having a spectral density varying as $|f|^\alpha$ over an arbitrarily large range of spectral frequency $f$ only for $-2 \leqslant \alpha \leqslant 0$. A class is the set of all perturbations which are equivalent under some individual independent scaling of amplitude, scaling of time, and translation of time. A subclass is characterized by $P(\tau)$ and $A^2(\tau)$. $P(\tau)$ is the lifetime probability density. $A^2(\tau)$ is a mean square amplitude of perturbations having lifetime $\tau$. For a given class, $|f|^{\alpha\infty}$ and $|f|^{\alpha 0}$ are the frequency-smoothed laws in the limits of infinite and zero frequencies, respectively. Any reasonable perturbation has $\alpha_\infty \leqslant -2$ and $\alpha_0 \geqslant 0$. To generate random noise having an $|f|^\alpha$ law over an arbitrarily large range of $f$ from a subclass chosen from any class characterized by $\alpha_\infty$ and $\alpha_0$, it is necessary that $\alpha_\infty \leqslant \alpha \leqslant \alpha_0$. For $\alpha_\infty < \alpha < \alpha_0$, it is necessary and sufficient that such subclasses satisfy the condition, $P(\tau)A^2(\tau) \approx B\tau^{-\alpha-3}$ with $B$ constant, over a suitable range of $\tau$, and that $P(\tau)A^2(\tau)$ not be larger than $B\tau^{-\alpha-3}$ outside the range. This general mechanical model is of immediate value in the formulation and criticism of specific physical models of $|f|^\alpha$ noise, including flicker noise, and in computer simulation of $|f|^\alpha$ noise.

**10556.** Hall, L. H., Spijkerman, J. J., Lambert, J. L., **Preparation and coordination studies of the complex acid, dihydrogen diethylenetriaminepentaacetatoferrate(III) dihydrate, and several of its metal (I) salts,** *J. Am. Chem. Soc.* **90,** No. 8, 2044-2048 (Apr. 10, 1968).

Key words: Coordination; infrared spectroscopy; magnetic susceptibility; Mössbauer spectroscopy; $M_2$FeDTRDS; photodecomposition; preparation; thermogravimetric analysis.

The coordination numbers of the central metal ion which exists in iron (III) chelated with diethylenetriaminepentaacetic acid, $H_5$DTPA have been investigated by the following methods: (a) infrared spectroscopy, (b) magnetic susceptibility, (c) Mössbauer spectroscopy, (d) photodecomposition and (e) thermogravimetric analysis. The iron(III) DTPA complexes were found to exist in three different forms in the solid phase; the complex acid, the mono-salt and the di-salt. All three forms were found to be high spin complexes. The complex acid $H_2FeDTPA \cdot 2H_2O$ was shown to have a coordination number of six around the central metal atom. The monoammonium salt, $NH_4HFeDTPA \cdot 1H_2O$ was found to be seven coordinated. However, the di-alkali metal salts $M_2FeDTPA \cdot nH_2O$ were found to have a coordination number of eight around the central atom but one of the iron(III) carboxylate bonds is different than the remaining four.

The cation in the salt of the complex interacts with the metal d-orbitals, and appears to decrease the size of the metal d-orbitals, which results in a concentration of the d-electron density nearer the nucleus.

**10557.** Hamer, W. J., **Battery, electric,** *Encyclopedia Americana* **3,** 357-363 (1967).

Key words: Battery; electric battery.

A brief description of the electric battery.

**10558.** Hamer, W. J., **Using standard cells,** *Meas. Data* **1,** No. 6, 64-67 (Nov.-Dec. 1967).

Key words: Early types of standard cells; life of standard cells; standard cells; temperature coefficient of standard cells.

This paper contains information on effects of temperature, pressure, electric current, light, shock, and vibration on standard cells. The paper also includes some information on the temperature range for which standard cells can be used and some information on their life.

**10559.** Hamer, W. J., Wood, R. E., **Electrolytic conductivity and electrode processes,** Chapter 9 in *Handbook of Physics, Second Ed., Part 4, Electricity and Magnetism,* E. U. Condon and H. Odishaw, eds., pp. 4-146–4-171 (McGraw-Hill Book Co., New York, N.Y., 1967).

Key words: Batteries; Debye-Hückel-Onsager theory of conductance; electrochemical thermodynamics; electrode mechanisms; electrolytic conductivity; fuel cells; ionic charge; ionization; standard cells; transference numbers.

This article deals with the general principles of electrolytic conductance and the mechanism of the processes that occur at the interfaces between electrodes and electrolytes. *Topics covered include:* Comparisons of electrolytic and electronic conductors, classes of electrolytic conductors, the process of ionization in conducting solutions, the determination of the degree of ionization in strong and weak electrolytes, ionic charge, values of the Faraday, equations for electrolytic conductivity, meaning of equivalent and molar conductance, ionic conductances and transference numbers, ionic mobilities, effects of interionic attraction on electrolytic conductance including a discussion of the Debye-Hückel-Onsager relations, high-field effects in conductance, conductance at high frequencies, electrochemical thermodynamics, activity coefficients, standard electrode potentials in aqueous solutions and molten electrolytes, standard cells, pH determinations, irreversible phenomena at electrodes, electrode polarization, hydrogen overvoltage, and electric cells and batteries including discussions of primary batteries, secondary batteries, reserve or delayed-action batteries, and fuel cells.

**10560.** Hammond, H. K., III, **Phototube response evaluation,** *Appl. Opt.* **7,** No. 5, 985 (May 1968).

Key words: Color temperature standards; phototube response evaluation; total irradiance standards.

Phototube response has been reported for many years on a photometric instead of a radiometric base. Theoretically a radiometric base would be preferable, but practically it appears to offer little advantage. Color temperature would still be required to specify the spectral distribution of each standard lamp. A conversion factor can be computed to go from a photometric to a radiometric base for a given color temperature, 2870 °K being the most frequently used.

**10561.** Harvey, M. E., **Precision temperature-controlled water bath,** *Rev. Sci. Instr.* **39,** No. 1, 13-18 (Jan. 1968).

Key words: Bath; control; temperature; water.

The water bath described was designed primarily to furnish an improved environment for microwave microcalorimeters but would also be useful for thermometer calibration, standard cells (suitably insulated), and other physical and chemical measurement systems. The bath and its associated temperature controller operate at any bath temperature between 18 °C to 28 °C which is not more than 6 °C below the ambient temperature. The bath provides a temperature stability of $\pm 25\mu$ °C over a 24-hour period when measured with a 100-second time constant. The short-term stability measured with a 0.7-second time constant is between $\pm 70\mu$ °C and $\pm 7\mu$ °C, depending on the location within the bath and the magnitude of the energy exchange between the heating and cooling mechanisms. The bath temperature change caused by an ambient temperature change of 2 °C is less than $5\mu$ °C.

**10562.** Hayward, R. W., **Nuclear electromagnetic radiation,** Chapter 6 in *Handbook of Physics, Second Ed., Part 9, Nuclear Physics,* E. U. Condon and H. Odishaw, eds., pp. 9-172–9-194 (McGraw-Hill Book Co., New York, N.Y., 1967).

Key words: Gamma rays; internal conversion; nuclear electromagnetic radiation.

An elementary treatment of interactions of nuclei with the electromagnetic field.

**10563.** Heydemann, P. L. M., **An ultrasonic pressure gage,** *J. Basic Eng.* **89,** No. 3, 551-553 (Sept. 1967).

Key words: Fluid range; measure pressures; pressure gages; pressure-sensitive components; regenerating circuits; transit time; ultrasonic pulses.

The transit time of short ultrasonic pulses in solid rods is used to measure pressures throughout the fluid range. Self-excited regenerating circuits are used. Measurements to 3500 bar with an uncertainty of 0.3 bar and to 20 kb with an uncertainty of 2 bar are reported. Further improvements, temperature compensation, and stability are discussed.

**10564.** Huget, E. F., Brauer, G. M., Loebenstein, W. V., **Apparent heats of wetting and heats of reaction of the components of tooth structure and synthetic fluorapatite,** *J. Dental Res.* **47,** No. 2, 291-301 (Mar.-Apr. 1968).

Key words: Anorganic whole tooth; components of tooth structure; dentin; enamel; fluorapatite; heats of reaction of components of tooth structure; heats of wetting of components of tooth structure.

The apparent heats of wetting $\Delta H_w$ and heats of reaction $\Delta H_R$ of ground dentin, enamel, anorganic tooth and synthetic fluorapatite of known specific surface were determined calorimetrically. The values of $\Delta H_w$ in water are affected by the presence of collagenous matter. Dentin saturated with water vapor gave $\Delta H_w$ of 0.31 cal/gm compared to 12 cal/gm for powder dried at $10^{-3}$ mm Hg. Dry dentin reacts with 0.006-0.6 M aqueous $NH_4$ citrate, malonic, ascorbic, citric and methacrylic acid as evidenced by heats of reaction $\Delta H_R$ ranging from 29-56 cal/gm. These reactions at the surface are caused mainly by organic groups since the $\Delta H_R$ for anorganic tooth, enamel and fluorapatite are much smaller on exposure to these reagents. On the other hand, disodium EDTA and the phosphoric acid in cola beverages react primarily with the mineral components of tooth structure. Harkins method for surface area determination applied to water vapor saturated samples gave approximately the same specific values for dentin as those obtained by the BET method, but gave smaller values for anorganic whole tooth tissue. These results of the heats of reaction of odontic powders are useful for studying the modification of tooth surface and in determining those groups that will bond to tooth structure in an aqueous environment.

**10565.** Hutchinson, J. M. R., Naas, C. R., Walker, D. H., Mann, W. B., **Backscattering of alpha particles from thick metal backings as a function of atomic weight,** *Intern. J. Appl. Radiation Isotopes* **19,** No. 6, 517-522 (June 1968).

Key words: Alpha particles; backscattering; $1\eta$; $\alpha$-counter.

Alpha-particle backscattering from thick metal backings has been studied using two separate counters with geometries of 2 percent and approximately 1 percent steradians.

**10566.** Ives, L. K., Ruff, A. W., Jr., **Studies of the effect of annealing on extended dislocation nodes in silver-tin alloys,** *Phys. Stat. Sol.* **27,** 117-123 (1968).

Key words: Dislocations; electron microscopy; oxygen impurities; silver-tin alloys; stacking fault energy.

Extended dislocation nodes have been observed by transmission electron microscopy and measured in several solid solution silver-tin alloys after annealing at elevated temperatures. The intrinsic stacking fault energies were determined and compared with previously reported values for freshly deformed specimens. Only small irreversible changes in the fault energy were found after annealing up to 600 °C, in contrast to results found in some other alloy systems. The effect of oxygen on the node extensions in pure silver was also studied.

**10567.** Jensen, M. W., **The Fair Packaging and Labeling Act of 1966 – its history and its implementation,** *Monthly Rev. J. Inst. Weights Measures Admin.* **76,** No. 4, 3-6 (Apr. 1968).

Key words: Commerce; consumers; labeling; measures; packages; weights.

The Fair Packaging and Labeling Act of 1966 was enacted by the Congress and signed into law by the President after some six years of legislative history. The Act gives certain regulatory responsibilities to the Department of Health, Education, and Welfare and the Federal Trade Commission, and makes the Secretary of Commerce responsible for the reduction of the quantities in which particular consumer commodities are offered for sale when such quantities are deemed by him to be unduly proliferated through voluntary action by the packaging industry. The weights and measures agencies of the individual States will play significant roles in the implementation of both the regulatory activities and the activities that will result in voluntary action by industry.

**10568.** Johannesen, R. B., **Relative signs of NMR coupling constants and isotope shifts in ammonium ions,** *J. Chem. Phys.* **48,** No. 3, 1414-1415 (Feb. 1, 1968).

Key words: Double resonance; isotopes; nitrogen-15; nuclear magnetic resonance; relative signs.

The NMR spectra of $^{14}NH_3DCl$ and $^{15}NH_3DCl$ have been measured and the signs of all coupling constants have been measured. Isotope shifts in the proton and nitrogen spectra are reported.

**10569.** Judd, D. B., **Color vision and colorimetry,** Chapter 4 in *Handbook of Physics, Second Ed., Part 6, Optics,* E. U. Condon and H. Odishaw, eds., pp. 6-65 – 6-77 (McGraw-Hill Book Co., New York, N.Y., 1967).

Key words: Anomalous trichromatism; color; colorimeter; dichromatism; luminous efficiency; photoelectric colorimetry.

The response functions of wavelengths defining the various types of human vision are given in terms of luminous-efficiency and color-matching functions. The types are trichromatic (normal, protanomalous, deuteranomalous), dichromatic (protanopic, deuteranopic, tritanopic), and monochromatic (twilight or rod vision). Measurement of color consists of determining the amounts of three primary colors defined by the Commission Internationale de l'Eclairage (CIE) required to match an unknown color. Equations are given to transform these amounts, called tristimulus values, from the CIE primary colors to any others. Theories of color vision are defined by the coefficients in the equations required to transfer the tristimulus values of a color from the CIE primaries to the set of primaries implied by that theory. The main theories are three-component (Young, Ladd-Franklin, and early König for cone photopigments; Helmholtz, late König for cone responses), opponent-color (Hering for optic-nerve processes), and zone or stage theories (v. Kries-Schrödinger, Adams, and Müller). Coefficients are also given for ten often used transformations of the CIE coordinate system. The uses are experimental determination of color-matching functions, color television, improved uniformity of color spacing, and measurement of color by photoelectric colorimeters.

**10570.** Keller, R. A., **Intramolecular energy transfer between triplet states of weakly interacting chromophores. II. Compounds in which the chromophores are perpendicular to each other,** *J. Am. Chem. Soc.* **90,** No. 8, 1940-1944 (Apr. 10, 1968).

Key words: Energy transfer; fluorescence; phosphorescence; triplet states.

The intramolecular energy transfer properties of the following two molecules were investigated at 77 °K. The spiro linkage holds the two chromophors perpendicular to each other. Complete transfer of both singlet and triplet excitation energy to the chromophor with the lowest excited state of a particular multiplicity was observed for both of these molecules. No absorption or emission bands were observed which could not be attributed to one of the chromophors.

**10571.** Kneissl, G. J., Richmond, J. C., Wiebelt, J. A., **A laser source integrating sphere for the measurement of directional hemispherical reflectance at high temperatures,** (Proc. Thermophysics Specialist Conf. of AIAA, New Orleans, La., Apr. 17-20, 1967), Chapter 1 in *Thermophysics of Spacecraft and Planetary Bodies, Radiation Properties of Solids and Their Measurement* **20,** 177-202 (Academic Press Inc., New York, N.Y., Dec. 1967).

Key words: Graphite; high temperature reflectance; integrating sphere; laser; reflectance; sodium chloride coating; thoria; tungsten.

The purpose of this research was to evaluate the high-temperature spectral emittance of refractory metals and ceramics by measuring their reflectance very accurately at high temperatures. An integrating sphere was used to measure the directional, hemispherical reflectance at temperatures up to 2000 °K. The accuracy of the measurement was practically independent of the directional distribution of the reflected flux, which made it possible to measure accurately any material of any surface texture. The source used for this instrument was an He-Ne CW laser operated at 0.6328, 1.15 and 3.39 $\mu$m. A narrow bandpass filter, whose peak transmittance coincided with the lasing wavelength, was placed in front of the detector to increase the signal-to-noise ratio. Since conventional sphere coatings could not be used for this high-temperature integrating sphere, a new sphere coating had to be developed. This coating exhibits a high reflectance at all three wavelengths in question, is a very good diffuser, possesses good mechanical properties, and can be used in a low-pressure system. Preliminary data are shown for materials such as graphite, tungsten, and thorium oxide.

**10572.** Kokoszka, G. F., Brinckman, F. E., **Electron paramagnetic resonance studies of phosphorus-containing reactive intermediates,** *Chem. Commun.* **7,** 349-350 (Apr. 10, 1968).

Key words: E.p.r.; free radicals; low-energy irradiation; low temperature; $PCl_3$; $PCl_2$; $PCl_4$; $sp^2$ hybrids; trigonal bipyramid.

The electron paramagnetic resonance (e.p.r) spectrum of the irradiation products of $PCl_3$ has been recorded at 77 °K with an X-band spectrometer. In the neat material two species have been identified. The first is $PCl_2$ with magnetic parameters $g = 2.017$ and $A_p \approx 33$ gauss. The second species is $PCl_4$ with parameters $g = 2.0124$, $A_p = 2106$ gauss, $A_{Cl} = 62$ gauss (2 chlorine atoms) and $A'_{Cl} = 7$ gauss (2 chlorine atoms). The uncertainties are believed to be less than 1 gauss in the A values and within 0.0005 for the g values.

When $PCl_3$ is diluted in a Xe matrix ($PCl_3$:Xe = 1:9) a large $PCl_2$ signal again develops but there is no evidence for $PCl_4$. In a mixture of $PCl_3$ and $PF_3$ ($\sim$10:1) the anisotropic spectrum associated with $PCl_2$ displays a seven-line chloride hyperfine pattern in the parallel portion.

In neat $MePCl_2$ a pentatomic phosphorus-containing species s produced. The data are constant with a formulation as $Me_2PCl_2$ or $MePCl_3$ but the former is believed to be more likely.

**10573.** Kuriyama, M., **Dynamical calculation of the x-ray diffraction profile from a distorted crystal,** *J. Appl. Phys.* **39,** No. 4, 2162-2163 (Mar. 1968).

Key words: Absorption; distortion; lattice sum; line broadening; perfect crystal; scattering amplitude; theory; x-ray diffraction.

A dynamical line-shape calculation for a distorted, parallel-sided crystal is given for the Laue geometry. The scattering amplitude previously formulated by the author is demonstrated to be indeed valid for an arbitrarily large distortion.

**10574.** Larsen, N. T., **50 microdegree temperature controller,** *Rev. Sci. Instr.* **39,** No. 1, 1-12 (Jan. 1968).

Key words: Controller; temperature control.

A temperature controller has been developed using a platinum resistance thermometer in a bridge with inductively-coupled ratio arms. It is capable of maintaining water bath temperatures constant to within ±25 microdegrees Celsius for 24 hours in an environment varying as much as ±1.5 °C at any temperature from 18 °C to 28 °C. The sensitivity of the controller approaches the theoretical limitation imposed by Johnson noise. The design makes possible control dials which are direct-reading in °C.

**10575.** Little, J. L., Mooers, C. N., **Standards for user procedures and data formats in automated information systems and networks,** *AFIPS Conf. Proc. Spring Joint Computer Conf., Atlantic City, N.J., Apr. 30-May 2, 1968,* **32,** 89-94 (Thompson Book Co., Washington, D.C., 1968).

Key words: Automated networks; automated systems; data formats; distributed data base; information networks; information system standards; on-line system reactive typewriters; retrieval; time-sharing computers; user procedures.

In the brave new world of the publicly accessible "on-line" computers and automated information systems, users are finding a rapidly growing chaos of incompatible control languages and methods of operation. Almost every automated system has been provided with a different language and method. The resulting chaos promises effectively to destroy much of the potential value of nationwide networks of such information systems. The community of users – and potential users – of such systems are the ones most seriously affected. In order to remedy this intolerable situation, the users must initiate immediate action to introduce standards for user control methods and languages which will permit easy and compatible utilization of automated information systems. This paper is devoted to an examination of twelve elementary logical functions for user control, and suggested keyboard assignment for these functions is reported.

**10576.** Lundgren, F. A., Nargolwalla, S. S., **Use of a dual sample-biaxial rotating assembly with a pneumatic tube transfer system for high precision 14-MeV neutron activation analysis,** *Anal. Chem.* **40,** No. 4, 672-677 (Apr. 1968).

Key words: Accuracy; activation analysis; design; oxygen; precision; sample rotator; 14 MeV neutrons.

Imprecision in 14-MeV neutron activation analysis is primarily due to nonhomogeneity and anisotropy in the usable neutron flux. This fact is considerably magnified in analyses pertaining to short-lived radioactivity such as in the determination of oxygen by $^{16}O(n,p)^{16}N$ reaction.

A design for a variable-speed dual sample rotating assembly is described. This assembly allows reproducible placement of pneumatically injected samples and permits both sample and standard to be exposed to an identical neutron flux as a result of biaxial rotation. The analytical precision, which is now most often limited by the total number of counts accumulated, is about 10 times better than that which standard normalization techniques can provide. The system permits the analyst to determine both neutron and gamma attenuation in dense samples.

This irradiation assembly is currently being utilized for the accurate and precise determination of oxygen in NBS Standard Reference Materials.

**10577.** Mahler, R. J., James, L. W., **Nuclear electric hexadecapole-phonon interaction,** (Proc. XIV Colloque Ampere, Sept. 6-11, 1966, Ljubljana, Yugoslavia) Chapter in *Magnetic Resonance and Relaxation,* R. Blinc, ed., pp. 938-945 (North-Holland Publ. Co., Amsterdam, The Netherlands, 1967).

Key words: Angular dependence; hexadecapole; hexadecapole transitions; phonon-nuclear interactions; saturation factor; ultrasonically induced transitions.

A nucleus with spin 5/2 or larger may possess an electric hexadecapole as well as an electric quadrupole moment. These electric moments can interact with the lattice to yield a static shift in the nuclear energy levels, or with the lattice vibrations (phonons) to produce transitions between the nuclear energy levels.

One can show theoretically that the hexadecapole interaction can give rise to $\Delta m = \pm 1,2,3,$ and 4 nuclear transitions, but experimentally the $\Delta m = \pm 1$ and 2 transitions would be masked by the much larger quadrupole interactions. Since a $\Delta m = \pm 3$ or 4 nuclear transition gives rise to a net change in the nuclear magnetization, pulsed NMR techniques are ideally suited to observe these interactions.

A theoretical expression for the hexadecapole-phonon interactions is derived, and the experimental procedure used to observe the interactions is discussed. Results of these and related experiments are given.

**10578.** Maki, A. G., Thibault, R., **Analysis of some perturbations in the $\nu_4$ band of methyl chloride,** *J. Chem. Phys.* **48,** No. 5, 2163-2167 (Mar. 1, 1968).

Key words: Absorption spectra; infrared; methyl chloride; perturbations; spectra; vibrational resonance.

The $\nu_4$ band of $CH_3Cl$ has been analyzed in detail. It is found that there is a weak but important, vibrational resonance between $\nu_4^1$ and $3\nu_6^1$. The resonance is quantitatively taken into account in order to determine the unperturbed rotational constants for both $\nu_4^1$ and $3\nu_6^1$. Both chlorine isotopes are resolved and treated separately. The interaction parameter is found to be given by $3.519\ (\pm 0.006) + 0.028\ ki\ (\pm 0.003)\ cm^{-1}$. The k dependent term is evidently due to a Coriolis-like interaction which is also possible between $\nu_4^1$ (E) and $3\nu_6^1$ (E).

**10579.** Manning, J. R., **Correlation factors for diffusion of vacancies in binary alloys,** (Proc. Subconference on Lattice Defects, Honolulu, Hawaii, Sept. 1965) Chapter in *Lattice Defects and Their Interactions,* R. R. Hasiguti, ed., pp. 269-289 (Gordon and Breach, New York, N.Y., 1967).

Key words: Binary alloys; calculations; correlation factors; diffusion; Kirkendall shift; thermodynamic equations for diffusion; vacancies.

A vacancy in a pure cubic crystal follows a random walk. In a binary alloy however, a vacancy usually has a higher jump frequency when exchanging with one type of atom than with the other. As a result, a vacancy in a binary alloy does not follow a random walk. Partial correlation factors $f_v^A$ and $f_v^B$ can be defined for vacancy jumps with A and B atoms, respectively. Then, the correlation factor for diffusion of vacancies is given by the weighted average $f_v = (w_A N_A f_v^A + w_B N_B f_v^B/(w_A N_A + w_B N_B)$, where $w_A$, $w_B$ are vacancy jump frequencies for exchange with A and B atoms, while $N_A$, $N_B$ are the mole fractions of A and B atoms. The partial correlation factors also enter into the equations for the vacancy flux in a Kirkendall shift experiment, but in a different combination than that for $f_v$. Consideration of this flux and the theory of correlated walks in a driving force allows $f_v^A$, $f_v^B$, and $f_v$ to be calculated. Experimental applications are considered.

**10580.** Manning, J. R., **Reply to comments on "Diffusion and the Kirkendall shift in binary alloys,"** *Scripta Met.* **2,** 177-178 (1968).

Key words: Binary alloys; diffusion; diffusion coefficients; kinetic theory; Onsager reciprocal relation; thermodynamic theory.

It is noted that Yao in his calculation of the parameter $\epsilon$ has not taken into account the relation $\partial c_A/\partial x = -\partial c_B/\partial x$ between the concentration gradients in a binary A-B alloy. As a result, Yao's calculation of $\epsilon$ is not correct. A kinetic equation for $\epsilon$ is calculated.

**10581.** Margoshes, M., Scribner, B. F., **Emission spectrometry,** *Anal. Chem.* **40,** No. 5, 223R-246R (Apr. 1968).

Key words: Atomic absorption spectrometry; atomic fluorescence spectrometry; emission spectrometry; flame photometry; isotopic analysis; microanalysis; review; spectrometry.

A review is given of emission spectrometry and flame emission, atomic absorption, and atomic fluorescence spectrometry for the years 1966-67. Emphasis is placed on analytical applications, but some theoretical papers are included. The major subjects included are books and reviews; spectral descriptions and classifications; instrumentation; standards, samples, calibration, and calculation; excitation sources; flame emission, absorption, and fluorescence; trace analysis; lasers and microanalysis; and other applications. Six hundred and seventy-six references are listed.

**10582.** Marron, B. A., deMaine, P. A. D., **Automatic Data Compression,** *Commun. ACM* **10,** No. 11, 711-715 (Nov. 1967).

Key words: Alphanumeric; automatic; compressor; computer; data; information handling; numeric.

The "Information Explosion" noted in recent years makes it essential that storage requirements for all information be kept to a minimum. A fully automic and rapid compressor, COPAK, developed for the SOLID SYSTEM, can be used with *any* body of information to greatly reduce slow external storage requirements and to increase the rate of information transmission through a computer. COPAK will also automatically decode the compressed information on an item by item basis when it is required.

The three components of COPAK, which can be used separately to accomplish their specific tasks, are described in this paper: NUPAK for the automatic compression of numerical data, ANPAK for the automatic compression of *any* information, and IOPAK for further compression of information to be stored on tape or cards.

**10583.** Marvin, R. S., **Twenty years of rheology,** *Phys. Today (20th Anniversary Edition)* **21,** No. 5, 52-53 (May 1968).

Key words: Rheology.

A summary of the principal activities in the field of rheology over the last twenty years.

**10584.** Mattis, R. L., Phillips, W. E., Bullis, W. M., **Measurement and interpretation of carrier lifetime in silicon and germanium,** *Tech. Rept.* **AFML-TR-68-81,** (Air Force Materials Laboratory, Air Force Systems Command, Wright-Patterson Air Force Base, Ohio, July 1968).

Key words: Carrier lifetime; diode recovery time; germanium; photoconductive decay; photomagnetoelectric effect; silicon; surface photovoltage.

Minority carrier lifetime is a basic parameter for the specification of semiconductor materials for transistors, diodes, and similar devices. Photoconductive decay measurements are routinely made on many crystals used in the fabrication of these devices. Although this measurement suffers both from lack of precision and from limitations in the range of applicability it is the only method for determination of carrier lifetime which has been accepted as standard. This report describes the results obtained during the first year of a continuing research project which was undertaken in order to determine the fundamental limitations on the precision and applicability of this method and to develop alternate methods which might be more suitable under various conditions. Detailed studies of the photoconductive decay method were accompanied by preliminary studies of the photomagnetoelectric method, the diode recovery time method, and the surface photovoltage method and a critical survey of the various methods which have been reported in the literature. The photoconductive decay method was studied in greatest detail.

**10585.** Melmed, A. J., **Field emission shadow microscopy,** *Appl. Phys. Letters* **12,** No. 3, 100-102 (Feb. 1, 1968).

Key words: Field electron microscope; field emission; microscope.

A microscope has been constructed which produces an electron shadow "image" of small electrically conducting objects in ultra-high vacuum. The microscope uses an electron field emitter as an approximate point source of electrons and casts a shadow of the object by direct projection onto a phosphor screen. When the object is also a field emitter, a second screen may be used to view its surface in the manner of a conventional field electron microscope. Thus far, magnifications up to 6,500, with a resolution of about 300 Å, have been realized. Magnifications of 20,000 or greater should easily be feasible with resolution of 10-30 Å possible.

**10586.** Menke, J. L., Schrack, R. A., **Feeble field feeler,** *Nucl. Instr. Methods* **57,** 158-159 (Dec. 1967).

Key words: Detector; magnetic field; magnetic null; null measurable; remanent field; saturable ferrite.

A simple magnetic field detector is described which allows measurement of magnetic fields to within .1 gauss. Together with its associated circuits it can be used to adjust an electromagnetic system for minimum remanent field.

**10587.** Milligan, D. E., Jacox, M. E., **Matrix-isolation study of the reaction of atomic and molecular fluorine with carbon atoms. The infrared spectra of normal and $^{13}$C-substituted $CF_2$ and $CF_3$,** *J. Chem. Phys.* **48,** No. 5, 2265-2271 (Mar. 1, 1968).

Key words: C atom reaction; F atom reaction; $F_2$ reaction; force constants; free radical; infrared spectrum; matrix isolation; $NF_2$; photolysis, thermodynamic properties; ultraviolet spectrum; $^{12}CF_2$; $^{13}CF_2$; $^{12}CF_3$; $^{13}CF_3$.

Carbon atoms, resulting from the photolysis of cyanogen azide, are found to react with molecular fluorine in an argon matrix at 14 °K to produce $CF_2$. The use of carbon-13 has led to confirmation of the previous assignment of features at 1073 and 191 $cm^{-1}$ to $^{13}CF_2$ present in natural abundance. Using recent structural data on $CF_2$ and the $^{12}CF_2$ and $^{13}CF_2$ frequencies, it has been possible to calculate the complete valence force potential of $CF_2$. Values of the potential constants are compared with those of the related species $NF_2$ and $OF_2$. When the sample is subjected to radiation of wavelengths effective in photolyzing $F_2$, $CF_3$ is also produced. Sufficient yields of both $^{12}CF_3$ and $^{13}CF_3$ have been obtained for observation of all four vibrational fundamentals. Data have been fitted to a four-constant valence force potential. Agreement is most satisfactory for a $C_{3v}$ structure with a deviation of 13° from planarity. Using this structure, the thermodynamic properties of $CF_3$ have been estimated.

**0588.** Moore-Sitterly, C., **IAU Commission 14—Fundamental spectroscopic data report of meetings, Aug. 23-25, 1967,** *Proc. XIIIth General Assembly Intern. Astronomical Union, Prague, Czechoslovakia, Aug. 22-31, 1967,* **13B,** 87-91 (1968).

Key words: Laboratory spectra; molecular spectra; solar spectrum; standards, wavelength; transition probabilities; wavelength standards.

During the 13th General Assembly of the International Astronomical Union, held in Prague August 22-31, 1967, there were four meetings of IAU Commission 14—Fundamental Spectroscopic Data. The present paper is a report on the business meeting and four scientific sessions of the Commission.

The Index of Refraction of Air, wavelength standards, laser sources, transition probabilities, molecular spectra and future trends in spectroscopy were the chief topics discussed.

**0589.** Nargolwalla, S. S., Crambes, M. R., DeVoe, J. R., **A technique for the evaluation of systematic errors in the activation analysis for oxygen with 14-MeV neutrons,** *Anal. Chem.* **40,** No. 4, 666-671 (Apr. 1968).

Key words: Correction factors; neutron and gamma-ray attenuation; oxygen; removal cross section; systematic errors; 14-MeV activation analysis.

In comparative 14-MeV neutron activation analysis of oxygen, the neutron and gamma ray attenuation differences in the sample and standard introduce systematic errors. A quantitative evaluation of these attenuation processes in a wide range of matrices and for three sample diameters is given.

The experimentally determined correction factor, in each case, shows an exponential dependence on the calculated difference between the appropriate attenuation coefficients for sample and standard. Over the range of sample diameters tested, the slope of each calibration line is linearly dependent on the sample diameter. For comparable diameters, the magnitude of the slope for neutron attenuation is approximately ten times greater than for gamma attenuation. These calibration lines are used to predict attenuation correction factors for the determination of oxygen in other matrices. Some typical analyses of Standard Reference Materials, corrected for attenuation, illustrate the high degree of accuracy and precision obtained.

**10590.** Newman, M., **Pairs of matrices generating discrete free groups and free products,** *Mich. Math. J.* **15,** 155-160 (1968).

Key words: Discrete matrix groups; free groups; free products.

It is shown that if

$$A=\left(\begin{smallmatrix} -a & b \\ -c & d \end{smallmatrix}\right),\ B=\left(\begin{smallmatrix} -\alpha & -\beta \\ \gamma & \delta \end{smallmatrix}\right)$$

are elements of SL(2,R) such that a, b, c, d, $\alpha$, $\beta$, $\gamma$, $\delta \geqslant$ and d-a $\geqslant 2$, $\delta-\alpha \geqslant 2$, then the group {A,B} is a free discrete subgroup of SL(2,R). Generalizations to free products are given.

**10591.** Oppenheim, I., Shuler, K. E., Weiss, G. H., **On the decay of initial correlations in stochastic processes,** *J. Chem. Phys.* **46,** No. 10, 4100-4111 (May 15, 1967).

Key words: Eigenvalue spectrum; initial correlation; r-particle Ursell functions; stochastic process.

We study the relaxation of a non-interacting, initially correlated many particle system in contact with an infinite reservoir. We use the master equation to study the time development of the r-particle distribution function $P_r(n;t)$ and assume that the relaxation process is Markovian. We study the decay of the correlations by investigating the time development of the r-particle Ursell functions, $U_r(n;t)$. We show that the correlation function $U_r(n;t)$ goes to zero much more rapidly with time than the r-particle distribution function approaches its equilibrium value $P_r(n;\infty)=\prod_{i=1}^{r} P(n_i;\infty)$. The exact forms of the relaxation of $P_r(n;t)$ and $U_r(n;t)$ depend upon the eigenvalue spectrum of the transition rate matrix of the master equation. The general theory is developed and then applied to a number of examples.

**10592.** Osgood, C. F., **A method in diophantine approximation (II),** *Acta Arith.* **XIII,** 383-393 (1968).

Key words: Convolution product; differential equations; diophantine approximation; integers; irrational numbers; linear operators.

This paper applies the general method of approachh developed in *A Method in Diophantine Approximation* to obtain further results about the diophantine approximation of values of certain functions. Examples of such functions are the inverse Laplace transforms of all functions of the form $z^{-\alpha} \exp\left(\sum_{i=1}^{l=1} r_i z^{-i}\right)$ where $\alpha$ and the $r_i$ are each rational, $\alpha > l+1$, $\alpha$ is not an integer and $r_{i=1} \neq 0$. For these latter functions we conclude that at any nonzero rational point the zeroth thru l-1 st derivatives are linearly independent over the rationals.

**10593.** Page, C. H., **Electronic circuits,** Chapter 4 in *Handbook of Physics, Second Ed., Part 4., Electricity and Magnetism,* E. U. Condon and H. Odishaw, eds., pp. 4-45—4-52 (McGraw-Hill Book Co., New York, N.Y., 1967).

Key words: Active; demodulation; gyrator; harmonic generation; modulation; nonlinear; parametric amplifier.

A brief outline of the properties and analysis of *nonlinear* and *active* electrical circuit elements, with reference to modulation, demodulation, harmonic generation, parametric amplifiers, and gyrators.

**10594.** Pichanick, F. M. J., Simpson, J. A., **Resonances in the total cross sections for metastable excitation of noble gases by electron impact,** *Phys. Rev.* **168,** No. 1, 64-70 (Apr. 5, 1968).

Key words: Cross sections; electron impact; excitation; helium; metastable.

Total cross sections for excitation by electron impact of metastable states in the noble gases helium, neon, argon, krypton and xenon have been measured as a function of impact energies. A 180° spherical monochromator was used to obtain incident beams of electrons with energy resolutions between 0.035 eV and 0.050 eV. Metastable atoms were detected in the scattering chamber by electron ejection from a metal surface. The detector was biassed negatively to repel scattered electrons, and was electrostatically shielded from the incident electron beam. The cross sections were measured for impact energies up to 5 eV above the metastable thresholds. Several narrow resonances associated with negative ion states were observed, and where possible their shapes and positions on the energy scale were compared with similar results obtained by different techniques.

**10595.** Radford, H. E., Evenson, K. M., **Paramagnetic-resonance spectrum of metastable ($^2$D) atomic nitrogen,** *Phys. Rev.* **168,** No. 1, 70-74 (Apr. 5, 1968).

Key words: Electric discharge; electron paramagnetic resonance; fine structure separation; g factors; metastable atomic nitrogen; Zeeman spectroscopy.

The paramagnetic resonance spectrum of free metastable ($^2$D) nitrogen atoms has been observed in the flowing products of an electric discharge in nitrogen-helium gas mixture. An analysis of the Zeeman effect and hyperfine structure yields the following values for the atomic g-factors and radial integrals: $g_j(^2D_{5/2}) = 1.20036 \pm 0.00001$; $g_j(^2D_{3/2}) = 0.79949 \pm 0.00002$; $\langle r_l^{-3} \rangle = (20.21 \pm 0.02) \times 10^{24}$ cm$^{-3}$; $\langle r_s^{-3} \rangle = (22.22 \pm 0.02) \times 10^{24}$ cm$^{-3}$. The $^2$D fine structure separation is found to be $-8.69 \pm 0.02$ cm$^{-1}$. Evidence is found of a small electric quadrupole hyperfine structure interaction.

**10596.** Reimann, C. W., Zocchi, M., **The structure of the trinuclear cation bis-[$\mu$-(tri-1,2,4-triazolo-N$^1$,N$^2$)-triquonickel]-nickel,** *Chem. Commun.* **5,** 272 (Mar. 6, 1968).

Key words: Bis[triaquo tri $\mu$(1,2,4 triazolo($-N_1$ $-N_2$)) nickel] nickel; crystal structure; trinuclear complex.

The complex bis[triaquo tri $\mu$(1,2,4 triazolo($-N_1$ $-N_2$)) nickel] nickel hexanitrate dihydrate has been prepared and the crystal structure was determined by single crystal x-ray diffraction techniques. This complex crystallizes in the monoclinic system with a = 14.261, b = 11.745, c = 14.948 Å, $\beta = 127.9°$, space group $P2_1/c$, $\rho_o = 1.85$ g cm$^{-3}$, $\rho_c = 1.84$ g cm$^{-3}$ and z = 2.

The bis[triaquo tri $\mu$(1,2,4 triazolo($-N_1$ $-N_2$)) nickel] nickel cation was found to contain three colinear nickel atoms with the central nickel atom bridged to the terminal nickel atoms by three 1,2,4 triazole rings. The Ni – Ni separation was found to be 3.73 Å. The coordination about each nickel atom is octahedral. The octahedral coordination of the terminal nickel atoms is completed by three molecules of water.

**10597.** Rosenstock, H. M., **Theory of mass spectra – A general review,** (Proc. Conf. on Mass Spectrometry, Berlin, Germany, Sept. 1967), Chapter in *Advances in Mass Spectrometry* **4,** 523-545 (The Institute of Petroleum, London, England, 1968).

Key words: Franck-Condon factors; theory of mass spectra; unimolecular dissociation.

In this paper we shall discuss developments in the theory of mass spectra since 1961. At that time an appraisal of the status of theory was presented, the main conclusions of which were as follows: (1) Quasi-equilibrium theory can reasonably account for the general features of mass spectra. (2) Quantitative disagreement between theory and experiment was in large measure due to poor mathematical approximations made in enumerating densities of states of reactants and activated complexes. (3) Non-equilibrium or non-equilibration effects were difficult to predict *a priori,* but some meaningful tests could be made by designing experiments to study the effects of different initial preparation on the subsequent kinetic behavior of ions.

Since the publication of these conclusions, considerable work has been done on enumeration of states, calculation of mass spectra and breakdown curves, detailed energization and fragmentation mechanisms, behaviour of metastable transitions, initial preparation effects, and quantum-mechanical theory of ion decomposition. These subjects will be discussed in detail.

**10598.** Rush, J. J., Flotow, H. E., **Vibration spectra of vanadium hydride in three crystal phases by inelastic neutron scattering,** *J. Chem. Phys.* **48,** No. 8, 3795-3804 (Apr. 15, 1968).

Key words: Crystal structure; frequency distribution; hydrogen positions; hydrogen vibration; metal hydride; neutron inelastic scattering; phase transformation; vanadium hydride; vibration spectra.

The vibration spectra of vanadium hydride in three crystal phases have been investigated by the energy-gain scattering of cold neutrons. The measured spectra are generally split into two broad bands above and below about 300 cm$^{-1}$, which are primarily associated with optical hydrogen vibrations and metal-atom vibrations, respectively. Pseudo-frequency distributions for the hydrogen vibrations were derived from the measured neutron spectra. These indicate broad optical vibration bands peaked at $970 \pm 50$ and $\sim 1400$ cm$^{-1}$ in the $\alpha$ (bcc) phase, $440 \pm 20$, 970 and $\sim 1400$ cm$^{-1}$ in the $\beta$ (bct) phase and $\sim 1300$ cm$^{-1}$ in the $\gamma$ (fcc) phase. The width of the 440 cm$^{-1}$ band increases with hydrogen concentration, possibly due to hydrogen-hydrogen interactions. The "metal-atom" vibration spectra also show changes in peak positions and widths as the distribution of phases is changed. The changes in the neutron spectra with temperature and as a function of composition between $VH_{0.20}$ and $VH_{1.71}$ correlate quite well with the previously measured phase diagram.

A comparison of the present results with neutron spectra for hydrides with known hydrogen positions suggests that in the $\alpha$ phase hydrogens only occupy tetrahedral-type sites, while in the $\beta$ phase both octahedral and tetrahedral sites are occupied. The results for $VH_{1.49}$ and $VH_{1.71}$ indicate that in the $\gamma$ phase the hydrogens occupy regular tetrahedral sites corresponding to the fluorine positions in a $CaF_2$-type structure.

**10599.** Saunders, J. B., **Precision measurements,** Chapter 1 in *Advanced Optical Techniques,* pp. 3-22 (North-Holland Publ. Co., Amsterdam, The Netherlands, 1967).

Key words: Double stars, measurement; expansion measurements; lens and mirror testing; optical engineering; optical surfaces; precision measurements; refractive indices; surface plate testing; temperature measurement; wavelength measurement.

This chapter contains methods and instrumentation for making precision measurements in a limited field of optical engineering. The fundamentals of all the included material has been published previously. The subjects that have been covered here are: refractive indices, wavelength measurement, testing of optical surfaces, surface plate testing, temperature measurement by optical methods, expansion measurements, lens and mirror testing, and the measurement of double stars.

**10600.** Schneider, W. E., Garvey, J. A., **Procedures for determining the spectral responsivity of an infrared radiometer,** *Appl. Opt.* **7,** No. 6, 1141-1148 (June 1968).

Key words: Calibration techniques; infrared radiometers; radiometric standards; radiometry; spectral responsivity.

With the increasing number of commercial radiometers employing rather varied and sophisticated optical designs, the determination of the spectral responsivity of these radiometers has accordingly become more involved. A joint National Bureau of Standards – U.S. Army calibration of an infrared radiometer was conducted at the White Sands Missile Range facility. The radiometer chosen for the measurements employed an uncooled PbS detector with an 8 inch Cassegrainian optical system. The selection of this particular type of instrument permitted two methods of measurement (each employing different standards and techniques) to be investigated. The methods of calibration and the uncertainties associated with each method are described and the application of the responsivity values to field measurements is discussed. The agreement of the spectral responsivity values as determined by each method is within the estimated uncertainty computed for each procedure.

**10601.** Sengers, J. M. H. L., **On the determination of virial coefficients from PVT data,** *Proc. 4th Symp. Thermophysical Pro-*

*perties, University of Maryland, College Park, Md., Apr. 1-4, 1968*, pp. 37-44 (American Society of Mechanical Engineers, New York, N.Y., 1968).

Key words: Density expansion; gas thermometry; power series coefficients; PVT; statistical analysis; virial coefficients.

In calculating coefficients of a power series expansion from experimental data, several factors besides experimental precision affect the standard error of these coefficients. Using the principles of statistical analysis, the effects of the factors: interval size, extrapolation, number, relative weight and distribution of experimental points have been studied by high-speed computer experiments.

For gas PVT data a density expansion is possible and approximate theoretical knowledge of the first five virials is available. This enables formulation of experimental conditions – other than improved precision – leading to decreased standard error in one or more of the first four virials.

**10602.** Sengers, J. V., Sengers, J. M. H. L., **The critical region,** *Chem. Eng. News* **46,** No. 25, 104-118 (June 10, 1968).

Key words: Critical phenomena; binary alloys; binary liquid mixture; critical opalescence; gas liquid transition; laser light scattering; magnets; superfluids; transport processes.

A comparative discussion is given of critical phenomena in gases, binary liquids, binary alloys, magnets and superfluids. Experiments show a striking similarity in thermodynamic behavior in widely different systems and transitions. The experimental results are in disagreement with the prediction of the classical theories of Van der Waals, Weiss and Bragg and Williams, but very similar to the theoretical predictions for the Ising model. The possibility of a universal equation of state, describing the various critical anomalies, is discussed. The behavior of transport properties near the critical point is summarized for gases and binary liquids. The paper concludes with a discussion of the phenomenon of critical opalescence and introduces the reader to the new possibilities for studying critical fluctuations with the aid of laser light scattering.

**10603.** Sengers, J. M. H. L., Vicentini-Missoni, M., **Thermodynamic anomalies near the gas-liquid critical point,** *Proc. 4th Symp. Thermophysical Properties, University of Maryland, College Park, Md., Apr. 1-4, 1968*, pp. 79-86 (American Society of Mechanical Engineers, New York, N.Y., 1968).

Key words: Chemical potential; critical region; lattice gas; scaling law; specific heat; thermodynamic anomalies; vapor pressure.

Thermodynamic anomalies near the gas-liquid critical point are more correctly described by the Ising model theory of the ferromagnet and the lattice gas than by Van der Waals-type theories. The inherent symmetries and the critical anomalies of the lattice gas are discussed using the proper variables, namely chemical potential, density and temperature. Part of the lattice gas symmetries are shown to be retained in the real gas if the same variables are used. The range of validity and some of the properties of a non-analytic equation-of-state in these variables, recently proposed by Widom, Kadanoff and Griffiths and representing successfully PVT data and density vs height isotherms in the critical region, are discussed.

**10604.** Shuler, K. E., **Microscopic and macroscopic approach to chemical rate processes,** (Proc. 7th AGARD Colloquium, Oslo, Norway, May 16-20, 1966), Chapter in *Recent Advances in Aerothermochemistry,* I. Glassman, ed., **1,** No. 12, 1-21 (Technical Editing and Reproduction Ltd., London, England, 1967).

Key words: Chemical kinetics; cross sections; rate theory; scattering theory; trajectory calculations; transport processes.

Chemical rate processes, like all other transport processes, can be considered on two levels – the molecular one and the statistical one. On the molecular (microscopic) level one is concerned with binary (or higher order) collisions between single atoms and/or molecules. Such elementary processes can best be studied through the scattering of the reactant species in atomic and molecular beams. The quantity of interest is the reactive scattering cross section; the theoretical approach involves the quantum theory of scattering. On the statistical (macroscopic) level one is concerned with the interactions of an ensemble of atoms and molecules characterized by their velocity and internal energy distribution functions. The experimental quantity of interest is now the rate coefficient; the theoretical approach involves the derivation and solution of the appropriate macroscopic transport equation in terms of the (microscopic) scattering cross sections and the distribution functions of reactants and products. In this paper, we will discuss these two approaches to the study of rate processes and their connection.

**10605.** Smit, J., Ogburn, F., Bechtoldt, C. J., **Multiple twin structures in electrodeposited silver dendrites,** *J. Electrochem. Soc.* **115,** No. 4, 372-374 (Apr. 1968).

Key words: Dendrites; electrocrystallization; faceting; silver; twinning; x-ray diffraction.

Silver dendrites, formed by electrocrystallization from aqueous solution were examined for twinning using optical goniometric, x-ray diffraction and metallographic techniques. The dendrites, in every case, were found to be twinned with a maximum of eight orientations in twin relation in a single dendrite. The growth axis of the dendrites was observed to be in the 110 direction. Dominant facets were found to be {111} planes on the 110 zone of the growth axis.

**10606.** Spijkerman, J. J., Hall, L. H., Lambert, J. L., **Coordination studies by Mössbauer spectroscopy of some metal(I) salts of the complex acid, hydrogen aquoethylenediaminetetraacetatoferrate (III),** *J. Am. Chem. Soc.* **90,** No. 8, 2039-2043 (Apr. 10, 1968).

Key words: Coordination studies; hydrogen aquoethylenediaminetetraacetatoferrate(III) infrared spectroscopy; magnetic susceptibility; MFe(OH$_2$)EDTA · nH$_2$O; Mössbauer spectroscopy; photodecomposition; thermogravimetric analysis.

The coordination numbers of the central metal ion that exist when iron(III) is chelated with ethylenediaminetetraacetic acid, H$_4$EDTA, have been investigated by the following methods: (a) infrared spectroscopy, (b) magnetic susceptibility, (c) Mössbauer spectroscopy, (d) photodecomposition, and (e) thermogravimetric analysis.

The iron(III) EDTA complexes were found to exist in two different forms in the solid phase, the complex acid and its M$^{+1}$ salt. Both forms were found to be high spin complexes. The complex acid, HFe(OH$_2$)EDTA, was found to be six coordinate; however, the M$^{+1}$ salts, MFe(OH$_2$)EDTA·nH$_2$O, were found to have a coordination number of seven around the central metal ion.

An interesting effect, ascribed to the influence of the cation in the salts of these complexes, was also observed. It is believed that this effect arises either from an interaction of the cation with the metal d-orbitals or with one of the carboxylate groups or both. Each interaction appears to result in a decrease of the size of the metal d-orbitals of the central metal ion. The results in a concentration of the d-electron density nearer the nucleus.

10607. Stern, K. H., **Ion diffusion into fused silica from molten salts,** *J. Phys. Chem.* **72,** No. 6, 2256-2259 (June 1968).

Key words: Glass; ion exchange; molten salts.

Compositional changes of fused silica containing a few ppm impurities resulting from immersion of the glass in molten salts were studied. At 570 °C immersion in AgCl and AgBr results in 1:1 exchange of $Ag^+$ with $Na^+$(glass). At 890° immersion in NaCl, KCl, and AgCl, respectively, increases the ionic concentration in $Na^+$, $K^+$, and $Ag^+$ above the initial total ($Na^+ + K^+ + Li^+$). $Cl^-$ diffusion is virtually absent. Possible interpretations of these results are presented.

10608. Stern, K. H., **Membrane potentials and ion selectivity of fused silica in molten salts,** *J. Phys. Chem.* **72,** No. 6, 1963-1975 (June 1968).

Key words: Fused silica; ion selectivity; membrane potentials; molten salts.

The effect of alkali metal cations on membrane potentials at the molten salt-fused silica interface has been studied using the concentration cell $Ag|AgCl, M_1Cl, M_2Cl \ldots |glass|M_1Cl, M_2Cl \ldots, AgCl|Ag$ where $M_1, M_2 \ldots$ are alkali metal cations and several types of fused silica and Vycor. The ion exchange theory is more appropriate for the interpretation of the data than the liquid junction theory, but the application of the theory requires detailed data on ion exchange and ionic mobility in fused silica which are not yet available.

The effect of anions on the membrane potential was studied with the cell M|MCl, NaCl|fused silica|MBr, NaBr|M where M = Ag, Tl, and Pb. The results for the three metals are quite analogous. The emf of the cells could be calculated by straightforward thermodynamic methods, without the assumption of specific anion-glass interactions. The emf measurement of these cells at low sodium halide concentration can also serve as an analytical tool for sodium determinations down to $10^{-3}$ mole percent, but not lower.

10609. Swanson, N., Powell, C. J., **Excitation of L-shell electrons in Al and $Al_2O_3$ by 20-keV electrons,** *Phys. Rev.* **167,** No. 3, 592-600 (Mar. 15, 1968).

Key words: Aluminum; amorphous $Al_2O_3$; cross sections; electron energy loss spectra; L-shell electrons; oscillator strengths; x-ray mass absorption coefficients; $\gamma$-$Al_2O_3$.

The energy loss distributions of ≈ 20 keV electrons transmitted through 210 to 575 Å thick specimens of Al and $Al_2O_3$ have been measured at zero scattering angle. Two types of $Al_2O_3$ were used: films of the $\gamma$-phase and amorphous films prepared by anodization. Loss spectra were obtained for an energy loss range of zero to 160 eV, in which structure due to L-shell excitation in Al and $Al_2O_3$ was observed. The positions of the absorption edges and of the peaks on the high-energy loss side of each edge agreed well with recent x-ray absorption measurements. Slightly different structure for the two forms of $Al_2O_3$ was found near the edge, as recently found by x-ray absorption. From the observed intensities, values of oscillator strengths, mass absorption coefficients and electron scattering cross sections have been derived for each material up to ≈ 85 eV beyond the absorption edge. The Al results are in good agreement with recent x-ray measurements and are consistent with the $Al_2O_3$ data. The similarity in the electron energy loss and x-ray absorption measurements are consistent with the equality of the longitudinal and transverse dielectric constants $[\epsilon(\omega)]$ and the expectation that in this energy loss region $IM(\epsilon)$ equals $-Im(1/\epsilon)$ to a good approximation.

10610. Swartzendruber, L. J., Bennett, L. H., **Hyperfine field distributions in $(ZrCo_2)_x(ZrFe_2)_{1-x}$ alloys,** *J. Appl. Phys.* **39,** No. 2, Part II, 1323-1324 (Feb. 1, 1968).

Key words: Alloys; cobalt; hyperfine fields; iron; Mössbauer effect; zirconium.

Mössbauer effect measurements in the cubic Laves phase pseudo-binary magnetic alloys $(ZrCo_2)_x(ZrFe_2)_{1-x}$ yield complex spectra. Magnetization curves on these alloys have been previously reported. $ZrFe_2$, with a saturation moment at 4 °K of about 1.6 $\mu_B$ per Fe atom and a Brillouin type magnetization curve, displays a Mössbauer spectrum consisting of two six line patterns, each with a hyperfine field of about 200 kOe. ZrFeCo has been reported to show only a quadrupole splitting at 78 °K, although this is well below the Curie temperature. We have observed resolved hyperfine splitting in this composition at 78 °K and at 4 °K. The magnetization curves in $(ZrCo_2)_x(ZrFe_2)_{1-x}$ for x = 0.2, 0.4, 0.5 and 0.6 imply magnetic moment distributions. The Mössbauer spectra for these alloys show hyperfine field distributions that are strong functions of temperature over a wide range below the Curie temperatures.

10611. Swartzendruber, L. J., Bennett, L. H., **Line profiles in the nuclear magnetic resonance and Mössbauer effect of $TiFe_{1-x}Co_x$ alloys,** *J. Appl. Phys.* **39,** No. 5, 2215-2220 (Apr. 1968).

Key words: Co; Fe; intermetallic compounds; internal oxidation; line structure; Mössbauer effect; nuclear magnetic resonance.

The $^{57}$Fe Mössbauer effect (ME) and the $^{59}$Co nuclear magnetic resonance (NMR) have been investigated as a function of alloy concentration, temperature, and stoichiometry in $TiFe_{1-x}Co_x$ alloys over most of the range $0 \leq X \leq 1$. At room temperature, in carefully prepared samples, a single narrow $^{57}$Fe ME line was observed for all values of x. This line broadened only slightly at low temperatures although the magnetic properties of these alloys would have led one to expect a larger broadening at certain compositions. The $^{59}$Co NMR line width was relatively narrow for x close to 0 or 1 and was a strong function of x as well as of magnetic field. The intermediate compositions displayed resolved satellite structures. Annealing reduced both the ME and NMR linewidths. Deviations from stoichiometry and internal oxidation were readily observable from their effect on the ME line profile. Both the ME and NMR results are consistent with a CsCl structure over the entire composition range. The NMR results indicate a lack of ordering on the Co, Fe sublattice.

10612. Swartzendruber, L. J., Bennett, L. H., **Mössbauer line structure in "non-magnetic" Cu-Fe and Cu-Ni-Fe alloys,** *Physics Letters* **27A,** 141-142 (1968).

Key words: Alloys; copper; iron; local moments; magnetism; Mössbauer effect; nickel.

The high temperature $^{57}$Fe Mössbauer effect residual line structure in Cu-rich Cu-Fe and Cu-Ni-Fe alloys is reinterpreted as being of magnetic origin, rather than arising from quadrupole interactions or lack of solubility.

10613. Swindells, J. F., **Thermometry and pyrometry,** Chapter 3 in *Handbook of Physics, Second Ed., Part 5, Heat and Thermodynamics,* E. U. Condon and H. Odishaw, eds., pp. 5-34—5-44 (McGraw-Hill Book Co., New York, N.Y., 1967).

Key words: Acoustical thermometry; black-body radiation; gas thermometry; Kirchoff's law; magnetic thermometry; "noise" thermometry; nuclear resonance thermometry; radiation thermometry; temperature measurement; temperature scales; temperature uncertainties; thermodynamic temperature scales.

The chapter defines an absolute thermodynamic temperature scale and describes methods for the realization of such a scale. The internationally accepted Kelvin scale is defined. Practical scales are discussed, and the International Practical Temperaure Scale of 1948 is defined. Temperature differences between ractical scales and the Thermodynamic Kelvin Scale are iscussed. Estimated limits of uncertainty in realizing both therhodynamic and practical scales are tabulated. Uncertainties asociated with the calibration and use of commonly used temperaure measuring instruments are also tabulated.

**0614.** Sze, W. C., **Comparator for calibration of inductive voltage dividers from 1 to 10 kHz,** *ISA Trans.* **6,** No. 4, 263-267 (Oct. 1967).

> Key words: Calibration; comparator; high permeability core; inductive voltage divider; phase angle; R-C network; shielded transformer; toroidal core; voltage divider; voltage ratio.

A high accuracy comparator is described for measuring the elative deviations in voltage ratios and phase angles of inductive oltage dividers. The new technique overcomes several inherent imitations of the existing comparison methods. The balance is accomplished by utilizing special shielded transformers and a resistance-capacitance network for in-phase and quadrature voltage injections. The measurements are accurate to within $1 \times 10^{-7}$ of input in the frequency range from 1 to 10 kHz. Resolution is better than $2 \times 10^{-10}$.

**10615.** Watson, R. E., Bennett, L. H., Freeman, A. J., **Origin of solvent Knight shifts in alloys,** *Phys. Rev. Letters* **20,** No. 13, 653-656 (Mar. 25, 1968).

> Key words: Alloys; charge impurity screening; hyperfine fields; Knight shift; noble metals; orthogonalized plane waves.

Consideration of the effects of conduction electron orthogonalization to the ion cores on the hyperfine field leads to the conclusion that current screening theories of Knight shifts of impurities in alloys require modification.

**10616.** Wiederhorn, S. M.,, Shorb, A. M., Moses, R. L., **Critical analysis of the theory of the double cantilever method of measuring fracture-surface energies,** *J. Appl. Phys.* **39,** No. 3, 1569-1572 (Feb. 15, 1968).

> Key words: Cleavage; crack propagation; elasticity; fracture; fracture energy; surface energy.

This paper presents a critical discussion of the double cantilever method of measuring fracture surface energies. It was found that the equation developed by Gillis and Gilman is valid for crack lengths greater than 1.5 times the crack arm height. The constants in this equation were evaluated and were found to be practically independent of the elastic constants of the material for which they were evaluated, suggesting the equation could be used on any material. The Gilman and Gillis approach to the double cantilever problem was found to be consistent with the approach used by Gross and Srawley.

**10617.** Yakowitz, H., **Evaluation of specimen preparation and the use of standards in electron probe microanalysis,** *Am. Soc. Testing Mater. Spec. Tech. Publ.* **430,** Fifty Years of Progress in Metallographic Techniques, 383-408 (1968).

> Key words: Electron probes; metallography; microanalysis; petrography; specimen preparation; x-ray analysis.

The magnitude of systematic and statistical errors in electron probe microanalysis due to faulty specimen preparation is discussed theoretically and experimentally. It is shown that this error increases as the energy of the x-ray line being monitored decreases and also as the x-ray emergence angle decreases. Specific specimens are chosen to illustrate various preparation problems in metallurgy, petrography, and biology. Generalizing from these, certain useful instrumental adjuncts can be listed; these adjuncts tend to allow the effects of the specimen surface on the analysis to be controlled more rigorously. Several conductive coatings commonly used are evaluated in terms of electron and optical transparency, adherence, x-ray attenuation, and thermal and electrical conductivity. Finally, a brief survey of standards employed in electron probe microanalysis is made. Situations for which nonelemental standards are required are outlined. The choice of standards for various types of work is discussed.

**10618.** Youden, W. J., **Statistical design of experiments,** Chapter 13 in *Handbook of Physics, Second Ed., Part 1, Mathematics,* E. U. Condon and H. Odishaw, eds., pp. 1-198—1-201 (McGraw-Hill Book Co., New York, N.Y., 1967).

> Key words: Block design; design of experiments; experimental design; factorial design; Latin square; statistical design; Youden square.

Statistical design of experiments involves the scheduling or grouping of measurements with respect to experimental or environmental factors such as instruments, procedure, temperature or time so as to minimize the effect of extraneous factors on the value of the sought-after quantity. The extension of the simple example of drift elimination in the ABBA arrangement for intercomparing two objects, A and B, to the intercomparison of many objects is illustrated by arrangements that account for one source of variability (Block designs) and two sources of variability (Latin squares, Youden squares). A second class of designs for studying the effect of many factors on a single quantity, called factorial designs are illustrated. For both classes of designs the use of fractional designs to reduce the total number of observations is discussed.

**10619.** Ambs, W. J., **Field-emission studies of the oxidation of clean nickel surfaces,** *Proc. Second Intern. Congress on Metallic Corrosion, New York, N.Y., Mar. 11-15, 1963,* pp. 815-821 (Natl. Assoc. Corrosion Engr., Houston, Texas, 1966).

> Key words: Emission microscopy; field-emission; nickel surfaces; oxidation.

The adsorption of oxygen on clean and slightly contaminated nickel surfaces and the subsequent oxidation of nickel have been studied by field-emission microscopy. The adsorption at room temperature depends strongly on crystal face, showing a considerable relative enhancement of emission on planes close to the {110}. This is interpreted as an independent confirmation of some of Germer's low energy electron diffraction results. Adsorption at 77 °K shows no such phenomenon. Formation of oxide whiskers at 600 °C and of epitaxial oxide layers at higher temperatures have also been observed. Preliminary experiments on iron show that iron whiskers can be grown by heating iron field emitters to about 900 °C in the electric field. The phase transition at 910 °C has also been observed.

**10620.** Armstrong, G. T., **Calorimetry,** *Encyclopaedic Dictionary of Physics, 2nd Supplementary Volume* **2,** 1-8 (Pergamon Press Inc., New York, N.Y., Oct. 1967).

> Key words: Calorimetric instruments and procedures; calorimetric measurements; calorimetry; calorimetry to thermodynamics; standard samples for chemistry.

This survey deals in separate sections with materials supplementary to articles on calorimetry appearing in the main work of the Encyclopaedic Dictionary of Physics. Separate sections treat the relationship of calorimetry to thermodynamics, applications of the results of calorimetric measurements, current (1965) areas of activity in the development of calorimetric instruments and procedures, and the scope of calorimetric work including national and international coordination.

A short article on Standard Samples for Calorimetry is appended.

**10621.** Bates, A. A., **Responsibility in building research,** *Proc. Third Australian Building Research Cong., Melbourne, Australia, Aug. 1967,* pp. 27-34 (1968).

Key words: Building research; corporate; historical; humane; individual; international; national; urban.

The aspects of building research are traced through the four historical periods of man's quest for an understanding and mastery of nature or "scientific research." These periods are identified as (1) individual, (2) the corporate, (3) the national, and (4) the international. The philosophic search for truth by individuals such as Archimedes, Galen, Bacon, Galileo, Newton and Faraday led to the industrial revolution and corporate investment in science and research for profit by the more industrially advanced nations. Motivated by public concern for national security and for the well being of people, organized building research developed during this period. This national concern expended to the international period which is now under way thereby establishing formal channels for cooperation between nations in building as well as other technology. The major broad objective of international research is to advance the welfare of mankind by providing food and shelter. Humane housing for every individual of whatever economic and social status is the urban problem of highest priority.

**10622.** Beaty, E. C., Patterson, P. L., **Mobilities and reaction rates in neon ions in neon,** *Phys. Rev.* **170,** No. 1, 116-121 (June 5, 1968).

Key words: Ion; mobilities; neon; rates; reaction.

The mobilities of $Ne^+$ and $Ne_2^+$ ions in neon has been measured at 300 °K. The mobility of $Ne^+$ and $Ne_2^+$ at low $E/p_o$ are given by the equations: $K(Ne^+) = 4.07\ [1 + 8.0 \times 10^3\ (E/p_o)^2 + 2.0 \times 10^{-6}\ (E/p_o)^4]^{-1/8}$ and $K(Ne_2^+) = 6.14\ [(1 + 8.3 \times 10^{-3}\ (E/p_o)^2/(1 + 2.0 \times 10^{-3}\ (E/p_o)^2 + 8.4 \times 10^{-6}\ (E/p_o)^4)]^{1/4}$. The $Ne^+$ was observed to convert to $Ne_2^+$ by a three-body reaction with a rate coefficient ranging from about $7 \times 10^{-32}$ cm$^6$/sec at $E/p_o = 2.0$ to about $5 \times 10^{-32}$ cm$^6$/sec at $E/p_o = 6.0$.

**10623.** Bennett, H. S., **F center in ionic crystals: semicontinuum polaron models,** *Phys. Rev.* **169,** No. 3, 729-745 (May 15, 1968).

Key words: Alkali halide; alkaline earth fluoride; alkaline earth oxide; F center; ionic crystal; polaron; semi-continuum model.

The states of the F center are considered on the basis of a model which treats the movement of the nearest neighbors to the F center and the F electron in a self-consistent manner. The lattice is described in terms of classical ionic crystal theory and the F electron is treated according to the semi-continuum polaron theory. The absorption energy, the emission energy, the lifetime of the first excited state, the thermal activation energies, and the Huang Rhys factor are evaluated for two models (Hartree and quasi-adiabatic) which differ in the evaluation of the optical polarization. It is shown that the Hartree semi-continuum polaron model agrees best with the experimental results for NaCl, KCl, $CaF_2$, $SrF_2$, and $BaF_2$. In addition, these models show that among the above quantities the thermal activation energies and the lifetime of the first excited state are most sensitive to the physical content of a given model.

**10624.** Bevan, A. W., Jr., Daniel, A. C., Mahler, R. J., **Indication of the effect of a magnon gap in the $^{19}F$ relaxation rate in antiferromagnetic $CoF_2$,** *Physics Letters* **25A,** No. 7, 555-556 (Oct. 9, 1967).

Key words: Antiferromagnetism; $CoF_2$; magnon gap; relaxation times.

The $^{19}F$ nuclear spin-lattice relaxation time in a $CoF_2$ single crystal has been measured in zero external magnetic field over the temperature range of 4° to 16 °K. The relaxation rate falls off exponentially, but faster than the $T^2 \exp(-T_{AE}/T)$ predicted using a simplified spin wave theory.

**10625.** Branscomb, L. M., **The misinformation explosion: Is the literature worth reviewing?,** *Sci. Res.* **3,** No. 11, 49-52 (May 1968).

Key words: Manuscripts; publications; scientific literature.

The exponentially increasing scientific literature contains data on properties of matter needed by science and technology. Bold inventions, such as the National Standard Reference Data System, help the user pick his way through this morass. Urgent need exists for quality control as follows: the development (and adoption by investigators) of criteria to delimit systematic errors; the rejection by journal editors of manuscripts which report data but do not contain sufficient information to permit their evaluation.

**10626.** Broberg, J., Leiss, J., Schrack, R. A., Wyckoff, J. M., **On-line handling system for the NBS linac,** *IEEE Trans. Nucl. Sci.* **NS-11,** No. 3, 331-337 (June 1964).

Key words: Building blocks; computer control; digital computer; Linac, NBS; multiplex register unit; nuclear physics experiments.

To meet the needs of the new Linac facility at the National Bureau of Standards an SDS 920 digital computer has been obtained for concurrent on-line processing of data from several independent experiments. The system surrounding the computer contains several novel devices for allowing convenient real time operator control of computer functions and to provide privacy of programs by means of priority interrupt lines controlling the sequence of operations. A family of building blocks is being developed for the input of information. Surprisingly, the requirements of all nuclear physics experiments projected for the facility can be met with only six different blocks; an Analog Voltage Analog to Digital Converter, a Digital Register Unit, a Spectrum Analog to Digital Converter, a Scalar and a Group Enable Unit. These devices all feed information into the computer via a Multiplex Register Unit. The man machine interface is made flexible by the use of two decoding units, one for outgoing signals and one for sense switch type information to be used in computer control. The conventional computer output devices are supplemented in this system by direct analog, digital, graphic and scope output of data.

**10627.** Bussey, H. E., **Instrumentation and measurement,** *1966 Digest of Literature on Dielectrics* **30,** Publ. 1496, 1-21 (National Academy of Sciences—National Research Council Washington, D.C., 1966).

Key words: Breakdown; dielectric constant measurements; discharges in dielectrics; instrumentation for dielectrics; permittivity measurements.

A bibliography of 200 literature references is given on the instrumentation for and measurements of complex dielectric constant and discharge or breakdown of dielectrics. Applicable theoretical topics are included.

**10628.** Chang, T., Yang, G. C., **Temperature dependence of paramagnetic relaxation of $Mo^{5+}$ in $TiO_2$,** *J. Chem. Phys.* **48** No. 6, 2546-2549 (Mar. 15, 1968).

Key words: $Mo^{5+}$; paramagnetic relaxation; temperature dependence; $TiO_2$.

The relaxation rate of $Mo^{5+}$ in $TiO_2$ was measured, by the measurement of line width at temperatures between 77 °K and 240 °K, and by the saturation and recovery method at temperatures at and below 4.2 °K. The line width is about 300 gauss at 240 °K, and 0.5 gauss at 77 °K. The relaxation time is about ec. at 4.2 °K and about 100 min. at 1.05 °K. The temperature deendence of the relaxation rate is $T^9$ between 3 °K and 200 °K, $^5$ between 1.5 °K and 3 °K, and T below 1.5 °K. At the linear ependence region, i.e., ~ 1 °K, the magnetic field dependence s $H^4$ as verified by experiments.

**0629.** Chappell, S. E., Humphreys, J. C., Motz, J. W., Berger, M. J., Seltzer, S. M., **Response of silicon transmission detectors to monoenergetic electrons,** *IEEE Trans. Nuclear Sci.* **NS-15,** No. 3, 359-362 (June 1968).

Key words: Monoenergetic electrons; Monte Carlo calculations; response function; semiconductor detectors; silicon.

Silicon transmission semiconductor detectors with thicknesses f 191 and 530 $\mu$m were exposed to normally incident electrons vith energies of 0.25, 0.50, 0.75, and 1.00 MeV. When the detecor thickness is less than the incident electron range, the pulseeight distributions produced by the electrons in these detectors vere characterized by an absorption peak and a relatively broad scape peak which was associated with transmission and reflecion of electrons. Comparisons were made between the experimental pulse-height distributions and Monte Carlo results calcuated for identical conditions. Good agreement was found etween theory and experiment at 0.75 and 1.00 MeV; however, ifferences, that remain to be explained, appeared in the position of the escape peak at 0.25 and 0.50 MeV.

**10630.** Cooper, M. J., **Electric field effect on critical opalescence of dipolar binary mixture,** *J. Chem. Phys.* **48,** No. 9, 4272-4277 (May 1, 1968).

Key words: Binary mixture; critical opalescence; electric field effect; excess concentration; van der Waals.

A modified van der Waals model is used to describe the effect of a time varying external electric field on the critical mixing point properties of a dipolar binary mixture. Assuming that the behavior of the concentration fluctuations about equilibrium is governed by linearized hydrodynamic equations and that the diffusion coefficient is determined by the instantaneous equilibrium state, the decay of the fluctuations is described. The relaxation time characterizing the electric field effect upon the light scattering by critical opalescence is related to the free relaxation of the concentration fluctuations.

**10631.** Corliss, E. L. R., **A mechanistic model for the limits of auditory perception,** *Proc. Symp. on Models for the Perception of Speech and Visual Form, Boston, Mass., Nov. 11-14, 1964,* pp. 339-343 (Massachusetts Institute of Technology, Boston, Mass., 1967).

Key words: Auditory detection; auditory discrimination; hearing; mechanistic model for hearing.

From a number of apparently diverse experiments on human hearing it has proved possible to construct a simple model describing the limits of auditory perception for normal and impaired ears. The model has been applied to interpret the perception of distorted speech by persons with normal and impaired hearing.

Two mechanisms are required: One element emits unit responses whose number is proportional to the amplitude of a sound. It is followed by a selector mechanism, analogous to a resonant circuit, that integrates the responses. Correspondingly, just two parameters are involved: the threshold of hearing and the "Q" of the selector mechanism. The theory of the selector mechanism is based upon a recently published study of the limits of performance of a system capable of storing oscillatory energy reversibly, but the remainder of the theoretical description makes use of ordinary communication theory.

The discriminating power of the normal ear is shown to be proportional to the one-fourth power of the level above threshold, and to relate closely to the sensation of loudness. This dependency results from considering the responses of the receptor mechanism to be integrated in random coherence by the selector mechanism, with the threshold of normal hearing representing a basic "least count" in the selector mechanism.

The model permits prediction of the influence of noise upon perception by normal and impaired ears. Experimental evidence from noise-masked audiometry indicates that the selector mechanism is unimpaired in many cases of sensorineural loss. In fact, the model is consistent with the selector mechanism having the same "least count" for normal and impaired ears; the observations on the effects of hearing loss can be referred to defects in the receptor mechanism alone. Loss with recruitment corresponds to emission of spontaneous responses from the receptor mechanism in addition to responses to the incoming sound. The classical type of loss without significant recruitment corresponds to a depression in the number of unit responses to sound of a given amplitude.

The model indicates quantitatively what has been recognized qualitatively: that amplification does not restore full discrimination in the presence of sensorineural loss. The application of the model to an experiment on the perception of distorted speech will be discussed.

**10632.** Davis, J. C., Faison, T. K., Achenbach, P. R., **Errors in temperature measurement in moving air under isothermal conditions using thermocouples, thermistors and thermometers,** *ASHRAE Trans.* **73,** Pt. I, VII 1.1 (1967).

Key words: Air in ducts; measurement errors; temperature measurement; thermistors; thermocouples; thermometers.

A study was made of the errors in measurement of the temperature of air moving in a duct at velocities from approximately 300 to 2000 fpm under isothermal conditions using copper-constantan thermocouples, thermistors, and mercury-in-glass thermometers. Generally, the indications of the three types of sensors agreed within 0.10 °F and in many cases to within 0.05 °F when installed in a test duct. Experience during this study showed, however, that such agreement is not attainable during laboratory use unless special calibration, application, and observation techniques are used. The change in calibration of the three types of sensors during successive annual intervals was also investigated. The annual drift in indicated temperature of the sensors was usually less than 0.05 °F except that the drift of the copper-constantan thermocouples approached 0.10 °F during the first year of the study. This investigation indicated that the accuracy in the measurement of temperature specified in testing standards for heating and air-conditioning equipment should be greater than 0.10 °F.

**10633.** Drechsel, D., Maximon, L. C., **Potential model calculation for coplanar and non-coplanar proton-proton bremsstrahlung,** *Physics Letters* **26B,** No. 8, 477-479 (Mar. 1968).

Key words: Coplanar and non-coplanar events; differential cross section; double scattering term; off-the-energy-shell behaviour; potential model calculation; proton-proton bremsstrahlung; scattering amplitude.

The cross section for proton-proton bremsstrahlung for both coplanar and non-coplanar events has been calculated using both Hamada-Johnston and Reid potentials. Prior calculations which disagreed with experiments left out double scattering terms. These terms, which are negligible in the center of momentum system, are shown to be particularly important when the calculation is performed in the lab system for non-coplanar events, even at high energies. The importance of these terms is, however, not reflected in the cross section for coplanar events integrated over photon angle at high energies, which accounts for the agreement between high energy experiments and calculations performed with this neglect. The present calculations show good agreement with the available experiments between 30 and 200 MeV and thus demonstrate that the local potentials in use all have the correct behaviour off the energy shell.

**10634.** Drechsel, D., Seaborn, J. B., Greiner, W., **Collective correlations in spherical nuclei and the structure of giant resonances,** *Phys. Rev.* **162,** No. 4, 983-991 (Oct. 1967).

Key words: Collective correlations; collective intermediate structure; dipole vibrations; giant resonance; particle-hole structure; photoabsorption; surface vibrations.

The theory of collective correlations in nuclei is formulated for giant resonances interacting with surface vibrations. The giant dipole states are treated in the particle-hole framework while the surface phonons are treated within the collective model. Consequently this treatment of nuclear structure goes as well beyond the common particle-hole model (including its various improvements which take groundstate correlations into account) as the pure collective model. The interaction between giant resonances and surface degrees of freedom as known from the dynamic collective theory is formulated in the particle-hole language. The theory contains therefore the particle-hole structures of giant resonances. Detailed calculations are performed for $C^{12}$, $Si^{28}$, and $Ni^{60}$. A good detailed agreement between theory and experiment is obtained for all these nuclei although only $Ni^{60}$ is in the region where one would expect the theory to work well ($50 < A < 110$).

**10635.** Durst, R. A., Ross, J. W., Jr., **Electrochemical generation of fluoride ion by solid-state transference,** *Anal. Chem.* **40,** No. 8, 1343-1344 (July 1968).

Key words: Constant-current coulometry; electrochemical generation; fluoride; lanthanum fluoride membrane; solid-state transference.

Fluoride ion is electrochemically generated by the solid-state transport of fluoride ions through a permselective membrane of europium-doped lanthanum fluoride. Under the conditions described, a constant-current generation efficiency of 99.2 percent is achieved. Potential uses for this technique include coulometric analysis and fluoridation of water supplies.

**10636.** Evenson, K. M., **The optical detection of stimulated emission in CN at 20-CM wavelength,** *Appl. Phys. Letters* **12,** No. 8, 253-254 (Apr. 15, 1968).

Key words: CN; microwave spectra; optical detection; stimulated emission.

Six of the seven allowed electric dipole transitions between the hyperfine levels of the $J = 7/2$ lambda doublet in the 10th vibrational level of the excited $A^2\pi_{3/2}$ state of CN were observed. The transitions at frequencies between 1580 and 1650 MHz were between the more populated negative parity levels and the positive parity levels. The stimulated emission was detected by measuring an increase in the intensity of the $B^2\Sigma^+ \rightarrow X^2\Sigma^+(0,0)$ violet band of CN near 3875°. A similar optical detection technique was attempted on the 337 $\mu$m "so-called" CN laser in order to discover which of the proposed laser mechanisms was correct; there was no indication that any of the proposed mechanisms were correct.

**10637.** Forbes, E. J., **A graphic method of economic feasibility analysis,** (Proc. Inst. Electronics and Automation in Publishing, Washington, D.C., 1965), Chapter 13 in *Automation and Electronics in Publishing,* L. H. Hattery and G. P. Bush, eds., **3,** Part IV, 129-140 (Spartan Books, Washington, D.C., 1965).

Key words: Computer-typesetting; cost studies or economic feasibility; estimating complex keyboarding; micropublishing; photocomposition; printing.

A recently developed graphic method for visually presenting the results of computer composition production experiments and economic feasibility studies is demonstrated. Following an explanation of the method and use of the new cost curves, performance characteristics of two new types of high speed photocomposers are summarized. Then, feasibility predictions are shown for by-product computer photocomposition of a large document center's announcement journal and alternate indices.

**10638.** Forman, R. A., Cardona, M., **Exciton electroreflectance in II-VI compounds,** *Proc. Intern. Conf. II-VI Semiconducting Compounds, Brown University, Providence, Rhode Island, Sept. 6-8, 1967,* pp. 100-111 (W. A. Benjamin, Inc., New York, N.Y., 1967).

Key words: CdS; differential techniques; electric field broadening; electroreflectance; excitons; Stark effect; ZnS; ZnSe; II-VI compounds.

We have applied the method of differential reflectivity to high resistivity samples of CdS, ZnS, and ZnSe. We modulate the reflectivity by means of a transverse electric field applied between two evaporated gold films on the reflecting surface with small spacing between them. As has been found in other differential reflectivity measurements, the sensitivity is quite high, thus enabling us to observe structure which is not easily seen in the dc reflectivity. The high sensitivity facilitates the study of the exciton line-shapes as a function of electric field and temperature; differences between various types of line-shapes (e.g., Gaussian and Lorentzian) are more apparent in differential spectra than in dc spectra. Our measurements have been performed with square-wave modulation; the spectra obtained are the direct difference between field-on and field-off. At low fields, the spectra resemble derivatives of dispersive signals but as the field is increased, the spectra become closer to the dispersive signals themselves. At low fields a Stark-like shift of the exciton binding energy and a broadening is obtained. At high fields, the exciton is destroyed (ionized).

**10639.** Freeman, D. H., Aiyar, A. S., **Studies of ion exchange materials: homogeneous fractional sulfonation of copolymers of styrene and divinylbenzene,** *Anal. Chem.* **39,** No. 10, 1141-1144 (Aug. 1967).

Key words: Copolymer; divinylbenzene; homogeneity; ion-exchange; kinetics; nitrobenzene; styrene; sulfonation; sulfuric acid.

The feasibility of slow sulfonation of bead-copolymers of styrene and divinylbenzene to give homogeneous and fractionally substituted ion-exchange materials is shown. The reaction of copolymer with dilute solutions of sulfuric acid in nitrobenzene at 23.5° approaches second order kinetics at less than 60 percent sulfonation; at higher values the rate constant falls toward a value of zero at 100 percent sulfonation. Volume swelling measurements of the fractionally substituted ion-exchangers agree by extrapolation to corresponding measurements by Wiley on the fully substituted materials.

**10640.** Freeman, D. H., Paulson, R. A., **Chemical microstandards from ion exchange resin,** *Nature* **218,** 563-564 (May 11, 1968).

Key words: Analytical detection limits; ion exchange resins; measurements; microstandards; standards.

Ion exchange resins are available in the form of small spherical articles. These can be used to provide mass standards that in- vidually contain extremely small and precisely defined quanti- es of matter. Their capabilities include the determination of alytical detection limits and the performance of chemical libration down to, and below the level of one picogram.

**0641.** Gammon, W. H., **Remotes and displays,** *Proc. A Pioneer Presentation of a National Symposium on the Impact of Automation and Documentation, Denver, Colo., Apr. 27-29, 1967,* p. 119 (1968).

Key words: Archives; displays; information retrieval; remote input devices.

Briefly describes equipment available for recording and dis- laying material in archives. The conclusion is reached that hile remote stations, such as teletypes, may become regularly part of archive service, display consoles (cathode ray tubes) ay not because of the economics involved in putting the materi- in the data bank for later display.

**0642.** Gammon, W. H., **Security and privacy problems brought on by automation,** *Proc. A Pioneer Presentation of a National Symposium on the Impact of Automation and Documentation, Denver, Colo., Apr. 27-29, 1967,* pp. 74-75 (1968).

Key words: Computer data banks; privacy of data.

There has recently been considerable public notice of the roblems of the protection of privacy of the individual in connec- on with computer data banks. Three different Committees of he Congress have held hearings on this subject. Data banks for hatever purpose will have to protect the privacy of the data hey collect. The presentation discusses six areas where precau- ons will have to be taken to assure the privacy of information. ne illustration (showing all of the areas discussed) is included.

**0643.** Gammon, W. H., **Software as it relates to documentation,** *Proc. A Pioneer Presentation of a National Symposium on the Impact of Automation and Documentation, Denver, Colo., Apr. 27-29, 1967,* pp. 14-22 (1968).

Key words: Archives; computer programs; documentation; software.

An archivist receiving a reel of tape may find that the record- ng was made on any one of 174 different makes and models of computers, each one with its own executive routine and operat- ng system. Thus, in order to read the tape, he would have to know the characteristics of the tape transport on which it was produced. This contrasts with the situation when a reel of microfilm is accessioned, where he can visually determine the width of the film and the magnification required to make it readable.

As an indication of the content of the applicable software documentation with which archivists need to be concerned, the presentation describes (using slides in the oral presentation) the components of a COBOL program. The paper includes illustrations of a flow chart, the machine language program and the COBOL version of a program to "compute FICA" (Federal Insurance Contributions Act).

**10644.** Gates, D. M., Keegan, H. J., Weidner, V. R., **Spectral reflectance and planetary reconnaissance,** (Proc. Third Goddard Memorial Symp. Scientific Experiments—Manned Orbital Flights, Washington, D.C., Mar. 18-19, 1965), Chapter 4 in *Scientific Experiments for Manned Orbital Flights,* pp. 71-86 (Western Periodicals Co., North Hollywood, Calif., 1965).

Key words: Planetary reconnaissance; spectral reflectance; spectrum of reflected sunlights; ultraviolet and visible wavelengths.

The spectral reflectance of selected vegetation, animal integuments, and minerals from 0.26 to 22.2 microns was measured and reported. Strong absorption by the material of incident radiation is caused by pigmentation at ultraviolet and visible wavelengths due to electronic quantum transitions. Strong absorption in the infrared beyond about 2.0 microns is caused by vibration-rotation quantum transitions due to water and organic molecules. A distinct absorption gap exists in the spectrum between these two wavelength regions which is exhibited by a strong reflectance in the 1.0 to 2.0 micron region. Plants with chlorophyll pigmentation display a very abrupt change in reflectance at 0.7 micron. Animal integuments and the bark of some trees do not exhibit this sharp edge. The reflectance spectra of plants and animals have a characteristic absorption band at about 3.5 microns due to C-H stretching.

If there is life on Mars it may be detected by searching with spectral reconnaissance for the presence of a sharp edge in the spectrum of reflected sunlight. The spectral characteristics of sunlight reflected from vegetation on the Earth's surface is described and the expected reflectance from Mars is discussed.

**10645.** Gould, H. A., Guernsey, R. L., Williams, R. H., **Comment on "the kinetic equation of a dilute gas with repulsive and attractive interactions,"** *J. Chem. Phys. Letter* **47,** No. 2, 872-873 (July 15, 1967).

Key words: Boltzmann equation; correlation term; dilute gas; Fokker-Planck equation; hard-core potential; Rice-Allnatt equation.

The Rice-Allnatt assumption has not been confirmed for a low density gas.

**10646.** Greenberg, L., **Kleinian groups,** *Proc. Am. Math. Soc.* **17,** No. 5, 1195-1198 (Oct. 1966).

Key words: Domain of discontinuity; Euler characteristic; fundamental polyhedron; Hilbert nullstellensatz; hyperbolic space; Kleinian group; limit set; parabolic triangle group; prime ideal.

A gap in a theorem by L. Ahlfors is filled, and further theorems on Kleinian groups are proved.

**10647.** Gugler, A. L., **A study of the adherence of porcelain enamel to aluminum,** *Proc. Porcelain Enamel Institute Forum* **29,** 202-208 (Nov. 1967).

Key words: Adherence; aluminum; chromium; electron microprobe; electron microscope; interface; magnesium; porcelain enamel; spall.

A study of the mechanism of adherence of porcelain enamel to aluminum has yielded some interesting observations. Various alloys of aluminum react quite differently when they are porcelain enameled. Enameled specimens which spall, exhibit an intermediate layer between the enamel and the base metal. When the layer is not present, adherence and spall resistance are good. Magnesium bearing alloys tend to form a layer of MgO on the outer surface of the alloy which the enamel does not completely take into solution. Chromium applied to the surface of the aluminum before enameling is beneficial, particularly on magnesium bearing alloys.

**10648.** Hall, M. B., Little, W. E., **A directional coupler with a readily calculable coupling ratio,** *IEEE Trans. Microwave Theory Tech.* **MTT-15,** No. 11, 598-603 (Nov. 1967).

Key words: Coupling ratio calculation; directional coupler; microwave.

A microwave (X-band) directional coupler consisting of two adjacent parallel waveguides with a common tantalum wall about four skin depths in thickness has been fabricated and studied. The coupler is of interest, particularly in Standards work, because its coupling ratio can be calculated by a straight forward procedure to within experimental error (currently a few tenths of a dB in 70 + dB).

**10649.** Harris, W. P., **Low frequency dielectric behavior,** (Proc. Seventh Electrical Insulation Conf., Chicago, Ill., Oct. 16-19, 1967), *IEEE Publ.* **32C79-42,** 123-125 (1967).

Key words: Bridge; dielectrics; dielectric measurements; dielectric phenomena; electrical measurements; low frequency; measurements; operational amplifiers; ultra low frequency.

Electrical engineers, as well as polymer physicists and materials researchers, can gain useful information from a study of the behavior of dielectrics, and of high-megohm resistors at very low frequencies. This is illustrated by examples.

There are two main methods of obtaining ultra-low-frequency data. One is to apply a d.c. voltage producing a time-dependent current which corresponds to an inverse frequency plot. The other is to use an alternating voltage, usually sinusoidal, and apply this to a bridge circuit including the material under study. Recent developments in the latter methods are presented, along with some typical results.

**10650.** Heinrich, K. F. J., **Electron probe microanalysis by specimen current measurement,** (Proc. Fourth Intern. Symp. X-ray Optics and Microanalysis, Orsay, France, Sept. 7-10, 1965), Chapter in *X-ray Optics and Microanalysis,* R. Castaing, P. Deschamps, and J. Philibert, eds., pp. 159-167 (Hermann, Paris, France, 1966).

Key words: Electron backscatter; electron probe microanalysis; microanalysis; specimen current.

Under appropriate instrumental conditions, electron backscatter coefficients of elements and compounds can be determined quantitatively in the electron probe microanalyzer, without interference of low energy electrons. It is shown that there is a simple relation between the backscatter coefficient of a binary target and those of its constituents. This relation can be used for quantitative analysis of binary specimens. The advantages and limitations of this method are discussed, and a practical application of the technique for quantitative metallography is demonstrated. The backscatter coefficients of several elements have been experimentally determined at electron energies of 10, 20, 30, 40, and 49 keV.

**10651.** Heinrich, K. F. J., **Scanning electron probe microanalysis,** *Am. Soc. Testing Mater. Spec. Tech. Publ.* **430,** 315-342 (1968).

Key words: Cathodoluminescence; electron backscatter; electron probe; microanalysis; scanning electron microscopy; x-ray spectrometry.

The combination of electron microprobe x-ray emission spectrometry with the scanning techniques first developed for the scanning electron microscope permits using the scanning electron probe as a microscope sensitive to elemental composition. This technique is particularly useful in the many applications in which spatial distribution of one or more elements in a specimen is more important than local composition. Although oscilloscope representation of probe scanning is usually obtained by the simple technique of producing a dot of light for each arriving photon, more sophisticated scanning techniques such as expanded contrast registration and concentration mapping can provide more quantitative information. Signals other than x-rays, such as target current, electron backscatter, or cathodoluminescence may be used for image formation. Electron beam scanning can also be performed in a discontinuous fashion, so that the electronn beam irradiates in succession a number of spots arranged in a square or rectangular pattern, and the number of photons registered in each position is retained in the memory of a multichannel analyzer. The application of these diverse scanning techniques is illustrated.

**10652.** Heinrich, K. F. J., Vieth, D., Yakowitz, H., **Correction for non-linearity of proportional counter systems in electron probe x-ray microanalysis,** *Advan. X-ray Anal.* **9,** 208-220 (1966).

Key words: Electron probe x-ray microanalysis; spectrometers; x-ray microanalysis.

While the theoretical basis for the correction of non-linearity or detector systems is well known, methods for the determination of dead time effects must be adapted to electron probe microanalyzer systems. Two such methods, one employing both x-ray and current measurements, and the other, simultaneous x-ray measurements on two spectrometers, are described. The effect of pulse height shrinkage at high counting rates on the linearity of the detector system is discussed. When the proposed corrections for the dead-time of x-ray detector systems employing proportional counters are applied to the x-ray intensity measurements obtained with the electron probe microanalyzer count rates as high as 50,000 cts/sec can be used.

**10653.** Herron, J. T., Huie, R. E., **Arrhenius parameters for the reactions of atomic nitrogen with some olefins and acetylenes,** *J. Phys. Chem.* **72,** No. 7, 2538-2540 (July 1968).

Key words: Acetylene; activation energy; atomic nitrogen; chemical kinetics; olefin; rate constant.

The rates of reaction of atomic nitrogen with a series of olefins and acetylenes have been measured from 320 to 550 K. Pre-exponential factors and activation energies have been derived. In addition, upper limits are given for the rates of reaction of atomic nitrogen with several miscellaneous organic compounds.

**10654.** Herron, J. T., Huie, R. E., **On the reaction of atomi nitrogen with carbon dioxide,** *J. Phys. Chem.* **72,** No. 6, 2235 2236 (June 1968).

Key words: Active nitrogen; atomic nitrogen; carbon dioxide; mass spectrometry; rate constant.

The rate constant for the reaction of atomic nitrogen with carbon dioxide has been found to be less than about $10^8$ cm$^3$ mol$^{-}$ s$^{-1}$ from 330 to 550 K. This result is in serious disagreement wit the results of L. I. Avramenko and V. M. Krasnen'kov (Izv Akad. Nauk. SSSR Ser. Khim. 516 (1967)).

**10655.** Hetzer, H. B., Robinson, R. A., Bates, R. G., **Dissociatio constants of piperazinium ion and related thermodynamic quantities from 0 to 50°,** *J. Phys. Chem.* **72,** 2081-2086 (1968).

Key words: Acid-base equilibria; dissociation constant electrolyte; ionization; piperazine; piperazinium ion; thermodynamics of ionization.

The two thermodynamic dissociation constants of piperazinium ion at 11 temperatures from 0 to 50° have been determine from emf measurements of hydrogen-silver chloride cell thout liquid junction. The first (acidic) dissociation constant $_1$) for the process $PzH_2^{++} + H_2O = H_3O^+ + PzH^+$ is given as function of T (°K) by the equation $-\log K_1 = 952.111/T +$ 3919 $- 0.007555T$. At 25°, $-\log K_1$ is 5.333, $\Delta H°$ is 31,080 J ole$^{-1}$, $\Delta S°$ is + 2.2 J deg$^{-1}$ mole$^{-1}$, and $\Delta C_p^\circ$ is 86 J deg$^{-1}$ ole$^{-1}$. The second (acidic) dissociation constant ($K_2$) for the ocess $PzH^+ + H_2O = H_3O^+ + Pz$ is given by the equation $-\log$ $_2 = 1656.59/T + 6.1316 - 0.006556T$. At 25°, $-\log K_2$ is $9.73_1$, H° is 42,870 J mole$^{-1}$, $\Delta S°$ is $-42.6$ J deg$^{-1}$ mole$^{-1}$, and $\Delta C_p^\circ$ 75 J deg$^{-1}$ mole$^{-1}$. The results are compared with those for her protonated bases of similar structure.

**656.** Hobbs, A. M., **Remarks on network simplification,** *J. Operations Res.* **15,** No. 3, 548-551 (May-June 1967).

Key words: Capacitated vertices; delta-wye network reductions; flows in networks; graph theory; mathematics; network simplification; single commodity flows; wye-delta network reductions.

In "The Use of Wye-Delta Transformation in Network Simfication," *8 OR* 1960, Sheldon B. Akers, Jr. stated two condins which together were supposedly sufficient for delta-wye ansformations in networks with finite node capacities. This ter gives a counter-example to the sufficiency of the two contions and emphasizes that the first condition must be satisfied any network before delta-wye transformations can be carried t.

**657.** Hughes, E. E., Dorko, W. D., **Direct mass spectrometric determination of atmospheric carbon dioxide,** *Anal. Chem.* **40,** No. 6, 866-869 (May 1968).

Key words: Atmospheric carbon dioxide; carbon dioxide; gas analysis; mass spectrometric atmosphere analysis.

The direct mass spectrometric determination of atmospheric rbon dioxide cannot be performed with any useful degree of curacy because of the high concentration of oxygen in the atosphere. By removing the oxygen with phosphorus it is possie to admit sufficiently high pressures of the remaining gas to etermine the carbon dioxide with an inaccuracy of less than 1 ercent. Since the argon content of the atmosphere is presumed onstant, a direct comparison of the carbon dioxide to argon tio should provide a fixed reference for future surveys. The ethod is rapid and requires little equipment other than a mass ectrometer. Results obtained on analysis of rural air in the icinity of Washington, D.C., are presented.

**0658.** Hummer, D. G., Mihalas, D., **Line formation with noncoherent electron scattering in O and B stars,** *Astrophys. J.* **150,** No. 1, L57-L59 (Oct. 1967).

Key words: Doppler noncoherence in electron scattering; electron scattering; line formation; O and B stars.

The importance of Doppler noncoherence in electron scatterng is stressed for lines formed in the outer regions of O and B tars. The redistribution function is derived and the implications f the scattering mechanism are discussed.

**0659.** Ito, J., **Strontium rare-earth hydro- and germanate garnets,** *Mater. Res. Bull.* **3,** 495-500 (1968).

Key words: Garnet; hydrogarnet; inorganic synthesis; rare earths; germanate; x-ray powder analysis.

New strontium and lutetium and ytterbium hydrogarnets, $Sr_3(Yb, Lu)_2(OH)_{12}$ and anhydrous ytterbium germanate garnet, $Sr_3Yb_2Ge_3O_{12}$ were synthesized by precipitation in 1M NaOH solution in air at 115 °C. Partial solid solubility was found in the $Sr_3Yb_2Ge_3O_{12}$ and $Sr_3Yb_2(OH)_{12}$ series.

**10660.** Kerns, D. M., Beatty, R. W., **Basic theory of waveguide junctions and introductory microwave network analysis,** Chapter in *International Series of Monographs on Electromagnetic Waves* **13,** 150 pgs. (Pergamon Press, Inc., New York, N. Y., 1967).

Key words: Matrix description of waveguide junctions; microwave network analysis; waveguide junction.

This monograph presents material developed for a graduate course and found useful for reference as well. It consists of two main parts. Part 1, which is a relatively rigorous introduction to the matrix description of waveguide junctions, is the foundation for Part 2, which is an introductory presentation of microwave network analysis with particular emphasis on concepts and techniques needed in precise measurements.

In Part 1, starting with Maxwell's equations, the theory of ideal waveguides of arbitrary cross section is developed briefly, and relevant general properties are summarized. "Voltage" and "current" are defined for waveguides, and the requisite normalizations are stated as power and impedance normalizations. Impedance, admittance, and scattering matrices are defined for waveguide junctions; realizability and reciprocity conditions for these matrices are stated in general terms. Renormalization, sources, and joining equations are considered.

In Part 2, specific applications of these fundamental relationships are made and additional analytical tools are developed. In particular, expressions are obtained for the conditions of realizability and losslessness for 2-ports, using scattering coefficients. The concepts of available power, efficiency, mismatch loss, attenuation, intrinsic attenuation, and phase shift are carefully examined and equations are given. Transformation of reflection coefficients by 2-ports is discussed and a brief treatment of 3 and 4-ports is presented. Finally, rules for using signal flow graphs are given and a few examples are worked.

**10661.** Koch, H. W., Caswell, R. S., Muehlhause, C. O., **Neutron measurement at the National Bureau of Standards,** *Nuclear News* **10,** No. 11, 48-53 (Nov. 1967).

Key words: Neutron cross sections; neutron measurement standards; neutron radiation fields; neutron sources; standard reference materials.

The national requirements for neutron measurement standards are being satisfied by the present research and service programs of the National Bureau of Standards. These programs are based primarily on an NBS role as a custodian and developer of the equipment for neutron measurement standards. Future requirements can be met by enlarging this role and by adding the role of a participant in information exchange and measurements of standard neutron cross sections.

**10662.** Kokoszka, G. F., Allen, H. C., Jr., Gordon, G., **Magnetic and optical spectra of copper monochloroacetate 2.5 hydrate,** *J. Chem. Phys.* **47,** No. 1, 10-13 (July 1, 1967).

Key words: Copper monochloroacetate 2.5 hydrate; copper pairs; copper-zinc pairs; e.p.r. spectra; exchange coupled; optical spectra.

The electron paramagnetic resonance spectra of copper monochloroacetate 2.5 hydrate, $Cu(O_2CCH_2Cl)_2 \cdot 2.5H_2O$, $[Cu(ClAc)_2]$ and zinc-doped $Cu(ClAc)_2$ have been observed at both K-band and X-band frequencies. The e.p.r. spectrum of the pure material was characteristic of a species with a spin of one, while the spectrum from zinc-doped $Cu(ClAc)_2$ revealed an additional spectrum due to a species with a spin of 1/2. The g-values for both the copper-copper pairs and the copper-zinc pairs were identical with values $g_z = 2.38$ and $g_x = g_y = 2.07$. The hyperfine coupling constant for the copper-copper pairs was about $84 \times 10^{-4}$ cm$^{-1}$, while in the copper-zinc spectrum it was about $158 \times 10^{-4}$ cm$^{-1}$. These results are consistent with the assumption of a weakly coupled interaction. The temperature variation of the doubly integrated intensity of the derivative spectrum indicated that the triplet state lies some 230 cm$^{-1}$ above the singlet ground state.

In the optical absorption spectrum of $Cu(ClAc)_2$ three bands were observed. A very intense band was found at 14,000 cm$^{-1}$, while two other bands were centered at 11,000 cm$^{-1}$ and 26,000 cm$^{-1}$.

**10663.** Krauss, M., **Use of approximate Hartree-Fock calculations to estimate ionization potentials,** Chapter in *Advances in Mass Spectrometry* **4,** 575-578 (Elsevier Publ. Co., Amsterdam, The Netherlands, Aug. 14, 1967).

Key words: $CH_3F$; $CH_3Cl$; correlation energy; $H_2O$; Hartree-Fock energy; ionization potential.

Accuracy of calculation of the inner ionization potentials of polyatomic molecules is examined for the Hartree-Fock orbital energies and for the Hartree-Fock ionization potential determined from neutral and ion calculations of the total energy. The routine ease of the orbital energy procedure is emphasized as well as the approximate accuracy of the orbital differences.

Correlation energy estimates are made to correct the calculated Hartree-Fock ionization potential for $H_2O$. Although reasonable estimates can be obtained in this case, generally it is very difficult to estimate or calculate the correlation energy defined relative to the restricted Hartree-Fock energy.

**10664.** Landgrebe, A. R., Pella, P. A., McClendon, L. T., DeVoe, J. R., Purdy, W. C., **The application of substoichiometric radioisotopic dilution principles to controlled potential coulometry and solvent extraction,** *Anal. Chim. Acta* **39,** 151-159 (1967).

Key words: Cadmium; coulometry; extraction; microanalysis; solvent; substoichiometric radioisotope dilution; trace; zinc.

A radioisotope dilution principle has been applied to controlled-potential electrolysis and solvent extraction with dithizone for the analysis of trace amounts of cadmium. A method has been developed to verify whether or not the substoichiometric principle is obeyed. If the substoichiometric principle is not obeyed, an analysis is still possible through the use of calibration curves. In order to obtain independent verification of the series controlled-potential method and to establish a means of comparison with the radioisotope dilution technique a current integration procedure was also employed. A microtechnique was used to extend the sensitivity of the solvent extraction system for cadmium. To demonstrate the application to real samples, a Standard Reference Material No. 108 (zinc spelter) and a high purity zinc was analyzed for cadmium after separation by a method of standard addition.

**10665.** Larsen, S. Y., **Quantum-mechanical pair-correlation function of hard spheres,** *J. Chem. Phys.* **48,** No. 4, 1701-1708 (Feb. 15, 1968).

Key words: Correlation functions; hard spheres; quantum mechanical.

The density independent part of the quantum mechanical direct and exchange pair correlation functions for hard spheres have been calculated for $\lambda_T/\sigma = 1.4, 2, 2.93761, 4, 6, 8$ and 10. I addition, points were obtained very near the surface of th sphere for $\lambda_T/\sigma = .025$ and .05. The results delineate the approach of the direct (Boltzmann) correlation function to the classical limit, and emphasize the rapid disappearance of the effect of statistics with increasing temperature. These features are explained using Wiener (path) integrals. Analytical expressio valid near the surface of the sphere are derived and compare we with numerical results. Virial coefficients obtained from the co relation functions are in satisfactory agreement with very precis value calculated by Boyd, Larsen and Kilpatrick.

**10666.** Lederer, P. S., **Performance testing, pressure transducer** *Instr. Control System* **40,** No. 9, 93-99 (Sept. 1967).

Key words: Calibration; dynamic calibration; electr mechanical; performance; pressure; telemetering; te method; transducer.

This publication describes methods in one particular progra at NBS for the performance-testing of electro-mechanical pre sure transducers (such as telemetering transducers used i aerospace testing). It covers static and dynamic calibratio procedures in detail, delineates environmental and other test and describes the test equipment used. Examples of dynam calibration results are interpreted.

**10667.** Leiss, J. E., **Electron linear accelerators as sources of hig intensity neutron bursts,** *Proc. Seminar on Intense Neutr Sources, Santa Fe, New Mexico, Sept. 19-23, 1966,* Repo No. CONF-660925, pp. 605-616 (1966).

Key words: Electron linear accelerator; high intensi neutron bursts.

Electron linear accelerators are used as non-booster sourc of neutrons in two distinct modes of accelerator operation, in t accelerator steady-state and in the transient or stored-ener mode.

The basic neutron production process in heavy elements is e amined and example accelerators proposed for each mode of a celerator operation which illustrate the present state of the art.

**10668.** Leiss, J. E., **The NBS linac,** *Proc. Linear Accelerat Conf., Los Alamos, New Mexico, Oct. 3-7, 1966,* Report N LA-3609, p. 20 (1966).

Key words: Linac, NBS; linear electron accelerat nuclear and radiation physics.

The NBS linear electron accelerator is a facility designed f a varied program in nuclear and radiation physics. Considerab attention has been spent in the design of the facility to the nee of experiments, the ability to rapidly (10-20 minute) switch t electron beam from one experimental area to another, and providing experiments with high intensity electron beams havi good energy resolution and stability.

The NBS linac and beam handling system are now ope tional. The linac has been in use for an experimental progr since March, 1966 with experimental set-ups at the end of the a celerator. While we still have problems typical of a new facili the general operation has been quite good. Variation of bea energy from below 10 MeV to 150 MeV without loss of bea has proven extremely easy and fast by back-phasing the last se tions of the accelerator. The highest beam currents at which have operated have been 0.6 milliampere average with about kilowatts of beam power.

**10669.** Lenzi, M., Okabe, H., **Photodissociation of NOCl and N in the vacuum ultraviolet,** (Proc. Intern. Conf. Photochem try, Munich, Germany, Sept. 6-9, 1967), *Ber. deut. Bunsenges. Phys. Chem.* **72,** No. 2, 169-173 (1968).

Key words: Absorption spectra; fluorescence excited states; nitrogen dioxide; photodissociation; vacuum ultraviolet nitrosyl chloride.

The photodissociation of NOCl and $NO_2$ in the vacuum ulviolet yields the electronically excited NO molecule which oresces in the near ultraviolet. The fluorescence spectrum, ich lies mostly in the region 2200 to 4000 Å, extends below 00 Å as the wavelength of incident light decreases. This is inpreted in terms of the production of the NO $C^2\Pi$, $D^2\Sigma^+$, $B'^2\Delta$, $\Sigma^+$ along with the production of the NO $A^2\Sigma^+$, $B^2\Pi$ molecule. e fluorescence intensity and the yield are measured as a funcn of incident wavelength. The fluorescence curves thus obned are correlated with the absorption spectrum. The absorpn coefficient of NOCl in the region 1100 to 2000 Å has been easured. The absorption spectrum between 1100 and 1700 Å y be divided into three regions each corresponding to the nsitions providing the NO $A^2\Sigma^+$, NO $C^2\Pi$, $D^2\Sigma^+$ and NO $\Delta$, $E^2\Sigma^+$ molecule along with the ground state NO or other oducts. On the other hand the absorption by $NO_2$ in the specl region from 1100 to 1450 Å involves not only transitions elding the NO $A^2\Sigma^+$, $B^2\Pi$, NO $C^2\Pi$, $D^2\Sigma^+$ and NO $B'^2\Delta$, $E^2\Sigma^+$ t also those yielding different states which give products other an the electronically excited NO. The threshold energy of the cident photon producing the NO $A^2\Sigma^+$, $B^2\Pi$ gives an upper nit for the bond dissociation energy. The bond energies obned are D(NO-Cl) $\leqslant 1.77 \pm 0.05$ eV and D(NO-O) $\leqslant 3.22 \pm$ 05 eV which are 0.17 eV and 0.10 eV higher than the respece values obtained from the heat of formation.

670. Leslie, R. T., Kuehner, E. C., **Ebulliometry,** Chapter 89 in *Treatise on Analytical Chemistry* **8,** Part D-5, 5085-5109 (1968).

Key words: Boiling points; chemical analytical applications; ebulliometry.

The definition and physical significance of the temperature lled the boiling point is discussed. It is pointed out that the mperature of the boiling point is sometimes confused with connsation temperature, the temperature of a boiling liquid, and nilar phenomena.

Approximate and precise methods of observing boiling points e described, including the use of thermal analysis and gasquid chromatography.

Some chemical analytical applications of boiling point determinations are described.

671. Lightbody, J. W., Jr., Penner, S., **A 12-channel semiconductor counter system for the NBS electron scattering spectrometer,** *IEEE Trans. Nucl. Sci.* **NS-15,** 419-425 (June 1968).

Key words: Backup detectors; counting rate corrections; electron scattering; relative efficiencies; semiconductor array; stepping motor.

A 12-channel array of lithium-drifted silicon detectors for decting high energy electrons in the focal plane of a magnetic ectrometer is described. The detectors are movable along the cal plane and are backed up by two large stationary plastic intillators. The scintillators are placed one behind the other, ich that a count is recorded when a triple coincidence occurs etween both scintillators and a single semiconductor detector. he system has a momentum resolution of 0.036 percent, determined by the detector size and the spectrometer momentum spersion. Discriminator curves have been obtained which ow sufficiently flat plateaus to afford stable counting condions over the entire energy range of the spectrometer. Detector ficiency measurements have also been made which show that the relative efficiencies of the detectors are stable and known to better than two percent of their values. An electron scattering experiment is now in progress using these detectors.

**10672.** Linzer, M., Forman, R. A., **NMR studies of single crystal $ND_4Cl$,** *J. Chem. Phys.* **46,** No. 12, 4690-4693 (June 15, 1968).

Key words: $ND_4Cl$; n.m.r.; quadrupole; single crystal.

The $^2D$ and $^{14}N$ n.m.r. spectra in single crystals of $ND_4Cl$ have been studied from room temperature to $-175$ °C. At high temperatures, motion of the ammonium ion narrows the n.m.r. resonances and averages out both dipole-dipole and quadrupole interactions. As the temperature is lowered, a linewidth transition occurs and quadrupole splittings of the $^2D$ spectrum appear. No splitting is found for the $^{14}N$ spectrum in both $NH_4Cl$ and $ND_4Cl$. From crystal rotation studies, the $^2D$ quadrupole coupling is determined to be $180.1 \pm 1.0$ KHz and the asymmetry parameter to be $0.00 \pm 0.01$, where the stated uncertainties are the estimated maximum errors.

**10673.** Litovitz, I., Macedo, P. B., **Ultrasonic relaxation, viscosity, and free volume in molten glasses,** (Proc. Intern. Conf. Physics of Non-Crystalline Solids, Delft, The Netherlands, July 6-10, 1964), Chapter in *Physics of Non-Crystalline Solids,* J. A. Prins, ed., p. 220 (North Holland Publ. Co., Amsterdam, The Netherlands, 1965).

Key words: Glasses; liquid viscosities; molten glasses; ultrasonic relaxation; viscosity.

Previous investigation by the authors have shown the connection between a distribution of structural relaxation times and the non-Arrhenius temperature dependence of the viscosity. The rate theory for liquid viscosities has been reformulated using the Cohen and Turnbull expression for the probability of finding a vacant site and yields an equation of the form,

$$\eta = A_0 \exp (E_v/RT + V_0/VF.$$

Consistent fits to both temperature and pressure dependence of viscosity were obtained. Using this "hybrid" equation as a basis, the relative role of activation energy and free volume were studied at the glass transition temperature. Once the reasons for non-Arrhenius temperature dependence of the viscosity was obtained, from the "hybrid" equation, it was compared with the origin of the distribution of relaxation times. This comparison seemed reasonable.

**10674.** Loftus, T. P., **Services and facilities for the calibration of soft x-ray detection instruments at the National Bureau of Standards,** (Proc. Conf. Detection and Measurement of X-Radiation from Color Television Receivers, Washington, D.C., Mar. 28-29, 1968), Chapter in *Conference on Detection and Measurement of X-Radiation from Color Television Receivers,* pp. 129-134 (U.S. Dept. Health, Education, and Welfare, Washington, D.C., Mar. 1968).

Key words: Calibration techniques; cavity ionization chamber; free-air chamber; soft x-rays.

The responsibility for the maintenance of national standards of measurement and the provision for access to these standards, for those requiring such services, is a statutory function of the National Bureau of Standards. In the field of x-ray exposure measurements, this responsibility is fulfilled by providing calibration services which reflect the needs of the public.

The standard free-air chamber is the primary standard used for the realization of the unit of x-ray exposure, the roentgen. In the energy range pertinent to the problems associated with stray radiation from color TV sets, two calibration ranges are available which include specially designed free-air chambers and x-ray tubes.

The equipment and calibration techniques set up, for these low-energy x-ray measurements, are designed to provide a calibration service for instruments such as those used in skin therapy. Modification of these methods will be necessary to establish a calibration service for instruments used in protection measurements where vastly different exposure rates are encountered. Investigations are being carried out which will provide information regarding the limitations of the equipment and the modifications required.

The instrument submitted for calibration should be appropriate for low-energy x-ray measurements, have a range within the limitations of the calibration equipment, and be of sufficiently high quality that it would be expected to retain its calibration.

**10675.** Lutz, G. J., DeSoete, D. A., **Determination of carbon in sodium by photon activation analysis,** *Anal. Chem.* **40,** No. 4, 820-822 (Apr. 1968).

> Key words: Carbon; carbon separation; detection limit; internal standard; photon activation analysis; sodium matrix.

A photon activation analysis method has been developed for the determination of carbon in sodium. The method utilizes the photonuclear reaction $^{12}C(\gamma,n)^{11}C$. The $^{22}Na$ or $^{24}Na$ activity produced in the matrix by $^{23}Na(\gamma,n)^{22}Na$ or $^{23}Na(n,\gamma)^{24}Na$ reaction is used as an internal standard. The carbon separation is effected by combustion of the sample in oxygen, treatment with dilute acid and collection of the radioactive carbon as $CO_2$. The time of separation is about 15 minutes. The detection limit is 0.5 micrograms of carbon. A series of five samples at the 48ppm level gave a standard deviation of 10 percent. A series of five samples at the 4ppm level gave a standard deviation of 33 percent.

**10676.** McCulloh, K. E., **Franck-Condon calculations for double ionization of molecular hydrogen,** *J. Chem. Phys.* **48,** No. 4, 2090-2093 (Mar. 1, 1968).

> Key words: Double ionization; Franck-Condon principle; $H_2$; kinetic energy; proton; reflection approximation; theoretical.

The Franck-Condon radial overlap integral for transition from the ground vibronic state of $H_2$ to a state in the $H_2^{++}$ continuum is expanded as an asymptotic series in powers of a small parameter. The initial semi-convergence of the series is sufficiently rapid to provide a convenient basis for computing the kinetic energy distribution for protons formed by double ionization of $H_2$. The results of these computations are presented. The analysis includes a derivation of the reflection approximation for the particular case of transition to the repulsive Coulomb potential curve. Preliminary results of a more general study indicate that this approximation can be applied to a much larger class of repulsive potentials. Previous forms of the reflection approximation, which have heretofore lacked theoretical foundation, are classified and discussed in relation to the derived approximation.

**10677.** McCulloh, K. E., Rosenstock, H. M., **Experimental test of the Franck-Condon principle: Double ionization of molecular hydrogen,** *J. Chem. Phys.* **48,** No. 4, 2084-2089 (Mar. 1, 1968).

> Key words: Double ionization; experimental; Franck-Condon principle; $H_2$; kinetic energy; proton.

The double ionization of molecular hydrogen by electron impact has been observed by coincidence detection of the resulting proton pairs in a system especially designed for absolute kinetic energy measurements. Monte Carlo calculations provided an accurate knowledge of the resolution with which the kinetic energy measurements were made. Experimental results agree closely with predictions based on accurate Franck-Condon overlap integrals for a model involving Morse oscillator wave functions f the molecule and Coulomb wave functions for the ion. In co trast, the reflection approximation and the harmonic oscillat approximation for molecular vibration, two approximatio frequently made in such Franck-Condon calculations, do n agree well either with experiment or accurate calculations. O servations at electron energies of 0.5, 0.75, and 1 keV show th the kinetic energy distribution is independent of electron energ and suggest that the double ionization cross section is inverse proportional to electron energy in this range. These results are be expected for a direct two-electron ejection mechanism f double ionization of $H_2$.

**10678.** McMurdie, H. F., **Progress in x-ray diffraction data co pilations,** Chapter in *Fifty Years of Progress in Metallograph Techniques, Am. Soc. Testing Mater. Spec. Tech. Publ.* **43** 192-200 (1968).

> Key words: Compilations; crystallographic data; diffra tion; x-ray diffraction.

Crystallography is a very active field for compilation effort the largest one being concerned with phase identification. The *Ray Powder Data File* and *Crystal Data* are the principal on for this use. *Structure Reports* and *Crystal Structures* are t major continuous series reporting crystal structures. Details the methods and procedures of producing data at NBS for the Ray Powder Data File are given.

**10679.** Mahaffey, C. T., **Basic construction standards and technical information center recommended at a Pan Americ seminar,** *ASA Mag. Std.* **36,** No. 12, 375-377 (Dec. 1965).

> Key words: COPANT; housing problems; industrializ building; Latin America; technical information center.

Agreements reached at the COPANT construction semin will help provide Latin American countries with the basic to they need to industrialize building and stimulate their economi A by product of this meeting was the enthusiastic endorseme of a resolution proposing the establishment of a Pan Americ technical information center. Gathering existing data pertaini to construction and making it readily available at the point of u is considered of primary importance in meeting the growi housing problems in Latin America.

**10680.** Maienthal, E. J., Taylor, J. K., **Improvement of pola graphic precision by a comparative technique,** *Mikrochim. Ac* **5,** 939-945 (1967).

> Key words: Cadmium, determination of; chemical analys copper, determination of; polarography; zinc, determinati of.

Comparative techniques are described which give an increa in precision of 100-fold over conventional polarography. By terchanging cells during measurement, certain electrode and c inequalities are minimized. Major constituents of many matric may be determined on microgram-amounts of sample with precision as good as 2 parts in 10,000. The technique is ill trated by the determination of copper, cadmium, and zinc several materials.

**10681.** Maki, A. G., **Interpretation of the $CS_2$ laser transitio** *Appl. Phys. Letters* **11,** No. 6, 204-205 (Sept. 1967).

> Key words: Carbon disulfide; $CS_2$; excitation mechanis infrared; lasers; spectra.

The $N_2$-$CS_2$ laser lines are identified as P-branch transiti with $J = 28$ to 46 for the 001-100 vibrational transition. A po lation ratio of $N_{001}/N_{100} = 1.07$ is determined for the system suming a temperature of 300 °K. The mechanism of selectiv populating the 001 level of $CS_2$ is discussed.

**0682.** Mann, D. E., Acquista, N., Linevsky, M. J., **An electronic band spectrum of yttrium monofluoride,** (Proc. 4th Rare Earth Research Conf., Phoenix, Ariz., Apr. 22-25, 1964). Chapter in *Proceedings of the Fourth Conference on Rare Earth Research,* pp. 363-372 (Gordon and Breach, New York, N.Y., 1965).

Key words: Electronic band spectrum; rare earth research; yttrium monofluoride.

A system of 19 double-headed red-degraded bands has been bserved in absorption in the range 3075-3300 A when $YF_3$ is eated to about 2000 °C in a King furnace. They have been atibuted to YF and a vibrational analysis made. The constants etermined from measurements on the R heads are (in $cm^{-1}$): $\nu_{00}$ = 31218.0, $\omega''_e = 633.5$, $\omega''_e x''_e = 2.0$, $\omega'_e = 539.0$, $\omega'_e x'_e = 2.0$. A eries of 10 diffuse bands in the range 2500-3000 A was also een in absorption. They have been tentatively ascribed to $YF_2$.

**0683.** Mann, D. E., White, D., Seshadri, K. S., Dever, D. F., Linevsky, M. J., **The infrared spectra, structures and thermodynamics of gaseous LiO, $Li_2O$ and $Li_2O_2$,** *J. Chem. Phys.* **39,** 2463-2473 (1963).

Key words: Infrared matrix; infrared spectra; isolation spectroscopy; lithium oxide species; matrix spectra; spectroscopy.

The vapor above heated lithium oxide ($Li_2O$) has been inestigated mass spectrometrically and by infrared matrix-isolaon spectroscopy. The vapor composition and Knudsen effusion ates were measured as functions of temperature, and the matrix pectra of the principal lithium oxide species—$Li_2O$, LiO, $i_2O_2$—identified and analyzed for different isotopic bundances. The predominant vapor species $Li^7_2O$ is probably near with r (Li-O) = 1.59 Å, and has fundamentals $\nu_1, \nu_2, \nu_3$ at 760], [140], and 987 $cm^{-1}$, respectively. Its heat of formation $H^{\circ}_{0}$(f) = −43.7 ± 2.5 kcal/mole. The diatomic molecule $Li^7O$ as $\nu = 745$ $cm^{-1}$, an estimated bond length r = 1.62A, and $H^{\circ}_{0}$(f) = +16.0 ± 5 kcal/mole. The previously undetected olecule $Li^7_2O_2$ is shown to resemble the alkali halide dimers in aving a planar rhombic ($V_h$) structure for which the O-Li-O ngle and Li-O bond length are estimated to be 116° and 1.90 Å, espectively. Its $B_{2u}$ and $B_{3u}$ frequencies are found at 324 and 22 $cm^{-1}$, respectively, in a krypton matrix. The remaining unoberved modes are estimated in $cm^{-1}$ as follows: $\nu_1(Ag) = 400$, $_2(A'_g) = 250$, $\nu_3(B_{1g}) = 300$, $\nu_4(B_{1u}) = 270$. Its $\Delta H^{0}_{0}$(f) = +27.5+ kcal/mole.

**0684.** Margoshes, M., **Selection of wavelengths for atomic absorption spectrometry,** *Anal. Chem.* **39,** No. 10, 1093-1096 (Aug. 1967).

Key words: Analysis; atomic absorption; Beer-Lambert law; continuum source; curve of growth; oscillator strength; wavelengths.

A method is described for the selection of wavelengths for tomic absorption spectrometry. The assumptions are made that he Beer-Lambert law applies approximately to the conditions of tomic absorption spectrometry and that the absorptivity is proortional to the oscillator strength of the line. The method pernits selection of the most sensitive line or, if the absorbance neasured with this line is too large, the selection of another line aving an appropriate sensitivity. A test of the assumptions is nade using published atomic absorption data, and it is shown hat the accuracies of the predictions are adequate for the purose of line selection. Modification of the theory for the case of tomic absorption with a continuum source is considered.

**0685.** Marton, L., **Photoelectricity,** *Encyclopedia of Physics,* R. M. Besancon, ed., pp. 512-514 (1966).

Key words: Photoelectricity; physics.

A short introduction into the principles of photoelectricity.

**10686.** Maryott, A. A., Birnbaum, G., **Line shape and collision effects in the microwave wing of far-infrared rotational lines,** *J. Chem. Phys.* **47,** No. 9, 3200-3205 (Nov. 1967).

Key words: Interacting molecular pairs; low frequency; microwave absorption; rotational spectra.

The microwave absorption located very far in the low frequency wings of the rotational spectra of HCl and DCl has been measured in order to test the applicability of the Van Vleck-Weisskopf relation for pressure broadening in the region many line widths removed from the resonance frequencies. Data for mixtures of HCl with the foreign gases, He, $H_2$, Ar, $N_2$, $CH_4$, $C_2H_6$, CO, $SF_6$, and $CO_2$, are also reported. Results for the mixtures with He and $H_2$ are in accord with theory. Results for the remaining mixtures and the pure gases do not agree with predictions, the observed absorption being from two to eight times greater. These discrepancies suggest the presence of an additional absorption region which is centered at a lower frequency than the normal rotational spectrum and which may by attributed to interacting molecular pairs.

**10687.** Mather, J. N., **Invariance of the homology of a lattice,** *Proc. Am. Math. Soc.* **17,** No. 5, 1120-1124 (Oct. 1966).

Key words: Combinatorics; cross-cut; homology; homotopy; lattice; simplicial complex.

Rota, Kan, Peterson and Whitehead have developed a homology theory for finite lattices which *a priori* depends upon the choice of a cross-cut of the lattice. It is shown here that the different cross-cuts of a lattice lead to simplicial complexes which have the same homotopy type and are therefore homology equivalent.

**10688.** Melmed, A. J., **Field emission microscopy,** Chapter in *Advances in Materials Research,* **Vol. 1,** *Experimental Methods,* H. Herman, ed., pp. 103-143 (Interscience Publ. Inc., New York, N.Y., 1967).

Key words: Field electron microscopy; field emission microscopy; field ion microscopy.

Field emission microscopy is reviewed. The field-electron-emission microscope and the field-ion microscope are treated separately, with a discussion of the imaging process, the capabilities, limitations, and research applications of each type of instrument.

**10689.** Melmed, A. J., **Whiskers, thin films, and applications (real and imagined) to mass spectrometry and biological molecule imaging,** Chapter in *Field-Ion Microscopy,* J. J. Hren and S. Ranganathan, eds., pp. 183-212 (Plenum Press Inc., New York, N.Y., 1968).

Key words: Field-ion microscopy; mass spectrometry ionization sources; organic molecule imaging; thin films; whiskers.

Four separate topics in field-ion microscopy are discussed. These are: Field-ion microscopy of whiskers, field-ion microscopy of thin films, field-ionization mass spectrometry, and biological molecule imaging with the field-ion microscope. Emphasis is placed on depicting the current state of the art and the techniques, capabilities and limitations.

**10690.** Melmed, A. J., Layer, H. P., Kruger, J., **Ellipsometry, low energy electron diffraction and field emission microscopy combined,** *Surface Sci.* **9,** 476-483 (1968).

Key words. Ellipsometry; field electron emission microscopy; low energy electron diffraction; surface physics.

An experimental approach has been developed which simultaneously applies three techniques to the study of surface phenomena. This approach was designed to exploit the complimentary features of the techniques as well as to compare the measurements of each where they provide similar information. The observational techniques that are included in the experimental apparatus are: ellipsometry, low energy electron diffraction, and field electron emission microscopy. Preliminary results obtained for the adsorption of oxygen on the (001) plane of tungsten are presented.

**10691.** Miller, K. J., Krauss, M., **Inapplicability of the Born exchange scattering amplitude for He ($1^1S \rightarrow 2^3S$) transition,** *J. Chem. Phys.* **48,** No. 6, 2611-2614 (Mar. 15, 1968).

Key words: Bonham-Ochkur approximation; Born exchange scattering amplitude; differential cross-section; helium ($1^1S \rightarrow 2^3S$).

Differential cross-sections are calculated for the He ($1^1S \rightarrow 2^3S$) transition within the Born-Oppenheimer approximation. The Bonham-Ochkur (OB) approximation is compared to the exact exchange scattering amplitude and it is found to yield semiquantitative agreement, especially at high incident energies. However, the theoretical results show qualitatively different behavior from recent experimental results. Experimental differential cross-sections peak in the forward direction while theory predicts a maximum at large angles.

**10692.** Moiseiwitsch, B., Smith, S. J., **Electron impact excitation of atoms,** *Rev. Mod. Phys.* **40,** No. 2, 238-358 (Apr. 1968).

Key words: Atom; electron; excitation; experimental; helium; hydrogen; impact; review; theoretical.

The experimental and theoretical literature about the electron impact excitation of atoms is reviewed. Theoretical methods ranging from the Bethe and Born approximations to the close coupling approximations are discussed and intercompared. Where possible, on theoretical grounds or through intercomparison, the reliability of the various methods is discussed.

A general critique of the optical method of measuring excitation functions is given, with the objective of promoting higher quality future experimental work. A critical study of existing experimental work leads to the conclusion that most workers have ignored important physical and instrumental effects, and it may be presumed that the data in the literature is subject to many unrecognized systematic errors. The literature on hydrogen and helium is discussed critically. The literature on alkalis, heavy rare gases, mercury, cadmium and zinc is surveyed but the quality of the literature does not support critical review beyond some general comments about the physics of these atoms.

**10693.** Moore, G. A., **Automatic scanning and computer processes for the quantitative analysis of micrographs and equivalent subjects,** (Proc. Symp. Automatic Photo Interpretation, Washington, D.C., May 31-June 2, 1967), Chapter in *Pictorial Pattern Recognition,* G. C. Cheng, R. S. Ledley, D. K. Pollock, and A. Rosenfeld, eds., pp. 275-326 (Thompson Book Co., Washington, D.C., 1968).

Key words: Analysis of microstructures; automatic scanning (of micrographs); computer processing (of micrographs); logical modification of pictures; precision scanning (of micrographs); quantitative microscopy.

Basically identical measurement problems are treated in the microscopic branches of all material sciences and in microbiology and medical diagnosis. Visual-manual methods, in use over a century, permit determination of the relative volume of a material phase, and of the average size and spacing of particles of this phase. Redefining a phase as the set of all areas having similar nature and a distinctive tone or color in a photograph, thes established methods can be extended to several varieties of non micrographic pictures.

Statistical considerations require the order of one million ob servations per picture to attain reasonable precision, dictatin automatic scanning and computer processing. Treatment o phase images in binary format permits feasible memory capaci ties and processing time. Production of a valid binary imag requires both high precision scanning and a battery of logic processes which can substitute for darkroom operations and log cal discriminating normally made by a human analyst. Other log cal processes permit dissection and description of individu phase areas. Presently attainable measurement precision is a order of magnitude greater than is normally attained by manu methods.

**10694.** Mopsik, F. I., **Molecular and ionic interactions,** Chapter in *1966 Digest of Literature on Dielectrics* **30,** 62-90 (Nation Academy of Sciences – National Research Council, Washing ton, D.C., 1966).

Key words: Dielectrics literature; dielectric theory; Dige of Literature; molecular and ionic interactions; review literature; 1966 dielectrics literature.

This year's chapter includes the literature covered by Physic Abstracts and Chemical Abstracts for the year 1966. The paper included are those, both theoretical and experimental, that ar concerned with underlying dielectric phenomena. Papers that r port values for dielectric parameters have been omitted unle there was a significant contribution to the understanding dielectric theory. In particular, papers that should be adequatel covered by the tables were not included.

**10695.** Mountain, R. D., **Relaxation times for the volume viscosi of simple fluids,** *J. Chem. Phys.* **48,** No. 5, 2189-2190 (Mar. 1968).

Key words: Corresponding states fluid; elastic moduli liquids; relaxation time for volume viscosity; shear relax tion time; time correlation function; volume viscosity.

Effective relaxation times for the volume viscosity of a co responding states fluid in the dense gas region are calculat using low frequency volume viscosity data and previous developed estimates of high frequency elastic moduli The tim are found to be on the order of $10^{-13}$ seconds.

**10696.** Mountain, R. D., Zwanzig, R., **Anomalous transport pr perties of a van der Waals gas,** *J. Chem. Phys.* **48,** No. 4, 145 1458 (Feb. 15, 1968).

Key words: Critical phenomena; fluctuation and time c relation function; heat capacity; shear viscosity; therm conductivity; van der Waals gas; volume viscosity.

The contribution of the long range potential to the transp coefficients of a van der Waals gas in the critical region are cal lated using the time correlation function methods. The mic scopic currents are expanded in terms of wave vector depend density fluctuations (found previously by van Kampen), wh time dependence is assumed to be described by the lineari hydrodynamic equations. Self consistent solutions for the th mal conductivity and volume viscosity are found to diverge n the critical point. The fluctuation correction to the specific h at constant volume is found to diverge as $|T\text{-}T_c|^{-1/2}$. The fluct tion correction to the equation of state indicated that these cal lations are at best meaningful only in the critical region beca the critical point is an apparent rather than a true critical point.

**10697.** Olver, F. W. J., **An extension of Miller's algorit** *Aplikace Mat.* **13,** 174-176 (1968).

Key words: Chebyshev series; difference equations; error analysis; Miller algorithm; recurrence methods; special functions.

A new algorithm is described for computing the solution of any second-order linear difference equation which is applicable when simple recurrence procedures cannot be used because of instability.

**10698.** Parker, R. L., **Report on the 1966 Boston International Conference on Crystal Growth,** *Proc. 1966 Intern. Union Crystallography, Moscow, U.S.S.R., July 12-21, 1966,* **7,** 341-354 (Academy of Sciences, Moscow, U.S.S.R., 1968).

Key words: Crystal; crystal growth; crystal morphology; interface kinetics; International Conference; ICCG; 1966 ICCG.

A report on the 1966 Boston International Conference on Crystal Growth (ICCG) is presented. The purpose of the interdisciplinary conference was to further the science and art of crystal growth by providing a forum for reporting and discussing recent original research in this field. Some data on the ICCG itself are given—its purpose and organization, registrants, and countries represented. Then brief summaries are given of 22 papers selected from the 170 papers presented at the conference. These papers dealt with such subjects as: Stability, Kinetics, Nucleation, Solidification, Whisker Growth, Phase Diagrams, Growth and Perfection. At the conference, particular attention was paid to certain macroscopic problems involved in crystallization, especially morphological stability and thermal convection.

**10699.** Patty, O. L., Little, W. E., Zanboorie, M. H., **Waveguide connector measurements with a millimeter wave reflectometer,** *IEEE Trans. Microwave Theory Tech.* **MTT-16,** No. 2, 121-123 (Feb. 1968).

Key words: Connector; millimeterwave; reflectometer; WR-12.

A system is described which extends reflection coefficient measurement techniques to (60-90 GHz) "E-band." Special apparatus and procedures are discussed. A new graphical presentation of reflectometer data is given which simplifies the measurement of connector impedance. Examples of the measured reflection coefficient of some common E-band connectors are given.

**10700.** Penner, S., **Handling high power electron beams,** *IEEE. Trans. Nucl. Sci.* **NS-14,** 908 (June 1967).

Key words: Accelerators; beam handling; electron beams; high power electron beams.

In recent years accelerators have been designed and built which produce beams of extremely high power, current, and charge-per-pulse. The handling of these beams presents a number of difficult problems. Among these problems are: removal of large heat flux, fatigue failure of components due to pulsed nature of the beam, radiation damage of materials, corrosion, residual radioactivity, and chemical effects such as radiolysis of water and production of noxious gases. Consideration of these problems strongly influences the overall design of beam handling systems, as well as the designs of specific components. Examples of the problems encountered and the solutions adopted in various electron accelerator laboratories will be discussed.

**10701.** Penney, R. W., Phillips, C. W., **Refrigeration requirements for truck bodies—effects of door usage,** *U.S. Department of Agriculture Tech. Bull.* No. 1375 (Superintendent of Documents, Government Printing Office, Washington, D.C., 20402, Nov. 1967, 10 cents).

Key words: Air exchange; calculation method; cooling load; door usage; helium trace measurement; refrigerated trucks; testing method.

The selection of a refrigerating system of adequate capacity for use in a refrigerated truck body requires knowledge of system capacity and the total cooling load. Rating and testing methods to establish system capacity and body cooling load due to heat transmission and air infiltration are now available. The cooling load casued by air exchange during door usage in a refrigerated truck used in local delivery service can be the largest part of the total cooling load. A means to determine this door-usage cooling load is needed and this technical bulletin presents such a method. Laboratory tests of four refrigerated truck bodies were made under controlled conditions of 0 °F temperature in the truck body and 100 °F temperature and 50 percent relative humidity in the test room to determine the air exchange and cooling load resulting from door openings of one to three minutes in duration. The effect of cargo loading on air exchange was determined. A brine refrigerating system was used to obtain the initial steady-state temperature conditions, and liquid nitrogen was then used to determine increases in cooling loads caused by opening the door. Helium gas was used as a tracer to measure the air exchange resulting from door usage. Tests showed that a 1-minute door opening can cause air temperature inside the truck body to rise as much as 60 degrees F with more than two complete air changes, and a cooling load of more than 2000 B.t.u. Formulas were developed to estimate the amount of air exchange and the cooling load caused by door opening.

**10702.** Persson, K-B., Johnson, E. G., Jr., Uhlenbrock, D. A., **Theory for cyclotron harmonic radiation from plasmas,** *Phys. Fluids* **11,** No. 3, 619-628 (Mar. 1968).

Key words: Electron cyclotron frequency; emission; harmonic; microwave; theory.

A highly simplified hydrodynamic model for the cause of cyclotron harmonics radiation in a magnetized abnormal glow helium plasma is proposed. The high velocity electrons are treated as sources for the charge density waves in the plasma. With the very crucial existence of statistical fluctuations in the ion density, these waves act as sources for electromagnetic radiation. This radiation contains the cyclotron harmonics. Some numerical curves of the radiation spectra are shown for a number of plasma parameters.

**10703.** Peterson, R. L., **Ising chain as the basic cluster in effective-field theories of magnetism,** *Physics Letters* **27A,** 177 (June 10, 1968).

Key words: Effective-field theory; Ising interaction; magnetism.

A linear chain is used as the basic cluster in effective-field theories of Ising systems. The chain gives limited improvement over the finite clusters in a molecular-field approach. Results are independent of cluster size in a "constant coupling" approach.

**10704.** Peterson, R. L., **Suppressed spin-lattice relaxation,** *Phys. Rev. Letters* **20,** No. 24, 1346-1348 (June 10, 1968).

Key words: Gadolinium hexa-antipyrene iodide; spin-lattice relaxation.

A possible explanation of some power-dependent spin-lattice relaxation effects observed in gadolinium hexa-antipyrene iodide is offered.

**10705.** Roder, H. M., **The thermal conductivity of helium gas at moderate pressures,** *Proc. Thermodynamik Symp., Heidelberg, Germany, Sept. 1967, Sponsored by the International Union on Pure and Applied Chemistry,* K. L. Schafer, ed., **Paper No. VI-3,** pp. 1-8 (1968).

Key words: Capacitance method; critical density; experimental measurement; helium gas; parallel plate method; thermal conductivity.

The apparatus used is a doubly-guarded flat plate calorimeter in which the cell constant is determined by a capacitance method. Experimental values of the thermal conductivity of helium gas are presented for 15 isotherms between 20 and 282 °K at pressures from 1 to 30 atmospheres, except for the 50 °K isotherm which extends to 50 atmospheres. The highest density is, thus, just under the critical density. The results are analyzed in terms of their density and temperature dependence.

**10706.** Ronn, A. M., **Laser induced infrared fluorescense,** *J. Chem. Phys.* **48,** No. 1, 511-513 (Jan. 1968).

Key words: Ammonia; carbon dioxide; emission; ethylene; infrared; laser.

Laser induced infrared emission has been observed in several gases which have absorption bands in the vicinity of the $CO_2$ laser's frequency. Ethylene showed an intense emission spectrum at an optimal pressure of 50 mm demonstrating that the efficiency of collisional transfer is sufficient to populate all, or most, members of a room temperature vibrational band when one or two vibration-rotation lines are strongly irradiated by the laser. Ammonia showed some irregularities in the emission spectrum which are currently under investigation.

**10707.** Rybicki, G. B., Hummer, D. G., **Spectral line formation in variable-property media: the Riccati method,** *Astrophys. J.* **150,** No. 2, 607-635 (Nov. 1967).

Key words: Doppler width; radiative transfer media; Riccati method; spectral line formation; variable-property media.

A numerical method, based on the generalized Ricatti transformation of Rybicki and Usher, is presented for the integration of the radiative transfer equation for spectral line formation by non-coherent scattering in inhomogeneous plane-parallel media. An asymptotic theory is developed which permits the application of this method to problems involving semi-infinite media. Numerical results obtained by the Riccati method are used to discuss the effects of spatial variations in the Doppler width on lines formed by pure Doppler broadening.

**10708.** Scribner, B. F., **Advances in excitation sources for spectrochemical analysis,** *Pure Appl. Chem.* **10,** 579-594 (July 21, 1967).

Key words: Arc discharge; excitation sources; fuel-rich flames; high-frequency torch; laser probe; plasma jet; spark discharge; spectrochemical analysis.

Recent developments are reviewed in methods of exciting spectra, with emphasis on sources for spectrochemical analysis. The subjects discussed include fuel-rich flames, the high-frequency torch, the plasma jet, arc and spark discharges in controlled atmospheres, and the laser probe.

**10709.** Sengers, J. V., **Triple collision contribution to the transport coefficients of gases,** (Lectures presented at the Theoretical Physics Institute, University of Colorado, Boulder, Colo., Summer 1966), Chapter in *Lectures in Theoretical Physics,* **Vol. IXC,** *Kinetic Theory,* E. E. Brittin, ed., pp. 335-374 (Gordon and Breach, New York, N.Y., 1967).

Key words: Dense gases; diffusion; rigid disks; rigid spheres; thermal conductivity; transport properties; triple collisions; viscosity.

The effect of triple collisions on the transport coefficients of gases is discussed. In particular the triple collision integrals determining the first density correction to the viscosity and thermal conductivity of a gas of rigid spheres are derived and estimates are presented for these integrals. By applying the metho to a two dimensional gas of rigid disks, an analysis is given of th logarithmic density dependence of the transport coefficients.

**10710.** Simmons, J. H., Macedo, P. B., **High temperature shea ultrasonic interferometer using sensitive phase-lock detectio system,** *J. Acoust. Soc. Am.* **43,** No. 6, 1295-1301 (June 1968)

Key words: High temperature ultrasonic interferometer lock-in amplifier system; measurements in molten glasses phase-lock detection system; shear relaxation; ultrasonic interferometer.

A high temperature (up to 1600 °C) ultrasonic (3 to 23 MHz interferometer having two single-crystal molybdenum transmission lines was used to study the propagation properties of shea waves through molten glasses. Shear velocity and absorption o the transmitted echoes were measured in a temperature rang which covered the major part of the relaxation region of a molte glass. The highest value of absorption per wave length for whic measurements were still possible was 5.4 nepers/cycle; ove twice the value from previously reported equipment.

A feature which made this work possible was the use of a lock in amplifier in the video circuit. This method of handling th transmitted echoes not only suppressed noise by 25 dB, but als permitted measurements of pulse heights to better than 0.1 dB The video circuit is independent of the r.f. and can be used wit most existing pulsed ultrasonic systems.

**10711.** Spokas, O. E., **The NBS linac master control and personn protection system,** *IEEE Trans. Nucl. Sci.* **NS-14,** 1016 (Jun 1967).

Key words: Linear accelerator safety; linear accelerat utilization; personnel and equipment protection system.

The operation of the NBS linear accelerator and its beam ha dling equipment has been integrated with personnel and equi ment protection safeguards and with the occupancy requirements of the linac complex. A mode switch is used to selec beam direction and experimental area, and to program th requirements for personnel protection interlocks, beam handlin system conditions, building mechanical services, experiment area services, and linac operation. The system includes visu and audible devices to indicate degree of readiness, hazard faults, interlock information, zone of operation and emergenc situations. A forced inspection of potentially dangerous zone programmed cued taped warning announcements, key inte locks, and flexibility are built-in features. It offers the capabilit of providing maximum protection to personnel against enviro mental radiation hazards, and allows utilization of a maximum laboratory space for varied beam conditions.

**10712.** Stern, J., **Aspect systems,** *Encyclopedia of Library and I formation Science* **1,** 669-671 (1967).

Key words: Aspect systems; index organization; inform tion retrieval systems; inverted index organization; inverte systems; Peek-a-Boo.

This encyclopedia entry defines the term aspect systems an describes briefly the type of index organization that chara terizes these systems and some of the techniques applicable them. The reader is referred to a number of other entries f more detailed information.

**10713.** Sukle, D. J., Wells, J. S., **An EPR sample servo,** *Rev. S Instr. Notes* **39,** No. 4, 604-605 (Apr. 1968).

Key words: Crystal alignment; electron paramagnet resonance; EPR sample orientation.

A device which permits one to change the orientation of an 'R sample with respect to the cavity without removing either m the spectrometer is described.

The sample orienter is essentially a mechanical servo com- sed of two ball and socket joints which are constrained by four igths of cotton thread to move together.

714. Tighe, N. J., Hyman, A., **Transmission electron microscopy of alumina ceramics,** (Proc. Intern. Symp. Anisotropy in Single-Crystal Refractory Compounds, Dayton, Ohio, June 13-15, 1967), Chapter in *Anisotropy in Single-Crystal Refractory Compounds,* F. W. Vahldiek and S. A. Mersol, eds., **2,** 121-136 (Plenum Press Inc., New York, N.Y., 1968).

> Key words: Alumina; defects; dislocations; electron microscopy; ionic bombardment; polycrystalline $Al_2O_3$.

Transmission electron microscopic studies have been carried t on two samples of sintered alumina having different density 99g/cm$^3$ and 3.78g/cm$^3$), composition and grain size. ecimens were thinned by an ionic-bombardment method ich preserved the grain boundaries and allowed observation relatively large areas. The sample of nearly full density $Al_2O_3$ d very few dislocations or small angle boundaries. It did have ains of second phase material (spinel) and these grains con- ned faults. The sample of lower density, had many small angle undaries, pores and extensive dislocation networks. A number the networks were composed of dislocations with Burgers ctors: 1/3 ⟨1120⟩ and 1/3 ⟨1011⟩.

715. Tisone, G. C., Branscomb, L. M., **Detachment of electrons from $H^-$ and $O^-$ negative ions by electron impact,** *Phys. Rev.* **170,** No. 1, 169-183 (June 5, 1968).

> Key words: Crossed-charged beams; electron collisions; hydrogen negative ion; ionization cross section; negative oxygen ion.

The energy range for the electron detachment cross section for $^-$ has been extended from 500 eV down to 8.4 eV. The ab- lute cross section for detachment of electrons from atomic ox- en negative ions has been measured in the energy range of 7.1 487.1 eV. Results of these measurements are compared with ethe-Born calculations of the cross section. This calculation ith the semiclassical Coulomb correction is in qualitative agree- ent with the experimental results above 20 eV electron energy r both $H^-$ and $O^-$, although the energy dependence of the H oss section from 100 to 500 eV is not consistent with the slope edicted theoretically for the high energy limit.

716. VanderHart, D. L., Gutowsky, H. S., Farrar, T. C., **Dipole-dipole interactions of a spin 1/2 nucleus with a quadrupole-coupled nucleus,** *J. Am. Chem. Soc.* **89,** No. 19, 5056-5057 (Sept. 13, 1967).

> Key words: Bond-distance; frequency-dependent proton NMR line shapes; indirect quadrupole interaction; solids.

Line shapes for two-spin (1/2, 7/2) system having axial sym- etry along the internuclear vector and quadrupole coupling at e spin 7/2 nucleus are calculated as a function of the ratio of e Zeeman to quadrupole interaction energies. It is shown that e spin-1/2 NMR line shape is frequency dependent and that e second moment of the spin-1/2 NMR spectrum may be as uch as 1.84 times its value in the absence of quadrupole oupling. Reported values for M-H bond distances via NMR udies in transition-metal carbonyl hydrides may be too small.

717. Vriens, L., Kuyatt, C. E., Mielczarek, S. R., **Tests of Born approximations; differential and total cross sections for elastic scattering of 100- to 400-eV electrons by helium,** *Phys. Rev.* **170,** No. 1, 163-169 (June 1968).

> Key words: Born approximation; differential and total cross sections; elastic scattering; electrons; exchange; helium.

The angular dependence for elastic scattering of 100 to 400 eV electrons by helium atoms has been measured with a high resolution electron spectrometer. The angular range in the present measurement extends from 5° to 30°. The relative differential cross sections were put on an absolute basis using measured ratios of elastic and $2^1P$ scattered currents and known $2^1P$ cross sections. The differential cross sections were integrated to get total elastic scattering cross sections. Large deviations from the Born approximation are found, especially for small incident energies and small scattering angles. The agreement with more sophisticated calculations of Khare and Moiseiwitsch is better, but not yet satisfactory. Our results are in reasonable qualitative agreement with results of earlier experiments, but are quantitatively quite different and extended to smaller scattering angles.

**10718.** Wachtman, J. B., Jr., Brower, W. S., Farabaugh, E. N., **Elastic constants of single crystal calcium molybdate ($CaMoO_4$),** *J. Am. Ceram. Soc.* **51,** No. 6, 341-344 (June 1968).

> Key words: Calcium molybdate; compressibility; Debye temperature; elastic constants; shear modulus; Young's modulus.

The seven elastic compliances (and seven elastic constants) of single crystal calcium molybdate were determined by a resonance method. The compliance $s_{16}$, which is zero for higher symmetry tetragonal crystals, need not be zero for crystals of lower tetragonal symmetry and contributes significantly to the orientation dependence of the elastic moduli of calcium molybdate. The values of the compliances and their standard errors (based on 41 measurements) in units of $10^{-11}m^2/N(10^{-12}cm^2/dyn)$ are $s_{11} = .974 \pm .005$, $s_{33} = .958 \pm .004$, $s_{44} = 2.720 \pm .009$, $s_{55} = 2.276 \pm .024$. $s_{12} = -.308 \pm .009$, $s_{13} = -.249 \pm .009$, and $s_{18} = .418 \pm .011$.

**10719.** Wassink, H. W., **Cyclotron harmonic emission along the field from a plasma,** *Phys. Fluids* **11,** No. 3, 629-637 (Mar. 1968).

> Key words: Electron cyclotron frequency; emission; harmonic; magnetic field; plasma.

Electron cyclotron harmonic (ECH) radiation from an abnormal negative glow plasma has been measured along the magnetic field with the following results: Single peaks of ECH radiation were observed at the harmonic frequencies which slowly decreased in amplitude with increasing harmonic number; these peaks were almost completely circularly polarized with a polarization opposite to that of an electron; a large peak was observed near the fundamental in the electron polarization only; ECH emission appeared only in the presence of the hot electrons produced by electron beams; the difference in the emission between the two polarizations indicated that most of the ECH radiation came from the interior of the plasma. A theory proposed by Persson, Johnson, and Uhlenbrock showed detailed agreement with these measurements.

**10720.** Watson, T. H., Flynn, D. R., **Thermal conductivity and electrical resistivity of beryllium copper foil,** *Trans. Met. Soc. AIME* **242,** 876-880 (May 1968).

> Key words: Beryllium copper; conductivity; copper alloys; electrical conductivity; heat conductivity; Lorenz function; resistivity; thermal conductivity.

Measurements have been made of the thermal conductivity and electrical resistivity of two specimens of 0.005 cm (2 mil) beryllium copper strip over the temperature range −140 to +200 °C. The thermal conductivity of beryllium copper Alloy 125 was found to be significantly higher that that of Alloy 25, which had a higher impurity content. The thermal conductivity and electrical resistivity values obtained were in concordance with the Smith and Palmer relation for copper alloys which states that $\lambda = 0.0239\ (T/\rho) + 0.075$ where $\lambda$ is thermal conductivity (W cm$^{-1}$deg$^{-1}$), $\rho$ is electrical resistivity ($\mu\Omega$ cm), and T is absolute temperature (°K), indicating that the Smith and Palmer relation can be used to predict the thermal conductivity of this type of beryllium copper alloy over the temperature range −140 to +200 °C to within an accuracy suitable for most engineering applications.

**10721.** Watson, T. W., Flynn, D. R., **Thermal conductivity of four heat-resistant alloys,** *Trans. Met. Soc. AIME* **242,** 844-846 (May 1968).

Key words: Conductivity; heat conductivity; heat-resistant alloys; heat transfer; stainless steel; temperature-resistant alloys; thermal conductivity.

Measurements are reported for the thermal conductivity of four heat-resistant alloys which were measured at the National Bureau of Standards. Data are given for two samples of AISI Type 316 stainless steel covering a combined temperature range from −150 to +800 °C. The thermal conductivities of three samples of AISI Type 347 were measured over the temperature range from −150 to +150 °C. Thermal conductivity values are given for Carpenter 20 stainless steel from 100 to 800 °C. Data are given for Inconel 702, in both the solution-annealed and the age-hardened condition, over the temperature range from −150 to +800 °C.

**10722.** Wiederhorn, S. M., **The influence of water vapor on crack propagation in soda-lime glass,** *J. Am. Ceram. Soc.* **50,** No. 8, 407 (1967).

Key words: Cleavage; crack propagation; cracks; delayed failure; fracture; glass; static fatigue.

This paper presents the results of a new experimental approach to the subject of static fatigue of glass. Using the double-cantilever cleavage technique, it was possible to observe crack motion and to accurately measure crack velocities in glass. The measured crack velocity is observed to be a complicated function of stress and of water vapor concentration in the environment. Experimental results are discussed with reference to current theories of static fatigue.

**10723.** Wiese, W. L., **Transition probabilities for prominent Ar I lines,** (Proc. 8th Intern. Conf. Phenomena in Ionized Gases, Vienna, Austria, Aug. 27-Sept. 2, 1967), Chapter in *8th International Conference on Phenomena in Ionized Gases,* p. 447 (Springer Verlag, Vienna, Austria, Sept. 1967).

Key words: Ar I; intermediate coupling; lifetime measurements; local thermal equilibrium; spectra; transition probabilities.

The transition probabilities of the prominent Ar I lines have been the subject of numerous studies. Nevertheless, many discrepancies remain between the various results. It is the aim of this paper to clear these up. To this end, new measurements have been undertaken for three selected Ar I lines which seem to be particularly suited to shed light on the cause of the disagreements. With these and other very recent data at the disposal, all available material is then critically assessed and a set of best values is suggested.

**10724.** Winogradoff, N. H., Neill, A. H., **Band tailing effects and the temperature dependence of radiative recombination in compensated, epitaxial GaAs laser junctions,** *IEEE J. Quantum Elect.* **QE-4,** No. 4, 111-113 (Apr. 1968).

Key words: Band pinch effect; band tailing; Fermi level; GaAs laser; internal quantum efficiency; radiative recombination.

An increase in threshold current and decrease in power outpu of GaAs laser diodes has been observed. In highly doped mater al, an exponential density of states "tail" is formed at the neares band edge. The nature of these tails and the temperature induce shift of the Fermi level may account for the temperature de pendance of the spontaneous and stimulated spectra through reduction in the internal quantum efficiency for radiative reco bination. Three semi-logarithmic curves of the spontaneou emission are presented to confirm a narrowing of the spectru and a decrease in light output with increasing temperatures. Pa kove's model for the behavior of the Fermi level in highl degenerate GaAs can account for the shape and temperature de pendance of spontaneous emission from highly doped p-n jun tions. The temperature dependance of the Fermi level in th band tails of such materials results in a narrowing of the spo taneous spectrum with increasing temperatures.

**10725.** Wyckoff, J. M., **On-line transformations of high resolutio spectra,** *IEEE Trans. Nucl. Sci.* **NS-14,** 634 (Feb. 1967).

Key words: Computer; gamma-ray; germanium-detecto on-line; pulse-height-distribution; spectra.

A new technique has been devised for transforming the puls height distribution obtained from a lithium drifted germaniu crystal used as a gamma-ray spectrometer into an energy, pe area vector. The computer operations required are simp enough to be performed by an on-line computer in about fi seconds. The vector is generated from the raw pulse height di tribution by the subtraction of a smoothed version of the ra vector. In order to remove the statistically insignificant portio of the difference, all values less than twice the square root of t original element of the data are set equal to zero. The on remanent of the Compton contribution to the raw data is a sm peak at the Compton edge. The resulting vector may be plott directly or further transformed to sum the area under each pe providing a convenient graphic or tabular means of presenti the gamma-ray energy and relative intensity information.

**10726.** Wyckoff, J. M., **Radioactivity produced by a linac,** *IE Trans. Nucl. Sci.* **NS-14,** 990 (June 1967).

Key words: Gamma rays; health physics; linac; radioacti ty; relative yield.

Over 40 different materials have been irradiated in the 1 MeV bremsstrahlung beam from the NBS linac. The major co tributions to the gamma ray spectrum from the radioacti products have been measured using a Ge(Li) detector. Measu ments have been made of gamma rays of concern in the minute to 30 day time interval but this includes in some cas gamma rays from nuclides with half lives as long as 30 yea Eighteen of the samples were pure materials and 25 were co monly used structural, shielding, electrical and mechanical co ponents. In several important cases nuclides produced by mul ple particle emission dominate the picture.

**10727.** Abrams, M. D., **A comparative sampling of the systems producing computer-drawn flow charts,** *Proc. 1968 Assoc tion for Computing Machinery National Conf., Las Veg Nevada, Aug. 27-29, 1968,* pp. 743-750 (Brandon/Syste Press, Inc., Princeton, N.J., 1968).

Key words: Algorithmic languages; computer graphi flowchart; graphical output; graphics.

Several programs which produce computer-drawn flowcha from assembly language and algorithmic compiler language compared. As a background, the applications, implementati and information transferral properties of flowcharts are brie treated. The strengths and restrictions of flowcharts as graphi communications media are also briefly discussed. Three p grams to draw flowcharts of compiler language programs directly compared; sample flowcharts and a tabular summary are provided.

**0728.** Ausloos, P., Lias, S. G., **Primary modes of decomposition of superexcited n-alkane molecules,** (Proc. Intern. Conf. Photochemistry, Munchen, Germany, Sept. 6-9, 1967), *Ber. deut. Gunsenges.* **72,** No. 2, 187-195 (1968).

Key words: Alkanes; free radical reaction; ion-molecule reactions; photoionization; photolysis; primary processes; superexcited molecules.

Information is summarized concerning fragmentation of superexcited propane and n-butane molecules produced by photolysis of these compounds with 11.6-11.8 eV photons, which is about 0.5 and 1.0 eV above the ionization energies of the two compounds. The decomposition of the excited $[C_3H_8^+]^*$ and $[C_4H_{10}]^*$ ions which are formed either by direct ionization or by autoionization are quenched at pressures around 10 Torr. These ions can then be removed from the photolysis system through a charge transfer reaction with added NO or an $H_2$ transfer reaction with low concentrations of added ethylene. The modes of decomposition of the superexcited alkane molecules are derived from the isotopic analysis of the products formed upon irradiation of $CD_3CH_2CD_3$, $CH_3CD_2CH_3$, $CD_3CH_2CH_2CD_3$ and of the equimolar mixtures $C_3H_8$-$C_3D_8$ and $C_4H_{10}$-$C_4D_{10}$. Comparison of these results with studies at longer wavelengths demonstrates that although the modes of decomposition observed at the superexcitation energies are the same as those observed at excitation energies below the ionization energy, free radical producing processes occur with higher probability when the energy of the photon is increased.

**10729.** Ausloos, P., Rebbert, R. E., Lias, S. G., **Structure and reactivity of propyl ions in gas-phase radiolysis,** *J. Am. Chem. Soc.* **90,** No. 18, 5031-5033 (Aug. 28, 1968).

Key words: Ion-molecule reactions; hydrocarbons; radiolysis; reaction rates; structure of ions.

This is a preliminary report concerning the structure of the propyl ions formed in the radiolysis of alkanes. It is demonstrated that there are two distinct propyl isomers; the normal propyl ion and the secondary propyl ion. The normal propyl ion is shown to react with alkanes at a considerably higher rate than the secondary propyl ions. In the radiolysis of normal butane-$NH_3$ mixture the normal propyl ion reacts with $NH_3$ to form cyclopropane as a product.

**10730.** Averbuch, P., James, L. W., Mahler, R. J., **Nuclear ultrasonic fast passage,** *Appl. Phys. Letters* **11,** N. 11, 339-340 (Dec. 1, 1967).

Key words: Nuclear spin; ultrasonic.

An ultrasonic fast passage experiment is described and the small resulting 16 percent nuclear spin inversion is explained as an inability to obtain ideal experimental conditions.

**10731.** Bates, R. G., **Measurement of pH,** *Handbook of Biochemistry,* H. A. Sober, ed., pp. J190-J194 (Chemical Rubber Company, Cleveland, Ohio, 1967).

Key words: Acidity; glass electrode; indicators; pH; standardization.

The operational definition of pH, in the form endorsed by the International Union of Pure and Applied Chemistry, is presented. The preparation of standard reference solutions for pH measurements is described and the choice of electrodes and measurement techniques is discussed. The proper interpretation of pH numbers is set forth briefly, and procedures for pH measurement with indicators are described.

**10732.** Bechtoldt, C. J., Ogburn, F., Smit, J., **Structure and morphology of electrodeposited molybdenum dendrites,** *J. Electrochem. Soc.* **115,** No. 8, 814-816 (Aug. 1968).

Key words: Electrodeposition; molybdenum dendrites; twin growth; twinning; twin plane reentrant edge; x-ray diffraction.

Twin growth has not been reported previously in molybdenum dendrites nor has growth by the "twin plane reentrant edge" (T-PRE) mechanism been reported for the body centered cubic lattice W-type structure. Electrodeposited molybdenum dendrites were examined using optical and x-ray diffraction techniques and found to be twinned. The dendrites were found to have been bounded by their closest packed {110} planes forming a hexagonal rod with extended growth in a ⟨111⟩ direction. The growth appeared to have been initiated by a TPRE mechanism with twin composition planes forming in two or three of the {112} planes which are parallel to the ⟨111⟩ growth direction. Although the two crystal parts were in an exact twin relation, the boundary appeared as a grain boundary except within the small region of TPRE growth. Crystal growth appears to be by means of a TPRE mechanism since it meets the requirements proposed by Faust and John.

**10733.** Bender, P. L., Alley, C. O., Currie, D. G., Faller, J. E., **Satellite geodesy using laser range measurements only,** *J. Geophys. Res.* **73,** No. 16, 5353-5358 (Aug. 15, 1968).

Key words: Continental drift; distance measurements; geodesy; geodetic satellite; geophysics; laser; worldwide geodetic network.

We have investigated the potential accuracy with which the distances between 12 observing stations spread fairly uniformly over the earth can be determined by using laser range measurements to a high altitude satellite equipped with optical retroreflectors. For each of 30 satellite positions, it was assumed that range measurements were made at about the same time from the 4 closest stations. For ideal distribution of the stations, the expected uncertainty in the distance between any two stations was found to be less than 45 cm, with little dependence on satellite altitude over the range of 20,000 to 110,000 km. With 12 stations chosen from the Pageos Worldwide Geometric Satellite Network, the expected accuracy for a satellite altitude of 110,000 km is 60 cm or better between any two stations.

**10734.** Bender, P. L., Branscomb, L. M., **Credit for gravity apparatus,** *Phys. Today Letter* **20,** No. 10, 17 (Oct. 1967).

Key words: Absolute gravity; gravity.

In his article on Geophysics Instrumentation in the July issue of Physics Today, J. N. Howard of the Air Force Cambridge Research Laboratories refers to an "absolute gravity apparatus developed jointly by AFCRL and NBS (which) uses a freely falling rotation-insensitive corner cube as one element of an optical interferometer." This project was initiated by Prof. James E. Faller while he was a NAS-NRC Research Associate at NBS and was a direct outgrowth of earlier absolute gravity measurements which he had made at Princeton Univ. (J. Geophys. Res. **70**, 4035; 1965). The experiments are now being carried out at Wesleyan Univ. by Prof. Faller and Mr. James A. Hammond.

**10735.** Bennett, J. A., **The initiation of fatigue microcracks under sequential bending and torsional loads,** *Trans. ASM* **61,** No. 2, 210-218 (June 1968).

Key words: Aluminum alloy; bending; fatigue strength; microcracks; shear stress; torsion.

Specimens of 6061-T6 aluminum alloy were stressed first in alternating torsion, then in reversed bending or vice versa. The development of cracks was observed by microscopic examination of replicas taken of the specimen surfaces at intervals during the tests. The results indicate that fatigue damage under uniaxial stress did not reduce the resistance to crack initiation in pure shear; the reverse was also true. Based on the number of cycles to initiate microcracks, the fatigue strength in terms of shear stress amplitude was 14 percent higher in torsion than in bending. Comparison of these results with earlier studies of environmental effects suggests that moisture influences the fatigue behavior of this alloy only after microcracks have formed.

**10736.** Bullis, W. M., Brewer, F. H., Kolstad, C. D., Swartzendruber, L. J., **Temperature coefficient or resistivity of silicon and germanium near room temperature,** *Solid-State Electron.* **11,** No. 7, 639-646 (July 1968).

> Key words: Extrinsic exhaustion region; germanium; n-type; p-type; resistivity; silicon; temperature coefficients.

Temperature coefficients for the resistivity of n- and p-type germanium and silicon in the neighborhood of room temperature have been determined over a wide range of resistivity. Linear temperature coefficients have been found for the extrinsic exhaustion region ($<5$ Ω·cm for germanium and $<5000$ Ω·cm for silicon). The results are presented as plots of temperature coefficient against resistivity at 23 °C. The plots may be used in connection with measurements of resistivity on extrinsic germanium and silicon doped with the usual shallow impurities such as boron, aluminum, gallium, phosphorus, arsenic, and antimony. Accurate linear coefficients cannot be found for specimens doped with deep-lying impurities in sufficient amounts to affect the carrier density nor for specimens with resistivity in the transition region between extrinsic and intrinsic conduction.

**10737.** Burke, P. G., Cooper, J. W., Ormonde, S., **Electron-impact excitation of $n = 2$ states in He,** *Phys. Rev. Letters* **17,** No. 7, 345-348 (Aug. 15, 1966).

> Key words: Close-coupling; electron excitation; multi-channel; polarization; resonance; threshold.

Calculations have been performed on the excitation of $n = 2$ states in He by electron impact at energies close to thresholds using close-coupling methods. The cross sections obtained for these processes are compared with experimental results and provide an explanation of resonance phenomena observed in 3 separate experiments. The excitation cross section $2^1S-2^3S$ was also calculated and found to agree with experimental results. The calculations show that 3 separate resonances play an important role in the vicinity of the $n = 2$ thresholds and that, due to strong polarization effects, $2^3P$ and $2^1P$ states must be included in calculations of this type in order to obtain the resonance structure.

**10738.** Codling, K., Madden, R. P., **Structure in the $L_{II,III}$ absorption of aluminum and its oxides,** *Phys. Rev.* **167,** No. 3, 587-591 (Mar. 1968).

> Key words: Absorption spectrum; aluminum; aluminum oxide; $L_{II,III}$ edges; soft x-ray.

The $L_{II,III}$ region of absorption has been observed for thin films of evaporated aluminum, for amorphous (anodized) $Al_2O_3$ and for crystalline ($\gamma$ alumina) $Al_2O_3$. The spectra were obtained in high resolution (0.06 Å) using the NBS 180 MeV electron synchrotron as a background source. The $L_{II,III}$ absorption edges of Al are located with improved accuracy at 169.49 (±0.05)Å (estimated probable error) and 170.49(± 0.05)Å. Structure on the high energy side is compatible with other recent observations. The $L_{II,III}$ absorption edge in $Al_2O_3$ is not split in high resolution and is located at 162.11(± 0.15)Å for the amorphous form and 160.15(± 0.15)Å for the $\gamma$ alumina. Both forms show considerable structure on the high energy side of the edge. That observed for the amorphous form is in agreement with other recent observations, while the absorption structure in $\gamma$ alumina (showing maxima at 78.0, 78.6, 79.5, 84 and 99 eV) has been found to be more complex.

**10739.** Corliss, C. H., **Relative oscillator strengths for lines of TbI,** *J. Quant. Spectry, Radiative Transfer* **8,** 1185-1191 (1968).

> Key words: Oscillator strengths; spectra, atomic; terbium; transition probabilities.

Relative oscillator strengths are derived for 250 lines of the first spectrum of terbium by using the relative intensities from the Tables of Spectral-Line Intensities by Meggers, Corliss and Scribner and the line classifications by Klinkenberg.

**10740.** Daniel, A. C., Bevan, A. W., Jr., Mahler, R. J., **Nuclea spin-lattice relaxation in the antiferromagnets $CoCl_2 \cdot O2H_2C$ and $FeCl_2 \cdot O2H_2O$,** *J. Appl. Phys.* **39,** No. 2, Part I, 496 497 (Feb. 1, 1968).

> Key words: Antiferromagnetism; magnon energy gap; mag nons; spin-lattice relaxation time.

Spin-lattice relaxation of protons in $CoCl_2 \cdot 2H_2O$ an $FeCl_2 \cdot 2H_2O$ has been measured over a temperature range of 1.3 to 12 °K in zero external magnetic field. The temperature depen dence of the relaxation rate exhibits two relaxation processes neither of which is adequately characterized by the T and T laws previously reported for $CuCl_2 \cdot 2H_2O$. Additional $T^{11}$ an $AT^2 \exp(-T_{AE}/T)$ dependences are required to fit our data whic predicts a $T_{AE} = (42.8 \pm 1)$°K for $CoCl_2 \cdot 2H_2O$ and a $T_{AE} = (4.1$ $\pm 0.2)$°K for $FeCl_2 \cdot 2H_2O$.

**10741.** Dean, J. W., Richards, R. J., **Hydrostatic pressure effect in carbon and germanium thermometers,** (Proc. 196 Cryogenic Engineering Conf., Stanford University, Stanfor Calif., Aug. 21-23, 1967), Chapter in *Advances in Cryogeni Engineering* **13,** 505-508 (Plenum Press Inc., New Yor N.Y., 1968).

> Key words: Carbon; germanium; pressure effect; the mometer.

This work describes measurements of the hydrostatic pressur coefficient of electrical resistivity for carbon and germaniu thermometers in the range of 4 to 295 °K with experimental pre sures up to 1000 psig($7.0 \times 10^6 N/m^2$). Pressure coefficients wer found to be independent of pressure but to vary with temperatu from $-0.65)$ $10^{-5}$ to $-1.1 \times 10^{-5}$ psi$^{-1}$ ($-0.944 \times 10^{-9}$ to $-1$ $\times 10^{-9}$ m$^2$/N) for germanium and from $-1.2 \times 10^{-5}$ to $-1.5 \times 10$ psi$^{-1}$ ($-1.74 \times 10^{-9}$ to $-2.18 \times 10^{-9}$ m$^2$/N) for carbon. The pressure coefficients result in resistance changes for a 10 psig($7.0 \times 10^6 N/m^2$) pressure at 20 °K that may be interpreted temperature errors of 0.3 °K for carbon and 0.03 °K for germa um.

**10742.** Dunn, G. H., **Photodissociation of $H_2^+$ and $D_2^+$: theo** *Phys. Rev.* **172,** No. 1, 172-178 (Aug. 5, 1968).

> Key words: Cross sections; $D_2^+$; $H_2^+$; photodissociatio theory; vibrational levels.

Theory is described and calculations made for photodissoc tion cross sections of $H_2^+$ ($D_2^+$) from each of the ion's 19 (2 vibrational levels. Cross sections are summed over an assum Franck-Condon distribution of initial vibrational states to giv predicted cross section for comparison with experiment. Auxil ry calculations are made of some of the cross sections using t common δ function approximation to the continuum radial wa functions, and a comparison made with the results using m exact wave functions, shows very good agreement for photod sociation from the lowest vibrational levels, but very poor agr ment for photodissociation from higher levels.

0743. Fano, U., **Introductory remarks,** *Proc. Intern. Conf. Radiation Research, Cortina, Italy, June 26, 1966,* pp. 13-19 (North-Holland Publ. Co., Amsterdam, The Netherlands, 1967).

Key words: Chemical activation; degradation; ionization; radiation effects.

This symposium constitutes, in effect, the report of a study group. The group met last September to consider aspects particularly relevant at this time. Various questions have been reviewed in some detail following that meeting and calculations performed as needed, with a steady exchange of correspondence, consultation and visits.

0744. Fowler, H. A., **Experiments in electron scattering. 1,** (Proc. Symp. Quantitative Aspects of Electron Microscopy, Walter Reed Institute of Pathology, Washington, D.C., 1965), *Lab. Investigations* **14,** No. 6, Part 2, 9-16 (1965).

Key words: Electron scattering; solids.

This paper contains a review of National Bureau of Standards work on electron scattering in solids.

0745. Franklin, A. D., **NBS dedicates new laboratory,** *J. Am. Ceramic Soc.* **45,** No. 10, 841-842 (1966).

Key words: Complex; laboratory; standards.

General discussion of the plans of the National Bureau of Standards for the dedication of its Gaithersburg, Maryland laboratory complex on November 15, 1966.

0746. Gallagher, A., **Rubidium and cesium excitation transfer in nearly adiabatic collisions with inert gases,** *Phys. Rev.* **172,** No. 1, 88-96 (Aug. 5, 1968).

Key words: Alkali resonance; cesium; collisions; cross sections; line broadening; rubidium; velocity dependence.

The cross sections for rubidium $5^2P_{1/2} \leftrightarrow 5^2P_{3/2}$ and cesium $6^2P_{1/2} \leftrightarrow 6^2P_{3/2}$ excitation transfer due to inert gas collisions have been measured. The temperature of the collision vessel has been varied from 300 °K to partially establish the velocity dependence of these cross sections (the alkali resonance line optical depths were always much less than one). The various cross sections exhibit a systematic behavior that can be combined to find the general shape of a "universal" cross section that ranges across six orders of magnitude, starting just below the threshold for "sudden" collisions. The surprisingly large influence of line broadening on these excitation transfer measurements has been removed as a source of error.

10747. Gammon, W. H., **What educators can expect from the Center for Computer Sciences and Technology,** *Proc. Gen. Conf. Midwestern States Educational Information Project, Des Moines, Iowa, June 20, 1967,* **P.L. 89-10,** Title V, Sect. 505, pp. 30-45, (Department of Public Instruction, State of Iowa, Des Moines, Iowa, 1967).

Key words: Computer applications; computer instruction; data processing; education; standard data elements.

This presentation was made to the Midwestern States Educational Information Project (MSEIP)—a group working under contract from the U.S. Office of Education—in order to establish a dialogue with the group and to let them know what the Federal Government is doing in the area of data processing standards and how this may assist them in their work.

The computer is becoming a very important tool to educators since it is estimated that upwards of 1/4 of the teachers' and counselors' time is spent in clerical tasks involved in handling educational data. ADP standards resulting from development work done by the Center for Computer Sciences and Technology of NBS will be mandatory on the Federal Government only, but will be of benefit to MSEIP and similar educational groups. As an example, state school systems will have to determine items of information to be maintained and standards for uniform documentation within each of the thousands of local school districts. Such data will sometimes have to be fed from the individual school to the school district, and in some cases to the state and national level. In order to be able to exchange such information, there need to be agreed upon standards for documentation. NBS is presently working in the area of program documentation standards and will share its findings with MSEIP and others as they become available.

10748. Glasgow, A. R., Jr., **High-temperature value for corrosive gases,** *Anal. Chem.* **38,** 1104 (July 1966).

Key words: Fluoride; high-temperature; high-vacuum; metal; nickel-Monel; non-corrosive; value.

Alterations in a commercially available, bellows-type valve are described which extends its usage with fluorides to higher-temperatures (250 °F to 1000 °F). The altered valve of nickel and Monel parts only was tested with a helium-leak detector from room temperature to 1000 °F and found to be high-vacuum tight across the closed valve seat and at its bellows gasket. The valve has performed well in systems where beryllium fluoride vapors, or fluorine gas, or hydrogen fluoride gas have been present.

10749. Goldman, D. T., **Reactor physicists emphasize need for neutron data, Phys. Today 21,** No. 8, 85-89 (Aug. 21, 1968).

Key words: Cross sections; meeting; neutrons; nuclear technology; reactors; shielding.

This is a summary of the Neutron Cross Sections and Technology Conference written by the Conference Chairman. It summarizes the meeting and describes very briefly each of the eight sections of the Conference.

10750. Gross, D., Loftus, J. L., Lee, T. G., Gray, V. E., **Smoke and gases produced by burning aircraft interior materials,** *FAA NA-68-36 (DS-68-16)* 50 pages (Federal Aviation Agency, Washington, D.C., June 1968).

Key words: Aircraft materials; combustion products; fire tests; interior finish; smoke; thermal degradation; toxic gases.

Measurements are reported of the smoke produced during both flaming and smoldering exposures on nearly 150 aircraft interior materials. Smoke is reported in terms of specific optical density, a dimensionless attenuation coefficient which defines the photometric obscuration produced by a quantity of smoke accumulated from a specimen of given thickness and unit surface area within a chamber of unit volume. A very wide range in the maximum specific optical density was observed. For the majority of materials, more smoke was produced during the flaming exposure test. However, certain materials produced significantly more smoke in the absence of open flaming.

During the smoke chamber tests, indications of the maximum concentrations of CO, HCl, HCN and other selected potentially toxic combustion products were obtained using commercial colorimetric detector tubes. A study was made of the operation, accuracy and limitations of the detector tubes used. Measurements of the concentrations of HCl were also made using specific ion electrode techniques.

The elevated temperature thermal degradation of selected materials was studied in a number of ways including thermogravimetry and differential scanning calorimetry.

Qualitative identification of the major components of the original test materials was accomplished primarily by infrared absorption spectrophotometry.

Of the materials tested, a number were found to possess good heat stability properties, and did not generate large quantities of smoke or high concentrations of the combustion products selected for analysis.

**10751.** Haber, S., **A combination of Monte Carlo and classical methods for evaluating multiple integrals,** *Bull. Am. Math. Soc.* **74,** No. 4, 683-686 (July 1968).

Key words: Integral; integration; modified Monte Carlo; Monte Carlo; multiple integral; numerical analysis; numerical integration; quadrature.

This is a preliminary announcement, stating results without proof. A class of formulas for multiple integration, called "Stochastic Quadrature Formulas," is defined, and an error estimate given. Some constant-coefficient formulas of this class are described.

**10752.** Herber, R. H., Spijkerman, J. J., **Narrow-line source for $^{119}$Sn Mössbauer spectroscopy,** *J. Chem. Phys.* **43,** No. 11, 4057-4059 (Dec. 1, 1965).

Key words: Isomeric state nuclide; Mössbauer spectroscopy; palladium matrix; spectroscopy.

Mössbauer spectroscopy with $Sn^{119m}$ has usually involved either $SnO_2$ or $Mg_2Sn$ as a host matrix for the 250 day isomeric state nuclide, although both of these materials have distinct disadvantages under normal applications.

A palladium matrix for $Sn^{119m}$ was chosen after a correlation between the recoil free fraction and the chemical shift was noted. Such a prepared source was to be usable at room temperature with a recoil free fraction of 0.80 and a line width of $0.71 \pm 0.07$ mm-sec$^{-1}$ compared to the natural line width 0.62 mm-sec$^{-1}$.

From the data presented it can be inferred that dilute solutions of tin in Pt,V, and Cu will constitute matrices which are suitable for use as Mössbauer sources at room temperature, while dilute solutions of tin in Ti, In, and Pb offer little advantage in such applications.

**10753.** Hertelendy, P., **An approximate theory governing symmetric motions of elastic rods of rectangular or square cross section,** *J. Appl. Mech. Paper No.* **68—APM-10,** pp. 333-341 (June 1968).

Key words: Longitudinal modes; theory of symmetric deformations of plates; thickness-shear modes; thickness-stretch modes; variational equations frequency as wave numbers; vibrations of square bars.

Variational equations of motion are developed for symmetric motions of linear elastic bars of rectangular cross-section. In the finite term approximation, sufficient terms are retained to allow a longitudinal mode, two thickness-stretch modes, and two thickness-shear modes of vibration in an infinite bar of square cross-section. Modes for complex wave numbers are also investigated. Adjustment factors in the strain energy and kinetic energy potentials are used to match exact and experimental solutions. Experimental frequency vs wave number results for four modes are reduced by Fourier synthesis and compared both to the approximate theory and to the exact solution for circular cylinders. Theory is intended to predict behavior of thick rectangular bars for which the plane stress solution is not accurate.

**10754.** Hiza, M. J., Heck, C. K., Kidnay, A. J., **Liquid-vapor and solid-vapor equilibrium in the system hydrogen-ethane,** (Proc. 1967 Cryogenic Engineering Conf., Stanford University, Stanford, Calif., Aug. 21-23, 1967), Chapter in *Advances in Cryogenic Engineering* **13,** 343-356 (Plenum Press Inc., New York, N.Y., 1968).

Key words: Ethane; hydrogen; hydrogen-ethane system; liquid-vapor equilibrium; low temperature phase equilibrium; solid-vapor equilibrium; solubility of hydrogen in liquid ethane.

Equilibrium gas phase compositions in the system hydrogen-ethane were measured for nine isotherms from 83° to 190 °K up to 150 atmospheres; equilibrium liquid phase compositions were measured for six of the isotherms from 108° to 190 °K. Gas phase compositions up to 130 °K were measured in a single-pass solid-vapor apparatus using continuous analysis with a hydrogen flame ionization detector. The remainder of the measurements were made in a vapor-recirculating liquid-vapor apparatus using chromatographic analysis with a thermal conductivity detector

Isobaric comparison of enhancement factors, $y_1\pi/p_{01}$, shows the gas phase data obtained by the two methods to be in excellen agreement. These data are in excellent agreement with the ga phase data of Williams and Katz at 185.93 °K. However, th only gas phase data of Williams and Katz below the normal boiling point of ethane (184.52 °K) at 144.26 °K appear to be a much as 25 percent too high in the concentration of ethane. Th liquid phase data are generally higher in hydrogen concentratio than the data of Williams and Katz by little more than the combined experimental errors. Very poor agreement was found wit the older gas and liquid phase data of Levitskaya from 158.15° t 188.15 °K. The present investigation provides the only gas phas data in the region of the ethane triple point, 89.89 °K.

**10755.** Hummer, D. G., **Radiative transfer processes in planetar nebulae,** (Proc. Intern. Astronomical Union, Symp. No. 34 Tatranska Lomnica, Czechoslovakia, Sept. 4-8, 1967 Chapter in *Planetary Nebulae*, D. E. Osterbrock and C. R O'Dell, eds., pp. 166-184 (D. Reidel Publ. Co., Dordrech Amsterdam, The Netherlands, 1968).

Key words: Balmer lines; Lyman continuum; non-coherer scattering; optical depth; planetary nebulae; radiativ transfer; velocity gradients.

The physical aspects of radiative transfer processes that ma be of importance in planetary nebulae are discussed and rece work on these problems is summarized.

**10756.** Ito, J., **Silicate apatites and oxyapatites,** *Am. Mineralogi* **53,** 890-907 (May-June 1968).

Key words: Condensation; field emission; hydroge molecular beam; tungsten.

Various synthetic compounds of the silicate apatite grou which are isomorphous with the minerals abukumalite, beckelit britholite and lessingite were investigated. Three different typ were synthesized hydrothermally at temperatures from 550 ° to 720 °C under 2 kilobars pressure: (Ca, Sr, Ba, Pb, Mn ar $Cd)^{2+}{}_4$ $(Ln, Y)_6{}^{3+}Si_6O_{24}(OH)_2$, $(Na, Li)_2$ $(Ln, Y)^{3+}{}_8Si_6O_{24}(OH$ and $Na_2Ca_X$ $(Ln, Y)_{8-X}Si_{6-X}P_XO_{24}(OH)_2$, X = 0 to 6.

Complete solid solution exists between hydroxyapatit $Ca_{10}P_6O_{24}(OH)_2$, and $Ca_4Y_6Si_6O_{24}(OH)_2$ (abukumalite). Unit c dimensions of all compounds and indexed x-ray powder data the typical end compounds are tabulated.

Anhydrous silicate apatite, oxyapatites with the probable fo mulae $M^{2+}{}_2$ $(Ln, Y)^{3+}{}_8Si_6O_{26}$ and $M^{1+}{}_1$ $(Ln, Y)^{3+}{}_9Si_6O_{26}$, a more generally ($M^{1+}$, $M^{2+}$, Ln, Y and $Th^{3+})_{10}$ (Si, P and $B)_6$ were prepared at temperatures from 950 °C to 1260 °C in a The following solid solution systems of oxyapatite we established: $Ca_2La_8Si_6O_{26} \rightleftharpoons Ca_8La_2P_6O_{26}$, $Ca_2Y_8Si_6O_{26}$ $Ca_iY_2P_6O_{26}$, $Pb^{4+}{}_3Pb^{2+}{}_5Y_2Si_6O_{26} \rightleftharpoons Pb^{2+}{}_2Y_8Si_6O_{26}$, a $Mg_2Y_8Si_6O_{26} \rightleftharpoons Y_{10}Si_4B_2O_{26}$.

Results of the infrared spectroscopic analysis, water det mination by two different methods and differential thermal an sis of selected compounds all agree well with the presence of OH in silicate apatite and its absence in oxyapatite.

$NaLa_9Si_6O_{26}$ was obtained as transparent needles up to ~0.2 mm by the slow cooling of the flux ($Na_2WO_4$) from 1,150 °C to 50 °C. Euhedral transparent crystals of $Na_2La_8Si_6O_{24}F_2$ up to mm were grown by the combination of slow cooling and vaporation of the flux (NaF) at temperatures from 1350 °C to 00 °C.

New fluorescent yttrium and gadolinium analogues of oxapatites, activated by europium and terbium, were prepared.

**0757.** Jackson, J. L., Coriell, S. R., **Transport coefficients of composite materials,** *J. Appl. Phys.* **39,** No. 5, 2349-2354 (Apr. 1968).

Key words: Composite material; dielectric constant; diffusion constant; electrical conductivity; eutectic; heat conductivity; magnetic permeability; transport coefficient.

The problem of the effective electrical conductivity of a composite material whose local conductivity is a function of position s treated. Using the analogy between this problem and the diffuion of ions in a periodic potential, upper and lower bounds are obtained for the effective conductivity. These bounds are shown o be the conductivities obtained in certain commonly used quivalent circuit approximations. Although the discussion in he paper is in terms of the electrical conductivity, the theory is qually applicable to many transport coefficients, e.g., the heat onductivity, magnetic permeability, dielectric constant, or diffuion constant.

**0758.** Johannesen, R. B., Candela, G. A., Tsang, T., **Jahn-Teller distortion: magnetic studies of vanadium tetrachloride,** *J. Chem. Phys.* **48,** No. 12, 5544-5549 (June 15, 1968).

Key words: Jahn-Teller distortion; ligand field; magnetic susceptibility; paramagnetic relaxation; paramagnetic resonance; vanadium tetrachloride.

Paramagnetic resonance of polycrystalline $VCl_4$ diluted with $TiCl_4$ has been observed near 9, 24, and 36 GHz below 9 °K. Both g-values and hyperfine A-tensors are axially symmetric and emperature independent with the same principal axes; $g_{\|} = .920$, $g_{\perp} = 1.899$, $|A_{\|}| = 72$ G, $|A_{\perp}| = 120$ G. The average g-value obtained from susceptibility data is in agreement with the resonance value. The paramagnetic relaxation time $T_1$ varies with temperature as shown by the relation $T_1 = 2 \times 10^{-9} \exp(25/T)$, indicating the presence of a potential barrier approximately 18 $cm^{-1}$ in height. The results indicate a static Jahn-Teller distortion, but with large zero-point vibrations. This situaion is in between Ballhausen-de Heer's ligand field and Ballhausen-Liehr's crystal field calculations.

**0759.** Kidnay, A. J., Hiza, M. J., Dickson, P. F., **The adsorption isotherms of methane, nitrogen, hydrogen and their mixtures on charcoal at 76 °K,** (Proc. 1967 Cryogenic Engineering Conf., Stanford University, Stanford, Calif., Aug. 21-23, 1967), Chapter in *Advances in Cryogenic Engineering* **13,** 397-408 (Plenum Press Inc., New York, N.Y., 1968).

Key words: Adsorption; charcoal; hydrogen; isotherms; methane; mixture adsorption; nitrogen.

The pure component adsorption isotherms of nitrogen, methane, and hydrogen were measured at 76 °K and in the pressure range of 0.19 to 13.5 mm Hg, 0.082 to 6.808 mm Hg and 1.45 to 95.00 atm, respectively. Binary adsorption isotherms for mixtures of 340 ppm nitrogen, 1450 ppm nitrogen, 352 ppm methane, and 770 ppm methane in hydrogen were measured at 76 °K and in the pressure range of 5 to 82 atm. A ternary sotherm for a mixture of 415 ppm methane + 686 ppm nitrogen in hydrogen was also determined in the pressure range of 6 to 48 atm.

The empirical adsorption enhancement factor may be used in conjunction with the pure component isotherms to predict the adsorption of nitrogen and methane from the binary gas mixtures with an accuracy that should be sufficient for most engineering calculations. The adsorption of nitrogen and methane from the ternary gas mixtures can be predicted quite accurately through the use of the prediction technique proposed by Kidnay and Myers.

**10760.** Klein, R., **The deposition of hydrogen beams on tungsten,** *Surface Sci.* **11,** No. 2, 227-241 (July 1968).

Key words: Condensation; field emission; hydrogen; molecular beam; tungsten.

The deposition and chemisorption of hydrogen on tungsten have been investigated with a molecular beam apparatus to which a field emission microscope is attached. The FEM is operated immersed in liquid helium. The surface temperature of both the surface on which the deposition is made, and the beam, can be varied independently. Advantage is taken of the formation of a sharp boundary line after spreading on a shadowed emitter to evaluate the effect of beam temperature on the condensation process. There is a very marked effect which suggests that the deposition depends on a critical velocity for the hydrogen molecule in the beam. This effect is found only for the second layer where the adsorption forces are relatively weak. The course of the deposition in the first layer can be followed from the characteristics of the electron emission from the tip as coverage proceeds.

**10761.** Klemens, P. G., Jackson, J. L., **Diffusion of electrons on the Fermi surface. II. Longitudinal magnetoresistance of Ib metals,** *Physica* **31,** 1421-1427 (1965).

Key words: Fermi surface; high-field magnetoresistance; magnetoresistance.

Following Pippard the longitudinal high-field magnetoresistance is discussed in terms of belts on the Fermi sphere on which the deviation of the electron distribution from equilibrium must vanish. For the ideal resistance case the electron diffusion equation is solved with appropriate boundary conditions for a number of directions and neck radii, and the magnetoresistance is pointed out.

**10762.** Kopec, C. S., **Measurement of gears,** Chapter 15 in *Handbook of Industrial Metrology,* pp. 424-450 (Prentice-Hall, Inc., Englewood Cliffs, N.J., 1967).

Key words: Analytical inspection; composite inspection; gears; index; involute; lead; metrology; process control.

This chapter contains 26 pages of information on gear measuring methods, practices and basic definitions. The data presented cover only those practices and inspection methods which are recognized and accepted throughout the gear industry as being reliable. The methods described provide measurements which are accurate and repeatable to a degree compatible with the specified quality. Experienced personnel, using calibrated instruments in suitable environment, are required. Process control is the method by which gear accuracy is maintained through control of manufacturing equipment, methods, and processes. When analytical inspection of gear elements is required, methods are described for measuring the following tooth elements: runout, pitch, profile, lead, backlash, tooth thickness and composite method of gear inspection.

**10763.** Kokoszka, G. F., Allen, H. C., Jr., Gordon, G., **Electron paramagnetic resonance spectra of two zinc-doped and nickel-**

**doped copper chloride pyridine-N-oxide complexes,** *J. Chem. Phys.* **46,** No. 8, 3020-3024 (Apr. 15, 1967).

Key words: Copper chloride-pyridine-N-oxide; copper-nickel pairs; copper-zinc pairs; e.p.r. pair spectra; magnetic resonance.

The electron paramagnetic resonance spectra of zinc-doped dichlorobispyridine-N-oxidecopper(II) [$(C_5H_5NO)_2Cu(Zn)Cl_2$] and zinc-doped dichloromonoaquopyridine-N-oxidecopper(II) [$C_5H_5NOCu(Zn)Cl_2 \cdot H_2O$] have been observed at liquid nitrogen temperature. The data could be fit to the usual $S = 1/2$ Spin Hamiltonian. The g values obtained in this study for the copper-zinc pairs agree with the g values obtained for the copper-copper pairs in the pure material to within experimental uncertainty. Copper hyperfine splitting and chlorine superhyperfine splitting were also observed. The magnetic parameters for $(C_5H_5NO)_2Cu(Zn)Cl_2$ are $g_z = 2.332$, $g_x = 2.056$, $g_y = 2.080$, $A_z = 129 \times 10^{-4}$ cm$^{-1}$, $A_x = A_y < 10 \times 10^{-4}$ cm$^{-1}$, $A' = 25 \times 10^{-4}$ cm$^{-1}$, and $B' = 7 \times 10^{-4}$ cm$^{-1}$, while for $C_5H_5NOCu(Zn)Cl_2 \cdot H_2O$ we obtain $g_z = 2.306$, $g_x = 2.056$, $g_y = 2.083$, $A_z = 139 \times 10^{-4}$ cm$^{-1}$, and $A_x = A_y < 10 \times 10^{-4}$ cm$^{-1}$. An analysis of the data using a simple LCAO-MO approach suggests relatively strong metal-ligand bonds.

The data obtained from the study of nickel-doped $(C_5H_5NO)_2CuCl_2$ could be dit to an $S = 1/2$ Spin Hamiltonian with the following magnetic parameters: $g_z = 2.14$, $g_x = 2.54$, $g_y = 2.49$, $A_z = 35 \times 10^{-4}$ cm$^{-1}$, and $A_x = A_y < 7 \times 10^{-4}$ cm$^{-1}$. For nickel-doped $C_5H_5NOCuCl_2 \cdot H_2O$ we obtain $g_z = 2.15$, $g_x = 2.61$, $g_y = 2.50$, $A_z = 40 \times 10^{-4}$ cm$^{-1}$, and $A_x = A_y < 7 \times 10^{-4}$ cm$^{-1}$. These are the first reported magnetic parameters from dimers which contain exchange coupled dissimilar transition metal ions.

**10764.** Kruger, J., **The spectrum of corrosion research of the Corrosion Section of the National Bureau of Standards,** (Proc. 12th Annual Appalachian Underground Corrosion Short Course, West Virginia University, Morgantown, West Virginia, Oct. 1967), *West Virginia University Tech. Bull.* **86,** 11-13, (1967).

Key words: Corrosion; National Bureau of Standards.

A non-technical description of the research carried out in the Corrosion Section of the National Bureau of Standards is given.

**10765.** Lonie, M., **A report on body sizing for boys and students,** *Boys' and Young Men's Apparel Buyers' Assoc. J.,* p. 8 (1967).

Key words: Body sizing standards; boys' size standards; "student" boys'.

Body Sizing Standards are discussed in general and the program involving the development of such standards for "Student" Boys is discussed specifically. Reference is made to the participation of the Boys' and Young Men's Apparel Buyers' Association in the development of this and other standards.

**10766.** Macek, J. H., **Application of the Fock expansion to doubly excited states of the helium atom,** *Phys. Rev.* **160,** No. 1, 170-174 (Aug. 5, 1967).

Key words: Atomic physics; classification; levels; lifetimes; spectroscopy; theoretical physics.

The origin of the plus and minus character of the $^1P$ and $^3P$ doubly excited states of helium which converge to the $n = 2$ level is investigated in the close coupling approximation. It is found that the close coupling wave functions do exhibit the plus and minus character, and that the widths of these states are related to their plus and minus character in the case of the $^1P$, but not for $^3P$.

**10767.** Maeda, K., Young, J., **Propagation of the pressure waves produced by auroras,** *J. Geomagnetism Geoelectricity* **18,** No. 2, 275-299 (1966).

Key words: Acoustic modes; auroras; gravity (thermobaric) mode; pressure waves; propagation.

It is shown that the traveling pressure waves associated with auroral activity are not necessarily limited to the acoustic mode, but sometimes extend to the gravity (thermobaric) mode. This is partly due to the existence of large positive lapse rate (i.e. very stable) layers such as in the upper part of the stratosphere and in the thermosphere. As a consequence, clear sinusoidal oscillations which appear occasionally with periods of group velocity minimum (around 5 min) can be ascribed to the Airy phase. As an example, the data obtained at the NBS stations in Washington, D.C. on July 15, 1960 are shown with preliminary results of power spectrum analyses.

**10768.** Marezio, M., Remeika, J. P., Zocchi, M., **Cation distribution in the garnet $Eu_3Fe_{1.94}Ga_{3.06}O_{12}$,** *J. Chem. Phys.* **48,** No. 3, 1094-1096 (Feb. 1968).

Key words: Single crystal x-ray diffraction; study $Eu_3Fe_{1.94}Ga_{3.06}O_{12}$.

A single crystal x-ray diffraction study of the cation distribution in the garnet $Eu_3Fe_{1.94}Ga_{3.06}O_{12}$ has been made. The greater preference of the $Ga^{+3}$ ions for the tetrahedral sites with respect to the one of the $Fe^{+3}$ ions, already postulated from magnetic measurements, has been confirmed. The fraction of $Ga^{+3}$ ions in tetrahedral site is $f_t = 0.91 \pm 0.03$.

**10769.** Mulroy, W. J., Kusuda, T., Phillips, C. W., **Survey on digital computer programs for heating and cooling load calculations,** *SICCAP Bull.* **2,** No. 2, 4-8 (May 1968).

Key words: Digital computer programs; energy-usage calculations for buildings; heating and cooling load calculations for buildings.

A summarization is made of findings obtained from a questionnaire sent out to ascertain the current state of activity in development and use of computer programs for calculating the heating and cooling loads of buildings. About 2500 questionnaries were sent out, and 489 replies were received. Sixty-one independently prepared computer programs were identified, the majority being based on the ASHRAE Guide and Data Book method. About 250 other replies came from people interested in such calculations but who have not developed a program for the purpose.

**10770.** Newman, M., **A bound for the number of cojugacy classes in a group,** *J. London Math. Soc.* **43,** 108-110 (1968).

Key words: Bounds; conjugacy classes; groups; matrix representations.

It is shown that if the group G is of order h and has k conjugacy classes, then $k \geqslant \log \log h/\log 4$.

**10771.** Odabasi, H., **Spectrum of doubly ionized lanthanum (La III),** *J. Opt. Soc. Am.* **57,** 1459-1463 (1967).

Key words: Fine-structure splitting; hyperfine structure ionization energy; lanthanum; spectrum.

Sixty-five new spectral lines of doubly ionized lanthanum in the interval from 2000 to 12000 Å are reported. Four newly discovered terms (10s, 9p, 9d, 9f) are given. Fine-structure splittings of 5g, 6g, 7g, and 8g terms are determined, and thei peculiar behavior discussed. The hyperfine structure of the $6s^2S_{1/2}$ level is observed to be $1.03 \pm 0.10$ cm$^{-1}$. By using the new terms, the previously reported ionization energy is corrected to $154664 \pm 15$ cm$^{-1}$. The theoretical values of spin-orbi coupling constants are calculated for the first three elements o the Cs isoelectronic sequence.

**10772.** Otto, E. M., **Rates of dissociation of $Ag_2O_2$,** *J. Electrochem. Soc.* **115,** No. 9, 878-881 (Sept. 1968).

Key words: $Ag_2O$; $Ag_2O_2$; aqueous potassium hydroxide; dissociation; rates; silver oxides.

The dissociation of $Ag_2O_2$ into $Ag_2O$ and $O_2$ has been investigated over the temperature range from 22 to 100 °C for the dry material, for water slurries and for slurries in KOH of concentrations from 1 to 13 molar. The method consisted in measuring the $O_2$ volume while the dissociation was progressing, and in most cases very smooth curves were obtained when the volume of dry $O_2$ corrected to 0 °C, 760 torr, per gram of sample was plotted against time. $Ag_2O_2$ in water had the lowest rate of evolution, dry $Ag_2O_2$ had an intermediate rate and the high concentrations of KOH solution, such as are used in Ag-Cd cells, had the highest rate. The rates ranged from .0001 to 1.8 ml $hr^{-1}g^{-1}$.

**10773.** Penner, S., **Handling high-energy high-power electron beams,** *Record IEEE 9th Annual Symp. Electron, Ion and Laser Beam Technology, Berkeley, Calif., May 9-11, 1967,* No. F-79, pp. 50-61 (1967).

Key words: Beam handling; electron accelerators; high power beams.

Linear electron accelerators (linacs) produce high power pulsed electron beams at energies from a few MeV to 20 GeV. These machines are used in a wide variety of industrial and research applications including radiography, food processing, radiation chemistry, and nuclear physics. Linacs are in use which produce electron beam powers of hundreds of kilowatts and average currents of the order of one milliampere. Existing linacs operate as pulsed devices with peak currents in the ampere range and energy per pulse as high as 300 joules. In the larger laboratories multiple target areas are used. The electron beam is guided from the linac to the target areas by complex ion-optical systems employing numerous deflection and focussing magnets. The beam paths are often hundreds of feet long. Beam spot sizes at the target are often required to be as small as one square millimeter. The design of targets, collimators, transmission windows, and absorbers for these high energy beams is dominated by problems associated with the heat load. The most difficult aspects of these problems are the extremely high heat transfer rates required and the metal fatigue problem due to the pulsed nature of the beam.

**10774.** Rhodes, I., **The importance of the glossary storage in machine translation,** Chapter in *Machine Translation,* A. D. Booth, ed., pp. 431-449 (North-Holland Publ. Co., Amsterdam, The Netherlands, 1967).

Key words: Glossary storage; machine translation; mechanical translation.

It is imperative that the "blueprints" of the entire scheme for Mechanical Translation be completed, before venturing to embark upon the extremely time- and money-consuming task of constructing the accompanying Machine Glossary. Moreover, this gigantic undertaking needs the full cooperation of all competent workers in this field. A brief outline of the NBS scheme, as well as excerpts from the proposed Glossary, are given in order to highlight the reasons for the above assertions.

**10775.** Rhodes, I., **The mighty man-computer team,** *Blanch Anniversary Volume,* pp. 277-284 (Aerospace Research Laboratories, Office of Aerospace Research, U.S. Air Force, Arlington, Va., Feb. 1967).

Key words: Achievements of automators; automators; electronic machines; failings of automators; human mind; tyro coders.

With the aid of electronic machines, the unsurpassable human brain can attain sublime achievements. We, automators, must first purge ourselves of three failings: the usurpation of the million-dollar instruments by tyro coders; the scandalous waste of time and money by the use of artificial languages; and the mulcting of Government funds by spurious schemes.

**10776.** Robbins, C. R., **Synthetic $CaTiSiO_5$ and its germanium analogue ($CaTiGeO_5$),** *Mater. Res. Bull.* **3,** 693-698 (1968).

Key words: $CaTiGeO_5$; $CaTiSiO_5$; crystal; mineral; space group; synthetic sphene; x-ray.

Synthetic, anhydrous $CaTiSiO_5$ (sphene) and $CaTiGeO_5$ are monoclinic with lattice constants $a = 6.567$, $b = 8.723$, $c = 7.454$ Å, $\beta = 119°52'$ and $a = 6.65$, $b = 8.92$, $c = 7.49$ Å, $\beta = 119°45'$ respectively. There are four formula units per cell. Cell dimensions of the silicate are close to those of natural sphene. The space group is $P2_1/n$ as compared with space group $C2/c$ reported for natural minerals of variable composition and general formula $CaTiSiO_4(OH,F,Cl)$. Although x-ray intensities indicate a structural similarity, some of the low-order (h + k odd) reflections of the synthetic crystals are fairly strong, indicating appreciable shifts from the $C2/c$ structure.

**10777.** Robbins, R. F., Reed, R. P., **Tensile properties of neoprene below the glass transition temperature,** (Proc. 1967 Cryogenic Engineering Conf., Stanford University, Stanford, Calif., Aug. 21-23, 1967), Chapter in *Advances in Cryogenic Engineering* **13,** 252-258 (Plenum Press Inc., New York, N.Y., 1968).

Key words: Glassy state; low temperature; mechanical property; modulus; neoprene; rubber; tensile strength; ultimate strength.

This paper describes tensile tests on two neoprene compounds at low temperatures. The neoprene compounds were chosen to determine the effect of carbon black filler material on the tensile properties below the glass transition temperature. Stress-strain curves were obtained at 4, 76, and 195 °K, and at strain rates between 0.01 and 10 inches per inch per minute. Results include the following: (1) Neoprene was ductile at temperatures 40 °K below the glass transition temperature ($T_g$); (2) The ultimate strength of the filled neoprene was less than the unfilled below $T_g$; (3) The ultimate strength of the filled neoprene was lower at 4 °K than at 76 °K; (4) The ultimate strength of neoprene at 195 °K was strain-rate dependent, and the ultimate strength of the filled neoprene showed a maximum at an intermediate strain rate.

**10778.** Rubin, R. J., **Momentum autocorrelation function of a heavy particle in a finite crystal,** *J. Am. Chem. Soc.* **90,** 3061-3063 (1968).

Key words: Brownian motion; correlation function; lattice dynamics.

The momentum autocorrelation function of a heavy particle in a finite one-dimensional crystal, $\rho_0^{(N)}(\tau)$, is compared with the same function in an infinite crystal, $\rho_0^{(\infty)}(\tau)$, by obtaining an explicit upper bound for the magnitude of the difference, $|\rho_0^{(N)}(\tau) - \rho_0^{(\infty)}(\tau)|$. The precise meaning of the statement that $\rho_0^{(\infty)}(\tau)$ is approximately a simple exponential is reviewed, and precise meaning is given to the statement that $\rho_0^{(N)}(\tau)$ decays exponentially.

**10779.** Ruch, R. R., DeVoe, J. R., **Radiochemical separation of copper by amalgam exchange,** *Anal. Chem.* **39,** No. 11, 1333-1335 (Sept. 1967).

Key words: Activation analysis; amalgam exchange; copper; radiochemical separation.

The technique of amalgam-exchange has been extended to and evaluated for the radiochemical separation of copper. The mercury phase is composed primarily of a finely divided suspension of electrodeposited copper in an extremely dilute solution of copper amalgam. Optimum conditions for separation are presented. The effect of some chemical interferences such as acids and salt have been observed. The evolved procedure has been evaluated for overall yield, precision, and decontamination. Generally recoveries greater than 98 percent may be obtained with better than 1 percent precision, accompanied by good decontamination ($> 10^5$) for most elements above copper in the electromotive series. This technique has been successfully applied to the activation analysis of low copper concentrations in NBS Standard Reference Material cast iron and magnesium alloy.

**10780.** Sadowski, W. L., **On some aspects of the eigenfunction expansion of the solution of the nonlinear Vlasov equation,** (Proc. Computer Simulation of Plasma and Many-Body Problems, Williamsburg, Va., Apr. 19-21, 1967), *Natl. Aeronaut. Space Agency Spec. Publ.* **153,** 433-440 (1967).

Key words: Eigenfunction; Landau damping; non-linear; numerical solution; plasma physics; truncation; Vlasov equation.

The non-linear Vlasov equation governing a one-dimensional periodic plasma was solved numerically. The solutions were expanded into a double set of eigenfunctions. The x-dependence of the distribution function was expressed by Fourier series, while Hermite polynomials were used to express the v-dependence. These two sets are eigenfunctions of the differential operators and the partial differential equation reduces to an ordinary differential equation on a matrix of expansion coefficients.

Some of the results are discussed as well as the closure problems arising from the attempts to represent an infinite expansion in terms of a finite matrix. The effect of the Fokker-Planck term or the detailed description of particle trapping and on Landau damping is also discussed.

**10781.** Schafft, H. A., **Avoiding second breakdown,** *Proc. XIII Intern. Scientific Congress on Electronics, Rome, Italy, June 1966,* pp. 119-130 (Rassegna Internazionale Elettronica Nucleare Teleradiocinematografica, Rome, Italy, 1966).

Key words: Electronics; failure mechanism; p-n junctions; reliability; second breakdown; transistors.

The problems that are encountered in avoiding second breakdown are discussed; they appear in three areas: (1) the design and fabrication of the transistor, (2) the specification of operations free of second breakdown, and (3) the interpretation of these specifications. In order to minimize the second breakdown problem in the transistor, it is vital that non-uniformities in the current density be minimized. The implications of this requirement to the design and fabrication of the transistor are considered. Generally the specifications that have appeared in data sheets are meant to apply to one of three types of operations: forward base drive operation, reverse base drive operation with a clamped inductive load, and reverse base drive operation with an unclamped inductive load. These specifications are examined to help the circuit designer to recognize the intent and limitation of a given specification and to interpret the specification for his particular application.

**10782.** Schindler, P. W., **Heterogeneous equilibria involving oxides, hydroxides, carbonates and hydroxide carbonates,** (Proc. Symp. Division of Water, Air, and Waste Chemistry, 151st Meeting of the American Chemical Society, Pittsburgh, Pa., Mar. 1966), Chapter in *Equilibrium Concepts in Natural Water Systems, Advances in Chemistry Series* **67,** 196-221 (American Chemical Society, New York, N.Y., 1967).

Key words: Carbonates; equilibria; hydroxide carbonates; hydroxides; oxides; sea water; solubility.

Part I discusses the experimental determination and graphical presentation of equilibrium data. , Some emphasis is placed on the connection between "thermodynamic" constants (referring to pure water as standard state) and "stoichiometric" constants relating to aqueous solutions of constant ionic strength. Part II compares equilibria in stable and metastable systems. Recent experimental work on the effect of particle size upon solubility is summarized, and the changes of solubility in the presence of metastable modifications is discussed. An attempt is made to classify some major and minor constituents of sea water with respect to a possible control of their concentrations by simple solubility equilibria.

**10783.** Schwerdtfeger, W. J., **Discussion of the paper "Method of estimating corrosion of highway culverts by means of polarization curves," by R. I. Lindberg,** *Highway Research Record No. 204, Metal Corrosion, Publ.* **1535,** p. 8 (Natl. Acad. Sci.—Natl. Res. Council, Washington, D.C., 1967).

Key words: Corrosion; corrosive soil; highway culverts; polarization curves; underground aluminum culverts.

The corrosion rate data obtained by Lindberg on actual underground aluminum culverts are evaluated on the basis of proven data obtained by the National Bureau of Standards upon which Lindberg's work is based. NBS polarization curves are also presented to show how a corrosive soil can be differentiated from a relatively non-corrosive soil.

Comments are made pertaining to the measuring circuit used in obtaining the polarization curves.

**10784.** Shapiro, J. T., Madden, R. P., **On the optical constants of polystyrene in the vacuum ultraviolet,** *J. Opt. Soc. Am.* **58,** No. 6, 771-775 (June 1968).

Key words: Optical constants; polystyrene; reflectance electron energy loss; vacuum ultraviolet.

The optical constants n and k for polystyrene in both thin film and bulk form have been measured by the reflectance vs angle of incidence technique in the wavelength region from 584 Å to 2000 Å. Four angles of incidence were used, and the effects of monochromator polarization were eliminated experimentally. The results differ from previously published data for the bulk form. The energy loss function $-\mathrm{Im}(1/\epsilon)$ was calculated from n and k determined for the thin films and compared with values obtained previously by characteristic electron energy loss techniques. These two methods yield the same structure in the energy loss function; however there remains some difference in the magnitude of the 6.9 eV loss relative to the background.

**10785.** Shideler, R. W., **Interfacing a teletypewriter to nuclear instruments used for computer-coupled activation analysis,** *Proc. 1965 Intern. Conf. Modern Trends in Activation Analysis, College Station, Texas, Apr. 1965,* pp. 236-242 (1965).

Key words: Digital instruments; digital multichannel pulse-height analyzer; multichannel analyzers; nuclear instruments; teletypewriter.

In performing activation analysis using modern digital instruments the volumes of numerical data dictate that an expedient data handling system be used.

The primary concern of this paper is to discuss the techniques and actual designs involved in the interfacing of a teletype to a digital multichannel pulse-height analyzer and to an automatic sample changer.

Two separate designs are discussed for interfacing to the multichannel analyzers. The first involves only minor changes to the analyzer. The second provides interfacing with no modification to the standard analyzer, and includes the additional capability of reading precursor data from external units including a time-of-year clock and programmed data groups. These additional data are included in the output format along with the analyzer data and serve to identify the data as well as to instruct the computer in its subsequent analysis.

Of primary importance in this paper is a discussion of the merits and advantages to be found in adopting the use of the teletype machine as an input-output device. As well as providing typed copy, it will punch and read a paper tape coded in the new ASCII code. The automatic inclusion of precursor data and an appropriate readout format brings on-line computer operation to a reality.

**10786.** Shimizu, A., **Calculations of the penetration of gamma rays through slabs by the method of invariant imbedding,** *Nucl. Sci. Eng.* **32,** 184-194 (May 1968).

Key words: Angular distributions; energy spectrum; gamma rays; invariant imbedding; shielding; transport.

The method of invariant imbedding has been applied to the penetration problem of gamma rays through slabs. The accuracy of the method was examined by comparison with other reliable calculations and proved to be competitive with other well developed methods. The method has the advantages that it is much more efficient than the Monte Carlo method and that it is readily applicable to the multi-layer problems. An extensive series of calculations on the transmission of gamma rays through homogeneous slabs was carried out. The energy and angular distributions of transmitted photons from mono-energetic and oblique sources were obtained for slab thickness up to fifteen mean free paths and for seven materials. The results of calculations were compared with experiments.

**10787.** Shimizu, A., **Calculation of the penetration of gamma rays through two-layer slabs,** *Nucl. Sci. Eng.* **32,** 385-391 (June 1968).

Key words: Dose transmission; gamma-rays; invariant imbedding; penetration; transport theory; two-layer slabs.

The method of invariant imbedding has been applied to the penetration problem of gamma rays through two-layer slabs, and turned out to be accurate and less time consuming than the Monte Carlo method. A series of calculations were made for two-layer slabs of water, iron and lead for plane oblique sources. An approximate formula for synthesizing the buildup factor of a composite slab from those of elementary layers is derived from numerical solutions by modifying the formula originally proposed by Kalos.

**10788.** Shuler, K. E., **Reaction cross sections, rate coefficients and nonequilibrium kinetics,** (Lecture, NATO Summer School on Theoretical Chemistry, Constance, Germany, Summer 1965), Chapter in *Chemische Elementarprozesse,* H. Hartmann, ed., pp. 1-22 (Springer-Verlag, Berlin, Germany, 1968).

Key words: Cross sections; nonequilibrium kinetics; rate coefficients; reaction cross sections.

The observed rate of a chemical reaction is usually expressed through an empirical equation involving the concentration of reactants and/or products and a proportionality constant $k$, the *rate coefficient*. This rate coefficient is determined experimentally from measurements of the change of concentration of reactants and/or products with time. If the empirical rate equation correctly describes, *in all aspects*, the reaction under investigation, the rate coefficient should be independent of the concentration of the reactants and/or products and of the time and should depend only upon the temperature of the (isothermal) reaction system.

Recent advances in experimental techniques permit the measurement of the "efficiency" of elementary chemical collision processes leading to product formation as a function of the energy of the reactants (kinetic and internal) and the geometry of the encounter. The results of these measurements are expressed as *reaction cross sections*, $\sigma_R$. It is the purpose of these lectures to explore the relation between the macroscopic rate coefficient k and the microscopic reaction cross section $\sigma_R$.

**10789.** Silverman, S., **Reflections on bioengineering,** (Proc. Symp. Engineering Significance of the Biological Sciences, Pittsburgh, Pa., Jan. 25-27, 1967), Chapter in *Bioengineering—An Engineering View,* pp. 103-106 (San Francisco Press Inc., San Francisco, Calif., June 1968).

Key words: Bioengineering; budgetary environment; social needs; technology; trends in science.

The role of Bioengineering in the contemporary scene is examined. The conviction is expressed that there is a real need for such an interdisciplinary development at this time. It is pointed out that Bioengineering must compete with other well-entrenched trends in science and technology in a budgetary environment that calls for thorough analysis and justification. There is, however, good evidence that the social needs should draw the necessary interest of gifted and competent people, and therefore sufficient Federal interest to support a growing program.

**10790.** Smith, G. W., Becker, D. A., **Preparation of an NBS biological standard reference material for trace elemental analysis,** *Proc. Nuclear Activation Techniques in the Life Sciences, Amsterdam, The Netherlands, May 8-12, 1967,* pp. 197-207 (International Atomic Energy Agency, Vienna, Austria, 1967).

Key words: Activation; analysis; biological; blood; bone; botanical; destructive; homogeneity; leaves; liver; neutron; non-destructive; reference; tissue; trace; variance.

A survey of leading U.S. biological, medical and forensic laboratories confirms the need for well characterized botanical, soft mammalian tissue, bone tissue and blood standards with elemental constituents at the 100 ppm level and below. The only sources of dried and sterilized tissue and blood known to the authors are certain U.S. drug concerns, whereas H. J. M. Bowen's kale has only been available since 1964 as a botanical comparison sample.

Before reliable analytical data can be obtained on a reference material, homogeneity must be established. Examples are given of this procedure, which is carried out routinely by the NBS on Standard Reference Materials. Homogeneity of Bowen's kale for chlorine ( ~ 4000 ppm), manganese ( ~ 14 ppm) and copper (~ 6 ppm) as well as for manganese in beef liver (~ 10 ppm) citrus leaf (~ 28 ppm) and oak leaf (~ 1000 ppm) are given. Measurements were made by neutron activation analysis both with and without chemical separation, using a Ge(Li) semiconductor detector. This technique was also used for the quantitative determination of the trace constituents chlorine and manganese, nondestructively. In addition, a destructive method was used for the elements arsenic and copper.

Analyses of variance, using the activation analysis data, indicate that all of the biological materials except the citrus leaves are homogeneous. Therefore, preparation under contract, of large lots of deciduous leaves and beef liver, will begin. Analyses for homogeneity and elemental content certification will be made by NBS activation analysis and other analytical competencies.

**10791.** Spijkerman, J. J., Ruegg, F. C., May, L., **The use of Mössbauer spectroscopy in iron coordination chemistry,** Chapter in *Mössbauer Effect Methodology* **2,** 85-93 (Plenum Press Inc., New York, N.Y., 1966).

Key words: Interpretation of chemical shift; iron coordination chemistry; Mössbauer spectroscopy; quadrupole splitting.

The application of Mössbauer Spectroscopy to the study of iron coordination chemistry is discussed. The chemical shifts of iron compounds are adjusted to the new standard, sodium nitroprusside, and this differential chemical shift is correlated with the 4s electron contribution to the bonding in the compounds. A new interpretation of the chemical shift – 4s electron contribution diagram is proposed including the latest results of Molecular Orbital calculations. The quadrupole splitting is related to the total spin and structure of the compound. The asymmetry of the doublet intensities can be used to obtain additional information about the structure of the compound and the spin-spin relaxation time. The relationships between the Mössbauer parameters and the data from other spectroscopic measurements are discussed.

**10792.** Stevens, M. E., **Information scientist, H. P. Luhn,** Chapter in *H. P. Luhn: Pioneer of Information Science – Selected Works,* C. K. Schultz, ed., pp. 24-30 (Spartan Books, New York, N.Y., 1968).

Key words: Auto-encoding; automatic abstracting; automatic indexing; KWIC indexing; Luhn; selective dissemination systems.

The contributions of H. P. Luhn to information science and technology, in the development of KWIC *k*ey-*w*ords-*i*n-*c*ontext (KWIC) indexing and of selective dissemination of information (SDI) systems, in "auto-encoding" principles for both automatic indexing and abstracting, and in other ways, are reflected not only in selected papers but in experimental demonstrations and in reductions to practice. In addition, he provided leadership for the American Documentation Institute in such areas as novel techniques for the preparation and advance distribution of Conference papers and the establishment of Special Interest Groups.

**10793.** Suzuki, G., **Quantitative methods for decision making,** Chapter VIII in *Management: Concepts and Practices,* F. R. Brown, ed., pp. 155-193 (Industrial College of the Armed Forces, Washington, D.C., 1967).

Key words: Decision-making; education; management; operations research; quantitative analysis.

An elementary treatment of some of the better known and widely used analytical methods in operations research/systems analysis. The material is presented in a manner which attempts to indicate why quantitative methods are useful in managerial decision-making situations. Some basic references are provided.

**10794.** Truesdell, C., **The non-linear field theories of mechanics,** *Encyclopedia of Physics* **III,** Part 3, 602 pages (Springer-Verlag, Berlin, Germany, 1965).

Key words: Elastic strain; field theories; finite elastic strain; mechanical response; mechanics.

This treatise presents an organized development of theories of mechanical response of materials subject to large deformations. It contains as one of its chapters an exposition of everything now known about the general theory of finite elastic strain.

**10795.** Tschuikow-Roux, E., **Photolysis of propene at 1470 Å,** *J. Phys. Chem. Note* **71,** 2355 (1967).

Key words: Photolysis; propylene; vacuum ultraviolet.

The photolysis of propylene at 1470 Å has been reexamined with the following new results. (1) Evidence is presented for the reaction

$$C_3H_6^* \rightarrow 2H + C_3H_4$$

(2) The previously postulated, but unidentified intermediate, methylcyclopropane (from the reaction of $CH_2$ with propylene), has been identified in the reaction products. Some basic references are provided. (3) The molecular elimination of hydrogen from the methyl group in propylene produces allylidene which may either isomerize to form allene and propyne or cyclyze to form cyclopropene. The latter was shown definitely to be absent and that isomerization of allylidene dominates over cyclization.

**10796.** Ugiansky, G. M., Ellinger, G. A., **Corrosion of Monel 400 in high $CO_2$ well water,** *Corrosion* **24,** No. 5, 134-136 (May 1968).

Key words: Corrosion; dezincification; electron probe microanalysis; Monel.

The dezincification type corrosion of a Monel well screen in natural water is discussed in detail. The second phase present in the corroded grain boundaries was determined by electron probe microanalysis to be nearly pure copper with little or no nickel present. It is concluded that Monel may be susceptible to dezincification type corrosion when used in certain environments.

**10797.** Ugiansky, G. M., Skolnick, L. P., Kruger, J., Stiefel, S. W., **Rate-controlling step in stress corrosion cracking,** *Nature* **218,** No. 5147, 1156-1157 (June 22, 1968).

Key words: Aluminum alloys; crack initiation; crack propagation; rate-controlling step; stress corrosion.

Experimental evidence is reported which shows that crack propagation, rather than crack initiation, is the rate limiting step in the intergranular stress corrosion of the high strength aluminum alloy 7075-T651. The directional susceptibility of certain aluminum alloys is explained on the basis of the crack propagation in an elongated grain structure.

**10798.** Utech, H. P., Early, J. G., **On the presence of thermal convection in the kinetics experiments of Rigney and Blakely,** *Acta Met.* **15,** No. 7, 1238-1239 (1967).

Key words: Interface; kinetics; thermal convection; thermal wave; tin; turbulence.

An experiment was conducted to test for the presence of thermal convection in the horizontal tube system employed by Rigney and Blakely to determine the interface kinetics of tin by the thermal wave technique. Thermal convection was found to be present.

**10799.** Utech, H. P., Parker, R. L., Early, J. G., Coriell, S. R., **The cam equation for a thermal-wave generator,** *J. Appl. Phys.* **38,** No. 9, 3799-3800 (Aug. 1967).

Key words: Cam; equation; generator; sine wave; thermal diffusivity; thermal-wave.

The cam equation for sinusoidal thermal-wave generator is derived, correcting an equation previously reported in the literature by Abeles, Cody, and Beers.

**10800.** Waclawski, B. J., Hughey, L. R., Madden, R. P., **Effect of oxygen adsorption on the photoelectron yield from tungsten in the vacuum ultraviolet,** *Appl. Phys. Letters* **10,** No. 11, 305-307 (June 1968).

Key words: Oxygen adsorption; photoelectric effect; tungsten; vacuum ultraviolet.

The effect of adsorbedd oxygen on the photoelectron yield of bulk polycrystalline tungsten was studied at photon energies of 7.7, 10.2, 11.8, 16.9, and 21.2 eV. Use of ultra-high vacua $\sim 3 \times 10^{-10}$ torr ensured sample cleanliness prior to oxygen exposure. The photoelectron yield decreases with oxygen exposure because of the increase in the electronic work function of the ngsten photocathode. However, at $h\nu = 21.2$ eV, an increase photoelectron yield with oxygen exposure also appears and is elieved to be due to photoelectron emission from the adsorbed xygen atoms.

**0801.** Wahsweiler, H. G., Greiner, W., Danos, M., **Continuum nuclear structure of $O^{16}$ in the Eigenchannel Reaction Theory,** *Phys. Rev.* **170,** No. 4, 893-906 (June 20, 1968).

Key words: Continuum states; coupled channels; interacting continua; nuclear structure; $O^{16}$; photo absorption.

The total particle-particle $S^J$-matrix of $O^{16}$ for spin $J = 1^-$ and xcitation energies between 15 and 27 MeV has been calculated the Eigenchannel Reaction Theory for several parameters of e Saxon-Woods potential and the two-body force. The many-ody problem has been treated in the one-particle one-hole aproximation. The photon channels have been included by perturation theory. Surprisingly, the most important structure of the xperimental cross sections is reproduced quite well in this sime approximation.

**0802.** Wang, F. E., DeSavage, B. F., Buehler, W. J., **The irreversible critical range in the TiNi transition,** *J. Appl. Phys.* **39,** No. 5, 2166-2175 (Apr. 1968).

Key Words: Covalent; delocalized; electronic conduction; Hall effect; localized; magnetic susceptibility; martensitic transition; order-disorder; phase transformation; resistivity.

Through an investigation of the transport and other related iermodynamic properties of TiNi at and around its "martentic" transition temperature, the existence of a critical range exnding over a 60 degree interval is characterized. Within this itical range, phase transition is second-order with anomalous eat capacity changes. Irreversibility of various properties ithin the critical range is interpreted in terms of irreversible near movement of atoms.

By inference, based on transport data, the band structure of iNi is a single or "nearly" single positive band within the temerature range investigated. The postulate that part of the alence electrons undergo a "covalent" ↔ "conduction" eleconic state transformation, in the course of the 60 degree interal second-order transition, is consistent in large measure with xperimental data.

**0803.** Weisman, H. M., **Information and the discipline of communication sciences,** (Proc. American Documentation Institute Annual Meeting, New York, N.Y., Oct. 22-27, 1967), Chapter in *Levels of Interaction Between Man and Information* **4,** 8-12 (Thompson Book Co., Washington, D.C., 1968).

Key words: Communication; communication sciences; documentation; information; information science.

This paper discusses the place of information in the field of ommunications. Documentation, information science, informaon, and communication are defined. The study of communicaon intersects many fields. Some of the significant fields within he communication sciences are identified. As a basic comonent of communication, information science has the major roblems that have prevented cohesion and unification of the iverse fields that comprise communication. The happenstances nat have created professional practitioners in information ciences are too haphazard to meet constantly growing requirements. Recommendations are made to develop a discipline of ommunication sciences through university academic programs.

**0804.** Weitzel, D. H., Sindt, C. F., Daney, D. E., **Hydrogen slush density reference system,** (Proc. 1967 Cryogenic Engineering Conf., Stanford University, Stanford, Calif., Aug. 21-23, 1967), Chapter in *Advances in Cryogenic Engineering* **13,** 523-533 (Plenum Press Inc., New York, N.Y., 1968).

Key words: Densitometer; density reference system; liquid hydrogen; nuclear radiation attenuation; slush hydrogen.

A hydrogen slush density reference system has been designed for calibration of field-type instruments and/or transfer standards. The device is based on the buoyancy principle of Archimedes. The solids are weighed in a light-weight container so arranged that solids and container are buoyed by triple-point liquid hydrogen during the weighing process. Nuclear radiation attenuation is considered as the most likely candidate for a transfer standard, and preliminary results obtained with a NRA densitometer are presented. The densitometer was used as an aid to determine pressure drop data for various slush hydrogen concentrations.

**10805.** Winogradoff, N. N., Kessler, H. K., **Compensation and band tailing effects in high power room temperature GaAs lasers,** *Solid State Commun.* **5,** 155-158 (1967).

Key words: Compensation with donors; expitaxial gallium arsenide lasers; laser characteristics.

A reduction in the density of states of a two level system would facilitate the production of an inverted electron population. Such a low density of states system can be produced by the incorporation of shallow donors into p-type material in such concentrations that mergence of the impurity bands with the intrinsic bands result in the formation of "tails" of states at the bottom and top of the intrinsic conduction and valence bands respectively.

The low density of states in these tails results in low room temperature thresholds, negligible time delays between the leading edge of the current pulse and the onset of lasing and high peak power outputs.

The behaviour of a series of vapour phase, epitaxially formed, p-n junctions with and without compensation will be discussed and recent achievements in high power outputs with compensated lasers will be described and correlated with field effect experiments, the results of which show that the enhanced light output in compensated material is not due to radiative transitions between acceptor and donor impurity centers.

**10806.** Yakowitz, H., Vieth, D. L., Heinrich, F. J., Michaelis, R. E., **Homogeneity characterization of NBS spectrometric standards. II: Cartridge brass and low-alloy steel,** (Proc. 14th Annual Conf. Applications of X-ray Analysis, University of Denver, Denver Research Inst., Denver, Colo., Aug. 25-27, 1965), Chapter in *Advances in X-ray Analysis,* G. R. Mallett, M. Fay, and W. M. Mueller, eds., **9,** 289-303 (Plenum Press Inc., New York, N.Y., 1966).

Key words: Electron probe microanalyzer; homogeneity—standards; NBS cartridge brass; NBS low-alloy steel; optical metallography; solids mass spectrometer; standards of composition.

Most modern instrumental methods of analysis depend on the use of known standards of composition for calibration. Newer analytical techniques such as the solids mass spectrometer, laser probe and, especially, the electron probe microanalyzer have reduced the amount of a sample which can be analyzed quantitatively to a range of about 0.1 micrograms to as little as 0.00005 micrograms. Corollary to these microanalytical advances, homogeneity requirements have become severe for the analytical standards. This paper describes a continuation of the NBS effort to more fully characterize existing standards as to suitability for the new microanalytical techniques (1). An NBS cartridge brass sample in both the wrought (NBS-1102) and chill cast forms (NBS-C1102), as well as a low alloy steel sample (NBS-463), have been investigated by means of electron probe microanalysis and optical metallography. Some seventeen elements are contained in the brass while twenty-five elements are in the steel. Results for ten elements in the steel are presented while results for six elements in the brass are given. In the steel, Fe, Ni, Cu, and Si are essentially distributed homogeneously at micron levels while Mn, Ta, Nb, Zr, S, and Cr are not. In the brass, Cu and Zn are distributed homogeneously at micron levels while Pb, S, Al, and Si are not. Electron probe microanalyzer results indicate that both NBS-1102 and NBS-C1102 brass are suitable for use as a calibration standard for electron probe microanalysis as well as other microanalytical techniques such as the solids mass spectrometer. The results for brass have been corroborated by a number of laboratories using the electron probe analyzer.

**10807.** Yee, K. W., Deslattes, R. D., **Transistorized current stabilizer for x-ray tubes with directly heated cathodes,** *Rev. Sci. Instr.* **38,** No. 5, 637-638 (May 1967).

Key words: Controlled; current; emission; impedance; regulator; stabilizer; x-ray tube.

An instrument is described which stabilizes the emission current in x-ray tubes with directly heated cathodes. Transistors are used in the amplifier and loading circuits. Emission currents from 20 mA to 1 A are maintained constant to within 0.1 percent for periods of about a half-hour.

**10808.** Yolken, H. T., Kruger, J., **Thermal regeneration of oxide covered iron {100} and {110} surfaces,** *J. Electrochem. Soc.* **114,** No. 8, 796-799 (Aug. 1967).

Key words: Ellipsometer; iron; oxidation; thermal regeneration.

The effects of ultra-high vacuum annealing on thin oxide films grown to a limiting thickness at room temperature on {100} and {110} iron surfaces were studied using an ellipsometer. After vacuum annealing at 400 °C or above, these films grew when reexposed to $1 \times 10^{-5}$ torr of oxygen at 25 °C. This process could be repeated several times, with the film each time exhibiting a greater limiting thickness until a thickness was reached which could not be appreciably increased by further annealing.

The thermal regeneration of oxide covered iron can be explained by a phase change of the oxide film from $Fe_3O_4$ to FeO on annealing at about 400 °C or above. Cooling to room temperature causes the reappearance of $Fe_3O_4$. Thin areas in the oxide film and some enrichment of iron in the film are the results of the phase changes. Concurrently, the adsorbed monolayer of oxygen anions is incorporated into the oxide during annealing.

**10809.** Yolken, H. T., Kruger, J., Calvert, J. P., **Hydrogen in passive films on Fe,** *Corrosion Sci.* **8,** 103-108 (1968).

Key words: $\gamma$-$Fe_2O_3$: iron passivity; tritium.

The use of radiochemical techniques involving tritium has shown that when a passive potential is observed for iron passivated either by immersion in a 0.1N $NaNO_2$ aqueous solution or by anodic polarization in a $Na_2B_4O_7 - H_3BO_3$ aqueous solution (pH 8.4) hydrogen is found in the film formed. By potentiostatic reduction of this film it was found that most of the hydrogen was in the outer layer, which was reducible at potentials less negative than that required to reduce $Fe_3O_4$. Approximately 0.06 percent hydrogen was found in the outer layer. Besides cathodic reduction, hydrogen could be removed from the film by using chloride ions or lowering the pH.

**10810.** Younglove, B. A., **Polarizability, dielectric constant, pressure, and density of solid parahydrogen on the melting line,** *J. Chem. Phys.* **48,** No. 9, 4181-4186 (May 1, 1968).

Key words: Dielectric constant; melting pressure; parahydrogen; polarizability; solid density.

Polarizibilities, calculated from measurements of the dielectric constant, are reported for solid parahydrogen on the melting line between 18 and 320 atmospheres (14.4 to 22.2 °K). Also new melting pressures below 17 °K are presented. Previously reported solid densities are adjusted slightly, using the new resulting pressure data. Liquid parahydrogen polarizibilities were determined over part of the density range of the solid and are seen to be slightly less than the solid polarizibilities.

**10811.** Zwanzig, R., Lauritzen, J. I., Jr., **Exact calculation of the partition function for a model of two-dimensional polymer crystallization by chain folding,** *J. Chem. Phys.* **48,** No. 8, 3351-3360 (Apr. 15, 1968).

Key words: Chain-folding; equilibrium statistical mechanics; partition function; phase transition; polymer crystals.

A model of two-dimensional polymer crystallization by chain folding is treated by equilibrium statistical mechanics. The Laplace transform of the partition function with respect to the length of the polymer chain is obtained in exact analytical form. The model leads to thermodynamically well defined chain folded crystals. Under certain circumstances in the limit of an infinitely long polymer chain, the model shows a second order phase transition from an "extended chain" crystal to the chain folded crystal.

**10812.** Weissberg, A., **Data handling systems,** (Proc. Second Conf Technical Information Center Adminstration, St. David's Pa., June 14-17, 1965), Chapter 7 in ***TICA* 2,** A. W. Elias, ed., pp. 75-89 (Spartan Books, Washington, D.C., 1965).

Key words: Data systems; information handling experts technical information.

The discussion emphasizes the intellectual organization o data systems and covers briefly the equipment used in suc systems. It concentrates on the reason why a particular dat system is needed, how it is defined and developed, and the organizational relationships in its development and operation.

The conclusions suggested are that the data system b adequately funded, established on the basis of a well understoo need, organized and operated by subject matter specialists, hav proper guidance from information handling experts, work withi well defined subject and organizational boundaries, and b responsive to the continuing needs of the technical community

**10813.** Acquista, N., Abramowitz, S., Lide, D. R., **Structure o the alkali hydroxides. II. The infrared spectra of matrix isolate CsOH and CsOD,** *J. Chem. Phys.* **49,** No. 2, 780-782 (July 15 1968).

Key words: CsOH; high temperature; infrared; molecula geometry; vibrational assignment.

The infrared spectra of matrix isolated CsOH and CsOD hav been observed. Both the CsO stretching mode and the bendin mode have been assigned for each isotopic species. $\nu_1$ of CsOH is at 335.6 cm$^{-1}$, while a value of 330.5 cm$^{-1}$ is found for CsOD $\nu_2$ is found at 306 cm$^{-1}$ for CsOH and at 226 cm$^{-1}$ for CsOD The isotope shift observed for $\nu_2$ confirms the essentially linea structure which was indicated by the microwave spectrum.

**10814.** Ahearn, A. J., Paulsen, P. J., **Workshop on mass spe trometric analysis of solids at the National Bureau of Standard in Gaithersburg, Md., Nov. 18 and 19, 1968,** *Anal. Chem.* **4** No. 2, 79A-81A (Feb. 1969).

Key words: Background; electrical detection; electric discharge; ion probe; ion sensitive plates; mass spe trometry; pelletizing; precision; relative sensitivity; sampl homogeneity; solids; statistics.

A Workshop on Mass Spectrometric Analysis of Solids was ponsored by and held at the National Bureau of Standards on Nov. 18, 19, 1968. The purpose of the workshop was to discuss roblems and factors that influence the accuracy and precision f analysis of solids by mass spectrometric techniques.

The topics considered, each led by a discussion leader, were 1) accuracy and precision problems, (2) surface analysis, (3) ample problems, (4) electrical discharge type ion sources, and 5) ion sensitive plate problems.

Five committees of four people each met during the first eveing or at the end of the workshop to summarize the treatment of he five topics. Abstracts of these summaries are presented.

**0815.** Altschuler, H. M., **Comments on "An improved method for measuring scattering parameters of nonreciprocal two-ports,"** *IEEE Trans. Microwave Theory Tech.* **MTT-16,** No. 4, 261-262 (Apr. 1968).

> Key words: Measurement; microwave; network; nonreciprocal; scattering parameters; two-port.

This letter points out that part of work described as new by Hoffman and Willem was already published by this author five ears ago and that the new aspect of their work most likely can e expected to reduce measurement uncertainty only if certain recautions are taken.

**0816.** Amano, T., Saito, S., Hirota, E., Morino, Y., Johnson, D. R., Powell, F. X., **Microwave spectrum of the ClO radical,** *J. Mol. Spectry.* **30,** No. 2, 275-289 (May 1969).

> Key words: Chlorine monoxide; free radical; hyperfine structure; microwave spectrum; rotational transitions; Stark effect.

Rotational transitions in the $^2\Pi_{3/2}$ and $^2\Pi_{1/2}$ electronic states have been investigated for both the $^{35}$ClO and $^{37}$ClO radicals by means of Stark modulated microwave spectrometers. Improved values were obtained for the rotational constants, Λ-doubling parameter and hyperfine constants of both radicals. It was found necessary to consider the effect of centrifugal distortion in order to determine the dependence of the spin-orbit coupling constant A on the internuclear distance. The distortion constant $D_e$ was found to be 0.077 ± 0.016 MHz and the value of $A' = (r\,dA/dr)$ at the equilibrium internuclear distance was 320 ± 60 cm$^{-1}$, assuming a value for A determined from electron-paramagnetic-resonance data.

The equilibrium internuclear distance $r_e$ was calculated to be .569±0.001 Å from the rotational constants $B_0$ for $^{35}$ClO and $^{7}$ClO. A detailed analysis of the second order Stark effect of the $F = 0 \leftarrow 1$ and $F = 1 \leftarrow 1$ components of the upper series of the $J = 3/2 \leftarrow 1/2$ rotational transition in the $^2\Pi_{1/2}$ state of $^{35}$ClO was performed and the electric dipole moment was determined to be .239±0.010 D. This value was confirmed for the $^2\Pi_{3/2}$ state of $^{5}$ClO where the Stark effect is first-order for weak electric fields. The indicated uncertainties are three times the standard errors of the reported value.

**0817.** Ambler, E., Schooley, J. F., Colwell, J. H., Pfeiffer, E. R., Frederikse, H. R., Hosler, W. R., Thurber, W. R., **Transition temperatures and critical fields of $SrTiO_3$ and mixed titanates,** *Proc. Xth Intern. Conf. Low Temperature Physics, Moscow, U.S.S.R., Aug. 31-Sept. 6, 1966,* **Vol. 2B,** *Superconductivity,* Paper S123, 142-148 (1968).

> Key words: $(Ba_xSr_{1-x})TiO_3$; $(Ca_ySr_{1-y})TiO_3$; critical fields; magnetic moment; penetration depth; semiconducting systems; $SrTiO_3$; superconducting; transition temperature.

The experimental investigation of the superconducting properies of the semiconducting systems $SrTiO_3$, $(Ba_xSr_{1-x})TiO_3$, and $(Ca_ySr_{1-y})TiO_3$ is reviewed. The studies of a.c. magnetic susceptibility, which yields transition temperature and penetration depth; of heat capacity, which yields the electronic density of states and transition temperature; and of magnetic moment, which yields first and second critical fields and transition temperature, are discussed briefly. Tables of experimental values of the parameters mentioned above are included.

**10818.** Anderson, H. J., Brenner, A., **Preparation of rhenium hexafluoroacetylacetonate,** *J. Electrochem. Soc.* **116,** No. 4, 513 (Apr. 1969).

> Key words: Hexafluoroacetylacetonate; rhenium; vapor deposition.

A brief account is given of the work now in progress on methods of preparing the rhenium derivative of hexafluoroacetylacetone. This compound can be vaporized without decomposition.

**10819.** Arenhovel, H., **General formulas for describing the absorption of polarized photons by oriented nuclei,** *Phys. Rev.* **171,** No. 4, 1212-1216 (July 20, 1968).

> Key words: Electromagnetic transition; matrix elements; nuclear orientation; orientation parameter; photo absorption; photon polarization; polarizabilities.

The absorption cross section of polarized photons by oriented nuclei is given in terms of the nuclear orientation parameters and the photon polarization parameters for linear and circular polarization. All quantities are given in terms of the nuclear polarizabilities which contain the electric and magnetic transition matrix elements.

**10820.** Arenhovel, H., Danos, M., **Baryon resonances in nuclei: Magnetic moment anomaly in $^3$H and $^3$He,** *Physics Letters* **28B,** No. 5, 299-301 (Dec. 23, 1968).

> Key words: Exchange currents; magnetic moment anomaly; nuclear magnetic moments; nuclear structure baryon resonances; resonance photoproduction.

The exchange current contributions to the static magnetic moments of $^3$H and $^3$He are described by the admixture of baryon resonance to the ground state. It is found that the dominant contribution comes from the admixture of the N*(1470) in a spatial symmetric $^2S_{1/2}$ states by means of the magnetic photon-production matrix element. An admixture of about 1 percent would be sufficient to account for the magnetic moment anomaly.

**10821.** Arp, V., **Properties and preparation of high-purity aluminum,** *Proc. 1968 Summer Study on Superconducting Devices and Accelerators, Brookhaven National Laboratory, Upton, N.Y., June 10-July 19, 1968,* Part III, **BNL 50155 (C-55),** pp. 1095-11144 (Clearinghouse for Federal Scientific and Technical Information, Springfield, Va., Apr. 1969, $3.00).

> Key words: Aluminum; impurity; resistivity; skin effect; thermal conductivity.

The potential economy of using aluminum magnets operating at cryogenic temperatures was suggested by Post and Taylor in 1959, before the advent of high field superconductivity. A liquid hydrogen-cooled aluminum magnet was built and operated not long thereafter (Purcell and Payne, 1963), but by this time superconducting magnets seemed to be generally more attractive. Nevertheless, a small effort was carried on, since for some low duty cycle conditions aluminum appears to be more attractive than superconductors (Arp, 1965). We have continued a study of the properties of aluminum which are related to this type of application, and a major part of this paper summarizes this study and knowledge in a tutorial fashion. The final and minor section of the paper reports the current status on the availability of high-purity aluminum in technologically useful quantities.

**10822.** Arp, V. D., Kasen, M. B., Reed, R. P., **Magnetic energy storage and cryogenic aluminum magnets,** *Tech. Rept.* **AFAPL-TR-68-87** 122 pages (Air Force Systems Command, Wright-Patterson Air Force Base, Ohio, Feb. 1969).

Key words: Aluminum; cryogenics; magnetic energy storage; magnets; metallurgy.

Factors pertaining to aluminum magnet technology have been investigated. Industrial competence and capacity to produce super-purity aluminum have been improved. Methods of analyzing super-purity aluminum have been studied; in particular, the eddy-current decay technique of measuring electrical resistivity ratios between 4 and 295 K have been improved and used extensively. New devices used to sensitively measure stress, strain, and resistivity at 4 K have been developed.

Two major experimental programs were conducted. One pertains to the effects of internal defects, particularly grain boundaries and impurity elements, on the residual resistance ratio. It was found that no one process can be ascribed to the linear relationship between increasing grain size and decreasing resistance ratio. One significant mechanism proposed is that, in super-purity aluminum, grain boundary motion acts to sweep away impurity elements in solid solution, thus having a purifying effect.

The second program involved the relationships between applied stress, plastic strain, and electrical resistivity changes due to the introduction of dislocations and vacancies at 4 K. It was found that the change in resistivity at 4 K is related to $\epsilon^{1.19}$ where $\epsilon$ is the plastic strain.

**10823.** Ausloos, P., Rebbert, R. E., Lias, S. G., **Gas-phase photolysis of cyclohexane in the photoionization region,** *J. Phys. Chem.* **72,** No. 11, 3904-3914 (Oct. 1968).

Key words: Cyclohexane; free radicals; ions; photoionization; photolysis; superexcited molecules.

The photolysis of cyclohexane (I.P. = 9.88 eV) has been studied in the gas phase using 1470 Å(8.4 eV), 1236 Å(10.03 eV), and 1067-48 Å(11.6-11.8 eV) radiation. At the latter two wavelengths, ions and superexcited molecules are formed. Emphasis is placed on the measurement of accurate quantum yields at all three wavelengths through both chemical actinometry and saturation current measurements. The primary decomposition of the excited cyclohexane molecule: cyclo-$C_6H_{12}^* \rightarrow C_6H_{10} + H_2$ reported earlier for the photolyses at 8.4 eV and 10.03 eV, is also seen to occur at 11.6-11.8 eV. In addition, evidence is presented for ring opening, and rearrangement of the excited hexamethylene intermediate, followed by decomposition of excited intermediates are readily quenched by an increase in pressure, the quenching being more effective for deuterated than for non-deuterated species. On the other hand, little or no pressure effect on product formation is observed in the photolysis at 1067-48 Å. In the photolysis at 1067-48 Å, although the parent cyclohexane ions have sufficient energy to undergo fragmentation processes, it is demonstrated that fragmentation is negligible at pressures above 1 torr. Using the photoionization results, it also demonstrated that in the radiolysis, $M(C_6H_{12}^+)/N_i$ is 0.3 at 13 torr and 0.34 at 90 torr. Assuming that the fragmentation of the excited cyclohexane molecule observed in the photolysis at 11.6-11.8 eV is roughly representative of the superexcited molecule dissociation which occurs in the radiolysis, the 1067-48 Å photolysis product yields are used to derive a value of $N_{ex}/N_i$ of 0.1-0.3 for the radiolysis.

**10824.** Bach, R. L., Caswell, R. S., **Energy transfer to matter by neutrons,** *Radiation Res.* **35,** N. 1, 1-25 (July 1968).

Key words: Energy transfer coefficient; first collision dose; kerma; neutron dosimetry; neutron energy transfer; nuclear reactions.

Calculations of energy transfer (kerma) for neutrons from thermal to 18 MeV energy have been carried out for hydrogen, carbon, nitrogen, and oxygen and for ten compounds or mixtures including tissue. All pertinent nuclear reaction processes are included. The calculation demonstrates the importance of (n,charged particle) reaction processes which have been neglected in nearly all previous calculations. These processes dominate the energy transfer process in carbon, nitrogen, and oxygen above roughly ten MeV.

**10825.** Barber, D. J., Tighe, N. J., **Neutron damage in single crystal aluminum oxide,** *J. Am. Ceram. Soc.* **51,** No. 11, 611-617 (Nov. 1968).

Key words: Aluminium oxide; defects; electron microscopy; neutron damage dislocations; sapphire.

Synthetic aluminium oxide crystals were irradiated with fast neutrons to a dose of $1.8 \times 10^{20}$ nvt and examined by transmission electron microscopy. As-irradiated crystals contained damage on a fine scale, revealed by diffraction contrast and showed a 28 percent increase in Knoop diamond hardness compared with un-irradiated material. Annealing above 600 °C, which decreased the hardness, caused the small defect clusters to grow, forming dislocation loops on {1010} planes, with ⟨1010⟩ Burgers vectors. Vacancy and interstitial loops occurred. High temperature annealing caused the loops to interact to give dislocation segments; these tended to align with the ⟨1010⟩ and ⟨1120⟩ directions. Grown-in dislocations also began to climb at high temperatures but showed evidence of impurity pinning. Isolated platelike precipitates on {1010} planes were also observed in samples annealed at high temperatures. Possible effects of the observed damage on physical properties are considered and there is qualitative agreement between predictions and existing data.

**10826.** Barger, R. L., Hall, J. L., **Pressure shift and broadening of methane line at $3.39\mu$ studied by laser-saturated molecular absorption,** *Phys. Rev. Letters* **22,** No. 1, 4-8 (Jan. 6, 1969).

Key words: Laser; methane; pressure broadening; saturated molecular absorption; wavelength standard.

We study broadening and shift of a rotation-vibration line of methane at millitorr pressures. Saturation by the laser intracavity field allows investigation of the *very* sharp natural linewidth without Doppler broadening. Two lasers were independently locked to this transition with an offset of less than 3 kc/s, a reproducibility of $3:10^{11}$!

**10827.** Bates, R. G., **Equilibrium properties of acids and bases in amphiprotic mixed solvents,** (Proc. Symp. Equilibria and Reaction Kinetics in Hydrogen Bonded Solvent Systems, University of New Castle, Upon Tyne, England, Jan. 10-12, 1968) Chapter in *Hydrogen-Bonded Solvent Systems,* A. K. Covington and P. Jones, eds., pp. 49-86 (Taylor and Francis, London, England, 1968).

Key words: Acidity; medium effects; mixed solvents; solvation of ions; solvent effect; transfer energy.

Binary mixed solvents which contain water as one componen possess the capacity to react protolytically both with hydroge acids and with their conjugate bases. Although the acid-bas behaviour of many of these solvent mixtures resembles that o water in kind, wide differences of degree are observed. Futher more, there is evidence that solute-solvent interactions becom more complex as the dielectric constant of the mixed medium i lowered. The effect of adding an organic constituent to aqueou solutions of acids and bases is examined through summaries o data for standard electromotive forces, equilibrium constants, medium effects, and thermodynamic functions for the transfe rom water to mixed solvents of various compositions. Systems onsisting of strong and weak electrolytes in mixed solvents are onsidered. An attempt is made to identify the factors on which he observed solvent effect depends. In particular, the roles of ielectric constant, solvent basicity, hydrogen bonding, sorting f the two types of solvent molecules by the ions, and the formaion of ion pairs and higher aggregates are discussed. Recent roposals for the establishment of a useful scale of individual onic transfer energies for mixed solvents are reviewed.

**0828.** Bay, Z., Luther, G. C., **Locking a laser frequency to the time standard,** *Appl. Phys. Letters* **13,** No. 9, 303-304 (Nov. 1, 1968).

Key words: Electrooptic modulation; optical frequencies; velocity of light.

On the basis of high frequency modulation experiments and vell known locking techniques, a scheme is described for staiilizing a visible laser frequency and simultaneously determining hat frequency in terms of the time standard. The importance of his method for a refined determination of the velocity of light nd the possibility of establishment of reference lines for specroscopy and for length measurements, throughout the spectrum vherever laser lines are available, is discussed.

**0829.** Beatty, R. W., **Discussion of effect of realizability conditions upon estimated limits of mismatch error in the calibration of fixed attenuators,** *IEEE Trans. Microwave Theory Tech.* **MTT-16,** No. 11, 976 (Nov. 1968).

Key words: Attenuation; microwave; mismatch error; realizability; 2-ports.

The effect or realizability conditions for 2-ports upon the estimation of mismatch error is discussed. Only the case of the inserion of fixed, symmetrical, reciprocal 2-ports is considered. It is shown that the effect of realizability conditions needs to be considered only for certain ranges of attenuation and VSWR. Most ttenuators encountered in practice do not fall within those anges so that the conventional method of estimating mismatch rror limits is usually satisfactory.

**10830.** Beatty, R. W., Fentress, G. H., **An attenuation and phase shift divider circuit,** *Proc. IEEE* **56,** No. 11, 2063-2064 (Nov. 1968).

Key words: Attenuation; circuit; rotary vane attenuator.

An attenuation divider circuit is described. The theory is resented for accurate division of small attenuation changes by arbitrarily selected ratios, and the procedure for adjusting the circuit is described. The circuit is useful for accurately producing small attenuation changes such as 0.0001 decibel, which is outside the capability of most attenuators.

**10831.** Beckett, C. W., Cezairliyan, A., **High-speed thermodynamic measurements and related techniques,** Chapter 14 in *Experimental Thermodynamics,* J. P. McCullough and D. W. Scott, eds., **Vol. I,** *Calorimetry of Non-reacting Systems,* 551-585 (Butterworth and Co., London, England, 1968).

Key words: Experimental thermodynamics; high-speed thermodynamic measurements; shock wave techniques; thermodynamic measurements; thermodynamic properties.

The needs and requirements of high-speed measurement of thermodynamic properties and related high-speed techniques in millisecond and microsecond time domain are presented. High-speed generation of heat by electrical pulse methods is reviewed. The technique of the measurement of heat through the measurement of electrical quantities is discussed and the factors causing error are summarized. High-speed temperature measurement methods, both photoelectric and photographic, are discussed. Other related subjects, such as high-speed photography, dynamic pressure measurements, fast x-ray and interferometry, are reviewed briefly. Applications of high-speed measurements to the determination of properties, such as specific heat, thermal diffusivity, electrical conductivity, are presented. Measurement of thermodynamic properties by shock wave techniques is reviewed. Other applications of high-speed measurement techniques in the areas of exploding conductors and high-temperature sources are also discussed.

**10832.** Bekkedahl, N., **Crystallization of natural rubber,** *Rev. Gen. Caoutchouc Plastiques* **45,** No. 3, 341-6—463-9 (1968).

Key words: Chain folding; contractility; crystallization; dilatometry; heat engine; melting; polymers; rubber; stark rubber.

This review article presents a resume of the research work that has been done at the National Bureau of Standards during the past thirty-five years in the field of crystallization of polymeris materials, with special emphasis on natural rubber. It contains only information on results of research work that has already been published.

**10833.** Bennett, H. S., **Diffuse and propagating modes in the Heisenberg paramagnet,** *Phys. Rev.* **174,** No. 2, 629-639 (Oct. 10, 1968).

Key words: Brillouin component; dynamic scaling theory; Heisenberg paramagnet; pair correlations; Rayleigh component; spectral weight function.

The spectral weight function for pair correlations is studied as a function of frequency $\omega$ and wave vector $q$ within the framework of the Heisenberg model for magnetism. The frequency regions $\omega\tau(q) \ll 1$ and $\omega\tau(q) \gg 1$ are examined for both the ferromagnet and the antiferromagnet in the paramagnetic state. The quantity $\tau(q)$ is a characteristic time of the system. It is shown that when $\omega\tau \ll 1$ a diffuse mode (Rayleigh component) dominates the spectral weight function and that when $\omega\tau \gg 1$ a propagating mode (Brillouin component) dominates the spectral weight function. A critical wave vector $q_c$ which separates these two regions is computed from microscopic theory and is found to scale according to the square root of the static susceptibility near the critical point. This latter microscopic result is identical in form to the result for the critical wave vector which separates the hydrodynamic and critical domains of dynamic scaling theory when the critical exponents are $\gamma = (413)$ and $\eta = 0$.

**10834.** Bennett, H. S., **Magnet scattering of neutrons from Heisenberg antiferromagnets,** *J. Appl. Phys.* **40,** No. 3, 1552-1553 (Mar. 1, 1969).

Key words: Heisenberg magnets; longitudinal diffusivity; longitudinal spectral weight function; moments; neutron scattering; $RbMnF_3$; sum rules.

The magnetic scattering of neutrons from Heisenberg antiferromagnets in the paramagnetic state is discussed within the rigorous framework of a spectral representation for the longitudinal spectral weight function, low order moments of this function, and sum rules. The longitudinal spectral weight function is expressed as a functional of the longitudinal diffusivity. The exact framework leads naturally to a phenomenological description of the neutron scattering cross section in Heisenberg antiferromagnets. It is shown that replacing the longitudinal diffusivity by the sum of a Gaussian function and a resonating function, which satisfies the sum rules, gives the essential features for neutron scattering in the Heisenberg antiferromagnet $RbMnF_3$.

**10835.** Bennett, H. S., **Phenomenology of neutron scattering in Heisenberg systems,** *Phys. Rev.* **176,** No. 2, 650-654 (Dec. 10, 1968).

Key words: Critical magnetic scattering; diffusivity; Heisenberg magnets; neutron cross section.

The critical magnetic scattering of neutrons from Heisenberg systems is discussed within the rigorous framework of spectral representations for the longitudinal and transverse spectral weight functions, low order moments of these functions, and their sum rules. The spectral weight functions are expressed as functionals of longitudinal and transverse diffusivities. This exact framework leads naturally to a two parameter phenomenological description of the neutron scattering cross section in Heisenberg ferromagnets. It is shown that replacing the diffusivities by two parameter Gaussian functions, which satisfy the first two sum rules, gives reasonable values for the neutron scattering cross section in ferromagnets.

**10836.** Bennett, L. H., **Nuclear magnetism,** Chapter 14 in *Magnetism and Magnetic Materials 1968 Digest,* H. Chang and T. R. McGuire, eds., pp. 201-221 (Academic Press, Inc., New York, N.Y., 1968).

Key words: Magnetic materials; Mössbauer effect; nuclear magnetic resonance; nuclear magnetism; nuclear specific heat; perturbed angular correlation.

This chapter reviews the 1967 literature that was devoted to the study of magnetism and magnetic materials taking advantage of the atomic nucleus as a probe. The bulk of the experimental papers utilize nuclear magnetic resonance (NMR or FNR) or recoilless-ray absorption, i.e. the Mössbauer effect (ME), as in previous years. Most of the NMR papers reviewed here are for ferromagnetic materials in the ordered state, for which we use the special abbreviation FNR. Other techniques for determining hyperfine (hf) magnetic fields ($H_{hf}$) include nuclear specific heat and perturbed angular correlation.

**10837.** Bennett, L. H., Mebs, R. W., Watson, R. E., **Solute Knight shifts in noble metals,** *Phys. Rev.* **171,** No. 3, 611-626 (July 15, 1968).

Key words: Ag; Al; alloys; Au; Cd; Cu; Ga; Hg; hyperfine fields; In; Knight shift; noble metals; P; Sn; susceptibility; Zn.

Knight shifts of Cu, Cd, Al, In, Sn and Ga as dilute solutes in Au/Hg and Al as dilute solutes in Ag; In as a dilute solute in Cu; and Sn as a dilute solute in Ag-Au alloys, are reported. These data are considered together with all other Knight shift data on dilute solutes in the 3 noble metals. Assuming the solute atom to be situated most nearly in a free conduction electron state when dissolved in Ag, the changes in Knight shift when dissolved in Cu or Au indicate a valence effect which is opposite in sense for these latter 2 noble metals. The Cd resonance linewidths for Au-Cd alloys show appreciable broadening with increase in alloy content or test frequency. Values of hyperfine fields for the free atom are presented together with alternative values of the paramagnetic spin susceptibility of the host. The problem of exchange enhancement of the spin susceptibility is discussed. Values for Knight's parameter $\xi$ usually considered as a measure of the amount of s-character in the metal are tabulated and discussed. The valence effects found in the Knight shifts, are also evident in the $\xi$ values. The requirement of orthogonalization of the conduction electron states to the metallic ion cores leads to a reconsideration of the origin of the solvent Knight shifts in noble metal alloys.

**10838.** Bennett, L. H., Swartzendruber, L. J., **Some comments on "The corrosion of materials in desalination plants,"** *Desalination* **4,** 389-390 (1968).

Key words: Alloys; copper; corrosion; desalination; iron; nickel.

The implications to testing and use of cupro-nickel alloys for desalination are described.

**10839.** Berger, M. J., Seltzer, S. M., Chappell, S. E., Humphreys, J. C., Motz, J. W., **Response of silicon detectors to monoenergetic electrons with energies between 0.15 and 5.0 MeV,** *Nucl. Instr. Methods* **69,** No. 2, 181-193 (Apr. 1969).

Key words: Detector response function; electron absorption; electron backscattering; electron transmission; silicon transmission detector.

By means of measurements as well as Monte Carlo calculations, response functions have been obtained which describe the pulse-height distributions produced by monoenergetic electrons incident perpendicularly on silicon detectors. Generally good agreement has been found between experimental and Monte Carlo results at energies of 0.25, 0.50, 0.75, and 1.00 MeV for detectors with thicknesses of 0.061, 0.105, 0.191, 0.530, 1.0, and 3.0 mm. Additional calculated results have been obtained as follows: (1) response functions at fifteen energies between 0.15 and 5.0 MeV for detectors with ten thicknesses between 0.05 and 10.0 mm; (2) response functions for arrangements in which the silicon detector is shielded partially or completely by other detectors operating in anticoincidence; (3) reflection, transmission and absorption coefficients of electrons for plane-parallel silicon targets.

**10840.** Berman, H. A., West, E. D., **Heat capacity of liquid nitromethane from 35° to 200 °C,** *J. Chem. Eng. Data* **14,** No. 1, 107-109 (Jan. 1969).

Key words: Heat capacity; nitromethane.

The heat capacity of saturated liquid nitromethane (under its own vapor pressure) has been determined in an adiabatic calorimeter to a precision of 0.1 percent between 35 and 200 °C, and may be represented in this range by the polynomial: $C_{sat} = 104.4_4 + 6.381_1 \times 10^{-2}t + 3.175_3 \times 10^{-4}t^2 - 8.131_8 \times 10^{-7}t^3 - 4.073_9 \times 10^{-9}t^4$, where $C_{sat}$ is in J/mol-deg C and t is in °C.

**10841.** Birmingham, B. W., ed., **A Report on the 1967 Applied Superconductivity Conference,** *Cryogenics* **8,** No. 3, 176-179 (June 1968).

Key words: Cryogenic refrigeration; superconducting electronics; superconducting magnets; superconducting materials; superconducting phenomena; superconducting power transmission; superconductivity.

The 1967 Applied Superconductivity Conference met at the University of Texas in Austin in response to a growing need for improved communications between researchers in superconductivity and potential users of new knowledge from industry government, private and national laboratories, and universities Invited papers presented the U.S. Bureau of Mines helium program, U.S. government programs in superconductivity, and superconductivity in Europe. Subjects covered in contributed papers included magnets and materials, computer devices, and phenomena and other devices. Two panel discussions highlighted superconducting power transmission and refrigeration. An exhibition of apparatus demonstrated superconducting phenomena and applications in addition to the latest cryogenic refrigerator developments and high field magnet materials and designs.

**10842.** Birmingham, B. W., Flynn, T. M., **National programs an the compressed gas industry,** (Proc. 55th Annual Meeting o the Compressed Gas Association, New York, N.Y., Jan 1968), Chapter in *The Future of the Compressed Gas Industry,* pp. 39-49 (Compressed Gas Assoc. Inc., New York N.Y., 1969).

Key words: Agriculture; compressed gases; conservation; cryogenics; education; health; national goals; space; transportation.

The object is to discuss a segment of the compressed gas instry, namely the cryogenic industry, and its relation to lected national programs, such as space, health, agriculture, ansportation, conservation, and education.

843. Blandford, J. M., Bensing, P. L., *Testing Programs for the Apparel Industry. Evaluation of Material and Components*, Part I, 31 pages; Part II, 222 pages (Apparel Research Foundation, Inc., Washington, D.C., Oct. 1, 1968).

Key words: Apparel materials; equipment, textile testing; fabric defects; physical properties, fabrics; programs, textile testing; test methods, textile; testing equipment, textile; textile testing.

This publication presents the details of minimum, interediate, and advanced textile testing programs for evaluating the pearance and performance properties of materials and compnents used by the apparel industries. Tabulations give testing quipment, properties its use may determine, testing procedures nd evaluation materials employed, and sources of supply and pproximate prices of the equipment and evaluation materials.

Included are: (1) sections on the significance of a textile testg program, conditioning for testing textiles, performance equirements for textile fabrics ((USA) Standard L22), and the vailability of short laboratory training courses for apparel comany employees; (2) reprints of the fifty-nine referenced test ethods.

0844. Blandford, J. M., **NBS-ARF apparel materials testing and evaluation project,** *Second Annual Conf. Apparel Research Foundation, Washington, D.C., Oct. 7-9, 1968*, 4 pages (Apparel Research Foundation, Washington, D.C., 1968).

Key words: Apparel materials; equipment, textile testing; physical properties, fabrics; programs, textile testing; test methods, textile; testing equipment, textile.

This address is a summary and final progress report of the Aparel Materials Evaluation Project on which the NBS and the pparel Research Foundation, Inc. (ARF) collaborated. It resents a discussion of the development and accomplishments f the Project with especial emphasis on its achievements which re two "firsts" for the apparel industry: (1) publication of the ook "Testing Programs for the Apparel Industry—Evaluation f Materials and Components" (published by the Apparel Research Foundation, Inc.); and (2) making available to the aparel industry (through nationally-recognized educational, esearch, and testing organizations) a short laboratory training rogram for apparel company employees. The book and training ourse complement one another.

10845. Botter, R., Rosenstock, H. M., **Franck-Condon factors for $NH_3$ and $H_2O$,** Chapter in *Advances in Mass Spectrometry* **4,** 579-589 (Institute of Petroleum, London, England, 1968).

Key words: Bond angle; bond length; Franck-Condon factors; $H_2O$; $NH_3$ ion; photo-electron; photo-ionization; spectroscopy.

10846. Boutillon, M., Henry, W. H., Lamperti, P. J., **Comparison of exposure standards in the 10–50 kV x-ray region,** *Metrologia* **5,** No. 1, 1-11 (Jan. 1969).

Key words: Air attenuation; analysis of uncertainties; correction factors; direct comparison; exposure standards; low-energy x rays.

Direct comparisons of the low-energy x-ray exposure standards of the International Bureau of Weights and Measures (BIPM) and the National Research Council of Canada (NRC), the BIPM and the National Bureau of Standards of the U.S.A. (NBS), were made, using x rays generated by 10, 30, and 50 kilovolts. The half-value layers for these qualities of radiation were $0.03_6$, $0.17_6$, and $2.25_7$ mm aluminum respectively. The results indicate that a direct comparison between two free-air chambers, in the low-energy x-ray region, can be precise to better than 0.3 percent. The uncertainties and errors in the geometric and correction factors used for the comparison measurements, as well as other systematic and statistical errors, were examined in detail and are reported. The results of preliminary work on the definition of the quality of radiation, air attenuation correction, diaphragm comparisons and saturation correction are included.

10847. Bowen, R. L., Cleek, G. W., **X-ray-opaque reinforcing fillers for composite materials,** *J. Dental Res.* **48,** No. 1, 79-82 (Jan-Feb. 1969).

Key words: Barium fluoride; composite materials; dental restorations; refractive index; reinforcing fillers; x-ray-opaque.

Clear, colorless glasses designed for use as part of the reinforcing fillers for composite dental restorative materials were prepared. They were formulated by melting together materials such as silica, boric oxide, alumina, barium oxide, and barium fluoride. Barium made the glasses radiopaque, fluoride lowered the refractive index, and alumina tended to stabilize the glasses.

10848. Bowen, R. L., Paffenbarger, G. C., Mullineaux, A. L., **A laboratory and clinical comparison of silicate cements and a direct-filling resin: A progress report,** *J. Prosthetic Dentistry* **20,** No. 5, 426-437 (Nov. 1968).

Key words: Clinical research; composites; color stability; dental materials; reinforced resins; silicate cements; solubility.

Two silicate cements showing a difference of about 0.7 percent solubility and disintegration in distilled water for 24 hours, showed approximately the same durability in clinical service during a four-to-six year period. There was more disintegration in the interproximal areas of the silicate restorations than there was in the self-cleansing areas.

An experimental reinforced resin gave sufficiently good results to warrent further clinical investigations of more recent and perhaps better composite formulations. Both unreinforced and reinforced resin materials appear to benefit from the use of a primer or "cavity seal."

10849. Bowen, R. L., Mullineaux, A. L., **Adhesive restorative materials,** *Dental Abstr.* **14,** No. 80, 80-82 (Feb. 1969).

Key words: Adhesion; alkylboron; coupling agents; cyanoacrylates; dental restorative materials; expoxy resins; isocyanates.

Available dental literature on adhesive dental restorative materials is reviewed.

10850. Branscomb, L. M., **Joint Institute for Laboratory Astrophysics of the National Bureau of Standards and the University of Colorado, Boulder, Colorado, observatory report,** *Bull. Am. Astron. Soc.* **1,** No. 1, 27-33 (Jan. 1969).

Key words: Annual summary; astrophysics; JILA.

This is an annual report of work accomplished in laboratory astrophysics at JILA (Joint Institute for Laboratory Astrophysics). No original technical material is presented.

**10851.** Branscomb, L. M., **Physics and the nation in a crystal ball,** *Phys. Today* **21,** No. 8, 23-28 (Aug. 1968).

Key words: Public policy in science.

This paper was prepared for presentation as part of a symposium on "The Coupling of Physics and Society in the Seventies" at a Special Joint Session of the American Physical Society and the American Association of Physics Teachers, Chicago, 30 January 1968.

**10852.** Brauer, G. M., McLaughlin, R., Huget, E. F., **Aluminum oxide as a reinforcing agent for zinc oxide-eugenol-o-ethoxybenzoic acid cements,** *J. Dental Res.* **47,** No. 4, 622-628 (July-Aug. 1968).

Key words: Alumina as a reinforcing agent; $Al_2O_3$ reinforced cements; crown and bridge; dental cements; EBA cements; zinc oxide-eugenol-EBA cements.

Aluminum oxide is a very effective reinforcing agent for *o*-ethoxybenzoic acid (EBA) cements. Addition of $Al_2O_3$ increases the amount of powder that can be incorporated into the mix. The compressive strength of the hardened cement is increased up to 1055 kg/cm$^2$ (15,000 psi) and the ADA film thickness decreased to 26$\mu$. The materials adhere to tooth structure as well as zinc phosphate cements and are suitable as crown and bridge cements. With higher powder-liquid ratios their high 10-minute compressive strength and excellent tissue tolerance suggests their use as bases under metallic restorations. These materials may also be employed as temporary restoratives. Mixes of $Al_2O_3$ and eugenol or glycerine may be of interest as a temporary non-hardening crown and bridge cement. Incorporation of $Al_2O_3$ whiskers did not improve the physical properties of these cements.

**10853.** Brinckman, F. E., Gordon, G., **Energetic intermediates in inorganic synthesis: characterization of transport species in electric discharge,** *Proc. Intern. Symp. Decomposition of Organometallic Compounds to Refractory Ceramics, Metals, and Metal Alloys, Dayton, Ohio, Nov. 1967,* pp. 29-46 (University of Dayton Press, Dayton, Ohio, Oct. 1968).

Key words: Boron; electric discharge; germanium; oxyfluorides; reactive intermediates; silicon; time-of-flight mass spectrometry; transport species.

Commercial processes involving energetic chemical transport and deposition reactions are poorly understood with respect to the identity and mechanistic behavior of their intermediates. Work is presented resulting from recent development of a facility for *in situ* sampling of electric discharge reactions by time-of-flight mass spectrometry. With use of single or mixed reactant gases to sustain a microwave discharge plasma, both homogeneous and heterogeneous reactions have been examined for synthetic potential under conditions of optimized energy input. A number of new compounds thereby have been identified with aid of computerized polyisotopic mass spectral analyses, but also by independent syntheses where known. Several important cases are presented with emphasis on oxyfluorides since both hetero- and homo-$\mu$-oxy-metalloid products form. These systems include Si-O-Si, Si-O-B, B-O-B, Si-O-Ge, Ge-O-Ge, and Ge-O-B species for which some relative stability data can be derived. Extension of these findings to analogous carbon-containing materials (derived from organometals or organometalloids) is also discussed.

**10854.** Broadhurst, M. G., **The dielectric properties of leaves, sticks, and dirt at radio and microwave frequencies,** *Proc. 1968 Annual Report Conf. Electrical Insulation and Dielectric Phenomena, Oct. 21-23, 1968, Buck Hill Falls, Pa.,* pp. 146-152 (Natl. Acad. Sci.—Natl. Res. Council, Washington, D.C., 1969).

Key words: Dielectric constant; dielectric loss; dielectri measurements; soil; vegetation.

The dielectric constant and loss of a variety of fresh leave were measured at room temperature from 0.1 MHz to 4.2 GHz A water displacement method was used with a single thicknes of leaf in a coaxial line. Capacitance and conductance wer determined with a bridge up to 250 MHz and a slotted line abov 250 MHz. The leaf is a high admittance shunt in the line and bot the real and imaginary components of the admittance could b measured within a few percent accuracy. The accuracy of th dielectric constant and loss values is limited to about 10 percen mainly by uncertainties in the sample thickness measurements The main features of the data are a Maxwell-Wagner type relaxation at about 10 MHz with a tan δ maximum of about 2. Both $\kappa$ and $\kappa''$ rise to about 10,000 at 0.1 MHz with a second relaxatio at lower frequencies apparent in the tan δ curve. Above 10 MHz, $\kappa'$ levels off at about 50 and above $10^9$ Hz a third relaxation—presumably due to the dipolar relaxation in water—appears. The results are surprisingly consistent among all varietie of leaves measured. Measurements were also made with reduce precision on twigs and clay at various moisture contents. Th measurement techniques, and evaluation of errors of the metho will be described together with the data.

**10855.** Brockman, J. F., **Popular science writing,** *Proc. 1967 Ins Technical Industrial Communications, Colorado Stat University, Ft. Collins, Colo., June 12-16, 1967,* pp. 96-10 (1967).

Key words: Image of science; lead paragraphs; popula science writing; science writers; science writing; scienc writing goals.

The term popular science writing carries connotations of superficiality and inaccuracy. But, if we are to convey understanding of science to the public—and I think it critically importan that we do so—we must make the efforts required to reverse th concept. I believe that this requires thoughtful consideration o our basic goals and of the images which we create of our organization, of its staff, and of science in general. Thus, it require clear understanding on our part of what we want to say, of wha we actually say, and of why we handle a particular subject in certain fashion.

The development of our material must, of course, be clear, an it must be interesting. The interesting features which w emphasize, however, must be valid. They must grow from th subject matter and not be artificially imposed by the writer. Th must be true not only of the story as a whole but also of the lea paragraphs where the pressure to gain attention is greatest.

In conveying understanding of science, there is room for improvement in all groups involved in the process, but the greate burden of responsibility is our own as science writers.

**10856.** Brooks, R., Horton, A. T., Torgesen, J. L., **Occlusion o mother liquor in solution-growth crystals,** *J. Crystal Growth* 279-283 (1968).

Key words: Ammonium dihydrogen phosphate; crystal defects; crystal growth; crystal-growth forms; mother-liqu inclusions; occlusions in crystals; sodium chlorate; solutio grown crystals.

Inclusions of mother liquor, comprising major defects i crystals grown from solution, are sometimes formed when th level of the supersaturation increases. The change in crystallization driving force can cause irregular growth or hopper growt particularly on fast growing faces if they are present, even whe the solution is strongly stirred and when the change of supersaturation is relatively slight; and inclusions can be formed by ove growth of the irregularities either by faces contiguous to the a cted face, or, if supersaturation is diminished, by development a new face of the kind that was originally present. When am- onium dihydrogen phosphate crystals or sodium chlorate ystals are grown under such conditions that their habits are aracterized by several forms, those faces which grow most pidly provide the primary sites for occlusion of mother liquor hen supersaturation is increased.

The results can be explained if formation of growth centers on ystal faces is sensitive to supersaturation so that location of ese centers is dictated by considerations of solute supply if su- ersaturation rises above a limiting value.

857. Brown, P. J., **Human factors research in motor vehicle occupant restraint systems,** *IEEE Trans. Man-Machine Systems* **MMS-9,** No. 3, 88-89 (Sept. 1969).

> Key words: Highway safety; human factors research; motor vehicle restraint systems.

The national program in highway and motor vehicle safety has ovided a new stimulus to human factors research by agencies f the Federal Government. An important area included in their st was the protection of occupants of a motor vehicle from inju- during a crash. This paper will describe some results of human ctors research in motor vehicle occupant restraint systems by e Office of Vehicle Systems Research in the National Bureau f Standards.

0858. Bullis, W. M., **Measurement problems in microcircuit processing,** (Proc. Government Microcircuit Applications Conference, Gaithersburg, Md., Oct. 1-3, 1968), *GOMAC Digest* **1,** 215-217 (Office of Naval Research, Washington, D.C., Oct. 1968).

> Key words: Microelectronics; monolithic microcircuits; reliability; semiconductor devices; silicon; test methods.

Attempts to meet reliability and interchangeability requirements for microcircuits solely by post-fabrication testing have roven to be extremely expensive and, at the same time, not ompletely successful. Since variations in materials and rocessing cause a given type of circuit to have a range of haracteristics, both reliability and interchangeability are af- ected. With suitable measurement procedures, these variations ould be better controlled. The first step is the establishment of rocedures with adequate sensitivity and reproducibility at all tages of microcircuit fabrication from specification and evaluation of the starting materials through the final processing steps. n many cases this can be accomplished with only incremental mprovements in existing procedures although in other cases ew methods or even new tests must be developed. Once such rocedures are available, tests for relevance can be undertaken nd then the specification, evaluation, and process control equence can be refined. A broad program intended to assist in he development of improved test methods is now in progress at he National Bureau of Standards. This program will be iscussed briefly in order to indicate the scope of problems encountered and the approach being employed to solve them.

10859. Bur, A. J., Roberts, D. E., **Rodlike and random coil behavior of poly(n-butyl isocyanate) in dilute solution,** *Proc. 1968 Annual Report Conf. Electrical Insulation and Dielectric Phenomena, Oct. 21-23, 1968, Buck Hill Falls, Pa.,* pp. 17-21 (Natl. Acad. Sci.—Natl. Res. Council, Washington, D.C., 1969).

> Key words: Dielectric constant; dielectric relaxation time; dipole moment; molecular relaxation in dilute solution; poly(n-butyl isocyanate); rodlike molecules.

Measurements of the complex dielectric constant $\epsilon^* = \epsilon' - i\epsilon''$ have been made on dilute solutions of fractionated poly(n-butyl isocyanate) (PBIC) in $CCl_4$. The measurements, which were carried out at 23 °C and over a frequency range 0.05 Hz to 1 mHz, yielded relaxation times and dipole moments of PBIC as a function of molecular weight where $M_w$ varied from $2.0 \times 10^4$ to $10 \times 10^6$. For low $M_w$ ( $< 250{,}000$) the relaxation time data indicate that the molecule is in a rigid rod conformation. As $M_w$ increases this rodlike conformation can not be sustained and the effects of chain flexibility accumulate with the addition of each monomer unit to the chain. Finally at high $M_w$ ( $> 10^6$) the dominant mode of relaxation is a long-range Rouse-Zimm normal mode and the conformation of the molecule is random coil. For these two conformations of PBIC, rigid rod and random coil, the molecular dimensions and dipole moments are calculated.

**10860.** Cahill, K. E., **Pure states and the P representation,** *Phys. Rev.* **180,** No. 5, 1239-1243 (Apr. 25, 1969).

> Key words: Coherent states; density operator; distribution theory; electromagnetic field; photon statistics; P representation; pure states; quantum optics; representation theory.

The coherent-state P representation for the density operator of the electromagnetic field is studied for the case in which the density operator represents a pure state, $\rho = |\psi\rangle\,\langle\psi|$. An exact and complete characterization is given of the states for which the P representation exists with a weight function $P(\alpha)$ that is a tempered distribution. These states $|\phi\rangle$ form an exceedingly narrow class: each may be generated from a particular coherent state $|\alpha\rangle$ by the application of a finite number of creation operators, i.e., $|\phi\rangle = [c_0 + c_1 a^+ + \ldots + c_n (a^+)^n]|\alpha\rangle$, where $\alpha$ and the $c_n$ are arbitrary complex numbers. For them the weight function $P(\alpha)$ is a linear combination of the two-dimensional delta function and a finite number of its derivatives. For other pure states the function $P(\alpha)$ has singularities that are not compatible with the form of the P representation.

**10861.** Cameron, J. M., **The statistical consultant in a scientific laboratory,** *Technometrics* **11,** No. 2, 247-254 (May 1969).

> Key words: Consulting; statistical consultation; statistics.

The responsibilities of the statistical consultant who is a regular staff member of a scientific institution are discussed. The effects of the continuing nature of his association with the organization, and of the fact that extended collaboration with the individual scientists is the rule, not the exception, are described. The importance of the statistician's educational role in providing lectures, courses, manuals, etc., which are tailor made for the needs of his organization is emphasized, along with the duty to provide computer aids for statistical analysis and data handling designed for the convenience of the using scientist.

**10862.** Campbell, W. H., **Aurora,** *Encyclopedia of Atmospheric Sciences and Astrogeology,* R. W. Fairbridge, ed., pp. 105-106 (Reinhold Publ. Co., New York, N.Y., 1967).

> Key words: Atmospheric physics; aurora; solid-earth geophysics.

This "Aurora" article is a brief description, designed for mature scientists with no upper atmospheric physics background.

**10863.** Carter, G. C., **The NBS Alloy Data Center,** *Mater. Res. Bull.* 3, 919-922 (1968).

Key words: Alloys; automated; bibliography; data; files; indexing computer programs; information; metals; physical properties; reference books (material).

A summary of the detailed description of the Alloy Data Center is presented.

**10864.** Case, W. E., Harrington, R. D., **Hysteresis effects in the slope calibration method for magnetometers,** *Proc. IEEE* **56,** No. 10, 1733-1734 (Oct. 1968).

Key words: Magnetization; magnetometer calibration; vibrating-sample magnetometer.

The slope method for calibrating vibrating sample magnetometers requires spherical samples of high permeability such that

$$(\mu+2)/(\mu-1) \approx 1.$$

It is shown that the presence of a small remanence in the calibration spheres results in an effective permeability that is as great if not greater than the initial permeability which is often used in the above equation. This even higher permeability further increases the validity of this approximation.

**10865.** Casella, R. C., **Decay modes with coherent resonant-energy transfer between deep impurities in solids,** *Phys. Rev.* **174,** No. 3, 830-834 (Oct. 15, 1968).

Key words: Coherence; decay modes; impurities; resonant-energy transfer.

Attention is called to the existence of new decay modes for deep impurities in solids associated with coherence in the resonant-energy transfer between them. The theoretical decay rate R of the two-impurity complex is of the form, $R(t) = C_1 \exp(-\gamma_1 t) + C_2 \exp(-\gamma_2 t) + \exp[-1/2\ (\gamma_1+\gamma_2)t] \times \mathrm{Re}\ D \exp(-i\Delta t)$, with $C_n$ and $\gamma_n$ real positive and D complex. The oscillations in time, t exhibited by the third term in the expression for R provide an experimental test for the coherence effect. The partial rate $R_\nu(t)$ for radiative decay is of the same form as R(t). In the analysis, use is made of an analogy between the decay of the excited impurity complex and that of K° mesons in particle physics, where similar coherent oscillations have been observed experimentally.

**10866.** Casella, R. C., **Time reversal and the K° meson decays. I,** *Phys. Rev. Letters* **21,** No. 15, 1128-1131 (Oct. 7, 1968).

Key words: Decay rates; symmetry; TCP; time reversal.

Based upon present data, we show that time reversal symmetry is violated, independently of how the vital question concerning possible TCP asymmetry is ultimately resolved.

**10867.** Casella, R. C., **Time reversal and the K° meson decays. II,** *Phys. Rev. Letters* **22,** No. 11, 554-556 (Mar. 17, 1969).

Key words: CPT theorem; decays; mesons; time reversal; weak interactions.

Current data on the $K^\circ \rightarrow 2\pi$ decays are used to extend the results of an earlier analysis testing these reactions for T invariance irrespective of CPT symmetry. The extended analysis together with recent work on pion production data allow us to establish that T is not conserved in these decays.

**10868.** Cassel, J. M., Gallagher, J., Reynolds, J. A., Steinhard J., **The role of transport ion binding studies of serum albumi** *Biochemistry* **8,** No. 4, 1706-1713 (Apr. 1969).

Key words: Albumin; binding; detergent; dialysis; kineti anomalies in dialysis; long-chain ligands; protein concentration effects.

Two hypotheses previously suggested to explain the apparen dependency on protein concentration of equilibrium dialysi measured binding of long-chain ionic ligands to bovine serum a bumin have been tested and disproved. Of greater importance, i is shown that the apparent protein concentration effect was a experimental artifact which originated in the anomalously slo approach to equilibrium with these ligands under the condition of the earlier experiments. The effects of protein concentratio ligand size, supporting electrolyte and temperature on the approach to dialysis equilibrium is examined. Hitherto unobserve and only partially understood kinetic anomalies occur when ioni ligands of high affinity are dialyzed *into* protein solutions whic are appreciably more concentrated than 0.1 percent.

**10869.** Cassel, J. M., Steinhardt, J., **Limitations inherent in th ΔpH method of determining binding isotherms of bovine seru albumin,** *Biochemistry* **8,** No. 6, 2603-2609 (June 1969).

Key words: Anion binding; anionic detergents; bovin serum albumin; electrostatic interaction factor; equilibriu dialysis; hydrophobic interaction; permselective membran Scatchard-Black method.

Binding isotherms, determined by the ΔpH method o Scatchard and Black, of a large variety of aliphatic and aromati anions, containing up to 14 carbon atoms, have been compare with isotherms obtained with the same substances by equilibriu dialysis and in two instances by measurement of potentia across permselective membranes. With symmetric non-deformable ions e.g., aromatic anions, the ΔpH method gives results i good agreement with those determined by dialysis. Wit aliphatic long chain anions, the amount of binding and the binding constants are systematically underestimated by factors whic increase with the affinity. In these comparisons due regard ha been taken of (a) the effects of the necessary differences in th amounts of competing electrolyte present when each of the thre methods is used, and (b) need to correct for the lack of bufferin capacity in very dilute solutions of unbuffered protein. Tw methods for evaluation of an empirical electrostatic factor from the ΔpH binding measurements in 0.001 M NaCl a discussed. Explanation of the much lower ω so computed fro that calculated by application of Debye-Hückel theory is soug in terms of applicability of the Linderström-Lang model to no covalently bound long chain ions with hydrophobic tails and ( differences between the effective charge Z of the macroion an the charge computed stoichiometrically. It is shown that as practical matter the ΔpH method cannot be applied to any ligan of high affinity ($K > 10^5$) because of the large effect in th method of small errors in determining concentration or prote molecular weight.

**10870.** Cassidy, E. C., Abramowitz, S., **Time-resolved emissio and absorption studies of exploding wire spectra,** (Proc. 4 Conf. Exploding Wires, Boston, Mass., Oct. 18-21, 1967

Chapter in *Exploding Wires* **4,** 109-124 (Plenum Press Inc., New York, N.Y., 1968).

Key words: AlO; electrical discharges; exploding wire; time-resolved spectroscopy; TiO.

Emission and absorption studies of the spectra produced by ploding wires in oxygen, nitrogen, hydrogen, or argon at- ospheres are described. A drum camera and a rotating shutter e used for continuous and time-resolved recording of the explo- on spectra. A high-intensity light source (a second exploding re or Lyman flashtube), synchronized with the rotating utter, is flashed through the explosion vapor for the absorption udies. Results from experiments performed under a variety of ntrolled conditions are presented. Effects of environment, essure, and electrical energy on the spectrum are discussed, d conditions found conducive to production of selected fea- res are indicated. The exploding wire is shown to be a rich urce for study of the AlO molecule, and observation of a umber of new bands (believed to be part of the B $^2\Pi_i - X\ ^2\Sigma^-$ ansition) is reported. Preliminary experiments with titanium ires exploded in oxygen suggest that the exploding wire may so be a desirable source for spectral studies of the TiO olecule. Some results from this work are included.

**0871.** Cassidy, E. C., Cones, H. N., Wunsch, D. C., Booker, S. R., **Calibration of a Kerr cell system for high-voltage pulse measurements,** *IEEE Trans. Instr. Meas.* **IM-17,** No. 4, 313-320 (Dec. 1968).

Key words: Electro-optical measurements; high voltage measurements; Kerr cell; pulse measurements.

Several techniques for calibration of an electro-optical (Kerr ell) high voltage pulse measuring system are described. Inde- endent calibrations, without reference to pulse divider measure- ents, are achieved by application of a direct bias voltage to the err cell. After calibration, experiments with voltages as high as 00 kV demonstrate reasonable agreement (to within 1 percent) etween simultaneous Kerr cell and calibrated pulse divider easurements.

**0872.** Chang, S. S., **Switch arrangement and power averaging in constant current calorimetric heating,** *Rev. Sci. Instr.* **40,** 822-825 (1969).

Key words: Calorimetry; constant current power supply; energy measurement; power averaging; switch contact arrangement; transient.

In order to minimize the transient effect associated with witching a constant current power supply to different loads, a reak-before-make type of switch contact arrangement is shown o be preferable to a make-before-break type of arrangement. Se- es resistance in the load circuit may be required for low current pplications.

With a constant heater current, the average heater power for he entire heating period can be precisely determined as the roduct of the current and the mean value of two particular otential readings. These two readings, symmetrical about the mid-point of the heating period, should be taken at specified in- ervals as determined by the exponential heat conduction charac- eristics of the calorimeter assembly.

**0873.** Christ, B. W., Giles, P. M., **On the detection of retained austenite in high-carbon steels by Fe$^{57}$ Mössbauer spectroscopy, with appendix,** *Trans. Met. Soc. AIME* **242,** 1915-1925 (Sept. 1968).

Key words: Chemical shift; hyperfine peaks; Mössbauer spectra; retained austenite; singlet center peak; x-rays; 10105 steel.

Mössbauer effect measurements have been made on 1-mil- hick foils of commercial 1 wt pct C steel and Fe-2 wt. pct C alloy. The experimental method required about 3 to 5 vol pct of a phase in the multiphase steel sample for detection. Room-temperature Mössbauer patterns obtained on austenitized and quenched samples exhibit fifteen, and possibly twenty-one, lines. A sharp paramagnetic singlet and a quadrupole doublet, poorly resolved from the singlet, are attributed to austenite. Remaining lines are due to martensite. Accurate evaluation of austenite line parameters is not feasible if significant amounts of other phases such as carbides or martensite occur simultaneously with austenite. This is demonstrated by comparison of hyperfine interactions determined for austenite in multiphase high-carbon samples with those reported for Fe – C austenite in a nearly 100 pct austenitic sample. Lines from carbides are incompletely resolved from austenite lines, as demonstrated by comparison of austenite line positions with carbide line positions calculated from published values of hyperfine interactions. One martensite line overlaps an austenite line in the pattern for commercial 1 wt pct C steel. Results of this study suggest that the usefulness of Fe$^{57}$ Mössbauer spectroscopy for quantitative analysis of austenite in bulk samples of quenched and tempered high-carbon steels is restricted by poor resolution. Use of Mössbauer spectroscopy for phase identification and for evaluation of atomic and electronic structures appears quite feasible.

**10874.** Christ, B. W., Smith, G. V., **Effects of impurities on yield and flow strength of zone refined iron,** *Mem. Sci. Rev. Met.* **LXV,** 208-223 (June 15, 1968).

Key words: Alloys; dilute, binary alloys; hydrogen-purified; hydrogen-purified iron; iron; zone-refined iron.

Effects of impurities on yield and flow strength of hydrogen-purified, zone-refined iron and of dilute, binary alloys made from it in the temperature range 77-300 °K have been examined. Data from the literature are compared with new data obtained on hydrogen-purified iron and iron-0.01 and 0.026 wt. percent nitrogen alloys. In 300 °K tensile tests, hydrogen purification causes substantial changes in the shape of the upper yield, the magnitude of yield stress, the grain-size dependence of yield stress and the response to strain aging treatments. However, hydrogen purification decreases total interstitial impurity by only 0.0008 wt. percent.

Dilute iron alloys are found to exhibit unusual, but widely documented solution strengthening behavior. The room temperature strength is proportional to impurity concentration. However, low-temperature strength is inversely proportional to impurity concentration. This phenomenon, termed "alloy softening," is more pronounced in poly- than in monocrystals, and for interstitial than substitutional impurities.

It is concluded that hydrogen-purification of zone-refined iron affects mechanical behavior by modifying interstitial impurity distribution, rather than by total removal of interstitial impurity. Alloy softening may be due to an increase in mobile dislocation density related to solute rearrangements during thermal treatments.

**10875.** Chung, K., Danos, M., Huber, M. G., **Microscopic description of the absorption of bound $\pi$-mesons,** *Physics Letters* **29B,** No. 5, 265-267 (May 16, 1969).

Key words: Correlated pairs; high momentum components; meson nucleus interactions; nuclear wave function; $\pi$ mesons; short range correlations.

The absorption rates of bound 1s and 2p pions in $^{16}$O have been calculated on the basis of an extended shell model treatment. The effects of the short range part of the nucleon-nucleon interaction are introduced by a two-body correlation factor. It turns out that these correlations are essential; in particular the high momentum exchange between two nucleons seems to be the basic mechanism needed to account for the experimental $\pi$-absorption rate. It is possible to explain both 1s and 2p absorption rates in a consistent picture. Furthermore, the spectra of the emitted nucleons contain useful information about the details of the correlation factor.

**10876.** Clark, A. F., **Low temperature thermal expansion of some metallic alloys,** *Cryogenics* **8,** No. 5, 282-289 (Oct. 1968).

Key words: Alloys; aluminum; copper; expansivity; iron; metals; nickel; thermal expansion.

The low temperature thermal expansion of several aluminum, nickel, copper, and iron base alloys was measured from liquid hydrogen temperature, 20 K, to room temperature, 293 K. Both the thermal contraction from room temperature, $(L_{293} - L_T)/L_{293}$, and the thermal expansion coefficient, $1/L_{293}\, dL/dT$, are tabulated as a function of temperature. Comparison of similar alloys and alloy conditions led to the general conclusions that relatively large changes in composition are required to produce significant changes in the thermal expansion, thermal treatment or condition has little effect except when it produces a basic structure change, and the thermal expansion coefficient at room temperature is a good indicator of the total length change to a low temperature.

**10877.** Clark, A. F., Fickett, F. R., **A nonsuperconducting detection system for low level dc voltages,** *Rev. Sci. Instr.* **40,** No. 3, 465-468 (Mar. 1969).

Key words: DC voltage; low level; measurement.

A low level DC detection system with an attainable precision of 25 pV is described. The system utilizes only normal metal components and commercially available equipment. Measurements can be made automatically, in the presence of large (microvolt) spurious voltages, with switched inputs, and in a non "null" configuration. A typical application is described in detail.

**10878.** Clark, A. F., Powell, R. L., **Longitudinal magnetoresistance of pure single-crystal copper,** *Phys. Rev. Letters* **21,** No. 12, 802-804 (Sept. 16, 1968).

Key words: Copper; electronic scattering; magnetoresistance.

The longitudinal magnetoresistance was measured along the [100] direction of a pure single crystal of copper. The temperature dependence of the saturation ratio, $\rho$ (B= sat.)/$\rho$ (B = 0), is given between 4 and 35 K. A limit is placed on the diffusion approximation for small angle electron scattering and it is suggested that the assumption of a relaxation time or of a mean-free-path parallel to the velocity is not valid for some types of impurity or low temperature phonon scattering.

**10879.** Clark, H. E., Young, R. D., **Field emission through single strontium atoms adsorbed on a tungsten surface,** *Surface Sci.* **12,** 385-389 (1968).

Key words: Adsorption; energy distribution; field emission; Fowler-Nordheim curves; resonance tunneling; strontium; tungsten.

Measurements of the total-energy distribution and current-voltage characteristics (Fowler-Nordheim curves) are reported for electron emission through single strontium adatoms. A number of interpretations of these data are considered; resonance tunneling appears to be the most satisfactory.

**10880.** Cole, A. R. H., Lafferty, W. J., Thibault, R. J., **Rotational fine structure of the perpendicular band, $\nu_7$, of ethane,** *J. Mol. Spectry.* **29,** No. 3, 365-374 (Mar. 1969).

Key words: C–H stretching region; Coriolis interaction; ethane; ground state rotational constants; perpendicular band; $\nu_7$; upper state rotational constants.

The perpendicular band, $\nu_7$, of ethane has been studied, and in dividual lines assigned in the sub-bands with $K\Delta K = +12$ to $-5$ An improved set of ground state constants has been obtained and upper state constants are reported for the individual sub bands.

**10881.** Coleman, J. A., Love, D. P., Trainor, J. H., Williams, D J., **Effects of damage of 0.8 MeV-5.0 MeV protons in silicon sur face-barrier detectors,** *NASA Rept.* No. x-611-68-221, 3 pages (National Aeronautics and Space Administration, God dard Space Flight Center, Greenbelt, Md., June 1968).

Key words: Detector; proton; radiation effect; semiconduc tor; silicon.

Changes in the performance of silicon surface-barrier detec tors after irradiation with protons at energies between 0.80 Me and 5.00 MeV have been investigated for fluences up to 10 protons cm$^{-2}$. Irradiations of the front, surface-barrier contact and the rear, ohmic contacts of these transmission detector were performed. In general, the detector current and noise in creased with fluence. When the rear, ohmic contact was i radiated with protons which stopped within the detector, th changes in the current and noise after irradiation were several o ders of magnitude smaller than after a similar irradiation of th front contact. For protons with energies greater than about MeV, the detector capacitance decreased at low reverse biase and increased at high biases with increasing fluence. The result indicate that a significant reduction in the increase of detecto current and noise can be obtained if the density or radiatio produced defects in the region of the junction is minimized.

**10882.** Cooper, M. J., Green, M. S., **Generalized scaling and th critical eigenvector in ideal Bose condensation,** *Phys. Rev.* **17** No. 1, 302-309 (Dec. 5, 1968).

Key words: Bose condensation; critical eigenvector; critic phenomena; scaled equation of state.

We consider the condensation of a perfect Bose gas in whic the phase symmetry of the Boson states has been removed by linear coupling of the creation/annihilation operators $\psi^+(r)$, $\psi($ to a fictitious external field C($r$) as a model of a second-ord phase transition. In the vicinity of the transition, the spontaneo order parameter (thermal expectation value of $\psi$) is related to th conjugate field by a series of terms of which the first represen a scaled equation of state that exhibits a power-law behavi with non-classical exponents. The expectation value for th ordered product of Boson operators $\langle\psi^+(1)\psi^+(2)\ldots\psi^+(M)\psi($ $\ldots\psi(N')\rangle$ is determined and its behavior across the coexisten curve discussed. The existence of a conjectured critical eige vector is demonstrated and a related asymptotic property of th ordered product determined.

**10883.** Cooper, M. J., **Point transformation of classical hard-co potential,** *J. Math. Phys.* **9,** No. 4, 571-578 (Apr. 1968).

Key words: Canonical point-transformation; dependent i teractions; equivalent non-singular potential; hard-sphe gas; kinetic equation; many-body analysis; non-loc velocity.

The method of an extended canonical point-transformation used to reformulate the singular repulsions in a classical har sphere gas as equivalent velocity dependent interactions. Th approach provides a Hamiltonian in which the repulsions appe as non-local potential interactions between the particles and m therefore be treated within any of the conventional perturbati methods of many-body analysis. Application of the technique obtain a kinetic equation for a hard-sphere gas is obtained.

**10884.** Coriell, S. R., Jackson, J. L., **Bounds on transport coef cients of two-phase materials,** *J. Appl. Phys.* **39,** No. 10, 473 4736 (Sept. 1968).

Key words: Composite materials; effective conductivity; transport coefficients; two phase materials; upper and lower bounds.

reviously derived upper and lower bound expressions for the ctive conductivity of composite materials are applied to two se materials. Results are presented for several simple metrical arrangements and for certain limiting cases.

85. Corruccini, R. J., **Principles of thermometry (measurement temperature),** Chapter 87 in *Treatise on Analytical Chemisy. Part I, Theory and Practice,* I. M. Kolthoff, P. J. Ebring, nd E. B. Sandell, eds., **8,** 4937-4990 (Interscience Publ., Inc., ew York, N.Y., 1968).

Key words: Temperature; temperature measurement; thermometry.

rom fundamental thermodynamic concepts the idea of temature as a quantitative parameter is developed. It is shown scales of temperature are defined, and how they are acculy realized in practice and transmitted to lower orders of ctical thermometers. The operating principles and characstics of expansion thermometers, resistance thermometers, mocouples, and radiometric thermometers are presented in ne detail.

86. Coxon, B., **P.M.R. evidence for the conformations of 1,2-O-enzylidene-α-D-glucofuranose derivatives,** *Carbohydrate Res.* , 125-134 (1968).

Key words: Benzylidene acetals; chemical shifts; conformations; D-glucofuranose derivatives; p.m.r. spectroscopy; proton coupling constants.

roton coupling constants and chemical shifts of two 1,2-*O*-zylidene- and four 1,2:3,5-di-*O*-benzylidene-α-D-glucofuose derivatives have been measured by p.m.r. spectroscopy 00 MHz. From these parameters, it is deduced that the furad rings of the mono- and di-benzylidene acetals exist mainly symmetric and non-symmetric twist conformations, respecly. The *m*-dioxane ring of the dibenzylidene acetals adopts t chair conformation in which C-6 is axially attached.

87. Creitz, E. C., **Construction details and measurements of esponse of a gas density balance,** *J. Chromatog. Sci.* **7,** 137-44 (Mar. 1969).

Key words: Chromatographic detector; density detector; gas density; gas detector.

he measured response of the Nerheim gas density balance ng hot wire anemometers as sensing elements, was compared h the predicted response for such variables as anemometer tch, resistance to flow in the exit branches of the duct system, anges in bridge current and reference gas flow rate. Criteria given for selecting matched pairs of anemometers and for ir calibration in the gas flow system. Proper selection of an erating point, in terms of reference gas velocity, permitted detion of differences in flow rates as small as $1.4 \times 10^{-3}$ cm s$^{-1}$. e measured overall sensitivity for oxygen and for methane, ng nitrogen as the reference gas, was $0.534 \times 10^6$ and $0.616 \times$ $^5$ millivolts per density unit (g cm$^{-3}$), respectively.

888. Crumlish, J. D., **Notes on U.S. Government information systems,** *Law Computer Technol.* **1,** No. 11, 15-21 (Nov. 1968).

Key words: Computer technology; documentation, federal systems; Government research and development information; information systems; scientific communication.

U.S. Government agencies have developed a number of infortion systems to help fulfill their statutory missions. Of the two mary types of non-military systems, one is outlined in this article: research and development information systems; telling who is doing what, where, and in some cases, how. The second major classification, statistical information systems; for the development, collection, analysis, and dissemination of data, are reserved for later treatment.

A sampling is described here to aid those interested in developing new systems or in making better use of, and coordinating with, those outlined herein.

10889. Cuthill, J. R., Dobbyn, R. C., McAlister, A. J., Williams, M. L., **Search for plasmaron structure in the soft x-ray $L_{2,3}$ emission spectrum of Al,** *Phys. Rev.* **174,** No. 2, 515-517 (Oct. 10, 1968).

Key words: Aluminum; electron gas; emission spectrum; excitations; plasmaron; soft x-ray.

The $L_{2,3}$ soft x-ray emission spectrum of Al has been carefully scanned for a weak low energy edge predicted by recent theoretical studies of the interacting electron gas. A very weak structure, near the predicted location, but just within the noise, is seen. An upper limit to the magnitude of such structures is established, and it is suggested that the light alkali metals should provide a better test of the theory.

10890. Cuthill, J R., McAlister, A. J., Williams, M. L., Dobbyn, R. C., **Soft x-ray spectra and comparison with the theoretical density of states,** (Proc. Conf. Soft X-ray Band Spectra and the Electronic Structure of Metals and Materials, Strathclyde, Scotland, Sept. 18-21, 1967), Chapter in *Soft X-ray Band Spectra and the Electronic Structure of Metals and Materials. Part II. Heavy Metal and Alloy Spectra and Comparison with other Optical Methods,* pp. 151-162 (Academic Press Inc., New York, N.Y., 1968).

Key words: Aluminum; density of states; L-emission band, M-emission band; Ni-Al system; nickel; soft x-ray spectroscopy; TiNi intermetallic compound; transition probability energy.

Emission spectra are being obtained with a 2-meter grazing incidence glass grating (30,000 lines/inch) spectrometer with photoelectron detection and digital recording. The long range objective is information pertaining to the changes in the density of states with alloying and intermetallic compound formation. However, most of the effort to date has been on the determination of the nickel-$M_{2,3}$ spectrum and its relation to the density of states in nickel. The temperature was held at 960 ± 7 °C to insure an oxide-free surface. A number of scans were summed to resolve detail that has not been resolved heretofore. Calculated transition probabilities appear to account for the observed L band always being narrower than the M.

A comparison of Al-$L_{2,3}$ and Ni-$M_{2,3}$ overlapping spectra from $NiAl_3$, NiAl, and 8 and 4 percent Al in nickel solid solutions together with the spectra of the pure metals, reveals certain major features of the soft x-ray spectra to be unrelated to crystal structure. The observed spectra suggest that the electronic structure of the aluminum undergoes a progressive change with increasing nickel content whereas the high energy x-ray L emission edge remains unshifted at least up to 50 percent Ni. In contrast to the Ni-Al system there is no overlap of the titanium-$M_{2,3}$ spectrum with the nickel-$M_{2,3}$ spectrum in the case of the Ti-Ni system. The nickel-$M_{2,3}$ from Ni in TiNi exhibits a peak at the same energy as that of the peak in the pure Ni spectrum but also exhibits a much larger peak about 3 eV lower in energy.

10891. Cutkosky, R. D., **A varactor null detector for audio frequency capacitance bridges,** *IEEE Trans. Instr. Meas.* **IM-17,** No. 4, 232-238 (Dec. 1968).

Key words: Audio amplifier; capacitance bridge detector; noise reduction; null detector; parametric amplifier; varactor amplifier.

A two-varactor, double sideband up-converter pumped at 30 MHz has been constructed. Operated at room temperature with a signal frequency of $10^4$ radians per second, the device has an optimum source resistance of $10^5$ ohms and a minimum noise figure of 0.01 dB. Immersed in liquid $N_2$, minimum noise figures below 0.001 dB referred to a room temperature source have been measured. The device is particularly useful as a null detector for audio frequency capacitance bridges. At $10^4$ radians per second, a signal current of $10^{-14}$ A through a capacitance of 1000 pF can be detected in less than one second with this instrument. Techniques for suppressing microphonics and other extraneous sources of noise are described.

**10892.** Czyz, W., Maximon, L. C., **High energy scattering of strongly interacting composite particles,** *Physics Letters* **27B,** No. 6, 354-357 (Aug. 19, 1968).

Key words: Hadron-hadron scattering; high-energy cross sections; high energy scattering; nucleon-nucleus scattering.

High energy electron-nucleus, nucleon-nucleus and nucleus-nucleus scattering are analyzed in the framework of geometrical optics. It is shown that good agreement with experimental cross sections is obtained provided that a correction for the center of mass motion is included.

**10893.** Czyz, W., Maximon, L. C., **High energy small angle elastic scattering of strongly interacting composite particles,** *Ann. Phys.* **52,** No. 1, 59-121 (Mar. 1969).

Key words: Deuteron-deuteron scattering; elastic scattering; hadrons; high energy scattering; proton-nucleus scattering; strongly interacting particles.

Starting from a simple-minded formulation of the Glauber model of the high energy multiple scattering of strongly interacting composite particles, several generalizations and limiting expressions are derived from the elastic scattering amplitudes at small scattering angles. An extensive discussion of the many possible applications to nucleon-nucleus, nucleus-nucleus and other composite hadron elastic scattering processes is given.

**10894.** Danielson, B. L., **An optical Faraday rotation technique for the determination of magnetic relaxation times,** *IEEE Trans. Mag.* **MAG-4,** No. 2, 176-178 (June 1968).

Key words: Faraday effect; paramagnetic relaxation.

A technique is described for the measurement of spin-spin and spin-lattice relaxation times in crystals using the optical Faraday rotation as a monitor of the magnetization. The method is applied to the paramagnetic $Eu^{2+}$ ion in $CaF_2$:$Eu^{2+}$. In this experiment the crystal is placed between a crossed polarizer and analyzer and subjected to a pulsed magnetic field. The transmitted light from a cw argon-ion laser gives a direct indication of the spin relaxation time. Some possible advantages of this technique for the determination of fast relaxation times in concentrated systems are discussed.

**10895.** Davis, D. D., Braun, W., **Intense vacuum ultraviolet atomic line sources,** *Appl. Opt.* **7,** No. 10, 2071-2074 (Oct. 1968).

Key words: Atomic lines; Br; C; flow lamp; N; O; photochemistry; vacuum ultraviolet.

Intense atomic lines (O, N, S, C, Br, Cl, H, Xe, Kr) have been produced by microwave excitation of mixtures of various gases in helium under flow conditions. The intensities generally obtained are greater than $10^{14}$ quanta/sec and are suitable for atomic fluorescence studies and as photochemical light sources in the vacuum ultraviolet. Conditions for producing these high purity line sources are discussed.

**10896.** Davis, D. D., Okabe, H., **Determination of bond dissoc tion energies in hydrogen cyanide. Cyanogen and cyanogen lides by the photodissociation method,** *J. Chem. Phys.* **49,** N 12, 5526-5531 (Dec. 15, 1968).

Key words: Bond dissociation energies; BrCN; ClCN; C $C_2N_2$; FCN; fluorescence; HCN; ICN; photodissociati vacuum ultraviolet.

The photodissociation process yielding CN B$^2\Sigma^+$ from varic cyanogen compounds has been studied in the vacuum ultraviol Threshold energies of incident photon to produce the CN B$^2$ are measured by monitoring the fluorescence due to the trar tion CN B$^2\Sigma^+$ – X$^2\Sigma^+$. The upper bounds of bond energies c be obtained from these thresholds and the electronic energy CN B$^2\Sigma^+$. The average heat of formation of CN and its estima overall uncertainty, $\Delta Hf_0^\circ(CN) = 418 \pm 4$ kJ mol$^{-1}$ (100 ± 1 k mol$^{-1}$), is computed using these bond energies together with v ous $\Delta Hf_0^\circ$. This value is within an estimated error in excell agreement with the photoionization value recently obtained Dibeler and Liston. The bond energies based on $\Delta Hf_0^\circ$(CN 418 kJ mol$^{-1}$ (100 kcal mol$^{-1}$) for various cyanogen compou are D(H–CN) = 497 (119), D(Cl–CN) = 401 (96), D(Br–C = 343 (82), D(I–CN) = 301 (72), D(NC–CN) = 531 (1 D(C–N) = 765 (183) all in kJ mol$^{-1}$ (kcal mol$^{-1}$) with an ove estimated error of ± 4 kJ mol$^{-1}$ (1 kcal mol$^{-1}$). Because of weak fluorescence intensity, no reliable bond energy was tained for $CH_3CN$. Other values obtained are D(F–CN) $\leqslant$ kJ mol$^{-1}$ (111 kcal mol$^{-1}$) and $\Delta Hf_0^\circ$(FCN) $\geqslant$ 30.9 kJ mol$^{-1}$ ( kcal mol$^{-1}$). A correlation of the dissociation process with the sorption spectrum is briefly discussed. A comparison is mad bond energies obtained by the photodissociation, photoion tion, and electron impact methods. Limitations of the photo sociation method to determine bond energies are discussed.

**10897.** Davis, G. T., Eby, R. K., Martin, G. M., **Variations of unit cell dimensions of polyethylene: effect of crystallization ditions, annealing, and deformation,** *J. Appl. Phys.* **39,** No. 4973-4981 (Oct. 1968).

Key words: Annealing; crystallization; deformation; de ty; fold surface; melt; polyethylene; solvent; temperat time; unit cell.

It is shown that the orthorhombic unit cell dimensions given polyethylene are not unique but depend upon physical thermal history. For polymer crystallized from a 3/4 percen xylene solution, the values of *a* and *b* determined by the pow camera technique vary (up to 0.6 percent) systematically crystallization temperature (50 °C, 70 °C, 90 °C) and the t perature of annealing (up to 127 °C). For "undeformed" cryst the changes with annealing appear to accompany the increas crystal thickness and for deformed crystals, they occur ov wider range of temperatures—even below the crystalliza temperature. The dimensions change within the first two min of annealing and appear to be independent of time therea The only exception observed is a slow decrease of *b* with upon annealing at 100 °C. Crystals grown from other solvent hibit very nearly identical effects and the presence of solv does not alter the cell dimensions at room temperature. Sin effects are observed for crystals grown from the melt by cooling, quenching in ice water, and quenching in a dry acetone suspension. The main difference is that cold wor does not appear to alter the effects of annealing. The mecha of the effects cannot be safely assigned but changes in the surface probably play a role and a discussion relevant to this other mechanisms is presented. Corresponding to the chang cell dimension are changes in cell density which are, howe too small to account for the frequently reported discrep between crystal and unit cell density. The effects of cell vari must be considered in interpreting the variation of physical perties.

98. Delaplane, R. G., Ibers, J. A., Ferraro, J. R., Rush, J. J., **iffraction and spectroscopic studies of the cobaltic acid system CoO$_2$-DCoO$_2$,** *J. Chem. Phys.* **50,** No. 5, 1920-1927 (Mar. 1, 969).

Key words: Cobaltic acid; crystal structure; hydrogen bond; infrared spectra; isotope effect; lattice vibrations; neutron spectra; selection rules.

obaltic acid, HCoO$_2$, and deuterated cobaltic acid, DCoO$_2$, e been prepared and studied by x-ray and neutron diffraction iniques, and by infrared spectroscopy and cold-neutron scatng. The materials crystallize in apparent space group $D_{3d}^5$-m of the trigonal system with three molecules in a hexagonal of dimensions: HCoO$_2$, a = 2.851 ± 001, c = 13.150 ± 005 DCoO$_2$, a = 2.854 ± 001, c = 13.354 ± 005 Å. The O-O ance, as determined by neutron powder studies, of HCoO$_2$ is ) ± 02 Å. On this basis and the fact that there are three O-H-onds along the *c* direction, the O-D-O distance is 2.57 ± 02 Hence, the isotope effect here is as large as in the system rO$_2$ – DCrO$_2$. Infrared studies at room temperature and at 95 C over the region 70 to 4000 cm$^{-1}$ may be interpreted in ns of an effectively symmetric O-H-O bond and an effective-symmetric O-D-O bond. Although the neutron inelastic scatng measurements are not inconsistent with this interpreta-ı. there is an intense band centered at 264 cm$^{-1}$ in the neutron ctrum for HCoO$_2$ that remains unexplained. Model calculais, based on a two-dimensional potential function in which the mmetric stretching frequency is coupled to the symmetric tching frequency, were unsuccessful owing to the magnitude the coupling term required to account for the very large ope effect.

99. Deslattes, R. D., **Estimates of x-ray attenuation coefficients or the elements and their compounds,** *Acta Cryst.* **A25,** Part 1, 9-93 (Jan. 1969).

Key words: Absorption fine structure; mixture rule; x-ray attenuation.

ome recent developments leading to improved knowledge of distribution of oscillator strength in the photoionization conia of atoms are briefly reviewed. Selective comparisons ween the experiments and calculations are indicated. Esties for attenuation by compounds and solids, insofar as they art from the mixture rule, require an understanding of x-ray structure or, at least of its limiting form, which is not yet at id. Some of the mechanism leading to fine structure in solids molecules are briefly reviewed.

00. Dibeler, V. H., Walker, J. A., **Mass spectrometric study of hotoionization. XIII. Boron trichloride and diboron etrachloride,** *Inorg. Chem.* **8,** No. 1, 50-55 (Jan. 1969).

Key words: BCl$_3$; bond dissociation energies; B$_2$Cl$_4$; heats of formation; ions; mass spectrometry; radicals; vacuum ultraviolet.

Mass spectra and ion-yield curves for the molecule ions and ious fragment ions of BCl$_3$ and B$_2$Cl$_4$ are obtained by means a combined vacuum ultraviolet monochromator and mass ectrometer. Shapes of ion-yield curves measured over the velength region from threshold to 600 Å, are discussed efly. Ionization threshold values are used to calculate heats of mation of ions and radicals and to derive bond dissociation rgies, including the boron-boron bond dissociation energy, (Cl$_2$B – BCl$_2$) = 3.80 eV (87.6 kcal mol$^{-1}$).

01. Dibeler, V. H., Liston, S. K., **Mass spectrometric study of hotoionization. XII. Boron trifluoride and diboron etrafluoride,** *Inorg. Chem.* **7,** No. 9, 1742-1746 (Sept. 1968).

Key words: BF$_3$; bond energies; B$_2$F$_4$; heats of formation; ionization; mass spectra; photoionization; vacuum ultraviolet.

Mass spectra and photon yield curves for the molecular and principal fragment ions of BF$_3$ and B$_2$F$_4$ are reported. The threshold regions only are measured for B$_2$F$_3^+$ and BF$^+$ from B$_2$F$_4$. These observations are intercompared in order to derive heats of formation of ions and radicals and bond dissociation energies. The boron-boron bond dissociation energy in B$_2$F$_4$ is calculated to be 431 kJ mol$^{-1}$ (103 kcal mol$^{-1}$).

10902. Dibeler, V. H., Liston, S. K., **Mass spectrometric study of photoionization. IX. Hydrogen cyanide and acetonitrile,** *J. Chem. Phys.* **48,** No. 10, 4765-4768 (May 15, 1968).

Key words: CH$_3$CN; dissociation; HCN; heats of formation; ionization; mass spectrometry; threshold energies; vacuum ultraviolet.

Photoionization yield curves are obtained from threshold to 600 Å for the HCN$^+$ and CN$^+$ ions of HCN and for the principal ions of CH$_3$CN. The first ionization energy of HCN is 13.59 eV. The threshold for CN$^+$ ion permits calculation of $\Delta Hf_0^\circ(CN) = 100$ kcal mol$^{-1}$, $D_0(CN) = 182.5$ kcal mol$^{-1}$, $D_0(H-CN) = 119.2$ kcal mol$^{-1}$, and $D_0(NC-CN) = 126.6$ kcal mol$^{-1}$. Dissociative photoionization processes in acetonitrile do not produce methyl or cyanogen radical ions in sufficient abundance for direct verification of the above. Nevertheless, threshold values of the principal photoions of CH$_3$CN are tabulated, and some thermodynamic values are calculated, including $\Delta Hf_0^\circ(CH_2) = 94$ kcal mol$^{-1}$.

10903. Dibeler, V. H., Liston, S. K., **Mass spectrometric study of photoionization. XI. Hydrogen sulfide and sulfur dioxide,** *J. Chem. Phys.* **49,** No. 2, 482-485 (July 15, 1968).

Key words: Dissociation; heats of formation; H$_2$S; ionization; mass spectrometer; photoionization; SO$_2$; vacuum ultraviolet.

Photoionization yield curves are obtained for the molecule and fragment ions of H$_2$S and SO$_2$ from onsets of ionization to 600 Å. Structural features of the curves are discussed. Ionization thresholds are tabulated and heats of formation of ions and radicals are calculated. Derived quantities (in kcal mol$^{-1}$) include: $D_0(HS-H) = 89.3$, $D_0(SH) = 83.2$, $\Delta Hf_0^\circ(S) = 65.0$, $D_0(S_2) = 99.4$, and $D_0(OS-O) = 129.1$. The ionization energy, I(SO) = 10.21 eV is obtained by indirect means.

10904. Dick, C. E., Motz, J. W., **Inelastic scattering cross sections for 200- and 400-keV electrons,** *Phys. Rev.* **171,** No. 1, 75-80 (July 5, 1968).

Key words: Aluminum; atomic binding effects; copper; gold; inelastic cross sections; ionization processes; large angle electron scattering; tin; 200 keV; 400 keV.

With 200 and 400 keV electrons incident on thin targets of aluminum, copper, tin, and gold, experimental data are given for the pulse height distributions produced in a silicon detector by the electrons scattered at angles of 40, 90, 120 and 140 degrees. These distributions were analyzed to determine the inelastic cross sections integrated over the energies of the scattered electrons in the energy region below the elastic peak. This lower energy region involves energy transfers that are large compared to the atomic binding energies and most probably involves atomic ionization processes. The results show that these inelastic scattering cross sections increase sharply for angles larger than 90 degrees, so that the ratio of the inelastic to the elastic cross sections becomes larger than unity. In addition, these large angle inelastic cross sections increase with the atomic number of the target and with the average binding energy per target electron. Because of the unavailability of accurate calculations for this process, comparisons are made with the Møller cross sections for electron-electron scattering in order to demonstrate how atomic binding influences large angle inelastic scattering.

**10905.** Dickson, R. W., Spinner, S., **An improved method for the determination of torsional and flexural resonance frequencies of cylindrical specimens,** *J. Mater.* **3,** No. 3, 716-724 (1968).

Key words: Cylinders; loop; suspension; torsional mechanical resonance frequency.

A suspension method is described for obtaining torsional as well as flexural mechanical resonance frequencies of cylindrical specimens which overcomes many of the difficulties previously encountered in determining the torsional modes for such specimens. The method is readily adaptable for such measurements as a function of temperature. Also internal friction measurements using this method yield responses having less suspension losses than other suspension systems, resulting in more reliable values of internal friction from the specimen.

**10906.** Diller, D. E., **Refractive index of gaseous and liquid hydrogen,** *J. Chem. Phys.* **49,** No. 7, 3096-3105 (Oct. 1, 1968).

Key words: Clausius-Mossotti function; Lorentz-Lorenz function; molecular polarizability; orthopara composition; parahydrogen; refractive index.

The refractive index of gaseous and liquid hydrogen has been measured by an interferometric method at temperatures between 15 and 298.15 °K and at pressures up to 230 atm. The measurements have been analyzed in terms of the density and temperature dependence of the Lorentz-Lorenz function,

$$L-L \equiv (n^2_\lambda - 1)/(n^2_\lambda + 2) \cdot 1/\rho,$$

where $n_\lambda$ is the refractive index at $\lambda = 5462$ Å and $\rho$ is the fluid density in g/cm³. The precision and reproducibility of $L-L$ is better than 0.05 percent in most cases.

$L-L$ for gaseous parahydrogen first increases with increasing density to a maximum and then decreases to a value below the low density limit. $L-L$ is also slightly temperature dependent; the low density limit increases with increasing temperature; the maximum on the $L-L$ isotherms decreases with increasing temperature. $L-L$ for saturated liquid parahydrogen decreases with increasing density by about 0.1 percent at temperatures between 15 and 32 °K. The difference in $L-L$ for normal and parahydrogen is consistent with previous theoretical and experimental estimates of the molecular polarizability difference.

**10907.** Dise, J. R., **Significance of the test for normal consistency of hydraulic cement,** *Am. Soc. Testing Mater. Spec. Tech. Publ.* **441,** *Cement, Comparison of Standards and Significance of Particular Tests,* pp. 3-15 (Aug. 1968).

Key words: Autoclave soundness; hydraulic cement; normal consistency; tensile strength; time of setting; Vicat.

The Vicat Test for Normal Consistency was devised in France approximately 150 years ago and has been in use as a standard ASTM method of test for hydraulic cements since 1904. Much has been learned about the relationship between normal consistency and various other properties of these materials from the numerous studies of related questions that have been carried out over the years. A summation of the information that has been developed concerning time of setting, autoclave soundness and tensile strength tests, and other subjects of potential interest to those engaged in the development of specifications and methods of test for cements, is presented in this review.

**10908.** Douglas, T. B., King, E. G., **High-temperature drop calorimetry,** Chapter 8 in *Experimental Thermodynamics,* **Vol. I,** *Calorimetry of Non-reacting Systems,* J. P. McCullough and D. W. Scott, eds., pp. 293-331 (Butterworth and Co., London, England, 1968).

Key words: Calorimetric methods; calorimetry; drop calorimetry; thermodynamic properties.

The principles and techniques of the drop method of determ
ing relative enthalpies of solids and liquids above room tempe
ture are discussed in detail and critically, with particular att
tion to those features which lead to the most accurate resul
Typical precise results are compared with those obtained usi
other calorimetric methods, and the advantages and dis
vantages of the drop method are considered. While alternati
accessories are referenced and discussed briefly, two import
types of furnace (with and without a good thermal conduct
and two types of calorimeter (the "ice" and "copper-block")
treated in detail with respect to their design, construction, a
operation with accuracy and convenience. Numerous sam
and container problems peculiar to high temperatures are c
sidered. Finally, various aspects of treating the data are de
with. These aspects include correcting to standard conditio
correcting for chemical impurities and irrelevant phase chang
smoothing and representing enthalpy values, derivation of ot
thermodynamic properties from enthalpies, and the evaluat
and representation of simple expressions of precision and ac
racy.

**10909.** Dragoo, A. L., **Diffusion rates in solids,** Chapter IV
*Atomic Energy Review,* O. Kubaschewski, ed., **2,** 187-202
ternational Atomic Energy Agency, Vienna, Austria, 1968)

Key words: Borides; carbides; diffusion rates; nitrides;
ides of nuclear materials.

A discussion of the types of diffusion coefficients and of
experimental techniques for their determination is presented
inclusion in the International Atomic Energy Agency Mo
graph Series on the Physicochemical Properties of Nuc
Materials. The diffusion coefficients for tracer diffusion, self-
fusion, intrinsic diffusion, chemical inter-diffusion and gr
boundary diffusion are described. Experimental methods
limitations are discussed for (1) metallic and metalloid ion di
sion in borides, carbides, nitrides and oxides of Be, Ti, Zr,
Nb, Ta, Mo, Th and U; (2) diffusion of B, C, N and O in met
and (3) rare gas diffusion from compounds used as nuclear fu

**10910.** Drechsel, D., **On the model-independent evaluation o
elastic electron scattering data at low momentum transfer,** *N
Phys.* **A113,** No. 3, 665-675 (June 7, 1968).

Key words: Correction factors; Coulomb effects; elec
excitation; low momentum transfer; magnetic transiti
model-independent evaluation; phase shift analysis; tra
tion radius.

At low momentum transfer, electro-excitation experim
may be corrected for the static Coulomb effects in a model-i
pendent way. This is demonstrated in the case of magnetic tra
tions for various phenomenological current and magnetiza
distributions. The inclusion of a finite excitation energy g
mainly a kinematical effect. It is further shown that for tr
verse transitions the notion of a "transition radius" has
model-independent physical meaning and should be avoided.

**10911.** Drechsel, D., Maximon, L. C., **Potential model calcul
for coplanar and noncoplanar proton-proton bremsstrahl**
*Ann. Phys.* **49,** No. 3, 403-444 (Oct. 1968).

Key words: Angular distributions; low energy approx
tion; non-coplanarity; off-the-energy-shell matrix elem
photon; potential model calculations; proton-proton bre
trahlung.

The cross section for proton-proton bremsstrahlung is c
lated for both coplanar and non-coplanar events using
Hamada-Johnston and Reid (soft-core) potentials. Agreeme
obtained with the experimental data for angular distribution
cross sections integrated over the photon directions. We pr
a detailed analysis of the kinematics, the phase space an

trix element in the neighborhood of the kinematic limit of non-planarity. We find a rapid decrease of the cross section in- rated over photon angles as this limit is approached. This is e, not to a strong variation of the phase space, which is essen- lly constant, but to the fact that near the kinematic limit for n-coplanarity of the protons, the photon is restricted to angles which the probability for emission is small. For low energies 30 MeV) of the incident proton we give analytic expressions the scattering amplitude, valid for coplanar as well as the non-planar events.

912. Driver, L. D., Arthur, M. G., **A wideband RF voltmeter-comparator,** *IEEE Trans. Instr. Meas.* **IM-17,** No. 2, 146-150 June 1968).

> Key words: Detector networks; differential voltmeter; voltage comparator; voltage monitor; voltmeter.

This paper describes a new, wide-band RF voltmeter/com- rator for the frequency range dc to 1 GHz and the voltage nge 1 to 15 volts. The device employs matched hot-carrier odes in a dual channel 50 ohm coaxial configuration. Power ex- ction from the signal under test is negligible and the coaxial e sections are impedance compensated so that the maximum SWR is 1.02. Applications include the following: (1) Measure- ent of RF voltage with 3 percent uncertainty limit. (2) Mea- rement of differential RF voltage. (3) High resolution RF volt- e comparator-monitor. (4) Leveler-detector, with flat sponse, for swept or fixed frequency operation.

913. Duerst, R. W., Baum, S. J., Kokoszka, G. F., **Exchange coupling in two dimeric copper adenine complexes,** *Nature* **222,** 665-666 (May 17, 1969).

> Key words: Adenine; copper(II); EPR spectra; exchange coupling; metal ion pairs; optical spectra; purine bases.

The electron paramagnetic resonance spectra of two pper(II)-adenine complexes, $Cu_2(C_5H_5N_5)_4(ClO)_4 \cdot nH_2O$(I) d $Cu_2(C_5H_4N_5)_4 \cdot 4H_2O$ (II), are characteristic of a species th a spin of one, a condition which may arise if two copper(II) ns, each with a spin of one-half, are exchange coupled. Further idence for the dimeric complex is furnished by the seven line perfine pattern in the parallel and zero field regions of the ectrum, observed for both complexes. The magnetic parame- rs are $g_{||}=2.22\pm.03$, $g_{\perp}=2.05\pm.01$, $D=(0.110\pm.005)$ n$^{-1}$, $E<0.03$ cm$^{-1}$, $(A_{||})/2=(88\pm3)\cdot10^{-4}$ cm$^{-1}$, and $A_{\perp}<$ 002 cm$^{-1}$ for I, and $g_{||}=2.19\pm.03$, $g_{\perp}=2.05\pm.01$, $D=$ .121±.005) cm$^{-1}$, $E<0.03$ cm$^{-1}$, $(A_{||})2=(81\pm8)\cdot10^{-4}$ cm$^{-1}$, d $A_{\perp}<0.002$ cm$^{-1}$ for II. The indicated error limits are esti- ated uncertainties. A temperature variation study of the line in- nsity over the range 77 to 300 K indicates that the triplet ate lies 300±60 cm$^{-1}$ and 160±60 cm$^{-1}$ above the singlet ound state for I and II respectively.

914. Dunn, G. H., **Colliding beams,** (Proc. First Intern. Conf. Atomic Physics, New York, N.Y., June 3-7, 1968), Chapter in *Atomic Physics,* B. Bederson, V. W. Cohen, F. M. J. Pichanick, eds., pp. 417-433 (Plenum Press Inc., New York, N.Y., 1969).

> Key words: Atomic physics; colliding beams; review; technique.

Variations of the colliding beams technique are compared with e another from the standpoint of energy range accessible, ener- spread in the beams, and systematic errors in the experiments. dvantages and disadvantages of different variations are pointed t.

915. Edelman, S., Roth, S., Grisham, L., **Electrical generation of motion in elastomers,** *Shock and Vibration Bull.* **39,** Part 2, 18 pages (Shock and Vibration Information Center, Naval Research Laboratory, Washington, D.C., Feb. 1969).

> Key words: Elastomers; electrets; electrically controlled damping; electrostriction; piezoelectricity; polymers; vibration generation.

Motion occurring in response to an applied electrical signal was studied in a number of elastomers. Motion at double the exciting frequency (electrostriction) was common. Linear response was found in a few materials. A few showed linear response in their original condition. Treatment with heat and intense electric fields caused linear response to appear or to increase in others. Superposition of a d.c. bias on the driving signal linearized the double frequency response and increased the linear response.

10916. Edmiston, C., Krauss, M., **Pseudonatural orbitals as a basis for the superposition of configurations. II. Energy surface for linear $H_3$,** *J. Chem. Phys.* **49,** No. 1, 192-205 (July 1, 1968).

> Key words: Correlation energy; electronic energy surface; Gaussian-type functions; Hartree-Fock; $H_3$; superposition of configurations.

A superposition of configurations (SOC) trial function is applied to the $H_3$ energy surface. The convergence of the SOC trial function is improved by constructing the configurations with approximate or pseudo-natural orbitals (PNO). For a given atomic function basis the PNO exhaust the accuracy of that basis in relatively few configurations compared to the total of all possible configurations. Gaussian-type functions (GTF) are then practicable as a basis for a SOC trial function.

Results are presented for the linear $H_3$ energy surface. The error when one hydrogen is removed to infinity is 0.1 eV and an extrapolation of this error yields a "probable" activation energy of 0.53 eV or 12 kcal.

10917. Edmonds, J., **Matroid partition,** Chapter in *Mathematics of the Decision Sciences, American Mathematical Society Lectures in Applied Mathematics* **11,** 335-345 (American Mathematical Society, Providence, R.I., 1968).

> Key words: Algorithm; combinatorics; forests; matroid; partition; transversals.

For an indexed family of matroids, $M_i=(E,F_i)$, all defined on the same set E, an algorithm is described for partitioning any H $\subseteq$ E, if possible, into sets $I_i$ such that $I_i \epsilon F_i$. Some applications are described. It is shown that the subsets H which can be partitioned in this way comprise the independent sets of a matroid which we denote as $M=\Sigma M_i$, the sum of matroids $M_i$. So-called *transversal matroids* are described as sums of rank-one matroids.

10918. Ehrlich, M., **Influence of irradiation rate on the production of F centers in LiF (TLD grade),** (Proc. Second Intern. Conf. Luminescence Dosimetry, Gatlinburg, Tenn., Sept. 23-26, 1968), J. A. Auxier, K. Becker, E. M. Robinson, eds., Paper No. CONF-680920 Health and Safety (TID-4500), pp. 322-326 (Oak Ridge National Laboratory, Oak Ridge, Tennessee, Sept. 1968); *J. Appl. Phys.* **40,** No. 2, 891-892 (Feb. 1969).

> Key words: F-center formation; LiF(TLD grade); rate dependence; thermoluminescence; $^{60}$Co gamma radiation.

Optically polished samples of extruded plaques of LiF(TLD grade) were given $^{60}$Co gamma-ray exposures ranging from about 30 000 R(9 C/kg) to 450 000 R(120 C/kg), at exposure rates between about $1.5\times10^3$ R/h (0.39 C/kg h) and $5\times10^6$ R/h 1300 C/kg h). Over this range of exposures and exposure rates, the resulting absorption in the F band was found to be independent of exposure rate, and to increase with exposure, even for exposures for which the thermoluminesence exhibited saturation effects. After thermoluminescence readout at about 235 °C, practically all the absorption in the F band created by the $^{60}$Co gamma-ray exposures had disappeared. These results are compatible with the dominant role given F centers in some of the current models for the thermoluminescence process in LiF(TLD grade).

**10919.** Unassigned.

**10920.** Ehrlich, M., **Personal dosimetry: methods other than T.L.D.,** *Proc. First Intern. Congress Radiation Protection, Rome, Italy, Sept. 5-10, 1966,* Part 1, pp. 69-76 (Pergamon Press Inc., New York, N.Y., 1968).

Key words: Calibration; data processing; evaluation; gamma rays; intercomparison; performance; personnel dosimetry; phosphate glass; photographic film; radioactive sources; thermal neutrons; x rays.

This is the rapporteur paper that was presented by the author on September 5, 1966, at the first International Congress of the International Radiation Protection Association, in Rome, Italy. The following eight papers were covered: Photographic dosimetry: beta-gamma calibration, M. P. Olivares, S. Perez-Modrego (Spain); Transportable calibration facility for film dosimetry of x-rays by means of radioactive sources, V. Paič (Yugoslavia); A new concept in film badge design, J. D. Eastes, M. L. Maurer, F. L. Paschal (U.S.A.); A phosphate glass dosimeter adapted to the requirements of health physics applications, W. Buttler, R. Maushart, E. Piesch (Federal Republic of Germany); Personnel film monitoring in Poland: organization, method, results, T. Musiałowicz (Poland); Practical personnel dosimetry of thermal neutrons, D. Nachtigall (Switzerland), E. Rose (Federal Republic of Germany); Automatic data processing of a film badge service, W. Benari, M. Schatz, G. Ben-David (Israel); Expérience pratique de dosimétrie comparée dans les six pays d'Euratom (premiers résultats), M. Collet, P. Recht (Euratom).

**10921.** Ehrlich, M., **Thermoluminescence response of LiF to x and gamma rays; a study of rate energy dependence over a wide range of exposures,** *Proc. First. Intern. Congress Radiation Protection, Rome, Italy, Sept. 5-10, 1966,* pp. 429-434 (Pergamon Press Inc., New York, N.Y., 1968).

Key words: Bremsstrahlung; Co$^{60}$ photons; energy dependence; F centers; impurities; LiF (TLD); rate dependence; superlinearity; thermoluminescence; trap formation.

The total thermoluminescence light emission ("response") of LiF (TLD grade) was studied as a function of exposure and exposure rate, and as a function of photon energy. Co$^{60}$ gamma rays and a broad spectrum of low-energy bremsstrahlung were employed. No rate dependence of the response was detected over the entire range of exposures and exposure rates employed (from about $10^2$ R to $2 \times 10^7$ R, and from about $10^2$ R/h to $7 \times 10^6$ R/h, respectively). This represents further evidence that centers other than F centers are involved in the thermoluminescence of LiF (TLD grade).

A comparison of the curves of response versus exposure for the two spectra confirms Naylor's findings that the superlinearity region is steeper for Co$^{60}$ gamma radiation than for low-energy x rays, and reveals that the effect is indeed dependent on photon energy rather than on exposure rate. These findings are compatible with an explanation of superlinearity as being due to the formation of additional traps by the radiation proper. For exposures above those causing superlinearity, the difference in curve shape again disappears. Also, there is no dependence on energy of the location and height of the response maximum, which suggests that the inhibiting mechanism is independent of photon energy.

**10922.** Ehrlich, M., Lamperti, P. J., **Uniformity of high-energy electron-beam calibrations,** *Phys. Med. Biol.* **14,** No. 2, 305-314 (Sept. 1968).

Key words: Calibration methods; facilities of users; ferrous sulfate; Fricke; high-energy electrons; NBS service; spectrophotometry; uniformity of dosimetry.

This is a report on the first year of operation of a new servic offered by the National Bureau of Standards (NBS). Dosimete units consisting of polystyrene blocks holding stoppered quart spectrophotometer cells filled with Fricke solution are bein shipped periodically to groups requesting assistance with ab sorbed-dose measurements in high-energy electron beams. As check on their stability, all dosimeters are pre-exposed to abou 6000 R (about 1.55 C/Kg) of $^{60}$Co gamma radiation, and thos with densities farthest from the average are excluded from a further work. The participants irradiate the dosimeters with elec trons, using energies of their choosing between about 5 and 5 MeV, and doses between 4000 and 8000 rads (between 5 and $\times 10^{-4}$ J/Kg) in water. The exposed dosimeters are returned t NBS for evaluation, along with unexposed controls. During th first year of operation, slightly more than one-half of the dose reported by the participants were within ±5 percent of the NB dose interpretation, but some differed by as much as 30 percer or more. Only little correlation was found between a partic pant's method of beam calibration and agreement with NBS dos interpretation.

**10923.** Ehrlich, M., Placious, R. C., **Thermoluminescen response of CaF$_2$:Mn in polytetrafluoroethylene to electron** *Health Phys.* **15,** 341-350 (1968).

Key words: CaF$_2$:Mn; electrons, 20 to 400 keV; energy d pendence; fluence response; response per unit electr energy absorbed; sample-thickness dependence; thermol minescence; thin foils; $^{60}$Co gamma radiation.

Foils of powdered CaF$_2$:Mn in polytetrafluoroethylene, wi thicknesses from 15 to 150 μm, were exposed to monoenerget electrons having energies in the region between 20 and 400 ke The thermoluminescence response of the foil was studied as function of the energy and the fluence of the incident electror the foil thickness, and the electron energy absorbed in the foi The dependence on electron energy of the response per u fluence was found to change considerably with foil thickness, t maximum response occurring at approximately the energy of t incident electrons whose ranges are equal to the thickness of foil layers. From the lowest incident-electron energy employ (20 keV) up to this energy (200 keV for the 150 μm laye response per unit fluence increased linearly with electron energ Therefore, response per unit energy fluence (in this energy ran approximately equal to total energy absorbed in the foils) was dependent of the energy of the incident electrons, at least wit the large error of the experiment. The response per unit of el tron energy absorbed also agreed, within the limits of experim tal error, with that obtained for foils exposed to $^{60}$Co gam radiation.

**10924.** Eick, J. D., Hegdahl, T., **Segregation in dental gold casti alloys,** *J. Dental Res.* **47,** No. 6, Part 2, 1118-1127 (Nov.-D 1968).

Key words: Casting gold; composition; dental gold allo electron microprobe; grain reduction; grain size; segre tion.

The purpose of this investigation was to establish a quant tive method for determining the degree of segregation in der gold casting alloys. The electron microprobe was employed analyze concentration differences. A line scan was used to de mine the variations in concentration present in the alloy. The ture of the segregation was expressed by the coefficient of relation and the coefficient of variation. Segregation occur between Ag and Cu in the Type I alloys. In the Type II and alloys Ag and Pd segregated together and opposed Cu, while Cu, and Pt opposed Pd in the Type IV alloys. Au and Zn did appear to segregate to a significant degree with the other ments. The coefficient of variation was used to define the deg of segregation on a quantitative basis. The degree of segregat tween the fine grained alloys and coarse grained alloys of the me type was not significantly different. Pd was found to have highest degree of segregation, while Au and Pt segregated the st. As the concentration of Cu was increased in the alloy, the gree of segregation decreased.

925. Eicke, W. G., **The zener diode, a working D-C voltage standard,** *1968 IEEE Intern. Convention Digest,* p. 71 (Mar. 1968).

Key words: Electrical measurements; instrumentation; standard cell; voltage standard; zener diode.

This is a summary of a Tutorial paper to be presented at the 68 IEEE International Convention in New York, N.Y. in arch 1968. The summary discusses zener diodes as a working C voltage standard.

926. Eisenhart, C., Zelen, M., **Elements of probability,** Chapter 12 in *Handbook of Physics, Second Ed., Mathematics,* E. U. Condon and H. Odishaw, eds., Part 1, pp. 1-163—1-197 (McGraw-Hill Book Co., Inc., New York, N.Y., 1967).

Key words: Bayes' theorem; central limit theorem; characteristic function of a distribution; mathematical probability; mean values of random variables; probability distributions; probability inequalities; probability limit theorems; propagation of error; random variables; statistical distributions; tables of probability distributions; transformation of variables in probability distributions.

This chapter provides a concise exposition of the axiomatic finition of (mathematical) probability; of the theory of random riables and distribution functions in one, two, and *n* nensions; of the properties of mean values of random variables d of characteristic functions, generating functions, and mo- ents; of measures of location, dispersion, skewness and kurto- of probability distributions; of weak and strong convergence probability; of the central-limit theorem and its applications; d of the special properties of the normal, chi-square, Student's Snedecor's F, binomial, negative binomial, hypergeometric d Poisson-exponential distributions. The annotated bibliog- phy of 132 entries serves as a guide not only to the principal xtbooks, treatises, and monographs on probability theory and applications, but also to authoritative individual tables of par- ular probability distributions as well as to general collections probability and statistical tables.

927. Enemark, E. A., Gallagher, A., **A Pockels cell light modulator for wide angle radiation,** *Rev. Sci. Instr.* **40,** No. 1, 40-41 (Jan. 1969).

Key words: Isotropic radiation; KDP light modulator; light modulator.

A Pockels cell light modulator which operates at radio equencies is described. It transmits more isotropic radiation an other Pockels cell or water cell modulators that operate at ese frequencies. In addition, the modulated light has less phase riation between different components of the radiation than do ater cell modulators.

928. Engen, G. F., **A method of calibrating coaxial noise sources in terms of a waveguide standard,** *IEEE Trans. Microwave Theory Tech.* **MTT-16,** No. 9, 636-639 (Sept. 1968).

Key words: Noise; noise calibration; radiometer.

The UHF and microwave portion of the radio frequency spec- um is characterized by the use of several different types of ansmission lines, the most common being coaxial line and ctangular waveguide. A frequent and recurring problem is that calibrating an item which is fitted with one type of output (or put) terminals, in terms of a "standard" having a different set terminals or connector.

By an extension of certain techniques which were developed in an earlier paper on power calibration transfer, it is possible to make a similar comparison of noise sources. The procedure requires a suitable adaptor and a pair of measurements which are combined in such a way that the adaptor losses approximately cancel.

10929. Engen, G. F., **A method of determining the mismatch correction in microwave power measurements,** *IEEE Trans. Instr. Meas.* **IM-17,** No. 4, 392-395 (Dec. 1968).

Key words: Microwave measurements; mismatch; power measurement.

With the increasing demands for accuracy in microwave measurements, mismatch corrections are assuming an increased importance. In the application of a terminating type power meter, the appropriate mismatch factor involves the *complex* reflection coefficients of the generator, load, and power meter.

Instead of measuring the individual reflection coefficients, which usually calls for the use of a slotted line, this paper describes a directional coupler technique which obtains the mismatch factor directly.

10930. Ensign, T. C., Chang, T. T., **Low temperature optical-EPR sample probe using tunable coaxial coupling,** *Rev. Sci. Instr.* **40,** No. 2, 268-270 (Feb. 1969).

Key words: EPR-optical double resonance; low temperature; magnetic resonance (EPR); tunable coaxially-coupled microwave cavity.

An optical-EPR sample probe using tunable coaxial coupling, for use at fixed temperatures in the range 1-300 K, has been designed and constructed. It allows both critical coupling of the resonant cavity to the microwave system and good sample illumination, while minimizing thermal agitation.

10931. Ernst, M. H., **Transport coefficients from time correlation functions,** *Lectures in Theoretical Physics, Kinetic Theory,* **IXC,** 417-441 (Gordon and Breach Science Publ. Inc., New York, N.Y., 1967).

Key words: Cluster expansion method; dense gases; projection operator method; self diffusion coefficient; time correlation function; transport coefficient.

Transport coefficients are calculated for a classical dense gas using time correlation functions. In particular two formal methods are discussed both of which lead to a systematic expansion of the transport coefficients in powers of the density. One method is an application of the projection operator method developed by Zwanzig; the second one uses the cluster expansion technique of Green and Cohen. A comparison between the results of both methods is given.

10932. Evans, J. P., Sweger, D. M., **Immersion cooler for freezing ice mantles on triple-point-of-water cells,** *Rev. Sci. Instr.* **40,** No. 2, 376-377 (Feb. 1969).

Key words: Ice mantle; immersion cooler; triple-point cell.

This note describes a simple immersion cooler designed to freeze an ice mantle on the reentrant well of a triple-point-of-water cell. The cooler consists of a thin wall metal tube, closed at one end and connected to a condenser at the other, filled with a liquid of low boiling point. When the cooler is inserted in the well of the triple point cell and the condenser is chilled with dry ice and alcohol, the liquid-vapor phase transition extracts heat from the cell, producing a uniform ice mantle in 30 minutes.

10933. Evenson, K. M., Broida, H. P., Wells, J. S., Mahler, R. J., Mizushima, M., **Electron paramagnetic resonance absorption in oxygen with the HCN laser,** *Phys. Rev. Letters* **21,** No. 15, 1038-1040 (Oct. 7, 1968).

Key words: Electron paramagnetic resonance; HCN laser; molecular oxygen; Zeeman levels.

Paramagnetic resonance absorption between the N = 3, J = 4, M = −4 and N = 5, J = 5, M = 4 levels of ground state $O_2$ was observed at the HCN laser frequency of 890, 759 ± 3 MHz in a 16,418 ± 1 gauss magnetic field. This is the first observation of absorption in a gaseous sample in which laser electron paramagnetic resonance techniques (LEPR) were used.

**10934.** Fano, U., Cooper, J. W., **Spectral distribution of atomic oscillator strengths,** *Rev. Mod. Phys.* **40,** No. 3, 441-507 (July 1968).

Key words: Absorption; light; oscillator strength; spectra distribution; x-ray.

Information on the spectrum of oscillator strength for neutral atoms in their ground states is surveyed with particular regard to recent progress in the far uv-soft x-ray range and to the theoretical interpretation of data from experiments and from numerical calculations. The analysis brings out numerous aspects of atomic mechanics and problems that remain unsolved. An effort is made to interconnect different theoretical approaches within the framework of the theory of atomic spectra.

**10935.** Farrar, T. C., Johannesen, R. B., Coyle, T. D., **Magnetic nonequivalence in the high-resolution NMR spectra of diborane,** *J. Chem. Phys.* **49,** No. 1, 281-285 (July 1, 1968).

Key words: Boron; computer-calculated spectra; diborane; magnetic non-equivalence; proton magnetic resonance; spin coupling.

Proton and boron-11 nuclear magnetic resonance spectra of $^{11}$B-enriched neat diborane have been measured over the temperature range from −7 to −60 °C. The terminal-proton resonance and the $^{11}$B spectrum exhibit partially-resolved fine structure which arises from the magnetic non-equivalence of the terminal protons and of the boron nuclei due to long-range spin coupling. Spectra were calculated which agree quite well with the observed spectra and result in a reasonably accurate determination of the magnitudes and most of the relative signs of the various coupling constants. These values are: $J_{BB}=\mp 5$ Hz, $J_{BH_b}=+47.0$ Hz, $J_{BH_t}=+133$ Hz, $J'_{BH_t}=+4$ Hz, $|J_{H_tH_b}|=7.2$ Hz, $J_{H_tH_t}$(trans or cis) $=\pm 14$ Hz, $J_{H_tH_t}$(cis or trans) $=\pm 6$ Hz, $|J^{gem}_{H_tH_t}| < 3$ Hz, $\delta(H_t-H_b)=-4.50$ ppm.

**10936.** Fatiadi, A. J., **Acylation of tetrahydroxy-p-benzoquinone,** *J. Chem. Eng. Data* **13,** No. 4, 591-593 (Oct. 1968).

Key words: Acetates; benzenehexol; disproportionation; esters; rhodizonic acid; tetrahydroxyquinone.

Procedures are described for preparation of previously unreported di- and tetraacetates of tetrahydroxyquinone. Chemical proof is presented for disproportionation of tetrahydroxyquinone into benzenehexol (hexahydroxy-benzene) and rhodizonic acid in a slightly basic solution. By use of this reaction, a series of acyl derivatives of benzenehexol has been prepared; certain esters of tetrahydroxyquinone also disproportionate in a slightly basic medium.

**10937.** Fatiadi, A. J., **Bromine oxidation of inositols for preparation of inosose phenylhydrazones and phenylosazones,** *Carbohydrate Res.* **8,** 135-147 (1968).

Key words: Bromine; inositol; inosose phenylhydrazone; inosose phenylosazone; mutarotation; oxidation.

The application of bromine oxidation of inositols to give inososes, followed by conversion of the latter into phenylhydrazones or phenylosazones, is described. The diketone from *myo*-inositol gives a phenylosazone in 22-30 percent yield, and L-inositol gives a monoketone phenylhydrazone (12 percent yield) and a diketone phenylosazone (28 percent yield); the co responding enantiomorphs were obtained in 8 and 29 percen yield, respectively. The diketone from quebrachitol yields a ne phenylosazone (29 percent yield) and no monoketone was iso lated. Pinitol gave a new diketone phenylosazone (10-15 percen yield) which showed rapid mutarotation in 1:1 (v/v) ethanol− dioxane. In addition, a new phenylosazone has been obtaine from DL-*epi*-inosose-2 phenylhydrazone. (+)-*proto*-Quebrachit (from acorns) has been converted into a phenylosazone (2 percent yield). *myo*-Inositol has been converted by bromi oxidation into DL-*xylo*-pentahydroxy-2-cyclohexen-1-one in lo yield.

**10938.** Fatiadi, A. J., **Esters of benzenepentol(pentahydrox benzene),** *J. Chem. Eng. Data* **14,** 118-119 (1969).

Key words: Acetic anhydride; aromatization; benzenepe tol (pentahydroxybenzene); ester; methyl sulfoxide; *myo*-i ositol.

Several esters of benzenepentol (pentahydroxybenzene) ha been prepared by one-step aromatization of *myo*-inositol, ar characterized.

**10939.** Fatiadi, A. J., **Evidence for a chair conformation of certa osotriazoles of inositols,** *Chem. Ind.* **19,** 617-619 (May 1 1969).

Key words: Computer; diketoinositol phenylosotriazol half-chair conformation; mercuric acetate; p.m.r. spectr symmetrical.

D-, L-, and DL-Inositol phenylosotriazoles were prepared wi a new reagent, namely, mercuric acetate. Proton magne resonance spectra showed the ring protons as an AA′B system. The favored conformation of the compounds as tet acetates in solution was found to be that of the half-chair. T observed ring proton p.m.r. spectrum of the DL-tetraacetate w found to be in good agreement with that calculated by comput

**10940.** Fatiadi, A. J., **Nature of a colored by-product found crude inosose phenylosazones,** *Carbohydrate Res.* **9,** 177-1 (1969).

Key words: Crude inosose; enols; formation; inositol; idation; phenylosazone.

It has been shown that the crude inosose phenylosazones fr D- and L-*myo*-inosose-1, *myo*-inosose-2, and DL-*epi*-inosos contain a red, enolic impurity having a known structure, name *xylo*-2-oxo-1,3-bis(phenylhydrazono)cyclohexane-4,5,6-tr Similarly, the crude inosose phenylosazones from quebrachi (1-*O*-methyl-*levo*-inositol) and pinitol (5-*O*-methyl-*dextro* ositol) also contain a colored, enolic impurity having a struct analogous to that obtained from the above nonmethylated osose phenylosazones.

**10941.** Feldman, A., Horowitz, D., **Dispersion of piezobirefringence of GaAs,** *J. Appl. Phys.* **39,** No. 12, 55 5599 (Nov. 1968).

Key words: Absorption edge; birefringence; dispersion piezobirefringence; gallium arsenide; nonlinear pie birefringence; photo-elasticity; piezobirefringence; pie optical coefficients; resonance-photoelasticity; str birefringence.

The piezobirefringence of GaAs shows a large anomal dispersion near the absorption edge and exhibits a nonlin stress dependence. The coefficient $\pi_{11} - \pi_{12}$ reverses si Lowering the temperature from 298 K to 77 K shifts the dis sion curves +0.088 eV which is approximately equal to the s of the energy gap with temperature. These effects, which h not been observed previously in GaAs, are related to the str pendence of transitions associated with the absorption edge d resonance photo-elasticity described by Kaplyanskii and zovskaya.

42. Feldman, A., Horowitz, D., **Stress-induced dichroism at he absorption edge of $SrTiO_3$,** *Solid State Commun.* **6,** 607-612 1968).

Key words: Absorption edge; dichroism; rotary transmission method; selection rules; $SrTiO_3$; uniaxial stress.

The stress-induced dichroism at the absorption edge of $SrTiO_3$ s been measured at room temperature by the rotary transmis- n method. Stress- and strain-absorption coefficients were termined for the range of photon energies 3.15 – 3.22 eV. Our ults, together with the selection rules derived by Casella, cast ubt upon the assignment of the absorption edge of $SrTiO_3$ to transition $X_{5'} \rightarrow X_3$.

943. Florin, R. E., Sicilio, F., Wall, L. A., **The paramagnetic species from titanous salts and hydrogen peroxide,** *J. Phys. Chem.* **72,** No. 9, 3154-3161 (Sept. 1968).

Key words: Electron spin resonance; free radicals; hydroperoxyl radical; hydroxyl radical; titanic complexes; titanium trichloride.

The radical species giving ESR spectra on mixing titanous ts and hydrogen peroxide cannot be hydroxyl as formerly sup- sed. Observed kinetics are inconsistent with simple generation d disappearance schemes. In organic substrate mixtures the ecies increases with time while organic radicals decrease. The o "hydroxyl" species are probably forms of $HO_2$ complexed th $Ti^{4+}$. The rate constant $k_1$ of the initial reaction $Ti^{3+} + H_2O_2$ $OH + OH^- + Ti^{4+}$ is estimated as equal to or greater than 0 $M^{-1}$ $sec^{-1}$ from appearance rate of $Ti^{4+} \cdot H_2O_2$, and 800- 00 $M^{-1}$ $sec^{-1}$ from indirect analysis of radical concentration- ne curves.

944. Flynn, D. R., Watson, T. W., **High temperature thermal conductivity of soils,** (Proc. 8th Conf. Thermal Conductivity, Purdue University, West Lafayette, Ind., Oct. 7-10, 1968), Chapter in *Thermal Conductivity,* pp. 913-939 (Plenum Press Inc., New York, N.Y., Apr. 1969).

Key words: Conductance; conductivity; heat transfer; nuclear safety; soils; temperature; thermal conductance; thermal conductivity.

A description is given of an apparatus which has been used to easure the thermal conductivity of soil samples at hot-side tem- ratures to 1600 °C. The method utilizes radial heat flow in a llow cylinder 1.3 cm inside diameter, 7.6 outside diameter, and cm long. The outside of the sample is maintained near room mperature while the inside is heated to the desired temperature means of a specially designed heater. The mathematical anal- is of the method is given. Thermal conductivity values are ven for nine natural or artificial soils which are representative most of the subsoils found on earth.

The method used shows considerable promise as a means of pid and cheap generation of engineering data on the thermal nductivity of loose-fill materials.

945. Folman, M., Klein, R., **Second layer migration with trapping on first layer sites: hydrogen, nitrogen, and carbon monoxide on tungsten,** *Surface Sci.* **11,** No. 3, 430-442 (Aug. 1968).

Key words: Carbon monoxide; field emission; hydrogen; nitrogen; second layer migration; tungsten.

Second layer migration of hydrogen, nitrogen, and carbon onoxide on tungsten is observed with a field emission icroscope. The initial deposition on the tungsten surface at 4.2 °K is made with molecular beams with the tungsten emitter axis perpendicular to the beam direction. The migration of the deposit is effected at temperatures far below those for which the chemisorbed layer is mobile. The shapes of the sharp line boundaries as the second layer migrates over the chemisorbed layer and onto the clean tungsten substrate are quite different for the three gases observed. It is proposed that, in addition to the barrier effects of certain planes of the tungsten, the density of trap sites on the clean surface dictates the boundary configuration. The trap site densities differ for the different gases.

10946. Foster, B. E., Blaine, R. L., **A comparison of ISO and ASTM tests for cement strength,** *Am. Soc. Testing Mater. Spec. Tech. Publ.* **441,** 33-60 (1968).

Key words: Cement strength; ISO cement standards; sand gradation; testing sand.

A comparison of compressive strength tests of 6 portland cements shows that the proposed ISO procedure gave results from 25 to 95 percent higher than ASTM Method C109, depending upon strength level, test age, and cement fineness. The testing sand is seen as the major problem in developing a truly international standard for cement strength, and it is concluded that the selection of equivalent sands is complicated by the prescribed mechanical compaction, which causes forced bleeding. ISO tests using Ottawa-type, round-grain sands are described.

10947. Fraction, G. F., Walker, J. C., Tauber, S. J., **Connection tables from Wiswesser line notation: A partial algorithm,** (Proc. Wiswesser Line Notation Meeting, Army Chemical Information and Data Systems Program, Edgewood Arsenal, Aberdeen, Md., Oct. 6-7, 1966, Spec. Publ. 400-8), *AD665397,* pp. 139-195 (Clearinghouse for Federal Scientific and Technical Information, Springfield, Va., Jan. 1968, $3.00).

Key words: Acyclic; benzene; chemical structure notations; connection tables; contractions; ring system; syntax analysis; transformation algorithm; Wiswesser.

An algorithm has been developed for transforming certain types of Wiswesser organic structure notations into connection tables. Acyclic and benzene structures are treated, and provision has been made for all of the types of contractions used by the Wiswesser notation system. A separate algorithm is presented for treating linearly fused ring aggregates. A syntax has been developed to describe those portions of Wiswesser notations which refer to non-benzene ring systems.

10948. Freeman, D. H., Paulson, R. A., **Chemical microstandards from ion exchange resin,** *Nature* **218,** 563 (1968).

Key words: Analytical detection limits; ion exchange resins; measurements; microstandards; standards.

10949. Frisch, R. C., Forman, R. A., **Nuclear magnetic resonance of Ti in Ti-H systems,** *J. Chem. Phys.* **48,** No. 11, 5187-5190 (June 1, 1968).

Key words: Hydrides; hydrogen; nuclear magnetic resonance; titanium.

The nuclear magnetic resonance spectrum of $^{47,49}$Ti in powder samples of metallic titanium hydride $TiH_x$ has been studied over the range of hydrogen concentrations corresponding to $1.7 \leq x \leq 2.0$. For $TiH_2$ the Knight shift is found to be $+0.26 \pm .04$ percent, and there is no change in the Knight shift as a function of hydrogen concentration over the range studied. The titanium resonance in all samples was quite broad, 20 Oe, so that the lines from the two isotopes were not resolved. As a function of hydrogen concentration, lineshape was found to remain constant, but a rapid decrease of line intensity was noted.

In order to investigate the possibility of magnetic ordering suggested by earlier studies of the magnetic susceptibility of $TiH_2$, studies of the magnetic field dependence and temperature dependence of the resonance were also performed. No dependence of Knight shift or lineshape on magnetic field was observed over the range of 9.0 to 15.0 kOe. No changes in Knight shift or lineshape were observed in the temperature region from 170 to 525 °K, thoroughly encompassing the region of the magnetic susceptibility maximum at approximately 300 °K. These results strongly suggest that the cause of the maximum in the magnetic susceptibility is not magnetic ordering.

Results on hydrogen and deuterium resonances in these samples are also reported.

**10950.** Gadsden, M., **Airglow,** *Encyclopedia of Atmospheric Sciences and Astrogeology,* R. W. Fairbridge, ed., pp. 8-10 (Reinhold Publ. Co., New York, N.Y., 1967).

Key words: Airglow; atmosphere.

A short article on the general topic of the airglow.

**10951.** Gadsden, M., **Airglow motions,** *International Dictionary of Geophysics* **I,** 50-56 (1967).

Key words: Airglow emissions; atmosphere; nightglow emission.

A critical review is presented of the available information on movements of the high atmosphere deduced from observations of airglow emissions. Some of the first results of an analysis to extend knowledge of movements disclosed by nightglow emissions are presented.

**10952.** Gallagher, A., **Excitation transfer in nearly adiabatic thermal collisions,** *Phys. Rev.* **179,** No. 1, 105-110 (Mar. 5, 1969).

Key words: Cs; excitation-transfer collisions; He; Rb; Stuckelberg Equation.

Some sources of error that arise in the use of Stuckelberg's formula for excitation-transfer calculations are pointed out. To demonstrate these difficulties. Stuckelberg's formula for noncrossing levels is used to calculate adiabatic excitation-transfer cross sections for $He^*$, $Rb^*$, and $Cs^*$ collisions with inert gases and for $Alkali^*$-Alkali collisions. In contradiction with another (erroneous) calculation for $He^*$, these cross sections generally disagree with experimental observations by orders of magnitude. The reasons for this, and some conditions for the validity of this method of calculating adiabatic cross sections are given.

**10953.** Gardner, T. V., Jr., Dickson, G., Kumpula, J. W., **Application of diffraction gratings to measurement of strain of dental materials,** *J. Dental Res.* **47,** No. 6, Part 2, 1104-1110 (Nov.-Dec. 1968).

Key words: Dental amalgam; dental materials; diffraction gratings; modulus of elasticity; strain gage; stress-strain measurement.

A system for measurement of strain by means of diffraction gratings ruled on small specimens has been applied to dental materials. The method gives a rapid response to stress, is effective over very short gage lengths, and does not require the attachment of a measuring device to the specimens. Gratings with a spacing of approximately 16,000 lines per inch are ruled on polished specimens. When the specimen is stressed, this spacing is changed resulting in a change in the angle of diffraction of a beam of light directed onto the grating. The change in angle of diffraction is measured by means of photomultiplier tubes behind "V" slits, and from the change in angle, the magnitude of the strain is calculated.

**10954.** Garfinkel, S. B., Mann, W. B., **A method for obtaining large numbers of measured time intervals in radioactive decay,** *Intern. J. Appl. Radiation Isotopes* **19,** No. 9, 707-709 (Sep 1968).

Key words: Multichannel multiscaler analyzer; Poisson di tribution; radioactive decay.

A method is described for the acquisition of large numbers measured time intervals between consecutive alpha-partic emissions in radioactive decay. A multichannel multiscal analyzer was used in a modified multiscaler mode. The data a to be analyzed to see if they conform to a Poisson distribution.

**10955.** Gatterer, L. E., Bottone, P. W., Morgan, A. H **Worldwide clock synchronization using a synchronous satellit** *IEEE Trans. Instr. Meas.* **IM-17,** No. 4, 372-378 (Dec. 196

Key words: Atomic clocks; clock synchronizatio geodesy; ionospheric propagation; navigation; satelli tracking; VHF satellite transponder.

An experiment performed in late 1967 is reported in which t synchronization of widely separated atomic clocks was i vestigated. One-way VHF radio transmissions from t reference clock were relayed to remote clocks using a geo-st tionary satellite transponder. This is in contrast to experimen described in the literature where two-way satellite communic tions were used. The problem of measuring the time differen between a remote clock and a reference clock using one-w radio transmissions reduces to the problem of predicting t propagation delay experienced by the radio wave. For exampl the accuracy with which a user's clock can be set using WWV limited by the predictability of the propagation delay from WW to the user's receiver. The principal advantage of using a geo-st tionary satellite transponder is that the radio path predominately a free space, line-of-sight path, which is predict ble. Those portions of the path for which radio refractive ind is variable constitute only a small percentage of the total path. this experiment predicted values of propagation delay were co pared to measured values. The accuracy of predictability, a hence of clock synchronization, was 10 μsec. or 60 μsec., d pending on the prediction method used. The technique may off an alternative to transporting atomic standards to geodetic a tracking stations around the world fulfilling their clo synchronization requirements. Several methods were used check the time differences between the station clocks. These i cluded transported atomic clocks, a satellite technique using tw way communications, and a one-way microwave link using t moon as a passive reflector.

**10956.** Gautier, T. N., Zacharisen, D. H., **Use of space and ti correlations in short-term ionospheric predictions,** *First A IEEE Commun. Convention,* pp. 671-676 (June 1965).

Key words: Ionospheric prediction; linear regression; spa and time correlations; sunspot cycle trends.

A scheme for short-term ionospheric prediction based on st dard methods of linear regression and least squares is present Emphasis is placed on the use of current observations of ionospheric characteristics themselves in the prediction of th future values or their values at other places. Predictions monthly median values for each hour of the day of cert characteristics, based on diurnal, seasonal, and sunspot cy trends, and their geographical variations, have been made many years. The short-term prediction scheme described h applies to the departures of daily values for a particular hour the day from the monthly median for that hour. The predicti equation, adjusted for a minimum mean square prediction err involves the correlation coefficients of the departures at differ times of the day at the same station as well as the correlati coefficients for the departures at different stations. Correlat coefficients computed from some actual observations presented to show how the correlation coefficient decreases w me separation of the observations at the same station, and with istance separation in the case of observations made simultaneusly at different stations. In the case of time separation of inividual stations, the median correlation coefficient for the staons studied fell below 0.7 at a time separation of about 2 hours, nd below 0.5 at about 4 hours. In the case of distance separaon, the median correlation coefficient for simultaneous oberations fell below 0.7 at a distance separation of about 1000 km nd below 0.5 at about 2000 km.

957. Gebbie, K. B., Thomas, R. N., **Non-LTE diagnostic stellar spectroscopy. I. Conceptual and analytical background,** *Astrophys. J.* **154,** No. 1, 271-283 (Oct. 1968).

Key words: Collisional processes; LTE; radiation field; state parameters; stellar atmosphere; thermodynamic equilibrium.

Seeking a non-restrictive determination of the state of a stellar mosphere, defined as the occupation numbers describing the nergy states of the directly-observable parts of the star, we elineate those regions where thermodynamic equilibrium state arameters can be adopted for internal energy states either ecause collisional processes predominate or because the radiaon field satisfies certain homogeneity conditions. The bounda- values for the state parameters of the LTE stellar interior ust generally be determined in a lower atmospheric region tisfying these homogeneity conditions on the radiation field; pectroscopic diagnostics generally refer to an upper atmospher- region not satisfying the homogeneity conditions. We sumarize an approach to specifying the state parameters describing ese latter regions, and the analytical basis for determining their alues. This paper then provides the background for the specific pplications in following papers.

958. Gebbie, K. B., Thomas, R. N., **Non-LTE diagnostic stellar spectroscopy. II. On the Schuster mechanism for the production of emission lines,** *Astrophys. J.* **154,** No. 1, 285-296 (Oct. 1968).

Key words: Collisional processes; LTE; radiation field; state parameters; stellar atmosphere; thermodynamic equilibrium.

We investigate the conditions under which the Schuster echanism can produce emission lines. We consider Schuster's riginal formulation, together with Milne's modification and a eneral non-LTE formulation. We conclude that while emission nes may result in particular circumstances, it is unlikely that obervations of bright lines can be interpreted by this mechanism.

0959. Geltman, S., **Topics in atomic collision theory, 30,** 247 pages (Academic Press Inc., New York, N.Y., 1969).

Key words: Atom-atom collisions; electron-atom collisions; static field scattering.

This book is based on a course of graduate lectures given at he University of Colorado, Boulder, Colorado (U.S.A.) and at niversity College in London, England. It concerns the applicaon of quantum scattering theory to low-energy atomic collision henomena. It is divided into the three parts—static field scatterng, electron-atom collisions, and atom-atom collisions—and here are ten sections in each of these parts.

0960. Ginnings, D. C., **Introduction,** Chapter 1 in *Experimental Thermodynamics,* **Vol. I,** *Calorimetry of Nonreacting Systems,* J. P. McCullough and D. W. Scott, eds., pp. 1-13 (Butterworth & Co., London, England, 1968).

Key words: Definitions; heat constants; heat units; methods of calorimetry; standard reference substances; symbols; terminology.

**10961.** Ginnings, D. C., West, E. D., **Principles of calorimetric design,** Chapter 4 in *Experimental Thermodynamics,* **Vol. I,** *Calorimetry of Nonreacting Systems,* J. P. McCullough and D. W. Scott, eds., pp. 85-131 (Butterworth & Co., London, England, 1968).

Key words: Design principles; heat leak errors; heat transfer; temperature gradients in calorimeters; tempering of leads.

**10962.** Ginnings, D. C., Stimson, H. F., **Calorimetry of saturated fluids including determination of enthalpies of vaporization,** Chapter 11 in *Experimental Thermodynamics,* **Vol. I,** *Calorimetry of Nonreacting Systems,* J. P. McCullough and D. W. Scott, eds., pp. 395-420 (Butterworth & Co., London, England, 1968).

Key words: Adiabatic calorimetry; heat capacity; heats of vaporization.

**10963.** Glasgow, A. R., Jr., Ross, G. S., **Cryoscopy,** Chapter 88 in *Treatise on Analytical Chemistry, Part I, Theory and Practice,* I. M. Kolthoff, P. J. Elving, E. B. Sandell, eds., **8,** 4991-5083 (Interscience Publ., New York, N.Y., 1968).

Key words: Calorimetry; cryoscopy; dilatometry; freezing; heat of fusion; melting; melting point molecular weight; purity.

The general principles of cryoscopy as applied to purity analysis, molecular weight determination, and phase investigation are described. The phase rule as it applies to both ideal and non-ideal solutions is discussed. The uses and descriptions of various cryoscopic apparatus are described in some detail. The use of resulting data in the calculation of melting point, sample purity, molecular weight, heat of fusion, heat capacity, and phase diagrams is discussed. The chapter primarily centers around the authors' own work in the field, but includes a bibliography of 175 references.

**10964.** Golub, S., Steiner, B., **Photodetachment of $[OH(H_2O)]^-$,** *J. Chem. Phys.* **49,** No. 11, 5191-5192 (Dec. 1, 1968).

Key words: Electron affinity; negative ion; photodetachment; water.

The relative photodetachment cross section of $H_3O_2^-$ has been measured from threshold near 2.95 eV to 4 eV. The continuously rising cross section is consistent with detachment to a repulsive state of the neutral $H_3O_2$. An upper limit on the weakest bond is shown to be 1.2 eV.

**10965.** Grabner, L., **Photoluminescence in $SrTiO_3$,** *Phys. Rev.* **177,** No. 3, 1315-1323 (Jan. 15, 1969).

Key words: Energy transfer; infrared emission; lattice phonons; photoluminescence; strontium titanate; visible emission.

At 77 K photoluminescence from nominally pure, 0.05 percent Sm-doped, and 0.005 percent Cr-doped $SrTiO_3$ give identical spectra in the infrared (I.R.) with an intensity ratio of 1:20:400, respectively. In undoped and Sm-doped specimens the intensity of emission is vanishingly weak at 4 K in constrast to Cr-doped $SrTiO_3$ in which it is practically unchanged relative to that at 77 K. At 77 K the spectrum consists of a narrow line at 1.5625 eV of half-width $0.5 \times 10^{-3}$ eV which we identify as the zero-phonon line and 31 satellite lines which are shown to be vibronics due to lattice phonons from the center and edge of the Brillouin zone. At 4 K the zero-phonon is a doublet. Comparison with the reported lattice phonon spectrum is satisfactory. In addition, the data suggest the energy of several zone boundary phonons which have not been reported.

In spite of identical emission spectra, undoped, Sm-doped, and Cr-doped specimens have different excitation spectra. This suggests energy transfer from Sm or Cr to a tightly bound center, isolated from the electronic energy bands, such as typically arise from rare earth ions in ionic crystals. It is suggested that the center is an intrinsic defect or intrinsic per se, viz., an exciton.

In undoped $SrTiO_3$ an emission band in the visible—2.175 eV (77 K), 2.475 eV (4 K)—and its excitation spectrum are reported. The temperature dependence of both are anomalous. In contrast to the infrared emission, it is broad (half-width 0.63 eV) and structureless. Application of a dc electric field ~ 100 V/cm, at 4 K, induces oscillations in time of the visible emission, a property not shared by the I.R. emission.

**10966.** Green, M. S., **Generalized Ornstein-Zernike approach to critical phenomena,** *J. Math. Phys.* **9,** No. 6, 875-890 (June 1968).

Key words: Critical phenomena; entropy-energy-volume; fluctuations; fundamental maximum principle; generalized Ornstein-Zernike equation; molecular distribution functions; Ornstein-Zernike theory; Percus-Yevick equation; phase transitions; potentials of average force.

A generalization of the Ornstein-Zernike integral equation is derived and suggestions are made about a possible application to an improved theory of critical phenomena. A fundamental maximum principle of statistical mechanics is used to place the generalized equation in the context of phase transitions and critical points. The equation is a relationship between a generalized correlation matrix by means of which the average fluctuation product of any two sum functions may be expressed and a generalized direct correlation matrix which is the second functional derivative of the functional in the maximum principle. The existence of a critical eigenvector of the direct correlation matrix is proposed and three physical meanings of this vector are given. An explicit formula for the direct correlation matrix is given and is used to derive two asymptotic properties. This formula exhibits an unexpected relationship between the generalized Ornstein-Zernike equation and the Percus-Yevick equation.

**10967.** Haber, S., Osgood, C. F., **On a theorem of Piatetsky-Shapiro and approximation of multiple integrals,** *Math. Comput.* **23,** No. 105, 165-168 (Jan. 1969).

Key words: Approximation; Banach-Steinhaus Theorem; Fourier Series; multiple integrals; number theory; numerical analysis; periodic functions; quadrature.

Quadrature formulas are derived for certain classes of functions of several variables having absolutely convergent Fourier Series. A limitation on formulas of the type considered is proven.

**10968.** Halford, D., Wainwright, A. E., Barnes, J. A., **Flicker noise of phase in RF amplifiers and frequency multipliers: characterization, cause, and cure,** *Proc. 22nd Annual Symp. Frequency Control, Atlantic City, New Jersey, Apr. 22-24, 1968,* pp. 340-341 (Solid State and Frequency Control Division, Electronic Components Laboratory, U.S. Army Electronics Command, Fort Monmouth, New Jersey, Apr. 1968).

Key words: Atomic frequency standards; capacitor noise; cesium beam; flicker phase noise; frequency multipliers; frequency standards; hydrogen maser; negative feedback; noise; phase noise; RF amplifiers; transistor noise.

**10969.** Hall, J. L., **The laser absolute wavelength standard problem,** *IEEE J. Quantum Elect.* **QE-4,** No. 10, 638-641 (Oct. 1968).

Key words: Laser wavelength standards; saturated molecular absorption; wavelength stabilization.

Stabilized lasers usually exhibit systematic frequency shifts larger than their resettability; this phenomenon is illustrated well by the 6328 Å Helium Neon laser. We describe a Lamb-dip stabilized laser which operates at 1.15259 microns in pure, low-pressure (0.12 torr) neon. Optical heterodyne experiments indicate an accuracy exceeding 1 part in $10^9$; short and mediu term precisions of $1:10^{10}$ are easily achieved. We also report the successful operation of a wavelength reference based on the saturation of sharp molecular absorption. In the first experiments the P(7) line of the $\nu_3$ band of methane is saturated insid the cavity of a 3.39 micron Helium-neon laser. The saturatio maximum at molecular line center produces an "emission" feature whose linewidth is less than 5 parts in $10^9$. The pressure-induced offset is expected to be less than 1 part in $10^{10}$. Size scalin is expected to improve these first results by at least 1 decade.

**10970.** Haller, W., Macedo, P. B., **The origin of phase connectivit in microheterogeneous glasses,** *Phys. Chem. Glasses* **9,** No. 5 153-155 (Oct. 1968).

Key words: Connectivity of microphases; fluctuatio theory; glass; intersecting growth theory; microheterogeneous glass; spinoidal decomposition theory.

Recently published electron micrographic studies have show that microheterogeneous glasses with interconnected phases ca form from early stages which consist of randomly distributed is lated spheres. These observations lend support to the previousl postulated Intersecting Growth Theory, and not to the Spinoid Decomposition Theory. While a classic diffusion model predict that the terminal growth rate at approaching surfaces of growin spheres becomes infinitely small due to diffusional depletion the separating matrix, the experimental facts do not show an such limitations since the approaching growth fronts join rapidl Various mechanisms are discussed by which a finite joining-ra can be achieved. A mechanism is suggested which is based upo the fact that the classic boundary concept of diffusion is not an more applicable to bodies of small magnitudes and has to replaced by the concept of a transitional fluctuating boundar From ultrasonic and electron microscopic evidence it is es mated that the fluctuations in the investigated systems are of t order of 50 Å.

It is furthermore shown that for systems having close to equ volume fraction the criterion for the terminal formation of an i terconnected network or of isolated spheroids will be the nucle tion density.

**10971.** Hanley, H. J. M., Childs, G. E., **Interim values for t viscosity and thermal conductivity coefficients of fluid H between 2 and 50 K,** *Cryogenics* **9,** No. 2, 106-111 (Apr. 196

Key words: Corresponding states; Enskog theory; heliu four; kinetic theory; quantum fluid; thermal conductivit viscosity.

We discuss the estimation of viscosity and thermal conducti ty coefficients of $He^4$ between 2 and 50 K for densities up to g/cm³. The literature is reviewed and data sources listed. Inter estimates of the coefficients are given based on limited expe mental data, dilute gas kinetic theory, the Enskog theory, a corresponding states.

**10972.** Hanley, H. J. M., McCarty, R. D., Sengers, J. V., **Dens dependence of experimental transport coefficients of gases,** *Chem. Phys.* **50,** No. 2, 857-870 (Jan. 15, 1969).

Key words: Correlation; density dependence; kine theory; least squares analysis; logarithmic expansion; th mal conductivity; viscosity.

We analyze experimental transport data for several gases a function of density and temperature. Necessary conditions proposed to check if the data are consistent with a given dens ction at fixed temperature. It is found that the theoretically gested density function, which involves terms logarithmic in density, satisfies the conditions for the data examined in the perature and pressure ranges considered. A power series in density does not. Based on the analyses, first density coeffints of thermal conductivity and viscosity are reported, ether with an estimate of their precision, at reduced tempera:s up to T* ≈ 30.

73. Hardy, S. C., Coriell, S. R., **Morphological stability and ne ice-water interfacial free energy,** *J. Crystal Growth* **3,** No. , 569-573 (1968).

Key words: Cylinder; heat flow; ice; interfacial free energy; perturbations; stability; surface tension; water.

he growth rates of slightly perturbed single crystal ice cylins in supercooled water have been measured. Using rphological stability theory, the ice-water interfacial free eners calculated from the experimental observations. A value of 21 J/m² (21 erg/cm²) is obtained. This is in good agreement h values previously obtained from nucleation experiments.

74. Hardy, S. C., Coriell, S. R., **Morphological stability of a rowing cylindrical crystal of ice,** *J. Appl. Phys.* **39,** No. 7, 505-3507 (June 1968).

Key words: Cylinder; heat flow; ice; morphology; perturbations; stability; surface tension; water.

he morphological stability of an ice cylinder growing radially slightly supercooled water is studied. The experimental ults are in agreement with theory.

75. Harris, W. P., Roberts, D. E., **New standard reference ielectric specimens at NBS,** *Proc. 1968 Annual Report Conf. lectrical Insulation and Dielectric Phenomena, Oct. 21-23, 968, Buck Hill Falls, Pa.,* pp. 80-84 (Natl. Acad. Sci. – Natl. es. Council, Washington, D.C., 1969).

Key words: Dielectric constant standards; fluorinated ethylene-propylene; fluorinated polymers; precise dielectric measurements; standard dielectric; standard of dielectric constant; standard reference materials.

number of specimens of FEP (fluorinated ethylenepylene copolymer) have been prepared and measured by the ymer Dielectrics Section of NBS. Several diameters and knesses are available. Values of dielectric constant, dissipa factor and thickness are supplied with each specimen.

ll values are obtained from two-fluid, three-terminal meaements. The estimated uncertainty of the dielectric constant thickness measurement is ±0.05 percent. The dissipation or is accurate to within about $\pm 10 \times 10^{-6}$. (This is a low-loss erial, with dissipation factor about $55 \times 10^{-6}$ at 1 kHz.)

hese specimens are expected to remain mechanically and ctrically stable over a long period of time, and to be relatively from changes due to humidity. They will not have to be kept dessicator.

he technique of measurement is discussed, and data are sented to support the accuracy claim.

76. Hartman, W. J., **Feasibility of communication with a satelte by means of tropospheric scatter,** *IEEE Trans. Commun. echnol.* **COM-14,** No. 3, 251 (June 1966).

Key words: Radio horizon; satellite; tropospheric scatter.

heoretical methods are developed for predicting the transsion loss over a tropospheric scatter path from a point on the th to a satellite. The results indicate that presently available ipment allows reliable communication to only very slightly ond the radio horizon. Some of the difficulties encountered in designing experiments to test the theoretical predictions are investigated.

10977. Hein, R. A., Cox, J. E., Blaugher, R. D., Waterstrat, R. M., **Superconducting behavior of A-15 compounds,** *Solid State Commun.* **7,** 381-384 (1969).

Key words: A-15 type phases; atomic ordering; beta-tungsten compounds; critical magnetic fields; critical temperatures; superconductors.

Superconductivity has been discovered in the A-15 type compounds $V_{1-x}Ni_x$, $V_3Pd$ and $Ta_{85}Pt_{15}$ and a new feature has been observed in the $T_c$ versus e/a correlation for these compounds. Evidence is presented to show that the anomalously low value of $T_c$ for $V_3Pd$ probably results from magnetic interactions which tend to depress $T_c$. Differences in the behavior of 3d compounds as compared with 4d compounds can be explained by the theory of McMillan.

10978. Heinrich, K. F. J., **Common sources of error in electron probe microanalysis,** *Advan. X-ray Anal.* **11,** 40-55 (1968).

Key words: Absorption correction; atomic number correction; electron probe microanalysis; fluorescence correction; quantitative analysis.

In order to reduce the error of quantitative electron probe microanalysis, error sources in the preparation and measurement of specimens and standards must be minimized. These sources of error are described, and literature references for detailed study are given. A critical analysis is made of 150 analytical measurements of binary specimens previously discussed by Poole and Thomas. It is shown that the cases of serious errors reported by these authors are mainly due to poorly characterized or measured specimens and in some cases to the omission of characteristic fluorescence corrections. If these sources of error are eliminated, a much more favorable error distribution can be obtained through relatively simple correction calculations. Further progress in quantitative microprobe analysis is dependent upon measurements using well-controlled conditions and standard materials of experimentally proven micro-homogeneity and reliably determined composition.

10979. Heinrich, K. F. J., **Electron probe microanalysis: a review,** *Appl. Spectry.* **22,** No. 5, Part 1, 395-403 (Sept.-Oct. 1968).

Key words: Analysis; electron probe; microanalysis; spectrometry; x-rays.

This review covers the development of electron probe microanalysis in the last ten years. After a brief description of the instrument, the following subjects are discussed: progress in instrumentation, progress in the theory of quantitative analysis, and the future development of microprobe analysis.

10980. Heinrich, K. F. J., Yakowitz, H., **Quantitative electron probe microanalysis: fluorescence correction uncertainty,** *Mikrochim. Acta* **5,** 905-916 (1968).

Key words: Electron probe microanalysis; error analysis; fluorescence corrections; quantitative analysis; x-ray fluorescence.

In order to evaluate the fluorescence correction uncertainty in electron probe microanalysis, effects of two general types were investigated. The effects of uncertainty in (1) microprobe operational variables, including x-ray emergence angle and operating voltage, and (2) errors in model input parameters, such as fluorescence yield factors and mass attenuation coefficients, were evaluated. The major conclusion of this study is, that even in cases requiring large fluorescence corrections, microprobe operation at high (≥30°) x-ray emergence angles, and at the lowest voltage compatible with a reasonable x-ray output is entirely satisfactory. This conclusion is reached by substituting into existing fluorescence correction models reasonable input parameter errors, x-ray emergence angles, and operating voltages. Results show that absolute compositional errors vary quite slowly with x-ray emergence angle and operating voltage. The chief source of error among input parameters is the fluorescence yield factor. The role of model selection as a source of potential error is also discussed.

**10981.** Henderson, M. M., **Introductory remarks and summary of discussion for symposium on critical reviews,** *J. Chem. Doc.* **8,** 231 and 245 (Nov. 1968).

Key words: Authors of reviews; critical reviews; editorial problems; information requirements; publication problems; review journals.

Critical reviews will be examined in terms of the quality and quantity of their present production, and the measure of their value and utility to scientists in meeting information needs. The papers first present the viewpoints of user, sponsor, author, and editor. The speakers and the audience then discussed present problems and possible future solutions to this aspect of information and communication.

**10982.** Herron, J. T., Penzhorn, R. D., **Mass spectrometric study of the reactions of atomic oxygen with ethylene and formaldehyde,** *J. Phys. Chem.* **73,** No. 1, 191-196 (Jan. 1969).

Key words: Atomic oxygen; ethylene; formaldehyde; kinetics; mass spectrometry; mechanisms; rate constant.

A mass spectrometric study has been made of the reactions of atomic oxygen with ethylene and formaldehyde. The formation of formaldehyde in the ethylene reaction is shown to be independent of the presence of molecular oxygen, and is attributed to a reaction between atomic oxygen and methyl radicals. The formaldehyde reaction has a rate constant at 300 K of $9.0 \times 10^{10}$ cm$^3$ mol$^{-1}$ s$^{-1}$, with an estimated uncertainty of $\pm 3.0 \times 10^{10}$ cm$^3$ mol$^{-1}$ s$^{-1}$.

**10983.** Heydemann, P. L. M., Houck, J. C., **Self-consistent ultrasonic method for the determination of the equation of state of liquids at very high pressures,** *J. Appl. Phys.* **40,** No. 4, 1609-1613 (Mar. 15, 1969).

Key words: Bulk modulus; density; equation of state; high pressure; velocity of sound; water.

Ultrasonic measurements on liquids at very high pressures and an accurate self-consistent ultrasonic method for the determination of the equation of state of liquids at very high pressures are described. The liquid sample is contained in a polyethylene-lined piston and cylinder device. The method described requires only the measurement of the transit time of an ultrasonic pulse through the liquid as a function of pressure. The difficulties and errors connected with a direct volumetric determination are thus avoided and a high accuracy is achieved. A computation of the uncertainties in the determination of the bulk moduli, the density and the velocity of sound is presented. Experimental results are given for water at 22 °C and pressures up to 12.6 kbar. Data for the density of water reported by P. W. Bridgman and by L. H. Adams, and for the velocity of sound reported by Holton, *et al.*, are found to be in good agreement with the present work.

**10984.** Hicho, G. E., Meyerson, M. R., Geil, G. W., **Effect of slack-quenched structures on the tensile properties of AISI 5140 steel,** (Proc. Intern. Conf. Strength of Metals and Alloys, Tokyo, Japan, Sept. 4-8, 1967), *Suppl. Trans. Japan Inst. Metals* **9,** 134-142 (1968).

Key words: AISI 5140 steel; hardness; heat treatment; reduction of area; slack-quenched structures; tempering temperature; tensile strength; yield strength.

Slack-quenched structures in steels are generally believed t
be detrimental even though adequate data on the tensile behavic
of these structures are not available. Results are reported of a
investigation on the tensile behavior of specimens of AISI 514
steel slack-quenched to different hardness levels and tested i
the conditions as (1) slack quenched and stress relieved at 27
°F, (2) slack quenched and tempered at 400, 550, 700, 850 an
1000 °F, and (3) slack quenched and tempered to selected harc
ness levels. The tempering of the slack-quenched specimens ha
a very beneficial effect on the yield behavior and ductility; ten
pering slack-quenched specimens to a reduction of $R_c$ 5 to 7 i
hardness generally produced a maximum increase in the yiel
strength. Moreover, the yield strength and reduction of area
the slack-quenced specimens tempered to a reduction of $R_c$ 5 t
7 or more in hardness were nearly equal to those of full
hardened specimens tempered to the same hardness level.

**10985.** Hiza, M. J., Duncan, A. G., **A simple gas recirculati
pump for low flow and high pressure applications,** *Rev. Sc
Instr.* **40,** No. 3, 513-514 (Mar. 1969).

Key words: High pressure; low flow rate; pump; recircul
tion.

A simple pump is described which was designed to recircula
the gas phase in vapor-liquid phase equilibrium studies at flo
rates approximately 100 cc/min and at pressures up to 200
mospheres.

**10986.** Hiza, M. J., Heck, C. K., Kidnay, A. J., **Liquid-vapor a
solid-vapor equilibrium in the system hydrogen-ethylene,** *Pr
Symp. Cryogenic Advance in the Space Program, Tam
Florida, May 19-22, 1968,* **64,** No. 88, 57-65 (American I
stitute of Chemical Engineering, New York, N.Y., 1968).

Key words: Ethylene; hydrogen; hydrogen-ethyle
system; liquid-vapor equilibrium; low-temperature pha
equilibrium; solid-vapor equilibrium; solubility of hydrog
in liquid ethylene.

Equilibrium gas phase compositions in the system hydrog
ethylene were measured for nine isotherms from 80 to 170
generally to 130 atm.; equilibrium liquid phase compositi
were measured for four of the isotherms from 122 to 170 K
150 atm. Gas phase compositions up to 130 K were determin
with a single-pass solid-vapor apparatus using continuous an
sis with a hydrogen flame-ionization detector. The remainder
the measurements were made in a vapor-recirculating liqu
vapor apparatus using chromatographic analysis with a therr
conductivity detector.

Isobaric comparison of enhancement factors, $y_1\pi/p_{01}$, sho
the gas phase data obtained by the two methods to be in excell
agreement. Poor agreement was found with the earlier gas
liquid phase data of Williams and Katz and of Likhter and T
honovich. The present investigation provides the only gas ph
data below the ethylene triple point, 103.97 K.

**10987.** Hogben, D., **The distribution of the sample variance fr
a two-point binomial population,** *Am. Stat.* **32,** No. 5, 30 (D
1968).

Key words: Distribution; parameter; probabilities; rand
sample; two-point binomial; variance.

In a random sample of size n the sample variance is $S^2 = \Sigma$
$(\overline{X}_i - \overline{X})^2/(n-1)$. For the two-point binomial distribution, i
shown that for $c = i(n-i)/n(n-1)$ and $i = 0, 1, \ldots,$ [n

$$\Pr\{S^2 = c\} = \binom{n}{i}\ p^i q^i\ \ (p^{n-2i} + q^{n-2i}),\ \ i < n/2. = \binom{n}{n/2}\ p^{n/2}$$

n even and $i = n/2$.

Two examples are given.

**988.** Hoover, T. B., **The N-methylpropionamide-water system. Densities and dielectric constants at 20-40°**, *J. Phys. Chem.* **73,** No. 1, 57-61 (Jan. 1969).

Key words: Density; dielectric constant; excess molar volume; Kirkwood correlation parameter; N-methylpropionamide; structure; water.

Densities and dielectric constants of the N-methylpropiona-ide (NMP)—water system were measured at 20, 30 and 40 °C. he curve of excess molar volume of the system *vs.* mole frac-n of water was essentially independent of temperature and had minimum of −1.32 cm$^3$ at 0.6 mole fraction of water. The olar volume of transfer of NMP from the pure liquid to a dilute lution in water had a minimum of −6.0 cm$^3$ at 0.9 mole frac-n of water. The dielectric data for the system were analyzed in rms of pseudo-Kirkwood correlation factors, calculated on the sis that the square of the gas-phase moment and the high-equency dielectric constant for the mixture were linear func-ns of the mole fractions of the components. The structural pro-rties of the system are discussed with respect to the cor-sponding data for the mixtures of water with N-methylaceta-ide, ethanol, or acetic acid. NMP and water each exerts a rong effect on the structure of the other.

**989.** Hubbell, J. H., Berger, M. J., **Photon attenuation. Attenuation coefficients, energy absorption coefficients, and related quantities,** Chapter 4 in *Engineering Compendium on Radiation Shielding,* R. G. Jaeger, E. P. Blizard, A. B. Chilton, M. Grotenhuis, A. Honig, T. A. Jaeger, H. Eisenlohr, eds., **1,** 167-202 (International Atomic Energy Agency, Vienna, Austria, 1968).

Key words: Attenuation coefficient; Compton scattering; cross section; energy absorption coefficient; gamma rays; pair production; photoelectric absorption; photons; x-rays.

This paper consists of two parts. The first part contains tabula-ons of the photon attenuation coefficient and the energy ansfer coefficient. The values of the attenuation coefficient present a revision which takes into account new theoretical ata on the photoelectric effect and on radiative corrections to ompton scattering and pair production. Rayleigh (coherent) attering and the photonuclear effect are disregarded, but can included by use of auxiliary tables. The main tables cover the ergy range 10 keV to 100 MeV for 21 elements and four mix-res. This range is extended to 10 GeV for 16 elements by inter-olation from experimental data. The energy transfer coefficient ata were taken directly from tabulations in the literature, and ver the energy range 10 keV to 100 MeV. In the second part, formation is given on the individual processes (photoelectric sorption, Compton scattering, pair production and other in-ractions of photons with matter) which combine to give the at-nuation coefficient. Theoretical and experimental data are viewed, and numerical tables and approximation formulas are ven.

**990.** Hudson, R. P., **The delta campaign. An account of the controversy surrounding the temperature scale for CMN,** *Cryogenics* **9,** No. 2, 76-79 (Apr. 1969).

Key words: CMN; low temperature; paramagnetic susceptibility; thermometry.

Theory predicts that the susceptibility of cerous magnesium trate will closely approximate Curie's law below 1 K and into e millikelvin region. Specifically, $\chi = c(T - \theta)^{-1}$, with $\theta =$ 0.27 mK. Single crystal specimens substantiate this prediction own to about 6 mK, below which strong deviations begin to ap-ear and the susceptibility reaches a limiting, maximum value for mperatures below 2 mK. On the other hand, thermometers shioned (for convenience) from powdered CMN and shaped into cylinders of diameter equal to height, appear—from the properties of $^3$He and expectations as to their temperature-dependence—to obey Curie's law down to 3 mK and below. Such drastic differences are of considerable importance, inasmuch as CMN is the only practical thermometer currently available for this region of temperature.

At various times, interested parties have expressed strong views that either the single crystal thermometric results or those for powder cylinders were wrong, or speculated that both might be correct. A condensed survey is here presented of the details of the dilemma, recent attempts to resolve it, and the situation at present.

**10991.** Hudson, R. P., Kaeser, R. S., **Magnetic temperature scale 0.002–5 K,** *Proc. Xth Intern. Conf. Low Temperature Physics, Moscow, U.S.S.R., Aug. 31-Sept. 6, 1966,* **Vol. 1,** *Properties of Helium,* Paper H4, pp. 171-173 (1968).

Key words: Cerous magnesium nitrate; low temperatures; magnetic cooling; magnetic thermometer; paramagnetic salt; temperature scale.

Our previous measurements of the heat capacity of cerous magnesium nitrate (CMN) as a function of susceptibility using gamma-ray heating have been superseded by new data obtained with a new single-crystal sphere following various improvements in apparatus and procedure. The entropy-susceptibility relation is the same for all specimens and is thus independent of ellipsoid axial ratio; the indicated value of b (coefficient of $T^{-2}$ for "high temperature" heat capacity) is 15 percent smaller than calculated by Cooke, Duffus and Wolf. Combining the heat capacity and entropy data led to values of absolute temperature, which fall below 0.002 K for the lowest entropy obtained, viz. $S/R = 0.25$. In the region between 0.02 and 0.2 K where both dipole-dipole and lattice specific heat are very small, an anomalous and apparently nonmagnetic contribution to the heat capacity was detected. No explanation for this has been found, but its existence undoubtedly accounts for the apparently non-isentropic demagnetizations experienced for "starting conditions" H/T less than 0.37 oersteds deg$^{-1}$.

**10992.** Huget, E. F., Brauer, G. M., **Reactivity of the components of tooth structure,** *J. Colloid Interface Sci.* **27,** No. 4, 714-721 (Aug. 1968).

Key words: Anorganic whole tooth; components of tooth; dentin; heat of reaction; reactivity of anorganic whole tooth surfaces; reactivity of dentin surfaces.

A restorative material capable of adhering to tooth structure is greatly needed. Bonding is complicated by the complex nature of tooth structure as well as the mechanical, toxicologic and bacteriologic conditions which occur in the oral cavity. Heats of immersion ($-\Delta H_w$) measurements for dentin, enamel and anorganic whole tooth tissue of known specific surface have been used to study the reactivity and degree of surface modification produced by various ions and functional groups in an aqueous environment. A decrease in the $-\Delta H_w$ value of dentin in water from 10.3 cal/g (4100 ergs/cm$^2$) to 4.0 cal/g (1590 ergs/cm$^2$) in 2-40 percent aqueous solutions of organic solvents suggests the strengthening of electrostatic bonds between polar groups of the collagenous matrix of dentin. In absolute ethanol and hexane, dentin absorbs heat indicating the weakening of hydrophobic bonds. $-\Delta H_w$ values for anorganic whole tooth in aqueous solutions of organic solvents are not appreciably different from those obtained in water (109 ergs/cm$^2$). The presence of $NO_3^-$, $NO_2^-$, $CNS^-$, ${}_2SO_4^=$, and $I^-$, at pH 5 depressed the $-\Delta H_w$ of dentin to 4.8 cal/g (1910 ergs/cm$^2$). Other anions ($F^-$ and $Cl^-$) had no appreciable effect. At pH 8, however, anions did not appreciably alter the $-\Delta H_w$ of dentin. The addition of aldehyde groups to the liquid adsorbate at pH 8 resulted in the lowering of the apparent $-\Delta H_w$ value of dentin. Changes in $-\Delta H_w$ values for anorganic whole tooth in the presence of anions or aldehyde groups were relatively small.

**10993.** Hummer, D. G., **Non-coherent scattering-IV. Doppler redistribution functions in moving atmospheres,** *Monthly Notices Roy. Astron. Soc.* **141,** 479-488 (Dec. 1968).

Key words: Non-coherent scattering; radiation transfer; redistribution function; spectral line.

Redistribution functions and their directional averages are derived for scattering by an assembly of atoms possessing a Maxwellian distribution in a frame moving with respect to the observer. Various assumptions concerning the form of the absorption coefficient and the coherence properties in the atom's rest frame are considered. The exact redistribution function for pure Doppler broadening is expanded in Legendre polynomials to facilitate evaluation of the source function. From the expansion it is clear that the use of direction-averaged redistribution functions will be significantly less accurate for moving than for static media.

**10994.** Hummer, D. G., Rybicki, G. B., **Line formation in differentially moving media with temperature gradients,** *Proc. Natl. Center for Atmospheric Research Conf. Resonance Lines in Astrophysics, Sept. 9-12, 1968, Boulder, Colo.*, pp. 315-330 (National Center for Atmospheric Research, Boulder, Colo., Dec. 1968).

Key words: Planetary nebulae; radiative transfer; spectral lines; velocity fields.

The line formation problem for two-level atoms scattering with complete redistribution is solved numerically for plane parallel media in which the macroscopic velocity, electron temperature and all other properties of the atmosphere are arbitrary functions of optical depth.

**10995.** Hummer, D. G., Rybicki, G. B., **Red-shifted line profiles from differentially expanding atmospheres,** *Astrophys. J.* **153,** No. 2, L107-L110 (Aug. 1968).

Key words: Expanding atmosphere; red-shift; spectral line.

Solutions of non-LTE line transfer methods for a differentially expanding atmosphere are shown to possess a red-shifted intensity peak in cases when a substantial fraction of the atmosphere is moving towards the observer. This phenomenon arises because photons in the red wing of the line see a smaller opacity than do those in the blue wing and therefore escape more readily.

**10996.** Hutchinson, J. M. R., Mann, W. B., Smith, C. N., Whittaker, J. K., **The half lives of two excited states in $^{239}$Np,** *Intern. J. Appl. Radiation Isotopes* **20,** No. 7, 493-498 (July 1969).

Key words: Alpha-particle; americium-243; excited states; gamma-ray; half-life; neptunium-239.

The half-life of the 74 keV(5/2-) state of $^{239}$Np has been determined to be 1.380 ns ± 0.032 ns where the uncertainty represents the sum of estimated bounds to the systematic error, ±0.010 ns, and twice the standard error of the mean, ±0.022 ns. The half-life of the 118 keV(7/2-) states of $^{239}$Np has been found to be less than 0.04 ns.

**10997.** Hyde, K. E., Gordon, G., Kokoszka, G. F., **Magnetic properties of some binuclear copper(II) complexes,** *J. Inorg. Nucl. Chem.* **30,** 2155-2161 (1968).

Key words: Copper monochloroacetate 2.5 hydrate; dichlorobis-(pyridine-N-oxide)copper(II); dichloromonoaquo-(pyridine-N-oxide)copper(II); exchange interactions; J values; magnetic susceptibility; spin-spin coupling.

The magnetic susceptibility of three binuclear copper compounds, dichloromonoaquo-(pyridine-N-oxide)copper(II), [$CuCl_2$(pno)], dichlorobis(pyridine - N - oxide)copper(II), [$CuCl_2(pno)_2$, and copper monochloroacetate 2.5 hydrate, [$Cu(ClAc)_2$], has been measured as a function of temperature. The exchange integral, J, has been determined to be 943 $cm^{-1}$, 770 $cm^{-1}$, and 292 $cm^{-1}$ for $CuCl_2$(pno), $CuCl_2(pno)_2$, and $Cu(ClAc)_2$, respectively. These values are compared to the J values determined by electron spin resonance on the same three compounds. A brief discussion of the accuracy of these values is presented. In addition, for two of the compounds, $Cu(ClAc)_2$ and Cu(pno), a better fit of the data was possible by assuming the presence of a small amount of monomeric ion in the samples. This was verified by additional ESR measurements.

**10998.** Ito, J., Johnson, H., **Synthesis and study of yttrialite,** *Am. Mineralogist* **53,** 1940-1952 (Nov. 1968).

Key words: Crystal chemistry; gel-preparation; inorganic synthesis; mineral identification; polymorphism; rare-earth silicate; solid solubility; x-ray powder analysis.

The rare-earth pyrosilicates, $R_2^3\ Si_2O_7(R^3 =$ Sc, In, Lu, Yb, Tm, Er, Ho, Y, Dy, and Gd) were synthesized at temperatures from 900-1,600 °C in air. "High-yttrialite" was identified as $\alpha$-$(Y,RE)_2Si_2O_7$ from the results of recrystallization of the natura mineral and by direct synthesis from gels both in air and unde water pressure.

A solid solution series exists between $Sc_2Si_2O_7$(thortveitite and $\rho$-$Y_2Si_2O_7$ at 1,300 °C in air and at 700 °C under 2.5 kb. The compositional range from $Y_2SiO_5-Y_2Si_2O_7-Y_2Si_3O_9$ was investigated at temperatures from 900-1,500 °C.

The phase described as "low-yttrialite" is a complex silicate o approximate formula $R(Y,RE)_5Si_6O_2$ where R includes ions o great variety, such as Na, $Mg^2$, $Fe^2$, $Fe^3$, $Al^3$, $Mn^2$, $Th^4$ and $Zr^4$

**10999.** Iverson, W. P., **Mechanisms of microbial corrosion,** (Proc First Intern. Biodeterioration Symp., Southhampton, England Sept. 9-14, 1968), Chapter in *Biodeterioration of Materials Microbiological and Allied Aspects,* pp. 28-43 (Elsevier Publ Co., Ltd., Essex, England, 1968).

Key words: Anaerobic corrosion; cathodic depolarization corrosion mechanisms; metabolic products; microbial corrosion; oxygen concentration cells.

A discussion of the general and specific mechanisms c microbial corrosion with special emphasis on anaerobic corrosion. General mechanisms include the production of corrosiv metabolic products, the initiation of oxygen concentration cell and cathodic depolarization. Recent evidence to be presented indicates that the cathodic depolarization theory may at least i part explain the corrosion due to microorganisms in an anaerobi environment.

**11000.** Iverson, W. P., **Microbiological corrosion,** *Proc. Con Corrosion and Protection of Pipes and Pipelines, Londo England, June 13, 1968,* 6 pages (Technical Exhibited Ltd London, England, 1968).

Key words: Anaerobic corrosion; cathodic depolarizatio desulfovibrio; microbial corrosion; sulfate-reducing ba teria; thiobacilli; underground pipeline corrosion.

A discussion of the microorganisms associated with microbi corrosion with emphasis on the sulfate reducers. Th mechanisms by which these microorganisms can cause corrosic include: (a) the production of corrosive metabolic products; ( the formation of concentration cells; (c) cathodic depolarizatio (d) combinations of (a), (b) and (c); (e) miscellaneo mechanisms. Corrosive metabolic products which are formed i clude hydrogen sulfide, ammonia and various acids. The form tion of concentration cells will be discussed as it relates to the e rior and interior of pipelines. As the mechanism of cathodic polarization by bacterial action has been so generally postu-ted to explain anaerobic corrosion of buried structures, recent idence for and against this mechanism will be elaborated upon. ractical measures to be instituted in preventing microbial corro-on involve placing underground structures, whenever possible, "non-aggressive" soil or protection of structures in "aggres-ve" soil by cathodic protection, protective coatings, or both.

**001.** Ives, J. M., Hughes, E. E., Taylor, J. K., **Absolute determination of low concentrations of oxygen in inert gases by means of galvanic cells,** *Anal. Chem.* **40,** No. 12, 1853-1856 (Oct. 1968).

Key words: Galvanic cells; gas analysis; gas analysis using electrochemical methods; oxygen determination; trace gas analysis; trace oxygen determination.

A method has been developed for the absolute determination oxygen in inert gases over the range from about 1 to 1000 ppm ygen. The gas to be analyzed is caused to flow through a series galvanic cells similar to the type developed by Hersch. Under e conditions used, most of the oxygen in a stream of gas is moved in the first cell; subsequent cells reduce oxygen concen-ations to virtually zero in the effluent gas. Measurement of the crease in all cell current outputs when the gas flow rate is in-eased by a known increment allows calculation of the absolute ygen concentration.

**1002.** Jacox, M. E., Milligan, D. E., **Matrix-isolation study of the infrared spectrum of the free radical $F_2CN$,** *J. Chem. Phys.* **48,** No. 9, 4040-4046 (May 1, 1968).

Key words: $CF_2NF$; $CF_3NF_2$; F atom reaction; FCN; $F_2CN$; FC=NF; free radical; infrared spectrum; matrix isolation; photolysis; ultraviolet spectrum.

In studies of the reaction of photolytically produced F atoms ith FCN in Ar and $N_2$ matrices at 14 K, the free radical $F_2CN$ stabilized in sufficient concentration for observation of its elec-onic spectrum and of six infrared absorptions. A vibrational as-gnment has been made. The carbon-nitrogen bond is found to ossess double bond character. Products of further F atom at-ick on $F_2CN$, including $CF_2NF$ and $CF_3NF_2$, are observed in ese experiments. Evidence is presented suggesting that the pecies FC=NF may also be stabilized.

**1003.** Jacox, M. E., Milligan, D. E., **Matrix-isolation study of the vacuum-ultraviolet photolysis of trichlorosilane. The infrared spectrum of the free radical $SiCl_3$,** *J. Chem. Phys.* **49,** No. 7, 3130-3135 (Oct. 1, 1968).

Key words: Force constants; free radical; infrared spectrum; matrix isolation; photolysis; $SiCl_3$; trichlorosilane; ultraviolet spectrum.

In studies of the vacuum-ultraviolet photolysis of $HSiCl_3$ in rgon and nitrogen matrices at 14 K, features appear near 470 nd 582 cm$^{-1}$ which may be identified with the two stretching undamentals of $SiCl_3$. Evidence supporting primary hotodecomposition by detachment of the H atom has been ob-ained in CO matrix experiments, in which HCO is a major roduct. The observed frequencies permit estimation of an angle f 72 ± 5° between the threefold axis and each of the Si-Cl bonds. orce constants have also been estimated. The FG-matrix treat-nent is presented for the stretching modes of a nonplanar $X_2YZ$ pecies with equal XYX and XYZ valence angles. The calcu-ated frequency and intensity pattern for the mixed chlorine sotopic species is in excellent correspondence with the observed attern, providing strong support for the identification and roposed vibrational assignment. Unstructured absorptions etween 2900 and 3300 Å and between 2150 and 2450 Å are entatively attributed to $SiCl_3$.

**11004.** Jespersen, J. L., Kamas, G., Gatterer, L. E., MacDoran, P. F., **Satellite VHF transponder time synchronization,** *Proc. IEEE* **56,** No. 7, 1202-1206 (July 1968).

Key words: Atomic oscillators; clock synchronization; VHF satellite transponder.

This paper describes an experiment designed to transfer accurate time between two widely separated clocks using a VHF satellite transponder. The satellite used was the NASA Application Technology Satellite ATS-1. The experiment used atomic oscillators to maintain accurate time at each station and the synchronization was accomplished by measuring the round trip delay times between the stations. The goal of the experiment was to evaluate a VHF system because of the low cost ground equipment involved. This was in contrast to microwave systems. The paper discusses the results and the various factors that contributed to the timing errors.

**11005.** Johannesen, R. B., Gordon, C. L., **Titanium(IV) bromide (titanium tetrabromide),** Chapter IV in *Inorganic Syntheses* **IX,** 46-50 (McGraw-Hill Book Co. Inc., New York, N.Y., 1967).

Key words: Hydrogen bromide; titanium; titanium tetrabromide; titanium tetrachloride.

Directions are given for the preparation of titanium tetrabromide. Distilled titanium tetrachloride is treated with an excess of gaseous hydrogen bromide and the product distilled under dry nitrogen into a container which can be sealed. Titanium tetrabromide prepared in this manner was found to contain 0.03 percent of chloride. The yield was 85 percent.

**11006.** Johnson, V. J., **Development and operation of a specialized technical information and data center (The Cryogenic Data Center),** *J. Chem. Doc.* **8,** No. 4, 219-224 (Nov. 1968).

Key words: Bibliography service; cryogenics; current awareness; data center; data evaluation; development; information retrieval; operation; technical information center.

As is typical of many specialized areas of science and technology, cryogenics has had an explosive development in the last decade and a half. The Cryogenic Data Center was established in 1958 to cope with the problem of organizing the world's literature pertinent to the field of cryogenics and furnishing this rapidly developing industry with reliable information and data. The development of this facility over the ten year period of its existence is discussed. Included is a description of the conversion from a manual to an automated bibliographic retrieval system, the development of cataloging and indexing techniques, the development of comprehensive awareness and literature acquisition procedures with public announcement of new literature, procedures for selecting and compiling data, and finally how the needs of the sponsors and the industry are being served. The discussion emphasizes the problems that are typical in facilities of this type and the need to consider standard or generally accepted solutions. The growing trend for a network system of technical information and data centers requires a high order of compatibility among them.

**11007.** Joiner, B. L., Rosenblatt, J. R., **The mean deviation and range for n = 3,** *Am. Stat.* **22,** No. 4, 37-38 (Oct. 1968).

Key words: Mean deviation; range; samples of size 3; statistics.

Although it is well known that the mean deviation from the sample median is identical to one-third the range for samples of size three from *any* distribution, it is not so well known that the mean deviation from the sample mean has the same distribution as $2/\sqrt{27}$ times the range for samples of size three from the *normal* distribution. In this note a simple method of proving the relationship between the distributions is given, based on the fact that linear functions of normal random variables are normally distributed.

**11008.** Jones, M. C., Giarratano, P. H., Simpson, A. U., **Flow and heat transfer characteristics of sub-triple-point cryogens in heated tubes,** *Proc. Second Intern. Cryogenic Enineering Conf., Brighton, England, May 7-10, 1968,* pp. 83-88 (Iliffe Science and Technology Publ., Ltd., Guilford, Surrey, England, 1968).

Key words: Flow; hydrogen; nitrogen; solid plug; solid-vapor mixture; sub-triple point; tubes.

When liquids are expanded to pressures below their triple point pressures they form two-phase, solid-vapor mixtures. The continuous discharge of such mixtures through tubes is important in a variety of situations in space vehicles, but this can only be assured if the tubes are heated. By studying heat transfer some insight has been gained into the mechanism of particle-wall interaction, which leads eventually, at low heat input, to a tube completely plugged with solid. A similarity criterion is proposed by which minimum adequate heating conditions might be correlated. Experimental values are given.

**11009.** Judd, D. B., **1964 CIE supplementary observer applied to the colorimetry of rutile and anatase forms of titanium dioxide,** *J. Opt. Soc. Am.* **58,** No. 12, 1638-1649 (Dec. 1968).

Key words: Color difference; colorimetry; color-matching functions; titanium dioxide; whiteness.

The study by White and Jacobsen of the applicability of the 1964 CIE supplementary observer to large-field colorimetry of the rutile and anatase crystal forms of titanium dioxide has been repeated. The six painted panels used by them were remeasured on a Hardy-type spectrophotometer with closely agreeing results. The arrangement of the panels in order of whiteness by north-sky light was made by 24 observers, yielding 45 arrangements, and these too were in good inverse agreement with the 26 yellowness arrangements made by 13 observers by White and Jacobsen. The spectrophotometric data were reduced to values of $U^*$, $V^*$, $W^*$ of the 1964 CIE uniform color space, and the sizes of the chromaticity differences between each panel and the magnesium oxide whiteness standard were computed. By substituting, for CIE illuminant $C$, the newly recommended CIE illuminants $D_{6500}$ and $D_{25000}$, representative of overcast sky and clear sky, respectively, and by taking account of normal variations of amount of lens pigment from one observer to another, we found that the 1964 CIE supplementary observer yields correct predictions of the frequency of the various whiteness arrangements of the six panels.

**11010.** Judd, D. B., **Color science and the paint industry,** *J. Paint Technol.* **40,** No. 525, 470-477 (Oct. 1968).

Key words: Absorption; color; colorant; metamerism; paint; scattering; spectrophotometry.

The principal color problems of the paint industry are color control, color permanence, colorant formulation, and filing of paint information according to color. To assist in solving these problems, color science has to offer, first and foremost, the spectrophotometer; second, the weighting functions defining the 1931 CIE standard observer for colorimetry; third, various tridimensional systems of color notation; and finally, the Kubelka-Munk theory of the light reflected by a layer which both absorbs and back-scatters the incident light. The spectrophotometer assists in color control by providing a permanent record of the reflectance of the paint chip as originally prepared. It also provides the basic data by means of which colorant formulation by instruments is possible. Tridimensional systems of color notation provide convenient forms for filing of paint recipes and production notes. The Kubelka-Munk theory provides the basic structure by which colorant formulation by instrumentation becomes routinely practical for large organizations.

**11011.** Kahn, A. H., **Polarons in anisotropic energy bands,** *Phys. Rev.* **172,** No. 3, 813-815 (Aug. 15, 1968).

Key words: Effective mass; energy bands; ionic crystals; polarons; semiconductors; strontium titanate.

The polaron weak coupling approximation has been applied to the problem of an electron on a spheroidal energy surface interacting with longitudinal optical phonons. The binding energy and effective masses are calculated. For $SrTiO_3$, where the observed masses are $m_l^*/m_o = 6.0$ and $m_t^*/m_o = 1.5$, the calculated bare masses are 4.7 and 0.96, respectively, and the binding energy is 0.26 eV. It is also shown how the polaron properties may be calculated when the band edge is of the degenerate type.

**11012.** Kamper, R. A., **Cryoelectronics,** *Cryogenics* **9,** No. 1, 20-25 (Feb. 1969).

Key words: Electronics; low temperature; superconductin devices.

This is a review of the progress to date in applying superconductivity to electronics.

**11013.** Kaufman, V., Radziemski, L. J., **Redetermined level value and interaction parameters of S I and Cl II ground configurations,** *J. Opt. Soc. Am.* **59,** No. 2, 227-228 (Feb. 1969).

Key words: Chlorine; energy levels; ground configurations Slater-parameters; sulfur; vacuum-ultraviolet.

Values for the levels of the ground configurations of S I and C II have been determined from new wavelength measurements i the vuv spectral region. Calculations of the Slater parameters t fit these levels were made and indicate the need for the configuration interaction parameter, $\alpha$.

**11014.** Keller, R. A., **Excited triplet → singlet intersyste crossing,** *Chem. Phys. Letters* **3,** No. 1, 27-29 (Jan. 1969).

Key words: Delayed fluorescence; fluorescence; i tersystem crossing; phosphorescence; triplet states.

The quantum yield for intersystem crossing from excite triplet states into the singlet manifold was estimated for sever molecules by observing the fluorescence emission from th lowest excited singlet state which resulted from photo-excitatic of metastable triplet states. In all cases these quantum yiel were very small.

**11015.** Keller, R. A., Dolby, L. J., **Intramolecular energy transf between triplet states of weakly interacting chromophores. II Compounds in which the chromophores are separated by a rig steroid bridge,** *J. Am. Chem. Soc.* **91,** No. 6, 1293-1299 (Sep 1969).

Key words: Energy transfer; fluorescence; phospho escence; triplet state.

The intramolecular transfer of triplet excitation betwe chromophores held approximately 15A apart by a rigid stero bridge was measured for two molecules. The acceptor in bo cases is the naphthalene chromophore. In I the donor is t benzophenone chromophor and in II the donor is the carbaz chromophore. The rate constant for transfer is 25 $s^{-1}$ for I a $0.04\ s^{-1}$ for II. The 1000 fold difference in these rate consta is paralleled by the 1000 fold difference in the triplet st lifetime for two donor chromophores. In both cases the trans of singlet excitation energy was more than the transfer of trip excitation energy.

1016. Kelley, R. D., Klein, R., Scheer, M. D., **The *cis-trans* effect in the H-atom addition to olefins,** *J. Phys. Chem.* **73,** No. 4, 1169-1170 (Apr. 1969).

Key words: Addition reactions; *cis, trans*; hydrogen atom; octadiene.

The relative rate of addition of hydrogen atoms to the two $\pi$-onds in *cis, trans* 2,6-octadiene has been measured in the yogenic temperature region. It has been found that the addition eaction at the *trans* double bond is 20 percent faster than at the *s* double bond. This effect is independent of temperature in the egion 90 to 143 K. Similar results by other workers for other *cis-uns* systems suggest that this effect be ascribed to steric hindance of the approach of the hydrogen atom.

1017. Kim, Y-K., Inokuti, M., Chamberlain, G. E., Mielczarek, S. R., **Minima of generalized oscillator strengths,** *Phys. Rev. Letters* **21,** No. 16, 1146-1148 (Oct. 14, 1968).

Key words: Absolute; cross section; electron; generalized oscillator strengths; theory; xenon.

Frequent occurrence of zero or near-zero minima of the eneralized oscillator strength is closely connected with the odes of the radial wave functions for the states involved. Some eneral implications of the minima are discussed, and, as an exmple, experimental and theoretical results for a transition in Xe re presented.

1018. King, R. J., Maley, S. W., Wait, J. R., **Experimental and theoretical studies of propagation of ground waves across mixed paths,** (Proc. URSI Symp. Electromagnetic Wave Theory, Delft, Holland, Sept. 1965), Chapter in *Electromagnetic Wave Theory,* J. Brown, ed., pp. 217-224 (Pergamon Press Inc., New York, N.Y., 1965).

Key words: Electromagnetic ground waves; ground waves; nonhomogeneous paths; propagation of ground waves.

The propagation of electromagnetic ground waves along nonhomogeneous paths has received considerable interest in the ast three decades. As a result, several empirical and semi-empirical solutions have been developed and proven useful in calcuating the portion of a ground wave transmitted across a coast ine. These methods generally have been replaced by more igorous formulations. Experimental results have been rather meager since ground waves are primarily important at low and very low frequencies where the distances involved are large. Furthermore, it is difficult to evaluate the unwanted effects of other nearby terrain and objects. Therefore, the experiments described here have utilized small laboratory models which simulate, as closely as possible, the mathematical model used in he theoretical formulations. In this way, distances and other parameters can be carefully measured and controlled. If the experimental results compare favorably with the theoretical solution, the theory can then be applied to naturally occurring mixed paths with considerably more confidence.

11019. Kirby, R. K., Rothrock, B. D., **Thermal expansion of vitreous selenium from −190 to +30 °C,** *J. Am. Ceram. Soc.* **51,** No. 9, 535 (Sept. 1968).

Key words: Grüneisen's parameter; linear thermal expansion; vitreous-selenium.

A vitreous-silica dilatometer was used to measure the linear thermal expansion of selenium glass from −190 to +30 °C. An attempt to measure the expansion above 30 °C with an optical comparator did not produce satisfactory results. The coefficients of linear thermal expansion at −190, 0, 20, and 30 °C are 32.4, 45.5, 51.3 and $93 \times 10^{-6}$ °C respectively. Grüneisen's parameter was determined to be constant, $\gamma = 1.0 \pm 0.1$, over the temperature range −190 to +20 °C.

11020. Kirchhoff, W. H., **The microwave spectrum, structure, and dipole moment of *cis*-thionylimide,** *J. Am. Chem. Soc.* **91,** 2437-2442 (1969).

Key words: Dipole moment; HNSO; isotopic species; microwave spectrum; Stark effect; structural parameters.

The microwave spectrum of thionylimide, HNSO, has been observed and assigned to the planar, *cis* form. The structural parameters are $d_{NH} = 1.029 \pm 0.01$ Å, $d_{NS} = 1.512 \pm 0.005$ Å, $d_{SO} = 1.451 \pm 0.005$ Å, $<$HNS$= 115.8° \pm 1°$ and $<$NSO$= 120.4° \pm 0.5°$ where the uncertainties are estimated to account for the effects of zero point vibrations. The dipole moment and its components along the principal axes in the HN$^{15}$SO isotopic species are $\mu_a = 0.893 \pm 0.003$ Debyes, $\mu_b = 0.181 \pm 0.005$ Debyes and $\mu = 0.911 \pm 0.003$ Debyes where the uncertainties are the standard deviations of the reported values, from the least squares analysis. Since no attempts were made to make a complete assignment of the impure sample, no comments can be made about the possible existence of *trans*-NSO.

11021. Klein, M., Hanley, H. J. M., **Selection of the intermolecular potential. Part 2. From data of state and transport properties taken in pairs,** *Trans. Faraday Soc.* **64,** Part 2, No. 551, 2927-2938 (Nov. 1968).

Key words: Equilibrium properties; experimental data; intermolecular potential function; simultaneous correlation; theory; transport properties.

In a previous paper we developed a method to evaluate quantitatively the relationship between intermolecular potential functions and macroscopic properties. This method was applied to a study of the second virial, Joule-Thomson, viscosity and diffusion coefficients. In this work the method has been extended to the simultaneous fit of all possible pair combinations of these properties. As before the relationship between function families available at this time has been clarified. New results from this investigation give important information on the possible simultaneous fit of a simple function to more than one property. The function families studied were the m-6, Kihara, exp-6 and Morse functions.

11022. Klose, J. Z., **Atomic lifetime measurements with pulsed electron beams,** (Proc. Beam-Foil Spectroscopy Conf., Univ. of Arizona, Tucson, Arizona, Nov. 20-22, 1967), Chapter in *Beam-Foil Spectroscopy* **II,** 285-304 (Gordon and Breach Science Publ. Inc., New York, N.Y., 1968).

Key words: Argon; atomic lifetimes; atomic spectra; helium; laser; neon.

Following a short discussion of the general method of measuring atomic lifetimes using pulsed electron beams, four separate determinations of the mean lives of the ten 2p levels (Paschen notation) in Ne I are presented for comparison. These four sets of results from different experimental groups are found to be in general agreement. Mention is next made of the published lifetime measurements in Ar I (2p levels) and Ar II without presentation of results. Finally, measurements of the pressure-dependent lifetime of the $3s_2$ laser level in Ne I are analyzed using the Holstein theory of the imprisonment of resonance radiation. The analysis yields information about transition probabilities from which are derived the $3s_2$ lifetimes for absence of imprisonment ($28 \pm 5$ nsec) and complete imprisonment ($52 \pm 2$ nsec) of the 600.04 Å ($3s_2 \rightarrow {}^1S_0$) resonance radiation.

11011A. Klose, J. Z., **Experimental lifetimes of the 5p levels in argon I,** *J. Opt. Soc. Am.* **58,** No. 11, 1509-1512 (Nov. 1968).

Key words: Argon; atomic lifetimes; atomic spectra.

Mean lives of seven of the ten 5p atomic levels in Ar I have been determined using electronic excitation and a method of delayed coincidence. The measured values and standard deviations in ns of the mean lives of the $3p_1$ and $3p_5$ through $3p_{10}$ (Paschen notation) levels in neutral argon are as follows: $3p_1$, 80 ± 1; $3p_5$, 96 ± 2; $3p_6$, 124 ± 3; $3p_7$, 136 ± 2; $3p_8$, 180 ± 5; $3p_9$, 141 ± 2; and $3p_{10}$, 189 ± 3. Wavelengths used in the determinations ranged from 4159 to 4702 Å. The lifetimes were estimated to contain systematic errors varying from 5 to 15 percent and are presented in comparison with values obtained by combining theoretical calculations with other experimental results.

**11023.** Koidan, W., **Calibration of standard condenser microphones: coupler versus electrostatic actuator,** *J. Acoust. Soc. Am.* **4,** No. 5, 1451-1453 (Nov. 1968).

Key words: Calibration of microphones; microphone calibration standards.

The response-frequency characteristic of a "one-inch" condenser microphone measured by an electrostatic actuator is likely to be significantly different from that measured by reciprocity in an acoustic coupler because of the radiation impedance of the microphone diaphragm with the actuator in place. It cannot be assumed, except at low frequencies, that the radiation impedance is negligible and that the actuator calibration yields the pressure response. Such an assumption also is apt to lead to errors in the determination of the free-field response when calculated with the aid of the free-field correction.

**11024.** Kokoszka, G. F., Linzer, M., Gordon, G., **Electron paramagnetic resonance spectra of polycrystalline dimeric complexes. Copper propionate monohydrate and zinc-doped copper propionate monohydrate,** *Inorg. Chem.* **7,** No. 9, 1730-1735 (Sept. 1968).

Key words: Copper propionate monohydrate; dimeric complexes; e.p.r.; exchange coupled; polycrystalline samples.

The electron paramagnetic resonance spectra have been observed in the polycrystalline form of copper propionate monohydrate and zinc-doped copper propionate monohydrate. The studies were carried out at liquid nitrogen temperature and at both X-band and K-band frequencies. The K-band $S=1$ spectrum arises from $\Delta m=1$ and $\Delta m=2$ transitions. Copper nuclear-hyperfine structure was observed in the parallel spectra at X-band and K-band frequencies as well as in the $\Delta m=2$ spectral region at K-band. The magnetic parameters for the exchange-coupled copper-copper pairs are $g_{\|}=2.348$, $g_{\perp}=2.060$, $A_{\|}=0.0073$ cm$^{-1}$, $A_{\perp}<0.001$ cm$^{-1}$, $D=0.327$ cm$^{-1}$, and $E<0.001$ cm$^{-1}$. For the $S=1/2$ spectra associated with the copper-zinc pairs, the magnetic parameters are $g_{\|}=2.348$, $g_{\perp}=2.064$, $A_{\|}=0.0152$ cm$^{-1}$, and $A_{\perp}=<0.001$ cm$^{-1}$. A consistent interpretation of the data is presented on the basis of a weak metal-metal interaction. A simple model is used to estimate covalency parameters for the metal-ligand bonds. Upper limits for the exchange integrals and the supertransferred hyperfine interaction are also derived from the data.

**11025.** Koonce, C. S., Cohen, M. L., **Theory of superconducting semiconductors and semimetals,** *Phys. Rev.* **177,** No. 2, 707-719 (Jan. 10, 1969).

Key words: Dielectric function; Green's function; semiconductors; semimetals; superconductivity.

A Green's function method is used to derive a superconducting energy gap equation without the assumption that the Fermi energy is much larger than phonon energies. This equation is then approximated using two separate methods. The first method applies when the screened electron-phonon interaction is almost independent of wavevector and the Fermi energy is of the order of, or larger than phonon energies. The gap equation obtained in this way takes account of the variation in the density of electron states with energy. The second approximation method applies when the screened electron-phonon interaction depends strongly on wavelength or when the Fermi energy is small compared to phonon energies. In this case, the gap equation takes account of the wavevector dependence of the interaction, the wavevector and frequency dependence of the electronic screening, the energy dependence of the density of states, and the wavevector dependence of the superconducting energy gap. In addition, the effects of the retardation of the electron-electron interaction are also included.

**11026.** Kraft, R., **An unusual mixed initial boundary problem in two independent variables,** *J. Math. Anal. Appl.* **25,** No. 2, 233-249 (Feb. 1969).

Key words: Hyperbolic system; mixed initial boundary; outgoing data; partial differential equations.

Consider for the hyperbolic system with constant coefficients (1) $(\alpha_i \cdot \nabla)\ U^i - \Sigma_{j=1}^{4} A_{ij} U^j \equiv (\alpha_{i1}\ \partial_x + \alpha_{i2}\ \partial_y) U^i - \Sigma_{j=1}^{4} A_{ij} U^j = 0$ $i=1, . : . 4$ where $A_{ii}=0$, $i=1, . . . 4$ and the unit vectors $\alpha_i \equiv (\alpha_{i1}, \alpha_{i2})$ satisfy $\alpha_{11} > \alpha_{21} > 0 > \alpha_{31} > \alpha_{41}$; $\alpha_{i2} > 0$ the initial boundary problem in the first quadrant with $U \equiv (U^1, . . . U^4) \epsilon C^2$ given on the positive x-axis and *outgoing* data $U^3$, $U^4 \epsilon C^2$ given on the positive y-axis. Theorem: If $A_{31}A_{42}/\cdot\alpha_1 N_3)(\alpha_2 \cdot N_4) - A_{22}A_{41}/(\alpha_2 \cdot N_3)(\alpha_1 \cdot N_4) \neq 0$ where $N_j \equiv (\alpha_{j21} - \alpha_{j1})$ and certain consistency conditions at the origin are satisfied, then a solutio of (1) of class $C^1$ exists in the first quadrant. Using Rieman functions the incoming data is calculated on the y-axis and this i used to find the solution by the standard method of successiv approximations.

**11027.** Krause, R. F., Jr., Douglas, T. B., **The heats of formatio of $AlClF_2$ and $AlCl_2F$ from subliming $AlF_3$ in the presence o $AlCl_3$ vapor,** *J. Phys. Chem.* **72,** No. 10, 3444-3451 (Oct 1968).

Key words: $AlCl_3$; $AlF_3$; dimerization correction; entrain ment method; heat of reaction; mixed halides; sublimation

The volatility of $AlF_3$, which was measured between 1196 an 1256 K by an entrainment method, was enhanced by th presence of $AlCl_3$ vapor. When the $AlCl_3$ vapor was generated a 373 or 394 K, the amount of sublimed $AlF_3$ was observed to b from 1.7 to 7.4 times that expected in an inert medium. Th vapor mixture saturated with $AlF_3$ was considered to include th two mixed-halide monomers formed according to:

$$(m/3)AlCl_3 + (1\text{-}3/m)AlF_3 = AlCl_mF_{(3-m)},$$

where $m$ is 1 or 2. After correcting for the formation of $Al_2F$ $Al_2Cl_6$, and the 22 possible mixed-halide dimers, a least-squar fit to the entrainment data yielded $\Delta H^\circ_{1225} = 0.5$ kcal with an est mated uncertainty of ±1 kcal for both the above all-monome reactions.

**11028.** Kropschot, R. H., **Report on the fourteenth cryogenic er gineering conference,** *Cryogenics* **8,** No. 6, 346-348 (De 1968).

Key words: Cryogenics; cryogenic engineering conferenc

Delegates from the United States and 6 foreign countries a sembled in Cleveland, Ohio, August 19-21, 1968 to discuss ne advances in cryogenics. The Case Western Reserve Universit was host to the 14th Annual Cryogenic Engineering Conferenc The technical program was divided into 12 technical sessio and eight seminars. This review presents the highlights of th conference.

**11029.** Ku, H. H., **Expressions of imprecision, systematic erro and uncertainty associated with a reported value,** *Meas. Da* **2,** No. 4, 72-77 (July-Aug. 1968).

Key words: Accuracy; calibrations; expression of unce tainty; measurements; precision; standard error; systemat error; uncertainty.

The work of a calibration laboratory is described in terms of a equence of operations that results in the collection, storage and ansmittal of information. Since the information content of the atements of uncertainty determines the worth of a reported alue, these statements deserve to be well formulated. An anotated guide to such commonly used expressions of uncertain-es is given in table form for convenient reference.

**1030.** Kuehner, E. C., Freeman, D. H., **Containers for pure substances,** Chapter in *Purification of Inorganic and Organic Materials*, M. Yief, ed., pp. 297-306 (Marcel Dekker Inc., New York, N.Y., 1969).

Key words: Container impurities; pure containers.

This is a brief discussion and summary of criteria used in the election of a pure container for pure chemical substances. The arious sources of contamination are classified according to conainer purity, container stability, and container inertness. A brief iscussion of container cleaning is included. A tabular summary f various container materials is presented according to the elevant sources of container imperfection or failure.

**1031.** Kuriyama, M., **Theory of x-ray diffraction by a distorted crystal. II. Scattering amplitude for a wave packet of finite size,** *J. Phys. Soc. Japan* **25,** No. 3, 846-856 (Sept. 1968).

Key words: Atom; displacement; distorted crystal; energy flow; finite beam; theory; wave field; wave packet; x-ray diffraction.

The x-ray scattering amplitude for a finite wave packet difracted by a distorted crystal has been calculated by the use of a previously formulated theory (M. Kuriyama, J. Phys. Soc. Japan 3, 1369 (1967)). An approximation used for deriving the final expression of the scattering amplitude is that the lateral sizes of an incident beam of ordinary x-ray energy are greater than everal hundred microns. When the beam is finite in its lateral ize, only a limited portion of the crystal is responsible for scatering. The geometrical arrangement of the limited region has been discussed in terms of an observation point on the crystal exit surface, an incident (glancing) angle and an observation (deector) angle. The internal wave fields and paths of classical energy flow are also discussed from the viewpoint of the present formulation.

**11032.** Kushner, L. M., **The National Bureau of Standards and the Fire Research and Safety Act of 1968,** *Fire J.* **62,** No. 5, 32-33, 118 (Sept. 1968).

Key words: Fire research; fire technology.

The National Bureau of Standards, which has a long history of activity in the fire research field, will have broadened responsibilities under the terms of the Fire Research and Safety Act of 1968. NBS will not only serve as a research resource, but as a center for administration in new areas of work including technical application to reduce fire losses. The Bureau will seek to avoid duplication of activities underway, and views the new program as a cooperative attack of Government and the private sector on the national fire problem. The levels of activity attained will depend on funding provided, and the short term objective will be to initiate projects for using existing technology to the fullest for reducing losses and improving fire services effectiveness. The development of new techniques for reducing fire losses is a longer term objective.

**11033.** Kusuda, T., **Thermal response factors for multilayer structures of various heat condition systems,** *ASHRAE Trans.* **75,** No. 1, V.3.1-V.3.25 (1969).

Key words: Cylinder; multilayer structures; response factors; sphere; transient head conduction.

The thermal response factor method for calculating transient heat conduction through multilayer slabs is generalized to include the solutions for many other important engineering heat transfer problems. Response factor formulas for multilayer structures of cylindrical and spherical objects (hollow as well as solid), plane and curved surface walls adjacent to infinitely thick heat conduction medium, such as ground, and plane slabs are presented in this paper. Numerical evaluation of these formulas are carried out for selected multilayer structures and the results are tabulated.

**11034.** Kuyatt, C. E., **Measurement of electron scattering from a static gas target,** Chapter 1 in *Methods of Experimental Physics*. **Vol. 7.** *Atomic and Electron Physics, Electron-Atom Interactions*, B. Pederson and W. L. Fite, eds., pp. 1-43 (Academic Press Inc., New York, N.Y., 1968).

Key words: Absolute electron energy; calculation of scattering geometries; differential electron scattering cross section; Doppler broadening; elastic electron scattering cross sections; electron multiplier; Faraday cup; generalized oscillator strength; inelastic electron scattering cross section; scattering chambers; transmission of energy analyzers.

The quantitative aspects of the measurement of elastic and inelastic scattering of electrons from static gas targets is discussed. Basic arrangements for the measurement of total and differential cross sections are reviewed, followed by a critical discussion of the calculation of scattering geometries, of the transmission of energy analyzers, of Faraday cup electron collectors, and of electron multiplier detectors. Other topics treated are scattering chambers, use of generalized oscillator strengths to express cross section data, Doppler broadening of energy distributions, pressure variation of scattered signals, and calibration methods for cross section and absolute electron energy.

**11035.** Lafferty, W. J., Maki, A. G., Pringle, W. C., Jr., **Comments on "two rotational lines of allene $C_3H_4$,"** *J. Chem. Phys.* **50,** No. 1, 564-565 (Jan. 1, 1969).

Key words: Allene; E vibrational state; microwave spectrum; rotational transitions; Stark effect; vibrational states.

Goertz (J. Chem. Phys. **48,** 523 (1968)) has claimed to have observed two rotational lines of allene arising from $J=3 \rightarrow 4$ transitions in the $K=0$ levels of the vibrational states of allene. A number of theoretical considerations are presented which cast doubt on the validity of Goertz's assignment of these lines to allene. A thorough search of the microwave spectrum of allene in the regions where the lines resulting from the $1 \rightarrow 2$ and the $3 \rightarrow 4$ transitions should fall produced no evidence for the lines observed by Goertz.

**11036.** Lance, H. W., **Metrology and national goals,** (Proc. 22nd ISA Conf. and Exhibit, Chicago, Ill., Sept. 11-14, 1967), *ISA Preprint* No. M4-1-MESTIND-67, 1-14 (1967); excerpt in *Meas. Data* **2,** No. 2, 68-71 (Mar.-Apr. 1968).

Key words: Calibration; cost-effectiveness; data; economic growth; information centers; measurements; metrology; National Bureau of Standards; National Measurement System; National Standard Reference Data System; Radio Standards Laboratory; reference data.

The ability to measure accurately and reliably is vital to the advancement of science and technology, and advanced science and technology are more and more essential in our large national programs. Therefore metrology is of prime importance to the achievement of national goals. Measurements in the United States take place within a loosely organized measurement system, which is not working as well as it should. Hence there are unnecessary expenditures of time and money on our national programs. The system could be improved by establishing comprehensive information centers, adopting new approaches to calibration, and implementing an existing standard reference data plan. However, carrying out these tasks will require additional resources for metrology. Funding problems arise because neither the layman nor the manager understand well the role of measurements, and the metrologist lacks data for demonstrating quantitatively the economic impact of his work. Therefore metrologists need to help the economists devise better ways of getting economic data on measurements and to mount a program for better understanding of the role of measurements, especially by policy makers. Such action would provide a basis of better national planning for measurements and exploitation of measurements for the economical attainment of national goals.

**11037.** Lang, S. B., Shaw, S. A., Rice, L. H., Timmerhaus, K. D., **Pyroelectric thermometer for use at low temperatures,** *Rev. Sci. Instr.* **40,** No. 2, 274-248 (Feb. 1969).

Key words: Calorimetry; cryogenics; dielectric constant; ferroelectric ceramic; pyroelectric coefficient; thermometry; volume resistivity.

The applicability of pyroelectric thermometry to temperature change or temperature rate measurement at cryogenic levels was studied, with particular emphasis on calorimetry. The pyroelectric coefficients, dc dielectric constants, and volume resistivities of three ferroelectric ceramic materials, Clevite Ceramic B, PZT-4 and PZT-5A, were measured over the temperature range 4.2 to 300 °K The pyroelectric coefficients were found to be reproducible, but large electric fields, thermal shock, and aging affected the pyroelectric coefficient. Expressions are derived for the temperature responsivity (voltage output per unit temperature change), noise equivalent temperature change (temperature change equivalent to the electrical noise in a pyroelectric thermometer), and figure-of-merit (a parameter characterizing the physical properties of a pyroelectric material). Typical temperature responsivities of 8.0 and 165 volts/°K, and values of noise equivalent temperature change of 2.5 and 0.12 microdegrees K, at 5 and 300 °K respectively, are calculated. Recommendations concerning the usage of a pyroelectric thermometer in a cryogenic calorimeter are given.

**11038.** Lashof, T. W., **Standardization and application of accuracy and precision statements: TAPPI Standards Committee – ASTM Committee D-6 policy,** *Tappi* **4,** 732-739 (Apr. 1969).

Key words: Accuracy; paper; precision; standards; test methods.

This paper states the present policy for the use of the terms precision and accuracy for TAPPI and ASTM D-6 Standards and Suggested Methods. Several questions involved in establishing the policy are discussed. Brief examples show how to compute precision from available data, how to state the precision of a test method, and how to apply this information in practical cases.

**11039.** Latanision, R. M., Staehle, R. W., **Plastic deformation of electrochemically polarized nickel single crystals,** *Acta Met.* **17,** 307-319 (Mar. 1969).

Key words: Active potentials; critical resolved shear stress; near surface dislocation sources; passive potentials; single crystals.

Nickel single crystals were deformed in uniaxial tension under active and passive conditions in a 1N $H_2SO_4$ solution at room temperature. $\tau_o$ increases and Stages I and II are suppressed in the presence of the thin passive film formed at 800 mV (SCE). In contrast, surface removal prior to deformation lowers $\tau_o$ in comparison to crystals deformed in the laboratory atmosphere. Continuous surface removal during deformation only slightly affects $\theta_I$, but does increase the extent of easy glide and Stage II. Abrupt changes in the stress for further plastic deformation occur when crystals are unloaded and held at constant potential in interrupted tests. Electron microscope studies of surface replicas show that slip lines formed under dissolution conditions are stronger and more widely spaced than those produced on crystals deformed in air. The spacing and step height on passivated crystals appear to be intermediate between two extremes. A model of plastic deformation based upon the activation of *near surface* dislocation sources is presented in the context of the above observations.

**11040.** Laufer, A. H., **Photolysis of ketene. Mechanism of hydrogen production and the reaction of methylene with methane,** *J. Phys. Chem.* **73,** No. 4, 959-963 (Apr. 1969).

Key words: Excited state; hydrogen formation; ketene; methylene; photodecomposition.

The photolysis of ketene has been investigated at photon energies from 3130 Å (3.96 eV) to 1470 Å (8.43 eV). Hydrogen is produced at all wavelengths. Based upon the photolysis of $CD_2CO$-$CH_2CO$ mixtures the reaction

$$CH_2CO \rightarrow H_2 + C_2O$$

is suggested as a primary process.

The sequence of reactions (1) and (2) has also been examined.

$$CH_2 + CH_4 \rightarrow C_2H_6^* \qquad (1)$$

$$C_2H_6^* \rightarrow H_2 + C_2H_4 \qquad (2)$$

It is concluded that of the decomposition paths available to $C_2H_6^*$ fewer than 6 percent proceed via reaction (2) over a wide energy range. The significance of this finding with respect to the photodecomposition of methane is discussed.

**11041.** Laufer, A. H., McNesby, J. R., **Photolysis of methane at 1236-A: quantum yield of hydrogen formation,** *J. Chem. Phys.* **49,** No. 5, 2272-2278 (Sept. 1, 1968).

Key words: Isotope effect; methane; quantum yields; vacuum ultraviolet.

Pure $CH_4$ and $CD_4$ have been separately but simultaneously photolyzed at 1236 Å by means of a split cell technique in order to obtain accurate relative quantum yields for the various modes of production of $H_2$ and $D_2$. The split cell technique has been used to obtain absolute quantum yields by comparison with the $CO_2$ actinometer. Molecular elimination yields for $CD_4$ and $CH_4$ (0.58) are found to be nearly equal while the H atom yield greatly exceeds the D atom yield. It is concluded from the results that a significant fraction of the atoms produced disappears by the association reaction $M + H + CH_3 \rightarrow CH_4 + M$. The effect o scavengers and inert gas have been studied and the absolute quantum yields measured by comparison with the $CO_2$ actinometer. The total quantum yield for H and $H_2$ formation is at least 1.29 and fragmentation of $CH_2$ or $CH_3$ formed in the primary process is suggested.

$$CH_3 \rightarrow H + CH_2$$

$$CH_2 \rightarrow H + CH$$

However, the lower limit for the quantum yield for D and $D_2$ formation is 0.76 and evidence for fragmentation of $CD_2$ or CD is absent.

**11042.** Lederer, P. S., **Pressure,** Chapter 1 in *ISA Transduce Compendium*, Part 1, 2nd ed., pp. 5-8 (1969).

Key words: Evaluation; measurement; performance; pressure; test methods; transducer calibration.

A chapter for the "ISA Transducer Compendium" briefly introducing the reader to the field of pressure and its measuremen means of electrical output transducers. The purpose of this apter is to assist the reader to select the transducer most suita- for his application from those listed in the compendium.

**043.** Lee, T. G., **A system for continuously monitoring hydrogen hloride concentrations in gaseous mixtures using a chloride ion-selective electrode,** *Anal. Chem.* **41,** 391-392 (Feb. 1969).

> Key words: Aerosol; chloride selective electrode; decomposition product; HCl gas analyzer; polyvinyl chloride.

A continuous recording aqueous chloride ion concentration alyzer for the determination of HCl in gas and aerosol samples described. It consists of a gas scrubber to absorb the HCl in gas sample and a chloride-ion selective electrode of the ion change type to measure the chloride ion in solution. At a gas mpling rate of 100 cm$^3$/min, range of detection was about 20- ,000 ppm HCl; reproducibility was within ±5 percent and time response to 99 percent of equilibrium was about 1.5 min.

**044.** Levin, E. M., **X-ray determination of the thermal expansion of silver nitrate,** *J. Am. Ceramic Soc.* **52,** No. 1, 53-54 (Jan. 1969).

> Key words: $AgNO_3$; density $AgNO_3$; polymorphism $AgNO_3$; thermal expansion $AgNO_3$; unit cell dimensions $AgNO_3$.

An x-ray diffractometer furnace was used to obtain powder tterns of orthorhombic (low) $AgNO_3$ between 25 and 140 °C d of rhombohedral (high) $AgNO_3$ between 25 and 175 °C. Unit ll dimensions are given for selected temperatures and are esntially a linear function of temperature. The values for the efficient of expansion of low $AgNO_3$ along a, b, and c, respecely, are $126 \times 10^{-6}$ deg$^{-1}$, $57 \times 10^{-6}$ deg$^{-1}$, $-0.4 \times 10^{-6}$ deg$^{-1}$. or high $AgNo_3$ the values along a and c, respectively, are 30 × $^{-6}$ deg$^{-1}$ and $134 \times 10^{-6}$ deg$^{-1}$. X-ray density of the high form a given temperature is greater than that of the low form and, in neral, does not agree with previous reported results. The value dT/dP calculated from the Clausius-Clapeyron equation is $6.9 \times 10^{-3}$ K/bar, at atmospheric pressure, vs Bridgman's exrimental value of $-7.6 \times 10^{-3}$ K/bar.

**045.** Lide, D. R., Jr., **Structure of the alkali hydroxides. IV. Interpretation of vibration-rotation interactions in CsOH and RbOH and refinement of structures,** *J. Chem. Phys.* **50,** No. 7, 3080-3086 (Apr. 1, 1969).

> Key words: Alkali hydroxides; anharmonicity; force constants; microwave spectrum; molecular structure; vibration-rotation interaction.

The unusual vibration dependence of $B_v$ in CsOH and RbOH found to be due to a somewhat accidental cancellation of harionic and anharmonic contributions to the interaction constant $_2$. A rather different formulation of the vibration-rotation interactions in linear molecules, which explicitly takes into acount the curvilinear nature of the motions, clarifies the physical asons for the apparent anomalies in the microwave spectra of e alkali hydroxides. This formulation also shows that the domiant contribution to $\alpha_2$ in most linear triatomic molecules is harionic in nature and may be ascribed to the direct averaging of e moment of inertia over the harmonic bending vibration; this in contrast to the usual viewpoint, in which the anharmonic ontribution is considered dominant. All of the microwave and nfrared data on CsOh and RbOh are consistent with a reasonale force field, although uncertainties in the harmonic force contants prevent a quantitative determination of anharmonic contants. In the absence of contrary evidence, we conclude that the lkali hydroxides very probably have a linear equilibrium conguration. The equilibrium bond lengths in CsOh are estimated o be: $r_{CsO}=2.391$ Å, $r_{OH}=0.96_0$ Å, in RbOH: $r_{RbO}=2.301$ Å, $_{OH}=0.95_7$ Å.

**11046.** Linzer, M., **Line parameters of Lorentzian curves containing arbitrary mixtures of absorption and dispersion,** *J. Appl. Phys.* **40,** No. 1, 372-376 (Jan. 1969).

> Key words: Absorption-dispersion mixtures; Lorentzian lineshape; spectroscopy.

A brief description is presented of various ways in which mixed absorption-dispersion modes can arise. Exact closed-form solutions are derived for the line parameters of zeroth derivatives of Lorentz shape functions containing arbitrary mixtures of absorption and dispersion. The parameters are obtained as functions of $\epsilon$, where $\epsilon$ represents the fractional admixture of one signal component relative to the other and may be determined experimentally from the signal amplitude asymmetry. Very simple expressions are also derived for the mixed first derivative curves if terms of the order of $\epsilon^3$ and higher are neglected. In the case of the 1:1 admixture, this procedure introduces an uncertainty in the position of the line center of approximately 1 percent of the halfwidth of the pure absorption curve. The implications of this analysis for practical spectroscopic measurements are discussed. In particular, a very simple relationship is shown to exist between the degree of admixture and the experimental variables.

**11047.** Lipkin, H. J., Meshkov, S., **The importance of the $\eta\pi$ decay mode in the split $A_2$ decay,** *Phys. Rev. Letters* **2,** No. 5, 212-213 (Feb. 3, 1969).

> Key words: $A_2$; boson; decay; octet; selection rule; symmetry.

If SU(3) symmetry is assumed and singlet-octet mixing is neglected, (a) the $\eta\pi$ decay mode is forbidden for all negative CP states including the $J^P = 1^{-+}$ state suggested by the Gell-Mann Zweig model; (b) $\eta\pi$ cannot appear in decays where the $K\bar{K}$ mode is absent; (c) the $\eta\pi/K\bar{K}$ branching ratio is the same for all isovector octet bosons allowed to decay into$\rho\pi$. Violation of these predictions would imply either SU(3) symmetry breaking or a singlet contribution in the decay and suggest serious re-examination of other SU(3) decay predictions. Prediction (b) seems to be violated by preliminary data. If there are no violations and $\eta\pi$ and $\rho\pi$ are both allowed, the only possible classification for either $A_2$ peak with $J < 4$ is $2^{++}$.

**11048.** Lippincott, E. R., Stromber, R. R., Grant, W. H., Cessac, G. L., **Polywater,** *Science* **164,** 1482-1487 (June 27, 1969).

> Key words: Anomalous water; infrared spectrum of polywater; polywater; Raman spectrum of polywater; water.

The infrared and Raman spectra of a form of water prepared in quartz capillaries and previously designated as "anomalous" water have been obtained. The spectra appear to be unique with the apparent absence of the O-H stretching bands prominent in normal water spectra, and the appearance of new bands near 1600 and 1400 cm$^{-1}$. The interpretation is that new and previously unreported strong symmetric O-H-O bonds are formed, isoelectronic with $FHF^-$. The approximate bond distances are given as 2.3 Å for 0 · · · 0, and 1.5 Å for H-O. These bonds are regarded as responsible for the remarkable properties of the material and have considerable covalent character. These bonds are so strong that they cannot be considered as normal 0 · · · H hydrogen bonds. Extensive electron delocalization could occur in structures which involve oxygen atoms in three equivalent bonds. The bond energy per O-H-O unit is given as approximately 30-50 kcal/mole, and an energy of 60-100 kcal per $H_2O$ structural unit. Several structures are proposed which are consistent with the spectral data and the remarkable properties and stability of the material. It is concluded that the material is a true polymer of water, and therefore named polywater.

**11049.** Little, W. E., Patty, O. L., Zanboorie, M. H., **A millimeter**

**wave reflectometer,** *IEEE Trans. Microwave Theory Tech.* **MTT-16,** No. 2, 121 (Feb. 1968).

Key words: Millimeter wave; reflectometer; WR-12 waveguide.

This paper describes a millimeter wave reflectometer system that has been developed in WR-12 waveguide. A detailed description of the system circuitry, a discussion of sources of measurement error and some measurement results are presented.

**11050.** Lloyd, E. C., **Erasable trace recording methods for chart recorders,** *Rev. Sci. Instr.* **39,** No. 12, 1953-1954 (Dec. 1968).

Key words: Automatic; chart recorders; erasable.

Citation of methods described in the technical and patent literature, and description of two new methods, for renewing the chart of closed-chart recorders by automatically removing the trace.

**11051.** Lloyd, E. C., **Standards for improved measurement of pressure and vacuum,** (Proc. 4th Intern. Measurement Conf., Warsaw, Poland, July 2-7, 1967), *Acta Imeko,* pp. 451-468 (Hungarian Academy of Sciences, Budapest, Hungary, 1967).

Key words: Accuracy; calibration; measurement; pressure; standards; vacuum.

Results of NBS developments are outlined in a number of projects relating to standards for improved measurement of pressures throughout the range from vacuum to very-high pressures. In the vacuum range this includes techniques for generation of stable reference pressures, and improved absolute instruments for force per unit area measurement down to $10^{-9}$ torr. In the range from a few millibars to hundreds of kilobars the use of fixed points, and the performance of improved piston gages and interpolation instruments, are described. Problems presently limiting accuracy of calibration and NBS investigations of possible solutions are mentioned. Two new "accuracy charts" are presented showing present and possible future NBS capabilities.

**11052.** Lloyd, E. C., Beckett, C. W., Boyd, F. R., Jr., **Measurements in the high-pressure environment,** *Science* **164,** 860-861 (May 16, 1969).

Key words: Equation of state; phase transformations as fixed points; pressure coefficients of thermocouples; pressure scale.

The highlights of the Symposium on Accurate Characterization of the High Pressure Environment are described. The Symposium was attended by 140 participants from the United States and abroad. Thirty-eight papers were presented and four panel sessions held covering current research at high pressures in static systems and in shock wave experiments. In panel sessions five fixed points below 100,000 bars were proposed, and values for these points recommended. The equation of state of sodium chloride was recommended as a standard for the x-ray determination of pressure. The measurement of temperature in high pressure apparatus and the measurement of phase transformations as a function of temperature and pressure using static and dynamic techniques were presented. Dynamic methods included studies of phase transformations ranging from 20,000 bars up to several million bars. Recent developments in the static high pressure techniques were also presented.

**11053.** Lutz, G. J., **Calculation of sensitivities in photon activation analysis,** *Anal. Chem.* **41,** No. 3, 424-427 (Mar. 1969).

Key words: Calculated sensitivities; cross section parameters; photon activation analysis; photon flux distribution; relative production rate; specific activities.

Estimates have been made of specific activities to be expecte from bremsstrahlung produced by an electron accelerator. Th photon flux distribution from electrons striking a 0.6 cm. tungsten target at different energies and included in the con described by a five degree angle from the forward direction is calculated. Flux times cross section for photonuclear reactions o analytical utility was integrated and disintegration rates of th reaction products for most of the elements under conditions o different electron energies and irradiation times were calculate Relative values for the specific activities were calculated an compared with the experimental results of Oka and co-worker and found to be in satisfactory agreement.

**11054.** McCaa, W. D., Jr., Nahman, N. S., **Phenomena and devices, frequency and time-domain analysis of a superconducti coaxial line using the two fluid model,** *J. Appl. Phys.* **39,** No. 2592-2596 (May 1968).

Key words: Frequency response; Gorter-Casimir two flui model; step response; superconductive coaxial line.

A miniature 80-ft superconductive coaxial line (Nb inner co ductor 0.01 in. od, Pb outer conductor 0.034 in. i.c polytetrafluoroethylene dielectric) has been analyzed in terms the Gorter-Casimir two-fluid superconductivity model, conside ing the anomalous and classical cases (without relaxation effect for the normal components. The dielectric and the metal fl trapping losses are assumed to be negligible. The $10^6$-$10^{12}$ line attenuation and the 1-100 psec step responses are presente for the temperature range of 2.3-10 °K. Predictions are compar with the experimental results of several independent investig tors. It is concluded that if the dielectric and the metal flu trapping losses are negligible, then (1) the model provid bounds between which the responses of physically realized lin will fall, and (2) the normal conductivity of the conductors mu be very good if the maximum bandwidth and minimum riseti are to be obtained.

**11055.** McCamy, C. S., **A half century of photographic st dardization in the United States,** *Photo. Sci. Engr.* **12,** No. 308-312 (Nov.-Dec. 1968).

Key words: Motion picture standards; photographic st dards.

Over the past 50 years, photography and cinematography ha reached a high level of standardization in the United States America. This has been accomplished through cooperative forts of the photographic industry, interested consumers, and t government. These efforts have been organized by societies su as the Society of Motion Picture and Television Engineers, a by the United States of America Standards Institute and predecessors. The USA program is coordinated with those other nations by the International Organization for Standardi tion. Besides the documentary standards which record the c sensus of interested parties with regard to specifications and t methods, there are physical standards, from various sourc which serve as the basis of measurement.

**11056.** McCamy, C. S., **Photographic image structure evaluati** Chapter in *Ultra-Microminiaturization Precision Phot raphy for Electronic Circuity,* pp. 130-140 (Society for Ph graphic Scientists and Engineers, Washington, D.C., 1968).

Key words: Photochemical fabrication; photographic im structure.

Photographic images are usually evaluated with respect visual applications. Photochemical fabrication can benefit fr the accumulated experience in this field, but introduces its c complications. The kind of optical density to be used or m sured must be precisely known. The nature of light limits amount of detail that can be reproduced. Photographic mater re limited with respect to resolving power, acutance, and granurity. These quantities can be useful in evaluating photochemial fabrication systems. Although modulation transfer theory has een applied to photographic systems, nonlinearities raise roblems which may require more rigorous treatment.

**1057.** McCamy, C. S., **Units for logarithmic scales,** *Phys. Today* **22,** No. 4, 42-44 (Apr. 1969).

Key words: Brigg; logarithmic scales; octave; optical density; order; symbols; units.

The following definition is proposed: If $\log_b(a/c) = n$, then a is orders to base b greater than c. One order is regarded as a unit f a logarithmic scale, the symbol $\text{ord}_b$ is proposed, and a number f existing applications are described in these terms. The brigg symbol: Br) is recommended as the name of one order to base 0. The symbols oc and st are recommended for octave and step.

**1058.** McClintock, M., Jennings, D. A., Mizushima, M., **Contribution to the Raman line profile in liquids from molecular reorientation,** *Phys. Rev. Letters* **21,** No. 5, 276-278 (July 29, 1968).

Key words: Benzene; carbon tetrachloride; Raman scattering.

The profiles of several Raman lines arising from nontotally ymmetric molecular vibrations in liquid benzene and carbon etrachloride have been measured using 4880 Å radiation from n argon ion laser as a source of illumination. These profiles have een analyzed on the assumption that scattering occurs from ime-dependent molecular reorientations of small angle in the iquid, analagous to those producing depolarized scattering at the Rayleigh line. On this basis, the half width at half maximum of he 606 $\text{cm}^{-1}$ Raman line in benzene was found to be 3.3 $\text{cm}^{-1}$, nd the half width of the "orientation" line underlying this Raman line was found to be 24.3 $\text{cm}^{-1}$. The rotational relaxation ime calculated for the $\nu_{18}$ vibrationally excited molecule is therefore $1.38 \times 10^{-12}$ seconds. This short compared with a period of otation and supports the assumption of rotational Brownian moion. It is also shorter than the rotational relaxation time for the nolecule in the ground vibrational state, and indicates that there s weaker rotational coupling between molecules in the ground state than between vibrationally excited molecules and those in he ground state. The depolarization ratios of the Raman and the orientation components of the 606 $\text{cm}^{-1}$ line for linearly oolarized incident light were found to be 0.748 and 0.749 respecively, in agreement with the theoretically predicted 0.750.

**11059.** McIntyre, D., Mazur, J.; Wims, A. M., **Effects of excluded volume on light scattered from flexible macromolecules,** *J. Chem. Phys.* **49,** No. 7, 2887-2895 (Oct. 1, 1968).

Key words: Chain-end distribution; excluded volume; light scattering; particle scattering factor; polydispersity.

The effect of the non-Gaussian behavior of the chain segment distribution in flexible polymer coils on the angular distribution of scattered light is discussed. The explicit form of a general spherical segment distribution function,

$$W(r,N)dr = \frac{t}{\Gamma(3/t)} \left[\frac{\Gamma(5/t)}{\Gamma(3/t)\,\langle R_N^2\rangle}\right]^{3/2} \exp - \left[\frac{\Gamma(5/t)r^2}{\Gamma(3/t)\,\langle R_N^2\rangle}\right]^{t/2} r^2 dr,$$

with different values of t, is used to evaluate the general scattering equation for the particle scattering factor P(Θ).

$$P(\Theta) = \frac{1}{N^2} \sum_{i>j}\sum \frac{\sin Ksr_{ij}}{ksr_{ij}}.$$

In addition, the effects of excluded volume on the mean end-toend chain separation $\langle r^2_N\rangle$ is taken to be of the form $\langle r^2_N\rangle \approx N^{1+\epsilon}$, where N is the number of chain steps and $\epsilon$ is a parameter, which measures the excluded volume effect on the $\langle r^2_N\rangle$. In this paper, an expansion of the P(Θ) function to the first few terms is carried out and numerically evaluated for the dependence of P(Θ) on the variable x, where $x = ks\langle r_{exp}\rangle$, k is the wave number of the incident light, s is related to the scattering angle and $\langle r_{exp}\rangle$ is the radius of gyration determined from experimental data of the scattering cross section. The computations were carried out for the polymer in good solvent, for which data for $\epsilon$ and t were adopted, based on the lattice model of non-self intersecting chain, and for polymer in theta solvent, for which Gaussian chain model was adopted. The computations were carried out for various degrees of polydispersity. A comparison was made between the theoretical and the experimental results on a polystyrene sample of molecular weight of $4.10^6$ in cyclohexane at 35, 45, and 55 °C, and in benzene at 40 °C.

**11060.** McIntyre, D., Sengers, J. V., **Study of fluids by light scattering,** Chapter 11 in *Physics of Simple Liquids,* H. N. V. Temperley, J. S. Rowlinson, G. S. Rushbrooke, eds., pp. 449-505 (North Holland Publ. Co., Amsterdam, The Netherlands, 1968).

Key words: Brillouin scattering; critical opalescence; fluctuations; gases; light scattering; liquids; Rayleigh scattering.

After introducing the basic scattering equations, the first part of the paper is devoted to a discussion of measurements of the intensity of scattered light. A survey is presented of the experimental verification of the Einstein scattering equations. Furthermore, the experimental angular dependence of the scattered intensity near the critical point is discussed, in particular for binary liquid mixtures near the critical mixing point.

The second part of the paper is devoted to the spectrum of scattered light. The Landau-Placzek theory, as worked out by Mountain, is discussed in detail for one component fluids and estimates are presented for several characteristic properties of the spectrum as a function of density and temperature. The experimental verification of the Landau-Placzek theory is surveyed. The paper concludes with a discussion of the spectrum of critical opalescence.

**11061.** McKinley, J. D., Jr., **Mass spectrometric investigation of the surface reaction of tungsten with chlorine-oxygen mixtures,** (Proc. 6th Intern. Symp. Reactivity of Solids, Schenectady, N.Y., Aug. 25-30, 1968). Chapter in *Reactivity of Solids,* J. W. Mitchell, R. C. DeVries, R. W. Roberts, and F. Cannon, eds., pp. 345-351 (John Wiley and Sons, Inc., New York, N.Y., 1969).

Key words: Chlorine; high temperature; mass spectrometry; oxygen; reaction kinetics; tungsten.

The rapid erosive attack of chlorine, oxygen mixtures on hot tungsten has been studied mass spectrometrically. At surface temperatures between 1000 and 2400 K the major product is gaseous tungsten dioxydichloride. Volatile tungsten dioxide and trioxide also form at lower rates. Oxide desorption exhibits the same pressure and temperature dependence as in pure oxygen. No evidence was obtained for simple tungsten chlorides or for chlorine oxides among the products.

**11062.** McNesby, J. R., Kelley, R. V., **High temperature vacuum ultraviolet photolysis of n-butane,** *J. Phys. Chem.* **73,** No. 4, 789-793 (Apr. 1969).

Key words: Chain reaction; n-butane; n-butane-$d_{10}$; photolysis; vacuum ultraviolet.

Mixtures of n-butane and n-butane-$d_{10}$ have been photolyzed at 1470 Å over the temperature range 35-398 °C. The mechanism of methane formation is shown to be largely intramolecular at 35 °C and becoming increasingly dominated by a chain reaction carried by methyl radicals as the temperature is raised. At 398 °C, the mechanism of methane formation is almost entirely free radical. Estimates have been made of average chain lengths as a function of temperature and from this, the chain length in the pyrolysis of n-butane is calculated to be about 2000. It is suggested that none of the methods of detecting molecular elimination of methane in the pyrolysis of butane have been sufficiently sensitive. Molecular elimination of methane in pyrolysis may be at least as important as methyl radical formation and still escape detection.

**11063.** Macedo, P. B., Napolitano, A., **Inadequacies of viscosity theories for $B_2O_3$,** *J. Chem. Phys.* **49,** No. 4, 1887-1895 (Aug. 15, 1968).

Key words: Activation energy; Arrhenius behavior; $B_2O_3$ glass; configuration entropy; distribution of relaxation times; free volume; Fulcher equation; viscosity.

The viscosity of $B_2O_3$ glass was measured from $10^{10}$ to $10^{14}$ poises by the fiber elongation method and found to be Arrhenius with an activation energy of 94 kcal/mol. These new data were combined with previously reported rotation data ($10^1$ to $10^{10}$ poises) and gave a smooth plot. Considering the best known viscosity theories, in view of the new additional viscosity data, and finding no reasonable fits, an examination of the validity of the basic assumptions underlying these theories was made. As a result of this study, it was found that the temperature dependence of the viscosity is not controlled by structural effects such as free volume, configuration entropy, etc. but by activation energy effects in the viscous flow process. The onset of the non-Arrhenius region is a direct consequence of the appearance of a symmetric distribution of relaxation times and/or a distribution of activation energies which can not be explained by existing viscosity theories. Finally, all theories are in error in predicting that the viscosity goes to infinity (in the annealing region) much faster than the measured values indicate.

**11064.** Macedo, P. B., Simmons, J. H., Haller, W., **Spectrum of relaxation times and fluctuation theory: ultrasonic studies on an alkali-borosilicate melt,** *Phys. Chem. Glasses* **9,** No. 5, 156-164 (Oct. 1968).

Key words: Alkali-borosilicate glass; composition fluctuations; immiscible alkali-borosilicate glass; spectrum of relaxation times; ultrasonic relaxation.

Ultrasonic relaxation measurements (3 to 23 MHz and 750 to 1200 °C) were made using shear waves on a molten glass of 6.72 percent $Na_2O$, 25.31 percent $B_2O_3$ and 67.97 percent $SiO_2$ with a solubility temperature of 749 °C. The spectrum of shear relaxation times was determined between 840 and 1200 °C, where it was found to be highly temperature dependent. A model was proposed which predicts the observed temperature dependence of the spectrum in terms of composition fluctuations. The model is based upon the concept that the activation energy of a molecule depends on the environment within a sphere of radius $r_o$ about the molecule. The value of $r_o \sim 50$ Å obtained from the supercritical composition fluctuations is of the same order as sizes of microheterogeneities directly observed with an electron microscope in single oxide glasses by other workers.

**11065.** Madden, R. P., Ederer, D. L., Codling, K., **Resonances in the photoionization continuum of Ar I (20-150 eV),** *Phys. Rev.* **177,** No. 1, 136-151 (Jan. 5, 1969).

Key words: Absorption cross-section; absorption spectra; argon; photoionization; vacuum ultraviolet.

The absorption spectrum of argon in the region 20-150 eV has been studied photographically and photoelectrically, using synchrotron light as a background source and a resolution of 0.06 Å. Many resonances have been observed in the photoionization continuum which are caused by electronic excitation to high autoionizing states of Ar I. In the region between 27 and 40 eV the observed structure is due to two types of electronic excitation: (i) the excitation of a single sub-shell 3s electron, resulting in the configuration $3s3p^6np$ and (ii) the excitation of two of the outer 3p electrons simultaneously, resulting in configurations of the type $3s^23p^4n\ell n'\ell'$. Between 44 and 59 eV weak structures have been observed in the absorption continuum due to the simultaneous excitation of a 3s and a 3p electron, resulting in configurations of the type $3s3p^5n\ell n'\ell'$. All of the observed resonances have been tabulated, and a partial classification has been given. The profiles of the resonances caused by transitions to states $3s3p^6(^2S_{1/2})np\ ^1P_1^o$, for n=4, 5, and 6, and the two electron excitation states $3s^23p^4(^3P)4s(^2P_{3/2})4p$ and $3s^23p^4(^3P)3d(^2P_{3/2})4p$, have been studied quantitatively. The values of q, $\rho^2$, and $\Gamma$ have been determined for each of these resonances, and the continuum cross-section has been measured between 24 and 36 eV.

**11066.** Mopsik, F. I., **Dielectric properties of slightly polar organic liquids as a function of pressure, volume, and temperature,** *J. Chem. Phys.* **50,** No. 6, 2559-2569 (Mar. 15, 1969).

Key words: Carbon disulfide; carbon tetrachloride; Clausius-Mossotti; density; dielectric constant; dipole moment; isopentane; polarizability pressure; slightly polar liquids; Tait equation; toluene.

The dielectric constant and density have been measured simultaneously for carbon tetrachloride, carbon disulfide, isopentane and toluene. The Clausius-Mossotti polarization for all liquids at constant temperature shows a linear decrease with density. Only isopentane and toluene show a temperature dependence of the Clausius-Mossotti polarization at constant density consistent with the presence of a permanent dipole moment. The dipole moments derived from the constant density data are 0.105 D fo isopentane and 0.332 D for toluene. Also, the Bottcher-Onsage equation is shown to be incompatible with the measured data.

**11067.** Mopsik, F. I., **The effect of pressure, volume and temperature on the dielectric constant of simple organic liquids,** *Proc 1967 Annual Report Conf. Electrical Insulation and Dielec tric Phenomena, Buck Hill Falls, Pa., Sept. 18-20, 1967,* pp 66-69 (Natl. Acad. Sci.—Natl. Res. Council, Washington D.C., 1968).

Key words: Carbon disulfide; carbon tetrachloride; density dielectric constant; n-hexane; polarizability; pressure.

Measurements have been made on carbon tetrachloride, car bon disulfide and hexane over a wide range of temperature an pressure for both density and dielectric constant. For all liquid there is a general decrease in the polarizability with an increas in density. N-hexane alone has shown a temperature dependenc of its dielectric constant consistent with a dipole moment.

**11068.** Mountain, R. D., Deutch, J. M., **Light scattering from bi nary solutions,** *J. Chem. Phys.* **50,** No. 3, 1103-1108 (Feb. 1 1969).

Key words: Binary mixtures; Brillouin scattering; diffusio coefficient; light scattering; optical mixing spectroscop Rayleigh scattering.

The spectrum of the light scattered by a binary solution is ca culated from thermodynamic fluctuation theory and th linearized hydrodynamic equations appropriate to a two con ponent fluid. The spectrum consists of three peaks. Expressio are obtained for the positions and widths of the two side, Bri louin peaks. In general the central, unshifted Rayleigh peak found to consist of a superposition of two Lorentzians that i volve the combined dynamical effects of heat conduction and di fusion. The condition is stated under which it is possible separate the central peak simply into two contributions, one ari ing from diffusion and one from thermal conduction. For ma binary systems this separation is justified. In these cases me ement of the spectrum of the scattered light should prove to an attractive alternative means of measuring the diffusion fficient of binary solutions.

69. Mozer, B., **Localized modes, resonant modes and impurity ibrational bands in vanadium alloys,** Chapter in *Neutron Inlastic Scattering* **1,** 55-63 (International Atomic Energy Agency, Vienna, Austria, 1968).

> Key words: Alloys; bound states; inelastic neutron scattering; local modes; resonant modes.

nelastic neutron scattering data have been obtained on Be-V, -V, W-V, Ni-V, and Cr-V alloys in a search for defect modes vibration, impurity vibrational bands, and effects on the vibranal spectrum arising from perturbed electron energy bands in ne of these alloys. The results of these experiments show for light mass beryllium atoms a single localized mode at 0.047 at low concentration and in agreement with theory for an topic defect; impurity bands with structure are observed at her concentrations. A decay constant of 2.5 $a_o^{-1}$ for the amtude of a localized mode can be obtained from the observed itting. Evidence is scant for resonant modes from heavy mass ms in vanadium as observed in the very small difference tween alloy vibrational spectra and the pure vanadium specm. Very small peaks are observed corresponding to a splitting the resonant modes with no theoretical explanation available. -V and Cr-V alloys of equal electron concentration show nilar spectra but differing greatly from the pure vanadium ectrum. Arguments on how the electron density influences the gnitude of the high frequency vibrational spectra of the ions ovide an indirect proof of the absence of bound electron states calized states) associated with nickel ions in vanadium.

70. Munis, R. H., Finkel, M. W., **Goniometric measurements of infrared transmitting materials,** *Appl. Opt.* **7,** No. 10, 2001-2004 (Oct. 1968).

> Key words: Angular scattering instrument; infrared scattering; polycrystalline scattering.

An angular infrared scattering instrument has been conucted. Measurements at infrared wavelengths have been made a polycrystalline specimen. A radiative balance equation has en written and an angular scattering function has been defined. e total scattered radiation is calculated by summation of the attering function over all solid angles.

071. Nemoto, T., Wait, D. F., **Microwave circuit analysis using the equivalent generator concept,** *IEEE Trans. Microwave Theory Tech.* **MTT-16,** No. 10, 866-873 (Oct. 1968).

> Key words: Cascaded multiports; equivalent generator; generalized reflectometers; multiports; reduced multiports; scattering matrix analysis.

To facilitate a scattering matrix analysis of complicated icrowave circuit problems, an equivalent generator approach s been developed. The equivalent generator parameters are ated in terms of the parameters of the actual circuit elements. hese statements are expressed in terms of special determinants hich make the results easier to remember, and easier to use. hree different types of problems are solved to demonstrate the ility of the method; the response from generalized reflectomers, the properties of cascaded multiports in terms of its eleents, and the properties of multiports whose number of availae ports have been reduced.

1072. Newman, M., **Maximal normal subgroups of the modular group,** *Proc. Am. Math. Soc.* **19,** No. 5, 1138-1144 (Oct. 1968).

> Key words: Linear fractional groups; maximal normal subgroups; simple groups.

The principal results of this paper are: (1) the modular group Γ contains infinitely many maximal normal subgroups of finite index which are not congruence groups, and (2) any element of LF(2,q) other than ±I may be written as the product of an element of period 2 and an element of period 3, provided that $p > 3$, where $q = p^n$.

11073. Nimeroff, I., **A survey of papers on degree of metamerism,** *Color Eng.* **6,** No. 6, 44-46 (Nov.-Dec. 1968).

> Key words: Colorimetric matches; colorimetry; color vision; index of metamerism; metamerism; spectrophotometric matches.

Generally, colorimetric matches are metameric, not spectral. The degree of metamerism between a pair of metameric colors is determined by the differences between the spectral distributions of light from these colors. A survey of work reported on metamerism revealed that colorimetric indexes of metamerism have been devised on the basis of observed color differences that appear with change of illuminating and viewing conditions. These indexes are, however, limited in scope and applicability. A general and fundamental metamerism index should depend directly on the spectral differences of the matched metameric colors. A description is given of an index of metamerism that depends directly on spectral differences, is independent of color lightness, and correlates well with the spread of chromaticity coordinates of metameric matches made by a number of observers for a variety of colors.

11074. Norton, R. B., **Aeronomy,** *Encyclopedia of Atmospheric Sciences and Astrogeology,* R. W. Fairbridge, ed., pp. 3-7 (Reinhold Publ. Co., New York, N.Y., 1967).

> Key words: Aeronomy; atmosphere; atmospheric; structure; theory.

The definition and general scope of aeronomy is indicated and the division of the atmosphere into regions is discussed. Atmospheric structure and theory is briefly reviewed.

11075. Okabe, H., **Photodissociation of $HN_3$ in the vacuum-ultraviolet production and reactivity of electronically excited NH,** *J. Chem. Phys.* **49,** No. 6, 2726-2733 (Sept. 15, 1968).

> Key words: Absorption spectrum; $A^3\Pi_i$; fluorescence; fluorescence quenching; $HN_3$; NH $c^1\Pi$; photodissociation; vacuum ultraviolet.

Photodissociation processes of $HN_3$ yielding electronically excited species have been studied in the vacuum ultraviolet. The fluorescence originating from these species has been investigated in the spectral region from 1700 to 6000 Å. The predominant excited species are NH $c^1\Pi$, NH $A^3\Pi_i$ and probably $N_2$ $B^3\Pi_g$. The yield of the NH $c^1\Pi$ is produced mainly in $v = 0$ levels with only 7 percent in $v = 1$ levels both at the Kr and Xe lines. However, it is rotationally excited up to $K = 18$. Direct formation of the NH $A^3\Pi_i$, a spin forbidden process, appears to be minor. The pressure dependence of the ratio, NH $A^3\Pi_i$ to NH $c^1\Pi$, indicates that the NH $A^3\Pi_i$ may be formed largely by the reaction of electronically excited $N_2$, most probably $N_2$ $B^3\Pi_g$, with $HN_3$. The absorption coefficient of $HN_3$ has been measured in the vacuum ultraviolet region in order to examine its correlation with dissociation processes. It was concluded that the NH $c^1\Pi$ may be formed from predissociation of electronically excited $HN_3$ below 1450 Å, while above 1450 Å from direct dissociation. The NH $c^1\Pi$ is quenched almost in every collision with $H_2$, CO, $O_2$, and NO. It was found that the main quenching process by paramagnetic gases, $O_2$ and NO, is the conversion of the $c^1\Pi$ to the $A^3\Pi_i$. Other primary processes are discussed in conjunction with the present work.

11076. Olver, F. W. J., **Error bounds for the Laplace approximation for definite integrals,** *J. Approx. Theory* **1,** 293-313 (1968).

Key words: Asymptotic expansions; Bessel functions; definite integrals; error bounds; gamma function; Laplace approximation.

Explicit error bounds are obtained for the well-known asymptotic expansion of integrals of the form

$$\int_a^b e^{\;\lambda p(x)} q(x)dx$$

in which λ is a large positive parameter, p(x) and q(x) are real differentiable functions, and p′(x) has a simple zero in the finite or infinite range [a,b]. The bounds are expressed in terms of the supremum of a certain function taken over [a,b], and are asymptotic to the absolute value of the first neglected term in the expansion as $\lambda \to \infty$. Several illustrative examples are given, including modified Bessel functions and the gamma function.

**11077.** Omar, A., Peterson, R. L., **On the validity of the Boltzmann relaxation equation,** *Physica* **39,** No. 1, 156-160 (July 1, 1968).

Key words: Boltzmann relaxation equation; Boltzmann transport equation; relaxation time approximation; transport theory.

A paper by Guénault and MacDonald, which shows that the "relaxation time approximation" is almost never strictly consistent with the "master equation," and which suggests that therefore this approximation can seldom be used in transport theory with confidence, is criticized. It is shown that the "Boltzmann relaxation equation" (BRE) in fact is often a direct consequence of the master equation in the steady state. We also point out that in those cases for which the BRE can be justified, the corresponding relaxation time is not generally sufficient in the Boltzmann transport equation if terms of higher order than the first in the driving field are desired.

**11078.** O'Reilly, D. E., Tsang, T., **On the order-disorder transition in ferroelectric ammonium sulfate,** *J. Chem. Phys. Letter to Editor* **50,** No. 5, 2274-2275 (Mar. 1, 1969).

Key words: Ammonium sulfate; deuteron magnetic resonance; ferroelectricity; neutron diffraction; order-disorder transition.

Divergent conclusions about the nature of ferroelectric transition in ammonium sulfate have been arrived at from the deuteron magnetic resonance and neutron studies. In this note, we review the evidence that the ferroelectric phase transition is an order-disorder phenomenon and suggest that the divergent conclusions are a result of the large thermal vibrations of the hydrogen atoms.

**11079.** Paabo, M., Bates, R. G., **Standards for a practical scale of pD in heavy water,** *Anal. Chem.* **41,** No. 2, 283-285 (Feb. 1969).

Key words: Acidity; carbonate; citrate; deuterium ion; deuterium oxide; glass electrode; heavy water; pD; phosphate; standards for pD.

The glass electrode has been found to respond to deuterium ion in heavy water solutions as well as to hydrogen ion in ordinary water. Futhermore, the glass-calomel pH assembly is useful for practical measurements of pD in heavy water. Several standard reference solutions for pD are needed, however, as the response of individual glass electrodes is not constant over the entire useful pD range. A suitable phosphate solution (pD 7.428 at 25 °C) composed of $KD_2PO_4$ and $Na_2DPO_4$ (each 0.025 molal) was established in earlier work. This reference has now been supplemented by two other useful buffer solutions, namely 0.05m $KD_2$ citrate (pD 4.293 at 25 °C) and a mixture of $NaDCO_3$ and $Na_2CO_3$ (each 0.025 molal) which has a pD of 10.736 at 25 °C. Values have been assigned at 10 temperatures from 5 to 50 °C. The conventional pD scale fixed by these three standards has been shown to have a satisfactory internal consistency.

**11080.** Pechukas, P., **Generalized Langevin equation of Mori an Kubo,** *Phys. Rev.* **164,** No. 1, 164-175 (Dec. 5, 1967).

Key words: Fluctuation-dissipation theorem; Langevi equation; stationary stochastic process.

We derive and discuss the generalized Langevin equation o Mori and Kubo for an arbitrary stationary stochastic proces with continuously differentiable correlation function.

**11081.** Pecker, J. C., Thomas, R. N., **Saturation in Fraunhofe lines,** *Observatory Letter* **88,** No. 964, 115-117 (June 1968).

Key words: Absorption tube profiles; equivalent-width; lin depth; line-profiles; non-LTE; optical thickness; saturatio source-function.

We take issue with an interpretation of line-profiles in terms absorption tube profiles, as suggested in a Letter to the Editor *Observatory* by Gussmann, and a critique of Pecker's saturatio function to represent equivalent-width by Gussmann. W present a more correct interpretation in terms of a complete no LTE formulation of the problem, introducing an "equivalent" "effective" source-function.

**11082.** Peiser, H. S., **The relative magnitude of jump rates f point-defect paths between equivalent sites around a trap,** *Korean Phys. Soc.* **1,** No. 1, 5-8 (Mar. 1968).

Key words: Crystal relaxation; crystal symmetry; cryst trap; defect mobility crystal; point-defect; point group.

To a limited but significant extent, the relative magnitude jump rates for point-defect paths between equivalent sit around a trap of non-cubic symmetry in crystals is governed cross-over points of equivalent paths on the stereograph representation of the trap environment and by true intersectio of paths caused by mirror planes of symmetry. The chief co sequence is that in simple experiments the number of defect pa types that cause observable internal-friction effects is grea limited. Moreover, a closer estimate than is otherwise possi can be made of the number of distinct paths needed for compl or partial relaxations, associated with an external influence.

**11083.** Peterson, R. L., **Short-range magnetic order in a modifi Weiss molecular-field theory,** *Phys. Rev.* **171,** No. 2, 586-5 (July 10, 1968).

Key words: Magnetism; molecular field theory; short-ra order.

The Weiss molecular field theory (WMFT) of ferromagneti as commonly used, has the well-known defect that the sh range order and heat capacity vanish in zero applied field temperatures above the Curie point. We here point out that same use of the WMFT also gives an isentropic susceptibi equal to zero at all fields and temperatures, and two differ results for the isothermal susceptibility, depending upon wh of two direct methods of calculation are used. These difficult are all traced to the use of the assumption that different spins uncorrelated. We argue that this assumption is not consist within the framework of the WMFT, and show that the mole lar field assumption by itself provides a measure of the spin c relations. The assumption that only nearest neighbor spins correlated is shown to be consistent at high temperature an yield the correct high-temperature expression for the short-ra order and heat capacity. Thus we argue that when corre used, the WMFT does not possess the gross defects usually tributed to it. The discussion applies also to antiferromagneti

**11084.** Plummer, E. W., Gadzuk, J. W., Young, R. D., **Resona tunneling of field emitted electrons through adsorbates on m surfaces,** *Solid State Commun.* **7,** 487-491 (1969).

Key words: Adsorption; energy distribution; field emission; surface; tunneling resonance.

Tunneling resonance of field emitted electrons through the ergy levels of single Zr atoms and $\chi$ nitrogen adsorbed on a ngsten surface has been observed. The enhanced tunneling obability through the Zr atoms on tungsten shows that the tomic band" of Zr is shifted by $\Delta E \sim 1.0-1.5$ eV with a width $\sim$ 1 eV. The resonance in $\chi$ nitrogen demonstrates that this trogen complex is probably negatively ionized.

**085.** Pong, W., **Photoemission from Al-$Al_2O_3$ films in the vacuum ultraviolet region,** *J. Appl. Phys.* **40,** 1733-1739 (1969).

Key words: $Al_2O_3$ films; electron attenuation length; electron mean free path; photoelectric effect; photoelectric threshold; thin films; vacuum ultraviolet.

Measurements of quantum yield of Al-$Al_2O_3$ films were made photon energies between 7 and 22 eV. The photoelectric reshold for intrinsic photoemission from amorphous $Al_2O_3$ ppeared to be about 8 eV. Approximately 1 eV was estimated r the electron affinity of $Al_2O_3$. The yield of anodic oxide film n aluminum at 10.2 eV decreased with increasing oxide ickness while the yield at 21.2 eV increased. The decrease in eld at 10.2 eV was attributed to photoelectrons originating om the aluminum film beneath the oxide layer. Attempts were ade to study the escape probability function for electrons moving through the oxide into the vacuum. An attenuation length of bout 129 Å for the photoelectrons in the oxide was obtained by sing the exponential-function approximation. The maximum initial energy of the electrons was estimated to be 7.8 eV above the acuum level. The electron mean free path for electron-phonon ollisions in the oxide was estimated to be approximately 16 Å.

**1086.** Pool, K. H., Bates, R. G., **Thermodynamics of hydrochloric acid in 95 volume percent (92.41 mass percent) ethanol from e.m.f. measurements at 5 to 50 °C,** *J. Chem. Thermodynamics* 1, 21-29 (1969).

Key words: Activity coefficients; emf measurements; enthalpy; entropy; ethanol-water solvents; hydrochloric acid; thermodynamics.

Electromotive-force measurements of cells of the type Pt;$H_2$, HCl(m) in EtOH-$H_2O$, AgCl;Ag at 10 temperatures from 5 to 50 C have been used to derive (a) the standard emf of the cell in 2.41 wt. percent ethanol, (b) the activity coefficient of ydrochloric acid, (c) the relative partial molal enthalpy and heat apacity of HCl, and (d) the thermodynamic constants for the ransfer of HCl from water to 92.41 wt. percent ethanol. The nolality of the acid ranged from 0.0099 to 1.085 mol $kg^{-1}$. To obain the standard emf it was necessary to correct for ion-pair fornation and to use the extended terms of the Debye-Hückel heory. The ion-size parameter, chosen to minimize the sum of he squares of the deviations, varied only slightly with temperaure, from 3.97 Å at 5 °C to 4.31 Å at 50 °C.

**1087.** Potzick, J., **Ac-dc regulator-modulator,** *Rev. Sci. Instr.* **39,** No. 8, 1219-1220 (Aug. 1968).

Key words: Feedback; modulator; regulator.

A general purpose regulator-modulator is described in which he gain of a d-c amplifier is determined by a control voltage lerived through an external feedback loop.

**1088.** Powell, C. J., **Characteristic energy losses of 8-keV electrons in liquid Al, Bi, In, Ga, Hg, and Au,** *Phys. Rev.* **175,** No. 3, 972-982 (Nov. 15, 1968).

Key words: Aluminum; bismuth; electron energy loss; gallium; gold; indium; liquids; mercury; solids.

Characteristic loss spectra have been obtained in a reflection scattering geometry for liquid Al, Bi, In, Ga, Hg and Au and, in the case of Al, Bi and Au, for the same specimens in the solid phase. Peaks due to surface and volume plasmon excitation dominated the loss spectra for all elements except Au. The relative intensity of these peaks varied rapidly with scattering angle for the liquid and frozen specimens but there was little angular variation when Al, Bi, or Au was evaporated onto a frozen substrate of the same element. The Al plasmon losses varied with temperature and changed at the mp as would be expected from the known density variation. Changes in the Bi plasmon energy losses on melting and changes in other structure on melting have been interpreted in terms of band-structure changes. The peaks in the gold loss spectra appeared to become broader and less distinct on melting from which it was concluded that the Au excited states had shorter lifetimes with increased disorder. In general, however, the liquid and solid-state spectra of the same element were similar, thereby showing that for these materials there was not a large change in band structure on melting.

**11089.** Powell, C. J., **Interaction of electrons with solids,** Chapter 9.2 in *Atomic and Electron Physics, Atomic Interactions,* **Vol. 7,** *Methods of Experimental Physics,* B. Bederson, ed., Part B, pp. 275-305 (Academic Press Inc., New York, N.Y., 1968).

Key words: Cross-sections; elastic scattering; electron detectors; electron energy analyzers; electron guns; electron scattering; electron-solid interactions; experimental techniques; inelastic scattering; multiple scattering; secondary processes; specimen preparation.

A review is given of methods and techniques useful in experiments where electrons of energy between 0 and 100 keV interact with solids. A general discussion is given firstly of common experimental components and procedures: electron guns, energy analyzers, and electron detectors; specimen preparation; and experimental strategy. The interaction of electrons with solids is considered firstly by assuming that the solid can be represented as an assemblage of atoms, thereby simplifying the analysis. Elastic and inelastic scattering measurements are discussed, followed by a survey of methods useful in situations where multiple scattering occurs and where secondary or higher order electrons and photons are generated. Finally, the relevance of angular anisotropies in elastic and inelastic electron scattering by crystalline solids is described.

**11090.** Powell, R. L., Clark, A. F., Fickett, F. R., **Longitudinal magnetoresistance of pure copper,** (Proc. Conf. Electron Mean Free Paths in Metals, Zurich, Switzerland, Sept. 3-5, 1968), *Phys. kondens. Materie* 9, 104-112 (Lange and Springer, Berlin, West Germany, 1969).

Key words: Copper; electronic scattering; magnetoresistance.

Pippard suggested that the longitudinal magnetoresistance for metal crystals should give information about electronic scattering mechanisms on the Fermi surface. Therefore we have determined the magnetoresistance saturation ratio $(R\{B = \text{saturation}\}/R\{B=0\})$ for copper crystals of different orientations at varying temperatures in order to test several hypotheses concerning the anisotropy of mean-free-paths and the validity of diffusion or relaxation-time approximations. The temperature dependence of the saturation ratios along the [100] and [110] directions has been determined from 4 to 35 K. Near 35 K experimental ratios are well below theoretical values calculated using even wide (5 to 1) variations for the mean-free-path. As the temperature decreases from 35 K and the average scattering angle decreases, the ratio rises as would be expected from an approach to the diffusion approximation, but then decreases again as impurity scattering, which would be expected to be more isotropic, begins to dominate.

**11091.** Przybylowicz, E. P., Smith, G. W., Suddueth, J. E., Nargolwalla, S. S., **Activation analysis of halogens in photographic**

**emulsions using a neutron generator,** *Anal. Chem.* **41,** No. 6, 819-823 (May 1969).

Key words: Chloride; iodide; nondestructive neutron activation analysis; photographic emulsions; silver bromide; 2.8-MeV neutrons; 14.7-MeV neutrons.

A nondestructive neutron activation technique for the analysis of chloride and iodide in a silver bromide matrix is described. Chlorine was measured after activation with 14.7-MeV neutrons. The 3.1-MeV gamma rays from $^{37}S$ were measured without interference. Calibrations were carried out using photographic emulsions containing 10- to 200 milligrams of chlorine. The relative standard deviation of a single determination at the 10 milligram level is 5 percent; at the 200 milligram level it approaches 1 percent. Iodine was measured via $^{128}I$ produced by (n,γ) activation with 2.8-MeV neutrons. A straight line curve was established for 2- to 420 milligrams of iodine. The relative standard deviation of a single determination at these two levels was 20 and 1 percent respectively. The method offers an attractive alternate to existing chemical and instrumental methods for the determination of iodide and chloride in silver halide mixtures since it has the potential for providing rapid analysis with reasonably good precision. With an order of magnitude increase in neutron flux, the method would be unquestionably superior to other instrumental methods for the halides.

**11092.** Quindry, T. L., **Transmissibility measurements for the determination of structural damping,** (Proc. Vibrations Conf., Philadelphia, Pa., Mar. 30-Apr. 2, 1969), *Preprint* No. 69-VIBR-36, 7 pages (American Society of Mechanical Engineers, New York, N.Y., 1969).

Key words: Air; antiresonances; cantilever beam; damping; mass-loading; resonances; tip rotary inertia; transmissibility; vacuum.

A straightforward means of determining the damping coefficient of structural metals by the use of a mass-loaded cantilever beam is described. In order to determine the structural damping coefficient, δ, from the form $E^* = E(1 + j\delta)$, experimental data is normalized to fit the non-dimensional equations of transmissibility. Only the experimental values of frequency for the first and second resonance and of transmissibility for the first antiresonance and second resonance are needed to determine the structural damping coefficient. The boundary conditions account for the effects of mass-loading and tip rotary inertia. For the same alloys, root stress and temperature did not vary appreciably during the conditions of the test.

Good repeatability was obtained for tests in air and in vacuum from specimens of ZK60A T5 magnesium alloy and 2024 T4 aluminum alloy.

Advantages of mass-loading and obtaining the structural damping coefficient from transmissibility at the second resonance are cited.

**11093.** Radford, H. E., **Scanning microwave echo box spectrometer,** *Rev. Sci. Instr.* **39,** No. 11, 1687-1691 (Nov. 1968).

Key words: Cavity spectrometer; echo box; free radicals; hydroxyl radical; microwave absorption.

A resonant cavity microwave spectrometer for wavelengths between 3 and 30 cm, which uses radar echo boxes as absorption cells, is described. The minimum detectable absorption coefficient at 10 cm wavelength is $10^{-10}$ cm$^{-1}$, and this sensitivity is maintained during frequency scans by automatic feedback tuning of the echo box. The spectrometer is well suited to studies of gaseous chemical reactions, and some preliminary observations are reported, including the negative results of a search for the 10 cm spectrum of CH, and measurements of OH spectra at 4.7 and 6.0 GHz.

**11094.** Ray, C. D., Tsukishima, T., Hyland, R. N., McLane, K., Carpenter, R. J., **Analysis of a frequency-swept one-b digital correlator,** *J. Appl. Phys.* **39,** No. 8, 3534-3542 (Jul 1968).

Key words: Correlator; cross-correlator; diffusion coefficient; digital correlator; frequency-swept; plasma.

An instrument for measuring the cross spectral density of tw random variables which are correlated is described. It was cor structed to study the relationship between electron densit fluctuations and the ambipolar diffusion coefficient in a plasm A stability in the zero correlation level of $10^{-3}$ is achieved b use of one-bit digital electronics in the multiplier and integrato An analysis of the design and function of the instrument is give together with a discussion of possible instrumental errors an statistical uncertainties in the measurements.

**11095.** Rebbert, R. E., Ausloos, P., **The photolysis of methane 584 Å,** *J. Am. Chem. Soc.* **90,** 7370-7371 (1968).

Key words: Charge transfer; ion-molecule reaction methane; photolysis; rare gas.

The photolysis experiments described in this paper have bee carried out with an enclosed helium resonance lamp. To o knowledge those are the first studies carried out with such a lig source. The experimental results obtained at pressures varyi from one to 15 torr are in general agreement with the publish mass spectrometric data which are generally obtained arou $10^{-5}$ torr.

**11096.** Risley, E. W., **Discontinuity capacitance of a coaxial li terminated in a circular waveguide,** *IEEE Trans. Microwa Theory Tech.* **MTT-17,** No. 2, 86-92 (Feb. 1969).

Key words: Discontinuity capacitance; open circuited coa ial line; Rayleigh-Ritz variational method; solid center co ductor.

This calculation evaluates the discontinuity capacitance of coaxial line terminated in a circular waveguide using t Rayleigh-Ritz variational technique. A 50 ohm, 3/4 inch, coaxi line termination with solid center conductor was fabricated wi center and outer conductor dimensions of 0.32568 ± 0.000 and 0.74995 ± 0.00002 inches respectively. The measured val of capacitance of this termination at 1000 Hz was 2.164 × 10 farads as compared with the calculated value of 2.177093 × 10 farads. Calculated values of capacitance for other line sizes we also compared with measured values and in each case the calc lated value agreed with the measured value to within the expe mental error of the measured value.

**11097.** Roach, F. E., **Diffuse galactic light,** Chapter in *Modern trophysics: A Memorial to Otto Struve,* M. Hack, ed., pp. 4 66 (Gordon and Breach, New York, N.Y., 1967).

Key words: Airglow continuum; diffuse starlight; galac light; light; starlight.

The observational evidence for the existence of diffuse st light scattered by interstellar dust is reviewed. The observatio difficulty in the measurement lies in the fact that the so-call galactic light is a relatively faint component of the light of t night sky in competition with the zodiacal light, the integrat starlight and the airglow continuum. Recent observations ma at Haleakala (Hawaii) indicate a galactic light with a dependen on galactic latitude in only partial agreement with a theoreti paper by Wang Shih-Ky.

**11098.** Roach, F. E., **The brightness of the zodiacal light at ecliptic pole,** (Proc. Symp. Meteor Orbits and Dust, Ca bridge, Mass., Aug. 9-19, 1965), *Smithsonian Contributi to Astrophysics,* F. L. Whipple, ed., **11,** 225-226 (Smithson nstitution Astrophysics Observatory, Cambridge, Mass., 967).

Key words: Photometry; zodiacal light.

A review of current photometric studies of the zodiacal light icates that it has a brightness at the pole of the ecliptic of 110 0(vis) units compared with 250 in the plane of the ecliptic at an ngation of 90°. The ratio of brightness (250/110 = 2.3) is a asure of the concentration of the zodiacal cloud toward the iptic.

**99.** Robbins, C. R., **Growth of strontium titanate from a silica flux,** *J. Crystal Growth* **2,** 402-404 (1968).

Key words: Flux growth; high temperature microscopy; silica flux; single crystals; strontium titanate.

A survey of selected compositions in the ternary system SrO-$O_2$-$SiO_2$ by high-temperature microscopy has shown that sin- crystals of $SrTiO_3$ may be grown from a silica flux. Crystals to 2.5 mm in longest dimension were obtained in a small scale periment by slow cooling of a 20 g melt of mole ratio 1 $TiO_3$:1 $SiO_2$. The crystals are clear, colorless to pale brown, of od optical quality, free from inclusions and show no evidence solid solution by x-ray powder diffractometry.

**100.** Romanoff, M., **Performance of ductile-iron pipe in soils,** *J. Am. Water Works Assoc.* **60,** No. 6, 645-655 (June 1968).

Key words: Cast iron; corrosion; ductile iron; exposure sites; ferrous metals; gray iron; pipe; pipelines; underground; soil corrosion.

This is a progress report on the behavior of specimens of duc- cast-iron pipe after exposures for 1, 2, 4 and 8 years at five ational Bureau of Standards soil corrosion test sites. It can be ncluded from the data that ductile cast-iron and gray cast- n corrode at nearly the same rate in a given soil environment, d that the pattern of corrosion and nature of the graphitic cor- sion products are also similar for the two materials in a given il.

**101.** Rossmassler, S. A., **Modification of dissemination channels for scientific information,** *J. Chem. Doc.* **9,** No. 1, 17-19 (Feb. 1969).

Key words: Abstract journal; evaluation; dissemination; information analysis; redesign; scientific information; technical literature.

Traditional channels for the dissemination of scientific infor- ation are based on primary publication in a scientific journal, th reader guidance provided by an abstract journal. These annels are designed primarily to meet the author's requirement d are document-oriented. The present growth of scientific in- rmation calls for a redesign of the technical literature. It is oposed that the single piece of scientific information be recog- zed as the unit of flow into the distribution system. The result- g need for organized efforts for selection and evaluation of in- rmation, and increased emphasis on users' requirements lead modification of dissemination channels. Possible changes in esent publication practices are considered.

**102.** Rothwell, G. J., **The performance concept: a basis for standards development,** *ASTME Vectors* **1969/2,** 23-25 (Mar.-Apr. 1969).

Key words: Engineering standards; performance concept; performance standards.

Technological measurements and standards are use-related d at the interface between science and its application in indus- y and government. They extend the principles of good mea- rement to the engineering world and to the complex needs of day's society.

But it is increasingly important that such measurements and standards do not hamper the introduction of new technologies or innovations for accomplishing society's objectives. One way to avoid such restrictions is suggested by the concept of using performance requirements as the basis for standards. This concept includes a concern for subjective factors which of necessity enter measurement problems as soon as man becomes part of the system to be measured.

**11103.** Rush, J. J., Melveger, A. J., Farrar, T. C., Tsang, T., **Laser-Raman spectra and hindered rotation in the phosphonium halides,** *Chem. Phys. Letters* **2,** No. 8, 621-624 (1968).

Key words: Crystal structure; force field; hindered rotation; laser; phosphonium halides; Raman spectra; torsional oscillation; vibration.

Laser Raman spectra have been measured for $PH_4Cl$, $PH_4Br$ and $PH_4I$. Intense peaks in all the halide spectra are assigned to torsional ($E_g$) oscillations and to the internal vibrations of the $PH_4^+$ ions. Barriers to $PH_4^+$ rotation are calculated and discussed in comparison with recent spectroscopic and structural results.

**11104.** Ryan, J. V., **Flammable Fabrics Act and its implementation,** *Mod. Textiles Mag.* **L,** No. 3, 67-70 (Mar. 1969).

Key words: Fabrics; flammability; Flammable Fabrics Act; interior furnishings; National Advisory Committee; textiles; textile technology· wearing apparel.

The provisions of the Amendments to the Flammable Fabrics Act are reviewed against the background of the original Act plus experiences with its effectiveness. Cooperation with the accident investigation efforts of the Public Health Service is described. Acquisition of data from additional sources has been somewhat successful.

The Department's procedures for rulemaking involve several steps with opportunity for comment from interested parties at two different times, followed by consultation with the National Advisory Committee for the Flammable Fabrics Act.

A general program approach is described, but the level of funding for the current fiscal year will place serious limitations on the ability to implement the program fully.

**11105.** Ryan, J. V., **The Flammable Fabrics Act and its implementation,** *Proc. Second Annual Meeting Information Council on Fabric Flammability, New York, N.Y., Dec. 3, 1968,* pp. 231-237 (Information Council on Fabric Flammability, New York, N.Y., 1968).

Key words: Carpets; fabrics; Flammable Fabrics Act; National Advisory Committee; procedures; regulations; textiles; wearing apparel.

The 1967 Amendments to the Flammable Fabrics Act delegated authority for establishment of regulations, research, investigations and test method development, and called for a National Advisory Committee with which the Secretary of Commerce must consult.

The National Bureau of Standards has been coordinating with Public Health Service in studying burn cases, and has established a Fabric Flammability Section to carry out the research responsibilities, the coordination, data analysis, and the formulation or recommendations for new or amended standards and regulations. Research will start with basic consideration of what happens in fires that represent hazards to life and property. Data will be considered from any competent source, in or out of government. Consumers Union has provided data on carpets and blankets. The Department has published Procedures for developing standards, and findings that there may be need for standards for wearing apparel and for rugs and carpets. Announcement of the membership of the National Advisory Committee is expected in the near future.

**11106.** Sanderson, B. T., Romanoff, M., **Performance of commercially pure titanium in corrosive soils,** *Mater. Production* **8,** No. 4, 29-32 (Apr. 1969).

Key words: Corrosion; exposure sites; pipe; soil corrosion; steel; titanium; underground.

This is a progress report on the behavior of specimens of titanium tubing with welded seams after exposure in the soils at six National Bureau of Standards corrosion test sites for exposures up to 8 years. The data show that the titanium tubing as well as the weld and heat affected zones are unaffected by corrosion with respect to pitting or metal attack in any of the soil environments to which they were exposed. Weight losses on the specimens were negligible in all soils. Data for carbon steel pipe specimens which were used as a reference material to determine the corrosiveness of the soils are included.

**11107.** Santoro, A., Mighell, A. D., Zocchi, M., Reimann, C. W., **The crystal and molecular structure of hexakis (imidazole)Ni (II) nitrate,** *Acta Cryst.* **B25,** No. 3, 842-847 (Apr. 1969).

Key words: Imidazole; ligand; octahedral coordination complex; trigonal symmetry; x-ray structure determination.

The crystal and molecular structure of hexakis(imidazole) nickel(II)nitrate, $(C_3H_4N_2)_6Ni(NO_3)_2$, was determined by single-crystal x-ray diffraction techniques. This compound crystallizes in the trigonal system, space group $R\bar{3}$. The lattice parameters (hexagonal axes) are $a = 12.353 \pm 0.001$, $c = 14.803 \pm 0.002$A, $Z = 3$, $\rho_o = 1.51$ g cm$^{-3}$, $\rho_c = 1.506$ g cm$^{-3}$. Three dimensional data were used (905 reflections) and the structure solved by an analysis of the Patterson map. The complex cation $(C_3H_4N_2)_6Ni^{++}$ has $\bar{3}$ point symmetry with the nickel atom at the center of a slightly compressed octahedron of nitrogen atom. The imidazole rings are planar to within experimental error. The final refinement by a three-dimensional least-squares analysis resulted in a R value 7.1 percent.

**11108.** Santoro, A., Weir, C. E., Block, S., Piermarini, G. J., **Absorption corrections in complex cases. Application to single crystal diffraction studies at high pressure,** *J. Appl. Cryst.* **1,** Part 2, 101-107 (June 1968).

Key words: Absorption correction; bromine; crystal structure; high-pressure; x-ray diffraction.

A method is described for evaluating the absorption corrections in complex cases in which objects other than the crystal itself take part in the absorption. The method has been applied to the high-pressure cell developed in this laboratory, and it has been tested on a set of intensities obtained from a single crystal of bromine grown and maintained under 10 kbar pressure.

**11109.** Sarachman, T. N., **Microwave spectrum of *cis*-2-butene,** *J. Chem. Phys.* **49,** No. 7, 3146-3149 (Oct. 1, 1968).

Key words: Barrier; *cis*-2-butene; dipole moment; internal rotation; microwave spectrum; molecular structure.

The microwave spectrum of the *cis*-2-butene molecule has been studied between 20 and 40 Gc/sec. Analysis of internal rotation splittings yields an effective three-fold barrier of .73 kcal/mol or 26 cm$^{-1}$. The principal moments of inertia of the normal isotopic species are 31.479, 98.370, and 123.659 amu Å$^2$. The electric dipole moment is $.25_7$ and lies along the b axis of the molecule.

**11110.** Saunders, J. B., Bruening, R. J., **A new interferometric test and its application to the 84-in. reflecting telescope at Kitt Peak National Observatory,** *Astron. J.* **73,** No. 6, 415-531 (Aug. 1968).

Key words: Aberration of telescopes; interferometer; shearing interferometer; telescopes; wavefront shearing interferometer.

The 84 inch aperture, Cassegrainian type telescope at Kit Peak National Observatory was tested with a wavefront shear ing interferometer. This test provided the optical path differenc between 538 uniformly spaced rays in the annular beam of ligh transmitted by the telescope. Independent tests were made fror photographs taken on each of two consecutive nights. The following results were obtained from this test: (a) the coordinates c the points of incidence of each of the 538 rays on the focal plan (a spot diagram); (b) a measure of primary astigmatism; and ( the deviation of the wavefront, at 538 uniformly spaced point from a sphere that is centered on the ideal image point.

A description of the mathematical operations is given with th results. The results show a measurable change in the wavefor during the test periods (approximately 30 minutes) each nigl and a larger difference from one night to the next.

**11111.** Saylor, C. P., **The freezing staircase method,** Chapter 11 *Purification of Inorganic and Organic Materials,* M. Zief, ec pp. 125-138 (Marcel Dekker Inc., New York, N.Y., 1969).

Key words: Crystallization; entrapment; impurity; pha equilibrium; purification; purity; solid solution.

In the freezing staircase method of purification, frozen pc tions of the material being purified are attached to the walls the vessel. They move slowly with the rotating apparatus, trar porting matter in that direction. An equal mass of liquid flows the opposite direction. The solid portions are maintained in crystalline state by stationary coolers outside the containe Since the growing front and the melting surfaces of each so portion remain stationary, the solid is caused to grow on one si and melt on the other until, under good conditions, it becom monocrystalline. By this means there is a close approach theoretical distribution coefficient of impurity between the liqu and solid phases except at locations in the apparatus where t concentration of solid insoluble impurities is at a high le (>5%). During the greater part of any run under good conditio there is no spontaneous nucleation. Encapsulation and entra ment are nearly or entirely eliminated. There is no back mixi of rejected impurities. Purification factors can easily be achiev in each stage which are clearly in excess of one thousand.

**11112.** Scala, A. A., Ausloos, P., **Gas-phase photolysis and radi ysis of cyclopropane,** *J. Chem. Phys.* **49,** No. 5, 2282-22 (Sept. 1, 1968).

Key words: Cyclopropane; free radical reactions; i molecule reactions; photolysis; radiolysis.

The gas phase photolysis of c-$C_3H_6$-$O_2$, $C_3H_6$-NO and c-$C_3$ $H_2S$ mixtures has been investigated at 1470 Å (8.4 eV), 123 (10 eV) and at 1048-67 Å (11.6-11.8 eV), that is at photon er gies below and above the ionization energy of cyclopropane (I = 10.06 eV). Examination of the products formed in the phase experiments at 1470 and 1236 Å as well as of th formed in a few solid phase photolysis experiments indicate t the major primary act of the neutral excited cycloprop molecule can be written as follows: c-$C_3H_6$ + $h\nu$ $CH_2CH_2CH_2^*$. The highly excited trimethylene decompo mainly to form $CH_2$ and $C_2H_4$. There is, however, also evide for rearrangement $CH_2CH_2CH_2^* \rightarrow CH_3CHCH_2^*$ which, at densities, is always followed by fragmentation of $CH_3CHCH$

**11113.** Schafer, G. E., **Precision microwave measurements — to and tomorrow,** *Microwave J.* **12,** No. 6, 25-28 (June 1969).

Key words: Measurements; microwave.

This is an invited guest editorial. The request called fc review of the state-of-the-art of measurements and some spe n on the trends of standards and measurements. This is done ne paper by examples only, since an in-depth review would itly exceed the two or three printed pages allowed by the rowave Journal.

14. Scharf, K., **Steady-state response of silicon radiation detec- rs to x and gamma rays,** *Proc. Symp. Physics and Non- estructive Testing, ITT Research Institute, Chicago, Ill., ept. 27-30, 1966,* **1,** 235-298 (Air Force Materials Laborato- . Wright-Patterson Air Force Base, Ohio, 1968).

Key words: Dosimetry; gamma rays; photodiodes; photovoltaic effects; radiation detection; radiation detectors; semiconducting devices; silicon; x rays.

review is given of investigations of the steady-state response ilicon radiation detectors to x and gamma rays which were ied out in the Radiation Physics Division of the National Bu- u of Standards. Theoretical relations between photocurrents erated in such detectors by x and gamma rays and exposure and quality of radiation are explained. Measurements of the endence of the generated photocurrent on exposure rate, lity of radiation, voltage applied, and detector temperature ied out on different types of detectors are presented, and dif- nt modes of operation of silicon radiation detectors are cussed. By using a special electrical compensation method, osure rates were measured ranging from 100 mR/hr of $^{137}$Cs nma rays to $10^5$ R/hr of 30-kV x rays.

15. Scheer, M. D., Fine, J., **The reaction of carbon monoxide ith a tantalum surface heated above 2000 °K,** *Surface Sci.* **12,** o. 1, 102-107 (Sept. 1968).

Key words: Activation energy; carbon monoxide; high temperature; mass spectrometry; surface reaction; tantalum.

he high temperature surface interaction between carbon noxide and tantalum has been studied with mass spectromet- detection of the gaseous products. It has been shown that car- monoxide is reduced by tantalum to form TaO above 2200 This process is first order in its dependence on carbon noxide pressure and proceeds with an activation energy of 5.1 .

16. Scheer, M. D., Klein, R., **Low-temperature oxygen atom ddition to olefins. III. Transition state and the reaction with *cis-* nd *trans*-2-butenes,** *J. Phys. Chem.* **73,** No. 3, 597-601 (Mar. 969).

Key words: Chemistry; low temperature; olefins; oxygen atom; 2-butene.

he reaction of ground state oxygen atoms O($^3$P), with either or *trans* 2 butene at cryogenic temperatures produces *cis* and *ns* 2,3 epoxybutane, 2 butanone, and isobutyraldehyde. oduct ratios are different for the two butenes. Two precursor tes, one leading to the *trans* epoxide and 2 butanone, and the er to the *cis* epoxide and isobutyraldehyde, are implied by the nstancy of the ratios *trans* 2,3 epoxybutane/2 butanone and *cis* epoxybutane/isobutyraldehyde. A new transition state for O atom-olefin reaction is proposed. A prediction based on new transition state for the O atom reaction with 2 methyl 2 ene was consistent with the experimental finding.

117. Schmidt, L. B., Case, W. E., Harrington, R. D., **Surface dependence of ferrimagnetic resonance fields in polycrystalline NiAl ferrite,** *Proc. IEEE* **56,** No. 7, 1236-1237 (July 1968).

Key words: Ferrite; ferrimagnetic resonance; ferrimagnetic resonance surface effect; nickel aluminum ferrite.

Data obtained at 1107 MHz demonstrates that the ferrimag- tic resonance field of polycrystalline Nickel Aluminum Ferrite pends upon the surface finish of the disk samples used in the measurement. Verification of this surface dependence at 3140 MHz is also reported.

**11118.** Schweitzer, W. G., Jr., **Saturated absorption by neon inside a 6328 Å laser with a mixture of neon isotopes in its gain tube,** *Appl. Phys. Letters* **13,** No. 11, 367-368 (Dec. 1, 1968).

Key words: Laser; neon; isotope shift; saturated absorption; wavelength standard.

In a saturated absorption experiment with neon in a 6328 Å He-Ne laser one can select a combination of isotopes of neon in the gain tube and the proper isotope in the loss tube so as to bring the maximum of the gain curve to the same frequency as that of the saturated absorption peak.

**11119.** Sengers, J. V., **Transport properties of compressed gases,** Chapter in *Recent Advances in Engineering Science,* A. C. Eringen, ed., **III,** 153-196 (Gordon and Breach Science Publ. Inc., New York, N.Y., 1968).

Key words: Compressed gases; thermal conductivity; transport properties; viscosity.

This paper reviews the experimental information on the viscosity and thermal conductivity of compressed one-component gases. The common features in the pressure and density dependence of these transport coefficients observed for various simple gases are summarized. An assessment is made of some methods used to predict the transport coefficients of a compressed gas and the relation between experiment and theory is discussed. A survey is included of the behavior of viscosity and thermal conductivity in the critical region and of the anomalous behavior of the dimensionless Rayleigh and Prandtl number, frequently encountered in the description of certain heat transfer processes. A new method to study transport processes by observing the spectrum of scattered light is discussed and some applications are indicated.

**11120.** Shah, J. A., Huber, M. G., Danos, M., **Separability of the nuclear residual two-body interaction,** *Physics Letters* **28B,** No. 6, 381-383 (Jan. 6, 1969).

Key words: Effective forces; nuclear forces; nuclear shell model; residual forces; separable forces.

The separability of a residual two-body interaction with finite range has been studied by calculating the giant resonance states of O$^{16}$. From the comparison of the effect of an appropriate separable force with the results of an exact calculation it seems that the residual nucleon-nucleon interaction can be represented quite well by a simple separable force which corresponds to the exchange of just one value of momentum between the two particles.

**11121.** Sher, A. H., **Lithium-ion drift mobility in germanium,** *J. Appl. Phys.* **40,** No. 6, 2600-2607 (May 1969).

Key words: Germanium; lithium ion mobility; radiation detectors.

The mobility of lithium in germanium has been determined at several temperatures between 23.8 and 61.2 °C by measuring the change of the capacitance with time of a reverse-biased p-i-n diode. The mobilities of lithium thus obtained (at the specified temperatures) were: $3.04 \times 10^{-10}$ cm$^2$/V-s (23.8 °C), $5.30 \times 10^{-10}$ cm$^2$/V-s (36.2 °C), $7.96 \times 10^{-10}$ cm$^2$/V-s (46.2 °C), and $16.86 \times 10^{-10}$ cm$^2$/V-s (61.2 °C). These values are higher than those which are obtained by the extrapolation of the results of others determined at higher temperatures into this temperature range. The results also suggest that at least three distinct field configurations exist during the early stages of the lithium drifting process rather than the two normally considered.

**11122.** Shirk, J. S., Bass, A. M., **Matrix-isolation spectra of discharge "sputtered" metals,** *J. Chem. Phys.* **49,** No. 11, 5156-5160 (Dec. 1, 1968).

Key words: Atomic spectra; high temperature materials; low temperature; matrix isolation; sputtering; ultraviolet spectroscopy.

Atomic Cu, Ag, Cd and Fe are produced by bombarding the appropriate metal with positive ions from a microwave discharge. The process is similar to sputtering. The metal atoms are trapped in an inert gas matrix on a cold window and their UV spectra observed. This is a new method for isolating high melting materials in a matrix for spectroscopic study.

**11123.** Shirley, J. H., **Dynamics of a simple maser model,** *Am. J. Phys.* **36,** Part 1, No. 11, 949-963 (Nov. 1968).

Key words: Laser dynamics; maser amplifier; maser dynamics.

A simple maser model consisting of a single mode field coupled to N identical two-level atoms is presented. The assumption of negligible statistical correlation between the atoms and the field permits the Heisenberg equations of motion to be replaced by a self-consistent set of ordinary nonlinear differential equations. Relaxation terms and an energy source are introduced phenomenologically. The resulting equations exhibit a threshold, stable and unstable steady states, and relaxation oscillations. The dynamic equations for the hydrogen maser and the rate equations of laser theory are derived as special cases. Also discussed are the maser amplifier, locking of a maser to an external signal and the effects of cavity thermal noise.

**11124.** Shives, T. R., Bennett, J. A., **The effect of environment on the fatigue properties of selected engineering alloys,** *J. Mater.* **3,** No. 3, 695-715 (1968).

Key words: Crack initiation; engineering alloys; environment; fatigue; humidity; oxygen.

Rotating beam fatigue tests were conducted in controlled environments on specimens of free cutting brass, titanium alloy Ti-4Al-4Mn, magnesium alloy AZ61A, and AISI 4340 steel. The fatigue strengths of all the alloys were lower in a moist atmosphere than in a dry one, although the difference was small for the brass specimens. The effect of oxygen on the fatigue behavior of the titanium alloy and a vacuum-melted 4340 steel was investigated by conducting tests both in air and in an inert gas; the influence of oxygen was found to depend on whether or not moisture was present. In many of the vacuum-melted steel specimens the fatigue crack started below the surface, and the performance of these individual specimens was related to the size of the inclusion at the origin of the crack. A coating of dodecyl alcohol had a beneficial effect on the two materials (magnesium alloy and steel) on which its influence was investigated. An interesting tarnishing effect was observed on the fatigue portion of the magnesium alloy fracture surfaces.

**11125.** Shumaker, J. B., Jr., **Franck-Condon factors for high rotational levels of nitrogen,** *J. Quant. Spectry. Radiative Transfer* **9,** 153-156 (1969).

Key words: Band strength; Franck-Condon factor; nitrogen; rotation-vibration interactions.

Franck-Condon factors and band strengths of some strong bands of the first negative, first positive, and second positive systems of nitrogen are calculated in the Morse potential approximation and are shown to exhibit little dependence upon rotational level up to rotational quantum number 100.

**11126.** Shumaker, J. B., Jr., Popenoe, C. H., **Experimental test of $H_\beta$ Stark-broadening theory at high electron densities,** *Phys. Rev. Letters* **21,** No. 15, 1046-1048 (Oct. 7, 1968).

Key words: $H_\beta$ profiles; plasma arcs; Stark broadening; temperature measurement.

$H_\beta$ spectral line profiles produced in atmospheric pressur
high current arc experiments at the Fowler-Milne normal elec
tron density are compared with theory and found to agree withi
the approximately 10 percent uncertainty of the theory unde
these conditions.

**11127.** Sieck, L. W., **Continuum emission from xenon in the vapo**
**phase induced by absorption of 1470 Å radiation,** *J. Phy*
*Chem.* **72,** No. 9, 3129-3133 (Sept. 1968).

Key words: Emission spectroscopy; energy level
diatomic molecules; energy transfer; gas phase kinetics; ra
gas photosensitization; vacuum ultraviolet photochemistr

When xenon is exposed to a source of its own lowest energ
resonance radiation (1470 Å) in the vapor phase a symmetr
continuum is observed in emission which exhibits a maximum
approximately 1715 Å. The addition of excess krypton to lo
pressures of xenon increases the continuum intensity substa
tially, and that "quenching" effects of other additives which a
transparent to the resonance radiation are also reported. T
kinetic data are generally, although not uniquely, consistent wi
the mechanism proposed by others to describe the origin of
molecular emission found in the afterglow of a pulsed dischar
through krypton. In spite of the apparent kinetic agreeme
however, marked dissimilarities exist in the contours of t
respective bands and the positions of the continua when co
pared to the wavelength (energy) of the appropriate $^3P_1 \leftrightarrow$
resonance transition.

**11128.** Sieck, L. W., **Xenon-photosensitized decomposition**
**methane at 1470 Å,** *J. Chem. Phys.* **50,** No. 4, 1748-17
(Feb. 15, 1969).

Key words: Energy transfer; hydrocarbons; photochem
try; quantum yields; rare gas levels; (vacuum ultravio
sensitized decomposition.

The xenon sensitized decomposition of methane and metha
ethylene mixtures has been investigated in the vapor phase
1470 Å.

Quantum yield determinations and analyses of the isoto
composition of the hydrogens and ethanes obtained fr
$CH_4-CD_4$ (1:1) mixtures under various conditions indicate t
sensitization occurs by at least two concurrent mechanisms. T
role of internal photolysis by resonating 1470 Å radiation w
found to be negligible in all mixtures, and the existence of X
as an important intermediate was inferred by chemical metho

**11129.** Simmons, J. A., Coriell, S. R., **Solution of the Ste**
**problem for whisker evaporation,** *J. Appl. Phys.* **39,** No.
3459-3463 (June 1968).

Key words: Mean adatom stay time; moving bounda
Stefan problem; surface diffusion; surface diffusion c
stant; whisker; whisker evaporation.

The moving boundary problem for whisker evaporation
solved numerically, using techniques previously developed
whisker growth. Curves of whisker length as a function of ti
are calculated for several values of the evaporation parame
The possibility of determining the surface diffusion constant
the mean adatom stay time from whisker experiments
discussed.

**11130.** Simmons, J. D., Bass, A. M., Tilford, S. G., **The fou**
**positive system of carbon monoxide observed in absorptio**
**high resolution in the vacuum ultraviolet region,** *Astrophys*
**155,** 345-358 (Jan. 1969).

Key words: Carbon monoxide; diatomic spectrum; mole
lar constants; perturbations; rotational analysis; vacuum
traviolet region.

he absorption spectrum of the fourth positive system ($A^1\Pi$ – ) of carbon monoxide has been observed at high resolution he region 1550-1060 Å. The rotational and vibration struc- : of 21 bands has been analyzed, viz the $\nu'' = 0$ progression for = 0-18, 20 and the (0-1) band.

detailed assignment of the numerous perturbation in $A^1\Pi$ e is given. Most of these perturbations can easily be assigned he five known states in the region of the $A^1\Pi$ state. However erturbation at low J-values in the (6-0) A-X band suggests the sence of another state in this region which has not as yet been erved directly.

31. Smith, E. W., Hooper, C. F., Jr., **Comments on ion icrofield distributions as used in plasma line broadening theo- ies,** *J. Quant. Spectry. Radiative Transfer* **8,** No. 9, 1617- 619 (Sept. 1968).

Key words: Asymptotic wings; ion microfield; line center; line shape; transition region.

is shown that the use of an extended ion microfield function s rise to improved line shapes in the transition region veen the line center and the asymptotic wings.

32. Smith, S. J., **Photodetachment,** Chapter in *Methods in Ex- erimental Physics,* **Vol. 7,** *Atomic and Electron Physics,* B. ederson and W. L. Fite, eds., pp. 179-208 (Academic Press nc., New York, N.Y., 1968).

Key words: Crossed beam method; drift tube experiments; $I^-$; negative ion; photodetachment; radiative attachment experiments.

33. Smith, R. V., **Current developments in cryomedicine,** *ryogenics* **9,** No. 2, 84-89 (Apr. 1969).

Key words: Cryobiology; cryomedicine; cryopreservation; cryoprotectants; cryosurgery; freezing; thawing.

he paper reviews current developments in the field by sum- rizing papers presented in the Fifth Annual Meeting of the ciety for Cryobiology. Cryomedicine is divided into two areas the purpose of discussion; cryosurgery and cryopreservation biological material for clinical use.

34. Smith, R. V., **Review of heat transfer to helium I,** *ryogenics* **9,** No. 1, 11-19 (Feb. 1969).

Key words: Boiling; convection; critical; heat transfer; helium I; supercritical.

This paper reviews heat transfer to helium I. Recommenda- ns are made for expressions to be used in design studies and further work required to produce needed information.

135. Smith, R. V., **Review of heat transfer to helium I,** *Proc. 1968 Summer Study on Superconducting Devices and Ac- celerators, Brookhaven National Laboratory, Upton, N.Y., une 10-July 19, 1968,* Part I, BNL 50155 (C-55), pp. 249-292 Clearinghouse for Federal Scientific and Technical Informa- ion, Springfield, Va., Apr. 1969, $3.00).

Key words: Boiling; convection; critical; heat transfer; helium I; supercritical.

This paper reviews heat transfer to Helium I. The data were llected, complied, and the results discussed. Recommenda- ns are made for expressions for use in design studies and for rther work required to produce needed information.

136. Steel, M. N., **Production of synthetic food materials: A statistical survey,** *Proc. Second Intern. Conf. Women Engineers and Scientists,* 30 pages (Women's Engineering Society, London, England, 1968).

Key words: Amino acids; food additives; food problem; production of synthetic food; synthetic food materials; urea; yeast.

This paper summarizes statistics on the production, sale, and value of synthetic vitamins, flavors, and amino acids in the United States from 1945 to 1965 and discusses the observed trends. In absence of statistics on the production in other countries, U.S. import statistics and information from industrial journals are examined for indications regarding quantities manufactured in other countries. U.S. shipment statistics are given for yeasts and are evaluated as a measure of the quantities being made. Production statistics for feed grade synthetic urea are also presented. The foregoing data are discussed in relation to the potential roles of synthetic and biosynthetic materials in meeting the world food deficit.

**11137.** Steiner, B., **The cross section for the photodetachment of electrons from $I^-$,** *Phys. Rev.* **173,** No. 1, 136-142 (Sept. 5, 1968).

Key words: Absolute cross section; iodine; negative ions; photodetachment.

The cross section for photodetachment of $I^-$ at 347 nm, 0.5 eV above threshold, has been determined to be $2.9 \pm 0.5 \times 10^{17}$ cm². This value has been obtained in a crossed beam experiment by comparison with photodetachment from $H^-$ at 993 nm, 0.5 eV above its threshold. The present determination permits placement of the previously determined relative cross section curve for the first electron volt above threshold on an absolute scale. The entire experimental curve is compared with the recent calculation of Robinson and Geltman. Although the shapes of the two curves are very similar, the new experimental cross section exceeds the calculation by a factor of two.

**11138.** Steiner, B., **Photodetachment of electrons from $SH^-$,** *J. Chem. Phys.* **49,** No. 11, 5097-5104 (Dec. 1, 1968).

Key words: Electron affinity; free radical; negative ions; photodetachment; SH.

The cross section for photodetachment of electrons from $SH^-$ for the first 0.75 eV above threshold ($\lambda = 534.7$ to 403.0 nm) has been measured in a crossed beam experiment. The cross section rises rapidly in the first 0.15 eV ($\Delta\lambda = 35$ nm) to the value $1.9 \times 10^{-17}$ cm² determined with a total uncertainty of $\pm 0.4 \times 10^{-17}$ cm² given by the square root of the sum of the squares of the maximum observed deviation and the allowances for various systematic factors; over the rest of the observed range it is constant. The detailed shape of the cross section vs. λ curve has been employed to derive the $SH^-$ structural parameters (and their upper limits of uncertainty), which are indistinguishable from those of the neutral free radical: $R = 0.135 \pm 0.002$ nm, $\omega_e = 2700 \pm 290$ cm⁻¹, and $B_e = 9.46 \pm 0.32$ cm⁻¹. The electron affinity is identified with the observed photodetachment threshold, $2.319 \pm 0.010$ eV. These results are in general agreement with the recent calculations of Cade. Evidence is presented for the importance of inclusion of long range forces in dealing with the threshold behavior of photodetachment from heteronuclear diatomic negative ions.

**11139.** Stephens, R. E., Sutton, L. E., **Diffraction image of a point in the focal plane and several out-of-focus planes,** *J. Opt. Soc. Am.* **58,** No. 7, 1001-1002 (July 1968).

Key words: Diffraction image; image evaluation; lens analysis.

For the case of an aberration-free lens system with circular aperture, a table is presented which gives the fraction of maximum irradiance in the diffraction image of a point. The columns of the table correspond to variations in location of the focal plane; the rows to variations in the distance from the center of a diffraction pattern. These values were obtained, to an accuracy of five decimal places, through Gaussian integration of the required Bessel function expressions, the calculations being performed on a digital computer.

**11140.** Stevens, M. E., **Automatic analysis,** *Encyclopedia of Library and Information Science,* A. Kent and H. Lancour, eds., **2,** 144-184 (Marcel Dekker Inc., New York, N.Y., 1969).

Key words: Automatic character recognition; automatic classification; automatic content analysis; automatic indexing; automatic pattern recognition; key word indexing; linguistic data processing; question-answering; statistical association.

Progress in techniques and applications of automatic analysis are discussed in terms of library and information science interests. Topics discussed include automatic pattern recognition, machine indexing by extraction of key words, automatic indexing and classification, statistical association techniques, linguistic data processing, automatic content analysis and question-answering systems.

**11141.** Stevens, M. E., **Progress and prospects in mechanized indexing,** (Proc. Symp. on Mechanized Abstracting and Indexing, Moscow, U.S.S.R., Sept. 28-Oct. 1, 1966), *UNESCO/NS/209,* 51 pages (United Nations Educational Scientific and Cultural Organization, Paris, France, Apr. 1967).

Key words: Automatic classification; automatic indexing; indexer inconsistency; mechanized indexing; selective dissemination systems.

Recent progress and problems in mechanized indexing, both for machine-compiled and machine-generated indexes, are reviewed. Results of automatic indexing and classification experiments reported after issuance of the NBS State-of-the-Art Report are briefly reviewed. It is concluded that the progress and prospects of automatic indexing are provocative because of practical and theoretical accomplishments that have been demonstrated and challenging because much remains to be done.

**11142.** Stevens, M. E., **Selected pattern recognition projects in Europe,** *Pattern Recognition* **1,** No. 2, 103-118 (Nov. 1968).

Key words: Optical character; pattern recognition; recognition; research; speaker identification; speech recognition; standardized fonts; U.S.S.R.; Western Europe.

In August-September, 1966, a survey of selected non-numeric data processing projects in Western Europe was conducted. Some of the projects active in various areas of pattern recognition research and development that were visited are discussed. In addition, details are given of an operational character recognition system in the U.S.S.R.

**11143.** Steward, W. G., Smith, R. V., Brennan, J. A., **Cooldown time for simple cryogenic pipelines,** (Proc. Tenth Midwestern Mechanics Conf., Colorado State University, Fort Collins, Colo., Aug. 21-23, 1967), Chapter in *Developments in Mechanics* **4,** 1513-1525 (Johnson Publ. Co., Boulder, Colo., 1968).

Key words: Chilldown, cooldown time; cryogenic fluids; transfer lines.

An uncooled pipeline which is used to transfer a cryogenic fluid from one point to another, must ordinarily go through a period of cooling down from ambient temperature to near the liquid boiling temperature. During most of this period the liquid boils and the pipe delivers only warm gas. Some effective methods of estimating this cooldown time have been proposed but they are all laborious. This paper offers a quick method by which cooldown time for a simple system can be calculated fron a dimensionless parameter read from a graph. To use the metho it is necessary to know the fluid and pipe enthalpy, density, an velocity of sound in the warm gas. The idealized model an closed form solution are described, and comparison with experi mental results is shown.

**11144.** Stiehler, R. D., Parks, E. J., Linnig, F. J., **Stiffening o elastomers by organic fillers,** *Appl. Poly. Symp.* No. 7, 143-15 (1968).

Key words: Anisotropic; beta-naphthyl group; bloc polymers; bonds; crystallization; elastomers; expansivity forces; phenyl-beta-naphthylamine; stiffening; vulcaniza tion; x-ray diffraction.

Elastomers can be stiffened in various ways. Self-stiffening oc curs in elastomers that crystallize or in block copolymers com posed of one block in the elastomeric state and two or mo blocks in the glassy or crystalline state. Fillers also cause stiffe ing. Some crystalline organic compounds which contain a bet naphthyl group are particularly effective. The conditions und which the crystals form in the elastomer affect the degree of sti fening. Under favorable conditions, about 3 percent crystalli phenyl-beta-naphthylamine (PBNA) stiffens rubber to about th same degree as 40 phr carbon black. Since the crystals can be e tracted with organic solvents, the stiffening effect is reversibl Studies with PBNA and results in the literature suggest that ( stiffening of elastomers by fillers is primarily a physic phenomenon, (2) the effectiveness of a filler is determined l both surface area and interfacial forces between the filler a elastomer, (3) surface area is determined by the geometry of t particles, (4) interfacial forces depend on the number of ato per unit surface area that are sufficiently close to atoms in t elastomer molecule to develop a substantial force, (5) interfac forces are maximized when the atoms in the surface layer of t filler have a geometric structure similar to the atoms in t elastomer, and (6) the elastomer molecule or segments of it mu have sufficient mobility to permit alignment with the filler su face to achieve attraction at as many points as possible.

**11145.** Straty, G. C., **Bellows-sealed valve for reactive gases moderately high pressures,** *Rev. Sci. Instr.* **40,** No. 2, 378-3 (Feb. 1969).

Key words: Bellows; fluorine; high pressure; packless; re tive; valve.

A relatively simple and inexpensive laboratory size bello sealed valve for use at pressures in excess of 3000 psi described. The valve is a modification of one of several comm cially available, small high pressure valves and uses a numbe standard components.

**11146.** Strobridge, T. R., **Refrigeration at 4 K,** *Proc. 19 Summer Study on Superconducting Devices and Accelerat Brookhaven National Laboratory, Upton, Long Island, N. June 10-July 19, 1968,* Part I, BNL 50155 (C-55), pp. 193-2 (Clearinghouse for Federal Scientific and Technical Infor tion, Springfield, Va., Apr. 1969, $3.00).

Key words: Claude; cryogenics; Gifford-McMahon; h um; Joule-Thomson; liquid; power; refrigeration; Sim size; Stirling.

Superconducting accelerators and support elements are be considered for the next generation of particle accelerators. U practical materials with higher transition temperatures bec a reality, refrigeration in the neighborhood of 4 K will required for these superconducting devices. This paper s marizes a lecture given on 4 K refrigeration covering evapora liquid helium baths, the Simon process, the Joule-Thoms Brayton, Claude, Stirling, and Gifford McMahon cycles. A uded were examples of analysis and descriptions of modern igerators and their components.

47. Strobridge, T. R., **Review of the cryogenics session – second eek of the Brookhaven summer study on superconducting evices and accelerators,** *Proc. 1968 Summer Study on Superonducting Devices and Accelerators, Brookhaven National aboratory, Upton, Long Island, N.Y., June 10-July 19, 1968,* art I, BNL 50155 (C-55), pp. 368-375 (Clearinghouse for ederal Scientific and Technical Information, Springfield, a., Apr. 1969, $3.00).

Key words: Cryogenics; cryopump; cryostat; electrical lead; heat transfer; mechanical properties; refrigeration; safety; superconductivity; superfluid.

his paper reviews the lectures given during the cryogenics sion at the Brookhaven Summer Study on Superconducting vices and Accelerators. Lectures were given on the low temature mechanical properties of both metallic and nonmetallic ctural materials, cryostat design, cryopumping, electrical d design, safety, superfluid helium, heat transfer to helium i finally three talks were given on refrigeration. The experts nions are outlined and the areas which most urgently require her research and development are listed.

48. Stromberg, R. R., **Polymer adsorption on substrates,** (Proc. ymp. Interface Conversion Polymer Coatings, General Mobrs Research Laboratories, Detroit, Mich., Oct. 1967), hapter in *Interface Conversion for Polymer Coatings*, P. Veiss and G. D. Cheever, eds., pp. 321-337 (American Elseier Publ. Co., Inc., New York, N.Y., 1969).

Key words: Adsorption; configuration of adsorbed polymer; interface; polymer adsorption.

olymer adsorption studies, theoretical and experimental, at National Bureau of Standards are reviewed. Both of these dies are primarily concerned with changes in the configuran of the molecule upon adsorption and with the nature of the eraction with the surface. The experimental methods include dies of the extension of the adsorbed polymer molecule norl to the surface and the concentration of polymer in the film. e measurement techniques are ellipsometry and internal ection spectroscopy. Also discussed are studies of the fracn of segments of the polymer chain attached to a surface. This antity is determined by measuring a shift of an absorption peak he infrared spectra that is caused by the attachment. Reversity of adsorption and rates of adsorption and desorption, meared using radioactive tracer techniques are also briefly menned.

49. Sugar, J., **Nuclear magnetic dipole moment of $^{165}$Ho,** *J. Opt. oc. Am.* **58,** No. 11, 1519-1523 (Nov. 1968).

Key words: Holmium; hyperfine structure; nuclear moment.

The first energy interval of the $4f^{11}6s$ configuration of Ho II s recently found by N. Spector and J. Sugar to be 637.8 cm$^{-1}$. e hfs of four of the lines defining this interval have been meaed with an HYPEAC spectrometer at a resolution of 600 000. ven independent equations relating the splitting factors $a_{6s}$, $a_{4f}$, d $b_{4f}$ to the measured hfs were derived. Known values of $a_{4f}$ d $b_{4f}$ from Ho I (deduced in an atomic beam magnetic onance experiment) were inserted in these equations, giving = 0.4437 cm$^{-1}$ (corrected for core polarization) with a probaerror of 0.0004 cm$^{-1}$. From $a_{6s}$, a value for the nuclear magtic dipole moment $\mu_I = (3.94 \pm 0.05)\mu_N$ was derived ($1\ \mu_N =$ 5050 × $10^{-27}$ JT$^{-1}$). The uncertainty in $\mu_I$ is the rms deviation e to uncertainties in $a_{6s}$ and in $\psi_{6s}^2(0)$, the value of the probaity density of the 6s-electron at the nucleus.

**11150.** Swanson, N., Codling, K., **Excitation of K-shell electrons in Be by soft x-rays and 20-keV electrons,** *J. Opt. Soc. Am.* **58,** No. 9, 1192-1194 (Sept. 1968).

Key words: Be; BeO; electron energy loss; fine structure; K edge; x-ray absorption.

The soft x-ray absorption spectra of Be and BeO were measured near the K edge using the NBS 180 meV synchrotron as a background continuum source. The energy loss spectrum of 20 keV electrons transmitted through thin Be films at zero scattering angle was measured in the corresponding 100-170 eV energy loss range. The K edges of Be and BeO measured by x-ray absorption were at 112.1 ± 0.2 eV and 118.4 ± 0.2 eV respectively. The Be K edge in the electron energy loss spectrum was at 111.7 ± 0.4 eV. The positions of maxima in the absorption fine structure determined by the two techniques were also in good agreement. The indicated uncertainties represent extended probable errors.

**11151.** Swartzendruber, L. J., **Variable temperature Mössbauer effect spectrometer with provision for longitudinal external fields,** *Nucl. Instr. Methods* **69,** 101-105 (1969).

Key words: Instrumentation; iron; low temperature; magnetic field; Mössbauer effect; spectrometry.

A Mössbauer effect spectrometer design for obtaining spectra with the absorber in a longitudinal external magnetic field is described. A superconducting magnet is the source of the field. The absorber temperature can be varied between 300 K and about 1.5 K and, independently, the source temperature can be varied between 300 K and about 10 K above the absorber temperature.

**11152.** Tanttila, W. H., Mahler, R. J., James, L. W., **Magnetic parametric nuclear spin saturation,** *Appl. Phys. Letters* **13,** No. 1, 27-29 (July 1, 1968).

Key words: Magnetic transitions; magnetic and quadrupole split energy levels; nuclear magnetic resonance; parametric.

Magnetic $\Delta m = \pm 2$ nuclear spin transitions are observed when an r.f. magnetic field at the frequency $(Em_{m-2} - E_m)/h$ is applied parallel to an external magnetic field in a crystal where the c-axis is perpendicular to the external magnetic field.

**11153.** Tauber, S. J., **Imprecision – problems for information processing,** *Am. Doc.* **19,** No. 4, 413-414 (Oct. 1968).

Key words: Experimental conditions; imprecision; information system design; levels of abstraction; mnemotechnics; semantics; specificity.

Some of the characteristics of imprecision which affect information storage and retrieval are pointed out and discussed in the areas of numeric values, experimental conditions, and semantics.

**11154.** Taylor, J. K., **Modern electrochemistry,** *Ind. Res.* **10,** No. 10, 68-74 (Oct. 1968).

Key words: Chemical analysis; coulometry; electrochemical analysis; electrochemical instrumentation; ion-selective electrodes; polarography.

Electrochemical methods of analysis are especially attractive because of the sensitivity and accuracy they provide. Methods based on measurement of resistance, current, and voltage singly or in combination provide a variety of techniques applicable from trace determinations to assays for major constituents. The methods are especially applicable to automation, process control, and remote-location monitoring situations. The recent advent of ion-selective electrodes promises to increase the scope of electroanalysis, especially for routine determination of moderate accuracy. The techniques most frequently used at the present time are described and discussed with reference to the areas of their greatest utility.

**11155.** Thomas, A. M., **Monte Carlo study of vacuum vane gauge design criteria,** *J. Vacuum Sci. Technol.* **5,** No. 6, 187-193 (Nov.-Dec. 1968).

Key words: Molecular flow; Monte Carlo; vacuum; vacuum gauge; vane gauge.

A Monte Carlo method is presented by which the effects of molecular motion in free molecular flow systems of various geometries may be studied. The geometry used in this study is that of a straight tube of circular cross section with a circular vane co-axial with and placed at various distances from the end of the tube. Calculations are made of the ratio of the force on the vane to the isotropic pressure at the opposite end of the tube. Parameters which are varied are tube length, tube wall thickness, distance to the vane, and radius of the vane; all of which are measured in terms of one tube radius. This study revealed that, for short, thin walled tubes and for a large vane, the force on the vane is fairly insensitive to the amount of separation between the tube and the vane as long as this separation is less than about one half a tube radius. However, for longer tubes, the force on the vane falls off quite rapidly as the vane is moved away from the tube end. Also, for tubes with thicker walls, the force-to-pressure ratio increases as the vane is first moved away from the tube and reaches a maximum which may be greater than twice the original value.

**11156.** Thomas, R. N., **Symposium on Wolf-Rayet stars: a summary,** *Astrophysical Letters* **2,** No. 3, 147-148 (Oct. 4, 1968).

Key words: Wolf-Rayet stars.

This paper is a brief summary of the Symposium on Wolf-Rayet stars held at the Joint Institute for Laboratory Astrophysics 10-15 July 1968 under joint sponsorship of JILA, the Smithsonian Astrophysical Observatory, Harvard College Observatory, and American Astronomical Society. The complete symposium was published in National Bureau of Standards Special Publication 307, Wolf-Rayet Stars, issued December 1968, available by purchase from the Superintendent of Documents, Government Printing Office, Washington, D.C. 20402 at $3.00 a copy.

**11157.** Thompson, B. A., LaFleur, P. D., **Rapid group radiochemical separations for activation analysis of steels,** *Anal. Chem.* **41,** No. 6, 852-855 (May 1969).

Key words: Activation analysis; group separations; radiochemical separations; steels.

Rapid group radiochemical separation procedures based on solvent extraction have been developed for the determination of W, Mo, Cu, Cr, As, Co, Sb, and Ga in steel and cast iron. The procedures have been applied to the analysis of NBS Standard Reference Material steels and give results in agreement with the NBS certified values. The precision obtained is routinely ±10 percent at the 95 percent confidence level and in favorable situations can be ±2 percent.

**11158.** Tipson, R. S., Cohen, A., **Reaction of some sulfonic esters of D-mannitol with methoxide; synthesis of 2,3:4,5-dianhydro-D-iditol,** *Carbohydrate Res.* **7,** 232-243 (1968).

Key words: Expoxide formation; D-mannitol; methoxide; sulfonic esters; 2,3:4,5-dianhydro-D-iditol.

3,4-Di-*O*-(methylsulfonyl)- and 3,4-di-*O*-*p*-tolylsulfonyl-D-mannitol and their 1,2,5,6-tetraacetates have been synthesized and crystallized. By the action of methanolic barium methoxide during 2 h at 25°, each of these compounds is converted into 2,3:4,5-dianhydro-D-iditol, the structure of which is assigned on the basis of chemical and physical properties, including n.m.r. evidence.

**11159.** Tipson, R. S., West, B. F., Brady, R. F., **Acid-catalyzed hydrolysis of isopropylidene acetals of some 2-pentuloses and 2-hexuloses,** *Carbohydrate Res.* **10,** 181-183 (1969).

Key words: Acid catalysis; hydrolysis; isopropylidene-acetals; *spiro*-fused structures; 2-hexuloses; 2-pentuloses.

The rate of hydrolysis with 100 m*M* oxalic acid (aqueous) at 65 °C was determined for the isopropylidene acetals of two 2-pentuloses and four 2-hexuloses. The compounds studied were found to fall into three groups according to the time to complet hydrolysis to the parent sugar: (a) 1,2:3,4-diacetal of D-*erythro*-pentulofuranose (~1.25 hr); (b) 1,2:4,5-diacetals of β-D-*ribo* hexulopyranose, β-D-*erythro*-2,3-hexodiulo-2,6-pyranose, an β-D-*arabino*-hexulopyranose (2-3 hr); and (c) 2,3-acetal of β-D *threo*-pentulofuranose and 2,3:4,5-diacetal of β-D-*arabino*-hexu lopyranose (8 hr). This shows that the presence of two *spiro* fused, 5-membered rings induces instability in the 1,2-isopropy lidene group. If the 1,2-*spiro* structure is absent and there is hydroxymethyl group attached at C-2, the rate of hydrolysis i lowest. Thus, determination of the rate of acid-catalyzed hydrol ysis is a simple, rapid method for determining (a) the presence o absence of a *spiro* structure involving C-1 and C-2 in cycli acetals of 2-ketoses, and (b) the presence of a furanoid ring if th *spiro* structure is present.

**11160.** Toots, J., Fowler, H. A., Marton, L., **Reflectance and 1/ resonance of beryllium in the far ultraviolet,** *Phys. Rev.* **17** No. 3, 670-676 (Aug. 15, 1968).

Key words: Beryllium; far-ultraviolet; optical propertie reflectance; stopping power.

The reflectance of evaporated Be layers has been measure after 3 min. exposure to ambient pressures of $\leqslant 3 \times 10^{-7}$ torr, f the wavelength range of 480-1200 Å, for a spread of angl between 20 and 80°. These values give n and k by calculatio also, from these, $\epsilon_1$, $\epsilon_2$, Re $(1/\epsilon)$, and Im $(1/\epsilon)$. The last two fun tions show good agreement with an inverted Drude-Sellmei resonance formula. The center-frequency of the resonance fa precisely on 18.4 eV ± 0.1 eV, corresponding to the natur plasma-resonance frequency of a free-electron-gas with 2.0 ele trons per atom; this confirms a 1948 prediction by A. Bohr. Ha width of the resonance is measured as 4.7 eV; this value is al obtained, within ±10 percent, from a sum-rule approximatic The value corresponds to a decay time (for intensity) of t plasma oscillation of about $1.3 \times 10^{-16}$ seconds. Argand-diagra display, and the "longitudinal" Kramers-Kronig relationship, a developed from the data.

**11161.** Torrance, K. E., Orloff, L., Rockett, J. A., **Experiments natural convection in enclosures with localized heating fr below,** *J. Fluid Mech.* **36,** Part 1, 21-31 (1969).

Key words: Enclosures; flow visualization; modeling; na ral convection.

An experimental study was made of the steady state natu convection induced in enclosures by a small hot spot centra located on the floor. Enclosures of rectangular and circular fl plan were employed, with height equal to major radius of floor plan. The movement of air within the chambers was m visible by adding metaldehyde dust particles and illuminat with an intense light beam. The Grashof number (Gr) based hot spot temperature and enclosure height ranged from $8 \times 10$ $1 \times 10^{10}$. Laminar flows were observed for Gr $\lesssim 1.2 \times 10^9$. T experimental flows in the circular chamber are compared i companion paper with theoretically calculated flows (Torra and Rockett (1968)). In the region of laminar flows the agr ment was excellent. The present paper notes certain similarit in the flows in rectangular and circular geometries. The distu ing effect of a slight heating of one wall of the rectangular enc e was also investigated. Measurements were made of heat nsfer from the hot spot to the air in the chamber.

62. Torrance, K. E., Orloff, L., Rockett, J. A., **Numerical tudy of natural convection in an enclosure with localized heat- ng from below – creeping flow to the onset of laminar instabili- y,** *J. Fluid Mech.* **36,** Part 1, 33-54 (1969).

Key words: Circular cylinder; enclosures; natural convection; numerical.

n analytical study was made of the natural convection in- ced in an enclosure by a small hot spot centrally located on the or. The enclosure was a circular cylinder, vertically oriented, h height equal to radius. A Prandtl number of 0.7 (air) was as- ned; the Grashof number (Gr) was based on cylinder height l hot spot temperature. The equations of fluid flow in axisym- tric cylindrical coordinates were simplified with the ussinesq approximation. The equations were solved numeri- ly with a computationally stable, explicit method. The compu- on, starting from quiescent conditions, proceeded through the ial transient to the fully developed flow. Solutions were ob- ned for Gr from $4 \times 10^4$ to $4 \times 10^{10}$. The calculated flows were mpared with the experimental flows presented in a companion per, Torrance, Orloff and Rockett (1968). The experimental ws were laminar for $Gr \lesssim 1.2 \times 10^9$; turbulence was observed ove this value. In the laminar flow region ($Gr \lesssim 1.2 \times 10^9$) eement between the theoretical and experimental flow pat- ns was excellent. When extended into the experimentally ob- ved turbulent range ($Gr = 4 \times 10^{10}$) the theoretical flow veloped a periodic vortex shedding, suggestive of the onset of nsition.

163. Travis, J. C., Spijkerman, J. J., **Mössbauer spectroscopy with $Ni^{61}$**, Chapter in *Mössbauer Effect Methodology* **4,** 237- 259 (Plenum Press Inc., New York, N.Y., 1968).

Key words: Chemical shifts; electronic configurations; internal magnetic fields; magnetic fields; magnetic moment ratio; nickel Mössbauer spectroscopy; nuclear hyperfine interactions; quadrupole splitting; single line source.

The practical application of Mössbauer spectroscopy to the udy of nickel compounds has been retarded by two factors: (1) e late discovery of a suitable, single line source, and (2) the ort half lives of both possible parent isotopes of $^{61}Ni$. A suita- e source of 15 percent Cr in Ni is activated by one hour of ex- sure to 100 MeV bremsstrahlung in the NBS linear electron celerator. The source has a fractional effect of $0.1 \pm 0.02$, and elds an experimental linewidth of $0.097 \pm 0.002$ cm/s when ex- apolated to zero thickness in source and absorber.

Adequate data have been obtained to determine a magnetic oment ratio, $\mu_e\mu_g = -0.568 \pm 0.055$, and an estimate for the ange in the nuclear charge radius, $\delta R/R = -2.5 \times 10^{-4}$. The ound state quadrupole moment is negligible for Mössbauer ectroscopy. Spectra which illustrate pure magnetic, pure adrupolar, and mixed (Laves phase) interactions have been tained.

This paper discusses the preparation of a single line source, e evaluation of nuclear parameters, theoretical studies of the clear hyperfine interactions, and theoretical prediction of the ectric field gradient tensor.

164. Trembath, C. L., Wait, D. F., Engen, G. F., Foote, W. J., **A low-temperature microwave noise standard,** *IEEE Trans. Microwave Theory Tech.* **MTT-16,** No. 9, 709-714 (Sept. 1968).

Key words: Cryogenic; microwave; noise; standard.

An x-band thermal noise source is described which consists of waveguide termination, cooled in a cryogenic environment, ong with temperature and pressure monitors and controls. With liquid helium as the cryogen, the effective noise output at the room temperature flange can be set to values around the boiling point of helium (4.2 K) with an accuracy of ±0.03 K. With liquid nitrogen as the cryogen, the output temperature can be set to values around 77 K with an accuracy of ±0.16 K.

This accuracy is made possible by several unique features. First, the terminating waveguide section is a vapor bulb thermometer with the absorbing load surrounded with the cryogenic liquid. Second, heat exchangers are used to permit an unusually short waveguide transition section between cryogenic and room temperature. Third, an absolute pressure regulator is used to control the cryogen boil-off rate resulting in a temperature stability of 0.002 K for helium and 0.02 K for nitrogen.

At present, the useful accuracy of the standard is limited to ±0.1 K because of uncertainties in the insertion loss (about 0.001 dB) of mating room temperature flanges.

11165. Tsai, D. H., Beckett, C. W., **Shock wave propagation in a two-dimensional crystalline lattice,** (Proc. Intern. Union of Theoretical and Applied Mechanics: Intern. Symp. Behavior of Dense Media Under High Dynamic Pressure, Paris, France, Sept. 11-15, 1967), Chapter in *The Behavior of Dense Media Under High Dynamic Pressure,* pp. 99-108 (Gordon and Breach, Science Publ. Inc., New York, N.Y., 1968).

Key words: Energy calculations; Grüneisen parameter; lattice stability; shock wave propagation; thermal oscillations; two-dimensional lattice dynamics.

Lattice dynamics has been applied to the study of the propagation of a strong, one-dimensional shock wave in a two-dimensional face-centered cubic lattice. The shock was generated at the free surface of the lattice by impact, and propagated into the lattice in the longitudinal direction perpendicular to the free surface. The transverse motion of the lattice points allowed the shock wave to be scattered and the compressive energy to be distributed between the longitudinal and transverse degrees of freedom. In our calculation, a Morse type potential function between pairs of lattice points was employed, and the interactions were assumed to extend to the fourth-neighbors. The equations of motion of the lattice points were solved by an approximate numerical method, and from the solutions, the dynamical behavior of the shock wave, the vibrational energy, and the Grüneisen parameter in the shock compressed region were obtained. These results were compared with similar results for a one-dimensional lattice model.

11166. Tsang, T., **Self-consistent correlation function approximation in Ising ferromagnets,** *Physica* **42,** 1-11 (1969).

Key words: Ising ferromagnet; molecular field approximation; pair correlation function; three-dimensional ferromagnet; two-dimensional ferromagnet.

Two modifications have been proposed to improve the Weiss molecular field approximation of Ising ferromagnets: a pair of central spins were examined to yield self-consistent equations for pair correlation functions; the nearest neighbors of the central spins are also taken in account. The method, which needs very little computational work, has been applied to the square and cubic Ising ferromagnets, and the results are in good agreement with Onsager's exact solution and the power series expansions.

11167. Tsang, T., Farrar, T. C., **Nuclear magnetic relaxation studies of internal rotations and phase transitions in borohydrides of lithium, sodium, and potassium,** *J. Chem. Phys.* **50,** No. 8, 3498-3502 (Apr. 15, 1969).

Key words: Lithium borohydride; nuclear magnetic relaxation; phase transition; potassium borohydride; sodium borohydride; spin lattice relaxation time.

Proton spin-lattice relaxation times, $T_1$, have been measured as a function of temperature for $KBH_4$, $NaBH_4$ and $LiBH_4$. For $NaBH_4$ and $KBH_4$, $^{23}Na$ and $^{11}B$ relaxation measurements were also made. In all cases, the magnetization recovery is approximately exponential. Correlation times, $\tau_c$, derived from $T_1$ data were used to calculate activation energies, V, for $BH_4^-$ ion reorientations, and the corresponding rms errors of the individual values involved. For the cubic phase of $KBH_4$, $V = 14.8 \pm 0.4$ kJ/mol ($3.55 \pm 0.1$ kcal/mol) from measurements on proton and $^{11}B$. For $NaBH_4$, V was found to be $11.2 \pm 0.5$ and $14.8 \pm 0.7$ kJ/mol ($2.7 \pm 0.1$ and $3.5 \pm 0.2$ kcal/mol) for the high (cubic) and low temperature (tetragonal) phases; an anomaly in $\tau_c$ was observed at temperatures slightly below the phase transition, and may be interpreted as a relatively sudden change in V associated with the phase transition. In $LiBH_4$, a rather broad minimum was observed for the proton $T_1$ vs. temperature; this has been interpreted as due to two inequivalent $BH_4^-$ tetrahedra with activation energies of $20 \pm 1$ and $16 \pm 1$ kJ/mol ($4.7 \pm 0.3$ and $3.8 \pm 0.3$ kcal/mol). The proton and $^{11}B$ nuclei are relaxed by magnetic dipolar interactions, but quadrupolar fluctuations are the dominating relaxation mechanism for $^{23}Na$ in the cubic phase of $NaBH_4$.

**11168.** Tsang, T., Farrar, T. C., Rush, J. J., **Proton magnetic resonance and hindered rotation in phosphonium halides and ammonium iodide,** *J. Chem. Phys.* **49,** No. 10, 4403-4406 (Nov. 1968).

Key words: Activation energy; ammonium iodide; hindered rotation; nuclear magnetic relaxation; phosphonium halides; proton; proton second moment; spin-lattice relaxation.

Proton spin-lattice relaxation times, $T_1$, and second moments have been measured as a function of temperature for the phosphonium halides and ammonium iodide. Correlation times $\tau_c$ derived from the relaxation data were used to obtain activation energies for the reorientation of the phosphonium and ammonium ions. The activation energies for $PH_4Cl$, $PH_4Br$, and $PH_4I$ are $(3.0 \pm 0.2) \times 10^4$, $(3.1 \pm 0.1) \times 10^4$ and $(3.06 \pm 0.04) \times 10^4$ joules per mole respectively, indicating little change in barrier with halide ion. The frequency factors, however, do appear to vary significantly from crystal to crystal. These results are in marked contrast with previous results for the ammonium halides and suggest that non-electrostatic repulsive forces are important in the phosphonium salts. The activation energy for $NH_4^+$ ion reorientation in the tetragonal phase (Phase III) of $NH_4I$ is found to be $(1.34 \pm 0.04) \times 10^4$ joules per mole. The present results are compared with previous spectroscopic and structural results.

**11169.** Tsang, W., **Thermal decomposition of 3,4-dimethylpentene-1, 2,3,3-trimethylpentane, 3,3-dimethylpentane, and isobutylbenzene in a single pulse shock tube,** *Intern. J. Chem. Kinetics* **1,** 245-278 (1969).

Key words: Bond energy; decomposition; free radicals; heat of formation; hydrocarbon; isobutylbenzene; pre-exponential factor; pyrolysis; single pulse shock tube; 3,3-dimethylpentane; 3,4-dimethylpentene-1; 2,3,3-trimethylpentane.

Several hydrocarbons have been pyrolyzed in a single pulse shock tube. Rate parameters for the main bond breaking step have been found to be

$$k\{iC_3H_7-CH(CH_3)CH{=}CH_2 \rightarrow iC_3H_7\cdot +$$
$$\cdot\, CH(CH_3)CH{=}CH_2\} = 10^{15.70} \exp(-32{,}500/T)\ \text{sec}^{-1}$$

$$k\{iC_3H_7-C(CH_3)_2C_2H_5 \rightarrow iC_3H_7\cdot +$$
$$\cdot\, C(CH_3)_2C_2H_5\} = 10^{16.15} \exp(-35{,}900/T)\ \text{sec}^{-1}$$

$$k\{C_2H_5-C(CH_3)_2C_2H_5 \rightarrow C_2H_5\cdot +$$
$$\cdot\, C(CH_3)_2C_2H_5\} = 10^{16.57} \exp(-38{,}800/T)\ \text{sec}^{-1}$$

$$k\{iC_3H_7-CH_2C_6H_5 \rightarrow iC_3H_7\cdot +$$
$$\cdot\, CH_2C_6H_5\} = 10^{15.23} \exp(-34{,}800/T)\ \text{sec}^{-1}$$

In combination with similar studies carried out earlier and through application of the well-established experimental rule $(k_r^2(AB)/k_r(AA)k_r(BB))^{1/2} \sim 2$ where A and B are radicals and the rate constants are for the combination of these radicals, rate parameters for the thermal decomposition of all the hydrocarbons formed from any pair of the following radicals: methyl, ethyl, isopropyl, *t*-butyl, *t*-amyl, allyl, methylallyl, and benzyl have been calculated. The available calculated and experimental values of the decomposition rate constants are in excellent agreement. It appears that, with the possible exception of reactions involving the ejection of methyl radicals, the frequency factors per bond are nearly constant, depending only upon the type of carbon–carbon bond that is being broken. These values are all lower than those expected from the radical recombination rates.

Heats of formation of ethyl, *t*-amyl, benzyl, methylallyl, n-propyl, *s*-butyl, isobutyl, neopentyl, and 3-pentyl radicals have been derived.

Rate parameters for the decomposition of some simple ketones and ethers have also been estimated.

**11170.** Turgel, R. S., **A comparator for thermal ac-dc transfe standards,** *ISA Trans.* **6,** No. 4, 286-292 (1967).

Key words: Ac; calibration; dc; intercomparison; ther moelement; transfer standard.

Thermal transfer standards play an important role in precisio a-c measurements. They are calibrated by intercomparison wit standards of known ac-dc difference. A comparator is describe that simplifies such routine calibrations. A sequence of nul balances in the measuring circuit operates a simple analog com puter which indicates the result of the intercomparison directl in parts per million of ac-dc difference.

**11171.** Van Blerkom, D., Hummer, D. G., **A non-LTE theory overlapping lines near the series limit,** *Astrophys. J.* **154,** No. 741-750 (Nov. 1968).

Key words: Band model; line formation; planetary nebula

The effects of overlapping on the formation of spectral line near the series limit are investigated through the introduction a band model. Numerical solutions are obtained which show th the source function can be increased by a factor two for $\epsilon = 0.$ and by much larger amounts for smaller $\epsilon$. A criterion presented to check when overlapping is likely to be important.

**11172.** Veillon, C., Margoshes, M., **An evaluation of th induction-coupled, radio-frequency plasma torch for atom emission and atomic absorption spectrometry,** *Spectrochi Acta* **23B,** 503-512 (1968).

Key words: Atomic absorption spectrometry; atomic emi sion spectrometry; detection limits; interelement effect plasma torch; radio-frequency; spectrochemical analysis.

A study has been made of the radio-frequency plasma torch a source of atoms for emission and absorption spectrochemic analysis. The factors evaluated include sensitivity, limits of d tection, interelement effects, limitations, and general co venience. In agreement with other reports, the plasma torch w found to give useful emission signals for several elements whi are difficult to excite in chemical flames, such as B, Ta, and The value of the source for atomic absorption spectrometry w found to depend on the availability of bright line sourc Pronounced interelement effects were found, affecting partic larly the emission signals. In most cases, these interelement fects were enhancements of the emission, although in one cas suppression was observed. Except for a few refractory elemen plasma torch does not appear to be a suitable replacement for chemical flame.

73. Veillon, C., Margoshes, M., **A pneumatic solution nebu-zation system producing dry aerosol for spectroscopy,** *pectrochim. Acta* **23B,** 553-555 (1968).

Key words: Atomizer; nebulizer; pneumatic aspirator; sample introduction; solvent removal; spray.

An efficient sample introduction system was developed for ieous solutions. It is made up of a pneumatic nebulizer, a ited chamber for solvent evaporation, and a chilled condenser solvent removal. Features include low gas flow rate, high effi-incy, and elimination of the solvent. Overall efficiency is 35 rcent.

74. Vicentini-Missoni, M., Sengers, J. M. H. L., Green, M. S., **Thermodynamic anomalies of $CO_2$, Xe, and $He^4$ in the critical egion,** *Phys. Rev. Letters* **22,** No. 9, 389-393 (Mar. 3, 1969).

Key words: Chemical potential; critical exponents; critical parameters; critical region; equation-of-state; fluids; scaling law; specific heat.

A closed-form equation for the chemical potential as function density and temperature, based on the scaling idea is fitted to perimental data in the critical regions of $CO_2$, Xe and He-4, timizing $\delta$, $T_c$ and two adjustable constants. Values obtained the critical exponents and the two constants vary only ghtly from substance to substance; we find $\beta = .35 - .36$, $\delta =$ $4 - 4.6$, $\gamma = 1.24 - 1.26$, $\alpha = 0.04 - 0.05$, $\Gamma/\Gamma' = 3.6 - 4.4$, $= 2.6 - 3.3$. Agreement with previous estimates and with inde-ndent $C_r$ and optical density gradient measurements is cussed.

175. Vieth, D. L., Yakowitz, H., **Tensile loading device for Kossel microdiffraction and metallography,** *Rev. Sci. Instr.* **39,** No. 12, 1929-1931 (Dec. 1968).

Key words: Instrument design; Kossel x-ray method; metallography; strain measurement; tensile testing; x-ray microdiffraction.

A loading device used primarily in conjunction with Kossel ivergent beam) x-ray diffraction is described. The device is mpatible with any standard upright metallograph as well. It is ur inches (10.1 cm) in diameter and accommodates specimens ie inch in reduced section by 1/4 inch wide. The device utilizes nall load cells having ranges of 0 to 10 pounds (44.5N) and 0 to 0 pounds (445N) respectively. Load cell error is ±0.5 percent the full load capacity. Load changes of 0.2 percent of load pacity can be observed. The load device is mechanically and ectrically stable. Loads are read on a standard commercial iversal indicator.

176. Wait, D. F., **Thermal noise from a passive linear multiport,** *IEEE Trans. Microwave Theory Tech.* **MTT-16,** No. 9, 687-691 (Sept. 1968).

Key words: Available power ratio; microwave multiport; nonreciprocal multiports; thermal noise.

The effective noise temperature $T_n$ of a linear passive mul-port at uniform temperature T is shown to be $T_n = AT$, where $_n$ is referred to the output port. The absorption coefficient A is ven for arbitrarily mismatched input-ports in terms of scatter-g matrices and reflection coefficients. A simplified expression given for multiports with nearly reflectionless port termina-ons. A method for precise measurement of A is pointed out. he results apply to either reciprocal or nonreciprocal junctions. he noise correlation between ports was calculated for mul-ports having reflectionless port terminations. The correlation shown to be proportional to the physical temperature of the ultiport and to the appropriate matrix element of $\mathbf{B} \equiv \mathbf{1} - \mathbf{SS}^{\dagger}$, where **S** is the scattering matrix of the junction and $\mathbf{S}^{\dagger}$ is the Hermitian conjugate of the scattering matrix.

11177. Wait, D. F., Nemoto, T., **Measurement of the noise temperature of a mismatched noise source,** *IEEE Trans. Microwave Theory Tech.* **MTT-16,** No. 9, 670-675 (Sept. 1968).

Key words: Effective temperature; measurement; mismatched generators; noise.

A method is suggested which can measure the available power (or the effective temperature) of a noise generator independent of its reflection coefficient. A system utilizing a compensation generator and a tuned three-port circulator, is constructed at X-band and evaluated for a noise generator of about 10,000 K. The error analysis and the experimental results indicate that the effective temperature of this generator, with a reflection coefficient of 0.5, can be measured within one-half of one percent in addition to the uncertainty of a standard needed to calibrate the system.

11178. Waterstrat, R. M., **Crystal structure transformations in VPt produced by plastic deformation at room temperature,** *Trans. Met. Soc. AIME* **245,** 1360-1361 (June 1969).

Key words: Atomic ordering; crystal structure; phase transformations; plastic deformation.

A crystallographic transformation has been produced in the phase VPt by plastic deformation at room temperature. In alloys annealed at 1300 °C the phase VPt has a B19 (AuCd) type structure but plastic deformation of this phase produces a transformation to either an ordered structure of the $Ll_0$ (CuAu) type or to a disordered face-centered cubic structure. It appears that alloy composition and the extent of cold working may be factors which determine the type of structure formed.

11179. Waterstrat, R. M., **Evaluation of a gallium-palladium-tin alloy for restorative dentistry,** *J. Am. Dental Assoc.* **78,** No. 3, 536-541 (Mar. 1969).

Key words: Dental amalgam; dental materials; gallium alloy; palladium alloy; restorative dentistry.

A gallium-palladium-tin alloy has been developed which may possibly be used for restorative dentistry. The alloy is handled using techniques very similar to those used with conventional dental amalgams. The gallium alloy, however, has a higher strength and a much greater resistance to flow or creep under an applied load. In addition the gallium alloy wets tooth structure and has a thermal expansion coefficient which is fairly close to that of human teeth. Much more clinical and biological testing will be needed before the alloy can be recommended for general use.

11180. Weir, C. E., Piermarini, G. J., Block, S., **Crystallography of some high-pressure forms of $C_6H_6$, $CS_2$, $Br_2$, $CCl_4$, and $KNO_3$,** *J. Chem. Phys.* **50,** No. 5, 2089-2093 (Mar. 1, 1969).

Key words: High-pressure; polymorphism; single-crystal; x-ray diffraction.

From single crystal x-ray diffraction at high pressure and room temperature, unit-cell and space-group data were obtained for the following materials: $C_6H_6$, I–orthorhombic, a = 7.17, b = 9.28, c = 6.65, Pbca; $CS_2$–orthorhombic, a = 6.16, b = 5.38, c = 8.53, Cmca; $Br_2$–orthorhombic, a = 8.54, b = 6.75, c = 8.63, Cmca; $CCl_4$, I–rhombohedral, a = 14.27, $\alpha = 90°$; $CCl_4$, II–monoclinic, a = 22.10, b = 11.05, c = 25.0, $\beta = 114°$, Cc or $C2/_c$; $CCl_4$, III–orthorhombic, a = 11.16, b = 14.32, c = 5.74, $C222_1$; $KNO_3$, III–rhombohedral, a = 4.31, $\alpha = 78°54'$; $KNO_3$, IV(?)–orthorhombic, a = 5.58, b = 7.52, c = 6.58, $P2_1nb$ or Pmnb. All unit-cell dimensions are given in Å with estimated uncertainties of ± 2 in the last decimal place given and uncertainties of ± 0.5 deg. in angles.

**11181.** Weisman, I. D., Swartzendruber, L. J., Bennett, L. H., **Resonance studies in ferromagnetic $Fe_2B$ and $Fe_2Zr$,** *Phys. Rev.* **177,** No. 2, 465-471 (Jan. 10, 1969).

> Key words: Anisotropy; electric field gradient; $Fe_2B$; $Fe_2Zr$; ferromagnetism; hyperfine field; nuclear magnetic resonance; quadrupole interactions; spin waves.

The hyperfine magnetic fields and quadrupole interactions in $Fe_2B$ and $Fe_2Zr$ are explored by nuclear magnetic resonance and the Mössbauer effect. As in previous work, an anisotropy is found in the Mössbauer spectra which can be interpreted as a superposition of an anisotropic magnetic field and electric field gradient from two magnetically inequivalent Fe sites. The two magnetic fields are found (with indicated extended uncertainties) to be (252 ± 2) dT and (244 ± 2) dT at 4.2 K. The resonance frequency shows a $T^{3/2}$ dependence with some low temperature deviations which can be understood in terms of a gap arising from magnetocrystalline anisotropy and spin wave demagnetization. The measured pressure variations, $\delta\gamma/\delta p$, of the $^{11}B$ and $^{91}Zr$ frequencies (and their extended uncertainties) are respectively $(-21 \pm 2)$ and $(31 \pm 2)$ Hz-(bar)$^{-1}$.

**11182.** Weiss, A. W., **Series perturbations and atomic oscillator strengths: the $^2D$ series of Al I,** *Phys. Rev.* **178,** No. 1, 82-89 (Feb. 5, 1969).

> Key words: Configuration interaction; oscillator strength; series perturbations.

A model calculation has been made of the effects of perturbations of the $3s^2nd$ series of aluminum by the $3s3p^2$ $^2D$-term. The model employed is the traditional one of configuration interaction among the independent particle model representations of the relevant discrete states, with Hartree-Fock functions being used to compute the necessary matrix elements. It is found that, while in the Hartree-Fock approximation the $3s3p^2$ term is bound and embedded in the $3s^2nd$ series, the configuration interaction gives rise to a new autoionizing state just beyond the series limit. This state, which is approximately 50 percent $3s3p^2$, is found to have most of the $^2D$ absorption oscillator strength (f = 1.1). The general properties of this model of series perturbations are also discussed in some detail.

**11183.** Weiss, B-Z., Meyerson, M. R., **Localized microstructural changes and fatigue crack propagation,** *Trans. Met. Soc. AIME* **242,** 2515-2518 (1968).

> Key words: Austenitic steels; carbide precipitation; fatigue crack propagation; plastic deformation; plastic zone size; temper embrittlement.

Changes of plastic zone size during fatigue crack propagation in fully reversed cyclic bending at constant load amplitude for conditions of plain strain were investigated by two different techniques. It appears that the rate of fatigue crack propagation cannot be expressed as a continuous simple function of plastic zone size. This was related to the anisotropic conditions of plastic deformation in the plastic zone preceding the crack. A theoretical-mathematical evaluation was formulated for fatigue crack propagation during repeated cyclic bending under conditions of plane strain. The theory is based on an elastic model and the assumption that the plastic deformation at the tip of the propagating crack does not cause drastic redistribution of stresses in the stress field around the tip of the crack. It was found that fatigue crack propagation can be expressed as a function of stress intensity factor.

Experimental results are in good agreement with the presented theoretical evaluation.

The effect of localized (heterogenous) structural changes su as selective precipitation of carbides in austenitic steels, temp embrittlement in a low alloy steel, and partial martensitic tra formation in a metastable austenitic steel have been investiga and are discussed.

**11184.** Weiss, B-Z., Meyerson, M. R., **The effect of mean stress fatigue crack propagation in plates under extension and be ing,** *J. Basic Eng.* **90,** Series D, No. 3, 414-417 (Sept. 1968).

> Key words: Crack propagation; fatigue; plastic zone.

This discussion presents comments on a paper by R. Robe and F. Erdogan, "The Effect of Mean Stress on Fatigue Cr Propagation in Plates Under Extension and Bending." So original data are presented to support the views of the discuss

**11185.** Weissberg, S. G., Brown, J. E., **Osmometry of polym** *Encyclopedia of Polymer Science and Technology* **9,** 659- (Interscience Publs. Inc., New York, N.Y., 1969).

> Key words: High speed osmometer; number-aver molecular weight; osmometer; osmotic pressu semipermeable membranes.

Brief summary of principles and methods of measuremen osmotic pressures of polymer solutions, with survey of mod high speed instruments.

**11186.** Weissler, P. G., **International standard reference zero audiometers,** *J. Acoust. Soc. Am.* **44,** No. 1, 264-275 (J 1968).

> Key words: Artificial ear; earphones; international diometric reference zero; pure-tone audiometers; thresh of hearing; uncertainty of threshold of hearing standard.

This is a detailed report on the technical activities of IS Technical Committee on Acoustics No. 43, Working Grou Threshold of Hearing, which led to the ISO Recommenda R389, "Standard Reference Zero for the Calibration of P Tone Audiometers," November 1964.

The activities described are the determinations of the tran factors from loudness balancing experiments between the earphone-coupler combinations in R389, the incorporation o transfer data into the computation of the reference equiva threshold sound pressure levels (RETSPL) in R389, and details of the weighting of the original threshold determinati A statistical analysis estimates the average standard deviatio the RETSPL in R389 to be 2 dB due in large part to the vari in the transfer factors. The present USASI standards definitely outside the ISO uncertainty limits at all frequen The standard deviation of the differences between colum R389, (or the equivalence of the RETSPL for the diffe earphone-coupler combinations) was estimated to be 2.5 dB improve accuracy in audiometry it is suggested that the vari due to the transfer factors be eliminated by agreement on standard earphone type.

**11187.** West, E. D., Churney, K. L., **A two-body model fo calorimeters with constant-temperature environment,** *J.* *Phys.* **39,** No. 9, 4206-4215 (Aug. 1968).

> Key words: Calorimeter; "drop" calorimeter; enthalpy surements; heat content measurements; isoperibol calor ter.

Equations are derived describing a model of a model isoperibol calorimeter in which the calorimeter proper co of two parts thermally connected, one surrounding the othe exchanging heat with the constant temperature environ These solutions provide insights into the behavior of calorimeters. Inferences are drawn relative to the effect of th cations of the thermometer and heat source on the er quivalent of the calorimeter and some possible errors are pointed out. Macleod's application of the two-body theory of ing and Grover to high temperature enthalpy measurements is iscussed and weaknesses in theory and experiment are pointed ut. Procedures having a better theoretical basis are outlined.

1188. West, E. D., Westrum, E. F., Jr., **Adiabatic calorimetry from 300 to 800 K,** Chapter 9 in *Experimental Thermodynamics,* **Vol. I,** *Calorimetry of Nonreacting Systems,* J. P. McCullough and D. W. Scott, eds., pp. 333-367 (Butterworth and Co., London, England, 1968).

> Key words: Adiabatic calorimetry; calorimeter; calorimetry; cryoscopy; melting; phase transition; purity; thermodynamics.

Adiabatic heat capacity calorimetry in the range 300 to 800 K reviewed with discussions of principles and two particular alorimeters. The general heat flow problem is discussed qualita-vely as it pertains to the design of calorimeters of this type. onstruction details are included in the examples and related to ne principles. The advantages and disadvantages of different methods of operation are discussed.

1189. Westrum, E. F., Jr., Furukawa, G. T., McCullough, J. P., **Adiabatic low-temperature calorimetry,** Chapter 5 in *Experimental Thermodynamics,* **Vol. I,** *Calorimetry of Nonreacting Systems,* J. P. McCullough and D. W. Scott, eds., pp. 133-214 (Butterworth and Co., London, England, 1968).

> Key words: Adiabatic calorimetry; calorimeters; calorimetry; cryoscopy; cryostats; curvature correction; heat-leak correction; low temperature calorimetry; phase studies; phase transitions; power; premelting correction; purity; smoothing of observations; temperature; thermodynamic properties; thermodynamics; thermometry; time vaporization correction.

Adiabatic heat-capacity calorimetry in the range 4 to about 50 K is reviewed with discussions in principles of calorimeter esign, measurements, and analysis of data obtained. Measurements of temperature, power, and time are discussed with critical analysis of expected accuracy of circuitry and equipment used. Methods for transferring samples into the calorimeter vessel and arious heat treatments in the calorimeter prior to measurements are suggested for substances that undergo phase transitions. Procedures are given for heat-leak, premelting, curvature, and aporization corrections. Methods for smoothing the observed heat-capacity data and calculation of thermodynamic properties re discussed.

1190. Wexler, A., **Calibration of humidity-measuring instruments at the National Bureau of Standards,** *ISA Trans.* **7,** No. 4, 356-362 (1968).

> Key words: Calibration accuracies; gravimetric hygrometer; humidity calibration; humidity generator; hygrometry.

The National Bureau of Standards provides a service to Government agencies and the public for the calibration of humidity measuring instruments. The equipment and procedures mployed in making these calibrations and the available ranges and accuracies are described. Calibrations are performed by subecting the instrument under test to atmospheres of known moisture content produced by the NBS two-pressure humidity generator. The most accurate calibrations are made with the NBS standard hygrometer, a device based on the gravimetric method. With the latter, a measurement can be made with an estimated uncertainty (estimated systematic error plus three times the standard deviation) of 13 parts in $10^4$.

1191. White, H. S., Jr., **Data management and standardization,** *Mod. Data* **2,** No. 5, 52-56 (May 1969).

> Key words: Codes; data; data elements; data management; data standardization; information; information management; standardization.

A critical review is made of the current state of affairs as concerns the subject of data management and data standardization. A proposal is offered as an initial attempt to define a technique for the systematic management of data. The role of data standardization as a management tool is discussed. Various standardization efforts at the government, national, and international levels are described.

11192. Wiederhorn, S. M., **Fracture surface energy of glass,** *J. Am. Ceramic Soc.* **52,** No. 2, 99-105 (1969).

> Key words: Cleavage; cohesive strength; cracks; double cantilever cleavage technique; fracture; fracture mechanics; glass; stress intensity factor; surface energy.

Fracture surface energies of six different glasses were measured using the double-cantilever cleavage technique. Values obtained ranged from 3.5 to 5.3 J/m$^2$ depending on the chemical composition of the glass and the temperature of the test. The fracture surface energy increased with decreasing temperature and increasing Young's modulus, however, exceptions to this behavior were noted. The magnitude of the values obtained are discussed with respect to the theoretical strength of glass, and possible irreversible effects at the crack tip such as stress corrosion and plastic deformation are considered.

11193. Wiederhorn, S. M., **Moisture assisted crack growth in ceramics,** *Intern. J. Fracture Mech.* **4,** No. 2, 171-177 (June 1968).

> Key words: Ceramics; crack growth; delayed failure; fracture; glass; sapphire; static fatigue; stress corrosion.

A method is described to study subcritical crack growth in ceramic materials. Large, macroscopic size cracks were used and quantitative crack velocity measurements were made on glass and sapphire as a function of applied force, temperature and environment. The measured crack velocity was a complex function of stress and water vapor concentration in the environment and portions of the data could be adequately explained by the stress corrosion theory of Charles and Hillig.

11194. Wiese, W. L., **Dependence of atomic f-values on nuclear charge,** (Proc. Conf. Beam-Foil Spectroscopy, University of Arizona, Tucson, Arizona, Nov. 20-22, 1967), Chapter in *Beam Foil Spectroscopy* **II,** 386-406 (Gordon and Breach Science Publ. Inc., New York, N.Y., 1968).

> Key words: Nuclear charge; oscillator strength; perturbation theory; systematic trend.

Conventional perturbation theory predicts a simple relationship between atomic oscillator strength and nuclear charge, which is rederived and discussed in some detail. By utilizing available f-value data for the lighter elements, it is then shown that this dependence is clearly evident in the numerical material supplied by theory as well as experiment. Several representative examples are given in graphical form and discussed.

11195. Wiese, W. L., **Systematic trends of atomic oscillator strengths in isoelectronic sequences,** *Appl. Opt.* **7,** No. 12, 2361-2366 (Dec. 1968).

> Key words: Atomic oscillator strengths; beam foil spectroscopy; isoelectronic sequences; nuclear charge dependence; systematic trends.

The dependence of atomic oscillator strengths (f-values) on nuclear charge, which leads to systematic trends along isoelectronic sequences, is discussed with particular reference to beam foil spectroscopy. The theoretical background for the nuclear charge dependence is given first, and then several characteristic examples are reviewed in detail. The beam foil technique of measuring lifetimes is one of the most important data sources, because it readily permits reliable experimental determinations of f-values over several stages of ionization within isoelectronic sequences. It is shown that experimental data are most urgently needed when f-values are affected by cancellation in the transition integral or configuration interaction effects, since in these cases most theoretical approaches run into great difficulties.

**11196.** Wiese, W. L., Weiss, A. W., **Regularities in atomic oscillator strengths,** *Phys. Rev.* **175,** No. 1, 50-65 (Nov. 5, 1968).

> Key words: Atomic oscillator strengths; atomic spectroscopy; isoelectronic sequences; spectral series; spectroscopic regularities.

Many regularities and systematic trends among atomic oscillator strengths have been studied using the extensive material which has recently become available for the lighter elements. The quantum mechanical background for the existence of these regularities is discussed, and in particular the relationship between oscillator strength and nuclear charge as predicted from conventional perturbation theory is reviewed in detail. A number of characteristic numerical examples are then presented. The regularities are of great practical importance since they may be exploited to obtain additional oscillator strengths by simple interpolation techniques as well as to evaluate the reliability of existing data by the degree of fit into established systematic trends.

**11197.** Wilcox, R. M., **Bounds for the isothermal, adiabatic, and isolated static susceptibility tensors,** *Phys. Rev.* **174,** No. 2, 624-629 (Oct. 10, 1968).

> Key words: Bounds; dielectric; inequalities; magnetic; susceptibilities.

Quantum statistical proofs are given that: (1) the isolated (or Kubo) susceptibility tensor is positive indefinite and is bounded from above by the adiabatic susceptibility tensor; (2) the isothermal susceptibility tensor is positive definite and is bounded from below by the adiabatic susceptibility tensor. The results apply to either the static dielectric or magnetic cases. Biasing fields and permanent dipole moments may be present if desired. Criteria for equality of the various susceptibilities is established.

**11198.** Wildhack, W. A., **Improving measurement accuracy for high systems reliability,** *Electronics* **41,** No. 5, 280 (Mar. 4, 1968).

> Key words: Accuracy; accuracy chart; calibration uncertainties; measurement; measurement systems; reliability; system reliability; uncertainty.

The accuracy actually attained in measurements, at any stage, may critically limit the actual reliability of an operational item or system, as well as the confidence in both predictions and demonstrations of performance and reliability. Measurement uncertainty increases with each successive echelon of calibration, with intervals between calibrations or checks, with environmental fluctuations, and with rigors of use in laboratory, plant or field. Available and developing resources and techniques for improving achieved accuracy in practical measurements are discussed.

**11199.** Wildhack, W. A., Mason, H. L., Powers, R. S., Jr., **Accuracy charts for RF measurements,** *Proc. IEEE* **55,** No. 6, 1056-1063 (June 1967).

> Key words: Accuracy; calibration; IEEE; measurements; radio; radio frequency.

The general factors involved in the estimation of uncertainties in calibration or measurement are reviewed briefly. Twenty-five accuracy charts are presented showing the estimated uncertainties in National Bureau of Standards calibrations of laboratory standards or measuring instruments for electrical and radic frequency quantities.

**11200.** Williams, E. S., **A voltage converter for a new era,** *Meas Data* **2,** No. 6, 75-79 (Nov.-Dec. 1968).

> Key words: Emf comparator; frequency compensation temperature compensation; thermoelement; transfer volt meter; voltage converter.

A set of thermal voltage converters recently developed a NBS consists of five series resistor units and two thermole ments, each of which can be used with any one of the resistors The thermoelements have rated currents of 2.5 and 5 mA. Thi arrangement permits each resistor to be used for two voltag ranges. The ac-dc difference or frequency influence of eac range is less than 20 ppm at 50 kHz from 1 to 600 volts. Ad jacent ranges can also be intercompared, so that all ranges can b evaluated relative to any one in only six steps. The thermoele ments are compensated for temperature changes to reduc warm-up drift. Difficulties with reversed d-c differences in th thermoelements and power supply instability are minimized b the test procedure used and by the special emf comparators which are also described.

**11201.** Wims, A. M., McIntyre, D., Hynne, F., **Coexistence curv for 3-methylpentane-nitroethane near the critical point,** *Chem. Phys.* **50,** No. 2, 616-620 (Jan. 15, 1969).

> Key words: Coexistence curve; critical phenomena; der sitometer; magnetic suspension; nitroethane; 3-methylper tane.

The coexistence curve for the liquid mixture 3-methylpentan nitroethane has been obtained using a visual and a flo technique. A detailed analysis of the data shows that the con position differences of the coexisting liquid phases are propo tional to $(t_c\text{-}t)\beta$, where $\beta = 0.340$ with a standard deviation 0.010. As a result of this analysis and an analysis of the earli work of Rice and Zimm it is shown that the value of $\beta$ for binar liquids is not significantly different from the value for gas-liqu systems.

**11202.** Wolcott, N. M., Falge, R. L., Jr., **Ferromagnetism $CrBe_{12}$,** *Phys. Rev.* **171,** No. 2, 591-595 (July 10, 1968).

> Key words: Curie point; ferromagnetism; magnetic m ment; susceptibility.

The intermetallic compound $CrBe_{12}$ has been found to exhil ferromagnetism. The ferromagnetic and paramagnetic Cu temperatures are in close agreement, each about 50 K. The spo taneous moment is 0.15 or 0.22 Bohr magnetons per chromiu atom depending on the scheme assumed. In the paramagne temperature range, one finds an effective magneton number 2.22 Bohr magnetons per chromium atom.

**11203.** Wolcott, N. M., Falge, R. L., Jr., Bennett, L. H., **NM studies in paramagnetic and ferromagnetic $CrBe_{12}$,** *Phys. R Letters* **21,** No. 8, 546-549 (Aug. 19, 1968).

> Key words: Be; Cr; ferromagnetism; hyperfine fiel nuclear magnetic resonance; paramagnetism.

The occurrence of bulk ferromagnetism, with a Curie point about 50 K, is verified for $CrBe_{12}$ by nuclear magnetic resonar experiments. The magnetic properties are explored by means *conventional* high field NMR in the ferromagnetic as well as paramagnetic state.

**11204.** Wolfe, W. C., **Field study of floor coverings,** *Flooring* , No. 11, 52-58 (Nov. 1968).

> Key words: Adhesion; floor coverings; orangic coatin performance characteristics; specifications; wear.

The National Bureau of Standards has made observations of performance of floor coverings in areas of severe exposure in partment of Defense installations and some civilian applica-s over a period of 13 years (1955-68). Valuable information the adhesion of coatings and coverings to their substrates, on ar and other performance characteristics was obtained. This rmation has been used by Federal agencies in preparing cifications and in selecting materials for specific applications. wever, it is evident that the incomplete observations were not quate to properly evaluate the relative performance of the dif-ent systems. Therefore recommendations are made for better-trolled field observations leading to laboratory investigations.

**05.** Wolfgang, R., Zare, R. N., Branscomb, L. M., **Chemical ccelerators,** *Science* **162,** No. 3855, 818-822 (Nov. 15, 1968).

Key words: Chemical accelerators.

This is a brief account of a conference on chemical accelera-s held at the University of Colorado March 28-29, 1968, sup-ted by the Advanced Research Projects Agency.

**06.** Unassigned.

**07.** Yakowitz, H., Heinrich, K. F. J., **Inclusion identification y means of electron probe microanalysis,** *Metallography* **1,** No. 1, 55-78 (Sept. 1968).

Key words: Concentration mapping; electron probe microanalysis; experiment design; inclusion analysis; microscopy; quantitative data scanning.

Each stage in the analysis of inclusions by electron probe troanalysis is evaluated. These stages include experimental ign and instrument operation, specimen preparation, element ntification, element distribution mapping and quantitative a scanning. The use of signals other than x-rays for inclusion lysis is considered as well as the analysis of submicron inclu-ns. The approach taken assumes that microprobe analysis will used in conjunction with careful optical microscopy and that ntitative microscopy may be used to classify the inclusions er microprobe analysis is carried out.

**08.** Yonemura, G. T., Kasuya, M., **Color discrimination under educed angular subtense and luminance,** *J. Opt. Soc. Am.* **59,** No. 2, 131-135 (Feb. 1969).

Key words: Color discrimination; signal lights; vision.

Under reduced visual conditions, small area and low lu-nance, color discrimination for normal eyes deteriorates in a nner similar to that observed for tritanopic vision. The pur-e of this study was to investigate and quantify the reciprocal ation between area and luminance for conditions where this s in color discrimination occurs for people with normal vision. adratic equations, $\ln s = a(\ln F)^2 + b(\ln F) + C$, were ob-ned from the empirical data to describe the relationship ween chromaticity discriminability s, with luminous flux F; ere s = the standard deviation of color matches and $F = \omega^{3/4}L$ get solid angular subtense $\omega$, and luminance L). The con-nts a, b, and c are different for the red-green and blue-yellow ections on the chromaticity diagram. The results of this study d their most obvious application in the field of signal lights.

**09.** Young, K. F., Forman, R. A., **Use of polystyrene beads for manufacture of low loss coaxial lines for low temperature esearch,** *Rev. Sci. Instr.* **39,** No. 12, 1964-1965 (Dec. 1968).

Key words: Coaxial cable; low-dielectric-loss coaxial lines; low temperature; transmission lines.

A new inexpensive technique is described for the production experimental coaxial transmission lines for low temperature e. These lines have been tested in both nuclear quadrupole onance and dielectric loss measurements and have proven to be as good electrically as commercial coaxial cable, with a large decrease in thermal conduction into the experimental system.

**11210.** Young, R. D., Kuyatt, C. E., **Resolution determination in field emission energy analyzers,** *Rev. Sci. Instr.* **39,** No. 10, 1477-1480 (Oct. 1968).

Key words: Analyzer resolution; energy analyzer; energy distribution; field emission.

The influence of energy analyzer transmission function on measured field emission energy distributions has been evaluated by folding a Gaussian transmission function into the field emission total-energy distribution. The resulting distributions at 0, 4.2, 20.3, 77, and 300 K are plotted as a function of the field- and work function-dependent parameter d, and for the special case $\varphi = 4.40$ eV, $F = 3.0 \times 10^7$ V/cm. A criterion is established for determining the width of an analyzer transmission function from distributions measured at the above temperatures. It is shown that the slope of the log of the energy distribution is changed by less than 1 percent when the analyzer width is changed from 0 to 100 mV.

**11211.** Zalubas, R., **Present state of analysis of the first spectrum of thorium (Th I),** *J. Opt. Soc. Am.* **58,** No. 9, 1195-1199 (Sept. 1968).

Key words: Energy levels Th I; first spectrum; thorium.

To date 268 even and 255 odd atomic energy levels in Th I have been found. The lowest level of the configuration $5f\,6d\,7s^2$ is ${}^3H_4^\circ$ and lies 7795.27 cm$^{-1}$ above the ground level ${}^3F_2$ of $6d^2$ $7s^2$. Some levels of $5f\,6d^2\,7s$ and $6d^2\,7s\,7p$ are identified.

**11212.** Madey, T. E., Yates, J. T., Jr., **Desorption by electron impact: oxygen adsorbed on tungsten,** *Surface Sci.* **11,** No. 2, 327-351 (July 1968).

Key words: Binding states; chemisorption; cross section; desorption; electronic desorption; electron impact; oxygen; physisorption; tungsten.

The interaction of oxygen with a polycrystalline tungsten ribbon has been examined using electron stimulated desorption. At least three binding states of adsorbed oxygen have been identified: a physically adsorbed state which forms at 20 K, and two chemisorbed states designated $\beta_1$ and $\beta_2$. Both the physisorbed state and the $\beta_1$ state liberate positive ions when bombarded by 100 eV electrons; no positive ions were observed on electron bombardment of the $\beta_2$ state. The results indicate that the physisorbed state and the $\beta_1$ state are molecular. There is an enhanced adsorption of oxygen above 500 K which is primarily due to the creation of binding sites by thermal rearrangement of the oxygen covered surface. The maximum in the ion energy distribution is at 6.5 volts for $\beta_1$ oxygen and at 0.5 volts for physisorbed oxygen. The total cross section $Q_{\beta_1}$ for electronic desorption from the $\beta_1$ state is $7 \times 10^{-19}$ cm$^2$; the ionic cross section $Q^+_{\beta_1}$ is $\gtrsim 3.4 \times 10^{-20}$ cm$^2$. The maximum ion yields $g^+$ (ions/electron) are $g^+ = 1.5 \times 10^{-6}$ for 300 K adsorption, $g^+ = 3.3 \times 10^{-6}$ for adsorption at 730 K, and $g^+ = 5 \times 10^{-5}$ for adsorption at 20 K.

**11213.** Maki, A. G., **Comment on the Fermi resonance constant in ICN,** *J. Chem. Phys.* **50,** No. 5, 2273 (Mar. 1, 1969).

Key words: Energy levels; ICN; infrared spectroscopy; microwave spectroscopy; molecular structure; vibrational resonance.

From microwave data the value of the Fermi resonance constant for ICN is found to be $W_{12} = 35$ cm$^{-1}$. This is in fairly good agreement with the value of $W_{12} = 32.5$ cm$^{-1}$ which was calculated from a harmonic internal-coordinate force field obtained using vibrational frequencies which were not corrected for anharmonicity.

**11214.** Manning, J. R., **Vacancy-wind effect in diffusion and deviations from thermodynamic equilibrium conditions,** *Can. J. Phys.* **46,** No. 23, 2633-2643 (1968).

> Key words: Correlation factor; deviations from thermodynamic equilibrium; diffusion; distortions of vacancy flux; vacancy concentrations; vacancy flow; vacancy wind.

The vacancy flow (or "wind') term which appears in kinetic treatments of the diffusion equations is discussed in terms of the vacancy concentrations which appear when a vacancy flow is distorted by an impurity. It is pointed out that this term arises from local distortions in the vacancy concentration profile and not from any overall deviation of the material from equilibrium vacancy concentrations. Thus, the thermodynamic treatment of Kirkaldy and Lane does not include the vacancy wind term. Several physical analogies help to describe the basic process.

The vacancy wind effect arises from motion of atoms other than the particular diffusing atom. In addition, motion of the diffusing atom itself can introduce distortions in the local vacancy distribution. For a slow-diffusing impurity, mobile-impurity effects are unimportant; but, for a fast-diffusing impurity, they become very important, both in their effect on the diffusion equations and in their effect on local vacancy distributions. Equations are given for the resulting deviations from equilibrium at sites neighboring on an impurity. The close relationship between mobile-impurity effects and the correlation factor is shown. For self-diffusion, mobile-impurity and vacancy wind effects exactly cancel in their influence on vacancy distributions.

**11215.** Marinenko, G., Taylor, J. K., **Electrochemical equivalents of benzoic and oxalic acid,** *Anal. Chem.* **40,** No. 11, 1645-1651 (Sept. 1968).

> Key words: Benzoic acid coulometer; electrochemical equivalent; faraday; oxalic acid coulometer.

Accurate values of the electrochemical equivalents of benzoic and oxalic acid dihydrate have been determined using a coulometer based on the electrochemical reaction $H^+ + e \rightarrow 1/2\ H_2$. The values of electrochemical equivalents of benzoic and oxalic acid dihydrate are 1.265715 ± 0.000036 mg/C and 0.653293 ± 0.000023 mg/C, respectively. The standards of electric current, mass, and time as maintained by the National Bureau of Standards were utilized in these determinations. The electric current was measured in terms of the emf of saturated Weston cells and electrical resistance. Benzoic acid ($99.995_5\%$ pure) and oxalic acid ($99.987_1\%$ pure) were used in this work. On the basis of these determinations, using the 1967 unified atomic weight scale, the faraday is calculated to be 96,486.7 ± 2.5 C/g-equiv. and 96,485.4 ± 3.4 C/g-equiv. for benzoic and oxalic acid coulometers, respectively. The indicated uncertainties are the overall limits of error based on the sum of the 95 percent confidence limits for the mean and an allowance for the effects of known sources of possible systematic error. It is proposed that conformance of material to its theoretical electrochemical equivalent should define the absolute purity and the faraday be used as the primary chemical standard of purity.

**11216.** Marzetta, L. A., **Noise limitations in signal detectors,** *Instr. Technol.* **16,** No. 2, 51-53 (Feb. 1969).

> Key words: Low-frequency detector; noise power; noise temperature; operational amplifiers; thermal noise.

A vigorous development program pursued in recent years by industry has resulted in a number of interesting electropotential detectors. The large void in a performance plot of available signal amplifiers of yesteryear has been almost completely occupied by devices that in some cases approach the theoretical thermal-noise limit, over a signal source resistance range from $10^0$ to $10^{16}$ ohms. There is good reason to expect the small remaining area marked for improvement will be filled in the near future.

**11217.** Matsumura, C., Lide, D. R., Jr., **Structure of the all**
**hydroxides. III. Microwave spectra of RbOH and RbOD.**
*Chem. Phys.* **50,** No. 1, 71-75 (Jan. 1, 1969).

> Key words: Bond distances; high temperature; microwa
> quadrupole; RbOH; rotational constants; spectra.

The microwave spectra of gaseous RbOH and RbOD h
been measured with a high-temperature spectrometer. The sp
tra are generally similar to those observed in CsOH and indic
an essentially linear structure for rubidium hydroxide. The va
tion of rotational constant with excitation of the bending m
shows anomalies similar to those found in CsOH. The Rb
bond length is found to be $2.30_5$ Å. while the O – H distanc
$0.96_5$ Å. Analysis of the nuclear quadrupole hyperfine struc
give eqQ values of –67.9 Mc/s in $Rb^{85}OH$ and –35 Mc/
$Rb^{87}OH$.

**11218.** Mazur, J., McCrackin, F. L., **Monte Carlo studies of**
**figurational and thermodynamic properties of self-interac**
**linear polymer chains,** *J. Chem. Phys.* **49,** No. 2, 648-665 (
15, 1968).

> Key words: Excluded volume; lattice; Monte Ca
> polymers; random walks; thermodynamics.

Non-self-intersecting walks on the simple cubic and face
tered cubic lattices are used as a model for the linear poly
chain with excluded volume. The statistical properties of
model with nearest neighbor interactions between the chain
ments are investigated by the Monte Carlo technique. The
lowing properties are investigated: the limiting distribution f
tion of chain-end dimensions, the dependence of mean sq
length of the chain on the number of chain elements, and
thermodynamic properties of the chain. A particular valu
the nearest-neighbor interaction parameter was found w
uniquely defines the Flory's theta point of the single c
Evidence for the phase transitions in the infinitely long cha
also presented.

**11219.** Mazur, J., McIntyre, D., Wims, A. M., **Asymp**
**behavior of the light-scattering function of coiled molecul**
*Chem. Phys.* **49,** No. 7, 2896-2904 (Oct. 1, 1968).

> Key words: Chain-end distribution; excluded volume;
> scattering; particle scattering factor; polydispersity.

This paper discusses the asymptotic solution of the scatt
function P(Θ) for large x where x is proportional to the scatt
angle, radius of gyration and the wave number. The theore
model employed for the calculation of the P(Θ) vs. x curves
presented in the preceding paper. The results are discussed
respect to the experimental data, after the results for P(Θ
corrected for various values of polydispersity.

A general analysis of the theoretical P(Θ) vs. x curv
presented, and the effect of the shape of the chain-end dis
tion function on the asymptotic behavior of the light scatt
function is discussed.

**11220.** Mears, T. W., Young, D. S., **Measurement and star**
**reference materials in clinical chemistry,** *Am. J. Clin. P*
**50,** No. 4, 411-421 (Oct. 1968).

> Key words: Clinical; measurement; medicine; sta
> reference materials.

The concept of the measurement system based upon th
parameters – length (meter), mass (kilogram), time (second
temperature (kelvin) – is developed. The proper daily oper
of an analytical laboratory depends on these basic mea
ments, and several derived from them, e.g., the liter. An
tional component of chemical measurement which direct

uences accuracy is the purity of the standards and reagents emloyed. The Standard Reference Materials program of the Naonal Bureau of Standards provides a central source of guaraneed high-purity reference materials which are available to all. he reliability of chemical measurements will increase as new tandard Reference Materials such as cholesterol, uric acid, rea, and creatinine are utilized to standardize methods and inruments in the clinical laboratories of this country.

1221. Mendlowitz, H., **Calculated line strengths for the transitions between the configurations ($3d^3 + 3d^24s$) and $3d^24p$ in Ti II,** *Astrophys. J.* **154,** 1099-1110 (Dec. 1968).

Key words: Calculated line strengths; configuration interaction; intermediate coupling; Ti II; $3d^3$; $3d^24s$; $3d^24p$ configurations.

We have calculated the relative line strengths in Ti II for the ansitions between the configurations ($3d^3 + 3d^24s$) and $3d^24p$. he strengths have been calculated in the intermediate coupling cheme while also taking into account the interaction between onfigurations. The relative magnitude and phase of the radial ansition integrals (s-p) and (d-p) for the jumping electron in the S coupling scheme have been obtained empirically from the ata of King and that of Wobig by means of a least-squares fit to ach set of data separately. From both sets of data we determined the relative phase to be −1, and the ratio of the magnitudes of the radial integral parameters obtained from King's ata differed from that obtained from Wobig's data by 10 perent. We have normalized the strengths in our paper to the abolute strengths of a group of lines corresponding to the transions of the $a^4P - z^4D^0$ multiplet given by Wobig. A comparison f the calculated and experimentally determined line strengths re made. An analysis of the data indicates that a number of the xperimentally determined lines are obtained under optically hick conditions.

1222. Meshkov, S., Ponzini, R., **$Su(6)_W$ and high-energy photoproduction,** *Phys. Rev.* **175,** No. 5, 2030-2034 (Nov. 25, 1968).

Key words: Dominance; meson; photoproduction-meson; $SU(6)_W$; symmetry; vector.

$SU(6)_W$ is used to make quantitative predictions for forward hotoproduction cross sections at high energies. The predicted atios for $\sigma(\gamma p|K^+\Sigma^0)/\sigma(\gamma p|K^+\Lambda)$ which vary from 0.5-1.0 for inident photons of energy 5-16 GeV are in good agreement with he SLAC experiments. This is in contrast to the quark model rediction of 1/27. Forward $\rho^0p$ and $\omega p$ photoproduction cross ections also agree very well with experiment, but $\varphi p$ is too large y a factor of two.

1223. Meyerson, M. R., Giles, P. M., Newfeld, P. F., **Dimensional stability of gage block materials,** *J. Mater.* **3,** No. 4, 727-743 (1968).

Key words: Ceramic; cermets; dimensional stability; gage blocks; length standards; precipitation hardening steel; secondary hardening steel; tempering; through hardening steel.

Gage blocks which are necessary for the production of dimenionally precise items may undergo a change of dimensions with ime. These changes are often extensive enough to cause the age block to lose its value as a standard of length. This paper lescribes the program carried out at the National Bureau of Standards, Institute for Materials Research over the past eight ears which has been successful in producing gage blocks which xhibit dimensional changes of less than $\pm 2 \times 10^{-7}$ in./in./yr.

Studies have been made on the effect on long term dimensional tability of variation of thermal and mechanical processing rocedures of gage blocks produced from four general categories of material. These four categories include (1) through hardened steels, (2) steels with hard cases and annealed cores, (3) steels with hard cases and partially hardened cores, and (4) ceramic and cermet materials.

11224. Mielenz, K. D., **Gas lasers and conventional sources in interferometry,** Chapter in *Electron Beam and Laser Beam Technology,* pp. 89-137 (Academic Press Inc., New York, N.Y., 1968).

Key words: Coherence; interferometers; lasers; light sources; multiple-beam; two-beam.

The theory of length interferometers is derived from the point of view of coherence theory. The performance of gas lasers and conventional sources in length interferometry is discussed.

11225. Mielenz, K. D., **Length measurement and laser wavelength stability,** *ISA Trans.* **6,** No. 4, 293-297 (1967).

Key words: Coherence; interferometry; lasers; length measurement; length standards; wavelength stability.

The application of gas lasers as light sources for interferometric length metrology, and the limitations imposed by variations of laser wavelengths, are discussed.

11226. Mies, F. H., **Configuration interaction theory. Effects of overlapping resonances,** *Phys. Rev.* **175,** No. 1, 164-175 (Nov. 5, 1968).

Key words: Autoionization; configuration interaction; electron scattering; photoionization; overlapping resonances; resonances; resonant scattering.

A generalized version of Fano's configuration interaction theory is presented which includes the interaction of many resonances with many continua and inelastic couplings between continuum states. In particular a new parameter is introduced; the overlap matrix between the continua to which neighboring resonances are coupled. Resonances which are coupled to the same channel states may be said to overlap. If their widths are comparable to their spacings the resultant effects on photoabsorption or on the scattering matrix can be quite profound. The apparent widths may bear little relation to the widths due to configuration interaction, and the resultant structure may not fit the usual Fano shapes for isolated resonances.

The effects of overlapping are examined for various models which are representative of atomic photoabsorption and electron-diatomic molecule scattering. It is demonstrated that without prior knowledge of the overlap matrix it is impossible to uniquely characterize a resonance from limited experimental observations. Scattering and photoabsorption experiments should be designed to examine all possible channels; both differential cross-sections and inelastic cross-sections. Even so, without the parallel support of theoretical estimates of partial widths, and the signs of the configuration interaction matrix elements, the interpretation of resonance phenomena and in particular the parameters which are extracted must be accepted with severe reservations.

11227. Mighell, A. D., Reimann, C. W., Mauer, F. A., **The crystal and molecular structure of diaquobis-(2,2′-biimidazole) nickel (II) dinitrate, $Ni(C_6H_6N_4)_2(H_2O)_2(NO_3)_2$,** *Acta Cryst.* **B25,** Part 1, 60-66 (Jan. 1969).

Key words: Biimidazole and water ligands; hydrogen bonding; transition metal coordination complex; x-ray structure determination.

The crystal and molecular structure of diaquobis(2,2′ biimidazole nickel (II) dinitrate, $Ni(C_6H_6N_4)_2(H_2O)_2(NO_3)_2$, was determined by single crystal x-ray diffraction techniques. This compound crystallizes in the monoclinic system with $a = 10.3925 \pm 0.0004$ Å, $b = 9.6284 \pm 0.0004$ Å, $c = 9.9615 \pm$

0.0003 Å, $\beta = 96.308 \pm 003$ Å, space group $P2_1/n$, $\rho_c = 1.68$ g $cm^{-3}$, and $z = 2$. The indicated uncertainties are the standard deviations of the sets of individual measurements involved. Three-dimensional data (3151 reflections) were used and the structure solved by the heavy atom method. The $Ni(biimidazole)_2(H_2O)_2(NO_3)_2$ molecule is centrosymmetric with the nickel atom at the center of an octahedron formed by two oxygen atoms and four nitrogen atoms. The four coordinating nitrogen atoms, two from each biimidazole molecule, form a rectangle (3.193 × 2.711 Å) and the water molecules lie above and below this plane. The structure consists of these complex cations linked by hydrogen bonds formed between coordinated water molecules, the noncoordinating nitrogen atoms in the biimidazole molecules and the nitrate anions.

**11228.** Mighell, A. D., Reimann, C. W., Santoro, A., **The crystal and molecule structure of dibromotetrapyrazole nickel(II), $Ni(C_3H_4N_2)_4Br_2$,** *Acta Cryst.* **B25,** Part 3, 595-599 (Mar. 1969).

Key words: Coordination complex; tetragonal nickel(II); x-ray crystal structure.

The crystal and molecular structure of dibromotetrapyrazole nickel(II), $Ni(C_3H_4N_2)_4Br_2$, was determined by single crystal x-ray diffraction techniques. $Ni(C_3H_4N_2)_4Br_2$ crystallizes in the monoclinic system with $a = 14.127 \pm .007$, $b = 9.334 \pm .003$, $c = 14.702 \pm .002$, $b = 118.62 \pm .03°$, space group $C2/c$, $p = 1.94$ gm $cm^{-3}$ and $Z = 4$. The structure was found to be isomorphous with dichlorotetrapyrazole nickel(II). The indicated uncertainties are the corresponding standard errors.

**11229.** Mighell, A. D., Smith, J. P., Brown, W. E., **The crystal structure of phosphoric acid hemihydrate, $H_3PO_4 \cdot 1/2H_2O$,** *Acta Cryst.* **25,** 776 (1969).

Key words: Crystal structure; monoclinic crystals; phosphoric acid hemihydrate.

The crystal structure of phosphoric acid hemihydrate, $H_3PO_4 \cdot 1/2H_2O$, was determined from three-dimensional Weissenberg data. Its crystals are monoclinic, with $a = 7.922 \pm 0.010$, $b = 12.987 \pm 0.02$, $c = 7.470 \pm 0.010$ Å, $\beta = 109.9 \pm 0.1°$, space group $P2_1/a$, and $Z = 4$. The structure was solved by vector methods and was then refined by full-matrix, isotropic, least-squares analysis. The two crystallographically independent phosphoric acid molecules are geometrically very similar to each other. Each is approximately tetrahedral with the P—O bond length significantly shorter than the P—OH bonds. Each phosphoryl oxygen atom, moreover, is the acceptor in two strong hydrogen bonds. The phosphoric acid and water molecules are linked into a three-dimensional network by hydrogen bonding, with each oxygen atom participating in at least one relatively strong intermolecular hydrogen bond.

**11230.** Miller, C. E., Lipsicas, M., **Nuclear spin-lattice relaxation in very dilute solutions of orthohydrogen in parahydrogen,** *Phys. Rev.* **176,** No. 1, 273-279 (Dec. 5, 1968).

Key words: Nuclear magnetic resonance; ortho hydrogen; relaxation time.

Measurements have been made of the proton spin lattice relaxation time in very dilute solutions of orthohydrogen in parahydrogen, as a function of temperature, density and fractional orthohydrogen concentration. Both the liquid phase, between 20 and 32 K, and the gas phase, between 34 and 40 K, have been studied. The salient features of the temperature and density dependences, qualitatively, fit an interpretation in terms of contributions from two particle and three particle correlations, as proposed by Deutch and Oppenheim.

**11231.** Milligan, D. E., Jacox, M. E., **Matrix-isolation study of the reaction of $F_2$ and of F atoms with NCN. The infrared spectra of the species $NF_2CN$ and FNCN,** *J. Chem. Phys.* **48,** No. 11 4811-4816 (June 1, 1968).

Key words: $CF_2$; $CF_3$; cyanogen azide; difluorocyanamide F atom reaction; $F_2$ reaction; FNCN; infrared spectrum isotopic substitution; matrix isolation; NCN reaction photolysis.

NCN produced by the photolysis of cyanogen azide isolate in an Ar matrix at 14 K has been found to react readily with F also present in the system, leading to the stabilization of $NF_2CN$ The absorption patterns observed for the most prominent in frared absorptions of $NF_2{}^{13}CN$ and of the two singly $^{15}N$-sub stituted difluorocyanamides are consistent with the previou vibrational assignment. When both NCN and F atoms ar present in appreciable concentration, absorptions appear at 87 and at 2068 $cm^{-1}$ which may be tentatively assigned to th FNCN free radical. Upon prolonged photolysis, incompletel characterized products of more extensive fluorination reaction are observed.

**11232.** Milligan, D. E., Jacox, M. E., **Matrix-isolation study of th vacuum-ultraviolet photolysis of dichlorosilane. The infrare spectrum of the free radical $SiCl_2$,** *J. Chem. Phys.* **49,** No. 1938-1942 (Aug. 15, 1968).

Key words: Dichlorosilane; dichlorosilane-$d_2$; force co stants; infrared spectrum; matrix isolation; photolysis; SiC free radical; ultraviolet spectrum.

In the studies of the vacuum-ultraviolet photolysis of $SiH_2C$ and of $SiD_2CL_2$ suspended in an argon matrix at 14 K, new a sorptions appear at 502 and at 513 $cm^{-1}$ which may be assign as the two stretching fundamentals of $SiCl_2$. A broad, unstru tured absorption is also observed in the region of the ultraviol spectrum in which features tentatively ascribed to $SiCl_2$ were o served in earlier gas-phase emission studies. The detailed assig ment of the observed infrared features is considered, and valu of the valence angle, the Si-Cl stretching force constant, and t stretching-interaction force constant are estimated, correspon ing to the two possible assignments for the infrared absorptio

**11233.** Milligan, D. E., Jacox, M. E., **Matrix-isolation study of t vacuum-ultraviolet photolysis of difluorosilane. The infrar and ultraviolet spectra of the free radical $SiF_2$,** *J. Chem. Ph* **49,** No. 10, 4269-4275 (Nov. 15, 1968).

Key words: Difluorosilane; free radical; $HSiF_2$; infrar spectrum; matrix isolation; $SiF_2$; ultraviolet spectru vacuum-ultraviolet photolysis.

The vacuum-ultraviolet photolysis of difluorosilane in in matrices at cryogenic temperatures has been found to lead to t stabilization of an appreciable concentration of $SiF_2$. A syst of ultraviolet absorption bands observed in a neon matrix c responds very well with the $Ov_2'O$-OOO bands recently report for gas-phase $SiF_2$ produced by another technique. In an arg matrix the bending fundamental of $SiF_2$ appears at 343 $cm^{-1}$ a the two stretching fundamentals at 843 and at 855 cm Evidence is presented supporting a previous assignment of the two fundamentals to the symmetric and antisymmetric stretchi modes, respectively. Carbon monoxide matrix observations dicate that H-atom detachment plays an important role in photolysis of difluorosilane. There is no evidence for the occ rence of processes involving F-atom detachment. It appears lil ly that an appreciable concentration of $HSiF_2$ is also stabilize the present experiments.

**11234.** Milligan, D. E., Jacox, M. E., Guillory, W. A., **Matr isolation study of the vacuum-ultraviolet photolysis trifluorosilane. The infrared spectrum of the free radical $SiF_3$** *Chem. Phys.* **49,** No. 12, 5330-5335 (Dec. 15, 1968).

Key words: Force constants; infrared spectrum; matrix isolation; $SiF_3$ free radical; thermodynamic properties; trifluorosilane; ultraviolet spectrum; vacuum-ultraviolet photolysis.

n studies of the vacuum-ultraviolet photolysis of $SiHF_3$ pended in argon, nitrogen, and carbon monoxide matrices at K, evidence has been obtained indicating that H-atom achment occurs and that the $SiF_3$ free radical is stabilized. All the vibrational fundamentals of $SiF_3$ have been observed in se experiments. The appearance of two stretching fundamen- s requires that the molecule be nonplanar. A more detailed nsideration of the pattern of vibrational absorptions indicates t the angle between each Si-F bond and the threefold sym- try axis of the molecule is approximately 71°, close to the ue characteristic of $sp^3$ hybridization of the valence electrons out the central atom. Force constants have been estimated ng a four-constant valence-force potential, and the ther- dynamic properties of $SiF_3$ have been calculated.

35. Mills, R. M., **Flame inhibition with electron attachment as he first step,** *Combustion and Flame* **12,** No. 2, 513-520 (Dec. 968).

Key words: Electron attachment; flame free radicals; flame inhibition mechanism.

The suggestion is made that combustion inhibition of the type served with the use of most halogenated hydrocarbons is due a two-step process: (1) negative ions and free radicals are med by dissociative electron attachment with the inhibitor olecules, and then (2) these negative ions and/or free radicals act with the free radicals found in flames. Considerable idence from the literature is presented which supports this ea. It is concluded that, while the evidence is not conclusive, a ious consideration of the idea is justified.

236. Moore, C. E., **Annual report on spectroscopy,** *Bull. Am. Astron. Soc.* **1,** No. 1, 85-86 (Jan. 1969).

Key words: Analyses of optical spectra; atomic spectra; data centers; molecular spectra; rare earth spectra; transition probabilities.

The present report has been prepared especially for as- physicists who are interested in the spectroscopic program at s Bureau. It is submitted annually and will be published with e Observatory Reports.

237. Moore, G. A., **Application of computers to quantitative analysis of microstructures,** (Proc. Third Intern. Materials Symp., Berkeley, Calif., June 13, 1966), Chapter 3 in *Ceramic Microstructures,* R. M. Fulrath and J. A. Pask, eds., pp. 71-120 (John Wiley and Sons, Inc., New York, N.Y., 1968).

Key words: Analysis of microstructures; automatic scanning (of micrographs); computer processing (of micrographs); logical modification of pictures; precision scanning (of micrographs); quantitative microscopy.

The problems and methods of quantitative microscopy are sically identical in all microscopic sciences. Results are limited the finite resolution of real micrographs and real observations d by the statistical necessity of processing a very large number observations, thus dictating automatic scanning and computer ocessing methods.

The presence or absence of a specific phase can be presented by a two-dimensional binary array which can be pidly processed to yield the required measurements. Logical odification by the computer is frequently necessary to sub- itute for some of the logical discriminations normally made by e human analyst and to facilitate the desired measurements.

Using high precision scanning equipment, the inaccuracies of easurement remain comparable to the limits imposed by statistics. Presently attainable precision is, however, an order o magnitude better than can normally be obtained by manual methods.

11238. Moore, G. A., Wyman, L. L., Joseph, H. M., **Comments on the possibilities of performing quantitative metallographic analyses with a digital computer,** Chapter 13 in *Quantitative Microscopy,* pp. 380-403 (McGraw-Hill Book Co. Inc., New York, N.Y., 1968).

Key words: Computer analysis of micrographs; grain size; micrographic analysis; pictorial analysis; quantitative microscopy; size distribution.

Preliminary experiments in the analysis of photographic information by means of a digital computer have shown that it is entirely feasible to analyze photomicrographs of metals by this means. The computer may be expected to become the quickest and most economical means of analysis whenever complete grain size or particle size distributions are to be obtained from 80 or more square inches of photomicrograph and when these distributions are to be translated into volume and weight terms.

11239. Mopsik, F. I., **Dielectric constant and loss,** *Digest of Literature on Dielectrics* **31,** 56-79 (1969).

Key words: Dielectric literature; dielectric literature in 1967; dielectric properties; digest of literature on dielectrics; literature compilation; survey of dielectric literature.

A compilation has been made of the literature appearing in 1967 on the subject of dielectric properties of materials. A summary of the highlights is included.

11240. Abramowitz, S., Levin, I. W., **Raman spectrum of $ONF_3$,** *J. Chem. Phys.* **51,** No. 1, 463-464 (July 1, 1969).

Key words: Infrared; laser; low temperature; Raman; trifluoramine oxide; vibrational assignment.

The Raman spectrum of a polycrystalline film of trifluoramine oxide at 78 K has been observed. The fundamental frequencies of the bending modes $\nu_3(A_1)$ and $\nu_5(E)$ are found at 535 and 522 $cm^{-1}$. The doubly degenerate $NF_2$ stretching mode, $\nu_4$, is thought to be complicated by a resonance between $\nu_4$ and $\nu_5 + \nu_6$.

11241. Allan, D. W., Guétrot, A., Higbie, L. S., Lavanceau, J. D., **An application of statistical smoothing techniques on VLF signals for comparison of time between USNO and NBS,** *Proc. 23rd Frequency Control Symp., Atlantic City, N.J., May 6-8, 1969,* p. 248 (1969).

Key words: Effect of mass on frequency; flicker noise; NBS; noise correlation; NSS; optimum filter; phase noise; radio propagation; time comparison; USNO; VLF propagation; WWVL.

Recent developments have provided a method for obtaining submicrosecond time comparisons over continental distances. The method was applied to a time comparison between the master clocks at the United States Naval Observatory (USNO) and at the National Bureau of Standards (NBS) in Boulder, Colorado.

There were the following developments. First, if two signals show a reasonable degree of correlation in their fluctuations, then one may derive an optimum linear combination of the two with a mean square error less than for either signal individually. The two signals studied were the transmissions on 21.4 kHz from NSS in Annapolis, Maryland, and on 20.0 kHz from WWVL in Fort Collins, Colorado. It is necessary that receivers be located for both signals at the locations of the controlling clocks. Existence of positive correlation was shown. The positive cross correlation probably was due to the near reciprocal path and the very close transmission frequencies.

Second, the phase fluctuations due to the propagation medium were consistent with a spectral density of the random phase noise proportional to $|f|^{-1}$, commonly called flicker of phase noise. This persisted for Fourier frequencies from one cycle per day down to one cycle per several weeks. The fluctuations on the linear combination of the two signals still behaved as flicker of phase noise but at a lower level.

The phase or time fluctuations of the master clocks however followed a spectral density law proportional to $|f|^{-3}$, flicker of frequency noise, for frequencies lower than one cycle per day.

Third, an optimum linear filter (Wiener filter) giving the minimum mean square error estimate (MMSEE) of the signal has been determined for a random walk of phase signal (spectral density proportional to $|f|^{-2}$) imbedded in white noise (spectral density proportional to $|f|^{0}$). The same filter was shown to be still optimum for spectral densities proportional to $|f|^{-3}$ for the signal and $|f|^{-1}$ for the noise.

Application of the above filter to the appropriate linear combination, defined through correlation properties, of NBS and WWVL signals showed an improvement of 15 dB in the rms day-to-day phase fluctuations. The day-to-day rms time deviations were about 70 ns on the final results. The output estimate of the filter, compared with portable clock measurements, gave a disparity of the order of the final output noise.

The experiment provided an opportunity to determine if there is an effect of mass on frequency and within the uncertainties of the experiment a null result was obtained.

**11242.** Alvarez, R., Paulsen, P. J., Kelleher, D. E., **Simultaneous determination of trace elements in platinum by isotope dilution and spark source mass spectrometry,** *Anal. Chem.* **41,** No. 7, 955-958 (June 1969).

Key words: Cation-exchange; electrodeposition; high-purity metal analysis; multi-element; spark source mass spectrometry; stable isotope dilution; trace determinations.

An isotope dilution technique using the spark source mass spectrograph was investigated for applicability to simultaneous, multi-element trace determinations. Isotopically altered Ag, Cu, Ni, Pb and Pd were separated from a 250-mg sample of platinum by cation exchange, and electrodeposited onto gold electrodes for sparking in the spectrograph. Electrodeposition provided the spiked analytes in an adherent form, relatively free of anions and organic residue from the ion exchange resin, both of which could complicate the spectrum. Contamination, the principal limitation of the method, was minimized by isothermally distilling the reagent acids and by isolating the operations from the laboratory environment. After determining the isotope ratios, the concentrations were computed, ranging from 0.5 ppm ($\mu$g/g) for Ni to 14 ppm for Pb. Improved precision and accuracy was obtained compared to conventional spark source analysis. The results were compared with those of other methods and the platinum material was issued by NBS as Standard Reference Material 681.

**11243.** Angeles, R., Aldridge, M., Freeman, D., Wall, L., **Cryodegradation of polyelectrolyte networks,** *Polymer Letters* 7, No. 8, 609-611 (1969).

Key words: Cryodegradation; freeze-thawing; polyelectrolyte networks; sulfonated polystyrene-divinylbenzene.

The cryodegradation of sulfonated polystyrene-divinylbenzene and the quaternary ammonium derivatives of the same copolymer was investigated by a swelling-ratio method. The results indicate that the networks swollen by water are extensively degraded by 150 freeze-thawing cycles. With these networks the effect of freeze-thawing is significantly greater than that observed with aqueously soluble linear sulfonate polystyrene.

**11244.** Armstrong, G. T., **Hydrogen fluoride and the thermochemistry of fluorine,** (Proc. Conf. Interagency Chemica Rocket Propulsion Group, Thermochemistry Working Grou Cleveland, Ohio, Apr. 9-11, 1969), *Seventh Meeting Bulleti* **1,** 119-135 (Chemical Propulsion Information Agency, John Hopkins University, Applied Physics Laboratory, Silve Spring, Maryland, Aug. 1969).

Key words: Fluorides, heat of formation; fluorine dissoci tion energy; fluorine thermochemistry; hydrofluoric aci hydrogen fluoride.

The thermochemistry of hydrogen fluoride is reviewed. Th principal emphasis is on the experimental basis of the heats formation of HF(g) and of HF(aq). Data from flame calorimet in which HF(g) and HF(aq) are formed, evidence from process involving other fluorine compounds, and some evidence fro spectroscopic and photodissociation studies are broug together.

**11245.** Armstrong, G. T., King, R. C., **The heats of formation some fluorine-containing oxidizers,** (Proc. Conf. Interagen Chemical Rocket Propulsion Group, Thermochemistry Wor ing Group, Cleveland, Ohio, Apr. 9-11, 1969), *Seventh Mee ing Bulletin* **1,** 19-40, (Chemical Propulsion Information Age cy, Johns Hopkins University, Applied Physics Laborator Silver Spring, Maryland, Aug. 1969).

Key words: Chlorine pentafluroide; chlorine trifluoride; C F bond energy; flow calorimetry of gases; heats of formati of fluorine-containing oxidizers; hydrogen chloride; N- bond energy; trifluoramine oxide.

A calorimetric apparatus previously developed for measuri enthalpy changes of constant pressure combustion reactions corrosive, fluorine-containing materials and the enthalpy of so tion of the acid products of combustion has been applied to t determination of the enthalpies of formation of chlori trifluoride, chlorine pentafluoride, and trifluoramine oxide. T reactions of hydrogen with fluorine, chlorine, chlori trifluoride, chlorine pentafluoride and trifluoramine oxide, f lowed by absorption of the HCl, HF, and $H_2O$ formed in wa or aqueous acid solution were studied. Preliminary values for t enthalpies of formation in kcal mol$^{-1}$ are: $\Delta H_f[ClF_3(g)]$, $-38.$ $\pm 0.5$; $\Delta H_f[ClF_5(g)]$, $-56.61 \pm 1.0$; and $\Delta H_f[NF_3O(g)]$, $-44.$ $\pm$ 1.5, in which the uncertainties are our estimates of proba total systematic and random errors. The average Cl-F bond en gy is 19.5 kcal mol$^{-1}$ less in $ClF_3$ than in ClF and 5.5 kcal mo less in $ClF_5$ than in $ClF_3$. The addition of an O atom to $NF_3$ form $NF_3O$ increases the binding energy by 74.4 kcal mol$^{-1}$.

**11246.** Astin, A. V., **Management and the metric system,** *Defe Management J.* **5,** No. 2, 27-34 (1969).

Key words: Accommodation; adaptation; conversi customary units (U.S.); economic costs; interchangeabil international cooperation; metric system; SI units.

A decision on whether or not the United States will conver the metric system may be facilitated by a current Cong sionally-authorized study of the problem, described here by N Director Astin. Scientific, military, industrial, economic, tra and educational considerations are discussed in detail, with il trative material drawn from the experience of U.S. industrie well as those in foreign countries. Attention is focused on th kinds of interaction which would be involved in a metric ch geover: accommodation, adaptation, and conversion.

**11247.** Bates, R. G., **Inner reference electrodes and their cha teristics,** Chapter in *Glass Microelectrodes,* M. Lavallee, O

Schanne, and N. C. Hebert, eds., pp. 1-24 (John Wiley and Sons, Inc., New York, N.Y., 1969).

Key words: Glass electrode; inner solutions; pH measurement calomel electrode; reference electrodes; temperature coefficients of e.m.f.; silver-silver chloride electrode.

The principles governing the selection of the most suitable ctrodes and inner solutions for making electrical contact with reference side of the glass electrode are set forth. Particular ention is given to choice of the best electrode and solution mposition to minimize, or even to nullify, the temperature iation of the standard e.m.f. of the pH cell. Temperature coef- ients of the e.m.f. of glass electrode pH cells of various designs listed and other useful characteristics of inner electrodes and ner solutions are summarized.

**248.** Bates, R. G., **Measurement of pH,** *Handbook of Biochemistry,* H. A. Sober, ed., pp. J190-J194 (Chemical Rubber Company, Cleveland, Ohio, 1967).

Key words: Acidity; glass electrode; indicators; pH; standardization.

The operational definition of pH, in the form endorsed by the ternational Union of Pure and Applied Chemistry, is esented. The preparation of standard reference solutions for I measurements is described and the choice of electrodes and asurement techniques is discussed. The proper interpretation pH numbers is set forth briefly, and procedures for pH mea- rement with indicators are described.

The revised version includes the addition of two new primary I standards to tables 1 and 3, coefficients for calculating the mperature dependence of pH in table 2, and a collection of pH lues for miscellaneous buffer solutions.

**249.** Bates, R. G., **Medium effects and pH in nonaqueous solvents,** Chapter in *Solute-Solvent Interactions,* C. D. Ritchie and J. F. Coetzee, eds., pp. 45-96 (Marcel Dekker Inc., New York, N.Y., 1969).

Key words: Acidity; ion activity; medium effect; nonaqueous solvents; pH; thermodynamics.

The nature of acidity in nonaqueous solvents of various types discussed and the implications of acid-base behavior on the asibility of establishing useful scales for experimental pH and idity measurement are considered. The Brønsted concept pro- des a useful approach to the quantitative expression of acid- se potential in many solvent media with some acidic or basic aracter but is of doubtful value in aprotic or inert solvents. A neral scale of acidity or electrode potential applicable to more an one solvent requires a knowledge of the medium effect of e proton or the free energy of transfer of the proton from one lvent to another. Various methods of determining medium ef- cts for ions are considered and shown to be inadequate at the esent time. The role of dielectric constant and solvation henomena in the medium effect are discussed, and suggestions e made for the practical measurement of acidity in deuterium ide and alcohol-water solvents.

**1250.** Beatty, R. W., **Coaxial power, impedance and attenuation calibration at the National Bureau of Standards,** *Microwave J.* **11,** No. 5, 65-75 (May 1968).

Key words: Attenuation; calibration; coaxial; impedance; microwave; power; standards.

NBS calibration methods are described for coaxial power, im- edance, and attenuation at microwave frequencies. Present and ture NBS capabilities in these areas are discussed. An indica- on is given of the state of the art, how NBS arrives at its quoted mits of error, and how it develops confidence in its reference andards. Details of some measurement procedures are given and a list of references is given for those who wish more information.

**11251.** Beatty, R. W., Yates, B. C., **A graph of return loss versus frequency for quarter-wavelength short-circuited waveguide impedance standards,** *IEEE Trans. Microwave Theory Tech.* **MTT-17,** No. 5, 282-284 (May 1969).

Key words: Coaxial short-circuit; impedance standards; microwave; return loss; waveguide short-circuit.

Formulas and a graph are presented for determining return losses of microwave impedance standards consisting of quarter wavelength sections of short-circuited waveguide. Most standard sizes of coaxial line and rectangular waveguide are included on the graph, which covers a frequency range from 0.2 to 330 GHz. The graph is based upon a conductivity of $10^7$ mho per meter. Values of return loss read from the graph must then be divided by the square root of the actual conductivity relative to the above value. A table of bulk conductivities of various metals is given.

**11252.** Bender, P. L., **Optical orientation experiments at Princeton,** Chapter in *Polarisation Matiere et Rayonnement, Volume Jubilaire en L'Honneur D'Alfred Kastler,* pp. 346-441 (Presses Universitaires de France, Paris, 1969).

Key words: Atomic collisions; atomic orientation; collisional disorientation; optical pumping; resonance fluorescence; sodium.

A brief historical review of early optical orientation experiments at Princeton is given in this article. *It contains no new technical information.*

**11253.** Bennett, H. S., **Ultrasonic attenuation in Heisenberg magnets,** *Phys. Rev.* **181,** No. 2, 978 (May 10, 1969).

Key words: Antiferromagnet; critical fluctuations; ferromagnet; Gd; Heisenberg magnet; $MnF_2$; $RbMnF_3$; ultrasonic attenuation.

The microscopic theory developed by H. S. Bennett and E. Pytte to treat ultrasonic attenuation in Heisenberg magnets overestimates the critical fluctuations. It is shown that much better agreement with experiment obtains when this fact is explicitly taken into account.

**11254.** Bennett, L. H., **"Charge transfer" in intermetallic compounds: Example—The sodium thallide structure,** Chapter in *Structural Developments in Alloy Phases,* B. C. Giessen, ed., Discussion I, 41-44 (Plenum Press Inc., New York, N.Y., 1969).

Key words: Alloys; charge transfer; intermetallic compounds; ionic bond; metallic bond; sodium thallide.

It has been usual to speak of an ionic bond coexisting with the metallic bond in metals. NaTl was one of the earliest examples of such a description. It is pointed out that NaTl can be described by an energy band structure not requiring ionic bonding. The color of LiCd is discussed.

**11255.** Birmingham, B. W., Flynn, T. W., **Cryogenics in United States National Programs,** *Cryogenics* **9,** No. 1, 3-10 (Feb. 1969).

Key words: Agriculture; compressed gases; conservation; cryogenics; education; health; national goals; space; transportation.

The object is to discuss a segment of the compressed gas industry, namely the cryogenic industry, and its relation to selected national programs, such as space, health, agriculture, transportation, conservation, and education.

**11256.** Boone, T. H., Skoda, L. F., Cullen, W. C., **Laboratory-field comparisons of built-up roofing membranes,** *Roofing Siding Insul. Mag.* **46,** No. 4, 28-33 (Apr. 1969).

> Key words: Bituminous adhesive; bituminous built-up membranes; engineering properties; laboratory-field comparison; strength-thickness.

The values of breaking load, elongation and thermal expansion of nine bituminous built-up membranes prepared by roofing contractors under field conditions and by technicians in the laboratory were measured at subfreezing temperatures. The data indicated that the field-prepared specimens agreed favorably with laboratory-prepared specimens, although the samples from the field frequently reflected higher values for thermal-shock resistance than did their laboratory-prepared counterparts. The higher values were attributed to the smaller amounts of bitumen used between the piles of the field specimens. The results appeared to support the validity of the application of the "strength-thickness rule" to bituminous built-up membranes.

**11257.** Boyd, M. E., Larsen, S. Y., Kilpatrick, J. E., **Quantum mechanical second virial coefficient of a Lennard-Jones gas. Helium,** *J. Chem. Phys.* **50,** No. 9, 4034-4055 (May 1, 1969).

> Key words: Equation of state; helium; Lennard-Jones gas exchange effects; quantum mechanics; second virial coefficient; Wigner-Kirkwood expansion.

The quantum mechanical second virial coefficients of Lennard-Jones $He^3$ and $He^4$ gases with the De Boer parameters have been obtained over the complete temperature range from near absolute zero to the classical region. A formalism separating the virial into direct (Boltzmann) and exchange (spin and quantum statistics) contributions has been employed. The calculation is based on phase shifts except at the very highest temperatures where a Wigner-Kirkwood method has been used. Examinations of the exchange term shows in detail the rapid suppression of the statistical effects with rising temperature, their contribution dropping to less than .001 $cm^3$ by 7 K ($He^4$). Comparison of the high temperature (Boltzmann) results with those obtained by a third order Wigner-Kirkwood expansion shows excellent agreement down to about 50 K for $He^4$ and 60 ° for $He^3$. The Wigner-Kirkwood expansion is shown to be unsuitable for determining the behavior of the exchange terms.

**11258.** Braun, W., Bass, A. M., Davis, D. D., Simmons, J. D., **Flash photolysis of carbon suboxide: absolute rate constants for reactions of $C(^3P)$ and $C(^1D)$ with $H_2$, $N_2$, CO, NO, $O_2$ and $CH_4$,** *Proc. Roy. Soc.* **A312,** 417-434 (1969).

> Key words: Absolute rate constants; carbon suboxide; flash photolysis; primary processes; reactions $C(^3P)$, $C(^1D)$.

The vacuum ultraviolet flash photolysis of $C_3O_2$ in the 159.0 nm absorption band has been investigated. The major primary products are $C(^1S)$, $C(^1D)$, $C(^3P)$, and CO. The species $C_2$ and $C_3$ have also been observed but are of minor importance in the overall reaction scheme. A number of pressure independent reactions involving $C(^3P)$, $C(^1D)$, and $C(^1S)$ with CO, $CH_4$, $N_2$, NO, $O_2$, and $H_2$ have been observed by means of the kinetic-spectroscopic method. The rate constants measured at room temperature in units of $cm^3\ sec^{-1} molec^{-1}$ are summarized here:

(7) $C(^3P) + CH_4 \rightarrow C_2H_4$ (?); $k < 5 \times 10^{-15}$
(8) $C(^1D) + CH_4 \rightarrow C_2H_2 + H_2$; $k = 3.2 \times 10^{-11}$
(10) $C(^1D) + N_2 \rightarrow C(^3P) + N_2$; $k \approx 2.5 \times 10^{-12}$
(12) $C(^3P) + NO \rightarrow CN + O$; $k = 1.1 \times 10^{-10}$
(13) $C(^1D) + NO \rightarrow CN + O$; $k = 9.2 \times 10^{-11}$
(18) $C(^1D) + H_2 \rightarrow CH + H$; $k = 4.15 \times 10^{-11}$
(19) $C(^1S) + H_2 \rightarrow CH + H$ (?); $k < 5 \times 10^{-12}$
(20) $C(^3P) + O_2 \rightarrow CO + O$; $k = 3.3 \times 10^{-11}$
(22) $C(^1D) + O_2 \rightarrow CO + O$ (?); $k < 5 \times 10^{-12}$

The pressure dependent reaction rates of $C(^3P)$ with $N_2$, CO, and $H_2$ have been qualitatively measured and are discussed in detail.

**11259.** Brennan, J. A., Edmonds, D. K., Smith, R. V., **Two-phase (liquid-vapor), mass-limiting flow with hydrogen and nitrogen,** (Proc. 1968 Cryogenic Engineering Conf., Case Western Reserve Univ., Cleveland, Ohio, Aug. 19-21, 1968), Chapter in *Advances in Cryogenic Engineering* **14,** Paper G-6, 294-298 (Plenum Press Inc., New York, N.Y., 1969).

> Key words: Choking; critical; hydrogen; nitrogen; two-phase flow.

Experimental data on choked or mass-limiting flow at the exit of a constant area test section are presented. The data are compared to some simple analytical models which have been recommended to indicate upper and lower limits of the flow rates.

**11260.** Brower, W. S., Robbins, C. R., **Growth of $CaTiSiO_5$ by the Czochralski method,** *J. Crystal Growth* **5,** 233-234 (1969).

> Key words: $CaTiSiO_5$; crystal growth; Czochralski method; single crystals.

Crystals of $CaTiSiO_5$ suitable for physical property measurements have been grown by the Czochralski method. Best result were obtained with relatively high rotation rates (100-150 rpm and a linear growth rate of 0.15 cm/hr. The crystals ar monoclinic with space group $P2_1/n$, the symmetry previously observed for anhydrous synthetic $CaTiSiO_5$, as compared wit space group $C2/c$ reported for natural sphene (titanite) mineral of general formula $CaTiSiO_4$ (O, OH, F).

**11261.** Brown, J. E., Tryon, M., Horowitz, E., **Thermal decomposition of Cu(II)-bis(8-hydroxy-5-quinolyl) methane coordination polymer,** *J. Appl. Poly. Sci.* **13,** 1937-1947 (1969).

> Key words: Bis(8-hydroxy-5-quinolyl)methane; coordination; copper; decomposition; infrared spectrophotometry ligand; mass spectrometry; polymer; thermal; 8-hydroxy quinoline.

The volatile products formed when the coordination polyme of copper(II) and bis(8-hydroxy-5-quinolyl)methane wa heated in vacuum at elevated preselected temperatures were examined. The amount of weight loss at each temperature wa determined with a recording thermal balance. Infrared spectrophotometry was used to aid in the identification of the majo volatile component. A sample was pyrolyzed directly into th mass spectrometer. The results show that the volatile product i for the most part the organic ligand, bis(8-hydroxy-5-quinolyl)methane and not derivatives of the copper complex or fragments of the ligand. The mechanism for the decomposition reaction previously proposed is supported.

**11262.** Bur, A. J., Roberts, D. E., **Rodlike and random-co behavior of poly(n-butyl isocyanate) in dilute solution,** *J. Chem Phys.* **51,** No. 1, 406-420 (July 1. 1969).

> Key words: Dielectric constant; dielectric relaxation time dipole moment; Kratky-Porod worm-like model; molecula relaxation in dilute solution; poly(butyl-isocyanate polymer chain configuration; polypeptides; rodlik molecules.

The polymer chain configuration, molecular relaxation and th dipole moment of poly(n-butyl isocyanate), $(\text{-CO-NR-})_n$ wher $R = C_4 H_9$, have been studied by dielectric measurements of th polymer in dilute solution. The complex dielectric constant, $\epsilon^* =$ $\epsilon' - j\epsilon''$, was measured at room temperature over a frequenc range $10^{-1}$ Hz to $1 \times 10^6$ Hz for fractionated samples whos molecular weights cover a very broad range, $20 \times 10^3$ to $10 \times 10$ From observation of the dielectric relaxation time as a functio of molecular weight we deduce that the low molecular weig olecule ($M_w < 80 \times 10^3$) is rodlike and helical. Upon increasing e molecular weight, this rodlike conformation can not be stained and chain flexibility accumulates with the addition of ch monomer unit to the chain. Finally at high molecular eight, $M_w > 10^6$, the polymer chain configuration can be scribed as random coil. The relaxation time and dipole mo-ent measurements indicate that there is a one-to-one cor-respondence between the end-to-end distance and the dipole mo-ent of the poly(n-butyl isocyanate) (PBIC)s molecule. Using e dipole moment data alone, we are able to show that the PBIC ain configuration as a function of molecular weight can be escribed by the Kratky-Porod worm-like model. The relation-ip between PBIC and biological molecules, especially the olypeptides, is discussed.

263. Burke, P. G., Cooper, J. W., Ormonde, S., **Low energy scattering of electrons by helium,** *Phys. Rev.* **183,** No. 1, 245-264 (July 5, 1969).

Key words: Close coupling; eigenphase; electron helium scattering; excitation; polarization; resonance.

The close coupling equations for electron-helium scattering ave been solved in the energy range near the n = 2 thresholds. ross sections for elastic scattering from both ground and xcited states, for excitation of the ground state to the n = 2 ates ($2^3S$, $2^1S$, $2^3P$ and $2^1P$) and for excitation and de-excita-on processes involving only the n = 2 levels are presented and ompared with experimental evidence on total metastable pro-uction, on angular distributions of excitation cross sections to e n = 2 levels and on processes involving only the n = 2 states. he percentage polarization of light emitted by electron impact xcitation to the $2^3P$ and $2^1P$ states is computed and compared ith experiment. The calculations indicate the importance of esonances in near threshold excitation and de-excitation rocesses in He. An attempt has been made to understand the esonant structure by considering both the energy dependence f the eigenphases of the many-channel S matrix produced by olving the close coupling equations and the energy dependence f eigenvalues of the related time delay matrix.

1264. Butterfield, M. A., **OCR standards today,** Chapter 37 in *Optical Character Recognition and the Years Ahead,* pp. 318-335 (Business Press, Elmhurst, Ill., July 1969).

Key words: Information processing standards; ISO DR966 OCR character sets National Bureau of Standards; OCR; OCR-A character set; OCR-B character set; OCR character sets; OCR forms; OCR paper; optical character recognition; USASI X3.1.

Standards are agreed upon solutions to recurring problems. Character reading devices contain the five basic components for Paper Handling, Scanner Unit, Recognition Unit, Control Unit, and Output Unit. The requirements of paper handling and canning define the mechanical properties and optical properties equired in OCR paper and the reflective or non-reflective inks used to produce OCR forms.

Forms used in OCR systems are categorized as Journal Tapes, Documents or Pages. Character sets have been tentatively categorized by the USASI X3.1 Committee into four groups of zero, one, two, or three dimension properties. Typical OCR character sets in use include among others the Perry Publishing Co., Farrington 12L/12F, IBM 1401, IBM 1428, NCR NOF, OCR-B, and OCR-A Character Sets.

Current OCR standards work programs at the National Bureau of Standards are described along with reasons therefor. Organizations active in USA national and international ADP standards efforts are described.

1265. Cahill, K. E., **Regularization of the P representation,** *Phys. Rev.* **180,** No. 5, 1244-1255 (Apr. 25, 1969).

Key words: Density operator; electromagnetic field; P representation.

A representation is introduced for the density operator of the electromagnetic field that is suitable for all density operators and that reduces to the coherent-state P representation when the latter exists. It expresses the density operator $\rho$ as the sum of four terms, each of which is a two-dimensional weighted integral over outer products of coherent states. The first integral has the form of the P representation, i.e., the outer products are project operators. The absence of singularities in this term is achieved by the presence of the three supplementary integrals which vanish when the density operator possesses the P representation. In general, for stationary density operators only the first two terms of the regularized P representation are necessary.

A simple prescription is given for obtaining the four weight functions of this representation from the function $\langle \alpha|\rho|\alpha \rangle$, where $|\alpha\rangle$ is a coherent state and $\rho$ the density operator. According to this prescription, the P representation does not exist and one or more of the supplementary, regularizing terms is necessary when the function $\langle \alpha|\rho|\alpha \rangle$ contains a term that decreases more rapidly than exp $(-|\alpha|^2)$ as $|\alpha| \rightarrow \infty$. The regularized P representation affords non-singular integral expressions for all density operators and for most expectation values, including, when they are finite, those of the normally ordered products of the creation and annihilation operators $\alpha$ and $\alpha^+$. The construction and use of this representation is illustrated with the aid of simple examples in which the density operator does not possess the P representation.

11266. Carpenter, B. S., Cheek, C. H., **Trace determination of uranium in biological material by fission track counting,** *Anal. Chem.* **42,** No. 1, 121-123 (Jan. 1970).

Key words: Activation analysis; biological material; fission track; microanalysis; nuclear track; uranium.

The nuclear track technique for determining micro quantities of uranium in material, which consists of counting fission tracks produced in solid-state detectors as a result of neutron irradiation, is employed to determine trace quantities of uranium in such biological materials as mammalian blood and plasma and oak leaves. Dry-ashed samples of the material are dissolved in dilute acid and made up to standard volumes. Aliquots of these solutions are placed on Lexan polycarbonate detectors, evaporated to dryness, and enclosed in polyethylene bags. After irradiation in a thermal neutron flux, the bag is removed and the Lexan detectors are etched in a sodium hydroxide solution. The amount of uranium present in the biological matrices is determined by counting the etched fission tracks with an optical microscope and comparing the results with those obtained for simultaneously irradiated reference standards containing known amounts of uranium. Average results obtained from thermal neutron irradiations for the blood and plasma samples were 86.1 ppb and 60.5 ppb, respectively, while the values for oak leaves ranged from 1.62 to 15.2 ppm.

11267. Carroll, J. J., Melmed, A. J., **Ellipsometry-LEED study of the adsorption of oxygen on (011) tungsten,** *Surface Sci.* **16,** 251-264 (Aug. 1969).

Key words: Ellipsometry; low-energy-electron-diffraction; optical constants; oxidation of tungsten.

The direct combination of ellipsometry and low-energy-diffraction (LEED) techniques has been extended to a study of room temperature oxygen adsorption on (011) tungsten. It is shown that, by use of a special continuous data-taking method, ellipsometry is easily capable of detecting small fractions of a monolayer of adsorbed oxygen on this metal crystal face. From the partial correlation of LEED and ellipsometry data, average sticking probability for oxygen adsorption in the first 1/2 monolayer of atoms is deduced to be 0.2 or 0.4, depending on the choice of adsorption model.

The experimental ellipsometry results are not understandable in detail in terms of existing ellipsometry theory. Consequently, and in view of the LEED results, it is tentatively concluded that the present results support a previously published complicated adsorption model involving oxygen atom-tungsten atom rearrangements.

**11268.** Champion, C. E., Marinenko, G., **Errors in coulometric chloride titrations due to photodecomposition of silver chloride,** *Anal. Chem.* **41,** No. 1, 205-207 (Jan. 1969).

Key words: Coulometric titration; high accuracy analysis; high precision analysis; photodecomposition; silver chloride.

Photodecomposition of silver chloride is a significant source of error in high accuracy argentimetric coulometry. A potentiometric method is described for the determination of the rate of photodecomposition under the conditions of a specific experiment. In a typical analysis, an initial rate of 0.5 $\mu$eq/hr was found which introduced an error of 0.02 percent in the coulometric analysis of a 2-meq sample during a titration period of one hour. A cubic equation, fitted to the rate data, was found to provide corrections for the photodecomposition effect with an accuracy of about 0.005 percent. However, to obtain an accuracy of the order of 0.001 percent it is necessary to exclude light from the coulometric titration cell.

**11269.** Colwell, J. H., **Molecular reorientation and nuclear spin conversion in the solid deuteromethanes at low temperature,** *J. Chem. Phys.* **51,** No. 9, 3820-3832 (Nov. 1, 1969).

Key words: $CD_4$; $CHD_3$; $CH_3D$; $CH_2D_2$; heat capacity; heat capacity anomaly; residual entropy; zero-point entropy.

The heat capacities of the solid deuteromethanes have been measured down to 0.3 K, tracing out the low temperature heat capacity anomalies which had been detected in the earlier work of Colwell, Gill, and Morrison. The anomalies in $CH_3D$ and $CHD_3$ have maxima at 0.43 and 0.48 K respectively, but the $CH_2D_2$ heat capacity is still increasing with decreasing temperature at 0.3 K. A small anomaly was found in $CD_4$ but this is ascribed to chemical and isotopic impurities present in the sample.

The observed anomalies are attributed to the removal of the orientational degeneracies of the molecules on the lattice sites which give rise to the well known residual entropies of Rln4 in $CH_3D$ and $CHD_3$ and Rln6 in $CH_2D_2$. Nuclear spin conversion also occurs in $CH_3D$. This is substantiated by the measured entropy change of $\Delta S = 1.614R$ over the range 0.3 to 4 K which exceeds the maximum value of Rln4 (1.386R) for molecular reorientation occurring separately. The occurrence of conversion was also indicated by a slow process characterized by a relaxation time ranging from 75 to 35 seconds in going from 0.3 to 4 K. There was no indication of conversion occurring in either $CH_2D_2$ or $CHD_3$.

The heat capacity anomalies are of the Schottky form and the results have been analysed on the basis that the energy levels available to the molecules are independent of the extent of order in the system. Precise values of the energy level splittings are obtained for $CH_3D$ and $CHD_3$, but there is some ambiguity as to which symmetry species the rotational states in $CH_3D$ belong. Poor agreement between the calculated heat capacity and the observed anomaly in $CH_2D_2$ is taken as an indication that there may be cooperative effects occurring in this transition.

**11270.** Colwell, J. H., **The performance of a mechanical heat switch at low temperatures,** *Rev. Sci. Instr.* **40,** No. 9, 1182-1186 (Sept. 1969).

Key words: Low temperature; low temperature calorimetry; mechanical heat switch; pressed contacts; thermal conductance of contacts; $^3$He cryostat.

A mechanical heat switch used in calorimetry experiments down to 0.3 K is described and its performance analyzed in sufficient detail to be useful for design purposes. The thermal conductance of the indium-copper switch contacts was determined as a function of applied force and temperature over the range 0.3 to 2 K. These results are compared with other conductance measurements to evaluate choices of materials for heat switch contacts.

**11271.** Colwell, J. H., Mangum, B. W., Utton, D. B., **The low temperature magnetic properties of some hexagonal rare-earth trihalides,** *Phys. Rev.* **181,** No. 2, 842-854 (May 10, 1969).

Key words: Heat capacity; linear chain models; low temperature; magnetic properties; magnetic susceptibility; nuclear quadrupole resonance; rare-earth trihalides; spontaneous magnetization.

We have made measurements of the low temperature heat capacity, magnetic susceptibility, and chlorine nuclear quadrupole resonance (NQR) of $CeCl_3$, $PrCl_3$, $NdCl_3$, $SmCl_3$ and $CeBr_3$. Some measurements have been made on $PrBr_3$ and $NdBr_3$. The experimental results can be closely correlated with antiferromagnetic linear chain models. The NQR shows that long-range order occurs in $PrCl_3$ at 0.428 K. In $NdCl_3$ the NQR line disappeared at 0.50 K and the resonances produced by an internal field appeared at 0.17 K. In $CeCl_3$ the NQR resonance disappeared at 0.110 K. In $CeCl_3$ the NQR resonance disappeared at 0.110 K and no lines were found above 0.054 K. In $SmCl_3$ the NQR line disappeared at 0.21 K and no resonance was observed above 0.1 K. In $PrCl_3$ and $NdCl_3$ we have measured the internal field, which is proportional to the sublattice magnetization, at the chlorine nucleus below their Néel temperatures and have determined the magnitude and the direction of the internal field at the chlorine nucleus relative to the principal axes of the electric field gradient.

**11272.** Cook, A. R., Matarrese, L. M., **Zero-field EPR of $Fe^{3+}$ i quartz,** *J. Chem. Phys.* **50,** No. 6, 2361-2364 (Mar. 15, 1969)

Key words: Amethyst; ferric ion; iron-doped quartz synthetic brown quartz; zero-field EPR.

The zero-field EPR transition frequencies of $Fe^{3+}$ in syntheti brown quartz (SBQ) and natural amethyst (NA) have been measured directly. The values obtained, 7113.2 ± 0.2 and 8812.5 ± 0.2 MHz for SBQ, and 24157.5 ± 0.5 and 35365 ± 2 MHz fo NA, are in excellent agreement with those calculated from th spin Hamiltonians derived from ordinary high-field EPR spectroscopy.

**11273.** Cooper, M. J., Vicentini-Missoni, M., Joseph, R. I, **Linear parameterization of the equation of state near the critica point,** *Phys. Rev. Letters* **23,** No. 2, 70-73 (July 14, 1969).

Key words: Critical point; equation of state; scaling laws Schofield parameterization.

A linear parameterization of the equation of state near th critical point proposed by Schofield is tested. We find the available experimental data in the critical regions of a number of magnets ($CrBr_3$, Ni, Gd) and fluids ($Co_2$, Xe, $He^4$) is *not* generall consistent with an assumption of linearity. Agreement with suc a linear form can be obtained only by locating the critic isochore asymptotically close to the coexistence line.

**11274.** Coriell, S. R., Hardy, S. C., **Morphology of unstable ic cylinders,** *J. Appl. Phys.* **40,** No. 4, 1652-1655 (Mar. 1969).

Key words: Crystal growth; cylinder; ice; morphologic stability; morphology; water.

ne wavelengths of sinusoidal perturbations in the shape of ice
ders growing in supercooled water have been measured as
nction of the experimental variables, primarily bath super-
ing. The experimental results are in good agreement with
ry.

5. Coxon, B., **Studies of $^{15}$N-labeled aminosugars. Synthesis
d spectroscopy of derivatives of 6-amino-6-deoxy-D-glucose-6-**
, *Carbohydrate Res.* **11,** 153-155 (1969).

Key words: Mass spectroscopy; N.M.R. spectroscopy; 6-
amino-6-deoxy-D-glucose-$^{15}$N; $^{15}$N-labeled aminosugars.

erivatives of 6-amino-6-deoxy-D-glucose-$^{15}$N (or-$^{14}$N) have
synthesized by reaction of 1,2:3,5-di-*O*-isopropylidene-6-
lylsulfonyl-α-D-glucofuranose or 6-deoxy-6-iodo-1,2:3,5-di-
opropylidene-α-D-glucofuranose with potassium phthali-
-$^{15}$N (or-$^{14}$N) in *N,N*-dimethylformamide or hex-
thylphosphoramide. The amino sugar derivatives have been
ied by nuclear magnetic resonance and mass spectroscopy.

6. Crawford, B. H., Nimeroff, I., **Radiation sources and their
wer supplies,** Chapter in *Techniques of Photostimulation in
ology,* (North-Holland Publ. Co., Amsterdam, Holland) pp.
-48 (1968).

Key words: Photostimulation; power supplies; radiation.

7. Crawford, M. L., **A new RF-DC substitution calorimeter
th automatically controlled reference power,** *IEEE Trans.
str. Meas.* **IM-17,** No. 4, 378-384 (Dec. 1968).

Key words: Coaxial dry-load calorimeter; feed-back con-
trol; radio-frequency power.

new dual-dry-load calorimeter, incorporating automatically
rolled reference dc input power, has been developed at the
onal Bureau of Standards. The calorimeter will be used as a
rence standard at frequencies up to 4.0 GHz in the power
e, 10 mW to 1 W. The maximum measurement uncertainty
26 percent at frequencies below 1 GHz and 0.35 percent at
uencies above 1 GHz. The time required for the measure-
t system to reach equilibrium is less than two minutes. Con-
ction details and design of the calorimetric and feedback con-
system are given along with an error analysis and results of
rcomparisons with other standards.

78. Crissman, J. M., **Mechanical relaxation in polypropylene
a function of polymorphism and degree of lamellar orienta-
on,** *J. Poly. Sci.* **7,** Part A2, 389-404 (1969).

Key words: Isotactic polypropylene; mechanical relaxation;
oriented lamella; torsion pendulum; α-modification; β-
modification.

echanical relaxation data as a function of temperature (≃
) have been obtained for several samples of isotactic
propylene crystallized from the melt, which exhibit both α-
β-forms as well as varying degrees of lamella orientation.
samples ranged in morphology from an unoriented sample
wing only the α-form to one highly oriented having approxi-
ely 90 percent the β-form. Results for the logarithmic decre-
nt (Δ) and loss modulus (G″) indicate that the low temperature
−75 °C) and glass temperature (≃ 0 °C) relaxations show lit-
or no sensitivity to orientation in the α-form, but that the in-
sity of the two processes is different in the α-form than in the
orm for samples of nearly equal overall percent crystallinity.
oth Δ and G″, the low temperature peak decreased and the
s-temperature peak increased in intensity as the fraction of
orm crystallinity present increased. Data for the high-tem-
ature relaxation (≃ 80 °C) indicate a dependence upon orien-
on and/or crystal form in addition to a dependence upon per-
t crystallinity.

**11279.** Cushen, W. E., **Systems analysis activities at the Technical Analysis Division of the National Bureau of Standards,** *C-E Newsletter* **4,** No. 3, 4-5 (June 1969).

Key words: Cost-effectiveness; systems analysis; Technical Analysis Division.

A general summary of the work of the Technical Analysis Division of the National Bureau of Standards is presented, with special emphasis on its studies in cost-effectiveness analysis. One of the novel studies now being initiated is the cost-effectiveness analysis of systems analysis studies; 12 kinds of needs in government are listed.

**11280.** Daney, D. E., Ludtke, P. E., Sindt, C. F., **Slush hydrogen pumping characteristics using a centrifugal-type pump,** (Proc. 1968 Cryogenic Engineering Conf., Case Western Reserve Univ., Cleveland, Ohio, Aug. 19-21, 1968), Chapter in *Advances in Cryogenic Engineering* **14,** Paper J-2, 438-445 (Plenum Press Inc., New York, N.Y., 1969).

Key words: Cavitation; centrifugal pumps; cryogenic pump; liquid-solid hydrogen mixtures; slush hydrogen.

The pumping characteristics of liquid-solid mixtures of parahydrogen (slush hydrogen) were investigated using a centrifugal type liquid hydrogen pump with a design specific speed of approximately 2200. Performance tests from 8,000 to 19,000 rpm and cavitation tests at 11,000 and 14,000 rpm were made. The slush solid fraction varied from 0.19 to 0.55. As predicted by theory, the developed head for liquid and slush hydrogen are the same when the difference in density is considered. The pump efficiency, cavitation constant and NPSH requirements are also the same for slush hydrogen and triple-point liquid. After 34 minutes running time with slush hydrogen out of a total running time of 79 minutes, the pump components showed no wear over that expected from operation in liquid.

**11281.** Davis H. A., Jr., Hastings, J. R., Waxman, M., **An improved tool for refinishing the conical ends of high pressure tubing,** *Rev. Sci. Instr.* **40,** No. 9, 1238 (Sept. 1969).

Key words: Coning tool; high-pressure tubing; pressure seal.

A simple tool has been developed for refinishing the conical ends of high-pressure tubing in order to obtain a satisfactory seal in a coned-and-threaded connection. The tool uses the threaded portion of the tubing as the reference for alignment and can be used to refinish tubing that has a bend very close to the end of the tubing.

**11282.** Dean, J. W., Brennan, J. A., Mann, D. B., **Cryogenic flow research facility of the National Bureau of Standards,** (Proc. 1968 Cryogenic Engineering Conf., Case Western Reserve Univ., Cleveland, Ohio, Aug. 19-21, 1968), Chapter in *Advances in Cryogenic Engineering* **14,** Paper H-1, 299-305 (Plenum Press Inc., New York, N.Y., 1969).

Key words: Cryogenic fluid metering; cryogenics; flow loop, cryogenic.

The Cryogenics Division of the NBS Institute for Basic Standards is currently involved in an extensive cryogenic fluid metering program. The objectives of this program are to study cryogenic fluid measuring practices, to develop recommended practices for the most effective transfer of cryogenic fluids of interest in commerce, and to allow testing of new concepts in measurement.

This paper describes the experimental facility built to implement this program. The facility consists of a cryogenic flow loop with a dynamic gravimetric mass flow calibration capability. A pump delivers from .00126 to .0126 m$^3$/s (20 to 200 GPM) of nitrogen or argon at pressures up to 1.9 MN/m$^2$ (275 psia). 15 kw of refrigeration is available at 63 K (113 R) to remove the pump and heat leak energy and thus controls the temperature environment in the test section. An analysis of the system errors is presented to provide an understanding of the system operation.

**11283.** Dehl, R. E., Hoeve, C. A. J., **Broadline NMR study of $H_2O$ and $D_2O$ in collagen fibers,** *J. Chem. Phys.* **50,** No. 8, 3245-3251 (1969).

Key words: Anisotropic molecular motion; broadline NMR; $D_2O$ in collagen; $H_2O$ in collagen; proton exchange; quadrupole splitting.

The deuterium NMR spectra of $D_2O$ absorbed in parallel collagen fibers have been recorded for samples containing four different percentages of $D_2O$. In all cases, the spectra consisted of a pair of lines, the separation of which is given by $K(3\cos^2\Theta-1)$, where K is small compared to the rigid-lattice value and decreases with increasing moisture content of the fibers, and $\Theta$ is the angle between the fiber axis and the magnetic field. The splitting is ascribed to quadrupole perturbation of the Zeeman levels of deuterium, caused by slightly anisotropic but rapid reorientation of $D_2O$ molecules in the fiber lattice. Contrary to the interpretation by others, we have concluded from a comparison of the spectra of $D_2O$ and $H_2O$ in collagen (1) that the center line in the $H_2O$ spectra is not due to water, and (2) that line broadening in the $H_2O$ spectra, both at high temperatures and in the presence of added salts, is due to proton exchange between the water molecules. Molecular motion causes both $H_2O$ and $D_2O$ splittings to be reduced to approximately the same fraction of their respective rigid-lattice splittings.

**11284.** DeLancey, G. B., **Analysis of multicomponent diaphragm cell data,** *J. Phys. Chem.* **73,** No. 5, 1591-1593 (May 1969).

Key words: Coefficients; diaphragm cell; matrix logarithm; multicomponent diffusion.

An analytical technique is presented for the evaluation of multicomponent diffusion coefficients from standard diaphragm cell data. Unlike computational procedures now in use, (i) no experimental or mathematical restrictions are imposed, (ii) the number of chemical species in the experiment does not complicate the calculations, and (iii) the diffusion coefficients are explicitly related to experimentally measured quantities. The method employes the generalization of the scalar logarithm to matrix arguments.

**11285.** DeRis, J. N., **Spread of a laminar diffusion flame,** *Proc. Conf. Twelfth Symp. (International) on Combustion, Poitiers, France, July 17, 1968,* pp. 241-252 (Combustion Institute, Pittsburgh, Pa., 1969).

Key words: Combustion; conduction; diffusion flames; flame spread; heat transfer; integral equations; mass transfer; radiation; reaction kinetics; thermal properties.

This work considers the problem of a gas-phase laminar diffusion flame spreading against the wind over a solid or liquid fuel bed. Both a thin sheet and a semi-infinite fuel bed are considered. The burning process is described as follows. The hot flame heats the unburnt fuel bed, which subsequently vaporizes. The resulting fuel vapor reacts with the oxygen supplied by the induced air; thus producing the heat which maintains the flame spreading process.

A simplified model is formulated and subjected to mathematical analysis. This model treats the combustion as a diffusion flame for which the reaction kinetics can be ignored. The model includes the effects of gas-phase chemical combustion, gas-phase conductive heat transfer, radiation, mass transfer, fuel vaporization, and fuel bed thermal properties.

The calculated flame spread formulas are consistent wit available experimental data. These results reveal much of th physics involved in a spreading flame. For instance, the reactio chemistry affects the flame speed only through the adiabati stoichiometric flame temperature. While most of the fuel be thermal properties are very important to the flame spread, th parallel fuel bed conductivity does not significantly affect th flame speed.

**11286.** Deslattes, R. D., Paretzkin, B., **A small set of referen crystals for double-crystal topography,** *J. Appl. Cryst.* **1,** Part 176-178 (Sept. 1968).

Key words: Crystal perfection; silicon; topography.

A set of six reference crystals of silicon makes possible doub crystal topography in the grating space range of 1-2 Å with C $K\alpha_1$ radiation.

**11287.** deWit, R., **Differential geometry of the nonlinear co tinuum theory of dislocation,** (Proc. IUTAM Conf. Stuttga Germany, Aug. 28-Sept. 2, 1967), Chapter in *Mechanics Generalized Continua*, pp. 251-261 (Springer-Verlag, Berli Germany, 1968).

Key words: Affine connection; continuum; defect; deform tion; dislocation; nonlinear; non-Riemannian geometry; to sion.

The differential geometric aspects of the limited nonlinear co tinuum theory of crystal dislocations are developed in terms a non-Riemannian geometry with vanishing Riemann-Christof curvature. The emphasis is on a general notation and a covaria formulation of the theory. Comparisons are made with the wor of Kröner and Eringen. The drawback of nondistant paralleli in passing to the general theory with nonvanishing curvature discussed.

**11288.** Dibeler, V. H., Walker, J. A., **Mass spectrometric study photoionization. XIV. Nitrogen trifluoride and trifluoramine ide,** *Inorg. Chem.* **8,** 1728-1733 (1969).

Key words: Bond dissociation energies; heats of formati ionization energies; mass spectra; $NF_3$; $ONF_3$; vacuum traviolet.

Photoionization yield curves for the $NF_3^+$, $NF_2^+$, and N ions of nitrogen trifluoride and the $ONF_3^+$, $ONF_2^+$, and N ions of trifluoramine oxide were obtained from threshold to Å. Ionization energies were used to calculate heats of format of ions, ionization energies of radicals, and bond dissociat energies. The high precision of the photoionization measu ments were not fully utilized because of uncertainties in, or l of, supporting thermal and spectral data. The following bond sociation energies (in eV) were derived: $D(NF_2\text{-}F) = 2.$ $D(NF\text{-}F) = 3.6$, and $D(NF) = 2.3$. The heat of formati $\Delta Hf_0^\circ(ONF_3) = -2.87$ eV ($-66$ kcal mol$^{-1}$) was derived fr ionization threshold data and used to estimate $D(O\text{-}NF_3) =$ eV, $D(ONF_2\text{-}F) = 1.9$ eV, and related thermodynamic pro ties.

**11289.** Dickens, B., Brown, W. E., **The crystal structures $CaNa_2(CO_3)_2 \cdot 5H_2O$, synthetic gaylussite and $CaNa_2(CO$ $2H_2O$, synthetic pirrsonite,** *Inorg. Chem.* **8,** No. 10, 2 2103 (Oct. 1969).

Key words: Carbonates; crystal structure; gayluss hydrated carbonates; hydrates; pirrsonite.

The crystal structure of gaylussite has been determined f single-crystal x-ray diffraction data. The unit cell is $a = 14.36$ .004, $b = 7.781 \pm .002$, $c = 11.209 \pm .004$A, $\beta = 127.84 \pm$ and the space group is C2/c. $R_w = (\Sigma(w\|F_o|-|F_c\|)^2)/\Sigma(w|F_o|$ 0.043. The hydrogen atoms have been located. Two $CO_3$ an re coordinated to a Ca ion and form a dihedral angle of 134.3°. ach $CO_3$ group is coordinated to four Na ions and four water olecules, but to only one Ca ion. Each Na is coordinated to ur $CO_3$ groups and two water molecules. Two water molecules rm hydrogen bonds to neighboring $CO_3$, anions. The remaining ater forms hydrogen bonds with the oxygens of two other ater molecules.

The crystal structure of pirrsonite has also been determined om single-crystal x-ray diffraction data. The unit cell is $a$ = 1.340 ± .004, $b$ = 20.096 ± .005, $c$ = 6.034 ± .002A and the pace group is Fdd2. $R_w = 0.029$. The hydrogen atoms have been cated. As in gaylussite, two $CO_3$ anions are coordinated to a a ion but with a dihedral angle of 95.5°. In contrast to gayssite, the $CO_3$ anions are also coordinated to a second Ca ion, well as to four Na ions and two water molecules. Each Na ion coordinated to four $CO_3$ anions and loosely to two water olecules. The water molecules complete the coordination of Ca ons and form hydrogen bonds with neighboring $CO_3$ anions.

1290. Dickson, R. W., Wachtman, J. B., Jr., Copley, S. M., **Elastic constants of single crystal $Ni_3Al$ from 10 to 850 °C,** *J. Appl. Phys.* **40,** No. 5, 2276-2279 (Apr. 1969).

Key words: Aluminum; elastic constants; elastic moduli; nickel; single crystals; superalloy.

The elastic constants of single-crystal $Ni_3Al$ were determined 0 to 850 °C by a resonance technique. The values of the comliance and their standard errors at 25 °C are $s_{11} = 0.927 \pm 0.015$, $= 0.825 \pm 0.027$ and $s_{12} = -0.319 \pm 0.050$ in units of $10^{-11}$ $^2$/N.

1291. DiMarzio, E. A., Guttman, C. M., **Separation by flow,** *J. Polymer Sci. Polymer Letters* **7,** 267-272 (1969).

Key words: Chromatography; gel permeation chromatography; polymer fractionation.

It is proposed that the separation in Gel Permeation Chroatography is due in part to the fact that polymer molecules of ifferent volumes entertaining Brownian motion flow down apillary tubes with different mean velocities. The velocity of the olymer, $v_p$, for each position in the tube is found to be a linear unction of the fluid's velocity at the polymer's center of mass. he average velocity of the polymer is then the average of $v_p$ ver those positions in the tube available to the polymer's center f mass. If one assumes a model in which a column is viewed as bundle of capillary tubes then agreement with experiment is obained. It is suggested fine capillary tubes or a bed of impermeale beads could be used to fractionate polymers.

1292. Dodd, J. N., Enemark, E., Gallagher, A., **Quenching of cesium resonance radiation by helium,** *J. Chem. Phys.* **50,** No. 11, 4838-4842 (June 1, 1969).

Key words: Cesium quenching; lifetimes.

Using the phase-shift technique to measure excited state ifetimes, upper limits of $1.5 \times 10^{-14}$ cm³/sec and $3 \times 10^{-14}$ m³/sec have been established for the $Cs(6\ ^2P_{1/2\ or\ 3/2}) + He \rightarrow$ $s(6\ ^2S_{1/2}) + He$ quenching rate constants at 350 and 820 K. (In "cross section" units these are equivalent to $10^{-19}$ cm² upper limits.) The natural lifetimes were measured to be $30.8 \pm 1.5 \times 10^{-9}$ sec and $35.2 \pm 1.5 \times 10^{-9}$ sec for the Cs $6\ ^2P_{3/2}$ and $6\ ^2P_{1/2}$ states.

11293. Domen, S. R., **Heat loss compensated calorimeter,** *Nature* **222,** No. 5198, 1061 (June 14, 1969).

Key words: Absorbed dose; calorimeter; heat loss compensation; heat flow theorem.

A new calorimetric design and measuring technique are proposed for reducing uncertainties caused by temperature gradients. A theoretical analysis revealed a mathematical theorem concerning heat transfer among the calorimetric elements.

11294. Donovan, R. J., Husain, D., Bass, A. M., Braun, W., Davis, D. D., **Kinetic spectroscopic studies of $Cl(3p^5\ ^2P_{3/2,\ 1/2})$ in the vacuum ultraviolet,** *J. Chem. Phys.* **50,** No. 9, 4115-4116 (May 1, 1969).

Key words: Atoms; chlorine; deactivation; kinetic; relaxation; vacuum ultraviolet.

Collisionally induced spin orbit relaxation of $CL(3^2P_{1/2})$ to $Cl(3^2P_{3/2})$ by various species M at room temperature have been measured and the results are summarized.

11295. Drechsel, D., Maximon, L. C., Warner, R. E., **Noncoplanar p-p bremsstrahlung calculations at 48 and 30 MeV,** *Phys. Rev.* **181,** No. 4, 1720-1722 (May 20, 1969).

Key words: Differential cross section; noncoplanar proton bremsstrahlung; off-the-energy-shell behavior; potential model calculation; proton-proton bremsstrahlung.

Cross sections for coplanar and noncoplanar proton-proton bremsstrahlung were calculated at 48 and 30 MeV, using the Hamada-Johnston potential. The coplanar results agree with those of Signell and Marker. The University of Manitoba p-p bremsstrahlung data were reanalyzed and new coplanar cross sections were extracted.

11296. Duerst, R. W., Kokoszka, G. F., **Hyperfine fields in dimeric metal ion complexes,** *J. Chem. Phys.* **51,** No. 4, 1673-1674 (Aug. 15, 1969).

Key words: Antisymmetrical exchange; copper(II)-nickel(II) pairs; dimeric complexes; e.p.r.; exchange-coupled metal ions; hyperfine fields; super-transferred hyperfine fields.

The electron paramagnetic resonance of dichlorobis(pyridine-N-oxide)copper(II) doped with metal ions in their plus two oxidation state has been observed at 77 K. The host lattice consists of complexes containing pairs of exchange-coupled copper(II) ions. The dopant ions enter the lattice substitutionally.

The A values observed in a plane perpendicular to the crystallographic c axis for Cu(II)-Ni(II) pairs, for Cu(II)-Pd(II) pairs (in which the Pd(II) ion's ground state is diamagnetic), and for Cu(II)-M(II) pairs (M may be Zn, Cd, or Pb) were 0.0102 cm⁻¹, 0.0128 cm⁻¹, and 0.0118 cm⁻¹ respectively.

An elementary model accounts for the variations in the A values depending on the dopant metal ion. For Cu(II)-Ni(II) pairs, a small angular deviation of the principal z axis of the g tensor was also observed. An explanation of this effect is suggested in terms of the Dzyaloshinsky-Moriya antisymmetrical exchange term $[d \cdot (S_1 \times S_2)]$.

11297. Durst, R. A., **Determination of fluoride by analate additions potentiometry,** *Mikrochim. Acta,* pp. 611-614 (1969).

Key words: Analate additions potentiometry; fluoride; fluoride ion selective electrode; potentiometry.

A novel direct potentiometric technique called analate additions potentiometry has been applied to the determination of fluoride using a fluoride ion selective indicator electrode. As expected, the analytical results are comparable to those obtained by the standard additions technique. An error of less than 1 part in 1000 and a precision of about 0.5 percent was achieved. The technique should be most useful in the determination of small sample volumes which cannot be done by the standard additions method without prior dilution.

11298. Edmonds, D. K., Hork, J., **Cavitation in liquid cryogens,** (Proc. 1968 Cryogenic Engineering Conf., Case Western

Reserve Univ., Cleveland, Ohio, Aug. 19-21, 1968), Chapter in *Advances in Cryogenic Engineering* **14,** Paper G-4, 274-282 (Plenum Press Inc., New York, N.Y., 1969).

Key words: Cavitation; cavitation inception; cryogenic; cryogenic cavitation; developed cavitation; thermodynamic cavitation.

Cavitation characteristics of liquid hydrogen and liquid nitrogen flowing in a transparent plastic venturi have been determined and conventional cavitation inception parameter curves are given. Representative thermodynamic data, consisting of pressure and temperature measurements within fully-developed cavities, are also given; measured temperatures and pressures within the cavities were generally not in thermodynamic equilibrium. Existing theory was used to obtain equations which correlate the experimental data for developed cavities in liquid hydrogen or liquid nitrogen. The theory is extended to include the effect of cavity thickness and the experimental data are used to evaluate the results. Some recommendations for future work are given.

**11299.** Ehrlich, M., **Proposed National Bureau of Standards Program for the calibration of instruments used in high-energy electron and x-ray beams,** (Proc. Conf. High-Energy Radiation Therapy Dosimetry, New York, N.Y., June 1967), *Annal. N.Y. Acad. Sci.* **161,** No. 1, 139-145 (July 3, 1969).

Key words: Absorbed dose; calibration; electrons; ferrous-sulfate system; graphite calorimeter; interim program; photons; transfer standard; uniformity checks; ~1 to 50 MeV

The NBS Radiation Physics Division plans to develop services for calibrating suitable measuring instruments in terms of absorbed dose in low-atomic number materials, for use with electrons and photons in the energy range from approximately 1 to 50 MeV. As the standard instrument, NBS plans to use a graphite calorimeter, surrounded by a graphite block. For use in routine calibrations, a stable transfer instrument will be developed which requires less exacting measurements than the calorimeter.

Since the absorbed-dose calibration services based on calorimetry will not be immediately available, an interim program has been initiated for uniformity checks of high-energy electron-beam calibrations. Starting in July 1967, NBS will prepare and mail ferrous-sulfate solutions in sealed radiation-resistant spectrophotometer cells. A minimum of four cells will be supplied to each participant, two of them to be used as controls, and the other two to be exposed by the participant in a polystyrene phantom. Upon their return, NBS will evaluate the dose received by the ferrous-sulfate solutions, using the G-value recommended by the American Association of Physicists in Medicine.

**11300.** Evenson, K. M., **Microwave magnetic-dipole transitions between excited electronic states of CN,** *Phys. Rev.* **178,** No. 1, 1-4 (Feb. 5, 1969).

Key words: CN; double resonance; excited state; magnetic dipole transitions; microwave spectroscopy.

Eleven microwave transitions in the frequency range from 10.5 to 11.5 GHz have been observed between excited electronic states of CN. These correspond to 11 of 13 allowed magnetic dipole transitions, $\Delta F = 0, \pm 1$, in the $K' = 4$ perturbation complex between the three hyperfine levels of the perturbed component of the $\Lambda$ doublet of the $A^2\Pi^{+}_{3/2}(v = 10)$ level and the three hyperfine levels in each of the perturbed and the unperturbed components of the spin doublet of the $B^2\Sigma^+$ $(v = 0)$ level. These transitions and the previously measured 13 electric dipole transitions determine all twelve hyperfine energy levels of this perturbation complex. The experiment is the first microwave measurement of magnetic dipole transitions between excited electronic states of a molecule. CN was produced predominately in the metastable $A^2\Pi$ state by a chemical reaction when methylene chloride was added to a nitrogen afterglow. Resonant microwave pumping from the $\Pi$ state increased the population of the three hyperfine levels of each $\Sigma$ state. The population change was detected by measuring an increase in the intensity of the $B^2\Sigma^+ \rightarrow X^2\Sigma^+$ (0,0) violet band of CN near 3875 Å.

**11301.** Fatiadi, A. J., **Acylation of tetrahydroxy-*p*-benzoquinone,** *J. Chem. Eng. Data* **13,** No. 4, 591-593 (Oct. 1969).

Key words: Acetates; benzenehexol; disproportionation; esters; rhodizonic acid; tetrahydroxyquinone.

Procedures are described for preparation of previously unreported di- and tetraacetates of tetrahydroxyquinone. Chemical proof is presented for disproportionation of tetrahydroxyquinone into benzenehexol (hexahydroxybenzene) and rhodizonic acic in a slightly basic solution. By use of this reaction, a series of acy derivatives of benzenehexol has been prepared; certain esters o tetrahydroxyquinone also disproportionate in a slightly basic medium.

**11302.** Fatiadi, A. J., **Novel iodination of the $\alpha$-methylene group i 1,3-diphenylpropane-1,3-dione and related $\beta$-diketones wit periodic acid,** *Chem. Commun.,* p. 11 (1970).

Key words: Acyclic; iodic acid; iodo derivatives; periodi acid; $\beta$-diketones.

On treatment with iodic acid, 1,3-diphenyl-1,3-propanedion is converted into the 2-iodo derivative in about 50 percent yield When periodic acid is used the diketone can be converted eithe into the 2-iodo or the 2,2-diiodo derivative. Formation of 2-iod derivatives has been observed for other acyclic $\beta$-diketones.

**11303.** Fenstermaker, C. A., McCrackin, F. L., **Errors arisin from surface roughness in ellipsometric measurement of th refractive index of a surface,** *Surface Sci.* **16,** 85-96 (1969).

Key words: Ellipsometry; index of refraction; light reflec tion; optical properties; rough surfaces.

The roughness of a surface is generally neglected when th refractive index of a material is calculated from ellipsomet measurements. Errors produced by neglecting the roughness the surface are evaluated for three models of the topography the surface (square ridges, triangular ridges, and pyramids). range of roughness from 0 to 500 Å and six substrate materia (glass, silicon, chrome, mercury, gold, and silver) are considere Large errors in determination of indices, even for small values roughness (50 Å), were found.

**11304.** Flynn, D. R., O'Hagan, M. E., **Measurements of the the mal conductivity and electrical resistivity of platinum from 1 to 900 °C,** *Engelhard Indust. Tech. Bull.* **8,** No. 4, 117-1 (Mar. 1968).

Key words: Conductivity; electrical conductivity; electric resistivity; heat conductivity; Lorenz function; pla num; reference material; resistivity; standard; therm conductivity.

Measurements have been made of the thermal conductiv and the electrical resistivity of commercial grade platin (99.98% pure) in the temperature range 100 to 900 °C. The me surements have been made with a view to providing accur data on the thermal conductivity of platinum to serve as a ba for establishing platinum as a thermal conductivity stand reference material. Two methods of measuring the thermal c ductivity have been employed, one an electrical method and other a nonelectrical method. In the electrical method, a dir nt passed through a necked-down portion of the specimen ne thermal conductivity was determined in terms of the tem- ure and electrical potential distribution in the necked-down n. The second method was of the absolute guarded longitu- ; heat flow type. The experiment was designed to permit urements by both methods in the same apparatus and on the specimen thereby providing as direct a comparison as ble between the methods. The data given by the two ods agree within experimental error and show the thermal uctivity of platinum to be a smoothly increasing function of erature in the measured range. Additional measurements on les of differing purities are necessary before platinum could opted as a thermal conductivity reference material.

5. Flynn, D. R., Watson, T. W., **Measurement of the thermal nductivity of soils at high temperature,** *Atomic Energy Re- rt SC-CR-69-3059* (Apr. 1969).

Key words: Conductance; conductivity; heat transfer; nuclear safety; soils; temperature; thermal conductance; thermal conductivity.

n apparatus is described which has been designed and built able measurement of the thermal conductance of soils at hot temperatures approaching 1700 °C. The method utilizes l heat flow through a hollow cylinder of soil contained een a central ceramic core and an outer water-cooled metal . Thermal conductivity values are reported for nine natural tificial soils representative of subsoils found on most of the h's surface. For each of these soils, measurements have been pleted on two different specimens under particular but oducible conditions of preparation.

6. Flynn, T. M., Birmingham, B. W., **Cryogenics and na- onal goals,** (Proc. 1968 Cryogenic Engineering Conf., Case estern Reserve Univ., Cleveland, Ohio, Aug. 19-21, 1968). hapter in *Advances in Cryogenic Engineering* **14,** Paper A-1, 12 (Plenum Press Inc., New York, N.Y., 1969).

Key words: Agriculture; compressed gases; conservation; cryogenics; education; health; national goals; space; transportation.

he object is to discuss a segment of the compressed gas in- try, namely the cryogenic industry, and its relation to cted national programs, such as space, health, agriculture, sportation, conservation, and education.

07. Frederick, N. V., **A low loss sliding short of limited travel r precision coaxial transmission lines,** *Proc. IEEE* **56,** No. 12, . 2188 (Dec. 1968).

Key words: Coaxial cavity tuning; coaxial short; precision transmission line; reflection coefficient; sliding short.

precisely adjustable sliding short with high reflection coeffi- nt is described. The reflection coefficient is approximately 6 at 4 GHz. Instructions are given for fabrication. The device specially useful for measuring electrical lengths and for tuning oaxial cavities and for coaxial line bridge work.

08. Frederick, N. V., **A new high-frequency current standard,** *EEE Trans. Instr. Meas.* **IM-17,** No. 4, 285-290 (Dec. 1968).

Key words: Ammeter; electrodynamometer; high frequency current; short-circuited ring; torsion balance.

short-circuited-ring electrodynamic ammeter is described. e short-circuited-ring is supported by a fine quartz fiber and is pended midway between the inner and outer conductors of a xial transmission line. The current on the line is measured by asuring the torque exerted against the ring by the current on coaxial line. A new technique is given for determining the ationship between the torque on the ring and the current on the transmission line and is compared with the technique which has been used in the past. The new method is an application of the resonator action theorem used by A. L. Cullen for calibrating a torque operated microwave wattmeter. The major weakness in the previous evaluations of the torque current relation is discussed. The ammeter is useful for measuring current from one to one hundred amperes over the frequency range 1 MHz to 1 GHz with an uncertainty of the order of 0.5 percent.

11309. Frederikse, H. P. R., Hosler, W. R., Casella, R. C., **Piezoresistive effects in semiconducting strontium titanate,** *Proc. Ninth Intern. Conf. Physics of Semiconductors, Moscow, USSR, July 23-29, 1968,* pp. 1175-1180 (NAUKA, Leningrad, USSR, 1968).

Key words: Piezoresistive effects; semiconductors; strontium titanate.

Piezoresistive effects in doped $SrTiO_3$ measured at 300, 77, and 4 K are interpreted in terms of many-valleyed energy band model [spheroids along $\langle 100 \rangle$ directions]. Low temperature saturation is explained by assuming domain flipping under stress.

11310. Furukawa, G. T., **Automation problems in thermometry and calorimetry,** (Proc. 2nd & 3rd Japanese Calorimetry Conf., Osaka, Japan, Nov. 27-28, 1967). Chapter 1 in *Calorimetry, Thermometry, and Differential Thermal Analysis,* Y. Otsubo, H. Kanbe, and S. Seki, eds., **2,** 1-35 (Kagaku Gijitsu-Sha, Tokyo, Japan, 1969).

Key words: Automatic calorimetry; calorimetry; heat capacity; Mueller bridge; thermometry.

For high-precision low-temperature calorimetry, the techniques used in measurement periods of temperature and of power are discussed separately. The application of electronic preset counters to automatic control of the calorimetric process is proposed. The thermometer resistances are measured by means of an automated Mueller bridge and the measurements are analyzed on a high-speed digital computer to obtain temperature-time observations. The electrical power introduced is automatically determined using a commercially available intergrating digital voltmeter (IDVM) to measure a small fraction of the total calorimeter heater voltage biased by a stable reference voltage. A modification of the IDVM to integrate over the heating interval to obtain the total electrical energy input is described.

11311. Gadzuk, J. W., **Band-structure effects in the field-induced tunneling of electrons from metals,** *Phys. Rev.* **182,** No. 2, 416-426 (June 10, 1969).

Key words: Band structure; density of states; field emission; surface physics; tunneling.

The theory of electron tunneling from metals into vacuum is investigated. Certain ambiguous conclusions reached in previous theoretical treatments are reconsidered. It is found that band structure information is contained in the total energy distribution of field emitted electrons.

The problem of electron tunneling from narrow energy bands with a high density of states, well described in the tight binding approximation, is treated. Expressions for the tunneling matrix element of electrons in tight binding d bands tunneling to free electron states outside the metal are obtained within the field ionization approximation of Oppenheimer.

Calculations are then given for the energy distribution of field emitted electrons coming from a model of a real metal in which the band structure is a superposition of a free s like band and a tight binding d band. This is a reasonable qualitative model for the band structure of a noble metal. The relationship between energy distribution and the band structure is established.

**11312.** Gadzuk, J. W., **Many-body tunneling-theory approach to field emission of electrons from solids,** *Surface Sci.* **15,** 446-482 (1969).

Key words: Electrons in solids; electron tunneling; field emission; many-body theory; surface physics.

The equation of motion and thermodynamic Green's function method for describing tunneling processes in normal and Josephson junctions is here adapted to the problem of field emission of electrons from solids. The formal developments lead to an equation for the emission current in terms of both the Fowler-Nordheim quantities and the spectral weight function of the single particle Green's function in the solid. The formal results are examined in detail for three specific examples.

In the case when the spectral function is that of a free, noninteracting electron gas, the formal results obtained here reduce to the usual Fowler-Nordheim result for the current and the energy distribution.

Expressions are then obtained for the current and energy distribution of field emitted electrons from superconductors. The consequences of these results are discussed.

The last example here is probably the most interesting from the experimental point of view. The emission current characteristics from an electron gas in which collisions between electrons and phonons, electrons, impurities, or imperfections occur are analyzed. The damping of the electron energy eigenstates, which is present in all real metals, results in new current characteristics for energies near the Fermi surface. The derived energy distributions are smeared about the Fermi energy. The degree of smearing is a function of the temperature dependent electron-phonon or electron-electron collision time. It is thus shown how to go backwards from the smeared energy distributions to obtain information pertinent to the electron-phonon interaction and the imaginary part of the bare electron self energy in the phonon field.

**11313.** Garvin, D., **Suggestion: the minireview,** *Phys. Today* **22,** No. 10, 13-15 (Oct. 1969).

Key words: Chemistry; evaluation of data; information retrieval; physics; publication; reference data; review.

It is suggested that the need for substantive reviews and evaluated data can be met, in part, by encouraging research scientists to write short evaluations based on topics that grow out of their own work. The preferred publication medium would be evaluation sections in the journals that normally cover the pertinent field.

**11314.** Gatterer, L. E., **Clock synchronization experiments at VHF utilizing the ATS-1 and ATS-3 transponders,** *Natl. Aeronaut. Space Admin. Report ATS Tech. Summary* (National Aeronautics and Space Administration, Greenbelt, Md., Feb. 16, 1968).

Key words: Atomic standards; ATS-1; clock synchronization; time dissemination; VHF propagation satellite timing.

Experiments are described which repeat demonstrations of the effectiveness of a technique for synchronizing widely separated clocks to better than 10 μsec, and which investigate extensions of this technique. Preliminary results are described. These experiments utilized the VHF transponder on ATS-1.

**11315.** Grenley, D. G., **Study of the effect of certain modified mortars on compressive and flexural strength of masonry,** (Proc. Intern. Conf. Masonry Structural Systems, University of Texas, Austin, Texas, Nov. 30-Dec. 2, 1967), Chapter in *Designing Engineering and Constructing with Masonry Products,* F. B. Johnson, ed., Paper 5, pp. 28-33 (Gulf Publ. Co., Houston, Texas, May 1969).

Key words: Compressive strength of clay masonry; flexur strength of clay masonry; high strength mortars; improve mortars; masonry; modified mortars.

The use of high strength mortars materially improves the fle ural and compressive strength of small masonry assemblage This is found to be true with a variety of brick although there indication that low quality brick will not experience a gre degree of improvement in their structure strength. Brick a mortar strength are shown to be important factors in dete mining structure strength, however these variables alone w not permit a quantitative prediction of structure performanc

**11316.** Grenley, D. G., Cattaneo, L. E., Pfrang, E. O., **Effect edge load on flexural strength of clay masonry systems utilizi improved mortars,** (Proc. Intern. Conf. Masonry Structu Systems, University of Texas, Austin, Texas, Nov. 30-De 2, 1967), Chapter in *Designing Engineering and Constructi with Masonry Products,* F. B. Johnson, ed., Paper 17, pp. 11 128 (Gulf Publ. Co., Houston, Texas, May 1969).

Key words: Compressive interaction in walls; compressi strength of walls; flexural interaction in walls; flexu strength of walls; high bond strength mortars; improv mortars; masonry walls.

This paper proposes a theoretical interaction diagram for t effect of edge load and flexural load on the ultimate strength masonry wall panels. Four experimental systems show go agreement with the theory and suggest a new approach to the tional design of masonry systems. The paper also indicates t substantial improvement in the strengths of masonry syste can be realized by improving the mortars used in their constru tion.

**11317.** Gugeler, A. L., Ballard, D. B., **The aluminum-porcel enamel interface as observed by electron microscopy,** *A Ceramic Soc. Bull.* **48,** No. 9, 842-845 (Sept. 1969).

Key words: Adherence; aluminum; electron microscope; terface; porcelain enamel; spall resistance.

The electron microscope was used in a study of the adhere of porcelain enamel to aluminum. Various combinations of minum alloys and metal pretreatments were studied. Shado plastic surface replicas of the porcelain enamel-aluminum in face were taken from polished and etched cross sections. Th combinations which had poor adherence, as indicated by low sistance to spalling, had a layered structure at the interface. T thin layer was not observed in those specimens which were c sidered to have good adherence. The susceptibility of the laye structure at the interface to corrosive attack appears to hav direct relationship to spall resistance.

**11318.** Halldane, J. F., **Visual responses of travelers in urban vironments,** (Proc. Symp. Man-Machine Systems, Cambric England, Sept. 8-12, 1969), Chapter in *Transport Syste Vehicle Control* **2,** Paper No. 8, 17 pages (1969).

Key words: Environmental design; human factors; in disciplinary study; relative motion; transportation; ur design; visual responses.

The contribution of a psychophysical discipline is discusse relation to the visual problems of urban design and vehicle c trol. In town planning, the visual fields of urban observers h mainly been considered from the aspect of architectural form the designer has had difficulty in communicating those proble in the context of other planning disciplines. While we h developed sophisticated physical techniques of measuring vis stimuli in transportation engineering, we do lack knowledge b in the implications of the response criteria adopted for sens investigations and in the methods of analysing experimental d

The paper contributes to planning and transportation by inducing a psychophysical synthesis as an interdisciplinary ans of posing and solving the visual problems of people mov- within urban environments. A planning philosophy is veloped where the response problems are derived from the havioral goals inherent within the planning program. A ychophysical synthesis is then applied to establish a valid nge of physical stimuli. Those stimuli in turn suggest possible tributions of the environmental systems to achieve the design. hether the responses are to be minimised, maximised, op- aised or negated become the prerogative of the designer ac- rding to the original goals.

**319.** Hanley, H. J. M., Childs, G. E., **Dilute gas viscosities at low temperatures,** *J. Chem. Phys.* **50,** No. 10, 4600-4601 (May 15, 1969).

Key words: Argon; correlation; dilute gas viscosity; kinetic theory; potential functions.

We recently reported that the tabulated and generally accepted scosity coefficients for simple gases could be systematically in ror at high temperatures (>300 K). We have extended our ork to cover viscosity data at low temperatures. We again find ctors indicating possible errors in experimental data (although t as great as before) which reinforce our opinion that the whole bject of dilute gas viscosities needs careful reexamination.

**320.** Hanley, H. J. M., Klein, M., **Selection of the intermolecular potential function, III. From the isotopic thermal diffusion factor,** *J. Chem. Phys.* **50,** No. 11, 4765-4770 (June 1, 1969).

Key words: Fitting of experimental data; isotopic thermal diffusion coefficient; potential function families; sensitivity of coefficient.

A method developed previously to evaluate quantitatively the lationship between intermolecular potential functions and acroscopic properties is extended to the isotopic thermal diffu- on factor. As before, the relationship between function families as been clarified. In particular, an insensitive temperature nge, here about $2 \leqslant T^*_{12,6} \leqslant 4$, was found in which the data do ot permit the selection of a function. The function families stu- ied were the m-6, Kihara, and exp-6. A quantitative evaluation f the sensitivity of the thermal diffusion coefficient to the poten- al function is presented.

**1321.** Hardy, S. C., Coriell, S. R., **Morphological stability of cylindrical ice crystals,** *J. Crystal Growth* **5,** 329-337 (1969).

Key words: Crystal growth; cylinder; ice; morphological stability; surface tension; water.

Small, single crystal ice cylinders have been grown into un- ercooled water. The initially smooth crystals develop sinusoidal erturbations about the circumference and parallel to the axis. he growth rates and wavelengths of these perturbations are in uantitative agreement with the predictions of a Mullins-Sekerka tability analysis. The growth rates of the perturbations along the xis yield a value of .022 J/m$^2$ (22 erg/cm$^2$) for the ice-water sur- ace tension.

**1322.** Hendricks, R. C., Simoneau, R., Smith, R. V., **Heat transfer with a near-critical fluid,** *Natl. Aeronaut. Space Admin. Report TNX 52612* (National Aeronautics and Space Administration, Greenbelt, Maryland, June 16, 1969).

Key words: Choking; critical; fluid flow; heat transfer; oscillations.

The three authors have reviewed the field and added some new material. The intent of the paper is to bring the literature together, to provide information for designers, and to suggest needed research.

**11323.** Herbert, R. L., Tryon, M., Wilson, W. K., **Differential thermal analysis of some papers and carbohydrate materials,** *Tappi* **52,** No. 6, 1183-1188 (June 1969).

Key words: Carbohydrate materials; differential thermal analysis; papers.

A study of the thermal degradation of various types of papers by differential thermal analysis (DTA) showed two distinct endothermic peaks, one at 135-155 °C, indicating loss of sorbed moisture, and the other at 310-365 °C, indicating massive decomposition. When the papers are ranked in order of decreasing temperature of the decomposition endotherm, and in decreasing pH values, a high correlation is indicated. Data on the DTA of several carbohydrate compounds related to cellulose also are presented.

**11324.** Herron, J. T., Huie, R. E., **Rates of reaction of atomic oxygen. II. Some $C_2$ to $C_8$ alkanes,** *J. Phys. Chem.* **73,** No. 10, **chloroalkanes and bromoalkanes,** *J. Phys. Chem.* **75,** No. 5, 1326-1335 (May 1969).

Key words: Atomic oxygen; bromoalkane; chemical kinetics; chloroalkane; mass spectrometry; organic compounds; rate constant.

A method for measuring rate constants for the reactions of atomic oxygen ($^3P$) with organic compounds is described. Rate constants and Arrhenius parameters are reported for the reactions of atomic oxygen with twelve chloroalkanes and bromoalkanes from 336 to 622 K.

**11325.** Herron, J. T., Huie, R. E., **Rates of reaction of atomic oxygen, II. Some $C_2$ to $C_8$ alkanes,** *J. Phys. Chem.* **73,** No. 10, 3327-3337 (Oct. 1969).

Key words: Alkane; atomic oxygen; chemical kinetics; mass spectrometry; organic compounds; rate constant.

Rate constants have been measured for the reactions of atomic oxygen ($O^3P$) with eight straight and branched chain alkanes from 250 to 600 K, and for six other branched chain alkanes at 307 K. The reactions are interpreted on the basis of a hydrogen atom abstraction mechanism, and Arrhenius parameters are derived for abstraction of primary, secondary, and tertiary hydrogen atoms. The activation energies are found to be in the order primary > secondary > tertiary. For abstraction at secondary C – H bonds, the activation energy is observed to decrease with increasing molecular complexity of the alkane.

A method of estimating rate constants is given.

**11326.** Hiza, M. J., Duncan, A. G., **Comments on "Intermolecular forces: Thermal diffusion and diffusion in He-Kr and $H_2$-Kr,"** *Phys. Fluids* **12,** No. 7, 1531-1532 (July 1969).

Key words: Beam scattering data; characteristic energy parameters; deviations from geometric mean diffusion properties; equilibrium properties.

Comments on a paper, "Intermolecular Forces: Thermal Diffusion and Diffusion in He-Kr and $H_2$-Kr" by Annis, Humphreys, and Mason published in "The Physics of Fluids," October 1968.

**11327.** Hiza, M. J., Duncan, A. G., **Equilibrium gas-phase compositions of ethane and ethylene in binary mixtures with helium and neon below 150 K and a correlation for deviations from the geometric mean combining rule,** (Proc. 1968 Cryogenic Engineering Conf., Case Western Reserve Univ., Cleveland, Ohio, Aug. 19-21, 1968), Chapter in *Advances in Cryogenic Engineering* **14,** Paper B-1, 30-40 (Plenum Press Inc., New York, N.Y., 1969).

Key words: Correlation for deviations from geometric mean combining rule; equilibrium gas-phase compositions;

ethane; ethylene; helium; helium-ethane system; helium-ethylene system; liquid-vapor equilibrium; low-temperature phase equilibrium; neon.

Equilibrium gas-phase compositions in the systems helium-ethane and helium-ethylene were measured along six and seven isotherms, respectively, between 90 and 150 K up to 130 atm pressure. Corresponding measurements were made in the systems neon-ethane and neon-ethylene along two isotherms each, but only up to 50 atm pressure. A single-pass flow apparatus was used with continuous anlaysis for ethane or ethylene by means of a hydrogen flame-ionization detector. These data complete a set of nine binary systems containing hydrogen, helium, and neon with light hydrocarbons which are the basis of a correlation relating the deviations from the geometric mean combining rule to the ionization potentials of the component species.

**11328.** Hoer, C. A., Smith, W. L., **A 1-MHz binary inductive voltage divider with ratios of $2^n$ to 1 or 6n dB,** *IEEE Trans. Instr. Meas.* **IM-17,** No. 4, 278-284 (Dec. 1968).

Key words: Attenuator; binary divider; inductive voltage divider; ratio transformer; voltage comparator; voltage divider.

A voltage divider with ratios of $2^n$:1 or 6n dB is obtained by cascading n binary dividers, each having a voltage ratio 2:1. A theoretical analysis results in an expression for the ratio error. Several techniques are given for reducing this error. A voltage comparator is described for eliminating errors due to external loading of the divider. An experimental cascaded binary divider with a total of 42 dB in seven 6 dB steps is described. The attenuation of the divider was measured with a precision waveguide below-cutoff attenuator at 1 MHz. The divider and attenuator values agree within the uncertainty of the attenuator and measuring system at 1 MHz.

**11329.** Hoffman, J. D., Lauritzen, J. I., Jr., Passaglia, E., Ross, G. S., Frolen, L. J., Weeks, J. J., **Kinetics of polymer crystallization from solution and the melt,** *Kolloid-Z. Polymere* **231,** Nos. 1-2, 564-592 (1969).

Key words: Bulk; chain fold; crystallization; fluctuation; growth; heat of melting; homogeneous nucleation; kinetics; lamella thickness; melt; melting point; nucleation; polymer; solution; surface free energy; theory; thermodynamics.

Kinetic nucleation theories of the growth of chain-folded polymer crystals from the melt and dilute solution are reviewed, and attention focussed on the recent treatment of Lauritzen and Passaglia (LP), which includes the effect of fluctuations in the fold period. The LP fold surface is rough, and contains terms resulting from the $\sigma$-type surface of the projecting folds, and the entropy of mixing. The relationship to earlier theories is indicated. The LP theory predicts that the "kinetic" value of the fold surface free energy, $\sigma_{e(k)}$ increases with increasing undercooling. An adjunct theory is given that approximately predicts the temperature dependence of the lateral surface free energy, $\sigma$, as $x=0.01$ in $\sigma=\sigma_1(1+x\cdot\Delta T)$. After review of the input data, expressions of the form $\sigma_{e(k)}=\sigma_{e(1)}[1+y\cdot\Delta T]$ and $\sigma=\sigma_1[1+x\cdot\Delta T]$ are employed to analyse homogeneous nucleation and growth rate data on polyethylene (bulk and dilute solution) to obtain fairly close estimates of y and $\sigma_1$. Melting point data give the approximate value of $\sigma_{e(1)}$. Predictions are then made for single crystals of the initial lamellar thickness $l^*_g$, the melting point $T_m$, and the heat of fusion defect, $\lambda_H$. Good agreement is obtained with $x=0.01$ deg$^{-1}$, $y=0.0135$ deg$^{-1}$, $\sigma_1=13.0$ erg cm$^{-2}$ and $\sigma_{e(1)}=67.5$ erg cm$^{-2}$. The LP theory is capable of predicting the temperature dependence found for $\sigma_{e(k)}$. The nature of the fold surface in single crystals and bulk is discussed in some detail. The roughness of the fold surface associated with $\sigma_{e(k)}$ is calculated to have a rms deviation from the mean of 5.6 Å at the melting point, and about twice this figure at the homogeneous nucleation temperature. These estimates are consistent with the existence of a density defect. It is concluded that the LP form of the kinetic nucleation theory explains the growth rates observed for polyethylene, gives the lamellar thickness, and leads to the thermodynamic properties of the crystal produced by the growth mechanism.

**11330.** Hubbell, J. H., **Gamma-ray cross-section evaluation and compilation,** *Proc. Special Sessions on Gamma-Ray Production and Transport and on Civil Defense Shielding, Winter Meeting of the American Nuclear Society, Nov. 5-9, 1967, Chicago, Ill.,* A. E. Straker, ed., ANS-SD-7, AEC TID-4500 Series, pp. 71-77, 82-100 (Aug. 1969).

Key words: Compilations; energy absorption coefficients; gamma ray coefficients; photon attenuation coefficients; photon cross sections; x-ray attenuation coefficients.

A brief history of compilation activity in the field of photon attenuation coefficients is given. Available experimental attenuation coefficient data are reviewed for Z = 1 to 100 and photon energies 10 eV to 100 GeV with indications given of gaps and uncertainties. Mention is made of recent and in-progress compilations at NBS, LRL (Livermore) and elsewhere, and of the existence of an NSRDS (National Standard Reference Data System) "X-ray attenuation coefficient information center" at the NBS.

**11331.** Hudson, G. E., Allan, D. W., Barnes, J. A., Hall, R. G., Lavanceau, J. D., Winkler, G. M. R., **A coordinate frequency and time system,** *Proc. 23rd Frequency Control Symp., Atlantic City, N.J., May 6-8 1969,* p. 249 (1969).

Key words: Coordinate time; local atomic standards; metric time; national unified atomic standards; proper time; universal coordinated time.

A coordinate frequency and time system, suitable for extension to worldwide coverage, is described in relation to the form evolving in the United States. It consists of a network of component primary and associated stations, at fixed locations and altitudes, and a reference coordinating component at a reference location and altitude. A unified local atomic standard for the system serves as the coordinating component.

The system could be extended internationally, by regarding the national unified standards as components of an international one whose assigned frequency would equal f(Cs).

**11332.** Hudson, G. E., Barnes, J. A., **Clock error statistics as a renewal process,** *Proc. 22nd Frequency Control Annual Symp., Atlantic City, N.J., Apr. 22-24, 1968,* pp. 384-413 (1968).

Key words: Clock errors; dispersion of clock reading; flicker noise; random-walk noise; renewal equation; renewal processes; statistics of clock ensembles; white noise; zero crossings.

A model ensemble specifying the distribution of its clock readings about their average obeys an integral equation of renewal type. Renewal processes ordinarily describe when mechanical or electrical components need to be replaced. In this case, clocks in the ensemble may repeatedly read correctly and "renew" themselves. Solutions of the equation are discussed and are related to other error statistics.

**11333.** Hudson, R. P., **The CMN temperature scale,** *Proc. XI Conf. Low Temperature Physics, St. Andrews, Scotland, Aug. 21-28, 1968,* **I,** 501-504, Paper D1.8 (University of St. Andrews, Scotland, 1968).

Key words: Adiabatic demagnetization; cerous magnesium nitrate; low temperature scales.

A re-examination of adiabatic demagnetization results for ous magnesium nitrate (CMN) shows them to agree with Van ck's theory of dipole-dipole interaction for the region above 1 K. To pursue the examination to lower temperatures, one uires fourth order and higher terms in the 1/T expansion, ich are not yet available. They have therefore been obtained least squares fitting and so provide a polynomial formula for entropy which may be used to calculate the heat capacity. e latter is of interest in comparing magnetic temperature les for CMN obtained by different methods.

**34.** Huget, E. F., Brauer, G. M., Kumpula, J. W., Civjan, S., **A filled cold-curing acrylic resin as a splinting material,** *J. Am. Dent. Assoc.* **79,** 645-648 (Sept. 1969).

Key words: Acrylic splint; auto-polymerizing acrylics; biomaterial containing filled acrylic resin; low peak temperature polymers; stabilizing material for fractures and implants.

A polymeric material suitable for the rapid fabrication of splint pe appliances has been developed. The dough-like product med on mixing a powder and liquid can be readily adapted to cervical third of the intact teeth. Auto-polymerization occurs the mouth within 6 minutes at peak temperatures not exceed- 50 °C. The polymerized product exhibits sufficient strength, idity and dimensional stability to function as a splint.

This material may also find application for the fabrication of hopedic splints and other medical uses.

**335.** Hummer, D. G., **Noncoherent scattering—VI. Solutions of the transfer problem with a frequency-dependent source function,** *Mon. Not. R. Astr. Soc.* **145,** 95-120 (1969).

Key words: Doppler broadening; noncoherent scattering; radiation scattering; spectral line.

A generalized discrete-ordinate method is used to obtain accu- te numerical solutions of the line transfer problem in what the attering is described by a redistribution function. Extensive sults are obtained and discussed for the cases of pure Doppler oadening and of Doppler and natural broadening combined. It shown that, in the latter case, the intensity of radiation emerg- g from a semi-infinite isothermal atmosphere approaches that r coherent scattering in the line wings instead of approaching e value of the Planck function.

**336.** Hust, J. G., Powell, R. L., **Thermal conductivity of aerospace alloys at cryogenic temperatures,** (Proc. 8th Conf. Thermal Conductivity, Purdue University, West Lafayette, Ind., Oct. 7-10, 1968), Chapter in *Thermal Conductivity,* C. Y. Ho and R. E. Taylor, eds., pp. 197-208 (Plenum Press Inc., New York, N.Y., 1969).

Key words: Aluminum alloy; electrical resistivity; Lorenz ratio; nickel alloy; thermal conductivity; thermopower; titanium alloy.

The apparatus described at the last Thermal Conductivity onference has been used to determine the thermal conductivi- , electrical resistivity, Lorenz ratio, and thermopower of everal aerospace alloys between 4 and 300 K: titanium A-110 T, Inconel 718*, Hastelloy X*, and aluminum 7039. These ata are presented graphically. By utilizing detailed numerical nd theoretical analyses, we have been able to separate the elec- onic and lattice contributions to the total thermal conductivity. arious scattering mechanisms have also been resolved for both pes of conduction. The first three alloys are predominately lat- ce conductors at low temperatures, with total Lorenz numbers s high as $15 V^2/K^2$ near 20 K.

**1337.** Isbell, H. S., Fatiadi, A. J., **Phenylhydrazone-phenylazo tautomerism. Part III. Reactions of phenylformazans and certain bis(phenylhydrazones) with strong acids,** *Carbohydrate Res.* **11,** 303-311 (1969).

Key words: Cation; charge-resonance; diphenylformazan; heteropolar; protonation; structure; 1,3-bis(phenylhydrazone).

The behavior of diphenylformazans, 2-oxo-1,3-bis(phenylhydrazones), 1,2-bis(phenylazo)ethylene, and the phenylhydrazone of 4-oxo-1-phenyl-5-phenylazo-3-pyridazinecarboxaldehyde on protonation has been examined spectrophotometrically. These compounds form purple, blue, or green protonated cations. The nature of the spectral changes suggest that the highly colored cations have extended, heteropolar, charge-resonance structures. Phenylosazones and bis(phenylhydrazono) compounds that cannot form extended charge-resonance structures involving the phenyl groups and the adjoining nitrogen atoms do not usually give the blue color reaction. Structures are proposed for the cations derived from diphenylformazans, and certain 2-oxo-1,3-bis(phenylhydrazones).

**11338.** Isbell, H. S., Frush, H. L., Wade, C. W. R., Hunter, C. E., **Transformations of sugars in alkaline solutions,** *Carbohydrate Res.* **9,** 163-175 (1969).

Key words: Acyclic intermediates in mutarotation of sugars; aldoses, enolization of; alkaline rearrangement of sugars; enediols of sugars; enolization, measurement by tritium exchange; inososes, enolization of; ketoses, enolization of; mutarotation of sugars; rearrangement of sugars in alkali; sugars, enolization and rearrangement of; tritium exchange, measurement of enolization by; 2-deoxy sugars, enolization of.

A comparative study has been made of the rates of enolization of sugars in alkaline tritiated water, by measurement of their rates of tritium exchange. Based on the rate for D-glucose as unity, the rates of tritium exchange under a specific set of conditions range from 0.5 to 4.5 for aldohexoses, 0.5 to 10.7 for adloheptoses, 4.1 to 28 for aldopentoses, 2.6 to 25 for various ketoses, 0.3 to 0.8 for some 6-deoxy sugars, 90 to 155 for some 2-deoxy sugars, 2.0 to 240 for some disaccharides, and 1000 to 1500 for some inososes. To account for differences in the behavior of epimeric sugars in alkaline solution, it is suggested that the mutarotation reaction proceeds through pseudoacyclic intermediates that possess some characteristics of the respective ring forms. This new concept, applied to the interpretation of enolization reactions, leads to the possibility of formation of *cis-* and *trans-*enediols, the proportions of which may differ from sugar to sugar.

**11339.** Jackson, J. L., Lifson, S., Coriell, S. R., **Association times of counterions to polyelectrolytes in solution,** *J. Chem. Phys.* **50,** No. 11, 5045 (June 1, 1969).

Key words: Conductivity; counterion; diffusion; polyelectrolyte; transference; transit time.

The experiments of Wall on the transference of sodium ion in polyelectrolyte solutions indicated that the counterion was associated with the polyion for a relatively long time. A calculation of Lifson and Jackson indicated that electrostatic forces could not explain these long association times. Recently, Manning has calculated the counterion current in a polyelectrolyte solution in the presence of an applied field. In this comment, we discuss the transference experiments in light of the calculations of Lifson and Jackson and Manning.

**11340.** Jacox, M. E., Milligan, D. E., **Matrix-isolation study of the infrared and ultraviolet spectra of several first-series transition-metal dichlorides,** *J. Chem. Phys.* **51,** No. 9, 4143-4155 (Nov. 1, 1969).

Key words: $Cl_2$ reactions; $CoCl_2$; $CrCl_2$; emission spectrum; $FeCl_2$; infrared spectrum; matrix isolation; $MnCl_2$;

molecular orbitals; $NiCl_2$; transition-metal reactions; ultraviolet spectrum.

Individual molecules of $CrCl_2$, $MnCl_2$, $FeCl_2$, $CoCl_2$, and $NiCl_2$ have been isolated in an argon matrix at 14 K in sufficient concentration for infrared and ultraviolet spectroscopic study not only by using the conventional effusion cell as a source of the $MCl_2$ species, but also by trapping the products of the reaction of chlorine with the hot transition-metal surface. Studies of the infrared spectra of all of these species in the 250-4000-cm$^{-1}$ spectral range are consistent with a linear structure. Ultraviolet absorptions in the 2000-5500 Å spectral range are in good agreement with the previously reported gas-phase absorptions. However, the absorption observed for matrix-isolated $NiCl_2$ between 4400 and 5000 Å must be attributed to three different electronic transitions, one of which exhibits extensive band structure. A molecular-orbital treatment involving participation of the 3d nickel electrons in the bonding of the molecule predicts the occurrence of several transitions in this energy range and provides a framework for understanding the appearance of extensive vibrational structure in several of the electronic transitions of $NiCl_2$.

**11341.** Jacox, M. E., Milligan, D. E., **Matrix-isolation study of the vacuum-ultraviolet photolysis of methyl fluoride. The infrared spectra of the free radicals CF, HCF, and $H_2CF$,** *J. Chem. Phys.* **50,** No. 8, 3252-3262 (Apr. 15, 1969).

Key words: Carbon atom reaction; CF; force constants; HCF; $H_2CF$; HF reaction; infrared spectrum; isotopic substitution; matrix isolation; methyl fluoride; thermodynamic properties; ultraviolet spectrum; vacuum-ultraviolet photolysis.

Upon vacuum-ultraviolet photolysis of methyl fluoride in an argon or a nitrogen matrix at 14 K, the free radicals CF, HCF, and $H_2CF$ are stabilized in sufficient concentration for observation of their infrared absorption spectra. Studies utilizing carbon-13 and deuterium substitution confirm the identification of these species. Visible-ultraviolet absorption spectra of photolyzed $Ar:CH_3F$ samples include bands which may be assigned to CH, to CF, and to HCF. The reaction of carbon atoms, produced by the photolysis of cyanogen azide isolated in an argon matrix, with HF trapped in the matrix has also been found to lead to the stabilization of sufficient HCF for infrared spectroscopic detection. Reaction of HCF with a second molecule of HF to form $CH_2F_2$ also occurs. The force constants and thermodynamic properties of HCF have been calculated, and a partial vibrational assignment is proposed for $H_2CF$. Although these experiments do not determine the primary photodecomposition processes important for methyl fluoride, there is evidence that both H atom and F atom detachment may occur under the conditions of these experiments.

**11342.** Jefferson, C. F., Baker, C. K., **Mechanism of electrical conductivity in nickel-iron ferrite,** *IEEE Trans. Magnetics* **MAG-4,** No. 3, 460-464 (Sept. 1968).

Key words: Conductivity; ferrites; Hall mobility; thermal emf; transition metal oxides.

Measurements of the frequency dependence of the dielectric conductivity, Hall mobility and thermal emf as a function of temperature on polycrystalline $Ni_{0.6}Fe_{0.4}Fe_2O_4$ indicate that this data can be interpreted in terms of the band model. Previous analyses of the semiconductor properties of ferrites according to the hopping model assume that the number of carriers, n, is identical with the concentration of divalent iron ions. Hall measurements indicate that this is not the case here and that n is best described by the equation

$$n^2=(N_D-n)N_o m^*/m^{3/2} g^{-1} \exp\text{-}E_p/kT.$$

Assigning a value of 2 to g, $m^*/m$ is 9.3 and $E_D$ is 0.034 eV.

The temperature dependence of the dc conductivity is considerably different from that of the ac conductivity. This difference is found for polycrystalline $Ni_{0.6}Fe_{0.4}Fe_2O_4$ and $LiFe_5O$ as well as for single crystal $LiFe_5O_8$. A Wagner type relaxation associated with interfacial polarization is present in all materials indicating that precautions must be taken in the interpretation o dc conductivity data even when single crystals are used.

The thermal emf, calculated from Hall data, shows that th measured value is considerably larger than the calculated value This implies that the measured values might contain a contribution from the phonon drag effect.

**11343.** Jellison, J. C., Collier, R. S., **Fluid phase and temperatur measurement with a single sensor,** (Proc. 1968 Cryogenic Engineering Conf., Case Western Reserve Univ., Clevelanc Ohio, Aug. 19-21, 1968), Chapter in *Advances in Cryogeni Engineering* **14,** Paper H-5, 322-330 (Plenum Press Inc., Ne York, N.Y., 1969).

Key words: Carbon; cryogenic; fluid phase; hydrogen; low gravity; resistance thermometry; temperature; thin film.

A technique is described, which permits a single sensor t measure temperature and the presence of liquid or vapor at specific point in cryogenic containers. This technique compensates for disturbances such as cryogen temperature variation and it offers indication of a gas to liquid transition in a fraction a second. Although designed and used for $LH_2$ instrumentatio the basic principle has been applied to $LN_2$ with slight modification. The system is able to discriminate liquid presence und normal and low-gravity conditions.

Optimum use of the system under low-gravity requires th development of a sensor having a fast thermal time constant, geometry capable of repelling cryogen films from its surface, ar which can be used as a resistance thermometer. Vacuu deposited thin films of carbon are discussed as a possibility f satisfying these requirements. The resistance-temperature cur for these carbon films is nearly log-log linear over a wide ter perature range, providing easy calibration of the sensor, and th have good stability on aging and thermal cycling.

**11344.** Johnson, V. J., **A memoir of Russell B. Scott,** (Pro CRYO/68 Conf., Chicago, Illinois, June 9-12, 1968), Chapt in *Applications of Cryogenic Technology,* R. W. Vance and Weinstock, eds., Introduction, pp. 1-11 (Tinnon-Brown In Los Angeles, California, 1969).

Key words: Biography; career; cryogenic engineerin memoir; Russell B. Scott; talk.

This is a review of the career of Russell B. Scott as Cryogenic Physicist and Cryogenic Engineer at the National B reau of Standards, as given at the Cryo/68 meeting in Chicag June 11, 1968. The memoir includes a brief mention of his ea home, family, and education. A few notes are included regardi the first 22 years of his life at NBS in Washington in the L Temperature Physics Laboratory. His career, in conjuncti with the development of the cryogenic industry, is discussed a little more detail along with the recognition he received a Cryogenic Engineer and as Manager of the Boulder Laboratories. It can be summed up by the inscription beneath his portr hanging in the lobby of the Cryogenic Laboratory to wit: "R sell B. Scott, April 17, 1902 – September 24, 1967, Founder a former Chief of the Cryogenics Division, An internationa recognized scientist and writer who served on the staff of the N tional Bureau of Standards from 1928-1965."

**11345.** Joiner, B. L., **The median significance level and other sm sample measures of test efficacy,** *J. Am. Statist. Assoc.* **64,** 9 985 (Sept. 1969).

Key words: Efficiency of tests; median significance le significance level; statistical tests.

The concepts of the "median significance level" (MSL) and "significance level of the average" (SLA) are introduced and me relationships among these measures and the recently inoduced "expected significance level" (ESL), "average critical lue" (ACV), and "median critical value" (MCV) are conlered. The median significance level is defined as the median the distribution of the observed significance level for a given ernative, and for one-sided tests is shown to be the sigficance level attained by the median of the test statistic. The ignificance level of the average" is analogously defined for e-sided tests to be the significance level attained by the erage (expectation) of the test statistic. For one-sided tests the SL and SLA are inverse functions of Geary's MCV and ACV. me relations between these small sample measures of test efacy, and Pitman's and Bahadur's asymptotic measures are scribed. The MCV is shown to be formally related to amaker's "indifference quality" method of classifying acptance sampling plans. Several simple examples are given ilstrating some relationships among the several criteria.

346. Jones, E., Yelon, W. B., Edelman, S., **Piezoelectric shakers for wide-frequency calibration of vibration pickups,** *J. Acoust. Soc. Am.* **45,** No. 6, 1556-1559 (June 1969).

Key words: Calibration; damped resonant cylinders; damping; piezoelectric shaker; stagger-tuned shaker; vibration; vibration pickup.

This paper describes a piezoelectric shaker consisting of a mbination of damped resonant cylindrical elements. Material aracteristics and design parameters are chosen so that the sonances of the combined elements overlap to provide "good" otion over a wide frequency range. Data from three shakers are esented to show how a suitable set of shakers can be used for libration of vibration pickups at frequencies up to 100 kHz.

347. Jones, M. C., Palmer, D. C., **A technique for the measurement of spectral reflectances at low temperatures in the infrared and far infrared,** (Proc. AIAA Third Thermophysics Conf., Los Angeles, Calif., June 24-26, 1968), Chapter in *Progress in Astronautics and Aeronautics.* **Vol. 21,** *Thermal Design Principles of Spacecraft and Entry Bodies,* pp. 543-557 (Academic Press Inc., New York, N.Y., 1969).

Key words: Infrared; low-temperature; measurement; spectral reflectance; stainless steel; technique.

An experimental technique is described for the measurement f normal, spectral, specular reflectance of materials at temperaures from room temperature down to a few degrees above liquid elium temperature. The reflectance of samples is measured by omparison with reference samples of ultra-high-vacuum eposited gold on glass substrates. The difficulty of maintaining ufficient parallelism between sample and reference has been vercome; also the problem of excessive delay between recordng sample and reference data has been reduced. Experimental etails are given and, in illustration of the technique, the eflectance of electropolished stainless steel is presented for the avelength range 3 μm to 300 μm at 297, 77, and 10.5 K.

1348. Kamper, R. A., **Possible contribution of superconducting devices to nuclear magnetic resonance detection,** *J. Appl. Phys.* **40,** No. 5, 2163 (Apr. 1969).

Key words: Magnetometers; nuclear magnetic resonance; superconducting devices.

We discuss the possible benefits of using superconducting omponents in a conventional NMR detection system, and of sing a superconducting magnetometer to detect the resonance y observing the change in steady state magnetization of the nuclei. It appears that the first approach is capable of improving he sensitivity of conventional techniques by one of two orders of magnitude for suitable specimens. The second would only offer an advantage if the relaxation time $\tau_1$ is very long.

11349. Kasen, M. B., **A method for producing small grain size in super-purity aluminum,** *Trans. Met. Soc.* **AIME 245,** No. 7, 1660-1661 (July 1969).

Key words: Aluminum; grain size; recrystallization; resistivity ratio; super-purity metals.

A method has been developed for recrystallizing super-purity aluminum to produce a very small, uniformly distributed grain size. The method involves (a) introducing a very large amount of cold work at 76 K, (b) a very short time exposure in a salt bath operating at 400 °C, and (c) a water quench. Grain sizes of 30 microns mean diameter may be reproducibly obtained in aluminum having a resistivity ratio, $\rho_{293K}/\rho_{4K}$, in excess of 16,000.

11350. Keller, R. A., **Intersystem crossing from excited triplet states into the singlet manifold,** (Proc. Intern. Conf. Molecular Luminescence, Loyola Univ., Chicago, Ill., Aug. 20-23, 1968), Chapter in *Molecular Luminescence,* E. C. Lim, ed., pp. 453-468 (W. A. Benjamin Inc., New York, N.Y., 1969).

Key words: Fluorescence; intersystem crossing; quantum yield; triplet states.

The quantum yield for intersystem crossing from excited triplet states into the singlet manifold was estimated for several molecules by observing the intensity of the fluorescence emission which resulted from photo-excitation of metastable triplet states. For naphthalene, about one out of every million triplet-triplet excitations crossed over into the singlet manifold. Similar results were obtained for fluorene, quinoline, and isoquinoline. No emission was observed from triphenylene, phenanthrene, or carbazole. A very small signal may have been observed from benzene.

11351. Kidnay, A. J., Hiza, M. J., Dickson, P. F., **The kinetics of adsorption of methane and nitrogen from hydrogen gas,** (Proc. 1968 Cryogenic Engineering Conf., Case Western Reserve Univ., Cleveland, Ohio, Aug. 19-21, 1968), Chapter in *Advances in Cryogenic Engineering* **14,** Paper B-2, 41-48 (Plenum Press Inc., New York, N.Y., 1969).

Key words: Adsorption; hydrogen; kinetics; low temperature; methane; nitrogen.

The breakthrough curves for 4 binary mixtures (2 nitrogen-hydrogen and 2 methane-hydrogen) and one ternary mixture (nitrogen-methane-hydrogen) were measured on an activated coconut shell charcoal at 76 K and over a wide range of flow rates. The equations of Eagleton and Bliss were used to obtain gas phase and adsorbed phase mass transfer coefficients from the breakthrough curves. Comparison of the mass transfer coefficients shows that in all cases diffusion in the pores of the adsorbent is the rate controlling step. The values for the gas phase mass transfer coefficient, when converted to $j_d$ values, are in good agreement with the general curve proposed by DeAcetis and Thodos. The breakthrough curves were also correlated using the empirical method proposed by Engel and Coull, with good results.

The results show that it is possible to predict with reasonable accuracy, the breakthrough curves of the binary mixtures using the relations of Eagleton and Bliss. The equation of Engel and Coull provides good representation of the breakthrough curves for the ternary mixture, but its empirical nature limits its usefulness.

11352. Kieffer, L. J., **The reliability of property data, or, whose guess shall we use?,** *J. Chem. Doc.* **9,** No. 3, 167-168 (Aug. 1969).

Key words: Data; information center; reliability.

Increased reliability of property data can be achieved by critical evaluation of the techniques used in making measurements. The necessity for an implementation of such evaluations are explored.

The material in this paper was presented in a talk to the Middle Atlantic Regional Meeting of the American Chemical Society, February 12-15, 1969, Washington, D.C. It does not include any new technical information.

11353. Klein, R., Scheer, M. D., **Reaction of $O(^3P)$ with 2-methyl-2-pentene at low temperatures and its implication for the transition state,** *J. Phys. Chem.* **73,** 1598-1599 (1969).

Key words: Low temperature chemistry; olefins; oxygen atoms.

A formulation of a new transition complex in the reaction of oxygen atoms with olefins, recently proposed, requires an interaction between O and neighboring hydrogens at the reaction site. An experimental assessment of the strength of this interaction, obtained with 2 methyl 2 pentene, shows that the interaction is indeed strong but not strong enough to prevent some H migration in the passage to final products. The ratio of addition to the two positions at the olefinic bond is in the same sense, but considerably less for O than for H.

11354. Klose, J. Z., **Transition probabilities and mean lives of the $2s_2$ laser level in neon I,** *J. Quant. Spec. Rad. Trans.* **9,** No. 6, 881-883 (June 1969).

Key words: Atomic lifetimes; atomic spectra; atomic transition probabilities; laser; neon.

Values of sums of transition probabilities and mean lives associated with the $2s_2$ (Paschen notation) laser level in Ne I have been determined under various theoretical assumptions and are presented in comparison with available experimental results. Also, using intermediate coupling and the Hartree-Fock-Slater approximation, the probability of the $2s_2 \rightarrow 2p^6\ {}^1S_0$ (626.8 Å) transition was calculated and found to be $8.8 \times 10^7$ sec$^{-1}$. The theoretical values were found to be in agreement with an extrapolation to zero pressure of a series of line-width measurements of the 11520 Å laser transition but in disagreement with the lifetime of the $2s_2$ level as determined from a delayed-coincidence experiment.

11355. Knoeck. J., **Vibrational spectrometric and electrochemical evidence for lanthanum(III)-nitrate complexes in aqueous solution,** *Anal. Chem.* **41,** No. 14, 2069-2071 (Dec. 1969).

Key words: Combining ratio; complex; infrared; ion selective electrode; lanthanum; nitrate; polarography; Raman.

Raman and infrared spectra of aqueous lanthanum nitrate solutions are consistent with nitratolanthanum complexes. The observation of a polarized Raman band at 1475 cm$^{-1}$ indicates that nitrate is a bidentate ligand in these complexes. Nitrate ion selective electrode measurements show that at least two complexes of 1:1 and 1:3 lanthanum to nitrate ratio exist in aqueous solution. The formation constant of the 1:1 complex is $30.0 \pm 4.0$ at 25 °C. The lanthanum catalyzed reduction of nitrate at a DME appears to involve reduction of the bound nitrate in the nitratolanthanum(III) complex ion.

11356. Knoeck, J., Taylor, J. K., **Aqueous boric acid-borate-mannitol equilibria,** *Anal. Chem.* **41,** No. 13, 1730-1734 (Nov. 1969).

Key words: Borate; boric acid; combining ratio; complex; formation constant; mannitol.

Despite recent reports to the contrary, the stoichiometry of the aqueous boric acid-borate-mannitol system has been shown to involve both a 1:1 and 2:1 mannitol-borate complex. Reliable values of the formation constants of these complexes have been determined from electrometric pH measurements. Widely dive
gent results obtained by previous workers in this area have bee
shown to be largely the result of misinterpretation of experime
tal data rather than anomalous behavior of the system. Reliab
data taken from previous work has been shown to give the san
results as data obtained in this laboratory thus providing a co
sistent model for boric acid-borate-mannitol equilibria.

11357. Koonce, C. S., **Tunneling into low carrier density supe
conductors,** *Phys. Rev.* **182,** No. 2, 5407 (June 10, 1969).

Key words: Density of states; low density superconducto
semiconductor; superconducting semiconductor; superco
ductivity; tunneling.

A theory of tunneling between a normal metal and a low car
er density superconductor at zero temperature is develope
Because of the small Fermi energy of low carrier density supe
conductors and the energy dependence of the tunneling matr
elements for these junctions, the conductance vs. voltage curv
are quite different from tunneling between a metal and a hi
density (metallic) superconductor. The tunneling displays bo
the voltage-dependent conductance associated with tunneli
between a metal and a degenerate semiconductor and the pea
in conductance arising from the large quasiparticle density
states at voltages slightly larger than the superconducting ener
gap.

11358. Kropschot, R. H., **Thermal diffusivity of powder insul
tion,** (Proc. 1968 Cryogenic Engineering Conf., Case Weste
Reserve Univ., Cleveland, Ohio, Aug. 19-21, 1968), Chapt
in *Advances in Cryogenic Engineering* **14,** Paper F-4, 224-2
(Plenum Press Inc., New York, N.Y., 1969).

Key words: Cryogenics; conductivity; diffusivity; powder
thermal insulation.

The thermal diffusivity of selected powder insulations (carbo
silica-magnesia and a silica-aluminum mix) has been experime
tally determined over the temperature range 76-300 K. The
results were used, along with the estimated specific heat, to c
culate the thermal conductivity. Good agreement is obtain
between these data and thermal conductivities obtained fro
steady state measurements. As expected, the diffusivity of high
evacuated 50-50 weight percent silica-aluminum powder vari
by a factor of three over this temperature range. These data al
enhance the justification for assuming the specific heat for bu
and powdered materials to be the same in this temperature rang

Experimentally, the diffusivities were determined fro
transient temperature response to a step input change in te
perature. Mathematical solution of the problem for constant d
fusivity is known, and it is shown here that the same basic math
matical approach is valid for the case of a temperature depende
diffusivity. The experimental apparatus is briefly described a
details of the experimental results and the mathematical analys
are included.

11359. Ku, H. H., Kullback, S., **Approximating discrete probabi
ty distributions,** *IEEE Trans. Info. Theory* **IT-15,** No. 4, 44
447 (July 1969).

Key words: Approximating discrete distributions; depe
dence trees; minimum discrimination information estin
tion.

The method of minimum discrimination information estin
tion is applied to the problem of estimating an n-dimensional d
crete probability distribution in terms of lower-order margi
distributions. The procedure provides a convergent iterative
gorithm. The method yields best asymptotically normal (BA
estimates. The general procedure includes as a particular ca
that proposed by a method using dependence trees. An exam
is given.

**60.** Kuriyama. M., **X-ray diffraction from a crystal containing solated imperfections,** *Acta Cryst.* **A,** No. 25, 682-693 (Nov. 969).

Key words: Anomalous absorption; contrast; diffuse scattering; dynamical diffraction; extinction; imperfect crystal; kinematical diffraction; topography.

The x-ray scattering amplitude from a crystal containing isoed imperfections is expressed in terms of the Fourier transm of the atomic displacement vectors. The amplitude contains y the local properties of the imperfections which are "seen" the incident beam of a finite size. The disruption of the Borrnn transmitted (or diffracted) beam, the narrowing of the namical diffraction range and the "diffuse" scattering caused dynamically diffracted x-rays are some of the results obtained m the scattering amplitude. The formations of black, white d black-white images in topographs are explained by the esent theory. Image contrast is also discussed in terms of the ckness of the crystal.

**361.** Kuriyama, M., Miyakawa, T., **Theory of x-ray diffraction by a vibrating crystal,** *J. Appl. Phys.* **40,** No. 4, 1697-1702 Mar. 15, 1969).

Key words: Dynamical diffraction; extinction; kinematical diffraction; piezoelectricity; theory; thickness vibration; vibrational modes; x-ray diffraction.

The scattering amplitude for x-ray diffraction by a vibrating ystal is obtained. The Bragg diffracted propagators for the peret crystal are replaced by new propagators in which the Fouritransform of the polarizability of the crystal is multiplied by $\mathbf{H} \cdot \mathbf{A}_q$) for the vibrational amplitude $\mathbf{A}_q$, as is corrected by the bye-Waller factor in the thermal problem. The scattering amtude contains not only dynamical scattering but kinematical attering.

The case of ideal thickness vibration is studied in detail. The l part of the perturbed scattering amplitude is proportional to $\mathbf{H} \cdot \mathbf{A}_q$ multiplied by the H-th Fourier transform of the larizability. The transient process from dynamical to kinemati scattering, that is, a decrease in extinction, is clearly demonated in terms of the vibrational amplitude.

**362.** Kushner, L. M., **The NBS contribution to technological measurements and standards,** *Mater. Res. Std.* **9,** No. 10, 8-10 (Oct. 1969).

Key words: Performance standards; technological measurements and standards.

Our national system of measurement incorporates physical, aterial and technological measurements and standards. hereas the first two are concerned largely with enabling us to scribe the physical world, technological measurements and andards are use-related and are at the interface between ence and its application in industry and Government. The BS program in technological measurements and standards is an ort to extend the principles of good measurement to the enneering fields and to the complex needs of today's society. This al is pursued mainly through projects designed to enable the vernment to use technology effectively in its role as a conmer and employer of innovative resources.

With government at all levels becoming more and more inlved in developing and setting standards in a variety of fields lated to public health and safety, it becomes increasingly imrtant that the standards be of such a nature that they do not mper the introduction of new technology for accomplishing ogram objectives. This leads to a need to develop more fully e concept of performance requirements as the basis for stanrds. This must include a concern with subjective factors which of necessity enter the measurement problems as soon as man becomes part of the system to be measured.

A related phenomenon is the "systems" nature of many of our national problems. These problems to which physical scientists and engineers are now being directed are not purely technical but have large and important social and economic components. Completely new measurement criteria are required to specify the problem and provide measures of progress toward its amelioration. The development of this new measurement methodology is being undertaken in a relatively new field of applied science, systems analysis. This is a new technology for the decision making process in business, industry and government.

The NBS technological measurements and standards program attempts to support and stimulate these activities as effective means for bringing our national scientific and engineering skills to bear on current problems.

**11363.** Kasuda, T., **Proposed procedures for determining building heating and cooling loads for energy calculations,** *ASHRAE Symposium Bulletin,* pp. 1-75 (1969).

Key words: ASHRAE; building heating and cooling load; energy requirements.

Hour by hour calculations of heating and cooling load are essential for the accurate evaluation of annual energy requirements needed to maintain a desired thermal environment within a building. There is a need for rigorous computer algorithms in calculating the transient thermal behavior of building structures under fluctuating climatic conditions. This paper describes most up-to-date computational algorithms for solar heat gain through fenestration, transient wall-heat conduction, psychrometrics, shadow movement, and others, which are recommended for the computer calculations of hourly heating and cooling loads.

**11364.** LaFleur, P. D., **Activation Analysis Section at the National Bureau of Standards, Washington, D.C., U.S.A., Laboratory of the Issue,** *J. Radioanalytical Chem.* **3,** No. 1-2, 127-133 (July 1969).

Key words: Activation analysis; Cockcroft-Walton neutron generator; LINAC; radiochemical separations; reactor; standard reference material.

The history and facilities of the Activation Analysis Section, Analytical Chemistry Division of the National Bureau of Standards are described. The Section is divided into three projects, each having application to a specific irradiation source and a project in radiochemical separations. Several examples of work in progress and of past accomplishments are included, as well as planned activities in the future.

**11365.** LaFleur, P. D., **Determination of molybdenum in steels and biological materials by activation analysis,** *Radiochem. Radioanal. Letters* **1,** No. 3, 225-229 (July 1969).

Key words: Activation analysis; biological materials; hydrogen bis(2-ethylhexyl) phosphate; molybdenum; radiochemical separations; steels.

A procedure for determining molybdenum by activation analysis in steels and biological matrices is described. The procedure involves a chemical separation of molybdenum by solvent extraction using the reagent hydrogen bis(2-ethylhexyl) phosphate, and subsequent back extraction with $HNO_3$-$H_2O_2$. Using the procedure as described precisions of 1-2 percent (at the 95% confidence level) are possible and 3-4 percent are routine.

**11366.** Lamb, V. A., **Electroplating with current pulses in the microsecond range,** *Plating* **56,** No. 8, 909-913 (Aug. 1969).

Key words: Electroplating with current in microsecond pulses; pulse plating.

Exploratory experiments were carried out on electrodeposition of copper and silver by use of pulsed direct current, with pulse periods from 0.1 to 50 microsecond and with very high current density. The microstructure and hardness of copper deposits made under these conditions were not significantly different than those of deposits plated under conventional conditions. Possible reasons are discussed. Current efficiency of copper deposition was low with the shortest pulses, but remained high for deposition of silver. Two experiments relating pulse duration to "reaction time" for the electrode reactions are described.

**11367.** LaVilla, R. E., Mendlowitz, H., **Optical properties of germanium,** *J. Appl. Phys.* **40,** No. 8, 3297-3300 (July 1969).

> Key words: Electron energy losses; germanium; $M_{IV,V}$ edge; optical constants; oscillator; strengths; sum rules; vacuum ultraviolet.

The set of optical constants of germanium reported by Marton and Toots, from 8 to 25 eV, have been assessed, and found to be consistent to within ±5 percent. An extension of the n and k values up to photon energy of 100 eV using Hunter's k values also has been studied. The analysis consisted of an internal consistency check by applying the Kronig-Kramers dispersion relations to the optical constants and an evaluation and study of the optical and electron oscillator strength distributions. From an application of the general sum rules to the oscillator strength distribution, the computed effective number of electrons per germanium atoms suggests a redetermination of the k values in the spectral region covered by Hunter.

**11368.** Lehner, J., Newman, M., **On Reimann surfaces with maximal automorphism groups,** *Glasgow Math. J.* **8,** Part 2, 102-112 (July 1967).

> Key words: Automorphisms; Fuchsian groups; modular group; Riemann surfaces.

Families of Fuchsian groups with associated Riemann surfaces having maximal automorphism groups are constructed, by a method which goes from the noncompact case to the compact case.

**11369.** Leiss, J. E., Penner, S., Rose, J. E., Broberg, J. B., **Transient beam loading in electron linear accelerators,** (Proc. 1969 Particle Accelerator Conf., Washington, D.C., March 5-7, 1969), *IEEE Trans. Nucl. Sci.* **NS-16,** Part I, No. 3, 1027-1030 (June 1969).

> Key words: Electron; energy loss; linear accelerator; short pulse; transient beam-loading; waveguide.

An experiment has been devised to measure directly the beam loading in electron linear accelerators operating with very short beam pulses. A well momentum analyzed and phase bunched electron beam is sent through either an unexcited waveguide or a vacuum pipe. Electron energy loss due to beam loading in the waveguide is detected by measuring the resulting energy shift of elastically scattered electrons with the NBS electron scattering spectrometer. Energy shifts of a few parts in $10^5$ can be measured at 60 MeV. Measurements made to date at 61 MeV and for beam pulse lengths of 5, 10, and 20 nanoseconds appear to confirm the existence of enhanced beam loading relative to the usual nondispersive linac theory. An attempt is made to compare the measurements to theoretical estimates of this enhancement.

**11370.** Levin, I. W., Abramowitz, S., **Vibrational spectra and force field for ruthenium tetroxide,** *J. Chem. Phys.* **50,** No. 11, 4860 (June 1, 1969).

> Key words: Coriolis constant; force field; infrared; isotopic shift; ruthenium tetroxide; vibrational amplitude; vibrational spectra.

Measurement of the infrared gas-phase spectrum of the $\nu$ vibration for $RuO_4$ provides values for both the Coriolis zeta constant $\zeta_3$ and the isotopic frequency shift $\Delta\nu_3$ for the $^{101}$Ru-$^{102}$Ru exchange. These data, in addition to the vibrational amplitudes l(Ru-O) and l(O-O), serve as constraints in specifying unique force fields for the $F_2$ symmetry species of $RuO_4$. Agreement among the sets of force constants separately determined by the supplemental information confirms the potential function fo this system.

**11371.** Logan, H. L., **Studies of hot salt cracking of the titanium percent-Al-1 percent Mo = 1 percent V alloy,** *Proc. Ohio Stat Stress Corrosion Symp., Ohio State University, Columbus Ohio, September 11-15, 1967,* pp. 662-672, (National Association of Corrosion Engineers, Houston, Texas, 1969).

> Key words: Hot salt cracking; LiCl-KCl eutectic; stress corrosion; titanium oxides; Ti-8-1-1 alloy.

Two approaches to the problem of hot salt cracking of th titanium alloy are reported. In the first of these the susceptibilit of the alloy to cracking in contact with a number of chlorides wa studied. Only NaCl, LiCl and a molten eutectic mixture of LiC and KCl were found to severely crack stressed specimens exposed in air at 800 °F.

In the second phase of the program the effects of environments on the alloy in contact with NaCl were investigated. Dat indicate that the oxide or series of oxides formed on the allo surface were important in determining whether specimen developed stress-corrosion cracks.

Data also indicate that little or no chlorine was produced in th corrosion reaction.

**11372.** Lutz, G. J., LaFleur, P. D., **Determination of yttrium i rare earths by photon activation analyis,** *Talanta* **16,** 1457-146 (1969).

> Key words: Coincidence spectrometry; photon activatio analysis; rare earths; yttrium.

The determination of yttrium in the presence of large amount of the rare earths by the thermal neutron reaction $^{89}Y(n,\gamma)^{90}Y$ i complicated because of frequent problems of sample self shielding from major constituents of the sample and the difficulty c separating $^{90}Y$, a pure beta emitter, from other elements whic are very similar chemically.

A nondestructive photon activation analysis method has bee developed for this determination. Bremsstrahlung from a 35-$\mu$ beam of 35-MeV electrons induces the photonuclear reactio $^{89}Y(\gamma,n)^{88}Y$. Optimum sensitivity is obtained by coincidenc counting of the 0.90 and 1.83 MeV gamma rays associated wit the decay of $^{88}Y$. The detection limit is less than one micrograr of yttrium.

**11373.** McBee, C. L., Kruger, J., **Ellipsometric-spectroscopy c films formed on metals in solution,** *Surface Sci.* **16,** 340-35 (1969).

> Key words: Ellipsometry; iron; optical constants; passiv films; spectra.

The computational problems involved in the analysis of "ellisometric-spectroscopic" data are considered, including the existence of multiple values of the optical constants for a sing wavelength.

Suggestions are made for eliminating the extra values. Examples of pertinent experiments to study corrosion processes a given for passive films grown on single crystals of iron in sodiu borate-boric acid solution.

**11374.** McCaa, W. D., Jr., Nahman, N. S., **Frequency and tir domain analysis of a superconductive coaxial line using the BC theory,** *J. Appl. Phys.* **40,** No. 5, 2098-2100 (April 1969).

Key words: BCS theory; superconductive lines; time and frequency response; two-fluid model.

A miniature superconductive lead-teflon-niobium coaxial line been analyzed in terms of the complete BCS theory of superductivity. The surface impedance of both superconductors. line attenuation and the picosecond step responses have been culated for a temperature of 4.24 K. The dielectric has been umed lossless.

n addition, the frequency and time domain responses obed with the BCS theory are compared with those predicted the same line parameters by the two-fluid model.

75. McNesby, J. R., **The photochemistry of Jupiter above 200,** *J. Atmospheric Sci.* **26,** No. 3, 594-599 (May 1969).

Key words: Ammonia; Jupiter; methane; photochemistry; vacuum ultraviolet.

ovian photochemistry is shown to consist of four zones: (1) otolysis of methane at 1216 Å and a total pressure of about $^{-6}$ atmospheres and 130 km above the ammonia cloud top; (2) otolysis of ammonia at 1700-2200 Å and a total pressure of out $10^{-4}$ atmospheres at 100 km; (3) Photolysis of both thane and ammonia at 1350-1450 Å at 100 km; and (4) otolysis of ammonia at 1450-1700 Å around $10^{-2}$ atmospheres 50 km. No photolysis occurs below this level. The large exs of hydrogen suggests that all radicals ultimately react with drogen, the net result being production of H atoms. It is conded that complex C-H-N molecules are not formed in Jovian otochemistry because of the reducing atmosphere. Methane d ammonia persist in the atmosphere because there is no chanism available for their disappearance.

76. Madey, T. E., Yates, J. T., Jr., **Temperature effects in lesorption by electron impact: molecular vibrations in the hemisorbed layer,** *J. Chem. Phys.* **51,** No. 3, 1264-1265 (Aug. , 1969).

Key words: Chemisorption; desorption; electron impact; molecular vibration; neutralization; oxygen; tungsten; (110) tungsten.

The method of desorption by electron impact is used to study ygen chemisorbed on a (110) tungsten crystal. The positive s desorbed from the crystal are energy-analyzed using a hemierical retarding potential analyzer, and the resulting ion ener distribution (IED) is observed. The shape of the IED is reed to the population of the various vibrational states of those sorbed species which produce positive ions on electron imct, and to their associated vibrational wave functions. A crude m of surface spectroscopy may therefore be carried out by asuring the change in shape of the IED with temperature and erring the change in population of the first excited vibrational te of the (surface-oxygen) oscillator. The frequency obtained this way is ~950 cm$^{-1}$ for the $\beta_1$ oxygen state; unequivocal ntification of the oscillator as a W–O stretch or an O–O etch is not possible.

The total positive ion yield from the surface decreases with inasing temperature. This is interpreted as arising from increase the neutralization rate with increasing temperature.

377. Madey, T. E., Yates, J. T., Jr., **The measurement of sticking coefficients at high temperature using the isotopic mixing method,** (Proc. Sixth Intern. Symp. Rarefied Gas Dynamcs, Cambridge, Mass., July 22-26, 1968), Chapter in *The Measurement of Sticking Coefficients at High Temperatures Using the Isotopic Mixing Method* **II,** 1345-1348 (Academic Press Inc., New York, N.Y., 1969).

Key words: Carbon monoxide; high temperature; isotopic mixing; molybdenum; nitrogen; rhenium; sticking coefficient; tungsten.

The reactive sticking coefficients for CO on Re and $N_2$ and CO on W have been determined at high temperatures and low coverages by studying the surface reactions: $^{14}N_2 + {}^{15}N_2$, $2{}^{14}N^{15}N$ and $^{12}C^{18}O + {}^{13}C^{16}O$, $^{12}C^{16}O + k\,{}^{13}C^{18}O$. At T > 1500 K, is nearly unity for CO on W and Re; ~.01 for $N_2$ on W.

11378. Mahler, R. J., **Interaction of Gunn domains with the Ga$^{71}$ nuclei in GaAs,** *Appl. Phys. Letters* **14,** No. 9, 277-279 (May 1, 1969).

Key words: Gunn effect; nuclear magnetic resonance; time dependent electric field gradients.

The application of an electric field of more than 3.2kV/cm across n-type GaAs results in the formation of high voltage approximately triangular domains which travel across the sample with a frequency determined by the length of the sample. A Ga$^{71}$ nuclear spin transition frequency was brought within the domain frequency bandwidth and an interaction between the domains and the nuclei was observed.

11379. Maki, A. G., Jr., **Vibrational spectroscopy,** *Ann. Rev. Phys. Chem.* **20,** 273-292 (1969).

Key words: Absorption spectra; infrared; instrumentation; potential functions; spectroscopy; vibration.

A review is given of the recent scientific literature on the subject of vibrational spectroscopy. Topics which are covered include instrumentation, gas phase spectra including band contour calculations, condensed phase spectra, and vibrational potential functions.

11380. Mandel, J., **A method for fitting empirical surfaces to physical or chemical data,** *Technometrics* **II,** No. 3, 411-429 (Aug. 1969).

Key words: Curve fitting; data analysis; empirical fitting of curves and surfaces; model, mathematical; response surface; surface fitting; two-way tables.

This paper presents an illustration of a recently developed method of surface fitting. Data on the specific volume of two types of rubber, measured at various temperatures and pressures, are used to establish empirical relationships between specific volume, temperature, and pressure.

An important feature of the method is that, to a considerable extent, it evolves the model from the data. Another basic feature is that it reduces the problem of surface fitting to that of fitting a few functions of one variable each.

11381. Mangum, B. W., Soulen, R. J., Utton, D. B., **Magnetic ordering in cerium trichloride at low temperatures,** *Proc. XI Conf. Low Temperature Physics, St. Andrews, Scotland, Aug. 21-28, 1968,* **2,** 1361-1363, Paper C10.9 (University of St. Andrews, Scotland, 1968).

Key words: Dilution refrigerator; low temperature; magnetic ordering; nuclear quadrupole resonance; nuclear resonance; thermometers.

We have used the nuclear quadrupole resonance (NQR) of $^{35}Cl$ as a means of detecting the onset of long range magnetic ordering in $CeCl_3$. A $^3He-{}^4He$ dilution refrigerator was used to attain the low temperatures, CMN was used as a thermometer and the nuclear resonance was detected with a Robinson oscillator. The $^{35}Cl$ pure quadrupole resonance line at 4.32 MHz was observable down to 0.110 K. The signal intensity was inversely proportional to the temperature above 0.20 K. The signal to noise ratio at 0.15 K was greater than 100:1. An unsuccessful search was made for nuclear resonances in the frequency range 3.47-5.18 MHz at 0.054 K which was our lowest operating temperature. We conclude that the specific heat anomaly at 0.268 K, reported by Keen et al., is not due to long range, but rather short range, magnetic ordering. Calculations show that any static arrangement of the cerium spins will result in a magnetic field at the chlorine site. A field of 3 oersteds (1 oe$=(4\pi)^{-1}10^3$AM$^{-1}$) would produce a measurable effect on the NQR signal; none was observed. Although the disappearance of the signal below 0.110 K indicates the presence of an appreciable magnetic field at the chlorine site, the present measurements do not permit the assignment of a long range magnetic ordering temperature.

**11382.** Mangum, B. W., Thornton, D. D., **Nuclear relaxation measurements of $^{35}$Cl in $PrCl_3$,** *Phys. Rev. Letters* **22,** No. 21, 1105-1107 (May 26, 1969).

Key words: Antiferromagnet; NMR; NQR; nuclear spin-spin relaxation; nuclear spin-lattice relaxation; $PrCl_3$.

We have made spin-spin, $T_2$, and spin-lattice, $T_1$, relaxation measurements of $^{35}$Cl in $PrCl_3$ from 4.2 to 0.08 K. $T_1$ and $T_2$ show unusual temperature dependences in both the paramagnetic and antiferromagnetic states.

**11383.** Marcus, M., Newman, M., **Doubly stochastic associated matrices,** *Duke Math. J.* **34,** No. 3, 591-598 (Sept. 1967).

Key words: Associated matrices; compounds; doubly stochastic matrices; induced powers; tensor products.

It is proved that the associated matrix K(A) is doubly stochastic if and only if A is a scalar multiple of a permutation matrix, unless K(A) is a Kronecker power. In this case K(A) is doubly stochastic if and only if A is a scalar multiple of a doubly stochastic matrix.

**11384.** Margoshes, M., **Remarks on linearization of characteristic curves in photographic photometry,** *Appl. Opt.* **8,** No. 4, 818 (April 1969).

Key words: Arrak transform; Baker transform; emulsion calibration; Kaiser transform; photographic emulsions; Sampson transform; Seidel transform; spectrochemical analysis.

A discussion is given of the transformation $\Delta = \log(10^D\text{-}1)$, where $D = \log(1/T)$ and T is the transmittance of the photographic image, recently rediscovered by de Vaucouleurs, who claimed that $\Delta$ is a linear function of the relative exposure, log(E), over the range of values of D which are of interest. It is pointed out that this transform has been independently discovered three or more times, and that it is well known in spectrochemical analysis as the Seidel transform. Previously published and new data are cited to illustrate that $\Delta$ is only rarely a linear function of log(E). Other transforms are noted which do appear to give a linear relation with log(E) in many cases.

**11385.** Margoshes, M., Rasberry, S. D., **Application of digital computers in spectrochemical analysis—computational methods in photographic microphotometry,** *Spectrochim. Acta* **24B,** 497-513 (Jan. 14, 1969).

Key words: Computers; microphotometry; photographic emulsion; photographic photometry; programs; spectrochemical analysis.

A new method is described for calibration of photographic emulsions and conversion of microphotometer readings to relative intensities on a digital computer with special application to spectrochemical analysis. The method for emulsion calibration replaces graphical procedures by a numerical method which is well suited for digital computations. The method of computation and its underlying assumptions are described, and results are given of tests of the procedure. It is recognized that the entire experimental arrangement is being calibrated, not merely the photographic emulsion, and it is shown how malfunctions of the microphotometer which affect the calibration can be recognized from the output of the computer. The program for conversion microphotometer readings to relative intensities provides several alternate calculations, including selection of the prop calibration parameters according to the wavelength of the li when these data are supplied for more than one wavelength gion, as well as correction for step and background whe required. The program is written to provide for automatic sele tion of the required alternative calculation, based on prelimina analysis of the input data.

**11386.** Margoshes, M., Rasberry, S. D., **Fitting of analytical fu tions with digital computers in spectrochemical analysis,** *An Chem.* **41,** 1163-1172 (Aug. 1969).

Key words: Analytical curves; analytical functions; em sion spectrometry; fluorescence spectrometry; spe trochemical analysis; statistics; x-ray.

Two procedures are described for fitting spectromet analytical functions on a digital computer and conversion of strument readings to element concentrations. The first procedu is intended for computers giving rapid response, and particula those which can operate in the conversational mode. During t running of the program the user decides on the equation to used and whether data for any standards are to be rejected. T second procedure is intended for use on batch-loading comp ters; these decisions are incorporated in the program. Results a given of the use of both procedures. The occasional failures the procedures are discussed, and methods are described for d tecting such failures. A discussion is given of a method for cluding an estimate of the uncertainty of the analytical functi in the estimated analytical error.

**11387.** Marinenko, G., **On the atomic weight of potassiu** *Talanta* **16,** 1339-1340 (1969).

Key words: Atomic weight; potassium.

A brief survey of data is made, which indicates the possibil that the internationally accepted value for the atomic weight potassium (39.109) is too high. Additional experimen evidence is brought to light, which also supports the above co clusion.

**11388.** Marinenko, G., Champion, C. E., **Difference between inflection point and the equivalence point in coulometric tit tions of weak acids,** *Anal. Chem.* **41,** No. 10, 1208-1211 (A 1969).

Key words: Boric acid; equivalence point; inflection poi Roller equation.

Mannitoboric acids of varying p$K_a$ were successfully used test independently the validity of the Roller equation for eval tion of the error due to noncoincidence of the inflection point a the equivalence point of acid base titration. The use of m nitoboric acid in media of different mannitol concentrations h provided the first test of the Roller equation under conditio where both parameters, c and $K_a$, are varied for a single acid known stoichiometry. Moreover, the applicability of the Rol equation to complex systems such as boric acid-mannitol has been established prior to this investigation.

**11389.** Marron, B. A., Tauber, S. J., **Evolution of a general co puter-based information system from pharmacological requi ments,** *Proc. Conf. 32nd Annual Meeting of the Americ Society for Information Science, San Francisco, Califor Oct. 1-4, 1969,* **6,** 223-230 (Greenwood Publ. Corp., We port, Conn., 1969).

Key words: Chemical data; computers; informat retrieval; information storage; information syste parameter control; pharmacological data.

A general information storage and retrieval system capable handling most kinds of information by parameter control escribed. The system is characterized by user description of ata processing requirements and the capability of attaching odules for handling special processing problems. A specific imementation of the system for representative data types taken om chemistry and pharmacology is detailed.

1390. Martin, W. C., Sugar, J., **Perturbations and coupling in the $d^9sp$ configurations of Cu I, Zn II, Ag I, Cd II, and Tl III,** *J. Opt. Soc. Am.* **59,** No. 10, 1266-1280 (Oct. 1969).

> Key words: Atomic spectra; cadmium; copper; energy levels; energy parameters; silver; thallium; zinc.

Application of intermediate coupling theory to $3d^94s4p$ in Cu and Zn II revealed perturbations which could not be due to conguration types $3d^{10}nl$. The $3d^94s4p$ levels except $4s4p(^1P^\circ)3d^9$ $P^\circ$ were then fitted by including interaction with $3d^84s^24p$. Inial values for the configuration interaction parameters were ased on M. Wilson's Hartree-Fock calculations, and energy arameters for $3d^84s^24p$ (not known experimentally) were fixed values based on related spectra. The results show that this ineraction accounts for the major distortions of $3d^94s4p$ in Cu I nd Zn II. The resulting interaction parameter values appear constent with Roth's values for related iron-group spectra. The disepancies between calculated and experimental positions for $P^\circ)3d^9\ ^2P^\circ_{1/2,\ 3/2}$ are qualitatively consistent with known $3d^{10}np$ $P^\circ$ series perturbations in Cu I, Zn II. Calculations without ineraction for $4d^95s5p$ in Ag I and Cd II indicate interaction with $d^85s^25p$ weaker than the corresponding interaction in the Cu I equence. The levels of Tl III ($5d^96s6p + 5d^{10}7p$) were fitted with onfiguration interaction. One experimental $d^9sp$ level is rejected Zn II, Ag I, and Tl III. Corresponding new levels are found for n II and Ag I. Leading eigenvector components for the $d^9sp$ vels in the $[sp(S_lL_l),d^9]SL$ and $[sp(S_lL_l)J_l,(d^9)J_{ll}]J$ coupling hemes are given for all five spectra. The Tl III levels are asgned $J_lJ_{ll}$ names as most appropriate.

1391. Martin, W. C., Tech, J. L., Wilson, M., **Note on the $3p^54s3d$ configuration in neutral potassium** (K I), *Phys. Rev.* **181,** No. 1, 66-69 (May 5, 1969).

> Key words: Absorption spectrum; autoionization; atomic energy levels; electron configuration; potassium.

Intermediate coupling matrices for $p^5sd$ were diagonalized ith energy parameters based on restricted Hartree-Fock avefunctions for K I $3p^54s3d$. The resulting energies and Rusell-Saunders percentage compositions for the levels are given. he average energy of the configuration was taken as 170644 $m^{-1}$, the baricenter position relative to $3p^64s$ as calculated by ne Hartree-Fock method. Four autoionization lines previously bserved in the vacuum ultraviolet absorption spectrum of K I re classified as transitions to levels of this configuration. An aproximate correction of $-3400\ cm^{-1}$ to the above baricenter is us obtained, and predicted positions for six other transitions to $p^54s3d$ expected below 600 Å are given. The doublet $3p^64s$ $S_{1/2} \rightarrow 3p^53d(^1P^\circ)4s\ ^2P^\circ_{1/2,\ 1\ 1/2}$ (calculated position ~ 480 Å) is redicted to absorb most of the oscillator strength of the array. he level percentage compositions also serve to confirm a conlusion of Sprott and Novick that the $^4D_{3\ 1/2}$ level observed by hem does not belong to $3p^54s3d$. Calculated positions for $p^54s3d$ and $3p^54s4p$ are consistent, within the approximations, ith the conclusion of Sprott and Novick that $3p^54s3d\ ^4F^\circ_{4\ 1/2}$ nd $3p^54s4p\ ^4D_{3\ 1/2}$ are not separated by more than ~ 0.15 eV.

1392. Mason, S. T., **Dependence of the phase shift on energy and atomic number for electron scattering by atomic fields,** *Phys. Rev.* **182,** No. 1, 97-101 (June 5, 1969).

> Key words: Atomic number; central potential; electron scattering; phase shift; Z-dependence.

Phase shifts of s-, p-, d-, and f-electrons scattered elastically by potential appropriate to singly charged positive ions have been calculated for energies ranging up to 2 Rydbergs above threshold and for selected elements throughout the periodic system. The results are discussed in terms of characteristics of the model potential.

11393. Matarrese, L. M., Wells, J. S., Peterson, R. L., **EPR spectrum of $Fe^{3+}$ in synthetic brown quartz,** *J. Chem. Phys.* **50,** No. 6, 2350-2360 (Mar. 15, 1969).

> Key words: Amethyst; electron paramagnetic resonance; ferric ion; quartz; synthetic brown quartz.

A detailed description is given of the EPR spectrum of $Fe^{3+}$ in synthetic brown quartz (the so-called I center, presumed to be interstitial). There are three, equally populated, inequivalent sites differing only in the orientation of their principal axes, which coincide with the three two-fold axes of quartz. The values of the Hamiltonian parameters that fit the data best are: $g = 2.0039 \pm 0.0003$, $C_{20}(\equiv D) = 734.1$ G, $C_{22}(\equiv(6^{1/2}/2)|E|) = 401.3$ G, $C_{40} = 2.5$ G, $C_{44} = 1.65$ G, $\lambda_{22} = 91.0°$, $\lambda_{44} = 71.5°$. The meaning of the latter two values is that lobes of the $V_{22}$ and $V_{44}$ parts of the crystal-field potential point 1° and 26.5°, respectively, from the optic axis of quartz. The occurrence of irregular off-axis extrema of the line positions when the magnetic field is directed in the vicinity of the optic axis precludes the assignment of magnetic axes of the paramagnetic center in the usual way. All features of the spectrum are predicted accurately by machine calculations based on the derived Hamiltonian. Although the data are not conclusive evidence, they are believed to be more consistent with an assignment of the I center to a substitutional site.

11394. Maximon, L. C., **Comments on radiative corrections,** *Rev. Mod. Phys.* **41,** No. 1, 193-204 (Jan. 1969).

> Key words: Corrections, radiative; electron scattering; essential elements; radiative corrections.

We present a review of the literature on radiative corrections to electron scattering, a summary of the essential elements of the theory in a manner hopefully useful to experimenters, and comments on certain aspects of the subject that need further investigation.

11395. May, L., Spijkerman, J. J., **On the relationship between Mössbauer spectroscopy and the nuclear magnetic resonance of organotin compounds,** *J. Chem. Phys. Letter to the Editor* **46,** No. 8, 3272-3273 (Apr. 15, 1967).

> Key words: Mössbauer spectroscopy; nuclear magnetic resonance; organotin compounds; relationship.

A relationship between the Mössbauer Spectroscopy chemical shift and the nuclear magnetic resonance coupling coefficient has been obtained for organotion compounds. By partitioning the total s-electron density at the tin nucleus in terms of the ligand contributions, the MS chemical shift can be calculated from the NMR coupling coefficient. This model was tested for the methylstannanes by a least square fit of the Mössbauer and NMR data. The fit was within the experimental error. The calculations also provided the ligand contribution to the total s-electron density at the tin nucleus, which explained the absence of a quadrupole splitting.

11396. Melmed, A. J., **Single-specimen FEM-LEED studies: carbon on tungsten,** *J. Appl. Phys.* **40,** No. 5, 2330-2334 (Apr. 1969).

> Key words: Carbon on tungsten; field emission microscopy; low-energy electron diffraction; surface study.

Field-electron microscopy and low-energy-electron diffraction can be used in a complementary manner. A method of making such a direct combination on a single specimen is described and applied to a study of the problem of carbon contamination of tungsten surfaces. It is shown that, within the sensitivity of the apparatus used, carbon may be present and undetected by LEED on a (nonperfect) (011)-oriented W LEED specimen.

**11397.** Melmed, A. J., **Surface characterization by ellipsometry low-energy electron diffraction, and field-electron microscopy,** (Proc. Conf. Third Battelle Memorial Institute Materials Science Colloquium, Kronberg, Germany, May 6-11, 1968), Chapter in *Molecular Processes on Solid Surfaces,* pp. 105-127 (McGraw-Hill Book Co., Inc., New York, N.Y., 1969).

Key words: Ellipsometry; field-emission; low-energy-electron diffraction; microscopy; optical constants; oxidation; surface characterization.

Two types of experiments are described. In the first ellipsometry and LEED are combined in a study of the room temperature interaction of oxygen with (011)-oriented tungsten. Based on published interpretations concerning the LEED aspects of this experiment, the ellipsometer is shown to be capable of detecting small fractions of a monolayer of adsorbed oxygen, and the average sticking probability for oxygen is estimated to be 0.2 or 0.4 for the first half monolayer of oxygen atoms. Inability to completely understand the ellipsometry data is encountered and is attributed to inadequacy of existing theory to cope with phenomena occurring in the sub-monolayer coverage range. In the second type experiment a technique is introduced which enables FEM and LEED observations to be made on a single specimen with reasonable assurance that the entire specimen undergoes the same thermal and environmental history. Oxidation of tungsten and the adsorption and removal of carbon on tungsten are used to demonstrate surface characterization with this FEM-LEED combination.

**11398.** Mendlowitz, H., **Calculated transition array for the configurations $3d^2$-3d4p in Ti** III, *Astrophys. J.* **158,** 385-388 (Oct. 1969).

Key words: Configurations $3d^2$3d4p; Ti III; transition strengths.

An intermediate coupling calculation has been carried out on the line strengths for the transitions between the configurations $3d^2$ and 3d4p in Ti III.

**11399.** Menis, O., Rains, T. C., **Determination of arsenic by atomic absorption spectrometry with an electrodeless discharge lamp as a source of radiation,** *Anal. Chem.* **41,** No. 7, 952-954 (June 1969).

Key words: Arsenic; atomic absorption; electrodeless; extraction-displacement reaction; standard reference materials; 4i,j and selenium 726.

The determination of arsenic in cast iron and high-purity selenium metal by atomic absorption spectrometry was facilitated by the extraction of the arsenic with diethylammonium diethyldithiocarbamate (DDDC) followed by a stripping process from the organic phase by displacement reaction. In addition, the high background absorption of arsenic radiation encountered in various oxidant-fuel systems was overcome with an argon (entrained air)-hydrogen. flame. The electrodeless discharge lamp was found to be an excellent high intensity source of radiation for use in atomic absorption in the far ultraviolet region. The detection limits for arsenic in an aqueous medium free of interfering cations was 0.1 $\mu$g/ml.

**11400.** Menke, J. L., **Beam monitoring at the NBS linac—energy, positioning, current, charge,** (Proc. 1969 Particle Accelerator Conf., Washington, D.C., March 5-7, 1969), *IEEE Trans. Nucl. Sci.* **NS-16,** Part 1, No. 3, 921-922 (June 1969).

Key words: Beam current; beam energy; beam position; ferrite coils; integrator.

We describe some of the beam monitoring systems used at th NBS Linac. These include an energy display system using pulsed magnet with 200 scanned-gate electronic readout. Shiel ing and electronics for use with ferrite loaded position and cu rent monitors are discussed; and the use of a fast, wide-range in tegrator with ferrite current pick-ups is outlined.

**11401.** Mies, F. H., **Resonant scattering theory of association rea tions and unimolecular decomposition. I. A united theory radiative and collisional recombination,** *J. Chem. Phys.* **51,** N 2, 787-797 (July 1969).

Key words: Absolute rate theory; association; configuratic interaction; optical potential; predissociation; quantu mechanics; resonance scattering; scattering theor unimolecular kinetics.

A complete quantum mechanical theory of unimolecul kinetics and of predissociation is developed using a generalize version of Fano's Theory of Resonant Scattering. An importa feature of the theory is that it treats the irreversible couplin between the activated molecules and either the photon fie (predissociation) or the inelastic collisions with bath molecul (unimolecular decomposition) by means of an optical potenti and leads to very concise and certainly in the case of predissoci tion exact results.

The final form of the rate expressions are expressed in a for resembling the Eyring Absolute Rate Theory (ART), with th important result that explicit theoretical expressions are give for the "transmission coefficients" as a function of temperatu and pressure, which in principle allows us to calculate the rate

**11402.** Miller, K. J., Mielczarek, S. R., Krauss, M., **Energy su face and generalized oscillator strength of the $^1A''$ Rydberg sta of $H_2O$,** *J. Chem. Phys.* **51,** No. 1, 26-32 (July 1969).

Key words: Born approximation; energy surface; genera ized oscillator strength; Hartree-Fock; $H_2O$; photodissoci tion; Rydberg.

The energies and wave functions of the lowest singlet ar triplet Rydberg states in $H_2O$ were calculated in the expansic basis self-consistent field procedure for a single configuration. portion of the energy surface of the $^1A''$ Rydberg state for a OHO angle of 105° was determined that shows the asymmetr dissociation of this state into ground state H($^2$S) and OH($^2$I fragments. The energy along the reaction coordinate is almo separable into a repulsion depending only on the center of ma separation and an attractive potential that depends only on th OH internuclear separation.

For the $C_{2v}$ conformation a large basis set was used to ap proach the Hartree-Fock limit. Using these functions a minimu was calculated in the generalized oscillator strength for the $^1A$ $\rightarrow$ $^1B_1$ transition as a function of the momentum transfer functic or the electron scattering angle. This behavior was then co firmed experimentally for an energy loss of 7.4 eV with an i cident electron energy of 500 eV. Such a minimum is a gener characteristic of Rydberg transitions and is not an essential molecular phenomena. The good agreement between experime and theory indicates a reasonable fit to the Rydberg wave fun tion by the approximate Hartree-Fock calculation.

**11403.** Miller, R. C., Prausnitz, J. M., **Statistical thermodynami of simple liquid mixtures. Henry's constants,** *Ind. Eng. Che Fundamentals* **8,** No. 3, 449-452 (Aug. 1969).

Key words: Henry's constants; liquid mixtures; partitic function; phase equilibria; statistical thermodynamics; su percritical component; van der Waals'/Percus and Yevic

The cell-theory partition function of Eckert and Renon is us ful for calculating Henry's constants for solutes provided that th perature is well below the solute's critical. For higher tem- tures a new partition function is developed based on a ified van der Waals' model. The potential energy of the te molecule in solution is related to a perturbation of the -sphere radial distribution function. calculations are ented for Henry's constants for methane, nitrogen and ogen in several simple liquid solvents.

4. Milligan, D. E., Jacox, M. E., **Matrix-isolation study of the frared and ultraviolet spectra of the free radical HCO. The drocarbon flame bands,** *J. Chem. Phys.* **51,** No. 1, 277-288 uly 1, 1969).

Key words: Absorption; DCO; emission; force constants; formaldehyde; free radical; HCO; hydrocarbon flame bands; infrared spectrum; matrix isolation; photolysis; ultraviolet spectrum.

he photoproduction of H or D atoms from a variety of ces in a carbon monoxide matrix or in an argon matrix to h a small concentration of carbon monoxide has been added s to the appearance of prominent ultraviolet absorptions veen 2100 and 2600 Å, all of which may be assigned to HCO DCO. Both the CO-stretching and the bending vibrational es are appreciably excited in the transition. Evidence is ented indicating that the transition observed in the matrix riments is the same one responsible for the hydrocarbon e bands. Using the frequencies observed in the matrix exnents, a tentative assignment for the hydrocarbon flame ls has been proposed which is in reasonable agreement with observed band structure of the emission system. In the upper , the carbon and oxygen atoms of HCO are approximately y bonded. Observation of the infrared absorption frequen- of isotopically substituted HCO in an argon matrix, has npted reconsideration of the valence force field appropriate round-state HCO. Interaction between the CH-stretching the CO-stretching modes has been found to play an impor- role. Factors leading to the stabilization of HCO in an argon ix in the present experiments, in contrast to the results of ious studies, are discussed.

5. Milligan, D. E., Jacox, M. E., **Studies of the photoproducon of electrons in inert solid matrices. The electronic spectrum the species $C_2^-$,** *J. Chem. Phys.* **51,** No. 5, 1952-1955 (Sept. 1969).

Key words: Acetylene; $C_2$ radical, $C_2^-$ ion; cesium; electron affinity; matrix isolation; photoionization; Swan bands; ultraviolet spectrum; vacuum-ultraviolet photolysis.

he vacuum-ultraviolet photolysis of acetylene isolated in an n matrix at 14 K in the presence of a small concentration of otoelectron source leads to a marked enhancement in the inity of the 5206 Å band system previously assigned to the n transition of $C_2$. Cesium atoms have been found to provide specially abundant electron source for these studies. The ational band spacings observed for the 5206 Å band system e much more closely with those recently reported by Herz- and Lagerqvist for the 5416 Å band system of a species tenely identified as $C_2^-$ produced upon flash discharge through nane than with the band spacings observed in the gas phase he Swan transition of $C_2$. Accordingly, it is suggested that 5416 Å band system of the gas-phase studies and the 5206 Å d system of the argon matrix experiments correspond to the e transition. The enhancement of this band system in the ence of a photoelectron source supports the hypothesis that species which contributes it is negatively charged.

6. Motz, J. W., Olsen, H. A., Koch, H. W., **Pair production photons,** *Rev. Mod. Phys.* **41,** No. 4, Part I, 581-639 (Oct. 969).

Key words: Electrons; pair production; photon polarization; photons; positrons; triplet production.

The present report reviews, analyzes, and integrates the various quantitative results that have been obtained for the process of pair production by photons. This summary includes a detailed review of total and differential pair cross sections with a critical evaluation of the conditions of validity and the accuracy of the results. In addition, a summary is given of the important kinematic relations and the polarization effects that occur in pair production.

**11407.** Mullen, L. O., Sullivan, D. B., **Fabrication of tunnel junctions on niobium films,** *J. Appl. Phys.* **40,** No. 5, 2115-2117 (April 1969).

Key words: Josephson effect; niobium; superconducting device; thin films; tunnel junctions.

High background currents, often observed in tunnel junctions when the barrier is formed by oxidizing niobium, probably stem from the fact that one oxide of niobium (NbO) is not an insulator. The fabrication process described in this paper uses an active layer of gas adsorbed on the niobium surface that reacts with the upper film (e.g. lead) and forms the junction barrier. This technique avoids the problem above and results in tunnel junctions with low background currents.

**11408.** Nahman, N. S., **Superconducting transmission lines – communication and power,** *Proc. 1968 Summer Study on Superconducting Devices and Accelerators, Brookhaven National Laboratory, Upton, L.I., New York, June 10-July 19, 1968,* **BNL-50155,** pp. 622-627 (1968).

Key words: Superconductive; transmission.

Reviews are given on (1) the experimental and theoretical work on S.C. signal transmission lines and (2) theoretical designs of S.C. power transmission lines. A brief exposition is presented on the constituents of a generalized data communication system. Elements of the above described topics are drawn together in a consideration of the idea of combining S.C. power and communication lines into one system.

**11409.** Nargolwalla, S. S., Przybylowicz, E. P., Suddueth, J. E., Birkhead, S. L., **Solution of blank problems in 14-MeV neutron activation analysis for trace oxygen,** *Anal. Chem.* **41,** No. 1, 168-170 (Jan. 1969).

Key words: Blank; Cockcroft-Walton neutron generator; "flow through" container; gamma-attenuation; geometrical correction; neutron attenuation; systematic error analysis; trace oxygen; 14-MeV neutron activation analysis.

A major difficulty in the analysis for trace oxygen by 14-MeV neutron activation analysis is the accurate determination of the oxygen contribution from the blank. If the count from the oxygen in the container is merely subtracted from the total sample-in-container count, errors greater than 100 percent in the oxygen content of the sample may result.

This work describes a procedure for accurately establishing the blank contribution. The method takes into consideration the attenuation of the activity produced in the polyethylene container by the sample during irradiation and counting. A proposed model permits corrections for the sample-in-container geometries with respect to the neutron source and detector system for different rod diameters. For metal rods, a "flow through" container propelled with nitrogen in the pneumatic transfer system was used to eliminate oxygen contribution from the container void volume. Within the precision of measurement, the experimental results agree with those predicted from theory.

**11410.** Nemoto, T., Beatty, R. W., Fentress, G. H., **A two-channel off-null technique for measuring small changes of attenua-**

**tion,** *IEEE Trans. Microwave Theory Tech.* **MTT-17,** No. 7, 396-397 (July 1969).

Key words: Attenuation; microwave; off-null technique; small attenuation changes; two-channel.

A technique is described for measuring small changes of attenuation which are not accompanied by significant changes in phase shift. It is a two-channel technique in which a small off-null output signal undergoes relatively large changes upon making small changes in a test attenuator in one of the channels.

The procedure is described and measurements from 0.01 to 0.1 decibel on a rotary vane attenuator are compared with similar measurements by a different method. Agreement is within 4 percent.

**11411.** Newman, M., **A diophantine equation,** *J. London Math. Soc.* **43,** 105-107 (1968).

Key words: Automorphisms; cyclotomic fields; diophantine equations; roots of unity.

An effective method for determining all rational solutions $x_1$, $x_2, \ldots, x_t$ of the equation $\sin\pi x_1 \sin\pi x_2 \ldots \sin\pi x_t$ = positive rational is given.

**11412.** Newman, M., **Some results on roots of unity, with an application to a diophantine problem,** *Aequat. Math.* **2,** No. 2/3, 163-166 (Nov. 28, 1967).

Key words: Cyclotomic fields; diophantine equations; multiplicative functions.

The principal result of this note is the determination of all rationals x, y such that $\sin\pi x \sin\pi y$ is rational.

**11413.** Newton, C. J., Ruff, A. W., Jr., **X-ray studies of plastically deformed silver alloys—effects due to oxygen, hydrogen, and tin solutes,** *Advan. X-ray Anal.* **12,** 316-328 (1969).

Key words: Alloys; plastics; silver alloys; x-ray studies.

Solid specimens of silver were charged at different temperatures in atmospheres of oxygen and of hydrogen. X-ray diffraction line profiles were obtained using powders filed from the treated specimens. Fourier analysis of the diffraction lines was conducted following the method of Warren. The effective particle sizes and root-mean-square strains were obtained from the line shape analysis. Stacking fault and twin fault probabilities were determined from peak-position and center-of-gravity displacements, respectively. For the purpose of comparison, two vacuum-melted silver samples and two different silver-tin alloys were studied. The stacking fault and twin fault probabilities were observed to be nearly unaffected by charging in either oxygen or hydrogen. These results are consistent with recent direct determinations of the effect of oxygen on the stacking fault energy of silver. In contrast, the rms strains and particle sizes changed significantly after charging in oxygen. A decrease in the root-mean-square strain and a corresponding increase in the particle size was found. These effects were opposite to those obtained by adding substitutional solute to silver. These findings are interpreted to indicate the effect of oxygen clustered with impurities on the dislocations and stacking faults in silver.

**11414.** Nimeroff, I., Schleter, J. C., **Professor Harry J. Keegan: Colorimetrist's spectrophotometrist,** *J. Appl. Opt.* **8,** No. 4, 757-761 (Apr. 1969).

Key words: Colorimetry; Keegan, Harry J.; photointerpretation; safety color codes; spectrophotometry; standards for spectrophotometers.

This paper is a tribute to Professor Harry J. Keegan (October 11, 1903 to April 19, 1968), prepared by two of his close associates at the National Bureau of Standards. The significance of his scientific and academic careers is reviewed and a subs
tially complete collection of references to his works is presen

**11415.** O'Connell, J. S., **An isospin sum rule for photonuc
reactions,** *Phys. Rev. Letters* **22,** No. 24, 1314-1316 (June
1969).

Key words: Correlations; electric dipole; isos
photonuclear; radii; sum rule.

A relationship is derived between proton and neutron m
square radii and a pair correlation function in stable nuclei.
energy weighted sums of the electric photodisintegration c
section to the two final isospin states.

**11416.** O'Connell, J. S., Prats, F., **Isospin sum rules and
photodisintegration of the A = 3 nuclei,** *Phys. Rev.* **184,** N
1007-1012 (Aug. 20, 1969).

Key words: Helium-3; isospin; photonuclear; radii;
rule; tritium.

Three sum rules for the electric dipole photodisintegra
cross section of the A = 3 nuclei are split into their final iso
components. The isospin doublet contribution to the th
nucleon breakup mode is found to be of the order of 10-20
cent and to originate primarily in the high energy region.

**11417.** Odom, J. V., **Problems of metric conversion,** *ASTME*
*tors* **4,** No. 4, 17-19 (July/Aug. 1969).

Key words: International system of units; measuren
systems; metric system; metric system study.

The increasing worldwide use of the metric system is cau
problems for manufacturers of hardware items. These probl
and the law that was recently enacted by Congress to study t
problems and seek sensible solutions are discussed, and
background that caused the law to be enacted is reviewed.

**11418.** Paabo, M., Bates, R. G., **Dissociation of deuteriocarbo
ion in deuterium oxide from 5 to 50°,** *J. Phys. Chem.* **73,** N
3014-3017 (Sept. 1969).

Key words: Acidic dissociation; bicarbonate ion; carb
acid; deuteriocarbonate ion; deuterium oxide; dissocia
of acids; emf measurements; heavy water; isotope eff
thermodynamics of dissociation.

Electromotive-force measurements of cells with deuterium
electrodes and silver-silver chloride electrodes have been
to determine the acidic dissociation constant of deuterio
bonate ion ($DCO_3^-$) in deuterium oxide from 5 to 50 °C at i
vals of 5 °C. In addition to the dissociation constant, the s
dard changes of enthalpy, entropy, and heat capacity for the
sociation process at 25 °C have been obtained. The isotop
fect, $pK(D_2O) - pK(H_2O)$, for bicarbonate ion is 0.748 at 2
and decreases with increasing temperature. This value is sig
cantly higher than is found for stronger acids. The entrop
ionization in deuterium oxide is smaller than that in water b
$K^{-1}$ $mol^{-1}$; this difference is the same as has been found for o
weak acids for which isotope effects have been determined.

**11419.** Peiser, H. S., Wachtman, J. B., Jr., **Jump rates for
defects in special positions held by a trapping centre of
symmetry,** Chapter 12 in *Physics of the Solid State,* S. B
rishna, M. Krishnamurty, and Rao B. Ramachandra, eds.
207-222 (Academic Press Inc., New York, N.Y., 1969).

Key words: Crystal; cubic; jump rate; point defect; rel
tion; symmetry; trapping center.

Point defects, held by a trapping center of cubic symmet
special positions relative to symmetry elements, generally
move between equivalent sites with more than one jump
For all possible symmetry groups of trap and point defe

inct paths are listed using a novel nomenclature. It is shown v such paths can give rise to relaxation phenomena by the ac- n of external influences. For all relevant symmetry combina- ns we list $J_{max}$, the maximum, and $J_{min}$, the minimum number jump rates for upsetting (or re-equalizing) the population ance between sites that are equivalent in the unstrained stal. $J_{max}$ often is the number of prime factors in the quotient ween the orders of the point groups of the trap and the defect. is the minimum number of operators that will raise the defect nt group to that of the trap.

20. Pella, P. A., DeVoe, J. R., Snediker, D. K., **Problems in sing Mössbauer spectrometry for quantitative analysis: appli- ation to tin,** *Anal. Chem.* **41,** No. 1, 46-50 (Jan. 1969).

Key words: High resolution detector; Mössbauer; quantitative analysis; source-sample-detector geometry; tin compounds; use of filters.

nitial studies for the application of Mössbauer spectroscopy he quantitative analysis of tin compounds are described. The ect of variables such as drift in detector response, sample ckness, and sample concentration on the spectral parameters s studied using $Pd_3Sn^{119m}$ as a source and synthetic samples of $D_2$ in an $Al_2O_3$ matrix. Under controlled conditions, the roducibility of the spectral parameters were studied for sam- sizes from 3 to 122 mg of $SnO_2$ with a relative standard devia- n (of a single measurement) for 3 replicates of 0.5 to 5 percent r this range of sample size. The data were well approximated an exponential absorption law. Such factors as source- nple-detector geometry, use of filters, and a high resolution ector were considered in an effort to optimize the ratio of the onant absorption intensity to the total transmitted intensity.

21. Pfeiffer, E. R., Schooley, J. F., **Superconducting transition emperatures of Nb-doped $SrTiO_3$,** *Phys. Letters* **29A,** No. 10, 89-590 (Aug. 11, 1969).

Key words: Charge carrier density; Nb-doped $SrTiO_3$; superconductivity; transition temperature maximum; transition temperatures.

Ve have observed superconducting transitions in Nb-doped $iO_3$ over the range of charge carrier densities $n = 0.13 - 2.2$ $0^{20}$ $cm^{-3}$. A $T_c$ maximum is observed similar to those previ- ly observed in reduced $SrTiO_3$ specimens.

22. Piermarini, G. J., Mighell, A. D., Weir, C. E., Block, S., **rystal structure of benzene II at 25 kilobars,** *Science* **165,** 250-1255 (Sept. 19, 1969).

Key words: Benzene II; high-pressure; single-crystal; structure determination; twinning.

t elevated temperatures and pressures, crystals of benzene nay be grown in the diamond-anvil high-pressure cell from er the liquidus or the solid I solid II transition. Depending n the conditions of growth, crystals were either single or nned. X-ray precession data were obtained from a single stal in the high-pressure cell. Benzene II crystallizes in the noclinic system with $a = 5.417 \pm .005$ Å (standard error), $b =$ 76 $\pm$ .019 Å, $c = 7.532 \pm .007$ Å, $\beta = 110.00 \pm .08°$, space up $P2_1/c$, $Z = 2$, $\rho_c = 1.26$ $g.cm^{-3}$ for the conditions 21 °C and 5 kbars. As only a limited amount of data were obtained, the cture was solved by generating all physically reasonable ecular packing configurations. For each configuration, struc- factors and a reliability factor were calculated. This cedure produced a unique solution for the molecular packing ne benzene molecules. The final R based on 19 unique reflec- s is 7.6 percent. This structure was confirmed by molecular king energy calculations.

23. Post, M. A., **Determination of styrene-butadiene and yrene-acrylate resins in solvent type paint,** *J. Paint Technol.* 1, No. 537, 567-580 (Oct. 1969).

Key words: Chlorinated paraffin; infrared spectroscopy; solvent type paint; styrene-acrylate resin; styrene-butadiene resin.

Styrene-butadiene and styrene-acrylate resins are determined quantitatively in solvent type paint by two methods. One, a short and convenient method, is useful in acceptance testing of Federal Specifications paints where the chlorinated paraffins 40 and 70 are used in 1:1 ratio. It involves determination of total benzene extractables and the styrene resin content therein. The latter is evaluated by measuring the 3.3 $\mu$m/3.5 $\mu$m absorbance ratio for styrene-butadiene and the 5.8 $\mu$m/3.5 $\mu$m absorbance ratio for styrene-acrylate, using the baseline method for both. The ratios are obtained from infrared spectrograms of cast films of benzene extracts. The styrene resin content then is determined from the appropriate standard curve. The second method separates the plasticizer (chlorinated paraffins) and styrene resin by Soxhlet extraction of the dried dispersed paint, first with n-pentane, which removes the plasticizers and 5-10 percent of the styrene resin, and then with benzene, which removes the remainder of the styrene resin. A combination of the two methods can be used for paints where the type and proportion of plasticizers are unknown. Methods are applicable to commercial materials.

11424. Powell, C. J., **Analysis of optican- and inelastic-electron-scattering data. Parametric calculations,** *J. Opt. Soc. Am.* **59,** No. 6, 738-743 (June 1969).

Key words: Complex dielectric constant; energy-loss interpretation; inelastic electron scattering; optical properties; parametric calculations.

Using a simple model for the complex frequency-dependent dielectric constant $\epsilon(\omega)$, calculations have been made of $-\mathrm{Im}[1/\epsilon(\omega)]$, the electron energy-loss function, as the model parameters were varied systematically in a physically-resonable range. It was found that the intensity as well as the position of structure in $-\mathrm{Im}[1/\epsilon(\omega)]$ were strongly influenced by the admixture of free-electron- and interband-transition-contributions to $\epsilon(\omega)$. Where such admixture-effects occur in real materials, it is not meaningful to identify structure in $-\mathrm{Im}[1/\epsilon(\omega)]$ as being exclusively due to plasmon excitation or to interband transitions.

11425. Qureshi, I. H., McClendon, L. T., LaFleur, P. D., **Extraction studies of the group of IIIB-VIIB elements and the lanthanides utilizing bis(2-ethyl-hexyl) orthophosphoric acid,** *Radiochim. Acta* **12,** No. 2, 107-111 (Aug. 1969).

Key words: Group IIIB-VIIB elements; HDEHP; hydrochloric acid; lanthanides; nitric acid; perchloric acid; solvent extraction.

The extraction behavior of the group IIIB-VIIB elements and the lanthanides from 1-11*M* hydrochloric, perchloric and nitric acid solutions into 0.75*M* bis(2-ethyl-hexyl) phosphoric acid solution has been studied. The group IVB elements and scandium exhibit high extraction which is independent of hydrogen ion concentration; the group VIIB elements are essentially unextracted. The extraction of some elements of group VB and VIB and of the lanthanides reaches a minimum and then increases with increasing acidity. This behavior is attributed to a change in extraction mechanism.

11426. Radziemski, L. J., Jr., Kaufman, V., **Wavelengths, energy levels, and analysis of neutral atomic chlorine (Cl I),** *J. Opt. Soc. Am.* **59,** No. 4, 424-443 (Apr. 1969).

Key words: Atomic spectra; chlorine; spectroscopy; wavelengths.

New wavelength measurements in the region from 950 to 12000 Å were combined with the infrared data of Humphreys and Paul (J. Opt. Soc. Am. **49,** 1180 (1959)) to extend the analysis of Cl I. Electrodeless discharge lamps containing $SiCl_4$, $GeCl_4$, $PbCl_2$, or chlorine gas were used to obtain wavelengths for 925 lines, of which 330 are interferometric values. The number of classified and observed lines has increased from about 550 and 780, to 1097 and 1173 respectively. Forty-three new even levels and 39 new odd levels were established, five levels rejected, and some J values and configuration assignments changed. The total number of known levels now stands at 112 odd and 128 even levels. The $3s3p^6\ {}^2S_{1/2}$ was found at 85679 $cm^{-1}$, and new levels belonging to each of the Cl II $3p^4$ limit levels were established. Most of the new levels belong to the $3p^46p$, $3p^4nf$ $n=6$ to 8, $3p^4ns$ $n=6$ to 8, and $3p^4nd$ $n=4$ to 8 configurations. The improved measurements and energy level values lead us to propose 108 vuv lines with uncertainties of less than 0.0015 Å as reference wavelengths. The accuracy of the series limit corresponding to Cl II $3p^4\ {}^3P_2$ was improved slightly; the newly calculated value is $104591.0 \pm 0.3$ $cm^{-1}$.

**11427.** Rains, T. C., **Chemical aspects of atomic absorption,** *Am. Soc. Testing Mater. Spec. Tech. Publ.* **443,** 19-36 (1969).

Key words: Analysis; atomic absorption; detection limits; electrodeless discharge; interferences; nebulizer-burner; organic ligands; releasing agents; solvents.

The phenomenal growth of atomic absorption spectrometry in the past 12 years can be attributed to many factors such as the high sensitivity of the method for a large number of elements, advances in overcoming interferences, saving of time required for analysis, and the rapid improvement of instrumentation. The major interferences in atomic absorption are of a chemical nature; however, physical interferences which are associated with the chemical matrix are often present. To overcome chemical interferences and to eliminate or minimize their influences from phosphate, aluminum, titanium and any other elements producing nonvolatile compounds, high temperature flames or releasing agents are used. Also, the use of a separation and preconcentration technique often becomes necessary when determining elements at the sub-trace level. A list of organic ligands and solvents used in solvent extraction for absorption are presented as a means of preconcentration and removal of chemical interferences.

**11428.** Rains, T. C., **Chemical interferences in condensed phase,** Chapter 12 in *Flame Emission and Atomic Absorption Spectrometry,* J A. Dean and T. C. Rains, eds., **1,** 349-379 (Marcel Dekker Inc., New York, N.Y., June 1969).

Key words: Atomic absorption; atomic fluorescence; flame emission; flame temperature; interference; oxidant-fuel; protective chelation; releasing agent.

In flame emission, atomic absorption or atomic fluorescence spectrometry, condensed phase type of interference is observed to occur for many analytes. The degree of interference on the analyte depends upon the interferent and the various parameters associated with the production of free atoms in the flame gas. Proposed mechanisms for the interference of $PO_4^{3-}$, $SO_4^{2-}$ and $Al^{3+}$ on the alkaline-earth metals are discussed together with methods for their elimination or control. The effect of flame temperature, choice of oxidant-fuel, nebulizer-burner systems and the use of releasing or protective chelating agents are reviewed as a method to minimize the condensed phase type of interference.

**11429.** Rains, T. C., Menis, O., **High-precision flame emission spectrometry,** *Spectroscopy Letters* **2,** No. 1, 1-7 (1969).

Key words: Attenuator; differential flame emission; phase shifter; precision; synchronous detector.

A new technique for differential flame emission spectrometry is described. The application of this method permits the determination of lithium as a major component in a glass matrix v a precision of one part per thousand.

**11430.** Raveché, H. J., Green, M. S., **On the consistency of Yvon-Born-Green hierarchy and its truncations,** *J. Chem. Pl* **50,** No. 12, 5334-5336 (June 1969).

Key words: Closure; consistency; hierarchy; Kirkwood perposition; potential of mean force.

The assumption of truncation of the hierarchy of reduced tributions for fluids at thermodynamic equilibrium is discus We consider the question of whether a truncated hierarchy yi expressions which are conservative for the mean force o molecule, in the presence of its neighbors. It is concluded tha general it does not, although the Kirkwood superposition and infinite hierarchy do. The conclusion is reached that, unless closure satisfies a certain condition, the truncated hierarch general has no solutions.

**11431.** Reader, J., **Optimizing Czerny-Turner spectrographs comparison between analytic theory and ray tracing,** *J. ( Soc. Am.* **59,** No. 9, 1189-1196 (Sept. 1969).

Key words: Aberrations; coma; Czerny-Turner; geom cal optics; plane grating; ray tracing; spectrograph.

The analytic theory of aberrations has been used to derive expression for the magnitude of the comatic width of the im in the meridional plane in a Czerny-Turner spectrograph w unequal mirror radii. The calculated properties of a 4-m spec graph with equal radii and a recently constructed 3.34-m spec graph with unequal radii are compared with the results obtai by tracing individual rays. The agreement is excellent, in c trast to the results of Chandler, J. Opt. Soc. Am. **58,** 895 (19 The lateral position of the grating for complete elimination coma found experimentally with the 3.34-m instrument is als good agreement with the theory. A correction to the $\sqrt{3}$ longi dinal grating position is given for a Czerny-Turner spectrogr which results in a flatter focal surface.

**11432.** Reed, R. P., **Low-temperature mechanical properties welded and brazed copper,** (Proc. 1968 Cryogenic Engineer Conf., Case Western Reserve Univ., Cleveland, Ohio, A 19-21, 1968), Chapter in *Advances in Cryogenic Engineer* **14,** Paper C-3, 83-87 (Plenum Press Inc., New York, N. 1969).

Key words: Brazed; copper; low temperature; notch-t sile; tensile; welded.

The tensile and notch-tensile properties of butt-welded overlap brazed copper plate were examined at test temperat 300, 195, 76, and 4 K. The brazed strengths were determined both 1/8 and 1/4 inch overlap widths. It was found that strength and ductility of copper joints increase at lower temp tures. Also, the joint strength decreases and elongation increa as the brazed overlap width is increased.

**11433.** Reed, R. P., Schramm, R. E., **Lattice parameters of n tensite and austenite in Fe-Ni alloys,** *J. Appl. Phys.* **40,** No 3453-3458 (Aug. 1969).

Key words: Fe-Ni alloys; lattice parameters; martensite.

The lattice parameters of the martensitic, body-centered c phase and the face-centered cubic phase were determined f series of Fe-Ni alloys. Compositions ranged from pure Fe to 35 at. percent Ni. Careful Debye-Scherer powder techni and computerized calculations and error analyses were ployed. The martensite lattice parameter has been preci determined for the first time as a function of composition in Ni alloys. Results indicate that the martensite lattice param reaches a maxmium between 9 and 15 at. percent Ni and room temperature lattice parameter of the face-centered c

se has a maximum in alloys having greater than 35 at. percent The face-centered cubic parameter was not measurable in al- having less than 27 at. percent Ni.

4. Reeve, G. R., **A heterodyne near-zone field-strength meter,** *EE Trans. Instr. Meas.* **IM-18,** No. 1, 32-37 (Mar. 1969).

Key words: Electric field strength; field, near zone electromagnetic; line, semiconducting plastic transmission; meter, radio field strength.

his paper describes a tunable field strength meter covering 12 to 30 MHz range which can be used to measure electric nsities from 0.1 to 1000 volts/meter in the near zone of an an- a with an estimated uncertainty of ±2 dB.

e use of high resistance plastic telemetry lines enables the to be probed without disturbance, while a novel detector it and meter enable a 40 dB display with minimal reading er- Laboratory and field test data on the device are presented.

5. Robbins, R. F., Weitzel, D.-H., **An automated resilience paratus for polymer studies from −196 to +180 °C,** *Rev. Sci. str.* **40,** No. 8, 1014-1017 (Aug. 1969).

Key words: Dynamic properties; low temperatures; polymers; resilience.

rebound resilience apparatus was developed to study the mic mechanical properties of polymeric materials from 6 to +180 °C. Resilience data at a frequency of about 3500 are obtained by measuring ball velocity near the sample with otoelectric device. Frequency of impact is estimated using icrophone pick-up. The results are recorded automatically a data acquisition system designed for the test.

e apparatus is virtually automatic in operation, and has wide bility in sample configuration, temperature range, and tem- ture control. The results can be related to other dynamic hanical properties data, and estimates of Young's modulus e regions of high resilience can be performed.

6. Roberts, D. E., **Recrystallization and melting of partially elted Stark rubber,** *Rubber Chem. Technol.* **42,** 540-546 ar. 1969).

Key words: Crystallized rubber; crystal size; heating rate; melting range; melting temperature; oriented; partial melting; recrystallization; rubber; slow melting; Stark rubber.

wo specimens from a piece of Stark rubber which had a melt- emperature originally at 41 °C were partially melted at 38 °C allowed to stand for 11 years, one at about 25 °C, the other °C. The first showed a continuous slow decrease in specific me, while the second increased slowly in volume for 5 ths and remained constant for about 5 months more before wing the continuous slow decrease. The melting temperature he first increased to 45 °C and the melting range was dened. The melting temperature of the second became 52 °C the range was narrowed. Perfecting or enlarging of crystals the effect of higher recrystallization temperatures have in- ced the melting temperatures. The effect of heating rate is ussed in connection with slow increases in volume, at- ted to relaxation of oriented regions, during melting.

7. Robinson, R. A., **An isopiestic vapor pressure study of the stem potassium chloride-sodium chloride in deuterium oxide lution at 25°,** *J. Phys. Chem.* **73,** No. 9, 3165-3166 (Sept. 69).

Key words: Deuterium oxide; potassium chloride; salt mixtures; sodium chloride; solutions.

apor pressure measurements of the system potassium ride-sodium chloride-deuterium oxide have been made at 25 °C and compared with similar data for the same salt system in ordinary water. There is no detectable difference in the behavior of this salt pair in the two solvents when the results are expressed on the aquamolality scale.

**11438.** Rockett, J. A., **Planned operation of the National Bureau of Standards Fire Research and Safety Office,** *Fire J.* **63,** No. 6, 41-43 (Nov. 1969).

Key words: Fire; research program.

The proposed program for the Fire Research and Safety Center is outlined. This consists of: (1) Statistical studies on deaths and injuries in fires and on the effectiveness of fire protection measures; (2) A study of the way in which fire grows and spreads in a building; and (3) Three programs related to fire service operations: (a) The use of Operations Research; (b) Improvement of breathing masks; and (c) A study of fire service training and education.

**11439.** Rubin, R. J., **Transmission properties of an isotopically disordered one-dimensional harmonic crystal,** *J. Math. Phys.* **9,** No. 12, 2252-2266 (Dec. 1968).

Key words: Crystal dynamics; defects; disordered crystals; multiple scattering; wave propogation in stochastic media.

The amplitude $\mathcal{T}_N(\omega)$ of a wave of frequency $\omega$ which is transmitted by a disordered array of N isotopic defects in a one-dimensional crystal has been investigated in the limit in which N $\rightarrow \infty$ while the overall concentration of the defects in the array remains fixed. The transmitted amplitude $\mathcal{T}_N(\omega)$ is proportional to the reciprocal of the magnitude of an Nth order determinant whose elements depend explicitly upon the spacings between defects, the incident frequency $\omega$, and the relative mass difference $Q = (M - m)/m$ between the defect particles and the particles of the host crystal. $\mathcal{T}_N(\omega)$ is represented as $\exp[-N\alpha_N(\omega, Q, c)]$ where C is the overall fractional concentration of defects; and two types of estimates of $\alpha_N(\omega, Q, c)$ are obtained. First, assuming that the spacings between nearest-neighbor pairs of defects are independent random variables, upper and lower bounds are obtained on $\alpha_N(\omega, Q, c)$ which are independent of N. Provided that C is sufficiently small, the lower bound is positive. Second, Monte Carlo estimates of $\alpha_M(\omega, Q, c)$ are obtained in the cases $Q = 1$, $C = 0.1$ and $Q = 1$, $C = 0.5$ for arrays of $3 \times 10^4$ defects. These Monte Carlo estimates are compared with the previously obtained bounds. It is also shown that at the special frequencies of Matsuda and for $Q \geqslant Q_{crit}$, the limiting value of $\alpha_M(\omega, Q, c)$ is positive in the entire concentration range $0 < C < 1$. Explicit upper and lower bounds are obtained on $\alpha[\sin(\pi/4), 1, c]$.

**11440.** Ruff, A. W., Jr., Ives, L. K., **Stacking fault energy determinations in HCP silver-tin alloys,** *Acta Met.* **17,** 1045-1055 (Aug. 1969).

Key words: Dislocation; dislocation double ribbons; dislocation nodes; hcp alloys; silver-tin alloys; stacking fault energy.

Measurements of the intrinsic stacking fault energy as a function of tin solute concentration are reported through the range of the intermediate hexagonal $\zeta$-phase. Four different alloy compositions in the range 12 to 17 atomic percent tin were studied. Extended dislocation nodes and dislocation double ribbons were observed and measured in order to determine the stacking fault energy. The stacking fault energy values obtained from measurements on these two configurations were in good agreement and indicated that the magnitude of the stacking fault energy increased linearly with solute concentration in the hcp phase. The results are compared with those of the cubic $\alpha$-phase alloys. The dislocation configurations in the hexagonal alloys are briefly described.

**11441.** Rush, J. J., Melveger, A. J., Lippincott, E. R., **Laser-Raman spectra of $PH_4I$, $PH_4Br$, and $PH_4Cl$,** *J. Chem. Phys.* **51,** No. 7, 2947-2955 (Oct. 1, 1969).

Key words: Barrier to rotation; crystal force field; crystal structure; lattice modes; phosphonium halides; Raman spectra; torsional frequency; vibration.

Laser-Raman spectra have been measured at 23 °C for $PH_4I$ and $PH_4Br$ and at ~5 °C for $PH_4Cl$. Peaks observed in the spectra of all the halides are assigned to "internal" $PH_4^+$ modes, $\nu_1(A_{1g})$, $\nu_2(A_{1g}, B_{1g})$, $\nu_3(E_g)$ and $\nu_4(E_g)$ and to torsional $[L_2(E_g)]$ and translational $[T_1(A_{1g})]$ lattice modes. The torsional frequencies are 326, 343 and $363 cm^{-1}$, respectively, for $PH_4I$, $PH_4Br$, and $PH_4Cl$, while the translational mode is observed at 55.5, 75 and $112 cm^{-1}$, respectively. Barriers to rotation are calculated from the torsional frequencies on the simple but unrealistic assumption of a "4-fold" cosine type potential for the $PH_4^+$ ions. The barriers obtained are 6.7, 7.4 and 8.2 kcal/mol, respectively for $PH_4I$, $PH_4Br$ and $PH_4Cl$. The spectral results and calculated barriers are compared in some detail with previous optical, NMR and neutron scattering results for both the phosphonium and ammonium halides. Suggested differences in force fields between the ammonium and phosphonium salts are discussed.

**11442.** Ruthberg, S., **Calibration to high precision in the medium vacuum range with stable environments and micromanometer,** *J. Vacuum Sci. Technol.* **6,** No. 3, 401-412 (May-June 1969).

Key words: Calibration; capacitance-diaphragm gauge; medium vacuum range; micromanometer; stable pressure generation; vacuum measurements.

Ultra stable vacuum environments are utilized with a micrometer point contact manometer as reference standard for measurement and calibration with an uncertainty of $1.2 \times 10^{-4}$ torr + 6 parts in $10^5$ of the reading from least count to several torr. The stable pressures are generated by dynamic vacuum systems and a servo control loop with cascaded error signals from a capacitance-diaphragm gauge for stabilities of better than 1 part in $10^5$ at 1 torr. Precise evaluation of systems and procedures is given. Operational factors affecting accuracy were studied, such as sorption in the manometer fluid, pressure distribution in the test chamber, time constants in the micromanometer, and thermal response of the control loop.

**11443.** Ryan, J. V., **Federal Government's role and activities in consumer safety. The role of the Fabric Flammability Section,** *Proc. Spring Workshop, Home Conf.,* 5 pages, National Safety Council, General Session, Washington, D.C., (May 26, 1969).

Key words: Fabrics; flammability; Flammable Fabrics Act; rugs; textiles; wearing apparel.

A review is given of consumer safety programs at the National Bureau of Standards, particularly those in response to legislation. The provisions of the Flammable Fabrics Act are listed and the chief items of implementation are discussed. Procedures for the development of standards have been published in the Federal Register. The initial step under the Procedures, a notice of finding that there may be need for new or amended flammability standards, has been taken for wearing apparel, carpets and rugs. Test method development in support of these findings is in progress. Research has been initiated in the flammability of materials. The National Advisory Committee for the Flammable Fabrics Act has been appointed and has met.

**11444.** Rybicki, G. B., Hummer, D. G., **Noncoherent scattering—V. Thermalization distances and their distribution function,** *Monthly Notices Roy. Astron. Soc.* **144,** 313-323 (1969).

Key words: Noncoherent scattering; radiative transfer; spectral line; thermalization length.

The distribution function for thermalization lengths is derive for an infinite atmosphere with a plane source. Precise defini tions of the thermalization length are discussed from the point o view of representing the distribution by a single characteristi length; of these a definition in terms of the median of the distribu tion seems to be most useful. The distribution of longest flight is derived and shown to provide a good approximation to the dis tribution of thermalization lengths at large distances from th source. Extensive numerical illustrations are provided.

**11445.** Santone, L. C., **Application of systems analysis to urba problems,** *International City Management Association, Th Municipal Yearbook,* pp. 225-232 (1969).

Key words: Accounting models; city management; facilit location; operations research; simulation technique systems analysis; urban problems.

At present, systems analysis is considered a potential tool t aid in the resolution of urban problems. It is possible for cit management to utilize the systems approach and perform certai techniques with minimum outside assistance. Three technique discussed in this paper are accounting models, simulatio models, and facility location models. Through these operation cities may develop a library of resources for application to futu problems. Because of similarity of problems, it may be possib to develop prototype models which would be available to all c ties. In essence, systems analysis offers urban areas a proce whereby it is possible to expand, validate, and organiz knowledge concerning a system so that given a problem withi the system, the alternative solutions may be more realistical evaluated.

**11446.** Scheer, M. D., Fine, J., **The desorption kinetics of $Cl^-$ an $I^-$ on Mo and Ta as determined by the pulsed-beam metho** (Proc. Sixth Intern. Symp. Rarefied Gas Dynamics, Can bridge, Mass., July 22-26, 1968), Chapter in *The Measur ment of Sticking Coefficients at High Temperatures Using th Isotopic Mixing Method* **II,** 1469-1477 (Academic Press Inc New York, N.Y., 1969).

Key words: Binding energies; $Cl^-$; desorption lifetimes; I Mo; Ta.

The desorption lifetimes of $K^+$ and $Cs^+$ on Mo were dete mined as a function of temperature. These results are in agre ment with previously reported lifetime measurements of thes ions on polycrystalline W and Re and hence appear to b independent of the metal substrate. A simple electrostat potential model can describe this alkali positive ion-met surface interaction.

In addition, desorption lifetime measurements were also mad for $I^-$ on and Ta and $Cl^-$ on Mo. These results are summarize It is seen that the binding energy between the halogen negati ions and the surface is strongly dependent upon the metal su strate. Further, the energy of a simple electrostatic bo between the halogen negative ion and the metal surface is abo half that which is actually observed. Consequently, unlike t case for the alkali positive ions, a covalent (M-X) or (M-X precursor is required to account for these large halogen negati ion desorption energies.

**11447.** Scheer, M. D., Fine, J., **The electron affinity of lithium,** *Chem. Phys.* **50,** No. 10, 4343-4347 (May 15, 1969).

Key words: Electron affinity; lithium; mass spectromet positive and negative surface ionization.

The positive and negative surface ionization of a lithium ato beam on a thin, heated, molybdenum ribbon was studied using specially designed mass spectrometer. At a constant incide beam flux, $Li^+$ yields were determined as a function of surfa temperature in the 1400 to 2100 K range. Using 5.39 eV for t lithium ionization potential (I), this data yielded an average tive ion work function ($\bar{\phi}_+$) of 4.38 eV with a standard devia- of 0.01 eV. The [Li$^+$/Li$^-$] ratio was then determined at n intensities and surface temperatures made sufficiently e to give measurable Li$^-$ yields. From the above values for I. T, and [Li$^+$/Li$^-$], it was found that A(Li)$=\bar{\phi}_- - 3.35$ eV a standard deviation of 0.05 eV. The quantity $\bar{\phi}_-$ is an age negative ion work function. This could not be measured any precision because of the very small Li$^-$ yields. A recent rmination of the single plane work functions of molybdenum vs a variation from 4.0 eV for the (116) plane to 5.0 eV for a ) surface. Since the negative ion work function average ac- uates the low work function patches, the maximum uncer- y in $\bar{\phi}_-$ is given by $4.0 < \bar{\phi}_- < 4.4$ eV. Consequently, the ron affinity of lithium is bounded by the following values: < A(Li) < 1.05 eV. From previously reported measure- ts of the polycrystalline work function of molybdenum, it is luded that A(Li) is more likely to be near the upper rather the lower limit of this range of uncertainty.

8. Schwartz, R. B., Schrack, R. A., Heaton, H. T., **A search r structure in the n-p scattering cross section,** *Physics Letters* B, No. 1, 36-38 (Sept. 1, 1969).

Key words: Cross section; hydrogen; neutron; neutron-proton scattering; structure; time-of-flight.

he n-p total cross section has been measured in the energy e 1.5 to 15 MeV with good energy resolution and high stical precision. No evidence of structure was found.

9. Seidel, G. P., **Neutron radiation hardening of polycrystal- ne iron,** *Radiation Effects* **1,** 177-190 (1969).

Key words: Annealing; impurities; iron; radiation hardening; strain ageing; yield stress.

ne dependence of the yield stress of vacuum-annealed and ogen purified iron polycrystals as a function of neutron dose annealing temperature and the influence of these parameters he effect of static strain-ageing has been investigated. The tion hardening was found to depend sensitively on the in- itial impurities N and C. This is explained by both a nuclea- of precipitation and a trapping of the impurities at radiation uced intrinsic defects. The radiation enhanced precipitation ominates in impurer iron and at low doses can be abolished ugh annealing below 190 °C. The trapping becomes effective gher doses or in purer iron. Below 400 °C two recovery s for the yield stress are observed (between 200 and 260 °C between 320 and 400 °C), which can be explained by the apping of N and C respectively. The static strain-ageing was d to be reduced by neutron irradiation. It reappears after an- ng at temperatures, at which the precipitates are thought to dissolved and the C and N atoms to be detrapped.

0. Shirley, J. H., **Validity of the semiclassical approximation maser theory,** *Phys. Rev.* **181**, No. 2, 600-609 (May 10, 69).

Key words: Correlations; laser; maser; phase fluctuations; semiclassical.

simple model of a maser or laser consisting of a single mode coupled to N identical two-level atoms is considered. The classical approximation is equivalent to neglecting the stical correlations between the atoms and the field. The ac- cy of this approximation is investigated by writing equations otion for the correlations. To obtain a complete, self-con- nt set of equations, it is necessary to include correlations of ield with itself (related to the coherence of the field) and cor- ions between different atoms. Relaxations and an energy ce are introduced phenomenologically into the equations of on. They are then solved for the case of steady state oscillation. It is found that the correlations are smaller than the terms kept in the semiclassical theory by the order of one over the number of photons present in the field, larger if thermal photons abound, but smaller if the field relaxation is dominant. Expressions are also found for the amplitude and phase fluctuations of the field. The latter yield a linewidth for the maser oscillator in agreement with earlier calculations, but obtained by a different method.

**11451.** Shumaker, J. B., Jr., Popenoe, C. H., **Arc measurement of some Ar II optical transition probabilities,** *J. Opt. Soc. Am.* **59,** No. 8, 980-985 (Aug. 1969).

Key words: Ar II; arc; argon; lifetimes; transition probabilities.

Wall-stabilized arc measurements employing the generalized Fowler-Milne diagnostic technique have been carried out in argon at atmospheric pressure. Transition probabilities are reported for all lines of the 4s-4p and 3d-4p Ar II arrays lying below 7200 Å.

**11452.** Simpson, J. A., **Electron impact spectrometry for gas phase chemical analysis,** *Mater. Res. Stand.* **9,** No. 8, 13-16 (Aug. 1969).

Key words: CO in air; electron impact spectrometer; gas analysis.

Electron impact spectrometry provides a new tool for gas phase chemical analysis. The data obtained is directly related to ultraviolet optical absorption but is easier to obtain and interpret. The instrument is briefly described and its performance demonstrated on CO in air at 15 ppm.

**11453.** Sitterly, C. M., **Forbidden transitions in atoms: catalogs and identifications,** *Mem. Soc. Roy. Sci. Liege* **V,** No. 16, 17-29 (1969).

Key words: Analyses of spectra, grades; atomic spectra, forbidden lines; celestial spectra, forbidden lines; corona, identifications; forbidden lines; nebular lines.

Forbidden lines identified in various celestial spectra are summarized in a general chart arranged by element and by the spectra of different stages of ionization for a given element.

The subject is reviewed by grading our present knowledge of atomic and ionic spectra in five general classes ranging from grades A to E. A chart of these grades is presented.

In view of the present advances in space technology, and future plans for observing stellar spectra in the vacuum ultraviolet, the needs of the astrophysicist are appraised.

Since forbidden lines can be identified in celestial spectra only as a result of laboratory analyses of spectra, the present programs on analyses are described. Progress in the preparation of tabular data needed to derive wavelengths of forbidden lines is outlined. Relevant bibliographical work being carried on as part of the "Atomic Energy Levels" Program at the National Bureau of Standards is reviewed.

**11454.** Sparks, L. L., Powell, R. L., Hall, W. J., **Progress on cryogenic thermocouples,** (Proc. 1968 Cryogenic Engineering Conf., Case Western Reserve Univ., Cleveland, Ohio, Aug. 19-21, 1968), Chapter in *Advances in Cryogenic Engineering* **14,** Paper H-4, 316-321 (Plenum Press Inc., New York, N.Y., 1969).

Key words: Cryogenics; gold alloy; thermocouples.

Experimental tests between 4 and 280 K have been completed on the following thermocouple materials: Chromel, copper, "normal" silver, platinum, *silver*-28 at. percent gold, constantan, Alumel, and *gold*-(0.02, 0.03, 0.07) at. percent Fe. Many thermocouple combinations can be made from the above materials; the four most important being Chromel vs constantan, copper vs constantan, Chromel vs Alumel, and Chromel vs gold-0.07 at. percent iron. Results on the last combination are of particular interest for measurements near liquid hydrogen temperatures and will be presented in some detail. The calibration cryostat is described briefly. Special methods of measurement and data analysis have been designed to study and minimize systematic errors. Simple illustrations of these measurement schemes are given.

**11455.** Stair, R., **Measurement of natural ultraviolet radiation; historical and general introduction,** (Proc. Conf. Fourth International Biometeorological Congress, Rutgers University, New Brunswick, N.J., 1966), Chapter in *The Biologic Effects of Ultraviolet Radiation,* Frederick Urbach, ed., pp. 377-390 (Pergamon Press Inc., New York, N.Y., August 1969).

Key words: Natural ultraviolet; radiometry; solar irradiance; spectroradiometry; ultraviolet.

The development of methods for the measurement of natural ultraviolet is interwoven with many fields of optics and electricity. Three hundred years ago Newton first observed that a crude glass prism would separate white light into colors or conversely combine colors. This was followed by the discoveries of ultraviolet and infrared by Ritter and Herschel. Then followed the work of Fraunhofer, Bunsen and Kirchhoff relating to the spectra. The discovery of the thermoelectric effect and its use in measurement by Nobili and Melloni opened the way for accurate measurements. Next came the discoveries in photography, photoelectricity, and great improvements in instrumentation which led the way for the measurements of solar radiation by Rowland, Langley, Fabry and Buisson, Pettit, Abbot, Nicolet, Allen, Mulders, Johnson, Coblentz, Stair and others.

**11456.** Stiehler, R. D., **History of measurement and the SI units,** *Mater. Res. Std.* **9,** No. 6, 14-18 (June 1969).

Key words: Ancient measures; history; measurement; SI units; units of measurement.

The evolution of the units of measurement from ancient Babylonia and Egypt to the present is briefly described. The so-called English units did not originate in England; they descended from antiquity. The confusion caused by the multiplicity of ancient units that were in use in Europe during the Renaissance was the stimulus that led to the development of the metric units. Similarly, the multiplicity of metric units for the same quantity that have arisen since 1800 led to the development of the rational and coherent International System of Units (SI) which were adopted in 1960 by the General Conference on Weights and Measures. The advantages and weaknesses of SI are discussed.

**11457.** Strobridge, T. R., **Refrigeration for superconducting and cryogenic systems,** (Proc. 1969 Particle Accelerator Conf., Washington, D.C., March 5-7, 1969), *IEEE Trans. Nuclear Sci.* **NS-16,** Part I, No. 3, 1104-1108 (June 1969).

Key words: Cost; cryogenic; efficiency; mass; refrigeration; volume; 1.8 to 90 K.

Cryogenics and high energy physics have been intimately associated for many years. The liquid hydrogen bubble chamber remains a primary detector for particle interactions and the recent successful development of superconducting RF cavities will vastly improve the duty cycle of linear accelerators. Aside from target and detection devices, it is not clear what role low temperature environments will play in the particle accelerators now being conceived. The amount of cooling required and the refrigeration temperatures may vary widely from concept to concept. To assist in planning, this survey of modern cryogenic refrigerators, covering refrigeration temperatures from about 1.8 to 90 K, gathers together performance, physical characterist and typical cost information from industry, academic, ar government sources both in the U.S. and abroad. Whenev possible, data on liquefiers are converted to an equivale refrigeration capacity. The capacities discussed range fro about one watt to kilowatts.

**11458.** Sukle, D. J., Wells, J. S., **Fine structure in EPR of $Mn^{2+}$ zinc sulfate,** *Phys. Rev.* **180,** No. 2, 445-450 (Apr. 10, 1969).

Key words: Anhydrous zinc sulfate; electron paramagnet resonance; manganese ion.

The electron spin resonance of 0.01 percent $Mn^{2+}$ in sing crystals of $ZnSO_4$ has been studied in order to investigate t crystal field interaction, which may be representative of the si gle ion anisotropy in $MnSO_4$. The symmetry group for the zi site, which the $Mn^{2+}$ ions are assumed to occupy, is $C_i$. There a in general, four inequivalent zinc sites, which produce a spe trum of 320 possible lines at an arbitrary orientation. Howeve data have been taken with $H_o$ in symmetry planes of the cryst so that pairs of inequivalent sites become equivalent. This resul in some simplification of the spectrum and provides a method f accurate alinement of the crystal.

The spectrum has been fitted to a low symmetry spin Ham tonian. Since crystal field terms are large, perturbation theo could not be used, and the spin Hamiltonian analysis of the spe trum was accomplished by computer programs which diagon ize the spin Hamiltonian parameters $C_{20} = 3.792 \pm 0.001$ $10^{-2}cm^{-1}$, $C_{21} = 3.815 \pm 0.001 \times 10^{-2}cm^{-1}$, $C_{22} = 5.808 \pm 0.0$ $\times 10^{-2}cm^{-1}$ with lobe orientations $\lambda_{21} = 152.6^o$ and $\lambda_{22} = 86.$ describe the room temperature spectrum reasonable well. T inclusion of the $C_{4q}$ terms improves the fit.

**11459.** Swartzendruber, L. J., Bennett, L. H., Watson, R. **Dilute $^5$Fe Mössbauer studies in Cu-Ni alloys,** *J. Appl. Ph* **40,** No. 3, 1489-1490 (Mar. 1, 1969).

Key words: Copper; invar effect; iron; magnetis Mössbauer; nickel.

The $^{57}$Fe Mössbauer effect has been used to study the prope ties of iron as a dilute impurity in Cu-Ni alloys. Using either 0 at. percent Fe as an absorber or $^{57}$Co as a source in Cu-Ni alloy we find a small, partially resolved magnetic hyperfine field what are normally considered nonmagnetic alloys. Previous the hyperfine field at 4 K was reported as undergoing a rap decrease in value near the equiatomic composition: from 243 d (243 kG) at 55 at. percent Ni to 0 dT (0 kG) at 45 at. percent (both alloys are ferromagnetic at 4 K). The present work exten this study and finds that the magnetic field drops instead to t small value of 10 dT (10 kG). This field is almost independent Ni concentrations between 10 and 45 percent Ni (i.e. in both fe romagnetic and paramagnetic regions). It is temperature ind pendent between 4.2 and 298 K, and is the same for either t source or absorber (0.5%). The Mössbauer results suggest invar-type effect occurs in this alloy system.

**11460.** Taggart, H. E., **Field strength and RFI standards at the N tional Bureau of Standards,** *Proc. IEEE Electromagne Compatibility Conf., Seattle, Washington, July 23-25, 196* pp. 149-158 (1968).

Key words: Antenna electromagnetic interference sta dards; calibration; measurement techniques.

Some of the calibration services offered to industry and ot governmental agencies by the National Bureau of Standar Radio Standards Laboratory are discussed. The emphasis placed on field strength measurements and related calibrati services at frequencies from 30 Hz to 12 GHz. These include t calibration of 3 basic types of antennas; (1) Loop antennas, Half-wave dipole antennas and (3) Horn antennas. Methods calibrating these antennas are described and illustrated.

discussion of calibration problems at microwave frequen-s emphasizing the measurements errors as related to the an-na and receiver voltage standing wave ratios (VSWR). Anten- and receiver VSWR's are exemplified, and corresponding asurement errors are shown. Methods of estimating errors are en.

The National Bureau of Standards recently designed and con-ucted some antenna standards for both the Air Force and the vy. These standards were designed to calibrate loop and half-ve dipole antennas. The frequency range is 10 kHz to 1000 Hz. These antenna standards are briefly described and illus-ted. The future plans for the development of antenna stan-ds and broadband EMC standards at the National Bureau of ndards are discussed. Work is in progress in areas of impulse nerators, random noise generators, and other instruments.

461. Tate, E. L., **Variations on a theme: government and library cooperation,** *D.C. Libraries* **39,** No. 3, 53-55 (1968).

Key words: Library cooperation.

ncreasing and changing demands for service are necessitating w cooperative programs among libraries in the Washington tropolitan area. These new programs, exemplified by the rk of the Library Technical Committee of the Metropolitan ashington Council of Governments or the Federal Library mmittee involve interagency rather than just interlibrary operation. Imaginative projects, like the High John project, ve been the result.

462. Thompson, B. A., LaFleur, P. D., **Activation analysis for molybdenum in samples containing large amounts of tungsten,** *Anal. Chem.* **41,** No. 13, 1888-1889 (Nov. 1969).

Key words: Activation analysis; molybdenum; radiochemistry; solvent extraction; technetium; tungsten.

Molybdenum has been determined by neutron activation analy- in the presence of large amounts of tungsten using a double ex-ction with bis (2-ethylhexyl) orthophosphoric acid (HDEHP). the first extraction W and Mo are separated from the trix elements. In the second extraction, made after equilibra-n of $^{99m}$Tc with $^{99}$Mo, the $^{99m}$Tc daughter of $^{99}$Mo is separated m W and Mo and used as a measure of the Mo present. The thod is very rapid and has good precision and accuracy.

463. Tipson, R. S., Brady, R. F., Jr., **Synthesis of the two D-2-pentuloses. New derivatives of D-*erythro*-pentulose,** *Carbohydrate Res.* **10,** 549-563 (Aug. 1969).

Key words: Acetonation; D-*erythro*-pentulose; D-*threo*-pentulose: isomerization; partition; pyridine.

The syrupy mixture of eight pentoses obtained by boiling a ution of either D-xylose (**1**) or D-arabinose (**2**) in pyridine for hours was freed of the four D-aldopentoses. The resulting xture of four D-pentuloses was resolved by condensation with etone, followed by partition between solvents or by distilla-n. In this way, crystalline 2,3-*0*-isopropylidene-*β*-D-*threo*-pen-ofuranose was readily prepared from **1**, and crystalline :3,4-di-*O*-isopropylidene-D-*erythro*-pentulofuranose (**14**) m **2**. Each of these isomerizations yielded a small proportion the epimeric D-2-pentulose, but the proportions of the D-3-ntuloses were much lower. The diacetal **14** was partially drolyzed, with dilute acid, to 3,4-*0*-isopropylidene-D-*erythro*-ntulofuranose (**17**), the *α*-D-anomer of which was obtained in ystalline form. The structure of **17** was proved by oxidation th periodate, to give the known, crystalline 2,3-*0*-isopropy-ene-D-erythrono-1,4-lactone. The anomers of the 1,3,4-acetate and 1,3,4-tribenzoate of methyl D-*erythro*-pentulofu-noside were prepared, and characterized by specific optical ation and n.m.r. spectroscopic evidence.

11464. Toots, J., Marton, L., **Optical properties of antimony and bismuth in the far ultraviolet,** *J. Opt. Soc. Am.* **59,** No. 10, 1305-1308 (Oct. 1969).

Key words: Antimony; bismuth; collective oscillations; dielectric constant electron-energy-losses; free-electron gas optical properties; plasma resonance; reflectance.

We have measured the multi-angle reflectance of Sb and Bi films in the region of collective oscillation resonance, for photon energies between 10 and 26 eV. Reflectances have been used to calculate the optical constants n and k, which in turn yield $\epsilon_1$ and $\epsilon_2$ as well as the real and imaginary parts of $\epsilon^{-1}$. F or Sb the $\epsilon^{-1}$ function can be closely fitted with the inverted Drude-Sellmeier resonance formula. The center of the resonance is at 16.0 eV, with a half-width of 5.2 eV corresponding to a decay time of $1.2 \times 10^{-16}$ s. The Bi data can not be fitted with a simple Drude-Sellmeier model, but it is in good qualitative agreement with the known electron energy absorption properties.

11465. Venable, W. H., Jr., Shumaker, J. B., Jr., **Observations of departures from equilibrium in a nitrogen arc,** *J. Quant. Spectr. Radiative Transfer* **9,** 1215-1226 (Sept. 1969).

Key words: Arc; nitrogen; nonequilibrium; spectral-intensity.

Atmospheric-pressure wall-stabilized arcs in nitrogen are found to exhibit molecular band intensities which are incompatible with the assumption of local thermodynamic equilibrium. Mechanisms to account for the departure from equilibrium are suggested.

11466. Verdier, P. H., **A simulation model for the study of the motion of random-coil polymer chains,** *J. Computational Phys.* **4,** No. 2, 204-210 (1969).

Key words: Chain dynamics; lattice model; Monte Carlo; polymer; simulation.

A lattice model of the dynamical behavior of a random-coil polymer chain in solution is described. Simulation of the model by a high-speed digital computer is discussed. The model appears especially suitable for the study of the effects of excluded volume interactions upon the motions of random-coil polymer chains.

11467. Viezbicke, P. P., **Interactions between nested receiving rhombic antennas,** *IEEE Trans. Ant. Prop.* **AP-17,** No. 1, 16-23 (Jan. 1969).

Key words: Antenna; comparison; co-planar; gain; interactions; mutuals; nested; patterns; planar; proximity; rhombic; spacing.

In order to install as many radiating circuits as possible in a given area, consideration has to be given to the operation of antennas in close proximity to one another. Therefore, mutual coupling between two nested rhombics and the effect of one rhombic on the radiation pattern of the other were measured.

For a ratio of antenna sizes of 2 to 1, the presence of either a coplanar or noncoplanar antenna had no influence on the gain and radiation pattern of the reference rhombic. To determine the minimum acceptable separation, measurements were extended to include rhombics almost equal in size and as close as practicable to each other. For wire separations of 0.5λ, the gain of the reference rhombic was reduced by 0.5 db. For 0.2λ separation the gain was reduced by 1 db, and for 0.04λ, by approximately 4 db. Except for very close spacings, the radiation patterns remained substantially unchanged.

Mutual coupling, expressed as transmission loss between the antennas in db, varied between −23 and −41 db.

11468. Viezbicke, P. P., **Why WWV moved to Colorado,** *Mark 5,* **13,** No. 3, 14-16 (June 1968).

Key words: High frequency broadcasts; standard frequencies; time signals; WWV.

This article outlines the reasons why WWV was moved from Greenbelt, Maryland to Fort Collins, Colorado. It summarizes the benefits resulting to the public.

**11469.** Waclawski, B. J., Hughey, L. R., **Effect of heating on the photoelectron yield of polycrystalline tungsten in the vacuum ultraviolet,** *J. Opt. Soc. Am.* **59,** 1494 (Nov. 1969).

Key words: Heating effects; photoelectron yield; spectral response; tungsten; ultra-high vacuum; vacuum ultraviolet.

The effect of heating on the spectral response of a previously atmosphere-exposed, polycrystalline tungsten photocathode was investigated for photon energies of 7.7, 10.2, 11.8, 16.9, and 21.2 eV. Use of ultra-high vacua $< 2 \times 10^{-9}$ torr precluded significant contamination of the sample after heating. The vacuum system bakeout at 630 K, as well as flashing the sample to 2200 K produced appreciable changes in the photoelectron yield (electrons per incident photon). The spectral response was modified by heating such that, compared to atmosphere-exposed tungsten, the yield decreased for photon energies greater than about 8 eV, but increased for lower photon energies.

**11470.** Waddell, W. J., Bates, R. G., **Intracellular pH,** *Physiol. Rev.* **49,** No. 2, 289-329 (1969).

Key words: Acidity; cell acidity; extracellular pH; glass electrode; intracellular pH.

Intracellular and extracellular pH are defined and methods for their determination are outlined. The literature on pH measurements in cells of the human body is summarized.

**11471.** Wagman, D. D., **Elements of chemical thermodynamics: introduction to thermal methods,** Chapter 86 in *Treatise on Analytical Chemistry,* Part I, *Theory and Practice,* I. M. Kolthoff, P. J. Elving, and E. B. Sandell, eds., **8,** 4909-4936 (Interscience Publ. Inc., New York, N.Y., 1968).

Key words: Equilibria; freezing point equation; ideal solution laws; thermal analyses; thermodynamic laws.

The chapter presents a short introductory statement of the principles of chemical thermodynamics, with special relevance to the laws used in the application of temperature and heat measurement to determinations of purity and extent of chemical reaction.

**11472.** Watson, R. E., Bennett, L. H., Freeman, A. J., **Comments on "origin of solvent Knight shifts in alloys,"** *Phys. Rev.* **179,** 590-592 (Mar. 10, 1969).

Key words: Alloys; charge impurity screening; hyperfine fields; Knight shift; noble metals; orthogonalized plane waves.

Objections, based on considerations of changes in electronic specific heat, to our proposal on the source of the changes in solvent Knight shift upon alloying, are examined and rejected.

**11473.** Weir, C. E., Piermarini, G. J., Block, S., **Instrumentation for single crystal x-ray diffraction at high pressures,** *Rev. Sci. Instr.* **40,** No. 9, 1133-1136 (Sept. 1969).

Key words: High pressure; single crystal; x-ray diffraction.

A diamond-anvil high pressure cell made of beryllium, a special goniometer head and a Buerger-type camera designed for x-ray diffraction by single crystals at high pressures are described in some detail. The most important problems still to be solved are discussed.

**11474.** Weir, C. E., Piermarini, G. J., Block, S., **Single crystal x-ray diffraction at high pressure,** *Proc. American Crystallographic Association/High Pressure X-ray Diffraction Sy posium, Seattle, Washington, Mar. 23-29, 1969,* **5,** 105-1 (1969).

Key words: High pressure; single crystal; x-ray diffractio

Apparatus and techniques used for single crystal x-ray diffra tion at high pressures are described briefly. The three types determinations carried out successfully are discussed. These ar (1) compressibility measurements; (2) unit cell and space gro determinations on high pressure phases; and (3) a structu determination.

**11475.** Weisman, I. D., Bennett, L. H., **Quadrupolar echoes solids,** *Phys. Rev.* **181,** No. 3, 1341-1350 (May 15, 1969).

Key words: KI; NiAl; nuclear magnetic resonance; puls nuclear resonance; quadrupolar interactions; spin echos.

In a classic paper, Solomon showed that the presence of i homogeneous, first order quadrupolar interactions leads to t formation of extra "allowed" spin echoes in nuclei for which t spin I = 5/2. We demonstrate (both theoretically and experime tally) that shifting the rf phase of the second pulse by 90° (in spin 5/2 system) enhances the allowed echoes by a factor of most 5 in amplitude over the unshifted case. Using the densi matrix formulation (and assuming no magnetic inhomogeneitie we have derived, for a 90° phase shift, the amplitude and sha dependence on the second pulse turning angle of the $3\tau/2$, $2\tau$ a $3\tau$ echoes. Experimental echo amplitudes and shapes (for bot and 90° phase shifts) were obtained, at room temperature, on in a fused sample of KI and these show quite good agreeme with the calculations. Due to the enhancement, this technique fords a much easier separation of the respective distributio arising from the 3/2 ↔ 5/2 and from the 1/2 ↔ 3/2 satellite tran tions than is possible in the unshifted case. Another feature the phase shifted case is that, in favorable circumstances, the echo may be observed although the $2\tau$ echo is obscured by t receiver recovery time. Preliminary data on quadrupole distrib tions at Al sites in NiAl intermetallic compounds are present

**11476.** Weiss, B-Z., Meyerson, M. R., **Effect of chromium dif sion coatings on fatigue in iron,** *Trans. Met. Soc. AIME* 2 1633-1643 (July 1969).

Key words: Armco iron; chromium diffusion coatin crack formation; crack propagation; fatigue.

Chromium diffusion coatings on commercial Armco Iron le to structural, compositional, and stress distributional changes the outer layers. These changes affect the mechanism of fati crack formation. In chromized samples, the crack initiates bel the Cr-rich zone after only a limited portion of the total lifeti (5 to 10%). The crack formation was observed at the grain bo daries, where precipitated Cr-carbides were found. Residual t sile stresses and a stress concentration caused by the carbi are considered as accelerating factors. In uncoated samples, cracks form at slip boundaries after 40 to 50 percent of t lifetime. The propagation process in coated samples is slo than in uncoated samples, as a result of the moderate rate propagation until such time as the crack proceeds complet through the coating. At best, the Cr-diffusion causes little if a increase in fatigue life, and in certain cases a severe deteriorat in fatigue life is observed.

**11477.** West, E. D., Ishihara S., **Experimental evaluation heater lead error in calorimetry,** *Rev. Sci. Instr.* **40,** No. 1356-1359 (Oct. 1969).

Key words: Calorimeter; energy measurement; errors calorimetry.

Improper location of the potential leads for calorime heaters can cause an appreciable systematic error. Calculati stimate limits on this error are usually based on greatly sim- ied heat flow problems. An easily understood experimental not involving such simplifications provides a more convinc- demonstration of a limit on the magnitude of the systematic r. Such a test is provided by measurements with the same or ivalent heater leads and heaters of very different resistances.

**78.** Wiederhorn, S. M., **Fracture of sapphire,** *J. Am. Ceram. oc.* **52,** No. 9, 485-491 (Sept. 21, 1969).

Key words: Cracks; crack propagation; double-cantilever-cleavage technique; fracture; fracture surface energy; sapphire.

he fracture of sapphire was studied using the double-cantil- r-cleavage technique. Fracture surface energies of 7.3 and J/m$^2$ were found for the $(10\bar{1}0)$ and $(\bar{1}012)$ planes respective- Attempts to measure the fracture surface energy on the 01) plane proved unsuccessful. The failure of sapphire to ture along the basal plane was attributed to the fact that these nes lack charge neutrality. The possibility of fracture induced ocation motion in sapphire at room temperature was in- tigated. No evidence for dislocation motion was found and it estimated that dislocations do not move in sapphire at room perature at stresses less than approximately $7 \times 10^9$ N/m$^2$ psi), Fracture behavior on $(\bar{1}012)$ planes was found to be er- c, varying from boule to boule. The topology of surfaces ned by crack propagation along this plane is described, but no lanation for the erratic behavior or the observed fracture fea- s is given.

**79.** Wiese, W. L., Bridges, J. M., Kornblith, R. L., Kelleher, D. E., **Transition probabilities for prominent Ar I lines in the ear infrared,** *J. Opt. Soc. Am.* **59,** No. 9, 1206-1212 (Sept. 969).

Key words: Atomic; infrared lines; neutral argon; transition probabilities; wall-stabilized arc.

elative transition probabilities of 81 infrared Ar I lines in the velength range from 9000-24000 Å have been measured with all-stabilized arc operating in argon at atmospheric pressure. large majority of the lines from the 4p-5s and 4p-3d transi- arrays has been observed and the measurements are con- ent with the J-file sum rule. The data have been normalized to absolute scale by utilizing other recent arc and lifetime values.

**80.** Wilson, W. K., Hebert, R. L., **Evaluation of the stability of ecord papers,** *Tappi* **52,** No. 8, 1523-1529 (Aug. 1969).

Key words: Accelerated aging; aging; deterioration; laboratory aging; preservation; records; stability.

nformation has been developed on the relative stabilities of pers made from a variety of pulps including groundwood, tral sulfite semichemical, bleached chemical wood and rag. er laboratory aging at 90 °C and 50 percent relative humidity various time periods, changes in reflectance, pH, folding en- ance, tear, burst, and tensile properties were determined. Al- ne papers as a group were more resistant to laboratory aging n any of the others. The papers made from groundwood also wed good resistance to aging. Papers containing large centages of neutral sulfite semichemical pulp covered a wide ge of stability depending on the pH. The pH was an important tor in laboratory aging, but the correlation between pH and rate of deterioration of physical properties was not high.

**81.** Wolcott, N. M., Falge, R. L., Bennett, L. H., **Magnetic ehavior of intermetallic compounds of beryllium,** *J. Appl. hys.* **40,** No. 3, 1377-1378 (Mar. 1, 1969).

Key words: Beryllium; ferromagnetism; intermetallic compounds; magnetic moment; nuclear magnetic resonance; paramagnetism.

The corroboration by NMR of the ferromagnetism of CrBe$_{12}$ has prompted an NMR investigation of the magnetic properties of other beryllium intermetallic compounds. Magnetic moment measurements of these materials show complex magnetic behavior at 4.2 K. All samples show strong paramagnetic moments and many exhibit remanence. To provide more information on this magnetic behavior, the $^9$Be resonance was observed in the following samples, listed in approximate order of their magnetic strength at 4.2 K: CrBe$_{12}$, ZrBe$_2$, MnBe$_8$, FeBe$_{11}$, MnBe$_{12}$, NbBe$_3$, ZrBe$_{13}$, TaBe$_3$, CrBe$_2$, Nb$_2$Be$_{17}$, TiBe$_{12}$, NbBe$_{12}$, VBe$_{12}$, MoBe$_{12}$, TaBe$_{12}$, WBe$_2$, Ta$_2$Be$_{17}$, WBe$_{12}$. Magnetization measurements are also reported for AgBe$_{12}$, FeBe$_{12}$, CoBe$_{12}$, PtBe$_{12}$, PdBe$_{12}$, and AuBe$_{12}$. Both the Knight shifts and the linewidths show correlation with the moment measurements. Most of the samples show small magnetic moments, positive Knight shifts, and small linewidths, $\Delta H$, less than (800 A/m = 10 Oe). ZrBe$_2$ and MnBe$_8$ have larger moments, negative values of K ($\sim -0.03\%$ at 300 K) and larger $\Delta H$ ($\sim$(12 kA/m = 15 Oe) at 300 K). CrBe$_{12}$, clearly ferromagnetic, with the largest moment (of the compounds studied) has the most negative value of K ($-0.19\%$ at 300 K) and the largest $\Delta H$ ((1.83 kA/m = 23 Oe) at 300 K). From the *temperature dependence* of the linewidths, it appears that NbBe$_3$ and CrBe$_2$ may be magnetic, although much weaker than CrBe$_{12}$. Anisotropic Knight shifts and first order quadrupole effects are noted.

**11482.** Woo, S. B., Branscomb, L. M., Beaty, E. C., **Sunlight photodetachment rate of ground state O$_2^-$,** *J. Geophys. Res. Space Physics* **74,** No. 11, 2933-2940 (June 1, 1969).

Key words: Drift tube; ion mobility; oxygen negative ion; O$_2^-$; photodetachment; photoionization.

Swarm, instead of the usual crossed-beam, technique is used to measure the sunlight photodetachment rate of O$_2^-$. The advantage of this technique is that the molecular negative ions can be relaxed through approximately $10^6$ collisions at thermal energy to ground vibrational and electronic state, before being introduced to the photodetachment chamber. Consequently, one can be confident of the applicability of data to the mesophere where the molecular negative ions are thought to be in thermal equilibrium with the temperature of the neutral gas. The measured absolute sunlight photodetachment rate of O$_2^-$ is $0.3 \pm 0.1$ per ion per second. This value is obtained through a relative measurement, calibrating against the 1.44 sec$^{-1}$ absolute sunlight photodetachment value of O$^-$, reported by Branscomb. A preliminary absolute solar-spectrum photodetachment rate of O$_3^-$ is reported. This value is 0.06 per ion per second, believed good to a factor of two.

**11483.** Yakowitz, H., Michaelis, R. E., Vieth, D. L., **Homogeneity characterization of NBS spectrometric standards. IV: Preparation and microprobe characterization of W-20% Mo alloy fabricated by powder metallurgical methods,** (Proc. 17th Annual Conf., Applications of X-ray Analysis, Estes Park, Colo., Aug. 21-23, 1968), Chapter in *Advances in X-ray Analysis,* C. S. Barett, G. R. Mallett, and J. B. Newkirk eds., **12,** 418-438 (Plenum Press Inc., New York, N.Y., 1969).

Key words: Homogeneity testing; metallography; microprobe analysis; NBS standards; powder metallurgy; tungsten-molybdenum alloys.

A significant problem of the National Bureau of Standards Standard Reference Materials program is the provision of standards suitable in homogeneity for use with microanalytical techniques such as the spark source mass spectrograph and the electron probe microanalyzer. An interim approach to the problem has been the extended homogeneity characterization of selected existing standards. This paper describes the preparation and evaluation of the first NBS standard tested specifically from the beginning for application to electron probe microanalyzers.

The standard designated SRM 480 is a tungsten-20 weight percent molybdenum alloy prepared by a powder metallurgy process. Based on the results of about 1500 determinations for both tungsten and molybdenum by electron probe microanalysis, the material was found to be of high homogeneity at about the micrometer level of spatial resolution. The coefficient of variation for molybdenum was 2.5 percent and that for tungsten 1.5 percent. Correction of relative intensity ratios to obtain concentrations is discussed in terms of input parameter uncertainties such as mass absorption coefficients, and electron backscatter factors. The result of studies for atomic number correction and effects on operating voltage on the microprobe absorption correction, will be given. It is concluded that SRM 480 should be a valuable addition to any microprobe laboratory doing quantitative analyses.

**11484.** Yates, J. T., Jr., Madey, T. E., **Chemisorption on rhenium: $N_2$ and CO,** *J. Chem. Phys.* **51,** No. 1, 334-337 (July 1, 1969).

Key words: Carbon monoxide; chemisorption; isotopic mixing, flash desorption; molybdenum; nitrogen; rhenium; sticking coefficient; tungsten.

The chemisorption of $N_2$ and CO on polycrystalline Re has been studied using flash desorption. A number of binding states have been identified and their binding energies have been estimated kinetically. Isotopic mixing between chemisorbed species has been observed for the $\beta$-$N_2$ and $\beta$-CO states on Re; there appears to be no evidence for dissociation of $\beta$-CO. The $\gamma$-$N_2$ and two $\alpha$-CO states on Re desorb without isotopic mixing.

In general, the distribution and properties of binding states for $N_2$ and CO on Re are remarkably similar to those found for these adsorbates on W.

An enhancement in nitrogen adsorption on Re occurs upon electron impact (150 eV) on $N_2(g)$. A new set of strongly-bound states are produced which are distinct from the $\beta$-$N_2$ states populated by adsorption of ground state $N_2(g)$.

A comparison of the sticking coefficients for $N_2$ and CO on Re is made, using two independent methods (uptake and isotopic mixing) over a wide temperature range. The sticking coefficient for $N_2$ on Re decreases markedly with increasing temperature; for CO on Re, there is little effect of temperature on the sticking coefficient.

A discussion is presented of migration-limited bimolecular kinetics at elevated temperatures in the chemisorbed layer.

**11485.** Yates, J. T., Jr., Madey, T. E., **Electron impact study of the $\gamma$-$N_2$ state chemisorbed on tungsten,** (Proc. Fourth International Materials Symp., Berkeley, California, June 1968), Chapter in *The Structure and Chemistry of Solid Surfaces,* Gabor A. Somorjai, ed., pp. 59-1, 59-27, (John Wiley and Sons, Inc., New York, N.Y., 1969).

Key words: Binding states; chemisorption; electron impact; flash desorption; nitrogen; tungsten.

Low energy (<75 eV) electron-impact conversion of the weakly-chemisorbed molecular $\gamma$-$N_2$ species on tungsten to more strongly bound chemisorbed species has been observed. It is possible to more than double the surface concentration of strongly bound nitrogen by this means. Neither $N_2^+$ nor $N^+$ were detected upon electron bombardment of $\gamma$-$N_2$ ($Q^+ < 1.4 \times 10^{-23}$cm$^2$). For 45 eV electron impact, the cross section for the depletion of the $\gamma$-$N_2$ state is $\sim 1 \times 10^{-19}$cm$^2$. Isotopic mixing between $^{14}N_2$ and $^{15}N_2$ does not occur in the $\gamma$-$N_2$ state upon electron impact.

**11486.** Young, D. S., Mears, T. W., **Measurement and standard reference materials in clinical chemistry,** *Clin. Chem.* **14,** No. 10, 929-943 (Oct. 1968).

Key words: Clinical; measurement; medicine; Standar Reference Materials.

The concept of the measurement system based upon the fou parameters – length (meter), mass (kilogram), time (second), an temperature (Kelvin) – is developed. The proper daily operatio of an analytical laboratory depends on these basic measurement and several derived from them, e.g., the liter. An additional com ponent of chemical measurement which directly influences accu racy is the purity of the standards and reagents employed. Th Standard Reference Materials program of the National Burea of Standards provides a central source of guaranteed high-purit reference materials which are available to all. The reliability chemical measurements will increase as new Standard Referenc Materials such as cholesterol, uric acid, urea, and creatinine a utilized to standardize methods and instruments in the clinic laboratories of this country.

**11487.** Beatty, R. W., ed., **Commission 1, Progress in radio mea surement methods and standards (Triennial report of progress** *Radio Sci.* **4,** No. 7, 579-590 (July 1969).

Key words: International Scientific Radio Union Repor measurement methods; radio measurements; radio sta dards; URSI XVIth General Assembly.

A review of progress within the USA in Radio Standards a Measurement Methods, covering the period 1966-1968, incl sive, is presented. This review is a part of the Triennial Report the U.S. National Committee of URSI (International Scientif Radio Union) to the XVIth General Assembly of URSI.

The following topics dealing with U.S.A. progress in Rad Standards and Measurement Methods are included: Time a Frequency; CW Power; CW Voltage; Noise; Pulsed Volta and Power; Attenuation, Phase Shift, and Time Delay; I pedance; Antenna Characteristics; Field Strength; RF Prope ties of Materials; Broadband Measurement Techniques; a Laser Measurements.

The report does not include all the developments which ha occurred in the U.S.A. in the period indicated, but rather has a tempted to include the most significant developments in ea field.

**11488.** Bennett, H. S., **F center in ionic crystals. II. Polarizable-i models,** *Phys. Rev.* **184,** No. 3, 918-935 (Aug. 15, 1969).

Key words: F center; Huang-Rhys factor; ionic cryst ($NaCl$, $KCl$, $MgO$, $CaO$, $SrO$, $CaF_2$, $SrF_2$, $BaF_2$); polariz ble ion; zero phonon transition.

The states of the *F* center are considered on the basis models which treat the movement of the nearest neighbors to t *F* center and the *F* electron in a self-consistent manner. The la tice is first described in terms of a classical ionic-crystal theo The theory is then extended to treat the nearest-neighbor ions a quantum-mechanical manner. The one defect electron (the electron) is treated according to polarizable-ion models. The a sorption energy, the emission energy, the lifetime of the fi excited state, the zero-phonon transition energies, and t Huang-Rhys factors are evaluated for two models, which dif in the rigor used to compute the polarization of the nearest a next-nearest neighbors. It is found that the model that contai the more rigorous evaluation of the polarization agrees best w the experimental results for CaO and perhaps MgO. In additi it is found that both these models are least successful for centers in NaCl and KCl. Not enough data exist to ma judgments about the agreement for $CaF_2$, $SrF_2$, and $BaF_2$.

**11489.** Bennett, H. S., **Frequency shifts of acoustic phonons Heisenberg paramagnets. III,** *Phys. Rev.* **185,** No. 2, 801-8 (1970).

Key words: Acoustic phonons; antiferromagnet; attenuation; EuO; ferromagnet; magnetic insulators; $MnF_2$; phonon frequency shift; $RbMnF_3$.

The propagation of sound waves in ferromagnetic and antifer-
nagnetic insulators is studied within the framework of two
dels which describe the interaction between the spin system
l the lattice. Expressions for the frequency shifts (phonon
ormalizations) at high temperatures and near the transition
nperatures are obtained in terms of time-dependent correla-
n functions. The frequency shifts for long-wavelength
onons are found to be negative, to increase rapidly in the
inity of the transition temperature, and to be less singular than
attenuation coefficients. The ratio of the frequency shift to
unperturbed phonon frequency is shown to be independent
the phonon frequency for long wavelengths. These results
ee qualitatively with present experiments.

90. Bennett, L. H., Swartzendruber, L. J., Watson, R. E.,
lagnetic clusters associated with isolated Fe atoms in paramagnetic Cu-Ni alloys,** *Phys. Rev. Letters* **23,** No. 20, 1171-1174
Nov. 17, 1969).

Key words: Alloys; Cu; Fe; magnetism; moments; Mössbauer effect; Ni.

small magnetic cluster is shown to exist around an isolated
atom in $Cu_{1-x}Ni_x$ alloys with a magnetic moment and satura-
n hyperfine field depending on the number $n$ of Ni near
ghbors. This small cluster changes abruptly from moments of
$5 + 0.6n) / \mu_B$ to large moments $[(\sim 17 \text{ to } 20)\mu_B]$ for Ni con-
trations near the critical composition. The moment compen-
on (Kondo effect) found for isolated Fe in Cu appears to per-
in Cu-Ni up to at least 10 at. percent Ni.

91. Berger, M. J., Seltzer, S. M., **Calculation of energy and
harge deposition and of the electron flux in a water medium
ombarded with 20-MeV electrons,** (Proc. Conf. High Energy
Radiation Therapy Dosimetry under the auspices of the
American Association of Physicists in Medicine, New York,
N.Y., June 15-17, 1967), *Ann. N.Y. Acad. Sci.* **161,** Art. 1, 8-
3 (July 3, 1969).

Key words: Charge deposition; electrons; energy deposition; flux; Monte Carlo; multiple scattering.

A combination of Monte Carlo and analytical techniques is
d to compute the penetration of fast electrons in water, taking
account multiple elastic scattering by atoms, multiple in-
stic scattering by atomic electrons, and the production of
msstrahlung. Secondary electrons are also considered which
ult from electron-electron collisions, or from the absorption
scattering of bremsstrahlung. The calculation provides infor-
tion about the spatial distribution of energy deposition, charge
osition and the electron flux (primary and secondary) down
a spectral energy of 400 eV. Representative results are
sented, mainly for 20-MeV electrons incident prependicu-
y on a semi-infinite water medium.

92. Blandford, J. M., **In-plant testing for wash-and-wear ap-
arel performance and labeling,** *Third Annual Tech. Conf. The
Apparel Research Foundation, Inc., Washington, D.C., Oct.
14-16, 1969,* 12 pages (Oct. 14, 1969).

Key words: Apparel; care instructions; labeling, apparel; performance, apparel; properties, apparel; testing textiles; wash-and-wear.

A distinction is made between washable garments, in general,
l wash-and-wear apparel, in particular, with reference to the
operties associated with appearance, performance, and ease of
e. The testing equipment, testing procedures, and evaluation
terials required by the apparel manufacturer in his assessment of these properties and formulation of ease-of-care instructions for labels and hang tags, are discussed. Tabulations and charts are included.

11493. Braun, W., Carrington, T., **Line emission sources for concentration measurements and photochemistry,** *J. Quant. Spectr. Radiative Transfer* **9,** 1133-1143 (1969).

Key words: Absorption; analysis; gas; photochemistry; spectroscopy; vacuum ultraviolet.

When a resonance line is absorbed in its own gas, measurements of this absorption can be used to derive a value of the product, *nf*, of concentration of the absorber and *f*-value of the transition. This line absorption process is also important in the study of fluorescence and photochemistry, where it is possible to produce atoms or molecules in a single quantum state without otherwise disturbing the system. The interpretation and success of these applications of line absorption depend critically on the shape of the line emitted by the light source. This is strongly influenced by the optical depth in the emitting region, and by the inevitable presence of a reversing layer through which the light must travel on its way out of the lamp. This paper presents a simple model which can be used to estimate the effects of these properties of the light source on the threshold and sensitivity of measurements of *nf*, and on the power which can be delivered to absorbing atoms outside the lamp. Emphasis is on the general principles of lamp design and diagnosis, rather than on accurate description of a particular lamp.

11494. Brenner, F. C., **Research for a uniform quality grading system for tires,** *Rubber Chem. Technol.* **42,** No. 5, 1446-1449 (Dec. 1969).

Key words: Bias ply; grading; passenger car tires; radial tires; speed capability; tires; winter tires.

The National Traffic and Motor Vehicle Safety Act of 1966 requires the establishment of a *uniform quality grading system.* This paper discusses the needs for the system and the complexity of the problem. The system proposed here will depend on five properties; tread wear, traction, impact resistance, endurance, and wheel speed capability.

11495. Brenner, F. C., Barton, F. W., **Cuts and cut growth in tires,** *Rubber Chem. Technol.* **42,** No. 5, 1462-1465 (Dec. 1969).

Key words: Cut growth; cutting; road test; tires.

Forty tires were subjected to severe road use on a course (approximately 3500 miles) that included Belgian block, over highways at turnpike speeds while overloaded. The course was repeated until the tires were worn smooth. At the end of each course, the number of new cuts and the length of all cuts in grooves was determined. Ten miles of Caliche (sharp stones) road was included between the first and second measuring period.

The tires experienced a total of 169 cuts. Forty seven (47) of these grew, 34 of which grew less than 0.11 inch. No cut grew continuously throughout the test. The cuts grew but not enough to cause tire failure except in one case where the cut exposed the fabric.

11496. Brenner, F. C., Mandel, J., Simson, B. G., **Research for a uniform quality grading system for tires. II. Wheel speed capability test,** *Rubber Chem. Technol.* **42,** No. 5, 1450-1461 (Dec. 1969).

Key words: Bias ply; grading; passenger car tires; radial tires; speed capability; tires; winter tires.

The wheel speed capability of a tire is defined by a test method which determines the speed at which the tire fails on a laboratory test wheel. Data is reported on over 100 different passenger car tires of all grades and types over a range of sizes.

A scaling system is devised for this property. It is found that the system produces consistent results for tires of given manufacturer's nominal grade across the size range tested and for samples produced several months apart.

**11497.** Deslattes, R. D., **Optical and x-ray interferometry of a silicon lattice spacing,** *Appl. Phys. Letters* **15,** No. 11, 386-388 (Dec. 1969).

Key words: Interferometer; lattice parameter; x-ray.

A device permitting simultaneous x-ray and optical interferometry over traverses in excess of 20 $\mu$m is reported. Results obtained to date suggest that such devices will permit measurements of certain crystal-lattice spacings with accuracies better than one part per million.

**11498.** Deslattes, R. D., **Relative energy measurements in the *K* series of argon,** *Phys. Rev.* **186,** No. 1, 1-4 (Oct. 5, 1969).

Key words: Argon; energy relation; x-ray spectra.

The relative positions of the principal features of the emission and absorption spectra of argon in its $K$ series have been measured. The energy difference between the $K$-series Rydberg limit and the peak of $K\beta_{1,3}$ is compared with the optical ionization potential. Location of the $K$-series limit via the experimental ionization potential leads to new values for the $L_{II}$ and $L_{III}$ terms from measurements of $K\alpha_2$ and $K\alpha_1$. These are in reasonable agreement with Hartree-Fock calculations, and with recent grating measurements from other laboratories and single-crystal measurements newly reported here.

**11499.** Ernst, M. H., Dorfman, J. R., Hoegy, W. R., Van Leeuwen, J. M. J., **Hard sphere dynamics and binary collision operators,** *Physica* **45,** 127-146 (1969).

Key words: Binary collision expansion; binary collision operator; hard sphere dynamics; N-body dynamics; overlap function W; overlapping configuration.

The dynamics of a classical hard sphere system has as peculiarties that the particles suffer instantaneous collisions and that certain ("overlapping") areas in phase space are not accessible to the particles. It is mainly the latter feature that prevents a straightforward application of the usual binary collision expansion, generating the particle trajectories. Depending on how the relevant streaming operators are extended to the overlapping area's binary collision expansions can be developed. The different expressions so far proposed are critically examined and the restrictions to their applicability are determined. The binary-collision expansion for potentials consisting of a hard core and a soft tail is also discussed.

**11500.** Farrar, T. C., Tsang, T., Johannesen, R. B., **Internal reorientations in $K_2ReH_9$ via wide-line and pulsed proton resonance studies,** *J. Chem. Phys.* **51,** No. 8, 3595-3596 (Oct. 15, 1969).

Key words: Internal reorientation; nuclear magnetic relaxation; potassium rhenium hydride; potential barrier; proton; second moment.

Proton spin-lattice relaxation times ($T_1$) and second moments ($M_2$) have been measured as a function of temperature for $K_2ReH_9$. The activation energies for internal reorientation of $ReH_9^=$ ions, and their rms errors, are $9.9 \pm 0.4$ and $25.0 \pm 0.8$ kJ/mole ($2.4 \pm 0.1$ and $6.0 \pm 0.2$ kcal/mole), respectively, for type *a* and *d* sites. Our results suggest that the barriers are determined by nearest-neighbor $ReH_9^= - ReH_9^=$ interactions.

**11501.** Fatiadi, A. J., **Novel aromatization of a trihydroxycyclohexanetrione (triketoinositol) to a dibenzo-*p*-dioxin derivati** *Carbohydrate Res.* **12,** 130-132 (1970).

Key words: Acetylation; aromatization; benzenehexol; c bonium ion; dibenzo-*p*-dioxin; hemiacetal; hydrogen shift

Novel aromatization of a triketoinositol on acetylation in presence of acidic catalyst is described. Treatment of 4, trihydroxy-1,2,3-cyclohexanetrione (a triketoinositol) w acetic anhydride and 100 percent phosphoric acid yields taacetoxy dibenzo-*p*-dioxin in 38-42 percent yield. It is belie that reaction proceeds by isomerization on a half triketoinositol to benzenehoxol followed by intramolec cycloaddition with the formation of a bishemiacetal intermedi Aromatization of a newly formed ring probably involves: (a) c bonium ion formation, (b) hydrogen shift, and (c) eliminatio two molecules of water. The structure was proved by ultravio infrared, nuclear magnetic resonance, and mass spectroscopy.

**11502.** Hoegy, W. R., **Convergent generalization of the Boltzm equation for a hard-sphere Lorentz gas,** *Phys. Rev.* **185,** No 210-218 (Sept. 5, 1969).

Key words: Binary collision expansion; generalized c sion integrals; multiple scattering system; physical exp sion; single scatter propagator.

A generalization of the Boltzmann equation for a class Lorentz gas with hard-core interaction is presented. The $N$-b streaming operator is evaluated directly from the dynam thereby avoiding the binary collision expansion. A cluster exp sion is developed in a form that results in exponential deca the dynamical correlations and regularizes all divergent grams. Virtual collisions, represented by virtual binary kern are related to configuration-space restrictions, which in turn responsible for the collisional damping. A prescription is gi for the convergent $l$-body collision integral.

**11503.** Hust, J. G., **A compilation and historical review of t perature scale differences,** *Cryogenics* **9,** No. 6, 443-455 (D 1969).

Key words: Temperature; temperature scales; th mometry.

A brief review is given of temperature scales, their definiti and measurement. Methods of practical temperature meas ment are described. Differences between internationally cepted temperature scales are presented graphically and in ta lar form; comparisons are also given for several national t perature scales. Emphasis has been placed on temperatu below 0 °C, but some information on temperatures above 0 has also been included. Suggested methods of convers between different temperature scales are described.

**11504.** Jones, M. C., **Far infrared absorption in liquid hydro** *J. Chem. Phys.* **51,** No. 9, 3833-3834 (Nov. 1, 1969).

Key words: Absorption coefficient; absorp mechanisms; infrared; liquid hydrogen; orthohydro parahydrogen; translational absorption.

The far-infrared spectra of liquid hydrogen at three para c centrations have been recorded in the wavenumber range 2 250 cm$^{-1}$. The observed variation of the absorption coeffici with composition is consistent with the theory of translatio absorption of Poll and Van Kranendonk.

**11505.** Jones, M. C., Giarratano, P. J., Simpson, A. U., H **transfer to solid-vapor mixtures of cryogens below their tr points flowing through heated tubes,** *AIChE J.* **15,** No. 5, 8 897 (Nov. 1969).

Key words: Boundary layer; cryogenic; heat trans hydrogen; low pressure; nitrogen; particle-wall interacti solid-vapor; tube; two-phase.

Data are presented for wall temperatures and heat transfer fficients for solid-vapor mixtures of parahydrogen and ogen flowing in an electrically heated straight tube of length times its diameter. These are interpreted by the application of plate, constant property boundary-layer theory to models in ich the solid particle geometrical distribution takes on simple iting forms. The observed enhancement of the heat transfer fficient over that for gas alone traveling at the same velocity ualitatively predicted as a function of a dimensionless heat x, the Sterman parameter $q_w/\rho_c U\lambda$.

**06.** Kamper, R. A., **The Josephson effect,** *IEEE Trans. Elec-ron Devices* **ED-16,** No. 10, 840-844 (Oct. 1969).

> Key words: Electron tunneling; electronics; low temperature; superconducting devices.

his is a review of the Josephson effect in superconductors, h emphasis on the electrical properties of Josephson junctions their application to devices and measurement techniques.

**07.** Ku, H. H., Varner, R. N., Kullback, S., **Analysis of multi-imensional contingency tables,** (Proc. 14th Conf. Design of xperiments in Army Research Development and Testing, dgewood Arsenal, Md., October 23, 1968), *ARO-D Report* **9-2,** 141-180, (U.S. Army Research Office-Durham, Dur-am, North Carolina, Sept. 1969).

> Key words: Contingency tables; computer programs; estimation of cell frequencies from marginals; generalized independence; higher-order interaction; hypothesis testing; information theory; interaction.

his is an expository paper on the analysis of contingency ta-s given at the Fourteenth Conference on the Design of Ex-iments. The principle of minimum discrimination information mation is described and used to generate estimates for tests ypotheses concerning second-order and higher-order interac-s. All classical hypotheses for contingency tables can be erated by the use of this principle when certain marginals are sidered as fixed.

xamples are given and two available computation programs described in detail.

**08.** McClintock, M., Balling, L. C., **Atomic and molecular uorescence from laser excited diatomic cesium and rubidium,** *. Quant. Spectro. Radiative Transfer* **9,** 1209-1214 (1969).

> Key words: Atomic fluorescence; cesium rubidium; laser induced fluorescence; molecular fluorescence.

t has been found that several argon laser lines and the 6328 Å um-neon laser line cause excitation of diatomic rubidium and ium in the vapor phase to excited electronic states. The ex-tion of only a few, well separated rotation levels in the upper e, and the resulting simple line fluorescence spectra will w determination of molecular constants not available by er methods. Atomic fluorescence was also present. Twenty-en atomic cesium lines were observed between 3611 and 6 Å under illumination at 4880 Å. The intensities of several mic lines were found to have a quadratic dependence upon r intensity, and are therefore attributed to excitation cesses involving two photons.

**09.** McDonald, D. G., Kose, V. E., Evenson, K. M., Wells, S., Cupp, J. D., **Harmonic generation and submillimeter wave ixing with the Josephson effect,** *Appl. Phys. Letters* **15,** No. 4, 21-122 (Aug. 15, 1969).

> Key words: Infrared; Josephson effect; lasers; submillimeter waves; superconductivity.

y observing constant-voltage steps from Josephson junctions voltages as high as 17 mV we deduce that junctions can generate harmonics up to frequencies as high as 8200 GHz. In consonance with this, submillimeter wave laser detection, harmonic generation and mixing are demonstrated. These results suggest a model for the upper frequency limit of the Josephson effect.

**11510.** Margoshes, M., Rasberry, S. D., **Application of digital computers in spectrochemical analysis—computational methods in photographic microphotometry,** *Spectrochim. Acta* **24B,** 497-513 (1969).

> Key words: Computers; emulsion; microphotometry; photographic emulsion; photographic photometry; photometry; programs; spectrochemical analysis.

A new method of computation is described for calibration of photographic emulsions and conversion of microphotometer readings to relative intensities on a digital computer with special application to spectrochemical analysis. The method for emulsion calibration replaces graphical procedures by a numerical method which is well suited for digital computations. The method of computation and its underlying assumptions are described, and results are given of tests of the procedure. It is recognized that the entire experimental arrangement is being calibrated, not merely the photographic emulsion, and it is shown how malfunctions of the microphotometer which affect the calibration can be recognized from the output of the computer. The program for conversion of microphotometer readings to relative intensities provides for several alternate calculations, including selection of the proper calibration parameters according to the wavelength of the line when these data are supplied for more than one wavelength region, as well as correction for step and background where required. The program is written to provide for automatic selection of the required alternative calculation, based on preliminary analysis of the input data.

**11511.** Meinke, W. W., **The NBS Standard Reference Materials Program: Past, present, and future,** *Mater. Res. Std.* **9,** No. 10, 15-18 (Oct. 1969).

> Key words: Primary standards; standards; standard reference material.

The past 60 years have been ones of rapid and sweeping technological change in the industrial world. During this time the National Bureau of Standards (NBS), has played a pivotal role in the orderly progress and quality control of the nation's productive process. One of the means by which this progress has been aided is through the production, certification, and issuance of Standard Reference Materials (SRM's) from NBS.

The development of our high-technology society is based in large part on the mass production of goods and services. In turn, mass production implies strict quality control of the means of production, an ever-increasing accuracy of measurement, interchangeability of parts, and stringent performance criteria for the wide variety of materials now used. The base of this structure rests firmly on a well-established standards program, national in scope, in which the NBS-SRM program plays a significant role. It is interesting to note that the national standards bodies, the ASTM being among the foremost, have interacted from the earliest days with the NBS-SRM program.

**11512.** Mies, F. H., **Resonant scattering theory of association reactions and unimolecular decomposition. II. Comparison of the collision theory and the absolute rate theory,** *J. Chem. Phys.* **51,** No. 2, 798-807 (July 1969).

> Key words: Absolute Rate Theory; association; configuration interaction; quantum mechanics; recombination decomposition; resonance scattering; scattering theory; unimolecular kinetics.

The rate expressions derived in the preceding paper using a resonant scattering theory (RST) to describe recombination and unimolecular decomposition are compared with the absolute rate theory (ART). A one-to-one correspondence exists between the resonance states in RST and the activated states in ART. The "states of the activated complex" are shown to be the channel states in RST, and using the adiabatic approximation to describe the continuum states it is shown that ART does give a proper *upper bound* to the rate even when nonadiabatic effects are included in RST, i.e., the mean transmission coefficient $\kappa$ is equal to or less than one. The collision theory gives explicit expressions for $\kappa(kT,P)$ which is a function of temperature and includes the dependence on pressure. Specific expressions are given for the "tight complex," where the "activated complex" occurs at some distorted region in configuration space, and for the "loose complex," where the activated complex is the rotational barrier in the asymptotic channel states. Particular attention is given to the high-pressure rate constant where the specific transmission coefficient can be simply related to the ratio of the mean widths to the mean spacings of the activated states. Criteria are given for the validity of ART, and it is shown that Light's statistical theory of reaction rates is a special microcanonical version of the ART for the "loose complex."

**11513.** Mullen, L. O., **On efficient use of selective vacuum pumping modes,** *J. Environ. Sci.* **12,** No. 5, 26-30 (Oct. 1969).

Key words: Cryopumps; getters; ion pumps; pumping efficiency; sublimation pumps; vacuum pumps; vapor pressure.

Most vacuum pumps are selective in the sense that they pump different molecular species at different speeds. Some pumps, such as sublimation pumps and cryopumps, are extremely selective. Efficient use of selective pumps requires that they be chosen to match the gas load. We present experimental data on some commonly encountered gas loads and discuss the choice of compatible pumps.

**11514.** Paulsen, P. J., Alvarez, R., Kelleher, D. E., **Determination of trace elements in zinc by isotope dilution spark source mass spectrometry,** *Spectrochim. Acta* **24B,** 535-544 (April 1969).

Key words: Electrodeposition; isotope dilution; preconcentration; spark source mass spectrometry; trace elements; zinc.

The applicability of the isotope dilution technique in spark source mass spectrometry has been investigated for the determination of Pb, Cu, Cd, Ag, Tl, and Sn in zinc metal. In the procedure developed, a solution of the zinc is spiked with known amounts of stable isotopes of the elements to be determined, and the elements are electrodeposited onto gold wires that subsequently serve as electrodes for the mass spectrographic isotopic analysis. Chemical operations, including isothermal distillation of reagents, dissolution of the zinc, and the electrodeposition step are conducted in a closed system to minimize contamination. The results of the analysis of two NBS zinc standard reference materials include determinations ranging from 11 ppm (11 $\mu$g/g) for Pb to as low as 0.02 ppm (20 ng/g) for Sn. It is concluded that this method is of general utility for simultaneous multi-element trace analysis and is especially applicable in providing much needed standardization in spark source mass spectrometry.

**11515.** Robbins, R. F., **Cryogenic properties of a polyurethane adhesive,** *J. Macromol. Sci.* **A3,** No. 7, 1367-1380 (Nov. 1969).

Key words: Adhesive; low temperature; mechanical properties; polymer; polyurethane; resilience; thermal properties.

Differential thermal analysis (DTA), rebound resilience, and tensile properties of a polyurethane adhesive were measured at cryogenic temperatures. The experimental methods are described, and test results which aid in evaluating the pol rethane for use at low temperatures are discussed. The D thermogram reveals that the glass transition temperature ($T_g$ 235 K. The resilience profile indicates a resilience minimum ( at 270 K and a frequency of 3800 Hz, which is consistent w the $T_g$ measured by DTA. The low resilience below $T_r$, cau by secondary low-temperature transitions, shows the high en gy absorption capabilities of the polyurethane. Considera plastic flow at 195 K (40 K below $T_g$) is evidenced in the resu of the tensile tests. The results of the three tests indicate that polyurethane adhesive will perform well at low temperatur The test methods should also be useful for evaluating the lc temperature performance of new polymers.

**11516.** Silverman, S., **The National Measurement System—a c cept to assist the private sector,** *Mater. Res. Std.* **9,** No. 10, 14 (Oct. 1969).

Key words: Measurement; National Bureau of Standar National Measurement System; national standards; s calibration; standards, national; systems concept.

The concept of a National Measurement System, involving entire complex of measurement activities within the Uni States, is developed. The central element of this Measurem System is the National Bureau of Standards. The role of N and of other functional elements of the System, such as priv laboratories, is discussed.

**11517.** Simpson, A. U., Timmerhaus, K. D., Kreith, F., Jor M. C., **Heat and mass transfer in dispersed, two-phase, sin component flow,** *Intern. J. Heat Mass Transfer* **12,** No. 1141-1155 (Sept. 1969).

Key words: Boundary layer; computation; dispersed flc heat transfer; solid-vapor; two-phase.

The process of heat transfer to a two-phase mixture of w dispersed subliming particles and vapor, flowing over a hea surface, is analyzed. It is shown by a laminar boundary analy that, when the surface-area per unit volume of the particle solid) phase is large enough, the phase change dominates heat-transfer process and hastens the development of the th mal boundary layer. Under these conditions, the thermal bo dary-layer thickness not only becomes uniform a short dista downstream from the starting point, but also is substantially l than it would be were the particle phase absent. For su systems, the equations describing the heat-transfer process be considerably simplified and, if the physical properties of b phases are uniform, a remarkably simple solution results. I systems in which the physical properties are not uniform, a sc tion involving integration across the boundary layer developed. The solutions are applicable to developing, as wel fully developed, laminar boundary layers over a flat plate; solutions also approximate conditions in flow through a tu provided that the tube radius is large compared to the therr boundary-layer thickness. The predictions of this theoreti analysis agree satisfactorily with experimental results. W slight modification, the same approach may possibly be appli ble for turbulent flow in the boundary layer.

**11518.** Smith, E. W., Cooper, J., Vidal, C. R., **A unified classi path treatment of Stark broadening in plasmas,** *Phys. Rev.* **1** No. 1, 140-151 (Sept. 5, 1969).

Key words: Classical path; spectral line broadening.

A theoretical treatment of spectral line broadening in plasr is developed using classical-path methods. This treatment uni certain aspects of the familiar impact, one-electron, and rela tion theories to produce results which are valid from the l center to the far line wings where the electrons may behave q sistatically. Calculations of the Lyman-$\alpha$ line of hydrogen used to illustrate the theory.

19. Smith. R. V.. **The influence of surface characteristics on the oiling of cryogenic fluids,** *J. Eng. Ind.* **91,** No. 4, 1217-1221 Nov. 1969).

Key words: Boiling; boiling hysteresis; boiling inception; boiling-site spreading; radiation.

his paper reviews the influence of the characteristics of the d surface on the boiling of cryogenic fluids. Particular emphas placed on papers presented in the cryogenics section of the 8 Annual ASME meeting.

ysteresis. boiling-site spreading and the influence of radiaon the surface are discussed in detail.

20. Strobridge. T. R., **Refrigeration techniques,** *U.S. Bureau ines Info. Circ.* No. 8417, pp. 39-56 (1969).

Key words: Applications; cryogenic; refrigeration; thermodynamic cycles.

he supply of helium accumulated through the conservation gram has allowed technology in many disciplines to freely e use of the unique behavior of helium. Helium is the only l that can be conveniently used as a refrigerant below about K and is often used at higher temperatures. The therlynamic cycles that modern helium refrigerators utilize are ewed. The Joule-Thomson process is important because it ns the lowest temperature stage of virtually all helium temture refrigerators. The various processes and cycles for cooling the helium stream prior to the Joule-Thomson cess form the essential differences between the closed cycle igerators operating today. Typical refrigeration and liquefacfacilities, both large and small. are discussed.

21. Vidal. C. R., Cooper. J., **Heat pipe oven: a new, wellefined metal vapor device for spectroscopic measurements,** *J. ppl. Phys.* **40,** No. 8. 3370-3374 (July 1969).

Key words: Absorption spectroscopy; heat pipe; metal vapor device; oven.

new, well-defined metal vapor device called the heat-pipe n has been developed on the basis of the heat pipe, a heat ductive element designed by Grover and his co-workers in Alamos. It continuously generates homogeneous vapors of -defined temperature, pressure, and optical path length. The or is confined by inert gas boundaries which remove the winproblem and allow a direct pressure measurement without ing on vapor pressure curves. Due to the continuous oration and condensation the vapor purifies itself during ration.

22. Wampler, R. H., **An evaluation of linear least squares computer programs: A summary report,** (Proc. 14th Conf. Design Experiments in Army Research Development and Testing, dgewood Arsenal, Md., October 23, 1968), *ARO-D Report* **-2,** 103-126 (U.S. Army Research Office-Durham, Durham, orth Carolina, Sept. 1969).

Key words: Computer programs; curve fitting; Gram-Schmidt orthogonalization; Householder transformations; iterative refinement; least squares; linear equations; orthogonalization; orthogonal polynomials; regression; rounding error; stepwise regression.

wo linear least squares test problems based on fifth degree nomials have been run on more than twenty different comr programs in order to assess their numerical accuracy. ong the programs tested were representatives from various istical packages as well as some from the SHARE library. entially four different algorithms were used in the various grams to obtain the coefficients of the least squares fits. The s were run on several different computers, in double precias well as single precision. By comparing the coefficients reported, it was found that those programs using orthogonal Householder transformations or Gram-Schmidt orthonormalization were much more accurate than those using elimination algorithms. Programs using orthogonal polynomials (suitable only for polynomial fits) also proved to be superior to those using elimination algorithms. The most successful programs accumulated inner products in double precision and made use of iterative refinement procedures. In a number of programs, the coefficients reported in one test problem were sometimes completely erroneous, containing not even one correct significant digit.

11523. Weber, L. A., **Saturation densities of oxygen in the critical region,** *Physics Letters* **30A,** No. 7, 390-391 (Dec. 1, 1969).

Key words: Critical density; critical point; critical temperature; oxygen; properties of fluids; P-V-T, saturation densities.

Dielectric measurements have been used to determine the saturation densities of oxygen in the critical region. Analysis of the data yields a value of 154.576 K for $T_c$ and 0.4362 g/cm$^3$ for $\rho_c$. The critical index $\beta = 0.353$

11524. Wiederhorn, S. M., **Crack propagation in polycrystalline ceramics,** (Proc. 15th Sagamore Army Materials Research Conf., Sagamore Conference Center, Raquette Lake, New York, Aug. 20-23, 1968), Chapter in *Ultrafine-Grain Ceramics* **15,** 317-338 (Syracuse University Press, Syracuse, N.Y., 1970).

Key words: Ceramics; fracture; fracture surface energy; strength; thermal shock.

In this chapter, the strength and shock resistance of ceramic materials will be related to microstructural details and the energy necessary to form fracture surfaces. The influence of grain size, grain orientation, crystal anisotropy and residual stresses on crack propagation will be discussed. It will be argued that the strength of ceramic materials is closely related to the grain boundary or single-crystal fracture surface energy, while shock resistance is related to the surface energy required to propagate large cracks through polycrystalline materials. The use of fracture surface energies as a research technique and as a design parameter will be discussed.

11525. Wilson, W. K., **Reflections on the stability of paper,** *Restaurator* **1,** No. 2, 79-86 (1969).

Key words: Degradation; paper; preservation of records; records; stability.

Variables in the composition of paper are discussed in relation to stability, and new approaches to research on preservation of records are described.

11526. Wood, R. E., Hamer, W. J., **Theoretical electromotive forces of metal-halogen cells: Some recalculations based on recent data,** *J. Electrochem. Soc.* **117,** No. 1, 82-83 (Jan. 1970).

Key words: Cells; emfs; free energies of formation; fused salts; halides; thermodynamics.

Comparison of the theoretical emfs for cells containing a single solid or molten halide published by Hamer, Malmberg and Rubin in 1956 and 1965 with emfs calculated from tabulations in the JANAF tables published in 1965, 1966, 1967 and 1968 reveals some rather large discrepancies. This note tabulates the 34 cases in which such discrepancies were found to exceed 100 millivolts, discrepancies equivalent to 2.3 kcal equiv$^{-1}$ or more.

11527. Yakowitz, H., **The divergent beam x-ray technique,** Chapter in *Advances in Electronics and Electron Physics, Suppl.* **6,** *Electron Probe Microanalysis,* A. J. Toksimis and L.

L. Marton, eds., pp. 361-431 (Academic Press Inc., New York, N.Y., 1969).

Key words: Kossel method; x-ray microdiffraction.

This is a review paper discussing the technique of divergent beam (Kossel) x-ray diffraction. The Kossel method is studied with regard to line intensities, photographic contrast, data reduction, specimen preparation, and contribution to scientific research.

**11528.** Adams, J. W., Jarvis, S., Jr., **Current distribution in barretters and its application to microwave power measurements,** *IEEE Trans. Micro. Theory Tech.* **MTT-17,** No. 10, 778-785 (Oct. 1969).

Key words: Barretter; bolometer; current distribution in barretter; microwave power measurement; substitution error.

This paper describes a mathematical analysis for determining the microwave current distribution in a barretter in a rectangular waveguide. This distribution, when used with another analysis which calculates substitution error for any given current distribution, provides a missing step necessary for the calibration of microwave and millimeterwave barretters for absolute power measurements.

**11529.** Balcom, M. M., **Influence of red and blue pre-adaptation on hue matching of purple samples,** *J. Opt. Soc. Am.* **60,** No. 1, 118-121 (Jan. 1970).

Key words: Adaptation; color; hue; vision.

This experiment was designed to show the effect, if any, of chromatic adaptation on hue matching of purple painted samples of different saturations. Five experienced observers were adapted for 1 min to a red field, then asked to find the hue match for each of three test samples from among a set of samples representing the complete hue circuit in 100 steps at middle saturation. The three test samples were of slightly greater saturation and representative of a range of purple samples. The entire procedure was repeated with blue and neutral pre-adapting fields, all under source C illumination. Results indicated that pre-adaptation did influence the hue-match selections, the average red-blue adaptive shift being about one Munsell hue step. Observers made systematically different hue matches for the same test sample, in accordance with their ages. A method for determining graphically the state of adaptation at the time when the hue judgments were made showed that the chromaticity of the test samples was at least as influential as either the neutral surround used or the pre-adaptation stimuli.

**11530.** Branscomb, L. M., **Truth in packaging of scientific information,** *Meas. Data* 3, No. 5, 104-105 (Sept.-Oct. 1969).

Key words: Reviews; science information; scientific literature.

This is an edited version of a talk presented to the Precision Measurements Association meeting in Boulder, Colorado, August 28, 1968.

**11531.** Brauer, G. M., Termini, D. J., Burns, C. L., **Characterization of components of dental materials and components of tooth structure by differential thermal analysis,** *J. Dental Res.* **49,** No. 1, 100-110 (Feb. 1970).

Key words: Characterization of dental materials; components of tooth structure; dental materials; differential thermal analysis (DTA); differential thermal analysis of calcium phosphates.

Differential thermal analysis (DTA) has been used to characterize a variety of dental materials and the components of tooth structure. The technic is useful for the rapid comparison similar materials, quality control, measurement of melti ranges, and the study of reactions occurring at elevated tempe tures.

**11532.** Brown, D. W., Wall, L. A., **Glass transition temperatu of several fluorine-containing polymers,** *J. Polymer Sci.: P A-2,* **7,** 601-608 (1969).

Key words: Fluorine-containing polymers; fluorine-conta ing styrene; glass temperature; high pressure; perfluo $\alpha,\omega$-dienes; perfluoro-$\alpha$-olefins.

The glass transition temperatures $T_g$ of several fluorine-co taining polymers were determined by use of the different scanning calorimeter. Values between −3 and 230 °C were c tained. In polymers of $\alpha$-olefins, $T_g$ increases with the fluori content of the backbone and the length of the *n*-perfluoroall branch. In styrene polymers $T_g$ also is higher if the backbo contains fluorine but nearly the same $T_g$'s are found for polym with phenyl and pentafluorophenyl groups. Saturated polym of perfluoro-$\alpha,\omega$-dienes have lower $T_g$'s than polyperfluoro olefins. The $T_g$'s of chloroperfluoropolymers are higher th those of perfluoropolymers. Polyperfluoropentadiene-1,3 has lowest $T_g$ of the polymers examined. Polyperfluoropentadie 1,3 forms by 1,4-addition.

**11533.** Demtroder, W., McClintock, M., Zare, R. **Spectroscopy of Na$_2$ using laser-induced fluorescence,** *J. Che Phys.* **51,** No. 12, 5495-5508 (Dec. 1969).

Key words: Alkali dimers; laser-induced fluorescen molecular fluorescence; molecular spectroscopy; N resonance fluorescence.

The argon-ion laser lines at 4658, 4727, 4765, 4880, 49 5017, and 5145 Å are each found to excite one or m resonance fluorescence series of the Na$_2$ ($X\ ^1\Sigma_g^+ - B\,^1\Pi_u$) bl green band system. Altogether, 19 different fluoresce progressions have been indentified and assigned *v*, *J* quant numbers. The absolute wavenumbers of many of these emissi lines have been measured interferometrically using a Fab Perot etalon crossed with a Bass-Kessler type spectrograph. revised set of spectroscopic constants has been determined both the upper and lower states which reproduce the observ term energies to better than 0.1 cm$^{-1}$ on the average. Using th improved spectroscopic data, potential curves have been c structed for the *B* and *X* states of Na$_2$ by the Rydberg-Kle Rees method. These potential curves are used in turn to comp Franck-Condon factors for the Na$_2$ B–X band system.

**11534.** Dickens, B., Brown, W. E., **The crystal structure of ca um carbonate hexahydrate at ~−120°,** *Inorg. Chem.* **9,** No 480-486 (Mar. 1970).

Key words: Calcium phosphate; calcium phosphate-calci silicate solid solution; calcium phosphosilicates; calcium icates; crystal structures; glaserite; hydroxyapatite; sin crystal x-ray diffraction.

The crystal structure of CaCO$_3$ 6H$_2$O has been determi from 1420 x-ray diffraction data collected photographically the oscillation technique from a single crystal held at ~−12 The unit cell parameters are $a = 8.87$ (2) Å, $b = 8.23$ (1) Å, 11.02 (2) Å, and $\beta = 110.2$ (2)°, and the space group is C2/c w $Z=4$. The calculated density at ~−120° is 1.80 g cm$^{-3}$, and observed density at ~0° is 1.82 g cm$^{-3}$. The final *R* factor is 0. The structure contains discrete CaCO$_3$ ion pairs, each s rounded by an envelope of 18 water molecules. Thus, Ca$^{2}$ coordinated to only one CO$_3^{2-}$. Six of the surrounding H molecules are bonded to Ca$^{2+}$, eight are hydrogen bonded to ygens of the CO$_3^{2-}$ group, and four are bonded to adjacent pairs and to other water molecules in the envelope. CaCO$_3$ 6H was found to be more stable than $CaCO_3 H_2O$ in water near 0°. The formation of $CaCO_3 6H_2O$ from an equivalent amount of calcite ($CaCO_3$) and water is accompained by a 20% decrease in volume. This may be important in explaining the scarcity of calcareous material in life in the ocean depths.

1535. Fatiadi, A. J., **Conversion of certain cyclic phenylhydrazino derivatives into phenylazo compounds with periodic acid,** *J. Org. Chem.* **35,** No. 3, 831-833 (Mar. 1970).

Key words: Action; cyclohexanedione; ene-hydrazine; enol; periodic acid; phenylazo compounds; phenylhydrazine.

Model ene-hydrazines (3-oxo-1-phenylhydrazino-1-cyclohexene and 5,5-dimethyl-3-oxo-1-phenylhydrazino-1-cyclohexene) have been prepared from the corresponding 1,3-cyclohexanediones (or their enols) and phenylhydrazine. Treatment of these ene-hydrazines with periodic acid at room temperature produces the corresponding azo compounds in 90 percent yield. It is probable that the action of periodic acid on a phenylhydrazino group proceeds by simultaneous attack of an electrophilic and a nucleophilic species (present in aqueous acetic—periodic acid) on vinyl and phenyl NH groups, respectively.

1536. Freeman, D. H., Currie, L. A., Kuehner, E. C., Dixon, H. D., Paulson, R. A., **Development and characterization of ion-exchange bead microstandards,** *Anal. Chem.* **42,** No. 2, 203-209 (Feb. 1970).

Key words: Ion exchange; microstandards; nanogram.

The encapsulation of Na or Ca by ion exchange beads is investigated in the counterion mass range below one nanogram. Preparative methods are described for obtaining the exchange in pure counterion form and for subsequent prevention of ion exchange so that the isolation of a single bead is possible in the absence of significant contamination. Activation analysis indicated that the network heterogeneity was characterized by a % relative standard deviation for Na in measurements extending to $3 \times 10^{-12}$ grams. A bead diameter measurement is equivalent to a counterion mass determination and this opens the door to the use of the beads as microstandards in the mass region where no other methods are applicable.

1537. Freeman, D. H., Goldstein, S., Schmuckler, G., **Homogeneous sulfonation of styrene-divinylbenzene copolymers with oleum in organic solvents,** *Israel J. Chem.* **7,** No. 6, 741-749 (1969).

Key words: Cation exchangers; ion exchangers; oleum; sulfonation.

In order to obtain homogeneously sulfonated cation exchangers, the copolymers were sulfonated by oleum in a mixture of methylene-chloride and nitromethane. The influences of the chemical interaction and of the diffusion process on the kinetic behavior of these systems were investigated, and it was shown that raising the temperature of the sulfonation mixture markedly increases the chemical reaction rate, while the effect on the diffusion is small. A curve-fitting technique was used for the interpretation of the degree-of-sulfonation-vs.-time curves. These investigations served as guidelines for the subsequent preparation of homogeneous highly sulfonated copolymers.

11538. Gadzuk, J. W., **Resonance tunneling through impurity states in metal-insulator-metal junctions,** *J. Appl. Phys.* **41,** No. 1, 286-291 (Jan. 1970).

Key words: Electron tunneling; impurities; junctions; metal-insulator-metal structures.

Motivated by the recent work of Parker and Mead on the effects of impurity trapping states in Schottky barriers, a theory of resonance tunneling through adsorbed atoms in field emission is modified to treat resonance tunneling through isolated and uniformly distributed impurities in the insulating layer of a metal-insulator-metal tunnel junction. In analogy with the magnetic impurity tunneling theory of Appelbaum, the effects of resonant tunneling through impurity states open up new tunneling channels with a concomitant change of slope in the current-voltage characteristics. These changes should be apparent as definite structure in curves of $d\sigma/dV$ versus voltage although depending upon the impurity concentrations and impurity level positions relative to the Fermi levels of the two metals, the height of the structure reflecting the impurity energy level spectrum may not rise above the noise level. In addition it is seen that the presence of impurities can alter the total conductance of a M-I-M tunnel junction. The new conductance versus voltage characteristics are calculated.

11539. Green, J. A. S., Mengelberg, H. D., Yolken, H. T., **Oxide growth on copper and alpha-brasses in aqueous ammonia,** *J. Electrochem. Soc.* **117,** No. 4, 433-437 (Apr. 1970).

Key words: Alpha-brass; copper; ellipsometry; oxide-growth; season-cracking; stress-corrosion.

An ellipsometric study of the kinetics of oxide growth for pure copper and a series of alpha-brasses immersed in tarnishing ammoniacal environments has established that the growth of the oxide, shown to be cuprous oxide, obeys a linear law in each case, and that the rate of growth increases significantly with (*a*) increasing zinc content of the solid, (*b*) increasing temperature, and (*c*) the application of anodic potentials. On the basis of these results it is suggested that the oxide is porous and that oxide growth involves the dissolution of metal ions at the base of the pore (anodic reaction) and their deposition at the oxide surface (cathodic reaction), electrons flowing through the oxide film. The influence of zinc content on the oxide-growth rate is attributed to its effect on the dissolution kinetics.

11540. Heinrich, K. F. J., Fiori, C., Yakowitz, H., **Image-formation technique for scanning electron microscopy and electron probe microanalysis,** *Science* **167,** 1129-1131 (Feb. 20, 1970).

Key words: Derivative signal; electron probe; image; scanning electron microscope; secondary electrons; target current.

A technique is described for producing improved topographic images on the scanning electron microscope and the scanning electron probe microanalyzer. In this technique, the brightness of the oscilloscope is modulated by a signal obtained by mixing the signal (from secondary electrons or target current) with its first derivative. This enhances minor topographic features which are poorly reproduced in the conventional technique.

11541. Ireland, C. T., Ku, H. H., Kullback, S., **Symmetry and marginal homogeneity of an r × r contingency table,** *J. Am. Statist. Assoc.* **64,** 1323-1341 (Dec. 1969).

Key words: Contingency table analysis; homogeneity of marginals; minimum discrimination information estimation; test for symmetry.

The principle of minimum discrimination information estimation is employed to obtain RBAN (Regular Best Asymptotically Normal) estimates of the cell frequencies of an $r \times r$ contingency table under hypotheses of either symmetry or marginal homogeneity. For the latter, a convergent iterative procedure is given to compute the estimates. The associated minimum discrimination information statistics are distributed asymptotically as $\chi^2$ under the null hypotheses. The procedures differ from those previously presented in the literature and permit of extension to multidimensional contingency tables. An example is given.

**11542.** Kaufman, V., Humphreys, C. J., **Accurate energy levels and calculated wavelengths of $^{86}$Kr I,** *J. Opt. Soc. Am.* **59,** No. 12, 1614-1628 (Dec. 1969).

Key words: Calculated wavelengths; energy levels; krypton 86; standard wavelengths.

A total of about 240 spectral lines of $^{86}$Kr I has been measured interferometrically during the past decade. Some have been measured in only one laboratory while others have been measured in as many as 12. On the whole, the agreement is good, but some discrepancies appear. For this work, almost all of the wavelengths have been averaged and used for the determination of a best set of energy-level values for this isotope of krypton. Forty-five even and 66 odd levels have been calculated by the method of least squares, with uncertainties ranging from $\pm 0.0001$ to $\pm 0.0016$ cm$^{-1}$. These interferometrically determined levels have, in turn, been used to calculate a completely consistent set of wavelengths that are preferable to any single set of measurements or averages of measurements of $^{86}$Kr I. The list of 530 lines contains only those calculable transitions that have been observed from krypton sources in the spectral region 3300-40 700 Å. With the exception of a number of weak lines and some close pairs, the final list of wavelengths is recommended for consideration for adoption as secondary standards.

**11543.** Kilgore, S. B., **Electronic circuit breaker for motor load protection,** *Rev. Sci. Instr.* **41,** No. 1, 40-41 (Jan. 1970).

Key words: Electronic circuit breaker; mechanical load protection; surge current; time delay.

An electronic circuit breaker, designed to switch off the power to an electric motor when the mechanical load increases beyond the normal load, is described. The circuit operates rapidly and can sense an increase in mechanical load before it reaches destructive proportions. The sensitivity of the electronic circuit makes it necessary to incorporate a time delay that prevents the initial surge current from turning the motor off before it gets started.

**11544.** Klein, R., Scheer, M. D., **Addition of oxygen atoms to olefins at low temperature. IV. Rearrangements,** *J. Phys. Chem.* **74,** No. 3, 613-616 (Feb. 5, 1970).

Key words: Low temperature; olefins; oxygen atoms.

Rearrangements in the O($^3$P) atom addition to internal, straight-chain olefins involve, as one of the processes, internal rotations resulting in configurational changes. Symmetrical *cis*-olefins at 90 K were found to show greater stereospecificity in the oxygen atom addition reaction as the chain length was increased. Rearrangements involving migration of alkyl groups and localization of oxygen on one of the carbon atoms of the olefinic pair occur in a concerted manner. This was shown from the reactions of 3-ethyl-2-methyl-2-pentene and two of its isomers. Clearly, independent rates cannot be associated with migrating alkyl groups, and additional factors, other than electron density, determine the position of addition of the oxygen atom.

**11545.** Krauss, M., Mielczarek, S. R., **Minima in generalized oscillator strengths; $C_2H_4$,** *J. Chem. Phys.* **51,** No. 12, 5241-5243 (Dec. 15, 1969).

Key words: Configurational mixing; $C_2H_4$; differential cross section; electron impact; excitation; oscillator strength.

A characteristic of electron impact excitation of low-lying Rydberg states is a minimum in the generalized oscillator strength as a function of $K$, the momentum transfer. This characteristic is used as a probe of the Rydberg character of four transitions in $C_2H_4$. Three, the $^1A_g \to {}^1B_{3u}(\pi \to 3s+3s)$, $^1A_g \to {}^1B_{3u}(\pi \to 3p_z - 3p_z)$, and $^1A_g \to {}^1B_{3u}(\pi \to 4s)$ transitions, have long been identified as Rydberg and are found to exhibit the characteristic minimum. A fourth transition $^1A_g \to {}^1B_{1u}(\pi \to \pi^*)$ is normally termed a valence excitation, and a theoretical calculation using Hartree-Fock molecular orbitals had predicted no minimum. For an energy loss of 8.0 eV which is identified with the valence transition a definite minimum is observed. Speculation on the source of this anomaly centers on a type of valence-Rydberg configurational mixing which can occur in many molecules. It is suggested that the presence or absence of minima in generalized oscillator strength curves be used to probe this aspect of the character of the excited state.

**11546.** Latanision, R. M., **On the dislocation distribution near the surface of lightly deformed copper single crystals,** *Scripta Met.* **3,** No. 7, 465-470 (July 1969).

Key words: "Debris layer"; edge dislocation; near-surface source; screw dislocation; single crystals; surface source.

Two recent and essentially identical etch-pitting studies on oriented copper single crystals have produced contradictory results. An explanation for the discrepancy is not obvious, but the results of these investigations may be interpreted in terms of either the surface "debris" layer hypothesis or the activation of surface or near-surface dislocation sources. The purpose of this note is to emphasize the ambiguity involved in such studies.

**11547.** Lechner, R. E., Rowe, J. M., Sköld, K., Rush, J. J., **Study of molecular reorientation in solid neopentane by quasielastic neutron scattering,** *J. Chem. Phys. Letters* **4,** No. 7, 444-448 (Dec. 15, 1969).

Key words: Activation energy: Cold neutron: correlation time; diffusion constant; molecular reorientation; neopentane; neutron scattering; plastic crystal; quasielastic.

Results of cold neutron scattering by plastic neopentane at several temperatures are presented. The measured quasielastic peak widths are compared with calculations for two simple models of molecular reorientation. An activation energy for reorientation of $0.88 \pm 0.11$ kcal/mole is derived.

**11548.** Lide, D. R., Jr., **Determination of anharmonic potential constants in linear XYZ molecules,** *J. Mol. Spectr.* **33,** No. 3, 448-459 (Mar. 1970).

Key words: Anharmonic constants; Fermi resonance; linear molecules; vibrational potential function; vibration-rotation interactions.

A method for determining the anharmonic potential constants $k_{122}$, $k_{322}$, and $k_{2222}$ of linear triatomic molecules is formulated. The calculation makes use of experimental rotational constants $B_v$ and vibrational term values $G_v$ of low-lying vibrational levels. The anharmonic (Fermi) interactions among the triad ($10^00$), ($02^00$), ($00^01$) are treated explicitly, but otherwise the calculation is based on the usual second-order theory. The method is applied to four molecules for which sufficiently accurate experimental data are available: $N_2O$, ClCN, BrCN, and OCS. The internal consistency of the calculation is not very satisfactory, which suggests that higher-order terms in the vibration-rotation Hamiltonian cannot be neglected. However, a set of anharmonic constants is obtained for each molecule which is felt to be more reliable than those previously published.

**11549.** McClintock, M., Demtroder, W., Zare, R. N., **Level crossing studies of $Na_2$ using laser-induced fluorescence,** *J. Chem. Phys.* **51,** No. 12, 5509-5521 (Dec. 1969).

Key words: Laser-induced fluorescence; laser-molecular level crossing; level crossing; molecular fluorescence; molecular spectroscopy; $Na_2$.

The technique of using laser excitation to study level crossings in molecules has been developed and used to determine the radiative lifetime of an excited state of $Na_2$. Optical detection of evel crossing in the $v' = 10, J' = 12$ level of the $B\,^1\Pi_u$ electronic tate of $Na_2$, excited by the 4765-Å argon-ion laser line, has esulted in a precise measurement of the product $g_\tau = 4.11 \pm 0.12$ $10^{-11}$ sec, corresponding to a magnetic field half-width of 1385 42 G. If the $g$ value is calculated assuming Hund's coupling ase (a), the radiative lifetime is determined to be $_t = 6.41 \pm 0.38$ $10^{-9}$ sec. The influence of molecular hyperfine structure on his measurement is discussed and is found in general to contribute little uncertainty to the value of the radiative lifetime, proided the rotational angular momentum is much larger than the uclear spin and/or provided the hyperfine interaction is much maller than the natural width of the excited state.

1550. McCrackin, F. L., **Analyses and corrections of instrumental errors in ellipsometry,** *J. Opt. Soc. Am.* **60,** No. 1, 57-63 (Jan. 1970).

Key words: Birefringence; ellipsometer; thin films.

Expressions for the errors produced in an ellipsometer due to n imperfect compensator, due to birefringence in windows of a ell containing the sample, and due to tilting of the sample are derived. Methods of analyzing the ellipsometer readings to liminate these errors are given.

1551. McLaughlin, W. L., Hussmann, E. K., **The measurement of electron and gamma-ray dose distributions in various media,** (Proc. Symp. Utilization of Large Radiation Sources and Accelerators in Industrial Processing, Munich, Germany, Aug. 18-22, 1969), Chapter in *Large Radiation Sources for Industrial Processes,* **IAEA-SM-123/43,** pp. 579-590 (International Atomic Energy Agency, Vienna, Austria, 1969).

Key words: Depth dose; dose distributions; dosimetry; dyes; electron beams; films; gamma rays; microdosimetry; radiographic imaging.

New radiochromic dye films and gels are proposed as simple and relatively accurate devices for imaging and determining the energy deposited locally at different depths and across interfaces of various irradiated media. Depth-dose measurements show remarkable agreement with theoretical computations in various plastics and aluminum, even near the end of the electron range, ndicating that the dosimeter response is representative of the energy imparted to the medium over a wide range of electron energies.

11552. Unassigned.

11553. Pizer, R. S., Spinner, S., **An apparatus for determining the actual footprint area of tires,** *Mater. Res. Std.* **10,** No. 2, 20-23 (Feb. 1970).

Key words: Contact area; silicon solar cell; tires; tire footprint.

An apparatus for measuring the actual contact area of tires regardless of their tread design is described. The procedure is both rapid and accurate. The method utilizes a bank of lights, an opal glass plate, a simple light focusing system, and a silicon solar cell which linearly transforms the incident light to an electrical current. The reduction in current is the measure of the true contact area of the tire.

11554. Potzick, J., **Low-frequency sine-wave oscillator,** *EEE* **18,** No. 3, 130 (Mactier Publishing Corp., Mar. 1970).

Key words: Low frequency oscillator; oscillator.

A simple, inexpensive, low-frequency oscillator which generates a fairly low distortion sine wave at a frequency of about one hertz is described.

11555. Powell, C. J., **Analysis of optical- and inelastic-electron-scattering data. II. Application to Al,** *J. Opt. Soc. Am.* **60,** No. 1, 78-93 (Jan. 1970).

Key words: Complex dielectric constant; electron-energy-loss; electronic band structure; infrared; least-squares fit to optical data; optical constants; reflectance; ultraviolet; visible.

Optical and electron energy-loss data for aluminum between 0.04 and 72 eV have been critically analyzed and used to test the validity of models for $\epsilon(\omega)$, the complex frequency-dependent dielectric constant. Experimental data and models for $\epsilon(\omega)$ can be effectively compared by use of a nonlinear least-squares computer program and, at least in simple cases, the model parameters have physical significance. Though aluminum has been widely regarded as a relatively ideal free-electron metal, it has been found that a Drude model for $\epsilon(\omega)$ does not adequately describe the observed data. Deviations from the Drude model for photon energies greater than about 1 eV have been interpreted in terms of the effects of interband-electronic transitions and a significant $L$-shell contribution to the real part of $\epsilon(\omega)$ between 10 and 72 eV. From a fit of reflectance data between 0.2 and 12 eV it has been possible to derive parameters describing the interband-transition contribution $\epsilon^{(b)}(\omega)$ to $\epsilon(\omega)$; the imaginary part of $\epsilon^{(b)}(\omega)$ does not differ significantly from calculations based on the aluminum band structure. Optical constants have been derived in the range of fit and agree closely with the measurements of Hass and Waylonis between 1.9 and 5.6 eV. For photon energies less than 0.2 eV, the reflectance data can be fitted by the empirical formulation of Roberts. The optical absorption for photon energies greater than 12 eV is monotonic and greater than that expected from the tails of the electronic transitions at 1.5 – 2eV.

11556. Powell, C. J., **Analysis of optical- and inelastic-electron-scattering data. III. Reflectance data for beryllium, germanium, antimony, and bismuth,** *J. Opt. Soc. Am.* **60,** No. 2, 214-220 (Feb. 1970).

Key words: Antimony; beryllium; bismuth; complex dielectric constant; germanium; least-squares fit to reflectance; optical constants; reflectance; ultraviolet.

A procedure is described for simultaneously fitting reflectance data obtained for various photon energies and angles of incidence using a simple physical model for $\epsilon(\omega)$, the complex frequency-dependent dielectric constant. The mutual consistency of the model and of the experimental data is tested, within the accuracy of each measurement. As an example of the technique, reflectance data in the vacuum ultraviolet obtained by Toots, Fowler and Marton for beryllium, germanium, antimony and bismuth have been satisfactorily fitted. The model parameters have been used to derive the optical constants $n$ and $k$ (in satisfactory agreement with conventional determinations) and can be readily related to other relevant experimental results or theoretical calculations of $\epsilon(\omega)$ if these are available.

11557. Reader, J. Epstein, G. L., **Revised $4p^5\ ^2P^\circ_{1/2,3/3}$ splitting of Y v,** *J. Opt. Soc. Am.* **60,** No. 1, 140 (Jan. 1970).

Key words: Atomic spectroscopy; energy levels; resonance lines; yttrium.

The two resonance lines of Y v consisting of transitions from $4s4p^6\ ^2S_{1/2}$ to $4s^24p^5\ ^2P^\circ_{1/2,3/2}$ have been observed for the first time. Measurement of the wave number difference between these two lines proves that the existing analysis of the Y v spectrum by Paul and Rense [Phys. Rev. **56,** 1110 (1939)] is entirely in error; as had been suspected by Edlén [in Atomic Spectra, Handbuch der Physik (Springer-Verlag, Berlin, 1964), Vol. XXVII, p. 185.]

11558. Roth, R. S., Stephenson, N. C., **Chemical and structural investigations in the $Ta_2O_5$-$WO_3$ system,** (Proc. Institute for Advanced Study on the Chemistry of Extended Defects in Non-Metallic Solids, Scottsdale, Arizona, April 16-26, 1969), Chapter in *The Chemistry of Extended Defects in Non-Metal-*

*lic Solids*, L. Eyring and M. O'Keeffee, eds., pp. 167-182 (North Holland Publ. Co., Amsterdam, The Netherlands, 1970).

Key words: Crystal structure; non-stoichiometry; order oxygen vacancies; tantalum oxide; tantulum tungsten system.

Crystal structures have been determined for the compounds $Ta_{22}W_4O_{67}$, $Ta_{30}W_2O_{81}$, $Ta_{74}W_2O_{191}$, and $Ta_2O_5$. These compounds are stable phases in the $Ta_2O_5$-$WO_3$ system and have unit-cells which are based, respectively, on 13, 8, 19 and 11 $UO_3$-type subcell units. Metal atoms are either octahedrally coordinated to six oxygen atoms or else surrounded by seven oxygen atoms in the form of a pentagonal bipyramid.

On the basis of these structures a building-block scheme is developed which enables the *ideal*, or undistorted, structure to be predicted for any member of the hundreds of compounds which form a continuous series of structures in the region $Ta_2O_5 - 11Ta_2O_5 \cdot 4WO_3$.

Anionic packing distortions occur in the *ideal* structures. In the *real* structures these distortions are minimized by a reduction in the coordination number of *some* seven-coordinated metal atoms. These atoms form distortion-sheets throughout the structure. The importance and distribution of these distortion-sheets is discussed.

**11559.** Simpson, J. A., **Electron impact spectroscopy,** (Proc. 10th Symp. on Electron, Ion & Laser Beam Technology, Gaithersburg, Md., May 21-23, 1969), Chapter in *Record of 10th Symposium, Electron, Ion, and Laser Beam Technology*, L. Marton, ed., pp. 345-352 (San Francisco Press, San Francisco, Calif., 1969).

Key words: Chemical analysis; electron impact spectrometer; uv absorption.

Recent developments in electron spectrometer design have made the application of inelastic electron scattering measurements to gas analysis competitive with other techniques. The energy distribution of electrons of an initially monoenergetic electron beam after an encounter with a gas target (the loss spectrum) contains the optical absorption spectrum of the gas. The absorption data extend from the extreme vacuum ultraviolet into the visible with an energy resolution comparable to a 1/2-meter optical grating spectrometer. Its response is linear with concentration over a very wide range and contains between $10^3$ and $10^4$ resolution widths. This spectrum, by revealing the valence energy states of the gas, is the most intrinsic possible "fingerprint" of the atom or molecule. An instrument has been built to explore the potentialities of this method. The instrument is described and its performance as a trace analyzer for air pollution studies discussed.

**11560.** Snelleman, W., Menis, O., Rains, T. C., Yee, K. W., Cook, H. D., **Flame emission spectrometry with repetitive optical scanning in the derivative mode,** *Anal. Chem.* **42,** No. 3, 394-398 (Mar. 1970).

Key words: Ac scan; derivative mode; design; detection limits; flame emission spectrometry; interferences; matrix; microsamples.

A flame emission spectrometer using a rapid repetitive scan of a narrow wavelength region has been developed. By this method of wavelength scanning the second derivative of the output intensity is measured. The use of this approach to minimizing spectral interference in matrices and the use of microsamples greatly enhance the potentialities for flame emission spectrometry, and minimizes the need for a monochromator of high resolving power. A quartz plate, made to vibrate at 145 Hz, is mounted behind the entrance slit of the monochromator. The ac amplifier is synchronized with the oscillations of the quartz plate. When the amplifier is tuned to twice the frequency of vibration, the secon derivative of the spectrum is obtained. This permits the measurement of weak line spectra nested in or on a broad band or continuum. It is demonstrated that spectral interference due t CaOH bands and/or a continuum are minimized in the measurement of barium. The elimination of interferences from bands an flame structure led to an improvement in detection limits of alka and alkaline earth elements in the presence of many matrix ions An analysis can be performed with 50 $\mu$l of solution whic makes it applicable to biochemical and air pollution studies.

**11561.** Swartz, J. C., Swartzendruber, L. J., Bennett, L. H., Watson, R. E., **Nuclear magnetic resonance of $^{57}$Fe in the paramagnetic alloys $TiFe_{1-x}Co_x$,** *Phys. Rev.* **1,** No. 1, 146-152 (Jan. 1 1970).

Key words: Electronic structure; Knight shift; nuclear magnetic resonance; nuclear moment; TiFe; $^{57}$Fe.

Nuclear magnetic resonances (NMR) of $^{57}$Fe in isotopicall enriched specimens of TiFe, $TiFe_{0.8}Co_{0.2}$, and $FeCl_3$, and of T in TiCo are reported. The results supplement existing F Mössbauer and Co NMR information on the pseudobinar $TiFe_{1-x}Co_x$. The Knight shift (and estimated uncertainty) of iro in TiFe is +(1.29 ± 0.03)% at room temperature and +(1.34 0.03)% at 77 K, yielding a hyperfine coupling constant of +(3 2) kG/$\mu_B$ per formula unit. Similar values are obtained for iron i $TiFe_{0.8}Co_{0.2}$. The Knight shift of Ti in TiCo is +(0.07 ± 0.02)% at room temperature, and −(0.06 ± 0.03)% at 77 K, yielding hyperfine coupling constant of −(12 ± 3) kG/$\mu_B$ per formula uni for Ti in TiCo, contrasting with a near-zero coupling constant fo Ti in TiFe. Both the orbital shifts and the *d*-spin hyperfin coupling constants for the Fe and Ti sites are much less dependent on cobalt concentration than these same quantities at th cobalt site. The NMR results on the three constituents of $TiFe_{1-x}Co_x$ suggest: (i) *s-d* admixture in the wave-function character a the Fermi surface for the (Fe,Co) sublattice, (ii) greater admixture and perhaps a greater *d*-spin moment at an iron sit than at a cobalt site in the iron-rich compounds, and (iii) nuclear moment for cobalt corresponding to a nuclear gyromagnetic ratio $\gamma = 2\pi \times 1.003$ kHz/G. The Knight shift of dilute Fe i Ti as measured by the Mössbauer effect is (0 ± 1)%. The chemical shift of Fe in enriched aqueous $FeCl_3$ is found by NMR to b +(0.40 ± 0.04)%.

**11562.** Tighe, N. J., Kreglo, J. R., Jr., **Electron microscopy of periclase brick,** *J. Am. Ceram. Soc.* **49,** No. 2, 188-192 (Feb. 7 1970).

Key words: Ceramic; electron microscopy, MgO; microstructure; sea-water periclase.

Transmission electron microscopy was used to study microstructure of sea-water periclase brick. The material containe 98.0% MgO and had a porosity of 19%. Specimens were cu from the brick and thinned for microscopy by ionic bombardment. MgO was present as single grains (20 to 90 $\mu$m) and as fine precipitate (~100 Å) in an amorphous matrix. Dislocation in MgO grains were decorated with impurity precipitates Forsterite, monticellite and glass were found as second phase regions.

**11563.** Waclawski, B. J., Hughey, L. R., **Adsorption of wate vapor on polycrystalline tungsten,** *Surface Sci.* **19,** 464-46 (1970).

Key words: Adsorption; hydrogen evolution; polycrystalline tungsten; room temperature; ultra-high vacuum; wate vapor; work function.

Following an induction period, a spontaneous evolution o hydrogen was observed to occur in the initial stages of adsorption at room temperature when polycrystalline tungsten was ex osed to water vapor. Concurrent photoemission measurements ndicated that a change in the work function of the sample ocurred during the hydrogen evolution. Calculations of the rate of volution, and the amount of hydrogen evolved are presented.

1564. Wall, L. A., Flynn, J. H., Straus, S., **Rates of molecular vaporization of organic plasticizers,** *Polymer Eng. Sci.* **10,** No. 1, 19-23 (Jan. 1970).

Key words: Energy of vaporization; internal energies of vaporization; molecular vaporization; organic plasticizers; plasticizers; solubility parameters.

The kinetics of the molecular vaporization process of 21 lasticizers were investigated in detail. By both isothermal and onisothermal kinetic methods, it was evident that 11 were quite ure single compounds, while 10 were clearly mixtures of compounds. For the single component species internal energies for aporization and rates of volatilization are listed. The internal nergies of vaporization are about one-half or less of values one an estimate from the additive factor method of Small. Thus, olubility parameters based on our experimental values are low y about 30 percent. From this and previous work on linear alanes, it is concluded that in the molecular vaporization process, ne large organic molecules studied evaporate approximately as pheres and hence low values for the energy of vaporization are btained. Consequently, the difference between our experimenal energy and that estimated from solubility parameters is the nergy for extending the molecule in a vacuum environment.

1565. White, H. J., Jr., **Absorption of cationic surfactants by cellulosic substrates,** Chapter 9 in *Cationic Surfactants* **4,** 311-340 (Marcel Dekker, Inc., New York, N. Y., 1970).

Key words: Absorption; adsorption; cationic surfactants; cellulosic materials; review.

The physical chemistry of the interaction of cationic surfacants with cellulosic substrates is reviewed.

1566. Wilson, W. K., **Discussion of paper "New Approaches to Preservation," by Richard D. Smith,** *Library Quart.* **40,** No. 1, 171-175 (Jan. 1970).

Key words: Accelerated aging; acidity; aging; alkaline filler; aqueous deacidification; deacidification; degradation; laboratory aging; non-aqueous deacidification; pH.

A discussion of Mr. Smith's paper is followed by some renarks on the philosophy of the approach to research on the reservation of records and especially to the use of laboratory ging as a research tool.

1567. Becker, E. D., Ferretti, J. A., Farrar, T. C., **Driven equilibrium Fourier transform spectroscopy. A new method for nuclear magnetic resonance signal enhancement,** *J. Am. Chem. Soc.* **91,**7784-7785 (1969).

Key words: Driven-equilibrium; Fourier-transform; high resolution; nuclear magnetic resonance.

A new method using a high-resolution pulsed NMR specometer is described by which the equilibrium magnetization of uclei with long $T_1$ may be restored rapidly in order to take full dvantage of the Fourier transform technique.

1568. Bender, P. L., Alley, C. O., Currie, D. G., Dicke, R. J., Faller, J. B., **Some implications for physics and geophysics of laser range measurements from earth to a lunar retro-reflector,** (Proc. Conf. NATO Advanced Study Institute, University of Newcastle, Upon Tyne, England, Mar.-Apr. 1967). Chapter in *The Application of Modern Physics to the Earth and Planetary Interiors,* S. K. Runcorn, ed., pp. 523-530 (John Wiley and Sons Inc., London, England, 1969).

Key words: Astronomy; continental drift; geophysics; gravity; laser; lunar; moon.

The technique of high-accuracy laser range measurements to an optical retro-reflector package on the moon is discussed. The information which can be obtained by this method about the hypotheses of continental drift and ocean floor spreading and about the motion of the pole is described. A method for checking on the constancy of the gravitational constant is also given. The accuracy with which information on all of these questions can be obtained from lunar range measurements is higher than for any other methods which have been suggested.

11569. Bennett, L. H., **Comments on "Fe and Ni hyperfine fields in $Ni_3Fe$,"** *Phys. Rev.* **188,** No. 2, 1048 (Dec. 10, 1969).

Key words: Alloys; hyperfine fields; iron; nickel; nuclear magnetic resonance.

A model is presented to explain the observed hyperfine fields in $Ni_3Fe$.

11570. Berger, M. J., Seltzer, S. M., **Penetration of electrons and associated bremsstrahlung through aluminum targets,** Chapter in *Protection Against Space Radiation, NASA SP-169,* pp. 285-322 (National Aeronautics and Space Administration, Greenbelt, Maryland, 1968).

Key words: Aluminum transmission; bremsstrahlung; electrons; Monte Carlo; penetration; thick target bremsstrahlung; transport theory.

This paper contains a brief description of Monte Carlo programs designed to calculate the transport of fast electrons and associated bremsstrahlung through extended media. Two applications are discussed: (1) transmission of electrons through plane-parallel targets, and (2) emergence of secondary bremsstrahlung from such targets. It is shown that the predicted results are in reasonably good agreement with recent experiments for electron beams with energies up to 8 MeV incident normally on aluminum targets. Extensive new calculated data for transmission and thick-target bremsstrahlung production are presented for aluminum targets exposed to an isotropic electron flux.

11571. Birky, M. M., **Simultaneous recording of near-field and far-field patterns of lasers,** *Appl. Opt.* **8,** No. 11, 2249-2253 (Nov. 1969).

Key words: Far-field diffraction; laser; near-field diffraction; neodymium; ruby.

A technique for simultaneous recording of near-field and far-field diffraction patterns at several exposures for a single laser pulse has been developed. A ruby laser and a neodymium doped glass laser have been investigated. The $Nd^{+3}$ laser shows striking high order cylindrical mode operation as a result of thermal stress. The time resolved output of this laser shows the usual spikes about 500 nanoseconds wide. When the cylindrical mode operation takes place some of the spikes consist of a large number of ultrashort pulses.

11572. Brady, E. L., **The National Standard Reference Data System,** *Mater. Res. Std.* **9,** No. 10, 19-21 (Oct. 1969).

Key words: Critical evaluation; information centers; information services; NSRDS; physical properties; standard reference data.

The National Standard Reference Data System is a government-wide effort to give to the technical community of the United States optimum access to the quantitative data of physical science, critically evaluated and compiled for convenience. This program was established in 1963 by the President's Office of Science and Technology, acting upon the recommendation of The Federal Council for Science and Technology. The NBS has been assigned responsibility for administering the effort. The general objective of the NSRDS is to coordinate and integrate existing data evaluation and compilation activities into a systematic, comprehensive program, supplementing and expanding technical coverage when necessary, establishing and maintaining standards for the output of the participating groups and providing mechanisms for the dissemination of the output as required. The NSRDS is conducted as a decentralized operation of nationwide scope with central coordination by NBS. It comprises a complex of data centers and other activities carried on in government agencies, academic institutions and non-governmental laboratories. The independent operational status of existing critical data projects is maintained and encouraged. Data centers that are components of NSRDS produce compilations of critically evaluated data, critical reviews of the state of quantitative knowledge in specialized areas and computations of useful functions derived from standard reference data.

**11573.** Christ, B. W., **On the mechanism of interstitial-impurity-induced cross-slip in iron deformed near 175 K,** *Acta Met.* **17,** No. 10, 1317-1321 (Oct. 1969).

Key words: Cross-slip; ductility; interstitial impurity; iron; nitrogen; yield stress.

A mechanism is proposed whereby the elastic dipole distortion of stationary interstitial impurity atoms in lattice solution can promote nucleation and stabilization of double-kink-size dislocation segments on cross-slip planes. Stress relaxation accompanying interstitial-impurity-induced cross-slip can account for the experimental observations that small atom fractions of nitrogen in lattice solution in iron deformed around 175 K decrease yield and flow stresses and increase ductility.

**11574.** Christ, B. W., Gamble, R. P., Smith, G. V., **On the distinction between alloy softening due to nitrogen and nickel in dilute lattice solution in iron,** *Script. Met.* **3,** No. 8, 521-530 (Aug. 1969).

Key words: Alloy softening; elastic; electronic; Fe-N alloys; Fe-Ni alloys; flow stress; lower yield stress; mobile dislocation density; Peierls stress.

Alloy softening (AS) is the decrease in yield and flow stresses of iron and other b.c.c. metals which accompanies increasing quantities of solute in lattice solution, within critical ranges of solute concentration and temperature. This note is a comparison of existing alloy softening data on Fe-N and Fe-Ni. Whereas AS in each alloy system is due to a reduction in the thermal component of stress, the basic cause of the reduction is different in each system. This is inferred from differences in the concentration and temperature dependence of AS for each alloy system. AS in Fe-N is attributed to an increase in mobile dislocation density during yielding and flow, as compared with that of hydrogen-purified iron, arising from the mechanism of interstitial-impurity-induced cross-slip. AS in Fe-Ni is attributed to a systematic reduction in the Peierls stress of iron with increasing Ni. Whereas AS in Fe-N is primarily of elastic origin, AS in Fe-Ni is primarily of electronic origin.

**11575.** Cohen, M. I., Casella, R. C., Blunt, R. F., Forman, R. A., **Lattice absorption in strontium titanate,** *Phys. Rev.* **186,** No. 3, 834-838 (Oct. 15, 1969).

Key words: Brillouin zone; critical points; infrared; optical absorption; phonons; selection rules; strontium titanate.

The optical absorption spectrum of $SrTiO_3$ is presented over the energy range 0.05 eV to 0.3 eV, well below the fundamental edge. Nine absorption bands are observed. We interpret all but one of them as being due to multi-phonon creation processes. The sole exception is a band at 0.068 eV which we attribute to a single-phonon process. Selection rules for simultaneous creation of either two or three phonons are obtained in dipole approximation, at selected critical points in the Brillouin zone. The observed bands are assigned using these rules together with the experimental phonon dispersion curves of Cowley and other published values for the higher energy branches obtained at specific points in the zone by other techniques.

**11576.** Currie, L. A., **Indirect estimation of component variability in chemical and physical systems,** *Anal. Chem.* **41,** No. 14, 2051-2054 (Dec. 1969).

Key words: Chemical microstandards; correlation coefficient; indirect variability estimation; stoichiometry; two-component system.

An indirect method is presented for assessing the variability of a chemical component or a physical property, when that property may not be directly observed. The method is based upon a simple physical model incorporating stoichiometry and the observation of the variability of a second, related property and/or the ratio of the two properties. A principal result of the investigation is an expression giving limits for the relative standard deviation of component-A, $\phi_A$: $|\phi_{A/B}^2 - \phi_B^2| \leqslant \phi_A^2 \leqslant \phi_{A/B}^2 + \phi_B^2$ where $\phi_{A/B}$ and $\phi_B$ represent the relative standard deviations of the ratio of components -A and -B and of component-B, respectively. Information is also obtained on bounds for the correlation coefficient.

**11577.** Durst, R. A., **Fluoride microelectrode – fabrication and characteristics,** *Anal. Chem.* **41,** No. 14, 2089-2090 (Dec. 1969).

Key words: Fluoride analysis; fluoride microanalysis; fluoride microelectrode; ion-selective microelectrode; microelectrode; potentiometry.

A fluoride ion-selective microelectrode has been constructed with a volume requirement of less than 2 μl. This microelectrode has the advantage of being suitable for *in situ, in vivo,* and continuous analysis of microliter volumes of solution. Details of construction and the response characteristics are given. Nernstian response is observed down to less than 10-5*M* fluoride. Further miniaturization is feasible by extension and refinement of this design.

**11578.** Ederer, D. L., **Computer analysis of resonance profiles by the method of least squares,** *Appl. Opt.* **8,** No. 11, 2315-2325 (Nov. 1969).

Key words: Beutler-Fano resonance profiles; least squares analysis; parameter correlation; random errors; slit function; slit width-resonance width ratio; systematic errors.

The method of least squares has been applied to the analysis of resonance profiles described by the Beutler-Fano (BF) absorption cross-section. To illustrate the method, parameters were determined for experimental data having BF profiles of (a) the asymmetric, enhanced absorption type, (b) the "window" type, and (c) the Lorentzian absorption type. Systematic and random errors, and correlation among the parameters were studied as a function of the slit width to resonance width ratio by applying the least squares fitting method to data computed by folding the BF transmission profile with a gaussian slit function. High correlation among the parameters and parameter fractional standard deviations of 10% to 20% for data with a standard deviation of 0.01 are an incentive to keep the slit width to resonance width ratio less than two for "window" type resonances. In addition i was found that the parameters describing a resonance could be determined with the greatest precision in a given time when the slit width to resonance width ratio was of order one. It was found that systematic errors greater than about one percent resulted i the number of mesh points used to approximate the convolution integral in the fitting procedure was less than at least two pe sonance width. Also, for resonances whose width was equal to e slit width, systematic errors in the parameter values of order 1 percent resulted if the width of slit function used in the fitting ocedure differed from the "actual" slit function by ten percent.

**579.** Eick, J. D., Caul, H. J., Hegdahl, T., Dickson, G., **Chemical composition of dental gold casting alloy and dental wrought gold alloys,** *J. Dental Res.* **48,** No. 6, 1284-1289 (Nov.-Dec. 1969).

Key words: Casting gold alloys; chemical composition; dental gold alloys; gold; plantinum; wrought gold wire; x-ray emission.

The chemical composition of 136 dental casting gold alloys d 21 dental wrought gold wire alloys was determined by an x-y emission method. The changes in composition from 1928 and 32 to the present time are small. There has been a decrease in tinum content in both castings and wires. About 1% nickel is und in the present-day wire which was not present in 1928 and 32.

**580.** Fatiadi, A. J., **Preparation of inositol hexasulfate,** *Carbohydrate Res.* **12,** 293-296 (1970).

Key words: Acid; chlorosulfonic; fuming; hexapotassium; hexasulfate; salt; sulfuric.

Inositol hexasulfate has been prepared in 55-62% yield by ect interaction of *myo*-inositol with either fuming sulfuric acid chlorosulfonic acid at 60-75 °C. The hexasulfate was isolated m the reaction mixture by an exchange reaction with potassi- chromate or by direct neutralization with potassium hydrox-: the inositol hexasulfate hexapotassium salt crystallizes out st ("salting out").

**581.** Feldman, A., Horowitz, D., **Refractive index of cuprous chloride,** *J. Opt. Soc. Am.* **59,** No. 11, 1406-1408 (Nov. 1969).

Key words: CuCl; dispersion; interference fringes; refractive index; refractometer.

The refractive index of single crystal CuCl was measured in wavelength range 0.42 μm to 22 μm using a commercial V-ck refractometer and also by measuring the wavelength de-ndence of interference fringes in thin polished plates.

**582.** Frederikse, H. P. R., **Superconducting semiconductors,** Proc. Conf. International Advanced Study Institute: Elec-ronic Structures in Solids, Chania, Crete, Greece, June 30-July 14, 1968). Chapter in *Electronic Structures in Solids,* pp. 270-282 (Plenum Press Inc., New York, N. Y., 1969).

Key words: Semiconductors; solid state; strontium titanate; superconducting semiconductors.

The application of the BCS theory to multi-valley semiconduc-s as carried out by M. L. Cohen is described. The optimum nditions for finding superconductivity in semiconductors are ted. Application of these ideas to $SrTiO_3$ and the experiments ncerned with superconductivity in this compound are cussed. Other examples are mentioned.

**583.** Haber, S., **Stochastic quadrature formulas,** *Math. Computation* **23,** No. 108, 751-764 (Oct. 1969).

Key words: Degree of precision; Hadamard matrices; integration; Monte Carlo; multiple integrals; numerical integration; numerical methods; quadrature; random.

A class of formulas for the numerical evaluation of multiple in-grals is described, which combines features of the Monte Carlo d the classical methods. For certain classes of func-ns—defined by smoothness conditions—these formulas pro-de the fastest possible rate of convergence to the integral. symptotic error estimates are derived, and a method is described for obtaining good *a posteriori* error bounds when using these formulas. Equal-coefficients formulas of this class, of degrees up to 3, are constructed.

**11584.** Haber, S., Osgood, C. F., **On the sum $\Sigma \langle n\alpha \rangle^{-t}$ and numerical integration,** *Pacific J. Math.* **31,** No. 2, 383-394 (1969).

Key words: Continued fraction; diophantine approximation; integration; multiple integration; number theory; numerical analysis; numerical integration; periodic (functions); quadrature.

It is shown that a certain problem in Diophantine Approximation—the estimation of sums of the form $\sum_{n=k}^{Ak} \langle n\alpha \rangle^{-t}$, where $\alpha$ is an irrational number, "$\langle x \rangle$" denotes the distance from x to the nearest integer, and A is a fixed number greater than 1—is related to the estimation of the error in Korobov's method of numerical integration of periodic functions of several real variables. Some estimates of such sums are found, for certain classes of irrational numbers.

**11585.** Haller, W., Blackburn, D. H., Wagstaff, F. E., Charles, R. J., **Metastable immiscibility surface in the system $Na_2O$-$B_2O_3$-$SiO_2$,** *J. Am. Ceram. Soc.* **53,** No. 1, 34-39 (1970).

Key words: $B_2O_3$-$Na_2O$-$SiO_2$; glass; immiscibility; melts; microheterogeneities; $Na_2O$-$B_2O_3$-$SiO_2$; $SiO_2$-$B_2O_3$-$Na_2O$.

Opalescence and clearing techniques have been used to determine the metastable immiscibility surface for sodium borosilicate solutions. These results indicate that a three-liquid region, which may or may not be metastable to two-liquid regions, underlies the immiscibility surface.

**11586.** Heinrich, K. F. J., **Advances in the metallurgical application of electron probe microanalysis,** *Proc. Conf. 5th International Congress on X-ray Optics and Microanalysis, Tubingen, Germany, Sept. 9-14, 1968,* G. Mollebstedt and K. H. Gaukler, eds., pp. 415-423 (Springer-Verlag Publ. Co., Berlin, Germany, Dec. 1969).

Key words: Applications; electron probe; microanalysis; metallurgy; spectrometry; x-rays.

Electron probe microanalysis is widely used in the investigation of phenomena of general metallurgical interest as well as in the study of specific materials and processes. New devices for x-ray detection, and automatic data collection, increase the usefulness of the microprobe for such applications. Besides the well-known methods for qualitative and quantitative electron probe analysis, the instrument can also be used advantageously for quantitative metallography and related techniques.

**11587.** Heinrich, K. F. J., Yakowitz, H., **Propagation of errors in correction models for quantitative electron probe microanalysis,** *Proc. Conf. 5th International Congress on X-ray Optics and Microanalysis, Tubingen, Germany, Sept. 9-14, 1968,* G. Mollebstedt and K. H. Gaukler, eds., pp. 151-159 (Springer-Verlag Publ. Co., Berlin, Germany, Dec. 1969).

Key words: Absorption of x-rays; atomic number effects; error propagation; fluorescence; microprobe analysis; quantitative analysis.

Lack of appropriate standards frequently forces the analyst to use elemental standards. The usefulness of correction models is limited by the accuracy to which the input parameters are known. Uncertainties in presumably known quantities (mass absorption, coefficients, fluorescence yield, mean ionization potentials, etc.) are in many cases the limiting factors. The resulting analytical errors can be minimized by judicious choice of experimental conditions. This paper will give examples involving the corrections for absorption, fluorescence by characteristic lines, and atomic number effects.

**11588.** Henderson, B., Stokowski, S. E., Ensign, T. C., **Luminescence from F centers in calcium oxide,** *Phys. Rev.* **183,** No. 3, 826-831 (July 15, 1969).

Key words: Calcium oxide; color centres; F-centres; luminescence; optical absorption; radiative lifetimes.

This paper reports data on the luminescence spectra associated with F$^-$ and F$^+$-centres in calcium oxide. Irradation in the F-band excites emission bands at 500 nm and 627 nm, which we identify with the transitions $^1P \rightarrow {}^1S$ and $^3P \rightarrow {}^1S$ respectively of the F-centre. Radiative lifetime measurements are consistent with this assignment. It is suggested that the weakness of the 500 nm band relative to the 627 nm band is due to competition between the $^1P \rightarrow {}^1S$ transition and a radiationless decay from the $^1P \rightarrow {}^3P$-level. At 4 K well-resolved fine structure is observed on the high energy side of both the 627.0 nm band and the 369.7 nm (F$^+$-band) band. For both bands the phonon assisted structure can be reconstructed using only three vibrational modes.

**11589.** Hosler, W. R., Frederikse, H. P. R., **Magnetoresistive effects in KTaO$_3$,** *Solid State Commun.* **7,** 1443-1449 (1969).

Key words: Band structure; magnetoresistance; perovskites; potassium tantalate.

The magnetoresistance of semiconducting KTaO$_3$ has been investigated. Low field results indicate that the bottom of the conduction band consists of 3 or 6 ellipsoids along the ⟨100⟩ crystalline axes, similar to the energy band model predicted (and experimentally confirmed) for SrTiO$_3$. Contrary to expectations the high field magnetoresistance did *not* show Shubnikov-de Haas oscillations.

**11590.** Kieffer, L. J., **Low-energy electron-collision cross-section data. Part I: Ionization, dissociation, vibrational excitation,** *Atomic Data* **1,** 19-89 (1969).

Key words: Atom; cross section; electron; molecule.

Graphical displays of selected experimental data on cross sections as functions of electron energy are presented for some 60 targets important in aeronomy, astrophysics, and plasma physics. The processes covered are ionization, dissociation, and vibrational excitation. Criteria for data selection are discussed. The literature available up to September, 1968, has been searched.

**11591.** Klose, J. Z., **Transition probabilities and mean lives of the 3s$_2$ laser level in neon I,** *Phys. Rev.* **188,** No. 1, 45-49 (Dec. 5, 1969).

Key words: Atomic lifetimes; atomic spectra; atomic transition probabilities; laser; neon.

The mean life of the 3s$_2$ (Paschen notation) laser level in Ne I has been measured for a series of pressures in the range of 3 to 11 $\mu$m of Hg using a method of delayed coincidence. The lifetime values, obtained by means of the $3s_2 \rightarrow 2p_4$ (6328 Å) transition, show an increase in magnitude with increasing pressure. This pressure dependence was interpreted as being due to the imprisonment of the 600.04 Å spectral line emitted in the transition of the 3s$_2$ level to the ground state. The Holstein theory of the imprisonment of resonance radiation was applied to the analysis of the lifetime vs pressure data to yield the following results: $A_{600} = 1.8 \pm 0.5 \times 10^7$ sec$^{-1}$, $\Sigma' A = (\Sigma A - A_{600}) = 1.76 \pm 0.10 \times 10^7$ sec$^{-1}$, and lifetimes of 28 ± 4 and 57 ± 3 nanoseconds for the low-pressure and high-pressure limits respectively. The error limits are obtained from the maximum estimated errors in the measured lifetimes and the measured pressures. Experimental results of other workers along with theoretical values calculated under various assumptions are presented for comparison with the results of the present work.

**11592.** Kostkowski, H. J., Erminy, D. C., Hattenburg, A. T., **High-accuracy spectral radiance calibration of tungsten-strip lamps,** Chapter 4 in *Advances in Geophysics* **14,** 111–127 (Academic Press Inc., New York, N.Y., 1970).

Key words: Blackbody; high temperature measurement; radiometry; spectral radiance; standards calibrations; tungsten strip lamp.

The accuracy of calibrating tungsten strip lamps in terms of absolute spectral radiance has been significantly improved. The standard deviation uncertainty of these calibrations is estimatec to vary from 0.3 percent at 850 nm to 1.5 percent at 210 nm. This accuracy has been realized as a result of: (1) The development of a highly stable 3000 K blackbody and a detailed investigation of its quality. (2) Increasing the accuracy with which the blackbody temperature could be determined. (3) Reducing and evaluating errors resulting from scattered light, polarization, and slit-function effects. Highlights of the instrumentation, the temperature measurement and the various error investigations are presented

**11593.** Lang, S. B., Rice, L. H., Shaw, S. A., **Pyroelectric effect in barium titanate ceramic,** *J. Appl. Phys.* **40,** No. 11, 4335-434 (Oct. 1969).

Key words: Barium titanate; ceramics; ferroelectricity phase transitions; pyroelectricity; spontaneous polarization

The pyroelectric coefficient (at constant stress) of a 95 percen BaTiO$_3$, 5 percent CaTiO$_3$ ceramic composition (Clevite Ceramic B) was measured over the temperature range from 4.9 to 40 K. Extrema in the pyroelectric coefficient were observed at th rhombohedral-orthorhombic transition point (150 to 170 K), th orthorhombic-tetragonal transition point (240 to 260 K), and th tetragonal-cubic transition point (Curie point, at 387 K). Th pyroelectric coefficient showed no anomalous behavior belov 150 K. A spontaneous polarization curve derived from th pyroelectric results is compared with published single-crysta measurements. A model for ceramic polarization suggests tha domain switching at phase transitions is biased by electrical interactions arising from space charges and by mechanical interactions resulting from internal strains.

**11594.** McAlister, A. J., **Calculation of the soft x-ray K-emissio and absorption spectra of metallic Li,** *Phys. Rev.* **186,** No. 3 595-599 (Oct. 15, 1969).

Key words: Absorption spectrum; band calculation; emission spectrum; K-spectra; lithium; transition probability

In an attempt to account for the premature peaking of the L K-emission spectrum, detailed augmented plane wave calculations were performed for metallic Li, at many general points i the Brillouin zone as well as symmetry points. Wave function were extracted, and the one electron K-emission and absorptio transition densities evaluated. The screening arguments so commonly invoked were not employed. No early peaking was foun in the emission density. Various spectral broadenin mechanisms were assessed. A good fit to the experimental dat was obtained by including available estimates of K-stat broadening by the phonon field. At present, there is no basis fo claiming uniqueness for this agreement.

**11595.** Manning, J. R., **Cross terms in the thermodynamic diffusion equations for multicomponent alloys,** *Met. Trans. AIM* **1,** 499-505 (Feb. 1970).

Key words: Alloys; cross terms; diffusion; multicompone alloys; random alloys; thermodynamic equations.

The kinetic equations for the atom fluxes in a multicompone alloy are derived in terms of atomic driving forces for a rando alloy model. In this model, the contribution of each atom flu from the vacancy wind effect is directly proportional to th cancy flux. The kinetic equations allow the $L_{ik}$ coefficients to identified. The cross terms relating the flux of species *i* to the emical potential gradients of other species *k* are found to be n-zero. Neglecting the cross terms can lead to serious inaccucies since these terms can have an appreciable effect on the om fluxes and can lead to negative intrinsic diffusion coeffients even in ideal systems. The $L_{ik}$ in an n-component system pends on the n tracer diffusion coefficients. In this respect, it ll is possible to express the n atom fluxes in terms of only n efficients.

**596.** Meyerson, M. R., Friedman, L., Giles, P. M., **Dimensional stability of 12 nickel maraging steel at ambient temperatures,** *Trans. ASM* **62,** No. 3, 809-812 (Sept. 1969).

Key words: Gage blocks; maraging steel; nitriding; precision equipment; surface hardened; temporal dimensional stability; ultrastability.

The maraging steels attain high strength with a relatively sim- low temperature heat treatment. The nature of the heat treatent and the low carbon content of the steels indicated low sidual stress levels, small lattice distortions, nitridability and ner characteristics which are known to promote dimensional ability at high strength levels. A 12% nickel maraging steel was eated to produce a surface hardness of greater than $R_c$ 65 and dimensional stability at submicroinch levels was observed er a period of about 2 1/2 years. The steel as treated was found be ultrastable, with an average decrease in length of only 0.05 0.10 micrometers per meter per year. Its performance meets exceeds that of any of the many other materials previously instigated at NBS.

**597.** Mosburg, E. R., **Periodic potential probe configuration for plasma diagnostics,** *J. Appl. Phys.* **40,** No. 13, 5290-5300 (Dec. 1969).

Key words: Diffuse flux; plasma diagnostics; plasma probes.

A probe having a spacially periodic potential is created by a lar winding of small tungsten wire. This geometry results in electric field configuration having an extremely short penetran distance into the plasma. The behavior of this probe is stued in extended negative glow and back-diffusion type plasmas. e floating mode current-voltage characteristic curve is seen to quite different from that of the usual double probe in that no ects of the electrons are observed. The behavior of the riodic probe is controlled by the ion inertia established in the fusion region which lies just in front of the probe. The impornt parameter of the characteristic curve is the slope near zero plied voltage difference. This slope can be related in a simple anner to the flux of plasma diffusing to the probe and to the difsion drift energy of the ions as they reach the probe. The elecns make no contribution to this slope for low applied voltage ferences. This probe thus provides a very sensitive method for easuring the diffusive flux of plasma to a containing wall.

**598.** Mozer, B., Price, D. L., Keating, D. T., Meister, H., **Incoherent neutron scattering from liquid and solid CuNi,** *Physics Letters* **30A,** No. 3, 206-207 (Oct. 6, 1969).

Key words: Alloy; CuNi; incoherent; liquid; neutron; scattering; solid.

Incoherent inelastic neutron scattering measurements were rformed on $Cu_{.525}$ $Ni^{62}_{.475}$ alloy in the liquid and solid state. e excitation spectrum is strikingly similar between liquid and lid. The diffusion coefficient ($4 \times 10^{-5}$ cm²/sec.) in the liquid s determined from the broadened elastic peak.

**599.** Newman, M., **Isometric circles of congruence groups,** *Am. J. Math.* **XCI,** No. 3, 648-656 (July 1969).

Key words: Diophantine approximation; modular groups.

Let n be any positive integer, $\epsilon$ any positive number. The principal result of this paper is that the fundamental region of the principal congruence subgroup $\Gamma$ (n) of the modular group $\Gamma$ consists of circles of radii 1/r, where $r = O(n^{2+\epsilon})$.

**11600.** Ohashi, M., Paffenbarger, G. C., **Some flow characteristics at 37 °C of ternary wax mixtures that may have possible dental uses,** *J. Nihon University Dentistry* **11,** No. 3, 109-208 (Sept. 1969).

Key words: Dental; flow; wax.

One hundred and eighty two ternary diagrams of the flow at 37 °C of mixtures of commercial waxes indicate some of these mixtures may have dental use.

**11601.** Paabo, M., Bates, R. G., **Deuterium isotope effects and the dissociation of deuteriophosphoric acid from 5 to 50°,** *J. Phys. Chem.* **74,** No. 4, 706-710 (Feb. 19, 1970).

Key words: Acidity; deuteriophosphoric acid; deuterium oxide; dissociation constant; Emf measurements; isotope effects; phosphoric acid; pK; thermodynamics.

The first dissociation constant of deuteriophosphoric acid in deuterium oxide has been determined over the temperature range 5 to 50 °C from emf measurements of cells using deuterium gas electrodes and silver-silver chloride electrodes, with the following results: $pK_1 = 843.979/T - 4.5714 + 0.0139555T$, where T is the thermodynamic temperature. The changes of enthalpy, entropy, and heat capacity characterizing the dissociation process have been derived from $pK_1$ and its temperature coefficient. By comparison of the results with similar data for protiophosphoric acid in water, the deuterium isotope effects on $pK_1$ and the thermodynamic functions have been evaluated. The isotope effect $pK_1$(in $D_2O$)-$pK_1$(in $H_2O$) is 0.272 unit and almost unchanged over the temperature range studied. This value confirms a linear relationship between the isotope effect for inorganic acids and pK(in $H_2O$).

**11602.** Paabo, M., Bates, R. G., **Dissociation constant of protonated 2,2-bis(hydroxymethyl)-2,2′,2″-nitrilotriethanol (bis-tris) and related thermodynamic functions from 0 to 50°,** *J. Phys. Chem.* **74,** No. 4, 702-705 (Feb. 19, 1970).

Key words: Acidity: bis-tris: buffer solutions; dissociation constant; ionization constant; pH; pK; thermodynamics; 2,2-bis(hydroxymethyl)-2,2′2″-nitrilotriethanol.

The acidic dissociation constant of protonated 2,2-bis(hydroxymethyl.-2,2′2″-nitrilotriethanol ("bis-tris") has been determined at 11 temperatures from 0 to 50 °C by emf measurements of hydrogen-silver chloride cells without liquid junction. At 25 °C, $pK_a$ is 6.483, and consequently buffer solutions of the base and its hydrochloride are useful for pH control in the region pH 5.5 to 7.5. The values of $pK_a$ over the temperature range studied are given as a function of the thermodynamic temperature (T) by the equation $pK_a = 1287.855/T + 2.7905 - 0.00210396T$. Standard thermodynamic functions for the acidic dissociation process have been derived. At 25 °C, $\Delta H^\circ = 28{,}238$ J mol⁻¹, $\Delta S^\circ = -29.4$ J K⁻¹ mol⁻¹, and $\Delta C_p^\circ = 24$ J K⁻¹ mol⁻¹. Conventional $pa_H$ values for five equimolal buffer solutions composed of bis-tris and its hydrochloride have been calculated.

**11603.** Sieck, L. W., Searles, S. K., Ausloos, P., **High-pressure photoionization mass spectrometry. I. Unimolecular and bimolecular reactions of $C_4H_8^+$ from cyclobutane,** *J. Am. Chem. Soc.* **91,** No. 27, 7627-7634 (Dec. 31, 1969).

Key words: Cyclobutane; ion-molecule reactions; mass spectrometry; photoionization; reaction kinetics; vapor phase.

Various mixtures of cyclobutane with cyclohexane, methylcyclopentane, 2-methylpentane, and cyclopentane have been selectively photolyzed at either 1236 Å (10.0 eV) or 1165 Å (10.6 eV) in a mass spectrometer designed to provide specific information concerning thermal ion-molecule reactions occurring in the gas phase. The modes of reaction, as well as the total reactivity found for $C_4H_8^+$ from cyclobutane in mixtures with the various hydrocarbons have been compared with those determined for 1-$C_4H_8^+$ and 2-$C_4H_8^+$ ions produced by photoionization of the appropriate butene at 10.0 eV. Evaluation of these data, including the charge exchange pattern for $C_4H_8^+$ established by the addition of compounds with various ionization potentials (NO, trimethylamine, cyclohexane, etc.), indicate that the $C_4H_8^+$ ion from cyclobutane is non-cyclic and that the probability for isomerization to a 1-$C_4H_8^+$ ion structure is approximately 0.2. The reaction cyclo-$C_6H_{12}^+ + \square \rightarrow C_6H_{12} + C_4H_8^+$, where cyclo-$C_6H_{12}^+$ is produced by photoionization of cyclohexane at 10.0 eV, has also been found. The interesting feature of this process is that charge exchange is exothermic only if $C_4H_8^+$ acquires a butene ion structure during the lifetime of the collision complex.

**11604.** Skolnik, H., Tauber, S. J., **Introduction to the symposium on management and operation of information groups and centers,** *J. Chem. Doc.* **9,** No. 4, 195 (Nov. 1969).

Key words: Classification; data; distribution symposium; documents; evaluation; information systems; management; operation.

This paper serves to introduce a set of papers with the following titles: Literature Searching Activities in a Technical Information Center; Operation of duPont's Patent Index; Information Operations at Esso Research Engineering Company; The Management of Information Operations at Lederle Laboratories; Management of Operations and Services in the Hercules Technical Information Division; Some Administrative Considerations at Biosciences Information Services; Technical Information Management in the U.S. Patent Office; The Role of a Government Agency as Coordinator of a Large Information System; The Transfer of Security Classified Information; Clearinghouse Announcements; The Reliability of Property Data, or Whose Guess Shall We Use?; Development and Application of Selection Criteria for Computer Systems; Organization and Management of Smith, Kline & French's R & D Information Facility.

**11605.** Utech, H. P., **Growing crystals in space,** *Proc. Conf. Manufacturing Technology Unique to Zero Gravity Environment, George C. Marshall Space Flight Center, Nov. 1, 1968, Huntsville, Alabama,* pp. 197-214 (National Aeronautics and Space Administration, Greenbelt, Md., 1969).

Key words: Crystal growing; crystals; gravity; metal; space.

**11606.** Weiss, A. W., **Superposition of configurations and atomic oscillator strengths—boron isoelectronic sequence,** *Phys. Rev.* **188,** No. 1, 119-130 (Dec. 5, 1969).

Key words: Energy levels; oscillator strengths; superposition of configurations; wave functions.

Oscillator strengths have been computed for transitions between a number of low-lying levels in B I and Ne VI. The wavefunctions were computed by the method of superposition of configurations, utilizing the pseudonatural orbital technique to accelerate convergence. The asymptotic, large-Z limiting f-values were also computed, using the nuclear charge perturbation expansion. Together with previous theoretical data from C II, these results have been used to make a graphical study of the f-value behavior for these transitions along the isoelectronic sequence. Comparisons were made between experiment and the predictions of the Hartree-Fock and charge expansion method as well as the present calculations. Finally these theoretica curves were used to predict individual f-values for each membe of the sequence through $Z = 15$ (P XI).

**11607.** Wiederhorn, S. M., Moses, R. L., Bean, B. L., **Plasti deformation and the fracture surface energy of sodium chloride** *J. Am. Ceram. Soc.* **53,** No. 1, 18-23 (Jan. 21, 1970).

Key words: Cleavage; fracture; fracture energy; plasti deformation; sodium chloride; surface energy.

This paper presents a correlation between plastic deformation at crack tips in sodium chloride and the measured value of th fracture surface energy. It is shown that plastic deformation can either aid or hinder crack growth depending on the mode o deformation at the crack tip. If plane stress deformation occurs crack motion is hindered by step formation, dislocation generation and plastic blunting of the crack tip. If plane strain deformation occurs, crack motion is aided by stress fields that arise from the deformation. The specific surface free energy of sodium chloride, {100} plane, is estimated to lie between 0.3 and 0.3 J/m$^2$.

**11608.** Young, K. F., Frederikse, H. P. R., **Temperature an pressure dependence of dielectric constant of cadmium fluoride** *J. Appl. Phys.* **40,** No. 8, 3115-3118 (July 1969).

Key words: Cadmium fluoride; dielectric constant; pressure dependence; temperature dependence.

The temperature and pressure dependence of the dielectri constant $\epsilon'$ of $CdF_2$ has been measured for $T = 4$-$300$ K (at atmospheric pressure) and $P = 1$-$2000$ bar (at room temperature) The frequency dependence of the real and imaginary part ($\epsilon'$ and $\epsilon''$) has been investigated up to 100 MHz.

**11609.** Ballard, D. B., Yakowitz, H., **Investigation of secondary cracks from the failed Point Pleasant, West Virginia bridge** *Proc. Third Annual Scanning Electron Microscope Symp. April 1970,* pp. 321-328 (Illinois Institute of Technology Research Institute, Chicago, Ill., 1970).

Key words: Electron probe microanalysis; ion microanalysis; metallography; nondispersive x-ray analysis; Poin Pleasant, W. Va. bridge; scanning electron microscopy.

Secondary cracks in an eyebar of the Point Pleasant, Wes Virginia bridge were investigated by means of scanning electron microscopy, electron probe microanalysis, and optical metallographic techniques. The observed microstructure, surface topography, and sulfur gradient in the secondary cracks suggest th mechanism of stress corrosion as the cause for crack propagation.

**11610.** Blake, R. W., **Language of performance, an NBS project** *Mater. Res. Std.* **9,** No. 3, 11-14 (Mar. 1969).

Key words: Performance language; performance specifications; performance type tests; test development.

The Public Buildings Service, National Bureau of Standard Building Systems Project is an experimental effort to affect procurement on a performance basis of one million square feet o a building system for use in new construction of government office buildings. The building system proposed is a Floor-Ceilin Sandwich (FTS) and Space Divider System consisting of th floor, the ceiling below, the luminaires (lighting fixtures) in th ceiling and all components between the floor and ceiling planes The basis of procurement is a description of performance required, with the low bidder in terms of cost, being declared th winning bidder. The description of performance, i.e. the languag of performance is stated as *requirement, criteria,* and *test,* a without regard to material that might be employed. Lack of testing related to usage of the building by actual users is pointed ou a limitation on the future development of performance specifi- tions.

611. Brenner, A., Sligh, J. L., **Electrodeless electrolysis,** *J. Electrochem. Soc.* **117,** No. 5, 602-608 (May 1970).

> Key words: Electrodeless electrolysis; electrolysis; electrolysis of glass; electron beam electrolysis; fused salts; glow discharge.

Solid ionic conductors and fused salts were electrolyzed thout contact of solid electrical leads. The current was carried the materials to be electrolyzed either by means of electrons nitted by a hot filament or by a glow discharge. The materials ere made the separating wall between the anode and cathode mpartments of an apparatus constructed of glass or fused sil- a. Electrolysis of glass produced a white opaque material which d not seem to differ chemically from the original glass. endrites of several metals were obtained in the glow discharge ectrolysis of fused salts. The results of the latter process sembled conventional electrolysis with metal electrodes and as not similar to the glow discharge electrolysis of aqueous ectrolytes.

612. Bullough, R., Simmons, J. A., **On the deformation of an imperfect solid,** Chapter 5 in *Physics of Strength and Plastici- y,* A. S. Argon, ed., pp. 47-63 (Massachusetts Institute of Technology Press, Cambridge, Mass., 1969).

> Key words: Continuity equations; continuous distribution of dislocations; defect measures; deformations of connections; deformations of tensors; dislocations; imperfect continuum; nonlinear elasticity; nonlinear strain measures; point defects.

A new formalism is presented for treating the nonlinear pects of the elastic theory of continuous distributions of dislo- tions and point defects. The concept of deformations of ten- rs and connections associated with an imperfect continuum is roduced and used to obtain relevant geometric field equations gether with expressions for the change of defect content thout invoking either "non-Euclidean spaces or anholonomic ordinates." Attention is drawn to the fact that the ordinarily ed Cauchy strain is a generally invalid strain measure and the eory is therefore developed using both the correct Green strain d other appropriate strain measures. The correct defect mea- re is the Cauchy torsion tensor shown to be, in general, inde- ndent of the analogous Green torsion tensor which occurs in geometric field equation for the Green strain. The con- quent difficulties are discussed and procedures for solving two w types of nonlinear defect problems are given.

613. Caswell, R. S., Danos, M., **On the accuracy of the adiabatic separation method,** *J. Math. Phys.* **11,** No. 2, 349-354 (Feb. 1970).

> Key words: Adiabatic approximation; adiabatic separation method; coupled oscillators; matrix diagonalization; nuclear collective model.

Numerical experiments performed for a model of two strongly upled oscillators indicate that the adiabatic separation method elds accurate results even where the condition of adiabaticity violated to a very high degree, except in those cases where two els are degenerate in the adiabatic approximation. An accu- e solution for those cases can be obtained by diagonalizing the 2 Hamiltonian submatrix built on the two degenerate iabatic states. It is conjectured that the adiabatic separation thod can be expected quite generally to yield highly accurate sults, at least for states belonging to the discrete spectrum.

614. Colwell, J. H., Mangum, B. W., Thornton, D. D., Wright, . C., Moos, H. W., **Low-temperature magnetic properties of $DyPO_4$: An ideal three-dimensional Ising antiferromagnet,** *Phys. Rev. Letters* **23,** No. 21, 1245-1247 (Nov. 24, 1969).

> Key words: Antiferromagnet; $DyPO_4$; exchange interaction; Ising; magnetic; three-dimensional Ising antiferromagnetic.

We have measured the magnetic susceptibility and heat capacity of $DyPO_4$ at low temperatures and compared our results with the exact series expansions based on the three dimensional Ising model for the diamond lattice. There is excellent agreement between experiment and theory.

11615. Coxon, B., **The synthesis, equilibration, and conformation of diastereoisomeric 1,2-*O*-isopropylidene-3,5-*O*-(methoxymethylidene)-6-*O*-*p*-tolylsulfonyl-α-D-glucofuranoses. Conformational evidence from a nuclear Overhauser effect,** *Carbohydrate Res.* **12,** 313-334 (May 15, 1970).

> Key words: Conformations; equilibration; glucofuranoses; interaction energies; NMR spectroscopy; nuclear Overhauser effect.

The diastereoisomers of 1,2-*O*-isopropylidene-3,5-*O*-(methoxymethylidene)-6-*O*-*p*-tolylsulfonyl-α-D-glucofuranose have been prepared by treatment of 1,2-*O*-isopropylidene-6-*O*-*p*-tolylsulfonyl-α-D-glucofuranose with trimethyl orthoformate in acidified *N*,*N*-dimethylformamide. Treatment of an equilibrated mixture of these diastereoisomers with acetone gave 1,2:3,5-di-*O*-isopropylidene-6-*O*-*p*-tolylsulfonyl-α-D-glucofuranose and methyl formate. Equilibration reactions of the diastereoisomers in various solvents, at various temperatures, have been studied quantitatively by n.m.r. spectroscopy. The resulting thermodynamic data allow a decision as to the diastereoisomer that is stabilized by intramolecular dipole-dipole interactions, which, when used in conjunction with conformational evidence from vicinal coupling-constants obtained by a computed-spectrum analysis indicated the configuration of the new asymmetric carbon atom. The configurational assignments made for these diastereoisomers were supported by chemical-shift data and by the observation of a spin-coupling over five bonds. Evidence for a favored orientation of the methoxyl group in one of the diastereoisomers was obtained from nuclear Overhauser experiments in which a 25% enhancement of the signal intensity of the neighboring methylidene proton was observed. Van der Waals interaction energies have been calculated for the conformations assigned to the diastereoisomers and for the possible conformations of the closely related 1,2:3,5-di-*O*-benzylidene-α-D-glucofuranose derivatives. The nonbonded interactions in these conformations are discussed and compared.

11616. Coyle, T. D., **Silica,** *Kirk-Othmer Encyclopedia of Chemical Technology* **18,** 2nd Edition, 46-61 (1969).

> Key words: Silica; silicon dioxide.

An introduction is given to the properties of silicon dioxide, including aspects of structure and bonding, the forms of silica and their interconversions, and the chemical properties and reactions of the material.

11617. Cuthill, J. R., **A soft x-ray spectrometer with improved drive,** *Rev. Sci. Instr.* **41,** No. 3, 422-423 (Mar. 1970).

> Key words: Lubrication in vacuum; soft x-ray spectrometer; spectrometer drive.

The spectrometer described is a grazing incidence grating instrument with an improved drive system for moving the electronic detector around the Rowland circle. In this system the lead screw driving the detector always lies along a chord of the Rowland circle joining the grating and the detector. With this design there is less chance of error due to flexure of the components than in previous designs, and the resolution of the spectrometer is constant in wavelength.

**11618.** Eisenhart, C., **Anniversaries in 1970 of interest to statisticians,** *Am. Stat.* **24,** No. 1, 25-68 (Feb. 1970).

Key words: Abraham De Moivre; Avogadro's number; Brownian motion; Chauvenet's criterion; Coast and Geodetic Survey; Corrado Gini; Emile Borel; factorial moments; Ferdinand Rudolph Hassler; history of probability; Isaac Todhunter; Jean Perrin; Louis Bachelier; method of least squares; *Metron*; moments; Norbert Wiener; Office of Weights and Measures; path-space measure; Pierre Simon de Laplace; rejection of observations; Stirling's formula; Stirling's numbers; *Théorie analytique des probabilités*; William Chauvenet.

Brief recognition is given to bicentennials of the death of James Stirling (1692-1770) and birth of Ferdinand Rudolph Hassler (1770-1843); to sesquicentennials of the publication of the 3rd definitive edition of Laplace's *Théorie analytique des probabilités*, and of the births of William Chauvenet (1820-1870) and Isaac Todhunter (1820-1884); to centennials of the births of Louis Bachelier (1870-1946) and Jean Perrin (1870-1942); and to the semicentennial of the initial publication (1920) of *Metron*, an International Review of Statistics.

**11619.** Engen, G. F. **An evaluation of the "back-to-back" method of measuring adaptor efficiency,** *IEEE Trans. Instr. Meas.* **IM-19,** No. 1, 18-22 (Feb. 1970).

Key words: Adaptor; adaptor efficiency; adaptor evaluation; power measurement.

The problem of adaptor evaluation is of considerable interest in the UHF and microwave art where, because of the several different types of transmission line in common use, there is a frequent need to extend an established measurement capability in one type of line to other types of lines, e.g., from rectangular waveguide to coax.

In power and noise calibrations, it is the adaptor *efficiency* which is usually of interest, and one indication of the adaptor losses may be obtained by connecting an identical pair "back to back" and measuring the insertion loss of the combination by the usual techniques. If, then, the losses are assumed to divide equally between the two, the efficiency is thereby determined.

As a practical matter, the losses do not, in general, divide equally, which leads to an error whose evaluation is the subject of this paper. In particular it is shown that the method is capable of good accuracy provided that the assumed identity of the two adaptors is satisfied.

**11620.** Evenson, K. M., Wells, J. S., Matarrese, L. M., **Absolute frequency measurements of the $CO_2$ cw laser at 28 THz (10.6$\mu$m),** *Appl. Phys. Letters* **16,** No. 6, 251-253 (Mar. 15, 1970).

Key words: $CO_2$ laser; cw laser absolute frequency measurement; harmonic generation; high frequency mixing; $H_2O$ laser; metal on metal diode.

The two highest cw absolute frequency measurements as yet reported are described. Frequencies of the *P*(18) and *P*(20) 10.6-$\mu$m lines from a cw $CO_2$ laser were found to be 28.359800 THz and 28.306251 THz ±0.000025 THz, respectively. The frequencies were measured by beating each of these lines with 3.8-THz (78$\mu$m) and 10.7-THz (28$\mu$m) radiation from a water vapor laser and a 26- to 28-GHz klystron in a tungsten-on-nickel point contact diode.

**11621.** Evenson, K. M., Wells, J. S., Matarrese, L. M., Elwell, L. B., **Absolute frequency measurements of the 28- and 78-$\mu$m cw water vapor laser lines,** *Appl. Phys. Letters* **16,** No. 4, 159-161 (Feb. 15, 1970).

Key words: Laser frequency measurement; 10.7 and 3.8 THz frequency measurement; 28 and 78 micron water vapor laser.

The two highest frequency measurements as yet reported are described. Frequencies of the 28- and 78-$\mu$m cw water vapor laser lines were found to be 10.718073 ± 0.000002 THz and 3.821775 ± 0.000003 THz, respectively, by beating each of these radiations with the 337- and 373-$\mu$m (0.89- and 0.80-THz) radiation from an HCN laser, in a metal-on-metal point-contact diode. The frequencies of the HCN laser were in turn measured by beating the 337-$\mu$m radiation with 74-GHz radiation and by measuring the 337- and 373-$\mu$m frequency difference.

**11622.** DiMarzio, E. A., Guttman, C. M., **Separation by flow** *Macromolecules* **3,** No. 2, 131-146 (Mar.-Apr. 1970).

Key words: Chromatography; gel permeation chromatography; particle separation; polymer separation.

Dilute solutions of finite size particles undergoing Brownian motion and flowing through a capillary have average velocities which depend on the particle size. Thus one can obtain a separation of particles of different sizes due to fluid flow. The elution volumes of suspended particles or polymer molecules are derived for various tube geometries. Following Taylor, the effects of diffusional broadening of the volume elution peak for finite size particles are discussed and a criteria for separation is given. It is found that particles very similar in size can always be separated. A scheme for separation by flow on a continuous basis is proposed.

**11623.** Frederikse, H. P. R., **The electronic band structure of strontium titanate: Theory and experiment,** (Proc. Conf. International Advanced Study Institute: Electronic Structure in Solids, Chania, Crete, Greece, June 30-July 14, 1968). Chapter in *Electronic Structures in Solids,* pp. 259-269 (Plenum Press, New York, N.Y., 1969).

Key words: Electronic band structure; oxides; semiconductors; strontium titanate; transition metal compounds; transport measurements.

The approach used for calculating the electronic energy bands of $SrTiO_3$ is indicated. A number of experiments designed to test the result of this calculation is discussed. Among these are both transport measurements and optical investigations.

**11624.** Furukawa, G. T., Saba, W. G., Sweger, D. M., Plumb, H. H., **Normal boiling point and triple point temperatures of neon** *Metrologia* **6,** No. 1, 35-37 (Jan. 1970).

Key words: Boiling point; neon; triple point.

The normal boiling point and triple point temperatures and the triple point pressure of neon were found to be 27.096 ± 0.001 K and 24.553 ± 0.001 K, and 43332 ± 13 N/m² [325.02 ± 0.10 mm Hg (0 °C)], respectively. (The temperatures are in terms of the NBS-1955 provisional temperature scale. The figures after the ± symbol indicate estimated uncertainties.) The triple point pressure is in accord with the more recent values, but the normal boiling point and triple point temperature deviate significantly from those of previous investigators.

**11625.** Gadzuk, J. W., **Resonance transmission in electron emission from surfaces with adsorbed atoms,** *Surface Sci.* **18,** 193-203 (1969).

Key words: Adsorption; electron emission; reflection resonance; transmission resonance.

Recent work on the effects of resonance tunneling through virtual bound states of adsorbed atoms on metal surfaces in field emission is extended to treat possible resonance transmission effects over adsorbed atoms in thermionic, auger, and photoelectron emission. The resonance effects are illustrated through act calculations on model potentials for the metal and ad- rbed atom. Shortcomings of the pseudopotential formulation wave interference phenomenon are indicated. The transmis- on and transmission enhancement functions are calculated for electron coming from within the metal which then crosses the mbined potential of the metal surface and the adsorbed atom. esonances in the transmission, similar to Ramsauer peaks, are edicted for suitable choices of model potential parameters nich may be reasonable approximations to the parameters scribing alkali atoms adsorbed on metal surfaces.

626. Graminski, E. L., **The stress-strain behavior of accelerated and naturally aged papers,** *Tappi* **53**, No. 3, 406-410 (Mar. 1970).

Key words: Accelerating (process); aging; break resistance; cross-linking; crystal structure; dimensional stability; paper; strains; stiffness; stresses.

The extensional stiffness generally increases when paper is ed under accelerated conditions, indicating that either cross- king occurs or that the degree of crystallinity increases. Either these processes could be responsible for the increase in wet- ength when paper is heated. An increase in wet strength also curs in the course of natural aging, indicating that some milarity exists between accelerated and natural aging.

627. Gross, D., Natrella, M. G., **Interlaboratory comparison of the potential heat test method,** *Am. Soc. Testing Mater. Spec. Tech. Publ.* **464**, *Fire Test Performance*, pp. 127-152 (1970).

Key words: Calorimetry; combustibility; evaluation; fire tests; heat of combustion; interlaboratory tests; oxygen bomb; potential heat; tests.

Quantitative measurements of the total heat release by lected building materials were made during an interlaboratory ıdy of the Potential Heat Method. Seven of the eleven par- ipating laboratories ranked the five materials in the same der, and a single ranking change for three other laboratories ould yield identical rankings. The general magnitude of within- oratory repeatability and between-laboratory reproducibility composite materials of generally low potential heat are in- cated by statistical analysis of the results.

Results are reported on the effect of the amount of combustion omoter used and on differences in the first and second phase lues. A discussion is presented on the effects of material sam- ng and on certain features of the experimental procedure nich require special care. A tentative test method standard, ntaining complete details of the test procedure, is included as appendix.

628. Guildner, L. A., Stimson, H. F., Edsinger, R. E., Ander- son, R. L., **An accurate mercury manometer for the NBS gas thermometer,** *Metrologia* **6**, No. 1, 1-18 (Jan. 1970).

Key words: Capacitance; diaphragm pressure transducer; environment; meniscus characteristics; mercury manometer; pressure; pressure regulator; vacuum joints; vacuum valves; wring tests.

A mercury manometer using capacitance sensing of meniscus sitions has been refined to give an accuracy within 2 parts in $^6$ of the pressure in the range from $1 \times 10^4$ to $1.3 \times 10^5$ N/m$^2$. ie determination of pressure ratios is accurate within 1.5 parts $10^6$ for pressures in the same range.

529. Haber, S., **Sequences of numbers that are approximately completely equidistributed,** *J. Assoc. Computing Mach.* **17**, No. 2, 269-272 (Apr. 1970).

Key words: Equidistribution; numerical analysis; pseudo-random; quadrature; random numbers; sequences; uniform distribution.

For certain computational purposes, it is desirable to have sequences of numbers that are completely equidistributed, i.e. such that $t_1, t_2, \ldots$ is equidistributed in the interval $[0,1]$; $(t_1, t_2)$, $(t_2, t_3)$, . . . is equidistributed in the unit square; $(t_1, t_2, t_3)$, $(t_2, t_3, t_4)$, . . . is equidistributed in the unit cube; etc. The construction of such sequences is apparently quite complicated. For calculations using no more than a fixed number $l$ of significant figures, the numbers in such a sequence must be rounded or truncated, and this results in a certain unavoidable minimum error in their distribution. In the paper this error is defined, and a simple construction is given of some sequences of $l$-digit numbers completely equidistributed to within the minimum error.

11630. Handy, L. B., Brinckman, F. E., **Chemistry of the methoxyfluorotungsten(VI) series,** *Chem. Commun.* pp. 214-215 (1970).

Key words: Fluorine; methoxy; n.m.r.; siloxane; stereochemistry; synthesis; tungsten.

The series of compounds $(MeO)_nWF_{6-n}$, $n = 1-5$, has been prepared by the reaction of $WF_6$ and $Me_3SiOMe$ and the stereochemical configuration of each member has been assigned on the basis of $^{19}F$ and $^1H$ n.m.r. data.

11631. Heinrich, K. F. J., **Electron and ion microprobe analysis,** (Proc. 10th Symp. Electron, Ion, and Laser Beam Technology, Gaithersburg, Md., May 21-23, 1969). Chapter in *Record of the 10th Symposium on Electron, Ion, and Laser Beam Technology*, L. Marton, ed., pp. 353-360 (San Francisco Press, San Francisco, Calif., 1969).

Key words: Electron microprobe; ion microprobe; mass spectrography; microanalysis; scanning electron microscopy; x rays.

This review covers the principles and development of electron probe microanalysis, with particular emphasis on recent developments. The double function of the instrument as a spectrograph and as a microscope is considered. The salient characteristics of the ion beam microprobe are also indicated.

11632. Heinrich, K. F. J., Yakowitz, H., **Quantitative electron probe microanalysis: Uncertainty in the atomic number correction,** *Mikrochim. Acta* **7**, No. 1, 123-134 (Jan. 1970).

Key words: Atomic number correction; Bethe's Law; electron backscatter; error propagation; mean ionization potential; microprobe analysis.

The atomic number effect in quantitative electron probe microanalysis has been considered from the point of view of error propagation. The results indicate that the chief causes of analysis uncertainty are poorly known electron backscattering factors and mean ionization potential values. Operating variables such as working voltage or x-ray take-off angle cannot be manipulated so as to reduce the effect of the uncertainties. However, the overall analysis uncertainty remains nearly constant over the entire range of working voltages practical for microanalysis.

11633. Horn, W. A., **Optimal networks joining n points in the plane,** (Proc. IVth International Symp. The Theory of Traffic Flow, Karlsruhe, Germany, June 18-20, 1968). Chapter in *Strassenbau und Strassenverkehrstechnik* **86**, W. Leutzbach and P. Baron, eds., pp. 160-166 (Bundesminister für Verkehr, Germany, 1969).

Key words: Optimal interchange location; optimal networks; optimal road layout; planar graphs; planar networks; road location; Steiner's problem; street-network problem; transportation theory.

This report develops a number of results on the problem of connecting n points in the plane, with given travel demands between each pair, by a minimum-cost network. The critical assumptions are (a) constant construction costs per mile, (b) constant travel cost per mile per traveller, and (c) use of shortest paths in the network for all travel.

These results are adequate to give a complete solution when $n=3$. For this case, the possible optimal network configurations are identified, each is shown actually to arise as the optimum for suitable combinations of problem data, and the computations necessary to choose among them are described. One of the results for general n is an upper bound (roughly $n^4/4$) on the number of nodes, other than the original n points, in an optimal network. Another is the determination of an explicit threshold, for the ratio of construction cost to travel cost, beyond which each "auxiliary node" will lie on exactly three links.

**11634.** Hummer, D. G., **Observatory Report—Joint Institute for Laboratory Astrophysics of the National Bureau of Standards and the University of Colorado,** *Bull. Am. Astron. Soc.* **2,** No. 1, 59-65 (1970).

Key words: Annual summary of astrophysics at JILA.

This is an annual report of work at JILA in astrophysics, and work in atomic physics that is immediately relevant to astrophysics. A list of publications for the period July 1, 1968-June 30, 1969 is appended.

**11635.** Kasen, M. B., **Grain boundary resistivity of aluminum,** *Phil. Mag.* **21,** No. 171, 599-610 (Mar. 1970).

Key words: Aluminum; electrical resistivity; grain boundaries; recrystallization; solute segregation; super-purity metals.

Residual resistivity at 4 K has been studied as a function of grain boundary area per unit volume in aluminium of two differing purities. A positive correlation between residual resistivity and boundary area was observed above a minimum boundary area per unit volume. The resistivity attributable to the presence of grain boundaries was found to reflect both the defect structure of the boundaries and the solute redistribution due to boundary segregation. Elimination of the solute effect yielded a specific boundary resistivity of $1.35 \pm 0.5 \times 10^{-12}$ ohm-cm² for pure boundaries. Evidence of a purification effect due to grain boundary segregation was noted.

**11636.** Kokoszka, G. F., Brinckman, F. E., **Electron paramagnetic resonance studies of phosphorus-containing reactive intermediates,** *J. Am. Chem. Soc.* **92,** No. 5, 1199-1205 (1970).

Key words: EPR; free radicals; irradiation; low-temperature reaction; methylchlorophosphines; phosphorus halides.

Several novel phosphorus-containing radicals have been produced at $-196°$ by photolytic methods and characterized by epr spectrometry. In addition to the formation of $PCl_2$ ($A(P)=92$ MHz; $g=2.018$) in neat parent $PCl_3$, a secondary reaction has been observed which yields $PCl_4$ ($A(P)=3398$ MHz; $A'(Cl)=175$ MHz; $A''(Cl)=21$ MHz; $g=2.013$). Appropriate modification of the parent matrix by either cocondensation of inert diluent (Xe) or possibly reactive materials ($PF_3$, $SnCl_4$) results in useful additional spectral information. Thus in $PF_3$:$PCl_3$ (1:10) the full anisotropy of $PCl_2$ is revealed ($A_{\|}(P)=753$ MHz; $A_{\perp}(P)=78$ MHz; $A_{\|}(Cl)=41.5$ MHz; $A_{\perp}(Cl)=0$ MHz; $g_{\|}=2.001$; $g_{\perp}=2.021'$. In contrast to neat $PCl_3$, irradiation of Xe:$PCl_3$(9:1) does not result in formation of $PCl_4$, presumably from inhibition of $Cl + PCl_3 \rightarrow PCl_4$ by competitive Cl recombination. Irradiation of $SnCl_4$:$PCl_3$(6:1) results in formation both of $PCl_2$ and $PCl_4$. Several related organophosphines were also irradiated, but only with $CH_3PCl_2$ was evidence obtained suggesting formation of a four-coordinate radical similar to $PCl_4$ ($A(P)=3015$ MHz, $g=2.000$). In all cases, however, epr data are consistent with bond scission of the ternary phosphine to produce $PCl_2$-like fragments. The above results are discussed in light of their bearing on the role of reactive intermediates in synthetic chemistry, and considerations of molecular geometric and orbital composition are presented with reference to current MO and electrostatic models.

**11637.** Kose, V. E., Sullivan, D. B., **Influence of external noise on microwave-induced Josephson steps,** *J. Appl. Phys.* **41,** No. 1, 169-174 (Jan. 1970).

Key words: Electromagnetic noise; fundamental constant; Josephson effect; superconductivity.

The influence of fluctuations on microwave-induced Josephson steps is treated phenomenologically and it is found that the center voltage of these steps is not shifted by the disturbance. Expressions governing the step shape are obtained for various noise spectra. The theory was checked by subjecting niobium point-contact junctions to several forms of externally generated noise. The theory does not differentiate between internal and external noise sources, so that a number of the conclusions can be extended to intrinsic fluctuations.

**11638.** Kuriyama, M., **The dynamical scattering amplitude of an imperfect crystal,** *Acta Cryst.* **A26,** No. 6, 56-59 (Jan. 1970).

Key words: Dynamical theory; imperfect crystal; line broadening; scattering amplitude; x-ray diffraction.

A formal expression for the x-ray dynamical scattering amplitude of an imperfect crystal is obtained. The resultant expression includes the dynamical line broadening effect on the diffracted x rays caused by imperfections. The effect due to absorption in the crystal are also taken into account.

**11639.** Kushner, L. M., **Are there standards?,** (Proc. National Safety Congress Conf., Chicago, Ill., Oct. 28, 1969), *National Safety Congress Trans., Civic Leadership* **6,** 12-16 (1969).

Key words: Consumers; safety; standards; voluntary standards.

Safety standards for consumer products are too few and too concentrated on a few classes of products. Perhaps the best way for consumers to remedy this situation is to make their voice heard in an organized and effective manner in the existing voluntary standards-making procedure.

**11640.** Lafferty, W. J., Maki, A. G., Coyle, T. D., **High resolution infrared spectrum and structure of diborane,** *J. Mol. Spectr.* **33,** No. 2, 345-367 (1970).

Key words: Bond angles; boron-boron bond length; boron hydrogen bond lengths; diborane; high resolution; infrared spectrum; molecular structure; rotational constants.

The two infrared active terminal B–H stretching bands, $\nu_8$ and $\nu_{16}$, of $^{10}B_2H_6$ and $^{11}B_2H_6$ were studied with a resolution of $0.04-0.05$ cm$^{-1}$. The following ground state rotational constants were obtained: for $^{10}B_2H_6$, $A_0=2.65550 \pm 0.00056$ cm$^{-1}$, $B_0=0.642190 \pm 0.000080$ cm$^{-1}$, and $C_0=0.587372 \pm 0.000066$ cm$^{-1}$; for $^{11}B_2H_6$, $A_0=2.65569 \pm 0.00026$ cm$^{-1}$, $B_0=0.606463 \pm 0.000068$ cm$^{-1}$ and $C_0=0.557279 \pm 0.000056$ cm$^{-1}$. These constants were used to derive the following structural parameters: $B \cdots B=1.762_8 \pm 0.0026$ Å, $B-H_t=1.200_5 \pm 0.0036$ Å, $B-H_b=1.320_4 \pm 0.0010$ Å, $\angle H_tBH_t=121.0 \pm 0.6°$ and $\angle H_bBH_b=96.2 \pm 0.2°$. (All errors cited are twice standard deviations.) Upper state constants are reported.

**11641.** Lawton, R. A., Allred, C. M., Hudson, P. A., **A wide-range cw power measurement technique,** *IEEE Trans. Instr. Meas.* **IM-19,** No. 1, 28-34 (Feb. 1970).

Key words: Receiver calibration; RF power, measurement.

An accurate power measurement technique is described, which makes possible the determination of the net power delivered to a load of arbitrary impedance over a wide power range. A standard power meter is employed to fix a reference power level. Subsequent measurements consist of dimensionless ratios that can be obtained from precision attenuators.

The method is applicable to a very wide range of frequencies and was demonstrated at a frequency of 30 MHz with power measurements extending from $10^{-2}$ to $10^{-14}$ watt. Maximum uncertainties ranged from ~0.5 to 1.5 percent.

This technique is applicable in the measurement of the sensitivity of very-low-level detectors, receivers, radiometers, etc.

**11642.** Larson, W., Desch, R. F., Gillard, B. F., **Further analysis of the off-null versus power ratio method of attenuation measurement,** *IEEE Trans. Microwave Theory Tech.* **MTT-18,** No. 2, 112-113 (Feb. 1970).

Key words: Attenuation measurement; microwave; rotary-vane attenuator.

Analysis of calibration data of a rotary-vane attenuator has yielded closer agreement between the recently developed off-null and the proven power ratio methods of attenuation measurement. A constant bias was discovered in the measured values of attenuation difference, and a procedure is described to correct for this bias. After the correction is applied, the average agreement between the two methods of measurements is improved an order of magnitude, namely, from a former 2.0 percent to 0.17 percent.

**11642A.** Lutz, G. J., **Determination of oxygen in sodium by photon activation analysis,** *Anal. Chem.* **42,** No. 4, 531-532 (Apr. 1970).

Key words: Coincidence spectrometry; oxygen; photon activation analysis; rapid radiochemical separation; sodium.

A photon activation analysis method has been developed for the determination of oxygen in sodium. The method utilizes the photonuclear reaction $^{16}O(\gamma,n)^{15}O$. A rapid separation of the oxygen activity is effected by dissolving the sample in a dilute sodium hydroxide solution under flowing nitrogen. The radioactive oxygen is converted to sodium hydroxide which exchanges with the water. A portion of the water is distilled from the mixture and counted. Yields are approximately 50% and the time of separation is about four minutes. The detection limit is about 2 ppm. Standard deviations are typically 10%.

**11643.** McLaughlin, W. L., **Photographic film dosimeters,** Chapter in *Manual on Radiation Dosimetry,* N. W. Holm and R. J. Berry, eds., pp. 387-394 (Marcel Dekker, Inc., New York, N.Y., 1970).

Key words: Dosimetry; gamma rays; hypersensitization; internal image; latensification; photographic development; photolysis; physical development; printout; radiographic films; silver halides.

A recipe and response curves are given for several dosimetry films, and their interpretation of $\gamma$-ray exposures over a wide range is discussed. The procedures include using a number of special optical and chemical treatments, in order to broaden the conventional response from $3 \times 10^{-2} - 10^{-3}$ roentgens to $10^{-3}$—$10^{8}$ roentgens. The special treatments include: Physical development, latensification plus physical development, stabilization processing. The advantages and disadvantages of these methods are outlined.

**11644.** McLaughlin, W. L., **Radiochromic dye-cyanide dosimeters,** Chapter in *Manual on Radiation Dosimetry,* N. W. Holm and R. J. Berry, eds., pp. 377-385 (Marcel Dekker, Inc., New York, N.Y., 1970).

Key words: Cyanides; dosimetry; dyes; electron beams; reflection densitometry; spectrophotometry; triphenyl methane; x- and $\gamma$-rays.

Triphenyl methane dye cyanide solutions (liquids, gels, films, and papers) have been developed for high-range dosimetry ($10^3$-$10^8$ rads). A recipe for their preparations, dose calibration by calorimetry, and spectrophotometric readout is included. The systems are shown to be highly versatile for radiation processing dosimetry.

**11645.** Mahler, R. J., **Nominal $\Delta m = \pm 1$, 2, 3, 4, 5 magnetic nuclear transition probabilities in ruby,** *Phys. Rev.* **188,** No. 2, 584-590 (Dec. 1969).

Key words: Electric field gradients; electric quadrupole; magnetic dipole; nuclear spin system.

The nominal $\Delta m = \pm 1$, 2, 3, 4, and 5 magnetic transition probabilities between $Al^{27}$ nuclear energy levels in ruby are calculated, and the energy-level populations are determined with the presence of an external perturbation connecting two energy levels. A simple model where the relaxation of the $Al^{27}$ spins is via a direct magnetic interaction with the $Cr^{3+}$ paramagnetic impurity is used to compare the calculated $\Delta m = \pm 2$ magnetic transition probability to the observed effects in a 4% $Cr^{3+}$-doped ruby sample. The calculated magnitude and angular dependence fit the experimental data and indicate that the effect is large enough to cause leakage effects when attempting a pure quadrupole saturation experiment in ruby.

**11646.** Mazur, J., **Higher order Markov chains and statistical thermodynamics of linear polymers,** Chapter 6 in *Markov Chains and Monte-Carlo Calculations in Polymer Science,* G. G. Lowry, ed., pp. 153-185 (Marcel Dekker, Inc., New York, N.Y., 1970).

Key words: Linear polymers; Markov chains; order-disorder transitions; random variables; restricted chains; Theta point; transition probabilities; volume exclusion.

The general theory of Markov chains is presented as it applies to linear polymer chains. The polymer chain is considered here as a linear sequence of consecutive events, upon which short-range intra-chain interactions are superimposed. The statistical and thermodynamic properties of these chains are obtained from the chain partition function, which is derived by the methods of averaging functions over the chains of random variables. The partition function and its various derivatives are calculated in terms of the eigenvalues and the eigenvectors of the matrices of the transition probabilities. In the various applications of the matrix method to the conformational properties of the linear polymer chains, the matrix of transition probabilities can be subsequently reduced by similarity transformations. The theory of Markov chains is applied, in particular, to the following problems: (1) the theory of the theta (ideal) point for lattice-simulated chains with short-range interactions, (2) volume exclusion problems for Markov chains, and (3) cooperative phenomena in linear polymers and the conditions for order-disorder transitions in self-interacting chains.

**11647.** Milligan, D. E., Jacox, M. E., **Infrared and ultraviolet spectra of the products of the vacuum-ultraviolet photolysis of silane isolated in an argon matrix,** *J. Chem. Phys.* **52,** No. 5, 2594-2608 (Mar. 1, 1970).

Key words: Disilane; free radical; infrared spectrum; matrix isolation; $Si_2$; SiH; $SiH_2$; $SiH_3$; silane; ultraviolet spectrum; vacuum-ultraviolet photolysis.

The vacuum-ultraviolet photolysis of silane and of the various deuterosilanes isolated in an argon matrix at 4 or at 14 K leads to the production of several reactive species. Infrared and ultraviolet spectroscopic evidence is presented indicating that $Si_2$, SiH, $SiH_2$, and $SiH_3$ are stabilized in these experiments. A previously unobserved transition of $Si_2$, tentatively identified as the $D(^3\Pi_u) - X(^3\Sigma_g^-)$ transition, is reported. Observation of the bending vibration absorption of $SiH_2$ at 1008 $cm^{-1}$ has confirmed that the lower state of the previously observed electronic transition of singlet $SiH_2$ is the ground state of this species. The stretching vibrations of $SiH_2$ have also been observed near 2000 $cm^{-1}$. Infrared absorptions at 925, 996, 1955, and 1999 $cm^{-1}$ have been tentatively assigned to $SiH_3$. The removal of one or more H atoms from $SiH_4$ leads to an appreciable lengthening of the remaining Si – H bonds. Disilane and incompletely characterized products of its photolysis contribute significantly to the infrared spectra observed at 14 K.

**11648.** Nargolwalla, S. S., Crambes, M. R., Suddueth, J. E., **Photon self-absorption corrections for the minimization of systematic errors in 14-MeV neutron activation analysis,** *Anal. Chim. Acta* **49,** No. 3, 425-436 (Mar. 1970).

Key words: Annihilation radiation; correction factors; neutron and gamma-ray attenuation; photopeak analysis; removal cross section; systematic errors; 14-MeV activation analysis.

In comparative 14-MeV neutron activation analysis for oxygen, systematic errors are evidenced if attenuation of incident neutrons and induced gamma radioactivity by a thick sample is ignored. The present study pertains to the general case of measurement where photopeaks resulting from either direct nuclear transitions or from positron annihilation are counted. A quantitative evaluation of these attenuation processes is presented. The results show that the photon attenuation correction factor is related to the difference between the calculated linear absorption coefficients for sample and standard through a simple exponential expression. The slopes of the respective correction factor lines are compared with that for integral gamma counting in oxygen analysis. Differences in the magnitudes of the slopes are discussed. The results of this study are consistent with the removal cross section theory describing 14-MeV neutron attenuation over a wide range of threshold energies. Typical analyses of Standard Reference Materials, using these correction factors, are given.

**11649.** Nargolwalla, S. S., LaFleur, P. D., **Characterization of standard reference materials for industry and research by neutron generator activation analysis,** *Proc. American Nuclear Society Topical Meeting, San Juan, Puerto Rico, May 4-6, 1969,* pp. 183-186 (1969). ●

Key words: Neutron generator activation analysis; organometallics; oxygen; standard reference materials; steels.

Described herein are examples which demonstrate the use of a low-cost neutron generator facility for materials characterization in the steel and oil industries. Analytical results for oxygen in steels and for the metallic component in a number of organometallic oil additives are given. The accuracy of these results is indicated by the close agreement of the activation data with that obtained by conventional and well proven chemical methods. These applications illustrate the utilization of standard materials useful for industrial and research needs.

**11650.** Newman, M., **A table of the first factor for prime cyclotomic fields,** *Math. Compt.* **24,** No. 109, 215-219 (Jan. 1970).

Key words: Class numbers; cyclotomic fields; factorization; first factor.

The first factor of the prime cyclotomic fields for all primes <200 is computed by means of a determinantal formula, correcting some errors in tables of Kummer.

**11651.** Powell, F. X., Johnson, D. R., **Microwave detection of $H_2{}^{18}O$,** *Phys. Rev. Letters* **24,** No. 12, 637 (Mar. 23, 1970).

Key words: Astrophysical; emission; galactic distribution of isotopes; $H_2{}^{18}O$; microwave absorption; rotational transition.

Laboratory detection of a microwave absorption in $H_2{}^{18}O$ near 5.33 cm is reported. This observed signal has been assigned to a pure rotational transition between the $6_{16}$ and $5_{23}$ levels in the ground vibrational state of $H_2{}^{18}O$. Signals from these same two rotational levels for $H_2{}^{16}O$ have been detected in emission from several sources in the galaxy.

**11652.** Rogers, E. E., Abramowitz, S., Jacox, M. E., Milligan, D. E., **Matrix-isolation studies of the infrared spectra of the free radicals $CCl_3$ and $CBr_3$,** *J. Chem. Phys.* **52,** No. 5, 2198-2204 (Mar. 1, 1970).

Key words: Bromoform; carbon tetrabromide; carbon tetrachloride; $CBr_3$; $CCl_3$; chloroform; infrared spectrum; lithium atoms; matrix isolation; vacuum-ultraviolet photolysis.

$CCl_3$ has been stabilized both by the reaction of lithium atoms with $CCl_4$ in an argon matrix at 20 K and by the vacuum-ultraviolet photolysis of $HCCl_3$ or of $DCCl_3$ in an argon or a nitrogen matrix at 14 K. The analogous techniques have been found to lead to the stabilization of $CBr_3$. The product spectra obtained in the lithium-atom experiments are considerably simpler than those obtained in the previous studies of the reaction of lithium atoms with matrix-isolated $CX_4$. In the vacuum-ultraviolet photolysis experiments, $DCCl_2$, $HCBr_2$, and $CBr_2$ have also been observed. The absorption frequencies and contours obtained for $\nu_3$ of $CCl_3$ and of $CBr_3$ are independent of the method used to produce these species, suggesting that lithium atoms and their reaction products do not appreciably perturb the degenerate stretching mode of either $CCl_3$ or $CBr_3$. Despite yields of these species comparable to those previously reported, absorptions at 674 and at 582 $cm^{-1}$, previously attributed to $\nu_1$ of $CCl_3$ and $CBr_3$, respectively, are completely missing from the present experiments. No other absorption attributable to $\nu_1$ of either species has been detected. It is concluded that a pyramidal $(C_{3v})$ structure for $CCl_3$ and for $CBr_3$ has not been established.

**11653.** Romanoff, M., **Corrosion evaluation of steel test piles exposed to permafrost soils,** *Proc. National Association of Corrosion Engineers 25th Conf., Houston, Texas, March 10-14, 1969,* pp. 6-13 (National Association of Corrosion Engineers, Houston, Texas, 1970).

Key words: Corrosion; permafrost; pilings; soil corrosion; steel; steel piles; underground.

This paper describes the results of inspections made to investigate the corrosion of steel pilings in permanently frozen soils, and in the active or thin layer of soil above the permafrost layer, as part of the joint investigation conducted by the National Bureau of Standards and the U.S. Army Office of the Chief Engineers on the corrosion of steel piles in underground environments.

Nine steel test piles exposed in 3 soil sites at the Alaska Field Station of the U.S. Army Cold Regions Research and Engineering Laboratory at Fairbanks, Alaska, were extracted to investigate the extent of corrosion on the piles. The pipe- and H-pile specimens were exposed underground for 6, 8, or 11 years in an active horizon, in which the soil thaws and freezes annually to a depth of approximately 5 feet (1.5 m), and in permanently frozen soil beneath the active layer.

The test piles were installed to depths of 21 feet (6.4 m) below ground surface by several different methods.

Results of the inspections show that the steel piles are unaffected by corrosion in the permafrost regions, and that there was no evidence of significant corrosion at the ground line, in the ac-live or thaw region, or at the boundary between the thaw and permafrost regions.

11654. Romanoff, M., **Performance of steel pilings in soils,** *Proc. National Association of Corrosion Engineers 25th Conf., Houston, Texas, March 10-14, 1969,* pp. 14-22 (National Association of Corrosion Engineers, Houston, Texas, 1970).

Key words: Corrosion; H-piles; sheet piles; soil corrosion; soils; steel piles; underground.

This paper consists of a summary of the results of inspections made on steel pilings in various underground structures to investigate the extent of corrosion on steel piles after many years of service in underground environments. This is part of an investigation being conducted by the National Bureau of Standards, in cooperation with the U.S. Army Corps of Engineers and the American Iron and Steel Institute.

Since the 1962 publication of the National Bureau of Standards Monograph 58, "Corrosion of Steel Pilings in Soils," additional data have been obtained from inspections of steel H- and sheet piles which have been exposed underground from 6 to 50 years in 35 structures in a wide variety of soil conditions.

At 18 locations the piles were pulled from the structures for inspection. At 17 locations, where it was not possible to pull the piles without disturbance to the existing structure, test holes were excavated adjacent to the sheet piling to expose at least an 8-ft width of steel on a section of the structure.

The results from the recent inspections are in agreement with, and substantiate, the observations previously made and published in Monograph 58.

The data show that, in general, pilings are not significantly affected by corrosion in undisturbed natural soils, regardless of the type of soil.

Piling exposed to fill soils, above or in the water table zone, appeared to be the most vulnerable to corrosion. However, only moderate corrosion in the form of localized pitting was generally found in these areas.

1655. Ruegg, F. C., Spijkerman, J. J., DeVoe, J. R., **A Mössbauer spectrometer for the structural analysis of materials,** (Proc. Symp. Radioisotope Instruments in Industry and Geophysics, Warsaw, Poland, Oct. 18-22, 1965), Chapter in *Radioisotope Instruments in Industry and Geophysics* **I,** 325-335 (International Atomic Energy Agency, Vienna, Austria, May 1966).

Key words: Materials; Mössbauer; spectrometer; structural analysis.

A Mössbauer spectrometer has been designed to provide high precision Mössbauer spectra. The instrument uses two electromechanical transducers, one driver and one sensor, in a feedback loop which incorporates an operational amplifier and a power amplifier. The transducer system is coupled to the scaler input of a multichannel analyzer. A high degree of synchronization between the channel number (which represents units of velocity) and the actual velocity produced by the transducer is obtained by using the analogue voltage of the channel number as the input to the electromechanical system. By advancing sequentially the channel number as a linear function of time, a motion of constant acceleration is produced. Gamma rays from the radiation detector proportional counter or the NaI(Tl) are then energy selected by a single channel pulse-height analyzer and these pulses are presented to the multiscaler input. The spectrometer can be used to accept high counting rates by using a unit scaler with a 10-MHz response.

The spectrometer can be used with a variety of auxiliary equipment to measure spectra at low temperature or high pressure.

The linearity of the spectrometer is found to be within ±0.1% relative standard deviation with the use of a voltage-to-frequency converter which is connected to the analyzer between the sensing transducer and the multiscaler input.

Some applications of this spectrometer to the analysis of materials are discussed.

11656. Santoro, A., Mighell, A. D., **Determination of reduced cells,** *Acta Cryst.* **A26,** No. 6, 124-127 (Jan. 1970).

Key words: Classification; identification; lattice; reduced cell.

An analysis is given of the relation between the reduced cells defined by Niggli and the cells obtained by applying Buerger's algorithm. It is shown that in many instances a cell based on the shortest three noncoplanar translations must be transformed to obtain the reduced cell. The required transformations for all cases have been derived and are presented in this paper.

11657. Schroeder, L. W., **Infrared and Raman spectra of $ClHCl^-$ and $BrHBr^-$ ions in $CsCl\cdot 1/3H_3OHCl_2$ and $CsBr\cdot 1/3H_3OHBr_2$,** *J. Chem. Phys.* **52,** No. 4, 1972-1978 (Feb. 1970).

Key words: $BrHBr^-$ ion; $ClHCl^-$ ion; environmental effects; infrared spectra; Raman spectra; symmetrical.

Infrared and Raman spectra of $CsCl\cdot 1/3H_3OHCl_2$ and $CsBr\cdot 1/3H_3OHBr_2$ have been measured in the 50-4000-$cm^{-1}$ region. The spectra show the bands expected for the oxonium ion plus bands due to the $XHX^-$ ion. The $XHX^-$ ions are in a symmetrical environment, and a consistent interpretation of the spectra suggests that the $XHX^-$ ions have a centrosymmetric structure in these salts.

11658. Schwerdtfeger, W. J., **Corrosion rates of metals, alloys, and galvanic couples as measured by polarization techniques,** *Mater. Res. Std.* **10,** No. 3, 22-28 (Mar. 1970).

Key words: Bridge circuit; change of pH; instantaneous corrosion rates; Pearson equation; pit depth; recorder; Stern-Geary equation; synthetic sea water; weight loss.

A variety of metals and alloys were exposed in the laboratory for 9 months in 340 gal. (1287 liter) of synthetic seawater held at 70 to 80 °F (21 to 27 °C). Corrosion currents calculated from polarization data obtained at periodic intervals were converted to weight losses by Faraday's law. The calculated weight losses were in reasonable agreement with the actual weight losses. Two techniques were used in calculating corrosion currents, namely, the Pearson method based on breaks in polarization curves and the Stern-Geary method based on polarization resistances. The two are considered to be complementary. The specimens, after cleaning and evaluating, were re-exposed to fresh synthetic seawater. The two polarization techniques were used to measure corrosion rates at periodically changed pH values of 8.5, 7.1, 5.6 and 4.2, and at pH 4.2 the effect on corrosion of water movement produced by compressed air was noted. It was observed that galvanic corrosion could be measured by the Pearson method when iron was coupled with other specimens which were cathodic.

11659. Snediker, D. K., **The Mössbauer effect of $Sn^{119}$ in palladium-rich palladium—tin solid solutions,** (Proc. 2nd Symp. Mössbauer Effect Methodology, New York, N.Y., Jan. 25, 1966), Chapter in *Mössbauer Effect Methodology* **2,** 161-170 (Jan. 1966).

Key words: Intermetallic; Mössbauer; palladium alloys; $Sn^{119m}$ source; solid solution; tin.

A study of the palladium-rich end of the palladium-tin alloy system has been conducted using the Mössbauer effect of $Sn^{119m}$. Alloy absorbers of composition from 1 to 16 atom % tin and the intermetallic $Pd_3Sn$ were studied.

The Mössbauer parameters, e.g. fractional effect, half-width and chemical shift are reported for the various compositions. The Mössbauer spectrum of the alloy absorber has been determined to be a doublet consisting of spectra with chemical shifts corresponding to $Pd_3Sn$ and the Sn-Pd solid solution.

A new source with a composition corresponding to $Pd_3Sn$ was synthesized. Using this source with a $\beta$-10 absorber a spectrum was obtained with a half-width of 0.08 cm/s and an effect of 24%.

**11660.** Snelleman, W., **The measurement and calculation of flame temperatures,** Chapter 7 in *Flame Emission and Atomic Absorption Spectrometry* **I,** 213-239 (Marcel Dekker, Inc., New York, N.Y., 1969).

Key words: Equilibrium; flame calculations; flame composition; flame temperature; line reversal.

The concept of thermodynamic equilibrium and temperature is briefly described and the deviations from this equilibrium that occur in actual flame gases are discussed. The various methods of measuring flame temperatures are considered, with special attention to the method of line-reversal as to systematic and random errors. Next a description is given of the calculation of flame temperatures (with some examples) and finally a comparison is made between calculated and measured flame temperatures.

**11661.** Swiggard, E. M., Clabaugh, W. S., **Preparation of barium titanate semiconductors containing controlled amounts of neodymium,** *Am. Ceram. Soc. Bull.* **45,** No. 9, 777-781 (Sept. 1966).

Key words: Barium titanate; barium titanyl oxalate; neodymium; rare earths; semiconductors.

A procedure is described for coprecipitating known amounts of neodymium with barium titanyl oxalate tetrahydrate. Semiconductors prepared from this doped barium titanate are shown to have predictable electrical properties. Neodymium added (mole percent), precipitation temperature, addition rate, and excess acid modify the amount of neodymium that is coprecipitated. Electrical properties depend not only on the amount of neodymium present but also on how the neodymium was precipitated with the barium titanyl oxalate. A method is described for determining the amount of rare earth present in barium titanate.

**11662.** Venable, W. H., Jr., **Effects upon radiant intensity measurements due to scattering by optical elements,** *Appl. Opt.* **9,** No. 3, 609-615 (Mar. 1970).

Key words: Instrument function; iterative computations; nitrogen arc; radiance; radiant sources; scattering.

Measurements to determine the radiance of one portion of a nonuniform source can be strongly influenced by radiation from other portions of the source scattered by the optical system used to transmit the radiation to the detector. Conditions under which such scattering is important and procedures to correct for it are discussed. An illustration is provided from measurements made on a nitrogen arc source.

**11663.** Wells, J. S., Evenson, K. M., **A new LEPR spectrometer,** *Rev. Sci. Instr.* **41,** No. 2, 226-227 (Feb. 1970).

Key words: Laser electron paramagnetic resonance spectrometer; oxygen.

A new spectrometer for conducting laser electron paramagnetic resonance experiments on gases is described. This spectrometer yields at least an order of magnitude better sensitivity than the first spectrometer used in this type of investigation.

**11664.** West, E. D., Jennings, D. A., **Power measurement of lar**
**laser beams with a small dual-cone calorimeter,** *Rev. Sci. Inst*
**41,** No. 1, 142 (Jan. 1970).

Key words: Calorimeter; laser; laser calorimeter; laser ene
gy; laser power.

Measurements of power and energy in large laser beams ca
be made with a small dual-cone calorimeter by covering the e
tire front surface with an aperture for the input cone. Irradiati
only part of the front surface gives an error in the measuremen

**11665.** Wilson, W. K., **Record papers and their preservatio**
*Chemistry* **43,** No. 3, 8-12 (Mar. 1970).

Key words: Degradation; paper; preservation of record
records; stability.

Variables in the papermaking process are discussed in relati
to the stability of the finished product. Restoration method
storage of records, and current research on preservation
records are described.

**11666.** Wims, A. M., Sengers, J. V., McIntyre, D., Shereshefsk
J., **Interfacial tension of 3-methylpentane-nitroethane near t**
**critical point,** *J. Chem. Phys.* **52,** No. 6, 3042-3049 (Mar. 1
1970).

Key words: Binary liquid mixtures; capillary rise; coe
istence curve; critical phenomena; nitroethane; surface te
sion; 3-methylpentane.

Experimental data are reported for the capillary rise of the i
terface between the two liquid phases of 3-methylpentan
nitroethane as a function of temperature. The data are i
terpreted in terms of a power law currently proposed for t
behavior of the interfacial tension near the critical mixing poi
The results seem to indicate that for 3-methylpentan
nitroethane the region of asymptotic behavior is limited to rath
small values of $\Delta T^* = (T_c - T)/T_c$. For $\Delta T^* \geqslant 10^{-2}$ Sugden
parameter $a^2$ can be represented by a power law $a^2 = A^2 \Delta T^*$
with an exponent $\phi = 1.00 \pm 0.01$. A comparison is made with t
behavior of the surface tension of simple one-component liqui
near the gas-liquid critical point.

**11667.** Alley, C. O., Chang, R. F., Currie, D. G., Poultney, S. K
Bender, P. L., Dicke, R. H., Wilkinson, D. T., Faller, J. E
Kaula, W. M., MacDonald, J. F., Mulholland, J. D., Plotki
H. H., Carrion, W., Wampler, E. J., **Laser ranging retro-refle**
**tor: Continuing measurements and expected results,** *Scien*
**167,** No. 3918, 458-460 (Jan. 30, 1970).

Key words: Geophysics; laser; lunar motion; selenology.

After successful acquisition in August of reflected ruby las
pulses from the Apollo 11 laser ranging retro-reflector (LRR
with the telescopes at the Lick and McDonald observatories, r
peated measurements of the round-trip travel time of light ha
been made from the McDonald Observatory in September wi
an equivalent range precision of ± 2.5 meters. These acquisiti
period observations demonstrated the performance of the LRR
through lunar night and during sunlit conditions on the moon. I
strumentation activated at the McDonald Observatory in O
tober has yielded a precision of ±0.3 meter, and improvement
±0.15 meter is expected shortly. Continued monitoring of t
changes in the earth-moon distance as measured by the roun
trip time of light from suitably distributed earth stations is e
pected to contribute to our knowledge of the earth-moon syste

**11668.** Astin, A. V., **Report on the symposium on an Internation**
**Standard Reference Materials Program,** *Metrologia* **6,** No.
33-34 (Jan. 1970).

Key words: Characterizing materials; measurement co
patibility; standard reference materials.

Standard Reference Materials (SRM's), through a certifiable hysical or chemical property of a given material, are an effecve means for achieving measurement compatibility. The proram has been highly successful in the United States, although ven in this country there is an identifiable need for well over 00 additional SRM's.

There is a growing recognition of the urgent need for a coorinated international SRM program. Such coordination will not nly reduce wasteful duplication but will greatly increase the orld supply of needed SRM's. The problem was recognized, cknowledged to be of great importance, and recommendations ere made to deal with it effectively.

1669. Baker, M. A., **Continuity of coating test and suggested applications,** Chapter in *Proceedings of the Porcelain Enamel Institute Technical Forum, Ohio State Univ., Columbus, Ohio, Nov. 4-6, 1969,* **31,** 71-84 (Porcelain Enamel Institute, Washington, D.C., 1969).

Key words: Continuity of coating; high-voltage; porcelain enamel; weather resistance.

The high-voltage method of determining the continuity of conentional porcelain enamel coatings has been developed into a andard test. Each high-voltage test instrument, either ac or dc, ust be calibrated. Once the instruments have been calibrated, ey can be used to locate both existing discontinuities and otential discontinuities, depending on the applied voltage. It has een shown that this test is effective in upgrading the quality of orcelain enamels used in exterior architectural applications and also capable of determining hot water tank and direct-on namels with good coverage.

1670. Baker, M. A., **A summary of the three year inspection of the 1964 exposure test of porcelain enamels on aluminum,** Chapter in *Proceedings of the Porcelain Enamel Institute Technical Forum, Ohio State Univ., Columbus, Ohio, Nov. 4-6, 1969,* **31,** 106-113 (Porcelain Enamel Institute, Washington, D.C., 1969).

Key words: Color; gloss; porcelain enamel on aluminum; weather resistance.

An exposure test of porcelain enamels on aluminum was iniated by the National Bureau of Standards and the Porcelain namel Institute in 1964. The enamels were returned from the xposure sites to the laboratory at NBS to be measured for nanges in gloss and color after six months', one year's and three ears' exposure. Changes were found to be greatest at Kure each and least at Montreal and Los Angeles, with moderate nanges occurring at Washington and New York.

Although the boiling citric acid test is used as an acceptance st for these enamels, the correlation with color change, particurly at Kure Beach, was not as good as expected. A cupric loride test was developed which shows an improvement in the orrelation.

1671. Bennett, L. H., Swartzendruber, L. J., **On the interpretation of Mössbauer effect spectra as related to the constitution of Cu-Ni-Fe alloys,** *Acta Met.* **18,** No. 5, 485-498 (May 1970).

Key words: Alloys; Cu; Fe; metallurgy; Mössbauer effect; Ni.

Iron Mössbauer effect data are presented for copper-rich Cui-Fe alloys containing up to 53 at.% Ni and up to 8 at.% Fe. he problem of interpreting the complex Mössbauer effect speca in these alloys is discussed in great detail. Phase separation, ecipitation and effects of heat treatments are analyzed. A new ature of the Mössbauer spectrum for rapidly quenched Fe in u is reported. The use of an external magnetic field is shown to e an aid in identification of spectral features. The possibility of relevance to the Weiss theory of $\gamma_1$-, $\gamma_2$-Fe is noted. Results in Cu-Fe give a new upper limit of 2 at. % for the maximum solubility of Fe in Cu for samples quenched from the melt or from 1000 °C.

11672. Bjorge, S. E., Urbach, P. F., Earl, P. H., King, D. W., Wiederkehr, R. R. V., **An experiment to determine the effectiveness of various announcement media on Clearinghouse for Federal Scientific and Technical Information sales,** *Proc. American Society for Information Science Annual Meeting, Columbus, Ohio, Oct. 20-24, 1968,* pp. 327-329 (Greenwood Publ. Corp., New York, N.Y., 1969).

Key words: Clearinghouse; document announcement; document sales; information centers.

The Clearinghouse for Federal Scientific and Technical Information (CFSTI) collects government sponsored research reports, announces their availability, and sells copies to the general public. An experiment was designed, conducted, and analyzed to determine the effect of the various announcement media on CFSTI sales. The results of this experiment were used to modify the Clearinghouse announcement system so as to improve the quality of service and to increase the number of sales.

11673. Bjorge, S. E., Urbach, P. F., Earl, P. H., King, D. W., Wiederkehr, R. R. V., **Experimentation, modeling and analysis to establish a new pricing policy at the Clearinghouse for Federal Scientific and Technical Information,** *Proc. American Society for Information Science Annual Meeting, Columbus, Ohio, Oct. 20-24, 1968,* pp. 311-314 (Greenwood Publ. Corp., New York, N.Y., 1969).

Key words: Clearinghouse; cost analysis; document sales; information center.

This paper summarizes the results of experimentation, modeling and analysis performed in 1966 to develop a new pricing policy at the Clearinghouse for Federal Scientific and Technical Information. Analysis of request processing activities at CFSTI indicated that for a high proportion of requests the processing times were unsatisfactorily long and costs were unsatisfactorily high. Preliminary investigation indicated that a single unit selling price for all titles instead of a sliding scale price and the use of prepaid coupons would solve both of these problems. However, the question remained whether a unit-price policy should be adopted since the impact of this policy on the public demand and the Clearinghouse income was not known. These questions were answered, in part, by measuring demand at various price levels by experimentation, modeling and analysis which determined the effect of demand at the various price levels on income and cost. A nearly optimum unit price was chosen by this means and the new pricing policy has been implemented.

11674. Boesch, L., Napolitano, A., Macedo, P. B., **Spectrum of volume relaxation times in $B_2O_3$,** *J. Am. Ceram. Soc.* **53,** No. 3, 148-153 (1970).

Key words: Activation energy; annealing; Arrhenius behavior; $B_2O_3$ glass; distribution of relaxation times; relaxation times; volume relaxation times.

Time-index of refraction isotherms were measured for $B_2O_3$ glass starting from both a high and a low temperature in the transformation region. The equilibrium index values at each temperature, obtained from both types of approach curve, were identical. As in the case of the density values, the equilibrium refractive index curve as a function of temperature for this glass is not a straight line. The two-relaxation-times (cross over) model was applied to $B_2O_3$ glass and fitted the data as well as it did in previous experiments with borosilicate crown and $GeO_2$ glasses. The reverse crossover which was predicted by the model was experimentally confirmed with the $B_2O_3$ glass. The spectrum of relaxation times narrowed with decreasing temperature, indicating approach to another region of single relaxation associated with the low-temperature Arrhenius region. The relaxation times for the low-temperature crossover agreed well with those from the high-temperature curves, indicating complete linearity in the experiments. The spectrum of relaxation times was slightly asymmetrical at constant pressure and very asymmetrical at constant volume.

**11675.** Boswarva, I. M., **Semiempirical calculations of ionic polarizabilities and van der Waals potential coefficients for the alkaline-earth chalcogenides,** *Phys. Rev. B.* **1,** No. 4, 1698-1701 (Feb. 15, 1970).

Key words: Alkaline earth chalcogenides; electronic polarizabilities; Lorentz factor; oxides; sulfides; van der Waals coefficients.

Electronic polarizabilities for the ions of the alkaline-earth chalcogenides have been calculated by assuming an additivity law within the family of salts and a Lorentz factor of $4/3\pi$, and using experimental refractive indices and interionic distances. It is shown that the additivity assumption is well obeyed, and the Lorentz factor value of $4/3\pi$ gives the best fit to the data. Each polarizability obtained has been related to a mean excitation or characteristic energy for the ion, and hence the coefficients of the dipole-dipole and dipole-quadrupole terms of the van der Waals interaction energy derived.

**11676.** Branscomb, L. M., **The photoionization of one- and two-electron atoms,** (Proc. Sommerfeld Centennial Memorial Meeting, Munich, Germany, Sept. 10-14, 1968), Chapter in *Physics of the One- and Two-Electron Atoms,* F. Bopp and H. Kleinpoppen, eds., pp. 669-699 (North Holland Publ. Co., Amsterdam, The Netherlands, 1969).

Key words: Helium and their ions; review of photoionization of hydrogen.

Major advances in the physics of photoionization of one- and two-electron atoms (the isoelectronic series starting with H and $H^-$) are reviewed, with an emphasis on the extent to which theory and experiment are independently reliable and relatively in agreement. Great progress has been made in the last ten years in both theory and experiment because of a number of relatively recent developments: extremely accurate two-electron wave functions and photoionization cross section calculations, made possible by the computer; crossed beam methods for photoionization studies; the use of synchrotron radiation as an ultraviolet continuous light source; the development of the theory of autoionizing states and resonances; the use of high energy resolution electron scattering experiments in the energy range of Born approximation validity to study the distribution of oscillator strength in the atomic continuum. A number of interesting problems, however, remain unsolved.

**11677.** Broadhurst, M. G., Mopsik, F. I., **Bulk modulus and Grüneiser parameters for linear polymers,** *J. Chem. Phys.* **52,** No. 7, 3634-3641 (Apr. 1, 1970).

Key words: Anderson-Grüneisen parameter; bulk modulus; compressibility; Grüneisen constant; pair potential; paraffins; polyethylene; polymers; pressure; volume.

Expressions are derived for the isothermal bulk modulus $B_T$ and Anderson-Grüneisen parameter $\delta$ for a simple two-dimensional bundle-of-chains model where parallel nearest-neighbor chains are assumed to interact with a simple separation-dependent potential. Bulk modulus data for general linear polymers are examined and shown to be essentially temperature independent at constant volume in accord with the model. The theory is shown to predict quite accurately for reasonable assumed pair potentials both $B_T$ and $\delta$ of high-density polyethylene and *n*-paraffins with no adjustable parameters. The values of $\delta$ obtain for polyethylene from $B_T$ data are in excellent agreement wi those reported from ultrasonic data. The analysis is also sho to provide a sensitive measure of the form of the effective ch pair potential near its minimum. Also, a close relationsh between $\delta$ and the Grüneisen constant $\gamma$ is derived for t model.

**11678.** Bur, A. J., **Extrapolation to single-relaxation-time behavi in solutions of poly(*n*-butylisocyanate),** *J. Chem. Phys.* **52,** N 7, 3813-3819 (Apr. 1, 1970).

Key words: Dielectric constant; dielectric relaxation tin dipole moment; distribution of molecular weights; distrib tion of relaxation times; poly(*n*-butylisocyanate); rodli molecule; single relaxation time.

The dielectric relaxation time of rodlike poly(*n*-butylis cyanate) (PBIC), $(-CO-NR-)_n$, where $R = C_4H_9$, has be observed for dilute solutions as a function of the polydispers in the PBIC molecular weight. The mode of relaxation is rotati about the minor axis of the rodlike molecule (end-over-end ro tion). The dielectric relaxation time for this mode is a sensiti function of molecular weight, and a distribution of relaxati times $\Phi(\tau)$ is observed whenever a distribution of molecu weights $\Psi(M)$ is present. A one-to-one correspondence betwe $\Phi(\tau)$ and $\Psi(M)$ is established by observing the half-width $W/2$ the dielectric dispersion on a log frequency plot as a function the ratio $M_w/M_n$, where $M_n$ and $M_w$ are the number and weig averages of $\Psi(M)$. Extrapolation of the $W/2$ vs $M_w/M_n$ data the monodispersed case ($M_w/M_n = 1.0$) is carried out in order determine whether or not a monodispersed sample has a sin relaxation time. The accuracy of the extrapolated half-width s fers because the estimated uncertainty of the measured ra $M_w/M_n$ is $\pm 10\%$. The data do, however, satisfy a necessary c dition for the presence of a single relaxation time. In the regi $M_w/M_n = 1.0$ to 1.6, the experimentally observed $M_w/M_n$ is good agreement with $M_w/M_n$ calculated from the observed Φ( For these calculations it is assumed that each molecular speci has a single relaxation time and that the molecular dipole m ment is proportional to the molecular weight. A distributi $\Psi(M)$ may be obtained from the observed $\Phi(\tau)$ if it can be sumed that all molecules have the same conformation.

**11679.** Burgess, A., Hummer, D. G., Tully, J. A., **Electron imp excitation of positive ions,** *Phil. Trans. Roy. Soc. London,* 2 Ser. A., No. 1175, 225-279 (April 23, 1970).

Key words: Cross section; electron impact excitati ionized helium; positive ion.

Non-relativistic Coulomb-Born-Oppenheimer reactan matrices and cross-sections are given for all transitions betwe the 1s, 2s and 2p states in $He^+$ and in hydrogen-like ions of la nuclear charge. From these results some cross-sections for int combination transitions in highly charged nonhydrogenic io are estimated.

**11680.** Burke, P. G., Gallaher, D. F., Geltman, S., **Electron sc tering by atomic hydrogen using a pseudo-state expansion. Elastic scattering,** *J. Phys. B. (Proc. Phys. Soc.)* **2,** 11 (1969).

Key words: Close coupling; elastic scattering; electr hydrogen atom; polarizability; pseudo-states.

A modified close coupling expansion has been developed a applied to calculate elastic electron-hydrogen atom scatteri phase shifts. This expansion into a complete, discrete, orthon mal basis set is a variant of the more usual close coupling exp sion into eigenstates of the target Hamiltonian. We retain t first few hydrogen atom eigenstates and augment these ter with pseudo-states chosen, in our particular case, to incorpor fully the ground state polarizability of the hydrogen atom. The resulting phase shifts are compared, where possible, with those obtained in the most accurate variational calculations available, and they indicate a distinctly improved convergence over those obtained in the close coupling expansion.

**11681.** Burke, R. W., **Exchange reactions of ternary ion association complexes directly in the organic phase,** *Talanta* **17,** 240-242 (1970).

> Key words: Directly in organic phase; exchange reactions; spectrofluorometric; spectrophotometric; ternary ion association complexes; trace.

A new approach has been developed that combines the advantages of solvent extraction with the inherently high sensitivities afforded through the incorporation of large organic dye cations into ternary ion-association complexes containing the metal ion of interest. Basically, the new technique involves the formation of a complex, $[ML_x^-]R^+$, where $R^+$ initially is either a non-colored or a non-fluorescent organic cation. Following extraction of $[ML_x^-]R^+$ a second cation, $R_1^+$, which is capable of exchanging with the first $R^+$ group, is added directly to the organic phase. In this instance, however, $R_1^+$ is purposely selected to be highly colored or fluorescent, thereby yielding the highly colored or fluorescent complex $[ML_x^-]R_1^+$. Unreacted $R_1^+$ is readily back-extracted, leaving only the dye-complex in the organic phase. In the present paper the determinations of gold and uranium are described to illustrate the advantages of the new technique.

**11682.** Burke, R. W., Deardorff, E. R., **Simultaneous spectrophotometric determination of cobalt, nickel and copper and 2,3-quinoxalinedithiol,** *Talanta* **17,** 255-264 (1970).

> Key words: Aqueous ethanol; cobalt; colored complexes; copper; least squares treatment data; nickel; simultaneous spectrophotometric; 2,3-quinoxalinedithiol.

In aqueous ethanol cobalt(II), nickel(II) and copper(I) react instantaneously with 2,3-quinoxalinedithiol at pH 2 to form strongly colored complexes exhibiting absorption maxima at 510, 606 and 665, and 625 nm, respectively. At pH 6 the reaction of copper can be virtually eliminated, while the cobalt and nickel reactions show only small decreases in sensitivity. This behavior has been made the basis of a rapid method for the simultaneous determination of these three elements. The absorbances of the complexes have been found to be additive for all combinations of these elements in which the individual concentrations have been varied from approximately 0.1 to 1 ppm. A least-squares estimate of the concentration of any of the elements may be readily obtained by using a simple linear equation based on the absorbance readings and a set of constants derived from the spectrophotometric data. The analyses of seven synthetic solutions and four NBS Standard Reference Materials yielded a maximum error of 6.0% and an average error of 1.6%.

**11683.** Burns, G. W., Hurst, W. S., **An investigation of W-3% Re and W-25% Re thermoelements in vacuum, argon and hydrogen,** *NASA Final Report* **CR-72639,** 1-28 (National Aeronautics and Space Administration, Greenbelt, Md., Mar. 10, 1970).

> Key words: Argon; evaporation; exposure; hydrogen and high vacuum environments; metallographic examination; stability; thermal emf; W-3% Re and W-25% Re thermoelements.

The effect of exposure of bare wire W-3% Re and W-25% Re thermoelements to environments of high vacuum ($< 1 \times 10^{-8}$ torr), Argon and Hydrogen at temperatures ranging from 2200 K to 2600 K for periods up to 1000 hours has been investigated. The individual thermoelements, and hence the W-3% Re versus W-25% Re thermocouple pair, experienced a shift in the emf-temperature relationship on initial heating. In Argon and Hydrogen, the shift was less than 1% at 2000 K for the thermocouple pair. After the initial shift, the thermoelements exposed in Argon and Hydrogen experienced no significant further change in their emf-temperature relationship for periods up to 1000 hours. Both the W-3% Re and the W-25% Re thermoelements, when exposed in vacuum at 2400 K and above, drifted continually from original calibration as a result of preferential loss of Re by evaporation. The thermoelements were examined for chemical and structural changes by electron microprobe analysis and by conventional metallographic techniques.

**11684.** Cassidy, E. C., Cones, H. N., **Electro-optical observations and measurements of distorted high-intensity electric fields,** *Proc. Conf. Electrical Insulation and Dielectric Phenomena, Buck Hill Falls, Pa., Oct. 20-22, 1969,* pp. 77-86 (National Academy of Sciences, Washington, D.C., 1970).

> Key words: Dielectric liquids; electro-optical measurements; electrostatic field measurements; high voltage measurements; Kerr cell.

The electric field between electrodes immersed in a dielectric liquid is often distorted by the presence of space charge, thus making analytical determination of the field distribution extremely difficult. This work utilizes laser light for Kerr electro-optical analysis of distorted electric fields imposed when high direct voltages are applied to nitrobenzene-filled Kerr cells. Two-dimensional fringe images, similar to those achieved in photoelastic mechanical stress analysis, are observed. Regions of high electrical stress are detected directly from concentrations of a greater number of fringes. Field profiles observed with voltages as high as 90 kV applied to cells with various interelectrode distances are presented. Space-resolved measurements of relative field strength, actual field strength (in V/cm) and potential are also derived. The measurement techniques employed are believed to be accurate within 1%.

**11685.** Cooper, M. J., **Critical indices of the Z-L polymer folding transition,** *J. Chem. Phys. Letter* **52,** No. 1, 473-474 (Jan. 1, 1970).

> Key words: Critical indices; critical phenomena; phase transition; polymer crystallization; Zwanzig-Lauritzen model.

The critical indices for the Zwanzig-Lauritzen polymer crystallization transition are identified and shown to satisfy the thermodynamic equalities.

**11686.** Fishman, L., Mountain, R. D., **Activity coefficients of solutions from the intensity ratio of Rayleigh to Brillouin scattering,** *J. Phys. Chem.* **74,** No. 10, 2178-2182 (May 14, 1970).

> Key words. Activity coefficients; binary mixture; Brillouin scattering; fluctuations; light scattering from solutions; Rayleigh scattering; thermal relaxation; volume viscosity.

The ratio of the intensity of Rayleigh to Brillouin scattered light for a binary mixture with internal degrees of freedom is determined by calculating the frequency spectrum of fluctuations in concentration, temperature, and pressure. Thermodynamic fluctuation theory and linearized hydrodynamic equations, modified to include the internal degrees of freedom through a frequency-dependent volume viscosity, are employed in the calculation. The intensity ratio is of interest as it may be used to determine activity coefficients. A method of doing so when the system contains internal degrees of freedom is described.

**11687.** Fraker, A. C., Ruff, A. W., Jr., **Microstructural studies of 7075 Al-relation to the directional sensitivity for stress corrosion cracking,** *Corrosion Sci.* **10,** 191-195 (1970).

Key words: Aluminum alloys; corrosion; dislocations; electron microscopy; precipitates; stress corrosion cracking.

Dislocation and precipitate distributions have been studied in stress corrosion samples produced from commercial 7075 Al rolled plate. Transmission electron microscopy results show that the dislocation and precipitate distributions are similar in thin sections parallel to the three principal planes and are relatively uniform from the grain boundaries to the inner grain regions. It is concluded that variations in the precipitate and dislocation structures in this alloy are not responsible for the pronounced directional sensitivity for s.c.c.

**11688.** Gadzuk, J. W., **Coupled surface-plasmon modes in metal-thin-film-vacuum sandwiches,** *Phys. Rev. B,* **1,** No. 3, 1267-1269 (Feb. 1, 1970).

Key words: Adsorption; electron emission; junctions; low energy electron diffraction; plasma oscillations.

The normal surface-plasmon modes for a thin-layered plasma bounded on one side by a semi-infinite plasma and on the other side by a vacuum are determined. The characteristic frequencies of the coupled modes resulting from surface oscillations of the plasma-plasma interface and the plasma-vacuum interface are found. The relevance of these results to recent experiments by MacRae, Müller, Lander, Morrison, and Phillips is indicated.

**11689.** Gallagher, A., **State-transfer collisions,** (Proc. Sommerfeld Centennial Memorial Meeting, Munich, Germany, Sept. 9-14, 1968), Chapter in *Physics of the One- and Two-Electron Atomics,* F. Bopp and H. Kleinpoppen, eds., pp. 788-794 (North Holland Publ. Co., Amsterdam, The Netherlands, 1969).

Key words: Alkalis; excitation transfer; helium.

The changes in state populations that occur in thermal atom-atom collisions will be discussed. Particular emphasis will be given to nearly adiabatic helium and alkali excitation transfer.

**11690.** Goltz, S. M., Tanner, C. B., Thurtell, G. W., Jones, F. E., **Evaporation measurements by an Eddy correlation method,** *Water Resources Res.* **6,** No. 2, 440-446 (Apr. 1970).

Key words: Eddy correlation; humidity sensor; vapor flux.

Eddy correlation measurements of water vapor flux density have been made using a barium fluoride film humidity sensor and a three-dimensional anemometer. During morning and evening periods, good agreement was obtained between Eddy correlation data and two independent methods. Serious disagreement between measurements occurred only when the humidity sensor was operating within a portion of the calibration curve which was not suited to the on-line computer calculations. The results indicate that the humidity sensor could be modified to allow operation at all times within linear segments of the calibration curve and permit successful on-line computer calculations of Eddy correlation vapor flux within one meter of the surface.

**11691.** Gugeler, A. L., **A study of the adherence of porcelain enamel to aluminum,** Chapter in *Proceedings of the Porcelain Enamel Institute Forum, Ohio State Univ., Columbus, Ohio, November 4-6, 1969,* **31,** 37-45 (Porcelain Enamel Institute, Washington, D.C., 1969).

Key words: Adherence; aluminum oxide; conversion chromate coating; electron microprobe; electron microscope; magnesium; porcelain enamel on aluminum.

The Porcelain Enameled Aluminum Council of the Porcelain Enamel Institute has been conducting a study of the adherence of porcelain enamels to aluminum. The work thus far indicates that the nature of the oxide layer on the metal is important to the adherence of porcelain enamel. If this layer is essentially pure aluminum oxide, the enamel adheres well. If the oxide layer contains magnesium, spalling may result. The adherence of enamels to alloys containing magnesium is improved if the metal surface is chromated before enameling.

**11692.** Hummer, D. G., **Spectral line formation by noncoheren scattering with a dipole phase-function,** *Astrophysical Letter* **5,** 1 (1970).

Key words: Anisotropic scattering; limb darkening; noncoherent scattering; Rayleigh scattering; spectral line formation.

Results are presented for lines formed by atoms scattering photons with complete redistribution in frequency and a dipole (Rayleigh) phase function. For optical thicknesses on the orde of unity the ratio of limb ($\mu \simeq 0.2$) to disc intensity for dipole scattering is about 5% larger than for isotropic scattering, at al frequencies. For larger optical thickness ($\geqslant 10^2$), the limb-to-disc ratio is about 2% lower for dipole than for isotropic scattering within a Doppler halfwidth of the line center and unity in the line wings. Some quantitative information is given on the angular distribution of the radiation field. An exact relation between two moments of the radiation field at the surface of a semi-infinite isothermal medium is presented.

**11693.** Landgrebe, W. B., Mann, W. B., Schima, F. J., **The distribution of 70-kV praseodymium ions in iron foil and a technique for removing thin layers of iron,** *Intern. J. Appl Radiation Isotopes* **21,** No. 3, 169-171 (Mar. 1970).

Key words: Barium-140; iron foils; praseodymium-142 thulium-170.

The NBS isotope separator has been used to implant barium-140, praseodymium-142 and thulium-170(1) into iron foils fo nuclear-orientation studies at low temperatures. In the case o praseodymium, stripping experiments were carried out to determine the depth of penetration. The profile of the beam was also determined.

**11694.** McKinney, J. E., Oser, H. J., **Stability of acoustic wave within a viscous compressible heat-conducting fluid,** *J. Acoust Soc. Am.* **47,** No. 3, 781-785 (March 1970).

Key words: Absorption; acoustic propagation; fluids Kirchhoff-Langevin; Navier-Stokes; stability; thermal conductivity; viscosity.

The question of stability of propagation of acoustic waves within a continuum of compressible viscous heat-conducting fluid has been investigated. A bounded solution (i.e., a stable solution) is assured if either of the following two conditions is satified:

$$\gamma = 1 \qquad (\mathrm{i}$$

or

$$\frac{3(2-\gamma)}{4[1+(3/4)(v/\eta)]P} \leqslant 1 \text{ (for } \gamma > 1\text{)}, \qquad (\mathrm{i}$$

where $P$ is the Prandtl number, $\gamma$ the ratio of specific heats, and $v$ and $\eta$ the bulk and shear viscosities, respectively. According to the theory, the above inequality must be obeyed for all passive fluids with $\gamma > 1$. Using experimental values for many differen fluids, it appears to be generally obeyed except for the molten metals including mercury and, possibly, the superfluids.

**11695.** Margoshes, M., Scribner, B. F., **Emission spectrometry** *Anal. Chem.* **42,** No. 5, 398R-417R (April 1970).

Key words: Emission spectrometry; excitation sources review; spectrochemical analysis; trace analysis.

The literature on optical emission spectrometry is reviewed for the period 1968-69, with emphasis on areas of importance to spectrochemical analysis. Major topics covered are books and reviews, spectral descriptions and classifications, instrumentation, calibration, excitation sources, trace analysis, lasers and microanalysis, and applications.

**11696.** Marton, L., **Survey of microanalysis—interpolation and extrapolation,** Chapter in *Electron Probe Microanalysis,* pp. 1-14 (Academic Press Inc., New York, N.Y., 1969).

Key words: Electron probe; microanalysis.

A review of the early history of the efforts to achieve a chemical analysis of very small areas of the surface of a specimen; besides the electron probe microanalyzer, it includes other less successful attempts. Looking in the future, a few possible improvements are discussed together with expected applications.

**11697.** Milligan, D. E., Jacox, M. E., Guillory, W. A., **Infrared spectrum of $NO_2$-ion isolated in an argon matrix,** *J. Chem. Phys.* **52,** No. 8, 3864-3868 (April 15, 1970).

Key words: Alkali metal atoms; electron bombardment; infrared spectrum; matrix isolation; nitrite anion; nitrogen dioxide; photodetachment; photoionization; vacuum-ultraviolet photolysis.

The molecular ion $NO_2^-$ has been stabilized in an argon matrix in sufficient concentration for detection of its antisymmetric stretching fundamental, $\nu_3$, at 1244 $cm^{-1}$ by electron bombardment or photoionization of matrix-isolated $NO_2$ and by the interaction of an alkali-metal atomic beam with $NO_2$ in an argon matrix. In contrast to the position of this fundamental in an inert, nonionic environment, a value of approximately 1275 $cm^{-1}$ is characteristic of the crystalline material. Isotopic data are consistent with a 115° valence angle for $NO_2^-$, independent of environment. Irradiation of the sample with light of wavelength near 3150 Å leads to the destruction of the $NO_2^-$ absorption in the studies of the electron bombardment and photoionization of $NO_2$, but not in the experiments in which the alkali metal atoms provide a reservoir of photoelectrons.

**11698.** Mountain, R. D., **Comments on fluctuation theory calculations of the specific heat near the critical point,** *J. Chem. Phys.* **52,** No. 7, 3852-3853 (April 1, 1970).

Key words: Cell model; correlation functions of fluids in the critical region; critical phenomena; distribution function; fluctuations in density; specific heat.

The failure of cell model calculations to correctly predict the critical region specific heat anomaly of a fluid is examined. The Gaussian assumption common to these calculations is seen to be the reason for the failure.

**11699.** Mountain, R. D., **Liquids: Dynamics of liquid structure,** *Critical Reviews in Solid State Sciences* **1,** No. 1, 5-46 (Chemical Rubber Co., Cleveland, Ohio, March 1970).

Key words: Infrared absorption; light scattering; liquids; magnetic resonance; molecular dynamics; neutron scattering; orientational correlation function; time correlation function.

The time correlation function formalism is used to bring out the interrelations existing for the experimental techniques of ultrasonic absorption, light scattering, neutron scattering, infrared absorption, dielectric absorption, magnetic resonance and molecular dynamics calculations. The dynamical effects in liquids associated with translational and rotational degrees of freedom are examined.

**11700.** Olver, F. W. J., **Why steepest descents?,** *SIAM Rev.* **12,** No. 2, 228-247 (April 19, 1970).

Key words: Airy integral; asymptotics; error bounds; gamma function; saddle-points; steepest descents; Watson's lemma.

A theorem is proved concerning the asymptotic expansion of contour integrals of the form

$$\int_a^b e^{-zp(t)}q(t)dt$$

in which *p(t)* and *q(t)* are analytic functions of *t*, and *z* is a large complex parameter. In comparison with the method of steepest descents, the essential condition imposed on the integration path by the new theorem is simply that Re$\{zp(t)\}$ attains its minimum at one of the endpoints. The theorem is illustrated by application to the Airy function of large complex argument.

Methods are given for the calculation of realistic bounds for the error terms in the asymptotic expansion. In this analysis the use of paths of steepest descent is necessary, at least in the neighborhood of the minimum of Re$\{zp(t)\}$. The error analysis is illustrated by some new results concerning Stirling's series.

**11701.** Osgood, C. F., **A method in diophantine approximation (III),** *Acta Arith.* **XVI,** 5-22 (1969).

Key words: Algebraic numbers; convolution product; differential equation; diophantine approximation.

In this paper the class of functions discussed in part II is investigated further. After introducing several normalizing conditions, it is shown to be a module under convolution multiplication from a certain ring of functions. Also algebraic coefficients and algebraic points can now be handled in our original type of differential equation.

**11702.** Osgood, C. F., **A method in diophantine approximation (IV),** *Acta Arith.* **XVI,** 23-40 (1969).

Key words: Convolution product; differential equations; diophantine approximation; irrational numbers; *n*-complex variables; rational numbers.

This paper generalizes the results in part III of this series of papers to $n > 1$ complex variables. It is shown that the values of a certain class of functions of *n* variables are poorly approximable at rational points in an appropriate domain. The algebraic structure of this class of functions is studied in an effort to determine the composition of the class. A module structure is exhibited under convolution product, i.e.

$$g_1(z_1, \ldots, z_n)*_k g_2(z_1, \ldots, z_n) = \int_0^{z_k}$$

$$g_1(z_1, \ldots, z_{k-1}, t_k, z_{k+1}, \ldots, z_n)$$

$$g_2(z_1, \ldots, z_{k-1}, z_k - t_k, z_{k+1}, \ldots, z_n)\partial t.$$

**11703.** Parke, W. C., Ponzini, R. G., Williams, H. T., **Remarks on finite-energy sum rules,** *Phys. Rev.* **1,** No. 1-D, 134-138 (Jan. 1, 1970).

Key words: Charge exchange; dispersion relations; duality; elementary particles; FESR; high energy scattering; pion-nucleon scattering; Regge parameters; sum rules.

Finite-energy sum rules with generalized weight functions are discussed with emphasis on methods for obtaining precise determination of high-energy parameters from low-energy data. Regge parameters for $t = 0$ $\pi N$ charge-exchange amplitudes are deduced as an example from a new sum rule.

**11704.** Paulsen, P. J., Alvarez, R., Mueller, C. W., **Spark source mass spectrographic analysis of ingot iron for silver, copper, molybdenum, and nickel by isotope dilution and for cobalt by an internal standard technique,** *Anal. Chem.* **42,** 673-675 (May 1970).

Key words: Ingot iron; isotope dilution; NBS standard reference material; preconcentration; spark source mass spectrometry; trace element.

Isotope dilution procedures using the spark source mass spectrograph have proven reliable for simultaneous trace element determinations in high-purity metals. The objective of this study was to extend the applicability of this method for determining trace and minor elements in a relatively impure matrix, ingot iron.

In the method developed, isotopically enriched spikes of Ag, Cu, Mo, and Ni were added to 100-mg samples being dissolved; and a known amount of mononuclidic Co was added to half of the samples. After extracting the iron with isopropyl ether, the elements in the aqueous layer were electrodeposited onto gold wire electrodes for sparking in the mass spectrograph. The Ag, Cu, Mo, and Ni concentrations were calculated after determining the altered isotope ratios for all samples. By using Ni as an internal standard and the known additions of Co, the Co concentration was obtained by measuring the Co to Ni ratios for each of the samples. Concentrations ranged from 0.0050% for Ag to 0.025% for Ni.

**11705.** Qureshi, I. H., McClendon, L. T., LaFleur, P. D., **Extraction studies of the group IIIB-VIIB elements and the lanthanides utilizing bis(2-ethyl-hexyl) orthophosphoric acid,** *Radiochim. Acta* **12,** No. 2, 107-111 (Aug. 1969).

Key words: Group VIII; HDEHP; hydrochloric acid; IB and IIB elements; nitric acid; perchloric acid; solvent extraction.

The extraction behavior of the group IIIB-VIIB elements and the lanthanides from 1-11*M* hydrochloric, perchloric and nitric acid solutions into 0.75*M* bis(2-ethyl-hexyl) phosphoric acid solution has been studied. The group IVB elements and scandium exhibit high extraction which is independent of hydrogen ion concentration; the group VIIB elements are essentially unextracted. The extraction of some elements of group VB and VIB and of the lanthanides reaches a minimum and the increases with increasing acidity. This behavior is attributed to a change in extraction mechanism.

**11706.** Randall, E. B., Jr., Lashof, T. W., **An interlaboratory study of the measurement of the bursting strength of paper,** *Tappi* **53,** No. 5, 799-809 (May 1970).

Key words: Analysis of variance; analyzing; bursting strength; burst testers; comparisons; evaluation; foil paper; instrument characteristics; materials testing; measuring instruments; mechanical properties; mechanical testing; paper; precision; reliability; reproducibility; standards; testing; testing equipment.

This paper reports on the results of an extensive interlaboratory study, involving more than 175 laboratories in North America and overseas using several different models of bursting strength testers to evaluate 34 papers and 6 foils. Significant differences, both in a statistical and in an economic sense, were found between results obtained on different models and those in different laboratories using the same model, confirming previous reports. There were also significant day-to-day variations within a laboratory, and aluminum foil specimens gave results relative to those of paper specimens that depended on the instrument model used. A convenient rule for the number of replications was obtained from the study: make 10 replications unless the range of the first 10 is greater than 20% of their average, then make an additional 10. Two test results, each with 10 or 20 replications, are expected to agree with each other within the following values 95% of the time: 5.4% for repeatability within a laboratory, 9.5% for comparability between materials, and 14.3% for reproducibility between laboratories. Between-laboratory comparisons may be standardized through the use of a composite reference material of paper, aluminum foils being of only marginal use for this standardization.

**11707.** Raveché, H. J., Mayer, J. E., **Theory of diffusion in simple liquid mixtures,** *J. Chem. Phys.* **52,** No. 8, 3990-4004 (April 15, 1970).

Key words: Binary liquid mixture; closure condition; diffusion coefficient; distribution function; liquids; reduced Liouville equations.

A method is presented for obtaining the diffusion coefficient in terms of functions of molecular properties for a liquid system of monatomic molecules near equilibrium. The approach considers the reduced probability density functions $W_n(\mathbf{r}_1 \cdots \mathbf{p}_n)$ for $n$ molecules ($n = 1$, 2, and 3) in the limit of a steady state. By operating on the complete probability density function $W_N$ with the conventional Liouville operator and by integrating over the phase space of $N-n$ molecules, we write the time dependence of $W_n$ in a form not explicity involving $W_m$ for $m > n$. The reduced probability densities and the average vector forces are developed as a power series in a small parameter $\lambda$. Starting with singlet functions corresponding to a gradient in the density of a binary isothermal solution at constant pressure and the corresponding flux of molecules, we determine a singlet momentum-dependent force which maintains the flux and gradient stationary in time. The force can only be consistent with a certain class of pair probability functions, and we write the required general forms. Repeating the operation, we compute the average pair force which maintains the fluid in a steady state. The operation may, in principle, be carried to $W_{n+1}$ for any $n$. From symmetry requirements we obtain a correction to the Kirkwood closure for the nonequilibrium factors in the triplet probability density. The closure fixes the ratio between the assumed density gradient and flux, which leads to the diffusion coefficient in terms of functions of pairs and triples of molecules and the intermolecular potential energy.

**11708.** Rosenblatt, J. R., Joiner, B. L., Hogben, D., **OMNITAB—Rapid statistical manipulation,** (Proc. Conf. Small-Area Statistics, American Statistical Association, New York, N.Y., Aug. 21, 1969), Paper in *Census Tract Papers Final 1970 Census Plans and Four Programming Systems for Computerized Data Retrieval and Manipulation, Series GE-40,* No. 6, pp. 46-59 (Superintendent of Documents, Government Printing Office, Washington, D.C., 20402, 65 cents, 1970).

Key words: Accuracy of computation; computing for non-programmers; computing system; data analysis; least squares computation; OMNITAB computing system; statistical computation; table making.

The nature of the OMNITAB computing system is illustrated and discussed, using several simple but realistic examples.

**11709.** Ryan, J. V., **Implementation of the Flammable Fabrics Act,** *Proc. Conf. Flame Retardant Cotton Batting Workshop, New Orleans, Louisiana, Nov. 15, 1968,* **ARS 72-72,** 1-77 (Oct. 1969).

Key words: Bedding; fabrics; flammability; hazards; mattresses; test methods; upholstered furniture.

Progress toward implementing the various provisions of the act will be described, along with the related problems. Ease of ignition, flame spread, transfer of heat, and development of smoke and other products of combustion are hazards, but not all apply to every product and use. New flammability standards will be based on risk to the public. Published procedures assure ample opportunity for all interested parties to participate in the development of standards. Most standards are expected to be for products, with industry free to choose fabrics and related materials to meet the requirements.

11710. Shipp, W. E., **Surface tension of binary mixtures of several organic liquids at 25 °C,** *J. Chem. Eng. Data* **15,** No. 2, 308-311 (April 1970).

Key words: Binary mixtures; density; organic liquids; surface tension.

The surface tension was determined for the following pairs of organic liquid mixtures over the entire range of concentration by he differential capillary rise method: benzene and ethyl acetate, carbon tetrachloride and ethyl acetate, benzene and carbon bisulfide, carbon tetrachloride and carbon bisulfide, benzene and carbon tetrachloride, and benzene and acetone. The first four pairs showed negative deviation and the last two, positive deviaion from the ideal mixture relationship. The density of the first hree pairs was also measured. Both surface tension and density were measured at 25 °C.

1711. Smith, S. J., **Survey on electron-atom collision experiments,** (Proc. Sommerfeld Centennial Memorial Meeting, Munich, Germany, Sept. 9-14, 1968), Chapter in *Physics of the One- and Two-Electron Atoms,* F. Bopp and H. Kleinpoppen, eds., pp. 574-597 (North Holland Publ. Co., Amsterdam, The Netherlands, 1969).

Key words: Atom; collisions; electron; helium; hydrogen; survey.

Within the last decade, application of the high-vacuum crossed-beam method to low energy collisions of electrons with hydrogen atoms has provided data on elastic, inelastic, and ionizing collisions. The experimental data appear to be largely internally consistent and to provide quite useful comparisons with theoretical results.

In helium, experimental elastic scattering and ionization data appears to be in a reasonable state, but the data on inelastic collisions are generally unsatisfactory. Opportunities for improvement through improved technique are noted.

1712. Vicentini-Missoni, M., Joseph, R. I., Green, M. S., Sengers, J. M. H. L., **Scaled equation of state and critical exponents in magnets and fluids,** *Phys. Rev. B.* **1,** No. 5, 2312-2331 (March 1, 1970).

Key words: Critical exponents; critical point fluids; Curie point; equation of state; ferromagnets; scaling laws.

A systematic analysis in the context of the scaled equation of state has been made of available experimental data in the critical egion of a number of ferromagnets [Gd, $CrBr_3$, $La_{0.5}Sr_{0.5}CoO_3$, Ni (two independent sets of data)] and fluids ($CO_2$, $He^4$, Xe) with the following assumed form for $h(x)=HM^{1}|M|^{1-\delta}$:

$$h(x)=E_1[(x+x_0)/x_0]\{1+E_2[(x+x_0]/x_0]^{2\beta}\}^{[\beta(\delta-1)-1]/2\beta},$$

where $h(x)$ is a scaling function, $x=t|M|^{-1/\beta}$, $t=(T-T_c)/T_c$, and $x=-x_0$ is the phase boundary. A nonlinear, least-squares method was used to simultaneously determine the six parameters $\beta$, $\delta$, $T_c$, $x_0$, $E_1$, $E_2$). Agreement between the proposed form for $h(x)$ and the experimental data was found. For both the magnets and fluids, we find that $\delta \approx 4.4$; for the magnets $\beta \approx 0.37$ and for the fluids $\beta \approx 0.35$. Reasons for the considerably different values eported elsewhere for these exponents in the materials $CrO_2$ and $YFeO_3$ are discussed.

1713. Weisman, H. M., **In the beginning was the word—Information needs and uses in science and technology,** Paper E4-2 in *Proceedings of the Seventeenth International Technical Communications Conference, Minneapolis, Minn., June 3-6, 1970,* B. F. Hylen and R. R. McDaniel, eds., pp. 1-5 (Society of Technical Writers and Publishers Inc., 1010 Vermont Ave., N.W., Washington, D.C., 20005, 1970).

Key words: Information; "information explosion"; information producer; information user; knowledge; scientific literature; word.

This paper traces the role of the Scientific Literature in the progress of Science and Technology. It notes the effect of the "information explosion," and poses a challenge to the Technical Writer and Editor on the part they might play in meeting the information problem.

11714. Yakowitz, H., **Comments on "application of color photography to electron microbeam probe samples,"** *Rev. Sci. Instr.* **41,** No. 4, 601 (April 1970).

Key words: Color metallography; electron microprobe scanning; electron microscopy.

11715. Zielinzki, W. L., Jr., Freeman, D. H., Martire, D. E., Chow, L. C., **Gas chromatography and thermodynamics of divinylbenzene separations on 4,4′-dihexoxyazoxybenzene liquid crystal,** *Anal. Chem.* **42,** No. 2, 176-180 (February 1970).

Key words: Chromatography; gas chromatography; gas liquid; nematic liquid.

Gas-liquid chromatography in the nematic region of 4-4′-dihexoxyazoxybenzene liquid crystal has shown base-line separations for the meta and para isomers of divinylbenzene and ethylvinylbenzene. Thermodynamic treatment of the data has illustrated that the meta isomers have a lower solubility (resulting in shorter retention times) than the respective para derivatives owing to a greater enthalpic requirement for solution in the rod-like ordered solvent. The para/meta separation factors depict a greater rate of decrease with increasing column temperature in the isotropic liquid region because of the loss of order which is present in the anisotropic nematic region. Data for naphthalene present as a contaminant in divinylbenzene samples, were included in the treatment. Chromatographic extension to preparative scale appears feasible.

11716. Anderson, R. L., Guildner, L. A., Edsinger, R. E., **Movable and fixed modular vacuum devices with confined fluorocarbon plastic seals,** *Rev. Sci. Instr.* **41,** No. 7, 1076-1082 (July 1970).

Key words: Fluorocarbon bearings; fluorocarbon gaskets; modular vacuum components; vacuum ball joints; vacuum cylinder joints; vacuum seals; vacuum techniques; vacuum valves.

Sealing techniques have been perfected which utilize the properties of fluorocarbon plastics to make high vacuum seals. Several designs are described in which confined gaskets are used instead of O-rings, with consequent reduction of contamination from outgassing and permeation. These sealing techniques have been incorporated into a series of modular components which may be used for assembly of high vacuum systems. Some of these components are movable joints which allow leak-free motion between parts of a system. While not suited for high temperature bakeout, systems constructed from these modular components are capable of being pumped below $10^{-7}$ Torr. Dependable systems can easily be assembled or modified using these components, with no detectable helium leaks at a level of $2 \times 10^{-10}$ std $cm^3$/sec.

11717. Arenhövel, H., Danos, M., Williams, H. T., **Baryon resonances in nuclei: Magnetic moments of the deuteron,** *Physics Letters* **31B,** No. 3, 109-112 (February 2, 1970).

Key words: Baryon resonances; deuteron; exchange currents; magnetic moments; nuclear structure; photodisintegration.

Baryon resonance admixtures to the p-n system have been calculated, as well as their effect on the static and transition magnetic moments of the deuteron.

**11718.** Arp, V., **Heat transport through helium II,** *Cryogenics* **10,** No. 2, 96-105 (April 1970).

Key words: Helium II, superfluid; thermal conductivity; thermal gradient; thermal flux; turbulence; two-fluid hydrodynamics; vorticity.

Heat transport through He II is summarized in terms of the hydrodynamics of the two-fluid model. With increasing thermal flux, three regimes are identified, depending on the development of vorticity in the superfluid component and the development of a classical turbulence in the normal component. Calculation of summary curves of thermal gradient as a function of thermal flux is explained, and graphical results presented. An estimate of the limiting thermal flux for inception of vapor formation within He II is made, and time-dependent effects are discussed. The presentation is oriented towards use of He II in the nominal range from 1.5 to 2.1 K; special effects near the λ-point (2.17 K) are not considered, nor are conductivity changes below about 0.6 K due to rapid decreases of roton contributions.

**11719.** Berger, M. J., **Spectrum of energy deposited electrons in spherical regions,** *Proc. 2nd Symp. Microdosimetry, Stresa, Italy, Oct. 20-24, 1969,* Euratom Document No. 4452 d-f-e, pp. 541-559 (1970).

Key words: Electrons; energy deposition, microdosimetry; Monte Carlo; multiple scattering; transport calculations.

Exploratory Monte Carlo calculations of electron transport in water have been made which are pertinent to microdosimetry. The objective of these calculations was to determine energy deposition spectra in spherical regions, i.e., the statistical distribution of the amounts of energy deposited as the result of the passage of electrons. Calculations were made for electrons with ranges comparable in magnitude to the size of the regions traversed, and the treatment therefore had to include certain phenomena that have been disregarded in previous microdosimetry calculations. These phenomena included (a) pathlength fluctuations and detours caused by multiple elastic scattering; (b) repeated passages of the same electron through the region as the result of backscattering; (c) the transport of energy into and out of the region of secondary knock-on electrons; and (d) the contributions to the energy deposition spectra from electrons born inside the region. Numerical results are presented for electrons with an initial energy of 5 keV that deposit their energy in spherical regions with diameters of 0.2 and 1.0 microns.

**11720.** Berger, M. J., Seltzer, S. M., Maeda, K., **Energy deposition by auroral electrons in the atmosphere,** *J. Atmospheric Terrest. Phys.* **32,** 1015-1045 (1970).

Key words: Atmosphere; aurora; electron; energy deposition; Monte Carlo; radiation transport.

The spatial distribution of the energy deposited by electrons in the atmosphere has been calculated by the Monte Carlo method. The distribution has been obtained as a function of the altitude and of the radial distance from the axis of the incident electron beam. The calculations take into account the deflection of the electrons by the geomagnetic field, and the scattering and slowing down due to multiple Coulomb interactions with atomic nuclei and orbital electrons. The assumed conditions were: (1) a semi-infinite air medium, extending downwards from a height of 300 km, with a composition and density corresponding to that of the CIRA (1965) Mean Atmosphere; (2) a vertical magnetic field with a strength of 0.6 G; (3) monoenergetic incident electron beams that are symmetric about a chosen field line; (4) incident electron energies between 20 keV and 2 keV; (5) various incident pitch-angles between 0° and 90°, or a pitch-angle distribution corresponding to an incident flux isotropic over th downward hemisphere. Calculations made with the same program, for a constant-density medium and no magnetic field, giv good agreement with the results of laboratory experiments. Th calculations are also in agreement with recent observations on a artificial aurora produced in the atmosphere with 8.7-keV electrons.

**11721.** Braun, W., Bass, A. M., Pilling, M., **Flash photolysis o ketene and diazomethane: The production and reaction kinetic of triplet and singlet methylene,** *J. Chem. Phys.* **52,** No. 10 5131-5143 (May 15, 1970).

Key words: Absolute reaction rates; diazomethane; flash photolysis; ketene; kinetics; methylene $CH_2$; vacuum UV

Ketene and diazomethane have been flash photolyzed in thei strongest absorption continua in the vacuum ultraviolet and fa ultraviolet. Triplet methylene was monitored by kinetic spectroscopy at 141.5 nm. Singlet methylene was not observe directly, but the growth of the triplet absorption as a function o inert-gas pressure indicates that singlet methylene was the majo primary product in both the ketene and diazomethane systems Various inert additives quantitatively quenched the singlet to th triplet state, while reactive additives were able to intercept th singlet before quenching occurred. A number of reactions an deactivations involving singlet methylene (${}^{1}CH_2$) and triple methylene (${}^{3}CH_2$) have been investigated at 298 K, and their rat constants are listed below (cm³ molecule · ⁻¹ second⁻¹):

$${}^{3}CH_2 + {}^{3}CH_2 \rightarrow C_2H_2 + n\,H_2 \qquad (5.3 \pm 1.5) \times 10^{-11}$$

(1a), (1b

$${}^{1}CH_2 + H_2 \rightarrow CH_4^* \rightarrow CH_3 + H \qquad (7.0 \pm 1.5) \times 10^{-12} \qquad (2$$

$${}^{1}CH_2 + H_2 \rightarrow {}^{3}CH_2 + H_2 \qquad < 1.5 \times 10^{-12} \qquad (3$$

$${}^{1}CH_2 + CH_4 \rightarrow C_2H_6^* \rightarrow CH_3 + CH_3 \qquad (1.9 \pm 0.5) \times 10^{-12} \qquad (4$$

$${}^{1}CH_2 + CH_4 \rightarrow {}^{3}CH_2 + CH_4 \qquad (1.6 \pm 0.5) \times 10^{-12} \qquad (5$$

$${}^{1}CH_2 + He \rightarrow {}^{3}CH_2 + He \qquad (3.0 \pm 0.7) \times 10^{-13} \qquad (11$$

$${}^{1}CH_2 + Ar \rightarrow {}^{3}CH_2 + Ar \qquad (6.7 \pm 1.3) \times 10^{-13} \qquad (12$$

$${}^{1}CH_2 + N_2 \rightarrow {}^{3}CH_2 + N_2 \qquad (9.0 \pm 2.0) \times 10^{-13} \qquad (13$$

$${}^{3}CH_2 + H_2 \rightarrow CH_3 + H \qquad < 5 \times 10^{-14} \qquad (18$$

$${}^{3}CH_2 + CH_4 \rightarrow CH_3 + CH_3 \qquad < 5 \times 10^{-14}. \qquad (19$$

The absolute reaction rates for the singlet are apparently independent of the source (i.e., ketene or diazomethane), suggestin that the reactions occur via vibrationally cold singlet methylene No evidence was found for deactivation of the triplet to th singlet, indicating that the energy difference between the tw states is greater than $kT$ ($T = 298$ K).

**11722.** Bridges, J. M., Wiese, W. L., **The oscillator-strength scal for Fe I,** *Astrophys. J.* **161,** L71-L75 (July 1970).

Key words: Arc; iron; oscillator strengths; spectrum; transition probabilities.

Extensive measurements of *f*-values for about 80 Fe I line have been performed photoelectrically with a wall-stabilized ar at electron densities of about $10^{16}$ cm$^{-3}$ and temperatures nea 10000 K. Our measurements include the majority of those line which have been recently investigated in a number of smaller, a yet unrelated experiments. All these measurements are thus tie together for the first time, and it is found that they generall agree with each other within a factor of 2 or better. On the othe hand, our measurements indicate very definitely a strong dependence on upper excitation potential in the widely used data o

Corliss and co-workers. While there is good agreement with their data for lines of low excitation potentials, the deviations become as large as factors of 25 for lines starting from higher excitation potentials.

**11723.** Brower, W. S., Jr., Fang, P. H., **Dielectric constants of zinc tungstate,** *J. Appl. Phys.* **41,** No. 5, 2266 (April 1970).

Key words: Dielectric constant; single crystal; zinc tungstate.

The dielectric constants ($\epsilon'$) of zinc tungstate were measured at 24.5 °C in air. The averages and deviations from the mean of he three determinations for each orientation are as follows:

| | a | b | c |
|---|---|---|---|
| $\epsilon'$ | $17.2 \pm 0.2$ | $20.6 \pm 0.3$ | $16.8 \pm 0.1$ |

**11724.** Brower, W. S., Jr., Fang, P. H., **Dielectric constants of scheelite structure crystals,** *J. Appl. Phys.* **40,** No. 12, 4988-4989 (November 1969).

Key words: Barium tungstate; dielectric constant; single crystal; strontium molybdate; strontium tungstate.

The dielectric constants ($\epsilon'$) of $SrMoO_4$, $SrWO_4$, and $BaWO_4$ were measured at 24.5 °C in air. The averages, and deviations from the mean, of two determinations are:

| | | |
|---|---|---|
| $SrMoO_4$ | $\epsilon' \| a = 31.7 \pm 0.2$ | $\epsilon' \| c = 41.7 \pm 0.2$ |
| $SrWO_4$ | $\epsilon' \| a = 25.7 \pm 0.2$ | $\epsilon' \| c = 34.1 \pm 0.2$ |
| $BaWO_4$ | $\epsilon' \| a = 35.5 \pm 0.2$ | $\epsilon' \| c = 37.2 \pm 0.2.$ |

**1725.** Brower, W. S., Jr., Farabaugh, E. N., **Dislocation etchant for single crystal $Y_2O_3$,** *J. Am. Ceram. Soc.* **53,** No. 4, 225 (April 1970).

Key words: Dislocations; etching; single crystal; $Y_2O_3$.

An etching technique has been developed to form dislocation etch pits on the {100} and {111} planes of single crystal $Y_2O_3$. Typical dislocation etch pit densities were of the order of $10^5$ to $0^6/cm^2$.

**1726.** Cassidy, E. C., Cones, H. N., **Use of expanded laser beam to analyze high-intensity electric fields,** *J. Soc. Motion Picture Television Engrs.* **79,** No. 7, 590-591 (July 1970).

Key words: Dielectric liquids; electric field measurements; electro-optical measurements; high voltage measurements; Kerr cell; laser applications; pulse measurements.

A Kerr electro-optical technique that permits direct observation and mapping of distorted high-intensity electric fields has been devised at NBS. Analysis of the field profile from two-dimensional fringe images, similar to those observed in photoelastic mechanical stress analysis, permits calibration of the Kerr System for measurement of high-voltage pulses, and determination of relative field strength, actual field strength, and potential.

**1727.** Cezairliyan, A., **High-speed methods of measuring specific heat of electrical conductors at high temperatures (A review),** *High Temperatures—High Pressures* **1,** 517-529 (1969).

Key words: High-speed measurements; high temperature; specific heat; thermodynamics; thermophysical properties.

Needs and advantages of high-speed methods (subsecond duration) for the measurement of specific heat of electrical conductors at high temperatures are presented. The high-speed methods are described and classified according to ambient and operational conditions. Measurement and recording of experimental quantities are discussed. A historical development and the major features of high-speed experiments are summarized. A discussion and conclusions regarding the advantages of various high-speed methods and their applications are given.

**11728.** Chandler, R. F., Christian, R. A., **Crash testing of humans in automobile seats,** *Proc. Society of Automotive Engineers Safety Conf. May 13-15, 1970, Detroit, Mich., and June 8-11, 1970, Brussels, Belgium,* Intern. Safety Conf. Conpendium No. P-30, 112-132 (Society of Automotive Engineers, Inc., New York, N.Y., June 1970).

Key words: Anthropometric; automobile; crash; displacement; forces; human; impact; velocity.

The design of the automobile interior is largely based upon design data gathered under static conditions, where the inertial properties of the human body do not enter into consideration. Anthropometric data based on static measurements are valid for design of clearance and access for normal operation of the vehicle, and have been widely collected and used for these purposes. The requirements of the human operator or passenger during a crash are not as well documented. Clearances, paths of travel, velocities along the path and other dynamic data are of vital interest to the designer. Because of the difficulties in obtaining information about humans under crash conditions, most of the available guidelines are based upon dummy or cadaver tests. Until adequate human data are available, the designer must use the information obtained from human simulators and consider it only an unconfirmed approximation.

To alleviate this shortage of human impact data, the National Bureau of Standards initiated a research program in cooperation with the 6571st Aeromedical Research Laboratory. Tests were conducted on the Daisy Decelerator at Holloman AFB to gather comparative data about human and dummy test subjects under crash conditions using automotive seating and restraint systems. The data presented in this report include 32 human tests of controlled impacts of approximately the same magnitude. Variables are the type of restraint, either lap belt or lap belt plus single diagonal, and subject size. All tests were conducted in the −Gx orientation using a production automobile bucket seat. Data presented include the displacement paths of the subjects during the impact, the maximum velocity along the path, anthropometric data, loads generated in the restraint system, and medical and subjective evaluation of the impacts.

**11729.** Childs, G. E., Diller, D. E., **Refractive index of liquid deuterium,** (Proc. 1969 Cryogenic Engineering Conf., June 16-18, 1969, Univ. of California, Los Angeles, Calif.), Chapter in *Advances in Cryogenic Engineering* **15,** Paper No. C-2, 65-69 (Plenum Press, Inc., New York, N.Y., 1970).

Key words: Deuterium; polarizability; refractive index; specific refraction.

The refractive index of liquid deuterium is often required for the analysis of data obtained from high-energy physics experiments which use bubble chambers containing this liquid as a radiating medium. Until recently no measurements of the refractive index of liquid deuterium had been published. Ayers et al. have recently determined a single value for the refractive index of the saturated liquid at 24.2 K at a radiation wavelength of 3200 Å. This paper describes a method which can be used to compute accurate refractive index values for deuterium throughout a wide range of temperatures, densities, and wavelengths. A few representative values of the refractive index of saturated liquid deuterium are presented for illustration.

**11730.** Christensen, R. G., Hoeve, C. A. J., **Comparison between theoretical and experimental values of the volume changes accompanying rubber extension,** *J. Polymer Sci.* **8,** Part A-1, 1503-1512 (1970).

Key words: Free energy; molecular theory; rubber elasticity.

The molecular theory of rubber elasticity assumes the free energy to consist of two parts: a liquidlike free energy that is governed by intermolecular interactions and is independent of strain at constant volume and an intramolecular interaction free energy equal to the sum of the free energies of the chains making up the network. The volume increases of rubber samples as a function of their length were found to be considerably larger than predicted by the molecular theory. Therefore, contrary to common belief, the values of $(\partial E/\partial L)_{V,T}$ might not be related solely to changes in intramolecular interactions with extension. Also, the usual procedure to obtain values of $(\partial E/\partial L)_{V,T}$ from measurements of $(\partial f/\partial T)_{p,L}$ with the aid of the molecular theory is not correct.

**11731.** Clark, A. F., Childs, G. E., Wallace, G. H., **Low-temperature electrical resistivity of some engineering alloys,** (Proc. 1969 Cryogenic Engineering Conf., June 16-18, 1969, Univ. of California, Los Angeles, Calif.), Chapter in *Advances in Cryogenic Engineering* **15,** Paper No. C-5, 85-90 (Plenum Press, Inc., New York, N.Y., 1970).

Key words: Aluminum alloys; copper alloys; electrical resistivity; iron alloys; nickel alloys; titanium alloys.

The electrical resistivities of several engineering alloys have been measured at 4K, 20K, 76K, 192K, and 273K. Different iron, nickel, copper, titanium and aluminum alloys have been measured, some of them in different heat treated conditions. Most of the alloys have a smooth decrease in resistivity with decreasing temperatures, but some unusual results are reported. Comparisons are made between different alloys and between different heat treatments of the same alloys.

**11732.** Coxon, B., **Model parameters for the analysis of skew conformations of carbohydrates by p.m.r. spectroscopy,** *Carbohydrate Res.* **13,** 321-330 (1970).

Key words: Carbohydrates; conformations; coupling constants; proton resonance; ribopyranose; skew.

The p.m.r. spectrum of 3-*O*-benzoyl-1,2,4-*O*-benzylidyne-α-D-ribopyranose (**1**) at 100 MHz has been analyzed by an iterative, least-squares method. The resulting geminal, vicinal, and long-range coupling-constants have been correlated with the stereochemistry of the locked, skew conformation of **1**, and used to test the applicability of equations that relate coupling constant to dihedral angle. The mean deviation of the approximate proton – proton dihedral angles as calculated from a Karplus equation from those measured from a molecular model was 11°.

**11733.** Daney, D. E., Rapial, A. S., **Preparation and characterization of slush hydrogen and nitrogen gels,** (Proc. 1969 Cryogenic Engineering Conf., June 16-18, 1969, Univ. of California, Los Angeles, Calif.), Chapter in *Advances in Cryogenic Engineering* **15,** Paper No. L-4, 467-475 (Plenum Press, Inc., New York, N.Y., 1970).

Key words: Gels, liquid hydrogen gels; liquid nitrogen gels; liquid-solid hydrogen mixtures; rocket propellants; slush hydrogen; slush hydrogen gels; slush nitrogen gels.

An experimental apparatus has been developed for the gelation of slush hydrogen, and slush hydrogen was gelled for the first time. Measurements of the weight-bearing capacity of the gel as a function of mass precent gelant were made for liquid and slush nitrogen and hydrogen. These measurements verify the simple models discussed here for gelled liquid and slush within the experimental accuracy; for the silica gelant used in this work the models predict a reduction in gelant concentration from 38 mass percent to 25 mass percent in going from Normal Boiling Point liquid hydrogen to slush hydrogen of 0.40 solid fraction. Reduction in the mass percent gelant for other gelants should be similar.

**11734.** Diller, D. E., Roder, H. M., **Thermal conductivity measurements on fluid hydrogen at 17 to 200 K and pressures to 10MN/m$^2$,** (Proc. 1969 Cryogenic Engineering Conf., June 16-18, 1969, Univ. of California, Los Angeles, Calif.), Chapter in *Advances in Cryogenic Engineering* **15,** Paper No. C-1, 58-64 (Plenum Press, Inc., New York, N.Y., 1970).

Key words: Critical region; parahydrogen; thermal conductivity.

New absolute thermal conductivity measurements on fluid normal and parahydrogen are reported. A nominal accuracy of 2% has been achieved using a parallel plate apparatus in the temperature range 17 to 200 K at pressures to 100 atm and densities to 2.6 times critical. A graphical presentation of the data is given along isotherms, isochores, and isobars in the following regions: (1) the dilute gas, (2) the moderately dense gas, (3) the saturated and compressed liquid, (4) the critical region. Several interesting features of the behavior of the thermal conductivity of this fluid are pointed out: (1) the thermal conductivity of saturated liquid hydrogen increases with temperature between the triple point and the normal boiling point in contrast to the temperature dependence for most liquids other than helium, (2) a large anomalous increase in the thermal conductivity of hydrogen was found in the vicinity of the critical point.

**11735.** Duncan, A. G., Hiza, M. J., **A multipurpose phase equilibrium apparatus to study mixtures of cryogenic fluids: Application to argon-methane,** (Proc. 1969 Cryogenic Engineering Conf., June 16-18, 1969, Univ. of California, Los Angeles, Calif.), Chapter in *Advances in Cryogenic Engineering* **15,** Paper No. B-2, 42-45 (Plenum Press, Inc., New York, N.Y., 1970).

Key words: Apparatus; argon-methane data; liquid-vapor; low temperature; phase equilibrium; solid-vapor; thermodynamic properties; three-phase loci.

A new phase equilibrium apparatus is described which is capable of providing data of sufficient accuracy for the derivation of meaningful thermodynamic properties of mixtures. It includes single-pass and recirculation flow options for measurement of solid-vapor and liquid-vapor equilibrium properties and the three-phase loci of mixtures from 10 to 150 K and up to 200 atm. Temperatures are measured with either a platinum or a germanium resistance thermometer, and phase compositions are determined by chromatographic or continuous analysis with appropriate detectors. Preliminary data for the $Ar\text{-}CH_4$ system are given as an example.

**11736.** Funkhouser, A. T., Mielenz, K. D., **High-speed holographic interferometry,** *Appl. Opt.* **9,** No. 5, 1215 (May 1970).

Key words: Holography; photography; ruby rod; solid-state laser rods.

A new method has been developed in which holographic interferometry and high-speed photography are combined to investigate rapid dynamic distortions. This method has been used for a time-resolved study of the distortions of solid-state laser rods which result from optical pumping. A ruby rod has been studied and convex distortions have been observed at several pumping levels.

**11737.** Gadzuk, J. W., **Resonance-tunneling spectroscopy of atoms adsorbed on metal surfaces: Theory,** *Phys. Rev. B.* **1,** No. 5, 2110-2129 (March 1, 1970).

Key words: Adsorption; atomic spectroscopy; electron tunneling; surface physics.

Using a perturbational approach, we consider the theory of resonance tunneling of field-emitted electrons through atoms adsorbed on metal surfaces, first treated by Duke and Alferieff. In shown how one can proceed from the observed total energy stributions to information concerning the energy-level spec- um of the atom perturbed by the metal surface. The major al- ration of the spectrum manifests itself in a shift and lifetime roadening of the atomic energy levels due to configuration in- ractions with the continuum of metal states. In past work, this ift and broadening have been theoretically calculated by vari- us workers. Theories have also been advanced for calculating pole moments and, consequently, work-function changes and nding energies in which the final expressions for these quanti- es require knowledge of the perturbed atomic energy-level heme. The plan in the present paper is to present a method of alyzing the data obtained in resonance-tunneling spectroscopy that values for the shift and broadening of the energy levels n be obtained. To proceed towards this end, a simplified model treated in a mathematically systematic manner We believe, owever, that the present approach maintains sufficiently close ntact with the physics of the processes involved and thus, ecause of its transparency, is a potentially more valuable tool an past theories. The first experimental data of resonance tun- ling in field emission, obtained by Plummer and Young and re- orted on in the preceding paper, are analyzed within the context the present theory. These data include tunneling through sin- e Zr atoms in which a single broad ground-state level is seen, nneling through Ba atoms in which both a broad ground state $6s^2$ character and two narrow excited $6s$ $5d$ states are seen, d tunneling through Ca in which a somewhat narrow $4s$ $4p$ cited state is seen. Most aspects of the data are satisfactorily counted for in the present theory, and the observed shifts and oadenings of the levels are in good agreement with past calcu- tions.

738. Geil. G. W., Feinberg, I J., **Temperature changes in specimens in microplasticity tests,** *Met. Trans.* **1,** No. 7, 1845-1851 (July 1970).

Key words: Capacitance gages; invar; loading rate; microplasticity; strain measurement; temperature changes in tensile specimens; 4340 steel.

A tensile specimen and a gage assembly were designed to mea- re plastic strain at room temperature. The assembly mounts ree capacitance strain gages 120 deg apart, and is held by ribs ith a 45 deg included angle so as to define a 2 in. (5.08 cm) gage ngth. This novel construction eliminates spurious effects due the fillets and shoulders of the specimen. The strain sensitivity $\pm 1 \times 10^{-7}$. The cooling and heating of a specimen, accompany- g the loading and unloading, respectively, in the elastic range, e shown to affect plastic strain readings in a manner not con- dered by other investigators of microplasticity. The thermal ntributions to apparent strain in specimens of normalized 4340 eel and annealed Invar were determined and were found to be gnificant at strains less than $10^{-5}$. Strain measurement chniques necessary for the exclusion of the thermal dimen- onal changes of the specimen from the measurement of very nall plastic strains are discussed.

739. Giacchetti, A., Stanley, R. W., Zalubas, R., **Proposed secondary-standard wavelengths in the spectrum of thorium,** *J. Opt. Soc. Am.* **69,** No. 4, 474-489 (April 1970).

Key words: Secondary standards in thorium spectrum; standards of wavelength; thorium; thorium standards of class B; wavelength standards.

Energy levels for Th I were computed from the weighted erages of wavelengths from seven sets of published inter- rometrically measured data. The most self-consistent energy vels obtained in this way were then employed to calculate avenumbers that have a standard deviation of less than 10 mK. e propose that these lines be adopted as class-B secondary andards. Calculated wavelengths of 1375 Th I lines and weighted averages of 181 interferometrically measured Th I and Th II lines between 2565 and 12 381 Å are given.

11740. Gonano, J. R., Adams, E. D., ***In Situ* vapor pressure measurement for low temperature thermometry,** *Rev. Sci. Instr.* **41,** No. 5, 716-719 (May 1970).

Key words: Capacitance manometer; cryogenic thermometry; manometry; pressure measurement; thermomolecular pressure difference; vapor pressure; vapor pressure thermometry.

By use of a capacitance diaphragm manometer operated at low temperatures, it is possible to measure the vapor pressure of cryogenic liquids without the uncertainties introduced by thermomolecular pressure gradients (thermal transpiration). Since the zero of this manometer is more stable at low temperature than at room temperature, useful sensitivity is increased. Because of the increased sensitivity at low pressure as well as great convenience and simplicity this technique appears to have wide application in precise vapor pressure thermometry and similar work.

11741. Greenspan, M., Tschiegg, C. E., **Cavitation nucleated by $^{10}$B(n,$\alpha$)$^{7}$Li,** *Nucl. Instr. Methods* **82,** No. 3, 310-312 (1970).

Key words: Acoustic cavitation; boron (n,$\alpha$) lithium reaction; cavitation; neutron detection; radiation-induced cavitation; thermal neutron detection.

Acoustic cavitation has been nucleated on the reaction $^{10}$B(n,$\alpha$)$^{7}$Li in methanol solution. Implications for a slow neutron detector or counter are discussed.

11742. Haar, L., Sengers, J. M. H. L., **The solubility of condensed substances in dense gases, and the effect on *PVT* properties,** *J. Chem. Phys.* **52,** No. 10, 5069-5079 (May 15, 1970).

Key words: Ammonia; dense gases; equation of state; hydrogen; mercury vapor; nitrogen; noble gases; solubility-enhancement; steam; van der Waals' equation.

An analytic relation is derived in terms of the molecular interactions for the density dependence of the solubility of a liquid or solid in dense gas using a modified van der Waals equation. It is shown that at high gas densities the solubility is sharply reduced. It is also shown that the effect of the solubility enhancement on high-density *PVT* measurements is smaller than previously thought. The analysis is applied to the case where the condensed material is liquid mercury. Solubility-vs-density isotherms and the effect of the solubility on *PVT* measurements are obtained at 50, 150, 250, and 400 °C for the following gaseous species: He, $H_2$, Ne, Ar, Kr, Xe, $N_2$, $NH_3$, $H_2O$. The need for accurate experimental data at high gas densities to test further the essential features of the analysis is discussed.

11743. Hamilton, W. C., Edmonds, J. W., Tippe, A., Rush, J. J., **Methyl group rotation and the low temperature transition in hexamethylbenzene. A neutron diffraction study,** *Discussions Faraday Soc.,* No. 48, 192-204 (1969).

Key words: Barrier to rotation; crystal; crystal structure; hexamethylbenzene; hindered rotation; phase transition; torsional oscillation; λ-point methyl group.

Neutron diffraction studies of single crystals of hexamethylbenzene at 298 K and at 130 K indicate that the molecule in e II has appromimate $D_{3d}$ symmetry. The amplitudes of libration of the methyl group and of rigid body motions of the molecule are consistent with earlier data, except that the barrier to methyl group rotation appears to be lower by about 0.5 kcal/mol (2100 J/mol).

Consideration of intra- and inter-molecular hydrogen atom contact distances and calculated potential energy curves using a 6-exp potential function suggest that intermolecular forces are important in determining the barrier to rotation of the methyl groups and that substantial changes in the intermolecular packing must be responsible for the lambda-point transition at 116 K and the consequent profound change in the potential barrier to internal rotation which has been previously observed.

**11744.** Hanson, D. W., **Quasi-optical components using total reflection in dielectrics,** *IEEE Trans. Microwave Theory Tech.* **MTT-18,** No. 4, 233-234 (April 1970).

Key words: Millimeter waves; polarizers; quasi-optics; total relection; turnstile junction.

Two quasi-optical components operating at 90 GHz which use the effects of a metal plate on total reflection are described. A circular polarizer and, with the addition of a metal plate grating, a device having properties similar to a tuned turnstile junction were constructed. Experimental results showed better than 99 percent polarization conversion for the polarizer.

**11745.** Hendricks, R. C., Simoneau, R. J., Smith, R. V., **Survey of heat transfer to near-critical fluids,** (Proc. 1969 Cryogenic Engineering Conf., June 16-18, 1969, Univ. of California, Los Angeles, Calif.), Chapter in *Advances in Cryogenic Engineering* **15,** Paper No. G-1, 197-237 (Plenum Press, Inc., New York, N.Y., 1970).

Key words: Choking; critical; fluid; fluid flow; heat transfer; oscillations.

The three authors have reviewed the field and added some new material. The intent of the paper is to bring the literature together, to provide information for designers, and to suggest needed research.

**11746.** Heydemann, P. L., **Ultrasonic measurements at pressures up to 50 kbar,** *Proc. Intern. Collog. Solids at High Pressures, Grenoble, France, Sept. 8, 1969,* No. 188, pp. 461-467 (Centre National de la Recherche Scientifique, Paris, France, 1970).

Key words: Bulk modulus; equation of state; high pressure; phase transitions; potassium chloride; tellurium; ultrasonics.

Ultrasonic measurements as a function of pressure or temperature provide one of the most accurate means to determine pressure or temperature dependence of the bulk modulus and the density of both liquids and solids. Such measurements are currently carried out with very high accuracy at pressures up to about 4 kbar (1 kbar = $10^8 N/m^2$) in several laboratories.

If the material under investigation undergoes transitions at higher pressures, or if the bulk modulus is noticeably non-linear with pressure, ultrasonic measurements at pressures higher than 4 kbar are needed. This report describes our method to carry out such measurements at pressures close to 50 kbar, both under hydrostatic and non-hydrostatic conditions.

For most materials the accuracy of the density and bulk modulus data obtained from such measurements is much higher than that obtained from isothermal dilatometric measurements. In the case of tellurium, the accuracies for the bulk modulus at 30 kbar are 1.6% and 23%, respectively.

Another interesting application of ultrasonics at high pressures is the detection of phase transitions and the measurement of the elastic properties as the material undergoes the transition. As an example for measurements through a transition range, our results of ultrasonic and isothermal dilatometric measurements on KCl are presented. We find that the ratio of specific heats also shows a sharp increase in the transition range.

**11747.** Hiza, M. J., **Solid-vapor equilibria research on systems of interest in cryogenics,** *Cryogenics* **10,** No. 2, 106-115 (April 1970).

Key words: Combining rule correlation; cryogenic enhancement factor theory; review; solid-vapor equilibria vapor pressures.

A review of research associated with solid-vapor equilibria o cryogenic systems is given with emphasis on the fundamenta value of such studies. Included are discussions of vapor pressures of solidified fluids, theory applicable to the prediction o solid-vapor equilibria, available data in the solid-vapor region fo systems of cryogenic interest, and a correlation derived fron selected solid-vapor equilibria data, which is offered as a significant improvement in the prediction of properties of two-component systems in general.

**11748.** Kidnay, A. J., Hiza, M. J., Dickson, P. F., **Adsorptio kinetics in a ternary system containing hydrogen,** (Proc. 196 Cryogenic Engineering Conf., June 16-18, 1969, Univ. o California, Los Angeles, Calif.), Chapter in *Advances i Cryogenic Engineering* **15,** Paper No. B-3, 46-49 (Plenun Press, Inc., New York, N.Y., 1970).

Key words: Adsorption; hydrogen; kinetics; methane nitrogen; ternary system.

The concentration-time (breakthrough) curves for a ternar mixture of nitrogen, methane, and hydrogen were measured o an activated coconut shell charcoal at 76 K over a range of flo rates. The equations of Eagleton and Bliss were used to obtai gas phase and adsorbed phase mass transfer coefficients from th breakthrough curves. The values for the gas phase mass transfe coefficient, when converted to *j* values, are in fair agreemen with the generalized correlations proposed by De Acetis an Thodos. The breakthrough curves were also correlated using th empirical method proposed by Engel and Coull, with goo results.

**11749.** Lawton, R. A., **New standard of electric field strength** *IEEE Trans. Instr. Meas.* **IM-19,** No. 1, 45-51 (Feb. 1970).

Key words: Antenna; electric field strength; measurement standard field.

A new technique is presented for establishing a standard electric field strength using a highly conducting sphere. An ana ysis is made to determine the current on the sphere as a functic of the electric field strength of an incident plane wave. A methc of measuring that current using electronic circuitry and an opt cal indicator within the sphere is described, and an intercon parison is made with an independent field-strength standard.

This technique is a significant improvement over previo ones in that it permits the absolute determination of field strengt with a maximum uncertainty of 1 percent or less at 30 MHz ar is applicable to a broad range of frequencies and field strength

**11750.** Levin, E. M., **X-ray determination of the thermal expa sion of silver nitrate,** *J. Am. Ceram. Soc.* **52,** No. 1, 53-5 (January 1969).

Key words: $AgNO_3$; density $AgNo_3$; polymorphis $AgNO_3$; thermal expansion $AgNO_3$; unit cell dimensio $AgNO_3$.

An x-ray diffractometer furnace was used to obtain powd patterns of orthorhombic (low) $AgNO_3$ between 25° and 140 ° and of rhombohedral (high) $AgNO_3$ between 25° and 175 °C Unit cell dimensions are given for selected temperatures and a essentially a linear function of temperature. The values for t coefficient of expansion of low $AgNo_3$ along *a, b,* and *c*, respe tively, are $126 \times 10^{-6}$ deg$^{-1}$, $57 \times 10^{-6}$ deg$^{-1}$, $-0.4 \times 10^{-6}$ deg For high $AgNO_3$ the values along *a* and *c*, respectively, are 30 $10^{-6}$ deg$^{-1}$ and $134 \times 10^{-6}$ deg$^{-1}$. X-ray density of the high for at a given temperature is greater than that of the low form and, general, does not agree with previous reported results. The val of $dT/dP$ calculated from the Clausius-Clapeyron equation

−6.9 × 10⁻³ K/bar, at atmospheric pressure, vs Bridgman's experimental value of −7.6 × 10⁻³ K/bar.

1751. Lutz, G. J., Masters, L. W., **Determination of carbon in high purity metals by photon activation analysis,** *Anal. Chem.* **42,** No. 8, 948-950 (July 1970).

Key words: Carbon; combustion separations; metals; photon activation analysis; radiochemical separations.

Photon activation anlaysis has been applied to the determination of carbon in a variety of pure metals. The samples are irradiated in the bremsstrahlung beam produced from electrons accelerated to 35 MeV. The reaction $^{12}C(\gamma,n)^{11}C$ is induced at these energies. The product nucleus has a half-life of 20.5 minutes and decays by positron emission. The separation of carbon is based on traditional high temperature combustion methods. The intrinsic sensitivity for the production of $^{11}C$, coupled with the absence of reagent and equipment blanks and the ability in some instances to etch the sample after irradiation but before separation and counting, allows determinations at levels below $10^{-7}$ grams of carbon. Precisions of 5-20 percent at levels of ppm or less are typical.

1752. Machta, L., Hughes, E., **Atmospheric oxygen in 1967-1970,** *Science* **168,** No. 3939, 1582-1584 (June 26, 1970).

Key words: Atmospheric composition; oxygen analysis; photosynthetic oxygen; oxygen variations.

Observations of atmospheric oxygen in clean air between 50 °N and 60 °S, mainly over the oceans, yield an almost constant value of 20.946 mole percent dry air. Since 1910 changes with time are either zero or smaller than the uncertainty in the measurements. Burning of fossil fuels since 1910 would have reduced the oxygen content by 0.005 mole percent while future combustion of all known recoverable fossil fuels could lower the oxygen content to about 20.8 mole percent.

1753. Madey, T. E., Yates, J. T., Jr., **Chemisorption on single crystals: $H_2$ on (100) tungsten,** *Proc. Colloque Intern. sur la Structure et les Proprietes des Surfaces des Solides, Paris, France, July 7-11, 1969,* No. 187, pp. 155-162 (Centre National de la Recherche Scientifique, Paris, France, 1970).

Key words: Binding state; chemisorption; hydrogen; isotopes; single crystal; tungsten; work function.

An ultrahigh vacuum apparatus has been constructed to study flash desorption of gaseous molecules from macroscopic single crystals. The crystals are in the form of thin discs, polished on both faces, whose total surface area is 95% of one orientation. A focussed light source external to the vacuum system is used to heat the nearly adiabatically suspended sample to T > 1200 K; temperature inhomogeneities and end effects which complicate kinetic measurements on resistively heated samples are not present here. The sample is cleaned by electron bombardment prior to making adsorption measurements. Work function changes upon adsorption are monitored using an electron gun; a quadrupole mass spectrometer is used as the detector of desorbed species.

The chemisorption of $H_2$ and $D_2$ on a (100) oriented tungsten disc has been examined with this apparatus. The hydrogen desorption spectra reveal that *two* binding states exist on the (100) surface. The first order $\beta_1$ state desorbs with an activation energy of ~25 kcal/mole and at saturation coverage, is twice as densely populated as the $\beta_2$ state. The coadsorption of an equimolar mixture of $H_2$ and $D_2$ shows that *both* states are isotopically mixed upon desorption. The work function-coverage relation is linear over the entire coverage range; the dipole moment per atom is 0.15 Debye, independent of binding state. Several models of $H_2$ chemisorption are discussed.

11754. Madey T. E., Yates, J. T., Jr., King, D. A., Uhlaner, C. J., **Isotope effect in electron stimulated desorption: oxygen chemisorbed on tungsten,** *J. Chem. Phys.* **52,** No. 10, 5215-5220 (May 15, 1970).

Key words: Adsorption; chemisorption; desorption; electron bombardment; isotope; oxygen; single crystal; tungsten.

Electron stimulated desorption (ESD) studies of oxygen chemisorbed on tungsten have revealed a large isotope effect in the desorption of ions. The probability of desorption of $^{16}O^+$ was found to be a factor of ~1.5 greater than the probability of desorption of $^{18}O^+$ upon bombardment of the adsorbed layer by 100-eV electrons. This observation is quantitatively consistent with the ESD mechanism proposed independently by Redhead and by Menzel and Gomer. On the other hand, the small isotope effect observed in ESD "total" desorption does not agree with this mechanism; possible reasons for this are discussed.

11755. Mahler, R. J., James L. W., **Acoustic and magnetic effects involving the $^{19}F$ nuclei in antiferromagnetic $KMnF_3$,** *J. Appl. Phys.* **41,** No. 4, 1633-1636 (March 15, 1970).

Key words: Interaction; nuclear spin system; phonons; transferred hyperfine.

A simple model which allows spin-1/2 nuclei in antiferromagnetic crystals to interact with phonons is presented and an order of magnitude calculation predicts the one- and two-phonon effects observed in $KMnF_3$.

11756. Margoshes, M., **Data acquistion and computation in spectrochemical analysis: A forecast,** *Spectrochim. Acta* **25B,** 113-122 (June 15, 1969).

Key words: Automation; computers; data acquisition; emission spectroscopy; microphotometers; spectrochemical analysis; television cameras.

Some new applications of automation and computerization in emission spectrochemical analysis are proposed. Automated microphotometers now make it possible to digitize complete photographically-recorded emission spectra in a reasonable time. Television techniques offer the prospect of digitally recording complete spectra photoelectrically, circumventing the problems and loss of time encountered with photographic spectroscopy. Reduction of the data with computers should make possible completely automatic qualitative analysis. Semiquantitative analysis without standards may also be possible. When standards are available, the use of computers for data reduction should improve the accuracy of analysis by allowing complex corrections to be made for interelement effects. The cost of programming could delay the development of these proposals, and a cooperative research program is suggested to reduce the cost to any one laboratory.

11757. Marvin, R. S., **Rheological models and measurements,** (Proc. 5th Intern. Congress on Rheology, Kyoto, Japan, Oct. 7-11, 1968), Chapter in *Fifth International Congress on Rheology,* S. Onogi, ed., **1,** 85-96, (University of Tokyo Press and University Park Press, Tokyo, Japan, 1969).

Key words: Measurements; model; rheology.

The evaluation of the rheological properties of a material requires certain assumptions from which the form of a constitutive equation can be deduced. The term model, whether molecular or phenomenological, here denotes the body of assumptions used in the development of a particular theory. The testing of these assumptions and the evaluation of the constants or functions in the resulting constitutive equation require the design and performance of various measurements. A single type of measurement may be adequate to evaluate functions occurring in a constitutive equation, but it is seldom sufficient to establish the validity of the assumptions on which that equation is based. Such results may simply establish an equation as a good empirical representation, a useful accomplishment, but one quite different from establishing the validity or adequacy of a model.

In carrying out measurements intended to check a model or some of the assumptions on which a model is based, certain factors which are deliberately ignored in the model (always an idealization of an actual material) must be considered, as must the effect of deviations from boundary conditions assumed in the measurement. And, a consideration often ignored, both the measurement and the manner in which the results are analyzed should be chosen to provide a sensitive check of the assumption or model. The history of experiments stimulated by the Weissenberg hypothesis about the equality of normal stress differences illustrates both the difficulty of satisfying these criteria and the danger of judging the correctness of a hypothesis or a model from the results of a single type of measurement.

**11758.** Mauvais, C. J., Latanision, R. M., Ruff, A. W., Jr., **On the anisotropy observed during the passivation of nickel monocrystals,** *J. Electrochem. Soc.* **117,** No. 7, 902-903 (July 1970).

Key words: Dislocations; nickel-single crystals; passive film; polarization; surfaces.

Potentiostatic polarization measurements on the three low index faces of a nickel monocrystal in 1*N* $H_2SO_4$ indicate a strong anisotropy in the passive region. Specifically, the degree of protection provided by the passive film on a {111} surface is greater than on either {110} or {100} faces, an orientation dependence identical to that observed for epitaxial films produced during gaseous oxidation. This behavior is discussed in terms of the creation of misfit dislocations at the crystal-passive film interface and the effect of misfit boundaries in the film.

**11759.** McNish, A. G., **The impact of increasing metric usage,** *Proc. Conf. Industrial Heating Equipment Association, Spring (77th Consecutive) Meeting, Hot Springs, Virginia, May 19-21, 1969,* Exhibit E, 12 pages (Industrial Heating Equipment Assoc., Washington, D.C., 1969).

Key words: Metric system; metric usage; Public Law 90-472.

Public Law 90-472 requires the Secretary of Commerce to determine the advantages and disadvantages of increased use of the metric system in the United States. Subsequent to its passage, the Secretary assigned responsibility for the Study to the National Bureau of Standards.

Degrees of increased use may be designated as accommodation, involving translation of measurement units where frequent use of measurements is not involved; adaptation, involving dual labelling of packaged goods and dual dimensioning of mechanical items; and conversion, involving design of products in the metric system yielding a final product which is completely metric.

Metric products are often produced in nonmetric shops and vice-versa, but with increased costs and difficulties. Many U.S. industries already make extensive use of the metric system. Difficulties experienced in producing metric products in U.S. factories arise because metric standard parts and metric stock sizes are not readily available in the United States. This is a particular difficulty experienced by companies which operate plants in the United States and abroad, which in many cases, require different designs for economical production.

On the other hand, there are many industries where U.S. based standards have found worldwide use and acceptance and change for many of these standards is undesirable, though the sizes and dimensions of the products involved may someday be expressed in metric language.

**11760.** McNish, A. G., **Progress on the Metric Study Program,** *Proc. Conf. 18th Annual Meeting of Standards Engineers Society, Washington, D.C., Sept. 17-19, 1969,* pp. 53-56 (Standards Engineers Society, Philadelphia, Pa., 1969).

Key words: Cost of transition; industrial cooperation; metric system; trade advantages.

The Metric Study Program is progressing at such a rate that it seems that completion of the Study on schedule can be accomplished. Techniques for the evaluation of the costs of increased metric usage have been developed in cooperation with industry. If transition to the metric system takes place at an optimum rate, the costs will not be as great as many of the estimates that have been made in the past. The Study is receiving cooperation from other branches of the government with an outstanding effort from the Department of Defense in evaluation of the costs of any possible change and its impact on our military posture. No great immediate advantage to our export trade is suggested by the statistics presently available, although international operations would be considerably helped by use of a single system of measurement.

**11761.** Melmed, A. J., Carroll, J. J., **Ellipsometry, LEED, and FEM study of evaporated epitaxial films of iron on (011) tungsten,** *Surface Science Letters to the Editor* **19,** No. 1, 243-248 (January 1970).

Key words: Ellipsometry; epitaxy; index of refraction; optical constants; thin films vapor deposition.

The structure, thickness, and optical constants of iron films vapor-deposited onto a single-crystal (011) tungsten substrate in ultra-high vacuum have been characterized by the ELF (ellipsometry, LEED, FEM) apparatus developed at NBS. It is shown that films of thickness 400 Å or greater have (after annealing) optical properties and surface structure indistinguishable from bulk iron.

**11762.** Mighell, A. D., Reimann, C. W., Santoro, A., **The crystal structure of the 2:1 dimer $[(\text{pyridine } N\text{-oxide})_2\text{CuBr}_2]_2$,** *Chem. Commun.* **4,** 204 (1970).

Key words: Crystal structure; pyridine *N*-oxide cupric bromide dimer.

The structure of the 2:1 dimer $[(\text{pyridine } N\text{-oxide})_2\text{CuBr}_2]_2$ is reported and is shown to differ significantly from that of the corresponding chloride complex as well as from other structure types in the aromatic *N*-oxide series.

**11763.** Melino, J. A., **Noise—the growing hazard,** *Dialog* **1,** No. 4, 26-28 (1970).

Key words: Hearing conservation; noise abatement; noise pollution.

Noise is a growing hazard. The private and public sectors of the country have responded to the problem in concrete ways. Hopefully the widespread concern over noise will lead to a forceful national program of noise control. But young people have created a special problem with the harmful sound levels of rock music. The damaging intensities of this kind of music should be further investigated.

**11764.** Negas, T., Roth, R. S., **The system $SrMnO_{3-x}$,** *J. Solid State Chem.* **1,** 409-418 (1970).

Key words: Four-layer $SrMnO_3$; perovskites; phase equilibria; strontium manganates; tetravalent manganese; trivalent manganese.

The system $SrMnO_{3-x}$ ($0 \leq x \leq 0.5$) was investigated by gravimetric and quenching experiments. Four-layer, hexagonal $SrMnO_3$ ($a = 5.449$ Å, $c = 9.078$ Å) is stable in air below 1035 °C. Above 1035 °C the basic structure becomes increasingly anion deficient, reaching the limiting composition $SrMnO_{2.89}$ near 1400 °C. Unit cell dimensions increase and distortion to orthorhombic symmetry occurs with decreasing oxygen content. Further reduction occurs from 1400 °C to a melting point at 1740 °C and a "perovskite" homogeneity range exists with limits $SrMnO_{2.74}$ and $SrMnO_{2.62}$. The anion-deficient perovskite phases can be rapidly reoxidized at low temperatures to yield a metastable cubic perovskite, $SrMnO_3$ ($a = 3.806$ Å). Stoichiometry and stability of phases are discussed from the standpoint of variation in the coordination of the manganese cation.

**11765.** Page, C. H., **The trolley problem,** *Am. J. Phys.* **38,** No. 5, 608-610 (May 1970).

Key words: Current density; electric current; electromagnetic field; Lorentz transformation; sliding circuit.

A rectangular current circuit in which one conductor is moving along its own axis is Lorentz equivalent to a two-trolley loop sliding along a stationary wire. The body and surface densities of charge and current are deduced on the basis of a simplifying idealization.

**11766.** Page, C. H., **Relations among systems of electromagnetic equations,** *Am. J. Phys.* **38,** No. 4, 421-424 (April 1970).

Key words: Coherent; dimension; quantity; rationalization; systems of equations; units.

The equations of electromagnetism, whether written in the electrostatic, electromagnetic, or symmetric system, whether in rationalized or nonrationalized from, express an invariant set of physical relationships. The same set of letter symbols is employed in each system of equations; these symbols represent related, but different, quantities in the various systems. The relationships among corresponding symbols are given and applied to precise statements about the relation between the oersted and the ampere per meter, the abampere and the ampere, etc.

**11767.** Pfeiffer, E. R., Schooley, J. F., **Effect of stress on the superconducting transition temperature of $SrTiO_3$,** *J. Low Temp. Phys.* **2,** No. 3/4, 333-352 (August 7, 1970).

Key words: Anisotropic stress effect; hydrostatic pressure; Nb-doped $SrTiO_3$; reduced $SrTiO_3$; superconductivity; transition temperatures; uniaxial compression; 0-1.8 kbars stress.

The superconducting transition temperatures of several specimens of reduced $SrTiO_3$ and of Nb-doped $SrTiO_3$ have been investigated as functions of hydrostatic and uniaxial compressive stresses up to 1.8 kbars. Decreases in $T_c$ as large as 0.12 K have been observed in specimens under hydrostatic pressure. Because of the low $T_c$ and small compressibility of $SrTiO_3$, $\Delta(\ln T_c/\Delta P$ and $\Delta(\ln T_c)/\Delta(\ln V)$ are orders of magnitude greater than the corresponding effects in elemental superconductors. The effect of uniaxial stress on $T_c$ varied with the direction of stress. Compression along a [111] direction caused large decreases in $T_c$, while both small increases and small decreases in $T_c$ have been observed for [100] compression. It is believed that the present results reveal the presence of a sensitive volume dependence in one or more of the parameters important to superconductivity in $SrTiO_3$, and that no significant electron-transfer effects occurred in the range of stresses of this experiment.

**11768.** Phillips, S. L., Johnson, C. E., **Effect of atmospheric exposure on the contact resistance of selected tin alloys,** *J. Electrochem. Soc.* **117,** No. 6, 827-830 (June 1970).

Key words: Contact resistance; corrosion; metal plating.

Atmospheric exposure of plated specimens in a rural outdoor location showed that both tin-zinc and tin-cadmium alloy coatings on steel maintained a lower contact resistance than did equal thicknesses of tin, tin-lead, or tin-antimony alloys. After exposure for over 2 months, the contact resistances under a 50g load for 5-38 $\mu$m thicknesses of tin-zinc and tin-cadmium ranged between 10-100 mohms, although both coatings rapidly lost their luster. The tin-lead alloy maintained the lowest contact resistance of all the coatings tested, although it failed to provide corrosion protection as good as equal thicknesses of tin-zinc or tin-cadmium.

**11769.** Plummer, E. W., Young, R. D., **Field-emission studies of electronic energy levels of adsorbed atoms,** *Phys. Rev. B.* **1,** No. 5, 2088-2109 (March 1, 1970).

Key words: Adsorption; alkaline earths; atomic energy levels; surface; tungsten; tunneling resonance.

The relative changes in the total energy distribution of field-emitted electrons upon adsorption of single atoms have been measured for adsorption of the alkaline-earth atoms (Ba, Sr, and Ca) on several crystal planes of tungsten. The expected perturbations of the energy distribution due to the tunneling resonance through an atomic "virtual level" at various positions relative to the Fermi surface and of various half-widths $\Gamma$ is demonstrated by a simple one-dimensional calculation. The measured energy-dependent structure in the current-enhancement factor due to the adsorbate has been interpreted in a tunneling-resonance model to yield the positions and shapes of the atomic "virtual levels." The ground-state $^1S$ $6s^2$ level of Ba is broadened to a half-width $\Gamma_S = 0.75$ eV and shifted upward by $\Delta E^S = 0.95$ eV. This causes it to overlap and mix with the first two excited states: a triplet $^3D$ $6s5d$ and a singlet $^1D$ $6s5d$. The observed $^3D$ and $^1D$ levels were not shifted and has a half-width $\Gamma_D = 0.1$ eV. Similarly, the first excited state of Ca, a triplet $^3P$ $4s4p$, was shifted by $\Delta E^{3P} \approx 0.4$ eV with a width $\Gamma_{3P} \approx 0.3$ eV ($2\Gamma =$ FWHM). The effect of the band structure of the substrate on tunneling is discussed.

**11770.** Powell, R. L., **Cryogenic materials needs,** (Proc. 5th Annual Natl. Conf. Industrial Research, Sept. 18-19, 1969, Chicago, Ill.), Chapter in *Applying Emerging Technologies,* pp. 102-107 (Industrial Research, Inc., Beverly Shores, Indiana, 1970).

Key words: Cryogenic fuels; food preservation; liquefied natural gas; medical technology.

Cryogenics has long been divided informally into three fields: superconductivity, liquid helium, and other. This talk is on the "other," with two special topics emphasized, cryogenic fuels and biological materials. The special fuel needs important now are hydrogen for space flight and liquefied natural gas for home use, industry, and transportation. Some applications of cryogenic techniques to medical operations and to preservation of gourmet foods are briefly described.

**11771.** Reed, R. P., Durcholz, R. L., **Cryostat and strain measurement for tensile tests to 1.5 K,** (Proc. 1969 Cryogenic Engineering Conf., June 16-18, 1969, Univ. of California, Los Angeles, Calif.), Chapter in *Advances in Cryogenic Engineering* **15,** Paper No. D-3, 109-116 (Plenum Press, Inc., New York, N.Y., 1970).

Key words: Capacitance extensometer; cryostat; strain measurement instruments; tensile properties.

A new tensile cryostat has been developed and tested at temperatures between 300 and 1.5 K. Better design, insulation, and vacuum-sealed environment reduces the heat leak to about 0.2 watts during continuous pumping above liquid helium. New capacitance strain-sensing equipment has been developed to provide ranges of strain sensitivities between $10^{-6}$ and $10^{-2}$ inches per inch. Details are presented of both devices.

**11772.** Ritter, J. J., Coyle, T. D., **Halogen exchange reactions of diboron tetrahalides,** *J. Chem. Soc.,* Sec. A, pp. 1303-1304 (1970).

Key words: Boron; boron subhalides; exchange; halides; halogen; redistribution.

Halogen exchange between $BCl_3$ and $B_2F_4$ at room temperature occurs in such a way as to concentrate chlorine on the diboron fragment and thus provides a convenient procedure for preparation of $B_2Cl_4$ in $> 80\%$ yield. Halogen exchange between $B_2Cl_4$ and $Me_2BF$ leads, however, to formation of $B_2F_4$ and $Me_2BCl$. I.r. and n.m.r. spectra indicate the presence of hitherto undetected diboron chlorofluorides in this system and in $B_2F_4-B_2Cl_4$ and $BF_3-B_2Cl_4$ mixtures.

**11773.** Robertson, A. F., Gross, D., **Fire load, fire severity, and fire endurance,** *Am. Soc. Testing Mater. ASTM Spec. Tech. Publ.* **464,** *Fire Test Performance,* pp. 3-29 (January 1970).

Key words: Burn out; experimental fires; fire endurance; fires in buildings; fire severity; fire ventilation.

A review is presented of fire studies beginning with the work of Ingberg at the National Bureau of Standards, who attempted to relate the severity of a fire endurance test in the laboratory to the conditions existing during actual building fires. He showed the importance of weight of combustibles per unit floor area as a major factor. He recognized the importance of ventilation in controlling fire behavior but did not specify it as a separate variable. Fujita in Japan is credited with emphasing the importance of ventilation. His work has been followed and enlarged by others around the world. Ventilation parameters, compartment geometry, and fuel arrangement have been shown to exert a powerful influence. The radiance from a burning building is dependent to a large extent on the nature of the ventilating openings. Fire severity is not well defined, since it depends on the interaction of the temperature-time curve developed during a fire and the themophysical properties of the materials exposed. There is a great need for further research on the influence of fuel arrangement, building geometry, and ventilation on fires in buildings.

**11774.** Rockett, J. A., **Objective and pitfalls in the simulation of building fires with a computer,** *Fire Tech.* **5,** No. 4, 311-322 (November 1969).

Key words: Building; computer; fire; simulation.

The complex interactions between a building and a fire are being studied using the National Bureau of Standards computer facility. By highlighting the information needs for a successful calculation, the fire simulation study provides a guide to future research.

**11775.** Schneider, W. E., **A one-solar-constant irradiance standard,** *Appl. Opt.* **9,** No. 6, 1410-1418 (June 1970).

Key words: Calibration techniques; radiometric standards; solar constant; spectral irradiance; total irradiance.

A new high-intensity standard of total and spectral irradiance has been developed recently at the National Bureau of Standards. The standard consists of a 1000-W tungsten-halogen lamp mounted in a ceramic reflector, the reflecting surface of which is coated with flame-sprayed $Al_2O_3$. The lamp-reflector combination results in a source having a relatively small (3 cm × 5 cm) radiating area yielding a total irradiance, at a distance of 40 cm, of about 136 mW $cm^{-2}$. The total irradiance calibrations are based on the radiance of a 1400-K blackbody and have an estimated maximum systematic error of 0.9% and a maximum estimated standard error of 0.19%. The spectral measurements were made over the wavelength range of 0.3 $\mu$m to 2.5 $\mu$m relative to the NBS 1000-W tungsten-halogen irradiance standards. The estimated uncertainty in these measurements ranges from 4% in the visible and near ir to 8% in the uv.

**11776.** Sher, A. H., Coleman, J. A., **Lithium driftability in detector-grade germanium,** *IEEE Trans. Nucl. Sci.* **NS-17,** No. 3, 125-129 (June 1970).

Key words: Gamma-ray spectrometers; Ge(Li) detectors; lithium driftability; lithium mobility; semiconductor nuclear radiation detectors.

The behavior of many germanium crystals during lithium-ion drift, in terms of compensated depth W as a function of drift time t, does not follow the prediction of the equation:

$$W = (2\mu_{Li} Vt)^{1/2}.$$

Modification of the lithium velocity expression to include the loss of mobile lithium ions during drift yields the expression:

$$W = \mu_{Li} V\tau(1\text{-}e^{-2t/\tau})^{1/2}$$

which seems to describe satisfactorily the experimental results. In addition to the loss mechanism, the effect of oxygen on lithium-ion drift mobility is considered.

**11777.** Sher, A. H., Keery, W. J., **Variation in the effective Fano factor in a Ge(Li) detector,** *IEEE Trans. Nucl. Sci.* **NS-17,** No. 1, 39-43 (February 1970).

Key words: Charge carrier trapping; effective Fano factor; gamma-radiation; Ge(Li) detector; intrinsic Fano factor; p-i-n junction.

Variations in the value of the effective Fano factor, F′, have been observed in Ge(Li) detectors using a collimated beam of $\gamma$-rays to irradiate selected areas in the sensitive region between the $n^+$- and p-contacts. For regions near the $n^+$-contact where the trapping of electrons is minimized, F′ was found to be statistically less than 0.11.

**11778.** Sindt, C. F., Ludtke, P. R., **Slush hydrogen flow characteristics and solid fraction upgrading,** (Proc. 1969 Cryogenic Engineering Conf., June 16-18, 1969, Univ. of California, Los Angeles, Calif.), Chapter in *Advances in Cryogenic Engineering* **15,** Paper No. I-6, 382-390 (Plenum Press, Inc., New York, N.Y., 1970).

Key words: Flow restrictions; liquid hydrogen; liquid-solid mixtures; plug flow; slurry flow; slush hydrogen; solid hydrogen.

Flow characteristics of liquid-solid mixtures of parahydrogen (slush hydrogen) were investigated in a 16.6 mm diameter pipe, a globe valve, two orifices, and a venturi. The pressure loss as a function of slush solid fraction and volume flow rate was determined for a 14.74 m test section of the pipe. Test results are presented as pressure loss versus volume flow and as friction factor versus Reynold number. Data for triple-point liquid and slush of solid fractions up to 0.5 are presented. When Reynolds numbers in the pipe were greater than $3 \times 10^5$, friction losses flowing slush hydrogen at mass solid fractions of 0.2 to 0.4 were greater than friction loss flowing triple-point liquid hydrogen. At a Reynolds number of $6 \times 10^4$ friction losses with liquid-solid mixtures of hydrogen in the test section were always greater than losses with triple-point liquid hydrogen.

Slush of solid fractions to 0.5 flowed through the valve, orifices and a venturi with the same pressure loss as with triple-point liquid hydrogen.

Upgrading of slush hydrogen solid fraction was achieved by retaining solids with a 30 mesh screen while drawing off triple-point liquid.

**11779.** Snyder, N. S., **Heat transport through helium II: Kapitza conductance,** *Cryogenics* **10,** No. 2, 89-95 (April 1970).

Key words: Heat transfer; helium II; Kapitza conductance; liquid-solid interface.

A review is presented of experimental and theoretical work on the Kapitza conductance, which limits the heat that can be transferred from a solid to helium II. A short derivation of the phonon radiation limit indicates that the reason for the approximate $T^3$ temperature dependence of the Kapitza conductance. The small size of this upper limit makes the Kapitza conductance a critical factor in He II heat transfer applications. Considerable qualitative and quantitative correspondence of the data with this limit is found. From the limited evidence available, the role of surface conditions and bulk parameters in determining the conductance are considered empirically. An examination of the theories of Kapitza conductance which have been proposed shows that none provide adequate explanations of the data, and that the underlying physical phenomena remain obscure. Because of the scarcity of available data, and discrepancies between experiments, the prediction of Kapitza conductance for design purposes from theory or experiment is difficult.

**11780.** Steward, W. G., Smith, R. V., Brennan, J. A., **Cooldown transients in cryogenic transfer lines,** (Proc. 1969 Cryogenic Engineering Conf., June 16-18, 1969, Univ. of California, Los Angeles, Calif.), Chapter in *Advances in Cryogenic Engineering* **15,** Paper No. I-2, 354-363 (Plenum Press, Inc., New York, N.Y., 1970).

Key words: Cooldown; cryogenic fluid flow; heat transfer; transfer pipelines; transients; surges.

A series of experiments in the cooldown of instrumented vacuum insulated pipelines has been performed using liquid nitrogen and liquid hydrogen. Downstream pressure surges greater than six times the inlet pressure were recorded. The observed pressure, temperature, and flow transients were reproduced within the experimental uncertainties by a digital computer program. The program can operate in one mode to obtain detailed histories of short period oscillations and in another mode to compute smoothed-out longer term transients such as wall cooldown. The program may be applied directly to pipelines fed by constant pressure sources and, with internal modification, should also be adaptable to more complex cryogenic apparatus.

**11781.** Stief, L. J., Payne, W. A., DeCarlo, V. J., Gorden, R., Jr., Ausloos, P., **Comment on "Xenon sensitized photolysis of carbon dioxide,"** *J. Chem. Phys.* **53,** No. 1, 475-476 (July 1, 1970).

Key words: $CO_2$; energy transfer; quantum yield; rare gas; sensitization; vacuum ultraviolet photolysis.

This Comment to the editor clarifies certain observations made in an earlier study of the xenon sensitized photolysis of $CO_2$. It is shown that contrary to earlier observations, the quantum yields of carbon monoxide in the photolysis of $CO_2$ - Xe (10:1) mixtures is equal to unity over the pressure range 10 to 100 torr.

**11782.** Straty, G. C., Prydz, R., **Melting curve and triple-point properties of fluorine,** *Physics Letters* **31A,** No. 6, 301-302 (March 23, 1970).

Key words: Density; fluorine; melting curve; β-fluorine.

The melting pressures of fluorine have been measured at 0.1 K intervals from the triple point to a maximum pressure of 13.7 $MN/m^2$ ($1\ MN/m^2 = 9.869\ 23$ atm). The density of solid $\beta$-$F_2$ at the triple point is calculated from the Clapeyron equation.

**11783.** Tighe, N. J., Hockey, B. J., **Ion thinning of electron microscope specimens,** (Proc. 10th Symp. Electron, Ion, and Laser Beam Tech., May 21-23, 1969, National Bureau of Standards, Gaithersburg, Md.), *Record of 10th Symposium on Electron, Ion, and Laser Beam Technology,* L. Marton, ed., pp. 375-380 (San Francisco Press Inc., San Francisco, Calif., 1970).

Key words: $Al_2O_3$; argon ion bombardment; ceramics; electron microscopy; hardness; ion thinning; $SiO_2$.

In recent years, it has been possible to prepare ceramic specimens for transmission electron microscopy using ionic bombardment for thinning bulk samples to less than $\sim 0.5\mu m$ thickness. Chemical inertness and electrical insulating properties of many ceramic materials make chemical and electrochemical methods, such as those used for metals, difficult to apply. Even when suitable chemical polishes are found they often are useful only for certain crystallographic orientations and not at all useful for polycrystalline bodies. In this laboratory, the ion-thinning technique has been applied to polycrystalline and single-crystalline ceramics including alumina, magnesia, silica and zirconia.

Prior to ion thinning, disk specimens 2.3 or 3 mm in diameter are cut from thin slices (40 to $150\mu m$) of the selected samples. When a specimen is particularly fragile because of large deformation, fractures, or porosity, a supporting rim is cemented to it. Specimens are thinned simultaneously from both sides and are rotated during thinning to eliminate or reduce directional grooving. They are thinned with argon ion beams using accelerating voltages of 4 to 8 kV and beam currents of 50 to $150\mu A$. Thinning rates vary from 1/2 to $4\mu m/hr$ depending on the specimen material and on the operating conditions.

The ion-thinned specimens have electron transparent regions which usually are more extensive than those in the best chemically thinned single crystal specimens. Studies of the microstructure of hot-pressed alumina, periclase brick, quartz and magnetite rocks and a number of sintered ceramics have been undertaken. The dislocation substructure, impurity precipitates, second phase grains, and voids have been revealed by transmission electron microscopy; and, in some cases, the defects have been related to the deformation sustained by specimens during forming or during mechanical testing. Because specimens can be thinned from only one side, it has been possible to study the damage in single and polycrystalline alumina specimens which is produced by hardness indents and by mechanical polishing with diamond abrasives.

**11784.** Torrance, K. E., Orloff, L., Rockett, J. A., **Numerical study of natural convection in an enclosure with localized heating from below—creeping flow to the onset of laminar instability,** *J. Fluid Mech.* 36, Part I, 33-54 (June 1969).

Key words: Circular cylinder; enclosures; natural convection; numerical.

An analytical study was made of the natural convection induced in an enclosure by a small hot spot centrally located on the floor. The enclosure was a circular cylinder, vertically oriented, with height equal to radius. A Prandtl number of 0.7 (air) was assumed; the Grashof number *(Gr)* was based on cylinder height and hot spot temperature. The equations of fluid flow in axisymmetric cylindrical co-ordinates were simplified with the Boussinesq approximation. The equations were solved numerically with a computationally stable, explicit method. The computation, starting from quiescent conditions, proceeded through the intial transient to the fully developed flow. Solutions were obtained for $Gr$ from $4 \times 10^4$ to $4 \times 10^{10}$. The theoretical flows are in excellent agreement with experimentally observed laminar flows ($Gr \leq 1.2 \times 10^9$) which are discussed in a companion paper, Torrance, Orloff & Rockett (1969). Turbulence was observed experimentally for $Gr \gtrsim 1.2 \times 10^9$. When the theoretical calculations were extended to $Gr = 4 \times 10^{10}$, a periodic vortex shedding developed, suggestive of the onset of laminar instability. The theoretical results reveal $a\sqrt{Gr}$ scaling for the initial flow transients and, at large $Gr$, the velocities and heat transfer rates.

**11785.** Torrance, K. E., Orloff, L., Rockett, J. A., **Experiments on natural convection in enclosures with localized heating from below,** *J. Fluid Mech.* **36,** Part I, 21-31 (1969).

Key words: Enclosures; flow visualization; modeling; natural convection.

An experimental study was made of the steady-state natural convection induced in enclosures by a small hot spot centrally located on the floor. Enclosures of rectangular and circular floor plan were employed, with height equal to one-half the major dimension of the floor plan. The movement of air within the chambers was made visible by adding metaldehyde dust particles and illuminating them with an intense light beam. The Grashof number *(Gr)* based on hot-spot temperature and enclosure height ranged from $8 \times 10^5$ to $1 \times 10^{10}$. Laminar flows were observed for $Gr \leq 1.2 \times 10^9$. The experimental flows in the circular chamber are compared in a companion paper with theoretically calculated flows (Torrance & Rockett 1969). In the region of laminar flows the agreement was excellent. The present paper notes certain similarities in the flows in rectangular and circular geometries. The disturbing effect of a slight heating of one wall of the rectangular enclosure was also investigated. Measurements were made of heat transfer from the hot spot to the air in the chamber.

**11786.** Verdier, P. H., **Relaxation behavior of the freely jointed chain,** *J. Chem. Phys.* **52,** No. 11, 5512-5517 (June 1, 1970).

Key words: Chain dynamics; polymers; random walk; relaxation; stochastic process.

A method is presented for treating the relaxation behavior of the freely jointed chain model of a random coil polymer. Exact results are exhibited for the relaxation of quantities linear in chain coordinates. For the treatment of quantities quadratic in chain coordinates, a numerical approach is employed and exemplified by obtaining the autocorrelation in the square of end-to-end length for chains of up to 16 beads. In both cases, the rapid approach of the behavior of the freely jointed chain of $N$ beads to that of the Rouse model of $N$ statistical segments is demonstrated.

**11787.** Weber, L. A., **The P-V-T surface of oxygen in the critical region; densities of saturated liquid and vapor,** (Proc. 1969 Cryogenic Engineering Conf., June 16-18, 1969, Univ. of California, Los Angeles, Calif.), Chapter in *Advances in Cryogenic Engineering* **15,** Paper No. B-4, 50-57 (Plenum Press, Inc., New York, N.Y., 1970).

Key words: Critical density; critical point; critical temperature; oxygen; properties of fluids; P-V-T; saturation densities.

A description is given of an apparatus used to determine the detailed nature of the *P-V-T* surface of fluids in the critical region by means of dielectric measurements. Preliminary data are presented for the saturation densities of oxygen within one degree of the critical temperature. Analysis of the data yields the following values of the critical parameters: $T_c = 154.575 \pm .010$ K, $\rho_c = 0.4361 \pm .0005$ gm/cm³.

**11788.** Weiss, A. W., Krauss, M., **Bound-state calculation of scattering resonance energies,** *J. Chem. Phys.* **52,** No. 9, 4363-4368 (May 1, 1970).

Key words: Ar; correlation energy; Feshbach resonance state; Hartree-Fock; He Ne; HF $H_2O$; $N_2$, resonance energy; Rydberg; valence.

Resonance energies in electron scattering are estimated by calculating bound trial functions which represent electron attachment to the lowest Rydberg state. The trial functions are kept orthonormal to a single-configuration description of the target state and so represent an approximation to the Feshbach procedure. Correlated trial functions are used for $He^-(^2S)$, $Ne^-(^2P)$, and $Ar^-(^2P)$. The resonant-energy predictions are in good agreement with observation. In addition, the correlation energy for the $ns^2$ pairs range from 0.55 to 0.75 eV. These correlation energies are used to correct Hartree-Fock estimates of resonance energies computed for the HF, $H_2O$, and $N_2$ molecules. Energy curves obtained for $HF^-(^2\Pi)$ indicate a dissociative attachment process is possible that leads to production of the $H^-$ ion. Only single points are calculated for $H_2O$ but the $^2B_1$ resonance state is assigned to a dissociative attachment at 6.5-eV incident electron energy that yields the $H^-$ ion. In addition to the attachment to Rydberg excited states, two $N_2$ valence-type Feshbach states are calculated. The results for $\sigma_g \pi_g^2$, $^4\Sigma_g^-$, and $^2\Delta_g$, when used with correlation energy estimates lead to the conclusion that valence-type Feshbach states are not bound relative to their concomitant neutral excited valence state. Sharp resonances would not then be expected below such neutral states.

**11789.** Wilson, W. K., **Development of specifications for archival record materials,** *Am. Archivist* **33,** No. 2, 219-223 (April 1970).

Key words: Acidity; aging; alum sorption; laboratory aging; manifold; paper; records; stability; stability of cellulose; stability of paper; thermal analysis.

Work in progress on the development of information on the stability of paper and modified cellulose is described in relation to the objectives of the program. Plans for calendar year 1970 are outlined.

**11790.** Winogradoff, N. N., Neill, A. H., Jr., **Temperature dependence of the power output of the spontaneous emission from GaAs laser diodes,** *Intern. J. Electron.* **28,** No. 5, 401-406 (1970).

Key words: Band filling; band tailing; GaAs; gallium arsenide; internal quantum efficiency; lasers; radiative recombination; temperature dependence; valence band.

Modulation of photoluminescence in *p*-type GaAs by a field effect indicated that the radiative recombination occurred through recombination centers. This suggested that the recombination rate in the depletion region of a luminescent *p-n* junction would be governed by Shockley-Read statistics. The resulting model showed that, with suitable diode parameters, an *increase* in temperature would produce an *increase* in the radiative efficiency of the diode. Such an effect was observed experimentally with vapor-grown GaAs *p-n* junctions, the *p*-type sides of which were heavily compensated.

**11791.** Winogradoff, N. N., Neill, A. H., Jr., Petrescu-Prahova, J. B., **Band tailing and the spontaneous spectra of compensated epitaxial GaAs laser junctions,** *IEEE J. Quantum Electron.* **Q.E. 6,** No. 6, 305-310 (June 1970).

Key words: Band tailing; GaAs lasers; non-radiative recombination centers; radiative recombination; temperature dependence; valence band.

The spectra of the spontaneous emission from GaAs laser diodes fabricated by vapor-phase epitaxy and containing a high degree of compensation in the *p*-type side of the junction are, in many respects, similar to those previously reported for the cathodoluminescence of homogeneous *p*-type material. The temperature dependence of the spectra of these diodes supports a model where the emission is attributed to radiative transitions between a narrow band of states near the conduction-band edge and an exponential distribution of states extending the valence band into the forbidden gap.

An increase in temperature then results in an *increase* or a decrease in the radiative power output depending on the position of the quasi-Fermi level for electrons relative to the above narrow band of states and a distribution of nonradiative levels below it.

**11792.** Wolfe, W. C., **Performance tests for floor coverings,** *Mater. Res. Stand.* **10,** No. 7, 15-18 (July 1970).

Key words: Carpet; floor coverings; foot comfort; performance requirements; resilient types; test methods; textile types; vehicle movement.

Well defined performance tests are an essential element of performance specifications, standards, and codes. The particular needs of the floor covering industry for such tests are pointed up by a discussion of the performance concept in terms of this industry. Performance requirements are listed by categories, to assist in identifying those requirements most important for inclusion in future performance specifications, and to provide guidance for research towards test methods of maximum possible usefulness and significance.

The National Bureau of Standards has recently developed two types of performance tests for floor coverings, considered from the standpoint of comfort, convenience, and efficiency. They are concerned with resistance to movement of wheeled vehicles and with resilience as related to foot comfort in hospitals. These are important factors to consider in deciding whether or not to use carpet.

Other performance requirements under study relate to health and safety, especially fire safety, and to economic criteria such as wear or durability.

Future work on performance tests needs extensive government-industry cooperation, encompassing interlaboratory comparisons and field-laboratory correlations.

**11793.** Wood, L. A., **Creep of "pure-gum" vulcanizates of natural rubber,** (Proc. Intern. Natural Rubber Conf., Kuala Lumpur, Malaya, Sept. 1968), *J. Rubber Res. Inst. Malaya* **22,** No. 3, 309-316 (1969).

Key words: Compliance; creep; dicumyl peroxide vulcanizates; indentation of rubber; modulus; natural; natural rubber; rubber; strain-time relations; vulcanizates.

The creep of vulcanizates of natural rubber cured with varying amounts of dicumyl peroxide was compared with that of vulcanizates cured by typical conventional sulphur-accelerator systems. The measurements involved indentation of a flat rubber disc as a function of time $t$ and temperature $T$. The product of shear compliance $J$ and $T$ as a function of log $t$ was represented by a family of curves with $T$ as the parameter. For the vulcanizates curved with the sulphur-accelerator system, previous work has shown that the individual curves could be shifted along the abscissa to yield a single continuous curve with a slope which increased from a negligible value to a maximum and then decreased, continuing through a region of minimum slope which extended over about 7 decades of time before ending in a region of increasing slope. The value of the creep was 1.5-2.0% per decade in the region of minimum slope.

When the same procedures were applied to the vulcanizates cured with dicumyl peroxide, the individual curves of $JT$ against log $t$ at each temperature did not yield a single continuous curve when shifted. In a limited region just above the glass transition temperature, the creep was appreciable, but neither a constant-activation-energy shift nor a Williams-Landle-Ferry shift was satisfactory. Above this region it was clearly impossible to obtain a single curve, since the compliance-temperature product at a given time increased with increasing temperature while the corresponding creep of the dicumyl peroxide vulcanizates was generally too small ($<0.5\%$ per decade) to be measured between 5 and 600 seconds, except when the compound contained less than 2.5 parts of effective dicumyl peroxide. Outside of these regions the shear modulus was found to increase linearly with temperature. The investigation included temperatures as high as 100 °C and effective dicumyl peroxide concentrations as high as 25 parts per hundred of rubber. The present results for the modulus and creep of dicumyl peroxide systems show good agreement with the published data of Chasset and Thirion (obtained by stress relaxation at 30 °C) and of Plazek (obtained by a torsion pendulum) over the ranges they investigated.

**11794.** Wood, L. A., Shouse, P. J., Passaglia, E., **How just appreciable fading of AATCC L-4 wool standard is related to exposure time,** *Textile Chem. Colorist* **2,** No. 11, 182-190 (June 3, 1970).

Key words: Appreciable fading; fading; light-sensitive paper; paper, light-sensitive; Standard Fading Hour; wool standards.

The color difference resulting from "just appreciable fading" of AATCC's L-4 Wool Standard, as judged by a panel of experts, is found to be about 1.5 units, as calculated by inserting the results of spectrophotometric measurements in the Adams chromatic-value relation, the Scofield-Hunter relation or the cube-root relation of Glasser, et al.

This value corresponds to about 3.0 NBS units of color difference. The change is equivalent to Step 4 of the International Geometric Gray Scale, which is defined by the Adams chromatic value relation. Fading of the wool standard to this extent was produced in slightly less than 14 hours in the NBS Master Carbon-Arc Lamp—an exposure equivalent to about 11 NBS Standard Fading Hours (SFH).

**11795.** Moore-Sitterly, C. E., **Rare-earth spectra—the 1966 picture,** *Proc. First International Conf. Spectroscopy, Bombay, India, January 9-18, 1967,* **1,** 1-13 (1967).

Key words: Astrophysical data on rare earths; atomic spectra; configurations; ground states; rare earth spectra.

The large and familiar program on the compilation of "Atomic Energy Levels" as derived from the analyses of optical spectra, continues. The last and fourth volume of the series will contain similar data on the atomic spectra of the two groups of rare earth elements: The lanthanon group, Ce thru Lu ($Z=58$ thru 71) and the action group, Th thru Lw ($Z=90$ thru 103).

The first spectra have low ionization potentials. Most of the earlier line lists do not separate the first and second spectra, and are wholly inadequate for analysis work. Suitable sources for separating spectra of different degrees of ionization have been developed, and the individual spectra are now being observed over a long spectral range. A number of homogeneous line lists exist, some of which contain more than 15,000 lines for a given spectrum.

Rare earth spectra are characterized by configurations involving f-electrons, and a number have overlapping configurations which explains the complexity of the spectra. So far, little is known beyond fourth spectra. The progress in this relatively new field of research is reported in some detail, along with brief mention of the present astrophysical needs for data on atomic spectra of the rare earths.

**11796.** Moore-Sitterly, C. E., **Fundamental spectroscopic data, IAU Commission 14, August 1967 Meeting,** *Trans. Intern. Astron. Union* **13A,** 229-266 (1967).

Key words: Cross sections; Draft Report IAU Commission 14; International Astronomical Union; spectroscopic data; transition probabilities; wavelength standards.

The present report summarizes important activities in the field since the Twelfth General Assembly of the Union held in Hamburg in 1964. The main topics deal with standards of wavelength, transition probabilities, line broadening, atomic collision cross sections, molecular spectra of astrophysical interest, general progress in studies of laboratory spectra and current work on the solar spectrum.

**11797.** Ku, H. H., **Statistical concepts in metrology,** Chapter 2 in *Handbook of Industrial Metrology,* pp. 20-54 (Prentice-Hall, Inc., Englewood Cliffs, N.J., 1967).

Key words: Control chart; data analysis; measurement process; metrology; precision; propagation of error; standard deviation; statistical concepts.

This chapter deals with statistical concepts of a measurement process and statistical analysis of measurement data, and is part of the text book *Industrial Metrology* sponsored by the American Society of Tool and Manufacturing Engineers.

Beginning with the differentiation between arithmetic and measurement numbers, the properties of the latter are developed and described, leading to a discussion of precision and accuracy.

A basic kit of tools for the comparison and manipulation of means and variances are given, including a collection of propagation of error formulas. The use of control chart techniques for monitoring stability is emphasized. Examples are given using actual calibration data of NBS.

Selected references are given for topics introduced but not treated in detail.

**11798.** Brauer, G. M., **Pyrolysis-gas chromatographic techniques for polymer identification,** Chapter 2 in *Thermal Characteristics Techniques in Techniques and Methods of Polymer Evaluations,* P. Slade, ed., **II,** 41-105 (Marcel Dekker Publ., New York, N.Y., 1970).

Key words: Chromatographic analysis of degradation products; polymer characterization; polymer identification; pyrolysis-gas chromatography of polymers; pyrolytic techniques.

Pyrolytic techniques used in conjunction with gas chromatography are very useful for elucidating the structure of macromolecules. These methods are a powerful tool in the qualitative characterization of the gross structure, the study of the thermal stability of polymers and the identification of their pyrolysis products, but have also found an increasing number of applications for the quantitative analysis of copolymeric systems and in studies of the kinetics of polymer degradation. The shape of the pyrograms is dependent on the structural characteristics such as the degree of branching or crosslinking, stereoregularity, crystallinity, and monomer sequence length distribution in block and graft copolymers. Thus the pyrolysis-gas chromatographic technique opens up new avenues in studying the ultimate arrangement of monomeric units within the polymer chain.

**11799.** Berger, M. J., Seltzer, S. M., **Bremsstrahlung and photoneutrons from thick tungsten and tantalum targets,** *Phys. Rev. C* **2,** No. 2, 621-631 (Aug. 1970).

Key words: Bremsstrahlung; bremsstrahlung efficiency; Monte Carlo; photon neutron; radiation transport; thick targets.

Monte Carlo calculations have been made of electron-photon cascades in thick tungsten targets bombarded by electrons with energies up to 60 MeV. The following information has been obtained: (1) the bremsstrahlung efficiency, (2) the angular distribution of the emitted bremsstrahlung intensity, (3) the spectra of the bremsstrahlung emitted in various directions, (4) the transmission of primary and secondary electrons through the target, (5) energy deposition as function of the depth in the target, (6) the differential photon track length distribution inside the target, and (7) the yield of photoneutrons. The paper also includes various comparisons with experimental data.

**11800.** Block, S., Weir, C. E., Piermarini, G. J., **Polymorphism in benzene, naphthalene, and anthracene at high pressure,** *Science* **169,** 586-587 (Aug. 7, 1970).

Key words: Anthracene; benzene; high-pressure; naphthalene; polymorphism.

Optical observations, in which a microscope was used with the diamond-anvil pressure cell, were carried out on benzene, naphthalene, and anthracene up to temperatures of about 600 °C and pressures of approximately 40 kilobars. New high-pressure phases of benzene (benzene III) and anthracene (anthracene II) were observed, and the existence of the high-pressure polymorph, naphthalene II, was verified. All three materials decompose initially to a reddish-orange liquid, and ultimately to amorphous carbon. The decomposition temperatures decrease with increasing molecular size.

**11801.** Borie, E., **Radiative corrections to back scattering,** *Phys. Rev. C* **2,** No. 2, 770-771 (Aug. 1970).

Key words: Anomalous moment; back scattering; electron; radiative correction.

It is shown that the anomalous magnetic moment of the electron contributes to the radiative correction to scattering by a charge, even at high energies, when the scattering angle is 180°. This effect increases the radiative correction slightly as compared with the usual Schwinger correction.

**11802.** Bowen, R. L., **Crystalline dimethacrylate monomers,** *J. Dental Res.* **49,** No. 4, 810-815 (July-Aug. 1970).

Key words: Biomaterials; dimethacrylates; phthalate monomers; purification methods; resins for composites; ternary eutectic; thermosetting monomers.

Certain dimethacrylate monomers can be prepared and purified by recrystallization. On mixing, the crystals liquefy by forming a ternary eutectic. The colorless oily liquid is suitable for use in composite formulations.

**11803.** Candela, G. A., **Spin relaxation process of chromium ion in potassium alum,** *J. Chem. Phys.* **52,** No. 7, 3754-3757 (Apr. 1, 1970).

Key words: Chromium alum; spin-lattice relaxation.

The electron spin relaxation process of potassium chrome alum and potassium chrome aluminum alum was investigated at 14.5 GHz by measuring the change in the static dc magnetization as a function of the cw microwave power absorbed at electron resonance. At liquid-helium temperatures, the direct spin-lattice relaxation process is the dominant rate-determining process for magnetically dilute potassium chrome aluminum alum, but for the magnetically concentrated crystals, the spin-lattice process can easily be obscured by the lattice-bath relaxation process. The spin-lattice relaxation measurements at 14.5 GHz and those of other workers at 9 GHz are in agreement with the calculations made by Van Vleck in 1940.

**11804.** Ensign, T. C., Chang, T. T., Kahn, A. H., **Hyperfine and nuclear quadrupole interactions in copper-doped $\mathbf{TiO_2}$,** *Phys. Rev.* **188,** No. 2, 703-709 (Dec. 10, 1969).

Key words: Copper; EPR; *g*-factors; hyperfine interaction; quadrupole coupling; rutile; titanium dioxide.

Single crystals of $TiO_2:Cu^{2+}$ have been investigated at 20 K using the technique of electron paramagnetic resonance. The major features of the EPR spectra can be attributed to divalent copper ($3d^9$) in substitutional ($Ti^{4+}$) sites. Information has been gained about both isotopes of copper and about the interactions which concern this ion. For the substitutional site, the spin-Hamiltonian parameters in the $S=1/2, I=3/2$ manifold are: $g_x=2.109$, $g_y=2.094$, $g_z=2.346$, $A_x^{63}=+18.7\times 10^{-4}$ cm$^{-1}$, $A_y^{63}=+27.2\times 10^{-4}$ cm$^{-1}$, $A_z^{63}=-87.5\times 10^{-4}$ cm$^{-1}$, $A_x^{65}=+18.8\times 10^{-4}$ cm$^{-1}$, $A_y^{65}=+28.7\times 10^{-4}$ cm$^{-1}$, $A_z^{65}=-93.7\times 10^{-4}$ cm$^{-1}$, $P_x=-2.56\times 10^{-4}$, $P_y=-2.37\times 10^{-4}$, and $P_z=+4.93\times 10^{-4}$ cm$^{-1}$. The magnitudes and relative signs of these parameters have been determined experimentally, while the absolute signs have been predicted theoretically from a model which gives a consistent picture of the ordering of the $d^9$ electronic states. In addition, the theoretical treatment gives a satisfactory estimate of $P$. Departure from tetragonality was taken into account. The covalency parameter $\alpha^2$ which measures the fraction of the hole wave function on the $Cu^{2+}$ ion is found to be 0.71, and the factor $\kappa$ giving rise to isotropic hyperfine structure is found to be 0.31.

**11805.** Ensign, T. C., Stokowski, S. E., **Shared holes trapped by charge defects in $SrTiO_3$,** *Phys. Rev. B* **1,** No. 6, 2799-2810 (Mar. 15, 1970).

Key words: Color centers; EPR; hole centers; optical absorption; shared holes; $SrTiO_3$.

Using the techniques of EPR and optical irradiation in conjunction with optical-absorption measurements, we have gained useful information about the nature of some hole centers in $SrTiO_3$. Primarily, we have investigated, at temperatures near 77 K, single crystals doped with aluminum. Two principal centers have been explored: (1) the Al-$O^-$ center—a hole shared among the oxygens which surround $Al^{3+}$, and (2) the $X$-$O^-$ center—a hole shared in a similar fashion, but more deeply trapped by a charge defect of unknown origin. The Al-$O^-$ center arises after band-gap irradiation and is characterized at 77 K by the following $g$ values and hyperfine constants: $g_{\parallel}=2.0137$, $g_{\perp}=2.0124$, $A_{\parallel}=8.3\times10^{-4}$ cm$^{-1}$, and $A_{\perp}=7.6\times10^{-4}$ cm$^{-1}$. The $X$-$O^-$ center is present before optical irradiation. No hyperfine structure is observed, but the isotropic $g$ value is 2.0130 at all temperatures from 4.2 to 300 K. An 800-nm absorption band arising after band-gap excitation has been correlated with the Al-$O^-$ center. 430- and 600-nm absorption bands have been correlated with the absence of $Fe^{3+}$ in the EPR spectrum, and a 500-nm band has also been observed. In addition, the role of iron in the photochromic processes of $SrTiO_3$ is presented. Finally, theoretical work utilizing the molecular orbital $\sigma$ and $\pi$ states in $O_h$ symmetry has provided a firm basis for the sharing model. The experimental $g$ values and hyperfine constants are discussed in light of this model and are found to be in good agreement.

**11806.** Evans, W., Garvin, D., **The evaluator versus the chemical literature,** *J. Chem. Doc.* **10,** No. 3, 147-150 (1970).

Key words: Abstracts; chemistry; content of articles; data; description of experiments; evaluation of data; numerical data; publication standards; titles.

The presentation of quantitative experimental results is discussed from the viewpoint of the evaluator of data. The principal needs are a detailed description of the experimentation and numerical results suitable for reanalysis. Suggestions are made for the improvement of the content of chemical papers and the retrieval of the results. Content may be improved by preparing guides that state the minimum acceptable detail for various types of measurements. Retrieval may be enhanced by judicious editing of titles and abstracts.

**11807.** Feldman, A., Brower, W. S., Jr., Horowitz, D., **Optical activity and Faraday rotation in bismuth oxide compounds,** *Appl. Phys. Letters* **16,** No. 5, 201-202 (Mar. 1, 1970).

Key words: $Bi_{34}Ga_2O_{54}$; $Bi_{12}GeO_{20}$; $Bi_{12}SiO_{20}$; $Bi_{12}TiO_{20}$; $Bi_{14}ZnO_{22}$; Faraday effect; modulator materials; optical activity; optical rotatory power; Verdet coefficient.

The optical rotatory power and Faraday rotation were measured in crystals of $17Bi_2O_3$: $Ga_2O_3$, $7Bi_2O_3$: ZnO, $Bi_{12}TiO_{20}$, $Bi_{12}GeO_{20}$, and $Bi_{12}SiO_{20}$ in the wavelength range 400 to 700 nm at room temperature. Our crystals were enantiomorphs of those reported previously. The large Verdet coefficients indicate that these crystals are potentially useful as magneto-optic modulator materials.

**11808.** Feldman, A., Kahn, A. H., **Landau diamagnetism from the coherent states of an electron in a uniform magnetic field,** *Phys. Rev. B* **1,** No. 12, 4584-4589 (June 15, 1970).

Key words: Coherent states; diamagnetism; electron in a magnetic field.

A complete set of coherent-state wave packets has been constructed for an electron in a uniform magnetic field. These states are nonspreading packets of minimum uncertainty that follow the classical motion. Use was made of the ladder operators that generate all the eigenstates of the Hamiltonian from any one energy eigenstate. The coherent states are the eigenstates of the two ladder operators that annihilate the zero-angular-momentum ground state. We have calculated the partition function, exploiting advantages of the coherent-state basis. The Landau diamagnetism and the de Haas-van Alphen oscillations are contained in the coherent-state framework.

**11809.** Frederikse, H. P. R., **Comments on electronic transport in transition metal oxides,** *J. Res. Develop.* **14,** No. 3, 295-300 (May 1970).

Key words: Electronic transport; $LaCoO_3$; magnetic ordering; transition metal oxides.

Several aspects of electronic transport in nonmagnetic and magnetic transition metal oxides are reviewed. These include high- and low-temperature measurements of conductivity, the Hall effect and the Seebeck effect, and their analysis in terms of the electronic energy structure. Particular emphasis is put on the temperature dependence of the Hall mobility, which gives essential information concerning the correct description of the energy states and the scattering of the charge carriers. The second half of the paper discusses the relation between the transport properties and the magnetic ordering. The properties of $LaCoO_3$ together with an interpretation suggested by Goodenough are presented to illustrate this point.

**11810.** Goldstein, J. I., Henderson, E. P., Yakowitz, H., **Investigation of lunar metal particles,** (Proc. Apollo 11 Lunar Science Conf., January 1970, Houston, Texas), *Geochim. Cosmochim. Acta* **1,** 499-512 (1970).

Key words: Electron probe microanalysis; lunar samples; lunar simulation; lunar thermal history; meteorites; scanning electron microscopy.

Several metallic particles from lunar fine samples 10084 and 10085-17M and from breccia sample 10046-18A were investigated by means of optical microscopy, scanning electron microscopy, and electron probe microanalysis. These particles consisted of two large globules, metal spread on glassy spheres, fragments and metal in the foamy vesicular-like fragments. The largest globule had a structure consisting of 40 $\mu$m Fe-Ni dendrites in a matrix of troilite. The dendrites showed typical Ni segregation, the composition at the outside being about 16 wt.% Ni with 13 wt.% Ni at the center. The troilite contained 0.1-1.5 wt.% Ni and appears to be in dis-equilibrium. A high Ni rim region was found at the troilite-dendrite interface. This region is taenite containing 29-46 wt.% Ni and about 0.3 wt.% S and was created by the rejection of Ni from the troilite. We were able to synthesize this globule; the same structure was obtained. From this simulation, the cooling rate was determined as 2.5 °C/sec. This globule probably was created by the impact of a chondrite on the moon.

A globule separated from the breccia rock apparently solidified quickly and then cooled slowly, the rock acting as a kind of crucible. This globule's metal regions contain 2 wt.% Ni, 1 wt.% P, 0.3 wt.% Co, balance Fe. There are also eutectic regions of phosphide with fine intergrowths of kamacite, troilite and carbides. This particle shows a striking similarity to spheroids from the Canyon Diablo iron. The evidence indicates that this globule was probably created by the impact of an iron meteorite on the moon.

The analysis of the metal particles makes it clear that both meteoritic and lunar Fe-FeS intergrowths are present in the lunar fines. The lunar metal is similar to the meteoritic material in that it is surrounded by sulfide; both metal constituents are of comparable structure and Co content. The two types of material can be differentiated by the significant Ni and P content of the transformed original meteoritic material.

**11811.** Holt, H. K., **Theory of gas lasers and its application to experiment,** *Phys. Rev. A* **2,** No. 1, 233-249 (July 1970).

Key words: Collisions; gas laser; line widths; power output; theory; tuning curves.

The semiclassical theory of gas lasers has been reformulated by adding rate terms to the density-matrix component differential equations. The solution to these equations, in the form of a Fourier series, is applicable at high laser intensities. A calculation of the effect of phase-changing collisions is also included so that the results can be compared to experimental data taken with a He-Ne laser operating at a wavelength of 1.15 $\mu$m.

**11812.** Hosler, W. R., **Low resistance contacts on semiconducting oxides,** *Solid-State Electron.* **13,** 517-519 (1970).

Key words: Contact resistance; oxide semiconductors; soldering; $TiH_2$.

A method using $TiH_2$ as a flux for a contacting metal in producing low resistance small area contacts in $KTaO_3$, $SrTiO_3$, $TiO_2$ and $BaTiO_3$ has been devised. The resulting contact resistances have been found to be near zero for $KTaO_3$ and to be greatly decreased for the other materials in comparison with conventional contacts.

**11813.** Howett, G. L., **Achromatic-point prediction,** *J. Opt. Soc. Am.* **60,** No. 7, 951-958 (July 1970).

Key words: Achromatic; appearance; brightness; chromatic adaptation; chromaticity; color; least squares; luminance; model; neutral; perception; vision.

This paper constitutes a mathematical elaboration, in a form permitting direct predictions of data, of the empirical discoveries of Helson and Michels concerning the "effect of chromatic adaptation on achromaticity." An equation is developed permitting the chromaticity of a test spot that appears achromatic against an extended chromatic background to be predicted from the background chromaticity and the luminance ratio of spot to background. The technique for numerical solution of the equation is explained, and a family of curves allowing approximate solution by interpolation is presented. If the luminance of the achromatic spot is no greater than that of the background, the achromatic chromaticity always lies more than 3/4 of the way along the line directed from the absolute (black background) neutral point to the background point, regardless of the color of the background. As part of a discussion of additional numerical methods useful in applying the model to data, general least-squares formulas are presented for the coordinates of the point best representing the common intersection of any set of given lines; and for the line, passing through a specified point, that best fits a set of given points by the criterion of perpendicular deviations.

**1814.** Hubbell, J. H., **X-ray absorption 75 years later,** *Phys. Bull.* **21,** 353-357 (1970).

Key words: Absorption corrections; attenuation coefficient; conference; crystallography; electron microprobe; fluorescence analysis; gamma rays; photons; Röntgen; x rays.

A Conference on X-Ray Absorption, organized jointly by the X-Ray Analysis Group, the Spectroscopy Group, and the Electron Microscopy and Analysis Group of the IPPS (Institute of Physics and the Physical Society) was held Nov. 14, 1969 in London. This article, besides reporting this conference, reviews some early developments in x-ray attenuation coefficient measurements starting with Röntgen (1895) and presents a graph of present coverage and uncertainties of measurements for elements $Z = 1$ to 100 and photon energies 10 eV to 100 GeV. The eleven presentations at the conference included, in addition to a paper on the present status of x-ray absorption data, papers on: (1) theoretical interpretations of these data including atomic photoeffect, phonon scattering and absorber grain-size effects, (2) measurement techniques including use of synchrotron light and Vodar discharge tubes as soft x-ray sources, and use and performance of various soft x-ray detectors, and (3) absorption data requirements in analysis applications including crystallography, fluorescence spectrometry, electron microprobe analysis, and x-ray reflection topography. Some possible directions of future experimental and theoretical work are indicated.

**11815.** Hummer, D. G., Mihalas, D., **Model atmospheres for the central stars of planetary nebulae,** *Monthly Notices Roy. Astron. Soc.* **147,** No. 4, 339-354 (1970).

Key words: Planetary nebulae; stellar atmospheres; transfer equation.

Approximately 70 model atmospheres for the central stars of planetary nebulae have been computed under the assumptions of hydrostatic, radiative and local thermodynamic equilibrium and of plane-parallel stratification. These models have effective temperatures and surface gravities in the range 30,000 K $\leq T_{eff} \leq$ 200,000 K and $3.4 \leq \log g \leq 7.5$. The atmospheres have been taken to consist of hydrogen, helium, oxygen, nitrogen, carbon and neon, and the opacity included contributions from both ground and excited states of each ion. The transfer equation is solved using Feautrier's method and the temperature correction is calculated by means of the Krook-Avrett procedure. Particular attention is given to the effects of gravity and chemical composition on the surface fluxes. The photon fluxes in the H I, He I and He II continua and the stellar flux at $H_\beta$ have been tabulated for use in the determination of Zanstra temperatures.

**11816.** Hust, J. G., **Thermal anchoring of wires in cryogenic apparatus,** *Rev. Sci. Instr.* **41,** No. 5, 622-624 (May 1970).

Key words: Cryogenics; equipment design; heat transmission; thermal contact.

Thermal anchoring of wires to heat sinks in cryogenic equipment is discussed. An analysis is presented to relate the length of tempered wire required and measurable parameters of the system. The solution of the problem is included along with tabular values for typical situations.

**11817.** Johnson, W. T. K., Chertok, B. T., Dick, C. E., **Study of nuclear states of several odd-*A* nuclei $68 \leq Z \leq 79$ through electromagnetic excitation from 2.3 to 3.6 MeV,** *Phys. Rev. Letters* **25,** No. 9, 599-602 (Aug. 31, 1970).

Key words: Electron and photon excitation; excited states; half-lives; isomeric levels; $^{197}$Au; $^{167}$Er; $^{179}$Hf; $^{191}$Ir.

Thirty-four excited states have been studied between 2.3 and 3.5 MeV in $^{167}$Er, $^{179}$Hf, $^{191}$Ir, and $^{197}$Au by observing the decay of the isomeric levels in these nuclei following electron and photon activation. Twenty-eight of these states are observed for the first time. Of the 34 observed transitions, $M1+E2$ multipolarity assignment is made to 20, two are identified as $E0$ transitions, and one is assigned $E1$ multipolarity. Accurate values for the isomeric half-lives are also presented.

**11818.** Kasen, M. B., **The effect of grain boundaries on the recovery of electrical properties during annealing,** *Scripta Met.* **4,** 575-580 (1970).

Key words: Aluminum; electrical resistivity; grain boundaries; solute segregation; super-purity metals.

The change in residual resistivity at 4 K has been studied as a function of annealing temperature during step-isochronal annealing of recrystallized, cold-worked, aluminum of two purities. The continued recovery of electrical properties and the eventual development of a resistivity minimum are shown to reflect the decreasing grain boundary area per unit volume as annealing progresses, combined with changes in the amount of solute segregated to the grain boundaries. The resistivity minimum is found to coincide with removal from solid solution of an amount of solute approximating that required to form 1/3 of a monolayer of segregate at the existing boundaries.

**11819.** Klein, R., **A field emission study of carbon monoxide on hcp metals rhenium and ruthenium,** *Surface Sci.* **20,** No. 1, 1-17 (Mar. 1970).

Key words: Carbon monoxide; desorption; field emission; monoxide; rhenium; ruthenium; surface migration.

The surface migration, work function increments, and desorption of carbon monoxide on two hcp metals, rhenium and ruthenium, were observed with field emission techniques. Carbon monoxide is weakly bound to ruthenium and more strongly bound to rhenium. For a complete monolayer, the work function increment is 1.3 eV for ruthenium and 0.8 eV for rhenium. Surface migration commences at a readily observable rate at about 125 K on ruthenium. The migration is characterized by a sharp boundary that becomes boundary free in the later stages. Because desorption precedes surface migration for CO on rhenium, the onset of migration is ill defined. Two well-defined binding states $\alpha$ and $\beta$, are seen for CO on rhenium.

**11820.** Ledbetter, H. M., Reed, R. P., **On the martensite crystallography of Fe-Ni alloys,** *Mater. Sci. Eng.* **5,** No. 6, 341-349 (June 1970).

Key words: Crystallographic theory; iron-nickel alloy; martensite.

For the first time lattice parameter data and habit plane measurements are available for an alloy system whose crystallographic features change continuously with composition. Other workers have produced this information for the plate-like martensitic transformation in Fe-base alloys containing between 29 and 35 wt.% Ni. This paper presents a careful examination of these data from the viewpoint of the Wechsler-Lieberman-Read, and equivalent, theories of martensite crystallography. It is found that these theories cannot explain the variation of the habit plane with composition. assuming a $\{110\}_F$ $\langle\bar{1}10\rangle_F$ deformation mode, without involving a varying $\delta$ (1.000 to 1.013), $\delta$ being an isotropic dilatation parameter. In addition to the habit plane, several quantities have been calculated as a function of composition: the volume change, the magnitude of the lattice invariant deformation, the magnitude and direction of the shape change, and the orientation relationship. The effects of errors in lattice parameters and of thermal expansion are considered.

**11821.** Mann, D. B., Roder, H. M., **Liquefied natural gas as a cryogenic fluid—instrumentation and properties,** *Proc. Transmission Conf. American Gas Association Operation Section, New Orleans, La., May 26-27, 1969,* pp. T-98-T-106 (American Gas Association, Arlington, Va., 1970).

Key words: Flowmeters; instrumentation; liquefied natural gas (LNG); methane; properties data.

The rapidly developing interest in liquefied natural gas as a fuel is based on existing and potential uses in a wide variety of fields. The advantages of liquefied natural gas have been explored by numerous interested parties and applied to transportation as a possible substitute for gasoline in internal combustion engines, public utility and industrial uses as a concentrated form of natural gas, and, more basically, as an attractive energy source which may be conveniently delivered throughout the world to those nations having insufficient energy producing resources.

Liquefied natural gas and methane are considered cryogenic fluids since their normal boiling temperatures lie within the cryogenic temperature range. A description of the current program of the Cryogenics Division in respect to methane and liquefied natural gas is presented. The program involves properties correlation, fluid measurement and instrumentation, and a study to determine the characteristics of high-density phases of liquefied natural gas and methane in the subcooled liquid or liquid-solid mixture states.

The presentation of material relating liquefied natural gas to the classical cryogenic fluids will be made in two parts. The first part by Douglas B. Mann will be a discussion of the measurement techniques currently being employed with varying degrees of success to cryogenic fluids. The purpose will be to illustrate what equipment and techniques might be utilized for LNG. Part II of this presentation by Hans M. Roder will deal with the situation that exists currently concerning the properties of liquefied natural gas.

**11822.** Meijer, P. H. E., O'Keeffe, D. J., **Low-temperature behavior of a pure dipole-dipole system,** *Phys. Rev. B* **1,** No. 9, 3786-3800 (May 1, 1970).

Key words: Cerous magnesium nitrate; dipole system; low temperature; paramagnetic salt; specific heat; susceptibility; thermometer scale.

The Van Vleck moment expansion is applied to a pure dipole system. On the basis of the long-range nature of the forces, sequences of diagrams are selected that give the dominant contributions in the lattice sums. A selection of diagrams contributing to the entropy and susceptibility is displayed. There are three different summations to be performed for each type of diagram: the trace over the spin variables, the lattice summation, and the summation over the Cartesian coordinates. The second was performed on a computer, and the last is obtained by means of the Kramers-Wannier diagonalization. In order to obtain the contributions of diagrams of higher order, a Fourier transform is employed. The calculations are performed for cerous magnesium nitrate using a $g$ factor that is zero along the $c$ axis. The results are compared with experiments. The susceptibility $\chi$ was calculated for a uniform and for a nonuniform field, and it is suggested that the critical temperature is determined by the infinity of $\chi(q)$ for $q \neq 0$, rather than by that of $\chi(0)$.

**11823.** Milligan, D. E., Jacox, M. E., **Spectra of radicals,** Chapter 5 in *Phys. Chem.* **4,** 193-231 (Academic Press Inc., New York, N.Y., 1970).

Key words: Electronic spectrum; flash photolysis; free radicals; matrix isolation; molecular orbitals; vibrational spectrum.

Problems arising in the direct spectroscopic detection of free radicals are surveyed. Apparatus used for the spectroscopic study of free radicals in the gas phase and trapped in inert solid matrices is described. The advantages and limitations of flash photolysis and of matrix isolation studies for the production and detection of free radicals are considered. Examples of radicals studied by these techniques are cited, and data on the structure and chemical bonding of these species derived from the observed spectra are correlated with the predictions of simple molecular orbital theory.

**11824.** Nimeroff, I., **Deuteranopic convergence point,** *J. Opt. Soc. Am.* **60,** No. 7, 966-969 (July 1970).

Key words: Color blindness; color vision; deuteranope; protanope.

The technique, described by Nuberg and Yustova in 1955 to determine the convergence points of dichromats, was used at the National Bureau of Standards for three deuteranopic eyes, to obtain data on the deuteranopic convergence point. A study of the convergence point for deuteranopes obtained at NBS and by several other investigators has indicated a fairly wide range of values for this convergence point (1.08 to 2.30 for $x$, $-0.08$ to

-1.30 for $y$). The NBS data for deuteranopic observers yield oints that fall within this range.

1825. Reed, R. P., Arp, V. D., **Techniques for measuring stress, strain, and resistivity at 4 K for very soft materials,** *Cryogenics Letter to Editor* **9,** No. 5, 362-364 (Oct. 1969).

> Key words: Cryostat; electrical resistance; soft materials; strain extensometer.

Existing techniques for conducting low temperature tensile ests have not proven satisfactory for super pure aluminum due o its extreme softness. The desire to concurrently measure pecimen resistivity during 4 K tests also provided experimental lifficulties, since the specimens had to be electrically isolated rom the metallic load assembly. This paper discusses these roblems and describes the apparatus designed to provide sensiive and accurate data on stress, strain, and resistivity at 4 K.

1826. Reimann, C. W., Santoro, A., Mighell, A. D., **The crystal molecular structure of hexapyrazolenickel(II)nitrate, $Ni(C_3H_4N_2)_6(NO_3)_2$,** *Acta Cryst.* **B26,** Part 5, 521-526 (May 1970).

> Key words: Inorganic coordination complex; octahedral coordination; pyrazole; trigonal symmetry; x-ray structure determination.

The crystal structure of hexapyrazolenickel(II)nitrate, $i(C_3H_4N_2)_6(NO_3)_2$, was determined by single-crystal diffraction echniques. Crystals of $Ni(C_3H_4N_2)_6(NO_3)_2$ are trigonal with $a=$ .958, $c=7.278$ Å, space group $P\bar{3}$, $Z=1$, $\rho_0=1.57$, $\rho_c=1.57$ cm$^{-3}$. Three-dimensional counter data were collected (1115 eflections) and the structure was solved by an analysis of the atterson map. The complex cation, $Ni(C_3H_4N_2)_6^{2+}$, formed by he coordination of six planar pyrazole molecules to the nickel on, has $\bar{3}$ point symmetry. The nickel ion lies at the center of a early regular octahedron of coordinated nitrogen atoms. These omplex cations and nitrate anions are linked by hydrogen bonds etween each pyrrole type nitrogen atom ($\rangle$N$-$H) in the yrazole ring and an oxygen atom in the nitrate group. The final efinement by full-matrix anisotropic least-squares analysis esulted in an $R$ value of 0.053.

1827. Roder, H. M., Diller, D. E., **Thermal conductivity of gaseous and liquid hydrogen,** *J. Chem. Phys.* **52,** No. 11, 5928-5949 (June 1, 1970).

> Key words: Critical region; normal hydrogen; parahydrogen; thermal conductivity.

The thermal conductivity of gaseous and liquid hydrogen has een measured with a guarded horizontal flat-plate calorimeter t temperatures between 17 and 200 K and at pressures to 15 1N/m². The data have been analyzed as a function of density at xed temperatures and as a function of temperature at fixed denties. Outside the critical region the thermal conductivity of both e gas and the liquid increases continuously with temperature nd density. In the compressed liquid the temperature derivative t fixed density is positive and unusually large compared to that or most other simple liquids. In the critical region the thermal onductivity increases rapidly with both temperature and density s these parameters approach their critical values. The thermal onductivity of the dilute gas is consistent with the kinetic theory xpression, $K_0(T)=f_{ME}(T)C_v^0(T)\eta_0(T)/M$, and the dilute gas iscosities to better than 3%.

1828. Ruff, A. W., Jr., **Measurement of stacking fault energy from dislocation interactions,** *Met. Trans.* **1,** No. 9, 2391-2413 (Sept. 1970).

> Key words: Dislocation nodes; dislocation ribbons; dislocations; faulted dislocation dipoles; stacking fault energy; stacking fault tetrahedra.

The theories and methods applied to the determination of the stacking fault energy ($\gamma$) using techniques of direct observation of dislocation configurations are reviewed. The four principal methods, utilizing dislocation nodes, multiple ribbons, stacking fault tetrahedra, and faulted dipoles, are discussed in detail. Different theoretical treatments are compared wherever possible. Experimental procedures and quantitative measurement methods are reviewed, concentrating on transmission electron microscopy techniques. Detailed examples of the application of each method are given. For $\gamma/\mu b$ in the range of $2\times10^{-4}$ to $5\times10^{-3}$ ($\mu$ the shear modulus, $b$ the Burgers vector), measurements on dislocation nodes or multiple ribbons in favorable cases should permit determinations of the stacking fault energy to a precision of 5 pct. For larger values of $\gamma/\mu b$ (up to $12\times10^{-3}$), measurements can be made on tetrahedra or faulted dipoles with less precision. Larger values of the stacking fault energy require high resolution studies of dislocations; these techniques are not yet well established. Possible sources of systematic bias are discussed. Two significant theoretical problems remain concerning the treatment of the dislocation core and the use of anisotropic elasticity. It is of prime importance to characterize as carefully as possible the materials studied if accurate results are desired.

11829. Searles, S. K., Sieck, L. W., **High pressure photoionization mass spectrometry, III. Reactions of $NO^+(X'\Sigma^+)$ with $C_3-C_7$ hydrocarbons at thermal kinetic energies,** *J. Chem. Phys.* **53,** No. 2, 794-797 (July 15, 1970).

> Key words: Alkanes; excited states; ion-molecule reactions; mass spectrometry; photoionization; rate constants.

The vapor phase reaction of $NO^+(X'\Sigma^+)$ with $C_3$ through $C_6$ normal, branched, or cyclic alkanes was found to proceed exclusively via an $H^-$ transfer mechanism:

$$NO^+(X'\Sigma^+)+RH_2-RH^++HNO. \qquad (I)$$

In addition to (I), $C_4H_9^+$ was also formed by a second order process in the reaction with 3-methylhexane. Absolute rate constants were determined for all systems at thermal kinetic energies. Isomers containing tertiary H atoms were found to be the most reactive, exhibiting rate constants on the order of $10^{-9}$ cm³/molecule-second. Isotopic labelling has verified that only the tertiary site is involved in the $H^-$ transfer reaction in those molecules having both secondary and tertiary H atoms. The rate constants found for $n$-alkanes and nonsubstituted cycloalkanes fall in the range $10^{-12}$ to $10^{-10}$ cm³/molecule-second. The bimolecular reaction cyclo-$C_6H_{11}^+ + NO - C_6H_{11}NO^+$ was also noted at higher pressures. No further reaction of the $RH^+$ species generated in (I) was found in any other $RH_2-NO$ combination at pressures up to 0.5 torr.

11830. Searles, S. K., Sieck, L. W., Ausloos, P., **Reactions of $C_2H_6^+$. Formation of the $(C_2H_6)_2^+$ ion,** *J. Chem. Phys.* **53,** No. 2, 849-850 (July 15, 1970).

> Key words: Alkane dimer ions; ethane; ion-molecule reactions; mass spectrometry; photoionization; protonated dimer ions.

This NOTE reports the discovery of a dimer alkane ion $(C_2H_6)_2^+$. To our knowledge this is the first time that such an ion has been observed in the mass spectrometer.

11831. Sharp, E. J., Weber, M. J., Cleek, G., **Energy transfer and fluorescence quenching in Eu- and Nd-doped silicate glasses,** *J. Appl. Phys.* **41,** No. 1, 364-369 (Jan. 1970).

> Key words: Energy transfer; Eu and Nd doped glass; fluorescence; fluorescence decay times; fluorescence quenching; laser glass; rare earth glass.

Radiative and nonradiative energy transfer and decay processes have been investigated in high silicate glass co-doped with Eu and Nd. Energy transfer from Eu to Nd was established from an examination of the excitation spectra and the increased

Eu decay rates in the presence of Nd. Measurements of the concentration dependences of the Eu$^{3+}$ and Nd$^{3+}$ fluorescence lifetimes reveal the presence of four distinct processes arising from various ion-ion interactions: (1) self-quenching of the Nd$^{3+}$ fluorescence, (2) self-quenching of the Eu$^{3+}$ fluorescence, (3) nonradiative energy transfer from Eu$^{3+}$ to Nd$^{3+}$, and (4) Eu quenching of the Nd$^{3+}$ fluorescence. This last process decreases the radiative quantum efficiency of the ${}^4F_{3/2}$ state of Nd$^{3+}$, thus limiting the attractiveness of Eu sensitization for Nd laser action.

**11832.** Shinyayev, A. Ya., Butrymowicz, D. B., **Interdiffusion in and the phase diagram for vanadium-rich alloys of the V-Al system at pressures 0 to 47 kbar,** *Met. Trans.* **1,** No. 7, 1905-1907 (July 1970).

Key words: Alloys; aluminum; diffusion; high-pressure; phase-diagram; vanadium.

The V-Al system between 16 and 39 at. pct Al was studied at 1400 °C under pressures of 0, 30, and 47 kbar. Electron microprobe analysis, x-ray diffraction, microhardness readings, and metallographic examination revealed only a single solid solution. Interdiffusion coefficients were determined as a function of composition and pressure. Concentration gradients were measured with an electron microprobe analyzer and the diffusion coefficients were calculated by the Matano analysis. At 1400 °C, the value of the interdiffusion coefficient varied from 1 to 12 × $10^{-9}$ sq cm per s, increasing with aluminum content and decreasing with increasing pressure.

**11833.** Simson, B. G., Mandel, J., Brenner, F. C., **Research for a uniform quality grading system for tires. III. Breaking energy,** *Rubber Chem. Tech.* **43,** No. 2, 356-369 (Mar. 1970).

Key words: Bias ply; breaking energy; passenger car; radial; tires; tire strength; winter.

A test procedure designed to classify tires according to their average breaking energy has been applied to a sample of passenger car tires. Data are reported on 127 different tires of all grades and types over a range of sizes.

A scaling system is devised and applied to the data. It is found that the system leads to conclusions similar to those derived from the original data.

**11834.** Stein, P. G., Lipkin, L. E., Shapiro, H. M., **Spectre II: General-purpose microscope input for a computer,** *Science* **166,** 328-333 (Oct. 17, 1969).

Key words: Biological structure; biomedical instrumentation; computer; image processing; microscope; microspectrophotometry; pattern recognition.

This paper describes a system of instruments used in biological and medical research for microspectrophotometry and computer analysis of microscopic images. The apparatus includes an optical microscope, spectrophotometer, a scanner, and a motor driven stage and monochromator all controlled by a small general-purpose computer. A keyboard permits manual operation of the equipment under computer control.

The system was constructed with great flexibility to permit its use in the evaluation and design of special-purpose apparatus for specific biomedical applications. A discussion of design criteria and a comparison with existing input devices for microscopic image analysis is included.

**11835.** Straty, G. C., Prydz, R., **The vapor pressure of liquid fluorine,** (Proc. 1969 Cryogenic Engineering Conf., June 16-18, 1969, Univ. of California, Los Angeles, Calif.), Chapter in *Advances in Cryogenic Engineering* **15,** Paper No. B-1, 36-41 (Plenum Press Inc., New York, N.Y., 1970).

Key words: Critical point pressure; fluorine; normal boiling point; vapor pressure data; vapor pressure equation.

This paper reports new vapor pressure measurements on liquid fluorine from the triple point to the critical point at 1 K intervals. Accuracies in both temperature and pressure approach a few hundredths of a percent. The data were fitted to a newly developed, nonanalytic vapor pressure equation and compared graphically to earlier, inconsistent measurements available in the literature. Of this earlier data, the estimated P-T values above the normal boiling point and the value given for the critical pressure are in error by as much as 10 to 15 percent.

**11836.** Sugar, J., **Spectrum of doubly ionized thulium (Tm III),** *J. Opt. Soc. Am.* **69,** No. 4, 454-466 (Apr. 1970).

Key words: Doubly ionized thulium; energy levels of Tm III; radial energy integrals of Tm III; spectrum of Tm III.

A list of 848 low-excitation spectral lines of Tm III has been obtained by utilizing the sliding-spark light source at a peak current of 6 A. An analysis of these lines yielded 108 energy levels belonging to the configurations $4f^{13}$, $4f^{12}5d$, $4f^{12}6s$, and $4f^{12}6p$. The classified lines and level values are presented as well as a theoretical interpretation of these configurations.

**11837.** Sugar, J., **Configuration $4f^{13}5d$ of doubly ionized ytterbium,** *J. Opt. Soc. Am.* **60,** No. 4, 571-572 (Apr. 1970).

Key words: Radial integrals; Sack correction; ytterbium.

The "effective" interaction parameters introduced by Sack are applied to the $4f^{13}5d$ configuration of Yb III, reducing the rms error of the calculated levels from 179 cm$^{-1}$ to 69 cm$^{-1}$.

**11838.** Swartzendruber, L. J., Bennett, L. H., **Clustering, cold work, and the Mössbauer effect doublet structure in Cu-Ni-Fe alloys,** *Physics Letters* **31A,** No. 10, 581-582 (May 18, 1970).

Key words: Alloys; clustering; cold work; Cu; Fe; magnetic moments; Mössbauer effect; Ni.

The doublet structure observed in the high temperature Mössbauer effect spectra of Cu-Ni-Fe alloys is present in a random alloy as well as in a metallurgically clustered alloy. The structure of the doublet is distorted by cold work.

**11839.** Ugiansky, G. M., Skolnick, L. P., Stiefel, S. W. **Directional effects in the stress corrosion cracking of an aluminum alloy,** *Corrosion* **25,** No. 2, 77-86 (Feb. 1969).

Key words: Aluminum alloy; corrosion; directional effects; grain morphology; preferred orientation; stress corrosion.

Studies of the relative effects of grain morphology and preferred orientation on the directional susceptibility to intergranular stress corrosion cracking of a 7075-T651 aluminum alloy plate have been conducted. The role of grain morphology was found to be of paramount importance in controlling crack propagation. It was found that a slow rate of propagation along grain boundaries parallel to the applied stress accounts for the low susceptibility of longitudinally stressed specimens. The results suggest that the threshold stress for short transverse specimens approximates the low stress necessary to crack grain boundaries normal to the applied stress, and the threshold stress for longitudinal specimens approximates the high stress needed to propagate cracks along boundaries parallel to the applied stress. Preferred orientation was found to be of secondary importance when compared to the effect of grain morphology. A high degree of preferred orientation, rather than any specific slip plane orientation, was found to increase the susceptibility of specimens with the same grain morphology. Pitting corrosion was found to occur to a much greater extent on unstressed than on stressed (undergoing stress corrosion cracking) specimens. This phenomenon is explained by what is termed an "internal cathodic protection mechanism."

**11840.** Wall, L. A., Flynn, J. H., Straus, S., **Rates of molecular**

**vaporization of linear alkanes,** *J. Phys. Chem.* **74,** No. 17, 3237-3242 (1970).

Key words: Alkanes; heats; *n*-hexatricontane; *n*-pristane; *n*-tetracosane; *n*-tetranonacontane; vaporization.

The rates of molecular vaporization of four linear alkanes, *n*-nonadecane ($C_{19}$), *n*-tetracosane ($C_{24}$), *n*-hexatricontane ($C_{36}$), and *n*-tetranonacontane ($C_{94}$), were measured. The tetranonacontane vaporized without detection of hydrocarbon decomposition products by mass spectral monitoring. The kinetics of the vaporization process showed zero-order behavior as a vaporization process proportional to the surface area should. The Arrhenius slope, $+3RT/2$, was compared to heats of vaporization of other *n*-alkanes in the literature. The data show that the heat of vaporization is closely proportional to the two-thirds power of the number *n*, of carbon atoms in the species and not to the first power. Our results and the majority of the known heats of vaporization are well fitted by the equation, $\Delta H_v = 13.43n^{2/3} - 0.08075T + 12.22$ kJ/mol. The results suggest a much higher upper limit to the size of species capable of molecular vaporization without decomposition than previously assumed.

**11841.** West, E. D., Churney, K. L., **Theory of isoperibol calorimetry for laser power and energy measurements,** *J. Appl. Phys.* **41,** No. 6, 2705-2712 (May 1970).

Key words: Calorimetry; laser calorimetry; lasers; thermodynamics.

Laser power and energy measurements are commonly made in calorimeters operating in a constant temperature environment. Calorimeters of this type are analyzed in terms of the first law of thermodynamics and the boundary value problem describing heat flow in the calorimeter. This theory of the measurement suggests design features of the calorimeter, sources of error to be avoided in design and operation, and tests to demonstrate experimentally the adequacy of the design. The analysis shows how time-temperature data can be used to allow for the temperature gradient on the calorimeter and the heat exchange due to transients in the temperature.

**11842.** Wilson, W. K., Fletcher, D. G., **Paper research at the National Bureau of Standards,** *Indian Pulp Paper* **24,** No. 7, 325-329 (Jan. 1970).

Key words: Appearance properties; paper research; preservation of records; tear reference; testing program.

A brief history of paper research at the National Bureau of Standards is followed by a description of the current program. Work is in progress on the preservation of records, currency paper, and optical properties of paper. A collaborative testing program enables participating laboratories to compare their test results with the results obtained in other laboratories. A tear reference standard also has been maintained for several years. Several staff members participate in a number of committees in the Technical Association of the Pulp and Paper Industry, American Society for Testing and Materials, USA Standards Institute and International Organization for Standardization.

**11843.** Wolcott, N. M., Falge, R. L., Jr., **Cluster specific heat in $Cu_{0.6}Ni_{0.4}$ alloy,** *J. Low Temp. Phys.* **2,** No. 314, 329-331 (1970).

Key words: Clustering; $Cu_{0.6}Ni_{0.4}$ alloy; electronic specific heat; specific heat; 0.48 to 10 K.

The specific heat of an alloy of copper with 40 at.% nickel has been measured. The "constant" or anomalous term is seen to decrease as the temperature is reduced below 1.4 K.

**11844.** Younglove, B. A., **Measurements of the dielectric constant of saturated liquid oxygen,** (Proc. 1969 Cryogenic Engineering Conf., June 16-18, 1969, Univ. of California, Los Angeles, Calif.), Chapter in *Advances in Cryogenic Engineering* **15,** Paper No. C-3, 70-75 (Plenum Press Inc., New York, N.Y., 1970).

Key words: Clausius-Mossotti function; dielectric constant; oxygen; polarizability; saturated liquid.

Dielectric constant measurements on saturated liquid oxygen ranged from 1.22 near the critical point to 1.57 near the triple point. The calculated "polarizability" (Clausius-Mossotti function) shows a variation of 1.3%, with the maximum occurring at about 150 K. The decrease in polarizability near critical is attributed to inaccuracies in the densities in this region. The uncertainty in dielectric constant is about 0.01%.

**11845.** Acquista, N., Abramowitz, S., **Structure of the alkali hydroxides. V. The infrared spectra of matrix-isolated RbOH, RbOD, NaOH, and NaOD,** *J. Chem. Phys.* **51,** No. 7, 2911-2914 (Oct. 1, 1969).

Key words: Alkali hydroxides; high temperature; infrared; matrix; NaOD; NaOH; RbOD; RbOH; vibrational assignment.

The infrared spectra of matrix-isolated RbOH, RbOD, NaOH, and NaOD have been observed. Both the alkali-metal-oxygen stretch $\nu_1$ and the bending mode $\nu_2$ have been assigned for each species. The metal-oxygen stretching mode is found at 354.4, 345, 431, and 422 $cm^{-1}$ for RbOH, RbOD, NaOH, and NaOD, respectively; the bending mode $\nu_2$ is observed at 309.0, 229, 337, and 250 $cm^{-1}$, respectively. Combination of the results of this study with the microwave measurements for RbOH and RbOD indicates an essentially linear structure for these species. The isotope shift for $\nu_2$ observed in NaOH coupled with reasonable bond lengths indicates an equilibrium configuration of NaOH which probably does not deviate significantly from linearity. The assumption of a linear model with a harmonic bending potential yields force constants of $0.046 \times 10^{-18}$ and $0.053 \times 10^{-18}$ Nm (0.046 and 0.053 mdyn·Å) for RbOH and NaOH, respectively. These results are consistent with our previously reported results for CsOH.

**11846.** Acquista, N., Schoen, L. J., **Matrix isolation spectrum of the SH radical,** *J. Chem. Phys.* **53,** No. 3, 1290-1291 (Aug. 1, 1970).

Key words: Infrared spectrum; isolated SH; low temperature; matrix; SH; ultraviolet.

The free radical SH is produced in sufficient quantities by photodeposition of $H_2S$ in argon matrices at 20 K for observation in the ultraviolet and infrared. Close agreement between the matrix data and the gas-phase work in the electronic region support the assignment.

**11847.** Ahearn, A. J., **Homogeneity of ion sensitive emulsions and precision of ion beam measurements in spark source mass spectrometry, (Summary),** *Proc. 16th Annual Conf. on Mass Spectrometry and Allied Topics, May 12-17, 1968, Pittsburgh, Pa., sponsored by ASTM Committee E14,* pp. 273-276 (1968).

Key words: Accuracy; circumvention; emulsions; homogeneity; ions; mass; platinum; precision; replicate; spark; spectrometry.

The precision and accuracy with which materials can be trace characterized by spark source mass spectrometry is determined in part by the precision with which ion beams can be measured with ion sensitive emulsions. Consequently, the homogeneity of the emulsion becomes an important factor. Replicate mass spectra of platinum extending over Q2 emulsions show that the sensitivity fluctuations about an average may be $\leqslant 5\%$, standard deviation in a 5 cm. length, or there may be as much as a 30% change in sensitivity over this distance.

**11848.** Anderson, H. J., Brenner, A., **Chemical vapor deposition**

**of rhenium,** *Proc. 2nd Intern. Conf. on Chemical Vapor Deposition, Los Angeles, Calif., May 1970,* pp. 356-366 (1970).

Key words: Chemical vapor deposition; rhenium; rhenium coatings; rhenium oxychlorides.

The chemical vapor deposition (CVD) of rhenium from a variety of compounds was investigated. The reduction of perrhenyl chloride and rhenium oxytetrachloride with hydrogen resulted in the production of deposits which ranged from bright to powdery, the latter being obtained at a temperature above 600 °C. The bright deposits were cracked and exfoliated from the substrate. The only ductile deposits were obtained by thermal decomposition of $ReOCl_4$ at about 1200 °C, which process has been previously described by Russian workers.

**11849.** Andrews, J. R., **Improved bias supply for tunnel-diode picosecond pulse generators,** *IEEE Trans. Instr. Meas.* **IM-19,** No. 3, 171-175 (Aug. 1970).

Key words: Jitter; picosecond; pulse generator bias supply; tunnel diode.

An improved bias supply for tunnel-diode (TD) picosecond-pulse generators is described. The supply is stable with temperature and, in a commercial 35-ps (nominal) risetime tunnel-diode pulse generator/sampling oscilloscope system, has produced a 4:1 reduction in time-base jitter and 2:1 reduction in time-base drift. Also described is a tunnel-diode pulse generator, which, when used with the bias supply, produces a stable pulse having a flat-top sag of no more than 2 percent in 1 $\mu$s.

**11850.** Armstrong, R. W., Waters, H. P., **Testing programs and research on restraint systems,** *Proc. Intern. Engineering Congress, Detroit, Michigan, January 13-17, 1969,* Report No. 690247, pp. 1-48 (Society of Automotive Engineers, New York, N.Y., 1969); Abstract in *SAE Trans.* **78,** 102 (1969).

Key words: Anthropomorphic dummies; auto seat tests; deceleration; human kinematics; human tests; restraint geometry; restraint systems; seat belt; sled tests; webbing abrasion; webbing degradation.

Extensive research in the field of occupant restraints has been made by the Office of Vehicle Systems Research at the National Bureau of Standards. Portions of that research, consisting of human dynamic sled tests at Holloman Air Force Base, tests of restraint systems on the NBS sled, and a variety of strength and degradation tests of seat belts are reported. The geometry of restraint systems in 1968 model production automobiles is documented.

Results of 75 human tests reported indicate the nature of human kinematic response to deceleration in seat belts and the forces the seat belt might be expected to withstand. Requirements for dynamic tests of seat belts have been investigated as well as degradation tests for improvement of the federal standards for seat belts for use in motor vehicles.

**11851.** Armstrong, R. W., Waters, H. P., Stapp, J. P., **Human muscular restraint during sled deceleration,** *Proc. 1968 Stapp Car Crash Conf., October 22-23, 1968, Detroit, Michigan,* Report No. 680793, pp. 440-462 (Society of Automotive Engineers, New York, N.Y., 1969); Abstract in *SAE Trans.* **77,** 179 (1969).

Key words: Acceleration (mechanical); biodynamics; biomechanics; human engineering; kinematics; occupant restraint systems; seat; seat belts.

The value of the restraint by legs and arms of a human being has been generally disregarded in the development of restraint systems for occupants of an automobile. As part of a series of tests on human beings in automotive restraints conducted for the National Bureau of Standards by the 6571st Aeromedical Research Laboratory, Holloman Air Force Base, New Mexico, measurements were made of the forces exerted on a foot rest during 15 g decelerations. Calculations revealed that for "lap belt only" configuration, 26% of the subject's kinetic energy absorbed was attributed to the seat belt and 55% attributed to the restraint by the legs.

**11852.** Arthur, M. G., **Impulse spectral intensity calibration at the National Bureau of Standards,** *Proc. Electromagnetic Compatability Symp., Ft. Monmouth, N.J., June 19-20, 1969,* pp. 133-138 (U.S. Army Electronics Command Hdq., Ft. Monmouth, N.J., 1969).

Key words: Fourier transform; impulse; impulse generator; impulse spectral intensity; impulse standards.

The National Bureau of Standards, in its Radio Standards Engineering Division, is working on standards and measurement techniques of impulsive signals. This work includes a study of impulse spectral intensity, the development of methods of measuring it, and the development of standard impulsive signal generators. These tasks are not yet completed, but certain useful accomplishments have been made.

An authoritative definition of impulse spectral intensity is lacking. Even so, two techniques are being developed at NBS for measuring the amplitude of the frequency spectrum of an impulsive signal. One technique involves the measurement of power spectral density, from which the spectrum amplitude is computed. The other technique involves the measurement of the relative amplitude of the spectrum, and makes use of the results of the first technique to obtain the actual spectrum amplitude. Also under development are two different types of precision impulse generators to be used as reference standards. Since none of this work is completed, no NBS calibration services for impulse spectral parameters are presently available.

**11853.** Ausloos, P., **Ion-molecule reactions and photoionization of hydrocarbons,** Chapter in *Progress in Reaction Kinetics,* G. Porter, ed., **5,** 113-179 (Mar.-Apr. 1970).

Key words: Hydrocarbons; ion-molecule reactions; photoionization; radiolysis; rate constants; theory.

This is a critical review of the literature on ion-molecule reactions in the radiolysis and photoionization of hydrocarbons.

**11854.** Ausloos, P., Lias, S. G., **Carbonium ions in radiation chemistry. Reactions of *t*-butyl ions with hydrocarbons,** *J. Am. Chem. Soc.* **92,** No. 17, 5037-5045 (Aug. 26, 1970).

Key words: Carbonium ions; ion-molecule reactions; neopentane; radiolysis; rate constants; *t*-butyl ion.

*t*-Butyl ions, generated by the $\gamma$ irradiation of neopentane, undergo hydride transfer reactions with alkanes having tertiary hydrogen atoms ($t\text{-}C_4H_9^+ + RH \rightarrow i\text{-}C_4H_{10} + R^+$) to form isobutane and a tertiary carbonium ion as products. By irradiating neopentane in the presence of mixtures of two reactant molecules, one deuterated and one nondeuterated, the relative rates of the hydride transfer reaction for 22 $C_5 - C_8$ alkanes were determined with an unusually high accuracy, from the observed ratios of $i\text{-}C_4H_9D$ to $i\text{-}C_4H_{10}$. Absolute rate constants for reactions, based on a determination of the rate of depletion of the isobutane yield when ammonia is added, are given. The rate constants are generally very low [$10^{-11} - 10^{-10}$ cm$^3$/(molecule sec)$^3$, but are shown to depend on the heat of reaction and steric factors involving van der Waals interactions between the approaching ion and hydrogen atoms or methyl groups on the carbon atom $\beta$ to the tertiary carbon. The evidence indicates that the hydride transfer reactions of the *t*-butyl ion have an activation energy, $E_{act} \leq 0.15$ eV. In another series of experiments, unsaturated hydrocarbons were added to neopentane-isopentane mixtures, and the rates of the condensation reaction of these additives with *t*-butyl ions were determined by measuring the rate of depletion of the isobutane yield. The rate constants for the condensation reactions are in the range $10^{-10} - 10^{-9}$ $cm^3$/(molecule sec). Some insight into processes occurring in the radiolysis of neopentane can be gained from these results. It is shown, for example, that in the absence of reactive additives, not more than about 14% of the *t*-butyl ions undergoes processes resulting in the formation of isobutene.

11855. Baird, R. C., **Recent theoretical and experimental results of the determination of antenna pattern and gain from near-field measurements, (Summary),** *Proc. Conf. Precision Electromagnetic Measurements, National Bureau of Standards, Boulder, Colo., June 2-5, 1970, CPEM Digest,* p. 60 (1970).

Key words: Gains; microwave antennas; near-field measurements; patterns.

Recent results based on a new method of determining antenna pattern and gain from near-field measurements are summarized. A brief description of the method covering the important new features (such as the ability to correct for the effects of the measuring probe) is included. Preliminary results of measurements made on three different horn antennas (gains = 6.8 dB, 21 dB, 47 dB) are presented. The accuracy of the method appears to be at least as good as conventional far-field measurements and may be significantly better for many antennas. Some potential applications of the method are mentioned and references of publications containing more complete discussions are given.

11856. Baird, R. C., Newell, A. C., Wacker, P. F., Kerns, D. M., **Recent experimental results in near-field antenna measurements,** *Electronics Letters* **6,** No. 11, 349-351 (May 28, 1969).

Key words: Antenna gain; antenna pattern; calculated far-field patterns; near-field measurements; new antenna theorems.

Recent experimental results on determination of antenna pattern and effective gain from near-field measurements are described. Two new antenna measurement theorems were applied. Measurements were made on an electrically large horn-lens, a standard-gain horn, and a nominal duplicate of the measuring antenna. Some comparisons with direct far-field measurement results were made.

11857. Barnes, J. A., **Frequency measurement errors of passive resonators caused by frequency-modulated exciting signals,** *IEEE Trans. Instr. Meas.* **IM-19,** No. 3, 147-152 (Aug. 1970).

Key words: Frequency; resonance; standards.

The condition of resonance for a signal with FM is defined in this paper as the condition of maximum power transfer by the resonant device. It is shown that if the width of the signal spectrum is small compared to the resonator's linewidth, then the frequency error is proportional to the third moment of the instantaneous signal frequency about its mean.

One expects that this treatment should, at least, give the leading term for a precise treatment of atomic resonances. Experimental results with a cesium beam frequency standard confirm this expectation and add caution to the idea that higher *Q* atomic resonances make better absolute frequency standards.

1858. Bates, R. D., Jr., Flynn, G. W., Ronn, A. M., **Laser-induced vibrational fluorescence in nitrous oxide,** *J. Chem. Phys.* **49,** No. 3, 1432-1433 (1968).

Key words: Fluorescence; infrared; laser; nitrous oxide; Q-switching; vibrational relaxation.

A laser induced fluorescence technique has been utilized to obtain the relaxation time of $N_2O$ in the 001 vibrational state. A thermalized $N_2O$ absorption cell was placed within an $N_2O$-$N_2$-He Q-switched laser cavity and the fluorescent emission monitored on a side window with a Au:Ge detector. A quenching rate for the 001 level was found to be ($672.6 \pm 8.9$ $sec^{-1}$ $torr^{-1}$) where the uncertainty is the estimated standard deviation. This corresponds to a cross section of $1.23 \times 10^{-19}$ $cm^2$.

11859. Bates, R. G., Staples, B. R., Robinson, R. A., **Ionic hydration and single ion activities in unassociated chlorides at high ionic strengths,** *Anal. Chem.* **42,** No. 8, 867-871 (July 1970).

Key words: Activity coefficients; activity scales of high concentrations; activity standard scales; chloride activity convention; ion activity standards; ionic activity; ion selective electrodes; single ion.

Although the convention on which standard reference values of pH are based is suitable at ionic strengths below 0.1, and extension of this formula is required to provide the single ionic activities needed for the standardization of ion-selective electrodes at high ionic strengths. This procedure must take into account the specific differences among activity coefficients of ions of the same charge, apparent at elevated concentrations but negligible at low ionic strengths. It is shown that a reasonable method for deriving single ionic activities can be based on the Stokes-Robinson hydration theory. The assumption is made that the chloride ion is not hydrated. Individual ionic activity coefficients in solutions of seven unassociated uni-univalent chlorides and four alkaline earth chlorides have been calculated. Advantages and limitations of the hydration treatment are discussed.

11860. Bennett, H. S., **Two-electron *F′* centers in the alkaline-earth oxides and in the alkali halides,** *Phys. Rev. B* **1,** No. 4, 1702-1715 (Feb. 15, 1970).

Key words: Alkali halides; alkaline earth oxides; *F* center; *F′* center; ionic crystals (NaCl, KCl, MgO, CaO).

The Hartree-Fock-Slater equations for the two electron orbitals localized about an anion vacancy in MgO, CaO, NaCl, and KCl have been solved numerically in the point-ion-lattice potential. The ionic polarization of the nearest-neighbor ions is treated in a self-consistent manner. It is found that the low lying $F'$ center states for MgO and CaO have the following order for increasing values of the energy: ${}^1S(1s,1s)$, ${}^3P(1s,2p)$, ${}^1P(1s,2p)$, and either ${}^3S(1s,2s)$ or ${}^1S(1s,2s)$. The states ${}^3S(1s,2s)$ and ${}^1S(1s,2s)$ both lie above the other three states, but whether the ${}^3S(1s,2s)$ state lies above or below the ${}^1S(1s,2s)$ state depends upon the ionic polarization of the crystal potential. The above ordering, the optical absorption and emission energies between the states ${}^1S(1s,1s)$ and ${}^1P(1s,2p)$, and the spin-forbidden emission energy from the state ${}^3P(1s,2p)$ to the state ${}^1S(1s,1s)$ agree reasonably with the experimental ordering of the states and with the experimental transition energy values of CaO, respectively. The same physical model gives very different results for the $F'$ center in NaCl and in KCl. It is found that only the ground state ${}^1S(1s,1s)$ contains spatially compact (bound) electronic orbitals. The ground-state energies of the $F'$ center in NaCl and KCl agree to within 20% of the experimental values. The existence of bound excited states for the $F'$ center in these monovalent crystals has been investigated. However, definitive statements on such states are not available at present.

11861. Berger, M. J., **Beta-ray dosimetry calculations with the use of point kernels,** (Proc. Symp. Medical Radionuclides: Radiation Dose and Effects, Oak Ridge Association Universities, Oak Ridge, Tennessee), *Atomic Energy Commission Report* **CONF-691212,** pp. 63-86 (June 1970).

Key words: Absorbed dose; beta ray; dosimetry; nuclear medicine; point kernel; radionuclide.

Some work on the evaluation, compilation, and use of point kernels in beta-ray dosimetry is described. Such kernels describe the distribution of absorbed dose around point sources. By the superposition of such kernels, one can determine the spatial pattern of absorbed dose in media in which a beta-emitting radionuclide is distributed in some specified fashion. The superposition method has the advantage of great economy. It is not completely realistic, however; its applicability is limited to media which are in effect unbounded and which are homogeneous in composition and uniform in density. Under the auspices of the Medical Internal Radiation Dose (MIRD) Committee of the Society of Nuclear Medicine, point kernels have been compiled for 75 radionuclides. These results are theoretical and are based on information about the shapes of beta spectra (obtained from the Oak Ridge National Laboratory Nuclear Data Group), data about electron stopping power and range values, and point kernels for monoenergetic sources calculated by Spencer. Confirming earlier findings by Cross, it is shown that the theoretical point kernels are in good agreement with corresponding experimental data for air and polystyrene. In a digression, a brief indication is given—derived from the analysis of Monte Carlo calculations—of how much the absorbed dose is reduced near a boundary through which the beta particles can escape from but not return to the medium, e.g., near an air-tissue interface. Finally, some considerations are presented concerning techniques useful for carrying out the numerical integrations for the superposition of point kernels. The examples discussed include the absorbed-dose distributions near line and plane sources, the absorbed-dose distributions inside and outside of volume sources with spherical and cylindrical shapes, and the self-absorption of beta-ray energy in slabs and spheres.

**11862.** Bergstrom, J. C., Bertozzi, W., Kowalski, S., Maruyama, X. K., Lightbody, J. W., Jr., Fivozinsky, S. P., Penner, S., **Electroexcitation of the low-lying states of $O^{16}$,** *Phys. Rev. Letters* **24,** No. 4, 152-155 (Jan. 26, 1970).

Key words: Electroexcitation; electron scattering; excited states of $O^{16}$; form factors; inelastic electron scattering; levels of $O^{16}$; low-lying states of $O^{16}$; $O^{16}$.

Measurements are reported of form factors for the electroexcitation of the $O^+$ (6.052-MeV), $3^-$ (6.131-MeV), $2^+$ (6.916-MeV), and $1^-$ (7.115-MeV) states of $0^{16}$, in the momentum-transfer region 0.5 to 1.0 $fm^{-1}$. The data are compared with the predictions of various particle-hole shell models and a two-component phenomenological model.

**11863.** Blaine, R. L., **A statistical study of the effects of trace elements on the properties of portland cement,** *Proc. 5th. Intern. Symp. on the Chemistry of Cements, Tokyo, Japan, October 7-11, 1968,* **3,** Part 3, 86-91 (Dec. 31, 1969).

Key words: Alkalies; concrete; durability; heat of hydration; portland cements; shrinkage; statistical evaluation; strength; sulfate expansion; trace elements.

A digital computer was used to find and evaluate significant relationships between the properties of a large number of portland cements and various independent variables which included chemical compounds, minor constituents, and trace elements. This article presents a review of the probable effects of minor constituents and trace elements on various properties including heat of hydration, sulfate expansion, compressive strength with different curing conditions, shrinkage, and durability. On the basis of the statistical study, $Na_2O$ or $K_2O$ were associated with most of the properties measured but not always to the same degree. Very few of the other individual trace elements had a highly significant relationship to the various properties measured, but when used in equations in addition to other commonly determined variables, there was usually a highly significant reduction in variance. The coefficients for Ba, Cu, SrO, P, and Li were significant at the 0.01 probability level in some tests and at the 0.05 probability level in other tests. The coefficients for Cr, Ni, Rb, Ti, V, and Zr were significant at the 0.05 probability level in equations for some of the tests. The effects of the alkalies and trace elements were generally small compared to the effects of major constituents and other independent variables.

**11864.** Blaugher, R. D., Hein, R. E., Cox, J. E., Waterstrat, R. M., **Atomic ordering and superconductivity in A-15 compounds,** *J. Low Temp. Phys.* **1,** No. 6, 539-561 (Dec. 1969).

Key words: Atomic ordering; binary A-15 compounds; superconductivity; transition elements.

Twenty-six different binary A-15 compounds were investigated to determine if superconductivity could be related to the degree of long-range atomic ordering on the crystallographic lattice sites. Significant changes in the superconducting transition temperatures and critical fields were produced by quenching from high temperatures followed by low-temperature annealing. These changes in $T_c$ were accompanied by changes in the degree of long-range ordering as determined using x-ray diffraction methods. The results can be interpreted within the framework of Weger's "linear-chain" model only when the B-element is a non-transition element. When both the A and B components are transition elements, however, the superconducting behavior will apparently depend on the nature of "*d*-electron" interactions between the component atoms. Complete ordering is not always an essential requirement for optimizing the superconducting properties.

**11865.** Boyne, H. S., Hall, J. L., Barger, R. L., Bender, P. L., Ward, J., Levine, J., Faller, J., **Absolute strain measurements with a 30-meter vacuum interferometer,** (Proc. Conf. Laser Applications in the Geosciences, Huntington Beach, Calif., June 1969), Chapter in *Laser Applications in the Geosciences,* J. Gauger and F. F. Hall, Jr., eds., pp. 215-225 (Western Periodicals, North Hollywood, Calif., 1970).

Key words: Earth strain; earth tide; geophysics; laser strainmeter; seismograph.

We present details on the design and performance of a 30-meter interferometric strain gauge. We also discuss a practical method for recording absolute earth strain measurements by comparing length changes in the interferometer with an absolute wavelength standard.

**11866.** Brady, R. F., Jr., **Cyclic acetals of ketoses. Part III. Re-investigation of the synthesis of the isomeric Di-*O*-isopropylidene-β-D-fructopyranoses,** *Carbohydrate Res.* **15,** No. 1, 35-40 (1970).

Key words: Fructose; gas-liquid chromatography; rare sugars; rearrangement; 1,3-dioxolane rings.

Condensation of D-fructose with acetone in the presence of sulfuric acid gave first 1,2:4,5-di-*O*-isopropylidene-β-D-fructopyranose. This compound isomerizes, at a rate dependent on the concentration of the acid, to 2,3:4,5-di-*O*-isopropylidene-β-D-fructopyranose. Careful selection of reaction conditions permits the synthesis of either isomer in satisfactory yield. In acetone containing 5% of sulfuric acid, either compound is converted into an equilibrium mixture (3:47) of 1,2:4,5- and 2,3:4,5-diacetal within 5 min at room temperature, but, when anhydrous zinc chloride is used as the catalyst, the 1,2:4,5-diacetal does not rearrange to the 2,3:4,5-diacetal.

**11867.** Bridges, J. M., Wiese, W. L., **Transition probabilities for the prominent red lines of Ne I,** *Phys. Rev. A* **2,** No. 2, 285-293 (Aug. 1970).

Key words: Neon; spectrum; transition probabilities.

Relative transition probabilities of all 30 lines belonging to the prominent $3s$-$3p$ transition array of Ne I have been measured in emission with a wall-stabilized arc operating in an argon-neon mixture at atmospheric pressure. The data have been normalized to an absolute scale provided by recent lifetime measurements o the $3p$ levels. Our results, as well as the data from other emission measurements, have been subjected to extensive comparisons and tests, including a check for fulfillment of the *J*-file sum rule. It is found that our data exhibit a much better consistency than ny other set of individual values. On the basis of this analysis as ell as our uncertainty estimates, we estimate that the accuracy f our individual transition probabilities for this transition array, xcept for a few weak lines, is of the order of 10% on an absolute asis.

1868. Brown, D. W., Lowry, R. E., Wall, L. A., **Radiation-induced copolymerization of tetrafluoroethylene and 3,3,4,4,5,5,5-heptafluoropentene-1 under pressure,** *J. Polymer Sci.* Part A-1, **8,** No. 9, 2441-2452 (1970).

Key words: Amorphous polymer; copolymerization; fluoropolymers; glass temperature; high pressure; radiation-induced; tetrafluoroethylene; 3,3,4,4,5,5,5-heptafluoropentene-1.

An investigation was made of the $\gamma$-ray-induced copolymerization of tetrafluoroethylene and 3,3,4,4,5,5,5-heptafluoropentene- At 22 °C at 5000 and 10 000 atm the polymerization rate anges little between 0 and 75 mole-% tetrafluoroethylene. bove 90 mole-% the rate increases greatly. Molecular weights ry with composition in a fashion similar to the variation of the tes. Crystallization occurs in the bulk pentene at 13 500 atm at °C. The polymerization rate is very low in the solid state. nder some conditions polymerization continues long after irdiation is ended. Both reactivity ratios favor the pentene. everal copolymer properties were studied. The polymers are norphous and soluble in perfluoro ethers, perfluoro alkanes, d perfluoro-aromatics if they contain less than 80% trafluoroethylene. The glass temperatures of the amorphous lymers decrease and the thermal and radiation stability ineases as the tetrafluoroethylene content increases.

869. Bullis, W. M., Scace, R. I., **Measurement standards for integrated circuit processing,** *Proc. IEEE* **57,** No. 9, 1639-1646 (Sept. 1969).

Key words: ASTM standards; integrated circuits; microelectronics; semiconductor devices; semiconductor materials; semiconductor process control; silicon.

Both yield and quality of silicon monolithic integrated circuits pend on adequate control at all stages of their manufacture. ch control depends on measurement at each step, beginning th the selection of the substrate wafer, process chemicals, and rts, through the fabrication, assembly, and packaging of the ished circuit. The American Society for Testing and Materials mmittee F-1 has developed standards for tests which have en widely used in the exchange of materials at various interces in the electron device industry. Many of these can be readi- adapted for in-process control as well as for materials and rts acceptance tests. These standards and the process by ich they were developed are reviewed; the importance of both dustrial participation and the technical support activities of the ational Bureau of Standards in this development is indicated. e need for additional standards is emphasized.

870. Casella, R. C., **Possible failure of the Pomeranchuck theorem—shrinkage of the forward elastic peak,** *Phys. Rev. Letters* **24,** No. 25, 1463-1466 (June 22, 1970).

Key words: Asymptotics; cross section; diffraction shrinkage; high energy; Pomeranchuck theorem.

Assuming constant but unequal asymptotic total cross secns $\sigma_{\pm}(\infty)$ leads to a $(\ln s)^2$ shrinkage of the forward elastic ak. Moreover, under rather general assumptions, $d\sigma^{el}/dt$ hibits an infinitude of oscillations in $t$ as $s \to \infty$, a result derived rlier by Finkelstein within the Regge-cut model.

871. Cezairliyan, A., McClure, J. L., Morse, M. S., Beckett, C. W., **Measurement of heat capacity of tantalum in the range 1900-3000 K by a pulse heating method,** Proc. 5th Symp. Thermophysical Properties, Newton, Massachusetts, September 30-October 2, 1960, C. F. Bonilla, ed., pp. 385-390 (American Society of Mechanical Engineers, New York, N.Y., 1970).

Key words: Heat capacity; high-speed measurements; high temperature; tantalum; thermodynamics.

A technique is described for the high-speed (millisecond resolution) measurement of heat capacity of electrical conductors at high temperatures (above 1900 K). Measurements on heat capacity of tantalum in the temperature range 1900 to 3000 K are reported and are compared with those in the literature. Duration of an individual experiment in which the specimen was heated from room temperature to near its melting point is less than one second. Temperature measurements were made with a high-speed photoelectric pyrometer. Experimental quantities (voltage, current, temperature) were recorded with a high-speed digital data acquisition system, which has a time resolution of 0.4 ms. Estimated inaccuracy of heat capacity measurements in the above temperature range is 2 to 3%.

11872. Champion, E. C., Marinenko, G., Taylor, J. K., Schmidt, W. E., **Determination of submicrogram amounts of chromium by coulometric titrimetry,** *Anal. Chem.* **42,** 11, 1210-1213 (Sept. 1970).

Key words: Chromium; coulometry; trace analysis.

An improved method has been developed for the determination of micro- and nanogram amounts of chromium by coulometric titrimetry. Samples containing 30 $\mu$g to 15 ng of chromium may be analyzed with an uncertainty limit of 1 ng. The method is bias-free within the uncertainty of the measurement due to random errors, and the end-point determination is the limiting factor for further improvements of the method.

11873. Clark, A. F., Childs, G. E., Wallace, G. H., **Electrical resistivity of some engineering alloys at low temperatures,** *Cryogenics* **10,** No. 4, 295-305 (Aug. 1970).

Key words: Aluminium alloys; copper alloys; cryogenics; electrical conductivity; iron alloys; nickel alloys; titanium alloys.

The electrical resistivities of several engineering alloys have been measured at 4, 20, 76, 192, and 273 K. Specimens of aluminium, nickel, copper, titanium, and iron alloys have been tested, some of them in different heat-treated conditions. Most of the alloys show a smooth decrease in resistivity with decreasing temperature, but some unusual results are reported. Comparisons are made between different alloys and between different heat treatments of the same alloys.

11874. Coxon, B., **The conformations of 1,2:4,6-Di-*O*-benzylidene-α-D-glucopyranose derivatives,** *Carbohydrate Res.* **14,** 9-15 (Oct. 1970).

Key words: Conformations; coupling constants; iterative analysis; *m*-dioxane ring; proton magnetic resonance; pyranoid ring; spectroscopy; 1,2:4,6-di-*O*-benzylidene-α-D-glucopyranoses.

The conformations of a series of 1,2:4,6-di-*O*-benzylidene-α-D-glucopyranose derivatives in solution have been studied by p.m.r. spectroscopy and double-resonance techniques at 100 MHz. The coupling constants obtained by first-order analysis of the spectra were compared with those computed by iterative analysis. It was concluded that these compounds adopt conformations in which the *m*-dioxane and pyranoid rings have chair and flattened-chair forms, respectively.

11875. Crissman, J. M., Passaglia, E., Eby, R. K., Colson, J. P.,

**Crystal data on n-eicosane ($C_{20}H_{42}$),** *J. Appl. Cryst.* **3,** 193-195 (1970).

Key words: Growth technique; n-eicosane; single crystal; unit cell.

A technique for growing relatively large crystals of n-eicosane ($C_{20}H_{42}$) is reported together with the unit cell parameters which are $a = 4.28_2$ Å, $b = 4.82_0$ Å, $c = 25.5_2$ Å, $d_{001} = 25.4_5$ Å, $\alpha = 91\ °_{10'}$, $\beta = 93\ °3_{2'}$, $\gamma = 107\ °2_{0'}$. The density of the unit cell is $0.935_5$ g/cm$^3$ at 24.5 °C and the macroscopic density is $0.93_6$ g/cm$^3$ at 24.2 °C.

**11876.** Cruz, J. E., Jellison, J. C., **A digital technique for generating variable frequency multiphase waveforms,** *Rev. Sci. Instr.* **41,** No. 7, 1098-1099 (July 1970).

Key words: Digital; logic gating; quasi-sinusoid.

To drive a two or three phase synchronous motor over a wide frequency range has, until now, required complex electronic networks to keep the proper phase relationships.

In this paper a technique is described for driving a two phase synchronous motor over a frequency range of three decades. This method consists of using digital techniques for generation of the two driving waveforms, with constant phase between them, over the specified frequency range.

Discussion of the feasibility of automatic control of the speed of the motor and expansion of the digital logic to generate n-phase waveforms is presented.

**11877.** Currie, L. A., **Radioactivity monitors and accuracy in photonuclear experiments, (Summary),** *Trans. Am. Nucl. Soc.* **13,** No. 1, 59 (1970).

Key words: Photonuclear experiments; radioactivity monitors.

**11878.** Davis, D. D., Jespersen, J. L., Kamas, G., **The use of television signals for time and frequency dissemination,** *Proc. IEEE* **58,** No. 6, 931-933 (June 1970).

Key words: Frequency and time code; television; time.

Measurements indicate that a television microwave path is stable to a few microseconds over a period of months. The paths measured are those used by the three major U.S. television networks between Washington, D.C., and Denver, Colo. Path stabilities of ± 5 ns (for half-hour periods) were measured by observing the phase of the television color subcarrier. A time dissemination system using the television signal format is described. Using locally broadcast VHF television signals, time information was recoverable with a resolution of several nanoseconds. This corresponds to a frequency stability of a few parts in $10^{12}$ for one hour averaging.

**11879.** Diller, D. E., Hanley, H. J. M., Roder, H. M., **The density and temperature dependence of the viscosity and thermal conductivity of dense simple fluids,** *Cryogenics* **10,** No. 4, 286-294 (Aug. 1970).

Key words: Density dependence; liquid state; simple fluids; temperature dependence; thermal conductivity; transport properties; viscosity.

This paper discusses the experimental information on the transport properties of dense simple fluids with emphasis on the compressed and saturated liquid states. Similarities and differences in the wide range density and temperature dependencies of the viscosity and thermal conductivity coefficients are summarized. The excess transport properties of argon, helium, hydrogen, oxygen, and carbon dioxide are graphically compared in the same reduced density and temperature ranges.

**11880.** Douglas, T. B., **New approach for evaluating lattice-configurational thermodynamic properties,** *J. Chem. Phys.* **51,** N 7, 2831-2839 (Oct. 1, 1969).

Key words: Configurational thermodynamic properties; excluded volume; extrapolations; lattice models; noncombinatorial method; statistical equilibrium.

As a generalization of earlier work of the author [J. Chen Phys. **40,** 2248 (1964); **45,** 1080 (1966)] a completely noncon binatorial method is derived which gives for any state the exa thermodynamic properties of a system of particles on a lattice i finite in one dimension. The method appears to be essentiall equivalent to, but somewhat simpler in development and applic tion than, the matrix method used for the same proble recently. Interaction of unit configurations is explicitly co sidered only at lattice boundaries, leading directly to a set of i dependent algebraic equations giving the complete solution f a specified state. Two simple examples are given to which alte native combinatorial procedures can be readily applied witho approximations, yielding identical explicit results. The gener method first given is modified for the imposition of artificial de sity constraints, and as an illustration it is shown how this vari tion improves markedly, over the range of disordered densitie the convergence to an infinite plane of the hard-core square-la tice fluid with nearest-neighbor exclusion.

**11881.** Engen, G. F., **A new method of characterizing amplifi noise performance (Summary),** (Proc. Conf. Precision Ele tromagnetic Measurements, National Bureau of Standard Boulder, Colo., June 2-5, 1970) *CPEM Digest,* pp. 20- (1970).

Key words: Amplifier noise; noise; noise measurement.

Although the use of a noise figure or noise temperature characterize amplifier performance is a well-established practic it is also recognized that this parameter provides only a parti description of the amplifier noise properties. In general, the noi figure (or temperature) depends upon the generator impedan and is thus a function of the signal source and amplifier combin tion.

Typically, the noise figure is measured by the Y-factor meth using hot and cold noise sources which are nominally match (reflectionless). The result of this measurement is of value a figure of merit; however, if optimum performance is to be re ized, the applications engineer must know whether to adjust t signal source impedance for maximum power transfer, minimu noise figure, or according to some other criteria, and the dete oration in performance which results if this is not done. It is t purpose of this paper to present an alternative method of chara terizing amplifier noise performance in terms of paramete which provide ready answers to these questions. In addition, t measurement of these parameters via a simple extension of t Y-factor method will be described.

**11882.** Farrar, T. C., **Pulsed and Fourier transform NMR sp troscopy,** *Anal. Chem.* **42,** No. 4, 109A-112A (Apr. 1970).

Key words: Fourier transform; nuclear magnetic; puls resonance.

Certain advantages in pulsed nmr spectroscopy, especially creased sensitivity, make it an attractive technique. With t solution of many of the problems in the spectrometers and sociated computer instrumentation, it is safe to predict it v rival continuous wave-nmr spectroscopy in usage.

**11883.** Frederick, N. V., Scott, W. W., Jr., **A simple technique metalizing boron nitride,** *Rev. Sci. Instr.* **40,** No. 9, 1240 (Se 1969).

Key words: Boron nitride; ceramic; metallizing; ultrason vacuum.

Boron nitride is a relatively new material, first develop bout ten years ago. It is a refractory ceramic of noteworthy hysical and dielectric properties. Successful metallization of oron nitride results in a product which should be very useful in he electronics industry.

A process is described for preparing the boron nitride surface which ultimately results in a strongly attached gold film surface which easily passes the accepted "scotch tape" test.

**1884.** Freeman, D. H., Zielinski, W. L., Jr., Rittner, W. F., **Recognition of crosslinking in the infrared spectra of poly(styrene-divinylbenzene),** *Proc. Ion Exchange in the Process Industries Conf., Imperial College of Science and Technology, London, England,* pp. 27-30 (1970).

> Key words: Copolymers; crosslinking; divinylbenzene; infrared; styrene.

Infrared spectra of polystyrene, poly(styrene/0.16 [mole raction] *p*-DVB), poly(styrene/0.16 *m*-DVB) and oly(styrene/0.16 [nominal mole fraction] technical DVB) are iven and discussed. Bands near 830 $cm^{-1}$ for *p*-DVB and echnical DVB copolymers, and near 797 $cm^{-1}$ for the *m*-DVB nd technical DVB copolymers are assigned to the *p*- and *m*- VB crosslinkages.

**1885.** Gebbie, H. A., Kuhn, P., Bohlander, R. A., **Scattering by high cirrus: Its effect on submillimeter wave determinations of atmospheric water vapor,** *Nature Letter to Editor* **226,** No. 5242, 71-72 (Apr. 4, 1970).

> Key words: Fourier spectroscopy; high cirrus; submillimeter waves; water vapor.

Submillimeter waves and, by implication in this context, the se of the pure rotation band, offer important advantages for etermining the distribution of water vapor with height in the at- osphere. The reasons are these. (1) We can readily resolve sin- e rotation lines in this region by Fourier spectroscopy using in- rferometers. The calibration for intensity of single lines is easi- made and a range of lines with different absorption strengths an then be chosen to match the requirements of the inversion ocedure used to construct the model radiating atmosphere. (2) he use of long wavelengths allows us to dispense with hot radia- on sources and use, for example, the radiation exchange etween a room temperature detector and cold sky.

**1886.** Gibson, B. F., O'Connell, J. S., **Angular distribution of the reaction $^1$H(d, $^3$He)$\gamma$,** *Physics Letters* **32B,** No. 5, 331-332 (Aug. 3, 1970).

> Key words: Angular distribution; cross section; helium-3; photonuclear; radiative capture.

The angular distribution of the proton-deuteron radiative cap- re cross section is calculated using the plane wave form of the ectromagnetic interaction operator and model wave functions r the $^3$He S, S′ and D-states and a plane wave continuum state.

**887.** Haar, L., Shenker, S. H., **A phenomenological equation of state,** *Proc. 5th Symp. Thermophysical Properties, Boston, Mass., September 30-October 2, 1970,* C. F. Bonilla, ed., pp. 223-226 (American Society of Mechanical Engineers, New York, N.Y. 1970).

> Key words: Compressibility factors; equation of state; high density; high temperature; pairwise potentials; Redlich Kwong; second virial coefficient; thermodynamics.

A simple phenomenological equation of state for high tempera- re gases is proposed. It is developed in terms of a gas interact- g as hard spheres with a superimposed Lennard-Jones attrac- e well. There are no arbitrary parameters as the equation is ed by the values of the second virial coefficient and its tem- rature derivative. The equation has been appplied to two sim- gases, nitrogen and argon. The results agree at least semiquantitatively with experimental data up to 10,000 bar and in the range of temperatures greater than twice the critical. Also included for comparison is the widely used Redlich Kwong equation. The present work compares favorably with the Redlich Kwong at the lowest temperature; however, as temperature is increased the present work becomes increasingly more accurate, whereas the corresponding states equation tends to degrade with temperature.

**11888.** Halford, D., **Frequency stability of quality quartz crystal oscillators: Performance and some critical applications,** *Proc. Intern. Colloq. Chronometrie, Paris, France, September 16-20, 1969,* **Serie A,** pp. A-11-1-A-11-3 (Sept. 1969).

> Key words: Atomic frequency standards; cesium beam; flicker noise; frequency stability; frequency standards; hydrogen maser; long baseline interferometry; quartz crystal oscillators; time standards.

For time intervals, tau, of one second or less, the short-term fractional frequency stability of high quality quartz crystal oscillators is superior to all other known frequency sources. For time intervals in the range of 1 to 10 seconds, these quartz crystal oscillators are at least as good as all other devices, such as hydrogen maser oscillators and rubidium gas cell frequency standards. For time intervals in the range from 10 to 1000 seconds, only hydrogen maser oscillators and the best cesium beam frequency standards are capable of frequency stabilities which exceed those of the best quartz crystal oscillators.

The stability of good quartz crystal oscillators has been found to be at least as good as 2 parts in $10^{13}$ for time intervals, tau, in the vicinity of 10 seconds, and is not much different for tau equal to 100 seconds.

This superb stability of quartz crystal oscillators, together with their other desirable features, indicates their use in several critical applications. These include long baseline interferometry, stable frequency reference for the cavity tuning servo in the hydrogen maser frequency standard, and stable frequency reference for evaluating the accuracy capability of cesium beam frequency standards, as well as the slaved oscillator in even the finest atomic frequency standards.

At the Colloque, I will discuss the measured frequency stability of commercially available quartz crystal oscillators, and some of their critical applications (accomplished and proposed). I will also mention some possibilities of achieving fractional frequency stabilities in the few parts in $10^{14}$ range with quartz crystal oscillators in the future. The nature of the flicker of frequency noise of quartz crystal oscillators will be discussed.

**11889.** Hardy, S. C., Coriell, S. R., **Morphological stability of ice cylinders in aqueous solution,** *J. Crystal Growth* **7,** No. 2, 147-154 (Sept.-Oct. 1970).

> Key words: Aqueous solutions; cylinder; ice; solute; stability; surface tension.

Cylindrical ice crystals oriented with the axis normal to the basal plane have been grown into slightly undercooled 0.1 molar HCl solution. The crystals develop approximately sinusoidal perturbations along the axis. The growth rates of these perturbations are in quantitative agreement with the predictions of a Mullins-Sekerka analysis of a cylinder growing into a binary melt. The ice-solution surface tension calculated from the perturbation growth rate is 23 $mJ/m^2$, essentially the same value found with distilled water. A number of other ionic solutes were studied at concentrations below $10^{-3}$ molar. Most solutes appear to have little effect on morphology or surface tension. However, ammonium compounds other than $NH_4F$ and $NH_4OH$ produce extreme changes in crystal morphology.

**11890.** Hayward, E., Schwartz, R. B., Murray, K. M., **Comments**

**on isospin of the $B^{11}$ giant resonance,** *Phys. Rev.* **2,** No. 2, 761-762 (Aug. 1970).

Key words: Boron eleven; giant resonance; isobaric spin splitting; photonuclear.

It was recently shown that in the photodisintegration of $B^{11}$ certain expected $\gamma$ rays were missing. A partial explanation is offered here for the failure to observe these transitions. It is also pointed out that no conclusions about the strength of the $T=3/2$ giant resonance can be drawn from this experiment.

11891. Hellwig, H., **The hydrogen storage beam tube, a proposal for a new frequency standard,** *Metrologia* **6,** No. 2, 56-60 (Apr. 1970).

Key words: Atomic beam tube; cavity pulling; frequency stability; frequency standard; hydrogen maser.

The basic design features and the frequency stability and accuracy capabilities of a proposed new frequency standard are projected. The hydrogen storage beam tube combines the virtues of the hydrogen maser with those of beam tubes eliminating most of the problems associated with these devices. The projected frequency stability for one second averaging is better than $10^{-14}$. The long term stability should be equally good. Ways for investigating the wall shift are discussed.

11892. Hellwig, H., Allan, D. W., Glaze, D. J., Vessot, R. F. C., Levin, M., Zitzewitz, P. W., Peters, H. E., **Measurement of the unperturbed hydrogen hyperfine transition frequency (Summary),** (Proc. Conf. Precision Electromagnetic Measurements, National Bureau of Standards, Boulder, Colo., June 2-5, 1970), *CPEM Digest*, pp. 72-73 (1970).

Key words: Frequency accuracy;hydrogen maser; wall shift.

We report the results of a joint experiment which was aimed at the determination of the frequency of the $H^1$ hyperfine transition $(F=1,\ m_F=0) \leftrightarrow (F=0,\ m_F=0)$. In terms of the frequency of the $Cs^{133}$ hyperfine transition $(F=4,\ m_F=0) \leftrightarrow (F=3,\ m_F=0)$, defined as 9192 631 770 hertz, we obtain for the unperturbed hydrogen transition frequency the value

$$\nu_H = 1420\,405\,751.769 \text{ Hz}.$$

This result is the mean of two independent evaluations which differ by only $2 \times 10^{-3}$ Hz. One evaluation is based on the wall shift experiments at Harvard University, the other is a result of a new measurement using many storage bulbs of different sizes at the National Bureau of Standards. We will describe the experimental procedures and the appplied corrections. We will compare our results with previously published values and discuss the error limits of our experiments.

11893. Hoer, C., Agy, D., **A broadhurst resistive coupler (Summary)** (Proc. Conf. Precision Electromagnetic Measurements, National Bureau of Standards, Boulder, Colo., June 2-5, 1970), *CPEM Digest*, pp. 18-19 (1970).

Key words: Coupler; directional coupler; directivity; impedance measurements; power measurements.

A new lumped circuit directional coupler is described for the 1 to 30 MHz frequency range. Directivity greater than 50 dB is achieved over this frequency range for coupling ratios of 30, 40, and 50 dB. Greater directivity can be achieved over a narrower frequency range, and the coupler can be tuned for essentially infinite directivity at a fixed frequency. The couplers, although resistive, can pass 100, 300, or 1000 Watts for the coupling ratios of 30, 40, and 50 dB respectively with less than 0.01 dB change in coupling ratio. The coupling ratios are constant with frequency to ±.25 dB.

11894. Homan, D. N., Zapf, T. L., **Two-stage guarded inductive voltage division for use at 100 kHz,** *Proc. 1969 Instrumen Society of America Conf., Houston, Texas, October 27-30 1969*, pp. 69-614 (1969); *ISA Trans.* **9,** No. 3, 201-209 (1970)

Key words: Divider; inductive voltage divider; ratio; voltage divider; voltage ratio.

A single decade inductive voltage divider with output tap corrections less than $5 \times 10^{-7}$ of input voltage at a frequency of 10 kHz is described and evaluated both experimentally an theoretically. The divider is a two-stage device which is als guarded section by section. These two techniques greatly reduc errors caused by unequal leakage inductance and interwindin capacitances, which otherwise cause significant errors at 10 kHz. Design and construction details are presented for th dividers and for the bridge circuit used to make the measurements of the output tap corrections to the divider.

11895. Hunt, C. M., Woolf, A. R., **Comparison of some differen methods for measuring particle size using microscopicall calibrated glass beads,** *Powder Technol.* **3,** 9-23 (1969).

Key words: Air elutriation; air permeability; Andrease pipette; calibrated glass beads; Coulter counter; electroformed sieves; microscopic size measurement; particle siz measurement.

Measurements of particle size distribution by the microscop and by a number of other methods were compared using sample of glass beads from a single blended batch as the referenc material. The other methods included a Coulter counter, elec troformed sieves, the Andreasen pipette, and the Roll analyzer. Surface average particle size calculated from micr scopic and Lea-Nurse air-permeability measurements were als compared. As an independent check of diameter measuremen with the microscope, comparisons were made with an inte ferometer, using fibers drawn from a melt of the same glas These comparisons afforded an opportunity to assess some the sources of error in each of the methods.

Differences between the averages of results obtained with th microscope and those obtained with the Coulter counter, th Lea-Nurse apparatus, the Andreasen pipette as well as the inte ferometer were comparable in magnitude with the norm statistical variations inherent in the methods themselves. How ever, small systematic biases were observed. Agreeme between results by the microscope and the Roller analyzer w satisfactory, although the latter is subject to greater uncertainti than the other methods investigated. Disagreements were o tained with fine electroformed sieves, which passed more mate al than predicted from the size distribution by the microscope.

11896. Jennings, D. A., West, E. D., **A laser power meter for lar beams,** *Rev. Sci. Instr.* **41,** No. 1, 565-567 (Apr. 1970).

Key words: Calorimetry; laser; laser calorimetry; las power.

A power meter is described in detail for large or diverge laser beams, either cw or repetitively pulsed. The meter me sures the flow of heat generated by the beam and is calibrat with an electrical heater wound just behind the absorbing su face. The meter is capable of power measurements of 1 to 30 accurate to ±2.5%.

11897. Johannesen, R. B., Ferretti, J. A., Harris, R. K., **UEAIT A new computer program for analysis of NMR spectra analy of the proton spectrum of triisopropylphosphine,** *J. Magne Resonance* **3,** No. 1, 84-93 (July 1970).

Key words: Computer program; isopropyl; NMR; nucle magnetic resonance; phosphorus; spectral analysis.

A new computer program for the analysis of NMR spectra reported. It adds iterative evaluation of input parameters to earlier program (UEANMR II) which makes use of magne quivalence factoring to reduce the size of certain matrices. The resent program, by iterating on line frequencies rather than nergy levels, and by using magnetic equivalence factoring, offers advantages of speed and convenience over previously escribed computer programs for NMR analysis. The analysis f the proton spectrum of triisopropylphosphine is described as n example and the trend of $^2J_{H\text{-}P}$ with increased alkyl substituon is found to be opposite to that of the trend of $^2J_{H\text{-}X}$ for all ther hetero-atoms, $X$, reported in the literature.

1898. Kidnay, A. J., Hiza, M. J., **Physical adsorption in cryogenic engineering,** *Cryogenics* **10,** No. 4, 271-277 (Aug. 1970).

Key words: Adsorbent-reaction; adsorption; heat transfer; isotherm; kinetics; mass transfer.

This article is a selective review of the literature on physical dsorption that is pertinent to cryogenic engineering. Included re tabulations of references to experimental adsorption otherms on high surface area adsorbents, both for pure materis and mixtures, and brief discussions of the more important chniques for correlating and predicting adsorption isotherms. dsorption kinetics, heat and mass transfer in packed beds, and dsorbent bed reactivation techniques are also discussed.

1899. Krauss, M., Mies, F. H., **Molecular-orbital calculation of the shape resonance in $N_2^-$,** *Phys. Rev. A* **1,** No. 6, 1592-1598 (June 1970).

Key words: Electron scatter; energy curve; local potential; $N_2$; resonance width; shape resonance; spectroscopic constant; valence orbital.

The 2-eV shape resonance in $N_2$-electron scattering is calcuted by a self-consistent-field energy-variational procedure. The sonance state corresponds to the attachment of an incident $d$-ave electron to the $1\pi_g$ valence orbital of the metastable $^2\Pi_g$ ate of $N_2^-$. The resonant behavior is due to the tunnelling of the ectron through a $2(2+1)/r^2$ centrifugal barrier and temporary apping in an attractive field. This tunnelling is reflected in the modal behavior of the calculated $1\pi_g$ orbitals; the inner portion the orbital defines the resonance state. The "potential" curve r $N_2^-$ is calculated in the Hartree-Fock approximation; a sonance threshold of 2.5 eV is predicted, with $R_e = 2.27$ a.u. d $\omega_e \approx 2000$ cm$^{-1}$. Expected correlation-energy corrections ould improve the agreement with experiment. A local potential r electron scattering is generated by inverting the $1\pi_g$ orbital, d resonance widths are calculated. The widths vary from 0.13 V at the equilibrium distance of $N_2^-$ to 0.8 eV at the $N_2$ quilibrium distance.

900. Lance, H. W., **Report on metrology sessions at the 24th annual ISA conference,** *Appl. Opt.* **9,** No. 6, 1497-1498 (June 1970).

Key words: Education for metrology; measurements; measurement techniques; metrology.

This report is primarily about the ISA sessions on "Education r Metrology." These sessions described (1) metrology training ograms in the military establishment and in industry—at least me of which are necessary because the nation's educational intutions largely neglect the subject of metrology—and (2) etrology courses being given or planned by a few universities. e latter verified the need for better measurement training, inted the way toward revitalized courses, and hinted that the iversities may be beginning to give more attention to this subt. The report also mentions selected papers from other sesns and summarizes briefly a Conference on Measurement lucation held in England in July 1969.

901. Lesclaux, R., Searles, S., Sieck, L. W., Ausloos, P., **Irradiation of cyclohexene with 8.4, 10.0 and 11.6-11.8 eV photons. Dissociation of neutral excited cyclohexene and reactions of $C_6H_{10}^+$,** *J. Chem. Phys.* **53,** No. 8, 3336-43 (Oct. 15, 1970).

Key words: Cyclohexene; ion-molecule reactions; photoionization; photolysis; unimolecular-dissociation.

The photolysis of cyclohexene has been investigated at photon energies above (10.0 eV, 11.6-11.8 eV) and below (8.4 eV) its ionization potential (8.9 eV). The ionic processes were studied in a mass spectrometer equipped with a photon source. The parent $C_6H_{10}^+$ ion was seen to undergo the following reactions with cyclohexene:

$$C_6H_{10}^+ + \text{cyclo-}C_6H_{10} \rightarrow \text{cyclo-}C_6H_{12} + C_6H_8^+ \; k = 0.7 \times 10^{-10} \text{ cm}^3\text{/molecule-sec}$$

$$\rightarrow C_{12}H_{20}^+ \; k = 4.1 \times 10^{-10} \text{ cm}^3\text{/molecule-sec.}$$

Analysis of the yields of cyclohexane formed in the first of these reactions in the photolysis at 10.0 eV over the pressure range from 1 to 10 torr indicates that the relative importance of the two reactions is the same in this pressure range as in the ion source of the mass spectrometer at a pressure of $10^{-2}$ torr. At 11.6-11.8 eV, the parent ion also dissociates, mainly to form $C_5H_7^+$ and $CH_3$. Evidence is presented which indicates that at these energies, the majority of the $C_6H_{10}^+$ ions retain a cyclic structure. The neutral, electronically excited cyclohexene molecule dissociates mainly as follows:

$$C_6H_{10}^* \rightarrow 1,3\text{-}C_4H_6 + C_2H_4, \text{ at } 8.4 \text{ eV}, \Phi = 0.82$$

$$\rightarrow C_5H_7 + CH_3, \text{ at } 8.4 \text{ eV}, \Phi = 0.08$$

The photolysis of 3,3,6,6-$d_4$-cyclohexene demonstrated that the first of these processes occurs predominantly by the "symmetrical" cleavage of the 3-4 and 5-6 C—C bonds, at all energies.

11902. Levin, E. M., **Liquid immiscibility in oxide systems,** Chapter in *Phase Diagrams Materials Science and Technology,* **Volume 3.** *The Use of Phase Diagrams in Ceramics, Glass and Metal Technology,* pp. 143-236, (Academic Press Inc., New York, N.Y., 1970).

Key words: Glass chromatography; immiscibility and courses of crystallization; immiscibility and practical applications; immiscibility and thermodynamics; immiscibility in oxides; liquid immiscibility; $Ln_2O_3 - B_2O_3$ phase diagrams; mechanism of phase separation; metastable liquid immiscibility; microphase separation; phase diagrams of metastable immiscibility; spinodal; structural interpretation of immiscibility; super-duty silica brick.

Stable and metastable liquid immiscibility in oxide systems is discussed from the standpoint of thermodynamics, interpretation, and application. The classic Gibbs free energy of formation-composition diagrams are used to illustrate the difference between a stable and a metastable immiscibility gap and to define the spinodal. Phase equilibrium principles are applied to liquid immiscibility and typical courses of crystallization are described. Structural interpretation is applied to the occurrence and extent of immiscibility including the temperature of the monotectic and the effect of homogenizers. The general incompatibility of compound formation and liquid immiscibility is demonstrated for the rare earth oxide-boric oxide systems. Occurrence and methods of study of microphase separation are elucidated. Three mechanisms of microphase separation are discussed briefly: nucleation and growth, spinodal decomposition, and intersecting growth theory. Binary and ternary phase diagrams showing liquid immiscibility are presented. Application to the following commercial products are discussed: super-duty silica brick, Vycor glass, Pyrex glass, glass ceramics, and glass chromatography.

**11903.** Levin, E. M., Roth, R. S., **The system niobium pentoxide-phosphorus pentoxide,** *J. Solid State Chem.* **2,** No. 2, 250-261 (1970).

Key words: $Nb_2O_5-P_2O_5$; $NbPO_5$; $Nb_2P_4O_{15}$; $Nb_9PO_{25}$; $Nb_{44}P_2O_{115}$; $P_2O_5-Nb_2O_5$; phase diagram; $ReO_3$-type compounds.

A partial phase diagram of the system $Nb_2O_5-P_2O_5$ has been determined experimentally, using the quenching technique and identifying the phases by x-ray powder diffractometry. The major phase, $NbPO_5$, has a melting point above 1650 °C. It transforms at about 1253 °C from a low-temperature, tetragonal phase to a high-temperature, monoclinic phase, isostructural with $TaPO_5$. The $9Nb_2O_5 \cdot P_2O_5$ phase shows a limited solid solution range and melts incongruently at 1435 °C. The eutectic between 9:1 and $NbPO_5$ is at 1365 °C and 67 mole % $Nb_2O_5$. At 96.4 mole % $Nb_2O_5$ another phase was found, stable between ~ 1340 and 1420 °C and isostructural with the 9:1 phase. A new monoclinic phase, "22:1" *ss* was found, with a limited stability field in both temperature and composition. It is most likely composed of 3 × 3 and 3 × 4 $ReO_6$-type blocks of octahedrally oxygen-coordinated niobium. In the subsystem $NbPO_5-P_2O_5$ liquidus values could not be determined even in sealed Pt tubes because of reactivity and high vapor pressure of $P_2O_5$. One compound was identified of probable composition $Nb_2O_5 \cdot 2P_2O_5$, with pseudocubic symmetry and melting incongruently at about 1025 °C. X-ray powder diffraction data and unit cell dimensions are listed for the phases.

**11904.** Lias, S. G., Collin, G. J., Rebbert, R. E., Ausloos, P., **Photolysis of ethane at 11.6-11.8 eV,** *J. Chem. Phys.* **52,** No. 4, 1841-1851 (Feb. 15, 1970).

Key words: Ethane; free radicals; ions; photolysis; primary processes; vacuum ultraviolet.

The photolysis of ethane, carried out with an argon resonance lamp, has been reinvestigated with the related purposes of (1) measuring quantum yields of all fragments formed in the dissociation of excited ethane, and (2) associating these fragments with the primary processes occurring in the photolysis of ethane. These, and their relative abundances are:

$$C_2H_6^* \rightarrow C_2H_6^+, 5\%$$

$$\rightarrow CH_4 + CH_2, 16\%$$

$$\rightarrow C_2H_5 + H, 41\%$$

$$\rightarrow C_2H_4 + H_2, 23\%$$

$$\rightarrow CH_3 + CH_3, 15\%$$

These results are compared with conclusions reached in earlier studies on the photolysis of ethane with xenon and krypton lamps in order to determine the effect of energy on the relative probabilities of the primary processes. It is found that direct bond scission increases in importance with increasing energy, while processes involving rearrangement decrease in importance.

The radical and molecular fragments formed in the dissociation of excited ethane were determined by (a) analyzing the products formed in $C_2H_6-C_2D_6-NO$ (1:1:0.1) mixtures and (b) $C_2D_6$ in the presence of $H_2S$, which scavenges free radicals to form isotopically-unique hydrocarbon products, and (c) $C_2H_6$ in the presence of $C_3D_6$, which scavenges H-atoms to form propyl radicals which in turn, react with radicals in the system to form characteristic products. Such experiments, as well as quantum yield determinations, were also carried out at tne krypton and xenon lines.

**11905.** Lias, S. G., Rebbert, R. E., Ausloos, P., **Irradiation of xenon-propane and argon-propane mixtures with gamma ray and 21.2 eV photons,** *J. Chem. Phys.* **52,** No. 2, 773-783 (Jan 15, 1970).

Key words: Deactivation; ion-molecule reactions photoionization; radiolysis; unimolecular ion fragmentation

Mixtures of xenon or argon with propane (20:1) are irradiate in the presence of radical scavengers by $\gamma$-rays and by 21.2 e photons from a helium resonance lamp. The ion-pair yields o products originating in ionic fragmentation reactions or ion molecule reactions are derived from isotopic analyses of produc molecules formed with $C_3D_8-C_3H_8$ mixtures or wit $CD_3CH_2CD_3$. At a given pressure, only minor differences ar seen between the radiolysis and photolysis in the modes of dissociation of parent propane ions formed by charge transfer wit a particular rare gas. Higher energy ionic fragmentatio processes are seen to be quenched with increasing pressure; i the case of xenon-propane mixtures, it is demonstrated that th parent ion yield increases as primary fragmentation processe are quenched. In the irradiated argon-propane-scavenger mixtures, isotope effects in the ionic fragmentation mechanism ar seen which indicate that collisional deactivation of the excite deuterated fragment ions is more efficient than that of the corresponding protonated ions. In the photolytic experiments, was deduced that the decomposition of neutral excited propan molecules constitutes about 10% of the product formin processes in the xenon mixtures, while in the radiolytic exper ments, the maximum contribution of neutral excited molecul decomposition is 5%. Similar deductions for the argon mixture were not feasible.

**11906.** Mandel, J., Paule, R. C., **Interlaboratory evaluation of material with unequal numbers of replicates,** *Anal. Chem.* 4 No. 11, 1194-1197 (Sept. 1970).

Key words: Analysis of variance; average (weighted); inte laboratory evaluation; round robin; single classificatio statistics; variance components; weighting.

Frequently, a "best value" has to be estimated on the basis measurements from different sources, such as different laborat ries. When the number of replicate measurements varies fro source to source, a problem of proper weighting arises. The usu formulas cover only one or the other of two extreme situation equal weighting of individual measurements, or equal weighti of source averages. The problem is described in detail, includi the interpretation of the analysis of variance, and an iterati procedure is presented for obtaining a properly weighte average. Formulas are also given for the estimation of the unce tainty of the weighted average. An illustrative example presented.

**11907.** Martin, W. C., Kaufman, V., **$4p^2$ configuration in neut zinc (Zn I),** *J. Opt. Soc. Am.* **60,** No. 8, 1096-1099 (Aug. 197

Key words: Atomic spectra; emission spectroscop wavelengths; zinc.

The Zn I $4s4p\ ^3P^\circ-p^2\ ^3P$ multiplet (2070–2105 Å) was reme sured on spectrograms from 10.7-m grating spectrographs. T new wavelengths are used to determine improved values for t $4p^2\ ^3P$ levels. Predicted positions and percentage compositio for the unknown $4p^2\ ^1D_2$ and $^1S_0$ levels are calculated in a pu configuration approximation. These results are combined wi our measurement of the autoionization width for the $^3P_2$ level, obtain a predicted autoionization probability of $1.3 \times 10^{15}\ s^{-1}$ f the $^1D_2$ level. The autoionization probability for the $^1S_0$ level similarly estimated to be $< 3 \times 10^{13}\ s^{-1}$. Wavelengths are giv for five new Zn I transitions (2040-2053 Å) from unknown a toionizing levels, probably belonging to the $4p4d$ configurati

11908. Mazur, J., **Non-self-intersecting random walks in lattices with nearest-neighbor interactions,** Chapter in *Stochastic Processes in Chemical Physics,* pp. 261-280 (John Wiley & Sons Inc., New York, N.Y., 1969).

Key words: Chain partition function; Monte-Carlo computations; near-neighbor interactions; phase transition; stochastic matrix; theta point.

A polymer chain is simulated as a self-avoiding walk on a lattice with forces of attraction between nonbonded chain elements which are mutually separated by a distance equal to a spacing between nearest lattice sites. The chain partition function and the related thermodynamic functions are investigated. Two different approaches are discussed: (1) Monte-Carlo investigations, based on random samples of self-avoiding walks, and (2) stochastic matrix method. Monte-Carlo investigations point to the possibility of configurational transitions in the chain and to the existence of the ideal, a theta, point. At the theta point, the dependence of the chain partition function on the number of chain elements is the same as if the chain were simulated by an equivalent Markovian chain model. The stochastic matrix method is formulated with the idea to verify and explain these Monte-Carlo results by investigation of the distribution of eigenvalues and eigenvectors of certain transition matrices, and their dependence on the near-neighbor forces of attraction. In this method, the chain is treated as a Markovian, multidimensional chain of dependent events. Some preliminary results of the investigation of chain partition function by the stochastic matrix method are presented.

1909. Meijer, P. H. E., **The importance of dipole-dipole interactions in ultralow temperature physics,** (Proc. 1970 Ultralow Temperature Symp. sponsored by Office of Naval Research and Naval Research Laboratory, April 23-24, 1970), R. A. Hein, D. U. Gubser, E. H. Takken, eds., *NRL Report 7133,* pp. 123-128 (Apr. 1970).

Key words: Cerous magnesium nitrate; cesium titanium alum; dipole-dipole interaction; neodymium ethyl sulphate; shape dependent; specific heat.

Preliminary results are given for the entropy corrections for cerous magnesium nitrate, cesium titanium alum, and neodymium ethyl sulphate. The entropy corrections were computed for the dipole interaction using the known g-factors and lattice constants. Also explains why the zero field specific heat is shape independent.

1910. Meinke, W. W., **Analytical chemistry – a fading discipline? No!,** *Anal. Chem.* **42,** 26A-38A (June 1970).

Key words: Analysis; analytical chemistry; analytical chemistry as a discipline; analytical chemistry as a profession.

Early in this century university curricula were built around detailed analytical courses, and the major chemical contributions of a national laboratory such as NBS were primarily analytical. The 20's brought a blossoming of organic chemistry, the 30's saw physical chemistry come into its own, the 40's saw a renewed emphasis put on inorganic chemistry, while in the 50's borderline fields such as biochemistry, nuclear chemistry, and geochemistry developed their followings. Despite this explosive growth of diverse chemical disciplines, the spirit of analytical chemistry is today much more pervasive than at any time in the last 50 years. The analytical chemist must determine over a wide range of concentrations not only what and how much is present, but in what valence form, how it is bound, and where it located spatially. Procedures must be rapid and easily automated, nondestructive if possible, and must give accurate and precise results. This demand for improved analytical measurement comes from fields as diverse as semiconductors and structural steel, air pollution and oceanography, clinical chemistry and lunar analysis.

11911. Melmed, A. J., Carroll, J. J., **Some initial observations of TiNi in the field-ion microscope,** *Appl. Phys. Letters* **17,** No. 6, 247-249 (Sept. 15, 1970).

Key words: Field-ion microscope; hydrogen; ion; liquid nitrogen temperature.

It is demonstrated that TiNi specimens can be successfully imaged with the field-ion microscope using liquid-nitrogen cooling, with hydrogen as the imaging gas. The material examined is shown to be structurally inhomogeneous, with relatively well-ordered regions in a less-ordered matrix. It is also shown that alternate atomic planes are different within some ordered regions.

11912. Meshkov, S., **Comments on baryon spectroscopy,** *Proc. Hyperon Resonances Conf., Duke University, Durham, N.C.,* pp. 471-500 (Apr. 24-25, 1970).

Key words: Baryons; configuration mixing; hyperons; resonances; rotations; $SU(6) \times 0(3)$.

A summary of the Hyperon Resonances Conference, together with various observations on the state of baryon spectroscopy is given.

11913. Nargolwalla, S. S., Niewodniczanski, J., Suddueth, J. E., **Experimental sensitivities for 3-MeV neutron activation analysis,** *J. Radioanal. Chem.* **5,** 403-423 (1970).

Key words: Absolute flux; Cockcroft-Walton neutron generator; sample attenuation corrections; sensitivity and gamma-ray spectra of the elements; 3-MeV neutron activation analysis.

The experimental sensitivity for 72 different elements using 3 MeV neutron activation has been investigated. Using a 200 kV Cockcroft-Walton neutron generator with a 3 MeV neutron flux of about $1.5 \cdot 10^6 n \cdot cm^{-2} \cdot sec^{-1}$, $\gamma$-ray spectra of 51 elements were obtained with a sufficient number of photopeak counts for sensitivity calculations using a photopeak integration method. A useful table summarizing the sensitivity results is given. That 3 MeV neutron activation analysis is practical, is demonstrated by the experimental sensitivities obtained.

11914. Nargolwalla, S. S., Suddueth, J. E., Rook, H. L., **Determination of pulse pileup and nuclear interferences in 14-MeV neutron activation analysis for trace oxygen, (Summary),** *Trans. Am. Nucl. Soc.* **13,** No. 1, 78-79 (1970).

Key words: Activation analysis; nuclear interferences; trace oxygen.

11915. Newton, C. J., Ruff, A. W., Jr., **X-ray study of annealing in plastically deformed Ag-Sn (silver-tin) alloys,** *Met. Trans.* **1,** No. 10, 2833-2838 (Oct. 1970).

Key words: Silver; silver-tin alloys; stacking fault probability; x-ray diffraction data.

The stacking fault probability, root-mean-square strain, and effective domain size are determined for pure silver and three Ag-Sn alloys using x-ray diffraction data. Both isochronal and isothermal annealing experiments were conducted to determine the nature of the recovery of plastic deformation in the filed powder specimens. An abrupt recovery of the above quantities was observed during isochronal annealing at temperatures that increased with solute concentration. Three recovery stages were observed in Ag-9 at. % Sn annealed at 165 °C for varying times. The principal stage is probably associated with recrystallization since both the stacking fault probability and rms strain recover together. An activation energy of 25 kcal per mol is determined for this stage.

11916. O'Connell, J. S., **Electron scattering sum rule for $^2$H, $^3$H, $^3$He and $^4$He,** *Physics Letters* **32B,** No. 5, 323-325 (Aug. 3, 1970).

Key words: Correlation; electron scattering; form factor; helium; hydrogen; sum rule.

A sum rule is derived for the spatially symmetric part of the 1s shell nuclei. The result depends on the mean square nucleon momentum in the ground state, the nucleon pair correlation form factor and, for the helium isotopes, a momentum pair correlation form factor.

**11917.** Otoshi, T. Y., Stelzried, C. T., Yates, B. C., Beatty, R. W., **Comparisons of waveguide losses calibrated by the dc potentiometer, ac ratio transformer, and reflectometer techniques,** *IEEE Trans. Microwave Theory Tech.* **MTT-18,** No. 7, 406-409 (July 1970).

Key words: Comparison of results; dc potentiometer test set; dual channel system; modulated subcarrier; ratio transformer test set; small attenuation measurement; small insertion loss measurement; small reflection coefficient measurements; stainless steel waveguide.

Comparisons are made of the losses of two precision waveguide sections that were calibrated by three independent attenuation measurement methods. The loss measurement systems involved were the (1) dual-channel system which uses thermistors and a dc potentiometer test set, (2) dual-channel system which uses barretters and an ac ratio transformer test set, and (3) National Bureau of Standards reflectometer system which utilizes a quarter-wave short circuit and an IF attenuation standard. Loss values of about 0.05 dB, as calibrated by the three independent methods, typically agreed to within 0.0006 dB. It is believed that the results of these calibrations are representative of the best that can be achieved with current state-of-the-art techniques and available instrumentation for low-loss waveguide measurements.

**11918.** Parker, R. L., **Crystal growth mechanisms: Energetics, kinetics, and transport,** *Solid State Phys.* **25,** 151-299 (Academic Press Inc., New York, N.Y., 1970).

Key words: Crystal; crystal growth; crystallization; growth mechanisms; morphological stability; nucleation; phase changes; transport processes.

A review is given of the mechanisms of crystal growth. Subjects discussed include thermodynamics and statistical mechanics of phase changes; the mathematical physics of crystal growth transport processes; nucleation; interface structure and interface kinetics; morphological stability; impurity effects; and fluid flow effects in crystallization. Particularly emphasized are the results of quantitative studies, both theoretical and experimental, on well defined systems. Experimental techniques and apparatus are not covered, nor are solid-solid transformations or the crystallization of polymers.

**11919.** Perel, J., Deslattes, R. D., **Extended fine-structure in x-ray absorption spectra of certain perovskites,** *Phys. Rev. B* **2,** No. 5, 1317-1323 (Sept. 1, 1970).

Key words: Absorption; fine-structure; perovskites; x ray.

In this paper we attempt to test the validity of the short-range-order (SRO) and the long-range-order (LRO) theories of the extended fine structure (EFS) in x-ray absorption spectra. This is done by comparing the EFS's of Ti, Ca, Zr, and Sr in the perovskitelike compounds $SrTiO_3$, $CaTiO_3$, $SrZrO_3$, and $CaZrO_3$. The regularities which have been anticipated from SRO or LRO theories have not been observed. We are thus led to suggest that models are required other than those which have been used to explain the EFS.

**11920.** Powell, C. J., **Validity of inelastic-electron-scattering data in determining the metallic or insulating properties of adsorbed atomic layers,** *Phys. Rev. B* **1,** No. 10, 4191-4192 (May 1970).

Key words: Adsorbed atomic layers; cesium; inelastic-electron scattering; metal-insulator transition; plasmon energy losses; tungsten.

It is pointed out that the observation of plasmon energy-loss peaks and determination of peak breadths in inelastic-electron-scattering experiments cannot be used to distinguish metallic or insulating materials. The recent claim, based on inelastic-electron-scattering data, by MacRae, Müller, Lander, Morrison, and Phillips that the initial (low-density) second layer of cesium adsorbed on a tungsten (100) surface is in an insulating state is considered not proved.

**11921.** Powell, C. J., **Comparison of optical data for sodium and potassium with interband-transition absorption theory,** *Optics Commun.* **2,** No. 2, 87-89 (July 1970).

Key words: Interband transition theory; optical absorption; potassium; pseudopotential; sodium.

Smith's optical data for Na and K have been used to test the validity of the Wilson-Butcher interband-transition absorption theory and recent theoretical modifications. Values of "optical" pseudopotential ($V_{110}$) have been obtained which deviate qualitatively from the pseudopotentials derived from de Haas-van Alphen data in the manner predicted by Animalu. Good agreement is found between the derived values of interband conductivity for Na and Animalu's calculations but the derived values for K are about a factor of two smaller than Animalu's result.

**11922.** Risley, A. S., Allan, D. W., Peters, H. E., Johnson, E. H., Vessot, R. F. C., Levine, M., Gray, J. E., Shoaf, J. H., **Stability characteristics of some atomic frequency standards (Summary)** (Proc. Conf. Precision Electromagnetic Measurements, National Bureau of Standards, Boulder, Colo., June 2-5, 1970), *CPEM Digest,* **pp. 74-75 (1970).**

Key words: Allan variance; cesium beam; frequency stability; hydrogen maser; NBS frequency standard; time scale.

Over a period of three and one-half months a frequency stability comparison was made between seven commercial cesium beams and a NASA (Goddard Space Flight Center) hydrogen maser. Two of the prime purposes in bringing the NASA maser to Boulder were: (1) to determine the general effect upon the NBS Time Scale of including the H maser as a part and (2) to determine the stability of the H maser for sampling times $\tau$ longer than $10^3$ seconds.

Two of the major results of the time scale and NASA maser comparison were, first, $\sigma_y(N=2,\ T=\tau,\ \tau=1\ \text{day})$ of the time scale—*including the maser*—was less than $1\times10^{-13}$, where $y\equiv\delta\nu/\nu$. Second, the inclusion of the maser in the time scale improved the precision about 30 percent.

Another hydrogen maser (from the Smithsonian Astrophysical Observatory) and a new four-foot long cesium beam (NBS-X4) were used along with the NASA maser to measure stabilities, $\sigma_y(N=2,\ T=\tau,\ \tau)$ $(\tau\approx1\ \text{day})$. The stabilities for both masers and for NBS-X4 were better than one part in $10^{13}$.

**11923.** Robertson, B., **Quantum statistical mechanical derivation of generalized hydrodynamic equations,** *J. Math. Phys.* **11,** No. 8, 2482-2488 (Aug. 1970).

Key words: Conservation equations; equation of motion; hydrodynamic equations; quantum fluids; quantum mechanical density distribution; quantum statistical mechanics.

Exact differential conservation equations are derived for the mass, momentum, and energy density operators for a one-com ponent simple fluid of Bose or Fermi particles with arbitrary pairwise interactions. These equations are used in a statistical mechanical derivation of exact equations of motion for the expectations of these operators. The equations of motion are coupled to the exact equations relating the local temperature, chemical potential, and fluid velocity to these expectations. The coupled equations are closed in the sense that the expectations and their thermodynamic conjugates listed above are the only unknowns, although some of the dependence in the equations on the conjugates is expressed only implicitly. The equations of motion are memory-retaining nonlocal generalizations of the classical hydrodynamic equations and apply to a normal fluid arbitrarily far from equilibrium. The formalism is not carried as far as has the corresponding classical formalism.

**11924.** Schneider, S. J., **Cooperative determination of the melting point of alumina,** *J. Pure Appl. Chem.* **21,** No. 1, 117-122 (1970).

Key words: $Al_2O_3$; alumina; IUPAC; melting point of $Al_2O_3$; melting point standards.

A task force on secondary temperature standards, sponsored by the Commission on High Temperatures and Refractories, International Union of Pure and Applied Chemistry, has undertaken a programme to investigate various inorganic nonmetallic substances for use as high-temperature reference materials. As part of this programme a cooperative determination of the melting point of $Al_2O_3$ (alumina) was conducted by the task force. In all, nine scientific groups representing seven countries contributed experimental data. All work was performed utilizing a common supply of $Al_2O_3$ of nominal 99.9 percent purity. Experimental techniques varied depending upon the individual investigator. The value for the alumina point as recommended by the task force is $2054 \pm 6$ °C (IPTS 1968).

**11925.** Schooley, J. F., Soulen, R. J., Koonce, C. S., **Surface potential barrier in $SrTiO_3$,** *Solid State Commun.* **7,** 1077-1079 (1969).

Key words: Indium; semiconductors; $SrTiO_3$; strontium titanate; superconductivity; surface potential barrier; tunneling.

We have observed supercurrent flow in tunneling measurements in In-$SrTiO_3$ junctions. Applying the coherence-distance criterion to these results, we can set an upper bound of 100 Å on the thickness of the indium-$SrTiO_3$ potential barrier.

**11926.** Selby, M. C., **The Bolovac and its applications (Summary),** (Proc. Conf. Precision Electromagnetic Measurements, National Bureau of Standards, Boulder, Colo., June 2-5, 1970) *CPEM Digest,* pp. 14-15 (1970).

Key words: Bolovac; current measurement (HF & MW); (HF & MW); microwave currents; microwave voltages; power measurement; voltage measurement (HF & MW).

The Bolovac is a new device for the standardization and measurement of TEM voltage, current and power through 18 GHz (potentially through 36 GHz). It can be used for attenuation measurement and as a near perfect impedance termination. It is the first and only anywhere practical means of calibrating microwave current indicators and of evaluating oscilloscopes displaying 25-ps or shorter rise-time pulses.

The application of the Bolovac will revolutionize power measurements. It eliminates (1) "mismatch errors," the major present source of uncertainty in power measurement, (2) the measurement of complex reflection coefficients, (3) complex computations, (4) the use of "error-limit" charts, and (5) the measurement of "effective efficiency" and "calibration factor." Its application may radically increase optimum accuracy and measurement-time efficiency.

The Bolovac can be used as a source of voltage or as an absorption power meter. It needs no rf calibration. It has a 15 to 40 dB range depending on the desired precision and on whether one or more sensors (special bolometric disks) are used.

**11927.** Sieck, L. W., Searles, S. K., **High-pressure photoionization mass spectrometry. Reactions of alkane and cycloalkane molecular ions with water vapor at thermal kinetic energies,** *J. Chem. Phys.* **53,** No. 1, 2601-2604 (Oct. 1, 1970).

Key words: Hydrocarbons; ion-molecule reactions; mass spectrometry; photoionization; proton transfer; water.

The reactions of alkane molecular ions ($RH_2^+$) with water vapor were found to proceed via a bimolecular mechanism in both ethane and propane. Parent ions from cyclohexane, cyclopentane, *i*-butane, *n*-butane, *i*-pentane, *n*-pentane, and *n*-hexane were observed to react exclusively via a termolecular mechanism involving two water molecules: $RH_2^+ + 2H_2O \rightarrow H^+(H_2O)_2 + RH$. Thermal rate constants of 1.2 and $1.4 \times 10^{-9}$ cm$^3$/molecule·sec, respectively, were derived for the bimolecular reactions of $C_2H_6^+$ and $C_3H_8^+$ with $H_2O$. The termolecular rate constants found in other $RH_2^+ - H_2O$ combinations were quite high, falling in the range $10^{-25} - 10^{-27}$ cm$^6$/molecule·sec. The nature of the collision complex is discussed, and new limits are estimated for $\Delta H_f(H_3O^+)$.

**11928.** Sieck, L. W., Searles, S. K., Rebbert, R. E., Ausloos, P., **Reactivity of the cyclohexane ion,** *J. Phys. Chem.* **74,** No. 21, 3829-3831 (Oct. 15, 1970).

Key words: Cyclohexane; effects impurity; ion-molecule reactions; mass spectrometry; radiolysis.

It is shown that contrary to the findings reported in a recent study (reference 2 cited in this communication) the cyclohexane ion reacts with cyclohexane very slowly ($k \leq 5 \times 10^{-14}$ cm$^3$/molecule-sec). Cyclohexane has been studied very extensively by radiation chemists who consider it as a key compound in the interpretation of energy deposition mechanisms. It is therefore important that the misconception recently introduced in the literature be rectified as soon as possible.

**11929.** Simmons, J. H., Napolitano, A., Macedo, P. B., **Supercritical viscosity anomaly in oxide mixtures,** *J. Chem. Phys.* **53,** No. 3, 1165-1170 (Aug. 1, 1970).

Key words: Anomaly in oxide mixtures; oxide mixtures; viscosity anomaly.

The viscosity anomaly, previously detected above the critical point of some fluid binary mixtures, is investigated in the sodium-borosilicate oxide system. At the sodium-borosilicate dome, the critical composition is selected with small CaO and $Al_2O_3$ doping additions to obtain samples whose critical temperatures range over 190 °C and have minimum high-temperature structural differences. Viscosities between $10^2$ and $10^9$ P ($10^{-1}$ N·sec/m$^2$) are measured. A fractional excess viscosity is defined as the difference between the viscosity of each melt and a normal viscosity function, divided by the normal viscosity. The normal viscosity function is taken to have the form of the viscosity curve from the sample with the lowest critical temperature. The fractional excess viscosity then shows an anomalous increase near the critical point. The fractional excess viscosity, $\Delta\eta/\eta_0$, attains a value of 2 near the consolute temperature but appears to remain finite at the critical point. This critical-point effect can be detected 200 °C above the critical temperature. Such results indicate that the viscosity is quite sensitive to the presence of composition fluctuations above the critical point of this system, and represents a good tool for investigating supercritical phenomena.

**11930.** Straty, G. C., Prydz, R., **Fluorine compatible apparatus**

**for accurate PVT measurements,** *Rev. Sci. Instr.* **41,** No. 8, 1223-1227 (Aug. 1970).

Key words: Cryostat; fabrication techniques; fluorine, materials compatibility; PVT apparatus; PVT method.

A fluorine compatible apparatus, incorporating numerous safety features, is described. This apparatus has been used to make accurate determinations of the PVT properties of gaseous and liquid fluorine from 53.5 K (the triple point) to 300 K and to pressures of 20 MN/m$^2$ (3000 psi). The experimental method is similar to the isochoric one used previously in this laboratory for oxygen and hydrogen. A limited testing program, to determine the suitability of various materials for use with high pressure fluorine, is described and the test results tabulated. Some general fabrication techniques, suitable for construction of fluorine handling apparatus, are discussed.

**11931.** Thomas, A. M., **Further study of vacuum vane gauge criteria: Effects of port-vane geometry,** *J. Vacuum Sci. Technol.* **7,** No. 4, 501-503 (July-Aug. 1970).

Key words: Design criteria; port-vane geometry; vacuum vane gauge.

The force on a movable vane which covers the exit of a tube is related to the pressure at the tube entrance. This principle can be utilized in the construction of a "vane" gauge. The Monte Carlo method has previously been used to determine the correlation between the force on the vane and the pressure at the tube inlet. An extension of that work to a more complex and realistic geometry, which includes an elbow and a conical section, is presented here. This geometry represents the port structure of a gauge presently under construction in our laboratory. Details of the molecular motion, such as density and flux distributions throughout the system, were calculated. Under certain conditions, the geometry upstream of the port was shown to have negligible effect on the force imparted to the vane and a calibration curve is presented relating this force to the vane-to-port distance over a limited range.

**11932.** Waxman, M., Hastings, J. R., Chen, W. T., **Nonlinear statistical analysis of Burnett PVT data,** *Proc. 5th Symp. Thermophysical Properties, Boston, Massachusetts, September 30-October 2, 1970,* C. F. Bonilla, ed., pp. 248-261 (American Society of Mechanical Engineers, New York, N.Y., 1970).

Key words: Burnett; gas; model dependency; nonlinear; PVT; statistical.

The Burnett method, which requires only temperature and isothermal pressure measurements made before and after stepwise expansions between two volumes, is being used extensively for determining gas compressibilities and density or pressure virial coefficients. The measurements are simple, but the data reduction involves rather formidable nonlinear statistical analysis of relationships containing the compressibility factor, defined by a density or a pressure virial expansion, and optional constants. In this paper we compare the results of analyzing different Burnett relationships with independent parameters and no restrictions on the data, using two nonlinear statistical methods, due to Gauss and to Deming, and argon data at 25 °C for pressures up to 250 atm. We discuss the computational difficulties and present background information on the experimental and analytical methods.

**11933.** Yokel, F. Y., Somes, N. F., **Proposed revision of ACI 318-63 Building Code Requirements for Reinforced Concrete,** *J. Am. Concrete Inst.* **67,** No. 9, 723-725 (Sept. 1970).

Key words: Axial load (force); bending moment; building codes; end-fixity; reinforced concrete; slenderness; strength; structural analysis; walls.

This contribution discusses Chapters 10 and 14 of the Proposed Revision of ACI 318-63 Building Code Requirements of Reinforced Concrete Reported by ACI Committee 318 in the Journal of the American Concrete Institute, February 1970. It points out some inconsistencies in the respective ways in which these two Chapters cover bearing walls. Some changes are recommended which, if adopted, would extend the coverage of Chapter 10 to include those walls covered only by Chapter 14.

**11934.** Young, J. P., Lamb, V. A., Reid, G. I., Berkeley, J. F., Ng, W., **Electroplated coatings on maraging steel for retarding catalytic decomposition of hydrazine rocket fuel,** *Plating* **57,** No. 9, 921-926 (Sept. 1970).

Key words: Compatibility tests; electrolytic protection; hydrazine; maraging steel; metallic coatings; missiles; rocket-fuel tanks.

Hydrazine and methyl hydrazine are catalytically decomposed in contact with certain metals, e.g., Maraging steel, yielding gaseous decomposition products. As a result, dangerous pressures develop during prolonged storage of rockets that employ hydrazine-type fuels contained in Maraging steel tanks. The tanks therefore require a coating on their internal surfaces that will not be corroded by hydrazine nor cause it to decompose. The work reported is a general survey of a variety of materials, most of them applied as plated coatings, to determine their suitability for this application. Cadmium and electroless nickel are the most practicable of a number of materials that were found to have low catalytic effect and that were not significantly corroded.

**11935.** Younglove, B. A., Straty, G. C., **A capacitor for accurate wide range dielectric constant measurements on compressed fluids,** *Rev. Sci. Instr.* **41,** No. 7, 1087-1089 (July 1970).

Key words: Capacitance; dielectric constant; stable capacitance; temperature variation of capacitance.

A capacitor is described which has been used to make accurate measurements of the dielectric constant of liquid and gaseous oxygen over a wide temperature (55-300 K) and pressure (0.2-34 MN/m$^2$) range. The capacitor is simple to construct and its stability is unaffected by large hydrostatic pressure variations. The temperature variation of the vacuum capacitance is small and remains reproducible even after repeated temperature and pressure cycling.

**11936.** Zimmerman, J. E., **Low cost sensors with millikelvin temperatures and other virtues (Summary),** (Proc. Conf. Precision Electromagnetic Measurements, National Bureau of Standards, Boulder, Colorado, June 2-5, 1970), *CPEM Digest,* p. 1 (1970).

Key words: Josephson effect; magnetometry; superconducting devices.

This paper is a 280-word summary of a talk to be given at the Conference on Precision Electrical Measurements. It summarizes the simple theory of the superconducting quantum devices known as weak links or Josephson junctions, and reviews some applications to magnetometry, high-frequency radiation sensing, and dc and rf current and voltage standards. The inherent low-noise, absolute calibration, versatility, and low-cost of the devices are emphasized.

**11937.** Unassigned.

**11938.** Bagg, T. C., **Factors dictating characteristics of systems utilizing microforms,** *J. Micrographs* **3,** No. 3, 143-146 (1970); *ABFM Format* **1,** No. 2, 1-2 (May 1970).

Key words: Document storage and retrieval; microform-microfilm systems.

There is a wide variety of microform formats and equipment vailable for handling microimages. The systems designer thereore has the opportunity to select those procedures and equipment that will assure the fulfillment of the system's requirements. This paper will briefly discuss some questions he must nswer before establishing the most effective design. Each appliation of microforms has its particular requirements; therefore he questions can serve only as guidelines. It cannot be over mphasized that the most useful systems are the simplest that will produce legible output images.

**1939.** Birky, M. M., **Simultaneous recording of near-field and far-field patterns of lasers,** *Appl. Opt.* **8,** No. 11, 2249-2253 (Nov. 1969).

Key words: Laser; near-field and far-field diffraction; neodymium; ruby.

A technique for simultaneous recording of near-field and far-ield diffraction patterns at several exposures for a single laser ulse has been developed. A ruby laser and a neodymium doped lass laser have been investigated. The $\mathrm{Nd}^{+3}$ laser shows striking igh order cylindrical mode operation as a result of thermal stress. The time resolved output of this laser shows the usual spikes about 500 nsec wide. When the cylindrical mode operaon takes place some of the spikes consist of a large number of ltrashort pulses.

**1940.** Branscomb, L. M., **A fully integrated partnership between government laboratory and university,** *Proc. Education on Federal Laboratory-University Relationships Symp. sponsored by the Federal Council for Science and Technology and the American Council on Education, Washington, D.C., October 29-31, 1968,* pp. 139-151 (May 1969).

Key words: *Research management* principles embodied in *government-university collaboration* in the *Joint Institute for Laboratory Astrophysics.*

Invited talk to symposium "Education and Federal Laboratory-University Relationships" sponsored by the Federal Council or Science and Technology, at the Smithsonian Institution, Oct. 9-31, 1968.

The pattern of government laboratory-university collaboration herent in the Joint Institute for Laboratory Astrophysics ILA) is described, with emphasis on its advantages and shortcomings and the relevant management principles. (No technical formation is included.)

**1941.** Branscomb, L. M., **Discussion,** *Can. J. Chem.* **47,** No. 10, 1703-1941 (May 15, 1969).

Key words: Aeronomy; editorial comments.

This manuscript contains the edited comments on invited apers by A. Dalgarno, A. V. Phelps, and E. E. Ferguson which ill appear in Transactions of the IAGA (International Associaon of Geomagnetism and Aeronomy) Symposium on Laborato Measurements of Aeronomic Interest, September 3-4, 1968, ork University, Toronto, Canada. The Transactions are to be ublished in the Canadian Journal of Chemistry.

**942.** Brenner, A., Anderson, H. J., **Chemical vapor deposition of rhenium,** *Proc. Interfinish 1968 7th International Metal Finishing Conf., May 5-9, 1968, Hanover, Germany,* pp. 28-31 (1968).

Key words: Carbonyl; chemical vapor deposition; electrodeposition; hexafluoroacetylacetone; rhenium coatings; trifluorophosphine.

Methods of depositing rhenium coatings are reviewed, and a rief account is given of work now in progress at NBS on the deposition of rhenium. The electrodeposition of rhenium from an aqueous perrhenate bath does not yield a satisfactory coating; work at NBS with various rhenium compounds in both aqueous and nonaqueous solutions did not lead to a better plating process. The chemical vapor deposition (CVD) of rhenium is more promising, particularly the reduction of rhenium hexafluoride with hydrogen. At NBS work has been done with the CVD of rhenium from the carbonyl, the hexafluoroacetylacetone derivative, and work is in progress with the trifluorophosphine derivatives.

**11943.** Carrington, T., Garvin, D., **The chemical production of excited states,** Chapter 3 in *Comprehensive Chemical Kinetics,* **Volume 3.** *The Formation and Decay of Excited Species,* pp. 107-181 (1969).

Key words: Atom-transfer reaction; chemical activation; chemical kinetics; chemi-excitation; gas phase; potential energy surfaces; recombination; review; unimolecular decomposition.

Chemical excitation, the production of molecules in nonequilibrium population distributions in electronic, vibrational and rotational states is described.

The applicable parts of reaction rate theory are reviewed. Typical cases are used as examples of chemi-excitation in combination, group transfer and decomposition reactions. Reactions involving excited electronic states are discussed in terms of the interaction of potential surfaces. Applications to lasers and to the study of unimolecular decompositions are described.

**11944.** Chandler, H. H., Bowen, R. L., Paffenbarger, G. C., Mullineaux, A. L., **Clinical investigation of a radiopaque composite restorative material,** *J. Am. Dental Assoc.* **81,** No. 4, 935-940 (Oct. 1970).

Key words: Clinical research (dental); composite restorations; diagnosis; physical properties of fillings; x-ray opaque.

A radiopaque composite restorative material was developed using a ternary eutectic dimethacrylate liquid formulation as the binder and a $\mathrm{BaF_2}$-containing glass and fused silica as the reinforcing fillers. One hundred and ten restorations were placed with this newly developed material. The restorations will be observed for an extended time. They had sufficient radiopacity and yet were esthetically pleasing. Postoperative radiographs showed comparatively radiolucent areas in and around many of the restorations. These radiolucencies were usually caused by unfilled spaces at the tooth restoration interface.

**11945.** Chandler, R. F., Christian, R. A., **Comparative evaluation of dummy performance under $-\mathrm{G}_x$ impact,** *Proc. 13th Stapp Car Crash Conf., Boston, Mass., December 2-4, 1969,* Report No. 690798, pp. 61-75 (Society of Automotive Engineers, New York, N.Y., 1970); Abstract in *SAE Trans.* **78,** 171-172 (1969).

Key words: Automobiles; dummies; dynamic; impact; performance; restraints.

Comparative evaluations of a variety of anthropomorphic dummies undertaken by the Office of Vehicle Systems Research at the National Bureau of Standards indicates a wide range of dummy performance. Dynamic tests, which were conducted on the NBS Dynamic Seat Belt Tester, simulated an impact environment with the dummies restrained by lap belt alone, or combined lap and torso diagonal belts of the type used in American automobiles. A variety of dummies, varying in construction from the most rudimentary to the most sophisticated were tested. Test parameters included variations in impact velocity and acceleration. Each dummy was tested with both types of restraints, and sufficient tests were made to demonstrate the ability of the dummy to reproduce its reaction performance.

These tests indicate that even when dummies are subjected to carefully controlled impacts with skilled technical personnel following identical procedures, it is difficult to reproduce test results. Techniques which were used to control dummy performance and modifications which were incorporated to improve reliability of the dummies are discussed.

**11946.** Christ, B. W., Smith, G. V., **Effects of nitrogen in lattice solution on the yielding and flow of zone-refined iron polycrystals between 128 and 300 K,** *Trans. Met. Soc. AIME* **1,** No. 4, 827-833 (Apr. 1970).

Key words: Flow stress; impurity softening; lattice solution; lower yield stress; nitrogen; polycrystals; solution hardening; upper yield point; zone-refined iron.

Up to 0.18 at. pct N was introduced into lattice solution in hydrogen-purified, zone-refined iron polycrystals. Tensile tests were conducted at 128, 173, 223, and 300 K on quenched samples at constant strain rate, $7 \times 10^{-4}$ sec$^{-1}$. The following dynamic effects due to increasing nitrogen in lattice solution were found: (1) the temperature dependence of the flow stress at strains beyond the end of the Luder's plateau decreased, (2) serrated flow occurred at 300 K, but not at lower temperatures, (3) elongation to maximum load decreased at 300 K, but increased at 173 K, and (4) the magnitude of the yield drop at 173 K decreased substantially. These dynamic effects are interpreted in terms of a change in the relative mobility of nitrogen atoms and dislocations between 128 and 300 K.

**11947.** Coriell, S. R., Jackson, J. L., **Probability distribution of the radius of gyration for two statistical segments,** *J. Chem. Phys.* **53,** No. 8, 3389 (Oct. 15, 1970).

Key words: Distribution; gyration; polymer; radius; two segments.

An analytic expression is obtained for the distribution of the one-dimensional radius of gyration of a random flight polymer chain of two statistical segments. The result is a product of an exponential function and a modified Bessel function of order zero.

**11948.** Cornog, D. Y., Cornog, J. R., **Human factors engineering in the sorting and handling of mail,** *Proc. NATO Advanced Study Institute on "Human Factors/Ergonomics," Mondello, Sicily, September 29, 1969,* pp. 1-34 (Jan. 21, 1970).

Key words: Human factors; mail handling; mail processing; mail sorting; methodology.

A case study is used to illustrate both the technical and management aspects of human factors in a unique American organization—an organization which combines a government agency with the typical operations of a gigantic materials handling industry—the United States Post Office Department. Mail handling operations are described with an enumeration of the types of human factors problems to be found. The various approaches to solving human factors problems include: in-house Human Factors Engineering Laboratory research, field studies in postal installations, and contract research performed by industry, private research firms and university departments. Future human factors research in mail handling problem areas is discussed. Information is provided about data sources for American human factors research activities and personnel.

**11949.** Davis, D. D., **Transmission of time/frequency signals in the vertical interval,** *Proc. 108th Technical Conference and Equipment Exhibit, New York, N.Y., October 4-9, 1970,* Article No. 43, p. 3 (Society of Motion Picture and Television Engineers, New York, N.Y., 1970).

Key words: Frequency and time dissemination; television; vertical interval signals.

An abstract will be prepared from the synopsis, by the Society of Motion Picture and Television Engineers, subject to the author's clearance.

**11950.** Dick, C. E., Lucas, A. C., ***K*-shell fluorescence yields fo light elements,** *Phys. Rev. A* **2,** No. 3, 580-586 (Sept. 1970).

Key words: Beryllium; boron; carbon; fluorescence yield fluorine; *K* shell; magnesium; $\omega_K$.

The *K*-shell fluorescence yield $\omega_K$ has been measured for the low-atomic-number elements beryllium, boron, carbon, fluorine and magnesium. The primary vacancies in the *K* shell were produced by an intense beam of *K* x rays generated by electron bombardment of aluminum and carbon targets. The measured values of $\omega_K$ agree quite well with values calculated from a theoretical prediction of Wenzel. They exhibit only fair agreement with semiempirical formulas which include screening and relativistic effects, and with a recent calculation by McGuire based on the *K*-shell Auger transition rate.

**11951.** Dickens, B., Brown, W. E., **The crystal structure of calcium carbonate hexahydrate at ~ – 120°,** *Inorg. Chem.* **9,** No 3, 480-486 (Mar. 1970).

Key words: Calcification; calcium carbonate; crystal structure; hydrate; ion pairs; mineralization.

The crystal structure of $CaCO_3 \cdot 6H_2O$ has been determined from 1420 x-ray diffraction data collected photographically by the oscillation technique from a single crystal held at ~ – 120° The unit cell parameters are $a = 8.87$ (2) Å, $b = 8.23$ (1) Å, $c =$ 11.02 (2) Å, and $\beta = 110.2$ (2)°, and the space group is C2/c with $Z = 4$. The calculated density at ~ – 120° is 1.80 g cm$^{-3}$, and the observed density at ~ 0° is 1.82 g cm$^{-3}$. The final *R* factor i 0.10. The structure contains discrete $CaCO_3$ ion pairs, each surrounded by an envelope of 18 water molecules. Thus, $Ca^{2+}$ i coordinated to only one $CO_3^{2-}$. Six of the surrounding $H_2O$ molecules are bonded to $Ca^{2+}$, eight are hydrogen bonded to oxygens of the $CO_3^{2-}$ group, and four are bonded to adjacent io pairs and to other water molecules in the envelope $CaCO_3 \cdot 6H_2O$ was found to be more stable than $CaCO_3 \cdot H_2O$ i water near 0°. The formation of $CaCO_3 \cdot 6H_2O$ from a equivalent amount of calcite ($CaCO_3$) and water is accompanie by a 20% decrease in volume. This may be important in explaining the scarcity of calcareous material in life in the ocean depths

**11952.** Dobbyn, R. C., Williams, M. L., Cuthill, J. R., McAlister A. J., **Occupied band structure of Cu: Soft-x-ray spectrum an comparison with other deep-band-probe studies,** *Phys. Rev.* **2,** No. 6, 1563-1575 (Sept. 15, 1970).

Key words: Band structure; Cu; deep probes; emission; occupied bands; soft x ray.

We report a new measurement of the soft-x-ray $M_{2,3}$ emissio spectrum of Cu, using improved experimental techniques. Prev ously unreported fine structure was observed in the spectrum Although exact correction for satellite and subband overlap an self-absorption effects is not yet possible, careful consideratio has been given to them, with the result that the $M_3$ band profil can be resolved from the accompanying structure in a plausibl way. Its features can be taken with reasonable confidence to b characteristic of the true $M_3$ profile. Comparison is made wit the complementary $L_3$ soft-x-ray profile, with band-theoretica estimates of both experimental x-ray profiles, and with th results of ultraviolet-photoemission, x-ray-photoemission, an ion-neutralization measurements. These comparisons favor single-particle description of the occupied bands of Cu.

**11953.** Egelstaff, P. A., **Cooperative rotation of spheric molecules,** *J. Chem. Phys.* **53,** No. 7, 2590-2598 (Oct. 1970).

Key words: Diffusion; light scattering; neutron scattering plastic crystal; rotational; spherical molecules.

The rotational diffusion of molecules in the liquid and solid tates can be studied by radiation scattering experiments. Both neutron and light scattering data are interpreted, conventionally, on the basis of rotation of single molecules, although in dense ystems cooperative rotation is a possibility. It is pointed out hat a comparison of incoherent neutron data and depolarized ght data allows the cooperative nature of molecular rotational iffusion to be verified. The method is applied to the plastic rystal phase of cyclohexane, and it is shown that individual molecules rotate about 10 times as rapidly as the relaxation rate f the mean orientation of a group of molecules.

1954. Evenson, K. M., Wells, J. S., Radford, H. E., **Infrared resonance of OH with the $H_2O$ laser: A galactic maser pump?** *Phys. Rev. Letters* **25,** No. 4, 199-202 (July 27, 1970).

Key words: Astronomical OH emission; $H_2O$ laser; magnetic resonance; OH; spectroscopy.

The 79-μm electric dipole spectrum of OH ($^2\Pi_{3/2}$, $J=3/2 \leftrightarrow$ $\Pi_{1/2}$, $J=1/2$) has been measured by a magnetic-resonance aborption method, with a water-vapor laser as the source oscillaor. Corresponding magnetic dipole spectra are calculated from he data. A near overlap of the water line on one magnetic-dipole ransition suggests a possible pumping mechanism for the 18-cm maser emission of stellar OH.

1955. Florin, R. E., Wall, L. A., **Small and large radicals in thin-film polymer depolymerization,** *Macromolecules* **3,** No. 5, 560-566 (Sept.-Oct. 1970).

Key words: Diffusion effects; free radicals; polymer decomposition; polymer depolymerization; polymer irradiation; polymer pyrolysis.

Rates of polymer decomposition are enhanced or retarded as result of the escape of small free radical or other species hrough the surface of thin films. Solutions for the rate equations re given as a function of thickness for a mechanism involving he competitive diffusion of small and large radicals. The nhancement of the rates of depolymerization of olytetrafluoroethylene observed with thin films is explained by he model. Comparison of the experimental results with theory ndicates that the irradiation of polytetrafluoroethylene produces omparable amounts of both large and small radicals. The mechanisms discussed are undoubtedly operative in many other tuations involving the radiolysis or pyrolysis of polymers, for xample, the radiation-induced cross-linking of polymers.

956. Franklin, A. D., Marzullo, S., **Orientation kinetics of $Gd^{3+}$-$F^-$ interstitial pairs in $CaF_2$,** *J. Phys. C. Solid State Phys. Letters to Editor* **3,** L171-L174 (Sept. 1970).

Key words: Calcium fluoride; defect dipoles; dielectric relaxation; ESR line broadening; gadolinium; orientational relaxation.

A calculation of approximate density of states for a disordered valent semiconductor shows that the energy gap is due to the resence of short range order.

1957. Freeman, D. H., Goldstein, S., Schmuckler, C., **Homogeneous sulfonation of styrene-divinylbenzene copolymers with oleum in organic solvents,** *Israel J. Chem.* **7,** No. 6, 741-749 (1969).

Key words: Cation exchangers; ion exchangers; oleum; sulfonation.

In order to obtain homogeneously sulfonated cation exchaners, the copolymers were sulfonated by oleum in a mixture of ethylene-chloride and nitromethane. The influences of the hemical interaction and of the diffusion process on the kinetic ehavior of these systems were investigated, and it was shown hat raising the temperature of the sulfonation mixture markedly increases the chemical reaction rate, while the effect on the diffusion is small. A curve-fitting technique was used for the interpretation of the degree-of-sulfonation-vs.-time curves. These investigations served as guidelines for the subsequent preparation of homogeneous highly sulfonated copolymers.

11958. French, B. M., Walter, L. S., Heinrich, K. F. J., **Quantitative mineralogy of an Apollo 11 lunar sample,** (Proc. Apollo 11 Lunar Science Conf., January 1970, Houston, Texas), *Geochim. Cosmochim. Suppl. 1,* **Vol. 34,** 433-444 (Feb. 1970).

Key words: Apollo 11; electron probe analysis; mineralogy; moon; petrography; rocks.

Petrography and mineral analyses of Sample 10017, collected by the Apollo 11 mission, are reported. They indicate formation by relatively rapid crystallization of a silicate melt. Major components are clinopyroxene, plagioclase and ilmenite. Minor components include troilite, native iron, and apatite. The mineral compositions indicate differentiation during magmatic crystallization, leading to Fe enrichment in the pyroxenes and to alkali enrichment in the feldspars. The mesostasis, the residual liquid produced during crystallization, is strongly enriched in K and Si, but strikingly low in Na; this may be due to volatilization during the later stages of crystallization. The compositional trends, similar to those in other lunar samples, indicate formation by relatively rapid magmatic crystallization, which developed significant chemical fractionation, at low oxygen fugacity and under virtually anhydrous conditions.

11959. Glaze, D. J., **Improvements in atomic cesium beam frequency standards at the National Bureau of Standards,** *IEEE Trans. Instr. Meas.* **IM-19,** No. 3, 156-160 (Aug. 1970).

Key words: Atomic frequency standard; cesium beam; figure of merit; frequency accuracy; frequency multiplier; frequency precision; NBS-III; NBS-5; phase noise; quartz crystal oscillator; Ramsey cavity; slave oscillator.

The National Bureau of Standards Frequency Standard, NBS-III, a cesium beam with a 3.66-meter interaction region, has been in operation since 1963. The last published (1966) accuracy capability for NBS-III was $1.1\times10^{-12}(1\sigma)$. Recently, several new solid-state broad-band frequency-multiplier chains have been constructed. Reduction of the random phase noise by more than 20 dB compared to the previous state of the art has been obtained consistently. In addition, a solid-state servo system has been installed to control the frequency of the 5-MHz slave oscillator.

Comparisons were made between NBS-III and one of the commercial cesium standards in the NBS clock ensemble. The relative fractional frequency stability $\sigma(N=2,\ T=7$ days, $\tau=1$ day$)=1\times10^{-13}$ was observed for nine weekly comparisons. The very-long-term frequency stability for the recently improved NBS-III system has not been evaluated fully. Due to the improvements both in electronic systems and evaluative techniques, however, an accuracy of $5\times10^{-13}(1\sigma)$ for a single evaluative experiment is reported.

Substantial effort is being expended toward improvement of the accuracy and figure of merit (presently 10) of the NBS cesium standard. The modified system, to be called NBS-5, is expected to be in operation in the latter half of 1970 and to exhibit a figure of merit in excess of 500.

11960. Goldman, A. J., **Analysis of a capacity concept for runway and final-approach path airspace,** *Proc. Ion National Air Meeting on Air Traffic Control in the 1970's, Institute of Navigation, St. Louis, Mo., April 14-16, 1970,* pp. 119-131 (1970).

Key words: Airport; air traffic control; capacity concept; Markov renewal process; runway.

This paper describes some highlights of a short-term analytical study leading: (a) to a "maximum throughput-rate" capacity concept in the context of a service facility handling a stream of customers of various types, and (b) to the specialization of this concept to a stream of IFR landings at a runway. The specialization is shown to be representable by a simple mathematical formula, of potential value (for example) in connection with cost-effectiveness analyses of proposed changes in ATC equipment or procedures. Directions for further research are identified, and the paper concludes with some general remarks on conceptual difficulties associated with the notion of "capacity."

**11961.** Hastie, J. W., Hauge, R. H., Margrave, J. L., **High temperature chemistry: Stabilities and structures of high temperature species,** *Ann. Rev. Phys. Chem.* **21,** 475-498 (1970).

Key words: High temperature species; stability structure.

Recent experimental and theoretical work on the stabilities and structures of high temperature species has been reviewed. Emphasis was given to data which may be used for the thermodynamic characterization of a high temperature species, such as molecular geometry vibrational and electronic energy levels. The techniques from which stability and structural data have been obtained for high temperature species are also discussed. These include, Knudsen effusion and photoionization mass spectrometry, matrix isolation infrared spectroscopy, electron diffraction, electric dipole deflection, electronic spectroscopy, microwave spectroscopy and semiempirical and abinitio molecular orbital calculations.

**11962.** Hiza, M. J., Duncan, A. G., **A correlation for the prediction of interaction energy parameters for mixtures of small molecules,** *AIChE J.* **16,** No. 5, 733-738 (Sept. 1970).

Key words: Binary fluid mixtures; correlation; deviations from geometric mean rule; interaction energy parameters; ionization potentials.

Low temperature, phase-equilibria data for binary systems containing hydrogen, helium, and neon were used to develop a correlation relating deviations from the geometric mean combining rule for the characteristic energy parameter to the ionization potentials of the component species. With the exception of oxygen systems, this relatively simple relationship correctly predicts published deviations, determined by different methods, for a number of systems within expected uncertainties. It is shown that consideration of attractive forces only, as done by Hudson and McCoubrey, is inadequate for such predictions.

**11963.** Hudson, R. P., **Conference Reports—Ultra-low temperatures 1970,** *Cryogenics* **10,** No. 5, 445 (Oct. 1970).

Key words: Cryogenics; low temperature physics.

A survey is given of a recent symposium at the Naval Research Laboratory on physics below 0.3 K.

**11964.** Jacox, M. E., Milligan, D. E., **Matrix-isolation study of the vacuum-ultraviolet photolysis of methyl chloride and methylene chloride. Infrared and ultraviolet spectra of the free radicals CCl, $H_2CCl$, and $CCl_2$,** *J. Chem. Phys.* **53,** No. 7, 2688-2701 (Oct. 1, 1970).

Key words: CCl; $CCl_2$; force constants; free radical; HCCl; $HCCl_2$; infrared spectrum; matrix isolation; photolysis; ultraviolet spectrum.

Infrared and ultraviolet spectroscopic studies have been conducted on the products of the vacuum-ultraviolet photolysis of normal and isotopically substituted methyl chloride and methylene chloride isolated in argon and nitrogen matrices at 14 K. The cage effect has been found to inhibit halogen detachment processes in these systems. Infrared absorptions attributable to CCl, HCCl, and $H_2CCl$ and the 2800-Å ultraviolet absorption of CCl appear in the methyl chloride photolysis studies. Observation of a "negative anharmonicity" for the lowest-frequency infrared absorption of $H_2CCl$ can be explained by postulating that the molecule is planar. The C–Cl stretching force constant of $H_2CCl$ is exceptionally high. The implications of $(p\text{-}d)\pi$ bonding, which may account for the large C–Cl stretching force constant, are explored. An absorption near 2300 Å behaves appropriately for assignment to a second electronic transition of CCl, providing support for the previous tentative assignment of a group of emission bands to such a transition. Photolysis of methylene chloride in a matrix environment leads principally to the stabilization of $CCl_2$. A revised estimate of the force constants of $CCl_2$ is given.

**11965.** Johnson, D. R., Powell, F. X., **Microwave detection of thioformaldehyde,** *Science* **169,** 679-680 (Aug. 14, 1970).

Key words: Astronomically important; electrical discharge; interstellar medium; microwave spectroscopy; rotational spectrum; thioformaldehyde.

Thioformaldehyde ($H_2CS$) has been detected and characterized from its microwave spectrum. Preliminary analysis of rotational transitions for the sulfur-32-containing form of $H_2CS$ shows this new species to have $C_{2v}$ symmetry with rotational constants (in megahertz) of $A = 292{,}729$, $B = 17{,}698$, and $C = 16{,}652$. The possibility of detection of thioformaldehyde in the interstellar medium is discussed, and a table of transitions expected to be of importance for that detection is presented.

**11966.** Kearsley, E. A., **Intrinsic errors for pressure measurements in a slot along a flow,** (Proc. Fifth Intern. Congress on Rheology, Kyoto, Japan, October 1968), *Trans. Soc. Rheology* **14:3,** 419-424 (1970).

Key words: Hole pressure; nonlinear rheology; normal stresses; pressure error; second order fluid.

Any rectilinear flow dynamically possible for a Newtonian fluid is shown to be possible also for a second order fluid. The stress which satisfies the condition of equilibrium is explicitly calculated. The component of stress normal to a wall bounding a shear flow is expressed in terms of the reading of a pressure gauge connected to a narrow slot in the wall, oriented in the direction of flow.

**11967.** Kerns, D. M., **Correction of near-field antenna measurements made with an arbitrary but known measuring antenna,** *Electronics Letters* **6,** No. 11, 346-347 (May 28, 1970).

Key words: Antenna gain; antenna gain measurement; antenna measurements; antenna pattern; antenna pattern measurement; near-field antenna measurements.

We describe a technique for rigorously correcting for the effects of an arbitrary but known measuring antenna (or "probe" in determination of vectorial far-field antenna pattern and power gain function from near-field measurements.

**11968.** Kerns, D. M., **New method of gain measurement using tw identical antennas,** *Electronics Letters* **6,** No. 11, 348-34 (May 28, 1970).

Key words: Antenna gain; antenna gain measurement; antenna measurements; antenna pattern; antenna pattern measurement; near-field antenna measurements.

A new method for the measurement of on-axis pattern vecto and power gain using two identical antennas is described. Th antennas must obey reciprocity, but may be otherwise arbitrary the usual requirements in the conventional 2-antenna gain-measurement method, that the polarization be known *a priori* an that the separation be large compared with the Rayleig distance, are eliminated.

1969. Krauss, M., **Potential energy surfaces,** *Ann. Rev. Phys. Chem.* **21,** 39-46 (1970).

Key words: Activation energy; configuration interaction; correlation energy surface; Hartree-Fock; $H_3^+$; $H_3$; $H_3^-$; $H_4$; $LiH_2$; LiHF; HNO; $HeH_2^+$; proton transfer.

*Ab initio* energy surfaces applicable to chemical kinetics and ollisional phenomena are reviewed. The calculations are diided into two categories, Hartree-Fock and beyond. It is noted nat Hartree-Fock calculations are routine but that correlation echniques are necessary for reactive collisions. Definitive work xists for $H_3^+$ and $H_4$, but the activation energy of $H_3$ is still inacurate relative to the scattering calculational requirements. ther qualitative work is described for H or Li interaction with iatomics.

1970. Lafferty, W. J., **Microwave spectrum, dipole moment, and conformation of cyclopentene oxide,** *J. Mol. Spectry.* **36,** No. 1, 84-93 (Oct. 1, 1970).

Key words: Cyclopentene oxide; dipole moment; epoxy cyclopentene; microwave spectrum; ring conformation; rotational constants.

The microwave spectrum of cyclopentene oxide has been stuied. Rotational constants for the ground state and two excited ibrational states of one ring conformation have been obtained. round state constants are $A_0 = 5709.38 \pm 0.02$, $B_0 = 4541.12 \pm$ .02, and $C_0 = 3248.97 \pm 0.02$ (errors are 2 standard deviations). he dipole moment components of the molecule are $\mu_a = 1.16_3 \pm$ .033, $\mu_c = 1.63_0 \pm 0.031$, and $\mu = 2.00_2 \pm 0.042$. The rotational onstants and dipole moment components obtained experimenlly can be satisfactorily explained only if the boat form is the ost stable conformation of the ring.

1971. Lamb, V. A., **Evidence for a complex chloromolybdate ion in a molten salt medium from transference experiments,** *J. Electrochem. Soc.* **117,** No. 10, 1269-1270 (Oct. 1970).

Key words: Hexachloromolybdate complex ion; molten salt; transference numbers.

Transference experiments have been performed with solutions potassium hexachloromolybdate in molten eutectic mixtures potassium chloride and lithium chloride. The results indicate at a complex molybdenum-containing anion exists at 800 °C.

1972. Latanision, R. M., Westwood, A. R. C., **Surface- and environment-sensitive mechanical behavior,** Chapter in *Advances in Corrosion Sciences and Technology* **1,** 51-145 (Plenum Press, New York, N.Y., 1970).

Key words: Complex-ion embrittlement; dislocations; liquid metal embrittlement; surface; surface active agent.

The influences of surface structure and environment on the echanical behavior of crystalline inorganic solids are reviewed nd possible mechanisms discussed. In particular, the various oles of such factors as the atomic, electronic, and defect strucres of the near-surface regions, the presence of adsorbed urface-active species, alloyed layers, oxide films, gaseous r liquid environments, etc., are considered in connection with oscoe, Rebinder, and Joffe effects, liquid-metal embrittlement, omplex-ion embrittlement, hydrogen embrittlement, and other henomena.

1973. Maki, A. G., Hexter, R. M., **Resonance interactions with $\nu_5$ of $CH_3I$; A method of determining $A_0$,** *J. Chem. Phys.* **53,** No. 1, 453-454 (July 1, 1970).

Key words: Absorption; gas; infrared; methyl iodide; molecular geometry; molecular structure; spectra.

Using a band contour computer program an analysis has been ade of the Fermi resonance between the two perpendicular bands $\nu_5$ and $\nu_3 + \nu_6$ of methyl iodide. A weak Coriolis interaction was found between the $K = 4, -l$ levels of $\nu_3 + \nu_6$ and the $K = 3, +l$ levels of $\nu_5$. From an analysis of this Coriolis interaction it is shown that $A_0 = 5.15_8 \pm 0.02$ cm$^{-1}$ where the uncertainty is an estimated 95% confidence limit. The ratio of the transition moments for $\nu_5$ and $\nu_3 + \nu_6$ was found to be $|M_{3+6}| / |M_5| = 0.17 \pm 0.05$.

11974. Meshkov, S., **How good are symmetry predictions?,** *Proc. Intern. Conf. on Symmetries and Quark Models, Wayne State University, Detroit, Michigan, June 18-20, 1969,* Ramesh Chand, ed., pp. 199-212 (Nov. 1970).

Key words: Exotic; mesons; reactions; structure; $SU(6)_W$; symmetry.

A summary discussion of the comparison of experiment and $SU(6)_W$ reaction predictions is presented.

11975. Milligan, D. E., Jacox, M. E., **Infrared spectrum of the ClHCl-ion isolated in an argon matrix,** *J. Chem. Phys.* **53,** No. 5, 2034-2040 (Sept. 1, 1970).

Key words: Bichloride anion; ClHCl free radical; electron attachment; HCl dimer; hydrogen bonding; infrared spectrum; matrix isolation; ultraviolet spectrum; vacuum-ultraviolet photolysis.

Upon vacuum-ultraviolet photolysis at 14 K of samples of HCl isolated in an argon matrix at mole ratios favorable for the presence of an appreciable concentration of dimeric HCl, prominent absorptions appear at 696 and 956 cm$^{-1}$. The positions, contours, and relative intensities of these absorptions correspond within experimental error with those previously attributed to the ClHCl free radical isolated in an argon matrix. Studies of a chlorine-37 enriched sample have confirmed the presence of two chlorine atoms in the molecule. A broad, unstructured absorption at 2870 Å may also be contributed by this ClHCl species. When a small concentration of atomic potassium or cesium is codeposited with the Ar:HCl sample, evidence is obtained for the formation of an alkali-metal-containing complex. Photoionization of the alkali-metal atoms upon exposure of the resulting sample to the radiation of a medium-pressure mercury arc leads to the appearance of very prominent absorptions at 696 and 956 cm$^{-1}$. It is proposed that these absorptions may more suitably be assigned to the $ClHCl^-$ ion, trapped in an inert, essentially nonionic environment. Implications of this reassignment with regard to the nature of the hydrogen bonding of $ClHCl^-$ are discussed, and possible mechanisms for the production of $ClHCl^-$ under the conditions of these experiments are considered.

11976. Moore, C. E., **Annual Report, July 1, 1968-June 30, 1969, The National Bureau of Standards, Washington, D.C.,** *Bull. Am. Astron. Soc.* **2,** No. 1, 99-100 (1970).

Key words: Annual report, National Bureau of Standards; astrophysical work, National Bureau of Standards.

As each fiscal year ends, it is an established custom to submit an annual report covering work of interest to astronomers. A number of Bureau programs are useful astrophysically. The present report is a current summary of work in selected areas of the Bureau.

11977. Moore, G. A., **Is quantitative metallography quantitative?** *Am. Soc. Testing Mater. Spec. Publ.* **480,** pp. 3-48 (1970).

Key words: Evaluation; measurement; metallography; metallurgical analysis; microscopy; photogrammetry.

While the basic principles of quantitative metallography have been firmly established, the practice of such measurements yields highly variable results. Simple laws define the statistical limitation on any measuring method. Serious errors arise from improper selection and preparation of specimens. Anticipated gradients must be encompassed by a planned sampling scheme which guarantees unbiased representation and permits measurement of actual variation in the material studied. Specimen preparation must give a truthful image of the structure. Any free choices by the operator introduce bias. The precision of measurement of one micrograph is primarily controlled by a combination of statistical uncertainty and observational error at the edges of particles. The statistical uncertainty conforms to the ideal when the apparent particle size is small, but observation becomes inefficient as the average intercept width increases and the number of particles in the field decreases. Edge errors are maximum with small particles and vary with the observer or the instrument used. Maximum precision is obtained when these two errors are approximately equal. While quantitative metallography is a statistical, rather than exact, process and subject to serious or fatal errors when practiced crudely, carefully controlled measurements can yield several structural parameters with a precision adequate to satisfy any practical metallurgist.

**11978.** Pella, P. A., DeVoe, J. R., **The determination of tin in copper-base alloys by Mössbauer spectrometry,** *Anal. Chem.* 42, No. 14, 1833-1835 (Dec. 1970).

Key words: Alloys; analysis; internal standard; Mössbauer spectrometry; stannic oxide.

The Mössbauer spectrometric method was applied to the determination of tin as stannic oxide in NBS SRM copper-base alloys. After converting the Sn in the alloy to $SnO_2$ the absorption intensity of $SnO_2$ was measured versus $\beta$-Sn as an internal standard absorber. Stannic oxide was obtained by the dissolution of the alloys in nitric acid. This produces a precipitate contaminated by the coprecipitation of a number of elements. Through the use of an appropriate standard, it was shown that the Mössbauer technique can measure the $SnO_2$ concentration without interference. The results for alloys 52c, 184, and 37e were 7.82±.05% (7.85), 6.31±.06% (6.38), and 0.99±.01% (1.00), respectively, where the uncertainties are the relative standard deviation of the mean values and the numbers in parentheses are the NBS certified values.

**11979.** Perloff, A., **The crystal structure of sodium hexamolybdochromate(III) octahydrate, $Na_3(CrMo_6O_{24}H_6)\cdot 8H_2O$,** *Inorganic Chem.* 9, No. 10, 2228-2239 (1970).

Key words: Heteropolymolybdate; x-ray crystal structure.

The detailed structure of the heteropoly salt $Na_3(CrMo_6O_{24}H_6)\cdot 8H_2O$ has been determined using three-dimensional x-ray diffraction data. The crystals are triclinic, space group $P\bar{1}$, with cell dimensions $a = 10.9080$ (4) Å, $b = 10.9807$ (4) Å, $c = 6.4679$ (2) Å, $\alpha = 107.594$ (2)°, $\beta = 84.438$ (2)°, and $\gamma = 112.465$ (3)° at 25°. There is one formula unit per unit cell. Final refinement by least-squares analysis with anisotropic temperature factors resulted in an $R$ value of 3.3%. The anion has the same structure as the $TeMo_6O_{24}^{6-}$ anion with excellent agreement of comparable bond distances. Charge balance and hydrogen-bonding arguments suggest that the hydrogen atoms of the anion are bonded to the oxygen atoms which are coordinated to the Cr atom. The anions are linked together through sodium octahedra and hydrogen bonding. No hydrogen atoms could be located directly, but a reasonable hydrogen-bonding scheme was inferred from short oxygen-oxygen distances.

**11980.** Prydz, R., Straty, G. C., Timmerhaus, K. D., **Properties of fluorine along the vapor-liquid coexistence boundary,** *J. Chem. Phys.* 53, No. 6, 2359-2363 (Sept. 15, 1970).

Key words: Critical point; fluorine; latent heats of vaporization; saturated liquid densities; saturated vapor densities vapor pressure.

Saturated liquid and vapor densities from the triple point to th critical points are reported. These data were derived from experimental PVT isochores and an accurate vapor pressure equation. The critical point parameters were estimated by fitting a equation to all experimental data within 20% of the critical temperature. Separate equations, each constrained to the new critical point parameters, were fitted to the saturated liquid an vapor densities. Latent heats of vaporization were calculate from the Clapeyron equation and compared to other publishe values. A vapor pressure equation based on the IPTS 1968 temperature scale is reported.

**11981.** Radebaugh, R., Siegwarth, J. D., **Theory of $He^3$-He dilution refrigerators,** (Proc. 1970 Ultralow Temperatur Symp., Washington, D.C., April 23-24, 1970), *NRL Repo 7133*, pp. 63-81 (1970).

Key words: Cryogenics; dilution refrigerator; Fermi-Dira statistics; heat exchangers; helium-3; helium-4; liquid helium; mixtures; quantum fluid; thermodynamic properties.

A review is given concerning the theoretical analysis of th dilution refrigerator. The weakly interacting Fermi-Dirac ga model for $He^3$ dissolved in superfluid $He^4$ is developed in deta to give accurate and self-consistent values for thermodynami properties of the dilute solutions. These calculated propertie along with measured properties of pure $He^3$, are used to analyz the behavior of the dilution refrigerator in the continuous mode The temperature which can be reached with a given number c perfect discrete heat exchangers is derived. The analysis of typical discrete heat exchanger taking thermal conductivity c the liquids into account shows it behaves nearly like the extrem of small length to area ratio, $l/A \ll 1$. The other extreme of zer liquid conductivity, or $l/A \gg 1$, is shown to be much more efficient for the same liquid volume but is difficult to make with lo flow impedance. The optimum ratio of dilute to concentrate liquid volumes is found to be 2.1 for the heat exchange analyzed.

**11982.** Reader, J., Sugar, J., **Ionization energies of Ce I and Gd** *J. Opt. Soc. Am. Letter to Editor* **60,** No. 10, 1421-1422 (Oc 1970).

Key words: Cerium; gadolinium; ionization energy.

The ionization energies of neutral cerium and gadolinium ar derived using a semi-empirical method.

**11983.** Rush, J. J., Schroeder, L. W., Melveger, A. J., **Infrare and Raman spectra of sodium bifluoride: Isotope dilution studies,** *Chem. Phys. Letters* **6,** No. 5, 533-536 (Sept. 1, 1970).

Key words: Bending vibration; hydrogen bond; infrared isotope dilution; lattice mode; Raman; sodium bifluoride stretching vibration.

IR and Raman spectra for sodium bifluoride containing 2, 1 and ≈ 80% $DF_2^-$ are presented. Changes in the $DF_2^-$ $\nu_2$ and $\nu$ IR bands with deuteration are related to coupling between lik oscillators or states. Raman assignments are made for the $HF_2$ $\nu_1$ and lattice librational ($E_g$) modes.

**11984.** Saylor, C. P., **Broken Virtue,** *Capital Chem.* **20,** No. 6 137-140 (Sept. 1970).

Key words: Art restoration; Cellini; chemical microscop National Gallery of Art; Renaissance bronzes; Widener collection.

A bronze statuette now named Virtue Overcoming Vice, assigned to Benvenuto Cellini was broken on arrival at the National Gallery of Art. Chemical microscopical studie established that the break was not new. The piece had bee broken before and repaired. Spectroscopic studies were compatible with the attribution to Cellini.

11985. Sengers, J. M. H. L., **Scaling predictions for thermodynamic anomalies near the gas-liquid critical point,** *Ind. Eng. Chem. Fundamentals,* **9,** No. 3, 470-480 (Nov. 9, 1970).

Key words: Argon; carbon dioxide; classical equation; coexistence curve; critical exponents; critical point; lattice gas; power laws; rectilinear diameter; steam; thermodynamic anomalies; vapor pressure.

Most empirical equations of state for gases have derivatives of all order in density and temperature at the critical point. This implies definite asymptotic characteristics ('classical') for thermodynamic anomalies in the critical region. Classical critical anomalies and symmetries are treated in some detail. The Ising model of statistical mechanics reveals an essentially different kind of critical behavior (nonclassical). A brief discussion is given. Real gases behave nonclassically. Therefore, classical equations of state cannot be valid in the critical region. The homogeneous or scaled equation of state, recently proposed by Widom, Kadanoff, and Griffiths, incorporates nonclassical critical anomalies. Its form and some of its consequences are discussed. Scaling ideas are applied to the correlation of coexistence curve data (for argon and steam) and vapor pressure data (for $CO_2$).

11986. Simmons, J. H., Macedo, P. B., **Viscous relaxation above the liquid-liquid phase transition of some oxide mixtures,** *J. Chem. Phys.* **53,** No. 7, 2914-2922 (Oct. 1, 1970).

Key words: Immiscibility; oxide glasses; relaxation times; supercritical fluctuations; ultrasonic spectroscopy; viscous relaxation.

The viscosity anomaly observed above the critical points of a series of sodium borosilicate melts is investigated by ultrasonic shear relaxation spectroscopy. The measurements were conducted at frequencies between 3 and 25 MHz and temperatures between 800 and 1300 °C. The samples tested have different critical temperatures as a result of small doping additions to the critical composition of the immiscibility surface in the phase diagram of the sodium borosilicate system. This permitted measurements over a wide range of reduced temperatures. Analysis of the data yields three structural relaxation parameters which are: the instantaneous shear modulus, the most probable relaxation time, and the width of the distribution of shear relaxation times. These parameters are related to the viscosity. It is found that while the instantaneous modulus and the most probable relaxation time appear unaffected by the presence of supercritical composition fluctuations, the width of the spectrum of shear relaxation times broadens drastically as the critical temperature is approached from above. Similar and parallel curves are formed from the widths of the distributions of relaxation times of all four samples when the temperature is properly normalized by the critical temperature. The general behavior of these curves exhibits the three reduced temperature regions predicted in a previously published relaxation model. The supercritical broadening of the width of the distribution of relaxation times accounts for the observed viscosity anomaly.

11987. Sitterly, C. M., **The present state of atomic spectra,** *J. Opt. Pura Aplicada* **11,** No. 3, 103-113 (1969).

Key words: Atomic spectra; coronal spectra; rare-earth spectra; solar spectra; spectra, atomic; spectra, rare-earth.

The present state of the analysis of atomic spectra is presented with special reference to the grades of analysis of all known spectra, the present work on rare-earth spectra and the needs for future work of astrophysical interest.

11988. Spencer, L. V., Stanley, W., **On neutron penetration in duct systems with large cross section,** *Proc. Special Session on Gamma-Ray Production and Transport and on Civil Defense Shielding, American Nuclear Society,* pp. 199-221 (Aug. 1969).

Key words: Albedo; civil defense; ducts; neutron penetration; nuclear weapons data; structure shielding.

Neutron albedo data for nonhydrogenous wall materials is insensitive to total cross section energy variations and to some extent details of cross section angular distributions. As a result, it makes sense to explore models in which the differential albedo is factored into energy dependent and direction dependent parts. This approximation results in a factoring of the transport equation for large enclosures into two parts, a one-velocity type of problem and a general problem of determining spectra for different orders of reflection. We extend this further to identify suitable parameters in terms of which data for elementary types of enclosure can be applied to complex configurations. These parameters are given, the procedure for combining duct sections is sketched, and calculations for a 3-legged duct are compared with Monte Carlo data for such a duct.

11989. Staveley, L. A. K., **Hard-sphere model applied to the solubility of gases in low-boiling liquids,** *J. Chem. Phys.* **53,** No. 8, 3136-3138 (Oct. 15, 1970).

Key words: Gas solubility; hard-sphere model; liquefied gases; phase equilibria; predicted thermodynamic parameters.

The hard-sphere model for fluids has been applied by Snider and Herrington to the calculation of the excess thermodynamic functions of binary liquid mixtures and also to the problem of the solubility of gases in liquids. While remarkably successful in the first case, it appeared to fail rather badly when applied to gas solubility. It is shown that this apparent failure was due to Snider and Herrington's choice of experimental data, and that in fact the approach is much more effective than they concluded in correlating and predicting the thermodynamic parameters for solutions of gases in low-boiling liquids. Results of calculations are presented for the systems argon-neon, nitrogen-hydrogen, methane-helium, and hydrogen-helium, where the first named component is the liquid solvent.

11990. Stein, P. G., **Image-analyzing microscopes,** *Anal. Chem.* **42,** No. 13, 103A-107A (Nov. 1970).

Key words: Computers; digital logic; image processing; microscope; microspectrophotometry; pattern recognition.

Image-processing technology, through expanded data gathering and storage capabilities, now has the potential to solve difficult problems in metallurgy, polymer and fiber chemistry, and cell biology. Many studies involving the counting and sizing of particles or fibers can be automated through the use of image-processing techniques.

11991. Wexler, A., **Measurement of humidity in the free atmosphere near the surface of the earth,** (Proc. American Meterological Society Symp. on Meterological Observations and Instrumentation, Washington, D.C., February 10-14, 1969), *Meterological Monographs* **11,** No. 33, 262-282 (Oct. 1970).

Key words: Dew point; hygrometry; meterology; moisture measurement in gases; psychrometry.

This paper is a survev of the state of the art in hygrometry as applied to humidity measurement in gases near atmospheric pressure. Hygrometric methods, techniques and instruments are divided arbitrarily into the following six classes involving methods dependent on: (1) the total removal of water vapor from a moist gas; (2) the addition of water vapor to produce a saturated gas; (3) the reversible sorption of water vapor by a sensor;

(4) the measurement of a physical property of a gas; (5) attaining the liquid-vapor or the solid-vapor equilibrium state of the water substance; and (6) chemical reactions and procedures. The methods of each class are further subdivided by principles of operation and are examined to assess such characteristics as range, accuracy, sensitivity, speed of response, effect of environmental conditions, and limitations in behavior and utility.

**11992.** Wiederhorn, S. M., Bolz, L. H., **Stress corrosion and static fatigue of glass,** *J. Am. Ceram. Soc.* **53,** No. 10, 543-548 (Oct. 1970).

Key words: Crack propagation; fracture; glass; static fatigue; stress corrosion.

Stress corrosion cracking of six glasses was studied using fracture mechanics techniques. Crack velocities in water were measured as a function of applied stress intensity factor and temperature, and apparent activation energies for crack motion were obtained. Data were consistent with the universal fatigue curve for static fatigue of glass, which depended on glass composition. Of the glasses tested, silica glass was most resistant to static fatigue, followed by the low-alkali aluminosilicate and borosilicate glasses. Sodium was detrimental to stress corrosion resistance. The crack velocity data could be explained by the Charles and Hillig theory of stress corrosion. It is probable that stress corrosion of glass is normally caused and controlled by a chemical reaction between the glass and water.

**11993.** Wiederhorn, S. M., Townsend, P. R., **Crack healing in glass,** *J. Am. Ceram. Soc.* **53,** No. 9, 486-489 (Sept. 1970).

Key words: Crack healing; fracture; glass; strength; surface.

Cracks in soda-lime-silica glass specimens closed spontaneously; the recovery in strength was determined by fracture mechanics techniques. Approximately 80% strength was recovered in cracks formed by mechanical shock, whereas approximately 20% was recovered in cracks that closed after being held open to the atmosphere for several minutes. The high strength recovery in the mechanically shocked specimens is attributed to the very active surface formed during fracture. If the surface is allowed to adsorb $O_2$ or $H_2O$ vapor, the activity is reduced, and healing is less complete. Crack healing can introduce surface flaws into glass that cannot be detected by current methods of nondestructive testing.

**11994.** Yakowitz, H., **Some uses of color in metallography,** *Am. Soc. Testing Mater., Spec. Publ.* **480,** pp. 49-66 (1970).

Key words: Color photography; electron microscopy; electron probes; evaluation; metallography; microscopy; polarized electromagnetic radiation.

The application of various methods for using color in metallography is outlined. The methods include plane and circularly polarized light, color etching, and color separation photography. Instruments used to obtain subjects for the color metallography examples shown in this paper include the optical microscope, the electron probe microanalyzer, the scanning electron microscope, and the transmission electron microscope. A brief discussion of color films is given. The technique used to obtain color photographs is given in detail for each aspect of color metallography discussed.

**11995.** Adler, I., Walter, L. S., Lowman, P. D., Glass, B. P., French, B. M., Philpotts, J. A., Heinrich, K. F. J., Goldstein, J. I., **Electron microprobe analysis of Apollo 11 lunar samples,** (Proc. Apollo 11 Lunar Science Conf., January 1970, Houston, Texas), *Geochim. Cosmochim.* **34,** Suppl. 1, 87-92 (Jan. 30, 1970).

Key words: Analysis; electron probe; lunar samples; microanalysis; minerals; rocks.

Plagioclase feldspar, clinopyroxene and ilmenite in a polished thin section of a "Type A" crystalline rock were analyzed. The clinopyroxene grains are compositionally variable and both high Ca and low Ca phases are present. The plagioclase is compositionally homogeneous. The ilmenite is chemically homogeneous except for occasional, small areas of high local chromium concentration. Accessory minerals are: apatite (containing Cl, F, Y and Ce), troilite, and metallic iron.

Glassy spherules from the lunar soil are mostly similar in composition to the crystalline rocks; however, some appear to have been monomineralic.

The crystalline rock has apparently formed by relatively rapid cooling of a silicate melt under conditions of low oxygen partial pressure. Many components of the soil appear to have formed by meteoritic impact.

**11996.** Brauer, G. M., Huget, E. F., Termini, D. J., **Plastic modified *o*-ethoxybenzoic acid cements as temporary restorative materials,** *J. Dental Res.* **49,** No. 6, 1487-1494 (Nov.-Dec. 1970).

Key words: Dental restorative materials; EBA cements; plastic reinforced restoratives; restorative materials; temporary dental cements.

Effects of adding polymeric materials to powder components of EBA cements were studied. The most suitable additives for reducing the brittleness of EBA cements were acrylic and vinyl chloride copolymers.

**11997.** Davis, M. M., **Bronsted acid-base behavior in "inert" organic solvents,** Chapter 1 in *The Chemistry of Nonaqueous Solvents* **III,** 1-135 (Academic Press Inc., New York, N.Y., 1970).

Key words: Acid-base behavior; acidity and basicity scales; aprotic organic solvents; hydrogen bonding; titrations.

A unified picture of acid-base behavior in aprotic organic solvents is presented, based on an extensive survey of the literature and experimental results of the author and associates. Evidence given to support this picture includes data pertaining to colligative properties of acids, bases, and salts and also conductance, dielectric constants, distribution between immiscible solvents, and spectral absorption in the infrared, visible, and ultraviolet. The acids upon which attention is centered are proton-donor compounds that are measurably ionized in water, such as aliphatic and aromatic carboxylic acids, substituted phenols, and mineral acids. The bases of principal interest are likewise compounds capable of forming ions in water, for example, aliphatic and aromatic amines and derivatives of guanidine or pyridine. The solvents emphasized are hydrocarbons and halohydrocarbons, but data for dipolar aprotic solvents (for example, acetone, acetonitrile, and nitrobenzene) are included. Contrasts in acid-base behavior and in acidity and basicity scales in aprotic and water-like solvents are discussed.

The role of hydrogen bonding in aprotic solvents is discussed at length. Important types of hydrogen-bonded structures include chelate rings; self-associated acids, bases, and salts; hydrogen-bonded ion pairs; and homo- and heteroconjugate cations and anions. Examples are given in which hydrogen bonding of these types affects such properties as the absorption spectrum of a salt, the catalytic effect of an acid, and the accurate location of a titration endpoint.

**11998.** Dehl, R. E., **Collagen: Mobile water content of frozen fibers,** *Science* **170,** 738-739 (Nov. 13, 1970).

Key words: Adsorbed water; calorimetry; collagen; frozen collagen; mobile water; NMR.

The NMR spectra of frozen wet collagen fibers indicate the presence of a considerable amount of unfrozen, mobile water.

The quantity of mobile water may be estimated from the approximate convergence of the low temperature NMR splitting constants. An independent estimate of the mobile water content by calorimetry agrees well with the NMR estimate.

**11999.** Durst R. A., **Pick an ion, any ion,** *Ind. Res.* pp. 36-39 (Nov. 1970).

Key words: Electrode monitoring; industrial monitoring; ion-selective electrodes; pollutant monitoring.

A brief discussion is given of the types of ion-selective electrodes and the basic principles of their operation. The advantages of these sensors for industrial and environmental pollution monitoring are given, such as, the continuous direct-reading nature of the measurement, fast response time, and portability. Examples of typical industrial and environmental monitoring applications are included, for example, sulfide ion in pulp processing, nitrogen oxides and fluoride in air pollution, and nitrate in soil slurries. Care is necessary in applying these sensors to complex systems where interferences could be a problem and ingenuity is required in modifying the analysis parameters to obtain reliable results. The specificity and sensitivity of these sensors to several serious pollutants will probably result in their future use in pollution-monitoring systems.

**12000.** Gills, T. E., Marlow, W. F., Thompson, B. A., **Determination of trace elements in glass by activation analysis using hydrated antimony pentoxide for sodium removal,** *Anal. Chem.* **42,** 1831-1833 (Dec. 1970).

Key words: Activation analysis; glass; hydrated antimony pentoxide (HAP); radiochemical separations; sodium; trace elements.

A method has been developed for the determination of a number of trace elements at the ppm and ppb levels in high-sodium glass by neutron activation analysis. For glass containing about 10% sodium, neutron irradiation at levels sufficient to allow determination of trace constituents results in production of 10 mCi or more of $^{24}$Na. If the $^{24}$Na is allowed to decay before analysis, information about elements producing short-lived radioisotopes is lost. In the procedure described the radiosodium is removed by passing the dissolved glass through a column of hydrated antimony pentoxide (HAP). The effluent can be counted directly with a Ge(Li) or NaI(Tl) detector. The method has been applied to the analysis of NBS Standard Reference Material (SRM) glass which was found to contain 1 ppm of Cu and sub-ppm levels of Mn, Au, Ga, Sb, La, Co, and Ir.

**12001.** Greenberg, L., Newman, M., **Some results on solvable groups,** *Arch. Math.* **21,** No. 4, 349-352 (1970).

Key words: Density; solvable groups; 2-generator groups.

Let $a$, $b$ be fixed relatively prime integers $> 1$. Let $s(n) = 1$ if a solvable group of order $n$ exists generated by elements $x$, $y$ such that $x^a / y^b = 1$; and 0 otherwise. It is proved that

$$1/x \sum_{n \leq x} s(n) \rightarrow 0 \qquad x \rightarrow \infty.$$

**12002.** Grosch, H. R. J., **A view of computers from the Bureau of Standards,** *Input* **6,** No. 2, 3-7 (1970).

Key words: Computer activities, NBS; computers; computer science at NBS.

A brief review is given of the activities of the Center for Computer Sciences at the National Bureau of Standards, in a popularized, informal treatment.

**12003.** Guttman, C. M., DiMarzio, E. A., **Separation by flow. II. Application to gel permeation chromatography,** *Macromolecules* **3,** No. 5, 681-691 (Sept.-Oct. 1970).

Key words: Chromatography; gel filtration; gel permeation chromatography; macromolecules; separation by flow.

Models of a gel permeation chromatography column are proposed in which there is flow through each of the beads as well as around them. Diffusion is allowed within and outside of the beads. By making general arguments on particle current flow, the volume elution is computed as a function of solute particle size for a simplified view of the column. The equation for the location of volume elution peaks thus derived shows functional dependences on the particle radius and the column geometry very much like equations derived by previous workers for models in which there was no flow in the beads. The method of Hermans to calculate the peak broadening is extended to allow for flow within the beads. Two times characterize the system; the time for a particle to diffuse into and out of the bead and the time to flush the particle out of the bead. The width of the volume elution peak no longer becomes infinite as the diffusion coefficient goes to zero (in contradistinction to the work of Hermans) since the residence time within the bead is never larger than the flush time. Explicit formulas are given for the first three moments of the volume elution; it is shown that the elution volume for a monodisperse species is Gaussian. In all cases systems with open pores which allow flow show better separation capabilities than those which do not allow flow.

**12004.** Henderson, M., Berry, P. L., **Progress of federal library automation,** *Drexel Library Quart.* **6,** Nos. 3 & 4, 249-263 (July-Oct. 1970).

Key words: Automatic data processing; automation of library functions; Federal libraries; Federal Library Committee (FLC); library automation; system design for libraries; Task Force on Automation.

Progress in automation for Federal libraries other than the three National libraries is the concern of the Federal Library Committee's Task Force on Automation. Its mission is to review automation developments in Federal libraries, to encourage compatible systems design, and to provide liasion between Federal libraries and other groups involved in automation of library functions and services. To fulfill this mission the Task Force has undertaken a phased program with four objectives: to review library automation developments; to define library functions not yet automated, but which benefit from automation; to develop a generalized system design for functions of the Federal Library community; and to establish a study and design sequence, for stepwise implementation of the system within that community. The first objective has been realized through the medium of two studies; the third phase, about to get underway, will work toward the longer-range objectives while building on and extending the earlier studies.

**12005.** Hirshfeld, A. T., Hoppes, D. D., **Transition mixing ratios determined from a study of the electron and gamma-ray distributions from oriented $^{192}$Ir,** *Phys. Rev. C* **2,** No. 6, 2341-2349 (Dec. 1970).

Key words: Beta rays, angular distribution of; gamma rays, angular distribution of; hyperfine field in iron; nuclear orientation; transition mixing ratios; $^{192}$Ir, magnetic moment of.

The angular distributions measured for 12 $\gamma$ rays in $^{192}$Os and $^{192}$Pt resulting from the decay of cryogenically oriented $^{192}$Ir have been used to determine the following $E2/M1$ mixing ratios: 201 keV, $\delta^2 > 3.7$; 296 keV, $\delta = -(6^{+3}_{-1})$; 308 keV, $\delta = -(7.1 \pm 0.6)$; 417 keV, $\delta = 4^{+7}_{-3}$; 485 keV, $\delta = 5.8 \pm 0.8$; 604 keV, $\delta = 1.5 \pm 0.1$, following the Rose-Brink sign convention. The angular distribution of the 672-keV $\beta$ group and the above $\gamma$ measurements limit the relative contribution, $I_L$, of different operator tensor ranks, $L$, involved in each $\beta$ transition. The results for electron-capture transitions terminating at levels in osmium are: 694-keV level, $I_1 > 0.9$; 584-keV level, $I_0 > 0.6$, $I_2 < 0.1$. For $\beta$ transitions feeding platinum states, we determine: 921-keV level, $I_1 > 0.8$; 785-keV level, $I_1 > 0.92$, $I_2 < 0.03$. The $^{192}$Ir ground-state magnetic moment is determined to be positive.

**12006.** Ledbetter, H. M., **On the martensite crystallography of the cubic to orthorhombic transformation in Au-47.5 Cd,** *Scripta Met.* **4,** No. 11, 931-937 (Nov. 1970).

Key words: Crystallography; gold-cadmium alloy; martensite; phase transformation; twinning.

Complete calculations of the geometrical features of the cubic to orthorhombic martensitic transformation in the Au-47.5 Cd alloy system have been made for both Type I and Type II transformation twinning. None of the usual crystallographic features are sufficiently sensitive to distinguish between these two possible modes of lattice invariant deformation. Alternatives are offered which are believed to be experimentally simpler than those previously proposed.

**12007.** Marshak, H., Langsford, A., Tamura, T., Wong, C. Y., **Total neutron cross section of oriented $^{165}$Ho from 2 to 135 MeV,** *Phys. Rev. C* **2,** No. 5, 1862-1881 (Nov. 1970).

Key words: Black-nucleus model; coupled channel calculation; nuclear orientation; nuclear Ramsauer effect; nuclear shape; optical-model; total neutron cross section; $^{165}$Ho.

The difference in the total neutron cross section due to nuclear orientation, $\Delta\sigma_{def}$, has been measured for $^{165}$Ho over the energy range of 2 to 135 MeV. The results show that $\Delta\sigma_{def}$ oscillates as well as changing sign, contrary to our classical concept of the interaction. The data, both $\sigma_t$ and $\Delta\sigma_{def}$, are successfully fitted by adiabatic coupled-channel calculations using the optical model. The parameters for the optical model were determined by fitting $\sigma_t$ and $\sigma_R$ data (over approximately the same energy range as in the present work) for the two spherical nuclei Cd and Pb. The only additional quantity introduced was the quadrupole deformation parameter for $^{165}$Ho which is known to be 0.33. The data for $\Delta\sigma_{def}$ can also be explained quite well by a simple semiempirical model which makes use of the black-nucleus model, the nuclear Ramsauer effect, and the experimental $\sigma_t$ data. The temperature dependence of $\Delta\sigma_{def}$ agrees very well with our calculated values for the degree of nuclear orientation, which is consistent with $^{165}$Ho being almost a pure quadrupole-shaped nucleus.

**12008.** Meadow, C. T., Meadow, H. R., **Organization, maintenance, and search of machine files,** Chapter 7 in *Annual Review of Information Science and Technology,* C. A. Cuadra, ed., pp. 169-191 (Encyclopedia Britannica, Chicago, Ill., 1970).

Key words: Data management; data structures; file organization; information retrieval; information systems; programming languages.

This article reviews the most significant literature in the field of file organization and search procedures that appeared during 1969. Among the points noted are the differences between total information systems and data management support systems and the separate development of several instances of each. The most important development is the trend toward data independence—separation of the concepts of logical and physical data organization.

**12009.** Meshkov, S., **Commentary on meson spectroscopy,** Chapter in *Experimental Meson Spectroscopy,* C. Baltay and A. H. Rosenfeld, eds., pp. 535-546 (Columbia Univ. Press, New York, N.Y., 1970).

Key words: $A_2$; mesons; resonances; spectroscopy; SU(3); $SU(6)_W$.

A description of a method for describing the split $A_2$ is presented, as well as some comments on the general problem of describing mesons and analyzing their structure.

**12010.** Moore-Sitterly, C. E., **Silicon in the sun,** Chapter in *Vistas in Astronomy (Commemoration of H. N. Russell),* A. Beer, ed., **12,** 307-312 (Pergamon Press Inc., New York, N.Y., 1970).

Key words: Silicon spectra in the sun's atmosphere; spectra of silicon, atomic and ionic in the sun; sun, silicon in the.

A brief survey is given of silicon lines in the spectra of the solar photosphere, chromosphere and corona. These lines arise not only from the spectrum of the neutral atom, but also from the ionic spectra of every stage of ionization, i.e., Si I through Si XIV. The ionization potentials range from 8 to 2673 eV, and the wavelengths of the solar identifications span the interval from 6 to 25129 Å. The wide range of excitation and ionization thus represented makes silicon a suitable element for detailed study of solar models, fluxes, abundances and the like.

**12011.** Neill, A. H., Jr., **High-energy light detector for use with pulsed ruby and glass lasers,** *Appl. Opt.* **9,** No. 10, 2392-2393 (Oct. 1970).

Key words: Calorimeter; detector; energy; laser; power; ruby.

A portable solid state light detector capable of measuring up to 100 joules of laser energy in the conventional mode has been designed and tested. Details on construction and operation are presented along with results of calibration.

**12012.** Okabe, H., **Photodissociation of HNCO in the vacuum ultraviolet; production of NCO $A^2\Sigma$ and NH ($A^3\pi$, $c^1\pi$),** *J. Chem. Phys.* **53,** No. 9, 3507-3515 (Nov. 1, 1970).

Key words: Bond dissociation energy; fluorescence; HNCO; NCO $A^2\Sigma$; NH $A^3\pi$, $c^1\pi$; photodissociation; vacuum ultraviolet.

Strong emissions bands originating from NCO $A^2\Sigma$ and NH ($A^3\pi$, $c^1\pi$) were found in the photodissociation of HNCO in the vacuum ultraviolet. In addition, weak bands coming from NCO $B^2\pi$ were observed. Threshold energies of incident photons to produce these bands were measured, from which the following bond dissociation energies and heats of formation were obtained: $D(\text{H-NCO}) = 4.90 \pm 0.01$ eV, $D(\text{HN-CO}) = 3.38 \pm 01$ eV, $D(\text{N-CO}) = 2.14 \pm 0.15$ eV, $\Delta H_f(\text{HNCO}) = -1.0 \pm 0.14$ eV, $\Delta H_f(\text{NCO}) = 1.6 \pm 0.15$ eV. The emission spectrum, NCO $A^2\Sigma \rightarrow X^2\pi$, produced from the photolysis at the Xe and Kr lines shows that NCO $A^2\Sigma$ is highly excited in bending vibration, indicating that the upper state of HNCO from which NCO $A^2\Sigma$ predissociates has a bent NCO configuration. NH $c^1\Pi$ formed is highly rotationally excited. Experimental evidence is presented to show that NH $A^3\pi$ is produced primarily by a secondary process, CO $a^3\pi$ + NH $X^3\Sigma \rightarrow$ CO $X^1\Sigma$ + NH $A^3\pi$. Primary processes in the near-ultraviolet photolysis of HNCO are discussed on the basis of bond dissociation energies obtained in the present work.

**12013.** Parker, H. S., Harding, C. A., **Vapor growth of $Al_2O_3$ bicrystals,** *J. Am. Ceram. Soc.* **53,** No. 11, 583-585 (Nov. 11, 1970).

Key words: Aluminum oxide; bicrystals; crystal growth; vapor crystal growth.

Bicrystals containing symmetrical tilt boundaries with either the $[10\bar{1}0]$ or the $[11\bar{2}0]$ direction as the rotation axis were vapor-grown at 1740 °C using the reaction $2AlCl_3(g) + 3CO_2(g) + 3H_2(g) \rightarrow Al_2O_3(s) + 6HCl(g) + 3CO(g)$. Specimens as large as 3 by 5 by 20 mm were produced in 24 h. Chemical purity of the specimens is high, with $< 0.1$ ppm total cation impurities, as determined by activation analysis.

**12014.** Plante, E. R., Paule, R. C., **Explanation of the $\Delta H^\circ$ vs $\Delta S^\circ$ correlation,** *J. Chem. Phys.* **53,** No. 9, 3770-3771 (Nov. 1, 1970).

Key words: Heat of vaporization; least squares fits; second and third heats; ΔH-ΔS correlation.

A correlation of $\Delta H^\circ$ vs $\Delta S^\circ$ proposed in the literature as a means of evaluating best heats of vaporization is examined. The correlation which seems to employ second law heats is found to be a modification of the familiar third law method. It utilizes a different method of averaging experimental free energy changes than that employed by the usual third law method. It is shown that the correlation will normally produce a less precise heat than that obtained by averaging the usual third law heats.

12015. Rasmussen, A. L., **Laser energy and power measurement with a double reflecting plate calorimeter,** *Rev. Sci. Instr.* **41,** No. 10, 1479-1484 (Oct. 1970).

Key words: Calorimetry; laser; laser calorimetry; laser energy; laser power.

In a double reflecting plate calorimeter, the energy from a laser beam is partially absorbed by metal mirrors. The rest is reflected through an exit where it is free to interact with some medium. Characteristics of this calorimeter with a pair of aluminum plate mirrors are (1) wavelength range $\sim 0.1 - \sim 1\mu$, (2) energy input range $\sim 0.1 - \sim 50$ J/cm$^2$ (pulsed normal mode) and estimated power $\sim 100 - \sim 1000$ MW/cm$^2$ (pulsed Q switched) depending upon energy density, (3) estimated error $\pm 2\%$ over most of the ranges given, (4) 5 sec for the plates to reach a uniform temperature and to make measurements, and 2-4 min required cooling time between inputs, and (5) both absorption and reflection determined from plate calorimetric data. The sensitivity and the wavelength, energy, and power ranges may be increased by using different plate dimensions and materials. Data from an intercomparison between this calorimeter and an NBS liquid cell calorimeter yield agreement of about 0.6% at 0.6943 $\mu$. The light was *p* polarized (electric vector parallel to the plane of incidence). The energy of the components of polarization parallel and perpendicular to the plane of incidence of a light beam may be evaluated.

12016. Raveché, H. J., Mountain, R. D., **Three body correlations in simple dense fluids,** *J. Chem. Phys.* **53,** No. 8, 3101-3107 (Oct. 15, 1970).

Key words: Neutron diffraction; Percus-Yevick equation; radial distribution function; simple liquids; superposition approximation; three body correlation function; x-ray diffraction.

Correlations between triples of molecules in simple fluids at thermodynamic equilibrium are studied through their contribution to the isothermal density derivative of the pair probability density. Explicit computations are performed to indicate the role of the triplet function in accounting for the structure of the density derivative of the radial distribution function. The results imply that contributions from triplet correlations are in general quite appreciable. Various consequences of the results are discussed, and the procedure is examined in general as a method for studying correlations between triples of molecules in simple fluids.

12017. Roth, R. S., Waring, J. L., Parker, H. S., **Effect of oxide additions on the polymorphism of tantalum pentoxide. IV. The system $Ta_2O_5$-$Ta_2WO_8$,** *J. Solid State Chem.* **2,** 445-461 (1970).

Key words: Melting points; phase equilibria; system tantalum oxide-tantalum tungstate.

The low-temperature form of pure $Ta_2O_5$ has been found to exist in two slightly different modifications. The lowest temperature form has a *b* axis multiplicity of 14 whereas the highest temperature form (about 1350 °C) has a multiplicity of 11. At intermediate temperatures an "infinite" number of at least partially ordered sequences of these two modifications exist in equilibrium.

The addition of $WO_3$ to $Ta_2O_5$ causes the "stabilization" of an "infinite" number of phases similar in structure to the low temperature form of $Ta_2O_5$. From just less than 10 mol% $WO_3$ to the last compound in the series at 26 2/3 mol% $WO_3$ these phases are in equilibrium with liquid, and the high temperature structure type of pure $Ta_2O_5$ is eliminated from the phase diagram. One compound, $15Ta_2O_5 \cdot 2WO_3$ with a multiplicity of 8, was found to melt congruently at about 1815 °C and the last phase, $11Ta_2O_5 \cdot 4WO_3$ with a multiplicity of 13, melts incongruently at about 1605 °C.

12018. Santone, L. C., Berlin, G., **Location of fire stations,** *Proc. WORC Symp. Systems Analysis for Social Problems, National Bureau of Standards, Gaithersburg, Maryland, May 26-28, 1969,* pp. 79-91 (Dec. 3, 1970).

Key words: East Lansing, Mich.; facility location; fire station; simulation model; systems analysis; urban analysis.

This study was part of a project to demonstrate how a city staff, given adequate technical assistance and guidance, could use the methods of systems analysis to solve a particular problem. The city of East Lansing, Michigan, with the Technical Analysis Division of the National Bureau of Standards serving as "technical coach," developed a simulation model to aid in determining the number and location of fire stations necessary to protect the city adequately now and in future years.

12019. Sleater, G. A., Freeman, D. H., **Rapid desorption of chromium (III) from cation exchanger with hydrogen peroxide solutions,** *Anal. Chem.* **42,** No. 13, 1666-1668 (Nov. 1970).

Key words: Cation exchanger; chromium; hydrogen peroxide.

Conventional cation exchange resin is readily saturated with one Cr(III) cation per three exchange sites, but the adsorbed metal ion is then very difficult to desorb. This problem is solved by utilizing the rapid, irreversible and quantitative desorption that can be obtained with basic aqueous hydrogen peroxide. Under these conditions the desorption is caused by charge reversal, and the lack of affinity in the exchanger for the chromate anion. As expected, hydrogen peroxide in neutral or acid media is much less effective.

12020. Stevens, M. E., **Introduction to the Special Issue on Optical Character Recognition (OCR),** *Pattern Recog.* **2,** No. 3, 147-150 (Sept. 1970).

Key words: Automatic pattern recognition; handprinted characters; OCR standards; optical character recognition.

A brief introduction, stressing some aspects of the state of the art and the state of the practice of optical character recognition (OCR), is provided for a special issue of the journal, Pattern Recognition.

12021. Stevens, M. E., **Selected R&D requirements in the computer and information sciences,** *Proc. Fall Joint Computer Conf., Houston, Texas, November 17-19, 1970,* pp. 159-168 (AFIPS Press, Montvale, N.J., 1970).

Key words: Communication; information processing; languages; man-machine relationships; teleprocessing.

This paper presents an advance overview of a series of reports on R&D requirements in the computer and information sciences, based upon selective reviews of the literature. Examples of topics include: information acquisition, sensing and input, including pattern recognition; some overall systems design requirements with emphasis upon programming languages and advanced hardware technologies, and communication problems of machine-with-machine, man-with-machine, and man-with-man. Some of the possible contributions of the computer sciences to the more traditional library and information sciences are noted, but there are fundamental problems of human preception, learning, concept formation, and knowledge requiring interdisciplinary attack.

12022. Tsai, D. H., Bullough, R., Perrin, R. C., **Molecular dynamical studies of the motion of point defects in a crystalline**

**lattice,** *Proc. Phys. Soc. (London) C: Solid State Phys.* **3,** 2022-2036 (1970).

Key words: Atomic diffusion; defect motion; interstitial motion; jump frequency; lattice model; migration energy; migration entropy; molecular dynamics; random-walk theory; vacancy motion.

We have applied molecular dynamical type of calculations to the study of the motion of interstitials and vacancies in a crystalline lattice. Our purpose was to investigate the effects of lattice thermal oscillations on the motion and the interactions of these simple defects and to study the "random walk" problem of defect motion on an atomic scale. The lattice model was a three dimensional body centered cubic (bcc) model with a central force interaction potential which extended to second neighbours and simulated the interaction energies in $\alpha$-iron. The lattice containing one or more defects was first relaxed statically to a configuration of minimum energy, corresponding to the condition of zero absolute temperature. A temperature was then given to the lattice by assigning a Maxwellian distribution to the velocity of components of the lattice points in a random order. The subsequent motion of the lattice points and of the defects was calculated according to classical mechanics.

Our dynamical results showed that the temperature dependence of the jump frequency of the defects was in general agreement with the random walk theory of atomic diffusion. From this temperature dependence, the energy and the entropy of defect migration were obtained. For interstitial motion, the migration energy from the dynamical model (0.23 eV) was the same as that from static calculations. For vacancy motion, the migration energy from the dynamical model (0.42 eV) was lower than that from static calculations (0.60 eV). Possible reasons for this difference are discussed.

**12023.** Wasik, S. P., Tsang, W., **Determination of trace amounts of contaminants in water by isotope dilution gas chromatography,** *Anal. Chem.* **42,** No. 13, 1649-1651 (Nov. 1970).

Key words: Aromatics; gas chromatography; isotope dilution; olefins; water analysis.

An isotope dilution technique using gas liquid chromatography is proposed for the quantitative analysis of trace organic pollutants in water supplies. The method was demonstrated using benzene with perdeuterated benzene as the isotope with both substances in the ppb concentration range. Columns with aqueous silver nitrate as the stationary phase were used to determine the ratio of the concentration of benzene to perdeuterated benzene.

**12024.** Wasik, S. P., Tsang, W., **Gas-liquid chromatography separations of hydrocarbons using columns with aqueous solutions of complexing metal ions as stationary phases,** *Anal. Chem.* **42,** No. 13, 1648-1649 (Nov. 1970).

Key words: Aliphatics; aromatics; complexing effects; gas chromatography; group separation; mercuric nitrate; olefins; silver nitrate; surface effect.

Interesting hydrocarbon selectivity was obtained in gas-liquid chromatography using aqueous solutions of $Ag^+$ and $Hg^{++}$ ions as the stationary phases. This was achieved by taking advantage of the complexing properties of these ions and the large surface effect of the solution. Columns may be designed to be specific for certain hydrocarbon groups using this technique.

**12025.** Weir, C. E., Block, S., Piermarini, G. J., **Compressibility of inorganic azides,** *J. Chem. Phys.* **53,** No. 1, 4265-4269 (Dec. 1970).

Key words: Anisotropic compressibility; azides; compressibility; high pressure; single crystal; x-ray diffraction.

The compressibility of $\alpha$ lead azide, $\beta$ lead azide, barium azide, potassium azide, sodium azide, and thallium azide have been measured by single-crystal x-ray diffraction techniques for the first time in a new application of the diamond anvil pressure cell. Both the anisotropic and volume compressibilities are reported. The pressures were determined by measurements at the known freezing points of $n$-hexane and ethanol. A phase transition occurs in thallium azide at a pressure between the freezing points of chloroform (5390 bar) and $n$-decane (2990 bar). Pressure-temperature observations in the diamond cell of lead azide were carried out to 300 °C and approximately 30 kbar. No phase transitions were observed. Radiation damage to azide crystals under high pressures is reduced significantly.

**12026.** Unassigned.

**12027.** Brenner, A., **Note on the electrodeposition of magnesium from an organic solution of a magnesium-boron complex,** *J. Electrochem. Soc.* **118,** No. 1, 99-100 (Jan. 1971).

Key words: Decaborane; electrodeposition of magnesium; lithium deposition; nonaqueous electroplating; organometallic compound.

A magnesium electroplating bath which yields smooth, white deposits, has been prepared from lithium methyl, decaborane, and magnesium chloride. The solvent consisted mostly of tetrahydrofuran.

**12028.** Cezairliyan, A., **High-speed methods of measuring thermophysical properties at high temperatures,** (Proc. Conf. Thermophysical Properties, Manchester, England, April 7-10, 1970), *Rev. Inst. Hautes Temper. Refract.* **T.7,** 215-229 (1970).

Key words: High-speed measurement methods; high temperatures; thermodynamics; thermophysical properties.

In this paper, "high-speed" refers to experiments which are of subsecond duration. However, in some cases quasi-dynamic experiments with durations greater than one second are also included. Advantages of high-speed measurement of thermophysical properties of substances at high temperatures (above 2000 K) are presented. Requirements of high-speed measurements are given. Methods used for the generation and measurement of thermal energy in short times are described. Various techniques (photoelectric, photographic, and others) used for the measurement of the temperature of rapidly heating or cooling specimen are presented. Techniques for high-speed recording of quantities are described. Particular attention is given to millisecond-resolution digital data acquisition systems. Application of the high-speed techniques to the measurement of specific heat, electrical resistivity, thermal radiation properties, melting point, thermal diffusivity and others are described. Accuracy of high-speed measurements are discussed and are compared with those of conventional methods. Potential applications of high-speed methods are presented.

**12029.** Chamberlain, G. E., Mielczarek, S. R., Kuyatt, C. E., **Absolute measurement of differential cross sections for electron scattering in helium,** *Phys. Rev. A* **2,** No. 5, 1905-1922 (Nov. 1970).

Key words: Absolute differential cross section; Born; elastic; electron impact; helium; inelastic.

Absolute measurements of cross sections for electron-impact scattering in helium at an angle of 5° have been made for elastic scattering and excitation of the $2^1P$ and $2^1S$ states and for incident energies of 50-400 eV. Cross-section values of $\sigma(2^1P,5°)$ are found to be lower than theoretical Born values by $(9.5\pm5.4)\%$ at 400 eV, $(31.5\pm4.6)\%$ at 100 eV, and $(62.5\pm3.4)\%$ at 50 eV. Deduced values of total $2^1P$ excitation cross sections ($E\geqslant 100$ eV) are in agreement with other experimental values. Our measurements for elastic scattering agree well with recent theoretical calculations.

**12030.** Colson, J. P., Reneker, D. H., **Polyoxymethylene crystals grown within irradiated trioxane crystals,** *J. Appl. Phys.* **41,** No. 11, 4296-4312 (Oct. 1970).

Key words: Chain folded crystals; crystal growth mechanisms; electron diffraction of polymers; electron microscopy of polymers; polymer crystals; polymer morphology; polyoxymethylene crystals; post irradiation heat treatment; $\alpha$-particle initiation.

The morphological development of polyoxymethylene crystals polymerized from and grown within trioxane crystals was observed following irradiation of the trioxane with alpha particles and a subsequent heat treatment. A novel method of sample preparation enabled the morphology to be observed in detail and resulted in the discovery of new forms of polyoxymethylene crystals as well as an improved description of previously reported forms. A solid-gas-solid crystal growth mechanism was postulated to account for the predominantly acicular habit of the polyoxymethylene crystals.

**12031.** Czyz, W., Maximon, L. C., **Coulomb effects in high energy $He^4$-$He^4$ elastic scattering,** *Ann. Phys.* **60,** No. 2, 484-486 (Oct. 1970).

Key words: Diffraction scattering; Glauber model; $He^4$-$He^4$ elastic scattering; high energy Coulomb effects; high energy scattering.

In this note we extend the results of previous work (Ref. [1]) for high energy $He^4$-$He^4$ elastic scattering to include the Coulomb corrections. We find these corrections important around the diffractive minima.

**12032.** Day, G. W., Gruzensky, P. M., **Some optical properties of cesium cupric chloride,** *Appl. Opt.* **9,** No. 12, 2794-2795 (Dec. 1970).

Key words: Crystal growth; $CsCuCl_3$; electrooptic effect; index of refraction; nonlinear optics; transmission.

Cesium cupric chloride has been suggested as a possible material for nonlinear optical processes in the wavelength region near 10 $\mu$m. However, insufficient information about the optical properties of this material has been available to evaluate its suitability for these applications. This paper reports data on the transmission characteristics and index of refraction of $CsCuCl_3$ as well as method of growth. Possible applications are discussed, based on this information.

**12033.** Dillon, T. A., Smith, E. W., Cooper, J., Mizushima, M., **Semiclassical treatment of strong collisions in pressure broadening,** *Phys. Rev. A* **2,** No. 5, 1839-1846 (Nov. 1970).

Key words: Classical path approximation; intermolecular potential; pressure broadening; strong collision.

The classical-path approximation reduces the problem of pressure broadening of spectral lines to the evaluation of matrix elements of the scattering operator. If the intermolecular potential is long range and the interaction volume is large, the broadening is caused by distant or weak collisions. In this case, the scattering operator can be approximated by a second-order expansion, and the perturber trajectories can be taken to be straight paths. For neutral atoms or molecules, the intermolecular potential is short range and broadening arises from close or "strong" collisions. In this paper it is shown how classical trajectories, determined by a "scalar interaction" (i.e., one that does not depend upon the state of the radiator), can be used to expand the scattering operator in the sum of operators characteristic of the radiator's internal states.

**12034.** Ederer, D. L., Lucatorto, T., Madden, R. P., **Autoionization spectra of lithium,** *Phys. Rev. Letters* **25,** No. 22, 1537-1540 (Nov. 30, 1970).

Key words: Absorption spectroscopy; autoionization; configuration interaction; K electron excitation; lithium vapor; two electron excitation.

Resonances have been observed in neutral lithium vapor by absorption spectroscopy for photons in the 50- to 70-eV energy range. These resonances are due to the excitation of a *K*-shell electron, or the simultaneous excitation of a *K*-shell electron and an outer electron to final states of the type $(1s2pnl)$ or $(1snln'l')$. Several well-developed series have been observed as well as resonances where energy position and intensity are perturbed by neighboring configurations.

**12035.** Gadzuk, J. W., **A comparison between the Fermi-Thomas and quantum dielectric response of a metal surface to a static point charge,** *Surface Sci.* **23,** 58-68 (1970).

Key words: Adsorption; electron gas; impurities; surface physics.

Recently published theoretical treatments of the screening of a point charge in the surface region of a bounded electron gas are considered. The Fermi-Thomas semi-classical electrostatic screening theory of Newns is compared with the quantum screening theory of the present author. Simple formulae for dipole moments and binding energies are given. The results are essentially equivalent for the two cases aside from numerical factors which are manifestations of the fact that Fermi-Thomas screening is too efficient.

**12036.** Hahn, T. A., **Thermal expansion of copper from 20 to 800 K—Standard Reference Material 736,** *J. Appl. Phys.* **41,** No. 13, 5096-5101 (Dec. 1970).

Key words: Components of error (within and between samples); copper; interferometer; standard reference material; thermal expansion.

Copper is the first of a series of materials that will be certified as thermal-expansion standards by the National Bureau of Standards. The results of tests on five specimens indicate the stock is of consistent quality so that it may be certified as Standard Reference Material 736. A Fizeau interferometer was used for the expansion measurements. Above room temperature a controlled-atmosphere furnace using a calibrated Pt vs Pt-10% Rh thermocouple was used. Below room temperature a cryostat capable of operation with both liquid nitrogen and helium was used with a calibrated platinum resistance thermometer. Values of expansivity were calculated between equilibrium temperatures. The expansivity was used in the analysis of the data. Third-order polynomials were fitted to the data for each of the five specimens in the overlapping temperature ranges from 0 to 70 K, 50 to 270 K, and 210 to 800 K to test for variations between the specimens. The deviations between the five equations were well within the standard deviations of the data for each of the specimens in the respective temperature intervals. All the expansivity data were then pooled and used to obtain an equation for each of the temperature ranges given above. These equations and their integrals were used to calculate the final values of expansivity and expansion, respectively. The results of the statistical analysis of the expansion and expansivity data are presented. A comparison is made with the data in the literature.

**12037.** Hamer, W. J., **Standard cells,** *The Primary Battery,* George W. Heise and N. Corey Cahoon, eds., **1,** No. 12, 433-477 (John Wiley & Sons Inc., New York, N.Y., Jan. 1971).

Key words: Electromotive force; saturated standard cells; standard cells; unsaturated standard cells.

This paper gives a survey of saturated and unsaturated standard cells including descriptions of their construction and their behavior under diversified conditions. The survey also includes a discussion of the role standard cells play in the maintenance of the unit of electromotive force. A discussion of the Hulett standard battery is also included.

**12038.** Harvey, J. L., Milliken L. T., Forthofer, R. J., **Trends in motor vehicle brake fluids and their standards,** *Proc. Society of Automotive Engineering Conf.,* Paper No. 710253, pp. 1-17, (Jan. 11-15, 1971).

Key words: Brake fluids; brake fluid standards; motor vehicle brake fluid; passenger car braking systems.

The development of motor vehicle brake fluids (MVBF's) and of their specification requirements is reviewed and discussed with emphasis on the major problems encountered in service. Those factors held to be of major importance in establishing performance requirements for MVBF's are considered also, and applied to the major changes that have recently been proposed for revision of Federal Motor Vehicle Safety Standard No. 116. The needs and possibilities for further revisions in the MVBF safety standard are examined. Finally, potential effects of some current trends in the design of passenger car braking systems are considered.

**12039.** Heydemann, P. L. M., **A simple and dependable electrical feedthrough for high pressures,** *Rev. Sci. Instr.* **41,** No. 12, 1896 (Dec. 1970).

Key words: Closure; feedthrough; high pressure; leads.

This note describes a novel type of high pressure feedthrough capable of withstanding more than 25 kbar repeatedly. It can be used for measurements with DC requiring very high insulation resistance as well as for RF up to 30 MHz.

**12040.** Kelley, R. D., Klein, R., Scheer, M. D., **Isotope effects in the hydrogen-atom addition to olefins at low temperatures,** *J. Phys. Chem.* **74,** No. 25, 4301-4309 (1970).

Key words: Atom addition; hydrogen isotopes; low temperatures; olefins; orientation; quantum tunneling.

The ratio of rates of addition of atomic hydrogen to the two possible sites of the double bond for several olefins has been measured over the temperature range 63-143 K. A pronounced isotope effect was found. In the comparison of addition ratios at a given temperature, the data show that the isotope effect is related to the value of the addition ratio, large ratios showing relatively large effects. The ratio of terminal to nonterminal addition of H to propylene at 90 K is 126, while for D it is 398. The ratio of H addition to carbon 2 relative to carbon 3 in *cis*-2-pentene at 90 K is 1.5 and that of D is the same. The results of these finds are discussed in terms of a one and two barrier model for the reaction of H with the olefinic bond. Both zero point energy effects and quantum tunneling of H through the reaction barriers are considered. It is concluded that a two barrier model with tunneling is most appropriate. The data generated from the H atom-olefin addition reactions in the low temperature region support the existence of chemical quantum tunneling. This is apart from the more equivocal arguments based on curvature of Arrhenius plots although indeed such curvature is found in the low-temperature H-atom additions.

**12041.** Lamb, V. A., Johnson, C. E., Valentine, D. R., **Physical and mechanical properties of electrodeposited copper, III. Deposits from sulfate, fluoborate, pyrophosphate, cyanide, and amine baths,** *J. Electrochem. Soc.* **117,** Nos. 9, 10, 11, 291C-318C, 341C-352C, 381C-404C (Sept., Oct., Nov. 1970).

Key words: Annealing-electrolylic copper; electrodeposited copper; impurity content; properties of mechanical structure.

This paper is the third published report on the results of broad program on properties of electrodeposited copper, spor sored jointly by the American Electroplaters' Society, The Inte national Copper Research Association, Inc., The Coppe Development Association, and the National Bureau of Star dards. The first paper is a comprehensive review of the literatur to 1965. The second paper is an interim report on experiment results. The present and final paper, which incorporates the dat in the second, includes data from the baths designated in the titl for deposits prepared under a wide range of operating condition and with use of a variety of addition agents. Properties measure include tensile strength, yield strength, elongation, modulus elasticity, fatigue strength, hardness, internal stress, densit electrical resistivity, and thermal expansivity. Properties wer measured for as-plated deposits, deposits after annealing several temperatures, after cold-working, and at low and hig ambient temperatures. Structure of deposits was examined b optical, electron micrograph, and x-ray methods. Content of im purities in deposits was determined. Correlations are develope among properties, structure, impurity content, type of bath, an operating conditions.

**12042.** Larsen, N. T., Clague, F. R., **The NBS type II power me surement system,** *Proc. 25th Annual 1970 Instrument Societ of America Conf. and Exhibit, Philadelphia, Pa., October 2 29, 1970,* 11 pages (1970).

Key words: Bridge; leveler; microwave; power; self balan ing; stabilizer.

The design, construction, and performance of a new solid stat microwave power measuring system are described. The instru ment consists of two modules—a self-balancing bolometer bridg and a reference generator. The reference generator is a mult function module which may be used as either a 0.01 percent d voltmeter with a 0 to 10 volt range, a 0 to 10 volt dc referenc voltage source of 0.01 percent absolute accuracy, or a precisio microwave power leveler. A six-decade divider provides hig precision in all three functions.

A comprehensive error analysis and complete schematic di grams are included.

**12043.** Lightbody, J. W., Jr., **Electron scattering sum rule for $^{12}$ experiment and theory,** *Physics Letters* **33B,** No. 2, 129-13 (Sept. 1970).

Key words: Electron scattering; momentum transfer; pa correlation; shell model; spurious; sum rule.

Inelastic electron scattering cross sections for $^{12}$C have bee integrated to form the longitudinal and transverse sums as a fun tion of momentum transfer. Comparison is made with sum rul calculated in the harmonic oscillator model. The various tw body correlation functions which enter the sum are evaluated f $^{4}$He, $^{12}$C and $^{16}$O in the oscillator model.

**12044.** Maki, A. G., Olson, W. B., Sams, R. L., **HCN rotationa vibrational energy levels and intensity anomalies determine from infrared measurements,** *J. Mol. Spectry.* **36,** No. 3, 43 447 (Dec. 1970).

Key words: Absorption; energy levels; gas laser; HC hydrogen cyanide; infrared; rotational constants; spectr vibrational constants.

New measurements have been made on the infrared trans tions $11^{1}0$-$00^{0}0$, $04^{0}0$-$00^{0}0$, $12^{0}0$-$01^{1}0$, $12^{2}0$-$01^{1}0$, $05^{1}0$-$01^{1}$ $13^{3}0$-$02^{2}0$, $13^{1}0$-$02^{0}0$, $12^{2}0$-$00^{0}0$, and $20^{0}0$-$00^{0}0$ for HCN and o the $11^{1}0$-$00^{0}0$ transitions for both $H^{13}C^{14}N$ and $H^{12}C^{15}N$. Whe ever possible those measurements were combined with las measurements to obtain the best set of constants for describin the energy levels. Unusual intensity distributions were observe and attributed to intensity mixing through $l$-type resonance. Several $P$-branch lines of a $\Delta$-$\Sigma$ ($12^20$-$00^00$) transition were also observed although the intensity was somewhat less than predicted from $l$-type resonance effects.

2045. McCaa, W. D., Jr., Nahman, N. S., **Generation of reference waveforms by uniform lossy transmission lines,** *IEEE Trans. Instr. Meas.* **IM-19,** No. 4, 382-390 (Nov. 1970).

Key words: Lossy uniform transmission lines; oscilloscope errors; pulse generators; standard waveforms.

This paper describes a method for generating fractional nanosecond pulsed waveforms of known shape thereby providing an a priori means for establishing reference waveform generators or standards to be used in pulsed measurements and other applications. The method employs the band-limiting properties of a lossy uniform transmission line to produce a known waveform and generator impedance. A theory for generator characterization and application is presented that defines a given generator in terms of time-domain or frequency-domain functions. A new term called the "available" waveform is defined. Rms error is employed as the error criteria.

An example of generator design is given that employs planar skin-effect loss and provides an output response having 0.2 percent rms error over the interval $0 \leq t \leq 600$ ps referred to the inherent step response of the waveshaping line. The input transition generator is assumed to be a 30-ps unit ramp generator. Also, an application example is given that employs a reference waveform generator to evaluate a sampling oscilloscope. The reference waveform generator uses a Debye dielectric lossy transmission line. The rms error of the oscilloscope time-domain response is determined as a function of time.

2046. Mangum, B. W., Thornton, D. D., **Vibrating sample magnetometer for use at very low temperatures and in high magnetic fields,** *Rev. Sci. Instr.* **41,** No. 12, 1764-1766 (Dec. 1970).

Key words: Bimorph; cryogenic; low-temperature; magnetometer; piezoelectric; vibrating-sample magnetometer.

A high sensitivity vibrating sample magnetometer for use at very low temperatures is described. It can be made extremely compact by the use of a piezoelectric element as the vibrator. The complete magnetometer can be placed in the cryostat between the poles of an electromagnet and can be operated at high applied magnetic fields.

2047. Meinke, W. W., **The universal analytical instrument,** *Proc. 5th Annual National Conference on Industrial Research, Applying Emerging Technologies, Industrial Research, Inc., Chicago, Ill., September 18, 1969,* pp. 31-41 (1970).

Key words: Automated analysis; clinical chemistry; instrumentation; standard reference materials.

The Fifth Annual National Conference on Industrial Research focused attention on the "Application of Emerging Technologies." As part of a panel discussion on "Instrumentation Applications," the author was asked to discuss "The Universal Analytical Instrument." This topic has been interpreted as applying to the overall field of automated laboratory instrumentation.

A summary was given of the experience in automation of the NBS Analytical Chemistry Division consisting of nine sections and approximately sixty different analytical competences. Several specific areas, such as clinical chemistry, where standardized instrumentation has not kept pace with the needs were discussed. Automation in optimum operation should free a scientist for the important and essential decision-making process rather than replacing him entirely. Furthermore, when automated systems become the rule rather than the exception, it is absolutely essential that there be some kind of standardization (often using standard reference materials) built into the system so that one can get a measurement that really means something. Finally, there is a need for finding new ideas for automation rather than extending old ones.

12048. Murphey, W. M., Caswell, R. S., **Analysis of results of the Bureau International des Poids et Mesures thermal neutron flux density intercomparison,** *Metrologia* **6,** No. 4, 111-115 (Oct. 1970).

Key words: Data analysis; flux density; intercomparisons; least squares; standards; thermal neutrons.

The results of an international comparison of thermal neutron flux density standards sponsored by the Neutron Working Group of the Bureau International des Poids et Mesures have been analyzed using a method conceptually different from a companion analysis by Axton. Both methods, however, yield closely the same results. All individual values are within ±2.6% of the adjusted value, the average absolute deviation being about 1%.

12049. Plummer, E. W., Gadzuk, J. W., **Surface states on tungsten,** *Phys. Rev. Letters* **25,** No. 21, 1493-1495 (Nov. 23, 1970).

Key words: Electrons; single crystal faces of tungsten; spin-orbit split bands; tungsten.

The energy distribution of field-emitted electrons from single-crystal faces of tungsten exhibits structure which is extremely sensitive to surface contaminants. The structure for the (100) plane has the correct shape and energy expected for surface states resulting from spin-orbit-split bands. These results are in good agreement with recent theoretical predictions.

12050. Potzik, J., **A method for determining the dynamic response of an elastic load cell element,** *Rev. Sci. Instr.* **41,** No. 12, 1726-1731 (Dec. 1970).

Key words: Dynamic force; load cell; viscoelastic damping.

A method has been developed for determining the dynamic characteristics of a load cell element by subjecting it to sinusoidally time dependent forces, and an experiment using a piezoelectric shaker is described which illustrates the feasibility of the method. At present a simple viscoelastic model is assumed for the load cell element, and relaxation times on the order of $10^{-7}$ sec have been measured. The application of this information to load cells subjected to other types of dynamic forces is also discussed.

12051. Preston, J. D., Forthofer, R. J., **Correlation of vehicle, dynamometer and other laboratory tests for brake friction materials,** *Proc. Society of Automotive Engineers Conf., Detroit, Michigan, January 11-15, 1971,* Paper No. 710250, pp. 1-10 (1971).

Key words: Brake friction materials; coefficient of friction; friction assessment screening test machine; friction materials test machine; Girling scale dynamometer; inertia brake dynamometer; vehicle road tests.

The frictional properties of brake lining materials are greatly influenced by the manner in which they are used. Test procedures designed to measure the coefficient of friction of these materials can likewise produce widely differing results depending on the type of test conducted. This paper presents data illustrating the performance correlation of three commercially available brake lining materials when subjected to vehicle tests and some of the more commonly used laboratory test procedures.

**12052.** Radlinski, R. W., Forthofer, R. J., Harvey, J. L., **Operating performance of motor vehicle braking systems as affected by fluid water content,** *Proc. Society of Automotive Engineering Conf.,* Paper No. 710253, pp. 1-11 (Jan. 11-15, 1971).

Key words: Automotive hydraulic brake fluids; brake fluids performance; braking systems; low temperature viscosity.

Automotive hydraulic fluids are known to pick up water in service. This paper shows that a major portion of the water picked up by the brake fluid in a braking system is transmitted through the hoses. It discusses two major effects of water pick-up on brake fluid performance—reduction in vapor lock temperature and increase in low temperature viscosity. Performance data for several "wet" brake fluids operating in actual braking systems at high and low temperatures are presented.

**12053.** Santoro, A., **Absorption correction for diffraction measurements in complex cases,** (Proc. Intern. Summer School organized by the Commission on Crystallographic Computing of the Intern. Union of Crystallography, Ottawa, Canada, August 4-11, 1969), Chapter in *Crystallographic Computing,* F. R. Ahmed, S. R. Hall, and C. P. Huber, eds., pp. 283-290 (Munksgaard, Copenhagen, Denmark, 1970).

Key words: Absorption correction; diffraction; x ray.

A method is described for evaluating the absorption corrections in those cases in which, in addition to the crystal, other objects take part in the absorption.

The method is applied to the most commonly used diffraction technique.

**12054.** Santoro, A., Mighell, A. D., Reimann, C. W., **The crystal structure of a 1:1 cupric nitrate-pyrazine complex $Cu(NO_3)_2{\cdot}(C_4N_2H_4)$,** *Acta Cryst.* **B26,** 979-984 (July 7, 1970).

Key words: Coordination complex; inorganic polymer; pyrazine ligand; x-ray structure determination.

The crystal structure of a 1:1 cupric nitrate-pyrazine complex, $Cu(NO_3)_2{\cdot}(C_4N_2H_4)$, was determined by single-crystal x-ray diffraction techniques. This compound crystallizes in the orthorhombic system with $a = 6.712$, $b = 5.142$, and $c = 11.732$ Å, space group *Pmna*, $\rho = 2.19$ g.cm$^{-3}$ and $Z = 2$. The intensities of 642 unique reflections were recorded by the $2\theta$-scan method and the structure was solved by an analysis of the three-dimensional Patterson map. The structure is a coordination polymer and consists of linear —Cu—pyrazine—Cu—pyrazine— chains. The nitrate groups lie in mirror planes normal to the chain axes and they are coordinated to the $Cu^{II}$ ion unsymmetrically through two oxygen atoms. Refinement by anisotropic least-squares analysis gave an $R$ value of 0.04.

**12055.** Selby, M. C., **The Bolovac and its applications,** *IEEE Trans. Instr. Meas.* **IM-19,** No. 4, 324-331 (Nov. 1970).

Key words: BOLOVAC; microwave current measurements; microwave power measurements; microwave voltage measurements.

The Bolovac is a novel device for the standardization and measurement of TEM voltage, current, and power from below 1 MHz through 18 GHz (potentially through 36 GHz). It can be used for attentuation measurement and as a superior impedance termination at all the above-mentioned frequencies. To date it is the first and only practical means of calibrating microwave current indicators and of evaluating oscilloscopes displaying 25-ps or shorter rise-time pulses.

It is felt that application of the Bolovac will radically improve power measurements. It reduces the problems arising from mismatch-error uncertainties, one of the major present sources of concern in power measurement; measurement of complex reflection coefficients; complex computations; use of error-limi charts; and measurement of effective efficiency and calibration factors. Its application should radically increase optimum accuracy and measurement-time efficiency in calibration facilities outside the National Bureau of Standards.

The Bolovac together with an RF generator can be used as a source of known voltage. It can also be used as an absorption power meter. It needs no RF calibration. It has a range as high as 40 dB depending on the desired precision and on whether one or more sensors (special bolometric disks) are used. Voltages down to 0.1 volt with accuracies of 0.5 percent and better (and corresponding power in 50-ohm systems) have been measured.

The paper describes the general features and application of the Bolovac and lists references to more comprehensive papers on the subject.

**12056.** Tjon, J. A., Gibson, B. F., O'Connell, J. S., **Trinucleon form factors calculated from realistic local potentials,** *Phys. Rev. Letters* **25,** No. 8, 540-542 (Aug. 24, 1970).

Key words: Charge; form factor; magnetic; nucleon potentials; repulsive core; $^3$He; $^3$H.

Charge and magnetic form factors are calculated using solutions of the three-nucleon Faddeev equations with the local two-nucleon potentials of Reid and of Malfliet and Tjon. The results give reasonable agreement with the data up to 9-fm$^{-2}$ transfer, but do not reproduce the minimum at 11.8 fm$^{-2}$ in the $^3$He charge form factor.

**12057.** Van Brunt, R. J., Kieffer, L. J., **Angular distribution of $O^-$ from dissociative electron attachment to $O_2$,** *Phys. Rev. A* **2,** No. 5, 1899-1905 (Nov. 1970).

Key words: Angular distribution of $O_2$; dissociative electron attachment; electron energy.

The angular distribution of $O^-$ produced by electron bombardment of $O_2$ has been measured in the electron energy range 5.75-8.40 eV. The results show a strong energy dependence and are consistent with the theory of O'Malley and Taylor if the final $O_2^-$ repulsive resonance state is assumed to have the symmetry $^2\Pi_u$, and if only the first two allowed partial waves of the incident electron corresponding to $L = 1$ and $L = 3$ contribute. The results indicate that the $L = 3$ term becomes more important as energy increases and thereby demonstrate that the single-term approximation for the angular distribution does not apply for this process.

**12058.** Van Brunt, R. J., Kieffer, L. J., **Angular distribution of protons and deuterons produced by dissociative ionization of $H_2$ and $D_2$ near threshold,** *Phys. Rev. A* **2,** No. 4, 1293-1304 (Oct. 1970).

Key words: Deuterium; dissociation; electron; hydrogen; molecule.

From observations of the kinetic-energy distribution of protons and deuterons at corresponding forward and backward angles with respect to the electron-beam direction, the forward momentum imparted to the dissociating $H_2$ ($D_2$) molecule by the incident electrons has been determined for electron energies up to 300 eV. The momentum transfer along the beam was found to remain nearly constant at all energies above threshold, although above 100 eV the values obtained for $D_2$ were systematically higher than the values for $H_2$. When corrected to the center-of-mass system, the angular distribution of $H^+$ ($D^+$) near threshold was found to contain a large isotropic component and an anisotropic component which deviates, in a manner suggested by Zare, from the $\cos^2\Theta$ dependence predicted from a simple dipole Born approximation.

**12059.** Allpress, J. G., Roth, R. S., **Structural studies by electron microscopy: Polymorphism of $ZrO_2 \cdot 12Nb_2O_5$,** *J. Solid State Chem.* **2,** 366-376 (1970).

Key words: Electron microscopy; lattice images; niobia; polymorphism; zirconia; $ZrO_2 \cdot 12Nb_2O_5$.

Three polymorphs of $ZrO_2 \cdot 12Nb_2O_5$ have been identified by the combined use of x-ray diffraction and electron optical techniques. The $\alpha$ form, which is the initial product of the reaction of $ZrO_2$ with $Nb_2O_5$ in the molar ratio 1:12, is isostructural with $TiNb_{24}O_{62}$. The monoclinic $\beta$ form, produced by long annealing, has a more complex structure, and may contain intergrowths of a third, $\gamma$, polymorph. Lattice images of the $\beta$ form, together with the diffraction data, are used to derive possible structures for these materials.

**12060.** Ballard, D., Yakowitz, H., **Spectrometer shield for stray iron x-ray radiation in the scanning electron microscope,** *Rev. Sci. Instr.* **42,** No. 1, 14-15 (Jan. 1971).

Key words: Increased sensitivity of touch alarm; scanning electron microscope; x-ray spectrometer shield.

A spectrometer shield for stray iron x-ray radiation was devised and installed in the scanning electron microscope. A modification to the touch alarm was also made to make the system operative.

**12061.** Boyd, M. E., Mountain, R. D., **Methods for determining the second virial coefficient of a gas from speed-of-sound data,** *Phys. Rev. A* **2,** No. 5, 2164-2167 (Nov. 1970).

Key words: Acoustic thermometry; equation of state; equilibrium gas properties; helium; second virial coefficient; speed of sound in gases.

Two methods of analyzing speed-of-sound data in gases to obtain the second virial coefficients $B(T)$ are compared. The older method, which assumes a form for the temperature dependence of $B$, is shown to correspond to finding an exact solution to an approximate differential equation for $B$, while a method recently proposed by Bruch solves the exact equation, but in an approximate manner. Examination of the errors in each method indicates that the first method is preferable.

**12062.** Brenner, A., Anderson, H. J., **Note on the preparation of rhenium oxychlorides,** *J. Electrochem. Soc.* **118,** No. 2, 373-374 (Feb. 1971).

Key words: Chemical vapor deposition; perrhenyl chloride; rhenium heptaoxide; rhenium oxytetrachloride.

This note describes a new method of preparing perrhenyl chloride, $ReO_3Cl$, by the reaction of rhenium heptaoxide with hydrogen chloride.

**12063.** Chappell, S. E., Humphreys, J. C., **Energy deposition in surface layers of silicon by monoenergetic electrons,** *Proc. 4th Intern. Conf. Electron and Ion Beam Science and Technology, May 10-14, 1970, Los Angeles, Calif.,* pp. 655-666 (The Electrochemical Society Inc., New York, N.Y., 1970).

Key words: Absorbed dose; absorbed-energy distributions; electron beams; energy deposition; silicon detectors; surface layers.

The energy absorbed from a normally incident electron beam by a thin silicon layer has been measured. The silicon layer was a transmission, semiconductor detector having a thickness less than the mean range of the incident electrons which had energies of 0.25, 0.50, 0.75, and 1.0 MeV. The fraction of beam energy absorbed in the silicon layer was determined from absorbed-energy distributions which were derived from pulse-height distributions measured with the detector. Measurements were made for two different cases: (1) energy absorbed in the specific layer alone and (2) the energy absorbed in the same layer as a part of a homogeneous, semi-infinite medium, i.e., a surface layer. In the latter case, a larger fraction of energy is absorbed for each incident energy. The results were compared with Monte Carlo calculations, with the measurements and calculations showing agreement better than 10 percent.

**12064.** Dibeler, V. H., Walker, J. A., McCulloh, K. E., **Photoionization study of chlorine monofluoride and the dissociation energy of fluorine,** *J. Chem. Phys.* **53,** No. 12, 4414-4417 (Dec. 15, 1970).

Key words: Chlorine monofluoride; dissociation energy; ionization energy; mass spectrometry; photoionization; vacuum ultraviolet.

Mass spectra and photoionization yield curves are obtained for the molecular and atomic ions of chlorine monofluoride. The atomic ions are formed both by ion-pair and by dissociative ionization processes, although the $F^+$ ion formed by the latter process is too weak for quantitative measurements. The $ClF^+$ curve exhibits a weak onset at 12.55 eV, ascribed to a hot band. An intense onset at 12.65 eV is ascribed to the (0, 0) transition. The observed thresholds for the $Cl^+$ ion support the spectroscopic determination of $D(ClF) = 2.558$ eV and, combined with a recent determination of the heat of formation of ClF, support the previously reported photoionization value of $D_0°(F_2) = 1.34$ eV.

**12065.** Edqvist, O., Lindholm, E., Selin, L. E., Asbrink, L., Kuyatt, C. E., Mielczarek, S. R., Simpson, J. A., Fischer-Hjalmars, I., **Rydberg series of small molecules. VIII. Photoelectron spectroscopy and electron spectroscopy of $NO_2$,** *Phys. Scrip.* **1,** 172-178 (1970).

Key words: Electron spectroscopy; $NO_2$; photoelectron spectroscopy; Rydberg series.

The photoelectron spectrum of $NO_2$ has been measured with high resolution up to 27.5 eV and interpreted by use of molecular orbital theory, taking especially the vibrational structure into account. The electron impact energy loss spectrum has been measured with electron energy 100 eV. The spectrum above 6.5 eV has been interpreted as due to Rydberg transitions and comparison with spectroscopic measurements have been made.

**12066.** Farabaugh, E. N., Mauer, F. A., **Application of a modified technique for x-ray topography of large crystals,** *J. Crystal Growth* **7,** 282-284 (1970).

Key words: Laser rod; orientation; ruby; single crystal; topography; x ray.

A transmission x-ray topography technique has been developed which is suitable for examining large, uncut crystals. A relatively large volume is represented in each photograph, and regions that are misoriented by more than 0.3° can be detected. Examination of single crystal ruby laser rods is used to illustrate the capabilities and limitations of the method.

**12067.** Harris, F. K., Fowler. H. A., Olsen, P. T., **Accurate Hamon-pair potentiometer for Josephson frequency-to-voltage measurements,** *Metrologia* **6,** No. 4, 134-142 (Oct. 1970).

Key words: Frequency-to-voltage ratio; Josephson effect; potentiometer; voltage standard.

Accuracy and precision of parts in $10^7$ have been demonstrated in a potentiometer which compares dc signals in the 2 to 10 millivolts range from Josephson junctions, against the U.S. "legal volt," as maintained by a group of standard cells. The circuit comprises two ($10 \times 100$ ohms) Hamon networks in series-to-parallel transposition, linked by a calibrated Kelvin-Varley current divider. The critical Hamon-circuit contacts are made through mercury-wetted amalgams; the entire circuit operates in smoothly stirred oil. Observations indicate the pair of Hamon boxes to be initially matched within 0.2 ppm at the operating temperature. Typical standard deviation in the day-to-day, run-to-run scatter of Josephson frequency-to-voltage ratio, measured with this instrument, is 0.3 ppm or less. Preliminary values for the observed ratio are in general accord with the quoted values of Parker et al., Petley and Morris, and Finnegan et al.

**12068.** Hellwig, H., **Areas of promise for the development of future primary frequency standards,** *Metrologia* **6,** No. 4, 118-126 (Oct. 1970).

> Key words: Ion storage; laser stabilization; maser oscillator; metrology; quantum electronics; saturated absorption; slave oscillators.

This paper discusses possibilities which may lead to the development of future primary frequency standards of superior accuracy capability. Aspects of costs and field-usage are totally neglected. A review is given of the various methods and techniques which are currently employed in quantum electronic frequency standards or which have a potential usefulness. Various effects which influence the output frequency of a primary standard are associated with these methods. They are discussed in detail, and expectation values for the related uncertainties are given. For selected particles certain methods of interrogation, confinement, and particle preparation can be combined such as to minimize the net uncertainty due to all applicable effects. Different technical solutions are the result. A review of existing and proposed devices is given, including quantitative data on the stability and accuracy capability. Aspects of the most promising devices are discussed, and it is concluded that accuracy capabilities of $10^{-14}$ should be within reach of today's research and development.

**12069.** Hellwig, H., Vessot, R. F. C., Levine, M. W., Zitzewitz, P. W., Allan, D. W., Glaze, D. J., **Measurement of the unperturbed hydrogen hyperfine transition frequency,** *IEEE Trans. Instr. Meas.* **IM-19,** No. 4, 200-209 (Nov. 1970).

> Key words: Frequency shift; frequency stability; hydrogen hyperfine transition; hydrogen maser; hydrogen storage; hydrogen wall collisions; NBS-III; teflon; universal time.

The results of a joint experiment aimed primarily at the determination of the frequency of the $H^1$ hyperfine transition $(F=1, m_F=0) \leftrightarrow (F=0, m_F=0)$ is reported. In terms of the frequency of the $Cs^{133}$ hyperfine transition $(F=4, m_F=0) \leftrightarrow (F=3, m_F=0)$, defined as 9192 631 770 Hz, for the unperturbed hydrogen transition frequency the value

$$\nu_H = 1420\,405\,751.768 \text{ Hz}$$

is obtained. This result is the mean of two independent evaluations against the same cesium reference, which differ by $2 \times 10^{-3}$ Hz. We estimate the one-sigma uncertainty of the value $\nu_H$ also to be $2 \times 10^{-3}$ Hz. One evaluation is based on wall-shift experiments at Harvard University; the other is a result of a new wall-shift measurement using many storage bulbs of different sizes at the National Bureau of Standards. The experimental procedures and the applied corrections are described. Results for the wall shift and for the frequency of hydrogen are compared with previously published values, and error limits of the experiments are discussed.

**12070.** Hoer, C. A., Agy, D. L., **Broad-band resistive-divider-type directional coupler,** *IEEE Trans. Instr. Meas.* **IM-19,** No. 4, 336-343 (Nov. 1970).

> Key words: Coupler; directional coupler; directivity; impedance measurements; power measurements.

A new lumped-circuit directional coupler is described for the 1-30 MHz frequency range. Directivity greater than 50 dB is achieved over this frequency range for coupling ratios of 30, 40, and 50 dB. Greater directivity can be achieved over a narrower frequency range, and the coupler can be tuned for essentially infinite directivity at a fixed frequency. The couplers, although resistive, can pass 100, 300, or 1000 watts for the coupling ratios of 30, 40, and 50 dB, respectively, with less than a 0.01-dB change in coupling ratio. The coupling ratios are constant with frequency to ±0.25 dB. Equations and curves are given for obtaining component values needed to design a resistive-divider-type coupler with any coupling from 3 to 60 dB.

**12071.** Hummer, D. G., Rybicki, G. B., **Noncoherent scattering-VII. Frequency-dependent thermalization lengths and scattering with continuous absorption,** *Monthly Notices Roy. Astron. Soc.* **150,** No. 4, 419-434 (1970).

> Key words: Activation energy; H atoms; $H_2S$; rate constant; resonance fluorescence; vacuum-uv.

Our previous definition of the thermalization length is generalized to cases in which the initial photon frequency is prescribed. This permits treatment of cases in which the emissivity does not have a unique frequency dependence. This definition is then applied to the case of a line formed by scattering in the presence of continuous opacity. In this case the emissivity in the line has a unique frequency dependence but the total emissivity does not. Equations for the distribution of thermalization distances are derived both by a diagrammatic technique and by use of resolvents. Median thermalization lengths are defined in terms of these distributions. Extensive numerical results are reported and the utility of this approach is discussed.

**12072.** Ives, L. K., Ruff, A. W., Jr., **Extended dislocation configurations in hcp silver-tin alloys of low stacking-fault energy,** *Metal Sci. J.* **4,** 201-209 (May 1970).

> Key words: Dislocation multipoles; dislocation networks; dislocation nodes; dislocations; electron microscopy; hexagonal alloys; silver-tin alloys.

Configurations resulting from the interaction of extended dislocations in hcp silver-tin alloys of low stacking-fault energy have been studied by means of transmission electron microscopy. The interactions of all possible sets of two different extended dislocations are considered. Since there are two distinct modes by which dislocations extend in the hcp structure, these interactions fall into two classes: Class I interactions occur between two extended dislocations having the same fault shear vector; Class II interactions involve two extended dislocations having opposite fault shear vectors. Interactions between two arrays of extended dislocations lead to the formation of networks. Among the configurations studied were two different types each of dipoles, dipole networks, multipoles, and extended nodes. The observed configurations are compared to those reported in hexagonal graphite. The Class I configurations are similar to those found in low-stacking-fault-energy fcc metals.

**12073.** Kuriyama, M., Miyakawa, T., **Primary and secondary extinctions in the dynamical theory for an imperfect crystal,** *Acta Cryst.* **A26,** Part 6, 667-673 (Nov. 1970).

> Key words: Dynamical diffraction; imperfections; kinematical scattering; piezoelectric vibration; secondary extinction; theory; x-ray diffraction.

Primary and secondary extinction are studied using the dynamical theory of x rays diffracted by imperfect crystals. The transition from dynamical to kinematical scattering is explained in terms of fundamental processes in diffraction. Contrary to existing extinction theories, where the intensities diffracted dynamically by single coherent domains of a mosaic are combined using an *ad hoc* assumption of mosaic distributions, the present theory permits the dynamical *amplitudes* to change in response to disturbances of the dynamical interactions by imperfections. Neither the mosaic block model nor the statistical treatment of imperfections is used. The extinction of diffracted intensities is thereby treated as caused solely by *inhomogeneous* strains in a single coherent domain.

12074. Kurylo, M. J., Peterson, N. C., Braun, W., **Absolute rate of the reaction $H + H_2S$,** *J. Chem. Phys.* **54,** No. 3, 943-946 (Feb. 1, 1971).

Key words: Activation energy; H atoms; $H_2S$; rate constant; resonance fluorescence; vacuum-uv.

Flash photolysis coupled with resonance fluorescence of Lyman-$\alpha$ radiation at 121.6 nm has been used to investigate the rate of reaction of H atoms with $H_2S$ over the temperature range 190-464 K. Conditions were chosen under which atom-radical and radical-radical reactions were unimportant and only the H-atom-$H_2S$ reaction occurred. The rate constant thus obtained can be expressed as $k_1 = (1.29 \pm 0.15) \times 10^{-11} \exp[-(1709 \pm 60)/1.987\ T]$ cm$^3$ molecule$^{-1}$·sec$^{-1}$. Comparison of the Arrhenius *A* factor with that predicted by entropy considerations suggests a somewhat loose activated complex, but not as loose as expected on the basis of the exothermicity of the $H + H_2S$ reaction.

12075. Laufer, A. H., Keller, R. A., **Lowest excited states of ketene,** *J. Am. Chem. Soc.* **93,** No. 1, 61-63 (Jan. 1971).

Key words: Absorption spectrum; excited states; ketene; spectroscopy; triplet state.

Analysis of the vibrational progression evident in the absorption spectrum of ketene suggests the absorption is due to a singlet-singlet transition and indicates the energy of the lowest singlet state is less than 61 kcal/mol (2.65 eV) above the ground state. Reasonable singlet-triplet energy splittings place the energy of the lowest triplet at less than 55 kcal/mol (2.39 eV). This conclusion is in agreement with recent results which demonstrate that ketene quenches the triplet state of biacetyl. Attempts to directly observe the triplet state of ketene by a variety of spectroscopic methods, including gas- and liquid-phase absorption spectroscopy, oxygen enhancement techniques, and triplet ← triplet absorption spectroscopy, were unsuccessful.

12076. Lutz, G. J., **Photon activation analysis—A review,** *Anal. Chem.* **43,** No. 1, 93-104 (Jan. 1971).

Key words: Bremsstrahlung; carbon; electron accelerators; nitrogen; oxygen; photon activation analysis; review; sensitivities.

Prior to the availability of high-energy electron accelerators, photon activation analysis was limited to the determination of deuterium and beryllium with isotopic gamma-ray sources. During the past 15 years, however, the development of high-current cyclic and linear electron accelerators has made possible many analyses not readily acomplished by other methods. These include the determination of carbon, nitrogen, and oxygen at levels well below 1 $\mu$g. This review discusses the determination of beryllium and deuterium with isotope sources; accelerator-produced photons and nuclear considerations in photon activation analysis; the determination of carbon, nitrogen, and oxygen; the determination of heavier elements, with emphasis on biological, geochemical, oceanographic, and forensic matrices; and errors and corrections in photon activation analysis.

12077. Meijer, P. H. E., **Influence of the dipole-dipole coupling on the specific heat of cesium titanium alum,** *Phys. Rev. B* **3,** No. 1, 182-185 (Jan. 1, 1971).

Key words: Cesium titanium alum; critical temperature; face centered cubic lattice; magnetic dipole-dipole coupling; specific heats.

To find the influence of the magnetic dipole-dipole coupling on the specific heat in a fcc lattice, the Hamiltonian was computed in a straightforward way. If one omits the nonring diagrams, the successive terms in $1/kT$ can be obtained from the Fourier transform. We found that the third-order term was different from the results quoted in the literature, both in sign and in magnitude. Some discussion is devoted to the question of what magnetic state will be realized below the critical temperature.

12078. Peterson, R. L., **Numerical study of deformation-potential scattering of electrons by optical phonons in a longitudinal magnetic field,** *Phys. Rev. B* **2,** No. 10, 4135-4144 (Nov. 15, 1970).

Key words: Magnetic field; Maxwellian distribution; scattering; semiconductor.

A detailed numerical study of the influence of a longitudinal magnetic field on carrier scattering is presented for the simple model of the band structure of a semiconductor and for deformation-potential scattering of carriers by optical phonons. A drifted Maxwellian distribution is used, and parallel electric and magnetic fields of arbitrary magnitude are considered. Interesting results of this study include magnetic-field-induced negative differential mobility, magnetic-field-induced "runaway" in the quantum limit, although not for ordinarily large magnetic fields, and longitudinal magnetoresistance resonances whose amplitudes are quite sensitive to electric field strength.

12079. Pierce, S., **Orthogonal groups of positive definite multilinear functionals,** *Pacific J. Math.* **33,** No. 1, 183-189 (1970).

Key words: Elementary divisors; multilinear functional; isometry.

Let $V$ be a finite dimensional vector space over the real numbers $R$ and let $T: V \to V$ be a linear transformation. If $\phi: \times_1^m V \to R$ is a real multilinear functional and

$$\phi(Tx_1, \ldots, Tx_m) = \phi(x_1, \ldots, x_m),$$

$x_1, \ldots, x_m \in V$, $T$ is called an isometry with respect to $\phi$. We say $\phi$ is positive definite if $\phi(x, \ldots, x) > 0$ for all nonzero $x \in V$. In this paper we prove that if $\phi$ is positive definite and $T$ is an isometry with respect to $\phi$, then all eigenvalues of $T$ have modulus one and all elementary divisors of $T$ over the complex numbers are linear.

12080. Robinson, D. C., **Determination of load errors in universal testing machines due to speed of testing,** *Mater. Res. Stand.* **11,** No. 1, 14-17 (Jan. 1971).

Key words: Compression tests; dynamic loads; high-speed photography; indicating instruments; indicator characteristics; loading rate; loads (forces); motion picture cameras; photographic equipment; static loads; test equipment.

A modification of an ASTM Proposed Method of Determining Errors in Testing Machines was used as the basis to measure the indicator errors caused by dynamic loading for three universal machines of different design. For each of the machines, load errors due to the lag of the indicator were found to be linearly related to the rate of applied load. Based on the experimental results, it appears that for testing machines of various design the response of the indicating system to uniformly increasing loads resembles that of a proportional error servomechanism which has a velocity-lag steady state error when following a ramp function input. A discussion is given of the variables which were found to be significant in determining the load errors for the three machines investigated. The essential components in the auxiliary load measuring system were a load cell, a fast response digital voltmeter, and a high-speed still camera. The modified method was found to provide higher quality photographic information from which to determine indicator errors than that obtained when using a moving picture camera as proposed in the ASTM procedure.

**12081.** Rowland, G. A., **The increasing role of states in building codes and standards,** *Proc. 26th Annual Conf. Reinforced Plastics, Composites Division, Washington, D.C., February 9-12, 1971,* Section 5-B, pp. 1-3 (Feb. 10, 1971).

Key words: Interstate; intrastate; "National Conference of States on Building and Standards"; uniformity.

Building codes promulgated, modified, and interpreted on a local basis have been deemed to be major deterrents to the development of reasonably large aggregated markets for many new or little-used materials needed in meeting the country's present and future building and housing requirements.

Since its inception in 1967, the National Conference of States on Building Codes and Standards has been increasingly active in promoting greater involvement of the States in the complex building regulatory system. The hope of more competent technical procedures for accrediting new materials, including reinforced plastics, for acceptance statewide, and possibly nationwide, rather than city-by-city will be a very important contribution toward progress.

The responsibilities of health and safety constitutionally rests in the several states and the differences in their administration of this responsibility is now being seriously reviewed. The Conference in its three years of existence has been able to bring together delegates from the several states, establish working arrangements, and proceed in developing a program of study and recommendations for consideration by the Conference in solving many of the present building regulatory problems.

The national effort is a new, refreshing, coordinated approach toward what has been a rather chaotic, restrictive, individual approach to building regulations.

A current report of the National Conference of States on Building Codes and Standards and the aforementioned organizational structure and activities will be presented.

**12082.** Sullivan, D. B., Peterson, R. L., Kose, V. E., Zimmerman, J. E., **Generation of harmonics and subharmonics of the Josephson oscillation,** *J. Appl. Phys.* **41,** No. 12, 4865-4873 (Nov. 1970).

Key words: Josephson effect; superconductivity.

The observation of harmonics and subharmonics of the Josephson oscillation is shown to be in agreement with a rather simple model of the junction. The generation of harmonics provides an explanation of induced steps in the current-voltage characteristic which occur at submultiples of the usual induced step voltages. The subharmonic oscillation is seen to be a relaxation-like process which can be easily understood in terms of a mechanical analog.

**12083.** Tighe, N. J., **Microstructure of fine-grain ceramics,** (Proc. 15th Sagamore Army Materials Research Conf., Sagamore Conference Center, Raquette Lake, N.Y., Aug. 20-23, 1968), Chapter in *Ultrafine-Grain Ceramics,* pp. 109-133 (Syracuse University Press, Syracuse, N.Y., 1970).

Key words: Alumina; $Al_2O_3$; ceramics; electron microscopy; fine-grain ceramic; ion bombardment; magnesia; MgO; microstructure; rock; zirconia.

This chapter describes the use of transmission electron-microscopy to characterize the microstructure of fine-grain ceramics. Observations have been made on a number of polycrystalline materials including alumina, magnesia, zirconia, metal-ceramic composites, and rock specimens.

Thin sections were prepared by ion bombardment. In these sections grain boundaries, pores, impurity precipitates, and dislocations could be observed directly. Crystalline second-phase material formed as grains and small precipitates could be identified by means of electron diffraction. The method of specimen preparation and the results obtained from the observation of the specimens will be discussed.

**12084.** Vidal, C. R., Cooper, J., Smith, E. W., **Hydrogen Stark broadening calculations with the unified classical path theory,** *J. Quant. Spectry. Radiative Transfer* **10,** No. 9, 1011-1063 (Sept. 1970).

Key words: Classical path; hydrogen lines; line wings; one-electron theory; Stark broadening; unified theory.

The unified theory has been generalized for the case of upper and lower state interaction by introducing a more compact tetradic notation. The general result is then applied to the Stark broadening of hydrogen. The thermal average of the time development operator for upper and lower state interaction is presented. Except for the time ordering it contains the effect of finite interaction time between the radiator and perturbers to all orders, thus avoiding a Lewis type cutoff. A simple technique for evaluating the Fourier transform of the thermal average has been developed. The final calculations based on the unified theory and on the one-electron theory are compared with measurements in the high and low electron density regime. The unified theory calculations cover the entire line profile from the line center to the static wing and the simpler one-electron theory calculations provide the line intensities only in the line wings.

**12085.** Watson, R. E., Bennett, L. H., Carter, G. C., Weisman, I. D., **Comments on the Knight shift in bismuth and other *p*-band diamagnetic metals,** *Phys. Rev. B* **3,** No. 1, 222-225 (Jan. 1971).

Key words: $AuGa_2$; BiIn; bismuth; diamagnetism; Knight shift; NaTl; polarization; $V_3Ga$.

The role of *p*-polarization and conduction-electron diamagnetism in some diamagnetic metals and intermetallic compounds, which have negative Knight shifts, is examined.

**12086.** Weiss, A. W., **Symmetry-adapted pair correlations in Ne, $F^-$, $Ne^+$, and F,** *Phys. Rev. A* **3,** No. 1, 126-129 (Jan. 1971).

Key words: Electron affinity; electron correlation; ionization potential; superposition of configurations.

The superposition-of-configurations method has been used to calculate, a single pair at a time, the pair correlation energies for Ne, $Ne^+$, $F^-$, and F. The approach is essentially a symmetry-adapted variation of Nesbet's formulation of the Bethe-Goldstone scheme for the atomic correlation problem, and the aim of this research was to test the usefulness of the method for predicting such physically observable quantities as ionization potentials and electron affinities. The calculations predict an ionization potential for neon of 21.52 eV, compared with a 21.56-eV experimental value, and a fluorine electron affinity of 3.47 eV, for which the experimental value is 3.45 eV.

**12087.** Weiss, B. Z., Meyerson, M. R., **Fatigue crack initiation and propagation in chromium diffusion coated Ti bearing steel,** *J. Iron Steel Inst.* **208,** No. 12, 1069-1077 (Dec. 1970).

Key words: Chromium diffusion coating; columnar grains; fatigue crack initiation; fatigue crack propagation; residual stress; titanium bearing steels.

Chromium diffusion coatings on Ti-bearing steel frequently lead to columnar growth beneath the Cr-rich layer. The grains are preferentially oriented. The depth of the columnar zone does not depend on the chromizing time. A high rate of cooling prevents columnar growth. No grain boundary diffusion or carbide formation at the grain boundaries was observed. The Cr-rich layer is structurally homogenous and consists of $\alpha$-solid solution. The hardness of the coating does not vary with the chromizing time.

Compressive residual stresses were found in the Cr-rich layer. The stresses, whose magnitude does not change with the depth of the layer, may be decreased by additional heat treatment.

Three modes of fatigue crack nucleation were observed all beneath the Cr-rich layer. Cracks were formed after 10 to 18% of total fatigue lifetime. Crack propagation in its initial stages is primarily dependent on the mode of nucleation. In the later stage propagation is dependent on stress and grain size. Fatigue properties may be improved considerably by a factor of 3 to 5 by additional "normalizing" after chromizing.

**12088.** Brenner, A., **Note on an organic-electrolyte cell with a high voltage,** *J. Electrochem. Soc.* **118,** No. 3, 461-462 (Mar. 1971).

Key words: Graphite electrode; high energy density cell; lithium deposition; organic electrolyte.

An unusually high back EMF of 5.2 volts was obtained after electrolysis of a 10% solution of lithium fluoborate in sulfolane with a graphite anode.

**12089.** Brown, D. W., Lowry, R. E., Wall, L. A., **The radiation-induced polymerization of 3,3,4,4,5,5,5-heptafluoropentene-1 at high pressure,** *J. Polymer Sci.,* Part A-1, **8,** 3483-3493 (1970).

Key words: Irradiation; polymerization; pressure; 3,3,4,4,5,5,5-heptafluoropentene-1.

A study was made of the radiation-induced polymerization under pressure of 3,3,4,4,5,5,5-heptafluoropentene-1. Polymerization rates increase with pressure (activation volume equals − 11 cc/mol) and temperature (activation enthalpy equals 6.5 kcal/mol) in liquid phase. At 13800 atm and 25 °C freezing occurs; the polymerization rate in the solid is very small. In liquid phase polymerization can continue for many hours after the irradiation is terminated. An active species is formed by radiation which initiates polymerization in the dark period.

**12090.** Brown, R. L., **An upper limit for the rate of destruction of $O_2(^1\Delta_g)$ by atomic hydrogen,** *J. Geophys. Res. Space Phys.* **75,** No. 19, 3935-3936 (July 1, 1970).

Key words: Hydrogen atoms; nitrogen atoms; $O_2(^1\Delta_g)$; oxygen atoms; quenching reactions; upper atmosphere.

From an analysis by EPR spectroscopy of the products of a microwave discharge through wet $O_2$, an upper limit of $6.5 \times 10^{-15}$ cm$^3$ molecule$^{-1}$ sec$^{-1}$ was obtained for the rate constant of a reaction between $O_2(^1\Delta_g)$ and H which destroys H. Also determined was an upper limit of $1.5 \times 10^{-14}$ for the rate constant of a reaction which destroys $O_2(^1\Delta_g)$ but not H.

**12091.** Brown, R. L., **Diffusion of a trace gas into a flowing carrier,** *Intern. J. Chem. Kinetics* **2,** 475-477 (1970).

Key words: Diffusion equation; diffusion of gases; flow reactor; gas mixing; mixing by diffusion; relaxation methods.

Numerical methods were used to solve the differential equation for diffusion of a trace gas into a flowing carrier gas having a parabolic velocity profile in a cylindrical tube. Steady state solutions are given in the form of contour diagrams of constant trace gas concentration.

**12092.** Chandler, H. H., Rupp, N. W., Paffenbarger, G. C., **Poor mercury hygiene from ultrasonic amalgam condensation,** *J. Am. Dental Assoc.* **82,** 553-557 (Mar. 1971).

Key words: Amalgam condensation; mercury; mercury vapor levels; threshold limit.

A cloud of mercury droplets and alloy particles was emitted from the soft amalgam at the working tip of the ultrasonic instrument tested. Mercury vapor levels were 20% of the allowable threshold limit value and probably are not hazardous. However, continued use of the ultrasonic instrument would result in deposition of numerous mercury droplets throughout the dental operatory and could thereby cause higher mercury vapor levels, especially in poorly ventilated places. Inhalation of the emitted material by the patient and the dental health personnel is not good hygiene. Therefore, the use of this instrument for amalgam condensation is contraindicated until the safety of the instrument for this purpose is firmly established.

**12093.** Cohen, J., Edelman, S., **Direct piezoelectric effect in polyvinylchloride films,** *J. Appl. Phys.* **42,** No. 2, 893-894 (Feb. 1971).

Key words: G modulus; piezoelectricity; polymers; polyvinylchloride films.

The piezoelectric modulus, $g_{31}$, of polyvinylchloride films has been measured at 20 Hz. Values are in the range of approximately 0.4 to 3 $Vm^{-1}/Nm^{-2}$, which are larger than the g values of conventional piezoelectric materials.

**12094.** Cooper, J. W., Conneely, M. J., Smith, K., Ormonde, S., **Resonant structure of lithium between the $2^3S$ and $2^1P$ thresholds,** *Phys. Rev. Letters* **25,** No. 22, 1540-1543 (Nov. 30, 1970).

Key words: Atomic absorption; close coupling; configuration; interaction; resonant structure.

Close coupling calculations of the optically allowed states in the 60-70 eV range above the ground state of atomic lithium have been performed. An interpretation of the resonant structure in this region is given based upon these calculations and recent experimental evidence.

**12095.** Fatiadi, A. J., **Oxidative cleavage of aromatic azines with periodic acid: e.s.r. evidence for the liberation of nitrogen dioxide,** *Chem. Ind.,* pp. 64-66 (Jan. 9, 1971).

Key words: Aromatic; azines; cleavage; complex; nitrogen paramagnetic; periodic acid; radical.

Aromatic azines were cleaved by periodic acid to the parent aldehyde or ketone in over 95% yield. The oxidative cleavage proceeds through a paramagnetic intermediate, as evidenced by trapping of the nitrogen dioxide at 77 K (e.s.r. evidence).

**12096.** Garvin, D., **The information analysis center and the library,** *Spec. Libraries* **62,** No. 1, 17-23 (Jan. 1971).

Key words: Standard reference data.

The information analysis center and the library have complementary functions. The former is both a user of library services and a source of information for libraries. How they can cooperate to their mutual profit is described. The evaluation of information is the principal task of the information analysis center. This process, and the organized program in the USA to foster it, are described.

**12097.** Gebbie, K. B., Thomas, R. N., **On the dependence of $T_e$ upon quantity versus quality of the radiation field in a stellar atmosphere,** *Astrophys. J.* **161,** No. 1, 229-241 (July 1970).

Key words: Electron temperature; line-blanketing; mechanical heating; radiation quality; radiation quantity.

We derive a simple algebraic expression for $T_e(\tau)$ that demonstrates as a function of collisions how and where the control of $T_e$ shifts from the quantity to the quality of the radiation field in a stellar atmosphere. We obtain explicit formulae for the gray case and show that mechanical heating and nongray processes can be treated algebraically as perturbations. We illustrate the size and effect of these processes by applying them to the Sun in the region $10^{-2} > \tau_5 > 10^{-5}$.

**12098.** Unassigned.

**12099.** Hellwig, H., **Areas of promise for the development of future primary frequency standards,** *Proc. 24th Annual Symp. on Frequency Control, Atlantic City, N.J., April 27-29, 1970,* pp. 246-258 (Electronic Industries Assn., Washington, D.C. 1970).

Key words: Accurate frequency standards; accurate length standards; accurate time standards; accurate voltage standards; ion storage; laser stabilization; maser oscillator; metrology; quantum electronics; saturated absorption; slave oscillators.

In this paper possibilities are discussed which may lead to the development of future primary frequency standards of superior accuracy capability. As the reference in performance today's most advanced primary frequency standard, the laboratory type cesium beam tube, is used. Aspects of costs and field-usage are totally neglected. A review is given of the various methods and techniques which are currently employed in quantum electronic frequency standards or which have a potential usefulness. Various effects which influence the output frequency of a primary standard are associated with these methods. A classification is given: (a) Effects associated with the interrogation of particles (atoms or molecules), (b) effects related to the method of confining the particles, and (c) effects associated with the particles themselves and the way in which they are treated for an effective interrogation by electromagnetic radiation. These classes of effects are discussed in detail, and expectation values for the related uncertainties are given. For selected particles certain methods of interrogation, confinement, and particle preparation can be combined such as to minimize the net uncertainty due to all applicable effects. Different technical solutions are the result. A review of existing and proposed devices is given, including quantitative data on the stability and accuracy capability. Aspects of the most promising devices are discussed, and it is concluded that accuracy capabilities of ten to the minus fourteen should be within reach of today's research and development.

**12100.** Hussman, E. K., **A holographic interferometer for measuring radiation energy deposition profiles in transparent liquids,** *Appl. Opt.* **10,** No. 1, 182-186 (Jan. 1971).

Key words: Absorbed dose; calorimetry; dose distribution; electron beams; holography; interferometry; pulsed beams; radiation.

An apparatus has been designed for real-time and double-exposure holographic interferometry to determine radiation absorbed dose distributions in transparent liquids. The change in refractive index of the liquid due to a temperature rise after irradiation is measured interferometrically. In a cylindrically symmetrical radiation field, the dose distribution can be computed from data supplied by the reconstruction of the holographic interferogram taken as a side-view profile of the change in optical pathlength. Relatively inexpensive components such as a low-powered He-Ne laser together with a conventional photographic shutter and low-cost mirrors and lenses were used. The mathematical procedure for unfolding the three-dimensional dose distribution is described, and an example is given for use with a high-intensity, pulsed, 2-MV electron source.

**12101.** Jacox, M. E., Milligan, D. E., **Infrared spectrum and structure of the species $CO_3$,** *J. Chem. Phys.* **54,** No. 3, 919-926 (Feb. 1, 1971).

Key words: $CO_2$; $CO_3$; force constants; infrared spectrum; matrix isolation; O-atom reaction; structure; ultraviolet spectrum; vacuum-ultraviolet photolysis.

Upon photolysis of solid $CO_2$ by 1216-Å radiation, very high yields of $CO_3$ have been obtained. There is no evidence for the production of hydrogen-containing species in experiments in which photolytically produced H or D atoms are also present. Experimental evidence supports a $C_{2v}$ structure for $CO_3$ in its ground state, as predicted by molecular orbital calculations. The vibrational frequency pattern for the planar modes of isotopically substituted species of $CO_3$ has been fitted to a valence force potential having a minimal number of interaction force constants, assuming both an open structure having an O-C-O angle of 80° and a three-membered ring structure having an O-C-O angle of 65°. Although the force constants obtained for the ring structure appear to be quite reasonable, exceptionally large values have been obtained for the O-C-O bending force constant and for all of the interaction constants for the open structure. On this basis, the three-membered ring structure is favored for $CO_3$ in its ground state.

**12102.** Julienne, P. S., **Predissociation of the $H_2$ $D^1\Pi_u$ state,** *Chem. Phys. Letters* **8,** No. 1, 27-28 (Jan. 1, 1971).

Key words: Born-Oppenheimer; Hartree-Fock; molecular hydrogen; partial widths; potential curve; predissociation; vibrational overlap.

The electronic nondiagonal Born-Oppenheimer coupling matrix elements between the molecular hydrogen $D^1\Pi_u$ state and the $B'^1\Sigma_u$ and $B^1\Sigma_u$ states were calculated in the Hartree-Fock approximation at $R = 1.0$, 1.2, 1.6, and 2.0 au. These were used to calculate the predissociation widths for the $v = 3$ to 12 levels of the D state with $J = 1$. The predissociation can only be caused by B′ state. The widths are around 1 cm$^{-1}$.

**12103.** Kamas, G., Hanson, D. W., **Recent VHF/UHF satellite timing experiments at the National Bureau of Standards,** *Proc. Precise Time and Time Interval (PTTI) Strategic Planning Meeting (U), Washington, D.C., December 10-11, 1970,* **1,** 79-82 (1970).

Key words: ATS satellite; LES-6 satellite; NBS satellite timing; satellites; TACSAT satellite; time; timing accuracy.

A summary discussion is presented of the current work accomplished by NBS in the field of time dissemination by geostationary satellites. The results of that program and its implication for the future are given.

**12104.** Kruger, J., Frankenthal, R. P., **B. Corrosion of metals,** Chapter in **Volume IV,** *Techniques in Metals Research,* Chapter 10B **Oxidation and corrosion,** R. A. Rapp, ed., R. F. Bunshah, Series ed., **14,** Part 2, 571-667 (John Wiley and Sons Inc., New York, N.Y. 1970).

Key words: Corrosion; electron diffraction; electron microscopy; research techniques.

The application of nonelectrochemical techniques to corrosion research are discussed. These include optical techniques, x-ray techniques, electron microscopy and diffraction, tracer techniques and mechanical techniques.

**12105.** Latanision, R. M., Ruff, A. W., **The temperature dependence of stacking fault energy in Fe-Cr-Ni alloys,** *Met. Trans.* **2,** 505-509 (Feb. 1971).

Key words: Dislocations; electron microscopy; iron alloys; stacking fault energy; temperature.

The variation of intrinsic stacking fault energy ($\gamma_i$) in two austenitic Fe-Cr-Ni alloys has been determined from dislocation node measurements over the range 25 to 325 °C by means of high temperature transmission electron microscopy. In both alloys $\gamma_i$ increases with temperature. Both reversible and irreversible effects have been observed in cyclic heating-cooling experiments. After the first heating to elevated temperature the irreversible component is removed and thereafter cyclic annealing produces essentially reversible changes in $\gamma_i$. The large reversible changes are best understood in terms of the variation in the bility of austenite with temperature. The smaller irreversible ect appears to arise from the formation of substitutional solute nospheres around partial dislocations at elevated temperature.

06. Linsky, J. L., Avrett, E. H., **The solar H and K lines,** *Astron. Soc. Pacific* **82,** 169-248 (Apr. 1970).

Key words: Ca H and K lines; non-LTE line formation; plages; radiative transport; solar chromosphere; solar spectrum; sunspots; Wilson-Bappu effect.

Ve review our current understanding of the formation of the II H and K resonance and infrared triplet subordinate lines in sun in view of the wealth of observations of these lines and development of non-LTE line formation theory. We describe low- and high-spatial resolution data of these lines on the ar disk, off the limb, and in stellar spectra. We also describe ervations on the analogous Mg II resonance lines.

Ve review the various explanations proposed for the observed tures of the lines including the double reversal, limb darken- , plage and spot profiles, and the anomalous line ratios. Line files are computed according to a first-order steady-state ory in which we assume a one-component atmosphere in drostatic equilibrium, noncoherent scattering, and a five-level m and continuum representation for Ca II. The chromospher- nodel chosen is meant to be representative rather than defini- , but it produces profiles of all five lines and a microwave tinuum in agreement with observations at the center of the k. We then discuss extensions of this first-order theory.

07. Liu, Y. M., Coleman, J. A., **Electron radiation damage ef- ects in silicon surface-barrier detectors,** *IEEE Trans. Nucl. ci.* **NS-18,** No. 1, 192-199 (Feb. 1971)

Key words: Alpha particles counting response; capacitance; detector noise; electron fluence; electrons radiation damage; front and rear contact; leakage current; silicon surface-barrier detector.

ilicon surface-barrier detectors have been irradiated at room perature with monoenergetic electrons in the energy range of keV to 1 MeV. The changes of detector reverse leakage cur- t, noise, capacitance and alpha-particle counting response e determined. In general, detector current and noise in- ased with electron fluence and energy for electron energies of keV and above. Detector capacitances tended to decrease htly for electron fluences up to $10^{13}$ cm$^{-2}$ and increase at ner fluences. No significant degradation of detector per- nance was observed as a result of irradiation with 200-keV trons for fluences up to $10^{16}$ cm$^{-2}$. The effects of damage on ector performance were reduced when the rear, aluminum tact was irradiated rather than the front, gold contact.

08. Madey, T. E., Yates, J. T., Jr., **Electron-stimulated desorp- on and work function studies of clean and cesiated (110) GaAs,** *Vacuum Sci. Technol.* **8,** No. 1, 39-44 (Jan.-Feb. 1971).

Key words: Adsorption; cesium; desorption; electron reflection; electron stimulated desorption; gallium arsenide; work function.

he surface of a degenerate *p*-type GaAs crystal, cleaved in ahigh vacuum to expose the (110) plane, has been examined function of cesium coverage using several methods. Electron ulated desorption (ESD) of ions upon bombardment of the ace by 100-eV electrons is found to be extremely sensitive to e quantities of adsorbed impurities. The work function- erage relation for $Cs^+$ deposited from a Cs zeolite ion gun determined using a retarding potential method; the energy endence of electron reflection in the range 0-10 eV was found iffer markedly between the clean and cesiated surfaces.

9. Mandel, J., **A new analysis of variance model for nonaddi- ve data,** *Technometrics* **13,** No. 1, 1-18 (Feb. 1971).

Key words: Factorial experiments; interaction; nonadditivity; principal components; surface fitting; two-way arrays.

A method is presented for the analysis of data representing functions of two variables, when the response can be tabulated in a rectangular array. The procedure is based on a partitioning of the row by column interaction effects into a sum of terms, each of which is the product of a row factor by a column factor. The factors in each term are estimated by a method involving the extraction of characteristic roots.

The method contains as special cases a number of procedures used for the handling of nonadditivity in two-way arrays. It is very useful for the fitting of empirical surfaces, but is also applicable to cases in which the data depend on qualitative rather than quantitative factors.

Comparisons with other techniques are made and an illustrative example is given.

**12110.** Menis, O., McClellan, B. E., Bright, D. S., **Determination of the formation constants of iron(III) and vanadium(V) with $\beta$-isopropyltropolone using the extraction method,** *Anal. Chem.* **43,** No. 3, 431-435 (Mar. 1971).

Key words: Chelate; equilibrium constants; extraction method; ferric; graphical; least squares computer calculations; vanadyl; $\beta$-isopropyltropolone.

Equilibrium constants of ferric and vanadyl ions for the formation of the chelate with $\beta$-isopropyltropolone (HIPT) were determined by the extraction method. The values for these constants were derived by graphic and least squares computer calculations. The constants for the vanadyl system are reported for the first time. It is postulated that an adduct $VO_2IPT \cdot HIPT$ is formed and its formation constant, log $\beta_N = K_1K'$, was determined as 13.8 and 13.6 ± 0.8 by graphic and least squares calculations, respectively. The partition constant, $K_{DC}$, was 2.45 and 2.6 ± 0.4, respectively. The values for $Fe(IPT)_3$ complex were for log $\beta_N$, 37.7 and 37.8 ± 0.1, respectively, while the log $K_{DC}$ was 2 and 2.0 ± 0.1, respectively. It was also possible to calculate the overall stepwise constants, log $\beta_1 = 13.0 \pm 0.2$ and log $K_2K_3 = 24.8 \pm 0.1$ by the least squares method. The other experimental parameters which were studied were the effect of solvent and ionic strength.

**12111.** Menis, O., Rains, T. C., **Sensitivity, detection limit, precision, and accuracy in flame emission and atomic absorption spectrometry,** Chapter 2 in *Analytical Flame Spectroscopy, Selected Topics,* R. Mavrodineanu, ed., pp. 47-77 (Springer-Verlag Publishing Co., New York, N.Y., 1970).

Key words: Accuracy; atomic absorption; detection limits; differential method; flame emission; nonaqueous media; precision; sensitivity; tables.

This chapter on sensitivity, detection limits, precision, and accuracy in flame emission and atomic absorption spectrometry discusses the principles, definitions, and methodology in establishing and evaluating these criteria. The various instrumental components and their optimum operation are described to enable the analyst to achieve these goals. Tables of data for all reported elements are presented for the current results on detection limits and sensitivity. The problem associated with the environment of the analyte and the effect of nonaqueous media are discussed from the standpoint of enhanced sensitivity. Finally the criteria for attaining improved precision and accuracy are discussed and the role of the differential method, ionization buffers and standard additions is discussed.

**12112.** Milligan, D. E., Jacox, M. E., **Infrared spectrum and structure of intermediates in the reaction of OH with CO,** *J. Chem. Phys.* **54,** No. 3, 927-942 (Feb. 1, 1971).

Key words: $CHO_2$ free radical; force constants; infrared spectrum; matrix isolation; reaction of OH with CO; stereoisomers; vacuum-ultraviolet photolysis.

Upon vacuum-ultraviolet photolysis of $H_2O$ in a CO matrix at 14 K, infrared absorptions of HCO, $H_2CO$, HCOOH, and $CO_2$ become prominent. Furthermore, new absorptions due to reactive product species appear at 615, 620, 1077, 1088, 1160, 1261, 1797, 1833, 3316, and 3456 $cm^{-1}$. These absorptions diminish in intensity when the sample is subjected to radiation in the 2000-3000-Å spectral range. Detailed consideration of the processes which may occur in this system and extensive isotopic substitution studies support the assignment of these absorptions to the *cis* and *trans* stereoisomers of $H-O-C=O$, produced by the reaction of OH with the CO matrix. Valence force potentials having only small contributions from interaction terms have been found which correspond to a physically reasonable vibrational assignment and which satisfactorily reproduce the pattern of observed frequencies for the various isotopic species of both *cis*- and *trans*-HOCO. Evidence suggests that *cis*- and *trans*-HOCO photodecompose to produce H atoms and $CO_2$.

**12113.** Missoni, G., Dick, C. E., Placious, R. C., Motz, J. W., **Inelastic atomic scattering of 0.1-, 0.2-, 0.4-, and 3.0-MeV electrons,** *Phys. Rev. A* **2,** No. 6, 2309-2317 (Dec. 1970).

Key words: Carbon; copper; experimental cross sections; gold; inelastic electron scattering; multiple scattering; 0.1 to 3.0 MeV.

Spectral data obtained with a magnetic spectrometer are presented for inelastic electron scattering from thin targets of carbon, copper, and gold at incident electron energies of 0.1, 0.2, 0.4, and 3.0 MeV, for scattering angles between 20 and 120°. For angles less than 90°, each spectrum consists of (a) a Møller line which has a half-width that increases with atomic number and which yields an experimental cross section that agrees within experimental error with the theoretical Møller cross section, and (b) a low-energy continuum which rises steeply at energies less than 40 keV. For angles greater than 90°, the Møller line which is kinematically forbidden vanishes, but the steeply rising continuum remains. This continuum may arise from single electron-atom scattering and from multiple scattering in the target. The latter process depends on target thickness. The experimental results for this low-energy continuum tend to confirm that the multiple-scattering effects as calculated by Ford and Mullin dominate the single-scattering process as calculated by Weber, Deck, and Mullin, and by Kolbenstvedt and Cooper even for an 11-$\mu g/cm^2$ carbon target which was the most favorable case for studying the single-scattering process. Because of multiple scattering, accurate experimental data for the low-energy continuum produced by single electron-atom inelastic scattering can best be obtained with gas targets.

**12114.** Mohan, R., Danos, M., Biedenharn, L. C., **Isospin impurities in the nuclear ground states,** *Phys. Rev. C* **3,** No. 2, 468-479 (Feb. 1971).

Key words: Excess neutrons; isospin; nuclear charge distribution; nuclear structure; three-fluid model; two-fluid model.

Isospin impurities in the ground states of some even-even nuclei are calculated in the shell model including the effective residual interactions and in the three-fluid model. It is shown that the residual interactions reduce the calculated impurities by an order of magnitude. The impurities given by the three-fluid model are even smaller. Comparison of the present results is made with those of the two-fluid model.

**12115.** McClellan, B. E., Menis, O., **Kinetics and mechanism of extraction of iron(III) with $\beta$-isopropyltropolone,** *Anal. Chem.* **43,** No. 3, 436-438 (Mar. 1971).

Key words: Fe(III)-$\beta$-isopropyltropolone (HIPT) complex; first order in Fe(III) and in HIPT; kinetics.

The kinetics and mechanism of the reaction between Fe(III) and $\beta$-isopropyltropolone (HIPT) were studied by the extraction technique. The reaction was found to be first order in Fe(III) a in HIPT, indicating the addition of the first ligand to the Fe( to be the rate-controlling step in the reaction. A first-order pendence on $NaClO_4$ was observed. No dependence on [H was observed in the rate under the acid (1M) conditions of t extraction. The rate constant for the reaction was $1.5 \times 10^{10}$ M Addition of ethanol prior to extraction greatly enhances the re tion rate.

**12116.** Noack, M., Kokoszka, G. F., Gordon, G., **Dynamic Ja Teller effects and magnetic anisotropies in aqueous solutions a water-ethanol glasses of copper(II) solvates and complexes w 2,2′-dipyridine,** *J. Chem. Phys.* **54,** No. 3, 1342-1350 (Feb. 1971).

Key words: Aqueous solutions; EPR; exponential tempe ture dependence; intramolecular relaxation; Jahn-Teller fect; tris(2,2 ′ -dipyridine)copper(II).

Dynamic Jahn-Teller effects have been recognized previou in solids which contain copper(II) ions in octahedral envir ments. In solutions, dynamic Jahn-Teller effects have n been observed in the EPR spectrum of the tris(2, dipyridine)copper(II) complex. This is shown by the small te perature coefficient of the apparent tumbling correlation time, which is associated with anisotropy contributions to the E linewidth and by the insensitivity of $\tau_c$ to variations of the solv viscosity. In partially substituted complexes, such as tetraaquo(2,2′-dipyridine)copper(II) species which has also be studied here, the dynamic Jahn-Teller effects are inhibited due the inhomogeneous nature of the first coordination sphere. T possible importance of dynamic Jahn-Teller effects homogeneous solvates of copper(II) is discussed. Evidence presented to show that addition of ethanol to aqueous soluti of copper(II) nitrate results in the formation of inhomogene species.

**12117.** Redding, R. W., Hougen, J. T., **Calculation of the Euler angles and large amplitude vibrational coordinate correspo ing to an arbitrary instantaneous molecular configuration** *Mol. Spectry.* **37,** No. 2, 366-370 (Feb. 1971).

Key words: Constraint equations; Eckart conditions; lerian angles; large amplitude vibrational coordin molecule-fixed axes; reference configuration.

The three Eulerian angles and the large amplitude vibratio coordinate of a nonrigid molecule are determined implicitly, a given configuration in space of the nuclei, by four equation four unknowns. A method is presented for reducing this progr to the solution of a single equation in the large amplitude c dinate. Once a value is determined for the large amplitude c dinate, numerical values for the direction cosine functions, hence for the three Eulerian angles, can be calculated immedi ly from expressions derived. For rigid molecules, i.e., those having a large amplitude vibrational coordinate, the met presented reduces to a set of explicit expressions for calcula the direction cosine functions for a given configuration in sp of the nuclei of the molecule.

**12118.** Rosenstock, H. M., Botter, R., **Franck-Condon princ for the ionization of polyatomic molecules** (Proc. Intern. C on Mass Spectroscopy, Kyoto, Japan, Sept. 1969), Chapte *Recent Development in Mass Spectroscopy,* K. Ogata an Hayakawa, eds., pp. 797-806 (University of Tokyo Pr Tokyo, Japan, 1970).

Key words: $C_2H_2$; Franck-Condon principle; $H_2O$; N $N_2O$; photoelectrons; photoionization.; spectroscopy.

Recent work on the application of the Franck-Condon pri ple to the ionization of polyatomic molecules is reviewed. vibrational structure of ionization curves in $C_2H_2$ $H_2O$, $NH_3$ $N_2O$, is discussed. Examples are given illustrating vari blems encountered in Franck-Condon problems, including ice of frequencies and force fields and the importance of nor- coordinate transformations between two states of different metry and symmetry.

19. Schroeder, L. W., Rush, J. J., **Neutron diffraction study of he structure and thermal motion of phosphonium bromide,** *J. hem. Phys.* **54,** No. 5, 1968-1973 (Mar. 1, 1971).

Key words: Crystal structure; neutron diffraction; $PH_4Br$; rigid-body analysis; thermal motion.

he crystal structure of $PH_4Br$ has been determined by a sin- crystal neutron diffraction study. The tetragonal structure is ilar to that determined previously for $PH_4I$ with the $P-H$ ds of the phosphonium ions directed at the four *next-nearest- ghbor* halide ions. The corresponding $P-H$ and $H \cdots Br$ ances are 1.414 and 2.65 Å, respectively, with a $P-H \cdots Br$ le of 172°. The orientation of the $PH_4^+$ ions (90° away from orientation of $NH_4^+$ in the analogous phase III ($NH_4Br$)) gests that hydrogen bonding plays a minor role in determining crystal structure. A "rigid-body" analysis of the motion of $PH_4^+$ ion was performed using the anisotropic thermal ameters of the phosphonium and hydrogen atoms derived n the $PH_4Br$ and $PH_4I$ diffraction data. The resulting mean- are amplitudes of translational and torsional motion of the $_4^+$ ion lead to frequencies which are in good agreement with ctroscopic observations.

20. Simmons, J. H., Macedo, P. B., **Analysis of viscous relaxa- on in critical oxide mixtures,** *J. Chem. Phys.* **54,** No. 3, 1325- 331 (Feb. 1, 1971).

Key words: Critical transport; critical viscosity; critical viscous flow; structural relaxation; ultrasonic spectroscopy.

n analysis of shear viscosity and ultrasonic measurements on ries of critical oxide mixtures shows that the supercritical, ess static viscosity is associated with a broadening in the dis- ution of structural relaxation times, rather than with an in- ction between the long-wavelength components of the fluc- ions and the shear flow processes. The broadening saturates the critical point, and the excess static viscosity approaches nite limit as a function of reduced temperature. These results in disagreement with existing excess-viscosity theories. A model is proposed which relates the distribution of relaxa- times to microstructure in the melt resulting from the super- cal fluctuations in composition. It also limits the range of in- ction associated with structural relaxation to a finite value. resulting conclusions are consistent with the observed lack ivergence in the excess viscosity and width of the distribu- of relaxation times at $T_c$.

1. Tipson, R. S., Brady, R. F., Jr., West, B. F., **Cyclic acetals ketoses. Part IV. Re-investigation of the oxidation of 1,2:4,5- i-*O*-isopropylidene-β-D-fructopyranose with methyl sulfoxide- etic anhydride,** *Carbohydrate Res.* **16,** 383-393 (Mar. 1971).

Key words: Acetals; fructose; ketoses; oxidation; psicose; reduction; ruthenium tetraoxide; sodium borohydride.

or the preparation of pure D-psicose **(5a)** via oxidation of 4,5-di-*O*-isopropylidene-β-D-fructopyranose **(2a)**, the latter t be free from its 2,3:4,5 isomer **(6a)**, which is oxidized to the esponding aldosulose acetal. Pure 1,2:4,5-di-*O*-isopropy- ne-β-D-*erythro*-2,3-hexodiulo-2,6-pyranose **(3)** undergoes eospecific reduction with sodium borohydride to give only 4,5-di-*O*-isopropylidene-β-D-*ribo*-hexulopyranose **(4a)**, h exists as two different crystal modifications. Compounds d **4a** have been characterized, and discrepancies in the litera- have been explained.

2. Walther, H., Hall, J. L., **Tunable dye laser with narrow ectral output,** *Appl. Phys. Letters* **17,** No. 6, 239-242 (Sept. , 1970).

Key words: Birefringent filter; dye laser; frequency control.

A tunable dye laser with narrow-banded spectral output in the order of 0.01 Å or smaller is described. This narrow spectral output is obtained by means of a birefringent filter (Lyot filter) which was inserted into the laser cavity. The properties of this laser setup have been investigated and are described.

**12123.** Weiss, A. W., **A review of theoretical developments in atomic *f*-values,** (Proc. 2nd Intern. Conf. Beam-Foil Spectroscopy in Nuclear Instruments and Methods, Lysekil, Sweden, June 8-12, 1970), Part III, *Theoretical transition probabilities, Nucl. Instr. Methods* **90,** 121-131 (North-Holland Publ. Co., Amsterdam, The Netherlands, 1970).

Key words: Atomic lifetimes; atomic spectra; configuration interaction; oscillator strengths.

Theoretical work on atomic *f*-values are reviewed with particular emphasis on the relation to recent beam-foil measurements. One-electron models currently in use are reviewed and their limitations and range of applicability are discussed. Many-electron, or multi-configuration, models are also described and their results compared with experiment. Regularities and irregularities along isoelectronic sequences will be discussed, and some current problems will be presented.

**12124.** Wiese, W. L., **Atomic transition probabilities—A survey of our present knowledge and future needs,** (Proc. 2nd Intern. Conf. Beam-Foil Spectroscopy in Nuclear Instruments and Methods, Lysekil, Sweden, June 8-12, 1970). Part II, *Lifetimes and transition probabilities, Nucl. Instr. Methods* **90,** 25-33 (North-Holland Publ. Co., Amsterdam, The Netherlands, 1970).

Key words: Atomic transition probabilities; beam foil spectroscopy; lifetimes; regularities; review.

A general survey of the present status of our knowledge of atomic transition probabilities is given and the principal methods for obtaining the numerical data are briefly reviewed on a critical basis. Areas of particular relevance to beam foil spectroscopy are emphasized. Using a number of numerical examples and employing systematic trends and comparison data, some general problems encountered with beam foil data are pointed out. Finally, some of the most pressing future needs for new and improved transition probabilities are indicated.

**12125.** Yates, J. T., Jr., Madey, T. E., **Interactions between chemisorbed species: $H_2$ and $N_2$ on (100) tungsten,** *J. Vacuum Sci. Technol.* **8,** No. 1, 63-68 (Jan.-Feb. 1971).

Key words: Chemisorption; flash desorption; hydrogen; nitrogen; tungsten; tungsten (100) plane; work function.

The interactions between hydrogen and nitrogen adsorbed species on a (100) tungsten crystal have been investigated by flash desorption methods. When the crystal covered with a monolayer of hydrogen is exposed to gaseous $N_2$, the nitrogen slowly replaces the two chemisorbed hydrogen $\beta$ states by means of a slight lowering of the hydrogen desorption energy. This displacement process occurs via slow thermal desorption of hydrogen in the presence of gaseous $N_2$ when the surface temperature is $\gtrsim$ 300 K; no such replacement is observed at 273 K. Coverage measurements indicate that there is a stoichiometric ratio between N atoms adsorbed and H atoms displaced from the crystal at ~ 300 K. Although virtually no hydrogen will adsorb on the nitrogen-covered surface at 300 K, several weakly bound hydrogen states are populated at 100 K on this surface. No chemical difference between the $\beta_1$ and $\beta_2$ hydrogen species was detected, suggesting that both states originate from adsorbed atoms.

**12126.** Wright, J. C., Moos, H. W., Colwell, J. H., Mangum, B.

W., Thornton, D. D., **$DyPO_4$: A three-dimensional Ising antiferromagnet,** *Phys. Rev. B* **3,** No. 3, 843-858 (Feb. 1, 1970).

Key words: Critical phenomena; diamond lattice; $DyPO_4$; Ising system; low temperature; magnetic susceptibility; metamagnetism; optical absorption.

The magnetic susceptibility, heat capacity, and optical-absorption spectrum of $DyPO_4$ have been measured as a function of temperature and magnetic field. The optical-absorption spectrum indicates that the magnetic interactions in $DyPO_4$ have the form of the Ising interaction and occur primarily between nearest neighbors. The magnetic-susceptibility and heat-capacity measurements have been compared with exact series expansions for a diamond lattice assuming an Ising system with nearest-neighbor interactions. The theoretical calculations are in agreement with the measurements. The nature of the divergence of the heat capacity at the critical point is examined. Our data do not permit us to distinguish between the applicability of the logarithmic and power-law divergencies since they are indistinguishable in the region of our measurements. The temperature dependence of the critical field for the metamagnetic phase transition has also been determined and compared with the calculated value for the critical field at 0 K obtained from the spectroscopic measurements.

**12127.** Ahearn, A. J., **Quantitative analysis of solids by spark source mass spectrometry,** (Proc. Intern. Conf. on Mass Spectroscopy, Kyoto, Japan, Sept. 6-13, 1969), Chapter in *Recent Development in Mass Spectroscopy,* K. Ogata and T. Hayakawa, eds., pp. 150-157 (University of Tokyo Press, Tokyo, Japan, 1970).

Key words: Fluctuations; homogeneity; ion sensitive emulsion; mass spectrometry; precision; quantitative analysis; solids; spark source; trace elements.

In spark source mass spectrometry, the ion sample generally misrepresents the solid sample. Consequently, standard reference materials are needed for direct comparison with the unknown or for the determination of correction factors. The precision in measurement of matrix element ions, trace element ions and their ratio is dependent on the homogeneity of the ion sensitive emulsion used. Methods for testing emulsion uniformity and results on Q2 plates are presented. In some the nonuniformity is less than 5%; in others up to a 60% change in 8 cm has been detected. Under optimum conditions, matrix ions are measured with an RSD $\leq$ 5% but with trace ions this precision is usually poorer. This means that the trace element contents of the recorded ion sample fluctuate. The trace ions in a spark source ion sample from NBS SRM Platinum 681 fluctuate but not independently. Ion microprobe and other tests should indicate whether the observed fluctuations arise in solid sample inhomogeneities or in fluctuations in the production and/or transmission of trace ions in SSMS.

**12128.** Armstrong, G. T., **Gibbs energy vs. free energy,** *Chem. Eng. News Letter to the Editor,* p. 3 (Apr. 26, 1971).

Key words: Energy; free energy; Gibbs energy; Helmholtz energy.

A rationale is given for the change of name of free energy to Gibbs energy, and the change of symbol from F to G, in answer to a letter of protest by E. J. Davis.

**12129.** Ausloos, P., Rebbert, R. E., Sieck, L. W., **Ion-molecule reactions in the radiolysis of ethane,** *J. Chem. Phys.* **54,** No. 6, 2612-2618 (Mar. 15, 1971).

Key words: Charge transfer; deactivation; ethane; ion-molecule reactions; mass spectrometry; radiolysis.

The reactions of ions generated in ethane irradiated with gamma rays have been studied by analyzing the neutral produ
formed in reactions with ethane and with other molecul
In experiments in the presence of added $(C_2D_5)_2CDC$
for example, it is shown that the following reactions ta
place: $C_2H_5^+ + C_2H_6 \rightarrow (C_4H_{11}^+)^* \rightarrow$ *sec*-$C_4H_9^+ + H_2$; *se*
$C_4H_9^+ + (C_2D_5)_2CDCD_3 \rightarrow$ *n*-$C_4H_9D + C_6D_{13}^+$. The interme
ate $(C_4H_{11}^+)^*$ ion can be stabilized by collisions and will th
undergo an undetermined reaction (neutralization or prot
transfer) to give *n*-$C_4H_{10}$ as a product. The over-all rate const
for reaction of the ethyl ion with ethane is shown to be $\leq$ 10
cm³/molecule·sec. Similarly, it is demonstrated that the reacti
$C_2H_3^+ + C_2H_6 \rightarrow C_4H_9^+$ leads predominantly to the formation
*t*-butyl ions under these conditions: $C_4H_9^+ + (C_2D5)_2CDCD_3$
$(CH_3)_3CD + C_6D_{13}^+$. Supplementary experiments performed
a photoionization mass spectrometer demonstrate that ethyle
ions undergo a "resonance $H_2^-$ transfer" reaction with etha
$C_2H_4^+ + C_2D_6 \rightarrow C_2D_4^+ + C_2H_4D_2$, with a rate constant of 1.
$10^{-10}$ cm³/molecule·sec. Similarly, the ethane parent ion rea
with ethylene: $C_2H_6^+ + C_2D_4 \rightarrow C_2H_4^+ + C_2H_2D_4$.

**12130.** Baker, M. A., **Study of the adherence of porcelain enan
to aluminum-use of the electron microscope and electr
microprobe,** *Proc. Porcelain Enamel Institute Techni
Forum, University of Illinois, Urbana, Ill., Oct. 7-9, 1970,*
48-51 (Porcelain Enamel Institute, Washington, D.C., 197

Key words: Adherence; aluminum; electron micropro
electron microscope; interaction zone.

The interfacial zone between porcelain enamel and alumin
has been examined with the electron microprobe and the el
tron microscope to gain insight into the mechanism of adheren
of the porcelain enamel to aluminum. The results obtained
dicate that good adherence may be associated with an interacti
between the enamel and the aluminum.

**12131.** Ballard, D. B., Yakowitz, H., Goldstein, J. I., **Study
metal in the lunar soil,** *Proc. 4th Annual Scanning Elect
Microscope Symposium, ITT Research Institute, Chica
Ill., April 29, 1971,* Part 1, 169-176 (Apr. 29, 1971).

Key words: Lunar soil; metal inclusions; meteorite; micr
tructure; SEM.

Metal particles and metallic inclusions in lunar (Apollo 11
12) soil particles were investigated using a SEM with a s
state detector. Many of the metallic particles were coated w
nonmetallic lunar material and had impact craters on the surfa
The SEM was used specifically to identify the type of lu
material in the craters and the exposed dendrites on the surfa
Slip bands indicating plastic deformation were observed
several metal particles.

Several glassy spherules in the Apollo 11 soil were stud
because the surfaces contained metal particles. Metal (Fe-
Co), as identified with the solid state x-ray detector, was spr
on the surface presumably as a result of the same impact ev
which produced the spherule. Other impacts may have form
the craters on the surface.

Several nonmetallic soil particles were sectioned
metallographically polished. Metallic inclusions in these soil p
ticles are small, < 100 $\mu$m in their largest dimension. The S
was employed to study the microstructure of these inclusio
Evidence of various degrees of shock damage in the metal
obtained.

**12132.** Becker, D. A., LaFleur, P. D., **Production and certif
tion of NBS biological standard reference materials,** *Proc.
Annual Conf. on Trace Substances in Environmental Hea
June 1970,* pp. 433-435 (University of Missouri, Colum
Mo., Mar. 1971).

Key words: Biological standards; blood standard; botan standards; environmental samples; Standard Reference Material; tissue standard; trace analysis.

The use of adequate standards is important in the trace ele- ent analyses of complex biological materials comprising many vironmental and biomedical samples. Available biological aterials for interlaboratory comparisons are almost exclusively ound-robin" type samples, and have failed to provide a well- aracterized widely distributed and easily available standard. he NBS Office of Standard Reference Materials is in the ocess of acquiring, analyzing and certifying a series of biologi- l standards. These standards, when issued, will include six otanical standards, a blood standard and a tissue standard.

133. Bennett, H. S., **Absorbing centers in laser materials,** *J. Appl. Phys.* **42,** No. 2, 619-630 (Feb. 1971).

Key words: Antimony; heat conduction; laser materials; Nd-doped glass; platinum; stress components; thermoelastic theory.

One of the severe problems encountered in high-power-solid- ate laser systems is the thermal damage to laser rods and opti- l elements arising from metallic or dielectric inclusions; i.e., purities with physical and optical properties which differ sub- antially from those of the host material. Such inclusions may sorb an appreciable amount of the incident radiation and ereby may produce major stresses within the host material. In is paper, the dependence of the maximum value of the tensile ess upon the size of the inclusion and upon the physical pro- rties of the host is examined. The feasibility of using optical chniques to detect metallic and dielectric inclusions in laser aterials before they cause damage also is studied. The compu- ions suggest that the use of laser pulse widths of the order of croseconds or longer may be more promising for the detection small incipient absorbing centers than the use of nanosecond lse widths.

134. Bennett, H. S., ***F* centers in ionic crystals: semicontinuum-polaron models and polarizable-ion models,** *Phys. Rev. B* **3,** No. 8, 2763-2777 (Apr. 15, 1971).

Key words: $CaF_2$; CaO; *F* center; internal Stark effect; KCl; optical phonons; polarizable ion model; semicontinuum polaron model.

The three lowest-lying *F*-center states for KCl, CaO, and $F_2$ are calculated within the framework of five micontinuum-polaron models and one polarizable-ion model. e movement of the nearest-neighbor ions to the *F* center and *F* electron are treated in a self-consistent manner in these odels. Exact solutions to these models for the states involved the transitions of optical absorption and emission are obtained merically. In addition, the internal Stark effect due to noncu- phonons is estimated. The absorption energy, the emission ergy, and the lifetime of the first excited state are evaluated for six models. It is shown that a semicontinuum-polaron model ees best with the experimental results for KCl and that the larizable-ion model gives the best results for CaO and $CaF_2$. addition, the semicontinuum-polaron model and the internal rk effect predict that the relaxed excited state in KCl consists a strong mixing of 2*p*-like and 2*s*-like states which are spatially fuse.

135. Boyne, H. S., **Laser frequency stabilization techniques and pplications,** *Proc. 24th Annual Frequency Control Symp., At- antic City, N.J., April 27-29, 1970,* pp. 233-339 (U.S. Army Electronics Command, Fort Monmouth, N.J., 1970), *IEEE Trans. Instr. Meas.* **IM-20,** No. 1, 19-22 (Feb. 1971).

Key words: Frequency; laser; laser frequency measurement; stabilization; techniques; time standard.

A review of progress in laser stabilization techniques and laser quency measurement is given. Methods for relating laser frequencies to the time standard and methods for absolute laser frequency stabilization are described. Experimental information on reproducibility and noise characteristics is reported. Application to frequency and wavelength standards is discussed.

12136. Unassigned.

12137. Brower, W. S., Jr., Parker, H. S., **Growth of single crystal cuprous oxide,** *J. Crystal Growth* **8,** 227-229 (1971).

Key words: Crystal growth; cuprous oxide; single crystal.

Single crystals of $Cu_2O$ in sizes up to 1 cm dia and several cm long have been grown by a floating zone technique in a controlled oxygen pressure of 0.4 torr. Total cation impurities in the crystals were determined to be $< 40$ ppm.

12138. Burdick, M. D., **An instrumental procedure for evaluating adherence of porcelain enamel cover coats direct-to-steel,** *Proc. Porcelain Enamel Institute Technical Forum, University of Illinois, Urbana, Ill., Oct. 7-9, 1970,* **32,** 160-167 (Porcelain Enamel Institute, Washington, D.C., 1971).

Key words: Adherence; instrumental evaluation; porcelain enamel direct-to-steel.

An instrumental method for rating the quality of direct-on adherence is described. It is appropriate either for monitoring day-to-day production or for making interlaboratory comparisons. The method is based on present practices, is rapid and eliminates subjective judgments. Other approaches to direct-on adherence measurements will be discussed.

12139. Cezairliyan, A., **A high speed method of measuring thermal expansion of electrical conductors,** *Rev. Sci. Instr.* **42,** No. 4, 540-541 (Apr. 1971).

Key words: High-speed measurements; high temperature; platinum; thermal expansion.

A transient method for the measurement of thermal expansion of electrical conductors is described. The method is based on detecting the change in radiance coming from a constant radiation source as a result of the expansion of the specimen placed between the radiation source and a radiation detecting system. The specimen can be pulse heated from room temperature to near its melting point in less than one second and pertinent experimental quantities can be measured with a time resolution of 0.4 ms and a full-scale signal resolution of one part in 8000. To check the method, preliminary experiments were performed on platinum in the temperature range 300 to 700 K. The estimated inaccuracy of the results is within 5 percent. The agreement of the results with those in the literature is within 3 percent.

12140. Chappell, S. E., Humphreys, J. C., **Silicon detector measurements of energy deposition in aluminum by monoenergetic electrons,** (Proc. Annual Conf. Nuclear Space Radiation, La Jolla, Calif., July 1970), *IEEE Trans, Nucl. Sci.* **NS-17,** No. 6, 272-277 (Dec. 1970).

Key words: Absorbed energy vs depth; absorbed-energy distributions; incident monoenergetic electrons; Monte Carlo calculations; semi-infinite aluminum medium; silicon detector.

The energy deposited at various depths in aluminum by incident monoenergetic electrons has been measured with a silicon-semiconductor, transmission detector. Beams of monoenergetic electrons with incident energies of 0.50, 0.75, and 1.0 MeV were directed normally on a semi-infinite slab of aluminum in which a 0.196-mm silicon detector was positioned at various depths. The pulse-height distributions recorded with the detector were converted to absorbed-energy distributions from which the probability of energy absorption per incident electron in the specific layer, as well as the absorbed energy as a function of depth in the material, could be determined. The curves of absorbed energy as a function of depth obtained for aluminum at each energy were compared to those calculated by Berger and Seltzer, employing a Monte Carlo method. Good agreement is shown between calculations and measurements.

12141. Collin, G. J., Ausloos, P., **Ion-molecule reactions in the condensed-phase radiolysis of hydrocarbon mixtures. III. Reactions of $i$-$C_4H_8^+$ and $tert$-$C_4H_9^+$ ions originating from neopentane,** *J. Am. Chem. Soc.* **93,** No. 6, 1336-1340 (Mar. 24, 1971).

Key words: Ion-molecule reactions; neopentane; neutralization; radiolysis; unimolecular fragmentation.

The liquid-phase radiolysis of neopentane has been investigated in the presence of various hydrocarbons and electron scavengers. It is found that the neopentane parent ion dissociates to yield $tert$-$C_4H_9^+$ and $i$-$C_4H_8^+$ ions. The yields of these ions which are intercepted in these experiments under optimum conditions are $\sim 2.4$ and $\sim 0.9$, respectively. The $i$-$C_4H_8^+$ ion reacts with various added alkanes by the $H_2^-$ transfer mechanism: $C_4H_8^+ + RH_2 \rightarrow i$-$C_4H_{10} + R^+$. The relative rates of reaction with different $RH_2$ additives have been determined and show the same trends as those observed for these reactions in the gas phase. That is, the rate is seen to increase with an increase in the exothermicity of the reaction (as calculated from gas-phase thermodynamic data). The effect of the $\Delta H$ of reaction is, however, more pronounced in the liquid than in the gas phase. The *tert*-butyl ion reacts more slowly with alkane additives than does the isobutylene ion, but reacts effectively with a negative ion from $CCl_4$ to form $tert$-$C_4H_9Cl$. Neutralization of the *tert*-butyl ion leads to the formation of isobutylene and propylene.

12142. Costrell, L., **CAMAC instrumentation system—introduction and general description,** (Proc. Nuclear Science Symp., New York, N.Y., Nov. 6, 1970), *IEEE Trans. Nucl. Sci.* **NS-18,** No. 2, 1-6 (Apr. 1971).

Key words: CAMAC; data; dataway; digital; instrumentation; modules; nuclear; standards.

The CAMAC instrumentation system developed by the ESONE Committee on European laboratories has been endorsed by the U.S. AEC NIM Committee as a dataway system complementary to the NIM (Nuclear Instrument Module) system. CAMAC is described in a general way in this introductory paper which is followed by papers that discuss the system in greater detail and describe typical implementation.

12143. Currie, L. A., Rodríguez-Pasqués, R. H., **Photonuclear tritium yields at 90 MeV,** *Nucl. Phys.* **A157,** 49-60 (1971).

Key words: Absolute tritium yields; hydrogen extraction; nuclear evaporation calculations; photonuclear reactions; 90 MeV bremsstrahlung; $^{64}$Cu, $^{61}$Cu, $^{11}$C activation monitor yields.

Photonuclear ($\gamma$,t) yields have been determined for Al, Zn, Sn and Bi using 90 MeV bremsstrahlung from the NBS electron synchrotron. The National Bureau of Standards P2 ionization chamber was used for primary monitoring of the bremsstrahlung beam; supplementary C and Cu activation foils, whose absolute yields are reported, were employed for relative intensity measurements. Tritium yields were determined by quantitative extraction from the molten samples with hydrogen carrier followed by activity measurement by means of low-level gas counters. The observed yields were generally consistent with those of other workers at lower energies. Comparison of the tritium yields with the results of statistical model calculations suggests the predominance of non-evaporative processes in the higher mass region ($A \gtrapprox 100$).

12144. Danos, M., Gibson, B. F., **Very high-momentum components in nuclei and far "subthreshold" production of quarks,** *Phys. Rev. Letters* **26,** No. 8, 473-476 (Feb. 22, 1971).

Key words: Coherent production; cosmic rays; high momentum components; many-body clusters; nuclei; quarks.

An estimate, valid for inelastic processes, of the probabilities of the high-momentum components in nuclei resulting from many-body correlations, together with data from Serpukhov, is used to derive upper limits for the quark-production cross section near threshold.

12145. Danos, M., Gillet, V., **Evidence for quartet structure in medium and heavy nuclei,** *Physics Letters* **34B,** No. 1, 24-26 (Jan. 18, 1971).

Key words: Binding energy; mass formulae; nuclei; particle-hole energy; quartet structure; rearrangement.

The second differences of the nuclear masses keeping *T* constant are discussed for even-even nuclei throughout the mass table. They are shown to be consistent with the quartet picture of weakly interacting tight two-proton two-neutron structures.

12146. Danos, M., Spicer, B. M., **Quartet structure in light nuclei** *Z. Physik* **237,** 320-326 (1970).

Key words: Collective correlations; four particle-four hole states; light nuclei; quartets; rotational states; vibrationa states.

The nature of the low-lying even parity, even spin states of $4n$ nuclei are discussed in terms of the quartet scheme, and many o their properties can be given by it. These states are also the low lying states important in the collective correlations model of th giant dipole resonance, and the quartet scheme thus provides description of them.

12147. DeVoe, J. R., Spijkerman, J. J., **Mössbauer spectrometry** *Anal. Chem. Annual Reviews* **42,** No. 5, 366R-388R (Apr 1970).

Key words: Chemical applications; literature; Mössbaue spectroscopy; review.

A review of the literature on chemical applications o Mössbauer Spectrometry for 1968 and 1969 are presented. Thi is done primarily with a table of pertinent information on com pounds and techniques. New developments in the field are als presented.

12148. Dibeler, V. H., **Photoionization studies and thermodynam ic properties of some halogen molecules,** (Proc. Intern. Conf. o Mass Spectroscopy, Kyoto, Japan, Sept. 8-13, 1969), Chapte in *Recent Development in Mass Spectroscopy,* K. Ogata an T. Hayakawa, eds., pp. 781-790 (University of Tokyo Press Tokyo, Japan, 1970).

Key words: Chlorine monofluoride; dissociative ionizatio fluorine; heats of formation; hot bands; hydrogen fluorid ion pairs; mass spectrometry; molecular ionizatio photoionization; vacuum ultraviolet.

Mass spectra and ion yield curves for molecular and dissocia tive ionization processes are measured for fluorine, hydroge fluoride, chlorine, and chlorine monofluoride by means of a com bined vacuum uv monochromator and mass spectromete Ionization and dissociation energies and heats of formation the molecules are obtained and compared with values derive from thermochemical and spectroscopic studies.

12149. DiMarzio, E. A., Guttman, C. M., **Separation by flow an its application to gel permeation chromatography,** *J. Chro matog.* **55,** 83-97 (1971).

Key words: Chromatography; elution volume; flow; gel per meation chromatography; hydrodynamic volume; polyme polymer separation.

When dilute solutions of finite size particles undergoin Brownian motion flow through a capillary, the larger particle ave higher average velocities than the smaller particles. Thus he can obtain a separation of particles of different sizes due to uid flow. The elution volumes of suspended particles or olymer molecules are derived for various tube geometries. Following TAYLOR, the effects of diffusional broadening of the olume elution peak for finite size particles are discussed and the ocess is shown to be chromatographic.

Models of a gel permeation chromatographic column are oposed in which there is fluid and particle flow through each of e beads as well as around them. Diffusion is allowed within and utside of the beads. Equations for the location of the volume ution peaks are computed for such models and shown to yield nctional dependence on the polymer radius and column ometry very much like equations derived by previous workers r models of gel permeation chromatographic columns in which ere was no flow allowed within the beads. Explicit formulae e given for the second and third moments for the above odels. It is shown that for a monodisperse species the volume ution peak is always a gaussian of a finite width. It is shown at beads with open pores that allow for flow always have better paration capabilities than beads with pores that do not allow r flow.

**150.** Dziuba, R. F., Dunfee, B. L., **Resistive voltage-ratio standard and measuring circuit,** *IEEE Trans. Instr. Meas.* **IM-19,** No. 4, 266-277 (Nov. 1970).

Key words: Divider; measurement system; ratio; ratio standard; resistive divider; voltage ratio.

This paper describes a highly stable, guarded dc voltage-ratio andard and the measuring network and techniques used to tablish the values of its ratios to an accuracy of 0.2 ppm. The tire system is housed within a dry-air enclosure whose temrature is maintained at 23 ± 0.05 °C. Discrete ratios from 1:1 1000:1 are provided, with maximum rated voltage set at 1000 lts. The design of the standard was chosen so that a redundan- of measurement could be incorporated in the system. Thus ch successive ratio is measured by a substitution or "bootrap" method and by satisfying the conditions of the seriesrallel principle, the 10:1, 100:1, and 1000:1 ratios are meared by a second independent method. The design also admits ditional checks on the validity of the measurements. An analy- of measurement errors and a discussion of their possible igin are included. Since the intent also was to design the ratio andard for low-frequency operation some preliminary data are cluded on its ac performance.

**151.** Fatiadi, A. J., **Determination of inososes with an alkaline solution of copper (II) oxalate-tartrate complex (the Somogyi reagent) and reaction mechanisms involved,** *Carbohydrate Res.* **17,** 419-430 (Mar. 1971).

Key words: Determination; electron-transfer; inosose; oxidation; quantitative; radical; reagent.

Four inososes have been analyzed with the Somogyi reagent d empirical equations for their quantitative determination were rived. Results from spectrophotometric and electron-spin sonance studies of the mechanism of oxidation of inososes th the Somogyi reagent at 25 to 55° are in agreement with a e-electron transfer process; however, at 90 to 100°, extensive gradation of inososes by the Somogyi reagent occurs, doubtss caused by generation of transient radicals during the oxidan, as evidenced by results of a radical-scavenging experiment.

**152.** Fickett, F. R., **Resistivity of polycrystalline aluminum and copper in high magnetic fields: The effect of temperature and purity,** *Appl. Phys. Letters* **17,** No. 12, 525-527 (Dec. 15, 1970).

Key words: Aluminum; copper; magnetoresistance.

Data are presented on the resistivity of polycrystalline aluminum and copper at 40 kOe and at temperatures from 4 to 30 K. Specimen purity varies over three decades of residual resistance ratio. For either metal, the actual resistivity measured in the field at a given temperature decreases with increasing specimen purity. This result is important for proposed high magnetic field applications of these metals.

**12153.** Fickett, F. R., Clark, A. F., **Longitudinal magnetoresistance anomalies,** *J. Appl. Phys.* **42,** No. 1, 217-219 (Jan. 1971).

Key words: Copper; magnetoresistance.

We have observed the anomalous longitudinal magnetoresistance conditions $R(H)=0$ and $0 < R(H) < R(0)$ on a [111]-oriented copper crystal specimen. The magnetoresistance voltages measured by two probe sets on mutually perpendicular faces of the specimen are observed to have a significant difference. Both of these effects are shown to be due to very slight misorientations of the specimen with respect to the magnetic field. In light of the observations, we present some precautions which should be observed in making longitudinal magnetoresistance measurements on high-purity materials.

**12154.** Gadzuk, J. W., Plummer, E. W., **Hot-hole-electron cascades in field emission from metals,** *Phys. Rev. Letters* **26,** No. 2, 92-95 (Jan. 11, 1971).

Key words: Attenuation length; electron gas theory; field emission; surface physics; tunneling.

Recent field-emission tunneling experiments have shown a current-dependent tail in the energy distribution for energies above the Fermi energy. This tail can be understood in terms of the products of a cascade process initiated by the injection of hot holes (removal of electrons by field emission) into the interacting electron gas or metal conduction band. The derived shapes of the tails, numerical values of the high-energy distributions, and field dependences of the current in the tails are in good agreement with our experimentally observed results.

**12155.** Geltman, S., Burke, P. G., **Electron scattering by atomic hydrogen using a pseudo-state expansion II. Excitation of 2s and 2p states near threshold,** *J. Phys. B: Atom. Molec. Phys.* **3,** No. 8, 1062-1072 (Aug. 1970).

Key words: Close coupling calculation; electron scattering; pseudo-state expansion.

The pseudo-state modification of the close-coupling expansion is applied to the 2s and 2p excitation of atomic hydrogen by electron impact. Pseudo-states are used which ensure the implicit inclusion of all important excited state polarizabilities. A detailed comparison is made with results obtained from other modifications of the close-coupling expansion and the eigenphase minimum principle is used to determine the best result for each partial cross section. Comparison of the theory and experiment in the first electron volt above the $n=2$ threshold shows very good agreement in the ratio $Q(1s-2s)/Q(1s-2p)$, but a 20% discrepancy exists between the individual cross section magnitudes when experiment is normalized to the Born approximation at higher energies.

**12156.** Green, M. S., Cooper, M. J., Sengers, J. M. H. L., **Extended thermodynamic scaling from a generalized parametric form,** *Phys. Rev. Letters* **26,** No. 9, 492-495 (Mar. 1, 1971).

Key words: Coexistence curve; critical point; liquid-gas phase transition; parametric form; scaling; thermodynamic properties.

A generalization of the parametric representation for thermodynamic scaling is proposed, introducing a new critical exponent $\epsilon$. Expansions about the critical point are deduced for the fluids, and to lowest order the asymptotic power-law forms are recovered. An exponent $1-\alpha'$ is obtained for the diameter of the coexistence curve. Experimental data are shown to support the predicted forms.

**12157.** Hastie, J. W., Hauge, R. H., Margrave, J. L., **Infrared spectra and geometries of heavy metal halides: $SrCl_2$, $BaCl_2$, $EuCl_2$, $EuF_2$, $PbCl_2$, and $UCl_2$,** *High Temp. Sci.* **3,** No. 1, 56-71 (Jan. 1971).

Key words: Heavy metal halides; infrared spectra; matrix isolation; molecular geometries.

The heavy metal dihalide species $SrCl_2$, $BaCl_2$, $EuCl_2$, $EuF_2$, $PbCl_2$, and $UCl_2$, generated under thermodynamic equilibrium conditions, have been isolated in matrices of solid Ne, Ar, Kr, and $N_2$. Methods of production varied from simple Knudsen vaporization for $SrCl_2$, $BaCl_2$, and $PbCl_2$, and decomposition vaporization, i.e.,

$$EuX_3(s) \rightarrow EuX_2(g) + 1/2\ X_2,$$

to oxidation vaporization, i.e.,

$$CaCl_2(g) + U(s) \rightarrow UCl_2(g) + Ca(g),$$

$$Cl_2(g) + U(s) \rightarrow UCl_2(g),$$

$$\text{and } 2HCl(g) + U(s) \rightarrow UCl_2(g) + H_2.$$

Infrared spectra for these matrix-isolated species were obtained ($33-4000$ cm$^{-1}$) and the symmetric ($\nu_1$) and the antisymmetric ($\nu_3$) vibrations observed in each case. For the chlorides the extreme low-intensity nature of the bending frequency ($\nu_2$), the numerous extraneous low-frequency absorptions associated with lattice modes of the solid matrices, and the ever-present HCl impurities resulted in a less reliable assignment of $\nu_2$ values. In some cases frequency measurement of the various naturally occurring $Cl^{35}$, $Cl^{37}$ isotopic species allowed definite assignments of the stretching frequencies to be made and the following bond angles were calculated: $SrCl_2$ ($130 \pm 8°$), $EuCl_2$ ($135 \pm 8°$), and $PbCl_2$ ($96 \pm 3°$). Fermi interactions between $\nu_1$ and $\nu_3$ for the unsymmetrical isotopic species were observable in these cases and provided added verification of the frequency assignments. From the relative intensities of $\nu_1$ and $\nu_3$ the following bond angle estimates were made: $BaCl_2$ ($120 \pm 10°$), $EuF_2$ ($110 \pm 15°$), and $UCl_2$ ($100 \pm 15°$). These bond angles were also in accord with a consistent set of force-constant data.

**12158.** Herron, J. T., Huie, R. E., **Mass spectrometric studies of the reactions of singlet oxygen in the gas phase,** *Ann. N. Y. Acad. Sci.* **171,** Article 1, 229-238 (Oct. 15, 1970).

Key words: Air pollution; chemical kinetics; chemistry; gas kinetics; olefins; singlet oxygen.

The reactions of singlet molecular oxygen ($0_2{}^1\Delta_g$) with some olefins and other organic reactants have been studied in the gas phase. Rate constants have been measured and the mechanisms of the reactions investigated. The significance of these reactions in air pollution is discussed.

**12159.** Kamper, R. A., Zimmerman, J. E., **Noise thermometry with the Josephson effect,** *J. Appl. Phys.* **42,** No. 1, 132-136 (Jan. 1971).

Key words: Josephson effect; noise; superconductivity; thermometry.

Thermal noise causes a random frequency modulation of the self-oscillation of a Josephson junction, and the temperature of the noise source can be determined by analysis of the generated signal. We show that a thermometer based on this principle would be theoretically capable of measuring temperatures in the microkelvin range, and describe a prototype thermometer which has recorded noise temperatures down to 0.075 K.

**12160.** Kidnay, A. J., Hiza, M. J., **The purification of helium gas by physical adsorption at 76 °K,** *AIChE J.* **16,** No. 7, 949-95 (Nov. 1970).

Key words: Breakthrough time; helium; mixture adsorption nitrogen methane.

The physical adsorption isotherms for three methane-heliu mixtures, two nitrogen-helium mixtures, and one methane nitrogen-helium mixture were measured at 76 °K, and pressure of 2 to 65 atm on a coconut shell charcoal. The adsorptio isotherms of the pure components (nitrogen, methane, and heli um) were also determined over the appropriate pressure range

Methods for predicting the mixture adsorption isotherms b using only the pure component isotherms are discussed and ar shown to be adequate for these systems.

The concentration vs. time or breakthrough curves were als measured for both the binary and ternary mixtures at a numbe of different flow rates. Mass transfer coefficients for both the ga phase and the adsorbed phase were obtained from thes breakthrough curves.

**12161.** Kieffer, L. J., **Low energy electron collision cross sectio data. Part II. Electronic excitation level and line cross section** *Atomic Data* **1,** No. 2, 121-287 (Nov. 1969).

Key words: Atom; cross section; electron; molecule.

This is the second part of a comprehensive compilation of lo energy electron collision cross section data. The compilation i limited to experimental measurements and includes data for a atomic species and for those molecules which are important i aeronomy, astrophysics, and plasma physics. The data include were taken from literature published through December 1968.

**12162.** Klein, M., Hanley, H. J. M., **The m-6-8 potential functio** *J. Chem. Phys.* **53,** No. 12, 4722-4723 (Dec. 15, 1970).

Key words: Gas; intermolecular potential; potential fun tion; scattering; second virial; viscosity.

We have studied the four parameter, semitheoretical m-6- potential as a potential function for some simple molecules. W find that the addition of the inverse eighth term to a thre parameter function substantially improves the relation foun previously between theory and experiment. We show here th with the m-6-8 potential we essentially duplicate the experime tal viscosity data for argon both at very high and very low te peratures. With the same parameters we were also able t reproduce the experimental second virial coefficient data for a gon. This improvement would appear to be due specifically t the addition of an eighth power attraction. It was further foun that the value of the repulsive exponent is consistent with th obtained from the analysis of scattering data. Based on co parisons between our results and those obtained for the mo elaborate function of Barker and Pompe we feel that modific tion of the repulsive term would not significantly alter th behavior of our results with respect to data.

**12163.** Lane, N. F., Geltman, S., **Differential elastic and rot tional excitation cross sections for electron-$H_2$ scattering,** *Phy Rev.* **184,** No. 1, 46-51 (Aug. 5, 1969).

Key words: Close coupling calculation; differential cro sections; elastic scattering; electron; $H_2$ (hydroge molecule); rotational excitation.

Differential elastic and rotational excitation cross sections f electron-$H_2$ scattering have been calculated in the close-couplin approximation with electron exchange neglected. The resulti elastic angular distributions are found to be in very good agre ment with measurements. An apparent oscillation in the me sured differential cross section for rotational excitation is n found in the calculation.

**12164.** Laufer, A. H., **Low-temperature chromatographic dete**

**mination of ketene and methyl ketene,** *J. Chromatogr. Sci.* **8,** 677-678 (Nov. 1970).

Key words: Analysis; gas chromatography; ketene; methyl ketene.

A quantitative chromatographic technique for the analysis of mall quantities of ketene and methyl ketene has been eveloped. The method involves low temperature separation of he components on a "Haloport-F" column.

2165. McConnell, P. M., Daney, D. E., Kirgis, J. B., **Thermoelastic expansion and creep of polyethylene terephthalate and polypyromelitimide film and polyethylene terephthalate fibers from 20 to 295 K,** *J. Appl. Phys.* **41,** No. 13, 5066-5070 (Dec. 1970).

Key words: Longitudinal; polyethylene terephthlate; polypyromelitimide; relative creep; thermoelastic; transverse.

A quartz tube dilatometer was used to measure the lineal thermal expansion and creep of single lengths of polyethylene erephthalate (PETP) film, polypyromelitimide (PPMI) film, and ETP multifiber yarn, while stressed under constant tension. ensions below and above the conventionally defined yield trength were used and the sample temperature ranged from 20 o 295 K. Relative creep strain measurements, taken at the constant temperatures 77, 195, and 295 K were found to obey the equation

$$\epsilon=\exp\left[-2.3\exp(A'y)\right],$$

where $y$ is a function of stress, time, and temperature and $A'$ is a onstant depending on the material. This equation was used to orrect the thermoelastic expansion measurements for creep at he higher stresses. PETP multifiber yarn subjected to a slight ension was found to elongate during cooldown from 293 to 20 K. Higher stresses caused less elongation; i.e., the coefficient of xpansion increased with stress. This result is believed to be due o changes in crystallinity at the higher stresses. A similar stress ffect was found with PETP film but not with PPMI film. The hermoelastic expansion of the film samples was also found to be ensitive to the thickness.

2166. McDonald, D. G., Evenson, K. M., Wells, J. S., Cupp, J. D., **High-frequency limit of the Josephson effect,** *J. Appl. Phys.* **42,** No. 1, 179-181 (Jan. 1971).

Key words: Detectors; infrared; Josephson effect; lasers; superconductivity.

Coherent detection of applied radiation via a Josephson current step has been achieved with an applied frequency approximately a factor of 3 higher than heretofore reported. The detected signal is at 2.5 THz (118 $\mu$). The inadequacy of existing heory to predict the frequency dependence of the Josephson effect is discussed.

2167. Manning, J. R., **Correlation effects and activation energies for diffusion in alloys,** (Proc. Conf. Atomic Transport in Solids and Liquids, Marstand, Sweden, June 1970), *Z. Naturforsch.* **26A,** No. 1, 69-76 (Jan. 1971).

Key words: Activation analysis; concentrated alloys; correlation factor; diffusion; random alloy; vacancies.

The problems involved in calculating correlation factors for iffusion in dilute alloys can be contrasted to those arising in oncentrated solid solutions. As one moves from the pure element to the dilute alloy to the concentrated alloy, the calculation ecomes progressively more difficult. Because of the complex tom configurations which can occur in concentrated alloys, it sually is not possible to calculate correlation factors in these alloys exactly.

Several important simplifications are available in non-dilute random alloys. A large reduction in complexity can be secured by using a random alloy model where each atom is treated as diffusing in a uniform matrix, with the matrix properties being determined by the composition and jump frequencies in the alloy. Resulting equations in this random alloy model can be expressed directly in terms of the experimentally measurable tracer diffusion coefficients with no unknown vacancy jump frequencies appearing. Also these equations have the advantage of being in simple analytic form and not requiring numerical methods to evaluate the correlation factors. These two features make possible the direct expression of the temperature dependence of the correlation factor in terms of the experimental activation energies.

Equations are found for $\Delta H/\Delta Q$ in random binary cubic alloys, where $\Delta H$ is the difference between the activation enthalpies for diffusion of the two species and $\Delta Q$ is the difference between the experimentally measured activation energies of the two species. This ratio is never less than unity and can be much larger than unity. Values are plotted for diamond, body-centered cubic and face-centered cubic structures. From the magnitude and composition dependence of $\Delta H/\Delta Q$, it is concluded that the temperature dependence of the correlation factor cannot by itself explain the difference between the activation energies measured from tracer diffusion and from internal friction in the non-dilute range.

12168. Matarrese, L. M., Evenson, K. M., **Improved coupling to infrared whisker diodes by use of antenna theory,** *Appl. Phys. Letters* **17,** No. 1, 8-10 (July 1, 1970).

Key words: Antenna theory; infrared detectors; lasers; whisker diode.

It is shown that the dependence of the output of a whisker diode on its orientation in the polarized beam of an infrared laser can be explained on the basis of simple long-wire antenna theory. Outstanding improvements in coupling the diode to the radiation field can result when this fact is utilized in applications.

12169. Moore, C. E., **Annual report on spectroscopy, July 1, 1969-June 30, 1970,** *Bull. Am. Astron. Soc.* **3,** No. 1, 154-155 (1971).

Key words: Atomic spectra; references; spectroscopy; transition probabilities.

A report of the activities at the National Bureau of Standards that are of special interest to astronomers and astrophysicists, is submitted annually for publication, along with observatory reports. The present report covers the fiscal year 1970.

12170. Olson, W. B., Papousek, D., **High-resolution infrared spectra of ethanelike molecules and the barrier to internal rotation: the $\nu_9,\nu_{13}$ band of dimethylacetylene,** *J. Mol. Spectry.* **37,** No. 3, 527-534 (Mar. 1971).

Key words: Dimethylacetylene; internal rotation; rotational constants; spectrum; vibration-rotation.

The infrared spectrum of dimethylacetylene was measured with high resolution in the region of the perpendicular band of the C – H stretching vibration and the $Q$ branches were partially resolved in the bunches of $Q$ branches. The upper limit to the torsional barrier was estimated to be 4 cm$^{-1}$.

12171. Pecker, J. C., Thomas, R. N., **Personal libraries and publication policies,** *Atoms* **25,** 37-38 (Jan. 1970).

Key words: Astronomy, working library; libraries, astronomy; publication policies, astronomy.

The authors have been concerned for some time with the difficulties involved in maintaining an adequate personal, working library in the field of astronomy. The problem is especially acute for younger astronomers and for students and researchers working in less affluent geographical areas or institutions. In this discussion, we present some thoughts on the relation of the current situation to the problem of publishing in our field, and some proposals which we believe will improve it.

12172. Ramboz, J. D., **A link-compensated ratio transformer bridge,** *Rev. Sci. Instr.* **42,** No. 4, 522-524 (Apr. 1971).

Key words: Bridge; impedance; impedance bridge; measurement; ratio transformer; ratio transformer bridge.

A ratio transformer impedance bridge that is capable of measuring either capacitive or inductive impedances is described. It is made of commercially available laboratory apparatus and can yield measurements to an uncertainty of less than ±0.1 percent. The unique feature is an injection transformer which reduces the effect of the interconnecting "link-resistance" between the unknown impedance and the bridge reference reactance. Five circuit variations of the bridge are shown and the equations which yield the solutions for the unknown resistance, capacitance, or inductance and phase angle are given.

12173. Ruegg, F. C., **A circuit which expands the count storage capacity of a multichannel analyzer,** *Nucl. Instr. Methods* **92,** 7-11 (1971).

Key words: Multichannel scaler; nuclear instrumentation; overflow counter.

A circuit has been designed which allows the experimenter to store up to $10^{10}$ counts/channel in a $10^5$ count capacity multichannel analyzer. The circuit uses the analyzer's second subgroup to store the overflow counts of the first subgroup. The circuit was designed to be used with an analyzer operating in the multichannel scaling mode.

12174. Scharf, K., **Spectrophotometric measurement of ferric ion concentration in the ferrous sulphate (Fricke) dosimeter,** *Phys. Med. Biol.* **16,** No. 1, 77-86 (1971).

Key words: Chemical dosimeter; chemical dosimetry, ferrous sulfate; ferrous sulfate dosimeter; ferric ions; Fricke dosimeter; radiation dosimeter; radiation dosimetry; spectrophotometry; spectrophotometric measurements.

A systematic error in the spectrophotometric measurement of ferric ion concentrations in the ferrous sulphate dosimeter may be made by an incorrect evaluation of a non-linear spectrophotometric calibration curve. Methods are discussed for determining the radiation-produced change in molarity from the actual calibration curve, and a method of normalization of measured absorbances is suggested. Normalization factors, converting measured absorbances into normalized values, can either be calculated by choosing a reference value of the molar extinction coefficient, or can be determined by comparative absorbance measurements on two spectrophotometers, one of them to be a precision instrument. Normalized absorbances are proportional to molarity and may be considered to be free of errors due to instrumental parameters and inaccuracies in acidity and temperature of solutions, and of errors in molarity if derived by comparative measurements.

12175. Sieck, L. W., Searles, S., Ausloos, P., **High-pressure photoionization mass spectrometry. Photoionization of propane at 11.6-11.8 eV. Formation and reactivity of the $(C_3H_8)_2{}^+$ dimer ion,** *J. Chem. Phys.* **54,** No. 1, 91-95 (Jan. 1, 1971).

Key words: Ion-molecule reaction; kinetics; mass spectrometry; photoionization; propane; radiation chemistry.

The major reaction path of the propane molecular ion with propane was found to be the formation of the dimer ion $(C_3H_8)_2{}^+$ via a termolecular mechanism,

$$C_3H_8$$

$$C_3H_8{}^+ + C_3H_8 \rightarrow (C_3H_8)_2{}^+ + C_3H_8.$$

In addition, $C_3H_6{}^+$ and $C_3H_7{}^+$ were also found as minor reaction products at lower pressures. The reactions of the dimeric ions with ethylene and NO were also investigated. The charg exchange reaction, $(C_3H_8)_2{}^+ + NO \rightarrow NO^+ + 2C_3H_8$, was foun in propane-NO mixtures, suggesting a recombination energy i excess of 9.24 eV. The formation of $C_3H_8NO^+$ was also detecte at higher total pressures. The dimeric ion was also found t transfer $H_2$ to ethylene without affecting the structural integrit of the carbon skeleton, $(C_3H_8)_2{}^+ + C_2H_4 \rightarrow C_6H_{14}{}^+ + C_2H_6$, indicating that this species exhibits the chemical behavior of saturated hydrocarbon ion.

12176. Sixsmith, H., Giarratano, P., **A minature centrifuga pump,** *Rev. Sci. Instr.* **41,** No. 11, 1570-1573 (Nov. 1970).

Key words: Centrifugal; helium; nitrogen; pump; pum design; pump performance.

A miniature centrifugal pump designed to circulate helium i a flow loop is described. It is designed to operate in the liqui helium temperature range under ambient pressures up to 100 atn ($10^7$ N/m$^2$), producing a maximum flow rate of 50 cm$^3$/sec and maximum pressure rise of 3400 N/m$^2$. The operating characteristics obtained from preliminary tests with cold nitrogen ga and an analysis of the performance are included.

12177. Spiegel, V., Jr., Murphey, W. M., **Calculation of therma neutron absorption in cylindrical and spherical neutron sources** *Metrologia* **7,** No. 1, 34-38 (Jan. 1971).

Key words: Manganous sulfate bath; neutron sourc absorption; neutron source calibration; thermal neutron absorption.

A calculation of the thermal neutron self-absorption for cylindrical or spherical neutron sources has been made. The calculations are confirmed by the experimentally-measured differenc in manganous sulfate bath activity for bare and cadmium covered Pu-Be and Am-Be neutron sources. The calculation i done in single interaction approximation and assumes that the incident thermal neutron flux is isotropic. The source material ma be fissionable and be covered by up to three cladding materials A computer program has been written for the numerical calculations.

12178. Tate, E. L., **Improving library collections by weeding** *Proc. U.S. Department of Interior, 1970 Departmental Library Workshop, Washington, D.C., Sept. 28-Oct. 2-1970,* pp. 54 61 (U.S. Department of Interior, Office of Library Services Washington, D.C., Feb. 1971).

Key words: Scientists' use of literature; weeding a scientifi library; weeding criteria.

Four recommendations for weeding a scientific and technica library are given: (1) develop written criteria for weeding specific collection; (2) involve in the selection process the scientific staff of the agency served by the library; (3) take ample tim to make the weeding a collection improvement program; and (4 do not regret the loss of one or two titles needed later but consider the overall benefits in terms of dynamic use of the library Specific suggestions based on research on the use of scientifi and technical literature are included as an aid in formulatin weeding criteria.

12179. Uzgiris, E. E., Hall, J. L., Barger, R. L., **Precision infrare Zeeman spectra of $CH_4$ studied by laser-saturated absorption** *Phys. Rev. Letters* **26,** No. 6, 289-293 (Feb. 8, 1971).

Key words: Lasers; methane; saturated absorption; Zeema effect.

Zeeman splitting of the methane 2947.912-cm$^{-1}$ $F_1$ line wa studied. The $g$ factor of the rotational magnetic moment o methane was measured to be $g_J = +0.311 \pm 0.006$ and it wa found that $g_J(\nu_3 = 1)$ is equal to $g_J(\nu_3 = 0)$. A Doppler-generate "level-crossing" saturated absorption signal was observed an is described.

2180. Van Blerkom, D., Hummer, D. G., **The normalized on-the-spot approximation for line transfer problems,** *J. Quant. Spectrosc. Radiat. Transfer Note* **9,** No. 11, 1567-1571 (Nov. 1969).

Key words: Doppler broadening; escape probability; planetary nebula; spectral line formation.

A simple approximation for line transfer problems is presented hich is useful when photons scatter only a few times before eing destroyed. Comparison is made to solutions of high accuacy.

2181. Wachtman, J. B., Jr., **Standard materials for measurements on ceramics,** *Am. Ceram. Soc. Bull.* **50,** No. 3, 242-247 (Mar. 1971).

Key words: Ceramics; chemical composition; mechanical properties; pressure; properties; standards; standard reference materials; temperature; thermal.

Standard materials having well determined values of specific roperties are useful in establishing the validity of techniques for haracterization and property measurements on ceramics. For ome properties certified materials are available "off-the-shelf"; or other properties certification is in progress and a few pecimens may be available on a collaborative basis. Recent rogress and current work on standardized materials are briefly eviewed for temperature, pressure, chemical composition, theral emittance, thermal expansion, thermal conductivity, vapor essure, elasticity and viscosity.

2182. Wait, D. F., **The precision measurement of noise temperature of mismatched noise generators,** *IEEE Trans. Microwave Theory Tech.* **MTT-18,** No. 10, 715-724 (Oct. 1970).

Key words: Compensation method; cryogenic noise generators; mismatch error; noise temperature measurement.

By refining the technique and analysis of an earlier paper, it is hown that a compensation method is the basis of the most ecise measurement of noise temperature, especially for yogenic noise generators. The measurement system is adjusted that it is in thermal equilibrium with the generator under test. s is typical for the compensation method, the generator under st may be mismatched, and the comparison errors and detector mitations can be verified experimentally. For generators with nall reflection coefficients ($|\Gamma| \leqslant 0.1$), the comparison error is ery close to the theoretical minimum, namely, twice the system solution. For reflection coefficients as large as 0.5, the comarison error increases in a typical system to about four times the stem resolution.

2183. Wallace, B., Brown, W. E., **Stoichiometric composition of whitlockite,** *J. Dental Res.* **50,** No. 2, 343-346 (Mar.-Apr. 1971).

Key words: Ca/P ratio; pyrolysis; pyrophosphate; stoichiometry; tricalcium phosphate; whitlockite.

The mineral whitlockite has been described as having Ca/P tios of 3:2 and 10:7. This study used the pyrolytic formation of yrophosphate and whitlockite from calcium orthophosphates nd their mixtures with $CaCO_3$ to determine this Ca/P ratio. Its ean value of $1.506 \pm 0.0015$ indicated a formula of $Ca_3(PO_4)_2$.

2184. Wampler, R. H., **A report on the accuracy of some widely used least squares computer programs,** *J. Am. Stat. Assoc.* **65,** No. 330, 549-565 (June 1970).

Key words: Computer programs; curve fitting; Gram-Schmidt orthogonalization; Householder transformations; iterative refinement; least squares; linear equations; orthogonalization; orthogonal polynomials; regression; rounding error; stepwise regression.

Linear least squares test problems based on fifth degree olynomials have been run on more than twenty different computer programs in order to assess their numerical accuracy. The programs tested, all in present-day use, included representatives from several statistical packages as well as some from the SHARE library. Essentially five different algorithms were used in the various programs to obtain the coefficients of the least squares fits. The tests were run on several different computers, in double precision as well as single precision. By comparing the coefficients reported, it was found that those programs using orthogonal Householder transformations, classical Gram-Schmidt orthonormalization or modified Gram-Schmidt orthogonalization were generally much more accurate than those using elimination algorithms. Programs using orthogonal polynomials (suitable only for polynomial fits) also proved to be superior to those using elimination algorithms. The most successful programs accumulated inner products in double precision and made use of iterative refinement procedures.

12185. Weber, L. A., **Density and compressibility of oxygen in the critical region,** *Phys. Rev. A* **2,** No. 6, 2379-2388 (Dec. 1970).

Key words: Chemical potential; coexistence curve; compressibility; critical point; oxygen; PVT.

Density-versus-height profiles have been measured in the critical region of oxygen by means of capacitance techniques. Results are given for the liquid and vapor densities at coexistence, for compressibilities along the coexistence curve to within $t \equiv (T-T_c)/T_c = -6 \times 10^{-5}$, for compressibilities along the critical isotherm to within $(\rho - \rho_c)/\rho_c = 5 \times 10^{-2}$, and for compressibilities along the critical isochore to within $t = 2 \times 10^{-4}$. The data are analyzed in terms of power-law descriptions and are shown to be in excellent agreement with recent scaling-law analyses of data for other fluids.

12186. Weber, L. A., **Some vapor pressure and *P,V,T* data on nitrogen in the range 65 to 140 K,** *J. Chem. Thermodynamics* **2,** No. 6, 839-846 (Nov. 1970).

Key words: Density; liquids; nitrogen; *P,V,T;* phase boundary; saturation density; vapor pressure.

New results are presented for the vapor pressure of nitrogen from 65 to 126 K and for seven *P,V,T* isochores between 80 and 140 K. The isochores range in density from 0.85 to 2.6 times the critical. The vapor pressures are compared with existing literature values, and an equation is given for the vapor pressure on the IPTS-68 temperature scale between the triple point and the critical point.

12187. Weir, C. E., Piermarini, G. J., Block, S., **On the crystal structures of Cs II and Ga II,** *J. Chem. Phys.* **54,** No. 6, 2768-2770 (Mar. 15, 1971).

Key words: Cesium; gallium; high-pressure; polymorph; single crystal; x-ray diffraction.

The structures of Cs II and Ga II have been confirmed by high pressure single crystal x-ray studies. Cs II is Face Centered Cubic with $a = 6.465 \pm 0.015$ Å and Ga II is Body Centered Tetragonal with $a = 2.808 \pm 0.003$ Å and $c = 4.458 \pm 0.0003$ Å.

12188. Wiederhorn, S. M., Johnson, H., **Effect of pressure on the fracture of glass,** *J. Appl. Phys.* **42,** No. 2, 681-684 (Feb. 1971).

Key words: Deep submergence; fracture; fracture energy; glass; high pressure; strength.

The fracture surface energy of three glass compositions was measured as a function of hydrostatic pressure and was found to be independent of pressure to 20 kbar. This suggests that no change in the fracture mechanism occurs. The brittle behavior of glass thus differs from plastics and metals which are observed to become stronger and more ductile with increasing pressure.

12189. Woelfel, J. B., Paffenbarger, G. C., **Expanding and shrinking 7-year-old dentures: report of cases,** *J. Am. Dental Assoc.* **81,** No. 6, 1342-1348 (Dec. 1970).

Key words: Adaption; acrylic; contraction; dentures; epoxy; expansion; hard rubber; retention; serviceability; stability.

Two sets of upper and lower complete dentures, one made of vulcanite and one made of epoxy resin, were evaluated for serviceability and for dimensional changes from the time they were made until they had been worn seven years. Deterioration in serviceability was caused by changes in the tissues of the patient rather than by dimensional changes in the dentures. The epoxy resin dentures expanded gradually but there was practically no warpage. There was warpage in the vulcanite dentures, possibly caused by the differences in water absorption between the two types of rubber than were used for the facial sides and for the bases.

12190. Zimmerman, J. E., **Recent developments in superconducting devices,** *J. Appl. Phys.* **42,** No. 1, 30-71 (Jan. 1971).

Key words: Cardiography; instrumentation; Josephson effect; magnetometry; superconductivity.

A simple model of the electrical characteristics of thin-film-bridge, point-contact, and tunnel junction Josephson devices is given, along with some comments on their relative performance at very low and at very high frequencies. A particular example is the dc *IV* characteristic of a point contact at the center of a parallel-disk microwave cavity. Some recent developments in devices and the application of a point-contact loop (SQUID) device to magnetocardiography is described.

12191. Engen, G. F., **A new method of characterizing amplifier noise performance,** *IEEE Trans. Meas. Instr.* **IM-19,** No. 4, 344-349 (Nov. 1970).

Key words: Amplifier noise; noise; noise factor; noise temperature; Y-factor.

Although the use of noise figure or noise temperature to characterize amplifier performance is a well-established practice, it is also recognized that this parameter provides only a partial description of the amplifier noise properties. In general, the noise figure (or temperature) depends upon the generator impedance and is thus a function of the signal-source and amplifier combination.

Typically, the noise figure is measured by the Y-factor method using hot and cold noise sources that are nominally matched (reflectionless). The result of this measurement is of value as a figure of merit; however, if optimum performance is to be realized, the applications engineer must know whether to adjust the signal source impedance for maximum power transfer, minimum noise figure, or some other criterion, and he must know the deterioration in performance that results if this is not done. It is the purpose of this paper to present an alternative method of characterizing amplifier noise performance in terms of parameters that provide ready answers to these questions. In addition, the measurement of these parameters via a simple extension of the Y-factor method will be described.

12192. Gadzuk, J. W., Plummer, E. W., **Energy distributions for thermal field emission,** *Phys. Rev. B* **3,** No. 7, 2125-2129 (Apr. 1, 1971).

Key words: Field emission; surfaces; tunneling.

A sequence of total energy distribution curves for field emission was experimentally obtained for a tungsten emitter heated to 1570 K. Theoretical curves using the Miller-Good WKB-type approximation for tunneling probabilities are in good agreement with the experimental measurements. A significant feature of both sets of curves is a change in slope corresponding to electron emission near the top of the surface barrier where the emission mechanism changes from tunneling to thermionic emission. This feature is in accord with the classical-image force model for the surface potential which appears to be valid for distances approaching 3-4 Å to the metal surface.

12193. McLaughlin, W. L., Hussmann, E. K., Eisenlohr, H. H. Chalkley, L., **A chemical dosimeter for monitoring gamma radiation doses of 1-100 krad,** *Intern. J. Appl. Radiation Isotopes* **22,** 135-140 (1971).

Key words: Chemical dosimeter; disinfestation; dosimetry dyes; gamma rays; insect sterilization; shelf-life extension sprouting inhibition.

A simple chemical dosimeter is described for measuring gamma-ray doses useful for insect sterilization, seed-sprouting inhibition, and food shelf-life extension. The solutions, colorles before irradiation, assume a stable blue-violet color when irradiated to absorbed doses from 1-100 krad. The readout may be made either visually, colorimetrically, or spectrophotometrically. The optical density is linear with dose, and the response does not vary with dose rate.

12194. Meinke, W. W., **Standard reference materials for clinica measurements,** *Anal. Chem.* **43,** 28A-47A (May 1971).

Key words: Clinical chemistry; organic SRMs; spectrophotometry SRMs; standard reference materials.

The NBS Program in Standard Reference Materials for Clinical Chemistry measurements is described. Each of the SRMs issued in this area in the last five years is discussed. Future directions of the program are also mentioned.

12195. Mountain, R. D., **Comment on "rotational diffusion o spherical-top molecules in liquids,"** *J. Chem. Phys.* **54,** No. 7 3243 (Apr. 1, 1971).

Key words: Angular relaxation; $ClO_3F$; magnetic resonance; relaxation times; rotational diffusion; spherical-top molecules.

The formal equivalence of the J- and M-diffusion models for rotational diffusion of spherical-top molecules with two models worked out by Fixman and Ryder is noted.

12196. Nimeroff, I., **Color-match classification by variable parameters,** *Color. Engr.* **9,** No. 2, 13-17 (Mar.-Apr. 1971).

Key words: Color-match classification; color; isomerism metamerism.

There is an increasing need for standard procedures by which to assess the nature of achieved color matches. It has been found that there are seven different classes of color matches in which the colorimetric parameters, the spectral characteristics of observer, source and specimen, are variable. The different classes result from the seven possible combinations of these three variable parameters, taken one, two and three at a time. Those matches in which one parameter varies are called, in accord with the variable parameter, observer-variable, source-variable or specimen-variable matches; those in which two parameters vary are called source-specimen-variable, source-observer-variable or specimen-observer-variable matches; those in which all three vary are called source-specimen-observer-variable matches. Three of these classes of color match are currently designated metameric matches, one class is currently designated spectral match, while the other three classes have no current designation. The colorimetric effect of spectral differences in all of these classes of color matches may be characterized by an index of spectral difference. Such an index has been developed by Nimeroff and Yurow for matches that are currently designated metameric matches. A generalization of this index and its applications are presented.

12197. Robertson, B., Mitchell, W. C., **Equations of motion in nonequilibrium statistical mechanics. III. Open systems,** *J Math. Phys.* **12,** No. 3, 563-568 (Mar. 1971).

Key words: Equations of motion; nonequilibrium statistical mechanics; open systems; thermal transport.

A simple hypothesis on the effect of the interaction between a stem and its surroundings is used to generalize nonequilibrium tistical mechanics to apply to open systems. Thermal driving a system by its surroundings is defined in statistical mechanics analogy with the first law of thermodynamics, which scribes exchange of heat between the system and an external urce. The assumption that an isolated system is thermally ven is used to derive a Liouville equation with an additional m that is linear in the external source strength. The general- d Liouville equation is used to derive closed equations of mo- n that are the same as for an isolated system except for an ad- ional term, which is just the source strength. This formalism attractive because the source strength, which is assumed own, appears in the equation linearly just as in classical ther- dynamics or hydrodynamics. A microscopic expression for source strength is obtained by comparing the thermal driving malism with an exact dynamical analysis of the system in- acting with its surroundings.

98. Scott, W. W., Jr., **New coaxial RF-DC ammeter,** *IEEE Trans. Instr. Meas.* **IM-19,** No. 4, 318-323 (Nov. 1970).

Key words: Ammeter; coax; infrared; rf-dc; thermopile radiation.

A unique new type of RF ammeter is described. The ammeter mbines broad frequency coverage with broad current range d is designed for use in a 50-ohm coaxial transmission line.

The ammeter consists of an elliptic-cylinder silver reflector of rared energy with a cylindrical thick-film heater along one cus and a heat-sensing thermopile along the other focus. Ad- ntages over older ammeter designs include a shielded con- uction with inherent electrical isolation between the RF and circuits, a large dc output (approximately 1-100 mV) cor- sponding to a decade dynamic range (0.25-2.5 amperes), and requency range from dc to about 1 GHz.

This coaxial ammeter is believed to be the first to have very v standing-wave ratio (SWR) (1.03) in a 50-ohm transmission e. Ammeters of lower current range can be built, but at a nalty of increased SWR due to the larger heater resistance quired.

199. Bennett, L. H., Swartzendruber, L. J., Watson, R. E., **nteractions between small magnetic clusters in copper-rich Cu-Ni-Fe alloys,** *J. Appl. Phys.* **42,** No. 4, 1547-1548 (Mar. 15, 1971).

Key words: Alloys; clustering; copper; iron; local moments; Mössbauer effect; nickel.

Traces of iron in "nonmagnetic" Cu-rich Cu-Ni alloys oduce small magnetic clusters largely limited to an Fe site and Ni nearest neighbors, as observed in Mössbauer *source* periments. The present work concerns $^{57}$Fe Mössbauer sorber data for higher Fe concentrations (1/4-3%), in the 10- % Ni range, which demonstrates the existence of a magnetic- ment distribution centered about *two* distinct moment values. r the lower Fe concentrations, the smaller and more abundant these moments is identical to that observed in the source ex- riments and is associated with isolated small Fe-Ni clusters. e other moment is about twice as large and can be ascribed to upled pairs of these small clusters. These results are almost e of effects of metallurgical clustering. By appropriate heat atment, clustered samples are obtained with different moment tributions and higher Curie temperatures.

200. Brenner, F. C., Kondo, A., **Research for a uniform quality grading system for tires IV. Tread wear,** *Rubber Chem. Technol.* **44,** No. 1, 106-121 (Mar. 1971).

Key words: Automobile tires; grading; rating; test method; tread wear.

This research had as its objective the development of a test procedure for rating tires for tread wear. The results of preliminary experiments on roads of different composition and severity are discussed. The authors conclude that the course on which tires are to be rated should include several different pavements and a variety of maneuvers of unequal severity.

Two courses, one near Bryan, Texas and the other near San Antonio, Texas, were designed on this principle. Eighteen brands of tires including bias, radial and G-78 belted-bias tires were run on each course. The tires ranked in order of decreasing projected mileage on each course were highly correlated, although the mileages were not equal.

12201. Cezairliyan, A., **Short-time (msec) fluctuations of radiance temperature of graphite arc,** *Appl. Opt.* **10,** No. 5, 1178 (May 1971).

Key words: Graphite arc; high-speed measurements; high temperatures; pyrometry; radiance; standards.

Short-time fluctuations of the radiance temperature of graphite arcs are investigated with a millisecond resolution photoelectric pyrometer. Standard deviation of the fluctuations around their mean is found to be 4 K. The range of low and high temperatures for four experiments extended from 3799 to 3808 K, with an average of 3804 K on IPTS-68.

12202. Colwell, J. H., Mangum, B. W., Thornton, D. D., **Low-temperature magnetic susceptibility and heat capacity of $GdAsO_4$,** *Phys. Rev. B* **3,** No. 11, 3855-3861 (June 1, 1971).

Key words: Antiferromagnetism; exchange interactions; $GdAsO_4$; heat capacity; Heisenberg; Ising model; low temperature.

We report measurements obtained in zero applied magnetic field of the magnetic susceptibility and heat capacity of $GdAsO_4$ in the temperature range 0.3-20 K. This material is antiferromagnetic below 1.262 K. A detailed comparison of the experimental results is made with those reported for the isomorphic compound $GdVO_4$. The entropy and energy of $GdAsO_4$ above and below the Néel temperature are in close agreement with the predictions of the Heisenberg model suggesting that the interactions are not only isotropic, but predominantly with the nearest neighbors as well. The magnetic measurements, on the other hand, indicate considerable anisotropy such that $GdAsO_4$ does not undergo a spin-flop transition. Attempts to explain this discrepancy are given. We have derived a value of the exchange-interaction constant $J/k \approx -0.04$ K, assuming a coordination number of 4 where $J$ is defined by the Hamiltonian

$$\mathscr{H} = -2 \sum_{i<j} J_{ij}\vec{S}_i \cdot \vec{S}_j - g\mu_B \sum_i \vec{H}_0 \cdot \vec{S}_i.$$

12203. Day, G. W., **Linear and nonlinear optical properties of trigonal selenium,** *Appl. Phys. Letters* **18,** No. 8, 347-349 (Apr. 15, 1971).

Key words: Nonlinear optics; optical activity; optical properties; second harmonic generation; selenium.

Measurement of the second-order nonlinear optical susceptibility of trigonal selenium yielded $d_{11} = (9.7 \pm 2.5) \times 10^{-11}$ m/V. This value was obtained by cw SHG with a 106-$\mu$m $CO_2$ laser at a phase-matching angle of $5.5 \pm 0.3°$ to the optic axis. Factors affecting this measurement are discussed along with data on absorption, optical activity, and birefringence.

12204. Domalski, E. S., **Thermochemical properties of peroxyacetyl (PAN) and peroxybenzoyl nitrate (PBN),** *Environ. Sci. Tech. Communications* **5,** 443-444 (1971).

Key words: Bond additivity method; group additivity method; peroxyacetyl nitrate; peroxybenzoyl nitrate; thermochemical properties.

The thermochemical properties of peroxyacetyl nitrate (PAN) and peroxybenzoyl nitrate (PBN) were estimated by means of bond and group additivity schemes. Values are given at 298.15 K for the following properties: ΔHf°(g), Cp°(g), S°(g), Cp°(liq), ΔHvap, and ΔHsublim.; these values were used to calculate ΔSf°(g), ΔGf°(g), ΔCp°[(liq) − (g)], ΔHf°(liq), and ΔHf°(s), which are also cited.

**12205.** Evans, B. J., Swartzendruber, L. J., **Mössbauer study of local molecular fields, cation distributions and recoilless fractions in Sb-substituted lithium ferrite,** *J. Appl. Phys.* **42,** No. 4, 1628-1630 (Mar. 15, 1971).

Key words: Antimony; ferrites; hyperfine fields; iron; isomer shift; lithium; Mössbauer effect; recoilless fraction.

Previous studies of the *B*-site hyperfine field distribution in spinel ferrites utilizing a local-molecular-field model have demonstrated that *A*-site cation disorder has a pronounced effect on $H_{eff}(B)$ and virtually no influence on $H_{eff}(A)$. The influence of *B*-site disorder on these hyperfine fields is less well known. We have made $^{57}$Fe Mössbauer measurements on $Li_{1.2}Fe_{4.6}Sb_{0.2}O_8$ in which *B*-site disorder greatly predominates over *A*-site disorder. From the near natural linewidths for the *A* and *B*-site patterns we conclude that, in this material, *B*-site cation disorder is not nearly as effective as *A*-site cation disorder in producing inhomogeneities in $H_{eff}$ at either site. The area ratio of the two hyperfine field patterns, which are well resolved in an applied field, yields equal recoilless fractions for the two sites.

**12206.** Evenson, K. M., Radford, H. E., Moran, M. M., Jr., **CH free radicals detected by infrared laser magnetic resonance,** *Appl. Phys. Letters* **18,** No. 10, 426-429 (May 15, 1971).

Key words: CH; far infrared; free radical; laser; laser magnetic resonance.

CH radicals in an oxyacetylene flame have been detected by a magnetic resonance absorption method, with a water-vapor laser as the source oscillator at a frequency of 2.5 THz. The absorption spectrum is identified with the pure rotational transition, $J, K = (5/2,2) \rightarrow (7/2,3)$ at a wavelength of 118.6 μm.

**12207.** Evenson, K. M., Wells, J. S., Matarrese, L. M., Jennings, D. A., **Variable output-coupling far-infrared Michelson laser,** *J. Appl. Phys.* **42,** No. 3, 1233-1234 (Mar. 1, 1971).

Key words: HCN lasers; $H_2O$ lasers; infrared lasers; variable laser coupling.

A method for varying the coupling out of far-infrared gas lasers is described. It is based on the Michelson interferometer principle and has the advantage of increasing the power available from the laser by providing a smooth variation of the coupling.

**12208.** Godfrey, J. T., Vidal, C. R., Smith, E. W., Cooper, J., **Effect of time ordering in the unified theory,** *Phys. Rev. A* **3,** No. 5, 1543-1546 (May 1971).

Key words: Lyman-α; Stark-broadening; time-ordering; unified theory.

Using a previously developed unified theory of spectral line broadening, the effects of time ordering over the complete line profile are investigated. The results of calculations for the Lyman-α line are presented.

**12209.** Greenspan, M., **Comment on "response of ideal circuit elements to sinusoidal excitations,"** *Am. J. Phys.* **39,** No. 5, 586-587 (May 1971).

Key words: Transients.

In treating the response of a capacitor (say) to a suddenly impressed half-sinusoidal voltage, the original authors err and so not predict the spike-like transient. The algebra is corrected a oscillograms of the phenomenon are presented.

**12210.** Hudson, R. D., Kieffer, L. J., **Compilation of atomic traviolet photoabsorption cross sections for wavelengths betwe 3000 and 10 Å,** *Atomic Data* **2,** No. 3, 205-262 (May 1971).

Key words: Atoms; compilation; cross section dat photoabsorption; photoionization; photon.

In the past several years the Information Center of the Joi Institute for Laboratory Astrophysics, University of Colorad Boulder, Colorado, has been engaged in a program of critical evaluating the reliability of cross section data for many atom and molecular processes, and in producing comprehensive cor pilations of these data. This report, the result of a joint effo between the JILA Information Center and NASA Mann Spacecraft Center, is a compilation of ultraviolet photoabsor tion cross sections for atoms between 3000 and 10 Å. The cor pilation is limited to experimental measurements only and i cludes data for all atomic species that have been measured with this energy range. The literature was searched for data throu October 1969, but because the Information Center covers son material through abstracting journals, a few recent measur ments may not be included.

**12211.** Klose, J. Z., **Mean lives and absolute *f*= values in neutr iron,** *Astrophys. J.* **165,** No. 3, 637-642 (May 1, 1971).

Key words: Atomic lifetimes; atomic spectra; *f*-values; iro

Mean lives of three levels in Fe I have been determined using electronic excitation and a method of delayed coincidenc By the use of known relative *f*-values, absolute *f*-values we derived from the lifetime results for the transitions used in t lifetime measurements. The experimental results are sur marized in the following table.

| Level | λ (Å) | Mean Life (nsec) | *f*-Value |
|---|---|---|---|
| $z^5F_5^o$............ | 3719.9 | 61.5 ± 0.4 | 0.0410 ± 0.000 |
| $z^5F_4^o$............ | 3737.1 | 67.1 ± 1.1 | 0.034 |
| $y^5F_5^o$............ | 3734.9 | 11.5 ± 1.5 | 0.14 |

The error given with each quantity is the standard deviation determined from the dispersion of the individual measurement In addition, the experimental results are estimated to conta systematic errors of up to 2 percent. Both the lifetimes and the values are presented in comparison with experimental results other workers.

**12212.** Kurylo, M. J., Peterson, N. C., Braun, W., **Temperatu and pressure effects in the addition of H atoms to propylene,** *Chem. Phys.* **54,** No. 11, 4662-4666 (June 1, 1971).

Key words: Absolute rate constant; activation energ fluorescence; H atom; propylene; reaction kinetics.

The effect of He pressure on the rate of addition of hydroge atoms to propylene was measured at 298 °K. H-atom concentr tion was measured by the method of resonance fluorescence Lyman α radiation at 121.6 nm. The results are consistent wi the $1/p^{1/2}$ dependence of $k_{bi}$ recently observed in the H-aton ethylene system. The limiting high-pressure rate constant o tained in this work is $H + C_3H_6 \rightarrow C_3H_7$, $k_1 = 1.61 \pm 0.04 \times 10^{-}$ cm$^3$ molecule$^{-1}$·sec$^{-1}$. The temperature dependence of the atom addition was investigated at 50 torr total pressure over t temperature range 177-473 K. Analysis of the data below roo temperature gives the following Arrhenius parameters for add tion to the terminal olefinic position: $k_{bi}^{50} = (10.18 \pm 0.26)$ $10^{-12}$ exp$[-(1211 \pm 11)/1.987T]$ cm$^3$ molecule$^{-1}$·sec$^{-1}$. Devi tions from this dependence above 298 K can be assigned to no terminal addition, H-atom abstraction, and increased decompos tion of the excited propyl radicals.

13. Merris, R., Pierce, S., **A class of representations of the full near group,** *J. Algebra* **17,** No. 3, 346-351 (Mar. 1971).

Key words: Full linear group; irreducible character; symmetry class of tensors.

et $V$ be a finite dimensional complex inner product space and $\oplus^m V$ be the $m$th tensor space over $V$. Given a subgroup of $S_m$ and an irreducible character $\chi$ on $H$, we define a ain subspace $V_\chi^m(H)$ of $\oplus^m V$. If $T: V \rightarrow V$ is linear, let $\Pi \cdot T$: $V \rightarrow \oplus^m V$ be the $m$th Kronecker power of $T$. Then $V_\chi^m(H)$ variant under $\Pi \cdot T$ and let $K(T)$ be the restriction of $\Pi \cdot T$ to $(H)$. The map $T \rightarrow K(T)$ is a representation of the full ar group. We prove that if $\chi$ is not linear, then this representa- is reducible.

14. Motz, J. W., Dick, C. E., Lucas, A. C., Placious, R. C., parrow, J. H., **Production of high-intensity *K* x-ray beams,** *J. ppl. Phys.* **42,** No. 5, 2131-2133 (Apr. 1971).

Key words: Beryllium to gold; electron produced; high intensity; monochromatic yields; purity; x-ray beams.

x-ray beams are produced by direct electron excitation in llium, carbon, aluminum, titanium, copper, silver, and gold ets. With excitation currents of 10 milliamperes from dc elec- accelerators or 1000 amperes from single pulse machines, *K* x-ray yields are respectively 4 to 9 orders of magnitude er than the yields produced by the conventional fluorescence hod. The bremsstrahlung contamination in the *K* x-ray beam ninimized by observing the *K* x-rays at 180 degrees with ect to the incident electron beam, in order to exploit the fact the bremsstrahlung intensities become more peaked in the vard direction as the electron energy increases. Values are n for the maximum yields and purities of the *K* x-ray beams the corresponding electron energies, and a comparison is le with values obtained by other methods involving atomic or photon excitation of *K* x-rays.

15. Ogburn, F., Shives, T. R., Brady, C. H., **Calibration of a lar micrometer,** *J. Mater.* **6,** No. 1, 60-66 (Mar. 1971).

Key words: Metal coatings; micrometers; microscopes; optical equipment; optical microscopes; thickness; thickness gages.

he precision with which a filar micrometer can be calibrated nst a fixed interval of a stage micrometer was determined at nifications of about 175 and 1900 for a group of 15 in- duals familiar with microscopes. At each magnification the ad of measurements among the 15 operators was about 0.8 cent, whereas the spreads for the individual operators were stantially less.

16. Osinsky, V. I., Winogradoff, N. N., **Excitation and tem- erature dependence of band-edge photoluminescence in gallium senide,** *Phys. Rev. B* **3,** No. 10, 3341-3346 (May 15, 1971).

Key words: Band-to-band recombination; concentration dependence; excitation dependence; gallium arsenide; impurity effects; photoluminescence; temperature dependence.

hotoluminescent spectra of *n*-type GaAs were studied as a ction of the excitation intensity, temperature, and doping l. The spectra consisted of two major bands representing ative band-to-band recombination and radiative transitions ugh impurity centers, respectively. The intensity of the peak he former went through a minimum and a maximum as the perature was increased from 175 to 500 K. The temperature esponding to the above maximum increased as the excitation nsity was decreased or the doping level increased. These ilts suggest that the temperature dependence of the peak in- ity in band-to-band transitions is primarily due to the thermal ribution of the carriers over the available energy states. The k intensity would therefore normally be expected to decrease monotonically with an increase in temperature, while the above maxima and minima represent perturbations imposed by the presence of temperature-dependent transitions through radiative or nonradiative impurity recombination centers.

**12217.** Page, C. H., **Comments on "nonlinear resistors that generate subharmonics,"** *Proc. IEEE Letters* **59,** No. 2, 301 (Feb. 1971).

Key words: Nonlinear; subharmonics.

The analysis reported by Erdey is shown to be incorrect.

**12218.** Parks, E. J., **Thermal analysis of modified cellulose,** *Tappi* **54,** No. 4, 537-544 (Apr. 1971).

Key words: Alum; aluminum; apparent activation energy; calcium; cellulose; crosslinking; differential thermal analysis; ion exchange; organic acid; oxycellulose; stability; sulfuric acid; thermogravimetric analysis.

Differential thermal analysis (DTA) and thermogravimetric analysis (TGA) techniques have been applied to characterize thermal properties of cellulose and modifications of the type that might reasonably occur in papermaking pulps. Periodate, periodate-chlorite, chromate, chromate-chlorite, hypochlorous acid, and hypochlorous acid – chlorite oxycelluloses all were examined, as were their calcium and aluminum exchange products. In addition, the effects on thermal properties of cellulose exerted by alum, sulfuric acid, and two organic acids that cause color reversion all were investigated. The peak temperature of a massive decomposition endotherm ($T_3$), the apparent activation energy of this endothermic reaction ($E^*$), and the integral procedural decomposition temperatures (IPDT) seem to be the best suited of the thermal variables to denote stability. Oxidation usually destabilizes cellulose slightly. An exception is exhaustive oxidation of periodate oxycellulose with chlorous acid. This causes $T_3$ and $E^*$ to increase, although the IPDT drops. Exchange with calcium greatly stabilizes cellulose containing carboxyl groups, whereas aluminum destabilizes the same material. Each effect is concentration dependent. The importance of pH in these relationships is not known. Sulfuric acid has a destabilizing effect qualitatively different from that of aluminum covering carboxyls and that of alum added to cellulose. Destabilization by alum is probably a result of contributions both by sulfate and by aluminum. Organic acids have little effect. Each treatment has resulted in a higher percentage of residue than that of cellulose, which may indicate the promotion of crosslinking by oxygen, metals, and acid.

**12219.** Smith, C. E., Milligan, D. E., Jacox, M. E., **Matrix-isolation study of the vacuum-ultraviolet photolysis of chlorofluoromethane. The infrared and ultraviolet spectra of the free radical ClCF,** *J. Chem. Phys.* **54,** No. 7, 2780-2793 (Apr. 1, 1971).

Key words: ClCF; chlorofluoromethane; chlorofluoromethane-$d_2$; fluorescence spectrum; free radical; infrared spectrum; matrix isolation; photolysis; ultraviolet spectrum.

The vacuum-ultraviolet photolysis of $CH_2ClF$ and of $CD_2ClF$ isolated in an argon matrix at 14 K leads to the appearance of prominent absorptions at 742 and at 1146 $cm^{-1}$ which have been assigned to the two stretching fundamentals of ClCF. A weak absorption band system between 3900 and 3400 Å, with a $376 \pm 10$ $cm^{-1}$ average band spacing, may be tentatively attributed to ClCF, as may be an emission band system which appears between 4000 and 4900 Å when the sample is excited by 3650 Å radiation. The $379 \pm 10$ $cm^{-1}$ average band spacing associated with this emission band system has been tentatively attributed to the bending mode of ground-state ClCF, permitting a normal coordinate analysis for this molecule. The bending and the C-Cl stretching modes are appreciably mixed. Several other groups of absorptions also have been observed in these experiments, but the species responsible for them have not been definitively identified.

**12220.** Swartzendruber, L. J., **Localized moments on Fe impurities in Nb-Mo alloys: Mössbauer-effect absorber study,** *J. Appl. Phys.* **42,** No. 4 (Mar. 15, 1971).

Key words: Alloys; magnetism; Mo; Mössbauer Effect; Nb.

Mössbauer-effect spectra for absorbers of Mo and $Mo_{0.8}Nb_{0.2}$ alloys containing $^{57}Fe$ impurities have been obtained in an external field as a function of temperature. The spectra for the Mo-Fe alloys are in close agreement with the results of Kitchens *et al.* for ($^{57}Co$) Mo sources. The $Mo_{0.8}Nb_{0.2}$ spectra show directly the presence of two distinct moment values for the Fe impurities, one with a moment of $1.9\mu_B$ and one with a moment of less than $0.6\mu_B$, with the two moments present in roughly equal proportions. This result gives support for a discontinuous formation model of the type proposed by Jaccarino and Walker. The saturation hyperfine field of 115 kG for Fe in Mo is apparently reduced to 90 kG for moment bearing Fe in $Mo_{0.8}Nb_{0.2}$. There appears to be no quenching of the Fe moment for Fe-Fe pairs such as that observed for Co-Co pairs in Mo-Nb alloys.

**12221.** Taylor, B. N., **Report on the International Conference on Precision Measurement and Fundamental Constants,** held at the National Bureau of Standards, Gaithersburg, Md., August 3-7, 1970, *Metrologia* **7,** No. 1, 39-42 (Jan. 1971).

Key words: Fundamental constants; least squares adjustments; precision measurements.

This is a report on the International Conference on Precision Measurement and Fundamental Constants held at the National Bureau of Standards, Gaithersburg, Maryland, August 3–7, 1970. It includes a brief discussion of the purpose and significance of the Conference as well as some of the organizational details as they pertain to the Conference sponsors, topics covered, publication of the Conference Proceedings, etc. The bulk of the report is devoted to a summary by topic of the Conference highlights and conclusions.

**12222.** Vidal, C. R., Cooper, J., Smith, E. W., **Unified theory calculations of Stark broadened hydrogen lines including lower state interactions, (Short Version),** *J. Quant. Spectry. Radiative Transfer* **11,** 263-281 (1970).

Key words: Hydrogen lines; line wings; Stark broadening; theory; unified classical path.

Recently published calculations of hydrogen Stark broadening on the basis of the unified classical path theory have been extended to include lower state interactions in the final line profile. A detailed comparison with experiments in the density range $10^{13}-10^{17}$ cm$^{-3}$ is given.

**12223.** Waxler, R. M., **Laser glass composition and the possibility of eliminating electrostrictive effects,** *IEEE, J. Quantum Electron.* **QE-7,** No. 4, 166-167 (Apr. 1971).

Key words: Electrostrictive; glass; lasers; photoelasticity.

Many authors have stated that electrostrictive self-trapping of the light beam initiates laser damage in solid transparent dielectrics. By systematically varying composition, it may be possible to find a glass in which electrostrictive effects are eliminated.

**12224.** Weiss, M. J., Kuyatt, C. E., Mielczarek, S., **Inelastic electron scattering from formaldehyde,** *J. Chem. Phys.* **54,** No. 10, 4147-4150 (May 15, 1971).

Key words: Formaldehyde; inelastic electron scattering; ultraviolet absorption.

The electron scattering spectrum of $H_2CO$ has been determined in the energy loss range between 0 and 16.0 eV. Three Rydberg series in the region 7-11 eV can be identified with the *p*, and *d* series reported in the literature by ultraviolet absorptio studies. Oscillator strengths are determined for some of the Ry berg states and comparison is made with recent ultraviolet a sorption work employing photoelectric methods of detection. serious disagreement exists between the *f* values obtained by th two methods for the $3sa_1$ Rydberg. Another Rydberg serie probably converging to the third ionization potential of $H_2CO$, observed in the electron scattering spectrum in the region 12. 14.0-eV energy loss. Erratic behavior of the quantum defects the first Rydberg series as well as failure to detect the $\pi \rightarrow \pi$ transition in $H_2CO$ is discussed in the light of recent theories i volving valence states which can seriously perturb members a Rydberg series.

**12225.** Weiss, M. J., Mielczarek, S. R., Kuyatt, C. E., **Inelast electron scattering from nitrous oxide between 5.0 and 20.0 e energy loss,** *J. Chem. Phys.* **54,** No. 3, 1412-1414 (Feb. 1971).

Key words: Far uv absorption; inelastic electron scatterin nitrous oxide; oscillator strengths.

The electron impact spectrum of $N_2O$ is reported between 5. and 20.0 eV energy loss. A number of Rydberg series, conver ing to the second and fourth ionization potentials of $N_2O$, are o served in the spectra above the first i.p. Relative *f*-values, dete mined for some of the transitions in the 13-17 eV region, are i excellent agreement with those derived from recent vacuum u traviolet absorption measurements.

**12226.** Wiese, W. L., Kelleher, D. E., **On the cause of the redshif in white-dwarf spectra,** *Astrophys. J.* **166,** L59-L63 (June 1971).

Key words: Balmer lines $H_\alpha$, $H_\beta$, and $H_\gamma$; gravitational re shift; Stark broadening; Stark-induced red shift; white dwa spectra.

Detailed laboratory measurements of the profiles of som Stark-broadened Balmer lines reveal systematic slight shifts these lines to the red, which are linear functions of the electro density. It appears that the Stark-induced redshift accounts f a portion of the observed redshift in white dwarfs which ha previously been attributed entirely to gravitation.

**12227.** Yokel, F. Y., Dikkers, R. D., **Strength of load beari masonry walls,** *J. Struct. Div. Am. Soc. Civil Engineers* **97,** N ST5, 1593-1609 (May 1971).

Key words: Bricks; buckling; deflection; loads (forces masonry; moments; slenderness ratio; stability; structur engineering; walls.

A theory is presented, for the rational analysis of mason walls under eccentric vertical compressive load, or under a co bination of vertical compressive and transverse load. The theo is based on established concepts, which have been modified account for the properties of masonry. Similar methods of r tional analysis have been adopted for the design of steel colum and are in the process of being adopted for reinforced concre columns. An investigation of the results of 192 tests of full-sca walls of various types of masonry construction established t feasibility of applying this theory to closely predict the streng of these walls. The analysis accounts for variables not present considered in the design of masonry structures. The correlati between test results and theory is illustrated by several typic examples.

**12228.** Barnes, J. A., Chi, A. R., Cutler, L. S., Healey, D. J Leeson, D. B., McGunigal, T. E., Mullen, J. A. Jr., Smith, L., Sydnor, R. L., Vessot, R. F. C., Winkler, G. M. R **Characterization of frequency stability,** *IEEE Trans. Inst Meas.* **IM-20,** No. 2, 105-120 (May 1971).

Key words: Allan variance; frequency; frequency stability; sample variance; spectral density; variance.

Consider a signal generator whose instantaneous output voltage $V(t)$ may be written as

$$V(t)=[V_0+\epsilon(t)]\sin[2\pi\nu_0 t+\phi(t)]$$

where $V_0$ and $\nu_0$ are the nominal amplitude and frequency, respectively, of the output. Provided that $\epsilon(t)$ and $\phi(t)=(d\phi)/(dt)$ are sufficiently small for all time $t$, one may define the fractional instantaneous frequency deviation from nominal by the relation

$$y(t)\equiv\frac{\dot{\varphi}(t)}{2\pi\nu_0}.$$

A proposed definition for the measure of frequency stability is the spectral density $S_y(f)$ of the function $y(t)$ where the spectrum is considered to be one sided on a per hertz basis.

An alternative definition for the measure of stability is the infinite time average of the sample variance of two adjacent averages of $y(t)$; that is, if

$$\bar{y}_k=\frac{1}{\tau}\int_{tk}^{tk+\tau}y(t)\ dt$$

where $\tau$ is the averaging period, $t_{k+1}=t_k+T, k=0, 1, 2 \ldots, t_0$ is arbitrary, and $T$ is the time interval between the beginnings of two successive measurements of average frequency; then the second measure of stability is

$$\sigma_y^2(\tau)\equiv\left\langle\frac{(\bar{y}_{k+1}-\bar{y}_k)^2}{2}\right\rangle$$

where $\langle\ \rangle$ denotes infinite time average and where $T=\tau$.

In practice, data records are of finite length and the infinite time averages implied in the definitions are normally not available; thus estimates for the two measures must be used. Estimates of $S_y(f)$ would be obtained from suitable averages either in the time domain or the frequency domain. An obvious estimate for $\sigma_y{}^2(\tau)$ is

$$\sigma_y^2(\tau)\approx\frac{1}{m}\sum_{k=1}^{m}\frac{(\bar{y}_{k+1}-\bar{y}_k)^2}{2}.$$

Parameters of the measuring system and estimating procedure are of critical importance in the specification of frequency stability. In practice, one should experimentally establish confidence limits for an estimate of frequency stability by repeated trials.

**12229.** Beatty, R. W., Fentress, G. H., **A simple tuning circuit for waveguide and transmission line systems,** *IEEE Trans. Microwave Theory Tech.* **MTT-19,** No. 3, 337-338 (Mar. 1971).

Key words: Impedance measurement; microwaves; mm-waves; reflection coefficient measurement; tuners; tuning circuit.

A simple tuning circuit for source or load matching is described that makes possible smooth and sensitive adjustments with no "holes" in frequency coverage over a complete waveguide band. Energy is coupled out of the mainline, the phase and magnitude adjusted with phase shifter and attenuator and fed back into the mainline to cancel the reflected signal. A simple analysis of the circuit is presented, and a graph given for estimating the maximum voltage standing-wave (VSWR) that can be "tuned out." Application to measurement of reflection coefficient or to impedance is proposed.

**12230.** Brauer, G. M., Huget, E. F., **Heats of immersion of the components of tooth structure,** *J. Dental Res.* **50,** No. 3, 776 (May-June 1971).

Key words: Heats of immersion; heats of immersion of tooth structure; reactivity of anorganic whole tooth; reactivity of dentin.

The apparent heat of immersion of dentin and anorganic whole tooth in aqueous solutions of phenol, urea, hydrogen peroxide, potassium permanganate and silver nitrate were determined at 30 °C. Phenol and urea solutions react either endothermically with the dentinal protein or are bound preferentially to charged sites at the expense of water. Potassium permanganate and silver nitrate react exothermically with dentin surfaces. For anorganic whole tooth, the apparent heat of immersion in water did not differ from those values obtained on exposure to the aqueous solutions considered in this study.

**12231.** Cezairliyan, A., Morse, M. S., Beckett, C. W., **Measurement of melting point and electrical resistivity (above 2,840 K) of molybdenum by a pulse heating method,** (Proc. Conf. Thermophysical Properties, Manchester, England, April 7-10, 1970), *Rev. Int. Hautes Tempér. et Réfract.,* **t. 7,** 382-388 (1970).

Key words: Electrical resistivity; high-speed methods; high temperature; melting point; metals; molybdenum; premelting; thermodynamics.

A pulse heating method is used to measure the melting point and electrical resistivity of molybdenum in the temperature range 2,840 to 2,889 K. The specimen is heated from room temperature to its melting point in approximately 0.8 s. Specimen temperature is measured with a high-speed photoelectric pyrometer. During the heating period, voltage, current, and temperature are recorded with a high-speed digital data acquisition system which has a full-scale signal resolution of approximately one part in 8,000, and a time resolution of 0.4 ms. Results are compared with those in the literature. Estimated inaccuracy in the melting point (2,889 K) and in electrical resistivity is 10 K and 0.5 percent, respectively.

**12232.** Chandler, H. H., Bowen, R. L., Paffenbarger, G. C., **Development of a radiopaque denture base material,** *J. Biomed. Mater. Res.* **5,** 253-265 (Mar. 1971).

Key words: Bonding; composites; denture base materials; diagnosis; light translucency; physical properties; radiopacity.

Radiopaque glass-resin composites were made for evaluation as denture base materials. The addition of silane-treated, radiopaque, powdered glass to clear poly(methyl methacrylate) resulted in composites that had greater optical translucency than commercially available pink denture base resins. These formulations could be pigmented and opacified to produce materials that simulated oral soft tissues in color and translucency.

Other composites were made using various monomer, polymer and glass combinations. Those made from mixes of BIS – GMA, methyl methacrylate, poly(methyl methacrylate), and radiopaque glass had excellent translucency but handling characteristics were less than ideal.

Removal of very small glass particles (less than a few μm) appeared to improve optical translucency.

A radiographic survey of 12 specimens that contained from 29 to 57% of the radiopaque glass, indicated that all had sufficient radiopacity to aid in localization of swallowed or aspirated dentures made from such materials.

Finishing procedures on composite specimens were more difficult and time-consuming and did not produce surfaces as smooth as those obtained on poly(methyl methacrylate). The finished surfaces felt smooth to the tongue but might stain more easily in the mouth.

**12233.** Chandler, H. H., Bowen, R. L., Paffenbarger, G. C., **The need for radiopaque denture base materials: A review of the literature,** *J. Biomed. Mater. Res.* **5,** 245-252 (Mar. 1971).

Key words: Denture foreign bodies: type, cause, prevention; prosthetic materials: radiopaquing agents; radiopaque denture base materials.

The need for esthetic and functionally acceptable radiopaque denture base materials is reflected by numerous reports of patients who ingested or aspirated portions of dentures and reports of difficulties encountered in the removal of these dentures because they could not be located radiographically.

The type of denture most commonly ingested or aspirated is a maxillary partial consisting of a palatal piece to which is attached one or more anterior teeth. It may or may not have clasps. Ingestion or aspiration of the foreign body commonly occurs when either broken or ill-fitting dentures are being worn. Few cases have been reported where patients swallowed portions of complete dentures.

Previous attempts at providing radiopacity have included addition of heavy metal salts or radiopaque inserts to denture base resins. None of these attempts has been entirely successful.

Elimination of dentures as foreign bodies requires a greater effort toward preventive measures by the dentist and the patient. When dentures are swallowed or inhaled, the dentist should immediately seek medical assistance for the patient. The common symptomless period following ingestion or aspiration should not lead the dentist to believe that there will not be serious subsequent complications.

**12234.** Davis, D. D., **Frequency standard hides in every color TV set,** *Electronics,* pp. 96-98 (May 10, 1971).

Key words: Dissemination; frequency; frequency synthesizers; linear phase comparators; television color subcarrier; time.

In color television broadcasting, a color "subcarrier" is transmitted at about 3.58 MHz. It is used as a reference signal in the color television receiver to demodulate the chrominance sidebands. The major U.S. networks use rubidium frequency standards to generate the color subcarrier. This paper describes a method for making use of the color subcarrier as a frequency standard. The output of a 1 MHz local standard synthesized to 3.58 MHz is used as one input to a phase comparator and is adjusted to agree with the received subcarrier signal. Results of actual network measurements are given.

**12235.** Dove, R. B., Marshak, H., **Shaft seal for mechanical pump,** *J. Vacuum Sci. Technol.* **8,** No. 3, 519 (May-June 1971).

Key words: Closed pumping system; $He^3$-$He^4$ dilution refrigerator; mass spectrometer leak detector; mechanical pump; shaft seal.

A simple vacuum shaft seal for a mechanical pump is described.

**12236.** Engen, G. F., **Power equations: A new concept in the description and evaluation of microwave systems,** *IEEE Trans. Instr. Meas.* **IM-20,** No. 1, 49-57 (Feb. 1971).

Key words: Attenuation; impedance; microwave power; mismatch error.

In the existing art, the description and evaluation of microwave systems is usually in terms of the complex wave amplitudes in the (assumed) uniform waveguide by which the components are interconnected. The interrelationships among these amplitudes are given by the scattering equations or indirectly by impedance parameters.

This paper introduces an alternative description, based on *power equations*, where the basic parameter is the net power in the waveguide of interest. Compared with the circuit description, there is a substantial suppression of detail and the remaining parameters are placed in better perspective. In particular, the technique provides a simplified method of describing and evaluating mismatch corrections, in which the precision connector and uniform waveguide requirements have been eliminated.

**12237.** Franklin, A. D., Marzullo, S., **9.—EPR study of point-defect equilibria in $CaF_2$ containing $GdF_3$,** *Proc. No. 19. British Ceramic Society, "Role of Point Defects in Solid State Mass," Mass Transport Proc. Non-Metallic Solids, London, England, Dec. 17-18, 1969,* pp. 135-150 (British Ceramic Society, Stoke-on-Trent, England, 1971).

Key words: Calcium fluoride; defect equilibria; electron paramagnetic resonance; point defects.

Room-temperature measurements have been made of E.P.R. spectra at 9.5 GHz arising from tetragonal and cubic centres in $CaF_2$ containing between 0.01 and 0.45 mol % $GdF_3$. The crystals were annealed in a 30:1 He-HF atmosphere at temperatures ranging from 500 to 1100 °C and then rapidly cooled to room temperature. The annealing times were long enough to achieve steady-state E.P.R. data, and the cooling was rapid enough so that a considerably slower cooling gave essentially the same result. The ratio of the concentration of tetragonal centres to that of cubic centres diminished as the total $GdF_3$ concentration increased. At a given $GdF_3$ concentration, this ratio passed over a maximum as the annealing temperature increased. This behaviour is inconsistent with a model including only anion interstitials and vacancies. If cation vacancies are included, and if they are assumed to be immobile while the anions can move during cooling, the qualitative features of the data can be produced by the model. Direct experimental confirmation of these assumptions and of the presence of cation vacancies has not been obtained.

**12238.** Haller, W., Simmons, J. H., Napolitano, A., **Viscosity-drift technique for determination of critical liquid-liquid immiscibility temperature of glasses,** *J. Am. Ceram. Soc.* **54,** No. 6, 299-302 (1971).

Key words: Glass; immiscibility; phase-separation; viscosity; viscosity-drift.

The time dependence of the low-temperature viscosity was used to determine the occurrence of phase separation in glass systems and to measure the critical immiscibility temperature. The technique is fast and easily performed and can be applied to materials with very low immiscibility gaps. Immiscibility temperatures for several technically important glass compositions are given.

**12239.** Haller, W., Winogradoff, N. N., **Explosive vapor release as cause of laser-induced surface damage of glass,** *J. Am. Ceram. Soc.* **54,** No. 6, 314-315 (1971).

Key words: Glass; laser damage; surface.

Gigawatt laser pulse produced surface lesions on an alkali lead silicate glass were investigated. Macroscopically, the lesions resemble thermal spall fractures. Electromicroscopic pictures and electron microprobe profiles, however, reveal that the damage is caused by the explosive release of alkali oxide vapors from the shock molten glass surface.

**12240.** Hoeve, C. A. J., **On the general theory of polymer absorption at a surface,** *J. Polymer Sci. Symposia,* **Part C,** No. 30, 361-367 (1970).

Key words: Configurations; excluded volume effect; loops; polymer adsorption; surface layer; trains; Θ-point.

Previous theoretical work dealt with polymer adsorption in which the adsorbed segments (trains) interact in the surface layer only. In this work the treatment is extended to include also interaction between the loops dangling in solution. Fortunately, the excluded volume effects for adsorbed polymer chains are found to be small. Therefore an approximate treatment is possible that leads to equations that govern polymer chains under a wide variety of conditions.

**12241.** Hummer, D. G., Rybicki, G. B., **Radiative transfer in**

**spherically symmetric systems. The conservative grey case,** *Monthly Notices Roy. Astron. Soc.* **152,** No. 1, 1-19 (1971).

Key words: Eddington factor; model atmospheres; spherical radiative transfer.

A practical computational method is presented for the solution of radiative transfer problems in spherically symmetric systems. This procedure involves iteration on the "Eddington factor" $f=K/J$ and is designed to handle the outward peaking of the radiation field in extended spherical systems. Extensive numerical results are obtained and discussed for systems in which $\kappa\rho=r^{-n}$, $0<r\leq R$, for $n=3/2$, 2 and 3.

12242. Jacox, M. E., Milligan, D. E., **Matrix-isolation study of the vacuum-ultraviolet photolysis of chloroform. Infrared spectra of the $CCl_3^-$, $HCCl_2^-$, and $HCCl_2^-$ molecular ions,** *J. Chem. Phys.* **54,** No. 9, 3935-3950 (May 1, 1971).

Key words: $CCl_3^-$; chloroform; electron attachment; $HCCl_2^-$; $HCCl_2^-$; $HCCl_3^-$; infrared spectrum; matrix isolation; photoionization; vacuum ultraviolet photolysis.

Photolysis of samples of $HCCl_3$ isolated in an argon matrix at 14 K using 1216-Å radiation leads not only to the isolation of a high yield of $CCl_3$, but also to the photoionization of $CCl_3$, resulting in the stabilization of a sufficient concentration of $CCl_3^-$ for direct infrared spectroscopic identification. The assignment of still other infrared absorptions which appear in this system to negatively charged species has been confirmed by experiments in which a small concentration of an alkali metal atom is also present in the matrix, providing a photoelectron source. When matrix-isolated $HCCl_3$ is subjected to photolysis by 1067-Å argon resonance radiation, very little $CCl_3$ is produced, but $HCCl_2$, $HCCl_2^+$, and the same negatively charged species are stabilized in significant concentration. Studies of chloroform samples enriched in carbon-13 and of $DCCl_3$ samples have provided support for these identifications and have yielded data necessary for obtaining several of the force constants of these species. The infrared spectrum of the negatively charged species can most satisfactorily be explained by postulating that dissociative electron attachment to chloroform occurs, resulting in the stabilization of $HCCl_2^-$ in the matrix environment.

12243. Karp, S. S., Matteson, T. T., **The integrated team concept of simulation model development,** *Proc. 1971 Summer Computer Simulation Conf., Boston, Mass., July 19-21, 1971,* pp. 1301-1307 (July 1971).

Key words: Coast Guard; development; interdisciplinary team; management science; model building; organization; search and rescue; simulation; team development.

The ultimate measure of a simulation model's effectiveness is the extent to which it provides meaningful insight towards the solutions of management's problem. Participation in model development by analysts from the management organization has proven to be highly beneficial in producing an effective simulation. An integrated team concept is a successful means of achieving management participation in the model development. This concept involves varying degrees of client (management) participation throughout the entire period of simulation development, with maximum interaction occurring during the conceptualization/modeling and validation/exercise phases. The participants in this integrated development team are personnel from both the client and consultant organizations. The integrated client-consultant approach to model development was used by the National Bureau of Standards and the U.S. Coast Guard to successfully develop an effective simulation model of the Coast Guard Search and Rescue system.

12244. Klein, M., **Practical treatment of coupled gas equilibrium,** Chapter 7 in *Physical Chemistry,* **Vol. 1.** Thermodynamics, 489-544 (Academic Press, Inc., New York, N.Y., 1971).

Key words: Chemical equilibrium; chemical reactions; equilibrium; gases; mass action; non-linear search.

Equations are derived for the species concentrations in coupled chemical equilibria in the gas phase. This is done both for the method of the direct minimization of the free energy as well as for the equilibrium constant method. The relations developed are such as to allow for the inclusion of detailed real gas effects. The emphasis is on practical problems encountered in the actual calculation of the species and the thermodynamic properties. Expressions are derived for the direct calculation of the concentration derivatives with respect to temperature and density required for the calculation of the derived properties (i.e., specific heats, sound velocities, etc.) Considerable space is given to discussions of the non-linear numerical methods available for the solution of the non-linear equations for the species concentrations.

12245. Kushner, L. M., **Welcoming address,** *Proc. Footwear Manufacturing Executives Conf. held at the King's Grant Motor Inn, Danvers, Mass., Dec. 1, 1970,* pp. 7-11 (Sponsored by the COMTECH, American Footwear Manufacturers Association, and the New England Footwear Association, December 1970).

Key words: New technology; performance standards; product standards; standardization.

12246. Linsky, J. L., **Can the ion $H_3^+$ account for missing opacity in the solar ultraviolet?** *Solar Physics* **11,** No. 2, 198-207 (Feb. 1970).

Key words: $H_3^+$; opacity, continuous; solar photosphere; solar ultraviolet spectrum.

Limb darkening and specific intensity data imply more continuous opacity in the solar photosphere between 2000 A and 3500 Å than has been predicted theoretically. The temperature dependence and wavelength dependence of this missing opacity are in qualitative agreement with those deduced for the ion $H_3^+$, but it is unlikely that $H_3^+$ is sufficiently abundant to account for this opacity.

12247. Linsky, J. L., **On the relative residual intensities of the calcium H and K lines,** *Solid Physics* **11,** No. 3, 355-373 (Mar. 1970).

Key words: Non-LTE radiative transfer; resonance lines, Ca II; solar chromosphere, physical properties; solar chromosphere, structure; spectral line formation; spectroscopic diagnostics.

We have observed the solar Ca II H and K lines to obtain well-calibrated ratios of their core residual intensities. From three independent calibrations, one using a standard lamp, we conclude that the residual intensity ratio $r(K_3)/r(H_3)$ is $1.048\pm0.03$ in the quiet chromosphere and $1.20\pm0.03$ in a plage region. These ratios correspond closely to those observed in stars with quiet and active chromospheres, respectively. For a chromospheric model suggested by the calcium lines and a four-level Ca II ion, we compute H and K line profiles varying the direct collisional coupling and indirect radiative and collisional coupling via the 3 $^2D$ level. We conclude that enhanced chromospheric activity in the sun and late-type stars results more from a steepening of the chromospheric thermal gradient than from a change in density.

12248. Linsky, J. L., Teske, R. G., Wilkinson, C. W., **Observations of the infrared triplet of singly ionized calcium,** *Solar Physics* **11,** No. 3, 374-383 (Mar. 1970).

Key words: Non-LTE radiative transfer; resonance lines, Ca II; solar chromosphere, physical properties; spectral line formation; spectroscopic diagnostics.

Observations are presented of the Ca II infrared triplet (8498 Å, 8542 Å, and 8662 Å) at three positions on the solar disk to make possible direct analyses of the lines and comparisons with theoretical computations. The source functions for the two strongest lines (8542 Å and 8662 Å) are equal at those heights corresponding to the wings of the lines ($|\Delta\lambda| > 0.4$ Å) but not to those of the cores. We suggest that the apparent source function inequality in the cores is due to limb darkening caused by inhomogeneities in the chromosphere.

**12249.** Loebenstein, W. V., **The exchange of $^{45}$Ca and $^{32}$P with hydroxyapatite as interpreted by adsorption from solution,** *J. Colloid Interface Sci.* **36,** No. 2, 234-246 (June 1971).

Key words: Adsorption from solution; calcium phosphate; composite adsorption; isotopic exchange; kinetics of adsorption; mechanism of adsorption; solution adsorption.

A theory has been developed based on Langmuir kinetics for the adsorption of a component from solution by a reversible and an irreversible process, simultaneously. The theory has been applied to the removal of traces of $^{45}$Ca and of $^{32}$P from saturated solutions of their nonradioactive counterparts as calcium and phosphate ions by isotopic exchange at the surface of hydroxyapatite. In testing the theory, a computer-programmed nonlinear least-square fit was used to evaluate the physically significant characteristic parameters. This has been accomplished for a number of similar experiments, each of which had a different pH, slurry density, and tagged ion concentration. The results of this study confirm that the approach is feasible and that the assumed model is reasonable. Not only does the theory fit the data, but the magnitude of the derived quantities is internally consistent. No change in calcium to phosphate ratio of the respective surface sites was evident from one experiment to another.

**12250.** Means, C. R., Rupp, N. W., Paffenbarger, G. C., **Clinical evaluation of two types of resilient liners on dentures,** *J. Am. Dental Assoc.* **82,** 1375-1380 (June 1971).

Key words: Denture base; protective; resilient liners; temporary expedients; tissue bearing.

This is a report of observations made on the clinical experiences of 14 patients wearing 23 dentures. The dentures were lined with one of these two resilient liners, Coe Super Soft or Silastic 616. These observations yielded results on which the following conclusions or recommendations are based. 1. Both materials are safe to use against oral tissues. 2. Since deterioration and loss of resilience reduce their effectiveness in a relatively short time, dentures lined with these materials should be observed every 3 months. 3. The border junction between the resilient liner and the denture base should be a butt joint. A thin tapered junction is unsatisfactory. The finish line should be well away from the borders of the flanges. 4. These resilient liners should be considered as temporary expedients to be used only in selected cases which require a protective resilient surface on the tissue bearing side of the denture base. 5. A denture that carries a resilient liner should be sufficiently thick in cross section to resist fracture. Thinning of a denture to make room for a resilient liner may lead to fracture in service.

**12251.** Myklebust, R. L., Heinrich, K. F. J., **Rapid quantitative electron probe microanalysis with a nondiffractive detector system,** *Am. Soc. Testing Mater. Spec. Tech. Publ.* **485,** pp. 232-242 (1971).

Key words: Electron diffraction; electron probes; evaluation; gas flow; lithium; microanalysis; multichannel analyzer; proportional counters; quantitative analysis; solid state counters; tests; x-ray spectra; x-ray spectrometers.

Nondiffractive detector systems on electron probe microanalyzers have decreased the time required for a qualitative analysis from 30 or 40 min to 1 or 2 min. The nondiffractive technique may be extended to the quantitative determination of an element by comparing either the peak height or the area beneath the peak of the signal from the specimen with that from the pure chemical element or a standard of known composition run under identical conditions. Results are given for quantitative analyses of several materials with a lithium-drifted silicon detector, used for x-ray lines above 1 keV, and a gas flow proportional detector, for x-ray lines from 0.16 to 1.5 keV. Quantitative analyses can be accomplished only when the experimental conditions are carefully selected and maintained throughout the measurement. They are then sufficiently precise to warrant the use of a "matrix" correction procedure to obtain concentrations. An analog curve analyzer is useful for resolving overlapping peaks and for integrating the areas beneath the peaks.

**12252.** Nuttall, R. L., Laufer, A. H., Kilday, M. V., **The enthalpy of formation of ketene,** *J. Chem. Thermodynamics,* No. 3, 167-174 (1971).

Key words: Bond energy; enthalpy of formation; heat of formation; ketene; methylene.

The enthalpy of reaction of ketene gas with aqueous sodium hydroxide was measured in an adiabatic solution calorimeter. For the reaction

$$\mathrm{CH_2CO(g) + NaOH(aq,500H_2O) = CH_3CO_2Na(aq,NaOH\ soln),}$$

$\Delta H(298\ \mathrm{K}) = -(208.2 \pm 1.6)\ \mathrm{kJ\ mol^{-1}} = -(49.75 \pm 0.38)\ \mathrm{kcal\ mol^{-1}}$. The uncertainties indicated include estimated systematic errors and a 95 percent confidence interval of $\pm 1.34\ \mathrm{kJ\ mol^{-1}}$. This value of $\Delta H$ was combined with published values for the enthalpy of formation of aqueous sodium hydroxide and of aqueous sodium acetate to calculate the enthalpy of formation of ketene gas:

$$\Delta H_f^\circ(298\ \mathrm{K}) = -(47.7 \pm 1.6)\ \mathrm{kJ\ mol^{-1}} = -(11.4 \pm 0.4)\ \mathrm{kcal\ mol^{-1}}.$$

**12253.** Peterson, N. C., Kurylo, M. J., Braun, W., Bass, A. M., Keller, R. A., **Enhancement of absorption spectra by dye-laser quenching,** *J. Opt. Soc. Am.* **61,** No. 6, 746-750 (June 1971).

Key words: Absorption; laser; spectra.

A new technique has been developed to enhance the detection of absorption spectra of weak absorbers. Preliminary experiments, which illustrate the technique, are described. An organic-dye laser normally emits a continuous spectrum with a bandwidth of 2-10 nm. The effect of placing an absorbing-gas sample inside a dye-laser cavity results in laser quenching at those wavelengths where the sample absorption exceeds a minimum threshold absorption. The threshold for absorption quenching appears to be very low; absorption of the order of 0.5% can cause spoiling of laser action at the absorbing wavelengths and displacement of laser emission to wavelengths where absorption is below the critical switching level. Detection limits for atoms and molecules by means of absorption spectroscopy inside a laser cavity can be more than two orders of magnitude lower than those attainable through conventional absorption spectroscopy. Experiments with $I_2$ and sodium both inside and outside the cavity of a rhodamine 6-G laser are described. A qualitative consideration of the proposed mechanism indicates that the technique can be significantly improved with further development.

**12254.** Rupp, N. W., Paffenbarger, G. C., **Significance to health of mercury used in dental practice: A review,** *J. Am. Dental Assoc.* **82,** 1401-1407 (June 1971).

Key words: Contamination; dental amalgam; environment; hazards; hygiene; mercury; vapor.

This is a literature review of the hazards of mercury to the patient, to the dental office personnel and the environment. Mercury content of urine is most frequently used and is reliable measure for evaluating exposure to mercury. The urine level drops however with the onset of toxic symptoms so this test is not reliable in diagnosing toxic responses. Patients have slightly elevated mercury levels in their urine after dental amalgam restorations are placed. After a few weeks this level returns to "normal." Scrap amalgam is usually collected and salvaged for the mercury and silver content. Mercury vapor from the surfaces of droplets, heating and other sources, is potentially hazardous to dental personnel since they are exposed to it for prolonged periods. Proper mercury hygiene practice includes prevention of spills, adequate ventilation and never heating mercury or its compounds. There is little danger to the patient, environment or dental personnel as long as all who handle it realize the potential hazard and observe good mercury hygiene.

**12255.** Sher, A. H., **Carrier trapping in Ge(Li) detectors,** *IEEE Trans. Nucl. Sci.* **NS-18,** No. 1, 175-183 (Feb. 1971).

Key words: Charge carriers; electrons; gamma rays; Ge(Li) detectors; germanium gamma-ray spectrometers; holes; lifetime; theoretical model; trapping.

The results of previously published studies relating to the trapping of charge carriers in semiconductor nuclear radiation detectors, including theoretical models and experimental data, have been used to construct a more realistic operational model which can be used to describe the trapping process. Specifically, the model has been developed for the situation most commonly reported in the literature, that of electron trapping in planar Ge(Li) detectors. The success of the present model has been judged on its ability to predict the variation of the peak shape resulting from $\gamma$-irradiation of a planar Ge(Li) detector as a function of applied bias. Full-energy $\gamma$-ray peaks have been calculated with digital computation techniques by incorporating the variation of peak amplitude as a function of charge collection efficiency as well as the variation of carrier lifetime with applied field into a previously published model.

**12256.** Souders, T. M., **A wide range current comparator system for calibrating current transformers,** *IEEE Trans. Power Appar. Syst.* **PAS-90,** No. 1, 318-324 (Jan.-Feb. 1971).

Key words: Calibration; current comparator; current transformer; overload testing; self-balancing current comparator; transformer; wide-range.

This paper describes a new measurement system for the calibration of current transformers at 60 Hz for all ratios up to 10000/5 and higher and at four time rated current. For ratios up to 1200/5, no reference transformer is needed and the system is accurate to five parts per million (ppm). Most higher ratios can be measured using only one reference transformer. Included is an example of how a laboratory could use such a system to measure all ratios up to 8000/5, requiring a calibration of only one reference transformer on one ratio (4000/5).

**12257.** Sugar, J., **New energy levels of triply ionized praseodymium,** *J. Opt. Soc. Am.* **61,** No. 6, 727-732 (June 1971).

Key words: Praseodymium; spectra; wavelengths.

Measurements of the spectrum of triply ionized praseodymium produced by a 500-A sliding-spark discharge revealed new high-lying energy levels of both even and odd parity. Nearly all levels of the $4f5f$ configuration were found as well as portions of $4f6d$, $4f7s$, and $5d6p$. Radial parameters were fitted to $4f5f$ and $4f6d$. A value for the ionization limit of $314\ 200 \pm 200$ cm$^{-1}$ was deduced from the $4f6s$, $7s$ series.

**12258.** Utton, D. B., **Temperature dependence of $^{35}$Cl NQR sodium chlorate,** *J. Chem. Phys.* **54,** No. 12, 5441-5442 (June 15, 1971).

Key words: Nuclear quadrupole resonance; sodium chlorate; temperature dependence 14-90 K; $^{35}$chlorine.

The temperature dependence of the $^{35}$Cl NQR in sodium chlorate has been measured in the temperature range 14-90 K. It is shown that the Bayer-Kushida theory satisfactorily explains the data if two distinct lattice vibrations are active. The results are compared with the Raman spectrum and the crystal structure.

**12259.** Vadelund, E. A., **The role of the Department of Commerce under the fair packaging and labeling act,** (Proc. Conf. 11th Annual Meeting—Food Distribution Research Society, St. Louis, Mo., Oct. 25-28, 1970), *J. Food Distribution Res.* **2,** No. 1, 103-106 (The Food Distribution Research Society, Inc., Hyattsville, Md., Feb. 1971).

Key words: Consumer commodities; labeling; packaging; proliferation; quantity standards; regulations.

A description of the responsibilities and activities of the NBS in the FPLA program to date. The paper details the responsibilities assigned to the NBS and the steps taken to implement the Act. A brief compilation of results in the various program areas is also presented.

**12260.** Weissler, P. G., **ANSI-1969 standard reference threshold sound-pressure levels for audiometers: Some comments,** *J. Acoust. Soc. Am.* **49,** No. 4, Part 2, 1319-1320 (Apr. 1971).

Key words: Audiometry; earphones; NBS 9-A coupler; reference threshold sound pressure levels; standards for audiometers; threshold of hearing.

New standard reference threshold sound pressure levels for four audiometric earphones are given in Appendix F of ANS Specification for Audiometers S3.6-1969 effective September 1, 1970. The change in reference level from ASA-1951 to ANSI-1969 is shown to be different for each earphone type. The sources of data for these new reference levels and the relationship of these new levels to ISO standards is discussed.

**12261.** Yates, J. T., Jr., Madey, T. E., **Interactions between chemisorbed species: $H_2$ and CO on (100) tungsten,** *J. Chem. Phys.* **54,** No. 12, 4969-4978 (June 15, 1971).

Key words: Carbon monoxide; chemisorption; co-adsorption; displacement reaction; hydrogen; single crystal; tungsten; work function.

The interaction of CO with chemisorbed $\beta$-hydrogen on the (100) plane of tungsten has been investigated using flash desorption and work function methods. CO efficiently displaces chemisorbed hydrogen from tungsten at temperatures near 300 K. This is a result of the CO-induced lowering of the activation energy for $H_2$ desorption, with CO chemisorbing initially on sites other than those occupied by hydrogen. At ~ 100 K, little CO-induced displacement of chemisorbed hydrogen occurs, and the production of three weakly bound hydrogen states (designated $\nu$-hydrogen) is observed. Each $\nu$ state exhibits a range of desorption energies. During the CO-induced surface conversion of $\beta$-hydrogen to $\nu$-hydrogen, a decrease in work function is observed. All of this behavior is indicative of a major interaction between adsorbed CO and adsorbed hydrogen. A weakly-bound molecular $H_2$ state ($\delta$-hydrogen) may be populated by adsorption of $H_2$ on top of partial CO layers on W(100) at ~ 100 K. The sites adsorbing the molecular state of hydrogen are related to the presence of $\beta$-CO species, and are probably the same sites which could adsorb $\alpha$-CO at higher CO coverages. In thermal desorption, the liberation of two discrete hydrogen binding states ($\beta_1$ and $\beta_2$) from pure hydrogen layers on W(100) is probably a result of coverage-dependent interactions between identical adsorbed H-atom species. No chemical differences are observed in this work between hydrogen species responsible for the two $\beta$-hydrogen binding states. No catalytic production of $H_2CO$, HCO, $CH_4$, or $C_2H_6$ was observed in coadsorption of hydrogen and CO on W(100).

12262. Abramowitz, S., Acquista, N., Thompson, K. R., **The infrared spectrum of matrix-isolated uranium monoxide,** *J. Phys. Chem.* **75,** No. 15, 2283-2285 (1971).

Key words: High temperature matrix isolation; infrared; uranium monoxide; uranium oxides; vibrational frequency.

The infrared spectra of matrix-isolated uranium oxides have been observed. By varying the O/U ratio of the condensed phase from 1.5 to 3.0 and comparing the observed spectra of the matrix-isolated vapors in equilibrium with the condensed phases it has been possible to assign a frequency of 776.0 cm$^{-1}$ to $U^{16}O$. Verification of this assignment has been obtained in similar experiments using oxygen-18 enriched uranium oxides; a frequency of 736.2 cm$^{-1}$ has been observed for $U^{18}O$. This yields a force constant to the harmonic approximation of 5.32 mdyn/Å for this species. A stretching mode of $UO_2$ has also been assigned for $U^{16}O_2$, $U^{18}O_2$, and $U^{16}O^{18}O$.

12263. Allpress, J. G., Roth, R. S., **The effect of annealing on the concentration of Wadsley defects in the $Nb_2O_5$-$WO_3$ system,** *J. Solid State Chem.* **3,** 209-216 (1971).

Key words: Annealing equilibria; electron microscopy; niobium tungsten system; Wadsley defects.

Mixtures of $xNb_2O_5 \cdot yWO_3$ with $x:y = 9:8$, 8:5, and 8:1 have been annealed at high temperatures for prolonged periods before quenching to room temperature. The concentration of Wadsley defects, estimated from lattice image electron micrographs of a few fragments in each sample, is reduced during this treatment. The results indicate that (1) the high temperature equilibrium is attained very slowly, and in stoichiometric samples probably involves the complete removal of Wadsley defects; (2) the high temperature situation is not seriously affected by the quenching treatment; and (3) variations in stoichiometry may be accommodated by means other than the presence of Wadsley defects.

12264. Barnes, J. A., **A non-mathematical discussion of some basic concepts of precise time measurement,** *Frequency* **2,** No. 2, 1-6 (Tracor Inc., Austin, Texas, May 1971).

Key words: Atomic time; standards; time; time standards, universal time.

A non-mathematical discussion of some of the basic concepts which must be understood by scientists and engineers who need to use precise time. It distinguishes between the concepts of date and time interval, describes the various scales used to measure astronomical and atomic time, and compares some major characteristics of astronomical and atomic time.

12265. Bennett, H. S., **Acoustic phonons in Heisenberg paramagnets,** *J. Phys.* **32,** No. C1, 526-527 (Feb.-Mar. 1971).

Key words: Frequency shift; Heisenberg paramagnet; specific heat; spin-diffusion; susceptibility; ultrasonic attenuation.

The propagation of sound waves in ferromagnetic and antiferromagnetic insulators is examined in terms of a volume magnetostrictive interaction. Expressions for the ultrasonic attenuation coefficients and for the phonon frequency shifts near the transition temperature are given as functions of the static susceptibilities, the spin diffusion coefficients, and the specific heats. The results agree with scaling law calculations and qualitatively with experiment.

12266. Bloom, D. W., Finegold, L., Lye, R. G., Radebaugh, R., Siegwarth, J. D., **Upper limit on electron-phonon interaction in vanadium carbide,** *Physics Letters* **33A,** No. 3, 137-138 (Oct. 19, 1970).

Key words: Band structure of solids; cryogenics; superconductivity; transition temperatures; vanadium carbides.

Single crystals of $VC_x$ ($x$ 0.87, 0.84, 0.81, 0.76) were not superconducting above 30 mK, indicating that the electron-phonon enhancement of the densities of states determined from electronic specific heats is less than 30%.

12267. Braun, W., Peterson, N. C., Bass, A. M., Kurylo, M. J., **A vacuum ultraviolet atomic emission detector: Quantitative and qualitative chromatographic analysis of typical C, N, and S containing compounds,** *J. Chromatog.* **55,** 237-248 (1971).

Key words: Analytical; atomic emission; detector; gas chromatography; spectroscopy; vacuum ultraviolet.

Vacuum ultraviolet atomic emission detection of effluent gases from a chromatographic column is a very sensitive and selective method for qualitative and quantitative elemental analysis of carbon, nitrogen, and sulfur compounds. A low pressure microwave discharge through helium, with added trace amounts of molecular oxygen, produced complete fragmentation of all compounds used and generated intense atomic emissions in the vacuum ultraviolet. Photometric measurement of these monochromator-isolated atomic emissions was successfully used to establish absolute concentration calibrations for the elements carbon, sulfur and nitrogen in various compounds. This detection method is sensitive, highly selective, and has a range of linearity greater than four decades.

12268. Byerly, R., Jr., Beaty, E. C., **Sunlight photodetachment of $O_3^-$,** *J. Geophys. Res.* **76,** No. 19, 4596-4601 (July 1, 1971).

Key words: Ion mobility; $O_3^-$; photodetachment; photodetachment rate measurement; sunlight.

The rate of photodetachment of $O_3^-$ by sunlight has been determined. The $O_3^-$ ions were identified by their mobility as they drifted in a weak field in 1 torr of $O_2$ buffer gas. This allowed the ions to lose any vibrational or electronic excitation through collisions with the buffer gas. Energy dependence of the cross section was estimated by the use of colored filters in the photon beam. The sunlight photodetachment rate measured was $0.2 \pm 0.1$ sec$^{-1}$.

12269. Carpenter, B. S., **The use of the nuclear track technique for boron and uranium analyses in botanical material,** (Proc. American Nuclear Society Meeting, Boston, Mass., June 17, 1971), *Trans. Am. Nucl. Soc.* **14,** No. 1, 130-131 (1971).

Key words: Alpha tracks; boron; botanical material; fission tracks; kale; orchard leaves; uranium.

The Nuclear Track Technique is used to determine trace quantities of boron and uranium in botanical materials. This technique uses both method of standard additions and the absolute method in its determinations.

12270. Carroll, J. J., Melmed, A. J., **Optical constants of (011) tungsten in the visible region,** *J. Opt. Soc. Am.* **61,** No. 4, 470-473 (Apr. 1971).

Key words: Absorption; ellipsometry; refractive index; tungsten.

Optical constants for tungsten measured ellipsometrically at room temperature in the visible spectrum are reported. Results are given for (011)-oriented tungsten characterized as clean by low-energy-electron diffraction, for the same surface saturated with oxygen, and for the surface after exposure to air at atmospheric pressure for several hours. Results are compared with earlier work and differences are attributed primarily to differences of surface contamination.

12271. Cohen, J., Edelman, S., **Piezoelectric effect in oriented polyvinylchloride and polyvinylfluoride,** *J. Appl. Phys.* **42,** No. 8, 3072-3074 (July 1971).

Key words: g moduli; piezoelectricity; polyvinylchloride; polyvinylfluoride.

The direct piezoelectric effect has been observed in roll-elongated films of polyvinylchloride and polyvinylfluoride. The effect was produced by applying tensile stress to a clamped specimen at a fixed frequency of 20 Hz. The piezoelectric modulus $g_{31}$ was determined to be 0.2 to 0.7 V $m^{-1}/N$ $m^{-2}$ in polyvinylchloride; in polyvinylfluoride $g_{31} \approx 0.2$ V $m^{-1}/N$ $m^{-2}$ and $g_{32} \approx 1$ V $m^{-1}/N$ $m^{-2}$. The piezoelectric effect in these films is believed to be due to mechanical distortion of oriented dipoles, resulting from the tensile stress, and the orientation appears to differ in the two materials.

12272. Coxon, B., **Application of internuclear, double-resonance techniques to carbohydrates. Detection of small coupling-constants,** *Carbohydrate Res.* **18,** No. 3, 427-442 (1971).

Key words: General Overhauser effect; internuclear double resonance; long-range coupling; magnetic equivalence factoring; spin-tickling; transient nutations; 6-Deoxy-α-D-glucofuranose derivative.

6-Deoxy-1, 2:3, 5-di-*O*-isopropylidene-α-D-glucofuranose-$d_{12}$ 1-$d_{12}$) has been synthesized by exchange of its non-deuterated nalog (1) with acetone-$d_6$. The p.m.r. spectrum of 1-$d_{12}$ at 90 MHz has been analyzed iteratively by means of a computer program for magnetic-equivalence factoring. Confirmation of the assignments of lines in the analysis has been investigated by proton-proton, internuclear, double-resonance (i.n.d.o.r.) echniques, which served also for the detection of a small long-range coupling-constant.

Examples of i.n.d.o.r. spectra containing general Overhauser effects, spin-tickling effects, or transient nutations are shown, and are discussed in relation to the experimental power-levels of the observing and double-resonance frequencies, and their weep-rates.

2273. Dickens, B., Brown, W. E., **The crystal structure of $Ca_5(PO_4)_2SiO_4$ (silico-carnotite),** *Tschermaks Mineral. Petrog. Mitt.* **16,** 1-27 (June 1971).

Key words: Calcium phosphate; calcium phosphate-calcium silicate solid solution; calcium phosphosilicates; calcium silicates; crystal structures; glaserite; hydroxyapatite; single crystal x-ray diffraction.

The crystal structure of $Ca_5(PO_4)_2SiO_4$ (silico-carnotite) has een determined from 3358 x-ray diffraction data collected by a ounter method and has been refined to $R_w = 0.038$, $R = 0.045$, n space group Pnma. The unit cell parameters are $a = 6.737$ (1) Å, $b = 15.508$ (2) Å and $c = 10.132$ (1) Å at 24 °C; $Z = 4$. The bserved density is 3.06 and the calculated density is 3.03 $\cdot cm^{-3}$. The crystal contains about 2.5% $V_2O_5$ as an impurity. he bond lengths within the tetrahedral anions suggest that subtitution or disorder of $PO_4^{3-}$, $SiO_4^{4-}$ and possibly $VO_4^{3-}$ occurs mong the anion sites. The structure has some relationship to hat of $Ca_5(PO_4)_3OH$, the predominant inorganic phase in the uman body, but suggests that the $Ca_5(PO_4)_3OH$ type structure nay not be stable without some of the OH positions being filled. $a_5(PO_4)_2SiO_4$ is more closely related to $K_3Na(SO_4)_2$ (glaserite) f it is considered that there are systematic cation vacancies in $a_5(PO_4)_2SiO_4$.

This type of structure is consistent with the view that cation acancies in the glaserite-type structure account for solid soluions between $Ca_2SiO_4$ and $Ca_3(PO_4)_2$ and between $Ca_3(PO_4)_2$ nd $CaNaPO_4$.

2274. Dickens, B., Brown, W. E., **The crystal structure of $Ca_7Mg_9(Ca,Mg)_2(PO_4)_{12}$,** *Tschermaks Mineral. Petrog. Mitt.* **16,** 79-104 (June 1971).

Key words: Calcium magnesium phosphate; cation vacancies; glaserite; single crystal x-ray diffraction; $\alpha$-$Ca_3(PO_4)_2$.

The unit cell of $Ca_7Mg_9(Ca,Mg)_2(PO_4)_{12}$ is $a = 22.841(3)$ Å, $b$ 9.994(1) Å, $c = 17.088(5)$ Å and $\beta = 99.63(3)°$ at 24 °C. The space-group is C2/c with four formula weights per cell. The crystal structure has been determined from 6330 x-ray reflections measured from a single crystal by a counter method and has been refined to $R_w = 0.044$, $R = 0.046$ (based on 4227 observed reflections and 322 of the unobserved reflections). One cation site may be occupied by Ca or Mg and gives rise to variability in composition as is reflected in the formula given above. In the sample studied, Ca and Mg occupy the site approximately equally. The $[10\bar{2}]$ direction in the unit cell is pseudo-hexagonal. The structure of $Ca_7Mg_9(Ca,Mg)_2(PO_4)_{12}$ is related to that of $K_3Na(SO_4)_2$ in that along $[10\bar{2}]$ it has columns of cations and columns of cations and anions. These columns are arranged in a $K_3Na(SO_4)_2$-type pseudo-cell. In the cation-anion columns, every other cation site in $K_3Na(SO_4)_2$ is vacant in $Ca_7Mg_9(Ca,Mg)_2(PO_4)_{12}$.

12275. Dehmer, J. L., Starace, A. F., Fano, U., Sugar, J., Cooper, J. W., **Raising of discrete levels into the far continuum,** *Phys. Rev. Letters* **26,** No. 25, 1521-1525 (June 21, 1971).

Key words: Autoionization; exchange interaction; photoabsorption transition elements; rare earths.

Broad peaks observed in the photoabsorption spectra of rare earths ~ 10-20 eV above the $4d$ edge are attributed to transitions $4d^{10}4f^N \rightarrow 4d^9 4f^{N+1}$. Exchange interaction splits the $4d^9 4f^{N+1}$ configuration and raises some multiplets by ~ 20 eV. Autoionization to $4d^9 - 4f^N \epsilon f$ broadens the high levels. The interpretation extends to $p \rightarrow d$ processes observed in the absorption of synchrotron light by transition elements.

12276. Edelman, S., Grisham, L. R., Roth, S. C., Cohen, J., **Improved piezoelectric effect in polymers,** *J. Acoust. Soc. Am.* **48,** No. 5, Part 1, 1040-1043 (Nov. 1970).

Key words: Piezoelectricity; piezoelectric modulus; polymer; polyvinylchloride; transducer; underwater sound.

Improved poling techniques have led to improvement in the piezoelectric activity of bulk polymers. Results now achieved approach the activity of conventional piezoelectric materials such as quartz, and further improvement is anticipated. The measured value of the piezoelectric strain modulus $d_{31}$ of a length expander bar of polyvinylchloride was $0.6 \times 10^{-12}$ m $V^{-1}$ and the electromechanical coupling factor $k_{31}$ was 0.6%. The response of a sample as an underwater sound receiver was −112 dB *re* 1V/μbar.

12277. Edsinger, R. E., Guildner, L. A., Anderson, R. L., **Precision measurement of internal diameters of long, small bore metal tubing,** *Rev. Sci. Instr.* **42,** No. 7, 945-950 (July 1971).

Key words: Capacitance probe; cylindrical gauge blocks; inside diameters; small-bore tubes; standard hole; wringing.

Internal diameters of a long, small bore metal tube were calculated from the measured capacitances between it and a cylindrical coaxial probe of known characteristics. The tube and the probe were used as the electrodes of a three-lead capacitor, measurable with high accuracy in a transformer ratio arm bridge. For tubes of 0.1 cm bore or less, average diameters as a function of position can be determined by this method with an over-all uncertainty of $\pm 6 \times 10^{-5}$ cm over lengths of 1 m. The method can readily be extended to larger bores and greater lengths.

12278. Fickett, F. R., **Magnetoresistance of very pure polycrystalline aluminum,** *Phys. Rev. B* **3,** No. 6, 1941-1952 (Mar. 15, 1971).

Key words: Aluminum; electron scattering; magnetoresistance; resistance.

The behavior of the resistance of polycrystalline aluminum wires as a function of magnetic field and purity at temperatures of 4, 15, and 19.6 K is reported. Both longitudinal and transverse configurations were measured. The residual resistance ratios of the specimens varied from 1600 to 31 000. The measured magnetoresistance ($\Delta R/R_0$) is separated into a saturating and a linear part. The value of the saturating component is high at 19.6 K but is shown to be less than 6, even in the limit of infinite specimen purity. The linear component varies with both temperature and purity. Possible sources for the large saturating magnetoresistance values and for the variations observed in the linear portion are discussed. An analysis scheme is presented which allows prediction of the saturating component from zero-field resistance values. A deviation from Matthiessen's rule observed here, and by several other experimenters, is presented and discussed.

12279. Gibson, B. F., Williams, H. T., **Virtual photon cross sections for two-body electrodisintegration,** *Nucl. Phys.* **A163, 193-202 (1971).**

Key words: Cross section; electric transition; electrodisintegration; few nucleon systems; long wavelength.

Two-body electrodisintegration cross sections (differential with respect to the angles of the ejected nuclear fragment) are developed in the long wavelength limit of virtual photon theory for the few-nucleon system. Only the non-spin-flip electric transitions are considered. Contributions from the multipole expansion through the E1-E3 interference terms are retained. Comparable photodisintegration expressions are included to facilitate the extraction of photo cross sections from appropriate inelastic electron scattering data.

12280. Hastie, J. W., **Thermodynamic studies, by mass spectrometry, of molten mixed halide systems,** Chapter 5 in *Advances in Molten Salt Chemistry* **1,** 225-257 (Plenum Press, Inc., New York, N. Y., 1971).

Key words: Complex molecules; mass spectrometry; molten salt halides; thermodynamics.

The thermodynamic properties of the complex vapors, present in molten mixed halide systems, are reviewed and evaluated. Also, the special techniques required for these studies are critically discussed. A model, based on entropy and enthalpy correlations, is proposed whereby the complex vaporization phenomenon can be rationalized and predictions made for unstudied systems.

12281. Hastie, J. W., Hauge, R. H., Margrave, J. L., **Infrared spectra and geometries for the dichlorides of Ca, Sc, Ti, V, Cr, Mn, Fe, and Ni,** *High Temp. Sci.* **3,** No. 3, 257-274 (May 1971).

Key words: Dichlorides of Ca, Sc, Ti, V, Cr, Mn, Fe, Ni; geometry; infrared spectra of species; matrix isolation; $ScCl_3$; $TiCl_3$; $TiCl_4$.

The dichloride species of Ca, Sc, Ti, V, Cr, Mn, Fe, and Ni, prepared by Knudsen cell techniques have been isolated in solid inert gas matrices and infrared spectra obtained over the range 33-1000 $cm^{-1}$. Spectra were also observed for $ScCl_3$, $TiCl_3$ and $TiCl_4$. Isotope shift measurements and the infrared selection rules indicate each of the dichlorides to be linear $D_{\infty h}$ species within the experimental bond angle uncertainty of about 10°. In several instances, the results implied a significant anharmonic effect on the isotope shifts. Significant differences in the geometry and vibrational data between the dichlorides and the corresponding difluorides are noted.

12282. Heuer, A. H., Hockey, B. J., Wiederhorn, S. M., **Discussion of "Observation of plastic deformation in sapphire base ceramics,"** *Metallurgical Trans.* **2,** 1475-1476 (May 1971).

Key words: Alumina; fracture; mechanical properties; plastic deformation; sapphire; strength.

A paper presented in Metallurgical Transactions by George F. Hurley is discussed. It is concluded that the observations concerning plastic deformation in sapphire-based ceramics are incorrect and that there is no evidence at present to link plastic deformation and fracture to alumina ceramics.

12283. Kieffer, L. J., **Low-energy electron-collision cross-section data Part III: Total scattering; differential elastic scattering** *Atomic Data* **2,** No. 4, 293-391 **(June 1971).**

Key words: Atom; cross section; elastic scattering; electron; molecule.

This is the final part of a three part compilation of low-energy electron-collision cross-section data issued by the Joint Institute for Laboratory Astrophysics (JILA) Information Center. Only experimental values are included for all atomic species and for those molecules which are important for aeronomy, astrophysics and plasma physics. The data included here were taken from literature published through July 1970.

12284. Kirsch, R. A., **Computer determination of the constituent structure of biological images,** *Comput. Biomed. Res.* **4,** 315-328 (1971).

Key words: Biological images; image processing; morphology; pattern recognition.

A class of algorithms is described which enables computer quantized images to be decomposed into constituent parts reflecting the structure of the images. This decomposition is viewed as the morphological precursor to a higher level syntactic analysis. Numerical results for a typical biological image are presented.

12285. Kuriyama, M., **On the principle of x-ray interferometry** *Acta Cryst.* **A27,** 273-280 (1971).

Key words: Diffraction theory; lattice constants; measurements; wave optics; x-ray interferometry.

The scattering amplitude of an x-ray interferometer is calculated using a general theory of x-ray diffraction. Analytic expressions are given for the intensities of diffracted beams in interferometry; these expressions include the effect of the positions of each crystal lattice in addition to ordinary dynamical effects. It is concluded that the fringes observed in x-ray interferometry of a lattice spacing are accounted for by an optical (Moiré) effec rather than by dynamical effects of x-ray diffraction.

12286. LaVilla, R. E., **Neon *K* emission spectrum,** *Phys. Rev. A* **4,** No. 2, 476-480 (Aug. 1971).

Key words: Electron excitation; neon *K* emission spectrum x-ray emission; x-ray satellites.

The neon *K* emission spectrum, excited by direct electron bombardment of the neon gas, has been obtained with photon counting on a single-crystal potassium-acid-phthalate (KAP planar spectrometer. The measured relative integrated intensity of the $\alpha'\alpha_3\alpha_4$ and $\alpha_5\alpha_6$ satellite groups was found to be larger than theoretical prediction, but in accord with the trend of previous comparisons for *K* satellites of neonlike ions in solids. A comparison of the present results for electron excitation and the preliminary results by O. Keski-Rahkonen and T. Åberg fo photon excitation indicates that the relative integrated intensity of the neon *K* satellites is independent of excitation mode at the excess excitation energies employed. A weak increase of intensity on the low-energy side of $K\alpha_{1,2}$ in the (803 – 809)-eV region was recorded and can be attributed to a radiative Auger transition.

12287. Mohan, R., Danos, M., Biedenharn, L. C., **Three-fluid hydrodynamical model of nuclei,** *Phys. Rev. C* **3,** No. 5, 1740-1749 (May 1971).

Key words: Charge distribution; collective model; giant resonance; hydrodynamic model; isospin; nuclear structure.

A three-fluid model of nuclei is introduced, the three fluids eing the protons, the neutrons of the same orbitals as protons, nd the excess neutrons, to account for the fact that the excess eutrons interact less strongly with the protons than do the eutrons which occupy the same space-spin states as the rotons. Calculations of proton and neutron density distribuions, of isotope shifts, and of isospin impurities have been caried out. The giant-dipole phenomenon is also studied in the resent model. It is found that considerable improvement is chieved in the results for the proton density distribution and for he isospin impurities as compared with the two-fluid model. The ther results are found to be consistent with previous calculaons.

2288. Moore-Sitterly, C., **The periodic table interpreted from atomic spectra,** *Proc. Mendeleev Conf., Torino-Rome, Italy, September 15-21, 1969,* pp. 163-188 (1969).

Key words: Atomic spectra; coronal spectra; periodicities, atomic spectra; rare-earth spectra; regularities, atomic spectra; solar spectra.

The properties of the valence electrons as revealed by the congurations and energy levels in atomic and ionic spectra are iscussed by considering four aspects of the Periodic Chart of he Atoms.

The series in first spectra of three *vertical* groups are escribed: similarities in the doublet series Li I, Na I etc.; the sigificance of the double-electron jump in the spectra Ca I, Sr I, Ba the pair-coupling in Ne I, Ar I etc. The importance of Zeeman bservations in interpreting spectra of magnetic stars, and imilarities in complex spectra such as Mn I and Tc I reveal diferent types of regularities.

In the *horizontal* grouping, the effect of building on electrons ith increasing atomic number is illustrated by considering onization potentials from H through Ca, and by inverted terms n complex spectra.

*Isoelectronic sequences* are extremely important for the nalyses of spectra of highly-ionized atoms. The observations of he solar spectrum and of other stellar spectra from rockets and rbiting telescopes has created a sudden demand for laboratory ata on these spectra. Extrapolation of intervals along the equences of light elements has led to the identification of strong nes in the solar corona. Coronal lines recently identified by B. dlén are described. A summary of spectra detected in the sun om H through Ni is presented.

Finally, the inherent regularities in electron structure revealed y known spectra furnish methods that are a valuable guide in ocating overlapping configurations in the complex *rare-earth pectra*. The theoretical work of G. Racah and the analysis of Yb are used as examples.

2289. Okabe, H., Laufer, A. H., Ball, J. J., **Photodissociation of $OCCl_2$ in the vacuum ultraviolet: Production and electronic energy of excited $Cl_2$,** *J. Chem. Phys.* **55,** No. 1, 373-378 (July 1, 1971).

Key words: Absorption coefficient; $Cl_2$; emission; electronic energy; $OCCl_2$; photodissociation; vacuum ultraviolet.

The photodissociation of $OCCl_2$ in the vacuum ultraviolet ields electronically excited $Cl_2$ producing emission continua in ne region 2000-3100 Å. A curve obtained by plotting uorescence efficiencies as a function of incident wavelength nows diffuse vibrational structure corresponding to the $\nu_1$ ymmetric stretching mode of $OCCl_2$, indicating that the process predissociative. Three main continua at 3063, 2565, and 2460 Å were observed by the photolysis of $OCCl_2$ with the Kr 1236-Å line, while only one continuum at 2580 Å was obtained by the Xe 1470-Å line. From threshold energies of the incident photons to produce each continuum it was possible to obtain electronic energies of excited $Cl_2$. Electronic energies thus obtained are $7.21 \pm 0.05$ eV and $7.93 \pm 0.03$ eV for the upper states associated with the 2580- and 3063-Å continua, respectively. The electronic energy of the upper state responsible for the 2460-Å continuum lies between 7.33 and 8.93 eV. The effect of inert gas on the emission continua was investigated. A comparison has been made of the emission continua obtained by the photolysis of $OCCl_2$ and those produced by an electric discharge of $Cl_2$. The absorption coefficient of $OCCl_2$ has been measured in the region 1170-1600 Å.

12290. Pilling, M. J., Bass, A. M., Braun, W., **Oscillator strengths of $CH_2$ and $CH_3$ in the vacuum ultraviolet,** *Chem. Phys. Letters* **9,** No. 2, 147-148 (Apr. 15, 1971).

Key words: Methyl radicals; methylene; oscillator strengths; spectroscopy; vacuum UV.

Maximum extinction coefficients and oscillator strength were measured for several $CH_2$ and $CH_3$ transitions in the vacuum UV. The method employed involved in the vacuum UV flash photolysis of ketene and diazomethane and vacuum UV spectrophotometry.

12291. Reimann, C. W., Zocchi, M., **The crystal structure of Bis-[$\mu$-(tri-1,2,4-triazolo-N$^1$,N$^2$)-triaquonickel]nickel hexanitrate dihydrate, $[(H_2O)_3(C_2H_3N_3)_3Ni]_2Ni(NO_3)_6(H_2O)_2$,** *Acta Cryst.* **B27,** Part 3, 682-691 (Mar. 1971).

Key words: Bis-[$\mu$-(tri-,1,2,4-triazolo-N$^1$,N$^2$)-triaquonickel] nickel hexanitrate dihydrate; trinuclear nickel(II) complex; x-ray structure analysis.

The crystal structure of bis-[$\mu$-(tri-1,2,4-triazolo-$N^1$,$N^2$)-triaquonickel]nickel hexanitrate dihydrate, $[(H_2O)_3(C_2H_3N_3)_3Ni]_2Ni(NO_3)_6(H_2O)_2$, has been solved by the Patterson method. This compound crystallizes in the monoclinic system with $a = 14.261$ (8), $b = 11.745$ (6), $c = 14.948$ (8) Å, $\beta = 127.13$ (4)°, space group $P2_1/c$, $\rho_c = 1.84$ g.cm$^{-3}$, and $Z = 2$. The structure consists of discrete centrosymmetric trinuclear cations, $[(H_2O)_3(C_2H_3N_3)_3Ni]_2Ni^{6+}$, in which the central nickel ion is joined to each terminal nickel ion by three planar triazole molecule bridges. The nickel-nickel distance is 3.737 Å. Three molecules of water complete the octahedral coordination of the terminal nickel ions. The N-H groups in the triazole rings and the coordinated water molecules participate in hydrogen bonding with the nitrate groups and non-coordinating water molecules. All hydrogen atoms in this structure were located in a difference map. Final refinement by three-dimensional anisotropic least-squares analysis resulted in an $R$ value of 0.045 based upon 5201 observed reflections.

12292. Ritter, J. J., Coyle, T. D., Bellama, J. M., **Reactions of diboron tetrahalides with haloolefins. Formation of poly(dihaloboryl) ethanes,** *J. Organometal. Chem.* **29,** 175-184 (1971).

Key words: Boron; boron subhalides; halides; haloolefins; organoboron compounds; tetrachlorodiborane(4); tetrafluorodiborane(4).

Tetrachlorodiborane(4) reacts with vinyl chloride in 2/1 ratio to yield 1,1,2-tris-(dichloroboryl)ethane and boron trichloride. The reaction appears to be general for a variety of haloolefins. Both $B_2Cl_4$ and $B_2F_4$ react similarly with haloethylenes containing halogens heavier than the halogen on the diboron moiety. Evidence has been obtained for a reaction sequence involving addition of $B_2X_4$ to the haloolefin, elimination of trihaloborane, and subsequent addition of $B_2X_4$ to the resulting vinyldihaloborane.

12293. Sanchez, I. C., DiMarzio, E. A., **Dilute solution theory of polymer crystal growth: A kinetic theory of chain folding,** *J. Chem. Phys.* **55,** No. 2, 893-908 (July 15, 1971).

Key words: Cilia; conformational entropy; free energy; nucleation rate; rate constants; self-nucleation; steady-state.

A kinetic theory of polymer crystallization from dilute solution is formulated for linear chain molecules of finite molecular weight (monodisperse). Two models of crystal growth are considered; both are essentially "regular" chain folding type models. Formulas for the crystal growth rates are derived as a function of the fundamental rate constants associated with the various states of molecular crystallization. These rate constants are evaluated as a function of polymer concentration, molecular weight, crystallization temperature, and crystal thickness. Consideration of finite molecular weight molecules requires an understanding of how these molecules are incorporated into the crystal and what happens to chain ends. Attention is focused on these problems and a description of how "cilia" are formed in polymer crystals is given. A remarkable aspect of cilia formation is that the uncrystallized portion of a chain molecule which dangles in the solution can participate in nucleating a new growth strip (fold plane) on the crystal face—a kind of "self-nucleating" mechanism.

12294. Simmons, J. H., Macedo, P. B., Napolitano, A., Haller, W. K., **Investigation of liquid-liquid phase transitions in oxide melts by viscosity measurements,** *Discussions Faraday Soc., Bristol, England, September 1970,* No. 50, 155-165 (1970).

Key words: Critical phenomena; immiscibility; oxide glasses; viscosity.

Results from viscosity measurements conducted both above and below the liquid-liquid phase transition of a series of molten oxide glasses are reported in order to analyze the effect of supercritical composition fluctuations on viscous flow, and to investigate the mechanisms of phase separation. Measurements of four oxide mixtures with similar high temperature structures and widely different critical temperatures, revealed an anomalous increase in viscosity at temperatures above the critical point. The anomalous increase occurs when large composition fluctuations characterizing the critical point are present. The effect is explained in terms of an interaction between viscous flow and the supercritical fluctuations through the structural relaxation process. An analysis of this interaction is presented.

Measurements conducted at temperatures slightly below the critical point of one of these glasses indicate that the microstructure resulting from the phase separation is highly sensitive to the preceding heat-treatment. Phase separation by the formation of isolated spheres of the silica-rich component is identified a few degrees below the critical point. Further measurements of viscosity by a fibre elongation method, conducted far below the critical temperature, are reported in order to analyze the growth mechanisms occurring in the separated phases. In this case, the rearrangement stage of phase separation is characterized by a growing interconnected structure.

12295. Simpson, P. A., Ondrejka, A. R., **Improvements to the NBS rf peak-pulse power standard,** *Instrument Society of America Silver Jubilee International Conference and Exhibit, October 26-29, 1970, Philadelphia, Pa.,* Paper **709-70,** 1-7 (Oct. 26-29, 1970).

Key words: Peak pulse power measurement; sampling power measurement; solid state switch.

The National Bureau of Standards maintains a standard for measuring rf peak-pulse power. This standard employs a sampling-comparison method in which a solid state diode switch is used to intercompare equal time-interval samples of cw and pulsed rf power. Recently a new type diode switch has bee developed which, when coupled with a sensitive peak detectio system, has greatly improved the performance of the standard i two general areas.

The first major improvement is in the frequency coverage. Th earlier version of the standard used two separate diode switche to cover the frequency bands 300 to 500 MHz and 950 to 120 MHz. The new diode switch permits measurements to be mad over the frequency range 0.1 to 4.4 GHz because of its lo VSWR (typically 1.1 or less).

The other major improvement is in the dynamic power rang of the system. The basic range of the earlier version was 0.1 t 1.2 watts. The new version operates over a power range of 5 m to 2 W.

This paper reviews the history of the system, describes its performance characteristics, and gives some of its more importan constructional details.

12296. Smith, S. J., **Lasers and lengths,** *Comments At. Mol. Phys* **2,** No. 3, 92-97 (Aug. 1970).

Key words: Coherence; laser stabilization; length; methane saturated absorption.

We review here developments which strongly suggest tha laser stabilization techniques fully complementary to the amazing coherence properties of the laser will ultimately be found. Indeed progress in hand assures an advance more revolutionar than evolutionary, and discussions of a possible redefinition o the standard of length are now beginning to be taken seriously.

12297. Spencer, L. V., **Remarks on the theory of energy depositio in cavities,** *Acta Radiol.* **10,** No. 1, 1-20 (Feb. 1971).

Key words: Bragg-Gray principle; cavity; detector respons functions; dosimetry; electron-energy deposition; Gra medal; ionization.

The contributions of Gray and Bragg to the theory of energ deposition in cavities are reviewed in connection with a mathematical formulation of the problem. The two principal contributors to the Bragg-Gray theory apparently used approaches tha were equivalent but dual in the sense of involving adjoint expressions of the energy deposition. Burch has later attempted an extension of Gray's ideas and Spencer-Attix have extended th theory by applying Bragg's point of view. Some comments on future cavity theory research are included.

12298. Yokel, F. Y., **Stability and load capacity of members wit no tensile strength,** *J. Struct. Div. Am. Soc. Civil Engineers* **97** No. ST7, 1913-1926 (July 1, 1971).

Key words: Buckling; compression members, concrete deflection; equilibrium; load eccentricity; masonry; sectio cracking; stability; stress distribution; unreinforce concrete.

A mathematical solution is derived, which permits the computation of critical load, deflection and stresses for eccentricall loaded slender prismatic compression members, made of materials that have compressive strength but no tensile strength. A graphical presentation of the solution facilitates its application In an example of application, the solution is used to compute th strength of masonry walls which were tested by the Structura Clay Products Institute. Even though there are limitations to ou ability of predicting the behavior of a complex material such a masonry by a mathematical solution based on a simplified model there is good agreement between computed and measure strength.

12299. Abramowitz, S., Levin, I. W., **Raman spectra of the hexahalogenated benzenes in the solid phase,** *Spectrochim. Acta* **26A,** 2261-2268 (1970).

Key words: $C_6F_6$; $C_6Cl_6$; $C_6Br_6$; $C_6I_6$; hexahalogenated benzenes; laser; Raman; vibrational assignment.

Solid Raman spectra of the hexahalogenated benzenes are examined at both room and liquid nitrogen temperatures. Tentative assignments for $C_6Cl_6$, $C_6Br_6$ and $C_6I_6$ are proposed on the basis of a puckered ($D_{3d}$) geometry.

**2300.** Bardos, D. I., Waterstrat, R. M., Rowland, T. J., Darby, J. B., Jr., **The magnetic susceptibility of transition-metal A15-type phases,** *J. Low Temp. Phys.* **3,** No. 5, 509-518 (1970).

Key words: Atomic ordering; intermetallic compounds; magnetic susceptibility; superconductors.

The temperature dependence of the paramagnetic susceptibiliy was measured for several binary A15-type compounds of ransition elements. Measurements were made between room emperature and either 3 K or the superconducting transition emperature, whichever was higher. The susceptibilities were ound to have, in most cases, a small linear temperature dependence. Molar susceptibilities $X_M$, superconducting transition emperatures $T_c$, and electronic heat coefficients $\gamma$ for these ompounds, when plotted as a function of the valence-electron oncentration *e*/*a*, reveal peaks at an *e*/*a* of about 6.5 for all three roperties. Compounds containing the 4*d*-series transition-elements molybdenum or niobium have higher Tc and lower $X_M$ alues than compounds containing the 3*d* transition-element hromium or vanadium. It appears that an increased mixing of toms on either of the two crystallographic sites in the A15-type tructure can be associated with a significant decrease in the aramagnetic susceptibility of the compound.

**2301.** Bennett, H. S., **Two-electron $F^-$ centers in the alkaline-earth fluorides,** *Phys. Rev. B* **4,** No. 4, 1327-1335 (Aug. 15, 1971).

Key words: Alkaline earth; color centers; $F^-$ centers; fluorides.

The Hartree-Fock-Slater (HFS) equations for the two-elecron orbitals localized about an anion vacancy in $CaF_2$, $SrF_2$, and $BaF_2$ have been solved numerically in the point-ion-lattice potenial. It is found that the ground state ${}^1S(1s,\ 1s)$ contains bound electronic orbitals which are spatially compact. The existence of bound excited states for the $F^-$ center in these crystals has been investigated. However, definitive statements on such excited tates are not available at present.

**2302.** Bowen, R. L., Argentar, H., **Amine accelerators for methacrylate resin systems,** *J. Dental Res.* **50,** No. 4, 923-928 (July/Aug. 1971).

Key words: Accelerators; amines; color-stable composites; methacrylates; polymerization; resins; synthesis.

Tertiary aromatic amines were synthesized with various itrogen and ring substituents. They were compared with commercial homologues using composites based on dimethacrylate monomer formulations containing benzoyl peroxide. Equimolar mounts of the different amines were the only variables. Although accelerating ability was a function of both ring and itrogen substitution, color stability was influenced more by the substituents on the ring than by the substituents on the nitrogen.

**2303.** Boyd, M. E., Larsen, S. Y., **First quantum-mechanical correction to the classical viscosity cross section of hard spheres,** *Phys. Rev. A* **4,** No. 3, 1155-1163 (Sept. 1971).

Key words: Boltzmann gas; cross-section for viscosity; hard sphere gas; quantum corrections; statistical mechanics; viscosity.

The classical and first quantum correction terms in a high-energy expansion of the viscosity cross section $Q^{(2)}$ for a Boltzmann gas of hard spheres is derived. The first correction is found o be proportional to $(1/k\sigma)^{4/3}$, which is a term nonanalytic in $\hbar$ (i.e., $\hbar^{4/3}$), and results from scattering near the edge of the sphere. A bound is established showing the remainder of the asymptotic series to be of $O[(\ln k\sigma)/(k\sigma)^2]$. This asymptotic formula is compared with calculations based on the exact phase-shift expressions and its range of validity is established. The next correction terms are deduced to be proportional to $(\ln k\sigma)/(k\sigma)^2$ and $1/(k\sigma)^2$ which involve $\hbar^2\ln\hbar$ and $\hbar^2$, respectively.

**12304.** Brenner, A., Sligh, J. L., **Electrodeposition of magnesium and beryllium from organic baths,** *Trans. Inst. Metal Finishing* **49,** 71-78 (May 1971).

Key words: Beryllium, electrodeposition of; beryllium azide; beryllium thiocyanate, decaborane; dimethyl beryllium; magnesium, electrodeposition of; nonaqueous plating baths; Grignard reagents; organic plating baths; triethylboron.

Solutions that are feasible for electrodepositing magnesium were prepared from Grignard reagents with the addition of boranes in ether solutions. A typical bath consisted of methylmagnesium chloride, 3-molar (dissolved in tetrahydrofuran), and 1-molar in triethylboron. The deposits were white, ductile and contained at least 99% of Mg. Cathode and anode current efficiencies were 100%. A similar beryllium plating solution, prepared with beryllium dimethyl and decaborane, yielded dark grey, coherent deposits containing 85% to 90% beryllium.

**12305.** Broadhurst, M. G., Mopsik, F. I., **Normal mode calculation of Grüneisen thermal expansion in *n*-alkanes,** *J. Chem. Phys.* **54,** No. 10, 4239-4246 (May 15, 1971).

Key words: Bulk modulus; Grüneisen; *n*-alkanes; normal mode; polyethylene; quasiharmonic specific heat; string of beads; thermal expansion; thermal properties; volume.

The normal mode problem is solved for a semirigid chain of beads in a quasiharmonic potential in order to separate the inter- and intrachain parts of the specific heat. The effects of lattice vibrations are included in an approximate way. The usual Grüneisen relation, $\alpha B_T = \gamma C_v/V$, valid only for acoustical modes, is generalized for optical modes to give $\alpha B_T = \Sigma_j(\gamma_j/V)$ $(\partial S_j/\partial ln\omega_{jmax})$, where $s_j$ and $\omega_{jmax}$ are the entropy and frequency cutoff of mode *j*. The predicted thermodynamic properties of the system are unusually sensitive to chain length because of interchain thermal energy effects. The parameters are given values from independent solid *n*-alkane data, and the calculated results are shown to predict quite well experimental $C_p$ and $V-T$ behavior of the *n*-alkanes.

**12306.** Cassidy, E. C., Cones, H. N., Booker, S. R., **Development and evaluation of electrooptical high-voltage pulse measurement techniques,** *IEEE Trans. Instr. Meas.* **IM-19,** No. 4, 395-402 (Nov. 1970).

Key words: Dielectric liquids; electric field measurements; electrooptical measurements; high voltage measurements; Kerr cell; laser applications; pulse measurements.

Use of the Kerr electrooptical effect for time-resolved pulse measurements is extended to the 300-kV level. Pulse durations are as short as 5 μs. The performance of systems equipped with Kerr cells of various designs is investigated under a variety of operating conditions. Calibrations are achieved using both pulse-divider and high direct-voltage techniques. Methods are devised for measurement and correction of errors resulting from the fringing electric field at the ends of the Kerr-cell electrodes. Measurements of the temperature coefficient of the Kerr-cell constant are also included.

The pulse waveform is reconstructed from typical Kerr-system results by automatic computation and compared with simultaneous time-resolved pulse-divider measurements. Comparisons at the peak of the pulse, where a "slideback" technique is used to enhance the resolution of the divider measurement, demonstrate agreement to better than 1 percent.

In addition, a novel technique is developed for measurement of the pulse magnitude from photographs of the Kerr-effect fringe patterns produced by passing an expanded, pulsed laser beam through the system. By this approach, voltage is measured optically without use of sophisticated electrical metering instrumentation.

**12307.** Cezairliyan, A., **Measurement of the variation of normal spectral emittance of tantalum during melting by a pulse heating method,** *High Temperatures-High Pressures* **2,** 501-506 (1970).

Key words: Emittance; high-speed measurements; melting; normal spectral emittance; tantalum; thermal radiation properties.

A pulse heating method was used to measure the change in normal spectral emittance (at 650 nm) of tantalum as a function of the change in electrical resistance during the initial melting period. Duration of an individual experiment, in which the specimen was heated from room temperature to its melting point, was approximately 400 ms. The partial melting period was approximately 100 ms. A millisecond resolution photoelectric pyrometer was used for temperature measurements. The recordings of experimental quantities were made with a digital data acquisition system, which has a full-scale signal resolution of approximately one part in 8000 and a time resolution of 0.4 ms. Results of the study show that normal spectral emittance decreased by approximately 3.5% during the initial one third of the melting period.

**12308.** Chandler, H. H., Bowen, R. L., Paffenbarger, G. C., **Method for finishing composite restorative materials,** *J. Am. Dental Assoc.* **83,** No. 2, 344-348 (Aug. 1971).

Key words: Composite restorative materials; finishing; operative dentistry; polishing instruments; surface finish.

An instrument, designed to finish the surface of composite restorative materials, was made by bonding 1$\mu$ to 5$\mu$ diamond particles to flexible paper disks. The surface finish produced by this instrument was superior to that obtained by fine cuttle-fish disks and inferior to surfaces obtained by the hardening of the material in contact with polished glass. Results are presented with use of scanning electron photomicrographs.

**12309.** Chandler, H. H., Bowen, R. L., Paffenbarger, G. C., **Physical properties of a radiopaque denture base material,** *J. Biomed. Mater. Res.* **5,** 335-337 (July 1971).

Key words: Composite materials; denture base materials; physical properties; prosthetic materials; radiopacity-radiopaque.

Physical properties were determined for radiopaque composite denture base materials consisting of poly(methyl methacrylate) as the matrix and 30, 40, and 50% by weight of a silane-treated barium fluoride-containing glass powder as the reinforcing filler. Specimens without glass were included for comparison.

All of the materials met the requirements of American Dental Association Specification No. 12 for Denture Base Polymer except that the material containing 50% glass had less deflection than the minimum required at the 5000-gm load in transverse testing.

There was little or no difference among the materials with respect to hardness, indentation resistance, water sorption, color stability, and resistance to drop impact.

Addition of glass to the 30% level decreased the transverse strength while 50% glass specimens had slightly greater transverse strengths as compared to specimens with no glass. I general, the addition of glass increased the time to reach th packing stage, densities, and Young's, bulk, shear, and flexura moduli, had only slight effect on solubility and decreased th cold-cure repairability and the coefficient of linear thermal expansion.

The solubility of the glass powder was about four times that o powdered porcelain teeth after 24 hr, and totaled 0.55% after days.

**12310.** Chandler, H. H., Bowen, R. L., Paffenbarger, G. C. **Radiopaque denture base materials technic dentures,** *J. Biomed Mater. Res.* **5,** 359-371 (July 1971).

Key words: Composites; denture base materials; dentures dimensional stability; foreign bodies; prosthetics; radiopacity; silane bonding.

Technic dentures were made using composite base material containing 30, 40, and 50 weight percent of a silane-treated radiopaque, powdered glass as the reinforcing filler an poly(methyl methacrylate) as the matrix. Dentures containing n glass were included for comparison. Molar-to-molar dimensiona changes, effects of silane treatment of the porcelain teeth an handling and finishing characteristics were determined.

Dentures containing glass had less dimensional change durin curing and subsequent water storage than those without glass Thick upper dentures exhibited the least change and thin lowers the most. The differences in the magnitudes of the change would not be clinically noticeable.

Silane treatment of the porcelain teeth in thick upper denture resulted in breakage of the posterior teeth in almost all instances Posterior teeth also fractured in thick upper dentures containin 40 and 50% of the silane-treated glass even though the teet were not treated with silane.

Mixing and molding properties of the composite materials while acceptable, were slightly inferior to the material containin no glass. Finishing characteristics were definitely inferior in tha it was more difficult and time-consuming to attain the final surfaces and these surfaces were not as smooth as those in denture without glass.

**12311.** Chang, S. S., Bestul, A. B., **Heat capacities of cubic monoclinic, and vitreous arsenious oxide from 5 to 360 K,** *J Chem. Phys.* **55,** No. 2, 933-946 (July 15, 1971).

Key words: Arsenious oxide; arsenolite; claudetite; crysta transition; cubic crystal; glass; heat capacity; monoclini crystal; low temperature; planar molecular structure; spherical shell molecules; vitreous state.

Experimentally determined heat capacities, $C_p$, precise t better than 0.1%, and derived thermal data are reported for cubi and monoclinic crystalline and vitreous arsenious oxide at temperatures from 5 to 360 K. $C_p$ for the glass is higher than fo either crystal at all temperatures. $C_p$'s for the cubic crystal ar lower than those for the monoclinic between about 20 and 310 K and higher at temperatures below and above this range. $C_p/T^3$ fo the glass is still increasing with decreasing temperature at 5 K although $C_p/T^3$ for both crystals peaks a few degrees above this $C_p$'s reported here for the monoclinic crystal are grossly differen from those previously reported by Stranski's school. The corresponding entropy difference between the two crystals a 298.15 K reported here is $5.9 \pm 0.2$ J $\text{deg}^{-1} \cdot \text{mole}^{-1}$, whereas tha previously reported from $C_p$ measurements by Stranski's schoo was 14.4 $\text{deg}^{-1} \cdot \text{mole}^{-1}$. Combined with a value newly obtaine elsewhere for the enthalpy difference between the two crystal at 298.15 K, the value reported here for the entropy differenc yields a transition temperature between them of $311 \pm 30$ K which is in the range currently cited on other bases. $C_p$ values reported here for the cubic crystal and the glass are consistently 4-5% lower than those previously reported by Tarasov's school, suggesting a systematic proportional effect of the magnitude in those previous values. The proportionality of $C_p$ to $T$ for the cubic crystal from 65 to 160 K, previously erroneously attributed to the monoclinic crystal by Tarasov on the basis of Anderson's $C_p$ data, are discussed.

**12312.** Chang, T-T., Cohen, M. I., Hosler, W. R., **Superhyperfine interactions in $CdF_2$:Yb,** *J. Chem. Phys.* **54**, No. 10, 4278-4280 (May 15, 1971).

Key words: Cadmium fluoride; EPR; superhyperfine interaction; ytterbium.

The superhyperfine structure of $Yb^{3+}$ in $CdF_2$ has been observed. Fitting of the structure was done according to the model of Ranon and Hyde. The principal values of the interaction tensor $T$ were approximated to be $-$ 16.7 MHz for $T_\perp$ and 37.8 MHz for $T_\parallel$.

**12313.** Creutzberg, F., Hougen, J. T., **Rotational line intensities for singlet-triplet transitions in molecules belonging to the point groups $D_{2h}$, $C_{2v}$, and $D_2$,** *J. Mol. Spectry.* **38**, No. 2, 257-272 (1971).

Key words: Asymmetric rotors; matrix elements; rotational line intensities; singlet-triplet transitions; spin forbidden transitions; transition calculations.

Explicit expressions are presented for transition moment matrix elements and Hamiltonian matrix elements which can be used directly in computer programs for calculating rigid rotor line intensities for singlet-triplet transitions in molecules belonging to the point groups $D_{2h}$, $C_{2v}$, and $D_2$. The calculational procedure outlined and the various matrix elements presented can be used for triplet states exhibiting large or small spin splittings in the nonrotating molecule.

**12314.** Fatiadi, A. J., **Evidence for adsorption as the first step in the solid-state oxidation of benzenehexol with active manganese dioxide,** *J. Chem. Soc.* Section B, 889-894 (1971).

Key words: Adsorption; amorphous; free-radical; ionic; manganese dioxide; polycrystalline; structure; surface.

Oxidation of benzenehexol on the surface of amorphous, precipitated ('active') manganese dioxide proceeds by a concerted mechanism, involving ionic and free-radical pathways, to give a croconic acid derivative. This manganese dioxide has a polycrystalline chain structure, in contrast to the crystalline oxidant prepared in deuterium oxide.

**12315.** Fraker, A. C., Ruff, A. W., Jr., **Observations of hot saline water corrosion of aluminum alloys,** *Corrosion* **27**, No. 4, 151-156 (Apr. 1971).

Key words: Aluminum alloys; hot saline water corrosion; oxide films; precipitates; transmission microscopy.

Corrosion films formed on aluminum in hot salt water (100 to 177 °C) after short time tests of thirty seconds to one hour were studied by transmission electron microscopy and diffraction. It was concluded from observation of 6061, 5454, 2024, Al-1.52Mn and Al-1.66Ni alloys that one controlling factor in the initiation and growth of the outer film of the duplex oxide film is the alloy composition. The outer film formed earlier on alloys containing copper and the film growth was also more rapid on these alloys. Additions of magnesium, manganese and nickel retarded this outer film formation but with nickel additions, pitting attack was more severe and deposition of copper from solution was increased. The formation and growth of the outer film was slowest on the 5454 alloy which was also the most resistant alloy tested.

**12316.** Frenkiel, F. N., Klebanoff, P. S., **Statistical properties of velocity derivatives in a turbulent field,** *J. Fluid Mech.* **48**, Part 1, 183-208 (July 13, 1971).

Key words: Computer; correlations; grid; intermittency; isotropy; moments; probability-distributions; turbulence; velocity-gradients.

High-speed digital computing methods are applied to the study of the statistical behaviour of turbulent velocity derivatives in a nearly isotropic turbulent field downstream of a grid. Higher-order correlations of turbulent velocity gradients, up to the eighth order, are measured. Contrary to the case of *velocities*, the higher even-order correlations of *velocity gradients* more clearly evidence the departure from a two-dimensional Gaussian probability distribution. Using non-Gaussian probability distribution laws the relations between different odd- and even-order correlations are obtained and compared with the experimental measurements. The conditions of a similarity and isotropy are evaluated for the small-scale structure as evidenced by the behaviour of the turbulent velocity gradients. The concept of intermittency of the small-scale structure is also discussed.

**12317.** Gadzuk, J. W., Hartman, J. K., Rhodin, T. N., **Approach to alkali-metal chemisorption within the Anderson model,** *Phys. Rev. B* **4**. No. 2, 241-255 (July 15, 1971).

Key words: Chemisorption; impurities; surface physics.

A theory of chemisorption relevant to alkali atoms on metal surfaces is presented. The virtual-impurity-state problem is modeled in the manner presented by Kjöllerström, Scalapino, and Schrieffer by solving the Anderson impurity problem in the low-density approximation (LDA). It is assumed that the binding or chemisorption energy of the alkali metal is composed of two parts, a metallic and an ionic component. Since considerable charge transfer from the alkali atom to the metal occurs, the LDA is appropriate for describing the metallic part of the binding. Another consequence of the large charge transfer is that the major portion of the binding results from an ionic type of bond between the partially charged alkali ion on the surface and a polarization or screening charge inside the metal. The results of the theoretical calculations indicate that binding energies for alkali atoms adsorbed on clean single-crystal faces of metals generally fall within the range of 1.5 $-$ 2.5 eV, in accord with available experimental data on metals such as W, Mo, Ta, and Ni.

**12318.** Grabner, L., Stokowski, S. E., **Photoluminescence of Cr-doped CaTiO,** *Phys. Rev. B* **2**, No. 11, 4351-4353 (Dec. 1, 1970).

Key words: $Cr^{3+}$; energy transfer; excitation; lifetime; photoluminescence.

At 4 and 77 K, photoluminescence from nominally undoped and 0.0025% Cr-doped $CaTiO_3$ shows identical spectra in the infrared with an intensity ratio of 1:2. The emission is attributed to the ${}^2E \rightarrow {}^4A_2$ transition of the $Cr^{3+}$ ion at a $Ti^{4+}$ site. At 4 K it consists of a single no-phonon line at 1.744 eV of half-width 1.5 MeV and a complex vibronic spectrum which is anomalously intense. Data at 77 K show a 2-MeV splitting of the ${}^2E$ state. The absorption spectrum of $CaTiO_3$:Cr is dominated by a "background absorption" by unknown defects. From the coincidence of the excitation spectrum with the absorption spectrum, we conclude that the excitation is dominated by absorption by these unknown defects which transfer energy into $Cr^{3+}$. In undoped $CaTiO_3$ a single-exponential decay of the emission is reported, with decay time 700 $\mu$sec. In $CaTiO_3$:0.0025% Cr, on the other hand, two exponentials with decay times 700 $\mu$sec and 11 msec were observed. The former is assigned to $Cr^{3+}$, the latter to the time of energy transfer from defects responsible for the background absorption to the $Cr^{3+}$. We also report a visible emission consisting of a broad structureless band centered at 2.7 eV, with half-width 0.7 eV. Presumably, it is recombination radiation caused by the recombination of a free charge carrier with a trapped charge at an unknown defect. Its excitation spectrum gives a band gap for $CaTiO_3$ of 3.70 eV at 4 K.

**12319.** Grabner, L., Stokowski, S. E., Brower, W. S., Jr., **No-phonon $^4T_2g$—$^4A_2g$ transitions of $Cr^{3+}$ in $TiO_2$,** *Phys. Rev. B* **2,** No. 3, 590-598 (Aug. 1, 1970).

Key words: Absorption; defect phonon; emission; excitation; lifetime; $^4T_2$ state.

Absorption and emission at 4 and 77 K are observed in Cr-doped $TiO_2$ consisting of two sharp no-phonon lines at 12685 and 12732 $cm^{-1}$, and vibronic sidebands with an integrated intensity $10^4$ times that of the no-phonon lines. In undoped $TiO_2$, identical spectra are observed but are a factor of 100 less intense. The center responsible for these spectra is identified as substitutional $Cr^{3+}$ by observing, in emission, a splitting of the 12685-$cm^{-1}$ line of 1.4 $cm^{-1}$, a value previously determined by EPR measurements. The vibronic sidebands have some structure superposed on a broad band. The vibronics are different in emission and absorption and have a lifetime of 45 $\mu$sec, equal to that of the no-phonon line. They are shown to be principally due to defect-induced phonons arising from the $Cr^{3+}$ defect. We argue that the spectra observed are not characteristic of the usual $^2E_g$-$^4A_{2g}$ transition, and propose that the $^4T_2$ lies lower in energy than the $^2E_g$ state. If so, the new results of this work are (1) no-phonon line emission for the $^4T_2$-$^4A_2$ transition and (2) defect phonon states which are different for the $^4A_2$ and $^4T_2$ states. The excitation spectrum is also presented. It shows that the excitation of the $Cr^{3+}$ emission occurs mainly by the transfer of energy from excited trapping centers rather than by direct excitation.

**12320.** Grimes, D. N., **Imaging of tri-bar targets and the theoretical resolution limit in partially coherent illumination,** *J. Opt. Soc. Am.* **61,** No. 7, 870-876 (July 1971).

Key words: Coherence; partially coherent imaging; resolution; resolving power; tri-bar targets.

In viewing systems that employ critical, Kohler, or collimated illumination, the illumination may frequently be characterized by the complex degree of coherence in the form of a first-order Bessel function divided by its argument. The anomalies that occur in the image of a tri-bar target viewed in partially coherent illumination of this form are discussed for a two-dimensional circular diffraction-limited imaging system. The Sparrow criterion, which in this case correlates with experimental measurements of resolving power, is applied to determine the resolution limit. The computed resolution-limit curve for a tri-bar target is shown and compared to the previously published two-point resolution-limit curve for a one-dimensional system and to the limiting values obtained in a two-dimensional system for coherent and incoherent illumination. In the latter case, the full curve is shown as a special case of the application of the Sparrow criterion to the partially coherent imaging equations for a circular two-dimensional system. Experimental confirmation of the calculations is given.

**12321.** Grimes, D. N., **Measurement of the second-order degree of coherence by means of a wavefront shearing interferometer,** *Appl. Opt.* **10,** No. 7, 1567-1570 (July 1971).

Key words: Coherence; coherence measurement; interferometry; wavefront shearing interferometer.

A method of measuring the second-order degree of coherence in an arbitrary plane by means of a compact wavefront shearing interferometer is described. The prism interferometer previously described by Saunders produces two sheared images that interfere, allowing measurement of the degree of spatial coherence. If the degree of coherence is a function of coordinate differences only, the visibility is constant; otherwise it varies over the field. Experimental results are given.

**12322.** Heydemann, P. L. M., **A fringe-counting pulsed ultrasonic interferometer,** *Rev. Sci. Instr.* **42,** No. 7, 983-986 (July 1971).

Key words: Phase sensitive detection; speed of sound; ultrasonic interferometer; ultrasonics.

A new ultrasonic interferometer for the automatic measurement of transit times is described. Its main advantage is its ability to follow very large changes of the transit time (1-20) and still maintain a resolution of typically $2.5 \times 10^{-10}$ sec. The method is based on the phase sensitive detection of multiple echoes, counting of the output signal at the rate of four counts per full cycle, and an additional interpolation.

**12323.** Hougen, J. T., **Interpretation of molecular-beam radiofrequency ortho-para transitions in methane,** *J. Chem. Phys.* **55,** No. 3, 1122-1127 (Aug. 1, 1971).

Key words: Group theory; inversion splitting; methane; molecular-beam data; ortho-para transitions; radio frequency.

A modified formalism, involving primarily changes in certain group-theoretical arguments, is presented for the data leading to the recent report that the splitting between the two inversion levels of methane has been resolved.

**12324.** Hussman, E. K., McLaughlin, W. L., **Dose-distribution measurement of high-intensity pulsed radiation by means of holographic interferometry,** *Radiation Res.* **47,** No. 1, 1-14 (July 1971).

Key words: Absorbed dose; calorimetry; electron beams; interference fringes; interferometry; pulsed beams; refractive-index holography; temperature profile.

A novel calorimetric method has been developed for evaluating the spatial distribution of radiation absorbed dose in transparent liquids, particularly for dosimetry in pulsed high-intensity electron beams. Local temperature change is determined without the introduction of temperature sensors that may disturb the radiation field. The change in a liquid's refractive index, which is a function of temperature, is measured by an interferometric method employing holographic wavefront reconstruction. For radiation beams essentially symmetric to the direction of propagation, the dose distribution can be derived from the information given by the interferogram. Dose distributions in water have been evaluated for short electron pulses of different energy spectra.

**12325.** Johnson, D. R., Powell, F. X., Kirchhoff, W. H., **Microwave spectrum, ground state structure, and dipole moment of thioformaldehyde,** *J. Mol. Spectry.* **39,** No. 1, 136-145 (July 1971).

Key words: Dipole moment; microwave spectrum; reactive species; rotational spectra; structure; thioformaldehyde.

The microwave spectrum of the reactive species thioformaldehyde ($H_2CS$) has been studied in the ground vibrational state. Rotational transitions in $H_2{}^{12}C^{32}S$, $H_2{}^{13}C^{32}S$, $H_2{}^{12}C^{34}S$, and $D_2{}^{12}C^{32}S$ have been measured and assigned. A detailed centrifugal distortion analysis has been carried out on the species $H_2{}^{12}C^{32}S$ with a total of 27 transitions up to $J=27$ fit to a standard deviation of 26 kHz. Rotational constants obtained from these four isotopic species have been used to obtain the following completely substituted structure: $r_{S=C}=1.6108(9)$Å, $r_{C-H}=1.0925(9)$Å, and $<HCH=116.85(5)°$. The dipole moment of $H_2CS$ was found to be $\mu=1.6474(14)$ Debye from Stark effect measurements on the $J=1_{01} \leftarrow 0_{00}$ transition. The typical reactive half-life of this new species was found to be about 6 min in a static system.

**12326.** Krauss, M., Maldonado, P., Wahl, A. C., **Interaction energy curves of LiHe and NaHe ($X\ ^2\Sigma^+$, $A\ ^2\Pi$, $B\ ^2\Sigma^+$) and $X\ ^1\Sigma^+$ ions,** *J. Chem. Phys.* **54,** No. 11, 4944-4953 (June 1, 1971).

Key words: Hartree-Fock; interaction energy; LiHe; NaHe; transition probabilities.

Hartree-Fock interaction energy curves have been calculated for the $X\,^2\Sigma^+$, $A\,^2\Pi$, and $B\,^2\Sigma^+$ states of neutral LiHe and NaHe as well as for the ground state $X\,^1\Sigma^+$ ions over a range of distances from 3 to 10 a.u. Since it is intended to apply these results to scattering problems, the variation of the dipole and quadrupole moments and the electronic transition probabilities with internuclear distance were also obtained. Both Slater-type functions and Gaussian-type functions were used as variational trial functions with the intention of gauging the efficacy of the Gaussian basis. Except for situations involving small energy minima the Gaussian basis yielded results accurate relative to the Slater basis. The features of the Hartree-Fock interaction energy curves can be summarized as follows:

(1) The $X\,^2\Sigma^+$ interaction energy is purely repulsive for both molecules to the accuracy of the present calculation.

(2) The $A\,^2\Pi$ and $X\,^1\Sigma^+$ curves are strikingly similar for both Li and Na confirming the penetration of the He for this interatomic orientation.

(3) The long-range repulsive behavior of the $B\,^2\Sigma^+$ curve compared with estimates of the correlation energy shows that the internuclear distance dependence of the energy in the region of 10 a.u. is dominated by the Hartree-Fock repulsive curve.

Charge-density plots have been obtained for all states and distances. These are used to illustrate the physical basis of the energy curves.

2327. Krauss, M., Mielczarek, S. R., Neumann, D., Kuyatt, C. E., **Mechanism for production of the fourth positive band system of CO by electron impact on $CO_2$**, *J. Geophys. Res.* **76**, No. 16, 3733-3737 (June 1, 1971).

Key words: CO; $CO_2$; electron impact; fourth positive bands; oscillator strength; Rydberg state; valence state.

The electron impact energy loss spectrum for $CO_2$ is presented over an energy range of 10 to 20 eV. Analysis of this spectrum and molecular orbital calculations indicate that valence state perturbers of $^1\Sigma_u^+$ and $^1\Pi_u$ symmetry contribute significantly to the oscillator strength in the range from 11 to 14 eV. The $^1\Sigma_u^+$ state is then determined to be the predominant contributor to the reaction $CO_2+e\rightarrow CO_2(^1\Sigma_u^+)+e\rightarrow CO(A^1\Pi)+O(^3P)+e$. Unusual intensity distributions in the observed fluorescence of the vibrational states of $CO(A^1\Pi)$ observed by M. J. Mumma, E. J. Stone, and E. C. Zipf (1970) are explained on the basis of competition between predissociation and autoionization from this single state. This mechanism would be one means for production of the fourth positive bands of CO in the ultraviolet dayglow of the upper atmosphere of Mars.

2328. Lafferty, W. J., Ritter, J. J., **Microwave spectrum, dipole moment, and structure of ethynyldifluoroborane**, *J. Mol. Spectry.* **38**, No. 1, 181-194 (Apr. 1971).

Key words: Dipole moment; ethynyldifluoroborane; microwave spectrum; molecular structure; rotational spectrum; Stark effect.

The microwave spectrum of ten isotopic species of ethynyldifluoroborane ($HCCBF_2$) has been measured. Rotational constants of the ground state and the lowest excited vibrational state have been obtained. Structural parameters obtained are: $r_{C-H}=.058\pm0.003$ Å, $r_{C\equiv C}=1.206\pm0.003$ Å, $r_{C-B}=1.513\pm0.005$ Å, $r_{B-F}=1.323\pm0.005$ Å, and $\angle FBF=116.5\pm1.0°$. The dipole moment is $1.87_6\pm0.010\ D$.

2329. Leasure, W. A., Jr., **Truck tire noise—preliminary results of a field measurement program**, *Proc. Purdue Noise Control Conference, Purdue University, West Lafayette, Indiana, July 14-16, 1971*, pp. 41-48 (July 1971).

Key words: Acoustics; noise measurement; noise pollution; noise (sound); sound transmission; tires; transportation noise; trucks; urban planning.

This paper presents an inventory of peak A-weighted sound levels measured during an extensive parametric study conducted to characterize the noise generated by typical rib, cross-bar, and retread type truck tires in actual use. A test sample of nine tread designs, estimated to represent 70-80% (these exact designs) of the truck tire population on the road today, was investigated considering the following variables: wear, loading, speed, pavement surface, and tire location. Test vehicles included both single-chassis vehicles and a tractor-trailer.

The results show that the A-weighted sound level increased with either an increase in load or speed. The pocket retread design always produced the highest level followed by the cross-bar tires and then the rib tires. This ranking held for both new and half-worn tires. The influence of wear and pavement surface is more complex. For all of the tread designs except one there was an increase in noise level between the new and half-worn states. The results for different pavement surfaces are much the same as with wear. The generated noise appears to depend on both the specific tread design and the surface roughness. Individual tires do contribute differently to the overall level depending on their location on the vehicle. In some cases, significant reductions in the noise level were observed when "noisy" tires were mounted inboard of "quieter" tires.

The paper includes a discussion of the measurement and analysis techniques utilized for the establishment of this data base.

12330. Loebenstein, W. V., **Calculations and comparisons of nonideal gas corrections for use in gas adsorption**, *J. Colloid Interface Sci.* **36**, No. 3, 397-400 (July 1971).

Key words: Adsorption; correction for gas; gas; gas law correction; imperfect gas; second virial coefficient.

Volumetric gas adsorption measurements have become increasingly popular in recent years. The techniques for determination of surface area and pore size distribution have become so commonplace that they can almost be termed routine. At the temperature of the adsorption experiment, it is necessary at each equilibrium pressure to correct for the nonideal behavior of the gas surrounding the sample in order to obtain by difference an accurate evaluation of the amount of gas actually adsorbed. The correction factors that are continually used by most adsorption chemists have not been critically reexamined by these ultimate users since they were originally recommended more than thirty years ago. Indeed, textbooks published more than 25 years later continue to perpetuate the same correction factors. It is the purpose of this paper, by comparing correction factors derived from various sources, to avoid gross inaccuracies and to suggest a procedure whereby the investigator may estimate his own factor in instances where tabulated values are not readily available to him.

12331. McNesby, J. R., Kelly, R. V., **Abstraction of hydrogen by methylene**, *Intern. J. Chem. Kinetics* **3**, 293-305 (1971).

Key words: Abstraction; deuterium; isotope effect; ketene; kinetics; methylene.

The photolysis of $CD_2CO$ at 313 nm in the presence of neopentane was carried out over the temperature range 576-706 K. Analysis of the products and isotopic analysis of the methanes demonstrate abstraction of H from neopentane and D from $CD_2CO$ by methylene. The relative kinetics of abstraction of H and D have been measured over the temperature range, and the absolute value for the collision yield of the abstraction of H from neopentane by $CD_2$ at 653 K has been estimated to be about $1.5 \times 10^{11}$ mole$^{-1}$ cm$^3$ sec$^{-1}$, a value $10^3$ times larger than the corresponding reaction of $CH_3$.

**12332.** Madey, T. E., Yates, J. T., Jr., **Electron-stimulated desorption as a tool for studies of chemisorption: A review,** *J. Vacuum Sci. Technol.* **8,** No. 4, 525-555 (July/Aug. 1971).

Key words: Adsorption; chemisorption; cross section; desorption; electron stimulated desorption; hydrogen; nickel; nitrogen; oxygen; surface; tungsten.

Bombardment of solids by low-energy electrons (< 500 eV) can cause various changes in the surface region, particularly if the surface contains an adsorbed layer. Electron bombardment can promote the desorption of energetic neutral and ionic fragments from the surface, can alter the bonding of surface species, and in some cases can cause decomposition of the surface region. These processes are termed electron-stimulated desorption (ESD) phenomena, and this review is primarily concerned with the use of ESD in studies of species adsorbed on surfaces. Topics covered include experimental methods, a theoretical discussion of physical mechanisms, and a detailed discussion of certain specific and well-studied adsorbate-substrate systems.

**12333.** Mandel, J., **Repeatability and reproducibility,** *Mater. Res. Stand.* **11,** No. 8, 8-16 (Aug. 1971).

Key words: Interlaboratory testing; precision; repeatability; reproducibility; test methods, evaluation of.

A simple method is presented for the evaluation of the repeatability and the reproducibility of test methods. The method obviates such difficulties as transformations of scale or weighted analysis of variance.

It is shown, furthermore, that the concepts of repeatability and reproducibility are, by themselves, insufficient to answer the major questions related to interlaboratory testing. Alternative procedures are mentioned. Finally, the paper presents a rationale for a proper choice of the number of laboratories and the number of replicate determinations required for an adequate interlaboratory study.

**12334.** Marlow, W. F., LaFleur, P. D., **Standard reference materials for the analysis of environmental samples,** *Proc. Symp. Nuclear Techniques in Measurement and Control of Environmental Pollution, Salzburg, Austria, Oct. 26-30, 1970,* pp. 91-94 (International Atomic Energy Agency, Vienna, Austria, March 1971).

Key words: Activation analysis; biological; botanical; environment; Standard Reference Material.

As is evidenced by the large number of publications on the subject, especially at this Symposium, many groups are engaged in the analysis of environmental samples of all kinds for their trace element content, as well as for their major constituent content. Perhaps the most versatile and popular method for the rapid, economical analysis of environmental samples for a large number of elements is neutron activation analysis. Also extensively used are x-ray fluorescence analysis, atomic absorption spectroscopy, spark-source mass spectrometry, and emission spectrometry. In many cases, meaningful results for multielement analysis have been difficult to obtain because of the lack of adequate standard materials, despite the limited efforts by some investigators to produce them. Particularly, in the cases of neutron activation analysis and spark-source mass spectrometry the matrix of the sample can have a pronounced effect upon the analysis. It is extremely important that the standard material have a matrix as similar as possible to that of the sample. At present such suitable standard materials are not widely available. Therefore, the U.S. Atomic Energy Commission and the U.S. National Bureau of Standards have instituted a program for the production of a series of special Standard Reference Materials, fully characterized for at least 22 and possibly 30 elements, suitable for use in the analysis of environmental samples, particularly biological samples. These Standard Reference Materials will be available for purchase by all laboratories. Multilaboratory intercomparisons of these Standard Reference Materials will be encouraged.

Details of the nature of these materials, elements for which they will be characterized and analytical techniques used in standardizing them are discussed.

**12335.** Menis, O., Iyer, C. S. P., **Spectrophotometric determination of vanadium and iron with β-isopropyltropolone,** *Anal. Chem. Acta* **55,** 89-95 (1971).

Key words: Analysis of steel samples; extraction with β-isopropyltropolone; simultaneous determination of vanadium and iron; spectrophotometric determination of vanadium.

A spectrophotometric procedure is described for the determination of vanadium and for the simultaneous determination of iron and vanadium using two wavelength measurements, at 470 and 540 nm or 418 and 470 nm. It is based on the formation of chelate complex with β-isopropyltropolone. The complex is extracted with chloroform and in the presence of alcohol the color develops rapidly and is stable for at least 24 hours. The precision of the calibration curve is 1 per cent relative standard deviation. The application and results of the analysis of NBS Standard Reference Material steel samples are presented.

**12336.** Milligan, D. E., Jacox, M. E., **Infrared spectrum and structure of the $SO_2^-$ radical ion,** *J. Chem. Phys.* **55,** No. 3, 1003-1012 (Aug. 1, 1971).

Key words: Alkali metal reactions; charge transfer; electron capture; infrared spectrum; matrix isolation; molecular orbitals; $SO_2^-$ anion; sulfur dioxide.

When a sample of $SO_2$ in a large excess of argon is codeposited at 4 or at 14 K with an atomic beam of an alkali metal, prominent new absorptions appear near 500 cm$^{-1}$ and between 975 and 1100 cm$^{-1}$. The pattern of absorptions is somewhat dependent both upon the alkali metal and upon the temperature at which the sample is deposited. Product absorptions which appear at 495, 985, and 1042 cm$^{-1}$ in samples containing a small concentration of cesium atoms have been demonstrated to be contributed by a single species, shown by isotopic substitution studies to contain one sulfur and two oxygen atoms. A slight splitting in the absorptions of the mixed oxygen isotopic species indicates that the two oxygen atoms are not symmetrically equivalent, either because of a site perturbation or because of a slight nonequivalence of the two S-O bonds. The absorptions have been assigned to the three $SO_2^-$ vibrational fundamentals of a charge-transfer complex in which the residual interaction of the cation is sufficiently small that all of the vibrational data can be fitted within experimental error without considering the motion of the cation. The data are consistent with an O-S-O valence angle of 110±5°. The S-O stretching force constant is significantly lower than that of $SO_2$, consistent with the addition of an electron to an orbital which is antibonding between the sulfur and two oxygen atoms.

**12337.** Ming, T-K., Tauber, S. J., **Chemical structure and substructure search by set reduction,** *J. Chem. Doc.* **11,** No. 1, 47-51 (Feb. 1971).

Key words: Ambiguity; binary matrices; bond adjacency; chemical information; computer; control vector; set reduction; structure search; substructure search.

The set reduction method of Sussenguth for chemical structure and substructure searching has been adapted: structure search and substructure search have been separated into distinct

›routines; first-order and second-order degree have been in-ded in the control vector. This method has been tested on uctures with greater symmetry than has been done previously, l it has been verified for disjoint substructures. A method has en demonstrated for removing the ambiguity inherent in using ond adjacency matrix.

38. Newman, M., **Invariant factors of combinatorial matrices,** *srael J. Math.* **10,** No. 1, 126-130 (1971).

Key words: Designs; incidence matrices; invariant factors; Smith normal form.

The Smith normal forms of an Hadamard matrix of order $4m$ square-free), and of the incidence matrix of a $(v, k, \lambda)$ configu-on ($n=k-\lambda$ square-free $(n,\lambda)=1$), are determined.

39. Rukwied, A., Ruff, A. W., Willard, W. A., **Study of the cel-lular solidification structure in continuously cast high purity opper,** *Metallurgical Trans.* **2,** 2105-2114 (Aug. 1971).

Key words: Cavities; cellular solidification; constitutional supercooling; copper (99.999%); dislocation arrangements; distribution of impurities; precipitate particles; thermomechanical treatment.

he aim of this paper is to characterize the principal micro-ctural features of continuously cast high purity copper 999 pct Cu), particularly those which might influence high perature creep. This material contains a cellular solidification cture resulting from impurity segregation due to constitu-al supercooling of the melt during solidification. This struc- could not be eliminated from the solid copper by ther-mechanical treatment. The grown-in structure was studied ıg optical and electron metallography as well as etch-pitting hniques. In the as-cast material a loose network of dislocation gles was observed, and in certain locations, preferential ing attack. In addition, small voids were found within the ocation tangles. Thermomechanical treatment eliminated the ocation tangles almost entirely, but left locations susceptible referential etching attack. At those locations impurities were bably concentrated into zones of a size of a few 1000 Å. m solubility and concentration considerations, small cipitates (less than 80 Å in size) or clusters of carbon are pected.

40. Rupp, N. W., Bowen, R. L., Paffenbarger, G. C., **Bonding ld-curing denture base acrylic resin to acrylic resin teeth,** *J. m. Dental Assoc.* **83,** 601-606 (Sept. 1971).

Key words: Acrylic teeth; adhesion; autoadhesion; bonding; cold-curing methyl methacrylate; dentures; tensile strength.

onding of cold-curing acrylic resin to acrylic resin teeth in-ses tooth retention and strengthens denture bases because plastic teeth become an integral part of the denture base. ding was effected in this manner: the necks of the teeth were ed with a solution of equal parts by volume of methylene ride and cold-curing methyl methacrylate monomer. This tment combines a solvent attack on the teeth with merization bonding and develops tensile strengths of more 80% of those of the acrylic resin denture base materials. bonding was verified in experimental dentures made of a pression molded and a pour type poly(methyl methacrylate). resin teeth became integral parts of the denture as evidenced eir retention in the base. On application of stresses, the frac-lines went through the teeth rather than through the tooth-ure base interfaces as before. The technique adds neither nor equipment to currently used laboratory procedures.

1. Sengers, J. M. H. L., Straub, J., Vicentini-Missoni, M., **existence curves of $CO_2$, $N_2O$, and $CClF_3$ in the critical re-n,** *J. Chem. Phys.* **54,** No. 12, 5034-5050 (June 15, 1971).

Key words: $CClF_3$; $CO_2$; coexistence curve; critical region; $N_2O$; rectilinear diameter; refractive index.

The coexistence curves of $CO_2$, $N_2O$, and $CClF_3$ are analyzed in the critical region. The curves were obtained by refractive index measurements which are virtually free of gravity effects and contain much detail near $T_c$. After proper weight assignment, it is established that the top of the coexistence curve is asymptotically symmetric: $\rho^{\pm}=\rho_c \pm Bt^{\beta}$; that the exponent $\beta$ is independent of the range, varies little from substance to substance, and is insensitive to impurities; and that the data are in agreement with the law of the rectilinear diameter. "Best" values for $\beta$, $B$, and for the slope of the diameter are presented. An analysis of earlier coexistence curves for $CO_2$ and $N_2O$, including a weight assignment, is presented; there is agreement between the older and newer data.

12342. Winnewisser, G., Maki, A. G., Johnson, D. R., **Rotational constants for HCN and DCN,** *J. Mol. Spectry.* **39,** No. 1, 149-158 (1971).

Key words: Bond distances; hydrogen cyanide; infrared; microwave; molecular structure; rotational constants; spectra.

Microwave measurements of rotational transitions within vibrationally excited states of several isotopic species of HCN have given improved values for the pertinent $B_v$ constants. These new data have been combined with infrared measurements given in the literature (including $D_v$ terms) to arrive at a set of rovibrational constants ($\alpha$ and $\gamma$ constants) which is consistent with all available data. Bond distances resulting from several different $B_e$ approximations are intercompared to assess the variability of the $r_e$ values and the importance of the $\gamma$ terms. The latest $r_0$ and $r_s$ bond distances are also given.

12343. Winogradoff, N. N., Osinsky, V. I., **Density-of-states tails associated with the ⟨100⟩ conduction band minima in heavily doped n-type GaAs,** *Solid State Commun.* **8,** No. 23, 2001-2003 (Dec. 1, 1970).

Key words: Band tailing; gallium arsenide; indirect valleys; *n*-type gallium arsenide; photoluminescence; temperature dependence.

In contrast with the photoluminescence of lightly doped *n*-type GaAs, a *reduction* in the temperature of heavily doped material produced an intensification and a *broadening* of the spectrum on the high-energy side of the band gap. This effect is attributed to the presence of 'density-of-states' tails associated with the indirect ⟨100⟩ minima in the conduction band of the heavily doped material.

12344. Yule, H. P., **Computer data reduction in activation analysis,** *Proc. NATO Advanced Study Institute on Activation Analysis in Geochemistry and Cosmochemistry, Kjeller, Norway, Sept. 7-12, 1970,* pp. 145-166 (1971).

Key words: Activation analysis; component identification; result computation; spectral resolution.

Methods of result computation with activation analysis gamma-ray spectra are reviewed, emphasizing recent developments. For NaI(Tl) detector spectra, the multiple linear regression technique is reported. For Ge(Li) detector, methods of peak location, net peak area computation, and complex peak resolution are indicated. Each technique is discussed for applicability and difficulties in utilization. General features of result computation and of various numerical analytic techniques are discussed.

12345. Alexandropoulos, N. G., Parks, S. H., Kuriyama, M., **Polarization of the x-ray Compton-Raman radiation,** *Physics Letters* **35A,** No. 5, 369-370 (June 28, 1971).

Key words: Azimuthal angle; Compton-Raman interaction; Hamiltonian; polarization; radiation; spectrometer.

The polarization of x-ray photons in the Compton-Raman scattering from polycrystalline lithium has been analyzed by a crystal-polarizer to show that the inelastically scattered photons satisfy the law of Malus, $\cos^2 \phi$ dependence, where $\phi$ is the azimuthal angle of the crystal-polarizer. This result indicates that the $A^2$ term in the interaction Hamiltonian is dominant in the elastic scattering when the transferred energy is different from the binding energy of atomic electrons.

**12346.** Ballantyne, J. P., Yakowitz, H., Munro, E., Nixon, W. C., **Analysis of a variable geometry cylindrical detector for the scanning electron microscope,** *Proc. 25th Anniversary Meeting of the Electronmicroscopy and Analysis Institute Physics Group Conference, Cambridge, England, June 29-July 1, 1971,* pp. 194-197 (1971).

Key words: Electron detector; image contrast; magnetic domains; scanning electron microscope.

The cylindrical detector described by Banbury and Nixon (1969) provides enhanced contrast and directional information from many SEM specimens. This paper describes an initial theoretical analysis of such a detector.

**12347.** Benjamin, I. A., **Research needs in fire and smoke control,** *Proc. Symp. Fire Hazards in Buildings, Semiannual Meeting, American Society of Heating, Refrigerating and Air-Conditioning Engineers, San Francisco, Calif., Jan. 19-22, 1970,* pp. 35-38 (1971).

Key words: Building design; dampers; ducts; fire control; fire spread; smoke movement.

The author discusses problems associated with the movement of smoke and fire in buildings and reviews some of the current design requirements. Selected areas of needed research are pointed out and mention is made of some of the work being conducted by the Fire Research Section of the National Bureau of Standards.

**12348.** Blunt, R. F., Candela, G. A., Forman, R. A., Kahn, A. H., Mangum, B. W., **Magnetic susceptibility and optical studies of $Cr^{3+}$ in $Al_2O_3$ (ruby): Magnetic method for determining concentration,** *J. Appl. Phys.* **42,** No. 8, 3058-3062 (July 1971).

Key words: Concentration determination; magnetic susceptibility; optical absorption coefficient; radiation damage; ruby.

Magnetic-susceptibility and optical-absorption measurements were performed on ruby samples of varying chromium concentration. Susceptibilities were measured by the Faraday method, both with and without selective microwave saturation of the $Cr^{3+}$ susceptibility at resonance. The susceptibility values were used to calculate the $Cr^{3+}$ concentrations, and these together with the optical absorption were used to obtain the "molar" absorption coefficients. The absorption coefficient of 50 $cm^{-1}$/wt% equivalent $Cr_2O_3$, for both the 0.40- and 0.56-$\mu$m band maxima ($E \perp c$), resulted. A $Co^{60}$ $\gamma$ irradiation was performed and the susceptibility was unchanged within experimental error.

**12349.** Cali, J. P., Seward, R. W., **The challenge of the 70's NBS standard reference materials program,** *Am. Lab.* **3,** No. 6, 10-14 (June 1971).

Key words: Agriculture; air and water pollution; biology; botany; health and medicine; instrument calibration; metrology; research materials; standard reference materials; SRM's; Standard Reference Materials Program.

The direction the National Bureau of Standards' Standard Reference Materials Program will take in the next decade is outlined with emphasis on those areas that have only recently been included in the SRM program such as health, pollution, botany, biology and agriculture, and also on areas in which no SRM now exist. As the program moves into these new areas, the tra tional industry-oriented aspects of the program will be ma tained and improved through close cooperation with such sta dards-making bodies as ASTM and ANSI.

**12350.** Carpenter, R. J., Forman, R. A., **Zeeman modulator nuclear quadrupole resonance spectroscopy,** *J. Phys. E: S Instr.* **3,** 922-924 (Nov. 1970).

Key words: Current; modulator; nuclear; pulse; quad pole; resonance; spectroscopy; transistor; Zeeman.

An instrument has been developed to drive modulation co to produce Zeeman modulation in nuclear quadrupole resonar spectroscopy. A sequence of alternately negative and posit current pulses of up to 4 A, spaced by no-current intervals produced. The frequency may be as high as 500 Hz, since electromechanical components are employed. The instrumen described in detail and sample resonance curves are presented

**12351.** Carter, R. S., **The NBS reactor as a source of neutro** *Proc. American Nuclear Society Topical Meeting on Neut Sources and Applications, April 19-21, 1971, Augusta, Ga. I-10–17 (Apr. 1971).*

Key words: Cold neutron source; high flux; irradiati neutron diffraction; research reactor; split core.

The NBS Reactor (NBSR) is a 10 Mw $D_2O$ moderated a reflected reactor. The fuel elements are located seven inch apart in hexagonal arrays around experimental irradiation fac ties. In order to support the broad range of research progra typical of a laboratory like the NBS, the reactor has extensive core, beam tube, and pneumatic tube facilities. Thermal neut fluxes in the beam tubes and higher-flux irradiation facilities about $10^{14}$ n/$cm^2$ -s. Several unique features of the NBSR c tribute to its versatility. They include a thermal column with c mium ratios for gold foils as high as 30,000 to 1, a split core minimize the intensity of very high energy neutrons in the be tubes, and a cold neutron source to enhance the intensity of v low energy neutrons available for certain inelastic scattering periments. Extensive, automated experimental facilities h been developed to fully utilize the neutron beams and irrad tions provided by the NBSR.

**12352.** Cohen, J., Edelman, S., Vezzetti, C. F., **Pyroelectric ef in polyvinylfluoride,** *Nature (London) Phys. Sci.* **233,** (Sept. 6, 1971).

Key words: Infrared; piezoelectricity; polymers; polyvi fluoride; pyroelectricity.

Significant infrared sensitivity has been obtained in orier polyvinylfluoride, apparently due to pyroelectricity.

**12353.** Durst, R. A., Duhart, B. T., **Ion-selective electrode st of trace silver ion adsorption on selected surfaces,** *Anal. Ch* **42,** No. 9, 1002-1004 (1970).

Key words: Electrometric study of silver adsorption; si adsorption; silver ion-selective electrode; trace silver de mination.

This study demonstrates the feasibility of using a silver selective electrode for monitoring silver ion losses in long-t investigations of trace silver adsorption on various container faces. The electrometric technique offers the advantages of complex and costly equipment, simplified procedure, and proved precision over the radiometric method. Nernstian e trode response was observed down to $4 \times 10^{-7}$ *M* silver. maximum sensitivity, $2 \times 10^{-6}$ *M* (0.2 ppm) silver was sele as the concentration for the test solution which was place Pyrex, Desicoted Pyrex, polyethylene, Vycor, and Teflon tainers. At various intervals up to 46 days, duplicate E readings were made on each of the five solutions with peri tandardization of the electrode to permit drift corrections. sorption levels at the end of 30 days increased in the order: cor < polyethylene ≈ Teflon < Desicoted Pyrex < Pyrex; ging from 28 percent adsorption for Vycor to 48 percent for rex. Although for periods of up to a day, silver losses on lon were less than 2 percent, this study indicates that none of above materials is suitable for long-term storage of solutions taining low levels of silver.

**54.** Evans, J. P., Wood, S. D., **An intercomparison of high tem-erature platinum resistance thermometers and standard ther-nocouples,** *Metrologia* **7,** No. 3, 108-130 (July 1971).

Key words: Calibration; fixed point; freezing point; furnaces; high temperature; IPTS-68; platinum resistance thermometer; temperature scale; thermocouple; triple point.

o obtain some of the information necessary for redefining a ctical temperature scale in terms of resistance thermometry to the gold point, we have intercompared nine high tempera-e platinum resistance thermometers and eight standard ther-couples at 50 degree intervals over the range 630.74 to 4.43 °C. Values of temperature were derived from "before after" calibrations of the instruments at the freezing points gold, silver, antimony, zinc, and tin, and at the triple point of er. Analysis of the data showed that the standard deviation of peratures measured with thermometers was about 4 mK, le with thermocouples it ranged from 25 to 30 mK. When tematic errors were accounted for, we found that values of peratures on IPTS-68 could be determined with a single ther-meter, using an interpolation formula analogous to that used ow 630.74 °C, with about one-third the uncertainty usually at-uted to a single thermocouple determination (± 200 mK). The a also revealed that there is a lack of "smoothness" in the le at 630.74 °C—first derivatives with respect to $t_{68}$ are continuous by about 0.1 percent at this temperature. We con-de from the results of this work that if a practical temperature e were redefined in terms of presently available high tem-ature platinum resistance thermometers, it could be realized n significantly less uncertainty (± 12 mK for a single deter-ation) than IPTS-68, as it is now realized with thermocouples 00 mK for a single determination). We recommend, how-r, that the adoption of such a scale be deferred until indicated rovements in thermometers have been made, and until cur-researches in gas thermometry have provided new values of modynamic temperatures for calibrating fixed points.

**55.** Fetters, L. J., Yu, H., **Equilibrium conformation and worm-like coil" configuration of poly(*n*-alkyl isocyanates),** *acromolecules* **4,** No. 4, 385-389 (July-Aug. 1971).

Key words: Configuration; conformation; Kratky-Porod model; light scattering; osmotic pressure; poly(*n*-alkyl isocyanates); radii of gyration; second virial coefficients.

smotic pressure and light-scattering measurements of the mers of *n*-butyl, *n*-hexyl, and *n*-octyl isocyanates are ented. The molecular weight dependence of the osmotic ond virial coefficients and the radii of gyration is analyzed in ns of the worm-like-coil model of Kratky and Porod. The acterization of the *n*-butyl polymer, which has been studied t extensively, results in 500-600 Å for the persistence length 1.8-2.1 Å for the monomeric projection along the contour ction of the chain. The dependence of the radii of gyration on weight-average molecular weights for the *n*-hexyl and *n*-octyl mers is found to be similar to that for the *n*-butyl polymer. s, although our analysis has focused on the *n*-butyl species, pears that a similar set of Kratky-Porod parameters should pplicable to the other polymers with normal aliphatic side ns of moderate length.

**6.** Flynn, J. H., **The historical development of applied nisothermal kinetics,** (Proc. 2nd Intern. Conf. on Thermal Analysis, Holy Cross College, Worcester, Mass., Aug. 19-23, 1969), *Thermal Analysis* **2,** 1111-1126 (Academic Press, Inc., New York, N.Y., 1969).

Key words: Applied nonisothermal kinetics; generalized techniques; historical review; isoconversional and isokinetic methods; isothermal; kinetic parameters; thermogravimetric analysis.

In spite of a surprisingly extensive literature prior to 1950 on nonisothermal kinetic methods, this field was long ignored by chemical kineticists who were preoccupied with simple systems in the gas phase or in homogeneous solution. In such systems, the equations of state of each involved species change with temperature so that isothermal restrictions were often necessary.

However, the advent of wide interest in thermogravimetric techniques applied to condensed phase volatilization reactions has helped the kineticist shake off the shackles of isothermicity and has fostered the development of new and powerful methods of kinetic analysis.

The neglected early literature is reviewed briefly in light of modern developments. Generalized techniques for determining kinetic parameters under isothermal, isoconversional and isokinetic conditions are outlined and illustrated.

**12357.** Franklin, A. D., Crissman, J., **Reorientation of trivalent cation-interstitial fluorine pair in $CaF_2$,** *Letters to the Editor, J. Phys. C: Solid State Phys.* **4,** L239-L242 (July 12, 1971).

Key words: Anelastic relaxation; calcium fluoride; defect pairs; dielectric relaxation; relaxation modes; reorientation.

A simple model based on the synthesis of de Gennes' double exchange concept and Hubbard's treatment of correlation in narrow band systems is proposed to account for the transition from the antiferromagnetic insulating state to the metallic state observed in various transition metal compounds.

**12358.** French, J. L., **Discussion of "Are individual current-meter ratings necessary,"** *J. Hydraulics Div. Proc. Am. Soc. Civil Engrs.* **HY1,** 507-511 (Jan. 1969).

Key words: Calibration; current meters (fluids); hydraulics; measurement; open-channel flow; standards.

This is a discussion of the paper "Are Individual Current-Meter Ratings Necessary?", Journal of the Hydraulics Division, American Society of Civil Engineers, March 1968. Experimental data relating to the performance of a Price current meter are presented. The data were obtained in a simulated working section of a water tunnel. It is concluded that the precision with which a Price meter responds to a given water flow is greater than might be expected from the data listed in the authors' tables 1 and 2.

**12359.** French, J. L., **Nonenlarged box culvert inlets,** *J. Hydraulics Div. Proc. Am. Soc. Civil Engrs.* **HY6,** 2115-2137 (Nov. 1969).

Key words: Culverts; entrance control; hydraulics; inlets.

The effect of variation in the dimensions of beveled leading edges on the discharge capacity of box culvert inlets of rectangular cross section is investigated. It is demonstrated that the effective control surface of a beveled edge may be either the face of the headwall or the beveled surface of the edge geometry, depending on the relative dimensions of the beveled edge. The bevel dimensions required to ensure bevel surface control are determined. The dependence of the discharge coefficient on the dimensions of the beveled leading edge and on the cross-sectional shape of the barrel is demonstrated. Methods for estimating the capacity in submerged entrance flow of box culvert inlets operating in entrance control are developed for various beveled leading edge geometries.

**12360.** Gebbie, K. B., Thomas, R. N., **The temperature control bracket,** *Astrophys. J.* **168,** No. 3, 461-479 (Sept. 15, 1971).

Key words: Boundary temperature; collisional-control; non-LTE; radiative-control; temperature-control-bracket.

The factors determining the temperature distribution in a stellar atmosphere are divided into transfer effects and population effects. As a measure of the latter, we introduce the Temperature Control Bracket [TCB], which, in radiative equilibrium, describes the control of $T_e$ by the quantity and spectral distribution of the radiation field. Algebraic expressions for the [TCB] are given in terms of the microscopic rate processes for a pure hydrogen atmosphere. A caricatured computation is presented to demonstrate the influence of the various physical effects on the distribution of $T_e$ in radiative equilibrium.

**12361.** Gravatt, C. C., **The application of light scattering,** *Appl. Spectry.* **25,** No. 5, 509-516 (Sept.-Oct. 1971).

Key words: Air pollution; Brillouin spectroscopy; lasers; light scattering; macromolecules; optical mixing spectroscopy; review.

Light scattering provides information concerning the size, shape, number, and time dependence of the physical nonuniformities of a system. Measurements of the scattered intensity as a function of both scattering angle and wavelength describe static properties, whereas the spectral distribution of the scattered radiation is related to time dependent phenomena. The applications of light scattering are discussed, including critical phenomena, molecular weight determination, air pollution analysis, and diffusion phenomena.

**12362.** Grimes, D. N., **Linear microdensitometry,** *J. Opt. Soc. Am.* **61,** No. 9, 1263 (Sept. 1971).

Key words: Diffuse density measurement; linear microdensitometer; microdensitometry.

A linear microdensitometer is proposed whose operation is independent of the coherence of the source used and which measures diffuse density. A theoretical analysis is given.

**12363.** Grundl, J. A., **Fission-neutron spectra: macroscopic and integral results,** *Proc. Neutron Standards and Flux Normalization, Symp. Argonne National Laboratory, Argonne, Ill., Oct. 21-23, 1970, sponsored by the European American Nuclear Data Committee,* pp. 417-451 (Aug. 1971).

Key words: Fission cross sections; fission neutron spectra; integral measurements.

Certain integral measurements performed with pure fission neutrons, and also with macroscopic systems that are dominated by the fission spectrum, locate an important area of difficulty for differential microscopic data. The classic measured value for the $^{238}$U average fission cross section for $^{235}$U thermal-neutron-induced fission neutrons, $\sigma_f(\chi_{25}, {}^{238}\mathrm{U}) = 310 \pm 4$ mb, is in serious disagreement with predicted values which fall between 270 and 282 mb depending upon the choice of $^{238}$U fission cross section and fission spectrum shape. Critical consideration is given to direct absolute determinations of $\sigma_f(\chi_{25}, {}^{238}\mathrm{U})$, and to indirect values obtained from fission ratio measurements with activation detectors. The latter substantiate the classic value and also provide a new value for the $^{239}$Pu fission spectrum. Equivalent disagreements with prediction occur in the interpretation fission ratio measurements performed in $^{235}$U and $^{239}$Pu metal critical spheres, and the discrepancy between calculated and measured age-to-indium-resonance of fission neutrons in water is in a direction consistent with the fission spectrum discrepancy. The growing importance of integral measurements for the technology of nuclear energy, and the consequent need for fast-neutron standardization to serve it, is assumed to emphasize the difficulties summarized in this review.

**12364.** Hall, J. T., Dixon, R. G., **Getting it all together cybernetic way,** *Management Rev.* pp. 16-22 (Americ Management Association, Inc., New York, N.Y., July 197

Key words: Brainstorming; cybernetic technique; data c lection; group dynamics; interpersonal relationshi management research; opinion survey.

This paper describes a number of management research periments with a technique for generating and gathering ide quickly and effectively, from people in moderate to large s groups. The experiments were conducted by the Managem and Organization Division of the National Bureau of Standar The paper also describes applications of this technique by reau staff members to various community related situations.

The mechanics by which this technique works involve the lection of inputs and feedbacks from individuals arrayed i variety of configurations. As the collection process proceed process of synthesis and a process of evaluation also occur. T primary value of the technique, again, is the ease with which it lows us to comprehend and capture complex ideas from gro of people.

Through the dynamics of capture, feedback, and recaptur thoughts in a changing interpersonal environment, users much closer to the reality or at least to the shape of gr opinions and ideas; closer than any survey or questionn techniques we have used or seen used in the management field

**12365.** Hellwig, H., Barnes, J. A., Glaze, D. J., **Frequency bi in a beam tube caused by Ramsey excitation phase differen** *Proc. 25th Annual Symp. on Frequency Control, Atlantic C N. J., April 26-28, 1971,* pp. 309-312 (Electronic Indust Association, Washington, D.C., April 1971).

Key words: Cavity phase shift; cesium beam tube; frequ cy accuracy; frequency modulation; frequency stand power shift; resonance line shape.

A phase difference between the two interaction regions Ramsey excitation resonance structure results in a freque bias in the measured beam resonance. A simple mathemat model is discussed which describes the dependence of this on the phase difference, the microwave power level, the mod tion amplitude, and the resonance linewidth. This depende results from the interaction of the modulated microwave ex tion frequency with the asymmetric shape of the slightly shi resonance line. In a first order approximation, no dependenc the frequency modulation amplitude is expected. Near-linear pendencies on the linewidth and microwave power level wl are quite pronounced even at relatively small cavity phase ferences are predicted.

The theoretical results are compared with one set of exp mental data on the microwave power dependence as meas in 1969 with the primary cesium beam standard NBS-III. A a correction is applied to remove the power dependence du spectral impurity of the microwave excitation, the remai measured power dependence agrees quantitatively with that culated using a cavity phase difference of about 3 milliradians

**12366.** Kulin, G., **Discussion of the paper "Triangular br crested weir," by C. D. Smith and W. S. Liang,** *Proc. Am. Civil Engrs., Irrigation Drainage Div. 96,* **IR4,** 494-497 ( 1970).

Key words: Flow measurement; weirs, broad-crested.

Published data on discharge coefficients for triangular br crested weirs are analyzed using a boundary layer model. Eff of changing the critical Reynolds number for boundary transition and possible scale effects are pointed out.

367. Laufer, A. H., Okabe, H., **Heat of formation and bond dissociation energy of diazomethane by a photodissociation method,** *J. Am. Chem. Soc.* **93,** 4137-4140 (1971).

Key words: Bond dissociation energy; diazomethane; heat of formation; vacuum ultraviolet.

A lower limit for the heat of formation of diazomethane has en obtained from measurement of the minimum energy quired to produce the $A^2\Delta$ state of CH in the low-intensity cuum-ultraviolet photolysis of diazomethane. The value obned is $\Delta H_f{}^\circ{}_0(CH_2N_2) \geqslant 51.3$ kcal/mol (2.22 eV). In conjuncn with $\Delta H_f{}^\circ{}_0$ $(CH_2) = 93.0$ kcal/mol, the dissociation energy the C=N bond in diazomethane is $\leqslant 41.7$ kcal/mol (1.81 eV). easonable upper limits for $\Delta H_f{}^\circ{}_0(CH_2N_2)$ are discussed.

368. Lawless, W. N., Radebaugh, R., Soulen, R. J., **Studies of a glass-ceramic capacitance thermometer btween 0.025 and 2.4 K,** *Rev. Sci. Instr.* **42,** No. 5, 567-570 (May 1971).

Key words: Capacitor; depolarization; dielectric; dilution refrigerator; glass ceramic; phase transition; strontium titanate; thermometer.

Capacitance measurements from 0.025 to 2.4 K are reported capacitance thermometers (made from an $SrTiO_3$ glassramic crystallized at 1100 and 1203 °C), two of which were ones reported in the previous article. It was found that the 00-type thermometer has a useful thermometric range down 0.06 K and a linear *C-T* region down to 0.5 K. The 1100-type ermometer has a useful range down to 0.110 K and a linear reon down to 1.1 K. The measured data do not appear to be inenced by self-heating or adiabatic correction effects. Both ermometers display an unexpected increase in capacitance th decreasing temperature below their monotonically decreas ranges. The 1100-type thermometer displays the more onounced increase, with $C \propto T^{-1}$ from 0.100 to 0.025 K. It is gued that this $T^{-1}$ behavior is due to the onset of an ultralow nperature phase transition in the glass crystallized $SrTiO_3$, and possibility of using this effect to achieve adiabatic depolarizan cooling is discussed.

369. Milligan, D. E., Jacox, M. E., **Infrared spectrum of the BrHBr$^-$ ion isolated in an argon matrix,** *J. Chem. Phys.* **55,** No. 5, 2550-2560 (Sept. 1, 1971).

Key words: Alkali metal reactions; $BrHBr^-$; charge transfer; $ClHCl^-$; electron attachment; infrared spectrum; matrix isolation; molecular rotation; vacuum-ultraviolet photolysis; vibrational potential function.

nfrared absorptions assigned to $\nu_3, (\nu_3 + \nu_1)$, and $(\nu_3 + 2\nu_1)$ of HBr$^-$ have been observed in samples of HBr in an argon trix which have been subjected to 1216-Å photolysis or which ve been co-deposited with an alkali metal atomic beam and n subjected to mercury-arc radiation. The corresponding eximents on deuterium-enriched samples support this identifica. Mechanisms by which $BrHBr^-$ is produced in these experints are considered in detail. An atomic mechanism leading to stabilization of the uncharged species is shown to be inquate. However, several ionic processes may contribute to observed production of the anion. As previously postulated, sociative electron attachment to $(HBr)_2$ may occur. In addin, it is necessary to postulate the production of $Br^-$ by various rge-transfer processes, followed by the reaction of $Br^-$ with r. Analysis of the infrared spectra of $BrHBr^-$ and of $BrDBr^-$ icates that the vibrational potential function must include sigcant contributions from both cubic and quartic terms.

70. Mountain, R. D., Raveché, H. J., **Entropy and molecular orrelation functions in open systems. II. Two- and three-body orrelations,** *J. Chem. Phys.* **55,** No. 5, 2250-2255 (Sept. 1, 971).

Key words: Configuration entropy; correlation function; entropy; hard sphere; liquid state; neon; Percus-Yevick equation.

We consider the contributions from the correlation of pairs and triples of molecules to the configurational entropy per molecule of a simple fluid system. Using numerical values of the pair function and only certain moments of the triplet function, we have computed the first few terms in an expression for the entropy in terms of the correlation functions. The results, which compare favorably with experimental values over a range of densities including that of the liquid, indicate that the contributions from the correlations of triples of molecules can be appreciable. The computations are done for a fluid of hard spheres and liquid neon and the results are discussed in terms of the molecular correlations in a simple fluid.

12371. Page, C. H., **External field of an ideal toroid,** *Am. J. Phys.* **39,** No. 9, 1039-1043 (Sept. 1971).

Key words: Leakage flux; magnetic field; toroid; transformer; vector potential.

The external magnetic field of an ideal toroid vanishes for dc excitation but not for an ac excitation. The external static field has a nonvanishing vector potential; the emf in a transformer winding is due to the time variation of this vector potential. An expression for the external magnetic field is derived, and it is shown that the external flux density is a negligible fraction of the flux density in the core.

12372. Page, C. H., **On the external magnetic field of a closed-loop core,** *Am. J. Phys.* **39,** No. 10, 1206-1209 (Oct. 1971).

Key words: Magnetic field; solenoid; toroid; transformer; vector potential.

An infinite solenoid, or a toroidal coil, has no external magnetic field for dc excitation but has a nonvanishing vector potential field. The development of the steady-state condition from the transient response to step excitation is discussed. Under ac excitation, an external magnetic field must be present, but in practical cases its magnitude is negligible.

12373. Raveché, H. J., **Entropy and molecular correlation functions in open systems. I. Derivation,** *J. Chem. Phys.* **55, No. 5,** 2242-2250 (Sept. 1, 1971).

Key words: Activity derivatives; closed system; correlation functions; entropy; open system; potentials of mean force.

A method is presented for obtaining an expression for the entropy in terms of molecular correlation functions defined in the grand canonical ensemble. The procedure is for a system of a single molecular species whose dynamics are determined by classical equations of motion. The entropy is obtained as a sum of two different classes of functions each involving the correlations between *n*-tuples of molecules. One class contains logarithmic terms similar to those obtained for the closed system; the other class involves isothermal activity derivatives of potentials of mean force. The latter terms, which are moments of the correlations between disjoint sets of molecules, can make appreciable contributions to the entropy. The method leads to results similar to those obtained from a different procedure by Nettleton and Green. The expression for the entropy is obtained and properties of the results are discussed for a simple fluid system.

12374. Rubin, R. J., **Comment on "Conformation of adsorbed polymeric chain. II,"** *J. Chem. Phys.* **51,** No. 10, 4681 (Nov. 15, 1969).

Key words: Adsorption; chain polymer; lattice model; partition function; random walk.

There is an error in one of the results in a recent paper by Motomura and Matuura [K. Motomura and R. Matuura, Mem.

Fac. Sci., Kyushu University **6**, 97 (1968)]. The result in question, which concerns the mean square end-to-end separation of an adsorbed polymer chain, is quoted in a subsequent paper [K. Motomura and R. Matuura, J. Chem. Phys. **50**, 1281 (1969)]. In this Comment, the origin of the error is identified and the form of the correct result is indicated.

**12375.** Rubin, R. J., **Transmission properties of an isotopically disordered one-dimensional harmonic crystal. II. Solution of a functional equation,** *J. Math. Phys.* **11,** No. 6, 1857-1867 (June 1970).

Key words: Defects in harmonic crystal; functional equation; many-body problem; multiple scattering; statistical physics; transmission coefficient.

The amplitude of a wave of frequency $\omega$ which is transmitted by a disordered array of $N$ isotopic defects in a 1-dimensional harmonic crystal is investigated in the limit $N \rightarrow \infty$. In particular, the ratio $\hat{T}_N(\omega)$ of the amplitude of the $N$th defect to the amplitude of the first defect is represented as $\exp [-N\hat{\alpha}_N(\omega, Q, \{a_n\})]$, where $\{a_n\}$, $n=2, \cdots, N$, is the sequence of nearest-neighbor spacings and $Q=(M-m)/m$. It is known from earlier work that $\hat{\alpha}_N(\omega, Q, \{a_n\})$ is the logarithm of the $N$th root of the magnitude of a continuant determinant of order $N$. The value of the continuant is expressed formally as a product of $N$ factors $\hat{g}_n$ which are recursively related. In the present case, the $\hat{g}_n$ happen to lie on a circle $K_0$ in the complex $\hat{g}$ plane. Assuming that the spacings between defects are independent identically distributed random variables with the mean value $c^{-1}$ and going to the limit $N \rightarrow \infty$, a functional equation for the limiting distribution function of the $\hat{g}_n$ on $K_0$ is derived. The limiting value $\alpha(\omega, Q, c)=\lim \hat{\alpha}_N(\omega, Q, \{a_n\})$, as $N \rightarrow \infty$, can be determined from the limiting distribution function of the $\hat{g}_n$. We determine the solution of the functional equation in three different ways for three different cases: (a) In the case of the special frequency of Matsuda, $\omega = 2^{-1/2}$ and $Q=1$, we obtain exact values of the integral of the $\hat{g}$ distribution function which are in excellent agreement with Monte Carlo estimates; (b) in the physically interesting case where the mean spacing between defects is small compared to the incident wavelength, i.e., $c^{-1}\omega \ll 1$, we obtain the solution of the functional equation correct to first order in $c^{-1}\omega$ and we calculate the lowest-order nonzero value of $\alpha(\omega, Q, c)$; (c) for the general case of moderate values of $\omega$, $Q$, and $c$, we develop a numerical method for solving the functional equation and present the results of the numerical calculations in several representative cases. These numerical results are in good agreement with Monte Carlo estimates. One of the principal results, obtained by solving the functional equation, is that $\alpha(\omega, Q, c) > 0$ for $\omega \ll c < 1$ and $\omega(|Q| + c^{-1}) \ll 1$ with $Q \neq 0$.

**12376.** Rubin, R. J., Greer, W. L., **Abnormal lattice thermal conductivity of a one-dimensional, harmonic, isotopically disordered crystal,** *J. Math Phys.* **12,** No. 8, 1686-1701 (Aug. 1971).

Key words: Disordered one-dimensional crystal; multiple scattering; statistical physics; thermal conductivity; transport properties.

Energy transport is investigated in a model system for which exact analytic results can be obtained. The system is an infinite, one-dimensional harmonic crystal which is perfect everywhere except in a finite segment which contains $N$ isotopic defects. Initially, the momenta and displacements of all atoms to the left of the defect region are canonically distributed at a temperature $T$, and the right half of the crystal is at a lower temperature. This initial nonequilibrium state evolves according to the equations of motion, and ultimately a steady state is established in the vicinity of the region containing the defects. The thermal conductivity is calculated from exact expressions for the steady state energy flux and thermal gradient. For a crystal in which the $N$ isotopic defects are distributed at random but in which the overall defect concentration is fixed, we demonstrate that the thermal conductivity approaches infinity as least as fast as $N^{1/2}$. A Monte C
evaluation of the thermal conductivity for a given defect-to-h
mass ratio and concentration is carried out for a series of rand
configurations of $N$ defects for $N$ in the range, $25 \leq N \leq 6$
The thermal conductivity is proportional to $N^{1/2}$ within
statistical uncertainty except for slight deviations at the smal
values of $N$.

**12377.** Saylor, C. P., **Return of the prodigal,** *Capital Chem.*
No. 6, 95-99 (Sept. 1971).

Key words: Cathedral; deformation; lead; roof; Washing
Cathedral; "1921."

The Washington Cathedral, built in the English style,
given a lead roof. Under the hot Washington sun, it crept.
caused it to leak. E. W. Washburn, Chief Chemist of NBS, d
nosed the difficulty and suggested correction. The eve
recounted in this article took place shortly after 1921.

**12378.** Shoup, R. R., VanderHart, D. L., **Effect of CH sc
coupling on $^{13}$C transverse relaxation times,** *J. Am. Chem.*
**93,** 2053-2054 (1971).

Key words: Fourier transform; nmr; relaxation; sc
coupling; sensitivity; $^{13}$C.

Experimental $^{13}$C NMR relaxation rates are reported fo
percent enriched $^{13}CH_3I$, $^{13}CH_3COOCD_3$, and $^{13}CS_2$. Excep
$CS_2$ transverse relaxation rates, $R_{2C}$'s, are found to be subs
tially higher than the corresponding longitudinal relaxation ra
This effect is shown, on the basis of the variation of $R_{2C}$
Carr-Purcell pulse repetition rate, to arise from scalar coup
of $^{13}$C with relaxing protons. Implications for $^{13}$C spectrosc
particularly Fourier transform techniques, are discussed.

**12379.** Smith. J. C., Kermish, G. A., Fenstermaker, C.
**Separation of filler particles from the matrix in a particul
loaded composite subjected to tensile stress,** *Proc. 162nd M
ing American Chemical Society, Organic Coatings
Plastics Chemistry, Washington, D.C., Sept. 13-15, 1971*
No. 2, 149-155 (Sept. 1971).

Key words: Composite materials; coupling agents; ep
polymer; parting agents; poisson's ratio; release age
stress-strain curve; volume dilation.

Simultaneous measurements of tensile stress, longitud
strain, and transverse strain were obtained on particulate-fi
composites. The matrix was a flexible epoxy polymer. S
glass spheres were used as filler in various volume ratios u
.35. The spheres were pretreated as follows: clean, coated
a parting agent, coated with either of two silane coupling age
The volume expansion behavior of composites containing p
ing agent treated spheres could readily be distinguished from
of composites containing clean glass spheres, but differe
caused by coating the spheres with coupling agents could no
distinguished. Stress-strain behaviors for the various comp
systems also showed differences. These differences in both k
of data are taken as indicative of matrix-filler separation and
sequent vacuole formation.

**12380.** Tech, J. L., Ward, J. F., **Accurate wavelength meas
ment of the $1s2p\,^3P^{\circ}-2p^2\,^3P$ transition in $^4$He I,** *Phys. Rev.
ters* **27,** No. 7, 367-370 (Aug. 16, 1971).

Key words: Atomic energy levels; atomic theory;
toionization; helium; wavelength measurement.

An accurate spectroscopic measurement has yielded 320.2
±0.0010 Å for the wavelength of the $1s2p\,^3P^{\circ}-2p^2\,^3P$ transi
in $^4$He I. Combining this wavelength with the well-known p
tion of the $1s2p$ term gives an experimental value of 481301
1.2 cm$^{-1}$ for the position of the doubly excited $2p^2\,^3P$ term
tive to the ground $1s^2\,^1S$. The new measurement is in exce
agreement with Aashamar's theoretical calculation of 4813
cm$^{-1}$ for the energy of the term.

**2381.** Ambler, E., **Measurement standards, physical constants, and science teaching,** *Sci. Teacher* **38,** No. 8, 63-71 (Nov. 1971).

Key words: Measurement standards; physical constants; science teaching.

Man's intuitive ability to perceive and recognize such con-
epts as temperature and distance is well-developed even before
s formal education begins. The inherited internal measurement,
- sensory, systems are extremely sensitive and lead to a direct
wareness and comprehension of the physical world in ways we
o not yet completely understand. Man's need to measure and
uantify more formally and less intuitively goes back as far as
corded history itself.

Man's ability to measure physical quantities in a coherent and
tional manner grew with the development of physics as a
ience. Indeed our very basic concepts of the nature of the
hysical world, such as mass, time, temperature, entropy and so
n, related as they are through the laws of physics, provide the
asis for a coherent and internationally recognized system of
easurement. The need to root our measurement system deeply
our understanding of natural phenomena was recognized from
e very outset of organized metrology ("un Nouveau système
étrique") long before our understanding of relativity, atomic
ructure, quantum theory and the significance of fundamental
ysical constants, such as the speed of light, Planck's quantum
action and the basic unit of electric charge, developed. Yet the
me general principle applies today as it did two hundred years
o, as we strive to incorporate the latest developments, such as
e coherent light from lasers and the coherent electric currents
superconduction, into a better physical measurement system.

As matters now stand our ability to measure physical quanti-
s is extremely refined and has been extended far beyond the
nges of intuitive perception, so that we can measure the diame-
of atoms that we cannot see, and the distance to the moon
at we cannot reach. It is strange that some quantities that were
atively recently only poorly understood, such as electric cur-
nt, are now almost universally understood and are measured
th utmost confidence and precision every day, while in other
antities, such as the difference between sound that is pleasing
d sound that is annoying, to which man has surely responded
ice time immemorial, we measure with much less unanimous
nfidence. Yet now we are called upon to measure more com-
x quantities such as noisiness of sounds in connection with
asuring and controlling our environment. We are faced with
king physical phenomena, which we understand quite well,
th human response which we understand less well. It seems
rly clear that a deeper scientific study of the workings of man's
nses and an understanding of reasonable limits of his adapta-
ity to variations in the stimulation of his senses is a challenging
ld in which there is great need to devise new methods of
aningful measurement.

**382.** Blandford, J. M., Baker, H. A., **Sewing threads for the apparel industry,** *Apparel Research Foundation, Inc., Washington, D.C.*, pp. 1-153 (May 15, 1971).

Key words: Apparel industry; industry, apparel; performance, sewing thread; properties, sewing thread; quality control, sewing threads; sewing threads; testing programs, sewing thread tests, sewing thread; thread properties; threads, sewing.

The objectives, development, and achievements of the National Bureau of Standards (NBS) Sewing Thread Project, carried out in collaboration with The Apparel Research Foundation, Inc. (ARF) are discussed.

The results of two questionnaire-surveys conducted among thread and apparel companies are summarized, as are the opinions expressed by thread and apparel manufacturers on industry-wide adoption of a uniform thread-sizing system.

Included are tabulations, graphs, and a statistical analysis of NBS tests of threads representative of those currently used by the apparel industry: soft and mercerized cotton; core and spun polyester; and nylon.

Testing programs for evaluating (1) the quality of threads purchased by the apparel manufacturer; and (2) the performance of threads in the apparel product, are discussed in detail. The following information is tabulated: testing equipment; properties which may be determined by its use; testing procedures and evaluation materials employed; and sources of supply and approximate prices of the equipment and evaluation materials. Supplementing the text are reprints of the 21 referenced test methods.

**12383.** Brandenberger, H., Hadron, F., Halford, D., Shoaf, J. H., **High quality quartz crystal oscillators: Frequency domain and time domain stability,** *Proc. 25th Frequency Control Annual Symp., Atlantic City, N.J., Apr. 26-28, 1971,* pp. 226-234 (Electronic Industries Association, Washington, D.C., Apr. 1971).

Key words: Allan variance; flicker of phase noise; frequency stability; oscillator noise models; phase noise spectral density; quartz crystal oscillator; time domain stability.

We measured the frequency stability of a pair of commercial 5-MHz quartz crystal oscillators which incorporate improved electronic design for enhanced short-term stability. The spectral density (frequency domain) of the phase noise, per oscillator, measured by each of our two laboratories, is

$$S_{\delta\phi} = +(10^{-11.8}\text{ radians}^2\text{ Hz}^2)(1/f^3) + (10^{-12.5}\text{ radians}^2)(1/f) + (10^{-14.4}\text{ radians}^2\text{ Hz}^{-1})f^0.$$

over the range of about $10^{-2}$ Hz to $10^{+3}$ Hz.

**12384.** Brown, D. W., Lowry, R. E., Wall, L. O., **Radiation-induced polymerization at high pressure of 2,3,3,3-tetrafluoropropene in bulk and with tetrafluoroethylene,** *J. Polymer Sci.* **9,** Part A-1, 1999-2007 (1971).

Key words: Polymerization; pressure; radiation-induced; tetrafluoroethylene; 2,3,3,3-tetrafluoropropene.

The radiation-induced polymerization of 2,3,3,3-tetrafluoropropene was studied as a function of temperature (22 − 100 °C) and pressure (autogenous to $10^4$ atm). Rates have varied 100-fold for the same reaction conditions probably because of trace impurities. The most rapidly polymerizing material has a rate of 4.5%/hr at 6000 atm, 22 °C, and 1500 rad/hr. The activation enthalpy and volume are 4 kcal/mole and −13 cc/mole, respectively. Rates are proportional to the square root of the radiation intensity. Degrees of polymerization varied between $2\times10^3$ and $2\times10^6$. In copolymerization with tetrafluoroethylene the reactivity ratios at 22 °C and 5000 atm are 0.37 (the ratio for addition to the tetrafluoroethylene-ended radical) and 5.4 (the ratio for addition to the tetrafluoropropene-ended radical). Comparison of ratios for the copolymerization of other fluorine-containing monomers with tetrafluoroethylene shows that they generally disfavor incorporation of the latter.

**12385.** Clifton, J. R., **The infrared spectra of supposed $\alpha$ and $\beta$ forms of calcium sulphate hemihydrate,** *Nature (London), Phys. Sci.* **232,** No. 32, 125-126 (Aug. 9, 1971).

Key words: $\alpha$-$CaSO_4\cdot1/2H_2O$; $\beta$-$CaSO_4\cdot1/2H_2O$; gypsum, infrared spectra; lattice water.

The infrared absorption spectra of supposed $\alpha$ and $\beta$ forms of calcium sulfate hemihydrate were measured from 580 to 4000 $cm^{-1}$, using doped potassium bromide pellets and mineral oil mulls.

It was impossible to differentiate between the two supposed forms of calcium sulfate hemihydrate because their infrared spectra were closely similar. The spectra of the supposed forms dispersed in potassium bromide consisted of 13 absorptions and the maximum difference in position between analogous bands of the two spectra was 5 $cm^{-1}$ while 8 absorptions had identical frequencies. Both supposed forms gave the same spectral features when made into mineral mulls.

Because of the high frequencies of $\nu_1(H_2O)$, 3528 $cm^{-1}$, and $\nu_3(H_2O)$, 3604 $cm^{-1}$, for calcium sulfate hemihydrate, it has been proposed that the water molecules are only interstitially held in the hemihydrate.

**12386.** Coriell, S. R., Hardy, S. C., Sekerka, R. F., **A non-linear analysis of experiments on the morphological stability of ice cylinders freezing from aqueous solutions,** *J. Crystal Growth* **11,** 53-67 (May 1971).

Key words: Cylinder; ice; morphology; non-linear; stability; surface tension.

A non-linear theory of morphological stability of a solid circular cylinder growing in a supercooled melt is developed and applied to recent experiments on the growth of ice cylinders in distilled water and in aqueous solution. The cylinders develop $\Phi$ perturbations in the circular shape and $z$ perturbations parallel to the axes of the cylinders. The theory successfully predicts the growth rate of the $z$ perturbations. The non-linearity arises because the $\Phi$ perturbations have grown to a substantial size before the $z$ perturbations are measured. From an analysis of the $z$ perturbation growth rates, a value of 25 $mJ/m^2$ is obtained for the ice-water surface tension on surfaces parallel to the $c$-axis; the corresponding value obtained from a less-satisfactory linear analysis was 22 $mJ/m^2$.

**12387.** Coxon, B., Schaffer, R., **Characterization and quantitative analysis of D-glucose for use in clinical analysis,** *Anal. Chem.* **43,** No. 12, 1565-1570 (Oct. 1971).

Key words: $\alpha$-D-glucose; anomerization; $\beta$-D-glucose; calorimetry; clinical analysis; differential scanning calorimetry; equilibration; gas chromatography; polarimetry; proton magnetic resonance spectroscopy.

The results from analysis of $\alpha$-D-glucose and $\beta$-D-glucose by a variety of spectrometric, chromatographic, and polarimetric techniques are presented and discussed. The apparent values of purity obtained for $\alpha$-D-glucose by differential scanning calorimetry are discussed in relation to the content of $\beta$ anomer as determined by gas chromatography and proton magnetic resonance spectrometry. It is shown that, during melting, both $\alpha$-D-glucose and $\beta$-D-glucose anomerize rapidly to give an equilibrated mixture of these anomers.

**12388.** Danos, M., **One physicist's view of special functions,** (Pro SIAM National Meeting, Washington, D.C., June 10-1 1969), Chapter in *Studies in Applied Mathematics* **6,** pp. 18- (1970).

Key words: Analytical continuation; electron scatterin potential scattering; recoupling coefficients; Regge pole special functions.

The need for presently unavailable information is illustrat with three examples taken from physics problems of present i terest. They involve both the evaluation of integrals over speci functions and the analytic continuation in one or several vari bles of diverse quantities which can be defined by differential difference equations. Of particular interest would be the soluti of the Schrödinger equation for the scattering of a particle in Yukawa potential.

**12389.** deWit, R., **Relation between dislocations and disclinatio** *J. Appl. Phys.* **42,** No. 9, 3304-3308 (Aug. 1971).

Key words: Burgers vector; crystal; disclination; disloc tion; distant parallelism; hexagonal; wedge.

The theory of disclinations contains the equation $\partial_i\alpha_{ij}+e$ $\theta_{mn}=0$, where $\alpha$ and $\theta$ are the dislocation and disclination den ty tensors, respectively. This expression is interpreted to me that dislocations can end on twist disclinations. A concrete ample in a hexagonal crystal is discussed to illustrate this c cept. It contains a 60° wedge disclination normal to the ba plane. By basic geometrical construction it is shown how a dis cation can be made to end on a jog in the wedge disclination. T jog is a small segment of twist disclination. Several ramificatio of this concept are that disclinations can act as sources and sin of dislocations, that dislocations change their Burgers vectors they glide around disclinations, that a dislocation which cross a disclination remains connected to it by a dislocation, that dis cations encircling a disclination must have a node, and that local Burgers vector is not conserved on following a dislocati around a disclination.

**12390.** Dibeler, V. H., **Photoionization studies and thermodyna ic properties of some halogen molecules,** (Proc. Intern. Conf. Mass Spectroscopy, Kyoto, Japan, Sept. 6-13, 1969), Chap in *Recent Development in Mass Spectroscopy,* K. Ogata a T. Hayakawa, eds., pp. 781-790 (University of Tokyo Pre Tokyo, Japan, 1970).

Key words: Chlorine monofluoride; dissociative ionizati fluorine; heats of formation; hot bands; hydrogen fluori ion pairs; mass spectrometry; molecular ionizati photoionization; vacuum ultraviolet.

Mass spectra and ion yield curves for molecular and disso tive ionization processes are measured for fluorine, hydro fluoride, chlorine, and chlorine monofluoride by means of a c bined vacuum uv monochromator and mass spectrome Ionization and dissociation energies and heats of formation the molecules are obtained and compared with values deri from thermochemical and spectroscopic studies.

**12391.** Dibeler, V. H., Walker, J. A., McCulloh, K. **Dissociation energy of fluorine,** *J. Chem. Phys. Letters to E tor* **50,** No. 10, 4592-4593 (May 15, 1969).

Key words: Dissociation energy; fluorine; mass sp trometry; photoionization; vacuum ultraviolet.

Photoionization and mass analysis are used to determine dissociation energy and estimated uncertainty, $D\,0°(F_2)=1.3$ 0.03 eV. The molecular ionization energy is also determine be $15.69\pm0.01$ eV. Both $F^+$ and $F^-$ ions are obtained by the i pair process.

392. Dibeler, V. H., Walker, J. A., McCulloh, K. E., **Photoionization study of the dissociation energy of fluorine and the heat of formation of hydrogen fluoride,** *J. Chem. Phys.* **51,** No. 10, 4230-4235 (Nov. 15, 1969).

> Key words: Bond dissociation energies; fluorine; heats of formation; hydrogen fluoride; ionization thresholds; mass spectra; photoionization; vacuum uv.

Mass spectra and photoionization yield curves are obtained r the molecular and atomic ions of fluorine and hydrogen oride. The atomic ions of both molecules are formed by ion-ir and by dissociative ionization processes. The $F_2^+$ curve has weak onset at 15.58 eV, ascribed to a hot band, followed by an rupt, intense onset at 15.69 eV, ascribed to the 0 – 0 transi-n. Several broad bands of autoionization are observed. The set of the dissociative ionization process occurs at 18.76 eV, om which we calculate $D_0°(F_2) = 1.34 \pm 0.03$ eV (30.9 kcal ol$^{-1}$). The only observed ion-pair process is spin forbidden, oducing $F^+(^3P) + F^-(^1S)$, for which the thermodynamic reshold is not reached. The $HF^+$ curve has a slightly tailing set at 15.92 eV. No $F^+$ ion is observed. The dissociative ization process yielding $H^+$ occurs at 19.34 eV, permitting the lculation of $D_0°(HF) = 5.74$ eV, and $\Delta Hf_0°(HF) = -2.83 \pm$ 03 eV ($-65.3$ kcal mol$^{-1}$). Identical ion-pair curves have a reshold at 15.87 eV resulting in *EA* (F) = 3.47 eV. The in-ated uncertainties are estimated limits of error.

393. Dibeler, V. H., Walker, J. A., McCulloh, K. E., **Threshold for molecular photoionization of bromine,** *J. Chem. Phys.* **53,** No. 12, 4715-4716 (Dec. 15, 1970).

> Key words: Bromine; hot-bands; mass spectrometry; molecular ionization; photoionization.

This brief communication reports on a photoionization mea-rement of the threshold for molecular ionization of bromine. nization of vibrationally-excited molecules is resolved from 0,0 transition and a value of $I(Br_2) = 10.52 \pm 0.01$ eV is ob-ned.

394. Douglas, C. A., **A survey of the use of flashing lights in aviation,** *Proc. Intern. Symp. on Perception and Application of Flashing Lights, London, England, Apr. 1971,* pp. 251-270 Adam Hilger Ltd., London, England, Apr. 1971).

> Key words: Aerodrome lighting; aircraft lighting; anti-collision lights; beacons; effective intensity; flashing lights.

Flashing lights have been used as beacons since the first days night flying. They are also used as identification lights in ap-oach and runway light systems. They have been used for many ars to mark obstructions and other hazards by night and are w being introduced as daytime markers. Flashing lights have en used since the 1940's to supplement the navigation lights on craft. Photometric performance of these lights is usually ecified in terms of steady state intensity and minimum flash ration or in terms of the candela seconds in the flash. Use of integral form of the Blondel-Rey relation was introduced in 1950's and use of this relation is increasing.

395. Douglas, T. B., **Summary of recent thermodynamic measurements by calorimetric, transpiration, mass spectrometric microwave, and infrared techniques,** *Proc. Conf. Interagency Chemical Rocket Propulsion Group, Thermochemistry Work-ing Group, Huntington Beach, Calif., Mar. 25-27, 1968, 6th Meeting Bulletin 173,* **1,** 93-104, (Chemical Propulsion Information Agency, The Johns Hopkins University, Applied Physics Laboratory, Silver Spring, Md., Aug. 1968).

> Key words: Absorption spectrometry; calorimetry; mass spectrometry; propulsion applications; thermodynamic measurements; transpiration equilibria.

This paper summarizes recent precise thermodynamic measurements, completed or in progress, by several research groups at the National Bureau of Standards (NBS). The heats of formation of $ClF3(g)$ and $BeO(c)$ are being measured by reaction calorimetry. "Heat-capacity calorimetry" has been completed at low temperatures on $Be_3N_2(c)$ and on $BeO(c)$ (larger crystals than usual), and at high temperatures on tungsten (to 2600 K) and on $BeO \cdot Al_2O_3(c,l)$ (to 2350 K). A new technique of fast dynamic calorimetry at high temperature has become operational for millisecond heating, with preliminary measurements on molybdenum and other electrically conducting refractories. Transpiration data on the $AlF_3 - AlCl_3$ system have been analyzed to give the heats of formation of $AlF_2Cl(g)$ and $AlFCl_2(g)$. High-temperature mass spectrometry is underway on the $BeF_2 - BeCl_2$ and the $BeO - H_2O$ systems. In the high-temperature microwave and the matrix-isolation infrared investigations of the alkali-hydroxide molecules, spectra have recently been observed and analyzed for RbOH (microwave and infrared) and for NaOH (infrared).

12396. Driscoll, R. L., Olsen, P. T., **Compensation of earth's field variations by field controlled rubidium oscillator,** *Rev. Sci. Instr.* **42,** No. 10, 1427-1431 (Oct. 1971).

> Key words: Absorption cell; earth's magnetic field; Helmholtz coil; magnetometer; optical pumping; resonance line; rubidium oscillator; solenoid.

The east-west variations of the earth's magnetic field over the working volume of the NBS precision solenoid are being canceled out by a closed loop system featuring a field controlled rubidium oscillator. The rubidium oscillator and solenoid are sufficiently separated in distance and do not affect each other's operation. Each system is enclosed in three-dimensional Helmholtz coils. Vertical and north-south components of earth's field are canceled. An east-west bias field is provided for rubidium oscillator operation at 10 kHz. The output of a phase sensitive detector locked to the 10 kHz frequency standard provides current for the electrically series connected east-west Helmholtz coils at both locations. The magnitude of this current is proportional to the phase difference of oscillator and reference. The full range of compensation is 100 nT. The rate of compensation is limited by a time constant of 0.002 sec, an adequate rate for most disturbances. To the extent that the two separated components of the closed loop system can be oriented directionally the same at any given time, the earth's field east-west variation is compensated exactly.

12397. Ekstrom, M. P., McCaa, W. D., Jr., Nahman, N. S., **The measured time and frequency response of a miniature superconducting coaxial line,** *IEEE Trans. Nucl. Sci.* **NS-18,** No. 5, 18-25 (Oct. 1971).

> Key words: Cable; step response; superconducting transmission line; time domain deconvolution.

A miniature superconducting 52 ohm coaxial transmission line 278 meters long, having a lead outer conductor (0.129 cm id), a teflon dielectric, and a niobium center conductor (0.038 cm), has been measured in both the time and frequency domains. The observed system step response (10% – 90%) times were 1.5 $\mu$s at room temperature, 375 ns at 77 K, and 255 ps at 4.2 K. The system step response data for 4.2 K was processed by a numerical system identification routine to determine the step response of the miniature superconducting line; the processed data gave a 220 ps risetime. Although the observed step responses at 4.2 K were smooth transitions, the observed swept frequency (0.1 GHz – 12 GHz) attenuation at 4.2 K was a quasi-periodic function of frequency, which indicated that the nonuniformity of the superconducting line was significant. For example, near 5 GHz and at 4.2 K, the attenuation minimum was 1.1 dB while about

0.5 MHz away the attenuation was 5 dB. By making normal conductivity measurements of the Nb conductor and incorporating the results into the two fluid model, the uniform line attenuation for 5 and 10 GHz was calculated with the classical and anomalous limits. The lowest observed attenuation values in the vicinity of 5 and 10 GHz fell between the computed classical and anomalous limit attenuation values.

**12398.** Forthofer, R. J., **Developing standards technology for automotive braking systems,** *Proc. 1969 18th Annual Meeting Standards Engineers Society, Washington, D.C., Sept. 15-17, 1969,* pp. 27-42 (Sept. 1969).

Key words: Automotive; brake; brake fluid; brake lining; standards; testing.

The Office of Vehicle Systems Research (OVSR) of the National Bureau of Standards, U.S. Department of Commerce, is concerned with the research, development, testing and evaluation necessary to provide the technical basis for recommended safety performance standards issued by the National Highway Safety Bureau of the Department of Transportation.

This paper discusses briefly the history of the Government's interest in automotive braking safety standards. Problems associated with the collection of research data for the performance of brake systems, brake linings, and brake fluid are discussed in more detail. The author comments on the direction that research is expected to take in the 1970's.

**12399.** Freeman, D. H., Enagonio, D. P., **Interactive gel networks for organic separations,** *Nature (London), Phys. Sci.* **230,** 135-136 (Apr. 1971).

Key words: Chromatography; interactive gel networks; liquid chromatography; organic separations.

Conventional organic networks, such as crosslinked polyvinylpyridine, can be used or modified so that chemical interactions of various specific types are obtained. They show excellent resolution and high capacity. The chromatographic properties are related to complexative interactions whose understanding in liquid media is independently established.

**12400.** Geist, J., **Note on the quality of freezing point blackbodies,** *Appl. Opt.* **10,** No. 9, 2188-2190 (Sept. 1971).

Key words: Blackbody; emmissivity; freezing point blackbody; heat pipe blackbody; quality.

It is shown that for freezing point blackbodies whose wall materials have thermal radiative properties which are independent of wavelength, a quantity can be defined which satisfies all of the intuitive ideas of the concept of the quality of the blackbody and which satisfies an integral equation which provides physical insight into the interaction of the reflectance and thermal resistance of the wall material of the blackbody in reducing its quality from unity.

**12401.** Hermach, F. L., **Testing hospital electric equipment for safe performance,** *Proc. National Research Council Workshop on Electric Hazards in Hospitals, Washington, D.C., Apr. 4-5, 1968,* pp. 175-177 (National Academy of Sciences, Washington, D.C., 1970).

Key words: Electric equipment; electrical safety; hospital safety; leakage currents; testing; test sets.

Electric equipment for use on patients must be evaluated to determine if it meets the requirements of safety codes—otherwise the codes are of little value. This can best be done by safety-testing labs which follow established test methods to determine compliance with broad performance requirements of such codes. A test set to which the user can connect electric equipment to determine if leakage currents are less than allowable limits woul be valuable additional protection, particularly in the interi period before approved equipment is available.

**12402.** Herron, J. T., **Mass spectrometric studies of atomic an free radical reactions,** *Advan. Mass Spectrometry* **5,** 453-46 (1971).

Key words: Atomic; chemical kinetics; free radicals; mas spectrometry; mechanism; review.

The applications of mass spectrometry to the study of th kinetics and mechanisms of atomic and free radical reactions i the gas phase are reviewed.

**12403.** Hudson, R. P., Mangum, B. W., **Effects of applied magnetic fields on cooperative Jahn-Teller transition temperatur of $DyAsO_4$ and $DyVO_4$,** *Physics Letters* **36A,** No. 3, 157-15 (Aug. 30, 1971).

Key words: Jahn-Teller effect; magnetic susceptibility.

We have measured the effects of applied magnetic fields on th cooperative Jahn-Teller transition temperatures of $DyAsO_4$ an $DyVO_4$. We find that even relatively weak fields produce a ver pronounced increase in the transition temperature of $DyAsO_4$.

**12404.** Hudson, P. A., Saulsbery, L. F., **An adjustable-slot-lengt UHF coaxial coupler with decade bandwidth,** *IEEE Tran. Micro. Theory Tech.* **MTT-19,** No. 9, 781-783 (Sept. 1971).

Key words: Attenuator; directional coupler, coaxial; powe measurement, rf.

A coaxial directional coupler has been developed which allow adjustment of the length of the coupling slot to λ/4 or 3λ/ throughout the frequency range 0.3 to 8.5 GHz. Coupling is fl to within 0.05 dB from 0.3 to 3 GHz (λ/4 mode) and 0.1 dB fro 0.9 to 8.5 GHz (3λ/4 mode). The coupler has 50-dB couplin 30- to 40-dB directivity and was designed primarily for hig power measurement (1 to 1000 W) using a low-power meter c the sidearm. The VSWR for the two modes of operation is 1.0 to 1.05. Five octave bandwidth-type couplers would be require to cover this same frequency range.

**12405.** King, D. A., Madey, T. E., Yates, J. T., Jr., **Interaction oxygen with polycrystalline tungsten. II. Corrosive oxidation,** *Chem. Phys.* **55,** No. 7, 3247-3253 (Oct. 1, 1971).

Key words: Adsorption; chemisorption; corrosion; flas desorption; oxidation; oxygen; tungsten; tungsten oxides.

The kinetics of formation of a corrosive oxide layer of apparently unlimited thickness during the interaction of oxyge with a polycrystalline tungsten filament at temperatures betwee 500 and 1000 K has been investigated by line-of-sight flas desorption mass spectrometry. The major desorption produ from this multilayer oxide film is $WO_2$, which desorbs over th temperature range 1000 to 1300 K. The rate of formation of th oxide film was shown to be directly proportional to the oxyge gas phase pressure at pressures $\leqslant 10^{-4}$ torr. A study of the temperature dependence of the oxidation rate revealed that the fo mation of the $WO_2$-producing oxide layer proceeds through tw distinct steps: these occur subsequent to the first three stages the interaction of oxygen with W characterized in Paper I. In th final stage of oxidation, the rate is shown to be independent the thickness of the oxide film. The results are in qualitative accord with the theoretical model of Mott. Desorption of the oxi film is a zero order process, with a desorption activation energ of 420 kJ $mol^{-1}$.

**12406.** Koonce, C. S., Mangum, B. W., Thornton, D. D., **Lo temperature properties of $DyPO_4$ in a magnetic field,** *Proc. 12 Intern. Conf. on Low Temperature Physics, Kyoto, Japa*

*Sept. 4-10, 1970,* pp. 705-707 (Keigaku Publishing Co., Japan, Mar. 1971).

Key words: Antiferromagnetic; dipolar interaction; $DyPO_4$; low temperature; magnetic field; paramagnetic.

The magnetization and the peaks in the heat capacity at con- nt applied field of $DyPO_4$, a material for which the Ising odel is particularly appropriate, have been measured, and com- red with a Bethe-Peierls approximation including dipolar in- actions.

407. Kranbuehl, D. E., **Atomic, molecular, and ionic interac- tions,** *Dig. Lit. Dielectrics* **33,** No. 2, 84-118 (1969).

Key words: Dielectric; ionic; polarizability; relaxation.

A review of those papers in the 1969 literature on dielectrics nich make a significant contribution toward understanding the ndamental dielectric properties of atoms, molecules and ions.

408. Kranbuehl, D. E., Verdier, P. H., **Stochastic molecular model studies of the relaxation of vector end-to-end length in polymer chains,** *Am. Chem. Soc. Polymer Preprints* **12,** No. 2, 525-628 (1971).

Key words: End-to-end length; excluded volume; Monte Carlo; polymer chain dynamics; relaxation.

The effects of excluded volume interactions upon the dynami- behavior of random-coil polymer chains are studied by ob- ning autocorrelation functions for the vector end-to-end length lattice model chains of 9, 15, 33, and 63 beads by a Monte rlo simulation technique. The configuration of the polymer ain, N-1 units long, is represented by a string of N connected ints on a 3-dimensional cubic lattice. Excluded volume is counted for by not allowing two beads to occupy the same tice site. It is found that the relaxation of vector end-to-end gth for a lattice chain with excluded volume varies substan- lly from that of a lattice chain without excluded volume. Re- ation of the vector end-to-end length requires from four to ven times as long as relaxation of its square, contrary to the edictions of simple models without excluded volume effects. is behavior suggests that the ratio of the relaxation time of ctor end-to-end length to that of its square is a measure of the esence or absence of excluded volume effects.

409. Kuriyama, M., Alexandropoulos, N. G., **On the relation- ship between x-ray inelastic scattering and absorption spectra,** *. Phys. Soc. Japan* **31,** No. 2, 561-562 (Aug. 1971).

Key words: Compton scattering; plasmon scattering; Raman scattering; relation between spectra; x-ray absorption; x-ray inelastic scattering.

The cross section for x-ray inelastic scattering from crystals been derived from first principles to explain the coexisting mpton and Raman scattering in solids. This derivation makes possible to express the inelastic scattering cross section in ms of the current correlation of electrons in a crystal. The terion for having a distinct Raman scattering is obtained ough the dependence of the current correlation on the mo- ntum transfer.

410. Lee, J. N., Moos, H. W., Mangum, B. W., **Magnetic pro- perties of $TbPO_4$, a canted antiferromagnet,** *Solid State Com- mun.* **9,** No. 13, 1139-1141 (1971).

Key words: Antiferromagnet; canted antiferromagnet; heat capacity; magnetic moment; magnetic susceptibility; metamagnet; optical spectroscopy; $TbPO_4$.

The magnetic properties of $TbPO_4$ at low temperatures have been investigated by high resolution optical spectroscopy, magnetic susceptibility, magnetization, and heat capacity measurements. $TbPO_4$ orders antiferromagnetically into a canted spin structure with zero net moment at 2.17 K. Metamagnetic behavior is observed. A magnetically induced lattice distortion mechanism is probably responsible for the detailed behavior.

12411. Manning, J. R., **Correlation factors for diffusion in nondilute alloys,** *Phys. Rev. B* **4,** No. 4, 1111-1121 (Aug. 15, 1971).

Key words: Alloys; atom jump frequencies; binary alloys; correlation factor; diffusion; multicomponent alloys; random alloy model; vacancies.

Correlation factors for diffusion in binary and multicomponent alloys are calculated for a random-alloy model with diffusion by a vacancy mechanism. This model, which should apply best for nondilute alloys, assumes that atoms and vacancies are randomly distributed and that suitable average values can be used to represent the actual atom and vacancy jump frequencies in the crystal. In alloys, both atoms and vacancies follow correlated walks. Also, the atom correlation factors are influenced by the nonrandom motion of the vacancies. Thus, in order to treat correlation effects in concentrated alloys properly, one must consider not only the correlation factors $f_i$ for diffusion of atoms but also the correlation factor $f_v$ for diffusion of vacancies. In specific calculations, one also must find the partial correlation factors $f_v^i$ for diffusion of vacancies by exchange with atoms of the particular species *i*. Analytic expressions for all of these correlation factors are calculated. These equations can be expressed directly in terms of the measureable tracer-diffusion-coefficient ratios $D_i^*/D_k^*$ with no unknown jump frequencies appearing. The calculations also yield a forbidden region in the plot of diffusion-coefficient ratio as a function of alloy composition, with correlation factors going to zero at the boundary of this region. Specific applications to binary alloys are discussed.

12412. Marzetta, L. A., **A high-performance phase-sensitive detector,** *IEEE Trans. Instr. Meas* **IM-20,** No. 4, 296-301 (Nov. 1971).

Key words: Op amp; operational amplifier; operational rectifier; phase-sensitive detector; signal extraction ratio.

A phase-sensitive detector is described that enables the retrieval of signals submerged 90 dB (voltage) below the noise level. Operation over four decades of signal amplitude (a full-scale linearity error of 0.01 percent) is possible for a frequency range of 0 – 150 Hz. Design features are offered allowing an experimenter to construct the device from inexpensive components and be assured a predictable performance.

12413. Mason, H. L., **Pounds, atoms, papers, and laws,** *Instrument Society of America Silver Jubilee International Conference and Exhibit, Oct. 26-29, 1970, Philadelphia, Pa.,* **25,** Part II, Paper 70-662, 1-5 (1970).

Key words: Calibration; instrument specifications; international standards; measurement history; measuring instruments; physical constants; physical standards.

Reviews three centuries, from William Penn to Richard Simpson, in the development of four kinds of technical standards – physical artifacts, natural phenomena, written agreements, and legal codes. Traces the influence of industrial practices, governmental agencies, and international organizations, on standards which specify quantities, and commercial products.

12414. Mighell. A. D., Santoro, A., Donnay, J. D. H., **Reduced cells,** Chapter in *International Tables for X-Ray Crystallog-*

*raphy*, N. F. Henry and K. Lonsdale, eds., **II**, 530-535 (The Kynoch Press, Birmingham, England, 1969).

Key words: Bravais lattice; identification; reduced cells; transformation matrix.

Tables and text are given that make it possible to determine the reduced cell for any lattice. Finally, a detailed table is presented which establishes the relationship of each of the 44 reduced cell types to one of the Bravais lattices.

**12415.** Milligan, D. E., Jacox, M. E., **Matrix-isolation study of the interaction of electrons and alkali metal atoms with various nitrogen oxides. Infrared spectra of the species $NO^-$, $NO_2^-$, and** $N_2O_2^-$, *J. Chem. Phys.* **55,** No. 7, 3404-3418 (Oct. 1, 1971).

Key words: Alkali metal reactions; charge transfer; electron attachment; infrared spectrum; matrix isolation; $NO^-$; $NO_2^-$; $N_2O_2^-$; $O^-$ reactions.

The infrared spectra which result when samples of $NO_2$ are codeposited with the various alkali metals in an argon matrix at 4 or at 14 K are consistent with the occurrence of strong charge-transfer interaction. In addition to isolated $NO_2^-$, previously identified in this system, ion pairs of general formula $M_x{}^+NO_2^-$ are stabilized. When NO is substituted for $NO_2$, the infrared spectrum of the initial deposit shows an absorption between 1350 and 1375 cm$^{-1}$ which can be assigned to the $NO^-$ stretching fundamental of $M_x{}^+NO^-$ ion pairs, in good agreement with the vibrational spacing recently reported for ground-state $NO^-$ in the gas phase. Weak charge-transfer interaction occurs between alkali-metal atoms and $N_2O$ in an argon matrix environment. Results of the present experiments can be explained by postulating that the upper, predominantly ionic state of the charge-transfer complex decomposes producing $O^-$, which may diffuse through the matrix. A new absorption which appears at 1205 cm$^{-1}$ has tentatively been assigned to $\nu_4(b_1)$ of a planar $O_2N=N^-$ anion. In studies of the interaction of sodium atoms with Ar:NO:$N_2O$ mixtures, mercury-arc irradiation of the sample leads to the appearance not only of the $N_2O_2^-$ absorption, but also of absorptions due to isolated $NO_2^-$ and to $Na_x{}^+NO_2^-$.

**12416.** Moore, G. A., **Design of a practical scanner unit for precision analysis of micrographs,** *Pattern Recognition* **3,** 91-122 (Oct. 1971).

Key words: Analysis of microstructures; automatic scanning (of micrographs); precision scanning (of micrographs); quantitative microscopy.

A precision mechanical scanner has been constructed for the purpose of preparing digital transcriptions of micrographs for computer analysis, and of performing elementary analysis without resort to a computer. Design criteria include convenience of operation and precision sufficient to correctly record all of the real information in one micrographic field.

Performance data are included. An analysis is given of the precision which may be expected in estimating area and volume percentage of a phase under various conditions. The attained precision is at least an order of magnitude greater than is normally obtained by manual methods.

**12417.** Post, M. A., **Copolymer determination in surface filler,** *Paint Varnish Prod.* **61,** No. 9, 31-38 (Sept. 1971).

Key words: Absorbance ratio method; infrared spectroscopy; resins; styrene-butadiene; surface fillers; vinyl toluene-acrylate; vinyl toluene-butadiene.

Styrene-butadiene, vinyl toluene-butadiene and vinyl toluene-acrylate copolymers in surface fillers are quantitatively determined by two methods. In one, a dual extraction method, which should be useful in acceptance testing of solvent type fillers, the resin is determined as the difference between the total benzene and n-pentane extractables. The second method, a combination of single extraction and infrared analysis, involves determination of the total benzene extractables and the resin content therein. The latter is determined by measuring the 3.3 $\mu$m/3.5 $\mu$m absorbance ratio of cast films from the benzene extract, using the baseline method, and reading the weight percent resin from the appropriate standard curve. This method depends on a constant ratio of styrene to butadiene, vinyl toluene to butadiene or vinyl toluene to acrylate. Its use is restricted to resins of a particular monomer ratio for which a standard curve has been made. These methods were developed and confirmed using commercially prepared fillers of known resin content.

**12418.** Prince, E., **Refinement of the crystal structure of apophyllite. III. Determination of the hydrogen positions by neutron diffraction,** *Am. Mineralogist* **56,** 1243-1251 (July-Aug. 1971).

Key words: Apophyllite; fluoro silicate; hydrated minerals; hydrogen bonds; mineral structure; neutron diffraction.

The crystal structure of apophyllite, a mineral with the ideal formula $KCa_4(Si_4O_{10})_2F\cdot 8H_2O$, has been refined using three-dimensional neutron diffraction data. 671 independent reflections were observed on a 4-circle diffractometer. Of these 516 had observable intensities. A least-squares refinement, with anisotropic temperature factors, led to an *R* index of 0.046. However, a difference Fourier synthesis revealed a region of negative scattering density in the vicinity of the fluorine atom. Accordingly a further refinement was carried out assuming a model in which 1/8 of the water molecules are replaced by OH$-$ions, with the remaining proton bonded to fluorine to form an HF molecule. This model refined quickly to an *R* value of 0.037. The water molecules and OH ions are hydrogen bonded to the silicate framework. A preliminary mass spectrometric analysis of the gases evolved when apophyllite is heated revealed that the higher temperature specific-heat anomaly is due to the evolution of hydrogen fluoride. This suggests that the structural formula is $KCa_4(Si_4O_{10})_2F_{1-x}(HF)_x\cdot[(H_2O)_{8-x}(OH)_x]$ with $x \approx 1$.

**12419.** Scheer, M. D., Klein, R., McKinley, J. D., **Surface lifetimes of alkali metals on molybdenum,** *J. Chem. Phys.* **55,** No. 7, 3577-3584 (Oct. 1, 1971).

Key words: Alkali atoms; desorption energies; modulated beam method; polycrystalline molybdenum; surface ionization; surface lifetimes.

The surface lifetimes ($\bar{\tau}$) of all the alkali metals on a polycrystalline molybdenum surface in the temperature region 900 − 1350 K were measured. The temperature dependence followed an Arrhenius expression of the form $\bar{\tau}^\circ$ exp ($\bar{l}/kT$). Desorption energies ($\bar{l}$) were found to be 3.14, 2.60, 2.53, 2.31, and 2.10 eV for Li, Na, K, Rb, and Cs. The corresponding pre-exponential factors ($\bar{\tau}^\circ$) were $3\times10^{-16}$, $3\times10^{-15}$, $2\times10^{-14}$, $1\times10^{-13}$, and $3\times10^{-13}$ sec. From these data, ion and neutral desorption energies were calculated using a model employing a partial surface charge for the adsorbed particle and the Schottky relation. The validity of the Schottky relation for an adsorbed alkali was supported by analysis of recently available theory of partial charges. An explanation of the variation of the pre-exponential factors is presented on the basis of relative mobility of the adsorbed species. A pre-exponential factor was calculated using a partition function for an adsorbate with mixed localized and nonlocalized character. The extremes of completely localized and completely nonlocalized adsorption led to pre-exponentials that spanned the experimental values.

**12420.** Sher, A. H., Croll, W. K., Thurber, W. R., **Determination of oxygen in germanium below 20 parts per billion by measure-**

**ments of lithium mobility and precipitation,** *Anal. Chem.* **43,** No. 13, 1831-1834 (Nov. 1971).

Key words: Ge(Li) detectors; germanium; infrared absorption; lithium mobility; lithium precipitation; oxygen concentration.

The range of sensitivity and the expected degree of precision r the analysis of oxygen concentration in germanium by mea- rements of lithium-ion drift mobility and lithium precipitation ve been determined. The relative sample standard deviations ve been found to be ±10% and ±15%, respectively, in the nge of oxygen concentration from 20 ppb (atomic) to 0.2 ppb tomic). However, the lithium precipitation method alone can- t be used unambiguously in the determination of oxygen con- ntration in germanium. The sole previously-published value r the dissociation constant of the $LiO^+$ complex in germanium 295 K has been confirmed. A newly-observed feature in the hium precipitation curve is shown to give semiquantitative in- rmation about oxygen concentration.

**2421.** Sher, A. H., Thurber, W. R., **Minority carrier and lithium-ion drift mobilities and oxygen concentration in *p*-type germanium,** *J. Appl. Phys.* **42,** No. 11, 4508-4509 (Oct. 1971).

Key words: Electron drift mobility; germanium diode; lithium-ion drift mobility; lithium precipitation; oxygen concentration; *p*-type germanium.

No correlations have been experimentally observed between ectron drift mobility and lithium drift mobility nor between ectron drift mobility and oxygen concentration in *p*-type ger- anium single crystals, as had been previously suggested.

**2422.** Shirk, J. S., **Laser excited fluorescence of $CCl_2$,** *J. Chem. Phys.* **55,** No. 7, 3608-3609 (Oct. 1, 1971).

Key words: Fluorescence; force field; matrix.

Laser-excited fluorescence of $CCl_2$ trapped in a low tempera- re matrix was observed in the 6000-8500 Å region. A normal oordinate analysis was carried out, using a Urey-Bradley force eld, to determine the molecular force constants.

**2423.** Simpson, J. A., **Use of a microscope as a noncontacting microdisplacement measurement device,** *Rev. Sci. Instr.* **42,** No. 9, 1378-1380 (Sept. 1971).

Key words: Dimensional metrology; displacement measurement; microscope; noncontact sensing; optical surface probe; surface detection.

It is shown that a common research microscope with vertical luminator can be easily converted to noncontacting measuring evice of submicroinch resolution.

**2424.** Smith, S. J., **Molecular negative ion structure,** *Comments At. Mol. Phys.* **2,** No. 6, 175-180 (Feb.-Mar. 1971).

Key words: Elastic scattering; electron affinity; high resolution; internuclear distance; molecular negative ions; photodetachment.

This paper is a commentary on the reasons for limited progress obtaining mechanical constants for molecular negative ions. It oints out that two experimental technologies, one a sophistica- on of the photodetachment technique which incorporates ener- y analysis of detached electrons, the other a refinement of elec- ron-neutral molecule scattering measurements with high energy esolution, now are yielding complementary data on molecular egative ion constants. In principle, these methods are widely pplicable.

**2425.** Thomas, D. B., **Some studies on the reproducibility of tungsten-rhenium type thermocouples,** *Proc. 26th Intern. Instrument Society of America Conf. and Exhibit on Advances in Instrumentation, Chicago, Ill., Oct. 4-7, 1971,* **26,** Part II, Paper 71-611 (Oct. 1971).

Key words: Anneal; argon; beryllium-oxide; calibrations; emf; helium; thermal-cycling; thermocouple; tungsten-rhenium; vacuum.

Representative samples of commercially available tungsten-rhenium type thermocouples were obtained from American manufacturers and calibrated in an argon atmosphere up to 2100 °C. After the initial calibrations were performed, the thermocouples were subjected to thermal-cycling between 1000 and 2100 °C and were also annealed for periods up to 420 hours at 2300 °C in argon. A comparison is made between the emfs of the thermocouples before and after the thermal-cycling and annealing periods. In general, the tungsten versus tungsten-26% rhenium thermocouples indicated the largest changes in emf after the thermal cycling and annealing periods while the tungsten-3% rhenium versus tungsten-25% rhenium thermocouples indicated the least change in emf. Some of the thermocouples were calibrated with and without beryllium-oxide insulation in argon, helium, and vacuum and a comparison is made between the thermocouple emfs under these conditions.

**12426.** Tsai, D. H., MacDonald, R. A., **Molecular dynamical studies of the phase transformation of iron under pressure,** (Proc. Symp. Mechanisms of the Phase Transitions, University of South Carolina, Columbia, S.C., Feb. 1, 1971), *Trans. Am. Crystallogr. Assoc.* **7,** 107-129 (Feb. 1, 1971).

Key words: Iron; lattice structure; martensitic transformation; molecular dynamics; phase diagram; P-V-T data.

We have applied molecular dynamics to the study of the transformation of iron from the $\alpha$ phase (bcc) to the $\epsilon$ phase (hcp) under hydrostatic pressure. The atomic interaction energy in both phases was represented by a two-body, central-force potential fitted (1) to the elastic properties of the $\alpha$ phase at zero pressure and zero absolute temperature, and (2) to an assumed transition pressure of 130 kb at zero absolute temperature, with a volume decrease of 0.2 $cm^3$/mol upon transition from the $\alpha$ to the $\epsilon$ phase. The classical equations of motion of the lattice points were solved by numerical computation, and the equation of state and specific heat data were obtained from the appropriate time-averages of the dynamical solutions. From these quantities, the Gibbs free energies of the two phases were calculated and a phase diagram for the $\alpha$ to $\epsilon$ transition was constructed. We found that the phase diagram thus obtained was in satisfactory agreement with experimental results. By observing the details of the lattice point motion given by the dynamical solutions, it was possible to follow the process of phase transformation when it occurred in the model. We describe here a martensitic type of buckling mechanism which was observed to transform the $\alpha$ phase to the $\epsilon$ phase.

**12427.** Tsang, W., Wasik, S. P., **The application of the isotope dilution GLC technique to air pollution analysis,** *J. Chromatog. Sci.* **9,** 567-569 (Sept. 1971).

Key words: Air pollution; benzene; benzene-$d_6$; gas analysis; gas chromatography; isotope dilution; sampling.

It is shown that the isotope dilution technique provides a simple means of accurately determining air pollutant concentrations under adverse conditions. This is demonstrated in various simulated situations with a sample of approximately 20 ppm benzene in argon.

**12428.** Wagner, H. L., Hoeve, C. A. J., **Effect of molecular weight on the refractive increment of polyethylene and *n*-alkanes,** *J. Polymer Sci.* **9,** Part A-2, 1763-1776 (1971).

Key words: Differential refractive index; differential refractometer; Lorentz-Lorenz; molecular weight; $n$-alkanes; polyethylene; polystyrene.

As in the case with other polymers previously reported, the values of the refractive index increment $dn/dc$ of polyethylene and the $n$-alkanes change with molecular weight. Most of the variation may be understood by examination of the role of density in the Lorentz-Lorenz mixing equation of specific refractivity, $R_{12}=p_1R_1+P_2R_2$ used to calculate $dn/dc$. It may also be shown that as the absolute refractive index difference between solute and solvent becomes smaller, $dn/dc$ becomes more sensitive to density change of the solute.

**12429.** Weir, C. E., **Concerning the maximum melting point,** *Japanese J. Appl. Phys.* **10,** No. 6, 714-716 (June 1971).

Key words: High pressure; melting point.

The theory of Kawai and Inokuti of the behavior of the melting point of solids as a function of pressure is discussed. The general theory is not considered applicable to the vast majority of materials known to date.

**12430.** Wexler, A., **Book review on "Modern Hygrometry" by A. Pande,** *Bull. Am. Meteorol. Soc.* **52,** No. 9, 897-898 (Sept. 1971).

Key words: Humidity; hygrometry; moisture; water vapor.

Book review on a monograph on the subject of hygrometry.

**12431.** Argentar, H., **Determination of the degree of polymerization of a polymeric amine from NMR data using a "least-squares" approach,** *J. Polymer Sci.* **9,** Part B, 657-659 (1971).

Key words: Aromatic amine; multiple regression analysis; nuclear magnetic resonance; polymer; proton magnetic resonance; spectroscopy.

A polymeric amine, the reaction product of 3,5-xylidine and the diglycidyl ether of bisphenol A, which had been synthesized and reported elsewhere, was analyzed by nuclear magnetic resonance spectroscopy (NMR). A statistical method was derived to estimate the degree of polymerization based on linear multiple regression analysis of the intensity of the NMR absorption peaks.

**12432.** Barnes, I. L., Sappenfield, K. M., Shields, W. R., **The mass spectrometric analysis of subpicogram quantities of lead,** (Proc. Int. Conf. Mass Spectroscopy, Kyoto, Japan, 1970), Chapter in *Recent Developments in Mass Spectroscopy,* K. Ogata and T. Hayakawa, eds., pp. 682-687 (University of Tokyo Press, Tokyo, Japan, 1970).

Key words: Lead; mass spectrometer; microsample.

An analytical method has been developed which gives stable measurable ion beams from samples containing $10^{-8}$ to $10^{-14}$ grams of lead.

Using a two stage twelve inch radius mass spectrometer equipped with an ion multiplier and electronics for fast pulse counting, a series of chemical microstandards loaded with known quantities of NBS standard lead samples (as small as $10^{-14}$ grams of lead) were analyzed. These analyses showed that accuracy and precision of better than 0.5 percent (95% L. E. for a single analyses) could be obtained and that usually, the accuracy and precision were limited only by random counting statistics.

A series of quantitative analyses were done with two microgram or smaller samples taken from a single wafer of a silicate glass of known composition by the method of isotopic dilution. The required "spiking" of the sample was done utilizing an NBS Microstandard Ion Exchange Bead loaded with lead of known weight and composition.

The results obtained show severe cross-sectional variations of lead in the sample and demonstrate the importance of careful handling of samples for trace element analysis.

The use of the technique for the direct analyses of small crystals and/or particles is described. In this use only minimal chemical treatment is necessary thus eliminating most, if not all, of the usual sources of contamination and all chemical treatment may be performed directly on the mass spectrometer filament.

**12433.** Bederson, B., Kieffer, L. J., **Total electron-atom collision cross sections at low energies—A critical review,** *Rev. Mod. Phys.* **43,** No. 4, 601-641 (Oct. 1971).

Key words: Critical review; cross section measurement; electron-atom collisions; total cross section data.

Experiments relating to measurements of total and momentum-transfer cross sections for the scattering of low-energy electrons by atoms and diatomic molecules are critically reviewed. Principal emphasis is placed upon the Ramsauer method, dc swarms, and crossed-beams experiments, which account for the bulk of the reliable data in the literature although other techniques including differential measurements are also discussed. The theories of the various methods and possible sources of error are discussed. The case of low-energy electron scattering by helium is exhaustively reviewed since this system has been most intensively studied experimentally and is particularly amenable as well to theoretical calculations. The best available cross section values, along with comments on individual experiments, are presented in several tables.

**12434.** Bennett, L. H., Carter, G. C., **Enhanced lever rule for high-precision phase diagram determination,** *Met. Trans.* 2 3079-3081 (Nov. 1971).

Key words: Alloys; high precision; lever rule; nuclear magnetic resonance; phase diagrams.

A description is given of the conditions under which high precision phase boundary determinations result from the application of the lever rule. This high precision results from a multiplication factor to the lever rule ratio, which is present only for experiments sampling one elemental site at a time. The multiplication factor is larger for smaller solubility limits. Precision o tenths of a percent can be readily attained under the indicate conditions. An example involving the $^{115}$In nuclear magneti resonance for the determination of the solubility of AuIn$_2$ i AuAl$_2$ is presented.

**12435.** Blandford, J. M., Bensing, P. L., **Part I. Testing program for the apparel industry. Part II. Evaluation of material an components,** Part I, 35 pages; Part II, 249 pages (2d ed.) (Apparel Research Foundation, Inc., Washington, D.C., May 1 1971).

Key words: Apparel industry; equipment, textile testing; industry, apparel; performance, apparel materials; propertie apparel; quality control, apparel industry; test methods, textile; testing programs, apparel industry; textile testing, apparel materials.

This publication presents the details of minimum, inte mediate, and advanced textile testing programs for evaluating th appearance and performance of materials and components use by the apparel industries. Tabulations give testing equipmen properties its use may determine, testing procedures and evalu tion materials employed, and sources of supply and approxima prices of the equipment and evaluation materials.

Included are: (1) sections on the significance of a textile tes ing program, conditioning for testing textiles, performanc requirements for textile fabrics, (American National Standa

22), evaluation of fabric defects, and the availability of short boratory training courses for apparel company employees; (2) bliography; (3) reprints of the sixty-eight referenced test ethods.

**436.** Brady, R. F., Jr., **Enolization of hexodiulose acetals. Synthesis of derivatives of D-psicose by reduction of a hex-3-enulopyranose,** *Carbohydrate Res.* **20,** 170-175 (Nov. 1971).

Key words: Cyclic acetals; hex-3-enulopyranose; hexodiulose; hexulose; psicose; stereospecific reduction; tagatose.

Previous papers from this laboratory have reported the nthesis of isopropylidene acetals of D-*erythro*-pentulose, D-*reo*-pentulose, D-fructose, and D-psicose, and have demonrated their utility in the synthesis and purification of rare etoses. The present work describes an attempt to synthesize milar acetals of D-tagatose (D-*lyxo*-hexulose). 1,2:4,5-Di-*O*-opropylidene-$\beta$-D-*erythro*-2,3-hexodiulo-2,6-pyranose (**1**), an termediate previously used, was converted into a 3,4-enediol cetate, namely, 1,2:4,5-di-*O*-isopropylidene-$\beta$-D-*glycero*-hex-3-ulopyranose (**2**). Reduction of **2** with hydrogen over palladium ave, however, only 3-*O*-acetyl-1,2:4,5-di-*O*-isopropylidene-$\beta$--psicopyranose (**3**), and none of the D-tagatose derivative.

The synthesis and synthetic applications of fully protected alosuloses and diuloses have received much attention, but the hemistry of enediol acetates, as obtained from these compounds y the action of acetic anhydride-triethylamine, is largely unexlored. Stereospecific reduction or addition reactions of these nsaturated derivatives offer attractive possibilities for the ynthesis of rare and unusual sugars.

**2437.** Brauer, G. M., **A review of recent studies of in vitro reactivity of surfaces of calcified tissues,** (Proc. Int. Symp. Calcified Tissues, Dental and Surgical Materials and Tissue Material Interactions, University of Nijmegen, Nijmegen, The Netherlands, 1970), *Dent. Tissues Mater.*, pp. 193-231 (1971).

Key words: Adhesion to tooth surfaces; adsorption on calcified tissues; bone; calcified tissues; dentin; enamel; modification of tooth surfaces; reactivity of calcified tissues.

Studies of the reactivity and modification of tooth surfaces ffer an attractive approach for obtaining useful information to educe dental caries and improve adhesion between tooth strucure and restoratives. Investigation of the interaction of gases on uch surfaces provides considerable insight into the structural etails of surfaces of hard tissues. Effectiveness of potential conlitioning agents can be demonstrated from alterations of the surace properties of teeth as indicated by changes in: critical surace tension, oil-wettability, adsorption isotherms and adheionability. Measurement and evaluation of heats of immersion nd heats of reaction are useful for observing modifications and letermining those groups that bond to tooth structure in aqueous nvironments. Application of dilute polyfunctional acids emoves debris, etches enamel and increases surface wettability. tching creates an increased surface area and opens pores into which resin can flow. Excellent adhesion is obtained after ardening because of mechanical interlocking of resin at the namel-resin interphase. Long side chains have been grafted to ollagenous surfaces (collagen powder or film, bone). Grafting monomers containing additional functional groups that are otential reactive centers for further modification is feasible. Surfaces with the desired degree of hydrophil-lipophil balance to uit specific applications can be prepared.

**12438.** Brown, W. E., **Physicochemical aspects of decay and decalcification,** (Proc. Int. Symp. Calcified Tissues, Dental and Surgical Materials and Tissue Material Interactions, University of Nijmegen, Nijmegen, The Netherlands, 1970), *Dent. Tissues Mater.*, pp. 69-97 (1971).

Key words: Calcium phosphate; caries; caries mechanism; enamel; hydroxyapatite; tooth mineral; solubility.

Much of the research directed toward understanding the "mechanism" of dental caries has been etiological in nature and has delineated the importance of certain micro-organisms and their products in producing caries. However, attempts to provide physicochemical models have been few in number, and because of the complexity of the system and lack of knowledge about some of the most important parameters, these models have been relatively primitive. Our increasing knowledge about the character of carious lesions, enamel surfaces, and plaque now make such a model more attainable. The purpose of such a model is not to describe quantitatively the caries process, *per se*, but instead to identify the essential or rate controlling steps that can then be modified to prevent caries.

The objective of this paper is to provide a thermodynamic and kinetic basis for developing such models. The phase diagrams for calcium phosphates in ternary and more complex systems are shown to be an essential basis and they have important implications regarding (1) the observation that $\beta$-$Ca_3(PO_4)_2$ is found in the carious lesion, and (2) the possible significance of variations in the solubility of the mineral phase relative to caries susceptibility. Transport mechanisms may prove to be crucial to the formation of caries, particularly when coupled with the fact that the isotherms for calcium phosphates have positive slopes in the (Ca) vs. (P) solubility diagrams. A model intermediate to the Donnan-membrane and the strictly diffusional types may prove to be the most appropriate.

**12439.** Burdick, M. D., **A test for the cleanability of surfaces finishes,** *Porcelain Enamel Inst. Bull.* **T-28,** pp. 1-17 (1971).

Key words: Cleanability; fluorescence; porcelain enamel.

A detailed procedure is given to permit a numerical evaluation of the cleanability of surfaces. The method employs a fluorescent, water soluble soiling agent, a mechanized procedure for its application and partial removal, the water extraction of the retained soil and the calculation of a cleanability index through the use of a standard reference surface.

**12440.** Casella, R. C., **The reversal symmetry and its breaking in physics,** *Phys. Teacher* **8,** No. 3, 114-123 (Mar. 1970).

Key words: *CPT*; K° meson; symmetry; time-reversal; weak decays.

A review of symmetry principles in physics including charge conjugation (*C*), parity (*P*), and time reversal (*T*) is given, with emphasis on *T* symmetry and its breaking in K° meson decay. Following the 1956 discovery of *P* violation, *CP*, *T*, and *CPT* were assumed valid. The discovery in 1964 of *CP* breaking in K° decay into pions coupled with the *CPT* theorem implies *T* violation there, but *T* symmetry remains intact in several closely related experiments, suggesting the need for a direct demonstration of *T* violation. An account is included of the author's analysis which provides this demonstration.

**12441.** Cooper, M. J., **Generalized scaling and the parametric equation of state in the critical region,** Chapter in *Critical Phenomena in Alloys, Magnets, and Superconductors*, pp. 77-87 (McGraw-Hill Book Co., Inc., New York, N.Y., 1971).

Key words: Critical phenomena; equation of state; parametric equation of state; scaling laws.

A description of the critical region is developed using a local parametric characterization of the thermodynamic potential surface. The physical consequences of the formalism are presented and its predictions compared with some of the experimental data. Results indicate an extended description of the thermodynamic properties over a much enlarged region about the critical point.

**12442.** Corliss, E. L. R., **Estimate of the inherent channel capacity of the ear,** *J. Acoust. Soc. Am.* **50,** No. 2, 671-677 (1971).

Key words: Articulation function of ear; "bit" capacity of ear; channel capacity of ear; distinctive features of ear and hearing; intelligibility vs word lengths as block codes; speech; word lengths as block codes; speech intelligibility as channel capacity.

The growth of intelligibility of speech stimuli as a function of level above hearing threshold can be computed from the "circuit parameters" of the hearing mechanism by applying Shannon's concepts of channel capacity, equivocation, and "bits." In the ear, the unit response is an effective "least count," derived from experimental data on hearing by means of the equations for a model resembling a frequency-selective circuit [E. Corliss, J. Acoust. Soc. Amer. **41,** 1500-1516 (1967)]. The model predicts that the number of least counts available rises as the one-fourth power of the signal intensity above threshold. Experimentally, this growth rate is observed for the intensity-resolving power of the ear. Approximately the same power law is observed for the sensation of loudness. The model ascribes both effects to the same mechanism. From the observed integration time of the ear, the model predicts the rate at which transitions of single counts can be detected. From the counting rate and the integration time, the channel capacity available at the ear and its increase with level above the threshold can be computed. The information content of speech as a source function is evaluated from the rate at which single "distinctive features" of speech phonemes are produced. Intelligibility scores can be predicted from the ratio between the rate at which information is being produced by the source and the rate at which the receptor can accept the source material. The scores predicted agree fairly closely with experimental data on random-word and random-syllable intelligibilities. This agreement shows that the listener need recognize no more than a single distinctive feature of each phoneme to display the recognition functions that have been observed. From a theorem of C. Shannon [Inform. and Control **1,** 6-25 (1957)] relating code length and error probability, one can show that the channel capacity required for polysyllabic words is lower than the channel capacity required for monosyllabic words because the duration of correlated utterance may be taken as a code length. Evidently, contextual effects are not prominent in the intelligibility of random-word lists; the hearing process involved is primarily recognition of groups of sounds; meaning is secondary. The results also lead to the inference that a direct relation may exist between channel capacity and perceived loudness when speech is transmitted over a broad-band system, and suggest that loudness functions for impaired ears might prove to be correlated with intelligibility functions.

**12443.** Coxon, B., **Studies of $^{15}$N-labeled amino sugars. The synthesis and mass spectrometry of derivatives of 6-amino-6-deoxy-D-glucose-6-$^{15}N$,** *Carbohydrate Res.* **19,** 197-210 (1971).

Key words: Derivatives of 6-amino-6-deoxy-D-glucose-6-$^{15}N$; differential scanning calorimetry; infrared isotopic shift; mass spectrometry; nucleophilic substitution; $^{15}$N-labeled amino sugars; $^{15}N$-trifluoroacetyl derivative.

Derivatives of 6-amino-6-deoxy-D-glucose-6-$^{15}N$ have been synthesized in high yield and high chemical and isotopic purity by reaction of the 6-*O*-*p*-tolylsulfonyl or 6-deoxy-6-iodo derivative of 1,2:3,5-di-*O*-isopropylidene-$\alpha$-D-glucofuranose with potassium phthalimide-$^{15}N$. The infrared and mass spectra of some of these derivatives are discussed. Comparisons of the mass spectra of the $^{14}$N compounds and $^{15}$N-labeled derivatives afforded confirmation of the pathways of fragmentation.

**12444.** Coxon, B., Johnson, L. F., **The N.M.R. spectroscopy of derivatives of 6-amino-6-deoxy-D-glucose-6-$^{15}N$. $^{13}$C Fourier-transform and internuclear, double- and triple-resonance studies,** *Carbohydrate Res.* **20,** 105-122 (Nov. 1971).

Key words: Internuclear double resonance; internuclear triple resonance; nitrogen-15 coupling constants; nuclea Overhauser effects; p.m.r. spectroscopy; 6-amino-6-deoxy D-glucose-6-$^{15}N$ derivatives; $^{13}$C n.m.r. spectroscopy; $^{19}$F n.m.r. spectroscopy.

A series of $^{15}$N-labeled 6-amino-6-deoxy-1,2:3,5-di-*O* isopropylidene-$\alpha$-D-glucofuranose derivatives and their $^{14}$N analogs has been studied by continuous-wave proton, $^{13}$C, an $^{19}$F magnetic resonance spectroscopy, and by $^{13}$C Fourier-transform techniques. Characteristic chemical shifts and the magnitudes of $^1H-^1H$, $^1H-^{15}N$, $^1H-^{19}F$, $^{13}C-^{15}N$, and $^{15}N-^{19}$ coupling-constants are reported and discussed. The $^1H-^{15}$ and $^{13}C-^{15}N$ coupling-constants over one bond have bee used to assess the hybridization of the $^{15}$N atom in three of th derivatives. Heteronuclear, internuclear, double-resonance (ir dor) and triple-resonance ("intripler") experiments have bee performed in which $^{15}$NH proton transitions were monitore while the $^{15}$N or $^{19}$F frequencies were swept or maintained o resonance. Replicas of the computed, theoretical $^{15}$N spectrui were recorded indirectly, and are discussed in relation to nucle Overhauser effects.

**12445.** Davis, J. E., **The dry and wet bulb psychrometer,** (Pro ASHRAE Symp. Humidity Measurement, Columbus, Ohi Feb. 5-8, 1968), Chapter in *ASHRAE (Amer. Soc. Hea Refrig. Air-Cond. Eng.) Bull. Humidity Measurement*, pp. 17 (May 1970).

Key words: Aspirating psychrometers; dry- and wet-bu psychrometers; errors in psychrometric measurement psychrometric formulas; thermocouple psychrometer thermodynamic wet bulb temperature.

A paper describing the state of the art of dry and wet bu psychrometry is presented. Mathematical relationships applic ble to a sling psychrometer (or a dry and wet bulb thermomet in a test duct) are given. Short discussions of the univers psychrometric formula and three equations for use with the sli psychrometer are presented. Two of these equations consider fects which cause the reading of the wet-bulb to deviate from t true thermodynamic wet bulb temperature, but they have limi tions which are described. The aspirating psychrometer discussed and the performance of a simple thermocou psychrometer devised at the National Bureau of Standards described. Accuracy, precision, and laboratory fabricati techniques are also discussed. Results of tests at NBS usi techniques published by earlier investigators at temperatures 32 °F (0 °C) or below are given. Reference is made to inst ments developed which measure true thermodynamic wet bu temperature, but in their present stage of development are t large to be used in a test duct.

**12446.** Dibeler, V. H., Walker, J. A., McCulloh, K. E., Ros stock, H. M., **Effect of hot bands on the ionization threshold some diatomic halogen molecules,** *Intern. J. Mass Spectro Ion Phys.* **7,** 209-219 (1971).

Key words: Halogen molecules; hot bands; ionizati threshold; mass spectrometry; monochromator; vacuum traviolet.

Photoion-yield curves are obtained for the molecular ions the homonuclear diatomic halogens and for iodine monochlor and iodine monobromide. Excepting iodine, ionizat thresholds of ground-state and vibrationally-excited molecu are separately identified by measurements made at several i source temperatures. The adiabatic ionization energies (in e are: $I(F_2)=15.69$, $I(Cl_2)=11.48$, $I(Br_2)=10.52$, $I(ICl)=10.$

and $I(\mathrm{IBr})=9.79$. A preferred value of $I(\mathrm{I}_2)=9.37$ eV is proposed.

**12447.** DiMarzio, E. A., Rubin, R. J., **Adsorption of a chain polymer between two plates,** *J. Chem. Phys.* **55,** No. 9, 4318-4336 (Nov. 1, 1971).

Key words: Adhesion; grand canonical ensemble formalism; polymer adsorption; random walk model.

A lattice model of adsorption of an isolated chain polymer between two plates is investigated using a matrix formalism and a grand canonical ensemble (GCE) formalism. The matrix formalism is particularly convenient for calculating the polymer segment density as a function of the distance from one of the plates for different fixed plate separations. The GCE formalism can be used to calculate the fraction of loops (sequences of polymer segments whose ends are in contact with one plate and whose intermediate segments lie between the two plates), bridges (sequences of polymer segments whose ends are in contact with different plates and whose intermediate segments lie between the two plates), and trains (sequences of polymer segments which are wholly in contact with one plate or the other). All of the foregoing quantities have been calculated in the limit of infinite molecular weight as a function of the distance of separation between the plates and the energy of adsorption of a polymer segment on a plate. The self-excluded volume of the polymer chain is ignored. In addition the average sizes of loops, bridges, and trains, and the effective force of attraction between the plates are calculated.

**12448.** Distefano, G., Dibeler, V. H., **Photoionization study of the dimethyl compounds of zinc, cadmium, and mercury,** *Intern. J. Mass Spectrom. Ion Phys.* **4,** 59-68 (1970).

Key words: Heats of formation; ionization thresholds; mass spectrometry; metal alkyls; photoionization.

Photoionization yield curves from onset to 600 Å and ionization threshold values have been obtained for the ions $\mathrm{M(CH_3)_2^+}$, $\mathrm{CH_3M^+}$ and $\mathrm{M^+}$ of the dimethyl compounds of zinc, cadmium, and mercury, and the $\mathrm{CH_3^+}$ from dimethyl-mercury. Bond dissociation energies and heats of formation of the ions are also reported.

**12449.** Durst, R. A., **Ion-selective electrodes in science, medicine, and technology,** *Am. Sci.* **59,** No. 3, 353-361 (May-June 1971).

Key words: Electrodes; ion-selective electrodes; ion-selective electrode review; membrane electrodes; potentiometry.

The state of the art of the newer, non-glass types of ion-selective electrodes is reviewed. This brief survey includes discussions of the characteristics of the solid-state, liquid ion-exchange, and heterogeneous membrane electrodes. Applications of these sensors to a wide variety of scientific disciplines is presented, including biomedical research and industrial monitoring and control systems.

**12450.** Fatiadi, A. J., **(*p*-Bromophenyl)osotriazoles from inositols,** *Carbohydrate Res.* **20,** 179-184 (Nov. 1971).

Key words: Infrared; inositol; osotriazole; parabromophenyl; preparation; spectra; study.

(*p*-Bromophenyl)osotriazoles from inositols (D,L and DL), (+) *proto*-quercitol and their derivatives have been prepared and characterized. The KBr matrix i.r. spectra of *D, L* and *DL* forms revealed some differences.

**12451.** Flynn, T. M., Smith, C. N., **Trends in cryogenic fluid production in the United States,** (Proc. Int. Institute of Refrigeration, Tokyo, Japan, 1970), *Int. Inst. Refrig. Bull. Suppl. Commission* **I,** pp. 241-247 (Annex 1970-2).

Key words: Argon; cryogenics; forecasts; helium; hydrogen; liquefied natural gas; nitrogen; oxygen; trends.

The cryogenic industry in the United States has changed dramatically in both scope and character during the last decade. It has progressed from a liquid hydrogen technology to a liquid helium technology to developing new technologies dependent upon both the upper and lower extremes of the cryogenic scale. Among these are practical applications of superconductivity and the use of liquefied natural gas as a major world energy source. This change in the nature of the industry, and some of its implications for the future, is seen in this paper which traces the production of the economically significant cryogens over the last decade and gives the present status of cryogen in the U.S.A.

**12452.** Franklin, A. D., **Theory of linear dielectrics,** Chapter 17 in *Proc. Conf. Electronic Phenomena in Ceramics, University of Florida, Gainesville, Fla., Nov. 10-14, 1969,* pp. 451-489 (1971).

Key words: Ceramics; dielectric constant; electronic polarization; interfacial polarization; lattice polarization; orientation polarization; theory.

A cursory review is given of the theory of the linear response of a dielectric to an impressed electric field, including the electronic, lattice, dipole orientation, and linear interfacial polarizations. Most emphasis is given to the crystalline ionic, insulating models appropriate for the more ionic ceramics. Modifications to the theory for semiconducting and vitreous materials are briefly touched upon.

**12453.** Haar, L., Shenker, S. H., **Equation of state for dense gases,** *J. Chem. Phys.* **55,** No. 10, 4951-4958 (Nov. 15, 1971).

Key words: Argon; compressibility factor; dense fluids; equation of state; molecular dynamics; molecular interactions; nitrogen; pair potentials; temperature perturbation theory.

A simple quantitative equation of state of the van der Waals type is proposed for dense fluids. The equation yields compressibility factors with a precision comparable to those from the more complicated temperature perturbation theory when tested against "computer experiments," including isotherms as low as 0.8 liquid-vapor critical temperature. The equation is capable of predicting compressibility factors for real gases as illustrated by calculations for argon and nitrogen at pressures up to 10,000 atm. The derivation of the equation is based on a rearrangement of the terms in the Ursell—Mayer density expansion of the configuration integral. The equation contains two temperature-dependent parameters, to be determined from the dilute gas second virial coefficients. A principal feature of our approach is that it does not require explicit knowledge of the details of the pair interaction.

**12454.** Hall, J. L., Barger, R. L., Bender, P. L., Boyne, H. S., Faller, J. E., Ward, J., **Precision long path interferometry and the velocity of light,** A. Smolinski and S. Hahn, eds., (Proc. URSI Conf. Laser Measurements, Warsaw, Poland, Sept. 24-26, 1968), *Electron Technol.* **2,** No. 2/3, 53-66 (Panstwowe Wydawnictwo Naukowe Polish Scientific Publ., Warsaw, Poland, 1969).

Key words: Interferometry; laser; optical heterodyne; velocity of light.

A JILA/NASA/NBS velocity of light experiment has recently been started using the 51 Gc neon laser doublet at 1.15 microns. An evacuated 30-meter Fabry-Perot interferometer has been servo-stabilized to ~1:10″.

**12455.** Hussmann, E. K., McLaughlin, W. L., **Dye films and gels for megarad dosimetry,** *Proc. United Kingdom Panel on Gamma and Electron Irradiation, The National Physical Laboratory, Teddington, England, July 1970,* pp. 35-60 (Apr. 1971).

Key words: Depth-dose dyes; dose distribution; dosimetry; electrons; films; gamma rays; gels; radiation beams; x rays.

Gel, liquid, and thin-film radiochromic dye systems developed by McLaughlin and Chalkley are shown to be useful for measuring large doses from electron and x- and gamma-irradiations. The thin films are particularly suited to imaging and measuring radiation field profiles and dose distributions in various materials, even across interfaces of media with different stopping powers and absorption coefficients.

**12456.** Johannesen, R. B., Duerst, R. W., **Nuclear magnetic resonance studies of inorganic fluorides. VI. Magnetic nonequivalence in *bis*(perfluorovinyl) mercury,** *J. Magn. Resonance* **5,** No. 3, 355-366 (Dec. 1971).

Key words: Double resonance; fluorine; INDOR; mercury; nuclear magnetic resonance.

Fluorine magnetic resonance and $^{19}F\{^{199}Hg\}$ resonance spectra of *bis*(perfluorovinyl)mercury and methyl(perfluorovinyl)mercury have been observed. Proton resonance and $^{1}H\{^{199}Hg\}$ spectra of methyl(perfluorovinyl)mercury and dimethylmercury have also been observed. The magnitudes and signs of all possible $F - F$, $F - Hg$, and $H - Hg$ coupling constants in these three compounds have been determined. The spectrum of *bis*(perfluorovinyl)mercury calculated from the determined parameters is in excellent agreement with observation and the presence of long-range $F - F$ coupling constants in this molecule, none of which are zero, verifies an earlier suggestion as to the reason for the complexity of the spectrum. The fluorine chemical shifts and $F - F$ coupling constants within a perfluorovinyl group are within the previously reported range for these parameters. The mercury chemical shifts determined by INDOR spectroscopy are as follows: dimethylmercury 0 (reference), methyl(perfluorovinyl)mercury $+482 \pm 3$ ppm, *bis*(perfluorovinyl)mercury $+957 \pm 3$ ppm.

**12457.** Julienne, P. S., Krauss, M., Donn, B., **Formation of OH through inverse predissociation,** *Astrophys. J.* **170,** 65-70 (Nov. 15, 1971).

Key words: Interstellar clouds; interstellar molecule formation; inverse predissociation; non-adiabatic mixing; OH radiative association rate; predissociation widths.

Formation of OH can occur by inverse predissociation from continuum levels to the $v = 1$, $k = 1$ level of the $A\ ^2\Sigma^+$ state. A rate constant of $1 - 3 \times 10^{-20}$ cm$^3$ s$^{-1}$ is calculated for temperatures greater than 20 K. Predicted OH densities are consistent with observations in dense, heavily obscured clouds but appear to be somewhat low for H I clouds.

**12458.** Julienne, P. S., Neumann, D., Krauss, M., **Calculation of the temperature dependence for absorption in $CO_2$ in the 1750 – 1200 Å region,** *J. Atmospheric Sci.* **28,** No. 6, 833-837 (Sept. 1971).

Key words: *Ab initio* potential curve; carbon dioxide; quasi-linear molecule; Renner splitting; temperature dependent absorption coefficient; transition moment; ultraviolet.

The absorption cross section of the diffuse absorption bands of $CO_2$ in the region 1750 – 1200 Å is of prime importance for understanding $CO_2$ photolysis, especially as a constituent of a planetary atmosphere. The upper state of the absorption is a $^1B_2$ state correlating with a $^1\Delta_u$ state in the linear geometry. Although the cross section for this vibronically allowed electric-dipole absorption will be temperature-dependent, there are no experimental studies of this temperature dependence, and room temperature values have been used in discussions of the atmospheres of Mars and Venus despite the widely disparate temperature distributions of their atmospheres.

We have calculated the temperature dependence of the integrated absorption coefficient for the 1750 – 1200 Å region. The electronic energies and transition moments were calculated *ab initio* as a function of the bending angle of the molecule; in this way the Renner type splitting of the degenerate $^1\Delta_u$ state into $^1B_2$ and $^1A_2$ energy curves is obtained. The integrated absorption cross section is proportional to the square of the transition moment averaged over the ground state vibrational wave functions. At room temperature the average of the transition moment squared over a Boltzmann distribution is $2.9 \times 10^{-3}\ (ea_0)^2$, which corresponds roughly to an oscillator strength of $6 \times 10^{-4}$. Although halving the temperature produces only about 10% decrease in absorption, there is a dramatic increase by 75% when the temperature is doubled. The temperature dependence of individual lines, particularly in the wings of the overall distribution, is likely to be even more sensitive.

**12459.** Kaldor, A., **Absorption spectrum of borazine in the vacuum ultraviolet,** *J. Chem. Phys.* **55,** No. 9, 4641-4643 (Nov. 1, 1971).

Key words: Borazine; gas phase; matrix isolation; photochemistry; spectra; vacuum ultraviolet; vibronic structure.

The absorption spectrum of both vapor-phase and matrix-isolated borazine has been investigated in the 2000–1500-Å region. Three electronic transitions have been observed. The strongest absorption, with a maximum at 1650 Å, is assigned to the allowed $^1E' - ^1A_1'$ transition. Two weaker absorptions, with forbidden origins at 1975 and 1889 Å, are assigned to the forbidden transitions $^1A_2' - ^1A_1'$ and $^1A_1' - ^1A_1'$, respectively. The $^1A_2' - ^1A_1'$ transition is made vibronically allowed by one quantum change in the $\nu_{16}$ and $\nu_{17}\ e'$ vibrations. The vibration making allowed the $^1A_1' - ^1A_1'$ transition could not be determined.

**12460.** Kao, R., Perrone, N., Capps, W., **Large-deflection solution of the coaxial-ring-circular-glass-plate flexure problem,** *J. Am. Ceramic Soc.* **54,** No. 11, 566-571 (Nov. 1971).

Key words: Coaxial; deflection; flexure; glass; numerical; plate; ring; solution; strength; stress.

Nonlinear deflections and radial surface stresses in thin elastic circular plates laterally deformed into symmetrical concave shapes are analyzed. The deformations are induced by loading each plate with a small center ring while the plate is resting on a ring of nearly the same diameter as the plate. The rings and plate are coaxial, i.e., concentric. Center deflections up to 3 and 4.5 times the plate thickness were predicted for ring-diameter ratios of 0.5 and 0.2, respectively. The predicted deflection profiles at various loads agreed quite well with those which were determined experimentally on a chemically strengthened glass plate. This analysis provides a new criterion for using the coaxial-ring loading method for flexural strength of brittle materials.

**12461** Kaufman, V., Sugar, J., **One-electron spectrum of doubly ionized lutetium (Lu III) and nuclear magnetic dipole moment of $^{175}$Lu,** *J. Opt. Soc. Am.* **61,** No. 12, 1693-1698 (Dec. 1971).

Key words: Lutetium; spectra; wavelengths.

Thirteen new terms of the $4f^{14}(^1S_0)nl$ doublet system of $Lu^{2+}$ have been found, comprising the *ns* series ($7 \leq n \leq 10$), the *nf* series ($5 \leq n \leq 9$), and the *5g*, *6d*, *7d*, and *7p* terms. Previously, only the *5d*, *6s*, and *6p* terms were known. The *ns* series was used to derive an ionization energy of 169049 ± 10 cm$^{-1}$. From the completely resolved hyperfine structure (hfs) of $6s\ ^2S_{1/2}$, the value $a(6s) = 0.436 \pm 0.002$ cm$^{-1}$ was obtained for the hyperfine splitting factor. With these data, the nuclear magnetic dipole moment $\mu_I$ was found to be $2.204 \pm 0.010\mu_N$, where the stated uncertainty includes only the experimental uncertainty for $a(6s)$.

**12462.** McBee, C. L., Kruger, J., **Optical changes in oxide films on iron prior to breakdown,** *Nature Phys. Sci.* **230,** No. 17, 194-195 (Apr. 26, 1971).

Key words: Chloride; ellipsometry; passive film; spectroscopy.

Evidence for optical changes in the passive film on iron prior to complete breakdown by chloride is presented. The technique of ellipsometric-spectroscopy is used to locate a wavelength affected by the chloride addition. The recovery of the passive film by removal of the chloride ion is also reported.

**12463.** McDowell, H., Brown, W. E., Sutter, J. R., **Solubility study of calcium hydrogen phosphate. Ion-pair formation,** *Inorg. Chem.* **10,** 1638-1643 (Aug. 1971).

Key words: Calcium-phosphate ion pairs; solubility of anhydrous dicalcium phosphate; solubility of calcium monohydrogen phosphate; solubility of dibasic calcium phosphate; solubility of dicalcium phosphates.

The solubility of $CaHPO_4$ has been determined in the ternary system $Ca(OH)_2 - H_3PO_4 - H_2O$, at 5, 15, 25, and 37°. The solubility product constant, $K_{sp} = (Ca^{2+})(HPO_4{}^{2-})$, varies with pH unless formation of ion pairs $CaHPO_4{}^0$ and $CaH_2PO_4{}^+$ is taken into consideration. Solubility product constants and their standard errors for $CaHPO_4$ are $(1.97 \pm 0.03) \times 10^{-7}$, $(1.64 \pm 0.01) \times 10^{-7}$, $(1.26 \pm 0.02) \times 10^{-7}$, and $(0.92 \pm 0.02\ \times 10^{-7}$ at 5, 15, 25, and 37°, respectively. Association constants and standard errors are $(2.4 \pm 0.3) \times 10^2$, $(1.9 \pm 0.2) \times 10^2$, $(3.8 \pm 0.5) \times 10^2$, and $(3.9 \pm 0.9) \times 10^2$ for $CaHPO_4{}^0$ and $5 \pm 1$, $10 \pm 1$, $10 \pm 1$, and $11 \pm 1$ for $CaH_2PO_4{}^+$ at the same respective temperatures. Thermodynamic functions for the dissolution reaction for $CaHPO_4$ and the association reactions for $CaHPO_4{}^0$ and $CaH_2PO_4{}^+$ are also presented.

**12464.** Martin, W. C., **Energy differences between two spectroscopic systems in neutral, singly ionized, and doubly ionized lanthanide atoms,** *J. Opt. Soc. Am.* **61,** No. 12, 1682-1686 (Dec. 1971).

Key words: Atomic spectra; electron configurations; energy levels; lanthanide elements; spectra.

Energy differences of the type $4f^{N-1}\,5d - 4f^N$ (doubly ionized atoms), $4f^{N-1}\,5d6s - 4f^N\,6s$ (singly ionized atoms), and $4f^{N-1}\,5d6s^2 - 4f^N\,6s^2$ (neutral atoms) are important for the interpretation of rare-earth spectra. Here $N = 1$ for La, . . . 14 for Yb, and each configuration is represented by its lowest level in these system differences (SD). Nineteen of these differences are now known exactly from analyses of the spectra. Five additional SD values are approximately fixed by a combination of observation and calculation. Regularities deduced from these known values allow predictions for the remaining 18 SD values. The estimated probable error for most of the predictions is either 1000 or 1500 cm$^{-1}$.

**12465.** Masters, L. W., Lutz, G. J., **Determination of thallium by photon activation analysis,** *Anal. Chim. Acta* **56,** 365-370 (1971).

Key words: Activation analysis; bremsstrahlung; determination; glass; photon activation analysis; thallium.

The determination of trace amounts of thallium by the thermal neutron reaction $^{203}Tl(n,\gamma)\ ^{204}Tl$ is complicated because $^{204}Tl$ is a pure beta-emitter, requiring a lengthy and rigorous separation. In addition the half-life of $^{204}Tl$ is too long to permit decay measurements. A photon activation analysis method has been developed for this determination. Bremsstrahlung from a beam of 35-MeV electrons induces the photonuclear reaction $^{203}Tl(\gamma,n)\ ^{202}Tl$. The detection limit is of the order of tens of nanograms. It was determined that there are no interfering photonuclear reactions from lead.

**12466.** Moore, R. T., **Determination of performance of digital data communication systems,** (Proc. IEEE, ICC 71 CIC Intern. Conf. Communications, Montreal, Canada, June 14-16, 1971), *IEEE, ICC 71 CIC Conf. Record VII, Session 12A,* **VIII,** 12-1 – 12-3 (1971).

Key words: Digital data communication; digital system performance; draft standard ANSI X3; RER; TOT; TRIB.

An overview is presented of the work of American National Standards Institute Task Group X3S3.5 in the development of a standard for the determination of the performance of data communication systems.

Four performance criteria are identified. These are: (1) Transfer Rate of Information Bits (TRIB), a measure of information throughput; (2) Transfer Overhead Time (TOT), a measure of delays associated with the communications process; (3) Residual Error Rate (RER); and (4) System Availability (A). These criteria, as defined, are independent and are both necessary and sufficient to express the performance of any Information Path operated in accordance with the applicability limitations of the document.

Data communications system description is developed on a functional rather than a physical basis, and only to the extent necessary for performance determination.

The five possible phases of data communication are identified as: (1) Connection Establishment, (2) Link Establishment, (3) Information Transfer, (4) Link Termination, and (5) Connection Disestablishment. The beginning and end of each of these phases is rigorously defined and these definitions support the methodology for determining values for the performance criteria TRIB and TOT.

**12467.** Nagasawa, T., Kobayashi, K., **Paracrystalline structure of polymer-crystal lattice distortion induced by electron irradiation,** *J. Appl. Phys.* **41,** No. 11, 4276-4284 (Oct. 1970).

Key words: Crystal; defects; irradiation; polyethylene; unit cell.

The melting temperature of polyethylene crystals decreases and the lattice constants (both *a* and *b*) and lattice distortion increase, but the macroscopic volume of the specimen does not change with electron irradiation. From these results a model of a deformed lattice structure with point defects produced by irradiation is proposed. Calculations indicate that the anisotropy of a polymer crystal (difference between the elastic modulus along the molecular axis and perpendicular to the axis) increases the range of the distortion in a crystal caused by a defect. The presence of lattice distortion in electron irradiated polymer single crystals produces observable features in the Moiré patterns obtained from the crystals.

**12468.** Negas, T., Roth, R. S., **Phase equilibria and structural relations in the system $BaMnO_{3-x}$,** *J. Solid State Chem.* **3,** 323-339 (1971).

Key words: Barium-manganese oxides; crystal structures; oxidation-reduction; phase equilibria; system $BaMnO_3$.

The system $BaMnO_{3-x}$ $(0 \leq x < 0.5)$ in air was investigated by gravimetric, quenching, single-crystal and powder-x-ray diffraction studies. Below 1150 °C hexagonal, two-layer $BaMnO_3$ ($a$= 5.699 Å, $c$=4.817 Å) is stable. Above 1150 °C a series of anion deficient $BaMnO_{3-x}$ phases exists. With increasing temperature, these include a rhombohedral 15-layer form ($a$=5.681 Å, $c$= 35.377 Å; hexagonal indexing) and hexagonal 8-layer ($a$=5.699 Å, $c$=18.767 Å), 6-layer ($a$=5.683 Å, $c$=14.096 Å), 10-layer ($a$=5.680 Å, $c$=23.373 Å) and 4-layer ($a$=5.672 Å, $c$=9.319 Å) forms. The 6-layer modification is not of the hexagonal $BaTiO_3$-type. A simple orderly structural sequence involving a progressive increase of cubic-type layer stacking with increasing temperature characterizes the phases prepared. Influence of anion stoichiometry on phase formation is considered.

**12469.** Newman, M., **Units in cyclotomic number fields,** *J. Reine Angew. Math.* **250,** 1-11 (1971).

Key words: Cyclotomic units; diophantine equations; roots of unity.

Conditions for a unit in a cyclotomic number field to be a power of another unit in that field are derived, and the results applied to show that equations such as $1+\zeta=\alpha^r$, $\zeta$ a primitive $n$th root of unity, $n$ odd and $>3$, have only the trivial solution $r=1$, $\alpha=1+\zeta$.

**12470.** Plitt, K. F., Utech, H. P., **Flammability of turnout coats tested,** *Fire Eng.* **124,** No. 10, 60 (Nov. 1971).

Key words: Bunker coats; fabric flammability; firefighter clothing; fireman; flame resistance; turnout coats.

Flame resistance tests (Vertical Burn Method) were conducted on four commercially purchased firefighters' turnout coats. Each coat had three fabric layers: outer shell, interlining, and inner lining. The results show that 2 of 3 fabric layers in each coat produced a char length of 12 inches.

**12471.** Powell, F. J., **Research needs in thermal insulation,** (Proc. Symp. Thermal Insulation, Columbus, Ohio, Feb. 5-8, 1968), ASHRAE (Amer. Soc. Heat. Refrig. Air-Cond. Eng.) *Bull. Thermal Insulation,* pp. 14-17 (1971).

Key words: Performance coefficients; thermal insulation; transient heat transfer.

The role that research in respect to thermal insulation can play will be examined in this paper. Efforts to develop better insultaion materials through research and to search for better methods of application need to be continued, and, in addition, the need to develop methods of measurement, performance coefficients, load calculations and applications based on transient or dynamic conditions of heat flow rather than steady-state concepts will be discussed. With the advent of computers, the sophistication required for treating the complex transient heat flow problems becomes feasible and the time has arrived for research to enable accurate estimation of transient loads that are indicative of actual performance.

**12472.** Rasberry, S. D., **Applications of x-ray analysis, 20th Annual Denver X-Ray Conference, Denver, Aug. 11-13, 1971,** *Appl. Opt.* **10,** No. 12, 2795 (Dec. 1971).

Key words: Applied x-ray analysis; conference report; material analysis; x-ray diffraction; x-ray fluorescence.

In this meeting report of the 20th Annual Denver X-ray Conference, the general nature of this series of meetings is outlined. Some details specific to the papers presented this year are reported.

**12473.** Rosenstock, H. M., **Harmonic oscillator Franck-Condon factors for the ionization of $N_2O$,** *Intern. J. Mass Spectrom. Ion Phys.* **7,** 33-39 (1971).

Key words: Franck-Condon factor; ionization; $N_2O$; $N_2O^+$; photoelectron spectroscopy.

Harmonic oscillator Franck-Condon factors have been calculated for the ionization of $N^2O$. The Franck-Condon factors are quite sensitive to the form of the valence force field for the ion. The results are in fair agreement with experimental values obtained by photoelectron spectroscopy.

**12474.** Rubin, S., Oettinger, F. F., **Thermal hysteresis and its possible effect in restricting the hot-spot-free operating range of some power transistors,** *IEEE Trans. Electron Devices* **ED-18,** No. 6, 393-394 (June 1971).

Key words: Current constriction; DC current gain; hot-spot screening; methods of measurement; power transistors; reliability; thermal hysteresis; thermal resistance; thermographic measurements; transistor screening.

Studies conducted on a number of silicon power transistors indicate that for some devices a hot spot, once formed, will remain even though the power dissipation is reduced to a level at which operation was previously free of hot spots. The hot spot can be eliminated only by a significant reduction in power dissipation from the level at which the hot spot first appeared. The effect of the hot spot on reliable device operation is discussed.

**12475.** Saylor, C. P., **Refractive index,** Chapter in *The Characterization of Chemical Purity of Organic Compounds,* L. A. K. Staveley, ed., pp. 67-79 (July 1971).

Key words: Contamination; differential refractometer; identification; impurity; interferometer; purity; refractive index; refractometer.

Refractive index is not particularly valuable in the measurement of purity because the effects of impurities upon the property are indeterminate. A given impurity may raise, lower, or leave the refractive index unchanged. Those impurities that will most probably be present are, ordinarily, least certain to affect the refractive index. Still, a sample that has exactly the same refractive index as the perfectly pure material can usually be presumed to have high purity, since contaminants are unlikely to compensate precisely, and the more accurately the property is measured the more valid is the presumption. The methods of determination using liquid samples and the limits of accuracy to which the measurements of refractive index can be pressed will be discussed.

The situation with solids is different. In most cases, an impurity influences the refractive index of a solid very little if at all. Refractive index differences can be used to recognize isolated pockets of impurity, however, and by estimation and summation of the volumes of such outcroppings useful clues to the degree of contamination on that are not otherwise available can be secured.

**12476.** Schade, P. A., **Signal decoder eliminates jitter,** *Electron. Design* **19,** No. 24, 1 (Nov. 25, 1971).

Key words: False counts; incremental encoder; jitter; up-down counter; 90° phase decoder.

The two main types of decoders used with incremental shaft encoders are discussed. Emphasis is given to the problem of decoding signals which result from an oscillating shaft. A particular decoder circuit designed and tested by the author is presented.

**12477.** Schwartz, R. B., Heaton, H. T., II., Schrack, R. A., **High-accuracy total-cross-section measurements with the NBS Linac,** (Proc. Symp. Neutron Standards and Flux Normalization, Argonne National Laboratory, Argonne, Ill., Oct. 21-23, 1970), *AEC Symp. Series Neutron Standards and Flux Normalization* **23,** 377-384 (Aug. 1971).

Key words: Cross section; MeV; neutron; time-of-flight.

A high-accuracy fast-neutron time-of-flight spectrometer used for neutron energies between 0.5 and 20 MeV is described. The neutrons are produced by a 2-nsec-wide electron-beam pulse from the National Bureau of Standards Linac. The resolution, with a 40-m flight path, is approximately 0.1 nsec/m, and the accuracy of the measurements is estimated to be 1%.

**12478.** Schwartz, R. B., Schrack, R. A., Heaton, H. T., II., **A search for structure in the *N-P* total cross section,** (Proc. Neutron Standards and Flux Normalization Symp., Argonne National Laboratory, Argonne, Ill., Oct. 21-23, 1970. Sponsored by the European American Nuclear Data Committee), *AEC Symposium Series* **23,** pp. 57-62 (Aug. 1971).

Key words: Cross section; hydrogen; neutron; *n-p*; scattering; time-of-flight.

High-precision measurements of the *n-p* total cross section below 30 MeV show no evidence of any structure. A careful measurement of the differential scattering cross section also shows no evidence of any anisotropy.

**12479.** Swartzendruber, L. J., Bennett, L. H., **Use of ultrasonics in laboratory development tests of cupro-nickel alloys for desalination,** *Desalination* **9,** 387-389 (June 1971).

Key words: Alloys; corrosion; cupro-nickel; high velocity; sea-water; ultrasonics.

Ultrasonic agitation of the salt-water bath is suggested as a simple laboratory corrosion test method for evaluating the relative performance of alloys intended for use at moderate or high-sea water velocities.

**12480.** Allan, D. W., Gray, J. E., **Comments on the October 1970 Metrologia paper "the U.S. Naval Observatory clock time reference and the performance of a sample of atomic clocks,"** *Metrologia* **7,** No. 2, 79-82 (Apr. 1971).

Key words: Atomic clock; clock weighting factors; flicker noise; frequency stability; noise; synchronization; time; time scale; time scale precision.

The paper cited in the title by Winkler, Hall, and Percival (WHP) documents some important aspects of the widely referenced United States Naval Observatory (USNO) Time Scale system. We augment the text of WHP regarding the mutual synchronization to within 5 $\mu$s of the Time Scale, UTC(USNO), with another widely referenced time scale, the National Bureau of Standard UTC(NBS) Time Scale. We show that some of the imformation available to WHP can be utilized to give even more precision to the USNO Time Scale system and that some of that information has been improperly interpreted causing some errors by WHP in their conclusions regarding time scale precision, clock weighting factors, and drift in rate of the time scale.

**12481.** Andrews, J. R., **Horizontal time base sweep generator for a traveling wave oscilloscope,** *IEEE Trans. Nucl. Sci.* **NS-18,** No. 5, 3-8 (Oct. 1971).

Key words: High voltage pulse; nanosecond; oscilloscope; pulse generator; sweep generator; time base; traveling wave oscilloscope.

This paper describes the design, construction, and performance of a time base generator for use with a cathode ray tube capable of displaying fractional nanosecond transients. The generator was designed for use with a traveling wave cathode ray tube having a simple electrostatic time base deflection structure. When operating into the deflection plates (total capacitive load of 25 pF), the generator produced a total ramp excursion of − 4 kV with a maximum average slope of about − 450 V/ns. with a maximum repetition rate of 10 kHz. The ramp slope may be decreased continuously by a control voltage. The generator may also be operated into a 50 ohm load for the production of a − 750 V transition with 10%-90% transition time of 4.8 ns.

**12482.** Bates, R. G., Paabo, M., **Measurement of pH,** *Handbook of Biochemistry,* H. A. Sober, ed., 2d Edition, pp. J227-J233 (Chemical Rubber Company, Cleveland, Ohio, Jan. 1971).

Key words: Acidity; glass electrode; indicators; pH; standardization.

The operational definition of pH, in the form endorsed by the International Union of Pure and Applied Chemistry, is presented. The preparation of standard reference solutions for pH measurements is described and the choice of electrodes and measurement techniques is discussed. The proper interpretation of pH numbers is set forth briefly, and procedures for pH measurement with indicators are described.

The revised version includes the addition of two new primary pH standards to tables 1 and 3, coefficients for calculating the temperature dependence of pH in table 2, and a collection of pH values for miscellaneous buffer solutions.

**12483.** Berry, R. J., Riddle, J. L., **Intercomparison of oxygen boiling point realizations in standards laboratories,** *Metrologia* **7,** No. 2, 56-58 (1971).

Key words: IPTS-68; oxygen point.

The experimental realizations of the normal boiling point of oxygen maintained in several national standards laboratories are compared.

**12484.** Block, S., **The user's viewpoint on x-ray diffraction safety standards,** *Proc. Conf. Radiation Safety in X-Ray Diffraction and Spectroscopy, University of Pennsylvania, Philadelphia, Pa., Jan. 6-7, 1970,* pp. 211-221 (Sept. 1971).

Key words: Diffraction; fluorescence analysis; radiation safety; x rays.

The user's point of view on safety standards for x-ray diffraction and fluorescence analysis equipment is presented as part of a panel discussion.

**12485.** Brady, G. W., Gravatt, C. C., Jr., **Determination of the radial distribution function and the direct correlation function of spheres by x-ray small-angle scattering,** *J. Chem. Phys.* **55,** No. 10, 5095-5101 (Nov. 15, 1971).

Key words: Hard sphere fluid; liquids; radial distribution function; small-angle x-ray scattering.

An experimental determination of the pair and direct correlation functions of polystyrene latex spheres in the high-density limit has been made. From these the pair potential for hard spheres has been calculated. The significance of the functions as they bear on the Percus-Vevick and the hypernetted chain approximation is discussed.

**12486.** Braun, W., Carlone, C., Carrington, T., Van Volkenburgh, G., Young, R. A., **Collisional deactivation of $H(2^2P)$ fluorescence,** *J. Chem. Phys.* **53,** No. 11, 4244-4248 (Dec. 1, 1970).

Key words: Deactivation; fluorescence; hydrogen atoms; quenching.

Collision cross sections for deactivation of $H^*(n=2)$ at 300 K have been measured by observations of the quenching of Lyman-$\alpha$ fluorescence in a discharge flow system. The quenchers (with cross section in Å$^2$) are $H_2(84\pm8)$, $D_2(84\pm8)$, $N_2(62\pm6)$, He $(<3)$. For $H^*+H_2$, less than 1% of the total quenching produces ions. Care has been taken to work with systems optically thin in Lyman $\alpha$ so that the rate of escape of radiation, which is the reference to which the quenching rate is compared, is not reduced by resonance trapping.

**12487.** Carter, G. C., Swartz, J. C., **Nuclear magnetic resonance Knight shifts and quadrupole effects in transition metal diborides,** *J. Phys. Chem. Solids* **32,** 2415-2421 (Jan. 1971).

> Key words: Electric quadrupole coupling constant; Knight shift; NMR; $ScB_2$; transition metal diborides.

Nuclear magnetic resonance data for $ScB_2$, $YB_2$ and $MnB_2$ are presented. These data together with earlier NMR data provide a complete picture of the 3*d* and 4*d* transition metal diborides: $ScB_2$ through $MnB_2$ and $YB_2$ through $MoB_2$. The Knight shifts, electric quadrupole coupling constants, and linewidths of the central resonance of the $^{45}Sc$ and $^{11}B$ nuclei in $ScB_2$ are essentially temperature independent in the range 4–300 K. The boron Knight shifts $\mathscr{K}(B)$ are 0.00(1)%, –0.004(10)% and –0.05(2)% in $ScB_2$, $YB_2$ and $MnB_2$, respectively. $\mathscr{K}(Sc) = 0.07(1)\%$ and $\mathscr{K}(Y) = 0.20(3)\%$ in the respective diborides. The difference between these values and the higher values for metallic Sc and Y is attributed primarily to reduced orbital and Pauli contributions. For the 3*d* series $ScB_2$ to $MnB_2$, the Knight shifts, electronic specific heats, magnetic susceptibilities and transport properties indicate increasing *d*-electron character with increasing group number. The quadrupole coupling constant of $^{11}B$ across both 3*d* and 4*d* series does not correlate with the c/a ratio or unit cell volume. This may indicate deviation of the boron atoms from a planar configuration.

**12488.** Cezairliyan, A., **Recent developments in thermophysical properties research,** *Proc. Committee Thermophysical Properties, Washington, D.C., Dec. 1, 1971,* **HTD-3,** 12-13 (American Society of Mechanical Engineers, New York, N.Y., 1971).

> Key words: High-speed measurements; high temperature; thermodynamics; thermophysical properties.

Recent developments in high-speed measurement of thermophysical properties at high temperatures are summarized. Emphasis is placed on methods that allow the performance of measurements in subsecond duration on electrically conducting substances in the solid phase. High-speed measurements of properties, such as specific heat, electrical resistivity, hemispherical total emittance, normal spectral emittance, and temperatures and energies of phase transitions and transformations are described.

**12489.** Cooper, M. J., **Various expansions in thermodynamic scaling,** *Phys. Rev. A* **5,** No. 1, 318-320 (Jan. 1972).

> Key words: Critical region; equation of state; scaling laws; thermodynamic scaling.

Several recently proposed general extensions of thermodynamic scaling are compared and a single comprehensive form suggested.

**12490.** Dean, J. A., Rains, T. C., **Standard solutions for flame spectrometry,** Chapter 13 in *Flame Emission and Atomic Absorption Spectrometry* **II,** 327-339 (Marcel Dekker, Inc., New York, N.Y., July 1971).

> Key words: Atomic absorption spectrometry; flame emission spectrometry; standard solutions; stock solutions.

The availability of standard samples and high-purity materials for preparing reference and standard solutions is an important criterion for the solution of an analytical method. For application in the fields of atomic absorption and flame emission spectrometry various types, as well as the source, of standard samples and high purity materials are listed. Procedures for preparing standard stock solutions for 74 elements and special solutions for a variety of matrices are described.

**12491.** De Simone, D. V., **Moving to metric makes dollars and sense,** *Harvard Bus. Rev.,* pp. 100-111 (Jan.-Feb. 1972).

> Key words: Business and industry; economy; education; international relations; international standards; international trade; metric; technology assessment.

The article will be a summary of the report, "A Metric America," which evaluates and distills the findings of the U.S. Metric Study in which thousands of individuals, firms and organized groups, representative of our society, participated. On the basis of all the evidence marshalled in the Study, the report concludes that the United States should change to the metric system through a coordinated national program.

**12492.** Dise, J. R., **Recent developments in cement testing,** *Proc. General Technical Committee, Portland Cement Association, San Francisco, Calif., Sept. 22, 1971, Mill Session Papers* **M-197,** 34-42 (1971).

> Key words: Hydraulic cement; testing of cement.

This review of recent developments in cement testing has been prepared for the purpose of recording some of the unpublished information about the testing of hydraulic cements that has come to the attention of the author through his work with Committee C-1 on Cement of the American Society for Testing and Materials, and the Cement and Concrete Reference Laboratory at the National Bureau of Standards.

**12493.** Escalante, E., Kruger, J., **Stress corrosion cracking of pure copper,** *J. Electrochem. Soc.* **118,** No. 7, 1062-1066 (July 1971).

> Key words: Copper; cupric acetate; kinetics; oxidation; stress corrosion; tarnish film.

It is known that the rate of tarnish film formation is an important factor in the stress corrosion cracking (SCC) of brass. Because copper immersed in cupric acetate and sulfate solutions has tarnish film growth rates comparable to those found for brasses susceptible to SCC, it should undergo cracking in such solutions if kinetics play a role. It was found that pure copper is susceptible to cracking in cupric acetate solution but not in cupric sulfate. Light, which retards film formation on copper, but not corrosion, prevents stress cracking in the cupric acetate solution. In the absence of stress, oxide forms all over the copper surface, while stress concentrates oxide formation at the grain boundaries. These experiments point to a brittle-film rupture mechanism of stress cracking.

**12494.** Fraker, A. C., Ruff, A. W., Jr., **Studies of oxide film formation on titanium alloys in saline water,** *Corrosion Sci.* **11,** 763-765 (Dec. 1971).

> Key words: Electron microscopy; hot saline water corrosion; oxide films; titanium; titanium alloy corrosion.

Oxide films formed on five titanium alloys were characterized after corrosion in 3.5wt.% NaCl solutions over the temperature range of 100-200 °C. Electron transmission microscopy and electron diffraction of corroded thin foils showed the oxide film to be TiO and $Ti_2O_3$ in the early corrosion stages and to change in the 150-200 °C temperature range to a final surface oxide, $TiO_2$ (anatase).

**12495.** Goldstein, J. I., Yakowitz, H., **Metallic inclusions and metal particles in the Apollo 12 lunar soil,** Chapter in *Proceedings 2d Lunar Science Conference, Houston, Texas, Jan. 1971,* **1,** 177-191 (MIT Press, Cambridge, Mass., Mar. 1971).

Key words: Electron probe microanalyzer; lunar age; lunar materials; meteorites; scanning electron microscopy.

Almost all the reduced metal in the Apollo 12 lunar soil was found as inclusions in the individual soil particles. The inclusions contain $< 0.1 - > 20.0$ weight% Ni and $< 0.1 - 2.5$ weight% Co. These Ni and Co contents are similar to those measured for metal grains in Apollo 12 igneous rocks. Curves of Ni vs. Co contents for meteoritic metal were used to differentiate the meteoritic metal component from the lunar component. On this basis over 80% of the metal areas examined had Ni and Co contents outside of the known meteoritic composition range and were derived from the lunar igneous rocks. The presence of the meteoritic inclusions in the soil particles can be explained by low velocity impacts in the lunar soil during major meteoritic bombardment on the moon.

Six individual metal particles $> 125$ μm in size, separated from 50 grams of Apollo 12 soil, were studied. Four of the six particles are meteoritic. Two of the meteoritic particles exhibit deformation bands produced by peak shock pressures $< 150$ kb. The other two meteoritic particles ~ 1/2 mm in diameter were remelted during impact on the moon. Dendrites of Fe-Ni are visible in one and a phosphide-kamacite eutectic structure is present in the other. The structures and compositions of the phases present in these particles indicate either slow cooling or a reheating of these particles on the moon's surface in the 500-600 °C temperature range for a year or more. Most of the meteoritic particles studied were probably originally pieces of chondrites.

**12496.** Hastie, J. W., Plante, E. R., **Entropy in isotopic systems,** *High Temp. Sci.* **3,** No. 5, 412-414 (Sept. 1971).

Key words: Entropy; isotopes; symmetry number; third law.

Many current textbooks and even the research literature appear inadequate in recognizing or discussing certain entropy conventions. The present article elaborates on this question with particular reference to a recent research article that amply demonstrates the errors that can result from the misunderstanding of entropy conventions in isotopic systems.

**12497.** Heydemann, P., **Ultrasonic measurements at very high pressures,** *Phys. Acoust.* **8,** 203-236 (1971).

Key words: Equation of state; high pressure; liquids; solids; ultrasonic measurements.

Ultrasonic measurements are used to determine equations of state for solids and liquids at very high pressures. These measurements are made in piston and cylinder, piston and die, belt or girdle and anvil apparatus. A particularly useful apparatus is the piston and die system with fluid container which is described in greater detail. Often ultrasonic measurements can be combined with isothermal compression measurements to give additional information on $c_p/c_v$, $\gamma_G$ and $\alpha$. Examples of results and estimates of the attainable accuracy are given.

**12498.** Hockey, B. J., **Plastic deformation of aluminum oxide by indentation and abrasion,** *J. Am. Ceram. Soc.* **54,** No. 5, 223-231 (May 1971).

Key words: Abrasion; alumina; annealing; dislocations; electron microscopy; indentation; plastic deformation; surface regions; transmission electron microscopy; twinning.

Transmission electron microscopy provided direct evidence that plastic deformation occurs during the room-temperature indentation and abrasion of $Al_2O_3$. Examination of single-crystal and polycrystalline specimens showed that high densities of dislocations are produced within the near-surface regions by mechanical polishing with a fine diamond compound (0.25 μm) and that plastic deformation by both slip and mechanical twinning occurs during the placement of Vickers microhardness indentations. The occurrence of plastic deformation in this normally brittle material is considered to be a consequence of the nature and magnitude of the local stresses developed under pointed indenters and irregularly shaped abrasive particles. Preliminary results on the effect of annealing on the retained substructure are also presented. Annealing at 900 °C and higher resulted in the reduction of residual stresses through the motion of dislocations and their rearrangement into lower-energy configurations.

**12499.** Huie, R. E., Herron, J. T., Davis, D. D., **Absolute rate constants for the reaction of atomic oxygen with 1-butene over the temperature range of 259-493 K,** *J. Phys. Chem.* **75,** No. 25, 3902-3903 (1971).

Key words: Atomic oxygen; flash photolysis; kinetics; 1-butene.

Rate constants for the reaction of atomic oxygen with 1-butene have been measured over a temperature range of 259 to 493 K using the flash photolysis-resonance fluorescence technique. No dependence of rate constants on pressure or reactant concentration was observed.

The rate constant for the reaction of atomic oxygen with 1-butene was found to be:

$$\kappa = 1.46 \pm 0.15 \times 10^{-11} \exp\left(\frac{-760 \pm 60 \text{ cal mol}^{-1}}{\text{RT}}\right) \text{cm}^3 \text{ molecule sec}^{-1}.$$

**12500.** Johns, J. W. C., Olson, W. B., **The infrared spectrum of thioformaldehyde,** *J. Mol. Spectry.* **39,** No. 3, 479-505 (Sept. 1971).

Key words: High resolution; infrared; rotational constants; short lived molecule; spectrum; thioformaldehyde.

The infrared spectrum of thioformaldehyde ($H_2CS$) has been observed in the C-H stretching region. The spectrum was obtained under conditions of high resolution and rotational analyses have been carried out on the three observed bands. The main results (in $cm^{-1}$) for the excited states are:

| *Band* | $\nu_0$ | *A* | *B* | *C* |
|---|---|---|---|---|
| $\nu_5$ | 3024.61 | 9.675 | 0.5893 | 0.5554 |
| $\nu_1$ | 2971.03 | 9.648 | 0.5907 | 0.5542 |
| $2\nu_6$(?) | 2877.11 | 9.821 | 0.5936 | 0.5533 |

Several local perturbations have been observed in the two fundamentals $\nu_5$ and $\nu_1$. These are presumably caused by overtones and combinations of the lower lying fundamentals but it has not been possible to make specific assignments of the perturbing levels.

**12501.** Johnson, D. R., Lovas, F., **A new look at the laboratory microwave spectrum of cyanoacetylene,** *Astrophys. J.* **169,** 617-619 (Nov. 1, 1971).

Key words: Cyanoacetylene; hyperfine structure; interstellar microwave emission; laboratory microwave spectrum; radio astronomy; rotational transitions.

Laboratory measurements have been made on several transitions in cyanoacetylene with potential application to radio astronomy. Observations of $J=1 \leftarrow 0$ and $J=2 \leftarrow 1$ rotational transitions are reported for the isotopic species $H^{12}C^{12}C^{12}C^{14}N$, $H^{13}C^{12}C^{12}C^{14}N$, and $H^{12}C^{12}C^{12}C^{15}N$. Measurement errors and resolution of hyperfine structure are discussed in some detail.

**12502.** Julienne, P. S., Krauss, M., Wahl, A. C., **Hartree-Fock energy curves for $X^2\Pi$ and $^2\Sigma^+$ states of $HF^+$,** *Chem. Phys. Letters* **11,** No. 1, 16-20 (Sept. 15, 1971).

Key words: $D_0^0$(HF); $D_e$($HF^+$); dissociation energy; Hartree-Fock; photoelectron spectra; vibrational energy levels.

Hartree-Fock energy curves have been calculated for the $X^2\Pi$ and $^2\Sigma^+$ states of $HF^+$ and applied to an analysis of the photoelectron spectra of HF. The $^2\Sigma^+$ energy curve is found to have a barrier about 0.07 eV high due primarily to a repulsive ion-quadrupole interaction, and a depth of 0.37 eV. This curve will support two bound states and one shape resonance with a half-width of 0.015 eV. The energy curves are probably accurate to 0.1 eV but the analysis shows that results accurate to within 0.03 eV are required to resolve the experimental questions on the dissociation energy for the ground state of HF. The most recent experimental photoelectron results of Berkowitz (following article) encouraged a model calculation of the vibrational states of the $^2\Sigma^+$ state. Assuming a dissociation energy of 0.45 eV and retaining the barrier three bound and one shape resonance vibrational levels are calculated for $HF^+$ in agreement with the results reported by Berkowitz.

**12503.** Kirby, R. K., Rothrock, B. D., **Thermal expansion of platinum to 1900 K and reference materials for thermophysical properties,** *Proc. European Conf. Thermophysical Properties of Solid Materials at High Temperatures, Baden-Baden, Germany, Nov. 11-13, 1968,* pp. 600-620 (Feb. 1970).

Key words: Platinum; standard reference materials; thermal expansion.

The thermal expansion of two specimens of platinum has been measured with a precision optical comparator. A controlled-gradient vacuum furnace was used to heat each specimen to temperatures between 1000 and 1900 K. Within this temperature range the linear thermal expansion of the two specimens is given by

$$\frac{L_t - L_{293}}{L_{293}} \times 10^6 = -2685 + 8.972\,T + 2.505 \times 10^{-4}\,T^2 + 4.641 \times 10^{-7}\,T^3.$$

The National Bureau of Standards is actively engaged in certifying several standard reference materials for thermophysical properties. These include expansivity standards of vitreous silica, borosilicate glass, single-crystal sapphire, copper and tungsten and a calorimetric standard of single-crystal sapphire.

**12504.** McAlister, A. J., Williams, M. L., Cuthill, J. R., Dobbyn, R. C., **Relation between the 5*d* band structure and soft x-ray $N_{6,7}$ emission spectrum of Au,** *Solid State Commun.* **9,** 1775-1777 (July 1971).

Key words: Band structure; emission spectrum; gold; *N* spectrum; soft x rays.

The $N_{6,7}$ soft x-ray emission spectrum of Au (5*d* to 4*f* transition) has been measured. Distinct structural features are observed. The absolute positions in photon energy of these features are derivable from x-ray and u.v. induced photo-emission spectra. In turn, these experiments agree well with recent band calculations for Au and thus offer further support of the utility of the single particle description of the occupied band structure of metals.

**12505.** Mentall, J. E., Gentieu, E. P., Krauss, M., Neumann, D., **Photoionization and absorption spectrum of formaldehyde in the vacuum ultraviolet,** *J. Chem. Phys.* **55,** No. 12, 5471-5479 (Dec. 15, 1971).

Key words: Formaldehyde; integrated oscillator strength; photoionization coefficient; Rydberg spectrum; SCF calculations; vacuum UV spectrum.

Absorption and photoionization coefficients have been measured for $H_2CO$ in the 600-2000-Å region. Integrated oscillator strengths were determined for a number of strong Rydberg transitions above 1200 Å. From the photoionization curve the first adiabatic ionization potential was found to be $10.87 \pm 0.01$ eV. As an aid in interpreting the absorption spectrum, theoretical calculations were made using a single-configuration self-consistent field procedure for the Rydberg states and a model which included mixing between the Rydberg and valence states. On this basis, weak absorption features between 1340 and 1430 Å have been assigned to the $^1B_1(\sigma \rightarrow \pi^*)$ valence state. The $^1A_1(\pi \rightarrow \pi^*)$ valence state is deduced to be strongly autoionized just above the $^2B_2$ ionization limit.

**12506.** Mielczarek, S. R., Miller, K. J., **Dependence of generalized oscillator strengths of $H_2O$ on momentum transfer,** *Chem. Phys. Letters* **10,** No. 4, 369-370 (Aug. 15, 1971).

Key words: Electronic excitation; generalized oscillator strength; $H_2O$; inelastic electron scattering; momentum transfer.

Experimental results on the dependence of generalized oscillator strengths of water on momentum transfer, showing the appearance of extrema and characteristic features in the electron scattering spectra are reported and discussed.

**12507.** Okabe, H., **Fluorescence predissociation of sulfur dioxide,** *J. Amer. Chem. Soc.* **93,** No. 25, 7095-7096 (1971).

Key words: Fluorescence; predissociation; quenching; $SO_2$.

The fluorescence intensity of $SO_2$ was measured as a function of incident wavelength in the region 2000 to 2300 Å where dissociation is expected to compete with fluorescence.

A sudden decrease of the fluorescence intensity was observed below the incident wavelength 2189 Å, corresponding to the photon energy of 5.66 eV which agrees almost exactly with the thermochemical threshold of 5.65 eV for dissociation. This indicates that the photodissociation starts to compete with the fluorescence above this photon energy. The quenching rate by Ar of the excited $SO_2$ produced at 2208 Å is $5 \times 10^{-11}$ cm$^3$ molecules$^{-1}$ sec$^{-1}$ on the basis of the lifetime of 9 ns calculated from the integrated absorption coefficient. The lifetime decreases to 3.2 ns for the excited state at 2189 Å because of the predissociation.

**12508.** Reneker, D. H., Colson, J. P., **Annealing and melting of polyoxymethylene crystals polymerized within irradiated trioxane crystals,** *J. Appl. Phys.* **42,** No. 12, 4606-4614 (Nov. 1971).

Key words: Annealing of polyoxymethylene; polyoxymethylene; polyoxymethylene crystals; solid state polymerization; trioxane.

Morphological changes produced by the annealing and melting of the polyoxymethylene crystals that polymerize inside irradiated trioxane crystals were observed. The crystals in which the polyoxymethylene chains were oriented parallel to the threefold axis of the trioxane underwent major reorganization when held at 184 °C for 30 sec. The polyoxymethylene crystals in which the chain axis was inclined at a large angle with respect to the threefold axis of the trioxane transformed and melted at temperatures approximately 5 °C lower.

**12509.** Robertson, B., **Wyler's expression for the fine-structure constant** $\alpha$, *Phys. Rev. Letters* **27,** No. 22, 1545-1547 (Nov. 29, 1971).

Key words: Conformal group; fine structure constant; relativistic quantum theory; symmetric spaces.

Wyler's expression for $\alpha$ in terms of the Euclidean volumes of certain bounded spaces agrees with experiment only if the radius of these spaces is arbitrarily chosen to equal 1. However, the relationship between these spaces and the invariance group *O(n,2)* of the *n*-dimensional wave equation is independent of the radius. There is no known reason for setting the radius equal to one.

**12510.** Romberg, E. F., Wall, N. S., Blum, D., Lightbody, J. W., Jr., Penner, S., **Elastic scattering of 60-120 MeV electrons from $^{46,48,50}$Ti,** *Nucl. Phys.* **A173,** 124-128 (1971).

Key words: Elastic electron scattering; nuclear charge distribution; nuclear radii; titanium isotopes.

The elastic electron scattering from the isotopes of $^{46,48,50}$Ti has been measured at an angle of 127.5°. The ratios of the cross sections were analysed with a partial-wave analysis for a Fermi-shaped charge distribution and the parameter variations were deduced. Some consequences of these results are discussed.

**12511.** Schooley, J. F., Soulen, R. J., Jr., **Superconductive transitions suitable as thermometric fixed points,** E. Kanda, ed., *Proc. XII Conf. Low Temperature Physics, Kyoto, Japan, Sept. 3-10, 1970,* pp. 833-834 (Keigaku Publishing Co., Tokyo, Japan, Mar. 1971).

Key words: Elements; fixed points; reproducibility; superconductors; thermometry; transition widths; wire samples.

We have shown that annealed wire samples of Pb, In, Al, Ga, and Zn, when simply prepared and mounted, exhibit superconductive transitions using A.C. susceptibility techniques which are sharper than one millikelvin. These transitions are reproducible to a millikelvin after many thermal cycles over a twenty-month period, suggesting their use as thermometric fixed points.

**12512.** Velapoldi, R. A., Menis, O., **Formation and stabilities of free bilirubin and bilirubin complexes with transition and rare-earth elements,** *Clin. Chem.* **17,** 1165-1170 (1971).

Key words: Bilirubin; bilirubin-lanthanide complexes; bilirubin-transition metal complexes; biliverdin; solvents; stability; tetrapyrroles.

We investigated complexes formed between bilirubin and transition or rare-earth elements, and their relative stabilities. Relative rates of complex formation were analogous to metalloporphyrin and metal complex stabilities, according to the Irving-Williams series. Transition metals that formed strong, square planar complexes caused rapid bilirubin degradation. Iron(II) was oxidized to iron(III) in the bilirubin complex. Of the lanthanide complexes, only samarium(III) showed covalent bonding tendencies. Comparative molar absorptivities were calculated for several of the metal-bilirubin complexes. The stability of bilirubin in several solvents and under various experimental conditions is reported. At room temperature, bilirubin photooxidizes to biliverdin on exposure to laboratory light.

**12513.** Wagner, H. L., **Standard reference materials for polymer characterization at the National Bureau of Standards,** *Polymer Preprints,* **ACS 12,** No. 2, 770-774 (1971).

Key words: Characterization; gel permeation chromatography; light scattering; molecular weight; molecular weight distribution; osmometry; SRM 705; SRM 706; SRM 1475; SRM 1476.

The National Bureau of Standards now has available a total of four Polymer Standard Reference Materials, designed for use in the calibration of instruments employed in polymer characterization. Polystyrene is available in narrow (SRM 705) and broad (SRM 706) molecular weight distributions, while polyethylene whole polymers are available in both high density linear (SRM 1475) and low density branched (SRM 1476) materials. After careful measurements of sample homogeneity, these materials were characterized with respect to weight and number average molecular weight, limiting viscosity number in several solvents, and for the polyethylenes, A.S.T.M. density and A.S.T.M. flow rate. The molecular weight of the branched material has not been certified. In addition, the molecular weight distribution of the linear polyethylene was carefully determined; consequently it is well suited for calibration of gel permeation chromatographs at high temperatures in the molecular weight range of $10^3$ to $10^6$.

**12514.** Waynant, R. W., Ali, A. W., Julienne, P. S., **Experimental observations and calculated band strength for the $D_2$ Lyman band laser,** *J. Appl. Phys.* **42,** No. 9, 3406-3408 (Aug. 1971).

Key words: Adiabatic approximation; band strengths; $D_2$ Lyman emission; emission wavelengths; traveling wave excitation; vacuum ultraviolet laser.

Experimental observations have been made of vacuum ultraviolet laser emission in the Lyman band of $D_2$. Fourteen lines from 1568 to 1614 Å have been measured to have a total peak power of nearly 1 MW in a short ($\sim$ 1 nsec) pulse. To facilitate identification of the laser wavelengths, optical functions were calculated using the adiabatic correction to the usual Born-Oppenheimer approximation. The theory predicts the most probable transitions and these wavelengths agree with experiment to within 0.1–0.2 Å.

**12515.** Wells, T. E., Gard, E. F., **An integrated system for the precise calibration of four-terminal standard resistors,** (Proc. Conf. Electronic and Electrical Measurements and Test Instrument Conference, Ottawa, Canada, June 1-3, 1971), *IEEE Trans. Inst. Meas.* **IM-20,** No. 4, 253-257 (Nov. 1971).

Key words: Ampere-turn balance; flux balance; standard resistor; voltage balance.

A description is given of the system currently in use at the National Bureau of Standards for measurements of 1 – Ω standard resistors of the Thomas type. A tenfold improvement in accuracy over the former method has been realized. Resistors of this type are now reported to eight decimal places with a total uncertainty of 0.08 ppm. The latter figure includes a three-standard-deviation limit for random errors plus an estimate of systematic errors.

The new system is not only more rapid in operation than the old one (fewer man hours required), but has consistently produced data of superior resolution while operating with a lower test power in resistors. A dc current-linkage balance is used to determine the standard-unknown differences while both are connected in series and totally immersed in a specially designed circular oil bath, which remains completely covered during all tests. Bath temperature is maintained constantly at 25,000 °C (± 0.003 °C) in a unique manner.

**12516.** Yokel, F. Y., Somes, N. F., **Performance criteria for innovative housing systems,** *J. Am. Soc. Eng. Ed.* **61,** No. 2, 105-107 (Nov. 1970).

Key words: Building code; building systems; housing; performance criteria; performance testing.

A philosophy for the application of the performance concept to the evaluation of innovative housing systems is evolved, and its application to Operation BREAKTHROUGH is illustrated by examples.

**12517.** Zalewski, E. F., Keller, R. A., **Tunable multiple wavelength organic-dye laser,** *Appl. Opt.* **10,** No. 12, 2773-2775 (Dec. 1971).

Key words: Dye laser; laser; organic dye laser; spectroscopy.

A technique for simultaneously tuning a dye laser at two different wavelengths has been developed. The apparatus consists of an optical cavity formed by two partially transparent, broadbanded mirrors. A diffraction grating is placed along the optical axis outside of each mirror to form a secondary cavity. When the gratings are at the proper angle, there is enough optical feedback through the partially transparent mirrors to cause the laser to emit only at the wavelengths corresponding to the grating angles. Two wavelength outputs with each wavelength separately tunable were obtained from a rhodamine 6G organic dye laser using this technique.

**12518.** Andrews, J. R., **An interfacing unit for a 28 psec feedthrough sampling head and a random sampling oscilloscope,** *Rev. Sci. Instr.* **42,** No. 12, 1882-1885 (Dec. 1971).

Key words: GHz; impulse; picoseconds; random sampling; sampling head; sampling oscilloscope; spark-gap.

In time domain measurements of repetitive pulses there are situations when a signal delay line cannot be tolerated and a signal pretrigger is not available. In such situations, a random sampling oscilloscope system must be used. In the course of recent research activities, the author encountered the need to employ a remote, 50 Ω feedthrough, 28 psec transition time, wide-band sampling head with a random sampling oscilloscope system. Because the sampling head and the random sampling system were incompatible units from different manufacturers, an interfacing system was required to connect the two units. Presented here are a working design for the interface and operating results.

**12519.** Cashion, J. K., Mees, J. L., Eastman, D. E., Simpson, J. A., Kuyatt, C. E., **Windowless photoelectron spectrometer for high resolution studies of solids and surfaces,** *Rev. Sci. Instr.* **42,** No. 11, 1670-1674 (Nov. 1971).

Key words: High resolution electron energy analyzer; photoelectron spectroscopy; photoemission from solids and chemisorbed gases; ultrahigh vacuum; ultraviolet source.

An ultrahigh vacuum photoelectron spectrometer capable of measuring electron energy distributions for solids and chemisorbed gases at photon energies of 16.8, 21.2, 26.9, and 40.8 eV is described.

**12520.** Chang, S. S., Bestul, A. B., **Heat capacity and thermodynamic properties of *o*-terphenyl crystal, glass, and liquid,** *J. Chem. Phys.* **56,** No. 1, 503-516 (Jan. 1, 1972).

Key words: Calorimetry; configurational entropy; glass; heat capacity; *o*-terphenyl; residual entropy; viscosity; vitreous state.

The heat capacity of *o*-terphenyl has been measured with an adiabatic calorimeter for the crystal from 2 K to $T_m$ (329.35 K), for the glasses from 2 K to $T_g$ (around 240 K) and for the liquid from $T_g$ to 360 K, on a sample with less than 0.005 mole % impurity. The heat of fusion and the entropy of fusion are 17 191 J mole$^{-1}$ and 52.20 J K$^{-1}$·mole$^{-1}$, respectively. The residual entropy of the glasses at 0 K is about 15 J K$^{-1}$·mole$^{-1}$. Above 170 K, the heat capacity of the *o*-terphenyl crystal is nearly proportional to the temperature to within 1%. Configurational entropy of the supercooled liquid, estimated from the result of this investigation, is used to relate the relaxation properties of glass-forming liquids according to the theory of Adam and Gibbs. Good agreement is found for both viscosity and NMR correlation frequency data.

**12521.** Cooper, J. W., Kolbenstvedt, H., **Differential energy and angular cross sections for ionization by several-hundred-keV electrons: Theory and comparison and experiment,** *Phys. Rev. A* **5,** No. 2, 677-687 (Feb. 1972).

Key words: Differential cross section; ioniziation; kilovolt electrons; Møller scattering.

A procedure for calculating cross sections for ionization of electrons in various shells of an atom differential in both angle and final electron energy is developed. Calculations for ionization of carbon, copper, and gold for incident energies in the range 100–400 keV are presented and compared with recent experimental results.

**12522.** Dalke, J. L., **International standards for magnetic materials and components,** *IEEE Trans. Magnetics* **MAG-7,** No. 3, 545-548 (Sept. 1971).

Key words: IEC; international standards; magnetic components; magnetic materials; magnetic measurements; magnetic standards.

In practically all of the industrially developed countries of the world there are strong national standards organizations. The International Electrotechnical Commission (IEC) coordinates and unifies electrical and electronic standards by drafting international recommendations from which member countries may draw for national standards. The benefits derived from this work include better understanding among electrical and electronic engineers and scientists, and a means for initiating and expanding international trade. The upsurge in development and application of ferrites led the IEC to establish a committee on ferromagnetic oxide parts 15 years ago, which rapidly expanded into a full technical committee on magnetic materials and components (TC 51). The magnetic activities include recommendations for terms and definitions, dimensional standardization, measurement methods, inductors and transformers, data storage devices, strip-wound cores and laminations, variability (temperature and time), gyromagnetic applications (microwave), and antenna rods Eleven TC 51 IEC publications are now available. Numerous others are in process.

**12523.** Daney, D. E., **Thermal conductivity of solid argon, deuterium, and methane from one-dimensional freezing rates,** *Cryogenics* **11,** No. 4, 290-297 (Aug. 1971).

Key words: Instrument; solid argon; solid deuterium; solidified gases; solid methane; thermal conductivity.

The thermal conductivities of solid argon, deuterium, and methane have been determined near their triple points from measurements of one-dimensional freezing rates. In this new technique, a cylinder of liquid is frozen axially from one end, and the thermal conductivity of the freezing solid is evaluated from the freezing rate and the cylindrical cell end temperatures. A plastic cell wall offers the advantages of visual observation of the freezing solid and negligible cell wall conduction. The estimated random and systematic errors for the apparatus are 5 and 3% respectively. Improved instrumentation may reduce these errors by one-half.

**12524.** de Graaf, L. A., Mozer, B., **Structure study of liquid neon by neutron diffraction,** *J. Chem. Phys.* **55,** No. 10, 4967-497 (Nov. 15, 1971).

Key words: Correlation function; interatomic potentia neon; neutron diffraction; structure factor.

Neutron-diffraction measurements with high statistical accuracy were performed on liquid neon at 35.05 K and at three different densities. The structure factors $S(\kappa)$, measured to momentum transfers $\kappa$ of 13.2 Å$^{-1}$, show a density-dependent structure well beyond 6 Å$^{-1}$. The data have been used to calculate the radial distribution functions $g(r)$, the direct correlation function $c(r)$, and effective interatomic potentials.

12525. Diller, D. E., **The specific heats $(C_v)$ of dense simple fluids,** *Cryogenics* **11,** No. 3, 186-191 (June 1971).

Key words: Density dependence; molecular dynamics; simple fluids; specific heats; temperature dependence.

This paper examines the wide-range temperature and density dependences of the specific heats $(C_v)$ of a number of simple fluids (helium, neon, argon, krypton, parahydrogen, oxygen, and fluorine). The temperature range between the triple point and $2T_c$ at densities up to $3\rho_c$ is emphasized. The behaviour of the internal specific heats of the classical monatomic fluids is compared with that of the diatomic and quantum fluids and with internal specific heats derived from molecular dynamics calculations. This comparison shows that (to a first approximation) the internal specific heats of classical monatomic fluids depend only on the intermolecular pair potential energy.

12526. Domalski, E. S., **Evaluating experimental data on heats of combustion,** *J. Chem. Doc.* **11,** No. 4, 234-237 (1971).

Key words: Bomb calorimetry; corrections to the combustion data; data evaluation; evaluation process; flame calorimetry; heats of combustion of organic compounds; recommendations to authors.

The approach used by data evaluators at the Chemical Thermodynamic Data Center of the National Bureau of Standards for the interpretation of published articles reporting values of the heats of combustion is discussed. An appropriate set of corrections is applied to the values when required to bring all data under study to a common base. Corrections which must be considered are: changes in calibration, reduction of the sample mass to vacuum, changes in atomic mass, reduction to standard states, expression of the data in proper energy units, and bringing the reference temperature for the combustion process to 298.15 K. Some corrections must be estimated because insufficient information is given in the article for a standard reanalysis. Guidelines are offered to authors of papers which will provide a maximum amount of data for the reexamination of experimental results, but yet maintain conciseness in the overall presentation.

12527. Eisenhart, C., **Youden's burette experiment,** *J. Quality Technol.* **4,** No. 1, 20-23 (Jan. 1972).

Key words: Accuracy; analysis of variance; measurement process; precision; regression line; scheduling measurements; statistical design of experiments; systematic error; Youden's burette experiment.

This is a write-up of a lecture given by Dr. W. J. Youden at the National Bureau of Standards in 1947 which may be said to have had three objectives: first, to lay bare the fallaciousness of the all-too-common belief that statistical methods—and a statistician!—can be of no help unless one has a vast amount of data; second; to demonstrate that one can obtain valuable information on the precision—and even on the accuracy!—of a measurement process without making a large number of measurements on any single magnitude; and third, to show how in routine work one can often obtain useful auxiliary information on personnel, equipment, etc., at little or no additional cost, by skillful preliminary planning of the measurements to be taken. These precepts are demonstrated by an experiment involving only 8 volumes of liquid drawn from a burette by two different operators and subsequently subjected to chemical analysis by the same individuals.

12528. Ellerbruch, D. A., **Microwave methods for cryogenic liquid and slush instrumentation,** *IEEE Trans. Instr. Meas.* **IM-19,** No. 4, 412-416 (Nov. 1970).

Key words: Cryogenic fluids; densitometer; flowmeter; instrumentation; microwave.

Microwave instrumentation is being developed to measure densities and flow rates of nitrogen or hydrogen in either the single-phase liquid state or the liquid-solid (slush) state. The dielectric behavior exhibited by these fluids is the basis for using microwave systems for the measurement. These methods can also be applied to the measurement of fluids at ordinary temperatures.

The three density instrumentation techniques discussed here require that the microwave signal be propagated through a column of cryogenic fluid (from the top to the bottom of a cryostat, for example). All of the fluid in the column influences the behavior of the microwave signal, thus the sample is representative of the fluids at all levels within the cryostat.

A Doppler flowmeter is also discussed. Its main advantages are that no moving mechanical parts are involved and no probe need be installed in the flow stream. The flowmeter may give simultaneous density and velocity measurements so that the mass flow rate can be determined.

12529. Evenson, K. M., Day, G. W., Wells, J. S., Mullen, L. O., **Extension of absolute frequency measurements to the cw He-Ne laser at 88 THz (3.39 $\mu$),** *Appl. Phys. Letters* **20,** No. 3, 133-134 (Feb. 1, 1972).

Key words: $CO_2$ laser; helium neon laser; laser frequency measurement; MOM diode; 3.39 $\mu$m laser.

The highest absolute frequency measurement yet reported is described. The frequency of the 3.39-$\mu$ line from a He-Ne laser oscillating at the methane absorption frequency was found to be 88.376245 (55) THz. The frequency was measured by beating the 88-THz radiation with the $R(30)$ line from a cw $CO_2$ laser and a 48-GHz klystron in a tungsten-on-nickel point-contact diode. The speed of light calculated from this frequency and previous wavelength measurements is in agreement with the accepted value and of comparable accuracy.

12530. Fatiadi, A. J., Schaffer, R., **Periodic acid as a new oxidant for the degradation of bile pigments. Isolation of a biliverdine type of reaction intermediate on oxidation of bilirubin with periodic acid,** *Experientia* **27,** No. 10, 1139-1141 (Oct. 15, 1971).

Key words: Acid; bile; bilirubin; biliverdine; charge-transfer; complex; degradation; iodine; methyl-sulfoxide; periodic; pigment; structure.

Degradation of porphyrins and bile pigments can be performed with aqueous periodic acid by use of methyl sulfoxide, acetic acid, or tetrahydrofuran as the co-solvent. By the use of methyl sulfoxide as the co-solvent in the oxidation of bilirubin with periodic acid, it was possible to isolate a biliverdine—iodine complex to which a charge-transfer structure has been assigned.

12531. Fey, L., **Time dissemination capabilities of the Omega system,** *Proc. 25th Annual Frequency Control Symp., Atlantic City, N. J., Apr. 26-28, 1971,* pp. 167-170 (Electronic Industries Association, Washington, D.C., Apr. 1971).

Key words: Multiple frequency timing; Omega time code; precise time receiver; precise timing; time code receivers; VLF timing.

The Omega VLF navigation system affords an opportunity to disseminate time synchronization signals which could serve two classes of users: those who need precise timing and those who need time-of-day information in the form of a time code. This paper discusses precise timing use in terms of carrier pulse timing, multiple frequency techniques for carrier cycle ambiguity resolution, and Omega system capabilities in the microsecond region. For use where unattended automatic timing is needed, a time code giving second, minute, hour, and day number information could serve a variety of needs. These are described along with characteristics and constraints of such a code imposed by the existing navigation format. The paper concludes with desirable receiver characteristics and development requirements for these two timing uses.

**12532.** Fickett, F. R., **Aluminum. 1. A review of resistive mechanisms in aluminum,** *Cryogenics* **11,** No. 5, 349-367 (Oct. 1971).

Key words: Aluminum; electron scattering; magnetoresistivity; resistivity; superconductivity.

Various mechanisms affecting the electrical resistivity of aluminum are reviewed. Brief treatments are given of the theory, experimental techniques, and the results of experiments to measure the effect of phonons, electron–electron interactions, boundaries, vacancies and interstitials, chemical impurities, dislocations, and stacking faults on the resistivity of aluminum at room temperature and below. Also reviewed are experimental data on superconductivity, magnetoresistivity, and the effect of interactions between the various mechanisms. Where appropriate, suggested values are given for the resistivity contribution of a particular mechanism.

**12533.** Foote, W. J., **A new flange design for O-ring seals,** *Rev. Sci. Instr.* **41,** No. 8, 1237 (Aug. 1970).

Key words: Flange design; O-ring; seal; vacuum.

A new type of O-ring seal was designed to provide a vacuum-tight cover for a wide-mouth cylindrical dewar. Covers using this type of seal are cheaper to machine than conventional designs, and can be quickly installed or removed. The design may be used to vacuum seal almost any smooth walled cylindrical vessel or large tubing.

**12534.** Giarratano, P. J., Arp, V. D., Smith, R. V., **Forced convection heat transfer to supercritical helium,** *Cryogenics* **11,** No. 5, 385-393 (Oct. 1971).

Key words: Correlations; cryogenics; forced convection; heat transfer; helium; supercritical.

Heat transfer coefficients have been measured for supercritical helium, circulated around a closed flow loop by a miniature centrifugal pump. Reynolds numbers in the 0.208 cm i.d. by 10 cm long stainless steel test section ranged from $1 \times 10^4$ to $3.8 \times 10^5$ with pressures 3 to 20 atm (0.3 to 2 $MN/m^{-2}$) and fluid temperatures 4.4 to 30 K. Wall-to-bulk temperature ratios varied from approximately 1.03 to 3.0. Results indicate an enhancement in heat transfer as the bulk temperature of the fluid approaches the transposed critical temperature. This improvement is qualitatively predicted by classical correlations due to the increase of thermal conductivity and specific heat in this region. Over the range of variables included in the measurements it was found that a modification of the Dittus-Boelter heat transfer correlation can be used to predict the heat transfer coefficient satisfactorily for most engineering calculations.

**12535.** Guttman, C. M., **Low-temperature heat-capacity differences between glasses and their crystals,** *J. Chem. Phys.* **56,** No. 1, 627-630 (Jan. 1, 1972).

Key words: Crystals; disordered crystal; glasses; heat capacity; low temperature.

It is suggested that the low-temperature heat-capacity difference between glasses and their crystal may be computed by considering the simple process, $C_x(V_x) \xrightarrow[(a)]{} C_x(V_g) \xrightarrow[(b)]{} C_g(V_g)$, where $C_x(V_x)$ is the constant volume heat capacity of the crystal at its equilibrium volume at normal pressures, $V_x$, $C_x(V_g)$ is the heat capacity of the substance of identical structure as the crystal but of a volume, $V_g$, equivalent to that of the glass, and $C_g(V_g)$ is the constant volume heat capacity of the glass. Estimates are made of the change in heat capacity due to step (a) (the change in heat capacity at constant crystal structure due to a volume change) and to step (b) (the change in heat capacity due to disordering at constant volume) for a one-dimensional model of a glass and crystal. These suggest that step (a) contributes more to the heat-capacity difference than does step (b). Contributions to step (a) from a three-dimensional Debye model show reasonable agreement with experiment.

**12536.** Hanson, D. W., Hamilton, W. F., **One-way time synchronization via geostationary satellites at UHF,** *IEEE Trans. Instr. Meas.* **IM-20,** No. 3, 147-153 (Aug. 1971).

Key words: Clocks; delay; ranging measurements; satellites; synchronization; timing; UHF.

This paper describes an experiment designed to evaluate the accuracy of one-way clock synchronization using geostationary satellites with the propagation delays calculated from the satellite's orbital elements. Propagation delays from a ground transmitter via satellite to each of five locations in the North and South American continents were measured and compared with the calculated values. Three months of data are presented along with descriptions of the equipment, timing signal format, and methods for delay calculation and time recovery.

The results show that within two weeks of epoch for the orbital elements, clocks can be synchronized to 150 $\mu$s using the Tactical Communications Satellite (TACSAT). If one of the observers of the timing signals was already synchronized to the master clock, his delay measurement could improve the results for TACSAT to 75 $\mu$s. By the same method and within 12 hours of epoch, the results for the Lincoln Experimental Satellite-6 (LES-6) indicated that synchronization to 25 $\mu$s was possible.

**12537.** Heinrich, K. F. J., **Errors in theoretical correction systems in quantitative electron probe microanalysis–a synopsis,** *Anal. Chem.* **44,** No. 2, 350-354 (Feb. 1972).

Key words: Electron probe microanalysis; errors; fluorescence; iteration; x-ray absorption; x-ray emission.

Accurate electron probe microanalysis with simple reference materials requires the use of theoretical models describing the emission of direct and indirect characteristic x-radiation, and of an iterative calculation procedure. The presently accepted theoretical equations for the calculation of intensities are presented, with discussion of the main sources of error. An efficient iteration procedure which uses a hyperbolic approximation to the analytical calibration curve is discussed in detail.

**12538.** Hust, J. G., Clark, A. F., **The Lorenz ratio as a tool for predicting the thermal conductivity of metals and alloys,** *Mater. Res. Stand.* **11,** No. 8, 22-24 (Aug. 1971).

Key words: Alloys; cryogenics; electrical restivity; electron conductivity; Lorenz ratio; low temperature research; metals; thermal conductivity; thermal resistance.

From a knowledge of the Lorenz ratio of a given class of alloys and a simple electrical resistivity measurement, one can calculate the thermal conductivity of a specimen with reasonable accuracy. A discussion contrasts the characteristic temperature dependence of the Lorenz ratios, $\rho\lambda/T$($\rho$ = electrical resistivity, $\lambda$ = thermal conductivity, $T$ = temperature), of metals and alloys with high conductivity with that of metals and alloys with low conductivity. An additional classification of alloys in terms of Lorenz ratio further enhances the predictive capabilities of the method. The advantages as well as the limitations of the method are discussed.

**12539.** Jennings, D. A., Varga, A. J., **Efficient second harmonic generation in ADP with two new fluorescein dye lasers,** *J. Appl. Phys.* **42,** No. 12, 5171-5172 (Nov. 1971).

Key words: ADP crystals; dye laser; fluorescein dye; second harmonic generation; tunable UV source.

Two new fluorescein solutions for flashlamp-pumped dye lasers are reported, providing peak powers on the order of kilowatts, tunable from 550 to 580 nm. The 90° phase-matched second harmonic generation in ADP demonstrated with these and other dyes provides a flash excited UV source tunable from 250 to 290 nm with peak powers of about 10 watts.

**12540.** Kestin, J., Paykoc, E., Sengers, J. V., **On the density expansion for viscosity in gases,** *Physica* **54,** 1-19 (1971).

Key words: Argon; dense gases; helium; nitrogen; transport properties; viscosity.

The paper presents the results of new, precise measurements of the viscosity of nitrogen, argon, and helium at 25 °C. The measurements were performed over a nominal range of pressures 1–100 atm and at very closely spaced density intervals. The data were subjected to a stringent statistical analysis in order to determine whether the density expansion consists of a pure polynomial or whether a term of the form $\rho^2 \ln \rho$ must be included in it. The existence of such a term was discovered theoretically by several investigators. The analysis indicates that if such a term exists, its factor must be very small. Moreover, the statistically significant interval of values which this factor can assume includes zero in it.

This result is interpreted as indicating that correlations which extend over distances of the order of a mean free path are negligible when compared with correlations which extend over distances of the order of the range of molecular interactions.

**12541.** Koonce, C. S., Mangum, B. W., Thornton, D. D., **Magnetic properties of the antiferromagnet $DyPO_4$ in applied fields,** *Phys. Rev. B* **4,** No. 11, 4054-4069 (Dec. 1, 1971).

Key words: Antiferromagnet; dipolar interactions; $DyPO_4$; heat capacity; magnetization; metamagnet; phase transition; shape effects; susceptibility.

The magnetization and susceptibility of the Ising antiferromagnet $DyPO_4$ have been measured as a function of temperature and applied field for samples having demagnetization factors $D \approx 0.02$ and $D \approx 1.0$. Also, the temperature at which peaks in the heat capacity at constant applied field occurred were measured for a number of applied fields. These results have been compared with predictions of the molecular-field approximation and the Bethe-Peierls approximation including long-range dipolar interactions. The temperature below which the antiferromagnetic-paramagnetic transition is first order has been obtained within the molecular-field approximation. In addition, expressions are obtained for the magnitude of the discontinuity in the heat capacity at the transition between the intermediate (or mixed) state and the antiferromagnetic or paramagnetic states for samples having nonzero demagnetization factors. These expressions do not depend on the molecular-field or Bethe-Peierls approximations.

**12542.** Kuriyama, M., **X-ray Compton-Raman scattering,** *Acta Cryst.* **A27,** Part 6, 634-647 (Nov. 1971).

Key words: Absorption; charge correlation; Compton effect; core electrons; current correlation; inelastic scattering; solid; theory; valence electrons; x-ray Raman effect.

X-ray Compton-Raman scattering is reviewed from an original point of view. The differential cross section for x-ray inelastic scattering from crystals is derived from first principles to explain the coexisting Compton and Raman scattering in solids. This derivation makes it possible to express the cross section in terms of the current correlation of electrons in a crystal. All the electrons, including the core electrons, are treated on an equal basis in this formulation. The relationship between the x-ray absorption spectrum and the inelastic scattering spectrum is discussed in detail. This formulation provides a theoretical justification to the importance of x-ray inelastic scattering experiments in connection with an experimental determination of the two-particle Green's function. In the Appendices the theoretical formulations are given in detail, which apply not only to the ordinary inelastic scattering process, but also to the processes involving Bragg diffraction.

**12543.** Kushner, L. M., **Technology, product performance, and the consumer,** *Sci. Teacher* **38,** No. 8, 22-26 (Nov. 1971).

Key words: Product performance; technology; technology assessment.

The relationship between technology and the consumer is a complex one. Its most obvious manifestation is in the performance of the products he purchases; but one must also take into account the impact of technology on the manufacturing process and on the buying habits of the consumer. The overriding effect of technological advance, however, has been to put the consumer very much at a disadvantage relative to his former position as an equal in face-to-face bartering with an individual craftsman. The courts, through an increasingly strict view of manufacturer liability, and the Congress, through its consideration of a host of consumer protection bills, are attempting to redress this imbalance. Responsible business and industry are seeking, through the voluntary standardization process to improve the situation; but this process, developed to suit the industrial buyer and seller, appears to be ill-suited to the task without substantial modification. As with the other serious and intricate problems society faces today, there are no simple solutions but to the extent that the consumer begins to understand his situation vis-a-vis technological development he becomes better able to deal with it. This is one of the challenges facing the educational community in general and science teachers in particular.

**12544.** Maki, A. G., **A high resolution study of *l*-type resonance in cyclopropane,** *J. Mol. Spectrosc.* **41,** No. 1, 177-181 (Jan. 1972).

Key words: Cyclopropane; energy levels; infrared; *l*-type resonance; molecular structure; spectroscopy.

The $\nu_5 + \nu_{10}$ band of cyclopropane ($C_3H_6$) centered at 2089.52 $cm^{-1}$ has been measured and analyzed taking into account the *l*-type resonance effect described by Cartwright and Mills. A least-squares fit of more than 300 well-resolved transitions gave a set of band constants which reproduced the measurements with a standard deviation of 0.003 $cm^{-1}$. The analysis confirms the *l*-type resonance treatment given by Cartwright and Mills and shows that their band contour fit gave remarkably accurate constants for this band.

**12545.** Mann, D. B., **Cryogenic flow-metering research at NBS,** *Cryogenics* **11,** No. 3, 179-185 (June 1971).

Key words: Cryogenic-fluid-flow measurement; cryogenic flowmetering; liquid argon; liquid nitrogen.

One very pressing cryogenic problem is that of cryogenic fluid flow measurement. An NBS programme, which focuses attention on the problem, has as its objectives to (1) establish present state-of-the-art by evaluating existing measurement methods, (2) establish methodology to maintain precision and accuracy of field-measurement devices, and (3) establish a comprehensive programme to develop new cryogenic fluid-measurement systems. The scope of this programme includes a precision measurement capability for measuring the flow of liquid nitrogen and liquid argon, a transfer of technology from the traditional cryogenic fluids to measuring the flow of liquefied natural gas and methane, and a concerted effort to develop new mass-flow measurements for cryogenic fluids such as slush or liquid hydrogen. Cryogenic flow-metering history is given as well as a description of three flow facilities that establish experimental confirmation of the cryogenic flow-measurement system under investigation.

**12546.** Mighell, A. D., Santoro, A., **The crystal and molecular structures of hexakis(imidazole) cadmium(II) nitrate, $[Cd(C_3H_4N_2)_6](NO_3)_2$, and hexakis(imidazole)cadmium(II) hydroxide nitrate tetrahydrate, $[Cd(C_3H_4N_2)_6](OH)(NO_3)\cdot 4H_2O$,** *Acta Cryst.* **B27,** Part 11, 2089-2097 (Nov. 1971).

Key words: Cadmium; coordination complex; crystal structure; imidazole; x ray.

The crystal and molecular structures of hexakis(imidazole)cadmium(II) nitrate, $Cd(C_3H_4N_2)_6](NO_3)_2$, and hexakis(imidazole)cadmium(II) hydroxide nitrate tetrahydrate, $[Cd(C_3H_4N_2)_6](OH)\ (NO_3)\cdot 4H_2O$, have been determined by single-crystal x-ray diffraction techniques. $[Cd(C_3H_4N_2)_6](NO_3)_2$ crystallizes in the trigonal system, space group $R\overline{3}$. The lattice parameters (hexagonal axes) are $a = 12.633(2)$, $c = 15.049(2)$ Å, $Z = 3$, $\rho_0 = 1.54$ g·cm$^{-3}$, $\rho_c = 1.54$ g·cm$^{-3}$. The final three-dimensional full-matrix least-squares refinement resulted in an $R$ value of 3.6% based on 1343 observed reflections. $[Cd(C_3H_4N_2)_6](OH)(NO_3)\cdot 4H_2O$ crystallizes in the hexagonal system, space group $P6_3/m$. The lattice parameters are $a = 9.0376(8)$, $c = 21.729(3)$ Å, $Z = 2$, $\rho_c = 1.45$ g·cm$^{-3}$, $\rho_0 = 1.44$ g·cm$^{-3}$. The final three-dimensional full-matrix least-squares refinement resulted in an $R$ value of 5.4% based on 996 observed reflections. Both structures consist of discrete $Cd(C_3H_4N_2)_6^{2+}$ cations and $NO_3^-$ anions but as a result of the presence of water molecules and $OH^-$ ions in the hydroxide complex, the packing of the cations in the two structures is considerably different. The ligand imidazole molecules are coordinated through the pyridine type nitrogen atoms ($\geqslant$N) to the $Cd^{2+}$ ions with an average bond distance Cd...N of 2.363 Å and they are hydrogen bonded through the pyrrole type ($-$ N $-$ H) nitrogen atoms to the nitrate groups. However, to accommodate hydrogen bonding, there is considerable difference in the orientation of the imidazole rings in the two complexes. Specifically, each ring in one of the two complex cations is rotated, about the Cd $-$ N(1) direction, approximately 130° with respect to its counterpart in the other cation. The bond distances and angles between the atoms of the imidazole molecules are practically identical in the two structures.

**12547.** Page, C. H., **The International System of Units (SI),** *Phys. Teacher* **9,** No. 7, 379-381 (Oct. 1971).

Key words: Giorgi; IEC, MKSA, SI; units.

An elementary discussion of the SI and its development from the MKS system of Professor Giorgi and the IEC.

**12548.** Peterson, W. K., Beaty, E. C., Opal, C. B., **Measurements of energy and angular distributions of secondary electrons produced in electron-impact ionization of helium,** *Phys. Rev. A* **5,** No. 2, 712-723 (Feb. 1972).

Key words: Electron scattering; helium; ionization; secondary electrons.

The energy and angular distributions of electrons produced in the ionization of helium by electrons with energies between 100 eV and 2 keV have been measured in a crossed-beam apparatus consisting of a fixed hemispherical energy analyzer and a rotatable electron gun. Distributions of secondary electrons (those electrons departing with energies less than one-half that of the incident primary electrons) were obtained for a wide range of energies and for angles between 30 and 150° with respect to the direction of the incident primary electron beam. The observed angular distributions were significantly different from the results of two early electron-impact measurements; however, they agreed to the extent expected with more recent results and with similar proton-impact data. For secondary energies above about 50 eV and for primary energies greater than 300 eV, the energy distributions (the cross sections integrated over angle) were observed to be very nearly equal to the distribution given by the Mott formula for free-electron-free-electron scattering multiplied by the number of electrons in the target.

**12549.** Phelan, R. J., Jr., Mahler, R. J., Cook, A. R., **High $D^*$ pyroelectric polyvinylfluoride detectors,** *Appl. Phys. Letters* **19,** No. 9, 337-338 (Nov. 1, 1971).

Key words: Detector; infrared; polyvinylfluoride; pyroelectric.

Polyvinylfluoride plastic films exhibit a normalized detectivity, $D^*$ (500 K, 1, 1), of $3 \times 10^8$ cm Hz$^{1/2}$/W. This value for the infrared-detector figure of merit is close to the highest available from other pyroelectric materials. A pyroelectric coefficient of 1 nC/cm$^2$K was obtained from the optical response, and a material figure of merit of $1.3 \times 10^{-9}$ C cm/J was determined.

**12550.** Powell, R. L., Wagner, P., **Irradiation effects on low temperature thermal and electrical conductivities of two graphites,** *Carbon Letters to Editor* **8,** 690-692 (1970).

Key words: Electrical conductivity; graphite; neutron irradiation damage; thermal conductivity.

Experiments to determine the effect of radiation on the low temperature (6-100 K) thermal conductivities and electrical resistivities of two commercially available graphites have been performed. Two specimens of H4LM grade graphite with sample axes oriented parallel and perpendicular to the grain respectively and one specimen of Graph-i-tite G with the sample axis oriented parallel to the grain were used for the experiments. The specimens were irradiated in the core of the reactor at a power level of five megawatts for a total exposure of 120 megawatt-hours. Integrated neutron dose was computed to be $1.73 \times 10^{18}$ nvt and total gamma $3 \times 10^9$ rads. The irradiation treatment reduced the thermal conductivity by a factor of about eight at 100 K and was also effective in reducing the temperature coefficient of the thermal conductivity. Similarly, the irradiation caused an increase in the electrical resistivity.

**12551.** Proctor, T. M., Jr., **A passive analyzer for ultrasonic shear waves,** *J. Acoust. Soc. Amer.* **50,** No. 5, 1379-1381 (Nov. 1971).

Key words: Multiwaveguide; shear wave analyzer; shear wave orientation; shear wave transducer.

A device has been developed which allows the determination of the direction of shear particle motion generated by a single transducer. The normal ways of determining shear motion are to use another crystal of known polarization or to know the crystallographic geometry. This device analyzes the shear motion by use of reflection modes in a multiwaveguide assembly. The shear motion can be related to the geometry of this waveguide assembly.

**12552.** Radebaugh, R., Siegwarth, J. D., **Anomalous thermal resistance between sintered copper powder and dilute $He^3$-$He^4$** solutions, *Phys. Rev. Letters* **27,** No. 12, 796-799 (Sept. 20, 1971).

Key words: Copper; cryogenics; dilution refrigerator; helium-3-helium-4; Kapitza resistance; phonon-electron interaction; powder.

The thermal resistances between seven samples of sintered copper powder and a nearly saturated dilute $He^3$-$He^4$ solution were measured between 14 and 200 mK. All samples showed the anomalously high thermal resistances seen in metal foils, and the values are in semiquantitative agreement with recent calculations of Seiden. Reproducibility of samples was found to be excellent and oxide layers formed at room temperature had no detectable effect.

**12553.** Radebaugh, R., Siegwarth, J. D., **Dilution refrigerator technology,** *Cryogenics* **11,** No. 5, 368-384 (Oct. 1971).

Key words: Cryogenics; dilution refrigerator; Fermi-Dirac statistics; heat exchangers; helium-3; helium-4; liquid helium; mixtures; quantum fluid; thermodynamic properties.

This review discusses theoretical and practical developments concerning the $He^3$-$He^4$ dilution refrigerator. Properties of $He^3$-$He^4$ solutions are briefly discussed in terms of the weakly interacting Fermi-Dirac gas model and reused to calculate the behaviour of dilution refrigerators. The thermodynamic behaviour of the dilution process is first discussed, and then an analysis of various types of heat exchangers is presented. The use of nearly optimum heat exchangers, designed by the method outlined here, can significantly reduce the liquid volumes required and/or reduce the low temperature limit of the continuous dilution refrigerator. With smaller liquid volumes, the refrigerator can be cooled down and can reach thermal equilibrium more rapidly. Discussions of various practical considerations and recent developments in hardware are also included. Some suggestions for future work and speculations on trends are presented.

**12554.** Rasmussen, A. L., **Measurement of laser energy of linear components of polarization at 1.060** $\mu$, *Rev. Sci. Instr.* **42,** No. 11, 1590-1593 (Nov. 1971).

Key words: Laser calorimeter; laser energy; laser polarization; laser power; reflectivity measurement.

A double reflecting plate calorimeter [Rev. Sci. Instrum. **41,** 1479 (1970)] was used to evaluate the energy components of a pulsed 1.060 $\mu$ neodymium laser light beam entering the calorimeter polarized parallel ($E_H$) and perpendicular ($E_V$) to a horizontal plane. The relationship between these components varied from $E_H = 0.94\ E_V$ to $E_H = 1.25\ E_V$. Estimated error of $E_H$ and $E_V$ is 2.3%. As a check on the accuracy of polarization component measurements at 1.060 $\mu$, an intercomparison of data was made between this calorimeter and an NBS liquid cell calorimeter. The agreement was about 0.2%.

**12555.** Reed, R. P., **Materials at low temperatures (a series of review papers). Introduction,** *Cryogenics* **11,** No. 5, 347-348 (Oct. 1971).

Key words: Cryogenics; materials properties; survey.

We intend to present a number of review papers critically evaluating research on particular materials (for example, aluminum) or groups of materials (for example, composites) to assist in appraisal for cryogenic use. Well-qualified experts have been asked to contribute to this series during the next several years.

**12556.** Reed, R. P., Clark, A. F., Schramm, R. E., **Defect annealing (4 to 295 K) after martensitic phase transformation in an Fe-29 Ni alloy,** *Scripta Met.* **5,** No. 6, 485-488 (June 1971).

Key words: Electrical resistivity; iron-nickel alloys; martensite; point defects.

An Fe-29 Ni alloy has been cooled from room temperature to 4 K and the electrical resistance measured on warming. On cooling the alloy transformed from austenite to martensite. By comparing the immediate isochronal resistivity to the temperature dependent martensite resistivity, the recovery profile is obtained. Results indicate that a very considerable number (about 0.5 at.%) of point defects are introduced during a martensitic transformation.

**12557.** Reimann, C. W., Zocchi, M., Mighell, A. D., Santoro, A., **Crystal and molecular structure of nitratobis-(2,2′-dipyridyl)-cobalt(III) hydroxide nitrate tetrahydrate, $[Co(C_{10}H_8N_2)_2(NO_3)](NO_3)(OH)\cdot 4H_2O$,** *Acta Cryst.* **B27,** Part 11, 2211-2218 (Nov. 1971).

Key words: Dipyridine and nitrate ligands; hydrogen bonding; monoclinic symmetry; octahedral coordination; transition metal-Co(III)-coordination complex.

The structure of nitratobis-(2,2′-dipyridyl)cobalt(III) hydroxide nitrate tetrahydrate, $[Co(C_{10}H_8N_2)_2(NO_3)](NO_3)(OH)\cdot 4H_2O$, has been determined by single-crystal x-ray diffraction techniques. Crystals of this complex are monoclinic with $a = 10.923(2)$, $b = 15.998(4)$, $c = 14.442(2)$ Å, $\beta = 101.93(2)°$, space group $C2/c$, $\rho_c = 1.57\ g\cdot cm^{-3}$, $\rho_o = 1.54\ g\cdot cm^{-3}$, and $Z = 4$. The structure was solved by Patterson and Fourier methods. The cobalt atom is octahedrally coordinated by two molecules of 2,2′-dipyridyl and by a bidentate nitrate group. Water molecules, nitrate groups, and the hydroxide ions are involved in hydrogen bonds which extend continuously in the a and c directions. The final refinement of the structure by full-matrix anisotropic least-squares analysis resulted in an $R$ value of 6.2%, based on 2995 observed reflections.

**12558.** Sharp, K. G., Coyle, T. D., **Synthesis and some properties of trifluoro(trifluoromethyl)silane,** *J. Fluorine Chem.-Short Communication* **1,** 249-251 (1971).

Key words: Difluoroiodo(trifluoromethyl)silane; fluorine; fluoroalkylsilanes; silicon; silicon difluoride; trifluoro(trifluoromethyl)silane.

The simplest member of the perfluoroalkylfluorosilane series, $CF_3SiF_3$ has been prepared in high yield from $CF_3SiF_2I$ and has been definitively characterized. The compound decomposes at 78° to form $SiF_4$, $C_2F_4$, and cyclo-$C_3F_6$. The thermal lability of $CF_3SiF_3$ can account for equivocal reports in the existing literature regarding synthesis from perfluoroalkyl halides and Si/Cu alloy at high temperatures.

**12559.** Schroeder, L. W., de Graaf, L. A., Rush, J. J., **Neutron diffraction study of the trigonal and cubic phases of NaSH,** *J. Chem. Phys.* **55,** No. 11, 5363-5369 (Dec. 1, 1971).

Key words: Crystal structure; ion orientation; libration; neutron diffraction; phase transition; reorientation; sodium hydrosulfide.

Neutron diffraction powder patterns have been measured for the trigonal and cubic phases of NaSH at 296 and 379 K, respectively. Several possible models describing the orientations of the $SH^-$ ion in the trigonal phase were compared with the experimental results. A model in which the $SH^-$ ions are aligned along the trigonal axis gave the best agreement between calculated and observed structure factors. Thus the transition from the cubic to trigonal phase apparently results from the alignment of the $SH^-$ ions along one of the cube diagonals which then becomes shorter than the other resulting in the less symmetric trigonal structure. Several structural models were also considered for the cubic phase. The isotropic, free rotator mode describing the $SH^-$ orientations can be rejected in favor of a less randomly disordered model by comparison with preliminary neutron inelastic scattering data. The limited diffraction data in this phase, however, do not enable a distinction to be made between disordered models. The preliminary inelastic scattering results also indicate that the librational frequencies of the $SH^-$ ions are similar in both phases, but that reorientations of the $SH^-$ ion between equivalent directions occur at a much faster rate ($\sim 10^{12}$ sec$^{-1}$) in the cubic phase.

**12560.** Siegwarth, J. D., Radebaugh, R., **Analysis of heat exchangers for dilution refrigerators,** *Rev. Sci. Instr.* **42,** No. 8, 1111-1119 (Aug. 1971).

Key words: Cryogenics; dilution refrigerator; heat exchangers; helium-3; helium-4.

Numerical calculations of the behavior of dilution refrigerator heat exchangers are discussed and some results for both discrete and continuous exchangers are presented. It is shown that thermal conductance along the stream is negligible for a typical continuous exchanger of the coaxial tube type, but becomes a dominant feature of a typical discrete exchanger operating below about 50 mK and degrades the performance considerably. A simple design change can be made that reduces the conductance along the liquid and improves the performance of such an exchanger. A simple means of determining whether conductivity is important in either continuous or discrete exchangers is given.

**12561.** Sullivan, D. B., **Resistance of a silicon bronze at low temperatures,** *Rev. Sci. Instr.* **42,** No. 5, 612-613 (May 1971).

Key words: Alloy; bronze; magnetoresistance; resistance; temperature coefficient.

A specially prepared silicon bronze is shown to be quite insensitive to magnetic field and temperature change at liquid helium temperatures. The temperature coefficient of resistance is of the order of a few parts per million per degree over the range 2-10 K and the change in resistance at a flux density of 1 T ($10^4$ G) is about 10 ppm.

**12562.** Tsang, W., **Thermal decomposition of 3,4-dimethylhexane, 2,2,3-trimethylpentane, *tert*-butylcyclohexane, and related hydrocarbons,** *J. Phys. Chem.* **76,** No. 2, 143-156 (1972).

Key words: Bond energy; cyclohexyl radical; 3,4-dimethylhexane; heats of formation; *n*-propyl radical; *s*-butyl radical; shock tube; *t*-butyl radical; thermal decomposition; 2,2,3,-trimethylpentane.

3,4-Dimethylhexane, 2,2,3-trimethylpentane, and *tert*-butylcyclohexane have been decomposed in a single-pulse shock tube. Rate expressions for the main bond-breaking steps are: $k(sec\text{-}C_4H_9\text{-}sec\text{-}C_4H_9 \rightarrow 2\ sec\text{-}C_4H_9\cdot) = 10^{16.34} \exp(-37{,}900/T)\mathrm{sec}^{-1}$; $k(sec\text{-}C_4H_9\text{-}tert\text{-}C_4H_9 \rightarrow sec\text{-}C_4H_9\cdot + tert\text{-}C_4H_9\cdot) = 10^{16.30} \exp(-36{,}400/T)\ \mathrm{sec}^{-1}$; and $k(tert\text{-}C_4H_9 - c\text{-}C_6H_{11} \rightarrow tert\text{-}C_4H_p\cdot + c\text{-}C_6H_{11}\cdot) = 10^{16.31} \exp(-37{,}300/T)\ \mathrm{sec}^{-1}$. They lead to $\Delta H_{f,300}(sec\text{-}C_4H_9\cdot) = 55$ kJ/mol (13.2 kcal/mol), $\Delta H_{f,300}(tert\text{-}C_4H_9\cdot) = 39$ kJ/mol (9.3 kcal/mol), and $\Delta H_{f,300}(c\text{-}C_6H_{11}\cdot)$ 66 kJ/mol (15.8 kcal/mol). Rate expressions for the decomposition of all hydrocarbons formed from *sec*-butyl or cyclohexyl radicals and methyl, ethyl, isopropyl, *tert*-butyl, *tert*-amyl, allyl, 1-methylallyl, propynyl, and benzyl radicals have been calculated. Estimates are given for the rates of decomposition of hydrocarbons formed from *n*-propyl radicals and any of the compounds listed above. The accumulated single-pulse shock tube data can now give quantitative information on the initial cracking patterns of almost all aliphatic hydrocarbons. The *A* factors determined in this study provide striking confirmation for the earlier observation that this value, per $C-C$ bond, for alkanes is a constant. On this basis, it appears that $D(tert\text{-}C_5H_{11} - H) - D(tert\text{-}C_4H_9 - H) = 5.4$ kJ/mol; $D(sec\text{-}C_4H_9 - H) - D(i\text{-}C_3H_7 - H) = 3.5$ kJ/mol; $D(n\text{-}C_3H_7 - H) - D(C_2H_5 - H) \sim -1.5$ kJ/mol. The absolute magnitude of the *A* factors are all at least a factor of 10 lower than expected. It is demonstrated that recent chemical activation and very low pressure pyrolysis studies support the shock tube results.

**12563.** Wiederhorn, S. M., Johnson, H., **Effect of pressure on static fatigue of glass,** *J. Amer. Ceram. Soc.—Discussions and Notes* **54,** No. 11, 585 (Nov. 1971).

Key words: Fracture; glass; high pressure; static fatigue; strength.

The static fatigue behavior of glass at elevated pressures was studied using fracture mechanics techniques. Stress time-to-failure data were obtained on three different glass compositions exposed to high pressure water, 7 kbar. The fracture behavior of glass in water was observed to be insensitive to pressure. It is suggested that this insensitivity resulted from compensating mechanisms in which the increase in fracture resistance arising from a positive activation volume for stress corrosion cracking is balanced by a decrease in fracture resistance due to increased hydroxyl ion concentration at the crack tip.

**12564.** Zimmerman, J. E., Frederick, N. V., **Miniature ultrasensitive superconducting magnetic gradiometer and its use in cardiography and other applications,** *Appl. Phys. Letters* **19,** No. 1, 16-19 (July 1, 1971).

Key words: Cardiography; gradiometry; instrumentation; Josephson effect; magnetocardiography; magnetometry; superconducting devices.

A portable magnetic gradiometer was built using an rf-biased point contact device as a sensor and a superconducting flux transformer 2.5 cm in diameter by 10 cm long to couple to the gradient of the external field. The instrument is limited by fluctuations which are probably associated with an uneven boiling of the cryogenic liquids and by environmental fluctuations in some locations. It is shown that the inherent sensitivity can be increased by an order of magnitude by increasing the bias frequency from 30 to 300 MHz. A possible use of the instrument as a magnetocardiograph in an unshielded environment was demonstrated.

**12565.** Zimmerman, J. E., **Sensitivity enhancement of superconducting quantum interference devices through the use of fractional-turn loops,** *J. Appl. Phys.* **42,** No. 11, 4483-4487 (Oct. 1971).

Key words: Instrumentation; Josephson effect; magnetometry; superconducting devices.

A new "fractional-turn" configuration for superconducting quantum interference devices provides enhanced sensitivity, with large loop area and low loop inductance. By operating the new configuration at optimum bias frequency (300 MHz or higher), inherent field sensitivities of $10^{-15}$ T ($10^{-11}$ G) or better can reasonably be expected. The operational sensitivity of an instrument using such a device would probably be limited by externally generated noise in most applications. The configuration is readily adaptable to measurements of both diagonal and off-diagonal components of the field gradient.

**12566.** Andrews, J. R., Nahman, N. S., **Electron-beam deflection in traveling-wave oscilloscopes,** (Proc. 11th Symp. Electron, Ion, and Laser Beam Technology, Boulder, Colo., May 12-14, 1971), Chapter in *Record of 11th Symposium on Electron, Ion, and Laser Beam Technology,* pp. 141-146 (San Francisco Press, Inc., San Francisco, Calif., 1971).

Key words: Cathode ray tube; CRT; deflection; electron beam; GHz; oscilloscope; picosecond; slow-wave; traveling-wave.

A generalized electron-beam deflection theory is presented it is applicable to fast- or slow-wave deflection structures in veling-wave oscilloscopes. The theory includes the deflection ucture circuit properties and the electron beam dynamics. The sults of experiments on two traveling-wave deflectors are esented: (1) a fast-wave rectangular transmission line, and (2) low-wave serrated rectangular transmission line. The theoreti- and experimental results were correlated in the frequency d time domains. The rise times of the experimental traveling-ve oscilloscopes were in the range of 95 to 211 picoseconds ).

567. Barnes, I. L., Garfinkel, S. B., Mann, W. B., **Nickel-63: Standardization, half-life and neutron-capture cross-section,** *nt. J. Appl. Radiat. Isotop.* **22,** 777-781 (1971).

Key words: Half-life; mass-spectrometry; microcalorimetry; Ni-63 neutron capture cross-section; radioactivity standards.

Nickel-63 has been standardized for activity using the Nanal Bureau of Standards' radiation balance and a calculated ue for the average beta-particle energy. From the activity and topic abundance of nickel-63 in May 1968, the half-life has en calculated to be $100.0_7$ years (±2.0 percent). The neutron-ture cross-section of nickel-63 has been found to be 23±3 n.

68. Beehler, R. E., **Cesium atomic beam frequency standards: survey of laboratory standards development from 1949-71,** *Proc. 25th Frequency Control Annual Symp., Atlantic City, N.J., Apr. 26-28, 1971,* pp. 297-308 (Electronic Industries Asociation, Washington, D.C., 1971).

Key words: Atomic frequency standards; cesium beam frequency standards; laboratory cesium standards.

A review is presented of progress achieved in the development cesium atomic beam frequency standards during the past 20 rs, including both trends in design philosophy and actual permance achieved. The emphasis will be on laboratory-type ium standards, in which attempts are made to optimize both uracy and stability performance with lesser emphasis on such tures as size and weight, environmental sensitivity, operaal convenience, and cost. However, some comparisons are made with commercially-developed cesium standards in er to emphasize various tradeoffs that are made for different lications. Up-to-date information is included on the current us of cesium standards being used or developed in various onal standards laboratories throughout the world. Finally, e future trends in the development of improved laboratory ium standards are discussed briefly.

69. Bennett, H. S., **Damage to ceramics from high intensity Q witched lasers,** (Proc. Conf. on Ceramics in Severe Environnents, North Carolina State University, Raleigh, N.C., Dec. -9, 1970), Chapter in *Materials Science Research,* W. W. Kriegel, ed., **5,** 537-546 (Plenum Publ. Corp., New York, N.Y., 1971).

Key words: Extrinsic damage; intrinsic damage; laser materials; surface damage; switched lasers; thermal stresses.

One important factor limiting the advance of high power laser nology is the failure of laser materials due to optically ined damage. Examples of surface damage, extrinsic damage duced by inclusions, and intrinsic bulk damage (beam ping) are presented. A model to treat metallic inclusions ch absorb an appreciable amount of incident laser radiation glass laser rods is formulated and used to estimate thermal sses and changes in refractive indices due to the thermal stress field. The feasibility of optical techniques to detect incipient damage sites also is discussed.

**12570.** Branscomb, L. M., **Taming technology,** *Science* **171,** 972-977 (Mar. 12, 1971).

Key words: Environmental pollution; performance specifications; product performance; technology.

The public is frustrated with technology. Science, the father of technology, stands accused of failing the human society, while much of the frustration results from the failure of our social institutions to use wisely and distribute fairly the benefits of technology. The resolution of conflicts must come from a combination of research, of responsible private action, and astute public policy—all carried on within a rational framework.

**12571.** Branscomb, L. M., **The U.S. Metric Study,** *Sci. Teacher* **38,** No. 8, 58-62 (Nov. 1971).

Key words: International system (SI); measurement language; metric system.

The U.S. Metric Study showed conclusively that we have only two real alternatives in the face of rapidly increasing use of the metric system of measurement in the world and in this country: to convert to use of the metric system deliberately with a plan or to go metric eventually without a plan. It is plain that the American education system will have to improve its performance if we are to adjust, by whatever mechanism, to our increasingly metric world. It also appears that the metric system could be thoroughly introduced into the educational system at a relatively moderate cost.

**12572.** Broadhurst, M. G., **Dielectric properties of methyl stearate-A model crystalline polymer,** (Proc. Symp. Dielectric Properties of Polymers, American Chemical Society Meeting, Los Angeles, Calif., Mar. 30, 1971), Chapter in *Dielectric Properties of Polymers,* F. E. Karasz, ed., pp. 129-145 (Plenum Publ. Corp., New York, N.Y., 1972).

Key words: Crystalline polymers; dielectric measurements; dielectric relaxation; dynamical diffusion; Grüneisen constant; methyl stearate; pressure.

The dielectric properties of methyl stearate, $CH_3 - (CH_2)_{16} - C{=}O{-}O{-}CH_3$, have been measured as a function of pressure and temperature with special emphasis on the $\alpha$ loss maxima. The experimental techniques are described and the frequency position, amplitude and width of the $\alpha$ loss region are given at 213, 243 and 263 K and at 0, 1 and 2 kbars pressure. The activation parameters at $P=0$ are $\Delta H^{\neq} = 12.6$ kcal/mol, $\Delta S^{\neq} = 20$ e.u., $\Delta V^{\neq} = 29$ cm$^3$/mol and $\log A \doteq 16.4$. The ratio of constant volume to constant pressure activation energy was found to be 0.85 and $(\partial T/\partial P)_{f_{\max}} \approx 15$ °C/kbar. A general model suggested by the results is discussed, and a dynamical theory is presented which predicts the temperature, pressure, and chain length dependence of the relaxation frequency in terms of bulk thermodynamic functions. (1 kcal/mol = 4.184 kJ/mol, 1 e.u. = 4.184 J/mol-K, 1 kbar = $10^5$N/m$^2$).

**12573.** Carpenter, B. S., **Determination of trace concentration of boron and uranium in glass by the nuclear track technique,** *Anal. Chem.* **44,** No. 3, 600-603 (Mar. 1972).

Key words: Boron; fission track counting; glass; neutron activation analysis; nuclear track technique; uranium.

The direct determination of boron and uranium was made on the National Bureau of Standards four trace element glass standards, nominally 500 ppm, 50 ppm, 1 ppm, and 0.02 ppm. The track counting results are compared with data obtained by isotope-dilution mass spectrometry. In addition the radial distribution of boron and uranium across the surface of the glass is discussed.

**12574.** Carter, G. C., Bennett, L. H., **$^{115}$In Knight shifts in liquid alloys containing small amounts of Pb,** *Phys. Rev. B* **5,** No. 5, 2022-2023 (Mar. 1, 1972).

Key words: Anisotropic scattering; In-Pb; Knight shift; liquid alloys; many body effects; nuclear magnetic resonance.

Measurements of the nuclear magnetic resonance of $^{115}$In in very dilute Pb in In liquid alloys have been made. No structure was observed in the Knight shift vs composition behavior.

**12575.** Cohen, G. G., Alexandropoulos, N. G., Kuriyama, M., **Energy loss spectrum of lithium metal in the region of intermediate momentum transfer,** *Solid State Commun.* **10,** 95-98 (Mar. 1972).

Key words: Collective excitations; energy transfer; lithium; momentum transfer; x-ray inelastic scattering.

An x-ray inelastic scattering spectrum of polycrystalline lithium with Cu-K$\alpha$ radiations was taken at the scattering angle 25° which corresponds to an intermediate momentum transfer ($\kappa/k_f$= 1.59). The unfolded spectrum showed a steep fall-off on the large energy transfer side, indicating that individual excitations of electrons are suppressed strongly.

**12576.** Collier, R. S., Jellison, J. C., **Fluid-phase and temperature measurement with a single sensor. II,** (Proc. 1970 Cryogenic Engineering Conf., June 17-19, 1970, Colorado Univ., Boulder, Colo.), Chapter in *Advances in Cryogenic Engineering*, K. D. Timmerhause, ed., **16,** Paper F-3, 251-260 (Plenum Press, Inc., New York, N.Y., 1971).

Key words: Fluid phase discrimination; hydrogen; low gravity; resistance thermometer; thin carbon film.

A method is described for obtaining fluid phase and temperature measurement of hydrogen with a single sensor. The sensor is a 1/8-inch diameter, 3/4-inch long sapphire cylinder on which is deposited a thin carbon film which is stable on thermal cycling and sensitive as a resistance thermometer in the temperature range 4-300 K. The sensor is pulsed with an electrical power input and a fluid phase discrimination (FPD) circuit samples the transient response of the sensor. This transient is a function of the sensor being in liquid or gas. The sensor returns to equilibrium between power pulses and a temperature measurement is taken at the onset of the next power pulse. This dual measuring process can occur at a sample rate of 20 Hz.

A drop tower experiment is described which demonstrates the utility of these sensors in a dynamically changing situation. The sensor response time as the sensor goes from gas to liquid is 50 milliseconds (one sample time); the response time from liquid to gas varies from 50 milliseconds to 1.2 seconds in normal gravity and from 50 milliseconds to 3.0 seconds in low gravity.

**12577.** Colson, J. P., Eby, R. K., Sinnott, K. M., **Alpha relaxation in polyethylene,** *J. Appl. Phys.* **42,** 13, 5902-5903 (Dec. 1971).

Key words: Alpha; density; lamella thickness; polyethylene; relaxation; solvent; unit cell.

It has been shown previously that the strength and temperature (peak) of the relaxation in solution-grown crystals of polyethylene appear to correlate with a number of parameters including lamella thickness, unit-cell dimensions, density, and residual solvent content. However, it has been reported also that in two samples which had different thermal histories for which all the above parameters are equal, the strength of the relaxation was the same but the temperature of the relaxation peak differed by 15 °C. It is the purpose of this communication to confirm thi observation and to report that the difference in relaxation ten perature decreases with increasing annealing temperature an becomes zero at 130 °C, while the above parameters remai equal in the two samples.

**12578.** Colson, J. P., Reneker, D. H., **Electron irradiation effec in polyoxymethylene crystals grown inside trioxane crystals, (** J. Arceneaux, ed., *29th Annual Proc. Electron Microscop Society America, Boston, Mass.,* pp. 78-79 (1971).

Key words: Polyoxymethylene crystals; trioxane crystal

Polyoxymethylene (POM) crystals grow inside trioxar crystals which have been irradiated and heated to a temperatu slightly below their melting point. Detailed examination at high magnification showed that three distinct types of POM crysta grew in a typical sample. We have observed the sensitivity each type of crystal to irradiation with 80 kilovolt electrons.

**12579.** Corliss, E. L. R., Berendt, R. D., **Computers—A white cc lar hazard,** *Pollut. Eng.* pp. 27-30 (Jan.-Feb. 1972).

Key words: Computer noise; damage-risk criteria; heari loss; noise control; scanning analyzer; spectral distributio

Noise levels generated by modern computers are high enou in some circumstances to induce hearing loss. Attention w recently focused on noise problems in computer laborator because of the relatively simple and recurrent errors made l programmers possibly as a result of distraction induced by tl very high noise levels under which they were working. It turn out, however, that the first order of business proved to be tl protection of hearing itself.

**12580.** Costrell, L., **An introduction to CAMAC,** *CAMAC Bu* Issue No. 2, 3-6 (Nov. 1971).

Key words: CAMAC; computer interfacing; contı systems; instrumentation; instrumentation standarc nuclear instrumentation; standards.

The CAMAC instrumentation system developed by t ESONE Committee of European Laboratories has been endo ed by the U.S. AEC NIM Committee as a dataway system co plementary to the NIM (Nuclear Instrument Module) syste CAMAC is described in a general way in this condensed versi of the introductory paper of the CAMAC Tutorial Session the 1970 IEEE Nuclear Science Symposium.

**12581.** Crissman, J. M., Passaglia, E., **Internal-friction study high-purity single crystals of *n* eicosane $(C_{20}H_{42})$,** *J. Appl. Ph* **42,** No. 12, 4636-4644 (Nov. 1971).

Key words: Cold-work; dislocation relaxation; internal fi tion; *n*-alkane; relaxation process; Young's modulus.

Large pure single crystals of *n* eicosane ($C_{20}H_{42}$) with [21 growth axes have been prepared by slow crystallizations fr the melt. Internal-friction measurements covering temperatu from 100 to 300 K at ≃ 1 kHz reveal that in the as-grown sin crystals both the $\alpha$ and $\gamma$ loss peaks characteristic of polycrys line *n* alkanes of less purity are absent, from which we concl that, in polycrystals, these processes are a result of impurit and/or crystal defects. Two very weak loss maxima of obsc origin were observed at about 270 and 287 K for all the cryst studies. In one single crystal progressive stages of light c work induced a complex spectrum of small loss maxima betw 200 and 300 K. These maxima were found to be highly sensit to aging. We believe that the observed behavior provi evidence for dislocation motion in crystals of this type. No tectable $\gamma$ peak resulted from the cold work. Data are also cluded for one single crystal which was irradiated with $\gamma$ rays.

582. Cuthill, J. R., **Satellites in soft x-ray spectra,** J. Thewlis, ed., *Encyclopaedic Dictionary of Physics* **4,** 1-2 (1971).

Key words: Auger transition; Coster-Kronig theory; nondiagram lines; Wentzel theory; x-ray satellite lines.

"Satellites" in soft x-ray spectra are defined. The transitions sponsible for some common satellite lines are discussed.

583. Cuthill, J. R., **Soft x-ray spectroscopy,** J. Thewlis, ed., *Encyclopaedic Dictionary of Physics* **4,** 1-11 (1971).

Key words: Absorption spectra; electron transitions; emission spectra; $L_{2,3}$ emission spectra; shells; soft x-ray spectroscopy; valence bands.

The soft x-ray range is not precisely defined but for practical rposes can be said to begin where an air or helium path and nventional windows cannot be used and extends up to where e techniques of optical spectroscopy are applicable (approxiately 2.5 to 500 Å). Solid state x-ray emission spectra in this nge involve electron transitions from the valence band into one the outermost normally full shells. The corresponding absorpn spectra involve transitions from one of the outermost norlly full shells to available empty states in the conduction band. e emission and absorption spectra are thus a measure of the nsity of occupied and unoccupied states, respectively, in the lence band. Examples of the interpretation of metal and alloy ectra in relation to bonding and density of states are given. In ht elements ($Z < 10$) analysis by x-ray spectroscopy the K ectrum is the valence band spectrum and spectrochemical alysis loses its unique feature of being independent of the state chemical combination. The changes in shape and the shifts in peaks and edges in the emission band spectra that take place a result of alloying now have to be taken into account in emical analysis.

Another important application of soft x-ray spectroscopy is to study of the radiation due to the recombination of highly ized atoms in a plasma. An interesting example is the corona the sun. Examples of some of the first soft x-ray spectra obned of the sun's corona during solar flares, which are by means satellite mounted spectrometers, are given.

nstrumentation for the soft x-ray range is described.

584. Davis, D. D., Blair, B. E., Barnaba, J. F., **Long-term continental U.S. timing system via television networks,** *IEEE Spectrum* **8,** No. 8, 41-52 (Aug. 1971).

Key words: Atomic clock comparisons; clock comparisons; Loran-C; NBS time scale; portable clocks; time synchronization; TV timing; USNO time scale.

Hundreds of atomic frequency standards and precision crystal cillators exist in remote locations throughout the continental S. that are synchronized through fairly complex and costly ans. Today, however, an inexpensive synchronization system available in the form of live television broadcasts by commerl networks. In precision and accuracy, the television method comparable to the portable atomic clock and/or Loran-C, with erage day-to-day differential delays less than 1 $\mu$s. Based on results of the tests presented here, the use of nearly any solidte television receiver and a low-cost horizontal sync pulse nerator can provide 10-$\mu$s synchronizations at all times. The eration of a TV line-10 timing system, including the circuitry auxiliary equipment, is also included. This article gives about /2 years of substantiating data for the three major commercial works (ABC, CBS, and NBC). There is also provision for nchronization with the NBS and/or USNO Coordinated iversal Time (UTC) scales through regularly published rets.

12585. Deason, V. A., Clark, A. F., Powell, R. L., **Characterization of high purity metals by the residual resistivity ratio,** *Mater. Res. Stand.* **11,** No. 8, 25-28 and 52 (Aug. 1971).

Key words: Contaminants; cryogenics; eddy currents; eddy current tests; electrical resistivity; nondestructive tests; purity; scattering; time constant.

In recent years the residual resistivity ratio has been widely used as a sensitive indicator of chemical purity in high purity metals. The conventional four-terminal measurement of resistivity becomes difficult with large or irregular specimens or with increasing purity and decreasing temperature. The paper describes an alternative technique, called the eddy current decay method, which greatly reduces the above difficulties. The eddy current measurement process does not require any attachment of leads and, in fact, is totally nondestructive. The eddy current apparatus is described, and some typical applications are presented.

12586. De Simone, D. V., **Island in a metric world,** *Panhandle Mag.* **6,** No. 2, 18-22 (Winter 1971-72).

Key words: Business and industry; economy; education; international relations; international standards; international trade; metric; technology assessment.

The article is an adaptation of the report, "A Metric America," which evaluates and distills the findings of the U.S. Metric Study in which thousands of individuals, firms and organized groups, representative of our society, participated. On the basis of all the evidence marshalled in the Study, the report concludes that the United States should change to the metric system through a coordinated national program.

12587. Dillon, T. A., Godfrey, J. T., **Pressure broadening of the $O_2$ microwave spectrum,** *Phys. Rev. A* **5,** No. 2, 599-605 (Feb. 1972).

Key words: Classical trajectory; oxygen; pressure broadening; strong collision.

A general expression for the calculation of pressure broadening for vibrational-rotational lines is derived in the strong-collision model. Classical trajectories and a peaking approximation are used to calculate a unitary scattering operator avoiding perturbation expansions, impact-parameter cutoffs, and straight paths. The latter approximations are not expected to be good when short-range potentials dominate the collision interaction. Use of intermolecular-potential parameters determined from thermodynamics and a simple theory of dispersion forces for $O_2$ calculations gave excellent agreement with experimental data on the magnitude, temperature and quantum-number dependence of the linewidth parameter.

12588. Duncan, A. G., Hiza, M. J., **Heat of mixing derived from liquid-vapor equilibrium data: A study of the argon-methane, normal hydrogen-neon, and normal deuterium-neon systems,** *Ind. Eng. Chem. Fundam.* **11,** No. 1, 38-45 (Feb. 1972).

Key words: Argon-methane; binary liquid mixtures; excess Gibbs free energy; excess thermodynamic properties; heat of mixing; liquid-vapor equilibrium data; normal deuterium-neon; normal hydrogen-neon.

A study of three binary systems of interest in cryogenics was undertaken to demonstrate that an acceptable estimate of the heat of mixing may be derived from carefully measured equilibrium liquid and vapor phase compositions employing conventional gas analysis techniques. New data for the $Ar - CH_4$ system are presented from which derived excess Gibbs free energy and heat of mixing values were obtained. These data and derived properties are shown to be in good agreement with comparable data available in the literature. Excess Gibbs free energy and heat of mixing values were derived from phase equilibrium data available in the literature for the $n\mathrm{H}_2 - \mathrm{Ne}$ and $n\mathrm{D}_2 - \mathrm{Ne}$ systems in the region of complete liquid phase miscibility. Both of these systems exhibit azeotrope formation in the region studied. For the $n\mathrm{H}_2 - \mathrm{Ne}$ system, results obtained from the two different sets of data used also were in good agreement.

**12589.** Durst, R. A., Staples, B. R., **Tris/Tris·HCl: A standard buffer for use in the physiologic pH range,** *Clin. Chem.* **18,** No. 3, 206-208 (Mar. 1972).

Key words: Clinical pH standard; pH standard; physiologic pH; tris(hydroxymethyl)aminomethane and tris pH buffer.

A buffer solution containing tris(hydroxymethyl)aminomethane (0.01667 molal) and its hydrochloride salt (0.0500 molal) is proposed as a pH standard for the physiologically important pH range of 7.3 to 7.5. Standard pH values were assigned to this reference solution at temperatures from 0° to 50 °C by means of measurements of hydrogen/silver chloride cells without transference. At 37 °C, the pH(S) of this buffer solution is 7.382 with a temperature coefficient of −0.026pH/°C. This new standard is more compatible with biologic fluids than is the previously certified phosphate buffer.

**12590.** Erez, A., **A proposed light-coupled analog system for electrical measurements,** *Proc. Electro-Optic Systems Design Conf., New York, N.Y., Sept. 14-16, 1971,* pp. 183-188 (Industrial and Scientific Conference Management, Inc., Chicago, Ill., Sept. 1971).

Key words: Electro-optical coupling; high voltage measurements; light emitting diodes; operational amplifiers.

The combination of a light emitting diode (LED) and a light detector has been widely used to get electrical isolation of the measuring system from the main electrical circuit. The accuracy of a LED-detector couple is limited by nonlinearity, temperature coefficient, and aging of the LED, and by variations in optical coupling. Therefore, most linear measuring and transmitting systems use the light beam as a carrier. The signal, converted to light pulse frequency modulation, is not affected by optical conditions.

An analog system is proposed to measure relatively low frequency (60 Hz) current and voltage in high voltage systems which must be completely isolated from the measuring instruments. It employs an LED and light detector in an optical feedback path of an operation amplifier. The light emitted by the LED contains the measured signal superimposed on a fixed intensity beam which is controlled by a reference zener diode. Part of the emitted radiation is collected by a light detector which serves as the linear negative feedback element, thereby forcing the emitted LED radiation to follow the input signal. The remainder of the beam is collected and transmitted to a photomultiplier which measures the ratio between the ac signal and the steady-state reference beam. The accuracy of the system is limited by the zener diode and linearity of the feedback light detector. Special care must be taken to select a light detector and amplifier with small leakage and bias currents. Optimal pairing of the electro-optical components, in order to achieve maximum radiation-detection efficiency, is a gallium-phosphide LED (600 – 800 nm) and a photocathode with extended red range.

The expected accuracy of the systems is 0.1%. The mean current in the LED is 1–2 mA.

**12591.** Falge, R. L., Jr., Wolcott, N. M., **Cluster specific heats in copper-rich Cu-Ni alloys: The effect of iron,** *J. Low Temp. Phys.* **5,** No. 6, 617-650 (Dec. 1971).

Key words: Alloy; clustering; copper Ni iron; ferromagnetism; interactions; magnetic; specific heat; superparamagnetic particles.

The specific heats of three Cu-Ni and two Cu-Ni-Fe sample have been measured in the range 0.4-6 K at compositions in th range 20-43% Ni and ~ 0-.2% Fe. The results are described i terms of a Schottky function from which the number of level and the cluster concentration are determined for each composition. Addition of iron to the 20%-Ni sample results in ~ 1/ cluster per Fe atom added. The specific heat increases in a magnetic field (known for one sample), which is compatible with th Schottky-like function description of the anomalous term in th specific heat, but is incompatible with the Einstein functio description. Another possible interpretation of the observe specific heat anomalies is given in terms of an intercluste cooperative phenomenon.

**12592.** Farrar, T. C., Druck, S. J., Shoup, R. R., Becker, E. D **Temperature-dependent $^{13}$C relaxation studies of sma molecules,** *J. Amer. Chem. Soc.* **94,** 699-703 (Feb. 1972).

Key words: Chemical shift anisotropy; dipole-dipole; scala relaxation; spin-rotation; $T_1$; $T_2$; $^{13}$C relaxation.

$^{13}$C spin-lattice relaxation times ($T_1$) are reported for 60% er riched samples of $\mathrm{CH_3OH}$, $\mathrm{CH_3I}$, $\mathrm{CH_3Br}$, $\mathrm{CHBr_3}$, $\mathrm{CHCl_3}$, CH $^{13}$COOH, and $\mathrm{CS_2}$, each measured over a wide range of tempera tures at 15.1 MHz. Data are also given on the magnetic field de pendence of $T_1(^{13}\mathrm{C})$ in $\mathrm{CH_3OH}$, $\mathrm{CH_3I}$, and $\mathrm{CH_3\,^{13}COOH}$. Th $T_1$ results, together with nuclear Overhauser enhancements mea sured for the foregoing hydrogen-containing molecules, as we as for $\mathrm{CH_3\,^{13}COCH_3}$, $\mathrm{^{13}CH_3COOCD_3}$, and $\mathrm{(CH_3)_4Si}$, are in terpreted in terms of the probable relaxation mechanisms.

**12593.** Fatiadi, A. J., **Oxidative cleavage of aromatic azines wit periodic acid; MO model for the reaction intermediate,** *Chim* **26,** No. 2, 70-72 (Feb. 1972).

Key words: Acid; benzalazine; cleavage; complex; molec lar; orbital; periodic acid; rules; symmetry.

Cleavage of benzalazine (and other azines) with periodic aci may initially involve, as a single step, the addition of $\mathrm{IO_4^-}$ (or i hydrate) across the conjugated azine system, to give an ioda I(V) complex; this view is supported from MO symmetry rule

**12594.** Fey, L., **New signals from an old timer – WWV,** *Broadca Eng.* **13,** No. 7, 44-46 (July 1971).

Key words: Clocks; h. f. broadcasts; sunspot cycle; tin signals; WWV; WWVH.

Although many other changes have occurred in broadcastir over the years those who tune in to the National Bureau of Sta dards time broadcast stations WWV or WWVH have come expect the same familiar time signals year after year. But n much longer. Soon a new broadcast will be heard with mo kinds of services than before for a wider variety of time ar frequency users.

**12595.** Franklin, A. D., Spal, R., **A method for the precision co parison of the densities of small specimens,** *Rev. Sci. Instr.* 4 No. 12, 1827-1833 (Dec. 1971).

Key words: Density measurement; hydrostatic; precisio small specimens.

The density of an unknown is compared to that of a set several standard specimens (weighing about 40 mg each) with standard deviation in the ratio of densities from a single dete mination of $3 \times 10^{-4}$ or better. The apparatus consists of two i miscible liquids and a float in the upper, supporting the specim in the lower by a wire that passes through the interface. The w ɔvides a buoyant force gradient. From the change in position the float when the unknown is substituted for the standards, density of the unknown relative to that of the standards can calculated. Other contributions to the buoyant force gradient also present; their variation during the course of the measure- nt established the precision of the measurement.

596. Freeman, D. H., **Interactive gel networks. I. Treatment of imple complexation and masking phenomena,** *Anal. Chem.* **44,** 17-120 (Jan. 1972).

Key words: Acceptor; chromatography; donor complexation; interactive gels; liquid chromatography.

Chemical interactions provide an unlimited basis for extending separation capabilities provided by gel chromatography. This per concerns the theory of simple acceptor:donor complexa- n equilibria, which are treated as idealized associative ocesses. Equations are developed to predict and interpret romatographic measurements involving a diffusible solute and vent, and the nondiffusible gel functional group. Systems ated include: I. Inert species, II. Simple solute:gel complexa- n, III. Solute:gel complexation with solvent:gel masking, IV. lute:gel complexation with solvent:solute masking and, ally, consideration of the effects of solute dimerization and ute difunctionality. The results are directly applicable to the perimentally measured solute distribution coefficient.

597. Furukawa, G. T., **Vapor pressures of natural neon and of he isotopes $^{20}$Ne and $^{22}$Ne from the triple point to the normal boiling point,** *Metrologia* **8,** No. 1, 11-27 (Jan. 1972).

Key words: Boiling point; neon; neon isotopes; neon point; triple point; vapor pressure; $^{20}$Ne; $^{22}$Ne.

Apparatus design and procedures are described for the deter- nation of the vapor pressures of naturally occurring neon Ne) and the pure isotopes $^{20}$Ne and $^{22}$Ne from their triple nts (TP) to their normal boiling points (NBP). The data have en fitted to vapor-pressure equations with root-mean-square viations of ±2.5 to ±4.7 N/m$^2$ (±0.019 to ±0.035 mmHg). e TP pressures ($P$) and the TP and NBP temperatures ($T$) re found to be:

| | TP | | NBP |
|---|---|---|---|
| | $P$ | $T$, K | $T$, K |
| Ne | 43332±13 N/m$^2$<br>(325.02±0.10 mmHg) | 24.553±0.001 | 27.096±0.001 |
| Ne | 43326±13 N/m$^2$<br>(324.97±0.10 mmHg) | 24.540±0.001 | 27.084±0.001 |
| Ne | 43654±13 N/m$^2$<br>(327.43±0.10 mmHg) | 24.687±0.001 | 27.211±0.001 |

ıe temperatures are in terms of the NBS-1955 provisional ıperature scale. The figures after the ± symbol indicate esti- ted uncertainties.) The calculated vapor pressures of the topic $^{nat}$Ne, based on Raoult's law of solution and the ob- ved vapor pressures of the pure isotopes, are in agreement hin the combined precision of the measurements with the ob- ved values of $^{nat}$Ne.

98. Geltman, S., Hidalgo, M. B., **A high energy approxima- ion: II. Hydrogen atom excitation by electrons,** *J. Phys. B: At. Mol. Phys.* **4,** 1299-1307 (1971).

Key words: Born approximation; charge transfer; Coulomb wave; ground state; high energy; hydrogen; rearrangement process; theoretical proton.

The cross sections for the excitation of the 2s, 2p, and 3s tes of hydrogen by electron impact are evaluated at high energy in a first order approximation in which the interaction between the incident electron and target proton is represented by a Coulomb wave final state in the $T$ matrix. In the usual Born approximation this interaction has a vanishing contribution because of the orthogonality of the atomic states. The evaluated total cross sections converge to the boron result at high energies, but the differential cross sections at large angles show marked disagreement with the Born approximation and reasonable agreement with experiment. We conclude that for non-forward inelastic scattering the Born approximation does not converge to the correct result in the high energy limit.

**12599.** Haber, S., **The error in numerical integration of analytic functions,** *Quart. Appl. Math.* **XXIX,** No. 3, 411-420 (Oct. 1971).

Key words: Best quadrature; error functionals; minimum-norm formulas; numerical analysis; numerical integration; optimal quadrature; quadrature.

$R$ is a simply-connected region in the complex plane, containing the interval $(a,b)$ on the real axis; $B$ is a Hilbert space of functions analytic on $R$. If $n$ is a positive integer, the integral over $(a,b)$ of any $f \epsilon B$ may be approximated by linear quadrature formulas $Q(f)=a_1f(x_1)+\ldots+a_nf(x_n)$. The minimum, over all choices of the $a_i$ and $x_i$, of the norm of the error functional $E$ defined by

$$E(f)=\int_a^b f-Q(f)$$

is denoted $E_n^{MN}$. It is shown that in the most commonly considered cases, if the closed interval $[a,b]$ is contained in $R$, then $E_n^{MN}=O(C^{-n})$ as $n\rightarrow\infty$, for some $C>1$. In one case—previously studied by H. S. Wilf—in which $b \epsilon R$, it is shown that $E_n^{MN}=O(n^{-1/2})$. Bounds are also found for some error functionals of Gaussian quadrature formulas.

**12600.** Hillhouse, D. L., **Circuit for impulse testing of gas tube lightning arresters,** *Proc. IEEE Fall Electron. Conf., Chicago, Ill., Oct. 18-21, 1971,* pp. 240-245 (Oct. 1971).

Key words: Gas tube arresters, impulse testing; impulse test circuit, gas tube arresters; impulse testing, lightning arresters, telephone; lightning arrester, telephone; measurement, impulse, telephone arresters; telephone lightning arrester, impulse testing; test circuit, telephone arrester.

Telephone lines may be protected from lightning-induced surges by gas tube lightning arresters. Typical arresters break down at 250-400 volts dc. Breakdown voltage increases with the rate of rise of the applied voltage, and may be two or three times the dc value at a rate of rise of 10 kilovolts/microsecond (kV/$\mu$s). Lightning surges on telephone lines approach this rate of rise.

The circuit described in this paper generates and measures ramps with linear rates of rise from 0.5 to 10 kV/$\mu$s, chopped at 500 to 1500 volts. In order to achieve ramp linearity and to minimize oscillations after the chop, stray capacitances and inductances must be made as small as possible. Construction and layout required to achieve this are described in some detail, and typical test oscillograms at 0.5 and 10 kV/$\mu$s are presented in corroboration. Measurement accuracy is analyzed, and maximum errors are estimated to be, for breakdown voltage, 3% and 10% at 0.5 and 10 kV/$\mu$s, respectively; and for rate of rise, 5% for all ramps. If greater accuracy is required, it can be obtained by correction for divider time constant errors, and by further study of carbon resistor voltage coefficients.

**12601.** Hust, J. G., **Thermal conductivity standard reference materials from 4 to 300 K. I. Armco iron,** (Proc. 9th Conf. Thermal Conductivity, Iowa State University, Ames, Iowa, Oct. 6-8, 1969), Chapter in *Thermal Conductivity,* pp. 217-233 (National Technical Information Service, Springfield, Va., 1970).

Key words: Cryogenics; electrical resistivity; iron; Lorenz ratio; Seebeck effect; thermal conductivity; transport properties.

Thermal conductivity, electrical resistivity, Lorenz ratio, and thermopower data are reported for several specimens of Armco iron for temperatures from 4 to 300 K. At low temperatures the electrical resistivity and thermal conductivity vary from specimen to specimen by more than 10%. However, the Lorenz ratios of these specimens differ by less than 2.5%; and the intrinsic resistivities calculated using Matthiessen's rule differ by less than 0.5% of the total resistivities. Thus, Armco iron specimens can be used as standards by measuring the residual resistivities and utilizing the Lorenz ratio reported here.

**12602.** Johannesen, R. B., Coyle, T. D., **Nuclear magnetic double resonance,** *Endeavour* **XXXI,** No. 112, 10-15 (Jan. 1972).

Key words: Double resonance; nuclear magnetic resonance; review.

Double resonance procedures supplement the more conventional techniques of high-resolution nuclear magnetic resonance spectroscopy. Applications of this method allow simplification of complex spectra and facilitate spectrum interpretation and assignment of chemical structures. The technique also permits indirect observation of resonance signals from a wide variety of nuclei.

**12603.** Joiner, B. L., Rosenblatt, J. R., **Some properties of the range in samples from Tukey's symmetric lambda distributions,** *J. Amer. Statist. Ass.* **66,** No. 334, 394-399 (June 1971).

Key words: Approximations; distributions, non-normal; lambda distributions; logistic distribution; order statistics; range; statistics; tables; Tukey's lambda distributions.

Tukey introduced a family of random variables defined by the transformation $Z=[U^\lambda-(1-U)^\gamma]/\lambda$, where $U$ is uniformly distributed on [0,1]. Some of its properties are described with emphasis on properties of the sample range. The rectangular and logistic distributions are members of this family and distributions corresponding to certain values of $\lambda$ give useful approximations to the normal and $t$ distributions. Closed form expressions are given for the expectation and coefficient of variation of the range and numerical values are computed for $n=2(1)6(2)12, 15, 20$ for several values of $\lambda$. It is observed that Plackett's upper bound on the expectation of the range for samples of size $n$ is attained for a lambda distribution with $\lambda=n-1$.

**12604.** Kamper, R. A., **Superconducting materials,** Chapter 6 in *Electronics Design Materials,* pp. 71-79 (The Macmillan Press Ltd., United Kingdom, 1971).

Key words: Electronics; low temperature; materials; superconductors.

This is a brief survey of the properties of superconducting materials which are of interest for engineering purposes.

**12605.** Kamper, R. A., Siegwarth, J. D., Radebaugh, R., Zimmerman, J. E., **Observation of noise temperature in the millikelvin range,** *Proc. IEEE Lett.* **59,** No. 9, 1368-1369 (Sept. 1971).

Key words: Amplifier noise; Josephson effect; low temperature; noise temperature; superconductors.

We report some measurements of noise at very low temperatures, with emphasis on the design and performance of the system used. This system is based on the Josephson effect, and has an observed noise temperature less than 0.005 K.

**12606.** Kaufman, V., Minnhagen, L., **Accurate ground-term combinations in Ne I,** *J. Opt. Soc. Amer.* **62,** No. 1, 92-95 (Jan. 1972).

Key words: Neon; spectra; ultraviolet; wavelengths.

The Ne I resonance line $\lambda 743$ has been accurately measure in the fifth order of the NBS 10.7-m vacuum spectrograp against Ar II Ritz standards in the same order; the measure wavelength is $743.7195_5 \pm 0.0002$ Å. This gives for the lowes excited level, $2p^5(^2P_{1\ 1/2}{}^\circ)3s[1\ 1/2]_2{}^\circ$ ($1s_5$ in Paschen's not tion), the value $134{,}041.84 \pm 0.04$ cm$^{-1}$ relative to the groun level. This result was used to calculate all of the observed $2p^5$ levels relative to the ground level, by use of Ne I observation published during the last two decades and the dispersion formul for air adopted after the publication of *Atomic Energy Leve* (NBS 1949). The $2p^5\ ^2P_{1\ 1/2}{}^\circ$ ionization energy is 173,929.75 0.06 cm$^{-1}$. From the level system, 46 lines in the vacuum u traviolet (vuv) between 743 and 576 Å have been calculated a cording to the combination principle; these should be accurate $\pm 0.0002$ Å or better between 743 and 580 Å and to about 0.0003 Å for the few lines below 580 Å.

**12607.** Kirchhoff, W. H., **On the calculation and interpretation centrifugal distortion constants: A statistical basis for mod testing: The calculation of the force field,** *J. Mol. Spectrosc.* 4 No. 2, 333-380 (Feb. 1972).

Key words: Centrifugal distortion; error evaluation; for fields; least squares analysis; model testing; symmetr triatomic molecules.

Watson's treatment of the theory of centrifugal distortion fects is reviewed in detail and special attention is drawn to t relationship between Watson's treatment and the Kivelson-W son treatment. The relationship between the distortion param ters and the force field for XYZ-type molecules is also review in order to remove ambiguities and inconsistencies presen found in the literature. Finally, procedures for exploiting t statistics associated with a least-squares analysis of the data a presented as a guide for model testing and for detecting mis signments and mismeasurements. A series of examples illustr ing the results of these procedures are presented using t published spectra of $SO_2$, $OF_2$, $SiF_2$ and NSF. In the cases $OF_2$, $SiF_2$ and NSF, improved values for the rotational consta are obtained.

**12608.** Kropschot, R. H., **Advances in thermal insulation,** (Pr 1970 Cryogenic Engineering Conf., June 17-19, 19 Colorado Univ., Boulder, Colo.), Chapter in *Advances Cryogenic Engineering* **16,** Paper No. D-1, 104-108 (Plen Press, Inc., New York, N.Y., 1971).

Key words: Cryogenics; thermal insulation.

This paper highlights several recent developments in insu tion which have significant impact upon the cryogenic indust It emphasizes the gaps in existing data. Complete steady st and transient data are needed over a wide range of temperatu to aid in confirming (or refuting) existing theories. Standard paratus and standard samples are needed to evaluate the relat merits of competitive insulation schemes.

**12609.** Ledbetter, H. M., Patrician, T. J., **On the trace analysi planar features in electron microscopy,** *Phys. Status Solid* No. 1, 305-310 (July 1971).

Key words: Electron diffraction crystallography; twinni

The effect due to a deviation of the foil plane from the im plane on the trace analysis of planar features in elect microscopy is considered. Analytical expressions are derived predicting the effects of a known deviation and, conversely, calculating for some cases the deviation from the observab Conditions under which the deviation is extreme (maximal minimal) are enumerated.

2610. McDaniel, C. L., Schneider, S. J., **Phase relations in the $CaO-IrO_2-Ir$ system in air,** *J. Solid State Chem.* **4,** 275-280 (1972).

Key words: $CaO:IrO_2$ compounds; $CaO-IrO_2-Ir$ system; dissociation; equilibrium; phase relations.

The equilibrium phase relations for the $CaO-IrO_2-Ir$ system ere determined in air using the quenching technique. The ystem contains three stable compounds $4CaO \cdot IrO_2$, $CaO \cdot IrO_2$, and $CaO \cdot IrO_2$; they dissociate to an oxide phase, Ir etal, and oxygen at 1240, 1170, and 1135 °C, respectively. A etastable form of $CaO \cdot IrO_2$ occurs at temperatures between 00 and 1100 °C. Indexed x-ray diffraction powder patterns of l compounds are given.

2611. McDonald, D. G., Risley, A. S., Cupp, J. D., Evenson, K. M., **Harmonic mixing of microwave and far-infrared laser radiation using a Josephson junction,** *Appl. Phys. Lett.* **18,** No. 4, 162-164 (Feb. 15, 1971).

Key words: Cryotemperatures; frequency measurements; harmonic mixing; infrared; Josephson junction; superconductivity.

Simultaneous irradiation of a Josephson junction with ≈ 10 Hz microwave power and 891-GHz laser radiation produces 60-MHz beat between the fundamental laser frequency and armonics of the klystron, ranging from the 84th to the 100th as e klystron is tuned. Observation of such high-order harmonic ixing of klystron and laser signals is unprecedented.

2612. Merris, R., **Trace functions I,** *Duke Math. J.* **38,** No. 3, 527-530 (Sept. 1971).

Key words: Character; group; positive semidefinite hermitian matrix; trace.

This paper introduces a natural generalization of the trace of matrix. The generalization inherits many of the properties of ace and may be substituted for the word "trace" in many eorems, an example of which is: Let $H$ be a $pn \times pn$ positive midefinite hermitian matrix. Partition $H$ into $p^2$ $n \times n$ matrices ${}_{st}$. Let $\tau_{st} = \mathrm{tr}(H_{st})$, $s, t = 1, \ldots, p$, and let $T$ be the $p$-square atrix $T = (\tau_{st})$. Then $T$ is positive semidefinite hermitian.

2613. Moore-Sitterly, C., **Fundamental spectroscopic data,** *Vistas Astron.* **13,** 161-163 (Mar. 1972).

Key words: Atomic spectra; fundamental spectroscopic data; spectroscopic data.

The primary function of Commission 14 of the International stronomical Union is to serve in a liaison capacity, i.e. to ascerin the many astrophysical needs in spectroscopy and to survey tive laboratory programs with the idea of obtaining the quired data. Some aspects of present activity and future needs, voiced by the Commission, are briefly reviewed here.

614. Newell, A. C., Kern, D. M., **Determination of both polarisation and power gain of antennas by a generalised 3-antenna measurement method,** *Electronics Letters* **7,** No. 3, 68-70 (Jan. 4, 1971).

Key words: Antenna polarisation and gain measurement; extrapolation of near-zone antenna measurements; microwave antenna measurement; near-zone antenna measurement.

A method enabling determination of polarisation and power in of three unknown antennas, requiring no prior quantitative owledge of polarisation, is developed. An application of the ethod using a new near-zone extrapolation technique (inoduced by Wacker and Bowman), which permits accurate antenna measurements at reduced distances in spite of proximity effects, is described.

12615. Olien, N. A., **The Cryogenic Data Center, an information service in the field of cryogenics,** *Cryogenics* **11,** No. 1, 11-18 (Feb. 1971).

Key words: Critical data; cryogenics; current awareness service; data compilation; information storage and retrieval; information systems; literature searches; National Bureau of Standards.

The Cryogenic Data Center compiles and critically evaluates data on the thermodynamic and transport properties of materials at cryogenic temperatures. The Center also operates an automated information storage and retrieval system covering the field of cryogenics. The paper describes the historical background of the Center and gives a description of the operation of the automated system. There is a brief sketch of the rigorous procedures used in compiling and critically evaluating data. The Data Center has several services which it provides for the general public as well as the staff of the National Bureau of Standards. These services include: a Current Awareness Weekly, quarterly publications on Superconducting Devices and on Liquefied Natural Gas, and conducting literature searches. The Cryogenic Data Center is cooperating with a number of National and International groups in both the data compilation and documentation areas.

12616. Olien, N. A., Sarkes, L. A., **LNG-2, A report on the Second International Conference on Liquefied Natural Gas,** *Amer. Gas Ass. Monthly* **53,** No. 2, 12-14 (Feb. 1971).

Key words: Cryogenics; economic forecasts; international conferences; liquefied natural gas; world trade.

The Second International Conference was held in Paris, October 19-23, 1970. More than 1200 persons attended the conference and fifty-five technical papers were presented. The conference was divided into seven technical sessions which covered the following topics: historical background of LNG; future role of natural gas as an energy source; liquefaction cycles; safety and testing; properties of LNG and methane; large-scale storage vessels; sea-going tanker construction and classification; LNG pipelines; importation of LNG from the developing to the developed nations; peak load shaving with LNG, liquefied natural gas as a fuel for aircraft and automobiles; projections on the future growth of world trade involving LNG. The future of liquefied natural gas lies in its use in peak shaving and in importation as base load. The major areas for importation will be Japan and the United States Eastern Seaboard. This trade will increase to about 8 to 10 billion cfd by 1980. Applications of LNG such as an automotive fuel are difficult to predict, because of the dominance of non-qualitative factors such as public opinion in any calculations. The future of liquefied natural gas looks very bright.

12617. Peterson, R. L., Magnusson, B., Weissglas, P., **Magnetophonon resonances in polar semiconductors,** *Phys. Status Solidi* **46,** 729-734 (Apr. 14, 1971).

Key words: Acoustoelectric gain; hot electrons; indium antimonide; magnetoresistance; semiconductors; transport theory.

The first numerical calculations are reported of electrical transport properties in polar semiconductors in the non-ohmic regime, for large to intermediate magnetic fields parallel to an electric field. Magnetophonon resonances in such properties as magnetoresistance and acoustoelectric gain are demonstrated. The results obtained generally confirm the hot electron interpretation by Dolat and Bray of their magnetoacoustoelectric experiments in n-InSb.

**12618.** Powell, R. L., Sparks, L. L., **Cryogenic thermocouple research,** (Proc. 11th Intern. Conf. Low Temperature Physics, University of St. Andrews, Scotland, 1968), *Instr. Soc. Amer.* **1,** 477-480 (1968).

Key words: Cryogenics; gold alloys; standard reference data; thermocouples.

Experimental tests and calibrations between 4 and 280 K have been completed for the following materials: Chromel, copper, "normal" silver, constantan, Alumel and *gold*-0.07 at.% iron. Many thermocouple combinations can be made from these materials; however, three of the possible pairs are very widely used in the cryogenic temperature range. These are copper vs constantan (type T), Chromel vs Alumel (type K) and Chromel vs constantan (type E). Our tables for types T, E and K are proposed to be the national standard reference tables for these materials. A fourth combination which is receiving increasing use is Chromel vs *gold*-0.07 at.% iron. This thermocouple is particularly important because of its relatively high sensitivity even below the normal boiling point of liquid helium. Graphs of voltage and thermopower are presented for this combination. A brief description of the experimental system used in the calibrations will be given. Special methods of data acquisition and analysis have been used to study and minimize systematic errors. These methods are general, but are described as they apply to our particular system.

**12619.** Prydz, R., Straty, G. C., Timmerhaus, K. D., **Calculation of thermofunctions of fluorine,** (Proc. 1970 Cryogenic Engineering Conf., June 17-19, 1970, Colorado Univ., Boulder, Colo.), Chapter in *Advances in Cryogenic Engineering* **16,** Paper No. C-2, 64-77 (Plenum Press, Inc., New York, N.Y., 1971).

Key words: Fluorine; heats of vaporization; saturation; single-phase; thermodynamic properties.

Use is made of newly available *PVT* and specific heat data to calculate thermodynamic functions of gaseous and liquid fluorine to pressures of 21 MN/m$^2$ (1 MN/m$^2$ = 10$^6$ newton/m$^2$ = 9.86923 atm) and temperatures to 300 K. The calculational procedures are described in detail. Ideal gas properties, which constitute the starting point for the calculations, have been recomputed based on the latest available data. Derived thermo-functions, heat of vaporization and sound velocities, for the single and two phase regions are tabulated.

**12620.** Ruegg, F. W., Shafer, M. R., **Flow measurement: Procedures and facilities at National Bureau of Standards,** (Proc. Symp. Flow Measurement, San Francisco, Calif., Jan. 19-22, 1970), Chapter in *ASHRAE (Amer. Soc. Heat Refrig. Air-Cond. Eng.), Bull. Flow Measurement Part 1,* **SF70-7,** 1-8 (1972).

Key words: Calibration; flow measurement; flowmeters; flowrate; fluid flow; fluid meters; NBS flow capabilities.

General requirements of flowmeter calibration systems for both liquid and gaseous flow are considered. Possible sources of error are reviewed including those introduced by dynamic characteristics of certain portions of the calibration system. Flowmeter calibration systems in use by the Fluid Meters Section are described including the measurement techniques, operating ranges, and uncertainties associated with these systems.

**12621.** Siegwarth, J. D., Sullivan, D. B., **A mechanical superconducting switch for low temperature instrumentation,** *Rev. Sci. Instr.* **43,** No. 1, 153-154 (Jan. 1972).

Key words: Instrumentation; superconductivity switch.

This paper describes a reliable mechanical superconducting switch for a low temperature voltage divider.

**12622.** Sindt, C., **A summary of the characterization study of slush hydrogen,** *Cryogenics* **10,** No. 5, 372-380 (Oct. 1970).

Key words: Cryogenic pump; densitometer; liquid-solid mixtures; rocket propellant; slurry flow; slush hydrogen.

A programme to study the characteristics of slush hydrogen preparation, storage, transfer, and instrumentation is continuing at the Cryogenics Division of the National Bureau of Standards. Slush preparation by intermittent vacuum pumping was developed. Slush was aged 100 hours during which time solid particle size and structure were observed. The solid particle structure changes dramatically during aging, even though the particle size changes insignificantly. Slush with over 0.5 solid content can be transferred and pumped with losses similar to losses in triple-point liquid hydrogen if Reynolds numbers are high. Transfer losses in a smooth pipe were 10% less with slush of 0.3 solid content than with triple-point liquid when the Reynolds number was $7 \times 10^5$ or greater. Slush density and mass flow instrumentation are being investigated. Although some special techniques are required for handling slush hydrogen, it has the characteristics of a simple cryogenic fluid for most applications.

**12623.** Sparks, L. L., Powell, R. L., **Laboratory method for assessing homogeneity and interchangeability of thermocoupl wires,** *Mater. Res. Std.* **11,** No. 8, 19-21 and 52 (Aug. 1971).

Key words: Cryogenics; dipping; evaluation; heterogenity, liquid helium; liquid nitrogen; low temperature tests Seebeck effect; temperature measurement; thermocouples thermoelectric properties.

Chemical and physical imperfections in thermocouple wir cause spurious voltages to be generated whenever these imperfections are exposed to temperature gradients. For thermometr it is important to know the range of thermally generated spuriou voltages to be expected from a specific material. Significar variations usually exist in the thermoelectric properties of widel separated lengths of wire from the same spool or from differer melts or from different manufacturers. Simple laborator methods are described for determining the effect of short rang inhomogeneities or inter and intracompany variations. Applica tion of the results obtained from these simple tests is discusse in order to point out the usefulness and limitations of tl methods.

**12624.** Straty, G. C., Younglove, B. A., **A fluorine compatible lo temperature electrical feedthrough,** *Rev. Sci. Instr.* **43,** No. 156-7 (Jan. 1972).

Key words: Electrical feedthrough; fluorine compatibilit fluorine seal; seal.

A simple seal is described which has been used successfully seal electrical leads into a cell containing liquid or gaseou fluorine.

**12625.** Sullivan, D. B., Zimmerman, J. E., **Mechanical analogs time dependent Josephson phenomena,** *Amer. J. Phys.* **39,** N 12, 1504-1517 (Dec. 1971).

Key words: Josephson effect; mechanical analogy; supe conducting devices.

The pendulum analog of a small area Josephson junction coupled to the analogs of other circuit elements to demonstra a variety of time dependent phenomena observed with actu devices. The analogy between electrical circuit and mechanic device is established through a Lagrangian formalism. T nalog provides a simple and quick means of developing physical isight into this highly nonlinear system. To demonstrate the alue of the analog we consider, as one example, the problem of junction coupled to a resonant cavity and present a result hich was missed by a previous solution.

626. Weisman, H. M., **Technical librarians and the National Standard Reference Data System,** *Special Libraries* **63,** No. 2, 69-76 (Feb. 1972).

> Key words: Properties data; National Standard Reference Data System; scientific and technical librarians; Special Libraries Association; survey; users.

Because technical librarians often serve as intermediaries etween National Standard Reference Data System publications id their users, the Office of Standard Reference Data surveyed mail 2,700 selected members of the Special Libraries Asciation to check their knowledge and use of NSRDS publicaons as well as to learn the problems they encounter in providing e publications or their data to their users. On the basis of a 22% sponse, the survey results showed that almost 88% of the sponders have heard of the NSRDS and that about 59% have dicated that their libraries carry NSRDS publications, but less an 44% of the responders have used an NSRDS publication; owever, 94% of this latter percentage (the users) indicated that ey have found NSRDS publications very or to some extent seful. The survey revealed that distribution and dissemination ocedures of NSRDS publications need improvement and that etter ways need to be found to acquaint both librarians and sers with the data and information contained in NSRDS publitions.

627. Weiss, B-Z, Meyerson, M. R., **Plastic zone formation and fatigue crack extension during high cyclic bending of steels,** *Eng. Fract. Mech.* **3,** 475-491 (1971).

> Key words: Fatigue crack propagation; fatigue of steels; high cyclic bending; plastic zone sizes; stress intensity factor.

In repeated high cyclic bending, with constant load amplitude, e size and the shape of the plastic zone preceding the propagatg crack is controlled by local structural conditions near the tip ther than by stress intensity. No significant correlations were und between the experimentally determined sizes of plastic ne and the theoretically predicted values of Liu and Rice. The astic zone sizes ahead of the propagating crack cannot be mply expressed as proportional to the rate of fatigue crack opagation, though a simple relationship exists between the rate id the stress intensity factor. The relationship given by Paris, $/dN = Q\Delta K^n$, describes the rate of crack propagation only in a nited range of relative crack length, $x < 0.5$. The extent of this nge depends on the structure and on the level of applied cyclic ress. Beyond this range, the Paris equation could not be applied d the crack propagation cannot be related to the stress intensifactor.

628. Abramowitz, S., Acquista, N., **The infrared spectrum of matrix isolated $UO_2$(g) and its thermodynamic properties,** *J. Phys. Chem.* **76,** No. 5, 648-649 (1972).

> Key words: Entropy; infrared spectrum; matrix isolation; thermal functions; $UO_2$.

The far-infrared spectrum of $U^{16}O_2$ and $U^{18}O_2$ has been obrved and assigned. A value of the missing stretching fundaental has been estimated. These vibrational frequencies have en utilized to estimate the $S°_{2000}$ for reasonable molecular odels. A value of $S°_{2000}$ of $93.9 \pm 2.0$ eu is estimated for $UO_2$(g) the harmonic oscillator rigid rotor approximation. Any elecnic contributions to the $S°_{2000}$ have been neglected and a aglet ground state has been assumed.

12629. Arenhovel, H., Danos, M., Williams, H. T., **Baryon resonances in nuclei with applications to the two-nucleon system,** *Nucl. Phys.* **A162,** 12-34 (1971).

> Key words: Baryon resonances; exchange currents; high momentum components; nuclear functions; nuclear magnetic moments; nuclear structure; nuclear wave functions.

The non-relativistic description of the nucleus is presented which allows the possibility of excited baryon resonances within the nucleus via collision of the nucleons with exchanged mesons. A perturbative treatment for the intrinsically excited configurations is justified, and lowest order results for the wave functions of the excited configurations are derived. Detailed formulae for the two-nucleon system are presented and numerical results are given to show the effect of the baryon resonances on the magnetic moment and threshold photodisintegration of the deuteron.

12630. Berger, M. J., **Distribution of absorbed dose around point sources of electrons and beta particles in water and other media,** *J. Nucl. Med.* **9,** MIRD Supplement No. 5, 6-23 (Mar. 1971).

> Key words: Absorbed dose; beta-rays; electrons; internal dosimetry; tissue; water.

This pamphlet presents information about the distribution of absorbed dose around point-isotropic sources of electrons and beta particles. Tabular results are presented for monoenergetic sources with energies between 10 MeV and 25 keV, and for 75 radionuclide beta-ray sources. The data are given for a water medium. Information and procedures are also given by which the data can be adapted to other media of low atomic number, such as tissue, air or plastics.

12631. Berger, M. J., **Energy deposition by low-energy electrons: Delta-ray effects in track structure, and microdosimetric event-size spectra,** *Proc. 3d Symp. Microdosimetry, Stresa, Italy, Oct. 18-22, 1971,* **EUR No. 4810 d-f-e,** pp. 157-177 (1972).

> Key words: Delta-ray; electron; energy deposition; event-size spectra; microdosimetric; stopping power; track structure.

The slowing down, diffusion and penetration of low-energy electrons has been calculated by the Monte Carlo method, in order to obtain data of radiobiological interest in two areas. One calculation deals with the energy deposited by the delta-rays around the tracks of heavy charged particles. Absorbed-dose distributions with respect to distance from the primary track axis have been obtained for six initial electron energies (20, 10, 5, 2, 1 and 0.5 keV) and for ten emission angles with respect to the primary track (0°, 10°, . . . 90°). These data have been put in such a form that interpolation with respect to initial delta-ray energy and emission angle is easy. They can be used together with experimental or theoretical information about delta-ray production to study track structure for any heavy charged particle. The second problem is to determine microdosimetric event-size spectra in a medium containing a uniform concentration of the beta-emitter tritium. Comparisons are made with experimental results of Ellett and Braby for spherical sites, with diameters of 1.85 and 0.44 microns, in a propane medium.

12632. Blair, B. E., **Letter in response to comments by R. O. Whitaker about the paper, Long-Term Continental U.S. Timing System Via Television Networks,** *IEEE Spectrum* **8,** No. 10, 13 (Oct. 1971).

> Key words: Clocks; NBS TV timing; time system; TV time dissemination; TV timing system.

A responding communication to a published letter by R. O. Whitaker in IEEE Spectrum (Sept. 1971) concerning the published paper, "Long-Term Continental U.S. Timing System

Via Television Networks." (Spectrum-August 1971). We note that a real time system could be available to the general public via television networks. We imply that TV sets could be built with clocks capable of day to day time errors of less than 100 ms.

**12633.** Bloss, R. L., **An extensometer for use as a laboratory standard at temperatures to 1500 °C,** *ISA Trans.* **10,** No. 3, 242-249 (1971).

Key words: Extensometer; high temperature; laboratory standard; strain gage; transient temperature.

Accurate measurement of strain is important in determining mechanical properties of materials and structures and in verifying the capability of structures to meet service conditions. When service conditions include hostile environments, such as high and rapidly changing temperatures, knowledge of the effect of these conditions on the strain gages being used is essential.

An extensometer was developed for use as a laboratory standard for evaluating the performance of remote reading strain gages at high (up to 1500 °C) and rapidly changing (up to 55 °C/s) temperatures. This instrument has a range of more than 2.2 mm, a resolution of $2.5 \times 10^{-7}$ m, nonlinearity of less than 0.2 percent of range, and random errors of about $5 \times 10^{-7}$ m. The effect of intense thermal radiation was small. The design, evaluation, and performance of this type of extensometer is discussed.

**12634.** Borie, E., Maximon, L. C., Olsen, H., **Molecular coherence effects in radiation processes: Bremsstrahlung,** *Phys. Rev. A* 2, No. 4, 1443-1449 (Oct. 1970).

Key words: Bremsstrahlung; electron; interference; molecular coherence; photon spectrum; radiation.

The influence of molecular structure on the bremsstrahlung process at low energies has been studied for diatomic molecules. Interference effects give rise to an increase in the total radiation cross section which is large low electron energies. Although the various cross sections are calculated in Born approximation, the results are expected to be qualitatively correct.

**12635.** Bowen, R. L., Cleek, G. W., **A new series of x-ray-opaque reinforcing fillers for composite materials,** *J. Dental Res.* **51,** No. 1, 177-182 (Jan.-Feb. 1972).

Key words: "Aluminoborate anomaly"; barium; composites; dental materials; glasses; radiopaque; reinforcements.

Clear, colorless glasses that absorb roentgen rays were prepared by melting together compounds yielding silica, barium oxide, boric oxide, and alumina. Barium oxide made the glasses radiopaque and gave the desired refractive index. Boric oxide lowered the melt viscosity, and alumina tended to stabilize the glasses. Some of these glasses seem to be suitable for use as the reinforcing fillers for composite dental restorative materials.

**12636.** Brady, E. L., Branscomb, L. M., **Information for a changing society,** *Science* **175,** 961-966 (Mar. 3, 1972).

Key words: Information packages; information policy; information systems; information users; OECD; technical information.

For society's needs, technical information must be credible, interpreted for various user groups, and repackaged together with other kinds of information in order to be used effectively by decision-makers. Starting from these premises, an Advisory Committee appointed by the OECD Secretary General developed 13 conclusions and recommendations for action by the Organization for Economic Development and its Member States. This paper summarizes the conclusions and recommendations and suggests ways in which the recommendations might be applied in practice.

**12637.** Branscomb, L. M., **Why people fear technology,** *The Fu turist*, p. 232 (Dec. 1971).

Key words: Performance standards; pollution; technology

Many people are "up tight" about technology, due mainly t rising expectations outstripping technology's ability to satisf them. Six reasons are given for the current anxiety and frustra tions the public has toward science and technology.

**12638.** Brauer, G. M., Termini, D. J., **Bonding of bovine enam to restorative resin: Effect of pretreatment of enamel,** *J. Den Res.* **51,** No. 1, 151-160 (Jan.-Feb. 1972).

Key words: Adhesion to bovine enamel; bonding enamel t restorative resins; effect of enamel surface treatmen enamel etch; restorative resins; tensile adhesion.

The efficiency of simple treatments of the enamel surface wit various polyfunctional acids and chelating agents was studied t obtain adequate adhesion between tooth surfaces and con mercially available acrylic resins. Many water soluble acids in duced bonding to enamel. Two ten-second treatments at thre minute intervals with acid solutions such as 20% lactic acid ma be useful in the clinical treatment of precarious lesions.

**12639.** Carter, J. C., Coyne, J. J., ***SU*(6) Clebsch-Gordan coeff cients for the product 35 × 70,** *J. Math. Phys.* **10,** No. 7, 120 1210 (July 1969).

Key words: Coupling coefficients; permutation symmetry quark interchange; relative phases, *SU*(6) multiplets; 35 70.

A method is presented which makes explicit use of Young di grams to calculate $SU(3) \times SU(2)$ multiplet-coupling coefficien in $SU(6)$. The multiplet-coupling coefficients for $35 \times 70$ a given.

**12640.** Cassinelli, J. P., Hummer, D. G., **Radiative transfer i spherically symmetric systems—II. The non-conservative ca and linearly polarized radiation,** *Mon. Notic. Roy. Astron. So* **154,** No. 1, 9-21 (Oct. 1971).

Key words: Polarized radiation; radiative transfer; Rayleig scattering; spherical geometry; stellar atmospheres.

The method for the solution of transfer problems in sphericall symmetric systems developed recently by Hummer and Rybic is here generalized to the non-conservative case. This procedur which depends on the iterative determination of the Eddingto factor $f = K/J$, handles in a natural way the outward peaking the radiation field which occurs in extended atmospheres. To i lustrate the present extension of this method, soiutions are ol tained for the problem of scattering of linearly polarized radi tion by an extended electron-scattering atmosphere. Althoug the transfer of radiation through such an atmosphere is conserv tive, each of the component equations is not. For opacity laws the form $\kappa\rho = r^{-n}$, $o < r < R$, $n = 2$ and 3, very large values of th polarization are found as a general feature arising from the stror peaking of the radiation field. It is found that the temperature di tribution in such extended electron-scattering atmospheres di fers negligibly from that computed on the assumption of isotrop scattering, with the neglect of polarization. The procedure use for the polarization problem can also be applied directly problems with a non-grey opacity involving many frequenci simultaneously.

**12641.** Coyle, T. D., Ritter, J. J., **Organometallic aspects diboron chemistry,** Chapter in *Advances in Organometall Chemistry* **10,** 237-272 (Academic Press, New York, N.Y 1972).

Key words: Boron; boron chemistry; catenated boron con pounds; diboron chemistry; organoboron compounds; o ganometallic chemistry.

This article reviews features of the chemistry of diboron com- unds of particular interest from the organometallic viewpoint. me general features of diboron chemistry are surveyed, with nphasis on unique synthetic aspects and on properties particu- rly characteristic of compounds containing a simple electron- ir bond between boron atoms. More extensive consideration given to the interaction of diboron compounds with unsatu- ted organic systems, which is a major aspect of organometallic emistry based on boron-boron bonded compounds, and to me of the chemistry of particular organoboron compounds rived from diboron precursors.

642. Danos, M., **Fully consistent phase conventions in angular momentum theory,** *Ann. Phys.* **63,** No. 2, 319-334 (Apr. 1971).

Key words: Angular momentum theory; matrix elements; phase conventions; Racah algebra; recoupling graphs; recoupling transformations.

By a slight modification of the phase conventions of angular omentum algebra, all phases can be eliminated from the formu- s. Consequently, a simple, true graphical representation of the mplete Racah algebra can be constructed. This way all pological questions of the recoupling transformations can be lved graphically, enabling one to write directly the algebraic pression of the final result.

643. Eisenhart, C., **The assumptions underlying the analysis of variance,** Chapter 7.1 in *Statistical Issues: A Reader for the Behavioral Sciences,* R. E. Kirk, ed., pp. 226-240 (Brooks/Cole Publ. Co., Monterey, Calif., 1972).

Key words: Analysis of variance; chi-square distribution, F-distribution; components of variance; confidence intervals; estimation; fixed effects; Model I; Model II; random effects; tests of significance.

It is shown that familiar partition of "sums of squares" is sed on algebraic identities that are valid whatever the in- rpretation of the numbers involved. Two distinct classes of oblems solvable by analysis of variance are recognized: detec- on and estimation (1) of fixed (constant) relations among the eans of sub-sets of the universe of objects concerned; and (2) components of random variation associated with a composite iverse of objects. The corresponding mathematical models are signated *Model I* and *Model II*, respectively. In *Model I* the servations $X_{ij}$ are normally and independently distributed with common variance $\sigma^2$ about (population) mean values $m_{ij}$ that e conceived to be fixed *constants* satisfying the *additivity* lations $m_{ij}=m_{..}+(m_{i.}-m_{..})+(m_{.j}-m_{..})$ where the $m_{i.}$ and $m_{.j}$ e the corresponding ith row and jth column means, respective- , $(i=1,2,\ldots,r; j=1,2,\ldots,c)$. In *Model II* the same structure assumed except that the row deviations $(m_{i.}-m_{..})$, $(i=1,2,..$ r) are no longer conceived to be fixed constants, but normally d independently distributed about zero with common variance $^2$; and the column deviations, $(m_{.j}-m_{..})$, $(i=1,2,\ldots,c)$, nor- ally and independently distributed about zero with common riance $\sigma_c^2$. These two models provide necessary and sufficient ses for the two common groups of tests of significance and nfidence interval procedures associated with analysis of vari- ce. For purposes of mere unbiased estimation of fixed row and lumn effects (Model I), or of row and column components of riance (Model II), it is sufficient that the respective random riables $x_{ij}$ be uncorrelated; the normality assumption is un- cessary except for rigor of the common tests of significance d corresponding confidence interval procedures.

644. Franzen, D. L., Jennings, D. A., **Gain saturation measurements in $CO_2$, TEA amplifiers,** *J. Appl. Phys.* **43,** No. 2, 729-730 (Feb. 1972).

Key words: Atmospheric; $CO_2$; gain saturation; lasers.

Measurements of gain in $CO_2$, TEA pulsed amplifiers operating at a pressure of 330 torr are described. The energy gain in traversing a small amplifying section decreases to one-half the small-signal value at an energy flux density of $1.2 J cm^{-2}$.

12645. Geist, J., **The effect of wall roughness on the spectral density of radiation within symmetric closed cavities in good conductors,** *J. Opt. Soc. Amer.* **62,** No. 4, 602-604 (Apr. 1972).

Key words: Blackbody; electromagnetic radiation; radiometry.

It is shown that roughening the walls of highly symmetric closed cavities in good conductors reduces the deviations of the spectral energy density within the cavity from that predicted by Planck's law. Roughening is most effective at short wavelengths, and it has its most significant effect on de-polarizing the radiation in the cavity.

12646. Handy L. B., Sharp, K. G., Brinckman, F. E., **The metathetical chemistry of halotungsten(VI) compounds. Synthesis and geometry of organooxy fluorides and chlorides,** *Inorg. Chem.* **11,** No. 3, 523-531 (1972).

Key words: Alkoxy; chlorides; exchange reactions; fluorides; methoxy; nuclear magnetic resonance; organosilanes; organoxy; stereochemistry; synthesis; tungsten(VI) halides.

Tungsten(VI) halides can be selectively metathesized with organooxysilanes and, where appropriate, with methoxide ion. Reactions proceed without reduction of the metal and degree of substitution can be regulated by control of stoichiometry. In this manner, the compounds $(CH_3O)_nWX_{6-n}$, where $n=1-4$ and $X=F$ or Cl, can be synthesized from the reaction of $CH_3OSi(CH_3)_3$ and $WX_6$. Further substitution does not efficiently take place with $CH_3OSi(CH_3)_3$ but can be effected with $CH_3O^-$, again with maintenance of the W(VI) state, to give the $(CH_3O)_5WCl$ and $(CH_3O)_6W$ species. The two series may be interconverted *via* fluorination of W – Cl bonds with $SbF_3$ or chlorination of W – F bonds with $(CH_3)_3SiCl$. The stereochemical disposition of all products has been determined by $^1H$ and, where possible, $^{19}F$ nmr.

12647. Hanson, D. W., Hamilton, W. F., **Clock synchronization from satellite tracking,** *IEEE Trans. Aerosp. Electron. Syst.* **AES-7,** No. 5, 895-899 (Sept. 1971).

Key words: Clocks; propagation delay; satellites; synchronization; time dissemination; tracking.

The tracking of synchronous satellites to provide propagation delays for the synchronization of clocks is described. The tracking is accomplished by range measurements to the satellite from three stations using signals transponded by the satellite. These same signals also functioned as the timing signals for the synchronization of other stations' clocks. Although the range measurements were of low resolution by usual standards, approximately 3000 meters, they provided the delays necessary to synchronize clocks to 40 microseconds or better. These results were obtained over a 4-month period using two satellites with measurements from five stations in the United States and South America.

12648. Hubbell, J. H., **Photon cross section compilation activity in the U.S. in the range 1 keV to 100 GeV,** *J. Phys.* **32,** No. 10, C4-14–C4-20 (Oct. 1971).

Key words: Attention coefficient; compilation; Compton scattering; photo electric effect; photons; x rays.

A brief survey will be presented of photon cross section (attenuation coefficient) measurements available over the range of photon energies 10 eV to 100 GeV and elements $Z=1$ to 100. The results of these measurements, extracted from the 1909-1970 literature, are on file at the NSRDS (National Standard Reference Data Center) *(X-Ray Attenuation Coefficient Information Center)* at the NBS. These data, plus newly-available theoretical values for photoabsorption, scattering and pair-production cross sections, are the subject of continuing evaluation and compilation programs at the NBS, LRL (Lawrence Radiation Laboratory, Livermore) and elsewhere. Present compilation efforts by NBS (10 keV-100 GeV, 23 elements) and by LRL-NBS (1 keV-1 MeV, 87 elements) will be described and compared with input information. Compilation uncertainties from $Z$-interpolation and absorption-edge fine-structure will be discussed.

**12649.** Keller, R. A., Zalewski, E. F., Peterson, N. C., **Enhancement of absorption spectra by dye-laser quenching, II,** *J. Opt. Soc. Amer.* **62,** No. 3, 319-326 (Mar. 1972).

Key words: Absorption; lasers; spectra.

Insertion of samples into a broad-band dye-laser cavity enhances photographic detectability of trace absorptions by approximately three orders of magnitude. Optical densities as small as 0.0004 were readily detected in a dilute solution of $Eu(NO_3)_3$. In a modified technique the bandwidth of the dye laser was reduced by using prisms, and the wavelength of this narrow band was swept through the absorption. The modified technique permitted detection of optical densities as small as 0.01. Solutions of theoretical equations describing both processes give good agreement with experimental results, and they provide insight into the mechanism of the effect. The measurements with the broad-band laser could be made in 100 ns or less; therefore, this technique should provide a powerful tool for detection of short-lived transients in very small concentrations.

**12650.** Kraft, R., **Convergence of semidiscrete approximations of linear transport equations,** *J. Math. Anal. Appl.* **37,** No. 2, 412-431 (Feb. 1972).

Key words: A-priori bound; convergence; finite differences; hyperbolic equation; positive mapping; semi-discrete approximations; transport equation.

A technique will be presented for establishing the convergence of semi-discrete methods of approximating linear transport equations. The technique is based on the "positivity" property of the system of hyperbolic equations which approximate the transport equation. A-priori bounds are deduced by using 1) the properties of Riemann functions that are associated with the hyperbolic systems; and 2) the "positivity" of the hyperbolic systems. The a-priori bounds are then used to deduce convergence in the classical way and obtain decay rates.

**12651.** Kuyatt, C. E., Natali, S., Di Chio, D., **Accurate calculation of properties of the two-tube electrostatic lens. III. Aberration coefficients,** *Rev. Sci. Instr.* **43,** No. 1, 84-87 (Jan. 1972).

Key words: Fifth-order aberration coefficients; intrinsic aberration coefficients; meridional electron trajectories; third-order aberration coefficients; two-tube electrostatic lens.

Using numerical methods, electric fields and meridional electron trajectories have been calculated for the two-tube electrostatic lens with sufficient precision to determine values for all the third-order and several of the fifth-order aberration coefficients for meridional trajectories. The aberration coefficients are expressed in a form which is intrinsic to the lens and do not depend on a particular object and aperture position. Results were obtained for voltage ratios of 2, 5, 10, 20, and 40.

**12652.** Kuyatt, C. E., Natali, S. V., Di Chio, D., **Third-ord aberration coefficients of electron lenses,** (Proc. 11th Sym Electron, Ion, and Laser Beam Technology, University Colorado, Boulder, Colo., May 12-14, 1971), Chapter *Record of 11th Symposium on Electron, Ion, and Laser Be Technology,* R. F. M. Thornley, ed., pp. 177-181 (San Fra cisco Press, Inc., San Francisco, Calif., 1971).

Key words: Electron lenses; experiment; theory; thi order aberration.

In the standard treatments of aberration coefficients of el tron lenses, deviations from perfect imagery are expressed power series of the ray coordinates in the object and apert planes. The resulting aberration coefficients depend on the ject and aperture positions, and a complete description of aberrations of a lens would, in principle, require a doubly infin set of aberration coefficients.

Verster has formulated the third-order aberrations of electr lenses in an object- and aperture-independent way for meridio trajectories and has determined some of the coefficients. Usi highly precise numerical methods, we have calculated elect fields and electron trajectories in the two-tube electrostatic le for voltage ratios from 1.5 to 50, and have derived all Verster's third-order aberration coefficients.

**12653.** LaVilla, R. E., Deslattes, R. D., **Single and multi vacancy effects in molecular x-ray spectra,** *J. Phys.* **32,** No. C4-160 – C4-164 (Oct. 1971).

Key words: Cl $K\beta$, $CH_3Cl$; double electron process; $L_{23}$ argon, Cl and $K$ in KCl; molecular x-ray emission; multi vacancies.

The x-ray $K\beta$ emission spectra from molecular gases discussed with the use of a particular example, $CH_3Cl$. With help of a crude threshold experiment, the multiple vaca processes are shown to be on the high energy side of prominent spectral lines in Cl $K\beta$ emission from $CH_3Cl$. Fro recent molecular orbital calculation, the Cl $K\beta$ molecular em sion lines are identified as the 3 e and 7 $a_1$ orbitals of $CH_3Cl$. T valence $K$ emission spectra can be interpreted for the most p in terms of one electron single vacancy transitions from in shells to the various outer molecular orbitals, where the spec line position and intensity are dependent on the molecular te value, symmetry and orbital overlap. In the course of extend the x-ray molecular emission studies to the $L$ series of sulp and chlorine we measured the $L_{23}$ spectra from argon gas study the instrumental response in this region. A prominent *e* low energy emission feature was found in the Ar $L_{23}$ spectra similar feature is also observed in the $L_{23}$ emission of Cl an from KCl. These *extra* features are interpreted as evidence double electron process.

**12654.** Levin, I. W., Abramowitz, S., Müller, A., **Jahn-Te vibrations of $ReF_6$,** *J. Mol. Spectrosc.* **41,** No. 2, 415-419 (F 1972).

Key words: Coriolis constant; force fields; hexafluor Jahn-Teller; $ReF_6$.

Model force fields are investigated in order to estimate the published frequencies $\nu_2^\circ$ and $\nu_5^\circ$ of the molecule $ReF_6$ which hibits a dynamic Jahn-Teller effect. The force fields were mated using the Coriolis constant $\zeta_3$ observed from the resolved vibration rotation band contour of $\nu_3$ and the other served frequencies $\nu_1$, $\nu_3$, $\nu_4$, and $\nu_5$.

**12655.** Lutz, G. J., **Determination of lead in environmental s ples by photon activation analysis,** *Proc. Am. Nucl. Soc. T cal Meeting on Nuclear Methods in Environmental Resea Aug. 23-24, 1971, Columbia, Mo.,* pp. 144-149 (Aug. 1971

Key words: Biological samples; environmental samples; lead; photon activation analysis; soil.

Photon activation analysis has been applied to the determina- on of lead in environmental samples. Electrons are accelerated a suitable energy (20-45 MeV) with a linear accelerator and al- wed to strike a tungsten target. High energy photons, called emsstrahlung, are produced from the interaction of the elec- ons with the coulomb field of the tungsten atoms. Part of this emsstrahlung is of sufficiently high energy to induce the reac- on $^{204}$Pb(γ,n)$^{203}$Pb. $^{203}$Pb has a half-life of 52 hours and decays ith the emission of a 279 keV gamma ray.

After irradiation the sample is either counted nondestructively ith a Ge(Li) detector or the lead is separated after dissolution the sample by extraction into methyl isopropyl ketone or by ore rigorous methods and then counted with a Ge(Li) or aI(Tl) detector.

Precision and accuracy have been determined to be adequate analyzing some soil and biological samples which had been sayed for lead by other methods. Interfering photonuclear actions do not occur below 45 MeV.

The limit of nondestructive determination with a Ge(Li) detec- r is about 0.5 ppm. With a rigorous separation, about 10 nano- ams can be determined.

**656.** McCarter, R. J., **The cause of anomalous behavior in the vertical flammability test,** *Text. Chem. Color* **4,** No. 4, 91-93 (Apr. 1972).

Key words: Flammability; strip tests; testing; testing equipment; vertical tests.

Experiments were conducted to determine the cause of omalous results in vertical flammability testing. Some fabrics marginal flammability had indicated an increased tendency to pport flame propagation when the time of exposure to the test ame was decreased.

The severity of the vertical test procedure was found to be a aximum when the burner was applied for only the interval cessary for ignition of the sample. With a longer application of e burner to fabrics of marginal flammability, the burning of the bric may be extinguished by the less-than-ambient oxygen con- nt of the burner plume.

**657.** Mangum, B. W., Lee, J. N., Moos, H. W., **Magnetically controllable cooperative Jahn-Teller distortion in TmAsO$_4$,** *Phys. Rev. Lett.* **27,** No. 22, 1517-1520 (Nov. 29, 1971).

Key words: Cooperative distortion; Jahn-Teller distortion; magnetically controllable distortion; rare-earth; TmAsO$_4$.

TmAsO$_4$ undergoes a cooperative Jahn-Teller distortion at 6.0 At $T < 6$ K there is a temperature-dependent critical field $\vec{B}_c$ which a cooperative distortion back to the high-temperature ase occurs. For $B < B_c$, the distortion directions in the basal ane are the (110) and the (1$\bar{1}$0) directions and are magnetically ntrollable.

**658.** Mavrodineanu, R., **Discussion of some experimental and fundamental conditions in analytical flame spectroscopy,** *Proc. 3d Intern. Conf. Atomic Absorption and Atomic Fluorescence, Paris, France, Sept. 27-Oct. 1, 1971,* pp. 39-60 (1972).

Key words: Flame; hydrogen; long-path burner; multichannel spectrometer; non-metals; overexcitation; phosphorus; spectrometry; sulfur; triple pass on-axis.

A flexible multichannel flame spectrophotometer was signed and built to extend the measuring capabilities of alytical methods in which a combustion flame is used to emit or absorb specific radiations. This instrument is composed of a 1 meter spectrometer with its multichannel phototube housing, the appropriate electronic components for scanning and ac and dc signal measurement with integration and printout and a punch tape arrangement for computer calculations. A unique feature of the measurement system is an NBS designed burner and sprayer made of pure alumina with a water cooled tantalum flame plate, which provides an unusually stable flame and hence improved precision of measurement. The instrument can be used as a scanning monochrometer, a spectrograph, or a multichannel spectrometer, by appropriate arrangement at the focal plane of the spectrometer. The instrument is used for the simultaneous determination of Na, K, Ca and Mg in biological fluids using Li as an internal standard. The instrument provides the full advantages of specificity, sensitivity, speed and economy of sample in simultaneously obtaining data suitable for rapid computer evaluation. The water-chilled hydrogen flame is described and its capability to excite non-metals is illustrated using P and S as examples. The spectra of HPO and S$_2$ are presented together with the mechanism suggested for their production.

**12659.** Merris, R., **A dominance theorem for partitioned hermitian matrices,** *Trans. Amer. Math. Soc.* **164,** 341-352 (Feb. 1972).

Key words: Associated transformation; generalized matrix function; (group) character; Hadamard (Schur) product; Kronecker product; orthogonality relations; Schur function.

Let $A=(A_{ij})$ be a partitioned positive semidefinite hermitian matrix, where $A_{ij}$ is $n$-square, $1 \leqq i,j \leqq m$. A class of ordered pairs of functions $(f_1,f_2)$ is given such that $(f_1(A_{ij})) - (f_2(A_{ij}))$ is positive semidefinite hermitian. Applications are given.

**12660.** Mielenz, K. D., Eckerle, K. L., **Accuracy of polarization attenuators,** *Appl. Opt.* **11,** No. 3, 594-603 (Mar. 1972).

Key words: Accuracy; phase retardation plates; polarization attenuators; sheet polarizers; spectrophotometry; transmittance standards.

The accuracy of various polarization attenuators is discussed, including systematic errors due to imperfections of the polarizers, setting errors of the rotating elements, alignment errors of fixed elements, and errors caused by oblique incidence and partial polarization of the incident light. Whereas the accuracy of conventional three-polarizer attenuators is limited to 0.001 transmittance unit, at least ten times more accuracy can be achieved with two new types of attenuators, which employ either a half-wave or a quarter-wave retardation plate in conjunction with two sheet polarizers.

**12661.** Mighell, A. D., Reimann, C. W., Santoro, A., **The crystal and molecular structure of dimeric dibromobis(pyridine *N*-oxide) copper(II), [(pyridine *N*-oxide)$_2$ CuBr$_2$]$_2$,** *Acta Cryst.* **B28,** Part 1, 126-134 (Jan. 1972).

Key words: Bromine; copper; crystal; pyridine *N*-oxide; structure; x ray.

The crystal and molecular structure of dimeric dibromobis(pyridine *N*-oxide) copper(II), [(C$_5$H$_5$NO)$_2$CuBr$_2$]$_2$, was determined by single-crystal x-ray diffraction techniques. This compound crystallizes in the triclinic system with $a=$ 10.510 (2), $b=$ 10.883 (1), $c=$ 11.818 (5) Å, $\alpha=$ 78.57 (3), $\beta=$ 89.88 (3), $\gamma=$ 81.17 (1)°, space group $P1$, $\rho_0=2.08$, $\rho_c=2.10$ g · cm$^{-3}$ and $Z=2$. The structure was solved by Patterson and electron-density Fourier techniques and refined by block-diagonal least-squares analysis to a final $R$ value of 0.046 based on 4415 observed reflections. The structure consists of two centrosymmetric dimeric molecules crystallographically nonequivalent. The centers of symmetry of the two molecules are located at the origin and at the center of the unit cell. In both dimers each copper atom is coordinated by two bromine atoms, and by three oxygen atoms of which two are bridging. The bromine atoms are located above and below the plane defined by the copper atoms and the bridging oxygen atoms. The two dimeric molecules show significant differences in some bond distances and angles and in the relative orientation of the pyridine *N*-oxide molecules. The geometry of this complex differs markedly from that of its chloride analog, as well as from that of other members of the aromatic *N*-oxide copper(II) halide series. The magnetic properties of the bromide complex are discussed in relation to those of related compounds.

**12662.** Miles, B. M., Wiese, W. L., **Critical evaluation of transition probabilities for Ba I and Ba II,** *Atomic Data* **1,** 1-17 (1969).

Key words: Ba I; Ba II; line strengths; oscillator strengths; transition probabilities.

Transition probabilities for allowed lines of Ba I and II, based on a critical evaluation of available literature sources, are presented in order of increasing quantum numbers.

**12663.** Milligan, D. E., Jacox, M. E., **Infrared and ultraviolet spectroscopic studies of a number of small free radicals and molecular ions in a matrix environment,** Chapter 1 in *Advances in High Temperature Chemistry* **4,** 1-24 (Academic Press, Inc., New York, N.Y., 1971).

Key words: Free radicals; infrared spectrum; matrix isolation; molecular ions, photolysis; ultraviolet spectrum.

The development of the matrix isolation technique is summarized, and the principles which have been found to be important for the *in situ* photoproduction of free radicals trapped in inert solid matrices in sufficient concentration for direct infrared and ultraviolet spectroscopic observation are considered. A survey of the small free radical species heretofore studied using these techniques is given. Examples of the successful application of the technique are drawn from recent studies of the vacuum-ultraviolet photolysis of matrix-isolated methane and silane and of their chloro- and fluoro-derivatives. Results of experiments designed to permit the trapping in inert, non-ionic matrices of negatively charged molecular ions are presented.

**12664.** Moore, G. A., **Gestalt properties of aggregate materials,** *Prakt. Metallogr.* **IX,** No. 2, 76-97 (Feb. 1972).

Key words: Analysis of microstructures; automatic image analysis; Gestalt of a material; microarchitecture; patternness; scanning microscopes; television microscopes.

From the viewpoint of materials engineering and quality control the significant aspects of the microstructure of a material as a whole constitute a Gestalt which controls mechanical behavior. Such a Gestalt has in the past often been specified by the thermal-mechanical history of the material. Higher precision and sound scientific practice require that the specification should be in terms of a properly selected set of measurements of the microstructure. The Gestalt of any aggregate material can be adequately specified by six stereologically valid parameters measuring phase concentration ($V_V$), size ($\bar{l}_\beta$) and spacing ($\bar{l}_\alpha$) of particles, variability between portions of the material (V.I.), general anisotropy ($\bar{l}_1/\bar{l}_2/\bar{l}_3$), and degree of patternness (S.I.). Raster scanning devices of either the mechanical or television type are intrinsically capable of easily measuring these six parameters. Only minor changes are required to provide this common set of measurements from all scanning instruments and to improve accuracy. In contrast, microarchitectural processes which identify, measure, and selectively count individual object sections require massive effort and have limited relation to behavior; thus are to be avoided whenever feasible.

**12665.** Natali, S., Di Chio, D., Uva, E., Kuyatt, C. E., **Accura calculation of properties of the two-tube electrostatic lens. I First-order focal properties and *P-Q* curves,** *Rev. Sci. Instr.* 4 No. 1, 80-83 (Jan. 1972).

Key words: Electric field; first-order focal propertie paraxial electron trajectories; *P-Q* curves; two-tube electr static lens.

Using digital methods, electric fields and paraxial electr trajectories in the two-tube electrostatic lens have been calc lated, and the first-order (Gaussian) focal properties accurate at least 0.1% were obtained for voltage ratios from 1.5 to 50. Tl results are presented in the form of *P-Q* (object-image positio curves for maximum ease of use.

**12666.** Opal, C. B., Peterson, W. K., Beaty, E. C., **Measuremen of secondary-electron spectra produced by electron impa ionization of a number of simple gases,** *J. Chem. Phys.* **55,** N 8, 4100-4106 (Oct. 15, 1971).

Key words: Atmospheric gases; ionization; noble gase secondary electron collisions.

The energy distribution and angular dependence of seconda electrons generated by the impact of 100-2000-eV electrons He, $N_2$, and $O_2$ and by the impact of 500-eV electrons on Ne, Kr, Xe, $H_2$, NO, CO, $H_2O$, $NH_3$, $CH_4$, $C_2H_2$, and $CO_2$ ha been measured over the 4-200-eV range. The measuremer were made in a crossed-beam apparatus with the use of a fix hemispherical electrostatic analyzer and a rotatable electron g The observed spectra were integrated over angle to obtain re tive cross sections for secondary-electron production. It w found that the shapes of the spectra of all the gases (except Kr, and Xe, which contain intense electron emission features this energy range) were smooth and qualitatively similar, proaching a constant cross section at low secondary energi and falling off at high secondary energies slightly faster than $E_s$ where $E_s$ was the energy of the secondary. The shape of spectrum was found to be nearly independent of primary ener in He, $O_2$, and $N_2$.

**12667.** Ott, W. R., **Measurement of transition probabilities for in the vacuum ultraviolet,** *Phys. Rev. A* **4,** No. 1, 245-251 (J 1971).

Key words: Arc emission; oxygen; transition probabili vacuum ultraviolet.

Transition probabilities for O I lines emitted in the vacuum traviolet were measured using a wall-stabilized arc discha operating in a mixture of argon and oxygen. The lines w emitted from a column of plasma which was observed end and which was characterized by a nearly uniform temperatu Optically thin conditions were achieved by reducing the relat concentration of oxygen atoms in the discharge to levels of than one part per million. Absolute values for the O I transit probabilities were obtained by determining the oxygen-at density and plasma length through a measurement of the solute intensity of the O I $\lambda = 7773.4$ Å line, whose transit probability is known. The following values were measured lines in the resonance transition array: $A(^1D_2 - {}^1D^\circ_2, \lambda = 11$ Å$) = 5.5 \times 10^8$ sec$^{-1}$; $A(^1S_0 - {}^1P^\circ_1, \lambda = 1218$ Å$) = 1.8 \times$ sec$^{-1}$; $A(^3P_0 - {}^3S^\circ_1, \lambda = 1306$ Å$) = 0.66 \times 10^8$ sec$^{-1}$; $A(^3P_2,$ $- {}^3S^\circ{}_1, \lambda = 1303.5$ Å$) = 5.9 \times 10^8$ sec$^{-1}$. These values are in cellent agreement with recent lifetime measurements. Exist discrepancies in the literature concerning a previous arc de mination of the O I vacuum ultraviolet oscillator strengths Boldt and Labuhn are discussed. The present method is c sidered to be an improvement over the method used by Boldt Labuhn which relied, first of all, upon extrapolation techniq to reach the linear part of the curve of growth and, secon on a complex calculation of the oxygen-atom number density ing basic conservation equations.

668. Piccirelli, R. A., **Theory of the dynamics of simple fluids for large spatial gradients and long memory,** *Phys. Rev.* **175,** No. 1, 77-98 (Nov. 5, 1968).

> Key words: Current autocorrelations; noninstantaneous effects; nonlinear effects; nonlocal effects; statistical mechanical theory; transport properties.

A generalization of the classical fluid dynamics which scribes noninstantaneous, nonlocal, and nonlinear responses flows to the thermodynamic forces (gradients) is derived by tistical-mechanical methods. The conservation equations termining the mass, momentum, and energy densities are changed in form, but new expressions are given for the pres- e tensor and heat current vector. The new expressions are ecified functionals of the temperature, flow velocity, and lmholtz free energy density, are determined by microscopic antities (e.g., interparticle potential), and consist of a reversi- and an irreversible part. The reversible parts are the expected xes in a local-equilibrium ensemble that includes nonlocal ef- ts. The reversible contribution to the heat current is non- nishing for large enough gradients. The expressions for the ir- versible parts are the analog of the classical transport relations, d are linear combinations of integrals over space and time of rrelation-function kernels convoluted with the thermodynamic ces. The kernels, which are specified functionals of the fluid nsities and are a kind of local-equilibrium correlation of sub- cted fluxes, are natural generalizations of the autocorrelation pressions for the classical transport coefficients.

669. Powell, F. X., Johnson, D. R., **Microwave spectrum of the BrO free radical,** *J. Chem. Phys. Letters to Editor* **50,** No. 10, 4596 (May 15, 1969).

> Key words: BrO; free radical; magnetic hyperfine; microwave spectrum; rotational spectra; transient species.

The gas phase microwave spectrum of the BrO free radical has en detected in the ground $^2\Pi_{3/2}$ state. BrO was produced by the action of oxygen atoms with molecular bromine at low pres- res. Measurements have been made in the hyperfine patterns r the $J=5/2 \leftarrow 3/2$ rotational transitions of both $^{79}$BrO and rO. Effective rotational constants, lumped magnetic hyper- e parameters and nuclear quadrupole coupling constants were termined for each isotopic species.

670. Powell, R. C., **Precision coaxial connectors,** Chapter in *Advances in Microwaves* **6,** 1-28 (Academic Press, Inc., New York, N.Y., 1971).

> Key words: Coaxial; connectors; microwave; precision measurements; standards.

The evaluation and status of precision coaxial connectors are viewed. Discussed are: precision coaxial lines, general and oratory precision connectors, dielectric supports, and upling mechanisms. Applications are given and an extensive liography is included.

671. Price, D. L., Rowe, J. M., Rush, J. J., Prince, E., Hinks, D. G., Susman, S., **Single crystal neutron diffraction study of potassium cyanide,** *J. Chem. Phys.* **56,** No. 7, 3697-3702 (Apr. 1, 1972).

> Key words: Cyanide ion; disorder; ion displacements; lattice dynamics; libration; neutron diffraction; potassium cyanide.

Neutron diffraction measurements were made on single ystals of KCN to obtain information about the disorder of the $N^-$ ions in the cubic phase. The crystals were obtained by pulling from the melt by a modified Czochralski method. Data were collected on two four-circle diffractometers at room temperature and at 180 K, just above the cubic-orthorhombic phase transition. Structure factors were obtained for 24 inequivalent reflections. Free rotation of the $CN^-$ ions is ruled out by the different structure factors obtained for reflections with equal values of $(h^2+k^2+l^2)$ but different $(h, k, l)$. However, models fitted to the data assuming orientations along a particular symmetry direction did not establish a preferred direction. The fits indicated that both vibrational and librational thermal amplitudes are large and relatively independent of temperature. These amplitudes could not be reproduced by a dynamical model assuming harmonic forces even when rotational-translational coupling was included. A tentative explanation of these results is given in terms of rapid $CN^-$ reorientations caused by the low activation energy for rotation.

12672. Prydz, R., **An improved oxygen vapor pressure representation,** *Metrologia* **8,** No. 1, 1-4 (Jan. 1972).

> Key words: Critical point; oxygen; temperature scales; triple point; vapor pressure equation.

Oxygen vapor pressure measurements reported in the literature have been critically evaluated and the most consistent and reliable of the data sets have been correlated with a vapor pressure equation. However, the data were first adjusted for temperature scale differences to conform with the IPTS-68 temperature scale. "Best" values for the oxygen triple point and critical point parameters were selected for use as indirect constraints in the equation. Pressures obtained from this equation are compared to corresponding values calculated from other published oxygen vapor pressure equations. A new value for the critical pressure of oxygen of $5.043_2$ MN/m$^2$ ($49.77_2$ atm) is given.

12673. Rankin, K., Tauber, S. J., **Linguistics as a basis for analyzing chemical structure diagrams,** *J. Chem. Doc.* **11,** No. 3, 139-141 (1971).

> Key words: Atom symbols; bond symbols; chemical diagrams; formal grammar; language; linguistic analysis; natural groups; numerical subscripts; patterns; strings; vocabulary.

Chemical structure diagrams constitute a language in the same sense that English and Fortran are languages. A language consists of combinations of members of a vocabulary. For chemical structure diagrams the vocabulary includes atom symbols, bond symbols, and numerical subscripts. In contrast to languages such as English and Fortran, wherein utterances are linear strings, the chemical diagram language uses arrangements of vocabulary members in two dimensions. The linguist seeks to construct a grammar which reflects the chemist's ability to distinguish between valid chemical structure diagrams and other patterns built from the same vocabulary. Such grammar should also account for "natural groups" in valid diagrams.

12674. Reader, J., Ekberg, J. O., **Resonance lines of Ce v and Ce vi,** *J. Opt. Soc. Amer.* **62,** No. 3, 464 (Mar. 1972).

> Key words: Cerium; spectra.

The spectra of Ce v and vi were photographed with sliding sparks in the vacuum ultraviolet. The five resonance lines of the type $5p^6\ {}^1S_0 - 5p^55d$ and $6s, J=1$ for Ce v and the two resonance lines of the type $5p^5\ {}^2P_{1/2,3/2} - 5s5p^6\ {}^2S_{1/2}$ are reported here. Identifications of upper levels are based on isoelectronic comparisons.

12675. Reader, J., Epstein, G. L., Ekberg, J. O., **Spectra of Rb ii, Sr iii, Y iv, Zr v, Nb vi, and Mo vii in the vacuum ultraviolet,** *J. Opt. Soc. Amer.* **62,** No. 2, 273-284 (Feb. 1972).

Key words: Molybdenum; niobium; rubidium; spectra; strontium; ultraviolet; wavelengths; yttrium; zirconium.

The characteristic resonance-line spectrum in the Kr I isoelectronic sequence, consisting of the five transitions to the $4p^6\ {}^1S_0$ ground state from levels with $J=1$ in the $4p^54d$ and $5s$ configurations has been observed from Rb II to Mo VII. The observations were made with sliding sparks, on the 10.6-m normal-incidence spectrograph at NBS and 5-m grazing-incidence spectrograph in Lund. A number of transitions from higher levels of the type $4p^5nd$, $4p^5ns$, and $4s4p^65p$ were also observed. Isoelectronic comparisons are given for all observed levels. The ionization energies in electron volts are

| | | | | | |
|---|---|---|---|---|---|
| Rb II | 27.285 | Y IV | 60.60 | Nb VI | 102.06 |
| Sr III | 42.87 | Zr V | 80.36 | Mo VII | 125.66 |

Anomalous relative intensities observed for the $4p^54d$ transitions are found to be caused by excitation conditions within the light source.

12676. Rook, H. L., LaFleur, P. D., Gills, T. E., **Mercury in coal: A new Standard Reference Material,** *Environ. Letters* **2,** No. 4, 195-204 (1972).

Key words: Activation analysis; coal; mercury; pollution; standard reference material.

Sources of environmental mercury contamination are generally related to industrial and mining activity. However, close examination of the sources reveal how complex the task of dealing with mercury pollution is. For example, virtually none of the mercury in fossil fuel is trapped in the fly ash, instead it is released in gaseous form as a product of combustion. Evidence now exists that this gaseous mercury is washed from the air by rain, being cycled to rivers, lakes and oceans where further evidence indicates that it may be methylated to its most toxic form, methylmercury.

Mercury releases to the environment from burning of fossil fuels have been calculated to contribute a significant portion of the total mercury released. Unfortunately, mercury concentrations in coals used to calculate mercury release differ by a wide range. This paper presents the results of a concerted analytical program by the National Bureau of Standards to develop a coal standard of proven homogeneity with an accurate value of mercury concentration. This standard was used in determining the mercury level in a suite of coal samples issued by the U.S. Bureau of Mines. The results of this work indicate a range of mercury levels from approximately 0.05 to 0.5 ppm with the average level of 0.1 to 0.2 ppm.

12677. Ruthberg, S., **Standards and vacuum measurements accuracy,** *J. Vacuum Sci. Technol.* **9,** No. 1, 186-195 (Jan.-Feb. 1972).

Key words: Absolute vacuum reference standards; dynamic pressure division; manometry; McLeod gage; static pressure division; vacuum measurements accuracy; vacuum standards.

Present capabilities for precision and accuracy are compared with the needs at the working level. A measurements structure is sketched by which reference standards accuracies are propagated. Uncertainties are prescribed for a number of prevalent measurement methods including precision U-tube manometer, McLeod gage, volumetric pressure division, and dynamic expansion. The development at the National Bureau of Standards of direct absolute measurements standards of high precision and their use in dynamic environments stabilized to better than one part in $10^3$ and ranging from the medium to the ultrahigh vacuum are described. These methods include precision liquid columns for the upper pressure range, interferometer manometer and modified McLeod gages for the high vacuu range, and a torsion microbalance or vane gage for the ultrahi vacuum range.

12678. Saylor, C. P., **Case of the flowing roof,** *Chemistry* **44,** N 11, 19-20 (Dec. 1971).

Key words: Cathedral; deformation; lead; roof; Washingt Cathedral.

The Washington Cathedral, built in the English style, w given a lead roof. Under the hot Washington sun, it crept. Th caused it to leak. E. W. Washburn, Chief Chemist of NBS, dia nosed the difficulty and suggested correction.

12679. Shirk, J. S., Bass, A. M., **Absorption and laser-excit fluorescence of matrix-isolated CuO,** *J. Chem. Phys.* **52,** No. 1894-1901 (Feb. 15, 1970).

Key words: Absorption; laser-excited fluorescence; mat isolation.

Absorption and laser-excited fluorescence spectra of Cu trapped in various matrices have been observed. The matrix da and previously observed gas-phase data are consistent with

| | $\nu_{00}$ (matrix) (cm$^{-1}$) | $\nu_{00}$ (gas)$^5$ (cm$^{-1}$) | $\nu$ (matrix) (cm$^{-1}$) | (cm$^{-1}$) |
|---|---|---|---|---|
| $C$ | | 23 550 | | |
| $B(^2\Sigma ?)$ | 20 490 | 20 953 | 624 | |
| $A(^2\Pi ?)$ | 3 900 | 4 460 | 605 | $(^2\Pi_{1/2}-{}^2\Pi_{3/2}=$ 2 |
| $X(^2\Pi)$ | 0 | 0 | 665 | $(^2\Pi_{1/2}-{}^2\Pi_{3/2}$ 2 |

for the lowest states of CuO. It is shown that the matrix-isolati technique can be used to "tune" an absorption into coincider with a laser line in order to observe fluorescence. The vibratio relaxation of CuO in a solid matrix requires on the order of vibrations.

12680. Shirk, J. S., Bass, A. M., **Laser-excited fluorescence matrix-isolated molecules,** *Anal. Chem.* **41,** No. 11, 103 107A (Sept. 1969).

Key words: Absorption; analytical methods; laser-exci fluorescence; matrix-isolation; molecular emission spect resonance fluorescence.

Matrix isolation and laser-excited fluorescence combined fo highly specific, sensitive analytical techniques. The meth have great potential in solving analytical problems.

12681. Swing, R. E., **Conditions for microdensitometer linear** *J. Opt. Soc. Amer.* **62,** No. 2, 199-207 (Feb. 1972).

Key words: Coherence; microdensitometer.

A simple microdensitometer system is analyzed using the pr ciples and analytical techniques of the theory of par coherence. A specification of the physical conditions un which the instrument is linear is obtained, for incoherent i mination. The illuminating mutual intensity is then generaliz by the Van Cittert-Zernike theorem, and conditions on the p tial coherence of the preslit illumination necessary for effect incoherence are determined. The new conditions determin mode of linear operation for the microdensitometer for which optical transfer function may be unambiguously defined.

12682. Tauber, S. J., Rankin, K., **Valid structure diagrams a chemical gibberish,** *J. Chem. Doc.* **12,** No. 1, 30-34 (1972).

Key words: Chemical structure diagrams; compu storage; display; geometric; grammar; input; labeled gra overlap; topological; validation.

Chemical structure diagrams are considered as utterances in a written language. Two types of grammars are considered for this language: topological grammars which emphasize the connectivity of the diagrams and geometric grammars which emphasize the arrangement of the diagrams in a plane. The vocabulary associated with each grammar consists of entities like atomic symbols, numeric subscripts, and bond symbols. Examples are given of initialization, propagation, and terminalization rules from each type of grammar and of the application of such rules. The value of grammars for the validation of computer input and for generation of computer output are indicated. The hypothesis is presented that compact computer storage may become accessible via grammars.

**12683.** Tech, J. L., **Annual Reports of Observatories (National Bureau of Standards) 1970/71,** *Bull. Amer. Astron. Soc.* **4,** No. 1, 136-139 (1972).

Key words: Atomic spectra; cross section; *f*-values; molecular spectra; photoionization; rare-earths; review; spectroscopy; transition probabilities.

Research activities of astrophysical importance carried out by workers at the National Bureau of Standards during the past year are reviewed. A bibliography of publications is also presented.

**12684.** Tilford, S. G., Ginter, M. L., Bass, A. M., **Electronic spectra and structure of the hydrogen halides. The $b\ {}^3\Pi_i$ and $C\ {}^1\Pi$ states of HI and DI,** *J. Mol. Spectrosc.* **34,** No. 2, 327-340 (1970).

Key words: Absorption spectra; electronic spectra; high resolution; hydrogen halides; molecular constants.

The absorption spectra of HI and DI below 1900 Å have been photographed at high resolution. Analyses of the "$B$" $\leftarrow X$ and $C \leftarrow X$ transitions show that the "$B$" state is the ${}^3\Pi_1$ component of a ${}^3\Pi_i$ state (designated here as $b$) and the $C$ state is a ${}^1\Pi$ state. Both $b\ {}^3\Pi_i$ and $C\ {}^1\Pi$ originate from the same $\pi^3\sigma$ configuration, exhibit strong predissociations, and show some small Case c effects. The transition from approximately $\Lambda$, $S$ toward $\Omega$, $\omega$ coupling is discussed for the $b$ and $C$ states of hydrogen halides, HCl, DCl, HBr, DBr, HI, and DI. Effective molecular constants are presented for the $b$ and $C$ states of HI and DI.

**12685.** Vidal, C. R., Haller, F. B., **Heat pipe oven applications. I. Isothermal heater of well defined temperature. II. Production of metal vapor-gas mixtures,** *Rev. Sci. Instr.* **42,** No. 12, 1779-1784 (Dec. 1971).

Key words: Absorption and fluorescent cell; heat pipe oven; metal vapor-gas mixtures.

A concentric heat pipe oven is described, which serves as an oven with a highly homogeneous temperature distribution as required by such applications as crystal growing, thermal treatment of materials, and radiation standards. The design is simpler than conventional ovens with similar temperature stability and homogeneity. The temperature control is replaced by a pressure control. This device is used in a modification of the heat pipe oven that generates homogeneous mixtures of a vapor (such as a metal vapor) and an inert gas at well defined total pressure, partial pressure, temperature, and optical path length. All the features of the previously described heat pipe oven are maintained with the additional option that allows quantitative total and partial pressure measurements without relying on vapor pressure curves.

**12686.** Weise, W., Huber, M. G., Danos, M., **A microscopic description of the $(\gamma, pn)$-reaction,** *Z. Physik* **236,** 176-191 (1970).

Key words: Cluster expansion; high momentum components; Jastrow wave function; photonuclear effect; quasideuteron effect; short range correlations.

The quasideuteron process has been investigated for photon energies 40 MeV $< E_\gamma <$ 160 MeV on the basis of a shell model picture modified by short range nucleon-nucleon correlations. It turns out that the cross section for the $(\gamma, pn)$-reaction depends sensitively on the details of the correlation function, i.e. on the exchange of high momenta between otherwise independently moving nucleons. The final state interaction has been consistently taken care of by using optical model wave functions for the outgoing nucleons. The results of the calculations for ${}^{16}$O indicate that precise measurements of the $(\gamma, pn)$ cross section do contain information on the properties of the nuclear wave functions for small internucleonic distances.

**12687.** Weitzel, D. H., Cruz, J. E., Lowe, L. T., Richards, R. J., Mann, D. B., **Instrumentation for storage and transfer of hydrogen slush,** (Proc. 1970 Cryogenic Engineering Conf., June 17-19, 1970, Colorado Univ., Boulder, Colo.), Chapter in *Advances in Cryogenic Engineering,* K. D. Timmerhaus, ed., **16,** Paper No. F-1, 230-240 (Plenum Press, Inc., New York, N.Y., 1971).

Key words: Density; flow; hydrogen; instrumentation; slush hydrogen.

A program for development and testing of density and flow instrumentation for use in hydrogen liquid and liquid-solid mixtures (slush) is reviewed. Performance criteria are indicated along with experimental and analytical results which provide some basis for choices among the various candidate systems. The density work is nearing completion; the flow studies have not yet provided data beyond the demonstration of feasibility.

**12688.** Carpenter, B. S., **Quantitative applications of the nuclear track technique,** (Proc. Inter/Micro 71 Conf., London, England, Sept. 17-24, 1971), *Microscope* **20,** 175-182 (1972).

Key words: Boron; glasses; image analyzing system; liver; microscopy; neutron activation analysis; nitrogen; nuclear track technique; orchard leaves; steels; track etch method; uranium.

The nuclear track technique has been used since the early 1960's as a means of mapping the location of uranium and boron concentration in several matrices and in geochronology. This technique has now been applied to the quantitative determination of several elements that emit charged particles. The detector sample "sandwich" is exposed to the desired radiation source, fast or thermal neutrons, or high energy photons, and the charged particles emitted are registered in plastic detectors. The elements boron, lithium, nitrogen, thorium and uranium have been determined in various matrices; *e.g.* liver, orchard leaves, tomato leaves, blood, glass, soil, steel and minerals. The amount of material in these matrices is determined in three different ways, the absolute method, the method of standard additions and the comparative method. All three of these methods require that the plastic detectors be chemically etched and the resulting optically visible tracks are then counted with the aid of an image analyzing microscope.

**12689.** Carpenter, B. S., LaFleur, P. D., **Observing proton tracks in cellulose nitrate,** *Int. J. Appl. Radiat. Isotop.* **23,** 157-159 (1972).

Key words: Activation analysis; cellulose nitrate detectors; nitrogen; nuclear track technique; proton tracks.

Cellulose nitrate is used as a detector to observe monoenergetic proton tracks. These monoenergetic protons are produced from a ${}^{14}$N source placed in contact with the detector and irradiated in a thermal-neutron flux. After irradiation the detectors are chemically etched to produce optically visible tracks.

**12690.** Clough, R. B., **Mobile dislocation density and velocity in plastically deformed aluminum at room temperature,** *Scr. Met.* **6,** No. 4, 293-298 (1972).

Key words: Aluminum; dislocation velocity; mobile dislocation density.

Recently, Gillis and Hockett have calculated the Gilman drag stress in commercially-pure aluminum as a function of strain and temperature, basing their calculations on a model of yielding by Gillis and Gilman. The purpose of this note is to show that the Gillis-Gilman model used cannot properly be applied to yielding in aluminum at constant strain rate because it leads to an improbable dislocation velocity-stress relationship. Another more satisfactory model is proposed, and in addition it is pointed out that the entropy of plastic flow in aluminum is significant at 300 K.

**12691.** Codling, K., Madden, R. P., **Resonances in the photoionization continuum of Kr and Xe,** *Phys. Rev. A* **4,** No. 6, 2261-2263 (Dec. 1971).

Key words: Autoionization; far ultraviolet; krypton; photoionization; resonances; xenon.

A total of 153 krypton resonances in the spectral region $500-337$ Å, and 254 xenon resonances in the spectral region $600-375$ Å are reported. The disposition of the detailed line lists are indicated. The analysis is very incomplete and will require detailed theoretical calculations to advance. In krypton, 45 resonances and in xenon, 56 resonances have been grouped into probable Rydberg series, for which classifications are suggested. In general, the resonances observed are due to the excitation of the inner subshell "*s*" electron $(ns^2np^6 \rightarrow nsnp^6mp)$ or to the excitation of two of the outer electrons simultaneously $(ns^2np^6 \rightarrow ns^2np^4mll')$. These high-lying excited states autoionize, resulting in resonances with window-, asymmetric-, and absorption-type profiles. The detailed lists for the subshell "*s*" electron excitations are given.

**12692.** Cooper, J. W., LaVilla, R. E., **"Semi-Auger" processes in $L_{23}$ emission in Ar and KCl,** *Phys. Rev. Lett.* **25,** No. 26, 1745-1748 (Dec. 28, 1970).

Key words: Argon; configuration interaction; KCl; radiative process; two-electron processes; x-ray $L_{23}$ emission.

X-ray emission studies in Ar and KCl due to formation of an $L_{23}$ vacancy reveal a low-energy satellite below the main emission peak. Comparison with other data on related processes indicates that this satellite is due to two-electron effects (configuration interaction) in the final state of the emission process.

**12693.** Coxon, B., **Application of internuclear, double-resonance techniques to carbohydrates. Detection of small coupling-constants,** *Carbohydrate Res.* **18,** No. 3, 427-442 (1971).

Key words: General Overhaus effect; internuclear double resonance; long-range coupling; magnetic equivalence factoring; spin-tickling; transient nutations; 6-deoxy-$\alpha$-D-glucofuranose derivative.

6-Deoxy-1,2:3,5-di-*O*-isopropylidene-$\alpha$-D-glucofuranose-$d_{12}$ (**1**-$d_{12}$) has been synthesized by an exchange reaction of its non-deuterated analog (**1**) with acetone-$d_6$. The p.m.r. spectrum of **1**-$d_{12}$ at 90 MHz has been analyzed iteratively by means of a computer program for magnetic-equivalence factoring. Confirmation of the assignments of lines in the analysis has been investigated by proton-proton, internuclear, double-resonance (indor) techniques, which served also for the detection of a small long-range coupling-constant. Examples of indor spectra containing general Overhauser effects, spin-tickling effects, or transient nutations are shown, and are discussed in relation to the experimental power-levels of the observing and double-resonance frequencies, and their sweep-rates. The mass spectra of **1** and **1**-$d_{12}$ are analyzed and compared.

**12694.** Dodge, W. R., Murphy, J. J., II, **Ratio of the $^4$He$(\gamma,p)$ and $^4$He$(\gamma,n)$ cross sections,** *Phys. Rev. Lett.* **28,** No. 13, 839-843 (Mar. 27, 1972).

Key words: Differential cross section; electrodisintegration; isospin; light nuclei; photonuclear; ratio cross sections.

The $^4$He$(\gamma,p)^3$H and $^4$He$(\gamma,n)^3$He cross sections have been determined with a magnetic spectrometer in the energy interval of 30.0 to 51.8 MeV. We find that the average value of $\sigma(\gamma,p)/\sigma(\gamma,n)$ is $1.03 \pm 0.04$ in the above energy interval. The $^4$He$(\gamma,p)$ cross section decreases from $1.52 \pm 0.13$ mb at 31.7 MeV to $0.36 \pm 0.03$ mb at 51.8 MeV.

**12695.** Durst, R. A., Staples, B. R., Paabo, M., **Activity standards for ion-selective electrodes,** *Experientia Suppl.* **18,** 275-279 (1971).

Key words: Activity standards; clinical pH; electrodes; ion-selective electrodes; pH; potassium chloride; sodium chloride; standards.

Ion-selective electrodes, like the pH glass electrode, are finding growing use in various biomedical studies for monitoring the activities of ions such as Ca$^{2+}$, Na$^+$, K$^+$, Cl$^-$, F$^-$, etc. As in the case of the pH electrode, standards are also required for the reliable application of these sensors to complex biological fluids. Research is in progress to establish ionic activity scales and reference materials to permit the accurate use of ion-selective electrodes for biological and medical studies. At the present time, these investigations are concerned with aqueous standards and will progress to studies of these ions in mixed electrolyte systems and synthetic and real biologic fluids.

Studies are concurrently in progress to certify clinical pH standard buffers based on the tris/tris · HCl system [tris = tris(hydroxymethyl)aminomethane]. This buffer has been exhaustively studied to establish its behavior over wide temperature ranges and buffer ratios.

The standard reference materials resulting from these studies will serve the all-important purpose of calibrating ion-selective electrode analyzer systems for use in many areas of science and technology.

**12696.** Eisen, H., Rosenstein, M., Silverman, J., **2.00-MeV electron depth-dose measurements in aluminum, copper and tin absorbers using a radiochromic dye film,** *Int. J. Appl. Radiat. Isotop.* **23,** 97-108 (Apr. 1972).

Key words: Absorbed energy; depth dose; electron energy deposition; radiation dosimetry.

The use of radiochromic dye films for electron dosimetry has been extended to absorbers with atomic numbers in the range $13-50$. The depth-dose profiles in slab targets of aluminum, copper, and tin irradiated by a plane parallel 2.00-MeV electron beam are presented for incident beams at 0, 30, and 60 degrees with respect to the surface normal. Absolute energy deposition per unit fluence was determined by using calibrated films, a fluence measurement, and a stopping-power ratio correction. The results are compared to the ionization measurements of Nakai and to the theoretical calculations of Berger and Seltzer; all agree within 10 percent. The stopping-power ratio, necessary to convert dose in the dye film to absorber dose at that point, is determined three ways and the results compared. The three techniques range from a detailed computer transport calculation yielding a variable stopping-power ratio with depth to the use of a constant stopping-power ratio obtained from tabulations. It is demonstrated that the use of the constant stopping-power ratio gives depth-dose distributions that differ by no more than 1-2 percent for aluminum, 3-5 percent for copper, and 4-8 percent for tin from the results obtained with the more rigorously evaluated stopping-power ratios.

**12697.** Fulmer, C. B., Toth, K. S., Williams, I. R., Handley, T. H., Dell, G. F., Callis, E. L., Jenkins, T. M., Wyckoff, J. M., **Photonuclear reactions in iron and aluminum bombarded with high-energy electrons,** *Phys. Rev. C* **2,** No. 4, 1371-1378 (Oct. 1970).

Key words: Aluminum; GeV electrons; iron; photonuclear; production cross sections; radioactivity; spallation.

Previously reported evidence for photofission of iron is investigated by a more extensive study. Thin foils of iron were bombarded with beams of 1.5-, 3-, 5-, and 16-GeV electrons. $\gamma$-ray spectroscopy and radiochemical measurements were used to measure yields of radionuclides produced in the targets. The yields of 25 nuclides were measured for the bombarded iron foils; these include eight nuclides in the mass region $22 \leq A \leq 35$. A thin aluminum target was bombarded with 16-GeV electrons, and the yields of seven radionuclides were measured. The yield of $^{24}$Na in a thick iron target was measured as a function of target thickness and compared with that of radionuclides produced by cascade-evaporation reactions. The experimental evidence obtained in this series of experiments indicates that nuclides of mass $< 35$ produced in the iron targets are the result of a fissionlike process. For cascade-evaporation reaction products, there is a decrease in the variation of yield with $\Delta Z$ as the bremsstrahlung energy is increased.

**12698.** Gebbie, H. A., Bohlander, R. A., **Nonresonant cavity as a long path absorption cell,** *Appl. Opt.* **11,** No. 4, 723-728 (Apr. 1972).

Key words: Absorption cell; far infrared; nonresonant cavity; spectroscopy.

We have constructed spherical specularly reflecting nonresonant cavities for use as absorption cells in far ir spectroscopy. A theory of their performance is developed and shown to be in agreement with experiment. An example is given of their use in a research program to ascertain the composition of water vapor. The essential advantage of these cells is that they give long pathlengths with high energy throughput.

**12699.** Geltman, S., **A high energy approximation: I. Proton-hydrogen charge transfer,** *J. Phys. B: At. Mol. Phys.* **4,** No. 10, 1288-1298 (Oct. 1971).

Key words: Coulomb wave; Born approximation; electron; excitation; high energy; hydrogen; large angle; theoretical.

The proton-hydrogen ground state charge transfer process is studied in a first order approximation in which the proton-proton interaction is treated as belonging to the unperturbed part of the problem. This results in the appearance of a Coulomb wave rather than a plane wave in the final state of the $T$ matrix. The result is a cross section which lies between the Brinkmann-Kramers and Jackson-Schiff results, with the high energy limit of $0.810\,\sigma_{BK}$.

**12700.** Hayward, E., Gibson, B. F., O'Connell, J. S., **Consequences of isospin sum rules for photonuclear reactions,** *Phys. Rev. C* **5,** No. 3, 846-852 (Mar. 1972).

Key words: Giant resonance; isoscalar; isospin; isotensor; isovector; photonuclear; sum rules.

Isospin sum rules for photonuclear reactions are derived; they relate the strengths of the two isospin components of the giant resonance to the isoscalar, isovector, and isotensor radii of the nucleus. The connection between these radii and both the number and correlations of excess neutrons is discussed. A semiempirical formula for the fraction of the dipole strength in the $T+1$ giant resonance is derived and various experimental data are discussed in the light of the results obtained using this equation.

**12701.** MacDonald, R. A., **Neutron scattering due to lattice distortion around point defects,** *J. Phys. F: Metal Phys.* **2,** 209-218 (Mar. 1972).

Key words: Anisotropic elastic continuum; coherent scattering; differential scattering cross-section; elastic scattering; isotropic elastic continuum; lattice; local force model; long wavelength; neutron scattering; point defects; vacancy.

The distortions calculated from four different models of a vacancy, one discrete lattice model, two anisotropic continuum models and one isotropic continuum model are used to calculate the differential cross section for coherent elastic scattering of long wavelength neutrons by a single vacancy in copper. The results of the local force anisotropic continuum model and the isotropic continuum model are distinctly different from those of the discrete lattice and nonlocal force anisotropic continuum models. The effect of the distortion around the vacancy on the differential scattering cross section extends to at least 600 neighbouring atoms.

**12702.** Moore, G. A., **Recent progress in automatic image analysis,** *J. Micros.* **95,** Pt. 1, 105-118 (Feb. 1972).

Key words: Analysis of microstructures; automatic image analysis; Gestalt of a material; microarchitecture; patternness; scanning microscopes; television microscopes.

The utility of computing devices in stereology is evaluated with regard to three objectives. (1) Computer terminals permit easy and rapid prediction of 2-dimensional measurement distributions characteristic of any mathematically defined spatial structure. (2) The materials engineer can be satisfied by description of a Gestalt which characterizes the material as a whole and which can reasonably be presumed to control the behavior of the material in service. Six stereologically valid parameters are sufficient to define such a Gestalt. These are: volume fraction ($V_V$), mean free path in the matrix ($\bar{l}_\alpha$), mean intercept width of particles ($\bar{l}_\beta$), and measures of material variability, general anisotropy, and degree of patternness. Current scanner models are intrinsically suitable for these measurements but will benefit from standardized data outputs and improvements to increase measuring accuracy. (3) Microarchitectural observations such as counting and measuring, or identifying, individual object sections are inefficient in ordinary computers. Large program effort is required for limited machine intelligence and operating speeds are unsatisfactory. These machine operations are not yet competitive with human observers. New hardware systems appear to be necessary to economically simulate human processes of image recognition. Some proposed systems will be mentioned.

**12703.** Oneal, G., Jr., Harris, W. P., **Three-terminal cell for thin film dielectric measurements,** (Proc. Electrical Insulation and Dielectric Phenomena, Buck Hill Falls, Pa., Oct. 20-22, 1969), Chapter in *1969 Annual Report of the Conference Electrical Insulation and Dielectric Phenomena,* pp. 164-170 (National Research Council, National Academy of Sciences, Washington, D.C., 1970).

Key words: Dielectric constant; dissipation factor; electrical measurements; FEP fluorocarbon; polyethylene terephthalate; thin films; two fluid.

A new design of dielectric test cell for measuring the dielectric constant and dissipation factor of a thin film has been built. The two fluid principle is used and agreement better than 1% in dielectric constant is obtained. Measurements on films as thin as 1.2 μm (50 gage) and frequencies as high as 1 MHz are practicable. A byproduct of the calculation is the average thickness of the sample. Results of measurements on films such as "FEP" fluorocarbon and polyethylene terephthalate will be presented.

**12704.** Newman, M., **2-Generator groups and parabolic class numbers,** *Proc. Amer. Math. Soc.* **31,** No. 1, 51-53 (Jan. 1972).

Key words: Fuchsian groups; parabolic classes; 2-generator groups.

It is shown that if $x$, $y$ are generators of the finite group $G$ such $x^p = y^q = (xy)^n = 1$, where $p$, $q$, $n$ are integers $> 1$, $(p, q) = 1$, and $xy$ is of true order $n$, then the order $\mu = nt$ of $G$ satisfies $n \leqq pqt^p$. This result is used to show that if $F$ is a Fuchsian group of genus 0 generated by 2 elliptic elements of coprime order and with 1 parabolic class, then $F$ possesses only finitely many normal subgroups having a given number of parabolic classes.

**12705.** Reichard, T. W., **Mechanical properties of insulating concretes,** Paper in *American Concrete Spec. Publ. SP 29, Lightweight Concrete,* pp. 253-316 (American Concrete Institute, Detroit, Michigan, 1971).

Key words: Cellular concrete; drying shrinkage; foam concrete; low density concrete; perlite concrete; thermal expansion; vermiculite concrete.

A description is given of a series of tests with insulating concretes of several types. The tests were designed to develop data for the purpose of determining: (1) Elastic properties and strength as a function of size and shape of specimen, curing method, density, and composition; (2) drying shrinkage; (3) thermally induced movements; and (4) the behavior of reinforced insulating concrete slabs under short-term and long-term loads.

Data are presented which show that although the relative strengths of various size specimens were affected by the curing method, the cubical specimen consistently showed a significantly higher strength than a cylindrical one with a height to diameter ratio of about two when their sizes are comparable.

There are significant differences in the drying shrinkages of 3 types of concretes and also in the shrinkages of the concretes made from the 3 brands of perlite.

**12706.** Reimann, C. W., **The single crystal spectra of dichlorotetrapyrazolenickel(II), dibromotetrapyrazolenickel(II), and hexapyrazolenickel(II) nitrate,** *J. Chem. Phys.* **74,** No. 3, 561-568 (Feb. 5, 1970).

Key words: Crystal spectra; pyrazole complexes; tetragonal molecular symmetry.

The single crystal spectra of hexapyrazolenickel(II) nitrate, dichlorotetrapyrazolenickel(II), and dibromotetrapyrazolenickel(II) from 6000 to 30,000 cm$^{-1}$ have been measured. The spectra of the halide complexes have been assigned on the basis of tetragonal molecular symmetry using the spectrum of hexapyrazolenickel(II) nitrate as a comparison. The tetragonal splittings in the first octahedral bands are considerably larger than observed in related complexes. These large splittings are related to low values of the effective *Dq* of the halide ions. Detailed crystallographic data are presented which show that the low effective field of the halide ions arises through an internal hydrogen bond interaction with the coordinated pyrazole molecules.

**12707.** Ritter, J. J., Coyle, T. D., Bellama, J. M., **Synthesis of ethynylboron halides,** *Chem. Commun.*, pp. 908-909 (1969).

Key words: Acetylenic boranes; ethynyldichloroborane; ethynyldifluoroborane; organoboron halides.

The first examples of organoboron halides containing acetylenic groups have been prepared and characterized. Ethynyldichloroborane, $HC_2BCl_2$, was obtained by irradiation of *cis*-bis(dichloroboryl)ethylene or trans-2-chlorovinyldichloroborane with a medium pressure mercury lamp (85% 2537 Å). The corresponding fluoride, $HC_2BF_2$, was prepared by the reaction of boron trifluoride with ethynyltrimethyltin. The compounds were characterized by infrared and mass spectroscopy and by cleavage of the ethynyl group with propionic acid to produce acetylene. In contrast to most known ethynylboranes, the new compounds are apparently stable as uncomplexed three-coordinate boron species.

**12708.** Roberts, J. R., Voigt, P. A., **The continuous emission from hydrogen at the bound-to-free transition regions,** *Proc. Xth Int. Conf. Phenomena in Ionized Gases, Oxford, England, Sept. 13-18, 1971,* p. 375 (1971).

Key words: Emission coefficient; hydrogen; hydrogen continuum; LTE; Stark broadening.

The continuous emission coefficient of a dense hydrogen plasma is appreciably modified by high density effects such as the lowering of the ionization potential and the merging of broadened higher lines to form a quasicontinuum. Close to a series limit, these effects become quite significant. A method for calculating the hydrogen emission coefficient near a series limit is proposed. The results of this method are in good agreement with the measured intensity distribution of a wall-stabilized hydrogen arc in the Balmer limit wavelength region of the spectrum.

**12709.** Rosenblatt, J. R., Filliben, J. J., **Randomization and the draft lottery,** *Science* **171,** 306-308 (Jan. 22, 1971).

Key words: Draft lottery; randomization; random numbers; random permutations.

Fifty "random permutations" were prepared for use by the Selective Service System as a basis for a two-stage randomization that preceded the lottery drawing on 1 July 1970. This report identifies the permutations used. It also gives the orders in which calendar dates and numbers were put into and drawn from two drums and the correlations between them.

**12710.** Rossmassler, S. A., **Federal information programs,** *Chem. Eng. Prog.* **67,** No. 11, 75-76 (Nov. 1971).

Key words: Chemical engineering information; data; information analysis centers; information systems; survey; technical information sources.

Many Federal Government programs can provide technical information and data useful to chemical engineers. Such material is available through government reports of completed work, professional journals, current project information systems, information analysis centers, specifications, the Patent Office, etc. Specialized information systems are evolving to make this information more accessible.

**12711.** Sengers, J. M. H. Levelt, Chen, W. T., **Vapor pressure, critical isochore, and some metastable states of $CO_2$,** *J. Chem. Phys.* **56,** No. 1, 595-608 (Jan. 1, 1972).

Key words: Burnett method; $CO_2$; coexistence curve; controlled clearance gage; critical exponent; critical isochore; critical region; metastable states pressure calibration; scaling law; vapor pressure.

An experimental method for obtaining precise *PVT* properties for gases in the critical region is described. Main features are absence of noxious volumes, small height of sample volumes, precise temperature control, and high pressure sensitivity. Some results are presented for $CO_2$. The 0 °C fixed point and the vapor-pressure curve have been measured and compared with literature values. Three liquid isochores including their metastable extensions into the two-phase region are also presented. The vapor-pressure data and pressures on the critical isochore above $T_c$ are compared with the predictions of the thermodynamic scaling law and with those of a recently proposed extension of scaling. The equation of extended scaling fits the data between −2 and 46 °C with a standard deviation of $1.5 \times 10^{-3}$ bar, for a "best" critical exponent $\alpha = 0.09$.

**12712.** Simmons, J. D., McDonald, J. K., **The emission spectrum of AlN,** *J. Mol. Spectrosc.* **41,** 584-594 (1972).

Key words: AlN; electronic spectrum; emission spectrum; high resolution; hyperfine broadening.

A new system of emission bands has been observed in the visible region of the spectrum. The bands exhibit the characteristic rotational structure of a $^3\Pi_i - {}^3\Pi_i$ electronic transition. Rotational analysis and isotopic studies of these bands indicate that the carrier of the spectrum is the species AlN. The rotational analyses of the (0 − 0) and (0 − 1) $Al^{14}N$ bands yield the following rotational constants, band origins, and lower state vibrational frequency $\Delta G''_{1/2}$

$$\nu_0\,(0-0) = 19727.37\ \mathrm{cm}^{-1};\ \nu_0\,(0-1) = 18980.44\ \mathrm{cm}^{-1};$$

$$B_0' = 0.5811\ \mathrm{cm}^{-1};\ B_0'' = 0.5702\ \mathrm{cm}^{-1};\ B_1'' = 0.5646\ \mathrm{cm}^{-1};$$

$$A_0' \cong -23\ \mathrm{cm}^{-1};\ A_0'' \cong -33\ \mathrm{cm}^{-1};\ A_1'' \cong -34\ \mathrm{cm}^{-1};$$

$$\Delta G''_{1/2} = 746.8\ \mathrm{cm}^{-1}.$$

The rotational analysis of the (0 − 0) $Al^{15}N$ band yields:

$$\nu_0\,(0-0) = 19727.13\ \mathrm{cm}^{-1};$$

$$B_0' = 0.5559\ \mathrm{cm}^{-1};\ B_0'' = 0.5454\ \mathrm{cm}^{-1};$$

$$A_0' \cong -21\ \mathrm{cm}^{1};\ A_0'' \cong -31\ \mathrm{cm}^{-1}.$$

An interesting pattern of sharp and broadened lines observed throughout the bands will be discussed in terms of unresolved nuclear hyperfine splittings.

**12713.** Taylor, J. K., Ed., Alvarez, R. A., Paulson, R., Rains, T. C., Rook, H. L., **Interaction of nitrilotriacetic acid with suspended and bottom material,** *Water Pollution Control Research Series 16020 GFR 07-71—Environmental Protection Agency (Progress Report)*, pp. 1-31 (July 1971).

Key words: Detergent; nitrilotriacetic acid; water pollution.

An experimental investigation was made of the possible interaction of residual concentrations of nitrilotriacetic acid in surface waters with metallic elements contained in sediments and bottom materials. Samples of bottom materials from typical bodies of surface waters were analyzed for their major, minor, and trace constituents. Eight representative samples of these were equilibrated with distilled water and with water containing 20 ppm of NTA and the resulting solutions were analyzed by three analytical techniques. Elements showing essentially no increased solubility in the presence of NTA were: barium, antimony, molybdenum, strontium, chromium, silver, tin, iron, lead, cadmium, copper, and mercury. Elements showing small increases in solubility were: nickel, zinc, manganese, and cobalt. Calcium and magnesium concentrations were increased somewhat above their normal relatively high concentrations.

This report was submitted in fulfillment of Project No. 16020 GFR under sponsorship of the Water Quality Office, Environmental Protection Agency.

**12714.** Thom, H. C. S., Marshall, R. D., **Wind and surge damage due to hurricane Camille,** *J. Waterways, Harbors, Coastal Eng. Div. Proc. Amer. Soc. Civil Eng.* **WW2,** No. 8144, 355-363 (May 1971).

Key words: Coastal engineering; damage; hurricanes; ocean waves; probability theory; storms; storm surges; wind.

The wind speeds in hurricane Camille are evaluated to provide a structural engineering interpretation. These are compared to published design winds for the area. Similar evaluation is made of the storm surge heights. A new method of probability analysis is applied to the historical surge data for Biloxi. Surveys of the storm and surge damage are considered with reference to actual wind speeds and design values in various parts of the storm area.

**12715.** von Busch, F., Dunn, G. H., **Photodissociation of $H_2^+$ and $D_2^+$: Experiment,** *Phys. Rev. A* **5,** No. 4, 1726-1743 (Apr. 1972).

Key words: $D_2^+$; experiment; $H_2^+$; ionization; photodissociation; vibrational state populations.

Measurements are reported of the cross sections for photodissociation of $H_2^+$ and $D_2^+$ at 21 wavelengths ranging from 2472 to 13,613 Å. The measurements are compared with theory using normalized Franck-Condon factors for the vibrational populations of the ions. Deviations are found, which are interpreted as a failure of this latter approximation. A least-squares analysis of the data yields vibrational-state populations different from simple Franck-Condon factors and alleged to be those characteristic high-energy electron-impact ionization of $H_2$ and $D_2$. Interpretation of the data using a mechanism requiring that a fraction of the ions formed by electron impact be generated via the autoionization channel can qualitatively lead to the observations of this experiment. However, such an explanation would require about 2/3 of all $H_2^+$ and $D_2^+$ to be formed via autoionization—a seemingly unrealistic requirement. Interpretation of the data in terms of a variation with internuclear separation of the electronic matrix element involved in the electron-impact ionization process shows that a matrix element varying as $Q_e(r) = 1 + 0.56(r_{a.u.} - 0.99)^2$ can lead to the experimentally deduced populations of both $H_2^+$ and $D_2^+$. This latter interpretation is favored, though one cannot rule out the former or some combination of the two. The data and interpretation are consistent with other related experiments.

**12716.** Scheer, M. D., Klein, R., **The addition of $O(^3P)$ to olefins. The nature of the intermediate,** *J. Phys. Chem.* **74,** 2732-2733 (1970).

Key words: Intermediate; olefins; oxygen atoms.

The currently available evidence, particularly that obtained at low temperatures, tends to support the Klein-Scheer planar intermediate for the reaction of ground state O atoms with olefins. This structure subsequently undergoes a set of concerted rearrangements in which a given group migration and oxygen atom localization occurs simultaneously to produce the final reaction products. Since electron spin is *not* conserved in the total reaction, the argument that a "triplet biradical" must first be formed before rearranging to singlet products is not compelling. The path by which the intermediate for this process rearranges to form the final products probably involves both energy and steric effects whose details have yet to be entirely elucidated. The spin relaxation process may ultimately prove to be only a minor barrier to the successful completion of these complex intramolecular rearrangements.

**12717.** Yakowitz, H., Ballantyne, J. P., Munro, E., Nixon, W. C., **The cylindrical secondary electron detector as a voltage measuring device in the scanning electron microscope,** *Proc. 5th An-*

*nual Scanning Electron Microscope Symp., ITT Research Institute, Chicago, Ill., Apr. 1972,* Part 1, pp. 33-40 (1972).

Key words: Computer aided design; contamination resters; electron trajectories; scanning electron microscopy; secondary electron detection; voltage contrast.

Voltage effects at a specimen surface have been investigated using secondary electron detectors in which several electrodes can be independently biased with respect to the specimen. Different electrode arrangements and bias conditions were tested. Electron trajectories and equipotentials within the cylindrical region were computed for various arrangements of electrodes and electrode bias values. Using these calculations, a detector of equal radius and height, 23mm, was built. With this detector conditions were found where the collected secondary electron current varied by over 30% per volt in the range $-5$ volts to $+8$ volts of specimen bias. Results for various conditions of electrode bias are given. The observed voltage response arises primarily from the spread of the electron trajectories as a function of secondary electron energy.

**12718.** Ballard, D. B., **Comparison and evaluation of specimens for resolution standard,** *Proc. 5th Annual Scanning Electron Microscope Symp., ITT Research Institute, Chicago, Ill., Apr. 1972,* Part 1, pp. 121-128 (1972).

Key words: Resolution; resolution specimens; secondary emission; SEM; specimen criteria.

A need exists for resolution test specimens for the SEM. The criteria for such specimens are restrictive and depend on various electron beam-specimen interactions. These criteria include, secondary emission, contrast, low contamination, beam and vacuum resistance, variable spacing, tapered edges, coating, rigid structure, beam deflection, vacuum cleanliness, known surface topography, use and storage, cost and availability, and stigmator adjustment.

Some of the commonly used specimens to demonstrate resolution are silver, iron oxide, gold deposit, aluminum-tungsten alloy, pearlite, gallium arsenide-gallium arsenide phosphide, thoria, osmium tetraoxide crystals, graphite, magnetic recording tape, zinc oxide, opal, latex spheres and marine micro-fossils. No single sample meets all the criteria though the finely spaced dendritic structure of the metallic Al-W sample satisfies most specimen requirements except for independent magnification calibration. An accurate magnification standard is now required so that resolution of a particular SEM can be determined accurately.

**12719.** Rosenstein, M., McLaughlin, W. L., Silverman, J., **Energy deposition of electron beams in insulating materials,** (Proc. 4th Int. Conf. on Electron and Ion Beam Science and Technology, Los Angeles, Calif., May 1970), Chapter in *Electron and Ion Beam Science and Technology, 4th International Conference,* R. Bakish, ed., pp. 591-604 (The Electrochemical Society, New York, N.Y., 1970).

Key words: Charge deposition; depth dose; dielectrics; dose distribution; dosimetry; dye film dosimeter; electron beams; polystyrene; radiochromic dye.

Experimental depth-dose curves were obtained for semi-infinite thicknesses of ordinary and conducting polystyrene, irradiated in air by a 1.5-MeV electron beam in the dose range 5 to 20 Mrad. Radiochromic dye films were used as spatial dosimeters. By using a calibration of optical density versus dose, a microdensitometric reading of the irradiated dye films gave continuous depth-dose curves. No difference was observed between the depth-dose curves for the ordinary polystyrene and conducting polystyrene at absorbed dose rates between 2.5 and 10 Mrad/min. Within the limits of uncertainty for the present experiment, the results are in agreement with theoretical and experimental depth-dose data for 1.5-MeV electrons in polystyrene. Under the conditions studied, trapped charge does not measurably perturb the energy deposition of electrons in polystyrene.

**12720.** Powell, C. J., **Structure on the high-energy side of the $KL_{23}M$ Auger peak from solid aluminum: Internal photoemission,** *Appl. Phys. Lett.* **20,** No. 9, 335-337 (May 1, 1972).

Key words: Aluminum; Auger-peak; secondary-electron energy distribution; x-ray photoemission.

Some weak structure on the high-energy side of the $L_{23}MM$ Auger peaks for Al and Si has been recently interpreted as being possibly due to the simultaneous decay of an inner-shell vacancy and a volume plasmon. It is shown here that similar structure due to multiple ionization is to be expected and that photoemission caused by internally generated x rays can be observed if the fluorescent yield is not too small. Relatively strong structure of the latter type has been observed in the secondary-electron energy distribution of evaporated Al on the high-energy side of the $KL_{23}M$ Auger peak.

**12721.** Carter, G. C., Weisman, I. D., Bennett, L. H., Watson, R. E., **The $AuAl_2$-$AuGa_2$-$AuIn_2$ problem: Knight shifts and relaxation times in their pseudobinary alloys,** *Phys. Rev. B* **5,** No. 9, 3621-3638 (May 1, 1972).

Key words: Alloys; aluminum; gallium; gold; indium; intermetallic compound; Knight shift; relaxation time; soft x-ray spectroscopy; x-ray photoemission spectroscopy.

The nuclear-magnetic-resonance (NMR) and susceptibility behavior of the intermetallic compound $AuGa_2$ differs anomalously from the isoelectric and isostructural compounds $AuIn_2$ and $AuAl_2$. In an effort to test and extend the explanation offered by Jaccarino et al. and by Switendick and Narath, spin-lattice relaxation times and Knight shifts have been measured as a function of temperature and composition for the $AuAl_2$-$AuGa_2$, $AuAl_2$-$AuIn_2$, and $AuGa_2$-$AuIn_2$ pseudobinary alloy systems. At high temperature, the solute $X$ (Al, In, Ga) resonance properties are dominated by the host. Satellite resonances are observed with temperature dependences differing from the main resonance. The results are partially explainable on the basis of an average-band model and partially on a local atom model. The role of the Au *d* bands is discussed. Metallurgical results on alloying are obtained using the NMR data.

**12722.** Shapiro, H. M., Bryan, S. D., Lipkin, L. E., Stein, P. G., Lemkin, P. F., **Computer-aided microspectrophotometry of biological specimens,** *Exp. Cell Res.* **67,** No. 1, 81-89 (July 1971).

Key words: Cytochemistry; histochemistry; image processing; laboratory automation; microscopy; spectrophotometry.

A scanning microspectrophotometer controlled by a small digital computer is used to produce data which is analysed using a larger, remote digital computer. Programs have been written for the smaller machine to permit automatic scanning of a large number of preselected fields. Other programs, written for the larger machine, enable the experimenter to pick out cells in a scan field and measure their size and optical density, or automatically locate and measure cells within a scan field, and generate statistical analyses of size and optical density measures for a number of cells. The further implications of this work for cytochemistry are discussed.

2723. Semmelroth, C. C., **Adjustment of the Munsell-value and $W^*$-scales to uniform lightness steps for various background reflectances,** *Appl. Opt.* **10,** No. 1, 14-18 (Jan. 1971).

Key words: Background effect; Munsell-value; reflectance.

For background reflectances taken equal to, or slightly lower han, the specimen reflectances, the Munsell-value, *V*, and the CIE 1964, $W^*$, scales are found to be essentially linear with a power formulation for lightness previously shown to accord with ghtness-spacing data for a wide variety of specimen and background reflectances. Adjustments required to make the Munsell-value function accord precisely with the power formulation for this background condition are all less than 0.2 of a Munsell-value step between 1/ and 9/. The power formulation is used to construct a table to show in Munsell terms the influence of background reflectance on perceived lightness for all combinations of specimen and background reflectance including Takasaki crispening for specimen reflectance approaching that of the background.

2724. Bender, P. L., Dicke, R. H., Wilkinson, D. T., Alley, C. O., Currie, D. G., Faller, J. E., Mulholland, J. D., Silverberg, E. C., Plotkin, H. H., Kaula, W. M., MacDonald, G. J. F., **The lunar laser ranging experiment,** (Proc. Conf. on Experimental Tests of Gravitational Theories, Pasadena, Calif., Nov. 1970), *JPL Technical Memo* **33-499,** pp. 178-181 (Jet Propulsion Laboratories, Pasadena, Calif., Nov. 1971).

Key words: Gravity; laser; lunar motion; moon; relativity.

The emplacement of the Apollo II retro-reflector package on the lunar surface has made possible very accurate measurements f the lunar distance. A continuing program of range measurements to the package at nearly all phases of the moon is being arried out by the McDonald Observatory under NASA support. Returned signals have also been obtained by the Pic du Midi Observatory in France and by the AFCRL Lunar Laser Observatory near Tucson, Arizona. It is hoped that several other unar ranging stations will be in operation within the next year or wo, including ones in Japan, Hawaii, Russia, and the southern emisphere.

2725. Semmelroth, C. C., **Prediction of lightness and brightness on different backgrounds,** *J. Opt. Soc. Amer.* **60,** No. 12, 1685-1689 (Dec. 1970).

Key words: Color; vision.

Two psychophysical responses to surface or self-luminous timuli are hypothesized. A response to the luminance of the stimulus ($\alpha$) and a response to the luminance difference between he stimulus and its surround ($\beta$) are both considered to be power unctions. Lightness or brightness is taken to be an additive or ubtractive combination of these two responses ($\alpha \pm K\beta$) depending on whether the surround is darker or brighter than the timulus, respectively. This model is shown to produce a quantitatively adequate explanation of Takasaki's data on crispening. An attempt is made to use this formulation to fit scaling data rom previous magnitude-estimation and partitioning studies of ghtness and brightness in which different results have been obtained from different backgrounds. Data from matching experiments that involve different backgrounds for the comparison and tandard stimuli are also analyzed by means of the same formulaion. The model is compared with the Adams – Cobb – Judd formulation of background effect on lightness, the Takasaki empirical formula for crispening, and Stevens's power-law formulation or brightness and lightness.

2726. Mahler, R. J., Phelan, R. J., Jr., Cook, A. R., **High $D^*$, fast, lead zirconate titanate pyroelectric detectors,** *Infrared Phys.* **12,** 57-59 (1972).

Key words: Infrared; pyroelectric; room temperature detector.

Large area PZT detectors with $D^*$ (500 K, 1, 1,) $= 7 \times 10^8$ cm $\text{Hz}^{1/2}$/W and fast detectors with a response time of at least 5 nsec have been fabricated. The pyroelectric coefficient of 27 nC/cm$^2$ K and a materials figure of merit of $2.8 \times 10^{-9}$ C cm/J have been measured for these devices.

12727. Mulholland, J. D., Alley, C. O., Bender, P. L., Currie, D. G., Dicke, R. H., Faller, J. E., Kaula, W. M., MacDonald, G. J. F., Plotkin, H. H., Wilkinson, D. T., **Preliminary results of laser ranging to a reflector on the lunar surface,** (Proc. 13th Plenary Meeting of COSPAR, Leningrad, May 1970), *Space Research XI,* 97-104 (Academie-Verlag, Berlin, 1971).

Key words: Celestical mechanics; geophysics; laser; lunar ephemeris; selenology.

The first Lunar Ranging Experiment (LURE) retroreflector array was placed on the lunar surface during the Apollo 11 mission. Prior to this event, a special high-precision lunar ephemeris (designated LE 16) was developed by means of a composite numeric/analytic process, so as to provide more accurate predictions for use at the telescope. First returns were observed at the Lick Observatory on 1 August 1969 and at the McDonald Observatory shortly thereafter. The observing program is to continue for several years. Preliminary use of these data consists of their comparison with the LE 16 ephemeris, preparatory to a differential correction of the lunar elements. Present indications are that the ephemeris must undergo order-of-magnitude improvements before the full power of the laser data can be utilized. Other parameters in the predictive process are also capable of being corrected; an improvement in the coordinates of the Lick Observatory 120-inch telescope is already indicated.

12728. Sengers, J. V., **Triple collision effects in the transport properties for a gas of hard spheres,** (Proc. Symp. on Kinetic Equations, Cornell University, Ithaca, N.Y., 1969), Paper C-1 in *Kinetic Equations,* R. L. Kiboff and N. Rostoker, eds., pp. 137-193 (Gordon and Breach, New York, N.Y., 1971).

Key words: Collision integrals; hard spheres; thermodynamic conductivity transport properties; triple collisions; viscosity.

A study is made of the effect of successive correlated binary collisions on the transport properties of gases. In particular, triple collision transport integrals are derived for the thermal conductivity and viscosity of a gas of hard spheres. Preliminary numerical estimates for these collision integrals allow us to make an assessment of the contributions from the various triple collision events.

12729. Danos, M., **Baryon resonances in the nuclear ground state: How about double counting?,** (Proc. 3d Int. Conf. High-Energy Physics and Nuclear Structure, Columbia University, New York, N.Y., Sept. 7-12, 1969), Chapter in *High-Energy Physics and Nuclear Structure,* pp. 811-815 (Plenum Press, New York, N.Y., 1970).

Key words: Baryon resonances; exchange currents; nuclear magnetic moments; nucleons; $\pi$-mesons; relativistic nuclear physics.

In a relativistic treatment of nuclei one encounters serious problems of double or multiple counting. They are associated with the existence of baryon and meson resonances. A procedure is described for overcoming these difficulties.

12730. Flynn, D. R., **Considerations in launching effective noise control programs,** (Proc. EASCON 1971 Conf., Oct. 6-8, 1971, Washington, D.C.), *IEEE Trans. Aerosp. Electron. Syst.*, pp. 53-59 (Nov. 1971).

Key words: Acoustics; environmental control; measurement; noise; pollution; sound.

Measurement plays a pervasive role in assessing the consequences of noise, its effects and control. Both the assessment of noise problems and the assessment of alternative strategies for noise abatement and control ultimately rest on accurate, reliable, and relevant measurement capability. Accurate measurement is required in order to ascertain the effects of a given noise exposure, to establish trends in noise exposure, to permit selection of cost-effective solutions, to monitor the effectiveness of control programs, and to provide the factual (measurement) basis for legal regulation. While considerable information is presently available regarding measurement and monitoring of noise, further work which will lead to more accurate or less expensive measurement methods is clearly needed. This paper will include a brief discussion of the research needs in assessment of the effects of noise on people, in characterization of the noise generation or transmission characteristics of various products or systems, and in development of meaningful correlations between noise exposure and the related human responses.

**12731.** Nimeroff, I., **The psychology of color,** *Amer. Paint J.*, pp. 65-70 (Jan. 11, 1971).

Key words: Color aesthetics; color vision; psychology of color.

In recent years there has been an increase in the attention that is being given by scientists, particularly psychologists, to a field of study called "the psychology of color." Selected language that associates color with emotions, with neuroses and psychoses, with health and illness, with human endeavors, with aesthetics, and the like, are some of the topics that have been and are being studied. Some of these studies are reported here. The mental associations with color present a practical difficulty in that there is such great disparity in language usage and association among individuals and among groups of people. Other topics, more subject to conventional quantitative study, are also related to psychological effects of color. These include: uniform color spacing, color harmony, color naming or ordering, and color metamerism. If we can gather sufficient information about the psychology of color and the color of man's environments, we may look forward to a time when we can devise ideal decor for living and working quarters.

**12732.** Yule, H. P., **Study of gamma-ray spectrum distortion by mathematical smoothing,** *Anal. Chem.* **44,** No. 7, 1245-1249 (June 1972).

Key words: Digital data smoothing; digital filtering; distortion; gamma-ray spectra; mathematical smoothing.

Removal of statistical scatter from gamma-ray spectra is a considerable aid in the computerized reduction of spectral data. Application of mathematical filters to the data may result in erroneous results due to distortion introduced by the filter. Such distortion is often difficult to detect and even more difficult to measure. In the present paper, repeated filtering, or smoothing, is applied to different spectral situations to obtain indications of the amount of distortions introduced by smoothing. It is concluded that filtering one time, the usual number of smoothing, introduces little distortion in most cases, although overlapping peaks may suffer some distortion.

**12733.** Rook, H. L., Gills, T. E., LaFleur, P. D., **Method for the determination of mercury in biological materials by neutron activation analysis,** *Anal. Chem.* **44,** No. 7, 1114-1117 (June 1972).

Key words: Activation analysis; biological; environment; mercury; Standard Reference Material.

A method is described for the determination of mercury in a variety of matrices. Three significant improvements over currently used procedures have been achieved: The procedure has a minimum of chemical manipulations, thereby minimizing technique related errors; the radiomercury separation is quantitative, thus eliminating unnecessary errors involved in the determination of chemical yields; the procedure is based on a simple combustion separation of radiomercury allowing the same technique to be used on a wide variety of matrices. The method was tested using radiotracer experiments and by analyzing samples of flour and coal which had been independently analyzed. The procedure has been subsequently used to determine the mercury concentration of two new Standard Reference Materials being offered by the National Bureau of Standards.

**12734.** Rook, H. L., **Rapid, quantitative separation for the determination of selenium using neutron activation analysis,** *Anal. Chem.* **44,** No. 7, 1276-1278 (June 1972).

Key words: Biological; neutron activation analysis; selenium; standard.

The role selenium plays in the biochemistry of higher animals is complex and as yet, ill defined. A prerequisite for definitive studies is a sensitive, accurate analytical procedure for selenium. Relatively few analytical techniques fulfill both criteria of sensitivity and accuracy in biological and environmental matrices. This work describes a simple, effective method for the determination of selenium by neutron activation analysis using a combustion separation of volatile elements followed by liquid nitrogen freezing.

**12735.** Yates, J. T., Jr., Madey, T. E., **The adsorption of methane by tungsten (100),** *Surface Sci.* **28,** 437-459 (1971).

Key words: Adsorption; field emission; methane; physical adsorption; single crystal; tungsten; work function.

The adsorption of methane by the (100) plane of tungsten has been studied using flash desorption and work function methods. It has been found that $CH_4$ adsorbs to appreciable coverage as an undissociated molecular species at ~ 100 K. The activation energy for first order desorption from this state is 6.9 kcal/mole (0.30 eV/molecule). This observed binding energy is greater than expected for dispersion forces alone, and added contributions to the binding energy are discussed. An observed work function of − 0.34 eV on adsorption of $CH_4$ is consistent with the presence of a physically adsorbed $CH_4$ layer.

Related studies of $CH_4$ adsorbed on a tungsten field emission tip demonstrate that adsorption of $CH_4$ proceeds rapidly at 77 K, but is negligible at 300 K. At tungsten temperatures above 1200 K in $10^{-5}$ torr of $CH_4$, decomposition of the $CH_4$ to form a carbon layer occurs.

It is postulated that at elevated temperatures and at high $CH_4$ pressures the physically adsorbed state may be sufficiently populated to serve as a source of adsorbed $CH_4$ species which undergo activated surface decomposition, leading eventually to surface carbides.

**12736.** Madey, T. E., **Adsorption and displacement processes on W(111) involving $CH_4$, $H_2$, and $O_2$,** *Surface Sci.* **29,** 571-589 (1972).

Key words: Binding energy; chemisorption; displacement; hydrogen; methane; oxygen; tungsten; work function.

Adsorption and displacement processes involving $CH_4$, $H_2$, and $O_2$ on the (111) surface of tungsten have been examined using the thermal desorption method in conjunction with mass spectrometry and work function changes. Methane is physically adsorbed on W(111) at $T \sim 125$ K and desorbs with a binding energy of 8.0 kcal/mole. Neither adsorption nor decomposition of $CH_4$ is observed at 300 K on W(111). Hydrogen is chemisorbed on W(111); 4 atomic binding states having desorption energies from 12 kcal/mole to 31 kcal/mole are observed. The influence of oxygen on the binding of both $H_2$ and $CH_4$ has been examined. Oxygen specifically blocks the adsorption of certain hydrogen binding states; oxygen causes an increase in the $CH_4$ binding energy to ~ 10 kcal/mole. Coadsorption of hydrogen and $CH_4$ also exhibits site specificity.

2737. Comeford, J. J., **The spectral distribution of radiant energy of a gas-fired radiant panel and some diffusion flames,** *Combust. Flame* **18,** 125-132 (1972).

Key words: Diffusion flames; emission spectra; flame spectra; infrared spectra; radiant test panel; radiant test sources.

Measurements were made of the spectral distribution of energy from radiant sources employed in standard test methods of flammability. Radiant sources examined were a gas-fired radiant panel employed in ASTM Test E-162 and the electric heater employed in the Smoke Chamber Test. To afford a basis for comparison, the emission spectra of several diffusion flames in air were measured. The energy distribution of the flames occurred essentially in two narrow wavelength intervals corresponding to emission of carbon dioxide at 4.4 μm and water at 2.7 μm. Luminous diffusion flames containing large amounts of incandescent carbon, such as occur from the combustion of acetylene-in-air, show a blackbody background continuum with $CO_2$ and $H_2O$ emission peaks superimposed on the continuum. The radiant test sources exhibited an energy distribution approximating that of a blackbody with atmospheric $CO_2$ and $H_2O$ absorptions superimposed. The gas-fired radiant panel in addition showed a significant emission peak at 4.4 μm due to excited $CO_2$.

2738. LaVilla, R. E., **$K\alpha$ emission spectrum of gaseous $N_2$,** *J. Chem. Phys.* **56,** No. 5, 2345-2349 (Mar. 1, 1972).

Key words: Electron bombardment; lead myristate analyzing crystal; M. O. correlation; nitrogen $K$ emission spectrum; resonance radiation; x-ray emission.

The nitrogen $K\alpha$ emission spectrum excited by electron bombardment of nitrogen gas was obtained on a single planar crystal spectrometer with photon counting. The experimental profile is in fair agreement with a calculated profile based on molecular orbital theory and the single vacancy states measured by x-ray photoelectron spectroscopy. Evidence is presented to suggest that some of the emission intensity on the high-energy side of the main peak is due to "resonance radiation." To fix the energy scale of the spectrum, the effective $2d$ spacing of the analyzing lead myristate crystal was experimentally determined.

2739. Okabe, H., **Photodissociation of $OSCl_2$ in the vacuum ultraviolet; the heat of formation of SO,** *J. Chem. Phys.* **56,** No. 7, 3378-3381 (Apr. 1, 1972).

Key words: Heat of formation; $OSCl_2$; photodissociation; SO; vacuum ultraviolet.

The photodissociation of $OSCl_2$ at the Kr (1165-, 1236-Å) lines has resulted in the production of SO $A\ {}^3\Pi$, $B\ {}^3\Sigma$. The threshold energy of incident photons to produce the reaction,

$$OSCl_2 \xrightarrow{h\nu} SO A\ {}^3\Pi_0 + 2Cl\,{}^2P_{3/2},$$

was 9.41 ± 0.03 eV from which $\Delta H_{f0}°(SO) = 1.3 \pm 0.7$ kcal/mole is derived. The $I_f/I_0$-vs-incident wavelength curve shows many diffuse bands found in the absorption spectrum of $OSCl_2$ indicating that the process is predissociative. Various other methods to obtain $\Delta H_{f0}°(SO)$ are compared. It is concluded that the best value is $1.3 > \Delta H_{f0}°(SO) > 0.8$ kcal/mole.

12740. Stephenson, N. C., Roth, R. S., **The crystal structure of the high temperature form of $Ta_2O_5$,** *J. Solid State Chem.* **3,** 145-153 (1971).

Key words: Crystallographic shear; crystal structure; high temperature $Ta_2O_5$; nonstoichiometric.

The structure of the high temperature form of $Ta_2O_5$ can be stabilized by doping with 2 mole%$Sc_2O_3$ and single crystals have been prepared from a $Ta_2O_5-Sc_2O_3$ (98:2) composition by the Czochralski technique. The crystal system which at first appeared to be body-centered tetragonal has been determined to be face-centered monoclinic, space group $C2$ with $a = 35.966$ Å, $b = 3.810$ Å, $c = 3.810$ Å, $\beta = 96°7'$. Least-squares refinement cycles reduced the reliability index $R$ to 0.089.

The structure consists of $\alpha UO_3$-type blocks in which each tantalum atom is surrounded by a pentagonal bipyramid of oxygen atoms. These blocks are infinite in two directions and are separated from similar blocks along a third direction by shear planes. In the vicinity of these shear planes the tantalum atoms are surrounded by distorted octahedral coordination polyhedra. It is believed that the stabilizing effect of the $Sc_2O_3$ impurity is due to an increase in the concentration of shear planes. Random shear planes (Wadsley defects) are introduced at approximately 300 Å intervals along the large axis by doping with a substance ($Sc_2O_3$) which has cations (Sc) large enough to substitute for the host (Ta) but a lower oxygen:metal ratio than the host compound ($Ta_2O_5$).

12741. Schrack, R. A., Heaton, H. T., II, Schwartz, R. B., **Suppression of after-pulsing in the type 58AVP photomultiplier,** *Nucl. Instr. Methods* **77,** 175-176 (1970).

Key words: After-pulse; gamma flash; neutron; photomultiplier; pulse; time-of-flight.

A technique for eliminating the after-pulse observed in photomultipliers after intense light pulses is described.

12742. Thompson, B. A., Lutz, G. J., **Characterization of ancient bronze artifacts by neutron and photon activation analysis,** *Radiochem. Radioanal. Lett.* **9,** No. 5-6, 343-350 (Mar. 1972).

Key words: Archeological materials; bronze; neutron activation analysis; nondestructive analysis; photon activation analysis.

Concentrations of nine major and minor constituents have been determined in samples of two ancient bronze artifacts using neutron and photon activation analysis. The analysis was carried out without chemical separation on 10 mg samples of the material. The results demonstrate the unique capability of nuclear methods for the analysis of small portions of artifacts in archeology.

12743. Seltzer, S. M., Berger, M. J., **Response of NaI detectors to high-energy gamma rays,** *Trans. Amer. Nucl. Soc.* **14,** No. 1, 124-125 (June 1971).

Key words: Detector; electron; gamma ray; Monte Carlo; response function; sodium iodide.

The response of NaI detector to high energy gamma rays has been calculated and compared with experimental results. The calculation takes into account the escape of energy carried by electron, positron and bremsstrahlung.

12744. Sanchez, I. C., DiMarzio, E. A., **Dilute-solution theory of polymer crystal growth. Some thermodynamic and predictive aspects for polyethylene,** *Macromolecules* **4,** 677-687 (Nov.-Dec. 1971).

Key words: Activity; chain fold; cilia; equilibrium dissolution temperature; equilibrium melting temperature; free energy of crystallization; lamella thickness; nucleation rate; surface free energy; undercooling.

The kinetic theory of polymer crystallization from dilute solution is applied to the system polyethylene-xylene. Prerequisite free energy driving forces are derived for crystallization from solution. These naturally depend on bulk thermodynamic properties and three thermodynamic potentials are derived depending on what melt and crystalline properties are assumed. The commonly used $\Delta H \Delta T/T_m^0$ expression is shown to be an upper bound for all materials and a more accurate expression descriptive of polyethylene is used in the actual calculations. Growth rate and lamella thickness are computed as functions of undercooling, concentration, and molecular weight. It is found that the growth rate varies roughly as concentration raised to a power, the value of the power being a function of both molecular weight and temperature. The isothermal lamella thickness increases only slightly with decreasing molecular weight and is even less dependent on concentration. The isothermal growth rate as a function of molecular weight exhibits a broad maximum. An analysis of the temperature dependence of the growth rate is made in terms of classical nucleation theory using calculations of the present theory as data points. This leads to the concept of an apparent $\sigma\sigma_e$ which is seen to vary as a function of molecular weight. The theory makes definitive, as yet unverified, predictions which can be tested experimentally.

**12745.** Garvin, D., Evans, W. H., Duncan, B. C., **Some information processing techniques for the small, semi-automated, scientifically-oriented data center,** (Proc. Forum on the Management of Information Analysis Centers, National Bureau of Standards, Gaithersburg, Md., May 17-19, 1971), Chapter in *The Management of Information Analysis Centers,* W. A. Smith, ed., **72-1,** 40-57 (Sponsored by The COSATI Panel Information Analysis Centers, U.S. Atomic Energy Commission, Oak Ridge, Tenn., Publ., Jan. 1972).

Key words: Chemistry; codes for information interchange; editing; information analysis centers; information processing; information retrieval; text handling.

Solutions are presented for several of the problems encountered in handling scientific text in machine-readable form in small data centers. The problems discussed are the selection of an adequate character set for representation of scientific text, the essential and useful features of editing routines, and batch-mode information retrieval.

**12746.** Bridges, J. M., Richter, J., **Arc measurements of Fe I oscillator strengths with improved accuracy,** *Proc. Xth Int. Conf. on Phenomena in Ionized Gases, Oxford, England, 1971,* p. 384 (Donald Parsons and Company, Ltd., Oxford, England, 1971).

Key words: Arc; *f*-values; iron; oscillator strengths; wall-stabilized.

Measurements of relative Fe I *f*-values have been performed with greatly improved accuracy over similar previous measurements. The lines are measured in emission from a wall-stabilized argon arc, containing admixtures of $FeCl_3$ and hydrogen. Recent modifications of the arc allow better control over the iron density, and lead to improved accuracy in relative intensity measurements as well as in plasma diagnostics required for determination of the arc temperature. Results for some selected lines are given, and the program for further measurements is discussed.

**12747.** Scheer, M. D., Fine, J., **The positive and negative self-surface ionization of tantalum,** Chapter 39 in *The Structure and Chemistry of Solid Surfaces,* G. A. Somorjai, ed., pp. 39-1–39-15 (John Wiley & Sons, Inc., New York, N.Y., 1969).

Key words: Electron affinities; self-surface ionization; singly charged positive and negative atomic ions; sublimation energies; tantalum.

The sublimation of atoms, singly charged positive, and negative atomic ions of tantalum has been investigated in the 2000-2600 K temperature range with a specially designed mass spectrometer. It was shown that carbon contamination of the tantalum surface could account for the discrepancies previously reported for the energies of atom sublimation. Measurements made on a carbon-free tantalum surface gave values of $7.94 \pm 0.09$, $11.18 \pm 0.11$ and $11.2 \pm 0.5$ eV for the sublimation energies of atoms, positive, and negative ions, respectively. The electron affinity of tantalum was found to be $0.9 \pm 0.3$ eV. These sublimation processes were shown to be consistent with the assumption of thermal equilibration on the tantalum surface and hence can be described by a generalized form of the Saha-Langmuir equation.

**12748.** Milligan, D. E., Jacox, M. E., **Infrared and ultraviolet spectroscopic studies of free radicals and molecular ions isolated in inert solid matrices,** Paper in *Molecular Spectroscopy Modern Research,* pp. 259-286 (Academic Press, Inc., New York, N.Y., 1972).

Key words: Alkali metal reactions; cage effect; flash photolysis; free radicals; infrared spectrum; matrix isolation molecular ions; molecular orbitals; photolysis; ultraviolet spectrum.

The principles of the matrix isolation technique are reviewed and results of experiments leading to the stabilization of free radicals in inert solid matrices in concentration sufficient for direct infrared and ultraviolet spectroscopic observation are surveyed. Emphasis is placed on the correlation of the matrix data with data obtained in gas-phase flash photolysis studies. Conclusions regarding the structure and bonding of these species are compared with the predictions of simple molecular orbita theory. Recent results on the infrared and ultraviolet spectra o the $C_2^-$, $NO_2^-$, and $ClHCl^-$ ions isolated in an inert, non-ionic environment are also presented.

**12749.** Moore-Sitterly, C., **Committee 4: Structure of atomic spectra,** (Commission 14, International Astronomical Union Report), *Trans. I.A.U.* **14A,** 133-137 (1970).

Key words: Atomic spectra; spectra, atomic; structure atomic spectra.

The present paper is a review of current work on the genera subject of analysis of atomic spectra. It deals briefly with programs that are in progress, vacuum UV spectra, rare-earth spectra and theory. A useful bibliography is included.

**12750.** Swanson, N., Kuyatt, C. E., Cooper, J. W., Krauss, M. **Alternative decay channels of a $CO^-$ Feshbach resonance,** *Phys Rev. Lett.* **28,** No. 15, 948-951 (Apr. 10, 1972).

Key words: CO; $CO^-$; decay channels; energy loss spectra Feshbach resonance.

By means of on- and off-resonance energy-loss measurements we have observed the decay of the 10.04-eV resonance in CO to the $A\ {}^1\Pi$, $a\ {}^3\Pi$, and $a'\ {}^3\Sigma^+$ states. The measurements identify the resonance as a ${}^2\Sigma^+$ state of $CO^-$.

**12751.** Pope, C. I., **A simplified method for determining residua thiosulfate in processed microfilm,** *Photogr. Sci. Eng.* **13,** No 5, 278-279 (Sept.-Oct. 1969).

Key words: Archival record film; hypo testing; microfilm residual thiosulfate.

In the silver nitrate test for residual thiosulfate in processed film the silver ion reacts quantitatively with thiosulfate to form silver sulfide *in situ*. The excess silver ion is removed by treating the sample in solutions of sodium chloride and sodium thiosulfate followed by washing. The method is simplified by using a solution of ammonium hydroxide and sodium chloride to remove the excess silver ion; no washing is necessary. The new method takes half the time previously required.

12752. Schubauer, G. B., **Early developments in hot-wire anemometry at NBS and a look at some elsewhere,** (Proc. Int. Symp. on Hot-Wire Anemometry, University of Maryland, College Park, Md., Mar. 20-21, 1967), Chapter in *Advances in Hot-Wire Anemometry,* W. L. Melnik and J. R. Weske, eds., pp. 13-24 (July 1968).

Key words: Anemometer; hot-wire; measurement of turbulence; turbulence.

The paper reviews the history of hot-wire anemometer development at NBS as applied to the measurement of turbulence. It makes limited mention of work done elsewhere, mainly to place NBS work in proper perspective. The story begins in the middle 1920's with early attempts to measure turbulence, followed by an account of the work of Dryden and Kuethe, which suddenly advanced the hot-wire anemometer as a useful and productive instrument for turbulence measurement. Work at the Technische Hoogeschool at Delft along similar lines, but coming a little later, is described. This is followed by an account of subsequent development of hot-wire equipment at NBS. Finally, departing from NBS work entirely but furthering the theme, "How It Began," an account is given of the birth of the constant-temperature method.

12753. Smith, M. W., Wiese, W. L., **Graphical presentations of systematic trends of atomic oscillator strengths along isoelectronic sequences and new oscillator strengths derived by interpolation,** *Astrophys. J. Supplement Series* **23,** Supplement No. 196, 103-196 (June 1971).

Key words: Atomic oscillator strengths; interpolated data; systematic trends.

Recently detected systematic trends of atomic oscillator strengths along isoelectronic sequences are utilized for the determination of new numerical data and for the evaluation of the reliability of existing material. All well-established systematic trends, which number about 100, are presented graphically. New oscillator strengths are interpolated from the graphs, mainly for the higher ions with wavelengths located principally in the vacuum ultraviolet, and are tabulated with their estimated uncertainties. The graphs are ordered according to isoelectronic sequences and are given with full grids to allow the addition of future data.

12754. Simmons, J. H., Macedo, P. B., **Shear and volume structural relaxation in immiscible oxide melts,** (Proc. Conf. Physics of Non-Crystalline Solids, Sheffield, England, Sept. 1970), Chapter 7 in *Amorphous Materials,* R. W. Douglas and B. Ellis, eds., pp. 69-78 (John Wiley and Sons, London, 1972).

Key words: Critical-point effect; immiscible glasses; longitudinal ultrasonics; phase separation; shear ultrasonics; structural relaxation.

The influence of composition fluctuations on the structural relaxation mechanism above the critical point of a series of immiscible oxide glasses is investigated by shear and longitudinal ultrasonic spectroscopy. The results are analyzed to determine the nature of the interaction between the fluctuations in composition and the viscous flow processes.

12755. Rosasco, G. J., Benoit, C., Weber, A., **Light scattering study of the attenuation and dispersion of hypersound in ammonium bromide,** (Proc. 2d Int. Conf. on Light Scattering in Solids, Paris, France, July 19-23, 1971), Chapter in *Light Scattering in Solids,* M. Balkanski, ed., pp. 483-488 (Flammarion Sciences Publ., Paris, France, 1971).

Key words: Acoustic phonons; ammonium bromide; Brillouin scattering; elastic constants; light scattering; relaxation phenomena.

By means of Brillouin scattering, the attenuation and velocity dispersion of hypersonic acoustic waves have been measured in the disordered, cubic phase of $NH_4Br$. Shear waves determined by the elastic constant $C_{44}$ show no dispersion. Longitudinal waves propagating in the $\langle 001 \rangle$ plane show velocity dispersion and associated attenuation. The $L$-mode data are adequately fit by a single relaxation model for the dispersion and attenuation as a function of frequency at 24 °C. The strength of the relaxation, $[C(\infty) - C(0)]/C(0)$ for the elastic constant $C_{11}$ is 2.5%; for $C_{12}$, 8.8%; and for $(C_{11} - C_{12})/2$, 0.6%. The relaxation time measured in this experiment is $1.16 \times 10^{-11}$ sec. Data which shows that the dispersion increases as the temperature is lowered toward the order-disorder $\lambda$-type transition at 234.5 K is also presented. A model is introduced which qualitatively explains the features of this dispersion.

12756. Berger, M. J., Seltzer, S. M., Eisen, H. A., Silverman, J., **Absorption of electron energy in multi-layer targets,** *Trans. Amer. Nucl. Soc.* **14,** No. 1, 887-888 (June 1971).

Key words: Absorbed dose; dosimetry; electrons; gamma rays; inhomogeneous media; interface.

This is a report on calculations of electron depth dose distributions in plane-parallel targets consisting of two or more layers of different materials. The cases treated include irradiations with monoenergetic electron beams (0.125 MeV to 1.0 MeV) and cobalt-60 gamma rays.

12757. Sher, A. H., Keery, W. J., Dyson, H. E., **Improved infrared response measurements in semiconductor nuclear radiation detectors,** *IEEE Trans. Nucl. Sci.* **NS-19,** No. 1, 341-344 (Feb. 1972).

Key words: Defect level; germanium; impurity levels; infrared response; lithium-drifted diodes; semiconductors.

An infrared response technique has been developed which has been shown to yield more detailed spectra than previous techniques and which can be used to identify more specifically energy levels arising from unwanted impurities and defects in semiconductor diodes used as nuclear radiation detectors. The presence of known impurities in germanium detectors, both lithium-compensated and high purity (uncompensated), has been confirmed using this technique. Such impurities include copper, gold, and iron. Features in the spectra associated with crystalline defects have also been identified.

12758. Sher, A. H., Keery, W. J., **Improved infrared-response technique for determining impurity and defect levels in semiconductors,** *Appl. Phys. Lett.* **20,** No. 3, 120-122 (Feb. 1, 1972).

Key words: Defect level; germanium; impurity levels; infrared response; lithium-drifted diodes; semiconductors; silicon.

The response of reverse-biased germanium diodes to monochromatic infrared radiation has been studied. Specimens included those fabricated from crystals doped with either copper or gold, or subjected to heat treatment. Preliminary results are reported that show the technique to be useful for identifying such impurities or defects in both lithium-compensated and high purity germanium specimens.

**12759.** Stephenson, N. C., Roth, R. S., **Structural systematics in the binary system $Ta_2O_5$ - $WO_3$. V. The structure of the low-temperature form of tantalum oxide *L*-$Ta_2O_5$,** *Acta Cryst.* **B27,** 1037-1044 (1971).

Key words: Crystal structure; low temperature form of $Ta_2O_5$; system $Ta_2O_5$-$WO_3$.

The orthogonal unit cell of the compound *L*-$Ta_2O_5$ has dimensions $a=6.198$, $b=40.29$, $c=3.888$ Å and contains 11 formula units. The structure was solved in projection from the Patterson function and refined to a conventional *R* value of 0.088 using full-matrix least-squares methods. The metal atoms are arranged in sheets and are surrounded by oxygen atoms which form either distorted octahedral or pentagonal bipyramidal coordination polyhedra. The structure contains, on the average, three distortion planes per unit cell. These are statistically distributed over four sites, thereby giving the average unit cell a higher symmetry than the real unit cell. The thermal equilibration of the compound, involving detectable structural changes, is discussed in terms of the migration of distortion planes.

**12760.** Stephenson, N. C., Roth, R. S., **Structural systematics in the binary system $Ta_2O_5$-$WO_3$. IV. The structure of $Ta_{38}WO_{98}$,** *Acta Cryst.* **B27,** 1031-1036 (1971).

Key words: Crystal structure; system $Ta_2O_5$-$WO_3$; $Ta_{38}WO_{98}$.

The structure of the composition $Ta_{38}WO_{98}$ is described in terms of a 19 $UO_3$-type subcell unit containing 38 metal atoms and 95.5 oxygen atoms. The orthogonal unit cell has dimensions $a=6.188$, $b=69.57$, $c=3.880$ Å and the structure was solved in projection from the Patterson function utilizing photographically recorded data. Atomic positional and thermal parameters were refined by least-squares methods to a conventional *R* value of 0.118. The composition requires that the unit cell of the equilibrated compound be 429 $UO_3$-type subcells. As a result, the description of the structure in terms of an average 19 $UO_3$-type subcell unit introduces a splitting of certain atomic peaks. These effects are discussed.

**12761.** Stephenson, N. C., Roth, R. S., **Structural systematics in the binary system $Ta_2O_5$-$WO_3$. III. The structure of $45Ta_2O_5 \cdot Al_2O_3 \cdot 4WO_3$,** *Acta Cryst.* **B27,** 1025-1031 (1971).

Key words: Crystal structure; system $Ta_2O_5$-$WO_3$; $45Ta_2O_5 \cdot Al_2O_3 \cdot 4WO_3$.

The composition $45Ta_2O_5 \cdot Al_2O_3 \cdot 4WO_3$ has an orthogonal unit cell with dimensions $a=6.182$, $b=29.200$ and $c=3.876$ Å. This unit cell contains one sixth of a formula unit and differs from $Ta_{30}W_2O_{81}$ in that it contains a whole number of atoms. The metal atoms are surrounded by either an octahedron or pentagonal bipyramid of oxygen atoms and distortions occur in the shapes of these polyhedra depending on their positions in the unit cell. Metal atoms lie in slightly puckered sheets parallel to (001) and the space group, selected after refinement in a number of plane groups and space groups, is *P*2. Atomic parameter interactions are shown to be minimized by the use of extensive three-dimensional data. However the interdependence of parameters is determined mainly by the model that is being refined, and the use of the maximum amount of data serves only to minimize rather than remove this intractability.

**12762.** Stephenson, N. C., Roth, R. S., **Structural systematics in the binary system $Ta_2O_5$-$WO_3$. II. The structure of $Ta_{30}W_2O_{81}$,** *Acta Cryst.* **B27,** 1018-1024 (1971).

Key words: Crystal structure; system $Ta_2O_5$-$WO_3$; $Ta_{30}W_2O_{81}$.

The structure of the compound $Ta_{30}W_2O_{81}$ has been determined in projection using single-crystal diffractometer x-ray data. The orthogonal unit cell has dimensions $a=6.172$, $b=29.226$, $c=3.850$ Å and contains, on the average, one half of a formula unit. The structure of this unit cell represents the superposition of two structural blocks $M_{16}O_{40}$ and $M_{16}O_{42}$ (where M is a metal atom), which occur in the ratio 3:1. In both structural blocks the metal atoms are arranged in sheets and are surrounded by oxygen atoms forming either distorted octahedral or pentagonal bipyramidal coordination polyhedra. The difference in structure between the two blocks is that in $M_{16}O_{40}$ some metal atoms reduce their coordination numbers to minimize packing distortions. The resultant distortion planes are distributed so that three occur every two unit cell. The asymmetric structural unit was refined in two plane groups, *pm* and *pg*, using full-matrix least-squares methods. The final *R* value is 0.077 and *pm* was chosen as the correct plane group on the basis of noncrystallographic considerations.

**12763.** Stephenson, N. C., Roth, R. S., **Structural systematics in the binary system $Ta_2O_5$-$WO_3$. I. The structure of $Ta_{22}W_4O_{67}$,** *Acta Cryst.* **B27,** 1010-1017 (1971).

Key words: Crystal structure; system $Ta_{22}O_5$-$WO_3$; $Ta_{22}W_4O_{67}$.

The orthorhombic unit cell of the compound $Ta_{22}W_4O_{67}$ has dimensions $a=6.136$, $b=47.40$, $c=3.84$ Å and, on the average, contains one formula unit. The structure was solved in projection from the Patterson function and refined to a conventional *R* value of 0.089 using full-matrix least-squares methods. The metal atoms lie in sheets which are separated by $c=3.84$ Å. Within each sheet these atoms have a close-packed hexagonal arrangement. Oxygen atoms complete a coordination polyhedron around each metal atom in the form of either a distorted pentagonal bipyramid or octahedron. These polyhedra are joined by edge-sharing within the (001) planes. Extension of the structure along [001] occurs by corner-sharing. The structure differs from one having *C*-centered orthorhombic symmetry only in certain areas where metal atoms have reduced coordination numbers. These metal atoms lie in sheets parallel to (010) and the "distortion planes" minimize the anionic packing distortions that would otherwise arise. In this structure there is, on the average, one distortion plane per unit cell.

**12764.** Eisenhauer, C., Chilton, A. B., **Angular distribution of scattered gamma rays from a fan source,** *Trans. Amer. Nucl. Soc.* **14,** No. 1, 402-403 (June 1971).

Key words: Angular distributions; civil defense; fallout; gamma radiation; Monte Carlo; structure shielding.

The angular distribution of exposure flux due to scattered photons emerging from the wall was calculated by the Monte Carlo method, using the exponential transform technique. Calculations were made for a source energy of 1.25 MeV, concrete thicknesses of 0.5, 1, 1.5, 2, 3, 4, 5, and 6 mean free paths. In order to allow comparison to be made with the OCD Standard Method for Fallout Gamma Radiation Shielding Analysis, the angular distribution of scattered radiation emerging from the wall was tabulated in terms of a polar angle $\theta$ measured relative to the vertical direction and an azimuthal angle $\phi$ measured relative to the vertical plane perpendicular to the wall. The angular distribution was grouped into 10 intervals of the polar angle and 6 intervals of the azimuthal angle. A total of 24,000 histories were followed down to a cut-off energy of .02 MeV.

**12765.** Sher, A. H., Liu, Y. M., Keery, W. J., **Infrared response measurements on radiation-damaged Si(Li) detectors,** *IEEE Trans. Nucl. Sci.* **NS-19,** No. 3, 312-317 (1972).

Key words: Defect levels; impurity levels; infrared response; lithium-drifted radiation detectors; semiconductors; silicon.

The improved infrared response (IRR) technique has been to ualitatively compare radiation effects on Si(Li) detectors with nergy levels reported for silicon in the literature. Measurements iave been made on five commercial silicon detectors and one abricated in-house, both before and after irradiation with fast eutrons, 1.9-MeV protons, and 1.6-MeV electrons. Effects deendent upon the extent of radiation damage have been oberved.

It seems likely that the photo-EMF, or photovoltage effect, is he basic mechanism for the observation of IRR in *p-i-n* diodes vith a wide *i*-region. Experimental characteristics of the IRR neasurement are in agreement with those of the photovoltage efect.

**2766.** Meinke, W. W., **Some comments on activation analysis,** *Proc. 2d Inter-American Conference on Radiochemistry, Mexico City, Mexico, Apr. 22-25, 1968,* pp. 54-60 (Published by Secretaría General de la Organizacíon de Estados Americanos, Washington, D.C., 1971).

Key words: Activation analysis; neutron activation; trace analysis; trace characterization.

An overview of the current status of Activation Analysis is iven with special note made of the use of neutrons other than eactor-produced neutrons and to the use of separation rocedures including group separations. The relation of activaion analysis to other methods of analysis is discussed with paricular emphasis on the adeptness of the method to handle large umbers of samples for certain elements which are amenable to his method. Activation analysis is inherently an accurate nethod and its use for trace analysis should join forces with ther trace analysis competences to permit a much broader perpective to be applied to the trace analysis problems. The uclear reactor center with its capability for activation analysis s one facet of general trace competence is a logical focal point or the development of characterization centers to meet the eeds in a diverse number of scientific endeavours.

**2767.** Smith, C. N., **Limit of error calculations used in integrated safeguards experiment,** *Proc. 12th Annual Meeting of the Institute of Nuclear Materials Management, Palm Beach Shores, Fla., June 28-July 1, 1971,* **1,** 193-207 (June 1971).

Key words: Integrated Safeguards Experiment; limit of error calculations; nondestructive assay techniques; safeguards.

The Integrated Safeguards Experiment sponsored by the Atomic Energy Commission relied heavily on nondestructive ssay techniques to attain a measured material balance on the nixed oxide fabrication process. This paper describes the calcuations involved in determining the limit of error values for naterial measurements using calorimetry and neutron coinidence counting as well as conventional chemical assay nethods.

**2768.** Geist, J., Kendall, J. M., Sr., **Circumsolar radiation and the international pyrheliometric scale,** *Appl. Opt.* **11,** No. 6, 1437-1439 (June 1972).

Key words: Circumsolar radiation; Eppley Angstrom pyrheliometer; international pyrheliometric scale; Primary Absolute Cavity Radiometer.

The responsivity as a function of angle is calculated for Primay Absolute Cavity Radiometers (PACRAD) with 2.45 and .32° angular field of view limiting apertures, and for a simplified nodel of the Eppley Angstrom (E-A) pyrheliometer. From this lata, the response of the three instruments to various mathematial models of circumsolar radiation is calculated, and compared with experimental data obtained during simultaneous measurements of solar irradiance with the three radiometers. The conclusion is that the difference between the values of solar irradiance measured with the 2.45° PACRAD and with the E-A pyrheliometer is not due to circumsolar radiation.

**12769.** Rasberry, S. D., **Application of computers in electron probe and x-ray fluorescence analysis,** (Proc. 20th Annual Conf. on Applications of X-Ray Analysis, Denver, Colo., Aug. 11-13, 1971), Chapter in *Advances in X-Ray Analysis,* K. F. J. Heinrich, ed., **15,** 56-69 (Plenum Press, Inc., New York, N.Y., 1972).

Key words: Automatic data acquisition; computer automation of laboratory equipment; computer controlled electron probe; computer controlled x-ray analyzers; electron probe automation.

This paper is a review of automation of electron microprobe and x-ray fluorescence instrumentation. Such a review seems timely because of the great increase in the application of computer systems in this field over the past decade. Some of these applications have been conceived to meet true technological needs while in other cases they have been undertaken to "keep up with the Joneses." I would like to show not only what automated systems are now feasible but also when and how they should be employed. The "when" and "how" of automation are largely dependent upon the application being considered; in this study, x-ray applications have been divided into the following classes: (1) on-stream process-control, (2) off-line quality assurance, (3) routine service laboratory, (4) general-purpose analytical laboratory. Several phases are present in these classes, including: specimen preparation and loading, measurement, data acquisition and transfer, data processing and display, and finally, archival data storage. Various workers have undertaken the automation of all these operations in one or the other of the classes of applications; from a review of their work and by examining details of each operation within the framework of a given application, we can now draw conclusions on the extent of desirable automation.

**12770.** Sugar, J., Kaufman, V., **Fourth spectrum of lutetium,** *J. Opt. Soc. Amer.* **62,** No. 4, 562-570 (Apr. 1972).

Key words: Lutetium; spectra; theory.

Spectra of lutetium obtained with a sliding spark were photographed in the wavelength range 400-3200 Å. Wavelengths of 246 lines, comprising all lines identified as Lu IV appearing in the spark at 50-A peak current, are given. Fifty-seven energy levels were deduced from these lines, including nearly all levels of the $4f^{13}(5d, 6s, 6p, 6d,$ and $7s)$ configurations and their connection to the $4f^{14}\ {}^1S_0$ ground state. An ionization energy of $364\ 500 \pm 200$ cm$^{-1}$ was derived. The energy levels are interpreted by means of a theoretical analysis utilizing fitted radial parameters. With these results, trends of Slater and spin-orbit parameters and configuration energy differences for fourth spectra of the rare earths are found. The fundamental energy differences between lowest levels of the $4f^N$ and $4f^{N-1}5d$ configurations for the fourth and fifth spectra are deduced.

**12771.** Schaffer, R., **Documentation interest of the National Bureau of Standards and collaborating groups for communication of laboratory results in clinical analysis,** (Proc. Conf. Clinically Oriented Documentation of Laboratory Data, Buffalo, N.Y., May 10-12, 1971), Chapter in *Clinically Oriented Documentation of Laboratory Data,* E. R. Gabrieli, ed., pp. 419-424 (Academic Press, Inc., New York and London, 1972).

Key words: Clinical analysis; referee methods for clinical analysis; standard reference materials.

The National Bureau of Standards is actively at work to help clinical laboratories obtain analyses at the level of accuracy that they require and to secure inter-laboratory comparability of results. For achieving these objectives, the Bureau's principal effort has been the certification of Standard Reference Materials for the clinical laboratory. Secondly, a joint program has begun between clinical chemists and NBS for developing referee methods for clinical analysis (methods whose accuracy is known).

**12772.** Schaffer, R., **Isotopic methods,** Paper in *The Carbohydrates, Chemistry and Biochemistry, Second Edition,* W. Pigman and D. Horton, eds., **11B**, 765-776 (Academic Press, Inc., New York and London, 1970).

Key words: Isotope-dilution analysis; isotopic distribution; kinetic isotope effects; labeled carbohydrates.

Isotopically labeled carbohydrates are considered for use as quantitative analytical reagents and for tracing the course of the isotopic portion of a labeled carbohydrate through complex reactions.

**12773.** Shafer, M. R., **Discussion of ASME paper 64-WA/FM-1, density effect and Reynolds number effect on gas turbine flowmeters by W. F. Z. Lee and H. J. Evans,** *J. Basic Eng. Trans. ASME, Series D.* **87,** No. 4, 1052-1053 (Dec. 1965).

Key words: Flowmeters; gas turbine flowmeters; Reynolds number effect on gas turbine flowmeters.

In this discussion of the paper "Density Effect and Reynolds Number Effect on Turbine Meters" by W. F. Z. Lee and H. J. Evans a procedure is suggested for constructing a chart from which the performance of a turbine meter can be predicted when metering any fluid provided compressibility is insignificant. It is believed this suggested procedure may have advantages in some applications over other procedures described in the paper.

**12774.** Forman, R. A., Piermarini, G. J., Barnett, J. D., Block, S., **Pressure measurement made by the utilization of ruby sharp-line luminescence,** *Science* **176,** 284-285 (Apr. 21, 1972).

Key words: Calibration; diamond cell; high-pressure; luminescence.

A rapid, convenient technique for precision pressure measurement in the diamond-anvil high-pressure cell, which makes use of the sharp-line ($R$-line) luminescence of ruby, has been developed. The observed shift is $-0.77 \pm 0.03$ reciprocal centimeters per kilobar for $R_1$ and $-0.84 \pm 0.03$ reciprocal centimeters per kilobar for $R_2$ to lower energy and is approximately linear in the range studied (to 22 kilobars). Line-broadening has been observed in some instances and has been tentatively identified with nonhydrostatic conditions surrounding the ruby sample.

**12775.** Linsky, J. L., **A proof of the relation between reflectivity and emissivity in an isothermal scattering and absorptive atmosphere,** *J. Quant. Spectrosc. Radiat. Trans.* **12,** No. 5, 777-781 (May 1972).

Key words: Emissivity; planetary atmospheres; reflectivity; spectral line scattering.

A simple relation between directional emissivity and directional hemispherical reflectivity is proven for an isothermal coherent scattering and absorptive atmosphere and also for the case of complete redistribution in a line.

**12776.** Roberts, J. R., Voigt, P. A., Nagy, J. J., **Continuous emission from hydrogen plasmas. I. The theoretical hydrogen emission coefficients,** *Proc. 9th Int. Conf. Phenomena in Ionized Gases, Bucharest, Romania, Sept. 1-6, 1969,* p. 595 (Editura Academiei Republicii Socialiste Romania, Bucharest, Romania, 1969).

Key words: Continuum; emission coefficients; emission intensity; hydrogen.

Extensive calculations of the continuous hydrogen emission coefficient for a temperature range from 7,000 to 16,000 K and a wavelength range from 1,500 to 15,000 Å have been carried out. The four major reasons for this new calculation are: (a) some of the most recent calculations differ by at least 25 percent in certain spectral regions from these new calculations; (b) a high intensity wall-stabilized hydrogen arc is now available which would allow spectral radiance calibration by means of the accurately calculable hydrogen emission coefficient into the vacuum ultraviolet region and portions of the visible and infrared spectral regions; (c) the contribution of the far wings of Stark broadened hydrogen lines as an addition to this continuum is usually neglected, but will be considered here in detail; and (d) newly available absorption coefficients for $H^-$ and $H_2^+$.

**12777.** Coxon, B., **Conformational analysis via nuclear magnetic resonance spectroscopy,** Article 93 in *Methods in Carbohydrate Chemistry,* R. L. Whistler and J. N. BeMiller, eds., **VI,** 513-539 (Academic Press, Inc., New York, N.Y., 1972).

Key words: Conformational analysis; iterative analysis; long-range coupling constants; n.m.r. spectroscopy; nuclear Overhauser effects; spin-spin coupling constants; variable temperature studies.

Instrumentation for conformational analysis of carbohydrates by n.m.r. spectroscopy is described, together with the preparation of suitable solutions. Spectral assignments may be confirmed by (a) solvent shifts, (b) exchange processes, (c) isotopic substitution, (d) effects of temperature, and (e) double-resonance techniques. Iterative analysis of spectra and interpretation of spin-spin coupling constants over two to five bonds are discussed. The study of conformational equilibria by means of variable-temperature techniques and nuclear Overhauser effects is described. An indication of the potential values of the magnetic resonance of nuclei other than protons is given.

**12778.** Perls, T. A., Stern, J., **Motion,** Chapter 3 in *ISA Transducer Compendium, Second Edition,* Part II, 105-111 (IFI/Plenum, New York, N.Y., June 1970).

Key words: Acceleration transducers; displacement transducers; jerk transducers; measurement of motion; motion transducers; transducer compendium; velocity transducers; vibration transducers.

This introduction to the chapter on motion transducers of the *Second Edition* of the *ISA Transducer Compendium* discusses the various motion measurands covered by the chapter, the principles used for their transduction to electrical signals, and various considerations that enter into the choice of a transducer for specific application.

**12779.** Yokel, F. Y., Somes, N. F., **Performance criteria for tall buildings,** (Proc. 5th CIB Congress, Paris-Versailles, France, June 1971), Chapter in *Research Into Practice, The Challenge of Application* **1,** 587-592 (June 1971).

Key words: Building; performance criteria; performance evaluation; structure; tall buildings; user requirements.

The introduction of performance criteria would help to overcome some of the difficulties presently encountered in the design and evaluation of innovative concepts. Performance criteria must be derived from user requirements. The various levels at which performance can be defined result in a hierarchy of performance criteria. The level at which performance should be defined varies for various applications.

An example is presented of performance criteria for structural attributes of buildings and the relationship between these criteria and limit states in structural design.

Recently the Building Research Division of the Institute for Applied Technology, National Bureau of Standards, developed guide criteria for the design and evaluation of innovative housing systems. These criteria are now applied to design, develop, evaluate and certify industrialized housing systems.

Various problems associated with performance evaluation and performance testing are discussed and an example is presented from a structural performance evaluation of a building system that was carried out by the Building Research Division.

**12780.** Stiehler, R. D., **Letter to the Editor,** *Modern Plastics* **49,** No. 5, 8 (May 1972).

Key words: Specific strength; specific Young's modulus; units of measurement.

Letter to the Editor of *Modern Plastics* correcting the use of the unit "inch" for specific strength and specific Young's modulus.

**12781.** Smith, C. N., **X-ray standards for law enforcement,** *The Police Chief,* p. 46 (International Association of Chiefs of Police, Gaithersburg, Md., May 1972).

Key words: Law enforcement; voluntary standards; x ray.

Voluntary performance standards for x-ray systems applicable to law enforcement activities are being developed by the Applied Radiation Division of the National Bureau of Standards. The article describes the types of objects subject to x-ray surveillance, the various applications for x-ray systems, and the basic considerations in the formulation of the standards.

**12782.** Liu, Y. M., Coleman, J. A., **Radiation damage effects by electrons, protons, and neutrons in Si(Li) detectors,** *IEEE Trans. Nucl. Sci.* **NS-19,** No. 3, 346-352 (1972).

Key words: Electrons; lithium-drifted silicon detector; neutrons; protons; radiation damage; radiation effects; silicon.

The degradation of performance of lithium-compensated silicon nuclear particle detectors induced by irradiation at room temperature with 0.6-MeV and 1.5-MeV electrons, 1.9-MeV protons, and "fast" neutrons from a plutonium-beryllium [Pu-Be] source has been investigated. In general with increasing fluence, the irradiations produced an increase of detector leakage current, noise, capacitance, and a degradation in the performance of the detector as a charged-particle energy spectrometer. Following the irradiations, annealing effects were observed when the detectors were reverse-biased at their recommended operating voltages. Upon removal of bias, a continuous degradation of detector performance characteristics occurred. Detectors which had been damaged by electrons and protons exhibited a stabilization in their characteristics within two weeks after irradiation, whereas detectors damaged by neutrons had a continuous degradation of performance over a period of several months.

**12783.** Radebaugh, R., Siegwarth, J. D., **Numerical analysis of continuous and discrete heat exchangers for dilution refrigerators,** (Proc. Comm. I, Conf. on Cryophysics and Cryoengineering, Tokyo, Japan, Sept. 11-12, 1970), *Bull. Inst. Int. Froid, Annexe 1970-2,* pp. 57-62 (Int. Inst. of Refrigeration, Paris, France, 1970).

Key words: Cryogenics; dilution refrigerator; heat exchangers; helium-3; helium-4; liquid helium; mixtures.

The design of heat exchangers for dilution refrigerators has proceeded until now with little quantitative information concerning the behavior of the heat exchanger system. In this paper we present results of a numerical analysis on the behavior of both discrete and continuous heat exchangers. Thermal conduction in both the dilute and concentrated streams is taken into account and this requires the solution of two simultaneous second order differential equations for each heat exchanger to determine the temperature distribution. In the case of the discrete heat exchangers, which are required for temperatures below about 0.05 K, the relatively high thermal conductivity of the liquids has a very strong effect on the temperature distribution. In fact for typical dimensions, the liquid temperatures are reasonably constant throughout the heat exchanger and most of the temperature change in each stream occurs in the inlet tubes just before entering the heat exchanger. This implies that the impedance can be reduced by using shorter lengths and larger diameters with little sacrifice in the thermal behavior of the heat exchanger. Figures are presented to aid in the selection of heat exchanger sizes optimized for faster equilibrium times and lower temperatures.

**12784.** Clark, A. F., Kropschot, R. H., **Low temperature specific heat and thermal expansion of alloys,** (Proc. Comm. I, Conf. on Cryophysics and Cryoengineering, Tokyo, Japan, Sept. 11-12, 1970), *Bull. Inst. Int. Froid, Annexe 1970-2,* pp. 249-254 (Int. Inst. of Refrigeration, Paris, France, 1970).

Key words: Aluminum alloys; copper-nickel alloys; cryogenics; specific heat; stainless steel; thermal expansion; titanium alloys.

Grüneisen was the first to show that statistical thermodynamics could be used to relate thermal expansion and specific heat. Using these relations we have calculated the specific heats of several alloy systems of importance in cryogenic design. Specific heats of copper-nickel alloys, austenitic stainless steels, aluminum alloys and titanium alloys have been calculated in the temperature range 4-300 K and comparisons made with the limited amount of experimental data. Results indicate that, to engineering accuracy, the specific heat of an alloy system can be readily predicted over a large temperature range from the experimentally determined thermal expansion.

**12785.** Andrews, J. R., **A frequency calibrator for UHF using an avalanche transistor,** *QST* **LVI,** No. 5, 16-18 (May 1972).

Key words: Avalanche transistor; frequency calibration; impulse; picosecond; spectral intensity; UHF; VHF.

Amateurs have long been accustomed to using 100 KHz crystal oscillators as a source of frequency markers for the calibration of their HF receivers. The frequency calibration of VHF and especially UHF narrow-band receivers has not been as easy. This is because the spectral intensity at VHF of the output from ordinary 100 KHz crystal calibrators has rolled-off into the noise level. This article describes a simple frequency calibrator that provides usable 10 KHz markers to beyond the 1296 MHz band. The calibrator uses a transistor operating in the avalanche mode to generate a 14 volt, 420 picosecond ($10^{-12}$ seconds) wide impulse into a 50 ohm termination.

**12786.** Oser, H. J., Translator and Editor of the book: **Boundary layers of flow and temperature, by A. Walz,** 297 pages (MIT Press, Cambridge, Mass. 1969).

Key words: Airfoil theory; boundary layer; drag; heat transfer; laminar; lift; skin friction; subsonic; supersonic; transition; turbulent.

A translation of the monograph: Strömungs-und Temperaturgrenzschichten by Alfred Walz. The book describes theory and computation of laminar and turbulent boundary layers without and with heat transfer.

**12787.** Milligan, D. E., Jacox, M. E., **Infrared and ultraviolet spectroscopic studies of molecular ions trapped in inert solid matrices,** *Proc. 19th Annual Conf. on Mass Spectrometry and Allied Topics, Atlanta, Ga., May 2-7, 1971*, pp. 100-104 (American Society for Mass Spectrometry, ASTM Committee E-14 and Naval Research Laboratory, Washington, D.C., 1971).

Key words: Charge transfer; free radical; infrared spectrum; matrix isolation; molecular ion; ultraviolet spectrum; vacuum-ultraviolet photolysis.

Details of experiments in which diatomic and small polyatomic molecular ions have been trapped in solid argon in sufficient concentration for direct infrared and ultraviolet spectroscopic detection are presented. Among the species for which spectroscopic observations are discussed are $C_2^-$, $NO^-$, $NO_2^-$, $SO_2^-$, $ClHCl^-$, $BrHBr^-$, $CCl_3^+$, $HCCl_2^+$, and $HCCl_2^-$.

**12788.** Horton, W. S., Carson, C. C., **Gas analysis: Determination of gases in metals,** Chapter 103 in *Treatise on Analytical Chemistry,* I. M. Kolthoff and P. J. Elving, eds., **10,** Part 1, Section E, 6017-6144 (John Wiley & Sons, Inc., New York, N.Y., 1972).

Key words: Gases in metals; hot extraction; nydrogen; Kjeldahl; nitrogen; oxygen; vacuum-fusion analysis.

Methods for the determination of oxygen, hydrogen and nitrogen in metals are discussed. General historical and technical information as well as procedural details and assessment of accuracy for some methods are given. Methods include vacuum-fusion, inert gas fusion, hot extraction, Kjeldahl, spectrographic and isotopic as well as others. This is an invited contribution to form a chapter of Kolthoff and Elving's *Treatise on Analytical Chemistry*.

**12789.** Meyerson, M. R., **Ultrahigh-strength materials,** Chapter 19 in *Materials Science and Technology for Design Engineers,* pp. 366-389 (Hayden Book Company, Inc., New York, N.Y., 1972).

Key words: Alloy steels; ausformed steels; cold-drawn steels; dispersion hardened alloys; fiber and whisker reinforced materials; maraging steels; refractory alloys; stainless steels; strengthening mechanisms; superalloys; titanium alloys; tool steels; ultrahigh strength.

This state of art survey is to be a chapter in a book entitled "Materials Science and Technology for Design Engineers." Written for non-metallurgists, it offers a review of the known strengthening mechanisms and describes the characteristics and mechanical properties of current commercial alloys which attain ultrastrength levels at room and elevated temperatures. Included are alloy steels, tool steels, ausformed steels, cold-drawn steels, hardenable stainless steels, precipitation-hardened stainless steels, maraging steels, titanium alloys, superalloys, refractory alloys, dispersion hardened alloys, and fiber and whisker reinforced materials.

**12790.** Hougen, J. T., **An interesting example of Hund's coupling case (c) in HgAr⁺,** *J. Mol. Spectrosc.* **42,** 381-384 (1972).

Key words: $HgAr^+$; Hund's case (c); $\Omega$-type doubling; rotational levels.

The rotational energy levels of a diatomic molecule in a Hund's case (c) $\Omega = 1/2$ state arising from $^2D_{5/2} + {}^1S_0$ separated atoms are shown to be given by an expression of the form $B[(J+1/2)^2 + 8 \mp 1/2\ (p/B)\ (J+1/2)] - D[(J+1/2)^2 + 8 \mp 1/2\ (p/B)\ (J+1/2)]^2$, where the upper and lower sign choices correspond to rotational levels of parity $(-1)^{J-1/2}$ and $(-1)^{J+1/2}$, respectively, and where $p \cong +6B$.

**12791.** King, D. A., Madey, T. E., Yates, J. T., Jr., **Interaction of oxygen with polycrystalline tungsten, Part 3.—Electron stimulated desorption,** *J. Chem. Soc. Faraday Trans. I,* **68,** 1347-1359 (1972).

Key words: Adsorption; chemisorption; desorption; electron stimulated desorption; oxidation; oxygen; tungsten.

This paper is a sequel to a detailed study of the kinetics of adsorption and desorption in the interaction of $O_2$ with polycrystalline tungsten, in which a number of oxide and O atom states were identified by thermal desorption. In electron stimulated desorption (ESD) studies two states of adsorbed oxygen were distinguished, $\beta_1$ and $\beta_2$; the former has a high ESD cross section and the latter a low cross section. In this paper an attempt is made to correlate the states observed in the thermal desorption study with these $\beta_1$ and $\beta_2$ states. The ESD properties of the $\beta_1$ state are determined, and the sticking probability for readsorption onto an oxygen-saturated surface depleted of $\beta_1$ by ESD is determined as a function of the incremental oxygen coverage. The steady state between electronic desorption and readsorption from the gas phase is examined, and isotopic exchange between $^{16}O$ and $^{18}O$ in the $\beta_2$ and $\beta_1$ states is observed and characterized. The appearance of the $\beta_1$ state is related in a complex way to the formation of tungsten oxides which can be thermally desorbed in the temperature range 1200-1600 K.

**12792.** Cox, D. M., Smith, S. J., **Absolute measurement of 2*S* atom production by dissociative excitation of molecular deuterium,** *Phys. Rev. A* **5,** No. 6, 2428-2442 (June 1972).

Key words: Absolute measurement; cross section; deuterium; dissociative excitation; metastable.

We have measured the cross section for production of metastable (2*S*) atoms by the process of dissociative excitation of molecular deuterium by electron impact. The measurement includes the quantitative evaluation of detection efficiency, density, and geometrical factors necessary to establish an absolute scale on a purely experimental basis. The method depends on the application of an rf field at the Lamb-shift frequency (1059 MHz) to quench the metastables at the point of excitation. The radiation induced by the applied field is isotropic so that the absolute cross section depends on a simple solid-angle correction. The cross sections at 23.8 and 39.1 eV are $2.97 \times 10^{-18}$ and $3.40 \times 10^{-18}$ cm², respectively, with a probable error estimated to be ± 14%. The energy dependence of the cross section was also measured from threshold to 500 eV.

**12793.** Opal, C. B., Beaty, E. C., **Measurements of large angle inelastic scattering cross sections for electrons on helium,** *J. Phys. B: At. Mol. Phys.* **5,** No. 2, 627-635 (Mar. 1972).

Key words: Cross section measurements; helium; inelastic scattering.

The ratios of the inelastic electron scattering cross section for the $n=2$ levels of helium to the corresponding elastic scattering cross sections have been measured in a crossed beam apparatus over the 30 to 150° range for incident energies of 82 and 200 eV. In both cases, at angles greater than 40° the ratio of the sum of the inelastic cross sections to the elastic cross section was constant at a few percent, in qualitative agreement with a similar experiment in atomic hydrogen by Williams. The four $n=2$ states were observed to have markedly different angular dependencies at 82 eV incident energies. Only the $^1S$ and $^1P$ states were important at 200 eV; the ratio $^1S/^1P$ was very nearly 2 at all angles larger than 60°. Within experimental error, over the range of variables studied, the observed cross sections agreed with those predicted by the first Born approximation only for $^1P$ at angles less than 45° at 82 eV incident energy and for $^1S$ and $^1P$ at 30° and 200 eV incident energy.

794. Hidalgo, M. B., Geltman, S., **A high energy approximation: III. Helium excitation by electrons,** *J. Phys. B: At. Mol. Phys.* **5,** No. 3, 617-626 (Mar. 1972).

Key words: Coulomb-projected Born; electron impact; excitation; helium; high energy; theory.

The cross sections for the direct excitation of the $2^1S$ and $2^1P$ tes of helium by electron impact are evaluated in a first order proximation in which the interaction between the incident ctron and target nucleus is represented by a coulomb wave al state in the $T$ matrix. The results obtained for the dif- rential cross sections are much greater than those of the Born proximation for large scattering angles, and the present results in much better agreement with experiment. The present cal- lation predicts inelastic differential cross sections which have asymptotic energy dependence of $E^{-3}$ for all nonzero angles scattering. The total cross sections converge to the Born lues at high energy.

'95. Albers, J., Mountain, R. D., **Asymptotic form of the pair- orrelation function in liquids,** *Phys. Rev. A* **5,** No. 6, 2629- 632 (June 1972).

Key words: Density expansion; liquid structure factor; liquid theory; neutron diffraction; pair correlation function; x-ray diffraction.

Recently, several authors have contended that the pair-cor- ation function for a simple liquid asymptotically goes to zero a way proportional to the two-particle potential. We critically amine the basis of their assertion and find that the conclusion unfounded. Existing x-ray and neutron-diffraction data on uids are inconclusive insofar as the asymptotic form of the pair rrelation is concerned. We propose an experiment which may ed some light upon the large-$r$ behavior of this important quan-

796. Maienthal, E. J., **Polarographic analysis at NBS,** *Amer. Lab.* **4,** No. 6, 12-21 (June 1972).

Key words: Analyses; cathode ray polarography; environmental analyses; Standard Reference Materials; trace metals.

A number of applications of cathode ray polarography to the alysis of Standard Reference Materials, research materials, d environmental samples at National Bureau of Standards dur- the period of July 1968 to June 1970 are discussed. High cision comparative methods for the analyses of major con- uents, such as copper in the organo-metallic SRM and high sitivity subtractive polarographic methods for the determina- n of trace metals in samples such as fish protein concentrate described.

797. Bay, Z., White, J. A., **Frequency dependence of the speed of light in space,** *Phys. Rev. D* **5,** No. 4, 796-799 (Feb. 15, 1972).

Key words: Upper limit of frequency dependence; vacuum dispersion; velocity of light.

To characterize the possible dispersion of the velocity of light space (vacuum) a Cauchy-type formula, $n^2 = 1 + A/\nu^2 + B\nu^2$, is ed. It is shown that relativity only allows a nonzero $A$ term, in- pendent of the nature of the waves or a quantization thereof. cent experimental data provide upper bounds for $A$ and $B$, iting thereby the dispersion in the microwave, infrared, visi- , and ultraviolet regions of the spectrum to less than one part $10^{20}$.

798. Rathbone, D. Z., Jr., **Cutting the costs of cooling,** *Plant Eng.* **26,** No. 12, 88-90 (June 15, 1972).

Key words: Amps; condenser water; economy; energy input; outside air wet bulb; power savings; refrigeration production; tons.

Experience with refrigeration production at the NBS central chilled water generation facility has demonstrated that economies in electrical consumption can be achieved by a managed reduction of condenser water temperatures. This paper reports the analysis of refrigeration production using the 3000 ton capacity centrifugal refrigeration compressors during two extremes of condenser water temperatures, and relates that production to the input electrical energy requirements. The conclusion, subsequently verified by operation of the plant according to newly developed operating procedures based upon these observed economies, is that real savings in energy, and consequently money, can be realized by continually maintaining the lowest condenser water temperature (within limits set by the compressor manufacturer) that outdoor weather conditions will permit.

12799. Pilling, M. J., Bass, A. M., Braun, W., **A curve of growth determination of the *f*-values for the fourth positive system of CO and the Lyman-Birge-Hopfield system of $N_2$,** *J. Quant. Spectrosc. Radiat. Trans.* **11,** 1593-1604 (1971).

Key words: Carbon monoxide; *f*-value; nitrogen; transition probability.

The curve of growth method has been employed to determine *f*-values for the fourth positive system of CO and the magnetic dipole and electric quadrupole components of the Lyman-Birge-Hopfield system of $N_2$. The transition moments are, respectively, 0.83 $a_0e$, $5.9 \times 10^{-11}$ Bohr magnetons and 2.6 $a_0^2e$. No significant dependence on $r$-centroid was found. The mean value of the ratio of the electric quadrupole to magnetic dipole *f*-values was 0.076.

12800. Hubbell, J. H., **Survey of photon-attenuation-coefficient measurements 10 eV to 100 GeV,** *Atomic Data* **3,** No. 3, 241-297 (Nov. 1971).

Key words: Attenuation coefficient; bibliography; cross section; data index; gamma rays; photons; x rays.

A bibliography of 290 references containing measured absolute-value photon total cross-section data above 10 eV is presented, covering the period 1909 to June 1971. An index by element ($Z=1$ to $Z=94$) and energy range, characterizing experiments according to source, detector, and number of data points, is included. Graphs are presented for 17 elements ($Z=1$ to $Z=92$) over the energy range 100 eV to 10 MeV comparing some recent attenuation-coefficient tabulations [by the Lawrence Radiation Laboratory (Livermore), National Bureau of Standards, Los Alamos Scientific Laboratory, and others] with the above documented data points.

12801. Spiegel, V., Jr., **Evaluation of the neutron source absorption correction in a manganous sulfate bath,** (Proc. Amer. Nucl. Soc. National Topical Meeting on Neutron Sources and Applications, Augusta, Ga., Apr. 18-21, 1971), Chapter in *Neutron Sources and Applications,* **II,** 1-170—1-171 (1971).

Key words: Manganous sulfate bath; neutron source calibration; neutron source self-absorption.

A computer code has been written and experimentally verified for the correction to the Manganous Bath Technique for thermal neutron self absorption in spherical and cylindrical neutron sources. The correction is generally small for most absolutely calibrated neutron sources, but may be as large as four or five percent for some commercially available sources with large thermal-neutron cross sections. Neutron multiplication in Pu-Be sources may partially or even overcompensate for neutron absorption. The thermal-neutron flux at the source location, the source dimensions, and the macroscopic fission and absorption cross sections for all materials in the source are required as program input.

**12802.** Smith, J. M., **Automatic data evaluation, manipulation, display, and plotting with SPEED,** *Comput. Graphics* **4,** No. 2, 41-53 (Fall 1970).

Key words: Automatic data evaluation; data conversion; data display; data manipulation; data plotting; digital scanning systems.

SPEED is a system of computer programs written for use in processing data which were automatically recorded on paper or magnetic tape in an engineering laboratory. The basic input is a matrix of values; each row representing a particular time, and each column representing a particular instrument's readings. Since SPEED had been kept general in concept, anyone with such a matrix of input cam make use of the programs.

SPEED has three primary phases. In the initial phase data are converted from paper tape, the data from a given instrument may be multiplied by a given coefficient, the converted data are printed and also plotted on the printer. The second phase allows the user to form new artificial data which can be expressed in terms of the input data. This is done using vector arithmetic considering the readings of any given instrument as a vector. In this second phase the user may again obtain printer plots of data. The third phase of SPEED generates pen plots on a CalComp plotter as final, publication quality, output.

**12803.** Karp, S. S., Rath, G. J., Wright, G. P., **A simulation model of admission and discharge policies for an intensive care unit,** *Proc. 1970 Summer Computer Simulation Conference, Denver, Colo., June 10-12, 1970,* pp. 1108-1114 (June 1970).

Key words: Administration; health; hospital; managerial applications; model; policies; queuing model; scheduling; simulation; systems.

A computer simulation model of the admission and discharge policies for an Intensive Care Unit (ICU) of a hospital is described. As determined by the policies being simulated, the model simulates the flow of patients within the hospital, especially with regard to their admittance to and discharge from the ICU. These policies are principally based on the state of health of the individual patients. Thus, the effects of various policies may be predicted in order to select a near optimal set of policies for a given hospital. The description of the pertinent features of the associated General Purpose Simulation System (GPSS) program is also presented.

**12804.** Slattery, W. J., **Standards: Information and sources,** *Proc. 2d Annual Plant Engineering and Western Maintenance Conf., Anaheim, Calif., Sept. 23-25, 1969,* pp. 49-57 (American Institute of Plant Engineers, Region 6, Cincinnati, Ohio, 1969).

Key words: Information sources; KWIC Index; plant engineering; product standards; specifications; standardization; standards.

A brief history of standardization is given. Then four categories of sources of standards information are discussed. The standardization services of the National Bureau of Standards are singled out for discussion with special emphasis on the Product Standards and Information Sections of the Bureau's Office of Engineering Standards Services. A suggestion concerning the mutual exchange of information between the American Institute of Plant Engineers and the NBS is included.

**12805.** Paffenbarger, G. C., **Dental cements, direct filling resins. Composite and adhesive restorative materials: A resume,** (Proc. Engineering Foundation Research Conferences, Engineerir in Medicine-Bioceramics, New England College, Hennike New Hampshire, August 3-7, 1970), *J. Biomed. Mater. Re Symp.* No. 2, Part 2, 363-393 (John Wiley & Sons, Inc., Ne York, N.Y., Jan. 1972).

Key words: Adhesive; cements; composites; cyanoacr lates; dental; methacrylate; polyacrylate; polyurethane resins; restorative.

This resume concerns experimental and commercial dental c ments and restorative and adhesive materials usually containi nonmetallic inorganic components, the biocompatibility of t above with oral tissues, proposed methods of bioevaluation, t oral environment, the nature of the hard tooth tissue, cavi treatment, agents for bonding the restorative material to t tooth, and 112 references.

The cements include those based on (C-1) zinc oxide-eugen with additives such as zinc acetate, rosin, polymers and most i portant *o*-ethoxybenzoic acid (EBA); (C-2) metallic oxide phosphoric acid; (C-3) acid phosphate salts-water; (C-4) al minosilicate glass-phosphoric acid; (C-5) zinc oxide-polyacry acid; (C-6) methyl methacrylate-poly-(methyl methacrylate) wi or without inorganic fillers. Direct filling resins (C-6) witho filler and composite restorative materials (C-6) with filler a based on acrylic resins or reaction products of acrylic (methacr lates) with other resins. Coupling agents include cyanoacrylate epoxy-acrylic adducts and polyurethanes. The 10 tables gi composition, values for pertinent physical properties or den requirements. (C-2) Dominates the cements but (C-1) wi (EBA) and (C-5) which has some adhesion to hard tooth tissu and stainless steel may displace (C-2). (C-4) Restorative mate als are anticariogenic and widely used but are being supplant by composite restorative materials.

**12806.** Guevara, F. A., McInteer, B. B., Ottesen, D., Hanley, M., **A critique of the high-temperature viscosity measuremen of Trautz and Zink,** *Los Alamos Scientific Laboratory, Ur versity of California, Los Alamos, New Mexico, Report N LA-4643-MS,* pp. 1-10 (June 1971).

Key words: Discrepancy; experimental analysis; viscosi

Because there is a serious discrepancy between modern dilu gas viscosity measurements and the values established pioneering workers, the older experiments of Trautz and Zi are examined in detail. On critical evaluation, the following cc clusions seem justified. (1) In the Trautz and Zink measuremer there is a systematic error common to all gases. (2) This err may be accounted for by assuming an error in the furnace te perature. (3) No other obvious experimental variable is capat of resolving the systematic discrepancy with modern results. ( Study of the early apparatus and technique shows that such experimental error is plausible.

**12807.** Klebanoff, P. S., Tidstrom, K. D., **Mechanism by whicl two-dimensional roughness element induces boundary-lay transition,** *Phys. Fluids* **15,** No. 7, 1173-1188 (July 1972).

Key words: Boundary layer; roughness; two-dimension stability; transition.

An experimental investigation of the effect of two-dimensio roughness elements on boundary-layer transition is describ Primary emphasis is given to the nature of disturbances witl the recovery zone, i.e., that region in the immediate downstre of the roughness where the mean flow has been distorted by t presence of the roughness. Detailed measurements of me velocity distributions, of disturbance spectra, and intensi growth, and decay of disturbances at discrete frequencies we made for a range of unit Reynolds numbers. The measuremer nonstrate that the behavior can best be understood by con-ering wave-type disturbances, and the basic mechanism by ich a two-dimensional roughness element induces earlier nsition to turbulent flow is by the destabilizing influence of the w within the recovery zone. Comparison with the behavior ex-ted from stability theory supports this conclusion.

08. Greer, W. L., Rubin, R. J., **Quantum theory of heat trans-ort in an isotopically substituted, one-dimensional, harmonic rystal,** *J. Math. Phys.* **13,** No. 3, 379-385 (Mar. 1972).

Key words: Harmonic crystal; heat transport; isotopic disorder; Kapitsa resistance; scattering theory in one-dimension; statistical mechanics; thermal conduction; thermal transport; transport coefficient; wave transmission in random media.

We present a quantum mechanical treatment of thermal trans-t in a one-dimensional isotopically substituted harmonic lat-. This work is an extension of a classical mechanical treat-nt. We find that the difference between the quantum and clas-l expressions for the thermal conductivity of a random chain ishes in the limit $N \rightarrow \infty$, where $N$ is the number of isotopes. us, as in the classical treatment, the thermal conductivity erges as $N^{1/2}$. For a periodic diatomic lattice, we derive ex-it formulas for the heat current as a function of temperature. very low temperatures, this quantum mechanical current ex-ts Kapitsa behavior.

09. Jacox, M. E., Milligan, D. E., **Spectrum and structure of e $HO_2$ free radical,** *J. Mol. Spectrosc.* **42,** No. 3, 495-513 une 1972).

Key words: ClOO; H-atom reaction; $HO_2$; $H_2O_2$; infrared spectrum; matrix isolation; normal coordinate analysis; $O_3$; ultraviolet spectrum; vacuum-ultraviolet photolysis.

n studies of the vacuum-ultraviolet photolysis of $Ar:O_2:HCl$ $Ar:O_2:H_2O$ samples at 14 K the free radical $HO_2$ has been ilized in considerably greater concentrations than in earlier eriments, in which the mercury-arc photolysis of HBr or of had been used to provide a source of H atoms. Appreciable centrations of $H_2O_2$ and $O_3$ and, in the experiments using l as an H-atom source, of HOCl and ClOO were also stabil-. The infrared spectra of the mixed oxygen-isotopic species $DO_2$ have been reported for the first time. The data for the oxygen-isotopic species of $HO_2$ have been subjected to a mal coordinate analysis, using a four-constant valence-force l, and the calculated $DO_2$ frequencies have been compared n the observed values. The previous assignment of the 1389-$^{1}$ absorption as the OH deformation fundamental and of the 1-cm$^{-1}$ absorption as the oxygen—oxygen stretching funda-ntal has been definitively established. A satisfactory fit to the erved absorption pattern for the oxygen-isotopic species of $_2$ has been obtained for a valence angle of 105 ± 5°. The mag-des of the two stretching force constants of $HO_2$ suggest that electronic structure of $HO_2$ may approach that of $O_2^-$, lend-some support to the previous identification of an electronic sition of $HO_2$ near that of $O_2^-$.

10. Levine, J., Hall, J. L., **Design and operation of a methane bsorption stabilized laser strainmeter,** *J. Geophys. Res.* **77,** o. 14, 2595-2609 (May 10, 1972).

Key words: Interferometer; methane-absorption stabilized; strainmeter.

unique 30-meter laser strainmeter is described. The system s a Fabry-Perot geometry and dynamically adjusts the uency of the illuminating laser to follow a single fringe. The rence length for the system is provided by a second laser ose wavelength is stabilized by a vibration-rotation absorption line in methane. The system shows excellent sensitivity, wide bandwidth, and essentially no drift. A sample of the earth-tide record obtained with the laser strainmeter and the initial motion observed for the nuclear explosion Boxcar are shown. The instrument should also be useful for observing free oscillations of the earth.

**12811.** Winogradoff, N. M., Haller, W. K., Hockey, B. J., **Cross-sectional energy distributions in gigawatt laser pulses: Implications and determination,** *Opto-Electron. Lett.* **3,** 145-148 (1971).

Key words: Beam uniformity; glass damage; laser induced sputtering; neodymium glass laser.

Cross-sectional beam uniformity is essential for quantitative work on non-linear optical phenomena and in the measurement of the threshold for laser induced damage in glass. A technique of obtaining detailed information on the beam uniformity by using laser induced sputtering on suitable glass surfaces is described.

**12812.** Spencer, L. V., Woolf, S., **A "forced-reflection"-type of collimator design,** Paper in Chapter on Shielding and Dosimetry, *Trans. Amer. Nucl. Soc.* **14,** No. 1, 887 (June 1971).

Key words: Collimators; multiple neutron backscattering; neutron experimental equipment; neutron-neutron scattering; re-entrent holes; straight ducts.

A collimator design concept is discussed, whereby wall-scattered neutrons are attenuated by an arbitrary number of reflections which are made necessary by choice of tapered segments of appropriate length and angle.

**12813.** Jednačak, J., Hudomalj, M., Pravdić, V., Haller, W., **Electrokinetics of glass surfaces. I. Charge densities at the solid/gas and the solid/liquid interfaces of porous glasses,** *Croat. Chem. Acta* **44,** 149-156 (1972).

Key words: Charge; electrokinetics; glass; surface.

An attempt is described to determine the charge densities at different layers of the surfaces of glass. Three different techniques were used: the heat-of-immersion technique, the electron spin resonance hyperfine splitting measurements, and the electrokinetic streaming potential or current technique.

Estimates of the charge densities at the various interfaces show the structure can be subdivided into the high and low charge portions. The heat-of-immersion technique, looks into the actual solid surface: there the charge density is estimated at in excess of $10^{14}$ unit e-charges per cm$^2$. The hyperfine splitting of the $^{107}$Ag ESR spectrum assumed due to the electrostatic field at the site of the localized atom position: a charge density of 0.7 to $1.3 \times 10^{13}$ is estimated. It is assumed that the Ag atom is localized in the gel-like layer-solution interface. The excess counterion charge in the diffuse part of the double layer in the liquid phase is estimated at 3 to $7 \times 10^{12}$. Thus, the high charge density plane is the interface solid-gel layer. The estimates are based on independent models of the interface structure, widely accepted in literature, although not entirely free of arbitrary assumptions.

**12814.** Kuyatt, C. E., Plummer, E. W., **Field emission deflection energy analyzer,** *Rev. Sci. Instr.* **43,** No. 1, 109-111 (Jan. 1972).

Key words: Electrons; energy analyzer; field emission; high resolution.

A Simpson-Kuyatt type spherical deflection energy analyzer has been adapted to a field emission source. A special decelerating lens allows the analyzer to be used over a wide range of electron energies and energy resolutions. For an electron energy of

2000 eV, a resolution of 20 meV has been demonstrated, while better resolution can be obtained for lower energies (~ 10 meV at 1000 eV). Special techniques and new design features were employed to make the new analyzer compatible with ultrahigh vacuum ( ~ $10^{-12}$ torr).

**12815.** Liebman, J. F., **Comment on the paper "Oxygen monofluoride (OF, $^2\Pi$): Hartree-Fock wavefunction, binding energy, ionization potential, electron affinity, dipole and quadrupole moments, and spectroscopic constants. A comparison of theoretical and experimental results" by P. A. G. O'Hare and A. C. Wahl,** *J. Chem. Phys.* **56,** No. 8, 4242-4243 (Apr. 15, 1972).

Key words: Oxygen fluorides; quantum chemistry; spin conservation.

O'Hare and Wahl recently performed highly accurate calculations on the bonding and energetics of $^2\Pi$ OF, $^3\Sigma$ $OF^+$ and $^1\Sigma$ $OF^-$. They calculate for the reaction $^1\Sigma$ $OF^- \rightarrow {}^3P$ $O + {}^1S$ $F^-$ a $\Delta G^\circ_{298}$ of $-9.2$ kJ $mol^{-1}$ and hence $OF^-$ is considered only marginally stable. It is argued only spin-allowed processes should be considered giving a $\Delta G^\circ_{298}$ of nearly 200 kJ $mol^{-1}$. $^3\Sigma$ $OF^+$ is calculated to have a $D_e$ of 300 kJ $mol^{-1}$ and an EA of 1264 kJ $mol^{-1}$. The logical but failing, synthetic scheme: $OF_2 + SbF_5 \rightarrow OF^+$ $Sb_2F_{11}^-$ is discussed and the failure explained by spin conservation. One must form the $^1\Delta$ state of $OF^+$ and the $^3\Sigma - {}^1\Delta$ separation is estimated as 130 kJ $mol^{-1}$. We may thus conclude $OF^+$ salts are unlikely.

**12816.** Brinckman, F. E., Johannesen, R. B., Handy, L. B., **Pi-bonding effects in organoxytungsten(IV) fluorides,** *J. Fluorine Chem. Short Commun.* **1,** 493-497 (1971/72).

Key words: Chemical shifts; fluorine NMR; organosilanes; organoxytungsten(VI) fluorides, *Pi*-bonding; substituent parameters; synthesis; tungsten hexafluoride.

Preparation of new substituted phenoxytungsten(VI) pentafluorides by treatment of $WF_6$ with corresponding phenoxytrimethylsilanes permits evaluation of *sigma*- and *pi*-bonding characteristics. Application of $^{19}F$ NMR parameters obtained for these compounds to well-established correlations thereby yield substituent parameters for the $-OWF_5$ group; it is shown that results are consistent with a strong inductive withdrawal effect ($\sigma_I = +0.9$) and a small *pi*-acceptor effect ($\sigma_R^\circ = +0.07$). Alternatively, inspection of the $-WF_5$ moiety reveals the chemical shift of F *trans* to the ligand, as compared to that for equatorial F, shows a marked dependence on the *pi*-donor properties of the ligand.

**12817.** Becker, D. A., LaFleur, P. D., **Determination of trace quantities of uranium in biological materials by neutron activation analysis using a rapid radiochemical separation,** *Anal. Chem.* **44,** No. 8, 1508-1511 (July 1972).

Key words: Biological materials; neutron activation analysis; rapid radiochemical separation; solvent extraction; trace analysis; uranium.

Neutron activation analysis has been applied to the determination of trace quantities of uranium in biological materials, using the short-lived radioisotope $^{239}U$ ($T_{1/2} = 23.5m$). A solvent extraction technique was developed for the extraction of uranium by the reagent hydrogen bis(2-ethylhexyl) phosphate (HDEHP). The technique developed was found to be applicable also to the analysis of uranium in other materials such as aluminum, copper oxide and zirconium. Extraction efficiencies for uranium using HDEHP are presented for nitric, perchloric, hydrochloric and hydrofluoric acids. The analysis for uranium at levels of $10^{-6}$g to $10^{-9}$g was made in practical samples, and good agreement obtained with other analytical techniques.

**12818.** Leung, P. S., Rush, J. J., Taylor, T. I., **Study of hinde rotation in crystals by neutron transmission measureme Comparison of calculated and measured scattering cross tions,** *J. Chem. Phys.* **57,** No. 1, 175-182 (July 1, 1972).

Key words: Ammonium salts; cross section; crystals; l dered rotation; methylbenzenes; neutron scattering; sional vibrations.

Total neutron cross sections have been measured as a funct of neutron wavelength ($\lambda_n = 5 - 11$ Å) and sample temperat for $(NH_4)_2SiF_6$, $(NH_4)_2S_2O_8$, durene and hexamethylbenze The experimental results are compared to previous cross-sect data for other ammonium salts and methyl-substituted co pounds and are correlated with the rotational freedom of $NH_4^+$ ions and methyl groups. A relatively simple theoret procedure is described for calculating total scattering cross s tions of hydrogenous crystals using torsional and translatic lattice-mode frequencies obtained from neutron or optical sp tra. Cross-section variations vs wavelength ($\Delta\sigma_s/\Delta\lambda$) and te perature ($\Delta\sigma_s/\Delta T$) are calculated for a large group of ammoni salts and methyl-substituted organics (including those for wh experimental cross sections are presented here) and are dire compared with measured cross section results. In every case experimental and theoretical results agree within about 10% less. Thus the previously observed empirical relations between $\Delta\sigma_s/\Delta\lambda$ and $\Delta\sigma_s/\Delta T$ and the rotational and vibratio behavior of ions and molecules in solids is placed on a m quantitative basis. These comparisons reinforce the usefuln of the neutron cross-section method as a supplement to spec scopic techniques.

**12819.** Prince, E., **Configuration of the water molecule in cu fluoride dihydrate at 298 K,** *J. Chem. Phys.* **56,** No. 9, 43 4355 (May 1, 1972).

Key words: Bond angle; diffraction; fluoride; hydr hydrogen bond; neutron diffraction; structure refineme thermal motion; water molecule.

The crystal structure of cupric fluoride dihydrate at 298 K been redetermined from three-dimensional, single crys neutron diffraction data. Least-squares refinement of 163 in pendent, observed reflections gave a final, weighted *R* index $= 0.038$. The H–O–H angle in the water molecule is 110. 0.2°, which, in contrast to the value 115.5±0.4° found in earlier study, is not significantly different from the tetrahe angle of 109.5°. Thermal vibration is highly anisotropic, w much larger amplitudes perpendicular to infinite, hydrog bonded sheets than parallel to the sheets.

**12820.** Kurylo, M. J., **Absolute rate constants for the additio $O(^3P)$ atoms to propylene,** *Chem. Phys. Lett.* **14,** No. 1, 1 120 (May 1, 1972).

Key words: Hydrogen atoms; propylene; reaction r resonance fluorescence.

The rate of addition of oxygen ($^3P$) atoms to propylene been investigated by the flash photolysis resonance fluoresce technique. Using $O_2$ as the atom source, the reaction was stu from 201 to 424 K. A linear least squares treatment of the henius data gave: $k = (4.17 \pm 0.33) \times 10^{-12}$ exp[ – (7 44)/1.987$T$] in units of $cm^3$ $molecule^{-1}$ $sec^{-1}$.

**12821.** Marchetti, M. A., Krauss, M., Weiss, A. W., **Symme adapted pair correlations in O and $O^-$,** *Phys. Rev. A* **5,** No 2387-2390 (June 1972).

Key words: Electron affinity; O, $O^-$; pair-correlation e gy; shell-correlation energy; symmetry-adapted.

A symmetry-adapted pair-correlation approximation has b used to calculate the electron affinity of the oxygen atom.

culated electron affinity is 1.47 eV which is in reasonable eement with experimental values. The present results add to evidence that the energy difference between similar systems be calculated with reasonable accuracy using symmetry-pted pair energies.

22. de Graaf, L. A., Rush, J. J., Flotow, H. E., Rowe, J. M., **uasielastic thermal neutron scattering by hydrogen in $\alpha$-anadium hydride,** *J. Chem. Phys.* **56,** No. 9, 4574-4581 (May , 1972).

Key words: Debye-Waller factor; hydrogen diffusion, interstitial site; linewidth; momentum transfer; neutron scattering, quasielastic scattering; vanadium hydride; vibration.

he diffusion process of hydrogen in vanadium has been stu- d by quasielastic thermal neutron scattering. Neutron widths associated with diffusion broadening have been deter-ed at 485 K for $VH_{0.198}$ and $VH_{0.570}$. These measurements er a range of momentum transfers ($Q$) for elastic scattering up .1 $Å^{-1}$. This is much larger than the momentum transfers ob-ed in earlier cold-neutron experiments, where no conclusive nparison was possible between data and proposed models in-ving diffusive jumps between octahedral and tetrahedral sites. e linewidth results for $\alpha$-$VH_{0.57}$ are compared with these dels and with an extension developed in the present paper. hough no complete agreement was obtained, this comparison ds to the conclusion that jumps between tetrahedral sites are dominant in the diffusion process. Differences in the width behavior for $VH_{0.198}$ and $VH_{0.570}$, and the fact that the asured widths at large $Q$ increase rapidly with $Q$ rather than roaching an asymptotic value as predicted by the theory, are cussed. It is suggested that these effects and the large Debye-ller factors found in the present and previous neutron experi-nts are connected with the relative magnitudes of diffusion xation time and the jump time between sites.

23. Davis, D. D., Huie, R. E., Herron, J. T., Kurylo, M. J., raun, W., **Absolute rate constants for the reaction of atomic oxygen with ethylene over the temperature range 232-500 K,** *J. hem. Phys.* **56,** No. 10, 4868-4876 (May 15, 1972).

Key words: Absolute rate constants; atomic oxygen; ethylene; gas phase kinetics.

ate constants for the reaction of atomic oxygen with ethylene re measured over a temperature range of 232-500 K using the h photolysis-resonance fluorescence technique. The rate con-nt at room temperature was also determined using a flash tolysis-kinetic absorption spectroscopy system and a charge-flow system coupled to a mass spectrometer. Within experimental errors of the three techniques, good agreement s found for the rate constant at 298 K. The bimolecular rate istant was also found invariant to changes in both total pres-e and reactant concentration. Over the temperature range of experiments, the rate data could be fitted by a simple Arr-nius expression of the form,

$$= 5.42 \pm 0.30 \times 10^{-12} \exp[(-1130 \pm 32 \text{ cal mole}^{-1})/RT] \text{ cm}^3 \text{ molecule}^{-1} \cdot \text{sec}^{-1}.$$

24. Eby, R. K., Colson, J. P., **Alpha relaxation in polyethylene,** *Appl. Phys.* **41,** No. 11, 4313-4316 (Oct. 1970).

Key words: Annealing; density; lamella thickness; mechanical; polyethylene; relaxation; solvent; unit cell.

ata are presented to show that a previously reported correla-n of the strength of the alpha relaxation in annealed solution-wn crystals of polyethylene with the inverse of lamella kness is not unique. Nor is a previously reported dependence relaxation temperature on lamella thickness unique. As the ella thickness changes with annealing temperature, the unit cell dimensions, the macroscopic density, and the residual solvent content of the crystals also change. Thus, there are apparent correlations between these parameters and the relaxation strength and temperature. Since it is not obvious which, if any, of these correlations is the fundamental one with regard to the alpha relaxation, some caution must be exerted in interpreting them. As an example of this, data are discussed to suggest that there is at least one other presently unknown parameter of importance to the relaxation.

12825. Scheer, M. D., Klein, R., McKinley, J. D., **Halogens adsorbed on molybdenum: their surface lifetimes and desorption kinetics,** *Surface Sci.* **30,** No. 2, 251-262 (Apr. 1972).

Key words: Desorption kinetics; halogen surface lifetimes; molybdenum; negative surface ionization.

The surface lifetimes of fluorine, chlorine, bromine and iodine adsorbed on a molybdenum surface have been obtained from measurements of the halide ion desorption flux using the modulated molecular beam technique. Measurements were made at temperatures between 1350 and 1850 K and at surface coverages of less than $10^{10}$ halogen atoms $cm^{-2}$. The temperature-lifetime data were fitted to an Arrhenius expression from which the binding energies, $\bar{l}$, and pre-exponential factors $\bar{\tau}^0$, were obtained:

F: $\bar{l} = 4.65$ eV and $\bar{\tau}^0 = 3 \times 10^{-16}$ s;
Cl: $\bar{l} = 4.11$ eV and $\bar{\tau}^0 = 3 \times 10^{-16}$ s;
Br: $\bar{l} = 3.70$ eV and $\bar{\tau}^0 = 2 \times 10^{-15}$ s;
I: $\bar{l} = 3.15$ eV and $\bar{\tau}^0 = 1 \times 10^{-14}$ s.

It was concluded that the halogens are adsorbed as strongly bound surface compounds, MoX (where X is either F, Cl, Br, or I) from which gaseous ions and neutral atoms desorb at rates consistent with the Saha-Langmuir relationship. From that relationship and the above data, separate binding energies and pre-exponentials were calculated for ion and neutral desorption. The importance of the desorption of MoX was assessed.

12826. Reader, J., Epstein, G. L., **Analysis of the spectrum of quadruply ionized yttrium (Y v),** *J. Opt. Soc. Amer.* **62,** No. 5, 619-622 (May 1972).

Key words: Spectra; ultraviolet; wavelengths; yttrium.

The Y v spectrum has been observed in a sliding-spark discharge with the NBS 10.7-m normal-incidence vacuum spectrograph. The analysis has yielded all the levels of the $4p^45s$ configuration and nearly all levels of $4p^44d$ that can combine with the $4p^5\ ^2P$ ground term. The $4s^24p^44d + 4s^24p^45s + 4s4p^6$ levels have been theoretically interpreted, including configuration-interaction effects. The $4s4p^6\ ^2S_{1/2}$ level was found to have a 26% $4s^24p^44d(D)^2S$ character and the $4s^24p^44d(D)^2S_{1/2}$ level a 22% $4s4p^6\ ^2S$ character. The energy parameters determined from a least-squares fit of the observed level values are compared with Hartree-Fock calculations. The ionization energy is estimated to be $75.0 \pm 0.5$ eV.

12827. Barnes, J. D., Fanconi, B. M., **Raman spectroscopy, rotational isomerism, and the "rotator" phase transition in *n*-alkanes,** *J. Chem. Phys.* **56,** No. 10, 5190-5192 (May 15, 1972).

Key words: *n*-alkanes; Raman spectroscopy; rotator phase; rotational isomerism.

Raman spectra of *n*-nonadecane in the ordered and rotator phases are compared to that of the liquid phase to determine the amount of rotational isomerism in the rotator phase. It is concluded that there is little or no rotational isomerism in the rotator phase.

**12828.** Okabe, H., **Photodissociation of $CS_2$ in the vacuum ultraviolet; determination of $D_0°$(SC-S),** *J. Chem. Phys.* **56,** No. 9, 4381-4384 (May 1, 1972).

Key words: Bond dissociation energy; $CS_2$; $CSA^1\Pi$; $D_0°$(SC-S); fluorescence; photodissociation; vacuum ultraviolet.

It has been shown that a major primary photochemical process of $CS_2$ in the vacuum ultraviolet is the reaction,

$$CS_2 \xrightarrow{h\nu} CS\ A\ {}^1\Pi + S\,{}^3P_2,$$

in apparent violation of the spin conservation rule. From the threshold energy of incident photons required to produce the fluorescence, CS $A\ {}^1\Pi - X\ {}^1\Sigma$, $D_0°$(SC-S) = 4.463 ± 0.014 eV or 102.9 ± 0.32 kcal/mole has been obtained in excellent agreement with the value derived previously from the photoionization of $CS_2$. Other related thermochemical data are derived and are compared with those obtained by various methods. The fluorescence excitation spectrum shows peaks corresponding to Rydberg series I and II, indicating that the above reaction is mainly the result of predissociation from Rydberg states. The fluorescence efficiencies became quite small above incident photon energies corresponding to the first ionization potential of $CS_2$. The CS $A\ {}^1\Pi$ fluorescence spectrum produced by the 1236 Å line photolysis shows vibrational levels populated up to $v' = 5$. The absorption coefficient of $CS_2$ has been measured in the region 1200 – 1400 Å.

**12829.** Camus, P., Sugar, J., **Theoretical study and interpretation of the electronic configurations in TM II. II. Odd excited configurations $4f^{12}(5d+6s)6p$ and $4f^{13}7s$,** *Phys. Scr.* **4,** 263-268 (1971).

Key words: Energy levels; theory; thulium.

The calculation of the energy eigenvalues and the Lande $g$ factors of the configuration $4f^{12}(5d+6s)6p$ taken together has allowed the identification of 175 odd levels with a mean error of 97 cm⁻¹. The configuration $4f^{12}5d6p$ is identified at 44 838 cm⁻¹. The eigenvectors of $f^{12}sp$ and those of $f^{12}dp$ for the matrices with $J$ greater than or equal to 5 are given in the $^*J_1J_2$ coupling scheme where $^*J_1$ is an eigenvector of the real core of $f^{12}$. The four levels of the configuration $4f^{13}7s$ are interpreted and the value of the IP of Tm II fitted by interpolation with the neighbouring elements, which is 12.05 volts, is confirmed.

**12830.** Camus, P., Sugar, J., **Theoretical study and interpretation of the electronic configurations in Tm II. I. Even configurations $4f^{12}(5d+6s)^2+4f^{13}6p$,** *Phys. Scr.* **4,** 257-261 (1971).

Key words: Energy levels; theory; thulium.

The calculation of the energy eigenvalues and the Lande $g$ factors of the configurations $4f^{12}(5d+6s)^2+4f^{13}6p$ taken together has led to the interpretation of 155 even levels whose energies are predicted with an rms error of 105 cm⁻¹. The configuration $4f^{12}5d^2$ is correlated with 36 experimental levels, among which is the lowest level at 30 508 cm⁻¹. Eigenvectors of the subgroup of configurations $f^{12}ds + f^{13}p$ are given in the $J_1J_2$ coupling scheme, which is the closest to the physical coupling.

**12831.** Tsang, W., **Comparative rate single-pulse shock tube studies on the thermal decomposition of cyclohexene, 2,2,3-trimethylbutane, isopropyl bromide, and ethylcyclobutane,** *Int. J. Chem. Kinet.* **II,** 311-323 (1970).

Key words: Bond energy; cyclohexane; decomposition; gas phase; isopropyl bromide; shock tube; $t$-butyl radical decyclization; 2,2,3-trimethylbutane.

A check of the data from comparative rate single-pulse shock tube experiments has been carried out through the use of a new standard reaction, the decyclization reaction of ethylcyclo tane. The rate expressions for cyclohexane and 2,2,3-trimetł butane have been found to be

$$k(C_6H_{10} \rightarrow 1{,}3\text{-}C_4H_6 + C_2H_4) = 10^{15.3} \exp(-33{,}690/T)\ \text{sec}^{-}$$
$$950 - 1100\ \text{K},\ 2-6\ \text{atm}$$

$$k(tC_4H_9 - iC_3H_7 \rightarrow tC_4H_9\cdot + iC_3H_7\cdot)$$

$$= 10^{16.5}\ \exp(-36{,}830/T)\ \text{sec}^{-1},\ 1000-1100\ \text{K},\ 2-6\ \text{atm}$$

in excellent agreement with previously published results. M of the small discrepancy that does exist is apparently due to differences between the present and earlier (decomposition isopropyl bromide) "standard" reaction. For the latter proce the present study yields

$$k(iC_3H_7Br \rightarrow C_3H_6 + HBr)$$

$$\rightarrow 10^{13.73} \exp(-23{,}970/T)\ \text{sec}^{-1},\ 800-1000\ \text{K},\ 2-6\ \text{atm}$$

These results confirm the correctness of previously publisł comparative rate single-pulse shock tube experiments. Tł demonstrate once again that for the decomposition of paraf hydrocarbons, calculated preexponential factors are at least order of magnitude higher than the directly measured numl and that the accepted value of the heat of formation of $t$-bu radicals $\Delta H_{f300}$ ($tC_4H_9\cdot$) = 29 kJ (6.8 kcals) is at least 10 kJ low. Finally, attention is called to recent studies on neopenta decomposition in flow and static systems which are in compl agreement with the present conclusions.

**12832.** Tsang, W., **Rate and mechanism of thermal decomposit of 4-methyl-1-pentyne in a single-pulse shock tube,** *Int. J. Che Kinet.* **II,** 23-36 (1970).

Key words: Allene; bond energy; comparative rate; phase; heats of formation; kinetics; molecular reacti propynyl; pyrolysis; single-pulse shock tube; 4-methylp tyne-1.

Dilute mixtures of 4-methyl-1-pentyne have been pyroly in a single-pulse shock tube. The decomposition process volves bond breaking:

$$HC \equiv C - CH_2(i\text{-}C_3H_7) \xrightarrow{k_B} HC \equiv C - CH_2 \cdot (\text{propynyl}) + i\text{-}C_3$$

as well as a molecular reaction:

$$HC \equiv C - CH_2(i\text{-}C_3H_7) \xrightarrow{k_M} C_3H_4(\text{allene}) + C_3H_6.$$

The rate parameters are:

$$k_B = 10^{15.56} \exp(-34{,}940/T)\ (\text{sec}^{-1})$$

$$k_M = 10^{13.1} \exp(-29{,}670/T)\ (\text{sec}^{-1}) \qquad 1100\ \text{K},\ 1.5-5\ \text{atn}$$

The heat of formation of propynyl radical is thus $\Delta H_{f300}$ = 338 mol⁻¹ (80.7 kcal mol⁻¹). This leads to a propynyl resonance en gy of 40 kJ mol⁻¹ (9.6 kcal mol⁻¹).

**12833.** Ehrlich, M., **Response of thermoluminescent dosimeter 15 MeV electrons and $^{60}$Co gamma rays,** *Health Phys.* **18,** 2 289 (1970).

Key words: Absorbed dose; $CaF_2$:Dy; dosimeters; L response; thermoluminescence; 15 MeV electrons; $^{60}$ gamma rays.

Thermoluminescence dosimeters (TLD) were mailed al with Fricke dosimeters to some of the participants in the N electron-dosimetry uniformity studies, for irradiation with MeV electrons in a polystyrene block. The electron-irradia TLD and Fricke dosimeters then were returned to NBS evaluation along with similar dosimeters exposed at NBS to $^{60}$

nma rays. Three TLD systems were used: LiF TLD-100 ques, LiF TLD-100 powder in gelatine capsules, and $F_2$:Dy TLD-200 plaques. For the gamma rays, absorbed dose he TLD material was computed from exposure, and for the ctrons, it was computed from the absorbed dose measured in Fricke dosimeters. Within the limits of experimental preci- n and the reliability of the computations, the relative TL ponse per unit absorbed dose in the three systems was found pe the same for $^{60}$Co gamma rays and for 15 MeV electrons.

34. Wilson, W. K., Hebert, R. L., **Evaluation of the stability of anifold papers,** *Tappi* **55,** No. 7, 1103-1107 (July 1972).

Key words: Aging; alkalinity; burst strength; degradation; differential thermal analysis; durability; manifold papers; loads; pH; reflectance; stability; storage; tear strength; testing.

he relative stabilities of a group of seven manifold papers e determined by accelerated aging in flowing air at 90 °C and % relative humidity. One alkaline paper, one neutral-sized er, and five acid papers were included. Changes during aging e noted by monitoring folding endurance, pH, tearing ngth, bursting strength, load elongation, and reflectance. The aline paper was very stable, the neutral-sized paper somewhat stable, and the acid papers could be ranked in stability ap- ximately according to their pH values. The temperature at ch a massive decomposition endotherm (differential thermal lysis) occurred also appeared to be a function of pH.

85. Schaffer, R., **Occurence, properties, and preparation of aturally occurring monosaccharides (including 6-deoxy su- ars),** Chapter in *The Carbohydrates. Chemistry and iochemistry,* Second Edition, W. Pigman and D. Horton, Eds., **1A,** 69-111 (Academic Press, Inc., New York, N.Y., 972).

36. Young, R., Ward, J., Scire, F., **Observation of metal- acuum-metal tunneling, field emission, and the transition re- ion,** *Phys. Rev. Lett.* **27,** No. 14, 922-924 (Oct. 4, 1971).

Key words: Field emission; MVM tunneling; surface finish; surface physics; tunneling.

We report what we believe are the first observations of metal- uum-metal tunneling. A field emitter is brought close to a tal surface and the current-voltage characteristic is measured hree regions: the Fowler-Nordheim region, the intermediate ion, and the metal-vacuum-metal region.

37. Young, R. D., **Surface microtopography,** *Phys. Today* **24,** No. 11, 42-49 (Nov. 1971).

Key words: Microscope; microtopography; single-crystal surface; surface; surface finish; surface profile.

The growing field of surface science would benefit con- erably from measurements of surface microtopography down the atomic level. A brief review is presented of several instru- nts used to quantitatively characterize the surface crotopography of metallic surfaces. Techniques are discussed employing the transmission electron microscope, the anning electron microscope, the optical interference croscope and an engineering profile measuring instrument to asure surfaces suitable for surface science experiments. In ad- ion a new noncontacting instrument, which is presently under velopment will be described. It is concluded that several hniques are presently available for detecting single atom steps single-crystal surfaces.

38. Berger, M. J., Seltzer, S. M., **Bremsstrahlung in the atmosphere,** *J. Atmos. Terr. Phys.* **34,** 85-108 (1972).

Key words: Aurora; balloon experiments; bremsstrahlung; electrons; energy spectrum; sodium iodide detectors.

Calculations are described pertaining to the emission of bremsstrahlung by electrons in the upper atmosphere and the penetration of this radiation to atmospheric depths of 3-10 g $cm^{-2}$ where it can be measured by balloon-borne detectors. The calculations take into account the multiple scattering and slowing down of electrons, and the multiple Compton scattering and photoelectric absorption of bremsstrahlung photons. Numerical data have been generated for electron beams incident onto the atmosphere with energies between 20 keV and 2 MeV, assuming wide-area precipitation and an incident angular distribution isotropic over the downward hemisphere. The results relate the number and energy spectrum of the incident electrons to the bremsstrahlung flux spectrum at balloon heights. The interpretation of some observed bremsstrahlung flux spectra is attempted.

**12839.** Sugar, J., **Potential-barrier effects in photoabsorption. II. Interpretation of photoabsorption resonances in lanthanide metals at the 4*d*-electron threshold,** *Phys. Rev. B* **5,** No. 5, 1785-1792 (Mar. 1, 1972).

Key words: Lanthanides; metallic spectrum; photoabsorption.

The resonances in the photoabsorption spectra of the lanthanides near the 4*d* absorption edge are interpreted as transitions of the type $4d^{10}4f^{N} \rightarrow 4d^{9}4f^{N+1}$. Calculations of the $4d^{9}4f^{N+1}$ energy levels and relative *gf* values for these transitions are shown to be in good agreement with the observed absorption spectra. The assumption that the lanthanides occur in trivalent form (with the exception of Eu and Yb) in the metallic solid state is confirmed by these results.

**12840.** Srinivasan, G. R., Tweer, I., Macedo, P. B., Sarkar, A., Haller, W., **Phase separation in $SiO_2$-$B_2O_3$-$Na_2O$ system,** *J. Non-Cryst. Solids* **6,** 221-239 (1971).

Key words: Electron microscopy; immiscible oxide; nucleation and growth; phase decomposition; phase separation; sodium-borosilicate.

Isothermal studies of the phase separation occurring in the $SiO_2$-$B_2O_3$-$Na_2O$ system near the center of the miscibility gap are made at three temperatures. Early stage observations of the phase morphology indicate that phase interconnectivity is probably due to nucleation and subsequent intersecting growth of silica-rich particles. It is found also that the extent of interconnectivity is strongly dependent on the volume ratio of the coexisting phases. Evidence is also presented that the glass of present composition is in a two-phase region rather than the three-phase region previously reported. It is also shown that there is very little rotation of the tie-lines between 748 and 650 °C.

**12841.** Fuller, E. G., **Nuclear reaction theory and the photonuclear giant resonance,** (Proc. 5th Congress of Yugoslavian Mathematicians, Physicists and Astronomers, Skopje, Yugoslavia, Sept. 13-14, 1972), *Physics,* Vol. II, No. 5, 5-10 (Macedonian Society of Mathematicians, Physicists and Astronomers, Skopje, Yugoslavia, 1972).

Key words: Coupled-channel; eigenchannel; giant resonance; photonuclear; reaction theory.

A brief review is given of the continuum theory of nuclear reactions with particular emphasis on the eigenchannel and coupled channel approaches as applied to the photonuclear giant resonance. Comparison of the theoretical results with experimental data indicates that at best the existing theories can describe only the gross features of the giant resonance. The experimental data seem to indicate the existence of large coherence effects in the giant resonance region.

**12842.** Goldberg, R. N., Frank, H. S., **Liquid junction potentials and single-ion activities by computer simulation. I. The concentration cell with transference,** *J. Phys. Chem.* **76,** No. 12, 1758-1762 (1972).

Key words: Computer simulation; electrochemistry; ionic activities; liquid junction potentials; thermodynamics.

The liquid junction potentials in KCl, NaCl, and HCl concentration cells with transference have been evaluated by computer simulation, making use of Onsager flux coefficients tabulated by Miller, and of a convenient formalism for single-ion activity coefficients to make possible the representation of osmotic driving forces. Varying assumptions regarding single-ion activity coefficients lead to varying values of a computed steady-state junction potential, but these differences are canceled by corresponding differences in calculated electrode potentials, so that the computed overall cell potential remains unchanged—*i.e.*, measurement of the potential of a concentration cell with transference can give no information about single-ion activity coefficients. This expected result plus the agreement of computed cell potentials with experimental ones speaks both for the essential validity of the method and for the mutual self-consistency of the numerical values inserted for Onsager coefficients and for mean ionic activity coefficients. In contrast to the steady-state cell potential, the time rise of the calculated potential is sensitive to the choice made for the single-ion activity coefficient parameter. There would thus seem to exist a possibility for determining single-ion activities in an experiment, if the time rise of the cell potential, after the formation of the junction, could be measured on a nanosecond time scale.

**12843.** Currie, L. A., **On the interpretation of errors in counting experiments,** *Anal. Lett.* **4,** No. 12, 873-882 (1971).

Key words: Activation analysis; Binomial and Poisson distributions; chi-squared; compound distributions; dispersion test; radioactivity.

Digital experiments, such as the measurement of radioactivity, are usually characterized by random errors which follow the Binomial or Poisson distribution. Three types of difficulty which commonly arise in the statistical treatment of such experiments include: (a) failure to recognize that the uncertainty in the physical quantity of interest may be governed by a compound probability distribution, particularly when dealing with short-lived radioactivity; (b) the improper use of the chi-squared statistic when making standard error estimates in weighted least-squares calculations; and (c) selecting the correct number of degrees of freedom and choosing between the $\chi^2$ dispersion test and the goodness-of-fit test for grouped data. Examination of the nature of each of these difficulties has been followed by a recommended course of action.

**12844.** Carpenter, B. S., **Boron and uranium determination in simulated lunar glass by the nuclear track technique,** (Proc. American Nuclear Society 16th Annual Meeting, Los Angeles, Calif., June 28-July 2, 1970), *Trans. Amer. Nucl. Soc.* **13,** No. 1, 79 (1970).

Key words: Alpha particles; boron; fission; fragments; recoiling fission fragments; trace element glasses; uranium.

Recoiling fission fragments and alpha particles were used to determine sub-microgram quantities of uranium and boron in three (50, 1 and 0.02 ppm) Trace Element Glasses certified by the National Bureau of Standards. Procedures for preparing the sample, irradiating the sample in the NBS Reactor, counting and calculations of results are given.

**12845.** Kirstein, A. F., **Discussion of the paper "Behavior of fiber glass reinforced concrete beams" by E. G. Nawy, G. E. Neuwerth, and C. J. Phillips,** *J. Struct. Div. Proc. Amer. S Civil Eng.* **98,** No. ST5, 1206-1207 (May 1972).

Key words: Concrete (reinforced); deflection; disc; fil glass; flexure; structural engineering.

**12846.** Plummer, E. W., Bell, A. E., **Field emission energy c tributions of hydrogen and deuterium on the (100) and (1 planes of tungsten,** *J. Vac. Sci. Technol.* **9,** No. 2, 583-5 (Mar.-Apr. 1972).

Key words: Energy distribution; field emission; hydrog tungsten; tunneling.

Total energy distributions of field emitted electrons from tungsten (110) and (100) planes as a function of coverage hydrogen and deuterium have been recorded utilizing a spheri deflection energy analyzer. The elastic tunneling resonar spectrum gives a plot of the "local density of states" in the ads bate. The inelastic tunneling spectrum reveals those discrete citation energies available in the adsorbate—substrate compl These spectroscopic data have been used to infer the chemi nature of the binding states which have been observed in flash desorption spectrum of hydrogen from tungsten.

**12847.** Gadzuk, J. W., **Tunneling from Cambridge surface sta** *J. Vac. Sci. Technol.* **9,** No. 2, 591-596 (Mar.-Apr. 1972).

Key words: Field emission; metals; surface states; tunn ing.

Solids with electron band structures given by a simple analy function of wavenumber ($E \sim k^2$ for free electron bands; $E$ for tightbinding bands) possess localized electron states at th surfaces which are easily treated within the complex $k$ vector f malism developed especially by Heine and collaborators. Th surface states, which will be called Cambridge surface states, occur not only in energy gaps caused by Bragg reflections at B louin zone faces but also in spin-orbit split gaps and hybridi tion gaps within the zone. In this work a theory of tunneling a field emission of electrons from such surface states is develop The field emission energy distribution from *d*-band metal surfa states is calculated using Harrison's *d*-band pseudopoten theory, and the results are favorably compared with experim tal data. Since the existence conditions for Cambridge surfa states depend crucially upon the boundary conditions at the s face, the act of measurement via a tunneling process can su ciently alter the boundary conditions that "surface states" either created or destroyed by "looking" at them. In particu the strong coupling ion neutralization tunneling experiments Hagstrum are very susceptible to this effect.

**12848.** Marzetta, L. A., **An evaluation of the three-voltme method for ac power measurement,** (Proc. Conf. Digest Precision Electromagnetic Measurement, Boulder, Col June 26, 1972), *IEEE Trans. Instr. Meas.*, pp. 41-42 (June 1972).

Key words: Opamp; phase-sensitive detector; power-fact quadrature; three-voltmeter method; wattmeter.

The accuracy and frequency response limitations in t present square-law responding laboratory wattmeters ha promoted the search for alternate methods of ac power measu ment using electronic instrumentation. The three-voltme method is based on an old principle of operation implemented new analog circuitry. Results of the tests reported here show precision of power calculation with 0.01% error at frequenci below 5 kHz. A unique test procedure is described for the co parison of the three-voltmeter device and a time-division m tiplier wattmeter operating at zero power-factor.

**12849.** Lehman, D. R., **Quasielastic electron scattering from $^3$I and $^3$H,** *Phys. Rev. C* **3,** No. 5, 1827-1840 (May 1971).

Key words: Electron scattering; final state rescattering; helium-3; separable potential; three-body problem; tritium.

Quasielastic electron scattering from $^3$He and $^3$H is in- tigated with a model in which the two-nucleon interaction is scribed by a separable potential. Cross sections are given in impulse approximation for the ejected proton and scattered ctron detected in coincidence, and for detection of only the ttered electron. Both two- and three-body breakup of $^3$He and are considered, with final-state interactions between the spec- or nucleons included in three-body breakup. Good agreement obtained with all the electrodisintegration data, except the $^3$He ncidence data, for wave functions derived from separable tentials which reproduce the *s*-wave two-nucleon phase shifts low and medium energies. Rescattering corrections between spectator particles are found to be important in calculating ee-body disintegration. The need for more refined and reliable ncidence data is reaffirmed.

**50.** Menke, J. L., **A fast pulse-dc integrator,** *Nucl. Instrum. Methods* **64,** 61-68 (1968).

Key words: Fast integrator; high duty; integral linearity; stable converter; wide dynamic range.

This fast pulse-dc integrator accepts pulses from dc to less n 20 ns width, over an input dynamic range of 400:1 in am- ude (1 mV minimum) without range switching. The integral earity (maximum absolute error as fraction of full scale) is 0.1 n at constant pulse height, 0.2% at constant pulse width. Any ding is accurate to within 2%. Temperature compensation and feedback ensure stability of operation. A fast voltage-to-cur- t converter stable to 0.002% of full scale current provides the arge for capacitor storage.

**851.** Shah, J. A., Danos, M., **Study of the neutron-proton cor- relations in the shell model,** *Phys. Rev.* **183,** No. 4, 899-907 July 20, 1969).

Key words: Correlations; neutrons; pairing; quartetting; shell-model; structure; wave function.

A shell-model treatment is given for the spectra of the nuclei ere there are two protons and two neutrons outside a doubly sed shell. The only restriction is that like-nucleons are uired to occupy the same angular momentum state. In addi- n to this general wave function, more restricted wave func- ns also are investigated, viz., the pairing wave function (as st one pair of like nucleons is coupled to zero angular momen- n) which contain no *n-p* correlations; the quartetting wave iction (two unlike nucleons are first coupled to the maximum gular momentum, then the two pairs are coupled to *I*, the clear angular momentum) which does contain *n-p* correlations; d a superposition of pairing and quartetting wave functions. sults for $^{44}$Ti, $^{64}$Zn, and $^{204}$Hg are given. The ground states are produced quite well by the pairing wave function; it seems, wever, to fail for the excited states. The overlap between the neral and the quartetting wave function is quite large. Finally, ults are also given for the pairing force, which has only a $T=1$ mponent.

**852.** Casella, R. C., **Time reversal symmetry and its breaking in physics,** *Phys. Teacher* **8,** No. 3, 114-122 (Mar. 1970).

Key words: CP symmetry; CPT theorem; elementary particles; $K^\circ$ mesons; symmetry; time reversal.

We remark on the relevance of symmetries in Nature, with nphasis on time reversal symmetry, its meaning, relation to her symmetries, and its experimental breakdown in elementa- —particle physics.

**12853.** Lightbody, J. W., Jr., Penner, S., **Electroexcitation of the $C^{12}$ giant resonance,** *Phys. Rev. Lett.* **24,** No. 6, 274-276 (Feb. 9, 1970).

Key words: Electroexcitation; energy dependent potential; Goldhaber-Teller model; longitudinal; matrix elements; momentum transfer; particle-hole model; quasi-elastic model; radiation tail; transverse.

Electroexcitation of $C^{12}$ in and above the giant resonance has been measured at several angles and incident electron energies in order to obtain transverse and longitudinal reduced matrix elements. Results are presented for a $q$ range of from 0.35 to 0.84 fm$^{-1}$ and for excitation of 22-37 MeV. Comparison is made with the recent calculation by deForest of quasielastic scattering, as well as with earlier particle-hole and liquid-drop-model calculations.

**12854.** Mohan, R., Danos, M., Biedenharn, L. C., **Three-fluid hydrodynamical model and the proton distribution in $^{208}$Pb,** *Phys. Rev. Lett.* **23,** No. 15, 868-870 (Oct. 1969).

Key words: Electron scattering; hydrodynamic model; isospin mixing; nuclear charge distribution; nuclear structure; short range correlations.

A three-fluid hydrodynamical model for nuclei is proposed and it is shown that the observed rise in proton density near the surface of $^{208}$Pb can be accounted for in this model.

**12855.** Wyckoff, J. M., **Integrated cross sections for $^{209}$Bi($\gamma$,*xnyp*) reactions,** *Phys. Rev.* **159,** No. 4, 953-954 (July 20, 1967).

Key words: Bismuth; gamma rays; integrated cross section; isomer; lead; linac; lithium drifted germanium; photonuclear; spallation.

Integrated cross sections for the photoproduction of $^{200-206}$Bi and $^{200-204}$Pb from $^{209}$Bi have been measured. A single sample was activated during a 10-minute 137-MeV bremsstrahlung bombardment by the NBS Linac, and $\gamma$ rays from the daughter products were measured with a Ge(Li) spectrometer over a two-month period to obtain relative yields. The yield data were used along with the established ($\gamma$,2*n*) integrated cross section and a calculated thick-target bremsstrahlung spectrum to derive integrated cross sections as follows: $^{206}$Bi(168 ± 25), $^{205}$Bi(88 ± 22), $^{204}$Bi(55 ± 16), $^{203}$Bi(66 ± 23), $^{202}$Bi(31 ± 12), $^{201}$Bi(10.7 ± 5.9), $^{200}$Bi(5.7 ± 3.4), $^{204}$Pb(8.0 ± 2.4), $^{203}$Pb(3.8 ± 1.3), $^{202}$Pb(3.4 ± 1.3), $^{201}$Pb(15.3 ± 8.4), and $^{200}$Pb(1.62 ± .97) MeV mb. Evidence is also presented for an 11.5-h isomeric state in $^{200}$Pb.

**12856.** Wyckoff, J. M., **Photon energy emission from spallation products produced by 3-13 GeV electrons,** *Health Phys.* **18,** 693-704 (June 1970).

Key words: Photon energy; production cross sections; spallation products; 3-13 GeV electron beam.

A calculation of the energy emitted as photons from the ensemble of spallation products produced by a 3-13.3 GeV electron beam has been made. The time range of 1 hr-50 months after irradiation is encompassed using measured production cross sections for Al, Fe, Ni and Cu, major structural materials used around high energy particle accelerators. Similar calculations have been made for Mo, In, Ta and Pb by estimating production cross sections for some of the nuclides for which measured production cross sections were not available. Additional production cross sections measured for 3, 5 and 10 GeV electrons and comparisons with published 3-30 GeV proton spallation data are used to show the general applicability of the calculated decay curves. Graphs of the instantaneous irradiation case are included as well as some illustrative results for photon energy emitted following extended irradiation periods.

**12857.** Praderie, F., Thomas, R. N., **On estimates of the nonradiative energy input to the solar chromosphere from the $H^-$ emission,** *Astrophys. J.* **172,** No. 2, 485-490 (Mar. 1, 1972).

Key words: $H^-$ radiative losses; non-LTE effects on mechanical heating; solar chromospheres.

The inclusion of non-LTE effects in the computation of mechanical heating in a gray atmosphere changes previous LTE estimates by a factor of $4b_{H^-}$.

**12858.** O'Toole, W. E., III, Keplinger, M. S., **An experimental program for automatic indexing at the National Bureau of Standards,** *Proc. American Society for Information Science, Philadelphia, Pa., Oct. 11-15, 1970,* **7,** 301-308 (American Society for Information Science, Washington, D.C., Oct. 1970).

Key words: Automatic indexing; COBOL; document records; programming; statistical analysis; teaching sample; word-term pairing.

A simple approach to automatic indexing is described along with its implementation in a program system.

The two main programs of the system, TESAT and IBSAT, are described from an operating point of view. The background is given for the development of the system, CAIC (Computer-Assisted Indexing and Categorizing). Also included are brief descriptions of experiences with the system and possible future applications and modifications.

**12859.** Holt, H. K., Sellin, I. A., **Time-dependent theory of Stark quenching of 2*S* states in hydrogen and helium,** *Phys. Rev. A* **6,** No. 1, 508-512 (July 1972).

Key words: Lifetimes; one- and two-electron 2*S* states; Stark quenching; time-dependent theory.

A nonperturbative time-dependent theory which gives Stark-quenching lifetimes in agreement with experiment for both one- and two-electron 2*S* states is presented. This theory differs from the conventional Bethe-Lamb theory of Stark quenching, but reduces to this older theory, for one electron atoms only, when a well-known sum rule is applied.

**12860.** Wyckoff, H. O., Rossi, H. H., **Dosimetric fundamentals and irradiation limits. 1.1. Radiation quantities and units,** Chapter 1 in *Engineering Compendium on Radiation Shielding* **I,** 1-5 (Springer-Verlag, New York, N.Y., 1968).

Key words: Definitions; glossary; radiation quantities; radiation shielding; radiation units.

This is part of an introduction to a book on radiation shielding. It includes definitions of quantities and units to be used in the book.

**12861.** Wachtman, J. B., Jr., Capps, W., Mandel, J., **Biaxial flexure tests of ceramic substrates,** *J. Mater.* **7,** No. 2, 188-194 (1972).

Key words: Aluminum oxide; bending; brittleness; ceramics; electronics; flexural strength; fractures (materials); mechanical tests; modulus of rupture tests; substrates; surface properties.

A method for determining the strength of thin, circular disks of brittle materials utilizing an exact elastic solution for small deflections was developed and tested in an interlaboratory program. The method determines the strength in biaxial flexure by supporting the specimen on three equally spaced balls concentric with the load, which is applied to the center of the specimen by a flat piston. This allows slightly warped specimens to be tested and produces results unaffected by the edge condition of the specimen. These features make the method suitable for assessi the effect of surface condition on strength. Results on eight typ of polycrystalline alumina ceramics ranging in strength fr 46,000 to 96,000 psi show that a coefficient of variation of ab seven percent can be achieved by testing five specimens and th different laboratories generally obtain good agreement strength values.

**12862.** Hanley, H. J. M., Klein, M., **Application of the *m*- potential to simple gases,** *J. Phys. Chem.* **76,** No. 12, 1743-17 (1972).

Key words: Carbon dioxide; diffusion; dispersion coe cients; methane; *m*-6-8 potential; nitrogen; oxygen; ra gases; thermal conductivity; thermal diffusion; viscosity.

The *m*-6-8 model potential function is applied to the gases gon, krypton, xenon, nitrogen, methane, and carbon dioxide a to the properties viscosity coefficient, self-diffusion coefficie thermal conductivity coefficient, virial coefficient, and t isotopic thermal diffusion factor. The potential is shown to ha a considerable advantage over previous simple analytic mod in that it can satisfy two criteria: (a) it can be used to correlat given property for all the gases studied over a wide temperatu range with a single set of parameters, and (b) it can be used correlate both transport and equilibrium properties for t monatomic gases with a single set of parameters. Reasons for t failure of polyatomic gases to satisfy (b) are suggested. A br discussion on the relation of the potential to theory is given.

**12863.** Spencer, L. V., **On the accuracy of transport calculati using moments methods,** *Trans. Amer. Nucl. Soc.* **14,** No. 339 (June 1971).

Key words: Biorthogonal functions; gamma rays; mome methods; neutrons; shielding; truncation errors.

Expressions are given for bounds to the truncation error finite $U_n^k$ polynomial representations of $\gamma$-ray and neutron s tial flux distributions. An extension to representations of a cl including sums of exponentials is also noted.

**12864.** Leiss, J. E., **Beam loading and transient behavior in tra ing wave electron linear accelerators,** Chapter in *Linear celerators,* P. M. Lapostolle and A. L. Septier, eds., pp. 1 172 (North-Holland Publ. Co., Amsterdam, The Netherlan 1970).

Key words: Accelerators; beam loading; dispersive effec linear accelerator; transients.

In the linear accelerator the transfer of energy from the celerator to the beam, known as beam loading, can be so effici that the behavior of the accelerator can not be even qualitativ described without consideration of beam loading. The energy loading, and changes in the radio frequency power density some points in the accelerating waveguides of an order of m nitude are observed.

A review of methods to calculate beam loading in the travel wave linear accelerator is presented. Both steady state a transient conditions are examined in various approximations.

**12865.** Swartzendruber, L. J., Evans, B. J., **Hyperfine fields at antimony sites in the Heusler-type $\mathrm{ni}_x$MnSb alloys,** (Proc. 1 AIP Conf. on Magnetism and Magnetic Materials, Chica Ill., Nov. 15-18, 1971), Chapter in *Magnetism and Magne Materials*, C. D. Graham, Jr., and J. J. Rhyne, eds., No. 539-543 (June 1972).

Key words: Alloys; hyperfine fields; Mössbauer effe order-disorder; $^{121}$Sb.

The $^{121}$Sb Mössbauer effect has been utilized to study hyper- : fields in the ferromagnetic alloys Ni$_x$MnSb for $1 \leq x \leq 2$. x=2, the crystal structure is of the Cu$_2$MnAl (L2$_1$) type racteristic of Heusler alloys. As x is reduced, Ni vacancies ear until, for x=1, the ordered C1$_b$ structure is obtained. Our ults indicate a $^{121}$Sb saturation magnetic hyperfine field of ap- ximately +300 kG with a relatively small dependence on Ni centration. It is possible to understand this result by using assumptions: (i) the Ni atoms make only a small contribution he conduction band and (ii) the Sb hyperfine field samples the rage spin polarization of the material. The Mössbauer spectra n a sensitive probe to reveal disorder not easily observed by ay diffraction. A spin-echo measurement of $^{123}$Sb in NiMnSb es good agreement with the $^{121}$Sb Mössbauer effect results.

66. Swartzendruber, L. J., Bennett, L. H., Kinsman, K. R., **Crystallographic and magnetic transformations of Fe precipitates in Cu,** (Proc. 17th AIP Conf. on Magnetism and Magnetic Materials, Chicago, Ill., Nov. 15-18, 1971), Chapter n *Magnetism and Magnetic Materials,* C. D. Graham, Jr., nd J. J. Rhyne, eds., No. 5, 408-412 (June 1972).

Key words: Alloys; copper; crystallography; iron, Mössbauer effect; precipitation.

The Mössbauer effect has been used to characterize the mag- ic state, and hence the crystallographic form, of very small rich precipitates extracted from a Cu matrix. The precipitates m in the Cu matrix as antiferromagnetic (Néel temperature 0 K) metastable fcc crystals. When this two phase matrix is ormed or the precipitates selectively isolated from the matrix, ortion of the precipitates spontaneously transform (marten- cally), at least partially, to bcc Fe. By a newly developed cedure we have extracted these fcc precipitates from the trix, collected, and mounted them for observation by ssbauer spectroscopy. The samples observed consist of small ticles of Fe, containing ~ 0.5% Cu, in the size range 0.1- μm. Since the fcc and bcc crystal structures of Fe have wide- different magnetic properties, the Mössbauer effect can be d to quantitatively characterize the crystallographic transfor- tion. In the extracted precipitates conversion to bcc is essen- ly complete, in contrast to the only partial transformation in- ed by deformation. An upper limit (< 0.3%) can be placed on amount of retained antiferromagnetic phase.

67. Sharp, K. G., Coyle, T. D., **Perfluoro(alkylsilanes). II. Trifluoro(trifluoromethyl)silane and trifluoro(pen- afluoroethyl)silane,** *Inorg. Chem.* **11**, 1259-1264 (1972).

Key words: Alpha-elimination; carbenes; difluorocarbene; difluoroiodo(perfluoroalkyl)silanes; fluoroalkysilanes; fluoro(trifluoromethyl)carbene; silicon difluoride; trifluoro(pentafluoroethyl)silane; trifluoro(trifluoromethyl) silane.

The perfluoro(alkylsilanes) CF$_3$SiF$_3$ (I) and C$_2$F$_5$SiF$_3$ (II) e been prepared and characterized. Synthesis was effected by orination of the corresponding difluoroiodo(perfluoroal- )silanes, obtained by the reaction of SiF$_2$ with the appropriate fluoroalkyl iodide. Both compounds are stable at room tem- ature. Products from thermolysis of I at *ca.* 80° or above and I at 160° or above, as pure compounds or in the presence of led reagents, are consistent with a decomposition mechanism olving α-fluorine transfer and the intermediacy of the car- es :CF$_2$ and CF$_3$CF, respectively. Basic and aqueous drolytic behaviors are described.

68. McMaster, W. H., Del Grande, N. K., Mallett, J. H., Hubbell, J. H., **Compilation of x-ray cross sections,** *Sec. II, Rev. 1, University of California Radiation Laboratory Report 50174,* 353 pages, Lawrence Livermore Laboratory, Livermore, Calif. (May 1969).

Key words: Attenuation coefficient; coherent scattering; compilation; cross section; incoherent scattering; photoelectric absorption; photons; x-rays.

This report contains graphs and tables of x-ray cross sections in the range of 1 keV to 1 MeV. The total cross sections presented are the sum of computed scattering cross sections and a combination of the fit to derived experimental and theoretical photoelectric cross sections.

12869. Dikkers, R. D., Yokel, F. Y., **Strength of brick walls subject to axial compression and bending,** (Proc. 2d International Brick Masonry Conf., Stoke-on-Trent, England, Apr. 12-15, 1970), Chapter in *SIBMAC Proceedings,* H. W. H. West and K. H. Speed, eds., No. 19, 125-132 (The British Ceramic Research Association, Stoke-on-Trent, England, 1971).

Key words: Brick walls; combined loading; compressive strength; flexural strength; high bond mortar; masonry walls; moment magnifier effect; slenderness effects; structural stability.

Unreinforced brick wall panels, 4-in. thick, 4-ft wide, and 8-ft high, were tested by applying uniform transverse loads, uniform axial compressive loads, or a combination of both types of loading. Companion prisms were also tested to determine their strength in compression and flexure. Data from both the wall and prism tests were used to develop analytical procedures for predicting the strength of walls subjected to axial compression and bending.

A new analytical approach is proposed to evaluate both strength and slenderness effects in masonry walls. The application of this approach would lead to new design procedures, closely paralleling similar procedures recently introduced in the USA for other engineered materials, such as steel and reinforced concrete.

12870. Rowen, J. W., Murphey, W. M., Smith, C. N., **Assessment of material unaccounted for control criteria,** (Proc. Synp. Progress in Safeguards Techniques, International Atomic Energy Agency, Vienna, Austria, 1970), Chapter in *Safeguards Techniques* **II,** 291-310 (Dec. 1970).

Key words: Inventory fluctuations; measurement errors; normalization factors; process activity; unidentified process losses.

Some of the factors that affect the usefulness of Material Unaccounted For (MUF) control criteria include process activity, measurement errors, normalization factors, time frame, inventory fluctuations and unidentified process losses.

It is important to know whether and how such criteria vary with the character of the data source and with variations in facility situations. This paper theoretically analyzes MUF criteria corresponding to three types of data sources and two situations. The two situations differ in that measurement errors are known in one but unknown in the other. Quantitative criterion expressions are developed for the six possible conditions of evaluation resulting from the three types of data sources and the two measurement situations. The statistical expressions developed are compared with each other and some available data are presented. Tentative conclusions are drawn with respect to the comparative sensitivities of the criteria resulting from the six possibilities. These conclusions will be tested in the U.S. Atomic Energy Commission's integrated safeguards experiments. These experiments which will provide data for some of the situations will involve subprocess, batch and campaign balances in which information on measurement errors will be available.

**12871.** Kidnay, A. J., Miller, R. C., Hiza, M. J., **Solid-vapor and liquid-vapor phase equilibria for the helium-krypton system,** *Ind. Eng. Chem. Fundam.* **10,** No. 3, 459-465 (Aug. 1971).

Key words: Cryogenic; helium-krypton; liquid-vapor; phase equilibria; solid-vapor.

A vapor-recirculation equilibrium cell was used to investigate both the solid-vapor and liquid-vapor equilibria and the three-phase curve for the system helium-krypton. Gas-phase compositions were measured above solid krypton at 100.00, 105.00, 110.00, and 115.00 K and at pressures to 120 atm (12.16 MN/m$^2$). Both gas and liquid compositions were determined at 117.09, 120.85, 129.60, 139.56, and 150.00 K for the same range of pressures. Analysis of the gas-phase data by both the virial and modified Redlich-Kwong equations indicates that a deviation parameter of about 0.3 is necessary for the geometric-mean mixing rule for energy parameters. Comparison of the Henry's law constants for the liquid phase with the statistical model of Miller and Prausnitz indicates a somewhat larger deviation parameter.

**12872.** Eisenhauer, C., **Some current problems in OCD fallout shielding calculations,** *Proc. Special Sessions on Gamma-Ray Production and Transport and on Civil Defense Shielding, Winter Meeting American Nuclear Society, Chicago, Ill., Nov. 1967, A. E. Straker, ed.,* **ANS-SD-7,** (TID) 4500, pp. 143-156 (1969).

Key words: Civil Defense; engineering method; fallout; gamma rays; shelter; shielding.

A discussion is given of the general situations in which present OCD calculations seem to be adequate. This consists mainly of the case in which an infinite plane source of radiation surrounds a simple building with no interior walls or floors. Three cases in which present calculations appear to be inadequate will be discussed in detail. The first case in which calculations appear to be inadequate involves a finite source strip whose width is a few story heights (~ 50 feet). The two main problems are that the theory assumes that radiation emerging from the inner surface of the exterior walls is symmetric with respect to the horizontal plane, and that the barrier factor for radiation penetrating up through the floor is equivalent to the barrier factor for a plane isotropic source. Possible modifications of these two assumptions are discussed. The second case is the "in-and-down" problem, in which radiation from sources on the ground penetrates *in* through a wall and *down* through the basement ceiling. The two main problems here are that the variation of reduction factor with depth is incorrect and that experimental results on model and full-scale structures given barrier factors which are in apparent disagreement. A possible explanation of this disagreement is discussed, along with some recent experimental data. The third case in which calculations seem to be inadequate is that of a core shelter. This situation occurs when interior partitions are significantly greater than a mean free path in thickness. The particular case of a home fallout shelter in a basement is discussed. The paper concludes with a summary of plans for experiments and calculations in the near future.

**12873.** Johnson, W. T. K., Dick, C. E., **Half-life measurement of several short-lived nuclear isomers,** *Nucl. Instrum. Methods* **99,** No. 2, 221-226 (1972).

Key words: Bromine; cadmium; erbium; gold; half lives; iridium; measurement; nuclear isomers; solenium; tungsten.

Bremsstrahlung produced by 3.5 MeV electrons incident on a platinum target was used to populate nuclear isomers in several nuclei through excitation of higher lying states. A shuttle was constructed to transport targets of natural isotopic abundance from an irradiation position to a measuring position. Other than a low background the activity measured was due entirely to isomeric decay. The measured half-lives in seconds are $^{77m}$ 17.58±0.12, $^{79m}$Br: 4.97±0.10, $^{167m}$Er: 2.28±0.03, $^{179m}$ 18.77±0.07, $^{183m}$W: 5.56±0.25, $^{191m}$Ir: 4.88±0.03, and $^{197m}$ 7.86±0.04. The data are presented and the methods of analy are discussed. The results are compared to recent literat values.

**12874.** Kondo, A., Brenner, F. C., **Research for a uniform qual grading system for tires. VI. Comparison of the effect of fr and rear wheel drive vehicles on projected tread wear of a ti** *Rubber Chem. Technol.* **44,** No. 4, 960-961 (Sept. 1971).

Key words: Automobile tires; environment, grading; pa ment; rating; test method; tread wear.

The total number of miles that could be expected for a tire v projected and compared from a test involving a front axle dr and a rear axle drive vehicle. On the front axle drive vehicle tires wore at twice the rate on the front wheels as on the rear; the other vehicle they wore at about the same rate on both axl

The projected mileages for the tires on the two vehicles w 22,400 and 22,500 miles which is not significantly different.

**12875.** Linzer, M. A., **A frequency swept injection locked nuc induction spectrometer with signal averaging,** *Rev. Sci. strum.* **43,** No. 5, 723-726 (May 1972).

Key words: Frequency-sweep; injection-locking; nmr; n nuclear induction; signal averaging.

A frequency sweep injection technique, suitable for sig averaging and fast passage studies, has been developed for with a nuclear induction spectrometer.

**12876.** Treu, S., **A conceptual framework for the searcher-syst interface,** *Proc. Workshop on Interactive Bibliograp Search: The User/Computer Interface, Palo Alto, Calif., J 14-15, 1971,* D. E. Walker, ed., pp. 53-66 (AFIPS Pr Montvale, N.J., 1971).

Key words: Bibliographic search; conceptual framewo interactive search system; man-computer interaction; m machine system.

A conceptual framework for the searcher-system interfac portrayed as dependent on whether (and how) the real or virt capabilities of the search system can satisfy the natural char teristics of human interactive information-seeking behavior. pragmatic retain-rectify-reform approach is defined and carr out towards arriving at a set of twelve such characteristi Because empirical confirmation (or rebuttal) is desirable lacking, a "transparent stimulation" experiment is suggested broadly described.

**12877.** Petrescu-Prahova, I., Winogradoff, N. **Photoluminescence in compensated *n*-type, Si-doped gallium senide,** *J. Phys. Chem. Solids* **32,** 1873-1879 (1971).

Key words: Amphoteric compensation; band tailing; c lomb potential screening; gallium arseni photoluminescence; silicon doping.

Band tailing observed in highly doped GaAs and ot semiconductors has been attributed to screened coulomb pot tials. The amphoteric nature of melt-grown, Si-doped samp limiting the free electron concentration to below $n=5\times 1$ cm$^{-3}$, permitted the unequivocal study of the band tail para ters as a function of impurity concentration at virtually const free carrier screening over a silicon concentration range from $\times 10^{18}$ to $1.2\times 10^{20}$ cm$^{-3}$. The photoluminescent spectra of s samples consisted of two broad bands, one of which, centere 1.2 eV, decreased with increasing temperature and vanishe higher temperatures where accurate analysis of the shape of other band, centered at any energy close to the band gap, ld be made. The intensity of the low energy side of the latter nd was found to be exponential proportional to exp $(h\nu/E_0)$, the dependence of $E_0$ on the concentration of the silicon do- nt was determined. Since a change of the excitation intensity er two orders of magnitude did not change the position or pe of the band-to-band "line," it was concluded that the na- e of the spectra reflects exponential density-of-states tails at conduction band edge.

78. Skopik, D. M., Dodge, W. R., **${}^4$He$(e,d)e'{}^2$H angular-dis- ribution and cross-section measurements between 36 and 50 MeV,** *Phys. Rev. C* **6,** No. 1, 43-53 (July 1972).

Key words: E-2 angular distributions; electric-quadrupole transition; identical particles; virtual photons; ${}^4$He photodisintegration.

leasurements of the angular distributions in the "virtual oton" energy interval of 40 ± 1 MeV and the total cross sec- n in the energy interval of 35.7 – 49.4 MeV of the e$(e,d)e'{}^2$H reaction are presented. The data are compared h early calculations and with more recent cluster-model and persive calculations.

79. Robertson, A. F., **Discussion of paper "Fire and the cur- ain wall' by H. L. Malhotra, United Kingdom,** (Proc. Symp. f CIB Conf. on Curtain Walls, Paris, France, Mar. 3-6, 970), *Symp. Papers in Light Facades,* pp. 74-75 (June 1971).

Key words: Curtain walls; exterior walls; fire spread.

he paper, "Fire and the Curtain Wall" by H. L. Malhotra to presented in a symposium sponsored by Counseil Interna- nal du Batiment pour Reserche et Documentation on the cur- n wall has been discussed in the light of information currently ilable in the USA. It is suggested that the experiments quoted Malhotra may have failed to properly simulate fire behavior buildings of conventional shape. A word of caution is offered inst the proposal that current code requirements with respect height of spandrel walls or horizontal floor projections are un- y restrictive.

80. Caswell, R. S., **Review of measurements of absolute eutron emission rates and spectra from neutron sources,** (Proc. Amer. Nucl. Soc. National Topical Meeting on Neutron Sources and Applications, Augusta, Ga., Apr. 19-21, 1971), Chapter in *Neutron Sources and Applications, CONF- 710402,* **I,** 1-53 – 1-62 (1971).

Key words: Manganous sulfate bath; neutron emission rate; neutron sources; neutron spectra; neutron spectrum measurement methods; ${}^{252}$Cf.

The measurement of the absolute neutron emission rate of utron sources has been reviewed with emphasis on the man- nous sulfate bath method, and is found to be in good quantita- e shape. In precision applications, such as $\nu$ (neutrons/fission) d certain cross section measurements, higher accuracy would, vertheless, be desirable. Significant improvement in the accu- y of $(\beta,n)$ source calibrations could be obtained by resolution the discrepancy on the magnitude of the fast neutron loss to clear reactions in the manganous sulfate bath.

Recent developments in the techniques of measuring spectra neutron sources has led to the beginning of reliable measure- nts in the energy region below 1 MeV. The source spectrum asurement field is, nevertheless, in semi-quantitative state. rther intercomparisons of measurement methods are needed, d also, the resolution of a discrepancy on the neutron energy ectrum for the ${}^{252}$Cf spontaneous fission neutron source.

12881. Jacox, M. E., Milligan, D. E., **Vibrational and electronic spectra of the $O_3^-$ anion isolated in an argon matrix,** *J. Mol. Spectrosc.* **43,** No. 1, 148-167 (July 1972).

Key words: Charge transfer; electron attachment; infrared spectrum; matrix isolation; molecular orbitals; $O_2 + O^-$ reaction; $O_3^-$ anion; ultraviolet spectrum.

The $O_3^-$ anion has been stabilized in an argon matrix at 14 K in concentration sufficient for the detection of the antisymmetric stretching fundamental, $\nu_3$, and of a band system between 5100 and 3700 Å. Both the reaction of $O^-$ (produced by the interaction of photoelectrons with $N_2O$) with $O_2$ and the charge-transfer interaction between $O_3$ and K atoms have served as sources of $O_3^-$ in these studies. Although the $\nu_3$ absorption is slightly dependent upon the alkali metal used as the photoelectron source, the experiments suggest that the $\nu_3$ absorption of $P_3^-$ isolated in an argon lattice should lie very close to 800 cm$^{-1}$. Detailed isotopic studies support the proposed vibrational assignment and demonstrate that the valence angle of ground-state $O_3^-$ is 110±5° and that the oxygen-oxygen bonds are considerably weaker than those of $O_3$. The nature of the observed electronic transition of $O_3^-$ is discussed, and evidence is considered for the presence of a low-lying dissociative state.

12882. Celotta, R. J., Bennett, R. A., Hall, J. L., Siegel, M. W., Levine, J., **Molecular photodetachment spectrometry. II. The electron affinity of $O_2$ and the structure of $O_2$,** *Phys. Rev. A* **6,** No. 2, 631-642 (Aug. 1972).

Key words: Electron affinity; molecular constant; molecular oxygen; negative ions, photodetachment.

A beam of $O_2^-$ ions, extracted from a glow discharge in $N_2O$, is crossed with the linearly polarized intracavity photon beam of an argon-ion laser (4880 Å). Electrons photodetached at right angles to the crossed beams are energy filtered by a hemispherical analyzer. The electron energy spectra are characteristic of photodetachment from the $v'=0$ state of $O_2^-$ to the $X^3\Sigma_g^-$ and $a^1\Delta_g$ state of $O_2$. Vibrational state analysis is facilitated by the use of isotopes. The electron affinity obtained is 0.440± 0.008 eV. Additionally, we have measured the relative transition probabilities as a function of final vibrational state and the angular distributions of the outgoing electrons. The relative intensities, corrected by the angular distributions, determine through Franck-Condon-factor analysis the internuclear distance for the negative ion. We find $r_e''=1.341\pm0.010$ Å and therefore $B_e''=1.17\pm0.02$ cm$^{-1}$

12883. Siegel, M. W., Celotta, R. J., Hall, J. L., Levine, J., Bennett, R. A., **Molecular photodetachment spectrometry. I. The electron affinity of nitric oxide and the molecular constants of $NO^-$,** *Phys. Rev. A* **6,** No. 2, 607-631 (Aug. 1972).

Key words: Electron affinity; molecular constants; negative ions; nitric oxide; photodetachment.

We apply laser photodetachment and photoelectron spectrometry for the first time to the study of molecular negative ions. We describe in detail the study of the nitric oxide ion $NO^-$; a following paper reports results for $O_2^-$. We use the $NO^-$ results to develop and illustrate in detail the principles and applications of the technique. A mass-selected $NO^-$ beam (680 eV) is crossed with a linearly polarized monochromatic (4880 – Å) argon-ion laser beam, and electrons photodetached into a $4\pi/2000$-sr solid angle perpendicular to the crossed beams are energy analyzed using a hemispherical electrostatic monochromator. The data yield a set of vertical detachment energies between vibrational states of $NO^-$ and NO, and relative intensities for these transitions. Angular distributions about the polarization direction are studied by rotating the laser polarization while maintaining the mutually perpendicular ion-beam-laser-beam-electron-collection geometry. For each transition we measure the anisotropy parameter $\beta$, corresponding to the form $[1+\beta P_2(\cos\theta)]$ for the angular distribution. Several arguments, including data on $NO^{18-}$ photodetachment, are used to identify the initial and final vibrational states. Molecular rotational effects, and effects associated with the spin-orbit splitting of the final $NO(X^2\Pi)$ state are identified and included in the analysis. A Franck-Condon-factor analysis of the observed relative cross sections, parametrized by trial values of the $NO^-$ molecular constants, is used to determine that for $NO^-$ $\omega_e''=1470\pm200$ cm$^{-1}$, $r_e''=1.258\pm0.010$ Å, and $B_e''=1.427\pm0.02$ cm$^{-1}$. Using these constants, the measured vertical detachment energy is reduced by rotational and spin-orbit effects to the electron affinity $E_A(NO)=24^{+10}_{-5}$ meV.

**12884.** Utton, D. B., Tsang, T., **Coupled nuclear spin relaxation and internal rotations in magnesium fluosilicate hexahydrate,** *J. Chem. Phys.* **56,** No. 1, 116-119 (Jan. 1, 1972).

Key words: Internal motion; magnesium fluosilicate hexahydrate; nuclear magnetic resonance; relaxation.

Both proton and fluorine nuclear spin-lattice relaxations have been studied by the 180-90° pulse method in $MgSiF_6\cdot6H_2O$ at 25 and 13 MHz over the temperature range 170-350 K. Nonexponential behaviors have been observed. Both $^1H$ and $^{19}F$ relaxations may be characterized by the same pair of relaxation times, the shorter component due to the intermolecular H–F dipolar interaction. The results indicate that the $SiF_6^{2-}$ ions are reorienting with an activation energy, $V=31\pm4$ kJ/mole$=7.5\pm1.0$ kcal/mole, and a frequency factor $\tau_0=10^{-14\pm1}$ sec. These values are consistent with other hydrogen-bonded fluorine compounds.

**12885.** Hutchinson, J. M. R., Garfinkel, S. B., **Standardization of cadmium-109 sources for γ-ray emission rate,** *Int. J. Appl. Radiat. Isotop.* **22,** 405-414 (1971).

Key words: Cadmium-109; cobalt-57; gamma-ray emission rate; iron-57; photoelectron escape; silver-109M; standardization; well crystal counting.

The standardization of $^{109}Cd$ sources for 88-keV γ-ray emission rate has been performed using a NaI(Tl) well crystal which gives a nearly $4\pi$ geometry. Since the low-energy portion of the 88-keV γ-ray spectrum is obscured by 22-keV X-ray pulses, the total counting rate cannot be found by merely summing the counting rates for all the channels in the distribution. A method, in which the spectrum is broken down into eight components, is used to determine the number of degraded 88-keV γ-ray pulses. The calibration is performed by summing the counting rates of the various components below an arbitrarily chosen energy of 39 keV, and adding them to the total counting rate above 39 keV. The process in which photoelectrons escape into the aluminum liner of the well is found to be responsible for most of the degraded 88-keV γ-ray pulses which fall below 39 keV. The estimated systematic error in the measurement is ±0.9 percent.

Using $^{57}Co$ sources which have been accurately calibrated by coincidence counting, the 2-in. × 2-in. NaI(Tl) well crystal is shown to have a γ-ray detection efficiency of 100 percent with an uncertainty of ±0.2 percent (after corrections have been made for well-wall γ-ray absorption and escape out of the well). The total abundance for 122- and 136-keV $^{57}Fe$ photons emitted per decay from $^{57}Co$ has been measured to be $0.963\pm0.003$.

**12886.** Hutchinson, J. M. R., Lantz, J. L., Mann, W. B., Mullen, P. A., Rodríguez-Pasqués, R. H., **An anti-coincidence shielded NaI(Tl) system at NBS,** *IEEE Trans. Nucl. Sci.* **NS-19,** No. 1, 117-118 (Feb. 1972).

Key words: Anti-coincidence; anti-Compton; gamma rays; low level radioactivity; multidimensional; radioactivity.

An anti-Compton, anti-coincidence shielded NaI(Tl) s trometer is described.

**12887.** Rodríguez-Pasqués, R. H., **Microactivity radiochemi** *Proc. 2d Inter-American Conference on Radiochemi Mexico City, Mexico, Apr. 22-25, 1968,* pp. 278- (Published by Secretaría General de la Organización Estados Americanos, Washington, D.C., 1971).

Key words: Detection limits; high sensitivity count low-level; low-level separations; microacti radiochemistry; radionuclide identification; specific acti threshold.

Microactivity is taken as synonymous with low-level radi tivity, and is defined as 1 dpm/g, or less. The refinement technique developed to deal with these low levels have wide the field of radiochemical and nuclear chemistry research new subjects. Two general requirements are discussed, nan high sensitivity detection, and refined chemical techniques.

The difficult problem of radionuclide identification at micr tivity level is also examined.

**12888.** Hirshfeld, A. T., Hoppes, D. D., Mann, W. B., Schima J., **Nuclear orientation of $^{82}$Br in iron,** (Proc. Int. Conf. Hyperfine Interactions in Excited Nuclei, Rehovot, Isr Sept. 6-11, 1970), Chapter in *Hyperfine Interactions Excited Nuclei* **1,** 335-338 (Gordon and Breach Sci. P New York, London, Paris, 1971).

Key words: Beta rays; gamma rays; hyperfine interacti isotope separator; magnetic moment; nuclear orientat $^{82}Br$.

$^{82}Br$ was implanted in .025 mm thick iron foil, using the high-resolution isotope separator. The bromine was oriente cooling by adiabatic demagnetization and the anisotropy of emitted beta and gamma radiation observed. For the upper 4 of the $5^-\rightarrow4^-$ beta spectrum an asymmetry of $\pm.046\pm.004$ observed at a foil temperature of 35 mK. This, taken toge with the observed anisotropies for seven gamma peaks, indic an effective field of $400^{+400}_{-100}$ kG acting on a fraction of bromine atoms. The sign of the $^{82}Br$ magnetic dipole mome positive, assuming a positive value for the effective field.

**12889.** Soulen, R. J., Jr., Colwell, J. H., **The equivalence of the perconducting transition temperature of pure indium as de mined by electrical resistance, magnetic susceptibility, and h capacity measurements,** *J. Low Temp. Phys.* **5,** No. 3, 325- (1971).

Key words: Carbon resistance thermometry; electrical sistance; heat capacity; indium; magnetic susceptibility; perconductivity; thermometric fixed point; transition t perature.

The superconducting transition temperature of a well nealed polycrystalline sample of pure indium was determine three different techniques. The heat-capacity and susceptibi transitions are approximately 1 mK wide and span the same t perature interval. The resistance transition is less than 0.2 wide and occurs at the center of the other transitions. By ch ing the midpoint of each transition the three measurements identical to within 0.1 mK.

**12890.** Cook, C. C., Allred, C. M., **An excitation system for pis attenuators,** *IEEE Trans. Instr. Meas.* **IM-20,** No. 1, 10 (Feb. 1971).

Key words: High-power impedance matching; mode filt negative current feedback; waveguide-below-cutoff atten tor.

The problems of mode purity and the interaction effect nerally necessitate a large insertion loss in precision veguide-below-cutoff (piston) attenuators to obtain a linear tput. An attenuator excitation system, used on a precision at-uation measuring system, that reduces these problems is scribed. Experimental work as well as theoretical considera-ns is discussed and designs are presented that have produced tput voltages of the piston attenuator greater than 1 V while ll maintaining a linearity of 0.001 dB as a function of piston sition. This has been accomplished by (1) operating with large out power (100-200 W), (2) development of new exciting units th improved geometry for better field excitation and utilizing ter-cooled elements for high-power operation, (3) special im-dance matching networks having exceptional stability with gh power input, (4) use of current feedback to achieve effec-ely constant current excitation, and (5) a mode filter that at-uates the undesired $TM_{01}$ mode 98 dB while attenuating the sired $TE_{11}$ mode only 0.2 dB.

891. Gimmestad, G. G., Pardoe, G. W. F., Gebbie, H. A., **The study of dimeric molecules in ammonia vapour of submillimeter wave spectroscopy,** *J. Quant. Spectrosc. Radiat. Transfer* **12,** 559-567 (1972).

Key words: Ammonia; dimers; infrared.

Absorption by true dimers can be distinguished from that at-butable to transient pairs by being spectrally narrow and by ving a temperature dependence characterized by a well fined binding energy. Using these criteria, the presence of mers in ammonia gas under conditions near those of saturated por is deduced from the observation of narrow spectral fea-res near 10 $cm^{-1}$, and a heat of dimerization of 3.6 ± 0.8 kilo-lories per mole. This value, of the order of what would be ex-cted from breaking single hydrogen bonds, is a little lower than e values found by other methods. The presence of dimers ould be considered in interpreting line shape observations at gh pressures.

892. Zimmerman, J. E., **Josephson effect devices and low-frequency field sensing,** *Cryogenics* **12,** No. 1, 19-31 (Feb. 1972).

Key words: Cryogenics; Josephson effect; magnetometry; superconductivity.

Three major areas of application of the Josephson effect are cognized; absolute standards, millimetre and sub-millimetre ave sensing, and dc and low-frequency current, voltage, and agnetic field sensing. In the latter area, single junction rf-biased w-inductance loop devices in a number of different forms inction types and loop geometries) have been developed with nsitivities of the order of $10^{-15}$ $T(10^{-11}G)$ or $10^{-19}V$. These nsors are being used in applications as diverse as mag-tocardiography and absolute noise thermometry in the illikelvin range. As amplifiers, they are characterized by monstrated equivalent noise temperatures of less than a few illikelvin, and probably a few microkelvin (theoretical). Highly liable thin-film loop devices in a number of different forms ve been developed in several laboratories, but the more easily-ade point-contact devices are probably the most widely used. any of the characteristics of the devices can be easily in-rpreted with the aid of a pendulum analogue.

893. Ruff, A. W., Jr., **Interpretation of x-ray diffraction data with regard to stacking faults in silver-tin alloys,** *J. Appl. Phys. Commun.* **43,** No. 6, 2909-2911 (June 1972).

Key words: Alloys; dislocation; stacking-fault energy; stacking-fault probability; x ray.

Several alternative interpretations of data from fcc silver-tin loys are discussed in examining the relation between stacking-fault probability and stacking-fault energy. One important aspect concerns the true variation of dislocation density with alloy composition.

12894. Siegwarth, J. D., Radebaugh, R., **The design of optimum heat exchangers for dilution refrigerators,** *Rev. Sci. Instrum.* **43,** No. 2, 197-204 (Feb. 1972).

Key words: Cryogenics; dilution refrigerator; heat exchangers; helium-3; helium-4.

The behavior of discrete heat exchangers as a function of temperature, heat transfer area, and $^3He$ flow rate is shown for a general case by means of some machine calculated curves. From these curves, the appropriate heat exchanger size can be determined for the various steps of a discrete heat exchanger. Also, curves for the mixing chamber temperature $T_m$ as a function of total surface area divided by flow rate for various amounts of external heat to the mixer are shown for the continuous exchanger. From these curves the optimum $^3He$ flow rate for a given heat input and exchanger size can be determined. Viscous heating has been included in the calculation of one typical coaxial tube exchanger. It is found that heating in the dilute stream has negligible effect on $T_m$, whereas the viscous heating in the concentrated side, though several times smaller than that in the dilute side, has considerably more effect on $T_m$. Based on this behavior, an improved method of "heat sinking" heat leak paths to the mixer is suggested.

12895. Mizushima, M., Evenson, K. M., Wells, J. S., **Laser magnetic resonance of the NO molecule using 78-, 79-, and 119-μm $H_2O$ laser lines,** *Phys. Rev. A* **5,** No. 5, 2276-2287 (May 1972).

Key words: *g* Factor; laser magnetic resonance; NO; spin-orbit coupling constant; water vapor laser.

The magnetic resonance of the NO molecule is observed using the 78-, 79-, and 119-μm lines of the $H_2O$ laser as the radiation source. The resonances in three cases are due to the $(^2\Pi_{1/2}J=12.5) \rightarrow (^2\Pi_{3/2}J=12.5)$, $(^2\Pi_{1/2}J=11.5) \rightarrow (^2\Pi_{3/2}J=11.5)$, and $(^2\Pi_{1/2}J=12.5) \rightarrow (^2\Pi_{3/2}J=11.5)$ transitions, respectively. Most of them are magnetic dipole transitions, but a few electric dipole transitions are also observed. It is found that the calculated $g$ factors $g_{c2}(11.5)=g_{d2}(11.5)=-0.0064$, $g_{c1}(11.5)=g_{d1}(11.5)=0.0272$, $g_{c2}(12.5)=g_{d2}(12.5)=-0.0092$, $g_{c1}(12.5)=g_{d1}(12.5)=0.0270$, and the calculated Λ-doublet separations $f_{c2}(11.5)-f_{d2}(12.5)=243$ MHz, $f_{c1}(11.5)-f_{d1}(11.5)=4323$ MHz, are consistent with our experimental results. The hyperfine structure and the second-order effects are also in agreement with theoretical values. The average separation between the $^2\Pi_{3/2}$ and $^2\Pi_{1/2}$ states for a given $J$, which we call $X_J$, is found to be $126.4469 \pm 0.0005$ and $127.5786 \pm 0.0005$ $cm^{-1}$ for $J=11.5$ and 12.5, respectively. The conventional spin-orbit coupling constant is found to be $123.1580 \pm 0.0010$ $cm^{-1}$ when $J=12.5$ or 11.5. [The conventional spin-orbit coupling constant $A_c$, commonly referred to as $A$, is given by $A - \delta(J+1/2)^2 + 1/4\gamma$ in our notation.] The coupling constant $\mu_s$ for the $\vec{S} \cdot \vec{N}$ term is found to be $-0.006 \pm 0.002$ $cm^{-1}$.

12896. Prydz, R., Goodwin, R. D., **Experimental melting and vapor pressures of methane,** *J. Chem. Thermodyn.* **4,** No. 1, 127-133 (Jan. 1972).

Key words: Boiling point; critical-point pressure; melting pressure; methane; triple-point constants; vapor pressure.

Thirteen melting pressures to 210 atm are represented by the Simon equation with a root mean square deviation of 0.05 atm (0.08 percent). This representation is highly sensitive to the triple point temperature, yielding 90.680 K (IPTS-1968). These pressures agree within 0.5 percent with the less precise data of one other investigator at temperatures above 93 K. One hundred and five vapor pressures from the triple point to the critical point are represented by a new, non-analytic equation with a root mean square relative deviation of 0.01 percent. The derived triple point pressure is 0.1159 atm. At the assigned critical point temperature of 190.53 K the pressure is 45.356 atm. Deviations of some of the data from other sources exceed one percent at $T < 140$ K.

**12897.** Ledbetter, H. M., **An approximation of $\theta_{elastic}$ for cubic metals,** *J. Phys. F* **2,** No. 2, 262-269 (Mar. 1972).

Key words: Crystal properties; Debye temperature; elastic constants; velocity/elastic waves.

The Debye characteristic temperature $\theta$ has been calculated from the elastic coefficients for 24 cubic elements by an approximate method proposed previously by other workers. The approximation requires that the elastic secular equation be solved only for the three principal cubic directions. New weighting coefficients for these directions were determined by a least squares best-fit procedure, based on computationally "exact" values of $\theta$. Comparisons with the results of previous three term approximations indicate which set of weighting coefficients gives the best approximation to $\theta$.

**12898.** McDonald, D. G., Risley, A. S., Cupp, J. D., Evenson, K. M., Ashley, J. R., **Four-hundredth-order harmonic mixing of microwave and infrared laser radiation using a Josephson junction and a maser,** *Appl. Phys. Lett.* **20,** No. 8, 296-299 (Apr. 15, 1972).

Key words: Cryotemperatures; harmonic mixing; infrared detectors; Josephson junctions; laser frequency measurements; lasers; superconductivity.

For mixing in a Josephson junction at infrared frequencies, we have shown that the available power from the junction increases as the intermediate frequency is increased. Following this result an infrared receiver has been developed incorporating a 9-GHz maser preamplifier at the i.f. Using this system, the beat between the 401st harmonic of a high-quality microwave source and a 3.8-THz infrared laser has been observed. Also, for low-order mixing at 3.8 THz, a comparison of beat signals from a Josephson junction and a room-temperature mixer has been made.

**12899.** Ledbetter, H. M., Wayman, C. M., **The crystallography of the $\beta$-to-$\beta''$ AuCd martensitic transformation,** *Acta Met.* **20,** No. 1, 19-30 (Jan. 1972).

Key words: Crystallography; gold-cadmium alloys; martensite; phase transformations.

The crystallography of the martensitic transformation in near-equiatomic AuCd alloys is re-examined, experimentally and theoretically, from the viewpoint that the low-temperature $\beta''$ phase has either trigonal or hexagonal symmetry. The elements of the Bain strain accompanying the transformation are found to be smaller than those reported for any other metallic system. As a result, only the habit plane and the twin ratio are useful quantities for characterizing the transformation. Predictions of the present study are in accord with existing measurements of these quantities. The reported lattice correspondence is believed to be unique for the martensitic transformation of a beta phase alloy.

**12900.** Manning, J. R., **Impurity-correlation factors for diffusion in diamond-structure crystals,** *Phys. Rev. B* **6,** No. 4, 1344-1355 (Aug. 15, 1972).

Key words: Correlation factor; diamond structure; diffusion; impurity; jump frequency; vacancy.

The correlation equations for impurity diffusion in the diamond structure have much in common with the equations for self-diffusion in pure face-centered-cubic and diamond st tures. Comparison of these equations allows the four-freque expression for the impurity-correlation factor in the diam structure to be calculated to the same precision as the correla factor for self-diffusion in a pure face-centered-cubic struct This precision is an order of magnitude better than that for previous calculation of this impurity-correlation factor. The culation also illustrates an effect that choice of diffus direction can have on the form of the correlation-factor ec tions. In these calculations, a generalized method is develope calculating impurity-correlation factors in terms of effect vacancy-return probabilities $U_q$, including contributions fr vacancies which move far away from the impurity before ef tively returning to their original site. Connections between v ous calculational techniques are discussed. The accurate val obtained here are compared with previous calculations done a variety of other methods. This allows an evaluation of problems arising in various standard calculational techniques.

**12901.** Foote, W. J., Hunter, R. D., **Improved gearing for rot vane attenuators,** *Rev. Sci. Instrum.* **43,** No. 7, 1042-1043 (J 1972).

Key words: Attenuator; microwave; rotary vane; Spi (Reg. T.M.).

A WR15 rotary-vane attenuator is modified and driven b 180:1 precision gear set. This one step drive provides an ac rate, repeatable readout resolution 20 times better than that u on commercial attenuators.

**12902.** Swartzendruber, L. J., Bennett, L. H., **Retained auste developed during surface grinding of a carbon steel,** *Scr. M* **6,** 737-742 (Aug. 1972).

Key words: Electron conversion; Mössbauer; retai austenite; standard sample; steel.

Light surface grinding on a spheroidized Fe-C alloy of the tectoid composition raises the surface layer to a temperature ficient to dissolve the carbide particles. The rapid quenching p vided by the sample substrate and the cutting fluid retains a s face layer of austenite approximately 0.01 $\mu$m thick. Mössba scattering experiments, using electron conversion, can detect retained austenite.

**12903.** Hyman, A., Perloff, A., **The crystal structure of bism (2:1) borate, $2Bi_2O_3 \cdot B_2O_3$,** *Acta Crystallogr.* **B28,** Part 2007-2011 (1972).

Key words: Bismuth; borate; x-ray crystal structure.

The crystal structure of bismuth (2:1) borate ($2Bi_2O_3 \cdot B_2$ was determined by single-crystal x-ray diffraction analy Proper classification of this compound is as an oxide-orthobor with the formula $Bi_4O_3(BO_3)_2$. The material crystallizes in monoclinic system, $P2_1/c$, with 4 formula units in a cell of dim sions $a = 11.107$, $b = 6.627$, $c = 11.044$ Å and $\beta = 91.04°$. Int sity data were obtained on an automated diffractometer us Nb-filtered Mo $K\alpha$ radiation ($\lambda = 0.71069$ Å). Bismuth positi were established by direct phase determining procedures and remaining atomic positions found from a three-dimensional ference synthesis phased by the bismuth atoms. Full-matr least-squares, isotropic refinement of the structure yielde residual $R = 5.1\%$ for 2098 observed reflections. The struct contains discrete pianar $BO_3^{3-}$ anions held together by coordi tion to bismuth atoms. Additional oxygen atoms, coordina only to bismuth, are present. The average B – O distance 1.38 Å. The minimum Bi – O distance found is 2.14 Å. Some the bismuth atoms do not have a clearly delineated coordinati shell.

**2904.** Perloff, A., **The crystal structures of hydrated calcium and ammonium monofluorophosphates: $CaPO_3F \cdot 2H_2O$ and $(NH_4)_2PO_3F \cdot H_2O$,** *Acta Crystallogr.* **B28,** Part 7, 2183-2191 (1972).

Key words: Ammonium fluorophosphate monohydrate; calcium fluorophosphate dihydrate; crystal structure; fluorophosphate ion.

With the primary intention of establishing the dimensions and onfiguration of the monofluorophosphate ion, the crystal strucures of the calcium and ammonium salts have been determined y three-dimensional x-ray diffraction analysis. Data were meaured on an automated diffractometer using Nb-filtered Mo $K\alpha$ adiation, $\lambda = 0.71069$ Å. Both structures were established by irect phase determining techniques and refined by full-matrix east-squares analysis using anisotropic thermal parameters for ne nonhydrogen atoms and isotropic thermal parameters for the ydrogen atoms. All hydrogen atoms were located in difference aps and the hydrogen bonding in these structures could be nambiguously determined. The crystal data (at 25 °C) and final R values are: $CaPO_3F \cdot 2H_2O$; $P\bar{1}$, $a = 8.6497$ (7), $b = 6.4614$ 5), $c = 5.7353$ (4) Å, $\alpha = 119.003$ (7), $\beta = 110.853$ (7), $\gamma =$ 4.146 (8)°, $V = 249.94$ Å$^3$, $Z = 2$, $\rho_c = 2.313$ g.cm$^{-3}$, $R = 2.0\%$ 1254 observed data). $(NH_4)_2PO_3F \cdot H_2O$; $P2_1/c$, $a = 6.3042$ (5), $= 8.2942$ (7), $c = 12.7597$ (10) Å, $\beta = 98.415$ (8)° $V = 660.00$ Å$^3$, $Z = 4$, $\rho_c = 1.530$ g.cm$^{-3}$, $R = 3.6\%$ (1721 observed data). he average dimensions of the $PO_3F^{2-}$ ion are; P – F 1.585, P – O 1.506 Å, F – P – O 104.5 and O – P – O 114.0°.

**2905.** Cezairliyan, A., **Measurement of melting point and electrical resistivity (above 3600 K) of tungsten by a pulse heating method,** *High Temp. Sci.* **4,** No. 3, 248-252 (June 1972).

Key words: Electrical resistivity; high-speed measurements; high temperature; melting point; thermodynamics; tungsten.

A subsecond duration pulse heating method is used to measure he melting point, and electrical resistivity of tungsten above 600 K. The results yield a value of 3695 K (on the International Practical Temperature Scale of 1968) for the melting point with n estimated inaccuracy of 15 K. Estimated inaccuracy in elecrical resistivity measurements is 1%.

**2906.** Rubin, R. J., **Velocity autocorrelation function of a large cluster of particles in a one-dimensional crystal,** *J. Chem. Phys.* **57,** No. 1, 312-316 (July 1, 1972).

Key words: Diffusion coefficient; harmonic crystal; velocity autocorrelation function.

The velocity autocorrelation function of the center of gravity of a cluster of $Q$ particles in a one-dimensional harmonic crystal s determined in the limit $Q \rightarrow \infty$. In this limit, the autocorrelation decreases linearly from one to zero. In the continuum limit of the attice equations of motion the same linear form is obtained for he velocity autocorrelation function. The coefficient of self-diffusion of the cluster of $Q$ particles equals $kT$, a result which is exact and independent of cluster size.

**12907.** Vidal, C. R., Hessel, M. M., **Heat-pipe oven for homogeneous mixtures of saturated and unsaturated vapors; application to NaLi,** *J. Appl. Phys.* **43,** No. 6, 2776-2780 (June 1972).

Key words: Heat-pipe oven; laser induced resonance fluorescence; NaLi molecule; vapor mixtures.

A heat-pipe oven has been developed to produce homogeneous mixtures of a saturated vapor with an unsaturated vapor at any arbitrary well-defined ratio. The oven is able to handle materials of widely different vapor pressures and the zone containing the homogeneous vapor mixture can be made to extend over any desired path length. With this heat-pipe oven containing sodium and lithium, the laser- and collision-induced fluorescence spectrum of the NaLi molecule has been used to study the operation of the oven. The first observation of a "propensity rule" for a polar molecule (the $\Delta J = +1$ collision-induced NaLi line is stronger than the corresponding $\Delta J = -1$ or 0 line) is reported.

**12908.** Paule, R. C., **Low level calibration mixtures for gaseous pollutants,** *Anal. Chem.* **44,** No. 8, 1537-1539 (July 1972).

Key words: Air pollution standards; calibration mixtures (of gases); microbubbles; microstandards; NO; $SO_2$.

Low level $SO_2$ calibration mixtures have been produced using a technique of mixing known weight $SO_2$ microbubbles with a diluent gas. Procedures used in the production and measurement of the microbubbles of pure pollutant and in the subsequent on-the-spot dilution of the microbubbles are described. A necessary and effective passivation procedure for the dilution cylinder is given, along with a discussion of other factors that can affect the standard.

**12909.** Rubin, R. J., **Span of a polymer chain,** *J. Chem. Phys.* **56,** No. 12, 5747-5757 (June 15, 1972).

Key words: Chain polymer; degenerate Dvoretzky-Erdös problem; lattice model; random walk.

The $x$ span of a polymer chain is defined as the difference between the largest $x$ coordinate and the smallest $x$ coordinate of any segments in the chain. The polymer chain is represented by a nearest-neighbor lattice-model random walk in which the mean square displacement of each component of a single step is 1/3. The distribution function of the $x$ span of an $N$ step random walk is obtained; and the following asymptotic formulas are obtained for its first and second moments, respectively, $2(2N/3\pi)^{1/2}$ and $4 \ln 2\, N/3$. The corresponding moments of the magnitude of the $x$ component of the end-to-end distance are $(2N/3\pi)^{1/2}$ and $N/3$. Excluded volume effects are not considered. It is noted that the problem of calculating the first moment of the $x$ span is identical with the one-dimensional case of the Dvoretzky-Erdös problem, namely, the calculation of the average number of different lattice sites visited in an $N$-step random walk on a $d$-dimensional lattice.

**12910.** Jones, M. C., Palmer, D. C., Tien, C. L., **Infrared absorptivities of transition metals at room and liquid-helium temperatures,** *J. Opt. Soc. Amer.* **62,** No. 3, 353-360 (Mar. 1972).

Key words: Absorption; chromium; iron; mirror; nickel; platinum; reflection.

Experimental data are presented for the normal spectral absorptivities of the transition metals, nickel, iron, platinum, and chromium at both room and liquid-helium temperatures in the wavelength range 2.5-50 $\mu$m. The absorptivities were derived from reflectivity measurements made relative to a room-temperature vapor-deposited gold reference mirror. The absorptivity of the gold reference mirror was measured calorimetrically, by use of infrared laser sources. Investigation of various methods of sample-surface preparation resulted in the choice of a vacuum-annealing process as the final stage. The experimental results are discussed on the basis of the anomalous-skin-effect theory modified for multiple conduction bands. As predicted, the results approach a single-band model towards the longer wavelengths. Agreement between theory and experiment is considerably improved by taking into account the modification of the relaxation time due to the photon-electron-phonon interaction proposed by Holstein and Gurzhi; but, particularly at helium temperatures, the calculated curve is consistently below the experimental results.

**12911.** Greenspan, M., **Acoustic transmission line; Some impedance properties,** *J. Acoust. Soc. Amer. Letters to Editor* **52,** No. 1, Part 2, 455-457 (July 1972).

Key words: Acoustic impedance; acoustic transmission line; sound absorption.

The imaginary part of the effective density of a fluid or of a viscoelastic material is zero. The contrary notion arises from an inadequate definition of characteristic impedance. The attenuation cannot exceed $2\pi$ Np per wavelength.

**12912.** Smith, R. V., **Two-phase, two-component critical flow in a venturi,** *J. Basic Eng. Trans. ASME, Series D* **94,** No. 1, 147-155 (Mar. 1972).

Key words: Critical flow; droplet flow; liquid film flow; transport coefficients; two-component flow; two-phase flow; venturi flow.

This paper reports the results of an analytical and experimental investigation whose object was to test the hypothesis that the flow of the gas phase controls critical and near critical two-phase flow for cases where the gas flow is essentially in separate streams. The results substantiate the hypothesis. The analytical results also indicate that one-dimensional flow equations with reasonably accurate estimates for the droplet size and for the drag and heat transfer coefficients will adequately describe critical and near critical flow over a wide range of flow conditions.

**12913.** Patrician, T. J., Ledbetter, H. M., Reed, R. P., **On the apparent rotation of transformation twins in Fe-Ni martensites,** *Metallurgical Trans.* **3,** No. 4, 947-952 (Apr. 1972).

Key words: Crystal imperfections; electron diffraction crystallography; iron alloys; nickel alloys; phase transformations/solid-state; twinning.

Fe-Ni alloys containing 28 to 33 wt pct Ni have been studied by transmission electron microscopy and by selected area diffraction to elucidate the phenomenon of the apparent deviation of the twin interface from the twinning plane $\{112\}_m$. Trace analyses of the twin interfaces are reported for 35 cases. Deviations of the twin trace, as projected onto the image plane, of up to 46 deg from those expected from $\{122\}_m$ transformation twins were observed. Contrary to previous interpretations, the conclusion of this study is that the deviations are due to the uncertainty of the orientation of the foil surface with respect to the electron beam. Thus, it has not been shown explicitly that this phenomenon provides a basis either for invoking multiple lattice invariant shears or for explaining habit plane scatter.

**12914.** Dickens, B., Bowen, J. S., Brown, W. E., **A refinement of the crystal structure of $CaHPO_4$ (synthetic monetite),** *Acta Crystallogr.* **B28,** Part 3, 797-806 (Mar. 1972).

Key words: Calcium coordinations; calcium phosphates; hydrogen bonding; monetite single crystals; x-ray diffraction.

$CaHPO_4$, synthetic monetite, crystallizes in the triclinic unit cell $a=6.910$ (1), $b=6.627$ (2), $c=6.998$ (2) Å, $\alpha=96.34$ (2)°, $\beta=103.82$ (2)°, $\gamma=88.33$ (2)° at 25 °C with cell contents of 4[$CaHPO_4$]. The structure has been refined in space-group $P\bar{1}$ by the method of least-squares to $R_w=0.032$, $R=0.031$ using 3738 observed x-ray reflections measured on a diffractometer. Corrections were made for absorption, anomalous dispersion and isotropic secondary extinction.

The structure may be considered to consist of $CaHPO_4$ chains bonded together by Ca...O bonds and three types of hydrogen bonds. One type of hydrogen bond, O(1) – H(1)...O(5), is normal but is at the short end of the normal range with O(1)...O(5) = 2.565 (1) Å; one, O(7) – H(2)...O(7′), is very short with O(7)...O(7′) = 2.458 (2) Å and is across a nominal center of sy metry; and one, O(6) – H(3)...O(8) where O(6)...O(8) = 2.6 (1) Å, is in the normal range but is presumed to be statistica disordered, with hydrogen covalently bonded to half of the O( atoms on average. The P – O distances support the choice these hydrogen positions. Ca(1) is coordinated to seven oxyg atoms in an approximately pentagonal bipyramid with Ca(1)... distances ranging from 2.2951 (9) Å to 2.763 (1) Å. Ca(2) coordinated to eight oxygen atoms with Ca(2)...O distances ran ing from 2.379 (1) Å to 2.5718 (9) Å, which all indicate stro Ca...O bonding. The Ca coordinations in several calciu phosphates and related compounds are compared.

**12915.** Bowen, R. L., Argentar, H., **A stabilizing comonomer: Synthesis and confirmation of structure,** *J. Dent. Res.* **51,** N 4, 1071-1074 (July-Aug. 1972).

Key words: Antioxidants; biomaterials; comonomers; i hibitors; polymerization; stabilizers; toxicity.

A compound (BHM) was synthesized that can stabili monomers by inhibiting premature polymerization but that ca serve as a monomer in the polymerization after the initiat system is activated. The structural formula of BHM (3,5-di-*ter* butyl-4-hydroxybenzyl methacrylate) was confirmed by nucle magnetic resonance analysis.

**12916.** Paffenbarger, G. C., **Guide to Dental Materials an Devices: a historical review,** *J. Amer. Dent. Ass.* **84,** 1333-133 (June 1972).

Key words: Certification program; guide; list of certifie dental materials; specifications; Wilmer Souder.

The Guide to Dental Materials and Devices is a biennial publ cation of the American Dental Association. It started in 1955 a a publication of the ADA Specifications for Dental Material Dr. Wilmer Souder, a physicist who was the founder and forme chief of the Dental Research Section, National Bureau of Star dards, originated the idea and gave the motivation for the origin specification for dental materials and the subsequent Guide. Th Guide is not intended to replace dental materials textbooks, bu is a source of current information for dentists, assistants an dental prosthetic laboratory technicians to guide them in thei selection and use of dental materials. The Sixth Edition 1972 1973 will be published in May or June of this year. It is a profes sional book with extensive references and is prepared by professional society for its members and their auxiliaries.

**12917.** Mihalas, D., Hummer, D. G., Conti, P. S., **On the N II λλ4640, 4097 lines in Of stars,** *Astrophys. J.* **175,** No. 2, Part 2 L99-L104 (July 15, 1972).

Key words: Dielectronic recombination; ionized nitrogen Of stars; stellar atmospheres; stellar spectra.

Detailed calculations based on non-LTE plane-parallel mode atmospheres show that the N III emission lines at λλ4634, 4640 4641 observed in Of stars are produced primarily by dielectroni recombination to $3d\ ^3D$ followed by the $3d$-$3p$ transition in a *compact atmosphere*. The $3p$ state in turn is drained by two-electron transitions to the $2p^2$ levels. We find that λ4640 is in emission for $T_{eff} \leqslant 37{,}000$ K for main-sequence objects (33,000 K for giants), while λ4097 remains strongly in absorption, in accordance with observations. The calculated equivalent widths are in substantial agreement with the observed values for those Of stars with He II λ4686 in absorption, i.e., for those objects designated by Walborn as O((*f*)).

**12918.** Peterson, R. L., **Pseudoresonances in the magnetophonon structure of nondegenerate semiconductors,** *Phys. Rev. Lett.* **28,** No. 7, 431-434 (Feb. 14, 1972).

Key words: Boltzmann equation; magnetophonon effect; semiconductors; transport theory.

A new oscillatory behavior of semiconductor transport properties in quantizing magnetic fields is predicted on general arguments. The "pseudoresonances" are due to the pairing off of single-LO-phonon emission and absorption processes ending at the infinite density-of-states region. An exact calculation of Ohmic longitudinal magnetoresistance shows that at "high" temperatures, the pseudoresonance amplitudes are comparable to the usual magnetophonon resonances. The pseudoresonances have probably been seen, but attributed to 2LO-phonon scattering processes.

12919. Young, R., Ward, J., Scire, F., **The topografiner: An instrument for measuring surface microtopography,** *Rev. Sci. Instrum.* **43,** No. 7, 999-1011 (July 1972).

Key words: Diffraction grating; field emission; micrometrology; profile; surface; surface instrumentation; surface metrology; topography; tunneling.

A noncontacting instrument for measuring the microtopography of metallic surfaces has been developed to the point where the feasibility of constructing a prototype instrument has been demonstrated. The resolution of the preprototype unit is 30 Å perpendicular to the surface and 4000 Å in the plane of the surface. Inherent noise in the perpendicular direction corresponds to 3 Å or one atomic layer. By using a typical field emitter with radius of 100 Å, an ultimate limit of 200 Å would be expected for the horizontal resolution. Topographic maps of an infrared diffraction grating have been measured in order to demonstrate the performance of the instrument in measuring a well characterized surface. The instrument has been shown to conform to the Fowler-Nordheim description of field emission while spaced at the usual operating distances from the surface. When moved to within 30 Å of the surface, its performance is compatible with Simmons' theory of MVM tunneling. In the MVM mode, the instrument is capable of performing a noncontacting measurement of the position of a surface to within about 3 Å. The instrument can be used in surface science experiments to study the density of single and multiple atom steps on single crystal surfaces, adsorption of gases, and processes involving electronic excitations at surfaces.

12920. Opal, C. B., Beaty, E. C., Peterson, W. K., **Tables of secondary-electron-production cross sections,** *At. Data* **4,** No. 3, 209-253 (July 1972).

Key words: Atmospheric gases; cross section measurement; noble gases; secondary electrons.

The normalized results of relative measurements of electron-production cross sections differential in angle over the 30 to 150° range and in ejected energy over the 4 to 200 eV range are tabulated. Primary electron energies from 50 to 2000 eV were used in the study of He, $N_2$, and $O_2$. The remaining gases (Ne, Ar, Kr, Xe, $H_2$, $CH_4$, $NH_3$, $H_2O$, CO, $C_2H_2$, NO, and $CO_2$) were studied under 500 eV impact. Measurements were performed in a crossed-beam apparatus with the use of a rotatable electron gun and a fixed hemispherical electrostatic energy analyzer.

12921. Dickens, B., Bowen, J. S., **Refinement of the crystal structure of $Ca(H_2PO_4)_2 \cdot H_2O$,** *Acta Crystallogr.* **B27,** Part 11, 2247-2255 (Nov. 1971).

Key words: Calcium phosphates; crystal structure; hydrated calcium phosphate; hydrogen bonding; monocalcium phosphate monohydrate; single crystal x-ray diffraction.

$Ca(H_2PO_4)_2 \cdot H_2O$ crystallizes in space group $P\bar{1}$ in the triclinic unit cell $a = 5.6261$ (5), $b = 11.889$ (2), $c = 6.4731$ (8) Å, $\alpha = 98.633$ (6), $\beta = 118.262$ (6), and $\gamma = 83.344$ (6)° at 25 °C with $Z = 2$. The structure was refined with 3401 observed reflections measured on a diffractometer to $R_w = 0.033$, $R_o = 0.069$. Corrections were made for absorption, anomalous dispersion, and isotropic secondary extinction. The structure contains $Ca(H_2PO_4)^+$ chains which form corrugated layers. Between these layers are layers of $(H_2PO_4)^-$ ions and water molecules. Hydrogen atoms have been located approximately; ideal positions for the hydrogen atoms have been calculated. The two sets of hydrogen positions differ by ~ 0.28 Å. One hydrogen bond, in which the water molecule is the donor, is apparently bifurcated. All other hydrogen atoms form normal hydrogen bonds, with each hydrogen site seemingly fully occupied. The disorder of one hydrogen atom between the centrosymmetrically related atoms O(1) and O(1′) was postulated by earlier workers. The P – O and O...O distances and electron-density maps obtained here show that there is no hydrogen atom in this position.

12922. Bowen, R. L., Argentar, H., **Tertiary aromatic amine accelerators with molecular weights above 400,** *J. Dent. Res.* **51,** No. 2, 473-482 (Mar.-Apr. 1972).

Key words: Accelerators; amines; color-stable composites; crystalline amine polymerization accelerators; synthesis; toxicity.

With the proper ring substituents, tertiary aromatic amines with large substituents on the nitrogen atom can be effective accelerators in free radical polymerization. Resistance to discoloration appears to be primarily a function of the substituents on the aromatic ring of the amine, whereas the rate of polymerization is dependent on both the alkyl substituents on the ring and the groups attached to the nitrogen atom.

12923. Brauer, G. M., Huget, E. F., **Dental adhesives,** Chapter 16 in *The Chemistry of Biosurfaces,* M. L. Hair, ed., **2,** 731-800 (Marcel Dekker, New York, N.Y., 1972).

Key words: Adhesives; adhesive test methods; bioadhesives; dental adhesives; dental resins; reactivity of tooth surfaces; tooth surface treatments.

Reactions occurring at the tooth surfaces and methods for obtaining bonding of restorative resins to enamel and dentin are reviewed. The composition of the tooth structure and the physical and mechanical properties of enamel and dentin are given. Studies of the reactivity of tooth surfaces as determined from adsorption, heats of immersion and wettability measurements are discussed. The effectiveness of various surface treatments such as by etching agents, enzymes, coupling agents and surface grafting techniques are examined. The potential organic polymeric adhesive systems, including bioadhesives useful for dental applications, are summarized. Methods of testing the magnitude of the adhesive joint are described.

12924. Jefferies, J. T., Orrall, F. Q., Zirker, J. B., **The interpretation of total line intensities from optically thin gases. I. A general method,** *Solar Phys.* **22,** No. 2, 307-316 (Feb. 1972).

Key words: Optically thin line emission; radiative transfer; solar corona; spectroscopic diagnostics.

We describe a general method for inferring, from the line emission of an optically thin medium, the physical state of the gas along the column in the line of sight which is sampled by the observations. Since it is not possible to infer the distribution of the physical state parameters with position in the line of sight – any arbitrary rearrangement of material giving equivalent line emission – we seek instead to specify the state in another way. A unique specification is found in terms of the bivariate distribution function $\mu(n, T)$, describing the partitioning of the matter in the gas over the density and temperature. We show that, given sufficient observational data, it is in principle possible to determine both $\mu(n, T)$, and the chemical composition. With less complete data the acuity of the analysis is correspondingly reduced.

The method is devised for application to the astronomical case, especially for studies of the solar corona, the chromosphere-corona transition region, planetary nebulae and other optically thin sources. We illustrate the formulation for the situation encountered in the solar corona.

**12925.** Jefferies, J. T., Orrall, F. Q., Zirker, J. B., **The interpretation of total line intensities from optically thin gases. II. The coronal forbidden lines,** *Solar Phys.* **22,** No. 2, 317-326 (Feb. 1972).

Key words: Optically thin line emission; radiative transfer; solar corona; spectroscopic diagnostics.

We discuss the application of a general diagnostic procedure, developed in the preceding paper of this series, to the inference of the physical state of coronal condensations from a knowledge of their forbidden line emission. We consider the limitations set on such an analysis by inadequacies in existing data and indicate the additional observations in the infrared and ultraviolet, as well as the visible, which will be needed for development of the full power of the diagnostic method.

**12926.** Jefferies, J. T., Orrall, F. Q., Zirker, J. B., **The interpretation of total line intensities from optically thin gases. III. Application to coronal forbidden line spectra,** *Solar Phys.* **22,** No. 2, 327-343 (Feb. 1972).

Key words: Optically thin line emission; radiative transfer; solar corona; spectroscopic diagnostics.

The diagnostic method developed in the two preceding papers of this series is applied to coronal forbidden line intensity data obtained at eclipses in 1952, 1961, 1965, 1966, and 1970. The application of the method is limited by the nature of the data but allows a first inference of the relationship between electron density and temperature in the condensations observed at these eclipses, and of the distribution of the electrons within the temperature range samples by the observations—effectively $10^6$ to $2.4 \times 10^6$ K. We determine the relative abundance of nickel to iron in the corona, finding a value in agreement with latest photospheric determinations and with a similar (factor of two) uncertainty. We are also able to set lower limits to the abundance of iron with respect to hydrogen, again finding values consistent with recent photospheric determinations.

**12927.** Lightbody, J. W., Jr., **Electron scattering from one- and two-phonon vibrational states,** *Phys. Lett.* **38B,** No. 7, 475-479 (Apr. 3, 1972).

Key words: Admixture; anharmonicities; branching ratios; electron scattering; phonons; reorientation effect.

Admixtures of one- and two-phonon states are required to fit (e, e′) form factors for the lowest two $2^+$ states in several even-even vibrational nuclei. These anharmonic wave functions correctly reproduce radiative branching ratios and excited state quadrupole moments.

**12928.** Neuhausen, R., Lightbody, J. W., Jr., Fivozinsky, S. P., Penner, S., **Elastic electron scattering from Zn isotopes,** *Phys. Rev. C* **5,** No. 1, 124-128 (Jan. 1972).

Key words: Electron scattering; nuclear radii; nuclear sizes; zinc nuclei.

Elastic electron scattering from the stable even-even Zn isotopes was measured in the region of the first diffraction minimum ($0.3 \leq q \leq 1.1$ fm$^{-1}$). The cross-section ratios for each pair of isotopes were used to determine the change in the rms radius. The rms radius follows an $A^{1/3}$ law between $^{64}$Zn and $^{66}$Zn and between $^{68}$Zn and $^{70}$Zn; whereas, between $^{66}$Zn and $^{68}$Zn th rms radius decreases significantly.

**12929.** Bergstrom, J. C., Crannell, H., Kline, F. J., O'Brien, J. T Lightbody, J. W., Jr., Fivozinsky, S. P., **Electroexcitation of th giant resonance of $^{13}$C,** *Phys. Rev. C* **4,** No. 5, 1514-1532 (Nov 1971).

Key words: Continuum spectra; efficiencies; fine structure giant resonance; isospin splitting; pygmy; pygmy resonance radiative tails; resonance weak coupling; $^{12}$C, $^{13}$C.

The giant resonance of $^{13}$C has been investigated by means o inelastic electron scattering. The incident energies and scatterin angles employed were 77.0 MeV (75°), 106.0 MeV (75°), 55. MeV (145.7°), and 81.0 MeV (145.7°). The data show a distinc splitting of the resonance into two large peaks near 20.5 and 24. MeV. Some fine structure is observed which correlates well wit the position of excitations calculated by Easlea. Considerabl strength is observed in the region of 14-MeV excitation whic may correspond to the "pygmy" resonance seen in th photonuclear work of Cook. Data were also taken consecutivel on $^{12}$C. The form factors for $^{12}$C and $^{13}$C are compared. Th presence of the extra neutron in $^{13}$C results in a major restructuring of the giant-resonance strength. The possibility of an isotopi splitting in the $^{13}$C giant resonance is discussed.

**12930.** Pruitt, J. S., **Electron beam current monitoring system I** *Nucl. Instrum. Methods* **100,** 433-443 (1972).

Key words: Beam; calibration electron; Faraday-cup; ferrite; monitor.

A reliable method for absolute calibration of a ferrite electro beam current monitor with a pulse generator has been develope and tested. The absolute accuracy of pulser calibrations an Faraday cup calibrations of the National Bureau of Standard ferrite monitor has been compared by using them both to determine the Faraday cup error. These independent determination differ by a maximum of 0.11% and an average of 0.03% at six different energies in the 20-120 MeV range, using beam current between 0.6 and 25 μA. Variation of the Faraday cup error wit energy is shown to compare favorably with the predictions o other authors, and the good agreement is used to argue that th influence of beam microstructure on the ferrite calibration is les than 0.1%.

**12931.** Becker, D. A., **Trace analysis for platinum in glasses b neutron activation,** *Anal. Chim. Acta* **61,** 1-6 (1972).

Key words: Glasses; neutron activation analysis radiochemical separations; spontaneous deposition; trace analysis.

Trace amounts of platinum were determined in eight glasses These glasses had been prepared under special conditions, and information on both the surface and interior platinum was desired. Previous microscopic examination of the glass samples had identified platinum on the surface of at least four of the samples. The platinum was analyzed using the nuclear reaction $^{198}$P $(n,\gamma)^{199}$Pt $\xrightarrow{\beta}$ $^{199}$Au. The $^{199}$Au product has a 3.15 day $T_{1/2}$ and $E_\gamma$ of 158 and 208 keV. Samples were irradiated in the NBSR for hours at $1.3 \times 10^{13}$ n · cm$^{-2}$ sec$^{-1}$. After irradiation, the glasses were etched with aqua regia for the determination of surface platinum, and then dissolved in HF and $HClO_4$ for the determination of interior platinum. The radioactive $^{199}$Au was separated from the matrix by spontaneous deposition on metallic zinc. Experimental sensitivites of 0.02 μg platinum were obtained.

**12932.** Pringle, W. C., Jr., **Microwave spectrum, vibration-rotation interaction, and ring puckering vibration in silacyclobutane**

**and silacyclobutane-1,1-$d_2$,** *J. Chem. Phys.* **54,** No. 12, 4979-4988 (June 15, 1971).

Key words: Dipole moment; molecular structure; ring puckering vibration; rotational spectrum; silacyclobutane; vibrational potential functions; vibration-rotation interaction.

The microwave spectrum of the molecules silacyclobutane nd silacyclobutane-1, 1-$d_2$ has been observed between 8 and 55 GHz and the first four vibrational states assigned. The ground tate rotational constants of the former molecule are 8815.75, 289.00, and 4245.32 MHz. The first two inversionlike intervals of the ring puckering mode were determined to be 75.75 and 790 MHz in the normal isotopic species; the corresponding inervals in the deuterated species are 43.06 and 4430 MHz. The ffect of these frequencies on the determination of the potential nergy for the ring puckering vibration was investigated. The ing configuration was shown to be significantly puckered in the ground state. The *a* component of the dipole moment was found o be nearly constant in the four vibrational states of the normal molecule, $\mu_a = 0.4396$ D, while the out-of-plane transition moment between inversion doublets dropped rapidly as the inverion levels approached the top of the barrier.

**2933.** Peterson, R. L., **Longitudinal magnetoresistance in polar semiconductors: A displaced-Maxwellian analysis,** *Phys. Rev. B* **5,** No. 10, 3994-4000 (May 15, 1972).

Key words: InSb; magnetophonon; magnetoresistance; semiconductors; transport theory.

The displaced-Maxwellian distribution function is used to tudy longitudinal magnetoresistance in polar semiconductors, when several carrier scattering mechanisms are simultaneously active. Although both the $B=0$ and the quantum-limit expresions for the resistance are largely the same as those obtained rom the Boltzmann equation, numerical calculations show that the displaced Maxwellian is unable to account for longitudinal magnetoresistance minima often observed in the magnetophonon tructure of polar materials. In the hot-electron regime, the displaced Maxwellian can give maxima or minima, depending upon attice temperature and type of scattering mechanisms.

**2934.** Wiese, W. L., Kelleher, D. E., Paquette, D. R., **Detailed study of the Stark broadening of Balmer lines in a high-density plasma,** *Phys. Rev. A* **6,** No. 3, 1132-1153 (Sept. 1972).

Key words: Asymmetries; hydrogen lines; line profiles; shifts; stabilized arc; Stark broadening.

The Stark-broadened profiles of the Balmer lines $H_\alpha$, $H_\beta$, $H_\gamma$, and $H_\delta$ have been measured in a high-current, wall-stabilized arc operated in hydrogen. Temperatures and electron densities have been determined with a plasma model assuming partial local thermodynamic equilibrium (LTE), after a detailed plasma analysis revealed small deviations from complete LTE. The temperaures have been determined from line-to-continuum intensity ratios using $H_\beta$ and continuum points in the near uv, and the elecron densities were derived from absolute intensity measurements. The investigations cover the range of electron densities between $1.5 \times 10^{16}$ and $10^{17}$ cm$^{-3}$ and temperatures between $0.9 \times 10^4$ and $1.4 \times 10^4$ K. Extensive comparisons with recent Stark-broadening theories and other experiments have been undertaken with the following principal results: The most pronounced differences between this experiment and theory occur in and near the line centers, where the measured profiles show systematically less structure than the calculations predict. Comparisons of the calculated and precisely measured ratios between the 1/2, 1/4, and 1/8 widths within *each* line show that the recent theories are internally consistent within 6% for $H_\beta$ and $H_\gamma$, whereas for $H_\alpha$ inconsistencies of order 25% occur. Similar inconsistencies, somewhat larger respectively, are found for the theoretical values of the half-width ratios between *different* Balmer lines. For the most important line $H_\beta$, the measured half-widths agree within 7% with the calculated values. The total experimental error in this comparison, which originates predominantly in the electron-density measurement, is estimated not to exceed 6%. Very reproducible asymmetries and red shifts are observed for $H_\beta$ and $H_\gamma$. Somewhat smaller red shifts are also obtained for $H_\alpha$. The shifts are approximately linear functions of the electron density. Comparisons with other experimental data show appreciable scatter between the various results. We estimate that for the most-often-studied line $H_\beta$ the uncertainties in the theoretical Stark widths are of the order of (5-7)% for the range of our experiment.

**12935.** Moore, G. A., **Automatic methods for analysis of microstructures,** (American Society for Testing and Materials Symp. on Stereology and Quantitative Metallography, Atlantic City, N.J., June 28, 1971), *Amer. Soc. Test. Mater. Spec. Tech. Publ.* **504,** pp. 59-80 (July 1972).

Key words: Aggregates; anisotropy; automation; computers; mechanical properties; microscopes; microstructure; particle distribution; phase mapping; quality control; scanning; television systems; variability; variance (statistics).

From the viewpoint of materials engineering and quality control the significant aspects of the microstructure of a material as a whole constitute a gestalt which controls mechanical behavior. This gestalt can be specified by six sterologically valid parameters measuring phase percentage, size and spacing of particles, variability among portions of the material, general anisotropy, and degree of patternness. Raster scanning devices of either the mechanical or television type are intrinsically capable of easily measuring these six parameters. Provision for each is available in at least one of the present television scanners. Minor changes are desirable to provide this common set of measurements with all instruments and to improve accuracy.

In contrast, microarchitectural processes which identify, measure, and selectively count individual object sections require massive programming effort and are inefficient and time consuming in present computers. Selective specimen preparation and human designation of objects are preferable to machine identification. Some proposals for more efficient and more human-like machines are mentioned. Materials engineers should try to avoid these difficult processes whenever feasible.

**12936.** Curl, R. F., Jr., Evenson, K. M., Wells, J. S., **Laser magnetic resonance spectrum of $NO_2$ at 337 $\mu$m and 311 $\mu$m,** *J. Chem. Phys.* **56,** No. 10, 5143-5151 (May 15, 1972).

Key words: HCN laser; laser magnetic resonance; $NO_2$; spectroscopy.

The Zeeman components of several rotational transitions of nitrogen dioxide have been observed in absorption using the 311 and 337 $\mu$m lines of an HCN laser as a source. The Zeeman components of four rotational transitions (two at 311 $\mu$m and two at 337 $\mu$m) have been assigned. Two components of the *g* tensor have been determined from the spectrum by least square fitting. The anisotropic component $(aa)_g{}^{(S)}$, obtained as $-0.010$, agrees well with that predicted from theory, but the isotropic component $(0)_g{}^{(S)}$, obtained as 2.013, does not agree satisfactorily with theoretical prediction or with solid phase measurements both of which give 1.9997. The rotational frequencies of the four transitions have also been obtained.

**12937.** Billingsley, F. P., II, Krauss, M., **Coupled multiconfigurational self-consistent-field method for atomic dipole**

**polarizabilities. I. Theory and application to carbon,** *Phys. Rev. A* **6,** No. 3, 855-865 (Sept. 1972).

Key words: Carbon ($^1D$); carbon ($^3P$); carbon ($^1S$); multiconfiguration; static dipole polarizability; variation method.

A method for calculating static dipole polarizabilities of atoms within a multiconfigurational self-consistent-field (SCF) framework is presented. The method involves the direct solution of the multiconfigurational SCF equations of an atom in the presence of a perturbing field which is simulated by a charged particle. The use of a multiconfigurational framework allows this technique to be applied straightforwardly to any given state of both degenerate and nondegenerate atoms, and also allows the explicit introduction of correlation effects. Sample calculations are reported for the static dipole polarizabilities of the carbon atom in its $^1S$, $^1D$, and $^3P$ states with partial inclusion of correlation. The results are compared with those obtained from many-body perturbation theory, and other techniques. In addition, a prescription for specifying a sufficiently flexible set of polarization basis functions is described.

**12938.** Jacox, M. E., Milligan, D. E., **Spectrum and structure of the $O_3^-$ and $O_4^-$ anions isolated in an argon matrix,** *Chem. Phys. Lett.* **14,** No. 4, 518-521 (June 15, 1972).

Key words: Charge transfer; infrared spectrum; isotopic substitution; matrix isolation; $O^- + O_2$ reaction; $O_3^-$ anion; $O_4^-$ anion; structure; ultraviolet spectrum.

An absorption which appears near 800 cm$^{-1}$ upon reaction of $O^-$ with $O_2$ in an argon matrix has been assigned as $\nu_3$ of $O_3^-$, with a valence angle of $110 \pm 5°$, and an absorption near 1000 cm$^{-1}$ can be assigned to *trans*-$O_4^-$.

**12939.** Franklin, A. D., **Defect equilibria in alkaline earth fluorides containing rare earth ions,** *Tech. Rep.* **AFML-TR-72-31,** 48 pages (Air Force Materials Laboratory, Air Force Systems Command, Wright-Patterson Air Force Base, Ohio, Mar. 1972).

Key words: Anelastic relaxation; $CaF_2$; density; dielectric relaxation; EPR; equilibria; point defects; rare-earth doping.

The point defects present in $GdF_3$-doped $CaF_2$, with concentrations ranging from 0.01 to 0.46 mole percent $GdF_3$, have been studied using measurements of density, EPR, and dielectric and anelastic relaxation as a function of concentration and of annealing temperature in an He + HF atmosphere in the range 500 to 1100 °C. The density measurements showed no dependence upon annealing. The unit cell contents increased in mass with increasing $GdF_3$ concentration more rapidly than expected on the basis of substitutional $Gd^{3+}$ and interstitial $F^-$ ions, and suggest the incorporation of an HF molecule with each $GdF_3$ unit. The role previously suggested for cation vacancies in the annealing behavior appears untenable in light of these density results. The reorientation kinetics of the pair formed by association of the mobile interstitial $F^-$ ion with the immobile $Gd^{3+}$ ion were studied using EPR line-broadening and dielectric relaxation measurements, and some anelastic relaxation measurements were made as well. The EPR line-broadening and dielectric relaxation data could be fitted very well with the same model, in which reorientation takes place in a mode dominated by nearest-neighbor jumps of the interstitial $F^-$ ion. This jump frequency is given by $3.1 \times 10^{12} \exp(-0.38 \text{ ev/kT}) \text{ s}^{-1}$. Additional relaxation modes appear in both the dielectric and anelastic spectra, and at least 2 and perhaps 3 centers are involved, as yet unidentified.

**12940.** Richmond, J. C., Kneissl, G. J., **Procedures for the precise determination of thermal radiation properties,** *Tech. Rep.* **AFML-TR-70-121,** 104 pages (Air Force Materials Laboratory, Air Force Systems Command, Wright-Patterson Air Forc Base, Ohio, Oct. 1970).

Key words: Emittance; graphite; iridium; laser-source i tegrating sphere; reflectance; shallow cavity emittance; su face characterization; thoria; tungsten.

The broad objective of this program, which has continued f several years, is to develop equipment and procedures for mea suring the important thermal radiation properties of material particularly those used in aircraft, missiles, and space vehicle at temperatures up to the melting points of the most refractor materials. During the period covered by this report the specif objectives were to complete development of the laser-source i tegrating sphere reflectometer, and to prepare emittance sta dards for use at temperatures above 1400 K (2000 °F). Th laser-source integrating sphere reflectometer consisted of (1) helium-neon laser as a source, capable of operation at 0.632 1.15, and 3.39 $\mu$m; (2) a 35 cm (14 in.) diameter sphere coate with barium sulphate or sodium chloride; (3) a lead sulfide detec tor; and (4) a radio-frequency generator for heating the sampl by induction. A spike filter, transmitting at the laser-wavelengt placed in front of the detector, reflected or absorbed most of th background radiation from the hot sample, and a chopped i cident beam together with synchronous amplification of th signal from the detector was used to eliminate the effect of th remaining background radiation. The integrating sphere could b evacuated, or used with an atmosphere of purified helium. A error analysis showed that the measured absolute reflectance i measured with a bias of less than one percent of the measure value. Data are presented on the directional-hemispherica reflectance [$\rho(12°;2\pi)$] at temperatures in the range of 1300 t 2500 K of well characterized samples of thoria, iridium, two lot of graphite and two lots of tungsten. Precision of measuremen on the order of 0.0005 in reflectance units, expressed as the stan dard deviation of six replicate measurements, was attained. Sam ples of one lot of tungsten and one lot of graphite were supplie by Arthur D. Little, Inc., from the same lots as those for whic thermal conductivity data are reported in AFML-TR-69-2. Dat are also presented for the normal total emittance of alumina thoria, magnesia, zirconia, graphite, iridium and two lots of tung sten, obtained by the shallow cavity technique and modification thereof, at temperatures in the range of 1400 to 2500 K (abou 2000 to 4000 °F).

**12941.** Mountain, R. D., **Temperature dependence of depolarize scattered light near the critical point,** (Proc. of the Colloquiu on Light Scattering by Fluids, Paris, France, July 15-17 1971), *J. Phys.* **33,** Supplement 2-3, C1-265 – C1-268 (Feb. Mar. 1972).

Key words: Correlation length; critical opalescence; criti cal phenomena; depolarized scattering; light scattering Ornstein-Zernike correlation function.

The double scattering formalism of Frish and McKenna i used to investigate the temperature dependence of the depolarized scattering in the vicinity of the critical point of a one component fluid composed of spherical molecules. The terms involving two particle correlations are estimated using the Ornstein-Zernike correlation function. The ratio of the intensity of the *H-H* to *V-V* scattering is found to diverge as $k\xi \ln(1/k\xi)$. The possibility of using depolarized scattering as a probe of three and four particle correlations near the critical point is discussed.

**12942.** McNesby, J. R., Braun, W., Ball, J., **Vacuum ultraviolet techniques in photochemistry,** Chapter 11 in *Creation and Detection of Excited State,* A. A. Lamola, ed., **1,** 503-586 (Marcel Dekker, Inc., New York, N.Y., 1971).

Key words: Actinometry; experimental; light sources; photochemistry; vacuum ultraviolet; window materials.

Vacuum ultraviolet techniques in photochemistry are eviewed from the standpoint of light sources (both continuously perated and pulsed), window materials, actinometry and chemi-al applications. Emphasis is given to modern physical chniques.

**2943.** Leasure, W. A., Jr., **Considerations in the development of measurement procedures for the regulation and monitoring of noise pollution,** (Proc. 2d Urban Technology Conf. and Technical Display, San Francisco, Calif., July 24-26, 1972), *AIAA Paper No.* **72-622,** pp. 1-10 (American Institute of Aeronautics, New York, N.Y., 1972).

Key words: Acoustics; noise measurement; noise pollution; noise regulations; noise (sound).

A noise standard or regulation should be based on accurate, liable and relevant measurements. In this paper, an outline is ven of some of the basic considerations in developing measure-ent systems which are required in order to effectively regulate monitor noise pollution or to assess the alternative strategies r noise abatement and control. The importance of these con-derations is reinforced through a discussion of the questions ddressed during the design of a test procedure and measure-ent methodology for a specific program in the area of motor ehicle noise.

**2944.** Wood, L. A., Bullman, G. W., **Creep and other tensile properties of rubber crosslinked by dicumyl peroxide,** *J. Polym. Sci.:* Part A-2, **10,** 43-50 (Jan. 1972).

Key words: Creep; modulus; rubber, natural; tensile properties; tensile strength; ultimate elongation.

Natural rubber crosslinked by dicumyl peroxide in amounts up 25 parts per hundred of rubber (phr) showed a maximum in nsile strength near 1 phr, followed by a steep decrease to a inimum near 5 phr. The ultimate elongation decreased from 70% at 0.5 phr to about 10% above 10 phr. The modulus in-eased linearly with increase of crosslinking. The creep rate ecreased from 5.6% per decade at 0.5 phr to zero at 5 phr and igher values. Crystallization, with a resultant abrupt increase in eep, was noted in specimens held in the stretched condition for ore than one day. Between 5 and 25 phr this system (when ystallization is avoided) appears to function as an ideal elastic etwork and can be recommended for studies of rubber elasticity nce no variation of modulus with time is observed.

**2945.** Miller, A., McLaughlin, W. L., Lynggard, B., **A scanning spectrophotometer for reading thin-film dosimeters,** *Dan. At. Energy Comm. Risö Rep. No.* **M-1525,** pp. 1-21 (Aug. 1972).

Key words: Dose distribution; dosimetry; electron beams; microdensitometry; spectrophotometry; thin films.

It is possible to convert a conventional spectrophotometer into versatile scanning spectrophotometer, without great difficulty r expense. The improved instrument can be tailored to perform any electro-optical tasks by the appropriate arrangement of odular components. In this work, basic optical components ight sources, monochromator, and sample chamber) of a con-entional spectrophotometer were used on an optical bench. pecially designed accessories could be added to these com-onents in order to measure at given wavelengths (from 200 to 00 nm) spatial variation (down to less than 10 $\mu$m) of optical ansmission or reflection quantities in thin-film dosimeters, over wide dynamic range. For high-speed data acquisition, nalogue-to-digital conversion could be programmed to give bular or graphical absorbed dose readings from calibrated film s a function of optical or spatial variables.

**12946.** Beatty, R. W., **Efficiencies of microwave 2-ports from reflection coefficient measurements,** *IEEE Trans. Microwave Theory Tech.* **MTT-20,** No. 5, 343-344 (May 1972).

Key words: Efficiency of two-port; measurement of 2-port efficiency; microwave measurements.

It is well-known that one can determine the efficiency of a microwave 2-port by measuring the reflection coefficient $\Gamma_1$ at the input port when the output port is terminated by a sliding short circuit. The locus of $\Gamma_1$ is a circle whose radius equals the efficiency $\eta_{2m}$ for energy entering port 2 when port 1 is terminated in a nonreflecting load. Similarly $\eta_{1m}$ is the radius of the $\Gamma_2$ circle when port 1 is terminated in a sliding short circuit.

This note describes a procedure for obtaining, from the same measured data, new reflection coefficients $\Gamma_{1N}$ and $\Gamma_{2N}$, whose circular loci have radii $R_{1N}$ and $R_{2N}$ which give the efficiencies of the 2-port when connected to an arbitrary load of reflection coefficient $\Gamma_L$.

Thus the $\Gamma_1$ or $\Gamma_2$ data may be used to obtain the efficiency of the 2-port when terminated in any arbitrary load. The method is potentially more accurate than the 3-point method since errors can be reduced by drawing a circle through many measured points.

**12947.** Arthur, M. G., **A precision HF-noise power measurement system,** *ISA Trans.* **10,** No. 3, 264-268 (1971).

Key words: Measurement system; noise comparator; noise measurement; noise standards.

This paper describes a precision HF noise power measurement system used at the National Bureau of Standards. It includes reference standard noise generators operating at approximately 77 and 373 K and an instrument for comparing the noise power of a noise source against the reference standards. The comparison instrument is a sum-and-difference correlation radiometer. Both the standards and the comparison instrument operate at 3, 30, and 60 MHz, and can be used with noise sources having source impedances of 50 ohms, unbalanced. Measurement uncertainty is typically less than 1% for sources with noise temperatures from 75 to 30,000 K.

**12948.** Fong, J. T., Simmons, J. A., **A non-equilibrium thermodynamic theory of simple materials based on a single-integral entropic functional,** (Proc. Int. Symp. on Foundations of Plasticity, Warsaw, Poland, Aug. 1972), *Arch. Mech. Stos.* **24,** No. 3, 363-372 (1972).

Key words: Anisotropy; continuum mechanics; entaxy; entropy; irreversibility; non-equilibrium state; nonlinear theory; plasticity; thermodynamics; viscoelasticity; yielding.

Based on the notion of a single-integral entropic functional as first introduced by Bernstein, Kearsley, and Zapas for a class of simple fluids in 1964, we present a non-equilibrium, irreversible thermodynamic theory of simple materials with fading memory within the general framework of Coleman's thermodynamic theory. Our theory is then modified, in a heuristic approach, to include "plasticity" by identifying the single-integral entropic functional with Bridgman's notion of "generalized entropy" for plastic deformations.

**12949.** Karp, S. S., Matteson, T. T., Maltese, M. D., **A search and rescue simulation model (SARSIM),** *Proc. Tokyo 1971 AICA Symp. on Simulation of Complex Systems, Tokyo, Japan, Sept. 3-7, 1971,* pp. I-4/1 – I-4/8 (The Society of Analog Technique of Japan, Tokyo, Japan, Sept. 1971).

Key words: Manning levels; modeling; multiserver queuing system; resource locations; resource utilization; response system; simulation.

The United States National Bureau of Standards and the United States Coast Guard, in a joint endeavor, have designed and developed an effective simulation model of the Coast Guard's complex Search and Rescue system.

The Search and Rescue Simulation (SARSIM) simulates the operational selection of the preferred SAR resource(s) to respond to each distress client; clients' needs for Coast Guard assistance vary widely, both in type and amount. SARSIM is a discrete event digital simulation which is modularized to allow the user to prepare any demand scenario (with overall or selective growth factors) in the Preprocessor; to exercise that demand in the Operational Simulator, controlling such inputs as the mix of resources and the organizational operating structure (e.g., decentralization of facilities); to examine the summary results of the exercise through the automatic preparation of specified output statistics; and to employ the Postprocessor to retrieve additional information.

This paper describes the SARSIM model, including: some of its more interesting and flexible algorithms, some validation data and representative results of simulation exercises.

**12950.** Geltman, S., **Applications of pseudo-state expansions,** (Proc. VII Int. Conf. on the Physics of Electronic and Atomic Collisions, Amsterdam, July 26, 1971), Chapter in *Physics of Electronic and Atomic Collisions,* T. R. Gover and F. J. de Heer, eds. pp. 216-231 (North-Holland Publ. Co., Amsterdam, The Netherlands, 1972).

Key words: Close coupling; electron-atom scattering; polarizabilities; pseudo-states; Sturmians.

The various types of pseudo-state expansions which have been applied to the scattering of a charged particle by atoms are discussed. Of the applications so far made, greater success has been achieved in the case of low energy electron-hydrogen scattering than for high-energy proton-hydrogen scattering.

**12951.** Coyne, J. J., Meshkov, S., **High-energy total cross sections and symmetry relations,** *Phys. Rev. D* **6,** No. 1, 399-402 (July 1, 1972).

Key words: Barger-Rubin; Johnson-Treiman; SU(3), SU(6); symmetry; total cross sections.

Recent Serpukhov measurements of meson-baryon total cross sections allow comparisons with the Johnson-Treiman and Barger-Rubin relations. For 25-55-GeV/*c* incident meson momenta, the Johnson-Treiman relation, $1/2\Delta(Kp)=\Delta(\pi p)$, is well satisfied. The less restrictive Barger-Rubin relation holds for most of the Serpukhov points. Linear extrapolation of Serpukhov fits for $\Delta(Kp)$ and $\Delta(\pi p)$ to high momenta leads to the prediction of large violations of the Johnson-Treiman relations.

**12952.** Hockey, B. J., **Observations by transmission electron microscopy on the subsurface damage produced in aluminum oxide by mechanical polishing and grinding,** (Proc. British Ceramic Society Meeting, Textural Studies of Ceramics, London, England, Dec. 16-17, 1970), Paper No. 6 in *Textural Studies of Ceramics, Proceedings No.* **20,** pp. 95-115 (British Ceramic Society, Shelton, Stoke-on-Trent, Great Britain, June 1972).

Key words: Aluminum oxide; dislocations; mechanical polishing and grinding; microtwins; transmission electron microscopy.

Transmission electron microscopy was used to examine the near-surface regions of $Al_2O_3$ crystals which were: (1) polished with 0.25 $\mu$m diamond, (2) polished with 0.3 $\mu$m alumina powder, or (3) ground with a diamond-impregnated wheel.

Near-surface regions of diamond-polished polycrystalline and (0001) single-crystal sections contained a relatively uniform high density of dislocations generally in the form of half-loops a closely associated with surface scratches. Similar subsurfa damage, but to a lesser extent, was found in alumina-polish polycrystalline specimens. In both cases, depth of subsurfa damage was estimated to be 1-2 $\mu$m.

Observations on diamond-ground polycrystalline specime at a depth of 2-4 $\mu$m below the original surfaces (necessitated the residual stresses and irregular topography) revealed penetra ing arrays of dislocations and/or microtwins (basal and rho bohedral), depending on the orientation of the grain. Large nu bers of basal twins, in particular, were found in diamond-grou $(0\bar{1}12)$ specimens, while a (0001) section contained only no basal dislocations. Maximum depth of damage produced grinding was estimated to be $\approx 20\ \mu$m.

The effect of briefly (1-4 hrs) annealing diamond-polish specimens at temperatures between 700 and 1500 °C was al investigated. Dislocation activity (and stress relief) was appare after annealing at 900 °C and led to the development of lar dislocation networks at 1200 °C. Annealing at 1500 °C, ho ever, resulted in thermal etching and the elimination of nearly subsurface damage.

**12953.** Hellwig, H., Bell, H. E., Kartaschoff, P., Bergquist, J. **Frequency stability of methane-stabilized He-Ne lasers,** *J. Ap Phys.* **43,** No. 2, 450-452 (Feb. 1972).

Key words: Frequency stability; He-Ne laser; laser st bilization; length standard; methane frequency standar saturated absorption; time standard.

Free-running laser stabilities of $1.5 \times 10^{-11}$ for the millisecon region and methane-locked stabilities of $10^{-13}$ for 10-sec avera ing time are achieved with a minimum of shock and vibratio isolation in an ordinary laboratory environment. Superior stabil ty performance is obtained with dc excitation as compared to excitation. The experimental setup is described in some detail.

**12954.** Kamper, R. A., Simmonds, M. B., **Broadband superco ducting quantum magnetometer,** *Appl. Phys. Lett.* **20,** No. 270-272 (Apr. 15, 1972).

Key words: Magnetometer; microwaves; quantum inte ference; superconductivity.

We describe the design, operation, and performance of a s perconducting quantum interference device (SQUID) whic operates at a frequency of 9 GHz. It is sensitive to variations magnetic field in a frequency band from 0 to 1 GHz.

**12955.** Grimes, D. N., **Optical autocorrelator with special applic tion to MTF measurement,** *Appl. Opt.* **11,** No. 4, 914-918 (Ap 1972).

Key words: Autocorrelation; interferometry; lens testin modulation transfer function; optics; physical optics; Sa nac interferometer.

An optical autocorrelator is described which is based on modified Sagnac two-mirror interferometer that operates in th zero-fringe mode. The real-time radiant flux output is the squar of the autocorrelation of the aperture function. In a particular a plication, when the aperture function is the pupil function of lens under test, the autocorrelator output is the MTF of the len The system is not limited in focal length; aperture size is limite only by the sizes of the beam splitters and mirrors. Experiment results are given with comparison data for both infinite-conjugat MTF and the autocorrelation of an annular aperture. Methods c adapting the system for measurement of the phase of the transfe function and for finite conjugate testing are also described.

**12956.** Hils, D., McCusker, M. V., Kleinpoppen, H., Smith, S. J. **Differential and direct differential elastic scattering cross se**

**tions for electrons and potassium atoms,** *Phys. Rev. Lett.* **29,** No. 7, 398-401 (Aug. 14, 1972).

Key words: Cross sections; elastic scattering; spin polarization.

In a modulated crossed-beam experiment we have elastically cattered unpolarized electrons of 3.3 eV energy from spin-olarized K atoms. A measurement of the polarization of the cattered electron yields $|f(\theta)|^2/\sigma(\theta)$. Our measured values of $f|^2/\sigma(\theta)$ show a significant angular shift relative to the theoretical urve in forward-angle scattering ($\theta = 20 - 40°$). This shift is not pparent in measurements of the differential scattering cross secon $\sigma(\theta)$ over the same angular range, which, however, do show significant angular shift in the range $\theta = 50 - 120°$.

2957. Kartaschoff, P., Barnes, J. A., **Standard time and frequency generation,** *Proc. IEEE* **60,** No. 5, 493-501 (May 1972).

Key words: Accuracy; basic standards; frequency; frequency metrology; stability; standards; time scales.

The basic properties of atomic primary frequency standards re reviewed. A continuously running frequency source comined with counting, storage, and display devices results in a lock. Time scales are obtained by setting clocks with respect to convenient origin. The accuracy of a primary frequency stanard is a combined theoretical and experimental assessment of ne uncertainties of all known possible sources of bias from the lealized definition. Recommended standard measures for the ability are the spectral density of fractional frequency fluctuaons (frequency domain) and the two-sample no-dead time Allan ariance (time domain). The operation of atomic frequency stanards is based on various methods of particle interrogation to oberve the transitions, particle confinement to obtain sufficient inraction time, and particle preparation to obtain the desired nergy level populations. Passive resonator and active oscillator naser) modes of operation are discussed; the former has some ndamental advantages.

A review of the state of the art and current practice shows that esium beam resonator standards have the best documented acracy capability ($5 \times 10^{-13}$) and, in their commercial versions, e presently the best available clocks.

There are three concepts related to time: time interval, date, d synchronization. In order to assign dates to events, time ales have to be established. The steadily growing need for a ry precise and uniform time scale has resulted in a new intertionally coordinated time scale, IAT.

Frequency metrology will have increasing impact on both ngth and voltage metrology in the near future.

958. Wells, J. S., Evenson, K. M., Day, G. W., Halford, D., **Role of infrared frequency synthesis in metrology,** *Proc. IEEE* **60,** No. 5, 621-623 (May 1972).

Key words: Frequency metrology; frequency of lasers; infrared frequency synthesis; laser frequency stabilization; methane-stabilized He-Ne laser; speed of light.

Infrared frequency synthesis (IFS) techniques are briefly suryed, and some important results are summarized. The recent easurement of the frequency of the methane-stabilized He-Ne ser is significant due to the accurate measurement of the ethane wavelength and its fundamental role in metrology. The ssibilities of an improved value for the speed of light and of adional applications for frequency measurements at various vels of accuracy are discussed.

959. Allan, D. W., **Time transfer using near-synchronous reception of optical pulsar signals,** *Proc. IEEE* **60,** No. 5, 625-627 (May 1972).

Key words: Accurate time dissemination; optical pulsars; precision timing; simultaneous reception; synchronization; time transfer.

The concept of time transfer between two geographically separated locations by using nearly simultaneous reception times from a common transmission has been used very fruitfully, e.g., the TV line-10 time transfer system and Loran-C. Some germane aspects of the concept are discussed and use of a signal from the optical pulsar NP0532 as the common transmitter is considered.

Theoretical considerations suggest that time could be transferred using this mode to an accuracy of about 2 μs and with global coverage. Some data were made available from Lawrence Radiation Laboratory giving the dates of pulsar events received at their observatory and also at the Harvard Observatory. A precision of about 13 μs was inferred from the data analysis.

This optical pulsar time transfer system seems to be feasible and worthy of further consideration because of the high accuracy and precision (a few microseconds for both) potentially achievable. For this potential, the development costs appear to be favorably competitive.

12960. Halford, D., Hellwig, H., Wells, J. S., **Progress and feasibility for a unified standard for frequency, time, and length,** *Proc. IEEE* **60,** No. 5, 623-625 (May 1972).

Key words: Cesium beam frequency standard; dissemination systems; EMF standard; frequency and time metrology; frequency standards; infrared frequency synthesis; International System of Units; Josephson effect; length standards; methane frequency standard; speed of light; unified standard.

The recent successful extension of frequency synthesis upward in the infrared to the 88-THz frequency of the very stable methane frequency standard has implications for expanded uses of frequency/time metrology and hence of frequency/time dissemination systems. After further refinements of the infrared frequency synthesis techniques, metrologists will have the opportunity to define a value for the speed of light and to use a particular frequency standard—the most accurate one—as a unified standard for frequency, time, and length.

12961. Penn, R. W., **Volume changes accompanying the extension of rubber,** *Trans. Soc. Rheol.* **14,** No. 4, 509-517 (1970).

Key words: Compressibility; natural rubber; strain energy; volume-extension.

The volume changes accompanying extension of peroxide vulcanizates of natural gum rubber were measured using a dilatometer technique. Measurements of the force-extension behavior and compressibilities were made on the same samples for the range of extension and volume change covered in the volume experiments. A constant compressibility was found; however, the volume changes accompanying extension were not proportional to the isotropic part of the stress. Thus, the strain energy cannot be separated into a sum of two parts, one due to the shear and one due to the dilatation.

12962. Artru, M-C., Kaufman, V., **Analysis of the spectrum of triply-ionized magnesium (Mg IV),** *J. Opt. Soc. Amer.* **62,** No. 8, 949-957 (Aug. 1972).

Key words: Magnesium; source; spectra; ultraviolet; wavelengths.

A study of Mg IV between 80 and 2100 Å has led to the classification of 243 lines. A total of 23 odd and 64 even levels have been identified as belonging to the $2s^22p^5$, $2s2p^6$, $2s2p^53s$, $2s^22p^44p$, $2s^22p^4ns$, and $2s^22p^4nd$ ($n$=3, 4, 5) configurations. Matrix diagonalizations and least-squares fits to the observed levels lead to well-defined radial integrals and verify the level assignments. On the basis of comparisons in the F I isoelectronic sequence, designation changes are suggested for some $2p^4(^3P)3\ d$ levels of Na III, Al V, Si VI, P VII, and S VIII. New levels are given for Na III and Al V, and some previously listed levels in Na III and S VIII are rejected as unreal. An ionization energy of 880 800 cm$^{-1}$ is given for Mg IV.

**12963.** Ivey, D. L., Keese, C. J., Neill, A. H., Jr., Brenner, C., **Interaction of vehicle and road surface,** *Highw. Res. Rec., Anti-Skid Program Management and Related Papers, 22 Reports,* No. 376, 40-53 (1971).

Key words: Brakes; coefficient of friction; skid testers; tire construction; traction.

This paper presents various factors which influence friction forces in the interaction between the vehicle and the road surface. Emphasis has been directed toward interpretation of slip curves and how they relate to total vehicle handling.

The effects of braking systems, locked wheels, antilock brakes, and suspensions are related to actual vehicle performance data. Likewise, variations in construction and tread depth are evaluated on both wet and dry surfaces.

**12964.** Powell, C. J., **Internal x-ray photoemission in aluminum: Excitation of electrons from the valence bands,** *Solid State Commun.* **10,** No. 12, 1161-1164 (June 15, 1972).

Key words: Aluminum; electronic density of states; photoelectron energy distribution; x-ray photoemission.

Measurements are reported of Al valence-electron excitation by $K\alpha_{1,2}$ x-rays internally generated in evaporated specimens by electron bombardment. The x-ray photoelectron energy distribution is consistent with the u.v. distributions of Huen and Wooten. Weak structures are found in the energy distribution at positions corresponding to those in the calculated density of states.

**12965.** McDaniel, C. L., **Phase relations in the CaO-Pt system in air,** *J. Amer. Ceram. Soc. Discussions and Notes* **55,** No. 8, 426-427 (Aug. 1972).

Key words: CaO-Pt system; CaO:PtO$_2$ compounds; dissociation; equilibrium; phase relations.

The equilibrium phase relations for the CaO-Pt system were determined in an air environment. The system contains two compounds $4CaO \cdot PtO_2$ and $CaO \cdot PtO_2$ which dissociate to an oxide phase, Pt metal, and oxygen at 1035 and 905 °C, respectively. An indexed x-ray diffraction powder pattern is given for the $4CaO \cdot PtO_2$ compound.

**12966.** Franklin, A. D., **Statistical thermodynamics of point defects in crystals,** Chapter 1 in *Point Defects in Solids,* J. Crawford and L. Slifken, eds., **1,** 1-101 (Plenum Press, Inc., New York, N.Y., 1972).

Key words: Formation enthalpy; formation entropy; formation free energy; formation volume; ionic solids; metals; noble gas solids; point defects; semiconductors; statistical thermodynamics.

A review is given of the statistical and thermodynamic theory of point defects in dilute solution in noble gas solids, metals, semiconductors, and ionic solids. Experimental methods for determining the free energies, enthalpies, entropies, and volumes of formation of single and complexed point defects are reviewed, and a survey is given of the available values at the present time.

**12967.** Sullivan, D. B., **Low temperature voltage divider and null detector,** *Rev. Sci. Instrum.* **43,** No. 3, 499-505 (Mar. 1972).

Key words: Null detector; superconductivity; voltage divider.

This paper describes a low temperature voltage divider a null detector which are designed to accurately bring the low le voltage of the Josephson steps to the 1 V level. The divider us the series-parallel interchange of resistors. Preliminary tests i dicate that the resistors are stable to within one part in $10^7$ a that the ratio is accurate to within one part in $10^6$. The null dete tor utilizes a superconducting quantum interference magnetom ter and is limited only by the Johnson noise in the cooled sistors.

**12968.** Meijer, P. H. E., **Specific heat and susceptibility in chrom um methylammonium alum above the critical temperatu** *Phys. Rev. B* **6,** No. 1,214-222 (July 1, 1972).

Key words: Chromium methylammonium alum; cryst field; high-temperature expansion; specific heat; suscep bility.

The specific heat and susceptibility of chromium methyla monium alum is calculated above the critical temperature. T method is based on a high-temperature expansion of the partiti function in the presence of a crystal field, using a Laplace tra form. The results are worked out in first (for the susceptibilit and second (for the specific heat) order in the coupling Ham tonian. The summation over the four different sublattices worked out for the two different crystallographic phases whi seem to occur above and below 170 K. The lack of rotation sy metry of the crystal field in its local reference system, which w found by paramagnetic resonance, is taken into account. T result for the susceptibility is given explicitly in Eq. (4.18a) as function of a reduced temperature.

**12969.** Krauss, M., Neumann, D., **Energy curves of $CO_2^-$,** *Che Phys. Lett.* **14,** No. 1,26-28 (May 1, 1972).

Key words: $CO_2^-$; electron scatter; energy curve; excit tion energy; metastable; quantum chemistry.

*Ab initio* energy curves of the $^2A_1$ and $^2B_1$ states of $Co_2^-$ are r ported as a function of the bending angle. The $^2A_1$ curve is fou to be bound relative to the neutral curve at angles greater th 130° from the linear geometry. Both the $^2A_1$ and $^2B_1$ states a found to be valence in character for the geometries consider and the excitation energy for $^2A_1 \rightarrow {}^2B_1$ is calculated to be 3.2 e in the neighborhood of the $Co_2^-$ equilibrium geometry while t experimental value for the maximum in the lowest absorpti curve is almost 3.5 eV.

From the bending energy curve it is deduced that gaseo $CO_2^-$ in its ground vibrational level can have a relatively long li since the ion energy in the neighborhood of the ion equilibriu geometry is about 1 eV below the neutral molecule energy f that geometry.

**12970.** Linzer, M., Brown, R. L., **Line parameters of absorpti and dispersion Lorentzian curves under conditions of combin modulation and saturation distortion,** *J. Magn. Resonance* 335-358 (1972).

Key words: Line shapes; Lorentzian lines; magnet resonance.

Analytical and computer solutions for the parameters of th first Fourier coefficients of Lorentzian lines subject to simu taneous modulation and saturation distortion are presented. Bo absorption and dispersion shape functions are examined. Th system is assumed to be described by the saturation theory either Bloembergen, Purcell, and Pound (BPP), or Redfield. the BPP case, results are given for the modulation frequency, $\omega$ being much greater or less than $1/T_1$, while in the Redfield cas only $\omega_m \ll 1/T_1$ is considered. In all cases, it is assumed th $\omega_m/2\pi$ is much less than the inverse line width of the pure a orption curve and that the line is traversed during a time which slow compared to $T_1$ and $2\pi/\omega_m$.

Various methods are outlined for determining the true line idth, line intensity, saturation parameter, and modulation am- litude from measurements on the distorted line shapes under onditions of optimum sensitivity. Tests for verifying the haracter of the Lorentzian line shape are also suggested.

2971. Brown, R. L., **Use of fiber optics in the study of chemiluminescent reactions,** *Rev. Sci. Instrum.* **43,** No. 5, 756-758 (May 1972).

Key words: Chemiluminescent reactions; fiber optics; photochemistry.

The use of stationary light pipes and a stationary detector to easure light decay along a tube in a steady state flow system is escribed. This method exhibits a number of advantages over hat of moving the detector. A means of calibrating the transmis- on of the light pipes *in situ* by using the properties of the yellow trogen afterglow is discussed. The high degree of spatial esolution achievable by this technique should make it especially itable for studies of small flames and discharges.

2972. Mangum, B. W., Utton, D. B., **NMR of $^{14}$N in cerous magnesium nitrate hydrate,** *Physica* **60,** No. 1, 63-72 (1972).

Key words: CMN; ideal paramagnet; NMR; NQR.

We have measured the nuclear magnetic resonance of $^{14}$N in erous magnesium nitrate hydrate, $Ce_2Mg_3(NO_3)_{12} \cdot 24H_2O$, at K in a magnetic field of 18.335 kG. The dipolar field at the trogen nucleus due to the $Ce^{3+}$ ions is appreciable at that tem- erature and field and produces phase shifts in the angular de- endence of the spectra. This complicates the interpretation of e data and prevents one from using the customary techniques. rom the measurements we have derived values for the quadru- olar coupling constant ($A = 0.160 \pm 0.005$ MHz), the asym- etry parameter ($\eta = 0.50 \pm 0.05$) and the directions of the elec- ic-field gradient axes. The spectra show clearly that for the trate groups there is no center of inversion at the cerium ions.

2973. Allan, D. W., Blair, B. E., Davis, D. D., Machlan, H. E., **Precision and accuracy of remote synchronization via network television broadcasts, Loran-C, and portable clocks,** *Metrologia* 8, No. 2, 64-72 (Apr. 1972).

Key words: Allan variance; cesium beam standards; frequency stability; frequency standards; Loran-C; portable clocks; time dispersion; time synchronization; TV timing.

A comparison among three precise timing centers in the nited States has been conducted for more than 1 year using ree different synchronization methods. The timing centers in- olved were the United States Naval Observatory (USNO) in ashington, D.C., Newark Air Force Station (NAFS) in ewark, Ohio, and the National Bureau of Standards (NBS) in oulder, Colorado. The three methods were cesium beam porta- e clocks; Loran-C transmissions from Cape Fear, North arolina, and Dana, Indiana; and ABC, CBS, and NBC network levision broadcasts commonly received by the three timing nters.

Cesium beam portable clocks have the capability of accurately d precisely synchronizing remote clocks to within 0.1 μs. The oran-C data involved a 3500 km (2180 miles) ground wave ath—the longest Loran-C ground wave path that has been stu- ed with the precision and accuracy reported herein. The long- rm precision achieved was about 1 μs over 1 year. The accura- y is limited on occasion by inability to resolve the 10 μs am- guity of the 100-kHz pulse train. The precision capability of aintaining remote clock synchronization within the majority of the continental United States using network television broadcasts was inferred to be about 5 ns $\cdot \tau^{1/3} s^{-1/3}$ over the range of $\tau$ from 86400 s (1 day) to about $10^7$ s (324 days) but with definite accuracy limitations caused by such factors as occasional network re-routing of the television signals. Some estimates of the long-term frequency stabilities among the references used at the three timing centers were measured or inferred.

12974. Clark, A. F., Deason, V. A., Powell, R. L., **Characterization of high purity metals by the eddy current decay method,** *Cryogenics* **12,** No. 1, 35-39 (Feb. 1972).

Key words: Contaminants; cryogenics; eddy currents; eddy current tests; electrical resistivity; nondestructive tests; purity; scattering.

In recent years, the residual resistivity ratio has been widely used as a sensitive indicator of chemical purity in high purity metals. The conventional four terminal measurement of resistivity becomes difficult either with large or irregular specimens or with increasing purity and decreasing temperature. This paper describes an alternative technique, called the eddy current decay method, which greatly reduces the above difficulties. The eddy current measurements do not require any attachment of leads and, in fact, the measurement process is totally non-destructive to the specimen. The eddy current apparatus is described, and some typical applications are presented.

12975. Sparks, L. L., Powell, R. L., **Methods for assessing homogeneity and interchangeability of thermocouple wires,** *Cryogenics* 12, No. 1, 40-43 (Feb. 1972).

Key words: Cryogenics; dipping; evaluation; heterogeneity; liquid helium; liquid nitrogen; low temperature; Seebeck effect; temperature measurement; thermoelectric properties.

Chemical and physical imperfections and inhomogeneities in thermocouple wire cause spurious voltages whenever these imperfections are subjected to temperature gradients. Thermocouple wires from different spools (or even from widely separated lengths on the same spool) usually exhibit significant differences in their thermoelectric properties. For accurate thermometry it is important to know the range of spurious voltages to be expected from a specific material. Simple laboratory methods are described for determining the effects of short-range inhomogeneities or long-range variations. Examples of results from tests are discussed in order to point out both the usefulness and the limitations of the methods.

12976. Jackson, A. D., Maximon, L. C., **Integrals of products of Bessel functions,** *SIAM J. Math. Anal.* **3,** No. 3, 446-460 (Aug. 1972).

Key words: Angular momentum algebra; Bessel functions; integrals of Bessel functions; invariant triple products; spherical Bessel functions; spherical harmonics.

Simple expressions for a variety of integrals involving the product of three cylindrical or three spherical Bessel functions are obtained in terms of the angular functions arising in the decomposition of a plane wave in two or three dimensions.

12977. McKinney, J. E., Penn, R. W., **Composite dilatometer for measuring density of liquids and solids,** *Rev. Sci. Instrum.* **43,** No. 8, 1211-1213 (Aug. 1972).

Key words: Compressibility; density; dilatometer; pressure; specific volume; temperature; thermal expansion.

A composite dilatometer for measuring densities of liquids and solids over wide ranges of temperature and pressure is described. The dilatometer has a glass capillary and a mechanically removable seal at the base to facilitate loading. The seal is leakproof, and constant volume is maintained with successive loadings.

12978. Kelly, G. E., Sengers, J. V., **Kinetic theory of droplet growth in nucleation,** *J. Chem. Phys.* **57,** No. 4, 1441-1458 (Aug. 15, 1972).

Key words: Droplet growth; inverse Knudsen number expansion; kinetic theory; nearly-free molecular regime; nucleation.

A kinetic theory is presented for the mass flux to a liquid droplet surrounded by its pure vapor. When the mass flux $\Gamma$ is expanded in terms of a parameter $\alpha$ which is the ratio of the droplet size to the mean free path (inverse Knudsen number), one obtains a series of the form $\Gamma = \Gamma^{(0)} + \Gamma^{(1)}\alpha + \Gamma^{(2)}\alpha^2 \ln\alpha + ...$ The coefficients of the first three terms of this expansion are derived by solving the Boltzmann equation using a modified Knudsen number iteration procedure. It is shown that the coefficients are determined by integrals associated with sequences of successive collisions among a number of vapor molecules and the droplet. These collision integrals bear a close similarity to the collision integrals derived earlier from the *generalized* Boltzmann equation for the density dependence of the transport properties of gases.

12979. Waxman, M., Hastings, J. R., **Proposed experiment to determine the effect of pressure on the emf of thermocouples,** *J. Appl. Phys.* **43,** No. 6, 2629-2632 (June 1972).

Key words: emf, thermocouple, effect of pressure on; hot-junction temperature, nonlinear evaluation of; hot-junction temperature, pressurized furnace; indirect temperature measurements; nonlinear data analysis, pressurized emf of thermocouples; pressure, effect on emf of thermocouples; simulated experiment, pressurized emf of thermocouples; temperature, measurement at high pressure; thermocouples, effect of pressure on emf of.

A new experimental procedure to determine the effect of pressure on the emf-vs-temperature behavior of thermocouples has been conceived and tested with simulated data on a computer. An important advantage of this procedure is that the temperature of the hot junction can be accurately evaluated without the necessity of measuring it directly. Instead, the emf of the pressurized thermocouple is expressed parametrically as an appropriate function of several variables: (i) a measurable property related to the hot-junction temperature, such as the electric power to the pressurized furnace; (ii) the cold-junction temperature; and (iii) a reference temperature, such as 100 °C, at which the pressure effect is known. By variation of the experimental conditions, a set of overdetermined equations is obtained from which the parameters can be evaluated, and thus the emf-vs-temperature relationship of the pressurized thermocouple can be determined. Our experience with simulated data indicates that for the temperature range from 100 to 1200 °C and for pressures to about 7 GN/m$^2$ (70 kbar), the procedure should not introduce a temperature error greater than the error associated with the measurements of the emf, power, and cold-junction temperature.

12980. MacDonald, R. A., **Cauchy relations for second- and third-order elastic constants,** *Phys. Rev. B* **5,** No. 10, 4139-4143 (May 15, 1972).

Key words: Cauchy relations; central force interaction; cubic crystals; second- and third-order elastic constants; stress-free equilibrium; third-neighbor model.

The results of an earlier paper on the relation between elastic constants and second- and third-order force constants in face-centered-cubic and body-centered-cubic lattices appeared to conflict with the Cauchy relations $C_{12} = C_{44}$, $C_{112} = C_{166}$, $C_{123} = C_{456} = C_{144}$ obtained by Cousins. We show here that no confli exists when we ensure that the lattice is in stress-free equilibr um, a necessary condition for Cauchy relations to hold. Hov ever, for the case of nearest- and next-nearest-neighbor centra force interactions previously considered, we obtain only speci cases of these Cauchy relations. We extend our earlier work t include further neighbors and find that the Cauchy relations a obtained when third neighbors contribute to the elastic co stants.

12981. Cassidy, E. C., **Pulsed laser Kerr system polarimeter fo electro-optical fringe pattern measurement of transient electri parameters,** *Rev. Sci. Instrum.* **43,** No. 6, 886-893 (June 1972

Key words: Electric fields; electrical measurement electro-optics; high-speed photography; high-spee techniques; high-voltage techniques; Kerr effect; laser ap plication; optical techniques; pulse techniques.

Novel electro-optical fringe pattern methods are developed fo measurement of transient high voltages and electric field Several techniques employing the Kerr effect, a pulsed lase source, and high-speed photographic recording equipment ar described. Typical fringe pattern results are compared with co ventional resistive divider measurements.

12982. Hellwig, H., Bell, H. E., **Experimental results with atomi hydrogen storage beam systems,** *Proc. 26th Annual Symp. o Frequency Control, Atlantic City, N.J., June 6-8, 1972,* pp 242-247 (Electronic Industries Association, Washingto D.C., June 6-8, 1972).

Key words: Atomic hydrogen beam; atomic hydroge generation; dispersion; frequency stability; frequency sta dard; hydrogen atom detection; hydrogen flux calibratio hydrogen maser; relaxation measurements; spin exchang

Two atomic hydrogen storage beam devices are described, on based on the detection of hydrogen atoms, the other on the d tection of changes in the microwave signal due to the hydroge resonance. Electron bombardment ionization is used for the d tection of atomic hydrogen. Efficiencies of up to $10^{-3}$ are me sured using a method which is based on the study of pulse deca at maser oscillation threshold. Quantitative measurements of th atomic hydrogen beam intensity as a function of source pressu and RF discharge power are given. The overall efficiency of th atomic hydrogen detection in the hydrogen storage beam devic is estimated at $10^{-7}$. Ways to increase the efficiency are i dicated.

A frequency standard is described in which a quartz cryst oscillator is locked to the hydrogen hyperfine transition using th dispersion of this resonance. The hydrogen storage beam ap paratus closely resembles a hydrogen maser with a low-Q cavit below oscillation threshold. Cavity pulling can be reduced to point where environmental temperature fluctuations limit th stability mainly via the second-order Doppler effect. Locking t the dispersion feature of the resonance eliminates the need fo frequency modulation in order to find line-center. The stabilit of the frequency standard was measured against crystal oscill tors and cesium beam frequency standards; stabilities of 4 $10^{-13}$ were recorded for sampling times of 30 seconds and of hours.

12983. Mangum, B. W., Thornton, D. D., **Magnetic phase di grams of $GdVO_4$ and $GdAsO_4$,** (Proc. 17th AIP Conf. on Ma netism and Magnetic Materials, Chicago, Ill., Nov. 16-1 1971), Chapter in *Magnetism and Magnetic Materials,* C. Graham, Jr., and J. J. Rhyne, eds., No. 5, 311-315 (1972).

Key words: $GdAsO_4$; $GdVO_4$; Heisenberg antiferroma nets; low temperatures; magnetizations.

$GdAsO_4$ and $GdVO_4$ are Heisenberg antiferromagnets with elatively large anisotropy fields, about half of which are dipolar origin. The ratios of the anisotropy to the exchange fields for e salts, based on the molecular field theory and using the pub- shed values of the interaction constants, indicate that both salts ould have spin-flop phases. We have measured the magnetiza- on and its derivative of $GdVO_4$ and $GdAsO_4$ as a function of pplied magnetic field for various temperatures below $T_N$ and erived their magnetic phase diagrams. $GdVO_4$ ($T_N = 2.50$ K) is textbook type example of a system having a spin-flop phase ith $T_3 = 1.37$ K. The critical field for the transition from the an- ferromagnetic to the spin-flop phase is 10.5 kG and that for the ansition from the spin-flop to the ferromagnetic (or saturated aramagnetic) phase is 21.8 kG. $GdAsO_4$ ($T_N = 1.26$ K) does not ave a simple spin-flop phase but undergoes transitions to two termediate phases before undergoing a transition to the fer- magnetic (or saturated paramagnetic) phase. The critical point r $GdAsO_4$ is $T_c = 0.47$ K and the critical fields are: $B_{c1} = 6.1$ G, $B_{c2} = 6.4$ kG, and $B_{c3} \simeq 9$ kG.

**984.** Rubin, L. G., Powell, R. L., Anderson, A. C., **Conference Report—The Fifth Symposium on temperature,** *Cryogenics* **11,** No. 6, 489-493 (Dec. 1971).

Key words: Temperature scales; thermocouples; thermometry.

The review briefly describes the talks on thermocouples and mperature scales. The article mentions the authors, their af- iations, and brief synopses of the more significant talks.

**985.** Weiss, A. W., **Calculations of the $2sns\ ^1S$ and $2p3p\ ^{3,1}P$ levels of Be I,** *Phys. Rev. A* **6,** No. 4, 1261-1266 (Oct. 1972).

Key words: Atomic spectra; lifetimes; oscillator strengths; wavelengths.

Large scale configuration-interaction calculations are carried it on the $2sns\ ^1S$ series of Be I in an attempt to account for the omalous behavior of the measured $f$ values for the 3455-Å ie, which had been identified as the $2s2p\ ^1P - 2p^2\ ^1S$ transition. ıe calculations indicate that the series is very nearly purely ydberg in character and that $2p^2\ ^1S$ is not embedded in the se- s between $6s$ and $7s$, as had been previously assigned. Addi- nal variational calculations on the $2snp$ and $2p3p$ levels in- cate that a reidentification of the 3455-Å line with the $2s3p\ ^1P$ $2p3p\ ^1P$ transition is consistent with both lifetime and wave- ngth measurements. These calculations also predict lines at 48 and 4528 Å, which have recently been found in beam-foil ectra.

**986.** Allan, D. W., Machlan, H. E., Marshall, J., **Time transfer using nearly simultaneous reception times of a common transmission,** *Proc. 26th Annual Symp. on Frequency Control, Atlantic City, N. J., June 6-8, 1972,* pp. 309-316 (Electronic Industries Association, Washington, D.C., June 6-8, 1972).

Key words: Atomic clock; frequency calibration; frequency stability; optical pulsars; remote clock comparisons; simultaneous reception; time dissemination; time stability; time synchronization; time transfer; TV color subcarrier; 60-Hz power line.

The concept of time transfer between two geographically parated locations by using nearly simultaneous reception times a common transmission has been used very fruitfully, e.g., the V line-10 time transfer system and Loran-C. This paper scusses some germane aspects of the concept and then con- ders using as some common transmissions a 30-Hz pulserate gnal from the optical pulsar NP0532, the 60-Hz power-line gnal, and the 3.58-MHz television color subcarrier signal.

The theoretical accuracy of each of these methods is discussed along with its coverage and the system feasibility. The day-to-day stability of the differential path delay of each of the above methods was measured or inferred to be ~ 13 μs, ~ 1 ms, and ~ 20 ns respectively.

**12987.** Smith, J. C., Kermish, G. A., Fenstermaker, C. A., **Separation of filler particles from the matrix in a particulate-loaded composite subjected to tensile stress,** (Proc. ACS Symp. on Recent Advances in Adhesion, Washington, D.C., Sept. 13-15, 1971), *J. Adhes.* **4,** No. 2, 109-122 (1972).

Key words: Adhesion; composite materials; epoxy polymer; silane coupling agents; stress-strain properties.

Simultaneous measurements of tensile stress, longitudinal strain, and transverse strain were obtained on particulate-filled composites. The matrix was a flexible epoxy polymer. Small glass spheres were used as filler in various volume ratios up to 0.35. The spheres were pretreated as follows: clean, coated with a parting agent, coated with either of two silane coupling agents. The volume-expansion behaviors of these four systems of composites showed differences attributed to matrix-filler separation and subsequent vacuole formation. Stress-strain behaviors were especially sensitive to this dewetting process. These two types of data, obtained simultaneously and considered together, thus provide valuable information about interface adhesion.

**12988.** Schooley, J. F., Soulen, R. J., Jr., **Thermometric fixed points using superconductivity,** *Advan. Cryog. Eng.* **17,** 192-198 (1972).

Key words: Calibration techniques; cryogenic temperature scale; OSRM; pure elements; superconductivity; thermometric fixed points.

Superconductive transitions in lead, indium, aluminum, zinc, and cadmium samples have been found to be both narrow and reproducible, suggesting their use as calibrating fixed points on the cryogenic temperature scale. Devices based on these measurements have been constructed. These results and their use in cryogenic thermometry are discussed.

**12989.** Mangum, B. W., Utton, D. B., **Low-temperature transitions in tetramethylammonium manganese chloride,** *Phys. Rev. B* **6,** No. 7, 2790-2795 (Oct. 1, 1972).

Key words: Cooperative transition; magnetic susceptibility; NMR; TMC.

We have measured the proton nuclear magnetic resonance of tetramethylammonium manganese chloride, a linear chain antiferromagnet, in the temperature region 0.4-300 K. In addition, its ac magnetic susceptibility was measured in applied fields of 0 to 22 kG in the temperature range 0.3-4.2 K. When measured along the crystallographic $c$ axis, the zero-field susceptibility had an anomaly at 0.84 K. When the external field was applied perpendicularly to the $c$ axis below 0.8 K, a critical field of 11.5 kG was observed in $dM/dB$. The proton NMR did not indicate any *cooperative transition* to a magnetically ordered state of the $Mn^{2+}$ spins. It did indicate, however, a gradual diminution of fluctuations in the crystallographic $ab$ plane until a nonrandom order had been established between chains below approximately 0.8 K. We find that the tetramethylammonium groups cease all rotations below 39 K. In the region of 40 to 50 K, the tetramethylammonium groups not only undergo some hindered rotations, but their orientation is different from the published room-temperature x-ray diffraction results. Above 50 K only a single narrow NMR line is observed and, consequently, no additional information on the crystal structure could be obtained.

**12990.** Colwell, J. H., Mangum, B. W., **The heat capacity of $TmAsO_4$ near its Jahn-Teller transition; evidence of a low-lying excited state,** *Solid State Commun.* **11,** 83-87 (1972).

Key words: Heat capacity; Jahn-Teller effect; molecular field approximation; Schottky anomaly; thulium arsenate; $TmAsO_4$.

We have measured the heat capacity of $TmAsO_4$ between 2 and 12 K and have established that there is a singlet state at approximately 20 K (14 cm$^{-1}$) above the ground state doublet. The heat capacity is accounted for on the basis of models which, in addition to the contribution from the low-lying singlet state, use the molecular field model to approximate the heat capacity arising from the Jahn-Teller splitting of the ground state doublet.

**12991.** Branscomb, L. M., **A metric America—and the paper industry,** *Tappi* **55,** No. 8, 1227-1230 (Aug. 1972).

Key words: Changeover; foreign trade; metric system; paper machines; planning; standards; United States; units of measures.

A study by the U.S. Department of Commerce clearly favors changeover to the metric system. There are two alternatives for the United States: to convert deliberately with a plan, or to go metric eventually without a plan. The change to the metric system will be costly and is not enthusiastically supported by the paper industry. Moreover, problems of adjustment will be great for the consumer in the market place. However, economic benefits of "going metric" may be achieved for a long time by making products conform to international standards developed by IEC and ISO. By conversion to the metric system, American industry could eliminate the necessity of keeping inventories of metric parts alongside customary parts. For the paper industry, conversion provides an opportunity to rationalize and simplify paper sizes. In addition, large economic benefits may be achieved through a rational, simplified series of package sizes. Thus, the paper industry will not be forced to scrap existing machinery; only those parts essential to producing products conforming to international standards need be changed.

**12992.** Tate, E. L., **NBS and the field service libraries of the Department of Commerce and the Interior Department,** *Proc. U.S. Department of Interior, Sixth Annual Library Workshop, Vancouver, Wash., Sept. 27-Oct. 1, 1971,* pp. 65-68 (U.S. Department of Interior, Office of Library Services, Washington, D.C., 1972).

Key words: National Bureau of Standards publication; National Standard Reference Data System.

Describes NBS services and publications of potential utility to the Department of the Interior and the Department of Commerce and their field service libraries.

**12993.** Pfrang, E. O., Yokel, F. Y., **Evaluation of innovative structural systems with respect to creep buckling,** *Proc. RILEM Int. Symp. on Experimental Analysis of Instability Problems on Reduced and Full-Scale Models, Buenos Aires, Argentina, Sept. 13-18, 1971,* **3,** 229-255 (1971).

Key words: Buckling; columns; creep; creep buckling; full-scale testing; load capacity; performance criteria; performance evaluation; performance testing; structural analysis; structural testing.

A major effort is now underway in the United States to introduce industrialized housing systems. This effort was initiated by the Department of Housing and Urban Development and is known as Operation Breakthrough. As a part of this effort, performance criteria were developed which make it possible to evaluate the structural adequacy of innovative systems. The criteria, analysis, and testing with respect to creep buckling a discussed. A case history is presented of the evaluation of t structural adequacy with respect to creep buckling of an innov tive reinforced concrete system. The system was evaluated full-scale testing and by analysis. An analytical approach w developed to predict the adequacy of reinforced concrete stru tural systems with respect to creep buckling.

**12994.** Semmelroth, C. C., **Adjustment of the Munsell-value a $W^*$-scales to uniform lightness steps for various backgrou reflectances,** *Appl. Opt.* **10,** No. 1, 14-18 (Jan. 1971).

Key words: Color; lightness; vision.

For background reflectances taken equal to, or slightly low than, the specimen reflectances, the Munsell-value, $V$, and t CIE 1964, $W^*$, scales are found to be essentially linear with power formulation for lightness previously shown to accord w lightness-spacing data for a wide variety of specimen a background reflectances. Adjustments required to make t Munsell-value function accord precisely with the power formu tion for this background condition are all less than 0.2 of a Mu sell-value step between 1/ and 9/. The power formulation is us to construct a table to show in Munsell terms the influence background reflectance on perceived lightness for all combir tions of specimen and background reflectance includi Takasaki crispening for specimen reflectance approaching th of the background.

**12995.** Ritter, J. J., Coyle, T. D., Bellama, J. M., **Reactions tetrachlorodiborane (4) with fluoroolefins,** *J. Organome Chem.* **42,** 25-31 (1972).

Key words: Boron; boron subhalides; fluoroolefins; h lides; haloolefin; organoboron compounc tetrachlorodiborane (4); tetrafluorodiborane (4).

Tetrachlorodiborane (4) reacts with trifluoroethylene to gi dichloro-2,2-difluorovinylborane and both isomers of dichloro-chloro-2-fluorovinylborane. These compounds can be convert to the corresponding difluoro (halovinyl) boranes by treatme with $SbF_3$. Reaction of $B_2Cl_4$ with vinyl fluoride gives 1,1,2-t (dichloroboryl) ethane. A facile halogen exchange with $B_2C$ was observed for a number of fluoroolefins, including vir fluoride, 1,1-difluoroethylene, 2-fluoropropene, and 3,3 trifluoropropene. No reaction was observed with 2,3,3 tetrafluoropropene.

**12996.** Rebbert, R. E., Lias, S. G., Ausloos, P., **Vacuum traviolet photolysis of methane. Reaction of methylene,** *Che Phys. Lett.* **12,** No. 2, 323-326 (Dec. 15, 1971).

Key words: Deactivation; insertion reaction; lifetim methane; methylene; photolysis; quantum yields.

Methylene radicals formed in the photolysis of methane (123 and 104.8 – 106.7 nm) insert into the C – H bond of methane produce ethane molecules whose lifetime is independent of t energy of the photon. Deactivation of ethane by collision wi methane is stepwise, and the lifetime of the insertion product shorter than reported in previous $CH_2CO$ photolysis studies.

**12997.** deWit, R., **The relation between continuous and discr disclinations,** (Proc. Int. Symp. on Foundations of Plasticit Warsaw, Poland, Aug. 30-Sept. 2, 1972), *Arch. Mech.* **24,** N 3, 499-510 (Wolters-Noordhoff Publ. Co., 1972).

Key words: Continuous; continuum; defect; disclinatio discrete; dislocation; distortion; Green's function; inco patibility; plasticity; strain; Volterra.

A recent paper of Mura introduces plastic and elastic disto tions to describe a theory of disclinations. Our objection to th proach is that the "elastic distortion" is not a state quantity hen disclinations are present. Mura's "plastic distortion" for a e singularity is examined in the light of our theory and found represent a dislocation wall terminating inside the body on a slocation loop. Mura's "plastic rotation" is found to represent dislocation wall terminating on a disclination. The sum of these o gives the "disclination" loop. Explicit expressions are rived for the elastic strain and bend-twist in both the discrete d continuous cases, which show that, contrary to the "elastic stortion," they are indeed state quantities.

998. Forman, R. A., Brower, W. S., Jr., Parker, H. S., **Phonons and the green exciton series in cuprous oxide, $Cu_2O$,** *Phys. Lett.* **36A,** No. 5, 395-396 (Sept. 27, 1971).

Key words: Copper oxide; cuprous oxide; excitons; forbidden bandgap; phonons.

Examination of the optical absorption edge spectra of samples melt-grown cuprous oxide enables identification of features of e green exciton series overlying the yellow series. Identifican of the green series $n=1$ line allows new interpretations of rious features seen earlier by other workers.

999. Sieck, L. W., Hellner, L., Gorden, R., Jr., **Kinetic mass spectrometric determination of the absolute rate coefficient for the reaction $NH_3^+$ ($\nu=0$) $+ NH_3 \rightarrow NH_4^+ + NH_2$ at thermal kinetic energies,** *Chem. Phys. Lett.* **10,** No. 5, 502-503 (Sept. 1, 1971).

Key words: Ammonia; mass spectrometry; photoionization; rate constants; thermal energy; vibrational energy.

The absolute thermal rate coefficient for the reaction $NH_3^+ +$ $H_3 \rightarrow NH_4^+ + NH_2$ has been determined experimentally for e first time for $NH_3^+$ ($\nu=0$) reactant ions. An increase in $E_{vib}$ sults in a decrease in the rate coefficient for proton transfer.

000. Ausloos, P., **Far ultraviolet photolysis of alkanes,** *Mol. Photochem.* **4,** No. 1, 39-55 (1972).

Key words: Energy partitioning; energy transfer; excited states; fluorescence; photoionization; photolysis; quantum yields.

The effect of wavelength on the primary photophysical and otochemical processes is reviewed. Quantum yields of the otoionization and of the photochemical decomposition of lected alkanes are presented. The modes of dissociation of utral electronically excited alkanes are related to information rived from high resolution gas phase absorption spectra and om liquid phase fluorescence measurements. The effect of ase on the primary decomposition mechanism and on energy ansfer processes is examined in the light of recent findings. ew experimental information on the energy partitioning among agments produced in the primary dissociation of $CH_4$ and $C_3H_8$ presented.

001. Mandel, J., **The statistical validation of tests,** *Mater. Res. Stand.* **12,** No. 9, 8-13, 62 (Sept. 1972).

Key words: Experimental error; measurement; statistical control; statistical design; test methods.

Basic to the evaluation of test methods is an understanding of e behavior of measurements, and particularly of the sturbances caused by random and systematic experimental errs. The concept of statistical control is discussed in terms of easuring processes. Finally, the role of statistical models and signs is illustrated by an example dealing with certain physical aracteristics of a blood expander.

13002. Sieck, L. W., Ausloos, P., **Ion-molecule reaction chains in isobutene,** *J. Chem. Phys.* **56,** No. 2, 1010-1011 (Jan. 15, 1972).

Key words: Ion-molecule reactions; isobutene; photoionization; polymerization; radiolysis.

The vapor phase ionic-chain reaction occurring in isobutene and propylene have been investigated both in the NBS high pressure photoionization mass spectrometer and in the closed systems photolysis. We have determined for the first time that the formation of stable dimer ions $(C_4H_8)_2^+$ in isobutene competes effectively with formation of $C_4H_9^+$. Dimeric ions are also observed in propylene. These dimeric ions are found to transfer $H_2$ to isobutene and propylene to yield isobutane and propane, respectively. The failure of other investigators to observe these sequences is discussed.

13003. Sieck, L. W., Searles, S. K., **High-pressure photoionization mass spectrometry. II. A study of thermal $H^-$ ($H^0$) and $H_2^-$ ($H_2^0$) transfer reactions occurring in alkane-olefin mixtures,** *J. Amer. Chem. Soc.* **92,** 10, 2937-2943 (May 20, 1970).

Key words: Alkanes; ion-molecule reactions; mass spectrometry; photoionization; rate coefficient; vapor phase.

Following photoionization of the $C_nH_{2n}$ (olefin) or $RH_2$ (alkane or cycloalkane) component in $RH_2$-$C_nH_{2n}$ mixtures with either 1236-Å (10.0 eV) or 1165-Å (10.6 eV) radiation, the following two classes of reactions have been investigated: (I) $C_nH_{2n}^+ + RH_2 \rightarrow C_nH_{2n+1} + RH^+$ ($H^-$ transfer) or $C_nH_{2n+2} + R^+$ ($H_2^-$ transfer); (II) $RH_2^+ + C_nH_{2n} \rightarrow C_nH_{2n+1} + RH^+$ (H transfer) or $C_nH_{2n+2} + R^+$ ($H_2$ transfer). Although these processes have been subjected to considerable scrutiny, the relative rate constants $k(H^-)/k(H_2^-)$ or $k(H^0)/k(H_2^0)$ found previously by kinetic mass spectrometry for any given reaction pair have always been considerably higher than those derived from photoionization and radiolysis experiments conducted in static systems. However, the values derived in our instrument, which reflect the interactions of ions at thermal energy, are in excellent agreement with the relative transfer efficiencies and other rate parameters derived from static experiments and suggest that kinetic and/or internal energy effects may have been important in previous experiments carried out in mass spectrometers. Rate constants and relative transfer efficiencies found for a number of reaction pairs are reported, and the nature of the collision complex is discussed.

13004. McBee, C. L., Kruger, J., **Nature of passive films on iron-chromium alloys,** *Electrochim. Acta* **17,** 1337-1341 (Oct. 1972).

Key words: Amorphous; diffraction; Fe-Cr; lattice parameter; 1 N $H_2SO_4$; oxide; passive; spinel.

Fe-Cr foils of a range of Cr content were anodically polarized in 1 N $H_2SO_4$ for passive film growth. The resulting oxide films were then studied while still in contact with the metal substrate with transmission electron diffraction at 100 kV.

Comparisons were made between the diffraction results for the Fe-Cr foils and previous diffraction studies for Fe foils. The diffraction patterns obtained revealed that as Cr content increased the oxide films were generally less able to sustain an epitaxial relationship with the substrates. The lower Cr foils had oxide patterns that could be fitted to a spinel structure; the lattice parameter in these cases increased with increasing Cr content. The highest Cr-content alloy, Fe-24% Cr, did not show any oxide pattern. It is concluded that the films tend to become amorphous as the Cr content of the alloy is increased.

13005. Sindt, C. F., Ludtke, P. R., **Characteristics of slush and boiling methane and methane mixtures,** *Proc. XIIIth Int. Con-*

A constant volume valve is described for pressures to 1400 bar with a volume change between the open and closed positions of less than 0.15 mm$^3$. The leak rate through the seat is less than $5 \times 10^{-5}$ mole/sec. The valve is of a very simple design. The type described here is pneumatically operated.

**13014.** Cohen, M. I., Young, K. F., Chang, T-T., Brower, W. S., Jr., **Phase transitions in $CsPbCl_3$,** *J. Appl. Phys.* **42,** No. 13, 5267-5272 (Dec. 1971).

Key words: $CsPbCl_3$; EPR of $Gd^{3+}$; phase transitions.

Measurements of dielectric properties, pyroelectricity, and the electron paramagnetic resonance spectrum of $Gd^{3+}$ as a function of temperature have been used to examine the phase transitions in $CsPbCl_3$. The results indicate the presence of five phase transitions and the loss of a center of symmetry at 194 K. The results together with the apparent order of the transitions, and published data, enable the Landau criterion to be used so that the point group of each phase may be identified. A reasonable choice of space group is also made.

**13015.** Forman, R. A., Brower, W. S., Jr., **Optical spectra of thallium-doped ammonium chloride,** *J. Lumin.* **4,** No. 2, 98-104 (Sept. 1971).

Key words: Ammonium chloride; luminescence, optical absorption; optical spectra; thallium ion.

The low temperature optical spectra associated with the thallium ion in doped samples of ammonium chloride have been investigated. Absorption, photoluminescence and luminescence excitation spectra are presented for this CsCl-structure (cubic) phosphor.

**13016.** Feldman, A., Horowitz, D., Waxler, R. M., **Relative importance of electrostriction and the Kerr effect to self-focusing in optical glasses,** *Appl. Phys. Lett.* **21,** No. 6, 260-262 (Sept. 15, 1972).

Key words: Damage threshold; electrostriction; Kerr-effect; laser damage in glasses; optical glasses; self-focusing.

The damage threshold for three optical glasses was found to be higher for circularly polarized radiation than for linear polarization, using 26-nsec pulses from a Nd:glass laser. The damage was assumed to result from self-focusing. The fractional contribution of electrostriction to the total nonlinear index $n_2$ is estimated to be $0.8 \pm 0.2$ for borosilicate crown glass, $1.15 \pm 0.35$ for fused silica, and $0.4 \pm 0.1$ for dense flint glass, assuming the Kerr effect to be the only other self-focusing mechanism. The data are consistent with present concepts of glass structure. The high damage threshold in fused silica is attributed to its relatively small Kerr effect.

**13017.** Forman, R. A., Hosler, W. R., Blunt, R. F., **The bandgap of cadmium fluoride,** *Solid State Commun.* **10,** No. 1, 19-24 (1972).

Key words: Bandgap; band structure; cadmium fluoride excitons; optical absorption; reflectivity; semiconductor.

Measurements of optical absorption and reflection at and below room temperature have been used to indicate that cadmium fluoride is a direct allowed bandgap material. In absorption an Urbach-type edge is observed, with the extrapolations from various temperatures intersecting to indicate an excitonic bandedge of ~7.6 eV in agreement with the reflectivity data. The absorption data are in accord with the thermal behavior expected for an allowed excitonic transition.

**13018.** Mandel, J., **Principal components, analysis of variance and data structure,** *Statist. Neerlandica,* pp. 119-129 (Aug. 1972).

Key words: Analysis of variance; data structure; princip components; two-factor data.

The relation between principal components and analysis variance is examined. It is shown that the model underlying t extended analysis of variance developed by GOLLOB a MANDEL is useful also as a model for principal component anal sis. The elucidation of structure of two-factor data using the ne analysis of variance model is illustrated by an example tak from thermodynamics.

**13019.** Kraft, R., **Analyticity and reflectivity for first order syste of elliptic type in two independent variables,** *J. Math. An Appl.* **29,** No. 1, 1-17 (Jan. 1970).

Key words: Analytic continuation; analyticity; compl variables; elliptic type; first order systems; partial d ferential equations; semilinear.

Analyticity and reflectivity results are established for fi order elliptic semilinear systems in two independent variabl The results are obtained by adaption and modifications techniques used by Garabedian in establishing similar results f second order systems.

**13020.** Rockett, J. A., **Fire research and safety center and the fi marshal,** *Fire J.* **64,** No. 6, 50-53 (Nov. 1970).

Key words: Education; fire act; fire data; fire preventio fire protection; training.

The present status of the Fire Research and Safety program discussed. Programs which will be of particular interest to t Fire Marshal are described. These include assistance in: fi records; fire record management and the use of fire data; fire i vestigations; training and education.

**13021.** Dillon, T. A., Stephenson, J. C., **Multiquantum vib tional-energy exchange,** *Phys. Rev. A* **6,** No. 4, 1460-1468 (O 1972).

Key words: Born; CO; collisions; exchange; multiquantu

A theory for exchange of vibrational quanta betwe molecules is formulated which does not rely on the Born expa sion of the $S$ matrix. A transformation is derived which diagon izes the vibrational operators responsible for exchange. T scattering operator is then expanded in a series of rotational te sor operators which permits evaluation of $S$-matrix elements all orders. This formulation shows that multiquantum process both rotational and vibrational, play an important role wh transition moments are large. Numerical calculations for vib tional exchange rates of carbon monoxide are compared w results of the first Born approximation from which they diff significantly. The dependence of the cross section on vibration energy defect is much less drastic than that of the Born appro mation. The present calculations indicate that cross sections the exchange of more than one vibrational quantum are subst tial, in marked contrast to the Born approximation where th are forbidden. The size of these multiquantum cross sections dicates that they can play an important role in the detailed kine modeling of CO lasers.

**13022.** Harman, G. G., Leedy, K. O., **An experimental model the microelectronic ultrasonic wire bonding mechanism,** *Pr 10th Annual IEEE Reliability Physics Symposium, L Vegas, Nevada, Apr. 5-7, 1972,* pp. 49-56 (1972).

Key words: Aluminum; microelectronics; ultrasonic bo ing; wire bonding.

Various concepts of the microelectronic ultrasonic bondi mechanism have been expounded for many years. The pres work attempts to resolve some of the conflicts by experimenta *ress of the International Institute of Refrigeration, Washing- on, D.C., Aug. 27-Sept. 3, 1971*, pp. 1-6 (Int. Inst. of efrigeration, Paris, France, 1971).

Key words: Binary mixtures; cryogenic mixtures; liquefied natural gas; methane; slush methane; slush natural gas.

iquefied natural gas (LNG) and methane are in contention as ls for high performance aircraft, rocket engines, and motor icles. They have the advantages, over kerosene and gasoline, higher specific heat of combustion and cleaner combustion, they are six times more dense than liquid hydrogen. Some of applications for either methane or LNG would benefit from increased heat capacity and the increased density of mixtures iquid and solid such as slush. Because of these potential ad- tages, the characteristics of slush and boiling methane and bi- y mixtures of methane and other natural gas constituents e investigated. Subcooled liquid or slush would also serve to uce or eliminate fuel losses that would accompany reduction uel tank pressure as the aircraft gains altitude.

he scope of the program was the characterization of slush pared from pure methane and binary mixtures of methane n nitrogen, ethane, and propane, and the investigations of the ling characteristics of these mixtures.

**06.** Grabner, L., Forman, R. A., Wong, E. Y., **Spectroscopy f $Cr^{3+}$ in $CsCr(SO_4)_2 \cdot 12H_2O/D_2O$, a $\beta$-alum,** *Phys. Rev. B* **6,** o. 3, 797-801 (Aug. 1, 1972).

Key words: $\alpha$-, $\beta$-, $\gamma$-alums; crystal field splitting; disorder; energy transfer; inequivalent sites.

he trigonal-field splitting of $^2\bar{E}$ into $\bar{E}$ and $2\bar{A}$ states is found e $\bar{E}-2\bar{A}=-120\ \mathrm{cm}^{-1}$ by identifying $2\bar{A}$. The no-phonon lines euterated samples are isotope shifted 6 $\mathrm{cm}^{-1}$ to the red. The owing generalizations suffice to relate the spectra of the Cr- ms: (i) They are due to $^4A_2 \rightarrow \bar{E}$, $2\bar{A}(^2E)$ transitions. The tting of $^2E$ is large for the $\beta$-alums, small for the $\alpha$-alums. (ii) ate-group disorder, found in all $\alpha$-alums, complicates their ctra by adding inequivalent $Cr^{3+}$ sites.

**07.** Frederikse, H. P. R., Hosler, W. R., **Excitons in solid and quid thallous chloride,** *Solid State Commun.* **9,** No. 10, 709- 12 (1971).

Key words: Excitons; liquid state; thallous chloride.

he absorption edge of thallous chloride has been measured ow and above melting point. In the crystal this edge resents the low energy tail of a strongly absorbing Wannier iton. The similarity between the shape and temperature de- dence of this absorption in the solid and in the liquid states gests that Wannier-like excitons exist also in liquid thallous oride.

**08.** Grabner, L., **Exciton emission and donor-acceptor associa- on in thallium bromide,** *Phys. Rev. B* **4,** No. 4, 1335-1339 Aug. 15, 1971).

Key words: Donor-acceptor pairs; excitons; thallium bromide.

ree- and bound-exciton emission with longitudinal optical )) phonon cooperation is reported in undoped TlBr. The bind- energies of the bound excitons with respect to the free ex- n are 4 and 7 MeV, respectively. A photocurrent peak at the rgy of the free exciton at 4 K is interpreted as due to an Auger cess at the bound-exciton complexes. Extrinsic photocurrent eported. The temperature dependence of its excitation spec- m is anomalous from the point of view of the conventional hl-Schön recombination model and is shown to be consistent h a model involving donor-acceptor pairs.

**13009.** Forman, R. A., **Order-disorder transition in lithium imide, $Li_2NH$,** *J. Chem. Phys. Letters to Editor* **55,** No. 4, 1987-1988 (Aug. 15, 1971).

Key words: Dipole ordering; DTA; NMR; order-disorder; phase transition; thermal analysis.

On the basis of differential thermal analysis results and previous NMR studies, we believe we have discovered an order-disorder transition, possibly of the λ-type, of $NH^{2-}$ dipoles in the cubic anti-fluorite compound lithium imide, $Li_2NH$.

**13010.** Franzen, D. L., **CW gas breakdown in argon using 10.6-μm laser radiation,** *Appl. Phys. Lett.* **21,** No. 2, 62-64 (July 15, 1972).

Key words: Gas breakdown; plasma.

A very intense gas breakdown spark has been extended to a continuous arc in argon using a focused cw $CO_2$ laser. To achieve cw breakdown, the focal volume of a mirror focusing a high-power $CO_2$ laser was preionized by a single pulse from a $CO_2$ TEA laser. The electron density created by the pulsed laser is sufficient to start the cw plasma. This letter reports accurate measurements of pulsed thresholds as well as preionized cw thresholds for breakdown in argon. Also, a study of the time development of the cw plasma is presented.

**13011.** Hedges, R. E. M., Drummond, D. L., Gallagher, A., **Extreme-wing line broadening and Cs-inert-gas potentials,** *Phys. Rev. A* **6,** No. 4, 1519-1544 (Oct. 1972).

Key words: Cesium; inert gas; line broadening; molecules.

The emission profiles of the cesium resonance lines broadened by collisions with inert gases have been measured from about 50-1000 $\mathrm{cm}^{-1}$ from line center. The emission is observed from optically excited Cs in a cell whose temperature is varied from about 300-800 K. By measuring the wing intensity relative to the entire line intensity from optically thin Cs, the profiles can be related to theoretical models without knowledge of the cesium density. The quasistatic theory of line broadening, extended to include the distribution of perturber positions about the Cs, is used to analyze the data. The observed temperature dependence of the emission profiles is associated with the temperature dependence of the perturber distribution in the Cs-inert-gas adiabatic potential. The quasistatic spectrum depends on the difference between excited- and ground-state adiabatic potentials, so each potential is thereby separately determined from the data. The $X\Sigma$, $A\Pi$, and $B\Sigma$ potentials for the 3.5 – 5-Å region are given.

**13012.** Kitching, P., Moss, G. A., Olsen, W. C., Roberts, W. J., Alder, J. C., Dollhopf, W., Kossler, W. J., Perdrisat, C. F., Lehman, D. R., Priest, J. R., **Reactions $(p,pd)$ and $(p,2p)$ on helium-3 at 590 MeV,** *Phys. Rev. C* **6,** No. 3, 769-772 (Sept. 1972).

Key words: Confidence cross sections; $^3He(pd)$ vertex; plane wave impulse approximations; quasi-free scattering; separable potentials; three-body problem.

The reaction $^3He(p,pd)$ has been studied for recoil momenta of the spectator proton up to 230 MeV/$c$. The cross section of $^3He(p,2p)$ was measured up to 100 MeV/$c$. The results are interpreted in terms of the plane-wave impulse approximation and the form factors for $^3He \rightarrow dp$ and $^3He \rightarrow p(pn)$ are compared with a calculation of the $^3He$ wave function in which the two-nucleon interaction is described by a separable potential which reproduces the low-energy properties of the two-nucleon system.

**13013.** Markus, W., **A constant volume valve,** *Rev. Sci. Instrum. Notes* **43,** No. 1, 158-159 (Jan. 1972).

Key words: Constant volume; equation of state; pressure; vacuum; valve.

examining each step in the ultrasonic aluminum wire bonding process. Measurements made with a capacitor microphone during bonding are correlated with appropriate SEM pictures of bond lift-off patterns. A series of inductive experiments have been performed, the results of which can be summarized as follows: Heat generation in the weldments is insufficient to cause the observed welding. The deforming wire breaks up and sweeps aside oxide, exposing clean metal surfaces which are then able to form metallurgical welds. The bonding tool does not grip the wire and slide it back and forth across the bonding pad. The use of a grooved tool does not improve the welding process. The tool-to-wire coupling takes place by a series of microwelds that are repeatedly made and broken as the tool moves back and forth across the wire surface.

**13023.** Bennett, H. S., Stoneham, A. M., **Effects of random fields on radiative decay of color centers,** *Phys. Rev. B* **6,** No. 8, 3086-3090 (Oct. 15, 1972).

Key words: Charged impurities; *F* center; Gaussian distribution; Holtsmark distributions; lifetime; phonons; potassium chloride.

Transitions which are normally forbidden have been observed in a variety of defects in solids because of the electric fields associated with lattice vibrations or with random impurities. The radiative decay of an *F* center is a good example of this. We ask in this paper: When will the contribution of random impurities be important, and when will the decay be intrinsic? Several qualitatively distinct examples are analyzed, and tables for the transition probabilities in terms of dimensionless parameters characteristic of the host and the defects are given. Random fields should dominate in III-V and group-IV hosts, but they should prove less important in the alkali halides. Effects of random fields on related phenomena are also discussed.

**13024.** Baker, L. C. W., Baker, V. S., Wasfi, S. H., Candela, G. A., Kahn, A. H., **Isomorphous heteropoly complexes containing various pairs of paramagnetic atoms. Exchange-coupled differing spins with absence of long-range magnetic interactions. A new class of paramagnetic behavior. Theoretical treatment. Novel geometrical isomerism,** *J. Amer. Chem. Soc.* **94,** No. 15, 5499-5501 (July 26, 1972).

Key words: CO; exchange coupling; Fe; heteropoly complexes; Keggin structures; magnetic spins; magnetic susceptibility; paired spins; tungsto-heteropoly complexes.

Coupled pairs of differing magnetic ions in tungsto-heteropoly complexes have been studied by magnetic susceptibility over the temperature range 2 to 300 K. The two substitutional sites are surrounded by oxygen ions in octahedral and tetrahedral coordinations with one oxygen ion in common. The ions studied were $Co^{2+}$, $Co^{3+}$, and $Fe^{3+}$, in a total of five combinations on the two sites, offering a unique set of symmetries and ions for examining super-exchange effects. The susceptibility has been analyzed according to the spin Hamiltonian

$$\mathscr{H} = \beta(g_1\mathbf{S}_1 + g_2\mathbf{S}_2) \cdot \mathbf{H} - J\mathbf{S}_1 \cdot \mathbf{S}_2;$$

fitted values of $J$ range from $-6$ to $-70$ K depending on the combinations of ions. The experimental agreement with the spin Hamiltonian for all cases studied is satisfactory for this unique system.

**13025.** Linsky, J. L., Mount, G. H., **On the validity of a generalized Kirchhoff's Law for a nonisothermal scattering and absorptive medium,** *Icarus* **17,** 193-197 (1972).

Key words: Emissivity; Kirchhoff's Law; lunar surfaces; planetary atmospheres; reflectivity.

The relationship of directional hemispherical reflectivit emissivity is investigated for a nonisothermal medium isotropic coherent scattering and absorption. Departures fro generalized Kirchhoff's Law occur due to the long range na of the scattering process. Such departures occur in lunar the emission at microwave but not at infrared frequencies.

**13026.** Trombka, J. I., Eller, E., Oswald, G. A., Berger, M Seltzer, S. M., **$^{252}$Cf neutron induced radiative capture gan rays for high energy detector calibration,** (Proc. Amer. N Soc. National Topical Meeting on Neutron Sources and plications, Augusta, Ga., April 19-21, 1971), Chapte *Neutron Sources and Applications,* **CONF-710402,** III, 43–III-47 (National Technical Information Service, Spr field, Va. 22151, 1971).

Key words: California; gamma rays; neutrons; radia capture; response functions; sodium iodide detector.

High energy gamma ray sources produced by prompt neu radiative capture were developed in order to study the varia of pulse height, the shape of pulse height distribution, and res tion as a function of energy for scintillation detectors. system as described below has also been used to calibrate gamma ray spectrometers which will be flown aboard Apoll and 16.

Spectral distribution of gamma rays in the 3 to 12 MeV en region using a 3 in. × 3 in. NaI(Tl) detector have been studie a number of nuclear species such as: Nickel with lines at 8. and 8.533 MeV; Mercury–5.967, 4.842, 4.740, and 3. MeV; and Hydrogen–2.223 MeV. The neutron excitatio these samples was carried out by placing these samples neutron moderator near a $^{252}$Cf source ($\sim 2\ \mu$g).

Methods for inferring photon spectra from the pulse he spectra have been developed and are to be used to interpre gamma ray measurements carried out during the Apollo 15 16 flights. Detailed knowledge of the response of the flight de tors as a function of energy is required to perform the analysi the energy region above 3 MeV, it is extremely difficult to ob response functions for truly monoenergetic gamma rays. Th fore the following approach has been taken: Monte Carlo ca lations have been carried out to determine the nature of response functions in the 3 to 12 MeV region. These spe have been compared with the experimentally determined spe obtained using the $^{252}$Cf system described above. These parisons form a basis for predicting the shape of the pulse he spectrum for gamma rays of any energy in this range.

**13027.** Cowan, D. O., Candela, G. A., Kaufman, F., **The org solid state. V. Symmetry distortions in ferrocenium compou** *J. Amer. Chem. Soc.* **93,** No. 16, 3889-3893 (Aug. 11, 1971

Key words: Biferrocene; electron resonance; suscepti ty; symmetry changes.

The magnetic susceptibilities of biferrocene [Fe(II)Fe(I picrate (**1**) and biferrocene [Fe(III)Fe(III)] difluoroborate were determined from 2 to 300 K. The experimental curve the effective magnetic moment ($\mu_{eff}$) are compared with theo cal curves based on a model involving molecular distortion f axial symmetry. For compound **1**, in the temperature range 300 K, the best-fit temperature-independent distortion fact = 1000 $cm^{-1}$/ferrocenium unit) is large when compared to pr ously observed distortions. The deviation from the theore $\mu_{eff}$ curve for this compound is small. For compound **2** in temperature range 77-300 K the best-fit temperature-inde dent distortion factor is 750 $cm^{-1}$/ferrocenium unit; while in temperature range 2-4 K the distortion factor is consider smaller ($\delta = 150$ $cm^{-1}$/ferrocenium unit). The electron resonance spectra of compounds **1** and **2** were measured a

298 K. The observed $g$ values were used to calculate the ef- ve magnetic moments and the distortion factors for com- ıds 1 and 2. These values are in good agreement with those ined from the magnetic susceptibility measurements. The rved low-temperature collapse of the $g_x$, $g_y$ signal and the :arance of a new $g_z$ signal (compound 2) are consistent with rge reduction in the distortion parameter at low temperature.

**8.** Waclawski, B. J., Plummer, E. W., **Photoemission observa- n of a surface state of tungsten,** *Phys. Rev. Lett.* **29,** No. 12, 3-786 (Sept. 1972).

Key words: Adsorption; energy distribution; photoemis- sion; surface states.

ıotoelectron energy distributions from clean, polycrystalline sten reveal a surface-sensitive peak about 0.4 eV below the ıi energy. This peak, which is identified as a surface state, lly decays during gas adsorption, and concomitant growth of w peak at ~ 2.5 eV below the Fermi energy is observed. the energy range of the surface-state peak, the strength of ıce-state emission relative to bulk emission decreases with asing photon energy. These results quantitatively substan- existing field-emission data and qualitatively agree with el photoemission calculations.

**9.** Steiner, B., **Photodetachment: Cross sections and electron inities,** Chapter 7 in *Case Studies in Atomic Collision ysics,* E. W. McDaniel and M. R. C. McDowell, Eds., **2,** 5-545 (North-Holland Publ. Co., Amsterdam, The Nether- ıds, 1972).

Key words: Atomic; crossed beam; cross section; electron affinitive; molecular; photodetachment.

ıe status of negative ion photodetachment cross section mination is reviewed, both theory and experiment. A ted table of best values is derived. Threshold behavior is ex- ed separately. Crossed beam experimental techniques are ribed in detail. Finally, the status of atomic and molecular ron affinity determinations is reviewed and an extensive of preferred values is compiled.

**0.** Nargolwalla, S. S., **Application of neutron generators to ac- ation analysis,** (Proc. Second Oak Ridge Conf. on the Use of nall Accelerators for Teaching and Research, Oak Ridge, nn., Mar. 23-25, 1970), USAEC Rept. Conf. **700322,** 185- 4 (Oct. 1970).

Key words: Accuracy; activation analysis; element; generator; micro; precision; reactor; selectivity; semimicro; sensitivity.

eutron activation analysis has gained wide acceptance in nt years as a very sensitive and specific method for the tative and quantitative determination of most of the ele- s in the periodic table. Until very recently, however, activa- analysis was limited to the use of thermal neutrons rated in a nuclear reactor. Today, the development of low- neutron generators has considerably added to the scope of technique, and made it available to most well-equipped tical laboratories. This review summarizes some of the key lopments in neutron generator technology which have had nificant bearing in the acceptance of neutron generators for recise and accurate determination of a large number of ele- s at the semimicro and macro levels of concentration.

cent advances in the design and utilization of experimental ware such as sample-placement devices, experimental ns and special long-lived neutron producing targets are ıssed. Descriptions of some investigations pertaining to the ıation of systematic errors in activation analysis with ron generators are presented, and various aspects of analytical significance related to the use of this type of radiation source are emphasized. In this regard, advantages offered by the neutron generator for the analysis of light elements are given. Research in the area of cross section measurements and their implications in light of the practical sample due to degradation of the nominal 14.7 MeV neutrons is described. Typical sensitivities obtainable with present-day neutron outputs from neutron generators are critically examined and anomalies between expected theoretical sensitivities and experimental sample response in high energy neutrons are discussed.

Pertinent applications of neutron generator activation analysis techniques in the areas of metallurgy, biochemistry, mineralogy and standard materials are described. Special attention is drawn to the introduction of this technique to the solution of industrial quality control problems. A brief treatment of the on-line analytical capabilities of neutron generators, particularly of the sealed-tube type is given. In this connection, efforts made toward the computerization of analytical procedures and data reduction are emphasized. In conclusion, the contribution of this analytical technique in terms of sensitivity, specificity, accuracy and precision, and possible future developments of the fast neutron facility are discussed.

**13031.** Baker, L. C. W., Baker, V. E. S., Wasfi, S. H., Candela, G. A., Kahn, A. H., **Exchange interactions between pairs of differing magnetic spins in heteropoly complexes,** *J. Chem. Phys.* **56,** No. 10, 4917-4923 (May 15, 1972).

Key words: Co; Fe; heteropoly complexes; Keggin structures; magnetic spins; magnetic susceptibility; paired spins; tungsto-heteropoly complexes.

Coupled pairs of differing magnetic spins in tungsto-heteropoly complexes have been investigated by studying the magnetic susceptibility over the temperature range 2-300 K. The two sites of the magnetic ions are surrounded by oxygen ions in octahedral and tetrahedral coordinations with one oxygen ion in common. The ions studied were $Co^{2+}$, $Co^{3+}$, and $Fe^{3+}$ in a total of six combinations on the two sites, offering a unique set of symmetries and ions for examining super-exchange effects. A closed form for the susceptibility has been obtained on assuming the spin Hamiltonian

$$\mathscr{H}=\beta(g_1\mathbf{S}_1+g_2\mathbf{S}_2))\,\mathbf{H}-\mathbf{J}\mathbf{S}_1\cdot\mathbf{S}_2,$$

allowing for the possibility of $g_1 \neq g_2$, $S_1 \neq S_2$. Fitted values of $J/k$ range from $-6$ to $-70$ K depending on the combination of ions. The experimental agreement with the spin Hamiltonian for all cases studied is satisfactory for this system.

**13032.** McAlister, A. J., Cuthill, J. R., Dobbyn, R. C., Williams, M. L., Watson, R. E., **Soft-x-ray studies of ferromagnetic and paramagnetic iron,** *Phys. Rev. Lett.* **29,** No. 3, 179-182 (July 17, 1972).

Key words: Band ferromagnetism; Fe; magnetic transition; M spectrum; soft-x-ray.

The soft-x-ray $M_{2,3}$ emission spectrum of Fe has been measured below (560 °C, $T/T_c=0.8$) and above (840 °C, $T/T_c=1.07$) the Curie point, and has revealed motion of distinct structural features within the $d$ bands on passing through $T_c$. The results, taken with earlier photoemission data on Fe and Ni, are in excellent numerical agreement with, while in no sense providing verification of, the band ferromagnetism description of Stoner, Wohlfarth, and Slater for these metals.

**13033.** Reno, R. C., Swartzendruber, L. J., **Time-differential perturbed angular correlations on $^{57}$Fe in Cu-Ni alloys: Mössbauer doublets explained,** *Phys. Rev. Lett.* **29,** No. 11, 712-715 (Sept. 11, 1972)

Key words: Cu-Ni-Fe alloys; hyperfine fields; Mössbauer effect; perturbed angular correlation.

It is shown that when hyperfine interactions at $^{57}$Fe nuclei are studied by both Mössbauer effect and time-differential perturbed angular correlations, information is obtained which is unavailable from either technique alone. In particular, previous ambiguities in the interpretation of $^{57}$Fe Mössbauer spectra of Cu-Ni alloys are removed: The Mössbauer doublet is shown to be primarily due to a distribution of electric field gradients acting on the $^{57}$Fe nuclei.

**13034.** Nahman, N. S., Holt, D. R., **Transient analysis of coaxial cables using the skin effect approximation $A=B\sqrt{s}$,** *IEEE Trans. Circuit Theory* **CT-19,** No. 5, 443-451 (Sept. 1972).

Key words: Analysis; cables; coaxial; skin effect; time-domain; transient; transmission.

The purpose of this paper is to demonstrate the utility of the function $A+B\sqrt{s}$ for approximating the coaxial line series impedance (skin effect) in applications to transient analysis. The time domain response expansions of Holt are modified in terms of two adjustable parameters which replace the physical parameters $R$ and $K$. The modified expansions are truncated to yield condensed expressions useful for analysis and design. Two types of terminations are considered: 1) nonreflective, terminated in the characteristic impedance $Z_0(s)$, and 2) doubly reflective, sending and receiving ends each terminated in the nominal characteristic impedance $R_0=\lim_{s\to\infty}Z_0(s)=\sqrt{L/C}$. Experimental data are presented on the frequency and time domain insertion responses of three commercial cables: RG 5B/U—68.6 m (225 ft), RG 21/U—96.8 m (317 ft). and RG 58A/U—137 m (450 ft). Theoretical and experimental time domain responses for the sending- and receiving-end voltages are compared over the time interval from the order of 10 ns to that of 10$\mu$s. It is demonstrated that the parameters $A$ and $B$ can be adjusted to provide functions of time which closely approximate the actual time domain response over different intervals.

**13035.** Barbrow, L. E., **The mass-weight dilemma,** *Sci. Teacher* **39,** No. 7, 4 (Oct. 1972).

Key words: Free fall; gravity; mass vs. weight; weight; weightlessness; weight vs. mass.

The impending changeover to the metric system has again given prominence to the confusion that exists regarding what the term "weight" signifies. This term for centuries has been used synonymously with mass but it has also been used to signify many other concepts, each related to the force of gravitational attraction in some way. The multiplicity of meanings of the term "weight" has created a dilemma the suggested resolution of which is the use of the term exclusively as being synonymous with mass and to use the term force when discussing any of the concepts related to gravity. How to handle the popularized concept of "weightlessness" is dealt with separately.

**13036.** Ledbetter, H. M., Wayman, C. M., **On $\beta$ AuCd martensites,** *Met. Trans.* **3,** No. 9, 2349-2356 (Sept. 1972).

Key words: Crystallography; crystal structure/alloys; gold-cadmium alloys; phase transformations/solid state; x-ray-diffraction crystallography.

The martensites which form from $\beta$ AuCd alloys have been studied by x-ray diffraction using both powder and single-crystal techniques. Alloys containing 46.8 to 51.0 at.pct Cd were examined. Besides the parent phase $\beta$ only two other phases were observed: $\beta'$ and $\beta''$. A new unit cell is proposed for $\beta''$ which has 18 atoms and trigonal-hexagonal point symmetry. All previous $\beta''$ crystal structure proposals are reviewed critically. The relationship of the $\beta''$ crystal structure to the $\beta$-to-$\beta''$ martens transition is discussed.

**13037.** Kirby, R. K., Hahn, T. A., Rothrock, B. D., **Thermal pansion,** Section 4f in *American Institute of Physics Ha book, Third Ed.*, pp. 4-119—4-142 (1972).

Key words: Alloys; compounds; elements; Grüneis constant; linear thermal expansion; liquids.

New and revised tables for the 3d edition of the AIP Ha book. These tables are: Table TE-1, Linear Thermal Expans and Coefficients of Linear Thermal Expansion of Chemical I ments; Table TE-2, Coefficients of Linear Thermal Expans of Materials at Low Temperatures; Table TE-3, Linear Ther Expansion and Coefficients of Linear Thermal Expansion Some Compounds and Alloys; Table TE-4, Thermal Expans of Liquids; and Table TE-5, Constants in Grüneisen's Equa for Thermal Expansion (eight of the elements have been del from this table as it appeared in the 2d edition because the in mation is not consistent with the data given in TE-1).

**13038.** Reed, R. P., **Aluminium. 2. A review of deformation perties of high purity aluminium and dilute aluminium all** *Cryogenics* **12,** No. 4, 259-291 (Aug. 1972).

Key words: Elastic properties; high-purity aluminium; tice defects; mechanical properties; recovery; strengt ing.

The elastic and plastic deformation behaviour of high-pu aluminium and of dilute aluminium alloys is reviewed. Reli property data, including elastic moduli, elastic coefficients, sile, creep, fatigue, hardness, and impact are presented. Si crystal tensile results are discussed. Rather comprehen reference lists, containing publications of the past 20 years, included for each of the above categories. Defect structures mechanisms responsible for mechanical behaviour presented. Strengthening techniques (alloys, cold work, irra tion, quenching, composites) and recovery are briefly revie

**13039.** Clark, A. F., **Combination of a power transmission line an active track for a magnetically suspended high-speed trai** *Appl. Phys.* **43,** No. 8, 3598-3599 (Aug. 1972).

Key words: Cryogenic; high-speed ground transportat magnetic levitation; power transmission.

The idea of utilizing proposed cryogenic power transmis lines as an active track for magnetically suspended high-s ground transporation is briefly explored. The advantage transporting both people and power on the same right of wa many, and proposed transmission current levels are more adequate for suspension.

**13040.** Hanley, H. J. M., McCarty, R. D., **Argon third virial ficients,** *J. Chem. Phys.* **57,** No. 7, 3023-3025 (Oct. 1, 1972

Key words: Argon; m-6-8 potential; nonadditivity; virial coefficients.

Experimental third virial coefficients for argon, taken several sources, are presented. An approximate calculatio the third virial coefficient from the 11-6-8 potential, inclu nonadditivity effects, is also discussed and the result comp to experiment. Agreement between theory and experime good.

**13041.** Straty, G. C., Younglove, B. A., **Dielectric constant molar polarizability of compressed gaseous and liquid fluo** *J. Chem. Phys.* **57,** No. 6, 2255-2259 (Sept. 15, 1972).

Key words: Clausius-Mossotti function; compre liquid; dielectric constant; fluorine; polarizability; satur liquid.

this paper we present accurate wide-range measurements of lielectric constant of saturated liquid fluorine from 70 to 140 d of compressed fluid fluorine at temperatures between 100 300 K at pressures to 21 $\mathrm{MN/m^2}$(1 $\mathrm{MN/m^2} = 9.8692$ atm= 038 psi). The data are combined with previously measured ities to determine the molar polarizability and its depen- e on density and temperature. The density range examined nds to nearly 3 times the critical density. The molar polariza- is found to increase initially with density and then ease. Current theories of the dielectric constant are found to satisfactory qualitative interpretation of the density depen- e of the molar polarizability but do not give satisfactory titative predictions.

2. Hust, J. G., **Electrical resistance ratios of Evanohm heater re at low temperatures,** *Rev. Sci. Instrum.* **43,** No. 9, 1387-88 (Sept. 1972).

Key words: Electrical resistance; electrical resistance temperature coefficient; heater wire; material variability.

a consequence of using Evanohm wire as heater elements ır thermal conductivity apparatus we have obtained exten- resistance-temperature data for wires from several spools at eratures from 5 to 300 K. These data, reduced to resistance s, *R(T)/R*(273 K), show the variation of resistance with erature as well as the degree of material variability.

3. Berger, M. J., Seltzer, S. M., **Response functions for sodi- iodide scintillation detectors,** *Nucl. Instrum. Methods* **104,** 7-332 (1972).

Key words: Detection efficiency; energy deposition spec- rum; gamma ray spectrum; Monte Carlo calculations; resolution; response function; sodium iodide detector.

e response of sodium iodide detectors to gamma rays has calculated by a method that takes into account the multiple ering and escape from the detector of the incident gamma as well as of the secondary charged particles and bremss- ung. The method is applicable to gamma rays with arbitrari- gh energies, and its accuracy has been verified by com- ons with experimental response functions at energies up to eV. A systematic tabulation has been made of the response ions for 3″×3″ detectors irradiated with broad parallel s of gamma rays, at energies between 100 keV and 20 . These results are given in a parametrized form which s it easy to interpolate with respect to incident gamma-ray gy. A few response functions have also been calculated for tors irradiated with 50 MeV gamma rays. Exploratory cal- ions have shown that 3″×3″ detectors are "om- ectional" in the sense that the shape of the response func- depends very little on the direction of the incident gamma- eam. Therefore, the tabulated data for broad parallel beams ent perpendicularly can, in good approximation, also be ap- to other source geometries, e.g., the case of a detector ex- d to an isotropic gamma-ray flux.

4. Mielenz, K. D., Eckerle, K. L., **Spectrophotometer lineari- testing using the double-aperture method,** *Appl. Opt.* **11,** No. , 2294-2303 (Oct. 1972).

Key words: Double-aperture method; light addition; nonlinearity correction; photomultiplier nonlinearity; spectrophotometry.

ne double-aperture method has been used to determine the inearity correction for a new spectrophotometer having a ision of $\pm 4 \times 10^{-5}$ transmittance units. The random and ematic errors of the method are discussed, and techniques described that yield the additive nonlinearity correction to igh level of precision required for this spectrophotometer. The correction was found to be independent of source polarization, free from interference errors, but slightly dependent on wavelength.

13045. Sugar, J., **Interpretation of photoabsorption in the vicinity of the 3*d* edges in La, Er, and Tm,** *Phys. Rev. A* **6,** No. 5, 1764-1767 (Nov. 1972).

Key words: Erbium; photoabsorption; theory; thulium; 3*d* edges.

Line spectra at the 3*d* photoabsorption edges of La, Er, and Tm are interpreted as transitions of the type $3d^{10}4f^N \rightarrow 3d^9 4f^{N+1}$. Calculated relative *gf* values for these transitions are compared with published absorption curves.

13046. Buchalter, D. N., Hargreaves, J. H., Jr., **Angular displacement detector,** *Rev. Sci. Instrum. Notes* **43,** No. 11, 1711-1712 (Nov. 1972).

Key words: Angular displacement detector; light emitting diode; phototransistors.

This Note describes a detector for small angular deflections (0.1 $\mu$rad resolution). It uses a modulated infrared beam focused on a mirror whose angular deflection is to be measured. The beam is then reflected onto two phototransistors. The difference of the output voltages from these transistors is a measure of the angular displacement.

13047. Marzetta, L. A., **An evaluation of the three-voltmeter method for AC power measurement,** *IEEE Trans. Instr. Meas.* **IM-21,** No. 4, 353-357 (Nov. 1972).

Key words: Phase-sensitive detector; power-factor; quadrature; three-voltmeter method; wattmeter.

The accuracy and frequency response limitations in the present square-law responding laboratory wattmeters have promoted the search for alternate methods of ac power measurement using electronic instrumentation. The three-voltmeter method is based on an old principle of operation implemented by new analog circuitry. Results of the tests reported here show a precision of power calculation with 0.01 percent error at frequencies below 5 kHz. A unique test procedure is described for the comparison of the three-voltmeter device and a time-division multiplier wattmeter operating at zero power factor.

13048. Goodwin, R. D., **Thermophysical properties of methane,** *Proc. 2nd Conf. on Natural Gas Research and Technology, Atlanta, Ga., June 5-7, 1972, Session V, Paper 2,* pp. 1-12 (Institute of Gas Technology, Chicago, Ill., 1972).

Key words: Methane; pressure-density-temperature relations; thermodynamic properties.

This report describes briefly the rather direct methods recently used at this laboratory to prepare tables of provisional values of thermodynamic functions for methane. The basic data are spectroscopic specific heats for ideal gas states; the vapor pressure and melting curves; available virial coefficients for low density gas; and density (PVT) measurements over the domain from the triple point (90.68 K) to 400 K at pressures to 350 bar (1 atm = 1.01325 bar). References are given for the principal sources of PVT data.

The analytical descriptions of the PVT physical properties are emphasized in this report because they are needed for smoothing, for interpolation, and for the computation of derivatives. These have been developed here in recent years to be at least qualitatively consistent with known behavior about the critical point. The nonanalytic equation of state used here is qualitatively consistent with the experimental observation that specific heats $C_v$ increase beyond measure upon close approach to the critical point.

**13049.** Goodwin, R. D., **Thermophysical properties of methane,** *Proc. 3rd Int. Conf. and Exhibition on Liquefied Natural Gas, Washington, D.C., Sept. 24-28, 1972, Session II, Paper 10,* pp. 1-12 (Institute of Gas Technology, Chicago, Ill., 1972).

Key words: Dielectric constants; methane, specific heats; thermal conductivities; thermodynamic functions; viscosities.

This report describes briefly the methods recently used at this laboratory to prepare tables of provisional values of thermodynamic functions for methane. References are given for the principal sources of PVT data. Emphasis is placed on analytical descriptions of physical properties because these are needed for smoothing, for interpolation, and for the computation of derivatives.

**13050.** Branscomb, L. M., **To help advance our Nation's scientific and technical capability for the greatest public benefit,** *Mater. Res. Stand.* **12,** No. 5, 8-12 (May 1972).

Key words: Experimental incentive program; metrication; technology; standardization.

This interview presents an overview of the National Bureau of Standards in the context of its goal "to strengthen and advance the Nation's science and technology and to facilitate their effective application for public benefit."

**13051.** Kushner, L. M., **We have decided to become more active at the policy level in voluntary standardization activities,** *Mater. Res. Stand.* **12,** No. 5, 13-14 (May 1972).

Key words: Engineering standards; standardization process; voluntary standardization.

The role of NBS in the voluntary standardization process used in this country is briefly outlined.

**13052.** Andrus, W. E., **A focus for the Bureau and all voluntary standardization organizations,** *Mater. Res. Stand.* **12,** No. 5, 15-17 (May 1972).

Key words: Engineering standards; standardization; voluntary standards system.

In interview form, the role of the NBS program office for engineering and information processing standards is outlined. The voluntary product standards program is described, as are guidelines for NBS participation in standardizing bodies.

**13053.** Ambler, E., **A major innovation is our measurement assurance program,** *Mater. Res. Stand.* **12,** No. 5, 18-23 (May 1972).

Key words: Basic standards; Josephson effect; lasers; metrology.

The mission and program of the NBS Institute for Basic Standards is presented in brief form. Calibration services, measurement assurance programs, and such new programs as laser stabilization and use of the Josephson junction in voltage monitoring are discussed.

**13054.** Hoffman, J. D., **IMR emphasizes accurate measurem and standards for materials,** *Mater. Res. Stand.* **12,** No 24-33 (May 1972).

Key words: Air pollution measurements; failure an sis; materials research.

Such aspects of the NBS Institute for Materials Researc air pollution measurements, failure analysis, standard refere materials, high pressure research, surface research, collab tive research, and others are presented. The competence the various IMR groups are tabulated, and problems, spectives, and future opportunities are covered.

**13055.** Willenbrock, F. K., **We can never afford to be technic wrong,** *Mater. Res. Stand.* **12,** No. 5, 34-36, 71-72 (May 19

Key words: Communications; consumer informati standardization.

A brief description of the NBS Institute for Materials search is presented, especially as it impacts the public thro information services and standardization activities.

**13056.** Young, T. R., **Laboratory evaluation: Facing up to a tional problem,** *Mater. Res. Stand.* **12,** No. 11, 22-26 (N 1972).

Key words: Accreditation; certification; evaluati national system; reference samples; testing laboratori

A concept of a national system for evaluation and accred tion of testing laboratory functions is reviewed. Reques laboratories having need would be provided examinati involving on-site inspections and reference sample audits plied by national reference laboratories or task groups of viduals. The criteria used and the examiners would be re nized by a National Board who would also issue accreditati of testing functions having a public interest, based upon eva tion of laboratory examinations. Examples of existing refere laboratories are discussed.

**13057.** Rowland, G. A., **A program to assist the States in acc ing industrialized housing,** *Mater. Res. Stand.* **12,** No 17-21 (Nov. 1972).

Key words: Building codes; building manufactu Coordinated Evaluation System; engineering analy laboratory accreditation; Laboratory Evaluation Accreditation Program (LEAP); Model Code Standard tion Council; National Conference of States on Buil Codes and Standards; quality assurance testing; tes laboratory.

The Laboratory Evaluation and Accreditation Prog (LEAP) was established at the National Bureau of Standard assist the States in the development of technical criteria a methodology for the accreditation of institutions engaged in evaluation of manufactured housing units for compliance specified building codes. The needs of such a program divided into: (1) a uniform national standard of refere (2) a standard of laboratory competence; and (3) standards uniform documentation of information. The program is cerned with: (1) engineering analysis; (2) physical testing; (3) quality assurance.

8. Powell, C. J., Mandl, A., **High-resolution measurements of e $L_3M_{2,3}M_{4,5}$ Auger transitions in nickel and copper,** *Phys. ev. Lett.* **29,** No. 17, 1153-1156 (Oct. 23, 1972).

Key words: Aluminum; Auger transitions; copper; electronic density of states; nickel; secondary-electron energy distribution; x-ray photoemission.

easurements are reported (with ≈ 0.1-eV resolution) of the $_{2,3}M_{4,5}$ Auger-electron energy distributions from evaporated nd Cu using electron-beam excitation. The data reveal new cture (over an ≈ 20-eV range) that could be correlated in with the final states (for atomic Cu) and in part with overall ires of the 3*d*-band density of states determined by soft-x- emission spectroscopy and x-ray photoelectron spectrosco-

9. Sengers, J. M. H. L., Greer, S. C., **Thermodynamic nomalies near the critical point of steam,** *Int. J. Heat Mass ransfer* **15,** 1865-1886 (1972).

Key words: Coexistence curve; compressibility; critical anomalies; critical exponents; critical region; equation of state; scaling law; specific heat; steam; water.

eas about the character of critical anomalies obtained from attice gas model are tested on the thermodynamic properties eam, using methods developed for nonpolar gases. The criti- anomalies in steam are shown to be nonclassical and very lar to those of simple gases. Specifically, the exponents ob- ed by power-law analysis of the coexistence curve, specific $C_v$ and compressibility $K_T$ are $\beta = 0.347 \pm 0.005$, $\alpha = 0.1 \pm$ , $\gamma = 1.20 \pm 0.05$, implying $\delta = 4.45$. Since the critical point us a point of nonanalyticity in the thermodynamic behavior, scaled equation of state may be an appropriate means to ribe the critical region. Some results of such a scaled analy- of the *PVT* data are presented and shown to be consistent independently measured vapor pressure and specific heat and with the exponents quoted. The best value obtained for critical temperature by scaling is 373.9 °C ± 0.05°, values veen 0.322 and 0.327 g/cm$^3$ are obtained for the critical den- depending on the property analyzed.

0. Acquista, N., Abramowitz, S., **Infrared spectrum of atrix isolated $NbF_5$,** *J. Chem. Phys.* **56,** No. 11, 5221-5224 une 1, 1972).

Key words: Infrared spectrum; Knudsen effusion; matrix isolation; molecular structure, $NbF_5$; vibrational assignment.

ne infrared spectra of matrix isolated $NbF_5$ as well as some phase spectra have been observed. These spectra have been ined using double boiler Knudsen cells. An interpretation of spectra to yield the six infrared active frequencies of a $C_{4v}$ omeric structure for $NbF_5$ is advanced.

1. Wall, L. A., Brown, D. W., **High pressure polymerization perfluorostyrene,** *J. Fluorine Chem.* **2,** No. 1, 73-85 972/73).

Key words: High pressure; perfluorostyrene; polymerization; polyperfluorostyrene.

Perfluorostyrene was prepared by reaction between pentafluorophenyllithium and tetrafluoroethylene and its physical behavior and thermal polymerization were studied in the temperature and pressure ranges 17-155° and 6,800-20,000 atm respectively. When highly superpressed the monomer becomes viscous and often glassy. The polymerization rates range from $10^{-3}$ to more than $10^2$ percent $h^{-1}$. They generally increase with temperature and pressure. Polymer intrinsic viscosities range from 0.07 to 0.41 $dlg^{-1}$. In liquid phase polymerizations they increase with pressure and decrease with temperature. In the glassy phase, polymer of lower intrinsic viscosity is formed; in the crystalline phase, higher polymer is formed.

**13062.** Barnes, J. A., Winkler, G. M. R., **The standards of time and frequency in the U.S.A.,** *Proc. 26th Annual Symp. on Frequency Control, Atlantic City, N.J., June 6-8, 1972,* pp. 269-284 (Electronic Industries Association, Washington, D.C., 1972).

Key words: Astronomical time; atomic time; frequency; international atomic time; management; NBS; standard time; time; USNO.

The National Bureau of Standards (NBS) and the U.S. Naval Observatory (USNO) are the two organizations chiefly involved in distributing accurate and precise time and frequency information within the U.S.A. The NBS is responsible for the "custody, maintenance, and development of the national standards" of frequency and time (interval) as well as their dissemination to the general public. The mission of the USNO includes the "provision of accurate time" as an integral part of its work concerned with the publication of ephemerides in support of navigation and in the establishment of a fundamental reference system in space.

Both agencies provide the U.S. contribution to the Bureau International de l'Heure (BIH) [International Time Bureau], which has the responsibility of publishing definitive values of Universal Time (UT), International Atomic Time (IAT), and Coordinated Universal Time (UTC).

**13063.** Zapf, T. L., **Accuracy and precision,** Chapter 4 in *Basic Electronic Instrument Handbook,* C. F. Coombs, Jr., Ed., pp. 4-1 – 4-20 (McGraw-Hill Book Co., New York, N.Y., 1972).

Key words: Accuracy; error analysis; instrument errors; measurement errors; precision.

Topics in this chapter have been chosen to give the reader a basic understanding of many of the concepts, procedures, and mathematical tools used by metrologists to ascertain the accuracy and the precision of measurements. The chapter includes discussions of errors, corrections, precision, accuracy, systematic and random errors, statistical methods, measures of imprecision, computations based on samples, errors in the use of instruments, and scale-reading errors. Basic information for the treatment of errors in measurements, and in instruments, is given.

**13064.** Howe, D. A., **Nationwide precise time and frequency distribution utilizing an active code within network television broadcasts,** (Proc. 26th Annual Frequency Control Symp., Atlantic City, N.J., June 6-8, 1972, Electronic Industries Association, Washington, D.C., 1972) *IEEE Trans. Instr. Meas.* **IM-21,** No. 3, 263-276 (Aug. 1972).

Key words: Frequency standard; network path delay; stability; time and frequency dissemination; time code generator; time code receiver.

Because of the increasing interest in time and frequency dissemination via television signals, the National Bureau of Standards (NBS) has sponsored an experiment using an active time and frequency code transmitted on a U.S. television network encompassing nationwide coverage. Some history of the project is given. The format of the television code and the equipment necessary to generate and decode the transmitted information are discussed. Statistical results of system stability from New York City, N.Y., to Boulder, Colo., and to Los Angeles, Calif., are presented, and comparisons are made with earlier observations using the passive line-10 television time synchronization technique and the 3.58-MHz color-burst frequency reference used for colorcasts. Analysis of the frequency-transfer capability is presented, and the ability of a phase-locked oscillator to lock to the code's frequency reference is discussed. With the decoder's oscillator in a locked condition, plots of phase with respect to time, time domain stability using the Allan variance, and spectral noise reveal that the system permits calibration of a remote standard to one part in $10^{11}$ within one-half hour. Long-term stability (several days) is typically a few parts in $10^{12}$. Using an active time code, short-term stability is governed to a noticeable degree by the television industry's standard video format. Finally, a schematic diagram, with discussion, outlines how time-of-day information can be extracted from the television code used in this experiment.

**13065.** Faller, J. E., Bender, P. L., Alley, C. O., Currie, D. G., Dicke, R. H., Kaula, W. M., MacDonald, G. J. F., Mulholland, J. D., Plotkin, H. H., Silverberg, E. C., Wilkinson, D. T., **Geodesy results obtained with lunar retroreflectors,** S. W. Henriksen, A. Mancini, and B. H. Chovitz, Eds., (Proc. Symp. on the Use of Artificial Satellites for Geodesy, Washington, D.C., Apr. 1971), Paper 6, Extraterrestrial Geodesy in *Geophys. Mongr. Series* **15,** 261-264 (American Geophysical Union, Washington, D.C., 1972).

Key words: Earth rotation; geodesy; laser distance measurements; lunar range; polar motion.

Retroreflector packages have been carried to the moon by the Apollo 11, Apollo 14, and Apollo 15 missions, as well as by Luna 17. Laser ranging from the earth onto these packages should eventually yield information on polar motions and crustal movements accurate to a few centimeters, and on UT1 to 100 $\mu$sec. Present (1971) error of the range measurements is 30 cm, but accuracy to 3 cm should be obtainable with improvements in methods and equipment.

**13066.** Johnson, D. R., Lovas, F. J., **Microwave detection of the molecular transient methyleneimine ($CH_2=NH$),** *Chem. Phys. Lett.* **15,** No. 1, 65-68 (July 15, 1972).

Key words: Methyleneimine; microwave spectrum; pyrolysis; quadrupole structure; rotational transitions; transient species.

The molecular transient methyleneimine ($CH_2=NH$) has been identified in the gas phase from its microwave spectrum. Preliminary analysis of the rotational spectrum of $^{12}CH_2={}^{14}NH$ shows the molecule to be planar with rotational constants (in MHz) of $A=196\,211$, $B=34\,642$, and $C=29\,352$. Estimates of the nuclear quadrupole coupling constants and electric dipole moment for the molecule are given. The half-life of this transient molecule is estimated to be less than 0.1 sec under the conditions used in the experiment under discussion.

**13067.** Geist, J., **Waveform-independent lock-in detection,** *Rev. Sci. Instrum.* **43,** No. 11, 1704-1705 (Nov. 1972).

Key words: Lock-in detection; synchronously rectified
tection.

A modification of the commonly used lock-in detect
technique is proposed. This technique produces an output sig
that is independent of the waveform of the input signal.

**13068.** Mizushima, M., Wells, J. S., Evenson, K. M., Welch,
M., **Laser magnetic resonance of the $O_2$ molecule using the 3**
**$\mu$m HCN laser,** *Phys. Rev. Lett.* **29,** No. 13, 831-833 (Sept.
1972).

Key words: HCN laser; laser magnetic resonance; mole
lar constants of $O_2$; $O_2$ spectrum.

We observed thirteen laser magnetic resonance lines (tra
tions between $[n=3, J=4] \rightarrow [n=5, J=5]$) for the oxy
molecule, using the 337-$\mu$m line of the HCN laser. The magn
$g$ factors ($g_\perp = 2.0044$, $g_z = 2.0020$, and $g_n = 0.000\,125$) give
best fit to the data. The zero-field frequency for the transition
$=J=3) \rightarrow (N=J=5)$ obtained by using these sets of the m
netic $g$ factors all agree with theoretical value of 775.700 4
0.000 01 GHz if an experimental uncertainty of ± 1 G (± 10⁻
is allowed.

**13069.** Wells, J. S., Evenson, K. M., Day, G. W., Halford,
**Role of infrared frequency synthesis in metrology,** *Proc. IE*
*Letters* **60,** No. 5, 621-623 (May 1972).

Key words: Frequency metrology; frequency of lasers;
frared frequency synthesis; laser frequency stabilizati
methane-stabilized He-Ne laser; speed of light.

Infrared frequency synthesis (IFS) techniques are briefly
veyed, and some important results are summarized. The rec
measurement of the frequency of the methane-stabilized He-
laser is significant due to the accurate measurement of
methane wavelength and its fundamental role in metrology.
possibilities of an improved value for the speed of light and of
ditional applications for frequency measurements at vari
levels of accuracy are discussed.

**13070.** Howe, D. A., **Results of active line-1 TV timing,** *P*
*IEEE Letters* **60,** No. 5, 634-637 (May 1972).

Key words: Frequency standard; network path delay;
bility; time and frequency dissemination; time code gen
tor; time code receiver.

Because of the increasing interest in time and frequency
semination via television signals, NBS has sponsored an exp
ment using an active time and frequency code transmitted
U.S. television network encompassing nationwide coverage.
code format is discussed and statistical results of system stab
using the network path from New York City, N.Y., to Boul
Colo., are presented through plots of phase with respect to t
and plots of time domain stability using the Allan variance. C
parison is made of the frequency transfer capability of the lir
method to the 3.57954...MHz color subcarrier signal used
network colorcasts. The active line-1 TV time system of
distinct advantages over existing dissemination methods utili
within the continental U.S. of principal interest is the short m
surement period required for a time or frequency calibrat
The system typically permits calibration of a remote standar
1 part in $10^{11}$ within one-half hour.

**13071.** Phillips, W. E., **Interpretation of steady-state sur**
**photovoltage measurements in epitaxial semiconductor lay**
*Solid-State Electron.* **15,** No. 10-E, 1097-1102 (Oct. 1972).

Key words: Absorption coefficients; epitaxial silic
minority carrier diffusion length; minority carrier lifeti
semiconductor characterization; surface voltage.

nalysis of the steady-state surface photovoltage (SPV) hod of measuring minority carrier diffusion length ($L$) has n extended to the case of an epitaxial layer on a thick subte. In layers with thickness greater than four diffusion ths, the measurement yields the bulk value of $L$. For layers ner than $0.5L$, the measured value is that of the substrate. intermediate thickness, the bulk value of $L$ can be estimated. method also provides a sensitive means of observing the innce of surface conditions on the absorption characteristics of on.

2. Arp, V., **Forced flow, single-phase helium cooling systems,** hapter on Helium Heat Transfer in *Advances in Cryogenic ngineering.* A Collection of Invited Papers presented at Naonal Technical Meetings during 1970 and 1971, **17,** Paper J-342-351 (Plenum Press, Inc., New York, N.Y., 1972).

Key words: Forced flow; heat transfer; helium; refrigeration.

flow loop using pumped supercritical helium for transferring from a source to a sink is considered. General factors coning design of the loop are outlined, and pumping losses are sidered in some detail. It is concluded that pumping losses end very sensitively on the heat transfer requirements, and mization of design must be done carefully for any particular em. Further studies of combined heat transfer and refrigeracycles are encouraged.

3. Brennan, J. A., Mann, D. B., Dean, J. W., Kneebone, C. ., **Performance of NBS cryogenic flow research facility,** hapter on Measurement and Instrumentation in *Advances in ryogenic Engineering.* A Collection of Invited Papers resented at National Technical Meetings during 1970 and 971, **17,** Paper G-2, 199-205 (Plenum Press, Inc., New York, .Y., 1972).

Key words: Accuracy statement; cryogenic; flow facility; liquid nitrogen; measurement.

he National Bureau of Standards and the Compressed Gas ociation have jointly sponsored a research program on genic flow measurement. A cryogenic flow research facility constructed and was first used to evaluate commercially lable positive displacement cryogenic flowmeters operating liquid nitrogen.

he performance of the flow facility was simultaneously being uated during the meter tests. This is a summary report of the ormance evaluation of the flow facility. An accuracy statet is given for both totalized mass and volumetric flow.

4. Broadhurst, M. G., **Use and replaceability of lychlorinated biphenyls,** *Environ. Health Perspect.*, pp. 81-02 (Oct. 1972).

Key words: Dielectric fluids; heat transfer; plasticizers; polychlorinated biphenyl; transformers.

n September 1, 1971, an interdepartmental task force was ned to coordinate the U.S. Government's scientific studies of chlorinated biphenyl (PCB's). The task force was coorted by the Office of Science and Technology and the Council Environmental Quality. Represented on the task force were following agencies: the Environmental Protection Agency, Food and Drug Administration, the National Institute of Ennmental Health Services, and the Departments of Agricul, Commerce, Interior, and Justice.

n September 13, individual tasks were assigned to participatagencies, and the Department of Commerce was asked to cally explore the question of the utility and replaceability of 3's. Dr. Robert W. Cairns, Deputy Assistant Secretary of Commerce for Science and Technology, requested NBS to assist him in this task.

This study has included consideration of the uses and replaceability of PCB's in the following areas: (1) Dielectric fluids for capacitors and transformers; (2) Industrial fluids for hydraulic, gas turbine, and vacuum pump uses; (3) Heat transfer fluids; and (4) Plasticizers and miscellaneous uses.

**13075.** Suzuki, G., **Measurements and nuclear accountability methods,** *Proc. AEC Symp. on Safeguards Research and Development, Los Alamos, N. Mex., Oct. 27-29, 1969,* pp. 67-68 (Mar. 1970).

Key words: Nuclear material balance accountability; nuclear material control; nuclear safeguards.

The problem discussed is the need for better material accountability through the application of better measurements in nuclear safeguards. This paper points out that accountability has many aspects and compares two of them. One aspect is that accountability is considered in the sense of a tighter material balance, accomplished by more accurate measurements in material accounts of inputs, outputs, and in inventory. Although the material balance for a process or, if you will, the entire plant is a necessary tool in nuclear materials accountability, its usefulness is limited to an indication that there is an unaccounted for loss but such loss is not necessarily due to diversion of material or to an unusual situation. Since the material balance is an aggregative tool dealing with totals, it generally does not provide a clue as to whether the material unaccounted for is in one lump or in small pieces or some intermediate form. Another aspect is that accountability be considered in the same sense except that it be accomplished by maintaining material balances around subprocesses, thus serving the additional function of material control. It points out that material control data are important especially in areas where process losses are suspected. In this manner, the safeguards capability of a plant would be enhanced both from the safeguards and plant material control points of view.

**13076.** Huie, R. E., Herron, J. T., Davis, D. D., **Rates of reaction of atomic oxygen with $C_2H_3F$, $C_2H_3Cl$, $C_2H_3Br$, 1,1-$C_2H_2F_2$, and 1,2-$C_2H_2F_2$,** *Int. J. Chem. Kinet.* **IV,** 521-527 (1972).

Key words: Atomic oxygen; haloethylenes; kinetics.

Rate constants for the reactions of atomic oxygen ($O^3P$) with $C_2H_3F$, $C_2H_3Cl$, $C_2H_3Br$, 1,1-$C_2H_2F_2$, and 1,2-$C_2H_2F_2$ have been measured at 307 K using a discharge-flow system coupled to a mass spectrometer. The rate constants for these reactions are (in units of $10^{11}$ cm$^3$ mole$^{-1}$s$^{-1}$) $2.63 \pm 0.38$, $5.22 \pm 0.24$, $4.90 \pm 0.34$, $2.19 \pm 0.18$, and $2.70 \pm 0.34$, respectively. For some of these reactions, the product carbonyl halides were identified.

**13077.** Huie, R. E., Herron, J. T., Davis, D. D., **Absolute rate constants for the reaction $O + O_2 + M \rightarrow O_3 + M$ over the temperature range 200-346 K,** *J. Phys. Chem.* **76,** No. 19, 2653-2658 (1972).

Key words: Atomic oxygen; kinetics; oxygen.

Using the technique of flash photolysis-resonance fluorescence, absolute rate constants have been measured for the reaction $O + O_2 + M \rightarrow O_3 + M$. For the case of $M = Ar$ the temperature range covered was 200-346 K, and the total pressure was varied from 50 to 500 torr. Over the indicated temperature range, an Arrhenius plot of the data yielded the expression $k_{Ar} = (6.57 \pm 0.59) \times 10^{-35} \exp[(1014 \pm 46 \text{ cal mol}^{-1})/RT]$ cm$^6$ molecule$^{-2}$ sec$^{-1}$. A comparison of the third-order rate constants for $M = He$, Ar, and $N_2$ gave the relative efficiencies for these three gases as 0.92:1.0:1.6 at 298 K. At 218 K, the efficiencies of Ar to $N_2$ were in the ratio of 1.0:1.7. The reported rate measurements indicate that the rate of production of stratospheric ozone could be nearly a factor of 2 lower than that estimated from previously reported values of the third-order rate constant.

13078. Koidan, W., Hruska, G. R., Pickett, M. A., **Wedge design for National Bureau of Standards anechoic chamber,** *J. Acoust. Soc. Amer.* **52,** No. 4, Part 1, 1071-1076 (1972).

Key words: Anechoic chamber design; plane-wave tubes; wedges.

Design techniques for anechoic room wedges must always be used with caution because of the possibility that a manufacturer may change the properties of the material. This paper describes efforts at the National Bureau of Standards to adapt to relatively new glass wool manufactured in the United States. A "hybrid" wedge designed for a large anechoic chamber at NBS consists of glass wool of two densities: 3 $\text{lb/ft}^3$ for the 55-in-long tapered portion and 1.1 $\text{lb/ft}^3$ for the 11-in-long base. Experimental evidence indicates that the light-weight material and the 4-in air space behind the wedge, in conjunction with the heavier material, serve to produce a useful resonance absorption. The "cutoff frequency" attained for the 70-in-long structure was about 45 Hz as measured in a 31-ft plane-wave tube. Normal acoustic impedance measurements looking into the wedge from the tip were made for the hybrid wedge and a half-scale model.

13079. Kaldor, A., Olson, W. B., Maki, A. G., **Pollution monitor for nitric oxide: A laser device based on the Zeeman modulation of absorption,** *Science* **176,** 508-509 (May 5, 1972).

Key words: Air pollution; infrared spectroscopy; lasers; nitric oxide; Zeeman effect.

The concentration of nitric oxide can be monitored by a new device in which the Zeeman effect is used to shift an absorption line of nitric oxide into coincidence with a laser line of carbon monoxide. The absorption is modulated by a small, oscillating magnetic field. This device is specific for nitric oxide and is not subject to interference from other gases.

13080. Hougen, J. T., **On a vibration-rotation Hamiltonian for bimolecular collisions analogous to the Wilson-Howard vibration-rotation Hamiltonian for isolated molecules,** *J. Chem. Phys.* **56,** No. 12, 6245-6250 (June 15, 1972).

Key words: Angular momentum; bimolecular complex; collisions; group theory; molecule-fixed axes; selection rules; vibration-rotation Hamiltonian.

A bimolecular vibration-rotation Hamiltonian is derived which is analogous to the Wilson-Howard vibration-rotation Hamiltonian for isolated molecules. The bimolecular Hamiltonian involves the use of a "complex-fixed" axis system, i.e., a system with one of its axes along the line joining the centers of mass of the two interacting molecules. The bimolecular vibration-rotation Hamiltonian shows some similarities to the diatomic-molecule vibration-rotation-electronic Hamiltonian, the role of the two atoms in the diatomic molecule being played by the two interacting molecules, the role of the internuclear axis by the line joining the molecular centers of mass, and the role of electronic orbital and spin angular momenta by the vibration-rotation angular momenta of the two interacting molecules. The application of permutation-inversion molecular symmetry group ideas to a bimolecular complex is described.

13081. Steiner, B., **Photodetachment of $S^-$: Behavior of the cross section above threshold,** Paper in *Sixth International Conference on the Physics of Electronic and Atomic Collisions, Massachusetts Institute of Technology, Cambridge, Mass., July 28-Aug. 2, 1969, Abstracts of Papers, Session C-8,* pp. 535-537 (Massachusetts Institute of Technology Press, Cambridge, Mass., 1969).

Key words: Cross section behavior; electron affinity; ne tive ion; photodetachment; S.

The cross section for photodetachment of $S^-$ has been m sured over the region within 0.5 eV of threshold in a cros beam experiment. The behavior of the cross section in this ra seems to be distinct from that in the immediate vicinity threshold and cannot be predicted on the basis of known theo

13082. Marlowe, D. E., Steel, J. S., **A fatigue crack initiation tector,** *J. Mater.* **7,** No. 1, 28-31 (Mar. 1972).

Key words: Aircraft; bend tests; bolted joints; bo cracking (fracturing); crack initiation; cyclic loads; ferentiating circuits; digital to analog converters; failu fasteners; fatigue (materials); fatigue tests; linear syste loads (forces); shear; transformers.

An instrument which detects the initiation of a fatigue crac the head of a bolt, by measuring the change in relative positio the two ends of the double shear test joint at the maximum of cyclic load as the crack propagates, has been developed. creases in relative displacement of 0.00002 in. (0.0005 mm) be reliably detected using the output of a linear variable ferential transformer (LVDT). Detection of the initial head fi crack should be a more reliable fatigue failure criterion should result in less experimental scatter than catastrop failure of the bolt. A detailed description of the instrument examples of its use and performance are given.

13083. Ekberg, J. O., Hansen, J. E., Reader, J., **Analysis of spectrum of six-times-ionized niobium (Nb VII),** *J. Opt. S Amer.* **62,** No. 10, 1139-1142 (Oct. 1972).

Key words: Niobium; spectra; ultraviolet; wavelengths.

The spectrum of Nb VII has been observed in a sliding-sp discharge with a 5-m grazing-incidence spectrograph. The ana sis has yielded nearly all levels of the $4p^44d$ configuration can combine with the $4p^5\ ^2P$ ground term. Seven of the ei levels of the $4p^45s$ configuration given previously by Charles by Chaghtai were confirmed. A new value was found for eighth. The $4s^24p^44d+4s^24p^45s+4s4p^6$ level structure has b theoretically interpreted, with configuration-interaction eff included. The $4s4p^6\ ^2S_{1/2}$ level was found to have a 2 $4s^24p^4(^1D)4d\ ^2S$ character and the $4s^24p^4(^1D)4d\ ^2S_{1/2}$ level a 2 $4s4p^6\ ^2S$ character. The energy parameters determined b least-squares fit to the observed level values are compared Hartree-Fock (HF) calculations. The ionization energy is e mated to be 118.9 ± 0.7 eV.

13084. Ekberg, J. O., Hansen, J. E., Reader, J., **Analysis of spectrum of five-times-ionized zirconium (Zr VI),** *J. Opt. Amer.* **62,** No. 10, 1134-1139 (Oct. 1972).

Key words: Spectra; ultraviolet; wavelengths; zirconiu

The spectrum of Zr VI has been observed in a sliding-sp discharge with a 5-m grazing-incidence spectrograph. The an sis has yielded nearly all levels of the $4p^44d$ configuration can combine with the $4p^5\ ^2P$ ground term. All of the $4p^45s$ le as given by Chaghtai were confirmed. The $4s^24p^44d+4s^24p^4$ $4s4p^6$ level structure has been theoretically interpreted, configuration-interaction effects included. The $4s4p^6\ ^2S_{1/2}$ le was found to have a 24% $4s^24p^4(^1D)4d\ ^2S$ character and $4s^24p^4(^1D)4d\ ^2S_{1/2}$ level a 21% $4s4p^6\ ^2S$ character. The ene parameters determined from a least-squares fit to the obser level values are compared with Hartree-Fock (HF) calculati The ionization energy is estimated to be 95.8 ± 0.6 eV.

13085. Ekberg, J. O., Hansen, J. E., Reader, J., **Analysis of spectrum of seven-times-ionized molybdenum (Mo VIII)**

**oelectronic comparison of the spectra Y v – Mo viii,** *J. Opt. oc. Amer.* **62,** No. 10, 1143-1148 (Oct. 1972).

Key words: Molybdenum; spectra; ultraviolet; wavelengths.

he spectrum of Mo viii has been observed in a sliding-spark harge with a 5-m grazing-incidence spectrograph. The analy- has yielded nearly all levels of the $4p^44d$ configuration that combine with the $4p^5\ ^2P$ ground term. Six of the eight levels he $4p^45s$ configuration given previously by Charles and by ghtai were confirmed. New values were found for the aining two. The $4s^24p^44d+4s^24p^45s+4s4p^6$ level structure been theoretically interpreted, with configuration-interaction cts included. The $4s4p^6\ ^2S_{1/2}$ level was found to have a 21% $p^4(^1D)4d^2S$ character and the $4s^24p^4(^1D)4d^2S_{1/2}$ level a 19% $p^6\ ^2S$ character. The energy parameters determined by a t-squares fit to the observed level values are compared with tree-Fock (HF) calculations. The ionization energy is esti- ed to be 144.0 ± 1.0 eV. Isoelectronic comparisons for the l positions in Y v, Zr vi, Nb vii, and Mo v are given graphi- . The ratios of the fitted energy parameters to the HF values compared for these ions.

6. Chesler, S. N., Cram, S. P., **Digitization errors in the mea- rement of statistical moments of chromatographic peaks,** *nal. Chem.* **44,** No. 13, 2240-2243 (Nov. 1972).

Key words: Chromatography; statistical moments.

inimum error curves are calculated for measuring statistical ents of Gaussian and asymmetrical chromatographic peaks ch include the effects introduced by analog-to-digital conver- and the effect of locating the limits of integration.

7. Holt, H. K., **Theory of laser saturation spectroscopy,** *Phys. ev. Lett.* **29,** No. 17, 1138-1140 (Oct. 23, 1972).

Key words: Laser; saturated absorption; spectroscopy.

theory of the laser saturation spectroscopy experiments of sch et al. is presented which is applicable at high values of saturating laser beam. Phase- and velocity-changing colli- s are taken into account.

8. Kuehner, E. C., Alvarez, R., Paulsen, P. J., Murphy, T. J., **oduction and analysis of special high-purity acids purified by b-boiling distillation,** *Anal. Chem.* **44,** No. 12, 2050-2056 ct. 1972).

Key words: Distillation; isotope dilution; pure reagents; spark source mass spectrometry; sub-boiling; trace elements.

ub-boiling distillation from pure quartz or Teflon (Du Pont) has been investigated for the production of high-purity inor- c acids and water. Nitric, hydrochloric, hydrofluoric, hloric, and sulfuric acids produced by this method contained ificantly lower cationic impurities than high-purity acids commercial sources. A complete system, including the s 100 environment, production, and storage of these high- ty reagents is described. A method based on spark source s spectrographic isotope dilution analysis has been eloped for the simultaneous determination of 17 elements in e materials. Results of the analyses of both the acids purified ub-boiling distillation and the ACS reagent grade acids used tarting materials are reported. The sum of the common impu- elements determined in the purified acids ranged from 2.3 in nitric acid to 27 ppb in sulfuric acid. No element in any of purified acids exceeded 10 ppb and most were well below the b level.

9. Moore, L. J., Machlan, L. A., **High accuracy determination of calcium in blood serum by isotope dilution mass spectrometry,** *Anal. Chem.* **44,** No. 14, 2291-2296 (Dec. 1972).

Key words: Calcium; isotopes; mass spectrometry; serum.

An isotope dilution technique utilizing thermal ionization mass spectrometry has been developed for the accurate determination of calcium in synthetic and serum samples at the 100 $\mu$g/g level. Calcium was separated from a serum matrix by destruction of the organic matter with $HClO_4$ and $HNO_3$ followed by ion-exchange separation from interferences using AG 50W-X8 100-200 mesh resin. A mass spectrometric isotopic analysis procedure was developed using a $Ca(NO_3)_2$ solution deposited on Re sample filaments in a triple filament thermal ion source. The relative error between calculated and experimentally determined concentrations in synthetic calcium solutions was $\leqq\sim$ 0.1%. The 95% limit of error for a single analysis was ~ 0.2% for synthetic and serum samples. A comparison of the isotope dilution data with concurrently determined atomic absorption data from several clinical and independent laboratories is presented.

**13090.** Barnes, I. L., Carpenter, B. S., Garner, E. L., Gramlich, J. W., Kuehner, E. C., Machlan, L. A., Maienthal, E. J., Moody, J. R., Moore, L. J., Murphy, T. J., Paulsen, P. J., Sappenfield, K. M., Shields, W. R., **Isotopic abundance ratios and concentrations of selected elements in Apollo 14 samples,** (Proc. 3d Lunar Science Conference, Houston, Tex., Jan. 1972), Supplement 3, *Geochimica et Cosmochimica Acta* **2,** 1465-1472 (1972).

Key words: Absolute abundance ratios; Apollo 14; isotope dilution analyses; Lunar samples; mass spectrometry; relative abundance ratios.

Absolute or relative isotopic abundance ratios have been determined for U, Pb, Rb, Sr, Ca, and Cu on a representative fraction of the bulk fines 14163,159 and for a breccia 14321,221. No significant variations from terrestrial values were noted for the nonradiogenic isotopes. Concentrations were determined for the above elements as well as for Th, B, Ag, Cd, Fe, Ti, and Ni.

$^{207}Pb/^{206}Pb$ ages of about 4860 m.y. (million years) and 4420 m.y. were calculated for 14163 and 14321, respectively. The Pb-U and Pb-Th ages are very slightly discordant, the soils exhibit a reversed discordancy and the breccia a normal discordancy. Extreme inhomogeneity of Rb and Sr in the fines sample was found.

**13091.** Rukwied, A., **High temperature creep cavitation mechanisms in a continuously cast high purity copper,** *Metallurgical Trans.* **3,** 3009-3023 (Nov. 1972).

Key words: Angular distribution of cavities; cavitation; copper; creep; grain boundaries; grain boundary sliding; nucleation of cavities; segregation nodes; vacancy condensation.

Continuously cast high purity copper was used to study intergranular high temperature creep fracture mechanisms. With the help of an internal marker system due to impurity segregation, grain boundary sliding, GBS, was found to have occurred to a similar extent on cavitated and uncavitated boundaries. To explain this phenomenon a void nucleation model involving small nonwetting shearable particles is suggested. Metallographic observations and the apparent activation energy derived from fracture time data indicate the operation of the vacancy condensation mechanism at the lower temperatures and higher stresses. At the higher temperatures and lower stresses void growth is enhanced by GBS. This cavitation mechanism obtains strong support from measurements of the distribution of voids on grain boundaries as a function of the boundary angle with respect to the tensile direction. Computer analysis of these distributions, in terms of a model which properly accounts for the distribution of potential nuclei, yields bimodal curves exhibiting peaks at grain boundaries oriented for high shear stress (peak I), and for high normal stress (peak II). A phenomenological equation is proposed for the dependence of peak I on test conditions. Peak II is thought to be caused by nucleation by local GBS and growth by vacancy condensation under locally enhanced normal stress.

**13092.** Marzzacco, C. J., Zalewski, E. F., **The fluorescence and phosphorescence spectra of pyrazine in benzene at 4.2 K,** *J. Mol. Spectry.* **43,** No. 2, 239-247 (Aug. 1972).

Key words: Fluorescence; phosphorescence; pyrazine; singlet emission; spectrum of pyrazine in benzene; triplet emission; vibration spectrum.

The fluorescence and phosphorescence spectra of pyrazine-$h_4$ and pyrazine-$d_4$ in benzene at 4.2 K are presented and analyzed. The Frank-Condon patterns of $a_{1g}$ modes in the fluorescence spectrum are quite similar to those in the phosphorescence spectrum for both pyrazine-$h_4$ and pyrazine-$d_4$.

The $\nu_5$ $(b_{2g})$ and $\nu_{10a}$ $(b_{1g})$ out-of-plane bending modes appear with quite different intensities in the fluorescence and phosphorescence spectra. The $0 \rightarrow 1$ transitions in these modes only appear in the fluorescence spectra while the $0 \rightarrow 2$ transitions are more intense in the phosphorescence spectra. These results are interpreted in terms of a vibronic interaction between $^{1,3}B_{3u}$ $(n\pi^*)$ and the $^{1,3}B_{2u}$ $(\pi\pi^*)$ and $^{1,3}B_{1u}$ $(\pi\pi^*)$ states.

No spectroscopic evidence is found for a forbidden $^1n\pi^*$ state below $^1B_{3u}$ $(n\pi^*)$.

**13093.** Reimer, G. M., Wagner, G. A., Carpenter, B. S., **The thermal stability of fission tracks in the Standard Reference Material glass standard (National Bureau of Standards),** *Radiat. Eff. Communication* **15,** 273-274 (1972).

Key words: Fission track; glass; nuclear track technique; Standard Reference Material; thermal stability; uranium.

The relatively low thermal stability of fission tracks in the National Bureau of Standards Standard Reference Material glass indicates that those glasses that are to be used as fission track references should be stored at temperatures below 20 °C. The low track stability may be due to the relatively high sodium and calcium content of the glasses.

**13094.** Ballard, D. B., Bennett, L. H., Swartzendruber, L. J., **Intergranular embrittlement of copper-palladium alloys in salt water,** *Corrosion* **28,** No. 10, 368-373 (Oct. 1972).

Key words: Alloys; copper; corrosion, embrittlement; palladium; salt water.

Intergranular embrittlement occurs when copper-rich Cu-Pd alloys are exposed to an aqueous 3.5 wt% sodium chloride environment. There is no evidence that the embrittlement reaction requires the presence of external or internal stresses for 2, 5, and 15 at% Pd in Cu. Scanning electron microscope (SEM) fractographic observations are reported for as-rolled, vacuum annealed, and hydrogen annealed alloys of composition 95 Cu-5 Pd.

**13095.** Raveché, H. J., Mountain, R. D., **Three atom correlations in liquid neon,** *J. Chem. Phys.* **57,** No. 9, 3987-3992 (Nov. 1, 1972).

Key words: Closure approximation; isothermal/density derivative of pair correlation function; liquid neon; neutron scattering; pair correlation function; triplet correlation function.

We consider the correlation of three atoms in liquid neon fr
the neutron diffraction measurement of the isothermal dens
derivative of the pair correlation function. Several closure
proximations for the triplet correlation function are discuss
Three of the approximations are representations of the trip
correlation function as a functional of the pair correlation fu
tion, and the other is expressed as a simple function of the p
correlation function.

**13096.** Shafer, M. R., Jr., Baker, D. W., **Practical considerati
for gas flow measurement,** *Proc. 3d Annual Precision Measu
ment Association Metrology Conf., National Bureau of St
dards, Gaithersburg, Md., June 17-18, 1970,* **1,** 187-
(Precision Measurements Association, Burbank, Calif., 19

Key words: Flowmeter calibration; gas density; gas fl
measurement; gas viscosity; mass and volume flow; vo
metric proving.

Physical variables and relations encountered in the mete
of gases and the calibration of gas flowmeters are reviewed.
modified by the compressibility factor to account for
behavior of real gases, the equation of state is given and the r
tion between mass and volume rate in steady flow is discuss
Application of these relations to volumetric proving or calil
tion of meters is explained.

**13097.** Agy, D. L., Nelson, R. E., **An immittance transcompa
tor,** *Proc. 3d Annual Precision Measurement Associa
Metrology Conf., National Bureau of Standards, Gait
sburg, Md., June 17-18, 1970,* **1,** 147-154 (Precision Meas
ments Association, Burbank, Calif., 1970).

Key words: Capacitance; coaxial; high-Q; immittance
ductance; measurement; radio frequency; resonance.

The immittance transcomparator is an instrument which
izes resonance techniques to make high-Q immittance meas
ments over the frequency range from 50 MHz to 250 MHz.
basic component of the instrument is a short section of 50
coaxial transmission line with provisions for introducing pro
to induce and sample electromagnetic energy. Uncertaintie
the order of 0.1% are realizable for the reactive component of
measured immittance.

**13098.** Williams, E. S., **Calibration of thermal voltage convert
*Proc. 3d Annual Precision Measurement Associa
Metrology Conf., National Bureau of Standards, Gait
sburg, Md., June 17-18, 1970,* **1,** 131-139 (Precision Meas
ments Association, Burbank, Calif., 1970).

Key words: Ac-dc transfer; comparator; thermal vol
converter; transfer standard.

Ac-dc difference corrections for thermal voltage conve
are obtained by comparing one instrument with another wh
corrections are already known. Present methods of making
comparisons are reviewed, and a new TE (thermoelement) c
parator is described. This comparator is relatively simple an
expensive, reduces the effect of power supply instability,
gives accuracies better than 10 parts per million.

**13099.** Hilten, J. S., **Accelerometer calibration with the ea
field dynamic calibrator,** *Proc. 3d Annual Precision Meas
ment Association Metrology Conf., National Burea
Standards, Gaithersburg, Md., June 17-18, 1970,* **1,**
(Precision Measurements Association, Burbank, Calif., 19

Key words: Accelerometer; air bearings; calibrator
celerometer; dynamic; earth's field; Inter-Agency Tr

ducer Project; low frequency; rotational frequency response; transducer.

his paper describes a simple device for the precise dynamic bration of certain accelerometers at low frequencies. Calibra- of an accelerometer is achieved by rotating the instrument he earth's gravitational field at a number of constant rota- al speeds.

00. Williams, E. R., Olsen, P. T., **A noncontacting magnetic ickup probe for measuring the pitch of a precision solenoid,** Proc. Conf. Precision Electromagnetic Measurements, Na- onal Bureau of Standards, Boulder, Colo., July 1972), *IEEE rans. Instr. Meas.* **IM-21,** No. 4, 376-379 (Nov. 1972).

Key words: Fine structure constant; fundamental constant; gyromagnetic ratio of proton; NBS ampere; pitch measurement.

he magnetic-field gradients produced by a current sequen- y activating a few turns of wire of a precision solenoid are d to measure its pitch. The position of the activated portion vire can be resolved to 0.1 $\mu$m. Preliminary results are found e in agreement with an earlier measurement using a contact- probe to within the uncertainty of the latter determination. s new technique reduces many of the difficulties associated 1 conventional pitch measuring schemes and at the same time vides a method of obtaining increased accuracy.

01. LaVilla, R. E., **The sulfur $K$ and $L$ and fluorine $K$ x-ray nission and absorption spectra of gaseous $SF_6$,** *J. Chem. Phys.* 7, No. 2, 899-909 (July 15, 1972).

Key words: Molecular orbital model; photon and electron excited emission spectra; resonance radiation; semi-Auger process; $SF_6$; x-ray absorption of sulphur $K$, $L$ and fluorine $K$; x-ray emission of sulphur $K\alpha$, $K\beta$, $L$ and fluorine $K\alpha$.

ith the exception of the sulfur $L$-absorption spectrum, mea- ements of all the soft x-ray spectra from gaseous $SF_6$ in their ective threshold regions are reported. The valence emission y spectra are interpreted in terms of a molecular orbital lel of $SF_6$ with the inclusion of sulfur $d$ orbitals. The experi- tal emission profiles are in fair agreement with a calculated ile based on the assigned orbital ionization energies and ecular orbital theory. The sharp resonance structures in the orption spectra are found to result from the potential barrier ned by the surrounding fluorine atoms and are consistent the molecular orbital model. The identification of the ab- tion resonance structure in terms of transitions to "virtual" ccupied electronic levels is substantiated by the observation resonance radiation," i.e., x-ray emission in coincidence with peak positions in the absorption region. The sulfur $K\alpha$ ctrum is also presented and discussed. A notable feature in spectrum is a weak peak on the low energy side of the $K\alpha_{1,2}$ which is interpreted as a semi-Auger process.

2. Voth, R. O., **Safety of hydrogen pressure gauges,** Chapter n Safety Considerations in *Advances in Cryogenic Engineer- g*. A Collection of Invited Papers Presented at National echnical Meetings during 1970 and 1971, **17,** Paper F-2, 182- 37 (Plenum Press, Inc., New York, N.Y., 1972).

Key words: Gauge case design; hydrogen embrittlement; hydrogen gas; pressure gauges; safety.

o determine the relative safety of various gauge case designs, y-five pressure gauges were purchased and intentionally rup- d using high pressure hydrogen gas. Fire was emitted from rly all gauges; however, gauges with solid fronts and plastic tals emitted the fire and debris out the rear of the case making them safer for use in a hydrogen system. One brand of gauge ruptured at reduced pressure when tested with hydrogen. The reduced rupture pressure indicated possible hydrogen embrittlement of the pressure sensing element.

**13103.** Snyder, W. F., **Standards,** Chapter 2 in *Basic Electronic Instrument Handbook,* C. F. Coombs, Jr., Ed., pp. 2-1 – 2-16 (McGraw-Hill Book Co., New York, N.Y., 1972).

Key words: Echelon of standards; electrical quantities; environments for standards laboratories; International System derived units; National Bureau of Standards; standards.

Brief accounts are given of the electrical system of units, the International System (SI) of derived units, an echelon of standards, the role of the National Bureau of Standards, and environments for standards laboratories.

**13104.** Snyder, W. F., **Basic electronic standards,** Chapter 3 in *Basic Electronic Instrument Handbook,* C. F. Coombs, Jr., Ed., pp. 3-3 – 3-64 (McGraw-Hill Book Co., New York, N.Y., 1972).

Key words: Basic electronic standards; classification of electronic standards; DC standards; low frequency standards; standards (coaxial connectors); standards (waveguide or coaxial line); traceability of electrical standards.

A classification of "atlas" of electronic standards is presented by selection of frequency range, electrical quantity, and an echelon of standards. The reader is referred, by a classification key, to many hundreds of literature sources for detailed information on standards, calibration methods, and measurement techniques.

**13105.** Kelly, G. E., Sengers, J. V., **Collision integrals for the Knudsen number dependence of the growth rate of droplets in supersaturated vapor,** *AEDC-TR-72-172,* 82 pages (Arnold Engineering Development Center, Air Systems Command, Arnold Air Force Station, Tenn., Dec. 1972).

Key words: Growth of droplets; kinetic theory of gases; liquid-vapor phase transitions; mass transport; nucleation theory; phase transitions.

A method is developed for calculating the mass flux to a liquid droplet surrounded by its pure vapor as a function of the Knudsen number. The Knudsen number K is defined as the ratio of the mean free path to the droplet size. When the mass flux is expanded in terms of the inverse Knudsen number $\alpha = K^{-1}$, we obtain a series of the form

$$\Gamma = \Gamma^{(0)} + \Gamma^{(1)}\alpha + \bar{\Gamma}^{(2)}\alpha^2 \ln\alpha + \ldots .$$

It is shown that the coefficients are determined by integrals associated with sequences of successive collisions among a number of vapor molecules and the droplet. In particular, we derive the collision integrals for the first three coefficients of the inverse Knudsen number expansion for $\Gamma$. These collision integrals bear a close similarity to the collision integrals derived in earlier technical reports for the density dependence of the transport properties of gases. It will be demonstrated in a subsequent technical report that the same method can be used to calculate the aerodynamic force on an object in a gas stream as a function of the Knudsen number.

**13106.** Elbourn, R. D., Saunders, P. B., **Simulation of air traffic control radar beacon code assignment plan 3d1,** *FAA Report No. FAA-RD-72-103,* 56 pages (National Technical Information Service, Springfield, Va. 22151, Sept. 1972).

Key words: Air traffic control; beacon code assignment; digital simulation; radar beacon system; secondary surveillance radar.

During implementation of the National Airspace System En Route Stage A, some Air Route Traffic Control Centers will have complete radar data processing capability while other centers have only flight plan data processing capability. This report describes a digital computer simulation of three versions of a radar beacon code assignment plan designed for this situation. The simulation employs one peak day's IFR traffic in the U.S.A. It determines the number of codes required, the numbers of code changes in flight for various reasons, and the variation of the number of code conflicts with the number of codes used.

**13107.** Furukawa, G. T., Douglas, T. B., Pearlman, N., **Heat capacities,** Chapter 4e in *American Institute of Physics Handbook, Third Edition,* pp. 4-105–4-118 (McGraw-Hill Book Co., Inc., New York, N.Y., 1972).

Key words: Debye characteristic temperature; Einstein function, Debye function; electronic specific heat; heat capacity; specific heat.

The work presents compilations of specific heats of the elements up to 3000 K, Debye characteristic temperatures and electronic coefficients of specific heat of the elements and some compounds, Einstein functions to five decimals at 0.1 intervals of the argument, and Debye functions to six decimals at 0.1 intervals of the argument. A short bibliography is given.

**13108.** Sengers, J. M. H. L., Klein, M., Gallagher, J. S., **Pressure-volume-temperature relationships of gases; virial coefficients,** Chapter 4i in *American Institute of Physics Handbook, Third Edition,* pp. 4-204–4-221 (McGraw-Hill Book Co., Inc., New York, N.Y., 1972).

Key words: Air constituents; Boyle temperature; deuterium; hydrogen; intermolecular potential; inversion temperature; methane; noble gases; potential parameters; second virial coefficient; third virial coefficient; water vapor.

Tables of second virial coefficients as functions of temperature are presented for 14 gases. These gases are mainly noble gases and constituents of all. In most cases, these are based on a reexamination of the original P-V-T data. Where necessary and possible, these data have been refitted and improved experimental virials determined. In the case of eight of these gases, it has been possible to fit the experimental second virials to those predicted by the $(m, 6)$ potential function and potential parameters determined. In almost all cases, an optimum fit was obtained for $m$-18. The optimum potential function was used for extrapolating the tables somewhat beyond the experimental range, and for obtaining temperature derivatives of $B$. In the case of the other six substances virial coefficients predicted by the $(m, 6)$ functions were used as a smoothing aid. Experimental third virial coefficients are presented at the experimental temperatures. A table of Boyle and Joule-Thomson inversion temperatures is also presented.

**13109.** Parks, E. J., Hebert, R. L., **Thermal analysis of ion exchange reaction products of wood pulps with calcium and aluminum cations,** *Tappi* **55,** No. 10, 1510-1514 (Oct. 1972).

Key words: Aluminum; calcium; carboxylic acid; cellulose; differential thermal analysis; hemicellulose; ion exchange; pH; pyrolysis; thermal stability; thermogravimetric analysis; wood pulp.

Differential thermal analysis (DTA) and thermogravimetric analysis (TGA) indicate differences in the thermal stability of wood pulps of different compositions. Fourteen typical pap making pulps having a reported alpha-cellulose content of 95% and a carboxyl content ranging from about 2.0 to meq/100 g of pulp were purified by deashing with 0.1 $N$ H treated with calcium acetate to provide calcium exchan products and with alum to provide aluminum exchange produc The temperature of an endotherm ($T_3$) and that of the h volatilization temperature ($T_i$) were obtained from DTA a TGA data, respectively. The data indicate that $T_3$ and $T_i$ a directly related to the pH of the various pulps and that pH in t is a function of the number of carboxylic acid groups. $T_3$ and are consistently lower for pulp-aluminum exchange products a higher for pulp-calcium exchange products than for the c responding deashed pulps. These trends are interesting beca of possible correlations with permanence. Both $H^+$ and $Al^+$ promote volatilization as shown by shifts in $T_i$ to lower tempe tures. Calcium retards volatilization, with the result that values are shifted to higher temperatures. The same proces are probably also responsible in part for comparable shifts in There is evidence that hemicelluloses have an important bear on thermal instability, but this is inconclusive. The concent tions of carboxylic acid groups, which may also be responsi for instability, are closely related to the hemicellulose content the pulp.

**13110.** Plumb, H. H., Powell, R. L., Hall, W. J., Swindells, J. **Temperature scales, thermocouples, and resistance thermor ters,** Chapter 4a in *American Institute of Physics Handbo Third Edition,* pp. 4-2–4-21 (McGraw-Hill Book Co., In New York, N.Y., 1972).

Key words: Electrical resistivity; IPTS-68; temperat scale; thermal emf of elements; thermocouple tables; th mometry; thermometry fixed points.

An abbreviated version of the text of the International Pra cal Temperature is presented. The article includes the defin fixed points of the scale and the equations that are employe utilizing standard platinum resistance thermometers, stand thermocouples and optical pyrometers in realizing the tempe ture scale. A table giving values of temperature differen between IPTS-68 and IPTS-48 is presented. Also included tables of thermal emf of chemical elements, alloys and th mocouple materials relative to platinum. Thermocouple tab are listed for types S, R, E, J, K and T thermocouples at 10 °C tervals. Finally, the electrical resistivity of some elements and loys as a function of temperature are given at 100 °C intervals

**13111.** Enemark, E. A., Gallagher, A., **Electron excitation of sodium *D* lines,** *Phys. Rev. A* **6,** No. 1, 192-205 (July 1972).

Key words: Electron excitation; sodium.

The electron excitation of the sodium resonance lines (*D* lin has been measured in the energy range from threshold to 1 eV. The electron-beam full width at half-maximum was ~ eV, and the sodium-beam optical depth was small and vari After correction for minor cascade contributions and the m sured polarization, the excitation function has been normali to the Born theory in a high-energy limit where the energy dep dence converges to the theoretical behavior. The resulting r malized cross section and the polarization are in excellent ag ment with recent close-coupling calculations for the energy gion from threshold to 5 eV.

**13112.** Roder, H. M., Weber, L. A., Editors, **ASRDI Oxy Technology Survey: Volume I. Thermophysical Propert** *NASA Spec. Publ.* **3071,** 434 pages (National Aeronautics Space Administration, Washington, D.C., 1972).

Key words: Computer programs; gaseous oxygen; graphs; handbook thermophysical properties; liquid oxygen; oxygen; property value uncertainties; solid oxygen; tables.

This Handbook is the result of an extensive survey of the ther- physical properties of oxygen, including densities and the rmodynamic, transport, electrical, optical, and molecular pro- ties for the gaseous and fluid states. A thorough bibliography published work on each property is given. Recommended erences are cited for those properties which have been criti- ly surveyed. Other references are listed which were reviewed : not considered as basic source material. Each property is scribed and defined; selected values are presented for the re common properties; and, where appropriate, graphical sentation is also made. The major tables cover the range 100- ) °R for pressure to 5000 psia (55-340 K, 340 atmospheres or 5 × 10$^5$ Pa). In addition, for property values beyond this range, ommended references are given, where available. The Hand- ok is designed to provide a convenient reference for the user.

13. Abrams, M. D., **Data structures for computer graphics,** Proc. Symp. on Data Structures in Programming Languages, University of Florida, Gainesville, Fla., Feb. 25-27, 1971), *J. ss. Comput. Mach. SIGPLAN Notes* **6,** No. 2, 268-286 Feb. 1971).

Key words: Computer graphics; data structures; directed graph.

This paper introduces data structures as applied to computer phics. Design criteria for computer graphics data structures discussed, followed by a comparison of general-purpose and ored graphic data structures. A general graphic data structure ntroduced as an example of a structure meeting the preceding eria. The L$^6$ language is then examined as a tool for imple- nting the above data structure, and is compared to a few other guage systems.

14. Mountain, R. D., **Evaluation of liquid structure data,** *J. Chem. Phys.* **57,** No. 10, 4346-4350 (Nov. 5, 1972).

Key words: Liquid; liquid structure factor; neutron diffraction; pair correlation function; radial distribution function; x-ray diffraction.

A procedure for assessing the overall accuracy of liquid struc- e factor data is examined. The method makes use of the uirement that the two particle correlation function and its ivative vanish for separations smaller than the size of an m. A series of numerical experiments, designed to evaluate procedure, are discussed and a calibration of the method ed on these experiments is presented. The method is sensitive en the over-all uncertainties in the data are smaller than 1%. ce this is just the level which is now being achieved in liquid cture measurements, the method should be quite useful in the luation of liquid structure data. As an illustration, the method applied to recently published data for liquid neon and liquid ium.

15. Laufer, A. H., Okabe, H., **Determination of the heat of for- nation of diazirine by photon impact,** *J. Phys. Chem.* **76,** No. 3, 3504-3507 (1972).

Key words: Absorption spectrum; diazirine; heat of formation.

hreshold energies of the incident photons required to initiate ee primary processes in diazirine (I, II, and III) have been asured yielding 8.6, 7.6, and 11.8 eV, respectively. A lower limit for the heat of formation of diazirine may then be derived, namely, $\Delta H_f°(\text{c-CH}_2\text{N}_2) \geq 60.6$ kcal/mol. A probable upper limit of $\Delta H_f°(\text{c-CH}_2\text{N}_2) \leq 66$ kcal/mol is obtained from the observation that process I does not occur as a result of Xe (147 nm) photolysis. The difference between the photon impact and previous electron impact value is discussed. The absorption coefficient of diazirine in the region from 125 to 200 nm has been measured.

13116. Hudson, R. P., **Very low temperature data. Properties of paramagnetic salts,** Section 5f-15 in *American Institute of Physics Handbook, Third Edition,* pp. 5-224–5-242 (McGraw-Hill Book Co., Inc., New York, N.Y., 1972).

Key words: Low temperatures; paramagnetic salts.

Section 5f-15 of the American Institute of Physics Handbook has been revised and brought up to date.

13117. Hils, D., McCusker, M. V., Kleinpoppen, H., Smith, S. J., **Differential and direct differential elastic scattering cross sections for electrons and potassium atoms,** *Phys. Rev. Lett.* **29,** No. 7, 398-401 (Aug. 14, 1972).

Key words: Cross sections; elastic scattering; spin polarization.

In a modulated crossed-beam experiment we have elastically scattered unpolarized electrons of 3.3 eV energy from spin-polarized K atoms. A measurement of the polarization of the scattered electron yields $|f(\theta)|^2/\sigma(\theta)$. Our measured values of $|f|^2/\sigma(\theta)$ show a significant angular shift relative to the theoretical curve in forward-angle scattering ($\theta = 20 - 40°$). This shift is not apparent in measurements of the differential scattering cross section $\sigma(\theta)$ over the same angular range, which, however, do show a significant angular shift in the range $\theta = 50 - 120°$.

13118. Saylor, C. P., **Supercooling in the barnyard,** *Chemistry* **45,** No. 11, 19-20 (Dec. 1972).

Key words: Crystallization; notes.

Once a substance has crystallized some molecules may be held on the surface of some invisible foreign particle in a configuration favorable for crystallization. If bonding to the particle is enough, this configuration may persist even above the melting point and serve to reseed the system when it is cooled.

13119. Bay, Z., Luther, G. G., White, J. A., **Measurement of an optical frequency and the speed of light,** *Phys. Rev. Lett.* **29,** No. 3, 189-192 (July 17, 1972).

Key words: Optical frequency; single-standard time-length measurement system; speed of light.

We report the measurement of the frequency of the 633-nm red laser line. This is the first measurement of an optical frequency in the visible range without reference to the speed of light or to a measured wavelength. Combination of the optical frequency with the known wavelength yields *c* to an accuracy higher than previously known. This method demonstrates the practicability of a single-standard time-length measurement system unified via a defined value of the speed of light.

13120. Hogben, D., **OMNITAB II: A computing system for statistical problem solving using Dutch rather than FORTRAN or ALGOL,** *Stat. Neerlandica* **26,** No. 3, 85-99 (1972).

Key words: Distribution of first significant digit; Dutch; Graeco-Latin square; language translation; natural language; OMNITAB II computing system; regression; statistical problem solving.

A brief description is given of a new Dutch version of the OMNITAB II computing system. Basic ideas are illustrated in a simple example. Further details are given in a more sophisticated example in statistical computation. It is suggested that the use of OMNITAB in the user's own language enhances its utility.

13121. Barbrow, L. E., **The metric system and small business,** *Manage. Aids,* No. **214,** 9 pages (Small Business Administration, Washington, D.C., July 1972).

Key words: Foreign trade; harmonization of standards; measurement systems; metric system; U.S. metric study.

From time to time, a Management Aid is published to suggest that owner-managers look to the future—to the horizon. Trends or techniques may be appearing that will demand your attention at a future date. This Aid is such an article. It discusses the matter of the United States changing to the metric system of measurement. At the present time, this country is the only major nation not operating on it or committed to it. The basic material used in developing this Aid is contained in A Metric America—A Decision Whose Time Has Come, which is a Report to the Congress on the findings of a 3-year study on the impact that the increasing worldwide use of the metric system has had on the United States. A plan for national changeover to the metric system over a 10-year period has been recommended. This Aid discusses what led up to that recommendation and urges owner-managers to be alert to developments as the Nation considers this proposal through its Congress.

13122. Barbrow, L. E., **Metrication in the United States, a status report,** *Engineering Issues, Amer. Soc. Civil Eng.* **98,** PP4, 505-510 (Oct. 1972).

Key words: Foreign trade; harmonization of standards; measurement systems; metric system; U.S. metric study.

For 200 years the advantages to America of having an internationally harmonized system of measurements have been reviewed in the Congress. Now the first step in the latest reopening of this subject has been taken in the Congress. No one can predict when the Congress will take final action or what that action will be. However, in view of the increasing use of the metric system not only abroad but in the U.S. also, all sectors of our society should study and determine for themselves whether increasing their metric use would be advantageous and, if so, plan to do so most efficiently. The time may come, sooner or later, when these plans will be welded into a master plan for the Nation. The metric problem has gained top-level consideration; the time to prepare for the future is now.

13123. Branscomb, L. M., **Product performance in an affluent society,** (Proc. 7th Annual Meeting, Symposium and Workshops Arranged by the National Academy of Engineering, Washington, D.C., Apr. 29-30, 1972), Paper in *Product Quality, Performance, and Cost,* pp. 23-31 (1972).

Key words: Conservation; consumer satisfaction; economic design; product safety; standards; test methods.

A detailed discussion is presented of the ecologic, economic, sociological, and political (international as well as local) reasons why more attention must be paid to the way consumer products are designed, built, and promoted, used, repaired, discarded, etc. The paper follows the theme of the public statements of the current administration as regards concern for the consumer. It touches upon the role of standards and test methods – both existing and those still to be developed in protecting the consumer pocketbook, his health and well-being and what is more important the limited natural resources of the earth.

13124. Jesch, R. L., Berry, I. S., **Batteries used with law enforcement communications equipment: Comparison and performance characteristics,** *LESP-RPT-0201.00,* 42 pages (U.S.
Department of Justice, Law Enforcement Assistance A
ministration, National Institute of Law Enforcement a
Criminal Justice, Washington, D.C., May 1972).

Key words: Batteries; battery comparison; communic
tions; law enforcement; performance characteristics.

This report is the result of an extensive literature search co
ducted in the field of primary and secondary batteries. It lis
terms and definitions pertaining to batteries and their chara
teristics, reviews basic battery principles and types, and asse
bles performance characteristics of battery systems into ch
form for comparative purposes. Considered are recommend
batteries, basic precautions and references to pertinent lite
ture.

13125. O'Connell, J. S., Donnelly, T. W., Walecka, J. I
**Semileptonic weak interactions with $C^{12}$,** *Phys. Rev. C* **6,** No.
719-731 (Sept. 1972).

Key words: Beta decay; carbon; electromagnetic; form fa
tor; muon; neutrino; weak interaction.

A unified analysis of semileptonic weak and electromagne
interactions in nuclei is applied to the $A = 12$ system. The pa
cle-hole model is used to describe the nuclear dynamics of B
$C^{12}$, and $N^{12}$. Neutrino reaction cross sections are presented
comparison with future experiments.

13126. Lehman, D. R., **Quasifree proton-proton and proton-de
teron scattering on $^3$He,** *Phys. Rev. C* **6,** No. 6, 2023-20
(Dec. 1972).

Key words: Pole dominance; quasifree scattering; resc
tering effects; separable potentials; three-body proble
$^3$He.

Quasifree proton scattering from $^3$He is examined on the ba
of available data. Cross sections are given in the pole-dominan
approximation for either two protons or a proton and deute
detected in coincidence. The cross sections are evaluated fo
constant $^3$He vertex and a separable-potential model of the $^3$
vertex amplitude. Both two- and three-body breakup of $^3$He
considered, with final-state rescattering included between t
spectator nucleons in three-body breakup. It is shown that t
asymptotic form of the coordinate-space $^3$He wave functi
governs the shape of these low-momentum-transfer cross s
tions and that final-state rescattering between the spectator p
in $^3$He$(p, 2p)pn$ mainly affects the magnitude of this cross s
tion.

13127. Meshkov, S., Rosen, S. P., **Lepton symmetry,** *Phys. R
Lett.* **29,** No. 26, 1764-1767 (Dec. 25, 1972).

Key words: Lepton; *m*-spin; neutrino; $SU(2)_M \times SU($
trident production; weak interaction.

Assuming a weak interaction invariant under $SU(2)$
$SU(2)_I$, we show that $M$-spin conservation leads to the r
$A(\nu_e e^- | \nu_e e^-) - A(\nu_\mu e^- | \nu_\mu e^-) = A(\nu_e \mu^- | \nu_\mu e^-)$ and to other s
rules for leptonic, semileptonic, and trident product
processes. The additional assumption of total isospin conser
tion yields simple relations for lepton-hadron scattering. We a
show that $\mu$ decay is forbidden in lowest order for various sy
metry schemes such as the SU(3) and O(3) theories based up
the Konopinski-Mahmoud assignment of lepton number.

13128. Haber, S., **Experiments on optimal coefficients,** Chapte
*Applications of Number Theory to Numerical Analysis,*
11-37 (Pergamon Press, Inc., New York, N.Y., 1972).

Key words: Algebraic numbers; approximation; dioph
tine approximation; exponential sums; functions of seve

variables; geometry of numbers; good lattice points; numerical integration; optimal coefficients; periodicity; quadrature.

Methods for calculating parameters for quadrature formulas of e type defined by N. M. Korobov and E. Hlawka have been oposed by several authors. In this paper a number of quences of such parameter sets are found, by methods due to K. Hua and Y. Wang, and to N. M. Korobov. An error bound r the quadrature formula corresponding to each parameter set found, by a modification of a method of Korobov. Conjectures out the asymptotic properties of these error bounds are formuted. Practical questions about the various methods of calculatg parameters are discussed.

**129.** McCarter, R. J., **The pyrolysis of cellulose at rates approaching those in burning,** *Text. Res. J.* **42,** No. 12, 709-719 (Dec. 1972).

Key words: Accessibility; Arrhenius plots; burned celluloses; celluloses; combustion; crystallinity; decomposition; DP; DTA; flame-retardant; $KHCO_3$; kinetics; moisture; oxygen indexes; pyrolysis; reaction rates; temperature; TGA; thermal analysis.

The thermal decomposition of cellulose was studied by a new ermal method suited to the measurement of faster reaction tes and to the problem of detecting concurrent reactions.

The pyrolysis data for four types of relatively pure cellulose dicated successive supramolecular and molecular decompon steps, either of which may control the decomposition rate ntingent upon the temperature history. The molecular decomposition step is interpreted as a first-order depolymerization action with an activation energy of 40 1/2 kcal/gmol.

The data for cellulose treated with retardant (1.5 wt% $HCO_3$) indicated two principal decomposition reactions. An itial lower-temperature reaction evolved principally $H_2O$ and $O_2$ from well-dried samples. The following main decomposition action exhibited the same kinetic parameters as the counterart depolymerization step of the untreated cellulose, but volved different vapor products.

Tests and analyses of these celluloses at transitional stages of ecomposition are summarized. The implications of the data oncerning the mechanism by which the retardant functions are scussed.

**3130.** Shine, R. A., Linsky, J. L., **Physical properties of solar chromospheric plages. 1. Line profiles of the Ca II H, K and infrared triplet lines,** *Solar Phys.* **25,** 357-379 (Aug. 1972).

Key words: Observations of solar spectra lines; solar atmosphere; solar chromosphere; solar plages.

Double pass photoelectric observations are presented of five aII lines (H, K, 8498 Å, 8542 Å, and 8662 Å) in a number of olar plages of different degrees of activity, quiet regions, and a unspot. The data are compared with previous work. All five nes show increasing emission together in plages and the least paque of the infrared triplet lines appears to exhibit core emison prior to the more opaque members of the multiplet. The uestion of source function equality is considered and the differences and similarities among plage profiles and between plage nd quiet profiles are shown qualitatively and quantitatively.

**3131.** Youden, W. J., **Randomization and experimentation,** *Technometrics* **14,** No. 1, 13-22 (Feb. 1972).

Key words: Experimental design; philosophy of design; randomization; restricted randomization.

Randomization, often specified as an indispensable requirenent in experimental design, is required only when the order or position of the experimental unit influences the performance of the unit. Randomization, when required, may give an arrangement that is obviously undesirable and one that may doom the particular experimental program. A system of constrained randomization is proposed that eliminates the undesirable arrangements without sacrificing the customary gains achieved by randomization.

**13132.** Youden, W. J., **Enduring values,** *Technometrics* **14,** No. 1, 1-11 (Feb. 1972).

Key words: Interlaboratory comparisons; philosophy of design; physical constants; variance components.

Why do results obtained by different investigators characteristically disagree by more than would be expected by their estimates of uncertainty? Youden notes that everything gets changed in another laboratory, whereas the investigator can (or does) make only minor changes within his laboratory. The message of this paper—that only those bounds for uncertainty based on actual measurement will endure—is already beginning to have an impact on physical measurement. Designed experiments to estimate bounds to systematic error will replace fallible judgment based on feelings and not observation.

**13133.** Kurylo, M. J., **Absolute rate constants for the reactions $H+O_2+M \rightarrow HO_2+M$ over the temperature range 203-404 K,** *J. Phys. Chem.* **76,** No. 24, 3518-3526 (1972).

Key words: Flash photolysis; H atoms; reaction kinetics; resonance fluorescence.

Absolute rate constants for the reaction $H+O_2+M \rightarrow HO_2+M$ have been measured by the flash photolysis-resonance fluorescence technique. For M = He, rate measurements over the temperature range 203-404 K and pressure range 10-400 torr gave the Arrhenius expression $k_1^{He} = [6.66\,(+1.2,\,-1)] \times 10^{-33} \exp[(473 \pm 92)\mathrm{cal\ mol}^{-1}/1.987T]$ $\mathrm{cm}^6$ $\mathrm{molecule}^{-2}$ $\mathrm{sec}^{-1}$. Comparisons of third-order rate constants at 298 K gave relative deactivation efficiencies of $CH_4/N_2/He/Ar = 15.7{:}3.4{:}1.0{:}1.0$. The efficiency ratio of $N_2$ to He was 4.5 at 226 K.

**13134.** Sengers, J. V., **Transport properties of fluids near critical points,** (Proc. Int. School of Physics "Enrico Fermi," Varenna on Lake Como, Italy, July 27-Aug. 8, 1971), Chapter in *Critical Phenomena,* pp. 445-507 (Academic Press, Inc., New York, N.Y., 1971).

Key words: Binary liquids; critical phenomena; dense gases; phase transitions; thermal conductivity; transport properties; viscosity.

The paper reviews the situation concerning transport properties of fluids in the vicinity of critical points. Methods for measuring viscosity and thermal conductivity are examined and a critical assessment is presented of the experimental results. The paper covers the viscosity and thermal conductivity in binary liquid mixtures near the critical mixing point, in gases near the gas-liquid critical point and in liquid He I near the superfluid transition. The experimental results are interpreted in terms of current theoretical predictions.

**13135.** Martin, W. C., Sugar, J., Tech, J. L., **Application of Slater-Condon theory with configuration interaction to the $5d^{10}6s6p$, $5d^96s^26p$, $5d^{10}6s7p$, and $5d^{10}6s5f$ configurations in Hg I, Tl II, Pb III, and Bi IV,** *Phys. Rev. A* **6,** No. 6, 2022-2035 (Dec. 1972).

Key words: Atomic energy levels; atomic theory; bismuth; configuration interaction; lead; mercury; thallium.

The calculations were based on fitting radial parameters to the observed energy levels, but with a requirement of regularity in the behavior of each parameter value along the isoelectronic sequence. Some parameters or ratios of parameters were fixed at values based on isoelectronic comparisons or adjusted Hartree-Fock values. The calculated levels, $g$ values, and $LS$ percentage compositions are given for each atom, and comparisons with experimental data are made. The results support new $5d^96s^26p$ levels recently found in Hg I, Tl II, and Bi IV, and one experimental $5d^96s^26p$ level in Pb III is rejected as unreal. The calculated ratio of the lifetimes of the Hg I $5d^{10}6s6p\,^3P_1^0$ and $^1P_1^0$ levels is compared with the experimental value. Some comparisons of calculated and observed isotope shifts are made for Hg I, Tl II, and Pb III. The leading percentages in the $jj$ coupling scheme are listed for levels having assigned $jj$ names ($5d^96s^26p$ levels in all four atoms and $5d^{10}6s7p$ levels in three atoms).

**13136.** Rowe, J. M., Rush, J. J., de Graaf, L. A., Ferguson, G. A., **Neutron quasielastic scattering study of hydrogen diffusion in a single crystal of palladium,** *Phys. Rev. Lett.* **29,** No. 18, 1250-1253 (Oct. 30, 1972).

Key words: Hydrogen diffusion; hydrogen in metals; jump diffusion; neutron scattering; palladium hydride; quasielastic scattering; single crystal.

The diffusion of hydrogen in a single crystal of palladium ($PdH_{0.03}$) has been studied by quasielastic neutron scattering. The results provide the best evidence yet obtained for the applicability of a simple jump model of hydrogen diffusion in a metal and confirm the predominant occupation of octahedral sites in the Pd crystal, with a mean residence time at 623 K of 2.8 psec between jumps.

**13137.** Eisenhart, C., Rosenblatt, J. R., **W. J. Youden, 1900-1971,** *Ann. Math. Statist.* **43,** No. 4, 1035-1040 (1972).

Key words: Experiment design; interlaboratory tests; statistics; Youden, W. J.

Youden's contributions to statistics are summarized. In experiment design, he was the originator of "Youden Squares," linked block and chain block designs, partially replicated Latin squares, and calibration designs. He developed an important new technique, the two-sample chart for graphical diagnosis of interlaboratory test results.

**13138.** Hanley, H. J. M., Barker, J. A., Parson, J. M., Lee, Y. T., Klein, M., **Comments on the interatomic potential for argon,** *Mol. Phys.* **24,** No. 1, 11-15 (July 1972).

Key words: Argon; cross sections; potential functions; second virial coefficient; viscosity coefficients.

Argon viscosity coefficients and second virial coefficients have been calculated for the potentials of Barker, Fisher and Watts, and of Parson, Siska and Lee. These potentials have strong physical foundations based on the representation of several microscopic properties of argon including recently measured cross-section data. An apparent slight discrepancy exists between the calculated and experimental values of the coefficients. The $11-6-8$ potential is also discussed. This potential, which apparently gives a satisfactory correlation of the microscopic properties of argon, is shown to be insufficiently flexible to represent the cross-section data.

**13139.** Hamilton, C. A., Johnson, E. G., Jr., **Analog computer studies of subharmonic steps in superconducting weak links,** *Phys. Lett.* **41A,** No. 4, 393-394 (Oct. 9, 1972).

Key words: Josephson junction; subharmonic steps.

Microwave radiation applied to certain types of Josephson junctions produces steps in the $V-I$ curve at voltages corresponding to subharmonics of the applied radiation. Analog studies show the existence of these steps to be strongly dependent on reactive elements connected to the junction.

**13140.** Peterson, R. L., **Magnetophonon structure in the longit dinal magnetoresistance of nonpolar semiconductors,** *Phy Rev. B* **6,** No. 10, 3756-3764 (Nov. 15, 1972).

Key words: Boltzmann equation; magnetoresistanc semiconductors; transport theory.

The magnetophonon effect in nonpolar nondegenera semiconductors is investigated by solving the Boltzmann equ tion exactly in the Ohmic limit for combined optical- an acoustic-phonon scattering of carriers in parallel electric an magnetic fields. The solution is used in computing the longit dinal magnetoresistance at several temperatures and ratios acoustic-to-optical-phonon scattering. As this ratio increase from zero at intermediate temperatures, the Gurevich-Firso (GF) resonance maxima are found to broaden and shift towa higher magnetic field, with pronounced minima developing at th resonance fields before the magnetophonon structure vanishe at large acoustic-phonon scattering. As the temperature i creases, additional (pseudoresonance) minima develop betwee the GF extrema, and are comparable in amplitude to the latt when $kT$ approximates the optical-phonon energy. At these ten peratures the GF extrema are minima, even in the absence elastic scattering. The results are compared with displaced-Ma wellian computations. The various effects are explained b physical arguments, which suggest that the same effects shoul occur for polar materials also.

**13141.** Ogburn, F., **Microscopical measurements of thicknes Manipulation of the microscope,** *Plating,* pp. 1155-1157 (De 1972).

Key words: Coating thickness; measurement of coatin thickness; metallography; microscopy; thickness determin tion of coatings.

Measurements of coating thickness by the microscopic method are subject to large errors. Major sources of error aris in the manipulation of the microscope as opposed to sampl preparation. These sources include calibration of stage micrometer, calibration of micrometer eyepiece, spontaneous motion o stage, alignment of micrometer eyepiece, positioning of interva to be measured relative to optic axis, spacing of binocula eyepieces, level of focus where focusing can change tube length and chromatic aberrations.

**13142.** Olson, W. B., **The infrared spectrum of $CH_3D$. Groun state constants and perturbation allowed transitions,** *J. Mo Spectrosc.* **43,** No. 2, 190-198 (Aug. 1972).

Key words: Infrared; molecular geometry; monodeuteromethane; perturbations; rotational constants; symmetri top.

The ground state rotational constants of $CH_3D$ have bee determined by a simultaneous least squares fit of combinatio differences obtained from twelve infrared absorption band recorded in the region of 2380-3160 cm$^{-1}$. The direct determination of $A_0$ and $D_0^K$ has been accomplished through combinatio differences obtained from transitions not ordinarily allowed i the infrared spectrum of a symmetric top molecule, but mad possible through perturbations between excited rovibroni levels.

**13143.** Ruthberg, S., **The measurement of conductance to fre molecular flow by substitution procedures,** *J. Vac. Sci. Techno* **9,** No. 6, 1457-1469 (Nov.-Dec. 1972).

Key words: Clausing factors; free molecular flow; precisio ionization gauges; stable vacuum systems; transmissio probability; vacuum calibration; vacuum measurements.

A method is presented which yields an order of magnitude in- ease in precision in the measurement of conductance to free olecular flow. The technique utilizes a calibrated variable con- ictance as a reference in a true substitution procedure. A series e was used to study balanced and unbalanced conditions and explore the effects of various factors on precision, such as w stability, pump behavior, ionization gauge sensitivity and sponse, temperature, transients, and sorption. A parallel line as used for measurements on short tubes of small diameter. For is, an iteration technique was employed for the calibration of e variable conductance on an absolute basis. Ionization gauge solution of 0.02% and linearity of better than 0.1% were hieved. Relaxation effects were apparent. Conductance mea- rement precision of a few parts per 1000 was obtained. Trans- ission probabilities for the small diameter, short tubes showed viations of as much as 18% from the Clausing factors at ngth-to-radius ratios $\geq 1$, but approached the Clausing values $l/r \rightarrow 0$. Deviations of $< 1\%$ from the Clausing value required $\leq 0.05$.

144. Rush, J. J., Schroeder, L. W., Melveger, A. J., **Dynamics of sodium and potassium bifluoride: Infrared, Raman, and neutron studies,** *J. Chem. Phys.* **56,** No. 6, 2793-2800 (Mar. 15, 1972).

Key words: Bending vibration; bifluoride ion, hydrogen bonding; infrared; lattice modes; neutron scattering; Raman; stretching vibration.

The crystal and molecular dynamic of $NaHF_2$ and $KHF_2$ have een studied by infrared and Raman spectroscopy and by eutron inelastic scattering. Infrared absorption spectra have een measured in the region of the bending ($\nu_2$) and asymmetric retching ($\nu_3$) vibrations of $NaHF_2$ and $KHF_2$ containing 2%, 1%, and $\approx 80\%$ $DF_2^-$. The spectra show a rather striking eduction in the widths of the $DF_2^-$ absorption peaks as well as nifts in peak frequencies as the percent $DF_2^-$ is lowered toward "defect" concentration. These results indicate that the con- derable width of the infrared absorption bands assigned to the and $\nu_3$ modes in pure $NaHF_2$ and $KHF_2$ is associated with oupling of near-neighbor $HF_2^-$ oscillators having similar equencies or energy states. The Raman spectrum for $NaHF_2$ nows peaks at 630.5 and 145 cm$^{-1}$ which can be unambiguously ssigned, respectively, to the $HF_2^-$ symmetric stretching mode $_{1g}$) and the $E_g$ librational lattice mode. The $KHF_2$ Raman spec- um is similar to a previous result, with some differences in the equencies of the lattice-mode peaks. The combined neutron nd far-infrared spectra on $NaHF_2$ provide information on the coustic and optical translational lattice modes. An approximate ibrational frequency distribution is derived from the neutron pectrum and compared with previous spectroscopic and neoretical results on $NaN_3$. A detailed assignment of the inter- al and lattice modes for both sodium and potassium bifluoride presented.

3145. Powell, C. J., Mandl, A., **High-resolution measurements of Auger-electron and photoelectron structure in the secondary-electron energy distributions of aluminum, nickel, and copper,** *Phys. Rev. B* **6,** No. 12, 4418-4429 (Dec. 15, 1972).

Key words: Aluminum; Auger transitions; copper; electronic density of states; nickel; secondary-electron energy distribution; x-ray photoemission.

Measurements are reported of selected structure in the secon- lary-electron energy distributions of evaporated aluminum, ickel, and copper. The specimens were bombarded with 3-keV lectrons and the secondary structure was measured with a esolution of 0.1 eV. For each metal, it was hoped to measure uger transitions involving two relatively narrow inner-shell evels and the valence band in order to obtain information on the valence-band density of states. Attempts were made to observe the Al $KL_{2,3}M$ Auger-electron energy distribution expected at about 1470 eV. Structure was, however, observed with a high-energy edge of $1485.9 \pm 0.5$ eV and a breadth of 8-9 eV. This structure was interpreted as being due to photoemission of valence electrons by internally generated $K\alpha$ x rays and was similar to uv photoelectron energy distributions and to the calculated density of states. Inelastic scattering of the photoelectrons obscures the expected Al $KL_{2,3}M$ structure. Auger-electron peaks in the ranges 730-800 and 820-865 eV were measured in the secondary-electron energy spectra for nickel and copper, respectively. Structure was observed in the $L_3M_{2,3}M_{4,5}$ Auger transition (over a range of about 20 eV) that could be associated in part with the final atomic states and in part with over-all features of the 3*d*-band density of states as determined by soft-x-ray-emission spectroscopy and x-ray photoelectron spectroscopy. It is believed that Auger-electron spectra can yield useful data on changes of electronic structure (e.g., by alloying or by compounding) but, in general, density-of-states data cannot be derived from the Auger spectra without detailed knowledge of the final states expected after the Auger transition of interest.

13146. Redding, R. W., **Rotational levels of double-minimum potentials: The linear BAB molecule with unequal bond lengths,** *J. Mol. Spectrosc.* **38,** No. 2, 396-414 (May 1971).

Key words: Double-minimum potentials; large-amplitude vibrations; linear molecules; rotational constants; triatomic molecules; vibration-rotation Hamiltonian.

The rotational constants and energy levels for the linear BAB system are studied under the assumption of unequal A – B bond lengths. The quantum mechanical Hamiltonian is derived according to a formalism which allows for a large-amplitude antisymmetric stretching motion. A numerical integration technique is used to obtain solutions of the one-dimensional Schroedinger equation corresponding to a zeroth-order approximation of the Hamiltonian. The behavior of the resulting rotational constants for various heights of the barrier in the double-minimum potential is discussed.

13147. Brower, W. S., Parker, H. S., Roth, R. S., Waring, J. L., **Phase equilibrium and crystal growth in the system lithium oxide-molybdenum oxide,** *J. Crystal Growth* **16,** 115-120 (1972).

Key words: Alkali molybdates; crystal growth; phase equilibria.

The phase equilibrium relationships of the $Li_2MoO_4 - MoO_3$ system were determined in air. Two intermediate compounds were found to occur in the system and single crystals of these compounds were grown by the Czochralski technique. The first compound $Li_4Mo_5O_{17}$ was found to melt congruently at 544 °C. The x-ray pattern of $Li_4Mo_5O_{17}$ was indexed on the basis of a triclinic cell $a = 6.786$ Å, $b = 9.481$ Å, $c = 10.812$ Å, $\alpha = 107° 1'$, $\beta = 88° 48'$, $\gamma = 110° 12'$. The second intermediate compound $Li_2Mo_4O_{13}$ was found to melt incongruently at 568 °C, and to occur in two polymorphic forms. The x-ray pattern of the first form was indexed on the basis of a triclinic cell $a = 8.227$ Å, $b = 8.503$ Å, $c = 11.46$ Å, $\alpha = 95° 24'$, $\beta = 109° 17'$, $\gamma = 96° 31'$ and the second form was indexed on a similar triclinic cell $a = 8.192$ Å, $b = 8.597$ Å, $c = 11.580$ Å, $\alpha = 111° 17'$, $\beta = 93° 55'$ and $\gamma = 96° 5'$.

13148. Dick, C. E., Whittaker, J. K., Sparrow, J. H., **Kiloampere current and charge measurements of a 2 MeV pulsed electron source,** *Nucl. Instrum. Methods* **104,** 131-136 (1972).

Key words: Charge monitor; high frequency; integrator; low current monitor; 2 MeV electron accelerator.

A current monitor has been developed to measure the electron current pulse from the NBS 2 MeV pulsed electron generator. This monitor features low inductance and a risetime of the order of a hundred picoseconds, enabling it to faithfully reproduce high frequency components present in the electron beam pulse. In addition, a charge integrating system comprised of an integrating capacitor and a precision integrator has been developed to measure the total charge contained in the electron beam pulse.

**13149.** Choi, C. S., Mapes, J. E., Prince, E., **The structure of ammonium nitrate (IV),** *Acta Crystallogr.* **B 28,** Part 5, 1357-1361 (May 1972).

Key words: Ammonium nitrate; crystal structure.

The structure of ammonium nitrate (IV), the phase which is stable between − 18 and 32.3 °C, has been refined by least-squares methods with three-dimensional neutron diffraction data. 188 independent reflections were observed on a four-circle diffractometer with a neutron wavelength of 1.232 Å and a limiting $2\theta$ angle of 100°. The refinement, using anisotropic temperature factors and an isotropic secondary extinction parameter, gave a final weighted $R$ index of 0.028. The structure is orthorhombic, space group *Pmmn*, with two $NH_4NO_3$ formula units per unit cell. A two-dimensional network of hydrogen bonds between the nitrogen atoms of the ammonium group and the oxygen atoms at one corner of the nitrate groups forms infinite sheets parallel to the (001) planes of the crystal. Adjacent sheets are bound together by van der Waals forces. This structure is simply related to the structures of the higher temperature phases.

**13150.** Martin, W. C., Sugar, J., Tech, J. L., **Calculations of autoionizing $d^9s^2np$ levels in Zn I, Cd I, and Hg I,** *J. Opt. Soc. Amer.* **62,** No. 12, 1488-1492 (Dec. 1972).

Key words: Cadmium; mercury; spectra; zinc.

Three Rydberg series of the type $d^{10}s^2\ {}^1S_0 - d^9s^2np\ (J=1)$ are known in each of these spectra. We have made intermediate-coupling calculations for the configurations Zn I $3d^94s^24p$, $5p$; Cd I $4d^95s^25p$, $6p$; and Hg I $5d^96s^27p$. The Slater parameters were determined to about 15% accuracy by various methods, or were adopted from previous calculations. Percentage compositions in the *LS* coupling scheme and in the scheme of highest purity are given for the three levels having $J=1$ in each configuration. The results establish the most appropriate designations for these levels and for all of the higher $d^9s^2np$ series members. Although the Zn I $3d^94s^24p$ $(J=1)$ levels are found to be significantly perturbed, the calculated relative oscillator strengths of the three absorption transitions to these levels agree well with the experimental values. Some other comparisons with experiment are discussed, and the relative intensities of the three observed series within each spectrum are qualitatively explained.

**13151.** Casella, R. C., Trevino, S. F., **Group-theoretical selection rules in inelastic neutron scattering within the rigid-molecule model,** *Phys. Rev. B*6, No. 12, 4533-4539 (Dec. 15, 1972).

Key words: Group theory; inelastic; neutron; rigid-molecule; scattering; selection-rules.

The model-independent technique of Elliott and Thorpe (ET) is extended to apply to a class of models in which molecular units undergo translational vibrations with respect to each other and also librations, but in which the internal vibronics of the molecules are neglected. Within the model we find that the ET "structure function" $F^{(r)}(\mathbf{k})$, associated with irreducible representation $r$ and momentum transfer $\mathbf{k}$, can be written in the form $F^{(r)}(\mathbf{k}) = F^{(r)}(\mathbf{k}|R) + F^{(r)}(\mathbf{k}|\theta)$, where $R$ and $\theta$ signify translational and rotational oscillations. Moreover, the translational part is identical to that of ET except that the atomic scattering lengths $a_n$ which appear in their result are to be replaced by $\mathbf{k}$-dependent molecular form factors $a_n(\mathbf{k}')$. $F^{(r)}(\mathbf{k}|\theta)$ contains a vecto form factor equal to $i\nabla_{k'}a_n(\mathbf{k}')$, where $\mathbf{k}'$ is related to $\mathbf{k}$ via a rotation. Mathematically, their result is contained in ours as a specia case. Physically, we indicate how to use both procedures in concert, thereby aiding in the identification of $r$ as well as in separating the internal from external vibrations and among the latter, th translational and rotational parts thereof. At the Brillouin-zon boundary we employ the so-called multiplier representations thereby achieving a simplification both of our results and theirs By significantly reducing the number of phonon modes to be considered in complex molecular crystals, we have likewise increased the diagnostic power of this method which requires n detailed knowledge of force constants. It is hoped that ou results will receive wide application in the identification o phonons in such crystals.

**13152.** Manghnani, M. H., Fisher, E. S., Brower, W. S., Jr. **Temperature dependence of the elastic constants of single crystal rutile between 4 and 583 K,** *J. Phys. Chem. Solids* 33 2149-2159 (1972).

Key words: Elastic constants: oxide; rutile; single crystal temperature dependence.

Measurements of all the six principal elastic constants of single-crystal rutile were made in the temperature range of 298-58 K. The temperature derivatives (in kb/deg) at 298 K are $\mathrm{d}C_{11}/\mathrm{d}T = -0.510$, $\mathrm{d}C_{33}/\mathrm{d}T = -0.900$, $\mathrm{d}C_{44}/\mathrm{d}T = -0.220$ $\mathrm{d}C_{66}/\mathrm{d}T = -0.458$, $\mathrm{d}C_{12}/\mathrm{d}T = -0.580$, and $\mathrm{d}C_{13}/\mathrm{d}T = -0.330$ Measurements of the four modes, $C_{11}$, $C' = (C_{11} - C_{12})/2$, $C_{66}$ and $C_{110L} = (C_{11} + C_{12} + 2C_{66})/2$, were extended to 4 K. Two features related to the temperature and volume dependences of th lattice vibrational frequencies are revealed: first, all the measured $\mathrm{d}C_{ij}/\mathrm{d}T$ except $\mathrm{d}C'/\mathrm{d}T$ become less negative with increasing temperature above 100 K. Second, $\mathrm{d}C'/\mathrm{d}T$ is positive at al temperatures but decreases with increasing temperature at temperatures $> 300$ K. Indirectly shown is that $(\partial C'/\partial P)_T$ having value of − 1.32 at 298 K, decreases with decreasing temperatures. The significance of this latter fact is discussed in light o the computation of Grüneisen mode $\gamma$'s from the acoustic $(\partial C_{ij}/\partial P)_T$ values, and the results are compared with $\gamma(\alpha_V)$ value obtained by Kirby from thermal expansion data. It is conclude that the large increase in $\gamma(\alpha_V)$ at low temperatures cannot be ascribed to a large temperature dependence of $(\partial C'/\partial P)_T$. Therefore, Kirby's explanation, that the large increase in $\gamma(\alpha_V)$ i caused by the large volume dependence of the acoustical mod frequencies, is not substantiated.

**13153.** Raveché, H. J., Mountain, R. D., Streett, W. B., **Thre atom correlations in the Lennard-Jones fluid,** *J. Chem. Phys* **57,** No. 11, 4999-5006 (Dec. 1, 1972).

Key words: Closure approximation; high pressure; Lennard-Jones potential; liquid densities; Monte Carlo method triplet correlation function.

The Monte Carlo method has been used to compute the triple correlation function in a classical fluid with Lennard-Jones interactions. The computations were performed for particular configurations at five thermodynamic states of high density. Th structure of the triplet function is discussed in the liquid an dense gas regions. Several closure approximations, which express the triplet function in terms of the pair correlation function are compared to the Monte Carlo results.

**13154.** Choi, C. S., Prince, E., **The crystal structure o cyclotrimethylene-trinitramine,** *Acta Crystallogr.* **B 28,** Part 9 2857-2862 (Sept. 1972).

Key words: Crystal; crystal structure; cyclotrimethylene-trinitramine; explosives; neutron diffraction; organic compound; RDX.

The structure of cyclotrimethylene-trinitramine (RDX), $_3H_6N_6O_6$, has been refined from single-crystal neutron-diffrac- on data. The final weighted *R* index for 836 independent reflec- ons is 0.021. The compound crystallizes in the orthorhombic ace group *Pbca*, $a = 13.182$ (2), $b = 11.574$ (2), $c = 10.709$ (2) , $Z = 8$. The molecule consists of alternate $CH_2$ and $N - NO_2$ oups in a puckered ring. The environment of the carbon atoms essentially tetrahedral, and the $N - NO_2$ groups are planar. he molecule possesses a plane of approximate mirror symmetry rpendicular to the plane defined by the three carbon atoms. he thermal motion may be described by rigid-body motion of e ring and separate rigid-body motion of the nitro groups.

**155.** Bensema, W. D., **Coal mine magnetic-field noise measurements,** *Proc. First West Virginia Conf. on Coal Mine Electrotechnology, West Virginia University, Morgantown, W. Va., Aug. 2-4, 1972*, pp. XII-1–XII-12 (Aug. 1972).

Key words: Communication; field strength; measurement; mines; noise.

A semiportable measurement system was developed to mea- re the extremely low frequency magnetic noise spectrum in the equency range from 40 Hz to 10 kHz. Ambient noise spectra om 40 to 3000 Hz are shown in an underground coal mine loca- on. Magnetic field strengths vary from a high of − 20 dB rela- ve to 1.0 ampere/meter measured at 60 Hz near an AC power us, to a low of approximately − 138 dB measured at a quiet lo- ation underground at 500 Hz. Impulsive noise from nearby ectric locomotives raise the background levels by approximate- 34 dB. At locations remote from arcing locomotives, deep inima of 60 or more dB were found between harmonics of the 0 Hz powerline frequency. "Three dimensional" graphs are ven showing some typical spectra as a function of time.

**3156.** Fano, U., **Field configurations and parameters that identify states with $j=1$,** Chapter in *Spectroscopic and Group Theoretical Methods in Physics, Racah Memorial Volume*, F. Bloch, S. G. Cohen, A. De-Shalit, S. Sambursky, and I. Talmi, Eds., pp. 153-160 (North-Holland Publishing Co., Amsterdam, The Netherlands, 1968).

Key words: Angular momentum; atoms; molecules; nuclei; orientation.

This paper reviews the problem of identifying an arbitrary ate within the set of degenerate energy eigenstates of a system olated in space. For $j = 1$, it presents a description and in- rpretation of identifying parameters and of their ranges of ariation which is summarized in section 5.

**3157.** Florin, R. E., Wall, L. A., **Radicals detected by electron spin resonance during fluorination of polymers,** *J. Chem. Phys. Letters to Editor* **57,** No. 4, 1791-1792 (Aug. 15, 1972).

Key words: Electron spin resonance; fluorination; free radicals; polymer reactions.

Radicals of both peroxyl and fluorohydrocarbon structure are bserved by electron spin resonance when organic polymers uch as polystyrene and polyethylene are exposed to dilute uorine. The character of the reactions suggests that F-atoms re the initiation species in this type of direct fluorination rocess.

**3158.** Olver, F. W. J., Sookne, D. J., **Note on backward recurrence algorithms,** *Math. Computation* **26,** No. 120, 941-947 (Oct. 1972).

Key words: Bessel functions; difference equations; error bounds; FORTRAN; Miller's algorithm; recursion.

An algorithm is given for the computation of the recessive olution of a second-order linear difference equation, based upon a combination of algorithms due to J. C. P. Miller and F. W. J. Olver. A special feature is automatic and rigorous control of truncation error.

The method is illustrated by application to the well-used example of the Bessel functions $J_r(x)$.

**13159.** Hastie, J. W., **Formation of $H_2O_2$ by adiabatic expansion of $H_2 - O_2$ gas mixtures,** *Chem. Phys. Lett.* **17,** No. 2, 195-198 (Nov. 15, 1972).

Key words: Adiabatic expansion; hydrogen peroxide; mass spectrometry.

Mass-spectrometric studies of adiabatic expansions of $H_2 - O_2$ and $H_2 - O_2 - N_2$ gas mixtures have revealed the formation of the species $H_2 \cdot O_2$ at concentrations of the order of $10^{-5} - 10^{-4}$ mole fraction. This species is believed to be a relatively weakly bound isomer which is less stable than $H_2O_2$, the common form of hydrogen peroxide. A mechanism which is more consistent with the data is: $H_2 + H_2 + O_2 \rightarrow H_2 \cdot O_2 + H_2$.

**13160.** Rukwied, A., Ballard, D. B., **Scanning electron microscope fractography of continuously cast high purity copper after high temperature creep,** *Metallurgical Trans.* **3,** 2999-3008 (Nov. 1972).

Key words: Creep cavitation; fractography; high purity copper; impurity segregation structure; stereo scanning electron microscopy.

Fracture surfaces produced by high temperature creep were studied using the scanning electron microscope. The material investigated was continuously cast high purity copper containing a nodal impurity segregation structure at which grain boundary voids are formed during creep. The observed void shape suggests that vacancies are supplied mainly via grain boundaries, and also by enhanced diffusion via segregation nodes; the vacancies seem to originate mainly at internal sources. The known distribution of potential nucleation sites was used to study the efficiency of the segregation structure in nucleating voids under various test conditions. Within the range of conditions employed, three different fracture modes were observed in separate regions of the stress-temperature plane. The regions are sequentially denoted *A*, *B*, and *C* as the temperature is increased at a given stress; they shift to lower temperatures as the stress is increased. In region *A* fracture is initiated by extensive cavitation along grain edges (line of junction of three grains); cavitation at the segregation structure seems to be of secondary importance. In region *B* formation and growth to coalescence of voids at segregation nodes governs fracture; the change of growth mechanisms with test conditions is discussed. In region *C* fracture is controlled by plastic instability.

**13161.** Greer, S. C., Sengers, J. M. H. L., Furukawa, G. T., **Heat capacity near the consolute point in solid $CH_4 - Ar$,** *J. Chem. Phys.* **57,** No. 12, 5052-5058 (Dec. 15, 1972).

Key words: Argon; calorimetry; critical phenomena; heat capacity; methane; mixture, binary; solution, solid.

Measurements are reported of the heat capacity at saturated vapor pressure (essentially $C_p$) of the system $CH_4 - Ar$ near its solid-solid consolute point (62 K, 65% Ar). In contrast to the behavior of the heat capacity at binary liquid consolute points where there are striking anomalies, no large increase was observed for $CH_4 - Ar$. An abrupt increase of only about 13% occurred in the heat capacity near the transition. The possibility that the anomaly is suppressed by lattice strain effects is discussed.

**13162.** Leiss, J. E., **Modern electron linacs and new user needs,** *Proc. 1972 Proton Linear Accelerator Conference, Los*

*Alamos, N. Mex., Oct. 10-13, 1972,* Report No. LA-5115, UC-28, pp. 197-204 (Nov. 1972).

Key words: Accelerators; electron linacs; nuclear research; radiation applications.

Existing and future needs for linear accelerator developments and the possibility for linac technology to satisfy these needs are discussed. Two major needs for high duty cycle accelerators on the one hand and high peak pulse current accelerators on the other are identified.

**13163.** Rowe, J. M., Sköld, K., Flotow, H. E., Rush, J. J., **Quasielastic neutron scattering by hydrogen in the $\alpha$ and $\beta$ phases of vanadium hydride,** *J. Phys. Chem. Solids* **32,** 41-54 (Apr. 1971).

Key words: Activation energy; hydrogen diffusion; lattice sites; neutron scattering; phase transition; quasielastic scattering; vanadium hydride.

The diffusion of hydrogen in the $\alpha$ and $\beta$ phases of vanadium hydride has been studied by neutron inelastic scattering. Samples of $VH_{0.198}$, $VH_{0.403}$ and $VH_{0.570}$ were used to determine the temperature and concentration dependence of the diffusion in the $\alpha$-phase. An activation energy of 550 ± 50 K was derived from the temperature dependence of hydrogen diffusion in the $VH_{0.198}$ sample. The theoretical neutron scattering cross-section for jump diffusion among the octahedral and tetrahedral interstitial sites of body-centered cubic lattices has been derived and compared to the experimental results. No conclusions about the site occupation in the $\alpha$-phase can be drawn from these results. The data for the $\beta$-phase of $VH_{0.570}$ indicate an abrupt decrease in the diffusion rate at the $\alpha \rightarrow \beta$ transition.

**13164.** Czyz, W., Maximon, L. C., **Comments on high energy coherent diffractive production of multi-body states on nuclear targets,** *Acta Phys. Pol. Letters to Editor* **B3,** No. 6, 897-902 (1972).

Key words: Coherent production; diffractive production; Glauber model; hadron scattering; high energy scattering; multi-body states.

Arguments are given that the traditional, Glauber-like model for the multiple scattering of composite objects be modified to the extent of including relativistic deformation of the wave functions. It is argued that this modified formalism is a specific realization of Van Hove's model of coherent nuclear production of multi-body states and thus is sufficient to explain the astonishingly small nucleon total cross-sections that have been extracted from multi-boson production experiments. It is shown on the simple example of Lorentz-contracted oscillator wave functions that, to have Van Hove's effect present, the interaction between the components of the diffractively produced object must be of the order of magnitude of their masses.

**13165.** Harris, W. P., **A wide-range bridge for dielectric measurements,** *1971 Annual Report, Conf. on Electrical Insulation and Dielectric Phenomena, Williamsburg, Va., Nov. 1-3, 1971,* pp. 177-179 (National Academy of Sciences, Washington, D.C., 1972).

Key words: Amplifiers; capacitors; dielectric constant; dissipation factor; measurements.

By employing modern fast operational amplifiers (slewing rate of 1000 V/$\mu$sec) the useful frequency range of the bridge described several years ago as an ultra-low-frequency bridge, has been extended upward by approximately two decades. This gives it a frequency range of about nine decades, from $10^{-3}$ Hz to 1 MHz. A source capable of providing a second output shifted 90° from the primary output is required. Up to $10^5$ Hz, this is provided by a single commercial instrument. Above $10^5$ Hz, t sources are used, the second triggered by the first, with adjus ble phase. The accuracy of the dielectric constant measureme is chiefly limited by the 0.1% uncertainty of the variable capa tors used. Phase shift in the inverters produces an error in t dissipation factor measurements, roughly proportional frequency. The effect of this can be greatly reduced by using substitution method, or a correction can be applied to direct me surements. A fast FET operational amplifier forms the heart the detector, with high input impedance over the broad freque cy range. Except at lowest frequencies, this bridge is char terized by rapid balancing, and extremely simple calculations.

**13166.** Bertozzi, W., Cooper, T., Ensslin, N., Heisenberg, Kowalski, S., Mills, M., Turchinetz, W., Williamson, Fivozinsky, S. P., Lightbody, J. W., Jr., Penner, **Deformation parameters of $^{152}Sm$ by electron scattering,** *Ph Rev. Lett.* **28,** No. 26, 1711-1713 (June 26, 1972).

Key words: Charge distribution; deformation paramete electron scattering; high-energy electrons; rotational ban samarium-152.

We have measured the cross sections for excitation of t ground-state rotational band in $^{152}Sm$ by high-energy electro The ground-state charge distribution has been determined i cluding the deformation parameters $\beta_2$ and $\beta_4$ of the nuclear su face.

**13167.** Gillen, K. T., Douglass, D. C., Malmberg, M. Maryott, A. A., **NMR relaxation study of liquid $CCl_3F$. Reorie tational and angular momentum correlation times and rotatio diffusion,** *J. Chem. Phys.* **57,** No. 12, 5170-5179 (Dec. 1 1972).

Key words: Diffusion constant; dipole relaxation; molec lar; spin lattice; temperature dependent.

Using pulsed NMR techniques, values of the self-diffusi constant $D_s$ and the $^{19}F$ spin-lattice and rotating frame relaxati times, $T_1{}^F$ and $T_{1\rho}{}^F$, have been obtained for $CCl_3F$ over its enti liquid range. (~ 150 – 450 K). The dependence of $T_{1\rho}{}^F$ on t rotating field strength $\omega_1$ has been used to derive temperature-d pendent values of the $^{35}Cl$ spin-lattice relaxation time $T_1{}^{Cl}$ a the chlorine to fluorine spin-spin coupling constant $J_{^{19}F-^{35}Cl}$ 11.9 ± 0.4 Hz, independent of temperature). Except at low te peratures where the intermolecular dipole-dipole relaxati mechanism is important, $T_1{}^F$ is dominated by the spin-rotati interaction $(T_1{}^F)_{sr}$. Using $D_s$ data to separate the dipole-dipo contribution from $T_{1sr}{}^F$ allows us to estimate values of the ang lar momentum correlation time $\tau_J$ over a 300° temperature rang Over the same temperature range, values of $T_1{}^{Cl}$ give the correl tion times for molecular reorientation $\tau_{\theta,2}$. Although possib anisotropy in molecular motion and in the spin-rotation intera tion precludes rigorous quantitative comparisons with rotation diffusion theory, the results for $\tau_J$ and $\tau_{\theta,2}$ are shown to be co sistent with Gordon's extended $J$ diffusion model. In particul at high temperatures the molecular reorientation is no long described by the small angular steps in classical theory: near t critical temperature $\tau_J$ and $\tau_{\theta,2}$ become of comparable magnitu and correspond to angular steps approaching 1 rad.

**13168.** Pedersen, N. F., Finnegan, T. F., Langenberg, D. **Magnetic field dependence and $Q$ of the Josephson plas resonance,** *Phys. Rev. B* **6,** No. 11, 4151-4159 (Dec. 1, 197

Key words: Josephson tunnel junction; magnetic fie microwave losses; quasiparticle interference current.

The results of an experimental study of the magnetic field d pendence of the Josephson-plasma-resonance frequency a ewidth in Pb — Pb oxide — Pb tunnel junctions are reported. the presence of an external magnetic field, the plasma mode is nd to be sensitive to an antisymmetric component of super-rent density which is not observed in conventional measure-nts of the field-dependent critical current. The frequency and d dependence of the plasma-resonance linewidth are in-preted as evidence that the previously unobserved quasi-parti--pair-interference tunnel current predicted by Josephson ex-s and has the expected magnitude but the opposite sign.

169. Finnegan, T. F., Wahlsten, S., **Observation of coherent microwave radiation emitted by coupled Josephson junctions,** *Appl. Phys. Lett.* **21,** No. 11, 541-544 (Dec. 1, 1972).

Key words: Junction array; radiation emmission; resonant tunnel junction.

We report here the results of a preliminary study of coherent crowave radiation emitted by a small array of interacting sephson tunnel junctions, including the first direct observation the superradiant state in pairs of junctions.

170. Horton, W. S., Ballard, D. B., **Scanning electron microscope studies of oxidized pyrolytic graphite,** *Carbon* **10,** 499-502 (1972).

Key words: Circular holes; face versus edge oxidation; impurity effect on oxidation; layers; pyrolytic graphite; scanning electron microscope.

Specimens of pyrolytic graphite (PG) that had been previously ed for kinetic oxidation studies, as well as some unoxidized ecimens, were examined. The principal topographic features oxidized PG faces included circular holes with flat bottoms d various depths. Some holes were basin-like at the top. The le walls were striated showing layers parallel to the deposition face. The bottom side (i.e., nearest the substrate) was more tensively oxidized than the top, and the hole diameters were order of magnitude larger. In contrast to these essentially indrical pits were a few with the shape of a paraboloid of volution. The edges had indications of circular holes also. owever, a nibbled effect appeared more common. A major fea-e of a thick specimen was the nonuniformity of attack as a nction of distance from the substrate surface. The large scatter the earlier kinetic data is attributed to this varying reactivity.

171. Olin, J. S., Thompson, B. A., Sayre, E. V., **Characterization of medieval window glass by neutron activation analysis,** (Proc. Developments in Applied Spectroscopy, St. Louis, Mo., Oct. 18, 1971), Chapter in *Developments in Applied Spectroscopy,* A. J. Perkins, E. L. Grove, E. F. Kaelble, and J. E. Westermeyer, Eds., **10,** 33-55 (1972).

Key words: Activation analysis; archeology; glass; manganese; medieval windows; potassium; sodium.

Analytical data on medieval glasses are presented which in-cate that alkali ratios and manganese-alkali ratios may be aracteristic of the "ash" used in the glass manufacture. Thus, ch data may be helpful in establishing the provenance of dieval glasses.

172. Rebbert, R. E., Ausloos, P., **Photolysis of methane: Quantum yield of C($^1$D) and CH,** *J. Photochem.* **1,** 171-176 (1972/73).

Key words: C-atoms; collisional deactivation; free radical reactions; methane; photolysis; quantum yields.

It is demonstrated that C($^1$D) and CH($^2\pi$) species are formed the photodissociation of $CH_4$ at $\lambda = 123.6$ nm [$\Phi(C) = 0.4 \pm$ $\times 10^{-3}$, $\Phi(CH) = 5.9 \pm 0.5 \times 10^{-2}$] and at $\lambda = 104.8$-$106.7$ nm (C)$= 6.5 \pm 0.5 \times 10^{-3}$, $\Phi(CH) = 0.23 \pm 0.03$]. There is no evidence for C or CH production at wavelengths where the photoionization quantum yield is equal to unity.

13173. Seitz, M. G., Walker, R. M., Carpenter, B. S., **Improved methods for measurement of thermal neutron dose by the fission track technique,** *J. Appl. Phys.* **44,** No. 1, 510-512 (Jan. 1973).

Key words: Fission tracks; glass; mica; microscopy; neutron dose measurements; uranium.

We describe scanning electron microscope and reflected light observations of fission tracks that lead to highly reproducible track density measurements for different observers. These new observational techniques are used to calibrate two uranium-doped glasses for neutron dose measurements. The glasses are available to other investigators.

13174. Wiederhorn, S. M., **A chemical interpretation of static fatigue,** *J. Amer. Ceram. Soc.* **55,** No. 2, 81-85 (Feb. 1972).

Key words: Crack propagation; fracture; glass; mechanical properties; strength.

The effect of water on the growth of cracks in glass is discussed. Crack motion is believed to result from a stress-enhanced chemical reaction between water and glass and is influenced strongly by the crack-tip $OH^-$ ion concentration. This hypothesis is supported by the observation that crack-velocity data can be correlated with measurements of pH in slurries of ground glass and water. Variation of the measured pH from 5 to 12, depending on glass composition, suggests a wide pH variation at crack tips. The types of chemical reactions that establish the slurry pH are discussed, and it is noted that the slurries behave as weak acids, buffered solutions, or salts of weak acids, depending on glass composition.

13175. Lias, S. G., Rebbert, R. E., Ausloos, P., **Gas phase pulse radiolysis of hydrocarbon mixtures; determination of the charge recombination rate coefficient and absolute rate constants of ion-molecule reactions of the *t*-butyl ion through a competitive kinetic method,** *J. Chem. Phys.* **57,** No. 5, 2080-2086 (Sept. 1, 1972).

Key words: Carbonium ions; hydrocarbons; ion-molecule reactions; neutralization; pulse radiolysis.

The gas phase pulse radiolysis of several neopentane-$d_{12}$-alkane mixtures has been studied with the purpose of examining the competition between the reaction of the fragment *t*-butyl ion with the alkane to form isobutane, $t\text{-}C_4D_9^+ + RH_2 \rightarrow i\text{-}C_4D_9H + RH^+$, and the neutralization of the *t*-butyl ion by an electron or $SF_6^-$ ion, $t\text{-}C_4D_9^+ + X^- \rightarrow$ products. Using a computer calculation which takes into account the pulse characteristics as a function of time, the yield of isobutane observed in the reaction with 2,3-dimethylbutane (for which $k_{rn}$ was accurately determined to be $5.7 \pm 0.5 \times 10^{-11}$ cm$^3$/molecule·sec) and the dose per pulse, rate coefficients of the competing neutralization reactions were determined. These are $\alpha = 1.92 \pm 0.2 \times 10^{-6}$ cm$^3$/molecule·sec for neutralization by an electron, and $0.40 \pm 0.04 \times 10^{-6}$ cm$^3$/molecule·sec for neutralization by the $SF_6^-$ ion. The latter value is independent of $SF_6$ concentration and both are independent of pressure between 40 and 200 torr. Finally, these values of the neutralization rate coefficients and yields of isobutane measured in the pulse radiolysis of neopentane in the presence of other added alkanes (2-methylpentane, 3-methylpentane, methylcyclopentane) are used to calculate absolute rate coefficients of the hydride transfer reactions between the $t\text{-}C_4D_9^+$ ion and these compounds; the values determined are in good agreement with those measured by other techniques. The unique feature of the competitive method described here consists of the fact that the positive ion which is neutralized can be identified by the conventional analysis of a known reaction product.

**13176.** Sieck, L. W., Gorden, R., Jr., Ausloos, P., **Energy-dependent ring opening of cycloalkane parent ions,** *J. Amer. Chem. Soc.* **94,** No. 20, 7157-7159 (Oct. 4, 1972).

Key words: Cycloalkanes; ion-molecule reactions; isomerization; mass spectrometry; photoionization; proton transfer reactions.

In contradiction to a previously held view it is demonstrated that cyclopropane parent ions do undergo ring opening. The extent of ring opening depends on the internal energy content of the ion. It is shown that the cyclic ion reacts with $NH_3$ in the following manner

$$c\text{-}C_3D_6^+ + NH_3 \rightarrow CD_2H_2N^+ + C_2D_4H \rightarrow CD_2H_3N^+ + C_2D_4$$

while the linear $C_3D_6^+$ ion reacts exclusively by deutron transfer

$$C_3D_6^+ + NH_3 \rightarrow C_3D_5 + NH_3D^+$$

The total rate constant for reaction of the $C_3D_6^+$ ions formed by photoionization of cyclopropane-$d_6$ is independent of the internal energy content ($k_{total} = 9.4 \pm 0.4 \times 10^{-10}$ cm³/molecule-sec). However, the relative rates of reactions 1, 2, and 3 are strongly dependent upon the photon energy [$k_3/(k_1+k_2) = 0.18$ and 0.75 at 10 and 11.6 – 11.8 eV respectively]. Additional experiments performed on $C_3D_6 - CH_3OH$ mixtures support the view that the fraction of the $C_3D_6^+$ ions which transfer a deuteron to $NH_3$ is representative of the fraction of acyclic $C_3D_6^+$ in the system.

**13177.** Ausloos, P. J., Lias, S. G., **Photochemistry in the far ultraviolet,** *Annu. Rev. Phys. Chem.* **22,** 85-107 (1971).

Key words: Absorption and emission spectroscopy; far (vacuum) ultraviolet; ion-molecule reactions; matrix isolation; photochemistry; photoionization; reaction kinetics; thermodynamic.

The 1969-70 literature relating to far ultraviolet photochemistry has been reviewed. In the limited space allocated to this chapter, the more relevant and controversial developments are confronted. An attempt is made to relate information from various sources in order to obtain a comprehensive view of the entire field.

**13178.** Sieck, L. W., Ausloos, P., **Reactions of the acetone cation. Implications for the radiolysis of acetone,** *Radiat. Res.* **52,** No. 1, 47-58 (Oct. 1972).

Key words: Acetone; energy transfer; ion-molecule reactions; mass spectrometry; radiolysis.

The reactions of the acetone and acetyl cation with acetone have been investigated in a photoionization mass spectrometer. Reaction of the acetone cation with ≦ 0.3 eV internal energy occurs essentially at every collision ($k = 8.4 \times 10^{-10}$ ml/molecule sec), but decreases slightly with an increase in internal energy. Two reaction channels are observed for the acetone cation: (a) $CH_3COCH_3^+ + CH_3COCH_3 \rightarrow (CH_3)_2COH^+ + CH_3COCH_2$ and (b) $CH_3COCH_3^+ + CH_3COCH_3 \rightarrow CH_3COCH_3COCH_3^+ + CH_3$. The $CH_3CO^+$ ion reacts mainly as follows: $CH_3CO^+ + CH_3COCH_3 \rightarrow CH_3 \cdot COCH_3COCH_3^+$ ($k \cong 4.6 \times 10^{-10}$ml/molecule sec). At pressures above $10^{-3}$ torr $(CH_3)_2COH^+$ and $CH_3COCH_3COCH_3^+$ reacts further with acetone to produce $(CH_3COCH_3)_nH^+$. It is suggested that in liquid phase radiolysis experiments the acetone cation will react within $10^{-12} - 10^{-13}$ sec. Recent radiolysis experiments in which acetone was used as a solvent are discussed in the light of this premise.

**13179.** Allen, J. H., Bender, P. L., **Narrow line rubidium magnetometer for high accuracy field measurements,** *J. Geomagn. Geoelec.* **24,** No. 1, 105-125 (1972).

Key words: Geomagnetism; magnetometer; optical pumping.

Observations of Zeeman transitions in $Rb^{87}$ vapor can be us to make accurate measurements of the earth's magnetic field pı vided that the resonance lines are narrow enough so that t separate components of the transitions are resolved Howev the resulting relatively low signal-to-noise ratio makes it diffic to follow rapid changes in the field. Self-oscillating magneton ters have rapid response to magnetic field changes and high se sitivity, but poor long-term stability. The advantages of both a proaches can be obtained with a compound magnetometer which a self-oscillating magnetometer is locked with a long tir constant to a narrow and well-resolved Zeeman transition. V designed and built two prototype optically pumped Rl magnetometers of this kind, and carried out a stability test them. Half-hour means of the magnetic field difference betwe the two were obtained for a period of nine and a half days. Dı ing this time local magnetic field activity ranged from quiet disturbed and a sudden commencement occurred. The standa deviation of the individual half-hour difference values was 0. γ (= 0.02 nanoteslas, or 0.2 microgauss).

**13180.** Goldman, D. T., **Properties of nuclides,** Section 8b *American Institute of Physics Handbook, Third Edition,* D. Gray, Ed., pp. 8-6–8-91 (McGraw-Hill Book Co., Ne York, N.Y., 1972).

Key words: Absorption cross section; magnetic momeı mass defect; nuclides; quadrupole moment; *q*-values; radi tion.

All known nuclides both stable and radioactive are list together with the following properties where measured or a propriate: mass defect; half-life or abundance; magnetic m ment; quadrupole moment; type of radioactive decays and ene gies associated with them; thermal neutron activation cross se tion. Data available through 1968 have been used in prepari the Table.

**13181.** Haber, S., **On the existence of simple quadratures,** *Mic Math. J.* **19,** 401-410 (1972).

Key words: Approximation theory; conditional conve gence; infinite series; integration; quadrature; simpl quadratures.

If $S$ is a set of functions that are Riemann integrable on [0,1 and a formula

$$\int_0^1 f(x)dx = \sum_{i=1}^{\infty} a_i f(x_i),$$

holds for every $f \in S$ – with the $a_i$ and $x_i$ fixed complex number independent of $f$, and the $x_i$ all distinct – then the formula called a "simple quadrature for $S$". It is known that there is ı simple quadrature for the set of all functions continuous ( [0,1]; in this paper simple quadratures are constructed for ce tain large classes of continuous functions.

**13182.** Greenspan, M., **Acoustic properties of liquids,** Section in *American Institute of Physics Handbook, Third Edition,* I E. Gray, Ed., pp. 3-86–3-98 (McGraw-Hill Book Co., Ne York, N.Y., 1972).

Key words: Absorption; acoustics; attenuation; liquid sound; speed of sound; velocity of sound.

Values of the speed and attenuation of sound in selecte liquids, taken from the literature, are presented in a way which i lustrates the systematics. References to major compilations aı given.

**13183.** Coxon, B., **Proton magnetic resonance spectroscopy: Pa I,** Chapter in *Advances in Carbohydrate Chemistry an* *iochemistry*, **27,** 7-83 (Academic Press, New York, N.Y., 972).

Key words: Carbohydrates; Fourier transforms; instrumentation; iterative analysis of spectra; non-equivalence; proton magnetic resonance spectroscopy; superconducting solenoids.

ecent applications of proton magnetic resonance spectrosco- to the analysis of carbohydrates are discussed with particular phasis on the use of superconducting solenoids.

mprovements in magnets, probes, signal-averaging systems l spectrometer consoles are described and also the advantages ısing a variety of field frequency stabilization techniques and omatic control and data acquisition.

)etailed discussions of pulse-Fourier transform techniques l of computerized literature analysis of spectra are given.

84. Smith, R. L., Russell, T. W., Case, W. E., Rasmussen, A. .., **A calorimeter for high-power CW lasers,** *IEEE Trans. nstr. Meas.* **IM-21,** No. 4, 434-438 (Nov. 1972).

Key words: Calorimetry; laser; laser calorimetry; laser energy measurement; laser power measurement.

calorimeter is described that can measure megajoules of er energy from CW lasers whose output wavelength is in the ion from 1 to 11 μm. The calibration of this device is tracea- to NBS electrical standards. This calorimeter can measure al energies from $3 \times 10^4$ to $10^7$ J. The laser power range this ice can handle ranges from 300 to 100 000 W.

85. Jones, M. C., **Computed total radiation properties of com- ressed oxygen between 100 and 1000 K,** *Int. J. Heat Mass ransfer* **15,** No. 11, 2203-2215 (Nov. 1972).

Key words: Computations; oxygen; thermal radiation properties.

he total emissivity, total band absorptance and Planck mean orption coefficient of compressed oxygen have been com- ed in the temperature range 100-1000 K. Computations were ed on published data for the spectral absorption coefficient l extrapolations above and below room temperature were per- med in accordance with published theory. It was found possi- to represent all of the total band absorptance results with a -parameter correlation.

86. Negas, T., **The $Ba_{1-y}Sr_yMnO_{3-x}$ system,** *J. Solid State hem.* **6,** 136-150 (1973).

Key words: Alkaline earth oxides; nonstoichiometry; oxidation-reduction; phase equilibria; transition-metal oxides.

ubsolidus phase relations at ambient atmospheric pressure l elevated temperatures in the $Ba_{1-y}Sr_yMnO_{3-x}$ system were estigated by quenching, gravimetric, and x-ray diffraction thods. The system is not binary above ~ 1035 °C because of ctions with atmospheric oxygen. The air isobar, $P_{O_2} = 0.2$ atm. s characterized at 1225, 1375, 1490, and 1610 °C. Seven ox- n-deficient phases including a perovskite phase characterize system. Their stability depends on the values of *y* and *x* in $_{1-y}Sr_yMnO_{3-x}$. The cell dimensions of these phases expand as ıcreases at fixed *y*. These seven modifications can be retained toichiometric form by oxidation at lower temperatures.

87. Fuller, E. G., **Photonuclear physics, 1971,** *Proc. 5th Int. etatron Symp., Bucharest, Romania, Oct. 18-23, 1971,* pp. 97-205 (Institute for Atomic Physics, Bucharest, Romania, ec. 1972).

Key words: Experiment; neutrons; nuclear; photons; photonuclear; protons; reactions; theory.

A brief review is given of the present status of the photonuclear physics field. Recent new experimental data are described both in their historical context as well as in the light of recent theoretical work. Present trends in the field are indicated particularly with regard to new facilities and new techniques and their implication with regard to future experimental measurements and theoretical attempts to explain the data.

13188. Spencer, L. V., Simmons, G. L., **Improved moment method calculations of gamma-ray transport: Application to point isotropic sources in water,** *Nucl. Sci. Eng.* **50,** 20-31 (1973).

Key words: Gamma ray penetration; moments method; point gamma source in water; polynomial approximation; radiation transport; truncation error.

Estimated error bounds derived from polynomial calculations have been used to revise the truncation error estimates of published data on gamma-ray penetration in water. It is also shown that more efficient use of moment data is possible to obtain greater accuracy in specific penetration regions and to extend the accuracy of polynomial calculations to greater penetrations. The results also indicate that in addition to the asymptotic power law, data to perhaps 40 mean-free-paths may be needed to make accurate extrapolations to arbitrarily great penetrations.

13189. Unassigned.

13190. Turner, J. E., Dutrannois, J., Wright, H. A., Hamm, R. N., Baarli, J., Sullivan, A. H., Berger, M. J., Seltzer, S. M., **The computation of pion depth – dose curves in water and comparison with experiment,** *Radiat. Res.* **52,** 229-246 (1972).

Key words: Depth dose; dosimetry; ionization chambers; pions; radiobiology; transport calculations.

A Monte Carlo program has been written for calculating absorbed dose as a function of position in a water target irradiated by beams of pions ($\pi^+$ and $\pi^-$). The incident pions can have an arbitrary energy spectrum, at present limited to 125 MeV, this energy including most beams that have been used in radiobiological experiments. The presence of muons and electrons, which contaminate pion beams in practice, is also included. The incident particles may enter the target at any point and with any direction of travel. Calculations can thus be made for nonparallel, nonuniform beams. The size of cylindrical volumes in the target over which the absorbed energy is averaged can be varied to simulate the use of detectors of various dimensions. The calculations include pion-nucleus interactions, multiple coulomb scattering, pion and muon decay at rest, as well as the transport and further interactions of secondary protons and neutrons. Good agreement is obtained between calculated and measured depth-dose curves with $\pi^+$ and $\pi^-$ beams from the 600 MeV Synchrocyclotron at CERN. The program will be used to study various factors that affect the dose and LET patterns that can be obtained with realistic pion beams.

13191. Rains, T. C., Menis, O., **Determination of submicrogram amounts of mercury in standard reference materials by flameless atomic absorption spectrometry,** *J. Ass. Offic. Anal. Chem.* **55,** No. 6, 1339-1344 (Nov. 1972).

Key words: Flameless atomic absorption; liver and coal; loss of mercury; mercury in orchard leaves; standard reference materials.

In a study of the flameless atomic absorption method for the determination of nanogram amounts of mercury in organic materials, the technique was improved to provide greater precision and accuracy. The loss of mercury during the digestion of organic materials with nitric, sulfuric, and perchloric acids is prevented by controlled heating and a packed refluxing column. The reduction and absorption system was simplified by using a heated absorption cell which alleviates the interference of volatile vapors. This method has been applied to the determination of mercury in NBS standard reference materials of orchard leaves, liver, and coal, and the results were compared with results obtained with two other analytical methods.

**13192.** Maienthal, E. J., Taylor, J. K., **Electrochemical techniques in water analysis,** Chapter 32 in *Water and Water Pollution Handbook,* L. L. Ciaccio, Ed., **4,** 1751-1800 (Marcel Dekker, Inc., New York, N.Y., June 1972).

Key words: Amperometry; chronopotentiometry; conductivity; coulometry; electrochemical analysis; polarography; potentiometry; water analyses; water pollution.

The uses of a variety of electrochemical methods of water analysis are described. The improved accuracy, sensitivity, selectivity, and ease of automation make these techniques the prime choice in many analytical problems concerned with water pollution and water analyses. The principles and applications of such methods as conductivity, potentiometry, amperometry, coulometry, chronopotentiometry, and polarography are discussed.

**13193.** Horn, W. A., **Single-machine job sequencing with treelike precedence ordering and linear delay penalties,** *SIAM J. Appl. Math.* **23,** No. 2, 189-202 (Sept. 1972).

Key words: Decision networks; minimum delay programs; network; network optimization; optimal sorting; sorting networks.

The problem treated is one of job sequencing on a single machine, where there is a precedence ordering between certain of the jobs, as given by a directed network which is a tree or a set of disjoint trees (a forest). The jobs form the nodes of the forest. The rule of precedence states that no job may be done before all those preceding it in its particular tree have been finished, and a job schedule is allowable if it obeys this rule. A penalty is assigned to each allowable schedule and is defined as the sum of delays for jobs, each multiplied by a number which represents the "value" or importance of that job. All delays are measured from time 0. Simple algorithms are given to find an allowable solution with minimum penalty in the two cases where all precedence relations in each tree go "inward," toward the root, or "outward," away from the root (where the root is a particular tip node of the tree).

**13194.** Weisman, I. D., Bennett, L. H., Maxwell, L. R., Sr., Woods, M. W., Burk, D., **Recognition of cancer in vivo by nuclear magnetic resonance,** *Science* **178,** 1288-1290 (Dec. 22, 1972).

Key words: In vivo; mouse; nuclear magnetic resonance; relaxation time; tumor.

Pulsed nuclear magnetic resonance has been used to differentiate in vivo between normal mouse tail tissue and a malignant transplanted melanoma, S91, located on the tail. The tumor displayed a nuclear (proton) spin-lattice relaxation time of ~ 0.7 second contrasted with the simultaneously measured normal tail tissue relaxation time of ~ 0.3 second.

**13195.** Kuriyama, M., **The dynamical scattering amplitude of an imperfect crystal. II. A relation between Takagi's dynamical equation and a more exact dynamical equation,** *Acta Crystallogr.* **A28,** Part 6, 588-593 (Nov. 1972).

Key words: Dynamical diffraction; imperfect crystal; scattering matrix.

A basic equation of dynamical diffraction for an imperfe
crystal is derived based on a general dynamical theory of diffra
tion. This equation is given in the form of a differential equatio
and therefore can be considered to describe the diffracti
processes locally inside a crystal. A phenomenological i
terpretation of this equation helps to fill in the gap betwe
modern quantum mechanical treatments and ordinary treatmer
by dynamical theory of diffraction for a perfect crystal. In the a
proximation of poor resolution the more exact equation reduc
to Takagi's equation. A necessary condition which mak
Takagi's equation valid leads to the concept of local reciproc
lattice vectors.

**13196.** Reader, J., Epstein, G. L., **Analysis of the spectrum**
**doubly ionized rubidium (Rb III),** *J. Opt. Soc. Amer.* **62,** N
12, 1467-1476 (Dec. 1972).

Key words: Rubidium; spectra; ultraviolet; wavelength
Zeeman effect.

The spectrum of Rb III has been observed in a sliding-spa
discharge with the NBS 10.7-m normal-incidence vacuum spe
trograph, and in an electrodeless discharge in a magnetic fie
with the NBS 10.7-m Eagle spectrograph in air. The analysis h
yielded most of the levels of the $4p^44d$, $4p^45s$, and $4p^4$
configurations. The $4p^45p$ levels and the $4s^24p^44d+4s^24p^45s$
$4s4p^6$ group of levels have been theoretically interpreted, wi
configuration interaction included. The energy parameters dete
mined from a least-squares fit to the observed level values a
compared with Hartree-Fock calculations. The ionization ene
gy is estimated to be 39.0 ± 0.3 eV.

**13197.** Sadowski, W. L., Lozier, D. W., **Use of Olver's algorith**
**to evaluate certain definite integrals of plasma physics involvi**
**Chebyshev polynomials,** *J. Comput. Phys.* **10,** No. 3, 607-6
(Dec. 1972).

Key words: Asymptotic solutions; Chebyshev polynom
als; difference equations; evaluation of integrals; numeric
stability; Olver's algorithm; plasma physics; recurren
relations.

The paper presents three methods of evaluating a sequence
definite integrals involving Chebyshev polynomials of the fir
kind. The integrals arise in a nonlinear plasma physics proble
It is shown that the first algorithm suffers such a loss of precisi
that the computed sequence diverges. The second algorith
yields results that lose all significance for higher terms in t
sequence, although the sequence does not diverge.

The problem is then formulated in terms of a three-term i
homogeneous recursion. Asymptotic analysis shows that neith
forward nor backward recursion is stable. Olver's algorithm pr
vides a method with an a-priori error bound for calculating t
sequence of integrals.

Tables of values obtained by the three methods are compare

**13198.** Evenson, K. M., Mizushima, M., **Laser magne**
**resonance of the $O_2$ molecule using 119- and 78-$\mu$m $H_2O$ las**
**lines,** *Phys. Rev. A* **6,** No. 5, 2197-2204 (Dec. 1972).

Key words: $H_2O$ laser; laser magnetic resonance; las
spectroscopy; $O_2$; 119; 78 $\mu$m.

Laser magnetic resonance of the $O_2$ molecule is observ
using the 119- and 78-$\mu$m lines of the $H_2O$ laser. The releva
transitions for the 119-$\mu$m line are $(N=13, J=14, M) \rightarrow (N$
$15, J=14, M')$, and those for the 78-$\mu$m line are $(N=21, J=2$
$M) \rightarrow (N=23, J=22, M')$, where $M'=M$ or $M \pm 1$ dependi
on the polarization. It is found that $g_\perp = 2.0044 \pm 0.0008$, $g$
$2.0020 \pm 0.0001$, $g_n = 0.000125 \pm 0.000008$ give slightly bett

ement between theory and experiment than Hendrie and ch's values ($g_\perp = 2.005169$, $g_z = 2.001939$, $g_n = 0.000122$) Bauer, Kamper, and Lustig's values ($g_\perp = 2.004838$, $g_z =$ 2025, $g_n = 0.000126$), but the present experimental accuracy ot high enough to exclude these older g-factor values. Using existing microwave data and the known laser frequencies, the -field frequencies for the transitions $(N = J = 13) \rightarrow (N = J =$ and $(N = J = 21) \rightarrow (N = J = 23)$ are found to be 2496.283 ± and 3865.81 ± 0.03 GHz, respectively. Combining these lts with the frequency of the $(N = J = 1) \rightarrow (N = J = 3)$ transi- obtained by McKnight and Gordy, we obtain $B_0 =$ 00518 ± 0.000020 GHz, $B_1 = -0.14496 \pm 0.00030$ MHz, $B_2 = -0.17 \pm 1.00$ Hz.

9. Boyle, D. R., Clague, F. R., Reeve, G. R., Wait, D. F., anda, M., **An automated precision noise figure measurement stem at 60 GHz,** *IEEE Trans. Instrum. Meas.* **IM-21,** No. 4, 3-549 (Nov. 1972).

Key words: Analysis; automation; noise figure; Y-factor.

s part of a millimeter-wave development program at the Na- al Bureau of Standards, a precision measurement method system was devised to automatically measure the effective t noise temperature of 55-65-GHz receivers.

alient features of the system include a bolometric Y-factor surement, a working "hot" noise source consisting of a eguide argon gas tube mount developed at the National Bu- of Standards, and a minicomputer system controller operat- n Basic. System design considerations and measurement un- ainties are discussed.

00. Jennings, D. A., Keller, R. A., **Detection of trace amounts sodium by fluorescence emission excited by a continuous wave ganic dye laser,** *J. Amer. Chem. Soc.* **94,** 9249 (1972).

Key words: Analytical; cw organic dye laser; fluorescence; laser; sodium vapor.

cw organic dye laser was used to excite fluorescence in nic sodium vapor. Fluorescence was visible at 80 °C, which esponds to a vapor pressure of $1.5 \times 10^{-8}$ mm of Hg. The centration of sodium atoms at this pressure is 16 fg/cm$^3$ or $\times 10^8$ molecules/cm$^3$. Measurements were actually made in olume of approximately a mm$^3$, which corresponds to 0.016 r $4.2 \times 10^5$ molecules.

01. Chappell, S. E., Humphreys, J. C., **The dose-rate response a dye-polychlorostyrene film dosimeter,** (Proc. Annual Conf. n Nuclear and Space Radiation Effects, Seattle, Wash., July 4-27, 1972), *IEEE Trans. Nuclear Science* **NS-19,** No. 6, 75-180 (1972).

Key words: Absorbed dose; dye-polychlorostyrene film dosimeter; high-intensity pulsed electron source; thin aluminimum calorimeters; $^{60}$Co gamma-ray source.

he responses of dye-polychlorostyrene film dosimeters are npared at low (~ $10^3$ rad/sec) and high (~ $10^{15}$ rad/sec) dose s. Low dose rate exposures were obtained with a $^{60}$Co ma-ray pool source, and high dose rates were obtained with gh-intensity, pulsed electron source. The dosimeter is a solid ition of polychlorostyrene and malachite green methoxide ch changes color upon irradiation. Two broad absorption ks appear in the visible region with maxima at about 425 and nm. The change in optical density of the 625-nm peak was nitored and correlated to the absorbed dose received by the imeters. At low dose rates, the source output was determined the basis of a previous calibration with a carbon calorimeter a cavity ionization chamber; at high dose rates, a thin imeter calibration system was employed. The calibration system has as its primary measuring elements aluminum calorimeters whose temperatures after exposure were monitored by chromel-constantan thermocouples. Associated electronics recorded the outputs of the thermocouples at every 0.1 sec. In the two cases, the dosimeters were exposed in a different but homogeneous medium, carbon or polystyrene at the low dose rates and aluminum at the high dose rates. In addition, Monte Carlo calculated stopping power ratios of the dye-film dosimeter to the medium were required to interpret the dose received by the dosimeters. The results indicate that there is no significant difference in the response at the two different rates.

**13202.** Lide, D. R., Jr., Johnson, D. R., Sharp, K. G., Coyle, T. D., **Microwave spectrum and barrier to internal rotation in $CF_3SiF_3$,** *J. Chem. Phys.* **57,** No. 9, 3699-3703 (Nov. 1, 1972).

Key words: Barrier to internal rotation in $CF_3SiF_3$; microwave spectrum; torsional mode.

The microwave spectrum of $CF_3SiF_3$ has been analyzed. The ground-state constants are $B_0 = 1328.464 \pm 0.001$ MHz, and $D_J = 0.09 \pm 0.05$ kHz. An extensive series of torsional satellite lines has been studied in some detail. The barrier to internal rotation is found to be $489 \pm 50$ cm$^{-1}$, corresponding to a torsional frequency of $37.0 \pm 2.0$ cm$^{-1}$. The lowest degenerate rocking mode has been determined as $158 \pm 12$ cm$^{-1}$. Other vibrational fundamentals are discussed.

**13203.** Ogburn, F., Smit, J., **Fluorescent x-ray methods for the measurement of coating thickness,** *Plating,* pp. 149-152 (Feb. 1973).

Key words: Coating thickness; electroplating; fluorescent x rays; thickness: x-ray spectrometry.

The use of x-ray spectrometry to measure the thickness of electroplated coatings is outlined. Sources of errors are calibration standards, dead time of x-ray detector and associated electronics, deformation of specimen, nonuniformity of coating thickness, background radiation, polychromaticity of x-ray source, density variations, metallic impurities, and excitation of characteristic radiation of coating material by characteristic radiation from substrate material. Techniques of minimizing these errors are discussed.

**13204.** Fatiadi, A. J., **The mechanism of formation of tris(phenylhydrazones) on treatment of cyclohexane-1,3-diones with phenylhydrazine,** *Carbohydrate Res.* **25,** 173-186 (Dec. 1972).

Key words: Cyclohexane-1,3-dione; formation; free-radical; ionic; mechanism; phenylhydrazine.

Treatment of the enolic cyclohexane-1.3-diones in aqueous acetic acid with an excess of phenylhydrazine at room temperature gave mixtures of the corresponding 2-oxo-1,3-bis(phenylhydrazone) and tris(phenylhydrazone) derivatives in low to moderate yield. E.s.r. study of the reaction path indicated that free-radical anionic intermediates are partially involved. Treatment of an enolic cyclohexane-1,2-dione (or of α-hydroxy or α-acetoxycyclohexanones) with phenylhydrazine gave mixtures of the corresponding mono- and bis(phenylhydrazones); formation of radical-anions was also observed in these reactions.

**13205.** Miller, R. C., Kidnay, A. J., Hiza, M. J., **Liquid-vapor equilibria at 112.00 K for systems containing nitrogen, argon, and methane,** *AIChE J.* **19,** No. 1, 145-151 (Jan. 1973).

Key words: Argon; binary system; excess Gibbs energy; liquid-vapor; methane; nitrogen; phase equilibria; ternary system.

Liquid-vapor phase equilibria measurements were made at 112.00 K on the binary systems nitrogen-argon, nitrogen-methane, and argon-methane and the ternary system nitrogen-argon-methane. Values of $g^E$, the excess Gibbs free energy, have been calculated from the experimental data for all the systems studied. The data and derived $g^E$ values for the binary systems were compared with the results of previous investigations with satisfactory agreement.

**13206.** Krauss. M., Neumann, D., Wahl, A. C., D̄as, G., Zemke, W., **Excited electronic states of $O_2^-$,** *Phys. Rev. A* **7,** No. 1, 69-77 (Jan. 1973).

Key words: Adiabatic correlation; asymptotic states; configuration interaction; correlation energy; excited states; multiconfiguration self-consistent field; $O_2^-$.

Excited electronic states of the $O_2^-$ molecule have been calculated with configuration-interaction (CI) variational trial functions that assure formally correct asymptotic behavior as well as the single-configuration self-consistent-field (SCF) approximation. CI results were obtained by both multiconfiguration self-consistent-field (MC-SCF) and pseudonatural orbital (PNO) techniques. The MC-SCF results are most accurate and are used to analyze the energy curves and wave functions of these states for internuclear separations larger than 3 a.u. All the excited states are found to have equilibrium-internuclear separations at least 1 a.u. larger than the ground state. The two lowest energy states, the $^4\Sigma_u^-$ and $^2\Pi_u$, are characterized, respectively, as shape and valence Feshbach resonances. They are sufficiently bound to make it likely they play a role in low-energy-electron scattering by oxygen.

**13207.** Zalubas, R., Borchardt, B. R., **Energy levels of neutral praseodymium (Pr I),** *J. Opt. Soc. Amer. Letters to Editor* **63,** No. 1, 102-103 (Jan. 1973).

Key words: Atomic energy levels; first spectrum of praseodymium (Pr I); spectrum.

The spectrum of atomic praseodymium has been observed with variety of light sources and spectrographs. The Zeeman effect has also been recorded. Three levels of $4f^36s^2\ ^4I°$ ground term and 62 even high levels of Pr I have been found.

**13208.** Mauer, F. A., Hahn, T. A., **Thermal expansion of some azides by a single crystal x-ray method,** (Proc. AIP Conf. on Thermal Expansion, Corning, N.Y., Oct. 27, 1971), Chapter in *Thermal Expansion,* M. G. Graham and H. E. Hagy, Eds., No. 3, 139-150 (1972).

Key words: Azides; thermal expansion.

A modification of the Bond technique is used to measure the lattice constants of small crystals with an error of a few parts in $10^5$ throughout the temperature range − 180 to 325 °C. Temperature calibration has been investigated and the results of thermal expansion measurements on $KN_3$ and $Ba(N_3)_2$ are reported.

**13209.** Hahn, T. A., Kirby, R. K., **Thermal expansion of fused silica from 80 to 1000 K – Standard Reference Material 739,** (Proc. AIP Conf. on Thermal Expansion, Corning, N.Y., Oct. 27, 1971), Chapter in *Thermal Expansion,* M. G. Graham and H. E. Hagy, Eds., No. 3, 13-24 (1972).

Key words: Fused silica; standard reference material; thermal expansion.

Fused silica is the second of a series of materials to be certified as thermal expanion standards by the National Bureau of Standards. The results of tests of five samples indicate the stock to be consistent quality suitable for certification as Standard Reference Material 739. The same interferometer apparatus w used as in the certification of copper SRM 736. Expansivi values from each of the five samples were fitted using a lea squares third order spline polynomial with three separate ter perature intervals. The data from all the samples were th pooled and fit with the same type spline polynomial. Values ca culated from these equations and their integrals are present and also compared to literature data on fused silica.

**13210.** Huebner, R. H., Mielczarek, S. R., Kuyatt, C. E **Electron energy-loss spectroscopy of naphthalene vapor,** *Che Phys. Lett.* **16,** No. 3, 464-469 (Oct. 15, 1972).

Key words: Electron energy-loss spectroscopy: naphth lene vapor: Rydberg states: oscillator strength.

The naphthalene energy-loss spectrum from 3 to 16 eV ol tained for 100 eV incident electrons closely resembles photoal sorption results. The need to include Rydberg configurations f any theoretical analysis of the spectrum is emphasized. The da yield an integrated oscillator strength of 8.6 below 15.1 eV.

**13211.** Wachtman, J. B., Jr., Dundurs, J., **Large localized surfa stresses caused by thermal expansion anisotropy,** *J. Ame Ceram. Soc. Discussion and Notes* **54,** No. 10, 525-526 (Oc 1971).

Key words: Grain size; Griffith equation; Petch equatio thermal expansion anisotropy; strength; surface stress.

The stress in the surface of a polycrystalline solid arising fro thermal expansion anisotropy is calculated from a model of a elastic sphere in a homogeneous material. The results depen strongly on the distance of the sphere from the surface and suggest that the usual calculation, which ignores the effect of th surface, seriously underestimates this stress.

**13212.** Eisen, H., Rosenstein, M., Silverman, J., **Electron deptl dose distribution measurements in two-layer slab absorber** *Radiation Res.* **52,** No. 12, 429-447 (Dec. 1972).

Key words: Depth-dose; dose distribution; dosimetry; dy film; electron beams; film dosimeter; interfaces; Monte Ca lo; radiochromic dyes; two-layer slabs.

Electron depth-dose distribution measurements were mad using the Chalkley-McLaughlin dye film dosimeter in two-lay slab absorbers of polystyrene-copper, polystyrene-tin, and al minum-gold. A plane-parallel 2.0-MeV electron beam was use Data were obtained for 12 cases by varying the location of the interface and by reversing the order of the slab component Reproducibility of the measurements was ±6 percent ($2\sigma$). A investigation of stopping-power ratio evaluation methods base on the treatment of the film dosimeter as a nonperturbing cavit demonstrated that a constant value could be used for eac material in a two-layer absorber independent of the thickness c each layer. The error in absorbed dose determination introduce by the use of a constant value ranged up to 8 percent. A fil placed at the interface between the two components of the sla was used to estimate the dose at the interface surfaces. Corresponding theoretical calculations were made using a multilaye electron transport computer code developed by Berger. Agreement between the measured and the calculated doses was withi 10 percent for metal layers and within 15 percent fo polystyrene. The discrepancies for polystyrene can be attribute to the omission of energy loss straggling in the calculation.

**13213.** McNeil, M. B., Pearson, W. B., Bennett, L. H., Watson R. E., **Stabilization and chemical bonding in Zintl phases,** *J Phys. C* **6,** 1-10 (1973).

Key words: Chemical bonding; phase stabilization; pseudopotential; Zintl phases.

The factors affecting the formation of B32 Zintl phases are ex- ned. Evidence is presented that the pseudopotential effects cussed by others have not been shown to be essential, and t the structures must still be accounted for largely by geomet- factors.

**14.** Penner, S., Lightbody, J. W., Jr., Fivozinsky, S. P., Cran- ell, H., Hallowell, P. L., Finn, M., **Electron scattering studies f vibrator-spectrum nuclei,** (Proc. Int. Conf. on Nuclear tructure Studies Using Electron Scattering and Photoreac- ion, Sendai, Japan, Sept. 12-15, 1972), Paper in *Nuclear tructure Studies Using Electron Scattering and Photoreac- ion,* K. Shoda and H. Ui, Eds., **5,** 49-60 (Laboratory Report f Nuclear Science, Tohoku University, Tomizawa, Sendai, apan, 1972).

Key words: Anharmonic vibrators; electron scattering; form factors; quadrupole moments, vibrator nuclei, $^{52}$Cr, $^{110}$Pd, $^{114}$Cd, $^{116}$Sn.

nelastic electron scattering is being used to study vibrator- ctrum nuclei in the medium-A region. In many cases we find t the second $2^+$ ("two phonon") state is much more strongly ited than is predicted by the harmonic vibrator model. The pes and magnitudes of the form factors of these states can be ed by calculations based on an anharmonic model in which ing of one- and two-phonon wavefunctions is included. An eriment is underway to measure inelastic scattering form fac- s in $^{52}$Cr, $^{110}$Pd, $^{114}$Cd, and $^{116}$Sn. In all of these nuclei we find t the second $2^+$ state is strongly enhanced compared to the monic vibrator model prediction.

**15.** Clark, A. F., Tryon, P. V., **Material variability as mea- ured by low temperature electrical resistivity,** *Cryogenics* **12,** No. 6, 451-461 (Dec. 1972).

Key words: Aluminum alloys; cryogenic; electrical resistivity; low temperature; material variability; nickel alloy; stainless steels; statistics.

ow temperature electrical resistivity was used to determine material variability (a) between different manufacturers, (b) ween different heats from the same manufacturer, and (c) hin a given heat for Al 2024, Al-5 percent Mg alloys, Inconel 8, A286 stainless, and AISI 316. Generally, the coefficient of iation for solution annealed alloys ranged from 1.2 to 14 per- t between manufacturers, 0.8 to 5.1 percent between heats, 0.1 to 1.6 percent within a heat with stainless steels at the ends and Al 2024 at the high ends. The variability is in- ased if the material is in a precipitation-hardened condition. tatistical analysis suggests that the variability within a heat is -normal. It is also shown that precipitation increases the in- sic resistivity.

**16.** Bolz, L. H., Reneker, D. H., Yee, K. W., **Ultrasensitive ogarithmic picoammeter for exposure and dose measurement in lectron microscopy of polymer crystals,** *J. Phys. E* **5,** No. 11, 039-1041 (Nov. 1972).

Key words: Electron collection efficiency; electron microscope exposure meters; logarithmic picoammeter; polymer crystals; polymer electron microscopy; radiation damage to polymers.

Measurements of electron beam currents for determination of otographic exposure times and for determination of the radia- n dose to which the sample was subjected were facilitated by ogarithmic picoammeter which indicated currents as low as uld produce a useful image in a few seconds on a fast emul- n. Since the meter was logarithmic it also indicated the much her currents ordinarily used without a scale change. Calibration of the electron collection efficiency of the focusing screen used to collect the current enabled the actual current density at the sample to be determined.

**13217.** Caswell, R. S., Coyne, J. J., **Interaction of neutrons and secondary charged particles with tissue: Secondary particle spectra,** *Radiat. Res.* **52,** No. 3, 448-470 (Dec. 1972).

Key words: Energy deposition; microdosimetry; neutron interaction with tissue; secondary particle spectra.

Theoretical calculations have been made of the secondary particle spectra for $p$, $d$, $\alpha$, $^{9}$Be, $^{11}$B, $^{12,13,14}$C, $^{14,16}$N, and $^{16}$O produced by interactions of 1- and 14-MeV neutrons with a four-element tissue containing the elements H, C, N, O. Detailed neutron cross-section data have been used in the calculation. Both "initial" spectra of the secondary particles as produced by nuclear reactions and the "equilibrium" spectra produced by particles slowing down are determined. This work is the first step in development of a quantitative description of the "physical" stage in the action of neutron radiation on biological materials. The spectra are input information for energy deposition studies for neutron microdosimetry and for models of the biological action of neutron radiation.

**13218.** Kirchoff, W. H., Johnson, D. R., **An investigation of centrifugal distortion in the microwave spectrum of formamide,** *J. Mol. Spectrosc.* **45,** No. 1, 159-165 (Jan. 1973).

Key words: Astrophysical interest; centrifugal distortion; formamide; microwave spectrum; quadrupole splittings; rotational transitions; weighted fit.

Measurements of the microwave spectrum of formamide have been extended in order to account accurately for the effects of centrifugal distortion. A total of 22 new transitions involving $J \leq 29$ have been measured for $^{14}\mathrm{NH}_2{}^{12}\mathrm{CH}^{16}\mathrm{O}$ in the ground vibrational state. Combined with previous observations, these transitions have been fit to a model containing five quartic distortion terms and seven sextic terms with an rms deviation of 64 kHz. A large number of resolved quadrupole shifts were fit with an rms deviation of 42 kHz. The remainder of the spectrum for $J \leq 30$ has been calculated with standard deviations less than 3 MHz. Correct weighting of the observed transitions has been found to be important.

**13219.** Oettinger, F. F., Rubin, S., **The use of current gain as an indicator for the formation of hot spots due to current crowding in power transistors,** *Proc. 10th Annual IEEE Reliability Physics Symp., Las Vegas, Nev., Apr. 5-7, 1972,* pp. 12-18 (1972).

Key words: Current gain, hot spot detection; hot spots, current gain as indication of; power transistors, screening; screening for hot spots, transistors; thermal hysteresis, transistors; transistors, hot spot detection.

D-C current gain, $h_{FE}$, measured as a function of collector voltage, with the collector current held constant, is used as a nondestructive screening technique to indicate the formation of hot spots due to current crowding. Its correlation with and advantages over previously used techniques are described. Examples of the use of this technique are presented for a variety of transistor operating conditions.

**13220.** Edwards, J. C., Meijer, P. H. E., **Transition temperatures of systems with mixed ferro and antiferromagnetic coupling,** *Physica* **61,** 67-79 (1972).

Key words: Antiferromagnetism; Bethe constant-coupling; critical temperature; ferromagnetism; Heisenberg model; Ising model; next nearest neighbor interaction.

To study the influence of a mixture of ferromagnetic and antiferromagnetic couplings on the transition temperature of a spin-1/2 system we used the Bethe or constant-coupling method and applied it to two models: Model A, a system containing two types of atoms with different inter- and intra-spin coupling; Model B, a system which contains two antiferromagnetic sublattices that are ferromagnetically coupled. We find that for reasonable values of the parameters the Curie temperature has the tendency to increase when the antiferromagnetic coupling is present, at least for the models considered using Ising and anisotropic Heisenberg coupling. We also were able to develop an expression, based on Model B, for the critical temperature of a spin-1 system.

**13221.** Prince, E., Finger, L. W., **Use of constraints on thermal motion in structure refinement of molecules with librating side groups,** *Acta Crystallogr.* **B29,** 179-183 (Mar. 1973).

Key words: Constrained refinement; least-squares refinement; molecular crystal structures; molecular libration; rigid-bodies; thermal constraints.

Explicit formulae are derived which express, for molecules consisting of a rigid core to which side groups that are free to librate around a single bond are attached, the second and third cumulants of the scattering density function as functions of molecular translation and libration parameters. These formulae and their derivatives with respect to the molecular motion parameters have been incorporated into a least-squares refinement program which determines directly the values of the position and thermal-motion parameters which give the best fit to the observed data.

**13222.** Prince, E., Schroeder, L. W., Rush, J. J., **A constrained refinement of the structure of durene,** *Acta Crystallogr.* **B29,** 184-191 (Mar. 1973).

Key words: Barrier to rotation; conformation; crystal structure; durene; libration; methylbenzenes, methyl group; molecular structure; torsional oscillation.

The crystal structure of durene (1,2,4,5-tetramethylbenzene, $C_{10}H_{14}$) has been refined from three-dimensional, single-crystal neutron-diffraction data. The crystals are monoclinic, $a=11.57$, $b=5.77$, $c=7.03$ Å, $\beta=112.93°$, space group $P2_1/a$, $Z=2$. A conventional refinement, with anisotropic temperature factors and 485 independent, observed reflections measured with a four-circle diffractometer, gave a weighted residual $R$, on $F$, of 0.085, but the model contained some physically unreasonable thermal parameters. An alternative refinement in which the molecule was constrained to move as a rigid body, but with the methyl groups permitted to librate around the C – C bond, gave a weighted $R$ of 0.115. All differences in position parameters between the two models were small. All carbon atoms and 6 of the 14 hydrogen atoms in the molecule are essentially coplanar. The ring is somewhat distorted, with bond angles at the corners with no methyl groups of about 123° and those at the other corners of about 118.6°. The C – C bond length between two methylated corners is about 1.425 Å, compared with 1.395 Å for the other bonds in the ring. This long bond, combined with C – C – C bond angles of 121.5°, results in adjacent methyl groups being pushed apart. The methyl groups are in an eclipsed conformation. The eigenvectors of the L tensor correspond very closely to the axes of principal moments of inertia of the molecule. The hydrogen amplitudes derived from the refinement predict a methyl torsional frequency of 130 $cm^{-1}$, in satisfactory agreement with observed frequencies of 144 and 179 $cm^{-1}$. The whole molecule amplitudes and frequencies derived from the L and T components of the thermal ellipsoids are also generally consistent with spectroscopic results.

**13223.** Koyama, R. Y., Hughey, L. R., **Angular anisotropies the photoemission from polycrystalline gold,** *Phys. Rev. Le* **29,** No. 22, 1518-1521 (Nov. 27, 1972).

Key words: Emission angle; energy distributions; gold; i cidence angle; photoemission; polarization; polycrystalli film; synchrotron radiation.

Measurements of the photoelectron energy distributions frc gold indicate angular anisotropies of the emission even f evaporated films. In particular, relative intensities and positio of the *d*-band emission peaks depend on the electron emissi angle. We also observe the dependence of the energy distributi on the incidence angle and polarization of the photons.

**13224.** Brown, D. W., Wall, L. A., **High-temperature aging fluoropolymers,** *J. Polym. Sci.,* Part A-1, **10,** 2967-29 (1972).

Key words: Degradation; fluoro-elastomer; fluoropolyme tetrafluoroethylene.

Fluoropolymers including those of 3,3,3-trifluoroproper 2,3,3,3-tetrafluoropropene, 3,3,4,4,5,5,5-heptafluoropentene- and their copolymers with tetrafluoroethylene, were aged in and in its absence at 225 and 305 °C. Intrinsic viscosities we measured before and after aging. Polymers of hi tetrafluoroethylene content are most stable. In air the presen of tertiary hydrogens is associated with lowered stability but t presence of tetrafluoroethylene greatly mitigates this effe Stress-relaxation studies in air of a vulcanizate of 3,3 trifluoropropene and tetrafluoroethylene cured by $\gamma$-rays i dicate that the vulcanizate degrades much more rapidly than t untreated polymer.

**13225.** Crannell, H., Hallowell, P. L., O'Brien, J. T., Finn, J. Kline, F. J., Penner, S., Lightbody, J. W., Jr., Fivozinsky, P., **Electron scattering from low lying $2^+$ states in $^{14}C$,** (Proc. I Conf. on Nuclear Structure Studies Using Electron Scatteri and Photoreaction, Sendai, Japan, Sept. 12-15, 1972), Pap in *Nuclear Structure Studies Using Electron Scattering a Photoreaction*, K. Shoda and H. Ui, Eds., **5,** 375-384 (Labo tory Report of Nuclear Science, Tohoku Univers Tomizawa, Sendai, Japan, 1972).

Key words: Electron scattering; E2 excitations; transiti radii; $^{14}C$.

The excitation of levels below 12 MeV in $^{14}C$ has been vestigated at the National Bureau of Standards electron scatt ing facility. The target consists of 50 $mg/cm^2$ powdered mater enriched to 70 percent in $^{14}C$ contained between 0.025 mm foils. Spectra have been obtained for electron energies from to 120 MeV at scattering angles of 92.5, 127.5, and 145 degre Levels in $^{14}C$ at 6.09 ($1^-$), 6.59 ($0^+$), 6.73 ($3^-$), 7.01 ($2^+$), 8. ($2^+$), 10.43 and 11.35 MeV have been observed.

**13226.** Evenson, K. M., Wells, J. S., Petersen, F. R., Danielsc B. L., Day, G. W., Barger, R. L., Hall, J. L., **Speed of lig from direct frequency and wavelength measurements of t methane-stabilized laser,** *Phys. Rev. Lett.* **29,** No. 19, 134 1349 (Nov. 6, 1972).

Key words: Laser; light; methane-stabilized laser.

The frequency and wavelength of the methane-stabilized las at 3.39 $\mu m$ were directly measured against the respective prim ry standards. With infrared frequency synthesis techniques, obtain $\nu=88.376\,181\,627(50)$ THz. With frequency-controll interferometry, we find $\lambda=3.392\,231\,376(12)$ $\mu m$. Multiplic tion yields the speed of light $c=299\,792\,456.2(1.1)$ m/sec, agreement with and 100 times less uncertain than the previous epted value. The main limitation is asymmetry in the krypton 7-Å line defining the meter.

27. Evenson, K. M., Wells, J. S., Petersen, F. R., Danielson, . L., Day, G. W., **Accurate frequencies of molecular transi- ons used in laser stabilization: The 3.39-$\mu$m transition in $CH_4$ nd the 9.33- and 10.18-$\mu$m transitions in $CO_2$,** *Appl. Phys. Lett.* 2, No. 4, 192-195 (Feb. 15, 1973).

Key words: $CO_2$ and He-Ne laser frequency; methane; saturated absorption.

he frequencies of three lasers stabilized to molecular absorp- s were measured with an infrared-frequency synthesis chain ending upwards from the cesium frequency standard. The asured values are 29.442 483 315(25) THz for the 10.18-$\mu$m 0) transition in $CO_2$, 32.134 266 891(24) THz for the 9.33- $R(10)$ transition in $CO_2$, and 88.376 181 627(50) THz for the 9-$\mu$m $P(7)$ transition in $CH_4$. The frequency of methane, en multiplied by the measured wavelength reported in the fol- ing letter, yields 299 792 456.2(1.1) m/sec for the speed of t.

28. Barger, R. L., Hall, J. L., **Wavelength of the 3.39-$\mu$m laser- aturated absorption line of methane,** *Appl. Phys. Lett.* **22,** No. , 196-199 (Feb. 15, 1973).

Key words: Interferometry; laser; methane; saturated absorption; wavelength; wavelength standards.

he wavelength of the 3.39-$\mu$m line of methane has been mea- ed with respect to the $Kr^{86}$ 6057-Å standard by using a uency-controlled Fabry-Perot interferometer. We have ex- stively studied systematic offsets inherent in the experiment, uding effects due to asymmetry of the Kr standard line. king a convention relating the defined Kr wavelength 7.802 105 Å to observables of the krypton line (e.g., center gravity or fringe maximum intensity point), we report two hane wavelengths: $\lambda_{max\ I}=33\,922.314\,04$ Å and $\lambda_{cg}=33$ .313 76 Å. Both results have an uncertainty of $\delta\lambda=\pm 1.2\times$ Å or $\delta\lambda/\lambda=\pm 3.5\times 10^{-9}$. Multiplication by the frequency surement of the preceding letter gives the speed of light, $c_{cg}=$ 792 456.2(1.1) m/sec.

9. Ely, J. F., Hanley, H. J. M., **Analysis of the viscosity and cond virial coefficients of non-polar polyatomic gases using the -6-8 potential,** *Mol. Phys.* **24,** No. 3, 683-687 (Sept. 1972).

Key words: Nonspherical interactions; polarizability; m-6-8 potential; quadrupole moment; second virial coefficients; viscosity coefficient.

he viscosity and second virial coefficients were calculated $O_2$, $N_2$, and $CO_2$ using the m-6-8 potential. For the second al coefficients, the potentials were modified to allow for spherical effects by introducing the quadrupole-quadrupole quadrupole-induced dipole interactions. Independently mea- d values of the quadrupole moments and molecular polariza- ies were used without changing the spherical parameters as rmined by the viscosity coefficients. Agreement between ry and experiment over a wide temperature range is shown e satisfactory for the viscosity and improved for the second al coefficients.

30. Pigman, W., Isbell, H. S., **Mutarotation of sugars in solu- ons: Part I,** Chapter in *Advances in Carbohydrate Chemistry* , 11-57 (Academic Press, Inc., New York, N.Y., 1968).

Key words: Acyclic sugars; anomerization of sugars; kinetics of mutarotation reactions.

his paper is an invited chapter in the annual series "Ad- ces in Carbohydrate Chemistry." The principal facts concerning ring changes and the basis for the mutarotation reactions are reviewed; the basic kinetics are developed and the factors affecting the equilibrium of sugars in solution are discussed. Methods for studying mutarotation reactions are described and the authors' early measurements are summarized.

13231. Cook, R. K., **Generation and propagation of sound waves between the ionosphere and the lower atmosphere,** *Conf. Proc. No. 115 on Effects on Atmospheric Acoustic Gravity Waves on Electromagnetic Wave Propagation, Weisbaden, Germany, Apr. 17-21, 1972,* pp. 3-1–3-6 (AGARD of NATO, Neuilly Sur Seine, France, Nov. 1972).

Key words: Auroral; infrasound; ionosphere; microphones; sound waves.

Various physical processes generate sound waves at infrasonic frequencies (oscillation periods > 1.0 sec) in the lower atmosphere. Some typical sources are volcanic explosions, earthquakes, severe storms, and the shock waves from vehicles moving at supersonic speeds. In the ionosphere, sources of infrasound include auroral discharges and shock waves from satellites and meteorites moving at supersonic speeds. We present the results of an analysis for the generation of sound and propagation downwards due to the heating effects of auroral discharges, particularly those traveling at supersonic speeds in directions parallel to the earth's surface. The "shock" waves from such discharges are propagated steeply downward with very little loss of energy from absorption by viscosity and heat conduction, and are frequently observed at infrasonic stations located at high latitudes. An estimate of auroral heating is derived from the observed strengths of infrasound at the earth's surface.

13232. Miller, R. C., Kidnay, A. J., Hiza, M. J., **The solid + vapor and liquid + vapor phase equilibrium properties of neon + krypton,** *J. Chem. Thermodyn.* **4,** No. 6, 807-818 (Nov. 1972).

Key words: Krypton; melting line; neon; phase-equilibria.

A vapor-recirculation equilibrium cell was used to investigate the solid + vapor and liquid + vapor equilibria and the three-phase curve (equilibrium between solid, liquid, and vapor) for neon + krypton. Gas phase compositions were measured above solid krypton at 100.00, 110.00, and 115.00 K and at pressures to 95 atm (9.6 MPa). Both gas and liquid phase compositions were determined at 120.00, 130.00, 140.00, and 150.00 K at pressures to 106 atm (10.7 MPa). Comparison of cross second virial coefficients from the experimental gas phase results with values obtained from a corresponding states correlation indicate that a deviation parameter from the geometric mean mixing rule for energy parameters of approximately 0.23 is necessary to reconcile the experimental and predicted virial coefficients. Analysis of the Henry's law constants obtained from the liquid phase results indicates a deviation parameter of approximately 0.21.

13233. Weisman, H. M., **Reaching other people's minds through written language,** *Tech. Commun.* **20,** No. 1, 16-19 (1973).

Key words: Human communication; language; meaning; symbols; understanding; written language.

The process of communication is complicated, involving eight variables, and a message must be conveyed through symbols. With such complexity, it seems a wonder that communication ever takes place. By understanding the process, however, communicators may be able to do a better job. This article examines the process in some detail.

13234. Hanley, H. J. M., McCarty, R. D., Cohen, E. G. D., **Analysis of the transport coefficients for simple dense fluids: Ap-**

**plication of the modified Enskog theory,** *Physica* **60,** No. 2, 322-356 (Aug. 1972).

Key words: Excess transport property; modified Enskog theory; prediction of transport data; thermal conductivity; transport first density corrections.

The viscosity ($\eta$) and thermal-conductivity ($\lambda$) coefficients for argon, oxygen, and p-hydrogen have been calculated from the modified Enskog theory (i.e., the hard-sphere Enskog theory adapted to include experimental *PVT* data) and compared with experiment over a wide range of experimental conditions. Specifically, experimental data and theoretical predictions for the first density corrections, $\eta_1$ and $\lambda_1$, were examined and the temperature and density dependences of the experimental and theoretical transport coefficients in the liquid were studied. A brief comparison of the modified Enskog with some other theories is included. Overall, the modified Enskog theory, with the exception of the critical region for the thermal conductivity, is found to given reasonable agreement with experiment (to within about 10-15 percent) for densities generally not exceeding twice the critical density.

Qualitatively the theory does not distinguish between the viscosity and thermal conductivity in the liquid. This is discussed by comparing the experimental and theoretical derivatives $(\partial\Delta\eta/\partial T)_Q$ and $(\partial\Delta\lambda/\partial T)_Q$, where $\Delta\eta$ and $\Delta\lambda$ are excess functions. The qualitative features of the theory are discussed in some detail leading to a method by which the predictive capability of the theory can be improved.

**13235.** Ausloos, P., Rebbert, R. E., Sieck, L. W., Tiernan, T. O., **Experimental evidence for statistical randomization of hydrogen atoms in the ethyl cation,** *J. Amer. Chem. Soc. Communications to the Editor* **94,** No. 25, 8939-8941 (1972).

Key words: Alkyl halides; ethyl cations; 1,2-hydride shift; ion-molecule reactions; ionic structure; photoionization.

It is shown that the hydrogen atoms in the ethyl cations formed in the unimolecular decomposition of $CD_3CH_2I^+$, $CH_3CD_2I^+$, $CD_3CH_2Br^+$, $CD_3CH_2CD_3^+$, $CH_3CD_2CH_3^+$ and $CD_3CH_2CH_2CD_3$ are scrambled statistically at reactant gas pressures ranging from $10^{-5}$ to 1000 torr. Photon absorption (11.6-11.8 eV), electron impact and $^{60}Co$-$\gamma$ radiation have been used in the production of the ethyl cations. Two experimental approaches, kinetic mass spectrometry and chemical end product analysis, have been applied to this problem. The energy barrier for the 1,2-hydride shift in the ethyl cation is shown to be less than 5 kcal/mole.

**13236.** Hummer, D. G., Rybicki, G. B., **The formation of spectral lines,** Chapter in *Annual Review of Astronomy and Astrophysics* **9,** 237-270 (Annual Reviews, Palo Alto, Calif., 1971).

Key words: Plasma diagnostics; radiating gases; radiative transfer; spectral lines; transfer equation.

An introductory survey is given of the current theory of spectral line formation in optically thick systems.

**13237.** Kamper, R. A., **Cryoelectronics,** *Proc. Helium Society Symp., Washington, D.C., Mar. 23-24, 1970,* pp. 68-82 (1970).

Key words: Electronics; low temperature; measurements; superconductivity.

This talk reviews achievements and prospects in the application of superconductivity to electronics and measurement technique. There is a brief introduction to some of the unique properties of superconducting metals at very low temperatures, and a survey of recent developments in the areas of ma netometry, thermometry, infrared technology, amplifie switches, low level detectors and voltmeters, and the measu ment of fundamental constants. This is an exciting new field which many researchers have already made impressive achie ments.

**13238.** Souders, T. M., **Wide-band two-stage current transform of high accuracy,** *IEEE Trans. Instrum. Meas.* **IM-21,** No. 340-345 (Nov. 1972).

Key words: Current measurement, audio frequency; cu rent ratio measurement; current transformers, aud frequency; current transformers, precision; transforme amplifier-aided; transformers audio frequency curre transformers, calibration of; transformers, capacitive err trimming; transformers, precision current; transforme two-stage current.

The design and performance of two high-accuracy transfo mers, identified as amplifier-aided two-stage transformers, a described. Each operates from 50 Hz to 10 kHz, supporting bu dens up to 1 Ω. Self-contained ratios span from 5/5 to 100/5, wi a rated secondary current of 5 A.

Results indicate the errors at 10 kHz are within 30 and 15 pp for the respective transformers, decreasing to less than 1 ppm 1 kHz.

Analysis of high- and low-frequency errors is presented, well as a detailed description of a capacitance trimmi technique effecting a factor-of-ten reduction of capacitive error

Also described is a relatively simple step-up calibratio system for determining the transformer errors. Calibratio results are included.

**13239.** Eicke, W. G., Jr., Taylor, B. N., **Summary of internation comparisons of as-maintained units of voltage and values 2*e*/*h*,** *IEEE Trans. Instrum. Meas.* **IM-21,** No. 4, 316-31 (Nov. 1972).

Key words: As-maintained; international compariso Josephson effect; 2*e*/*h* measurements.

Using temperature-regulated transportable standard-cell en closures, the National Bureau of Standards (NBS), under th auspices of the Bureau International des Poids et Mesure (BIPM), during the period June 1971 through June 1972 has car ried out a series of direct comparisons of the units of voltage as maintained by NBS and BIPM, Sèvres, France; the Nationa Physical Laboratory, United Kingdom; the National Researc Council, Canada; the National Standards Laboratory, Australia and the Physikalisch-Technische Bundesanstalt, Germany. Th main purpose of these comparisons was to provide a sound basi for intercomparing values of 2*e*/*h* obtained at the various na tional laboratories via the ac Josephson effect in superconduc tors. It was found that when converted to a common unit of volt age, most measured values of 2*e*/*h* agreed with each other t within the 1 to 2 parts in $10^7$ estimated uncertainty (1 standar deviation) of the volt comparisons. This satisfying result woul seem to indicate that serious consideration should be given t adopting a single international value of 2*e*/*h* for use in maintaining units of voltage.

**13240.** French, B. M., Walter, L. S., Heinrich, K. F. J., Loman P. D., Jr., Doan, A. S., Jr., Adler, I., **Compositions of majo and minor minerals in five Apollo 12 crystalline rocks,** *NASA Spec. Publ. 306,* 142 pages (National Aeronautics and Spac Administration, Washington, D.C., 1972).

Key words: Apollo 12; electron probe analysis; lunar materials; mineral analysis; synthetic standards.

nalytical results are presented on polished thin selections of Apollo 12 lunar samples. The techniques used are petro- hic modal analysis and electron probe microanalysis, includ- energy-dispersive analysis. Natural minerals and synthetic les were used as standards for electron probe analysis.

**1.** Hord, J., **Cavitation in liquid cryogens II—Hydrofoil,** *ASA CR-2156*, 157 pages (National Aeronautics and Space lministration, Washington, D.C., Jan. 1973).

Key words: Cavitation; cryogenics; hydrofoil; nucleation; pumps; venturi.

is document constitutes the second of four volumes to be is- on the results of continuing cavitation studies. Boundary principles, and two-phase flow concepts, are used to im- e existing correlative theory for developed cavity data. ils concerning cavity instrumentation, data analysis, cor- ve techniques, and experimental and theoretical aspects of vitating hydrofoil are given. Both desinent and ther- namic data, using liquid hydrogen and liquid nitrogen, are ted here. The thermodynamic data indicated that stable nodynamic equilibrium exists throughout the vaporous gen cavities. The improved correlative formulae were used aluate these data. A new correlating parameter, based on deration of mass limiting two-phase flow flux across the y interface, is proposed. This correlating parameter appears ctive for future correlative and predictive applications. ement between theory and experiment is discussed, and tions for future analysis are suggested. The front half of the ies, developed on the hydrofoil, may be considered as polically-shaped.

**13 .** Schmidt, A. F., Editor, **ASRDI oxygen technology survey lume III. Heat transfer and fluid dynamics—abstracts of ected technical reports and publications,** *NASA Spec. Publ.* 76, 172 pages (National Aeronautics and Space Administra- n. Washington, D.C., 1972).

Key words: Boiling heat transfer; bubble dynamics; cavita- ion; condensing heat transfer; correlations; cryogenic fluid afety; fluid dynamics; fluid transfer; heat transfer; heat ransfer equipment; liquid helium; liquid hydrogen; liquid nitrogen; liquid oxygen; missiles and rockets; pressuriza- ion; radiation heat transfer; spacecraft tankage; stratifica- ion; supercritical storage; two-phase flow; zero gravity.

is survey constitutes selected information from an assem- of reports and publications on Heat Transfer and Fluid mics with direct applicability to oxygen systems. For each nent cited, an abstract has been prepared together with key s and a listing of most important references found in the nent. Additionally, an Author Index, a Subject Index, and y Word Index have been provided to simplify the retrieval ecific information from this work. In each subject area—e.g. ng Heat Transfer—the individual citations are listed betically by first author, with review papers dually noted the appropriate subject category and under Review rs.

the documents reviewed and evaluated for inclusion in this cation, coverage of existing information directly concerned oxygen was given primary emphasis. However, work not fically oxygen-designated but considered applicable to ox- by the reviewer—e.g., a two-phase friction factor correla- derived from nitrogen experiments—is occasionally given e no actual oxygen data exist, as an aid to the reader.

**13243.** Simmons, J. H., Macedo, P. B., Volterra, V., **Analysis of composition fluctuation lifetimes in a critical oxide mixture by volume relaxation spectroscopy,** *J. Non-Cryst. Solids* **11,** No. 4, 357-367 (Jan. 1973).

Key words: Composition fluctuations; critical point phenomena; immiscibility; oxide glasses; ultrasonic spectroscopy; volume relaxation.

The distribution of volume relaxation times in a critical oxide mixture is calculated from longitudinal and shear modulus measurements. Ultrasonic relaxation allows the investigation of two distinct effects in the distribution of relaxation times as the temperature is lowered toward the critical point. At high temperatures, a coupling between the compressional component of the ultrasonic wave and supercritical fluctuations in composition leads to an anomalous broadening of the distribution of volume relaxation times. This interaction allows a measure of the average composition fluctuation lifetime, $\tau_D$, as a function of temperature. At lower temperatures, as $\tau_D$ becomes longer than the volume relaxation times, the behavior of the distribution follows closely the predictions of an environmental relaxation model proposed by these authors for the analysis of shear relaxation processes in the same material.

**13244.** Kurylo, M. J., Huie, R. E., **Flash photolysis resonance fluorescence study of the addition of $O(^3P)$ atoms to $C_2H_4$ and $C_2D_4$ at 298 K,** *J. Chem. Phys. Letters to Editor* **58,** No. 3, 1258-1259 (Feb. 1, 1973).

Key words: Ethylene; flash photolysis; kinetics; oxygen atoms; resonance fluorescence.

The flash photolysis resonance-fluorescence technique has been used to measure the rates of the reactions $O+C_2H_4$ and $O+C_2D_4$ at atom concentrations near $10^{11}$ cm$^{-3}$. A computer simulation of the reaction system indicates that at values of $[C_2H_4]/[O] > 1000$ secondary reactions of the O atoms are nonexistent. Under these conditions we confirm our earlier number for $O+C_2H_4$ with $k_1(C_2H_4) = 7.96\times10^{-13}$ cm$^3$ molec$^{-1}$ s$^{-1}$ and find $k_1(C_2D_4) = 8.18\times10^{-13}$ cm$^3$ molec$^{-1}$ s$^{-1}$. The estimated precision is ± 10 percent.

**13245.** Beers, Y., Klein, G. P., Kirchhoff, W. H., Johnson, D. R., **Millimeter wave spectrum of thioformaldehyde,** *J. Mol. Spectrosc.* **44,** No. 3, 553-557 (Dec. 1972).

Key words: Centrifugal distortion; interstellar molecule; millimeter wave spectra; rotational transition thioformaldehyde.

The rotational spectrum of $H_2{}^{12}C^{32}S$ has been investigated in the millimeter region from 100 to 250 GHz. Twenty-five new *R*-branch transitions have been measured and combined with earlier data in a centrifugal distortion analysis of the spectrum. A set of rotational parameters are presented representing the best fit of all available data on the molecule. These rotational parameters allow reliable predictions for all transitions of $H_2{}^{12}C^{32}S$ up to $J = 30$ and $\nu < 300$ GHz.

**13246.** Melmed, A. J., Carroll, J. J., **Field-ion microscopy of osmium,** *J. Less-Common Metals* **30,** 199-204 (1973).

Key words: Field-ion microscopy; osmium.

Osmium has been successfully imaged in the field-ion microscope using helium ions at temperatures of about 87 K and lower. Specimen preparation procedures and details of image characteristics are described.

**13247.** Davis, D. D., Herron, J. T., Huie, R. E., **Absolute rate constants for the reaction $O(^3P) + NO_2 \rightarrow NO + O_2$ over the tem-**

**perature range 230-339 K,** *J. Chem. Phys.* **58,** No. 2, 530-535 (Jan. 15, 1973).

Key words: Kinetics; nitrogen dioxide; oxygen atoms; rate constants; stratosphere.

Using the technique of flash photolysis-resonance fluorescence, absolute rate constants have been measured for the reaction $O(^3P) + NO_2 \rightarrow NO + O_2$. Over the temperature range 230-339 K, the rate constant was found to have the value $k = 9.12 \pm 0.44 \times 10^{-12}$ cm³ molecule⁻¹ sec⁻¹, independent of temperature. At stratospheric temperatures, this rate constant is about a factor of two faster than indicated from previous measurements.

**13248.** Barrett, R. F., Biedenharn, L. C., Danos, M., Delsanto, P. P., Greiner, W., Wahsweiler, H. G., **The eigenchannel method and related theories for nuclear reactions,** *Rev. Mod. Phys.* **45,** No. 1, 44-108 (Jan. 1973).

Key words: Continuum shell model; nuclear reactions; nuclear structure; photonuclear reactions; *s*-matrix.

The theory of the treatment of particle hole states in the continuum is reviewed with emphasis on the eigenchannel method. The results of actual calculations are compared with experimental data. Some aspects of the experiments are rather well reproduced by the calculations. However, in certain other aspects a qualitative disagreement exists between theory and experiment, pointing to an essential inadequacy of the underlying nuclear model.

**13249.** Roth, R. S., Parker, H. S., Brower, W. S., **Crystal chemistry of lithium in octahedrally coordinated structures. III. A new structure-type in the system $K_2O$:$Li_2O$:$TiO_2$ ($K_xLi_xTi_{4-x/2}O_8$),** *Mater. Res. Bull.* **8,** 327-332 (1973).

Key words: Coordination of $Li^+$ ion; crystal structure; nonstoichiometric phase; system $K_2O$:$Li_2O$:$TiO_2$.

A new compound in the system $K_2O$:$Li_2O$:$TiO_2$ corresponding to the formula $K_xLi_xTi_{4-x/2}O_8$ was found to be orthorhombic with a = 3.821, b = 15.921, c = 2.973A space group Cmcm. The similarity between this unit cell and those of $Rb_xMn_xTi_{2-x}O_4$ and FeO(OH) has been used to predict the structure of this new phase. From the composition of this phase and that of the hollandite and ramsdellite phases in this system, it can be deduced that some of the $Li^+$ ions occur in the tunnels as well as in octahedral coordination substituting for titanium.

**13250.** Waclawski, B. J., Plummer, E. W., **Field emission and photoemission surface studies (Extended Abstract),** *J. Vac. Sci. Technol.* **10,** No. 1, 292 (Jan./Feb. 1973).

Key words: Adsorption; carbon monoxide; field emission; hydrogen; metal surfaces; oxygen photoemission; tungsten.

Since the earliest days of vacuum science, one of the major goals sought by numerous investigators has been the understanding of the nature of the surface bond. Fundamental to this understanding is a determination of the electronic energy levels of a given adsorbate-adsorbent system. Recent advances in experimental techniques show promise of developing a "surface spectroscopy" analogous to the fruitful optical spectroscopy of atoms and molecules. The application of field emission and photoemission to surface spectroscopy has been investigated at NBS for a number of years. Field emission and photoemission electron energy distributions have been measured for tungsten under ultrahigh vacuum conditions and with exposures to gaseous contaminants. The following discussion will illustrate the capabilities, limitations, and complementary features of the techniques.

**13251.** Roth, R. S., Parker, H. S., Brower, W. S., **Comments on the system $Ag_2S$-$In_2S_3$,** *Mater. Res. Bull.* **8,** 333-338 (1973).

Key words: Chalcopyrite-type; silver indium sulf
spinel-type; wurtzite-type.

The high temperature polymorph of $AgInS_2$ has been foun
be orthorhombic with $a = 7.001$, $b = 8.278$, $c = 6.698$Å, sp
group probably $Pna2_1$ with a distorted wurtzite structure.
phase transition temperature was found to be 620 ± 10 °C
the melting point 880 ± 10 °C. A new cubic spinel type pl
was found at the composition $AgIn_5S_8$ with $a = 10.827$Å.

**13252.** Kessler, E. G., Jr., **Determination of the Rydberg cons
from the He II $n$ = 3-4 (469-nm) line complex,** *Phys. Rev.*
No. 2, 408-415 (Feb. 1973).

Key words: Fine structure; helium; Rydberg constant.

The Rydberg constant has been determined from abso
wavelength measurements on two fine-structure component
the He II $n = 3$-4 transition. The He II transition was excite
a liquid-nitrogen-cooled hollow cathode. A pressure-scan
Fabry-Perot spectrometer was used to compare the H
wavelengths with a $^{198}$Hg standard source. The measured v
of the Rydberg is $R_\infty = 109\ 737.3208 \pm 0.0085$ cm⁻¹, where
uncertainty is one standard deviation.

**13253.** Chang, S. S., **A calorimetric method for studying g
transition in highly crystalline polyethylene,** (Papers Prese
at American Chemical Society Meeting, Boston, Mass., (
1971), *Polym. Prepr. Amer. Chem. Soc. Div. Polym. Ch*
J. E. McGrath, Ed., **13,** No. 1, 322-326 (Apr. 1972).

Key words: Calorimetry; glass transition temperature;
tially crystalline polymer; polyethylene; linear
branched; temperature drift method.

A sensitive calorimetric method is employed for the detec
of the glass transition phenomena in highly crystalline polym
This method is based upon the observation of the spontane
temperature drifts in the glass transition range. The occurre
of the glass transition in a polyethylene sample of 96 perc
degree of crystallinity can be demonstrated by this meth
Three linear and one branched polyethylene samples were
died. The glass transition in polyethylene is found to occu
235-240 K.

**13254.** Rasberry, S. D., **Investigation of portable x-
fluorescence analyzers for determining lead on painted surfa**
*Appl. Spectrosc.* **27,** No. 2, 102-108 (Mar.-Apr. 1973).

Key words: *In situ* lead detection; lead detection; lea
paint detection; portable lead detectors; portable x-
fluorescence analyzers.

Four portable x-ray fluorescence analyzers have been
amined to ascertain the detection limits and precision with wh
they can be used for determining lead on painted surfaces.
tests consisted of using the analyzers to determine the weigh
lead present (mg/cm²) on each of several substrates which
been coated with weighed quantities of paints of known comp
tion. All of the instruments tested had detection limits lower t
1.0 mg/cm². In some measurements, where lead was pres
between 1.0 and 6.6 mg/cm², errors as large as 30 to 50 perc
occurred; thus, it was concluded that the portable analyz
tested would be useful mainly for screening painted walls
high lead levels.

**13255.** Geist, J., Zalewski, E., **Chinese restaurant nomenclat
for radiometry,** *Appl. Opt.* **12,** No. 2, 435-436 (Feb. 1973).

Key words: Geometrical radiative transfer; nomenclat
optical radiation; phluometry; photometry; radiometry;
minology.

ew nomenclature system for radiometry is proposed.

Caswell, R. S., Coyne, J. J., **Secondary particle spectra duced by neutron interactions with tissue,** *Proc. 1st Symp. Neutron Dosimetry in Biology and Medicine, herberg/Munchen, Germany, May 15-19, 1972,* **1, EUR 5 d-f-e,** 25-41 (Commission of European Communities, enbourgh, Germany, Sept. 1972).

ey words: Energy deposition; neutron dosimetry; secon- ary particle spectra; tissue.

ne basic aspects of neutron interactions with tissue are sed: energy transfer to matter according to element it in the tissue and by type of charged particle produced; ations of secondary particle spectra produced when ons interact with tissue for 1 and 14 MeV neutron energy. he primary spectra of secondary particles as produced in uclear reactions, and the softer "slowing-down" or ibrium" spectra after particle slowing down are deter- . The relative importance of the various secondaries (p, d, B, C, N, O) are discussed. These spectra provide physical information for calculations of neutron energy deposition ples given) and for models of neutron radiation effects on ical materials.

. Waterstrat, R. M., **The vanadium-platinum constitution gram,** *Met. Trans.* **4,** 455-466 (Feb. 1973).

ey words: Alloys; constitution diagram; equilibrium dia- ram; phase diagram; platinum; vanadium.

: system V-Pt was investigated over the entire composition by metallography, x-ray diffraction and electron probe studies. There are at least four equilibrium inter- te phases in this system and they are stable to progressive- her temperatures with increasing vanadium concentration. phases which have been observed are: $\gamma'$, cubic, $Cu_3Au$ $\theta$, tetragonal, $TiAl_3$ type; $\delta$, orthorhombic, $MoPt_2$ type; $\zeta$, hombic, AuCd type; and $\beta$, cubic, $Cr_3Si$ type (A15). The ise is possibly metastable. A very stable ribbon-like growth nase in the fcc platinum terminal solid solution has been ob- d in alloys containing about 43 at. pct V. The platinum ter- solid solution forms a congruent melting maximum at 1805 °C. A eutectic reaction occurs at 1720 ± 10 °C and tectic reaction is indicated at 1800 ± 10 °C. Vanadium is e in the fcc platinum terminal solid solution up to about 57 at 1720 °C. Platinum dissolves only to the extent of about pct at 1800 °C in bcc $\alpha$-V.

. Mies, F. H., **Molecular theory of atomic collisions: Fine- cture transitions,** *Phys. Rev. A* **7,** No. 3, 942-957 (Mar. 3).

ey words: Atomic collisions; fine-structure transitions; $IF^+$ molecule; molecular states; quantum chemistry.

theory of fine-structure transitions in atom-atom colli- is formulated in terms of the molecular states of the nic collision complex. The Born-Oppenheimer (BO) elec- wave functions are implicit functions of the interatomic inate $R$, and the molecular theory is analogous to the "per- l-stationary-state" method. Expansion in *molecular* el states incorporates the effects of polarization, exchange, alence forces on the electronic portion of the scattering function and embodies the "adiabatic" contribution of the set of closed-channel excited states that are generated in ore usual asymptotic-atomic-state expansion. The channel are expressed explicitly in terms of the body-fixed molecu- ve functions, and the resultant interaction matrix elements close-coupling scattering formalism are related to the molecular potentials. The theory is developed specifically for proton collisions with the fluorine atom in its ground $^2P_{j,mj}$ state, with explicit account being taken of the spin-orbit splitting between the $j=3/2$ and $j=1/2$ multiplet states. Use is made of the accurate $HF^+(^2\Pi)$ and $HF^+(^2\Sigma)$ wave functions calculated by Wahl, Julienne, and Krauss. These molecular states asymptotically approach $H^+ + F(^2P)$, and accurate quadrupole and induced-dipole interaction parameters which describe the asymptotic interaction potentials are obtained from the calculations. Estimates are made of the BO coupling terms and they are found to be negligible compared to the spin-orbit couplings. In the following paper close-coupling calculations are made of the cross sections for the fine-structure transitions $(j,m_j \rightarrow j',m_j)$.

**13259.** Paffenbarger, G. C., Rupp, N. W., **Research techniques used in evaluating dental materials,** *J. Amer. Dent. Ass.* **86,** 643-651 (Mar. 1973).

Key words: Biological; chemical; physical; reliable; specification; use; valid.

Evaluation of dental materials is an exact science that is dependent on several disciplines to be effective. Physical, mechanical, chemical, biological and clinical or user tests must be coordinated with maximum and/or minimum values for each evaluation. In the acceptance of a material for use in dentistry each of these areas must be accurately defined. Then for specifications prescribing the quality of a material the pertinent or relevant properties are determined and tests established to measure these characteristics. The design of suitable specification tests that are both reliable and valid is no mean research task. By reliable it is meant that a test can be repeated satisfactorily by different laboratories. By valid is meant that the tests will predict the behavior of the materials in service. These tests of necessity must provide answers quickly within days as compared to years in service, thus are often abusive in nature. Silicate cements and acrylic resins are two materials used to illustrate various tests and their development.

**13260.** Loebenstein, W. V., **Heats of adsorption of ammonia and carbon dioxide on tooth components,** *J. Dent. Res.* **51,** No. 6, 1529-1536 (Nov.-Dec. 1972).

Key words: Adsorption; ammonia adsorption; carbon dioxide adsorption; dental adhesive; dentin; heats of adsorption; surface area.

The study demonstrates how heats of adsorption and area of coverage can be used as criteria for comparing the ultimate strength of chemically reactive groups for incorporation in potential dental adhesives. Carbon dioxide and ammonia were chosen as the reactants because they typified acidic and basic groups, respectively, and were both gases. Measurements were confined to the region of reversible adsorption in order to assure reproducibility of the adsorbent surface. The presence of collagen exerted a profound influence on the BET area depending upon the gas used when compared with nitrogen. Ammonia exhibited a higher surface area as well as a higher heat of adsorption on dentin than did carbon dioxide. It would therefore qualify as a better adhesive under the conditions of comparison. The surface area of dentin available to ammonia, however, was no greater than the surface area of anorganic dentin. The average heat of adsorption of ammonia on anorganic dentin based on anorganic whole teeth is estimated to be at least as large as it is for whole dentin. Thus, it would appear that the presence of collagen did not contribute to the adhesive strength of ammonia.

**13261.** Paffenbarger, G. C., **The role of dental materials in the prevention of dental diseases,** *Int. Dent. J.* **22,** No. 3, 343-349 (Sept. 1972).

Key words: Caries; dental materials; plastics; prevention; sealants; tooth loss.

The permanent tooth loss per hundred of 13 year olds averaged 6 for Norwegians and 100 for Americans because of early treatment of caries of the Norwegians with dental restorative materials.

Recurrent caries occurs less frequently around restorations of silicate cement than around any other restorative material. The same holds for caries of surfaces of adjacent teeth in contact with silicate cement restorations. The anticariogenic effect is probably caused by the transfer of fluoride ions to the dental enamel, thereby rendering it less soluble. Newly developed plastic formulations appear to seal developmental defects in teeth so as to greatly retard dental caries which so frequently occurs at such sites.

Recurrent caries around restorations should be reduced if a chemical bond of the tooth-filling interface could be achieved. Promising developments are available.

**13262.** Hougen, J. T., **Reinterpretation of molecular beam hyperfine data for $^{14}NH_3$ and $^{15}NH_3$,** *J. Chem. Phys.* **57,** No. 10, 4207-4217 (Nov. 15, 1972).

Key words: Centrifugal distortion; hyperfine structure; inversion doublet; molecular beam; $NH_3$; quadrupole splitting.

Reassignments are presented for the hyperfine patterns of six $^{15}NH_3$ inversion doublets. The new assignments alter the sign of the nitrogen-hydrogen spin-spin interaction constant. Previous disagreement between theory and experiment for the hyperfine pattern of the $J=3$, $K=2$ $^{14}NH_3$ inversion doublet is removed by including the effect of centrifugal distortion on the quadrupole splitting. An explanation is presented for a discrepancy remaining in the fit of the $J=K=6$ hyperfine pattern of $^{15}NH_3$.

**13263.** Seltzer, S. M., Berger, M. J., **Photoneutron production in thick targets,** *Phys. Rev. C* **7,** No. 2, 858-861 (Feb. 1973).

Key words: Bremsstrahlung; Monte Carlo; neutron yield; photonuclear cross sections; photoneutrons; radiation transport.

This paper reports new results on the yield of photoneutrons from thick targets bombarded with electron beams. Yields have been calculated for incident electron energies from 20 MeV down to the photonuclear cross section threshold, for tantalum and tungsten targets with thicknesses up to 12.5 gcm$^{-2}$. The increased yield from composite tungsten-beryllium targets has been explored.

**13264.** Chen, C. L., Phelps, A. V., **Absorption coefficients for the wings of the first two resonance doublets of cesium broadened by argon,** *Phys. Rev. A* **7,** No. 2, 470-479 (Feb. 1973).

Key words: Absorption coefficient; argon; broadening; cesium; resonance lines.

Measurements are reported of the absolute absorption coefficients in the wings of the 8944-, 8521-, 4593-, and 4555-Å resonance lines of cesium in the presence of argon at densities between about $6 \times 10^{18}$ and $2 \times 10^{19}$ atom cm$^{-3}$. The data extend from about 0.7 Å to as much as 600 Å from the line center and were obtained using cesium densities between $7 \times 10^{11}$ and $2 \times 10^{15}$ atom cm$^{-3}$ and temperatures between 390 and 470 °K. The measured absorption coefficients are proportional to the product of the cesium and argon densities as expected from line broadening produced by binary collisions between cesium and argon atoms. Using the quasistatic theory as a guide for interpretation, the line profiles for wings of the first resonance doublet show a transition from a wavelength dependence determined by range van der Waals forces to a dependence determined b short-range internuclear potentials discussed by Hedges, D mond, and Gallagher (HDG). The far-wing absorption pr obtained in the present experiments are in good agreement those calculated from the fluorescence data of HDG.

**13265.** Greer, S.C., **The $CH_4$-Kr solid phase diagram,** *Phys.* **43A,** No. 1, 73-74 (Feb. 12, 1973).

Key words: Crystal structure; krypton; methane; mix binary solid.

X-ray diffraction studies on solid mixtures of $CH_4$ an show complete miscibility on a face-centered cubic lattice 21K to the melting curve.

**13266.** Costrell, L., **CAMAC: A review and status report,** (I Symp. on Nuclear Science, Miami, Fla., Dec. 8, 1972), *I Trans. Nucl. Sci.* **NS-20,** No. 1, 557-561 (Feb. 1973).

Key words: CAMAC; computer interfacing; co systems; instrumentation; instrumentation stand nuclear instrumentation; standards.

CAMAC is a modular instrumentation system for tran sion of digital data between instruments and between in ments and computers and computer peripherals. The syst described in a general way and the history of the CAN development, its expanding utilization in various fields ar current status are discussed. This is an introductory p delivered at the 1972 Nuclear Science Symposium and i lowed by papers that discuss CAMAC in greater detail.

**13267.** Horn, W. A., **Some fixed point theorems for compact and flows in Banach spaces,** *Trans. Amer. Math. Soc.* **149,** 404 (June 1970).

Key words: Asymptotic fixed point theorems; Ba space; compact mappings, fixed points; flows; noneje fixed points; nonrepulsive fixed points.

Let $S_0 \subset S_1 \subset S_2$ be convex subsets of the Banach spac with $S_0$ and $S_2$ closed and $S_1$ open in $S_2$. If $f$ is a compact ma of $S_2$ into $X$ such that $\cup_{j}^{m}=1f^{j}(S_1) \subset S_2$ and $f^m(S_1) \cup f^{m+1}($ $S_0$ for some $m > 0$, then $f$ has a fixed point in $S_0$. (This exte result of F. E. Browder published in 1959.) Also, if $\{T_t : t \in$ is a continuous flow on the Banach space $X$, $S_0 \subset S_1 \subset S$ convex subsets of $X$ with $S_0$ and $S_2$ compact and $S_1$ open i and $T_{t_0}(S_1) \subset S_0$ for some $t_0 > 0$, where $T_t(S_1) \subset S_2$ for all $t$ then there exists $x_0 \in S_0$ such that $T_t(x_0) = x_0$ for all $t \geqq 0$. M extensions of Browder's work on "nonejective" and "nonr sive" fixed points are also given, with similar results for flow

**13268.** Stromberg, R. R., McCrackin, F. L., **Ellipsometry as for the characterization of surfaces,** (Proc. Symp. on Clear faces: Their Preparation and Characterization for Inter Studies, North Carolina State University, Raleigh, N.C., 1968), Chapter in *Clean Surfaces: Their Preparation Characterization for Interfacial Studies,* G. Goldfinger, pp. 65-76 (Marcel Dekker, Inc., New York, N.Y., 1970).

Key words: Characterization surface; ellipsometry; int cial studies; optical constants; polarization of light; r tivity.

The application of ellipsometry to the characterization o faces is discussed. The technique is very sensitive and is ap ble to the detection of very thin contaminating films. It is possible to characterize a surface under the same condi required for further interfacial studies of the surface. The sitivity of the method and the dependence of this sensitivi s such as refractive index differences, angle of incidence, umber of reflections are discussed relative to the problem face characterization and detection of contaminating films. echnique is not limited to highly reflecting surfaces and its ations to studies of surfaces of transparent materials are escribed.

. Zimmerman, J. E., **A review of the properties and applica- s of superconducting point contacts,** *Proc. Conf. Applied perconductivity, Annapolis, Md., May 1-3, 1972*, pp. 544- (IEEE, Inc., New York, N.Y., 1972).

ey words: Josephson effect; point contacts; superconduc- vity.

erconducting small-area ("point") contacts are easily made umber of forms, and are used in a wide variety of devices, of which are quite highly evolved. For many practical pur- no special contact surface preparation is required. Electri- operties are often said to be "tunnel-junction like" or l-bridge like," but the meaning of these terms is not clear. evidence shows that perfectly-clean metallic contacts often it all the features expected of low-capacitance tunnel junc- Permanently-stable point-contact devices have been made e or a combination of several techniques, but their vulnera- to electrical and other transients has led to the develop- of simple and effective adjusting mechanisms. Certain contacts, with minimum possible shunt capacitance and normal conductance, approach the ideal of pure Josephson nt elements (i = i, sin $\theta$) more closely than any other type of hson junction, and, for this reason, appear to be the best of junction for millimeter-wave and far-infrared applica- Paradoxically, the dc-IV characteristics of such pure hson elements can be very complex if they are closely cou- external circuit elements such as microwave cavities and ances of impurity molecules.

Kaldor, A., Maki, A. G., Dorney, A. J., Mills, I. M., **The gnment of $\nu_2$ and $\nu_4$ of $SO_3$,** *J. Mol. Spectrosc.* **45,** No. 2, -252 (Feb. 1973).

ey words: Air pollution; infrared spectra; molecular ructure; Raman spectra; spectra; sulfur trioxide.

ee experiments have been performed to resolve an uncer- in the assignment of $\nu_2$ and $\nu_4$ for $SO_3$: (i) the gas phase n spectrum has been measured; (ii) the infrared active com- on band $\nu_3 + \nu_4$ has been measured; (iii) a band contour cal- on has been performed taking account of the *l*-type ance in $\nu_4$ and a strong Coriolis resonance between $\nu_2$ and ese experiments establish beyond any doubt that $\nu_2$ lies at 497.5 cm$^{-1}$ and $\nu_4$ lies at about 530.2 cm$^{-1}$. The contour ation also shows that the Coriolis resonance gives rise to tive intensity perturbation.

. Das, E. S. P., Marcinkowski, M. J., Armstrong, R. W., de , R., **The movement of Volterra disclinations and the as- ated mechanical forces,** *Phil. Mag.* **27,** No. 2, 369-391 (Feb. 3).

ey words: Disclination; dislocation; glide; plasticity; wist; Volterra; wedge.

analysis is made of conservative and non-conservative ment of Volterra disclinations and the associated mechani- rces. It is shown that both disclination lines and their axes xperience a force under the action of an applied stress. A al equation is derived for the force on a disclination loop ts axis. The condition for conservative movement is d. Examples illustrating these principles are given. Glide es for disclination loops are defined. The motion is conservative on a surface generated by rotating the disclination line around its axis, and on a plane normal to the axis. It is shown how a twist loop can be converted to a wedge loop and, *vice versa*, conservatively.

**13272.** Meijer, P. H. E., Niemeijer, Th., **Search for the ground state of cerous magnesium nitrate by an extended Luttinger-Tisza method,** *Phys. Rev. B* **7,** No. 5, 1984-1988 (Mar. 1, 1973).

Key words: Antiferromagnetism; cerium magnesium nitrate; digital representation; dipole-dipole interaction; ground state; Luttinger-Tisza method; neodimium magnesium nitrate; superlattice.

The ground state of cerous magnesium nitrate is determined using the assumptions that the spins are coupled by purely dipolar forces, the magnetic structure is periodic after eight or less lattice periods, and the spins can be considered as classical vectors. The ground state has a layered antiferromagnetic structure as described in the text. A study is made to see whether this result is dependent on the assumption that the *g* factor parallel to the crystallographic *c* axis is zero or almost zero for this specific salt. The conclusion is that this is to a large extent not the case. The ground state lies at an energy − 1.867 mdeg K, using the lattice constants as given by Schiferl.

**13273.** Mies, F. H., **Molecular theory of atomic collisions: Calculated cross sections for $H^+ + F(^2P)$,** *Phys. Rev. A* **7,** No. 3, 957-967 (1973).

Key words: Atomic collisions; fine-structure transitions; $HF^+$ molecule; molecular states; quantum chemistry.

The results of a close-coupling calculation of the fine-structure transitions $(j,m_j \rightarrow j',m_j')$ are presented for collisions between photons and $F(^2P_{j,m_j})$. The theory is formulated in the perturbed-stationary-state approximation using accurate molecular wave functions for the ground $^2\Pi$ and $^2\Sigma$ states of $HF^+$. Comparison is made to the predictions of the Born approximation. The magnetic selection rule $(j,m_j \rightarrow j,\text{-}m_j)$ is strongly violated in the $j = 3/2$ state and less strongly violated in the $j = 1/2$ state. It is concluded that the important region of interaction for the $j = 1/2 \rightarrow j = 3/2$ transition is at short-to-intermediate distances where accurate molecular potentials are required and close-coupling effects are dominant.

**13274.** Bennett, J. J., Holman, M. A., Tumarkin, J. E., **The economic impact of noise,** *Environmental Protection Agency Report No. NTID 300.14,* 104 pages (available as PB206726 from the National Technical Information Service, Springfield, Va. 22151, Dec. 31, 1971).

Key words: Economic impact of noise; noise abatement.

A study has been undertaken to survey the economic impact of noise. Data available on the entire subject of noise and its abatement are so rudimentary that they do not lend themselves to even the most primitive economic analysis. It is demonstrated that the number of sources of noise in homes, in industry, on the highways, and in the air is growing at a dramatic rate. These noise sources are heterogeneous and transient, and therefore, a universal solution for abatement of noise at the source is not available. From the economic viewpoint, it has been demonstrated that substantial costs are associated with noise and its abatement. Costs such as those associated with equipment redesign, right-of-way, and receiver insulation are discussed in detail. The most glaring data gaps highlight the need for research into the relationship between noise, its abatement, and its impact on: wages, prices, productivity, production costs, employment, balance of payments, real property values, and health. Research using the principles of economics must identify and analyze the most cost-effective alternative solutions to noise. A discussion of spending for noise research is included in the study.

**13275.** Christ, B. W., Smith, L. C., **A chemical polish for quick removal of grinding and lapping scratches from iron and low-carbon steel,** *J. Iron Steel Inst. Tech. Note*, p. 155 (Feb. 1973).

Key words: Chemical polish; iron; low-carbon steel; single phase alloys; swabbing.

The composition and use of a chemical polish for iron and low-carbon steel is described. Swabbing metallographic samples with this polish completely removes scratches left by 600 grit silicon carbide in about 5 seconds. Furthermore, the polished surfaces are flat enough for grain size analysis via optical microscope observation.

**13276.** Cezairliyan, A., Beckett, C. W., **Pulse calorimetry of solids at high temperatures,** Chapter 6 in *Thermochemistry and Thermodynamics*, H. A. Skinner, Ed., **10,** 159-175 (Butterworths, London, 1972).

Key words: Measurements at high temperatures; millisecond resolution; pulse calorimetry; solid electrical conductors.

Pulse techniques for the measurement of specific heat of solid electrical conductors at high temperatures are described. Design and operational characteristics of pulse calorimetric systems reported in the literature are summarized. Details of an accurate millisecond resolution pulse calorimeter are given.

**13277.** Marshall, H. E., **Cost sharing and multiobjectives in water resource development,** *Water Resour. Res.* **9,** No. 1, 1-10 (Feb. 1973).

Key words: Cost allocation; cost sharing; environmental quality; efficiency; equity; multiobjectives; multi-purpose projects; regional development; water policy; water resources.

The U.S. Water Resources Council has considered objectives in addition to national economic development for the evaluation of water projects. Cost-sharing rules have not been proposed for the new objectives. A conceptual method is proposed for planning the nationally optimal project with multiobjectives. The data required for project evaluation with multiobjectives are used to apply a cost-sharing rule that induces local interests to choose nationally efficient projects. The rule is recommended for traditional project purposes and some new purposes. It can be applied to a multiple-purpose project without allocating project joint costs. A ceiling and a floor on local percentage cost shares of 100 percent and 20 percent of project costs, respectively, are considered for traditional purposes. Local percentage cost shares of 50 percent and 100 percent are considered for all costs allocated to environmental quality and regional development objectives, respectively.

**13278.** Radebaugh, R., Frederick, N. V., Siegwarth, J. D., **Flexible laminates for thermally grounded terminal strips and shielded electrical leads at low temperatures,** *Cryogenics* **13,** No. 1, 41-43 (Jan. 1973).

Key words: Cryostat; laminate; photoetching; thermal grounding; transmission line.

It is shown how to make compact, thermally grounded terminal strips for electrical leads in cryostats from flexible electrical laminates composed of copper foil bonded to a polyimide film. Laminates of lead foil and polyimide film are used to make a superconducting strip line, a type of transmission line in which it is easy to thermally ground both conductor and shield. thermal resistance across a laminate was measured between and 4 K from which the thermal conductivity of polyimide is deduced between 0.1 and 4 K.

**13279.** Danos, M., Greiner, W., Rafelski, J., **Fields nonloc Clifford space. I. Classical gauge-invariant nonlinear theory,** *Phys. Rev. D* **6,** No. 12, 3476-3491 (Dec. 15, 1972

Key words: Fermion-boson interactions; field the gauge invariance; hypercomplex coordinates; intera fields; nonlinear field theory; nonlocal field theory.

A fully gauge-invariant, Lorentz-covariant, nonlocal, and linear theory, for coupled spin-1/2 fields, $\psi$, and vector field i.e., "electrons" and "photons," is constructed. The field th is linear in the $\psi$ fields. The nonlinearity in the $A$ fields a unambiguously from the requirement of gauge invariance. coordinates are generalized to admit hypercomplex values, they are taken to be Clifford numbers. The nonlocality is lin to the hypercomplex component of the coordinates. As the of the nonlocality is reduced toward zero, the theory goes into the inhomogeneous Dirac theory. The nonlocality para ter corresponds to an inverse mass and induces self-regula properties of the propagators. It is argued that in a gauge-in ant theory a graph-by-graph convergence is impossible in pr ple, but it is possible that convergence may hold for the com solution, or for sums over classes of graphs.

**13280.** Armstrong, G. T., **Some current topics in thermochem and calorimetry at the National Bureau of Standards,** *Proc. loq. Int. de Thermochimie, Marseille, France, June 30-Ju 1971*, No. 201, 77-96 (Centre National de la Recherche S tifique, Colloques Internationaux, Paris, France, 1972).

Key words: Calorimetry, flow; calorimetry, solu chlorine monofluoride; fluorine dissociation; hydroflu acid solution calorimetry; microcalorimetry; quartz, s dard reference materials; standard reference material calorimetry.

The current program of the Thermochemistry Section a National Bureau of Standards includes approximately equal portions of experimental research and data compilation evaluation activities. Experimental studies of calorimetric a racy, reference materials for calorimetry, and the propertie selected key substances are in progress. The enthalpy of solu in aqueous hydrofluoric acid (24.4 percent and other concen tions) at 80 °C and as a function of temperature has been d mined for $\alpha$-quartz to permit its issuance as a reference mat for mineralogical calorimetry. A Calvet microcalorimeter been placed in operation with digital data-logging access with a sensitivity of about 0.1 $\mu$W. It has been shown to ope effectively in a temperature-scanning mode. Flow calorim using the reaction:

$$\Big[\mathrm{ClF}_n(\mathrm{g}) + \left(\frac{n+1}{2}\right) \mathrm{H_2(g)} + m\,\mathrm{H_2O(l)} = [\mathrm{HCl} + n\,\mathrm{HF} + m\,\mathrm{H_2O}$$

has led to enthalpies of formation of ClF, $ClF_3$ and $ClF_5$. binding energy per atom in the gaseous molecules varies from 128.0 to 122.3 kJ mol$^{-1}$ in the series. The enthalpy of mation of ClF provides some (inconclusive) evidence that zero point dissociation energy of fluorine is less than 153. mol$^{-1}$. Other experimental programs are also active but are covered here.

**13281.** Barnett, J. D., Block, S., Piermarini, G. J., **An op fluorescence system for quantitative pressure measureme the diamond-anvil cell,** *Rev. Sci. Instrum.* **44,** No. 1, 1-9 ( 1973).

ey words: Diamond-anvil cell; fluorescence; pressure easurement; ruby.

optical system for rapid routine pressure measurement is ped which utilizes a pressure shift in the sharp $R$-line scence spectrum of ruby or similar materials. The system, consists of a standard polarizing microscope and a 1/4 m hromator with associated photodetection system, is used he diamond-anvil pressure cell, but can be employed with e modification in any pressure system which has optical . The precision of the pressure measurement in a hydro- environment up to 100 kilobar is 0.5 kilobar using ruby as essure sensor. This precision is better than the accuracy of resent pressure scale above 40 kilobar. The merits of scent materials other than ruby as pressure sensors are iscussed. A description of a Waspaloy diamond cell with modifications in design is given. This improved cell and as- ed techniques extends the pressure range in gasketed ns up to 200 kilobar at room temperature and to moderate res at 700 °C.

Horn, W. A., **Determining optimal container inventory and ing,** *Transp. Sci.* **5,** No. 3, 225-231 (1971).

ey words: Containers; inventory; network flows; optimal ntainer routing; optimal routing; routing in a network.

eralizing work of Samuel and Ullmann, this paper how to determine the optimal number and routings of con- s used to move mail among several cities. Critical assump- are (a) periodic demand patterns and linear transportation (for full or empty containers, or uncontainerized mail) en each city-pair, and (b) constant fixed cost per container system. The optimization problem is transformed into a rk flow linear program for which efficient solution methods own.

Garvin, D., **Critical data for the physical sciences,** (Papers sented to the Council of Biology Editors, Carleton Univer- Ottawa, Canada, May 11, 1970), *CBE Newsletter,* pp. 6- Sept. 1970).

ey words: Chemistry; critical data; evaluation of delay; formation analysis; publication standards; standard ference data.

subject of this paper is critical data in the physical es. The topic is a broad one; only a few aspects can be sed, those of current interest. The topic is also diffuse and lt to define. The term "critical data" is a technical term misleading. What we are concerned with is "reliable data," , data that may be used with confidence in planning experi- , reducing results and interpreting phenomena. The term al data" is used in the sense of criticism; review, selection, arison and recommendation. This is part of the process of ling a discipline with that large body of information, in y accessible form, upon which it must build.

Maienthal, E. J., **Determination of trace elements in silicate rices by differential cathode ray polarography,** *Anal. Chem.* No. 4, 644-648 (Apr. 1973).

ey words: Alloys; analyses; cast irons; differential athode ray polarography; high-purity materials; metals; eels; trace elements.

thods are described for the analysis of some new Trace ents in Glass Standard Reference Materials by differential de ray polarography. Iron and titanium were determined in 0-, 50-, 1-, 0.02-ppm and base glasses after cupferron and nium hydroxide separations. Nickel was determined in the nd 1-ppm samples after extraction with dimethylglyoxime.

**13285.** Hagan, L., **Reports of observatories for 1971/72, National Bureau of Standards, Washington, D.C.,** *Bull. Amer. Astron. Soc.* **5,** No. 1, Part II, 201-204 (Jan. 1973).

Key words: Atomic energy levels; atomic line shapes; atomic spectra; atomic transition probabilities; bands, molecular; energy levels, atomic; line shapes, atomic; molecular bands; molecular spectra; rotational constants.

Research at the National Bureau of Standards in spectroscopy pertinent to astronomy is summarized. Publications on atomic spectra, atomic transition probabilities and line broadening, and molecular spectra are referenced and work in progress is discussed.

**13286.** Hall, J. L., **The lineshape problem in laser-saturated molecular absorption,** Paper in *Lectures in Theoretical Physics,* K. T. Mahanthappa and W. E. Brittin, Eds., **XII,** 161-210 (Gordon and Breach, Sci. Publ. Inc., New York, N.Y., Mar. 1973).

Key words: Absorption; laser; molecular; saturation.

The use of lasers makes it possible to observe non-linear optical absorption in molecules. Experiments involving two running waves represent a particularly interesting case, as they allow observation of a very sharp "emission" feature when the radiation frequency matches the natural molecular absorption frequency. This resonance feature has a width characteristic of *natural* rather than Doppler broadening. This paper presents a physical discussion of the main features of the saturated absorption process, with particular emphasis on realistically representing inherent experimental conditions as they affect the mathematical formulation. In a certain approximation, one finds a power-broadened Lorentzian lineshape, in agreement with a fairly broad class of experimental results. A pair of coupled differential equations is derived which should represent the lineshape under more general conditions. The saturation process provides a selection mechanism *against* particles which experience a collision during their coherent interaction with the radiation. The implications of this effect for laser collision physics experiments are examined in some details.

**13287.** Krauss, M., **Energy surfaces for energy transfer and chemical reaction,** *Proc. IBM Scientific Computing Symp. on Computers in Chemistry, Poughkeepsie, N.Y., October 6-17, 1968,* pp. 65-76 (1969).

Key words: *Ab initio* calculations; HF approximation; schematic mechanism; simple prototypes.

The calculations described are an indication of the possibilities of *ab initio* calculations. They provide the necessary data for an accurate scattering calculation or a test of a schematic mechanism deduced from experiment. For carefully chosen systems, the HF approximation is sufficient and the present results point to obviously analogous systems, for which these results would be useful. The extent to which this is done depends almost entirely on the cost. Table I gives the time on an IBM 7094-I for a representative point on the surface depicted herein. The systems are simple prototypes, and the extension to larger, more practicable ones would considerably increase the times. This is especially true for the correlated calculations which must be seriously considered for the general problem. But the present results and those from many other sources would strongly indicate that it is very worthwhile to spend the effort required to adapt these problems to the new generation of computers.

**13288.** Kurylo, M. J., Peterson, N. C., Braun, W., **Absolute rates of the reactions $\mathbf{H + C_2H_4}$ and $\mathbf{H + C_2H_5}$,** *J. Chem. Phys.* **53,** No. 7, 2776-2783 (Oct. 1, 1970).

Key words: Ethyl radicals; ethylene; hydrogen atoms; kinetics; resonance fluorescence.

The hydrogen atom-ethylene system was studied at 298 K employing the methods of resonance fluorescence and absorption by hydrogen atoms of Lyman $\alpha$ radiation at 1216 Å. The contribution of hydrogen atom-radical reactions was evaluated under varying experimental conditions, and the rate of disappearance of H atoms in ethylene was measured under conditions where stoichiometric corrections became significant. Measurements in the literature of reaction rates for $H + C_2H_4$ at low total pressure are now in good agreement; however the limiting high-pressure absolute rate constants thus far reported differ depending on the assignment of stoichiometric factors. Our results indicate that stoichiometric factors obtained under low-pressure conditions may not be applicable to high pressure. Furthermore, extrapolations based on plots of inverse rate constant vs inverse pressure may be in error due to significant curvature in such plots. Our high-pressure limiting rate constant for $H + C_2H_4$, extrapolated from data at pressures higher than those used by other workers, is free to stoichiometric corrections and is in agreement with our earlier measurements. Absolute rate constants obtained in this work are

$$H + C_2H_4 \rightarrow k_1 = 13.6 \pm 1.9 \times 10^{-13}\ (\text{cm}^3\ \text{molecule}^{-1} \cdot \text{sec}^{-1})$$
(extrapolated to infinite He pressure),

$$H + C_2H_5 \rightarrow k_4 = 6.0 \pm 2.0 \times 10^{-11}\ (\text{cm}^3\ \text{molecule}^{-1} \cdot \text{sec}^{-1})$$
(50 torr He).

The latter rate has been estimated from the variation of the rate of disappearance of H atoms as a function of initial H atom concentration at 50 torr total pressure.

**13289.** Ledbetter, H. M., **Poisson's ratio for polycrystals,** *J. Phys. Chem. Solids* **34,** No. 4, 721-723 (Apr. 1973).

Key words: Cauchy relations; elastic constants of solids; elasticity; Poisson ratio; polycrystals.

Accepted views concerning Poisson's ratio for central-force polycrystals are amended. For polycrystals the ratio can vary from 1/4, which is actually a lower limit. An upper limit of Poisson's ratio exists also. Both limits can be calculated from single-crystal elastic data. The limits correspond to Voigt's and Reuss's states of uniform local strain and of uniform local stress, respectively.

**13290.** Rowe, J. M., Hinks, D. G., Price, D. L., Susman, S., Rush, J. J., **Single crystal neutron diffraction study of sodium cyanide,** *J. Chem. Phys.* **58,** No. 5, 2039-2042 (Mar. 1, 1973).

Key words: Angular distribution; crystal structure; cyanide ion; Debye-Waller factor; neutron diffraction; orientational disorder; potassium cyanide; sodium cyanide.

The neutron diffraction pattern of a single crystal of cubic NaCN has been measured at 295 K. These data and earlier results for KCN at 180 and 295 K have been analyzed in terms of a model which expands the angular distribution of $CN^-$ orientations in symmetry-adapted spherical harmonics. From this analysis, the distributions of $CN^-$ in these crystals have been derived, and these indicate a monotonic trend in the series KCN (295 K) thru KCN (180 K) to NaCN (295 K) involving a shift in preferential orientation from the [111] toward the [100] directions in the crystal. Unusually large translational Debye-Waller factors have also been derived for NaCN and KCN from the fitting procedure, in agreement with earlier results and analysis on KCN. In addition, an average $C \equiv N$ bond distance of 1.18 Å is obtained.

**13291.** Wasik, S. P., Tsang, W., **Gas chromatographic determir tion of partition coefficients of some unsaturated hydrocarbo and their deuterated isomers in aqueous silver nitrate solutio** *J. Phys. Chem.* **74,** No. 15, 2970-2976 (1970).

Key words: Aromatics; gas analysis; gas chromatograph isotope effect; isotopic separation; olefins; silver nitrate.

Experiments using aqueous solutions of silver nitrate as a g chromatographic liquid phase have been carried out. Stabili constants for the reaction, $(Ag^+)_{aq} + (\text{Hydrocarbon})_{aq}$ $(Ag^+ \cdot \text{Hydrocarbon})_{aq}$, where $(\text{Hydrocarbon})_{aq}$ are various lig olefins, aromatics, or some of their deuterated isomers have be determined. For the olefins these values are in quantitati agreement with those obtained from conventional sta techniques. In the case of ethylene $\Delta H = -23$ kJ/mol and $\Delta S$ $-38$ J/mol deg. The isotope effect for the solubility of benzer $d_6$ (compared to the lightest isomer) in water is 1.05. Aqueo silver nitrate columns should also have interesting analytical a plications, particularly in the field of isotopic separations. Th appear to be more efficient than the conventional ethyle glycol-silver nitrate columns.

**13292.** Herron, J. T., **An evaluation of rate data for the reactio of atomic oxygen ($O^3P$) with methane and ethane,** *Int. J. Che Kinet.* **1,** 527-539 (1969).

Key words: Atomic oxygen; ethane; evaluation; methan rate data.

This review presents in tabular and graphical form rate data the reactions of atomic oxygen ($O^3P$) with methane and ethar The reliability of these data is discussed and suggested values the rate constants are given over specified temperature interva Specific values are given for 298 and 1000 K.

**13293.** Dibeler, V. H., Walker, J. A., **Photoionization of acetyle near threshold,** *Int. J. Mass Spectrom. Ion Phys.* **11,** 49- (1973).

Key words: Franck-Condon factors; mass spectrometr photoionization; Rydberg series; vacuum ultraviolet.

Photoion yield curves for $C_2H_2$ and $C_2D_2$ cooled to 118 K a remeasured at 0.2 Å intervals from ionization threshold to abo 0.6 eV above threshold. Clearly defined autoionization featur are observed superimposed on vibrational step structure. T latter observation suggests molecular predissociation occurri in competition with the autoionization process. A simple mea of estimating Franck-Condon factors for the direct ionization the presence of autoionization gives values in agreement wi photoelectron spectroscopy data. Comparisons of observed a calculated Rydberg levels converging to vibrationally excit states of the molecular ion are discussed briefly.

**13294.** Wasik, S. P., Roscher, N. M., **Diffusion coefficients paraffin-chain salts and the formation energetics of micelles,** *Phys. Chem.* **74,** No. 14, 2784-2787 (1970).

Key words: Decyltrimethyl ammonium bromide; diffusi coefficient; dodecyltrimethyl ammonium bromide; standa free energy; tetradecyltrimethyl ammonium bromide.

The diffusion coefficients of the colloidal electrolytes dec dodecyl, and tetradecyltrimethylammonium bromide have be measured as a function of concentration in aqueous solutions 25°. These values compared favorably with values obtained fro the theoretical expression derived by Hartley. A method presented for determining the standard Gibbs free energy chan of micelle formation from diffusion coefficient vs concentrati plots.

95. Meshkov, S., **Review of hadron spectroscopy,** (Proc. Int. onf. on Duality and Symmetry in Hadron Physics, Tel Aviv, srael, Apr. 5-7, 1971), Chapter 8 in *International Conference n Duality and Symmetry in Hadron Physics,* E. Gotsman, d., pp. 252-316 (The Weizmann Science Press of Israel, and he Jerusalem Academic Press, Jerusalem, Israel, 1971).

Key words: $A^2$; baryons, exotics; mesons; quarks; spectroscopy.

he present state of hadron spectroscopy is comprehensively iewed. Classifications of the mesons and baryons according he SU(6) × O(3) model are presented, as are discussions conning the $Z^*$, the $A^2$ and exotic amplitudes.

96. Yahalom, J., Ives, L. K., Kruger, J., **On the nature of films ver corrosion pits in stainless steel,** *J. Electrochem. Soc.* **120,** lo. 3, 384-386 (Mar. 1973).

Key words: Corrosion pits; electron microscopy; Fe-Cr alloys; passive films; stainless steel.

hin films over corrosion pits in two commercial austenitic nless steels, AISI 304 and 316, and three ferritic Fe-Cr als containing 5, 12 and 19 wt.% Cr were studied by means of nsmission electron microscopy and scanning electron roscopy. It is shown that these films originally existed as the sive film on the metal surface. Electron diffraction and rgy-dispersive x-ray analysis results are presented.

97. Keller, R. A., **Effect of quenching of molecular triplet states n organic dye lasers,** *IEEE J. Quantum Electron.* **QE-6,** No. 7, 11-416 (July 1970).

Key words: Dye lasers; lasers; quenching agents; triplet states.

The effect of quenching of metastable triplet states upon the iciency of organic dye lasers is considered in detail by solving coupled differential equations describing the laser process. It shown that specific quenching agents for excited triplet states n 1) cause a dramatic increase in the laser efficiency, 2) negate previous requirements of very fast pumping sources, and 3) rmit the use of dyes with relatively small fluorescence quann yields. The addition of quenching agents that quench both glet and triplet states (such as molecular oxygen) generally imves the efficiency although not as dramatically. Steady-state utions were developed that lead to analytical expressions for laser efficiency and the concentrations of the excited states a function of time.

298. Herron, J. T., Huie, R. E., **Rate constants for the reactions of $O_2$ $^1\Delta_g$ with 2,3-dimethyl-2-butene and 2,5-dimethylfuran,** *J. hem. Phys.* **51,** No. 9, 4164-4165 (Nov. 1, 1969).

Key words: Chemical kinetics; mass spectrometry; olefins; rate constant; singlet oxygen; $O_2$ $^1\Delta_g$.

Rate constants for the gas phase reactions of $O_2$ $^1\Delta_g$ have been asured using a mass spectrometric technique at 300 K. sults are $k$(2,5-dimethylfuran) = $1.6 \pm 0.4 \times 10^{10}$ cm$^3$ mol$^{-1}$ s$^{-1}$ d $k$(2,3-dimethyl-2-butene) = $1.0 \pm 0.3 \times 10^9$ cm$^3$ mol$^{-1}$ s$^{-1}$ timated uncertainties). Additional rate constants relative to rate constant for 2,3-dimethyl-2-butene have been measured follows: 2;3 dimethyl-2-pentene, 0.7; 1-methylcyclopentene, 15; 1,2-dimethylcyclopentene, 0.4; 1,2-dimethylcyclohexene, 4; and 1,3-cyclohexadiene, 0.09.

299. Rodriguez-Pasqués, R. H., Steinberg, H. L., Harding, J E., Mullen, P. A., Hutchinson, J. M. R., Mann, W. B., **Low-level radioactivity measurements on aluminum, steel and copper,** *Int. J. Appl. Radiat. Isotop.* **23,** No. 10, 445-464 (1972).

Key words: Contamination of aluminum; copper and steel; low-level radioactivity measurements.

The radioactive contamination levels in samples of aluminum, steel and copper, supplied by a number of producers of these materials have been measured and activities have been assigned to possible natural radioelements. These activities were found to lie in the range of 0.02-0.6 pCi/g of parent radionuclide. The decay with time of some contaminants has been observed. A few measurements were also made on a number of other materials.

**13300.** Young, R. H., Brewer, D., Keller, R. A., **The determination of rate constants of reaction and lifetimes of singlet oxygen in solution by a flash photolysis technique,** *J. Amer. Chem. Soc.* **95,** No. 2, 375-379 (Jan. 24, 1973).

Key words: Lasers; photochemistry; photooxidation; $^1\Delta O_2$.

A flash photolysis technique, employing a dye-laser as the flash excitation source, was developed to determine, directly, the rate constant of decay ($k_d$) of singlet oxygen ($O_2{}^1\Delta_g$) and rate constant of reaction ($k_{rx}$) between singlet oxygen and 1,3-diphenylisobenzofuran, DPBF, in a variety of solvents. Some results are the following: methanol, $k_d = (9.0 \pm 0.6) \times 10^4$ sec$^{-1}$, $k_{rx} = (1.3 \pm 0.1 \times 10^9$ sec$^{-1}$ $M^{-1}$, $k_d/k_{rx} = 7.2 \times 10^{-5}$ $M$; $n$-butyl alcohol, $k_d = (5.2 \pm 0.8) \times 10^4$ sec$^{-1}$, $k_{rx} = (0.80 \pm 0.2) \times 10^9$ sec$^{-1}$ $M^{-1}$, $k_d/k_{rx} = 6.5 \times 10^{-6}$ $M$; *tert*-butyl alcohol, $k_d = (3.0 \pm 0.4) \times 10^4$ sec$^{-1}$, $k_{rx} = (0.57 \pm 0.08) \times 10^9$ sec$^{-1}$ $M^{-1}$, $k_d/k_{rx} = 5.3 \times 10^{-5}$ $M$. Values in benzene:methanol(4:1), bromobenzene:methanol (4:1), pyridine, dioxane, methanol:water(1:1), methanol:glycol (1:1), and glycol were also obtained. The resulting $\beta$ values ($k_d/k_{rx}$) are in good agreement with $\beta$ values determined in other ways. The technique was also shown useful for determination of absolute rate constants of reaction with or quenching of singlet oxygen by compounds such as 2,5-diphenylfuran and $N,N$-dimethylaniline.

**13301.** Kulin, G., **Discussion of the paper "Free overfall as a flow measuring device" by S. W. Bauer and W. H. Graf,** *Proc. Amer. Soc. Civil Eng., Irrigation Drainage Div.* **98, IR1,** Paper 8750, 159-165 (Mar. 1972).

Key words: Hydraulic measurements; open-channel flow; overfalls.

Effects of wall friction and mild slopes on rectangular free overfalls used for measuring open channel flow are discussed. Additional research needs are pointed out.

**13302.** Dillon, T. A., Stephenson, J. C., **Calculation of vibrational and rotational energy transfer between HF, DF, HCl, and $CO_2$,** *J. Chem. Phys.* **58,** No. 5, 2056-2064 (Mar. 1, 1973).

Key words: Energy transfer; HF, DF, $CO_2$; linewidth; unitary.

A theory of vibrational energy transfer which retains the exponential form of the scattering operator is applied to energy transfer between vibrationally excited HF, DF, HCl, and $CO_2$. The calculations contain several new features, including use of curved classical trajectories and vibrational wavefunctions obtained numerically from an RKR potential. Cross sections for multiquantum pure rotational changes caused by the dipole-quadrupole interaction are calculated. These multiquantum rotational transitions play an important role in vibrational energy exchange by allowing large vibrational energy defects to be absorbed by the rotational degrees of freedom. Agreement between theory and experiment is excellent. Cross sections calculated for simultaneous transfer of two vibrational quanta from HF or HCl to $CO_2$ are very small. However, for DF-$CO_2$ the calculated two-quantum-transfer cross section is only a factor of 2-6 smaller than that for single-quantum transfer.

**13303.** Bowen, R. L., Argentar, H., **A stabilizing comonomer: II. Stabilization and polymerization characteristics,** *J. Dent. Res.* **51,** No. 6, 1614-1618 (Nov.-Dec. 1972).

Key words: Antioxidants; biomaterials; comonomers; inhibitors; polymerization; stabilizers; toxicity.

BHM (3,5-di-*t*-butyl-4-hydroxybenzyl methacrylate) was evaluated with regard to its effectiveness as a stabilizer (polymerization inhibitor). This sterically-hindered phenol containing a methacrylate moiety was an effective stabilizer but it had lower efficiency than BHT (2,6-di-*t*-butyl-4-methylphenol). This is attributed to the greater steric hindrance at the *para* position and lower electron-donating nature of the *para*-substituent of the phenol, BHM. The homopolymer of BHM was prepared by polymerization of the methacrylate group, under anaerobic conditions, even though, under aerobic conditions it is an effective stabilizer.

**13304.** Barton, J. A., Jr., Eick, J. D., Dickson, G., **Comparison of Brinell and Vickers hardness tests on dental casting gold alloys,** *J. Dent. Res.* **52,** No. 1, 163-169 (Jan.-Feb. 1973).

Key words: Brinell hardness number; dental casting; gold alloy; indentation; Rockwell superficial hardness tester; Vickers hardness number; Vickers hardness tester.

A large group of dental casting gold alloys representing all four types listed in American Dental Association Specification No-5 were indented, using the Brinell and Vickers methods. The relationship between Vickers and Brinell hardness numbers was found to be linear with the addition of 19 to the Brinell number approximating the Vickers number fairly well. The coefficient of variation for the Brinell test was found to be about 1 percent less than that of the Vickers test. Surface preparation, grain size, and the position of the indentation with respect to grain structure did not affect the precision of the Vickers method. The effects of reading error and sample inhomogeneity on the precision of the Vickers values were also evaluated. The reading error was a large portion of the total error for types I, II, and III, but only about 35 percent of the total error for type IV alloys.

**13305.** Hadley, S. G., Keller, R. A., **Direct determination of the singlet → triplet intersystem crossing quantum yield in naphthalene, phenanthrene, and triphenylene,** *J. Phys. Chem.* **73,** No. 12, 4356-4359 (1969).

Key words: Aromatics; electronic spectroscopy; intersystem crossing; quantum yields; triplet states.

Radiationless singlet → triplet intersystem crossing quantum yields have been directly determined. The technique used depends upon using previously determined extinction coefficients to relate the optical density of the triplet ← triplet absorption and the absolute intensity of the light used to generate triplet state molecules to the intersystem crossing quantum yield. The quantum yields at 77 K in a rigid matrix and their estimated uncertainties were found to be naphthalene-$h_8$, $0.25 \pm 0.05$; naphthalene-$d_8$, $0.25 \pm 0.05$; phenanthrene-$h_{10}$, $0.35 \pm 0.07$; phenanthrene-$d_{10}$, $0.45 \pm 0.09$; triphenylene-$h_{12}$, $0.54 \pm 0.11$; and triphenylene-$d_{12}$, $0.88 \pm 0.18$. No significant deuterium isotope effects were noted on the intersystem crossing quantum yields.

**13306.** Davis, D. D., Braun, W., Bass, A. M., **Reactions of $Cl^2P_{3/2}$: Absolute rate constants for reaction with $H_2$, $CH_4$, $C_2H_6$, $CH_2Cl_2$, $C_2Cl_4$, and c-$C_6H_{12}$,** *Int. J. Chem. Kinet.* **II,** 101-114 (1970).

Key words: Absolute rate constants; atom-molecule reactions; chlorine atoms; resonance fluorescence.

The absolute rate constants have been measured for several gas-phase chlorine atom-molecule reactions at 25 °C by resonance fluorescence. These reactions and their correspon rate constants in units of cm³ mole⁻¹ sec⁻¹ are:

$$Cl^2P_{3/2} + H_2 \xrightarrow{k_1} HCl + H \qquad k_1 = 1.4 \pm 0.1 \times 10^{-14}$$

$$Cl^2P_{3/2} + CH_4 \xrightarrow{k_2} HCl + CH_3 \qquad k_2 = 1.5 \pm 0.1 + 10^{-13}$$

$$Cl^2P_{3/2} + CH_2Cl_2 \xrightarrow{k_5} HCl + CHCl_2 \qquad k_5 = 5.5 \pm 0.5 \times 10^{-13}$$

$$Cl^2P_{3/2} + C_2Cl_4 \xrightarrow{k_6} C_2Cl_5 \qquad k_6 = 5.3 \pm 0.5 \times 10^{-12}$$

$$Cl^2P_{3/2} + C_2H_6 \xrightarrow{k_7} HCl + C_2H_5 \qquad k_7 = 6.7 \pm 0.7 \times 10^{-11}$$

$$Cl^2P_{3/2} + c\text{-}C_6H_{12} \xrightarrow{k_8} HCl + c\text{-}C_6H_{11} \qquad k_8 = 2.0 \pm 0.2 \times 10^{-10}$$

The effects of varying the substrate pressure, total pressu light intensity and chlorine-atom source on the value of bimolecular rate constants have been investigated for all th reactions. Conditions under which no competing side react occurs were established and the reported rate constants w measured under these conditions. For reactions (2), (5), (6), and (8), there is a discrepancy of a factor of two between the constants measured in this work and values in the literature; suggested that this is due to an error in the previously measu value of $k_{CH_4}/k_{H_2}$ upon which the relative measurements in literature ultimately depend.

**13307.** Lester, W. A., Jr., Krauss, M., **Interaction poten between Li and HF,** *J. Chem. Phys.* **52,** No. 9, 4775-4781 (M 1, 1970).

Key words: Hartree-Fock approximation; induction en gy; interaction potential; radial coefficients; scattering culations.

The interaction potential between Li and HF has been de mined in the Hartree-Fock approximation. An expression for interaction potential has been determined in the case of fixed ternuclear distance of HF in a form suitable for scattering cal lations. The results are tabulated as radial coefficients for the termolecular potential expressed as $V(r,\theta) = \Sigma_i v_i(r) P_i(\cos\theta)$. long range, the Hartree-Fock calculation determines the ind tion energy of a spherical atom Li interacting with a dip molecule HF. For the approach of the Li atom toward th atom, there is a minimum in the energy for a Li to HF center mass distance of 4 a.u. Most of the hemisphere on the F sid the surface ultimately leads to reaction. On the other hand, spherically symmetric component of the intermolecular pot tial, $(\nu_0(r)$, has a minimum at about 9 a.u. which is related to potential well deduced from glory scatter data.

**13308.** Meijer, P. H. E., Colwell, J. H., Shah, B. P., **A note on morphology of heat capacity curves,** *Amer. J. Phys.* **41,** Nc 332-339 (Mar. 1973).

Key words: Brillouin function; density of states; Eins function; energy levels; harmonic oscillator; heat capac molecular field; molecular rotation; Schottky anomaly.

In this article we try to relate the general features of sev types of heat capacity curves to the underlying energy level sp trum. We are interested in heat capacity "anomalies" (i.e., h capacities which occur in addition to the usual lattice vibra and conduction electron contributions) and restrict ourselve systems which can be described on an independent particle sis. We begin by considering Schottky anomalies and show effects on the heat capacity of varying the spacings degeneracies of the energy levels. The relation between Schottky anomaly arising from the equally spaced n generate levels of the Brillouin function and the heat capacity the Einstein function is discussed. The effects on the heat pacity of a marked local change in the density of states of an herwise uniform energy-level spectrum is considered. The heat pacities of the free rotor and the molecular field model are ed to exemplify particular points of the discussion.

309. Linzer, M., Stokesberry, D. P., **A frequency-lock method for the measurement of $Q$ factors of reflection and transmission resonators,** *IEEE Trans. Instrum. Meas.* **IM-22,** No. 1, 61-77 (Mar. 1973).

> Key words: Automatic $Q$ measurement; frequency-lock method; $Q$ measurement; reflection resonators; transmission resonators.

A new method for the measurement of $Q$ factors of reflection ngle-ended) and transmission (double-ended) resonators has en developed. The basis of the technique is the locking of an cillator to some point away from the center of the resonator sponse curve. This is accomplished by the introduction of a ase offset into a conventional oscillator-resonator stabilization rcuit so as to make the stabilizer sensitive to both the real and aginary portions of the voltage transfer coefficient of the sonator. From a determination of the phase and frequency ifts, the $Q$ factor may be evaluated.

The frequency-lock method shows promise of having signifi nt advantages in speed, convenience, and accuracy over previ s techniques. The basic features of this approach were suc ssfully demonstrated in a measurement of the $Q$ factor of an $X$-nd reflection cavity. A circuit for fully automatic $Q$ terminations is proposed. In this mode of operation, the device ould be insensitive to changes in the eigen-frequency of the sonator and should be capable of measuring very small anges in $Q$.

310. Levin, I. W., Abramowitz, S., **Isotopic splitting in matrix isolated BF$_3$,** *Chem. Phys. Lett.* **9,** No. 3, 247-248 (May 1, 1971).

> Key words: BF$_3$; Coriolis; isotope effects; vibrational force field.

Small isotopic frequency shift information, if precisely deter ined, provides an effective constraint on intramolecular force elds. The most precise data for these frequency shift parame rs $\Delta\nu$ are derived from high resolution, gas-phase infrared spec al analyses. In the present study, we compare for BF$_3$ the otopic frequency shift $\Delta\nu_4$ from a recently published gas-phase udy with the value for $\Delta\nu_4$ that we obtain from the spectrum of atrix isolated BF$_3$. The excellent agreement between the two ethods suggests further applications of the matrix technique for btaining precise frequency shift data.

3311. Page, C. H., **Ambiguities in the use of unit names,** *Science* **179,** 873-875 (Mar. 2, 1973).

> Key words: Gyromagnetic ratio; measurement units; physical constants; SI units.

Experimental determinations of physical constants are usually eported in the literature in accepted units, such as SI. The actual easurements are *not* made in terms of the reported units, but in erms of the units maintained by a standards laboratory. This ack of precise identification of the results leads to ambiguities in omparing data from different countries, and in adjusting con tants to make a most consistent set.

The semantics and algebra of the situation are presented, with tentative resolution of the problem.

3312. Burdick, M. D., **Test for the adherence of porcelain enamel cover coats direct-to-steel,** *Porcelain Enamel Inst. Bull.* **T-29,** 1-10 (1972).

> Key words: Adherence; direct-on porcelain enamels; impact.

An adherence test for direct-on-cover coat porcelain enamels has been developed. This test consists of deforming the porcelain enameled specimen with a 1/2 inch diameter ball with 80-inch pounds of energy into a 3/4 inch die. The adherence is then evaluated by determining the amount of enamel adhering after impact by measuring it with an adherence meter.

13313. Barnes, I. L., Garner, E. L., Gramlich, J. W., Moore, L. J., Murphy, T. J., Machlan, L. A., Shields, W. R., Tatsumoto, M., Knight, R. J., **Determination of lead, uranium, thorium, and thallium in silicate glass standard materials by isotope dilution mass spectrometry,** *Anal. Chem.* **45,** No. 6, 880-885 (May 1973).

> Key words: Isotope dilution; lead; mass spectrometry; silicate glass standard materials; standard reference materials; thallium; thorium; uranium.

A set of four standard glasses has been prepared which have been doped with 61 different elements at the 500-, 50-, 1-, and 0.02-ppm level. The concentrations of lead, uranium, thorium, and thallium have been determined by isotope dilution mass spectrometry at a number of points in each of the glasses. The results obtained from independent determinations in two laboratories demonstrate the homogeneity of the samples and that precision of the order of 0.5 percent (95 percent L.E.) may be obtained by the method even at the 20-ppb level for these elements. The chemical and mass spectrometric procedures necessary are presented.

13314. Kessler, B. V., Meijer, P. H. E., **Calculation of behavior of paramagnetic systems with dipolar and exchange interactions,** *Phys. Rev. B* **7,** No. 6, 2839-2850 (Mar. 15, 1973).

> Key words: Cerium ethyl sulfate; cerous magnesium nitrate; cobaltous fluosilicate; cupric potassium sulfate; dipole-dipole interaction; entropy; exchange interaction; ferric methyl ammonium alum; low temperature paramagnetism.

This paper deals with a precise calculation of the $b_2$ coefficients in the specific heat for a number of ultralow-temperature compounds. The result is given for the actual dipole-dipole interaction plus a varying amount of isotropic exchange $J$. Comparison with experimental data leads to a determination of $J$. Usually two values are possible as a result of the quadratic dependence of $b_2$ on $J$. Similar calculations are performed for the $T^{-3}$ term in the specific heat. In this case there are two types of contributions: one from the two-point summation and one from the three-point sum or ring diagram. The value of each is determined as a function of $J$. The values of $J$ as determined from the comparison of the experimental values of $b_2$ with the calculated values of $b_2$ are substituted in $b_3$ and the values thus predicted, on the basis of isotropic exchange, are given.

13315. Taragin, M. F., Eisenstein, J. C., Haller, W., **Mössbauer study of Fe$^{57}$ in an aluminophosphate glass,** *Phys. Chem. Glasses* **13,** No. 5, 149-152 (Oct. 1972).

> Key words: Aluminophosphate glass; Fe$^{57}$; glass; iron; Mössbauer spectra; phosphate glass.

Mössbauer spectra of an aluminophosphate glass which contains 10 percent Fe$_3$O$_4$ were obtained from room temperature to 450 °C. Fe$^{2+}$ and Fe$^{3+}$ ions are present. The isomer shift and quadrupole splitting for these ions are each given as a function of temperature, and it appears that both ions are in octahedral coordination. The ratio of the product of the Mössbauer fraction multiplied by the concentration ratio of $Fe^{3+}$ to $Fe^{2+}$ was determined. This ratio varies with temperature. A possible explanation is that the effective Debye temperatures are different for the two ionic species, being 385 K for $Fe^{3+}$ and 230 K for $Fe^{2+}$. The difference may possibly be attributed to differences in the sites occupied by $Fe^{3+}$ and $Fe^{2+}$ in the glass structure.

**13316.** Costrell, L., **CAMAC instrumentation system—introduction and general description,** *IEEE Trans. Nucl. Sci.* **NS-20,** No. 2, 3-8 (Apr. 1973).

Key words: CAMAC; dataway; instrumentation; modules; nuclear; standards.

The CAMAC instrumentation system developed by the ESONE Committee of European Laboratories has been endorsed by the U.S. AEC NIM Committee as a dataway system complementary to the NIM (Nuclear Instrument Module) system. CAMAC is described in a general way in this introductory paper which is followed by papers that discuss the system in greater detail. This paper is an updated version of the introductory paper that appeared in the April 1971 IEEE Transactions on Nuclear Science.

**13317.** Zalewski, E. F., Keller, R. A., **Pressure dependence of intersystem crossing and triplet internal conversion in naphthalene vapor,** (Proc. Int. Conf. on Luminescence, University of Delaware, Newark, Del., Aug. 25-29, 1969), *J. Lumin.* **1,2,** 143-153 (1970).

Key words: Internal conversion; intersystem crossing; naphthalene vapor absorption spectrum; pressure effect on absorption spectrum; radiationless transitions.

The pressure dependence of intersystem crossing and internal conversion in the triplet manifold of naphthalene vapor was studied by monitoring the concentration of both the singlet ground state at the peak of and one minute after flash excitation, and the lowest triplet state at the peak of the flash. Helium was used as the foreign gas up to pressures of 460 torr. The pressure of naphthalene was 0.026 torr in all cases. In summary, the experimental results are: (1) Ground state depletion during the flash is independent of pressure. (2) The population of the lowest triplet state, experimentally zero initially, increases with increasing helium pressure and becomes constant above 100 torr. (3) Photodecomposition decreases with increasing pressure of helium and finally approaches zero at pressures greater than 100 torr. The conclusions which result from these observations are: (1) In the absence of collisions, photochemical decomposition of excited triplet molecules can compete effectively with internal conversion. (2) Intersystem crossing is not pressure dependent in naphthalene.

**13318.** Okabe, H., Mele, A., **Photodissociation of $NCN_3$ in the vacuum-ultraviolet production of CN $B\ ^2\Sigma$ and NCN $A\ ^3\Pi$,** *J. Chem. Phys.* **51,** No. 5, 2100-2106 (Sept. 1, 1969).

Key words: Absorption coefficient; bond dissociation energies; CN $B\ ^2\Sigma$; NCN $A\ ^3\Pi$; $NCN_3$; photodissociation; vacuum ultraviolet.

The photodissociation of $NCN_3$ in the vacuum ultraviolet has yielded CN $B\ ^2\Sigma$ and NCN $A\ ^3\Pi$. No NCN $^1\Pi$ was detected. The fluorescence intensity of the CN violet emission, $I_f/I_0$, was measured as a function of incident wavelength, λ. The $I_f/I_0$-vs-λ curve shows structure, indicating that the process

$$NCH_3 \xrightarrow{h\nu} CN\ B\ ^2\Sigma + N_3,$$

is predissociative. The yield at 1216 Å is estimated to be approximately 2.5 percent. The threshold wavelength of incid photons to yield CN $B\ ^2\Sigma$ is 1685±20 Å. The production NCN $A\ ^3\Pi$ is attributed to the formation of $N_2\ A\ ^3\Sigma$

$$NCN_3 \xrightarrow{h\nu} NCN\ X\ ^3\Sigma + N_2\ A\ ^3\Sigma,$$

with the threshold wavelength of 1915±30 Å followed by sensitized reaction, $N_2\ A\ ^3\Sigma + NCN_3 \rightarrow NCN\ A\ ^3\Pi + 2N_2$. Bc dissociation energies obtained from threshold energies $D(NC-N_3) = 4.2 \pm 0.1$ eV $(= 96 \pm 2$ kcal mole$^{-1})$ $D(NCN-N_2) = 0.3 \pm 0.1$ eV $(= 7 \pm 2$ kcal mole$^{-1})$ where error limit indicates an experimental uncertainty of the thresh energy measurements. Estimated heats of formation $\Delta H_f°(NCN_3) = 4.7 \pm 0.2$ eV $(= 108 \pm 5$ kcal mole$^{-1})$ $\Delta H_f°(NCN) = 5.0 \pm 0.2$ eV $(= 115 \pm 5$ kcal mole$^{-1})$ from wh $D(N-CN)$ of $4.3 \pm 0.2$ eV $(= 99 \pm 5$ kcal mole$^{-1})$ is obtain The absorption coefficient of $NCN_3$ in the region 1200 to 2 Å has been measured. A comparison is made of bond energie several azide compounds.

**13319.** Mele, A., Okabe, H., **Distribution of the excess energ CN $B\ ^2\Sigma$ produced in photodissociation of cyanogen halides hydrogen cyanide,** *J. Chem. Phys.* **51,** No. 11, 4798-4808 (D 1, 1969).

Key words: BrCN; ClCN; CN $B\ ^2\Sigma$; energy partiti HCN; ICN; photodissociation; vacuum ultraviolet.

The vibrational and rotational excitations of CN $B$ produced in photodissociation of cyanogen halides and hydro cyanide in the vacuum ultraviolet have been measured as a fu tion of incident wavelengths. More than 70 percent of the to population is in levels up to $\nu' = 3$. No population inversion observed, indicating the photodissociation takes place with much change in the equilibrium C-N bond distance. The perc conversion of the excess energy to vibration is approximately percent for cyanogen halides and about 12 percent for hydro cyanide, irrespective of the amount of excess energy, whic much less than that expected from the equipartition of energ all vibrational degrees of freedom of the molecule. The rotatic levels of CN $B\ ^2\Sigma$ are highly excited for all molecules. The ext of conversion of the excess energy to rotation is of the orde 10-20 percent for ICN and ClCN, and only several percent BrCN and HCN. The remaining energy must be distribute kinetic energy between CN $B\ ^2\Sigma$ and atoms. The vibrational rotational distributions are discussed in terms of the equilibri geometries of the ground and excited molecules and of the f products. The CN $A\ ^2\Pi$ state is also formed in photodissociat and apparently not directly but through the CN $B\ ^2\Sigma$. The int sity of the CN red emission is much less than that of the vio Various other photodissociation processes are discussed. general, the extent of conversion of the excess energy to vi tion is much less than that expected from the equipartition the for most triatomic molecules. No vibrational population in sion has been observed.

**13320.** Kaldor, A., Maki, A. G., **High resolution infrared s trum and the molecular structure of sulfur trioxide,** *J. Struct.* **15,** 123-130 (1973).

Key words: Air pollution; bond distances; infrared s troscopy; molecular structure; spectra; sulfur trioxide.

The $2\nu_3{}^2(E')$ band of sulfur trioxide has been measured wi resolution of 0.03 cm$^{-1}$. The analysis of this band yields a se rotational constants which fit the data to within a standard de tion of 0.003 cm$^{-1}$ (which is the expected error limit). From rotational constant $B_0 = 0.34857 \pm 0.00006$ cm$^{-1}$ the S-O b distance is found to be $r_0 = 1.4198 \pm 0.0002$ Å. This value i agreement with earlier infrared measurements, but represen considerable improvement in accuracy.

21. Loebenstein, W. V., **Adsorption of water on tooth com- ponents and related materials,** *J. Dent. Res.* **52,** No. 2, 271-280 Mar.-Apr. 1973).

Key words: Adsorption; dental materials; hysteresis; sorption; surface area; teeth; water vapor.

By use of a novel, simply constructed, vapor-circulating ap- ratus, complete water adsorption isotherms, and surface areas ived therefrom, were obtained for tooth components and resentative dental materials. Characteristic hysteresis loops re found for all materials studied.

322. Hadley, S. G., Keller, R. A., **Direct determination of the xtinction coefficients for triplet ← triplet transitions in naphthalene, phenanthrene, and triphenylene,** *J. Phys. Chem.* 73, No. 12, 4351-4355 (Dec. 1969).

Key words: Aromatics; electronic spectroscopy; intersystem crossing; quantum yields; triplet states.

Extinction coefficients for triplet ← triplet absorption have en directly determined for several aromatic hydrocarbons. A gh intensity photolysis lamp was used to populate the triplet ate and the concentration of triplets was measured by monitor- the depletion of the ground state. The values of the extinction efficients $\epsilon \times 10^{-4}$ (l. mol$^{-1}$ cm$^{-1}$) and their estimated uncer- nties at the most prominent maximum λ(nm) are: naphthalene- 4.0 ± 0.6, 414.0; naphthalene-$d_8$, 4.0 ± 0.6, 414.0; enanthrene-$h_{10}$, 3.8 ± 0.6, 492.5; phenanthrene-$d_{10}$, 3.1 ± 0.5, 2.5; triphenylene-$h_{12}$, 1.56 ± 0.23, 430.0; and triphenylene-$d_{12}$, 20 ± 0.18, 431.0. For anthracene, $\epsilon_T \geqslant 9 \times 10^4$ l. mol$^{-1}$ cm$^{-1}$ at 7.3 nm.

323. Hampson, R. F., Jr., Okabe, H., **Collisional stimulation of the O($^1S$) – O($^1D$) emission of oxygen atoms formed in vacuum-ultraviolet photolysis of nitrous oxide,** *J. Chem. Phys.* **52,** No. 4, 1930-1933 (Feb. 15, 1970).

Key words: Collisional stimulations; $N_2O$; $O^1S - O^1D$ emission; photodissociation; vacuum ultraviolet.

Oxygen atoms in the $^1S$ state have been produced by the acuum-ultraviolet photolysis of $N_2O$ and observed by their nission at 5577 Å in the $^1S - {}^1D$ transition. The stimulation of is emission by collision with added gases has been studied. The nission has been found to be proportional to the pressure of the lded gas. Xenon is the most efficient stimulator of the gases sed, followed in order of decreasing efficiency by Kr, Ar, $N_2$, $_2$, and He. Data gotten by photolysis of $NO_2$ and $CO_2$ have een used to estimate their quantum yields for formation of ($^1S$).

324. Guttman, C. M., Flynn, J. H., **On the drawing of the base line for differential scanning calorimetric calculation of heats of transition,** *Anal. Chem.* **45,** No. 2, 408-410 (Feb. 1973).

Key words: Base line determination; differential scanning calorimetry (DSC); heats of transition; thermal analysis; thermoanalytical calorimetry.

The heat of transition has been computed from a Differential canning Calorimetry (DSC) trace by drawing a base line related nly to the heat capacity of the transition's upper state.

3325. Stein, P. G., **Communications protocols: The search for SYN,** *Datamation* **19,** No. 4, 55-57 (Apr. 1973).

Key words: Asynchronous; communications; computer; data transmission; errors, protocol; synchronous.

This article gives a brief review of the field of serial data trans- ission with emphasis on protocols for synchronous communications. An example of such a protocol is given while describing a specific system implemented by the author. The importance of good system coordination and planning is stressed.

13326. Swartzendruber, L. J., Evans, B. J., **Giant hyperfine field at the antimony site in the Heusler-alloy $Pd_2MnSb$,** *Phys. Lett.* **38A,** No. 7, 511-512 (Mar. 27, 1972).

Key words: Alloys; hyperfine field; Mn; Mössbauer effect; Pd; Sb.

The magnetic hyperfine field at $^{121}Sb$ in $Pd_2MnSb$ has the anomalously large value (at 100 K) of ± 579 ± 5 kG. In the closely related compound PdMnSb we find ± 302 ± 5 kG, similar to other ferromagnetic intermetallics containing Mn and Sb.

13327. Braun, W., Bass, A. M., Davis, D. D., **Experimental test of a two-layer model characterizing emission-line profiles,** *J. Opt. Soc. Amer.* **60,** No. 2, 166-170 (Feb. 1970).

Key words: Atoms; hydrogen; resonance; spectra.

Deuterium Lyman-α line profiles, generated from a microwave-powered lamp containing flowing mixtures of deuterium in helium, were examined spectroscopically under high resolution. The primary purpose was to test a simple two-layer model describing the line shape emerging from a discharge zone containing both emitting and absorbing atoms. This simple model characterized the experimentally obtained line shapes under varying conditions of atom densities and line self-reversal. The kinetic (translational) temperature of the discharge could be calculated from the data. Resonance interaction between ground-state D($^2$S) atoms and excited D($^2$P) atoms is offered as an explanation for the experimentally observed line asymmetries. The presence of line self-reversal significantly amplifies the small spectral shifts between the absorption and emission lines. These shifts can be calculated from the model.

13328. Franklin, A. D., **Point defects in alkaline earth fluorides,** (Proc. 3d Int. Conf. on Sintering and Related Phenomena, University of Notre Dame, Notre Dame, Ind., June 5-7, 1972), Paper in *Materials Science Research,* G. C. Kuczynski, Ed., **6,** 19-27 (Plenum Publ. Corp., New York, N.Y., 1973).

Key words: Alkaline earth fluorides; $CaF_2$; clusters; defect models; $GdF_3$; mass transport; point defects.

Alkaline earth fluorides containing substitutional trivalent cations are known to contain fluorine interstitials as well, providing charge balance. It has been customary to assume that at low temperatures association between these impurity cations and interstitial anions controls the anion interstitial concentrations. However, an examination of EPR and optical data on quenched specimens of $CaF_2$: $GdF_3$ shows that this is probably not the case. Rather, interstitial clusters are formed at low temperatures. Sample calculations with a model of quenched crystals based upon this notion reproduces the main features of our previous data on variation of the relative concentrations of associated and unassociated $Gd^{3+}$ ions with $GdF_3$ content and annealing temperature.

13329. Hall, J. L., **Saturated absorption spectroscopy with applications to the 3.39 μm methane transition,** (Proc. 3d Int. Conf. on Atomic Physics, Boulder, Colo., Aug. 1972), Chapter in *Atomic Physics,* S. J. Smith and G. K. Walters, Eds., **3,** 615-646 (Plenum Publ. Corp., New York, N.Y., Feb. 1973).

Key words: Laser; methane; optical frequency standards; saturated absorption; spectroscopy.

In basic research we are grateful to be able to pursue research in profitable directions, e.g., those directions where the boundaries of experimental or theoretical possibilities seem most susceptible to growth. Of course we know of some areas that could be investigated and many numerical data recorded, but we are uneasy in not knowing how to make use of the data. As physicists we especially like to make progress synthesizing specialized concepts into more general forms. We savor the similarities – and differences – when ideas developed in one area prove useful in another set of circumstances. Just now it is optical resonance physics that seems to be ripe for explosive growth using new laser techniques and "classical" resonance ideas. This paper represents a direct effort to sketch, in the opinion of a certain class of partisans, "where the action is." We begin with a brief discussion of experiments in which a laser is useful but not necessary, and a consideration of the basic optical facts of life. The bulk of the paper explores the exciting land beyond the Doppler limit.

**13330.** Shields, J. Q., **Phase-angle characteristics of cross capacitors,** *IEEE Trans. Instrum. Meas.* **IM-21,** No. 4, 365-368 (Nov. 1972).

> Key words: Capacitor; cross capacitor; dielectric films; loss angle; phase angle.

It has been found that under proper conditions thin dielectric films on the electrodes of certain types of cylindrical cross capacitors tend only to produce equal and opposite contributions to the phase angles of the two cross capacitances. To a lesser degree, this same type of cancellation effect has been found to be associated with toroidal cross capacitors.

**13331.** Caswell, R. S., Berger, M. J., **Theoretical aspects of radiation dosimetry,** (Proc. Conf. on Particle Accelerators in Radiation Therapy, Los Alamos, N. Mex., Oct. 2-5, 1972), Paper in *Conference on Particle Accelerators in Radiation Therapy,* **LA-5180-C,** 60-74 (Mar. 1973).

> Key words: Absorbed dose distribution; electrons; heavy ions; interpretation of measurements; neutrons; pions; protons; radiation dosimetry; radiation quality; radiation transport theory.

A review of made of the role of theoretical dosimetry in interpretation of measurements, determination of the spatial distribution of absorbed dose, and in providing detailed physical information about radiation quality. The state of the art in calculating absorbed dose distributions in homogeneous tissue equivalent media is examined by comparisons with experiments for electron, proton, neutron, and pion beams. In cases where physical properties of the beam and medium are particularly well known, the accuracy can sometimes approach 5 percent. In a larger number of cases the accuracy is 10-15 percent or worse. Knowledge of absorbed dose distributions in realistic inhomogeneous media is rudimentary: new methods, schematizations, and further calculations are required. For improved absorbed dose calculations, further neutron and pion medium energy cross section information is needed.

Radiation transport calculations are providing detailed physical information needed for the various models of radiation action on biological materials. Such detailed information is usually not available from experiment. Improvement in these calculations will depend on improved knowledge of the interaction of electrons and heavy ions with matter. New pertinent atomic data are being generated, but the cross section data base for low energy calculations is far from complete.

**13332.** Cezairliyan, A., **Measurement of melting point, normal spectral emittance (at melting point), and electrical resistivity (about 2650 K) of niobium by a pulse heating method,** *High Temp.-High Pressures* **4,** 453-458 (1972).

> Key words: Electrical resistivity; emittance; high-sp
> measurements; high temperature; melting point; niobium

A subsecond duration pulse heating method is used to meas
the melting point, normal spectral emittance (at the mel
point), and electrical resistivity (above 2650 K) of niobium.
results yield a value of 2750 K for the melting point on the In
national Practical Temperature Scale of 1968. Normal spec
emittance at the melting point is 0.338, and remained cons
during melting. At 2740 K electrical resistivity is 90.11 × 1
ohm m. Estimated inaccuracy is 10 K in the melting point, 3
cent in normal spectral emittance and 0.5 percent in electrical
sistivity.

**13333.** Goldberg, R. N., Prosen, E. J., **Evaluation of heat**
**transition in scanning calorimetry,** *Thermochimica Acta* **6,**
1, 1-11 (1973).

> Key words: Heats of transition; scanning calorime
> theory of calorimetry; thermal analysis.

A procedure for the evaluation of heats of transition
scanning calorimetry has been developed. A formula for eva
tion of the energy of fusion of a compound at its melting poi
derived that takes into account the baseline shift that is attrib
ble to the heat capacity change on melting. Several o
calorimeter parameters of importance are discussed. These
clude heat exchange between calorimeter vessel and jacket,
time constant of the instrument, the scanning rate, and the he
placement.

**13334.** Milligan, D. E., Jacox, M. E., McAuley, J. H., Smith
E., **Matrix isolation study of the vacuum-ultraviolet photol**
**of $HCClF_2$ and of $HCCl_2F$. Infrared spectra of the pa**
**molecules and of the $ClCF_2$ and $FCCl_2$ free radicals,** *J.*
*Spectrosc.* **45,** No. 3, 377-403 (Mar. 1973).

> Key words: $ClCF_2$; $DCClF_2$; $DCCl_2F$; $FCCl_2$; HCC
> $HCCl_2F$; infrared spectrum; matrix isolation; vacuum
> traviolet photolysis.

Studies of the vacuum-ultraviolet photolysis of $HCClF_2$
of $HCCl_2F$ isolated in argon and nitrogen matrices at 14 K h
led to the infrared spectroscopic identification of the free radi
$ClCF_2$ and $FCCl_2$, respectively. Support for this identifica
has been obtained from studies of the vacuum-ultraviolet ph
ysis of $DCClF_2$, of $DCCl_2F$, and of $H^{13}CCl_2F$, as well as f
studies of halogen-atom abstraction from $CClF_3$ and from C
by sodium atoms in an argon matrix environment. The C
bonds of $FCCl_2$, like those of $CCl_3$ and of $HCCl_2$, appear t
exceptionally strong. Gas-phase infrared spectral data are
reported for $DCClF_2$ and for $DCCl_2F$, not previously stud
Vibrational assignments are proposed for these two molec
and data supporting the reassignment of one of the C
stretching fundamentals of $HCClF_2$ are presented.

**13335.** Hutchinson, J. M. R., Lantz, J. L., Mann, W. B., Mul
P. A., Rodriguez-Pasqués, R. H., **An anti-coincidence shie**
**NaI(Tl) system at NBS,** *IEEE Trans. Nucl. Sci.* **NS-19, N**
117-118 (Feb. 1972).

> Key words: Anti-coincidence shielding; low-level radi
> tivity measurements; scintillation counting; sodium-io
> crystals.

The anti-Compton anti-coincidence shielded 8 in NaI
crystal system recently installed at N.B.S. is described. This
paratus is composed of 2 – 8 in × 4 in well crystals which ca
used in coincidence, and a 30 in diameter 20 in long cylindr
anti-Compton anti-coincidence scintillation plastic shield.
instrument is discussed as a particularly powerful tool for
level radioactivity calibration.

336. Cotton, I. W., **Intelligent terminals,** *Datamation* **19,** No. 5, 149 (May 1973).

Key words: Computer terminals; intelligent terminals.

This article is a description of a forthcoming panel session on telligent Terminals which the author will chair at the 1973 Na-onal Computer Conference. The theme of the session is ex-ained, and the paper authors and panelists are identified.

337. Taylor, B. N., **Determining the Avogadro constant to high accuracy via improved measurements of the absolute ampere,** *Metrologia* **9,** No. 1, 21-23 (1973).

Key words: Absolute ampere; Avogadro number; fundamental constants.

It is shown how an improved measurement of the absolute am-ere, that is, the ratio of a particular as-maintained unit of current the absolute or *Systeme International d'Unites* (SI) unit of urrent, can now lead to an improved value of the Avogadro con-ant.

338. Nahman, N. S., **Miniature superconductive coaxial transmission lines,** *Proc. IEEE* **61,** No. 1, 76-79 (Jan. 1973).

Key words: Cables; coaxial; cryogenic; miniature; pulse delay; superconducting; telecommunications; transmission lines.

This is a review paper concisely tracing the development of iniature superconductive coaxial transmission lines from the riginal invention as a vertical channel signal delay line for frac-onal nanosecond pulse oscillography to present-day work owards highly compact, broad-band, and low-loss telecommuni-ation cables. The present state of development yields a 1.6-mm oaxial line operating at 4.2 K and having Pb conductors, olyethylene dielectric, $Z_0 = 50 \pm 0.3$ Ω and a 1-GHz attenuation f the order of 1 dB/km. The attenuation up to 1 GHz is mainly ue to dielectric losses.

3339. Adler, A., Kahan, W., Novick, R., Lucatorto, T., **Measurement of the lifetime and the electron-impact excitation cross section and polarization of the $2^3P$ term of singly ionized lithium,** *Phys. Rev. A* **7,** No. 3, 967-872 (Mar. 1972).

Key words: Electron-excitation cross section; lifetime; rf resonance spectroscopy; $2^3P$ term of Li$^+$.

The lifetime of the 2 $^3P_j$ states in singly ionized lithium has een measured using an rf magnetic-resonance technique; the alue is $\tau = 45 \pm 5$ nsec. Neutral lithium was ionized and excited y a unidirectional beam of electrons which produced an align-nent in the excited state. The cross section for the electron-im-act excitation $1s^2\ 2s\ ^2S \rightarrow 1s2p\ ^3P$ near the threshold was mea-ured to be $10^{-22\pm1}$ cm$^2$. Implications for the feasibility of rf esonance spectroscopy on the fine and hyperfine structure of he $2^3P$ term will be discussed.

13340. Spicer, B. M., Danos, M., **Quartet structure and collective effects in the scandium isotopes,** *Z. Phys.* **246,** 97-103 (1971).

Key words: Core polarization; electromagnetic transitions; nuclear spectroscopy; nuclear structure; quadrupole moment; quartet structure.

The systematics of the excitation energies of the non-normal parity states of the scandium isotopes are interpreted in terms of the formation of a quartet of $1f_{7/2}$ nucleons. Calculation of the *B(E2)* value for a typical radiative transition between non-normal parity states in $^{43}$Sc, using this model, shows that the transition must involve more than the single quartet formed in the $1f_{7/2}$ shell; that is, that core polarization is an important factor in determining the *B(E2)* value.

13341. Spencer, L. V., Woolf, S., **"Forced-reflection" collimators and the n-n scattering experiment,** *Nucl. Instrum. Methods* **97,** 567-576 (1971).

Key words: Air ducts in shields; collimators; neutron instrumentation; neutron-neutron scattering; neutron penetration; re-entrant holes.

An approach to neutron collimator design is suggested in which wall-emergent neutrons are forced to reflect from the surface of each (tapered) segment beyond the point of emergence. Designs of this type, together with a suggested design for a proposed neutron-neutron scattering experiment, are compared in simple Monte Carlo and analytic studies.

13342. Dickens, B., Brown, W. E., **The crystal structure of $CaKAsO_4 \cdot 8H_2O$,** *Act. Crystallogr.* **B28,** Part 10, 3056-3065 (Oct. 1972).

Key words: Calcium arsenates; calcium phosphates; inorganic hydrate; ion hydration; single crystal x-ray diffraction.

$CaKAsO_4 \cdot 8H_2O$ crystallizes in the orthorhombic unit cell $a = 7.146(1)$, $b = 11.696(2)$, $c = 7.100\ (2)$ Å at 25 °C with cell contents of 2[$CaKAsO_4 \cdot 8H_2O$]. The density calculated from the x-ray data is 2.027 g.cm$^{-3}$; that calculated from the refractive indices is 2.10 g.cm$^{-3}$. The structure has been refined to $R_w = 0.037$, $R = 0.043$ in space group *Cm2m,* using 1023 observed reflections measured on an automated diffractometer and corrected for absorption. Allowance was made for anomalous dispersion and secondary isotropic extinction. All ions in $CaKAsO_4 \cdot 8H_2O$ are completely hydrated. Ca coordinates to eight water oxygen atoms with Ca...O distances in the range 2.460(5) to 2.490(3) Å. K coordinates to eight water oxygen atoms with K...O distances ranging from 2.756(3) to 2.960(7) Å. The coordination polyhedron of Ca shares one face of four water molecules and two edges with neighboring coordination polyhedra of K. Each oxygen atom of the $AsO_4$ ion is the acceptor in hydrogen bonds from four water molecules and forms no bonds with the cations. The two crystallographically different As-O distances in the $AsO_4^{3-}$ ion are 1.682(4) and 1.684(4) Å when uncorrected for thermal motion, and 1.690 and 1.692 Å with the riding model correction. The structure of $CaKAsO_4 \cdot 8H_2O$ is related to that of $MgNH_4PO_4 \cdot 6H_2O$, struvite. This structural type may be common to several calcium phosphates and related compounds.

13343. Fabry, A., Jenkins, J. D., **Calculation of the ΣΣ facility with ENDF/B-versions II and III and comparison with experiment,** *Trans. Amer. Nucl. Soc.* **15,** No. 2, 1 (Nov. 1972).

Key words: Comparison; fast; integral-measurements; neutron; nuclear-data; spectra; standard; theory.

The intermediate-energy standard neutron spectrum facility ΣΣ is a permanent, clean, and reproducible standard neutron source characterized by a central radiation field typical of zero-power fast breeder test assemblies. It consists of a spherical shell of natural uranium of 24.5-cm o.d. x 5-cm thickness embedded at the center of a 50-cm-diam spherical cavity in a graphite thermal column: it contains a spherical shell of natural boron carbide 15 mm thick, which surrounds the central exposure zone of 11-cm diam. The ΣΣ central neutron spectrum and reaction rates have been computed with the evaluated nuclear data files ENDF/B Versions II and III. The one-dimensional discrete ordinates transport calculations were performed in the $S_{16}P_3$ approximation. Extensive measurements of infinitely dilute reaction rates in ΣΣ are compared to these calculations using detector cross sections from a current neutron dosimetry library. Sizable discrepancies are apparent. For the detector ratios with major response in the energy range above 50 keV, theory is presently unable to reproduce the observed spectral indexes, especially the $^{238}U(n,f)/^{235}U(n,f)$ ratio: the deviation with respect to the trend indicated by the other threshold reactions is similar to the one previously suggested in cavity fission neutron spectrum integral measurements. The neutron spectrum between ~ 300 eV and 5 keV has been found very sensitive to the shape and intensity of the excitation function for the 45-keV $^{238}U$ level.

13344. Wiederhorn, S. M., Johnson, H., **Influence of sodium-hydrogen ion exchange on crack propagation in soda-lime silicate glass,** *J. Amer. Ceram. Soc. Discussions and Notes* **56,** No. 2, 108-109 (Feb. 1973).

Key words: Crack propagation; fracture; fracture mechanics; glass; strength; stress corrosion.

The effect of sodium-hydrogen ion exchange on crack propagation was studied. It was concluded that stresses arising from ion exchange play a minor role in determining the strength of glass when strength is controlled by crack propagation.

13345. Camarda, H. S., **Monte Carlo studies of $D_2O$ and $H_2O$ neutron moderators for time of flight experiments,** *Nucl. Instrum. Methods* **106,** 205-212 (1973).

Key words: Deuterium; moderator; Monte Carlo; neutrons; oxygen; protons, time delay; time smearing.

Calculations of neutron moderation in finite $D_2O$ and $H_2O$ media have been performed. Neutron spectrum shapes, time delays, and time smearings have been determined over a neutron energy range $1.8\ \text{keV} \leq E \leq 1\ \text{MeV}$.

13346. Bennett, J. A., Mindlin, H., **Metallurgical aspects of the failure of the Point Pleasant bridge,** *J. Test. Eval.* **1,** No. 2, 152-161 (Mar. 1973).

Key words: Bridge; failure; fracture toughness; Point Pleasant; stress corrosion cracking.

Examination of the fractured eyebar which caused the collapse of the bridge led to the conclusion that a stress-corrosion crack had penetrated to a depth of 1/8 inch during the 40 years that the bridge was in service. This flaw was sufficient to initiate fracture across the remainder of the 16 in.$^2$ area of the lower limb of the eye due to the high local stress and the low fracture toughness of the steel.

13347. Utech, H. P., **Injuries show what protection improved clothing should offer,** *Fire Eng.* **125,** No. 4, 47-49 (Apr. 1972).

Key words: Firefighter injuries; injury statistics; occupational injuries; protective clothing; protective equipment.

Firefighting continues to be one of this country's most hazardous occupations. Statistics on firefighter injuries are analyzed to identify the problem areas. This analysis indicates that improvement in the design of protective clothing and equipment can lead to the reduction of firefighter injuries. Improved respiratory protection, reduction in the weight and bulk of clothing and equipment, and better protection against impact, are the primary needs.

13348. Wiederhorn, S. M., **Prevention of failure in glass by proof-testing,** *J. Amer. Ceram. Soc.* **56,** No. 4, 227-228 (Apr. 1973).

Key words: Crack propagation; failure prevention; fracture; glass; proof testing.

A method of predicting the minimum lifetime of glass under static load is presented. The method involves proof testing and a knowledge of the growth behavior of cracks in glass.

13349. Wiederhorn, S. M., Johnson, H., **Effect of electrolyte on crack propagation in glass,** *J. Amer. Ceram. Soc.* **56,** No. 192-197 (Apr. 1973).

Key words: Crack propagation; fracture; fractu mechanics; glass; strength; stress corrosion.

Crack velocities in glass in various acids, bases, and neut solutions were studied using the double-cantilever-be technique. Results are explained in terms of crack-tip pH, whi is controlled by the electrolyte at low crack velocities and by t glass composition at high velocities. The crack-velocity data consistent with the known dependence of strength on pH soda-lime silicate glass. Results also suggest that the slope of t universal fatigue curve should depend on surface pH.

13350. Franklin, A. D., **Density of $CaF_2$ containing low concent tions of $GdF_3$,** *J. Nonmetals* **1,** 27-34 (1972).

Key words: Calcium fluoride; cation vacancies; densi gadolinium impurity; interstitial anions; lattice paramet point defects.

The density relative to that of pure crystals has been measur for $CaF_2$ crystals containing mole fractions from 0 to 4.6 × 1 of $GdF_3$, and the lattice parameters of these and also of p crystals were measured. The doped crystals had been anneal at temperatures from 500 to 1100 °C in an atmosphere of plus HF. No influence of annealing was seen on either the den ty or the lattice parameter. The precision of both measureme is, however, not quite good enough to rule out definitely an ea er suggestion that cation vacancies play an important role in t annealing behavior of this system. However, the density chan accompanying the incorporation of these amounts of $GdF_3$ $CaF_2$ are too large to be accounted for by the usual model which $Gd^{3+}$ occupies a cation site and is accompanied by extra $F^-$ ion in an interstitial site. The changes do agree wit model in which one HF molecule accompanies each $GdF_3$ u added, but attempts to detect the HF in nmr and infra-red sorption experiments were unsuccessful.

13351. Mabie, C. P., Jr., **Petrographic study of the refractory p formance of high-fusing dental alloy investments: I. High-fir phosphate-bonded investments,** *J. Dent. Res.* **52,** No. 1, 96-1 (Jan.-Feb. 1973).

Key words: Alloy; casting; dental; investment; petr raphy.

Detailed x-ray, optical microscopic, optical emission, a electron probe analyses of a phosphate-bonded investment fore and after firing and after casting were made. Complex sint ing reactions that involve incipient liquefaction generate bo in the fired investment. The refractory behavior of this inve ment, which is reflected by the extent of liquefaction induced casting, may influence casting roughness, fit, and porosity.

13352. Yule, H. P., **Conversational text editor for a laborat minicomputer,** *Anal. Chem.* **44,** No. 2, 430 (Feb. 1972).

Key words: Assembly; conversational; editor; langua minicomputer; text.

A conversational text editing program for the Varian 6 minicomputer is described. Virtually identical in operation w a commercially available, time-sharing, conversational text e tor, this program permits rapid and easy modification of text, cluding insertion, deletion, and editing of lines of text.

13353. Lang, R., Bender, P. L., **Analytic approximation for saturation behavior of OH emission regions,** *Astrophys. J.* **1** No. 2, 647-660 (Mar. 1, 1973).

Key words: OH microwave transition; radio astronomy; saturation; stimulated emission.

One of the simplest models for a cosmic maser consists of a homogeneous spherical region in which inverted population is created at a uniform rate. We have investigated the radiation transfer problem including saturation for this case under the following assumptions: (1) two levels only, without magnetic sublevels; (2) a square line shape; (3) excitation by spontaneous emission at a uniform rate through the region; and (4) no scattering in the medium or reflection at the boundary. An approximate analytic solution has been found which closely satisfies the radiation transfer equation under conditions of substantial saturation. This analytic solution has been checked against numerical solutions which are intended to approximate the flux and apparent size of the $-$ 43.7 km $s^{-1}$ feature in W3. Both the analytic solution and the numerical models show that the actual size of an emitting region can be considerably larger than for a region of uniform population difference which has the same apparent size.

**13354.** Deslattes, R. D., **L-series emission spectrum of germanium,** *Phys. Rev.* **172,** No. 3, 625-627 (Aug. 15, 1968).

Key words: Emission spectrum; germanium; profile measurement; valence emission bands.

Measurements are reported on the *L*-series emission spectrum of germanium which lead to line identifications at variance with other recent work. Some features of the *K*-emission spectrum were also recorded to confirm previous work there and aid in the location of the valence emission bands in the *L* series. It is shown that these are of extremely low intensity, so low in fact as to preclude for the present a detailed profile measurement.

**13355.** Fong, J. T., Simmons, J. A., **A decomposition theorem on the scalar potential of a compressible BKZ fluid,** *J. Appl. Math. Phys.* **23,** No. 5, 780-794 (1972).

Key words: Anisotropy; BKZ fluid; composite material; continuum mechanics; hyperelasticity; isothermal; nonlinear; variational principle; viscoelasticity.

Based on the existence of a caloric equation of state in the thermodynamic theory of a nonlinear viscoelastic fluid (Bernstein, Kearsley and Zapas, 1964), and the additional assumption that the local entropy production along any instantaneous deformation path is finite, we first show that such a fluid behaves as a perfectly elastic material whenever the deformation gradient suffers from a jump-type discontinuity. The nature of the apparently perfectly elastic material serving to interpret results in the instantaneous deformation depends on the previous history only through two parameters, namely, the density and the temperature of the fluid immediately prior to the jump. This result is then applied, in conjunction with the usual conditions of isotropy and objectivity as well as an application of Schur's Lemma on irreducible sets of matrices, to obtain a decomposition of the scalar potential of the compressible Bernstein-Kearsley-Zapas Fluid (abbrev. BKZ Fluid).

**13356.** Zimmerman, J. E., **Possible parametric capacitance in Josephson junctions,** *Phys. Lett.* **42A,** No. 5, 375-376 (Jan. 1, 1973).

Key words: Josephson effect; parametric capacitance.

The capacitance of a Josephson junction is much larger (at least in the low frequency limit) than the classical value $\epsilon A/l$, and is a function of the phase difference $\theta_0$.

**13357.** Reader, J., **Comment on "Configuration interaction in the x-ray photoelectron spectra of alkali halides,"** *Phys. Rev. A* **7,** No. 3, 1431-1433 (Apr. 1973).

Key words: Photoelectron spectra; potassium; rubidium; sodium; x-rays.

Recently obtained data on doubly ionized Rb in the free state indicate that the satellite of the Rb(4*s*) resonance in the photoelectron spectra of RbF and RbCl is primarily due to a $4s^24p^44d\ ^2S$ final state rather than a $4s^24p^45s\ ^2S$ one. For the potassium salts, the satellite of the K(3*s*) resonance is most likely due to a $3s^23p^43d\ ^2S$ final state. The absence of a satellite for the Na(2*s*) resonance for the sodium salt is due to the nonexistence of 2*d* electrons.

**13358.** Linsky, J. L., Ayres, T., **Stellar model chromospheres. I. On the temperature minima of F, G, and K stars,** *Astrophys. J.* **180,** No. 2, Part 1, 473-481 (Mar. 1, 1973).

Key words: Spectral line formation; stellar chromospheres.

Brightness temperatures are deduced for the $H_{1I}$ and $K_{1I}$ features of the Ca II resonance lines in Procyon (F5 IV-V), Arcturus (K2 IIIp), and the Sun (G2 V). The brightness temperatures of Procyon and the Sun are in the same ratio as their effective temperatures, suggesting a simple scaling law for the temperature minima of F and early G stars. Arcturus departs from this law in a way that can be explained by CO line blanketing.

**13359.** Kamper, R. A., Simmonds, M. B., Adair, R. T., Hoer, C. A., **A new technique for RF measurements using superconductors,** *Proc. IEEE* **61,** No. 1, 121-122 (Jan. 1973).

Key words: Josephson effect; quantum interference; rf attenuation; rf measurements; superconductivity.

The quantization of magnetic flux in a superconducting circuit can serve for the measurement of electrical quantities in the same way that we use the wavelength of light to measure length. We report a demonstration of this function in the measurement of attenuation ratio at a frequency of 30 MHz.

**13360.** Linsky, J. L., **The moon as a proposed radiometric standard for microwave and infrared observations of extended sources,** *Astrophys. J. Suppl. Ser.* **25,** No. 216, 163-204 (Feb. 1, 1973).

Key words: Absolute radiometric calibration—astronomical; absolute radiometric calibration—infrared; absolute radiometric calibration—microwave; lunar surface; lunar thermal emission; moon.

Measured values of the average midnight and morning terminator infrared brightness temperatures of the central portion of the lunar disk can quite accurately determine the mean surface temperature despite likely horizontal and vertical inhomogeneities of the thermal properties of the lunar soil. These data together with laboratory measurements on lunar soil and in situ temperature measurements in and on the lunar surface lead to a mean surface temperature of 220.5 K ± 2.5 percent and a mean temperature 35 K hotter at a depth of 1 m. The monthly average brightness temperature is then estimated as a function of wavelength between 10 $\mu$m and 100 cm taking into account likely temperature dependencies of the thermal conductivity and loss tangent, and the variation of emissivity with wavelength. The accuracy with which the Moon can be used as an absolute radiometric standard for extended sources is estimated based on the likely range of lunar thermal and electromagnetic properties.

**13361.** Danos, M., Gillet, V., **Quartet effects in the nuclear masses and excitations,** *Z. Phys.* **249,** 294-311 (1972).

Key words: Nuclear binding energies; nuclear quartets; nuclear reactions; nuclear structure; quartet model; supermultiplet theory.

The assumptions of the quartet model are given and it is shown that they are consistent with the fine structure of the nuclear mass curves throughout the table. It is also shown by an analysis of the nuclear masses that the quarteting effect accounts for 2/3 of the neutron binding energies. The consequences of the quartet picture for the existence of low-lying many-particle many-hole states in medium and heavy nuclei are discussed.

**13362.** Kushner, L. M., **Progress report on activities of the National Bureau of Standards under the 1967 Amendments to the Flammable Fabrics Act,** *Proc. 3d Annual Meeting of the Information Council on Fabric Flammability, New York, N.Y., Dec. 4, 1969,* pp. 156-163 (Information Council on Fabric Flammability, New York, N.Y., 1969).

Key words: Flammable fabrics; flammability standards; National Advisory Commission for the Flammable Fabrics Act; 1967 Amendments to the Flammable Fabrics Act.

Presents a summary of activities at the National Bureau of Standards since enactment of the 1967 Amendments to the Flammable Fabrics Act.

**13363.** LaVilla, R. E., **Carbon and fluorine x-ray emission and fluorine $K$ absorption spectra of the fluoromethane molecules, $CH_{4-n}F_n$ ($0 \leq n \leq 4$). II,** *J. Chem. Phys.* **58,** No. 9, 3841-3848 (May 1, 1973).

Key words: Calculated relative x-ray emission; carbon $K\alpha$ emission; fluorine $K$ absorption; fluorine $K\alpha$ emission; fluoromethane molecules; methane; molecular orbital level sequence.

The carbon and fluorine $K\alpha$ emission and the fluorine $K$ absorption spectra of the molecular gases $CH_{4-n}F_n (0 \leq n \leq 4)$ are reported. All the spectra were obtained on a single flat crystal spectrometer with photon counting. The emission spectra, which were excited by direct electron bombardment, are in fair agreement with an interpretation based on electric dipole transitions between single vacancy states and molecular orbital theory for the molecules. The applicability of x-ray emission spectra to the determination of orbital order of a molecule is illustrated. The proximity of the resonance structure in the fluorine $K$ absorption spectra for $CH_{4-n}F_n (1 \leq n \leq 4)$ to their respective fluorine $K$ shell thresholds suggests that the resonance structure is due to transitions to excited valance states $1a \rightarrow V^*$ rather than Rydberg states.

**13364.** Ku, H. H., **Analysis of information-an alternative approach to the detection of a correlation between the sexes of adjacent sibs in human families,** *Biometrics* **27,** 175-182 (Mar. 1971).

Key words: Analysis of information; categorial data; chi-square; contingency table; independence; Markov chain.

Through the use of an example given by Greenberg and White [1965], the analysis of a multiway contingency table by the information approach is illustrated. Analyses of information tables are given for independence, homogeneity, conditional independence and conditional homogeneity, and Markovity.

**13365.** Fabry, A., Jenkins, J. D., **Wall return neutron fluxes for high- and intermediate-energy cavity neutron sources,** *Trans. Amer. Nucl. Soc.* **15,** No. 2, 975-976 (Nov. 1972).

Key words: Carbon; cavity; fast neutron; spectra; theory.

Spherical cavities in graphite thermal columns of nuclear reactors provide an ideal environment for the production of comparatively intense, energy distributed neutron fields, i.e., either intended pure fission neutron spectrum sources or intermediate-energy standard neutron spectra. Cavities of 50 cm diameter are used in various laboratories; a 30 cm diameter cavity is operated at NBS and a 1 meter diameter cavity has recently been impl mented at CEN-SCK.

Numerical computations of graphite wall-return neutron spe tra have been performed by means of the discrete ordinates mu tigroup method in one-dimensional spherical geometry. Tl evaluated nuclear data files KEDAK, ENDF/B Version 3 hav been used and the convergence of the $S_n$ multigroup multitab treatment has been established systematically.

Within the cavity, a good approximation of the wall return is

$$\phi_{W}(r,\mu,E;r_s) = \phi_{W}(E).$$

This relationship is correct to better than 2% for r, $r_s \leq R$ where R is the cavity radius and $r_s$ the radius of a thin, fissi spectrum source shell. This fundamental property has led to tl development of an experimental method for determining wa return backgrounds.

**13366.** Roberts, J. R., Andersen, T., Sørensen, G., **Determinati of atomic lifetimes and absolute oscillator strengths for neutr and ionized titanium,** *Astrophys. J.* **181,** 567-586 (Apr. 1 1973).

Key words: Absolute transition probabilities; arc; bea foil; experimental; lifetimes; titanium.

Measurements of atomic lifetimes by the beam-foil techniqu and branching ratios by use of a gas-flow stabilized arc have le to an experimental determination of absolute oscillator strengtl of Ti II. Some lifetimes of Ti I, Ti III, and Ti IV are al presented.

**13367.** Roberts, J. R., Andersen, T., Sørensen, G., **Determinati of atomic lifetimes and absolute oscillator strengths for neutr and ionized vanadium,** *Astrophys. J.* **181,** 587-604 (Apr. 1 1973).

Key words: Absolute transition probabilities; arc; bea foil; experimental; lifetimes; vanadium.

Measurements of atomic lifetimes by the beam-foil techniqu and branching ratios by use of a gas-flow stabilized arc have le to an experimental determination of absolute and relative oscill tor strengths of V I and V II. Some lifetimes of V III are al presented.

**13368.** Liebman, J. F., Vanderspurt, T. H., **Polarization of X bonds,** *J. Fluorine Chem.* **2,** 413-424 (1972/73).

Key words: Fluorine; polarization of bonds; prot assisted reactions; X-F bonds.

We discuss in this paper several reactions of compounds co taining X-F (X=C, N, O, F, S and Xe) bonds. An attempt unify these reactions conceptually is made by suggesting the in portance of X-F bond polarization by protic media. Relate Lewis-acid-induced polarization reactions can usually be env sioned. Some new reactions and mechanisms are suggested as consequence of our analysis.

**13369.** Grundl, J. A., **Brief review of integral measurements wi fission spectrum neutrons,** (Proc. of the Consultants' Meetin Vienna, Austria, Aug. 1971), Paper in *Prompt Fissic Neutron Spectra,* pp. 29-32 (International Atomic Energ Agency, Vienna, Austria, 1972).

Key words: Fission spectra; integral measurements; cros sections.

The paper is an edited transcript of the introduction to th discussion of integral measurements of fission cross-sectior averaged over fission spectra given by the author at the meetin

13370. Artru, M-C., Kaufman, V., **Re-evaluation of parameters for even configurations of triply ionized magnesium,** *J. Opt. Soc. Amer.* **63,** No. 4, 449-450 (Apr. 1973).

Key words: Magnesium; source; spectra; ultraviolet; wavelengths.

In a previous publication, HF values for $2p^4\ 3s \leftrightarrow 2p^4\ 3d$ interaction parameters were misinterpreted. Correct HF values for these parameters have been used in a new calculation of these configurations.

13371. Jones, M. C., **Use of superconductors in thermal insulations,** *Cryogenics* **13,** No. 2, 83-84 (Feb. 1973).

Key words: Niobium; superconductors; thermal radiation shields; total emissivity.

A suggestion is made for using superconductors as thermal radiation shields at or below liquid helium temperatures. Calculations are described which predict total emissivities for niobium of $10^{-4}-10^{-5}$ at 4 K and $10^{-8}-10^{-7}$ for temperatures of $1-2$ K.

13372. Robertson, B., **Introduction to field operators in quantum mechanics,** *Amer. J. Phys.* **41,** 678-690 (May 1973).

Key words: Field operators and statistics; Fock space; occupation number; permutation symmetry of wave functions; quantum mechanics; second quantization.

The equivalence of the field operator formulation of quantum mechanics and ordinary wave mechanics is proved in an efficient and elementary way. The discussion proceeds algebraically from the (anti-) commutation relations, which the field operators are defined to satisfy. Although the paper is introductory and presumes only a knowledge of elementary wave mechanics, it is intended to cover all of the essential elements of the subject in a rigorous way.

13373. Cezairliyan, A., **High-speed (subsecond) simultaneous measurement of specific heat, electrical resistivity, and hemispherical total emittance of Ta-10 (wt.%)W alloy in the range 1500 to 3200 K,** *High Temp.-High Pressures* **4,** 541-550 (1972).

Key words: Electrical resistivity; emittance; high-speed measurement; high temperature; specific heat; Ta-W alloy.

Simultaneous measurements[a] of specific heat, electrical resistivity, and hemispherical total emittance of Ta-100(wt.%)W alloy in the temperature range 1500 to 3200 K by a subsecond-duration pulse-heating technique are described. Estimated inaccuracies of measured properties are: 3% for specific heat and hemispherical total emittance, and 0.5% for electrical resistivity. Properties of the alloy are compared with the properties of the constituent elements. The values of measured specific heat are approximately 2% higher than the values computed according to Kopp's additivity law. However, this difference is within the combined estimated errors. The electrical resistivity results indicate a significant departure from Matthiessen's law. Like tantalum, the alloy showed a negative departure from linearity in the temperature dependence of electrical resistivity.

13374. Fuller, G. H., **Problems of compiling and evaluating or what is the nuclear moment?** (Proc. Int. Conf. on Nuclear Moments and Nuclear Structure, Osaka, Japan, Sept. 4-8, 1972), *J. Phys. Soc. Jap.* **34,** Supplement, 153-154 (1973).

Key words: Compilation problems; nuclear magnetic moments.

A "best-value" list of nuclear magnetic moments to accuracies of 0.01% or better is unrealistic at this time. There are many fundamental problems which are associated with the measurement of a nuclear moment in the laboratory where the nucleus is part of an atom or molecule in a gas, liquid or solid mixture. These problems are compounded by poorly written papers with much important information needed for the re-evaluation of data missing.

13375. Waxman, M., Hilsenrath, J., Chen, W. T., **Compressibility factor and the second virial coefficient of boron trifluoride from 0 to 225 °C and for pressures up to 250 bar,** *J. Chem. Phys.* **58,** No. 9, 3692-3701 (May 1, 1973).

Key words: Boron trifluoride; density, second virial coefficients; gas, compressibility.

The isothermal compressibility factor of boron trifluoride has been determined from a regression analysis of Burnett PVT measurements to an accuracy of 0.1% at 13 temperatures from 0 to 225 °C and for pressures up to 250 bar. The analysis has also yielded the second virial coefficient for each temperature. A correction for the presence of sorption has been included in the data reduction.

13376. Coxon, B., Schaffer, R., **Analysis of a cortisol clinical standard by Fourier transform, proton magnetic resonance spectroscopy,** *Anal. Lett.* **6,** No. 4, 291-300 (1973).

Key words: Chemical shifts; clinical Standard Reference Materials; cortisol; Fourier transform, proton magnetic resonance spectroscopy.

Cortisol intended for use as a clinical Standard Reference Material has been subjected to liquid chromatography and the resulting fractions analyzed by thin layer chromatography and Fourier transform, proton magnetic resonance spectroscopy at 90 MHz. Four steroid impurities and one artifact have been characterized by means of computer measured chemical shifts.

13377. Grundl, J. A., Spiegel, V., Jr., Eisenhauer, C., **Measurement of $^{235}$U and $^{238}$U fission cross sections for $^{252}$Cf spontaneous fission neutrons,** *Trans. Amer. Nucl. Soc.* **15,** No. 2, 945-946 (1972).

Key words: Absolute fission cross section; californium neutron source.

Absolute $^{235}$U and $^{238}$U fission cross sections have been measured with a small, low-mass $^{252}$Cf spontaneous fission source and a lightweight, double fission ionization chamber.

13378. Nahman, N. S., **A note on the transition (rise) time versus line length in coaxial cables,** *IEEE Trans. Circuit Theory* **CT-20,** No. 2, 165-167 (Mar. 1973).

Key words: Cables; coaxial; pulse response; transient analysis; transmission lines.

A tutorial discussion is given on the relation between the shape of the transition (rise) time versus length curve and that of the frequency domain attenuation. An analysis is developed in terms of hypothetical cable attenuation responses having a frequency $f$ dependence of $f^m$, where $m$ is a constant $0 < m < 1$. It is shown that if the $f^m$ law prevails, then the transition time depends on the length $l$ as $l^{1/m}$. Practical applications are made to RG 58C/U, RG 59B/U, and RG 63B/U.

13379. Dodge, M. J., Malitson, I. H., Mahan, A. I., **A special method for precise refractive index measurement for uniaxial optical media,** *Appl. Opt.* **8,** No. 8, 1703-1705 (Aug. 1969).

Key words: Refractive index; refractometry; ruby.

A method was developed for measuring the refractive index of optical glasses and uniaxial crystalline solids when established refractometric methods are not feasible. A synthetic ruby cuboid was contacted to a prism of known refractive index and a spectrometer was used to measure the angles describing the optical path through the ruby-glass combination. Ray tracing equations were derived to compute the refractive index accurate within 3 × $10^{-5}$. Index values for both polarizations of ruby are given at selected wavelengths from 0.4358 $\mu$m to 0.7065 $\mu$m.

**13380.** Kirby, R. K., **Thermal expansion of tungsten from 293 to 1800 K,** *High Temp.-High Pressures* **4,** 459-462 (1972).

Key words: Standard Reference Materials; thermal expansion; tungsten.

Measurements on the thermal expansion of three samples of tungsten were made with a twin-microscope method in the range of 1000 to 1800 K. Measurements were also made on one of these samples with a Fizeau interferometer in the range below 1100 K. The results obtained indicated that the values for the expansion of the three samples, two prepared by sintering and one by arc melting, are in reasonable agreement with one another and with some of the data in the literature.

**13381.** Weisman, I. D., **$^{109}$Ag Knight shift in an $Ag_{0.96}Al_{0.04}$ alloy,** *J. Chem. Eng. Data* **18,** No. 2, 146 (Apr. 1973).

Key words: Absorption derivative; alloys; asymmetry; host; lineshape; $^{109}$Ag Knight shift.

The $^{109}$Ag Knight shift in a $Ag_{0.96}Al_{0.04}$ alloy has been measured with respect to $^{109}$Ag metal at room temperature. The change in shift is $-$ 0.015 (±3%).

**13382.** Ruff, A. W., Ives, L. K., **On the temperature dependence of stacking fault energy in cubic and hexagonal silver-tin alloys,** *Phys. Status Solidi A,* No. 16, 133-149 (1973).

Key words: Annealing; cubic alloy; dislocation; electron microscopy; hexagonal alloy; silver-tin alloy; stacking fault energy.

Measurements on extended dislocation nodes and double ribbons have been made between room temperature and 500 °C using transmission electron microscopy. Two low stacking fault energy (SFE) alloys with compositions near the mixed phase region were principally studied; 9 at% Sn (f.c.c.) and 11.9 at% Sn (hexagonal). The SFE in the cubic alloy increased *reversibly* with increasing temperature from 270 to 500 °C; a corresponding decrease in SFE was observed in the hexagonal alloy. Both alloys showed a substantial *irreversible* change in faulted defect size upon annealing, comparing results in as-deformed specimens with those from material annealed above 270 °C. The irreversible behavior is attributed to solute pinning of the partial dislocations. The dependence of SFE on composition throughout the f.c.c. and hexagonal phase regions is considered in light of these results.

**13383.** Baker, M. A., **Weatherability of porcelain enamels,** (Proc. Aluminum Finishing Seminar, Chicago, Ill., Mar. 19-21, 1973), Paper C12 in Applied Session: Technical Papers, pp. C12-1 – C12-16 (The Aluminum Ass., New York, N.Y., Mar. 1973).

Key words: Color; gloss; porcelain enamel on aluminum; weather resistance.

An exposure text of porcelain enamels on aluminum was initiated by the National Bureau of Standards and the Porcelain Enamel Institute in 1964. The enameled specimens were returned from exposure sites at Kure Beach, N.C.; Washington, D.C.; New York, N.Y.; Montreal, Canada; and Los Angeles, Calif., to the laboratory at NBS to be measured for changes in gloss and color after 6 months, and 1, 3, and 5 years' exposure. The 5-year data indicate no change in enamel thickness and good color retention at all sites except Kure Beach.

**13384.** Moore, R. T., **Penetration resistance tests of reinforced concrete barriers,** *NBSIR 73-101,* 83 pages (Dec. 1972). (Available as COM 73-10867 from the National Technical Information Service, Springfield, Va. 22151.)

Key words: Barrier penetration; intrusion detection; physical security; reinforced concrete.

This report describes the results of a series of penetration tests on six concrete slabs. The tests were conducted at the U.S. Army Corps of Engineers Construction Engineering Research Laboratory in Champaign, Ill., during the period October 31 through November 3, 1972. Several alternative methods of attack were employed, and the time to penetrate, and in some instances, to produce a 96-inch² opening, was measured, and estimates were developed regarding the acoustic, ultrasonic and vibrational disturbances produced by the attacks.

Depending upon the attack technique, a man-passable opening can be made in 4-inch thick reinforced concrete in times ranging from 4 to nearly 15 minutes. The corresponding times for 8-inch thick reinforced regular concrete range from about 7 to 25 minutes and from about 20 to 30 minutes fibrous concrete.

With the exception of the diamond core drill, detection should be relatively easy by the combined acoustic, ultrasonic or vibrational disturbances produced by the attacks even though not al techniques produce all three types of disturbances.

**13385.** Berg, C. A., **Energy conservation through effective utilization,** *NBSIR 73-102,* 53 pages (Feb. 1973). (Available as COM 73-10856 from the National Technical Information Service, Springfield, Va. 22151.)

Key words: Effective utilization; energy conservation.

In two major sectors of the economy (building services and industrial processes), accounting for approximately 75 percent o total national energy consumption, energy utilization is found t be inefficient. It is estimated that in these two sectors, as muc as 25 percent of the energy consumed annually by the nation a a whole may be lost through ineffective practices. Possible reasons for existence of ineffective utilization are considered and possible means of improving effectiveness of utilization ar discussed. Three possible levels of effort to promote effective utilization of energy are identified; one promotes effective use o present fuels in present processes; the second promotes utilization of presently unused energy sources; the third promote more effective investment of energy in durable and maintainable products.

Substantial latitude for improvement of effectiveness is show to be realizable through technological efforts at these three levels. It is finally recommended that a national program, incorporating efforts at the three levels identified, be undertaken wit the ultimate goal of creating and implementing a technology o improved energy utilization.

**13386.** Shaver, J. R., Masters, L. W., Reichard, T. W., Pielert, J H., **Environmental evaluation of polyurethane foam core sandwich panel construction,** *NBSIR 73-105,* 47 pages (Dec. 1972) (Available as PB 219118 from the National Technical Information Service, Springfield, Va. 22151.)

Key words: Accelerated aging; compression; environmental conditions; flexure; housing system; Operatio BREAKTHROUGH; polyurethane foam; sandwich construction; wall system.

An environmental evaluation of a sandwich panel bearing wal system for use in one of the Operation BREAKTHROUGH housing systems is described. Two samples of polyurethan foam core sandwich construction and four full size wall panel were evaluated.

The samples of the sandwich construction were used to evaluate the effect of extreme temperature and moisture on this type of sandwich construction. The full size panels were used to determine the behavior in service considering the effects of adverse environmental conditions on ultimate strength and mode of failure.

**13387.** Unassigned.

**13388.** Yokel, F. Y., **Study of the local resistance of conventional plywood subflooring to concentrated load,** *NBSIR 73-116,* 64 pages (Mar. 26, 1973). (Available as PB 220432 from the National Technical Information Service, Springfield, Va. 22151.)

Key words: Concentrated-load capacity; evaluation criteria; floors; hardboard; load capacity; Operation BREAKTHROUGH; performance criteria; plywood subflooring; subflooring; underlayment; wood-frame construction.

Five conventional plywood floor systems, constructed in accordance with the requirements of the FHA "Minimum Property Standards" were tested under concentrated loads in order to compare their performance with that stipulated by performance criteria developed on the basis of anticipated occupancy loads.

In 24 out of 26 tests the performance of the floor systems exceeded that stipulated by the criteria. Data on failure loads, load-deflection characteristics and failure modes are presented and discussed.

**13389.** Yancey, C. W., Somes, N. F., **Structural tests of a wood-frame housing module,** *NBSIR 73-121,* 111 pages (Mar. 26, 1973). (Available as COM 73-10860 from the National Technical Information Service, Springfield, Va. 22151.)

Key words: Deflection; housing; laboratory; module; racking; stiffness; strength; structural tests; sustained load; transportation; vibration; wood-frame.

This paper reports the results of tests to determine the structural strength and stiffness characteristics of a prototype wood-frame volumetric housing module. The series of six structural tests was performed at the NBS Structures Laboratory, Gaithersburg, Md., subsequent to a trial rail shipment, which included several coupling impacts. This report refers to the transportation study only to the extent that it concerns the module, and in particular, its condition at the start of the structural tests. The total sequence of the tests closely simulated the experience of a typical module as it undergoes manufacture, transportation, erection and in-service loading.

**13390.** Cattaneo, L. E., Yokel, F. Y., **Structural tests of mechanical connections for concrete panels,** *NBSIR 73-126,* 118 pages (Nov. 1972). (Available as PB 219124 from the National Technical Information Service, Springfield, Va. 22151.)

Key words: Concrete panels; connections; ductility; floor diaphragms; housing systems; insert connectors; Operation BREAKTHROUGH; precast concrete.

Structural evaluation tests were performed on prototype steel insert connectors proposed for joining floor and wall panels of a precast concrete housing system included in Operation BREAKTHROUGH. Descriptions are given of 25 tests conducted with 5 different types of connectors. Specimen connections were laboratory tested under simulated design loading conditions to evaluate their load capacity and ductility.

**13391.** Waksman, D., Skoda, L. F., Clark, E. J., Godette, M., **Evaluation of lead paint hazard elimination methods, Part II,** *NBSIR 73-127,* 77 pages (Mar. 1973). (Available as PB 213352 from the National Technical Information Service, Springfield, Va. 22151.)

Key words: Deleading methods; lead paint poisoning; performance; properties.

Four major classifications of procedures that should be considered when selecting a method for the elimination of the lead paint hazard are analyzed in this report. They are: surface repair methods, surface finish methods, cover up methods with unfinished membrane materials, and cover up methods with prefinished rigid materials. The attributes associated with each type of method were considered and analyzed in terms of inaccessibility of the leaded paint and implementation considerations. Recommendations are made for the in-use performance properties of surfaces.

**13392.** Halsey, N., Mitchell, R. A., Mordfin, L., **Evaluation of GRP rod and rope materials and associated end fittings,** *NBSIR 73-129,* 87 pages (Dec. 1972). (Available as AD 759931 from the National Technical Information Service, Springfield, Va. 22151.)

Key words: Aeolian vibration, simulated; composite materials; end fittings for GRP rod and rope; grips, guy; guys, antenna; humidity, effects on GRP; mechanical properties of GRP; pultruded rod; reinforced plastics, rod and rope; rope, GRP; static fatigue of GRP.

An extensive and varied test program was carried out on four GRP rod and rope materials to evaluate tensile strengths, moduli of elasticity, flexibility at low temperatures, effects of simulated Aeolian vibration, and stress-rupture properties at moderate elevated temperatures both with and without high humidity. The effects of elevated temperature on long-term storage capabilities were investigated, and diameter-temperature relationships were established for avoiding buckling due to storage in a coiled condition.

The performances of five commercially available end fittings on these materials were examined in terms of the breaking loads attained in tensile tests. Using finite-element analyses, an improved end fitting was developed which is capable of approaching the true tensile strengths of two of the GRP materials. An experimental stress analysis of the improved fitting was performed.

**13393.** Pezoldt, V. J., Persensky, J. J., **Human factors evaluation of a voice encoding system,** *NBSIR 73-131,* 57 pages (Mar. 1973). (Available as COM 73-10863 from the National Technical Information Service, Springfield, Va. 22151.)

Key words: Feasibility; keyboard alternative; man-machine interface; postal sorting; voice encoding.

The feasibility of employing voice encoding as an alternative to keyboard entry for postal sorting application was investigated in two phases. Phase I was a simulated parcel sorting situation. Phase II was performed to determine man-machine interface limitations. The results of this study led to the following conclusion and recommendations. Voice encoding would be of limited value to high speed parcel sorting unless it was used only during slack periods or the current facer and keyer both use a VES. Voice encoding could be applied to other sorting tasks. USPS tasks should be analyzed for the possibility of such application. Other voice encoding systems should be evaluated. These systems should have single command training capability, a cancel capability accessed by other than a unique verbal command, and should require infrequent system training.

**13394.** Son, B. C., **Fire endurance tests of steel sandwich panel exterior wall and roof/ceiling constructions,** *NBSIR 73-135,* 38 pages (Dec. 1972). (Available as PB 221310 from the National Technical Information Service, Springfield, Va. 22151.)

Key words: Exterior wall; fire endurance; fire test; housing systems; Operation BREAKTHROUGH; paper honeycomb; roof/ceiling assembly; structural sandwich panel.

As part of the evaluation of a housing system proposed under Operation BREAKTHROUGH, fire endurance tests were performed at the National Bureau of Standards on an exterior wall assembly and a roof/ceiling assembly. Both constructions were assemblies of sandwich panels composed of a paper honeycomb core with sheet steel facings.

The test method was in accordance with the requirements of ASTM E 119, Standard Methods of Fire Tests of Building Construction and Materials, for loadbearing structures. The applied live load was 237 pounds per linear foot (plf) for the wall assembly and 28.6 pounds per square foot (psf) on a 13 ft 5 in span for the roof/ceiling assembly. The results of these tests are valid only for walls and roof/ceilings of such constructions described in this report and loaded at or below the stress levels developed by these loadings.

The fire endurance of the wall assembly was 7 min 50 sec; and the roof/ceiling, 9 min 09 sec. In both cases, the failure was due to a maximum temperature rise of 181 °C (325 °F) above the initial temperature on the unexposed surface.

**13395.** Craw, A. R., **Time series forecasting of highway accident fatalities,** *NBSIR 73-138,* 37 pages (Mar. 1973). (Available as COM 73-10868 from the National Technical Information Service, Springfield, Va. 22151.)

Key words: Exponential smoothing; fatalities; highway accidents; time series.

Using twelve years of time series data on highway fatalities, the methodology currently employed by the National Highway Traffic Safety Administration (NHTSA) to forecast the annual (calendar year) total of highway accident fatalities were compared with those obtained by several computer routines based on exponential smoothing techniques and available at the National Bureau of Standards. The use of unadjusted and seasonally adjusted data was also examined.

It is found that there is no coercive evidence to lead to abandoning the present NHTSA methods in favor of readily available computer routines based on exponential smoothing methods.

Of the methods examined in this study, the best results were obtained with the EXPSMOOTHING routine using unadjusted fatality data.

**13396.** Son, B. C., **Fire endurance test of plywood-faced exterior walls for single family housing,** *NBSIR 73-140,* 24 pages (Mar. 1973). (Available as PB 22026/5 from the National Technical Information Service, Springfield, Va. 22151.)

Key words: Fire endurance; fire test; housing systems; interdwelling wall; Operation BREAKTHROUGH; single wall.

As a part of the testing and evaluation activities in Operation BREAKTHROUGH, a standard fire test conforming to ASTM E 119 was performed at the National Bureau of Standards on a wall assembly where half represented a nonbearing single exterior wall (as found in single family detached housing) and the other half represented a nonbearing double wall for an interdwelling separation which would occur at the interface of two parallel adjacent modules. Each wall contained a layer of gypsum board as an interior (room) surface and a layer of plywood as an exterior surface, and was framed with nominal 2 × 4 in wood studs on 16 in centers. No structural load was applied during the test.

The fire endurance of the single wall was 43 min. The initial mode of failure was by excessive average temperature rise on th unexposed surface of the wall.

Although the test results of the interdwelling wall were inco clusive, its fire endurance was considered to be 1 hr. 02 mi This fire endurance was based on visual observation during th test and was the time when the gypsum board on the unexpose side was observed to separate from the wood studs.

**13397.** Shoub, H., Son, B. C., **Fire endurance tests of plywood c steel joist floor assemblies, with and without ceiling,** *NBSIR 7 141,* 37 pages (Mar. 1972). (Available as PB 220430/3 fro the National Technical Information Service, Springfield, V 22151.)

Key words: Fire test; floor assembly; floor-ceiling a sembly; housing systems; modular construction; Operatic BREAKTHROUGH; steel framing; steel joist floor.

Fire endurance tests were conducted on two floor/ceiling a semblies intended for use in modular housing. One assemb simulated the combination of the floor of an upper story modu with the ceiling assembly of the module beneath; the other a sembly, the floor of a first floor module over a ceilingless cra or foundation space.

The floors were of plywood deck with vinyl or carpet overla on light gage steel "C" joists. In the floor-ceiling assembly, th ceiling was separately supported on its own joists, containe simulated HVAC (Heating, Ventilation, and Air Condition) du work and a layer of glass fiber batt insulation. During the tes which were conducted generally in accordance with the requir ments of ASTM E 119-71, Fire Tests of Building Constructic and Materials, the floors were loaded to represent the de weight of structural parts bearing on them and a live load applic tion of 40 psf. The test results are valid only for floors of simil construction loaded at or below the stress level developed by th loading.

Failure of the floor with the protective ceiling assembly o curred by flame-through to the unexposed surface at 29 mi with extensive structural failure (collapse under load) followi at 33 min. The unprotected floor over the crawl space had flame-through at 3 1/4 min, and structural failure following at 3/4 min.

**13398.** Kusuda, T., **Climatological data at the proposed prototy sites in the United States for the evaluation of HUD Operati BREAKTHROUGH housing systems,** *NBSIR 73-144,* 1 pages (Apr. 10, 1973). (Available as PB 220849/4 from t National Technical Information Service, Springfield, V 22151.)

Key words: Air contamination; design conditio earthquake risk; evaluation; ground temperature; humidit noise level; Operation BREAKTHROUGH; precipitatio solar radiation; temperature; wind direction; wind speed.

The purpose of this report is to provide preliminary inform tion on site climatology useful for the design and evaluation HUD Operation BREAKTHROUGH experimental buildi systems. In order to evaluate the design as well as the pe formance of building systems, the following environmen parameters are considered essential and are included in this r port for each of the selected sites: temperature, humidity, wi speed and direction, precipitation (snow and rain), solar radiati (direct and diffuse), ground temperature (depth and fros background noise level, air contamination, and earthquake ris

**13399.** Rossiter, W. J., Jr., **Outdoor performance of plastics. Final update of weathering data,** *NBSIR 73-146,* 104 pag (Mar. 1973). (Available as COM 73-10989 from the Natio Technical Information Service, Springfield, Va. 22151.)

Key words: Manufacturing Chemists' Association (MCS); performance of plastics outdoors; plastics; weathering of plastics.

Twenty plastics samples have been weathered in Arizona, Florida, and Washington, D.C. for 72 months. The weathering of these samples has been followed by measuring changes in the specimen's color, tensile, flexure, gloss, and haze properties. Computer-generated graphs of these changes with time are presented.

**13400.** Unassigned.

**13401.** Yokel, F. Y., Reichard, T. W., **Evaluation of the column connections used in a precast concrete modular housing system,** *NBSIR 73-148*, 90 pages (Mar. 26, 1973). Superseded by NBS Technical Note 811 (in press). (Available as PB 220366/7 from the National Technical Information Service. Springfield, Va. 22151.)

Key words: Building system; column connection; concrete triaxial strength; ductility; neoprene bearing pad; Operation BREAKTHROUGH; performance tests; precast concrete; structural design.

The column connections used in a housing system employing stacked precast concrete box modules were tested to evaluate their structural performance. The system was proposed for construction in Operation BREAKTHROUGH, a research and demonstration program sponsored by the Department of Housing and Urban Development. The system uses innovative structural design concepts, which include: confinement of the concrete in the vicinity of the column bearings by reinforcing ties in order to increase concrete compressive strength; neoprene pads between column bearings in the upper stories; steel-neoprene-steel sandwich in the lower stories; and a grouted dowel through the center of the columns to provide resistance to tension and shear.

The test program included the following: tests to determine the effect of various bearing pads on the load capacity of the connection; tests to determine the load-deformation characteristics of the neoprene pads; a test to determine the performance of a lower-story connection using a steel-neoprene-steel sandwich and a grouted dowel; and tests to evaluate the strength and ductility of the connections when subjected to a shear force. The test results are presented and interpreted and the findings are summarized.

**13402.** Donaldson, J. R., **On uncertainty in mass measurement,** *NBSIR 73-151*, 10 pages (Mar. 1973). (Available as COM 73-10866 from the National Technical Information Service, Springfield, Va. 22151.)

Key words: Mass measurement; random variability; standard deviation; systematic error; uncertainty.

This paper is a review of the factors which determine the total uncertainty of a measured mass value. It explains how to determine the standard deviation of the measurement process, how to combine error terms to provide a realistic estimate of the uncertainty, and how these error terms are propagated through a chain of mass measurements.

**13403.** Craw, A. R., **A summary of the relationships between accident indices and rates following a redefinition of "failure,"** *NBSIR 73-154*, 17 pages (Mar. 1973). (Available as COM 73-10865 from the National Technical Information Service, Springfield, Va. 22151.)

Key words: Accident indices; accident rates; failure indices; failure rates; highway accidents.

Using Cerrelli's association of "failure" with active involvements in the case of two vehicles accidents, one can define failure indices, accident involvement indices, failure rates, accident involvement rates for 1-vehicle, 2-vehicle and for the union class of 1- and 2-vehicle accidents. This note presents in a condensed form all of the definitions of these measures, and a number of useful relationships and interrelationships that exist between these different measures. These formulae should prove useful in the calculation of the resulting indices and rates and of converting from one set of measures to another.

**13404.** Finkel, P. W., Miller, T. R., **Executive summary of a proficiency test assessment of clinical laboratory capability in the United States,** *NBSIR 73-162*, 9 pages (May 1973). Superseded by NBSIR 73-163. (Available as COM 74-10542 from the National Technical Information Service, Springfield, Va. 22151.)

Key words: Accuracy; clinical chemistry; hematology; medical usefulness; microbiology, proficiency testing.

The proficiency of a selected sample of physician, hospital and independent laboratories was assessed with respect to their ability to analyze clinical chemistry and hematology samples and to identify microbiological organisms. For the assessment of clinical chemistry and hematology proficiency, the laboratories were grouped and determinations of group accuracy and group precision were made. Further analyses were performed to determine relative accuracy and precision of the techniques presently applied to these groups. There was no significant difference at the 95% confidence level in the accuracy achieved by the various laboratory groups involved in clinical chemistry and hematology analysis. In clinical chemistry, the Medicare-Certified Independent Laboratories, CDC Tested Laboratories and JCAH-Members generally proved more precise than Physicians' Office and Medicare-Certified Hospital Laboratories. However, none of the laboratory groups were sufficiently accurate to permit the monitoring over time of variation in an individual patient's constituent concentrations. It would appear that poor selection of techniques was an important contributor to this low performance level. In hematology the Physicians' Office Laboratories proved to be the least precise of the groups. There was no noticeable difference in precision between participants in the CDC proficiency testing program and nonparticipants. With respect to microbiology, 7.6% of the identifications by laboratories participating in the CDC testing program were incorrect, while 19.4% of all other identifications were incorrect.

**13405.** Son, B. C., **Fire endurance test of a steel sandwich panel floor construction,** *NBSIR 73-164*, 25 pages (Apr. 1973). (Available as PB 221642 from the National Technical Information Service, Springfield, Va. 22151.)

Key words: Fire endurance; fire test; flame penetration; floor assembly; housing systems; Operation BREAKTHROUGH; paper honeycomb; structural panel.

As a part of the evaluation of a housing system proposed under Operation BREAKTHROUGH, a fire endurance test was performed at the National Bureau of Standards on a floor, made up of sandwich panels consisting of a paper honeycomb core with steel and plywood surfaces, supported on steel joists.

The test method was generally in accordance with the requirements of ASTM E 119, Fire Tests of Building Construction and Materials, for loadbearing floor constructions. The applied live load was 40 psf and the test results are valid only for floors of similar construction loaded at or below the stress level developed by this loading.

Failure occurred by flame-through of the floor assembly in 8 min 45 sec, with structural failure (inability to sustain the applied load) following immediately.

**13406.** Son, B. C., **Fire endurance test on a steel tubular column protected with gypsum board,** *NBSIR 73-165*, 23 pages (Apr. 1973). (Available as PB 221474 from the National Technical Information Service, Springfield, Va. 22151.)

Key words: Fire endurance; fire test; housing system; multifamily housing; Operation BREAKTHROUGH; single family attached housing; steel tube column.

As a part of the evaluation of housing systems for Operation BREAKTHROUGH a standard fire endurance test was performed at the National Bureau of Standards on a load-bearing steel column construction for use in single-family attached and multifamily low-rise housing. The test method was generally in accord with the requirements of ASTM E 119, Standard Methods of Fire Tests of Building Construction and Materials, for a loaded column. The applied load was 7110 pounds per column and the test results are valid only for columns of such construction loaded at or below the stress level developed by this loading.

The 3 in × 2 in × 3/16 in rectangular hollow tubular steel column was protected with two layers of gypsum board.

The fire endurance of the column assembly was established at 59 min, when structural failure occurred.

**13407.** Son, B. C., **Fire endurance test of an interdwelling double wall construction of paper honeycomb and gypsum board,** *NBSIR 73-166*, 24 pages (Apr. 1973). (Available as PB 222297 from the National Technical Information Service, Springfield, Va. 22151.)

Key words: Fire endurance; fire test; flame penetration; glass reinforced plastic; housing systems; interdwelling wall; modular construction; Operation BREAKTHROUGH; paper honeycomb; structural panel.

As a part of the evaluation of a housing system proposed under Operation BREAKTHROUGH, a fire endurance test was performed at the National Bureau of Standards on a double wall assembly intended as an interdwelling separation for single family attached housing. Each wall of the assembly contained a core of paper honeycomb surfaced on both sides with glass fabric impregnated with polyester resin, and protective layers of gypsum board.

The test method was generally in accordance with the requirements of ASTM E 119, Fire Tests of Building Construction and Materials. The applied live load was 636 plf on each panel and the results of this test are valid only for walls of similar construction loaded at or below the stress levels developed by this loading.

The fire endurance of the first (fire-exposed) wall panel was 65 min:30 sec, based on flame penetration through cracks and openings formed on the back face of the first wall. The overall fire resistance of the double wall assembly was 79 min when pieces of the structural glass fabric of the front face of the second wall were observed falling into the furnace.

**13408.** Son, B. C., **Fire endurance test of a roof/ceiling construction of paper honeycomb and gypsum board,** *NBSIR 73-167*, 20 pages (Jan. 1973). (Available as PB 222298 from the National Technical Information Service, Springfield, Va. 22151.)

Key words: Fire endurance; fire test; flame-through failure, structural panel; glass-fabric reinforced plastic; housing systems; Operation BREAKTHROUGH; paper honeycomb; roof/ceiling assembly; structural panel.

In a program of evaluation of various housing systems proposed under Operation BREAKTHROUGH, a fire endurance test was performed at the National Bureau of Standards on a roof/ceiling assembly consisting of a paper honeycomb structural core surfaced both sides with glass-fabric impregnated with polyester resin and outer layers of gypsum board.

The test method was generally in accordance with the requirements of ASTM E 119, Fire Tests of Building Construction and Materials, for loadbearing roof assemblies. The applied load was 15.9 psf and the test results are valid only for roof/ceilings o similar construction loaded at or below the stress leve developed by this loading.

Under a loading of 15.9 psf on a 13 ft 5 in span, which produced a stress equivalent to the application of 20 psf on a 1 ft span, failure occurred by flame-through of the roof/ceiling assembly at 37 min 13 sec.

**13409.** Son, B. C., **Fire endurance test of a fiber glass reinforced polyester double wall assembly,** *NBSIR 73-168*, 27 pages (Apr 1973). (Available as PB 221184 from the National Technica Information Service, Springfield, Va. 22151.)

Key words: Fire endurance; fire test; glass fiber-reinforced plastic; housing systems; interdwelling wall; Operation BREAKTHROUGH.

As a part of the evaluation of a housing system proposed unde Operation BREAKTHROUGH a standard fire endurance tes was performed on a double wall assembly comprising a loadbearing interdwelling (party) wall for single family attached housing. The test method was in accordance with the requirements o ASTM E 119, and the applied load was 700 pounds per linea foot (plf) per wall. The test results are valid only for walls o similar construction loaded at or below the stress leve developed by this loading.

The double wall, representative of an interdwelling (party wall) separation, was made up of two identical parallel panel from two adjacent modules separated by a 2 1/4 in air space Each wall assembly contained glass fiber-reinforced polyeste (GRP) sheet faces, glued to a corrugated GRP stiffener core The GRP core members were painted with an intumescent typ fire retardant paint and the core spaces were filled with minera wool insulation.

The fire endurance of the first (fire-exposed) wall was 2 min:25 sec with the initial mode of failure by structural collapse

The second (unexposed) wall failed at 42 min when a ho (charred) spot was observed on the unexposed surface.

**13410.** Son, B. C., **Fire endurance test of a wood stud interdwelling double wall construction,** *NBSIR 73-169*, 21 pages (Apr 1973). (Available as PB 221185 from the National Technica Information Service, Springfield, Va. 22151.)

Key words: Fire endurance; fire test; flame-through failure of walls; housing systems; interdwelling wall; Operation BREAKTHROUGH.

As a part of the evaluation of a housing system proposed unde Operation BREAKTHROUGH a standard fire endurance tes was performed on a double wall construction representing a non-load-bearing interdwelling wall for single family attached housing. The test was conducted at the National Bureau of Standards and followed the requirements of ASTM E 119, Fire Tests o Building Construction and Materials.

The double wall which represented an interdwelling separation between two adjacent modules, was made up of two identical parallel walls separated by a 1/2 in air space. Each wall con ained two layers of fire-rated gypsum board attached to wood tud framing on the dwelling room side.

Since the test assembly represented a nonbearing wall, no load was applied during this test.

The failure of the first (fire exposed) wall occurred at 1 h:17 min when a joint in the second layer of gypsum board opened to allow passage of flame.

The second (unexposed) wall failed at 2 hr 19 min when the emperature rise at one point on the exposed surface exceeded he maximum allowable.

**13411.** Son, B. C., **Fire endurance test of an interdwelling double wall constructed of polyurethane foam-filled sandwich panels,** *NBSIR 73-170*, 27 pages (Apr. 1973). (Available as PB 221193 from the National Technical Information Service, Springfield, Va. 22151.)

> Key words: Fire endurance; fire test; housing systems; interdwelling wall; load failure; modular construction; Operation BREAKTHROUGH; polyurethane foam; toxic gases.

As a part of the evaluation of housing systems for Operation BREAKTHROUGH, a standard ASTM E 119 fire endurance est was performed on a double wall assembly comprising a loadbearing interdwelling (party) wall for single family attached housing.

The test was generally in accordance with the requirements of ASTM E 119, Fire Test of Building Construction and Materials. The applied live load was 678 pounds per linear foot (plf) per wall and the test results are valid only for walls of similar construction loaded at or below the stress level developed by this loading.

The fire endurance of the first (fire exposed) wall, based on structural load failure, was 1 hr and 4 min. The test was discontinued at 1 hr:06 min because of untenable conditions in the test building resulting from smoke and combustion gases released by the polyurethane foam insulation in the wall.

**13412.** Son, B. C., Shoub, H., **Fire endurance tests of double module walls of gypsum board and steel studs,** *NBSIR 73-173*, 32 pages (Apr. 1973). (Available as COM 73-10844 from the National Technical Information Service, Springfield, Va. 22151.)

> Key words: Fire endurance; fire tests; housing systems; modular construction; Operation BREAKTHROUGH; steel framing.

Standard fire endurance fire tests were conducted on two 8-ft high by 16-ft long assemblies, each consisting of double modular partition walls. In these tests, the applied loads represented the weight of modules supported by the walls, and other applicable design live loads. The partitions were of gypsum board on metal studs and simulated the juxtaposition of walls of two adjoining housing modules. As each of the parallel module walls was an independent load bearing member both were required to meet a specified fire endurance under the applied load in tests conducted in accordance with the requirements of ASTM E 119-71, Fire Tests of Building Construction and Materials.

The load applied was 1078 pounds per linear foot (plf) per wall and the test results are valid only for walls of similar construction loaded at or below the stress level developed by this loading.

The fire exposed wall of the first test specimen (with 3 in "C" type studs) failed structurally at 42 min and the outer wall failed structurally at 1 hr 13 min. In the second test specimen, with tubular studs for increased strength, the fire exposed wall failed structurally at 1 hr 7 min and the outer wall failed at 1 hr 37 min by passage of hot gas.

**13413.** Quigley, D. F., **USAC transferability,** *NBSIR 73-183*, 71 pages (Apr. 1973). (Available as COM 73-11177 from the National Technical Information Service, Springfield, Va. 22151.)

> Key words: Information systems; management information systems; municipal systems; technology transfer.

This is a report on the transferability of the USAC program technology. USAC is a Federal Urban Information Sytems Inter-Agency Committee which oversees a program of research and development of municipal information systems. This report examines the transferability of the program results from three perspectives: the technical results achieved *vis-a-vis* its research objectives, the technology products for transfer, and the organizations that could participate in the transfer. Proposals to enhance the transferability of USAC technology are made.

**13414.** Quindry, T. L., **Acoustical evaluation of a single family attached steel-frame modular housing system constructed on an Operation BREAKTHROUGH prototype site,** *NBSIR 73-190*, 21 pages (Apr. 1973). (Available as PB 221189 from the National Technical Information Service, Springfield, Va. 22151.)

> Key words: Acoustics; noise isolation class; Operation BREAKTHROUGH.

The acoustical performance of a single family attached steel-frame modular housing system was tested on an Operation BREAKTHROUGH prototype site.

Test results are given concerning the noise isolation of interdwelling walls, the noise isolation of intradwelling walls and floor-ceiling assemblies.

**13415.** Quindry, T. L., **Acoustical evaluation of a single family detached honeycomb panel housing system constructed on an Operation BREAKTHROUGH prototype site,** *NBSIR 73-192*, 19 pages (Apr. 1973). (Available as PB 222231 from the National Technical Information Service, Springfield, Va. 22151.)

> Key words: Acoustics; noise criterion curves; noise isolation class; Operation BREAKTHROUGH.

The acoustical performance of a single family detached honeycomb panel housing system was tested on an Operation BREAKTHROUGH prototype site.

Test results are given concerning the noise isolation of intradwelling walls and the noise levels within living units.

**13416.** Ludtke, P. R., **Development of insulation transfer-standards using a flat plate calorimeter,** *NBSIR 73-301*, 43 pages (Mar. 1973). (Available as COM 73-10762 from the National Technical Information Service, Springfield, Va. 22151.)

> Key words: Calorimeters; fiber glass; foam insulation; insulation transfer-standard; multilayer insulation; thermal insulation; transfer standards.

This program was initiated to develop insulation transfer-standards to be used for evaluating calorimeters at different locations throughout the country. Various types of insulation materials were evaluated for use as transfer-standards. Samples were prepared for preliminary evaluation from selected candidate insulation materials. A 30.5 cm diameter double guarded flat plate calorimeter at MSFC was provided for testing. The calorimeter was checked and the boiloff-gas instrumentation updated. Thermal conductivity screening tests were conducted using liquid nitrogen on open and closed cell foam and fiber glass samples. The mean thermal conductivity values of the samples tested during the screening tests are presented. Compliance with the proposed ASTM Standard Method of Test for Heat Flux Through Evacuated Insulations was stressed.

**13417.** Gans, W. L., Nahman, N. S., **Fast Fourier transform implementation for the calculation of network frequency domain transfer functions from time domain waveforms,** *NBSIR 73-303*, 53 pages (Dec. 1972). (Available as COM 73-10509 from the National Technical Information Service, Springfield, Va. 22151.)

Key words: Discrete Fourier transform; fast Fourier transform; frequency spectra, discrete; network transfer function; time domain waveform; transfer function.

This report is concerned with the software applications of the fast Fourier transform algorithm to the relationship between time domain waveforms and frequency domain spectra. The first chapter is devoted to a description of the discrete Fourier transform and the fast Fourier transform. Chapter 2 contains the text and a brief description of all FORTRAN II programs utilized in connection with this work. All computation was performed on the in-house time share computing system in the NBS facilities, Boulder, Colo. In Chapter 3, problems encountered using the fast Fourier transform algorithm are discussed, an example of a time domain to frequency domain calculation is presented, and future developmental considerations are mentioned. In addition, Appendix A contains a detailed example aimed at disclosing the inner mechanisms of the fast Fourier transform algorithm.

**13418.** Sindt, C. F., **Insulation of liquid oxygen dewars,** *NBSIR 73-308*, 44 pages (Apr. 1973). (Available as AD 763325 from the National Technical Information Service, Springfield, Va. 22151.)

Key words: Cryogenic insulation; insulation; LOX dewars; microspheres; polyurethane foam.

The Navy has experienced failure of vacuum insulation in dewars used for storage and handling of liquefied breathing oxygen for aircraft pilots. Because of the vacuum insulation failures, a search was made for a more rugged insulation that has thermal performance similar to the currently used vacuum with multilayer or powder. No system was found that compared in thermal performance and did not require a vacuum. Two systems were experimentally evaluated that did not require vacuum. One was polyurethane foam with an intermediate fiber glass shell and the other was glass bubbles in argon gas at one atmosphere pressure. The polyurethane foam system was successful in that no cracks penetrated to the outside surface; however, the average thermal conductivity was 160 $\mu$W/cm-K which is about 15 times greater than vacuum and powder. The glass bubbles in argon gas was also successful since the argon gas pressure always remained high enough to prevent air and moisture from entering the insulation through small leaks in the outer shell. The thermal performance was poorer than the polyurethane foam. The average thermal conductivity was 212 $\mu$W/cm-K or about 20 times greater than for the same glass bubbles in a vacuum.

**13419.** Thurber, W. R., Lewis, D. C., Bullis, W. M., **Resistivity and carrier lifetime in gold-doped silicon,** *NBSIR 73-128*, 56 pages (Jan. 31, 1973). (Available as AD 760150 from the National Technical Information Service, Springfield, Va. 22151.)

Key words: Carrier lifetime; gold-doped silicon; resistivity; semiconductor characterization; silicon.

This report describes the current status of a continuing study of the electrical properties of gold-doped silicon. Room temperature resistivity and Hall effect measurements were made on many sets of gold-diffused boron- or phosphorus-doped silicon wafers for a wide range of initial resistivities of both types. The general suitability of the proposed model was verified although an apparent discrepancy still remains between total and electrically active gold as confirmed by resistivity data as a function of gold density for phosphorus-doped silicon. Electrical measure ments were made to study the activation energies of the gol donor and acceptor. In addition, the activation energy of th gold-coupled shallow acceptor in the proposed model was ob served. The values found were in good agreement with other re ported observations of these levels. In the application of the sur face photovoltage method to the measurement of minority carri er lifetime, it was found that the optical absorption coefficient needed in the analysis of the data were dependent on the hea treatment given to the specimen. The uncertainty in diffusio length was determined to be about 2 $\mu$m which placed an effec tive lower limit on lifetime measurements of about 15 ns in *p* type and about 50 ns in *n*-type silicon. An analysis of the use o the surface photovoltage method for lifetime measurements i thin epitaxial layers is included as an appendix. The revers recovery (RR) technique for measuring lifetime was examine and it was observed that the dependence of diode storage time o the ratio of forward to reverse current varied with the base widt of the diode studied. While theory and experiment for open ci cuit voltage decay (OCVD) were in agreement for long bas width diodes, correlation for short base diodes was less satisfac tory; this study is continuing. Both the RR and OCV techniques give the same value of lifetime for long base diode but agreement for short base diodes is not as good. Addition entries are included as a supplement to an earlier bibliography o the properties of gold-doped silicon.

**13420.** Stoltenberg, R. E., **RF null detector NBS/SND,** *NBSIR 7 302*, 88 pages (June 1973). (Available as COM 73-10869 fro the National Technical Information Service, Springfield, V 22151.)

Key words: Detector; phase sensitive; RF null detector.

This report describes an ultrasensitive receiver for detecti low-level rf signals in the nanovolt region. The primary purpo of the instrument is to detect the balance condition in rf bridge however, it is useful in any comparison measurement in whic two or more signals can be adjusted in phase and magnitude suc that their summation results in a null.

The receiver frequency is determined by individual plug- units. Units have been built for selected frequencies from 1 kHz through 30 MHz. Detection is accomplished by double co version. The first converts the signal of interest to a common i termediate frequency; the second performs a dual synchrono (homodyne) conversion. The dual detectors are sensitive signals in quadrature with each other. A reference volta synchronous with the null signal is required. Thus, the dual d tection provides an indication of both the phase and the ma nitude of the null unbalance.

The output of each detector is displayed on a zero-center m ter, thus indicating the direction of unbalance as well as the ma nitude. This information is also available at a rear panel jack f use in servo control of the external system.

Gain adjustment over a 90 dB range is provided by a sing front panel control. Phase adjustment to compensate for d ferential phase delay between the reference and null signals is a complished with a front panel 360° continuous phase control.

**13421.** Unassigned.

**13422.** Milligan, D. E., Jacox, M. E., **Matrix isolation spectrosc py,** Chapter 1 in *MTP (Medical and Technical Publishing) I ternational Review of Science. Physical Chemistry Seri One. Vol. 3. Spectroscopy*, D. A. Ramsay, Ed., pp. 1-32 (B terworth & Co., Ltd., London, England and University Pa Press, Baltimore, Md., 1972).

Key words: Atomic spectra; electronic spectra; free radicals; high-temperature species; matrix isolation; molecular ions; reactive molecules; rotation in matrices; vibrational spectra.

Studies of the infrared and ultraviolet spectra of atoms and molecules isolated in inert solid matrices at cryogenic temperatures are reviewed, with emphasis on the basic principles of the technique and on publications during the period 1969-1971.

**3423.** Hudson, R. P., **Book: Principles and application of magnetic cooling,** *Series in Low Temperature Physics* **2,** 1-230 (North-Holland Publishing Co., Amsterdam, The Netherlands, 1972).

Key words: Adiabatic demagnetization; cryogenics; cryothermometry; magnetic cooling; magnetism.

Magnetic cooling is discussed in terms of basic thermodynamic principles, then supplemented by a review of paramagnetism theory, and descriptions of experimental techniques (including thermometry) involved in applying the magnetocaloric effect to real systems.

**3424.** Wong, C. Y., Tamura, T., Marshak, H., Langsford, A., **Effects of nuclear collectivity on the total neutron cross section,** *Particles Nucl.* **4,** 163-174 (1972).

Key words: Coupled channel calculations; holmium$^{165}$; nuclear collectivity; nuclear Ramsauer effect; optical model; total neutron cross section.

A study is made of the effect of the nuclear collectivity on the variation of the total neutron cross section with respect to the incident energy ranging from 4 to 20 MeV. It is found that the higher the collectivity, the smoother is the excitation function, for both deformed and vibrational nuclei. This feature is understood qualitatively in terms of the nuclear Ramsauer effect and is explained quantitatively by coupled-channel calculations. These calculations further reveal that deformed nuclei have larger total cross sections and smoother variations than do the vibrational nuclei. For vibrational nuclei, it is also found that the quadrupole deformation has a slightly larger effect on the smoothness than does the octupole deformation, if they have the same deformation parameter.

**13425.** Ehlers, V. J., Gallagher, A., **Electron excitation of the calcium 4227-Å resonance line,** *Phys. Rev. A* **7,** No. 5, 1573-1585 (May 1973).

Key words: Calcium; electron excitation.

We have measured the optical-excitation function and polarization of the 4227-Å line, using crossed electron and calcium beams, for electron energies from threshold to 1400 eV. In the high-energy region, from 100-450 times the threshold energy, we have used the Bethe theory to normalize our experimental results. An excellent signal-to-noise ratio combined with ~ 0.3-eV full width at half-maximum electron-energy resolution has enabled observation of structure in the excitation function and polarization curves below 5 eV. We observed a threshold polarization limit of (98 ± 3)%, consistent with the expected + 100%. The data are also consistent with a logarithmic approach to a high-energy polarization of − 100%.

**13426.** Kirchhoff, W. H., Lide, D. R., Jr., **Microwave spectrum, dipole moment, and quadrupole coupling constant of trifluoramine oxide,** *J. Chem. Phys.* **51,** No. 1, 467-468 (July 1, 1969).

Key words: Dipole moment; hyperfine structure; microwave spectrum; quadrupole coupling; Stark effect; symmetric top; trifluoramine.

The microwave spectrum of trifluoramine oxide, $NF_3O$, has been observed and is consistent with a symmetric top structure for the molecule. The dipole moment has been measured from the Stark effect of the $K = 1, J = 1 \rightarrow 2$ transition and its value is $0.0390 \pm 0.0004$ Debyes where the uncertainty indicated is twice the standard error obtained from a least squares fit of the data. The quadrupole coupling constant of the nitrogen nucleus was calculated from the hyperfine splitting of the $K = 1, J = 1 \rightarrow 2$ transition. Its value is $eqQ = -1.52 \pm 0.15$ MHz where the uncertainty is based on an estimated uncertainty of 0.05 MHz in the measured hyperfine splitting.

**13427.** Kirchhoff, W. H., **Microwave spectroscopy — a molecular probe,** *Ind. Res.* **12,** No. 2, 38-41 (Feb. 1970).

Key words: Chemical analysis; dipole moment; microwave; molecular structure; radio astronomy.

A brief state-of-the-art description of microwave spectroscopy is presented. The discussion includes a description of those molecular properties which may be derived from a microwave spectrum, the physical model describing the origin of a microwave spectrum and a discussion of some of the potential uses of microwave spectroscopy as a tool for chemical analysis.

**13428.** Flynn, H. G., Cook, R. K., **The effects of sonic boom and similar impulsive noise on structures,** *Environmental Protection Agency Report No. NTID300.12,* 19 pages (available as PB 206725 from the National Technical Information Service, Springfield, Va. 22151, Dec. 31, 1971).

Key words: Damage by sonic booms; noise pollution; sonic boom.

This report is a review and summary of recently published studies on the effects of sonic booms, mainly physical and financial effects on property. It has been prepared in partial response to Title IV — Noise Pollution, of the Clean Air Amendments of 1970 (Public Law 91-604). It will be published and distributed, concurrently with its presentation to the President and Congress, by the Environmental Protection Agency. A bibliography of recent papers and studies on the damage done by sonic booms is included.

**13429.** Yakowitz, H., Jacobs, M. H., Hunneyball, P. D., **Analysis of urban particulates by means of combined electron microscopy and x-ray microanalysis,** *Micron* **3,** 498-505 (1972).

Key words: Air pollution; composite dust; electron microanalysis; electron microscopy; submicrometer; urban particulates.

Particles from four samples of urban particulate matter collected in the U.S.A. were analysed by combined electron microscopy and microanalysis (EMMA). In the case of material collected at Baltimore, Md., lead was found to be present only in particles ranging from 0.05 μm to about 0.3 μm in size. The lead bearing particles did not seem to associate with other particles. Analysis of a fly ash specimen showed no qualitative or significant quantitative variation in chemistry as a function of size for the most prevalent type of particle found. Since it may be crucial to have information about particles smaller than 0.5 μm in air pollution studies, EMMA should be included with spectrometric analysis, x-ray diffraction, scanning electron microscopy and electron probe microanalysis as a primary tool for particulate analysis.

**13430.** Mihalas, D., Hummer, D. G., **Analyses of light-ion spectra in stellar atmospheres. III. Nitrogen III in the O stars,** *Astrophys. J.* **179,** No. 3, 827-845 (Feb. 1, 1973).

Key words: Dielectronic recombination; doubly ionized nitrogen; emission lines; O-stars; stellar atmospheres; stellar spectra.

An analysis of the N III emission lines in O stars has been carried out on the basis of a detailed solution of the coupled statistical-equilibrium and transfer equations for a multiline, miltilevel, multi-ion ensemble. Our calculations, using static, plane-parallel models reproduce successfully the observed emission at λλ4634, 4640, 4641 ($3p\,^2P^0 - 3d^2D$) and absorption at λλ4097, 4103 ($3s\,^2S - 3\mathrm{p}\,^2P^0$). The $^2P^{0-2}\,D$ multiplet is found to come into emission at the observed temperature for both main-sequence and low-gravity objects. The equivalent widths of the emission lines agree very well with those measured for the class of Of stars thought to have compact atmospheres, i.e., those classified as O((f)) by Walborn. In these stars the basic physical mechanism responsible for this phenomenon is the overpopulation of $3d$ by means of dielectronic recombinations from the low-lying $2s2p(^1P^0)3d$ autoionizing states with cascades $3d \rightarrow 3p$. The $3p$ state is drained by the "two-electron jumps" coupling $3p$ to the $2s2p^2(^2S,^2P,^2D)$ states, thus presenting emission in the $2s - 3p$ lines. $3s$-$3p$ lines. The possible importance of the Swings mechanism to the fully developed Of stars (in Walborn's sense) is pointed out, and the irrelevance of the Bowen mechanism to all Of stars is firmly demonstrated. The fact that the N III emission lines can be produced in static nonextended atmospheres in radiative equilibrium has the far-reaching significance that the presence of emission lines in a spectrum is not in itself sufficient evidence for the existence of a stellar chromosphere (i.e., an extended, nonradiatively heated region).

**13431.** Ku, H. H., Kullback, S., **Analysis of multidimensional contingency tables: An information theoretic approach,** *Contributed Papers 37th Session of the International Statistical Institute, London, England, Sept. 3-11, 1969,* pp. 156-158 (Sept. 11, 1969).

Key words: Contingency table; estimation of cell frequencies; hypothesis testing; information theory; interaction; residual analysis.

The principle of minimum discrimination information estimation is described and used for the analysis of multidimensional contingency tables. All classical hypothesis for contingency tables can be generated by the use of this principle and considered as "generalized" independence hypotheses when certain marginals are considered as fixed. The analysis is given in terms of effects and interactions. The practice of residual examination is stressed.

**13432.** Tate, E. L., **Anglo-American code implementation,** Paper in *Advances in Librarianship* **3,** 167-194 (Seminar Press, Inc., New York and London, 1972).

Key words: Anglo-American cataloging rules; cataloging rules; main entries.

"Anglo-American Code Implementation" relates the impact of the code on librarians and the effects it has had on the library world.

**13433.** Jespersen, J. L., Fey, L., **"Time-telling" techniques,** *IEEE Spectrum* **9,** No. 5, 51-58 (May 1972).

Key words: Automatic vehicle location; dissemination of time and frequency; portable clocks; radio propagation; satellite time dissemination; television time and frequency dissemination; time-frequency; time signal noise; system designs; transfer standards.

A brief, historical development of astronomical time scales and their use in navigation, including the present use of an atomic time scale. Frequency standards are compared in terms of accuracy, stability, and practical parameters such as cost.

Time and frequency dissemination methods are treated, including radio propagation effects, factors involved in precise time broadcasts, and use of radio navigation systems for time broadcasts. Various artificial satellite time broadcast techniques are compared. TV time techniques are discussed, as well as portable clock use and other specialized methods. The various time dissemination techniques are compared according to various parameters of interest to the user.

Some basic similarities of systems employing time and frequency are pointed out. Growing complexities of systems requiring time and frequency as an integral part are noted. This generates pressure toward diversification of the designer but emphasizes the need for further integration of time and frequency technology.

**13434.** Dillon, T. A., Stephenson, J. C., **Effect of the straight path approximation and exchange forces on vibrational energy transfer,** *J. Chem. Phys.* **58,** No. 9, 3849-3854 (May 1, 1973).

Key words: $CO_2$; exchange forces; hydrogen halides; line widths; straight path; vibrational energy transfer.

A wide variety of theories exist for calculating fundamental molecular collision processes such as line broadening or energy transfer rates. All of these theories involve evaluation of a "phase" integral or Fourier transform of the intermolecular potential. In this paper we consider two major sources of error that can occur in the evaluation of phase integrals. "Universal" phase integrals calculated in a straight path model are compared with calculations based on trajectories determined by solution of classical orbit equations. Serious discrepancies are pointed out and practical computational alternative is suggested. A simple empirical model for exchange forces is introduced in calculations of linewidths and $V$-$V$ transfer for hydrogen halides in a $CO_2$ atmosphere. These calculations show that exchange forces can have a large effect but that the simple procedure of adding "a short range" contribution to a cross section calculated from attractive multipolar forces gives a totally incorrect picture.

**13435.** Jespersen, J. L., Blair, B. E., Gatterer, L. E., **Characterization and concepts of time-frequency dissemination,** *Proc. IEEE* **60,** No. 5, 502-521 (May 1972).

Key words: Dissemination of time and frequency; portable clocks; radio propagation; satellite time dissemination; television time and frequency dissemination; time signal noise; time-frequency system designs; transfer standards.

Fundamental considerations that arise in designing a time or frequency dissemination system, are discussed and some dissemination methods are surveyed. A section on "Signal design for time and frequency dissemination" briefly summarizes radio propagation characteristics, discusses time signal format design, and considers how noise affects time and frequency signals.

We point out fundamental techniques of time and frequency dissemination and describe similarities between systems for time dissemination and navigation. The use of synchronous satellite transponders and commercial television systems for time dissemination is emphasized because of their great promise. No attempt is made to cover every existing dissemination system; some systems are treated elsewhere in this *Special Issue on Time Frequency*. The concluding section gives three categories of users according to their required accuracy and shows typical systems which can provide desired accuracies. Various dissemination techniques are charted and evaluated in terms of salient characteristics such as accuracy, geographical coverage, cost factors, and others. To alleviate an existing frequency spec-rum problem, we suggest that designers of communication and navigation systems consider opportunities for including time and frequency dissemination in their systems.

3436. Fey, L., **A time code for the Omega worldwide navigation system,** *Proc. IEEE* **60,** No. 5, 630 (May 1972).

Key words: Omega; precision time; time broadcasts; time code; VLF timing.

Time-of-day information could be added to the signals of the Omega worldwide VLF navigation system by means of a digital code. This could be valuable in resetting precision clocks and in monitoring them for malfunction. Also, Omega's worldwide coverage could then provide timing for automatic recording of data, such as geophysical information, in remote locations.

13437. Phelps, A. V., **Collision cross sections for electrons with atmospheric species,** (Proc. IAGA Symp. on Aurora and Airglow, Moscow, Aug. 1971), *Ann. Geophys.* **28,** No. 3, 611-625 (1972).

Key words: Atmospheric gases; cross sections; electron-ion recombination; electrons; review of data.

Recent laboratory measurements have yielded much detail concerning cross sections for the elastic and inelastic scattering of electrons by stable atmospheric species. Measurements of the energy and angular distributions of inelastically scattered electrons have yielded cross sections for excitation of the principal levels of $N_2$, $O_2$ and He and for the distribution of secondary electron energies resulting from collisional ionization of these gases. Electron beam measurements of cross sections for the production of radiation from $N_2$, $O_2$ and $N_2^+$ provide data of direct applicability to calculations of auroral intensities, etc. Similar data are also obtained from measurements of electron induced fluorescence. Swarm experiments provide cross section data for vibrational and rotational excitation of $O_2$ and $N_2$ at electron energies below about 1 eV. Afterglow and shock tube measurements have yielded the electron energy and temperature dependence of the electron-ion recombination for a few positive ions. Theoretical calculations of the cross sections for excitation of atomic oxygen and nitrogen are particularly important since laboratory measurements are not generally available.

13438. Frommer, M. A., Murday, J. S., Messalem, R. M., **Solubility and diffusivity of water and of salts in an aromatic polyamide film,** *Eur. Polym. J.* **9,** 367-373 (1973).

Key words: Aromatic polyamide membranes; desalination; diffusion; membranes; NMR; permeation in polymers; polymeric films; reverse osmosis; salt-polymer interactions.

The solubility and the diffusivity for water and NaCl in a fully aromatic polyamide (PA) film have been determined. From these the "intrinsic permeability characteristics" of this polymer have been calculated and its suitability for desalination by reverse osmosis is compared with that of the commonly used cellulose acetate (CA). It has been found that, although the solubility of NaCl in the PA film is higher than that in a CA film, PA membranes will reject salt better than CA membranes having identical structure and morphology. This is because the diffusivity of NaCl through the PA film is substantially lower, and the permeability of water through it (as well as the solubility and the diffusivity of water in it) are higher than the comparable values for CA films.

13439. Barger, R. L., Sorem, M. S., Hall, J. L., **Frequency stabilization of a cw dye laser,** *Appl. Phys. Lett.* **22,** No. 11, 573-575 (June 1, 1973).

Key words: Dye lasers; laser frequency stabilization; saturated absorption.

A cw dye laser system frequency stabilized to a high-finesse optical reference cavity is described. Laser frequency is servo controlled to the cavity resonance with residual fluctuations less than 50 kHz for short times (20 $\mu$sec) and 100 Hz for long times (10 sec). Drift in absolute laser frequency of about 1.5 MHz/min is observed due to drift of the unstabilized reference cavity. A saturated absorption spectrum of $I_2$ obtained with this system is shown.

13440. Stephenson, J. C., **Vibrational excitation and relaxation of the $CO(v=1)$ and $CO(v=2)$ states,** *Appl. Phys. Lett.* **22,** No. 11, 576-578 (June 1, 1973).

Key words: Carbon monoxide; infrared lasers; laser pumping of molecules; vibrational energy transfer.

Pulses from a $CO_2$ laser have been frequency doubled in a tellurium crystal and used to optically pump the first vibrational level in room-temperature CO. By monitoring infrared fluorescence from the $v=1$ and $v=2$ states, the rate constant for the process $CO(v=1)+CO(v=1)\rightarrow CO(v=0)+CO(v=2)$ has been determined. Other rate constants involving the $CO(v=1)$ level are also reported.

13441. Garvin, D., Hampson, R. F., **Atmospherical modelling and the chemical data problem,** *Proc. AIAA/AMS Int. Conf. on the Environmental Impact of Aerospace Operations in the High Atmosphere, Denver, Colo., June 11-13, 1973,* AIAA Paper No. 73-500, 1-6 (American Institute of Aeronautics and Astronautics, New York, N.Y., 1973).

Key words: Atmosphere; carbon monoxide; chemical kinetics; data evaluation; hydroxyl; nitric acid; nitric oxide; nitrogen dioxide; oxygen atom; ozone; photochemistry; stratosphere.

The chemistry of the stratosphere is determined by 50 to 100 reactions. Accurate data for these reactions are needed as input in models of the chemical dynamics of the stratosphere.

A program to provide reliable rate and photochemical data is described. The present status of some of the reactions involving O, $O_3$, $NO_2$, HO and $HNO_3$ is discussed. Recommended values are given for rate constants for a number of chemical reactions. Reactions requiring further study are indicated.

13442. Parker, R. L., **Crystal growth,** Article in *Yearbook of Science and Technology, McGraw-Hill Encyclopedia of Science and Technology,* pp. 158-160 (McGraw-Hill Book Co., New York, N.Y., 1973).

Key words: Crystal growth; crystallization; growth techniques; morphological stability.

The field of crystal growth is briefly reviewed and a number of new developments noted.

13443. Ehrlich, M., **Influence of size of $CaF_2$:Mn thermoluminescence dosimeters on $^{60}$Co gamma-ray dosimetry in extended media,** *Proc. 3d Int. Conf. on Luminescence Dosimetry, held at the Danish AEC Research Establishment Risø, Roskilde, Denmark, Oct. 11-14, 1971,* Risø Report No. 249, Part II, 550-560 (Dec. 1971).

Key words: Absorbed dose; $CaF_2$:Mn; $^{60}$Co gamma radiation; extended media; interface; theory.

Absorbed-dose distributions were measured in $CaF_2$:Mn TLD of thicknesses between 0.5 and 3.5 mm, irradiated with an essentially plane-parallel beam of $^{60}$Co gamma rays in media of aluminum (homogeneous case), polystyrene, copper, and lead. Change of average absorbed dose with dosimeter thickness was deduced from the dose distribution. Since dosimeter sizes were of the order of secondary-electron ranges, total energy absorption was found to be critically affected by interface effects, which caused a loss of linearity of energy absorbed with dosimeter thickness for polystyrene and lead. A relatively strong asymmetry in the absorbed-dose distributions was found near front and rear interfaces, absorbed dose being ~ 10 percent higher in front for polystyrene, and ~ 15 and ~ 30 percent lower for copper and lead, respectively. Comparisons of relative experimental values of average absorbed dose for different dosimeter thicknesses with values computed according to Burlin's scheme (which does not consider front-rear asymmetries) were not conclusive for polystyrene and lead, since the assumptions regarding the electron spectrum at the dosimeter site proved to be critical for polystyrene, and the assumptions regarding the photon spectrum critical for lead. For copper, there was agreement to within the limits of experimental reproducibility.

**13444.** Reed, R. P., Schramm, R. E., Clark, A. F., **Mechanical, thermal, and electrical properties of selected polymers,** *Cryogenics* **13,** No. 2, 67-82 (Feb. 1973).

Key words: Compilation; electrical properties; mechanical properties; plastics; polymers; thermal properties.

An extensive compilation has been completed on the mechanical, thermal, and electrical properties of six commercially available polymers. These data are discussed and summarized here as a function of temperature, radiation, and frequency. A brief description and characterization of each polymer is included.

**13445.** Ku, H. H., Varner, R., Kullback, S., **Analysis of multidimensional contingency tables,** *Proc. 14th Conf. on the Design of Experiments in Army Research Development and Testing, Edgewood Arsenal, Md., Oct. 23-25, 1968,* ARO-D Report 69-2, pp. 141-180 (1969).

Key words: Contingency tables; estimation of cell frequencies from marginals; generalized independence; hypothesis testing; information theory; interaction; higher-order interaction; computer programs.

This is an expository paper on the analysis of contingency tables given at the Fourteenth Conference on the Design of Experiments. The principle of minimum discrimination information estimation is described and used to generate estimates for tests of hypotheses concerning second-order and higher-order interactions. All classical hypotheses for contingency tables can be generated by the use of this principle when certain marginals are considered as fixed.

Examples are given and two available computation programs are described in detail.

**13446.** Ledbetter, H. M., **Estimation of Debye temperatures by averaging elastic coefficients,** *J. Appl. Phys.* **44,** No. 4, 1451-1454 (Apr. 1973).

Key words: Debye temperature; elastic constants of solids; elasticity.

Elastic Debye temperatures $\theta$ were calculated by averaging elastic stiffness coefficients. For cubic symmetry, eight averaging methods were evaluated with respect to a computationally exact $\theta$. Reuss's $\theta$, corresponding to uniform stress, gave better agreement than Voight's $\theta$, corresponding to uniform strain. Hill's geometrical $\theta$ gave the best agreement.

**13447.** Grundl, J. A., **Measurement of the average fission cross-section ratio, $\sigma_f(^{235}U)/\sigma_f(^{238}U)$ for $^{235}U$ and $^{239}Pu$ fission neutrons,** (Proc. Specialists's Meeting on Prompt Fission Neutron Spectra, Vienna, Austria, Aug. 1971), Paper in *Prompt Fission Neutron Spectra,* pp. 107-111 (International Atomic Energy Agency, Vienna, Austria, 1972).

Key words: Fission cross sections; fission neutrons; integral measurements.

Average fission cross-section ratios, $\sigma_f(^{235}U)/\sigma_f(^{238}U)$, have been measured for $^{235}U$ and $^{239}Pu$ fission neutrons. A cavity fission source, a fission ionization chamber, and a redundant determination of fission foil weight ratios were employed for the measurements. The result for $^{235}U$ fission neutrons is $3.71 \pm 0.17$, a value that confirms earlier integral microscopic results and is 12 to 20% discrepant with predictions based on differential microscopic data. The observed ratio of average cross-section ratios $\chi_{49}/\chi_{25}$, is $0.970 \pm 0.012$. This value represents a departure from unity that is less than one-half of that predicted by differentia microscopic data. The measurements described remain in progress.

**13448.** Drummond, D., Gallagher, A., **A low resolution scanning multiple Fabry-Perot spectrometer,** *Rev. Sci. Instrum.* **44,** No 4, 396-399 (Apr. 1973).

Key words: Fabry-Perot; spectrometer.

A low resolution scanning multiple Fabry-Perot spectrometer has been built for the observation of very weak extended light sources. The instrument consists of three sets of 7.6 cm diam Fabry-Perot plates operated in central order; their spacings are in a 3-4-5 ratio and are servo controlled using reference light provided by a single master grating monochromator. The instrument is scanned by varying the wavelength setting on the grating instrument. The resolution of the instrument is variable through the range 0.5-15 A, and its luminosity is equal to that of a 5 cm interference filter with a 65% peak transmittance. The free spectral range is about 125 times the peak half-width. Wavelengths in that range are transmitted at a level of $10^{-4}$ or less of the central transmission peak.

**13449.** Danos, M., **Baryon resonances in nuclei,** *J. Phys.* **33** Supplement to No. 8-9, 171-182 (Aug.-Sept. 1972).

Key words: Baryons; duality; exchange currents; magnetic moments; mesons; nuclear structure.

The problems one encounters when incorporating baryon resonances and mesons into the nuclear wave function are discussed. Since no workable strong interaction theory exists they must be attacked in a quasi-theoretical step-by-step manner The present status in the understanding is discussed and the possible future development suggested.

**13450.** Richmond, J. C., Walters, E. L., **Development of a standard for passive night vision devices, a progress report,** (Proc Carnahan Conf. on Electronic Crime Countermeasures, Lexington, Ky., Apr. 25-27, 1973), Paper in *Proceedings 1973 Carnahan Conference on Electronic Crime Countermeasures* UKY Bull. 102, 145-156 (Apr. 1973).

Key words: Contrast transfer function; distortion; flare image intensifiers; law enforcement; light equivalen background; light induced background; night vision devices optical gain.

The National Bureau of Standards is developing a standard for night vision devices for use by law enforcement agencies. This work is sponsored by the Law Enforcement Standards Laboratory of NBS, which is financed by the National Institute of Law Enforcement and Criminal Justice of the Department of Justice.

The paper discusses image quality criteria in general, and gives reasons for selecting contrast transfer function (CTF) and distortion as the primary criteria for image quality of night vision devices. The test equipment and procedures used at NBS for testing night vision devices will be described. Specific tests to be included are optical gain, light equivalent background, and flare in addition to contrast transfer function and distortion.

451. Stein, P. G., Boyle, D. R., **How to cope with nickel and diming in your minicomputer,** (Proc. IEEE Minicomputer Conf. on Trends and Applications, National Bureau of Standards, Gaithersburg, Md., Apr. 4, 1973). *Symposium Record,* IEEE Catalog No. 73CHO 760-9 C, pp. 5-7 (1973).

Key words: Computer, computer hardware; computer software; cross-assembler; cross-compiler; hardware; language; minicomputer; software.

Cost centers in minicomputer use are many, and some of them e not obvious to the fledgling user. Most newcomers to the eld concentrate on specifying machines for lowest system hardare cost, and sometimes just for lower CPU cost. When the oks are balanced at the end of the project, it is always clear at these factors played a small role in the total expense. Recurng maintenance, software development, software maintenance, stem changes after installation, and even costs of expendable pplies can all "nickel and dime" you to distraction or even to ankruptcy.

As usual, a careful systems approach, coupled with a realistic nderstanding of what it *really* costs to develop and operate a inicomputer system, can save a small project from the poor-ouse.

3452. Davis, R. M., **Automation technology for the retail industry (welcome address),** *Proc. Conf. Automation Technology for the Retail Industry, held at the National Bureau of Standards, Gaithersburg, Md., Mar. 15, 1972,* COM 72-10495, pp. 1-7 (National Technical Information Service, Springfield, Va., 1972).

Key words: Automated customer identification; automated merchandise identification; automatic reading technology; automation technology for retail industry; computers; National Retail Merchants Association; retail industry; retail merchandising; voluntary standards.

This report is made up of the papers presented at the March 5, 1972 conference on Automation Technology for the Retail ndustry which was cosponsored by the National Bureau of tandards and the National Retail Merchants Association. The urpose of the conference was to describe the retail industry's utomation technology objectives and voluntary standards plans o the manufacturers and suppliers of computer and automatic eading devices. The papers present a frame of reference and ummary of the NRMA efforts to apply computer and automated reading technologies to retail merchandising; the retail industry's automation problems; the functional requirements for utomated merchandise identification; the NRMA objectives for oluntary industry standards relative to automated merchandise nd credit customer identification; and recommended administrative procedures for industry liaison with the NRMA.

3453. Cotton, I. W., **A position paper—panel session on intelligent terminals—chairman's introduction,** (Proc. 1973 National Computer Conference and Exposition, New York, N.Y., June 4-8, 1973), Paper in *AFIPS Conference Proceedings* **42,** 217-218 (AFIPS Press, Montvale, N.J., 1973).

Key words: Computer terminals; intelligent terminals.

This article is a description of a forthcoming panel session on ntelligent Terminals which the author will chair at the 1973 National Computer Conference. The theme of the session is explained and the paper authors and panelists are identified.

13454. Stabler, T. M., **U.S. membership in the International Organization of Legal Metrology,** *NBSIR 73-159,* 12 pages (Apr. 1973). (Available as COM 73-11174 from the National Technical Information Service, Springfield, Va. 22151.)

Key words: Developing countries; International Bureau (BIML); International Committee (CIML); International Conference; International Organization of Legal Metrology; International Recommendations; legal metrology; OIML.

The International Organization of Legal Metrology (OIML) was formed in 1955 to promote intergovernmental cooperation in the field of weights and measures. In addition to its responsibilities as the center of documentation and information exchange in legal metrology, the OIML recommends uniform international requirements for measuring instruments and drafts model laws and regulations for consideration by the member states.

In October 1972 the United States became the 38th member nation of OIML, with NBS being assigned general responsibility for the development of U.S. positions for technical matters arising in the organization.

The benefits to the U.S. of participation in OIML are: (1) To improve opportunities for exporting measuring instruments, (2) To obtain better information regarding measurement techniques in the field, (3) To influence internationally adopted measurement technique so U.S. procedures will not be at a disadvantage, (4) To insure that the U.S. can influence the adoption by developing countries of model laws and uniform procedures, (5) To facilitate the development of an international standards program for the U.S. in legal metrology.

The U.S. Delegation participated in the International Conference of OIML held in London, October 23-28, 1972.

13455. Quindry, T. L., **Acoustical evaluation of a single family attached wood-frame modular housing system constructed on an Operation BREAKTHROUGH prototype site,** *NBSIR 73-191,* 21 pages (Apr. 1973). (Available as PB 221695 from the National Technical Information Service, Springfield, Va. 22151.)

Key words: Acoustics; field impact insulation class; noise criterion curve; noise isolation class; Operation BREAKTHROUGH.

The acoustical performance of a single family attached wood-frame modular housing system was tested on an Operation BREAKTHROUGH prototype site.

Test results are given concerning the noise isolation of intra-dwelling walls and floor-ceilings, as well as the noise levels within living units.

13456. Costrell, L., Editor, **CAMAC—A modular instrumentation system for data handling,** (AEC Committee on Nuclear Instrument Modules), *AEC Report No. TID-25875,* 66 pages (U.S. Atomic Energy Commission, Washington, D.C., July 1972).

Key words: CAMAC; computer interfacing; control systems; instrumentation; instrumentation standards; nuclear instrumentation; standards.

CAMAC is a digital data handling system in widespread use with on-line digital processors and computers. The system is based on a digital highway for data and control. Mechanical and signal standards are specified to ensure physical and operational compatibility between units from different sources. Except for pages i-vi, 46A and 46B, this report is identical to EURATOM Report EUR 4100e dated 1972. AEC Report TID-25877 constitutes a supplement to and is to be used in conjunction with this report. This revised specification introduces several new features but is consistent with the previous version (EUR 4100e, 1969).

The CAMAC system was specified by European laboratories through the ESONE Committee and has been endorsed by the U.S. AEC NIM Committee.

**13457.** Costrell, L., Editor, **Supplementary information on CAMAC instrumentation system,** (AEC Committee on Nuclear Instrument Modules), *AEC Report No. TID-25877,* 45 pages (U.S. Atomic Energy Commission, Washington, D.C., Dec. 1972).

Key words: CAMAC; computer interfacing; control systems; instrumentation; instrumentation standards; nuclear instrumentation; standards.

This report contains supplementary information to be used in conjunction with AEC Report TID-25875 (EUR 4100e, 1972), which describes the CAMAC modular instrumentation system for data handling, and AEC Report TID-25876 (EUR 4600e, 1972) which defines a CAMAC branch highway and crate controller. Included are recommendations concerning the implementation and interpretation of the specifications and descriptions of preferred practices and current applications. This report does not modify the specifications referred to above.

**13458.** Schroder, I. G., **Emission of long-range $\alpha$-particles in the subthermal-, thermal- and resonance-neutron fission of $^{239}$ Pu,** *Nucl. Phys.* **A195,** 257-268 (1972).

Key words: Alpha-particle; emission; fission; neutron; reactor; $^{239}$ Pu.

An investigation has been made of the possible dependence of the binary-to-ternary fission ratio as well as of the energy distribution of the long-range $\alpha$-particles emitted in the low-energy fission of $^{239}$ Pu on the energy of the incident neutron. To this effect a number of relative measurements have been made using three neutron filters covering, respectively, the subthermal-, thermal- and resonance-neutron regions. Furthermore, a measurement of the binary-to-ternary fission ratio has been performed for a reactor beam. The results obtained show no variation in the binary-to-ternary fission ratio or in the energy of the long-range $\alpha$-particles for the energy intervals considered to within the precision of these measurements. The measurement with the reactor beam yielded a value of the binary-to-ternary fission ratio of 412 ± 11.

**13459.** Franzen, D. L., **Continuous laser-sustained plasmas,** *J. Appl. Phys.* **44,** No. 4, 1727-1732 (Apr. 1973).

Key words: Gas breakdown; laser; plasma.

Continuous plasmas sustained by a focused high-power $CO_2$ laser are described. The power required for maintaining a cw plasma following preionization has been determined for Xe, Kr, and Ar, and attempted for Ne and He. Measurements indicate the noble gases with the lowest ionization potentials have the lowest sustaining thresholds. Radiative properties of some of the plasmas were studied with calorimetric techniques. Under certain conditions, more than half of the incident laser radiation can either be scattered or absorbed by the plasma. A major loss mechanism for the plasma is shown to be radiation in the visible and ultraviolet. Spectra of low-pressure Xe plasmas indicate the presence of ultraviolet transitions with a high contrast over the continuum.

**13460.** Le Neindre, B., Tufeu, R., Bury, P., Sengers, J. V., **Thermal conductivity of carbon dioxide and steam in the supercritical region,** *Ber. Bunsenges. Physik. Chem.* **77,** No. 4, 262-275 (1973).

Key words: Carbon dioxide; critical phenomena; steam; thermal conductivity; transport properties.

The thermal conductivity of carbon dioxide and steam has been measured as a function of temperature and density using a concentric cylinder method. Earlier measurements of the thermal conductivity of $CO_2$, obtained with a parallel plate method, covered a range of temperatures from 25 to 75 °C and reveale
the existence of an anomalous thermal conductivity in the critic
region. In this paper the experimental temperature range for th
thermal conductivity of $CO_2$ is extended to 700 °C. The hig
temperature data enable us to determine a "background" therm
conductivity needed for a quantitative analysis of the anomalo
thermal conductivity in the critical region. In addition, we pr
vide experimental evidence that the thermal conductivity
steam exhibits an anomalous increase in the critical regio
similar to the behavior observed for the thermal conductivity
$CO_2$.

**13461.** Armstrong, G. T., **Calorimetric reference mater
als—status of the primary standard,** *Proc. 1st Int. Conf. o
Calorimetry and Thermodynamics, Warsaw, Poland, Aug. 3
Sept. 4, 1969,* pp. 261-267 (Polish Scientific Publishers, Wa
saw, Poland, 1971).

Key words: Benzoic acid; calorimetric reference material

Reference materials for reaction calorimetry are briefl
reviewed. The value of 26434 $Jg^{-1}$ for the energy of combustio
of the primary standard, benzoic acid, has been confirmed b
three recent careful determinations, and give this value a ver
sound basis. Any future investigations leading to a possibl
change in this value will require extremely careful document
tion of precision and accuracy of measurement. Possible source
of systematic error are discussed.

**13462.** Hessel, M. M., Lucatorto, T. B., **The rotating heat-pip
oven; a universal device for the containment of atomic an
molecular vapors,** *Rev. Sci. Instrum.* **44,** No. 5, 561-563 (Ma
1973).

Key words: Heat pipe; indium iodide; laser applicatio
sodium; spectroscopic application.

A new type of heat-pipe oven has been developed that use
centrifugal force as a return mechanism for the condense
vapors in contrast to capillary return forces for the convention
heat-pipe oven. Since this new oven is no longer limited t
materials that wet wicks, it can be used to contain *any* materi
that does not react with the walls of the containing vessel. W
describe the operation of this oven with sodium and InI eve
when the InI is solid. Spectroscopic and laser applications of th
"rotating" heat-pipe oven are discussed.

**13463.** Lozier, D. W., Maximon, L. C., Sadowski, W. L., **A b
comparison program for algorithm testing,** *Comput. J.* **16, N
2, 111-117 (May 1973).

Key words: Algorithm testing; bit comparison testing; con
puter algorithm; mathematical function subroutines.

In view of the increasingly important role of the computer i
scientific calculations, the development of computer algorithn
for elementary and special functions has been given a great de
of attention. The development of algorithms cannot be divorce
from their evaluation, for a computer algorithm is judged sole
on the basis of its performance characteristics. These includ
storage requirements, speed and accuracy. The present pap
will deal only with the accuracy aspect of algorithm testing. Th
other two aspects must be evaluated in the context in which th
algorithm is used. In this paper by an algorithm we mean a con
puter algorithm, i.e., an implementation of a mathematical a
gorithm in a specific environment. The environment is taken t
include factors that may affect the algorithm, e.g., the operatin
system under which the program is run and hardware algorithm
for arithmetic operations. Whereas in some instances mathemat
cal algorithms have been successfully used to locate hardwar
malfunctions that were not traceable by normal trouble shootin

ts, any malfunctions of the software or hardware will not be nsidered here to be part of the environment.

**64.** Rosenstock, H. M., Larkins, J. T., Walker, J. A., **nterpretation of photoionization thresholds: Quasiequilibrium heory and the fragmentation of benzene,** *Int. J. Mass Spec-rom. Ion Phys.* **11,** 309-328 (1973).

> Key words: Appearance potential; benzene; photoionization; quasiequilibrium theory.

)uasiequilibrium theory has been applied to the parent ion gmentation of benzene. Assuming uniform excitation energy nsfer in the fragmentation threshold region and applicability he step-function photoionization threshold law, it is possible calculate fragment photoionization threshold curves in good eement with experiment. It is concluded that the unimolecu- decomposition occurs via two independent pairs of competing ctions. One pair of reactions leads to the formation of $C_6H_5^+$ $C_6H_4^+$, and involves the benzene ion ground state. The other r of reactions, leading to $C_4H_4^+$ and $C_3H_3^+$ involves the first ited state of $C_6H_6^+$ lying 2.25 eV above the ground state, or open chain isomer having a similar heat of formation. At eshold the $C_6H_5^+$ ion has a phenyl ion structure, the $C_3H_3^+$ ion yclopropenyl ion structure and the $C_4H_4^+$ ion may have a lobutene ion structure. A heat of formation of ~ 100 kcal/mol derived for the benzyne molecule, in good agreement with ni-empirical estimates. Kinetic shift effects on the fragmenta- n thresholds are found to be important. Some difficulties are ountered in the comparison of relative abundances of parent metastable transitions to the relative abundances of the ghter ions near threshold. The calculated energy dependence the unimolecular rate of formation of $C_4H_4^+$ ion is in good eement with experiment. However, the weak energy depen- nce of the rate of formation of $C_6H_5^+$ found experimentally nnot be explained. Suggestions for further work are outlined.

**65.** Zimmerman, J. E., Siegwarth, J. D., **Portable helium lewars for use with superconducting magnetometers,** *ryogenics* **13,** No. 3, 158-159 (Mar. 1973).

> Key words: Dewar; gas shielded; helium; liquid; magnetometer; multilayer insulated.

imple helium dewars have been constructed using gas-cooled iation shields and multilayer aluminized plastic insulation. ey will retain one litre of liquid for up to 40 hours. The shields y be made mostly non-conducting so the dewar can be used h ultrasensitive superconducting magnetometers. For most er applications thin sheet metal such as copper or aluminium uitable for the shields.

**66.** Roszman, L. J., Hooper, C. F., Jr., **Distribution of the ime-dependent microfield in a plasma,** *Phys. Rev. A* **7,** No. 6, 2121-2130 (June 1973).

> Key words: Distribution; Holtsmark; ion dynamics; microfield; plasma; time-average.

The theory of the distribution of the time average of the time- pendent microfield in a quantum plasma taken over a finite ne interval is introduced and developed. The short- and long- ne limits are derived. The Wigner phase-space representation employed to derive the correct distribution for a classical sma and to establish a formalism which can be used for low- der quantum corrections. Numerical results are presented for lassical gas of charged noninteracting particles. It is found that time-averaging intervals, which are larger than the time it kes a particle traveling with the average thermal velocity to oss the ion-sphere radius, the distribution deviates from the rresponding Holtsmark distribution for the quasistatic model.

**13467.** Edelsack, E. A., Kropschot, R. H., Olien, N. A., Olsen, J. L., **A Directory of European Low Temperature Research,** *Cryogenics* **13,** No. 3, 132-133 (Mar. 1973).

> Key words: Cryogenics; European low temperature research.

The publication of a Directory of Low Temperature Research in seventeen European countries is described. The Directory contains the names of some three hundred researchers, their addresses, telephone numbers, and brief descriptions of their research interests. Information for obtaining free copies of the Directory is included.

**13468.** Linsky, J. L., **A recalibration of the quiet sun millimeter spectrum based on the moon as an absolute radiometric standard,** *Solar Phys.* **28,** No. 2, 409-418 (Feb. 1973).

> Key words: Millimeter absolute radiometry; millimeter solar continuum; solar chromosphere.

The solar millimeter continuum between 1 and 20 mm is recalibrated using observations of the average lunar brightness temperature at the center of lunar disk and new Moon brightness temperatures. The solar data are placed on a common scale according to the average lunar brightness temperature distribution proposed by Linsky. A least-squares parabolic regression curve is proposed for the solar millimeter continuum. A small departure from this regression curve near 8 mm may indicate the existence of an absorption feature.

**13469.** Cezairliyan, A., **A high-speed (millisecond) system for studies of phase transitions and thermophysical properties of electrical conductors above 2000 K,** *Proc. Int. Conf. on Etude des Transformations Cristallines a Haute Température, Odeillo, France, Sept. 27-30, 1971,* No. 205, 25-32 (Centre National de la Recherche Scientifique, Paris, France, 1972).

> Key words: High-speed methods; high temperature; phase transitions; refractory metals; thermophysical properties.

A high-speed system is described for conducting studies on phase transitions, and for measuring selected thermophysical properties of electrical conductors at temperatures above 2000 K. The system can measure specific heat electrical resistivity, hemispherical total emittance, and melting point in subsecond duration experiments. Temperature measurements are made with a millisecond resolution photoelectric pyrometer. Experimental quantities are recorded with a high-speed digital data acquisition system. The entire system has a time resolution of approximately 0.4 millisecond. An experiment simulating the conditions of phase transitions is described. Results of measurements on solid-liquid phase transitions in niobium, molybdenum, and tungsten are presented. High-speed measurements of selected thermophysical properties of niobium, molybdenum, tantalum, and tungsten are summarized. Sources and magnitudes of errors are discussed.

**13470.** Straty, G. C., Younglove, B. A., **Velocity of sound in saturated and compressed fluid oxygen,** *J. Chem. Thermodyn.* **5,** No. 3, 305-312 (May 1973).

> Key words: Compressed liquid; compressibility; saturated liquid; sound velocity oxygen; specific heat ratio.

In a continuing effort to generate accurate thermodynamic and transport properties of cryogenic fluids, we have measured the velocity of sound in saturated liquid oxygen from 58 to 150 K and in compressed fluid oxygen along isotherms from 70 to 300 K at pressures to 34 MPa. The results have been used along with previously measured *p, ρ, T* results to obtain the isentropic compressibility and the heat capacity ratio, and to examine the quality of the *p*, *p*, *T* data by comparison of the measured velocities with velocities calculated from these data.

**13471.** Molino, J., **Perceiving the range of a sound source when the direction is known,** *J. Acoust. Soc. Amer.* **53,** No. 5, 1301-1304 (May 1973).

Key words: Audition and ranging; physiological and psychological acoustics; psychophysics; space perception.

A modification is proposed in Hirsch's equation for determining the range of a sound source of unknown strength [H. R. Hirsch, J. Acoust. Soc. Am. **43,** 373-374 (1968)]. The modified formula applies to the case where the direction of the sound source is known. Greene's comments on Hirsch's letter are investigated for their ability to predict the limitations on the resolution obtainable in human auditory ranging [D. C. Greene, J. Acoust. Soc. Am. **44,** 634 (1968)]. In a brief experiment, two subjects were unable to make distance judgments for sustained pure-tone sources over ranges of 3 to 48 ft.

**13472.** Lew, H. S., **The effect of impact loadings on the performance of wood joist subflooring systems,** *NBSIR 73-187,* 49 pages (May 1973). (Available as PB 221188 from the National Technical Information Service, Springfield, Va. 22151.)

Key words: Concentrated loads; deflection; floor hardboard; housing; impact energy; Operation BREAKTHROUGH; plywood; subfloors; underlayment; wood; wood joists.

This report presents the results of an experimental study of wood-joist subflooring systems subjected to impact load. Six different types of subflooring systems were tested following the test method described in the ASTM Standard Methods (ASTM Designation E-72). The magnitude of impact load was varied by dropping a 60-lb bag from different heights.

A concentrated static load of 400 lb was applied to the subfloor after it was exposed to impact load. It is suggested that the deflection under this concentrated load be used as a measure of the impact resistance of the subfloor.

**13473.** Reichard, T. W., Greene, W. E., Jr., Cattaneo, L. E., Masters, L. W., **Structural tests on housing components of glass fiber reinforced polyester laminate,** *NBSIR 73-188,* 98 pages (Apr. 1973). (Available as PB 221183 from the National Technical Information Service, Springfield, Va. 22151.)

Key words: Adhesive bond; aging; composites; compression; flexure; glass fiber; housing system; innovations; laminate; Operation BREAKTHROUGH; racking; reinforced plastics; reinforced polyester; sustained loading; tensile shear.

This report describes a series of structural evaluation tests performed on housing components made with a glass fiber reinforced polyester (FRP) laminate. The components tested were: (1) the FRP laminate used for the facings and the corrugated core of the basic panel; (2) the adhesive bond between the facing and core; (3) typical wall panels; and (4) typical roof panels. Test data include: (1) the effect of temperature and moisture on the tensile and compressive strength of the FRP laminate; (2) the effect of temperature, accelerated aging and sustained loads on the tensile shear strength of the facing-to-core polyester adhesive bond; (3) the short-term strength of the wall panels under compressive and in-plane shear loading; (4) the long-term strength of the wall panels under sustained compressive loading; and (5) the short-term and long-term performance of the roof panels under flexural loading.

**13474.** Churney, K. L., West, E. D., Armstrong, G. T., **A cell model for isoperibol calorimeters,** *NBSIR 73-184,* 100 pages (Apr. 1973). (Available as COM 73-11110 from the Natior Technical Information Service, Springfield, Va. 22151.)

Key words: Calorimetry; energy equivalents; energy me surement; heat transfer; internal energy measureme isoperibol calorimeters; measurement theory.

A calorimeter can be modeled as a large number of volume e ments or cells in each of which the temperature may be cc sidered uniform, and each of which can store heat and exchan heat with other cells. Application of the first law of th modynamics to this set of cells leads to representations of t usual calorimetric equations for internal energy change e pressed in terms of measurable or estimatable heat capaciti heat transfer coefficients, temperatures, and work terms for t individual cells. Analysis of the results yields a framework wit which most of the design and measurement problems isoperibol calorimeters can be treated.

**13475.** Somes, N. F., **Abnormal loading on buildings and progr sive collapse,** *NBSIR 73-221,* 76 pages (May 1973). (Availal as PB 220849 from the National Technical Information S vice, Springfield, Va. 22151.)

Key words: Abnormal loading; building; codes; desi criteria; multistory; progressive collapse; risk; stabili standards; strength; United States.

The document is an interim report of ongoing studies at National Bureau of Standards. It defines the several aspects abnormal loading on buildings and the problem of progress collapse. It documents the extent to which present U.S. Coc and Standards address the problem.

Abnormal loadings are identified, classified and discussed w regard to their characteristics and frequencies of occurren The report reviews the state of international knowledge of characteristics of abnormal loadings and the response buildings and building elements to these loadings. The latter cludes discussion of several incidents in which multist buildings have collapsed progressively.

Using currently available statistics an estimate is made of combined frequency of abnormal loadings on residen buildings in the U.S. For buildings susceptible to progress collapse, the corresponding risk of fatality is compared with levels of risk that society will generally accept. The risk is furt compared with the risk of mortality associated with fire in idential buildings, an area of considerable public concern expenditure.

It is concluded that U.S. standards-writing bodies sho adopt appropriate rational criteria as soon as possible to red the risks of progressive collapse. There are several areas which criteria might be introduced to reduce the risk of prog sive collapse. These are discussed; particular attention is gi to the philosophies behind the structural criteria implemente the USA and other countries.

**13476.** Peiser, H. S., Corruccini, R. J., Newman, S. **Standardization and measurement services in Turkey,** *NB 73-172,* 90 pages (Oct. 14-28, 1972). (Available as COM 11175 from the National Technical Information Serv Springfield, Va. 22151.)

Key words: AID; assistance; economics; LDC's ( developed countries); measurement services; standard tion; survey; Turkey.

The survey of standardization and measurement services developing industries in Turkey has been carried out by N with funding by AID, with participation by representative Ecuador and Korea, and under the guidance of the Turkish S dards Institute. The Survey Team spent two weeks in Tur here it inspected representative laboratories and plants, and d discussions with leaders of Government, the USAID Mis-n, principal universities and industry. The Report describes e preparation for the Survey, a summary of the economy of the untry soon to be a full member of the European Common Mar-t, notes on Turkish science and technology and the indepen-nt Turkish Standards Institute recognized by law as the na-nal standards body. Issues addressed are 1) Standards evelopment, 2) Test Methodology, 3) Product Certification, 4) oduct Testing, 5) Calibration, 6) Weights and Measures Con-l, 7) Export Control, 8) Quality Control, 9) Consumer Protec-n, 10) Industrial Extension, 11) Building Codes, 12) Interna-nal Contacts, and 13) Publications. The principal conclusion that the Turkish economy would benefit from a strengthening standardization and measurement services. Appropriate commendations are offered.

477. Tsai, D. H., MacDonald, R. A., **Second sound in a solid under shock compression,** *J. Phys. C: Solid State Phys. Letter to Editor* **6,** L171-L175 (1973).

Key words: Crystalline solid; iron; molecular dynamics; second sound; shockwave; thermal relaxation; three dimensions.

The propagation of a strong shock wave in a perfect, three-nensional crystalline lattice is studied by means of molecular-namical calculations. The results show that behind the shock nt there is a region of thermal relaxation which increases with ne. The thermally relaxed region, therefore, propagates with a locity lower than that of the shock front. It is believed that the ave-like propagation of this thermally equilibrated region is a tural extension of second sound from the conventional low-mperature, low-pressure régime to the high-temperature, high-essure régime. The implication of this phenomenon on *PVT* lculations from shock-wave data is discussed briefly.

478. Negas, T., **The $SrMnO_{3-x}$-$Mn_3O_4$ system,** *J. Solid State Chem.* **7,** 85-88 (1973).

Key words: Nonstoichiometry; phase equilibria; $SrMnO_{3-x}$-$Mn_3O_4$ system; $SrMn_3O_{6-x}$.

Phase relations were determined in the $SrMnO_{3-x}$-$Mn_3O_4$ stem at elevated temperatures in air using quenching, avimetric, and x-ray diffraction techniques. The system con-ns one intermediate compound, $SrMn_3O_{6-x}$ ($0 \leqslant x \leqslant 0.10$ tween 900-1200 °C), which decomposes to $SrMnO_{3-x}$ plus $n_3O_4$ near 1215 °C. The existence of an oxygen deficient $MnO_{3-x}$ having the hexagonal 4-layer structure was con-med. Crystals of perovskite-like $SrMnO_{3-x}$ ($x > 0.25$) were own from its primary field located in the system.

479. Dhez, P., Ederer, D. L., **Photoionization resonance profile parameters of the 3s3p $^1P_1$ two-electron excitation in He I,** *J. Phys. B: At. Mol. Phys. Letter to Editor* **6,** L59-L64 (Apr. 1973).

Key words: Autoionization; cross section; Fano parameters; helium; photoionization; resonance profile.

The cross section profile of the 3s3p $^1P_1$ two-electron excita-n has been measured in He I. The cross section was assumed have the form

$$\sigma(E)=C(E)+\frac{(E-E_0)\frac{1}{2}\Gamma a+(\frac{1}{2}\Gamma)^2 b}{(E-E_0)^2+(\frac{1}{2}\Gamma)^2}$$

nere the adjustable parameters $a$, $b$, $1/2\Gamma$ and $E_0$ were deter-ined by a least squares fitting process. The parameter values tained in the experiment were: $a=0.86\pm0.16$ cm$^{-1}$, $b=0.27$ 0.13 cm$^{-1}$, $1/2\Gamma=65.9\pm7.0$ meV, $E_0=69.919\pm0.007$ eV. ne Fano parameters $q$ and $\sigma_a$ were determined from $a$ and $b$ and had the values $1.36\pm0.20$ and $0.32\pm0.08$ cm$^{-1}$ respectively.

13480. Hamilton, C. A., **Analog-computer studies of mixing and parametric effects in Josephson junctions,** *J. Appl. Phys.* **44,** No. 5, 2371-2377 (May 1973).

Key words: Analog; Josephson junction; mixing; parametric.

Analog-computer studies are made on a variety of mixing and parametric effects in Josephson junctions. The predictions of the constant-voltage model are compared with the more general behavior of a junction in a resistive circuit. A simple approximate method is developed for calculating frequency conversion efficiency and the matching condition for a junction operating in the oscillator mixer mode. A similar calculation is made for the second mode of operation, in which an external local oscillator is used. In either of these modes, frequency conversion gain is possible even in a purely resistive circuit. The conditions for parametric amplification without frequency conversion are also studied and it is found that gain occurs only when the self-oscillation frequency is near the signal frequency.

13481. Smith, R. L., Phelan, R. J., Jr., **Limitations of the use of vacuum photodiodes in instruments for the measurement of laser power and energy,** *Appl. Opt.* **12,** No. 4, 795-798 (Apr. 1973).

Key words: Biplanar vacuum photodiodes; lasers; laser energy measurements; laser power measurements; vacuum photodiodes.

The effect of the variation in the area sensitivity upon the calibration of instruments incorporating biplanar vacuum photodiodes for the measurement of laser power and energy is discussed. A technique for the measurement of the area sensitivity is described, and the experimental results for several tubes are given. At the present time it would appear to be difficult to use biplanar vacuum photodiodes in devices to measure laser energy or power.

13482. Eisenhower, E. H., **Safety recommendations in ANSI documents,** (Proc. Symp. on Radiation Safety and Protection in Industrial Applications, Washington, D.C., Aug. 16-18, 1972), *DHEW Pub.* No. (FDA) 73-8012, H. F. Klein, Ed., pp. 240-252 (U.S. Department of Health, Education, and Welfare, Public Health Service, Food and Drug Administration, Bureau of Radiological Health, Rockville, Md., Oct. 1972).

Key words: Radiation safety; radiography; voluntary standards; x rays.

This paper discusses American National Standards relating to safety in industrial applications of ionizing radiation. It includes methods by which voluntary standards are produced, and outlines approval procedures required for designation as an American National Standard. The structure and relevant activities of Standards Committee N43, of the American National Standards Institute (ANSI) are described. Maximum permissible dose equivalent values recommended by the National Council on Radiation Protection and Measurements are presented as the basis for requirements in ANSI standards. Existing and future standards of interest to radiation safety in industrial applications are outlined.

13483. Powell, C. J., **High-resolution measurements of Auger-electron and photoelectron structure in the secondary-electron energy distributions of aluminum, nickel and copper,** (Proc. Int. Conf. on Inner Shell Ionization Phenomena and Future Applications, Atlanta, Ga., Apr. 17-22, 1972), Paper in *Proceedings of the International Conference on Inner Shell Ionization Phenomena and Future Applications,* R. W. Fink, S. T. Manson, J. M. Palms and P. V. Rao, Eds., CONF-720404, 1, 743-756 (U.S. Atomic Energy Commission, Technical Information Center, Oak Ridge, Tenn., Jan. 1973).

Key words: Aluminum; Auger-transitions; copper; electronic density of states; nickel; photoelectron energy distribution; secondary-electron energy distribution; x-ray photoemission.

Measurements are reported of selected structure in the secondary electron energy distributions of evaporated aluminum, nickel and copper. The specimens were bombarded with 3 keV electrons and the secondary structure was measured with a resolution of 0.1 eV. For each metal, attention was given primarily to data that could give information on the valence-band density of states.

Attempts were made to observe the $AlKL_{2,3}M$ Auger-electron energy distribution expected at about 1470 eV. Structure was, however, observed with a high-energy edge of $1485.9 \pm 0.5$ eV and a breadth of 8-9 eV. This structure was interpreted as being due to photoemission of valence electrons by internally generated $K\alpha$ x-rays and was similar to uv photoelectron distributions and to the calculated density of states. Inelastic scattering of the photoelectrons obscures the expected $AlKL_{2,3}M$ structure.

Auger electron peaks in the ranges 730-800 eV and 820 to 865 eV were measured in the energy spectra for nickel and copper, respectively. Structure was observed in the $L_3M_{2,3}M_{4,5}$ transition which could be associated in part with solid-state effects and in part with the final atomic states of each element. Density-of-states data could not be derived from the Auger spectra without more detailed knowledge of the final states expected after the Auger transition of interest.

**13484.** Garvin, D., **Progress in rate evaluations,** (Proc. 7th Thermochemistry Working Group, Interagency Chemical Rocket Propulsion Group, Cleveland, Ohio, Apr. 9-11, 1969), *CPIA Pub. 189*, **I**, 109-118 (Chemical Propulsion Information Agency, Johns Hopkins University, Applied Physics Laboratory, Silver Spring, Md., Aug. 1969).

Key words: Art of evaluation; chemical reactions; quality control measures; rate constants; rate evaluations.

A survey is given of recent activities in the area of evaluation of rates of chemical reactions. The problem of quality control is discussed. A recent evaluation of rates of reactions of oxygen is used to illustrate the uses of evaluated data and conclusions that can be drawn from them. A plan for expanding evaluation efforts is offered.

**13485.** Soulen, R. J., Jr., Schooley, J. F., **Superconducting transition widths and reproducibilities,** (Proc. XIIIth Int. Congress of Refrigeration, Washington, D.C., Aug. 27-Sept. 3, 1971), Paper in *Progress in Refrigeration Science and Technology* **1**, 399-403 (Avi Publ. Co., Inc., Westport, Conn., 1973).

Key words: Superconductivity; thermometry, transition temperature.

As part of a program to investigate the possibility of utilizing superconductive transitions as reference points on a cryogenic temperature scale, we are examining the transitions of samples with different purities and with various metallurgical histories. In our initial efforts, we examined the transition widths of Pb, Sn, In, Al, Ga, Zn and Cd wires using short mutual inductance coils to avoid end effects. As we reported at the XII Int. Conf. on Low Temperature Physics, all but the Sn and Cd samples showed transition widths of $10^{-3}$ K or less, and repeated examination of the widths over an extended period of temperature cycling showed no drift or broadening of the five narrow trar tions larger than $10^{-3}$ K.

We are now preparing samples of Pb, In, Al, Zn and Cd w various impurities and with various forming and anneal procedures in order to determine the practical boundary cor tions for obtaining a given transition temperature and transit width. We are attempting to extend this study to low temperat (Ir, $T_c \approx 0.1$ K) and high-temperature ($Nb_3X$, $V_3Si$, $T_c = 15$ – K) materials, although intitial experiments show transit widths of 0.1 – 0.3 K for the latter.

**13486.** Roth, R. S., Parker, H. S., Brower, W. S., Waring, J. **Phase equilibria, crystal chemistry and crystal growth of all oxide-metal oxide systems,** (Proc. NATO sponsored Advan Study Institute, Belgirate, Italy, Sept. 1972), Paper in *Fast Transport in Solids,* pp. 217-232 (North-Holland Publ. C Amsterdam, The Netherlands, 1973).

Key words: Alkali oxides; crystal chemistry; cry growth; phase equilibria; system $LiTaO_3$-$Ta_2O_5$; syst $NaTaO_3$-$Ta_2O_5$; system $KTaO_3$-$Ta_2O_5$.

In view of the recently discovered properties of the sodium in $\beta$-alumina, it is of some scientific and practical importanc review the chemistry of alkali ions in oxide systems in gene From a practical point of view, however, the number of syste of interest will necessarily be severely limited. For commer utilization of ionic conductivity it is necessary to limit system those which will contain little or no electronic conductivity therefore do not contain an element which is easily reduced ing the synthesis. For fast ion transport it is probably vantageous to have an alkalai ion in a "non-stoichiomet crystallographic position. Attention will be concentrated methods of study of alkali oxide-tantalum oxide systems as plied to the search for new crystallographic phases which ma of interest.

New results are presented of phase equilibria studies in systems $Li_2O$, $Na_2O$ and $K_2O$ with $Ta_2O_5$ and $Li_2O$ with Nb In addition preliminary results will be discussed of the terr systems involving the binaries with $MoO_3$. These terr systems have been utilized for flux-growth of single crystal many of the new phases in the binary systems. Each of the Ta systems has at least one interesting non-stoichiometric pl which deserves further study for conductivity properties phase in the $Li_2O$-$Ta_2O_5$ system has the structure of the low-t perature form of $Ta_2O_5$, the $Na_2O$-$Ta_2O_5$ system contair phase with a "tetragonal-bronze"-like structure and the K $Ta_2O_5$ system has both "tetragonal-" and "hexagonal-bron like phases. In the sub-system $Ta_2O_5$-$KTaO_3$ eleven dist phases have been found where only two were previously knc

**13487.** Pike, R. G., Hay, R. E., Clifton, J. R., Beeghly, H Mathey, R. G., **Nonmetallic coatings for concrete reinfor bars,** *Public Roads* **37,** No. 5, 185-197 (June 1973).

Key words: Chlorides; concrete; corrosion; ep coatings; organic coating; steel reinforcing bars.

The study reported here was conducted to determine the fe bility of using organic coatings, especially epoxies, to pro steel reinforcing bars embedded in concrete from corrosion celerated by chloride ions.

Coatings were evaluated on the basis of their chemical physical durabilities as well as their protective qualities. In study, attention was also directed to the application methods surface preparation of the steel reinforcing bars. Four diffe materials appear to be suitable for such coatings.

**13488.** Barnes, J. D., **Neutron inelastic scattering study of "rotator" phase transition in n-alkanes,** (Proc. 5th Symp

Neutron Inelastic Scattering, Grenoble, France, Mar. 6-10,
972), Chapter in *Neutron Inelastic Scattering*, pp. 287-299
International Atomic Energy Agency, Vienna, Austria,
972).

Key words: n-Alkanes; n-nonadecane; neutron inelastic scattering; phase transition; rotational diffusion; rotator phase.

Many n-alkanes exhibit a solid-solid phase transition a few
rees below their melting points. Such characteristics of the
se transition as transition temperatures, volume change on
nsition, and heats of transition are very sensitive to chain
gth in these materials. To characterize the role which molecu-
motions play in this phase transition, inelastic neutron scat-
ng experiments were carried out on the Fermi chopper time-
flight spectrometer at the National Bureau of Standards Reac-
Experiments were performed on n-nonadecane at tempera-
es of 77, 291, 297, 301 and 307 K and on n-eicosane at 301 K.
mentum transfers ranged between .42Å$^{-1}$ and 3.3 Å$^{-1}$ for
67 Å neutrons. The full width at half maximum of elastically
ttered neutrons was found to be 1.58 ps$^{-1}$ from measurements
cattering from vanadium ($\Delta\lambda/\lambda = 4.6\%$). 297 K and 301 K are
ve the temperature of the "rotator" phase transition for n-
adecane. The spectra taken under these conditions consist of
roadened elastic peak superimposed on a continuous spec-
m arising from the vibrational modes of the system. The
adening of the elastic peak is found to depend on momentum
nsfer and is analysed in terms of models involving rotational
fusion of the molecule about the long axis of the chain. The
a at 307 K, where the material is molten, reveal a further in-
ase in the quasi-elastic component of the scattering.

89. Kruger, J., **Application of ellipsometry to electrochemistry,**
Chapter in *Advances in Electrochemistry and Electrochemical*
*ngineering,* R. H. Muller, Ed., **9,** 227-280 (John Wiley &
ons, Inc., New York, N.Y. 1973).

Key words: Corrosion; electrochemistry; electropolishing; ellipsometry; electrodeposition.

A review of the application of ellipsometry to electrochemistry
iven which considers the electrochemical phenomena of pas-
ation and corrosion, electroadsorption, electrodeposition and
ctropolishing. The ellipsometry of bare surfaces and gaseous
orption as related to electrochemistry is discussed. Both the
antages and limitations of the techniques are considered.
er a hundred references are cited.

90. Maienthal, E. J., **Determination of trace elements in metals**
**y differential cathode ray polarography,** *Amer. Lab.*, pp. 25-33
1972).

Key words: Alloys; analyses; cast irons; differential cathode ray polarography; high purity materials; metals; steels; trace elements.

Some of the recent applications of cathode ray polarography
NBS to the determination of a number of trace elements in dif-
ent metal matrices will be discussed. Some of the elements
uld be determined directly with no separations. The elements
ermined included aluminum, antimony, copper, cadmium,
n, lead, bismuth, and tellurium in matrices such as steels, high
nperature alloys, white cast irons, brasses, bronzes, and high
ity metals. The results will be compared with those obtained
other techniques.

91. Garvin, D., Hampson, R. F., **Evaluated rate and**
**hotochemical data for modeling of the stratosphere,** (Proc. 2d
Conf. on Climatic Impact Assessment Program, Cambridge,
Mass., Nov. 14-17, 1972), *DOT Report* No. TSC-OST-73-4, 12 pages (Transportation Systems Center, Department of Transportation, Cambridge, Mass., 1972).

Key words: Atmospheric chemistry; chemical kinetics; data evaluation; nitrogen oxides; ozone; photochemistry; stratosphere; water.

Three important types of input data for studies of the chemistry of the stratosphere are rate constants, absorption coefficients, and quantum yields for elementary processes. About 135 of these data items are needed for studies that will define the chemistry of the stratosphere. These data are being obtained both by experiment and by review and evaluation of existing measurements.

The data-evaluation program has two parts: evaluation by a group at NBS, and a cooperative survey by a large number of gas kineticists. The evaluated data now available are summarized in a table. The possible interactions among 42 species that may be present in the stratosphere are displayed on a reaction grid. Where possible the importance of a reaction and the status of its data are indicated.

Pollutants introduced into the stratosphere will interact with the existing complex $O_3/O_2/NO_x/HO_x$ photolytic system. Laboratory studies of the $O_3/O_2$ and $O_3/H_2O_2$ photolytic systems and rate measurements in an $O/O_3/NO_x$ system illustrate the types and magnitudes of effects to be expected.

13492. Slattery, W. J., **Standards information for your company,** *Stand. Eng.* **25,** No. 3, p. 22, (June 1973).

Key words: Company; information; standardization; standards.

The Standards Information Services Section of the National Bureau of Standards (NBS-SIS) maintains the largest reference collection of engineering and related standards, specifications, test methods, codes and recommended practices in the United States. From its original holdings of several thousand standards, NBS-SIS now maintains an extensive reference collection of over 122,000 standards issued by U.S. industry associations, federal and state governmental organizations, and foreign national and international standardizing bodies. NBS-SIS serves primarily as a referral activity by identifying sources of standards, and directing inquirers to the respective standards-issuing organizations to obtain copies of standards. By means of a computer-produced Key-Word-In-Context (KWIC) Index, more than 4,000 inquiries are answered a year. Although the majority of these requests have to date come from agencies of the U.S. Federal Government, the staff is particularly interested in receiving an increase in the number of inquiries from the corporate sector. NBS-SIS also compiles computer-produced indexes designed to assist companies and other industry groups, government organizations and anyone interested in information on standards. Requests for information may be made by personal visit, telephone or letter.

13493. LaFleur, P. D., **Retention of mercury when freeze-drying biological materials,** *Anal. Chem.* **45,** No. 8, 1534-1536 (July 1973).

Key words: Freeze-drying; lyophilization; mercury; mercury loss; methylmercury; nuclear activation analysis; phenylmercuric acetate.

The retention on freeze-drying of three compounds of mercury tagged with mercury-203 and fed to experimental animals, has been measured. The compounds employed in the investigation were methylmercuric chloride, phenylmercuric acetate and mercuric nitrate. The retention of mercury was determined radiometrically on individual tissues and on blood and feces. The effect of prefreezing the samples, prior to the lyophilization cycle, was also studied.

**13494.** Reno, R. C., Swartzendruber, L. J., **Origin of Mössbauer linewidth in stainless steel,** (Proc. 18th AIP Conf. on Magnetism and Magnetic Materials, Denver, Colo., Nov. 28-Dec. 1, 1972), Paper in *Magnetism and Magnetic Materials,* C. D. Graham, Jr., and J. J. Rhyne, Eds., No. 10, 1350-1353 (American Institute of Physics, New York, N.Y., 1973).

Key words: Hyperfine fields; perturbed angular correlation, Mössbauer effect; stainless steel.

The hyperfine interactions which broaden the Mössbauer effect (ME) spectrum in austenitic stainless steel have been investigated with the aid of $^{57}$Fe time-differential perturbed angular correlations (TDPAC). The TDPAC measurements reveal a distribution of electric field gradients at the $^{57}$Fe nuclei with a mean value corresponding to a Mössbauer splitting of 0.14 mm/s. This splitting is not sufficient to explain the total line width and isomer shifts are invoked to account for the remaining width.

**13495.** Swartzendruber, L. J., Evans, B. J., **Local interactions and spin transfer mechanisms in the Heusler-type alloys $Pd_{1+x}MnSb$ and $Pd_2MnSb_{0.9}Sn_{0.1}$,** (Proc. 18th AIP Conf. on Magnetism and Magnetic Materials, Denver, Colo., Nov. 28-Dec. 1, 1972), Paper in *Magnetism and Magnetic Materials,* C. D. Graham, Jr., and J. J. Rhyne, Eds., No. 10, 1369-1373 (American Institute of Physics, New York, N.Y., 1973).

Key words: Alloys; antimony; hyperfine fields; manganese; Mössbauer effect; palladium, tin.

The magnetic hyperfine fields at $^{121}$Sb, $H_{eff}(Sb)$, in the Heusler-type alloys $Pd_{1+x}MnSb$ are found to be strongly dependent on x, varying from about 600 kG for $x = 1$ to about 300 kG for $x = 0$. As x is decreased from unity, the single unique value observed in $Pd_2MnSb$ is replaced by a distribution in $H_{eff}(Sb)$, with an average value which decreases in a regular manner with the number of Pd vacancies. In $Pd_2MnSb_{0.9}Sn_{0.1}$, $H_{eff}(Sn)$ is found to be similar in magnitude to $H_{eff}(Sn)$ in $Pd_2MnSn$. Both these results indicate that local spin transfer mechanisms are important in determining the magnitude and sign of $H_{eff}$ at the Sb site in Heusler-type alloys.

**13496.** Geltman, S., **Free-free radiation in electron-neutral atom collisions,** *J. Quant. Spectrosc. Radiat. Transfer* **13,** 601-613 (June 1973).

Key words: Bremsstrahlung; elastic scattering; free-free radiation.

Free-free absorption coefficients are calculated for the electron-neutral atom systems involving He, C, N, O, Ne, Ar, Kr, and Xe. The calculations are based upon model atomic potentials which have been adjusted to fit experimental scattering cross sections or electron affinities. Some angular distributions are presented and thermal averages are evaluated in the ranges $\lambda = 0.5 - 20\ \mu m$ and $T = 500 - 20{,}000$ K.

**13497.** Aras, N. K., Zoller, W. H., Gordon, G. E., Lutz, G. J., **Instrumental photon activation analysis of atmospheric particulate material,** *Anal. Chem.* **45,** No. 8, 1481-1489 (July 1973).

Key words: Air pollution; atmospheric particulate material; electron linac; photon activation analysis.

Concentrations of fourteen elements in atmospheric particulate matter have been measured by irradiation of the samples with bremsstrahlung from electrons of 35 MeV from the NBS electron linac and observation of $\gamma$ rays from the reaction products with Ge(Li) detectors. The elements routinely observed by this nondestructive method are: Na, Cl, Ca, Ti, Cr, Ni, Zn, As, Br, Zr, Sb, I, Ce, and Pb. Several other elements suc
Fe, Se, Rb, and Y are marginally observable. Although,
general, instrumental photon activation analysis (IPAA) is
sensitive than instrumental neutron activation analysis (INA
with IPAA one can measure concentrations of several eleme
that are difficult or impossible to measure in urban particul
with INAA, especially Ti, Ni, As, I, and Pb. Measurement
Ni, As, and Pb are quite important because of their known t
icities.

**13498.** Leasure, W. A., Jr., Rubin, A. I., Fath, J. M., Fisher
L., Flynn, D. R., **Fundamentals of noise: Measurement, ra
schemes, and standards,** *Environmental Protection Agency
port No. NTID300.15,* 163 pages (Available as PB 206
from the National Technical Information Service, Springfi
Va. 22151, Dec. 31, 1971).

Key words: Acoustics; environmental pollution; nc
sound.

This report is intended to serve as an introduction to noise
cluding the inter-relationship between physical measures
psychological responses. The basic principles of sound gen
tion and propagation are discussed as well as the measurem
of both the physical attributes of noise and the effects of nois
people. The suitability and effectiveness of various noise e
sure rating schemes, used to estimate or predict the effect
noise on man, are discussed and critiqued. Included are sa
calculations of sound level, loudness level, and perceived n
level for five selected spectra. The need is stressed for inclu
of well-defined environmental and operational requirements
measurement procedures for those devices where the n
produced is dependent on the surroundings and the operati
the device. Also presented are a glossary of pertinent aco
terminology and a compilation of existing standards relate
noise, including a brief description of the intent and scop
each.

**13499.** Omont, A., Smith, E. W., Cooper, J., **Redistributi
resonance radiation. I. The effect of collisions,** *Astrophys. J.*
No. 1, Part 1, 185-199 (July 1972).

Key words: Collisional depolarization; level degene
redistribution functions; resonance radiation.

The techniques of modern line-broadening theory are us
investigate the scattering of polarized radiation in the rest f
of an atom undergoing collisions. The formulation explicit
cludes both elastic and inelastic (quenching) collisions. Whe
lower state has zero width, a form for the redistribution fun
similar to that of Zanstra is obtained, but with the redistrib
in the neighborhood of the resonance line being caused sole
elastic collisions. In the limit of no collisions, but with both l
of finite lifetime, the result of Weisskopf and Woolley i
tained. The effect of level-degeneracy is also explicitly incl
in this case the results are a function of the polarization c
light and the different relaxation rates for the multipolar
ponents of the atomic states.

**13500.** Omont, A., Smith, E. W., Cooper, J., **Redistributi
resonance radiation. II. The effect of magnetic fields,** *Astro
J.* **182,** No. 1, Part 1, 283-300 (May 15, 1973).

Key words: Irreducible tensor formalism; magnetic f
resonance radiation.

Previously obtained results for scattering of radiation i
presence of collisions are restated in a density matrix form
which employs an irreducible-tensor description of the
tion field. This formalism is particularly useful for pro

ociated with radiative transfer theory. The redistribution is n extended to include the effect of a weak magnetic field. By eraging over a finite bandwidth which is on the order of the ppler width, simplified expressions of physical significance the scattering in the Doppler core and the Lorentz wings are tained. Expressions are also obtained for the corresponding urce function of radiative transfer theory.

01. Acquisita, N., Abramowitz, S., **Vibrational spectrum of MoF$_5$**, *J. Chem. Phys.* **58,** No. 12, 5484-5488 (June 15, 1973).

Key words: Infrared; matrix isolation; MoF$_5$; Raman spectroscopy.

The infrared spectrum of matrix isolated MoF$_5$ as well as the man spectra of the liquid and polycrystalline species have en observed. The use of double boiler Knudsen cells has ilitated a vibrational assignment for monomeric MoF$_5$ based a trigonal bipyramid ($D_{3h}$) structure.

502. Gadzuk, J. W., Lucas, A. A., **Field-emission tails and tunneling lifetimes,** *Phys. Rev. B* **7,** No. 11, 4770-4775 (June 1, 1973).

Key words: Field emission; surfaces; tunneling.

Recent observations of high- and low-energy tails in fieldission energy distributions can be interpreted in terms of asi-stationary-state single-particle tunneling. This imposes a triction on the observable range of energies in such studies. e tails result from the predicted breakdown of the transfer miltonian theory of tunneling when fourth-order terms in the rturbation expansion of the tunneling matrix element become ge. The tunneling lifetimes ~ $10^{-12}$ sec required to fit the exrimental data are consistent with both the *RC* time constant cussed by Thornber, McGill, and Mead and also a simple intive picture. Alternate theories of tunneling lifetimes are critilly evaluated.

503. Jones, F. E., **Air density and helicopter lift,** *Joint Army-Navy Aircraft Instrumentation Research, JANAIR Report No. 721201,* 54 pages (Available as AD 754420 from the National Technical Information Service, Springfield, Va. 22151, Jan. 1973).

Key words: Air density; helicopter lift; ideal gas law.

An analysis has been made of ideal and real gas equations as ey apply to the calculation of air density in the region of inrest for helicopter flight. The uncertainties in calculated air nsity due to uncertainties in measurements of temperature, essure and humidity have been investigated and estimates ve been made of measurement accuracies which would be quired to enable calculation of air density with a desired relae uncertainty. A reference system has been assembled to prode measurements of temperature, pressure and dew-point temrature aboard a helicopter. This system is to be used in making lculations of reference air density for flight tests of a system r computing hover lift margin and several devices for measurg air density. The effects on hover lift margin, defined by a sime equation, of relative uncertainties in air density and power ve been investigated. Nuclear statistics as they apply to direct" measurements of air density by application of nuclear diation are discussed.

504. Rubin, A. I., **The social impact of noise: A survey of medical, psychological, and social consequences,** *Environmental Protection Agency Report No. NTID300.11,* 25 pages (Available as PB206724 from the National Technical Information Service, Springfield, Va. 22151, Dec. 1971).

Key words: Noise; noise sources; social impact.

Noise is an environmental pollutant which shares many characteristics with other pollutants—its levels are increasing, more and more people are being affected; its consequences are medical, psychological and social. Man has been successful in producing labor-saving devices used during work and play as well as to provide many forms of transportation. However, an associated by-product is increasingly in evidence as the machines have become more powerful, namely *Noise*. Whereas only midcity areas, heavy industries and communities near airports were formerly recognized as being "special" problems because of the noise levels associated with them; this is no longer true. Intrusive noise pervades the home, industry and most recreation areas now since, where man has moved, he has taken his machines with him. This pervasiveness of noise has led to actions by individuals, groups, and many levels of government to "do something about the problem." Among the methods attempted have been regional planning, zoning ordinances, government standards and regulations, and individual law suits. Thus far these approaches have not been successful. The number of people exposed to hazardous noise levels is increasing, the quality of our auditory environment is being degraded, and the social impact of noise may substantially contribute to other problems in our society.

**13505.** Maki, A. G., Sams, R. L., Olson, W. B., **Infrared determination of $C_0$ for phosphine via perturbation-allowed $\Delta|k - l| = \pm 3$ transitions in the $3\nu_2$ band,** *J. Chem. Phys.* **58,** No. 10, 4502-4512 (May 15, 1973).

Key words: Forbidden transitions; ground state splitting; infrared spectrum; perturbation allowed transitions; phosphine; rotational constants.

The $3\nu_2(A_1)$ and $4\nu_2 - \nu_2(A_1)$ infrared bands of PH$_3$ have been measured with high resolution. In the $\nu_2 = 3$ state an interaction between the $K$ and $K \pm 3$ levels gives rise to perturbation allowed $\Delta K = 3$ transitions through a weak high order interaction. Since only one component of the $K = 3$ levels is of the proper symmetry to interact with the $K = 0$ levels there is a splitting of the $K = 3$ levels. Also detectable is the splitting of the $K = 3$ levels of the ground vibrational state. The measurements have been combined with microwave measurements to give accurate values for the ground state rotational constants $B_0$, $C_0$, $D_0{}^J$, $D_0{}^{JK}$, $D_0{}^K$, $H_0{}^J$, $H_0{}^{JJK}$, and $H_0{}^{JKK}$. The absence of observable inversion effects sets an upper limit of about 0.02 cm$^{-1}$ for the inversion splitting of the $4\nu_2$ level.

**13506.** Keplinger, M. S., **The case for invisible copies,** *Proc. 33d Annual Meeting of the American Society for Information Science, Philadelphia, Pa., Oct. 11-15, 1970,* **7,** 241-243 (1970).

Key words: Computers; copyright; information storage and retrieval; infringement; input; intellectual property; proprietary rights.

The problem of control of the use of copyrighted works in computerized information storage and retrieval systems is discussed. It is concluded that such input may be considered copyright infringement under the current Copyright Revision Bill as interpreted through the teachings of recent court decisions, as well as being an infringement under the current copyright statute.

**13507.** Albers, J., Deutch, J. M., **On the rate equation description of spectral lines,** *Chem. Phys.* **1,** No. 2, 89-98 (Mar./Apr. 1973).

Key words: Correlation function; density expansion; kinetic equations; Langevin equation; rate equations; scattering theory.

We present a derivation of an exact, low-density equation of motion for the generating operator $G_{ij}(t) = \exp(iLt)|j\rangle\langle i|$. For the case of foreign gas pressure broadening, the equation for $G_{ij}(t)$ may be used to obtain an exact rate equation for the line amplitude operator. Under certain well-defined approximations, this rate equation reduces to the form of an equation proposed by Gordon. The origin of the linear density term is considered. We discuss the implications of the use of only completed collisions to describe the spectrum.

**13508.** Martin, W. C., **Some aspects of the energy-level structures of lanthanide atoms and ions,** *Opt. Pura Apl.* **5,** No. 3, 181-191 (1972).

Key words: Atomic spectra; energy levels; rare earths.

The development of our understanding of some main features of these structures is reviewed, and the present degree of completeness of the analyses and theoretical interpretations of the spectra is indicated. Energy differences of the type $4f^{N-1}nl(6s^{M}) - 4f^{N}(6s^{M})$(with each configuration represented by its lowest level) are of special importance, both for the analyses of a number of the spectra and for the interpretation of certain basic data for metals and compounds of these elements. The general behavior of such differences as a function of N is understood, and the resulting graphs are very similar to the d-shell energy-difference graphs studied by Catalán, Rohrlich, and Shenstone, and by Racah. The data confirm striking regularities among the f-shell graphs, first used by Racah, that yield predictions of unknown system differences and, for third and higher spectra, of ionization energies (M = 0, n = ∞).

**13509.** Huggett, C., **Carpet flammability and the NBS corridor fire program,** *ASTM Stand. News* **1,** No. 5, 16-20 (May 1973).

Key words: Carpets; corridor fires; fire test; flammability; floor coverings.

The NBS corridor fire program was designed to study the effects of configuration, fuel loading and distribution, ventilation, and other design parameters on the spread of fire through corridors in multiple occupancy buildings. A fully instrumented 8 ft × 8 ft × 30 ft corridor is used to carry out full-scale experiments. Fires are started in a connecting 8 ft × 8 ft × 9 ft fire room and the rate and intensity of fire spread in the corridor is observed.

Floor coverings have received special attention during the initial phase of the program. With a sufficiently intense room fire source, fire can spread rapidly over the surface of a carpet in the corridor, even with noncombustible wall and ceiling surfaces. Radiative energy transfer to the carpet surface appears to be the controlling mechanism. When the carpet starts to burn, additional energy feedback causes an accelerated propagation down the corridor. The fire spread is characterized in terms of critical energy input necessary to cause propagation, rate of fire spread, and energy contribution of the carpet to the fire.

Results of typical experiments are described. Preliminary experiments relating to the development of a test method to assess the hazard potential of floor coverings in building, based on a critical energy concept, are described.

**13510.** Craw, A. R., **A comparison of several methods for forecasting U.S. traffic fatalities,** *NBSIR 73-189,* 45 pages (May 1973). (Available as COM 73-11173 from the National Technical Information Service, Springfield, Va. 22151.)

Key words: Exponential smoothing; forecasting; time-series; traffic fatalities.

This is a second report to the Mathematical Analysis Division of the National Highway Traffic Safety Administration (NHTSA) on the subject of forecasting annual highway fatalities. Th report concerns a comparison of several time series analysis pr grams based on exponential smoothing and nondecomposition methods currently employed by NHTSA for projecting the a nual *traffic* fatalities for the entire U.S. Several methods of da aggregation are studied.

It is found that there is some advantage in using lump (pooled) data for each region aggregated either quarterly or h yearly, and using the Sum of Regional estimates to estimate t national value.

Also, there does not appear to be any great difference in t results obtained using the nondecompositional methods a those obtained by time-series analysis programs based on e ponential smoothing methods.

Estimates for the 1972 and 1973 national traffic fatalities b variety of methods were made. For 1973 the estimates rang from a low of 54186 to a high of 55994, with a mean of 55055.

**13511.** Moriarty, J. E., **City I: Player's Manual,** *NBSIR 73-1* 149 pages (Mar. 1973). (Available as COM 73-11191 from t National Technical Information Service, Springfield, 22151.)

Key words: City; computer; directors; economic; gam government; metropolitan; players; sectors; simulation; cial; urban.

City I is an operational simulation game in which participa make economic, government, and social decisions affectin hypothetical metropolitan area. Through the use of a comput the simulated urban system responds to the participant's de sions as any real city would. Each player in City I is assigned a team which shares an economic and governmental role. T manual describes the player details for the economic and gove ment sectors along with general information required for ga play. It is one of three manuals necessary for game pl (Player's Manual, Director's Manual, Computer Operat Manual). Each of these manuals are designed to be used reference and by themselves will not describe enough details a complete game play.

**13512.** Peterson, R. L., **Kinks in the magnetophonon oscillati of semiconductors,** *Phys. Rev. B* **7,** No. 12, 5405-5408 (J 15, 1973).

Key words: Magnetophonon effect; semiconductors; tr port theory.

Exact expressions for the discontinuities in the magnetic f derivative of the longitudinal drift mobility at the m netophonon resonance and pseudoresonance fields are given nonpolar semiconductors with combined optic- and acou phonon scattering of carriers. The reasons for the discontinu are discussed in physical terms.

**13513.** McCamy, C. S., **Properties of photographic films rel to information recovery,** *SPIE Seminar Proc. on Image In mation Recovery, Philadelphia, Pa., Oct. 24-25, 1968,* **16,** 19 (Society of Photo-Optical Instrumentation Engineers, dondo Beach, Calif., 1969).

Key words: Image processing; photographic films; ph graphic information.

New concepts, terminology, and symbolic notation sim the precise treatment of optical density, which is the fundame quantity in information recovery. The resolving power of op and photographic systems may be treated as discrete or sta cal, visual or instrumental and may be a guide to informa capacity. The photographic spread function is the key to standing image formation. The ambiguity of the modulation nsfer function requires recourse to more rigorous analytic thods. Granularity, spatial effects of processing, temporal ef- ts, and dimensional stability are important considerations in ormation recovery.

14. Powell, C. J., **Contrasting valence-band Auger-electron pectra for silver and aluminum,** *Phys. Rev. Lett.* **30**, No. 23, 179-1182 (June 4, 1973).

Key words: Aluminum; Auger electron transitions; electronic density of states; final state effects; silver; transition probabilities.

Measurements of the $L_{2,3}VV$ ($V$=valence) Auger spectrum of minum and the $M_{4,5}VV$ Auger spectrum of silver cannot be ply related to the valence-band density of states. The data for indicate a strong energy variation of the transition probability. r silver, the position and shape of the Auger spectrum are as- ciated with multiplet splitting of localized double-$d$-hole al states.

15. Robertson, A. F., Rappaport, M. W., **Fire extinguishment n oxygen enriched atmospheres,** *NASA CR-121150*, 60 pages National Aeronautics and Space Administration, Washing- on, D.C., Feb. 1973).

Key words: Controlled atmospheres; extinguishing; fire extinguishers; fires; halons; oxygen; spacecraft cabin atmospheres; water.

Current state-of-the-art of fire suppression and extinguishment hnique in oxygen enriched atmosphere is reviewed. Four sses of extinguishment action are considered: cooling, separa- n of reactants, dilution or removal of fuel, and use of chemi- ly reactive agents. Current practice seems to show preference very fast acting water spray applications to all interior sur- es of earth-based chambers. In space, reliance has been ced on fire prevention methods through the removal of igni- n sources and use of nonflammable materials. Recommenda- ns are made for further work related to fire suppression and tinguishment in oxygen enriched atmospheres, and an exten- e bibliography is appended.

516. Pierce, E. T., Kelly, K. L., McPherson, M. A., Howett, G. L., Booker, R. L., **Emergency vehicle warning devices: Interim review of the state-of-the-art relative to performance standards,** *LESP-RPT-0501.00*, 73 pages. Available as PB211938 from the National Technical Information Service, Springfield, Va. 22151, (U.S. Department of Justice, Law Enforcement Assistance Administration, National Institute of Law Enforcement and Criminal Justice, Washington, D.C., May 1972).

Key words: Action; communication; conspicuity; controlled environment; effectiveness; flashing lights; guidelines; information; laboratory testing; people; response; sirens; standards.

This interim progress report describes the activities carried t, from the initiation of the program through July 1971, con- rning the preparation of performance standards for emergency hicle warning devices (lights and sirens). A partial survey of esent standards and specifications indicated that there now are ry few meaningful performance standards for emergency arning lights and essentially none for sirens. Brief descriptions those standards which were found are included. Manufac- rer's literature on available warning devices rarely includes eaningful quantitative data on the physical performance aracteristics of either lights or sirens. The program strategy scribed in this report includes (a) quantitative physical charac- ization of the spectral content, directionality, level, and time duration of the signals from a representative sampling of emergency vehicle warning equipment; (b) literature and laboratory study of the effectiveness of representative signals in alerting drivers to an emergency situation requiring appropriate reactions; and (c) development of draft standards. In conjunction with the physical characterization of lights and sirens, examples are given of the type of data which will be taken and detailed descriptions are given of the facilities which will be used for these measurements. A discussion is given of the various factors which influence the effectiveness of warning signals. It is proposed to study both the time elapsing between the occurrence of a signal and the completion of the required response (complex reaction time) and the distance at which an observer first notices and correctly interprets a signal (recognition distance). Performance standards can then be prepared which are clearly related to the appropriate human responses.

13517. Sullivan, D. B., **Precise electrical measurements at low temperature,** *Proc. 1972 Applied Superconductivity Conf., Annapolis, Md., May 1-3, 1972*, pp. 631-639 (IEEE, Inc., New York, N.Y., 1972).

Key words: Fundamental constants; Josephson effect; precise electrical measurements; superconductivity.

The application of low temperature phenomena to electrical metrology is reviewed. The review includes a number of recent developments which involve measurement systems based on the quantum of magnetic flux as well as adaptations of classical concepts to low temperature devices. Quantities considered include radio frequency current, infrared frequency, and direct current and voltage. Concepts for secondary emf standards are also discussed.

13518. Brower, W. S., Parker, H. S., Roth, R. S., **Synthesis of mercury bismuth sulfide $HgBi_2S_4$,** *Mater. Res. Bull.* **8**, 859-862 (1973).

Key words: Bismuth; mercury; sulfides; synthesis.

The compound $HgBi_2S_4$ was found to be the only phase present, other than the end members, in mixtures of HgS and $Bi_2S_3$. The compound is apparently a new structure type with monoclinic symmetry, space group C2, Cm or C2/m $a = 14.179$, $b = 4.0555$, $c = 13.986$ Å, $\beta = 118°13.8'$.

13519. Hall, J. L., Bordé, C., **Measurement of methane hyperfine structure using laser saturated absorption,** *Phys. Rev. Lett.* **30**, No. 22, 1101-1104 (May 28, 1973).

Key words: Hyperfine spectrum; laser stabilization; methane: spectroscopy.

With optical resolution above $10^{10}$, we study hyperfine structure in the methane vibration-rotation line at 3.39 $\mu$m. Doppler-generated crossing resonances were observed in addition to the resolved $\Delta F = 0$ and $-1$ lines. Splittings in both ground and excited states were determined. Differential saturation of such hyperfine structure will lead to an intensity-dependent shift in many molecularly stabilized lasers.

13520. McCamy, C. S., Pope, C. I., **The stability of silver-gelatin images,** (Proc. 2d Int. Congress on Reprography, Cologne, Germany, Oct. 25-31, 1967), Paper A3-1 in Section A3 of *Reprographie* **II**, 112-115 (Verlag Dr. Othmar Helwich, Darmstadt, Germany und Wien, Austria, 1969).

Key words: Aging blemishes; blemishes, microfilm; film storage; microfilm; microfilm image stability.

Though microfilm has been in commercial use in the United States for 40 years, recent observations of blemishes on film have occasioned a re-evaluation of factors affecting long-term stability. Six types of blemishes appear to be the result of oxidation-reduction reactions initiated by gaseous reactants. These reactants are traceable to the cardboard containers in which reels of film have been stored. Statistical analysis of data gathered by 100 film inspectors supports this conclusion. Laboratory experiments ruled out biological causes. Experiments prove the existence of oxidizing and reducing agents, formaldehyde, and formic acid in the atmosphere within cardboard containers. Appropriate films, properly processed and stored in inert containers, at a relative humidity under 40 percent and temperature under 21 °C, should be as durable as the best record paper.

**13521.** Brown, W. E., **Solubilities of phosphates and other sparingly soluble compounds,** Chapter 10 in *Environmental Phosphorus Handbook,* E. J. Griffith, A. Beeton, J. M. Spencer and D. T. Mitchell, Eds., pp. 203-239 (John Wiley & Sons, Inc., New York, N.Y., 1973).

Key words: Calcium carbonates; calcium phosphates; hydroxyapatite; limnetic phosphate; phase diagrams; phosphate pollution; solubility.

Solubilities of five calcium phosphates, $Ca_5(PO_4)_3OH$, $\beta-Ca_3(PO_4)_2$, $Ca_8H_2(PO_4)_6 \cdot 5H_2O$, $CaHPO_4$, and $CaHPO_4 \cdot 2H_2O$ must be considered as factors that may limit the concentrations of calcium and orthophosphate ions in natural waters. In the three-dimensional plot pH vs $[Ca(OH)_2]$ and $[H_3PO_4]$ for all solutions in the ternary system, $Ca(OH)_2$-$H_3PO_4$-$H_2O$, one obtains a surface that (i) has an important bearing on the positions of the isotherms for the five calcium phosphates and the fact that the isotherms have negative slopes, and (ii) is a consequence of the fact that $H_3PO_4$ is a polybasic, weak acid.

The phase diagram for the ternary system can be expanded to approximate a four component system in which the effects of all other components are incorporated into a single variable which is a measure of their net basicity or acidity. This diagram should have considerable value in the interpretation of field data. Lines of constant pH on this diagram can be used to determine whether a solution is undersaturated or supersaturated with respect to the salt under consideration. Other lines on this diagram define compositions along which the chemical potentials of $Ca(OH)_2$, $H_3PO_4$ and the various calcium phosphate salts are all constant.

Potential diagrams (− log of the activity of $Ca(OH)_2$ plotted vs that of $H_3PO_4$) are useful for establishing (i) the degree of saturation of a given solution with respect to anyone or all of the calcium phosphates, and (ii) the Ca/P ratio of the saturating solid phase.

A variety of theoretical and experimental factors must be taken into account in the design of solubility measurements and in the interpretation of results. Their application to calcium phosphates and other sparingly soluble salts of polybasic acids is described.

**13522.** Waterstrat, R. M., Dickens, B., **The crystal structure of $V_3Rh_5$,** *J. Less-Common Metals* **31,** 61-67 (1973).

Key words: Atomic ordering; crystal structures; intermetallic compounds; rhodium alloys; vanadium alloys.

The crystal structure of the phase $V_3Rh_5$ has been elucidated. The unit cell is orthorhombic with $a = 5.420$ Å, $b = 9.276$ Å, $c = 4.320$ Å and $Z = 2$; the space group is either *Cm2m* or *Cmcm*. The structure is close-packed and contains both ordered and disordered atomic sites. It is intermediate between the structures of the $Cu_3Au$ and CuAu types except that it possesses a two-layer stacking sequence.

**13523.** McCamy, C. S., Pope, C. I., **Redox blemishes— their cause and prevention,** (Proc. National Microfilm Association, Boston, Mass., May 7, 1969), *J. Micrógr.* **3,** No. 4, 165-170 (June 1970).

Key words: Archival records; microfilm; redox blemish

A type of small spots and character-associated defects some microfilm were investigated by a variety of techniqu The blemishes result from the displacement of image silver by oxidation-reduction reaction caused by peroxides and ot gaseous products of degradation of the paper cartons in wh the films are stored. A method of producing blemishes for t purposes was developed. Recommendations cover the materi processes, and storage conditions for microfilm preservation records of permanent value.

**13524.** Schneider, S. J., Levin, E. M., **Polymorphism of $K_2CO_3$** *Amer. Ceram. Soc.—Discussions and Notes* **56,** No. 4, 2 219 (1973).

Key words: DSC; DTA; high temperature x-ray; K₂C phase transformation; polymorphs.

The polymorphism of $K_2CO_3$ was investigated by differen thermal analysis, differential scanning calorimetry and high te perature x-ray diffraction techniques. The data indicate t $K_2CO_3$ is dimorphic with a 2nd order transformation fron monoclinic form to a hexagonal modification occurring at 42 5 °C. Unit cell dimensions as a function of temperature an representative x-ray powder pattern of hexagonal $K_2CO_3$ given.

**13525.** Okabe, H., Splitstone, P. L., Ball, J. J., **Ambient source $SO_2$ detector based on a fluorescence method,** *J. Air P lut. Contr. Ass.* **23,** No. 6, 514-516 (June 1973).

Key words: Air pollutant; detector, fluorescence; $SO_2$.

The principle of this detector is based on the measuremen the intensity of the ultraviolet fluorescence of $SO_2$ produced absorption of the Zn 2138 Å or Cd 2288 Å line. T fluorescence intensity was found to be linear from 0.1 to ppm of $SO_2$ in air with the Zn lamp and from 0.1 to 1600 p with the Cd lamp. The detection limit at present is about 20 p There is no detectable interference from $O_3$, $H_2S$, $NO_2$, C CO, or $H_2$, although the presence of a large concentration of (500 times as much as $SO_2$) NO (500 times) or $C_2H_4$ (4000 tim interferes with the measurement. The presence of 2 percent H reduces the signal by 25 percent, while up to 1 percent $CH_4$ almost no effect.

**13526.** Heinrich, K. F. J., **The application of Monte-Carlo calcu tions in electron probe microanalysis,** *Proc. of the Seminar Quantitative Analysis with Electron Microprobes and Sec dary Ion Mass Spectrometry, Jülich, Germany, Oct. 18- 1972,* pp. 149-155 (Mar. 1973).

Key words: Data reduction; electron probe; Monte-Ca calculations; thin layers.

The simulation of electron trajectories by means of the Mor Carlo calculations offers an attractive alternative to the conv tional data reduction procedures in electron probe microanaly It is particularly flexible with regard to specimen geometry, should be very useful for the analysis of thin films and sim materials. However, as in the conventional procedures, appr mations and empirical adjustments are necessary for development of a useful model. The experiences derived fr such a model can in turn be used to improve the conventional gebraic correction schemes.

**13527.** Frenkiel, F. N., Klebanoff, P. S., **Probability distributi and correlations in a turbulent boundary layer,** *Phys. Fluids* No. 6, 725-737 (June 1973).

Key words: Boundary layer; correlations; higher-order ments; high-speed computing; hot-wire anemometry; pro bility distributions.

ne-dimensional and joint probability density distributions for itudinal components of turbulent velocities as well as higher- er correlations are measured in a turbulent boundary layer on at plate using hot-wire anemometry and high-speed comput- methods. The effect of the nonlinear response of the hot-wire ken into account. Data pertaining to the general nature of the ulent boundary layer are presented and comparison is made veen the measured correlations and those corresponding to aussian probability distribution of turbulent velocities as well o non-Gaussian distributions of the Gram-Charlier type. ilar comparisons are made of the measured one-dimensional joint probability distributions. Probability distributions in boundary layer are also compared to those measured nstream of a grid. The closure of the tails of the probability ribution and its effect on the accuracy of the measurements igher-order moments is considered.

28. Atkinson, G. H., Laufer, A. H., Kurylo, M. J., **Detection f free radicals by an intracavity dye laser technique,** *J. Chem. hys.* **59,** No. 1, 350-354 (July 1, 1973).

> Key words: Absorption; flash photolysis; free radicals; laser; spectra.

new technique for the detection of free radicals inside the ity of a dye laser is described. This intracavity absorption nomenon has two important advantages: (1) It has the poten- for quantitative detection suitable for kinetic studies of isient chemical species and (2) it has a high degree of sen- vity. In the present work the technique is shown to be at least sensitive as, and most probably several orders of magnitude re sensitive than, previous methods for the detection of nsients. It is presently a powerful tool for obtaining high olution spectra as well as obtaining precise information about energy distribution of transient species produced photolyti- y or kinetically. Spectra for both $NH_2$ and HCO (produced h photolytically) are presented.

29. Feldman, A., Horowitz, D., Waxler, R. M., **Laser damage n materials,** *NBSIR 73-119,* 52 pages, (Feb. 1973). (Available s AD 757789 from the National Technical Information Ser- ice, Springfield, Va. 22151.)

> Key words: Absorption coefficient; damage threshold; electrostrictive self-focusing; electrostriction; Kerr effect; laser damage; nonlinear index of refraction; self-focusing; thermal self-focusing.

he relative contributions of the Kerr, electrostrictive, and rmal effects to the self-focusing thresholds of borosilicate wn glass, fused silica, and dense flint glass have been esti- ted from an analysis of damage threshold data for linearly arized and circularly polarized radiation. The measurements re made with a Nd:glass laser operating in the $TEM_{00}$ mode h a temporal pulse width of 25 ns. The Kerr effect appears to the largest effect. The thermal effect is also significant. The ctrostrictive effect is smallest. Reasonable values of absorp- n coefficient are calculated from the thermal contribution. The ults are in qualitative agreement with the work of others. Self- using data obtained with linearly polarized and circularly arized radiation are presented for yttrium aluminum garnet AG) and five commercial Nd:doped laser glasses. The YAG a agree with the theory of self-focusing. Near the threshold laser glass data appear to indicate intrinsic damage rather n self-focusing. Differences between the various laser glasses small. Self-focusing data obtained in dense flint glass with a ger focal length lens are also presented. An electro-optic itter actuated by a laser triggered spark gap is discussed.

13530. Lee, T. G., Huggett, C., **Interlaboratory evaluation of the tunnel test (ASTM E 84) applied to floor coverings,** *NBSIR 73-125,* 56 pages, (Mar. 1973). (Available as COM 73-11189 from the National Technical Information Service, Springfield, Va. 22151.)

> Key words: ASTM E 84; building materials; carpets; fire tests; flame spread tests; interlaboratory evaluation; round robin; statistical analysis; test method standard.

Results of an interlaboratory evaluation of the ASTM E 84 tunnel test method involving eleven laboratories and nine materials, including four carpets, are reported. Data on flame spread, smoke, and fuel contribution are analyzed statistically. Selected physical characteristics of each tunnel are tabulated and compared relative to specifications in the test method. The between-laboratory coefficient of variation (reproducibility) in flame spread classification (FSC) was found to range from 7 to 29% for the four carpets and from 18 to 43% for the other materials tested. The between-laboratory coefficients of variation for smoke developed and fuel contribution ranged from 34 to 85% and from 22 to 117% respectively for all materials tested. The causes of higher variability in smoke and fuel contribution measurement between laboratories is not definitely known but may reasonably be attributed to variations in tunnel construction, maintenance, and operation, in the location of photometers, and in the mounting of thermocouples in different laboratories. Some variability of results may possibly be due to variation in test specimens. Variation in construction and measurement techniques among tunnels may be minimized by updating the test method standard.

13531. Koonce, C. S., **Theory of superconducting semiconductors,** (Proc. of a Summer Course on The Science and Technology of Superconductivity, held at Georgetown University, Washington, D.C., Aug. 13-26, 1971), Paper in *The Science and Technology of Superconductivity,* W. D. Gregory, W. N. Mathews, Jr., and E. A. Edelsack, Eds., **1,** 373-387 (Plenum Press, New York, N.Y., 1973).

> Key words: Energy gap equation; semiconductors; superconductor; transition temperature.

The BCS theory of superconductivity will be applied to degenerate semiconductors. Methods of calculating superconducting properties of degenerate semi-conductors will be compared with methods used to calculate superconducting properties of metals. The normal state properties of degenerate semiconductors which are important in determining the superconducting properties will be discussed.

13532. Koonce, C. S., **Enhancement effects: Theory,** (Proc. of a Summer Course on The Science and Technology of Superconductivity, held at Georgetown University, Washington, D.C., Aug. 13-26, 1971), Paper in *The Science and Technology of Superconductivity,* W. D. Gregory, W. N. Mathews, Jr., and E. A. Edelsack, Eds., **1,** 389-403 (Plenum Press, New York, N.Y., 1973).

> Key words: Dielectric function; superconductor; transition metal; transition temperature.

A discussion of which modifications of normal state properties such as phonon frequencies and electronic density of states as a function of energy are likely to enhance the superconducting transition temperature will be given. A discussion of the methods of modification of the material properties such as alloying, doping applying pressure and forming thin films will also be given.

13533. McLaughlin, W. L., Kosanić, M., Draganić, I. G., **Extending the response of the pararosaniline dye system,** (Proc.

Int. Symp. on Dosimetry in Agriculture, Industry, Biology and Medicine, Vienna, Austria, Apr. 1972), Paper in *Dosimetry in Agriculture, Industry, Biology and Medicine*, pp. 362-366 (International Atomic Energy Agency, Vienna, Austria, 1973).

Key words: Dosimetry; dyes; gamma rays; nitrobenzene; oxidation; pararosaniline cyanide; radiochromic dyes; triphenylmethane dyes.

Organic solutions of triphenylmethane dye precursors, particularly pararosaniline cyanide (4, 4′, 4″ -triamino-triphenylacetonitrile) and hexa (hydroxyethyl) pararosaniline cyanide (4, 4″, 4″ -tris- (di-β-hydroxyethylamino) triphenylacetonitrile, have been used successfully in measuring gamma-ray absorbed doses in the range from 1 to 100 krad. With conventional slightly acidified and aerated ether alcohol solutions of the dye precursors, the optical density read at the absorption maximum in the visible portion of the spectrum increases linearly with dose up to about 100 krad. Saturation and bleaching of the solutions at doses between 100 and 200 krad limit the usefulness of these liquid systems. A recent study has been performed at the Boris Kidric Institute of Nuclear Sciences and the Danish Atomic Energy Commission, Research Establishment Risø, for the purpose of making chemical adjustments in the solutions so that higher absorbed doses may be measured with a linear optical density-versus-dose response.

**13534.** McCamy, C. S., **The evaluation and manipulation of photographic images,** Chapter in *Picture Processing and Psychopictorics,* A. Rosenfeld and B. S. Lipkin, Eds., 57-74 (Academic Press, Inc., New York, N.Y., 1970).

Key words: Image evaluation; image manipulation; image optics; photography.

The scientific use of photography in the study of the psychophysics of images requires a knowledge of the techniques employed in specifying the characteristics of optical and photographic systems and the available techniques for manipulating photographic images. The primary measure of the photographic effect is *optical density*, a quantity which depends on the method of measurement in a complex way. The photographic process is quantitatively characterized by sensitometry. Image structure is characterized by resolving power, spread function, modulation transfer function, pupil function, acutance, and granularity. Photographic images may be manipulated by various forms of dodging, masking, and special processing.

**13535.** Olien, N. A., Sarkes, L. A., **Keeping up with LNG—a new literary awareness service helps to do the job,** *Amer. Gas Ass. Mon.* **55,** No. 7-8, 29 and 31 (July-Aug. 1973).

Key words: Current awareness services; information retrieval; information systems; Liquefied Natural Gas; methane; methane mixtures.

A description is given of the methods used by the Cryogenic Data Center in covering the current published and patent literature. The services provided to the Cryogenic industry are also discussed. The *Liquefied Natural Gas Quarterly* which has been published since 1970 is covered in detail. It is noted that nearly 2,000 articles, papers, reports, and patents dealing with LNG have been listed in the twelve issues of the quarterly published to date. A series of comprehensive bibliographies on LNG, methane, and methane mixtures is also described.

**13536.** Kirchhoff, W. H., **Microwave spectroscopy,** *Chem. Eng. News* **47,** 88-98 (Mar. 24, 1969).

Key words: Dipole moment; microwave spectroscopy; molecular rotation; molecular structure; qualitative analysis; quantitative analysis.

A review of microwave spectroscopy is presented with speci
emphasis on its applications to problems of chemical intere
The fundamental concepts of molecular rotation are discuss
using classical mechanics, and the relationship of molecul
structure and forces with the molecular rotation is presente
The quantum mechanical model is then presented with sufficie
detail to understand the nature of rotational spectroscopy. T
Stark effect and its dependence on the molecular dipole mom
is briefly described. Recent instrumental advances as well as t
application of microwave spectroscopy to quantitative a
qualitative analysis are mentioned.

**13537.** Reed, R. P., Arvidson, J. M., Durcholz, R. L., **Tens
properties of polyurethane and polystyrene foams from 76 to 3
K,** (Proc. 1972 Cryogenic Engineering Conf., Boulder, Col
Aug. 9-11, 1972), Paper E-3 in *Advances in Cryogenic E
gineering* **18,** 184-193 (Plenum Press, New York, N.Y., 197

Key words: Foams; low temperature; tensile properties.

The tensile properties of 17 different polyurethane foams a
2 polystyrene foams have been measured at 300, 195 and 76
The Young's modulus, yield strength and tensile strength
creased with decreasing temperature, while the elongati
decreased. Strength and Young's modulus were found to be
proximately linearly dependent on temperature; however, at l
temperatures the density dependence was greater. Specime
whose long axis was cut parallel to the cell rise direction w
stronger than those whose long axis was cut normal to the c
rise direction. Comparisons between foam tensile and compr
sive properties are presented in the accompanying paper.

**13538.** Cruz, J. E., Rogers, E. H., Hiester, A. E., **Continu
liquid level measurements with time-domain reflectomet**
(Proc. 1972 Cryogenic Engineering Conf., Boulder, Col
Aug. 9-11, 1972), Paper H-4 in *Advances in Cryogenic E
gineering* **18,** 323-327 (Plenum Press, New York, N.Y., 197

Key words: Coaxial probe; emptying rate; fill rate; liq
level; time domain reflectometer.

A time domain reflectometer is considered a closed-loop, c
dimensional radar system. Applying the principle of time dom
reflectometry to the detection of cryogenic liquid levels, m
surements on the order of ±0.3% of total liquid level probe len
are possible.

The time domain reflectometer liquid level measurement is
dependent of liquid density variations and is simple to calibr
and operate. Construction of the liquid level sensing probe
described.

**13539.** Orcutt, R. H., **Interlot density variation of a silox
manometer fluid,** *J. Vac. Sci. Technol.* **10,** No. 4, p. 506 (Ju
Aug. 1973).

Key words: Diffusion pump fluid; micromanometry;
icone.

The mean value of density for six samples of a silox
manometer fluid is 1.06311 g/cm$^3$ with an estimated stand
deviation of $11 \times 10^{-5}$ g/cm$^3$ for the lot-to-lot variation in dens
of this fluid. From this result it is concluded that for use of t
material in manometry to the 0.01% level the density of the
tual fluid used must be determined.

**13540.** Schooley, J. F., **Superconductors in thermometry,** (Pr
Summer Course on The Science and Technology of Superc
ductivity held at Georgetown University, Washington, D.
Aug. 13-26, 1971), Paper in *Science and Technology of Sup
conductivity,* W. D. Gregory, W. N. Mathews, Jr., and E.

delsack, Eds., **2,** 625-630 (Plenum Press, New York, N.Y., 973).

Key words: Critical magnetic field; heat capacity; Josephson junctions; noise thermometry; superconductive fixed points; superconductivity; thermometry.

arious properties of superconductors show monotonic tem- ature dependences, so that in principle they may be used as mometric parameters. Other properties can be utilized in ices which find convenient application in thermometry. Of many possible examples, we will examine several which have nd some actual use either as thermometers or detectors in rmometry.

**41.** Arvidson, J. M., Durcholz, R. L., Reed, R. P., **ompressive properties of polyurethane and polystyrene foams om 76 to 300 K,** (Proc. 1972 Cryogenic Engineering Conf., oulder, Colo., Aug. 9-11, 1972), Paper E-4 in *Advances in ryogenic Engineering* **18,** 194-201 (Plenum Press, New ork, N.Y., 1973).

Key words: Compression; foams; temperature.

he compressive properties of 4 different polyurethane foams 2 polystyrene foams have been measured at 300, 195 and 76 Similar to tensile properties, the Young's modulus, yield ngth, and compressive strength increased with decreasing perature, while the elongation to fracture decreased. An ap- ximate linear dependence on density was found for Young's dulus in compression and the proportional limit. Longitudinal cimens were usually stronger than transverse specimens. cimens pulled in tension were considerably stronger than cimens loaded under compression, but these differences inished at lower temperatures.

**42.** Wells, J. S., **A stabilized HCN laser for infrared frequency ynthesis,** *IEEE Trans. Instrum. Meas.* **IM-22,** No. 2, 113-118 une 1973).

Key words: HCN laser; infrared frequency synthesis; laser frequency measurements; laser stabilization; laser metrology; phase locked laser.

nfrared frequencies have recently been synthesized in suita- diodes up to 88 THz with accuracies of parts in $10^9$. Stabil- d lasers are necessary in order to make frequency measure- nts of higher accuracy. The hydrogen-cyanide laser is the est frequency basis laser used in these synthesis schemes, l its stabilization has been the subject of recent interest. The er is stabilized by locking it to a phase-locked microwave erence chain. Two servo loops are utilized. The first loop is a atively slow frequency-lock loop with the correction applied a piezoelectric-translator driver. This loop not only accom- dates thermal expansion of the laser, but also serves as an uisition aiding loop for the second servo. The latter is a se-locked system with the correction applied to the laser charge current controller. Data regarding the system stability presented.

**43.** Geist, J., **Theoretical analysis of laboratory blackbodies. 1: A generalized integral equation,** *Appl. Opt.* **12,** No. 6, 1325- 330 (June 1973).

Key words: Blackbody; holrahm radiation; radiometry; thermal radiative transfer.

The integral equations describing radiative equilibrium in a ckbody cavity are presented. Solving these equations in terms he power sources in the furnace surrounding the cavity is not ctical. However, if provisions are made for measuring the temperature over some surface between the power sources and the cavity interior, the analysis is feasible. This restriction and some realistic assumptions lead to a single, linear, inhomogeneous integral equation that approximately describes the interaction of the cavity geometry, the thermal radiative properties of the cavity wall, and the temperature gradients within the cavity in reducing the quality of the blackbody. The formulation is general enough to accomodate realistic reflectance and temperature distributions for high quality blackbodies, and the accuracy of calculations based upon it will probably not be limited by approximations involved in its derivation, but by the present state of the art in the knowledge of the thermal radiative properties of materials.

**13544.** Schooley, J. F., **Enhancement effects,** (Proc. Summer Course on The Science and Technology of Superconductivity, held at Georgetown University, Washington, D.C., Aug. 13-26, 1971), Paper in *The Science and Technology of Superconductivity,* W. D. Gregory, W. N. Mathews, Jr., and E. A. Edelsack, Eds., **1,** 405-428 (Plenum Press, New York, N.Y., 1973).

Key words: High transition temperature; pressure effects; proximity effect; superconductive alloys; superconductive compounds; superconductivity.

Superconductivity research has had as one of its continuing aims the production of high-transition-temperature materials. This situation arises from the realization that superconductivity can be applied to transportation, communication, power transmission, and instrumentation on a wider and more efficient basis, the higher the transition temperature. Many of these applications will be discussed during this course by several of the lecturers.

In this lecture, I will discuss various ways in which experimenters have attempted to generate high transition temperatures.

**13545.** Milligan, D. E., Jacox, M. E., **Infrared spectroscopic evidence for the stabilization of HAr$_n^+$ in solid argon at 14 K,** *J. Mol. Spectrosc.* **46,** No. 3, 460-469 (June 1973).

Key words: Argon reactions; H($2^2S$) reaction with Ar: HAr$_n^+$; infrared spectrum; interstitial H atom spectrum; matrix isolation; proton affinity; vacuum ultraviolet photolysis.

Absorptions which have been observed at 905 and at 644 cm$^{-1}$ upon 1216-Å photolysis of hydrogen- and deuterium-containing compounds, respectively, in an argon matrix correspond well with similar absorptions reported in studies of the trapped products of a glow discharge through Ar:$H_2$ and Ar:$D_2$ mixtures. Evidence is presented supporting the assignment of these two absorptions to HAr$_n^+$ and to DAr$_n^+$ rather than to interstitial H and D atoms trapped in octahedral sites in the argon lattice.

**13546.** Cohen, J., Edelman, S., Vezzetti, C. F., **Pyroelectricity and piezoelectricity in oriented films of polyvinyl fluoride and polyvinylidene fluoride,** (Proc. Conf. on Electrets, Charge Storage and Transport in Dielectrics, Miami Beach, Fla., Oct. 8-13, 1972), Paper in *Electrets, Charge Storage and Transport in Dielectrics,* Martin M. Perlman, Ed., pp. 505-516 (The Electrochemical Society, Inc., Princeton, N.J., 1973).

Key words: Piezoelectricity; poling; polyvinyl fluoride; polyvinylidene fluoride; pyroelectric coefficient; pyroelectricity.

Improved pyroelectric and piezoelectric activities have been produced in films of polyvinyl fluoride (PVF) and polyvinylidene fluoride ($PVF_2$). The phenomena are ascribed to orientation of dipoles normal to the plane of the film. Activity is developed or enhanced by applying intense electrical fields across the films at elevated temperatures and cooling to room temperature with the field still applied (poling). The $PVF_2$ films are usually stretched before poling, and this is found to increase both pyroelectric and piezoelectric effects. Room temperature pyroelectric coefficients for these materials have been estimated from measurements of voltage responsivity, and pyroelectric coefficients comparable to that of triglycine sulfate (TGS) have been obtained. Observations of the correlation between the thermal radiation effects and the piezoelectric activity suggest that the former are pyroelectric. A method has been developed to study the poling process.

**13547.** Geist, J., **New NBS scale of irradiance,** *Appl. Opt.* **12,** No. 4, 907-908 (Apr. 1973).

Key words: Electrically calibrated detectors; irradiance; total irradiance.

This letter presents a short report on the new NBS scale of total irradiance that was recently realized with an electrically calibrated detector. The results of intercomparisons of two such detectors as well as a comparison of the new scale with the old scale as maintained at NBS are presented.

**13548.** Grabner, L., Wong, E. Y., **Zeeman effect of no-phonon $^4A_{2g}$ - $^4T_{2g}$ transition of $Cr^{3+}$ in $TiO_2$,** *Phys. Rev. B* **8,** No. 3, 1032-1037 (Aug. 1, 1973).

Key words: $Cr^{3+}$ in $TiO_2$; identification of excited state; $^4A_{2g}$ - $^4T_{2g}$ transition; Zeeman effect.

The site symmetry of $Cr^{3+}$ in $TiO_2$ is $D_{2h}$ which splits the cubic $(O_h)$ $^4T_{2g}$ state into $^4B_{1g}$, $^4B_{2g}$, and $^4B_{3g}$. Spin-orbit interaction further splits these states into six Kramers doublets all of symmetry $\Gamma_5^+$. Previous optical work on $TiO_2$: $Cr^{3+}$ established the lowest-lying sharp lines at 12685 and 12732 $cm^{-1}$ as no-phonon lines of magnetic dipole character. It proposed these lines as due to transitions between the $^4A_{2g}$ ground state and two of the above six states. The present report extends this work by a Zeeman study, in emission, at 4 K of the line at 12685 $cm^{-1}$. The results are: The Zeeman splitting of this line identifies the excited state of this transition as the $M_s = \pm 3/2$ spin-orbit component of an orbital state consisting of 77% $^4B_{2g}$, 17% $^4B_{1g}$, and 6% $^4B_{3g}$ with an effective $g = 1.73$. Furthermore, the line at 12732 $cm^{-1}$ is identified as the $M_s = \pm 1/2$ spin-orbit component by its effect in second order in the magnetic field on the Zeeman pattern of the line at 12685 $cm^{-1}$. For the excited state the spin is quantized along the $x$ direction of the magnetic axes while for the ground state it is quantized along the $z$ direction. The reason for spin quantization along the $x$ axis is discussed.

**13549.** Achenbach, P. R., Phillips, C. W., **Performance characteristics of pressure-actuated water-regulating valves for refrigerant condensers,** (Proc. XII Int. Congress of Refrigeration, Madrid, Spain, 1967), Paper in *Progress in Refrigeration Science and Technology* **2,** 1107-1118 (Gráficas Reunidas, Madrid, Spain, 1969).

Key words: Performance characteristics; refrigeration accessories; valves; water-flow regulation.

Water-regulating valves are used on the condensers of water-cooled refrigerating units to maintain a satisfactory refrigerant condensing pressure and to conserve water. Both pressure-actuated and temperature-actuated valves are used for this purpose. A study was made of three sizes of pressure-actuated water-regulating valves from each of three sources to determine their range of condenser pressure control, the change in condensing pressure required to move the valves from fully-closed to fully-open position, the hysteresis in the control mechanism, and the water-flow characteristics near the fully-closed position. These and other performance characteristics related to water conservation and reliable operation of refrigerating units were investigated to provide guidance to the U.S. Army Natick Laboratories in writing performance specifications. The study reveale that the nominal pipe size of the valves was not a good indicatio of water-flow capacity, that the sensitivity of the various valve to change in condensing pressure differed widely, and that th difference between opening and closing pressure was in exces of 10 psi (0.7 $kg/cm^2$) in some valves. Moreover, the condensin pressure at 90 percent maximum water flow rate ranged fro 118 to 172 psig (8.3 to 12.1 $kg/cm^2$) for the several valves whe the opening pressure was set at 80 psig (5.6 $kg/cm^2$).

**13550.** Canfield, L. R., Johnston, R. G., Madden, R. P., **NBS d tector standards for the far ultraviolet,** *Appl. Opt.* **12,** No. 1611-1617 (July 1973).

Key words: Detectors; far ultraviolet; ion chambe photodiodes; radiometry; thermopile.

A program at NBS leading to the realization of practical, st ble transfer detector standards for the far ultraviolet is reviewe Three basic detector types, one covering the region of 584-121 Å and the other two covering the region of 1164-2537 Å, a described. Examples of these detectors have been calibrated NBS and distributed to laboratories throughout the Unit States and Europe, where they are being used as prima radiometric calibration references in a variety of far-uv expe ments.

**13551.** Tilford, C. R., **A fringe counting laser interferomet manometer,** *Rev. Sci. Instrum.* **44,** No. 2, 180-182 (Feb. 197

Key words: Fringe counting; laser interferomete manometer.

A prototype standard mercury manometer using a frin counting laser interferometer to measure the differential heig of the mercury columns has been built and successfully operate The 10.6 $\mu$ wavelength radiation from a $CO_2$ laser and special treated manometer tubes have been used to reduce the effect disturbances on the mercury surface so that reliable operation the manometer is possible.

**13552.** Roder, H. M., **A new phase transition in solid hydroge** *Cryogenics Letter to Editors* **13,** No. 7, 439-440 (July 1973).

Key words: Hydrogen; phase transition.

Available but often discordant data on PVT, dielectric co stant, specific heat, velocity of sound, and melting pressures a interpreted to indicate the possibility of a transition in so hydrogen. This structural change, suggested by others pre ously, has not yet been investigated as thoroughly as the co responding transition in solid helium.

**13553.** Hsieh, C., Thomson, R., **Lattice theory of fracture a crack creep,** *J. Appl. Phys.* **44,** No. 5, 2051-2063 (May 197

Key words: Creep of crack; fracture; lattice theory.

A quasianalytic solution for the atomic displacements of a d crete two-dimensional lattice containing a crack is obtained. W assume that the force laws are linear up to a critical displacem when the bond snaps, which is the basic assumption of the latt static approximation. When compared to the classic Griffith co tinuum description, new results are: (i) a predicted and obser ble lattice trapping of the crack, (ii) difficulties with the terpretations of the crystal surface energy in a cleavage expe ment, and (iii) a predicted characteristic crack cre phenomenon under external constant stress. The present theo shows how two separate "surface energies" are inferred from t stress to open and to close a crack, and on our model these en differ from one another by a large factor of 5.7. The ther- ynamic "surface energy" is not related to either of these ntities. Experimental verification of the lattice trapping of ks is thought to be most readily and directly obtained by ob- ations of the creep of a crack under high vacuum conditions.

54. Fickett, F. R., **Properties of nonsuperconducting technical lids at low temperatures,** *Proc. 4th Int. Conf. on Magnet echnology,* Brookhaven National Laboratory, Upton, N.Y., ept. 19-22, 1972, pp. 498-516 (Atomic Energy Commission, ashington, D.C., 1972).

Key words: Composite materials; electrical properties; mechanical properties; metals; plastics; review; thermal properties.

number of physical and mechanical properties of materials d in low temperature applications are described with rences to both theory and compiled data. These properties, ch fall into three main groups, thermal, electrical, and hanical, are given for pure metals, alloys, and a few non- als. In essence, this paper is a review of concepts and availa- data for low temperature engineering applications of nonsu- conductors.

55. Fröhlich, C., Geist, J., Kendall, J., Sr., Marchgraber, R. 1., **The Third International Comparisons of Pyrheliometers nd a comparison of radiometric scales,** *Sol. Energy* **14,** 157- 66 (1973).

Key words: International Pyrheliometric Scale; irradiance; pyrheliometer; World Meteorological Organization.

he Third International Comparisons of Pyrheliometers or- ized by the World Meteorological Organization and the vos Observatory were held in September 1970 at Davos and arno. For this purpose the intensity of solar radiation was asured simultaneously by the standard radiometers gström compensation and silver-disc pyrheliometers) from over the world. For meteorological use the intensity values r to the International Pyrheliometric Scale 1956 represented the reference instruments of the Davos Observatory and of Swedish Meteorological and Hydrological Institute at ckholm. At the same time measurements were performed by instruments rendering an absolute value of high accuracy. se sophisticated instruments have been constructed by Ken- l and Geist respectively.

A fully-automatic data acquisition system together with a com- er was used to compare simultaneously the 22 Ångström Pyr- iometers and to monitor the auxiliary measurements necessa- for defining the state of the atmospheric conditions specified a turbidity coefficient of $0.03 < m\beta < 0.3$. The intensity ues covered a range of 55-100 mW/cm$^2$. The results show a nificant difference between the two radiometeric scales. The nsity value deduced from the absolute measurement is about ercent higher than the value based on the International Pyr- iometric Scale.

56. Corliss, E. L. R., **Remark on "Fixed-scale mechanism of bsolute pitch",** *J. Acoust. Soc. Amer. Letters to Editor* **53,** No. , 1737-1739 (June 1973).

Key words: Absolute pitch sense; audition; auditory memory; hearing; musical acoustics; pitch recognition.

Several aspects of this author's subjective experiences con- ned with perception of pitch are at variance with the ex- iences reported by Paul T. Brady, *J. Acoust. Soc. Am.* **48,** 3-887 (1970). In particular, my recognition is not tied to a ecific scale (though, of course, nomenclature must be); the cision of recognition shows little fluctuation, if any; and changes in tuning do not influence the recognition of pitch, although such changes may influence the performance of remembered music and the ease of transposition. Tonal memory overrides motor memory for the performance of music learned on instruments tuned to initially different keys.

13557. Kamper, R. A., Simmonds, M. B., Adair, R. T., Hoer, C. A., **Quantum mechanical measurement of rf attenuation,** *Proc. 1972 Applied Superconductivity Conf., Annapolis, Md., May 1-3, 1972,* pp. 696-700 (IEEE, Inc., New York, N.Y., 1972).

Key words: Josephson effect; quantum interference; rf attenuation; rf measurements; superconductivity.

We have used a broadband Superconducting QUantum Interference Device (SQUID), operating at a frequency of 9 GHz, as a sensor of current at lower radio frequencies. The periodic nature of the response of the SQUID enabled us to measure variations in rf attenuation directly. The results of such a measurement were in agreement with the NBS Calibration Service to within ±0.004 dB over a dynamic range of 40 dB. We also discuss other applications of this SQUID to rf measurements.

13558. Eisen, H., Rosenstein, M., Silverman, J., **Electron dosimetry using Chalkley-McLaughlin dye-cyanide thin films,** (Proc. Int. Symp. on Dosimetry in Agriculture, Industry, Biology and Medicine, Vienna, Austria, April 1972), Paper in *Dosimetry in Agriculture, Industry, Biology and Medicine,* pp. 615-625 (International Atomic Energy Agency, Vienna, Austria, 1973).

Key words: Calorimetry; depth dose; dose distributions; dye films; electron beams; interface; Monte Carlo transport; stopping power; thin films.

The purpose of this work was to measure electron energy deposition profiles in a variety of absorbing materials and to evaluate the Chalkley-McLaughlin radiochromic dye-cyanide film dosimeter. Information of this type is useful for effective utilization of electron beams in industry and medicine where adjustments in sample thickness, electron beam energy, angle of electron beam incidence, and backing materials may provide more advantageous beam utilization. Experimental depth-dose distributions were determined for broad beams of 2.00 MeV electrons incident on polystyrene, aluminium, copper, tin, gold, and several two-layer slab absorbers. Data were obtained for both semi-infinite and finite homogeneous absorbers at incident beam angles ranging from 0 (normal incidence) to 75 degrees. Radiochromic dye-cyanide films were used as solid-state cavity dosimeters, with an experimental reproducibility of ±6% ($2\sigma$). The stopping power ratio necessary to convert from film dose to absorber dose was evaluated several ways. Depth-dependent stopping power ratios, obtained by accounting for the changing electron energy spectrum with absorber depth by two methods, were compared with a constant stopping power ratio for each material. The difference between the constant ratio and a depth-dependent ratio was 1% to 2% for aluminium, 3% to 5% for copper, 3% to 7% for tin, and 3% to 8% for gold. The data demonstrate the decrease in the depth-dose distribution and the total absorbed dose in finite slabs as compared to equivalent layers in semi-infinite slabs. The effect of the atomic number of the absorber and the angle of beam incidence on the shape of the energy deposition profile is also demonstrated. The data for the two-component slab absorbers illustrate the modification of the depth-dose profile in a finite slab of material if a different material is placed adjacent to it. From the dose received by a film placed at the interface, the surface doses at that position were estimated using the material-to-film stopping-power ratio appropriate for each material. The data are compared to theoretical depth-dose profiles obtained using Monte Carlo transport codes.

The agreement is generally between 5% to 10% for homogeneous cases and in most cases better than 10% for the two-component cases.

**13559.** McLaughlin, W. L., Hjortenberg, P. E., Radak, B. B., **Absorbed-dose measurements with thin films,** (Proc. Int. Symp. on Dosimetry in Agriculture, Industry, Biology and Medicine, Vienna, Austria, April 1972), Paper in *Dosimetry in Agriculture, Industry, Biology and Medicine,* pp. 577-597 (International Atomic Energy Agency, Vienna, Austria, 1973).

Key words: Absorbed dose; calorimetry; cavity theory; depth dose; dosimetry; dye dosimeters; electron beams; gamma rays; plastic dosimeters; radiochromic dyes; thin films.

Thin films of plastic, coatings, papers, ceramics, emulsions, cleaved crystals, microtomed gel sections, and metal foils have all been used with advantage to measure large radiation absorbed doses. The three most successful methods of relating the radiation effects in the film to the dose are: Calorimetry, which measures temperature rise; photometry, which measures changes in light emission, transmission or reflection; and electrometry, which measures electrical changes such as variations in resistivity, e.m.f., current, etc. The chief problems in making good measurements of radiation dose or dose rate with thin films are: (1) quality control of the dosimeter itself; (2) discontinuity problems, that is, how the energy imparted to a thin probe is related to energy imparted to surrounding matter; (3) meaning of the calibration, that is, how the radiation effect in the film material is related to the absorbed energy as a function of spectrum dose rate, temperature, etc. The first of these can be dealt with effectively by control of film thickness, chemical composition and environmental influences. The second is often more complicated, especially if the thin probe differs appreciably in absolute density and atomic number from its surroundings, since proper application of cavity theory may be difficult for some geometrical arrangements. The third problem is usually the most difficult of all, because the radiation effect in a thin material used as a dosimeter often depends on many variables leading to systematic errors in dose interpretations. In this work, methods are given for calibrating in electron beams the radiation response of thin-film dosimeters calorimetrically, accounting for the sources of error cited above. The calibration procedures include the use of appropriate cavity-theory correction factors needed to relate the response of the thin probe of one material held in another medium. Finally, a suitable film dosimeter material is described. It consists of radiochromic dye films, which can measure doses from about $10^4$ to $10^8$ rad in various media under different irradiation conditions.

**13560.** Heinrich, K. F. J., **Errors in electron probe microanalysis,** *Proc. of the Seminar on Quantitative Analysis with Electron Microprobes and Secondary Ion Mass Spectrometry, Jülich, Germany, Oct. 18-20, 1972,* pp. 68-79 (Mar. 1973).

Key words: Data reduction; electron probe; errors; microanalysis; x-ray measurement.

Errors in quantitative electron probe microanalysis are due to errors in the measurement of relative characteristic x-ray intensities and in the interpretation of the experimental measurements. The random errors in the x-ray measurement include those due to Poisson's statistics, but other sources must not be excluded from consideration. Systematic errors may be committed in the estimation of coincidence losses (dead-time) and background. Those arising in the evaluation of the data may be due to the theoretical models, or to the parameters and constants which enter the calculation. Satisfactory models require adjustment to empirical measurements, and improvement in the accuracy of electron probe microanalysis requires the performing of critical experiments which can lead to further adjustment of the model It is also important to adjust the conditions of measurement so a to minimize the effects of uncertainties and errors in models an parameters.

**13561.** Flynn, D. R., **Inter-Noise 72 Panel: Noise measur ment – problems, perils and pitfalls,** *Noise/News* **2,** No. 1, 7- (Jan.-Feb. 1973).

Key words: Acoustics; noise measurements; sound level

This short paper discusses some of the problems involved i noise measurements. It is pointed out that noise measureme standards should specify environmental and operational co straints in addition to precise, accurate measurement and oper tional procedures. A few examples are given of sources of signi cant measurement errors. The Measurement Assurance Pr grams of NBS are briefly described as a means that has be used in other disciplines to improve measurements in a tot system context.

**13562.** Moore, R. T., **Penetration tests on J-SIIDS barrie** *NBSIR 73-223*, 86 pages, (June 4, 1973). (Available as CO 73-11120 from the National Technical Information Servic Springfield, Va. 22151.)

Key words: Barrier penetration; intrusion resistanc physical security.

A series of penetration tests were made on three simulat arms rooms which incorporated a variety of structural barrie which were intended to be representative of the broad range construction likely to be encountered in existing arms rooms.

The observed penetration times varied from 1.3 minutes fo double-planked wooden wall, 11.31 minutes for an eight-in thick, reinforced concrete wall and up to 18.27 minutes for GSA Class 6 vault door. All penetrations were made with port ble readily available tooling and produced acoustical or vib tional or both types of disturbances which are readily detectab

The test results provide a basis for estimating the time which response to an intrusion alarm must occur in order adequately safeguard an arms room, a computer room or a other sensitive area.

**13563.** Garvin, D., **Chemical kinetics data survey V. Sixty-six co tributed rate and photochemical data evaluations on ninety-fo reactions,** *NBSIR 73-206*, 121 pages, (May 1973). (Availa as COM 73-11262 from the National Technical Informati Service, Springfield, Va. 22151.)

Key words: Atmospheric chemistry; chemical kineti data evaluation; gas phase reactions; optical absorpti cross sections; photochemistry; quantum yields; rate c stants.

This report records the data evaluations contributed to the C matic Impact Assessment Program chemical kinetics surv during the period Nov. 1972-Apr. 1973 by various kinetici and photochemists. Data are included on reactions of O($^1$ O($^1$S), $O_2(^1\Delta)$, $CH_3ONO$, $CH_3O$, $CH_3O_2$, $H_2O_2$, $HO_2$, SO, S and the $H_2$-$N_2$-$O_2$ system.

**13564.** Finkel, P. W., Rowen, J. W., **Clinical laboratory p formance analysis using proficiency test statistics,** *NBSIR 197* Revised, 63 pages, (Dec. 1973). Supersedes PB21 287/6. (Available as COM 73-11253 from the Natio Technical Information Service, Springfield, Va. 22151.)

Key words: Accuracy; CLIA '67; clinical chemistry; matology; microbiology; precision; proficiency testing.

The proficiency testing aspects of the Clinical Laboratory I provement Act of 1967 program were assessed. The ove ility of licensed or volunteer laboratories to accurately deter- ne mean values for any of the 13 constituents was not signifi- ntly altered during the first two years of program operation. owever, the variability of the laboratories has decreased over e two-year period. It appears that the program has increased nsistency of laboratory performance.

The general level of laboratory capability seemed to be inde- ndent of involvement in state-supported or voluntary profi- ency testing programs other than the CDC program and of hether the working supervisor had a B.S., M.S., Ph.D., or .D. degree. Choice of analytical method did significantly affect rformance. Although insufficient evidence was available to ake a definitive statement, the data do not appear to support ar- ments favoring establishment of method-dependent reference oup target values.

Finally, it appears that consideration should be given to alter- ative sampling methods, such as reduced or skip-lot sampling, r those constituents which appear to present no analytical chal- nge to the licensed and volunteer laboratories. Greater empha- s might then be placed on those constituents which give the boratories the most difficulty (cholesterol and creatinine, for xample).

**3565.** Hust, J. G., Clark, A. F., **A survey of compatibility of materials with high pressure oxygen service,** *Cryogenics* **13,** No. 6, 325-336 (June 1973).

Key words: Compatibility data; high pressure; oxygen; safety; survey.

The literature on high pressure oxygen compatibility has been urveyed in order to present the existing state of knowledge. earches have been conducted of NASA and NBS data retrieval ystems. In addition, many individuals, active in the field, were ontacted in order to retrieve useful unpublished information. ompatibility data, such as mechanical impact, pneumatic im- act, ignition temperature, and flash-and-fire point, were com- iled for pressures above 200 bar ($2 \times 10^7$ $\mathrm{Nm}^{-2}$). Lower pres- ure data were included if they were useful for extrapolation to ressures above 200 bar. These data, too numerous to be given ere, are available from the authors. Brief descriptions of the rends of these data are given. Recommendations for additional igh pressure studies are included.

**3566.** McLaughlin, W. L., Bjergbakke, E., **Electrochemical dosimetry using ferric-fluoride ion complex formation,** (Proc. Int. Symp. on Dosimetry in Agriculture, Industry, Biology and Medicine, Vienna, Austria, Apr. 1972), Paper in *Dosimetry in Agriculture, Industry, Biology and Medicine,* pp. 383-396 (International Atomic Energy Agency, Vienna, Austria, 1973).

Key words: Dosimetry; electrochemistry; ferric-fluoride complex; ferrous sulfate solutions; fluorides; Fricke dosimeter; ion selective electrodes; lanthanum fluoride; potentiometry.

Irradiated aqueous ferrous sulphate solutions containing luoride ions can be analysed for ferric ion yield by means of lectrochemical potentiometry. For certain applications this ap- roach has advantages over the usual method of spec- rophotometric determination of ferric ion concentration, which also varies linearly with absorbed dose up to about 40 krad: (1) Small dosimeter volumes down to 10 microlitres are functional; 2) Solid gels may be used, thus allowing for thin-film geometries; (3) The potentiometric method permits real-time current readings) or integrated (EMF readings) measurement of radiation dose. The electrochemical analysis of ion-complex yield is fairly simple. A fluoride ion electrode of the solid-state type serves as an ion-selective sensor. The electrochemical potential (or its rate of change in some instances) between the fluoride ion electrode and the reference electrode is then read on a pH-meter. Since the $Fe^{3+}$ cation complex with $F^-$ is not passed by the lanthanum fluoride crystal membrane at the end of the electrode probe, and since the free $F^-$ ion concentration diminishes linearly with dose up to about 40 krad (corresponding to approximately 0.4m*M* $Fe^{3+}$ ion concentration at pH 2.7), the dose or dose rate can be determined from readings of linear change in millivoltage or rate of change of millivoltage. For cobalt-60 gamma-ray irradiation of a 1.00m*M* solution of $Fe^{2+}$ and $F^-$ made to pH 2.7 with $H_2SO_4$, the G-value of $Fe^{3+}$ -$F^-$ complex formation is $13.7 \pm 0.3$ per 100 eV energy absorbed. This G-value is in good agreement with the initial G-value 13.75 of the Fricke dosimeter at pH 2.74.

**13567.** Hauge, R. H., Margrave, J. L., Hastie, J. W., **Infrared spectra of matrix isolated $ZrF_2$, $ZrF_3$, and ZrF,** *High Temp. Sci.* **5,** 89-96 (1973).

Key words: Entropy; geometry; infrared spectra; matrix isolation; stability; $ZrF_2$, $ZrF_3$, $ZrF_4$, $CaF_2$.

By using the multiple Knudsen cell technique the equilibrium species $ZrF_2$, $ZrF_3$, and $ZrF_4$ have been produced and isolated in rare gas solid matrices. From infrared spectra, the antisymmetric stretch frequencies have been assigned for each species. Isotope shift measurements indicate a $120° \pm 4°$ bond angle for the $C_{2v}$-$ZrF_2$ species, the symmetry being verified by the observation of the symmetric stretch frequency. The results are compared with those of the Ti-F and similar systems. The measured frequencies and bond angle of $ZrF_2$ were used to determine the entropy and FEF data for $ZrF_2$ at various temperatures.

**13568.** Hastie, J. W., **Mass spectrometric studies of flame inhibition: Analysis of antimony trihalides in flames,** *Combust. Flame* **21,** 49-54 (1973).

Key words: Antimony trihalides; flame inhibition; flames; mass spectrometry.

The chemistry of $SbBr_3$ and $SbCl_3$ in 1 atm premixed fuel rich $CH_4$-$O_2$ and $CH_4$-$O_2$-$N_2$ flames has been studied. Using line-of-sight mass spectrometric techniques, concentration profiles were obtained for the major species $SbX_3$, HX, $CH_3X$, X, Sb, and SbO, where $X = Br$ or Cl. Reaction mechanisms are indicated and their relation to flame inhibition discussed. Evidence for a negligible perturbation of the flame kinetics by the sampling procedure is given.

**13569.** Mittag, K., **Kapitza conductance and thermal conductivity of copper niobium and aluminum in the range from 1.3 to 2.1 K,** *Cryogenics* **13,** No. 2, 94-99 (Feb. 1973).

Key words: Aluminum; copper; heat transfer; Kapitza conductance; niobium; superfluid helium; thermal conductivity.

The Kapitza conductance and thermal conductivity of ofhc-copper, niobium, ultra high purity aluminium, and of the aluminium alloy 6061 A1 have been measured in the temperature range from 1.3 to 2.1 K, yielding both quantities in the same steady state experiment. The temperature dependence of the Kapitza conductance, $h_0$, was between $T^{3.3}$ and $T^{4.6}$ for the different samples, which is higher than the most frequently observed $T^3$ dependence. The magnitude of $h_0$ for both ofhc-copper and aluminium agrees well at 1.9 K with an empirical prediction, but for niobium it is a factor of two to four lower than the value predicted. At 1.9 K, $h_0$ is higher by a factor of two for an annealed and chemically polished niobium sample than for an untreated sample. The thermal conductivity measured from ofhc-copper and 6061 A1 as in good agreement with the value calculated from the resistivity of these materials and the Wiedemann-Franz law. The measured thermal conductivity obtained for an annealed niobium sample is a factor of 2.8 higher than the highest published value.

**13570.** Daney, D. E., McConnell, P. M., Strobridge, T. R., **Low-temperature nitrogen ejector performance,** (Proc. 1972 Cryogenic Engineering Conf., Boulder, Colo., Aug. 9-11, 1972), Paper L-4 in *Advances in Cryogenic Engineering* **18,** 476-485 (Plenum Press, New York, N.Y., 1973).

Key words: Cryogenic ejector; ejector; ejector pump; jet pump; low temperature refrigeration; refrigeration.

The primary objective of the test program reported here was to obtain a nitrogen ejector to replace the Joule-Thomson valve in a Joule-Thomson refrigerator. The desired primary nozzle inlet conditions were 200 atm and 161 K with a flow rate of 16.6 g/s, and the required entrainment ratio was 0.145. In an attempt to find a near optimum ejector for the above conditions, and in order to obtain a more general knowledge of low temperature nitrogen ejector performance, the tests were run over a range of operating conditions. The primary nozzle supply pressure ranged from 35 to 200 atm with a temperature near 161 K. The discharge pressure varied from 1.2 to 1.6 atm, and the entrainment ratio varied from 0.0 to 0.5. Combinations of three primary nozzles with three mixing sections resulted in a range of 118 to 365 for the ratio of the mixing tube area to the primary nozzle throat area. For the design conditions given above, a suction pressure of 0.27 atm was obtained. This corresponds to a liquid nitrogen saturation temperature of 67.7 K.

**13571.** Evans, J. P., **High temperature platinum resistance thermometry,** (Proc. 5th Symp. on Temperature, Its Measurement and Control in Science and Industry, Washington, D.C., June 21-24, 1971), Paper in *Temperature, Its Measurement and Control in Science and Industry,* H. H. Plumb, Editor-in-Chief, **4,** Part 2, 899-906 (Instrument Society of America, Pittsburgh, Pa., 1972).

Key words: Freezing point; gold point; high temperature; platinum resistance thermometer; standard thermocouple; temperature scale.

During the past decade a number of investigators have worked on various aspects of high temperature platinum resistance thermometry with the aim of developing thermometers suitable for use as interpolating instruments on a practical temperature scale up to the gold point. Long-time stability studies have been made of thermometers employing several designs and a variety of insulating and protecting materials; factors affecting the use of thermometers for temperature measurement have been investigated; new electrical instruments, using both direct and alternating current, have been developed to facilitate the measurement of thermometer resistance; and the investigation of metal freezing points as fixed points for calibrating thermometers has been extended to higher temperatures. An intercomparison of standard thermocouples and high temperature platinum resistance thermometers has shown that a practical temperature scale based on resistance thermometry can be realized at least an order of magnitude more precisely than a scale based on thermocouples, and several workers have suggested interpolation schemes for resistance thermometer scales. This paper reviews recent developments in high temperature platinum resistance thermometry, its current status, and some of the problem areas that need further attention.

**13572.** Powell, R. L., **Revision of the standard reference data for thermocouples,** (Proc. 5th Symp. on Temperature, Its Measurement and Control in Science and Industry, Washington, D.C., June 21-24, 1971), Paper in *Temperature, Its Measurement and Control in Science and Industry,* H. H. Plumb, Editor-in-Chief, **4,** Part 3, 1579-1584 (Instrument Society o America, Pittsburgh, Pa., 1972).

Key words: Standard Reference Data; thermocouples.

Revision of the International Practical Temperature Scal requires that there be changes for all accurately tabulated thermophysical values. Revised reference data for thermocouple have been generated in a cooperative program between group of the National Bureau of Standards in Boulder and Gaithersburg. The new reference data reflect not only revisions in th temperature scale, but also slight changes in the materials themselves and improvements in data fitting methods. A new NB monograph that contains tables, analytic expressions, variou approximations, and explanatory text has been prepared. A general discussion of the project and some specific examples wil be given.

**13573.** Cezairliyan, A., **Measuring transient high temperatures b optical pyrometry,** (Proc. 5th Symp. on Temperature, Its Measurement and Control in Science and Industry, Washington D.C., June 21-24, 1971), Paper in *Temperature, Its Measurement and Control in Science and Industry,* H. H. Plumb, Editor-in-Chief, **4,** Part 1, 657-664 (Instrument Society of America, Pittsburgh, Pa., 1972).

Key words: High-speed measurements; high temperature pyrometry; radiation; temperature measurement.

Various pyrometric (optical) methods, using photoelectric an photographic detectors, are described for measuring high temperatures. Emphasis is placed on techniques of measurin transient temperature of solids above approximately 1500 K with subsecond (upper millisecond to upper microsecond resolution. Advantages and limitations of the various method are discussed and estimates of uncertainties are given. Example of application of the high-speed temperature measuremen methods to various fields of investigations, including determination of thermophysical properties, is presented.

**13574.** Meijer, P. H. E., **Calculations on the specific heat and th susceptibility of interacting spin systems,** (Proc. 5th Symp. o Temperature, Its Measurement and Control in Science and Industry, Washington, D.C., June 21-24, 1971), Paper i *Temperature, Its Measurement and Control in Science an Industry,* H. H. Plumb, Editor-in-Chief, **4,** Part 1, 1267-127 (Instrument Society of America, Pittsburgh, Pa., 1972).

Key words: Dipole-dipole interactions; low temperatur salts; specific heat; susceptibility.

The corrections on the specific heat and susceptibility due t dipole-dipole interactions in a number of low temperature compounds are calculated. A general description of the method i given, followed by a short discussion of the properties of th most used low temperature compounds. Eight representativ salts were chosen and the deviations from the ideal specific hea and susceptibility in second and third order were determined.

**13575.** Cataland, G., Plumb, H. H., **The realization of low temperature fixed points on the NBS acoustical and the NBS-195 temperature scales,** (Proc. 5th Symp. on Temperature, It Measurement and Control in Science and Industry, Washington, D.C., June 21-24, 1971), Paper in *Temperature, Its Measurement and Control in Science and Industry,* H. H. Plumb Editor-in-Chief, **4,** Part 1, 183-193 (Instrument Society o America, Pittsburgh, Pa., 1972).

Key words: Acoustical thermometry; e-$H_2$ NBP-e-$H_2$ T fixed points; neon NBP.

The normal boiling and triple points of equilibrium hydroge have been realized and related to the NBS (1955) temperatur ble. From isotherms that were determined with the NBS oustical thermometer, values of T(acoustical) can be asciated with the above fixed points and also with the normal iling point.

**576.** Quinn, T. J., Lee, R. D., **Vacuum tungsten strip lamps with improved stability as radiance temperature standards,** (Proc. 5th Symp. on Temperature, Its Measurement and Control in Science and Industry, Washington, D.C., June 21-24, 1971), Paper in *Temperature, Its Measurement and Control in Science and Industry,* H. H. Plumb, Editor-in-Chief, **4,** Part 1, 395-411 (Instrument Society of America, Pittsburgh, Pa., 1972).

Key words: Pyrometry; source; temperature; tungsten.

This paper describes the changes which take place in a piece tungsten strip as it is outgassed and aged during the processing a vacuum tungsten strip lamp. It is shown that by paying sufficient attention to the cleaning of the tungsten and the glass bulb, id to the outgassing and aging of the tungsten, a very stable rip lamp can be produced. Results are given of a series of stalility tests from 1064 to 1500 °C of a group of lamps made in this ay at NBS.

**577.** Bedford, R. E., Ma, C. K., Barber, C. R., Chandler, T. R., Quinn, T. J., Burns, G. W., Scroger, M., **New reference tables for platinum 10% rhodium/platinum and platinum 13% rhodium/platinum thermocouples,** (Proc. 5th Symp. on Temperature, Its Measurement and Control in Science and Industry, Washington, D.C., June 21-24, 1971), Paper in *Temperature, Its Measurement and Control in Science and Industry,* H. H. Plumb, Editor-in-Chief, **4,** Part 3, 1585-1602 (Instrument Society of America, Pittsburgh, Pa., 1972).

Key words: Blackbodies; calibrations; optical pyrometer; platinum resistance thermometer; platinum-rhodium vs platinum thermocouples; reference tables; thermometric fixed points.

New reference tables for platinum 10 percent rhodium/platinum and platinum 13 percent rhodium/platinum thermocouples have been prepared as a result of a cooperative program among the National Bureau of Standards (USA), the National Physical Laboratory (UK), and the National Research Council (Canada). High purity platinum wires ($\alpha \geq 1.3924 \times 0^{-3}$) and alloy wires of as closely as possible 10 percent and 13 ercent rhodium composition, respectively, were supplied by even American and British manufacturers, from which thirty-wo Pt10Rh/Pt and thirty-six Pt13Rh/Pt thermocouples were onstructed. Primary calibrations below 1064.43 °C were performed at NBS and NRC; primary calibrations above 1064.43 C were done at NPL; thermocouple intercomparisons over the whole temperature range were done at NBS and NRC. The eference tables derive from polynomials fitted, by means of east squares orthogonal polynomial techniques, to a selected group of thermocouples of each type.

**3578.** Hudson, R. P., Pfeiffer, E. R., **Temperature scale for cerous magnesium nitrate,** (Proc. 5th Symp. on Temperature, Its Measurement and Control in Science and Industry, Washington, D.C., June 21-24, 1971), Paper in *Temperature, Its Measurement and Control in Science and Industry,* H. H. Plumb, Editor-in-Chief, **4,** Part 2, 1279-1285 (Instrument Society of America, Pittsburgh, Pa., 1972).

Key words: Cerous magnesium nitrate; low temperature; magnetic temperature; temperature scale; thermometry.

Below 1 K, cerous magnesium nitrate (CMN) should obey the Curie Law over a wide temperature range and show deviations only in consequence of the dipolar coupling between ions. The susceptibility deviation should be accounted for by a very small Curie-Weiss $\theta$ (theoretical value, 0.27 mK) and the entropy should vary as $\ln 2 - AT^{-2} + BT^{-3} - CT^{-4} + ...$, with theoretical values now available for A, B and – somewhat less firmly based – C. These show that representation of S(T) by the term in A alone is justifiable only above 0.1 K. We present experimental values for A, B, and C arising from recent measurements together with new results for the magnetic temperature, T*, scale derived from $\gamma$-ray heating calorimetry.

**13579.** Anderson, R. L., **The high temperature stability of platinum resistance thermometers,** (Proc. 5th Symp. on Temperature, Its Measurement and Control in Science and Industry, Washington, D.C., June 21-24, 1971), Paper in *Temperature, Its Measurement and Control in Science and Industry,* H. H. Plumb, Editor-in-Chief, **4,** Part 2, 927-934 (Instrument Society of America, Pittsburgh, Pa., 1972).

Key words: Chemical changes in platinum resistance thermometers; high temperature platinum resistance thermometers; physical changes in platinum resistance thermometers; stability of platinum resistance thermometers.

Some of the chemical and physical parameters that affect the stability of platinum resistance thermometers have been studied, particularly at temperatures near the gold point (1064 °C). A simplified form of resistance thermometer sensor was designed to aid in these studies. The new design, designated as the "steeple," allowed the fabrication of some thermometers from single crystals. Measurements were made of the resistance at the triple point of water after the thermometers had been held above 1000 °C for extended periods. Further information on the aging of platinum wires at high temperatures was obtained with the scanning electron microscope. Some of the results are shown to be applicable to standard thermometers when used above 400 °C.

**13580.** Powell, R. L., Hall, W. J., Hust, J. G., **The fitting of resistance thermometer data by orthogonal functions,** (Proc. 5th Symp. on Temperature, Its Measurement and Control in Science and Industry, Washington, D.C., June 21-24, 1971), Paper in *Temperature, Its Measurement and Control in Science and Industry,* H. H. Plumb, Editor-in-Chief, **4,** Part 2, 1423-1431 (Instrument Society of America, Pittsburgh, Pa., 1972).

Key words: Numerical analysis; orthogonal functions; resistance thermometer.

Analyses of highly accurate thermal data require sophisticated fitting methods so that expensively obtained experimental precision will not be negated by inadequate mathematical techniques. This article describes fitting methods using orthogonal functions that have been used for several years to fit many types of data, including germanium resistance curves. The method is a generalization and extension of ideas suggested earlier by Lanczos for fitting noisy data. The method usually cleanly separates noise from the fundamental signal in a straightforward manner, allowing one to avoid either an oscillating overfit or an inaccurate underfit. The procedure consists of five parts: (1) transformation of variables so that the curve is as linear as possible in the transformed variables; (2) weighting of data to satisfy the Gauss-Markoff conditions with the weighting function inversely proportional to the experimental variance; (3) orthogonal function generation and coefficient determination using Gram-Schmidt type algorithms developed by Bjorck; (4) separation of noise coefficients from the fundamental signal coefficients based on their different dependence on the number of terms; and (5) calculation of smoothed data using the proper number of coefficients.

**13581.** Jacox, M. E., Milligan, D. E., **Matrix isolation study of the vacuum-ultraviolet photolysis of methanol. The infrared spectrum of the $CH_2OH$ free radical,** *J. Mol. Spectrosc.* **47,** No. 1, 148-162 (July 1973).

Key words: $CH_2OH$; force constants; infrared spectrum; matrix isolation; methanol; vacuum-ultraviolet photolysis.

Infrared studies of the products of the 1470 Å photolysis of normal and isotopically substituted methanol isolated in argon and nitrogen matrices at 14 K have provided evidence for the stabilization of a significant yield of $CH_2OH$. Assuming a slightly nonplanar structure for the molecule, it has been possible to obtain an approximate valence-force potential field which provides a reasonable fit to virtually all of the data. The C-O bond of $CH_2OH$ is slightly stronger than that of methanol, and the torsional barrier is significantly greater, in accord with previous electron spin resonance observations. There is no evidence for the production or stabilization of $CH_3O$ in the matrix. $CH_2OH$ undergoes photodecomposition upon exposure to radiation in the 2300-2800 Å spectral region, leading to a growth in the HCO absorptions.

**13582.** Liebman, J. F., **On the electron affinity of perfluorocycloalkanes and perfluoroalkanes,** *J. Fluorine Chem.* **3,** 27-33 (1973/74).

Key words: Electron affinity; fluorocarbons; orbital; perfluoroalkanes; perfluorocycloalkanes.

There is an increasing body of evidence showing that perfluorocycloalkanes have a higher electron affinity than their open chain analogs, the perfluoroalkanes. A new molecular orbital model is presented to explain these results and compared with the electrostatic model of Mittal and Libby. Explicit experiments are suggested which would allow comparison of the two models.

**13583.** Smith, R. L., Honda, T., **Impulse rise and fall times of biplanar vacuum photodiodes,** *Appl. Opt.* **12,** No. 7, 1606-1610 (July 1973).

Key words: Biplanar vacuum photodiodes; impulse fall time; impulse rise time; laser pulses.

The impulse rise and fall times of biplanar vacuum photodiodes are experimentally investigated by the use of a single ultrashort laser pulse from a train of mode-locked pulses. It was confirmed that the impulse rise time is a function of the photoelectrons' transit time from photocathode to anode, and that the impulse fall time is 2.2 times the capacitance of the photodiode and the resistive component of the load.

**13584.** Reader, J., **Comment on: How to mount a Pellin-Broca prism for laser work,** *Appl. Opt.* **12,** No. 7, 1405 (July 1973).

Key words: Pellin-Broca prism; spectroscope.

It is shown that a recently published mounting for constant deviation prisms is equivalent to one published in 1917. An example of the use of this mounting for a plane grating spectrograph at NBS is given.

**13585.** Burns, G. W., Hurst, W. S., **Studies of the performance of W-RE type thermocouples,** (Proc. 5th Symp. on Temperature, Its Measurement and Control in Science and Industry, Washington, D.C., June 21-24, 1971), Paper in *Temperature, Its Measurement and Control in Science and Industry,* H. H. Plumb, Editor-in-Chief, **4,** Part 3, 1751-1766 (Instrument Society of America, Pittsburgh, Pa., 1972).

Key words: Beryllium oxide; ductility; emf-temperature relationship; microstructure; thermocouple drift; W-Re alloys; W-Re type thermocouples; W-Re thermoelements.

The effect of exposure of bare-wire and BeO-insulated commercial W-Re thermocouple materials to high temperatures in gaseous environments has been investigated. The temperature range of interest has been primarily 2000 to 2400 K, and the investigations have been confined to thermocouple wires of 0.25 mm diameter. With high temperature exposure of the bare thermoelements, an initial shift in the emf-temperature relationship of the exposed thermoelements versus an unexposed "as received" thermoelement was exhibited, and thereafter no discernible drift occurred with exposure in environments of Ar He, $H_2$ or $N_2$ for periods up to 1000 hours. Aging studies were performed to determine the time-temperature parameters of the shift. Thermoelements were examined for metallurgical structural changes and chemical changes by conventional methods. In the temperature range of interest, grain growth was inhibited in the chemically doped W-3 percent Re alloy, and excellent room temperature ductility was retained subsequent to the exposure The compatibility of high purity (in excess of 99.8 percent), sintered BeO insulators with the thermoelements differed, depending upon whether the BeO-insulated thermoelement assemblies were self-heated electrically or heated in a furnace; in tests in argon environments, highly reliable performance occurred when the assemblies were heated in a furnace. BeO-insulated W-3 percent Re vs W-25 percent Re thermocouples, constructed with degassed and aged materials, exhibited drifts equivalent to about 3 mK/h during 1000 hours of exposure at 2073 K in argon while in the presence of tantalum.

**13586.** Furukawa, G. T., Bigge, W. R., Riddle, J. L., **Triple point of argon,** (Proc. 5th Symp. on Temperature, Its Measurement and Control in Science and Industry, Washington, D.C., June 21-24, 1971), Paper in *Temperature, Its Measurement and Control in Science and Industry,* H. H. Plumb, Editor-in-Chief, **4,** Part 1C, 231-243 (Instrument Society of America Pittsburgh, Pa., 1972).

Key words: Argon; fixed point; triple point; temperature scale.

The average triple-point (TP) temperature of two argon cells was determined to be $83.7997_7$K, the two cells being within 0.38 mK of each other and the estimated uncertainty of the value being ±0.5 mK. (The uncertainty includes imprecision of the measurements and possible systematic errors.) The temperature value is based on thermometers calibrated in terms of the NBS-1955 temperature scale adjusted to the International Practical Temperature Scale of 1968 (IPTS-68). The value of temperature obtained by extrapolating the deviation function, $\Delta W_4(T)$ specified for the temperature interval 90.188 K to 273.15 K by the IPTS-68, is about 0.3 mK lower. The argon TP is recommended as a defining fixed point to replace the oxygen normal boiling point.

**13587.** Kamper, R. A., **Survey of noise thermometry,** (Proc. 5th Symp. on Temperature, Its Measurement and Control in Science and Industry, Washington, D.C., June 21-24, 1971) Paper in *Temperature, Its Measurement and Control in Science and Industry,* H. H. Plumb, Editor-in-Chief, **4,** Part 1 349-354 (Instrument Society of America, Pittsburgh, Pa. 1972).

Key words: Absolute temperature; thermal noise; thermometry.

This survey covers various techniques which have been developed to estimate relative or absolute temperatures by measuring various parts of the spectrum of thermal noise at frequencies in the microwave range and below. It includes a report of the author's own work on absolute noise thermometry in the millikelvin range of temperature.

**3588.** Guildner, L. A., Anderson, R. L., Edsinger, R. E., **Effects of sorption on the realization of the thermodynamic scale,** (Proc. 5th Symp. on Temperature, Its Measurement and Control in Science and Industry, Washington, D.C., June 21-24, 1971), Paper in *Temperature, Its Measurement and Control in Science and Industry,* H. H. Plumb, Editor-in-Chief, **4,** Part 1E, 313-322 (Instrument Society of America, Pittsburgh, Pa., 1972).

Key words: Gas thermometer; sorption; steam point; thermodynamic temperature scale.

The NBS Gas Thermometer is of the constant volume type. It as a 450 cm³ platinum-20% rhodium bulb connected by a 0.9 mm internal diameter tube to a diaphragm at room temperature. he measured quantities contribute an estimated uncertainty of parts per million. The gas thermometer has such stability that, pon return to the fiducial temperature, the pressure is eproduced within one or two parts per million for periods of a eek or more. This stability is attributed to a marked reduction f sorption effects achieved by the following: (1) The thermomeer bulb is subjected to prolonged pumping at high temperatures rior to measurements. (2) With most of the contaminants emoved by this procedure, and the use of very pure helium as a hermometric fluid, there is too little active gas left to produce eratic results from sorption. The value of the temperature at the team point on the thermodynamic Celsius scale has been determined as 99.973 °C. A final certainty is not assigned.

**3589.** Gonano, R., **Isothermal comparisons of He³ and He⁴ vapor pressures,** (Proc. 5th Symp. on Temperature, Its Measurement and Control in Science and Industry, Washington, D.C., June 21-24, 1971), Paper in *Temperature, Its Measurement and Control in Science and Industry,* H. H. Plumb, Editor-in-Chief, **4,** Part 1, 121-126 (Instrument Society of America, Pittsburgh, Pa., 1972).

Key words: Helium; pressure measurement; temperature scale; vapor pressure.

Isothermal measurements of He³ and He⁴ vapor pressures are eing made in order to compare proposed vapor pressure scales n the region 0.90 to 3.32 K. Preliminary results in the range 1.40 o 3.25 K show that the currently accepted scales, $T_{62}$ and $T_{58}$, re in close agreement with each other as was intended during he construction of $T_{62}$. Observed differences are less than 0.6 mK (rms deviation = 0.22 mK), which is within the experimental uncertainty of the present comparison. No systematic pattern is detectable in the deviations. A comparison of germanium resistance thermometers calibrated on the NBS Provisional Scale 2-20 (1965) with the vapor pressure scales shows that $T_{2\text{-}20} - T_{vp}$ ranges from 6 mK at 2.3 K to 10 mK at 4.2 K, in agreement with other published values. We also discuss the techniques used o reduce or eliminate the effects on vapor pressure measurements of the aerostatic and thermomolecular pressure gradients and of the heat load due to superfluid film flow.

**13590.** Lee, R. D., Kostkowski, H. J., Quinn, T. J., Chandler, P. R., Jones, T. P., Tapping, J., Kunz, H., **Intercomparison of the IPTS 68 above 1064 °C by four national laboratories,** (Proc. 5th Symp. on Temperature, Its Measurement and Control in Science and Industry, Washington, D.C., June 21-24, 1971), Paper in *Temperature, Its Measurement and Control in Science and Industry,* H. H. Plumb, Editor-in-Chief, **4,** Part 1, 377-393 (Instrument Society of America, Pittsburgh, Pa., 1972).

Key words: International temperature scale; pyrometry; standards; temperature.

The International Practical Temperature Scale above the melting point of gold, as realized and maintained with high precision photoelectric pyrometers at NBS, NPL, NSL and PTB, has been intercompared. Six specially selected tungsten strip lamps, four vacuum and two gas, were used in the intercomparison. Determinations were made at a number of brightness temperatures from 1064 to 1700 °C and at 2200 °C with the laboratories agreeing to within a few tenths of a degree up to 1700 °C and 2.0 °C at 2200 °C.

**13591.** Schooley, J. F., Soulen, R. J., Jr., **The use of superconductors to provide fixed points on a cryogenic temperature scale,** (Proc. 5th Symp. on Temperature, Its Measurement and Control in Science and Industry, Washington, D.C., June 21-24, 1971), Paper in *Temperature, Its Measurement and Control in Science and Industry,* H. H. Plumb, Editor-in-Chief, **4,** Part 1, 169-174 (Instrument Society of America, Pittsburgh, Pa., 1972).

Key words: Fixed points; OSRM; superconductive devices; superconductive transition temperature; superconductivity; temperature scale.

It is suggested that reproducible superconductive transition temperatures be used as fixed points for temperature scales below 10K. The superconductive transitions of lead, indium, aluminum, zinc, and cadmium have been found to be as narrow as one millikelvin and reproducible to less than one millikelvin. It is planned that devices incorporating these elements will be made available through the NBS Office of Standard Reference Materials.

**13592.** Ginnings, D. C., Reilly, M. L., **Calorimetric measurement of thermodynamic temperatures above 0 °C using total blackbody radiation,** (Proc. 5th Symp. on Temperature, Its Measurement and Control in Science and Industry, Washington, D.C., June 21-24, 1971), Paper in *Temperature, Its Measurement and Control in Science and Industry,* H. H. Plumb, Editor-in-Chief, **4,** Part 1, 339-348 (Instrument Society of America, Pittsburgh, Pa., 1972).

Key words: Blackbody; calorimeter; ice point; steam point; Stefan-Boltzmann law; thermodynamic temperature scale.

Using the Stefan-Boltzmann law, a thermodynamic temperature can be determined by measuring the ratio of blackbody radiation at the unknown temperature to that at the triple point of water. This measurement requires no knowledge either of radiation constants or of geometry. For the above measurements, there has been developed a heat-flow calorimeter operating at liquid helium temperatures in which extremely small powers can be accurately measured. The radiant power absorbed by the calorimeter is measured by substituting known electrical power; if these powers are equal the substitution results in no change in the temperature of the calorimeter.

The calorimeter was originally intended for measuring the thermodynamic temperature of the melting point of gold, but as a check on its performance, measurements are being made of the ratio of radiation at 100 °C to that of 0 °C (IPTS-68). Performance tests show the calorimeter to be sensitive to a change of about 0.002 °C in the temperature of the radiator with the chosen aperture system. There is now in progress an investigation of possible errors of the measurements, including any effect of diffraction.

**13593.** Ely, J. F., Hanley, H. J. M., Straty, G. C., **Analysis of the pressure virials and Clausius-Mossotti function for polyatomic gases,** *J. Chem. Phys.* **59,** No. 2, 842-848 (July 15, 1973).

Key words: Clausius-Mossotti function; dielectric virial coefficients; m-6-8 potential; polarizability; polyatomic gases; pressure second virial coefficients; quadrupole moment; statistical mechanics.

Statistical mechanical equations for the second pressure virial coefficient and the second and third dielectric virial coefficients for quadrupolar molecules are evaluated using the *m*-6-8 potential function. The results are compared with experimental data for nitrogen and fluorine. An approximate value for the quadrupole moment of fluorine is estimated. Agreement between theory and experiment is generally good.

**13594.** Sugar, J., **Ionization energies of the neutral actinides,** *J. Chem. Phys.* **59,** No. 2, 788-791 (July 15, 1973).

Key words: Actinium; americium; berkelium; californium; curium; einsteinium; fermium; ionization energy; mendelevium; neptunium; nobelium; plutonium; protactinium; thorium; uranium.

Values for the ionization energies of the neutral actinides have been derived by utilizing interpolated spectral properties of these atoms. The results in electron volts are Ac: 5.17(12); Th: 6.08(12); Pa: 5.89(12); U: 6.05(7); Np: 6.20(12); Pu: 6.06(2); Am: 5.993(10); Cm: 6.09(2); Bk: 6.30(9); Cf: 6.41(10); Es: 6.52(10); Fm: 6.64(11); Md: 6.74(12); No: 6.84(12).

**13595.** Brown, W. C., Buchanan, C. J., **A study of the strength capabilities of children ages two through six,** *NBSIR 73-156,* 56 pages, (Aug. 7, 1973). (Available as COM 73-11286 from the National Technical Information Service, Springfield, Va. 22151.)

Key words: Children; children's strength; pull; push; safety; strength; squeeze; test methods; toys; toy safety; twist.

The Child Strength Study was conducted to provide information which can be used to develop reliable and realistic standards and test methods for children's toys. The study was conducted on over 550 children in the Washington Metropolitan area, and included both black and white children with varying economic and social backgrounds.

Four test devices were used to measure the forces exerted by children when pushing, pulling, twisting, and squeezing. Quantitative relationships were found to exist between these four types of measurements. The study also provided quantitatively precise and useful information about the effects of age and sex on the strength capability of children two through six years old. The results of the study are exhibited in tables of averages, standard deviations, coefficients of variation, and 95th percentiles for each age and sex group tested. A number of graphs are also included for a quick appraisal of the test results.

**13596.** Craw, A. R., **Analyses for decision in the office of flammable fabrics: the level of the standard,** *NBSIR 73-182,* 90 pages, (Apr. 1973). (Available as COM 73-11284 from the National Technical Information Service, Springfield, Va. 22151.)

Key words: Children's sleepwear; decision analysis; flammable fabrics; probability assessment; standards; utility theory.

The fundamentals of a single-stage decision problem are discussed and illustrated in the problem: The Level of the Standard for Children's Sleepwear, originally discussed by M. Tribus. Outcomes are identified, and various potential measures of disutility are discussed.

Given a particular alternative is in effect one must assign the conditional probabilities of arriving at each outcome. This process is aided by introducing intermediate events (extending the conversation). For the children's sleepwear problem this is done by considering for each of two age groups and three income levels the probability tree with branches: alternatives (a), technology (T), nightwear (N), additional cost to the consumer (C), Use (U) or non-use (u), existence of a hazard (H), exposur (E), ignition (I), burn (B) and burn-severity ($B_i$), survival (S) or death (D) and body image ($I_d$).

Attention is given to the preliminary assignment of each of th conditional probabilities needed. Suggestions are made as t sources of information. Much of the needed information is no available, especially that dealing with the social and behaviora aspects of the problem. The concept of exposure to an ignitio hazard, for which an operational definition does not exist, i discussed.

**13597.** Garvin, D., **Chemical kinetics data survey IV. Preliminar tables of chemical data for modelling of the stratosphere** *NBSIR-203,* 95 pages, (May 1973). (Available as COM 73 11288 from the National Technical Information Service Springfield, Va. 22151.)

Key words: Atmospheric chemistry; chemical kinetics data evaluation; energy transfer; gas phase; high temperature air chemistry; ion-molecule reactions; optical absorption cross sections; photochemistry; quantum yield; rat constants.

Chemical kinetic and photochemical data for gas phase reactions pertinent to the chemistry of the stratosphere are presente in four tables. These tables give recommended values and als cite recent experimental work. They give data in the followin subject areas: chemical reactions and photochemistry of neutra species, energy transfer reactions, high temperature air reactions, and ion-molecule reactions.

**13598.** McClenon, R., **General purpose scientific document cod operations under Exec 8,** *NBSIR 73-198,* 21 pages, (Ma 1973). (Available as COM73-11289 from the Nationa Technical Information Service, Springfield, Va. 22151.)

Key words: Character codes for scientific text; computerized text processing; NBS computer system; scientifi text; users manual.

Operating procedures for the use of the General Purpos Scientific Document Code text handling system are describe These apply to the use of the system on the NBS 1108 compute under control of the Exec 8 supervisor. Control cards, file defin tion and handling, compilation of routines and execution of programs are described. Examples of typical runs are given. The report is a manual for users of the system.

**13599.** Furukawa, G. T., Riddle, J. L., Bigge, W. R., **Investigatio of freezing temperatures of National Bureau of Standards ti standards,** (Proc. 5th Symp. on Temperature, Its Measurement and Control in Science and Industry, Washington, D.C June 21-24, 1971), Paper in *Temperature, Its Measuremen and Control in Science and Industry,* H. H. Plumb, Editor-in Chief, **4,** Part 1D, 247-263 (Instrument Society of Americ Pittsburgh, Pa., 1972).

Key words: Fixed point; freezing point; standards; tin; ti point.

The intercomparison of freezing points was made on selecte samples of tin from two series of standards that are nominall 99.9999 (6N) and 99.999 (5N) percent pure. The freezing poi of each tin-point cell prepared from the samples is reproducib within 0.05 mK from freeze to freeze; the freezing points of th cells from each series agree with each other within ±0.1 mK The freezing points of the 5N standard are on the average 0. mK lower than those of the 6N standard. On the basis of th chemical purity information on the samples, the freezing-point o the 6N samples is expected to be within less than ±0.7 mK o the freezing point of 100 percent pure tin.

600. Fraker, A. C., Ruff, A. W., Yeager, M. P., **Corrosion of itanium alloys in physiological solutions,** (Proc. 2nd Int. Conf. on Titanium, Boston, Mass., May 2-5, 1972), Paper in *Titanium Science and Technology,* R. I. Jaffee and H. M. Burte, Eds., **4,** 2447-2457 (Plenum Publishing Corp., New York, N.Y., 1973).

Key words: Alloys; biological; corrosion; electron microscopy; implant; saline solution; titanium.

This study intends to determine corrosive effects of saline and ganic solutions on several titanium alloys for potential use as ological implant materials. Experimental techniques included ectrochemical measurements and thin foil transmission elec- on microscopy and diffraction. The effects of varying alloy mposition, method of specimen preparation, and different or- nic and salt solutions were studied. Thin foil transmission elec- on microscopy was used to examine surfaces of specimens ex- sed to salt solutions containing albumin, cystine, alanine and ic acid.

601. Furukawa, G. T., **Vapor pressures of $^{20}$Ne and $^{22}$Ne,** (Proc. 5th Symp. on Temperature, Its Measurement and Control in Science and Industry, Washington, D.C., June 21-24, 1971), Paper in *Temperature, Its Measurement and Control in Science and Industry,* H. H. Plumb, Editor-in-Chief, **4,** Part 1B, 127-135 (Instrument Society of America, Pittsburgh, Pa., 1972).

Key words: Fixed point; $^{nat}$Ne; $^{20}$Ne; $^{22}$Ne; neon; vapor pressure.

The results of the vapor-pressure measurements with pure eon isotopes $^{20}$Ne and $^{22}$Ne are described. The measurement ecision is ±0.1 to ±0.2mK. The vapor pressures of $^{nat}$Ne cal- lated from the law for ideal solutions and the data on the pure eon isotopes are in agreement with the observed values on Ne within about ±0.5 mK. A table of normal boiling point mperature as a function of composition of "$^{nat}$Ne" is given.

602. Fraker, A. C., Ruff, A. W., **The effect of solution pH on the saline water corrosion of titanium alloys,** (Proc. 2nd Int. Conf. on Titanium, Boston, Mass., May 2-5, 1972), Paper in *Titanium Science and Technology,* R. I. Jaffee and H. M. Burte, Eds., **4,** 2655-2663 (Plenum Publishing Corp., New York, N.Y., 1973).

Key words: Corrosion; electron microscopy; pressure; salt water; titanium.

The initial stages of corrosion attack on several titanium alloys saline water solutions have been studied. Transmission elec- on microscopy and electron diffraction were used to study the orrosion films formed on the exposed surfaces of thin foil ecimens and to determine their degree of crystallinity and omposition. The corrosion sensitivity of each material to pH ariation was studied. Six different alloys were examined over e range 100-200 °C in a Hastelloy-C pressure vessel contain- g the 3.5 wt. pct. NaCl solution. Sulfuric acid, hydrochloric cid and sodium hydroxide were added singly to the saline solu- on for individual tests with pH values ranging from 1.8 to 12.5. e find that the surface oxide composition changes with dif- erent solution pH values. The oxide covering the surface after xposing in neutral and acid solutions does not occur in alkaline olutions. Examples of local pitting attack were found to occur t both high and low pH values but were more frequent when pecimens were corroded in the alkaline solutions.

3603. Hust, J. G., Powell, R. L., Sparks, L. L., **Methods for cryogenic thermocouple thermometry,** (Proc. 5th Symp. on Temperature, Its Measurement and Control in Science and Industry, Washington, D.C., June 21-24, 1971), Paper in *Temperature, Its Measurement and Control in Science and Industry,* H. H. Plumb, Editor-in-Chief, **4,** Part 3, 1525-1535 (Instrument Society of America, Pittsburgh, Pa., 1972).

Key words: Cryogenics; thermocouples; thermometry.

Accurate cryogenic thermocouple thermometry is only possible if care is taken in material selection, general experimental design, thermocouple calibration and assembly, and measurement techniques. After several years' research on both calibration and usage of thermocouples, we have developed procedures and tests that minimize experimental temperature errors and give realistic estimates of the inaccuracies.

Some material selection criteria are listed and recommendations are given for a few common experimental conditions. Simple experimental systems are described that may be used for tests to determine static or dynamic short range inhomogeneities, variability and interchangeability of different lots, and deviations from standard values. Methods for adding corrections to the standard tables are also given.

Good design criteria and methods of thermocouple assembly can lead to significant improvement in accuracies. Specific topics of discussion include reference junction placement, thermal tempering, heat conduction and radiation shielding, electrical connections, and electrical shielding.

**13604.** LaVilla, R. E., **$M_{2,3}$-Region x-ray emission spectrum from gaseous krypton,** *Phys. Rev. A* **8,** No. 2, 1143-1145 (Aug. 1973).

Key words: Double electron single vacancy process; final state configuration interaction; krypton; $M_{2,3}$ x-ray emission; single electron double vacancy process.

The $M_{2,3}$ x-ray emission spectrum of gaseous krypton excited by direct electron bombardment has been recorded with a scanning single-flat crystal spectrometer. The most prominent spectral features are two peaks at 187 and 203 eV, with the 187-eV peak having an extended low-energy tail. This low-energy tail is attributed to double-electron single-vacancy transitions owing to the strong mixing of the final-state configuration $4s4p^6\,{}^2S$ with the even levels $4s^24p^4ns\,{}^2S$ and $4s^24p^4nd\,{}^2S$. The 203-eV peak is identified as probably the single-electron double-vacancy $M_{2,3}M_{2,3} \rightarrow M_{2,3}N_1$ multiplet complex

**13605.** Kuriyama, M., **Dynamical diffraction equations for imperfect crystals,** *Z. Naturforsch.* **28a,** No. 5, 622-626 (1973).

Key words: Canonical transformation; dynamical diffraction; imperfect crystal.

The ray theory of Kato and Kambe for imperfect crystals is derived in a formal way from a general dynamical theory of diffraction. This development together with the results from a previous paper concerning Takagi's equation (the wave theory) helps to clarify the meaning and limits of various phenomenological theories that have been extended to an imperfect crystal from the dynamical diffraction theory for a perfect crystal.

**13606.** Fromhold, A. T., Jr., Kruger, J., **Space-charge and concentration-gradient effects on anodic oxide film formation,** *J. Electrochem. Soc.* **120,** No. 6, 722-729 (June 1973).

Key words: Anodization; corrosion; oxidation.

Numerical computations illustrate the effects of space charge and a concentration gradient on the steady-state mobile-defect concentration profile and the kinetics of anodic film formation. The position-dependence of the concentration of mobile defects producing growth is shown to vary with current density and film thickness. Of especial interest is a series of curves illustrating the total electrostatic potential developed across the oxide as a function of thickness for growth under constant current conditions.

Space charge is shown to have the capability of being a critical factor in retarding the growth rate of the anodic film.

**13607.** Mitchell, R. A., Woolley, R. M., Chwirut, D. J., **Composite-overlay reinforcement of cutouts and cracks in metal sheet,** *NBSIR 73-201*, 96 pages, (Feb. 1973). (Available as COM73-11121 from the National Technical Information Service, Springfield, Va. 22151.)

> Key words: Adhesively bonded joints; composite materials; composite-overlay reinforcement; contour plotting; cracks, reinforcement of; cutouts, reinforcement of; debond analysis, progressive; finite element analysis; joints, adhesively bonded; nonlinear analysis, shear; reinforcement, composite overlay; reinforcement, cutouts and cracks; shear analysis, nonlinear.

Finite element computer programs were developed for the planform analysis and the longitudinal cross-section analysis of metal sheet reinforced by adhesively bonded overlays of composite material. The analyses articulate the separate responses of the metal sheet, the composite overlays, and the adhesive layers. All materials are assumed to be orthotropic and linear elastic, with the provision that nonlinear interlaminar shear deformation can be approximated by a series of stepwise-linear solutions. The computer programs were developed specifically for the study of three general configurations: (1) a sheet with a reinforced cutout; (2) a sheet with a reinforced cutout with two symmetrical transverse cracks, within the sheet, radiating away from the cutout edge; and (3) a sheet with a reinforced transverse crack. The programs are also suitable for the study of bonded lap joints. The principal output of the computer programs is a set of contour plots of stress and strain fields throughout the sheet, the overlays, and the adhesive layers. A series of laboratory tests was conducted to demonstrate the validity of the analyses. Strains measured on the surfaces of specimens representing the general configurations studied were, for the most part, in good agreement with strains predicted by the finite element analyses. Significant correlations between certain failure modes and the stresses computed by the finite element analyses were apparent. Similarities between the modes of failure under static and fatigue loading were also evident.

**13608.** Peiser, H. S., Coyle, T. D., Eby, R. K., **A report on a survey in Korea on standardization and measurement services in support of industrialization goals of Korea.** *NBSIR 73-185*, 41 pages, (June 19-30, 1972).

> Key words: AID; assistance; economics; LDC's (less developed countries); measurement services; standardization; survey; Korea.

The survey of standardization and measurement services for developing industries in Korea has been carried out by NBS with funding by AID, participation by representatives of Ecuador and Turkey, and under the guidance of the Korean Ministers for Commerce and Industry, and for Science and Technology. The Korean Director of the Survey was backed by six Korean Survey Team members and seven senior staff. The Survey Team spent two weeks in Korea where it inspected representative laboratories and plants, and had discussions with leaders of government, the USAID Mission, principal universities and industry. The report describes the preparation for the Survey, a summary of the economy of the country, notes on Korean science and technology, and relevant Korean institutions and laws. Nineteen problems were identified as of concern to national capability for standardization and measurement services. A summary description is given of the various existing and needed functions that Korean government should provide. The idea is endorsed to create a single agency to address all thes functions.

**13609.** Ferguson, J. B., **Summary of flame spread and smok generation tests conducted for Operation BREAKTHROUGH** *NBSIR 73-228*, 27 pages, (July 1973). (Available as PB 222425 from the National Technical Information Service Springfield, Va. 22151.)

> Key words: Carpets; flame spread; kitchen cabinets Operation BREAKTHROUGH; smoke generation; wa and ceiling.

This document is a listing of the flame spread and smok generation results of a range of materials that were tested unde the Operation BREAKTHROUGH housing evaluation program. The test results reported here were obtained under differing conditions and should not be considered the results of a comprehensive and unified research program for evaluation of inter or finish materials. Tables of test results and a brief discussion o the results are presented for walls, ceilings, kitchen cabinets an floor coverings.

**13610.** Siu, C. I., Ellis, W. M., Kusuda, T., **Test of a polyeste composite wall panel for moisture accumulation and potenti removal of moisture through venting,** *NBSIR 73-220*, 18 page (May 1973). (Available as PB 222437 from the Nation Technical Information Service, Springfield, Va. 22151.)

> Key words: Composite wall panel; condensation; humidity moisture; pressure; temperature.

A polyester composite exterior wall panel was exposed to accelerated winter temperature and humidity conditions for th purpose of determining performance with respect to moisture accumulation and release as a result of pressure and temperatur differences. No moisture condensation within the wall syster was detected from visual examinations made at various times o the testing period; no significant increase in gross weight of th wall was found from the direct weighings of the wall system Results also indicate that a wet insulation in such a wall syster is unlikely to be dried out by natural thermal action and convective motion.

**13611.** Rupp, N. W., **Intermediary base and cementation,** Chapte 5 in *Operative Dentistry*, L. Baum, Ed., pp. 59-72 (W. B Saunders Co., Philadelphia, Pa., 1973).

> Key words: Cementation; intermediary base; pulp protection; retention; temporary cementation.

This is a literature review of the dental cements currentl being used for intermediary bases and cementation. Clinical applications of the various cements are discussed relative to phys cal properties and biological response of tooth tissues. Som recently introduced materials are included.

**13612.** Craw, A. R., Ku, R., **The sensitivity of certain indices associated with two-vehicle accidents,** *Accident Anal. Prev.* 5 137-146 (1973).

> Key words: Highway traffic accidents; indices; sensitivit analysis.

This study describes in mathematical terms a procedure employed by the National Highway Traffic Safety Administratio of the Department of Transportation for the analysis of two vehicle accidents. The procedure contains an Assignment Rul in which one of the involved driver-vehicle combinations is assigned to the class of active involvement and the other driver vehicle combination is assigned to the class of passive involvement. One case of interest is the Random Assignment Rule, an this is contrasted with the results of a Fixed Assignment Rul sults are derived that show the effect on specific indices of (1) ors in assignment and (2) a Composite Assignment Rule (a xture of Fixed and Random Rules).

613. Birky, M. M., **Calorimeter for laser energy measurements,** *ppl. Opt.* **10,** No. 1, 132-135 (Jan. 1971).

Key words: Calorimeter; energy; laser; neodymium; ruby.

A calorimeter enclosed in a constant temperature environment s been constructed to measure the output energy of a conven- nal mode ruby or neodymium laser. The calorimeter was signed according to the measurement theory and has an esti- ted uncertainty of ± 2% in the range 5J to 100J. The time-tem- rature curves were analyzed according to the theory with the l of a computer program.

614. Waterstrat, R. M., Manuszewski, R. C., **The chromium- rhodium constitution diagram,** *J. Less-Common Metals* **32,** 331-343 (1973).

Key words: Chromium alloys; constitution diagram; equilibrium diagram; phase diagram; rhodium alloys.

The Cr-Rh alloy system has been studied over the entire com- sition range by metallography, X-ray diffraction and electron croprobe methods. There are two intermediate phases in this stem. The $\epsilon$ phase has a hexagonal close-packed structure and stable over a broad composition range from about 20 at.% Cr 900 °C to 68 at.% Cr at 1475 °C. The $\beta$ phase possesses a $_3$Si(*A*15) type structure and is stable over a narrow composi- n range from about 77 to 78 at.% Cr. The location of the face- ntered cubic ($\gamma$ Rh) to hexagonal close-packed ($\epsilon$ phase) transi- n is strongly temperature dependent. Precipitation of a etastable hexagonal close-packed structure occurs during rapid oling of the body-centered cubic ($\alpha$-Cr) solid solution. A ritectic reaction exists at 1700 ± 10 °C, a eutectic reaction oc- rs at 1475 ± 10 °C, and peritectoid reaction is located at 1265 12 °C.

615. Cezairliyan, A., **Measurement of the heat capacity of graphite in the range 1500 to 3000 K by a pulse heating method,** (Proc. 6th Symp. on Thermophysical Properties, Palm Springs, Calif., Aug. 1973), Paper in *Proceedings of the 6th Symposium on Thermophysical Properties,* P. E. Liley, Ed., pp. 279-285 (American Society of Mechanical Engineers, New York, N.Y., 1973).

Key words: Graphite; heat capacity; high-speed measurements; specific heat; thermodynamics.

Measurement of the heat capacity of a grade of graphite XM-5Q, POCO) in the temperature range 1500 to 3000 K by subsecond-duration, pulse-heating technique is described. The moothed results for a single specimen corresponding to two dif- rent heating rates are in agreement within 0.1% on the average. he smoothed results for two different specimens are in agree- ent within 0.6%. The heat capacity of graphite in the tempera- re range 1500 to 3000 K based on the present results is ex- ressed by the following function (standard deviation = 0.5%):

$$c_p = 19.12 + 4.236 \times 10^{-3}\,T - 5.919 \times 10^{-7}T^2,$$

here T is in K and $c_p$ is in J mol$^{-1}$K$^{-1}$. The inaccuracy of the re- orted results is estimated to be not more than 3%.

3616. Barnes, I. L., Murphy, T. J., Gramlich, J. W., Shields, W. R., **Lead separation by anodic deposition and isotope ratio mass spectrometry of microgram and smaller samples,** *Anal. Chem.* **45,** No. 11, 1881-1884 (Sept. 1973).

Key words: Anodic deposition; isotopic analysis; lead; mass spectrometry.

A method is reported for the separation by anodic deposition and subsequent analyses by isotope ratio mass spectrometry of small samples of lead from a variety of matrices. The combined procedure is applicable to samples containing from 10 $\mu$g to less than 10 ng of lead and the electrodeposition is more than 95% efficient at these levels. Only a few elements interfere with the deposition, most notably iron and cerium, and procedures for removing the interfering elements are given. The optimum conditions for the anodic deposition of lead as $PbO_2$ were studied. The mass spectrometric procedure described permits a precision of 0.1% (95% limit of error) or better for the measured isotopic ratios.

13617. Hartman, A. W., Rosberry, F. W., Simpson, J. A., **A non-contacting length comparator with 10 nanometer precision,** *Opt. Eng.* **12,** No. 3, 95-101 (May/June 1973).

Key words: Dimensional metrology; displacement measurement; microscope; non-contact sensing; optical surface probe; surface detection.

A non-contacting length comparator utilizing two specially designed photo-electric microscopes has been constructed. Performance tests of this comparator, using lapped and polished steel surfaces demonstrate a resolution of ~ 1 nanometer, a precision of ~ 10 nanometers, and a linear range in excess of 50 micrometers.

13618. Creswell, R. A., Lafferty, W. J., **Microwave spectrum, dipole moment, and conformation of 3,6-dioxabicyclo[3.1.0] hexane,** *J. Mol. Spectrosc.* **46,** No. 3, 371-380 (June 1973).

Key words: Boat conformation; dipole moment; microwave spectrum; ring conformation; rotational constants; 3,6-dioxabicyclo[3.1.0]hexane.

The microwave spectrum of 3,6-dioxabicyclo[3.1.0]hexane has been obtained. The rotational lines of one ring conformation only have been observed and assigned. Ground state rotational constants are $A_0 = 6287.302 \pm 0.011$ MHa, $B_0 = 4683.546 \pm 0.008$ MHz, and $C_0 = 3358.517 \pm 0.089$ MHz. The dipole moment components obtained from Stark effect measurements are $\mu_a = 0.276 \pm 0.010$ D and $\mu_c = 2.47 \pm 0.04$ giving $\mu = 2.485 \pm 0.040$ for the dipole moment of the molecule. The rotational constants and dipole moment components obtained experimentally can be satisfactorily explained only if the boat form is the most stable ring conformation.

13619. Olson, W. B., **A precision photoelectric azimuthal polarimeter,** *Opt. Eng.* **12,** No. 3, 102-105 (May/June 1973).

Key words: Instrument; polarimeter; polarimetry quartz; signal-to-noise ratio; throughput.

A high precision photoelectric azimuthal polarimeter has been designed and constructed. The instrument is designed to determine the angle of rotation with an accuracy ($3\sigma$) of better than 1 part in $10^4$. The instrument is of a relatively compact design and quite simple in construction.

13620. Bowen, R. L., Chandler, H. H., **Metal-filled resin composites,** *J. Dental Res.* **52,** No. 3, 522-532 (May-June 1973).

Key words: Aluminum; composites; coupling agents gold; mercaptan; methacrylates; polymers; resin; silane; tantalum; zirconium.

Certain physical properties of metal-filled resin composite materials can be improved if properly selected and applied coupling agents are used in treating the surfaces of the metal particles.

13621. Waterstrat, R. M., **The chromium-platinum constitution diagram,** *Met. Trans.* **4,** 1585-1592 (June 1973).

Key words: Alloys; chromium; constitution diagram; equilibrium diagram; phase diagram; platinum.

The system Cr-Pt has been investigated over the entire composition range by metallography, x-ray diffraction, and electron microprobe studies. There is only one intermediate phase and it has a $Cr_3Si$(A15)-type crystal structure. The fcc platinum terminal solid solution extends to 71 at.pct Cr at 1530 °C and forms a congruent melting maximum at about 1790 °C. Atomic ordering within this solid solution range begins at about 17 at.pct Cr and there is a continuous change from the $Cu_3Au$-type structure to the CuAu-type structure with increasing chromium content. Two eutectic reactions at $1530 \pm 10$ °C and $1500 \pm 10$ °C were indicated and there is evidence of a syntectic reaction at $1580 \pm 10$ °C. Platinum is soluble in the bcc chromium terminal solid solution up to about 10 at.pct Pt at 1500 °C but the solubility decreases rapidly at lower temperatures.

**13622.** Waterstrat, R. M., Manuszewski, R. C., **The chromium-iridium constitution diagram,** *J. Less-Common Metals* **32,** 79-89 (1973).

Key words: Chromium alloys; constitution diagram; equilibrium diagram; iridium alloys; phase diagram.

The Cr-Ir alloy system has been investigated over the entire composition range by metallography, x-ray diffraction and electron microprobe studies. There are two intermediate phases in this system. The $\beta$ phase possesses a $Cr_3Si$ ($A15$)-type crystal structure and is stable from about 73 to 82 at.% Cr. The $\epsilon$ phase has a hexagonal close-packed crystal structure and is stable between 30 and 68 at.% Cr. The face-centered cubic iridium terminal solid solution can dissolve about 28 at.% Cr. Atomic ordering occurs within this solid solution, beginning at about 16 at.% Cr and forming a $Cu_3Au$ type structure up to the limit of solid solubility. Iridium is soluble in the body-centered cubic chromium terminal solid solution to the extent of about 12 at.% Ir at 1680 °C but the solubility decreases at lower temperatures. Two peritectic reactions were observed at $1750 \pm 10$ °C and at $2200 \pm 50$ °C. A eutectic reaction is indicated at $1680 \pm 10$ °C.

**13623.** Mosburg, E. R., Jr., **A study of the CW 28-$\mu$m water-vapor laser,** *IEEE J. Quantum Electron.* **QE-9,** No. 8, 843-851 (Aug. 1973).

Key words: Infrared laser; vibrational excitation; water vapor discharge; water vapor laser.

The low signal gain of a CW water-vapor laser at 28 $\mu$m was measured as a function of the discharge current and pressure. Together with the measurement of other quantities such as the axial electric field and the concentration of OH, a partial interpretation of the mechanisms involved in pumping the 28-$\mu$m transition was possible. Thermal equilibrium between the $\nu_0, 2\nu_2$, and $\nu_3$ vibrational levels will result in a large absorption at the elevated gas temperatures observed (800-1000 K). The strong dependence of gain on the electron temperature strongly suggests that the vibrational excitation proceeds through electron-impact excitation. Only the electron-impact excitation of $H_2O$ is quantitatively capable of overcoming the large thermally induced absorption. Although vibrational-excitation transfer from $H_2$ to $H_2O$ seems insufficient, by itself, to overcome this absorption, it may provide appreciable additional gain. Pumping of the 28-$\mu$m line through electron-ion recombination and by reactions involving OH can be ruled out.

**13624.** Sparks, L. L., Powell, R. L., **Calibration of capsule platinum resistance thermometers at the triple point of water,** (Proc. 5th Symp. on Temperature, Its Measurement and Control in Science and Industry, Washington, D.C., June 21-24, 1971), Paper in *Temperature, Its Measurement and Control in Science and Industry,* H. H. Plumb, Editor-in-Chief, **4,** Pa
2, 1415-1421 (Instrument Society of America, Pittsburgh, P
1972).

Key words: Resistance thermometers; temperature me
suring instruments; triple point; water.

Temperature determinations by means of a platinum r
sistance thermometer, both above and below the triple point te
perature of water, depend upon an accurate value for the r
sistance at the triple point, 0.01 °C. A good general methodolo
for making such a determination was described by H. F. Stims
at the 1955 Temperature Symposium. However, several aspec
of the method must be refined or modified for accurate measu
ments on capsule thermometers. After a series of developme
tests, we were able to isolate and correct for several types
systematic experimental errors that were significant, but not i
mediately obvious. Some of the effects that must be careful
controlled in order to guarantee high precision are (1) thermal
sistance between the thermometer and the freezing interface; (
thermal conductance down to the thermometer from the ambie
environment; (3) high-resistance electrical leakage betwe
leads in the heat exchange fluid; and (4) freezing conditions
the triple point cell itself. Using the procedures developed duri
the test program, we have been able to obtain reproducibiliti
and statistical imprecisions of about 10 $\mu\Omega$ or 100 $\mu$K.

**13625.** Molino, J. A., **Pure-tone equal-loudness contours for sta
dard tones of different frequencies,** *Perception Psychophysi*
**14,** No. 1, 1-4 (1973).

Key words: Loudness; noise; psychoacoustics; psych
physics.

Six Ss made judgments of equal loudness by adjusting the i
tensity of comparison tones of 10 different frequencies. T
comparison tones were presented diotically alternately w
standard tones. Each standard tone remained fixed at o
frequency (125, 1,000, or 8,000 Hz) and one intensity (10, 2
40, or 70 dB sensation level) while collecting the data for any s
gle equal-loudness contour. In this manner, families of equ
loudness contours were generated for each of the three standa
frequencies. The contours for the 1,000-Hz standard were co
pared with those in the literature. The families of contours for
125- and 8,000-Hz standards, determined by the same algorith
differed in the spacing of the contours from the 1,000-Hz st
dard family as well as from each other. Implications for t
reflexive, symmetric, and transitive properties of the equal-lo
ness relation are discussed.

**13626.** Furukawa, G. T., Reilly, M. L., **Application of prec
heat-capacity data to the analysis of the temperature intervals
the international practical temperature scale of 1968 in the
gion of 90 K,** (Proc. 5th Symp. on Temperature, Its Measu
ment and Control in Science and Industry, Washington, D.
June 21-24, 1971), Paper in *Temperature, Its Measureme
and Control in Science and Industry,* H. H. Plumb, Editor-
Chief, **4,** Part 1A, 27-36 (Instrument Society of America, Pi
sburgh, Pa., 1972).

Key words: Heat capacity; specific heat; temperature int
vals; temperature scale.

Precise heat-capacity data were employed to analyze the te
perature intervals or smoothness of the International Practi
Temperature Scale of 1968 (IPTS-68) between 15 and 380
particularly in the region of 90 K, as it is maintained at the N
tional Bureau of Standards. Results show that there are no lo
irregularities in the temperature scale within the precisi
($\pm$0.02 percent) of the heat-capacity data between 40 and 380
Below 40 to 15 K the uniformity of the temperature scale is le

tain because of the lower precision of the heat-capacity data he temperature range.

627. Newell, A. C., Baird, R. C., Wacker, P. F., **Accurate measurement of antenna gain and polarization at reduced distances by an extrapolation technique,** *IEEE Trans. Antennas Propagat.* **AP-21,** No. 4, 418-431 (July 1973).

Key words: Antenna gain; antenna polarization; extrapolation technique; 3-antenna technique.

A new technique is described for determining power gain and larization of antennas at reduced range distances. It is based a generalized three-antenna approach which, for the first time, rmits absolute gain and polarization measurements to be perrmed without quantitative *a priori* knowledge of the antennas. e required data are obtained by an extrapolation technique ich includes provisions for rigorously evaluating and correctg for errors due to proximity and multipath interference effects. e theoretical basis provides a convenient and powerful aproach for describing and solving antenna measurement oblems, and the experimental method employed illustrates the lity of this approach. Examples of measurements are included ich exhibit errors in gain as small as ± 0.11 dB ($3\sigma$).

628. Klein, W., **Perturbation solution of the Kirkwood-Salsburg equation,** *J. Math. Phys.* **14,** No. 8, 1049-1059 (Aug. 1973).

Key words: Asymptotic behavior at large cluster separations; Banach space; Kirkwood Salsburg equation; perturbation expansion; product property; strip operator approximation.

A formal series solution to the Kirkwood-Salsburg equation d its radius of convergence are derived. This solution leads turally to the establishment of an approximate hierarchy of uations for the distribution functions which needs no closure. e asymptotic behavior of the solutions to this approximate erarchy is studied as well as the behavior of the derivatives of e pair function with respect to the interparticle distance.

629. Mandel, J., **Structure analysis in two-way tables of measurement data,** *Proc. 39th Session of the International Statistical Institute, Vienna, Austria, Aug. 20-30, 1973,* **2,** 697-705 (International Statistical Institute, Vienna, Austria, 1973).

Key words: Analysis of variance; interaction; principal components; structure; two-way tables.

A general procedure is presented for the elucidation of the ructure of a two-way table. The method is based on a partitiong of the row by column interaction into a sum of multiplicative rms. To this partitioning corresponds a breakdown of the sum f squares of interaction and of the corresponding degrees of reedom in the analysis of variance table.

By studying the interrelationships of the parameters occurring the model, the internal structure of the data can generally be scertained. An illustrative example taken from an actual study discussed.

3630. Hjortenberg, P. E., McLaughlin, W. L., **Use of radiochromic dye systems for dosimetry,** (Proc. Regional Conf. on Radiation Protection, Jerusalem, Israel, Mar. 1973), Paper in *Radiation Protection,* Y. Feige and T. S. Schlesinger, Eds., **1,** 122-140 (Israel Atomic Energy Commission, Yavne, Israel, 1973).

Key words: Accelerator; blood irradiators; dosimetry; electron beams; gamma rays; radiochromic dyes; x-rays.

Radiochromic dye systems have been developed at the U.S. ational Bureau of Standards and have been further investigated at the Accelerator Department, The Danish Atomic Energy Commission Research Establishment Riso. Measurable absorbed doses range from $10^2$ to $10^8$ rads, depending on the particular system. Some characteristic properties are as follows: long shelf life, dose rate independence, low atomic number constituents (C, H, N, O), small temperature dependence, sensitivity to ultraviolet light, linear dose response, rather insensitive to organic impurities. In this paper a liquid system with a useful dose range of $10^2$-$10^5$ rads is described. Results demonstrate its capabilities for calibration of radiation fields including isotope irradiators and electron accelerators. Intercomparisons were made with Fricke- and thermoluminescence dosimetry.

13631. Benzinger, M., Benzinger, T. H., **Tympanic clinical temperature,** (Proc. 5th Symp. on Temperature, Its Measurement and Control in Science and Industry, Washington, D.C., June 21-24, 1971), Paper in *Temperature, Its Measurement and Control in Science and Industry,* H. H. Plumb, Editor-in-Chief, **4,** Part 3, 2089-2102 (Instrument Society of America, Pittsburgh, Pa., 1972).

Key words: Anesthesiology; brain temperature; carotid artery; clinical medicine; cold stress (diver); disposable thermometry; esophageal thermometer; fever; fulminant hyperpyrexia; heart temperature; hypothalamus heat stress; hypothermia; obstetrics; ovulation-detection; open heart surgery; pediatric surgery; pyrogens; sweating; temperature, central body; thermocouple disconnect; thermoelectric thermometry; thermometer; vasodilation; warm sensitive neurons.

Tympanic thermometry, first introduced in physiology where it was instrumental in finding the mechanisms of human temperature regulation, has passed the test of application to clinical medicine. In the clinical situations thus far tested, which included anesthesia of various types, hypothermia for surgery, extreme heat and cold stress, extracorporeal circulation for open heart procedure and one case of terminal cooling toward exitum after stroke, tympanic and esophageal patterns were found identical for practical purposes. Rectal tracings deviated grossly from the significant central patterns which monitor the temperature of the heart, the brain and the centers of thermoregulation. These central patterns can now be conveniently obtained, by way of the tympanic approach, with clean disposable probes on awake patients, and without embarrassment, discomfort or airway interference, in hospitals or at home. For hospital use, instruments are commercially available. For home use, small and inexpensive readout instruments have yet to be developed.

13632. Powell, C. J., **Semiautomated data-recording and control system for an electron energy analyzer,** *Rev. Sci. Instrum.* **44,** No. 8, 1031-1033 (Aug. 1973).

Key words: Auger-electron spectra; characteristic electron energy-loss spectra; digital data-recording and control system; electron energy analyzer; liquid aluminum; tungsten.

A description is given of a digital data-recording and control system that has been used with a high resolution low energy electron scattering apparatus for the measurement of characteristic electron energy-loss spectra and Auger-electron spectra of solids (at room and elevated temperatures) and liquids. This system is based on a multichannel analyzer and has the following features: (a) Specimens can be prepared many times with data accumulated in arbitrarily short times after preparation (prior to specimen contamination), and final spectra of high precision can be obtained by summation of individual runs; (b) the voltage sweep applied to the electron energy analyzer can be calibrated dynamically; and (c) data can be accumulated and the target heated by electron bombardment in a cyclic manner with variable accumulation and heating periods. Characteristic loss spectra of tungsten at 800 °C and of liquid aluminum are presented as examples of operation of the system.

**13633.** Gadzuk, J. W., Plummer, E. W., **Field emission energy distribution (FEED),** *Rev. Mod. Phys.* **45,** No. 3, 487-548 (July 1973).

Key words: Chemisorption; electronic properties of metals; field emission; surface physics.

The technique of measuring the energy distribution of electrons which have been field emitted from a cold cathode is considered. The general historical and introductory theory is presented. A survey of the experimental techniques and existing energy analyzers is given. Specific studies on clean metal surfaces in which work functions, band structure effects, surface states, thermal effects, and many-body effects have been studied are reviewed from both the experimental and theoretical points of view. Field emission energy distributions have been particularly valuable in studies of atoms chemisorbed on surfaces. Several theories of enhanced resonance tunneling due to chemisorbed atoms are discussed. Specific systems studied experimentally are reviewed. Inelastic adsorbate enhanced tunneling is also treated.

**13634.** Mullen, L. O., **High and ultra-high vacuum by pumping with cryocooled surfaces,** (Proc. American Institute of Chemical Engineers, Symp. Series on Cryogenic Pumping, Denver, Colo., 1971), Paper in *Vacuum Technology at Low Temperatures* **125,** No. 68, 24-30 (1972).

Key words: Cryopumping; cryosorption; gettering; vacuum pump; vapor pressures.

This presentation reviews the principles of pumping with cryogenically-cooled surfaces to produce high and ultra-high vacuum. The theory of cryopumping and entrapment by cryopumping, as well as some advantages and limitations are discussed.

**13635.** Morrissey, B. W., Powell, C. J., **Interpolation of refractive index data,** *Appl. Opt.* **12,** No. 7, 1588-1591 (July 1973).

Key words: Cubic-spline interpolation; cyclohexane; interpolation; polystyrene; refractive index; sapphire.

A comparison of the interpolation of index of refraction data for Czochralski sapphire, cyclohexane, and polystyrene dissolved in cyclohexane using a three-term Sellmeier equation, the Lorentz-Lorenz equation with six terms, third and fifth order polynomials, and a cubic-spline technique indicates that the cubic spline method is extremely valuable for simple interpolation. Not only were the magnitudes of the rms and average absolute residuals the smallest, but the fits showed no systematic errors.

**13636.** Unassigned.

**13637.** Masters, L. W., Wolfe, W. C., Rossiter, W. J., Jr., Shaver, J. R., **State of the art on durability testing of building components and materials,** *NBSIR 73-132,* 128 pages (Mar. 1973). (Available as PB222300 from the National Technical Information Service, Springfield, Va. 22151.)

Key words: Accelerated aging; aging of buildings; building components; climate; criteria; deterioration; durability; materials; mechanisms; nondestructive testing; testing.

This report is a summary of the present knowledge pertaining to durability predictions for building components and materials which are subjected to the effects of outdoor exposure. The various chapters of the report include discussions of the nature of aging, the measurement of properties to predict durability, nondestructive evaluation techniques, outdoor exposure technique accelerated aging techniques, techniques for applying testin data to durability predictions and difficulties which arise in pre dicting durability. Conclusions and recommendations are also i cluded.

An appendix, which summarizes ASTM Standards for dura bility testing of building components and materials, is include

**13638.** Cohen, E. R., Taylor, B. N., **A reevaluation of the funda mental physical constants,** (Proc. 4th Int. Conference o Atomic Masses and Fundamental Constants, Teddington, E gland, Sept. 3-7, 1971), Paper in *Atomic Masses and Funda mental Constants,* J. H. Sanders and A. H. Wapstra, Eds Part 13, 543-563 (Plenum Publishing Co., New York, N.Y 1972).

Key words: Data analysis; fundamental constants; leas squares adjustments.

This paper is a progress report on our current efforts to revis and update the comprehensive review of the fundamental phys cal constants by Taylor, Parker, and Langenberg (1), includin their set of best or recommended values. That such an updatin is necessary just two years after their review appeared is due t the extraordinary amount of new experimental and theoretic work which has since been completed. Here, we very briefl summarize the experimental and theoretical evidence, wit emphasis on the new results which have become available withi the last two years, and discuss various treatments of the dat However, no new set of recommended constants is given sinc such a set will necessarily require the inclusion of the new dat which has become available at this Conference.

**13639.** Haar, L., **The ideal gas-calorimetric thermometer,** *Scienc* **176,** 1293-1296 (June 23, 1972).

Key words: Ammonia; calorimetry; flow calorimeter; he capacity; ideal-gas; temperature; thermodynamic tempera ture; thermometer.

A new thermometer is suggested for probing the differenc between the thermodynamic temperature scale and a practic scale, say the International Practical Temperature Scale—196 The method is based on the fact that the fractional difference the heat capacity as measured on two scales is very nearly equ to the temperature derivative of the difference in hotne between the scales. Now, the heat capacity on the the modynamic scale is by definition that of the ideal gas calculate from the molecular structure using statistical mechanics. This w compare with the analogous quantity measured calorimetrical and extrapolated to the ideal gas limit. The feasibility of th method is illustrated using very accurate data for gaseous an monia.

**13640.** Barber, W. C., Hayward, E., Sazama, J., **Nuclear scatte ing of plane-polarized photons,** (Proc. Int. Conf. on Nucle Structure Studies using Electron Scattering and Photorea tion, Sendai, Japan, Sept. 12-15, 1972), Paper in *Nucle Structure Studies Using Electron Scattering and Photorea tion,* Supplement to *Research Report of Laboratory Nuclear Science,* K. Shoda and H. Ui, Eds., **5,** 313-31 (Tohoku University, Tomizawa, Sendai, Japan, 1972).

Key words: Dynamic collective model; giant resonanc photon scattering; polarized photons.

A beam of plane-polarized, monochromatic photons has bee produced by the resonance fluorescence of the well-known state in $^{12}$C. These have been scattered a second time from ta gets of cadmium, tin, tantalum, gold, and bismuth. A measur ment of the number of photons scattered along and perpendicul he polarization vector in the incident 15.1 MeV beam allows etermination of the relative contribution of incoherent and erent scattering to the total scattering cross section. These ults can be compared to the predictions of the dynamic collec- model.

41. LaFleur, P. D., Thompson, B. A., **Gamma-ray spectrosco- y**, Paper in the *Encyclopedia of Chemistry, Third Edition*, C. lampel and G. G. Hawley, Eds., pp. 1032-1033 (Van Nos- rand Reinhold Co., New York, N.Y., 1973).

Key words: Activation analysis; gamma-ray spectroscopy; Ge(Li) detectors; group separations; instrumentation.

his article has been prepared for the third edition of the En- lopedia of Chemistry. It is a revision of an article which ap- red in the previous edition, published by Reinhold Publishing mpany in 1966.

42. Gilman, F) J., Kugler, M., Meshkov, S., **Pionic transi- ions as tests of the connection between current and constituent uarks,** *Phys. Lett.* **45B,** No. 5, 481-486 (Aug. 20, 1973).

Key words: Baryon decays; constituent quarks; current quarks; pionic transitions; su(3); su(6)$_w$.

A proposed connection between current and constituent arks is discussed and tested through comparison with the mag- udes and signs of amplitudes for pionic transitions between drons.

643. Fatiadi, A. J., **Facile coupling of sterically hindered 2,6-di- alkylphenols with periodic acid,** *Synthesis Commun.* No. 6, 357-358 (June 1973).

Key words: Coupling; dialkylphenols; dimethylformamide; hindered; oxidation; periodic acid.

A procedure has been developed by which sterically hindered enols can produce coupling products (diphenoquinones) in 60 94 percent yield when treated with periodic acid in an aqueous N-dimethylformamide.

644. Saks, T. H., Yates, R. F., Goodman, K. M., **The Shirley Highway Express-Bus-on-Freeway demonstration project-users' reactions to innovative bus features,** *NBSIR 73-265*, 53 pages (June 1973). (Available as COM 73-11453 from the National Technical Information Service, Springfield, Va. 22151).

Key words: Attitudinal survey; bus-on-freeway; exclusive bus lanes; importance assessments; interior bus features; mass transit technology; satisfaction assessments; transit service features.

The Shirley Highway Express Bus-on-Freeway Project emonstrates the application of a new mass transit technology. he elements tested in this demonstration project include: an ex- usive bus lane in the median of a freeway and bus priority lanes the downtown distribution area; fringe parking facilities which re coordinated with the bus service; new-look/new-feature uses; and extension of service to additional residential areas in n overall systems approach to the improvement of mass transit. s part of the evaluation of this demonstration project, a survey f commuters on board these buses was undertaken in order to btain users attitudes concerning the special interior bus features s well as transit service features.

The results obtained from this study should be of interest to ersons considering how to allocate expenditures for new bus ehicles and transit service improvements.

Bus commuters perceptions of the relative importance of vari- us bus interior features (i.e., carpeting, special lighting, etc.) and ansit service features (i.e., reliable schedules, assurance of a seat, etc.) are analyzed in this report, along with their relative satisfaction assessments of the special bus interior features. Analyses were conducted to determine if marginal improvements in interior comfort and aesthetic features proved significantly more appealing to bus commuters. The relative impact of various project marketing and promotional techniques is also presented.

**13645.** Smith, M. W., Martin, G. A., Wiese, W. L., **Systematic trends and atomic oscillator strengths,** *Nucl. Instrum. Methods* **110,** 219-226 (1973).

Key words: Atomic oscillator strengths; homologous atoms; isoelectronic sequences; regularities; spectral series; systematic trends.

A number of newly established or significantly improved systematic trends of atomic oscillator strengths in isoelectronic sequences and spectral series are presented. For most of these trends, beam-foil experiments have played a prominent role in supplying critically needed points. Of particular interest are the changes in several transitions of the Be and C sequences brought about by improved beam-foil results and more refined theoretical calculations. Also of significance are newly detected trends in the Li and Al isoelectronic sequences. An example will be given where the analysis of the $f$-value dependence along a sequence, coupled with an understanding of the changes in the energy level structure, points out areas where future beam-foil experiments would be desirable in clearing up discrepancies. The $n^{*3}$ dependence of oscillator strengths for perturbed series will be illustrated with another interesting example.

**13646.** Ott, W. R., Wiese, W. L., **Far ultraviolet spectral radiance calibrations at NBS,** *Opt. Eng.* **12,** No. 3, 86-94 (May/June 1973).

Key words: Calibrations; deuterium lamp; far ultraviolet; hydrogen; Krefft-Rössler lamp; spectral radiance; transfer standards; wall-stabilized arc.

The range of NBS radiometric calibration services has been extended into the far ultraviolet region of the spectrum where a dc high power hydrogen wall-stabilized arc is used as a primary standard of spectral radiance. A capability in the range 130 nm to 360 nm (overlapping conventional tungsten strip lamp radiometry) is presently available with estimated uncertainties between 5 and 10 percent depending upon wavelength. The status of radiometric source standards in the far ultraviolet is briefly reviewed and the hydrogen arc and NBS calibration facility are described in detail. The use of commercially available mercury Krefft-Rössler lamps and deuterium arc lamps as transfer or secondary standards is discussed and the spectra of these lamps calibrated with the hydrogen arc standard are presented.

**13647.** Dellepiane, G., Gussoni, M., Hougen, J. T., **Hamiltonian, symmetry group, and vibrational coordinates for the nonrigid molecule $CXY_2 - C \equiv C - CXY_2$,** *J. Mol. Spectrosc.* **47,** No. 3, 515-530 (Sept. 1973).

Key words: Double-valued presentation; free internal rotation; Hamiltonian energy operator; non-rigid molecules; permutation-inversion group; vibrational coordinates.

A vibration-torsion-rotation Hamiltonian is derived for a molecule of the type $CXY_2 - C \equiv C - CXY_2$ exhibiting nearly free internal rotation. The Hamiltonian obtained preserves many of the features of the ordinary Wilson-Howard vibration-rotation Hamiltonian and is based qualitatively on the idea of a slowly varying torsional reference configuration from which the atoms make rapid vibrational displacements. The appropriate molecular symmetry group for this molecule is found to be a double group of the simple Longuet-Higgins permutation-inversion symmetry group. The indeterminacy of symmetry species (single-valued vs double-valued) for coordinates used to describe the small amplitude vibrations is illustrated and clarified using a simple model for the skeletal bending vibrations.

**13648.** Christ, B. W., **Effects of misalignment on the premacroyield region of the uniaxial stress-strain curve,** *Met. Trans.* **4,** 1961-1965 (Aug. 1973).

Key words: Bending; capacitance strain gage; tensile; Ti-6Al-4V; uniaxial loading; 4340 steel.

Some bending usually occurs in uniaxial testing systems due to small unavoidable misalignment. The resulting elastic strain gradient can lead to significant differences between axial strain and extreme surface bending strains, especially at small strains. A three-point microstrain measurement around a cylindrical sample permits evaluation of the extreme strains and of the precision of alignment. A three-point, parallel-plate capacitance strain gage having a linear output with displacement was designed to evaluate bending of tensile samples in the microstrain range. The resolution of the gage was 3 parts in 10,000 at plate separations of 0.010 in. Varying misalignment resulted in extreme elastic bending strains at the sample surface of the order of tens to hundreds of micro-in. per in. larger than the axial strain. Analysis of the mechanics of bending in uniaxial loading demonstrated that: 1) the average applied stress divided by the average elastic strain always gives a unique number, Young's modulus, and 2) the average microplastic strain is not uniquely related to the average applied stress, but rather depends upon precision of alignment. The influence of bending on the determination of the average stress at which microplastic flow initiates is discussed, and a method for making meaningful comparisons of plastic microstrain data generated with significant misalignment is suggested.

**13649.** Maki, A. G., **Infrared spectra of $CS_2$: Measurement of "hot" bands associated with the 2325 $cm^{-1}$ and 2962 $cm^{-1}$ bands,** *J. Mol. Spectrosc.* **47,** No. 2, 217-225 (Aug. 1973).

Key words: Absorption spectra; carbon disulfide; energy levels; high resolution; infrared; molecular spectra.

The $12^01 - 00^00$ and $02^01 - 00^00$ transitions of $CS_2$ have been measured with a resolution of 0.025 $cm^{-1}$. The following "hot" bands associated with these transitions were also measured $13^11 - 01^10$, $22^01 - 10^00$, $14^01 - 02^00$, $14^21 - 02^20$, $03^11 - 01^10$, $12^01 - 10^00$, $04^01 - 02^00$, $04^21 - 02^20$, $13^11 - 11^10$, and $22^01 - 20^00$. Improved rotational constants are given for the ground state and the first bending state. A consistent set of band constants is given for all the above vibrational transitions.

**13650.** Comeford, J. J., Birky, M., **A method for the measurement of smoke and HCl evolution from poly(vinyl chloride),** *Fire Technol.* **8,** No. 2, 85-90 (May 1972).

Key words: HCl: He-Ne laser; poly(vinyl chloride); pyrolysis; smoke; thermal decomposition.

As poly(vinyl chloride) becomes more popular as a building material and electrical insulation, it becomes more important to life safety to determine its smoke and hydrogen chloride evolution characteristics during pyrolysis. The authors have devised a method of measuring the two simultaneously.

**13651.** Creitz, E. C., **Extinction of fires by halogenated compounds—a suggested mechanism,** *Fire Technol.* **8,** No. 2, 131-141 (May 1972).

Key words: Extinguishment; flame inhibition; inhibition mechanisms.

It is suggested that halogenated compounds extinguish dif
sion flames by promoting recombination of reactive oxyg
atoms to form less reactive molecular oxygen. Oxygen atoms
important in the branching steps of the hydrogen-oxygen ch
reaction. For a fuel containing carbon, CO is an intermedi
product which appears in the region in which inhibition tak
place. Inhibition of its oxidation appears to take place because
the paucity of hydroxyl radicals which are a product of t
hydrogen-oxygen chain reaction. The mechanism is suggested
an attempt to rationalize a number of apparently disparate obs
vations reported in the literature of both normal and inhibit
flames. Data in support of the suggested mechanism
discussed.

**13652.** Ott, W. R., Fieffe-Prevost, P., Wiese, W. L., **V**
**radiometry with hydrogen arcs. I: Principle of the method a**
**comparisons with blackbody calibrations from 1650 Å to 3**
**Å,** *Appl. Opt.* **12,** No. 7, 1618-1629 (July 1973).

Key words: Continuum emission coefficient; hydrogen a
radiometry; vacuum ultraviolet.

A method is described that utilizes the continuum emissi
from a wall-stabilized arc discharge as a radiometric standard
the vuv. Ultimately, this standard will cover the waveleng
range from 500 Å to 3600 Å. Results of a first experiment co
paring this method to two other calibration methods in the regi
above 1650 Å are presented. A calibrated tungsten strip lamp
used between 2500 Å and 3600 Å; the method of blackbo
limited lines is applied at two wavelengths in the vuv. T
hydrogen arc method depends upon the fact that the continu
emission coefficient for a hydrogen plasma at typical arc te
peratures of about 14,000 K is calculable to within a few perc
since the essential spectroscopic constants, continuum abso
tion coefficients, and transition probabilities are exactly kno
The accuracy of the method depends primarily on the capabil
of spatially resolving in an end-on measurement the nea
homogeneous plasma layers near the axis of the cylindrica
symmetric arc column.

**13653.** Maki, A. G., Johnson, D. R., **Microwave spectra of c**
**bonyl sulfide: Measurements of ground state and vibrationa**
**excited $^{16}O^{13}C^{32}S$, $^{18}O^{12}C^{32}S$, and other isotopic species,** *J. M*
*Spectrosc.* **47,** No. 2, 226-233 (Aug. 1973).

Key words: Bond distances; carbonyl sulfide; microwa
spectra; molecular parameters; rotational transitions; sp
tra.

Microwave measurements have been made on isotopically
riched samples of $^{13}C$-carbonyl sulfide and $^{18}O$-carbonyl sulfi
Centrifugal distortion constants and *l*-type doubling consta
have been determined for these isotopically substitut
molecules. Rotational constants have been measured for
vibrational states below 2150 $cm^{-1}$ and $B_e$ values have be
determined. The equilibrium bond distances calculated from
ferent pairs of isotopes are compared and a substitution equili
um structure is given. Some new measurements are also report
for the isotopic species $^{18}O^{13}C^{32}S$, $^{18}O^{13}C^{34}S$, $^{18}O^{12}C^{34}S$, a
$^{16}O^{13}C^{34}S$.

**13654.** Bellet, J., Lafferty, W. J., Steenbeckeliers, G., **Microw**
**spectra of $D_2{}^{17}O$ and $D_2{}^{18}O$,** *J. Mol. Spectrosc.* **47,** No. 3, 3
402 (Sept. 1973).

Key words: Centrifugal distortion constants; $D_2{}^{17}O$; $D_2{}^{18}$
quadrupole coupling constants; rotational constants; ro
tional spectra.

Forty lines of the microwave spectra of $D_2{}^{17}O$ and $D_2{}^{18}O$ ha
been measured in the region from 8 to 400 GHz and analyzed

ding to Watson's centrifugal distortion theory. Comparison of results obtained for $D_2{}^{16}O$, $D_2{}^{17}O$, and $D_2{}^{18}O$ demonstrates ir internal consistency. The transferability of the parameters ording to the isotopic substitution rules is evidence for the idity of the model chosen for the study of the ground state of vy water.

he effective rotational constants deduced from the observed ctra are very close to the values calculated using Oka's ond order theory. The values obtained in MHz are:

$$A = 456766.9, B = 218041.0, C = 144701.5\ (D_2{}^{17}O);$$

$$A = 451891.9, B = 218045.2, C = 144201.7\ (D_2{}^{18}O).$$

e hyperfine structure of the $D_2{}^{17}O$ lines has been analyzed ng as a reference the corresponding quadrupole coupling ten- of $HD^{17}O$ with the appropriate rotation. The values of $\chi_{yy}$ in Hz used for the analysis are:

$$\chi_{xx} = -1.2104, \chi_{yy} = 10.1068, \chi_{zz} = -8.8964.$$

54A. Roberts, R. W., **1973 INTERMAG keynote address: NBS—The magnetic domain,** *IEEE Trans. Magn.* **MAG-9,** No. 3, 152-155 (Sept. 1973).

Key words: Magnetic research; magnetism.

The National Bureau of Standards has been active in magnetic earch for 70 years, in such areas as theory, development of gnetic devices, and use of magnetism in other scientific estigations. Highlights of NBS programs, past and present, featured.

**655.** Olf, H. G., Fanconi, B., **Low frequency Raman-active lattice vibrations of *n*-paraffins,** *J. Chem. Phys.* **59,** No. 1, 534-544 (July 1, 1973).

Key words: *n*-paraffins; polyethylene phonon dispersion curves; Raman spectroscopy-lattice vibrations.

Raman spectra in the frequency range 5 – 200 $cm^{-1}$ have en measured for a series of crystalline *n*-paraffins from *n*-$H_{12}$ to *n*-$C_{26}H_{54}$ and also *n*-$C_{32}H_{66}$, *n*-$C_{35}H_{72}$, and *n*-$C_{36}H_{74}$. It found that the spectral data may be grouped consonant with ystal structures exhibited by *n*-paraffins. The data are used to ap out portions of the transverse acoustical phonon dispersion rves of the orthorhombic polyethylenelike lattice and of one clinic crystalline form. A band whose frequency is independent of chain length is observed for the orthorhombic *n*-paraffins d is assigned to the $B_{3g}$ rotatory lattice mode of polyethylene.

**656.** Barnes, J. D., **Inelastic neutron scattering study of the "rotator" phase transition in *n*-nonadecane,** *J. Phys. Chem.* **58,** No. 12, 5193-5201 (June 15, 1973).

Key words: Molecular dynamics; *n*-alkanes; *n*-nonadecane; neutron scattering; paraffin; rotator phase.

A simple kinematic model for rotational jump diffusion of a ormal alkane about its long axis (circular random walk model) developed. Inelastic neutron scattering data obtained on the ermi chopper time-of-flight instrument at the National Bureau f Standards reactor using an incident neutron wavelength of .47 Å ($\Delta\lambda/\lambda \simeq 3.8$ %) are compared with the predictions of the odel. Data taken below the temperature of the "rotator" phase ansition in *n*-nonadecane (295 °K) show no quasielastic scattering due to diffusive motions. Data taken in *n*-nonadecane in its isordered solid phase show quasielastic scattering consistent ith the circular random walk model. Estimates for values of the odel parameters of 3.5 psec. for $\tau_1$ and $N \geq 8$ are obtained.

**13657.** Creitz, E. C., **Gas chromatographic determination of composition profiles of stable species around a propane diffusion flame,** *J. Chromatogr. Sci.* **10,** 168-173 (Mar. 1972).

Key words: Flame gases; flame inhibition; gas analysis; gas chromatographic techniques.

An analytical method was developed for determining, quantitatively, with a GC, the gases present around a 2.4 cm high propane diffusion flame burning in air. The method gives quantitative results on samples having some constituents which may not be eluted from the column. Outside the yellow mantle the only fuel species found were carbon, hydrogen and carbon monoxide. The oxygen concentration dropped to zero at a distance of 0.57 mm from the yellow mantle indicating that pyrolysis of the fuel was essentially without $O_2$. The absence of other fuel species implicates the hydrogen-oxygen chain reaction as having a part in the mechanism of inhibition. When $CF_3Br$ was added to the air, its decomposition was complete at a distance of 2.56 mm from the yellow mantle. The decomposition appeared to be chemical rather than thermal.

**13658.** Chertok, B. T., Sheffield, C., Lightbody, J. W., Jr., Penner, S., Blum, D., **Low-$q^2$ electron scattering from the 15.109-MeV state of $^{12}C$ and the conserved-vector-current test,** *Phys. Rev. C* **8,** No. 1, 23-36 (July 1973).

Key words: Electron scattering; extrapolation, $\Gamma_\gamma$; low $q^2$; $1^+$ state; 15.11 MeV.

High-precision electron scattering measurements from the 15.109-MeV $1^+$ state in $^{12}C$ are made at $\theta = 75$ and 110 ° with 35 $\leq E \leq 55$ MeV. From the measurements $B\,(M1)$ is extrapolated to the photon point and the radiative width is determined, $\Gamma_\gamma = 37.0 \pm 1.1$ eV. The corresponding weak magnetism results for $\beta$ decay and $\mu$ capture are given.

**13659.** Coriell, S. R., Sekerka, R. F., **Morphological stability near a grain boundary groove in a solid-liquid interface during solidification of a binary alloy,** *J. Cryst. Growth* **19,** 285-293 (1973).

Key words: Alloy; grain boundary; morphology; solidification; stability.

In order to further explore the influence of grain boundaries on the phenomenon of morphological stability, we have extended our previous treatment for a pure substance to a binary alloy. For unidirectional solidification at constant velocity, the shape, $y = W(x,t)$, of a nearly planar interface, intersected perpendicularly by a grain boundary, is calculated. The stability-instability criterion is identical to that for an interface without a grain boundary. If the interface is unstable, the main influence of the grain boundary is to provide an initial perturbation and the time evolution of the interface shape can be treated by approximate analytical methods. For times sufficiently large that initial transients have decayed but sufficiently small that linear theory is applicable, $W(x,t)$ is proportional to $\exp(t/\tau)\cos(\omega_0 x)\exp(-x^2/4\mathscr{D}t)$, where $\omega_0$, $\tau$, and $\mathscr{D}$ are constants that depend on experimental conditions. After initial transients have decayed, a stable interface attains a time-independent shape. For this case, $W(x, t \to \infty)$ is evaluated numerically; it is found that $W(x, t \to \infty)$ can be an oscillatory function of x. The size of the oscillations and the depth of the grain boundary groove increase as the stability-instability demarcation is approached, giving the specious appearance of premature instability.

**13660.** Kaufman, V., Sugar, J., **One-electron spectrum of singly ionized ytterbium (Yb II),** *J. Opt. Soc. Amer.* **63,** No. 9, 1168-1172 (Sept. 1973).

Key words: Energy levels; spectrum; ytterbium.

The spectrum produced by the hollow-cathode discharge was measured from 2107 to 1377 Å. With these new data and the previously published observations of Yb II at longer wavelengths, new $4f^{14}nl$ series terms were found, including $10s$, $7p$, $7-11d$, $5-14f$, and $5-6g$. A value of 98 269(50) cm$^{-1}$ was deduced for the ionization energy.

**13661.** Coriell, S. R., Sekerka, R. F., **Morphological stability near a grain boundary groove in a solid-liquid interface during solidification of a pure substance.** *J. Cryst. Growth* **19,** 90-104 (1972).

Key words: Crystal growth; grain boundary; morphological stability; solidification.

In order to explore the influence of a specific type of defect on the phenomenon of morphological instability, we have calculated the time-dependent shape of a nearly planar interface, intersected perpendicularly by a grain boundary, during solidification of a pure substance at constant velocity. The calculational methods and principal assumptions are similar to those employed in previous theories of morphological stability except that the slope of the interface is maintained at a finite and constant value, $s$, in the immediate vicinity of the grain boundary groove. The position of the solid-liquid interface is described by the equation $y = W(x,t)$ where $t$ is the time and $W(x,0) \to 0$ as $|x| \to \infty$ (all quantities are assumed independent of $z$). Whereas the stability-instability criterion is found to be identical to that for an interface without a grain boundary, the boundary is found to be an effective initial perturbation. Under conditions for instability the depth of the grain boundary groove increases exponentially with time and an oscillatory instability propagates laterally from the boundary. Under conditions for stability, the interface eventually attains a time-independent shape given by $W(x,t\to\infty) = (-s/a)\exp(-ax)$, where $a^2 = (\mathcal{G}_S + \mathcal{G}_l)/2T_M\Gamma$, $\mathcal{G}_S$ and $\mathcal{G}_l$ are conductivity-weighted temperature gradients in solid and liquid, respectively, $T_M$ is the melting temperature and $\Gamma$ is a capillary constant. For conditions corresponding to the demarcation between stability and instability, a mode of thermal grooving, similar to that previously described by Mullins, is found. A meaningful criterion for instability is shown to be the exponential growth of perturbations while, conversely, stability entails their exponential decay; phenomena such as the algebraic increase of amplitude characteristic of thermal grooving are shown to be manifestations of constraints. Finally, the situation where the interface shape is allowed to depend on $z$ is shown to be describable by a superposition of $W(x,t)$ with a function $W_0(x,z,t)$ that corresponds to the conventional case where the grain boundary is absent.

**13662.** Reader, J., Epstein, G., **Zeeman effect and revised analysis of singly ionized rubidium (Rb II),** *J. Opt. Soc. Amer.* **63, No. 9, 1153-1167 (Sept. 1973).**

Key words: Rubidium; spectra; ultraviolet; wavelengths; Zeeman effect.

The spectrum of Rb II has been observed in a sliding-spark discharge with the NBS 10.7-m normal-incidence vacuum spectrograph and in an electrodeless discharge with the NBS 10.7-m Eagle spectrograph in air. The Zeeman effect was observed from 2200 to 5200 Å with an electrodeless lamp in a magnetic field of 31 000 G. The analysis has confirmed all ten of the previously known levels of the $4p^55p$ configuration. The $4p^54d$, $4p^55s$, $4p^55d$, and $4p^56s$ configurations have been considerably revised and extended. Almost all levels of these configurations are now known, as well as those of $4p^56d$, $4p^57s$, and $4p^54f$, which were newly located. All configurations have been theoretically interpreted, with configuration interaction included. The energy parameters determined from a least-squares fit to the observed level values are compared with Hartree-Fock calculations. The ionization energy as derived from the $4p^5ns$ series, $n = 5, 6, 7,$ 220 070 ± 25 cm$^{-1}$ (27.285 ± 0.003 eV).

**13663.** Yates, J. T., Jr., Madey, T. E., Dresser, M. J., **Adsorpti and decomposition of formaldehyde on tungsten (100) and (11 crystal planes,** *J. Catal.* **30,** No. 2, 260-275 (Aug. 1973).

Key words: Carbon dioxide; catalytic; chemisorptio decomposition; formaldehyde; methane; tungsten.

The chemisorption of formaldehyde at ~ 100 K has been i vestigated on two single crystal planes of tungsten, W(100) a W(111). At low $H_2CO$ coverages, only $H_2$ and CO are observ as thermal desorption products. At higher $H_2CO$ coverages bo $CH_4$ and $CO_2$ are observed as additional desorption produc Work function and flash desorption measurements indicate th the dissociative adsorption of $H_2CO$ into H(ads) and CO(ads) accompanied at higher surface coverages by the formation other surface complexes.

A detailed comparison of W(100) with W(111) indicates th crystallographic differences play a minor role in the surface ca lyzed decomposition of $H_2CO$ by tungsten.

**13664.** Collier, R. S., Ellerbruch, D., Cruz, J. E., Stokes, R. V Luft, P. E., Peterson, R. G., Hiester, A. E., **Mass quant gauging by rf mode analysis,** *NBSIR 73-318,* 196 pages (Ju 1973). (Available as N73-27390 from the National Techni Information Service, Springfield, Va. 22151.)

Key words: Gauging; hydrogen; nitrogen; radio frequenc total mass.

This is a summary report of work done to date on NAS (Johnson Space Center) purchase order T-1738B concerni Radio Frequency (RF) Mass Quantity Gauging. Experimen apparatus has been designed and tested which measures t resonant frequencies of a tank in the "time domain." The frequencies correspond to the total mass of fluid within the ta Experimental results are discussed for nitrogen and hydrogen normal gravity both in the supercritical state and also in the t phase (liquid-gas) region. Theoretical discussions for m general cases are given.

**13665.** Bussey, H. E., **Wavelength of a slotted rectangular l containing two dielectrics,** *NBSIR 73-326,* 17 pages (J 1973). (Available as COM 73-11465-AS from the Natio Technical Information Service, Springfield, Va. 22151.)

Key words: Capacitance; dielectric measurement; slab li slotted line.

The titled electromagnetic wave property is obtained appro mately for a rectangular slab line with two dielectrics. The p turbing dielectric is a thin sheet set on the center conductor a slotted to permit travel of the probe when the line is used a slotted line. The purpose is to measure an unknown dielect filling most of the line, but perturbed by the thin sheet.

**13666.** Giarrantano, P. J., Hess, R. C., Jones, M. C., **Forced c vection heat transfer to subcritical helium I,** *NBSIR 73-322,* pages (May 1973). (Available as COM 73-11464-AS from t National Technical Information Service, Springfield, V 22151.)

Key words: Centrifugal pump; critical heat flux; film b ing; forced convection; heat transfer; helium; nucleate b ing; subcritical; supercritical.

Preliminary results of an experimental investigation of h transfer to liquid helium under forced flow conditions are ported for a 0.213 cm i.d. × 10 cm long test section subject to t following range of operating conditions:

System pressures  1.1 − 2.1 atm

Mass velocities  4 − 64 g/s-cm²

Heat fluxes  0.04 − 0.53 W/cm²

Inlet subcooling 0.03 − 0.10 K

effect of the above system parameters on the heat transfer critical heat flux is discussed; a comparison of forced con- tion boiling with other modes of heat transfer (pool boiling supercritical) and the performance of a centrifugal pump d for circulating the liquid helium are also included in the re- t.

67. Diller, D. E., Sarkes, L. A., **Properties data for LNG,** *mer. Gas Ass. Mon.* **55,** No. 9, 27-28 (Sept. 1973).

Key words: Calculation methods; densities; ethane; liquefied natural gas mixtures; methane; pure components; propane; properties data.

he need for new physical and thermodynamic properties data liquefied natural gas mixtures at low temperatures is cussed. A plan is given for calculating properties data for id mixtures at temperatures well below the critical tempera- e. The National Bureau of Standards Cryogenics Division's gram to provide accurate input data for calculating properties a for LNG is described.

68. Mabie, C. P., **Petrographic study of the refractory per- ormance of high-fusing dental alloy investments: II. Silica- onded investments,** *J. Dent. Res.* **52,** No. 4, 758-773 (1973).

Key words: Alloy; casting; chromium; investment; mold.

etrographic study of the refractory performance of silica- nded investments revealed that recrystallized silica bonds nsisting of tridymite and cristobalite are formed during bur- ut. The major reaction product created during casting is colaite. Liquefaction and sintering in the investment at and ar its interface with the casting plugs pores and may lower meability.

69. Bowen, R. L., Argentar, H., **A method for determining the ptimum peroxide-to-amine ratio for self-curing resins,** *J. Appl. Polym. Sci.* **17,** 2213-2222 (1973).

Key words: Accelerators; amines; dental materials; initiators; peroxides; polymerization.

The rate of polymerization of a methacrylate monomer was in- enced by the molar ratio of benzoyl peroxide to an aromatic tiary amine accelerator when the product of the concentra- ns of these was kept constant. The maximum rate, measured the minimum gel time, occurred in monomer solutions con- ning about 1.5 moles of peroxide per mole of amine.

670. Levine, J., Stebbins, R. T., **Ultrasensitive laser inter- ferometers and their application to problems of geophysical in- terest,** *Phil. Trans. Roy. Soc. London A* **274,** 279-284 (1973).

Key words: Earth tides; interferometer; normal modes; strainmeter.

A 30 m laser strainmeter is currently being operated in an un- orked gold mine near Boulder, Colorado. The strainmeter con- ts of an evacuated Fabry-Perot interferometer illuminated by 3.39 $\mu$m He-Ne laser. A second 3.39 $\mu$m laser is stabilized by eans of saturated absorption in methane and its wavelength rves as the reference length for the system. We shall describe e instrument in some detail and present the latest results in our vestigation of the Earth tides and the Earth normal modes.

13671. Penn, D. R., **The concept of the surface molecule in chemisorption,** *Surface Sci.* **39,** 333-340 (1973).

Key words: Density of states at the adsorbate; energy levels; S state adsorbate; surface molecule; tight binding calculation; W substrate.

Under certain circumstances the binding of an adsorbate to a metal surface may be thought of as the formation of a surface molecule composed of the adsorbate and the metal. This point of view is reasonable if the metal density of states at the adsorbate resembles that of an atom, i.e., exhibits a small number of well defined peaks as a function of energy. The width of these peaks must be small compared to the metal band width. Within the context of a simple tight binding model for the metal we find that for an S state adsorbate on W there are certain adsorbate positions for which the surface molecule concept should be valid.

13672. Hastie, J. W., **Mass spectrometric analysis of 1 atm flames: Apparatus and the $CH_4 - O_2$ system,** *Combust. Flame* **21,** 187-194 (1973).

Key words: $CH_3$; flames; H; mass spectrometry; OH; radicals.

A mass spectrometric system is described for the measurement of reactive intermediates in 1 atm flames. The system has been tested on $CH_4 - O_2$ and $CH_4 - O_2 - N_2$ flames and provides for the first time a complete analysis of such flames for species in excess of $10^{-5}$ mole fraction concentration.

13673. Levine, J., Stebbins, R., **Upper limit on the gravitational flux reaching the earth from the Crab pulsar,** *Phys. Rev. D* **5,** No. 7, 1465-1468 (Apr. 1, 1972).

Key words: Crab pulsar; gravitational waves; laser strainmeter; precision interferometry.

A 30-m laser interferometer has been used in a search for gravitational radiation from the Crab pulsar. The minimum detectable signal would be produced by an incident gravitational flux of $10^9$ ergs/sec cm² and we find no effect at this level.

13674. Barton, J. A., Jr., Burns, C. L., Chandler, H. H., Bowen, R. L., **An experimental radiopaque composite material,** *J. Dent. Res.* **52,** No. 4, 731-739 (1973).

Key words: Barium glass; dental composites; dental reinforcements; physical properties; resins; silica; x-ray opacity.

Physical properties of a composite material, developed for use as a temporary posterior restorative material, have been investigated. The material is based on isomeric phthalate esters of 2-hydroxyethyl methacrylate and reinforcing fillers consisting of particles of vitreous silica and an x-ray-opaque glass. Properties investigated include hardening time, tensile and compressive strengths, indentation and recovery, hardness, water sorption, solubility, polymerization shrinkage, optical and x-ray opacity, color stability and thermal expansion. All properties were studied using 3 different powder-liquid rations: 1.10, 1.35 and 1.45 Gm of powder to 0.4 ml of monomer, under wet and dry storage conditions. The powder-liquid ratio had little effect on compressive strength; e.g., 1.45 ratios, respectively. The tensile strength of the 1.10 ratio specimens was lower than those of the 1.35 and 1.45 ratio specimens (at six hours, 25.5 as compared to 30.4 MN/m²). Water sorption at one week was 0.2 to 0.3 mg/cm².

13675. Shirley, J. H., **Semiclassical theory of saturated absorption in gases,** *Phys. Rev. A* **8,** No. 1, 347-368 (July 1973).

Key words: Gas laser theory; lamb-dip; saturated absorption.

A three-dimensional theory for the resonant interaction of electromagnetic waves with a gas of two-level atoms is formulated in terms of macroscopic variables. The theory is utilized to find the steady-state attenuation of a plane wave in the presence of another plane wave running in the opposite direction with different amplitude. Contributions are included from the reflection of the oppositely running wave by an induced standing-wave inhomogeneity in the population inversion of the medium. The resulting attenuation and reflection coefficients are expressed as velocity integrals of continued fractions. Correspondence is made with existing gas-laser theories, yielding the formulation of a high-intensity ring-laser theory. Analytic approximations for the coefficients are presented for the Doppler-limit cases of both waves weak, one wave weak, and negligible reflection (rate-equation approximation). More-general cases have been calculated numerically. The attenuation coefficients exhibit a Lamb-dip feature. The relative depth of the dip increases rapidly with power at low saturation levels, slowly at high saturation, and is greater in the attenuation of the weaker wave. The width of the dip is nonlinearly power broadened. The shape of the dip is very nearly Lorentzian, except for one special case at high power in which the line splits. The propagation equations for the two waves are integrated over long absorption paths. A large resulting attenuation increases the relative size of the dip while decreasing the power broadening.

**13676.** Roberts, J. R., Andersen, T., Sørensen, G., **Determination of atomic lifetimes and absolute oscillator strengths for neutral and ionized titanium,** *Nucl. Instrum. Methods* **110,** 119-125 (1973).

Key words: Absolute transition probabilities; arc; beam foil; experimental; lifetimes; titanium.

Measurements of atomic lifetimes by the beam-foil technique and branching ratios by use of a gas-flow stabilized arc have led to an experimental determination of absolute oscillator strengths of Ti II. Some lifetimes of Ti I, Ti III and Ti IV are also presented.

**13677.** Robertson, A. F., **Tests indicate venting increases smoke from some polymerics,** *Fire Eng.* **126,** No. 9, 97-98 (Sept. 1973).

Key words: Buildings; cellulosics; fires; polymers; smoke; venting.

The problem of voluminous smoke production during burning of plastic or polymeric materials is considered. Experimental data on smoke density resulting from both smouldering and flaming pyrolysis of cellulosic and polymeric sheet and foam materials are presented and compared. It is concluded that in general, although exceptions occur for specific materials, cellulosics produce much less smoke than polymerics under flaming exposure. The smoke production under smouldering exposure is roughly comparable for the two classes of materials. However, the polymeric materials show a marked increase of smoke production for flaming vs. smouldering while the converse is true for cellulosics. It is suggested that the fire fighting ventilation tactics developed and used for fires involving cellulosic materials may aggravate rather than ameliorate the problem of fighting fires involving polymeric materials.

**13678.** Simmons, J. D., Keller, R. A., **Interferometric effects on the output of organic dye lasers,** *Appl. Opt.* **12,** No. 9, 2033 (Sept. 1973).

Key words: Dye laser continua; high resolution; interferometric effects; optical components; organic dye lasers; wedged optical surfaces.

This note illustrates the necessity of using wedged optica components in organic dye laser systems to avoid interferometric effects.

**13679.** Fatiadi, A. J., **Mechanism of formation of tris(phenylhydrazones) on treatment of cyclohexane-1,3-diones with phenylhydrazine,** *Chem. Ind.*, pp. 38-40 (Jan. 6, 1973).

Key words: Cyclohexane-1,3-dione; formation; free-radical; ionic; mechanism; phenylhydrazine.

The e.s.r. studies show that the formation of the 2-oxo-1,3 bis(phenylhydrazones) and tris(phenylhydrazones) fron cyclohexane-1,3-diones, and of bis(phenylhydrazones) fron cyclohexane-1,2-diones, following treatment with phenylhydrazine in polar solvents most likely proceeds by a concerte process, involving both ionic and free-radical pathways.

**13680.** Stephenson, J. C., **Vibrational energy transfer in NO,** *J Chem. Phys.* **59,** No. 3, 1523-1527 (Aug. 1, 1973).

Key words: Infrared lasers; laser pumping of molecules nitric oxide; vibrational energy transfer.

Laser-excited vibrational fluorescence measurements hav been used to obtain rate constants at room temperature for vibrational relaxation of the $V=1$ state of NO in collisions with He Ar, $H_2$, CO, NO, $N_2$, and $CO_2$. Pulses from a $CO_2$ laser, frequency doubled in a tellurium crystal, provided the excitation source The rate for the $V-V$ exchange $NO(1)+NO(1)\rightarrow NO(0)$- NO(2) was obtained.

**13681.** Judd, D. B., Eastman, A. A., **Prediction of target visibilit from the colors of target and surround,** *Illum. Eng.* **66,** No. 256-266 (Apr. 1971).

Key words: Color; contrast; detection; tritanopia; visibil ty; vision.

The target visibilities of each of 266 combinations of targe and surround colors have been measured by means of the Eas man contrast-threshold visibility meter. The targets and su rounds were Munsell papers, and the targets were of such siz and distance from the observer (AAE) that they subtended 1 minutes of arc. Analysis of these data shows that a modificatio of the 1964 CIE uniform color space applied to the fluxes leavin target and surround accounts for two-thirds of the observe variation in visibility among the 266 combinations. This modif cation for 10-minute targets consists of neglecting the viole greenyellow component of the color differences entirely and counting the red-green component less than one-tenth th proper for 60-minute targets. By taking into account the fact th the lens system of the human eye, because of chromatic aberr tion, causes some of the flux leaving the surround to fall on th retinal image of the target, this modified color space has bee shown to account for four-fifths of the observed variations visibility.

**13682.** Hougen, J. T., **Tabulation of hyperfine splittings in rot tional $F_1$ and $F_2$ levels of the ground vibrational state of $^{12}CH$ for $J \leqslant 20$,** *J. Mol. Spectrosc.* **46,** No. 3, 490-501 (June 1973

Key words: Computer tabulation; ground vibrational stat hyperfine splittings; methane; quantum mechanical Hamitonian; rotational levels.

To a good approximation, hyperfine splittings for $F_1$ and rotational levels of the ground vibrational state of $^{12}CH_4$ depen linearly on three hyperfine interaction parameters. Coefficien in these linear expressions have been computed in a relativel simple manner and tabulated for levels with $1 \leqslant J \leqslant 20$. Th hyperfine pattern for the $J=7$ $F_2^{(2)}$ level computed from thes expressions using values for the three hyperfine interactio meters reported recently by Yi, Ozier and Ramsey [1] es well with the pattern obtained from new He-Ne laser surements of Hall and Bordé [2] on the $P(7)\ F_2^{(2)}$ line of the nd of methane.

3. Frederikse, H. P. R., Hosler, W. R., **Electrical conductivi- of coal slag,** *J. Amer. Ceram. Soc.* **56**, No. 8, 418-419 (Aug. 73).

Key words: Electrical conductivity; slag; transfer.

ne electrical conductivity of natural and synthetic slags (con- ng 14 to 36 wt% Fe) was measured from 1200 to 1700 K at ressures from 1 to $2 \times 10^{-6}$ atm. The conductivity is relative- gh ($\approx 10^{-2}\ \Omega^{-1}\ cm^{-1}$ at 1700 K) and stems from the transfer ectrons between $Fe^{2+}$ and $Fe^{3+}$ ions. Anomalies in the con- ivity around 1600 K are the result of devitrification of the s samples.

4. Dewitt, D. P., Richmond, J. C., **Theory and measurement the thermal radiation properties of metals,** Chapter 1 in *easurement of Physical Properties: Some Special Proper- es,* E. Passaglia, Ed., **VI,** Part 1, 1-90 (Interscience Publ., ew York, N.Y., 1972).

Key words: Absorptance; electromagnetic theory; emittance; measurement techniques; metals; reflectance; surface effects; thermal radiation properties.

his is a general review of the thermal radiation properties of als, and includes (1) description and definition of the proper- and a discussion of their interrelationships, (2) a brief review ne physical laws relating to blackbody radiation, (3) discus- of the theory of the interaction of electromagnetic waves electrical conductors, (4) the effect of surface condi- – profile and surface films – on thermal radiation properties netals, and (5) a review of methods of measuring thermal ation properties of metals.

85. Straty, G. C., Younglove, B. A., **Some sound velocity mea- rements on liquid fluorine,** *J. Chem. Phys.* **58,** No. 5, 2191- 192 (Mar. 1, 1973).

Key words: Compressed liquid; fluorine; saturated liquid; sound velocity.

ome sound velocity measurements on liquid fluorine at 110 nd 130 K at pressures to 21 $MN/m^2$ are reported. Data were uired prior to a destructive reaction in the cell which vented further measurements.

86. Fickett, F. R., **Magnetoresistivity of copper and aluminum cryogenic temperatures,** *(Proc. 4th Int. Conf. on Magnet echnology, Brookhaven National Laboratory, Upton, N.Y., ept. 19-22, 1972),* pp. 539-541 (Atomic Energy Commission, ashington, D.C., 1972).

Key words: Aluminum; copper; electrical properties; magnetoresistance.

esults of recent measurements of the magnetoresistance of crystalline wires of aluminum and copper are presented. The surements were made in the temperature range 4 K to 35 K in magnetic fields to 100 kOe. The aluminum wires ranged urity from RRR = 1000 – 30 000 and the copper wires from R = 200 – 7000. RRR = R(273 K)/R(4 K).

87. Becker, D. A., LaFleur, P. D., **Neutron activation analy- s: Application to trace element analysis in biological and en- ironmental materials,** *Proc. 5th Annual Conf. on Trace Sub- tances in Environmental Health, University of Missouri, olumbia, Mo., 1971,* pp. 447-453 (1972).

Key words: Biological samples; biological standards; chemical separations; environmental samples; neutron activation analysis (NAA); nondestructive; reagent blanks; trace element analysis.

Neutron activation analysis (NAA) has been found useful for trace element analysis of biological and environmental samples. The favorable characteristics of this technique include high sensitivity, wide applicability, great specificity, and reduced contamination and reagent blank problems. The utilization of this technique for the analysis of several elements (Mn, Na, Cu, Zn, U) in the recently certified NBS Biological Standard Reference Material: Orchard Leaves, is described. Techniques used include both nondestructive analysis and destructive analysis using radiochemical separations. In addition, the analytical results obtained by NAA on the Orchard Leaves, is compared to that obtained by other analytical techniques.

**13688.** Hummer, D. G., Kunasz, C. V., Kunasz, P. B., **Numerical evaluation of the formal solution of radiative transfer problems in spherical geometries,** *Comput. Phys. Commun.* **6,** 38-57 (1973).

Key words: Early-type stars; model atmospheres; radiative transfer; spectral line formation; spherical geometry.

If the source function and opacity are specified numerically on a grid of radius and frequency points in a spherically symmetric atmosphere, the program described here calculates the formal solution of the radiative transfer equation, that is, the intensity of radiation on the corresponding grid, and evaluates the first three angular moments of the radiation field. Extensive use of cubic splines in the analysis has made possible an extremely rapid and compact procedure for this calculation. This program has been used extensively in the solution for line formation problems in spherically symmetric atmospheres.

**13689.** Lovejoy, R. W., Olson, W. B., **Ground state rotational constants for $^{28}SiH_3D$,** *J. Chem. Phys. Letters to Editor* **57,** No. 5, 2224-2225 (Sept. 1, 1972).

Key words: Infrared spectrum; monodeuterosilane; perturbation allowed transitions; rotational constants; stretching vibrations.

The infrared spectrum of the $\nu_1$ and $\nu_4$ stretching vibrations of $SiH_3D$ have been recorded with high resolution. The ground state rotational constants have been determined with much greater precision than has previously been reported. Observed perturbation allowed transitions have also made possible the determination of $A_o$-$B_o5D_o{}^K$.

**13690.** Field, R. W., Wicke, B. G., Simmons, J. D., Tilford, S. G., **Analysis of perturbations in the $a^3\Pi$ and $A^1\Pi$ states of CO,** *J. Mol. Spectrosc.* **44,** No. 2, 383-399 (Nov. 1972).

Key words: $a^3\Pi$, $A^1\Pi$ states; CO; configuration interaction; electronic perturbation parameters; matrix element; perturbation analysis.

The results of an analysis of perturbation of the CO $a^3\Pi$ and $A^1\Pi$ states of the...$(\pi 2p)^4(\sigma 2p)(\pi^* 2p)$ electronic configuration by states of the ...$(\pi 2p)^3(\sigma 2p)^2(\pi^* 2p)$ configuration provide evidence for the following conclusions: (i) For perturbations between vibronic levels of a given pair of electronic states, the perturbation matrix element is the product of a vibrational factor and a constant electronic factor, (ii) Simple single configuration arguments successfully predict that all the electronic factors for the perturbations between levels of each pair of states can be related to two constants which are joint properties of the two electronic configurations $\sigma\pi^*$ and $\pi^3\pi^*$.

**13691.** Field, R. W., Tilford, S. G., Howard, R. A., Simmons, J. D., **Fine structure and perturbation analysis of the $a^3\Pi$ state of CO,** *J. Mol. Spectrosc.* **44,** No. 2, 347-382 (Nov. 1972).

Key words: $a^3\Pi$ state; CO; electronic spectra; rotational analysis; vibrational analysis.

The Cameron absorption bands of CO($v' = 1 - 8$; $v'' = 0$) have been photographed at high resolution. The analysis of these bands along with a reanalysis of the $a^3\Pi$, $v = 0$ level and an analysis of the perturbations of the $a^3\Pi$ state by levels of the $a'^3\Sigma^+$, $e^3\Sigma^+$, $d^3\Delta_i$ and $I^1\Sigma^-$ states will be presented. Deperturbed molecular constants for the $a^3\Pi$ state and accurate perturbation parameters for the interactions of $a^3\Pi$ with nearby states have been determined by a last-squares matrix diagonalization technique. The input data included: (i) earlier measurements from triplet-triplet emission transitions, (ii) the new measurements of the Cameron bands, (iii) rf measurements of $a^3\Pi$ lambda doubling transitions, and (iv) measurements of absorption to the neighboring perturbing states.

**13692.** Seltzer, S. M., Berger, M. J., Rosenberg, T. J., **Auroral bremsstrahlung at balloon altitudes,** *NASA Spec. Publ. 3081,* 25 pages (National Aeronautics and Space Administration, Washington, D.C., 1973).

Key words: Atmosphere; auroral electrons; balloon experiment; bremsstrahlung; energy spectrum; transport calculation.

Data from a Monte Carlo calculation of the transport of electrons and secondary bremsstrahlung are presented in tabular and graphical form. These data describe bremsstrahlung flux spectra at various atmospheric depths between 3.0g/cm² and 15.0 g/cm² caused by a wide-area uniform precipitation into the atmosphere of electrons with energies between 30 and 2000 keV. The angular distribution of the incident electrons has been assumed to be isotropic over the downward hemisphere. A basic set of results is given for incident monoenergetic electron beams, which can be used to treat incident electron beams with any spectrum of interest. A comprehensive set of results, in the form of differential and integral bremsstrahlung flux spectra, has been obtained for the case of electron beams with exponential energy spectra, for e-folding energies between 5 and 200 keV.

**13693.** Prince, E., Donnay, G., Martin, R. F., **Neutron diffraction refinement of an ordered orthoclase structure,** *Amer. Mineral.* **58,** 500-507 (1973).

Key words: Aluminum silicate; feldspar; neutron refinement; orthoclase, silicate minerals; silicon aluminum ordering.

The crystal structure of a pegmatitic monoclinic potassium feldspar, $(K_{0.86}Na_{0.10}\square_{0.04})$ $(Si_{3.00}Al_{1.00})$ $[0_{7.96}(OH)_{0.04}]$, from the Himalaya mine in the Mesa Grande pegmatite district, Calif., has been refined with 3-dimensional neutron-diffraction data to an unweighted $R$ value of 0.031 for 721 symmetry-independent observed reflections. Atomic coordinates differ by no more than 3 estimated standard deviations from those of Spencer B adularia, yet the specimen does not have the adularia morphology, and no diffuse reflections with $(h+k)$ odd have been observed. Direct refinement of the tetrahedral cation distribution shows that the Al content of the $T(2)$ sites is not significantly different from zero (actually $-$ 0.016 with an e.s.d. of 0.029); in other words the Al-Si ordering in the tetrahedral sites is essentially complete. The mean Si-O distance in the $T(2)$ sites is 1.616 Å, appreciably greater than the values predicted by various regression lines relating bond distance to aluminum content. This indicates that the observed mean $T_1(m)$-O, $T_2$(O)-O, and $T_2(m)$-O bond lengths reported for low albite and maximum microcline are consistent with full Si occupancy. This ordered orthoclase occurs in gem pockets in a microcline-bearing pegmatite. The association suggests stable growth of ordered orthoclase above the field of stability of microcline and metastable persistence to lower temperatures. Perhaps because of more rapid crystal growth, the bulk of the pegmatitic K-feldspar ordered to common orthoclase, then transformed to maximum microcline.

**13694.** Currie, L. A., **The limit of precision in nuclear and analytical chemistry,** *Nucl. Instrum. Methods* **100,** 387-395 (1972).

Key words: Counting precision; excess variability; limiting precision; photonuclear chemistry; Poisson statistics; single and multiple parameter nuclear analyses; statistical weights; 14 MeV neutron activation.

The precision associated with an experiment in nuclea chemistry or activation analysis is commonly estimated b means of Poisson counting statistics. Such an estimate, as well a the conclusion that the precision may be indefinitely improve by increasing the number of counts obtained, is necessaril wrong when additional sources of random error are operating Knowledge of the additional, non-Poisson component of randon error is required for reliable estimates of parameters and thei standard errors, to detect model errors, to plan counting experi ments efficiently, and to establish the limit of precision when th Poisson counting error becomes negligible. For these purposes an iterative computation program – XESS – has been develope to take into account the additional variance and unequal statist cal weights. The significance and detectability of excess varianc is illustrated with data from studies of photonuclear reaction and activation analysis.

**13695.** Piganiol, M. P., Balke, S., Branscomb, L. M., Hamada, S Hookway, H. T., Tell, B. V., Ad Hoc Group on Scientific an Technical Information OECD, **INFORMATION for a chan ing society, some policy considerations,** *Organisation for Ec nomic Co-operation and Development,* 46 pages (OEC Publication, Paris, France, 1971).

Key words: Information packages; information policy; i formation systems; information users; OECD; technical i formation.

Early in 1969 the Secretary General of OECD established Ad Hoc Group on Scientific and Technical Informatio requesting the Group to "explore the nature, magnitude, and im plications of the needs for scientific and technical informatic and data in science, the economy and society, and how the needs may be met through changes in the structures, technol gies and policies, and management concepts." The Ad H Group reached 13 conclusions and recommendations deali with the scope of action of OECD, the usefulness and applic bility of scientific and technological information systems, quali control of content and procedure of information systems, educ tion for information system needs, and international cooperatic The report describes the observations and arguments leading the conclusions and recommendations.

**13696.** Myers, V. W., **Klein-Gordon equation for a charged par cle interacting with an electromagnetic wave,** *J. Franklin In Brief Commun.* **295,** No. 6, 497-499 (June 1973).

Key words: Expectation values; Klein-Gordon equatic plane electromagnetic wave.

A solution of the two-component Klein-Gordon equation obtained from a solution of the corresponding one-compon equation for the example of a charged particle interacting wit plane electromagnetic wave. Expectation values for moment components and the total energy of the particle are calculated.

**13697.** Santoro, A., Mighell, A. D., **Properties of crystal lattic The derivative lattices and their determination,** *Acta Crys logr.* **A28,** Part 3, 284-287 (May 1972).

Key words: Crystallography; lattices; sub-lattices; sup lattices.

erivative lattices are classified as super. sub and composite, the basis of the properties of the transformation matrices ting them to the lattice from which they are derived. A hod for obtaining the transformation matrices generating se lattices is given. The method has been applied to derivation he unique super and sublattices in a few important cases.

**98.** Rowe, J. M., Livingston, R. C., Rush, J. J., **Neutron uasielastic scattering study of $SH^-$ reorientation in the cubic hases of cesium and rubidium hydrosulfide,** *J. Chem. Phys.* **58,** o. 12, 5469-5473 (June 15, 1973).

Key words: Alkali hydrosulfides; hydrosulfide ion; ion reorientation; neutron scattering; phase transition; quasielastic scattering.

he orientational disorder of the hydrosulfide ions in CsSH Cl phase) and RbSH (NaCl phase) has been investigated quasielastic neutron scattering with high energy resolu- ($\Delta E_{1/2max}$=0.25 meV). The experimental results pro- e a clear demonstration of the theoretically predicted sepa- on of the quasielastic neutron peaks for rotating groups molecules into unbroadened and broadened components ch reflect, respectively, the geometric and time behavior he rotation. Jump reorientation of the ions between equi- ium directions is established as the dominant mechanism ating the rotational disorder in the hydrosulfides, and h small-step rotational diffusion and quasifree rotation clearly ruled out. Average residence times between re- entation jumps are derived from comparisons of the ex- imental results with theoretical calculations based on ip reorientation models, but it is not possible to determine equilibrium orientation of the $SH^-$ ions. Mean-square rational amplitudes for the hydrogen atoms are also ob- ied from the observed integrated intensities of the elastic ks. The present results are compared in detail with previous er-resolution neutron results on NaSH and CsSH. It is con- ded that in most cases measurements using single crystals will necessary to establish the details of orientation disorder in ds.

**99.** Santoro, A., Mighell, A. D., **Coincidence-site lattices,** *Acta rystallogr.* **A29,** Part 2, 169-175 (Mar. 1973).

Key words: Crystal aggregates; crystals; grain boundaries; lattices; sublattices; superlattices.

oincidence-site lattices are characterized mathematically, in general case, by a method that can be applied to a pair of ginal lattices of any symmetry, either metrically identical or trically different, does not involve inspection and is readily ptable to computer calculations. The procedure is illustrated several numerical examples. The proposed characterization coincidence-site lattices is based on the theory of derivative ices and makes extensive use of the concepts of superlattice l sublattice. Appended is a simple procedure for determining transformation matrices needed to generate superlattices and lattices of any multiplicity.

**00.** Rush, J. J., de Graaf, L. A., Livingston, R. C., **Neutron cattering investigation of the rotational dynamics and phase ransitions in sodium and cesium hydrosulfides,** *J. Chem. Phys.* **8,** No. 8, 3439-3448 (Apr. 15, 1973).

Key words: Cesium hydrosulfide; hydrosulfides; ion reorientation; libration; neutron scattering; phase transition; quasielastic; residence time; sodium hydrosulfide.

he rotational motions of the hydrosulfide ions in the trigonal l fcc phases of NaSH and in the pseudo-bcc (CsCl) phase of SH have been studied by quasielastic and inelastic neutron ttering. NaSH and CsSH are members of a broad group of compounds $M^+(XY^-)$ which have cubic symmetry in the solid phase just below the melting point and a lower symmetry in lower temperature crystal phases. The measured inelastic neutron spectra above and below the trigonal to cubic phase transition in NaSH show that $SH^-$ ion "librations" about equilibrium orientations persist in passing through the transition. The maximum of the broad librational bands for both NaSH and CsSH occurs near 400 $cm^{-1}$. A temperature and momentum-transfer ($Q$) dependent broadening is observed, however, in the quasielastic peaks in the cubic phases of the hydrosulfides, which indicates a rapid reorientation of the $SH^-$ ions. The experimental quasielastic scattering results are compared with theoretical calculations of quasielastic scattering behavior based on the assumption of instantaneous reorientational jumps between a limited number of quasiequilibrium orientations. The widths of the measured quasielastic peaks plotted vs $Q$ show an oscillatory behavior as predicted by the theoretical calculations. An isotropic reorientation model is ruled out, and the differences in the rotational disorder in NaSH and CsSH are discussed. Relaxation times ($\tau$) for the $SH^-$ motions are derived from the theoretical analysis. The $\tau$ values for fcc NaSH vary from 0.4 to 0.15 psec between 103 and 212 °C, while the values for pseudo-bcc CsSH vary from 2.0 to 0.75 psec between 23 and 140 °C.

**13701.** Siu, M. C. I., **Equations for thermal transpiration,** *J. Vac. Sci. Technol.* **10,** No. 2, 368-372 (Mar./Apr. 1973).

Key words: Anomalous Knudsen limit; diffuse scattering; irreversible thermodynamics; specular scattering; thermal transpiration.

A formalism for analytically obtaining an expression for the thermal transpiration pressure ratio $R$ is presented. An experimental parameter $\sigma$, which is associated with the type of molecule-solid surface collisions, is introduced. A completely diffuse scattering and a completely specular scattering from a solid surface correspond to $\sigma=0$ and $\sigma=1$, respectively. A known distribution function is used to derive a practical formula for $R$ in the case of long tubes and very low pressures. Quantitative results obtained from this formula indicate that deviations from completely diffuse scattering of molecules from solid surfaces give rise to an anomalous Knudsen limit.

**13702.** Petersen, F. R., McDonald, D. G., Cupp, J. D., Danielson, B. L., **Rotational constants for ${}_{12}C_{16}O_2$ from beats between Lamb-dip-stabilized lasers,** *Phys. Rev. Lett.* **31,** No. 9, 573-576 (Aug. 27, 1973).

Key words: Accurate rotational constants; carbon dioxide (${}^{12}C^{16}O_2$); Josephson junction; Lamb-dip-stabilized lasers.

New experimental measurements of the frequency separations of 30 pairs of ${}^{12}C^{16}O_2$ laser lines in the 10.4-$\mu$m band and 26 pairs in the 9.4-$\mu$m band have been made with Lamb-dip-stabilized lasers. The use of a Josephson junction as the frequency-mixing element simplified the measurements. Uncertainties in existing rotational constants for the laser vibrational levels were reduced 20 to 30 times and an additional rotational constant $H_v$ was determined for the first time.

**13703.** Sugar, J., Reader, J., **Ionization energies of doubly and triply ionized rare earths,** *J. Chem. Phys.* **59,** No. 4, 2083-2089 (Aug. 15, 1973).

Key words: Cerium; dysprosium; erbium; europium; gadolinium; hafnium; holmium; ionization energy; lanthanum; lutetium; neodymium; praseodymium; promethium; samarium; terbium; thulium; ytterbium.

Values for the ionization energies of the doubly and triply ionized rare earth atoms have been derived from interpolated spectroscopic properties of the $4f^Nns$ series, and from interpolated energy intervals relating the first series member, $4f^N6s$, to the ground state. The results in eV are

| | | |
|---|---|---|
| Tb III | 21.91(10) | IV 39.79(20) |
| Dy | 22.79(30) | 41.47(20) |
| Ho | 22.84(10) | 42.48(32) |
| Er | 22.74(10) | 42.65(21) |
| Tm | 23.68(10) | 42.69(20) |
| Yb | 25.03(2) | 43.74(20) |
| Lu | 20.9596(10) | 45.19(2) |
| Hf | | 33.33(2) |
| La III | 19.1774(6) | |
| Ce | 20.198(3) | IV 36.758(5) |
| Pr | 21.624(3) | 38.98(2) |
| Nd | 22.14(30) | 40.41(20) |
| Pm | 22.32(36) | 41.09(32) |
| Sm | 23.43(30) | 41.37(38) |
| Eu | 24.70(32) | 42.65(32) |
| Gd | 20.63(10) | 44.01(35) |

The values for the doubly ionized atoms agree to within ~ 1 percent with those deduced from thermodynamic measurements on lanthanide oxides. A value for the ionization energy of Gd II of 12.09(8) eV was determined by using new spectroscopic data for Gd II Gd III.

**13704.** Flynn, J. H., **Instrumental limitations upon the measurement of temperature and rate of energy production by differential scanning calorimetry,** (Proc. 3d Int. Conf. on Thermal Analysis, Davos, Switzerland, Aug. 23-28, 1971), Paper in *Thermal Analysis,* H. G. Wiedemann, Ed. **1,** 127-138 (Birkhäuser Verlag, Basel, Switzerland, 1972).

Key words: Cooling curve temperature calibration; differential scanning calorimetry; evaluation of thermal apparatus; temperature calibration; thermal analysis.

Instrumental time constants for rate of energy production response, temperature-programming response and temperature-averaging network response, time constants for a wide variety of conditions for interfacial conductivity between the sample and the calorimeter cup, and for the thermal conductivity of the sample are catalogued for the differential scanning calorimeter. Assessment of the effects of these factors upon the net rate of power production sensitivity and the temperature calibration results in the establishment of limits of precision in the measurement of temperature, specific heat and heats and rates of enthalpy change during chemical and physical transformations. The vulnerability of these calibrations to instrumental readjustment and variation in experimental techniques is also quantitatively evaluated.

**13705.** Milligan, D. E., Jacox, M. E., Guillory, W. A., **Infrared spectrum on the $NO_2^-$ ion isolated in an argon matrix,** *J. Chem. Phys.* **52,** No. 8, 3864-3868 (Apr. 15, 1970).

Key words: Alkali metal reactions; electron attachment; infrared spectrum; matrix isolation; $NO_2^-$; photodetachment; photoionization.

The molecular ion $NO_2^-$ has been stabilized in an argon matrix in sufficient concentration for detection of its antisymmetric stretching fundamental, $\nu_3$, at 1244 $cm^{-1}$ by electron bombardment or photoionization of matrix-isolated $NO_2$ and by the interaction of an alkali-metal atomic beam with $NO_2$ in an argon matrix. In contrast to the position of this fundamental in an inert, nonionic environment, a value of approximately 1275 $cm^{-1}$ is characteristic of the crystalline material. Isotopic data are consistent with a 115° valence angle for $NO_2^-$, independent of environment. Irradiation of the sample with light of wavelength near 3150 Å leads to the destruction of the $NO_2^-$ absorption in the studies of the electron bombardment and photoionization of $NO_2$, but not in the experiments in which the alkali metal atoms provide a reservoir of photoelectrons.

**13706.** Milligan, D. E., Jacox, M. E., **Infrared and ultraviolet spectroscopic studies of a number of small free radicals and molecular ions in a matrix environment,** (Proc. Symp. on Spectroscopic Methods in Cryochemistry and of the Chemistry of High Temperature Species, Minneapolis, Minn., Apr. 1969), Paper in *Advances in High Temperature Chemistry,* Leroy Eyring, Ed. **4,** 1-42 (Academic Press, Inc., New York, N.Y., 1971).

Key words: Free radicals; infrared spectrum; matrix isolation; molecular ions; photolysis; ultraviolet spectrum.

The development of the matrix isolation technique is summarized, and the principles which have been found to be important for the *in situ* photoproduction of free radicals trapped in inert solid matrices in sufficient concentration for direct infrared and ultraviolet spectroscopic observation are considered. A survey of the small free radical species heretofore studied using these techniques is given. Examples of the successful application of the technique are drawn from recent studies of the vacuum-ultraviolet photolysis of matrix-isolated methane and silane and of their chloro- and fluoro-derivatives. Results of experiments designed to permit the trapping in inert, nonionic matrices of negatively charged molecular ions are presented.

**13707.** Finnegan, T. F., Witt, T. J., Field, B. F., Toots, J., **Measurements of 2*e*/*h* via the AC Josephson effect.** (Proc. 4th Int. Conf. on Atomic Masses and Fundamental Constants, Teddington, England, Sept. 6-10, 1971), Paper in *Atomic Masses and Fundamental Constants* **4,** J. H. Sanders and A. H. Wapstra, Eds., pp. 403-410 (Plenum Press, New York N.Y., 1972).

Key words: Josephson junction; standard cell; voltage comparison.

Recent sub-part-per-million determinations of 2*e*/*h* have been reported by several groups. The accuracies of these determinations have been limited to a large extent by uncertainties in the local voltage standard (i.e., standard cells). The present state o agreement between the various 2*e*/*h* determinations will be reviewed by using the results of the triennial international vol comparisons at BIPM, as well as the results of direct volt comparisons between NBS and other national laboratories, to relate the various national as-maintained units of voltage.

Progress on the NBS project to maintain a unit of emf via Josephson junction device will also be reported. The results of series of 2*e*/*h* measurements made at the site of the NBS reference group of standard cells will be presented. The implications of these measurements on the stability of the NBS reference group of standard cells, and on the fundamental physical constants (i.e., the fine structure constant) will be discussed

**13708.** Nelson, J. D., Blair, W., Brinckman, F. E., Colwell, R. R Iverson, W. P., **Biodegradation of phenylmercuric acetate b mercury-resistant bacteria,** *Appl. Microbiol.* **26,** No. 3, 321 326 (Sept. 1973).

Key words: Atomic absorption; biodegradation; mercury resistant bacteria; mercury transformations; phenylmercuric acetate, Pseudomonas.

Selected cultures of mercury-resistant bacteria degrade th fungicide-slimicide phenylmercuric acetate. By means of closed system incorporating a flameless atomic absorption spectrophotometer and a vapor phase chromatograph, it was demonstrated that elemental mercury vapor and benzene were product of phenylmercuric acetate degradation.

09. Falge, R. L., Jr., Swartzendruber, L. J., **Influence of lustering on the paramagnetic behavior of a Cu-Ni alloy,** *Phys. ett.* **44A,** No. 4, 285-286 (June 18, 1973).

Key words: Clustering; critical phenomena; Cu-Ni alloy; heat treatment; magnetism; susceptibility.

The equation usually reserved for the critical behavior of a fer-nagnet just above $T_c$ also describes the susceptibility of $_{0.47}Ni_{0.53}$ over a very large temperature range. The parameters, ich vary with heat treatment suggest lamellar clustering.

10. Miller, G., **The Shirley Highway Express-Bus-on Freeway lemonstration project—Project description,** *Report DOT/UMTA 1,* 87 pages (Urban Mass Transportation Administration, Department of Transportation, Washington, D.C., Aug. 1971). (Available as PB 218983 from the National Technical nformation Service, Springfield, Va. 22151).

Key words: Bus fringe parking; bus priority lanes, bus priority lanes in District of Columbia; bus transit operation; exclusive bus lanes, express-bus-on freeway technology; Shirley Highway Corridor in Northern Virginia; Urban Mass Transit Demonstration Project.

This report describes the three major demonstration project ments: (1) the busway, including the exclusive lane on Shirley ghway and the bus priority lanes in the District; (2) the bus nsit operation, involving new buses (with special features) on w routes and schedules; and (3) the residential fringe parking, h shopping centers and new lots providing free parking for s riders. The existing roadway and bus operations are docu-nted and the improvements planned for 1971-72 are esented. The Shirley Highway Corridor where the bus and to commuters live is described, as is the major employment stination areas. Data are also presented on bus and auto travel lumes for 1970-1971, before the busway was completed and new buses placed into operation.

711. Wiederhorn, S. M., **Environmental stress corrosion racking of glass,** (Proc. Int. Conf. on Corrosion Fatigue, Chemistry, Mechanics and Microstructure, University of Connecticut, Storrs, Conn., June 14-18, 1971), Paper in *Corrosion Fatigue,* **NACE-2,** 731-742 (National Association of Corrosion Engineers, Houston, Texas, 1972).

Key words: Cracked propagation of glass; glass; glass fibers; hardness of glass; static fatigue of glass; strength of glass; stress corrosion cracking of glass; structure of glass.

A review is presented on the effect of environment on the ength of glass. The structure of glass and its strength in the sence of environment are discussed briefly. Experimental sults on environmental cracking of glass are presented. Finally, eroretical treatments are given and discussed with respect to ailable experimental data.

712. Etz, E. S., Robinson, R. A., Bates, R. G., **Dissociation constant of protonated tris(hydroxymethyl)aminomethane in N-methylpropionamide and related thermodynamic quantities from 10 to 55 °C,** *J. Solution Chem.* **2,** No. 4, 405-415 (1973).

Key words: Acidic dissociation; dissociation constant; emf measurements; ionization processes; N-methylpropionamide; solvation; tris(hydroxymethyl)aminomethane.

The dissociation constant of protonated tris(hydroxmethyl)aminomethane (tris $H^+$) in the solvent *N*-methylropionamide (*NMP*) has been determined at intervals of 5 °C om 10 to 55 °C by measurement of the emf of cells without quid junction using hydrogen and silver-silver chloride elecodes. At 25 °C, $pK_a$ was found to be 8.831, as compared with .075 in water. The standard changes in Gibbs energy, enthalpy, ad entropy for the dissociation process have been evaluated from the dissociation constant and its change with temperature. By comparison with similar data for the dissociation of tris · $H^+$ in water, thermodynamic functions for the transfer from water to *NMP* have been derived. The dissociation process is isoelectric, and the solvent dielectric constant is high ($\epsilon = 176$ at 25 °C). Consequently, electrostatic charging effects are expected to be minimal, and the change in dissociation constant depends primarily on solute-solvent interactions. The results, combined with transfer energies for *HCl*, tris, and tris · *HCl* from emf and solubility measurements, demonstrate that the decreased acidic strength of tris · $H^+$ in *NMP* is attributable in large part to the fact that *NMP* is less effective than water in stabilizing tris and its salts.

13713. Unassigned.

13714. Baker, M. A., **Observing porcelain enamels with a scanning electron microscope,** *Proc. Porcelain Enamel Institute Technical Forum, The Ohio State University, Columbus, Ohio, Oct. 6-8, 1971,* **33,** 84-90 (Porcelain Enamel Institute, Inc., Washington, D.C., 1971).

Key words: Corrosion; pinhole-type defects; porcelain enamel; scanning electron microscope; weathering tests; non-dispersive x-ray spectrometer.

Porcelain enamel surfaces and enamel-metal interfaces have been observed with a scanning electron microscope. The increased depth of field and the extended range of magnifications of the scanning electron microscope were utilized in studies of the enamel-metal interface and of weathering test specimens that corroded after relatively short periods of exposure. The non-dispersive x-ray spectrometer accessory for the scanning electron microscope was used to determine the elements present in the enamel surface and to obtain qualitative distributions of these elements.

13715. Baker, M. A., **Weathering tests of porcelain enamels on steel and aluminum,** *Proc. Porcelain Enamel Institute Technical Forum, The University of Illinois, Urbana, Ill., Oct. 11-13, 1972,* **34,** 186-198 (Porcelain Enamel Institute, Inc., Washington, D.C., 1972).

Key words: Accelerated tests; acid resistance; aluminum; color; gloss; porcelain enamel; steel; weather resistance.

The Porcelain Enamel Institute and the National Bureau of Standards have been conducting weathering tests of porcelain enamels since 1939. The four tests now in progress contain matte and glossy porcelain enamels on both steel and aluminum. When the data obtained from these weathering tests were compared with accelerated test data on laboratory specimens, an excellent correlation was found. It was also found that the enamels in all four tests changed gloss and color in practically the same manner.

13716. Dibeler, V. H., Walker, J. A., McCulloh, K. E., **Observations on hot bands in the molecular and dissociative photoionization of acetylene and the heat of formation of the ethynyl ion,** *J. Chem. Phys.* **59,** No. 5, 2264-2268 (Sept. 1, 1973).

Key words: Ethynyl ion; heat of formation; ionization threshold; mass spectrometry; vacuum ultraviolet.

Photoion yield curves in the vicinity of threshold are obtained for the molecular and the ethynyl ions of acetylene and acetylene-$d_2$ at ion source temperatures of 360, 298, and 130 K. Weak ionization below the adiabatic threshold for $C_2H_2^{+}$ and $C_2D_2^{+}$ is ascribed to the ionization of molecules excited by one quantum of the bending vibrations, $\nu_4$ and $\nu_5$. Consideration of selection rules suggests a change in symmetry from the linear ground state molecule to a bent ground state ion. The 0 K curves for $C_2H^+$ and $C_2D^+$ are estimated from the observed 130 K data. Satisfactory agreement is obtained when the 298 K data are compared with a curve calculated from the 0 K curve by convolution with vibrational and rotational distributions. The 0 K thresholds corrected for kinetic energy are used to calculate $\Delta Hf^\circ_0(C_2H^+) = 17.47 \pm 0.01$ eV ($402.8 \pm 0.2$ kcal $mol^{-1}$) and $\Delta Hf^\circ_0(C_2D^+) = 17.43 \pm 0.02$ eV ($402.0 \pm 0.5$ kcal $mol^{-1}$). The ionization energy of the ethynyl radical is estimated to be $11.96 \pm 0.05$ eV.

**13717.** Bur, A. J., **Dielectric properties of fluorine-containing polymers,** Chapter 15 in *Fluoropolymers,* L. A. Wall, Ed., **25,** 475-505 (John Wiley-Interscience, New York, N.Y., 1972).

Key words: Dielectric constant; dielectric loss; fluoropolymer; relaxation phenomena; review.

The dielectric properties of polytetrafluorethylene, polychorotrifluoroethylene, polyvinylidene fluoride, and fluorinated ethylene propylene copolymer are reviewed. Relaxation phenomena as a function of temperature and crystallinity is emphasized. Molecular interpretations of the data are discussed. The effects of humidity changes on the dielectric properties of polytetrafluoroethylene and fluorinated ethylene-propylene copolymer show that these polymers are insensitive to humidity changes. Eighty references are cited.

**13718.** Abrams, M. D., **Remote computing: The administrative side,** *Comput. Decisions,* pp. 42-46 (Oct. 1973).

Key words: Administration; batch; computing; documentation; remote; service; users.

The administration and management of remote computing services are discussed with the objective of making both users and administrators aware of the potential problems. Likely difficulties are anticipated and coupled with discussions of assistance, operation, documentation and other features which make it more possible to utilize the technical services. The response to technical questions is covered in terms of written, on-line, and direct contact assistance. A question and answer organization is employed.

**13719.** Krauss, M., Julienne, P. S., **Dissociative recombination of $e + CH^+ (X\ {}^1\Sigma^+)$,** *Astrophys. J.,* **183,** L139-L141 (Aug. 1, 1973).

Key words: CH, $CH^+$; dielectronic recombination; electron-ion recombination; energy curve; Rydberg excited state; valence excited state.

The ratio of the dissociative recombination rate for $e + CH^+$ to the dielectronic recombination rate is calculated to be of the order of $10^3$. These rates place a serious constraint on homogeneous gas-phase production of interstellar $CH^+$ and CH from ground-state atoms.

**13720.** Mielenz, K. D., Eckerle, K. L., Madden, R. P., Reader, J., **New reference spectrophotometer,** *Appl. Opt.* **12,** No. 7, 1630-1641 (July 1973).

Key words: Beam geometry; high accuracy; optical design; spectrophotometer; systematic errors; transmittance.

A new single beam spectrophotometer is described in which transmittance is measured by placing samples normal to a parallel beam of light. Collimation and focusing of the main beam are achieved by means of off-axis parabolic mirrors. The wavelength at which the transmittance is to be measured is selected by a plane grating monochromator having off-axis parabolic mirrors and circular holes as entrance and exit apertures. The instrument has an inherent *accuracy* estimated to be 0.0001 transmittance unit. Its *precision* is characterized by a repeatability of 0.00004 transmittance units for neutral-density filters with transmittances between 10 and 30 percent. The design philosophy used to achieve these results is presented. A discussion of some systematic errors commonly neglected in routine spectrophotometric measurements is given. Systematic errors such as detector nonlinearity and stray radiant energy are measured.

**13721.** Collins, R. C., Haller, W., **Protein-sodium dodecyl sulfate complexes: Determination of molecular weight, size and shape by controlled pore glass chromatography,** *Anal. Biochem.* **54,** 47-53 (1973).

Key words: Chromatography; controlled pore glass; molecular size; porous glass chromatography; protein; protein-sodium dodecyl sulfate complexes; sodium dodecyl sulfate-complexes.

The peak position vs log molecular weight curves of protein-SDS complexes chromatographed on controlled pore glass of narrow pore size distribution is linear over a molecular weight range of 17,000-385,000. A glass with a pore size of approximately 500 Å allows the inclusion of all complexes in this range. Peak position curves on glasses with broad pore distributions show decreased resolution and deviate from linearity at low elution coefficients.

Exclusion size analysis of the elution coefficients of individual complexes from different columns with pore diameters ranging from 197 to 650 Å gives from 120 to 423 Å as their longest dimension. Assuming constant hydration and SDS-to-protein ration, the found dimension suggests the shape of a football, rather than a sphere or rigid rod.

**13722.** Fuller, E. G., **Photonuclear Physics 1973. Where we are and how we got there,** (Proc. Int. Conf. on Photonuclear Reactions and Applications, Pacific Grove, Calif., Mar. 26-30, 1973), Paper in *International Conference on Photonuclear Reactions and Applications,* B. L. Berman, Ed., pp. 1201-1224 (Ernest O. Lawrence Livermore Laboratory, University of California, Livermore, Calif., 1973). (Available as CONF-730301 from the National Technical Information Service, Springfield, Va. 22151).

Key words: Data; experimental facilities; history; photonuclear reactions; research programs; survey.

A brief history is presented of the study of photonuclear reactions from the time of the first measurements in 1934 through the most recent measurements in 1972 and early 1973. Trends are indicated both for the specific types of measurements carried out, as well as for the geographic areas of the world active in the field. A review is given of the data obtained since 1955 as a function of element and isotope and the areas where data are missing are pointed out. Finally, the results of a survey made in early 1973 are given. This survey covered the existing experimental facilities, as well as the research programs directed toward the study of the interaction of electromagnetic radiation with nuclei.

**13723.** Hallowell, P. L., Bertozzi, W., Heisenberg, J., Kowalski, S., Maruyama, X., Sargent, C. P., Turchinetz, W., Williamson, C. F., Fivozinsky, S. P., Lightbody, J. W., Jr., Penner, S., **Electron scattering from $^{19}F$ and $^{40}Ca$,** *Phys. Rev. C* **7,** No. 4, 1396-1409 (Apr. 1973).

Key words: Electron scattering; inelastic; $^{19}F$; $^{40}Ca$; transition strengths.

Electron scattering form factors were measured for the low-lying levels of $^{19}F$ and $^{40}Ca$ for momentum transfers between 0.55 and 1.00 $fm^{-1}$. Elastic scattering from $^{19}F$ yields an rms charge radius of $2.885 \pm 0.015$ fm. Transition strengths and transition radii are obtained for the lowest $5/2^+$, $5/2^-$, and $3/2^+$ states in $^{19}F$. A deformed rotational model gives a very good fit to the form factors for the positive-parity levels with ground-te deformation parameters of $\beta_2=0.41$ and $\beta_4=0.17$. The m factors for excitation of the $3^-$ and $2^+$ states in $^{40}$Ca are alyzed by phase-shift analysis, and transition strengths and nsition radii are also obtained for these levels.

**724.** Martin, W. C., Sugar, J., **Classifications of the resonance ines of europium** III, *Astrophys. J.* **184**, 671-674 (Sept. 1, 1973).

Key words: Atomic ions; atomic spectra; classified lines; energy levels; europium; ionization energy; stellar spectra.

A first analysis of Eu III by Russell *et al.* in 1941 yielded clas-ications of seven lines (2350-2523 Å) as transitions from the $^8S^0_{7/2}$ ground level to upper levels identified only as belonging the $4f^6\,5d$ configuration. We have diagonalized a truncated ergy matrix for $4f^6(^7F)5d$, using parameter values appropriate Eu III. Comparison of the results with available data for the es allows identifications of the seven experimental upper vels. These show that the seven lines include the three lines of basic $4f^7\,{}^8S^0 - 4f^6(^7F)5d\,{}^8P$ multiplet, the strongest resonance es of Eu III, and account for most of the oscillator strength of $4f^7\,{}^8S^0 - 4f^6\,5d$ group.

**725.** Broadhurst, M. G., Malmberg, C. G., Mopsik, F. I., Harris, W. P., **Piezo- and pyroelectricity in polymer electrets,** (Proc. Conf. on Electrets, Charge Storage and Transport in Dielectrics, Miami Beach, Fla., Oct. 8-13, 1972), Paper in *Electrets, Charge Storage and Transport in Dielectrics,* M. M. Perlman, Ed., pp. 492-504 (The Electrochemical Society, Inc., Princeton, N.J., 1973). (Available as AD 758730 from the National Technical Information Service, Springfield, Va. 22151).

Key words: Electret; piezoelectric; polymer electret; poly(vinyl chloride); pyroelectric.

A model for a polymer electret, based on an elastically isotrop- solid with orientationally frozen molecular dipoles, was veloped and tested experimentally. This electret is shown to both piezoelectric and pyroelectric. The polarization is shown change with mechanically and thermally induced strains in the larization direction. The currents generated by the electret will proportional to the strain rate and, for thin contact electrodes d uniform strains, unaffected by the presence of real charges. ly(vinyl chloride) films were poled at 80 °C, just above their ass transition temperature. The pressure- and temperature-inced short-circuit currents in the polarization direction equalled 15 (pA/cm$^2$)/(bar/min) and 2.2 (pA/cm$^2$)/(K/min) respectively r a specimen poled at 320 kV/cm. These currents were 1) versible and proportional to the rate of temperature or pressure ange, 2) proportional to poling voltage up to 320 kV/cm, 3) in e direction corresponding to increasing polarization with in-easing pressure and decreasing temperature, 4) stable with me without special storage conditions, 5) about 1.6 times as eat for temperature induced strains as for equivalent pressure duced strains and 6) about 2-4 times as great in magnitude as pected from dielectric constant measurements. The apparent larization from temperature measurements for the 320 kV/cm ecimen was about 1.7 $\mu$C/cm$^2$, or about 1/3 the value expected r maximum alignment of dipoles. In the same specimen the yroelectric coefficient was found to be $p_3 = -0.39$ nC/cm$^2$ K d, assuming elastic isotropy, the piezoelectric strain coeffi-ents were found to be $d_{31}=d_{32}=d_{33}=-0.89$ pC/N.

**3726.** Blomquist, D. S., **An experimental investigation of foam windscreens,** (Proc. 1973 International Noise Control Engineering Conference, Copenhagen, Denmark, Aug. 22-24, 1973), Paper in *Inter-Noise 73 Proceedings,* O. J. Pedersen, Ed., pp. 589-593 (Inter-Noise 73, Technical University, Lyngby, Denmark, 1973).

Key words: Acoustic attenuation; foam windscreens; wind-generated noise.

The amount of reduction in wind-generated noise and the amount of acoustic attenuation of the signal as a function of frequency for four different pore sizes and various diameters of open-cell polyurethane foam windscreens is presented.

**13727.** Leasure, W. A., Jr., Bender, E. K., **Tire-road interaction noise,** (Proc. 1973 International Noise Control Engineering Conference, Copenhagen, Denmark, Aug. 22-24, 1973), Paper in *Inter-Noise 73 Proceedings,* O. J. Pedersen, Ed., pp. 421-425 (Inter-Noise 73, Technical University, Lyngby, Denmark, 1973).

Key words: Acoustics; noise (sound); tire noise; transportation noise.

The important parameters influencing tire noise are discussed and the basic mechanisms of tire-noise generation are briefly described from a theoretical viewpoint. Areas for future research are identified—based on gaps in the existing data base and a rather primitive level of understanding of tire noise-generating mechanisms.

**13728.** Blomquist, D. S., Leasure, W. A., Jr., **An hourly noise exposure meter,** (Proc. 1973 International Noise Control Engineering Conference, Copenhagen, Denmark, Aug. 22-24, 1973), Paper in *Inter-Noise 73 Proceedings,* O. J. Pedersen, Ed., pp. 67-69 (Inter-Noise 73, Technical University, Lyngby, Denmark, 1973).

Key words: Acoustics (sound); environmental acoustics; instrumentation; noise exposure.

An instrument has been designed which provides information regarding the average noise exposure over each hour rather than simply a singly measure of noise exposure over an 8-hour work period. The theory of operation and examples of practical measurements utilizing this device will be discussed in the verbal presentation.

**13729.** Benzinger, T. H., **A new concept in thermodynamics and its implication in molecular biology and pharmacology,** Chapter 14 in *Methods in Pharmacology* **2,** Part 2, 481-488 (Appleton-Century Crofts, New York, N.Y., 1972).

Key words: Characteristic function (Planck); chemical bonding energy; double helix; heat integrals; molecular biology; thermal free energy; thermodynamics.

An extended statement of chemical equilibrium of the integral $T\int_0^T (\Delta Cp/T)dT (= T\Delta S_T^\circ)$ and $\Delta H_T^\circ$—the classical terms of the equation $-\mathrm{RTlnK} = \Delta H_T^\circ - T\Delta S_T^\circ$. The integral $\int_0^T \Delta Cp\,dT$ is not negligible for macromolecules and particularly biopolymers, and its direct experimental determination at all temperatures down to 0 K is therefore indispensable for thermodynamic understanding of the objects of molecular biology.

**13730.** Chignell, C. F., Benzinger, T. H., **Heatburst microcalorimetry,** Chapter 14 in *Methods in Pharmacology* **2,** Part 1, 465-489 (Appleton-Century Crofts, New York, N.Y., 1972).

Key words: Adenosinetriphosphate-thermodynamics; chemical bond energy; coiled helix thermopiles; drug receptor complexing; entropy; enzyme detection+analysis; equilibrium; free energy; free entropy concept; heat of reaction; heatburst principle; hydrogen bonding; immunoreaction calorimetry; microcalorimetry; molecular biology;

pharmacology; protein calorimetry; polynucleotide calorimetry; purity assay; reaction coupling; thermodynamics; warfarin.

In this chapter the heatburst principle will be briefly discussed followed by a description of the construction and operation of the heatburst microcalorimeter. In the next section, it will be shown how heat can not only be used as an indicator for chemical or biochemical change but can also be used to derive thermodynamic data for the system under study. In a third section, some further possible applications of heatburst microcalorimetry to current problems in molecular biology and pharmacology will be suggested. In a separate section, following this article, the classical determination of the laws of chemical equilibrium and the driving energies of chemical change will be re-examined, and a new determination, more suited to the objects of molecular biology and pharmacology, will be derived.

**13731.** Newbury, D. E., Yakowitz, H., Myklebust, R. L., **Monte Carlo calculations of magnetic contrast from cubic materials in the scanning electron microscope,** *Appl. Phys. Lett.* **23,** No. 8, 488-490 (Oct. 15, 1973).

Key words: Contrast mechanism; electron backscattering energy filtering; iron; magnetic domains; Monte Carlo methods; scanning electron microscopy; transformer steel.

Monte Carlo calculations confirm that contrast observed in the scanning electron microscope from magnetic domains in materials of cubic anisotropy is due to the alteration of electron trajectories within the specimen. Results are presented for the effects of electron accelerating potential, specimen tilt, and rotation. The contrast arises mainly from the high-energy portion of the back-scattered electron distribution.

**13732.** Quindry, T. L., Flynn, D. R., **On a simplified field measurement of noise reduction between spaces,** (Proc. 1973 International Noise Control Engineering Conference, Copenhagen, Denmark, Aug. 22-24, 1973), Paper in *Inter-Noise 73 Proceedings,* O. J. Pedersen, Ed., pp. 199-207 (Inter-Noise 73, Technical University, Lyngby, Denmark, 1973).

Key words: Absorption coefficient; acoustics; airborne sound insulation index; frequency; noise reduction; transmission loss.

This paper investigates the relationships between ratings based on the 1/3-octave band data and more easily obtained ratings of isolation based on A-weighted or C-weighted sound level data. The effects of the source room sound power spectrum, source and receive room absorptions and other parameters on the correlation obtained are discussed.

**13733.** Brenner, F. C., Kondo, A., Cohen, G. B., **Research for a uniform quality grading system for tires V. Effect of environment on tread wear rate,** *Rubber Chem. Technol.* **44,** No. 4, 952-959 (Sept. 1971).

Key words: Automobile tires; environmental effects; test method; tread wear.

This paper is a continuation of work reported in *Rubber Chem. Tech.* **44,** (1971). The results of an additional tread wear test are reported. This and the earlier data are analyzed to determine environmental effects on rate of tread wear.

For all types of commercial passenger car tires our test results support the thesis that the rate of wear on the tire is independent of the extent of wear. Our results also indicated that the rate of tread wear is greater on wet pavements than on dry. An explanation for this phenomenon is discussed.

**13734.** Miller, G. K., Goodman, K. M., **The Shirley Highway Express-Bus-on Freeway demonstration project—first year results,** *DOT/UMTA* **2,** 120 pages (Urban Mass Transportation Administration, Department of Transportation, Washington, D.C., Nov. 1972). (Available as PB 214333 from the National Technical Information Service, Springfield, Va. 22151).

Key words: Bus fringe parking; bus priority lanes; bus priority lanes in District of Columbia; bus transit operation; exclusive bus lanes; express-bus-on-freeway technology; Shirley Highway Corridor in Northern Virginia; urban mass transit demonstration project.

The purpose of the Shirley Highway Express-Bus-On exclusive freeway lane demonstration project is to determine the effectiveness of this technology in easing urban traffic congestion and improving the urban environment. This project, jointly sponsored by the Urban Mass Transportation Administration and the Federal Highway Administration, Department of Transportation, is comprised of three elements—exclusive bus lanes, new feature buses, and park-ride lots coordinated with the express bus service.

The objectives of this demonstration project are: (1) Determine the magnitude of the modal shift (auto-to-bus) in the Shirley Highway Corridor and develop an effective planning tool that may be used to transfer the knowledge gained from the Bus-on-Freeway experiment to other geographic areas; (2) Promote economic viability of transit operation; (3) Reduce traffic congestion during peak periods; (4) Increase people-moving efficiency of Shirley Highway; (5) Reduce vehicle-related air pollution; (6) Reduce travel times for motorists and transit users; (7) Improve reliability of transit service; (8) Increase perceived value of transit; and (9) Improve mobility of young, old, physically handicapped, and low income travelers.

The Technical Analysis Division, National Bureau of Standards is evaluating the demonstration project by monitoring performance in terms of attaining the project objectives, and by determining the contributions of project features to increases in the percentage of commuter trips by bus.

This report presents the results of the evaluation at the end of the first eighteen month period (June 1972) of this multi-year demonstration project.

**13735.** Hord, J., **Cavitation in liquid cryogens. III—Ogives,** *NASA CR-2242,* 235 pages (National Aeronautics and Space Administration, Washington, D.C., May 1973).

Key words: Cavitation; cryogenics; hydrofoil; nucleation; ogives; pumps; venturi.

This document constitutes the third of four volumes to be issued on the results of continuing cavitation studies. Experimental results for three, scaled, quarter-caliber ogives are given. Both desinent and developed cavity data, using liquid hydrogen and liquid nitrogen, are reported here. The desinent data do no exhibit a consistent ogive size effect, but the developed cavity data were consistently influenced by ogive size—B-factor increases with increasing ogive diameter. The developed cavity data indicated that stable thermodynamic equilibrium exists throughout the vaporous cavities. These data were correlated using the extended theory derived in Volume II of this report series. The new correlating parameter, MTWO, improves data correlation for the ogives, hydrofoil, and venturi and appears attractive for future predictive applications. The cavitation coefficient $K_{c,min}$, and equipment size effects are shown to vary with specific equipment-fluid combinations. A method of estimating $K_{c,mi}$ from knowledge of the noncavitating pressure coefficient is suggested.

**13736.** O'Connell, J. S., **Neutrino disintegration of the deuteron** (Proc. Int. Conf. on Few Particle Problems in the Nuclear Interaction, Los Angeles, Calif., Aug. 28-Sept. 1, 1972). Pape

*Few Particle Problems in the Nuclear Interaction,* I. Slaus, . A. Moszkowski, R. P. Haddock, and W. T. H. van Oers, ds., pp. 906-909 (North Holland Publishing Co., Amsterlam, The Netherlands, 1972).

Key words: Carbon; deuteron; interaction neutrino; neutron.

he cross section for the reaction $D(\nu_e,e^-)2p$ averaged over neutrino spectrum expected from the beam stops of high-in- sity proton accelerators is given. Calculations were carried using a multipole expression for the neutrino-nucleus interac- n and the effective-range theory for the electromagnetic akup of the deuteron.

737. Freeman, D. H., Kuehner, E. C., **Laser detection of small articles in liquids,** *Annals N.Y. Acad. Sci.* **158,** Article 3, 731-740 (June 20, 1969).

Key words: Air pollution; laser; light scattering; liquid pollution; particulate matter; water pollution.

A 0.3 milliwatt He-Ne laser is used with a photomultiplier to vey the light scattered by particulate matter suspended in all (7 ml) samples of liquids. Estimates of weight compositions inferred by calibration against reference solutions of spended polystyrene latex. A small size dependence is ob- ved in the particle size range of 0.1 to 2.0 microns. The thod is useful in the range of one part per million (PPM) to e part per billion (PPB). Results are reproducible with relative ors of approximately twenty percent.

Samples of solid chemical reagents dissolved in distilled water ve been examined. The results show variable contamination els up to 1 ppm. A sample of NBS pond water indicated 1 m. The effect of ultra filtration is easily demonstrated. As a le benefit, the scattered laser beam is easily inspected in uids to show gross presence or absence of suspended matter.

738. Danielson, S. L., Howe, D. A., **Use of the television vertical interval to broadcast time for everyone and program captions for the deaf,** *Commun. Soc.* **11,** No. 5, 3-6 (Nov. 1973).

Key words: Digital code; integrated circuit chip; program captioning; television; time and frequency dissemination; TvTime.

This paper describes the events leading to the development of e NBS TvTime System for both time and frequency dissemina- n and program captioning for the deaf. It explains how the stem works, its advantages over other systems, and its cost. nally, it discusses the possible implications of such a system r future communication applications. The text is written in men's language to suit the publication.

739. Mopsik, F. I., Broadhurst, M. G., **Grüneisen constants of polymers,** *J. Appl. Phys.* **44,** No. 10, 4261-4264 (Oct. 1973).

Key words: Bulk modulus; Grüneisen constant; infrared; lattice vibrations; polyethylene; polymers.

One result of recent interest in Grüneisen constants, $\gamma = -d$ $\nu/d \ln V$, of polymers is a considerable spread of reported $\gamma$'s for lids like polyethylene. From elasticity data (bulk modulus or und velocities for example) one finds $\gamma \approx 6$ for linear polymer lids. Values of $\gamma$ from thermal data are much lower than 6 ecause the relationship usually employed, $\gamma = \alpha BV/C_v$, is not lid for polyatomic solids. Measurements of the shifts in lattice equencies with volume strains are the most direct way of mea- ring $\gamma$. However, the results for pressure-induced strains differ om those for temperature-induced strains, and both differ from e results from elasticity data. In this paper we consider vibra- ons in a simple anharmonic well and show how the apparent shifts in vibrational frequency with pressure and temperature can be derived from changes in force constants.

13740. Currie, L. A., **On the use of small calculators having stacked registers,** *Anal. Lett.* **6,** No. 9, 847-864 (1973).

Key words: Instruction list; iteration; memory register; operational stack; pop-up; Polish notation; push-down; radioactivity and isotopic calculations; recursion; statistical calculations.

The incorporation of an operational stack considerably enhances the potential of the small calculator. Full use of the stack permits calculations involving a stored constant or two or more intermediate results, but it requires careful planning and execution. Regardless of whether the calculator is "programmable," an explicit instruction list, preferably written down, may contribute greatly to the rapidity and accuracy of such calculations. The "pop-up" feature of the stack is of particular interest, for it can be utilized to increase the permanent storage capacity. A comparison between conventional (memory) storage and stack storage is given, and examples are presented for the application of a calculator having a 4-register stack (plus 1-memory register) to problems involving 2 parameters and/or summations, iterative solution of a transcendental equation, and recursion.

13741. Ederer, D. L., **Cross-section profiles of resonances in the photoionization continuum of krypton and xenon (600-400 Å),** *Phys. Rev. A* **4,** No. 6, 2263-2270 (Dec. 1971).

Key words: Autoionization; configuration interaction; inner shell excitation; photoionization cross section; resonance profiles; uv absorption spectroscopy.

The cross-section profiles in krypton and xenon have been measured for one- and two-electron excitations of the type $ns^2np^6(^1S_0) \rightarrow nsnp^6(^2S_{1/2})mp$ or $ns^2np^6(^1S_0) \rightarrow ns^2np^4(^3P, {}^1D, {}^1S)$ $mlm'l'$. These cross sections were assumed to have the form

$$\sigma(E) = C(E) + \sum_i \frac{(E-E_i)(\Gamma_i/2)a_i + (\Gamma_i/2)^2 b_i}{(E-E_i)^2 + (\Gamma_i/2)^2},$$

where the adjustable parameters $C(E)$, $b_i$, $a_i$, $E_i$, and $\Gamma_i$ were determined by a least-squares unfolding process which separated the smearing effect of the monochromator slit from the true optical density. Parameter values and cross-section curves are given for 12 krypton resonances and 11 xenon resonances.

13742. Negas, T., Roth, R. S., Parker, H. S., Brower, W. S., **Crystal chemistry of lithium in octahedrally coordinated structures. I. Synthesis of $Ba_8(Me_6Li_2)O_{24}$($Me = Nb$ or $Ta$) and $Ba_{10}(W_6Li_4)O_{30}$. II. The tetragonal bronze phase in the system $BaO$-$Nb_2O_5$-$Li_2O$,** *J. Solid State Chem.* **8,** No. 1, 1-13 (1973).

Key words: $Ba_8Nb_6Li_2O_{24}$; $BaO$-$Nb_2O_5$-$Li_2O$ systems; $Ba_8Ta_6Li_2O_{24}$; $Ba_{10}W_6Li_4O_{30}$; close-packed oxides; crystal growth; tetragonal bronzes.

The preparation, single crystal growth, and crystallographic properties of a close-packed, eight-layer, hexagonal ($a = 5.803$ Å, $c = 19.076$ Å) modification having the stoichiometry $Ba_8Nb_6Li_2O_{24}$ and of a close-packed, ten-layer, hexagonal ($a = 5.760$ Å, $c = 23.742$ Å) phase with $Ba_{10}W_6Li_4O_{30}$ stoichiometry are discussed. The isostructural $Ba_8Ta_6Li_2O_{24}$ form of the eight-layer phase was also prepared ($a = 5.802$ Å, $c = 19.085$ Å). Proposed crystal structures involve the pairing of lithium and metal (Nb, Ta, or W) octahedra to yield face-sharing units. The relationship of this phenomenon to other known close-packed phases containing Li is demonstrated. An investigation of the $Ba_8Nb_6Li_2O_{24} - Ba_{10}W_6Li_4O_{30}$ system is reported.

A tetragonal bronze phase homogeneity region was delimited at 1200 °C in the $BaO - Nb_2O_5 - Li_2O$ system. A new orthorhombic phase ($a=10.197$ Å, $b=14.882$ Å $c=7.942$ Å) was prepared with the stoichiometry $Ba_4Li_2Nb_{10}O_{30}$.

**13743.** Broadhurst, M. G., Mopsik, F. I., **Vibrational frequency spectrum for polymers,** *J. Chem. Phys.* **55,** No. 8, 3708-3711 (Oct. 15, 1971).

Key words: Frequency spectrum; linear chains; *n*-alkanes; polyethylene; polymer.

A method is given for calculating the vibrational frequency spectrum of a model linear polymer. The model is a chain of $N$ masses having bending and stretching force constants. Each mass is quasiharmonically coupled to a Debye lattice which has a cutoff frequency $\omega_L$. Each of the $3N$ free chain eigenfrequencies $\omega_j$ becomes a band with a low frequency cutoff $\omega_{jmin}{}^2=\omega_j^2$, a high frequency cutoff $\omega_{jmax}{}^2=\omega_j^2+\omega_L{}^2$, and a pseudo-$n$-dimensional Debye distribution $g_j(\omega)=n\omega^{n-1}/(\omega_{jmax}{}^n-\omega_{jmin}{}^n)$ for $\omega_{jmin}<\omega<\omega_{jmax}$. The total frequency distribution agrees closely with the results by Genensky and Newell for the Stockmayer and Hecht lattice using their force constants and compares reasonably well with results of GF matrix calculations for polyethylene.

**13744.** Evans, A. G., **Strength degradation by projectile impacts,** *J. Amer. Ceram. Soc.* **56,** No. 8, 405-409 (Aug. 1973).

Key words: Ceramics; fracture; impact; projectiles.

The impacting of ceramic components by small projectiles can lead to strength degradation caused by the formation of Hertzian cracks. The conditions which produce degradation are analyzed in terms of the momentum and elastic properties of the projectile. A critical momentum must be exceeded before strength loss can occur, and the critical condition depends on the surface condition of the ceramic. Comparison of the analytical predictions with data for SiC confirms the reliability of the analysis.

**13745.** Brauer, G. M., Termini, D. J., **Grafting of acrylates and vinyl chains onto collagen with ceric initiator,** *J. Appl. Polym. Sci.* **17,** 2557-2568 (1973).

Key words: Acrylate copolymers; ceric ion initiated; grafting collagen; graft polymerization; modification of collagenous surfaces.

To determine the scope of the grafting reaction, over 30 monomers were grafted to steer hide collagen and collagen films using ceric ammonium nitrate as initiator. High yields of apparent graft polymer were obtained with most acrylate and methacrylate esters. Yields were not changed greatly by employing the higher homologues. Moreover, monomers containing such diverse substituents as hydroxy, cyano, chloro, trifluoroethyl, or glycidyl groups may be grafted onto collagen. The presence of these functional groups in the products provides potential reaction centers to further modify the collagenous surface. Presence of vinyl polymer was confirmed by IR spectra. The large number of monomers of varying polarity which were found to undergo apparent grafting makes it possible to vary widely the surface properties of collagen. It was shown that certain monomers impart water and oil repellency to collagenous surfaces, whereas others increased the hydrophilicity or oleophilicity of the substrate. Thus, by proper selection of monomers, the desired degree of hydrophilic to hydrophobic or oleophilic to oleophobic balance of the collagen surface to suit specific applications can be obtained.

**13746.** Chesler, S. N., Cram, S. P., **Iterative curve fitting of chromatographic peaks,** *Anal. Chem.* **45,** No. 8, 1354-1359 (July 1973).

Key words: Chromatography; curve fittings; moment analysis.

Iterative curve fitting of an eight parameter function to chromatographic peak profiles by nonlinear residual least squares is reported. Gaussian, exponential, and hyperbolic tangent functions are convoluted and iteratively fit to any experimental chromatographic peak shape and integrated to give total statistical moments with errors as small as 1 percent, even for the higher order moments. Exponential and band broadening operators are deconvolved for measurement of physicochemical and analytical studies. The models and calculations may be extended to the resolution of overlapping peaks and complex elution profiles for the measurement of the rate of on-column chemical reactions.

**13747.** Candela, G. A., Kahn, A. H., Negas, T., **Magnetic susceptibility of $Co^{4+}(d^5)$ in octahedral and tetrahedral environments,** *J. Solid State Chem.* **7,** No. 4, 360-369 (1973).

Key words: $Co^{4+}$ compounds; crystal fields; magnetic susceptibility; theory of magnetic susceptibility.

Measurements of magnetic susceptibility on compounds containing stoichiometric $Co^{4+}$ are reported. The compound $Ba_2CoO_4$ has the $Co^{4+}(d^5)$ ion at a tetrahedral site and displays a susceptibility of the expected magnitude for $S=5/2$. The compounds $Ba_3Co_2CO_9$ and $BaCoO_3$ have the $Co^{4+}$ at an octahedra site and show a susceptibility expected for low spin, $S=1/2$. Fo the low spin case significant deviations from Kotani's calculate susceptibility were observed. Improvement of the theory wa made through incorporation of the effects of distortion from perfect octahedral symmetry and the inclusion of higher electroni configurations above $t_2{}^5$ in the $^2T_2$ ground state. A case of lo spin Ni in octahedral environment is also reported.

**13748.** Okabe, H., Dibeler, V. H., **Photon impact studies o $C_2HCN$ and $CH_3CN$ in the vacuum ultraviolet; heats of formation of $C_2H$ and $CH_3CN$,** *J. Chem. Phys.* **59,** No. 5, 2430-243 (Sept. 1, 1973).

Key words: Acetonitrile; cyanoacetylene; $C_2H$; heat of formation; photodissociation; photoionization; vacuum ultraviolet.

A photodissociation process to produce CN $B^2\Sigma$ from $C_2HC$ and $CH_3CN$ has been studied as a function of inciden wavelength. Threshold photon energies required for the produc tion of CN $B^2\Sigma$ from $C_2HCN$ and $CH_3CN$ are $9.41\pm0.04$ an $8.52\pm0.03$ eV, respectively, from which $D_0(C_2H-CN)\leqslant6.2$ $\pm0.04$ eV and $D_0(CH_3-CN)\leqslant5.32\pm0.03$ eV are obtaine The photoionization yield curves have been measured for th $C_2HCN^+$ and $C_2H^+$ ions. Threshold photon energies obtaine for the production of CN $B^2\Sigma$, $C_2HCN^+$, and $C_2H^+$ fro $C_2HCN$ lead to the following thermochemical value I.P.$(C_2HCN)=11.64\pm0.01$ eV, I.P.$(C_2H)=11.96\pm0.05$ e $\Delta Hf_0{}^\circ$ $(C_2HCN)\geqslant85\pm1$ kcal mol$^{-1}$ ($355\pm4$ kJ mol$^{-1}$). $\Delta Hf$ $(C_2H)=127\pm1$ kcal mol$^{-1}$ ($531\pm4$ kJ mol$^{-1}$) and $D_0(C_2H-$ $=5.38\pm0.05$ eV. $\Delta Hf_0{}^\circ$ $(C_2H)$ obtained is in good agreeme with the recent value obtained directly from a study of the hi temperature reactions of graphite with hydrocarbons. $\Delta Hf$ $(CH_2CN)\geqslant14\pm1$ kcal mol$^{-1}$ ($59\pm4$ kJ mol$^{-1}$) derived from $(CH_3-CN)$ agrees within the stated error limit with the val obtained recently by bomb calorimetry. The fluorescence ef ciency vs incident wavelength curves for $C_2HCN$ and $CH_3C$ show several peaks corresponding to Rydberg states indicati that the process is predissociative. The absorption coefficient $C_2HCN$ has been measured in the vacuum ultraviolet. T photoionization yield curve for $C_2HCN^+$ shows at least tw Rydberg series converging to vibrationally excited $C_2HC$ ions.

**13749.** Mulholland, G. W., **Line of symmetry for the classi equation of state,** *J. Chem. Phys.* **59,** No. 5, pp. 2738-27 (Sept. 1, 1973).

Key words: Classical equation of state; coexistence curve; critical phenomena; diameter of coexistence curve; line of symmetry; liquid-vapor phase transition.

The existence and properties of the Widom-Stillinger line of nmetry are examined for the "classical" equation of state, that an equation of state in which the chemical potential is ex- ssed as a power series in density and temperature. In doing s, the chemical potential is shown to be an analytic function of nperature in the two phase region. This analyticity has been icipated for a number of years.

50. Morris, J. C., Walker, J. H., **Electron-neutral transport ross section of mercury,** *J. Appl. Phys.* **44,** No. 10, 4558-4561 Oct. 1973).

Key words: Arc mercury; conductivity; cross section; electrical conductivity of mercury; electron-neutral; electron-neutral transport cross section of mercury; mercury arc.

The electron-neutral transport cross section and the electrical nductivity of Hg have been determined using a constricted dc arc. This arc has a novel configuration which permits the cise measurement of the pressure, the voltage gradient, the nperature profile, and the total current. For the temperature ige 5000-6500 K, the electron-neutral transport cross section s found to be $1 \times 10^{-14}$ cm² with a precision of ±6 percent and absolute accuracy of ±20 percent. A description of the ap- atus and technique is presented as well as a comparison with ier existing data.

751. Bowen, B. E., Cram, S. P., Leitner, J. E., Wade, R. L., **High precision sampling for chromatographic separations,** *Anal. Chem.* **45,** No. 13, 2185-2191 (Nov. 1973).

Key words: Computer-based data acquisition; gas chromatography.

The precision of several chromatographic sampling valves of ginal design is shown to approach 0.05 percent for unretained utes. Hybrid-fluidic, high pressure, and commercial valves ve been characterized by measuring the precision of their lumn input profiles and statistical moments. A computer- sed data acquisition and control system was developed for use th high precision algorithms.

752. Phelan, R. J., Jr., Cook, A. R., **Electrically calibrated yroelectric optical-radiation detector,** *Appl. Opt.* **12,** No. 10, 2494-2500 (Oct. 1973).

Key words: Calibration; detector; infrared; pyroelectric; radiometers; ultraviolet.

An electrically calibrated optical detector has been developed ing a pyroelectric response of the plastic, polyvinylfluoride. in-depth look at the modulation frequency response was per- med to substantiate the equivalence of the optical and electri- l inputs, indicate the optimum structure and allow for a clearer derstanding of the device limitations. The experimental results the dynamic range, linearity, uniformity, and detectivity con- m the device's utility.

753. Kidnay, A. J., Hiza, M. J., Miller, R. C., **Liquid-vapour equilibria research on systems of interest in cryogenics—A survey,** *Cryogenics* **13,** No. 10, 575-599 (Oct. 1973).

Key words: Annotated bibliography; binary systems; cryogenic fluid mixtures; liquid-vapour equilibria; multicomponent systems; survey.

This survey provides a convenient summary of available data liquid-vapour equilibria for systems of interest in cryogenics. n annotated bibliography of 392 references has been compiled, rrent to January 1973. These references have been scanned individually with few exceptions, and cross-indexed by system with notation of extent of data and other significant features. The systems included are those made up of the possible combinations of $H_2(D_2$, HD), $N_2$, $O_2$, $F_2$, CO, $H_2S$, He(He$^3$), Ne, Ar, Kr, Xe, and the saturated and unsaturated hydrocarbon through the $C_4$s.

13754. O'Connell, J. S., **Electromagnetic sum rules,** (Proc. Int. Conf. on Photonuclear Reactions and Applications, Pacific Grove, Calif., Mar. 26-30, 1973), Paper in *International Conference on Photonuclear Reactions and Applications,* B. L. Berman, Ed., pp. 71-94 (Ernest O. Lawrence Livermore Laboratory, University of California, Livermore, Calif., 1973). (Available as CONF-730301 from the National Technical Information Service, Springfield, Va. 22151).

Key words: Effective interaction; electron scattering; nucleon-nucleon correlations; photoabsorption; photon scattering; sum rules.

A survey of total and partial nuclear cross section sum rules for photoabsorption and electron scattering is presented. The sums are derived from closure or the dispersion relation and are compared with available data and discussed in the context of the single particle shell model. A few of the rules are model-independent or relate observables, but most are influenced either by the form of the effective two-nucleon interaction or by nucleon-nucleon correlations in the nuclear ground state. The relation of electron scattering sums in the low momentum transfer region to photo sums is emphasized. A new sum rule for elastic photon scattering is given.

13755. Pella, P. A., DeVoe, J. R., **Internal standardization in Mössbauer spectrometry,** *Appl. Spectrosc.* **25,** No. 4, 472-474 (July/Aug. 1971).

Key words: Beta-tin; internal standardization; Mössbauer spectroscopy.

The concept of internal standardization is applied in quantitative analytical studies using the Mössbauer spectrometric technique. The ratio of the absorption intensity of $SnO_2$ (analyte absorber) to that of $\beta-$Sn (internal standard absorber) is measured using $BaSn^{119m}O_3$ as the source. The results demonstrate that the systematic error which arises because of differences in the chemical composition between the analyte samples and standards can be eliminated by using an internal standard.

13756. Broadhurst, M. G., **Fluctuation-barrier model for rotational relaxation,** (Proc. Conf. Electrical Insulation and Dielectric Phenomena, Buck Hill Falls, Pa., Oct. 20-22, 1969), Chapter in *1969 Annual Report of the Conference Electrical Insulation and Dielectric Phenomena,* pp. 48-54 (National Research Council, National Academy of Sciences, Washington, D.C., 1970).

Key words: Elastic barrier; lattice; molecular rotation; relaxation; temperature dependence.

A model is presented where the barrier to molecular rotation in solids is taken to be the work to elastically expand the lattice around the molecule. This barrier is shown to increase with pressure and decrease with temperature. The model calculations are compared to data on long chain paraffin-like solids for the dielectrically active relaxation involving rotation of the entire molecule around its chain axis (analogous to the $\alpha$ relaxation in polymers). The model accurately predicts the temperature dependence of the relaxation time (the activation entropy in the Eyring Theory), and the Eyring activation energy (the activation energy does not equal the elastic barrier height). The predicted pressure dependence of the relaxation time is in error by a factor of 2 indicating the need for further refinement of the model. This paper reports the current status of this problem.

**13757.** Ederer, D. L., Lucatorto, T., Madden, R. P., **Resonances in the photoionization continuum of lithium I (55 to 70 eV),** *J. Phys.* 32, Supplement to No. 10, C4-85 – C4-87 (Oct. 1971).

Key words: Absorption; heat pipe; K-edge; lithium; resonances; spectrum.

Resonances in the photoionization continuum of lithium have been observed by absorption spectroscopy in the region of 55 to 70 eV. These resonances are associated with configurations of the type (1 s 2 snl) and (1 snln′l′) and lie more than 50 eV above the ionization potential; the lowest lying most prominent of these can be identified with configurations of the type (1 s 2 snp) $^2$P. A multiconfiguration calculation for the first five members of the series (performed by A. Weiss) has yielded values for the energies which agree with experimental results to within 2 eV.

The design of the lithium vapor absorption furnace was based on the heat-pipe principle. Argon, which has very little structure in the region from 55 to 70 eV, was used as a buffer gas and was contained inside the furnace by thin film aluminum windows. The light source was the 180 MeV NBS synchrotron.

**13758.** Carpenter, B. S., Samuel, D., Wasserman, I., **Quantitative applications of $^{17}$O tracer,** *Radiat. Eff. Short Commun.* **19,** 59 (1973).

Key words: Alpha tracks; alumina; cellulose acetate; citric acid; image analyzing system; nuclear track technique; oxygen tracer; thermal neutrons.

We describe the use of alpha tracks from the $^{17}$O($n$, $\alpha$)$^{14}$C as a means of oxygen determination and distribution in biological material. A determination of oxygen in alumina and citric acid using enriched tracer was made.

**13759.** Verdier, P. H., **Fluctuations in autocorrelation functions in diffusing systems,** Chapter in *Stochastic Processes in Chemical Physics,* K. E. Shuler, Ed., **15,** 137-148 (John Wiley & Sons, Inc., New York, N.Y. 1969).

Key words: Autocorrelation; correlation; diffusion; fluctuations; relaxation; time correlation.

The relative rates of relaxation of the autocorrelation function and the fluctuations in its sampled values are derived for several simple diffusing systems. It is found that in general, the autocorrelation function and its fluctuations relax at rates which are different, but of the same order of magnitude. In the cases studied, the ratio of the relaxation time for the fluctuations to that for the autocorrelation function varies from about 1/2 to about 1 1/6.

**13760.** Stillman, R. B., **The concept of weak substitution in theorem-proving,** *J. Ass. Comput. Mach.* **20,** No. 4, 648-667 (Oct. 1973).

Key words: Associative processing; first-order predicate calculus; resolution; subsumption; theorem-proving; unification.

Many of the centrally important predicates which occur within theorem-proving programs involve, in their computation, a subcalculation aimed at determining whether or not a substitution exists satisfying certain constraints. Some of the principal difficulties in achieving efficient theorem-proving programs are traceable to the amount of computation required by this "substitution-existence analysis." In this investigation, the concept of "weak substitution" is introduced and its utility and applicability in the subsumption and unification computations are examined. The main motivation for considering weak substitutions is this: the existence of a *weak* substitution having certain properties is relatively easy to detect, whereas the existence of a substitution proper having the same properties is not. Furthermore, the absence of such a weak substitution is a sufficient condition for the absence of the substitution proper. Using the concept of weak substitution, a particularly efficient implementation of the subsumption and unification computations on an associative processor is presented.

**13761.** Lyndon, R., McDonough, T., Newman, M., **On products of powers in groups,** *Proc. Amer. Math. Soc.* **40,** No. 2, 419-420 (Oct. 1973).

Key words: Free groups; powers.

In this note we show that a product of *N*th powers in a group cannot in general be expressed as a product of fewer *N*th powers. This extends a result of Lyndon and Newman.

**13762.** Ordman, E. T., **Convergence and abstract spaces in functional analysis,** *J. Undergraduate Math.* **1,** No. 2, 79-96 (Sept 1969); **2,** No. 1, 25-36 (Mar. 1970).

Key words: Convergence; filter; function space; limi space; linear topological space; net; topological space.

This paper is an expository survey of the theory of limi spaces, discussing and contrasting approaches by way of net and filters and considering a number of the extant ways of axiomatizing such a structure. Applications are given to a number o common notions of convergence of functions and to the topolog of function spaces linear topological spaces.

**13763.** Meinke, W. W., **Is radiochemistry the ultimate in trac analysis?,** *Pure Appl. Chem.* **34,** 93-104 (1973).

Key words: Accuracy error limits; activation analysis atomic absorption; instrument biases; isotope-dilutior method biases; nuclear track technique; practical sample radiochemistry; trace analysis techniques.

Proponents of widely-used analysis methods such as atomi absorption, spark source mass spectrometry, polarography, a tivation analysis, etc. often give the impression that the methods alone can solve a large fraction of the problems of trac analysis. In addition, from time to time new, specialized trac methods are reported and sometimes find use in solving speci analytical problems. However, the trace analyst deceives himse and, worse yet, gives false impressions to others unless he is ab to understand the biases of his methods and instruments in rel tion to other possible methods and instruments, – and in additi express these biases quantitatively as accuracy error limits. O experience at NBS in certifying trace element Standa Reference Materials in matrices as diverse as glass, orcha leaves, gold, zinc, beef liver, tuna fish and coal has given us an i sight into the optimum contributions which can be made of the methods. The advantages and disadvantages of activation anal sis as well as of several other types of radiochemical metho will be discussed in relation to other trace analysis technique based on our NBS experience in practical trace analysis. It concluded that activation analysis ranks high among the metho for trace analysis of real samples.

**13764.** Ballard, L. D., Edelman, S., Epstein, W. S., Smith, E. **A suggestion for determining g by a two interferomet technique,** *SPIE J.* **9,** No. 5, 166-168 (June/July 1971).

Key words: Acceleration; counter; filter; g; gravity; int ferometer; laser.

A method for determining the acceleration due to gravity suggested. Two falling interferometer reflectors illuminated a laser are used. The falling reflectors are separated by a $\Delta T$ a thus have a constant velocity differential, this generates frequency linearly proportional to acceleration ($g = kf = \Delta V/\Delta$

Thus, the metrology of measuring g is simplified by havin linearly proportional to frequency.

**3765.** Greenspan, M., **Transducer measurements: Use of the current probe,** *J. Acoust. Soc. Amer. Tech. Notes and Res. Briefs* **53,** No. 4, 1186-1187 (Apr. 1973).

Key words: Current probe; impedance measurements; piezoelectric transducer measurements; transducer measurements; ultrasonic instruments.

It has been found that various measurements commonly made n piezoelectric transducers are simplified by use of the current robe, a commercially available instrument. Examples are imedance, ultrasonic interferometry, and power.

**3766.** Spurgeon, J. C., **Response characteristics of a portable x-ray fluorescence lead detector: Detection of lead in paint,** *NBSIR 73-231,* 37 pages (June 1973). (Available as PB 224645 from the National Technical Information Service, Springfield, Va. 22151.)

Key words: Lead paint detection; portable x-ray fluorescence lead detector; portable x-ray fluorescence lead calibration standards.

The objective of this investigation was to obtain an indication the validity of the field data resulting from the use of portable -ray fluorescence lead detectors by local lead paint detection rograms. This report is intended to provide guidance in the use portable x-ray fluroescence lead detectors by housing and/or ealth authorities who are responsible for the collection and inerpretation of field data as part of lead paint control programs.

The response characteristics of such an instrument to condions that are related to those encountered in the field have been ivestigated and the results are presented in this report. The efcts of calibration standards, state of charge, paint overlayers, ubstrate, and distance on instrument response are discussed, in ddition to the limit of detection and precision. The accomplishent of these tasks required the development of panel-type lead alibration standards. These standards encompass the concenration range from 0.1 mg/cm$^2$ to 9.0 mg/cm$^2$.

**3767.** Boone, T. H., Ray, T. R., Street, W. G., **Pilot demonstration of lead based paint hazard elimination methods,** *NBSIR 73-242,* 38 pages (June 1973). (Available as PB 224654 from the National Technical Information Service, Springfield, Va. 22151.)

Key words: Cost analysis; hazard elimination; housing; lead based paint; materials; surface preparation; surface refinishing.

This report describes the elimination of the hazard of lead earing paints in a one bedroom apartment using materials and rocedures that are undergoing laboratory and field evaluation y the National Bureau of Standards (NBS). Paint removal was sed to eliminate the hazard from some surfaces and two non-azardous membrane type coverings were installed as barrier aterials over the residual leaded paint on other surfaces. The reparation and refinishing of the interior surfaces are described nd work rates and cost data are presented.

This pilot demonstration is the first of a series of studies that ill be used to determine the merits of various lead based paint azard elimination methods when applied to actual housing conitions.

Final recommendations for further use of materials and ystems, described in this report, are not presented due to the reliminary nature of this work. The completion of the projected eries of demonstrations and the long term evaluation of the inse performance of the materials and systems will be required efore final recommendations can be made.

**13768.** Paabo, M., **Analytical methods for the detection of toxic elements in dry paint matrices—a literature survey,** *NBSIR 73-251,* 49 pages (July 1973). (Available as PB 224688 from the National Technical Information Service, Springfield, Va. 22151.)

Key words: Analytical methods; antimony; arsenic; cadmium; lead; mercury; review; selenium; toxic elements in paints.

This report is a summary description of the chemical procedures currently available for the analysis of selected toxic elements in dried paint. The elements included in this report are lead, mercury, cadmium, antimony, arsenic, and selenium. The literature search upon which this report is based was directed primarily toward references pertaining to the analysis of dried paint. A bibliography of 57 references to wet chemical analysis, colorimetry, atomic absorption spectroscopy, electrochemistry, neutron activation analysis, and x-ray emission analysis is presented.

**13769.** Kruger, J., Ambrose, J. R., **The role of passive film growth kinetics and properties in stress corrosion and crevice corrosion susceptibility,** *NBSIR 73-244,* 75 pages (July 1973). (Available as AD 767326 from the National Technical Information Service, Springfield, Va. 22151.)

Key words: Chloride; crevice corrosion; dissolved oxygen; ellipsometry; nitrates; pH; repassivation kinetics; stainless steel; stress corrosion cracking; titanium alloys.

Repassivation kinetics of an AISI 304 stainless steel have been determined in 1.0N NaCl solutions using the triboellipsometry technique which permits measurement of film growth and total reaction rates following removal of the surface film by abrasion. Although deoxygenation of the solution resulted in little change in either film growth kinetics or the ratio of total change to film thickness ($R_p$), changing the solution pH affected both the mechanism and rate of film growth which resulted in increased rates of metal dissolution in acidic (pH3) and basic (pH11) solutions.

The triboellipsometry technique was also used to determine repassivation kinetics and stress corrosion cracking (SCC) susceptibility for Ti-8Al-1Mo-1V alloy. Repassivation transient behavior in a 1.0N NaCl solution, where cracks have been found to propagate, was compared to that in a 1.0N $NaNO_3$ solution where SCC susceptibility has never been detected. Susceptibility was found to be related to film growth kinetics in the two solutions.

The early stages of crevice corrosion of AISI 304 stainless steel in 1.0N NaCl solution have been detected using the ellipsometer to measure changes in optical properties occurring within the crevice between a polished metal surface and a glass plate. Changes in the ellipsometer parameters $\Delta$ and $\psi$ begin almost immediately upon creation of the crevice and can be interpreted as resulting from a build-up of soluble species within the crevice solution, followed by an overall thinning of the protective film and general corrosion attack.

**13770.** Hampson, R. F., Garvin, D., Herron, J. T., Huie, R. E., Kurylo, M. J., Laufer, A. H., Okabe, H., Scheer, M. D., Tsang, W., **Chemical kinetics data survey VI: Photochemical and rate data for twelve gas phase reactions of interest for atmospheric chemistry,** *NBSIR 73-207,* 127 pages (Aug. 1973). (Available as AD 769266 from the National Technical Information Service, Springfield, Va. 22151.)

Key words: Atmospheric chemistry; chemical kinetics; data evaluation; gas phase reaction; optical absorption cross section; photochemistry; quantum yield; rate constants.

Photochemical and rate data have been evaluated for twelve gas phase reactions of interest for the chemistry of the stratosphere. The results are presented in data sheets, one for each reaction. For each reaction the data are summarized. A preferred value is given for the rate constant or the primary quantum yield and photoabsorption cross section.

13771. Sanchez, I. C., Colson, J. P., Eby, R. K., **Theory and observations of polymer crystal thickening,** *J. Appl. Phys.* **44,** No. 10, 4332-4339 (Oct. 1973).

Key words: Annealing; comonomer inclusion; copolymers; lamella thickness; theoretical and experimental; thickening; unit cell.

The thickening of polymer crystals during isothermal annealing is usually observed to be an irreversible process. Phenomenological laws that govern such processes take the form of simple proportionalities – flux being proportional to force. For polymer crystals, a thermodynamic force capable of driving the thickening phenomenon arises from the unequal free energies of the fold and lateral surfaces. By analogy with other irreversible phenomena, the rate of crystal thickening is taken to be proportional to the derivative of the surface free energy with respect to crystal thickness. After certain assumptions, integration yields an equation in which three parameters characterize the system: an initial thickness $l_0$, and equilibrium thickness $l^*$, and a relaxation time $\tau$ which is a function of the "undercooling." The theory provides a basis for considering the effects of parameters such as time, temperature, thermal history, pressure, and liquids on the thickening rate. In particular, the theory adequately describes the time and temperature dependence of crystal thickening in random copolymers of tetrafluorethylene and hexafluoropropylene which exhibit thickening behavior completely analogous to that of homopolymers. During thickening, the unit cell dimensions of *these quenched-crystallized copolymers* decrease in a manner that is consistent with the concept of complete comonomer inclusion upon crystallization.

13772. Ogburn, F., Johnson, C. E., **Banded structure of electroless nickel,** *Plating Technical Brief,* pp. 1043-1044 (Oct. 1973).

Key words: Electroless nickel; electroless plating; nickel phosphorus.

The cross section of an electroless nickel deposit was scanned for phosphorus with an electron probe. The variations in phosphorus content corresponded inversely with the degree of etching with the usual nitric-acetic acid etchant, which develops the striations characteristic of electroless nickel deposits.

13773. Livingston, R. C., Rothschild, W. G., Rush, J. J., **Molecular reorientation in plastic crystals: Infrared and Raman band shape analysis of neopentane,** *J. Chem. Phys.* **59,** No. 5, 2498-2508 (Sept. 1, 1973).

Key words: Band shape analysis; diffusion models; infrared; jump diffusion; molecular reorientation; neopentane; phase transition; plastic crystal; Raman; and rotational diffusion.

An infrared and Raman band shape analysis of the broadened 924 $\text{cm}^{-1}$ fundamental for neopentane in its liquid and plastic crystal phases is presented. Correlation functions and times for molecular reorientation derived from both the infrared and Raman data show the liquidlike behavior of the plastic phase of neopentane, with the molecules rotating "freely" through $\sim 10°$ (175 K) to $\sim 30°$ (300 K) around an inertial axis with the corresponding reduced intermolecular torques $(< L^2 >^{1/2} kT)$ decreasing from 8.2 to 3.8. Furthermore, the linewidth and correlation time results show no indication of a change in rotational behavior in passing through the plastic crystal-liquid phase transition. Theoretical fits of our experimental infrared and Raman correlation function with Gordon's *M* and *J* diffusion models, as extended by McClung for spherical molecules, show that the experimental results lie between the functions predicted by these two models. The time between rotational "collisions" (angular momentum correlation time) varies continuously from $0.4 \times 10^{-12}$ sec for the room-temperature liquid to $0.2 \times 10^{-12}$ sec at the lowest temperature in the plastic phase. Activation energies for molecular reorientation of 4.1 and 3.6 kJ/mol are obtained, respectively, from the experimental half-widths and from the angular momentum correlation times, in good agreement with previous NMR and neutron scattering results. The results prove that neopentane melts in two stages: near 140 K, the rotational degrees of freedom of the (rigid) molecule are liberated, whereas near 253 K the translational degrees of freedom are liberated without observable change of the characteristics of the rotational motion.

13774. Davis, G. T., Eby, R. K., **Glass transition of polyethylene: Volume relaxation,** *J. Appl. Phys.* **44,** No. 10, 4274-4281 (Oct. 1973).

Key words: Dilatometer; isothermal volume change; polyethylene; specific volume; superposition; thermal expansion; volume relaxation, WLF.

Data are presented to show that when linear polyethylene is quenched from room temperature to temperatures below 273 K it exhibits a volume decrease for times long compared with tha required to establish temperature equilibrium. The time, temperature, and density dependence of this decrease is shown to b consistent with a relaxation occurring in the amorphous portio (lamella boundary layers) of the samples. The data can be superposed and the shift factors follow the WLF formalism. Analysi by this method yields a $T_g$ of $231 \pm 9$ K but the uncertainti preclude any correlation with specific volume over the rang $1.01 - 1.05\ \text{cm}^3\ \text{g}^{-1}$. The data indicate the absence of any comparably strong time dependence of the volume near 150 K. Thi method of detecting a glass transition in partially crystallin polymers is relatively freer of subjective judgment than most.

13775. Ballantyne, J. P., Yakowitz, H., Nixon, W. C **Simultaneous x-ray microanalysis and resistance measureme of electron beam induced direct metallic deposition,** (Proc. 6t Int. Conf. on X-Ray Optics and Microanalysis, Osaka, Japa Sept. 1971), Paper in *Proceedings of the Sixth Internation Conference on X-Ray Optics and Microanalysis,* G. Shinod K. Kohra and T. Ichinokawa, Eds., pp. 219-227 (University Tokyo Press, Tokyo, Japan, 1972).

Key words: Deposited thin film; electron beam met deposition; scanning electron microscopy; x-ray microana ysis.

The decomposition of thin film AgCl, vapor deposited onto a oxidized silicon substrate, was caused by electron bombardme in a scanning electron microscope operating at a pressure of 10 torr. This decomposition was monitored by nondispersive x-r analysis techniques. At the same time, the resistance of the fil was also recorded.

The curves of chlorine concentration and resistance as a fun tion of exposure are very similar in shape. The chlorine conte of the film reaches a level that does not alter with increasing e posure. At this point, film resistance is about 1000 Ω a remains essentially constant with increasing exposure. T residual chlorine can be removed by chemical treatment aft which the resistance values drop to less than 50 Ω.

The quantitation of the x-ray results must await new c rection procedures presently under study. However, a simp ection procedure has been employed in order to illustrate im- ant trends in the direct metallic deposition process.

6. Page, C. H., **Logarithmic quantities and units,** *Proc. IEEE tters* **61,** No. 10, 1516-1517 (Oct. 1973).

Key words: Decibel; logarithm.

ecent letters on *decibel* are commented upon, and stan- ization proposed by the International Electrotechnical Com- ion (IEC) is mentioned.

7. Stabler, T. M., **National program of metrology for uador,** *NBSIR 73-157,* 33 pages (Apr. 1973). (Available as OM74-10394 from the National Technical Information rvice, Springfield, Va. 22151.)

Key words: Calibration and testing; Ecuadorian Institute of Standardization (INEN); field inspections; mass, length, and volume standards; metrology laboratory; model law and regulations; technical education; U.S. AID.

t the request of the Ecuadorian Institute of Standardization EN) the U.S. AID made arrangements for a weights and sures advisor to assist in the development of a program for ntific and legal metrology, including the design of a metrolo- aboratory, inspection system, a training program, and other ntial features. A four week survey by an NBS representative resulted in recommendations for a metrology laboratory, sical standards, an Ecuadorian weights and measures law, ulations, and control program.

onsidered also were the Ecuadorian National Standards of s, length, and volume; precision balances, and other labora- instruments. A program of technical education was recom- nded for an INEN engineer (Program Administrator) and for er members of the INEN laboratory staff.

78. Wyly, R. S., Rorrer, D. E., **Field test of hydraulic per- rmance of a single-stack drainage system at the operation REAKTHROUGH prototype site in King County, Washing- on,** *NBSIR 73-161,* 66 pages (May 1973). (Available as B225-310 from the National Technical Information Service, pringfield, Va. 22151.)

Key words: Crossflow; field testing, plumbing; performance criteria, plumbing; performance, functional; single-stack drainage; siphonage, induced; siphonage, self; test loads, hydraulic; trap-seal reduction detector; trap-seal retention.

procedure for measuring the hydraulic performance of in-waste-vent (DWV) systems in the field is described, and results obtained with this procedure in a field demonstration the hydraulic performance of a single-stack DWV system are sented.

mong the most important criteria for hydraulic performance drain-waste-vent systems are the following: (1) Trap-seal re- tion in idle fixtures; (2) Ability of the system to resist the re- tion of suds, sewage, or foul gases due to hydrostatic or pneu- tic pressures in the DWV system; (3) Absence of cross flow tween fixtures; (4) Absence of self-siphonage in the individual ture traps.

onsidering the needs for minimization of maintenance in ser- e and for the continuation of venting during cold weather, the lowing additional criteria can be identified: (5) Ability to main- n adequate hydraulic performance over a long period of ser- e without excessive maintenance of branch piping; (6) equacy of performance under climatic conditions conducive frost closure of vent terminals.

The procedures for selection and application of hydraulic loads, based on state-of-the-art guidelines, are described as applied to the soil and waste stacks evaluated for conformance to criteria (1) through (4) above.

The results show adequate performance in relation to criteria (1) through (4), with a single example of non-conformance on criterion (3), subject to the limiting condition that some uncertainty exists as to the degree of leak resistance of the DWV systems made available for the tests.

Recommendations are offered concerning further work that could provide information to confirm estimated conformance to criteria (5) and (6).

13779. Finkel, P. W., Miller, T. R., **A proficiency test assessment of clinical laboratory capability in the United States,** *NBSIR 73-163,* 147 pages (May 1973). Supersedes COM73-11190, COM73,11193, and COM74-10552. (Available as COM-74-10542 from the National Technical Information Service, Springfield, Va. 22151.)

Key words: Accuracy; clinical chemistry; hematology; medical usefulness; microbiology; proficiency testing.

The proficiency of a representative sample of physician, hospital and independent laboratories was assessed with respect to their ability to analyse clinical chemistry and hematology samples and to identify microbiological organisms. For the assessment of clinical chemistry and hematology proficiency, the laboratories were grouped, and determinations of group accuracy and group precision were made. Further analyses were performed to determine relative accuracy and precision of the techniques presently applied by these groups. There was no significant difference at the 95 percent confidence level in the accuracy achieved by the various laboratory groups involved in clinical chemistry and hematology analysis. In clinical chemistry, the Medicare-Certified Independent Laboratories, CDC Tested Laboratories and JCAH-Members generally proved more precise than Physician's Office and Medicare-Certified Hospital Laboratories. However, none of the laboratory groups were sufficiently accurate to permit the monitoring over time of variation in an individual patient's constituent concentrations. It would appear that poor selection of techniques was an important contributor to this low performance level. In hematology the Physician's Office Laboratories proved to be the least precise of the groups. There was no noticeable difference in precision between participants in the CDC proficiency testing program and nonparticipants. With respect to microbiology, 76 percent of the identifications by laboratories participating in the CDC testing program were incorrect, while 19.4 percent of all other identifications were incorrect.

13780. Unassigned.

13781. Fribush, S. L., Bowser, D., Chapman, R., **Estimates of vehicular collisions with multistory residential buildings,** *NBSIR 73-175,* 72 pages (Apr. 1973). (Available as COM74-10395 from the National Technical Information Service, Springfield, Va. 22151.)

Key words: Collisions of vehicles with buildings; multistory buildings; progressive collapse of buildings; residential buildings; vehicular impact.

Through analysis of data from Oklahoma and Illinois along with national statistics, estimates are made of the number of vehicular collisions with buildings on an annual, nationwide basis. The best estimate is on the order of tens of thousands. However, since the impetus for the study was on multistory buildings and the likelihood of their being subject to progressive collapse the calculations have been refined to apply to substantial damage to multistory residential buildings. In 1970, such accidents were only on the order of 40, hence the probability of a given building being so affected in a single year is approximately one in 10,000. Some discussion is provided on improvement for data collection for the future.

**13782.** Burnett, E. F. P., Somes, N. F., Leyendecker, E. V., **Residential buildings and gas-related explosions,** *NBSIR 73-208,* 31 pages (June 1973). (Available as COM74-10127 from the National Technical Information Service, Springfield, Va. 22151.)

Key words: Building; explosion; frequency; gas; gas industry; progressive collapse; risk; statistics; structure.

The findings of an analysis of available statistics concerning the frequency of gas-related explosions in residential buildings are presented. The study was confined to incidents involving piped gas systems as they affect residential and commercial buildings. Though due regard has to be taken of the limitations inherent in the available statistics, it is concluded that in the USA the probability of occurrence of an explosion capable of causing significant structural damage could be 2.2 per million housing units per year.

**13783.** Greifer, B., Taylor, J. K., **Survey of various approaches to the chemical analysis of environmentally important materials,** *NBSIR 73-209,* 237 pages (July 1973). (Available as COM74-10469 from the National Technical Information Service, Springfield, Va. 22151.)

Key words: Air pollution; atomic absorption; electron microprobe; emission spectroscopy; environmental analysis; industrial effluents; ion-selective electrodes; nuclear activation analysis; particulate analysis; polarography; spark source mass spectrometry; spectrophotometry; trace elements; water pollution; x-ray fluorescence.

Various approaches to the chemical analysis of heavy industry process materials and effluents for trace element constituents that might contribute to environmental pollution are summarized.

The capabilities and costs of nuclear methods, spark source mass spectrometry, x-ray fluorescence and electron microprobe spectrometry, atomic absorption spectrometry, absorption spectrophotometry, atomic emission spectroscopy, voltammetry (polarography) and potentiometry (ion-selective electrodes) for determining traces (less than 100 parts per million) of mercury, beryllium, cadmium, arsenic, vanadium, manganese, nickel, antimony, chromium, zinc, copper, lead, selenium, boron, fluorine, lithium, silver, tin, iron, strontium, sodium, potassium, calcium, silicon, magnesium, uranium, and thorium in such matrices as fly ash, coal, oil, ores, minerals, metals, alloys, organometallics, incinerator particulates, slurry streams, and feeds to and from sedimentation processes have been assessed.

The report includes a critically selected bibliography of the current literature.

**13784.** Abrams, M. D., Hudson, J. A., Meissner, P., Pyke, T. N., Jr., Rosenthal, R. M., Ulmer, F. H., **Use of computer networks in support of interactive graphics for computer-aided design and engineering,** *NBSIR 73-217,* 47 pages (June 30, 1972). (Available as COM74-10470 from the National Technical Information Service, Springfield, Va. 22151.)

Key words: Computer-aided design; computer networks; interactive graphics, performance measurement; remote computer utilization.

This report covers work performed between 1 July 1971 and 30 June 1972 as part of a long-term study of interactive computer-aided techniques. The primary emphasis during th period has been on investigating the feasibility of using comput networks in support of interactive graphics for computer-aid design and engineering. Alternative means for providing remo computer service have been studied. An experimental configur tion has been devised taking advantage of the fact that there located at the National Bureau of Standards a node of the ARP Computer Network. Arrangements were made via this config ration for users at the Electronics Command to utilize a stru tural design program, NASTRAN, at a remote computer si Emphasis has been placed on the evaluation of performance interactive design techniques using displays supported by loc and remote computers in a hierarchical arrangement. A varie of problems are identified which must be considered in order support interactive graphics via a computer network; these a compounded where the network itself is in an evolving state development. The report includes an outline of a synchrono communication protocol which was developed for use betwe ECOM and NBS.

**13785.** Llewellyn, L. G., Peiser, C., **NEPA and the environmen movement: a brief history,** *NBSIR 73-218,* 40 pages (Ju 1973).(Available from the National Technical Informati Service, Springfield, Va. 22151.)

Key words: Environment; environmental impact sta ment; environmental movement; National Environmen Policy Act (NEPA); politics and the environment.

This paper traces some of the critical events leading up to t National Environmental Policy Act (NEPA) of 1969. The ope ing section spotlights the rapid growth of an environmental etl in this country, the impact of some highly visible ecological d asters, and the subsequent pressure for environmental reform e erted by opinion leaders and the mass media. The Fede Government's response to perceived changes in public priorit is the focal point of the second section. The activities of Co gress and the Nixon Administration are charted in a two-ye chronology spanning the 1968 and the 1970 elections, a k period in the development of environmental policy. The fi section provides a critique of NEPA with special attenti devoted to the controversial requirement for environmental i pact statements. The paper concludes with a brief discussion some of the challenges facing the environmental moveme today.

**13786.** Ogburn, F., Johnson, C. E., **Effects of electroless nic process variables on quality requirements,** *NBSIR 73-240,* pages (June 1973). (Available from the National Techni Information Service, Springfield, Va. 22151.)

Key words: Chemical nickel; coatings; electroless nick metal coatings; nickel; nickel-phosphorus.

Deposition rate, phosphorus content, hardness, appearan and metal distribution are reported for deposits from two ac hypophosphite type electroless nickel baths, one proprietary a one non-proprietary. The baths were operated under a variety conditions with variations of composition. Extensive data given on the relation of deposit hardness to phosphorus cont and to heat treatment at 100, 200, and 400 °C.

**13787.** Fried, C., Ramsburg, R., Butler, S., **A survey of the sani ry conditions of migrant labor camps,** *NBSIR 73-248,* 81 pa (Aug. 1973). (Available as COM74-10474 from the Natio Technical Information Service, Springfield, Va. 22151.)

Key words: Health standards; migrant labor cam questionnaire construction; regulations; survey design.

The Community Health Service (CHS) of the Department Health, Education, and Welfare has been assigned the respon y of providing health care services to migrant farmworkers. ce poor sanitation can be a major factor in the health of rants, CHS requested NBS' Technical Analysis Division AD) to perform a field survey of the current state of the sanita- onditions of migrant housing.

survey form was developed by TAD as an aid in evaluating grant housing. The form was derived from the checklist cedure employed by sanitarians to determine whether grant housing meets state and local housing regulations.

ield visits were made to migrant labor camps in five different ions of the United States. These regions were selected ause they contained a large number of camps open at the time the visits. Within each region, camps were selected on a dified random basis.

description of the findings of the survey is provided in both ular and narrative form. A discussion of the limitations in the cedures used in conducting the survey is also included, and anges are suggested which could be incorporated into future veys.

88. Holberton, F. E., Parker, E. G., **NBS Fortran test programs version 1 and version 3,** *NBSIR 73-250,* 267 pages (June 973). (Available as COM73-11955 from the National Techical Information Service, Springfield, Va. 22151.)

Key words: Computer programming language; FORTRAN; language validation; standard FORTRAN; test program design.

The NBS FORTRAN test programs, written in Standard RTRAN, are designed to test whether a FORTRAN comer accepts the forms and interpretations of the FORTRAN guage as described in the American National Standard FORRAN document × 3.9 – 1966. The test programs are recorded magnetic tape in approximately 14,500 punch card images, d comprise 116 test units. The test units may be used as parate executable FORTRAN programs, or may be linked end end with other test units, with a minimum of user effort, to imove operating efficiency. An additional copy of these 116 test its structured into 14 executable programs and the documentaon supporting the test programs are included in the distribution.

The test program design criteria was to: (1) Constrain all test ograms to the FORTRAN Standard × 3.9 – 1966; (2) Reduce e effect of those areas in which the FORTRAN Standard does ot prescribe a method or solution, e.g., range, precision, size of mputer, etc.; (3) Simplify the use of the FORTRAN test prorams; (4) Test FORTRAN language elements before they are sed in support of other tests; (5) Maintain an open ended stem so that tests may be changed or added.

The test programs require the use of a card reader, printer and ne intermediate unit.

3789. Shives, T. R., Willard, W. A., **MFPG detection, diagnosis, and prognosis,** *NBSIR 73-252,* 266 pages (Sept. 1973). (Available as AD772082 from the National Technical Information Service, Springfield, Va. 22151.)

Key words: Condition monitoring; failure detection; failure diagnosis; failure prevention; failure prognosis; diagnostic systems.

These proceedings consist of a group of sixteen submitted apers and discussions from the 18th meeting of the Mechanical ailures Prevention Group which was held at the National Bueau of Standards on November 8-10, 1972. Failure detection, iagnosis, and prognosis represent the central theme of the roceedings. Bearing condition monitoring, diagnostic systems echnology and applications, and new approaches in sensing and rocessing are discussed.

13790. Son, B. C., **Fire endurance tests of unprotected wood-floor constructions for single-family residences,** *NBSIR 73-263,* 65 pages (July 1973). (Available as PB225-284 from the National Technical Information Service, Springfield, Va. 22151.)

Key words: Fire endurance; fire test; flame through; full scale; housing; Operation BREAKTHROUGH; single family residence; small scale; thermal resistance; wood floor; wood joist.

Fire endurance tests were performed on two full-scale and twelve small scale wood floor constructions. The fire endurance ratings on unfinished wood joist and plywood subfloor constructions varied from 10 to 13 minutes and were mainly determined by the time to "flame through." In small-scale tests, the addition of carpeting with a hair pad delayed the time of "flame through" approximately 8 minutes. Time to "flame through" may be estimated from the thermal resistance of the construction, and may be modified by the effects of applied load or construction details such as gaps, joints, and penetrations.

13791. Son, B. C., Fang, J. B., **Fire spread on exterior walls due to flames emerging from a window in close proximity to a reentrant wall corner,** *NBSIR 73-266,* 35 pages (Apr. 1973). (Available as PB225-286 from the National Technical Information Service, Springfield, Va. 22151.)

Key words: Exterior wall; fire spread; fire test; ignition; Operation BREAKTHROUGH; reentrant corner.

As a part of the research program concerning the recommended criteria for fire safety in Operation BREAKTHROUGH, two full scale fire tests were performed on a mockup of a reentrant corner, i.e., the interior corner formed at the intersection of the exterior walls of adjacent buildings, such as townhouses and garden apartments.

In each test, two wall specimens representing exterior walls were erected perpendicular to a wall containing a window opening into a fire room. One wall was located 1 foot east and the other one 5 feet west of the edges of the window. The objective of the reentrant corner fire test was to study the potential ignition and spread of fire from the room to an adjacent exterior combustible wall.

In the first test, charring on the east wall, but no surface ignition was observed during the test. The peak temperature measured did not exceed 350 °C (660 °F). In the second test, surface ignition occurred on the east wall 9 minutes after the wood crib, representing the combustible contents of the room, was ignited. No significant changes were observed on the west wall during either test.

The instantaneous heat flux incident on the east wall just prior to ignition and the total heat energy absorbed were estimated to be on the order of 1.0 W/cm² and 175 Joules/cm² respectively.

13792. Issen, L. A., **Report of fire tests on flexible connectors in HVAC systems,** *NBSIR 73-267,* 67 Pages (July 1973). (Available as COM73-11955 from the National Technical Information Service, Springfield, Va. 22151.)

Key words: Aluminum; ductwork; fabric; fiberglass; fire tests; high rise buildings; HVAC systems; steel; terminal units.

The contemporary high rise building with its control air conditioning system and high content of synthetic materials presents a higher hazard than those erected prior to 1950. The ability of the duct work to resist fire breaking into it and spreading through the duct system is an important factor affecting the integrity of the building. Since they penetrate fire barriers, the flexible connectors between the main ducts and the terminal units are important elements in maintaining the desired fire resistance. Flexible connectors made of four different materials (aluminum, galvanized steel, felted fiberglass and woven fiberglass fabric) and two attachment techniques were subjected to fire tests in accordance with ASTM E119. The results show that the materials of the connectors must withstand the fire exposure, the connectors must remain tightly attached to the main duct, and the penetrations through the fire barrier must be suitably blocked in order to prevent fire from breaking into the duct system. The tests also showed that rubber and plastic materials in the terminal units can produce significant amounts of irritating smoke.

**13793.** Feldman, A., Horowitz, D., Waxler, R. M., **Laser damage in materials,** *NBSIR 73-268,* 44 pages (Aug. 1973). (Available as AD768-303 from the National Technical Information Service, Springfield, Va. 22151.)

Key words: Absorption coefficient; calcite; damage threshold; deuterated potassium dihydrogen phosphate; electrostriction; electrostrictive self-focusing; inclusion damage; Kerr effect; laser damage; lithium niobate; nonlinear index of refraction; potassium dihydrogen phosphate; self-focusing; thermal self-focusing; thoria:yttrium oxide ceramic; yttrium aluminum garnet.

Neodymium:glass laser induced damage is observed in lithium niobate ($LiNbO_3$), calcite ($CaCO_3$), potassium dihydrogen phosphate (KDP), and deuterated potassium dihydrogen phosphate (KD*P). The damage at the lowest power levels is caused by inclusions. At higher power levels, filamentary damage, which is indicative of self-focusing, is observed in $LiNbO_3$. An analysis of self-focusing data in yttrium aluminum garnet shows that the Kerr effect is the dominant self-focusing mechanism, with some contribution from the thermal effect. Bulk and surface damage thresholds in neodymium-doped thoria:yttrium oxide ceramic are obtained relative to bulk damage thresholds in several optical materials. For solid materials relationships are obtained between the stress-optic coefficients and the electrostrictive coefficients under different geometric boundary conditions.

**13794.** McNeil, M. B., **Report to AID on an NBS/AID workshop on standardization and measurement services in industrializing economics,** *NBSIR 73-275,* 64 pages (May 4-18, 1973). (Available as COM74-10126 from the National Technical Information Service, Springfield, Va. 22151.)

Key words: AID; assistance; economics; foreign relations; industrializing nations; LDC's; measurement services; standardization.

On May 4-18, 1973, a Workshop was held at the National Bureau of Standards (Gaithersburg), under the sponsorship of AID, whose object was to give standards officials of industrializing nations insight into the standards and measurement systems in the United States and the role of the National Bureau of Standards, so that these officials might consider what parts of the U.S. system might usefully be adapted to conditions in their home countries. The report contains copies of speeches and presentations by representatives of both the U.S. and the industrializing nations, in addition to a general agenda of talks, presentations, and tours of laboratories both of NBS and of other organizations.

**13795.** Fung, F. C. W., **Evaluation of a pressurized stairwell smoke control system for a 12 story apartment building,** *NBSIR 73-277,* 53 pages (June 1973). (Available as PB225-278 from the National Technical Information Service, Springfield, Va. 22151.)

Key words: Analysis; basic correlation formulas; computer calculations; high-rise building fire; Operation BREAKTHROUGH; pressurized stairwell; quantitative experiment; smoke control; smoke simulation.

An NBS study to evaluate the effectiveness of a pressurize stairwell smoke control system in a high rise apartment buildin is summarized and discussed in the light of experimental results analysis, and computer prediction. A quantitative experimenta technique of smoke simulation and smoke movement measurement is described, supplemented by basic physical laws necessary for correlation with small fires, and illustrated by the results c an actual field experiment. Experiments were conducted in a 1 story apartment building constructed on the Operatio BREAKTHROUGH prototype site in St. Louis, Missouri. Th experimental results are then further extended to a wider rang of ambient weather conditions by way of computer predictio calculations. General conclusions and relevant recommendations as a result of the study are also presented.

**13796.** Trechsel, H. R., **Swiss building and housing research a tivities,** *NBSIR 73-288,* 63 pages (Aug. 1973). (Available COM73-11861 from the National Technical Informatio Service, Springfield, Va. 22151.)

Key words: Building research; buildings; cooperatio housing; international; Switzerland.

Following up earlier contacts of CBT management wi representatives of Swiss building research organizations, th author visited Switzerland in the Fall of 1972 for two weeks.

This report discusses the results of meetings with represent tives of the Swiss Federal Commission for Housing Researc (FKW), major educational and research establishment architects, contractors, builders, and local building official Topics covered in the discussions included building economic modular coordination, pre-evaluation of performance of housir projects, pre-evaluation of research projects, building desig land use and planning, transportation, and building laws, code and standards.

It appears that cooperative programs in any or all of the areas could be profitable to NBS, and to the corresponding Swi organizations.

**13797.** Treu, S., **Characterization and testing of interacti graphics for computer-aided design and engineering,** *NBSI 73-289,* 36 pages (June 30, 1973). (Available as COM7 10475 from the National Technical Information Servic Springfield, Va. 22151.)

Key words: Characteristics; computer-aided design; i teractive graphics; man-machine interaction; performan measurement.

This report presents material developed as part of a long-te "Interactive Computer-Aided Techniques Study." The repo outlines the stages of development in the utilization of interacti graphics as a tool for Computer-Aided Design and Engineeri (CAD/E). A series of characteristics are presented which are significance to the designers and users of such systems and a s ries of questions of evaluative interest posed. These questio are intended to delineate the extent to which a system under e amination achieves its stated design objectives. The chara teristics are grouped in accordance with the nature and comple ity of the experiments which would need to be conducted establish values for them. The report suggests selected chara teristics of particular interest and suggests the design of expe ments for examining them in detail. The report makes speci reference to the MEDEA design terminal concept unc development within the Graphical Systems and Technolo Branch of ECOM.

**98.** Clifton, J. R., Beeghly, H. F., Mathey, R. G., **Interim Re- ort No. 7. Chemical resistance and physical durability testing f coating materials,** *NBSIR 73-295*, 22 pages (Aug. 1973). Available as COM74-10471 from the National Technical nformation Service, Springfield, Va. 22151.)

Key words: Bridge decks; corrosion; creep testing; epoxy coatings; polyvinylchloride coatings; steel reinforcing bars.

he possibilities of protecting steel reinforcing bars embedded oncrete of bridge decks from corrosion by using organic bar- -type coatings are being investigated in this project. This cor- ion is accelerated by the chloride ions of the two most com- nly applied deicing materials, sodium chloride and calcium oride.

n this report, physiochemical studies performed on coatings l coated bars are discussed, including: immersion studies of tings in corrosive solutions; impact and embedded in icrete.

**99.** Andrews, J. R., **Random sampling oscilloscope time base,** *BSIR 73-309*, 86 pages (June 1973). (Available as COM73- 1981 from the National Technical Information Service, pringfield, Va. 22151.)

Key words: Mercury switch; oscilloscope; picosecond; pulse; random sampling; risetime; sampling; time base; transition time.

Vith the advent of new miniaturized mercury (Hg) switches h reputed transition times of the order of 10 picoseconds, in- est has been rekindled in their use in high speed pulse mea- ements. Since there is no pre-trigger signal available from a switch, normal sequential sampling techniques are not usable measure the fast Hg switch transition time. For this reason a random sampling time base unit was designed to perform se measurements at the low repetition rate of Hg switches ( < ) Hz). The time base may be used with commercial sampling illoscope systems through suitable interconnection terminals possible interface equipment. It features three selectable time ndows of 1 $\mu$s, 100 ns, and 10 ns. Using its time magnifier, the test sweep rate is 10 ps/cm. A variable trigger lead time con- l is provided. The trigger sensitivity is 10 mV. The long term ing stability of the time base is excellent with less than 15 ps/h ft.

**800.** Kartaschoff, P., Jarvis, S., Jr., **Notes on infrared absorp- tion experiments in a methane molecular beam,** *NBSIR 73-312*, 32 pages (May 1973). (Available as COM73-11893/7AS from the National Technical Information Service, Springfield, Va. 22151.)

Key words: Frequency standard; methane resonance; molecular beam; Ramsey resonance; saturated absorption; stabilized laser; transition probability.

The problem of calculating the transition probability of methane molecules in a molecular beam interacting with an infrared (3.39 $\mu$) radiation beam is discussed. Contrary to the usual microwave molecular beam experiments, first-order Doppler frequency shifts cannot be neglected. This makes the solution of the wave-equations more difficult. Weak field approximations to the transition probability have been calculated. Single optical beam experiments analogous to the Rabi-type interaction result in a Doppler-broadened absorption line with an estimated half-power width of a few MHz. For separated multiple field experiments analogous to the Ramsey-type interaction, no observable response is predicted, the expected sharp resonance pattern being smeared out by the random Doppler shifts due to the spread of the molecular beam trajectories. Further investigations are required in order to predict the resonance line shapes for strong fields, i.e., saturated absorption.

**13801.** Woolley, M. L., **Bibliography of the Electromagnetics Division June 30, 1972 to June 30, 1973,** *NBSIR 73-320*, 22 pages (June 1973). (Available as COM73-11971 from the National Technical Information Service, Springfield, Va. 22151.)

Key words: Antenna parameters; attenuation; current; electromagnetic measurements; field strength; impedance; waveguide theory.

This bibliography lists the publications of the NBS Electromagnetics Division between June 30, 1972 and June 30, 1973.

**13802.** Unassigned.

**13803.** Parrish, W. R., Hiza, M. J., **Calculated liquid phase thermodynamic properties and liquid-vapor equilibria for fluorine-oxygen (FLOX) mixtures,** *NBSIR 73-338*, 30 pages (Sept. 1973). (Available as COM73-11660 from the National Technical Information Service, Springfield, Va. 22151.)

Key words: Calculated thermophysical properties; compressed liquid phase, fluorine-oxygen mixtures, hard-sphere model; liquid-vapor equilibria.

Liquid phase thermodynamic properties and liquid-vapor equilibria of fluorine-oxygen mixtures, for which no experimental data exist, have been calculated. The results are based on excess properties predicted from the Snider-Herrington equations, with an adjusted combining rule, and the corresponding data for the pure fluids. Mixtures considered are 0.6, 0.7, 0.8, 0.88, and 0.9 weight fraction of fluorine from 55 to 90 K up to 70 × $10^5$ Pa. In the compressed liquid, molar volumes, enthalpy, entropy, and constant pressure specific heat were determined. Along the saturation boundary, coexistent vapor compositions and solution vapor pressures were determined as well. Corresponding properties of pure fluorine from experimental data have also been included. Results are tabulated in both British and S.I. units.

**13804.** Romanoff, M., Gerhold, W. F., Schwerdtfeger, W. J., Iverson, W. P., Sanderson, B. T., Escalante, E., Watkins, L. L., Alumbaugh, R. L., **Protection of steel piles in a natural seawater environment—Part I,** (Proc. 3d Int. Congress on Marine Corrosion and Fouling, Gaithersburg, Md., Oct. 2-6, 1972), Paper in *Proceedings: Third International Congress on Marine Corrosion and Fouling,* pp. 103-119 (Northwestern University Press, Evanston, Ill., Oct. 1973).

Key words: cathodic protection; coating index; corrosion rates; marine environment; polarization techniques; protective coatings; steel piling.

In a joint research effort between the National Bureau of Standards, the U.S. Army Corps of Engineers, and the U.S. Naval Civil Engineering Laboratory, the corrosion behavior of protected carbon and low alloy steel piling in seawater is being investigated. Nine-three "H" and pipe pile specimens, 35 feet long, were jetted into the Atlantic Ocean floor off the coast of Dam Neck, Va. The results of this study, which will take about 15 years to complete, will demonstrate which of the systems tested are best for protecting steel piles in seawater. Many types of protective methods are included in the investigation consisting of coating systems (coal-tar epoxy, hot-dip zinc, flamesprayed aluminum and zinc, zinc-rich paints, epoxies, etc.), cathodic protection by zinc and aluminum sacrificial anodes, and combinations œ coatings and cathodic protection. At one-year intervals, polarization measurements and visual observations are made on the piles to determine the effectiveness of the coating systems and to measure the rates of corrosion. Potentials of cathodically protected piles are also measured. These data will be correlated with physical determinations made on the piles when they are removed from exposure. The first removal of one set of piles (31 in number) is scheduled for October 1972, after exposure for approximately 5 years.

**13805.** Bennett, L. H., Swartzendruber, L. J., McNeil, M. B., **On the electron-configuration theory of marine corrosion,** (Proc. 3d Int. Congress on Marine Corrosion and Fouling, Gaithersburg, Md., Oct. 2-6, 1972), Paper in *Proceedings: Third International Congress on Marine Corrosion and Fouling,* pp. 410-426 (Northwestern University Press, Evanston, Ill., Oct. 1973).

Key words: alloy theory; catalysis; chemisorption; Cu-Ni alloys; d-bands; electron-configuration; metallurgy; passivity; rigid-band model; saltwater corrosion; surfaces.

The electron-configuration theory of corrosion introduced by Uhlig relates chemisorption and passivity to alloy compositions having favorable d-electron configurations. This theory postulates a critical composition for passivity which coincides with a theoretical filling of the d-band in a "rigid-band" description of these alloys. Recently, detailed knowledge of the electronic structure of Cu-Ni alloys has been greatly increased, and it no longer appears that a strict band model alone can give an adequate description of the disordered alloys. Recent theories and modern spectroscopic methods, including soft x-ray and photoelectron spectroscopy and other techniques, have provided a great deal of new knowledge concerning the electronic structure of Cu-Ni alloys. In light of these experimental and theoretical developments, this paper investigates whether or not there is any evidence to support an electron-configuration theory of c rosion, without regard to the question of passivity, for Cu-Ni loys in saltwater. The addition of small amounts of Fe has imp tant effects on the corrosion rate in the copper-rich alloys and t relevance of this to the electron-configuration theory is c sidered. Effects of metallurgical variables and of film properti are noted. The related topic of heterogeneous catalysis discussed.

**13806.** Iverson, W. P., **The corrosion of mild steel by a mar strain of** ***Desulfovibrio,*** (Proc. 3d Int. Congress on Mari Corrosion and Fouling, Gaithersburg, Md., Oct. 2-6, 197 Paper in *Proceedings: Third International Congress Marine Corrosion and Fouling,* pp. 61-82 (Northwest University Press, Evanston, Ill., Oct. 1973). 340

Key words: anaerobic corrosion; depolarizing agent; ferr ions; marine corrosion; *marine Desulfovibrio*; polarizat techniques.

A marine strain of *Desulfovibrio* was isolated from steel pil detritus at Dam Neck, Va. A medium which provided good s face growth on 2 percent agar plates in a hydrogen atmosph was developed (Trypticase, 15 gm; Phytone, 5 gm; NaCl, 5 seawater, 1000 ml). The corrosion rate of mild steel in this m um, with and without the addition of Fe$^{++}$ ions, was investiga using polarization techniques. In the absence of added Fe$^{++}$ ic the corrosion rate was found to decrease and then either incre or remain at a low level. In one corrosion cell a high rate of c rosion was accompanied by the formation of a corrosion prod or products in the shape of "stalactite" formations. Analysis dicated free sulfur and an iron sulfur compound with iron in Fe$^{+++}$ state.

In the presence of added Fe$^{++}$ ions, the corrosion rate found to increase to 255 mdd in one corrosion cell and t decrease. Chemically prepared FeS produced little change in potential or the corrosion rate. Corrosion of mild steel in a b teria-free culture filtrate, to which Fe$^{++}$ ions were added in cess to remove the S$^{=}$ ions was extremely high. After an inc tion period of 3 days, the corrosion rate increased to a maxim of 1130 mdd 8 days after the start of the corrosion process. I ing the period of extensive corrosion, the potential of the s dropped to more noble values.

When the black precipitate, formed upon the addition of F ions, was removed, the resulting filtrate was still highly co sive, indicating that the depolarizing agent was water soluble not the precipitate. The depolarizing agent appears to act a electron carrier, removing electrons from the iron and trans ring them to an acceptor which is thereby reduced. The actio this depolarizing agent could account for the high anaerobic rosion rates observed in the field.

Inhibition of corrosion in cultures of *Desulfovibrio* appea be due to the action of H$_2$S which reacts with the iron to fo protective film and prevents the actions of the sol depolarizer.

**13807.** Leasure, W. A., Jr., **Automobile tire noise: A review of open literature,** (Proc. 1973 National Noise Control Engin ing Conf., Washington, D.C., Oct. 15-17, 1973), Pape *Noise-Con 73 Proceedings,* D. R. Tree, Ed., pp. 187-195 stitute of Noise Control Engineering, Noise/N s, Poughkeepsie, N.Y., Oct. 1973).

Key words: acoustics; automobile; noise (sound); tire noise; ransportation noise.

tomobiles, the primary mode of transportation in the ed States, contribute significantly to the noise environment o the large number in operation. In this paper, one aspect of mobile noise is discussed, namely the contribution to overall cle noise made by the interaction of the tires with the road ce. For passenger cars, tire noise can be a significant contor to overall levels at speeds as low as 35-40 mph and typi is the major contributor at higher speeds. Based on the ed data base available in the open literature, a discussion is of the effects of various vehicle operational modes, tire anical properties, and road surface texture on the noise rated by passenger car tires. Both community noise and the heard by the occupants of the vehicle are considered. ible noise generation mechanisms, although not well untood, are presented. Areas for future research and develop are identified based on gaps in present knowledge.

8. Corley, D. M., **Test of a proposed method for vehicle noise easurement,** (Proc. 1973 National Noise Control Engineerg Conf., Washington, D. C., Oct. 15-17, 1973), Paper in *oise-Con 73 Proceedings,* D. R. Tree, Ed., pp. 230-235 (Initute of Noise Control Engineering, Noise/News, oughkeepsie, N.Y., Oct. 1973).

Key words: directivity; noise source level; sound pressure level; truck tire.

a spherical pulsating source radiates into a infinite medium, sound pressure is inversely proportional to the distance from source. No real source exactly fulfills these conditions but it enerally assumed that far enough away from the source, rical spreading will result. It has been proposed [Hixon, r-Noise 72, Washington, D.C.] that a measurement indepen of distance results if both sound pressure level and distance the source are monitored and the sound pressure level is malized to a constant distance, e.g., 1 meter, from the source. s measurement is deemed Noise Source Level. Data exist for which can indicate the merit of this approach [W. Leasure l, DOT-OST-ONA 71-9]. These data consist of sound pres level and distance from the source simultaneously monid as unpowered trucks coast past an array of microphones. A-weighted Noise Source Level from three types of truck s with tread designs representative of tread patterns in com use today are presented. It is concluded that spherical eading is generally not the case even 500 feet from the source. r-dependence is not satisfactorily removed by this method analysis. Therefore considerable care should be exercised if ise Source Level is used to characterize truck tire noise els. Noise Source Level does appear to be useful for present source directivity.

09. **Bender, P. L., Currie, D. G., Dicke, R. H., Eckhardt, D. I., Faller, J. E., Kaula, W. M., Mulholland, J. D., Plotkin, H. I., Poultney, S. K., Silverberg, E. C., Wilkinson, D. T., Wilams, J. G., Alley, C. O., The lunar laser ranging experiment,** *cience* **182,** 229-238 (Oct. 1973).

Key words: celestial mechanics; crustal movements; earth rotation; geophysics; laser; moon; polar motion; selenodosy.

he data obtained so far by the McDonald Observatory have n used to generate a new lunar ephemeris based on direct nurical integration of the equations of motion for the moon and nets. With this ephemeris, the range to the three Apollo oreflectors can be fit to an accuracy of 5 meters by adjusting differences in momenta of inertia of the moon about its prinal axes, the selenocentric coordinates of the reflectors, and McDonald longitude. The accuracy of fitting the results is ited currently by errors of a few arc sec in the angular orientation of the moon, as derived from the best available theory of how the moon rotates in response to the torques acting on it. A new calculation of the moon's orientation as a function of time based on direct numerical integration of the torque equations is expected to considerably improve the accuracy of fitting the data.

**13810.** Unassigned.

**13811.** Thomas, R. N., Gebbie, K. B., **Theory of stellar atmospheres,** *Trans. Int. Astron. Union* **15A,** 537-569 (1973).

Key words: stellar atmospheres.

This report has been prepared by the President in collaboration with the Secretary of the Commission. It is based on (1) material supplied by those members and associates of the Commission who responded to requests made in our circulars, (2) a bibliographical search intended to supplement the above material, (3) discussions with other interested persons, and (4) our own knowledge and impressions of the activity within the province of the Commission over the last three years. The report is divided into three parts. Part A is a scientific review aimed not at a comprehensive summary of all work but at a selective review of that which has, in our opinion, introduced some significant change in our concept of a stellar atmosphere or in the likely direction of future developments. Part B is a bibliography. It is this part of the report that is intended to provide an exhaustive summary of work done in the field over the last three years. To authors of those papers we have inadvertently omitted, we offer our apologies: neither were they sent to us nor did we locate them ourselves. Finally, Part C is an outline of the aims and activities of the Commission.

The decision to write the entire report ourselves, rather than delegate specific sections to other people, was aimed at providing a more coherent approach to the subject as a whole. Clearly, this represents only one of many possible approaches, and the form of the report is highly individual. The choice of what to include without encroaching on the fields of other commissions has become increasingly difficult. No longer can Commission 36 confine itself to theoretical models of stellar atmospheres. Empirical analyses that reveal inconsistencies in our theoretical assumptions must also be included, as must some consideration of solar phenomena, which are now recognized as being relevant to a wide variety of stars. Reference must also be made to those results of physics that are immediately applicable to the theory of stellar atmospheres. Inevitably, the selection has to some extent been arbitrary.

**13812.** Flynn, D. R., Leasure, W. A., Jr., **Machinery noise: Measurement standards and test codes,** (Proc. 1973 National Noise Control Engineering Conf., Washington, D.C., Oct. 15-17, 1973), Paper in *Noise-Con 73 Proceedings,* D. R. Tree, Ed., pp. 257-260 (Institute of Noise Control Engineering, Noise/News, Poughkeepsie, N.Y., Oct. 1973).

Key words: acoustics; noise; soundpower.

Measurements of the sound power emitted by machinery, or of the sound pressure at specific locations, are needed for a variety of purposes. These include measurements for diagnostic and control purposes, measurements for labeling (explicitly or implicitly) the noise emission from a product, and measurements to determine compliance with specifications or regulations. A brief discussion is given of the general items which should be included in noise measurement standards and test codes. An example of standards addressing these points is the series of basic documents on sound power level measurements being prepared under the auspices of the International Organization for Standardization.

**13813.** Cameron, J. M., Plumb, H., **Traceability—with special**

**reference to temperature measurement,** *Soc. Automot. Eng. Trans.* **78,** Section 3, 1586-1590 (1969).

Key words: calibration; temperature; traceability.

The requirement that measurements be traceable to national standards arose in response to needs for consistency between different parts of the measurement system. There is one single agreed-upon definition for traceability, but it has been taken to mean the existence of some chain of intercomparisons or calibrations leading back to the National Bureau of Standards. Like all procedural or material requirements, its presence or absence may bear little relation to the performance characteristic one is really interested in. The scientific problem of expressing the desired performance requirements in terms of the amount and type of evidence needed to determine the degree of consistency of measurement processes is discussed and illustrated for the measurement of temperature. The importance of the study of measurement as a production process and the need for a program for the surveillance of the measurement process is discussed and plans for a new service for transfer of measurement capability in thermometry are presented.

**13814.** Cook, R. K., **The use of modulated reverberation for measurement of absorption and sound power,** (Proc. 1973 National Noise Control Engineering Conf., Washington, D.C., Oct. 15-17, 1973), Paper in *Noise-Con 73 Proceedings,* D. R. Tree, Ed., pp. 303-308 (Institute of Noise Control Engineering, Noise/News, Poughkeepsie, N.Y., Oct. 1973).

Key words: acoustical measurement; noise control; sound power.

A source of sound power modulated in amplitude 100 percent at a very low sinusoidal frequency $F$ is introduced into a reverberation chamber. The total acoustical energy in the sound field will have an amplitude modulation at the same frequency $F$, but lagging in phase by $\phi$ due to the absorption in the chamber. An analysis of the differential equation for energy and sound power balance yields (1) the absolute cross-section $A$ for absorption, and (2) the time-averaged absolute sound power $W_o$ of the source. Measurements $A$ and $W_o$ have been made at various audio frequencies in the 425 $m^3$ reverberation chamber of the Bureau. The modulated source of sound power was electroacoustical—an array of four loudspeakers having their audio input voltage waveforms amplitude-modulated at $F = 0.1$ to 0.4 Hz. The sound pressure $|p^2|$ was measured with an array of four microphones. The phase $\phi$ was obtained by means of an analog computer based on a least squares principle of design. For a steady source of sound power, e.g., a noisy machine, a modulated sound field can be produced by modulating (as a function of time) the absorption cross-section of the reverberation chamber. We present the analysis for energy and sound power balance, and examine some methods for achieving modulated absorption cross-sections.

**13815.** O'Connell, J. S., **Electromagnetic interactions of the few-nucleon systems,** *Proc. Seminar Electromagnetic Interactions of Nuclei at Low and Medium Energies, Moscow, U.S.S.R., Dec. 11-13, 1972,* pp. 299-309 (Dec. 1973).

Key words: deuterium; electron scattering; helium-3; helium-4; photonuclear; weak interactions.

Recent progress on the photodisintegration electron scattering reactions on the hydrogen and helium isotopes is reviewed. The connection to weak interactions and the effect of meson dynamics on few-nucleon properties and reactions are discussed.

**13816.** Post, M. A., **Liquid latex paint analysis,** *Paint Varnish Prod. Part 1,* **63,** No. 9, 21-25 (Sept. 1973); *Paint Varnish Prod. Part 2,* **63,** No. 10, 27-38 (Oct. 1973).

Key words: acrylic; alkyd modified latex paints; deep-tone latex paints; infrared spectroscopy; polyvinyl aceta styrene-acrylate; vinyl-acrylic; vinyl acetate-dibu maleate; vinyl acetate-ethylene; vinyl acetate-ethyl ac late; vinyl acetate-2-ethyl-hexyl acrylate; vinyl chlori acrylate.

The qualitative identification by infrared spectroscopy of la resins, the quantitative determination of the latex resin and alk modifier in alkyd modified latex paints and of the latex resir unmodified latex paints are discussed. Four procedures for la resin identification and two methods for quantitative determi tion of the latex resin are presented. One of the quantitat methods can be used for any latex paint. The other, whicl shorter is useful only for paints based on polyvinyl acetate, vi acetate-dibutyl maleate and vinyl-acrylic copolymers.

**13817.** Hummer, D. G., Seaton, M. J., **Interpretation of the sp tra of planetary nebulae.** Introductory Report, *Mem. Soc. R Sci. Liege* V, 225-238 (1973).

Key words: forbidden lines; nebular spectra; planet nebulae; recombination spectra.

Progress since 1967 in the interpretation of nebular spectr reviewed.

**13818.** Keller, R. A., **Tunable lasers for chemists,** *Ch Technol.,* 626-634 (Oct. 1973).

Key words: dye laser; isotope separation; photochemis review; saturation spectroscopy; spectroscopic analysis.

A general review of organic dye lasers and their use in fields of: analytical chemistry, chemical synthesis and sep tion, photobiology, and spectroscopy is presented. The tex cludes 47 references.

**13819.** Mordfin, L., Robusto, R., Jr., **Plastic deformation cha teristics of refractory metals above 3000 °F,** (Proc. 5th Nati Society for the Advancement of Material and Process gineering Technical Conf., Kiamesha Lake, N.Y., Oct. 9 1973), Paper in *Materials & Processes for the 70's* **5,** 378- (SAMPE, National Business Office, Azusa, Calif., Oct. 19

Key words: evaluation; high temperature tests; mo denum; plastic flow; Poisson ratio; refractory metals; st hardening; strain rate, stress strain diagrams; tantalum; sile properties.

Using a photographic strain-measuring technique, explora tensile tests were conducted to investigate the plastic beha of unalloyed molybdenum and tantalum in the hot-working perature range. Several unusual characteristics were obser including serrated flow, a negative strain-rate sensitivity an one case, considerable strain hardening. These observation dicate a need for further research in this area, before hot-wor processes for refractory metals can be made practical.

**13820.** Hayward, E., Barber, W. C., Sazama, J., **Nuclear sca ing of plane-polarized photons,** *Phys. Rev. C* **8,** No. 3, 1 1073 (Sept. 1973).

Key words: dynamic collective model; giant resona nuclear surface oscillations; photon scattering; pola photons; tensor polarizability.

A beam of plane-polarized monochromatic photons has produced by the resonance fluorescence of the well-know state at 15.1 MeV in $^{12}C$. These have been scattered a se time from natural targets of Cd, Sn, Ta, W, Pt, Au, and Bi. I surements were made with poor energy resolution of the rel number of photons scattered at 90° parallel and perpendicu the polarization vector in the incident 15.1-MeV beam. Th servation of photons scattered along the polarization v reflects the contribution of incoherent scattering to the dom coherent-scattering process and results either from perma ar deformation or from the dynamic deformation produced e coupling of the giant dipole resonance with the quadrupole ations of the nuclear surface. The observed intensities of in-rent scattering are of the same order of magnitude for the rmed nuclei and the spherical vibrators and agree roughly the predictions of the dynamic collective model. No in-rent scattering was observed from the rigid sphere $^{209}$Bi.

1. Tschiegg, C. E., Greenspan, M., **Helmholtz resonators as nic bubble chambers?,** *J. Acoust. Soc. Amer.* **54,** No. 4, 1112-13 (Oct. 1973).

Key words: bubble chamber; Helmholtz resonators; rapid-cycling bubble chamber; sonic bubble chamber.

has been found possible to develop alternating pressures of o 10 atm in liquid-filled Helmholtz resonators. Some ad-ages and disadvantages of the construction of a rapid-cycling le chamber along such lines are discussed.

2-13831. Unassigned.

2. Mies, F. H., **Stimulated emission and population inversion diatomic bound-continuum transitions,** *Mol. Phys.* **26,** No. 5, 33-1246 (1973).

Key words: continuum emission; lasers; line shapes; molecular spectroscopy; quantum chemistry; stimulated emission.

act expressions are derived for the rate of stimulated emis-and the conditions for population inversion in a diatomic d-continuum transition. The resultant formulae resemble of a simple, homogeneously broadened, discrete transition the Lorentzian lineshape replaced by a continuum hape, $g^C(h\nu = E_{v'} - \epsilon'')$, which is approximately equal to the re of the overlap between the initial, emitting, vibrational $v'$ and the final, energy-normalized continuum state $\epsilon''$, i.e. $(v'|\epsilon'')^2$. Using the "reflection method," which is most ap-ble to a strongly repulsive final state, equations are obtained h allow simple, but accurate, estimation of the pertinent meters which influence lasing action. Some general conclu-are extracted, and specific results are presented for the ulated vacuum ultraviolet emission in high pressure Xe.

3. Carrington, C. G., Drummond, D., Gallagher, A., Phelps, V., **Oscillations in continuum molecular spectra of alkali-tal–noble-gas molecules,** *Chem. Phys. Lett.* **22,** No. 3, 511-4 (Oct. 15, 1973).

Key words: alkali-metal; continuum; molecules; rare-gas; spectra.

gular intensity undulations in the continuum spectra of y diatomic molecules are reported. In particular, the -XΣ transition of the Rb–noble-gas Cs–noble-gas cules has been studied. Calculations as well as experimental rvations of absorption and emission spectra are reported.

4. Taylor, P. O., Dunn, G. H., **Absolute cross sections and larization for electron-impact excitation of the *K* and *H* onance lines of the Ca⁺ ion,** *Phys. Rev. A* **8,** No. 5, 2304-21 (Nov. 1973).

Key words: Ca II; electron impact; excitation cross sections; polarization; resonance lines.

rossed beams of electrons and $Ca^+$ ions have been used to sure absolute cross sections for electron-impact excitation e resonance *K* and *H* lines of Ca II at 3934 and 3968 Å, ectively. Polarization fractions of the light were also mea-d. The cross sections presented are absolute in the sense that neasurables including photon flux, have been compared to vant standards. The cross section for excitation of the *K* line oserved to have a value of about $(18 \pm 2)\pi a_0^2$ at the 3.15-eV shold, and to decrease to a magnitude of $(1.5 \pm 13)\pi a_0^2$ at 700-eV electron energy. Experimental uncertainties have been presented at the 98 percent confidence level, typically three standard deviations of random fluctuations combined in quadrature with the systematic uncertainties. The experimental results for both the *K* and *H* emissions are in agreement at 350 eV with the Coulomb distorted-wave calculation of Burgess and Sheorey but lie about 35 percent below the low-energy three-state close-coupling calculations of Burke and Moores. The ratio of the cross sections for the *K* and *H* emission is found to be 2.0 at all energies. Detailed study of the cross section at low energies demonstrates the expected finite value at threshold (within the accuracy allowed by the electron energy spread of 0.3 eV), and does not indicate the presence of a large (greater than 5%) contribution from cascade. Structure in the *K* cross section about 2 eV above threshold suggests interactions with autoionizing levels of Ca I, presumably belonging to the 5*snl* or 4*dnl* series. The polarization fraction at low energy is about 25 percent higher than the calculation of Saraph which is based on the Burke and Moores close-coupling calculation.

13835. Liebman, J. F., **Regularities and relations among ionization potentials of nontransition elements,** *J. Chem. Educ.* **50,** No. 12, 831-834 (Dec. 1973).

Key words: atoms; extrapolation; ionization potentials; nontransition elements; semiempirical rules.

In this paper, we ask "How does the ionization potential vary with increasing atomic number?" and in addition inquire about higher ionization potentials. Five classes of semiempirical procedures are given, utilized and discussed. Two new procedures are introduced and found to be reliable.

13836. Clough, S. A., Beers, Y., Klein, G. P., Rothman, L. S., **Dipole moment of water from Stark measurements of $H_2O$, HDO, and $D_2O$,** *J. Chem. Phys.* **59,** No. 5, 2254-2259 (Sept. 1, 1973).

Key words: dipole moment; Stark effect; water.

The equilibrium dipole moment of the water molecule has been determined from Stark effect measurements on two $H_2O$, one $D_2O$, and six HDO rotational transitions. The variation of the dipole moment projection operator with rotational state is taken into account and expressions are given for this operator evaluated in the ground vibrational states of the three isotopes. The value obtained for the equilibrium dipole moment is $|^0\mu_x| = 1.8473 \pm 0.0010$ D. The effective dipole moments in the principal axis energy representation are $|\mu_b(\mathrm{HOH})| = 1.8546 \pm 0.0006$ D, $|\mu_b(\mathrm{DOD})| = 1.8558 \pm 0.0021$ D and $|\mu_b(\mathrm{DOH})| = 1.7318 \pm 0.0009$ D, $|\mu_a(\mathrm{DOH})| = 0.6567 \pm 0.0004$ D.

13837. Weisman, I. D., Swartzendruber, L. J., Bennett, L. H., **Nuclear resonances in metals: Nuclear magnetic resonance and Mössbauer effect,** Chapter 9 in *Techniques in Metals Research,* E. Passaglia and E. Bunshah, Eds., **6,** Part 2, 165-504 (John Wiley and Sons, Inc., New York, N.Y., 1973).

Key words: experimental techniques; ferromagnetic nuclear resonance; metallurgy; Mössbauer effect; nuclear magnetic resonance; pure quadrupole resonance.

It is the purpose of this chapter to review nuclear magnetic resonance, nuclear quadrupole resonance, ferromagnetic nuclear resonance and the Mössbauer effect in metals, alloys and intermetallic compounds. The emphasis is on the technique of measurement, and includes only such theory as is deemed essential to understand the purpose of the measurement, its limitations, the sample preparation required, and when a particular kind of measurement is most appropriate.

13838. Soulen, R. J., Jr., Schooley, J. F., Evans, G. A., Jr., **Simple instrumentation for the inductive detection of supercon-**

**ductivity,** *Rev. Sci. Instrum.* **44,** No. 10, 1537-1538 (Oct. 1973).

Key words: ac susceptibility; superconductivity; temperature; thermometric fixed point.

A circuit is described which can be used to detect the superconductive transitions of several elements used as thermometric fixed points. The circuit is found to perform as well as much more elaborate mutual inductance bridges previously used for this research. Details for construction and operation for the circuit are given.

**13839.** Swanson, N., Cooper, J. W., Kuyatt, C. E., **Resonant structure in near-threshold electron excitation of krypton,** *Phys. Rev. A* **8,** No. 4, 1825-1834 (Oct. 1973).

Key words: electron excitation; high resolution; krypton; resonance.

By using a monochromator-analyzer combination, electron-excitation functions of the lowest-lying electronic states of krypton have been obtained at a scattering angle of 45° in the near-threshold region (9-14 eV). All excitation functions display a complex resonant structure. Additional data have been obtained on elastic scattering at 45° to provide further information on the resonances. In addition to the $4p^55s^2$ $J=3/2$, 1/2 resonance doublet, a number of narrow resonances appear below about 12 eV in both the excitation data and elastic scattering which correlate in energy with recent measurements on transmission by Sanche and Schulz. Broad resonant structure is found in a number of the excitation curves and the excitation process in the near-threshold region appears to be dominated by resonant effects. An analysis of the elastic-scattering data on the $4p^55s^2$ doublet is presented and resonance parameters obtained compared with theory. A comparison of the narrow resonant structure data with optical absorption data Rb I obtained by Beutler indicates that the narrow resonances in the 10.5 – 12-eV region are probably due to levels of the $4p^55s4d$ configuration.

**13840.** Jacox, M. E., Milligan, D. E., **Matrix-isolation study of the reaction of H atoms with NO. The infrared spectrum of HNO,** *J. Mol. Spectrosc.* **48,** No. 3, 536-559 (Dec. 1973).

Key words: force constants; H + NO reaction; HNO; infrared spectrum; matrix isolation; thermodynamic properties.

Studies of the reaction with NO in an argon or a nitrogen matrix at 4° or 14 K of H and D atoms produced either photolytically or in a microwave discharge have confirmed the previous identification of the ground-state NO stretching fundamental of HNO and of DNO but have dictated a reassignment of the deformation fundamental of these two species. An absorption at 1153 cm$^{-1}$ has been assigned as the deformation fundamental of DNO, and evidence is presented suggesting that the deformation fundamental of HNO lies very close to 1500 cm$^{-1}$. The assignment of an absorption at 2717 cm$^{-1}$ as the NH stretching fundamental of HNO and of an absorption at 2043 cm$^{-1}$ as the corresponding fundamental of DNO is consistent with the previous report of an exceptionally long NH bond for ground-state HNO. Detailed isotopic studies support this revised vibrational assignment, which is shown to be consistent with previous gas-phase studies. The force constants and thermodynamic properties of ground-state HNO derived from the matrix data are presented.

**13841.** Lovas, F. J., Johnson, D. R., **Reaction of $BF_3$ with $NH_3$: Microwave spectrum of $BF_2NH_2$,** *J. Chem. Phys.* **59,** No. 5, 2347-2353 (Sept. 1, 1973).

Key words: aminodifluoroborane; dipole moment; gas-phase reaction; microwave spectrum; molecular structure; rotational transitions.

Microwave spectra assignable to gas phase aminodifluoroborane ($BF_2NH_2$) have been detected in the re
tion of $BF_3$ with $NH_3$. A centrifugal distortion analysis has be
carried out on the species $^{11}BF_2{}^{14}NH_2$ and $^{10}BF_2{}^{14}NH_2$. Dist
tion corrected rotational constants have also been obtained
$^{11}BF_2{}^{15}NH_2$, $^{10}BF_2{}^{15}NH_2$, $^{11}BF_2{}^{14}ND_2$, and $^{10}BF_2{}^{14}ND_2$. T
molecule has been found to be planar with the follow
geometry: $r_{B-F}=1.325(12)$A, $r_{B-N}=1.402(24)$Å, $r_{N-}$
1.0029(18)Å, $\angle FBF=117.9(17)°$ and $\angle HNH=116.94(3$
The observed dipole moment of $BF_2NH_2$ is $\mu=2.595(30)$ D.

**13842.** Haynes, W. M., **Viscosity of gaseous and liquid arg**
*Physica* **67,** No. 3, 440-470 (Aug. 1973).

Key words: argon; compressed gas and liquid; dilute g
saturated liquid; torsional crystal viscometer; viscosity.

The coefficient of shear vicosity of fluid argon has been m
sured at temperatures from 85 to 298 K and at pressures up to
MN/m$^2$ using the torsional crystal viscometer. The precision
accuracy of these measurements were estimated to be 0.5 an
percent, respectively. A detailed description of the appara
and experimental measuring techniques is presented. Visco
data for the compressed gas were represented and analy
using density expansions. An empirical relation was develo
to represent the data over the entire fluid range as a functio
density and temperature. Also included is a comprehensive c
parison of the present results with previous experimental
and theoretical predictions.

**13843.** Weisman, I. D., Bennett, L. H., Maxwell, L. R., Sr.
**vivo NMR relaxation studies of tumors,** *IEEE Trans. M*
**MAG-9,** No. 3, 454-456 (Sept. 1973).

Key words: in vivo; melanoma; nuclear magn
resonance; spin-lattice relaxation; spin-spin relaxation;
mor.

Pulsed nuclear magnetic resonance has been used to
ferentiate between normal mouse tail tissue and a malig
transplanted melanoma S91 located on the tail of a live mo
Measurements of proton spin-lattice and spin-spin relaxa
serve to detect and monitor the tumor growth. The mature tu
exhibits a spin-lattice relaxation time $T_1$ of ~ 0.7-0.8 s cont
ing with the corresponding normal tail tissue $T_1$ of half this v
On the other hand spin-spin relaxation in normal tissue cann
characterized by a single relaxation time $T_2$. The correspon
relaxation in a mature tumor is found to be closer to a singl
ponential but still requires at least two superimposed expone
decays.

**13844.** deWit, R., **Continuous distribution of disclination l**
*Phys. Status Solidi (a)* **18,** 669-681 (Aug. 1973).

Key words: burgers vector; continuous defect distribu
disclination; dislocation; distortion elasticity; Frank ve
loop; plasticity.

Kroupa's theory of a continuous distribution of disloc
loops is extended to include disclination loops. The relati
the loop densities to the plastic strain and bend-twist are der
This provides the connection with the theory of the contin
distribution of dislocations and disclinations. Mura has rec
introduced the new concepts of "plastic distortion" and "pl
rotation," and they are identified in this paper as the disloca
and disclination-loop density tensors. The significance of
quantities for a finite loop is discussed.

**13845.** Johnson, C. R., **A Gersgorin inclusion set for the fi**
**values of a finite matrix,** *Proc. Amer. Math. Soc.* **41,** No.
60 (Nov. 1973).

Key words: eigenvalues; field of values; Geršgorin se
merical radius; spectrum; subadditive set valued functi

An easily computed Geršgorin type inclusion set for the lues of an *n* by *n* complex matrix is presented. Some func- l properties of this inclusion set parallel those of the field of s, and illustrative examples are given.

5. Ballard, D. B., **A resolution test sample for the scanning ctron microscope,** (Proc. 30th Annual Meeting on Electron croscopy Society of America, Los Angeles, Calif., Aug. 14- , 1972), Paper in *8th Annual Proceedings Electron croscopy Society of America,* C. J. Arceneaux, Ed., pp. 5-447 (Claitor's Publishing Division, Baton Rouge, La., ig. 1972).

Key words: Al-W alloy; resolution test specimen; SEM; specimen criteria.

test sample that satisfies the restrictive specimen criteria issed previously [1] for a resolution determination of the is essential. At present, the use of a resolution sample from a specimen well-known to the particular operator carries out measurements on the subsequent photomicro- h is the usual procedure. The aluminum-tungsten (Al-W) ritic structure (located at arrow) in figure 1 that remains on rystal surface of the bead resulting from the melting of alu- m on a hot tungsten filament, provides such a specimen.

7. Yates, J. T., Jr., Madey, T. E., Rook, H. L., **Wear of En- sh monumental brasses caused by brass rubbing,** *Nature* **243,** o. 5407, 422-424 (June 15, 1973).

Key words: monumental brasses; neutron activation; preservation of historical objects; wear.

easurements of the wear of English monumental brasses ng brass rubbing have been made using neutron activation ysis. The median rate of wear as determined from twenty-six surements corresponds to an average thickness of $1.8 \times 10^{-8}$ f brass removed per rubbing.

8. Johnson, V. J., **Thermodynamic and transport properties cryogenic propellants and related fluids,** (Proc. American ociety for Testing and Materials Symp. on Cryogens and ases: Testing Methods and Standards Development, Los ngeles, Calif., June 25-30, 1972), *Amer. Soc. Test. Mater. pec. Tech. Publ.* **537,** pp. 64-78 (1973).

Key words: argon; bibliography; compilations; critical evaluation; cryogens; experimental measurement; fluorine; helium; hydrogen; methane; nitrogen; oxygen; properties of fluids; review; thermodynamic.

gnificant advances have been made in recent years in the ity and range of thermophysical data for the cryogenic oellants, pressurants, and inertants. These advances have lted from improved evaluation and compilation techniques oled with better and more extensive experimental data and n a better theoretical understanding of the physical properties ases. A review of recently completed and current data com- tion projects for helium, hydrogen, argon, nitrogen, oxygen, rine, and methane will be given as well as recommended rences for thermodynamic and transport property data tables these fluids. Modern techniques in the plotting of ther- lynamic charts from tabular data (or from functions such as equation of state) have greatly improved their precision and le. A list of such charts is included.

49. Plummer, E. W., **Electronic characterization of sub- onolayer films,** (Proc. Symp. on Monolayer and Sub- onolayer Helium Films, Stevens Institute, Hoboken, N.J., une 7-8, 1973), Paper in *Proceedings of Symposium on Monolayer and Submonolayer Helium Films,* J. G. Daunt and . Lerner, Eds., pp. 157-160 (Plenum Press, New York, N.Y., 973).

Key words: electronic characterization; submonolayer films; surfaces; surface spectroscopy.

The complete characterization of a surface or a submonolayer film on a surface must specify the chemical identity of the atoms present, the geometrical or structural arrangement of these atoms, and the distribution in space and energy of electrons around these atoms. Various forms of electron emission spectroscopy are sensitive to the surface region, yet each technique has a different sensitvity and produces a different perturbation of the surface or adsorbed film. Several methods of probing the electronic properties of the surface and submonolayer films are described, and the advantages of each technique are discussed.

13850. Stern, K. H., **The effect of cations on the thermal decomposition of salts with oxyanions. A semi-empirical correlation,** *J. Chem. Educ.* **46, No. 10, 645-649 (Oct. 1969).**

Key words: inorganic oxyanions; thermal decomposition; thermodynamics.

Decomposition reaction enthalpies of sulfates, carbonates, nitrates and phosphates to the respective oxides are linear functions of the cation radius/electronegativity ($r/S$) ratio. Alkali metal salts are more stable than predicted by this relation since their oxides have the antifluorite structure which is less stable than the NaCl structure in which most of the other oxides crystallize.

13851. Stern, K. H., **The effect of anions on sodium-determined glass membrane potentials in molten salts,** *J. Phys. Chem.* **74,** No. 6, 1329-1337 (Mar. 19, 1970).

Key words: glass electrode; glass membrane potential; molten salts.

The effect of changing anion composition on the sodium-determined glass membrane potential was studied using the molten salt concentration cell

Ag/AgCl, AgA, Na$^+$/fused silica/AgCl, AgA, Na$^+$/Ag or Pyrex
I II

for low concentrations of Na$^+$, and $A = NO_3^-$, $SO_4^{2-}$, $CrO_4^{2-}$, $PO_4^{3-}$. For all of these anions the ion-exchange selectivity constant increases in a regular manner with increasing oxyanion concentration. Since the cation mobility ratio in the glass is unaffected by changing melt composition, the ion-exchange equilibrium constant similarly increases. These results are accounted for in terms of Eisenman's selectivity theory and the double layer at the glass-melt interface.

13852. Leiss, J. E., **Future accelerators for photonuclear studies,** (Proc. Int. Conf. on Photonuclear Reactions and Applications, Pacific Grove, Calif., Mar. 26-30, 1973), Paper in *International Conference on Photonuclear Reactions and Applications,* B. L. Berman, Ed., pp. 1241-1248 (Ernest O. Lawrence Livermore Laboratory, University of California, Livermore, Calif., 1973). (Available as CONF-730301 from the National Technical Information Service, Springfield, Va. 22151).

Key words: electron accelerators; linear accelerators; photonuclear physics; race track microtron; storage rings.

The status of electron accelerator developments and the need for new accelerators in photonuclear studies is discussed. The development of 100 percent duty cycle accelerators is identified as a major goal. Specific accelerators which would satisfy this goal are identified. The possibility of modifying existing facilities to enhance the application of photon activation analysis is given as an example of ways in which photonuclear applications can be encouraged.

13853. Wiederhorn, S. M., Hockey, B. J., Roberts, D. E., **Effect of temperature on the fracture of sapphire,** *Phil. Mag.* **28,** No. 4, 783-796 (Oct. 1973).

Key words: alumina; crack growth; critical stress intensity factor; fracture; plastic deformation; sapphire; strength; transmission electron microscopy.

At low temperatures, metastable crack growth dictates the environment free strength of sapphire. Plastic deformation by dislocation motion or twin formation and growth plays no role in the fracture process at temperatures below 400 °C. These conclusions are supported both by crack growth studies and critical stress intensity factor measurements on sapphire crystals, and by transmission electron microscopy studies of arrested cracks in sapphire and alumina.

**13854.** Chandler, H. H., Bowen, R. L., Paffenbarger, G. C., Mullineaux, A. L., **Clinical evaluation of a radiopaque composite restorative material after three and a half years,** *J. Dent. Res.* **52,** No. 5, 1128-1137 (Sept.-Oct. 1973).

Key words: clinical evaluation; clinical research; composite restorations; dental restorations; dentistry; monomers; operative dentistry; reinforcements.

A clinical comparison was made of an experimental radiopaque composite restorative material and Addent 35. The radiopaque experimental formulation contained a novel ternary eutectic dimethacrylate as the resin binder and fused silica and a novel $BaF_{2-}$ containing glass as the reinforcing fillers. Evaluation of restorations indicate that the experimental material compared favorably with the commercial material.

**13855.** Arni, H. T., **Precision of air-permeability, turbidimeter, and No. 325 sieve fineness data,** *Amer. Soc. Testing Mater. Spec. Tech. Publ.* **473,** pp. 20-44 (1970).

Key words: air-permeability; cements; fineness; No. 325 sieve; portland cements; precision; tests; Wagner turbidimeter.

Data on air-permeability and turbidimeter fineness from an interlaboratory test program involving eight different portland cements and from about 80 to 150 laboratories over a period of a year and a half are presented and analyzed from the standpoint of between-laboratory and within-laboratory precision. Scatter diagrams for the four pairs of samples are presented and used as an aid in the analysis. For six of the cements, results of determinations of fineness by the No. 325 sieve are also analyzed and scatter diagrams shown. The effect on the calculated standard deviation of the elimination of some outlying results is assessed. A method of determining within-laboratory or single-laboratory precision without the use of duplicate determinations is presented. Laboratory bias was found to be significantly larger than the random error for all three tests. There was no indication of any significant difference in precision or in laboratory bias between the Type I and Type IA cements for any of the tests.

**13856.** Chow, L. C., Brown, W. E., **Phosphoric acid conditioning of teeth for pit and fissure sealants,** *J. Dent. Res.* **52,** No. 5, 1158 (Sept.-Oct. 1973).

Key words: enamel; hydroxyapatite; monocalcium phosphate monohydrate; pit and fissure sealant; phosphoric acid.

It is shown that monocalcium phosphate monohydrate, $Ca(H_2PO_4)_2 \cdot H_2O$, forms on enamel surface during the $H_3PO_4$ conditioning of teeth administered prior to application of pit and fissure sealants. The $Ca(H_2PO_4)_2 \cdot H_2O$ coating appears to protect teeth from excessive dissolution during the pretreatment and is washed away subsequently to provide a clean surface available for adhesion to sealant. These phenomena are in complete accord with the phase diagram for the ternary system $Ca(OH)_2OH_3PO_4 - H_2O$.

**13857.** Flatto, L., Haber, S., **A quadrature formula of degree three,** *J. Approximation Theory* **9,** No. 1, 44-52 (Sept. 1973).

Key words: Hilbert basis; integration; invariants; multi integrals; numerical integration; quadrature; reflecti groups; symmetric groups; symmetries.

Let $R$ be a region in $n$-space and $Q$ a linear quadrature form for $R$ of the form

$$Q(f)=\sum_{r=1}^{k} a_r f(x_r).$$

It is known that if $Q(f)=\int_R f$ whenever $f$ is a polynomial degree 3 or lower, then $k \geqslant n+1$. It is known that the minim possible value of $k$ depends on the region $R$, being $2n$ for the cube and $n+2$ for the $n$-simplex ($n>1$). In 1956 Hammer Stroud conjectured that $k \geqslant n+2$ for every $R$, when $n>1$. this paper we construct an $R$, and a $Q$ with the required prope with $k=n+1$.

**13858.** Haber, S., Shisha, O., **An integral related to numerical tegration,** *Bull. Amer. Math. Soc.* **79,** No. 5, 930-932 (Se 1973).

Key words: bounded variation; improper integ monotonicity; numerical integration; quadrature; Reim integral.

The question of the convergence of numerical integration mulas (of Riemann sum type) to the improper Riemann inte $\int_0^\infty$ f(x)dx is studied. A new integral over [0, ∞), more restrict than the improper Riemann integral but not absolutely con gent, is introduced. Necessary and sufficient conditions found for a function to be integrable in the new sense; they stated in terms of property of functions similar to the propert being of bounded variation. A convergence theorem for the merical integration of such functions is given.

**13859.** McCulloh, K. E., **Photoionization of carbon dioxide** *Chem. Phys.* **59,** No. 8, 4250-4259 (Oct. 15, 1973).

Key words: carbon dioxide; $CO^+$; $CO_2^+$; dissocia ionization; $O^+$; photoionization.

The yields of photoions from $CO_2$ cooled to 150 K have b measured at a resolution of 0.22 Å for $CO_2^+$ and 0.4 Å for the and $CO^+$ fragments, in the photon energy region extending f onset for each species to approximately 20 eV. Most of the served structure of the molecular ion yield curve recapitul the well known features of the absorption spectrum, b number of anomalies are reported. Autoionization peak photon energies just above the first molecular ionization lim 13.773 ± 0.002 eV do not fit into a pattern characteristic of berg series converging to excited vibrational levels of the Although the Tanaka-Ogawa series and Henning's sharp se can be assigned as *ns* Rydberg series on the basis of quantum fects, the expected 3*s* members could not be observed in present study. The most prominent feature of the $O^+$ yield c is a step at 19.39 eV, suggesting that the principal mechanism production of this fragment is predissociation of $CO_2^+(C\ ^2\Sigma_g$ its ground vibrational state. Completeness of this predissocia is inferred, although the proposed explanation involves dou quartet mixing at large bending angles. The structure of the yield curve between 19.07 and 19.39 eV suggests that Ryd states converging to $CO_2^+(C)$ also undergo predissociation, spontaneous ionization, to produce this fragment ion. Evid pertaining to production of $CO^+$ fragments by predissociatic excited vibrational states of $CO_2^+(C)$ is also presented.

**13860.** Cezairliyan, A., **Change in normal spectral emittanc 650 nm) of niobium during melting and its relation to su roughness,** *Surface Sci.* **40,** 429-432 (1973).

Key words: high temperature; melting; niobium; no spectral emittance; surface roughness.

Investigations on the normal spectral emittance (at 650 nr ium during melting are reported. An attempt is made to re- the difference between the emittance of solid and liquid lium at the melting point to the roughness of the solid surface. results indicate that this difference is primarily due to condi- s of the solid surface.

1. Keller, R. A., Simmons, J. D., Jennings, D. A., **hancement of absorption spectra by dye-laser quenching, III: uantitative aspects and a comparison of flash-lamp-pumped d cw systems under high resolution,** *J. Opt. Soc. Amer.* **63,** o. 12, 1552-1555 (Dec. 1973).

Key words: dye laser; intra-cavity absorption; iodine detection; laser quenching; trace absorption detection; visible molecular absorption.

he enhancement of the detectability for trace absorptions by ing samples inside the laser cavity was found to be a factor 00 for a flash-lamp-pumped dye laser and one thousand for dye laser. High-resolution spectra showed that the holes in laser output were as narrow as the absorptions that caused n. An approximately linear relationship (rather than the step- tion behavior often associated with threshold phenomena) ts between pressures necessary to produce visually identical orption spectra from samples placed inside and outside of the r cavity. If such a relationship is of general occurrence, it will tly facilitate the use of intracavity absorption for quantitative ysis, determination of relative absorption cross section, and the study of the kinetics of appearance and disappearance of sient species.

62. Moore, L. J., Moody, J. R., Barnes, I. L., Gramlich, J. W., urphy, T. J., Paulsen, P. J., Shields, W. R., **Trace determina- on of rubidium and strontium in silicate glass standard eference materials,** *Anal. Chem.* **45,** No. 14, 2384-2387 (Dec. 973).

Key words: isotope dilution; mass spectrometry; rubidium; standards; strontium; trace analysis.

rocedures have been developed for the accurate trace analy- of Rb and Sr by mass spectrometric isotope dilution. A new sotopic assay technique capable of measuring the three abun- t Sr isotopes to $< 0.05$ percent (ts) was combined with ently available high purity reagents and absolute standards to duce accurate and reliable analytical techniques. Application hese techniques to the determination of Rb and Sr in silicate s standard reference materials has resulted in accuracies hin $< 0.25$ percent at the ppm (μg/g) level and within $< 0.6$ cent at the ppb (ng/g) level.

63. Smith, E. W., Cooper, J., Chappell, W. R., Dillon, T., **An npact theory for Doppler and pressure broadening – I. General eory,** *J. Quant. Spectrosc. Radiat. Transfer* **11,** 1547-1565 1971).

Key words: molecular collisions; scattering theory; spectral line widths.

quantum-mechanical impact theory for the combined effects Doppler and pressure broadening is developed from quantum iation theory. The results are compared with other semiclassi- theories and certain simplifying approximations relevant to es of experimental and theoretical interest are discussed.

64. Smith, E. W., Cooper, J., Vidal, C. R., **Comments on the alidity of the unified classical path theory of Stark broadening,** *. Phys. B* **5,** L33-L35 (1972).

Key words: electron gas; Stark broadening; unified theory.

n a recent paper by Frisch and Brissaud certain aspects of the fied classical path theory for Stark broadening are criticized; ce we feel that their results could be misleading, we offer ne comments on their paper.

13865. Vidal, C. R., **Spectroscopic observations of subsonic and sonic vapor flow inside an open-ended heat pipe,** *J. Appl. Phys.* **44,** No. 5, 2225-2232 (May 1973).

Key words: heat pipe oven; resonance fluorescence spectra; sonic flow.

Spectroscopic measurements of the vapor flow velocities inside a heat-pipe oven have been performed as a function of pressure, heater power, and radial position inside the pipe. For this purpose the relative intensity of the collision-induced satellite lines in laser-induced resonance fluorescence spectra of the $^{7}\mathrm{Li}_2$ molecule has been employed. A one-dimensional flow model is presented which determines the vapor parameters as a function of position along the pipe. It predicts the onset of the sonic flow which has been verified experimentally. A criterion is derived from which the parameters of the vapor can be obtained from the ideal gas relation, neglecting velocity-dependent terms.

13866. Smith, E. W., Cooper, J., Chappell, W. R., Dillon, T., **An impact theory for Doppler and pressure broadening – II. Atomic and molecular systems,** *J. Quant. Spectrosc. Radiat. Transfer* **11,** 1567-1576 (1971).

Key words: molecular collisions; scattering theory; spectral line widths.

A semiclassical theory for Doppler and pressure broadening in neutral gases is derived as a limiting case of a more general quantum mechanical theory. This theory is compared with other semiclassical theories and methods of calculation are discussed.

13867. Smith, E. W., Cooper, J., Roszman, L. J., **An analysis of the unified and scalar additivity theories of spectral line broadening,** *J. Quant. Spectrosc. Radiat. Transfer* **13,** 1523-1538 (1973).

Key words: relaxation theory; scalar additivity theory; spectral line broadening; unified theory.

A new derivation of both unified and scalar additivity theories is given. This derivation concentrates on their regions of validity and certain key differences are analyzed in detail.

13868. Nelson, C. A., Steele, D., **Symmetry relations among pionization cross sections,** *Phys. Rev. D* **8,** No. 9, 2908-2915 (Nov. 1, 1973).

Key words: inclusive reactions; pionization region; quark model; Regge residue; SU(3); symmetry relations.

From Mueller's Regge analysis of the *pionization region,* symmetry relations to order $s^{-1/4}$ among invariant cross sections at $x = 0$, in which a final pion is observed, are derived. SU(3) and quark universality are assumed to relate the Regge residues at the projectile-Reggeon vertex. There is good agreement with experiment to 10 – 15 percent indicating that the approximate symmetry pattern at nonasymptotic energies is that of total cross sections. The rising of the invariant cross sections to their asymptotic forms as $c - bs^{-1/4}$ can be understood in terms of *known* $j$-plane singularities if the $f$-Pomeron central vertex $g_{fp}^{\pi^+}(q_\perp^2) < 0$. Symmetry relations valid for final kaons and nucleons and for both the pionization and the target-fragmentation regions are also given.

13869. Morrissey, B. W., McCrackin, F. L., Stromberg, R. R., **Determination of distributions in inhomogeneous films,** *J. Colloid Interface Sci.* **42,** No. 1, 198-200 (Jan. 1973).

Key words: attenuated total reflection; distributions; ellipsometry; inhomogeneous films.

The distribution of material in an inhomogeneous film is an important parameter in many problems. By representing the inhomogeneous film as a stack of thin homogeneous films, we have developed a method for utilizing concomitant ellipsometric and attenuated total reflection measurements to determine the distribution of films whose thickness can be modified stepwise. We have compared our method to that of Beckman and Harrick, using their data for SiH impurity within an $SiO_2$ film. For two distributions, an exponential and a Gaussian, our method produced good fits with an accuracy limited only by the incremental thickness used for the calculations. Application of the method of Beckmann and Harrick yielded less accurate results which can also show artificial minima in the distribution.

**13870.** Hunt, C. M., **An analysis of roll filter operation based on panel filter measurements,** *ASHRAE Trans.* **78,** Part 2, 227-234 (1972).

Key words: air conditioning filters; air filters; particulate filters; roll filters.

The pressure drop across an air filter can usually be expressed as a linear function of the face velocity in a log-log plot. This is true for both clean and dirty filters. Use of this fact has been made to develop a descriptive model to predict the dust holding capacity of a roll filter from parameters measured with a panel filter of the same medium when the movement of the roll filter is controlled by a pressure switch. The model is applied to some test data obtained with a panel filter to explore the possible effect of varying pressure switch settings, air velocity, and other parameters on the predicted performance of a roll filter.

**13871.** Berger, M. J., **Beta-ray dose in tissue-equivalent material immersed in a radioactive cloud,** *Health Phys.* **26,** 1-12 (Jan. 1974).

Key words: beta-rays; depth-dose; dosimetry; electrons; immersion problem; radioactive cloud.

The radioactive-cloud immersion problem for beta-radiation has been treated schematically by assuming a semi-infinite air medium (source region) located adjacent to a semi-infinite water medium (tissue-equivalent target). The source region has been assumed to contain a uniform concentration of beta-emitting radionuclide, and calculations have been made of the absorbed-dose distribution (depth dose) in the water target. A leakage correction has also been made to estimate the reduction of absorbed dose that would occur if the target had lateral dimensions small compared to the beta-particle range in air. Depth-dose calculations have been carried out for various source spectra (including beta-ray as well as discrete electron spectra) for 15 radionuclides (rare gases) emitted by nuclear power plants into the atmosphere, and for 12 other commonly used radionulides.

**13872.** Gubser, D. U., Soulen, R. J., Jr., **Thermodynamic properties of superconducting iridium,** *J. Low Temp. Phys.* **13,** No. 3/4, 211-226 (1973).

Key words: critical magnetic field; iridium; superconductivity; transition temperatures.

The superconducting transition temperature of pure Ir is found to be 0.1125 K ($\pm 0.0005$ K). The critical magnetic field as a function of temperature $H_c(T)$ has also been measured. From these data it is determined that $H_c(O)$ is 16.00 G (1 G corresponds to $10^{-4}$ T), $(dH_c/dT)_{T=Tc}$ is 235 G/K, the linear coefficient of normal state electronic specific heat $\gamma$ is 3.19 mJ/mole-$K^2$, and the energy gap anisotropy parameter $\langle a^2 \rangle$ is 0.048. This value for $\langle a^2 \rangle$ is the largest of any superconducting element so far observed, and its significance in determining the superconducting properties of Ir is discussed. By using the large supercooling effects noticed near $T_c$, the Ginzburg-Landau parameter $\chi_0$ is found to be $8.6 \times 10^{-3}$. The effects of impurities on $T_c$ and on the magnetic behavior of Ir are also discussed.

**13873.** Blevin, W. R., **Sinusoidal radiation chopper,** *Appl. Opt.* **12,** No. 12, 2802 (Dec. 1973).

Key words: radiation chopper; sinusoidal modulation.

A description is given of a simple method for modulating
beam of optical radiation sinusoidally.

**13874.** Dickens, B., Prince, E., Schroeder, L. W., Brown, W. E
**$Ca(H_2PO_4)_2$, a crystal structure containing unusual hydrog**
**bonding,** *Acta Crystallogr.* **B29,** Part 10, 2057-2070 (Oc
1973).

Key words: calcium phosphate; centered hydrogen bond
hydrogen bonding; single crystal neutron diffraction; sing
crystal x-ray diffraction.

$Ca(H_2PO_4)_2$ crystallizes in the triclinic unit cell $a = 7.5577$ (
$b = 8.2531$ (6), $c = 5.5504$ (3) Å, $\alpha = 109.87$ (1)°, $\beta = 93.68$ (1
and $\gamma = 109.15$ (1)° at 25 °C with $Z = 2$. The structure was dete
mined by an automated $\Sigma_2$ method from x-ray data and refined
least-squares analysis to $R_w(F) = 0.048$, $R(F) = 0.020$ usi
3678 observed x-ray data and to $R_w(F) = 0{\cdot}055$, $R(F) = 0{\cdot}0$
using 843 observed neutron data. Corrections were made for a
sorption, isotropic secondary extinction and anomalous dispe
sion in the x-ray case and for anisotropic secondary extinction
the neutron case. Least-squares refinements proceeded to t
limits of the data sets in space group $P\bar{1}$. Rudimentary chai
$Ca \cdots [P(1)O_4] - H(1) \cdots [P(2)O_4] \cdots$ run parallel to $[1\bar{1}0]$. A
jacent chains are joined by $Ca \cdots O$ bonds on one side and
$O(8) - H(5) - O(8')$ hydrogen bonds on the other. Alternative
the structure may be considered to contain hydrogen-bond
layers of $PO_4$ groups; these layers are held together by hydrog
bonds on one side and by $Ca \cdots O$ bonds on the other. There
two very strong hydrogen bonds in the structu
$O(7) - - H(4) - - 0(7')$, $O(7) \cdots O(7') = 2.434$ (2) Å a
$O(8) - - H(5) - - 0(8')$, $O(8) \cdots O(8') = 2.423$ (2) Å. The
hydrogen bonds join the $P(2)O_4$ groups together to form and
finite chain. The very strong hydrogen bonds are across nomi
centers of symmetry, and diffraction results indicate that each
the H(4) and H(5) protons is effectively centered in a broad sy
metric potential well, possibly with a central barrier. A combi
tion of diffraction and infrared spectral considerations sugge
that the central barriers in the wells, if they exist, probably
below the zero-point energy of the hydrogens.

**13875.** Currie, L. A., **The evaluation of radiocarbon measureme**
**and inherent statistical limitations in age resolution,** (Proc.
International Conference on Radiocarbon Dating, Wellingt
New Zealand, Oct. 18-25, 1972), Paper in *Proceedings 8th*
*ternational Conference on Radiocarbon Dating,* T. A. Raf
and T. Grant-Taylor, Eds., **2,** 598-611 (Royal Society of N
Zealand, Wellington, New Zealand, 1973).

Key words: age resolution; extraneous random errors; f
tor of merit components; method performance char
teristics; minimum and maximum detectable ages; radioc
bon dating; statistical limitations.

A uniform approach, based upon the statistical behavior
random measurement errors, is suggested for assessing the re
tive merit of alternative methods of measuring radiocarbon
for interpreting and reporting the results of such measureme
The need for an objective, uniform approach is manifest beca
of the increasing concern with results which are close to
limits of precision or detection of the dating procedures.

The standard deviation of the estimated net signal (sam
counts) is first examined in terms of its dependence upon rand
errors arising in observations of background and gross sam
counts. Because of the high precision characterizing such ob
vations, it becomes vital to evaluate random errors additiona
the Poisson (counting) errors. The ability to discrimi
between samples of similar age, and minimum and maximum
tectable ages are discussed in terms of the statistical theor
hypothesis testing. An explicit approach results for the unif
treatment of detection, detectability and age limits.

The performance characteristics of alternative measure ıods cannot simply be stated in terms of a single "figure of t," because of the rather complex dependence upon count- imes, sample, background and modern standard counting , and non-Poisson sources of random errors. A "reduced ac- y" (sample activity/background equivalent activity) plot is ed as a means for planning experiments and for rapidly as- ng the capabilities of any specific measurement procedure. result of the particular choice of variables for this plot, alter- ve procedures may be represented by points in a fixed, two- ensional array, where simple translations of the entire array espond to changes in counting time or sample age.

6. Colson, J. P., Reneker, D. H., **Growth direction of polyox- nethylene crystals inside irradiated trioxane crystals,** *J. Appl. hys.* **44,** No. 10, 4293-4302 (Oct. 1973).

Key words: electret domains; polyoxymethylene crystals; radiation damage; solid state polymerization; trioxane.

ne long slender crystals of polyoxymethylene that grew in ir- ated trioxane crystals all grew toward the negative end of the ane crystal. The observed direction of growth was con- ent with the assumption that the ion at the growing end of the oxymethylene chain was a cation. Certain morphological ures such as facets and direction of taper of these polyox- thylene crystals indicated the direction in which the crystals v. Incidental observations of polyoxymethylene precursor tals, electret domains in trioxane, and the effects of electron diation on polyoxymethylene crystals were made.

7. Wiese, W. L., **Arc plasmas as radiation standards in the acuum ultraviolet,** (Proc. VI Yugoslav Symp. and Summer chool on the Physics of Ionized Gases, Miljevac by Split, ugoslavia, July 16-21, 1972), Paper in *Physics of Ionized ases,* M. V. Kurepa, Ed., pp. 597-625 (Institute of Physics, eograd, Yugoslavia, 1972).

Key words: hydrogen arc plasma; radiation standard; radiometric calibrations; vacuum ultraviolet.

he principle of using arc plasmas as radiation standards in the ıum ultraviolet is described, and it is shown that a hydrogen arc plasma has particularly suitable properties due to the fact that its atomic radiation constants are exactly known. The calibration work with a hydrogen arc plasma at NBS is discussed, and preliminary results with this recently established facility are presented.

**13878.** Hougen, J. T., **A modified ladder operator formalism for molecule-fixed components of the total angular momentum operator in linear molecules,** *J. Mol. Spectrosc. Notes* **48,** No. 3, 609-611 (Dec. 1973).

Key words: commutation relations; Eulerian angles; ladder operators; linear molecules; molecule-fixed components; total angular momentum.

Because molecule-fixed components of the total angular momentum operator for linear molecules do not obey angular momentum commutation relations (either with or without the anomalous sign of *i*), the traditional angular momentum ladder operator formalism cannot be applied. It is known that this difficulty can be overcome by introducing into the linear molecule problem an extra rotational angle, which has no physical significance, but which does lead to a formalism isomorphic with the normal formalism for nonlinear molecules. It is shown that the linear molecule angular-momentum problem is susceptible to treatment, without introduction of an extraneous variable, by a relatively straightforward extension of the conventional formalism, in which angular momentum operators are taken to be functions of an integral or half-integral parameter representing the projection of the total angular momentum along the linear axis.

**13879.** Vidal, C. R., Cooper, J., Smith, E. W., **Hydrogen Stark-broadening tables,** *Astrophys. J. Suppl. Ser.* **25,** No. 214, 37-135 (Jan. 1973).

Key words: Stark broadening of hydrogen.

Tables of Stark broadening of the first four Lyman lines and the first four Balmer lines of hydrogen are presented. They are based on a recently developed "unified theory" of line broadening which generates normalized profiles covering the entire profile from the impact limit in the line center to the quasi-static limit in the line wings. The tables are presented in a convenient form for accurate numerical interpolation.

**13880-13893.** Unassigned.

**13894.** Kearsley, E. A., **Measurement of normal stress by means of hole pressure,** *Trans. Soc. Rheol.* **17,** No. 4, 617-628 (1973).

Key words: hole pressure; normal stress; pressure hole errors; shearing flows.

A measurement of normal stress differences in a shearing elastic liquid is accomplished through direct measurement of hole pressure. Gravity flow down an inclined channel is used and hole pressure is measured for slots perpendicular and parallel to the flow, as well as for a circular hole. The first and second normal stress differences are calculated under the assumption of second-order fluid behavior. Dynamic data are compared and a discrepancy noted.

**13895.** Hardy, S. C., Coriell, S. R., **Surface tension and interface kinetics of ice crystals freezing and melting in sodium chloride solutions,** *J. Cryst. Growth* **20,** 292-300 (1973).

Key words: crystal growth; ice; interface kinetics; morphological stability; sodium chloride; surface tension.

Cylindrical ice crystals growing into supercooled 0.1 M sodium chloride solutions develop approximately sinusoidal perturbations parallel to the cylinder axis. Using a previously developed non-linear morphological stability theory, an analysis of the growth and melting rates of these perturbations yields values of the solid-liquid surface tension and linear interface kinetic coefficient. In contrast to previous results in 0.1 M hydrochloric acid solutions, the melting behavior in sodium chloride solutions is different from the growth behavior. From the growth data, the solid-liquid surface tension is 30 mJ/m$^2$ and the linear interface kinetic coefficient is $2.2 \times 10^{-4}$ m/s K for solutions with pH $> 6$. For solutions with pH $< 5.5$ and for all solutions on melting, the kinetic coefficients is too large ($> 10^{-3}$ m/s K) to measurably affect the perturbation velocities. From the melting data, the surface tension is 38 mJ/m$^2$. The difference in surface tension on melting and growth is attributed to ionic a sorption during growth. Experiments in which the crystal grown in one solution and is melted in a different solution i dicate that the surface tension depends on the chloride conte of the ice.

**13896.** Ferguson, E. E., Fehsenfeld, F. C., Phelps, A. V **Comment on photodetachment cross sections for $CO_3^-$ and i first hydrate,** *J. Chem. Phys.* **59,** No. 3, 1565-1566 (Aug. 1973).

Key words: $CO_3^-$; negative ions; photodetachment cros section; photodissociation.

Burt recently reported the photodetachment threshold ene gies for $CO_3^- + h\nu \rightarrow CO_3 + e$ and $CO_3^- \cdot H_2O + h\nu \rightarrow CO_3$ $H_2O + e$ to be 1.8 and 2.1 eV, respectively. It can be shown fro previously established thermochemistry that these reporte threshold energies are substantially too low unless the dissoci tion energy $D(CO_2 - O)$ is much larger ($> 1.5$ eV) than has bee previously reported.

**13897.** Julienne, P. S., **Nonadiabatic effects in the** $B$, $C$, $B'$, **and states of $H_2$,** *J. Mol. Spectrosc.* **48,** No. 3, 508-529 (Dec. 1973

Key words: Λ-doubling; heterogeneous interaction; molec lar hydrogen; nonadiabatic; pure precession; RKR pote tials.

The Kolos-Wolniewicz potentials for the $H_2$ $B^1\Sigma_u^+$ and $C^1$ states were used together with the hypothesis of pure precessi for the rotation-electronic interaction, to calculate t nonadiabatic energy levels of these states for $J = 1$ to 5. T complete coupling matrix was computed using accurate numer cal vibrational wavefunctions. The calculated Λ-doubling of t $v = 0$ to 12 $C$ vibrational levels generally agrees well with exper mental values, and the nonadiabatic shifts in the $B$ rotation constants qualitatively explain the difference between t theoretical and RKR potentials for this state.

The interaction of the $B'$ $^1\Sigma_u^+$ and $D$ $^1\Pi_u$ states was also i vestigated, but only qualitatively since adiabatic potentials of sufficient accuracy do not exist for these states. The Λ-doubling of the $Dv=0$ rotational levels agrees well with the experimental values. An appreciable "background" nonadiabatic shift in the $B'$ rotational constants was found. This shift, which is nearly 5 percent of $B_v$, is in addition to that of strong local two-level interactions and was not "deperturbed" in constructing the $B'$ RKR potential. The result is that the RKR turning points differ by about 0.04 au from the "true" adiabatic turning points. This conclusion is supported by a Hartree-Fock calculation of the $B'$ potential to the left of $R_e$.

13898. Lowke, J. J., Phelps, A. V., Irwin, B. W., **Predicted electron transport coefficients and operating characteristics of $CO_2$-$N_2$-He laser mixtures,** *J. Appl. Phys.* **44,** No. 10, 4664-4671 (Oct. 1973).

> Key words: attachment coefficient; $CO_2$ cross sections; $CO_2$ laser; electron distribution; electron transport; ionization coefficient.

Calculations have been made of transport coefficients of electrons in gas mixtures for ratios $CO_2$:$N_2$:He of 1:1:8, 1:2:3, 1:7:30, and 1:0.25:3. New cross sections for $CO_2$ derived from swarm experiments are used together with previously published cross sections for $N_2$ and He. Curves are presented of the predicted electron drift velocity, transverse and longitudinal diffusion coefficients, and ionization and attachment coefficients for $E/N$ values ranging from $10^{-18}$ to $1 \times 10^{-15}$ V cm$^2$; $E$ is the electric field strength and $N$ the gas number density. Examples are given of derived distribution functions and comparisons are made with a Maxwellian distribution function. The percentage of the input electrical power which excites vibrational processes coupled to the 001 upper laser level of $CO_2$ is given as a function of $E/N$. The maximum efficiency from these calculations increases for increasing ratios of $N_2$:$CO_2$, because the proportion of energy used to excite the bending and stretching modes of $CO_2$ is then reduced. By assuming a recombination coefficient of $10^{-7}$ cm$^3$ sec$^{-1}$, the operating $E/N$ for self-sustained glow discharges is predicted as a function of current density for various laser mixtures by equating the ionization rate to the attachment and recombination rate.

3899. Reimer, G. M., Carpenter, B. S., **Thorium determination in glasses using fission track technique,** *Nature* **247,** 101-102 (Jan. 11, 1974).

> Key words: fast flux; fission track technique; thorium determination; Th/U ratio; track excess.

The fission track technique has been applied for the determination of thorium in glasses. Two irradiations are performed. The first is with a thermalized flux to determine the uranium content by fission of $^{235}$U. The second irradiation is with a fast flux to induce fission of thorium in addition to uranium. By comparing track counts of both irradiations to a uranium standard, the "track excess" of the second irradiation is related to the thorium content. The accuracy is dependent on the Th/U ratio. The uncertainty for the Th/U ratio of 4 is approximately 20 percent and increases as the ratio decreases.

3900. Jennings, D. A., Braun, W., Broida, H. P., **Vibrational relaxation of hydrogen by direct detection of electronic and vibrational energy transfer with alkali metals,** *J. Chem. Phys.* 59, No. 8, 4305-4308 (Oct. 15, 1973).

> Key words: apparatus; energy transfer; metals; method; photochemistry; resonance fluorescence; vibrational relaxation.

A technique has been developed to measure the rate constant for vibrational relaxation of $H_2^{v=3,4}$ by $H_2^{v=0}$. The technique uses a mechanically chopped, tunable, cw dye laser coincident with either of the Na resonance lines at 589.6 or 589.0 nm. Sodium vapor is contained in a glass cell along with Cs atoms and $H_2$. Sodium atoms, excited by the dye laser radiation, collisionally transfer electronic energy to $H_2$ producing some $H_2^v$. Only vibrational energy in $H_2^v$ from levels $v=3,4$ can transfer to Cs as electronic energy and cause Cs resonance line emission at 894 and 852 nm. In this manner, using the observed emission as a detector of $H_2^{v=3,4}$, the vibrational relaxation rate constant was determined to be $3.9 \times 10^{-14}$ cm$^3$ sec$^{-1}$. Similar rate constants were measured, with somewhat less accuracy, for $D_2^v$ colliding with $D_2$ and for $H_2^v$ colliding with He. It was found that $N_2$, Na, and Cs also undergo electronic to vibration and vibration to electronic energy exchange.

13901. Davis, D. D., Klemm, R. B., Braun, W., Pilling, M., **A flash photolysis-resonance fluorescence kinetics study of ground-state sulfur atoms. II. Rate parameters for reaction of $S(^3P)$ with $C_2H_4$,** *Int. J. Chem. Kinet.* **4,** 383-394 (1972).

> Key words: chemistry; ethylene; flash-photolysis; kinetics; resonance-fluorescence; sulfur atoms.

Absolute rate constants for the reaction of $S(^3P)$ with ethylene were measured over an ethylene concentration range of 7, a total pressure of 50 to 400 torr, and a flash intensity range of 10. At 298 °K, the bimolecular rate constant was found to be invariant over this range of variables and had a measured value of $4.96 \times 10^{-13}$ cm$^3$ molec$^{-1}$ s$^{-1}$. Over the temperature range of 218° to 442 K, the rate data could be fit to a simple Arrhenius equation of the form

$$k_1 = (7.13 \pm 0.74) \times 10^{-12} \exp\left(\frac{-1.58 \pm 0.08 \text{ kcal/mole}}{RT}\right).$$

Units are cm$^3$ molec$^{-1}$ s$^{-1}$. The dependence of the measured value of $k_1$ on the concentration of the reaction product ethylene episulfide is discussed.

13902. Colwell, J. H., **Thermal contacts in a low temperature cryostat,** *Cryogenics* **13,** No. 11, 674-675 (Nov. 1973).

> Key words: cryogenics; electrical leads; low temperature; thermal conductivity; thermal contact.

The thermal conductances of an assembly used for thermally anchoring electrical leads in a low temperature cryostat are reported. Measurements were made between 0.3 and 4 K of the conductance across the contacts of miniature gold-plated electrical connectors, insulated copper wires varnished to a copper mounting, and its copper mounting bolted to a copper support.

13903. Lide, D. R., Jr., Rossmassler, S. A., **Status report on critical compilation of physical chemical data,** *Annu. Rev. Phys. Chem.* **24,** 135-158 (1973).

> Key words: compilation; critical evaluation; data; NSRDS; physical chemistry; reference data; status report.

The significance of data evaluation and the importance of sources of reliable reference data are pointed out. A review is provided of major past and present data compilation activities of interest to physical chemists, including early efforts (before 1930); isolated programs in the period 1930-1960; the National Standard Reference Data System; other government and non-government programs; other national programs; and international programs. A rationale and discussion of methodology of data evaluation are presented with brief illustrations. Finally, three types of data sources are listed: systematic publication series, data centers, and recent compendia.

13904. Mauer, F. A., Hubbard, C. R., Hahn, T. A., **Thermal expansion and low temperature phase transition of thallous azide,** *J. Chem. Phys.* **59,** No. 7, 3770-3776 (Oct. 1, 1973).

> Key words: bond method; phase transition; thallous azide; thermal expansion.

Thallous azide, $TlN_3$, is tetragonal at room temperature. It transforms at $248 \pm 5$ K to a phase that can be indexed on the basis of an orthorhombic cell. Lattice parameters of the tetragonal phase have been determined by the Bond single crystal method at intervals of approximately 25 K from 248 to 498 K. Single crystals do not survive the transition, so the parameters of the orthorhombic phase were measured by powder diffraction at intervals of 25 K down to 133 K. Representative parameters, after corrections for the effects of radiation damage, are $a = 6.2094$ Å, $c = 7.3583$ Å at 298.2 K for the tetragonal phase, and $a = 8.718$ Å, $b = 8.766$ Å, $c = 7.395$ Å at 238.2 K for the orthorhombic. Thermal expansion parameters show anomalies that are believed to be the result of changes in the orientation of azide ions. The linear expansion coefficients, $\alpha_a$ and $\alpha_c$, for the tetragonal phase are both approximately $5.2 \times 10^{-5}$ K$^{-1}$ at the transition. By 486 K, $\alpha_c$ has increased to $21 \times 10^{-5}$ K$^{-1}$ and $\alpha_a$ has decreased to $-1.2 \times 10^{-5}$ K$^{-1}$. For the orthorhombic phase $\alpha_b$ remains constant at $5.2 \times 10^{-5}$ K$^{-1}$ while $\alpha_a$ increases from $10 \times 10^{-5}$ K$^{-1}$ to $22 \times 10^{-5}$ K$^{-1}$ and $\alpha_c$ decreases from $-1.5 \times 10^{-5}$ K$^{-1}$ to $-11 \times 10^{-5}$ K$^{-1}$ in the temperature range 150 to 225 K. There does not appear to be a discontinuity in the volume at the transition. The volume expansion coefficient is approximately $17 \times 10^{-5}$ K$^{-1}$ for the orthorhombic phase and $15 \times 10^{-5}$ K$^{-1}$ for the tetragonal.

**13905.** Kirchhoff, W. H., Johnson, D. R., Powell, F. X., **Centrifugal distortion effects in $SF_2$: Calculation of the force field and infrared spectrum,** *J. Mol. Spectrosc.* **48,** No. 1, 157-164 (Oct. 1973).

Key words: centrifugal distortion; force field; microwave spectrum; $SF_2$; structure; vibrational fundamental.

Measurements of the microwave spectrum of $SF_2$ have been extended up to $J = 43$ in order to account for the effects of centrifugal distortion. Seventy-five transitions have been included in a weighted least squares fit of the measured spectrum with an rms deviation of 0.078 MHz. The force field for $SF_2$ has been determined from the centrifugal distortion constants. The vibrational spectrum, as yet unobserved, has been predicted from the force field as have been the Coriolis coupling constants and the average structure.

**13906.** Thomas, R. N., **Suggested interpretation of the correlations in intensity fluctuations in the lines Ca II H and K, magnesium b, and hydrogen H$\beta$,** *Solar Phys.* **27,** 303-304 (Dec. 1972).

Key words: intensity fluctuations; solar spectral lines.

In the preceding note, Evans and Catalano have found interesting behavior in the correlation between intensity fluctuations in the continuum and in the lines H and K of Ca II, b1 and b2 of MgI, and hydrogen H$\beta$. In the first four lines, the correlation drops smoothly from $\sim 0.9$ near the continuum to negative values; followed by a rise to about zero at line center. For H, the correlation is never negative, reaching zero at about 0.25 Å.

We suggest that this behavior reflects a combination of effects. First the source-sink terms in the source-functions depend on different physical parameters in the two sets of lines. In addition, the line center regions are dominated by transfer effects at the top of the atmosphere.

**13907.** Billingsley, F. P. II, **Calculation of the absolute infrared intensities for the 0-1, 0-2 and 1-2 vibration-rotation transitions in the ground state of $NO^+$,** *Chem. Phys. Lett.* **23,** No. 2, 160-166 (Nov. 15, 1973).

Key words: dipole moment function; infrared intensities; multiconfiguration; $NO^+$.

The absolute infrared intensities of the 0-1, 0-2 and 1-2 vibration-rotation bands in the $^1\Sigma^+$ ground state have been calculated from first principles. The dipole moment function for $NO^+$ was determined in the region of the equilibrium internuclear separation by an accurate multi-configuration self-consistent-fiel
procedure. The dipole matrix elements over vibration state
were solved exactly using numerical techniques. The ratio of th
calculated integrated absorption coefficients for the fundamenta
and first overtone (88.8 cm$^{-2}$ atm$^{-1}$ and 0.6 cm$^{-2}$ atm$^{-1}$, respec
tively, at 273.16 K) is in reasonable agreement with an estimat
based on observation of these bands in $NO^+$ at high altitudes i
the upper atmosphere.

**13908.** Cassidy, E. C., Anderson, W. E., Booker, S. R., **Recer
refinements and developments in Kerr system electrical mea
surement techniques,** *IEEE Trans. Inst. Meas.* **IM-21,** No.
504-510 (Nov. 1972).

Key words: electric fields; electrical measurements; electr
optics; high-speed photography; high-speed technique
high-voltage measurements; Kerr effect; laser application

Kerr system electrical measurement techniques are improve
by progress in two important areas: 1) in the development
methods for visualizing and measuring pulsed (microsecon
electric fields and high voltages from time-varying electro-optic
fringe patterns recorded using high-speed photograph
techniques, and 2) in the development of convenient experime
tal methods for evaluating and correcting path-dependent erro
in Kerr system response. Results demonstrate use of fringe-pa
tern measurements in achieving accurate pulse voltage measur
ments and in correction of errors resulting from sizeable en
field variations in existing 300-kV Kerr cells.

**13909.** Jacob, E. J., Lide, D. R., Jr., **Structural implications of t
microwave spectrum of hexafluoropropene,** *J. Chem. Phys.*
No. 11, 5877-5881 (Dec. 1, 1973).

Key words: ground vibrational state; microwave spectru
of hexafluoropropene; rotational constants.

Analysis of the microwave spectrum of hexafluoroprope
$C_3F_6$, has yielded rotational constants for the ground vibratio
state of 2557.88, 1255.033, and 987.082 MHz. Assignme
have also been made on the first four excited states of the C
torsional mode and on the first excited state of another low-ly
skeletal mode. A rough estimate of 350 cm$^{-1}$ has been obtain
for the barrier to internal rotation of the $CF_3$ group. The grou
state moments of inertia are consistent with the expec
geometry of the molecule, in which all atoms are coplanar exc
for two equivalent F atoms in the $CF_3$ group.

**13910.** Simmons, G. L., Eisenhauer, C., **Moments method cal
lations of neutron distributions in concrete,** *Nucl. Sci. Eng.*
197-219 (1974).

Key words: concrete; function fitting; moments; neut
transport; reactor shields; shielding.

The moments method is applied to the problem of calculat
neutron distributions in an infinite medium. Several comparis
are given of these results with similar data calculated by the
crete ordinates method. New calculations are presented on
distribution of doses from neutrons, originating in a plane-s
fission source and incident, at various angles, on concrete
ized in radiation measurements at the Tower Shielding Faci
of the Oak Ridge National Laboratory (TSF concrete). F
given set of neutron cross sections, these results give relia
estimates of the dose distribution at deep penetrations, i.e.
tenuation of six orders of magnitude or more. Functio
representations of the distributions are included in orde
facilitate the use of the data in shield design calculations.

**13911.** Rasberry, S. D., Heinrich, K. F. J., **Calibration for
terelement effects in x-ray fluorescence analysis,** *Anal. Ch*
**46,** No. 1, 81-89 (Jan. 1974).

Key words: calibration; empirical calibration; iron-nic chromium alloys; x-ray fluorescence; x-ray spectrochemical analysis.

A new empirical method for the calibration of x-ray uorescence analysis in the presence of interelement effects is iven. The effects of secondary fluorescence and of absorption re considered separately, with different expressions, in the alibration equation. The new approach is compared with empiral methods previously proposed by other authors, and is accu-ate and applicable over wide ranges of composition, even when he number of standards available is limited. An alloy system, in vhich the interelement effects are severe (Fe-Ni-Cr, over a ange of composition from 0 to 100%), is studied experimentally; lso evaluated are data, previously presented by other authors, or the calcium carbonate-silica system. With reference to 23 hemical determinations, in the two systems, the relative error is ±1 percent or less in 13 instances and ±4 percent or less in all ut two determinations.

3912. Hebner, R. E., Jr., Cassidy, E. C., **Measurement of 60 Hz voltages using the Kerr effect,** *Rev. Sci. Instrum.* **43,** No. 12, 1839-1841 (Dec. 1972).

Key words: electrical measurements; electro-optics; high voltage measurements; Kerr effect; laser applications; optical techniques.

The Kerr effect has been used to measure 60 Hz alternating oltage up to 30 kV peak. The system behaves much as it does nder the influence of a short high-voltage pulse except that in his case the frequency of the applied voltage is sufficiently low hat the space charge effects in the liquid are not negligible.

3913. Bagus, P. S., Krauss, M., LaVilla, R. E., **The threshold region of the methane carbon K-absorption spectrum,** *Chem. Phys. Lett.* **23,** No. 1, 13-17 (Nov. 1, 1973).

Key words: carbon-K-absorption threshold; first Rydberg transition; $1a_1^{-1}$ hole state calculation; methane; vibronic transition.

The carbon K-absorption of $CH_4$ is analyzed with the help of n ab initio calculation of the Rydberg states of $1a_1^{-1}$ hole state. he strong absorption peak at 288.3 eV is identified as the first ydberg $2t^* \leftarrow 1a_1$, whose calculated ionization potential is in ood agreement with experiment. Also, the oscillator strength or this transition was calculated to be $f=1.9\times 10^{-2}$, which is ithin the estimated margin of error of the experimental $f=0.6\times$ $0^{-2}$. The weak peak at 287.2 eV is interpreted as a vibronic ansition to the $3a_1(3s)$ Rydberg. An estimate of its oscillator trength as 10 percent of the allowed 2t(3p) Rydberg line is con-istent with experiment. For the case of $CD_4$, this weak forbid-en transition was estimated to be 20 percent of the allowed t(3p) Rydberg line.

3914. Drullinger, R. E., Zare, R. N., **Optical pumping of molecules II. Relaxation studies,** *J. Chem. Phys.* **59,** No. 8, 4225-4234 (Oct. 15, 1973).

Key words: molecules; optical pumping.

The ($v''=3$, $J''=43$) level of $Na_2$ has been optically aligned sing the 4880-Å line of a cw argon ion laser as a light source. he relaxation of this alignment is measured upon addition of oreign gas. In a low-pressure regime, where the mean free path xceeds the diameter of the light beam which both pumps and amples the alignment, the relaxation of the alignment versus ressure shows a "dog-leg shape" consisting of two linear re-ions. The first linear region corresponds to both elastic velocity-changing) and inelastic (primarily rotational transfer) ollisional relaxation whereas the second corresponds purely to nelastic collisional relaxation. The former process is dependent n the mode structure of the laser and shows saturation with in-reased pressure. In this low-pressure regime, the measured cross sections are shown to be lower bounds to the true cross sections and excitation by a multimode laser is shown to be inequivalent to excitation by a white light source when the width of the holes in the velocity distribution of the absorber molecules are nonoverlapping.

13915. Bass, A. M., Laufer, A. H., **The methyl radical combination rate constant as determined by kinetic spectroscopy,** *Int. J. Chem. Kinet.* **V,** 1053-1065 (1973); *Ber. Bunsenges. Phys. Chem.* **78,** No. 2, 198-200 (1974).

Key words: absorption spectroscopy; combination; f-number; methyl; radical; rate constant.

The rate constant for the reaction

$$CH_3+CH_3+M\xrightarrow{k_1}C_2H_6+M \qquad (M=He)$$

has been determined by means of vacuum ultraviolet flash photolysis and time-resolved kinetic spectroscopic observations of the 1504-Å absorption band of $CH_3$. The measurements made using three different sources of methyl radicals (azomethane, dimethylmercury, and ketene-hydrogen) were in accord and yielded a value for the rate constant of $k_1=(9.53\pm1.17)\times10^{-11}$ cc molec$^{-1}$ sec$^{-1}$. A detailed error analysis is presented. The $f$-value for the 1504-Å band of $CH_3$ is determined to be $(2.5\pm0.7)\times10^{-2}$.

13916. Chow, L. C., Brown, W. E., **Reaction of dicalcium phosphate dihydrate with fluoride,** *J. Dent. Res.* **52,** No. 6, 1220-1227 (Nov.-Dec. 1973).

Key words: calcium phosphates; dental caries; fluoride; fluorapatite; tooth enamel.

The intermediate formation of $CaHPO_4\cdot 2H_2O$ and its subsequent conversion to $Ca_5\,(PO_4)_3F$ or $CaF_2$ may be a major factor in increased fluoride uptake when tooth enamel is pretreated with acid solutions before being exposed to fluoride. To obtain information concerning the form of fluoride incorporation, the reactions of $CaHPO_4\cdot 2H_2O$ with solutions containing various amounts of $F-$ and $PO_4^{3-}$ ions were studied.

13917. Erez, A., **Low-frequency electrical signal measurement by electrooptical methods,** *IEEE Trans. Instr. Meas.* **IM-21,** No. 4, 358-360 (Nov. 1972).

Key words: electrooptical coupling; feedback amplifiers; light emitting diodes; photodetectors.

An analog system for the optical telemetry of voltage or current information using light-emitting diodes (LED) is described. Errors resulting from variations in the optical coupling efficiency are minimized because the light emitted by the LED contains the signal to be measured superimposed on a fixed intensity beam controlled by a reference zener diode. The nonlinearity of the LED is overcome by using part of its emitted light to control the feedback current of an operational amplifier that supplies the signal to the LED. The prototype system developed has a total error of approximately 0.2 percent of the input signal.

13918. Cassidy, E. C., Hebner, R. E., **Experimental study of the behavior of nitrobenzene under varied high voltage conditions,** (Proc. Electrical Insulation and Dielectric Phenomena, Buck Hill Falls, Pa., Oct. 23-25, 1972), Chapter *1972 Annual Report of the Conference Electrical Insulation and Dielectric Phenomena,* pp. 37-44 (National Research Council, National Academy of Sciences, Washington, D.C., 1973).

Key words: dielectric liquid; electrical properties of liquids; electro-optics; high voltage measurement; Kerr effect; laser applications; nitrobenzene; optical properties of liquids.

Recently developed fringe-pattern methods are employed for visualizing time and space variations in electric fields between electrodes immersed in nitrobenzene. Investigations are conducted with operation under high direct, pulsed (μs), and 60 Hz voltage. With minimization of effects resulting from variations in the fringing fields at the electrode ends, the fringe-pattern "mappings" of the field distribution enable observation of space-charge behavior. Applied voltages are measured simultaneously using calibrated (with state-of-the-art accuracy) devices. Results enable computation and plotting of electric field distribution and intensity, of charge distribution, and of the Kerr constant of nitrobenzene.

**13919.** Bur, A. J., Fetters, L. J., **Intrinsic viscosity measurements on rodlike poly(*n*-butyl isocyanate) and poly(*n*-octyl isocyanate),** *Macromolecules* **6,** No. 6, 874-879 (Nov.-Dec. 1973).

Key words: intrinsic viscosity; poly(*n*-butyl isocyanate); poly(*n*-octyl isocyanate); rodlike.

Previous calculations of the molecular length of rodlike poly(*n*-butyl isocyanate), $(-\mathrm{CO}-\mathrm{NC_4H_9}-)_n$, from dielectric relaxation time measurements have not shown satisfactory agreement with the results from x-ray and light-scattering measurements. Here, we examine this conflict by extending our hydrodynamic experiments to include intrinsic viscosity measurements on well-characterized low molecular weight samples of poly(*n*-butyl isocyanate) (PBIC) and poly(*n*-octyl isocyanate) (POIC), $(-\mathrm{CO}-\mathrm{NC_8H_{17}}-)_n$. Using the Kirkwood-Auer-Riseman equation relating intrinsic viscosity and rod dimensions, the intermonomer translation along the rod axis is calculated to be $1.66 \pm 0.12$ Å. This is lower than the 1.94-Å result from x-ray measurements, but higher than the $1.33 \pm 0.12$ Å result from dielectric relaxation time measurements. The root of the problem appears to be the application of hydrodynamic equations to a physical situation which does not satisfy the model assumptions.

**13920.** Evans, A. G., Fuller, E. R., **Crack propagation in ceramic materials under cyclic loading conditions,** *Met. Trans.* **5,** 27-33 (Jan. 1974).

Key words: ceramics; cyclic failure; relation to static failure; slow crack growth; tension/compression; time to failure.

An analysis is presented which enables crack propagation rates under cyclic loading conditions to be predicted from static slow crack growth parameters. A comparison of the predicted times to failure under cyclic conditions with available measured failure times, for several ceramic materials at ambient temperatures, suggests that there is no significant enhancement of the slow crack growth rate due to cycling. This is verified in a series of measurements of slow crack growth rates under static and cyclic conditions.

**13921.** Cowan, D. O., LeVanda, C., Collins, R. L., Candela, G. A., Mueller-Westerhoff, U. T., Eilbracht, P., **Mössbauer and magnetic susceptibility studies of biferrocenylene (II, III) picrate,** *J. Chem. Soc. Chem. Commun.*, pp. 329-330 (1973).

Key words: biferrocenylene (2,3) picrate; magnetic susceptibility; Mössbauer.

Mössbauer and magnetic susceptibility studies of biferrocenylene (II, III) picrate show that extensive donor-acceptor interactions occur in this mixed-valence molecule which result in fractional oxidation states for the iron atoms.

**13922.** Evans, A. G., Linzer, M., **Failure prediction in structural ceramics using acoustic emission,** *J. Amer. Ceram. Soc.* **56,** No. 11, 575-581 (Nov. 1973).

Key words: acoustic emission; ceramics; failure prediction; fracture.

Crack propagation in a typical structural ceramic (porcelain) is accompanied by acoustic emission. Two types of emission are detected. The first type is caused by slow growth of the fracture-initiating flaw; the emission rate depends primarily on crack velocity. Failure prediction using this source of emission can be effective, however, only if low-level emission, which may be related exclusively to crack growth, can be detected. The secon source of emission, which occurs during bulk stressing, is the cracking associated with second-phase particles (quartz particle in porcelain) as a result of the combined action of the applie stress and local thermal and mechanical stresses. An analysis fo predicting emission rates is developed and forms the basis fo using this source of acoustic emission in failure prediction.

**13923.** Dragoo, A. L., Paule, R. C., **Ultrapure materials: Containerless evaporation and the roles of diffusion and Marangon convection,** (Proc. 12th Aerospace Sciences Meeting Washington, D.C., Jan. 30-Feb. 1, 1974), *AIAA Paper No.* **74 209,** pp. 1-8 (American Institute of Aeronautics and Astronautics, New York, N.Y., 1974).

Key words: $\mathrm{Al_2O_3}$; complex equilibria; convective-diffusion; evaporative rate; purification (evaporative); soluta capillary; thermal capillary convection; vacuum vaporization.

Contamination from containers is a major problem in prepa ing ultrapure refractory materials. Space with its zero gravity an its high vacuum offers an opportunity for containerless purific tion of these materials. The evaporation of impurities from a me will involve many complex chemical equilibria. Thermodynam calculations have been modified to describe these equilibr when impurities in the melt evaporate into vacuum. The co tributions of diffusion and Marangoni convection to ma transfer rates in the bulk liquid have been estimated. Calcul tions for the evaporative purification of molten alumina a given.

**13924.** Geist, J., Blevin, W. R., **Chopper-stabilized null radiom ter based upon an electrically calibrated pyroelectric detecto** *Appl. Opt.* **12,** No. 11, 2532-2535 (Nov. 1973).

Key words: ac power measurements; electrically calibrat radiometer; pyroelectric detector; radiometer; radiometr

In this paper we will describe a new type of radiometr system that combines the high-accuracy characteristics of ele trical calibration and null detection with the noise a background discrimination of chopper-stabilized, synchrono detection. We start by outlining those characteristics required high accuracy and those required for good noise discriminati Next we show that these requirements are mutually inconsiste for certain types of detectors (thermopiles), but that they can be well satisfied by electrically-calibrated pyroelectric detecto Then we discuss the special requirements for a chopper-sta ized null radiometer, including wave-form independent, lock detection, and lastly we describe the performance of a syst that we have constructed.

**13925.** Geist, J., Schmidt, L. B., Case, W. E., **Comparison of laser power and total irradiance scales maintained by the N tional Bureau of Standards,** *Appl. Opt.* **12,** No. 11, 2773-27 (Nov. 1973).

Key words: intercomparison; irradiance scale; laser po scale.

The paper describes an intercomparison of the instrum used to realize and maintain the NBS laser power and ene scale with the instrument used to realize and maintain the up end of the NBS total irradiance scale. The intercomparison v conducted by performing simultaneous measurements of average power from a cw krypton laser with both instrume The procedure and apparatus of the comparison are describ The measured difference between the two instruments was v ithin the ~ 1.5 percent limit of error associated with the inter- omparison.

3926. McCarter, R. J., **A new technique for thermal analysis of vapor-producing reactions,** *J. Appl. Polym. Sci.* **17,** 1833-1846 (1973).

Key words: differential thermal analysis; DTA; kinetics; pyrolysis; TGA; thermal analysis; thermal degradation; thermogravimetric analysis.

An apparatus was developed for measuring the rate at which apors are evolved during the thermal degradation of materials nd thereby deriving the kinetics of such reactions. Requisite to ie operating scheme of the apparatus is the provision of a high- mperature zone to convert condensable or tarry vapors into oncondensable form. The apparatus yields a direct measure of eaction velocity, rather than the integrated indication obtained ith thermogravimetric analysis. This simplifies the identifica- on and calculation of kinetic parameters. Increases in sensitivi- and operating range are also achieved. Flexibility in operation obtained that permits the separate recording of reactions that end to overlap. Although the apparatus principally has been perated using a combustible gas indicator to meter the evolved apors, a number of options are available for the latter function, icluding flowmeters and various continuous gas analyzers. The pplicability of the method appears promising.

3927. Unassigned.

3928. Weiss, A. W., **Correlation in excited states of atoms,** *Advan. At. Mol. Phys.* **9,** 1-46 (1973).

Key words: correlation; energy levels; oscillator strengths; spectroscopy; wave functions.

This article reviews the current status of work on electron cor- elation in excited states of light atoms through approximately Z 20. The primary orientation is towards *ab initio* correlation cal- ulations, so that semiempirical methods are not discussed ex- ept insofar as they relate directly to the correlation problem. urthermore, the discussion is restricted to the effects of correla- on on only two properties, namely energies and oscillator trengths. After a brief statement and description of the correla- on problem in general, we concentrate on 1) methods currently mployed to attack excited state correlation, and 2) a description f some of the results obtained so far which appear to be peculiar o excited states.

Since most excited state correlation calculations have relied n the multiconfiguration expansion, this method is described at ome length. For convenience the variety of such approaches are lassified according to the choice of zeroth order, or reference tate, starting point, which may be the Hartree-Fock, Hartree- ock-Slater, or statistical model. Allowing the reference state or- itals to relax in the field of the virtual configuration leads to the nulticonfiguration self-consistent field approximation, and this iethod is described as well. The charge expansion scheme and ie pair correlation approach are also discussed from the stand- oint of providing a framework for analyzing much of the results vhich have been obtained.

Some of the more striking effects of excited state correlation re related to the readjustment of energy levels along an isoelec- ronic sequence. Not only are there anomalies associated with vel crossings, but the asymptotic degeneracy effects predicted y the charge expansion theory appear, very often, to persist long an entire sequence. One of the large correlation cor- ections in the ground state involves orbital polarization, and this lso happens with excited states, where it can often be un- erstood as a series perturbation phenomenon. Series perturba- ons represent a large and important correlation correction not nly for the series but for the perturbing state as well. These ef- ects are all discussed by way of examples. Finally, some discus- on is given of the role of pair correlations in excited states.

13929. Farabaugh, E. N., Parker, H. S., Armstrong, R. W., **Skew-reflection x-ray microscopy of the vapor-growth surface of an $Al_2O_3$ single crystal,** *J. Appl. Crystallogr.* **6,** Part 6, 482-486 (Dec. 1973).

Key words: $Al_2O_3$; Berg-Barrett; single crystal; skew reflection; vapor growth; x-ray diffraction microscopy.

The most commonly used geometry for the Berg-Barrett x-ray microscopy uses the zero-layer reflections as described by Newkirk. It can be shown that non-zero-layer reflections, skew-plane reflections, can be used equally well to obtain x-ray micrographs. The analysis of the stereographic representation of the skew-reflection geometry demonstrates the many usable reflections and gives the conditions for minimum image distortion. In these x-ray micrographs the contributions to diffraction contrast from shadowing and sub-boundaries can be identified. An estimate of the height of steps occurring on the crystal surface can also be made.

13930. Rowe, J. M., Livingston, R. C., Rush, J. J., **Neutron quasielastic scattering study of $SH^-$ reorientation in rubidium hydrosulfide in the intermediate temperature trigonal phase,** *J. Chem. Phys.* **59,** No. 12, 6652-6655 (Dec. 15, 1973).

Key words: neutron scattering; orientational disorder; phase transition; reorientation; residence time; rubidium hydrosulfide; vibration amplitude.

The reorientation of $(SH)^-$ ions in the trigonal phase of RbSH has been investigated by neutron quasielastic scattering at 373 and 393 K. The quasielastic peaks show a distinct two-component (elastic and broadened) structure, the behavior of which is used to establish that the ions are reorienting between two equilibrium sites (presumably by 180° flips along the trigonal axis) with average times between reorientation of $5.4 \pm 0.4$ psec and $4.0 \pm 0.4$ psec at 373 and 393 K. Mean square amplitudes of hydrogen vibration are determined from the momentum transfer dependence of the total intensity, and found to be higher than that found in the high temperature fcc phase, even though the rate of reorientation is an order magnitude faster in the cubic phase.

13931. Blunt, R. F., Candela, G. A., Forman, R. A., **Effect of $\gamma$ irradiation on the magnetic properties of ruby,** *J. Appl. Phys.* **44,** No. 4, 1753-1755 (Apr. 1973).

Key words: aluminum oxide; chromium; color centers; magnetic susceptibility; radiation damage; ruby.

The magnetic susceptibilities of ruby samples ($Cr^{3+}$ in $\alpha$-$Al_2O_3$) were measured before and after $Co^{60}$ $\gamma$ irradiation. Within the experimental error the magnetic susceptibility was found to be unchanged by the irradiation. The degree of microwave saturation possible for the $Cr^{3+}$ spin system, when at the resonance condition for complete saturation, showed a marked decrease after irradiation. Together, these results indicate that the $\gamma$ irradiation has changed the resonance condition for approximately 10-15 percent of the $Cr^{3+}$ in a 0.05 wt% $Cr_2O_3$ sample. A likely inference is that the oxidation state of at least 99 percent of the chromium is unaltered, and that less than 10 ppm Cr has valence differing from three in the irradiated sample. These experiments are in essential agreement with other experiments on ruby.

13932. Barnes, I. L., Garner, E. L., Gramlich, J. W., Machlan, L. A., Moody, J. R., Moore, L. J., Murphy, T. J., Shields, W. R., **Isotopic abundance ratios and concentrations of selected elements in some Apollo 15 and Apollo 16 samples,** (Proc. 4th Lunar Science Conf., March 5-8, 1973, Houston, Tex.), *Geochimica et Cosmochimica Acta, Suppl. 4,* **2,** 1197-1207 (1973).

Key words: chromium; isotopic ratios; lead; model ages; nickel; potassium; rubidium; strontium; thorium; uranium.

The elements Pb, U, Th, Rb, Sr, K, Cr, and Ni have been determined on a series of Apollo 15 and 16 rocks and soils. The elements U, Rb, Cr, and Ni show isotopic abundances identical with those of terrestrial materials in both types of samples but the $^{39}$K/$^{41}$K ratio is fractionated by about 1 percent in the soils and the extreme reversed discordancy of the Pb-U-Th ages in the Apollo 16 soils indicated that lead has also been fractionated in these.

The breccia 60335,36 has concordant Pb-U-Th model ages of 4075 MY and the basalt 15495,59 shows one slightly discordant age of around 4480 MY. The Rb-Sr model ages are in good agreement with the Pb-U-Th model ages.

**13933.** Lenzi, M., McNesby, J. R., Mele, A., Xuan, C. N., **Collisional deactivation of NH$_2$($\tilde{A}^2A_1$)**, *J. Chem. Phys.* **57**, No. 1, 319-323 (July 1, 1972).

Key words: ammonia; fluorescence; Jovian; vacuum ultraviolet.

NH$_2$($\tilde{A}\ ^2A_1$) was produced by photolysis of ammonia in the vacuum ultraviolet. Deactivation rates of this radical were measured by the quenching of fluorescence in NH$_3$, CH$_4$, H$_2$, N$_2$, He, Ne, Ar, Kr, Xe. An estimate of the lifetime of spontaneous radiative decay of $0.8 \times 10^{-5}$ sec is suggested. Application of the results to the dynamics of the Jovian atmosphere is reported.

**13934.** Laughlin, D. E., Cahn, J. W., **The crystal structure of the metastable precipitate in copper-based copper-titanium alloys,** *Scr. Met.* **8,** 75-78 (1974).

Key words: coherency; copper-titanium; D1$_a$; electron diffraction; L1$_2$.

Knight and Wilkes recently reported that the metastable ordered phase which forms by precipitation from copper-rich copper-titanium binary alloys is of the type L1$_2$. This note shows that this indexing is incorrect, and that the previously assigned structure of D1$_a$ is fully consistent with all experimental findings.

**13935.** Berger, H. W., **Polarography. Constant-current coulometry. Differential thermal analysis,** Parts 10.7, 10.8 and 10.9 in *Paint Testing Manual,* Gardner/Sward, 13th Edition, G. G. Sward, Ed., *Amer. Soc. Testing Mater. Spec. Tech. Publ.* **500,** pp. 556-563 (1972).

Key words: coulometric titration; coulometry; differential thermal analysis; diffusion current; dropping mercury electrode; half-wave potential; polarography.

Polarography is an instrumental method of analysis based on the evaluation of current-voltage curves that are obtained during the electro-reduction or oxidation of a chemical compound. The limiting current is diffusion controlled and is a function of concentration. The half-wave potential is the voltage at one-half the diffusion current and is characteristic of the reaction occurring. The dropping mercury electrode, used in polarography, has the particular advantage of being constantly renewed.

Constant current coulometry is a highly accurate analytical technique based on Faraday's Law and involves measuring the number of coulombs (current × time) that pass through a chemical cell. Coulometric titrations can be performed by electrogenerating the necessary titrant in situ.

Differential thermal analysis is used for identifying or measuring the physical and chemical changes that occur in materials as they are heated or cooled. The temperature of a test sample is compared to an inert reference and the differential temperature is recorded. Exothermic and endothermic temperature changes are related to chemical reactions or physical transformation.

**13936.** Rains, T. C., Epstein, M. S., Menis, O., **Automatic correction system for light scatter in atomic fluorescence spectrometry,** *Anal. Chem.* **46,** No. 2, 207-210 (Feb. 1974).

Key words: atomic fluorescence spectrometry; automatic correction; electrodeless discharge lamp; light scatter; standard reference material.

Light scattering of incident radiation by solvent droplets and unvaporized solute particles in the flame is a major interference in atomic fluorescence spectrometry (AFS). A technique for the automatic correction of light scatter is described which increases the speed and accuracy of analysis. The light from an electrodeless discharge lamp and a 150-W xenon lamp is alternately passed through the flame. The resulting signal from the multiplier phototube is fed to a lock-in amplifier which corrects for the contribution of the light scattering to the fluorescence signal. The principles of the technique and apparatus for making the automatic correction are described. To accomplish this correction, scatter of the incident radiation from the electrodeless discharge and xenon lamps is balanced initially while aspirating a 1 percent lanthanum solution. The method has been applied to the determination of 0.11 and 0.26 $\mu$g Cd/gram in SRM's Orchard Leaves and Liver, respectively, without any prior

**13937.** Newbury, D. E., Yakowitz, H., Yew, N. C., **Observation of magnetic domains in nickel using the scanning electron microscope,** *Appl. Phys. Lett.* **24,** No. 2, 98 (Jan. 15, 1974).

Key words: bitter patterns; contrast mechanisms; magnetic domains; nickel; scanning electron microscopy; transformer alloy.

Scanning electron microscope (SEM) observation of magnetic domains in a polycrystalline pure nickel sheet was made possible through the use of a 50-kV accelerating potential. The contrast was unobservable in an SEM capable of only a 30-kV accelerating potential.

**13938.** Costrell, L., Editor, **CAMAC – organization of multi-crate system,** (AEC Committee on Nuclear Instrument Modules) *AEC Report No. TID-25876,* 42 pages (U.S. Atomic Energy Commission, Washington, D.C., Mar. 1972).

Key words: CAMAC; computer interfacing; control systems; instrumentation; instrumentation standards nuclear instrumentation; standards.

CAMAC is a design for modular equipment systems used on line with digital processors and computers and incorporates comprehensive data transfer highway (Dataway). This extensio to the CAMAC specifications defines a Branch Highway and standard Crate Controller for communication between a syster controller or computer and as many as seven crates. The specification has been developed by the ESONE Committee of European Laboratories and has been endorsed by the U.S. AEC Committee on Nuclear Instrument Modules (NIM Committee Except for pages i-vii and page 30A, this report is identical t Euratom Report EUR 4600e dated October 1971. AEC Repor TID-25877 constitutes a supplement to and is to be used in conjunction with this report. The basic CAMAC specifications ar defined in AEC Report TID-25875.

**13939.** Gallagher, A., Lewis, E. L., **Determination of the vapo pressure of rubidium by optical absorption,** *J. Opt. Soc. Ame* **63,** No. 7, 864-869 (July 1973).

Key words: rubidium; vapor pressure.

The vapor pressure of rubidium was determined in th neighborhood of 330 K from measurements of optical absorptic of the resonance lines. A narrow-line source was used and a fu analysis of the line profiles was done. Measurements resonance-broadening depolarization give another check on th Rb vapor pressure in the 430-K range, assuming that theoretic cross section is correct. The results are very close to the analyt compromise previously suggested by Nesemeyanov.

**13940.** Wiese, W. L., **Regularities in atomic oscillator strengt**

(Proc. VI Yugoslav Symp. and Summer School on the Physics of Ionized Gases, Miljevac by Split, Yugoslavia, July 16-21, 1972), Paper in *Physics of Ionized Gases*, M. V. Kurepa, Ed., pp. 627-649 (Institute of Physics, Beograd, Yugoslavia, 1972).

Key words: atomic oscillator strengths; perturbation theory; regularities; systematic trends.

A review of the recently detected regularities and systematic trends among atomic oscillator strengths is presented. The quantum mechanical background for the existence of these regularities is discussed and, in particular, the relationship between oscillator strengths and nuclear charge as derived from perturbation theory is derived in detail. All regularities are illustrated by some typical graphical or tabular examples.

**13941.** Wiese, W. L., **Experimental studies of the Stark broadening of hydrogen lines,** (Proc. VI Yugoslav Symp. and Summer School on the Physics of Ionized Gases, Miljevac by Split, Yugoslavia, July 16-21, 1972), Paper in *Physics of Ionized Gases,* M. V. Kurepa, Ed., pp. 559-596 (Institute of Physics, Beograd, Yugoslavia, 1972).

Key words: atomic line shapes; critical review; hydrogen lines; plasma sources; Stark broadening.

Recent experimental investigations on the Stark broadening of hydrogen lines by high density plasma sources are critically viewed. The principal requirements for accurate Stark broadening experiments are discussed, and plasma sources, line profile measurements, and diagnostic techniques are reviewed in detail. The most recent experimental results are presented, compared with theory, and their significance for future theoretical work on Stark broadening is pointed out.

**13942.** Howell, B. F., Margolis, S., Schaffer, R., **Residual fluorescence as an index of purity of reduced nicotinamide adenine dinucleotide,** *Clin. Chem.* **19,** No. 11, 1280-1284 (1973).

Key words: alcohol dehydrogenase; fluorescence studies; nicotinamide adenine dinucleotide; optical rotation.

Determination of fluorescence remaining after reduced nicotinamide adenine dinucleotide (NADH) has reacted with excess acetaldehyde in the presence of alcohol dehydrogenase (EC 1.1.1.1) is useful as a criterion of NADH purity when used in conjunction with other methods for determining purity such as the rate of reaction, the ratio of ultraviolet absorbances at 260 nm and 340 nm, the color, and the chromatographic homogeneity of the preparation. Measurement of residual fluorescence monitors the enzymatically inactive material which absorbs at 340 nm. The specific optical rotations of NADH at several wavelengths are also reported.

**13943.** Raveché, H. J., Mountain, R. D., **Structure studies in liquid $^4$He,** *Phys. Rev. A* **9,** No. 1, 435-447 (Jan. 1974).

Key words: condensate fraction; ground state wave function; neutron diffraction; pair correlation function; triplet correlation function; $^4$He.

We investigate, using neutron-diffraction data, several properties of the local atomic structure in liquid $^4$He, both above and below the superfluid transition. Distinguishing features of the pair-correlation function are summarized and the diffraction data are employed to investigate a proposed form for the condensate fraction as a function of temperature. The pair-correlation function is used to examine an inequality that gives an upper bound that is close to the observed values, and also to examine the use of approximate integral equations for the ground-state wave function. Triplet correlations and closure approximations are studied from the isothermal density derivative of the pair-correlation function. The results sug st that, analogous to the pair-correlation function, the triple-correlation function shows a temperature dependence that is not observed in simple classical fluids.

**13944.** Kuriyama, M., Early, J. G., Burdette, H. E., **Fluid flow effects on crystalline perfection,** (Proc. 12th Aerospace Sciences Meeting, Washington, D.C., Jan. 30-Feb. 1, 1974), *AIAA Paper No. 74-204,* pp. 1-10 (American Institute of Aeronautics and Astronautics, New York, N.Y., 1974).

Key words: copper single crystals; crystal perfection; dislocations; fluid flow; thermal convection; x-ray topography.

In the absence of gravity, thermal convection, i.e., convection induced by gravity acting on density differences in the melt, would be expected to be negligible. Fluid flow in the melt, including thermal convection, probably affects the perfection of crystals grown from the melt. At present, the relationship between crystal growth conditions, in particular, fluid flow conditions, and the degree of crystal perfection has not been well established for metals. It is, therefore, highly desirable to document the perfection of crystals grown from the melt in terms of directly controllable process parameters, before one even begins to analyse the fluid flow conditions in the melt in terms of thermodynamical variables. In this paper, optimum solidification parameters for the production of highly perfect copper crystals by Czochralski growth are sought along with documentation of crystal imperfections under various growth conditions. A vital part of research of this type is the assessment of crystal perfection. X-ray techniques which do not in their application produce defects and which allow the characterization of imperfections in single crystals are chosen to assess crystal perfection. The properties of crystals grown from the melt are anticipated to vary over a large range, since the growth conditions, especially the fluid flow conditions, are deliberately changed. The x-ray techniques employed ranged from ordinary Laue photography through Borrmann topography to double-crystal scanning diffractometry, thus allowing crystals with a wide variation in perfection to be studied. As a set of controllable solidification parameters, the rotation of the seed and of the melt and the diameter of the bottle-neck are chosen. X-ray diffraction topographs are analysed along with the data obtained from rocking curve measurements. Tables of growth conditions and quantitative data of rocking curve widths are presented.

**13945.** Chang, S-S., **Thermal relaxation and glass transition in polyethylene,** *J. Polym. Sci.,* No. 43, 43-54 (1973).

Key words: annealed; crystallinity; glass transition; polyethylene; relaxation; temperature drifts.

Thermal relaxations in the glass transition region can be observed as spontaneous temperature drifts of the sample under adiabatic conditions. Upon the heating of a quenched glass, positive drifts are observed reaching a peak at some temperature just below its $T_g$. An annealed glass produces a peak in the negative drift at temperatures just above its $T_g$. Heat capacity measurements have been made on three linear polyethylene samples having 71 to 96 percent crystallinity and on one branched polyethylene sample, in an adiabatic calorimeter from 2 to 360 K. In all four samples, temperature drifts were detected with peaks occurring around 235-240 K. The temperature of the peaks is not significantly affected by the degree of crystallinity. However, the magnitude of the peaks decreases as the crystallinity is increased.

**13946.** Mielenz, K. D., **Eureka!,** *Appl. Opt.* **13,** No. 2, A14 and A16 (Feb. 1974).

Key words: Archimedes; Buffon; burning mirrors; feasibility; history of optics; Second Punic War; solar energy.

In view of the recently renewed controversy whether Archimedes could have used mirrors to defer the attacking Roman fleet during the siege of Syracuse in the Second Punic

War, it is pointed out that the feasibility of this has been demonstrated by Buffon in 1747. Additional facts are presented which also suggest that the use of burning mirrors could have presented a serious threat to the blockading Romans.

**13947.** Frommer, M. A., Shporer, M., Messalem, R. M., **Water binding and irreversible dehydration processes in cellulose acetate membranes,** *J. Appl. Polym. Sci.* **17,** 2263-2276 (1973).

> Key words: adsorption of water; cellulose acetate; dehydration; free induction decay; freezing of water; irreversible processes; membranes; NMR; porous membranes.

The relative amounts of freezing and nonfreezing water in various water-wet cellulose acetate (CA) membranes were determined by NMR techniques, from the initial heights of the water component in the free induction decay (NMR intensity). The results suggest that (1) a significant fraction of the water in various wet CA membranes does not freeze, probably because of strong interaction with the polymer; (2) the relaxation times $T_2$ of the nonfreezing water are of the order of milliseconds indicating that they are still highly mobile compared with ice; (3) all the water contained in dense CA films or in membranes equilibrated at relative humidity of 0.93 does not freeze upon cooling the membranes from room temperature to $-60$ °C; (4) the amounts of nonfreezing bound water in membranes is higher than the total amount of water absorbed from liquid water by a dense film of the same polymer. However, the amounts of nonfreezing water in various CA membranes as calculated from the "relative NMR intensities" is substantially lower than those calculated from DSC melting endotherms by assuming the heat of fusion of water in membranes to be identical to that of pure water. Various possible reasons for this discrepancy are discussed. Measurements on the first desorption-adsorption cycle of *wet* CA membranes have also been performed. They suggest that during the first dehydration process, irreversible changes are induced in the structure of the membrane which result in a significantly lower accessibility of the polymer to interact with water. The extent of these irreversible changes in membrane structure is dependent on the details of the dehydration process being more pronounced at higher temperatures.

**13948.** Fanconi, B., **Low-frequency vibrational spectra of some homopolypeptides in the solid state,** *Biopolymers* **12,** 2759-2776 (1973).

> Key words: far infrared spectroscopy; interchain hydrogen bonding; low frequency vibrations; polypeptides; Raman spectroscopy.

Low-frequency Raman and far-infrared spectra of polyglycine, poly-L-alanine, and poly-L-valine have been measured. The Raman spectra exhibit an intense band near 100 $cm^{-1}$ for these homopolypeptides. Lattice calculations of the polyglycines are used to assign the intense Raman band to a rotatory lattice mode. For homopolypeptides in the $\beta$ conformation, an infrared band is observed whose frequency varies inversely with the square root of the mass of the peptide repeating unit. This infrared band is assigned to the hydrogen bond stretching lattice vibration.

**13949.** Field, B. F., Finnegan, T. F., Toots, J., **Volt maintenance at NBS via $2e/h$: A new definition of the NBS volt,** *Metrologia* **9,** No. 4, 155-166 (1973).

> Key words: Josephson effect; standard cell; tunnel junction; voltage comparator; voltage standard.

This paper describes in detail the procedures, methods and measurements used to establish a new definition of the U.S. legal volt via the ac Josephson effect. This new definition has been made possible by the use of thin film tunnel junctions (capable of producing 10 mV outputs) and high accuracy voltage comparators. The Josephson junction is used as a precise frequency-to-voltage converter with a conversion factor equal to $2e/h$. A series of measurements of $2e/h$ have been carried out at NBS
referenced to the as-maintained unit of emf based on a larg
group of standard cells. Measurements made at regular interval
over a one year period (1971 to 1972) indicate that the mean em
of this group of standard cells has decreased about 4 parts in $10^7$
Primarily to remove the effects of this drift, on July 1, 1972
new as-maintained unit was defined by choosing a value of $2e/$
consistent with the existing unit of emf. The adopted value o
$2e/h$ is 483593.420 GHz/$V_{\mathrm{NBS}}$. The precision (one standar
deviation) with which the new unit of emf can be maintained wit
the present techniques and apparatus is about 2 parts in $10^8$. Th
accuracy of the present system is estimated to be 4 parts in 10
Comparisons of $2e/h$ systems at different national laboratorie
have been limited by uncertainties associated with the physic
transfer of standard cells. In order to determine the relativ
agreement of the various $2e/h$ systems with precision better tha
1 or 2 parts in $10^7$, it appears desirable to compare $2e/h$ system
directly by transporting one of them.

**13950.** Goldman, A. J., **Approximate localization theorems for op
timal facility placement,** *Transp. Sci.* **6,** No. 2, 195-201 (Ma
1972).

> Key words: facility location; optimal location.

The problem is that of locating a flow-receiving facility in a r
gion, so as to minimize the weighted sum of distances betwee
sources and facility. It is shown here that if a subregion S bo
generates "sufficiently much" of the region's total flow, and a
mits entry via specified "gate" points without "too much" circu
ty, then (a) S contains at least one "near-optimal" location for t
facility, and (b) no strictly optimal location can lie "too far" fro
S.

**13951.** Lee, P. H., Broida, H. P., Braun, W., Herron, J. T., **Dire
observation of vibrationally excited hydrogen produced by col
sional energy transfer from electronically excited sodium, r
bidium, caesium, and mercury,** *J. Photochem.* **2,** 165-1
(1973/74).

> Key words: absorption spectra; apparatus and metho
> energy transfer; gases; kinetics of reaction; photochemistr
> vacuum u.v.

Hydrogen has been vibrationally excited by direct ener
transfer from electronically excited sodium, rubidium and cae
um, and mercury. The vibrational excitation of the $B^1\Sigma^+_u$
$X^1\Sigma^+_g$ transitions in hydrogen was detected by absorption of t
vacuum u.v. radiation from a low pressure molecular hydrog
lamp.

**13952.** McAlister, A. J., Cuthill, J. R., Dobbyn, R. C., Willian
M. L., **Soft x-ray study of the *d*-bands in $AuAl_2$,** (Proc. I
Conf. on Band Structure Spectroscopy of Metals and Allo
Strathclyde, Glasgow, Scotland, Sept. 26-30, 1971), Paper
*Band Structure Spectroscopy of Metals and Alloys,* D.
Fabian and L. H. Watson, Eds., pp. 191-203 (Academic Pre
London, England, 1973).

> Key words: Au; $AuAl_2$; *d*-bands; emission spectrum; N
> soft x-ray.

The $N_{6,7}$ soft x-ray emission spectrum (5d to 4f transition)
Au in $AuAl_2$ has been measured. This work, together with the
ray photoemission results of Chan and Shirley, shows the
bands to be distributed over a range of approximately 4 eV, w
maxima at 5.0 and 7.1 eV below the Fermi level. These res
raise some questions about the interpretation of the Al L en
sion spectrum from the compound, which appeared to of
strong confirmation of nonrelativistic band calculations of
electronic structure of $AuAl_2$, and again raise the possibility o
band participation in the strong coloring of the compound, an
fect which the Al emission spectrum and nonrelativistic b
calculations appeared to exclude.

13953. Piermarini, G. J., Block, S., Barnett, J. D., **Hydrostatic limits in liquids and solids to 100 kbar,** *J. Appl. Phys.* **44,** No. 12, 5377-5382 (Dec. 1973).

Key words: diamond-anvil pressure cell; glass transition pressures; hydrostaticity; pressure gradients; pressure measurements; ruby fluorescence.

The hydrostatic properties of the materials methanol, isopropyl alcohol, water, sodium chloride, silver chloride, and the binary mixtures pentane-isopentane and methanol-ethanol have been determined in the diamond-anvil pressure cell up to 180 kbar by line-broadening and line-shift measurements of the sharp $R_1$ ruby fluorescence line. A liquid mixture 4:1 by volume of methanol:ethanol remains hydrostatic to almost 100 kbar at room temperature. This mixture exceeds the hydrostatic limit of the previous generally accepted fluid, 1:1 pentane:isopentane which has a hydrostatic limit of about 70 kbar. Silver chloride and water (ice VII) are better than sodium chloride as pressure-transmitting media, but do not even qualitatively approach hydrostatic conditions much above 70 kbar. The stress sensitivity level of the ruby limits the extent to which slight deviations from hydrostatic conditions can be determined in solid systems and suggests the qualitative nature of the method in characterization of quasihydrostatic states. The equilibrium freezing pressure of methanol at 24 °C was redetermined to be $35.8 \pm 0.8$ kbar.

13954. Arp, V. D., Clark, A. F., Flynn, T. M., **Superconducting levitation of high speed vehicles,** *Transp. Eng. J.* **99,** No. TE4, 873-885 (Nov. 1973).

Key words: fatigue life; magnetic properties; materials; refrigeration; superconducting magnets; suspension; transportation; urban transportation.

The current status (December 1972) of worldwide research on high speed ground transportation techniques is reviewed. Particular attention is given to studies of magnetic levitation using superconducting magnets, including comparison with alternative magnetic techniques and with air suspension systems. Superconducting levitation appears to be a strong contender in the U.S. Department of Transportation hopes to select in the late 1970's the best of the possible levitation techniques for subsequent advanced development. Cryogenic engineering research needed in support of major development of a superconducting levitated system is identified.

13955. Mandel, J., Lashof, T. W., **Interpretation and generalization of Youden's two-sample diagram,** *J. Qual. Technol.* **6,** No. 1, 22-36 (Jan. 1974).

Key words: collaborative reference programs; interlaboratory tests; test method evaluation; Youden diagram.

Youden's two sample diagram is a useful method for certain types of interlaboratory comparisons of test results. Generally, points in the plot fall within an elongated ellipse, the major axis of which makes a 45° angle, approximately, with the x, y axes. Occasionally it happens that the axes are not the bisectors of the coordinate axes. This paper (1) examines more closely the assumptions underlying the Youden diagram and presents a more general method of interpreting it and (2) generalizes the diagram to situations where the two samples do not have the same level and/or the axes of the ellipse definitely do not bisect the coordinate axes.

13956. Kurylo, M. J., **Kinetics of the reactions $OH(\upsilon=0) + NH_3 \rightarrow H_2O + NH_2$ and $OH(\upsilon=0) + O_3 \rightarrow HO_2 + O_2$ at 298 K,** *Chem. Phys. Lett.* **23,** No. 4, 467-471 (Dec. 15, 1973).

Key words: ammonia; kinetics; OH radical; ozone; stratosphere.

The rate constants for the reactions $OH(X^2\Pi,\ \upsilon=0) + NH_3 \xrightarrow{k_1} H_2O + NH_2$ and $OH(X^2\Pi,\ \upsilon=0) + O_3 \xrightarrow{k_2} HO_2 + O_2$ were measured at 298 K by the flash photolysis resonance fluorescence technique. The values of the rate constants thus obtained are $k_1 = (4.1 \pm 0.6) \times 10^{-14}$ and $k_2 = (6.5 \pm 1.0) \times 10^{-14}$ in units of $cm^3$ $molecule^{-1}$ $sec^{-1}$. The results are discussed in terms of understanding the dynamics of the perturbed stratosphere.

13957. Straty, G. C., Goodwin, R. D., **Dielectric constant and polarizability of saturated and compressed fluid methane,** *Cryogenics* **13,** No. 12, 712-715 (Dec. 1973).

Key words: dielectric constant; methane; polarizability.

Accurate measurements of the dielectric constant of methane have been made on the saturated liquid from near the triple point to 188 K and on the compressed fluid along selected isotherms from 100 K to 300 K and at pressures to 345 bar. The data are combined with accurate densities to obtain the molar polarizability and its dependence on density and temperature. The density range examined extends to nearly three times the critical density. The molar polarizability is found to increase initially with density and then decrease in qualitative agreement with theoretical predictions and the behaviour of other fluids.

13958. Goldman, A. J., **Minimax location of a facility in a network,** *Transp. Sci.* **6,** No. 4, 407-418 (Nov. 1972).

Key words: facility location; network theory; optimal location.

The problem is that of locating a facility in a network *N* so as to minimize the largest of its distances from the vertices of *N*. A method is given that either solves the problem, or else reduces it to an analogous problem for a single "cyclic component" of *N*. When *N* is acyclic (a tree), a very efficient solution algorithm results. Partial analogs of these results are given for a "weighted-distance" extension of the problem.

13959. Perlstein, J. H., Ferraris, J. P., Walatka, V. V., Jr., Cowan, D. O., Candela, G. A., **Electron transport and magnetic properties of new highly conducting TCNQ complexes,** (Proc. 18th AIP Conf. on Magnetism and Magnetic Materials, Denver, Colo., Nov. 28-Dec. 1, 1972), Paper in *Magnetism and Magnetic Materials,* C. D. Graham, Jr., and J. J. Rhyne, Eds., No. 10, 1494-1498 (American Institute of Physics, New York, N.Y., 1973).

Key words: electron transport; magnetic properties; metallic; TCNQ complexes.

Single crystals of the 1:1 complexes tetrathiafulvalinium tetracyanoquinodimethane (TTF-TCNQ) and tetrathianaphthacinium tetracyanoquinodimethane (TTN-TCNQ) have been synthesized and the electron transport properties and magnetic susceptibility have been measured from 2 K to room temperature. For TTN-TCNQ, $\sigma$ at room temperature is $1\Omega^{-1}\ cm^{-1}$. For TTF-TCNQ, $\sigma$ at room temperature along the long axis ($\sigma_\perp$) is in the range $192\text{-}652\Omega^{-1}\ cm^{-1}$ depending on sample whereas perpendicular to the long axis $\sigma_\perp$ is $1\Omega^{-1}\ cm^{-1}$. The conductivity remains metallic down to 66 K in both directions whereupon a continuous metal to insulator transition occurs. The activation energy in the insulating state is 0.0062 eV. The transition is associated with a small hysteresis between the heating and cooling curves suggesting a possible structural change. In the metallic region, $\rho_{\parallel}$ follows a $T^2$ dependence whereas $\rho_\perp$ follows a $T^{+1}$ behavior. The magnetic susceptibility is diamagnetic below 20 K becoming increasingly more paramagnetic with increasing T even in the metallic region. It is suggested that spin disorder scattering may account for the anomalous temperature dependence of $\rho_{\parallel}$.

13960. Brown, D. W., Florin, R. E., Wall, L. A., **The effect of dilute fluorine on certain fluoropolymers,** *Appl. Polym. Symp. No. 22,* 169-180 (1973).

Key words: crosslinking; fluorine; fluoropolymers.

Various fluoropolymers were exposed to 5 percent fluorine in helium at 25 °C and one atmosphere. About 10-100 percent as many fluorine molecules were charged as monomer units in each polymer. Certain polymers degraded as shown by decreases in their intrinsic viscosities. Degrading polymers had the structures

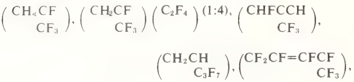

$$\left(\begin{smallmatrix}\mathrm{CH_2CF}\\ \quad\mathrm{CF_3}\end{smallmatrix}\right), \left(\begin{smallmatrix}\mathrm{CH_2CF}\\ \quad\mathrm{CF_3}\end{smallmatrix}\right)\left(\mathrm{C_2F_4}\right)(1{:}4), \left(\begin{smallmatrix}\mathrm{CHFCCH}\\ \quad\mathrm{CF_3}\end{smallmatrix}\right), \left(\begin{smallmatrix}\mathrm{CH_2CH}\\ \quad\mathrm{C_3F_7}\end{smallmatrix}\right), \left(\begin{smallmatrix}\mathrm{CF_2CF{=}CFCF}\\ \qquad\mathrm{CF_3}\end{smallmatrix}\right),$$

and

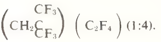

$$\left(\mathrm{CH_2C}\begin{smallmatrix}\mathrm{CF_3}\\ \mathrm{CF_3}\end{smallmatrix}\right)\left(\mathrm{C_2F_4}\right)(1{:}4).$$

The intrinsic viscosity of polyperfluoropropene was not changed. Other polymers cross-linked, as shown by formation of gel. These had the structures

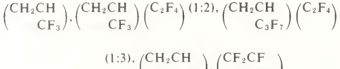

$$\left(\begin{smallmatrix}\mathrm{CH_2CH}\\ \quad\mathrm{CF_3}\end{smallmatrix}\right), \left(\begin{smallmatrix}\mathrm{CH_2CH}\\ \quad\mathrm{CF_3}\end{smallmatrix}\right)\left(\mathrm{C_2F_4}\right)(1{:}2), \left(\begin{smallmatrix}\mathrm{CH_2CH}\\ \quad\mathrm{C_3F_7}\end{smallmatrix}\right)\left(\mathrm{C_2F_4}\right)(1{:}3), \left(\begin{smallmatrix}\mathrm{CH_2CH}\\ \quad\mathrm{C_6F_5}\end{smallmatrix}\right), \left(\begin{smallmatrix}\mathrm{CF_2CF}\\ \quad\mathrm{C_6H_5}\end{smallmatrix}\right)$$

and

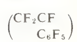

$$\left(\begin{smallmatrix}\mathrm{CF_2CF}\\ \quad\mathrm{C_6F_5}\end{smallmatrix}\right)$$

In homopolymers the greater the hydrogen content the more likely the polymer was to crosslink, suggesting that crosslinking proceeds via abstraction of hydrogen atoms. However, an increased content of tetrafluoroethylene in copolymers also was associated with greater crosslinking or reduced degradation. Viton and a copolymer of 3,3,3-trifluoropropene gave highly crosslinked materials. The vulkanizates of Viton are quite resistive to stress relaxation at 250 °C in air. Those of the trifluoropropene copolymer are very unstable.

13961. Goldberg, R. N., Armstrong, G. T., **Microcalorimetry: A tool for biochemical analysis,** *Med. Instrum.* **8,** No. 1, 30-36 (Jan.-Feb. 1974).

Key words: analytical chemistry; bacterial identification; biochemistry; cellular processes; clinical chemistry; enzyme activity; immunochemistry; medical instrumentation; microcalorimetery; thermochemistry.

In order for the application of heat measurements to analysis and clinical chemistry to be feasible, three requirements must be met: (1) specificity of reaction, (2) knowledge of the thermochemistry involved, and (3) adequate instrumentation. Instrumentation requirements are met by devices known as heat conduction microcalorimeters. Some of the principles underlying these instruments are reviewed. The current status of microcalorimetry regarding requirements of sensitivity, sample volume, accuracy, reproducibility, and speed is considered. A brief review of analytical applications that have utilized microcalorimetry is given. These applications include assays for enzymes and substrates, bacterial identifications, and investigation of cellular processes. The advantages and disadvantages of the method as well as possibilities for future development are considered.

13962. Kelleher, D. E., Wiese, W. L., **Observation of ion motion in hydrogen Stark profiles,** *Phys. Rev. Lett.* **31,** No. 24, 1431-1434 (Dec. 10, 1973).

Key words: Balmer; broadening; dynamic; ion; plasma; Stark.

We have measured the central part of the Balmer $H_\beta$ or $D_\beta$ line in similar stabilized arc plasmas, but of different chemical compositions. We have found an ion-motion effect which appears to scale with the inverse square root of the reduced mass of the radiator-perturber system and which, for $H_\beta$ at least, essentially removes one of the largest remaining discrepancies between experiment and Stark-broadening theory.

13963. Bennett, H. S., **Two-electron *U* centers in ionic crystals: Point-ion models,** *Phys. Rev. B* **6,** No. 10, 3936-3940 (Nov. 15, 1972).

Key words: $BaF_2$; $CaF_2$; $CdF_2$; ionic polarization; KCl; Mollwo-Ivey relations; NaCl; point-ion potential; $SrF_2$; *U* centers.

The Hartree-Fock-Slater (HFS) equations for the two-electron orbitals about a proton located substitutionally at an anion site have been solved numerically in the point-ion lattice potential. The lattice relaxation of the nearest-neighbor ions is included in the model. The five lowest-lying *U*-center states for NaCl, KCl, $CdF_2$, $CaF_2$, $SrF_2$, and $BaF_2$ have been calculated within the framework of the above model. It is found that the low-lying singlet states have the following order for increasing values of the energy: ${}^1S(1s,\ 1s)$, ${}^1P(1s,\ 2p)$, and ${}^1S(1s,\ 2s)$. The energy levels for the triplet states ${}^3S(1s,\ 2s)$ and ${}^3P(1s,\ 2p)$ lie between the energy levels for the ${}^1S(1s,\ 1s)$ and ${}^1P(1s,\ 2p)$ states. The ordering of the triplet states depends upon the host crystal and the lattice relaxation. In some cases, these triplet states may be degenerate or very nearly so. In addition, the extent to which the peak energies of the *U* bands obey Mollwo-Ivey relations is given for the alkali halides and for the alkaline-earth fluorides. The predictions based upon the numerical HFS wave functions are compared with the predictions based upon past variational wave functions and with experiment.

13964. Feldman, A., Horowitz, D., Waxler, R. M., **Mechanisms for self-focusing in optical glasses,** *IEEE J. Quantum Electron.* **QE-9,** No. 11, 1054-1061 (Nov. 1973).

Key words: absorption coefficient; damage threshold; electrostriction; electrostrictive self-focusing; Kerr effect; laser damage; nonlinear index of refraction; self-focusing; thermal self-focusing.

The relative contributions of the Kerr, electrostrictive, and thermal effects to the self-focusing thresholds of borosilicate crown glass, fused silica, and dense flint glass have been estimated from an analysis of damage-threshold data for linearl polarized and circularly polarized radiation. The measurement were made with a Nd:glass laser operating in the $TEM_{00}$ mod with a temporal pulsewidth of 25 ns. The Kerr effect appears t be the largest effect. The thermal effect is also significant. Th electrostrictive effect is smallest. Reasonable values of the absorption coefficient are calculated from the thermal contribution The results are in qualitative agreement with the work of others

13965. Hastie, J. W., Hauge, R. H., Margrave, J. L., **Infrare spectra of matrix-isolated species in the gallium-fluorine system** *J. Fluorine Chem.* **3,** 285-291 (1973/74).

Key words: aluminium; fluorides; gallium; infrared spectra matrix isolation.

The species $GaF_3$, GaF, $AlF_3$, AlF and $(AlF)_2$ have been iso lated in inert-gas matrices and their infrared absorption spectr obtained over the range 33-4000 cm$^{-1}$. The following technique were used to generate these species; (i) co-deposition of Ga o GaF and molecular $F_2$ or F atoms with an excess of inert gas; (i Knudsen cell effusion and matrix isolation of the vapors ove $GaF_3$, $GaF_3$ + Ga and $GaF_3$ + Al.

**3966.** Currie, L. A., DeVoe, J. R., **The isotope separator as a tool for low-level radioassay and trace activation analysis,** (Proc. Symp. on Nuclear Techniques in Measurement and Control of Environmental Pollution, Salzberg, Austria, Oct. 26-30, 1970), Paper in *Nuclear Techniques in Environmental Pollution,* pp. 183-190 (International Atomic Energy Agency, Vienna, Austria, 1971).

Key words: activation analysis; iodine; mass separation; physical-radiochemical separation.

Determinations of environmental radioactivity and of low-level products of nuclear activation are frequently limited in sensitivity because of isotopic contamination. Sensitivity may be limited by radioisotopes because of interfering radiations and by stable isotopes because of decreased specific activity. To overcome these limitations, electromagnetic isotope separation, which is applicable to most elements, has been investigated as a complement to radiochemical separation and decay scheme resolution. An added advantage of mass separation in environmental studies is the physical separation of a diluting radioisotope—radioisotope dilution being desirable because of the possibility of unknown initial amounts of stable isotopes.

The characteristics of the relatively new class of laboratory isotope separators having moderately large beam currents, 1-5 mA, are particularly suitable, for they include reasonable throughput (~mg/h), yield (~10%) and resolution (~$10^3$). Isotope separation was investigated in connection with the neutron activation analysis of trace quantities (~$10^9$ atoms) of iodine. The mass-separation step was found to be essential because of the production of interfering iodine fission products—even when uranium contamination was as low as 1 ppm. A particularly important result of our investigation was the absence of any detectable blank effect from prior separations. In addition, it has been shown that for certain problems electromagnetic separation, when combined with a high efficiency radiation detector, is far more sensitive and selective than a high resolution detector without mass separation.

**13967.** Richmond, J. C., **A standard for night vision devices for law enforcement,** (Proc. of the Society of Photo-Optical Instrumentation Engineers, San Diego, Calif., Aug. 27-29, 1973), Paper in *Image Intensifiers: Technology, Performance, Requirements and Applications,* A. D. Schnitzler and M. W. Klein, Eds., **42,** 109-115 (1974).

Key words: contrast transfer function; distortion; flare; image intensifiers; law enforcement; light equivalent background; light induced background; night vision; optical gain.

A draft Standard for Passive, Hand-Held Night Vision devices has been developed for the Law Enforcement Standards Laboratory of the National Bureau of Standards. This Standard is now being circulated for comment prior to adoption as a Standard of the National Institute of Law Enforcement and Criminal Justice of the Law Enforcement Assistance Administration of the Department of Justice.

The paper mentions some of the philosophy behind the standard, lists the performance requirements and describes briefly the test procedures for (A) focus adjustment, curvature of field and distortion of the eyepiece lens, (B) optical gain, optical gain stability, light equivalent background, light induced background, luminance of output screen, luminance uniformity, cathode and screen quality, contrast transfer function, distortion and flare of a night vision device complete with objective lens, but with the eyepiece removed, and (C) for resistance to vibration, high and low temperature storage, operation and thermal shock and humidity of night vision devices complete with both objective and eyepiece lenses, and (D) boresight adjustment, click movement and resistance to mechanical shock of night vision devices intended for use as rifle sights.

**13968.** Brown, D. W., Lowry, R. E., Wall, L. A., **Radiation-induced polymerization at high pressure of *cis-* and *trans-*1,3,3,3-tetrafluoropropene in bulk and with tetrafluoroethylene,** *J. Polym. Sci.* **11,** Part A-1, 1973-1984 (1973).

Key words: copolymerization; high pressure; polymerization; radiation; tetrafluoroethylene; tetrafluoropropene.

The radiation-induced polymerization of *cis-* and *trans-*1,3,3,3-tetrafluoropropene in bulk and with tetrafluoroethylene was studied at pressures between 5000 and 15000 atm and temperatures between 21 and 100 °C. At $10^3$ rad/hr the homopolymerization rates range from about $10^{-4}$ to 1 percent/hr. The activation enthalpy and volume are about 8 kcal/mole (33 kJ/mole) and $-10$ cm$^3$/mole, respectively, for both isomers. The *cis* isomer polymerizes about twice as rapidly as the *trans* isomer. The latter freezes in the experimental range of temperature and pressure; the polymerization rate is very low in solid phase. Polymer intrinsic viscosities increase with polymerization pressure and decrease with polymerization temperature; the largest value obtained was 0.23 dl/g. In the copolymerizations all reactivity ratios favor incorporation of tetrafluoroethylene by factors of 6-16. The preference is stronger when the *trans* isomer is used.

**13969.** Olsen, P. T., Driscoll, R. L., **Determination of $\gamma_p'$ at the National Bureau of Standards,** (Proc. 4th Int. Conf. on Atomic Masses and Fundamental Constants, Teddington, England, Sept. 6-10, 1971), Paper in *Atomic Masses and Fundamental Constants,* J. H. Sanders and A. H. Wapstra, Eds., pp. 471-484 (Plenum Press, London, England, 1972).

Key words: fine structure constant; gyromagnetic ratio of proton; nuclear induction; precision solenoid.

The gyromagnetic ratio of the proton, $\gamma_p'$ is one of our most important fundamental physical constants. (The prime indicates that the protons are in a spherical sample of pure $H_2O$.) Not only is it used for calibration purposes in nuclear magnetic resonance experiments, but it plays a crucial role in determining the fine structure constant from the measurement of 2e/h via the ac Josephson effect. Additionally the continued measurement of $\gamma_p'$ can be used to monitor as-maintained units of current.

The precision of $\gamma_p'$ measurements at the National Bureau of Standards (NBS) has improved significantly since the early measurements of the 1950's, from several parts per million (ppm) to the present 0.1 to 0.2 ppm. Current efforts are now being directed towards improving the present 3 to 4 ppm accuracy of the experiment by an order of magnitude. It is the purpose of this paper to briefly report the progress being made in this direction. First, a general discussion of the experiment is given, including (a) use of the method of nuclear induction to determine the precession frequency; (b) a description of a new and improved series of pitch measurements using a laser interferometer; (c) a discussion of the effect of the change in original winding tension on the effective diameter of the windings; and (d) an analysis of the effect of the finite susceptibility of the solenoid and water sample support structure on the calculated magnetic field. All of the known corrections to the field are then summarized, and finally, a brief analysis of the uncertainties in the experiment is given along with a value for $\gamma_p'$.

**13970.** Bower, V. E., **Determination of the Faraday by means of the iodine coulometer,** (Proc. 4th Int. Conf. on Atomic Masses and Fundamental Constants, Teddington, England, Sept. 6-10, 1971), Paper in *Atomic Masses and Fundamental Constants,* J. H. Sanders and A. H. Wapstra, Eds., pp. 516-520 (Plenum Press, London, England, 1972).

Key words: coulometry; Faraday; fundamental constants.

This paper describes briefly the work now in progress at NBS on the determination of the Faraday by means of the iodine coulometer. Results obtained to date are compared with a recent determination of the Faraday by means of the silver coulometer and with an adjusted value of the same constant derived from recent determinations of the gyromagnetic ratio of the proton and proton magnetic moment in nuclear magnetons.

**13971.** Galy, J., Roth, R. S., **The crystal structure of $Nb_2Zr_6O_{17}$,** *J. Solid State Chem.* **7,** 277-285 (1973).

Key words: anion excess fluorite; crystal structure; $Nb_2Zr_6O_{17}$; square anti-prism.

$Nb_2Zr_6O_{17}$ is orthorhombic, space group $Ima2$, with $a=40.91$, $b=4.93$, $c=5.27$ Å. The asymmetric structural unit contains one octahedron, three sevenfold coordinated ions, and one square antiprism, and its relations to the fluorite and $ZrO_2$ structures are discussed. Variations in compositions can be accounted for by increasing or decreasing the number of sevenfold coordinated ions in the structure.

**13972.** Sharman, L. J., Tovey, H., Vickers, A. K., **Current status and national priorities for flammable fabric standards,** *Proc. 6th Annual Meeting of Information Council on Fabric Flammability, New York, N.Y., Dec. 7, 1972,* pp. 265-306 (Information Council on Fabric Flammability, New York, N.Y., May 1, 1973).

Key words: blankets; children's sleepwear; fabric fires; fabric flammability standards; FFACTS; fire injuries; flammable fabrics; flammability standards priorities; garment flammability; garments; sampling plans; upholstered furniture.

The present status (calendar year 1972) of flammability standards issued by the Department of Commerce is described. During 1972, a sampling plan was developed for the Standard for the Flammability of Children's Sleepwear, DOC FF 3-71. The Standard was reissued with this plan included. A Flammability Standard for Mattresses was also issued. Work is in progress on a proposed flammability standard for blankets and flammability test methods for upholstered furniture. The approaches used in development of the standard and the current status of the work are discussed.

The results of a recent analysis of information available to the Fire Technology Division, National Bureau of Standards, on the relative need for specific flammability standards for wearing apparel are discussed. The system used for developing "candidate priorities" for standards is briefly described. A list of high priority garment types is presented, along with examples of compilations of data from the NBS-Flammable Fabrics Accident Case and Testing System (FFACTS) and other sources supporting the placement of the individual garment types on the list.

**13973.** Levin, E. M., Benedict, J. T., Sciarello, J. P., Monsour, S., **The system $K_2SO_4$-$Cs_2SO_4$,** *J. Amer. Ceram. Soc.* **56,** No. 8, 427-430 (Aug. 1973).

Key words: $Cs_2SO_4$; density $K_2SO_4$-$Cs_2SO_4$ solid solutions; equilibrium diagram $Cs_2SO_4$-$K_2SO_4$; hexagonal solid solutions; $K_2SO_4$; phase diagram $Cs_2SO_4$-$K_2SO_4$; polymorphism $Cs_2SO_4$-$K_2SO_4$ solid solutions; solid solutions.

The phase diagram for the system $K_2SO_4$-$Cs_2SO_4$ was determined by using DTA for melting relations and DTA and high-temperature x-ray diffractometry for subsolidus relations. At the solidus the system shows complete solid solubility, with a minimum at 940 °C and 50 mol% $Cs_2SO_4$. Orthorhombic $K_2SO_4$ and $Cs_2SO_4$, the stable low-temperature forms, show mutual solid solubility and form a eutectoid at 50 mol% $Cs_2SO_4$ and 430 °C, the lowest temperature of stability of the high-temperature hexagonal solid-solution phase. Isothermal plots of the $a$ and $c$ dimensions of this hexagonal phase vs composition show large positive deviations from linearity for $c$. These deviations are interpreted on the basis of the crystal structure of $KNaSO_4$ with similar unit cell.

**13974.** Goldman, D. T., Logan, D. A., **Solid wastes – a technological assessment,** *Chem. Eng. Progr.* **69,** No. 9, 33-35 (Sept 1973).

Key words: engineering education; solid waste disposal technology assessment.

A technology assessment is performed on the problem of th disposal of municipal refuse. Various alternative methods ar considered including proposed methods for the utilization o solid waste. The identification of those affected by the various alternatives and an evaluation of the impacts these alternative have on the affected parties are presented. The conclusions c this simple assessment is that sanitary landfills is the most desirable form of presently available disposal methods. For the futur new methods for the utilization of solid waste are required.

**13975.** Mauer, F. A., Hubbard, C. R., **Evaluation of the energ dispersive powder diffraction method for the determination quartz in dust samples,** (Proc. Roundtable Discussion o Analytical Techniques for Quartz, Cincinnati, Ohio, Dec. 6- 1972), Paper in *Analytical Techniques for Quartz,* pp. 17-2 (National Institute for Occupational Safety and Health, Ame ican Conference of Governmental Industrial Hygienists, Ci cinnati, Ohio, Jan. 1974).

Key words: analytical methods; industrial hygiene; quart silicosis; x-ray diffraction.

An energy dispersive powder diffractometer was assemble and used to determine the amount of quartz on six silver membrane filters, such as those used in sampling airborne dust. Th amount of quartz, which varied from 24 to 531 $\mu g$, was als determined by weighing. The results obtained indicate that th overall uncertainty in the weight of quartz obtained by the ene gy dispersive x-ray method is at least 50 $\mu g$. The method, ther fore, does not meet the National Institute for Occupation Safety and Health requirement for a practical lower limit of d tection of 20 $\mu g$ and an analytical range of 20 $\mu g$ to 4 mg.

**13976.** Newman, M., **Symmetric completions and products of symmetric matrices,** *Trans. Amer. Math. Soc.* **186,** 191-201 (De 1973).

Key words: fields; principal ideal rings; symmetric compl tion; symmetric matrices; unimodular matrices.

We show that any vector of $n$ relatively prime coordinat from a principal ideal ring $R$ may be completed to a symmet matrix of SL($n$, $R$), provided that $n \geqslant 4$. The result is also true f $n=3$ if $R$ is the ring of integers $Z$. This implies for example th if $F$ is a field, any matrix of SL($n$, $F$) is the product of a fix number of symmetric matrices of SL($n$, $F$) except when $n=2$, $=$ GF(3), which is a genuine exception.

**13977.** Huie, R. E., Herron, J. T., Davis, D. D., **Absolute ra constants for the addition and abstraction reactions of atom oxygen with 1-butene over the temperature range 190-491 K,** *Phys. Chem.* **76,** No. 23, 3311-3313 (1972).

Key words: abstraction reactions; addition reactio atomic oxygen; reaction kinetics; 1-butene.

Using the technique of flash photolysis-resonar fluorescence, absolute rate constants have been measured for t reaction of ground-state atomic oxygen with 1-butene over t temperature range 190-491 K. With a measured precision of percent at each temperature, it was found that the data could n be fit by a single straight line. It was concluded that the curvat in the Arrhenius plot was due to concurrent abstraction and ad tion reactions, the former process representing approximately percent of the total reaction at 300 K and 39 percent at 500 K. The rate expressions derived were $k_{addition} = (3.7 \pm 1.8) \times 10^{-12}$ $\exp(-50 \pm 210$ cal $\mathrm{mol}^{-1}/RT)$ $\mathrm{cm}^3$ $\mathrm{molecule}^{-1}$ $\mathrm{sec}^{-1}$ and $k_{abstraction} = (1.6 \pm 0.9) \times 10^{-11}$ $\exp(-1970 \pm 430$ cal $\mathrm{mol}^{-1}/RT)$ $\mathrm{cm}^3$ $\mathrm{molecule}^{-1}$ $\mathrm{sec}^{-1}$.

13978. Dragoo, A. L., **Diffusion**, Chapter IV in *Tantalum: Physico-Chemical Properties of Its Compounds and Alloys, Atomic Energy Review Special Issue*, O. Kubaschewski, Ed., No. 3, pp. 131-133 (International Atomic Energy Agency, Vienna, Austria, 1972).

Key words: chemical interdiffusion; grain-boundary diffusion; intrinsic diffusion; lattice diffusion; self-diffusion; tracer diffusion.

The tracer diffusion coefficient, the self-diffusion coefficient, the intrinsic diffusion coefficient and the interdiffusion coefficient are briefly described. Grain boundary and lattice (volume) diffusion are contrasted. The frequency factors ($D_0$) and activation energies (Q) are tabulated for diffusion in the borides, carbides, and oxides of Be, Hf, Mo, Nb, Ta, Th, Ti, and Zr and for diffusion of C, N, and O in these metals. The purity of the solvent media, the preparation and properties of the samples, the method, the type of diffusion coefficient measured and the temperature range are also specified.

13979. Dragoo, A. L., **Diffusion**, Chapter IV in *Beryllium: Physico-Chemical Properties of Its Compounds and Alloys, Atomic Energy Review Special Issue*, O. Kubaschewski, Ed., No. 4, pp. 173-175 (International Atomic Energy Agency, Vienna, Austria, 1973).

Key words: chemical interdiffusion; grain-boundary diffusion; intrinsic diffusion; lattice diffusion; self-diffusion; tracer diffusion.

The tracer diffusion coefficient, the self-diffusion coefficient, the intrinsic diffusion coefficient and the interdiffusion coefficient are briefly described. Grain boundary and lattice (volume) diffusion are contrasted. The frequency factors ($D_0$) and activation energies (Q) are tabulated for diffusion in the borides, carbides, and oxides of Be, Hf, Mo, Nb, Ta, Th, Ti, and Zr and for diffusion of C, N, and O in these metals. The purity of the solvent media, the preparation and properties of the samples, the method, the type of diffusion coefficient measured and the temperature range are also specified.

13980. Armstrong, G. T., **Recent developments in calorimetry and thermochemistry at the National Bureau of Standards**, (Proc. Plenary Lectures of 8th Symp. on Calorimetry and Thermal Analysis, Okayama, Japan, Nov. 1972), Paper in *Calorimetry, Thermometry and Thermal Analysis* **6**, 51-60 (Kagaku Gijitsu-Sha, Tokyo, Japan, 1973).

Key words: calorimetry; microcalorimetry of biological processes; standard reference materials for calorimetry; thermochemistry; thermodynamic data.

The thermochemistry work at the National Bureau of Standards provides standard reference data for the National Measurement System both in the form of critical compilations of work done elsewhere and also in the form of new measurements of key substances. A new electrolyte thermodynamic data center has been formed. On-going compilations of the properties of inorganic compounds are being systematized in the form of a catalog of thermochemical quantities. New measurements on organic halogen, nitrogen, and sulfur compounds are extending the range of certified standard reference materials for calorimetry.

A new program on the microcalorimetry of biological processes has shown the applicability of calorimetry to practically important problems of clinical chemistry, and has resulted in improvements in the accuracy of microcalorimetric measurements.

13981. Wampler, R. H., **Some recent developments in linear least-squares computations**, (Proc. Computer Science and Statistics 6th Annual Symp. on the Interface, University of California, Berkeley, Calif., Oct. 16-17, 1972), Paper in *Proceedings of the Computer Science and Statistics Sixth Annual Symposium on the Interface*, M. E. Tarter, Ed., 94-110 (Western Periodicals Co., North Hollywood, Calif., Oct. 1972).

Key words: analysis of variance; computer programs; Gram-Schmidt orthogonalization; Householder transformations; ill-conditioned test problems; iterative refinement; least squares computations; linear equations; OMNITAB; regression; rounding errors; statistics.

The results of an evaluation of linear least-squares computer programs (Wampler (174, 175)) are briefly summarized. Subsequent work, including problems encountered, to provide a more accurate least-squares routine for the OMNITAB II program is discussed. In this connection, the comparative results of running a number of ill-conditioned problems on OMNITAB II and two other reliable programs are presented. A bibliography of the recent literature on least-squares analysis has been prepared with special emphasis on the computational aspects of obtaining least-squares solutions.

13982. Douglas, W. M., Johannesen, R. B., Ruff, J. K., **Reactions of coordinated ligands. II. $\mu$-oxo-bis(difluorophosphineiron tetracarbonyl)**, *Inorg. Chem.* **13**, No. 2, 371-374 (1974)

Key words: carbonyl compounds; coordination compounds; fluorophosphine; iron carbonyl; nmr; nuclear magnetic resonance.

Reaction of $Fe(CO)_4PF_2Br$ with potential sources of the oxide ion (*e.g.*, $Ag_2O$, $Cu_2O$, etc.) yielded the new complex compound, $Fe(CO)_4PF_2OPF_2Fe(CO)_4$. A more convenient preparation of this material involved the use of $AgMnO_4$ instead of the metal oxides. The $^{31}P$ and $^{19}F$ nmr parameters for the complex were obtained by analysis of the spectra as a AA′XX′-X″X‴ spin system.

13983. Cohen, G. G., Alexandropoulos, N. G., Kuriyama, M., **Relation between x-ray-Raman and soft-x-ray-absorption spectra**, *Phys. Rev. B* **8**, No. 12, 5427-5431 (Dec. 15, 1973).

Key words: energy transfer; lithium; momentum transfer; x-ray absorption; x-ray inelastic scattering.

A spectrum of x-ray inelastic scattering of copper $K\alpha_1K\alpha_2$ radiation scattered by metallic lithium through $2\theta = 115°$ was obtained. (These conditions correspond to a momentum transfer $k = 6.87 \times 10^{10}\ \mathrm{m}^{-1}$.) The spectrum is compared quantitatively to an experimental soft-x-ray-absorption spectrum of lithium. This comparison serves as an experimental verification of the relation between x-ray-Raman spectra and soft-x-ray-absorption spectra. The method renders possible the study of solid-state effects via x-ray Compton-Raman experiments without *ad hoc* assumptions concerning the wave functions of the inner electrons. Also presented is some evidence of the failure of a random-phase approximation and the impulse approximation in the region under investigation.

13984. Mount, G. H., Linsky, J. L., Shine, R. A., **One- and multi-component models of the upper photosphere based on molecular spectra. I: The violet system of CN (0,0)**, *Solar Phys.* **32**, No. 1, 13-30 (Sept. 1973).

Key words: best-fit model; carbon abundance; molecular spectra; upper photosphere.

Spectroheliograms taken in the CN(0,0) violet band near λ3883 Å show very small scale network and cell structures with high contrast. The bandhead itself, which is a broad feature due to overlap of several CN lines, allows the diagnostic simplicity of a continuum since motions, magnetic fields, and broadening mechanisms are unimportant. We have obtained spectroheliograms in the bandhead and center-to-limb photoelectric spectra of CN(0,0) at Kitt Peak National Observatory. From the photoelectric spectra and a detailed analysis of the formation of the CN(0,0) spectrum we derive a best-fit one-component upper photospheric model differing from that of the HSRA and recommend a change in solar carbon abundance from the HSRA value of log $A_c=8.55$ to log $A_c=8.25$. From the calibrated spectroheliograms we consider a multi-component model to account for the observed fine structure intensity variations.

**13985.** Hellwig, H., Jarvis, S., Jr., Halford, D., Bell, H. E., **Evaluation and operation of atomic beam tube frequency standards using time domain velocity selection modulation,** *Metrologia* **9,** No. 3, 107-112 (1973).

Key words: atomic beams; cavity phase shift; cesium beam; frequency accuracy; frequency standard; pulsed excitation; second-order Doppler shift; velocity distribution.

Pulsed excitation of atomic and molecular beam devices with separated Ramsey-type interaction regions allows the observation of signals due to very narrow atomic velocity groups. The theoretical background of this method is discussed. Experimental operation of a near mono-velocity cesium beam tube is demonstrated. The velocity distribution of a commercial cesium beam tube is obtained using the pulse method. The normal Ramsey pattern of this beam tube is calculated from the velocity distribution and compared with the measured Ramsey pattern. The pulse method allows the direct determination of the cavity phase shift and of the second-order Doppler correction in beam devices. The pulse method thus shows promise for the evaluation of existing laboratory as well as commercial cesium beam tubes with respect to these effects.

**13986.** Haber, S., **Numerical evaluation of multiple integrals,** *SIAM Rev.* **12,** No. 4, 481-526 (Oct. 1970).

Key words: best integration formulas; diophantine approximation; Gaussian quadrature; integration; Monte Carlo; multiple integration; multiple quadrature; numerical analysis; numerical integration; optimal formulas; quadrature.

This paper is an expository survey of the main methods that have been developed for numerical evaluation of multiple integrals. Among the approaches discussed are: the Monte Carlo method and its generalizations; number-theoretical methods, based essentially on the ideas of diophantine approximation and equidistribution modulo 1; the functional analysis approach, in which the quadrature error is regarded as a linear functional and one attempts to minimize its norm; and the classical approach of designing formulas to be exact for polynomials of high degree while using as few values of the integrand as possible. Most of the research in this field is quite recent.

**13987.** Ledbetter, H. M., Naimon, E. R., **Relationship between single-crystal and polycrystal elastic constants,** *J. Appl. Phys.* **45,** No. 1, 66-69 (Jan. 1974).

Key words: Debye temperature; elastic constants; lattice-vibrational properties; polycrystal; single crystal; Voigt-Reuss-Hill.

A new method is given for computing effective polycrystalline elastic constants from single-crystal elastic coefficients. Agreement with observation is good. The method is based on the assumed equivalence of the lattice-vibrational properties of single crystals and polycrystals of the same material; single-crystal and polycrystal Debye temperatures are equated. Present predictions of polycrystal elastic moduli differ significantly from those of most other averaging methods by being lower than the familiar Voigt-Reuss-Hill results.

**13988.** Hellwig, H., Bell, H. E., **Some experimental results with an atomic hydrogen storage beam frequency standard,** *Metrologi*
**8,** 96-98 (1972).

Key words: atomic hydrogen beam; dispersion; frequenc
stability; frequency standard; hydrogen maser.

A frequency standard is described in which a quartz cryst
oscillator is locked to the hydrogen hyperfine transition using th
dispersion of this resonance. The hydrogen storage beam a
paratus closely resembles a hydrogen maser with a low-$Q$ cavit
below oscillation threshold. Cavity pulling can bé reduced to
point where environmental temperature fluctuations limit th
stability mainly via the second-order Doppler effect. Locking
the dispersion feature of the resonance eliminates the need f
frequency modulation in order to find line-center. The stabili
of the frequency standard was measured against crystal oscill
tors and cesium beam frequency standards; stabilities of 4
$10^{-13}$ were recorded for sampling times of 30 seconds and of
hours.

**13989.** Allan, D. W., Glaze, D. J., Machlan, H. E., Wainwrigh
A. E., Hellwig, H., Barnes, J. A., Gray, J. E., **Performanc
modeling, and simulation of some cesium beam clocks,** *Pro
27th Annual Symp, on Frequency Control, Cherry Hill, N.
June 12-14, 1973*, pp. 334-346 (Electronic Industries Associ
tion, Washington, D.C. 1973).

Key words: atomic clock; atomic clock modeling; atom
clock noise; atomic clock performance; atomic time sca
accuracy; comparison of atomic time scales; comparison
frequency standards; frequency calibration; frequency dri
simulation of clock performance.

With the availability of a new primary frequency standar
NBS-5 at the National Bureau of Standards, we have been ab
to evaluate with greater confidence than in the past the pe
formance characteristics of the commercial cesium beam cloc
used in the AT(NBS) atomic time scale. Two other techniqu
have also been employed to evaluate a clock's performance, vi
interclock comparisons and comparisons with other nation
laboratories.

Utilizing the above performance data we have construct
models for the behavior of cesium beam atomic clocks. Based
these models and appropriate optimization procedures,
gorithms have been developed to generate an atomic time sca
AT(NBS), from the ensemble of standards available to us. T
model is shown to well fit both individual clocks as well as clo
ensembles. This modeling provides a direct opportunity for clo
data simulation. Simulation techniques are developed and a
plied in the testing of some diagnostic tests for frequency and/
time steps. The results are very encouraging as a new effort f
even better clock modeling.

Rate calibrations of AT(NBS), UTC(NBS), TAI, and oth
national time scales are given with reference to NBS-5, and the
are compared with other past primary cesium beam frequen
standards. TAI was measured as too high in rate by 12 ± 5 pa
in $10^{13}$.

**13990.** Glaze, D. J., Hellwig, H., Jarvis, S., Jr., Wainwright,
E., Allan, D. W., **Recent progress on the NBS primary freque
cy standard,** *Proc. 27th Annual Symp. on Frequency Contr
Philadelphia, Pa., June 12-14, 1973*, pp. 347-356 (Electro
Industries Association, Washington, D.C., 1973).

Key words: cesium beam standard; Doppler effect; freque
cy accuracy; frequency stability; power shift; prima
frequency standard.

The design of NBS-5 is discussed in detail including its re
tion to previous NBS primary cesium beam frequency standar
The application of pulsed microwave excitation, and the use
the accuracy evaluation of frequency shifts due to kno
changes in the exciting microwave power are discussed. Sign

cant changes in the measured atomic velocity distribution with the beam alignment are reported and compared with measured Ramsey patterns. Stabilities of $3 \times 10^{-14}$ for one-day averaging are reported and data on accuracy are given. Preliminary results give an evaluated accuracy of $2 \times 10^{-13}$ with indications that this figure may be improved in the future.

The bias-corrected frequency of NBS-5 agrees to within $1 \times 10^{-13}$ with the value obtained with NBS-III in 1969 which is preserved in the rate of the NBS Atomic Time Scale.

**13991.** Hellwig, H., Jarvis, S., Jr., Glaze, D. J., Halford, D., Bell, H. E., **Time domain velocity selection modulation as a tool to evaluate cesium beam tubes,** *Proc. 27th Annual Symp. on Frequency Control, Philadelphia, Pa., June 12-14, 1973,* pp. 357-366 (Electronic Industries Association, Washington, D.C., 1973).

Key words: atomic beams; cavity phase shift; cesium beam; frequency standard; pulsed excitation; second-order Doppler shift; velocity distribution.

Pulsed excitation of atomic and molecular beam devices with separated Ramsey-type interaction regions allows the observation of signals due to very narrow atomic velocity groups. The theoretical background of this method is discussed. Experimental operation of a near mono-velocity cesium beam tube is demonstrated. The velocity distribution of a commercial cesium beam tube and of the primary laboratory standard NBS-5 are obtained using the pulse method. The normal Ramsey patterns are calculated from the velocity distribution and compared with the measured Ramsey patterns. The pulse method allows the direct determination of the cavity phase shift and of the second-order Doppler correction in beam devices. Velocity distributions obtained via the pulse method allow the use of microwave power shift results for accuracy evaluations. These aspects as well as the effects of modulation and different velocity distributions are discussed in detail. The pulse method thus shows promise for the evaluation of existing laboratory as well as commercial cesium beam tubes with respect to these effects.

**13992.** Simmonds, M. B., **Using the semiconductor junction in quantum interference devices,** *J. Appl. Phys.* **45,** No. 1, 366-368 (Jan. 1974).

Key words: Josephson junctions; quantum interference; SQUID.

We have fabricated small-area tunnel junctions of a lead-tellurium-lead structure. These have been used in conjunction with bulk superconductors to make hybrid interference devices. We have successfully operated these devices at bias frequencies of 30 MHz, 300 MHz, and 10 GHz.

**13993.** Lyon, G., **Syntax-directed least-errors analysis for context-free languages: A practical approach,** *Commun. ACM* **17,** No. 1, 3-14 (Jan. 1974).

Key words: arbitrary input strings; context-free grammars; dynamic programming; parsing.

A least-errors recognizer is developed informally using the well-known recognizer of Earley, along with elements of Bellman's dynamic programming. The analyzer takes a general class of context-free grammars as drivers, and any finite string as input. Recognition consists of a least-errors count for a corrected version of the input relative to the driver grammar. The algorithm design emphasizes practical aspects which help in programming it.

**13994.** Johnson, C. R., **Gersgorin sets and the field of values,** *J. Math. Anal. Appl.* **45,** No. 2, 416-419 (Feb. 1974).

Key words: D-stable matrix; diagonal; doubly stochastic matrix; field of values; Gersgorin circles; numerical radius; positive definite; spectrum.

Two links are drawn between two well-known inclusion sets for the characteristic roots of a complex matrix: the field of values and the Gersgorin circles. An application is made to the theory of D-stable matrices.

**13995.** Halford, D., **Infrared-microwave frequency synthesis design: Some relevant conceptual noise aspects,** (Proc. Frequency Standards and Metrology Seminar, Quebec, Canada, Aug. 30-Sept. 1, 1971), Paper in *Proceedings of the Frequency Standards and Metrology Seminar,* pp. 431-466 (Quantum Electronics Laboratory, Laval University, Quebec, Canada, 1972).

Key words: Allan variance; base units; fast linewidth; frequency multiplication; infrared frequency metrology; Josephson effect; linewidth; methane frequency standard; phase noise; unified standard.

Extremely accurate and precise frequency synthesis into the infrared and visible radiation regions will allow new vistas of metrology. Frequency and time measurements are the basic operations which will be affected, and impact is expected in such diverse areas as length standards and metrology, spectroscopy, timekeeping, communications, and relativistic tests. In addition the set of independent base units of measurement may change, and the speed of light may become a conventional (defined) quantity. The attainment of the desired high accuracy and precision will be easiest and cheapest if there is careful optimization of the synthesis design aspects involving noise. When frequencies in the terahertz region are considered, the linewidth of the signal becomes an important parameter. Due to the low-frequency-divergence of the instability of good signal sources, the concept of the *fast linewidth* becomes of particular importance. Some of the properties and importance of the *fast linewidth* in system design are discussed in this paper.

**13996.** Merris, R., Newman, M., **An explicit isomorphism with applications to inequalities for matrix functions,** *J. Algebra* **25,** No. 3, 468-474 (June 1973).

Key words: central idempotents; group algebras; irreducible representations; matrix functions.

Inequalities for matrix functions are derived in a uniform way for an explicit isomorphism.

**13997.** Beehler, R. E., **Recent progress on atomic frequency standards,** (Proc. 1972 Precision Electromagnetic Measurement Conf., Boulder, Colo., June 26-29, 1972), Paper in *CPEM Digest,* pp. 166-167 (IEEE, Inc., New York, N.Y., June 1972).

Key words: atomic frequency standards; cesium beam standards; hydrogen masers; rubidium standards.

A brief summary is presented of a paper reviewing progress achieved in the development of atomic frequency standards during recent years. Particular emphasis is placed on cesium, rubidium, and hydrogen maser standards.

**13998.** Allan, D. W., Gray, J. E., Machlan, H. E., **The National Bureau of Standards atomic time scales: Generation, dissemination, stability, and accuracy,** *IEEE Trans. Instrum. Meas.* **IM-21,** No. 4, 388-391 (Nov. 1972).

Key words: AT(NBS); clock dispersion; clock ensemble; frequency and time standards; International Atomic Time; Loran-C; model of clock stability; optimum time prediction; precision and accuracy of timing; time coordination, synchronization, and dissemination; UTC(NBS).

The independent atomic time scale at the National Bureau of Standards AT(NBS), is based upon an ensemble of continuously operating cesium clocks calibrated occasionally by an NBS primary frequency standard. The data of frequency calibrations and interclock comparisons are statistically processed to provide nearly optimum time stability and frequency accuracy. The long-term random fluctuation of AT(NBS) due to nondeterministic perturbations is estimated to be a few parts in $10^{14}$, and the present accuracy is inferred to be 1 part in $10^{12}$.

A small coordinate rate is added to the rate of AT(NBS) to generate UTC(NBS): this small addition is for the purpose of maintaining synchronization within a few microseconds of other international timing centers. UTC(NBS) is readily operationally available over a large part of the world via WWV, WWVH, WWVB, and telephone; also via some passive time transfer systems, e.g., Loran-C and the TV line-10 system; and also experimentally via satellite and WWVL. The precision and accuracy of these dissemination systems will be discussed.

**13999.** Risley, A. S., **The Josephson junction as applied to the measurement of the frequencies of several laser lines,** (Proc. Frequency Standards and Metrology Seminar, Quebec, Canada, Aug. 30-Sept. 1, 1971), Paper in *Proceedings of the Frequency Standards and Metrology Seminar,* pp. 325-328 (Quantum Electronics Laboratory, Laval University, Quebec, Canada, 1972).

Key words: harmonic generation; Josephson junction; laser frequencies; methane; microwave frequency stability.

The Josephson junction has been applied to the measurement of laser frequencies as high as 3.8 THz by direct multiplication from an x-band source. An attempt is being made to extend this technique to frequencies as high as 10.7 THz.

**14000.** Allan, D. W., **Statistical modeling and filtering for optimum atomic time scale generation,** (Proc. Frequency Standards and Metrology Seminar, Quebec, Canada, Aug. 30-Sept. 1, 1971), Paper in *Proceedings of the Frequency Standards and Metrology Seminar,* pp. 388-410 (Quantum Electronics Laboratory, Laval University, Quebec, Canada, 1972).

Key words: clock stability model; frequency calibration; frequency stability; international time scale; time scale accuracy; time scale stability.

Statistical models for the fractional frequency fluctuations in atomic clocks, clock ensembles, and some of the propagation media are developed. Using these models, near optimum time prediction algorithms are employed to generate time for a clock ensemble or for a set of laboratories' time scales. An example using data from the BIH Circular D bulletin is illustrated and the results compared with IAT.

Accuracy and uniformity problems are considered in light of the CCDS June 1970 recommendations. A model for an evaluable primary frequency standard is developed as well as for a time scale (flywheel frequency standard). It is shown that under certain conditions the accuracy of a time scale can be better than the accuracy of the primary standard for the current calibration, if there is a sufficient number of independent past calibrations. A method of simultaneously achieving accuracy and uniformity is discussed.

**14001.** Naimon, E. R., **Elastic constants of the perovskite $RbMnF_3$ using a Born model,** *Phys. Rev. B* **9,** No. 2, 737-740 (Jan. 15, 1974).

Key words: Born-Mayer repulsion; Born model; elastic constants; electrostatic interactions; perovskite; $RbMnF_3$.

The elastic constants of $RbMnF_3$ were calculated using a Born model, which consists of electrostatic and Born-Mayer repulsive interactions. This model has two adjustable parameters; these were determined from the equilibrium volume and one of the three second-order elastic constants. Calculated third-order elastic constants agreed reasonably well with experiment. Als calculated were the electrostatic contributions to the first-second-, and third-order elastic constants of the cubic perovskit structure for several values of ionic charge. Relationships o these constants to those of the NaCl- and CsCl-type structure are given.

**14002.** Costrell, L., **Highways for CAMAC systems—a brief in troduction,** *IEEE Trans. Nucl. Sci.* **NS-21,** No. 1, 870-87 (Feb. 1974).

Key words: CAMAC; computer interfacing; contr systems; instrumentation; instrumentation standards nuclear instrumentation; standards.

The interconnection between CAMAC crates and betwee the crates and a computer is called the CAMAC highway. Th purpose of this paper is to present a brief summary of CAMA highway configurations to put in perspective the highway paper that follow and to serve as a starting point for the panel discus sion on CAMAC highways.

**14003.** Diamond, J. J., Weissler, P. G., **Hearing protectors for us on firing ranges,** *NILECJ-STD-0102.00,* 11 pages (U.S. De partment of Justice, Law Enforcement Assistance Administra tion, National Institute of Law Enforcement and Crimin Justice, Washington, D.C., Mar. 1973).

Key words: earmuffs; earplugs; firing range noise; gunfir noise; hearing protectors.

This standard establishes performance requirements an methods of test for wearable devices used to protect the auditor system against the gunfire noise on firing ranges. The te method described measures hearing protection b psychoacoustic tests on human subjects, that is, the real-ear pr tection at threshold of audibility. It is based on ANSI Standar Z24.22-1957.

**14004.** Andrews, J. R., **Inexpensive laser diode pulse generator fo optical waveguide studies,** *Rev. Sci. Instrum.* **45,** No. 1, 22-2 (Jan. 1974).

Key words: fiber optics; GaAs; impulse; laser; optic picosecond; pulse; waveguide.

An inexpensive GaAs laser diode pulse generator i presented. This generator has found application in the evaluatio of optical pulse dispersion in glass fiber optical waveguide stu dies. It is capable of producing optical impulses as narrow as 11 psec at a wavelength of 0.9 $\mu$ and a pulse repetition rate of 5 kHz. With a slight modification, it may be used to produce opt cal pulses of considerably longer duration at reduced repetitio rates.

**14005.** Diamond, J. J., Calvano, N. J., **Ballistic resistance of poli body armor,** *NILECJ-STD-0101.00,* 10 pages (U.S. Depar ment of Justice, Law Enforcement Assistance Administratio National Institute of Law Enforcement and Criminal Justic Washington, D.C., Mar. 1972).

Key words: armor (wearable); ballistic deformation; ba listic penetration; body armor; bullet proof vests.

This standard establishes performance requirements for ba listic penetration, and methods of test for ballistic penetratic and deformation of police body armor intended to protect th torso against small arms gunfire. Standards are established f armors intended to provide three levels of protection: Armo protective against .30-06 armor piercing rifle fire, armors prote tive against .357 magnum revolver fire, and armors protecti against .22 long rifle high velocity rifle fire.

**14006.** Roberts, R. W., **Energy research: Scientists seek to ease t pinch,** *The Futurist* **VIII,** No. 1, 19-22 (Feb. 1974).

Key words: buildings; conservation, energy.

In this period of energy shortage, intensive research and velopment efforts are required for the development of viable ternatives to traditional energy sources. During the inevitable g time between energy need and new supply, conservation easures can do much to reduce the energy gap. This is espe- ally true in buildings, where vast amounts of energy are cur- ntly wasted. Various NBS programs bearing on the design and eration of more energy efficient buildings are summarized.

4007. Brown, R. L., **Effects of N-atom concentration, pressure, and carrier composition on some first positive band intensities in the yellow nitrogen afterglow,** *J. Chem. Phys.* **52,** No. 9, 4604-4617 (May 1, 1970).

Key words: energy transfer; first positive $N_2$ bands; Lewis-Rayleigh afterglow; nitrogen afterglow; nitrogen atoms; vibrational relaxation electronic quenching.

Absolute intensities of seven $N_2$ 1st positive bands with $\nu' = 6$-2 were measured as a function of carrier pressure, carrier com- osition, and N-atom concentration in the range 4.5-0.06 torr. or an Ar carrier large pressure-dependent shifts in the $B\ ^3\Pi_g$ ibrational distribution to higher levels were observed below 4 orr; similar but much smaller shifts were also found for $N_2$ and le carriers. With Ar, reducing the N-atom concentration shifted e vibrational distribution to lower levels. Changes in carrier omposition produced large pressure dependent changes in the osolute and relative band intensities. An attempt was made to t the results to a model involving vibrational relaxation and lectronic quenching in $B\ ^3\Pi$. While qualitatively successful, this odel could not account quantitatively for the observed relative tensity changes over the whole pressure range for which data re available and, in addition, implied physically unreasonable ibrational relaxation rates. It is suggested that the observed hanges in the $B\ ^3\Pi_g$ vibrational distribution below 4 torr may rise from vibrational relaxation in some precursor state.

4008. Scavennec, A., Nahman, N. S., **A simple passively mode-locked CW dye laser,** *IEEE J. Quantum Electron.* **QE-10,** No. 1, 95-96 (Jan. 1974).

Key words: DODCI; dye laser; laser; mode-lock; picosecond; rhodamine 6 G.

The operation of a simple passively mode-locked 5800-Å dye aser is reported. A single active medium, solution of rhodamine G and diethyloxadicarbocyanine iodide (DODCI) in glycol lowing as an unconfined liquid film, is used for the simultaneous roduction of gain and nonlinear absorption.

4009. Aminadav, N., Selig, H., Abramowitz, S., **Raman spectrum of $F_3NO$ gas,** *J. Chem. Phys.* **60,** No. 1, 325-326 (Jan. 1, 1974).

Key words: gas; $ONF_3$; Raman spectroscopy; thermodynamic properties; vibrational analysis.

The Raman spectrum of gaseous $F_3NO$ has been observed al- owing a definite vibrational assignment. The thermal functions ave been computed using this assignment and previous microwave and electron diffraction data.

4010. Brennen, W., Brown, R. L., **Measurements on the nitrogen atom and pressure dependences of the visible nitrogen afterglow intensity in a nitrogen carrier using EPR,** *J. Chem. Phys. Letters to Editor* **52,** No. 9, 4910-4911 (May 1, 1970).

Key words: atom recombination; energy transfer; Lewis-Rayleigh afterglow; N-atoms; $N_2$ first positive bands; nitrogen afterglow.

The relative visible nitrogen afterglow intensity in a $N_2$ carrier was measured as a function of pressure and N-atom concentra- ion using EPR detection over a range 0.12 to 75 torr. The specific intensity $I/[N]^2$ was found to be independent of pressure and [N], within the experimental uncertainty.

14011. Kaufman, V., Artru, M-C., Brillet, W-U L., **Revised analysis of the $2p^53s$, $3p$, $3d$, and $4s$ configurations of triply ionized aluminum (Al IV),** *J. Opt. Soc. Amer.* **64,** No. 2, 197-201 (Feb. 1974).

Key words: aluminum; energy levels; spectra; ultraviolet; wavelengths.

The spectrum of triply ionized aluminum (Al IV) was observed between 700 and 2200 Å. About 60 new lines have been identified as transitions between the $2p^53s$, $3p$, $3d$, and $4s$ configurations. The ground-state combinations have been remeasured (124-161 Å). Energies and designations are given for all levels of these configurations, and several changes and additions to the previous analysis have been made. Results of calculations of these configurations are included to support the level identifications. An isoelectronic comparison is discussed.

14012. McDaniel, C. L., **Phase relations in the systems $Na_2O$-$IrO_2$ and $Na_2O$-$PtO_2$ in air,** *J. Solid State Chem.* **9,** 139-146 (1974).

Key words: compounds; dissociation; $Na_2O$-$IrO_2$ system; $Na_2O$-$PtO_2$ system; phase relations.

The equilibrium phase relations for the $Na_2O$-$IrO_2$ and $Na_2O$-$PtO_2$ systems were determined in air using the quenching technique. The $Na_2O$-$IrO_2$ system contains two stable compounds $Na_2O \cdot IrO_2$ and $2Na_2O \cdot 3IrO_2$, which dissociate at 1235 and 1040 °C, respectively. The $Na_2O$-$PtO_2$ system contains three compounds: $Na_2O \cdot PtO_2$, metastable $2Na_2O \cdot 3PtO_2$, and $Na_xPt_3O_4$ $(0 \leq x \leq 1)$. Their dissociation temperatures are 890, 710, and 810 °C, respectively. Indexed x-ray diffraction powder patterns for $Na_2O \cdot IrO_2$ and $2Na_2O \cdot 3IrO_2$ are given.

14013. Kayser, B., Lipkin, H. J., Meshkov, S., **Tests of higher symmetries,** *Phys. Rev. D* **8,** No. 11, 4193-4198 (Dec. 1, 1973).

Key words: cross sections; reactions; Regge pole; SU(3); symmetry breaking; trajectory.

Model-independent cross-section relations predicted by unbroken SU(3) symmetry, and some predicted by $SU(6)_{W,strong}$, are compared with experiment. The relations are found to be satisfied, apart from deviations which follow, in every case, the pattern and rough size of symmetry breaking expected from Regge-pole exchange. Interestingly, this Regge symmetry breaking diverges with increasing energy. It is argued that this behavior, though contrary to intuition, is reasonable.

14014. Camarda, H. S., ***P*-wave neutron strength-function measurements and the low-energy optical potential,** *Phys. Rev. C* **9,** No. 1, 28-37 (Jan. 1974).

Key words: function; mass number; neutrons; optical potential; *R*-matrix; strength; time-of-flight.

Using the National Bureau of Standards electron linac and underground time-of-flight facility, precise average neutron-transmission measurements have been made in the energy range 1 keV $\leq E \leq$ 600 keV on the elements As, Br, Nb, Rh, Ag, In, Sb, I, La, Ho, Au, and Th. The samples were "thick" in that the *s*-wave self-protection had to be accounted for at low energies. However, the samples were still sufficiently thin that any errors introduced by neglecting *p*-wave self-protection were negligible. The average *R*-matrix theory was employed in the analysis and the $l = 0$ scattering length $R'$ and the *p*-wave strength function $S_1$ were extracted from the data. The behavior of $S_1$ vs mass number $A$ in the region of the $3P$ maximum was found to vary smoothly with no evidence of any splitting of the resonance. Using Moldauer's optical potential, which fits the $l = 0$ data well, the behavior of $S_1$ vs $A$ was calculated. The predicted behavior was found to differ significantly from experiment. In particular, experiment indicates $S_1$ peaks at a lower mass number and that the maximum is stronger than indicated by the calculations. When the constants of the potential were changed in order to reproduce the observed behavior of $S_1$, a significant discrepancy with the $l = 0$ data resulted. The results presented here imply an orbital angular momentum dependence of the low-energy optical potential.

**14015.** Mazur, J., Rubin, R. J., **Average span of self-avoiding walks on the simple cubic lattice,** *J. Chem. Phys. Letters to Editor* **60,** No. 1, 341-342 (Jan. 1, 1974).

Key words: polymer chains; ratio method; self-avoiding walks; span.

In a recent publication, Bellemans concluded that the average span of a self-avoiding walk has a different asymptotic dependence on the number of steps than does the root-mean-square end-to-end distance. In this paper, we reanalyse Bellemans' data and show that there is no basis for his conclusion.

**14016.** Mazur, J., Guttman, C. M., McCrackin, F. L., **Monte Carlo studies of self-interacting polymer chains with excluded volume. II. Shape of a chain,** *Macromolecules* **6,** No. 6, 872-874 (Nov.-Dec. 1973).

Key words: asymmetry of polymer configurations; excluded volume; principal moments; radius of gyration; self-interacting polymer chains.

The principal moments of the squared radius of gyration of polymer chains with excluded volume were computed for chains on the simple cubic and face-centered cubic lattices. The moments were ordered for each configuration by their magnitude, then averaged over a large number of chain configurations and divided by the squared radius of gyration to yield shape factors of the chain. These shape factors were found to be independent of chain length for long chains. The shape factors showed that the instantaneous shape of a polymer chain is very asymmetrical. With increasing interaction energy between the segments of the chains, the chains became less asymmetrical; at the $\Theta$ point the shape factors became equal to those of the random coil as previously calculated by Solc and Stockmayer. The relative variations of the principal moments were also calculated. The largest principal moments were found to have the largest relative variations.

**14017.** Penn, D. R., **An improved Anderson model,** *Phys. Rev. B* **9,** No. 3, 839-843 (Feb. 1, 1974).

Key words: adsorbates on metal surfaces; density of states; impurity wave function; magnetic impurities; phase shift; reformulation of the Anderson model.

The Anderson model has been very successful in the study of (magnetic) impurities in metals and has also proved useful for atoms adsorbed on metal surfaces. The model as originally formulated is phenomenological in that the position and width of the resonant impurity state cannot be calculated within the context of the model even in the absence of correlation effects. Anderson and McMillan and also Kanamori have proposed theories which are more quantitative. We show that the results of both theories follow from very simple assumptions. Moreover, we show that for the case of a free-electron-like metal and a spherical impurity potential both theories will give a correct density of states for the metal plus impurity if the wave function associated with the impurity is chosen properly. This is particularly important for the theory of Kanamori where the use of a non-Hermitian Hamiltonian raises questions about its validity. The best choice for the impurity wave function requires it to be energy dependent, unlike that one which appears in the usual Anderson model. However, it is shown that an energy-independent wave function can be chosen such that the Anderson-McMillan and Kanamori theories will yield a good density of states.

**14018.** Dehl, R. E., **NMR second moment of rotator-pha
polycrystalline $n$-$C_{19}H_{40}$,** *J. Chem. Phys. Letters to Editor* 6
No. 1, 339-340 (Jan. 1, 1974).

Key words: molecular rotation; NMR second moment; nonadecane; paraffin; rotator phase; wideline NMR.

The proton NMR second moment of polycrystalline $n$-$C_{19}H$
in the rotator phase at 25 °C was measured for several spectra
the as-received ("98.5%") and the solution-recrystallized para
fin. The average second moment of the as-received paraff
(0.060 $(\mathrm{mT})^2$) was considerably lower than that of the recrysta
lized paraffin (0.076 $(\mathrm{mT})^2$), indicating the importance of chem
cal purity in obtaining accurate second moments of paraffin
The results for the recrystallized paraffin were significant
lower than Andrew's theoretical prediction (0.088 $(\mathrm{mT})^2$), b
significantly higher than the value predicted by Olf and Peterl
(0.064 $(\mathrm{mT})^2$). Because of these discrepancies, the theoretic
NMR second moment of the "rotator" paraffin was reevaluate
using exact calculations of the most important dipolar contrib
tions and estimates of the smaller terms. The calculated and o
served values were thus found to differ by only 4 percent. T
NMR second moment is consistent with simple rotation or larg
amplitude oscillation of the chains about their long axes.

**14019.** Kessler, K. G., **Absolute measurements of differential cro
sections for electron scattering at intermediate energies (50-5
eV),** *Comments At. Mol. Phys.* **1,** No. 3, 70-72 (Aug.-Se
1969).

Key words: differential cross sections; elastic cross se
tions; electron scattering.

Technological improvements in the design and construction
electron impact spectrometers now make possible more reliab
absolute measurements of elastic and inelastic differential cro
sections for the scattering of electrons by atoms and molecule
Cross sections can now be determined with an imprecision o
percent or less, depending upon the degree to which systema
errors are brought under control.

**14020.** McCrackin, F. L., Mazur, J., Guttman, C. M., **Mon
Carlo studies of self-interacting polymer chains with exclud
volume. I. Squared radii of gyration and mean-square end-t
end distances and their moments,** *Macromolecules* **6,** No.
859-871 (Nov.-Dec. 1973).

Key words: excluded volume; Monte Carlo; polymer so
tion; radii of gyration; theta point.

Random walks that are not allowed to intersect themselv
were generated on the simple cubic and face-centered cubic l
tices and used as a model of a linear polymer chain in dilute sol
tion with excluded volume and attractive energies between cha
elements. The mean-square end-to-end distances and me
squared radii of gyration and their moments were computed f
chain lengths up to 2000 segments and for a wide range of attra
tive energies. The partition functions of the chains were al
computed. The attractive energy required for a given property
the chain to be the same as the given property of a random co
the $\theta$ point, was investigated. The required attractive energy
pended slightly on the particular property chosen for co
parison, so rather than a unique $\theta$ point, a narrow range o
points was found.

**14021.** Shumaker, J. B., **A spectroscopic study of equilibrium
nitrogen arcs,** *J. Quant. Spectrosc. Radiat. Transfer* **14,** 19-
(1974).

Key words: arc plasma; equilibrium; LTE; nitrogen.

Nitrogen arc measurements of the intensity of the 4915 Å
4935 Å NI doublet and of the 3995 Å NII line show that loc
thermodynamic equilibrium cannot be assumed in nitrogen ar
at electron densities below $1 \times 10^{17}$ cm$^{-3}$. Below this point, t

results suggest that gas and electron temperatures differ significantly and that ground states are overpopulated with respect to upper electronically excited states.

**14022.** Geltman, S., Teague, M. R., **Atomic absorption of ultra intense laser radiation,** *J. Phys. B: At. Mol. Phys. Letter to Editor* **7,** No. 1, L22-L27 (1974).

Key words: atoms; free-free absorption; ultra-intense laser radiation.

We derive an expression for the rate of absorption by an atomic system (bound or free) of radiation from an ultra intense laser beam. The absorption characteristics are radically different from those of conventional weak-field absorption theory.

**14023.** Mozer, B., De Graaf, L. A., Le Neindre, B., **Neutron-diffraction studies in liquid $^4$He,** *Phys. Rev. A* **9,** No. 1, 448-459 (Jan. 1974).

Key words: condensate fraction; density and temperature; liquid helium; neutron diffraction; pair correlation and three-atom correlation function; structure factor.

Structure factors of liquid helium have been determined from neutron-diffraction measurements of high statistical accuracy. Diffraction measurements were performed out to momentum transfers of 7 Å$^{-1}$ for three different densities of liquid helium at a constant temperature above the helium λ transition and at a nearly constant temperature below the λ transition for the same three densities. Statistically significant differences in the structure factors are observed as the density is varied at constant temperature and for temperatures above and below the λ transition at constant density. The radial pair-correlation functions have been calculated from the liquid-structure factors. The structure factors or the related radial pair-correlation functions can be used to obtain information about three-atom correlations in liquid helium above and below the λ transition from a construction of their isothermal density derivative. The temperature dependence of the constant-density structure factors or their derived pair-correlation functions can also be used to test a current theoretical estimate of the condensate fraction in liquid helium.

**14024.** Verdier, P. H., **Monte Carlo studies of lattice-model polymer chains. III. Relaxation of Rouse coordinates,** *J. Chem. Phys.* **59,** No. 11, 6119-6127 (Dec. 1, 1973).

Key words: excluded volume; lattice-model polymer chains; Monte Carlo; polymer chain dynamics; relaxation times.

The relaxation of the seven lowest Rouse coordinates for simple lattice models of polymer chains of up to 64 beads, with and without excluded volume, is studied by simulation on a digital computer. The similarity between the relaxation of the lattice-model chains without excluded volume and that of a statistical-bead model, noted in previous studies of end-to-end length, is confirmed and examined in greater detail. The effect of excluded volume in slowing down the relaxation of the Rouse coordinates is examined, and a simple picture is suggested which accounts qualitatively for the results obtained. The nonnormal coordinate nature of the Rouse coordinates for chains with excluded volume is demonstrated by their nonexponential autocorrelation functions. However, the results suggest that for each chain length, there is a unique longest internal relaxation time, corresponding to an internal coordinate closely resembling the lowest Rouse coordinate.

**14025.** Kranbuehl, D. E., Verdier, P. H., Spencer, J. M., **Relaxation of fluctuations in the shape of a random-coil polymer chain,** *J. Chem. Phys. Letter to Editor* **59,** No. 7, 3861-3862 (Oct. 1, 1973).

Key words: lattice-model polymer chains; Monte Carlo; polymer chain dynamics; relaxation times.

The relaxation times of deviations from spherical symmetry of random-coil polymer chains in dilute solution have been investigated by dynamical Monte Carlo studies of lattice-model chains without excluded volume. The deviations are found to persist for times of the order of the longest relaxation times of the internal motions of the chains.

**14026.** Dehl, R. E., **The effect of salts on the nmr spectra of $D_2O$ in collagen fibers,** *Biopolymers* **12,** 2329-2334 (1973).

Key words: collagen; $D_2O$ in collagen; deuterium nmr; $MgCl_2$ in collagen; $MgSO_4$ in collagen; wideline nmr.

The effects of two salts, $MgCl_2$ and $MgSO_4$, on the wide-line nmr spectrum of $D_2O$ in oriented, undenatured collagen fibers have been examined at four different $D_2O$ contents. $MgCl_2$ was found to decrease the nmr doublet splitting, as compared with equal quantities of pure $D_2O$, while the major effect of $MgSO_4$ was to inhibit the adsorption of $D_2O$ without significantly affecting its nmr spectrum. The results, together with a few observations of KCl and LiCl solutions, indicate that even fairly high concentrations of salt have only small effects on the nmr spectrum of $D_2O$ in fibrous collagen. It is considered unlikely that either "two-state" or "structured-water" models can satisfactorily account for the $D_2O$-nmr doublet spectrum or the effects of salts on it, over the entire range of observed $D_2O$ content.

**14027.** Madey, T. E., Yates, J. T., Jr., Erickson, N. E., **ESCA study of fractional monolayer quantities of chemisorbed gases on tungsten,** *Chem. Phys. Lett.* **19,** No. 4, 487-492 (Apr. 15, 1973).

Key words: carbon monoxide; ESCA; monolayer; oxygen; photoyields; sensitivity; tungsten.

X-ray photoelectron spectroscopy (ESCA) has been used in a study of CO and $O_2$ chemisorbed on a polycrystalline tungsten sample. Working under ultrahigh vacuum conditions, the surface was cleaned and then covered with known monolayer and fractional monolayer quantities of adsorbed CO and $O_2$. The O(ls) and C(ls) spectral features were detected, and the influence of an adsorbed layer on the tungsten spectral features was determined. A chemical shift of 3.4 eV in the O(ls) line from chemisorbed CO is related to the different modes of bonding of CO to tungsten. A model calculation of the photoelectron yields expected from an adsorbed monolayer is in good agreement with the experimental results.

**14028.** Halford, D., Shoaf, J. H., Risley, A. S., **Spectral density analysis: Frequency domain specification and measurement of signal stability,** *Proc. 27th Annual Symp. on Frequency Control, Cherry Hill, N.J., June 12-14, 1973,* pp. 421-431 (Electronic Industries Association, Washington, D.C. 10006).

Key words: amplitude fluctuations; cross-spectral density; frequency domain; frequency noise; modulation noise; noise specification and measurement; oscillator noise; phase noise; radio frequency power spectral density; script $\mathscr{L}$(f); script $\mathscr{M}$(f); script $\mathscr{N}$; sidebands; signal stability; spectral density.

Stability in the frequency domain is commonly specified in terms of spectral densities. The spectral density concept is simple, elegant, and very useful, but care must be exercised in its use. There are several different but closely related spectral densities, which are relevant to the specification and measurement of stability of the frequency, phase, period, amplitude, and power of signals. Concise, tutorial descriptions of useful spectral densities are given in this survey. These include the spectral densities of fluctuations of (a) phase, (b) frequency, (c) fractional frequency, (d) amplitude, (e) time interval, (f) angular frequency, and (g) voltage. Also included are the spectral densities of radio frequency power and its two normalized components, Script $\mathscr{L}$(f) and Script $\mathscr{M}$(f), the phase modulation and amplitude modulation portions, respectively. Some of the simple, often-needed relationships among these various spectral densities are given. The use of one-sided spectral densities is recommended. The relationship to two-sided spectral densities is explained. The concepts of cross-spectral densities, spectral densities of time-dependent spectral densities, and smoothed spectral densities are discussed.

**14029.** Thrower, P. A., Nagle, D. C., Horton, W. S., **The anisotropy of pyrolytic graphite,** *J. Appl. Crystallogr.* **6,** Part 5, 347-351 (Oct. 1973).

Key words: magnetic susceptibility; orientation function; perferred orientation; pyrolytic graphite.

Two proposed expressions, $I_1(\phi) = \cos^m \phi$ and $I_2(\phi) = (1 + b^2 \sin^2 \phi)^{-1}$, for the orientation function, $I(\phi)$, of pyrolytic graphites have been shown analytically to give quite different values for the Bacon anisotropy factor (BAF) for oriented materials. BAF values derived from the angle of half-maximum intensity using $I_1(\phi)$ are within 20 percent of numerically calculated values for the BAF range 10-90, whereas values obtained using $I_2(\phi)$ are smaller by as much as a factor of twenty. The effect of sample preparation on such measurements has been found to be negligible. Diamagnetic-susceptibility measurements on the graphites investigated validated the calculated BAF values in that the derived single-crystal susceptibilities were in reasonable agreement with known values. BAF values calculated *via* $I_2(\phi)$ produced unacceptable paramagnetic values parallel to the basal plane. It is suggested that $I_1(\phi)$ be used for rapid BAF determinations; although numerical calculation is preferred, the difficulty of measuring $I(\phi)$ at large $\phi$, for highly oriented materials, may make the full numerical procedure impracticable and this approximate procedure the more desirable.

**14030.** Gebbie, K. B., Steinitz, R., **On spatial variations in the intensity of chromospheric $H_\alpha$,** *Astrophys. J.* **188,** No. 2, 399-406 (Mar. 1, 1974).

Key words: features observed in $H_\alpha$; $H_\alpha$ filtergrams; lateral contrasts in intensity; profile variation mechanism.

We investigate the formation of patterns in $H_\alpha$ spectroheliograms and filtergrams. Introducing a *source-sink-control diagram,* we conclude that the $H_\alpha$ line source function in the quiet solar chromosphere is indirectly controlled by the photospheric radiation fields in the Balmer and Paschen continua. We demonstrate that in producing the observed patterns, horizontal spatial variations in the shape of the absorption profile are extremely effective compared to changes in the source and sink terms. Applying this mechanism, we compute asymptotic values for the contrasts and visibilities in chromospheric $H_\alpha$.

**14031.** Moos, H. W., Linsky, J. L., Henry, R. C., McClintock, W., **High-spectral-resolution measurements of the H I λ 1216 and Mg II λ 2800 emissions from arcturus,** *Astrophys. J.* **188,** No. 3, L93-L95 (Mar. 15, 1974).

Key words: late-type stars; OAO spectroscopic observations; stellar chromospheres; stellar ultraviolet observations.

High-spectral-resolution scans of H I λ 1216 and Mg II λλ 2796, 2803 obtained using the ultraviolet spectrometer aboard the *Copernicus* satellite show broad and very asymmetrical emission profiles. The ratio of the line widths to the solar values is consistent with a law similar to the Wilson-Bappu relation for the calcium K reversal. A fit of the interstellar absorption profile indicates that the average H density toward this nearby star is low, $0.02 - 0.1$ cm$^{-3}$.

**14032.** Frommer, M. A., Messalem, R. M., **Mechanism of membrane formation. VI. Convective flows and large void formation during membrane precipitation,** *I&EC Prod. Res. Develop.* **12,** 328-333 (Dec. 1973).

Key words: convection flows; desalination; interfacial tu bulence; membranes; membrane structures; polyme precipitation; scanning electron micrographs.

The factors governing the formation of voids and large cavitie in a wide variety of membranes made from different polyme cast from different solvents and precipitated in various nonso vents have been studied. It has been shown that the formation large voids in membranes can be eliminated by (1) lowering th tendency of the nonsolvent to penetrate into the casting solutic or (2) increasing the viscosity of the cast solution or creating thick gel layer on top of this cast solution. It is suggested that th formation of large finger-like cavities in membranes originate from convective flows formed within the cast (fluid) polym solution upon its immersion in the bath of nonsolvent for fin precipitation. It is also shown that the driving forces leading the formation of these convective flows are not densi gradients.

**14033.** Johnson, C. R., **A note on matrix solutions to** $A = XY$ $YX$, *Proc. Amer. Math. Soc.* **42,** No. 2, 351-353 (Feb. 1974).

Key words: commutator; eigenvalues; positive definit trace.

It is known that a square matrix $A$ can be written as a comm tator $XY - YX$ if and only if $\mathrm{Tr}(A) = 0$. In this note it is show further that for a fixed $A$ the spectrum of one of the factors m be taken to be arbitrary while the spectrum of the other factor arbitrary as long as the characteristic roots are distinct. T distinctness restriction on one of the factors may not in gene be relaxed.

**14034.** Radziemski, L. J., Jr., Kaufman, V., **Wavelengths, ener levels, and analysis of the second spectrum of chlorine (Cl II),** *Opt. Soc. Amer.* **64,** No. 3, 366-389 (Mar. 1974).

Key words: chlorine; energy levels; spectra; wavelengths.

We have observed the spectrum of singly ionized chlorine ( II) with grating spectrographs from 500 to 11 000 Å using a ri discharge and a pulsed rf-discharge source. The accuracy of t observed wavelengths is about 0.002 Å from 500 to 3000 Å a 0.01 Å from 3000 to 11 000 Å. The number of known ener levels has increased from 140 to 270 and the number of classifi lines from 600 to over 1100. We have found 25 levels of $3p^3\ ng$ $= 5$-$8)$ and 59 levels of $3p^3\ nf (n = 4$-$10)$, including all 20 levels $3p^3\ (^2D)4f$. Combinations with the latter levels gave new inf mation on the singlets in the $3p^3\ 3d$ configuration, which led the rejection of some levels, the establishment of others, a many changed assignments. *Ab initio* energy-level and spectr calculations and least-squares energy-level fits showed large i teractions between the $3s\ 3p^5$, $3s^2\ 3d$, and $3s^2\ 3p^3$ configurations. The ionization limit of $Cl^+$ is $192070 \pm 1$ cm$^{-1}$.

**14035.** Oettinger, F. F., Gladhill, R. L., **Thermal response m surements for semiconductor device die attachment evaluati** *1973 IEDM Tech. Digest,* pp. 47-50 (1973).

Key words: die attachment evaluation; diode die tachment; screen, die attachment; transistor die attachme

This paper discusses an improved technique, based transient thermal response measurements, to nondestructiv evaluate die attachment in semiconductor devices. T technique was confirmed with studies performed on dio bonded to TO-5 headers and transistors bonded to both TC and TO-66 headers with voids intentionally incorporated into t die attachment. The advantages of using the transient therm response technique for screening semiconductor devices poor die attachment are emphasized.

**14036.** Wagner, H. L., **The polymer standard reference materi program at the National Bureau of Standards,** *Adv. Chem.* *ries No.* **125,** pp. 17-24 (1973).

Key words: gel permeation chromatograph calibration; limiting viscosity number; molecular weight; molecular weight distribution; polyethylene standard; polystyrene standard; standard reference materials; standard reference polymers.

The National Bureau of Standards now distributes four llymer Standard Reference Materials designed for use in the libration of instruments employed in polymer characterization. lystyrene is available in narrow (SRM 705) and broad (SRM 6) distributions and polyethylene in high-density linear (SRM 75) and low-density branched (SRM 1476) whole polymer. nese materials are characterized with respect to many but not cessarily all of the following properties: weight and number-erage molecular weight, limiting viscosity number in several lvents, ASTM density, and ASTM melt flow rate. In addition e molecular-weight distribution of the linear polyethylene is ven, making it suitable for the calibration of gel-permeation romatographs at high temperatures.

037. Wachtman, J. B., Jr., **The influence of surface features on the strength of polycrystalline alumina,** (Proc. 1971 Int. Conf. Mechanical Behavior of Materials, Kyoto, Japan, Aug. 13-31, 1971), Chapter in *Mechanical Behavior of Materials* **4,** 432-442 (The Society of Materials Science, Kyoto, Japan, 1972).

Key words: fracture surface energy; machining damage; plastic deformation; polycrystalline alumina; strength; surface features; thermal expansion anisotropy.

Fracture surface energy of polycrystalline alumina measured ith large cracks ranges from 10 to 46 J/m$^2$; the critical surface ergy depends on the size of the fracture nucleus. For single ystals, values depend on the plane of the crack with a minimum 6 J/m$^2$ for (10$\bar{1}$1). On this basis failure results from surface icrocracks only one fourth the average grain diameter. The ermal expansion anisotropy stress acting on this size crack is 5 times the value calculated for an internal crack due to surface oximity. Hardness indentations produce cracks at high loads ut reduce strength only when a greater critical load, which increases with decreasing grain size, is exceeded. This behavior pparently corresponds to a range of safe machining.

038. Horton, W. S., **A relationship between the magnetic susceptibilities of pyrolytic and single crystal graphites,** *Proc. 11th Biennial Conf. on Carbon, Gatlinburg, Tenn., June 4-8, 1973,* Paper EP-2, pp. 2-3 (1973).

Key words: anisotropy; magnetic susceptibility; pyrolytic graphite; single crystal graphite.

Actual magnetic susceptibility data are compared with the elation $\chi_\perp + 2\chi_\parallel = 3\chi_r$ where the first two susceptibilities refer those perpendicular and parallel to the deposition plane, and $_r$ is that for a random mixture of perfect crystals. A parabolic ather than linear relation appears to fit better empirically. An inersection of the straight and curved lines appears to be close to ne measured values of principal magnetic susceptibilities of ood single crystal graphite.

4039. Gravatt, C. C., Jr., **Real time measurement of the size distribution of particulate matter by a light scattering method,** *APCA J.* **23,** No. 12, 1035-1038 (Dec. 1973).

Key words: air pollution; light scattering; particulate matter.

The body of information presented in this paper is directed to hose individuals concerned with the measurement of the size listribution of particulate matter in air. The light scattering intrument described herein is characterized by the fact that it can ccurately size particles almost independently of their index of efraction. The basic concept involves the simultaneous measurement of the intensity of light scattered by a single particle at wo small scattering angles. The ratio of the two intensities is directly related to the size of the particle, and for scattering angles of 5 and 10° the effective range of the instrument is 0.2 to 4 $\mu$m. The air flows through the optical system at such a rate that approximately 25 $\mu$s are required to determine the size of each particle, and concentrations as high as $10^4$ particles/cc can be measured without dilution and without serious coincidence effects. By employing a multichannel analyzer as the data storage and readout device it is possible to detect changes in particulate size distribution within a few seconds. Calibration of the instrument has been performed using polystyrene latex spheres and materials having a wide range of index of refraction and shape including carbon black, iron oxide and spores.

**14040.** McCall, R. C., Nelson, W. R., Wyckoff, J. M., Pruitt, J. S., **Angular distribution of thick target bremsstrahlung,** *Proc. Second Int. Conf. on Accelerator Dosimetry and Experience, SLAC, Stanford, Calif., Nov. 5-7, 1969,* Conference Report No. 691101, pp. 684-691 (1969).

Key words: angular distribution; depth-dose; photon energy; Ta target; thermoluminescent detectors; 30 and 57.4 MeV electrons.

The angular distributions of dose due to 30 and 57.4 MeV electron beams striking a thick Ta target have been measured using small thermoluminescent detectors. Depth-dose curves measured at 5 and 135° have been used to demonstrate the contribution of secondary electrons in free air, at a plexiglas surface and at 9.25 g/cm$^2$ inside the plexiglas. Comparisons are made with calculated angular distributions of the photon energy emitted showing fair agreement.

**14041.** Goldberg, S., Ogburn, F., **Plating standards and specifications,** Chapter 7 in *Electroplating Engineering Handbook (3d Edition),* pp. 258-271 (Van Nostrand Reinhold Co., New York, N.Y., 1972).

Key words: coating thickness; coatings; electrodeposited coatings; electrodeposits; metal coatings; plated coatings; plating specifications; plating standards; specifications.

The electroplated coating specifications of the ISO, the ASTM, and the U.S. Government are discussed in some detail. The requirements of the specifications and the test methods are reviewed and coating thickness requirements are tabulated. A number of the applications for which various types of plated coatings suitable are discussed.

**14042.** Filliben, J. J., **Comments on the paper "Treatment of null responses," by G. L. Meyer and R. L. Johnson,** *Proc. 17th Conf. on the Design of Experiments in Army Research Development and Testing, Washington, D.C., Oct. 27-29, 1971,* ARO-D Report 72-2, pp. 397-402 (Sept. 1972).

Key words: camouflage; design of experiment; null responses; paired comparisons; sign test; statistics.

Comments are given on the paper "Treatment of Null Responses" by G. L. Meyer and R. L. Johnson at the 17th Conference on the Design of Experiments in Army Research Development and Testing. The statistical limitations imposed by small sample sizes are discussed. A change in the design of the experiment is suggested which would reduce or eliminate altogether the number of ties (due to null responses). A modification of the Sign Test is proposed which allows the processing of the data even in the presence of ties.

**14043.** Brauer, G. M., **Adhesives and composites in dentistry—present and future,** *Proc. Symp. Dental Biomaterials-Research Priorities, Des Plaines, Ill., Aug. 1973,* DHEW Publ. No. (NIH) 74-548, pp. 63-99 (Department of Health, Education, and Welfare, Bethesda, Md., 1974).

Key words: adhesion to tooth structure; adhesives; dental composites; dental restorative materials.

Probably no subject matter affects as many facets of dental biomaterials as that of the modification of and adhesion to tissues. The many techniques that are available to gain valuable information of the structure of tooth surfaces and methods to vary their characteristics are reviewed. Materials and procedures have become available that exhibit clinically significant adhesion to enamel. Bonding to collagenous surfaces such as dentin under conditions encountered in the oral cavity appears to be a realizable goal. Composite restoratives possess unusually good esthetics and their overall properties are considerably better than those of unfilled resins. Investigations of reactions at the interfaces and optimization of the ingredients, as well as the rapidly expanding wealth of experience with these materials, should lead to further improvements. For many composite restorations a nonadhesive protective liner is needed. This requirement negates the use of a tooth-composite coupling agent unless this agent protects the pulp from the noxious effects of the composite. Nonetheless, the evidence today suggests that continuing progress will lead to clinically acceptable adhesive restoratives that will substantially improve the quality of dental services.

**14044.** Tsang, W., **Pyrolysis of 2,4-dimethylhexene-1 and the stability of isobutenyl radicals,** *Int. J. Chem. Kinet.* **5,** 929-946 (1973).

Key words: bond strength; combination rate; decomposition; isobutenyl; shock tube; 2,4-dimethylhexene-1.

2,4-Dimethylhexene-1 has been decomposed in single-pulse shock tube experiments. Rate expressions for the initial reactions are

$$k(C_4H_7\text{-}s\text{-}C_4H_9 \rightarrow C_4H_7\cdot(\text{isobutenyl}) + s\text{-}C_4H_9\cdot) = 10^{15.6} \exp(-33{,}200/T)\ \text{sec}^{-1}$$

and

$$k(C_4H_7\text{-}s\text{-}C_4H_8 \rightarrow iC_4H_8 + n\text{-}C_4H_8) = 10^{12.5} \exp(-26{,}900/T)\ \text{sec}^{-1}$$

at 1.5-5 atm and 1050 K. This leads to $\Delta H^\circ_{f300}$ ($CH_2{=}C(CH_3)CH_2$) = 124 kJ/mol, or an allylic resonance energy of 50 kJ/mol. Rate expressions for the decomposition of the appropriate olefins which yield isobutenyl radicals and methyl, ethyl, isopropyl, *n*-propyl, *t*-butyl, and *t*-amyl radicals, respectively, are presented. The rate expression for the decomposition of isobutenyl radical is

$$k(C_4H_7\cdot(\text{isobutenyl}) \rightarrow C_3H_4(\text{allene}) + CH_3\cdot) = 10^{13.3} \exp(-25{,}200/T)\ \text{sec}^{-1}$$

(at the beginning of the fall-off region). For the combination of isobutenyl and methyl radicals, the rate constant at 1020 K is

$$k(C_4H_7\cdot(\text{isobutenyl}) + CH_3\cdot \rightarrow \text{2-methylbutene-1}) = 10^{10.3}\ \text{l./mol sec}$$

Combination of this number and the calculated rate expression for 2-methylbutene-1 decomposition gives $S^{C_4H_7}.\ (1100) = 470$ J/mol K. This yields

$$k(CH_3\cdot + C_3H_4(\text{allene}) \rightarrow C_4H_7\cdot(\text{isobutenyl}) = 10^{8.2} \exp(-2{,}500/T)\ \text{l./mol sec}$$

It is demonstrated that an upper limit for the rate of hydrogen abstraction by isobutenyl from toluene is

$$k(C_4H_7\cdot + \phi CH_3 \rightarrow iC_4H_8 + \phi CH_2\cdot) \leqq 10^{8.3} \exp(-6{,}000/T)\ \text{l./mol sec.}$$

**14045.** Berger, M. J., Seltzer, S. M., Maeda, K., **Some new results on electron transport in the atmosphere,** *J. Atmos. Terrest. Phys.* **36,** 591-617 (1974).

Key words: atmosphere; backscattering; bremsstrahlung; electron; energy deposition; flux spectrum; Monte Ca calculations.

The penetration, diffusion and slowing down of electrons i semi-infinite air medium has been studied by the Monte Ca method. The results are applicable in the atmosphere at altitud up to ~ 300 km. Most of the results pertain to monoenerge electron beams, with energies between 2 keV and 2 MeV, jected into the atmosphere at a height of 300 km, either vertica downwards or with a pitch-angle distribution isotropic over downward hemisphere. Some results were also obtained for va ous initial pitch angles between 0 and 90°. Information has be generated concerning the following topics: (a) the backscatter of electrons from the atmosphere, expressed in terms backscattering coefficients, angular distributions and ene spectra; (b) the altitude dependence of energy deposition by el trons and by secondary bremsstrahlung, for incident elect beams that are monoenergetic or have exponential spectra w e-folding energies between 5 and 200 keV; (c) the evolution electron flux spectra as function of the atmospheric depth, for cident beam energies between 2 and 20 keV.

**14046.** Tsang, W., **Comparisons between experimental and cal lated rate constants for dissociation and combination reacti involving small polyatomic molecules,** *Int. J. Chem. Kinet* 947-963 (1973).

Key words: ammonia; combination; cyanogen; decompo tion kinetics; nitric acid; nitryl chloride; ozone; RRKM.

The experimental results on decomposition and combinat reactions involving $O_3$, $HNO_3$, $NH_3$, $C_2N_2$, and $NO_2Cl$ over tended temperature and pressure ranges are compared with deductions from RRKM calculations. Quantitative fits of data over the entire range are possible only if the exter (overall) rotations are assumed to be involved in the reactio Recommended rate constants for the reactions $O + O_2 + N_2 \rightarrow$ $+ N_2$ and $OH + NO_2 + N_2 \rightarrow HNO_3 + N_2$ are presented.

**14047.** Pummer, W. J., Wall, L. A., **The burning and thermal p perties of some γ-irradiated polymers,** *Proc. 165th Da Meeting of the American Chemical Society—Division of ganic Coatings and Plastic Chemistry, Dallas, Texas, Apr 13, 1973,* **33,** No. 1, 490-498 (1973).

Key words: combustion; DTA; γ-irradiation; L polymers; TGA.

Very little data are available which are concerned directly v the burning characteristics of γ-irradiated polymers. In this port, samples of six commercially available polymers were posed to γ-rays from a cobalt-60 source for 24 and 72 h periods of time. Data was collected and compared between nonirradiated and exposed polymers in the following areas: the limiting oxygen index values, (2) the differential thermal a ysis, (3) thermogravimetric analysis, and (4) temperature pro of the polymers burning at or near their oxygen index val The behavior of the polymers towards γ-rays is dependent u the structure of each polymer. For example, Plexiglas (PMM Celcon (acetal copolymer), and poly-α-methyl-styrene degraded by γ-rays, while polystyrene, polyethylene, and Su A ionomer undergo mainly crosslinking types of reacti although some degradation may also occur in the latter polymers. In turn, the changes that may occur in thermal pro ties of the γ-treated polymers depend upon the severity of radiation damage caused by the γ-rays to the polymers under conditions of exposure. The amount of radiation dam sustained by each polymer would also be expected to affect burning characteristics of each polymer. Thus, Celcon and P iglas, severely degraded by γ-rays, show the largest variation their LOI values. Polystyrene, poly-α-methylstyrene and ionomer, show no changes in their values after γ-irradiation.

yethylene shows a slight rise in the LOI value on longer expo-re times.

48. Yakowitz, H., **X-ray microanalysis in scanning electron microscopy,** *Proc. Annual Scanning Electron Microscopy ymp. sponsored by IITRI, Chicago, Ill., Apr. 7-9, 1974,* pp. 029-1042 (IIT Research Institute, Chicago, Ill., Apr. 1974).

> Key words: analytical accuracy; electron probe microanalysis; elemental mapping; energy dispersive analysis; scanning electron microscopy; specimen preparation.

This tutorial paper touches briefly on a number of aspects of alitative and quantitative x-ray analysis. The way in which ergy dispersive detectors can be used for qualitative and quan-tive analysis is described. Automatic qualitative analysis and ckground subtraction for energy dispersive methods are scribed. Crystal spectrometer systems are considered and mpared with energy dispersive techniques. The question of ntification and analysis of elements of atomic number eleven less is discussed. A great many practical problems can be ved by elemental distribution mapping. Therefore, this chnique is outlined and an example given. A brief compendium the classical theoretical basis for quantitative analysis is given; tograms of results indicate what accuracy can be expected m optimum specimens. Other quantitative analysis methods ch as the hyperbolic approximation are also touched upon. An -line quantitative analysis computer routine is outlined. Spe-l specimen geometries such as thin films, either free standing on a substrate or small spheres, or inclusions require special ndling. Finally, a few comments on specimen preparation are fered.

049. Fathers, D. J., Jakubovics, J. P., Joy, D. C., Newbury, D. E., Yakowitz, H., **A new method of observing magnetic domains by scanning electron microscopy. I. Theory of the image contrast,** *Phys. Status Solidi* **20,** 535-544 (1973).

> Key words: contrast measurement; image contrast; iron-silicon alloy; magnetic domains; nickel; scanning electron microscopy.

A theory is developed to explain the magnetic domain contrast served by scanning electron microscopy using the method re-rted recently. The theory is based on a model which assumes at the contrast is due to the Lorentz deflection of the incident ectrons inside the specimen. Using this model, the depend-ce of the image contrast on various experimental parame-rs was calculated analytically. The model was confirmed by eans of calculations carried out by computer simulation of elec-on trajectories (Monte Carlo techniques). The theory accounts tisfactorily for previous experimental results. A more detailed mparison of the theory with experimental results will be blished in a subsequent paper.

050. Marcus, M., Merris, R., **A relation between the permanen-tal and determinantal adjoints,** *J. Australian Math. Soc.* **XV,** Pt. 3, pp. 270-271 (1973).

> Key words: congruence; doubly stochastic matrix; positive definite hermitian matrix.

Let $A$ be an $n$-square positive definite hermitian matrix and $i|j)$ be the submatrix of $A$ obtained by deleting row $i$ and lumn $j$. Let $P(A)$ be the $n$-square matrix whose $i,j$ entry is per $j|i)$. If $D(A)$ is the classical adjoint of $A$ then $n$(per $A$) $A)-(\det A)\,P(A)$ is positive semidefinite.

051. Kessler, K. G., **Progress in the measurement of atomic transition probabilities and solar abundances,** *Comments At. Mol. Phys.* **11,** No. 5, Part D, 151-155 (Dec. 1970-Jan. 1971).

> Key words: astrophysics; *f*-values; oscillator strengths; transition probabilities.

The exploitation, over the past decade, of new approaches to the measurement of atomic transition probabilities has produced data of greater accuracy than was available before. The value of these new data to astronomy is well illustrated by the recent work on the iron spectrum. Though it is a somewhat atypical example, it serves as an excellent illustration of the great progress in this field and its effect on astrophysics.

14052. Wells, J. S., McDonald, D. G., Risley, A. S., Jarvis, S., Cupp, J. D., **Spectral analysis of a phase locked laser at 891 GHz, an application of Josephson junctions in the far infrared,** *Rev. Phys. Appl.* **9,** 285-292 (Jan. 1974).

> Key words: frequency noise; HCN laser; infrared frequency synthesis; Josephson junction; laser frequency measurements; laser linewidth; laser stabilization; phase locked laser.

We have used a Josephson junction to investigate the spectral purity of an HCN laser which is used in an infrared frequency synthesis chain. To obtain a narrower linewidth from the laser it has been phase locked to a multiplied microwave reference chain. A calculated value for this linewidth was based upon the measured noise spectrum of the microwave source and a theory due to Middleton. One can take advantage of the unique properties of the Josephson junction as a frequency multiplier and mixer for use in measuring this linewidth. The Josephson junction is driven by an x-band signal which is derived from a specially designed cavity stabilized klystron system of high spectral purity. The 92nd harmonic of the x-band signal is generated in the Josephson junction. In addition, the Josephson junction acts as a mixer of the harmonic signals and the 891 GHz output of the HCN laser. The 92nd harmonic beat signal is taken from the Josephson junction, amplified, and sent to a spectrum analyzer for frequency domain analysis. Details of the experiment, results, and relation to predicted linewidths are presented.

14053. Schoenwetter, H. K., **An ultra-stable ac power supply for an absolute volt determination,** *Metrologia* **10,** No. 1, 11-15 (Mar. 1974).

> Key words: absolute volt experiment; feedback control system; power amplifier; power supply oscillator; stable ac supply; voltage monitor.

A 159.2 Hz power supply with 85 VA power output and very stable amplitude was designed and constructed for use in an absolute volt experiment. The rms value of the ac voltage is regulated at the level of a dc reference voltage (based on unsaturated standard cells), using a feedback control circuit. The measured amplitude drift is less than 0.5 ppm/h and is typically less than 1 ppm in 4 h. The measured amplitude temperature coefficient is 0.6 ppm/°C and the distortion is less than 0.02 percent.

14054. Wagner, H. L., Hoeve, C. A. J., **Mark-Houwink relations for linear polyethylene in 1-chloronaphthalene and 1,2,4-trichlorobenzene,** *J. Polymer Sci.* **11,** 1189-1200 (1973).

> Key words: fractionation; limiting viscosity number; linear polyethylene; Mark-Houwink; molecular weight; Stockmayer-Fixman; unperturbed dimensions; viscosity; 1-chloronaphthalene; 1,2,4-trichlorobenzene.

The parameters in the Mark-Houwink relationship, $[\eta]=K'M_v{}^a$, for linear polyethylene in 1-chloronaphthalene and 1,2,4-trichlorobenzene at 130 °C have been estimated. They were found by measuring the limiting viscosity numbers of a series of fractions with molecular weights ranging from less than 10,000 to almost 700,000. The results are for 1-chloronaphthalene, $[\eta]=0.0555\ M_v{}^{0.684}$ (with a standard error of 0.0064 in $K'$ and 0.010 in $a$) and for 1,2,4-trichlorobenzene, $[\eta]=0.0392\ M_v{}^{0.725}$ (with a standard error of 0.00703 in $K'$ and 0.015 in $a$), where $[\eta]$ is expressed in ml/g. The unperturbed end-to-end distance calculated from the viscosity-molecular weight data agrees with the theoretically expected value.

**14055.** Ruff, A. W., **Grain orientation dependence of reactivity in polycrystalline titanium after anodic polarization,** *Met. Trans.* 5, 601-603 (Mar. 1974).

Key words: corrosion; crystallographic orientation; electrochemical polarization; electron channeling; titanium.

Selected area electron channeling patterns were obtained from individual grains down to 10 $\mu$m size in polycrystalline titanium after different anodic polarization treatments in 1 N $H_2SO_4$. The crystallographic orientations of the more resistant and less resistant grains were determined and correlated with their relative reactivity. The results were in agreement with previously reported single crystal studies on titanium.

**14056.** Colwell, J. H., **The heat capacity of cerous magnesium nitrate and some related materials between 0.3 and 4 K,** *J. Low Temp. Phys.* **14,** Nos. 1/2, 53-71 (Jan. 1974).

Key words: cerous magnesium nitrate; heat capacity; magnetic thermometry and adiabatic cooling.

Cerous magnesium nitrate (CMN) is the preeminent electronic paramagnet in use in cryogenic physics for magnetic thermometry and adiabatic cooling. In demagnetization experiments designed to establish the thermodynamic temperature relations for CMN, an inexplicable heat capacity anomaly was found to occur above 20 mK and is shown here to persist to temperatures near 1 K. The anomaly is small but its presence interferes with and may cause errors in the analysis of thermometric data. We have measured the heat capacity of CMN, lanthanum magnesium nitrate (LMN), cerous nitrate hexahydrate, and a saturated aqueous solution of CMN (CMN liquor) in the temperature range 0.3-4 K in an attempt to find the source of the anomaly. The LMN heat capacity shows no anomaly and is used to approximate the lattice heat capacity of CMN. At low temperatures the CMN heat capacity, exclusive of the lattice contribution, is some 2 1/2 times larger than the magnetic heat capacity predicted by other investigations. At high temperatures an exponentially increasing heat capacity due to the first excited electronic level is observed and indicates a splitting which is in accurate agreement with the spectroscopic value. There is evidence that the lattice heat capacity in CMN is about 1 percent smaller than in LMN, which is probably the result of the crystal-field interaction with the electronic states of the cerous ions. The lattice terms and the $T^{-2}$ term of the magnetic heat capacity for cerous nitrate have been determined, the latter being 25 times larger than the predicted $T^{-2}$ term in CMN. The CMN liquor measurements indicate that this sample had probably become a glass on cooling. The lattice heat capacity is considerably larger than could be predicted from the separate components and there is no indication of the exponential term which would be observable if appreciable crystalline CMN were present. These measurements help to define the nature of the anomalous heat capacity and remove from consideration some possible explanations, but they do not reveal the cause of the anomaly.

**14057.** Soulen, R. J., Finnegan, T. F., **A microwave resistive SQUID for noise thermometry,** *Rev. Phys. Appl.* **9,** No. 1, 305-307 (Jan. 1974).

Key words: Josephson junction; superconductivity; temperature.

A SQUID magnetometer has been shown to work at 10 GHz with a significant enhancement of signal-to-noise over 30 MHz devices. This article describes how such enhancement could lead to faster determinations of absolute temperature using a resistive SQUID, i.e., a noise thermometer. A prototype 10 GHz resistive SQUID is described and its performance evaluated. The feasibility of using a 10 GHz system is clearly established.

**14058.** Chandler, H. H., Bowen, R. L., Paffenbarger, G. C., Mu lineaux, A. L., **Clinical evaluation of a tooth-restoratio coupling agent,** *J. Am. Dental Assoc.* **88,** 114-118 (Jan. 1974

Key words: clinical evaluation; clinical research; composit restorations; dental restorations; dentistry; monomer operative dentistry; reinforcements.

The clinical effectiveness of a tooth-restoration coupling age (NPG-GMA) was tested by treatment of 54 Class III and cavity preparations with an acetone solution of this surface-a tive comonomer. Fifty-four additional preparations were treat with acetone alone for comparison. The teeth were restored wi an experimental composite material.

The restorations were observed by three dentists for 3 1 years. The evaluations indicated that the restorations plac over the NPG-GMA coupling agent had significantly better ma gins, and a significantly higher number of the NPG-GMA a sociated restorations were rated better compared to those plac over the acetone control.

**14059.** Unassigned.

**14060.** Hanson, D. W., Hamilton, W. F., Gatterer, L. E., T **NBS frequency and time satellite experiment using ATS-3,** *Pro 3d Precise Time and Time Interval Strategic Planning Me ing, Washington, D.C., Nov. 16-18, 1971,* pp. 155-165 (U. Naval Observatory, Washington, D.C., 1971).

Key words: frequency; satellites; time.

A frequency and time dissemination experiment usi NASA's ATS-3 synchronous satellite is explained. Details frequency, bandwidth, receiving equipment requirements a recovery techniques are given to allow reader to use syste Results and data concerning accuracy and expected performan are included.

**14061.** Sadowski, W. L., Lozier, D. W., **A unified standards proach to algorithm testing,** (Proc. ACM SIGPLAN Symp. Computer Program Test Methods, Chapel Hill, N.C., June 23, 1972), Paper in *Program Test Methods,* Part VIII, 277-290 (1973).

Key words: algorithms; mathematical functions; p formance; standards; testing; validation.

A system of standards is proposed for the testing and vali tion of mathematical function subroutines. The system is bas on a standards chain of the type that has been used successfu in metrology. This chain consists of a primary standard transfer standard, and a working standard. Their main char teristics are described and examples are given to illustrate considerations that determine the writing of each of the abo standards. The validation and testing process with the aid these standards is discussed.

**14062.** Leasure, W. A., Jr., **Performance evaluation of perso noise exposure meters,** *Sound Vib.* **8,** No. 3, 36-40 (Mar. 197

Key words: exposure meters, noise; meters noise exposu noise exposure meters; personal noise exposure meters.

The promulgation of Federal occupational noise expos regulations has resulted in a proliferation of personal noise ex sure meters. A wide variation in performance has been obser among the various instruments; therefore, the user should cautioned to carry out enough evaluation tests to determine t the devices are performing adequately for his purpose.

**14063.** Molino, J. A., **Psychophysical verification of predicted teraural differences in localizing distant sound sources,** *Acoust. Soc. Amer.* **55,** No. 1, 139-147 (Jan. 1974).

Key words: auditory localization; diffraction patter earphone simulation; human audition; interaural ferences; minimum audible angle; psychometric functions; psychophysics; space perception.

ubjects made forced choices to either side of a reference ection (0, 30, 60, and 75°) to locate the image of pure tones sented through earphones. Various combinations of interau- intensity differences (IID's) and interaural time differences D's) were used, including some combinations which do not ur in nature. Psychometric functions confirmed the expected parent azimuth of ITD/IID combinations based on free-field raction theory and microphone measurments. The relative ninance of the intensive and temporal cues was examined at h frequency (500, 1000, and 8000 Hz). The shape of the chometric plane for the bidimensional matrix at the 1000-Hz condition showed possible nonlinearities in the trading rela- n. Data were also collected from the same subjects using the ne signals presented by means of distant loudspeakers in an en field. When the free-field data were compared with the data m ear-phone-simulated sounds, they showed similar angular ities, being approximately the size of those reported in the rature.

**064.** DiMarzio, E. A., **Statistical mechanics of polymers with pplication to a polymer between plates,** (XXIII Int. Congress of Pure and Applied Chemistry, Special Lectures, Boston, Mass., July 26-30, 1971), *J. Pure Appl. Chem.* **8,** 239-263 1971).

Key words: polymer statistics; statistical mechanics of polymers.

It is shown that the customary separation of the classical parti- n function into a translational part and a configurational part invalid for polymers. However, the integration over momen- n coordinates can always be performed resulting in a configu- ion integral with effective potential energies. The problem of olymer molecule near a surface of arbitrary shape is formally ved. The polymer is allowed to experience a spacially varying tential (V(r) per segment). Kakutani's theorem of probabilistic tential theory is easily derived. Using both continuum and lat- e methods explicit formulae are obtained which describe the havior of a polymer molecule constrained to be (1) on one side an infinite plate, or (2) between two parallel plates, or (3) in a dge of arbitrary angle. These results are applied to the oblems of adsorption and adhesion and to the problem of ystallization. It is shown how an understanding of these sub- ts requires prerequisite knowledge of the appropriate lymer-interface problem. The notion of polymer size is not in- riant but rather depends on the process in which the polymer rticipates. If one thrusts a plate towards another plate on hich a polymer molecule resides until a first contact is made en the resulting plate separation defines a polymer size which relevant to the problems of adhesion and crystallization. It is ger than the root-mean-square end-to-end length.

**065.** Fatiadi, A. J., **Electron spin resonance studies of chemical changes of phenylhydrazones and osazones in alkaline solution,** *Adv. Chem. Ser., No. 117, Carbohydrates in Solution,* pp. 88-105 (1973).

Key words: alkaline solution; chemical changes; electron spin resonance; free radical mechanism; nitroxide radical; osazones; phenylhydrazones.

Treatment of a solution of a sugar phenylhydrazone or azone in methyl sulfoxide with potassium *tert*-butoxide and a ace of oxygen at room temperature gives products that have a ree-line electron spin resonance (ESR) spectrum characteristic a nitroxide radical. The apparent fragmentation of the phenyl- drazine moiety under reaction conditions used does not show idence of any paramagnetic species derived from glyoxal s(phenylhydrazone). The latter had been reported to be the oduct of degradation of the sugar phenylhydrazones under more vigorous alkaline treatment. Some inosose phenylhydrazones in alkaline methyl sulfoxide solution produce stable radical-anions in which the phenylhydrazine moiety remains intact. A free radical mechanism is advanced to account for the $\beta$-elimination reactions of the sugar phenylhydrazones under mildly basic conditions.

**14066.** Giarratano, P. J., **Supercritical helium heat transfer,** (Proc. CRYO-72 Conf., Chicago, Ill., Oct. 3-5, 1972), Chapter 4 in *Applications of Cryogenic Technology* **5,** 52-89 (Scholium Int. Inc., Whitestone, N.Y., 1973).

Key words: forced convection; heat transfer; helium; supercritical.

This paper reports part of the National Bureau of Standards Cryogenics Division's program to provide helium heat transfer information to designers of helium cooling systems. An experiment on supercritical helium heat transfer is described, and its results are compared with various standard and modified correlation expressions.

Extensive appendices give tables of helium viscosity, thermal conductivity, and Prandtl numbers from 3 to 300 K.

**14067.** Hall, J. L., **Saturated absorption line shape,** *Proc. Esfahan Symp. on Fundamental and Applied Laser Physics, Esfahan, Iran, Sept. 1971,* pp. 463-477 (1972).

Key words: laser spectrometer; pressure broadening; resonance line shape; saturated absorption.

In this paper we demonstrate optical frequency stability of $\pm 3 \times 10^{-14}$ obtained at 3.39 $\mu$m by use of saturated molecular absorption in methane. Through Frequency Offset Locking this stability can be transferred to other lasers, thus allowing construction of a very powerful laser spectrometer. A resolution of $2 \times 10^9$ FWHM and absolute resettability of $\pm 1/2 \times 10^{-11}$ have been achieved with this spectrometer. We have studied the power- and pressure-broadening of saturation resonances in methane for several different laser spot sizes. Except near zero power and pressure, the line shape is found to be accurately Lorentzian. Based on a saturation model, a 3-parameter formula is presented which accounts for the observed broadening. The residual line width (intercept at zero power and pressure, HWHM) times laser spot radius is found to be 70 kHz mm. The saturation power turns out to be 1 mW. Pressure broadening rates of 10 to 16 kHz (HWHM)/mT are observed.

**14068.** Haller, W., **A single equation relating molecular weight, pore-size, and elution coefficient in the controlled pore glass chromatography of protein-sodium dodecyl sulfate complexes,** *J. Chromatog.* **85,** 129-131 (1973).

Key words: chromatography; controlled pore glass; denaturing solvents; glass; molecular weight; permeation; porous glass; proteins; sodium duodecyl sulfate.

Permeation chromatography elution coefficients of the sodium duodecyl sulfate complexes of thirteen different proteins on controlled pore glass columns were analyzed. A master equation, relating elution coefficient, subunit molecular weight and pore diameter of glass is described. The equation allows estimating the subunit molecular weight of the proteins from elution results on colums of any known pore diameter, without the need for individual column calibration with a series of proteins with known subunit molecular weight.

**14069.** Cuthill, J. R., Dobbyn, R. C., McAlister, A. J., Williams, M. L., **Critical evaluation of soft x-ray emission spectra: Al metal,** *Proc. Int. Symp. X-Ray Spectra and Electronic Structure of Matter, Munchen, Germany, Sept. 18-22, 1972,* **II,** 208-219 (1973).

Key words: aluminum; critical evaluation; emission spectra; metals; soft x ray.

Measurements of the K and L valence band emission spectra of Al metal are critically compared in the light of current theory and experimental practice, and with the results of ultraviolet photoemission. The picture which emerges is one of essential agreement of experiment with one electron band theory. A number of discrepancies are noted within the existing body of data, and ascribed to inconsistencies in experimental practice.

**14070.** McAlister, A. J., Cuthill, J. R., Williams, M. L., Dobbyn, R. C., **Electronic structure of the diborides of the 3d metals,** *Proc. Int. Symp. X-Ray Spectra and Electronic Structure of Matter, Munchen, Germany, Sept. 18-22, 1972,* **II,** 426-448 (1973).

Key words: band structure; borides; density of states; emission spectra; soft x ray; transition metal diborides.

Reported here are the results of two studies of the electronic structure of the isostructural sequence of refractory hard metals $ScB_2$, $TiB_2$, $VB_2$, and $CrB_2$. Experimentally, we have obtained the Boron soft x-ray K-emission spectra of the series and, as in other physical properties, observed a systematic variation with metal atomic number. Computationally, we have carried out a model band calculation which predicts qualitatively both the observed soft x-ray behavior and other observed trends in the properties of these compounds.

**14071.** Mann, D. B., Diller, D. E., Olien, N. A., Hiza, M. J., **Measurements of liquefied natural gas in commerce,** *Proc. American Gas Association Operating Section, El Paso, Texas,* pp. D-206 – D-214 (American Gas Association, Inc., Arlington, Va., 1973).

Key words: cryogenic; density; flow; importation; liquefied natural gas; measurement; methane.

The Cryogenics Division of the NBS Institute for Basic Standards is currently involved in a number of programs dealing with liquefied natural gas (LNG). The objective of these NBS programs is to bring to bear over 20 years of cryogenic experience on certain selected LNG problem areas. A description of the programs will be given in the following sections as well as a summary of progress of this five-year effort.

In addition, the objectives of past, present and projected LNG programs at NBS will be related to one specific LNG problem area, custody transfer, and suggestions will be made about maximum utilization of present and expected research results.

**14072.** Penn, D. R., **Field emission from adsorbate covered surfaces. II,** *Phys. Rev. B* **9,** No. 3, 844-847 (Feb. 1, 1974).

Key words: adsorbate density of states; adsorbate energy level; chemisorb; field emission; surface; total electronic energy distribution.

A previous calculation of the total energy distribution of field-emitted electrons in the presence of chemisorbed atoms by Penn, Gomer, and Cohen (PGC) is reexamined with respect to the following point. PGC assumed that the metal-adsorbate system could be represented by the Anderson model; however, the Anderson model is phenomenological. Anderson and McMillan have shown how the model can be reformulated in a way which makes it more quantitative. Use of the reformulated model leads to a significant change in the PGC result for the field-emission current. We find $\Delta j(\omega)/j_0(\omega)=R^{-1}u'^2\rho_a$, where $\Delta j(\omega)$ is the change in the current at energy $\omega$ due to the presence of the adsorbate and $j_0(\omega)$ is the current in the absence of the adsorbate. $\rho_a$ is the density of states at the adsorbate and $u'^2$ and $R^{-1}$ are given in the text. This result differs from that of PGC by the factor $R=[1+\xi^{3/2}(\pi\alpha)^{-1/2}]^2$, where $\xi=(-2mE_F/\hbar^2)^{1/2}$ and $\alpha=2meF/\hbar^2$. Energies are measured from the vacuum level, $E_F$ is the metal Fermi energy, and $F$ is the strength of the external electric field. For typical experimental conditions $R^{-1}\approx 1/16$.

**14073.** Bennett, L. H., Swartzendruber, L. J., Watson, R. E. **Critical temperatures in Fe-doped copper-rich Cu-Ni alloys** (Proc. 17th AIP Conf. on Magnetism and Magnetic Materials Chicago, Ill., Nov. 15-18, 1971), Chapter in *Magnetism and Magnetic Materials,* C. D. Graham, Jr., and J. J. Rhyne, Eds. No. 5, pp. 1190-1194 (June 1972).

Key words: alloys; copper; critical temperatures; iron; magnetism; Mössbauer effect; nickel.

Systematics of magnetic ordering as a function of Fe and N content have been investigated by use of the Mössbauer effect i Cu-based alloys with up to a few percent Fe and up to 40 percen Ni. The halfwidth of the magnetic transition is ~ 1 K in all th "weak" ferromagnets (i.e., when the critical temperature, $T_c \leq$ 10 K), and is a similar, or smaller, fraction of $T_c$ for the stron ferromagnets. $T_c$ is sharply defined for all compositions, despit the distribution of hyperfine fields and magnetic moments existing in these alloys. For any Ni concentration, $T_c$ increases wit increasing Fe. As a function of Ni, a minimum in $T_c$ occurs nea 30 percent Ni. These results indicate that the long-range conduction electron interaction between Fe atoms in Cu is reduced b Ni addition, with strong short-range interactions becoming mor important for ferromagnetism at higher Ni concentrations.

**14074.** Wachtman, J. B., Jr., **Determination of elastic constan required for application of fracture mechanics to ceramic** (Proc. Symp. on Fracture Mechanics of Ceramics, Universit Park, Pa., July 11-13, 1973), Paper in *Fracture Mechanics Ceramics,* R. C. Brandt, D. P. H. Hasselman, and F. Lange, Eds., **1,** 49-68 (Plenum Publishing Corp., New Yor N.Y. 1974).

Key words: anisotropy; elastic constants; elasticity; fracture; fracture mechanics; Griffith criterion.

Elastic properties enter into fracture mechanics most simp in the case of plane stress in an elastically isotropic body f which $EG_1=\Pi K_1^2$ where $G_1$ is the energy release rate, $K_1$ is t stress intensity factor, and E is Young's modulus. For an elas cally orthotropic body the same result holds provided 1/E replaced by $(s_{11}s_{22}/2)^{1/2}\,[s_{22}/s_{11})^{1/2}+(2s_{12}+s_{66})/2s_{11}]^{1/2}$ where t $s_{ij}$ are the single crystal elastic compliances. These equatio may be used to establish a Griffith type fracture criterion setting $G_1=G_{1C}=2\gamma_f$ where $\gamma_f$ is the fracture surface energ Elastic moduli or compliances can usually be determined mo accurately than either $G_{1C}$ or $\gamma_f$. Methods for their determinati by resonance or by ultrasonic wave propagation are brie described. Values of the elastic factors in the energy relea rates for material in polycrystalline form are compared wi values for materials in single crystal form for various orthotro orientations of cracks to indicate the effectiveness of sin crystal elastic isotropy in causing variation in the fracture con tion. This theory is shown to predict an anisotropic fractu criterion for certain crystal planes.

**14075.** Allan, D. W., Gray, J. E., Machlan, H. E., **The Natio Bureau of Standards atomic time scale: Generation, dissemi tion, precision, and accuracy,** (Proc. Conf. Electromagne Measurement, Boulder, Colo., June 26-29, 1972), *19 CPEM Digest,* p. 165 (1972).

Key words: atomic clock; cesium clock; coordinate tin Flicker noise; frequency standard; time dissemination; ti scale.

The atomic time scale at the National Bureau of Standar AT(NBS), depends upon an ensemble of continuously operat cesium clocks calibrated occasionally by the NBS prim frequency standard. The data of interclock comparisons a frequency calibrations are statistically processed to provide n mum time stability and frequency accuracy. Each clock is esented by a simple mathematical model of its noise spec- n, with parameters determined by the behavior of that clock. se noise parameters are used in a nearly optimum procedure periodically recalibrating the frequency of each clock and for bining the clock readings to produce AT(NBS). The long- n fractional frequency stability of AT(NBS) is shown to be a parts in $10^{14}$, and the accuracy is inferred to be 1 part in $10^{12}$.

small coordinate rate is added to the rate of AT(NBS) to erate UTC(NBS); this small addition is for the purpose of ntaining synchronization within a few microseconds of other rnational timing centers. UTC(NBS) is readily and opera- ally available over a large part of the world via WWV, VH, WWVB, and telephone; also via some time transfer tems, e.g., Loran-C and the TV line-10 system; and also ex- imentally via satellite and WWVL. The precision and accura- of these dissemination systems will be discussed.

76. Hunt, C. M., **Simple observations of some common indoor ctivities as producers of airborne particulates,** (Proc. SHRAE Symp. Cleaner Indoor Air—Progress and roblems, Cincinnati, Ohio, Oct. 19-22, 1972), Chapter in *SHRAE*, pp. 8-14 (American Society of Heating, Refrigerat- ng, and Air-Conditioning Engineers, New York, N.Y., 1973).

> Key words: air cleaning; air pollution; dust generation; indoor pollution; particulates.

Observations were made of some common indoor particle erating and dispersing activities by performing them in a all closed room and measuring the changes in particle count as nction of time using a light scattering particle counter. Two ranges were measured, particles larger than 0.3 $\mu$m in meter, and particles larger than 3 $\mu$m. The activities examined re smoking, heating grease as in frying, operation of a vacuum aner, and use of household aerosol sprays. The particle count a closed room without activity was also observed as well as effect of an oscillating electric fan.

hermal operations such as smoking and the heating of grease duced a much larger number of particles smaller than 3 $\mu$m n the mechanical generating and dispersing activities. The chanical activities, by comparison, tended to produce more ticles larger than 3 $\mu$m. With no activity in the room the parti- count in both size ranges decreased with time, and with the ctric fan or vacuum sweeper operating an increase in particle unt was observed, followed by a decrease qualitatively similar that observed with no activity in the room. The increase in unt by the aerosol sprays appeared to be dominated by effects e to the propellant.

77. Lyerla, J. R., Jr., McIntyre, H. M., Torchia, D. A., **A $^{13}$C uclear magnetic resonance study of alkane motion,** *Macromolecules* **7,** 11-14 (Jan.-Feb. 1974).

> Key words: alkanes; carbon-13; magnetic resonance; molecular motion; polyethylene; rotational potentials; spin-lattice relaxation.

arbon-13 spin-lattice relaxation times ($T_1$) have been mea- ed for resolved carbons in neat *n*-alkanes ($n=7$, 10, 13, 15, 20) and 2-methylnonadecane, and effective correlation times ) have been calculated from the $T_1$ values. A self-consistent alysis of the $\tau_{eff}$ values is provided using a model which con- ers alkane carbon motion in terms of contributions from erall and internal rotations. This analysis yields values for the rriers to methyl rotation in the linear (2.6 kcal/mol) and anched (2.9 kcal/mol) alkanes that are in approximate agree- nt with previously reported values. One also obtains informa- n on the effects of chain ends and branches on internal motion d an estimate of the number of carbons involved in segmental tion of long alkanes.

**14078.** VanderHart, D. L., **Low capacitance electrical feedthrough and simple, reuseable closure seal for hydrostatic pressures to 7 kilobar and temperatures to 200 °C: Application to NMR,** *Rev. Sci. Instrum.* **45,** No. 1, 111-113 (Jan. 1974).

> Key words: closure seal; electrical feedthrough; high pressure; hydrostatic; NMR; temperature.

An electrical feedthrough having a capacitance of 7 pF is described. It consists of a stack of two right circular cylinders, one an insulator, and one a metal with polyimide gaskets appropriately placed. A very simple, reuseable, polymeric closure seal is also described. The seal is patterned after the "C" seal and features easy extraction and sealing on the small bore of the pressure vessel. The closure seal and feedthrough have been tested to 7 kilobar at room temperature and 5 kilobar at 200 °C without failure.

**14079.** Zwanzig, R., Bishop, M., **Tunnel model of liquid diffusion,** *J. Chem. Phys.* **60,** No. 1, 295-296 (Jan. 1974).

> Key words: liquid diffusion; tunnel model; velocity correlation function.

A tunnel model of liquid diffusion, analogous to Barker's thermodynamic model, is constructed by separating particle motion into components parallel and perpendicular to a tunnel axis. By combining exact results for hard rod systems, one is able to predict both the tunnel diffusion coefficient and the corresponding velocity correlation function. The ratio of the tunnel diffusion coefficient to the Enskog value at the same density and temperature is obtained by matching the virial and the temperature. The value predicted lies outside the range investigated by Alder *et al*; therefore direct comparison to molecular dynamics results is not possible. However, the velocity correlation function has the negative region characteristic of dense fluids. It is suggested that the derivation of the tunnel model dynamics may be valid at close packed densities.

**14080.** Beatty, R. W., **2-Port $\lambda_G/4$ waveguide standard of voltage standing-wave ratio,** *Electronics Letters* **9,** No. 2, 24-26 (Jan. 25, 1973).

> Key words: coaxial line; impedance standard; reflection coefficient standard; VSWR standard; waveguide.

A new calculable standard of voltage-reflection coefficient and voltage standing-wave ratio consists of a quarter-guide-wavelength section of waveguide having cross-sectional dimensions different from those of the waveguide system into which it is inserted. Design equations are given for waveguide of rectangular and coaxial cross-sections.

**14081.** Frederikse, H. P. R., Hosler, W. R., **Electrical conductivity of MHD-channel materials,** *Proc. 14th Symp. on Engineering Aspects of Magnetohydrodynamics, Tullahoma, Tenn., Apr. 8-10, 1974,* pp. IV.2.1-IV.2.3 (1974).

> Key words: coal slag; electrical conductivity; high temperature; magnetohydrodynamics; zirconates.

This paper deals with two aspects of MHD-channel materials. The first part reports on the electrical conductivity of mixtures of coal slag and $K_2SO_4$ seed. The second part discusses the problem of finding electronically conducting electrode materials and describes the results of conductivity measurements performed on Ce and Ti doped $SrZrO_3$.

**14082.** Candela, G. A., Forman, R. A., Kahn, A. H., Meadowcroft, D. B., Wimmer, J., **Magnetic susceptibility of lanthanum chromite doped with strontium,** *Proc. 14th Symp. on Engineering Aspects of Magnetohydrodynamics, Tullahoma, Tenn., Apr. 8-10, 1974,* pp. IV.5.1-IV.5.3 (1974).

> Key words: lanthanum chromite; lanthanum strontium chromite; magnetic susceptibility.

The magnetic susceptibility of sintered samples of Sr doped $LaCrO_3$ has been measured over the temperature range of 2 K to 365 K. All the samples were antiferromagnetic at low temperatures. Above 300 K all the doped samples exhibited a lower susceptibility than the pure material. Analysis of these results showed that in the doped samples not all of the chromium is in the $3^+$ oxidation state. These results support the view that Sr doping modifies the valence of the Cr and thereby enhances the electronic conduction.

**14083.** Becker, D. A., LaFleur, P. D., **Characterization of a nuclear reactor for neutron activation analysis,** (Proc. Int. Conf. on Modern Trends in Activation Analysis, Saclay, France, Oct. 1972), *J. Radioanal. Chem.* **19,** 149-157 (1974).

Key words: cadmium ratio; fast neutron flux; neutron activation analysis; sample pressure; thermal neutron flux; threshold foil.

Evaluation of some of the neutron activation analysis irradiation characteristics for the NBS Nuclear Reactor (NBSR) are reported, along with a description of a measurement technique developed. The characteristics discussed here are the thermal (sub-cadmium) neutron flux determination, neutron energy distribution measurements using cadmium ratios and threshold foil detectors, and the determination of excess sample pressures generated during irradiation.

**14084.** Grabner, L. H., Hosler, W. R., Frederikse, H. P. R., **Some optical and electrical properties of undoped and SR-doped $LaCrO_3$,** *Proc. 14th Symp. on Engineering Aspects of Magnetohydrodynamics, Tullahoma, Tenn., Apr. 8-10, 1974,* pp. IV.4.1-IV.4.3 (1974).

Key words: diffuse reflectivity; $LaCrO_3$; photoconductivity; photoexcitation; photoluminescence; transport data.

Transport data and optical data (photoluminescence, photoexcitation, diffuse reflectivity and photoconductivity) are presented for undoped, and Sr and Ca doped $LaCrO_3$. We conclude that $LaCrO_3$ is a wide band-gap semiconductor (~ 7 eV) in which an oxygen deficiency of the complex $Cr^{3+}$ octahedrally coordinated with $60^{=}$ gives rise to a donar with an activation energy of about 0.5 eV. This oxygen deficiency can be induced as a charge compensation mechanism when $LaCrO_3$ is doped with either Sr or Ca.

**14085.** Rook, H. L., Lutz, G. J., LaFleur, P. D., **The use of a high efficiency mass separator in activation analysis,** (Proc. Int. Conf. on Modern Trends in Activation Analysis, Saclay, France, Oct. 1972), *J. Radioanal. Chem.* **15,** 557-565 (1973).

Key words: activation analysis; cadmium; lead; mass separator.

The application of high yield mass separators to problems in activation analysis is discussed. The identification of separation parameters including separator yields, memory, resolution and overlap, and sputtering are considered. The use of the mass separator in determining lead by photon activation analysis is described.

**14086.** Mauer, F. A., Hubbard, C. R., Hahn, T. A., **Anisotropic thermal expansion of $\alpha$-$Pb(N_3)_2$,** *J. Chem. Phys.* **60,** No. 4, 1341-1344 (Feb. 15, 1974).

Key words: lead azide; thermal expansion.

The anisotropic expansion coefficients of orthorhombic $\alpha$-$Pb(N_3)_2$ in the temperature range 102-423 K were determined by a single crystal x-ray method. The cell parameters and rms deviations at 298.2 K are $a=11.33344[17]$, $b=16.28277[37]$, and $c=6.64058[10]$ Å. The linear expansion coefficients change gradually from $\alpha_a=5.7\times10^{-5}$, $\alpha_b=0.3\times10^{-5}$, and $\alpha_c=1.4\times10^{-5}$ $K^{-1}$ at 112, to $\alpha_a=8\times10^{-5}$, $\alpha_b=0.4\times10^{-5}$, and $\alpha_c=2.0\times10^{-5}$ $K^{-1}$ at 412 K. The largest expansion is in the *a* directio which is perpendicular to sheets of azide ions separated by le atoms.

**14087.** Mulholland, G. W., Rehr, J. J., **Coexistence curve prope ties of Mermin's decorated lattice gas,** *J. Chem. Phys.* **60,** N 4, 1297-1306 (Feb. 15, 1974).

Key words: coexistence curve; critical azeotrope; critic double point; decorated lattice gas; maxithermal poi renormalization.

Mermin's decorated lattice gas, noteworthy for its singul coexistence curve diameter and previously studied in connecti with the breakdown of the law of rectilinear diameters, is sho to display in addition a rich variety of coexistence curve shap and kinds of critical behavior as the interaction parameters of t model are varied. For an attractive decoration interaction, t coexistence curve of the model resembles, and can closely a proximate, the liquid-vapor coexistence curve of real fluids. F a sufficiently repulsive decoration interaction, however, t model is shown to possess (at fixed temperature) three tran tions to increasingly dense phases. These coexistence curv may feature peculiar shapes, such as necks and cusps, and th can appear inverted near the critical point; these curves t minate at either a critical point or at a maxithermal point ( analog of an azeotropic point). For discrete values of the intera tion parameters, the model possesses a critical double point (t coalescence of two critical points) or a *cuspoidal* critical po (critical azeotropy), in which cases the critical expone become renormalized. Qualitatively these results are found to independent of lattice structure and spatial dimensionality $d \geqslant$ and representative coexistence curves are plotted for the sim cubic lattice. Possible applications of these results are me tioned.

**14088.** Abrams, M. D., Lindamood, G. E., Pyke, T. N., J **Measuring and modelling man-computer interaction,** *Proc. Annual SIGME Symp. on Measurement and Evaluation, P Alto, Calif., Feb. 26-28, 1973,* pp. 136-142 (Feb. 1973).

Key words: dialogue; interaction; man-computer; measu model; monitor.

The Dialogue Monitor has been developed as a tool for t measurement of computer service. The objectives of such m surement are defined. A set of models and measures developed. Operation of the Dialogue Monitor and analysis the data obtained are briefly discussed.

**14089.** Beatty, R. W., **Methods for automatically measuring n work parameters,** *Microwave J.* **17,** No. 4, 45-49, 63 (A 1974).

Key words: automatic measurements; automatic netwo analyzer; complex reflection coefficients; complex tra mission coefficients; computer controlled measureme systems; computer-operated transmission measuremen envelope delay; group delay; network parameters.

A survey is presented of techniques, from 1934 to the prese time, used in the automatic measurement of network paramete Some of the computer-controlled measurement syste developed in the U.S.A. since 1968 are described. The directi that future developments may take is forecast. Numero references are given.

**14090.** Newell, A. C., Crawford, M. L., **Planar near-field m surements on high performance array antennas,** *Proc. 23d U Air Force Antenna Symp., Urbana, Ill., Oct. 10-12, 197* preprint 66 pages (Wright-Patterson Air Force Base, Dayto Ohio, Oct. 1973).

Key words: antennas; near-field measurements; phased rays.

he results of measurements are described which apply the nar near-field measurement technique to phased array anten- . Fast and efficient tests are used to determine the required n area and data point spacing. The use of these tests can uce the amount of data required for some antennas without ously increasing the errors in computed results.

Measurements were made at different distances from the an- nas, with the probe transmitting and receiving, and for both n and monopulse difference patterns. Comparisons between far-field patterns computed from the near-field data and those asured on far-field ranges are presented.

91. Lyndon, R. C., Newman, M., **Commutators as products of quares,** *Proc. Amer. Math. Soc.* **39,** No. 2, 267-272 (July 1973).

Key words: commutators; products of squares; squares, products.

t is shown that if $G$ is the free group of rank 2 freely generated $x$ and $y$, then $xyx^{-1}y^{-1}$ is never the product of two squares in although it is always the product of three squares in $G$. It is o shown that if $G$ is the free group of rank $n$ freely generated $x_1, x_2, \cdots, x_n$, then $x_1^2x_2^2\cdots x_n^2$ is never the product of fewer n $n$ squares in $G$.

092. Wachtman, J. B., Jr., Schneider, S. J., **Measurements and standards for high temperature materials in energy conversion and clean fuel production,** *Stand. News* **1,** No. 8, 16-23 (Aug. 1973).

Key words: clean fuel; coal; energy; gas; gas turbine; MHD; slag.

The serious energy situation in the United States requires eatly increased use of fossil fuel over the next thirty years spite the projected growth of nuclear power generating capaci- More efficient generation of electric power from coal and ry large production of clean fuel from coal are urgently eded. Both require high temperatures and highly reactive emical conditions.

The severe environments existing in high temperature gas tur- nes, MHD power generators, and coal gasifiers are briefly mmarized. Data and test methods needed for process op- nization, engineering design of hardware, and reliability as- rance are analyzed. Early results are presented on slag charac- rization and on reaction of slag components with refractories. ypical data on viscosity of slag and on electrical conductivity of ag and alumina insulating material are given. A procedure to in- re required lifetime under service stress is described. The im- ications of the present work for practical test methods for echanical lifetime assurance, corrosion resistance, electrical nductivity measurements, viscosity measurements, and wear e assessed.

093. Kusuda, T., **Effectiveness method for predicting the performance of finned tube coils,** *ASHRAE Symp. Bull.*, pp. 5-14 (1970).

Key words: air conditioning; cooling and dehumidifying capacities; effectiveness; finned tube coil; heat transfer; refrigeration.

In 1960 the author proposed using the effectiveness method r predicting the heat and mass transfer performance of chilled ater coils. This method is reviewed and elaborated. Com- arisons of predicted chilled water dehumidifying coil capacities sing this method with observed experimental values given by rof. Trapanese of Italy were made. The comparisons show that e effectiveness method is accurate if the parameters employed the effectiveness equation are properly evaluated.

The effectiveness method also appears to be a powerful concept for predicting the performance of finned tube coils at conditions other than those originally selected for design purposes.

**14094.** Burns, G. W., Hurst, W. S., **Some studies on the behavior of W-RE thermocouple materials at high temperatures,** *NASA CR-72884*, 42 pages (National Aeronautics and Space Administration, Washington, D.C., Feb. 1972). (Available as N 7220401 from the National Technical Information Service, Springfield, Va. 22151).

Key words: beryllium oxide; drift; microstructure; thermal emf-temperature; thermocouples; tungsten-rhenium alloys.

Bare 0.25 mm diameter W-Re alloy thermoelements (W, W-3% Re, W-5% Re and W-25% Re) and BeO-insulated W-3% Re and W-25% Re thermoelements have been examined for metallurgical, chemical and thermal emf changes after testing for periods up to 1000 hours at temperatures principally in the range 2000 to 2400 K. Environments for the tests consisted of high purity argon, hydrogen, helium or nitrogen gases. Commercially obtained bare-wire thermoelements typically exhibited a shift in their emf-temperature relationship upon initial exposure. The shift was completed by thermally aging the W-3% Re thermoelement for 1 hour and the W-25% Re thermoelement for 2 minutes at 2400 K in argon or hydrogen. Aged thermoelements experienced no appreciable drift with subsequent exposure at 2400 K in the gaseous environments. The chemically "doped" W-3% Re thermoelement retained a small-grained structure for exposure in excess of 50 hours at 2400 K. BeO-insulated thermoelement assemblies showed varied behavior that depended upon the method of exposure. However, when the assemblies were heated in a furnace, no serious material incompatibility problems were found if the materials were given prior thermal treatments. Thermocouples, assembled from aged W-3% Re and W-25% Re thermoelements and degassed sintered BeO insulators, exhibited a drift of only 2 to 3 K during exposure in argon at 2070 K for 1029 hours.

**14095.** Ehrlich, M., **Dosimetry performance tests,** (Proc. Panel on National and International Radiation Dose Intercomparisons, Vienna, Austria, Dec. 13-17, 1971), Paper IAEA-PL-479/8 in *National and International Radiation Dose Comparisons*, pp. 41-57 (International Atomic Energy Agency, Vienna, Austria, 1973).

Key words: choice of dosimeters; electrons; ferrous sulfate dosimeters; medical applications; performance criteria; personnel monitoring; photographic film; photons; radiation measurements; test patterns.

This report presents a discussion of the need for critical studies of radiation measurement techniques and routine measurement performance. The aim of such studies is to improve practical measurement performance by periodic testing and by the distribution of the knowledge gained by the participants in such tests. Besides general consideration, such items as test pattern, choice of dosimeters and examples from tests are discussed.

**14096.** Kropschot, R. H., **Helium heat transfer,** *Proc. Application of Superconducting Cable in Electrical Engineering and High Energy Physics, Titisee, Germany, Oct. 9-13, 1972*, pp. D1-D32 (Gesellschaft fuer Kernforschung, Karlsruhe, Germany, 1973).

Key words: cryogenics; heat transfer; helium; refrigeration; thermodynamic properties.

Design of an optimum superconducting device such as a magnet, cavity, generator, motor, transmission line or electronic device requires careful consideration of heat transfer. Any transient or oscillatory electrical behavior will cause heat generation which must be removed in order to permit continuous operation. Helium is the only cooling medium for most applications and as system size, cost and complexity increase it may not be practical to immerse the conductor in a container of helium and depend upon pool boiling, commonplace in small laboratory magnets. The purpose of this paper is to present the state of the art of reliable data on helium properties and helium heat transfer necessary for serious engineering studies of superconducting systems.

**14097.** Kessler, K. G., **The role of resonance interactions in some molecular far-infrared laser systems,** *Comments At. Mol. Phys.* **11**, No. 2, Part D, 67-72 (June-July 1970).

Key words: Coriolis interactions; infrared lasers; molecular lasers.

An analysis of the HCN laser system is presented and generalized to explain the operating mechanism for molecular lasers systems in general.

**14098.** Kanda, M., Adams, J. W., **Amplitude statistics of electromagnetic noise in coal mines,** *Proc. Thru-the-Earth Electromagnetics Workshop, Colorado School of Mines, Golden, Colo., Aug. 15-17, 1973,* pp. 156-160 (1973).

Key words: amplitude probability distributions; electromagnetic compatibility; electromagnetic interference in coal mines; field strength measurement.

A system for measuring amplitude probability distributions (APD's) of electromagnetic noise in coal mines is described and typical APD's from an underground coal mine are presented. The APD is a basic statistic required for the design and analysis of communication systems, especially those intended for use in noisy environments, and where neither overdesign nor underdesign is acceptable. The rms and average field strengths are obtained by integration of the APD, and examples are shown at several frequencies. All field strength levels are given in absolute units. Selected frequencies cover the range from 10 kHz to 32 MHz.

**14099.** Olver, F. W. J., **Error bounds for stationary phase approximations,** *SIAM J. Math. Anal.* **5**, No. 1, 19-29 (Feb. 1974).

Key words: asymptotic approximations; error analysis; generalized integrals; special functions; stationary phase; Watson's lemma.

An error theory is constructed for the method of stationary phase for integrals of the form

$$I(x) = \int_a^b e^{ixp(t)} q(t)\, dt.$$

Here $x$ is a large real parameter, the function $p(t)$ is real, and neither $p(t)$ nor $q(t)$ need be analytic in $t$. For both finite and infinite ranges of integration, explicit expressions are derived for the truncation errors associated with the asymptotic expansion of $I(x)$. The use of these explicit expressions for the computation of realistic error bounds is illustrated by means of an example.

**14100.** Hagen, L., **Report of The National Bureau of Standards 1972/73, for Reports of Observatories,** *Bull. Amer. Astronom. Soc.* **6**, No. 1, 140-144 (1974).

Key words: atomic energy levels; atomic line shapes; atomic spectra; atomic transition probabilities; bands, molecular; energy levels, atomic; line shapes, atomic; molecular bands; molecular spectra; rotational constants.

Research at the National Bureau of Standards in spectroscopy pertinent to astronomy is summarized. Publications on atomic spectra, atomic transition probabilities and line broadening, and molecular spectra are referenced and work in progress is discussed.

**14101.** Crenshaw, R., Thomas, C., Ramsey, R., Morgenroth,
**An approach to performance specifications for public buildin**
(Proc. Int. Conf. on Planning and Design of Tall Buildin
Lehigh Univ., Bethlehem, Pa., Aug. 21-26, 1972), Paper
*Tall Building System and Concepts,* **Ia,** 797-806 (1972).

Key words: office buildings; performance criteria; syste
building.

A progress report after one year on the use of *The PBS P*
*formance Specification for Office Buildings* for the construct
of three Social Security Payment Centers. The report is mai
concerned with the shift in responsibility for the architect, ind
try, research and management.

**14102.** Greene, W. E., Jr., **Stochastic models and live load surve**
(Proc. Int. Conf. on Planning and Design of Tall Buildin
Lehigh Univ., Bethlehem, Pa., Aug. 21-26, 1972), Paper
*Tall Building System and Concepts,* **Ib,** 35-58 (1972).

Key words: computer simulation; live and fire loads; oc
pancy; stochastic predictive models; survey; techniques.

Design fire loads and live loads for office buildings are ba
on data collected over 30 years ago. Maximum cost efficienc
gathering this loads data requires the use of stochastic mod
Explanatory models based on room characteristics such as ro
use, occupancy type, age of occupancy, etc. are used to de
mine (explain) room loads for the rooms not surveyed. O
about 10,000 rooms will be surveyed from about 100 of
buildings which will serve to provide information for estima
parameters for the predictive loads models (sustained, maxim
sustained, extraordinary). The explanatory models will prov
the remaining room loads. The topology of these 100 buildi
having been previously programed and stored in the compu
all rooms of the building population will be loaded thro
mathematical simulation. A pilot study, using a limited amo
of previously collected data has been initiated to verify th
models as much as possible, this will be followed by a redu
survey of about 25 buildings to further refine the models bef
the major survey of approximately 75 buildings will be c
ducted.

**14103.** Wright, R. N., **Survey of fire and live loads,** (Proc.
Conf. on Planning and Design of Tall Buildings, Lehigh Un
Bethlehem, Pa., Aug. 21-26, 1972), Paper in *Tall Buil*
*System and Concepts,* **Ib,** 128-130 (1972).

Key words: buildings; design; fire loads; fire rating; fl
loadings; live loads; stochastic models.

This discussion, presented at the session on gravity loads
temperature effects of the ASCE-IABSE Conference on
Buildings, outlines a program of survey of fire and live lo
which the National Bureau of Standards is beginning under
auspices of the Building Research Advisory Board and the sp
sorship of the Public Building Service of the General Serv
Administration. Its objectives are to improve the technical ba
for criteria for fire ratings of buildings and for floor loadings u
in building design. The surveying will employ stochastic mo
for representation of loadings developed at NBS. It will pro
a data base for immediate improvements in building standa
for fire resistance and design live loads. The information
veyed also will provide an information basis for long-range sc
tific studies to develop new design concepts for control of bu
ing fires and new criteria for mitigation of fire effects. The
loads information will allow theoretical studies of design l
configurations leading to more consistent probabilistic form
tions of combinations of loadings from the building's own wei
the effects of occupancy, effects of wind, effects of earthqu
etc.

04. Dalgliesh, W. A., Marshall, R. D., **Research eview—North and South America,** (Proc. Int. Conf. on Planning and Design of Tall Buildings, Lehigh Univ., Bethlehem, Pa., Aug. 21-26, 1972), Paper in *Tall Building ystem and Concepts,* **Ib,** 383-398 (1972).

Key words: climatological data; meteorology; tall buildings; wind effects; wind loads; wind tunnel.

The current status of research in North and South America evant to the prediction of tall building behavior in response to d is reviewed under four main headings: Meteorological earch—wind structure and climate; Full-scale investigations wind action on tall buildings; Development of wind tunnel hniques for building aerodynamics; Simplified theoretical dels of wind effects on tall buildings.

05. Somes, N. F., **Progressive collapse risk,** (Proc. Int. Conf. on Planning and Design of Tall Buildings, Lehigh Univ., Bethlehem, Pa., Aug. 21-26, 1972), Paper in *Tall Building System and Concepts,* **Ib,** 727 (1972).

Key words: accident occurrence; building; gas explosion; hazards; progressive collapse; tall buildings.

The National Bureau of Standards is undertaking an extensive dy on behalf of the U.S. Department of Housing and Urban evelopment. The objectives are to determine the nature and quency of occurrence of the various forms of extreme local ds on high rise buildings and to develop criteria necessary to duce the risk of progressive collapse to an acceptable level.

106. Yokel, F. Y., Wright, R. N., **Summary report—Technical Committee No. 26, Limit states design,** (Proc. Int. Conf. on Planning and Design of Tall Buildings, Lehigh Univ., Bethlehem, Pa., Aug. 21-26, 1972), Paper in *Tall Building System and Concepts,* **III,** 949-953 (1972).

Key words: deterioration; failure; limit states design; mode of failure; reliability; structural failures.

A limit state has been defined as "a particular state, in which structure ceases to fulfill the function or to satisfy the condition r which it is designed" (1). By this definition a limit state is a ode of failure, which includes failure to perform a specific funcon or to provide a desired attribute. The goal of limit states sign as presently defined is to give explicit consideration to all ilure modes and to assure a suitably low probability that the ructure or any of its components reach a limit state in service.

The state of the art reports presented in behalf of Committee identify limit states of reinforced concrete structures and sury our knowledge with respect to the application of limit states sign. In this paper the state of the art reports are summarized d some new definitions are suggested for consideration.

107. Dikkers, R. D., **Summary report—Technical Committee No. 27, Masonry structures,** (Proc. Int. Conf. on Planning and Design of Tall Buildings, Lehigh Univ., Bethlehem, Pa., Aug. 21-26, 1972), Paper in *Tall Building System and Concepts,* **III,** 1103-1114 (1972).

Key words: bricks; building codes; buildings; concrete blocks; masonry; research; reinforced masonry; structural engineering; walls.

The re-emergence of masonry as a modern and viable strucral material during the past decade is described. Buildings have een constructed up to a height of 206 ft (63 m) utilizing 10-in 54 mm) thick loadbearing masonry walls. Extensive research rograms have been recently conducted but high priority should e given to additional investigations of reinforced masonry. Varius needs in masonry standards and codes of practice are also entified. The use of prefabricated and prestressed masonry ould continue to increase in the future.

14108. Mandel, J., **The evaluation of referee methods in clinical chemistry,** *Med. Instrum.* **8,** No. 1, 26-29 (Jan.-Feb. 1974).

Key words: accuracy; calcium in serum; clinical testing; interlaboratory comparisons; precision.

The importance of clinical testing to health demands that both precision and accuracy be achieved. Proficiency testing has shown that generally this is not the case. The next task is to study some individual clinical methods in depth to provide the profession with well developed referee methods. An interlaboratory study of a test method involves five elements: the protocol, samples, laboratories, statistical design, and analysis of the data. These elements are discussed and illustrated in terms of determining calcium in serum by atomic absorption spectrometry, using isotope dilution mass spectrometry as a standard of accuracy. This study, consisting of five "exercises," shows that only through constant vigilance and an attitude of real concern can acceptable levels of precision and accuracy be achieved.

14109. Roberts, R. W., **Freedom and social responsibilities,** *IEEE Spectrum 11,* No. 4, 59-60 (Apr. 1974).

Key words: computer privacy; freedom of information; information; public information.

The guiding principle of the Freedom of Information Act is promotion of the public interest. Effective use of technical information requires more than "freedom," if by freedom one means merely unrestricted access. It requires a sense of responsibility and an activist approach toward evaluation and distribution to assure adequate dissemination of correct information. This is our approach at NBS.

14110. McClendon, L. T., LaFleur, P. D., **Determination of rare earths in standard reference material glass using neutron activation analysis and reversed-phase chromatography,** *J. Radioanal. Chem.* **16,** 123-126 (1973).

Key words: di(2-ethylhexyl) orthophosphoric acid, Corvic; NBS Standard Reference Material 480; neutron activation analysis; rare earths; reversed-phase chromatography.

Recently, the interest in quantitative determination of rare earth elements has grown considerably, especially in connection with the space programs. There has also been a need for quantitative methods for rare earth element determination in different matrices at the National Bureau of Standards. We have therefore applied some of our earlier qualititative investigations with di(2-ethylhexyl) orthophosphoric acid (HDEHP) to separations of these elements for their subsequent quantitative determination. The rare earth elements in NBS Standard Reference Material 480, Trace Elements in Glass, a sodium glass to which 61 trace elements, including the thirteen naturally occurring rare earths, were added, have been determined by neutron activation analysis with a chemical separation using a column (11 cm × 40 cm) of "Corvic" powder [poly(vinyl chloride-vinyl acetate)] loaded with HDEHP and operated at a constant temperature. Since our earlier solvent extraction studies with HDEHP had shown perchloric acid to be the most favorable of three acids (HCl, $HNO_3$, $HClO_4$) for rare earth separation, we established the best operating conditions (e.g., time, flow, acid concentration, etc.) using this acid.

14111. Wait, D. F., Beatty, R. W., **The 1973 International Microwave Symposium,** *IEEE Trans. Microwave Theory Tech.* **MTT-21,** No. 12, 747-751 (Dec. 1973).

Key words: exhibits; microwave; symposium.

The 1973 IEEE G-MTT International Microwave Symposium was held June 4-6, 1973, in Boulder, Colo. The theme was "Microwave Applications in the 70's."

**14112.** Risley, E. W., Jr., **Discontinuity capacitance of a coaxial line terminated in a circular waveguide. Part II—Lower bound solution,** *IEEE Trans. Microwave Theory Tech.* **MTT-21,** No. 8, 564-566 (Aug. 1973).

Key words: coaxial line; lower bound; open circuit termination.

This calculation provides a lower bound (complementing the upper bound solution given earlier) to the discontinuity capacitance of a coaxial line terminated in a circular waveguide. A 50-Ω 0.9525-cm (3/4-in) open-circuited coaxial termination with a solid center conductor was fabricated with center- and outer-conductor diameters of $0.82723 \pm 0.00005$ and $1.90487 \pm 0.00005$ cm (1 cm = 0.393703 in), respectively. The measured value of capacitance of this termination at 1000 Hz was $216.4 \pm 1.0$ fF, as compared with the calculated lower bound of 215.0 fF. (The upper bound for this case was 217.7 fF.)

**14113.** Maryott, A. A., Malmberg, M. S., Gillen, K. T., **Effective collision numbers for angular momentum relaxation from nuclear relaxation studies of simple liquids,** *Chem. Phys. Lett.* **25,** No. 2, 169-174 (Mar. 15, 1974).

Key words: angular momentum relaxation; collision numbers; liquids; NMR relaxation; rotational diffusion; spin-rotation.

Angular momentum correlation times, $\tau_J$, derived from nuclear relaxation studies of a number of liquids composed of small molecules of high symmetry are compared with hard sphere and cell model collision rates. Either model leads to the conclusion that collision efficiency is high (collision number of 1 to 2) and provides a useful and simple relationship for predicting $\tau_J$ semiquantitatively over the liquid range.

**14114.** Maximon, L. C., O'Connell, J. S., **Sum rules for forward elastic photon scattering,** *Physics Letters* **48B,** No. 5, 399-402 (Mar. 4, 1974).

Key words: Compton scattering; dispersion relations; photon; proton; scattering; sum rules.

Relations between integrals over forward elastic photon scattering amplitudes, forward elastic cross sections and total cross sections are derived from dispersion relations. A new photon-proton interaction sum rule is derived and evaluated.

**14115.** Lutz, G. J., **Determination of lead in paint with fast neutrons from a californium-252 source,** *Anal. Chem.* **46,** No. 4, 618-620 (Apr. 1974).

Key words: activation analysis; californium-252; lead; neutron irradiation; paint.

Large amounts of lead in the paint on walls in dwellings is potentially hazardous to children in certain susceptible age groups who may ingest it. Most analytical methods for screening suspect homes require lengthy dissolution or other chemical procedures. Activation analysis with unmoderated neutrons from a $^{252}$Cf source inducing the nuclear reaction $^{204}$Pb(n,n')$^{204m}$Pb followed by gamma spectrometry with a Ge(Li) detector is shown to be a convenient, reliable and potentially rapid nondestructive method for this determination. The lower limit of determination in a 1.5 gram sample of paint with a 600 μg source of $^{252}$Cf is of the order of one percent lead.

**14116.** Spiegel, V., **The effective half-life of californium-252,** *Nucl. Sci. Eng. Tech. Note* **53,** No. 3, 326 (Mar. 1974).

Key words: activation analysis; californium-252; manganese activity; neutron irradiation.

The effective half-life of $^{252}$Cf has been determined as $2.638 \pm 0.007$ yr. The method utilized the ratio of the manganese activity induced in a manganous-sulfate bath by a $^{252}$Cf spontaneous-fission neutron source and the National Bureau of Standa photoneutron source to measure the change in emission rate the $^{252}$Cf source over a period of 1.77 half-lives. The data w corrected for the activity of radium (1622-yr half-life) in photoneutron source (−0.2%) and for the competing neut production from $^{250}$Cf.

**14117.** Treu, S., Pyke, T. N., Jr., **Project-oriented collaborat via a computer network,** *Proc. Computer Science Confere Columbus, Ohio, Feb. 1973*, p. 27 (1973).

Key words: computer network; interpersonal commun tions; task group collaboration.

Given a commitment to collaborate on a particular project, hampered by geographical separation, a telecommunications angle was established within the context of the ARPA Netw The triangle consisted of NBS, Pitt and ECOM. Sev staff/faculty members at the first two institutions emplo facilities of the Network Information Center (SRI) in orde formulate plans, exchange ideas, and produce specific result support of a project at ECOM. That project involved interac graphics for computer-aided design and engineering. ECOM sonnel were able to "observe" and supply feedback when propriate. A set of written ground rules for participation and collection sheets for recording individual experiences designed in advance. Results of this project-oriented collab tion have been analyzed in terms of feasibility, productivity, required network capabilities.

**14118.** McLaughlin, W. L., Holm, N. W., **Physical characteri of ionizing radiation,** Chapter 1 in *Manual on Radia Sterilization of Medical and Biological Materials, Tech. ports Series No. 149*, pp. 5-12 (International Atomic En Agency, Vienna, Austria, 1973).

Key words: dosimetry; electrons; gamma rays; ioni radiation; microdosimetry; radiation physics; radia sterilization; radiobiology; x rays.

An important step in developing the background for the ra tion sterilization process is to review the physics and chemi of radiation interactions in matter and the quantities that are for monitoring radiation energy depositions. From this basis can go on in subsequent chapters to the practical considerat of how efficiently the most radiation-resistant living organi (fungi, bacteria, viruses, etc.) can be inactivated without cau excessive damage to the host material.

**14119.** Blanc, R., **Minicomputer trends and applications—1** *Computer* **6,** No. 6, 28-29 (June 1973).

Key words: minicomputer applications; minicomp maintenance; minicomputer peripherals; minicomputer ware.

The present trends in the growth and utilization of minicon ters as presented and discussed at a recent Symposium cos sored by NBS are reviewed. In addition, problems are identi in the areas of minicomputer software, peripherals, and m tenance.

**14120.** Jan, G., Mendlowitz, H., **Optical imaging with freque dependent spectral-density functions,** *J. Opt. Soc. Amer.* No. 7, 865-869 (July 1971).

Key words: coherence; image formation; modula transfer; optical transfer function.

In this investigation, the quasimonochromatic condition is assumed, and the spectral-density function of the radiation pends on frequency as well as on positions. We discuss var models for the impulse-response function of the optical sys and examine the results in temporal-frequency space. We proximate the integration by employing the method of stee escent. An explicit relation of the mutual coherence function ıd the spectral-density function of the source is established ith some correction factors that differ from the results of the ıasimonochromatic approximation.

**121.** Abrams, M. D., Rosenthal, R., **On the passing of MOBIDIC-B,** *Computer* **6,** No. 3, 10-18 (Mar. 1973).

> Key words: computer; MOBIDIC-B; teleprocessing system.

The history, design, hardware configuration, instruction set d operating system of the MOBIDIC-B used in the National ıreau of Standards (NBS) computer research facility is scribed using conventional methods and Bell and Newell's MS and ISP notations. As modified at NBS, MOBIDIC-B is e nucleus of an experimental remote access computer system, th variable partition multiprogramming capability, that supırts conversational terminal usage.

**122.** Pyke, T. N., Jr., Blanc, R. P., **Computer networking technology— A state of the art review,** *Computer* **6,** No. 6, 13-19 (Aug. 1973).

> Key words: computer-communications; computer network architecture; computer networks.

Computer networking technology as represented by existing ıd planned computer networks is reviewed. Functional capailities of alternative approaches to networking are considered ırticularly in terms of terminal and host computer system interces. Commonalities and differences in network architecture e identified. The limitations of existing network technology are scussed to clearly identify current problems and to indicate eas where further research and development is needed.

**123.** Brower, W. S., Parker, H. S., Roth, R. S., **Reexamination of synthetic parkerite and shandite,** *Amer. Mineral.* **59,** 296-301 (1974).

> Key words: chalcogenides; parkerite; shandite; subsulfides.

A reinvestigation of synthetic parkerite, $Ni_3Bi_2S_2$, has demonrated that the unit cell is 4 times the volume of that previously ported (Michener and Peacock, 1943). It has monoclinic symetry, most probable space group $C2/m$ with $a=11.066$, $b=$ 085, $c=7.965$ Å, $\beta=134.0°$. The larger cell was confirmed by ıgle crystal x-ray diffraction data, but can be deduced from the esence of extra lines in the powder pattern of a specimen ıich has been annealed after grinding. This same technique vealed the rhombohedral distortion of shandite, $Ni_3Pb_2S_2$, ace group $R\overline{3}m$, previously thought to be dimensionally cubic. ıe unit cell of shandite was found to be $a=5.591$, $c=13.579$ The Sn analogue of shandite, $Ni_3Sn_2S_2$, reported for the first ne, is hexagonal with $a=5.465$, $c=13.196$ Å. We were unable synthesize any Mn, Fe, Co, or Cu analogs of the parkeriteandite series.

**124.** Bass, A. M., Laufer, A. H., **Extinction coefficients of azomethane and dimethyl mercury in the near ultra-violet,** *J. Photochem. Short Communication* **2,** 465-470 (1973/74).

> Key words: absorption spectrum; azomethane; dimethyl mercury; extinction coefficient; ultraviolet.

The absorption spectra and extinction coefficients of omethane and dimethyl mercury have been measured between 0-360 nm. In each case the absorption consists of an intense ɔad band upon which is superimposed a vibrational sequence a single frequency. For azomethane the vibrational spacing is out 470 $cm^{-1}$; for dimethyl mercury it is about 347 $cm^{-1}$. The rational frequencies of the upper states have been tentatively signed.

**125.** Unassigned.

**14126.** Lutz, G. J., **The analysis of biological and environmental samples for lead by photon activation,** *J. Radioanal. Chem.* **19,** 239-244 (1974).

> Key words: biological samples; environmental samples; lead; photon activation analysis.

The photonuclear reaction $^{204}Pb(\gamma,n)$ $^{203}Pb$ is used for the determination of lead in biological and environmental samples. Precision and accuracy were determined to be adequate by analyzing some samples which have been assayed for lead by other methods. With a rigorous post-irradiation separation, the limit of detection is of the order of tens of nanograms.

**14127.** Hurlock, S. C., Lafferty, W. J., Rao, K. N., **Analysis of the $\nu_3$ band of $^{14}N^{16}O_2$,** *J. Mol. Spectrosc.* **50,** 246-256 (1974).

> Key words: air pollutant; fundamental vibrational band; high-resolution; molecular constants; spin-splittings; vibration-rotation.

The rotational structure of the $\nu_3$ fundamental of $^{14}N^{16}O_2$ has been recorded by employing a vacuum grating infrared spectrograph. The analysis has led to the assignment of over 500 $R$- and $P$-branch transitions in the spectral region 1650-1562 $cm^{-1}$. Molecular constants for the upper state, 001, have been presented. No $Q$-branch transitions were used in the evaluation of these constants. The presently obtained $\alpha_3{}^A=0.22517$ $cm^{-1}$ and the band center $\nu_0=1616.846$ $cm^{-1}$ differ significantly from previous determinations. Spin splitting was observed but no information was extracted about upper state spin splitting parameters.

**14128.** Kearsley, E. A., **A test sample to standardize measurements of normal stress,** *Rheol. Acta* **12,** No. 4, 546-549 (1973).

> Key words: molecular weight distribution; normal stress; polystyrene solutions; standard sample; streaming birefringence.

This paper is an account of the design of a test sample of polystyrene solution which will be distributed to research laboratories interested in participating in a comparison of techniques of measurement of normal stresses through a common sample. Questions of concentration, molecular weight distribution and solvent properties are considered.

**14129.** Carroll, J. J., Melmed, A. J., **Optical constants of titanium,** *J. Opt. Soc. Amer. Letters to Editor* **64,** No. 4, 514-515 (Apr. 1974).

> Key words: ellipsometry; optical constants; titanium.

Optical constants of (0001) titanium at $\lambda=5461$ Å were measured ellipsometrically under a variety of conditions. The results are compared to the appropriate literature values.

**14130.** Huebner, R. H., Celotta, R. J., Mielczarek, S. R., Kuyatt, C. E., **Electron energy loss spectroscopy of acetone vapor,** *J. Chem. Phys.* **59,** No. 10, 5434-5443 (Nov. 15, 1973).

> Key words: acetone vapor; electron energy-loss spectroscopy; oscillator strength.

High resolution, inelastic electron scattering data can provide new spectroscopic information on the electronic structure of polyatomic molecules. Features in the acetone energy loss spectrum from 0 to 15 eV obtained for 100 eV incident electrons correspond to vibrational, electronic discrete, and electronic continuum excitations. These data are compared with optical measurements in a wide spectral region extending from the infrared to the vacuum ultraviolet. A comprehensive interpretation of the energy loss spectra is attempted with the use of photochemical and photoelectron data, as well as quantum-chemical calculations in the literature. Three Rydberg series with quantum defects of 1.03, 0.81, and 0.315 join onto bands previously discussed in terms of transitions to valence orbitals. These series converge to an ionization limit of 9.705 eV in good agreement with previous optical determinations. Dissociative continua underlie the Rydberg region and give rise to a variety of neutral products observed in recent photolysis work. Broad features in the ionization continuum appear to correlate generally with higher ionization potentials observed by photoelectron spectroscopy. Apparent oscillator strengths derived from the energy loss data for the bands at 4.4 and 6.35 eV and for a region (9.7-11.78 eV) of the ionization continuum agree very well with the photoabsorption measurements. Integrated oscillator strengths of 0.46 below 9.7 eV and 3.93 below 15 eV were derived from the electron impact data.

**14131.** Wakeford, O. S., Robinson, D. E., **Lateralization of tonal stimuli by the cat,** *J. Acoust. Soc. Amer.* **55,** No. 3, 649-652 (Mar. 1974).

Key words: animal audition, cats; animal psychophysics; auditory lateralization; auditory localization; avoidance; binaural hearing; earphones for animals; interaural differences.

The ability of the cat to "lateralize" tonal signals having interaural intensive or interaural temporal disparities was measured. Interaural intensive differences were studied at 0.5, 1.0, and 3.0 kHz. Interaural temporal differences were studied at 0.5, 1.0, 2.0, and 3.0 kHz. Miniature audio transducers were employed to present the stimuli to the animals. The transducers were held in a fixed spatial relation to the auditory canal by means of "pinna inserts" and leather helmets. An avoidance response in a shuttle box was used as the dependent variable. The animals' task involved the detection of a right-left reversal in a gated sequence of tone bursts. The cat appears to be about as sensitive as the human to both interaural intensive and temporal disparities at each of the frequencies studied.

**14132.** Newman, M., **Diophantine equations in cyclotomic fields,** *J. Reine Angew. Math.* **265,** 84-89 (1974).

Key words: cyclotomic fields; diophantine equations; units.

Let $K_p$ be the cyclotomic field $Q(\zeta_p)$, where $\zeta_p = \exp(2\pi i/p)$, $Q$ is the field of rationals, and $p$ is a prime $> 3$. The principal result of this paper is that the equation $\xi = \eta^n - 1$ has no solutions in units $\xi, \eta$ of $K_p$ which are not roots of unity, provided that $n > 2$. MOS Numbers—10.66, 10.10.

**14133.** Celotta, R. J., Mielczarek, S. R., Kuyatt, C. E., **Electron energy loss spectrum of ozone,** *Chem. Phys. Lett.* **24,** No. 3, 428-430 (Feb. 1, 1974).

Key words: electron energy-loss; electron excitation; gas scattering; ozone.

Electron energy loss spectra for ozone are presented over the energy loss range 1-30 eV with an incident electron energy of 300 eV. The data are obtained using an electron monochromator-analyzer combination and a static gas cell, and have a resolution of 0.035 eV fwhm.

**14134.** Celotta, R. J., Bennett, R. A., Hall, J. L., **Laser photodetachment determination of the electron affinities of OH, $NH_2$, NH, $SO_2$, and $S_2$,** *J. Chem. Phys.* **60,** No. 5, 1740-1745 (Mar. 1, 1974).

Key words: electron affinity of $NH^-$; electron affinity of $NH_2^-$; electron affinity of $OH^-$; electron affinity of $S_2^-$; electron affinity of $SO_2^-$; photodetachment.

Using a fixed frequency argon ion laser we have studied the energy spectra of electrons photodetached from $OH^-$, $NH_2^-$, $NH^-$, $SO_2^-$, and $S_2^-$. We determined the following electron affinities: $E_A(OH) = 1.829_{-0.014}^{+0.010}$ eV, $E_A(NH_2) = 0.779 \pm 0.037$ eV, $E_A(NH) = 0.38 \pm 0.03$ eV, $E_A(SO_2) = 1.097 \pm 0.036$ eV, and $E_A(S_2) = 1.663 \pm 0.040$ eV. Additionally, the angular distribution anisotropy parameter $\beta$ was measured for $OH^-$ and $NH_2^-$ at 4880 Å, as $-0.993 \pm 0.040$, and $0.027 \pm 0.012$, respectively, and information about negative ion vibrational constants is presented.

**14135.** Gadzuk, J. W., **Valence-band Auger-electron spectra fo aluminum,** *Phys. Rev. B* **9,** No. 4, 1978-1980 (Feb. 15, 1974).

Key words: attenuation lengths; Auger effect; electro spectroscopy of solids; surfaces.

Recent measurements of the $L_{23}$ VV Auger spectrum of Al b Powell, have shown that the observed energy distributions d not correspond to the self-convolution of the Al bulk density c states. Attempts to account for this discrepancy in terms of ene gy-dependent matrix elements and inelastic scattering of th ejected electron are described here.

**14136.** Dobbyn, R. C., McAlister, A. J., Cuthill, J. R., Erickso N. E., **Valence band x-ray photoemission and soft x-ray emissio studies of Pt,** *Phys. Lett.* **47A,** No. 3, 251-252 (Mar. 25, 1974

Key words: electronic density of states; Pt; surface cleanl ness; valence-band; x-ray photoemission.

The soft x-ray $N_{6,7}$ (5d to 4f transition) emission spectrum a the x-ray photoemission spectrum of Pt (the latter under tv conditions of surface cleanliness) have been obtained, and a compared with the results of photoemission and band theoretic studies.

**14137.** Stevens, W. J., Billingsley, F. P. II, **Coupled multiconfig rational self-consistent-field method for atomic dipole polari bilities. II. Application to the first-row atoms, lithium throu neon,** *Phys. Rev. A* **8,** No. 5, 2236-2245 (Nov. 1973).

Key words: atoms; correlation; dipole polarizabiliti excited states; ground state; multiconfiguration.

Static dipole polarizabilities, accurate to within 5 percent presented for the ground states and some valence excited sta of the first-row atoms. The polarizabilities are obtained fr multiconfigurational self-consistent-field wave functions, wh were computed with the perturbing electric field incluc directly in the Hamiltonian. The use of the multiconfiguratio framework allows any state of both degenerate and n degenerate atoms to be considered, and also allows for the plicit introduction of electron-correlation effects. Detai discussions of basis-set selection and the effects of electron c relation are presented along with comparisons with experime and other theoretical polarizability results.

**14138.** Hougen, J. T., **Comment on the paper "About the s metries of the rotation-vibration wavefunction of molecules"** *Mol. Spectrosc.* **50,** 485-486 (1974).

Key words: group theory; methane; rovibronic symm species; selection rules; tetrahedral point group.

Qualitative observations are presented concerning the lc standing controversy over the correct use of group-theoret symmetry operations and symmetry species in the meth molecule. No new mathematical details are introduced; dis sion focuses rather on the merits of papers in the existing lit ture. The observations are presented in response to a comn by Professor J. Moret-Bailly, published simultaneously, in w an opposing point of view is given.

**14139.** Hellner, C., Keller, R. A., **Flash photolysis of sulfur c ide,** *J. Air Pollut. Contr. Ass.* **22,** No. 12, 959-963 (Dec. 19

Key words: air pollution; flash photolysis; sulfur dioxide traviolet absorption.

The body of information presented in this paper is directe photochemists and air pollution scientists interested in spe ich result from the interaction of $SO_2$ and light. When $SO_2$ at w pressures is subjected to an intense photolysis flash, the aracteristic, very structured $SO_2$ absorption spectrum disap- ars immediately after the flash and is replaced by a continuous sorption. The continuous absorption gradually decays and the rmal $SO_2$ absorption spectrum returns. The initial absorbance the continuous absorption is proportional to the square of the $_2$ pressure and the square of the flash irradiance. From these cts we propose the formation of a metastable dimer of $SO_2$ rmed by the collision of two excited molecules. Some proper- s of this dimer are: natural lifetime = 2 sec; energy above parated monomers = 4 kcal; lifetime at atmospheric pressure 1 sec (quenching coefficients with several foreign gases = $10^{-20}$ n$^3$/sec molecule); absorption of ultraviolet light results in otodecomposition of the dimer into monomeric $SO_2$. The long etime of this species and its low quenching cross section may ake it an important intermediate in photochemical reactions of $_2$. The relatively low excitation energy of the metastable spe- es indicates it may also be an intermediate in thermally excited actions and perhaps an important component of smoke stack luent.

140. Kuyatt, C. E., Celotta, R. J., Mielczarek, S. R., **Applications of electron spectroscopy to air pollution measurements,** (Proc. VIII Int. Conf. on Physics of Electronic and Atomic Collisions, Belgrade, Yugoslavia, July 16-21, 1973), Paper in *Proceedings VIII International Conference on Physics of Electronic and Atomic Collisions—Invited Lectures and Progress Reports,* B. C. Cobic and M. V. Kurepa, Eds., pp. 681-701 (Institute of Physics, Belgrade, Yugoslavia, 1974).

Key words: air pollution; electron spectroscopy; energy-loss spectroscopy.

Recent developments in electron spectrometer design have ade the application of inelastic electron scattering measure- ents to gas analysis competitive with other techniques. The ergy distribution (energy loss spectrum) of electrons of an ini- lly monoenergetic electron beam after an encounter with a gas get contains the optical absorption spectrum of the gas. This ectrum, by revealing the valence energy states of the gas, is an rinsic "fingerprint" of the atom or molecule. An instrument s been built to explore the potentialities of this method. Its sponse is linear with concentration over a very wide range. e instrument is described and its performance as a trace alyzer for air pollution studies discussed.

141. Brown, W. E., **Physicochemical mechanisms of dental caries,** *J. Dent. Res.* **53,** No. 2, 204-216 (Mar./Apr. 1974).

Key words: caries models; dental caries; phase diagrams; physicochemical mechanism; solubility of enamel.

A review of models for physicochemical mechanisms of dental ries is presented. The existing models belong to three general tegories: Equilibrium, steady-state and cyclic. A new in- rpretation is provided for these models by the application of ase diagram consideration in a generalized four component stem, $Ca(OH)_2$-$H_3PO_4$-HX-$H_2O$, in which HX is a bioorganic id; the role of important factors in caries process is evaluated d advantages and shortcomings of the existing models are scussed. New directions for future research are recommended.

142. Mitchell, R. A., Woolley, R. M., Chwirut, D. J., **Analysis of composite-reinforced cutouts and cracks,** (Proc. 15th Structures, Structural Dynamics and Materials Conference, Las Vegas, Nev., Apr. 17-19, 1974), AIAA Paper No. 74-377, pp. 1-13 (American Institute of Aeronautics and Astronautics, New York, N.Y., 1974).

Key words: adhesively bonded joints; composite materials; composite-overlay reinforcement; contour plotting; cracks, **reinforcement of; cutouts, reinforcement of; finite element analysis; joints, adhesively bonded; reinforcement, composite overlay; reinforcement, cutouts and cracks.**

Finite element computer analyses of the reinforcement of cutouts and cracks in metal sheet, by bonded overlays of composite material, are described. The analyses articulate the separate responses of the sheet, the overlays, and the adhesive. Contour plots of computed stress and strain fields are automatically generated by the computer programs. Strains measured on the surfaces of several reinforced-sheet tensile specimens were, for the most part, in good agreement with strains predicted by the analyses. Significant correlations between certain failure modes observed in the test specimens and the stress distributions given by finite element analysis are apparent. The same analytical approach is currently being used to study weld/bond and fastener/bond joints, and it could be used to study other problems such as hole repair in metal or composite sheet and embedded defects in laminar material.

14143. Okabe, H., **Production of electronically excited species in photodissociation of simple molecules in the vacuum ultraviolet,** (Proc. Advanced Study Institute on Chemical Spectroscopy and Photochemistry in the Vacuum Ultraviolet, NATO, Valmorin, Quebec, Canada, Aug. 1973), Paper in *Chemical Spectroscopy and Photochemistry in the Vacuum Ultraviolet,* C. Sandorfy, P. J. Ausloos, and M. B. Robin, Eds., **8,** Series C, 513-523 (D. Reidel Publishing Co., Dordrecht, Holland, 1974).

Key words: bond energy; fluorescence; photodissociation; predissociation; spin conservation rules; vacuum ultraviolet.

Recent studies of the primary process in the photodissociation of small molecules have been reviewed. The process of producing fluorescing excited species in photodissociation in particular has been studied as a function of incident wavelength. The determination of the threshold wavelength of incident photons required for the production of the excited species provides information on bond dissociation energies and other thermochemical data. The nature of the primary process (i.e., direct dissociation, predissociation, the spin conservation rule, and the configuration of an upper state) has been discussed for some small molecules.

14144. Mihalas, D., Hummer, D. G., **Some observational implications of extended static O-star model atmospheres,** *Astrophys. J.* **189,** L39-L43 (Apr. 1, 1974).

Key words: astrophysics; energy loss; O-stars; radiative transfer; stellar atmospheres.

Some results and observational implications are presented for the first extended spherical non-LTE model atmospheres in hydrostatic and radiative equilibrium. These models all correspond to a star with $\mathcal{M} = 60\ \mathcal{M}_{\odot}$, $L = 1.25 \times 10^6\ L_{\odot}$, and $R = 24\ R_{\odot}$, with an effective temperature $T_{eff} \simeq 39{,}500$ K and surface gravity log $g \simeq 3.45$ (spectral type near O6). They are differentiated by the magnitude and radial dependence of a radiation-force multiplier $\gamma$, inserted into the equation of hydrostatic equilibrium, to simulate the effect of radiation force on opacity sources (e.g., lines) that have not been included in the calculations. It has been possible to obtain models very close to the limit at which the radiation force balances the gravity. Hydrogen and helium ($Y = 0.1$) constitute the gas; six hydrogen lines are treated explicitly. These models show L$\alpha$ in emission, the lower Balmer lines in absorption, the Balmer jump in absorption, and both infrared and ultraviolet excesses relative to the visual. Continuum jumps and gradients, Strömgren-system colors, and equivalent widths of H$\alpha$, H$\beta$, and H$\gamma$ are tabulated and discussed briefly.

**14145.** Cunningham, G. W., Meijer, P. H. E., **Exact calculation of the energy and heat capacity for the triangular lattice with three different coupling constants,** *J. Math. Phys.* **15,** No. 1, 55-59 (Jan. 1974).

Key words: anisotropic coupling; elliptic integrals; heat capacity; internal energy; Ising model; triangular lattice.

Calculation of the internal energy and heat capacity of the general anisotropic triangular Ising lattice is derived from the double integral form of the partition function. The principal result is the reduction of the elliptic integrals to a standard form for three arbitrary coupling constants. Both the standard form and the method of reduction are due to Legendre. The method of reduction is one involving two linear transformations. A straightforward reduction of elliptic integrals to standard form could not be used in this application. This is because of the functional dependence of the two linear transformations on the many combinations and permutations of the signs and relative magnitudes of the coupling energies of the lattice. A relatively simple formulation is presented in which the many combinations and permutations previously mentioned are reduced to only two distinct cases. An independent numerical solution was calculated directly from the partition function as a means of verifying the formulation presented in this paper.

**14146.** Day, G. W., Hamilton, C. A., Peterson, R. L., Phelan, R. J., Jr., Mullen, L. O., **Effects of poling conditions on responsivity and uniformity of polarization of $PVF_2$ pyroelectric detectors,** *Appl. Phys. Lett.* **24,** No. 10, 456-458 (May 15, 1974).

Key words: infrared detectors; $PVF_2$; pyroelectric detectors; uniform polarization.

A large number of pyroelectric detectors, fabricated from commercially available $PVF_2$ and poled under a variety of conditions of voltage, temperature, and time have been evaluated for responsivity and uniformity of polarization in the direction of the poling field. Results show that uniformity of polarization (a requirement for flat frequency response) can be achieved and responsivities as high as 2.9 $\mu$A/W can be obtained.

**14147.** Coxon, B., **Studies of carbohydrates by Fourier transform NMR spectroscopy: Structural analysis of glycosyl cyanides,** *Ann. N.Y. Acad. Sci.* **222,** 952-970 (Dec. 31, 1973).

Key words: fluorinated chemical shift reagents; Fourier transform $^{13}C$ magnetic resonance spectroscopy; glycosyl cyanides; $^{13}C$-H coupling constants.

Acylated glycosyl cyanides are useful intermediates in the synthesis of C-nucleoside antibiotics, but the preparation of these intermediates from glycosyl halides and heavy metal cyanides may be complicated by the simultaneous formation of, and identification of isomeric 1,2-*O*-(cyanoalkylidene) derivatives. Hexopyranosyl, pentopyranosyl, and pentofuranosyl cyanides in the D-glucose, D-galactose, D-ribose, and D-xylose series and some isomeric cyanoalkylidene structures have been identified and distinguished by the characteristic chemical shifts of the CN, C-1, and alkylidene $^{13}C$ nuclei determined by pulse-Fourier methods at 22.6 MHz. The $^{13}C$-H coupling constants of the cyanoalkylidene derivatives are approximately proportional to the respective $^{13}C$ shifts from tetramethylsilane as measured by computer. The acetyl methyl $^{13}C$ signals of carbohydrate acetates are often coincident and afford little stereochemical information. For structural analysis, these resonances may be resolved by use of the $Eu(fod)_3$ or $Pr(fod)_3$ shift reagents.

**14148.** Daywitt, W. C., **A reference noise standard for millimeter waves,** *IEEE Trans. Microwave Theory Tech.* **MTT-21,** No. 12, 845-847 (Dec. 1973).

Key words: millimeter waves; noise calibration; standard; thermal noise.

The WR15 thermal noise standard that is used as the nationa reference standard of noise power in the frequency range fron 56 to 64 GHz is described in this short paper. The source form a basis for both the noise-power comparison service and noise figure service offered by the National Bureau of Standards in thi frequency range.

**14149.** Pyke, T. N., Jr., **Some technical considerations for improved service to computer network users,** (Proc. 7th Annua IEEE Computer Conference, San Francisco, Calif., Feb. 27 Mar. 1, 1973), Paper in *Computing Networks from Mini through Maxis—Are they Real?, Digest of Papers*, pp. 53-5 (1973).

Key words: computer network; computer service; mar computer interface.

A variety of required and desired communications support se vices to users of computer networks are described. The gener framework for these services is a large resource sharing networ in which a number of host computer systems provide service users through suitable communication facilities. Both interacti and noninteractive users are considered, and some alternativ are outlined for implementation necessary to provide these us services.

**14150.** Unassigned.

**14151.** DiChio, D., Natali, S. V., Kuyatt, C. E., Galejs, A., **U of matrices to represent electron lenses. Matrices for the tw tube electrostatic lens,** *Rev. Sci. Instrum.* **45,** No. 4, 566-5 (Apr. 1974).

Key words: focal properties; matrix elements; paraxi strong lenses; two-tube electrostatic lens; weak lenses.

The use of matrices to represent electron lenses is discuss It is shown that it is more convenient and natural to represen lens by a matrix and that the matrix elements show a more re lar behavior than do the focal properties. Thus matrices are m convenient to use in computer programs. Matrix elements for two-tube electrostatic lens are presented and their propert discussed. A simple analytical form for the matrix elements lenses with near-unity voltage ratios is given.

**14152.** Penn, D. R., Plummer, E. W., **Field emission as a prob the surface density of states,** *Phys. Rev. B* **9,** No. 4, 1216-12 (Feb. 15, 1974).

Key words: field emission; metal surface; photoemissi surface density of states; total energy distribution.

Field-emission measurements of the total-energy distribut from a clean metal surface are shown to provide informat about the density of states near the surface. Specifically, we f the field-emitted current per unit energy at energy $\omega$ to be gi approximately by $j(\omega) \simeq (2\hbar/m)S\lambda^{-2}(\omega)\Sigma_m$ $D_0^2(E$ $\times|\psi_m(\chi_m)|^2\delta(\omega-\epsilon_m)$, where $D_0^2$ is the usual barrier-penetra probability with image potential corrections, $E_\perp{}^m=$ $\hbar^2k_{\parallel}{}^2/2m$, where $k_{\parallel}$ is the electron momentum parallel to the face, $|\psi_m(\chi_m)|$ is the amplitude of the metal electron at the cla cal turning point ($\chi_m \sim$ 1-2 Å), $\lambda(\omega)$ is a slowly varying func of $\omega$, and $S$ is the metal surface area. The $D_0^2$ factor in strongly weights electron states with small $k_{\parallel}$ and conseque $j(\omega)$ measures the density of states at $\chi_m$ arising from the c ponent of the bulk band structure normal to the surface. M surements of $j(\omega)$ for several single-crystal planes of tungsten be presented and compared to the relevant photoemission d

**14153.** Fowlkes, C. W., **Fracture toughness tests of a rigid po rethane foam,** *Int. J. Fract.* **10,** No. 1, 99-108 (Mar. 1974).

Key words: fracture; fracture toughness; polyureth foam.

he results of some exploratory tests for determining the frac- toughness of a rigid polyurethane foam are presented. The cimen geometries used included center- and double-edge- cked plates, the single-edge-cracked tensile specimen and the ble cantilever beam specimen. The validity of applying the cepts of linear elastic fracture mechanics to the fracture of foam is discussed. Some unique features of the fracture of m are discussed.

54. Fatiadi, A. J., **New applications of periodic acid and eriodates in organic and bio-organic chemistry,** *Synthesis eviews,* No. 4, 229-272 (Apr. 1974).

Key words: application; bio-organic; methods; organic; oxidation; periodates; review.

ecent applications of periodic acid and periodates to organic bio-organic chemistry are reviewed. Unique periodate ox- ions and synthetic methods employing periodates are cussed.

55. Bagchi, A., Gomer, R., Penn, D. R., **The field emission otal energy distribution in the presence of adsorbates,** *Surface ci.* **41,** 555-558 (1974).

Key words: adsorbed molecules on metal surfaces; Anderson Model; energy distribution of field emitted electrons; field emission theory; metal surface; overcomplete states.

he total energy distribution (TED) of field-emitted electrons m an adsorbate-covered metal surface is studied within the nework of the Anderson Hamiltonian, but taking over- npleteness of states into account. The correct asymptotic avior of the adsorbate wavefunction, postulated in the previ- work, is now established, and a numerical correction factor 15) to the adsorbate induced current density is obtained.

56. Farabaugh, E. N., **X-ray microscopy of single-crystal otassium dideuterium phosphate,** *J. Appl. Phys. Commun.* **45,** o. 4, 1905-1907 (Apr. 1974).

Key words: dislocations; KD*P; Lang technique; solution grown; x-ray diffraction microscopy.

xamination of solution-grown KD*P single crystals by the ng technique has shown that the crystals are free from growth ls, impurity segregation, and subgrain boundaries. The densi- of dislocations varies throughout the volume of the crystals, ne areas being nearly dislocation free. One Burgers vector ntified as being parallel to ⟨100⟩ is common to the similar P and ADP single crystals.

57. Bonnelle, C., Karnatak, R. C., Sugar, J., **Photoabsorption n the vicinity of 3*d* absorption edges of La, $La_2O_3$, Ce, and $eO_2$,** *Phys. Rev. A* **9,** No. 5, 1920-1923 (May 1974).

Key words: absorption; Ce; La; x rays.

bservations of photoabsorption in La, $La_2O_3$, Ce, and $CeO_2$, he vicinity of the 3*d* edges are given. Calculations of relative orption intensities for Ce are shown to correspond well with experimental data.

58. Negas, T., Roth, R. S., Parker, H. S., Minor, D., **ubsolidus phase relations in the $BaTiO_3$-$TiO_2$ system,** *J. Solid tate Chem.* **9,** 297-307 (1974).

Key words: barium-titanium oxides; $BaTiO_3$-$TiO_2$ system; crystal structure; phase equilibria.

$a_6Ti_{17}O_{40}$, $Ba_4Ti_{13}O_{30}$, $BaTi_4O_9$, and $Ba_2Ti_9O_{20}$ are the only mpounds which were found to have a stability range in the osolidus of the $BaTiO_3$ - $TiO_2$ system. $BaTi_2O_5$ and $BaTi_5O_{11}$, orted in other studies, apparently are not stable. The com- und reported as $Ba_2Ti_5O_{12}$ appears to have been mistaken for $_6Ti_{17}O_{40}$. X-ray diffraction powder data are given for this phase which is monoclinic with $a = 9.890$, $b = 17.117$, $c = 18.933$ Å and $\beta = 98°42.6'$. The phase formulated previously as $BaTi_3O_7$ is shown to be $Ba_4Ti_{13}O_{30}$ based on structural and density considerations, phase equilibria, and single crystal and powder x-ray diffraction data. This compound is othorhombic with $a = 17.072$, $b = 9.862$, and $c = 14.059$ Å, probable space group, *Cmca.* An idealized structure for this phase is proposed. $Ba_2Ti_9O_{20}$ decomposes above 1300 °C in the solid state to $BaTi_4O_9$ plus rutile. Single crystals were grown using $BaF_2$ as a mineralizer.

14159. Jones, M. C., Giarratano, P. J., McConnell, P. M., Arp, V., **Refrigeration with forced flow of helium,** *Proc. Cryogenic Cooler Conf., USAF Academy, Colorado Springs, Colo., Oct. 16-17, 1973,* pp. 441-462 (Air Force Flight Dynamics Laboratory (FEC), Wright-Patterson Air Force Base, Ohio, Dec. 1973).

Key words: forced flow; heat transfer; helium; pump; refrigeration.

The operation of practical superconducting components usually generates some heat because on nonideality of the superconductors, particularly in a.c. applications. In many cases, e.g., pulsed magnets, system design and performance is strongly constrained by the available heat transfer between the superconductor and the surrounding helium. We have been studying the general problems of maintaining the required refrigeration by forced flow of helium.

The desired helium flow can be obtained either directly from the refrigerator system (i.e., room temperature compressors) or from auxiliary pumps which offer additional system flexibility at the cost of probable additional thermal load on the refrigerator. We have evaluated centrifugal pump performance in superfluid, normally boiling, and supercritical helium, with results in approximate accord with scaling laws and pump performance measurements in other fluids. Cavitation limits and other performance considerations in helium will be presented.

14160. Rook, H. L., LaFleur, P. D., Suddueth, J. E., **Trace element determination using a high yield electromagnetic isotope separator and neutron activation—the determination of cadmium,** *Nucl. Instrum. Methods* **116,** 579-586 (1974).

Key words: cadmium; high yield mass separator; neutron activation.

The use of isotope separators capable of producing high beam currents as applied to neutron activation analysis is discussed. The specificity of mass separation in this application allows beta or gross gamma counting to be used thereby providing increased sensitivity. The definition of instrument operational parameters and capabilities are discussed. Such parameters as yield, memory, resolution, overlap, and sputtering are considered. The optimized use of the mass separator as applied to the determination of cadmium in submicrogram quantities is presented.

14161. McCulloh, K. E., Walker, J. A., **Photodissociative formation of ion pairs from molecular hydrogen and the electron affinity of the hydrogen atom,** *Chem. Phys. Lett.* **25,** No. 3, 439-442 (Apr. 1, 1974).

Key words: deuterium; electron affinity; hydrogen atom; ion-pair formation; para-hydrogen; photodissociation.

Photodissociative production of ion pairs from $H_2$ has been observed in the wavelength range 706-718 Å at spectral resolutions of 0.4 and 0.22 Å. From measured thresholds for production of $H^-$ from $H_2$ molecules in each of the three lowest rotational states, the lower bound $EA(H) \geqslant 0.754 \pm 0.002$ eV is obtained, in excellent agreement with the theoretical electron affinity of 0.75421 eV. For formation of $D^-$ from $D_2$, a threshold assigned to molecules in the rotational state $J = 2$ has been measured, from which the bound EA(D) $\geqslant 0.757 \pm 0.005$ eV is obtained. Negative ion yield curves are presented for hydrogen.

**14162.** Yates, J. T., Jr., Madey, T. E., Erickson, N. E., **ESCA study of carbon monoxide and oxygen adsorption on tungsten,** *Surface Sci.* **43,** 257-274 (1974).

Key words: carbon monoxide; chemical shift; chemisorption; ESCA; oxygen; tungsten.

The chemisorption of both CO and $O_2$ on a clean tungsten ribbon has been studied using an ultrahigh vacuum x-ray photoelectron spectrometer. For CO, the energy and intensity of photoemission from O(ls) and C(ls) core levels have been studied for various adsorption temperatures.

At adsorption temperatures of ~ 100 K, the "virgin"-CO state was the dominant adsorbed species. Conversion of this state to more strongly-bound $\beta$-CO is observed upon heating the adsorbed layer to ~ 320 K. Thermal desorption of CO at $300 \leqslant T \leqslant 640$ K causes sequential loss of $\alpha_1$-CO and $\alpha_2$-CO as judged by the disappearance of O(ls) and C(ls) photoelectron peaks characteristic of these states.

Oxygen adsorption at 300 K gives a single main O(ls) peak at all coverages, although at high oxygen coverages there exist small auxiliary peaks at ~2 eV lower kinetic energy. The photoelectron C(ls) and O(ls) binding energies observed for these adsorbed species are all lower than for gaseous molecules containing C and O atoms. For CO adsorption states there is a systematic decrease in photoelectron binding energy as the strength of adsorption increases. These observations are in general accord with expectations based on electronic relaxation effects in condensed materials.

**14163.** Van Brunt, R. J., Kieffer, L. J., **Electron energy dependence of the energy and angular distributions of $O^-$ from dissociative ion pair formation in $O_2$,** *J. Chem. Phys.* **60,** No. 8, 3057-3063 (Apr. 15, 1974).

Key words: dissociation; electron; ionization; molecular oxygen.

The energy and angular distributions of $O^-$ produced from $O_2$ by dissociative ion pair formation have been measured at selected incident electron energies from threshold to 100 eV. The kinetic energy distributions show well-defined maxima near 2.0 and 3.3 eV with appearance potentials, respectively, at 20.0 and 23.0 eV. The angular distributions are peaked in the forward and backward directions relative to electron beam and exhibit nondipolar structure. The shape of the distributions depends on electron energy, becoming more isotropic with increasing energy. An attempt has been made to explain the behavior of the angular distributions in terms of a superposition of final states using a multipole expansion of the differential cross section which includes the effects of higher-order partial waves.

**14164.** Diller, D. E., **The Clausius-Mossotti functions (molar polarizabilities) of pure compressed gaseous and liquid methane, ethane, propane, butanes, and nitrogen,** *Cryogenics* **14,** No. 4, 215-216 (Apr. 1974).

Key words: butanes; Clausius-Mossotti function; density; dielectric constant; ethane; interpolation function; LNG components; methane; mixtures; nitrogen; propane.

This report gives accurate interpolation functions for the Clausius-Mossotti functions (molar polarizabilities) of pure compressed gaseous and liquid methane, ethane, propane, butanes and nitrogen; and suggests a method for calculating the dielectric constants or the densities of their mixtures. The accuracy of calculated Clausius-Mossotti functions for mixtures containing a high concentration of methane is expected to be better than 1 percent using only data for the pure components. Additional data for the dependence of the excess Clausius-Mossotti function on composition could reduce the uncertainty in Clausius-Mossotti functions for multicomponent mixtures to less then 0.2 percent.

**14165.** Gadzuk, J. W., **Surface molecules and chemisorption. I Adatom density of states,** *Surface Sci.* **43,** 44-60 (1974).

Key words: chemisorption; molecules; surfaces.

A useful picture of chemisorption on metal surfaces is one i which a localized molecule is formed between the adatom and it nearest neighbor substrate atoms. The interaction responsibl for the molecule formation is treated as the coupling between th adsorbate state and a group orbital formed from a linear com bination of atomic orbitals on the substrate atoms. Within th surface molecule picture, level width and level shift function given by Newns modification of the Anderson theory, have bee calculated and the resulting adatom density of states function ha been obtained. This has been done for model systems in whic the substrate is either a free electron metal or a tightbinding band metal and the adsorbate is s or p like. The results show ho it is possible to simultaneously have narrow virtual levels due t chemisorption (~ 1 eV) which previously implied weak intera tions and also high binding energies (> 3 eV) as are observed e perimentally.

**14166.** Gilman, F. J., Kugler, M., Meshkov, S., **Transformati between current and constituent quarks and transitions betwe hadrons,** *Phys. Rev. D* **9,** No. 3, 715-735 (Feb. 1, 1974).

Key words: cross sections; reactions; regge pole; SU(3 symmetry breaking; trajectory.

The transformation from current- to constituent-quark ba states is discussed. Certain algebraic properties of the tra formed vector and axial-vector currents are abstracted from t free-quark model and assumed to hold in nature. Supplement by the partially conserved axial-vector current hypothesis a assumptions about the identification of the observed hadro with simple constituent-quark states, the algebraic properties the transformed currents are used to compute the pion a photon transitions between any two hadron states. Gene selection rules are stated. Many specific matrix elements both meson and baryon decays are tabulated, and both their m nitudes and signs are compared with experiment.

**14167.** McDonald, D. G., Peterson, F. R., Cupp, J. D., Da son, B. L., Johnson, E. G., **Josephson junctions at 45 times energy-gap frequency,** *Appl. Phys. Lett.* **24,** No. 7, 335- (Apr. 1, 1974).

Key words: cryogenics; infrared; Josephson juncti lasers; superconductivity.

Superconductive Nb-Nb point contacts have been stu with 9.5-$\mu$m radiation from $CO_2$ lasers. Two models are c sidered to explain the experiments: one is Wertham Josephson junction model and the other is a thermally modul Josephson junction. The evidence favors Werthamer's model is not conclusive.

**14168.** Haque, S. S., Lees, R. M., Saint Clair, J. M., Beers, Johnson, D. R., **Microwave spectrum of $^{13}C$ metha** *Astrophys. J.* **187,** L-15 – L-17 (Jan. 1, 1974).

Key words: carbon-13; methanol.

Laboratory measurements of the frequencies of some tronomically interesting transitions of the $^{13}C$ isotopic specie methanol are reported. Most lines of the $J = 2 \leftarrow 1, 3 \leftarrow 2, 4$ $\mu_a$-type $\Delta k = 0$ transitions in the 94-, 142-, and 189-GHz regi have been measured, as well as a number of $\mu_b$-type transit in the 14-50 GHz region. The standard deviation of fit with constants given is 0.098 MHz. The remaining unmeasured in these $R$-branch patterns have been predicted with an un tainty of 0.3 MHz.

169. Unassigned.

170. DiChio, D., Natali, S. V., Kuyatt, C. E., **Focal properties of the two-tube electrostatic lens for large and near-unity voltage ratios,** *Rev. Sci. Instrum.* **45,** No. 4, 559-565 (Apr. 1974).

Key words: focal properties; near-unity voltage ratios; object-image curves; paraxial; two-tube electrostatic lens; weak lenses.

Accurate calculations of focal properties of the two-tube elec- static lens are extended to cover a range of voltage ratios from to 10000. The accuracy of the calculations is discussed in tail. For voltage ratios near 6400 the lens is found to be tele- opic. Results are given in tabular form and as *P-Q* (object- age) curves. A simple analytical form for the focal properties lenses with near-unity voltage ratios is given.

171. Roder, H. M., **ASRDI oxygen technology survey. Volume V: Density and liquid level measurement instrumentation for the cryogenic fluids oxygen, hydrogen, and nitrogen,** *NASA Spec. Publ.* **3083,** 67 pages (National Aeronautics and Space Administration, Washington, D.C., 1974).

Key words: density; instrumentation; liquid level; phase detection; quantity gaging.

This volume of the survey presents information on instrumen- ion for density measurement, liquid level measurement, quan- y gaging, and phase measurement. Information directly con- rned with oxygen was given primary emphasis, work not ecifically designated for oxygen, but considered of potential lue in oxygen service was included. The information available each instrument is presented under the headings: reference(s), strumentation type, physical principle, phase of operation, a scription of the instrument, materials of construction signifi- nt to oxygen compatibility, calibration method, performance aracteristics, oxygen service, and limitations. The report also esents a discussion of problem areas in density and liquid level easurement, and recommends areas for further research and velopment.

172. Naimon, E. R., Weston, W. F., Ledbetter, H. M., **Elastic properties of two titanium alloys at low temperatures,** *Cryogenics* **14,** No. 5, 246-249 (May 1974).

Key words: bulk modulus; compressibility; Debye temperature; elastic constant; Poisson's ratio; shear modulus; sound velocity; titanium alloys; Young's modulus.

Sound velocities and elastic constants were determined semi- ntinuously for two annealed polycrystalline titanium alloys tween 4 and 300 K. Results are given for: longitudinal sound locity, transverse sound velocity, Young's modulus, shear odulus, bulk modulus, Poisson's ratio, and elastic Debye tem- rature. A pulse-superposition technique was used.

173. McCarty, R. D., **A modified Benedict-Webb-Rubin equation of state for methane using recent experimental data,** *Cryogenics* **14,** No. 5, 276-280 (May 1974).

Key words: equation of state; methane.

A 33 term modified Benedict-Webb-Rubin equation of state is esented for methane. The adjustable parameters in the equa- on of state have been estimated using recent experimental data d least squares techniques which include the thermodynamic uilibrium conditions for the co-existing liquid and vapour ases. Comparisons of the new equation of state and an older odified Benedict-Webb-Rubin equation of state to experimen- l data are given.

174. Broadhurst, M. G., Malmberg, C. G., Mopsik, F. I., Harris, W. P., **Piezo- and pyroelectricity in polymer electrets,** (Proc. Conf. on Electrets, Charge Storage and Transport in Dielectrics, Miami Beach, Fla., Oct. 8-13, 1972), Chapter in *Electrets, Charge Storage and Transport in Dielectrics,* M. M. Perlman, Ed., pp. 492-504 (Electrochemical Society, New York, N.Y., 1973).

Key words: dipoles; electret; glass transition; polymer; pyroelectric.

A model for a polymer electret, based on an elastically isotropic solid with orientationally frozen molecular dipoles, was developed and tested experimentally. This electret is shown to be both piezoelectric and pyroelectric. The polarization is shown to change with mechanically and thermally induced strains in the polarization direction. The currents generated by the electret will be proportional to the strain rate and, for thin contact electrodes and uniform strains, unaffected by the presence of real charges. Poly (vinyl chloride) films were poled at 80 °C, just above their glass transition temperature. The pressure- and temperature-induced short-circuit currents in the polarization direction equalled 0.15(pA/cm$^2$)/(bar/min) and 2.2 (pA/cm$^2$)/(K/min) respectively for a specimen poled at 320 kV/cm. These currents were 1) reversible and proportional to the rate of temperature or pressure change, 2) proportional to poling voltage up to 320 kV/cm, 3) in the direction corresponding to increasing polarization with increasing pressure and decreasing temperature, 4) stable with time without special storage conditions, 5) about 1.6 times as great for temperature induced strains as for equivalent pressure induced strains and 6) about 2-4 times as great in magnitude as expected from dielectric constant measurements. The apparent polarization from temperature measurements for the 320 kV/cm specimen was about 1.7 $\mu$C/cm$^2$, or about 1/3 the value expected for maximum alignment of dipoles. In the same specimen the pyroelectric coefficient was found to be $p_3 = -0.39$ nC/cm$^2$ K and, assuming elastic isotropy, the piezoelectric strain coefficients were found to be $d_{31} = d_{32} = d_{33} = -0.89$ pC/N.

14175. Powell, R. L., Fickett, F. R., Birmingham, B. W., **Programs on large scale applications of superconductivity in the United States,** (Proc. NATO Advanced Study Institute, Superconducting Machines and Devices-Large Systems Applications, Entreves, Italy, Sept. 5-14, 1973), Chapter 17 in *Superconducting Machines and Devices-Large Systems Applications,* S. Foner and B. B. Schwartz, Eds., pp. 651-675 (Plenum Publishing Corp., New York, N.Y., 1974).

Key words: electrical machinery; land transportation; power transmission; propulsion systems; superconducting devices; superconducting magnets; superconductivity.

A brief overview is given of U.S. programs on large-scale applications of superconducivity. Tables are presented listing for each project: the organization; the manager; a description of the device; a comment on the type of program; the source and amount of funding; the current status and the projected plans. The seven major project categories are: (1) Generators for electric power systems; (2) Power transmission; (3) Machinery for propulsion systems; (4) Magnets for energy storage, MHD and CTR systems; (5) Magnets and cavities for high energy physics experiments; (6) Magnets for industrial and medical applications; (7) Land transportation systems.

14176. Brennan, J. A., **LNG measurement projects at NBS,** *Proc. 49th Int. School of Hydrocarbon Measurement, Norman, Okla., Apr. 16-18, 1974,* pp. 464-465 (1974).

Key words: description; LNG; projects.

This paper presents, in summary form, the projects at the Cryogenics Division of NBS involved with LNG or LNG related measurements. A brief description of each project is given along with identification of the sponsoring agency.

14177. Krauss, M., Neumann, D., **Multi-configuration self-consistent-field calculation of the dissociation energy and electronic structure of hydrogen fluoride,** *Mol. Phys.* **27,** No. 4, 917-921 (1974).

Key words: configuration interaction; dipole moment; dissociation energy; electronic structure; HF; quadrupole moment.

The optimized valence configuration method of Wahl and Das is applied to a study of the electronic structure of FH at the equilibrium internuclear separation. A compact eight configuration wave function is found to yield an accurate dissociation energy and dipole moment.

14178. Soulen, R. J., Jr., **Calibration of paramagnetic thermometers using superconductive fixed points,** *Cryogenics* **14,** No. 5, 250-252 (May 1974).

Key words: fixed points; paramagnetism; superconductivity; temperature.

A new method for calibration of paramagnetic materials is described. The technique consists of fitting the temperature-dependent mutual inductance of a coil set surrounding a paramagnetic material to a Curie Law using the superconductive transitions of several elements as thermometric fixed points. As a particular demonstration of this technique, the paramagnetic salt, cerous magnesium nitrate, was calibrated using the superconductive transitions of aluminium, zinc, and cadmium. The temperature scale obtained in this way was used in a study of the superconductive properties of iridium.

14179. Chang, S. S., Bestul, A. B., **Heat capacities of selenium crystal (trigonal), glass, and liquid from 5 to 360 K,** *J. Chem. Thermodyn.* **6,** 325-344 (1974).

Key words: annealed and quenched glasses; calorimetry; glass transformation; heat capacity; selenium; supercooled liquid; thermodynamic properties; trigonal selenium.

Heat capacities of high purity selenium (better than 99.999 moles percent) have been measured for the trigonal crystal from 5 to 360 K, for the quenched and annealed glasses from 5 K to $T_g$ (around 300 K) and for the supercooled liquid from $T_g$ to 340 K. The glass transformation temperature $T_g$, as determined from plots of $H$ against $T$, is 304 K for the quenched glass and 295 K for the annealed glass. $C_p$ of the glass is higher than that of the crystal over the entire temperature range of investigation. $C_p$ $\{H(T) - H(\mathrm{c}, 0)\}$, and $S$ for the trigonal form of Se at 298.15 K are 25.05 J $K^{-1}$ $mol^{-1}$, 5509 J $mol^{-1}$, and 42.27 J $K^{-1}$ $mol^{-1}$, respectively. The corresponding thermodynamic properties of the annealed Se glass at 298.15 K, evaluated by incorporating the present results with recently published high-temperature data, are 26.23 J $K^{-1}$ $mol^{-1}$, 9363 J $mol^{-1}$, and 48.60 J $K^{-1}$ $mol^{-1}$, respectively. The residual entropy of the annealed Se glass is estimated to be 3.6 J $K^{-1}$ $mol^{-1}$ at $T = 0$.

14180. Walls, F. L., Dunn, G. H., **Measurement of total cross sections for electron recombination with $NO^+$ and $O_2^+$ using ion storage techniques,** *J. Geophys. Res.* **79,** No. 13, 1911-1915 (May 1, 1974).

Key words: ion storage technique; recombination of $NO^+$; recombination of $O_2^+$.

The total cross section as a function of electron energy for recombination of electrons with room temperature $NO^+$ has been measured with a trapped ion technique. Measurements were made in the electron energy range 0.045-4 eV with an energy resolution between 0.045 and 0.120 eV, and the cross sections, which showed some structure, ranged from $1.25 \times 10^{-14}$ $cm^2$ at the lowest energy to $1.7 \times 10^{-16}$ $cm^2$ at the highest energy. Similar measurements were made on $O_2^+$, the species used to calibrate the apparatus geometry. A Maxwellian distribution of electron velocities was used with the measured cross sections to calculate rate constants, giving values extending to electron temperatures as high as 40,000 K. Comparison with previously measured rate coefficients at lower temperatures is quite satisfactory.

14181. Burke, J. M., Ritter, J. J., Lafferty, W. J., **Infrared and Raman spectra of ethynyldifluoroborane ($HC_2BF_2$) and ethynyldichloroborane ($HC_2BCl_2$),** *Spectrochim. Acta* **30A,** 993-999 (1974).

Key words: ethyldifluoroborane; ethynyldichloroborane; gas phase; infrared; Raman; spectra.

The vapor phase infrared and Raman spectra of several isotopic species of ethynyldifluoroborane ($HC_2BF_2$) and ethynyldichloroborane ($HC_2BCl_2$) have been obtained. Vapor phase band contours, Raman polarization data, characteristic group frequencies, and isotopic frequency shifts have been used to make the vibrational assignments for these molecules.

14182. Risley, E. W., Jr., **Discontinuity capacitance of a coaxial line terminated in a circular waveguide. II. Lower bound solution,** (Proc. Conf. Precision Electromagnetic Measurement
Boulder, Colo., June 26-29, 1972), *CPEM Digest,* p. 111
(1972).

Key words: coaxial line reactance termination; discontinui-
ty capacitance; lower bound.

The standard of reflection for coaxial line is the quarter wav
short circuit termination. There are shortcomings to this stan
dard; the fabrication cost is high and each termination is usabl
at only one frequency. However, an open-circuited coaxial lin
with extended outer conductor and solid inner conductor coul
be used advantageously as a standard termination because fabri
cation can be made using commercially available component
the device is broad-banded and losses are minimal. In addition t
the high-frequency application, the termination can also be use
at low frequencies as a standard of capacitance.

In an earlier paper (Discontinuity Capacitance of a Coaxi
Line Terminated in a Circular Waveguide, Vol. MTT-17, No.
Feb. 1969), the input admittance $y_{in}$ of this termination was ca
culated, assuming perfect conductivity, using a variation
technique. A stationary form was derived for $y_{in}$ which dete
mined an *upper bound* to the discontinuity capacitance of the te
mination.

14183. Drummond, D. L., Gallagher, A., **Potentials and co
tinuum spectra of Rb-noble gas molecules,** *J. Chem. Phys.* 6
No. 9, 3426-3435 (May 1, 1974).

Key words: molecules; rubidium.

Rubidium vapor is optically excited by either of the atom
resonance lines in the presence of typically 400 torr of He, N
Ar, Kr, or Xe. Normalized emission spectra of the far wings
these resonance lines are then measured as a function of te
perature. These far wings, extending as much as 1000 Å from t
resonance lines, are interpreted as molecular continuum rad
tion of Rb-noble gas molecules. Using the quasistatic theory
line broadening, or the classical Franck-Condon principle, the
spectra are analyzed to yield the ground and excited st
molecular potentials.

14184. Carrington, C. G., Gallagher, A., **Teratomic recombi
tion of excited RbXe,** *J. Chem. Phys.* **60,** No. 9, 3436-34
(May 1, 1974).

Key words: molecules; recombination.

Free Rb(5 $^2S$) is optically excited to Rb*(5 $^2P_{1/2}$) in
presence of Xe gas, and the RbXe*($A$ $^2\Pi_{1/2}$) → RbXe($X$ $^2\Sigma$
fluorescence is measured as a function of xenon pressure. T
teratomic recombination process, Rb* + 2Xe → RbXe* +
and other collision processes compete with radiative decay. T
radiative rate is known, so collisional rates can be inferred fr
the data. The molecular spectrum is observed as a continu
whose intensity profile yields the bound-state vibrational
tribution at each xenon pressure. The low-pressure limit of

stribution yields the teratomic recombination rate as a function vibrational state, and the total recombination rate constant $k_f$. ne recombination rate into a bound state increases with in-easing binding energy, but less rapidly than the increase in uilibrium population. The transition from this initially formed stribution to the high-pressure equilibrium distribution is re-orted. The ratio $k_f/K_{eq} = 2.4 \times 10^{-11}$ cm$^3$/sec and the equilibrium nstant $K_{eq} \simeq 3.4 \times 10^{-21}$ cm$^3$, corresponding to the experimen-l temperature of 300 K, are deduced from the data. The $A\ ^2\Pi_{1/2}$ nd $X\ ^2\Sigma_{1/2}$ potentials are also obtained from analysis of the spec-um in the low-pressure and high-pressure limits.

**4185.** Roth, R. S., Parker, H. S., Brower, W. S., Minor, D., **Alkali oxide-tantalum oxide and alkali oxide-niobium oxide ionic conductors,** *NASA CR-134599*, 60 pages (National Aeronautics and Space Administration, Washington, D.C., Apr. 1974).

Key words: alkali ions; ionic conductors; niobates; tantalates.

A search was made for new cationic conducting phases in al-ali-tantalate and niobate systems. The phase equilibrium dia-ams were constructed for the six binary systems $Nb_2O_5$-$iNbO_3$, $Nb_2O_5$-$NaNbO_3$, $Nb_2O_5$-$KNbO_3$, $Ta_2O_5$-$LiTaO_3$, $a_2O_5$-$NaTaO_3$ and $Ta_2O_5$-$KTaO_3$. Various other binary and ter-ary systems were also examined. Pellets of nineteen phases ere evaluated (by the sponsoring agency) by dielectric loss easurements. Attempts were made to grow large crystals of ght different phases. The system $Ta_2O_5$-$KTaO_3$ contains at ast three phases which showed peaks in dielectric loss vs. tem-erature. All three contain structures related to the tungsten onzes with alkali ions in nonstoichiometric crystallographic ositions.

**4186.** Fickett, F. R., **Oxygen annealing of copper: A review,** *Mater. Sci. Eng.* **14,** No. 3, 199-210 (June 1974).

Key words: annealing; copper; oxidation; purification.

A useful technique for significantly increasing the low tem-erature electrical conductivity of copper is heating in the resence of a reduced pressure of oxygen. The same technique sometimes used on dilute alloys to produce dispersion harden-g by oxide particles. This paper reviews the literature on the xidation process in copper. Particular emphasis is on oxidation increase conductivity. A set of conditions for a purifying an-eal are presented. A brief discussion of dispersion hardening by xidation and of several chemisorption experiments is included.

**4187.** Radford, H. E., Evenson, K. M., Howard, C. J., **$HO_2$ detected by laser magnetic resonance,** *J. Chem. Phys.* **60,** No. 8, 3178-3183 (Apr. 15, 1974).

Key words: free radical; $HO_2$; laser magnetic resonance.

Far-infrared absorption spectra of $HO_2$ in the gas phase have een detected at six wavelengths of a water vapor laser magnetic esonance spectrometer. The identification of $HO_2$ as the ab-orbing molecule is based on a partial analysis of the spectra and n a variety of different chemical methods used to produce the adical. Approximate values of rotational constants and spin oublet separations are derived from the spectra.

**4188.** Stephenson, J. C., Mosburg, E. R., Jr., **Vibrational energy transfer in CO from 100 to 300 K,** *J. Chem. Phys.* **60,** No. 9, 3562-3566 (May 1, 1974).

Key words: carbon monoxide; $CO_2$ lasers; combustion; optical pumping of molecules; vibrational relaxation.

The laser fluorescence method, whereby CO molecules are ptically pumped from the vibrational level $v=0$ to the $v=1$ tate by frequency-doubled pulses from a $CO_2$ laser, has been sed to determine vibrational energy transfer rate coefficients for O. Rates for the *V-V* exchange processes $CO(0)+N_2(1) \rightarrow CO(1)+N_2(0)$ and $CO(1)+CO(1) \rightarrow CO(0)+CO(2)$, and for the deactivation of CO(1) by $H_2$ have been measured in the range $100\ K \leq T \leq 300\ K$. The probability of energy transfer from $N_2$ to CO decreases slightly as $T$ decreases in this range, while the probability of the CO-CO *V-V* process is approximately proportional to $T^{-1}$. Rate coefficients were also measured at $T = 297$ K for the deactivation of CO(1) by the polyatomic molecules $CH_4$, $C_2H_4$, $C_2H_6$, HCOOH, $CH_3COOH$, $CH_3CHO$, $CH_3OH$, $C_2H_5OH$, $H_2O$, $D_2O$, $H_2S$, and $C_4H_{10}$.

**14189.** Ambrose, J. R., Kruger, J., **Tribo-ellipsometric study of the repassivation kinetics of a Ti 8Al-1Mo-1V alloy,** *J. Electrochem. Soc.* **121,** No. 5, 599-604 (May 1974).

Key words: repassivation kinetics; stress corrosion cracking; titanium alloy; tribo-ellipsometry.

The tribo-ellipsometric technique allows one to distinguish between film growth and other reactions that occur after removal of a film from a metal surface in a given environment. This technique was used to study the relationship between repassivation kinetics and stress corrosion cracking (SCC) susceptibility for Ti 8Al-1Mo-1V alloy. In these studies the effect of the rate of film growth on the amount of metal dissolution which occurs during the repassivation process was investigated by comparing the repassivation transient behavior in a 1.0*N* NaCl solution, where cracks have been found to propagate, to that in a 1.0*N* $NaNO_3$ solution where SCC susceptibility has never been detected. Film growth kinetics in both solutions were consistent with a Fleischmann-Thirsk mechanism of oxide patch nucleation and two-dimensional growth, although the film growth rate was significantly slower in the 1.0*N* NaCl solution. Low film growth rate led to an increase in metal dissolution in a solution where crack propagation velocities have been measured, but at an apparent rate slower than necessary to propagate such cracks by metal dissolution alone.

**14190.** Page, C. H., **Tetrahedral junction error contribution to a series-parallel four-terminal resistor,** *IEEE Trans. Instrum. Meas.* **IM-23,** No. 1, 5-8 (Mar. 1974).

Key words: four-terminal; Hamon divider; resistance network; series-parallel; tetrahedral junction.

The errors of a series-parallel four-terminal resistor build-up box due to imperfections in the tetrahedral junctions are analyzed. It is shown how these errors can be made negligible by choosing orientations of the junctions.

**14191.** Allpress, J. G., Iijima, S., Roth, R. S., Stephenson, N. C., **Structural studies by electron microscopy: High-resolution observations on $\beta$-$ZrO_2 \cdot 12Nb_2O_5$,** *J. Solid State Chem.* **7,** 89-93 (1973).

Key words: $\beta$-$ZrO_2 \cdot 12Nb_2O_5$; electron microscopy; high resolution; structural studies.

Reliable idealized structures for the $\beta$ and $\gamma$ forms of $ZrO_2 \cdot 12Nb_2O_5$ have been deduced following the observation of lattice images, recorded at a resolution of about 0.3 nm, from crystals oriented with their short *b* axes parallel to the incident electron beam. The structure of the $\beta$ form is confirmed by preliminary results from single crystal x-ray studies. The present observations are compared with previous work on these phases.

**14192.** Swartzendruber, L. J., Bennett, L. H., Schoefer, E. A., DeLong, W. T., Campbell, H. C., **Mössbauer-effect examination of ferrite in stainless steel welds and castings,** *Weld. J.* **39,** No. 1, 1-S-12-S (Jan. 1974).

Key words: backscattering; casting; ferrite; Mössbauer; stainless steel; welding.

The differences between wholly austenitic, single phase stainless steels and those with two phase, partially ferritic structures have assumed commercial importance in recent years, but full utilization of the benefits to be derived from such two phase materials has been hampered by difficulties in establishing their exact ferrite contents.

The Mössbauer-effect scattering method measures the relative amounts of the austenite and ferrite phases on the basis of their magnetic properties in a way which is relatively independent of the shape, size and orientation of the ferrite particles.

**14193.** Robertson, A. F., **Effluent fire product—A crude approach to fire gas hazard assessment,** *Fire Technol.*, pp. 115-128 (May 1974).

Key words: effluent fire product; fire gas; fire hazard; gas hazard; hazard analysis; insulation; loss on ignition; potential heat.

A method is proposed for classifying the various factors influencing the life safety hazard posed during fires. Five fire hazard components are identified; these include oxygen deficiency, toxic combustion products, smoke particulates, hot gases and flame exposure. It is shown that the relative importance of these can be influenced by a number of hazard modifiers. These have been subdivided into three classes, those related to the material or product under consideration, those influenced by the fire location or degree of confinement and those associated with the people exposed.

It seems premature to try to evaluate in a quantitative way the influence of these many modifiers on the overall life hazard. However, it may serve a useful purpose in ranking materials or products with regard to the fire gas hazard to assume this is a function of the loss on ignition or the effluent fire product (EFP). An example of the usefulness of this concept is presented by a method for use of EFP in ranking insulation materials in such a manner that proper recognition is taken of their thermal properties.

A procedure making use of the potential heat test is proposed to permit avoidance of erroneously high value of EFP as a result of weight loss resulting from combined water and other inert components.

**14194.** Newman, M., **Modular quotient groups,** *Ill. J. Math.* **18,** No. 2, 265-274 (June 1974).

Key words: commutator subgroups; inclusion theorems; modular groups; quotient groups; solvability.

Let $\Gamma = SL(t,Z)$, $\Gamma(n)$ the principal congruence subgroup of $\Gamma$ of level $n$. If $t > 2$ it is shown that the commutator subgroup of $\Gamma(n)/\Gamma(nm)$ is $\Gamma(n\delta)/\Gamma(nm)$, $\delta = (m,n)$. This implies that the number of 1-dimensional representations of $\Gamma(n)/\Gamma(nm)$ is $\delta^{t^2-1}$, and that $\Gamma(n)/\Gamma(nm)$ is solvable if and only if each prime dividing $m$ also divides $n$. Similar results are proved for $t = 2$, by means of inclusion theorems proved in the paper. Another noteworthy result is that if $t > 2$, then the commutator subgroup of $\Gamma(n)$ is just $\Gamma(n^2)$.

**14195.** Abraham, B. M., Ketterson, J. B., Roach, P. R., Pfeiffer, E. R., **Demagnetization experiments on some promising new compounds for very low-temperature refrigeration,** *J. Low Temp. Phys.* **14,** Nos. 3/4, 387-396 (1974).

Key words: adiabatic magnetization; cerium compounds; cerium magnesium nitrate; low temperature thermometry; magnetic temperature; paramagnetic compounds.

We have performed demagnetization experiments on spherical specimens of silver chloride-bonded, compacted powders of four different compounds. Pure and lanthanum-diluted cerium magnesium nitrate (CMN) was studied along with two new compounds formed from cerium iodide and antipyrine and from cerium thiocyanate and triphenyl phosphine oxide. The magnetic temperatures T* were determined from measurements of the magnetic susceptibility perpendicular to the axis of the initial magnetizing field. Both the lanthanum-diluted CMN and the triphenyl phosphine oxide compounds yielded significantly lower values of T* than that obtained with CMN. The problem of thermal equilibrium within the demagnetized sample is considered.

**14196.** Tsang, W., **Thermal decomposition of 1,1,2,2-tetramethylcyclopropane in a single-pulse shock tube,** *Int. J. Chem. Kinet.* V, 651-662 (1973).

Key words: cyclohexene; decomposition; decyclization shock tube; 2,4-dimethylpentene-2; 1,1,2,2-tetramethylcyclopropane.

1,1,2,2-Tetramethylcyclopropane (TTMC) has been decomposed in a single-pulse shock tube. The main reaction process i

$$\mathrm{TTMC} \xrightarrow{k_1} \text{2,4-dimethylpentene-2(2,4 DMP-2)} \xrightarrow{k_2} (CH_3)_2C-CH-CH(CH_3)+CH_3$$

Side reactions are unimportant. From comparative rate experiments (with cyclohexene decomposition as standard) the rate expression for these reactions are

$$k_1 = 10^{14.82} \exp(-\ 31{,}320/T)\ \mathrm{sec}^1$$

$$k_2 \sim 10^{16.0} \exp(-\ 35{,}050/T)\ \mathrm{sec}^1$$

These numbers are consistent with a "best" value for cyclohexene decomposition of

$$k(cC_6H_{10} \rightarrow 1{,}3\text{-}C_4H_6 + C_2H_4) = 10^{15.15} \exp(33{,}500/T)\ \mathrm{sec}^1$$

**14197.** Kuyatt, C. E., DiChio, D., Natali, S. V., **Third-orde aberration coefficients of electron lenses. II,** *J. Vac. Sc Technol.* **10,** No. 6, 1124-1126 (Nov./Dec. 1973).

Key words: aberration integrals; asymptotic trajectorie electron lens; third-order aberration coefficients.

In the standard treatments of aberration coefficients of ele tron lenses, deviations from perfect imagery are expressed power series of the ray coordinates in the object and apertu planes. The resulting aberration coefficients depend on the o ject and aperture positions, and a complete description of t aberrations of an electron lens would require a doubly infinite s of aberration coefficients for each voltage ratio of the len Hawkes has carried out a general treatment of the third-ord aberrations of electron lenses which is independent of object a aperture positions. Six quantities are sufficient to specify t third-order aberration properties of an electron lens. We ha derived equations for these six quantities in the form of integra involving derivatives of the axial potential no higher than t second, and using our previously calculated potentials have co puted aberration coefficients for the two-tube electrostatic le

**14198.** Galejs, A., Kuyatt, C. E., **Representation of focal prop ties of the equal-diameter two-tube electrostatic lens for co puter calculations,** *J. Vac. Sci. Technol.* **10,** No. 6, 1114-11 (Nov./Dec. 1973).

Key words: electron optics; electrostatic lenses; focal p perties; lens optimization.

Previous calculations have given accurate first-order fo properties for the two-tube electrostatic lens at discrete volta ratios. For computer optimization, calculations involvi systems of two-tube lenses, one must be able to calculate focal properties continuously over some arbitrary range of vo age ratios. Hence the data must be displayed in a continu manner, and a method of interpolation is needed which yie functions having a high degree of smoothness. Special care m be taken to describe the lens behavior correctly near z ength or for the voltage ratio approaching unity. A satisfactory ution to this problem has been achieved using cubic splines. e resulting functions of the focal properties are continuous l have continuous first and second derivatives. The total beam avior, and hence the system design, is determined by the nsfer matrix which is obtained from the focal properties. To ieve sufficient accuracy in the lens calculations over the en- range of required focal properties, the region near zero lens ength had to be treated separately.

**99.** Tsang, W., **Recalculation of data on the thermal decomposi- ion of 1,1-difluoroethane and 1,1,1-trifluoroethane,** *Int. J. hem. Kinet.* **V,** 643-649 (1973).

> Key words: elimination; fluoroethane; kinetics; single pulse shock tube; thermal decomposition; 1,1-difluoroethane; 1,1,1-trifluoroethane.

Disagreements in rate constants and parameters between blished results on the decomposition of 1,1-difluoroethane and ,1-trifluoroethane are shown to originate from incorrect ecification and setting of reaction conditions in one of the stu- s. When corrected, applicable results are in excellent agree- nt.

**200.** Kuyatt, C. E., DiChio, D., Natali, S. V., **Focal properties of the two-tube electrostatic lens for large voltage ratios,** *J. Vac. Sci. Technol.* **10,** No. 6, 1118-1119 (Nov./Dec. 1973).

> Key words: electron trajectories; focal properties; P-Q curves; two-tube electrostatic lens; ultra-focal refraction.

Previous calculations of electron trajectories and first-order cal properties of the two-tube electrostatic lens have been ex- nded to a voltage ratio of 1000. Considerable ultrafocal refrac- n occurs in these strong lenses, with the result that near the ghest voltage ratio studied the two focal points are both on the w-voltage side of the lens and nearly coincident. The results e presented in the form of a table and *P-Q* (image-object) rves.

**201.** Schweitzer, W. G., Jr., Kessler, E. G., Jr., Deslattes, R. D., Layer, H. P., Whetstone, J. R., **Description, performance, and wavelengths of iodine stabilized lasers,** *Appl. Opt.* **12,** No. 12, 2927-2938 (Dec. 1973).

> Key words: iodine stabilized lasers; krypton; pressure broadening; pressure shifts; saturated absorption; wavelengths.

A description is given of lasers stabilized to components of the $I_2$ spectrum in the region of the 633-nm laser lines for $^3$He-Ne and $^3$He-$^{22}$Ne. Relationships between operational charac- ristics such as power output, peak size, and peak width are own, along with their relationships to some of the controllable rameters such as excitation level, iodine absorption, and dine pressure. We found an iodine pressure broadening of out 13 MHz/torr with a 2.6-MHz zero-pressure intercept. The equency shift associated with iodine pressure is roughly $2 \times$ $)^{-9}$ $\nu$/torr to the red. Power broadening and power shifts are nall, about a 10 percent increase in width and about $2 \times 10^{-11}$ variation in frequency for a fivefold to sixfold increase in ower. These lasers exhibit a frequency stability for 10-sec sam- ing time of about $2 \times 10^{-12}$ $\nu$ and a resetability of about $1 \times$ $)^{-10}$ $\nu$. The absolute vacuum wavelength for one iodine com- onent has been measured against the $^{86}$Kr standard—$^3$He-Ne:$^{129}I_2$, $k$ $\lambda = 632\,991.2670 \pm 0.0009$ pm. The wavelengths of everal other iodine components have been determined by mea- ring the frequency difference between them and the $^{129}I_2$, $k$ omponent. Among these are $^3$He-$^{22}$Ne:$^{129}I_2$, $B$ $\lambda = 632\,990.0742$ 0.0009 pm: and $^3$He-$^{20}$Ne:$^{127}I_2$, $i$ $\lambda = 632\,991.3954 \pm 0.0009$ m. These results were obtained using the Rowley-Hamon odel for asymmetry in the krypton line and assume that the efined value for the standard is associated with the center of gravity of the line profile. The indicated uncertainties are statistical. No allowance has been included for imperfect realization of the krypton standard or for uncertainty in the asymmetry model.

**14202.** Waterstrat, R. M., van Reuth, E. C., **Effects of compositional variations on the atomic ordering in Al5 phases,** (Proc. 3d Bolton Landing Conf. on Ordered Alloys, Lake George, N.Y., Sept. 8, 1969), Chapter in *Ordered Alloys, Structural Application and Physical Metallurgy,* pp. 95-110 (Claitor's Publ. Div., Baton Rouge, La., 1970).

> Key words: A-elements; A-site atoms; band structure; B-elements; d-electron; electron-compound; wave-functions.

Binary Al5 phases containing only transition elements have been found to possess composition ranges which shift in a regular manner consistent with periodic table positions. This is suggestive of the so-called "electron-compound" behavior previously noted for the sigma phases and other complex structures. It has been shown that deviations from the "ideal" ($A_3B$) composition are accomplished by direct substitution of A-elements and B-elements rather than by vacancy formation. The degree of long-range atomic ordering decreases as one selects elements closer to the manganese column in the periodic table. This effect may be related to the extent of overlapping for d-electron wave-functions particularly along the chains of A-site atoms and is consistent with the band structure model proposed by Labbé and Friedel.

**14203.** Arnett, R. W., Voth, R. O., **A computer program for the calculation of thermal stratification and self-pressurization in a liquid hydrogen tank,** *NASA CR-2026,* 131 pages (National Aeronautics and Space Administration, Washington, D.C., May 1972).

> Key words: computer program; cryogenic; liquid hydrogen; mathematical model; self pressurization; thermal stratification.

This report describes an analysis and computer program used to calculate the thermal stratification and the associated self pressurization of a closed liquid hydrogen tank. A sample calculation is provided as well as a description and listing of the program. Fortran-IV language is used and runs have been made on IBM 360/65 and CDC 3600 computers. Comparisons are made between the program calculations and test results from both ground and orbital coast tests of a Centaur space vehicle.

**14204.** Stiehler, R. D., **Standards and standardization,** *Am. Soc. Testing Mater. Spec. Tech. Publ.* **553,** 87-103 (1974).

> Key words: interlaboratory testing; international standards; standardization; standards.

Standards are practices established by authority, custom, or common consent. The practices embrace all activities of society including social, religious educational, and technical practices. This paper deals with technical practices embodied in national or international engineering standards. A good engineering standard should: (1) stimulate competition and not restrict trade; (2) prescribe practices which conserve natural resources; (3) be abreast of technology and not be a deterrent to desirable change arising from new knowledge, new capabilities, or new environment; (4) be concise, explicit, and limited to essential provisions and requirements; and (5) be effective in achieving its purpose.

Due to the rapid increase in the number of standards both domestically and internationally, there is a movement to control proliferation through the development and use of international standards, primarily under the aegis of the International Organization for Standardization (ISO) and the International Electrotechnical Commission (IEC). Standards developed by ISO and IEC have now become sufficient in number to be a significant factor in international trade.

Standards development has varied considerably from one industry to another, and U.S. participation in ISO and IEC has also varied from industry to industry. ISO Technical Committee 45 on Rubber and Rubber Products has been among the ten most active committees, and U.S. participation has been exceptionally effective in it. Nearly 80 percent of the 102 standards developed by ISO/TC 45 through 1972 are in accord with ASTM Standards.

Recently, there has been a growing interest in standards for consumer products, both nationally and internationally. Eight of the 20 ISO committees most recently established deal with consumer products. There has also been a growing interest in ascertaining the ability of laboratories to obtain consistent results using standard methods, both nationally and internationally. The Standard Reference Materials issued by NBS and the NBS interlaboratory programs for testing were established for this purpose. Laboratory performance, international standardization, and the development of standards for consumer products are likely to become increasingly important in future standardization efforts.

**14205.** Wagman, D. D., Jobe, T. L., Domalski, E. S., Schumm, R. H., **Temperatures, pressures, and heats of transition, fusion and vaporization,** Chapter 4j in *American Institute of Physics Handbook, Third Edition,* D. E. Gray, Ed., pages 4-222—4-261 (McGraw-Hill Book Co., New York, N.Y. 1972).

Key words: fusion heat; fusion temperature; transition heat; transition temperature; vaporization heat; vaporization temperature.

Summary of values of temperatures, pressures and heats of phase change for a selected set of inorganic and organic substances. Data for over 500 compounds are tabulated, including all elements for which thermodynamic information is available, halides, oxides, and some sulfates, nitrates, etc.

**14206.** Haber, S., Shisha, O., **Improper integrals, simple integrals, and numerical quadrature,** *J. Approximation Theory* **11,** No. 1, 1-15 (May 1974).

Key words: improper integrals; integration; numerical integration; quadrature; Riemann integrals.

The question of the convergence of numerical integration formulas (of Riemann sum type) to the improper Riemann integral $\int_0^\infty f(x)dx$ is studied. A new integral over $[0, \infty)$, more restrictive than the improper Riemann integral but not absolutely convergent, is introduced. Necessary and sufficient conditions are found for a function to be integrable in the new sense; they are stated in terms of property of functions similar to the property of being of bounded variation. A convergence theorem for the numerical integration of such functions is given, and also weaker convergence theorems for the integration of improperly Riemann-integrable functions.

**14207.** Christ, B. W., Picklesimer, M. L., **The relationship between Luder's strain, testing system compliance and other phenomenological variables affecting serrated yielding of recrystallized iron,** *Acta Met.* **22,** 435-447 (Apr. 1974).

Key words: compliance; Luder's strain; recrystallized iron; serrated yielding; tensile test.

Constant cross-head speed uniaxial tensile tests were conducted on recrystallized iron wires (0.0016 m diameter) which exhibited serrated yielding as a single Luder's band front advanced intermittently from one grip to the other. The ranges of temperature and cross-head speed were, respectively, 383 and 508 K and $8.3 \times 10^{-7} - 8.3 \times 10^{-6}$ m/s. Average load drop amplitude, $\overline{\Delta L}$, was about 25 percent of the peak stress.

The effect of testing system compliance, $C$, on the number o equal load drops, $n$, during serrated yielding was determined. I was found that the number of load drops decreased as compliance increased. The following relationships for averag Luder's band front advance during a single load drop wa established,

$$\overline{a_i}=l_0/n$$

where $l_0$ = gage length. Furthermore, it was demonstrated tha average Luder's strain during the $i$th load drop, $\epsilon_i$, is given by

$$\epsilon_i=C_i\Delta L_i/\overline{a_i}=nC_i\Delta L_i/l_0.$$

It was concluded that analysis of the $i$th load drop is a valuabl new method for studying Luder's strain during serrated yieldin

**14208.** Cali, J. P., **An idea whose time has come** (guest editorial *Clin. Chem.* **19,** 291-293 (1973).

Key words: accuracy; clinical chemistry; health.

An editorial stressing the importance of achieving accuracy i the methods used in clinical chemistry. Meaningful measuremer systems have five requirements: (1) agreement on a ration system of base units; (2) well-characterized materials (e.g., NBS SRM's) that together with (3) referee methods of proven accur cy are used to realize these units and their derivatives; (4) fiel methods used in practical application to be tested for accurac by (2) and (3); and, (5) a quality control assurance program to i sure the long-term integrity of the measurement system.

Actions initiated and completed within the past 3 years a stated showing that the achievement of accuracy in clinic chemistry is underway. A plea for an acceleration of this proce is made.

**14209.** Cali, J. P., **Problems of standardization in clinical chemi try,** *Bull. Wld. Hlth. Org.* **48,** 721-726 (1973).

Key words: accuracy; analysis; clinical chemistry; measur ment; precision; referee methods; specificity; standa reference materials.

If analytical results in clinical chemistry are to be ma meaningful, i.e., accurate, precise, and specific, a systematic a proach to their attainment is necessary. Furthermore, becau this system is so complex in scope and the need for it is widespread, it will require international coordination. Agreeme on the units of measurement, the production and certification standard reference materials, and the development of referen methods of demonstrated accuracy will require the support of segments of clinical chemistry.

**14210.** Cali, J. P., **A systematic approach to accuracy in clini chemistry,** *Med. Instrum.* **8,** No. 1, 17-21 (1974).

Key words: accuracy; clinical chemistry; meaningful me surement.

When measurements made in clinical chemistry laborator are "meaningful," the values obtained are accurate, precise, a specific. The latter two characteristics, related to reproducibil and singularity respectively, represent no great problem in cli cal chemistry measurements. Accuracy, however, which is lated to the "true" value, remains a somewhat elusive goal. U less a measurement system is based on accuracy, comparison results obtained over time and distance in different laborator may lead to doubtful or misleading conclusions. A meaning measurement system consists of five parts: (1) a rational, se consistent, agreed-on system of units of measurement; (2) w characterized materials used in conjunction with; (3) refe methods of known accuracy to realize in practice the base ur and their derivative; (4) field or applied methods of measu ment, assessed for accuracy via parts 2 and 3; and (5) a proc whereby the long-term integrity of the measurement system assured.

211. Beatty, R. W., **A frequently reinvented circuit (abstract),** *IEEE Trans. Microwave Theory Tech. Letter to Editor* **MTT-22,** No. 5, 58 (May 1974).

Key words: directional couplers; impedance measurement.

Attention is called to published work describing an ipedance-measuring circuit that is frequently reinvented.

212. Arora, V. K., Peterson, R. L., **Theory of magnetophonon structure in the longitudinal magnetothermal emf,** *Phys. Rev. B* 9, No. 10, 4323-4328 (May 15, 1974).

Key words: magnetophonon effect; Seebeck effect; semiconductor; transport.

The magnetophonon effect, as manifested in the longitudinal agnetothermal emf (Seebeck coefficient $Q_{zz}$), is examined ialytically and numerically in the limit of no Landau-level oadening, for combined optic and acoustic-phonon scattering electrons in nonpolar semiconductors. In addition to off-sonance maxima occurring at magnetic fields somewhat larger ian those given by the Gurevich-Firsov resonance condition $\omega_c=\omega_0$, $N=1,2,...$, where $\omega_c$ and $\omega_0$ are the cyclotron and otic-phonon frequencies, discontinuities in the derivative of $Q_{zz}$ ith respect to magnetic field are found. The slope discontinuies lie precisely at $N\omega_c=\omega_0$ and at $(2n+1)\omega_c=2\omega_0$, $n=0,1,...$, elding additional structure characterized by $\partial|Q_{zz}|/\partial B_- > Q_{zz}|/\partial B_+$ at all temperatures and degrees of elastic scattering.

4213. Unassigned.

4214. Cezairliyan, A., **A high-speed (subsecond) system for accurate thermophysical measurements at high temperatures,** (Paper 73-743, Proc. AIAA 8th Thermophysics Conf., Palm Springs, Calif., July 16-18, 1973), Chapter in *Thermophysics and Spacecraft Thermal Control* **35,** 205-228 (MIT Press, Cambridge, Mass., 1974).

Key words: electrical resistivity; emittance; heat capacity; high-speed measurements; high temperatures; thermophysics.

A system is described for the high-speed (subsecond) accurate ieasurement of selected thermophysical and related properties f electrically conducting substances in the temperature range 500 K to the melting point of the specimen. The method is ased on rapid resistive self-heating of the specimen from room emperature to any desired high temperature in less than 1 sec by he passage of electrical currents through it and on measuring nd recording the experimental quantities every 0.4 msec with a ull-scale signal resolution of one part in 8000. The system has een used to measure heat capacity, electrical resistivity, hemipherical total emittance, normal spectral emittance, and the nelting point of niobium, molybdenum, tantalum, tungsten, some efractory alloys, and graphite. The results of preliminary experinents have shown the potential application of the system to meaurements of temperatures and energies of solid-solid phase ransformations, heat of fusion, and thermal expansion at high emperatures.

4215. Clark, A. F., Hust, J. G., **A review of the compatibility of structural materials with oxygen,** *AIAA J.* **12,** No. 4, 441-454 (Apr. 1974).

Key words: compatibility; materials; metals; oxygen; safety; survey.

The compatibility of structural materials, particularly metals, vith gaseous and liquid oxygen is reviewed. Various methods of esting for oxygen compatibility are described. The literature is eviewed with respect to accidents, experimental measurements of ignition and combustion, the effect of high pressure, theory, and properties data. The relative compatibility of various materials is discussed and a selection procedure recommended. Needed future research is also outlined.

14216. Coble, J. B., Achenbach, P. R., **Description of equipment and instrumentation for a field study of a total energy system in an apartment development,** *Proc. 7th Intersociety Energy Conversion Engineering Conf., San Diego, Calif., Sept. 25-29, 1972*, pp. 1-27 (Sept. 1972).

Key words: data acquisition system; electrical power system; energy conservation; fuel utilization; thermal efficiency; thermal energy system; total energy system; utility system performance; waste heat recovery.

The Department of Housing and Urban Development selected the BREAKTHROUGH site at Jersey City, N.J. as the location for an installation and field study of a total energy system. This development covers six acres, and is comprised of four buildings containing 488 dwelling units, a small building for commercial use, two small schools, a swimming pool, and the total energy plant. The field study of this installation is being carried out by the National Bureau of Standards to produce much-needed authoritative information on engineering performance, maintenance requirements, and load-and-cost data for total energy systems.

The central plant and the individual buildings are being extensively instrumented to provide digital data on fuel utilization, the generation of electrical and thermal energy, the excess heat rejected, and the utilization of electrical and thermal energy by all major segments of the load. A separate analog data system is being employed to obtain recordings of transient conditions of voltage, frequency, current, power factor, and load division during sudden load changes and to record interruptions of service due to overload or malfunction of equipment. The environmental impact of the total energy plant with respect to noise, vibration, air pollution, and aesthetics is also being evaluated.

14217. Gallagher, A. C., York, G., **A photoionization source of monoenergetic electrons,** *Rev. Sci. Instrum.* **45,** No. 5, 662-668 (May 1974).

Key words: monochromatic electrons; photoionization source.

A photoionization source of monoenergetic electrons is described and design criteria for such sources are discussed. The present design produces a beam of $\simeq 10^{-12}$-$10^{-13}$ A by photoionization of a metastable ($^1D_2$) barium beam inside the cavity of a He-Cd laser operating at 3250 Å. The photoelectrons are produced with 17 MeV kinetic energy and a calculated energy spread of < 1 MeV. Energy analysis is provided by measuring the width of the 11.08 eV argon resonance. The observed width of this resonance has, to date, been limited to ~ 6 MeV, but tests are reported which indicate that this width is largely due to Doppler spreading in the target atomic beam and potential gradients across the collision volume.

14218. Heinrich, K. F. J., Rasberry, S. D., **X-ray fluorescence analysis of high-temperature superalloys—calibration and standards,** Chapter in *Advances in X-Ray Analysis,* C. L. Grant, C. S. Barrett, J. B. Newkirk, and C. O. Ruud, Eds. **17,** 309-317 (Plenum Publ. Corp., New York, N.Y., June 1974).

Key words: calibration; empirical calibration; high-temperature superalloys; x-ray fluorescence; x-ray spectrochemical analysis.

The current experimental work extends our calibration concept of separating the effects of absorption and fluorescence to the high-temperature superalloys. The new calibration procedure produces calibration equations which are valid over wide ranges of composition—a feature which is useful in the analysis of high-temperature superalloys. For the specimens considered, the elements iron, nickel, chromium, cobalt and molybdenum can be present at levels greater than 10 percent; while tantalum, aluminum, titanium, manganese, silicon and vanadium may be present at levels between 1 and 6 percent. The calibration for this group of alloys has required, in the past, a large number of standards; the number is reduced by judicious application of the given correction equations. Analytical errors can be limited to 1 to 2 percent in the use of this method.

**14219.** Hosteny, R. P., Hinds, A. R., Wahl, A. C., Krauss, M., **MC SCF calculations on the lowest triplet state of $H_2O$,** *Chem. Phys. Letters* **23,** No. 1, 9-12 (Nov. 1, 1973).

Key words: electron impact; energy loss; energy surface; excitation energy; $H_2O$; repulsive curve; triplet state.

Recent electron impact work on $H_2O$ has shown a broad absorption peak near 4.5 eV which has generally been attributed to the lowest triplet ($^3B_1$) state of $H_2O$. However, the results of SCF and multiconfiguration SCF (MC SCF) calculations reported here indicate that the $^3B_1$ state is unbound with respect to the dissociative asymptotes $H(^2S)+OH(^2\Pi)$ and $O(^3P)+H_2(^1\Sigma_g^+)$, in disagreement with the experimental interpretation.

**14220.** Newman, M., **Units in arithmetic progression in an algebraic number field,** *Proc. Am. Mathematical Soc.* **43,** No. 2, 266-268 (Apr. 1974).

Key words: algebraic number fields; units.

It is shown that a given algebraic number field of degree $n \geqq 4$ over the rationals can contain at most $n$ units in arithmetic progression, and that this bound is sharp.

**14221.** Achenbach, P. R., Coble, J. B., **Site analysis for the application of total energy systems to housing developments,** *Proc. 7th Intersociety Energy Conversion Engineering Conf., San Diego, Calif., Sept. 25-29, 1972,* pp. 1-31 (Sept. 1972).

Key words: air conditioning; air pollution; central utility systems; electric power generation; energy conservation; energy costs; heat recovery, power systems; total energy systems; utilities for housing.

In early 1970 the Department of Housing and Urban Development approved a program to design and construct about 2800 dwelling units on eleven sites in the United States with the objective of encouraging the industrialization of the home-building process. It was also decided that as a part of this program, Operation BREAKTHROUGH, a full-scale field study would be made to determine whether or not total energy systems could provide economical and reliable energy services to apartment complexes and maintain a high level of environmental quality.

The characteristics of the eleven sites that were important in determining their suitability for a total energy system were studied by the National Bureau of Standards as a basis for selection. Fourteen parameters related to site planning, climate, building design, load factors, cost for fuel, equipment and maintenance, and the interest of the builders and developers were investigated in the feasibility study. The study resulted in the choice of Jersey City, New Jersey as the preferred location for the pilot installation of a total energy system and the identification of three other sites of lower priority.

**14222.** Ball, J. J., **Device for stabilizing electrodeless discharge lamps,** *Rev. Sci. Instrum.* **44,** No. 8, 1141 (Aug. 1973).

Key words: atomic spectroscopy; electrodeless lamps.

Increased stability for electrodeless discharge lamps used in atomic spectroscopy is attained by mounting a heater coil below the lamp. Heating by convection maintains the lamp at a constant temperature resulting in stable output within 2 percent.

**14223.** Blackburn, D. L., Schafft, H. A., Swartzendruber, L. J., **Nondestructive photovoltaic technique for the measurement of resistivity gradients in circular semiconductor wafers,** *J. Electrochem. Soc.* **119,** No. 12, 1773-1778 (Dec. 1972).

Key words: germanium; inhomogeneities; measurement methods; photovoltaic efffect; resistivity; semiconductors; silicon.

The bulk photovoltaic effect is applied to the measurement of radial resistivity gradients in circular semiconductor wafers. This nondestructive technique permits a continuous measurement of the resistivity variation to be made by contacting only the rim of the wafer. An expression relating the radial resistivity gradient to the photovoltage measured at the wafer rim is derived and used to calculate the resistivity profile. Photovoltaic resistivity profiles, which were made on silicon and germanium wafers with resistivities ranging from 1 Ω · cm to 5000 Ω · cm, generally agree well with two- and four-probe resistivity profiles in the central portion of the wafer. Lack of agreement observed at positions in the outer half of the wafer is discussed in terms of basic material parameters, electrical contact quality, and measuremen precision of the four-probe method.

**14224.** Perloff, A., **Quartz analysis by x-ray diffraction,** *Proc Roundtable Discussion on Analytical Techniques for Quartz Amer. Conf. Governmental Industrial Hygienists, Cincinnati Ohio, Dec. 6-7, 1972,* pp. 1b-6b (1973).

Key words: microanalysis by x-ray diffraction; quartz dust

Standard x-ray diffraction techniques can be readily used t measure small quantities of respirable-sized quartz dust. Unde idealized circumstances a practical lower limit of detection is 2 μg of quartz within ± 5 μg. No significant difference between x ray units of different manufacturers was observed.

**14225.** Brown, D. W., Lowry, R. E., Wall, L. A., **Radiation-in duced polymerization at high pressure of 2,3,3,3 tetrafluoropropene in bulk and with tetrafluoroethylene,** *J Polymer Sci.* **9,** Part A-1, 1999-2007 (1971).

Key words: polymerizing material; propene; radiation-in duced polymerization; tetrafluoroethylene; tetrafluor propene.

The radiation-induced polymerization of 2,3,3,3 tetrafluoropropene was studied as a function of temperature (22 100 °C) and pressure (autogenous to $10^4$ atm). Rates have varie 100-fold for the same reaction conditions probably because trace impurities. The most rapidly polymerizing material has rate of 4.5 percent/hr at 6000 atm, 22 °C, and 1500 rad/hr. Th activation enthalpy and volume are 4 kcal/mole and − 1 cc/mole, respectively. Rates are proportional to the square ro of the radiation intensity. Degrees of polymerization varie between $2 \times 10^3$ and $2 \times 10^6$. In copolymerization wit tetrafluoroethylene the reactivity ratios at 22 °C and 5000 at are 0.37 (the ratio for addition to the tetrafluoroethylene-ende radical) and 5.4 (the ratio for addition to the tetrafluoropropen ended radical). Comparison of ratios for the copolymerization other fluorine-containing monomers with tetrafluoroethyle shows that they generally disfavor incorporation of the latter.

**14226.** Buehler, M. G., **Thermally stimulated measurements: Th characterization of defects in silicon *p-n* junction** *Semiconductor Silicon,* pp. 549-560 (1973).

Key words: defect centers; *p-n* junction; semiconduct characterization; silicon; thermally stimulated measur ments.

Thermally stimulated capacitance and current measuremen utilize the ability of defects in the vicinity of a *p-n* junction to tra holes or electrons and to emit them after receiving sufficie thermal energy. Values for defect densities, energy levels, ar emission rates can be derived from these measurements whe the limit of detectability can be as low as $10^{10}$ defects/cm$^3$. Fro these values the atomic nature of the defects can be identified.

4227. Benjamin, I. A., Parker, W. J., **Fire spread potential of ABS plastic plumbing,** *Fire Technol.* **8,** No. 2, 104-119 (May 1972).

Key words: ABS, building fires; drain pipe; fire spread; pipe chase; smoke; temperature; vent pipe; waste pipe.

Eight chases, each with a different drain, waste, and vent pipe stallation, were subjected to the standard ASTM E119 fire exosure for up to 2 hours duration. These tests were designed to xamine the possibility of vertical fire spread from one room to nother via a chase containing ABS pipes and fittings; and to entify the type of installation least susceptible to fire spread.

The best performance should be obtained when the ABS teral enters the smoke-tight chase at a downward angle of 45° nd is enclosed in a steel sleeve at the point of penetration of the hase wall.

4228. Benjamin, I. A., **The criteria for fire safety in Operation BREAKTHROUGH,** *Bldg. Stand.* **40,** No. 6, 32-36 (Nov.-Dec. 1971).

Key words: fire resistance; fire safety; housing performance; life safety.

The presentation gives the philosophical background for some f the criteria which have been used for evaluation of innovative ousing in Operation BREAKTHROUGH. Particular attention s given to a modified concept of fire resistance, the introduction f new types of material controls and the concept of life safety ystem for residential construction.

4229. Benjamin, I. A., **The influence of fire-resistant design on survival,** *Proc. Symp. Designing to Survive Disaster, Illinois Institute of Technology Research Institute, Chicago, Ill., Nov. 6-8, 1973,* pp. 263-282 (1973).

Key words: building fires; design; evacuation; fire alarms; fire protection; fire resistance; fire safety; fire spread; fire statistics; fire suppression; high rise buildings; ignition source; life safety; refuge areas; smoke control.

Annual fire losses in the U.S. approximate 12,000 deaths and ver $2 billion direct property damage. New materials and new ethods of construction have produced new potential fire azards which increase the threat to life, especially in tall, densey-populated buildings. Data are presented showing the most ommon ignition sources for building fires. Fire safety must be ncluded at the earliest stages of building design, in order to asure that it is systematic and adequate to protect lives. Several ethods of dealing with the fire problem are described, including revention of ignition, containment of fire and smoke within a imited space, automatic and manual methods of fighting fire, and rovisions for life safety. Smoke often causes death before lames and heat reach the building occupants and, therefore, engineered smoke control design measures must be a major provision to protect lives. Problems with total evacuation of high rise nd institutional buildings are described, and new life safety concepts, such as refuge areas, are suggested as alternatives. As uildings become more complex and hazardous construction aterials become more prevalent, it is increasingly important to esign ahead for fire prevention so that protection is in the building when it is built, not as an afterthought.

14230. Blevin, W. R., Geist, J., **Influence of black coatings on pyroelectric detectors,** *Appl. Opt.* **13,** No. 5, 1171-1178 (May 1974).

Key words: black coatings; detectors; gold-black; pyroelectric; radiometry.

The extent to which the thermal capacitance and resistance of black coating on a pyroelectric detector offset the gain in optial absorptance is investigated. A black paint is shown to be of ittle value, but a coating of gold-black may increase the detector responsivity for modulation frequencies up to at least several kilohertz. When a coated pyroelectric detector is calibrated electrically, a correction is necessary for the thermal impedance of the black. For gold-blacks of superficial density 2 g m$^{-2}$, this correction is shown to be less than 2 percent for frequencies within the 0-100-Hz range.

14231. Cuthill, J. R., McAlister, A. J., Erickson, N. E., Watson, R. E., **X-ray photoemission studies of rare earth hard magnets,** (Proc. 19th AIP Conf. on Magnetism and Magnetic Materials, Boston, Mass., Nov. 13-16, 1973), Chapter in *Magnetism and Magnetic Materials,* C. D. Graham, Jr., and J. J. Rhyne, Eds., pp. 1039-1043 (American Institute of Physics, New York, N.Y., 1974).

Key words: electronic structure; ESCA; hard magnets; magnetic materials; photoelectron spectroscopy; rare-earth magnets; x-ray photoelectron.

In the present investigation we attempt to probe the electronic properties of the $RCo_5$ compounds by x-ray photoelectron spectroscopy studies of $SmCo_5$ and $PrCo_5$ and endeavor to relate the results to the properties of the pure metals and to the picture developed to describe the magnetism of the compounds. The results indicate a valence band structure which is similar to that of Co metal; there is the suggestion that if there is charge flow it is off the rare-earth sites; there appears to be significant change in the 4f spectra from that of the pure rare-earth metals; and there is a suggestion of f-d hybridization.

14232. Deslattes, R. D., Henins, A., **X-ray to visible wavelength ratios,** *Phys. Rev. Lett.* **31,** No. 16, 972-975 (Oct. 15, 1973).

Key words: conversion factor; interferometer; lattice repeat distance; x-ray; wavelength.

The lattice repeat distance of a nearly perfect single crystal of silicon has been measured in terms of the visible wavelength of a stabilized He-Ne laser. This crystal subsequently has been used to diffract reference x-ray lines (Cu $K\alpha_1$, Mo $K\alpha_1$) thereby establishing their wavelength relative to visible standards. In terms of the x-ray scale in which $\lambda(\text{Cu } K\alpha_1) = 1.537\,400$ kxu, the conversion factor is $\Lambda_{Cu} = 1.002\,0802$ Å/kxu (1 ppm); if $\lambda(\text{Mo } K\alpha_1) = 0.707\,831$ kxu, $\Lambda_{Mo} = 1{,}002\,1017$ Å/kxu (0.6 ppm).

14233. Gadzuk, J. W., **Chemisorption bond geometry determined by photoemission (Abstract),** *J. Vac. Sci. Technol.* **11,** No 1, 275 (Jan./Feb. 1974).

Key words: angular distributions; chemisorption; photoemission; photoionization; surfaces.

In this paper it is shown how a measurement of the angular distribution of electrons which are photoemitted from atoms chemisorbed on a metal surface can be used to determine the chemisorption bonding geometry.

14234. Haynes, W. M., **Viscosity of saturated liquid methane,** *Physica* **70,** No. 2, 410-412 (Dec. 1973).

Key words: comparisons; graph; methane; saturated liquid; table; torsional crystal; viscosity.

The results of absolute measurements of the viscosity of saturated liquid methane using a torsionally vibrating quartz crystal are reported for temperatures from 95 to 190 K. Comparisons are made with other data, all of which have been obtained with techniques different from that of the present work.

14235. Hein, R. A., Cox, J. E., Blaugher, R. D., Waterstrat, R. M., van Reuth, E. C., **Low-temperature annealing effects upon the superconducting properties of $V_3Au$,** *Physica* **55,** 523-533 (1971).

Key words: annealing; magnetic field; stoichiometry; superconductivity; transition temperature.

The superconducting transition temperature, $T_0$, and the initial slope of the upper critical magnetic field curve of $V_3Au$ have been measured as functions of low (400-800 °C) temperature annealing. $T_0$ ranges from no superconductivity down to 0.015 K to a $T_0$ as high as 3.22 K. X-ray diffractometer data indicated that all the samples employed in this study had the A15 structure. Metallographic studies indicated the presence of a few percent of a second Au rich phase in these equilibrated samples. The x-ray data also indicated that the low-temperature anneals did change the degree of crystallographic long range order present in the samples and our data clearly indicate that $T_0$ increases quite markedly as the Bragg-Williams long-range order parameter approaches the value of unity. The magnitude of the initial slope of the critical magnetic field curve also increases with increase in $T_0$ (from $-22 \times 10^3$ Oe/deg to $-37 \times 10^3$ Oe/deg for $T_0 = 0.89$ K and 3.1 K respectively) with one notable exception, and that is the sample with the highest $T_0$ for which the slope has its smallest value, namely $-16 \times 10^3$ Oe/deg.

**14236.** Heinrich, K. F. J., **Electron and ion probe microanalysis—physical bases,** (Proc. Symp. on Microprobe Analysis as Applied to Cells and Tissues, Seattle, Wash., Apr. 29-May 2, 1973), Chapter in *Microprobe Analysis as Applied to Cells and Tissues,* pp. 75-87 (June 1974).

> Key words: biological analysis; electron probe; ion probe; microprobe analysis; quantitation; soft tissue.

Both electron and ion probe analysis are tools for the detection and measurement of elements on a micrometer ($\mu$m) scale. The physical bases of electron probe microanalysis are now reasonably well known, but the special conditions prevalent in the analysis of biological tissue present specific difficulties. New data evaluation procedures, such as the Monte-Carlo computation technique, may be useful to attack these problems.

The ion probe is a novel tool of great promise for the analysis of biological tissue since it combines shallow sampling with very high sensitivity and capability for the analysis of elements of low atomic number.

**14237.** Jacox, M. E., Milligan, D. E., **Matrix isolation study of the vacuum ultraviolet photolysis of allene and methylacetylene vibrational and electronic spectra of the species $C_3$, $C_3H$, $C_3H_2$, and $C_3H_3$,** *Chem. Phys.* **4,** 45-61 (1974).

> Key words: allene; $C_3H_n$ ($n = 0$ to 3); infrared spectrum; isotopic substitution; matrix isolation; methylacetylene; ultraviolet spectrum; vacuum-ultraviolet photolysis.

Upon hydrogen-discharge photolysis of normal or deuterium-substituted allene or methylacetylene in an argon or a nitrogen matrix at 14 K, infrared absorptions of all of the $C_3H_n$ species with $n < 4$ appear. A hydrogen-deformation fundamental of $C_3H_2$ has been identified in the far infrared. Infrared studies of the partially deuterium-substituted methylacetylenes indicate that extensive photoisomerization occurs. The observed products are consistent with those predicted using the previously postulated gas-phase photolysis mechanism. The ultraviolet spectrum of $C_3H_3$ corresponds closely with that characteristic of the gas-phase molecule. Comparison of the spectrum between 1900 and 4000 Å of photolyzed methylacetylene with that of matrix-isolated graphite vapor has indicated that any new electronic transition of $C_3$ in this region must be weak.

**14238.** Kraft, R., **Uniqueness and existence for the integral equation of interreflections,** *SIAM J. Math. Anal.* **5,** No. 2, 293-302 (Apr. 1974).

> Key words: contractivity; existence of solutions; integral equations; interreflections; radiation transfer; uniqueness of solutions.

The integral equation of interreflections, determining radiant energy exchange in cavities, is shown to have a unique solution in the space on nonnegative functions defined over the cavity surface. The result is established by employing the contraction mapping principle.

**14239.** LaVilla, R. E., **$M_{4,5}$ emission spectra from $Gd_2O_3$ and $Yb_2O_3$,** *Phys. Rev. A* **9,** No. 5, 1801-1805 (May 1974).

> Key words: $Gd_2O_3$; fluorescence spectra; $M_{4,5}$ emission spectra; resonance radiation; $Yb_2O_3$.

The $M_{4,5}$ emission spectra from $Gd_2O_3$ and $Yb_2O_3$ have been obtained in fluorescence on a double-crystal spectrometer. The profiles differ from the $M_{4,5}$ emission spectra excited by electron impact. These differences are due to resonance radiation and substantiate the interpretation given by Bonnelle and Karnatak. The $M\alpha$ emission line was found to lie above (in energy) the $M_5$-absorption resonance line $Yb_2O_3$, which is in contrast to $Gd_2O_3$ and general experience. It is suggested that this observation is a result of the discrete nature of the absorption lines. With the help of estimated binding energies for the final configurations $5p^5{}_{1/2,3/2}4f^7$, the photoelectron spectrum of $Gd_2O_3$ is discussed.

**14240.** Levy, J., **The optimal size of a storage facility,** *Nav. Res Log. Quart.* **21,** No. 2, 319-326 (June 1974).

> Key words: building design; inventory theory.

The appropriate size for a piece of fixed capital equipmen (measured in units of capacity) depends on the anticipated demand for its services and on its cost. Using several models developed in the study of optimal inventory policy we derive the contribution to cost reduction that additional storage space makes under each of these models. Comparison of the sum of the discounted benefits (i.e., reduced operating cost) with construction costs for additional storage space then yields the optima size of the storage facility.

**14241.** Milligan, D. E., Jacox, M. E., **Spectra of free radicals and molecular ions produced by vacuum ultraviolet photolysis in low-temperature matrices,** (Proc. Advanced Study Institute NATO, Valmorin, Quebec, Canada, Aug. 5-17, 1973) Chapter in *Chemical Spectroscopy and Photochemistry in the Vacuum-Ultraviolet* **8,** Ser. C, 305-315 (D. Reidel Publ. Co. Boston, Mass., 1974).

> Key words: free radicals; $HAr_n{}^+$; infrared spectrum molecular ions; $NO_2{}^-$; reaction of OH with CO; ultraviolet spectrum; vacuum-ultraviolet photolysis of HCN, of halogen cyanides, of $CH_4$, of $CH_3Cl$, of $CH_3OH$, of $C_2H_2$ of $HCCl_3$.

The principles governing the stabilization of small free radicals and molecular ions in inert, rigid matrices will be reviewed Emphasis will be placed on the strengths and limitations of th technique in obtaining information of concern to th photochemist. Examples will be drawn from studies of th vacuum-ultraviolet photolysis of HCN, $CH_4$, $CH_3Cl$, $CH_3OH$, $C_2H_2$, $NO_2$, and $HCCl_3$ in a matrix environment.

**14242.** Block, S., Piermarini, G. J., **The melting curve of sulfur to 300 °C and 12 kbar,** *High Temp.-High Pressures* **5,** 567-57 (1973).

> Key words: diamond-anvil cell; high pressure; meltin curve; polymorphism; sulfur.

The melting curve of sulfur has been studied to 300 °C and 1 kbar using a diamond-anvil high-pressure cell and an optic system which utilizes the ruby-fluorescence $R_1$ line shift for measuring the pressure. Two triple points were determined in th temperature range: (i)L-IV-VI at $(235 \pm 5)$°C and $(8 \cdot 5 \pm$ kbar, and (ii)L-VI-VIII at $(290 \pm 5)$°C and $(12 \pm 5)$ kba Because of the nonequilibrium behavior of sulfur the meltin curve could not be characterized with any degree of certaint above 235 °C.

43. Unassigned.

244. Carpenter, B. S., **Lithium determination by the nuclear track technique,** (Proc. Int. Conf. Modern Trends in Activation Analysis, Saclay, France, Oct. 1-6, 1972), *J. Radionanal. Chem.* **19,** 233-234 (1974).

Key words: alpha tracks; biological material; image analyzing system; lithium; microscope; nuclear track technique; standard reference material.

The Nuclear Track Technique was used to determine lithium Biological Standard Reference Material 1571 (Orchard aves). Alpha tracks produced in cellulose acetate (CA) from e nuclear reaction $^6$Li(n,$\alpha$)$^3$H with thermal neutrons were unted to determine the concentration of lithium present. The ethod of standard additions was used and, with least squares alysis of the data, the lithium concentration was found to be .72 ± 1.50 ppm.

245. Cassel, J. M., **Aggregation phenomena of collagen,** Chapter 2 in *Biophysical Properties of the Skin,* H. R. Elden, Ed., pp. 63-100 (John Wiley & Sons, Inc., New York, N.Y., 1971).

Key words: aggregation; collagen; fibrils; hydrophobic bonding; native-type fibril formation; phase transition; precipitation kinetics.

Various aggregation phenomena exhibited by dissolved col- gen are reviewed. Main consideration is given to native-type ril formation. The kinetics and thermodynamics of this ecipitation process are examined. Subtopics included are ase diagram determinations, hydrophobic bonding aspects, me-dependent changes in the reversibility of native-type fibril ecipitation, and the role of polyanions. The review is con- uded with discussion of collagen fibril formation in vivo.

246. Clough, R. B., Simmons, J. A., **A theory of multiaxial plasticity based on integral dislocation dynamics,** *Acta Met.* **22,** 513-521 (May 1974).

Key words: dislocations; plasticity; thermal activation.

A macroscopic theory of isotropic plastic flow under multiaxi- stress states is developed from considerations of thermally activated dislocation motion on discrete randomly-oriented slip anes. The resulting equations are in agreement with classical asticity theory. Yielding is volume-preserving, pressure-inde- endent, and the principal stress and principal strain axes coin- de. The flow surface is constructed on the basis of constant ower dissipation of plastic flow, and has a variable shape and thogonal strain vector. For most materials, the predicted flow rface resembles the Tresca yield surface at low temperatures nd approaches the von Mises yield surface as its high tempera- re limit. Other applications are discussed.

247. Cook, R. K., **Foreword and introduction for the Symposium on Atmospheric Acoustics and Noise Propagation,** *J. Acoust. Soc. Am.* **55,** No. 5, 926 (May 1974).

Key words: acoustics; aircraft noise; atmospheric acoustics; infrasound; noise propagation; sound propagation.

Foreword and introduction for the Symposium on Atmospher- Acoustics and Noise Propagation.

248. Copley, J. R. D., Rowe, J. M., **Density fluctuations in liquid rubidium. I. Neutron-scattering measurements,** *Phys. Rev. A* **9,** No. 4, 1656-1666 (Apr. 1974).

Key words: coherent scattering function; density fluctuations; liquid rubidium; molecular dynamics; neutron scattering and potential.

We report neutron-scattering measurements of the coherent cattering function $S(Q,\omega)$ of liquid rubidium at 315 K, in the range of wave vectors $1.25 \leq Q \leq 5.5$ Å$^{-1}$. In this range there is no evidence of peaks at finite $\omega$ in $S(Q,\omega)$ plotted at constant $Q$. On the other hand the Fourier transform $F(Q,t)$ exhibits structure, notably for $Q = 2.0$ Å$^{-1}$, which indicates at least two characteristic (wavelength-dependent) relaxation times in the liquid. For wave vectors $> 3.0$ Å$^{-1}$, $F(Q,t)$ may be characterized by a single relaxation time. These results, in conjunction with our results for $Q < 1.0$ Å$^{-1}$, offer the possibility of detailed comparisons with models of the liquid state and with molecular-dynamics calculations.

14249. Cox, J. E., Hein, R. A., Waterstrat, R. M., **Superconducting properties of Al5 phase V-Pt alloys,** *Proc. 12th Int. Conf. on Low Temperature Physics, Kyoto, Japan, Sept. 4-10, 1970,* pp. 333-334 (Mar. 1971).

Key words: Al5 compounds; atomic ordering; critical magnetic field; superconducting; superconductivity; transition temperatures.

Superconducting transition temperatures, $T_0$, and initial slopes of the critical magnetic field curves are reported for V-Pt alloys of the Al5 crystal structure. Increased atomic ordering produces an increase in $T_0$, contrary to our previous results.

14250. Piermarini, G. J., Braun, A. B., **Crystal and molecular structure of $CCl_4$ III: A high pressure polymorph at 10 kbar,** *J. Chem. Phys.* **58,** No. 5, 1974-1982 (Mar. 1973).

Key words: carbon tetrachloride; crystal structure; diamond-anvil cell; high pressure; polymorphism.

The crystal and molecular structure of a high pressure form of carbon tetrachloride ($CCl_4$ III) was determined at approximately 10 kbar using a diamond-anvil beryllium pressure cell and a modified Buerger-type precession camera. $CCl_4$ III crystallizes in the monoclinic system with a unit cell of the following dimensions: $a = 9.079 \pm 0.012$ Å, $b = 5.764 \pm 0.003$ Å, $c = 9.201 \pm 0.004$ Å, and $\beta = 104.29 \pm 0.05°$. The space group is $P2_1/c$ with four molecules per unit cell. Observed infrared spectra indicate that the $CCl_4$ molecule exhibits regular tetrahedral symmetry at 10 kbar. By using an approximation to the repulsion energy in a least-squares refinement procedure considering only nonbonded Cl-Cl interactions, an approximate structure was obtained. Subsequent structure factor calculations using a grid-point sampling procedure yielded a final structure with a reliability factor of 9.56 percent. $CCl_4$ III is isostructural with $SnBr_4$, and contains closest nonbonded Cl-Cl distances of 3.49 Å, significantly less than the normal Van der Waals separation of 3.6 Å. Taking four molecules per unit cell, the calculated density is 2.190 g cm$^{-3}$. A more compact phase than $CCl_4$ III was predicted in the $CCl_4$ system on the basis of packing efficiency and the predicted phase ($CCl_4$ IV) was subsequently verified by visual observation in microscopic studies at pressures in the 35-40 kbar range and temperatures up to 500 °C.

14251. Righini, F., Cezairliyan, A., **Pulse method of thermal diffusivity measurements (a review),** *High Temp.-High Pressures* **5,** 481-501 (1973).

Key words: heat transfer; thermal conductivity; thermal diffusivity; thermophysical properties; transient techniques; transport properties.

The pulse (flash) method of measuring thermal diffusivity is reviewed. The basic theory of such measurements is presented and theoretical advances to account for departures from simplified assumptions are discussed. The experimental systems for thermal diffusivity measurements employing the pulse method are described and a summary of investigations reported in the literature is given. Emphasis is placed on the analysis of the accuracy of the method. Potentials of the technique for improved measurements at high temperatures are discussed.

**14252.** Achenbach, P. R., **Energy conservation in buildings: Its foundation, cost, and acceptance,** *Proc. Conf. Energy Conservation: Implications for Building Design and Operation, Bloomington, Minn., May 23, 1973,* pp. 44-73 (1973).

Key words: building design; building performance; building research; building systems; energy conservation; energy use; mechanical systems.

Changes in building practice could save substantial amounts of energy and ease the impending shortages of fuel in the United States. However, changes that are technically sound must also be economically sound, and they must be implemented on a broad scale by the building industry if they are to have a significant impact on fuel usage. The National Bureau of Standards is carrying out significant analytical, laboratory and field investigations of promising technology in energy-saving potential of these building practices. The more extensive field studies are collaborative efforts with other Federal agencies. Concurrently, existing technical information on energy conservation is being collected and prepared as brochures for convenient use by the building design profession and for use in building standards and specifications of various Federal agencies. The program of the National Bureau of Standards on energy conservation in building is summarized and research opportunities in the field are identified for both new and existing buildings.

**14253.** Tsai, D. H., MacDonald, R. A., **Heat pulse propagation in a crystal: A molecular dynamical calculation,** *Solid State Commun.* **14,** No. 11, 1269-1273 (1974).

Key words: anharmonicity; crystal; heat pulse; lattice; molecular dynamics; second sound; stress wave; temperature wave; thermal relaxation.

The propagation of a heat pulse into a perfect bcc crystal is studied by means of molecular dynamical calculations. We observe second sound waves associated with the heat pulse as well as with longitudinal and transverse elastic pulses. Our results explain a number of features observed in second sound experiments and suggest that second sound is a phenomenon of general occurrence.

**14254.** Treu, S., **Techniques and tools for improving the interactive system interface,** (Proc. Interactive Bibliographic Systems, Gaithersburg, Md., Oct. 4-5, 1971), *U.S. Atomic Energy Commission Symp. Series* **28,** pp. 32-38 (Apr. 1973).

Key words: data collection techniques; interactive system interface; retrieval systems; user-system interface.

This is an account of a brief talk presented to the User Interface Session of the Forum on Interactive Bibliographics Systems. Consistent with the planned panel format of that Session, it is not a formally prepared paper. After some assertions about the need for considering the user and his system to be a team and about having to recognize user behavior and satisfaction in assessment of team performance, the use of more unobtrusive techniques for pertinent data collection is advocated. Two tools for enabling these techniques are described: a dialogue monitor which can record the entire two-way message stream and certain related timing data, and a user stimulation system which can actively manipulate the interaction while collecting data on resulting user satisfaction.

**14255.** Taylor, P. O., Dolder, K. T., Kauppila, W. E., Dunn, G. H., **Measurement of spiraling in a magnetically confined electron beam for use in collision studies,** *Rev. Sci. Instrum.* **45,** No. 4, 538-544 (Apr. 1974).

Key words: electron gun; measurement of spiraling; spiraling.

A method is described to directly measure mean spiral diameter in a magnetically confined electron beam. In collision experiments, spiraling affects polarization measurements and effectiv path length assessment; and in experiments using collidin beams, the collision energy or energy spread can be significantl altered. The technique described here allows experimental co rection for these effects. Magnitudes of transverse velocitie from various causes leading to spiraling are estimated on th basis of models. A gun designed for use in crossed bea electron-ion excitation experiments is described, and results tests on spiraling and space charge effects for this gun are give The tests generally indicate the modeling to be correct. Judicio choice of operating conditions led to path length corrections small as 4 ± 2 percent at 3 eV, decreasing to 0.25 ± 0.2 perce at 200 eV.

**14256.** Watson, R. E., Bennett, L. H., **Charge transfer in alloy The blind men and the elephant,** (Proc. Twin Symp. sponsore by the Committee on Alloy Phases of the Inst. of Metal Univ. of Pennsylvania, Philadelphia, May 1973), Chapter *Charge Transfer/Electronic Structure of Alloys,* L. H. Benne and R. H. Willens, Eds., pp. 1-21 (Published by the Metallurg cal Society of AIME, Inc., New York, N.Y., 1974).

Key words: alloys; atomic volume; charge transfer; chem cal bonding; internal conversion; isomer shift.

This paper attempts to provide an introduction to the concep underlying much of the discussion in the papers presented at t Symposium on Charge Transfer in Alloys. It also concentrat on two related methods of obtaining charge transfer informati in alloys which are not covered elsewhere in the Symposiu namely, the Môssbauer isomer shift and internal conversion e periments.

**14257.** Sugar, J., **Revised ionization energies of the neutral ac nides,** *J. Chem. Phys.* **60,** No. 10, 4103 (May 15, 1974).

Key words: actinium; americium; berkelium; californiu curium; einsteinium; fermium; ionization energy; me delevium; neptunium; nobelium; plutonium; protactiniu thorium; uranium.

Revised values for the ionization energies of the neutral ac nide atoms based on new experimental data are given.

**14258.** Ryan, J. V., **Standards for textiles in the U.S.A.,** *Gottl Duttweiler Institutes J.* **2,** No. 5, 35-41 (May 1971); *Polyn News* **1,** Nos. 6-7, 10-18 (1973).

Key words: beds; carpets; Child Protection Act; fabri flammability; Flammable Fabrics Act; Hill-Burton Act.

Mandatory standards for flame-resistant textiles, or rela materials, are authorized under the Flammable Fabrics Act (I partment of Commerce), the Child Protection Act amendme to the Federal Hazardous Substances Act (Department Health, Education, and Welfare), the Hill-Burton and Medic Acts (Department of Health, Education, and Welfare), the N tional Highway Safety Act (Department of Transportation), a the basic Acts of the U.S. Coast Guard and the Federal Aviat Administration. Of these Statutes, the Flammable Fabrics is the most comprehensive, including within its scope all wear apparel and interior furnishings for homes, offices, and places assembly or accommodation. Standards are authorized a under State and local laws, particularly those relating to build or fire codes. Flammability requirements in purchase specifi tions have the force of law when made part of a contract.

Standards or proposed standards have been published wearing apparel, carpets and rugs, small carpets and rugs, to floor coverings in hospitals and long term care faciliti merchant ships, aircraft cabin liners and furnishings, and mo vehicles. Building and fire codes usually set requirements o for textile furnishings in places of assembly. Purchase specifi tions rarely include flammability requirements except when intended use is regulated by statutory requirements.

59. Unassigned.

60. Evans, A. G., **Fracture mechanics determinations,** (Proc. Conf. on Fracture Mechanics of Ceramics, Pennsylvania State Univ., University Park, Pa., July 11-13, 1973), Chapter in *Fracture Mechanics of Ceramics,* R. C. Bradt, D. P. H. Haselman, and F. F. Lange, Eds., **1,** 17-48 (Plenum Publ. Corp., New York, N.Y., 1974).

Key words: ceramics; failure prediction; fracture mechanics; materials development; techniques.

Techniques for the evaluation of fracture mechanics parame-s are described. The selection of techniques for various amic applications is discussed, emphasizing the particular blems encountered with these measurements in ceramic tems. Finally, the application of fracture mechanics parame-s to problems in both materials development and failure pretion in ceramic systems is described.

261. Dick, C. E., Lucas, A. C., Motz, J. W., Placious, R. C., Sparrow, J. H., **Large-angle $K$ x-ray production by electrons,** *J. Appl. Phys.* **44,** No. 2, 815-826 (Feb. 1973).

Key words: aluminum; beryllium; carbon; copper; electron excitation; gold; $K$ x-ray beams; purities; silver; titanium; yields.

Experimental values are given for the yields and spectral ener- purities of $K$ x-ray beams emitted at 120 and 180° from varis targets when bombarded by 0.01- to 3.0-MeV electron ams. Yields and purities are determined for beryllium, carbon, ıminum, titanium, copper, silver, and gold targets as a function the target thickness and target inclination angle.

262. Andrews, J. R., **Random sampling oscilloscope for the observation of mercury switch closure transition times,** *IEEE Trans. Instrum. Meas.* **IM-22,** No. 4, 375-381 (Dec. 1973).

Key words: mercury switch; oscilloscope; picosecond; pulse; random sampling; risetime; sampling; transition time.

With the advent of new miniaturized mercury (Hg) switches th reputed transition times of the order of 10 ps, interest has en rekindled in their use in high-speed pulse measurements. nce there is no pretrigger signal available from a Hg switch, rmal sequential sampling techniques are not useable to meare the fast Hg switch transition time. For this reason, a new ndom sampling time base unit was designed to perform these easurements at the low repetition rate of Hg switches. The ne base may be used with commercial sampling oscilloscope stems through suitable interconnection terminals or possible terface equipment. It features three selectable time windows of $\mu$s, 100 ns, and 10 ns. Using its time magnifier, the fastest veep rate is 10 ps/cm. A variable trigger lead time control is ovided. The trigger sensitivity is 5 mV.

263. Dickens, B., Brown, W. E., Kruger, G. J., Stewart, J. M., **$Ca_4(PO_4)_2O$, tetracalcium diphosphate monoxide. Crystal structure and relationships to $Ca_5(PO_4)_3OH$ and $K_3Na(SO_4)_2$,** *Acta Crystallog.* **B29,** Part 10, 2046-2056 (Oct. 1973).

Key words: crystal structure; hydroxyapatite; single crystal x-ray diffraction; structural relationships; tetracalcium phosphate; twinning.

$Ca_4(PO_4)_2O$, tetracalcium diphosphate monoxide, crystallizes the monoclinic unit cell $a=7\cdot023$ (1), $b=11\cdot986$ (4), $c=$ ·473 (2) Å, $\beta=90\cdot90$ (1)° (at 25 °C) in space group $P2_1$ with [$Ca_4(PO_4)_2O$] per cell. 3288 x-ray data were measured from a ngle crystal by $\theta$-$2\theta$ scans using Mo $K\alpha$ radiation; 56 of these eflections were of "unobservable" intensity. The structure was olved by an application of direct phasing methods and subequent calculation of an $E$ map. It was refined anisotropically y full-matrix least squares to $R_w(F)=0\cdot036$, $R(F)=0\cdot037$. Allowance was made for isotropic secondary extinction but not for anomalous scattering or absorption. The dimensions of the unit cells of $Ca_4(PO_4)_2O$ and $Ca_5(PO_4)_3OH$ (hydroxyapatite), an idealized form of the major inorganic phase in the hyman body, are simply related. Although this 3-dimensional relationship in the unit-cell shapes is not carried over into the details of the actual structures, $Ca_4(PO_4)_2O$ does contain a layer which is similar to a layer in $Ca_5(PO_4)_3OH$, and an epitaxic relationship between the two compounds is conceivable. $Ca_4(PO_4)_2O$ is also related to the $K_3Na(SO_4)_2$ (glaserite) structure. In this relationship the oxide ions are "extra" ions. One Ca ion in $Ca_4(PO_4)_2O$ is weakly coordinated to a face of a $PO_4$ group, a feature which has been previously observed for Ca only in a disordered cation site in $\beta$-$Ca_3(PO_4)_2$. The two crystallographically discrete oxide ions are surrounded by tetrahedra of Ca ions, with Ca···O distances in the range $2\cdot136$ (4) to $2\cdot277$ (3) Å. Thus, the oxide ions do not lie in a channel formed by cations in the structure and $Ca_4(PO_4)_2O$ cannot be considered to be an oxyapatite. The positions of the P atoms and the Ca and oxide ions lie close to those required by space group *Pmcn*. This explains the appreciable twinning exhibited by $Ca_4(PO_4)_2O$. It also makes the existence of a higher-symmetry modification feasible.

14264. DeVoe, J. R., Shideler, R. W., Ruegg, F. C., Aronson, J. P., Shoenfeld, P. S., **Computer utility for the analytical laboratory,** *Anal. Chem.* **46,** No. 4, 509-520 (Apr. 1974).

Key words: computer control; laboratory automation; teleprocessor.

The use of a parallel digital data bus as part of an elaborate teleprocessor system enables the analytical chemist to utilize computer control of his instrument in a manner which is simpler than has been previously described. The use of pushbuttons and thumbwheels with data display, plot, or print in the laboratory, coupled with interactive control of the experiment control program, provides a capability in computer control of instrumentation that approaches the concept of a computer utility. The teleprocessor and software used in a multiprogram environment are described.

14265. Barnes, J. A., Winkler, G. M. R., **The standards of time and frequency in the U.S.A.,** *Proc. 26th Annual Frequency Control Symp., Atlantic City, N. J., June 6-8, 1972,* pp. 269-278 (Electronic Industries Assn., Washington, D.C., 1972).

Key words: astronomical time; atomic time; frequency; International Atomic Time; management; NBS; standard time; time; USNO.

The National Bureau of Standards (NBS) and the U.S. Naval Observatory (USNO) are the two organizations chiefly involved in distributing accurate and precise time and frequency information within the U.S.A. The NBS is responsible for the "custody, maintenance, and development of the national standards" of frequency and time (interval) as well as their dissemination to the general public. The mission of the USNO includes the "provision of accurate time" as an integral part of its work concerned with the publication of ephemerides in support of navigation and in the establishment of a fundamental reference system in space.

Both agencies provide the U.S. contribution to the Bureau International de l'Heure (BIH) [International Time Bureau], which has the responsibility of publishing definitive values of Universal Time (UT), International Atomic Time (LAT), and Coordinated Universal Time (UTC).

14266. Davies, J. B., **A least-squares boundary residual method for the numerical solution of scattering problems,** *IEEE Trans. Microwave Theory Tech.* **MTT-21,** No. 2, 99-104 (Feb. 1973).

Key words: electromagnetic scattering; least-squares; numerical solution; point-matching.

An explicit least-squares criterion is put forward as an alternative to the point-matching method of numerically solving scattering problems. While being an established method of functional approximation, it has been largely ignored in numerical approaches to electromagnetic scattering.

In contrast to point matching, the least-squares approach has a rigorous proof of convergence. An electric/magnetic weighting factor is found useful in optimizing convergence. Finally, it allows use of perhaps the fastest and most compact matrix inversion algorithm.

**14267.** Deslattes, R. D., Sauder, W. C., **Intercomparison of micrometer, nanometer and picometer wavelengths,** (Proc. 4th Int. Conf. on Atomic Masses and Fundamental Constants, Teddington, England, Sept. 6-10, 1971), Chapter in *Atomic Masses and Fundamental Constants,* J. H. Sanders and A. H. Wapstra, Eds. **4,** 337-347 (Plenum Press, London, England, 1972).

Key words: Avogadro's number; Compton wavelength; gamma-ray wavelength; lattice parameters; x-ray conversion factor; x-ray wavelengths.

Reckoning of a common baseline by x-ray and optical interferometry impinges on several fundamental measurements. Our program involves successive wavelength—lattice parameter—lattice parameter—wavelength transfers. Aside from unification of the visible and x-ray and $\gamma$-ray wavelength scales, we aim at Avogadro's constant and the electron's Compton wavelength. This report outlines the program, gives current progress, and mentions residual problems.

Requirements for high resolution linear and angular measuring engines have been met by extensions of available technology. Similarly, density measurements as refined from classical bouyant weighings by Bowman and Schoonover appear adequate.

**14268.** Bay, Z., **The constancy of the velocity of light and prospects for a unified standardization of time, frequency and length,** (Proc. 4th Int. Conf. on Atomic Masses and Fundamental Constants, Teddington, England, Sept. 6-10, 1971), Chapter in *Atomic Masses and Fundamental Constants,* J. H. Sanders and A. H. Wapstra, Eds. **4,** 323-336 (Plenum Press, London, England, 1972).

Key words: accuracy limits in interferometry; experimental evidences for constancy of speed of light; unified primary standard for time and length.

Light propagation in vacuum is experimentally proven to be dispersionless to within accuracies exceeding by many orders those of measurements in metrology. The independence of c relative to the motion of the frame connected to the moving earth is established less accurately, but accurate enough for metrology; any departure from constancy would affect length measurements, based on wavelength standards, or based on c, in the same way. It can be expected that in the not too distant future 1) optical frequencies in the infrared and visible spectrum can be measured at least as accurately as length can be measured, and 2) that the speed of light will be known to the accuracy of the present length standard. If 1) and 2) materialize then, on both theoretical and practical grounds, the unified standardization of time interval, frequency and length via an agreed upon value of c will be preferable to a system based on a frequency standard and on a wavelength standard.

**14269.** Allan, D. W., Blair, B. E., Davis, D. D., Machlan, H. E., **Precision and accuracy of remote synchronization via portable clocks, Loran C, and network television broadcasts,** *Proc. 25th Annual Symp. on Frequency Control, Atlantic City, N.J., Apr. 26-28, 1971,* pp. 195-208 (Electronic Industries Assn., Washington, D.C., 1971).

Key words: cesium beam standards; frequency standards Loran C; portable clocks; time synchronization; TV timing

Three precise timing centers in the U.S. have made remot time comparisons for over a year using three differen synchronization methods. The timing centers were the U.S Naval Observatory (USNO), Washington, D.C.; Newark Ai Force Station (NAFS), Newark, Ohio; and the National Burea of Standards (NBS), Boulder, Colo. The synchronizatio methods were cesium beam portable clocks; Loran C transmis sions from North Carolina and Indiana; and ABC, CBS, an NBC live network TV broadcasts common to the three timin centers. Cesium beam portable clocks, having capabilities of ac curately and precisely synchronizing remote clocks to within 0. $\mu$s, formed the basis of comparison. This method is one of th most accurate now available. The Loran C data were taken ove a 3150 km (1958 mi) ground wave path, which is believed th longest such path studied with the precision and accuracy of ou results. The long term precision between the three remote tim centers was better than 2 $\mu$s via Loran C; the accuracy of thes data is limited by 10 $\mu$s ambiguity in identifying the proper cycl of the 100 kHz pulse train. The precision of the TV broadcast in synchronizing remote clocks was 30 ns $T^{12}$ $d^{-12}$, where T is i days. Factors such as occasional rerouting of TV networ signals limited the accuracy. Relative frequency stabilitie between ensembles of cesium beam standards at the three tim centers were a few parts in $10^{14}$ for sample times of about thre months.

**14270.** Fath, J. M., **The sound of America today,** *Proc. 26th Na tional Home Appliance Conference on Today's Realitie Boston, Mass., Nov. 29-Dec. 1, 1972,* pp. 115-117 (Associ tion of Home Appliance Manufacturers, Chicago, Ill., 1972

Key words: home noise; noise sources; recreational; wor

An audio/visual presentation of various noise sources encou tered in our daily lives at home, at work, and in recreational a tivities. The presentation was followed with a discussion of tl general problems associated with noise in America today.

**14271.** Madey, T. E., Yates, J. T., Jr., Erickson, N. E., **X-ra photoelectron spectroscopic study of the adsorption of $N_2$ an NO on tungsten,** *Surface Sci.* **43,** 526-544 (1974).

Key words: chemical shifts; chemisorption; ESCA; nitr oxide; nitrogen; spectroscopy; x-ray photoelectron.

X-ray photoelectron spectroscopy (ESCA) has been used a study of $N_2$ and NO adsorbed on a polycrystalline tungsten ri bon. The sample was flash cleaned under ultrahigh vacuum co ditions, and cooled to either 300 or 100 K for the adsorption st dies. Large chemical shifts, as great as 8 eV, were observe between the N(ls) spectra associated with the weakly chemi orbed $\gamma$-nitrogen states and the strongly chemisorbed $\beta$-nitrog states. Chemical shifts in both the N(ls) and O(ls) spectra sugge that NO is largely nondissociatively chemisorbed at 100 K. general, the binding energies of N(ls) and O(ls) electrons in t adsorbed layers are *smaller* than the binding energies for t same atoms in small gaseous molecules. In addition, the bindi energies associated with the weakly-bound states of NO and l are invariably greater than the binding energies associated wi strongly chemisorbed species.

**14272.** Page, C. H., **Definitions of electromagnetic field quantiti** *Amer. J. Phys.* **42,** 490-496 (June 1974).

Key words: definitions; electromagnetism; fields.

A logically consistent set of definitions of the electromagne field quantities is extremely difficult to find in the literatu Most textbooks either evade the problem, or present definitio that are applicable only to special cases. A philosophy of t problem is presented, and a consistent system developed.

273. Allan, D. W., Barnes, J. A., **Some statistical properties of LF and VLF propagation,** (Proc. AGARD/EPC 13th Symp., Ankara, Turkey, Oct. 9-12, 1967), Chapter 15 in *AGARD Conference Proceedings No. 33, Phase and Frequency Instabilities in Electromagnetic Wave Propagation*, K. Davies, Ed., pp. 219-230 (Technivision Services, Slough, England, July 1970).

Key words: flicker noise; phase fluctuations of VLF and LF transmissions; statistical analysis.

A statistical analysis has been conducted on the day-time ase fluctuations of the standard frequency and time Radio Sta- ns WWVB (60 kHz) and WWVL (20 kHz) as received at Palo to, Calif., and of WWVB as received at the National Research ouncil, Ottawa, Canada. The analysis technique allows a eaningful determination of the low frequency spectral density, the variance of the phase and frequency fluctuations, and of me cross-correlations. The analysis techniques used are ap- opriate for commonly encountered nonstationary as well as tionary noise processes.

The results of the analysis yielded a spectral density of the ne fluctuations proportional to the reciprocal spectral frequen- ($S_l(\omega)=h/|\omega|$, flicker noise) for the propagation noise on both WVL and WWVB. The value of h was equal to $7.9\times10^{-14}$ s$^2$ WWVL and $2.2\times10^{-14}$ s$^2$ for WWVB for the Palo Alto path, d h was $4.4\times10^{-14}$ s$^2$ for WWVB over the Ottawa path. For cker noise phase modulation a good model of the standard viation of the fractional frequency fluctuations is: $\sigma=k|\tau|^{-1}$, here $\tau$ is the sample time in days. The values of k were $2.4\times$ $^{-11}$ days for WWVL and $1.2\times10^{-11}$ days for WWVB over the lo Alto path and $1.8\times10^{-11}$ days for WWVB over the Ottawa th.

A cross-correlation coefficient of $-0.6$ was found between WVL and WWVB for the Palo Alto path. A linear combina- on of the two transmissions improved the flicker noise level by factor of 11.5 over WWVL and by a factor of 2.7 over WWVB, owing a precision of frequency measurement of $1\times10^{-12}$ for nine day average any time of the year and of $1\times10^{-12}$ for a five y average over the summer months.

274. Pyke, T. N., Jr., Blanc, R. P., **Networking challenges: The user's viewpoint,** (Proc. EDUCOM Fall Conf., Princeton, N.J., Oct. 9-11, 1973), Chapter 14 *Transportability of Instructional Systems in Facts and Future*, pp. 211-217 (EDUCOM, The Intercommunication Council, Princeton, N.J., 1974).

Key words: computer network; network access machine; network measurement machine; network user; resource sharing; user services.

A number of problems that impede the effective sharing of omputer and information resources are identified and scussed. Taking examples from the use of present research and perational resource sharing networks, the difficulties associated ith measuring and comparing performance of services pro- ded, identifying and comparing costs to the end user, and deter- ining the amount of effort required on the part of the user to ccessfully utilize a computer network are presented. Some ap- roaches toward the solution of these problems are also scussed.

4275. Field, R. W., English, A. D., Tanaka, T., Harris, D. O., Jennings, D. A., **Microwave optical double resonance spectroscopy with a cw dye laser: BaO $X\,{}^1\Sigma$ and $A\,{}^1\Sigma$,** *J. Chem. Phys.* **59,** No. 5, 2191-2203 (Sept. 1, 1973).

Key words: cw dye laser; double resonance; microwave; spectroscopy.

A tunable, single frequency, continuous wave, dye laser has een used to optically pump various lines of the BaO $A\,{}^1\Sigma - X$ $\Sigma$ electronic transition. Microwave optical double resonance (MODR) spectra are recorded as changes in the intensity of dye laser induced photoluminescence. Fourteen microwave rotational transitions in the $X\,{}^1\Sigma$ ($\nu=0,1$) and $A\,{}^1\Sigma$ ($\nu=0-5$) states of ${}^{138}$Ba${}^{16}$O and one transition in the $A\,{}^1\Sigma$ ($\nu=1$) state of ${}^{137}$Ba${}^{16}$O have been observed. Partially deperturbed rotational constants obtained for BaO $A\,{}^1\Sigma$ are $B(\nu)=0.25832(2)-0.001070(5)(\nu+1/2)$ cm$^{-1}$. Two physical models are described which account for microwave optical double resonance effects in the strong (nonlinear) and weak (linear) optical pumping limits. Observed changes in photoluminescence polarization caused by excited state microwave transitions are predicted by a semiclassical transition dipole model. A three level steady state kinetic treatment of microwave optical double resonance indicates that the BaO MODR transitions reported in this paper are observed near the strong optical pumping limit. It is shown that for most allowed transitions in diatomic molecules a 100 mW single frequency, dye laser is sufficiently intense to significantly deplete rotational levels of the electronic ground state with respect to neighboring rotational levels and to cause the populations of the depleted ground state and optically pumped excited state levels to become comparable.

14276. Velapoldi, R. A., Reisfeld, R., Boehm, L., **Quantum efficiencies and transition probabilities of Eu$^{3+}$ in silicate glasses,** *Phys. Chem. Glasses* **14,** No. 6, 101-106 (Dec. 1973).

Key words: europium; fluorescence; lifetimes; luminescence; nonradiative rates; oscillator strengths; quantum efficiencies; radiative rates; rare earths; silicate glasses.

Absorption, excitation, and emission spectra of Eu(III) in silicate glasses have been measured. The oscillator strengths for transitions from the populated $^7F$ multiplet have been calculated and compared with those in other matrices. Quantum efficiencies were determined by comparative and lifetime measurements. Percentage quantum efficiencies for the ${}^5D_i\rightarrow{}^5D_0$ transitions and radiative and nonradiative rate constants were calculated.

14277. Weinstein, B. A., Piermarini, G. J., **First and second order Raman scattering in GaP to 128 kbar,** *Physics Lett.* **48A,** No. 1, 14-16 (May 20, 1974).

Key words: diamond-anvil cell; gallium phosphide; Raman scattering.

One- and two-phonon room temperature Raman spectra of GaP were measured to 128 kbar using a diamond-anvil pressure cell. Linear and quadratic pressure coefficients were determined for phonons at $\Gamma$,L, (X → K), and $\Sigma$. The results suggest possible "soft" mode behavior for TA(L) and TA(X → K) phonons.

14278. Evans, A. G., Wiederhorn, S. M., **Crack propagation and failure prediction in silicon nitride at elevated temperatures,** *J. Mater. Sci.* **9,** 270-278 (1974).

Key words: elevated temperatures; failure prediction; silicon nitride; slow crack growth.

A technique for studying high temperature crack propagation in ceramic materials is developed. The technique is used to obtain relationships between the crack propagation rate and the stress intensity factor for hot-pressed silicon nitride up to 1400 °C. The data are then used to develop proof test diagrams which give values for the safe working stress levels for this material after proof testing (or any other flaw detection procedure).

14279. Franklin, A. D., Crissman, J., Young, K. F., **Point defect interactions in CaF$_2$:GdF$_3$,** *J. Phys.* **C9,** C9-179-C9-183 (Nov.-Dec. 1973).

Key words: anelastic relaxation; CaF$_2$; dielectric relaxation; EPR lifetime broadening; GdF$_3$; pairs; point defects.

The reorientation of the point-defect pair formed in CaF$_2$ crystals by substitutional Gd$^{3+}$ and interstitial F$^-$ ions has been studied using EPR lifetime broadening measurements and dielectric and anelastic relaxation studies at temperatures between liquid $N_2$ and room. The $GdF_3$ concentration ranged from 0.01 to 0.3 mole percent. The crystals were annealed in an atmosphere of He and HF at temperatures from 600 to 800 °C and quickly cooled. Three major relaxations were observed in the anelastic temperatures corresponding well to two major relaxations observed in the dielectric spectrum. The most important of these correlated both in relaxation parameters and intensity changes upon annealing and/or changing concentration of $GdF_3$ with the lifetime broadening and intensity of the EPR spectrum from the nearest-neighbor pair. The entire pattern has the proper symmetry for the pair with relaxation modes generated by excursions of the $F^-$ interstitial out to third-neighbor positions, assuming that the most stable positions are closest to the $Gd^{+3}$ ions. However, this model is inconsistent with the relative intensities of the dielectric relaxations, and it is concluded that at least two distinct centers must be present.

14280. Mandel, J., **The evaluation of standard test methods,** *Stand. News* **2,** No. 4, 17-20 (Apr. 1974).

> Key words: interlaboratory studies; measurement; precision accuracy; test methods.

Test methods can be classified into two types: those for which the quantity to be measured is defined independently of the test method and those for which it is defined in terms of the test method. In either case, the evaluation of the precision and accuracy of single measurements can be made only in terms of the characteristics of the method itself. The study of a test method requires the postulation of a mathematical model which in turn determines the proper statistical method of data analysis. The interpretation of the results must be made in terms of the requirements imposed on the method by its practical applications.

14281. Krell, J. M., Sams, R. L., **Vibration-rotation bands of nitrous oxide: 4.1 micron region,** *J. Mol. Spectrosc.* **51,** No. 3, 492-507 (June 1974).

> Key words: Coriolis interaction; Fermi resonance; high resolution; $H_2O$; infrared; perturbation allowed transitions.

The infrared spectrum of nitrous oxide has been measured and analyzed from 2265 $cm^{-1}$ to 2615 $cm^{-1}$. Newly refined effective rotational constants for twenty-one vibrational states of $^{14}N_2O$, three vibrational states each of $^{14}N_2{}^{18}O$ and $^{15}N^{14}N^{16}O$, two states of $^{14}N^{15}N^{16}O$ and one state of $^{14}N_2{}^{17}O$ have been calculated.

The most interesting features observed are two $\Delta$-$\Sigma$ "forbidden" bands, $04^{2c}0$-$00^00$ and $12^{2c}0$-$00^00$. These bands occur because of Coriolis interaction between unperturbed vibrational states having $l=0$ and $l=2$.

14282. Durig, J. R., Carreira, L. A., Lafferty, W. J., **Spectra and structure of small ring compounds. Microwave spectrum of cyanocyclobutane,** *J. Mol. Spectrosc.* **46,** No. 2, 187-193 (May 1973).

> Key words: cyanocyclobutane; dipole moment; microwave spectrum; molecular structure; ring conformation; rotational constants.

The rotational spectrum of cyanocyclobutane has been investigated in the region 18.0-40.0 GHz. Only A-type transitions were observed. R-branch assignments have been made for the ground state and the first three excited states of the ring puckering mode as well as the first two excited states of the out-of-plane cyano-bending mode. The microwave data are consistent with a bent equilibrium ground state for the ring with the cyano-group in the equatorial position. The dipole moment components were determined to be $\mu_a = 4.04 \pm 0.09$ D and $\mu_c = 0.92 \pm 0.03$ D with the total dipole moment, $\mu$, having a value of $4.14 \pm 0.09$ D.

14283. Ambrose, J. R., Kruger, J., **Tribo-ellipsometry: A new technique to study the relationship repassivation kinetics to stress corrosion,** *Corrosion* **28,** No. 1, 30-35 (Jan. 1972).

> Key words: repassivation kinetics; steel; stress corrosion; tribo-ellipsometry.

Since the susceptibility of a material to stress corrosion cracking (SCC) may be related to the rupture of a protective film and the repassivation rate of the material thus exposed, a technique, tribo-ellipsometry, has been developed which simulates film rupture by abrading off the surface oxide. During the subsequent repassivation of the exposed surface, this technique allows simultaneous determination of film growth kinetics by ellipsometry and current transients during that time interval following removal of the oxide film. The major advantage of the technique is that the ellipsometric transient allows one to determine which part of the current transient is responsible for repassivation and which part is involved in metal dissolution. Th utility of the technique is demonstrated by comparing repassivation rates for a low carbon steel in a sodium nitrate solution i which the metal is susceptible to SCC to those in a sodium nitrit solution, in which it is not. Results obtained using this method indicate that the repassivation rate is slower at elevated temperatures in the nitrate than it is in the nitrite, and that a larger proportion of the current is involved in metal dissolution in th nitrate. This may offer an insight into the reasons for observe susceptibility of mild steels to SCC in such nitrate environment

14284. Wiederhorn, S. M., Evans, A. G., Roberts, D. E., **A fracture mechanics study of the Skylab windows,** Chapter i *Fracture Mechanics of Ceramics,* R. C. Bradt, D. P. H. Hasselman, and F. F. Lange, Eds., **2,** 829-841 (Plenum Pub Corp., New York, N.Y., 1974).

> Key words: crack growth; fracture mechanics; glass; stati fatique; structural design; windows.

Design criteria based on fracture mechanics concepts ar developed for spacecraft windows. Critical stress intensity facto data and crack velocity data are used for lifetime predictions an for the development of acceptance tests for the eight candidat glass compositions for the Skylab. Design charts are presente which give the minimum time to failure of the Skylab windows a function of service stress and proof test stress. Surface a sorbed water is shown to be detrimental to the strength spacecraft windows, even after the spacecraft has left the earth atmosphere, because of the slow rate of evaporation of wat from surface cracks.

14285. Wilson, W., Swartzendruber, L. J., **A flexible least squar routine for general Mössbauer effect spectra fitting,** *Comput Phys. Commun.* **7,** 151-162 (1974).

> Key words: FORTRAN; least squares fitting; Mössbau effect; numerical analysis.

A FORTRAN version of a versatile and flexible least squar fitting routine for Mössbauer effect data is described.

14286. Fromhold, A. T., Jr., Coriell, S. R., Kruger, J., **Transpo and thermodynamic analyses of steady-state currents in soli** *J. Phys. Soc. Japan* **34,** No. 6, 1452-1459 (June 1973).

> Key words: electrochemistry; Gibbs-Duhem; lo equilibrium; nonequilibrium thermodynamics; oxidation metals; solid state diffusion; transport in solids.

The usual derivation of the well-known Gibbs-Duhem relati (or its electrochemical analog) from equilibrium thermodynam is based on certain assumptions which are only approximat met for nonhomogeneous systems; the postulate of lo equilibrium generally employed in nonequilibrium th modynamics is commonly utilized to extend the results to nonequilibrium domain. The application of the electrochemi bs-Duhem relation to the particular case of several charged sing species in a solid is utilized herein to obtain an expres- for the local electric field which is then compared with an ression for the field deduced by an ordinary phenomenologi- transport analysis. The two approaches yield consistent alts only in the limit of thermodynamic equilibrium. Implica- s of the analyses are pointed out for the special problem of growth of oxides and similar tarnish films on metals.

87. Bennett, L. H., Cuthill, J. R., McAlister, A. J., Erickson, . E., Watson, R. E., **Electronic structure and catalytic ehavior of tungsten carbide,** *Science* **184,** 563-565 (May 974).

Key words: catalysis; density of states; magnetic exchange enhancement; Pt; W; WC.

ungsten carbide has been shown to be an effective catalyst a number of reactions that are readily catalyzed by platinum, not at all by tungsten, and it was speculated that this behavior lue to changes in the electron distribution when carbon is ed to tungsten. A test of this hypothesis, made by measuring valence band x-ray photoelectron spectrum of tungsten car- e and comparing it with the spectra of tungsten and platinum, ws that, near the Fermi level, the electronic density of states ungsten carbide more nearly resembles that of platinum than of tungsten.

88. Tetelman, A. S., Evans, A. G., **Failure prediction in brittle aterials using fracture mechanics and acoustic emission,** hapter in *Fracture Mechanics of Ceramics,* R. C. Bradt, D. . H. Hasselman, and F. F. Lange, Eds. **2,** 895-924 (Plenum ubl. Corp., New York, N.Y., 1974).

Key words: acoustic emission; failure prediction; fast crack propagation; fracture mechanics; slow crack growth.

coustic emission testing has found many uses in recent years new applications are constantly being uncovered. The in- esting areas for application lie in failure prediction and the racterization of the microscopic processes of yielding and cture, and the macroscopic processes of slow crack growth onset of fast crack propagation. This paper has described se applications and emphasized that the total counts and nt rate depend on the energy released per event and the den- of events per unit of deformation. Where models are sented, they should be regarded as first order approximations ch await confirmation.

89. McNesby, J. R., **Standard reference materials for air pol- ution,** *Proc. Tech. Conf. on the Observation and Measure- nent of Atmospheric Pollution (TECOMAP), Helsinki, Fin- and, July 30-Aug. 4, 1973,* Special Environmental Report No. , 595-603 (World Meteorological Organization, Geneva, witzerland, 1974).

Key words: air pollution; Standard Reference Materials.

he compatibility and accuracy of air pollution measurements ends strongly upon the integrity of the measurement stan- ds to which calibration gases are referred. For this reason it ssential that great care be exercised in establishing scientifi- ly their integrity. The emphasis at the U.S. National Bureau Standards is being placed upon the development of Standard ference Materials for those air contaminants designated by U.S. Environmental Protection Agency as ambient air pollu- ts, i.e., particulate matter, $SO_2$, $NO_x$, CO, hydrocarbons, and otochemical oxidants. Standard Reference Materials must be eloped also in different concentration ranges for automobile aust and for point source effluents. All of these categories are der development at the National Bureau of Standards.

90. Wiederhorn, S. M., **Subcritical crack growth in ceramics,** hapter in *Fracture Mechanics of Ceramics,* R. C. Bradt, D. P. H. Hasselman, and F. F. Lange, Eds. **2,** 613-646 (Plenum Publ. Corp., New York, N.Y., 1974).

Key words: ceramics; crack growth; delayed failure; fracture; proof testing.

Subcritical crack growth that causes delayed failure is discussed in terms of fracture mechanics concepts. Techniques of characterizing subcritical crack growth are presented and the available crack growth data are discussed with particular emphasis on fracture mechanisms. Finally a design technique is presented to predict useful component lifetime from crack growth data after proof testing.

**14291.** Clark, J. E., **A proposed flammability standard for children's sleepwear,** *Proc. 4th Annual Meeting of the Information Council on Fabric Flammability, New York, N.Y., Dec. 3, 1970,* pp. 142-149 (1970).

Key words: accidents; children; clothing; fabrics; flammability; sleepwear; standards.

Developments toward a flammability standard for children's sleepwear are presented. The basis is reviewed for the legal finding that a standard is needed. The laboratory research studies and the analysis of accident investigation reports are summarized.

The proposed standard provides a vertical test method which uses char length and afterflame time criteria to determine the flammability of children's sleepwear. The procedure, apparatus and care lable requirements are outlined.

**14292.** McLaughlin, W. L., Kosanić, M., **The gamma-ray response of pararosaniline cyanide dosimeter solutions,** *Int. J. Appl. Radiat. Isotop.* **25,** No. 6, 249-262 (June 1974).

Key words: dosimetry; dyes; dye yield; gamma rays; pararosaniline cyanide; 4,4′,4″-triaminotriphenylacetonitrile; triphenyl-methane dyes.

Triphenylmethane dye derivatives, especially the colorless nitriles in organic or aqueous solution, serve as convenient radiation dosimeters. With large absorbed doses ($10^3$-$10^6$ rads), permanent ionized dye is produced with sufficient color for routine photometric measurement. If a polar solvent is used and the solution is oxygenated and stabilized by weak acid, the optical density measured at the absorption maximum of dye is a linear function of dose. Dye yield varies with the type of solvent, concentration of the dye precursor, temperature during irradiation, acid and oxygen content and batch of dye precursor used. Additions of small amounts of acid to solutions prevent back reactions. Dissolved oxygen or a weak oxidizing agent helps extend the dose range of response by scavenging free-radical agents formed in the solvent during irradiation. Suitable plastic containers may be used, without the need for ultraclean handling procedures or superdistilled solvents. Since the main sources of systematic error are easily controlled and since the new dosimeter solutions may be used over a wide dose range, they show advantages over other chemical dosimeters for many applications.

**14293.** Clark, J. E., Tovey, H., **Priorities for fabric flammability investigations,** *Proc. 5th Annual Meeting of the Information Council on Fabric Flammability, New York, N.Y., Dec. 9, 1971,* pp. 208-214 (1972).

Key words: accident data; apparel standard (CS 191-53); fire safety; Flammable Fabrics Act; ignition sources; mandatory standards.

A broad attack is necessary in order to reduce deaths, injuries, and property loss from fabric fires. Standards on the flammability of fabrics are greatly needed and careful study is necessary to ensure that these standards are, as the law requires, reasonable, appropriate, and technologically practicable.

In addition, improvements in standards and engineering design of common heat sources could well contribute to significant reduction of clothing ignitions.

Further study of use and packaging of flammable fluids can be expected to lead to reduced hazard. But much more knowledge is needed in this area before optimum recommendations can be made.

Improved and uniform building fire codes could also contribute to improved occupant safety, through wider use of smoke and fire detectors, audio-visual warning systems, self-closing doors, and automatic sprinklers.

Finally, we must continue and greatly increase our education efforts so that the consumer has an increased awareness of the fabric fire problem, and concomitant knowledge of proper fire prevention and extinguishment procedures.

**14294.** Currie, L. A., Filliben, J. J., DeVoe, J. R., **Statistical and mathematical methods in analytical chemistry,** *Anal. Chem. Ann. Rev.* **44,** 497R-512R (Apr. 1972).

Key words: chemical analysis; curve fitting; distribution functions; experiment planning and optimization; measurement process; on-line computers; recognition techniques; review; statistics; transforms.

The statistical and chemical literature are surveyed for the period October 1967 to October 1971, with emphasis on work related to the application of mathematical statistics to analytical chemistry. Principal categories covered include: Reviews, Conferences, Journal and Books; Method Characterization; Planning and Optimization of Experiments; Curve Fitting; Online Computers; and Other Topics (techniques for testing basic statistical assumptions; special distributions; transforms, correlation and signal/noise enhancement; recognition techniques). The bibliography, consisting of somewhat less than 600 references, contains mostly English-language journals and books, but important foreign-language articles—particularly French, German and Russian— also appear.

**14295.** DeVoe, J. R., **A laboratory based multi-instrument computer system,** (Proc. Int. Conf. on Modern Trends in Activation Analysis, Saclay France, Oct. 2-6, 1972), *J. Radioanal. Chem.* **15,** 657-667 (1973).

Key words: computer; digital communication system; laboratory automation; multi-program monitor.

Design of computer system for assistance in the operation of experiments contains certain factors unique to a particular laboratory. Details are given on the procedure that was used to generate design criteria and to implement such a design for a computer system in the Analytical Chemistry Division, NBS. The system is currently servicing ten instruments (ranging from spectrophotometers to mass spectrometers) with a projected capacity exceeding sixty depending upon the type of instruments connected.

**14296.** DeVoe, J. R., **Automation and computerization of analytical measurements,** *Proc. Seminar Series on Chemistry and Biology of Trace Metals in the Environment, University of Illinois, Urbana, Ill., Spring 1971,* pp. 147-162 (University of Illinois Press, Urbana, Ill., 1972).

Key words: computer; digital communication system; laboratory automation; multi-program monitor.

Design of computer systems for assistance in the operation of experiments contains certain factors unique to a particualr laboratory. Details are given on the procedure used to generate design criteria and to implement such a design for a computer system in the Analytical Chemistry Division, National Bureau of Standards.

**14297.** Garfinkel, S. B., Mann, W. B., Schima, F. J., Unterwege M. P., **Present status in the field of internal gas counting,** (Proc First Int. Summer School on Radionuclide Metrology, Herce Novi, Yugoslavia, Aug. 21-Sept. 1, 1972), *Nucl. Instrum Methods* **112,** No. 1/2, 59-67 (Sept.-Oct. 1973).

Key words: argon-37; carbon-14; internal gas counting radioactive standardization; tritium; xenon-131m.

The gas-counting equipment at the National Bureau c Standards has been recently modified and reconstructed. Th preparation of various radioactivity gaseous standards will b described. In some cases purity is assured by a prior separatio in the isotope separator.

**14298.** Selig, H., Sarig, S., Abramowitz, S., **Alkali fluorotellurat (VI),** *Inorg. Chem.* **13,** 1508-1511 (1974).

Key words: alkali hexafluorotellurates; inorganic comple intermediate phases; structure; thermodynamic analysis.

The reactions of tellurium hexafluoride with cesium fluori or rubidium fluoride go nearly to completion if the alka fluorides are suspended in the inert solvent, $C_6F_6$. With cesiu fluoride a limiting composition of $CsF \cdot TeF_6$ is approache while rubidium fluoride gives compounds of composition 2RbF $TeF_6$. Thermogravimetric analyses of the products show vario inflection points indicating the existence of intermedia products stable at higher temperatures. Complete decompositic of the complexes is not achieved up to the melting points of th alkali fluorides, except in some cases under prolonged pumpin The infrared and Raman spectra of the materials have been te tatively interpreted in terms of $D_{8h}$ and $D_{4d}$ structures for t $TeF_7^-$ and $TeF_8^{2-}$ anions, respectively.

**14299.** Hutchinson, J. M. R., Mann, W. B., Mullen, P. A., **Sur peak counting with two crystals,** (Proc. First. Int. Summ School on Radionuclide Metrology, Herceg Novi, Yugoslavi Aug. 21-Sept. 1, 1972), *Nucl. Instrum. Methods* **112,** No. 1/ 187-196 (Sept.-Oct. 1973).

Key words: aluminum-26; bismuth-207; cobalt-6 niobium-94; radioactivity standardization; sodium-22; su coincidence counting; yttrium-88.

Very great improvements in accuracy of measurements radioactivity by the sum-peak technique of coincidence counti have been achieved by the utilization of two NaI(Tl) crystals.

Taking advantage of the coincidence and anticoincidence po sibilities in this arrangement, equations and techniques ha been developed, so that accuracies obtainable by the sum-pe technique are improved by an order of magnitude, and becor comparable to those obtainable by means of conventional $\beta$ and $\gamma$-$\gamma$ coincidence counting.

Good statistical accuracy can be obtained quickly, and ma small but often laboriously determined corrections which appe in $\beta$-$\gamma$ and $\gamma$-$\gamma$ coincidence counting, are important in this n method, which has been applied to the standardization of $^{60}$C $^{94}$Nb, $^{88}$Y, $^{22}$Na, $^{26}$Al and $^{207}$Bi.

**14300.** Hutchinson, J. M. R., Mann, W. B., Perkins, R. W., **Lo level radioactivity measurements,** (Proc. First Int. Summ School on Radionuclide Metrology, Herceg Novi, Yugoslav Aug. 21-Sept. 1, 1972), *Nucl. Instrum. Methods* **112,** No. 1 305-318 (Sept.-Oct. 1973).

Key words: aluminum; anticoincidence shielding; bovi liver assay; copper; low-level radioactivity; radioactivity tercomparisons; steel.

Low-level radioactivity measurements are reviewed. Alp and $\beta$-particle, and $\gamma$-ray low-level-radioactivity counting discussed, and various detector systems are compared for det tion sensitivity. Low-level measurements on bovine liver st d reference material, and radioactive contamination in indus- l samples of aluminum, copper, and steel are reviewed. The ults of low-level radioactivity intercomparisons are discussed.

**01.** Garfinkel, S. B., Mann, W. B., Pararas, J. L., **The National ureau of Standard 4π β-γ coincidence-counting and γ-ray in- ercomparator automatic sample changers,** (Proc. First Int. ummer School on Radionuclide Metrology, Herceg Novi, ugoslavia, Aug. 21-Sept. 1, 1972), *Nucl. Instrum. Methods* **12**, No. 1/2, 213-217 (Sept.-Oct. 1973).

> Key words: radioactivity measurements; 4π β-γ coincidence counting; γ-ray intercomparator automatic sample changers.

nstruments of very simple and somewhat novel design will be cribed. The 4π β-γ changer holds from 1 to 30 carriers of rces, each of which can be counted for any preset number, up 0, of counting periods. The γ-ray changer accomodates from 24 source carriers. In comparing γ-ray source count rates, detector-to-source distances for individual sources are care- y controlled.

**02.** Mann, W. B., **Radioactive calorimetry—a review of the ork at The National Bureau of Standards,** (Proc. First Int. ummer School on Radionuclide Metrology, Herceg Novi, ugoslavia, Aug. 21-Sept. 1, 1972), *Nucl. Instrum. Methods* 12, No. 1/2, 273-277 (Sept.-Oct. 1973).

> Key words: intercomparative measurements; nickel-63; radioactive calorimetry; radioactive standardization.

alorimetric measurements in the field of radioactivity will be iewed with special reference to the standardization of $^{63}$Ni. ercomparative measurements with the National Research uncil of Canada and Atomic Energy of Canada Limited will discussed.

**03.** Cavallo, L. M., Coursey, B. M., Garfinkel, S. B., Hutchinson, J. M. R., Mann, W. B., **Needs for radioactivity tandards and measurements in different fields,** (Proc. First Int. ummer School on Radionuclide Metrology, Herceg Novi, ugoslavia, Aug. 21-Sept. 1, 1972), *Nucl. Instrum. Methods* 12, No. 1/2, 5-18 (Sept.-Oct. 1973).

> Key words: intercomparisons; radioactivity; standards; traceability.

Vith the enormous and world-wide increase in the applica- ns of radioactive materials in so many scientific and hnological fields, a corresponding need has arisen for in- ased skill and improved facilities for the assay of such materi- . In the U.S.A., the use of radioisotopes, including radiophar- ceuticals is about $80 million annually. The measurements lls and facilities must of necessity tend to lag behind such a id growth, and increasingly from many quarters we at the Na- nal Bureau of Standards are being requested for help in ablishing a consistent measurements system in radioactivity ceable both to us and through us to the international measure- nts system. This paper will discuss the measures that we are ing in order to achieve such traceability in a consistent mea- ements system in different fields of radioactivity, with special phasis on environmental and radiopharmaceutical measure- nts.

**04.** Lawless, W. N., **Dielectric cooling technology: 15—4.2 K,** Proc. Cryogenic Cooler Conf., USAF Academy, Colo., Oct. 16-17, 1973), Chapter in *Closed Cycle Cryogenic Cooler Technology and Applications* **1**, 417-440 (AF Flight Dynamics Lab., (FEC), Wright-Patterson AFB, Ohio, Dec. 1973).

> Key words: adiabatic polarization; cooling technology; dielectric cooling; glass-ceramics; magnetic thermal valve; mechanical thermal valve; refrigeration, solid-state; $SrTiO_3$.

A comprehensive analysis of a proposed dielectric refrigerator operating in a closed cycle between a load at 4.2 K and a reservoir at 15 K is presented. The working dielectric material is a $SrTiO_3$ glass-ceramic, for which the dielectric equation of state is experimentally determined. Hysteretic phenomena, breakdown strength, and phonon-polarization data are presented and discussed. A realistic engineering model for the refrigerator is described and analyzed, including parasitic thermal loads and losses. Some of the dimensional parameters of the model maximize the performance, and these optimal dimensions are physically reasonable. Computer analyses are made of these models, which are right circular cylinders of diameter D and height D. The results are that the net powers absorbed from the load at 4.2 K vary from 1 to 50 W for D-values between 5 and 20 cm and for cycle times ~ second. These results are shown to be relatively insensitive to the choice of metals used for the electrodes and heat conductors in the model (Rh, Pt, W, Cr, Cu) or to the approximations employed. A joint development program between the National Bureau of Standards and Corning Glass Works is underway to develop a prototype dielectric refrigerator along the lines discussed in this paper.

**14305.** Voth, R. O., Petropoulos, S. K., **Cryogenic refrigerators for shipboard forward looking infrared applications,** (Proc. Cryogenic Cooler Conf., USAF Academy, Colo., Oct. 16-17, 1973), Chapter in *Closed Cycle Cryogenic Cooler Technology and Applications* **1**, 27-33 (AF Flight Dynamics Lab., (FEC), Wright-Patterson AFB, Ohio, Dec. 1973).

> Key words: cryogenics; infrared detector; low capacity; reliability; shipboard; 77 K refrigerator.

The Naval Ordnance Laboratory (NOL) has asked the Cryogenics Division of the National Bureau of Standards to investigate and evaluate 1) commercially available refrigerators, 2) refrigerators under development, and 3) new or novel ideas applicable to a refrigerator to cool infrared detectors in a shipboard Forward Looking Infrared (FLIR) system. The FLIR requires a refrigerator capacity of approximately 2 watts at 77 K and a physical configuration allowing for an interface to the FLIR unit. Information was collected by interviewing FLIR manufacturers, surveying refrigerator manufacturers and by contacting users of similar systems. Correlation of this information with the NOL requirements is presented herein. The primary difference between airborne/spaceborne refrigerators and a shipborne refrigerator is the accessibility for minor repairs on-board ship although major repairs may be deferred for extended periods of time. It is anticipated that the shipboard units will operate away from major maintenance facilities, for periods as long as 6 months, with the refrigerator operating at least half of this time. Thus, reliability and ease of maintenance are emphasized when evaluating the various systems.

**14306.** Haller, W., Blackburn, D. H., Simmons, J. H., **Miscibility gaps in alkali-silicate binaries—data and thermodynamic interpretation,** *J. Amer. Ceram. Soc.* **57**, No. 3, 120-126 (1974).

> Key words: alkali-silicates; glass; immiscibility; lithium-silicate binary; melts; miscibility gaps; sodium-silicate binary; thermodynamics.

Measurements of the miscibility gaps in the $Li_2O$- and $Na_2O$-$SiO_2$ binaries are reported and compared to data of other workers. Heat treatments by brief immersion in liquid Sn were used for measuring the properties of glasses with a strong devitrification tendency. The miscibility-gap boundaries of both systems are successfully described by modified regular-mixing equations based on the concept that the thermodynamic mixing processes are controlled by complex but discrete molecular structures which exist in the melt. The assumptions and implications of the model are discussed.

**14307.** Collins, R. C., Haller, W., **Protein-sodium dodecyl sulfate complexes: Determination of molecular weight, size and shape by controlled pore glass chromatography,** *Anal. Biochem.* **54,** No. 1, 47-53 (July 1973).

Key words: chromatography; controlled pore glass chromatography; molecular size; porous glass chromatography; protein; protein-sodiumduodecylsulfate complexes; sodiumduodecylsulfate-complexes.

Protein-SDS complexes chromatographed on controlled pore glass elute linearly with log molecular weight over a range from 17,000 to 385,000 daltons. A glass with a pore size of approximately 500 Å allows the inclusion of all complexes in this range.

Exclusion size analysis of the individual complexes gives from 120 to 423 Å as their longest dimension.

**14308.** Cassidy, E. C., Hebner, R. E., Jr., Zahn, M., Sojka, R. J., **Kerr-effect studies of an insulating liquid under varied high-voltage conditions,** *IEEE Trans. Elec. Insul.* **EI-9,** No. 2, 43-56 (June 1974).

Key words: electric fields; electrical measurements; high voltage measurements; insulating liquids; Kerr effect; nitrobenzene; space charge.

Refined Kerr electrooptial fringe-pattern methods are used to study time and space variations in the electric field between the electrodes of parallel-plate capacitors filled with liquid nitrobenzene. Photographs of fringe-pattern data recorded during application of high direct (both positive and negative) and sinusoidal voltages, ranging in frequency from 40 to 200 Hz, are compiled to enable computation of space-charge distortions of the field bulk of the liquid during the stress of high-field (up to 85-kV/cm) operation. The measurements reveal significant differences between the field and charge behavior under short pulse (microsecond) voltage conditions, during prolonged dc operation, after sudden changes in the dc voltage level and polarity, and, for the first time, at various intervals over the course of entire cycles of sinusoidal voltage. The results show that space-charge distortion in the interelectrode field is influenced by the level, frequency, and duration of applied voltage. Discussions of effects believed due to particulate charge carriers, to electrohydrodynamic motion of the liquid, and to the electrode materials are also included.

**14309.** Unassigned.

**14310.** Iverson, W. P., **Tests in soils,** (Proc. Symp. on State-of-the-Art in Corrosion Testing ASTM Annual Meeting, June 21-26, 1970, Toronto, Canada), Chapter 21 in *Handbook on Corrosion Testing and Evaluation,* W. H. Ailor, Ed., pp. 575-597 (John Wiley & Sons, Inc., New York, N.Y., 1971).

Key words: biological activity; chemical tests; electrochemical tests; pH; polarization measurements; redox-potential; soil corrosivity; soil resistivity.

A review and discussion of various methods used in measuring the corrosivity of soils and thin relative significance.

Methods discussed include soil pH, total ductility redox-potential, redox-capacity, resistivity, chemical tests, biological activity, electrochemical tests, and polarization techniques.

**14311.** Mangum, B. W., **Standard Reference Materials 933 and 934: The National Bureau of Standards' precision thermometers for the clinical laboratory,** *Clin. Chem.* **20,** No. 6, 670-672 (1974).

Key words: clinical laboratory; enzymology; health care; standard reference material; SRM 933; SRM 934; thermometers.

Because many facets of clinical laboratory work, such as enzymatic reactions, pH measurements, and blood-gas analysis, are highly sensitive to temperature, there is a need to measure ten perature accurately and closely control it. To help satisfy thes needs and to aid in getting a usable temperature scale into th clinical laboratory, the National Bureau of Standards ha developed SRM 933 and SRM 934. These precision thermom ters are calibrated at 0, 25, 30, and 37 °C. Their value to th clinical laboratory is described.

**14312.** Newbury, D. E., Christ, B. W., Joy, D. C., **Relevance electron channeling patterns to embrittlement studies,** *Me Trans.* **5,** 1505-1508 (June 1974).

Key words: cleavage surfaces; electron channeling contras embrittled iron; grain surfaces; scanning electron microsc py.

The new technique of scanning electron microscopy utilizi electron channeling contrast has been applied to the study fracture surfaces of embrittled iron. The degradation of electr channeling patterns with increasing amounts of surface layer ( mn deep) deformation is an ideal tool for qualitatively measuri plastic flow in small areas (10 $\mu$m diameter) of fracture surfac Electron channeling patterns were obtained from grain surfac and cleavage surfaces. It was always possible to obtain chann ing patterns from grain surfaces, but there were many regions cleavage surfaces where electron channeling contrast w completely eliminated. Variations in the amount of plastic fl were evident from point to point on both grain surfaces a cleavage surfaces.

**14313.** Horn, W. A., **Some simple scheduling algorithms,** *N Res. Logistics Q.* **21,** No. 1, 177-185 (Mar. 1974).

Key words: job scheduling; minimizing maximum latene minimizing total delay; multimachine scheduling; sched ing; scheduling algorithms; single-machine scheduling.

This paper considers situations in which jobs require only operation on a single machine, or on one of a set of identi machines. Penalty-free interruption is allowed. Some simple gorithms are given for finding optimum schedules to minim maximum lateness and total delay, for the single-machine ca and maximum lateness for a restricted multimachine case. A s ple flow problem formulation permits minimizing maximum la ness for the more general multimachine case.

**14314.** Herzberg, G., Hugo, T. J., Tilford, S. G., Simmons, J. **Rotational analysis of the forbidden $d^3\Delta_i \leftarrow X^1\Sigma^+$ absorp bands of carbon monoxide,** *Can. J. Phys.* **48,** No. 24, 30- 3015 (1970).

Key words: absorption spectrum; carbon monoxide; e tronic spectrum; forbidden transition; rotational analy rotational perturbations.

The forbidden $d^3\Delta_i - X^1\Sigma^+$ transition of CO has been served in absorption at high resolution in the vacuum ultravi region. The intensity distribution in the rotational structur the observed bands in conformity with the assumption that transition occurs on account of the interaction between the state and a $^1\Pi$ state, presumably the $A^1\Pi$ state. Thirteen banc the $d - X$ system have been analyzed yielding more exten rotational data for the $d^3\Delta_i$ state than were previously know discussion of the local perturbations in the $d$ state by the $A^1\Pi$ $a^3\Pi$ states is included.

**14315.** Horn, W. A., **Minimizing average flow time with par el machines,** *Oper. Res.* **21,** No. 3, 846-847 (May-June 1973).

Key words: assignment problems; job scheduling; sche ing.

It is noted that the assignment and sequencing of one-mac ne jobs in a multimachine environment can be formulated a linear-programming assignment problem. Means for reducin ne size and computational difficulty of this problem are identifie

316. Dillon, T. A., Stephenson, J. C., **Calculation of vibrational and rotational energy transfer between HF, DF, HCl, and $CO_2$,** *. Chem. Phys.* **58,** No. 5, 2056-2064 (Mar. 1, 1973).

Key words: energy transfer; HF, DF, $CO_2$; linewidth; unitary.

A theory of vibrational energy transfer which retains the ex- nential form of the scattering operator is applied to energy nsfer between vibrationally excited HF, DF, HCl, and $CO_2$. e calculations contain several new features, including use of ved classical trajectories and vibrational wavefunctions ob- ned numerically from RKR potential. Cross sections for mul- uantum pure rotational changes caused by the dipole-quadru- le interaction are calculated. These multiquantum rotational nsitions play an important role in vibrational energy exchange allowing large vibrational energy defects to be absorbed by rotational degrees of freedom. Agreement between theory d experiment is excellent. Cross sections calculated for simul- neous transfer of two vibrational quanta from HF or HCl to $)_2$ are very small. However, for DF-$CO_2$ the calculated two- antum-transfer cross section is only a factor of 2-6 smaller an that for single-quantum transfer.

317. Billingsley, F. P. II, Krauss, M., **Quadrupole moment of CO, $N_2$, and $NO^+$,** *J. Chem. Phys.* **60,** No. 7, 2767-2772 (Apr. 1, 1974).

Key words: CO; hyperpolarizability; multiconfiguration SCF; $N_2$; $NO^+$; quadrupole moment.

Quadrupole moments obtained by a variety of experiments ex- bit a wide range of values even for molecules such as CO and . Previous theoretical values were obtained with Hartree- ck single-configuration wavefunctions. This study reports adrupole moments obtained with multiconfiguration self-con- tent-field wavefunctions chosen by the optimized valence con- uration approach of Wahl and Das. The theoretical MC-SCF adrupole moments are compared with both the experimental d Hartree-Fock values. Vibrationally averaged values of the adrupole moments were obtained for CO and $NO^+$. The sults for the $\nu = 0, J = 0$ vibrational level are $-2.23$ and $0.56 \times$ $^{-26}$ esu cm$^2$, respectively.

318. Albares, D. J., **Electron and ion momentum transfer from plasma electrical conductivity in a magnetic field,** *Phys. Fluids* **16,** No. 8, 1252-1258 (Aug. 1973).

Key words: Hall effect; helium; magnetic field; momentum transfer; negative glow plasma.

The electrical conductivity of a partially to strongly (Coulomb llision-dominated) ionized dc plasma in a dc magnetic field was vestigated at low frequency by two experimental methods, one tilizing the Hall effect and the other a plasma interaction with induced solenidal electric field. Electron-ion and electron- om momentum transfer collision frequencies and ion mobility the magnetic field (ion slip) were inferred. The helium abnor- al negative glow plasma was used at pressures of 0.5 to 2.5 rr, electron densities of 1 to $32 \times 10^{17}$ m$^{-3}$ and temperature ≈ 0 K; the magnetic field ranged up to 675 G. The data support akarofsky's theory of partial ionization. When ion motion ecomes dominant, the resulting ion mobility is 75 percent larger an $He^+$ mobility in helium taken from drift tube measurements. his disagreement suggests that further theoretical work on ion obility in a plasma is needed.

319. Gevantman, L. H., Garvin, D., **The compilation and evaluation of chemical kinetics data: A descriptive survey of current efforts,** *Int. J. Chem. Kinet.* V, 213-230 (1973).

Key words: chemical kinetics; CODATA kinetics task group; compilation; evaluation; kinetics; national programs; rate constant data.

A description of the current range of activities being pursued in the compilation and evaluation of chemical kinetic data is given. The roles of individual scientists, professional groups, and national and international programs are detailed. The special problems attending on kinetic parameters are enumerated and discussed. An appendix is included which gives a comprehensive list of compilations and evaluations extant in the field of chemical kinetics.

14320. Evans, B. J., Swartzendruber, L. J., **Supertransferred hyperfine fields and covalency at diamagnetic cations in magnetic insulators,** *Phys. Rev. B* **6,** No. 1, 223-231 (July 1, 1972).

Key words: antimony; ferrites; hyperfine fields; iron; Mössbauer effect; nickel; valency.

The sign and magnitude of the antimony hyperfine fields has been measured in Sb-substituted nickel ferrite using the $^{121}$Sb Mössbauer effect. We obtain a value of $-311 \pm 4$ kG for this field at 100 K. This result is compared with results obtained for Sn in yttrium iron garnet and, among the possible mechanisms, $3d$-$5s$ covalent spin transfer appears to make the predominant contribution to the hyperfine field.

14321. Evenson, K. M., Wells, J. S., Petersen, F. R., Danielson, B. L., Day, G. W., **Accurate frequencies of molecular transitions used in laser stabilization: The 3.39-μm transition in $CH_4$ and the 9.33- and 10.18-μm transitions in $CO_2$,** *Appl. Phys. Lett.* **22,** No. 4, 192-195 (Feb. 15, 1973).

Key words: $CO_2$ and He-Ne laser frequency; methane; saturated absorption.

The frequencies of three lasers stabilized to molecular absorptions were measured with an infrared-frequency synthesis chain extending upwards from the cesium frequency standard. The measured values are 29.442 483 315(25) THz for the 10.18-μm $R(30)$ transition in $CO_2$, 32.134 266 891(24) THz for the 9.33-μm $R(10)$ transition in $CO_2$, and 88.376 181 627(50) THz for the 3.39-μm $P(7)$ transition in $CH_4$. The frequency of methane, when multiplied by the measured wavelength reported in the following letter, yields 299 792 456.2 (1.1) m/sec for the speed of light.

14322. Ehrlich, M., **Influence of irradiation on the production of *F* centers in LiF (TLD grade),** *J. Appl. Phys.* **40,** No. 2, 891-892 (Feb. 1969).

Key words: annealing; *F* centers; $^{60}$Co gamma-ray irradiation; LiF (TLD grade) plaques; readout; thermoluminescence.

Optically polished samples of extruded plaques of LiF (TLD grade) were given $^{60}$Co gamma-ray exposures ranging from about 35 000-450 000 R, at exposure rates between about $1.5 \times 10^3$ and $5 \times 10^6$ R/h. Over this range of exposures and exposure rates, the resulting absorption in the *F* band was found to be independent of exposure rate, and to increase with exposure, even for exposures for which the thermoluminescence exhibited saturation effects. After thermoluminescence readout at about 235 °C, practically all the absorption in the *F* band created by the $^{60}$Co gamma-ray exposure had disappeared. These results are compatible with the dominant role given *F* centers in some of the current models for the thermoluminescence process in LiF (TLD grade).

14323. Dillon, T. A., Stephenson, J. C., **Energy transfer during "orbiting" collisions,** *J. Chem. Phys.* **60,** No. 11, 4286-4288 (June 1, 1974).

Key words: energy transfer; infrared lasers; molecular collisions; vibrational exchange.

Semiclassical collision theory is used to calculate the temperature dependence of cross sections for exchange of vibrational excitation from HF and DF to $CO_2$. For collisions with kinetic energy less than four-fifths of the intermolecular potential well depth there exists a narrow range of impact parameter for which the scattering angle exceeds $2\pi$ (i.e., more than one revolution). That part of the trajectory in excess of a single revolution can be accurately represented by a simple model of a circular orbit with a constant angular velocity replacing the instantaneous classical turning point. Calculations are compared to experimental data and illustrate the significance of multiple revolution collisions.

14324. Flynn, J. H., **Thermodynamic properties from differential scanning calorimetry by calorimetric methods,** *Thermochimica Acta* **8,** 69-81 (1974).

> Key words: DSC; enthalpy; glass transition; heat capacity; thermal analysis; thermodynamic properties.

Simple theory and techniques are explored and developed to utilize the differential scanning calorimeter for the determination of heat capacities, glass transition and enthalpies of transition between two thermodynamic states of substances. Effects due to the transition kinetics and thermal and electronic lags of the instrument are either corrected for or eliminated.

14325. Heydemann, P. L. M., Houck, J. C., **Bulk modulus and density of polyethylene to 30 kbar,** *J. Polym. Sci.* **10,** Part A-2, 1631-1637 (1972).

> Key words: bulk modulus; density; equation of state; glass transition temperature; polyethylene; pressure dependence.

The results of bulk modulus and density measurements on low-density polyethylene to 30 kbar are presented. From these data the pressure coefficient $dT_t/dp$ of the glass transition temperature is obtained, and a comparison is made with data calculated from Pastine's theoretical equation of state for polyethylene.

14326. Billingsley, F. P. II, Krauss, M., **Multiconfiguration self-consistent-field calculation of the dipole moment function of CO($X$ $^1\Sigma^+$),** *J. Chem. Phys.* **60,** No. 11, 4130-4144 (June 1, 1974).

> Key words: CO; dipole moment; dipole moment functions; infrared intensity; multiconfiguration SCF.

The dipole moment function for the $^1\Sigma^+$ ground state of CO in the vicinity of the equilibrium internuclear distance has been calculated by the optimized valence configurations (OVC) multiconfiguration self-consistent-field method. The results are compared with existing Hartree-Fock and configuration interaction treatments of this molecule at single points and also the dipole moment function deduced from experimental infrared intensities. At the experimental equilibrium separation, the calculated dipole moment is $-0.167$ D ($C^-O^+$) which is in reasonable agreement with the microwave value of $-0.112$ D ($C^-O^+$). The vibrationally averaged expectation value of the dipole moment based on the computed moment function and accurate vibrational wavefunctions is $-0.151$ D ($C^-O^+$) which is in better agreement with the observed microwave quantity and illustrates that the effect of vibrational averaging is not negligible in systems such as CO that possess small permanent dipole moments. A general prescription for constructing OVC wavefunctions for diatomic molecules is also presented.

14327. Holt, H. K., **Theory of gas lasers and its application to an experiment,** *Phys. Rev. A* **2,** No. 1, 233-249 (July 1970).

> Key words: collisions; gas laser; line widths; power output; theory; tuning curves.

The semiclassical theory of gas lasers has been reformulated by adding rate terms to the density-matrix component differential equations. The solution to these equations, in the form of a Fourier series, is applicable at high laser intensities. A calculation of the effect of phase-changing collisions is also included so that the results can be compared to experimental data take with a He-Ne laser operating at a wavelength of 1.15 $\mu$m.

14328. Heinrich, K. F. J., **Gegenwärtiger stand der klassische theorie der quantitativen elektronenstrahl-mikroanalys** *Mikrochim. Acta.*, Suppl. IV, pp. 252-262 (1970).

> Key words: corrections; electron probe microanalysi quantitative analysis; x-ray spectroscopy.

Although the foundations for a procedure of data reduction quantitative electron probe analysis have not been changed f several years, there has been progress in the choice of expre sions, parameters, and constants. A brief account of recon mended expressions and procedures is given. Reference is ma to the Standard Reference Materials of Au-Ag and Au-Cu allo issued for electron probe microanalysis. These are especial useful for investigating the application of correction procedure

14329. Gevantman, L. H., **Survey of analytical spectral da sources and related data compilation activities,** *Anal. Chem.* 4 No. 7, 30A-48A (June 1972).

> Key words: analytical spectral data; automated spect data sources; data centers; standard reference data.

A broad survey is made of analytical spectra data sources. T activities described include some description of the operati data systems, their location and the type of data issued. The port describes sources for infrared spectra, mass spectromet data, atomic absorption data, x-ray diffraction data, NMR spe tral data (chemical shift), ultraviolet spectra and others. New i itiatives for automation and easy access and retrieval in so spectral areas are mentioned.

14330. Harrison, J. O., Jr., **The role of standards in d processing,** (Proc. 1969 International Data Processing C ference and Business Exposition, Data Processing Mana ment Association, Montreal, Quebec, Canada, June 16-1 1969), Paper in *Data Processing,* **XIV**, 451-458 (D Processing Management Association, Park Ridge, Ill., 197

> Key words: codes; compatibility; computers; data terchange; information processing; standards.

Federal information processing standards are for use wit the data processing installations of the U.S. Government. Th are generally, but not always, adopted from approved U.S. standards, and they are reflected in U.S. Government A procurement specifications. Federal information processi standards are, for the most part, directed to the solution of co patibility problems such as the interchange of data between a among information systems, the interchange of programs am computers of different makes and models, the interchange devices and components among different product lines and interchange of computer related ideas among people. T authoritative source of information on Federal informat processing standards is the Federal Information Process Standards Register issued by the National Bureau of Standa and distributed by the U.S. Government Printing Office.

14331. Straty, G. C., **Velocity of sound in dense fluid metha** *Cryogenics* **14,** No. 7, 367-370 (July 1974).

> Key words: compressibility; methane; sound veloci specific heat ratio.

Measurements of the velocity of sound in saturated and c pressed fluid methane are reported. Measurements were m on the saturated liquid from 91 K to 186 K and on the c pressed fluid along selected isotherms from 100 K to 300 K pressures to about 35 MN $m^{-2}$. Data were combined with ne available $P\rho T$ data to obtain the isentropic compressibility the ratio of the specific heats. Measurements along the hig temperature isotherm were limited to densities greater t put 10 mole $l^{-1}$ at 300 K increasing to about 14 mole $l^{-1}$ at 210 due to the large low pressure sound attenuation in methane.

332. Cornell, D., Tsang, W., **Pyrolysis generation of dilute concentration of sulfur dioxide,** *Anal. Chem.* **46,** No. 7, 933-935 June 1974).

Key words: pollution; pyrolysis; $SO_2$; standards.

$SO_2$ has been produced in dilute concentrations by pyrolysis trimethylene sulfone. The decomposition is unimolecular and lds equimolar amounts of $SO_2$ and $C_3$ hydrocarbons. Adntages of the method for use in calibration of $SO_2$ monitors in utine field analytical determinations are discussed.

333. Davis, D. D., Huie, R. E., Herron, J. T., **Direct rate measurements showing negative temperature dependence for reaction of atomic oxygen with *cis*-2-butene and tetramethylethylene,** *I. Chem. Phys.* **59,** No. 2, 628–634 (July 15, 1973).

Key words: atomic oxygen; gas phase kinetics; olefins.

Reported in this paper are the first direct rate measurements owing a negative temperature dependence for the reaction of ound state atomic oxygen with *cis*-2-butene and ramethylethylene. Wide variations made in the experimental nditions (e.g., total pressure, O atom concentration, and olefin ncentration) of these two systems have shown that the measured rate constants were uninfluenced by secondary reactions. ne absence of any dependence of the measured rate constants total pressure at several temperatures indicate that the reacons investigated were bimolecular processes. When expressed the form of an Arrhenius equation, the observed negative temrature dependence results in an apparent negative activation ergy, i.e., $k_{cis\text{-}2\text{-}B} = (9.69 \pm 0.96) \times 10^{-12}$ exp $(319 \pm 63$ cal ol$^{-1}/RT)$ and $k_{TME} = (5.58 \pm 1.07) \times 10^{-12}$ exp $(1570 \pm 120$ cal ol$^{-1}/RT)$. Units are in cubic centimeters per molecule seconds. a threshold energy of 0.0 cal mole$^{-1}$ is assigned to the reaction $O(^3P)$ with TME, the temperature dependence of the pre-exonential term for a rate expression of the form $k = A(T)\exp(-$ $/RT), E \geqslant O)$ is calculated to be $T^{-2}$. These new results are scussed in terms of both collision and transition state theories.

334. Unassigned.

335. Geltman, S., Hidalgo, M. B., **The Coulomb-projected Born approximation. IV. Ionization of hydrogen,** *J. Phys. B: At. Mol. Phys.* **7,** No. 7, 831-839 (1974).

Key words: Born approximation; hydrogen; ionization; triple differential cross section.

The triple differential cross section for the electron impact nization of hydrogen atoms is calculated in the Coulomb-procted Born approximation, including exchange, and detailed omparison is made with the ordinary Born result. The calculaons are done for a variety of energies and angles of the two econdary electrons in coplanar and noncoplanar geometries. ppreciable differences occur in the results predicted by the arious approximations.

4336. Davis, D. D., **Frequency standard hides in every color TV set,** *Electronics* **44,** No. 10, 96-98 (May 10, 1971).

Key words: dissemination frequency; frequency synthesizers; linear phase comparators; television color subcarrier; time.

In color television broadcasting, a color "subcarrier" is transitted at about 3.58 MHz. It is used as a reference signal in the olor television receiver to demodulate the chrominance sidebands. The major U.S. networks use rubidium frequency standards to generate the color subcarrier. This paper describes a ethod for making use of the color subcarrier as a frequency standard. The output of a 1 MHz local standard synthesized to 3.58 MHz is used as one input to a phase comparator and is adjusted to agree with the received subcarrier signal. Results of actual network measurements are given.

**14337.** Unassigned.

**14338.** Cuthill, J. R., **Grating spectrometers and their application in emission spectroscopy,** Chapter 3 in *X-Ray Spectroscopy,* L. V. Azároff, Ed., pp. 133-172 (McGraw-Hill Book Co., New York, N.Y. 1974).

Key words: excitation methods; gratings; grating spectrometers; photon detectors; soft x rays.

This is a textbook-type chapter on the basic principles and characteristics of grazing incidence grating spectrometers and their components for use in obtaining soft x-ray emission spectra. Correction factors involved in relating the observed soft x-ray emission spectra to the valence band electron density of states is discussed briefly.

**14339.** Evans, W. H., Grimes, J. J., Jobe, T. L., Henderson, H. A., Beck, D., Beckwith, B., Boyd, R. N., Domalski, E. S., **Bibliography and substance-property index (inorganic), 1968-1973,** *Bull. Thermodyn. Thermochem. Section III. Inorganic Substances* **12,** 267-344, 447-549 (1969); **13,** 226-308, 391-483 (1970); **14,** 183-257, 319-382 (1971); **15,** 211-314, 389-485 (1972); **16,** 261-416, 497-639 (1973).

Key words: inorganic compounds; thermodynamic publications.

Bibliography (authors, title, journal, volume, page, year) and Substance-Property Index of material published from 1968 through 1973. This is a continuation of work done over the past several years and published in earlier editions of the Bulletin.

**14340.** Harrison, J. O., Jr., **Standards (Computer),** *McGraw-Hill Yearbook of Science and Technology,* pp. 392-396 (McGraw-Hill Book Co., New York, N.Y., 1973).

Key words: American National Standards Institute; ASCII; COBOL; computers; International Standards Organization; standards.

Computer standards are developed at the international level by ISO/TC 97, Computers and Information Processing, at the American national level by American National Standards Committee X3, and at the U.S. Federal Government level by NBS.

Such standards are devoted to many specific purposes, most of them related to the problems of interchanging data and interchanging programs among different computers. The American Standard Code for Information Interchange and the standardization of COBOL are given as examples.

**14341.** Filliben, J. J., **Techniques for tail length analysis,** (Proc. 18th Conf. on the Design of Experiments in Army Research Development and Testing, Aberdeen Proving Ground, Md., Oct. 25-27, 1972), *ARO Report 73-2,* Part 2, 425-450 (Department of Defense, Washington, D.C., 1973).

Key words: correlation coefficient; data analysis; distribution analysis; estimation; Fortran subroutine; Lambda distribution; medians; normality; order statistics; probability plot correlation coefficients; probability plots; statistics.

This paper concerns itself with the problem of estimating from a set of data the tail length of the underlying distribution. A probability plot technique for such distributional analysis is developed which makes use of order statistic medians. The probability plot correlation coefficient $r_D$ for a distribution D is introduced which gives a statistical measure of probability plot linearity. The output from a computerized version (written in machine-independent ANSI Fortran) of the proposed tail length analysis procedure is illustrated. Three examples are discussed.

**14342.** Sparks, L. L., **ASRDI oxygen technology survey. Volume IV: Low temperature measurement,** *NASA Spec. Publ. 3073,* 153 pages (National Aeronautics and Space Administration, Washington, D.C., 1974).

Key words: calibration; cryogenics; liquid helium; liquid hydrogen; liquid neon; liquid nitrogen; liquid oxygen; reference data; resistance thermometers; thermocouples; thermometry; vapor pressure.

The specific goal of this review is to present up-to-date information on temperature measurement between the triple and critical point of oxygen. Temperature transducers which can be used in this range are treated over their entire range of usefulness. Three broad types of thermometer are considered—resistance thermometers, thermocouples, and filled systems. In particular, platinum, indium, copper, germanium, carbon, and thermistor resistance thermometers are considered; thermocouple standard types E, K, T, and J plus various combinations utilizing *Au*-Co and *Au*-Fe alloys are considered; vapor pressure systems utilizing He, $H_2$, Ne, $N_2$, and $O_2$ as fill substances are discussed. Methods of low temperature thermometry are presented along with methods of calibration and analytical representation. Reference data are given in terms of Cragoe Z functions for indium and copper resistance thermometers and resistance ratios for carbon. Reference tables are included for each thermocouple type along with the power series coefficients necessary to generate the tabular data. Tabular vapor pressure data and analytical functions for each fill gas are also included. The relationship of the IPTS-68 temperature scale to previously used scales is discussed.

**14343.** Huie, R. E., Herron, J. T., **Kinetics of the reactions of singlet molecular oxygen ($O_2{}^1\Delta_g$) with organic compounds in the gas phase,** *Int. J. Chem. Kinet.* **V,** 197-211 (1973).

Key words: air pollution; kinetics, organic compounds; rate constant; reactions; singlet oxygen.

The reactions of singlet molecular oxygen ($O_2{}^1\Delta_g$) with a series of organic compounds have been studied in the gas phase at 298 K. The concentration of singlet molecular oxygen was determined by titration with 2,5-dimethylfuran. The titration technique was checked using a photoionization technique. Absolute rate constants were measured on the basis of the loss of organic reactant and, in some cases, of singlet molecular oxygen. It was found that the usual method of producing singlet molecular oxygen in the gas phase can also, under some conditions, allow reactive species other than singlet molecular oxygen to enter the reactor, leading to serious errors in the determination of rate constants. This problem was eliminated by carrying out the rate measurements in the presence of a small amount of nitrogen dioxide a radical scavenger.

**14344.** Huntoon, R. D., Lichtenstein, S., **The National Bureau of Standards prepares for the 1970's,** *Science* **165,** 867-874 (Aug. 29, 1969).

Key words: Astin-Branscomb transition; Astin legacy; compatibility and reproducibility of measurements; contributions to basic science; design and performance standards; fundamental constants; international standards; metric system study; National Standard Reference Data System; NBS in the coming decade; public health and safety; self-calibration by users; special NBS facilities.

A retirement story on Allen V. Astin covering his 17 year leadership of the National Bureau of Standards. Discusses Astin's role in acquiring the ultramodern Gaithersburg facility and the nomination of Lewis M. Branscomb as the new director.

**14345.** Johnson, C. R., **Hadamard products of matrices,** *Linea*
*and Multilinear Algebra* **1,** 295-307 (1974).

Key words: closure; diagonal matrix; *D*-stability; field c
values; Hadamard product; inclusion theorem; Kronecke
product; numerical radius; spectrum stable matrix.

The entry-wise product of arbitrary $n \times n$ complex matrices
studied. The principal tools used include the Kronecker produc
field of values and diagonal multiplications. Inclusion theorem
for the field of values and spectrum are developed in the gener
case and refined in special cases. These are employed to oba
inequalities involving the real parts of the characteristic roo
and the numerical radius, and previously known results a
found to be special cases of several of the theorems. In additio
the case of positive stable matrices is considered and a new cla
of nonnegative stable matrices is introduced, studied and relat
to *D*-stability.

**14346.** Quintiere, J., **Radioactive characteristics of fire fighte**
**coat fabrics,** *Fire Technol.* **10,** No. 2, 153-161 (May 1974).

Key words: firefighters; protective clothing; reflectanc
spectral radiation; transmittance.

The results of spectral reflectance measurements are report
for a number of typical and proposed fabrics for the outer shell
firemen's turnout coats. The spectral range of measurement w
from 0.35 to 22 μm. Spectral transmittance values are al
presented for some samples. From these data total reflectan
values were calculated for blackbody source distributions ov
a range of temperature from 300 to 6000 K and for a solar sp
tral distribution. The implications of these results are consider
for thermal protection and comfort of clothing worn
firefighters.

**14347.** Holt, D. R., Nahman, N. S., **Coaxial-line pulse-respo**
**error due to a planar skin-effect approximation,** *IEEE Tra*
*Instrum. Meas.* **IM-21,** No. 4, 515-519 (Nov. 1972).

Key words: asymptotic expansion; characteristic i
pedance; coaxial line; complimentary error function; c
ductor; cylindrical; dielectric; error; generator; los
microminiature; model; planar; propagation function; pul
receiving end; skin effect; step response; time domain; v
age divider.

The time-domain error introduced by the planar skin-effect
proximation is examined by comparing the approxim
response with the cylindrical skin-effect response. Expressi
are developed for the cylindrical skin-effect response and appl
to line outer conductor ID sizes ranging from a 0.1-
microminiature size to 10 mm. For 50-Ω air dielectric lines
cluding 3.5 and 7 mm) curves are given for the cylindrical sl
effect response transition (rise) time (0 to 50 percent and 10 t
percent) versus line length (0.01-100 m). Step responses
given for a 1-m length of 0.1-mm 50-Ω microminiature line v
relative dielectric constants of 1, 2, and 3.

**14348.** Kirchhoff, W. H., Lide, D. R., Jr., Powell, F. X.,
**microwave spectrum, force field and dipole moment of CF**
*Mol. Spectrosc.* **47,** No. 3, 491-498 (Sept. 1973).

Key words: $CF_2$; dipole moment; force field; microw
spectra; structure.

Measurements of the microwave spectrum of $CF_2$ have b
extended to include transitions up to $J = 40$. Using these
tended measurements, a centrifugal distortion analysis has b
performed and from the distortion constants, the force field
frared spectrum, average structure, Coriolis coupling consta
and inertial defect have been calculated. The original assignm
of the infrared spectrum has been confirmed. An improved v
for the dipole moment, 0.469 ± 0.026 D, has been obtained.

**19. Cohen, J., Vezzetti, C. F., Edelman, S., Polymeric
roelectric detector,** (Proc. of the Special Meeting on the
hysics of Detectors U.S. Naval Training Device Center, Or-
ndo, Fla., Mar. 15, 1972), Paper in *Proceedings of the Spe-
al Meeting on the Physics of Detectors*, pp. 113-117 (In-
ared Information and Analysis Center, Institute of Science
ıd Technology, Willow Run Laboratories, University of
lichigan, Ann Arbor, Mich., Aug. 1972).

Key words: detector; infrared; polymer; polyvinyl fluoride; polyvinylidene fluoride; pyroelectric.

olymers have a number of advantages over conventional
pelectric materials such as triglycine sulphate crystals; for ex-
ole, they are not hygroscopic, retain their polarization for long
es, and are simple and inexpensive to fabricate into detectors.
have been experimenting mainly with films of polyvinylidene
ride, and to a lesser extent, polyvinyl fluoride. These experi-
ıts will be described.

50. Kahn, A. H., Candela, G. A., Walatka, V., Jr., Perlstein,
H., **Magnetic susceptibility of the one-dimensional electron
as; application to BDP(TCNQ)$_2$,** *J. Chem. Phys.* **60,** No. 7,
664-2669 (Apr. 1, 1974).

Key words: magnetic susceptibility; organic conductors; paramagnetism; TCNQ compounds.

he magnetic susceptibility of the noninteracting electron gas
been studied on the basis of free electrons and the tight-bind-
model, with application to the properties of organic conduct-
materials. Theoretical curves of susceptibility versus tem-
ature are presented. The gradual transition from low tempera-
Pauli paramagnetism to the high temperature Curie law re-
n is shown. In the transition region, the one-dimensional
tems show a peak in the susceptibility of the order of 110 per-
t of the low temperature limit. The magnetic susceptibility of
compound BDP(TCNQ)$_2$ is interpreted in terms of a one-
ıensional tight-binding model with an energy bandwidth of
7 eV.

51. Weiss, A. W., **Series perturbations in atomic spectra: Su-
erposition-of-configurations calculations on Al I and Al II,**
*hys. Rev. A* **9,** No. 4, 1524-1536 (Apr. 1974).

Key words: atomic spectra; atomic wave functions; oscillator strengths; series perturbations.

onfiguration-interaction calculations, using only Hartree-
ck discrete-state configurations, are reported for the two per-
bed series, $3snf\,^3F$ of Al II and $3s^2nd\,^2D$ of Al I. While good
ults are obtained for term values and oscillator strengths in Al
this is not the case for Al I, where the calculations predict the
$p^2$ perturber to be expelled into the continuum. To study this
e more closely, superposition of configurations (SOC) calcu-
ons, which include all correlation effects, were carried out on
five lowest $^2D$ states of Al I. These results indicate that the
turber actually remains in the discrete spectrum, but loses its
ntity and is smeared out over the entire series. New Rydberg
oitals are extracted from the SOC wave functions which are
ite different from the Hartree-Fock but very similar to those
the Coulomb approximation. Various truncations of the SOC
ıctions are also analyzed and the implications for the correla-
n problem discussed.

352. Levin, E. M., **System $Y_2O_3$-$GeO_2$ below 1700 °C,** *J. Amer.
eram. Soc.* **57,** No. 4, 189-190 (Apr. 1974).

Key words: germania-yttria system; immiscibility; phase equilibrium; yttria-germania system.

The phase diagram for the system has been determined up to
00 °C using the quenching technique. Phases were identified
th the aid of the polarizing microscope and by x-ray powder
fraction. The system contains three compounds, $Y_4GeO_8$, $Y_2GeO_5$, and $Y_2Ge_2O_7$. A region of liquid immiscibility extends from 83.5 to 96.5 mol. percent $GeO_2$ at 1593 ± 5 °.

14353. Ju-Te Lin, L., Ausloos, P., **Gas phase photolysis of acetone in the far ultraviolet,** *J. Photochem.* **1,** 453-462 (1972/73).

Key words: acetone; far ultraviolet; photolysis; primary processes; quantum yields.

The photolysis of acetone (pressure: 2 to 25 torr, $T$:300 K) was investigated at 147 nm (8.4 eV), 123.6 nm (10 eV) and 106.7 – 104.8 nm (11.6 – 11.8 eV). The quantum yields of the products $H_2$, $CO$, $CH_4$, $C_2H_6$, $C_2H_4$, $C_2H_2$, $C_3H_8$, $C_3H_6$, $C_3H_4$, and $CH_3COC_2H_5$ were measured both in the presence and absence of free radical scavengers ($C_2H_4$ or NO). These data, in conjunction with the results of deuterium-labelling experiments, demonstrated the occurrence of the following primary processes:

$$CH_3COCH_3 + h\nu \rightarrow 2CH_3 + CO \qquad (a)$$

$$\rightarrow CH_3COCH_2 + H \qquad (b)$$

$$\rightarrow CH_3COCH + H_2 \qquad (c)$$

$$\rightarrow CH_4 + CH_2CO \qquad (d)$$

It is also suggested that the primary process:

$$CH_3COCH_3 + h\nu \rightarrow C_3H_4 + H_2O \text{ (or } H_2 + O) \qquad (e)$$

occurs with a quantum yield of ~ 0.02. The quantum yield of "molecular" methane (process d) is 0.02 (147 nm), 0.028 (123.6 nm) and 0.043 (104.8 – 106.7 nm). The quantum of "molecular" hydrogen is 0.03 (147 nm) 0.26 (123.6 nm) and 0.28 (104.8 – 106.7 nm). The quantum yield of process (a) is 0.7 ± 0.1 at 147 nm. At shorter wavelengths the quantum yield of the latter process could not be estimated because of the uncertain fate of the cations [$\Phi(CH_3COCH_3^+) = 0.25$ at 123.6 nm and 0.21 at 104.8 – 106.7 nm] and the extensive dissociation of the internally excited species formed in the primary processes.

14354. Heinrich, K. F. J., **Review 3d National Conference on Electron Microprobe Analysis and the 1st Annual Meeting of the Electron Probe Analysis Society of America,** *Applied Optics* **8,** No. 4, 862-863 (1969).

Key words: conference review; electron probe; microanalysis; microscopy; spectroscopy; x rays.

This paper is a review of the Conference mentioned in the title. The review has been requested by the Editorial Consultant of the journal Applied Optics, published by the Optical Society of America.

14355. Johnson, D. R., Powell, F. X., **Microwave spectrum and structure of sulfur difluoride,** *Science* **164,** 950-951 (May 23, 1969).

Key words: microwave spectroscopy; rotational spectrum; sulfur difluoride; molecular structure; dipole moment; electrical discharge.

Sulfur difluoride has been identified and characterized from its microwave spectrum. The analysis of rotational transitions for both sulfur difluoride-32 and sulfur difluoride-34 shows that this molecular species has $C_{2v}$ symmetry with a bond length of 1.589 angstroms, a bond angle of 98°16′, and a dipole moment of 1.05 Debye.

14356. Johnson, W. T. K., Dick, C. E., **Half-life measurement of several short-lived nuclear isomers,** *Nucl. Instrum. Methods* **99,** 221-226 (1972).

Key words: bromine; cadmium; erbium; gold; half lives; iridium; measurement; nuclear isomers; solenium; tungsten.

Brehmsstrahlung produced by 3.5 MeV electrons incident on a platinum target was used to populate nuclear isomers in several nuclei through excitation of higher lying states. A shuttle was constructed to transport targets of natural isotopic abundance from an irradiation position to a measuring position. Other than a low background the activity measured was due entirely to the isomeric decay. The measured half-lives in seconds are $^{77m}$Se $17.58 \pm 0.12$, $^{79m}$Br: $4.97 \pm 0.10$, $^{167m}$Er: $2.28 \pm 0.03$, $^{179m}$Hf: $18.77 \pm 0.07$, $^{183m}$W: $5.56 \pm 0.25$, $^{191m}$Ir: $4.88 \pm 0.03$, and $^{197m}$Au: $7.86 \pm 0.04$. The data are presented and the methods of analysis are discussed. The results are compared to recent literature values.

**14357.** Hougen, J. T., Bunker, P. R., Johns, J. W. C., **The vibration-rotation problem in triatomic molecules allowing for a large-amplitude bending vibration,** *J. Mol. Spectrosc.* **34,** No. 1, 136-172 (Apr. 1970).

Key words: bending vibration; large amplitude; quasi-linear; theory; triatomic; vibration-rotation.

In this paper we derive an expression for the vibration-rotation Hamiltonian of a triatomic molecule. In the derivation we use a curvilinear bending coordinate and two rectilinear stretching coordinates in such a way that the Hamiltonian obtained is applicable for any triatomic molecule, linear or bent, and allows for large displacements of the bending coordinate (sometimes said to result from the molecule being "quasi-linear" but, in fact, of general occurrence). We derive a zeroth-order Hamiltonian to describe the energy levels associated with the bending vibration, and are able to fit the experimental results on HCN and DCN better than if we had used the standard formalism of rectilinear (and small) displacements. We also use the formalism to describe the dependence of the rotational constant $B$ on the bending vibrational quantum number and apply the results to the microwave data on CsOH and CsOD.

**14358.** Sengers, J. M. H. L., **Compressibility, gas,** *Encycl. Phys. 2d Edition,* pp. 149-151 (1974).

Key words: adiabatic compressibility; density fluctuations; equation of state; isothermal compressibility; speed of sound.

This is an entry for the Encyclopedia of Physics. Isothermal and adiabatic compressibilities are defined. Their experimental behavior is discussed and an explanation of this behavior in terms of molecular theory is given. The most important experimental technique for obtaining these compressibilities are discussed. Some of the newer developments using the theory of the radial distribution functions are indicated. References to general material for further study are given.

**14359.** Koonce, C. S., **Peierls transitions in semimetallic one dimensional charge transfer salts,** *Solid State Commun.* **14,** No. 11, 1141-1144 (1974).

Key words: charge transfer salts; electronic energy band structure; electron-phonon coupling; one dimension; Peierls transition; tetrathiofulvalinium-tetracyanoquinodimethan (TTF-TCHNQ).

Peierls transitions in one dimensional charge transfer salts in which both donor and acceptor molecules have even valency such as TTF-TCNQ have been studied. Transitions involving macroscopic occupation of phonon states of wavevector $k_F(\text{TTF}) + k_F(\text{TCNQ}) = 1/2\, G$ and $|k_F(\text{TTF}) - k_F\,(\text{TCNQ})|$ can occur as well as transitions of wavevector $2k_F(\text{TTF})$ [and $2k_F(\text{TCNQ})$].

**14360.** Hoover, T. B., **The frequency extrapolation of conductance data for aqueous salt solutions,** *J. Phys. Chem.* **74,** No. 13, 2667-2673 (1970).

Key words: conductance; conductivity; extrapolation; faradaic process; frequency extrapolation; palladium black; platinum, polarization; polarization electrode; Standard Se Water.

Polarization phenomena in conductivity measurements we investigated in order to reduce systematic error in the sta dardization of solutions intended for the calibration of condu tivity cells and salinometers. Data for demal potassium chlori solutions and for Standard Sea Water were obtained with tw cells having constants of 37 and 86, respectively, both wi bright platinum and with palladium black-coated electrode Four empirical and three theoretical functions of resistance frequency were fitted to the data. Correctness of the extrapol tion was judged by the agreement of the limiting resistance o tained with bright electrodes with that obtained with coated ele trodes. All of the empirical formulas predicted limiting values f the bright electrodes that were lower by 0.02 to 0.15 percer Equations based on the model of Grahame for the farada process, as well as a simplified model, agreed within 0.01 perce while a third theoretical equation was intermediate in accurac

**14361.** Isler, M. A., Stenbakken, G., **Magnetic switches for bu glar alarm systems,** *NILECJ-STD-0301.00,* 20 pages (U. Department of Justice, Law Enforcement Assistance A ministration, National Institute of Law Enforcement a Criminal Justice, Washington, D.C., Mar. 1974).

Key words: burglar alarm sensor; burglar alarm syste door switch; magnetically actuated; perimeter sens switch.

This standard establishes performance criteria for magne cally-actuated switches intended for use in protective intrusi alarm circuits to monitor the position of doors, windows, et and to cause the initiation of a signal sufficient to cause auxili equipment to send an alarm to a police panel, central station, a local audible alarm device. Included are requirements a methods of test for materials, performance, and electrical prop ties. The performance characteristics selected are those that fect the false alarm susceptibility of the device. This stand does not provide performance criteria for resisting attempts defeat the device through physical or surreptitious attack. T standard is one of a series establishing standards for intrusi alarm sensors, installation, and operation.

**14362.** Kase, K. R., Domen, S. R., **Calorimetric and ionizat measurements of stopping power in carbon for 19.5 GeV el trons,** *Nucl. Instrum. Methods* **118,** 469-475 (1974).

Key words: absorbed dose; calorimeter; carbon; electro stopping power.

A portable carbon calorimeter built at the National Bureau Standards was used in a 19.5 GeV electron beam at the Stanf Linear Accelerator to measure absorbed dose. The dose m surements were normalized to a given number of incident el trons by monitoring the electron intensity with a transmission chamber previously calibrated against a quantameter in the sa beam. The simultaneous measurements of integrated electron tensity and absorbed dose allowed a direct determination stopping power in carbon for 19.5 GeV electrons. The measu value of 1.80 MeV cm$^2$/g is within 6 percent of the calcula value.

**14363.** Klein, R., **Preparation of contiguous chemisorbed adla by sequential deposition and surface migration,** *Surface Sci.* 309-316 (1972).

Key words: chemisorption; deposition; gas separation; p sisorption.

The separation of two sequentially deposited gases on a shadowed field emission tip by surface migration of the p sisorbed layer furnishes a convenient method for the product of distinct, contiguous layers. Oxygen and carbon monoxide gsten as well as ruthenium, and oxygen and nitrogen on henium have been separated in this manner.

64. Lauritzen, J. I., Jr., Hoffman, J. D., **Extension of theory of rowth of chain-folded polymer crystals to large undercoolings,** . *Appl. Phys.* **44,** No. 10, 4340-4352 (Oct. 1973).

Key words: chain folds; growth rate; isotactic; lamellar thickness; nucleation theory; polyethylene; polymer crystallization; polystyrene; undercooling.

he kinetic theory of the rate of growth $G$ and the initial lamel- thickness $l_g^*$ of chain-folded crystals is extended so that it is plicable at high undercoolings. Attention is centerd on the ails of how the first step element and the first fold are put wn on the substrate. A parameter $\phi$ that varies between zero d unity, which apportions the free energy of attachment of the p element between the forward and backward reactions, is ed to denote variations in this process. Expressions for $G$ are rived from flux equations for two limiting cases: regime I, sin- surface nucleation act with rapid substrate completion and ime II, numerous surface nucleation acts with very slow sub- ate completion. Data from the literature on $G$ for isotactic ystyrene (regime II) and polyethylene single crystals (regime re analyzed to obtain surface free energies, and these are used h the revised theory for $l_g^*$ to predict the lamellar thickness of se polymers. Good agreement between $l_g^*$ and published data found for $1 > \phi > O$. Values of $\phi$ below unity imply that the lecules are physically adsorbed onto the substrate prior to ac- l crystallographic attachment. A discussion is given of the gmental transport effects that dominate the behavior of $G$ at h undercoolings in bulk polymers.

365. Fickett, F. R., Sullivan, D. B., **Magnetic studies of oxidized mpurities in pure copper using a SQUID system,** *J. Phys. F: Metal Phys.* **4,** No. 6, 900-904 (June 1974).

Key words: copper; impurities; magnetism; quantum interference; susceptibility.

A magnetometer system utilizing a SQUID and a supercon- cting flux transformer has been used to monitor the internal idation process in very pure copper. Both remanent moment d low field susceptibility have been measured for copper con- ning 0.1-1 at ppm Fe and 70 at ppm Fe in various states of an- al. The results suggest that the oxidation process proceeds ite differently in the previously unobserved situation where ry dilute amounts of iron are present than in the case of rela- ely high impurity concentrations.

366. Lafferty, W. J., Ritter, J. J., **Microwave spectrum, structure, and dipole moment of ethynyldifluoroborane, $\text{H-C} \equiv \text{CBF}_2$,** *Chem. Commun.*, pp. 909-910 (1969).

Key words: dipole moment; ethynylditluoroborane; microwave spectrum; rotational constant; structure; vibrational frequency.

The microwave spectrum of enthynyldifluoroborane was stu- ed in the 18-33 GHz region. The molecule has been deter- ned to have $C_{2v}$ symmetry and estimates can be made for the B bond distance and the FBF angle. The dipole moment of the lecule was found to be 1.93D with a 20-uncertainty of ± 06D.

367. Kohayakawa, Y., **Contrast-difference thresholds with sinusoidal gratings,** *J. Opt. Soc. Amer.* **62,** No. 4, 584-587 (Apr. 1972).

Key words: vision; visual contrast.

Two halves of a sinusoidally modulated transparency were ojected on a diffusing surface. The contrast $C$ of one half of the ld was changed by defocusing until a definite difference of ntrast, $\Delta C$, was perceived. The contrast of either half of the field could be changed without changing the mean luminance. A plot of $\Delta C/C$ against $C$ declines monotonically with increasing contrast. On the other hand, $\Delta C$ against $C$ has a maximum at an intermediate contrast. The contrast difference $\Delta C$ can be interpreted as relative luminance difference $\Delta L/L$, to which the Weber law applies. A function relating subjective to objective contrast was obtained. The relation between modulation transfer function (MTF) with constant input and constant output is discussed.

14368. Rowe, J. M., Rush, J. J., Flotow, H. E., **Neutron-quasielastic-scattering study of hydrogen diffusion in a single crystal of tantalum,** *Phys. Rev. B* **9,** No. 12, 5039-5045 (June 15, 1974).

Key words: hydrogen diffusion; hydrogen in tantalum; interstitial sites; neutron scattering; quasielastic scattering; residence time; single crystal; vibration amplitudes.

The diffusion of hydrogen in a single crystal of bcc tantalum ($\text{TaH}_{0.02}$) at 584 K has been investigated by neutron-quasielastic scattering at a variety of crystal orientations, and over a range of wave-vector transfer $|\overrightarrow{Q}|$, from 0.8 to 2.5 Å$^{-1}$. A detailed analysis of the observed quasielastic line shapes and widths shows that the results cannot be fitted by any simple jump-diffusion model involving instantaneous jumps between octahedral and tetrahedral interstitial sites. The quasielastic width curves (full width at half-maximum versus $\overrightarrow{Q}$) are much more isotropic than those predicted by any of the hydrogen-jump models, although the general shape of the widths at large $Q$ is closer to that predicted by a tetrahedral-site model. These results are in distinct contrast to a recent neutron study of hydrogen diffusion in single-crystal (fcc) palladium, where the details of the quasielastic scattering were fitted well by a model assuming instantaneous jumps between octahedral sites. The $\text{TaH}_{0.02}$ quasielastic peaks suggest a diffusion "relaxation time" between 1 and 2 ps at 584 K. Analysis of the data also provides an average "mean-square hydrogen vibration amplitude" of 0.040 Å$^2$. The present single-crystal results are in reasonable agreement with the results of a previous neutron study of polycrystalline ($\alpha$-phase) $\text{TaH}_x$. In addition, a value for the macroscopic diffusion constant at 584 K of $2.8 \times 10^{-5}$ cm$^2$s$^{-1}$ is derived from the low-$Q$ results, which is in excellent agreement with the value predicted from Gorsky-effect measurement.

14369. Hanley, H., Klein, M., Liley, P. E., Saxena, S. C., Sengers, J. V., Thodos, G., White, H. J., Jr., **Recommendations for data compilations and for the reporting of measurements of the thermal conductivity of gases,** *J. Heat Transfer,* pp. 479-480 (Nov. 1971).

Key words: critical evaluation of data; gases; thermal conductivity.

Recommendations are made with respect to what features should be incorporated in compilations of critically evaluated data to provide the greatest reliability and utility. The information required by evaluators for an accurate assessment of the reliability of experimental measurements is also discussed and some recommendations made relating to the presentation of this information.

14370. Meijer, P. H. E., Scherer, W. D., **Phonons and lambda temperature in liquid $^4$He as obtained by the lattice model,** (Proc. 13th Int. Conf. on Low Temperature Physics, Boulder, Colo., Aug. 21-25, 1972), Paper in *Low Temperature Physics-LT 13,* K. D. Timmerhaus, W. J. O'Sullivan and E. F. Hammel, Eds., 1, 84-86 (Plenum Publ. Corp., New York, N.Y., 1974).

Key words: helium four; lambda temperature; lattice model; phonons.

This paper describes the density of the condensate in helium four from $T = 0$ to the lambda temperature using an extension of the Matsubara Matsuda Lattice model.

**14371.** Lilly, R. L., Rebbert, R. E., Ausloos, P., **Far ultra-violet photolysis of ammonia quantum yield determination for the primary process: $NH_3(ND_3) + h\nu \rightarrow NH(ND) + H_2(D_2)$,** *J. Photochem.* **2,** 49-61 (1973/74).

Key words: ammonia; extinction coefficients; far ultraviolet photochemistry; free radicals; primary processes; quantum yields.

The gas phase photolysis of $NH_3$-$C_2D_4$ and $ND_3$-$C_2H_4$ mixtures has been investigated at 147 nm (8.4 eV), 123.6 nm (10eV) and 104.8-106.7 nm (11.6-11.8 eV). The quantum yield of $D_2$ in the irradiation of $ND_3$-$C_2H_4$ mixtures is independent of the concentration of $C_2H_4$ and of the pressure of $ND_3$ (10 to 180 torr). It is concluded that in these mixtures $D_2$ is entirely formed by molecular elimination from excited $ND_3$. The quantum yields of such a process are as follows at these energies: 147 nm, 0.032 ± 0.005; 123.6 nm, 0.244 ± 0.01; and 104.8 – 106.7 nm, 0.306 ± 0.007 ($M/N_{ex} = 0.52 \pm 0.02$). Although the $NH_3 - C_2D_4$ photolysis data exhibit less reliability, it can be concluded that the quantum yield of molecular $H_2$ at 147 nm is twice that of molecular $D_2$. Isotope effects are much less pronounced at higher photon energies.

**14372.** Levin, E. M., Schneider, S. J., Plante, E. R., **Phase equilibria involving seed materials in MHD,** (Proc. 13th Symp. on Engineering Aspects of Magnetohydrodynamics, Stanford University, Stanford, Calif., Mar. 26-28, 1973), Paper in *13th Symposium on Engineering Aspects of Magnetohydrodynamics,* pp. IV.5.1-IV.5.9 (Department of Mechanical Engineering, University of Mississippi, University, Miss., 1973).

Key words: alkali seeds in MHD; condensation of $K_2CO_3$; $Cs_2SO_4$; $Cs_2SO_4$-$K_2SO_4$; $K_2CO_3$; $K_2SO_4$; $K_2CO_3$-$K_2SO_4$; $K_2CO_3$-MgO; MHD; phase equilibria.

This paper reports some of the first results in a systematic study of the phase relations involving seed materials. Polymorphism and thermal expansion of the following unary seed systems were studied by high temperature x-ray diffraction: $K_2CO_3$, $K_2SO_4$, and $Cs_2SO_4$. The binary systems $K_2SO_4$ - $Cs_2SO_4$ and $K_2CO_3$ - $K_2SO_4$ were determined by DTA and high temperature x-ray diffraction. Finally, the system $K_2CO_3$ - MgO (seed-insulator) was studied mainly by the quenching technique. $K_2CO_3$ is dimorphic, showing a second order transition at 420 ± 5 °C, between the low temperature monoclinic form and the high temperature hexagonal form. $K_2SO_4$ and $Cs_2SO_4$ are also dimorphic, but with orthorhombic low temperature forms transforming at 588 ± 5 °C and 718 ± 5 °C, respectively, to the hexagonal phase. However, whereas the $K_2SO_4$ transition is first order, that in $Cs_2SO_4$ is similar to $K_2CO_3$, i.e., shows no volume discontinuity, and is also most likely second order. In the system $K_2SO_4$ - $Cs_2SO_4$, the solidus curve shows continuous solid solution with a minimum at 940 °C and ~ 50 mol percent $Cs_2SO_4$. The subsolidus phase relations show a eutectoid at 430 ± 5 °C and ~ 50 mol percent $Cs_2SO_4$. In the $K_2CO_3$ - K.2SO4 system, the liquidus curve is almost horizontal near the $K_2CO_3$ component and rises from about 25 mol percent $K_2SO_4$. Subsolidus solid solution phase boundaries are delineated. The $K_2CO_3$ - MgO system, in equilibrium with its own vapor, behaves as a simple eutectic system, with the eutectic located at 895.5 °C and ~ 2 mol percent MgO. Thus, liquid will be formed anywhere in the MHD channel that condensed $K_2CO_3$ exists in contact with MgO above ~ 896 °C. Thermodynamic calculations involving activity of $K_2CO_3$ are applied to calculate approximate phase diagrams for several pressures of vaporized $K_2CO_3$ species. Similar arguments are used to predict whether or not liquid formation will occur in an MHD channel when additiona gases are present.

**14373.** Frederikse, H. P. R., Hosler, W. R., **Electrical conductivity of coal slag,** (Proc. 13th Symp. on Engineering Aspects o Magnetohydrodynamics, Stanford University, Standford Calif., Mar. 26-28, 1973), Paper in *13th Symposium on Engineering Aspects of Magnetohydrodynamics,* pp. IV.4.1 IV.4.3 (Department of Mechanical Engineering, University o Mississippi, University, Miss., 1973).

Key words: coal slag; electrical conductivity; high temperature; magnetohydrodynamics; oxides.

The efficiency of a coal fired MHD-generator will be influenced by the presence of slag layers condensed on the walls o the MHD-channel. Hence, there is a need for physical an chemical characterization of coal slags. As part of such a pr gram, the electrical conductivity of some natural and syntheti slag samples (containing 14-36 wt. % iron) has been measure over the temperature range 1200-1700 K and at oxygen pressures between 1 and $2 \times 10^{-6}$ atmosphere. The conductivity i relatively high (~ $10^{-2}$ $ohm^{-1}$ $cm^{-1}$ at 1700 K) and stems fro the transfer of electrons between ferrous and ferric ions. Anom lies in the conductivity around 1600 K are the result of devitrif cation of the glass samples.

**14374.** Latanision, R. M., Ruff, A. W., Jr., **Extrinsic-intrins stacking-fault pairs in an Fe-Cr-Ni alloy,** *J. Appl. Phys.* **40,** N 7, 2716-2720 (June 1969).

Key words: dislocations; electron microscopy; stacki fault energy; stacking fault pairs; stainless steel.

Transmission electron images of extrinsic-intrinsic fault pai in a Fe-Cr-Ni alloy are shown to be sensitive to changes in t sign of (**g**·**b**)*s* for reflections producing either line or stackin fault contrast. This is interpreted in terms of the overlappi strain fields of the three closely spaced partial dislocations. differential treatment of the measured widths of the intrinsic a extrinsic faults indicates that the stacking-fault energy ratio $\gamma_{ei}$ = 1.6 in this alloy.

**14375.** Rowe, J. M., Nicklow, R. M., Price, D. L., Zanio, **Lattice dynamics of cadmium telluride,** *Phys. Rev. B* **10,** No. 671-675 (July 15, 1974).

Key words: cadmium telluride; frequency dispersion; latti dynamics; neutron inelastic scattering; phonon dispersi relation; semiconductors.

The phonon dispersion relation of CdTe at 300 K has be measured for the [100], [111], and [110] directions of propa tion using neutron inelastic scattering. The CdTe single crys was grown from the melt with Cd present as $^{114}$Cd to reduce t neutron absorption of the specimen. The results have been fit to a 14-parameter shell model that represents both the neutr data and other measured properties well when the non-neutr data are included in the fit. The present results, along with earl measurements on α-Sn and InSb, complete the isoelectro sequence α-Sn → InSb → CdTe. The systematic trends in lattice dynamics of this series of semiconductors (which characterized by increasing band gap and ionicity) are brou out by comparison of frequency distributions calculated from shell-model fits.

**14376.** Lauritzen, J. I., Jr., **Effect of a finite substrate length u polymer crystal lamellar growth rate,** *J. Appl. Phys.* **44,** No. 4353-4359 (Oct. 1973).

Key words: crystallization; growth rate; nucleation s strate; polymer.

The polymer crystal lamellar growth rate *G* is an often-m sured property of semicrystalline polymers. In this paper, we

stigate the dependence of $G$ upon the length of the substrate,
the surface nucleation rate of new growth layers per unit
gth per unit time, $i$, the velocity with which the growth layer
vers the substrate, $g$, and the thickness of the growth layer, $b$.
r the purposes of this paper, $L$ is the average length where the
lymer segments in the substrate are in crystallographic re-
ter. We show that $G=biL/\overline{n}$, where $\overline{n}$ is the average number
nuclei that contribute to each growth layer. We show that $\overline{n}$
pends only on the dimensionless parameter $z=iL^2/4g$. We
ve not obtained $\overline{n}$ explicitly, but we can place upper and lower
nits on $\overline{n}$ that closely define $G$ in regime I, where $G \simeq biL$ and
o a transition region between regime I and regime II where $G$
$b(ig)^{1/2}$. The experimental results for several polymers are
alyzed and some are found to be in or near regime 1, and
ners in or near regime II.

377. Burns, G. W., Hurst, W. S., Scroger, M. G., **High reliabili-
ty sheathed, beryllia insulated, tungsten-rhenium alloy ther-
mocouple assemblies—their fabrication and EMF stability,**
*NASA CR-134549*, pp.1-36 (National Aeronautics and Space
Administration, Washington, D.C. June 1974).

Key words: beryllium oxide; emf drift; sheathed thermocouples; tantalum; temperature measurements; tungsten-rhenium alloys.

1.6 mm diameter tantalum sheathed, BeO insulated, W-3 per-
nt Re/W-25 percent Re thermocouple assemblies have been
bricated and their emf drift determined during 2059 hours of
posure at 2073 K in a gaseous helium environment. The
eathed thermocouple assemblies were constructed from aged
ermoelements, specially heat-treated BeO insulators, and spe-
ally cleaned and etched tantalum sheaths. Their thermal emf
lifts ranged from the equivalent of only − 0.3 to − 0.8 K drift
r 1000 hours of exposure at 2073 K. No evidence of any gross
emical attack or degradation of the component materials was
und. The emf drift and material behavior of some unsheathed,
eO insulated, W-3 percent Re/W-25 percent Re thermocouples
2250 and 2400 K were also determined. Unsheathed ther-
ocouples tested in an argon environment at 2250 K for 1100
ours and at 2400 K for 307 hours exhibited changes in thermal
nf that typically ranged from the equivalent of a few degrees K
as much as + 11 K. Post-test examinations of these ther-
ocouples revealed some undesirable material degradation and
teraction which included erosion of the BeO insulators and
ontamination of the thermoelements by tantalum from the tan-
lum blackbody enclosure in which the thermocouples were
ontained. Preliminary tests to examine the chemical compati-
lity of sintered BeO insulators with Ta sheaths in an argon en-
ronment at 2073, 2250, and 2400 K were also conducted. They
vealed gross erosion of the insulator after only 50 hours expo-
re at 2400 K. A 50 percent reduction in the insulator diameter
the open end of the sheath was typical. Well inside the sheath,
here gaseous reaction products were confined, the erosion was
onsiderably less. Similar behavior occurred with long exposure
100 hours) at 2250 K. Serious problems with the BeO insula-
rs were not apparent in tests at 2073 K.

4378. Hoer, C. A., **The six-port coupler: A new approach to measuring voltage, current, power, impedance, and phase,** *IEEE Trans. Instrum. Meas.* **IM-21,** No. 4, 466-470 (Nov. 1972).

Key words: admittance; current; directional coupler; hybrid junction; impedance; phase angle; reflection coefficient; six-port coupler; voltage.

A six-port coupler is described having four side arms whose
utputs are proportional to the voltage, current, incident voltage
vave, and reflected voltage wave at some desired measurement
lane in the transmission line. The phase relationship between
ne outputs is the same as between corresponding quantities at
ne measurement plane. Complex impedance and phase angle as well as voltage, current, and power can be obtained from simple power or voltage magnitude measurements at the four side arms. A vector voltmeter used with this six-port becomes a direct reading vector impedance meter, admittance meter, or reflection coefficient meter.

14379. Hudson, J., **Programming and control languages for automated laboratory experimentation,** *Astron. Astrophys. Suppl. Ser.* **15,** 487-495 (1974).

Key words: laboratory automation; process control; programming languages.

The problem of coding programs for computers used to control laboratory experiments is discussed. Several compilers which were developed for this purpose are described. The problem of developing "experimenter-proof" control languages is also addressed, and several approaches are mentioned.

14380. Schwarz, F. P., Okabe, H., Whittaker, J. K., **Fluorescence detection of sulfur dioxide in air at the parts per billion level,** *Anal. Chem.* **46,** No. 8, 1024-1028 (July 1974).

Key words: detection; fluorescence; $H_2O$; $SO_2$; Zn lamp.

A previously reported detector capable of rapid and continuous measurement of $SO_2$ in air has been modified to extend the detection limit to the low ppb range. The principle of detection is based on photon counting of the $SO_2$ fluorescence excited by the Zn 2138-Å line. Fluctuation of the lamp intensity was accounted for by measuring the ratio of the fluorescence photon counts to that of the excitation source. At 8.6 ppb, the standard deviation is 29 percent for a counting time of about 1 minute. The detector response is linear from at least 8.6 ppb to 1.8 ppm. The major source of measurement error at low ppb concentrations is the statistical fluctuation of the low scattered light and signal counts, whereas at high $SO_2$ levels, it is due to fluctuations in the sample preparation. The cell design was modified to reduce the scattered light. The inside of the cell was coated with a non-water-absorbing black Teflon to reduce possible $H_2O$-$SO_2$-wall interactions. With the Zn lamp as an excitation source, the quenching effect of water vapor on the $SO_2$ fluorescence signal previously observed with Cd 2288-Å excitation was found negligible. The result can be reasonably explained by the shorter life time of the $SO_2$ fluorescence.

14381. Hillhouse, D. L., Peterson, A. E., **A 300-kV compressed gas standard capacitor with negligible voltage dependence,** *IEEE Trans. Instrum. Meas.* **IM-22,** No. 4, 408-416 (Dec. 1973).

Key words: capacitor, compressed-gas, negligible voltage dependence; capacitor, high-voltage, negligible voltage dependence; capacitor, negligible voltage dependence; capacitor, standard, negligible voltage dependence; capacitor, 300-kV, negligible voltage dependence; voltage dependence, negligible 300-kV capacitor.

A compressed gas capacitor now in use at the National Bureau of Standards (NBS) changes capacitance by less than 2 parts per million from 0-300 kV. This extremely small variation results primarily from rugged construction, and thus requires only reasonably careful centering of its three cylindrical electrodes. It has a hallow cantilevered high-voltage electrode suspended between an outer 100-pF low-voltage electrode and a segmented inner low-voltage electrode having values of 1, 2, 4, 8, and 10 pF, or any parallel combination thereof. The capacitor's small voltage dependence was inferred from the following independent measurements: 1) comparison with another high-voltage capacitor having a small experimentally determined coefficient; 2) comparison of the inner and outer sections with each other; and 3) measurement of capacitance change resulting from application of known forces on the cantilevered electrodes, and correlating this with calculated high-voltage electrostatic forces. The capacitor is used in determining the voltage coefficients of NBS-owned commercial standard capacitors; in the calibration of customers' standard capacitors, voltage transformers, and dividers to 200 kV and above; and in research on coupling capacitor voltage transformers and other high-voltage devices and materials.

**14382.** Lovas, F. J., Johnson, D. R., **Microwave spectrum of BF,** *J. Chem. Phys.* **55,** No. 1, 41-44 (July 1, 1971).

Key words: boron monofluoride; dipole moment; discharge; microwave spectrum; quadrupole structure; rotational transitions; transient species.

Direct rotational transitions have been observed in the ground vibrational state of $^{10}B^{19}F$ and $^{11}B^{19}F$ produced in the gas phase by a discharge in flowing $BF_3$. Measurements on the $J = 1 \leftarrow 0$ transitions yield $B_0(^{10}BF) = 48\,022.63 \pm 0.08$ MHz, $eq_0Q(^{10}B) = -9.5 \pm 0.8$ MHz, $B_0(^{11}BF) = 45\,185.77 \pm 0.06$ MHz, and $eq_0Q(^{11}B) = -4.5 \pm 0.4$ MHz. New molecular parameters are derived for $^{11}BF$ including $B_e = 45\,481$ MHz, and $r_e = 1.2625$ Å. The electric dipole moment of BF is determined to be $0.5 \pm 0.2$ D.

**14383.** Seltzer, S. M., Berger, M. J., **Transmission and reflection of electrons by foils,** *Nucl. Instrum. Methods* **119,** 157-176 (May 1974).

Key words: angular distribution; electrons; energy spectra; reflection; transmission; transport calculation.

This paper describes Monte Carlo calculations pertaining to the penetration of electron beams through foils. The method of calculation is validated by comparisons with experimental transport data at energies between 50 keV and 1 MeV. New data are presented on the transmission and reflection of electrons through beryllium, mylar, aluminum, and titanium foils, for incident beam energies between 100 and 400 keV. The results given include transmission and reflection coefficients and the energy spectra and angular distributions of transmitted electron beams.

**14384.** Heinrich, K. F. J., Barrett, C. S., Newkirk, J. B., Ruud, C. O., Eds., **Advances in x-ray analysis,** *Proc. 20th Annual Conf. on Applications of X-Ray Analysis, Aug. 11-13, 1971,* **15,** 573 pages (Plenum Press, New York, N.Y., 1972).

Key words: automation; defraction; detectors; spectrometry; x-ray analysis; x-ray fluorescence.

The application of solid-state detectors of high energy resolution to x-ray spectrometry, and the increasing use of computers in both measurement and data evaluation, are giving a new stimulus to x-ray techniques in analytical chemistry. The Twentieth Annual Denver X-Ray Conference reflects this renewed interest in several ways.

The invited papers, grouped in Session I, review the characteristics of the detectors used in the measurement of x rays. One paper is dedicated to the detection of single ions. Although such a subject may appear to be marginal to the purposes of the Denver Conference, we must recognize the affinity of techniques applied to similar purposes. Ion probe mass spectrometry is dedicated to tasks similar to those performed by x-ray spectrometry with the electron probe microanalyzer. Scientists and technologists will see these two techniques discussed in the same meetings.

The discussion of automation and programming is not limited to the two invited speakers, but extends to papers presented in more than one session. The matter of fluorescence analysis by isotope- and tube-excitation will also be of great interest to those concerned with the practical applications of x-ray techniques.

The communications contained in this volume, and the lively discussions which frequently followed the presentation of papers, attest to the vitality of the subjects which are the concern of the Annual Denver X-Ray Conference.

**14385.** Kurylo, M. J., Braun, W., Kaldor, A., Freund, S. M. Wayne, R. P., **Infrared laser enhanced reactions: Chemistry o vibrationally excited $O_3$ with NO and $O_2(^1\Delta)$,** *J. Photochem.* 3 71-87 (1974/75).

Key words: kinetics; laser enhanced reactions; nitric oxide $O_2(^1\Delta)$; ozone; vibrationally energy.

Vibrationally excited ozone, produced by absorption of CO laser radiation, was found to react significantly faster with N and $O_2(^1\Delta)$ than thermal ozone. Using a modulation technique absolute and relative rate constants at 300 K for the followin reactions were calculated assuming rapid equilibration betwee the three closely spaced vibrationally excited levels of $O_3$, an that only the lowest level of these, the $\nu_2$ bending mode, is activ in reaction.

$$O_3 + NO \rightarrow NO_2^*(^2B_1) + O_2 \qquad \text{(}$$
$$O_3^\dagger + NO \rightarrow NO_2^*(^2B_1) + O_2 \qquad \text{(1}$$

$$O_3 + NO \rightarrow NO_2^\dagger(^2A_1) + O_2 \qquad \text{(}$$
$$O_3^\dagger + NO \rightarrow NO_2^\dagger(^2A_1) + O_2 \qquad \text{(2}$$

$$O_3 + O_2(^1\Delta) \rightarrow 2O_2 + O \qquad \text{(}$$
$$O_3^\dagger + O_2(^1\Delta) \rightarrow 2O_2 + O \qquad \text{(7}$$

$k_{1'} + k_{2'} = 2.7 \times 10^{-13}$ cm$^3$ molecule$^{-1}$ s$^{-1}$; $(k_{1'} + k_{2'})/(k_1 + k_2)$ $16.2 \pm 4.0$; $k_{1'}/k_1 = 4.1 \pm 2.0$; $k_{2'}/k_2 = 17.1 \pm 4.3$; $k_{7'}/k_7 = 38 \pm 2$ These rate constants must be modified if a different combinati of vibrationally excited levels is involved. The fraction of vibr tional energy usable in chemical reaction was found to be abo 15, 50 and ~ 100 percent respectively for processes 1′, 2′ and Our measurements clearly differentiate between the particip tion of vibrational energy and thermal energy but do not disti guish differences between the individual vibrationally excit states. Details of the modulation technique, involving chemil minscence detection of $NO_2$ and resonance fluorescence dete tion of oxygen atoms, are described. Comparison of our resu with a previous measurement of the summation reaction (1′ + shows excellent agreement.

**14386.** Dorman, D. E., Torchia, D. A., Bovey, F. A., **Carbon- and proton nuclear magnetic resonance observations of the co formation of poly(L-proline) in aqueous salt solutio** *Macromolecules* **6,** No. 1, 80-82 (Jan.-Feb. 1973).

Key words: carbon-13; nuclear magnetic resonance; poly- proline; polypeptides.

Proton nmr at 220 MHz and $^{13}C$ nmr at 25 and 15.08 M have been employed to confirm previous conclusions that t disordering of poly(L-proline) chains in concentrated aque salt solutions arises primarily from the formation of rand sequences of cis and trans peptide bonds. The effects of KI a $CaCl_2$ are essentially similar. The β- and γ-carbon resonances the proline ring appear to be the most reliable monitors of t isomerization process, giving distinct and well resolved peaks the cis and trans conformations.

**14387.** Jackson, R. H. F., Lechner, J. A., Sookne, D. J., **A syst for position-location based on ranges,** (Proc. 18th Conf. on Design of Experiments in Army Research Development a Testing, Aberdeen Proving Ground, Md., Oct. 25-27, 197 *ARO Report 73-2,* Part 2, 549-577 (Department of Defe Washington, D.C., 1973).

Key words: algorithms; least-squares; multilateration; p tion-location; ranges; simulation.

The system in question is intended to employ range-only in mation, or range-plus-altitude information, to track the positi p to hundreds of users (only some of which measure ranges ther users) in three dimensions or on the earth's surface. This er describes the structure, use and results of a simulation dy which focused, within a larger analysis, on the absolute relative adequacies of various mathematical position-estima- algorithms. The discussion will include comparisons among six different algorithms investigated, considering both accu- y and computer time required.

**88.** Hayward, R. W., **Parity,** Paper in *The Encyclopedia of hysics, 2d Edition,* R. M. Besancon, Ed., pp. 671-675 (Van ostrand Reinhold Co., New York, N.Y., 1974).

> Key words: charge conjugation; parity; relativity; space inversion; time reversal.

short encyclopedic article on the concept of parity and other continuous Lorentz transformations and their applications in sics.

**89.** Fanconi, B., **Lattice dynamics of polyglycine I,** *J. Chem. hys.* **57,** No. 5, 2109-2116 (Sept. 1, 1972).

> Key words: frequency distribution; lattice vibrations; normal mode analysis; polyglycine I.

he two-dimensional lattice vibrations of the extended form of yglycine have been calculated from a five mass model of the cine chemical repeat unit and with interchain hydrogen bond etching. The effects of hydrogen bond bending and torsion on lattice modes are determined using a model in which the en- chemical repeat unit is treated as a single dynamical unit. e valence force field for the latter model is found by fitting the tical frequencies determined from the five mass calculation. e density of phonon states for the two-dimensional lattice is ermined for the single mass model.

**90.** Brower, W. S., Minor, D. B., Parker, H. S., Roth, R. S., aring, J. L., **Flux synthesis of cubic potassium antimonate,** *ater. Res. Bull.* **9,** No. 8, 1045-1051 (1974).

> Key words: cubic potassium antimonate; flux synthesis; impurity stabilization; potassium antimonate; potassium fluoride-antimony oxide; single crystals.

Although the compound $KSbO_3$ has been reported to occur in igh temperature cubic polymorph, only the rhombohedral il- enite phase was obtained in this study for pure material at am- ent pressure and temperatures up to about 1350 °C in open Pt ucibles or sealed Pt tubes. With the addition of about 2 mole rcent $SiO_2$, $B_2O_3$ or other oxides of small cations a primitive bic phase was found with a $\simeq 9.578$ A. Small single crystals of ody centered cubic phase (a = 9.605 A) were easily synthes- ed by a flux evaporation technique at about 1000 °C in an open crucible from a composition of about 5 mole percent $Sb_2O_4$:95 ole percent KF. The exact composition and structure of this ase (presumably $K_{1-x}SbO_{3-x}F_x$, $0 < \chi \leqslant 0.5$) is now under in- stigation.

**391.** Kuriyama, M., Early, J. G., **The dynamical scattering amplitude of an imperfect crystal. III. A dynamical diffraction equation for topography in the spatial coordinate representation,** *Acta Crystallogr.* **A30,** 525-535 (Jan. 1974).

> Key words: dynamical diffraction; imperfect crystal; integral equation; topography.

Based on a general dynamical theory of diffraction, an integral uation for dynamical diffraction in imperfect crystals is ob- ined in the spatial coordinate representation. This equation is rived for diffraction topography in the symmetrical Laue ometry from the basic dynamical equation of diffraction previ- sly derived in the momentum representation. Discussion is esented on an interpretation of this integral equation beyond the given diffraction geometry. This equation can be considered as a basic equation for diffraction topography.

**14392.** Hockey, B. J., **Use of the hardness test in the study of the plastic deformation of single crystals,** (Proc. ASM-AIME Symp. on the Science of Hardness Testing and its Research Applications, Detroit, Mich., Oct. 18-21, 1971), Chapter 3 in *The Science of Hardness Testing and its Research Applications,* pp. 21-50 (American Society for Metals, Metals Park, Ohio, 1973).

> Key words: deformational twinning; dislocations; hardness test; lattice friction; plastic deformation; single crystals.

The use of the hardness test in the study of the plastic deformation of single crystals is reviewed and its applicability to materials of different mechanical behavior discussed. Emphasis is placed on those studies which demonstrate the unique or relative advantages of point loading. It is shown that valuable information on the conditions under which plastic flow occurs, on dislocation slip system identification, on deformational twinning, and on lattice friction effects have been obtained.

**14393.** Heuer, A. H., Cannon, R. M., Tighe, N. J., **Plastic deformation in fine-grain ceramics,** (Proc. 15th Sagamore Army Materials Research Conf., Sagamore Conference Center, Raquette Lake, N.Y., Aug. 20-23, 1968), Chapter 16 in *Ultrafine-Grain Ceramics,* pp. 339-365 (Syracuse University Press, Syracuse, N.Y., 1970).

> Key words: fine-grain ceramics; grain boundary; plastic deformation; polycrystalline.

Plastic deformation in fine-grain (i.e., $\leqslant 10\ \mu$) ceramics is discussed. It is shown that fine-grain polycrystals can be exceptionally ductile, the fine grain size enhancing diffusional deformation and grain boundary sliding processes. The deformation is sensitive to both grain size and temperature.

The influence of grain size (1-10 $\mu$), strain-rate ($2 \times 10^{-6} - 3 \times 10^{-4}$/sec), and temperature (1100-1700 °C) on the deformation of fine-grain alumina has been studied. It is suggested that the predominant deformation mechanism in the larger grained polycrystals is diffusional creep, and that grain boundary sliding makes an increasingly important contribution as the grain size is decreased; in addition, deformation twinning can also be important. These results are shown to be consistent with previous work on deformation in polycrystalline alumina. A brief review of the literature on plastic deformation in fine-grain magnesia, beryllia, thoria, and urania indicates that grain boundary sliding may be important for each of these materials as well.

**14394.** Ku, H. H., **Statistical methods applicable to counting experiments and evaluation of experimental data,** *Nucl. Instrum. Methods* **112,** 377-383 (1973).

> Key words: calibration; check standard; control chart on precision measure; data analysis; design of experiments; deporting of results; standards; statistical methods.

In an experiment a sequence of operations is performed that results in the collection, interpretation, and transmission of information on a topic of interest. Statistical methodology may be used to help in increasing the efficiency of collection, in checking the validity of interpretation, and in editing the presentation of results. Some such concepts and methods that are useful to counting experiments, and essential to the operations of standards and calibration laboratories, will be discussed.

**14395.** Lieblein, J., **Generalized propagation of error using a new approach,** *Proc. 11th Annual Meeting of the Institute of Nuclear Materials Management, Gatlinburg, Tenn., May 25-27, 1970,* pp. 190-211 (1970).

Key words: coefficients subject to error; determinant; error propagation; implicit functions; linear equations; matrix; propagation of error; variance.

Propagation of error formulas for the case of one function of several variables or several explicitly known functions have been studied. The only untreated case remaining is the one where the "dependent" variable is an implicit function and cannot readily (or at all) be solved in terms of the independent variables. This case is treated in the present paper which takes the general matrix viewpoint and thereby obtains results in concise form. A special case is application to linear (algebraic) system, arising in an idealization of a nuclear process flow, without the necessity for obtaining the explicit solution.

**14396.** Gallagher, A., Lewis, E. L., **Resonance broadening of Hanle-effect signals in rubidium,** *Phys. Rev. A.* **10,** No. 1, 231-241 (July 1974).

Key words: line broadening; rubidium.

We have measured the broadening of $Rb^{87}$ level-crossing signals due to collisions with $Rb^{85}$. The depolarization or broadening rates for the 5 $^2P_{1/2}$ state orientation, the 5 $^2P_{3/2}$ state orientation and alignment, and the 5 $^2P_{3/2}$ state 58-G crossing were measured. Theoretical resonance-broadening depolarization rates for the electronic angular momentum, due to Carrington, Stacey, and Cooper, have been incorporated into calculations of the Hanle-effect signals in the presence of nuclear-spin coupling. The experimental broadening rates are corrected for a minor amount of coherence narrowing. The measured broadening rate for the three 5 $^2P_{1/2}$ state level-crossing signals are in 20 percent agreement with the theory. The measured 5 $^2P_{1/2}$ state broadening rate exceeds the theoretical by about a factor of 2. This discrepancy may be due to the action of the hyperfine interaction during these unusually long duration collisions. The natural lifetimes of the 5 $^2P_{3/2}$ and 5 $^2P_{1/2}$ states are determined from the low-density linewidth to be $27.0 \pm 0.5$ and $29.4 \pm 0.7$ nsec, respectively.

**14397.** Kaldor, A., Hastie, J. W., **Infrared laser modulated molecular beam mass spectrometry,** *Chem. Phys. Lett.* **16,** No. 2, 328-331 (Oct. 1, 1972).

Key words: infrared laser; laser chemistry; mass spectrometry; molecular beam; phase spectroscopy; vibrational energy transfer.

A technique is described whereby a modulated molecular beam can be extracted from gas mixtures which are excited by infrared laser radiation. The method has been applied to time resolved mass spectrometric studies of laser induced molecular processes for systems containing $BCl_3$ and $SF_6$ as radiation absorbers, and shows general applicability to studies of laser induced chemical reaction.

**14398.** Khoury, F., Fanconi, B., Barnes, J. D., Bolz, L. H., **Effects of polymorphism on the Raman-active longitudinal acoustical mode frequencies of *n*-paraffins,** *J. Chem. Phys.* **59,** No. 11, 5849-5857 (Dec. 1, 1973).

Key words: chain-folded polyethylene crystals; longitudinal acoustical modes; *n*-paraffins; polymorphism; Raman spectroscopy.

Raman spectroscopic measurements on the orthorhombic and monoclinic crystalline forms of $n\text{-}C_{36}H_{74}$ and $n\text{-}C_{94}H_{190}$ show that the frequencies of the longitudinal acoustical modes depend on the orientation of the chain axis relative to the planes containing the terminal methyl groups as well as the chain length. The frequency differences between the orthorhombic and monoclinic forms of a given *n*-paraffin depend on the magnitude and direction of the regular stagger between neighboring end groups in the monoclinic forms. It is concluded that these frequency differences are most likely associated with variations in end gro packing associated with differences in crystalline form. The i plications of these observations to the use of Raman spectr scopic data to characterize the morphology of chain-fold polyethylene crystals are discussed.

**14399.** Halford, D., **Comparing frequencies,** *Phys. Today* **26,** 2, 15 (Feb. 1973).

Key words: cesium frequency; frequency multiplication; frared frequency synthesis; Josephson junction; lase methane frequency.

An incorrect and misleading statement was made in a ne item in Physics Today, April 1972, page 17, regarding infra frequency synthesis: "A chain of experiments is needed beca two frequencies differing by more than a factor of 12 cannot compared directly." This Letter to the Editor points out the istence and importance of some previously published papers, cluding as examples factors of 100 and of 401 obtained in direct step, respectively, by McDonald and coworkers in 1 and in 1971.

**14400.** LaVilla, R. E., **Semi-Auger electron transitions,** (Proc. Conf. on Inner Shell Ionization Phenomena and Future Ap cations, Atlanta, Ga., Apr. 17-22, 1972), Paper in *Proceedi of the International Conference on Inner Shell Ionizat Phenomena and Future Applications,* R. W. Fink, S. T. M son, J. M. Palms, and P. V. Rao, Eds., Conf. 720404, 1, 5 522 (U.S. Atomic Energy Commission, Technical Informat Center, Oak Ridge, Tenn., Jan. 1973).

Key words: argon, KCl, $CH_3Cl$, $SF_6$; L and K x-ray spec semi-Auger effect; x-ray photoelectron spectra.

The argon and KCl $L_{2,3}$ x-ray emission spectra excited direct electron bombardment have been recorded with pho counting on a planar single crystal spectrometer. A promin feature lying approximately 6, 11, and 14 eV below the pa emission peak in Cl, Ar and K respectively, was observed in spectra. Comparison with other data on related processes dicates that the low energy features are direct evidence "semi-Auger" two electron process, due to configuration teraction in the final state. The initial $L_{2,3}$ single vacancy is fi by an outer shell electron and simultaneously another outer electron is excited with the emission of a single photon. possible identification of this process in other systems will be discussed.

**14401.** Kranbuehl, D. E., Verdier, P. H., **Monte Carlo studi the relaxation of vector end-to-end length in random polymer chains,** *J. Chem. Phys.* **56,** No. 6, 3145-3149 (Mar. 1972).

Key words: end-to-end length; Monte Carlo; polymer c dynamics; random-coil.

The effects of excluded volume interactions upon the dyn cal behavior of random-coil polymer chains are studied by taining autocorrelation functions for vector end-to-end lengt lattice-model chains of 9, 15, 33, and 63 beads by a Monte C simulation technique. It is found that relaxation of the ve end-to-end length requires from 4 to 7 times as long as relaxa of its square, in contrast to the predictions of simple mo without excluded volume effects.

**14402.** Jacob, E. J., Lide, D. R., Jr., **Microwave investigatio methyl sulfone and methane sulfonyl fluoride,** *J. Chem. P* **54,** No. 11, 4591-4596 (June 1, 1971).

Key words: dipole moment; internal rotation; methane fonyl fluoride; methyl sulfone; microwave spectra; mol lar structure.

Rotational constants for the ground state of methyl sulfone d for the ground and first excited torsional state of methane fonyl fluoride have been derived from microwave spectra obved in the 18 000 – 37 000-MHz region. Molecular dipole oments of 4.50 ± 0.10 D for $(CH_3)_2SO_2$ and 3.88 ± 0.04 D for $H_3SO_2F$ were measured. Relative intensity measurements ce the barrier to methyl rotation in $CH_3SO_2F$ at 880 ± 120 $^{-1}$ (2.25 ± 0.35 kcal/mole). Alternate structures for $H_3)_2SO_2$, based on assumption of either the SO or the SC bond gth from a recent electron diffraction study, are presented. th reveal a significant discrepancy between the microwave d diffraction values for the OSO angle.

**403.** Giguere, P. T., Clark, F. O., Snyder, L. E., Buhl, D., Johnson, D. R., Lovas, F. J., **Upper limits for interstellar fulvene and nitric acid,** *Astrophys. J.* **182,** No. 2, 477-479 (June 1, 1973).

Key words: fulvene; interstellar molecules; nitric acid; radio astronomy; rotational transitions; telescope search.

Radio searches for the $1_{01}$-$0_{00}$ transition of fulvene (an isomer benzene) at 6399 MHz and for the $1_{10}$-$1_{11}$ transition of nitric id at 5839 MHz were not successful. Upper limits are reported fulvene against three galactic sources and for nitric acid ainst four. Our measurements indicate that nitric acid may be derabundant with respect to cyanoacetylene in the direction Sgr B2.

**404.** Lauritzen, J. I., Jr., Zwanzig, R., **Exact calculation of the partition function for a generalized model of two-dimensional polymer crystallization by chain folding,** *J. Chem. Phys.* **52,** No. 7, 3740-3751 (Apr. 1, 1970).

Key words: chain-folded crystal; partition function; phase transition; polymer.

A generalized model for two-dimensional polymer crystallization by chain folding is treated by equilibrium statistical echanics. A generating function for the partition function is obined in exact analytic form. The model leads to thermodynamilly well-defined chain-folded polymer crystals. Under certain rcumstances in the limit of an infinitely long polymer chain, the odel shows a second-order phase transition from an "extendedain" crystal to the chain-folded crystal.

**405.** Sengers, J. M. H. L., **From Van der Waals' equation to the scaling laws,** *Physica* **73,** 73-106 (1974).

Key words: coexistence curve; corresponding states; critical exponents; critical isotherm; rectilinear diameter; scaling laws; scaling symmetry; universality; Van der Waals' equation; vapor pressure curve.

From our present-day perspective, the most important results otained by Van der Waals for thermodynamic behavior in the itical region of gases are: the cubic critical isotherm and uadratic coexistence curve; the continuity of slope of the vaporressure curve; the law of the rectilinear diameter and the law of orresponding state. The critical behavior of Van der Waals' quation is typical for equations of state that are regular at the itical point in a sense to be discussed; those equations are resently called "classical." The confrontation with experiment ok place before 1900. At that time, the first power-law nalyses of data were made and their results disproved classical eory convincingly. It took, however, another 65 years before lassical theory was replaced by the scaling laws. The very mited validity of the law of corresponding states, however, ever posed a serious threat to the classical equation. On the ontrary, by generalizing this law in various ways, our insight nto the relation between molecular interaction and thermodynamic behaviour has been deepened considerably. In a ense, the principle of universality may be considered the latest eneralization of the law of corresponding states. The principle of continuity of slope of the vapor-pressure curve has been preserved; the direction of the vapor-pressure curve at the critical point is a very special one according to the thermodynamic theory of Wheeler and Griffiths and also in the theories of "extended scaling." The law of the rectilinear diameter, now under siege by theory, has not yet failed us experimentally.

The lines from the past to the present are sketched in this contribution, and the modern concepts of scaling will be developed from the classical equation of state. The consequences of the scaling laws for the description of thermodynamic data of fluids in the critical region will be discussed and illustrated with experimental material. Universality of critical behavior in fluids will be demonstrated.

**14406.** Mann, D. B., **ASRDI oxygen technology survey. Volume VI: Flow measurement instrumentation,** *NASA Spec. Publ.* **3084,** 104 pages (National Aeronautics and Space Administration, Washington, D.C. 1974).

Key words: argon; calibration; cryogenic; flowmeter, measurement; nitrogen; oxygen.

A survey of the literature combined with the results of a joint government-industry cooperative program on cryogenic flowmetering is presented. The objective was to establish the state of the technology and art of oxygen flowmetering in liquid and gaseous states.

Only those meters with demonstrated performance are considered. These were classified as quantity, head, momentum and velocity types. A comparison of the performance of these devices and a discussion of future requirements for flow reference systems and metering are given.

**14407.** Malmberg, M. S., Maryott, A. A., **Dipole moments of $ClSF_5$ and $CF_3SF_5$ from the dielectric relaxation spectra of the vapors,** *J. Chem. Phys.* **53,** No. 4, 1614-1615 (Aug. 15, 1970).

Key words: $CF_3SF_5$; ClSF; dielectric relaxation time; dipole moment; microwave absorption; vapor phase.

The microwave absorption associated with the dielectric relaxation spectra of the symmetric-top gases, $ClSF_5$ and $CF_3SF_5$, was measured at various pressures up to two atmospheres at a frequency of 1216 MHz at 298 K. Values of the electric dipole moments derived from these data are $0.51_1$ D for $ClSF_5$ and $0.38_4$ D for $CF_3SF_5$.

**14408.** Martin, W. C., **Low-energy level structure of neutral cerium (Ce I),** *Phys. Rev. A* **3,** No. 6, 1810-1815 (June 1971).

Key words: atomic energy levels; atomic spectra; electron configurations; neutral cerium; Zeeman effect.

The low portion of an extensive level structure derived from analysis of the optical spectrum is reported. Positions, $J$ values, and $g_J$ factors are given for 98 levels, including all 91 levels expected below 10 000 $cm^{-1}$. A previous report on this analysis showed the ground level to be $4f5d6s^2\ {}^1G_4^\circ$ and gave the lowest levels of $4f5d^26s$. Comparison of the observed odd-parity levels with calculations by Goldschmidt and Salomon shows that all 86 of the odd levels tabulated here belong to these configurations. All but seven of these odd levels are assigned $LS$ names, although the calculations show that many of them have low $LS$ purities, and a few have strong mixtures of the two configurations. The much simpler system of even levels below 10 000 $cm^{-1}$ includes only the six levels of $4f^26s^2\ {}^3H$ and ${}^3F$, beginning with ${}^3H_4$ at 4762.718 $cm^{-1}$ above the ground-state level. The table of even levels also includes $4f^26s^2\ {}^1G_4$ and the lowest two levels of each of the lowest two terms of $4f^25d6s$, ${}^5I_{4,5}$, and ${}^5K_{5,6}$.

**14409.** Layer, H. P., **Circuit design for an electronic self-nulling ellipsometer,** *Surface Sci.* **16,** 177-192 (1969).

Key words: corrosion; electronic ellipsometer; Faraday cells; self-nulling ellipsometer; thin films.

The importance of automating the ellipsometer has been recognized by researchers active in the field and considerable attention has been given to the development of a practical instrument. The present work was motivated by the belief that a more satisfactory automatic ellipsometer could be developed if the all-electronic approach suggested by Winterbottom was used. This approach has resulted in the design and construction of an instrument that is sensitive, stable, relatively inexpensive and which has a response time that is of the order of milliseconds. The electronic circuits will easily lend themselves to duplication by investigators interested in such a device and are of such a configuration that existing instruments need only minor modifications. An automatic gain stage circuit is included to maintain maximum sensitivity where spectral emission and sensitivity variations are encountered, as in continuous wavelength scanning ellipsometric measurements.

**14410.** Mahoney, R., Srinivasan, G. R., Macedo, P. B., Napolitano, A., Simmons, J. H., **Effect of subcritical microstructure on the viscosity of a sodium borosilicate glass,** *Phys. Chem. Glasses* **15,** No. 1, 24-31 (Feb. 1974).

Key words: borosilicate; environmental-relaxation model; glass; microstructure; phase-separation; viscosity.

Viscosity and electron microscopy measurements were made on a phase separating glass as a function of time, at various temperatures. The viscosity changed by five orders of magnitude during the phase separation in a time period identified to be solely in the coarsening stage by electron microscopy. The stage during which composition changes are dominant occurs very quickly despite the high starting viscosity ($10^{11}$ P) and, therefore, is nearly complete before reliable viscosity data can be obtained (2 min). Analysis of the rate of increase of the average particle size identified a rearrangement stage proceeding by bulk diffusion through the fluid phase with an apparent activation energy of 98 kcal/mole ($4.1 \times 10^5$ J/mole). Superposition of the viscosity-microstructure size curves for various temperatures demonstrated that the change in viscosity was totally controlled by the growth of the viscous phase whose activation energy for viscosity is 132 kcal/mole ($5.52 \times 10^5$ J/mole). The change of viscosity with time is explained in terms of changes in the size of the microstructure by applying an environmental relaxation model proposed by two of the authors. The significance of the good quantitative fit of the data by the model and the physical significance of the parameters are discussed.

**14411.** McClendon, L. T., DeVoe, J. R., **Substoichiometric radioisotope dilution analysis of tungsten as a major constituent in molybdenum containing materials using toluene-3,4-dithiol,** *Anal. Chem.* **41,** No. 11, 1454-1456 (Sept. 1969).

Key words: molybdenum; radioisotope dilution; substoichiometric; toluene-3,4-dithiol; tungsten.

A radioisotope dilution procedure was developed for tungsten determination in molybdenum containing materials using a substoichiometric amount of the complexing reagent, toluene-3,4-dithiol. Using this approach, an equal amount of tungsten is isolated before and after dilution of the radioisotope, thus avoiding serious interferences by eliminating the need for quantitative separation. This technique was used for tungsten determination in NBS tungsten-molybdenum alloy (SRM-480) indicate composition of alloy found by standard method where the average concentration found was 79.32 percent with a pooled estimate of the standard deviation (for a single determination) of ± 0.43 percent. The precision obtained is very good for this type of technique.

**14412.** Miller, L. D., Schima, F. J., **The half-life of $^{129m}$Xe,** *Int. J. Appl. Radiat. Isotop.* **24,** 353 (1973).

Key words: gamma-ray energy; half-life; isomeric $^{129}$Xe radioactivity; transition probability.

The decay of the isomeric level in $^{129}$Xe has been studied b means of Ge(Li) and Si(Li) detectors. Sources of the isomeric ac tivity were prepared by (n,$\gamma$) reaction on isotopically enhance $^{128}$Xe ion implanted in Al foil. Two $\gamma$-rays have been observed The energies and estimated standard errors were found to b $39.50 \pm .17$ and $196.46 \pm .02$ keV. The isomeric half-life an estimated standard error have been determined to be $8.89 \pm .0$ days. The reduced transition probabilities of the four M4 isome of Xe are compared to the quasiparticle theory.

**14413.** Hastie, J. W., **Mass spectrometric evidence for $HO_2$ in l atn flames,** *Chem. Phys. Lett.* **26,** No. 3, 338-343 (June 1, 1974).

Key words: flame inhibition; flames; $HO_2$; mass spec trometry.

The perhydroxyl species $HO_2$ has been observed in l atm H $- O_2 - N_2$ flames and its flame concentration determined as function of flame composition and position. Also the oxidatio of small additions of CO to these flames has been observed an the results favor the reaction, $OH + CO \rightarrow CO_2 + H$, rather tha the alternative process, $HO_2 + CO \rightarrow CO_2 + OH$.

**14414.** Molino, J. A., **Equal aversion levels for pure tones and 1/ octave bands of noise,** *J. Acoust. Soc. Amer.* **55,** No. 6, 128 1289 (June 1974).

Key words: audition; aversion for sound; escape an avoidance; loudness; noisiness; psychophysics; schedul of reinforcement.

College students tapped rapidly on a telegraph key to redu the intensity of a continuous acoustic stimulus presented throu earphones. Failure to respond resulted in an intensity of l d every 4 sec. A group of 14 students responded during 10-m sessions to eight pure tones and eight 1/3-octave bands of noi at octave frequencies from 63 Hz to 8 kHz. The average SP maintained by the subjects became stable after about 5 min. T different asymptotic levels observed from 5-10 min were tak as a measure of equal aversion levels for the stimuli. Equal ave sion levels were compared with other subjective weighting co tours: equal loudness level, *A*-weighted sound level, perceiv noise level, etc. They were closest to an *A*-weighted sound lev of 80-85 dB.

**14415.** Marezio, M., Dernier, P. D., Santoro, A., **Twinning in C doped $VO_2$,** *Crystallogr.* **A29,** 618-621 (1973).

Key words: chromium doping; metal-insulator transitio twinning; vanadium oxide; x rays.

Twinning has been studied in several samples of V containing substitution solid solution 0.5 and 2.5 at.% Cr. T twinning is by reticular pseudo-merohedry and it is controlled the tetragonal pseudo-symmetry of a superlattice obtained fr the original monoclinic cell ($a \simeq 9.1$, $b \simeq 5.8$, $\underline{c} \simeq 4.55$ Å, $\beta \simeq 9$ by means of the transformation $100/002/0\bar{1}0$. More than o twin law is found in every sample studied. All the theoretica possible twin laws, except one, have been observed. The pos bility of twinning simulating a lattice and a space group differe from the true ones has been pointed out and methods for dete ing twins in these cases are given.

**14416.** Santoro, A., **Characterization of twinning,** *Acta Cryst logr.* **A30,** Part 2, 224-231 (Mar. 1974).

Key words: coincidence-site lattices; determination of tv laws; equivalence of twin laws; lattices; oriented crys growths; twin obliquity and twinning.

A new twinning condition is derived. It is more general t Friedel's ratios [Friedel, G. (1964). *Leçons de Cristallograp* p. 249, Paris: Blanchard], and it allows one to predict not o e twin laws of a crystalline species, but also the regular asciations of crystals mutually oriented according to noncrystalgraphic rotations. The deviation suffered by the twin lattice at e composition surface is better described in terms of the new inning condition than in terms of the twin obliquity.

**417.** Molino, J. A., **Odor pollution detection and measurement,** *ASTM Stand. News Letter to Editor* **1,** No. 3, 47 (Mar. 1973).

Key words: pollution; psychophysics.

This paragraph proposes the organization of a committee, task rce, or working group to study psychophysical measurement chniques and data concerning human tolerance to and perssible standards for various sorts of pollution, e.g., odor, noise, are, vibration, etc.

**418.** Kunasz, P. B., Hummer, D. G., **Radiative transfer in spherically symmetric systems-IV. Solution of the line transfer problem with radial velocity fields,** *Mon. Notic. Roy. Astron. Soc.* **166,** No. 1, 57-78 (1974).

Key words: gas dynamics; radiative transfer; spectral line profiles; stellar atmospheres.

A numerical procedure is presented for solving the line ansfer problem with complete redistribution in spherically symetric atmospheres in which the radial velocity is an arbitrary nction of radius, limited by practical considerations to maxaum velocities a few times the mean thermal velocity. In this ocedure the transfer equation, written in the observer's frame, differenced along rays and the resulting very large set of coued linear equations is cast into the novel form, proposed by ybicki, that allows for extremely rapid solution of the system. umerical results are discussed for three sequences of models, vo with linear velocity laws and one with constant velocities, in hich the effect of the transverse velocity gradient is demonrated. It is shown that velocities as small as 0.05 of the mean ermal velocity produce observable asymmetries in the flux ofile.

**419.** Kunasz, P. B., Hummer, D. G., **Radiative transfer in spherically symmetric systems-III. Fundamentals of line formation,** *Mon. Notic. Roy. Astron. Soc.* **166,** No. 1, 19-55 (1974).

Key words: radiative energy loss; radiative transfer; spectral line profiles; spherically symmetric gas clouds; stellar atmospheres.

A generalization of the variable Eddington factor method is resented that makes possible the solution of line formation roblems in extended spherical atmospheres whose constitutive roperties depend on radius in an arbitrary way. Extensive nuierical results for Doppler broadening in models with power law pacities ($n=0,2,3$) are presented and interpreted. Very subantial deviations are found from the solutions of analogous lane-parallel models. The single-flight escape probability is erived for a general opacity law and is shown to exceed that for n analogous plane-parallel slab by no more than a factor of aproximately two for Doppler broadening, or three-halves for orentz broadening. However, it is shown that each time a hoton is scattered, it has a probability greater than one-half of nding its flight at a radius larger than that at which it was mitted. This effect is peculiar to spherical geometries and may e important in aiding the escape of photons from optically thick ystems. Finally the effects of dilution are considered and some roperties of the infinite radius, finite optical depth models are nferred. An appendix contains the solution of the line transfer roblem for a homogeneous sphere by the kernel-approximation nethod.

**4420.** Lloyd, A. C., **A critical review of kinetics of the dissociation-recombination reactions of fluorine and chlorine,** *Int. J. Chem. Kinet.* **III,** 39-68 (1971).

Key words: bimolecular; chlorine; dissociation; evaluation; fluorine; gas; recombination; review; termolecular; third body.

A critical evaluation of the rates of the dissociation and recombination reactions of fluorine and chlorine is given. Data are presented graphically and in tabular form. The effect of various third bodies is discussed. Rate expressions for specified temperature ranges are recommended, while comparison with theoretical values obtained from the Benson and Fueno theory is made where applicable.

**14421.** Frommer, M. A., Lancet, D., **Freezing and nonfreezing water in cellulose acetate membranes,** *J. Appl. Polym. Sci.* **16,** 1295-1303 (1972).

Key words: bound water; cellulose-acetate membranes; differential scanning calorimetry; freezing of water; membranes; nuclear magnetic resonance; reverse osmosis membranes; water in membranes.

The relative amounts of freezing and nonfreezing water in various cellulose acetate (CA) membranes were determined by differential scanning calorimetry. It was found that: (1) A significant fraction (17-40%) of the water (1.0-3.1 g $H_2O$ per gram dry CA) in any membrane does not freeze at temperatures as low as − 60 °C. (2) The amount of nonfreezing bound water (0.4-0.7 g nonfreezing water per gram dry CA) depends upon the nature of the membrane and is significantly higher than the total amount of water (all of which is nonfreezing) absorbed from liquid water by a *dense* film of the same polymer (~ 0.18 g water per gram dry CA). The structures of the membranes were studied by scanning electron microscopy. The results suggest that the amounts of nonfreezing water in cellulose acetate membranes decrease with the increase in the packing density (compactness) of the polymer within the membrane. In dense films, the extent of polymer-polymer interactions within the polymeric matrix is high, and therefore the macro-molecular chains are less accessible to bind water.

**14422.** Maryott, A. A., Farrar, T. C., Malmberg, M. S., **$^{35}$Cl and $^{19}$F NMR spin-lattice relaxation time measurements and rotational diffusion in liquid $ClO_3F$,** *J. Chem. Phys.* **54,** No. 1, 64-71 (Jan. 1, 1971).

Key words: angular-momentum; correlation-times; molecular-reorientation; NMR-relaxation-times; $^{19}$F; $^{35}$Cl.

The NMR spin-lattice relaxation times of $^{35}$Cl and been $^{19}$F have measured by pulse techniques over the entire liquid range of $ClO_3F$ (130-368 K). The chlorine relaxation which is due solely to the nuclear quadrupole interaction can be used together with the known quadrupole coupling constant to determine the correlation time for molecular orientation, $\tau_{\theta,2}$. The fluorine relaxation is dominated by the spin-rotation interaction with only a small intermolecular dipole contribution at the lowest temperatures. In order to obtain the angular momentum correlation time, $\tau_J$, an independent estimate of the spin-rotation tensor was made by combining gas-phase measurements of $T_1(^{19}F)$ with previous data on the chemical shift and gas-phase dielectric relaxation. The results for this quasispherical molecule are in accord with rotational diffusion theory and Hubbard's relation, $\tau_{\theta,2}\tau_J = I/6kT$, at the lowest temperatures and agree over the entire range with the extended treatment of McClung.

**14423.** Mackay, D. R., **NBS information services on engineering standards,** *Stand. Eng.*, pp. 17-19 (June 1971).

Key words: information services; standards.

This paper covers the history of the information services provided by the National Bureau of Standards on published standards and standardization activities and describes the current activities of the Information Section of the Bureau's Office of Engineering Standards Services.

**14424.** Marlowe, D. E., Sushinsky, G. F., Dexter, H. B., **Elastic torsional buckling of thin-walled composite cylinders,** *Amer. Soc. Test. Mater. Spec. Tech. Publ.* **546,** pp. 84-108 (1974).

Key words: composite materials; elastic buckling; reinforced aluminum; stability; thin shells; torsional buckling.

The elastic torsional buckling strength has been determined experimentally for thin-walled cylinders fabricated with glass/epoxy, boron/epoxy, and graphite/epoxy composite materials and composite-reinforced aluminum and titanium. Cylinders have been tested with several unidirectional-ply orientations and several cross-ply layups. Specimens were designed with diameter-to-thickness ($D/t$) ratios of approximately 150 and 300 and in two lengths ($L$), 10 in. (25.4 cm) and 20 in. (50.8 cm).

The results of these tests were compared with the buckling strengths predicted by the torsional buckling analysis of Chao. In this analysis, the instability loads of heterogeneous anisotropic cylinders are calculated with Timoshenko's equilibrium equations. The computer program associated with the analysis seeks the solution with the lowest buckling strength by iterating on the number of circumferential buckling waves. For the cylinders considered ($L/r=3.3$ and $L/r=6.7$), the experimental buckling torques were approximately 85 percent of the torques predicted by the Chao analysis. In the cross-ply laminate cylinders, the stacking sequence of the plies was found to have a marked effect on the elastic buckling torque.

Reversal of the stacking sequence of the cross-plied cylinders resulted in buckling torques which differed by a factor of 2. Similar results were obtained by reversal of the direction of twist on the original stacking sequence. This observation may be important in applications where reversal of loading can occur. The size effect of linear scaling was investigated for cylinders whose dimensions were different but whose $L/r$ and $D/t$ ratios were the same. As expected from the analysis, the experimental buckling stress remained constant.

**14425.** Meinke, W. W., **The ultimate contribution of nuclear activation to analysis,** *J. Radioanal. Chem.* **15,** 419-433 (1973).

Key words: accuracy limits; activation analysis; activation spectrometry; analytical chemistry; measurement biases; ppb; ppm; real samples; Standard Reference Materials; trace element analysis.

This paper challenges the implied accuracy of many of the analytical results below the ppm level reported in the literature. The present status of trace element techniques including activation analysis is evaluated. Practical experiences at NBS in the use of clean facilities, ultrapure reagents and special clean containers for obtaining trace composition values with known accuracy for the certification of Standard Reference Materials are described. The use of recently certified NBS Standard Reference Materials to aid the trace analyst in the biological and geochemical areas in understanding the biases of their methods is also described.

Activation spectrometry (i.e., nondestructive analysis) as opposed to activation analysis involving radiochemical separations, has the limitations of other spectrometries. However, nuclear activation analysis with careful attention to the principles of accurate measurement should be able to lower the limits of meaningful measurement of many inorganic elements several orders of magnitude during the next decade.

**14426.** Melmed, A. J., Carroll, J. J., **Oxidation of (011) iron at room temperature: Mainly LEED aspects,** *J. Vac. Sci. Technol.* **10,** No. 1, 164-169 (Jan.-Feb. 1973).

Key words: ellipsometry; low energy electron diffraction; metal oxidation; oxidation kinetics; oxide structure; surface potential.

The interaction of oxygen with (011) Fe at room temperature has been investigated using simultaneous combinations of LEED, ellipsometry, and surface potential measurements. This paper is concerned mainly with the LEED aspects. The sequence of LEED patterns found was either similar to that previously found or slightly different, depending on experimental conditions. In most experiments a new LEED pattern, $p(2\times1)$, was observed instead of the $c(3\times1)$ pattern previously reported. Direct keying of the LEED patterns to the ellipsometry-derived growth kinetics leads to further understanding of the oxidation mechanism. The occurrence of heterogeneous oxide nucleation is supported, and it is shown that an oxide consistent with the expected diffraction properties of FeO grows to a "limiting" thickness of about 25-30 Å in oxygen. The terminal oxide in the air is concluded to have about the same thickness but a significantly different structure.

**14427.** Crandall, D. H., Taylor, P. O., Dunn, G. H., **Electron-impact excitation of the Ba$^+$ ion,** *Phys. Rev. A* **10,** No. 1, 141-157 (July 1974).

Key words: absolute cross sections; Ba$^+$ ion; cross beams; electron impact; excitation; polarization.

Crossed beams of Ba$^+$ and electrons were used to measure the absolute emission cross sections for the Ba$^+$ lines, 455.4, 493.4, 490.0, and 413.1 + 416.6 nm. Polarization fractions of the light were also measured. The data were analyzed to extract level excitation cross sections. The excitation cross section for the 6 $^2P_{3/2}$ level has a value $34.7\times10^{-16}$ cm$^2$ at the 2.72-eV threshold, shows marked structure in the 3 – 10-eV interval, and decreases to $1.71\times10^{-16}$ cm$^2$ at 747 eV. The polarization fraction for the 455.4-nm light exhibits pronounced oscillatory structure in the interval 3 – 7 eV. Excitation cross section for the 6 $^2P_{1/2}$, 7 $^2S_{1/2}$ and 6 $^2D_{3/2+5/2}$ levels have values at threshold of $20.0\times10^{-16}$, 5.4 $\times10^{-16}$, and $4.3\times10^{-16}$ cm$^2$, respectively. Total uncertainties a a "high-confidence level" are about ±10 percent for the 6 $^2P_{1/}$ and 6 $^2P_{3/2}$ cross sections. Uncertainties range around ±30 percent for the 7 $^2S_{1/2}$ cross section and ±20 percent for the 6 $^2D_{3/2+5/2}$. Measurements for the 6 $^2P$ cross sections agree at hig energies with the Coulomb distorted-wave calculation c Sheorey and Burgess. Measurements for the 6 $^2P_{3/2}$ level are i quite good agreement with the measurements of Bacon an Hooper and of Pace and Hooper for energies 6 to 100 eV. However, the Pace and Hooper points at 3 and 4 eV are nearly twic the present values. Signals due to excitation of metastable 5 $^2$ ions in the ion beam were observed, and estimates could be mad of the cross section for excitation from this state to the fin states above. Cross sections at threshold were estimated to b $13.4\times10^{-16}$ cm$^2$ ± 34 percent, $9.8\times10^{-16}$ cm$^2$ ± 28 percent, 7. $\times10^{-16}$ cm$^2$ ± 100 percent, $6.9\times10^{-16}$ cm$^2$ ± 27 percent for excitation from the 5 $^2D$ levels to the 6 $^2P_{3/2}$, 6 $^2P_{1/2}$, 7 $^2S_{1/2}$, and $^2D_{5/2+3/2}$ levels, respectively. The rate coefficients for excitatic of 6 $^2P_{3/2}$ calculated from the data are in reasonable agreeme with the measurements of Hinnov *et al.*

**14428.** Mebs, R. W., Carter, G. C., Evans, B. J., Bennett, L. H **NMR chemical shifts in cuprous salts: The magnetic moment Cu,** *Solid State Commun.* **10,** No. 9, 769-774 (1972).

Key words: chemical shifts; copper (I) compounds; copp salts; Knight shift; magnetic moment; nuclear magnet resonance.

An extensive study has been made of chemical shifts of t $^{63}$Cu resonance in a number of cuprous salts. The observed tre in chemical shifts for the cuprous halides is in disagreement w theoretical ionicity estimates of either Pauling or Phillips. Tl trend has been explained by taking into account the relative i portance of $\pi$ bonding for the different halides. On the basis resent data, CuBr is the most suitable Knight shift reference pound. The measurements indicate $\mu=2.2206$ nm for $^{63}$Cu $\mu=2.3791$ nm for $^{63}$Cu for reference moment, without agnetic correction.

9. Danos, M., Rafelski, J., **Gauge invariance of the vacuum larization in quantum electrodynamics,** *Lett. Nuovo Cimento ries 2*, **10,** No. 3, 106-110 (May 18, 1974).

Key words: gauge invariance; quantum electrodynamics; renormalization; time-ordering operator; vacuum polarization; weak interactions.

is shown that the conventional perturbation formalism of theory treats incorrectly the equal time point in the nological products of field operators. If this imprecision is fied the contradictions between the results of the perturba- expansion of the *S*-matrix and of the predictions of axio- c field theory disappear. In particular, the gauge invariance ating quadratic divergence of the vacuum polarization loop not arise in the *S*-matrix formulation. This is of particular ortance for certain classes of the so-called nonrenormalizable theories, e.g., the Fermi-type theories of the weak interac-

.

0. Mount, G. H., Linsky, J. L., **One- and multicomponent odels of the upper photosphere based on molecular spectra. II: N(1,1) of the CN violet system,** *Solar Phys.* **35,** 259-276 974).

Key words: best-fit model; carbon abundance; molecular spectra; upper photosphere.

e have obtained center-to-limb photoelectric spectra of the 1,1) B-X bandhead region λ3868-3872 Å at Kitt Peak Na- al Observatory. From these spectra and a detailed analysis ne formation of the CN(1,1) spectrum we derive a best-fit er photospheric model differing from the HSRA which is sistent with our previous CN(0,0) λ3883 spectra. We derive lar carbon abundance of log $A_c=8.30\pm0.10$ compared to HSRA value of log $A_c=8.55\pm0.10$. In addition we specify regions of formation for the CN(0,0) λ3883.35 and CN(1,1) 71.38 bandheads at disc center and limb.

1. Decker, G. E., Stiehler, R. D., **Standardization of Mooney scometer and oscillating-disk cure meter,** *Amer. Soc. Test. ater. ASTM Spec. Tech. Publ.* **553,** pp. 19-30 (1974).

Key words: cure meter; Mooney viscometer; oscillating-disk cure meter; processability; rubber testing; standardization; vulcanization.

he Mooney viscometer has been the principal instrument d to control the processability of synthetic rubber production the past 30 years. The oscillating-disk cure meter is now oming the principal instrument for determining the vulcaniza- characteristics of standard compounds of raw rubbers and pounding materials and of factory compounds used for per products. Therefore, a large amount of effort has been ex- ded in their standardization. Nevertheless, both instruments ch have certain similarities are affected by the following fac- that still cause variability among instruments: 1. tempera- of the rubber in the die cavity; 2. friction between the oscil- g or rotating stem and the stationary lower die; 3. slippage at rubber-metal interfaces; 4. the pressure on the rubber during ; and 5. scale calibration. This paper summarizes past and ent studies on these factors and indicates from recent findings direction for further standardization.

easurements of the disk temperature in the oscillating-disk e meter were made. These measurements indicated that the rance between the oscillating or rotating stem and the lower is critical for temperature uniformity. Also, the present gn of the upper die in ASTM Measurement of Curing Characteristics with the Oscillating Disk Cure Meter (D 2084-71 T) substantially reduces the rate of heat transfer to the specimen. However, the design is reasonably effective for applying pressure on the specimen which reduces slippage at the rubber-metal interfaces. Other means of applying pressure may be used. Slippage also depends on the torque at the rubber-metal interfaces. In the Mooney viscometer, torque can be reduced by decreasing the speed of the rotor or by increasing the temperature. In the cure meter, torque is most effectively reduced by keeping the amplitude of oscillation as small as practical.

**14432.** Mavrodineanu, R., Lazar, J. W., **Standard Reference Materials: Standard quartz cuvettes for high-accuracy spectrophotometry,** *Clin. Chem.* **19,** No. 9, 1053-1057 (1973).

Key words: cuvette, spectrophotometry; lightpath; pathlength; quartz, cuvette; radiation pathlength.

Accurate knowledge of lightpath and parallelism of cuvettes used in spectrophotometry are indispensable parameters that must be determined when accurate transmittance measurements of liquid materials are considered. A description is given of the design and techniques developed at NBS for production of quartz cuvettes (SRM 932) having a nominal radiation pathlength of 10 mm ± 0.03 mm. For each cuvette, pathlength and parallelism are certified with an uncertainty of ± 0.0005 mm. The method and instrumentation used to determine these parameters are also described.

**14433.** Tiemann, E., Hoeft, J., Lovas, F. J., Johnson, D. R., **Spectroscopic studies of the $SO_2$ discharge system. I. The microwave spectrum and structure of $S_2O$,** *J. Chem. Phys.* **60,** No. 12, 5000-5004 (June 15, 1974).

Key words: centrifugal distortion; chemistry; disulfur monoxide; microwave spectra; structure; vibrational state.

The microwave spectrum of $S_2O$ has been reexamined in order to obtain reliable predictions of all rotational transitions up to $J=50$ in the frequency region 10-130 GHz and to determine the structure of the molecule. A centrifugal distortion analysis has been carried out on the ground state and lowest bending vibrational state of $^{32}S^{32}S^{16}O$. Centrifugal distortion corrected rotational constants have also been obtained for $^{34}S^{32}S^{16}O$ and $^{32}S^{34}S^{16}O$. These observations allowed the determination of the structure: $r_s(S-S)=1.88248(10)$ Å, $r(S-O)=1.4637(5)$ Å, $\angle SSO=118.26(7)°$.

**14434.** Lovas, F. J., Tiemann, E., Johnson, D. R., **Spectroscopic studies of the $SO_2$ discharge system. II. Microwave spectrum of the SO dimer,** *J. Chem. Phys.* **60,** No. 12, 5005-5010 (June 15, 1974).

Key words: centrifugal distortion; dipole moment; microwave spectrum; molecular structure; sulfur monoxide dimer; rotational spectrum.

Microwave spectra assignable to a dimer of SO have been detected in an electric discharge of $SO_2$. A centrifugal distortion analysis has been carried out on the spectra from the ground state and the lowest excited vibrational state of $^{16}O^{32}S^{32}S^{16}O$ and the ground vibrational state of $^{16}O^{32}S^{34}S^{16}O$. The molecule was found to have a planar *cis* configuration with the following geometry: $r(SO)=1.458(2)$ Å, $r_s(SS)=2.0245(6)$ Å, and $\angle SSO=112.7(5)°$. The observed dipole moment of OSSO is $\mu=3.17(10)$ D.

**14435.** Schwartz, R. B., Schrack, R. A., Heaton, H. T. II, **Total neutron cross sections of uranium-235, uranium-238, and plutonium-239 from 0.5 to 15 MeV,** *Nucl. Sci. Eng.* **54,** 322-326 (1974).

Key words: MeV neutrons; time-of-flight; total neutron cross sections; $^{239}$Pu; $^{235}$U; $^{238}$U.

The total neutron cross sections of $^{235}$U, $^{238}$U, and $^{239}$Pu were measured over the energy range 0.5 to 15 MeV, using the U.S. National Bureau of Standards electron linear accelerator as a pulsed neutron source. Neutron energies were measured by the time-of-flight method, with a resolution of 0.1 nsec/m. The measurement accuracy is estimated to be ± 1 percent. The cross-section curve is smooth, with no observable fine structure. The data are in excellent agreement with recent results from the Rensselaer Polytechnic Institute, and in satisfactory agreement with the ENDF/B-III data file, except at the high and low energy ends of our energy range.

**14436.** Fathers, D. J., Jakubovics, J. P., Joy, D. C., Newbury, D. E., Yakowitz, H., **A new method of observing magnetic domains by scanning electron microscopy. II. Experimental confirmation of the theory of image contrast,** *Phys. Status Solidi A*, No. 22, 609-619 (1974).

Key words: contrast measurement; image contrast; iron-silicon alloy; magnetic domains; nickel; scanning electron microscopy.

Experiments have been carried out to test the predictions of the theory of type II magnetic contrast, which is an effect enabling magnetic domains in materials including those with cubic anisotropy to be directly observed by scanning electron microscopy, previously presented in [1]. The experiments include measurements of the contrast as a function of the voltage and angle of incidence of the incident electron beam and of the angle of rotation of the specimen about its surface normal. The results are in good agreement with the theory and confirm beyond doubt that type II contrast arises from the alteration of incident electron trajectories within the solid by the internal magnetic induction. Domain images obtained by the use of type II contrast can be interpreted on the basis of this mechanism.

**14437.** Natrella, M. G., **Design and analysis of experiments,** Section 27 in *Quality Control Handbook, Third Edition,* J. M. Juran, F. M. Gryna, Jr., and R. S. Bingham, Jr., Eds., pp. 27-1 – 27-49 (McGraw Hill Book Co., New York, N.Y., 1974).

Key words: analysis of variance; block designs; design of experiments; factorial designs; interlaboratory tests; mixture designs.

This chapter provides an introduction to the design and analysis of experiments, including a classification of designs and a summary of important recent developments. Detailed designs and methods of analysis are given for factorial and fractional factorial designs, for completely randomized designs, and for the more common types of block designs (e.g., randomized blocks, balanced incomplete blocks, Latin Squares). Descriptions are given of some special-purpose designs, such as mixture designs, group screening designs and cross-over designs. Some simple techniques that are useful in planning and analyzing the results of interlaboratory tests are included.

**14438.** Marsden, C. P., **The formation and growth of Committee F-1,** *ASTM Stand. News* **1,** No. 4, 24-28 and 54 (Apr. 1973).

Key words: ASTM; history; semiconductors; vacuum tubes.

The organization of Committee F-1, an outgrowth of Committee B-4, was formalized on June 27, 1955. Since that time, the committee has tripled its membership and increased the number of documents under its jurisdiction by a factor of six to a total of 122 documents. While retaining the original number of ten subcommittees, it has reorganized these subcommittees away from the vacuum tube industry towards the semiconductor technology. It has assumed projects on lasers and memory cores and plans to assume other aspects of the electronic technology.

**14439.** Madey, T. E., **Chemisorption of $H_2$ on W(100): Absolute sticking probability, coverage, and electron stimulated desorption,** *Surface Sci.* **36,** 281-294 (1973).

Key words: deuterium; electron stimulated desorption; hydrogen; isotope effect; probability; tungsten.

Measurements of both the absolute sticking probability near normal incidence and the coverage of $H_2$ adsorbed on W(100) at ~ 300 K have been made using a precision gas dosing system; a known fraction of the molecules entering the vacuum chamber struck the sample crystal before reaching a mass spectrometer detector. The initial sticking probability $\mathscr{S}_0$ for $H_2$/W(100) is $0.51 \pm 0.03$; the hydrogen coverage extrapolated to $\mathscr{S}_0 = 0$ is 2.0 $\times 10^{15}$ atoms cm$^{-2}$. The initial sticking probability $\mathscr{S}_0$ for $D_2$/W(100) is $0.57 \pm 0.03$; the isotope effect for sticking probability is smaller than previously reported. Electron stimulated desorption (ESD) studies reveal that the low coverage $\beta$ hydrogen state on W(100) yields $H^+$ ions upon bombardment by 100 eV electrons; the ion desorption cross section is $\sim 1.8 \times$ $10^{-23}$ cm$^2$. The $H^+$ ion cross section at saturation hydrogen coverage when the $\beta_1$ state is fully populated is $\ll 10^{-25}$ cm$^2$. An isotope effect in electron stimulated desorption of $H^+$ and $D^+$ has been found. The $H^+$ ion yield is $\gtrsim 100 \times$ greater than the $D^+$ ion yield, in agreement with theory.

**14440.** Jacox, M. E., Milligan, D. E., Guillory, W. A., Smith, J J., **Matrix-isolation study of the vacuum-ultraviolet photolysis o $NF_3$. The electronic spectrum of the $NF_2$ free radical,** *J. Mo Spectrosc.* **52,** 322-327 (1974).

Key words: infrared spectrum; matrix isolation; NF; $NF_2$ $NF_3$; ultraviolet spectrum; vacuum ultraviolet photolysis.

The vacuum-ultraviolet of $NF_3$ in an argon or a carbon monox ide matrix at 14 K leads to the production of $NF_2$, identified b its infrared absorption. F-atom photodetachment also leads t the appearance of FCO in the carbon monoxide matrix studies The photodissociation of $NF_2$ by 2537 Å radiation has been con firmed. The appearance of a band system near 2600 Å with pos tion and band spacings close to those previously reported fo $NF_2$ in the gas phase demonstrates that the lower state of th gas-phase transition is the ground state of the molecule and con firms the assignment of the observed structure to a progressio in the upper-state bending vibration.

**14441.** Pruitt, J. S., **Electron beam current monitoring systen** *Nucl. Instrum. Methods* **92,** 285-297 (1971).

Key words: electron beam; errors; Faraday cup; ferrit linac; monitor.

A beam current monitoring system used with the NBS ele tron linac is described in detail. The system consists of a wate cooled Faraday cup designed to dissipate the energy in a 1 c diameter, 100 kW beam of 100 MeV electrons, and a non-inte cepting ferrite loaded toroidal coil. The ferrite is used for co tinuous-duty monitoring and can be calibrated in absolute uni with the Faraday cup. The Faraday cup errors have been me sured with an absolute accuracy of better than 0.1 percent b bucking the Faraday cup current against the beam current, usi the ferrite monitor as a null detector. The Faraday cup losses a about 0.5 percent at 30 MeV and decrease to less than 0.1 pe cent at 120 MeV. These losses are attributed to backscatter high energy electrons from the front face of the cup. In additio it is shown that secondary electrons produced by Møller scatte ing in the Faraday cup entrance foils may lead to spurious me surements of beam current, and a correction for this effect derived.

**14442.** Pruitt, J. S., **Correction to electron beam monitor pape** *Nucl. Instrum. Methods* **109,** 393-395 (1973).

Key words: beam; calibration electron; Faraday-cup; fe rite; monitor.

Two mistakes have been found in previously published papers out the electron beam monitor system of the NBS Linac. They validate the previously proposed explanation of the change in e measured Faraday cup error when vacuum foils are inoduced into the beam line. When these mistakes are corrected. is found that the generation of secondary electron by Møller atter in the vacuum foils accounts for only about one third of e observed change, rather than all of it, as originally claimed. dditional experiments at 50 MeV have shown that the obrved change is a non-linear function of foil thickness, and that e beam transmitted by the foils includes electrons with energes as small as 0.3 MeV. Electrons with this low an energy uld not have been generated by Møller scattering and must be e product of multiple processes in the foils.

443. Madey, T. E., **Adsorption of oxygen on W(100): Adsorption kinetics and electron stimulated desorption,** *Surface Sci.* **33,** 355-376 (1972).

Key words: adsorption; chemisorption; desorption; electron reflection; electron stimulated desorption; oxygen; single crystal W(100); surface; tungsten; work function.

The interaction of $O_2$ with a single crystal W(100) surface at ~ 00 K has been examined using a combination of techniques. A ecision gas dosing system was used to deposit $O_2$ onto the ystal; the absolute accuracy in the average flux $F$ (molecules $n^{-2}$ $s^1$) is ±6 percent. The initial sticking probability for $0_2$ on (100) is effectively unity; $\mathscr{S}_0 - 0.98 \pm 0.03$. The accuracy of is measurement arises from the fact that a known large fraction the $O_2$ molecules entering the experimental chamber strike the ystal before reaching the mass spectrometer detector. The ectron Stimulated Desorption (ESD) measurements of ablute $O^+$ ion yields and energy distributions as a function of oxgen exposure were made during bombardment by 100 eV elecons. A measurable ion yield is detectable at the earliest stages adsorption; a slight maximum in the ion yield of $\sim 5 \times 10^{-9}$ ns/electron occurs at about one half monolayer coverage. vidence of reconstruction of the substrate at this coverage follows from this and other work. At oxygen coverages $\gtrsim 4 \times 10^{14}$ olecules $cm^{-2}$, a high-ion yield ESD state appears ($\sim 10^{-6}$ $O^+$ ns/electron). An estimate of the angular distribution of ESDerated $O^-$ ions was made using a primitive two-segment colctor. The ion angular distribution is strongly peaked in the rection normal to the surface. The functional form of this disibution is not known, but if the distribution were of the form $s^n\theta$, the results are consistent with $n \gtrsim 14$. Implications of this servation for the possible identification of chemisorption sites e discussed. Work function changes and elastic electron reflecon characteristics have been measured for the oxygen-covered d clean W(100) surface.

444. Mopsik, F. I., **Dielectric constant and loss,** Chapter 3 in *Digest of Literature on Dielectrics* **32,** 76-99 (National Academy of Sciences, Washington, D.C. 1970).

Key words: dielectric constant; dielectric literature; dielectric loss; dielectric theory; digest of literature; ionic processes.

The coverage of this chapter is a direct continuation of last ar's chapter. The papers included are those abstracted during 968 by *Chemical Abstracts* and *Physics Abstracts* and are ose that are concerned with dielectric theory, either theoretical experimental. No attempt has been made to include papers at would adequately be covered by the preceding chapter.

445. Hebner, R. E., Jr., Cassidy, E. C., Zahn, M., Sojka, R., **Electric field distributions and space charge behavior in nitrobenzene under low frequency alternating voltage,** (Proc. 1973 Annual Conference on Electrical Insulation and Dielectric Phenomena, Varennes, Quebec, Canada, Oct. 29-31, 1973), Paper in *1973 Annual Conference on Electrical Insulation and Dielectric Phenomena*, pp. 112-119 (National Academy of Sciences, Washington, D.C., 1974).

Key words: dielectric liquids; electric field mapping; high voltage measurements; Kerr effect; nitrobenzene; space charge.

The measurement of electric field distributions in dielectric liquids during high voltage operation is of interest for applications ranging from high voltage measurements to the physics and chemistry of dielectric fluids to the prediction and control of electrical breakdown in high-voltage apparatus. For this reason, we have used the electro-optic Kerr effect to measure the spatial and temporal variations of electric fields in a nitrobenzene-filled parallel-plate capacitor. Results obtained during operation under low frequency alternating high voltages are emphasized because of the significance of studies in this frequency range for design and testing of high-voltage apparatus. The effects of voltage level and frequency on space charge density and distribution are investigated for voltage up to 20 kV rms and over a frequency range of 0-120 Hz.

The results obtained are compared both with pulses and direct voltage observations in the same system and with some recent discussions of the role of particulate charge carriers in the behavior of insulating liquids.

14446. Crandall, D. H., Kauppila, W. E., Phaneuf, R. A., Taylor, P. O., Dunn, G. H., **Absolute cross sections for electron-impact excitation of $N_2^+$,** *Phys. Rev. A* **9,** No. 6, 2545-2551 (June 1974).

Key words: crossed beams; cross sections; excitation of $N_2^+$; 1st negative band.

Crossed beams of $N_2^+$ and electrons were used to measure the absolute cross sections for the excitation, $N_2^+(X\ ^2\Sigma_g^+, \nu=0) + e \rightarrow N_2^+(B\ ^2\Sigma_u^+, \nu=0) + e$, over an electron energy range from below threshold (3.17 eV) to 91 eV. Absolute emissions of the 391.4-nm band were measured from impact of electrons on $N_2^+$ ions in various state mixtures. Corrections were made to the data to account for state mixtures and other effects to obtain the cross section for the above process. The cross section falls from its finite threshold value of $3.0 \times 10^{-16}$ to $0.30 \times 10^{-16}$ $cm^2$ at 91 eV. The present values are more than an order of magnitude smaller than either the 1968 values of Lee and Carleton or the 1973 values of Daschenko *et al.* At threshold the Gaunt-factor formula of Seaton predicts a value only 45 percent of that measured, but at the highest energy, the predictions of the Seaton formula have converged to within 20 percent of the present values of the cross section. Rate coefficients calculated from the present measurements are consistent with the recent rate-coefficient measurements of McLean *et al.* Total uncertainty at high confidence is about 18 percent, taken as a quadrature sum of random uncertainty (15% at 98% confidence level) with systematic uncertainties (about 8% at high confidence). The analysis leading to interpretation of the emission cross section in terms of an excitation cross section between specific states is subject to uncertainties which are not well defined, and are not included in the stated uncertainty.

14447. Morrissey, B. W., Stromberg, R. R., **The conformation of adsorbed blood proteins by infrared bound fraction measurements,** *J. Colloid Interface Sci.* **46,** No. 1, 152-164 (Jan. 1974).

Key words: blood proteins; infrared bound fraction; protein adsorption; protein conformation.

The likelihood that surface-induced blood coagulation results from specific protein-material interactions has led to a study of the conformation of adsorbed blood proteins. Infrared difference spectroscopy was used to determine the bound fraction, i.e., the fraction of carbonyl groups of an adsorbed molecule directly interacting with the surface, of serum albumin, prothrombin, and fibrinogen *in situ*. Measurements were carried out on individual proteins as a function of the amount adsorbed, time of absorption, pD, and ionic strength using a silica surface.

The results obtained for serum albumin and prothrombin indicate that the internal bonding of these globular proteins is sufficient to prevent changes in the structure while adsorbed, even at low surface population. The bound fraction of fibrinogen increases with increasing adsorbance, suggesting possible interfacial aggregation. The conformation of all three proteins was found to be independent of the time of adsorption, although major differences in the rates of adsorption were observed.

Studies of cross-linked and denatured serum albumin have provided information on the conformational changes concomitant with adsorption of the native protein. Qualitatively, such changes, if they occur, are small. This conclusion is supported by computer simulation studies of lysozyme adsorption. Studies of the effect of pD and ionic strength on the adsorbance and bound fraction of serum albumin show that caution must be exercised when identifying the plateau adsorbance of a protein isotherm with a close-packed monolayer.

**14448.** Marshall, R. D., **Surface pressure fluctuations near an axisymmetric stagnation point,** *Fluid Dyn. Trans.* **5**, Part II, 135-163 (1970).

Key words: disk; pressure fluctuations; turbulence.

Surface pressure fluctuations on a circular disk placed normal to a turbulent air stream have been investigated. Turbulence intensities of approximately 10 percent were produced by a coarse grid installed at the test-section entrance. The turbulent field in the neighborhood of the disk was homogeneous and nearly isotropic.

Experimental results indicate that existing linear theories which do not consider distortion of the flow fail to predict the nature of surface pressure fluctuations on a bluff body. Only for wavelengths which are large compared to the body do these theories yield satisfactory results. A strong attentuation of the high frequency components occurs as the flow stagnates. This is accompanied by a transfer of energy from short to long wavelengths. The opposite effect is observed as the flow attains a radial direction and approaches the edge of the disk. A neutral wavelength which undergoes little change in energy was observed. Integral scales of pressure fluctuations are much larger than the lateral integral scale of the free-stream turbulence.

Pressure-velocity correlations indicate the existance of two distinct regions, an inner region in which correlations and optimum delay times exhibit considerable change along the radius of the disk, and an outer region where there is little dependence on radial distance. Maximum values of the optimum correlations are found in the outer region. There is qualitative agreement between the experimental results and theoretical predictions which consider the effect of vortex stretching.

**14449.** Corliss, E. L. R., **Measurement of meter ballistics,** *J. Acoust. Soc. Amer.* **55**, No. 4, 889 (Apr. 1974).

Key words: impact sounds; meter ballistics; sound-level meters.

Measurements of transient phenomena such as impact sounds are influenced by the characteristics of the metering system used. This note describes a method for obtaining the undamped natural frequency and the relative damping of a meter. From this information and the measured electrical impedance of the meter circuit the ballistic behavior of the meter can be predicted.

**14450.** Newbury, D. E., Yakowitz, H., **Magnetic domain studies in iron-3 1/4 weight percent silicon transformer sheet using the scanning electron microscope,** (Proc. 18th AIP Conf. on Magnetism and Magnetic Materials, (19th Annual Conf.), Boston, Mass., Nov. 13-16, 1973), Paper in *Magnetism and Magneti Materials*, C. D. Graham, Jr., and J. J. Rhyne, Eds., pp. 1372-1376 (American Institute of Physics, New York, N.Y., 1974).

Key words: iron-silicon transformer alloy; magnetic contrast; magnetic domains; scanning electron microscope.

The form of the magnetic domain configuration of orientec transformer sheet plays an important role in determining th magnitude of power losses during use of the sheet. In the presen work, a recently developed technique for observation of magnetic domains in iron in the scanning electron microscope (SEM has been employed. The mechanism by which this magnetic contrast arises, and the electron-optical and signal processin requirements to obtain the contrast are described. The maximun value of the contrast is about 0.3 percent with an acceleratin potential of 30kV. Changes in the domain configuration due t residual strain gradients, inclusions, and applied magnetic field have been studied in the SEM using this contrast.

**14451.** Swartzendruber, L. J., Siegel, E., **The effect of cobalt o the formation of a non-magnetic surface developed in grindin carbon steel,** (Proc. 18th AIP Conf. on Magnetism and Magnetic Materials, (19th Annual Conf.), Boston, Mass., Nov. 13 16, 1973), Paper in *Magnetism and Magnetic Materials*, C. D Graham, Jr., and J. J. Rhyne, Eds., pp. 735-739 (American Institute of Physics, New York, N.Y., 1974).

Key words: cobalt; grinding; Mössbauer effect; scatterin steel; surfaces.

The effect of grinding on the metallurgical and magnetic structure of the surface of carbon steels containing cobalt has been investigated using $^{57}$Fe Mössbauer scattering. Difference between the surface and the bulk are revealed by comparin scattering spectra obtained by counting 14 keV gamma rays wit those obtained by counting conversion electrons. Light grindin produces a thin non-magnetic layer ($\lesssim 0.05\ \mu$m) of austenite (i.e $\gamma$ Fe) on the surface of a carbon steel. This layer is too thin to b observed by conventional techniques, including glancing angl x-ray diffraction and 14 keV $\gamma$-ray of 6 keV x-ray detecte Mössbauer scattering. A series of steels containing 3.6 a/o ca bon and from 0 to 12 a/o cobalt were given identical heat trea ments followed by identical grinding treatments. The cobalt found to have considerable influence on the composition of t surface layer.

**14452.** Seltzer, S. M., Berger, M. J., **Bremsstrahlung in the a mosphere at satellite altitudes,** *J. Atmos. Terr. Phys.* **36**, 128 1287 (1974).

Key words: atmosphere; auroral electrons; bremsstrahlun energy spectra; Monte Carlo calculation; satellite altitude

Transport calculations have been made to determine the emi sion of bremsstrahlung by electrons in the atmosphere and t penetration of this radiation to high altitudes where it can be d tected by satellite-borne instruments. The calculations we done assuming uniform wide-area precipitation into the a mosphere of an electron flux isotropic over the downward hen sphere. The intensity and energy spectrum of the bremsstrahlu have been obtained for the case of incident monoenergetic ele tron beams at energies between 20 keV and 2 MeV, for incide electron beams with exponential spectra with *e*-folding energi between 5 and 200 keV.

**14453.** Powell, C. J., **Attenuation lengths of low-energy electro in solids,** *Surface Sci.* **44**, 29-46 (1974).

Key words: attenuation lengths; Auger-electron spectrosc py; inelastic cross sections; inelastic electron scattering low energies; solids; x-ray photoelectron spectroscopy.

A compilation is presented of measured attenuation lengths low-energy electrons in solids in the energy range (40 to 20

V) normally employed in x-ray photoelectron and Auger-elec- on spectroscopy. The techniques used to obtain electron at- enuation lengths are summarized, and it is pointed out that the ccuracy of measurement needs both to be defined adequately nd to be improved for more meaningful intercomparisons of ata and theory. An approximate expression is derived to predict ttenuation lengths using either dielectric data (derived from op- cal or electron-energy-loss data) or average excitation energies stimated from electron binding energies for given materials at lectron energies greater than about 500 eV. Good agreement is ound between the predictions of this formula and some mea- ured attenuation lengths (e.g., for Al, C, Mo, W) but further ork is required to validate the formula and to extend it to lower lectron energies.

4454. Mopsik, F. I., **High pressure dielectric measurements and the theories for the dielectric constant of a liquid,** *Proc. Conf. Electrical Insulation and Dielectric Phenomena, Buck Hill Falls, Pa., Oct. 20-22, 1969,* pp. 64-68 (National Academy of Sciences, Washington, D.C., 1970).

> Key words: density; dielectric constant; dielectric theory; dipole moment; high pressure; liquids; polarizability.

The conventional approach to the examination of the validity f the theories for the dielectric constant of the liquid state is to se dielectric measurements over a range of temperature and erhaps, also refractive index measurements. However, density s one of the most important variables in these theories and the olecular parameters involved could be mildly density depen- ent. Therefore a more valid approach is to combine high pres- ure dilatometry with dielectric measurements so that tempera- ure and density dependencies of the dielectric constant can be eparated.

Results of measurements to 2 kbar over a moderate range of emperature for several liquids will be presented and examined n order to establish the validity of dielectric theory.

4455. Marshall, R. D., Hsi, G., **Techniques for measuring wind loads on full-scale buildings,** (Proc. U.S.-Japan Research Seminar on Wind Loads on Structures, Honolulu, Hawaii, Oct. 19-24, 1970), Paper in *Proc. of Seminar Wind Loads on Structures,* pp. 133-148 (University of Hawaii, Honolulu, Hawaii, 1970).

> Key words: buildings; full-scale tests; instrumentation; pressure fluctuations; statistical analysis; wind loads.

Wind pressure measurements are being made on a four-story uilding on the National Bureau of Standards campus at Gaither- sburg, Md. Field data will be used to develop new design criteria nd to improve wind tunnel modeling techniques. Simultaneous vind velocity measurements from six meteorological towers nake it possible to relate pressure distributions and fluctuations on the building to the undisturbed wind field.

4456. Isbell, H. S., Pigman, W., **Mutarotation of sugars in solution: Part II,** *Advan. Carbohyd. Chem.* **24,** 14-65 (1969).

> Key words: acid and base catalysts; catalysis of mutarotation; deuterium oxide mutarotation of; isotope effects in mutarotations; mechanism of mutarotation reaction; mutarotases; mutarotation of sugars; pseudo-acyclic intermediates in mutarotation; sugars, mutarotation of; thermodynamic data for mutarotations.

The publication is part of a comprehensive review describing nd interpreting the changes which occur with reducing sugars in queous solutions. It treats, in depth catalysis by acids and ases, isotope effects, equilibrium states, thermodynamic pro- erties, and reaction mechanisms. A new reaction mechanism is roposed in which the sugar ring is opened momentarily, forming a pseudo-acyclic intermediate, having a conformation resembling that of the parent sugar. This intermediate passes through characteristic transition states to the various tautomeric modifications of the sugar.

14457. Reader, J., **Position of the *sp*$^6$ configuration in the neutral halogens,** *J. Opt. Soc. Amer. Letters to Editor* **64,** No. 7, 1017-1018 (July 1974).

> Key words: bromine; chlorine; electronic configuration; halogen; iodine; spectra.

An extrapolation of the unperturbed position of the $4s4p^6\ {}^2S_{1/2}$ level in the Br I isoelectronic sequence shows that this level will most likely lie above the ionization limit in neutral Br. It is concluded that the $sp^6$ configuration cannot be identified in the neutral halogen atoms by isoelectronic extrapolation of observed level positions, thus calling into question the identification of this configuration in neutral chlorine, bromine, and iodine.

14458. Pyke, T. N., Jr., **Terminal requirements for interactive bibliographic retrieval,** *Proc. Forum on Interactive Bibliographic Retrieval, Oct. 4-5, 1971,* pp. 9-12 (U.S. Atomic Energy Commission, Technical Information Center, Oak Ridge, Tenn., 1973).

> Key words: bibliographic retrieval; computer terminals; remote computer systems.

General requirements placed on interactive terminals used for bibliographic retrieval are identified. These requirements include not only those for input/output and hard copy but also those resulting from constraints placed on the terminal by the attached communication line and computer system. The implications of these requirements on terminal design are then described, with emphasis on ideas for new, potentially useful terminal features.

14459. Evans, B. J., Swartzendruber, L. J., **Supertransferred hyperfine fields at $Sb^{5+}$ in insulating ferrites: Effects of local order and ion-specific properties,** (Proc. 18th AIP Conf. on Magnetism and Magnetic Materials, (19th Annual Conf.), Boston, Mass., Nov. 13-16, 1973), Paper in *Magnetism and Magnetic Materials,* C. D. Graham, Jr., and J. J. Rhyne, Eds., pp. 518-522 (American Institute of Physics, New York, N.Y., 1974).

> Key words: ferrites; hyperfine fields; Mössbauer; Sb; YIG.

The supertransferred hyperfine fields at $Sb^{5+}$ in $LiFe_5O_8$, $CoFe_2O_4$, and YIG have been determined using $^{121}Sb$ Mössbauer spectroscopy. In contrast to $CoFe_2O_4$, $NiFe_2O_4$, and YIG, the small, average hyperfine field of ~ 100 kOe at $Sb^{5+}$ in $LiFe_5O_8$ requires the existence of significant local order and indicates that the clustering of $Li^{1+}$ about $Sb^{5+}$ is approximately ten times as large as that expected for a random intrasite cation distribution, in agreement with the known strong influence of Sb substitution in destroying the Li:Fe ordering. The decrement in the hyperfine field at $Sb^{5+}$ due to an A-site $Co^{2+}$ is also found to be larger than that due to $Ni^{2+}$.

14460. Maki, A. G., Sams, R. L., **Infrared spectrum of $CS_2$: "Hot" bands associated with the 2185 $cm^{-1}$ band and evidence for the $CS_2$ laser assignment,** *J. Mol. Spectrosc.* **52,** 233-243 (1974).

> Key words: absorption spectra; carbon disulfide; energy levels; infrared; lasers; molecular spectra.

The $10^01 - 00^00$ band of $CS_2$ has been measured with a resolution of 0.030 $cm^{-1}$. The following "hot" bands associated with this transition were also measured and analyzed: $11^11 - 01^10$, $12^01 - 02^00$, $12^21 - 02^20$, $13^31 - 03^30$, $20^01 - 10^00$, $30^01 - 20^00$, $21^11 - 11^10$, and $22^01 - 12^00$. In addition, the $10^01 - 00^00$ bands of the isotopic species $^{13}C^{32}S_2$, $^{12}C^{32}S^{33}S$, and $^{12}C^{32}S^{34}S$ were measured in natural abundance. With the results of these measurements it is shown that the $0201 - 12^00$ transitions do indeed coincide with the $CS_2$ laser transitions, as do the $00^01 - 10^00$ transitions. New arguments are given favoring the latter assignment.

**14461.** King, D. A., Madey, T. E., Yates, J. T., Jr., **Interaction of oxygen with polycrystalline tungsten. I. Sticking probabilities and desorption spectra,** *J. Chem. Phys.* **55,** No. 7, 3236-3246 (Oct. 1, 1971).

Key words: adsorption; chemisorption; flash desorption; oxidation; oxygen; tungsten; tungsten oxides.

The interaction of oxygen with a polycrystalline W filament has been studied in the temperature range 300-1200 K and for exposures between $10^{-7}$ and 1 torr·sec. Both sticking probabilities and desorption spectra have been measured. After low exposures ($< 2 \times 10^{-6}$ torr·sec) the adsorbate is all desorbed as O atoms with first order kinetics. With higher exposures, oxygen is removed as oxides: WO, $WO_2$, $WO_3$, $W_2O_6$. The desorption spectra for each of these species are complex, and nine distinct and reproducible oxide states are identified. Saturation coverages in each of these states are independent of adsorption temperature in the range 300-1200 K. At a total coverage of $8.5 \times 10^{14}$ $O_2$ molecules $cm^{-2}$, $2.2 \times 10^{14}$ $O_2$ molecules $cm^{-2}$ are desorbed as oxides; after exposures $> 10^{-2}$ torr·sec at 300 K, the total uptake rises to $15 \times 10^{14}$ $O_2$ molecules $cm^{-2}$. At temperatures between 500 and 1000 K and exposures up to 1 torr·sec, a multilayer oxide film is formed of unlimited thickness. The desorption product from this oxide film is predominantly $WO_2$, which desorbs in the region of 1200 K. The kinetics of adsorption and desorption are evaluated and discussed.

**14462.** Rebbert, R. E., Lias, S. G., Ausloos, P., **Photolysis of alkyl iodides at 147.0 nm. The reaction $H + C_nH_{2n+1}I \rightarrow HI + C_nH_{2n+1}$,** *Int. J. Chem. Kinet.* V, 893-908 (1973).

Key words: alkylhalides; far ultraviolet photochemistry; free radicals; hydrogen atoms; photochemical dissociation; rate constants.

The 147 nm (8.4 eV) photolysis of gaseous $C_2H_5I$, n-$C_3H_7I$, and sec-$C_3H_7I$ was investigated in the presence of and absence of HI. The main overall processes are:

$$C_2H_5I + h\nu \rightarrow C_2H_4 + H + I \quad \Phi = 0.75$$

$$\text{n-}C_3H_7I + h\nu \rightarrow C_3H_6 + H + I \quad \Phi = 0.38$$

$$\rightarrow CH_3 + C_2H_4 + I \; \Phi = 0.47$$

$$\text{sec-}C_3H_7I + h\nu \rightarrow C_3H_6 + H + I \quad \Phi = 0.80$$

$$\rightarrow CH_3 + C_2H_4 + I \; \Phi = 0.07$$

These dissociative processes occur mainly as a result of initial cleavage of the weak C − I bond, followed by decomposition of the internally excited alkyl radicals. In all cases, approximately 5-10 percent of the alkyl radicals thus formed do not undergo dissociation at pressures around 3-7 torr. There is also evidence for the elimination of HI as well as C − C cleavage in the primary dissociation. The former is indicated by deuterium labeling experiments and the formation of cyclopropane ($\Phi = 0.04$) as a product in the photolysis of n-$C_3H_7I$. Because the processes listed above provide a constant source of H atoms whose quantum yield can be exactly determined, it was feasible to obtain accurate values for $k_a/k_b$:

$$H + C_nH_{2n+1}I \xrightarrow{a} C_nH_{2n+1} + HI$$

$$H + HI \xrightarrow{b} H_2 + I$$

For thermally equilibrated H atoms (300 K), $k_a/k_b$ is $0.44 \pm 0.04$, $0.57 \pm 0.06$, $0.95 \pm 0.1$, and $0.024 \pm 0.01$ for $C_2H_5I$, n-$C_3H_7I$, sec-$C_3H_7I$, and $C_2H_5Br$, respectively.

**14463.** Hellner, L., Sieck, L. W., **High-pressure photoionization mass spectrometry. Effect of internal energy and density on the ion-molecule reactions occurring in methyl, dimethyl, and trimethylamine,** *Int. J. Chem. Kinet.* **V,** 177-186 (1973).

Key words: amines; collisional stabilization; ionization energy effect; mass spectrometry; photoionization; rate constants.

The ion-molecule reactions of $CH_3NH_2^+$, $(CH_3)_2NH^+$, and $(CH_3)_3N^+$ with the respective amines have been investigated at thermal kinetic energies in a high-pressure photoionization mass spectrometer at several wavelengths (energies) in the vacuum ultraviolet. The absolute rate coefficient for proton transfer from $(CH_3)_3N^+$ to $(CH_3)_3N$ decreases from $8.2 \times 10^{-10}$ $cm^3$/molecule·sec at 147.0 nm (8.4 eV) to $4.9 \times 10^{-10}$ $cm^3$/molecule·sec at $106.7 - 104.8$ nm (11.7 eV). In dimethylamine, the rate coefficient decreases from $11.6 \times 10^{-10}$ $cm^3$/molecule·sec at 8.4 eV to $10.2 \times 10^{-10}$ $cm^3$/molecule·sec at 11.7 eV, while no significant effect of energy was detected in methylamine. The reactions of several fragment ions are also reported. Experiments were also carried out at pressures up to 0.5 torr in order to investigate the further solvation of $CH_3NH_2^+$, $(CH_3)_2NH_2^+$, and $(CH_3)_3NH^+$ It was found that the maximum proton solvation numbers in methyl-, dimethyl-, and trimethylamine are 4, 3, and 2, respectively, under these conditions.

**14464.** Sieck, L. W., Gorden, R., Jr., **Photoionization of $N_2O$ at 73.6 − 74.4 and 58.4 nm. Evidence for collision-induced dissociation at thermal kinetic energies,** *J. Chem. Phys.* **58,** No. 6, 2653-2654 (Mar. 15, 1973).

Key words: ion-molecule reaction; mass spectrometry; $N_2O$; rate constant; vapor phase.

The photoionization of $N_2O$ at 73.6-74.4 and 58.4 nm has been investigated in the NBS high pressure mass spectrometer up to approximately 0.1 torr. Evidence has been found for the collision-induced dissociation

$$N_2O^+ + M \rightarrow NO^+ + N + M$$

which occurs at thermal kinetic energies and involves excite levels with lifetimes $>> 10^{-5}$ s. Experiments with various additive gases have revealed that initial population of the $A^2\Sigma$ leve (certainty), and $B^2\pi$ and $C^2\Sigma$ (possibly) results in formation o the $N_2O^+$ states responsible for the dissociation. No evidenc was found for participation of vibrationally excited ground stat $X^2\pi$ states in this reaction.

**14465.** Sieck, L. W., Gorden, R., Jr., **Formation of association ion in the photoionization of alkyl halides,** *Int. J. Chem. Kinet.* 5 No. 3, 445-454 (May 1973).

Key words: alkyl halides; ion-molecule reactions; mas spectrometry; photoionization; radiolysis; rate constants.

The methyl and ethyl chlorides and bromides, as well a methyl iodide, were photoionized in the vacuum ultraviolet a 300 K in a mass spectrometer over the pressure range 0.5 to approximately 100 millitorr. Under these conditions, stabilize parent ion dimers are found in $CH_3Br$, $CH_3I$, and $C_2H_5Br$, bu not in the chlorides. Lower limits for the dissociative lifetimes the ion-molecule collision complexes were estimated and are a follows: $(CH_3Br)_2^+$, 1.6 μs; $(CH_3I)_2^+$, 1.9 μs; and $(C_2H_5Br)_2$ 5.4 μs. An increase in photon energy (internal energy content the reactant ion) decreases the dissociative lifetime of the coll sion complex in $CH_3I$.

**14466.** Little, J. L., **ASCII code applications to alphanumeric di play terminals,** *Proc. Society for Information Display Te minals, Gaithersburg, Md., Nov. 30-Dec. 1, 1971,* **14,** No. Second Quarter, 67-72 (1973).

Key words: alphanumeric displays; ASCII code; cathode-ray-tube displays; control functions; display terminals; interactive terminals; remote computer terminals; soft copy; text-editing displays; visual displays.

This paper reviews briefly the evolution of the American Stan-
rd Code for Information Interchange (ASCII) and its interna-
onal version (ISO R-646). It also reviews the evolutionary im-
ct of typewriters, teletypewriters and the ASCII code on con-
entions now employed in alphanumeric display terminals. It
ows a proposed keyboard layout, some approved graphic sub-
ts of ASCII, and some codes used in computers. Current
evelopments in the representation of extended versions of
SCII in 7 and 8 bits are given. Proposed standards for control
nctions for alphanumeric display terminals are also included,
ith a warning that their standardization is under the jurisdiction
the American National Standards Institute's Technical Com-
ittee X3L2 on Character Codes.

**4467.** Meyerson, M. R., **International voluntary standards,** *Food Technol.*, pp. 58 and 62 (Nov. 1972).

Key words: consumer standards; DoC-NBS voluntary product standards; international standardization; international trade; national standards.

Various aspects of the activities of the National Bureau of
tandards in national programs of voluntary consensus stan-
ards writing are discussed, and the operation of the DoC-NBS
oluntary Product Standards Program described. This is fol-
wed by observations and a discussion of the role of stan-
ardization in international trade.

**4468.** Rice, J. R., Thomson, R., **Ductile versus brittle behaviour of crystals,** *Phil. Mag.* **29,** No. 1, 73-97 (Jan. 1974).

Key words: dislocation nucleation; ductile vs. brittle; fracture; theoretical strength.

A necessary criterion for brittle fracture in crystals is
stablished in terms of the spontaneous emission of dislocations
om an atomically sharp cleavage crack. We have calculated the
ability of a sharp crack against emission of a blunting disloca-
on for a number of crystals and crystal types in two dimensions
nd the energy to form a stable loop of dislocation from the crack
p in three dimensions. We find that contrary to previous expec-
ations, an atomically sharp cleavage crack is stable in a wide
ange of crystal types, but that in the face centred cubic metals
vestigated, blunting reactions occur spontaneously. Of the
ody centred metals investigated, iron is an intermediate case
etween the brittle and ductile cases, and the ionic and covalent
rystals investigated are all stable against dislocation emission.
ualtitatively, we find that crystals whose dislocations have
ide cores, and small values of the parameter $\mu b/\gamma$ ($\mu b/\gamma \lesssim 7.5$
10) are ductile while crystals with narrow cores and large
alues of $\mu b/\gamma$ are brittle.

**4469.** Eyler, J. R., Ausloos, P., Lias, S. G., **A novel ion-molecule reaction involving cleavage of the carbonyl bond in ketones and aldehydes,** *J. Amer. Chem. Soc.* **96,** No. 11, 3673-3675 (May 29, 1974).

Key words: aldehyde-chlorocarbon ion; fluorocarbon ion; halocarbon ions; ion-cyclotron resonance; ion-molecule reaction; ketone; mass spectrometer.

The reactions of $CF_3^+$, $CCl_3^+$, and $C_2F_5^+$ with aldehydes and
etones have been investigated. Ninety-five percent or more of
he reactive encounters between $CF_3^+$ or $CCl_3^+$ and
$H_3COCH_3$, $CH_3CHO$, $C_2H_5COCH_3$, $C_2H_5COC_2H_5$, and *n*-
$_4H_9COCH_3$ result in a reaction in which an O atom and a $F^+$ or
$L^+$ are exchanged, in what is apparently a concerted
nechanism:

$$CX_3^+ + R'COR \rightarrow R'CXR^+ + CX_20$$

(where X is F or Cl, R and R′ are H, $CH_3$, $C_2H_5$, or $n$-$C_4H_9$ as appropriate). The product $R'CXR^+$ ions have a tendency to dissociate by losing HX; the stability of the $R'CXR^+$ ions vis-a-vis this dissociation is very sensitive to the exothermicity of the $CX_3^+$-$R'COR$ reaction, showing a greater tendency to dissociate for larger R′COR reactant molecules. Further, the rate constants of the reactions of $CCl_3^+$ are slower by 1-2 orders of magnitude ($10^{-11}$-$10^{-10}$ cm³/molecule-sec) than the rates of the corresponding reactions of $CF_3^+$ ($10^{-9}$ cm³/molecule-sec). The $C_2F_5$ ion undergoes a reaction analogous to I with these carbonyl compounds, but with ketones larger than acetone an important alternate reaction channel leads to the formation of $CF_3CO^+$ product ions.

**14470.** Spiegel, V., **Age of californium-252 fission neutrons to indium resonance energy in water,** *Nucl. Sci. Eng.* **54,** 28-34 (1974).

Key words: age; fission spectrum; neutron; neutron age; $^{252}$Cf.

The age of $^{252}$Cf fission neutrons to indium resonance energy (1.44 eV) was measured in water using a source encapsulated in a 7.6-mm-diam by 7.6-mm-high cylinder. The correction for the displacement of the moderator by the source was experimentally determined to be -0.13 cm² or about -0.5 percent in approximate agreement with calculation. The distribution of indium resonance energy neutrons close to the source was measured to be Gaussian. The age measured for this experiment was 28.69 ± 0.39 cm². An average energy for the $^{252}$Cf neutron spectrum of 2.21 ± 0.05 MeV is inferred from this age.

**14471.** Freeman, D. H., **The gels for liquid chromatography,** *J. Chromatogr. Sci. II*, 175-179 (Apr. 1973).

Key words: gel; ion exchange; liquid chromatography.

This paper attempts to unify an understanding of various chromatographic gels. First, all gels are reviewed for their common tendency to fractionate on the basis of steric exclusion. The chemical contribution to chromatographic affinity is superimposed. Descriptions of interactive effects and reactive ion exchange processes are referred to their major chemical equilibria. The use of this understanding for solving chemical separation problems is described.

**14472.** Freeman, D. H., Angeles, R. M., Enagonio, D. P., May, W., **Interactive gel networks. Chromatographic and analytical properties with a pyridine type functional group,** *Anal. Chem.* **45,** 768-774 (Apr. 1973).

Key words: chromatography (liquid); interactive gel; organic separations.

The gel is a copolymer of 2-methyl-5-vinyl pyridine with DVB cross-linking. The composition, infrared absorption, swelling, and gel permeation properties were measured. The pyridine moiety is basic, as indicated by its ability to complex ROH and RCOOH solutes. Chromatographic affinity is directly related to the strength of the solute:gel complex. Solvents mask the pyridine gel in the order EtOH > $CHCl_3$ > $CCl_4$. The resulting solute affinity varies oppositely with the strength of the solvent:gel complex. ROH affinity correlates systematically with the proton donor strength. Gel capacity is high and several applications are described.

**14473.** Roszman, L. J., Hooper, C. F., Jr., **Time-dependent plasma microfield distribution,** *Physica* **73,** 259-286 (1974).

Key words: cluster expansion; collective-coordinates; distribution; ion correlations; microfield; plasma; time-dependent microfield.

The theory of the distribution of the finite-interval time average of the time-dependent low-frequency microfield (ion produced) in a plasma containing ion-ion correlations is developed The plasma model contains ion-ion interactions in the appropriate statistical ensemble (statistical ion correlations), but does not contain ion interactions in its dynamics (free-streaming dynamics). The theory allows inclusion of statistical ion correlations to any order. A discussion of all approximations is included.

**14474.** Torchia, D. A., Piez, K. A., **Mobility of elastin chains as determined by $^{13}$C nuclear magnetic resonance,** *J. Mol. Biol. Letters to Editor* **76,** 419-424 (1973).

> Key words: carbon-13 relaxation times; collagen; configurational entropy; correlation times; elastic properties; elastin; ligamentum nuchae; rotational correlation times.

Relaxation times and integrated intensities of $^{13}$C have been obtained from nuclear magnetic resonance spectra of elastin in unstretched calf ligamentum nuchae and indicate that about 80 percent of the backbone carbonyl carbons have short rotational correlation times, $\tau_R \sim 40$ nanoseconds. $\tau_R$ is reduced by only a factor of two when the ligament is in contact with 2M-KCNS, a strong denaturant. By contrast, the highly ordered chains of collagen in insoluble calf achilles tendon give no spectrum until denatured in 2 M-KCNS, when $\tau_R$ decreases by many orders of magnitude. These results show that elastin is composed largely of highly mobile chains under physiological conditions, suggesting that configurational entropy has an important role in its elastic properties.

**14475.** Torchia, D. A., Lyerla, J. R., Jr., **Molecular mobility of polypeptides containing proline as determined by $^{13}$C magnetic resonance,** *Biopolymers* **13,** 97-114 (1974).

> Key words: biopolymers; carbon-13 magnetic resonance; polypeptides; relaxation times.

The molecular conformations and dynamics of poly(L-prolyl), poly(hydroxyl-L-prolyl), poly(L-prolyl-glycyl), poly(hydroxyl-L-prolyl), and poly(glycyl-glycyl-L-prolyl-glycyl), in aqueous solution, have been studied using $^{13}$C pulse Fourier transform nmr spectroscopy. From a measurement of the intensities of major and minor resonances in the spectra of the copolypeptides, it was determined that 15-20 percent of the glycyl-prolyl and glycyl-hydroxyprolyl peptide bonds are *cis.* Effective rotational correlation times ($\tau_{eff}$), obtained from measurements of spin-lattice relaxation times ($T_1$) of individual backbone and side-chain carbons, demonstrated that backbone reorientation is approximately isotropic for the five polypeptides and is characterized by correlation times of ca. 0.3-0.6 nanoseconds as a result of rapid segmental motion. In a given polypeptide glycyl and pyrrolidine residues were found to have the same backbone correlation times, but backbone carbon $\tau_{eff}$ values did decrease as the glycyl content of the peptides increased. A semi-quantitative analysis of $C^b$, $C^g$, and $C^d$ correlation times suggests that rapid ring motion in both prolyl and hydroxyprolyl involves primarily $C^g$ and $C^b$, with the prolyl ring being more mobile than the hydroxyprolyl ring.

**14476.** Thomson, R. M., **The fracture crack as an imperfection in a nearly perfect solid,** *Annu. Rev. Mater. Sci.* **3,** 31-51 (1973).

> Key words: brittle material; cleavage; deformation; fracture; hydrogen embrittlement; mechanical properties; stress corrosion; ultimate strength.

The field of fracture is reviewed from the standpoint of physical models which are used and appraisal is attempted of the major areas where new theoretical physical progress is required. Topics include fracture vs. ductility, Griffith criterion, nonlinear theories, atomic theories and effects of atmospheres.

**14477.** Simmons, J. H., **Miscibility gap in the system PbO-$B_2O_3$,** *J. Amer. Ceram. Soc.* **56,** No. 5, 284-285 (May 1973).

> Key words: glass; lead-borate; immiscibility temperatures

The immiscibility temperatures of lead-borate glasses are reported. The data indicate the existence of a $PbO \cdot 4B_2O_3$ structur in the melt. A fit of the data by a regular mixing equation leads t the calculation of miscibility gap and spinodal boundaries.

**14478.** Schaefer, A. R., Mohan, K., **A new gonioradiometer fo total flux measurements,** *J. Illum. Eng. Soc.* **3,** No. 4, 349-35 (July 1974).

> Key words: geometrically total luminous; gonioradiomete spectral radiant flux.

This paper describes the design, construction, and characterization of a new instrument for the measurement of geometr cally total flux. This is done by measuring the flux emanatin from a source in different directions and integrating it over an entire imaginary surface surrounding the source. A new approac is suggested for the realization of the scales of total luminous flu and geometrically total spectral flux. In this approach, thes scales would be derived from standards of irradiance and illuminance.

**14479.** Paffenbarger, G. C., Rupp, N. W., **Composite restorativ materials in dental practice: A review,** *Int. Dent. J.* **24,** No. 1, 1 11 (Mar. 1974).

> Key words: abrasion resistance; BIS-GMA; coefficient c thermal expansion; composite resin; compressive strength silane coupling agent; silicate filler.

This review of the literature concerning composite resin discusses the composition, physical properties, uses and th manipulation techniques for some current, 1973, commercia products. These restorative materials are based upon the BIS GMA resin reinforced with inorganic silicious fillers bonded t the resin matrix with a silane coupling agent. Their use is limite to the restoration of non-load bearing surfaces of the teeth.

**14480.** Simmons, J. H., Mills, S. A., Napolitano, A., **Interactio of microstrucure development with viscous flow processes i glass,** *J. Non-Cryst. Solids* **14,** 302-309 (Jan. 1974).

> Key words: microstructure; phase separation; viscosity.

Measurements in glasses undergoing phase separation showe a large increase of viscosity with heat-treatment time. A correlation of this effect with electron micrographs of the structure indicated that the change in viscosity was related to an increase i size of the microstructure. A theoretical analysis is presente which is based on a model relating point-to-point variations i molecular environments to viscous flow processes in glass.

**14481.** Siu, M. C. I., **Equations for thermal transpiration,** *J. Vac Sci. Technol.* **10,** No. 2, 368-372 (Mar.-Apr. 1973).

> Key words: anomalous Knudsen limit; de Brogli wavelength; diffuse scattering; distribution function; free molecular flow; irreversible thermodynamics; specula reflection.

A formalism for analytically obtaining an expression for th thermal transpiration pressure ratio $R$ is presented. An experimental parameter $\sigma$, which is associated with the type o molecule-solid surface collisions, is introduced. A completel diffuse scattering and a completely specular scattering from a solid surface correspond to $\sigma=0$ and $\sigma=1$, respectively. A known distribution function is used to derive a practical formul for $R$ in the case of long tubes and very low pressures. Quantitative results obtained from this formula indicate that deviation from completely diffuse scattering of molecules from solid surfaces give rise to an anomalous Knudsen limit.

**14482.** Sieck, L. W., Gorden, R., Jr., Ausloos, R., Lias, S. G. Field, F., **Ion-clustering of the cations in the high energy ir**

**radiation of nitrous oxide,** *Radiat. Res.* **56,** No. 3, 441-459 (Dec. 1973).

Key words: ion clustering; ion-molecule reactions; mass spectrometry; nitrous oxide; photoionization radiolysis.

The reactions of the positive ions in $N_2O$ have been studied ass spectrometrically at pressures up to approximately 2 torr id at temperatures in the vicinity of 300 K, that is, under condi- ons similar to those which prevail in a gas phase radiolysis ex- eriment.

The $N_2O^+$ parent ion associates with a $N_2O$ molecule to form $(N_2O)_2{}^+$ dimer, with a termolecular rate constant of $4.8 \pm 0.5 \times$ $)^{-28}$ cm$^6$/molecule$^2$-sec at 300 K. The ratio $(N_2O)_2{}^+/N_2O^+$ ows a sharp decrease with an increase in temperature. The $O^+$ fragment ion also associates with a $N_2O$ molecule to form e $NO^+ \cdot N_2O$ association ion. At pressures greater than 1 torr, is ion associates with a second molecule of $N_2O$ to form $O^+ \cdot (N_2O)_2$.

In order to investigate the effects of accumulated radiolytic oducts on the ionic mechanisms in $N_2O$, experiments were erformed in which small amounts (~ 0.1%) of $O_2$, NO, and $N_2$ ere added to $N_2O$. In the presence of 0.1 percent $O_2$, $O_2{}^+ \cdot N_2O$ formed. In the presence of 0.1 percent NO, $NO^+ \cdot N_2O$ and $_2O)_2NO^+$ were observed in much greater abundance than in ure $N_2O$, presumably from a reaction of $N_2O^+$ or $(N_2O)_2{}^+$ with O molecules. The $(NO)_2{}^+$ dimer ion was also observed in these periments. No reactions of the positive ions in $N_2O$ with $N_2$ ere observed.

The results obtained in earlier pulse radiolysis and conven- onal low dose rate radiolysis experiments are reevaluated in der to take into account the formation of association ions. If ne assumes that no dissociation occurs in the $N_2O$ species rmed by neutralization of $(N_2O)_n{}^+$ ions by $SF_6{}^-$, it can be own that observed pulse radiolysis results are consistent with e electron neutralization of $(N_2O)_n{}^+$ to give only one excited $_2O^*$ species which dissociates; an alternate assumption about e neutralization mechanism involving $SF_6{}^-$ leads to the conclu- on that, on the average, 1.8 $N_2O$ species dissociate for each $_2O)_n{}^+$ ion neutralized by an electron. In the low dose rate diolysis, accumulated products may be expected to modify the nic mechanism, so that radiolytic product yields will be depen- ent on dose.

**483.** Sieck, L. W., Gorden, R., Jr., Ausloos, P., **Effects of low concentrations of $O_2$ and CO on the ion-clustering reactions in the lower ionosphere of Mars,** *Planet. Space Sci. Research Notes* **21,** 2039-2041 (1973).

Key words: ion clusters; ion-molecule reactions; ionosphere; Martian atmosphere; mass spectrometry; photoionization.

It is demonstrated that under conditions which approximate ose of the Martian ionosphere traces of CO and $O_2$ can be ef- ctively incorporated in ion clusters via ion-molecule reaction hemes initiated by the $CO_2{}^+$ ion. For example, when 0.3 per- ent CO is added to $CO_2$, $(CO)_2{}^+$ and $[(CO)_2CO_2]^+$ appear as e major cations (584 Å radiation, 300 K). In mixtures contain- g $O_2$ in addition to CO, $(CO_2 \cdot O_2)^+$ and $[(CO_2)_2O_2]^+$ are impor- nt species. A recently proposed mechanism to account for the w abundance of CO and $O_2$ in the Martian atmosphere is scussed in the light of these observations.

**484.** Gadzuk, J. W., **Reply to comments on a theory of field-induced tunneling,** *Phys. Rev. B* **3,** No. 5, 1772-1773 (Mar. 1, 1971).

Key words: adsorption; field emission; surface physics; tunneling.

The implication of an observation by Glasser relevant to past eories of field emission are discussed.

**14485.** Kelley, R. D., Klein, R., **Cross disproportionation of alkyl radicals,** *J. Phys. Chem.* **78,** No. 16, 1586-1595 (1974).

Key words: alkyl radicals; cross disproportionation; steric effects.

The cross disproportionation of several alkyl radicals has been measured using a novel technique that eliminates most of the uncertainties characterizing previous gas-phase results. The radicals are prepared in the condensed phase at 90 K by the H atom addition to a mixture of two olefins. The concentrations are adjusted so that one of the two radicals produced is in great excess. The other radical, then, is involved only in cross and not in autodisproportionation. From the results of a number of measurements, it is shown that alkyl radical disproportionation is governed almost completely by steric factors whereby the hydrogen acceptor-donor characteristics of each radical of the cross-disproportionating pair are independent of the counter radical. The cross disproportionation of an alkyl radical containing a double bond shows that the double bond has an orienting effect on the approach to and reaction with a second radical.

**14486.** Swartzendruber, L. J., Bennett, L. H., **Retained austenite developed during surface grinding of a carbon steel,** *Scr. Met.* **6,** No. 8, 737-741 (1972).

Key words: electron conversion; Mössbauer; retained austenite; standard sample; steel.

Light surface grinding on a spheroidized Fe-C alloy of the eutectoid composition raises the surface layer to a temperature sufficient to dissolve the carbide particles. The rapid quenching provided by the sample substrate and the cutting fluid retains a surface layer of austenite approximately 0.01 $\mu$m thick. Mössbauer scattering experiments, using electron conversion, can detect the retained austenite.

**14487.** Swartzendruber, L. J., **Localized moments on Fe impurities in Nb-Mo alloys: Mössbauer effect absorber study,** *Int. J. Magn.* **2,** 129-138 (1972).

Key words: alloys; iron; magnetic moments; molybdenum; Mössbauer effect; niobium.

Mössbauer effect spectra for absorbers of Mo and $Mo_{0.8}Nb_{0.2}$ alloys containing $^{57}$Fe impurities have been obtained in an external field as a function of temperature. The spectra for the Mo-Fe alloys are in close agreement with the results of Kitchens *et al.* for ($^{57}$Co)Mo sources. The $Mo_{0.8}Nb_{0.2}$ spectra show the presence of two distinct moment values for the Fe impurities, one with a moment of 1.9 $\mu_B$ and one with a moment of zero (with experimental upper limit of 0.6 $\mu_B$). The two moment species are present in nearly equal proportions. This result gives direct support for a discontinuous moment formation model of the *type* proposed by Jaccarino and Walker. The saturation hyperfine field of 115 kG for Fe in Mo is apparently reduced to 90 kG for moment bearing Fe in $Mo_{0.8}Nb_{0.2}$. There appears to be no quenching of the Fe moment for Fe-Fe pairs such as that observed for Co-Co pairs in Mo-Nb alloys.

**14488.** Lesclaux, R., Searles, S., Sieck, L. W., Ausloos, P., **Modes and rates of reaction of cyclopentene and methylcyclopentene ions with their parent molecules,** *J. Chem. Phys.* **54,** No. 8, 3411-3418 (Apr. 15, 1971).

Key words: cyclopentene; ion-molecule reactions; mass spectrometry; methyl cyclopentene; photoionization; vacuum ultraviolet.

Cyclopentene and methylcyclopentene ions were generated by irradiating the respective parent compounds with 10.0-eV photons; cyclopentene was also irradiated with 11.6–11.8-eV photons. The ionic products of ion-molecule reactions were observed in the NBS high-pressure photoionization mass spectrometer, while the neutral products of these reactions were determined by chemical analysis of products formed in photolytic experiments in a closed system. The cyclopentene ion, which at 10.0 eV retains its cyclic structure, undergoes an $H_2$ transfer reaction ($c$-$C_5H_8^+ + c$-$C_6H_8 \rightarrow c$-$C_5H_{10} + c$-$C_5H_6^+$, $k = 3.3 \times 10^{-10}$ cm³/molecule·sec) and a condensation reaction ($c$-$C_5H_8^+ + c$-$C_5H_8 \rightarrow C_{10}H_{16}$, $k = 2.7 \times 10^{-10}$ cm³/molecule·sec) with the parent molecule. The same reactions are observed for ions formed at 11.6-11.8 eV, but at the higher energy, approximately 20 percent of the ions are observed to undergo ring opening to form 1,3-$C_5H_8^+$ ions; the latter ions undergo an $H_2$ transfer reaction with the cyclopentene molecule (1,3-$C_5H_8^+ + c$-$C_5H_8 \rightarrow$ 2-$C_5H_{10} + C_5H_6^+$, $k = 1 \times 10^{-10}$ cm³/molecule·sec). The three methylcylopentene ions also undergo $H_2$ transfer reactions with the corresponding parent molecules [$C_6H_{10}^+ + C_6H_{10} \rightarrow (CH_3)C_5H_9 + C_6H_8^+$, $k = 4.6$, 1.8, and $2.9 \times 10^{-10}$ cm³/molecule·sec for 1-, 3-, and 4-methylcylopentene, respectively]. Condensation reactions between these ions and their parent molecules are observed to only a minor extent, but a second major mode of reaction, namely H transfer, is observed ($C_6H_{10}^+ + C_6H_{10} \rightarrow C_6H_{11} + C_6H_9^+$, $k = 0.6$, 2.8, and $1.2 \times 10^{-10}$ cm³/molecule·sec for 1-, 3-, and 4-methylcyclopentene, respectively). Structural reasons for these rate variations are discussed.

14489. Burke, R. W., Diamondstone, B. I., Velapoldi, R. A., Menis, O., **Mechanisms of the Liebermann-Burchard and Zak color reactions for cholesterol,** *Clin. Chem.* **20,** No. 7, 794-801 (1974).

Key words: carbonium ion formation; cholestapolyenes; cholesterol; enylic cations; Liebermann-Burchard; oxidative reactions; reaction mechanisms; Zak.

Correlation of $SO_2$ and $Fe^{2+}$ measurements with new spectral data indicates that the Liebermann-Burchard (L-B) and Zak color reactions for cholesterol have similar oxidative mechanisms, each yielding, as oxidation products, a homologous series of conjugated cholestapolyenes. These studies further suggest that the colored species observed in these two systems are enylic carbonium ions formed by protonation of the parent polyenes. Thus, the red ($\lambda_{max}$, 563 nm) product typically measured in the Zak reaction is evidently a cholestatetraenylic cation, and the blue-green product in the L-B reaction ($\lambda_{max}$, near 620 nm) is evidently the pentaenylic cation. The effects of rate of carbonium ion formation and sulfuric acid concentration on sensitivity and color stability are discussed. A solvent extraction procedure is described for specifically converting cholesterol to 3,5-cholestadiene. Incorporating this step into the typical L-B method can increase the L-B sensitivity for cholesterol by several fold.

14490. Lias, S. G., Viscomi, A., Field, F. H., **Chemical ionization mass spectra. XXI. Reactions in $t$-$C_5H_{11}Cl$, $t$-$C_5H_{11}Br$, $t$-$C_5H_{11}OH$, and $t$-$C_5H_{11}SH$,** *J. Amer. Chem. Soc.* **96,** No. 2, 359-364 (Jan. 23, 1974).

Key words: alcohols; alkyl halides; chemical ionization; ion-molecule reactions; mass spectrometry; mercaptans.

Mixtures of isobutane with small amounts (0.01-1%) of added $t$-$C_5H_{11}Cl$, $t$-$C_5H_{11}Br$, $t$-$C_5H_{11}OH$, and $t$-$C_5H_{11}SH$ have been studied in a high-pressure mass spectrometer as a function of total pressure, temperature, and concentration of additive. It is seen that proton transfer occurs only to $t$-$C_5H_{11}SH$, and even in this case, proton transfer is a minor process. The major reaction observed with each of the four molecules is the formation of a condensation ion which dissociates rapidly to give ($C_9H_{19}^+ +$ HX) or ($C_5H_{11}^+ +$ neutral products) where X is Cl, Br, OH, or SH. The formation of $C_5H_{11}^+$ is favored under all conditions, but the formation of $C_9H_{19}^+$ becomes more important as the pressure is raised or the temperature is lowered. When $i$-$C_4D_{10}$ is substituted for $i$-$C_4H_{10}$, it is seen that in the mercaptan, where proton transfer may be slightly exothermic, the departing hydrogen s fide molecule carries away a D species from the reacting *te* butyl ion with a high probability; conversely, in $t$-$C_5H_{11}Br$, t departing hydrogen bromide molecule has a low probability containing a hydrogen species from the reacting *tert*-butyl io This result suggests that when proton transfer competes with t displacement reaction, the two reactions proceed through t same intermediate ion, a $C_9H_{20}X^+$ species, in which "interna proton transfer has occurred. The product $C_5H_{11}^+$ ion undergo an analogous displacement reaction with all of these molecul to form the following as products: ($C_{10}H_{21}^+ +$ HX) and ($C_6H_{13}^+$ neutral products). The $C_6H_{13}^+$ product ion also undergoes a d placement reaction with all of these molecules to form products ($C_{11}H_{23}^+ +$ HX).

14491. Sieck, L. W., Gorden, R., Jr., **Photoionization of sim hydrocarbons at 73.6-74.4 and 58.4 nm. Comparison wi Penning ionization,** *Chem. Phys. Lett.* **19,** No. 4, 509-512 (A 15, 1973).

Key words: energy transfer; hydrocarbons; ionic fragmen tion; mass spectra; photoionization; unimolecular reactio

Ionic fragmentation patterns have been determined for C $CD_4$, $C_2H_2$, $C_2H_6$, and $C_3H_8$ following photoabsorption at 73 74.4 (16.7-16.9 eV) and 58.4 nm (21.2 eV). These mass spec have been compared with previous spectra obtained via Penni ionization processes involving collisions of these same molecu with metastable Ne (16.6-16.7 eV) and He (19.8-20.6 eV). the basis of this comparison it is concluded that the molecu ions produced in Penning ionization have a higher internal en gy content than is produced by photoionization at the same en gy.

14492. Ausloos, P., Rebbert, R. E., Lias, S. G., **Prima processes in the photolysis of propane: The use of HI as a radi scavenger,** *J. Photochem.* **2,** 267-283 (1973-74).

Key words: equipartition of energy; hydrogen iodi methylene insertion reaction; propane; radical scavengi vacuum ultraviolet photolysis.

The photolysis of $C_3D_8$ has been investigated with 8.4, 1 and 11.6-11.8 eV photons, using HI to scavenge the radic through the reaction: $R_D + HI \rightarrow R_DH + I$ (where $R_D$ is a fu deuterated alkyl or alkenyl radical). Comparison of the resu with the results of analogous experiments using $H_2S$ as scavenger leads to the conclusion that HI is a more efficient ra cal scavenger than $H_2S$. The results are discussed with particu emphasis on determining whether the primary processes inclu direct C–C and C–H bond cleavage. An examination of the fects of HI concentration, conversion, and pressure on the yi of ethyl radicals intercepted indicates that the ethyl radicals formed in the primary process: $C_3D_8^* \rightarrow C_2D_5 + CD_3$. It is no that the relative importances of this process and the other prin ry processes involving breaking of the C–C bond ($C_3D_8^*$ $CD_4 + C_2D_4$ and $C_3D_8^* \rightarrow C_2D_6 + CD_2$) do not change w energy, and it is thus suggested that they all occur from an exci tion in the C–C bond, and that RRKM considerations relat to equipartition of energy are not applicable to the dissociati of electronically excited alkanes. It is pointed out that, as in photolysis of ethane, the dissociation leading to the formation a molecule of hydrogen (deuterium) ($C_3D_8^* \rightarrow D_2 + C_3$ which apparently occurs as a result of an excitation in a C– (C–D) bond, predominates in the 8.4 eV photolysis, diminishes sharply in importance with respect to the C–C b cleavage processes when the energy is increased. The insert of methylene into a primary C–H bond of $C_3H_8$ to give n-but is examined, and information concerning the internal energy the $CH_2$ species is derived and discussed in terms of the prim dissociation of propane.

14493. Sze, W. C., Kotter, F. R., **The design of near-perfect instrument transformers of simple and inexpensive construction,** *J. Appl. Meas.* **2,** No. 1, 22-27 (Jan.-Feb. 1974).

Key words: current ratio; leakage impedance; magnetizing impedance; ratio error; single-stage transformer; two-stage transformer; voltage ratio.

A brief discussion of the causes of ratio errors in single- and two-stage transformers is presented. The design and construction of two simple two-stage transformers, which can be used in either the voltage or current mode with an accuracy better than 10 ppm in ratios over the frequency band of 50 to 2000 Hz are described. Multiple ratios are obtained by series-parallel interconnections of windings.

14494. Simmons, J. H., Mills, S. A., Napolitano, A., **Viscous flow in glass during phase separation,** *J. Amer. Ceram. Soc.* **57,** No. 3, 109-117 (Mar. 1974).

Key words: glass; microstructure; phase separation; viscosity.

The isothermal viscosities of two borosilicate glasses, one a commercial glass widely used for chemical glassware, increase by 4 to 5 orders of magnitude with heat-treatment time near the annealing point. The glasses are basically sodium borosilicates but differ greatly in phase-separation characteristics. Electron micrographs were used to analyze the development of microstructure during the suspected phase separation. In both glasses, structure development is primarily responsible for the viscosity increase. An analysis of the data and a theoretical interpretation of the effect are presented.

14495. Saunders, J. B., **Reflection, transmission and phase shift of light at imbedded optical films,** *J. Opt. Soc. Amer.* **62,** No. 1, 6-9 (Jan. 1972).

Key words: interferometry; Kösters prism; optical films; phase shift; polarized light; reflection; thin films; transmission.

Reflectance and transmittance of polarized light at imbedded optical films are measured for films of different compositions and thicknesses. The reflectance/transmittance ratio of plane-polarized light from such films, whose reflectance equals the transmittance at normal incidence, can be varied from approximately 1/3 to 4 by rotating the plane of polarization. A method is described that permits measurement of differences of phase shift, between reflected and transmitted light, for optical films imbedded in dielectric media that are approximately homogeneous. Phase-shift differences were obtained for two different aluminum films. Whereas values approximately $\pi/2$ rad were expected, values of 106 and 74°, respectively, were found for light polarized parallel and perpendicular to the plane of incidence. The two interferograms, produced by light of these two polarizations, appear to be complementary. However, the two interferograms produced by either polarization and observed from opposite sides of the film are not complementary—thus indicating a variation of absorption of the film with optical-path difference.

4496. Schneider, S. J., McDaniel, C. L., **The BaO-Pt system in air,** *J. Amer. Ceram. Soc. Discussions and Notes* **52,** No. 9, 518-519 (Sept. 21, 1969).

Key words: BaO-Pt system; BaO-$PtO_2$ system; dissociation; phase equilibria.

The phase relations between BaO and Pt in air were studied by x-ray diffraction, differential thermal analysis, and quenching techniques. At lower temperatures the system can be represented by the BaO-$PtO_2$ pseudobinary. Prominent features of the system include a hexagonal 4BaO·$PtO_2$ compound, a phase of unknown composition and symmetry and a solid solution (orthorhombic) existing approximately between 33 and 50 mole % $PtO_2$ at 1025 °C. At higher temperatures all intermediate phases eventually dissociate to BaO and Pt. The dissociation temperature of $PtO_2$ in air was determined as 585 °C.

14497. Tiemann, E., **Isotope dependence of the rotational constant of sulfur monoxide in the $^3\Sigma$-ground state,** *J. Mol. Spectrosc.* **51,** 316-320 (1974).

Key words: Born-Oppenheimer approximation; isotopic effects; microwave spectra; molecular parameters; rotational transitions; sulfur monoxide.

The rotational spectra of $^{32}S^{16}O$, $^{34}S^{16}O$ and $^{32}S^{18}O$ were measured. The rotational constant $B_0$ was accurately determined for all three isotopes whereas the spin-spin coupling $\lambda_0$ and the spin-rotation coupling $\gamma_0$ have less accuracy due to the strong correlation of these constants for the observed transitions. The evaluated breakdown of the Born-Oppenheimer approximation can primarily be attributed to the nonadiabatic correction term found for $^1\Sigma$-diatomic molecules. The small adiabatic correction for SO is obtained with the opposite sign as usually derived in $^1\Sigma$-molecules.

14498. Weisman, H. M., **A survey on the use of National Standard Reference Data System publications,** *J. Chem. Doc.* **12,** No. 4, 211-216 (1972).

Key words: National Standard Reference Data System; properties data; survey; users.

The purpose of this mail survey to purchasers of National Standard Reference Data System publications was to assess what benefits the publications provided its users and to obtain feedback on user experience, requirements, and problems of use. Survey returns gave evidence that NSRDS publications were helpful to users in meeting their data requirements. Specific uses and benefits were identified. The greatest use of NSRDS publications was in connection with basic research. Because NSRDS compilations have utility in the applied areas as well, their usefulness needs to be promoted among applied workers and engineers.

14499. Clark, F. O., Johnson, D. R., **Magnetic fields in the Orion molecular cloud from the Zeeman effect in SO,** *Astrophys. J.* **191,** L87-L91 (July 15, 1974).

Key words: dense molecular clouds; magnetic field; Orion A; radio astronomy; sulfur monoxide; Zeeman effect.

Reported line widths of observed emission features from a variety of interstellar molecules are compared for the Orion A molecular cloud. All of the excess width observed for SO in Orion A is assumed to be due to Zeeman splitting of the energy levels in order to obtain an estimate of the upper limit for the ambient magnetic field in this source. From the available data, upper limit estimates yield a most probable value near 6 gauss for the magnetic field in the central feature of Orion A. This estimate can possibly be reduced by a factor of 2 or 3 if other effects such as kinematics are responsible for a portion of the observed widths. The implications of a field of this magnitude in a dense molecular cloud are discussed.

14500. Swing, R. E., **The optics of microdensitometry,** *Opt. Eng.* **12,** No. 6, 185-198 (Nov.-Dec. 1973).

Key words: linear optical systems; microdensitometry; optics; partial coherence.

A review of the current developments in microdensitometry is made, with emphasis on the investigations leading to the current level of understanding of optical performance. The classical microdensitometer is then analyzed according to the principles of the theory of partial coherence. Conditions for the insuring of linear operation are derived, and the idea of effective incoherence at the source aperture is presented with a discussion of the implications. The various microdensitometer configurations are subjected to analysis, and the four possible variations (viz., overfilling, underfilling, with two possible locations for the sampling aperture) are thoroughly evaluated. The new concept of linear microdensitometry is discussed and summarized briefly. The current concerns of microdensitometry are then presented and considered. The restrictions on maximum sample frequency as a result of the partial coherence in the illumination is a major concern of this paper, and tables are presented for typical microdensitometer configurations that delineate the kinds of limitations that can be expected.

**14501.** Freeman, D. H., **Interactive gel networks for organic chemical separations,** *Isr. J. Chem.* **10,** 889-891 (1972).

Key words: chromatography; interactive gel; separations.

A comparison is drawn between the fundamental logic of the origin of ion exchange affinity, and that of the newly discovered behavior of interactive gels. The basis for predicting interactive chromatographic affinity is examined.

**14502.** Winzer, G. E., **National Bureau of Standards mobile acoustical laboratory,** *Sound Vib.* **4,** No. 5, 12-15 (May 1970).

Key words: acoustical instrumentation; architectural acoustics; building research; field measurements; noise control; sound measurements; sound transmission.

A mobile laboratory has been designed for research and measurement of the acoustical performance of buildings and for the study of environmental noise. The measurement capabilities are of the quality usually associated only with fixed acoustical laboratories. Data may be collected, reduced and analyzed in the field, or stored on magnetic tape for future reduction.

**14503.** Vomhof, D. W., Thomas, J. H., **Determination of moisture in starch hydrolyzates by near-infrared and infrared spectrophotometry,** *Anal. Chem.* **42,** No. 11, 1230-1233 (Sept. 1970).

Key words: hydrolyzates; infrared; moisture; near-infrared; spectrophotometry; starch.

Evidence is presented that the near-infrared method, employing either DMF or $Me_2SO$ as the solvent, and the infrared method, with $Me_2SO$ as the solvent, are quite applicable to the determination of the moisture content of starch hydrolyzates. The near-infrared method is superior in terms of both accuracy and precision to both the present vacuum-oven method and the infrared method. These methods do not seem to be influenced by the method of manufacture, the saccharide distribution, or the ash content. They are sufficiently rapid that they could be used for quality control both by manufacturers and users of corn syrups and solid sugars.

**14504.** Cezairliyan, A., **Simultaneous measurements of heat capacity, electric resistivity, and hemispherical total emittance of an alloy of niobium, tantalum, and tungsten in the range 1500 to 2800 K,** *J. Chem. Thermodyn.* **6,** 735-742 (1974).

Key words: electrical resistivity; emittance; high-speed measurements; high temperature; refractory alloy; specific heat; thermodynamics.

Simultaneous measurements of the heat capacity, electric resistivity, and hemispherical total emittance of an alloy of niobium, tantalum, and tungsten (nominal composition: 80 mass percent Nb, 10 mass percent Ta, and 10 mass percent W) in the temperature range 1500 to 2800 K by a sub-second-duration transient technique are described. Estimated inaccuracies of measured properties are: 3 percent for heat capacity, 5 percent for hemispherical total emittance, and 0.5 percent for electric resistivity. Properties of the alloy are compared with the properties of the constituent elements. The measured heat capacities are approximately 2.6 percent (on the average) higher than th values computed according to Kopp's additivity law. Althoug this difference is within the combined estimated inaccuracies, is higher than the combined estimated imprecision of the me surements. Therefore, the alloy probably departs from Kopp law. The electric resistivities indicate a significant departu from Matthiessen's law. Like the major constituent niobium, th alloy showed a negative departure from linearity in the plot electric resistivity against temperature.

**14505.** Rossmassler, S. A., **Public/private cooperation in planni and developing reference data programs,** *J. Chem. Doc.* **13,** N 2, 65-68 (1973).

Key words: advisory services; consultation; cooperati programs, NSRDS; reference data.

The National Standard Reference Data System relies heavi on the advice of experts in special subject-areas of science a technology to plan and develop programs for compilation a evaluation of quantitative data. Advisory panels provide a mea of bringing together generators and evaluators of data to defi needs, recommend specific projects, determine priorities, a coordinate new activities with those already in process. Such a visory panels are the natural basis for the development cooperative programs, not only for data compilation and evalu tion, but also for improvement in the quality of original expe mental work, standardization of techniques, and agreement formats for the presentation of, e.g., spectroscopic data. Wh such panels are sponsored by the Federal Government, the pa membership includes people from universities, private industr professional societies, and consultant organizations. T cooperative nature of the undertakings fosters attention to us needs and public benefits.

**14506.** Griffin, R. J., Jr., **Pointing the finger at burn safety,** *I Res.* **16,** No. 6, 45 and 47 (June 1974).

Key words: burns; instrumentation; product safety; safe test.

Describes an instrument, developed by NBS, designed to te surfaces for burn hazards. Termed a "thermesthesiometer," t instrument is capable of duplicating the temperature that wo be experienced by human contact to heated surfaces.

**14507.** Zapas, L. J., **Nonlinear behavior of polyisobutylene so tions,** (Proc. Battelle Colloquium on Deformation and Fra ture of High Polymers, Kronberg, Germany, Sept. 11-1 1972), Paper in *Deformation and Fracture of High Polyme* H. H. Kausch, J. A. Hassell and R. I. Jaffee, Eds., pp. 381-3 (Plenum Press, New York, N.Y., 1974).

Key words: BKZ; nonlinear shear behavior; polyisob tylene.

Experiments on various histories of simple shear were c tained with a polyisobutylene solution. A possible inadequacy the BKZ theory is presented, together with a modified the whose predictions are in agreement with the experimental da

**14508.** Walls, F. L., Dunn, G. H., **Storing ions for collision s dies,** *Phys. Today* **27,** No. 8, 30-35 (Aug. 1974).

Key words: dissociative recombination; electron collisio ion trap.

Overcoming the limitations of plasma and colliding be techniques, the new ion storage methods have proved their eff tiveness in ion recombination studies.

**14509.** Mayer, I., Roth, R. S., Brown, W. E., **Rare earth s stituted fluoride-phosphate apatites,** *J. Solid State Chem.* 33-37 (1974).

Key words: crystal structure; $Ln_xM_{10-2x}Na_x(PO_4)_6F_2$; rare earth apatites.

Compositions with the general formula $n_xM_{10-2x}Na_x(PO_4)_6F_2$ (Ln = La, Pr, Nd, Sm, Eu, Dy, Er, Lu, nd *Y*; M = Ca, Sr, and Ba) have been prepared and studied by -ray diffraction methods. The hexagonal apatite like structure vas indicated by the powder patterns of all the compounds (with a compounds only when Ln = La through Sm). Single crystal recession data reveal that the crystal lattice of all the compositions in the Ca and Sr system have space group $P6_3/m$, the $n_2Ba_6Na_2(PO_4)_6F_2$ compounds crystallize in space group $P\bar{6}$ nd the $Ln_3Ba_4Na_3(PO_4)_6F_2$ compounds in the trigonal space roup *P*3. Order and disorder mechanisms of the substitution nd its dependence on size and polarization effects are iscussed.

4510. Ballard, D. B., **A low magnification-large sample holder for the SEM,** *Proc. 32d Annual Electron Microscope Society of America Meeting, St. Louis, Mo., Aug. 13-16, 1974*, pp. 446-447 (Aug. 1974).

Key words: large sample; low magnification; scanning electron microscope; stage.

A large specimen stage with low magnification capability was onstructed to fit the SEM. The specimen can be rotated for tereo pair photographs. All modes of signal processing and EM controls that are normally available can be used with this tage.

4511. Yates, J. T., Jr., King, D. A., **Chemisorption of carbon monoxide on tungsten: Correlation of reflection-absorption infrared spectra with CO binding state population,** *Surface Sci.* **30,** 601-616 (1972).

Key words: carbon monoxide; chemisorption; flash desorption; infrared spectroscopy; molecular vibration; tungsten.

The vibrational frequency of carbon monoxide chemisorbed n an atomically clean polycrystalline tungsten ribbon has been udied using reflectance-infrared spectroscopy and ultrahigh acuum techniques. The initial appearance of an infrared absorpon band at 2093 $cm^{-1}$ is unequivocally associated with the nset of adsorption of the weakly-bound $\alpha$-CO state, which ocrs at coverages where the more strongly-bound $\beta$-CO species e already extensively populated. As the $\alpha$-CO coverage is ineased to its maximum value, the infrared band shifts to 2117 $m^{-1}$. Partial thermal desorption of the $\alpha$-CO by pumping at 295 . for ~ 2000 sec causes the band to reversibly shift back to ~ 93 $cm^{-1}$. The band disappears rapidly and completely upon ermal desorption of CO at 403 K, confirming that the absorpon band observed in this region of the spectrum is due to $\alpha$-CO. he spectral frequency indicates that the $\alpha$-CO species on tungen are closely analogous to the linear CO moieties found in ansition metal carbonyls. The vibrational frequency observed in close agreement with low energy electron energy-loss measrements made for CO on W(100). A model is proposed for the ight strengthening of the carbon-oxygen bond in $\alpha$-CO as the O coverage increases. The model involves coverage-dependent ectronic back-donation from surface W atoms into $\Pi$-antibondg orbitals as originally proposed by Blyholder for adsorbed O, and by Jones for certain transition metal hexacarbonyls.

4512. Yolken, H. T., **Standard reference materials and meaningful x-ray measurements,** (Proc. Denver X-Ray Conference, Denver, Colo., Aug. 21-23, 1973), Paper in *Advances in X-Ray Analysis*, C. L. Grant, C. S. Barrett, J. B. Newkirk, and C. O. Ruud, Eds., **17,** 1-15 (1974).

Key words: standard reference materials; x-ray calibration; x-ray measurements.

A review of the procedures and efforts at the National Bureau Standards (NBS) to provide for meaningful measurements through the use of Standard Reference Materials (SRM's) is presented.

The examples of NBS standardization efforts for x-ray analysis range from basic metrology to applied environmental measurements. These examples include a determination of x-ray wavelength by a method which in part utilizes simultaneous x-ray and optical interferometry measurements of the atomic planes of near perfect silicon. In addition, Standard Reference Materials (SRM's) are being developed and applied to trace element analysis using x-ray fluorescence techniques. These efforts include development of SRM's for trace element analysis of air particulates. In another area, work is proceeding on the development of a silicon powder Standard Reference Material intended for x-ray diffractometer calibration. An effort to develop a suitable x-ray diffraction technique to determine the amount of quartz in mine dust is also underway. NBS efforts to provide SRM's for the calibration of electron microprobes and the validating of correction factor calculations are also described.

**14513.** Wright, J. R., **Performance criteria in building, Sci. Amer. 224,** No. 3, 16-25 (Mar. 1971).

Key words: agrément system; building code of New York State; building codes; human requirements; National Conference of States; performance approach; performance criteria; performance methodology;regulatory system.

The performance approach seeks the solution to building problems in terms of human requirement satisfaction, irrespective of the methods or materials employed. The approach has application both to the regulatory (building codes) system and to the full range of concerns in building, from research to design. The performance-oriented National Conference of States on Building Codes and Standards is expected to be instrumental in modernizing the regulatory system.

**14514.** Zief, M., Barnard, A. J., Jr., Rains, T. C., **Magnesium gluconate as a standard for the determination of serum magnesium,** *Clin. Chem.* **19,** No. 11, 1303-1304 (1973).

Key words: atomic absorption spectrometry; magnesium gluconate; serum magnesium; standard material.

Magnesium gluconate dihydrate has been prepared and tested as a source of material for a magnesium standard in atomic absorption spectrometry. This material meets the criteria for purity (99.9%), stability, weighing factor and flame characteristics and would serve as an ideal standard for serum magnesium. Magnesium gluconate dihydrate has a solubility of 16g/100 ml of water at 25 °C and can be acidified with a mineral acid to insure a long shelf life as a magnesium standard stock solution.

**14515.** Wu, Yung-Chi, **Young's mixture rule and its significance,** *J. Phys. Chem.* **74,** No. 21, 3781-3786 (1970).

Key words: electrolytes; excess thermodynamic properties of mixtures; mixture; ternary solutions; thermodynamics; Young's mixture rule.

Young's general mixing rule postulates that in the mixing of two binary solutions of the same ionic strength to produce a ternary solution an excess thermodynamic quantity of the ternary solution may be expressed accurately as the sum of the corresponding excess thermodynamic quantities of the pure binary solutions. Young's corollary to the general rule postulates further that deviations from the rule are a function both of the ionic strength and of the respective solute fractions of the mixture. In terms of Young's two postulates any mixing process at constant ionic strength may be treated as one of four special cases. Young's postulates may also be applied to ternary mixtures of different ionic strength in which the mixing ratio of the constituents is constant.

**14516.** Fraker, A. C., Ruff, A. W., Green, J. A. S., Bechtoldt, C. J., **Polarization measurements on titanium tube and sheet having preferred orientation textures,** *Corrosion* **30,** No. 6, 203-207 (June 1974).

Key words: corrosion; NaCl solution; passivation; sheet; sulfuric acid; titanium; tubing.

The influence of preferred orientation texture on the anodic polarization behavior of titanium tubing and sheet has been investigated. Potentiostatic polarization measurements were made on specimens in the annealed and deformed conditions during exposure to boiling NaCl solutions (pH = 1) and to 1N $H_2SO_4$ (pH = 0.3) solutions at 23 °C (73 °F). Results were correlated with single crystal data, and it was found basal (0001) orientation texture has a marked effect on the anodic polarization of titanium, especially in the active region where this texture gives lower current densities. Polarization curves and examples of the microstructures are shown and discussed.

**14517.** Wu, Yung-Chi, **Material properties criteria for thermal safety,** *J. Mater.* **7,** No. 4, 573-579 (1972).

Key words: heat conduction; thermal inertia; thermal injury; thermal safety; thermal tissue damage.

The purpose of this study is to establish the relationship between the thermal properties of materials and thermal injury to human tissue. The interdependency of temperature and time to the conditions required for thermal safety is based on the physiological process of thermal injury. By the application of Fourier's heat equation, the relationship between the permissible temperature and time of contact of a heated body and its thermal properties is determined.

**14518.** Alexandropoulos, N. G., Cohen, G. G., Kuriyama, M., **Evidence of optical transitions in x-ray inelastic scattering spectra: Li metal,** *Phys. Rev. Lett.* **33,** No. 12, 699-702 (Sept. 16, 1974).

Key words: Compton scattering; lithium; optical transitions; x-ray inelastic scattering; x-ray Raman scattering.

We report results of x-ray Compton-Raman scattering experiments. In addition to the expected Compton and Raman scattering, there is a prominent feature in the form of a peak near $E/E_F = 1$. The new peak can be explained qualitatively by considering the conduction band of lithium metal to be composed of hybridized orbital electrons, and it furnishes the first evidence of an *L*-x-ray Raman band.

**14519.** Orvini, E., Gills, T. E., LaFleur, P. D., **Method for determination of selenium, arsenic, zinc, cadmium, and mercury in environmental matrices by neutron activation analysis,** *Anal. Chem.* **46,** No. 9, 1294-1297 (Aug. 1974).

Key words: activation analysis; arsenic; cadmium; environment; mercury; pollution; radiochemical separations; selenium.

A procedure has been developed for the simultaneous determination of selenium, arsenic, zinc, cadmium, and mercury in different environmental matrices. The radiochemical separation method involves the combustion of the samples, followed by reduction with carbon monoxide and volatilization of the metals at high temperature. The method was initially tested with radiotracer experiments; then by analyzing some NBS Standard Reference Materials. The procedure has been used to determine the Se, As, Zn, Cd and Hg concentration of some new Standard Reference Materials being prepared by the National Bureau of Standards.

**14520.** Peterson, R. L., Day, G. W., Gruzensky, P. M., Phelan, R. J., Jr., **Analysis of response of pyroelectric optical detectors,** *J. Appl. Phys.* **45,** No. 8, 3296-3303 (Aug. 1974).

Key words: detectors; gold-blacks; optical radiation det tors; optics; polymers; pyroelectric detectors; pyroelectri ty; self-calibrated detectors.

Several configurations of pyroelectric optical-radiation det tors are mathematically modeled to determine their frequen response and current response to step-function heat inputs. cluded in the analysis are heat losses by conduction and rerad tion, effects of absorptive coatings, and an experimentally served nonuniformity of polarization through the thickness polymer pyroelectric films. Roll-off of the frequency response both low and high frequencies is carefully examined. Cu fitting to response data allows a quantitative determination of pyroelectric coefficient and the degree of nonuniformity of polarization. The thermal conductivities of gold blacks used absorbers are determined from the high-frequency data toget with independent measurements of the black thicknesses densities. The total emissivity of evaporated nickel films so times used as absorbers can be estimated from the low-freque data. The difference in response to optical and electrical heat puts is examined as a part of our effort in fabricating electric self-calibrating optical detectors.

**14521.** Pardoe, G. W. F., Larson, S. J., Gebbie, H. A., Strick S. J., Ingham, K. D., Johnson, D. G., **Far-infrared spectru *ortho*-xylene,** *J. Chem. Phys. Letters to Editor* **52,** 6426-6 (1970).

Key words: far infrared; *ortho*-xylene; torsional vibratio

Far infrared measurements have been made on *ortho*-xyl in the liquid and vapor phases. A band in the region of 180 c is plausibly assigned to a torsional vibration of methyl groups.

**14522.** Snyder, W. F., **Lord Kelvin on atoms as fundamental n ral standards (for base units),** *IEEE Trans. Instrum. Meas.* **22,** No. 1, 99, (Mar. 1973).

Key words: atomic frequency standards; fundamental st dards; Lord Kelvin; Maxwell; natural standa wavelength standards.

In the 1879 edition of *Elements of Natural Philosophy,* L Kelvin stated, at the suggestion of Maxwell, that atoms hydrogen and sodium could serve as natural standards of t (frequency) and length. This was a far-sighted view in term recent developments of atomic frequency standards and the of wavelengths of light as length standards.

**14523.** Young, R. D., **Surface microtopography,** *Phys. Today* No. 11, 42-49 (Nov. 1971).

Key words: microscope; microtopography; single-cry surface; surface; surface finish; surface profile.

The growing field of surface science would benefit siderably from measurements of surface microtopography d to the atomic level. A brief review is presented of several ins ments used to quantitatively characterize the sur microtopography of metallic surfaces. Techniques are discus for employing the transmission electron microscope, scanning electron microscope, the optical interfere microscope and an engineering profile measuring instrumen measure surfaces suitable for surface science experiments. In dition a new noncontacting instrument which is presently u development will be described. It is concluded that sev techniques are presently available for detecting single atom s on single-crystal surfaces.

**14524.** Boyle, D. R., Clague, F. R., Reeve, G. R., Wait, D. Kanda, M., **An automated precision noise figure measure system at 60 GHz,** *IEEE Trans. Instrum. Meas.* **IM-21, N** 543-549 (Nov. 1972).

Key words: analysis; automation; noise figure; *Y*-factor.

As part of a millimeter-wave development program at the Na-nal Bureau of Standards, a precision measurement method d system was devised to automatically measure the effective put noise temperature of 55-65-GHz receivers.

Salient features of the system include a bolometric *Y*-factor easurement, a working "hot" noise source consisting of a veguide argon gas tube mount developed at the National Bu-au of Standards, and a minicomputer system controller operat- in Basic. System design considerations and measurement un-rtainties are discussed.

**525.** Schafft, H. A., **Failure analysis of wire bonds,** *Proc. 11th Annual IEEE Reliability Physics Symp., Las Vegas, Nev., April 3-5, 1973, IEEE Catalog No. 73CHO 755-9PHY*, pp. 98-104 (1973).

Key words: electrical connection; failure analysis; intermetallic compounds; Kirkendall voids; microelectronics; reliability; semiconductor devices; wire bond.

Failure analysis of wire bonds has an important part to play in ermining the causes of microelectronic device failure and ys for making and using devices to achieve greater reliability. veral tests and procedures used in the failure analysis of wire nds are reviewed. Some of the inferences about possible uses of permanent or intermittent failure that can be drawn m such tests, particularly those involving inspection with an ical microscope and with a scanning electron microscope, are cussed. Some attention is paid to the effects on the reliability the wire bond of the growth of gold-aluminum intermetallic mpounds, of Kirkendall voids, and of the use of poor materi-, poor processes in making the wire bond, and poor control er the processes used. Also reviewed are some metallurgical tioning techniques and a variety of methods used in opening commonly used packages and in exposing wire bonds that are capsulated in epoxy, phenolic resin, or silicone materials.

**26.** Blair, W., Iverson, W. P., Brinckman, F. E., **Application f a gas chromatograph – atomic absorption detection system to survey of mercury transformations by Chesapeake Bay microorganisms,** *Chemosphere III*, No. 4, 167-174 (1974).

Key words: anaerobic bacteria; atomic absorption; Chesapeake Bay; dimethylmercury; estuary; faculative bacteria; gas chromatography; mercury; metabolites; methylmercury; sediments.

A flameless atomic absorption spectrophotometer coupled to apor phase chromatograph was developed which permits ciation of elemental mercury (Hg°) methylmercury $H_3HgCl$), and dimethylmercury in gaseous metabolites at en-onmental concentrations. Through use of this technique, a nber of mercury tolerant anaerobic and aerobic bacteria, iso-d from Chesapeake Bay sediments, were examined for their ity to produce these compounds in the presence of Hg as $Cl_2$ (1 ppm). Of the two faculative isolates examined in a $N_2$ osphere, one produced both methylmercury and Hg° and the er only Hg°. In the presence of air only one of these organ-s produced slight traces of Hg°. Of the five anaerobic iso-s, one produced Hg°, methylmercury, and dimethylmercury, produced only Hg°, and two evolved only very slight or no ectable traces of Hg°. These and previous results are con-ent with the view that biomethylation of Hg is a more likely cess under anoxic conditions.

**27.** Moldover, M. R., **Visual observation of the critical tem-erature and density: $CO_2$ and $C_2H_4$,** *J. Chem. Phys.* **61,** No. 5, 766-1778 (Sept. 1, 1974).

Key words: $C_2H_4$; carbon dioxide; $CO_2$; critical density; critical point; critical temperature; ethylene; temperature reference point.

The critical temperature ($T_c$) and density ($\rho_c$) of carbon dioxide ($CO_2$) and ethylene ($C_2H_4$) have been determined by a modern version of the classical technique of visual observation of the disappearance of the meniscus. We discuss in some detail what a "visual observation of the disappearance of the meniscus" is, a subject that is relevant to the possible use of critical temperatures as secondary temperature reference points. For $CO_2$ we find $T_c = 30.977 \pm 0.004$ °C and $\rho_c = 0.4678 \pm 0.0022$ g/cm³. For $C_2H_4$ we find $T_c = 9.194 \pm 0.004$ °C and $\rho_c = 0.2146 \pm 0.0006$ g/cm³. The errors quoted for $\rho_c$ are two standard deviations from a fit to an assumed symmetrical scaling equation of state. The errors quoted for $T_c$ are an "estimated" limit of error. A comparison of the values of $T_c$ which we have measured with recent *PVT* data yields new values for the critical pressures ($P_c$). We find that $P_c = 73.753$ bar (72.789 atm) for $CO_2$ and $P_c = 50.390$ bar (49.731 atm) for $C_2H_4$.

**14528.** Iverson, W. P., **Biological corrosion,** Chapter in *Advances in Corrosion Science and Technology*, M. G. Fontana and R. W. Staehle, Eds., **2,** 1-42 (Plenum Press, New York, N.Y., 1972).

Key words: algae; bacteria; biological corrosion; fungi; mechanisms; prevention; review.

A review article of biological corrosion. Includes a brief historical outline, a discussion of the organisms involved in, the mechanism of and methods for preventing biological corrosion. The organisms associated with biological corrosion include fungi, bacteria and algae. The bacteria involved in sulfur and iron transformations, the "sulfur" and "iron" bacteria are among the most important organisms involved in biological corrosion. The mechanisms reviewed include the formation of acids, sulfur and sulfur compounds, ammonia and other corrosive compounds by microorganisms, formation of differential oxygen and chemical concentration cells, cathodic depolarization, disruption of protective films and breakdown of corrosion inhibitors. The methods for control and prevention of biological corrosion discussed include proper selection of a suitable environment, modification of a corrosive environment, the use of microbial inhibitors, and the use of protective coatings and cathodic protection separately or jointly.

**14529.** Bagg, T. C., Editor, **A report of the micrographic Goodwill People-to-People tour through Europe, including the Soviet Union,** *J. Microgr.* **6,** No. 5, 219-229 (May-June 1973) and **6,** No. 6, 269-279 (July-Aug. 1973).

Key words: microfilm; libraries; microfiche; overseas.

During the fall of 1972 the National Microfilm Association organized and coordinated a delegation of 12 members and 8 of their wives on a visit to Europe and Soviet Union as part of the Goodwill People-to-People Program. The purpose of this trip was to give micrographic leaders in the U.S. an opportunity to meet their overseas counterparts. The major cities visited were, the Hague, Brussels, Paris, Prague, Moscow, Belgrade and London. This report consists of brief discussions by various delegates of the many professional groups visited.

**14530.** Schooley, J. F., **Superconductive transition in cadmium,** *J. Low Temp. Phys.* **12,** Nos. 5/6, 421-437 (1973).

Key words: cryogenics; pure cadmium; reproducibility; superconductivity; thermometric fixed point; transition temperature; transition widths.

Mutual inductance measurements of the superconductive transitions occurring in single-crystal and polycrystalline cadmium samples in magnetic fields of $0-10^{-4}T$ (0–1 G) are presented. The temperature at which the zero-field superconductive transition midpoints occur appears to be constant within ± 0.2 mK for transitions narrower than 2 mK, but $T_c$ increases for broader transitions. The transitions exhibited both narrowing and hysteresis, the latter perhaps due to supercooling, in fields of a few tenths of a gauss. $T_c$ has been measured as $0.515 \pm 0.002_5$ K on the $T_{62}$ temperature scale.

**14531.** Phelan, R. J., Peterson, R. L., Klein, G. P., Hamilton, C. A., Day, G. W., **Absolute, pyroelectric radiometers and two dimensional arrays,** *Proc. American Electro-Optical Systems Design Conference, New York, N.Y., Sept. 18-20, 1973,* pp. 117-123 (1973).

Key words: IR detectors; polyvinylfluoride; pyroelectrics; radiometers.

In pursuit of useful techniques for measurements of laser power and beam profiles, we have been developing some pyroelectric detector devices and systems. The power measurements are based on electrical substitution techniques and thus do not require standard optical sources. The beam profiles have been measured using two axis mirror scanners with a single detector, single axis scanners with linear arrays, and two dimensional arrays of pyroelectrics. We will briefly discuss the general calibration scheme to indicate why we are using pyroelectrics, give some of the properties of pyroelectrics, give some of the details of device construction, describe a few systems and give some experimental results.

**14532.** Finnegan, T. F., Wahlsten, S., **Microwave emission from coupled Josephson junctions,** (Proc. 13th Int. Conf. on Low Temperature Physics-LT 13, Boulder, Colo., Aug. 21-25, 1972), Paper in *Low Temperature Physics-LT 13,* K. D. Timmerhaus, W. J. O'Sullivan, and E. F. Hammel, Eds., **3,** 272-275 (Plenum Publishing Corp., New York, N.Y., 1974).

Key words: ac Josephson effect; frequency-pulling; tunnel-junction array.

Recently, much interest has developed in the possibility of using large arrays of Josephson junctions for various applications. To this end, the properties of the microwave radiation emitted by a pair of coupled Josephson tunnel junctions connected permanently in series but independently current biased have been investigated experimentally. The detected coherent radiation emitted by the individual junctions when biased on the self-resonant voltage steps was between $10^{-13}$ and $10^{-10}$ watts. When both junctions were biased to radiate at the same frequency, the radiation from the junctions combined coherently in one of two ways: (1) The total radiation was unusually large as would occur if the oscillations of the two junctions were in phase. When the bias point of one of the junctions was varied slightly, frequency-pulling and phase-locking effects were directly observed. (2) The total radiation was unusually small as would occur if the oscillations of the two junctions were out of phase (with a relative phase difference of $\pi$). The details of these results are discussed.

**14533.** Saunders, J. B., **A simple interferometric method for workshop testing of optics,** *Appl. Opt.* **9,** No. 7, 1623-1629 (July 1970).

Key words: interferometry; optical shop testing; shearing interferometer; testing of optics.

A simple step-by-step method is given for deriving the shapes of wavefronts from data obtained with a wavefront shearing interferometer. No mathematics, other than arithmetic, is used. The result is the accurate deviation of the wavefront from a reference sphere that coincides with it at three chosen reference points. The method is intended primarily for the use of opticians in optical workshops, but is also quite practical for the final testing of optics for performance rating. A method is given by which an optician can evaluate an optical surface by comparing the interferogram produced by it and a known prism interferometer, with a drawing of the desired interferogram. This procedure is analogous to using test plates for visual inspection of optical surfaces.

**14534.** Simiu, E., **Wind spectra and dynamic alongwind response,** *J. Struct. Div. Proc. Amer. Soc. Civil Eng.* **100,** No. ST9 1897-1910 (Sept. 1974).

Key words: acceleration; aerodynamics; building (codes) deflection; dynamic structural analysis; pressure; spectra structural engineering; tall buildings; turbulence; wind (meteorology).

Current methods for determining dynamic alongwind respons are based on the assumption that turbulence spectra are independent of height. The adequacy of this assumption is assessed in the light of recent theoretical and experimental results of boundary layer meteorology. Expressions for the alongwind response including deflections and accelerations, are proposed. It i shown that, in the case of tall, flexible, lightly damped structure (i.e., of structures for which the resonant response, as defined by Davenport and Vickery, is high), expressions of the spectrum which reflect its dependence upon height yield lower values o the alongwind fluctuating response than the expression currently used in building codes and standards, in which this dependence is ignored. Results of numerical calculations show that the value of the fluctuating deflections and of the gust factors obtained i the latter expression is used may be higher by as much as 50 an 25 percent, respectively, than those obtained if the variation o spectra with height is taken into account.

**14535.** Wright, R. N., Kramer, S., **Buildings in the 1972 Managu earthquake,** *Mil. Eng.* **65,** No. 428. 382-388 (Nov.-Dec. 1973

Key words: building; building codes; earthquakes; hazards natural disasters; structures.

Following the Managua, Nicaragua earthquake of Decembe 23, 1972, a team of engineers representing the U.S. Departmen of Commerce's National Bureau of Standards and the Nationa Academy of Engineering performed field investigations i Managua, Nicaragua, from December 26, 1972 to January 4 1973. The objectives were to assist the Nicaraguan governmen in surveying major buildings to determine whether each wa suitable for emergency use, repairable, or appropriate fo clearance. The team also viewed the patterns of successful pe formance and damage to identify needs for improvements i building practices for mitigation of earthquake hazards and opportunities for more detailed investigations which could provid information for future improvements in practices.

The Managua earthquake, estimated at Richter magnitud 6.25, was not a great earthquake, but the loss of life approache 10,000, approximately 75 percent of Managua's 450,000 occupants were rendered homeless, and property damages are est mated to approach $1 billion. In general, these damages canno be attributed to unusual intensities of ground shaking or severit of surface faulting. Most damages appeared to result from def ciencies in building practices; deficiencies which had been e hibited many times before in previous earthquakes, deficiencie which would be avoided by implementation of up-to-date prov sions for earthquake resistant design and construction. Ho ever, Managua did not employ a building code with seism design requirements appropriate to its earthquake risk, an furthermore, did not have a building regulatory system capab of effective implementation of its building code provisions.

The Managuan experience may serve as an incentive to improvement of building practices in many other areas which a subject to substantial earthquake risks and have not consistent accounted for these risks in their building codes and buildi regulatory system.

**14536.** Sakuma, E., Evenson, K. M., **Characteristics of tungste nickel point contact diodes used as laser harmonic-generat**

mixers, *IEEE J. Quantum Electron.* **QE-10,** No. 8, 599-603 Aug. 1974).

Key words: laser harmonic generator-mixer; tungsten-nickel point contact diodes.

Properties of tungsten-nickel point contact diodes, when used s harmonic-generator mixers, were measured. The measured roperties are those which will be useful to workers wishing to se these high-speed devices (faster than $10^{-14}$ s). Some of the roperties measured were: the decrease in signal with mixing rder; the detected signal as a function of laser frequency; and e power required to optimize the harmonic beat notes.

**537.** Rains, T. C., Menis, O., **Determination of submicrogram amounts of mercury in standard reference materials by flameless atomic absorption spectrometry,** *J. Ass. Offic. Anal. Chem.* **55,** No. 6, 1339-1344 (1972).

Key words: flameless atomic absorption; liver and coal; loss of mercury; mercury in orchard leaves; standard reference materials.

In a study of the flameless atomic absorption method for the etermination of nanogram amounts of mercury in organic aterials, the technique was improved to provide greater precion and accuracy. The loss of mercury during the digestion of rganic materials with nitric, sulfuric, and perchloric acids is revented by controlled heating and a packed refluxing column. he reduction and absorption system was simplified by using a eated absorption cell which alleviates the interference of olatile vapors. This method has been applied to the determinaon of mercury in NBS standard reference materials of orchard aves, liver, and coal, and the results were compared with esults obtained with two other analytical methods.

**538.** Merris, R. L., Pierce, S., **The Bell numbers and $r$-fold transitivity,** *J. Combinatorial Theory* **12,** No. 1, 155-157 (Jan. 1972).

Key words: Bell numbers; permutation group; $r$-fold transitivity; Stirling numbers.

Let $G$ be a permutation group of order $|G|$ acting on a set of elements. For $g \in G$, let $\theta(g)$ be the number of elements left ked by $g$. Then, for $1 \leq r \leq n$,

$$\sum_{g \in G} (\theta(g))^r > X_r |G|$$

th equality if and only if $G$ is $r$-fold transitive. Here, $X_r$ is the h Bell number.

**539.** Huie, R. E., Herron, J. T., **The rate constant for the reaction $O_3 + NO_2 \rightarrow O_2 + NO_3$ over the temperature range 259-362 K,** *Chem. Phys. Lett.* **27,** No. 3, 411-414 (Aug. 1, 1974).

Key words: air pollution; nitrogen dioxide; ozone; rate constant; stratosphere.

The rate constant for the reaction of ozone with nitrogen dioxe has been measured over the temperature range 259 to 362 K, ing a stopped-flow system coupled to a beam sampling mass ectrometer. A fit of the data to the Arrhenius equation gave: $k$ $9.44 \pm 2.46) \times 10^{10} \exp[(-2509 \pm 76)/T]$ cm$^3$ mol$^{-1}$ sec$^{-1}$.

**540.** Dickens, B., Schroeder, L. W., Brown, W. E., **Crystallographic studies of the role of Mg as a stabilizing impurity in $\beta$-$Ca_3(PO_4)_2$. I. The crystal structure of pure $\beta$-$Ca_3(PO_4)_2$,** *J. Solid State Chem.* **10,** 232-248 (1974).

Key words: beta tricalcium phosphates; cation vacancies; positional disorder; single crystal; x-ray diffraction.

$\beta$-$Ca_3(PO_4)_2$ crystallizes in the rhombohedral space group c with unit cell parameters $a = 10.439(1)$, $c = 37.375(6)$ Å exagonal setting) and cell contents of 21 $[Ca_3(PO_4)_2]$. The structure was refined to $R_w = 0.026$, $R = 0.030$ using 1143 x-ray intensities collected from a single crystal by counter methods. Corrections were made for absorption, secondary extinction, and anomalous dispersion.

The structure is related to that of $Ba_3(VO_4)_2$, but has lower symmetry because of the widely different ionic sizes of Ca and Ba. Seven $[Ca_3(PO_4)_2]$ units occupy a volume corresponding to eight $[Ba_3(PO_4)_2]$ units. The requirement of the $c$ glide in $\beta$-$Ca_3(PO_4)_2$ has been shown in the least squares refinements to be attained by disorder of one cation over two sites. This disorder has a far-reaching effect on the structure.

**14541.** Powell, C. J., **Internal x-ray photoemission in aluminum: Excitation of electrons from the valence band,** *Solid State Commun.* **10,** No. 12, 1161-1164 (1972).

Key words: aluminum; density of states; photoelectron energy distribution; x-ray photoemission.

Measurements are reported of Al valence-electron excitation by $K\alpha_{1,2}$ x-rays internally generated in evaporated specimens by electron bombardment. The x-ray photoelectron energy distribution is consistent with the u.v. distributions of Huen and Wooten. Weak structures are found in the energy distribution at positions corresponding to those in the calculated density of states.

**14542.** Merris, R., Pierce, S., **Monotonicity of positive semidefinite hermitian matrices,** *Proc. Amer. Math. Soc.* **31,** No. 2, 437-440 (Feb. 1972).

Key words: character; Kronecker power; symmetric group; tensor power.

Inequalities which compare elements of the convex cone of positive semidefinite hermitian matrices with products of roots of elements are proved. They yield inequalities for Schur functions (generalized matrix functions) which, when specialized to the determinant, give a result of R. Bellman and L. Mirsky.

**14543.** Meshkov, S., **How good are symmetry predictions?** (Proc. Int. Conf. on Symmetries and Quark Models, Wayne State University, Detroit, Mich., June 18-20, 1969), Paper in *Proceedings of the International Conference on Symmetries and Quark Models,* R. Chand, Ed., pp. 199-209 (Gordon and Breach, New York, N.Y., 1970).

Key words: exotic; mesons; reactions; structure; $SU(6)_W$; symmetry.

A summary discussion of the comparison of experiment and $SU(6)_W$ reaction predictions is presented.

**14544.** Yap, W., **Binding of ions to oligopeptides,** *Biophys. J.* **13,** 1160-1165 (1973).

Key words: ion binding; nearest-neighbor interaction; oligopeptide; titration curve.

A model for the binding of ions to oligopeptides, in which nearest neighbor interactions are considered is developed. Equations for the titration curves are derived. The apparent association constants are determined as a function of the degree of polymerization and of the interactions between nearest neighbors.

**14545.** Nyyssonen, D., **Partial coherence in imaging systems,** *Opt. Eng.* **13,** No. 4, 362-367 (July-Aug. 1974).

Key words: coherence measurement; microdensitometry; optical imaging; partial coherence.

An improved method of measuring spatial coherence is described and some sources of measurement errors are discussed. Partial coherence in the image plane of an optical system is discussed and results of coherence measurements are given that demonstrate the scaling of the coherence function for coherence intervals large compared to the diameter of the Airy disk and the limiting value for the coherence interval equal to the diameter of the Airy disk. The application of these results to microdensitometry is discussed and results of coherence measurements in the source plane of currently-used classical microdensitometers are given.

**14546.** Sawyer, D. E., **Prevalent error sources in transistor delay-time measurements,** (Proc. Annual Conf. on Nuclear and Space Radiation Effects, Seattle, Wash., July 24-27, 1972), *IEEE Trans. Nucl. Sci.* **NS-19,** No. 6, 121-124 (Dec. 1972).

Key words: delay time; measurement errors; radiation effects; transistors.

Measurements of bipolar transistor delay times are extensively employed to predict neutron vulnerability. Of the various possible delay times, phase delay is most commonly measured. Although this is the simplest delay measurement to implement, the measurement circuit may be quite susceptible to extraneous signal coupling at the measurement frequency and this can cause the accuracy to be severely degraded. A technique for minimizing this delay-time error has been developed. It employs simple, preferably nonreactive, but at least known, networks in place of the transistor. From the differences between the "delay times" measured on these known networks, the location and magnitude of the error sources in the circuit are found. This allows one to reduce greatly the effects of the error sources on all subsequent measurements.

To confirm the theory of the error-correcting technique, RC networks with known delay times were assembled on transistor headers. For a particular bridge configuration, the uncorrected delay times measured were quite frequency dependent, but this dependence was removed by adding a correction term to the delay times. The correction term is obtained from measurements on the nonreactive networks and does not at all depend on the measured RC network delay times.

The effects of error-sources are particularly severe when transistors with low or moderate $h_{fe}$ values are measured, as when measurements are made on transistors that have been degraded by subjecting them to neutron radiation. The delay time then observed may show significant frequency-dependence, but, as for the measurement described on the RC networks, this dependence is the signature of the measurement system rather than the transistor, and may be removed by adding an independently-obtained correction term. In the absence of this correction, erroneous conclusions may be reached as to the effects of the radiation on the devices under test.

**14547.** Powell, C. J., **Structure on the high-energy side of the $KL_{23}M$ Auger peak from solid aluminum: Internal photoemission,** *Appl. Phys. Lett.* **20,** No. 9, 335-337 (May 1, 1972).

Key words: aluminum; Auger-peak; secondary-electron energy distribution; x-ray photoemission.

Some weak structure on the high-energy side of the $L_{23}MM$ Auger peaks for Al and Si has been recently interpreted as being possibly due to the simultaneous decay of an inner-shell vacancy and a volume plasmon. It is shown here that similar structure due to multiple ionization is to be expected and that photoemission caused by internally generated x rays can be observed if the fluorescent yield is not too small. Relatively strong structure of the latter type has been observed in the secondary-electron energy distribution of evaporated Al on the high-energy side of the $KL_{23}M$ Auger peak.

**14548.** Kurylo, M. J., Braun, W., Kaldor, A., **A laser enhanced reaction technique for the measurement of V → T deactivation rates: Deactivation of vibrationally excited $O_3$,** *Chem. Phys. Lett.* **27,** No. 2, 249-253 (July 15, 1974).

Key words: apparatus and methods; deactivation; energy transfer; infrared laser; luminescence; ozone.

Rates of V → T transfer for vibrationally excited ozone ($O_3$† in the (100), (010) and (001) levels have been measured using laser enhanced chemiluminescent method for the deactivatin gases He, Ar, $H_2$, $N_2$, $O_2$, $H_2O$, $CO_2$, $SO_2$, $CH_4$, and $SF_6$. Th method takes advantage of an enhanced reaction rate betwee $O_3$† + NO producing electronically excited $NO_2$ and uses th $NO_2$ chemiluminescence as a tracer for the $O_3$† concentration Results obtained by this new method are compared with recen results obtained by an IR fluorescence method. Good agreement is obtained for all gases, except methane, and implication of these results on the mechanism for deactivation are describe

**14549.** Braun, W., Kurylo, M. J., Kaldor, A., Wayne, R. P. **Infrared laser enhanced reactions: Spectral distribution of th $NO_2$ chemiluminescence produced in the reaction of vibrationally excited $O_3$ with NO,** *J. Chem. Phys.* **61,** No. 2, 461-46 (July 15, 1974).

Key words: chemiluminescence reaction; emitting state; enhanced reaction; infrared laser; spectral distributio vibrationally excited.

Vibrationally excited ozone, produced by $CO_2$ laser radiatio was found to react significantly faster with NO than does the mal $O_3$. The emission spectrum of the laser enhanced chemiluminescence from this reaction was measured from 520 to 81 nm. The lowest lying $1^2B_2$ state was identified as the primar source of $NO^*_2$ emission in the NO + $O_3$ reaction. One quantu of vibrational excitation in the reactant $O_3$ was found to introduce one quantum of vibrational energy in the product NO ($1^2B_2$). The rate enhancement of the reaction channel producin $NO_2(1^2B_2)$ as a result of vibrational excitation of $O_3$ was 5.6 1.0. Thus, only about 50 percent of the available vibration energy is used to enhance this reaction.

**14550.** Eliason, L. K., Isler, M. A., Stenbakken, G. N., **Mercu switches for burglar alarm systems,** *NILECJ-STD-0303.00,* 1 pages (U.S. Department of Justice, Law Enforceme Assistance Administration, National Institute of Law E forcement and Criminal Justice, Washington, D.C., Ma 1974).

Key words: burglar alarm sensor; burglar alarm system; interior perimeter sensor; mercury; switch.

This standard establishes performance criteria for mercu switches intended for use in protective intrusion alarm circuits monitor the position of doors, windows, etc. These devices cau the initiation of an alarm signal to a police panel, central statio or local audible alarm device. Included are requirements and te methods for performance, electrical properties and materia The characteristics addressed are those which affect the reliabi ty of the device with emphasis on those performance chara teristics which affect its false alarm susceptibility. This standa does not provide performance criteria concerning the ability these devices to resist attempts to defeat them through physic or surreptitious attack.

**14551.** Richmond, J. C., **Test procedures for night vision devic** *LESP-RPT-0302.00,* 21 pages (U.S. Department of Justic Law Enforcement Assistance Administration, National I stitute of Law Enforcement and Criminal Justice, Washingto D.C., July 1974).

Key words: contrast transfer function; distortion; flare; lig equivalent background; light induced background; night sion devices; optical gain; test methods.

This report includes descriptions of the test procedures t will be used for testing image intensifier night vision devices the passive type, in a project sponsored by the Law Enforcem Standards Laboratory at NBS. These same procedur odified, if necessary, in the light of experience gained in testing number of the night vision devices, will be incorporated in a andard for such devices.

**552.** Treado, M. J., Taggart, H. E., Nelson, R. E., Workman, J. L., **Mobile antennas,** *NILECJ-STD-0205.00,* 9 pages (U.S. Department of Justice, Law Enforcement Assistance Administration, National Institute of Law Enforcement and Criminal Justice, Washington, D.C., May 1974).

Key words: antenna; communications; law enforcement; mobile; standard; transceiver.

This standard establishes minimum performance requirements d methods of test for mobile antennas mounted in vehicles nich are used by law enforcement agencies.

**553.** Dobbyn, R. C., Calvano, N. J., **Portable ballistic shields,** *NILECJ-STD-0103.00,* 7 pages (U.S. Department of Justice, Law Enforcement Assistance Administration, National Institute of Law Enforcement and Criminal Justice, Washington, D.C., May 1974).

Key words: armor; ballistic shields; standard.

The purpose of this document is to establish performance quirements and a method of test for the ballistic resistance of rtable ballistic shields intended to protect against small arms e.

**554.** Nicholson, W. L., **Some revised approaches to x-ray crystal structure analysis calculations,** (Proc. Conf. Critical Evaluation of Chemical and Physical Structural Information, Dartmouth, College, Hanover, N.H., (June 24-29, 1973), Paper in *Critical Evaluation of Chemical and Physical Structural Information,* D. R. Lide, Jr. and M. A. Paul, Eds., pp. 45-47 (National Academy of Sciences, Washington, D.C., 1974).

Key words: least squares; robust techniques; statistics.

This note is a progress report on a reanalysis of the Internaonal Union of Crystallography (IUCr) Single-Crystal Intensity easurement Project on d(+) – tartaric acid. X-ray structure facr data are currently being analyzed by classic least squares ocedures with complex pseudo-theoretical model components account for observed inadequacies of the classic model, a ear combination of Gaussian characteristic functions. The rpose of the present reanalysis is to illustrate that introduction terms for systematic error into the classic model and use of ting techniques not crucially dependent on the Gaussian error sumption may bring the results of supposedly discrepant colborative studies into agreement.

**555.** Malmberg, M. S., Kryder, S. J., Maryott, A. A., **Vapor phase dielectric relaxation spectra and dipole moments of paraldehyde and *cis*-1,3,5-trimethylcyclohexane,** *J. Chem. Phys. Letters to Editor* **61,** No. 6, 2476-2477 (Sept. 15, 1974).

Key words: *cis*-1,3,5-trimethylcyclohexane; dielectric; dipole moment, gas; microwave absorption; paraldehyde; relaxation.

Vapor phase dielectric relaxation spectra are obtained from easurements of microwave nonresonant absorption for parall hyde and *cis*-1,3,5-trimethylcyclohexane. Gas dipole moents are found to be 1.43 ± .02 D and 0.25 ± .01 D respective-

**556.** Howard, C. J., Evenson, K. M., **Laser magnetic resonance study of the gas phase reactions of OH with CO, NO, and $NO_2$,** *J. Chem. Phys.* **61,** No. 5, 1943-1952 (Sept. 1, 1974).

Key words: gas phase reactions of OH with CO, NO, and $NO_2$; laser magnetic resonance; rate constant.

A laser magnetic resonance spectrometer has been used in mbination with a discharge-flow system to measure the gas phase reaction rates of the OH radical with CO, NO, and $NO_2$ at 296 K and over a pressure range 0.4 – 5 torr. For the bimolecular reaction $OH + CO \rightarrow CO_2 + H$ we measure a rate constant, $k = 1.56 \times 10^{-13}$ cm³/molecule·sec. For the termolecular reactions $OH + NO + M \rightarrow HNO_2 + M$, $M = He$, $k = 4.0 \times 10^{-31}$ cm⁶/molecule² · sec; $M = Ar$, $k = 4.4 \times 10^{-31}$ cm⁶/molecule² · sec; $M = N_2$, $k = 7.8 \times 10^{-31}$ cm⁶/molecule² · sec. For the reaction $OH + NO_2 + N_2 \rightarrow HNO_3 + N_2$, $k = 2.9 \times 10^{-30}$ cm⁶/molecule² · sec. Laser magnetic resonance detection of radicals is shown to be extremely sensitive, linear, and versatile. A complete description of this technique is presented with a discussion of its potential in the study of the reactions of free radicals.

**14557.** Miller, E. F., Jr., Lindamood, G. E., **Structured programming: Top-down approach,** *Datamation* **19,** No. 12, 55-57 (Dec. 1973).

Key words: GOTO statements; hierarchical design; programming; structured programming; top-down design.

Structured programming is the topic of considerable current interest and discussion in computing circles. This informal, tutorial article explains the basic concepts of structured programming – GOTO-less programming, top-down design, and abstract resources – and traces their origins.

**14558.** Sullivan, D. B., Dziuba, R. F., **Low temperature direct current comparators,** *Rev. Sci. Instrum.* **45,** No. 4, 517-519 (Apr. 1974).

Key words: current comparator; current ratio; shielding; superconductivity; transformer.

This paper presents an improved version of the low temperature direct current comparator described originally by Harvey. The comparator described herein exhibits a resolution of 1.5 nA · turn and provides ratios which have uncertainties of less than 4 parts in $10^{10}$. An alternate approach to the shielding of the windings is discussed and a preliminary comparator based on this concept is shown to have equally good performance. The latter comparator is probably better suited to the attainment of large current ratios.

**14559.** Mies, F. H., **Ultraviolet fluorescent pumping of OH 18-centimeter radiation in comets,** *Astrophys. J.* **191,** L145-L148 (Aug. 1, 1974).

Key words: comet; fluorescence; OH; optical pumping; radiowave spectrum.

In the absence of collisions, optical pumping of cometary OH by solar ultraviolet radiation determines the relative population of OH molecules in the Λ-doubled levels of the $^2\Pi_{3/2}$ ground state. The distribution is extremely sensitive to the heliocentric radial velocity of the comet, and at appropriate velocities the level populations will be either inverted or anti-inverted. Thus the OH 18-cm spectrum of a comet, measured with respect to the 10 K galactic background at 1665 and 1667 MHz, may be observed either in *emission* or in *absorption* at different periods during the trajectory. Optical pumping also will produce an alignment of the magnetic sublevels along the axis of the incident solar radiation, and variable degrees of linear polarization are expected.

**14560.** Ely, J. F., Straty, G. C., **Dielectric constants and molar polarizabilities of saturated and compressed fluid nitrogen,** *J. Chem. Phys.* **61,** No. 4, 1480-1485 (Aug. 15, 1974).

Key words: Clausius-Mossotti function; dielectric constant; dielectric virial coefficients; molar polarizability; nitrogen; saturated liquid densities.

In this paper we present accurate, wide range measurements of the dielectric constant of saturated and compressed fluid nitrogen. Measurements were made from 65 to 125 K along the saturated liquid boundary and along selected liquid and gaseous isotherms ranging from 92 to 300 K at pressures to 34.5 MPa. Densities ranged from the dilute gas to nearly three times the critical density. Molar polarizabilities, thought to be accurate to better than 0.10 percent, were calculated by combining the dielectric constant measurements with densities obtained from least-squares analyses of experimental $pVT$ data. A correlation function based on selected experimental data is given for the saturated liquid densities. Dielectric virial coefficients, derived from the calculated molar polarizabilities, are also presented.

**14561.** Van Brunt, R. J., Lawrence, G. M., Kieffer, L. J., Slater, J. M., **Electron energy dependence of the kinetic energy and angular distributions of $O^+$ from dissociative ionization of $O_2$,** *J. Chem. Phys.* **61,** No. 5, 2032-2037 (Sept. 1, 1974).

Key words: dissociation; electron impact; ionization; oxygen.

The electron energy dependence of the kinetic energy and angular distributions of $O^+$ have been measured for the process of dissociative ionization of $O_2$. The kinetic energy distributions for energies above 0.5 eV are compared with other dissociative ionization measurements as well as results of dissociative photoionization and dissociative excitation by electrons leading to production of Rydberg excited neutral fragments. Angular distributions are interpreted in terms of symmetries of possible molecular ion states contributing to dissociation, and the results near threshold are compared with recent measurements of $O^-$ from dissociative ion pair formation in $O_2$. Information about the states of excitation of the dissociation fragments as a function of ion energy is obtained from appearance potential measurements. The results indicate that predissociation may be important and that dissociative ionization of $O_2$ is in general a complicated process involving many $O_2^+$ states.

**14562.** Madey, T. E., Yates, J. T., Jr., Erickson, N. E., **Use of x-ray photoelectron spectroscopy for studies of gases chemisorbed on metals,** *Electron. Fisc. Apl.* **17,** Nos. 1-2, 190-192 (1974).

Key words: carbon monoxide; chemical shifts; chemisorption; ESCA; nitric oxide; oxygen; photoelectron spectroscopy.

X-ray photoelectron spectroscopy (ESCA) has been used in a study of $O_2$, NO and CO adsorbed on polycrystalline tungsten. The adsorption and oxidation studies were carried out under ultrahigh vacuum conditions. Chemical shifts of several eV in the O(ls) spectra for each of these adsorbates were found to be correlated with different modes of bonding between adsorbate and substrate. In general, the core level binding energies associated with adsorbed species are smaller than the binding energies for the same atoms in small gaseous molecules.

**14563.** Jacox, M. E., Milligan, D. E., **Matrix-isolation study of the vibrational spectrum and structure of the $CO_3^-$ radical anion,** *J. Mol. Spectrosc.* **52,** 363-379 (1974).

Key words: charge transfer; $CO_2^-$; $CO_3^-$; $CO_3^{-2}$; infrared spectrum; K atom reactions; matrix isolation; molecular structure; $N_2O + CO_2^-$ reaction; $O^- + CO_2$ reaction; $O_2^- +$ CO reaction.

Charge-transfer interaction processes which occur upon codeposition at 14 K of an $AR:CO_2:N_2O$ or an $Ar:CO:O_2$ mixture with an atomic beam of potassium lead to the stabilization of $CO_3^-$ in the solid deposit. Infrared spectroscopic data require a $C_{2v}$ structure for this molecule. Although the deviation of the structure from the expected $D_{3h}$ symmetry may result in part from Jahn-Teller distortion, cation interactions have been found to play a significant role. Evidence is presented for the initial formation of $CO_3^-$ with trigonal symmetry. Upon mercury-arc irradiation of the deposit, absorptions due to $CO_3^{-2}$ grow in importance.

**14564.** Wright, J. R., **Building research in the National Bureau**
**Standards (U.S.A.): How it relates to other Federal agencies a**
**to industry,** *Proc. 2d South African Building Research Co*
*gress, Johannesburg, South Africa, May 5-8, 1969,* Paper N
S4/2, 1-23 (May 1969).

Key words: building research; building standards; measu
ment techniques; performance requirements.

The National Bureau of Standards (NBS) is the central me
surement laboratory for the USA, covering the entire spectr
of the physical sciences and many fields of engineering. N
serves as the focal point in the Federal Government for assuri
maximum application of the physical sciences and engineering
the advancement of technology in industry and commer
Building research constitutes a major activity and is carried
primarily in the Building Research Division of the Institute
Applied Technology, NBS. The Division conducts scientific a
technical investigations of the chemical, physical, and engine
ing properties of building materials, components and syste
and their interaction with the building occupants, as a basis
defining the performance requirements and the measurem
techniques required to better adapt the physical and functio
characteristics of buildings to user needs. The Division provi
laboratory and field support to: Federal agencies concerned w
building construction and technology; public and private
ganizations that draft, promulgate and distribute building st
dards and codes; and the building industry, primarily to stimul
industrial innovation in building systems. The building resea
program is sufficiently basic to maintain a resource capability
flexible enough to assist with the practical problems of
Federal agencies that construct buildings. The building indus
is supported in a major way through technical-committee act
ties (285 separate memberships), consultation, publication,
direct laboratory research (Industry Associates program). T
relationship of the NBS building research program to indus
and to other Federal agencies is presented, covering probl
selection, research programs and results, implementation of
put, and effectiveness feedback.

**14565.** Wall, L. A., Straus, S., Florin, R. E., Fetters, L.
**Pyrolysis of anionic and thermally prepared polystyre**
(Paper presented at American Chemical Society Meet
New York, N.Y., Aug. 28-31, 1972), *Polym. Prepr. Am*
*Chem. Soc. Div. Polym. Chem.* **13,** No. 2, 1044-1045 (A
1972).

Key words: anionic polystyrene; molecular weight distri
tions; polymers; polystyrene degradation; pyrolysis.

The changes in molecular weights and their distributions
ing pyrolysis have been examined for a series of polystyre
prepared by thermal and anionic procedures. The initial rate
weight loss for the thermal polymer showed a 0.25 power dep
dence on the reciprocal of the number average molecular wei
while the anionic polymer showed zero dependence. The in
mation obtained and previous results can be explained to a
large extent by a kinetic chain decomposition comprised of c
peting end and random initiation, depropagation, intra- and in
molecular transfer and termination by combination.

For thermal polystyrenes the ratio of rate constants for
dom to end initiation has a value of $3 \times 10^{-4}$ initially. The pre
treatment assumes this value is constant with conversion. O
other hand the anionic polymers initiate at random in the lim
zero time, after which end-initiation begins to occur, as
number of ends increases. The inter-molecular transfer cons
zip length and kinetic chain length are dependent on the st
state radical concentration and are functions of the mole
weight. Their values, at the molecular weights present whe
pyrolytic weight loss exceeds 5 percent, agree well with ea
estimates.

**566.** Zapas, L. J., **Non-linear behavior of concentrated polymer solutions,** (Paper presented at American Chemical Society Meeting, Atlantic City, N. J., Sept. 1974), *Polym. Prepr. Amer. Chem. Soc. Div. Polym. Chem.* **15,** No. 2, 131-136 (Sept. 1974).

Key words: BKZ theory; concentrated solutions; nonlinear behavior; polyisobutylene; polystyrene; superposition.

A phenomenological approach based on the elastic fluid eory of Bernstein, Kearsley and Zapas is discussed, with spect to the shear behavior of concentrated solutions. For cer- n systems a concentration superposition scheme can be found hich covers the linear and nonlinear region. This is true only hen the nonlinear stress relaxation modulus can be represented a product of a function of time and a function of strain.

**567.** Mount, G. H., Linsky, J. L., **One- and multi-component models of the upper photosphere based on molecular spectra. III: CH(O,O) λ3144 of the CH C-X system,** *Solar Phys.* **36,** No. 2, 287-298 (June 1974).

Key words: best-fit model; carbon abundance; molecular spectra; upper photosphere.

We have obtained accurate center-to-limb photoelectric spec- a of the CH(0,0) C-X bandhead region λ3143-3148 Å at Kitt ak National Observatory. From these spectra and a detailed alysis of the formation of the CH(0,0) spectrum we demon- ate that the best-fit upper photospheric model derived from r previous analyses of CN(0,0) and CN(1,1) spectra adequate- explains the CH C-X observations. In addition we derive a lar carbon abundance of log $A_c = 8.30 \pm 0.20$ compared to the SRA value of log $A_c = 8\ 55$. This confirms our previous CN alyses which demonstrated that if the HSRA nitrogen undance of log $A_N = 7.93 \pm 0.10$ is assumed, then log $A_c = 8.20$ 0.10. We also specify the regions of formation for the CH(0,0) 143.47 Å bandhead at disc center and limb.

**568.** Siddiqi, A. A., Chen, C. T., Meisels, G. G., Gorden, R., Jr., **On the ionization efficiencies of $C_4H_8$ isomers at 123.6 nm,** *J. Chem. Phys. Letters to Editor* **57,** No. 10, 4506-4507 (Nov. 15, 1972).

Key words: butene; ionization efficiency; isomers; krypton resonance line; quantum yield; ultraviolet.

The ionization efficiencies of the $C_4H_8$ isomers were deter- ned at the krypton resonance line at 123.6 nm using total ab- rption and attenuation techniques. Average ionization efficien- s (ionization quantum yields) obtained independently in both oratories are: isobutene, 0.206, 1-butene, 0.201, *cis*-2-butene, 201, *trans*-2-butene, 0.268, methylcyclopropane, 0.136, and clobutane, 0.0022.

**569.** Sebastian, K. J., Nelson, C. A., **$|\Delta I| = 1/2$ rule from the symmetric quark model,** *Phys. Rev. D* **8,** No. 9, 3144-3161 (Nov. 1, 1973).

Key words: color-quark model; current algebra and pcac; nonleptonic $\Omega^-$ decays; paraquark model; symmetric quark model; three-triplet quark model.

Two topics are treated in this paper: the explanation of the $I| = 1/2$ rule based on the symmetric quark model and the tests this explanation in $\Omega^-$ nonleptonic decays. From the "color- ark," the three-triplet, and the paraquark models, the $|\Delta I| =$ rule follows for the octet-hyperon, the $\Omega^-$, and the kaon weak nleptonic decays as a consequence of current algebra, pion AC (partially conserved axial-vector current), and dispersion ations. Gronau's successful numerical results for the octet- peron decay amplitudes also follow in these alternatives to the se-quark model. However, though the origin of both explana- ns is the Fierz reshuffling property of the $V \pm A$ interactions, explanations of the $|\Delta I| = 1/2$ rule are quite distinct, e.g., in the Bose-quark model this rule is *exact* whereas in the other versions it is only *approximate*, being violated by continuum contributions to the absorptive parts. Because $\langle 0|\mathscr{H}_w|K\rangle$ and $\langle \pi|\mathscr{H}_w|K\rangle$ vanish in the symmetric quark model, the usual current-algebra soft-pion argument for $|\Delta I| = 1/2$ rule and the $K^*$-pole-dominance assumption (as a Feynman diagram) for $K_1{}^0 \rightarrow 2\pi$ are *not* convincing. On the other hand, the ordinary Fermi-quark model supplemented with octet dominance can be excluded, as it predicts $D/F = 3$ in the SU(3) limit for the matrix element of the parity-conserving Hamiltonian for two baryons in the nucleon octet ($D/F \simeq -0.85$ from $P$-wave fits). The $\Lambda K^-$ decay mode of the $\Omega^-$ should be *predominantly* $P$ wave (parity-conserving), whereas the $\Xi\ \pi$ mode should have the $P$ wave strongly *suppressed* and comparable to the $D$ wave (parity-violating). This implies $\Gamma(\Omega^- \rightarrow \Xi\ \pi)/\Gamma(\Omega^- \rightarrow \Lambda K^-) << 1$. The estimated total $\Omega^-$ decay rate is consistent with the present experimental number.

**14570.** Brown, D. W., Lowry, R. E., Wall, L. A., **Glass and melting transitions of copolymers of tetrafluoroethylene with propylene and isobutylene,** *J. Polym. Sci. Part A-2* **12,** 1303-1318 (1974).

Key words: copolymer; fluoropolymer; glass temperature; isobutylene; melting temperature; polymer; propylene; tetrafluoroethylene.

Copolymers of tetrafluoroethylene and propylene were prepared that contained 30-65 mole-percent of the former. Reactivity ratios of tetrafluoroethylene- and propylene-ended radicals are 0.008 and 0.06, respectively, resulting in formation of highly alternating copolymers. The glass temperatures, $T_g$, were determined using a differential scanning calorimeter. Values ranged from 260 to 275 K. A plot of $T_g$ versus composition has a low maximum centered about the equimolar composition. Copolymers of tetrafluoroethylene and isobutylene were prepared that contained 30-56 mole-percent of the former. Reactivity ratios of tetrafluoroethylene- and isobutylene-ended radicals are 0.005 and 0.021, respectively. The glass temperatures of these copolymers range 257 to 313 K. A higher maximum at the equimolar composition is obtained when $T_g$ is plotted versus composition. Isobutylene-containing copolymers having 45-54 mole-percent tetrafluoroethylene are crystalline. Melting temperatures range from 416 to 476 K and have their maximum value at the equimolar composition. It is thought that long sequences of alternating units behave as a third entity in these copolymers, the other two being nonalternating units of the two monomers. Unless inhibited, ionic homopolymerization of isobutylene can be appreciable, sometimes resulting in the polymer having two $T_g$.

**14571.** Steiner, B., **Conference on photometry and colorimetry,** *Zlatni Piasatsi, 27-30 June 1973, Appl. Opt. Meeting Reports* **12,** No. 12, 2992-2993 (Dec. 1973).

Key words: colorimetry; photometry; review.

A personal view of the International Conference on Photometry and Colorimetry in Varna is given for inclusion in the meeting report column of Applied Optics.

**14572.** Wyckoff, J. M., Pruitt, J. S., Svensson, G., **Dose vs. angle and depth produced by 20 to 100 MeV electrons incident on thick targets,** (Proc. Int. Congress on Protection against Accelerator and Space Radiation, Cern, Geneva, Switzerland, Apr. 26-30, 1971), *Health Phys. CERN 71-16,* **2,** 773-797 (July 1, 1971).

Key words: electrons; MeV electrons; targets; thick targets.

When energetic electrons strike a thick target a number of processes lead to photons, electrons and neutrons leaving that target. The dose produced by this emerging radiation has been measured as a function of angle and depth in a polymethylmethacrylate phantom for incident 20 to 100 MeV electrons. While this is a special geometry, it is fairly typical and the general nature of the distribution may be of interest in planning of exposure and shielding against exposure. The measurement technique, involving the use of a large number of small thermoluminescent dosimeters, is shown to produce results that compare very favorably with recent calculations made for the particular 30 MeV electron target conditions.

**14573.** Ross, P. D., Goldberg, R. N., **A scanning microcalorimeter for thermally induced transitions in solution,** *Thermochimica Acta* **10,** 143-151 (1974).

Key words: biopolymer transitions; calorimetry; chemical instrumention; dipalmitoyl L-α-lecithin; microcalorimeter; thermochemistry.

A scanning microcalorimeter for the measurement of energies of transition in solution is described. The calorimeter utilizes semi-conductor thermoelectric modules and is of a very simple and inexpensive construction. The imprecision of measurement is three percent when measuring 25 to 250 mJ of heat associated with transitions over temperature intervals of up to 8 K. The calorimeter operates from ambient to 90 °C.

**14574.** Waterstrat, R. M., Dickens, B., **Atomic ordering in a 15-type phases in the vanadium-nickel and vanadium-cobalt systems,** *J. Appl. Phys.* **45,** No. 9, 3726-3728 (Sept. 1974).

Key words: A 15 phases; atomic ordering; magnetic structure; neutron diffraction; superconductivity; vanadium alloys.

Atomic ordering in the V-Ni and V-Co A 15-type phases has been studied using neutron diffraction. The V-Ni Structure is shown to be ordered to the maximum extent permitted by the "off stoichiometric" composition, $V_{77.5}Ni_{22.5}$. The V-Co structure possessing the "ideal" composition $V_{75.0}Co_{25.0}$ is also highly ordered. However, the V-Co diffraction data are less accurate due to neutron absorption by the cobalt atoms and interference from the sample holder. No magnetic structures were detected in the V-Co phase at 4.2 K.

**14575.** Leep, D., Gallagher, A., **Electron excitation of the lithium 6708-Å resonance line,** *Phys. Rev. A* **10,** No. 4, 1082-1090 (Oct. 1974).

Key words: electron excitation; lithium.

We have measured the relative optical excitation function and the polarization of the 6708-Å line, using crossed beams of electrons and lithium-6, for electron energies from threshold to 1400 eV. The electron energy resolution was ~ 0.25 eV, and the lithium-beam optical depth was small and varied. We have normalized our excitation function to Born theory at 1404 eV, where the energy dependence has converged to the theoretical behavior. Between 2 and 6 eV, the measured cross section is (10-45)percent smaller than the results of the most recent close-coupling calculations, but the measured polarization *P* agrees with these theories within 20 percent of *P*. The theoretical polarization at threshold is not observed with our energy resolution.

**14576.** Wiederhorn, S. M., Evans, A. G., Fuller, E. R., Johnson, H., **Application of fracture mechanics to space-shuttle windows,** *J. Amer. Ceram. Soc.* **57,** No. 7, 319-323 (July 1974).

Key words: fracture; glass; proof testing; static fatigue; stress corrosion.

The fracture properties of an ultralow-expansion glass intended for use in windows for the Space Shuttle were characterized by strength and fracture-mechanics techniques to provide reliable design data. Proof-test diagrams for predicting minimum times-to-failure under specified service loads were developed from measurements of subcritical crack growth in water and a
Failure predictions were confirmed from strength measuremer
in water. In vacuum ($< 10^{-4}$ torr), the fracture behavior w
similar to that of other high-$SiO_2$ glasses, as evidenced by t
absence of subcritical crack growth and by insensitivity of t
critical stress intensity factor to temperature.

**14577.** Evans, A. G., Linzer, M., Russell, L. R., **Acoustic em
sion and crack propagation in polycrystalline alumina,** *Mat
Sci. Eng.* **15,** 253-261 (1974).

Key words: acoustic emission; alumina; crack propagatio
failure prediction; microcracking.

Acoustic emission is measured during the fracture
polycrystalline alumina. It is shown that acoustic emission is o
tained during macrocrack growth, which can be used for failu
indication. Acoustic emission is also obtained owing to the fo
mation of non-propagating grain size microcracks at the surfac
This emission can mask that due to macrocrack growth, but or
for short failure times or at high stresses. Models are present
which relate the acoustic emission to the various crack propag
tion processes.

**14578.** Evans, A. G., Wiederhorn, S. M., **Proof testing of ceran
materials—an analytical basis for failure prediction,** *Int.
Fract.* **10,** No. 3, 379-392 (Sept. 1974).

Key words: ceramics; failure probability; minimum time-
failure; proof stress diagrams; proof testing.

An analysis is presented which permits the accurate predicti
of component lifetimes after proof testing. The analysis appl
to crack propagation controlled fracture but can be used a
conservative prediction when crack initiation is predomina
The analytical predictions are confirmed in a series of time-
failure measurements.

**14579.** Wiederhorn, S. M., Johnson, H., Diness, A. M., Heu
A. H., **Fracture of glass in vacuum,** *J. Amer. Ceram. Soc.*
No. 8, 336-341 (Aug. 1974).

Key words: crack propagation; fracture; fractu
mechanics; glass; strength.

The fracture of 6 glasses was studied in vacuum, $< 10^{-4}$ t
($10^{-2}$ N/m$^2$), as a function of temperature from 25 to 775
Subcritical crack growth was observed in 4 of the glasses.
tivation energies for crack motion ranged from 60 to 1
kcal/mol. The glasses which did not exhibit slow crack grov
were "anomalous" glasses with abnormal thermal and elas
properties. Critical stress intensity factors for these 2 glasses
creased ≈ 10 percent as the temperature increased to ≈ 600
It is felt that subcritical crack growth is not the result of alk
ion diffusion or viscous flow but rather of a thermally activa
growth process which depends on the crack-tip structure in
glass. A narrow cohesive region at the crack tip favors subcr
cal crack growth, whereas a wide region favors abrupt fractu

**14580.** Hoer, C. A., **The 6-port coupler; a new approach to m
suring V, I, P, Z, and θ, (Summary),** (Proc. Conf. Digest
Precision Electromagnetic Measurements, Boulder, Co
June 26-29, 1972), *CPEM Digest,* pp. 15-17 (1972).

Key words: current; directional coupler; impedance; pha
power; voltage.

A 6-port coupler is described having four side arms whose
puts are proportional to the voltage, current, incident volt
wave, and reflected voltage wave at some desired measurem
plane in the transmission line. The phase relationship betw
the outputs is the same as between corresponding quantitie
the measurement plane. Complex impedance and phase angl
well as voltage, current, and power can be obtained from sin
power or voltage magnitude measurements at the four side ar

4581. Levine, J., **Precision long-path interferometry and its application to geophysics and astrophysics,** (Proc. Conf. Digest on Precision Electromagnetic Measurements, Boulder, Colo., June 26-29, 1972), *CPEM Digest,* p. 115 (1972).

Key words: geophysics; interferometry; saturated absorption stabilizer; strainmeter.

We are currently operating a 30-meter Fabry-Perot inter- erometer as a strainmeter in an unworked gold mine near Boulder, Colorado. The interferometer is illuminated by a 3.39 m single mode helium-neon laser. The laser is locked to one of he transmission maxima of the Fabry-Perot by means of a servo oop which tunes the laser so as to maximize the power transmitted through the long path. The tuning is accomplished by nounting one of the laser mirrors on a piezoelectric ceramic and y applying a suitable voltage to the ceramic.

4582. Benjamin, E. A., **A review of methods and requirements for fire protection of steel-framed buildings,** *Proc. Structural Engineering Association of California, Coronado, Calif., Oct. 3, 1968,* pp. 24-28 (1968).

Key words: building codes; E-119 test; fire protection; fire research; steel construction.

Developments in materials and techniques to meet the current uilding code requirements for fire protection of steel-framed uildings are described. Included is a discussion of some of the st requirements in the ASTM Standard, Methods of Fire Tests f Building Construction and Materials. Research work that may ad to improvement in the Fire Test Method is described.

4583. Wyckoff, J. M., **Measurements for radiation safety,** *Proc. 19th Annual Meeting of the Institute of Environmental Sciences, Anaheim, Calif., Apr. 2-5, 1973,* pp. 130-135 (1973).

Key words: government agencies; measurement assurance program; permissible limits; radiation; regulations; standards; transfer standards.

Good measurements are the key to safe application of both nizing and nonionizing radiation in industry, medicine and con- umer products. The National Bureau of Standards, as the Na- on's primary source of physical measurement capability, is ex- anding its measurement services to radiation users. At the same me, it works closely with federal regulatory agencies such as EC, BRH, NIOSH, and EPA to assist them in preparation of gulations containing realistic measurement requirements. The ate of the measurement art in x-ray, nuclide, ultraviolet, laser, ectromagnetic and ultrasonic radiation measurements will be viewed highlighting the need for stable and accurate transfer andards to serve the safety community.

584. Warkulwiz, V. P., Mozer, B., Green, M. S., **Observation of the deviation from Ornstein-Zernike theory in the critical scattering of neutrons from neon,** *Phys. Rev. Lett.* **32,** No. 25, 1410-1413 (June 24, 1974).

Key words: critical exponent $\eta$; critical point; critical scattering; neon; neutron diffraction; Ornstein-Zernike.

A deviation from the Ornstein-Zernike theory of critical scat- ring has been observed in a neutron-diffraction study of neon ar its critical point. The critical exponent $\eta$ was determined to ve the value $0.11_{-0.02}^{+0.03}$.

585. Mabie, C. P., **Adhesive refractory protective coating for investment casting,** *J. Dent. Res.* **53,** No. 5, 1181-1188 (Sept.-Oct. 1974).

Key words: casting; coat; dental; investment; refractory.

A refractory protective coat has been developed that greatly duces scale formation and is capable of lowering sandblasted sting roughness 30 to 50 percent. When applied as a thin film to the refractory model, it remains as a tacky base which will fix wax and plastic.

14586. Hahn, T. A., Kirby, R. K., **Thermal expansion of a borosilicate glass from 80 to 680 K—Standard Reference Material 731,** (Proc. AIP Conf. on Thermal Expansion, Lake of the Ozarks, Mo., Nov. 7-9, 1973), Paper in *AIP Conference Proceedings No. 17, Thermal Expansions, 1973,* R. E. Taylor and G. L. Denman, Eds., No. 17, 93-101 (American Institute of Physics, New York, N.Y., 1974).

Key words: borosilicate glass; dilatometer calibration; standard reference material; thermal expansion.

This Borosilicate Glass is the third Standard Reference Material (SRM) to be certified for thermal expansion measurements by the National Bureau of Standards. Copper (SRM 736) and Fused Silica (SRM 739) are the other two materials. The results of tests on six samples taken from the stock will be reported in this paper. These results indicate the stock to be of consistent quality suitable for certification. Measurements were made in the temperature range from 80 to 680 K using an interferometer apparatus. At 293 K the expansivity is $4.78 \times 10^{-6}$ K$^{-1}$ and the standard deviation is $0.06 \times 10^{-6}$ K$^{-1}$ calculated from a least squares fit to the data over the entire temperature range. A description of the calibration of a fused quartz dilatometer using the three Standard Reference Materials will also be presented.

14587. Yonemura, G. T., **Opponent-color-theory treatment of the CIE 1960 (u,v) diagram: Chromaticness difference and constant-hue loci,** *J. Opt. Soc. Amer.* **60,** No. 10, 1407-1409 (Oct. 1970). (Oct. 1970).

Key words: chromaticity diagram; color difference; color hue; color theory.

An angular interpretation of the CIE 1960 $(u,v)$ system is presented. This new development of the CIE 1964 $(u,v)$ $(U^*, V^*, W^*)$ system results in improved chromaticness-difference predictions and is more in accord with empirical constant-hue loci than the $U^*$, $V^*$, $W^*$ system.

14588. Scott, W. W., Jr., **A new coaxial RF-DC ammeter, (Summary),** (Proc. Conf. Digest on Precision Electromagnetic Measurements, Boulder, Colo., June 2-5, 1970), Special Issue *CPEM Digest,* p. 13 (1970).

Key words: ammeter; compensation; radio-frequency; RF-DC difference; standard; thermal-current-convertor; thermopile.

A small, portable reference standard of radio-frequency current has been developed which, when calibrated with the NBS Standard Electrodynamometer, will serve as an interlaboratory standard of high accuracy between NBS and users in industry.

The ammeter is unique and has no precedence in principle of operation. It consists of an elliptic cylindrical silver reflector of infrared energy with a cylindrical thin-film quartz heater along one focus and a heat sensing thermopile along the other focus.

The ammeter has three times the current range of older ammeters with up to ten times larger output and unequalled broadband frequency range. The prototype covers 0.5 ampere to 5 amperes (heater burnout at about 9 amperes) with corresponding dc outputs from 1 millivolt to 100 millivolts for currents in the frequency range dc to 1 GHz.

14589. Marzetta, L. A., **A thermesthesiometer—an instrument for burn hazard measurement,** *IEEE Trans. Bio-Med. Eng.* **BME-21,** No. 5, 425-427 (Sept. 1974).

Key words: burn-hazard; heat-flow; thermal-inertia; thermesthesiometer.

Surface temperature measurement alone is insufficient to establish the hazard to the human of contact with a hot or cold object. A metal surface is more likely to cause thermal injury than a plastic surface at the same temperature. An instrument equipped with a measuring probe has been developed for indicating the temperature that would be experienced if human contact were made with the hot surface in question. The correct value of interface contact temperature can be read for a selected contact time without knowing the composition or temperature of the heated material under test.

14590. Crandall, D. H., Dunn, G. H., Gallagher, A., Hummer, D. G., Kunasz, C. V., Leep, D., Taylor, P. O., **Rate coefficients for electron excitation of the first resonance transition in H, Li, Na, Ca, Ca$^+$, and Ba$^+$ calculated from experimental data,** *Astrophys. J.* **191,** No. 3, 789-793 (Aug. 1, 1974).

Key words: atomic cross sections; atomic data; atomic physics; rate coefficients; resonance lines.

By fitting cubic spines augmented with special functional forms for low and high energies to cross-section data determined experimentally at discrete values of the electron energy, we obtain an interpolation that can be visually inspected and adjusted to prevent the appearance of spurious features. The familiar integral expressing the rate coefficient in terms of the cross-sections can then be evaluated with no further approximation. This procedure is applied here to cross-section data for the first resonance transition of H, Li, Na, Ca, Ca$^+$, and Ba$^+$. The resulting collisional de-excitation rate coefficient, from which the excitation-rate coefficient can be determined by the detailed balance relation, is tabulated in each case for electron temperatures in the interval from $10^3$ to $10^5$ K and is expressed in terms of a Chebyshev expansion valid for this range of temperature.

14591. Pilsworth, M. N., Jr., Hoge, H. J., Robinson, H. E., **The thermal conductivity of natural rubber from 134 to 314 K,** *J. Mater.* **7,** No. 4, 580-585 (Dec. 1972).

Key words: glass transition; heat transfer; Hevea rubber; thermal conductivity; thermophysical properties; transport properties.

The thermal conductivity of soft natural rubber, compounded and vulcanized as specified in ASTM recipe 2A, has been measured over a range extending from well below the glass transition to above room temperature. The glass-transition temperature deduced from the thermal-conductivity measurements is 212 K (– 78 F). Most of the measurements were made at the Natick Laboratories in a guarded-hot-plate apparatus, with silicone rubber pads on either side of the sample. The rest of the measurements were made at the National Bureau of Standards with apparatus and procedures that have been used for many years in reference-standard work. The thermal-conductivity data are believed to be accurate to 3 percent or better at room temperature and to about 6 percent at the glass transition and below.

14592. Willis, P. M., Fox, M. R., **Computers for the inexperienced and impecunious,** *Liberal Education* **55,** No. 4, 545-550 (Dec. 1969).

Key words: computer science; computers; Hood College; research tool; time sharing; undergraduate education.

Hood College, a small liberal arts college in Frederick, Md., collaborated with the National Bureau of Standards in Gaithersburg in developing a work-study program in computing science that has served to introduce students and faculty to the capabilities and limitations of the digital computer. The program, sponsored by the National Science Foundation, resulted in four small liberal arts colleges establishing a computer appreciation course at nominal cost that has wide applicability to similar colleges which have access to and assistance in instruction from nearby government or industrial laboratories with computer capability. Details of the experiment along with costs are provided i sequence for the two years it encompassed.

14593. Trechsel, H. R., **Structural performance testing of windows, curtain walls, and doors,** *Amer. Soc. Test. Mater. ASTM Spec. Tech. Publ.* **552,** pp. 36-41 (1974).

Key words: curtain walls; doors; test; walls; wind loads windows.

This paper is a commentary on the ASTM Test for Structura Performance of Exterior Windows, Curtain Walls, and Door under the Influence of Wind Loads, Designation E 330-70. A brief historical background of the development of the tes method is given, the procedure is summarized, some of its features are highlighted, and the use, application, and significanc of the method are discussed.

14594. McDonald, D. G., Risley, A. S., Cupp, J. D., **The relationship of Josephson junctions to a unified standard of lengt and time,** (Proc. 13th Int. Conf. on Low Temperature Physic Boulder, Colo., Aug. 21-25, 1972), Paper in *Low Temperatu Physics LT 13,* K. D. Timmerhaus, W. J. O Sullivan, and E. F Hammel, Eds., **4,** 542-549 (Plenum Press, New York, N.Y 1974).

Key words: cryogenics; infrared; Josephson junction lasers; superconductivity.

Recent developments have led to large improvements in th frequency stability of infrared lasers. The stability is now comparable with that of the primary frequency standard and great exceeds that of the length standard. Thus a stabilized infrare laser could become a unified standard of time (or frequency) an length and replace the two existing standards. A practic problem is that infrared frequency synthesis must be simplifie and Josephson junctions show promise for this purpose.

14595. Siegwarth, J. D., Radebaugh, R., **The Kapitza resistan between Cu(Cr) and $^4$He($^3$He) solutions and applications to he exchangers,** (Proc. 13th Int. Conf. on Low Temperatu Physics, Boulder, Colo., Aug. 21-25, 1972), Paper in *Lo Temperature Physics LT 13,* K. D. Timmerhaus, W. J. O'Su livan, and E. F. Hammel, Eds., **1,** 398-400 (Plenum Pres New York, N.Y., 1974).

Key words: alloy; copper; dilution refrigerator; Kapitza sistance.

The Kapitza resistance of work hardened copper has be found to be as much as ten times lower than that of anneal copper below 0.1 K. There are other hardening techniques whi can be used for copper, such as oxygen annealing of copper containing small amounts of such impurities as Al, Be or Si precipitation hardening of copper containing small amounts of or Zr. We have measured the Kapitza resistance betwee precipitation hardened alloy of Cu – 0.6 atomic percent Cr a the dilute He$^3$ stream in a dilution refrigerator. With the pro heat treatment, Cu(Cr) has a Kapitza resistance ten tim smaller than annealed OFHC copper. The thermal conductiv of Cu(Cr) is about 0.1 that of OFHC copper. This is suffici for use in heat exchangers in dilution refrigerators. Such exchanger may be fabricated by sintering in $H_2$ at ~ 750 °C, th heat treating at ~ 450 °C to obtain low Kapitza resistances.

14596. Wall, L. A., **Condensed phase combustion chemistry,** *F Res. Abstr. Rev.* **13,** 204-219 (1971).

Key words: burning of polymers; combustion; igniti polymer decomposition; pyrolytic decomposition.

The role of the chemical pyrolytic decomposition mechanis of polymer decomposition in the ignition, combustion and bu ing of polymers is outlined in the light of available informat The particular aspects discussed are: mechanism, effect of c tions, catalytic effects, energetics, types of decompositions in-uced and oxidative degradation, burning of polymers, heats of sification and regression rates.

597. Mahajan, B. M., **Safety standards for home playground equipment,** *Proc. 27th Annual Conf. for Engineering in Medicine and Biology, Philadelphia, Pa., Oct. 6-10, 1974,* **16,** 503 (Alliance for Engineering in Medicine and Biology, Chevy Chase, Md., Oct. 1974).

Key words: component; criteria; development; equipment; hazard; hazardousness; home playground; identification; mishap; misuse; product defect; safety standards; swing set; test method.

Summaries of swing set related accident investigations were amined in order to identify the hazards associated with swing ts. Approximately half of the swing set related mishaps were rectly attributed to the design and construction defects of the oducts. The other half of the recorded mishaps results from im-oper installation, deterioration or misuse of the product.

Some necessary information, such as anthropometric data, in-ry threshold data, loading conditions representing child-hazard teractions, and loads applied to certain components to swing ts is presented.

Quality criteria and test methods are suggested, to establish fety standards for reducing hazards due to design and con-ruction defects of the equipment.

598. Mahajan, B. M., **Standards for athletic helmets—a state-of-the-art,** *Proc. 27th Annual Conf. for Engineering in Medicine and Biology, Philadelphia, Pa., Oct. 6-10, 1974,* **16,** 181 (Alliance for Engineering in Medicine and Biology, Chevy Chase, Md., Oct. 1974).

Key words: athletic helmets; head injury; injury criteria; safety standards.

The available information on the types of impact induced head uries, their relative severity, and injury threshold values was llected from the literature. The search revealed that the reshold values are either questionable or are not available.

The literature search revealed that the information regarding e impact conditions which are generated by athletic mishaps is most non-existent.

A review of standards for helmets revealed that there are no tisfactory performance standards for athletic helmets and that e performance criteria and testing procedures used to evaluate ner helmets may be neither appropriate nor adequate for test- athletic helmets.

599. Klein, G. P., Hamilton, C. A., **Measure power with a calculator chip and a DPM. By direct multiplication of current and voltage, you can cover a dynamic range of almost seven decades,** *Electron. Des.* **21,** 112-114 (Oct. 11, 1974).

Key words: calculator chip; digital panel meter; laser power.

This paper discusses techniques used in developing a direct ading laser power meter. Minimum modifications to a digital nel meter and the proper interfacing with a decimal arithmetic ocessor make this task possible. Actual working models of this vice along with the power detectors are presently in use within BS.

600. Frederick, N. V., Stanley, W. D., Zimmerman, J. E., Dinger, R. J., **An application of superconducting quantum interference magnetometers to geophysical prospecting,** *IEEE Trans. Geosci. Electron.* **GE-12,** No. 3, 102-103 (July 1974).

Key words: geophysical prospecting; magnetometer; magnetotelluric; quantum interference; SQUID; superconductor.

Magnetotelluric field measurements were carried out at two geothermally interesting locations with two Superconducting QUantum Interference Device (SQUID) magnetometers. The tests demonstrated the very attractive combination of characteristics of these instruments for geophysical magnetic measurements. They have noise levels down to $10^{-14}$ T/Hz$^{1/2}$ ($10^{-5}$ gamma Hz$^{-1/2}$); frequency response from 0 to several kHz; dynamic range of at least 160 dB; and in addition are portable and easy to set up in the field.

14601. Harrison, C. A., **Utilization of cation-selective membranes in the study of caries formation,** *J. Dent. Res.* **53,** Suppl. to No. 5, 1023-1032 (1974).

Key words: activity; calcium hydroxide; dental caries; mechanism; permselective membrane.

A caries mechanism was tested in a model experiment in which cation-permselective membranes were used to simulate the outer enamel-plaque layer. According to this theory, preferential diffusion of $Ca^{2+}$ and $H^+$ accelerates caries formation. The results support the theory and confirm that activity of $Ca(OH)_2$ is of fundamental importance.

14602. Taylor, B. N., **Cryogenic metrology,** (Proc. 13th Int. Conf. on Low Temperature Physics, Boulder, Colo., Aug. 21-25, 1972), Paper in *Low Temperature Physics LT 13,* **4,** 465-482 (Plenum Press, New York, N.Y., 1974).

Key words: cryogenics; fundamental constants; instrumentation; metrology.

The application of cryogenic technology and phenomena to selected areas of metrology is discussed. While the several and varied uses of the Josephson effects in the solution of metrological problems is the main topic reviewed, some past and present metrological uses of non-Josephson related low temperature phenomena are included. Prognostications regarding the future of the field are also given.

14603. Yeh, K-N., Birky, M. M., Huggett, C., **Calorimetric study of flammable fabrics. II. Analysis of flame retardant-treated cotton,** *J. Appl. Polym. Sci.* **17,** 255-268 (1973).

Key words: calorimetric; cellulose; flammability; flame retardant; heat; phosphorus; rate.

Efficiencies of three flame retardants for cellulose; phosphoric acid, diammonium phosphate and THPOH ammonia finish, have been evaluated based on the heat-release value and the rate of heat-release of treated fabrics burning in air measured with the isoperibol calorimeter. The results were compared and correlated with those obtained previously with the bomb calorimetric technique. Complete heat balances were obtained for the systems studied by correlation of the calorimetric data and the measurement of combustible gases evolved from the fabric burning in air. The rate of heat-release was found to correlate with 45° flame propagation rate. The results from the heat, rate and combustible gas measurements were interpretable in terms of existing mechanisms of flame retardant action.

14604. Harrison, J. O., Jr., **New information processing standards,** (Proc. of the American Association of State Highway Officials Committee on Electronics National Conf., Seattle, Washington, May 6-7, 1969), Paper in *Committee on Electronics,* pp. 23-35 (1969).

Key words: Cobol; computers; information interchange; information processing; standards.

Information processing standards are needed for the interchange of machine sensible data, the interchange of computer programs, the interchange of computer components and devices, and the interchange of computer related ideas among people. Organizations for the development of such standards exist at four levels: international, national, Federal Government, and State Government. Two important standards recently adopted are the United States of America Standard Code for Information Interchange and United States of America Standard COBOL. Federal information processing standards are promulgated through the Federal Information Processing Standards Register.

**14605.** Wilson, W. K., Parks, E. J., **Research program on stability of records at the National Bureau of Standards,** (Proc. 22nd TAPPI Testing Conference, Savannah, Ga., Oct. 7, 1971), *TAPPI* **55,** No. 1, 151-161 (1972).

Key words: accelerated aging; dry breaking load; paper; pH; records; reflectance; specifications; stability; wet breaking load.

An outline is given of historical origins and the current status of research into records preservation at the National Bureau of Standards. The principal effort concerns causes of the degradation of paper in storage. As many compositional and environmental variables contribute to the degradation of paper, it is not practical to analyze every potential variable. Some representative data are given from which it is concluded that (1) aging processes in dry and humid gases are mechanistically different; (2) increases in acidity are concurrent with decreases in the dry breaking load of paper, but not *functionally* related; (3) blue reflectance decreases as acidity increases and the dry breaking load decreases; (4) thermal analyis may be a crude but useful tool for detecting impermanence in paper. While an interim specification for permanence may be based on pH, it appears that an accelerated aging test must eventually be specified. The validity of dry oven aging is questionable.

**14606.** Thurber, W. R., Bullis, W. M., **Resistivity and carrier lifetime in gold-doped silicon,** *Air Force Cambridge Research Laboratories Report AFCRL-72-0076,* 37 pages (Air Force Cambridge Research Laboratories, Air Force Systems Command, U.S. Air Force, Bedford, Mass. 01730, Jan. 31, 1972).

Key words: carrier lifetime; gallium arsenide; gold-doped silicon; resistivity; silicon; surface photovoltage.

This report describes the present status of an on-going study of the properties of gold-doped silicon. Resistivity, Hall effect, and carrier lifetime are being measured at room temperature in silicon wafers doped with varying amounts of gold and either phosphorus or boron. Reasons are being sought for the apparent discrepancy between total and electrically active gold, for the discrepancy between calculated and observed resistivity in both *n*-type and *p*-type specimens with very large gold concentration, and for the diversity in capture cross-section data reported in the literature. Although many questions still remain, progress has been made in resolving these discrepancies. There is considerable evidence that the low resistivity observed at large gold concentrations is associated with the introduction of shallow acceptor states in concentrations strongly dependent on the gold concentration. The origin of these states is being sought. Initial studies of the application of the surface photovoltage method to the measurement of carrier lifetime in gold-doped silicon have been completed. This method also appears to be suitable for use on gallium arsenide specimens. A bibliography of the literature on properties of gold-doped silicon that contains 136 entries is also included as an appendix.

**14607.** Waksman, D., Ferguson, J. B., **Fire tests of building interior covering systems,** *Fire Technol.* **10,** No. 3, 211-220 (Aug. 1974).

Key words: fire hazard properties; gaseous combustion products; interior covering systems; interior finishes; smoke generation; surface flammability.

The fire performance of assemblies consisting of surface coverings applied over two types of painted substrates was investigated. Relatively noncombustible asbestos cement boar (ACB) and painted plywood intended to represent a combustibl substrate were used. Properties measured included surfac flammability, and smoke density and gaseous combustio product levels. Considerable substrate dependence was foun for these properties. On the basis of the results observed in thi study, it is concluded that it would be advantageous to base fir safety ratings on the results of tests conducted on coverings ap plied to both combustible and noncombustible substrates.

**14608.** Huebner, R. H., Celotta, R. J., Mielczarek, S. R., Kuyat C. E., **Oscillator strength values derived from electron energ loss spectra of molecules,** (Proc. VIII Int. Conf. on the Physic of Electronic and Atomic Collisions, Beograd, Yugoslavi July 16-19, 1973), Abstracts of Papers of the *VIII Interna tional Conference on the Physics of Electronic and Atomi Collisions,* B. C. Cobic and M. V. Kurepa, Eds., **I** 435-436 (Ir stitute of Physics, Beograd, Yugoslavia, May 1973).

Key words: acetone; energy loss spectra; ethano methanol; oscillator strengths.

The method of obtaining oscillator strengths from electro energy loss data is described.

**14609.** Swanson, N., Celotta, R. J., Kuyatt, C. E., **Resonar structure in electron impact excitation of xenon,** (Proc. VIII In Conf. on the Physics of Electronic and Atomic Collision Beograd, Yugoslavia, July 16-19, 1973), Abstracts of Pape of the *VIII International Conference on the Physics of Ele tronic and Atomic Collisions,* B. C. Cobic and M. V. Kurep Eds., **I,** 478-479 (Institute of Physics, Beograd, Yugoslavi May 1973).

Key words: electron impact; uv lasers; xenon excitati functions.

Electron impact excitation functions for atomic xenon a presented.

**14610.** Rabinow, J., **Small business R&D – to be or not to be,** *Pro Conf. II on Survival and Growth: The Small R&D Firm, Se 27-29, 1972,* pp. 29-35 (Sept. 1972).

Key words: government contracts; government laborat ries; in-house research; patent rights; small company R&

The talk concerned small R&D research firms and the d ference between those who make a product and those that wo strictly as consultants. I discussed the nature of governme R&D contracting and the less-than-honorable practices indulg in both by the government and by contractors. The arguments how much R&D work should be done by government in-hou versus outside was touched upon and I pointed out that if t government people are to be competent they must do in-hou research and the small R&D firms would do better under su conditions. The question of patent rights was also discussed.

**14611.** Rabinow, J., **Improving the patent system,** (Proc. Conf. American Patent Law Association's Annual Meeti Washington, D.C., Oct. 19, 1972), *American Patent Law sociation's Bull.,* pp. 608-625 (Oct.-Nov. 1972).

Key words: antitrust; Department of Justice; human inert innovation; inventions; patents and the courts.

The talk touched on the subject of the attacks on the pat system and the recent interest in invention and innovation at high levels of Government. The relationship between mate wealth, the quality of life and the role of the inventor w discussed. The processes of invention and innovation were co pared to other games of chance and the effects of adjusting odds were discussed. A plea was made for raising the odds the inventor. The talk illustrated the attitude of some memb of the Department of Justice and the courts relative to the inv tor. The quality of patents as issued by the Patent Office entioned, together with a plea to keep the quality as high as ssible. The Patent Bar was also asked to improve its ethics and eliminate the attorneys and some organizations that now are ecing the unsophisticated inventor. The talk closed with a scussion of the difficulty of introducing an invention into the al world.

**612.** Wyly, R. S., Orloski, M. J., **Studies of reduced-size venting of sanitary drainage systems in the USA,** (Proc. CIB Commission W62 Symp. on Gravity Drainage, Stockholm, Sweden, Sept. 24-25, 1973), Paper 13 in *Drainage Services in Buildings, D14:1973,* pp. 13:1–13:19 (National Swedish Building Research, Stockholm, Sweden, 1973).

Key words: air demand; criteria for venting; reduced-size venting; trap performance; trap-seal retention/reduction; venting criteria; venting, reduced-size.

Results of experimental studies of reduced-size venting in the SA are summarized, tentative criteria are presented, and the ed for further work leading to a general method for computa- n of vent sizes is discussed. Experimentation with vents aller than customarily allowed has shown satisfactory per- mance under selected conditions that seem representative of e service environment.

Among the significant findings were: (1) trap-seal retention s adequate with peak fluctuating suction of as much as 75 mm ter column for a water closet trap, and about 38 mm for a lava- y P-trap, compared with the 25 mm presently assumed for sign, (2) air demand rates required to assure adequate trap-seal ention were significantly less than presently assumed, obably because of effective "slippage" between air and water short stacks and because of air circulation in systems com- sed of a piping "network," (3) discharge profile and accumula- e duration of test loading significantly affected idle trap-seal rformance, and (4) back pressure (blow-back) was a significant terion for system performance, particularly at the ground-floor vation of a high-rise system.

**13.** Yakowitz, H., Fiori, C. E., Newbury, D. E., **Implications f specimen current and time differentiated imaging in scanning lectron microscopy,** (Proc. Sixth Annual Scanning Electron Microscopy Symp., Chicago, Ill., Apr. 21-23, 1973), Chapter n *Scanning Electron Microscopy/1973, Part I,* pp. 173-180 IIT Research Institute, Chicago, Ill., Apr. 1973).

Key words: channelling patterns; iron; lunar samples; magnetic contrast; scanning electron microscope; signal differentiation; specimen current images.

The technique of specimen current imaging has not been wide- used in the SEM field, primarily because of a lack of an equate amplifier system to operate with the low beam current, ically $5 \times 10^{-11}$ amperes, used in high resolution work. A cur- t amplifier capable of providing images of the specimen cur- t signal when that signal is as low as $5 \times 10^{-12}$ amperes is cribed briefly. This instrument also provides differentiation h respect to time (time differentiation) of either the absorbed rent or secondary electron signals from the specimen.

Micrographs comparing the secondary electron and specimen rent images under various operating conditions are discussed terms of picture quality. Often, the specimen current image vides information which cannot be obtained from the emis- e mode (primary or secondary electrons) image or else is espe- lly difficult to obtain because of specimen/collector geometry. the past, direct current amplifiers were unable to operate with ficiently low specimen currents for high resolution photog- hy. Therefore, the impression that specimen current imaging s intrinsically inferior to secondary electron imaging was mulgated. The use of present day equipment indicates that s impression is not correct.

The extra flexibility added by a time differentiating device for both the secondary electron and specimen current modes is described. Mixing the normal signal with the time differentiated signal in all proportions is desirable in order to retain some field depth while reducing gray level disparity.

**14614.** Henderson, M. M., **Programs and services of the Federal Library Committee's task force on automation,** *Proc. 1st Annual Federal Interagency Field Librarians' Workshop, Washington, D.C., Sept. 24-28, 1972,* pp. 57-68 (Sept. 1972).

Key words: automation of library operations; Federal Library Committee; field libraries; FLC; library automation; task force on automation.

The Federal Library Committee's Task Force on Automation (TFA) has established a program which will contribute to effective and efficient improvement of Federal library and information services. The program is based on data collected during a recent survey of the Federal library community, for which the TFA served in a technical advisory capacity. Priorities include development of a tutorial workshop on techniques of evaluation for library automation, establishment of a reference file on current Federal library automation activities, and participation in a study of the feasibility of a Federal library service center operation. Such programs are of interest, and will prove of benefit, to field libraries within the Federal establishment.

**14615.** Wiese, W. L., McClelland, J. F., Kelleher, D. E., Paquette, D. R., **Continuous emission from hydrogen plasmas. II. Experimental studies with a wall-stabilized arc,** *Proc. 9th Int. Conf. on Phenomena in Ionized Gases, Bucharest, Romania,* p. 596 (Sept. 1969).

Key words: continuum; emission intensity; hydrogen; plasma.

A wall-stabilized arc operating in hydrogen is used for the measurement of the continuous hydrogen emission in the visible and near ultraviolet regions of the spectrum. The arc plasma is spectroscopically analyzed, and measured continuum intensities are compared with recent extensive calculated values. Consistency is observed at all measured wavelengths.

**14616.** Blackburn, D. L., Oettinger, F. F., **Transient thermal response measurements of power transistors,** *Proc. IEEE Power Electronics Specialists Conf., Bell Telephone Laboratories, Murray Hill, N.J., June 10-12, 1974, PESC '74 Record,* pp. 140-148 (IEEE, New York, N.Y., Oct. 1, 1974).

Key words: computer simulation (transient thermal); current crowding (transistors); power transistors; thermal impedance measurements; thermal response measurements; transistors (thermal measurements).

Differences between the measured thermal impedance of power transistors when determined by the pulsed heating curve and cooling curve techniques are discussed. These differences are shown to result primarily because the power density distributions of these devices change as the devices heat; as a result of these changes the heating curve and the cooling curve are not conjugate. It is shown that the cooling curve technique, when the cooling curve is initiated from the most non-uniform steady state thermal distribution, (maximum voltage, maximum power) will indicate a larger value for the thermal impedance than will the pulsed heating curve technique, even for pulses in excess of the d-c power level. A one dimensional model for power transistor cooling is described. The theoretical predictions of the model are shown to be in good agreement for practical applications with three-dimensional computer simulations and experimental results. Using this model, it is possible to estimate an average junction temperature and the area of power generation at steady state. Both TO-66 and TO-3 encased devices of mesa and planar structures were included in this study.

**14617.** Brauer, G. M., Termini, D. J., **Grafting of monomers to collagen and hard and soft tissues,** (Proc. XXIII International Congress of Pure and Applied Chemistry, Boston, Mass., July 1971), *Macromolecular Preprint* **1,** pp. 601-608 (1971).

> Key words: collagen; graft polymers; hard tissue; soft tissue; surface grafting; tissue modification.

Grafting of monomers to collagenous surfaces offers an attractive technique for modifying the surface properties of soft and hard tissues. Some 20 monomers were grafted to purified steelhide collagen powders or films using $1.10^{-3}$M ceric ammonium nitrate as initiator. Yields after extraction of homopolymer were greatly dependent on the monomer used. With the most reactive monomers, surface grafts were obtained within 15 minutes. The large variety of monomers, including those with additional reactive or crosslinking groups, graftable to collagen indicates that surfaces with the desired hydrophilichydrophobic balance to fit specific applications can be otained. Some monomers such as ethylene dimethacrylate or glycidyl methacrylate could be grafted to epidermal calfskin. No apparent grafting to calfskin was observed for most of the other monomers. Apparently, the presence of the keratinous layer reduces the reactivity toward graft polymerization. On grafting glycidyl-, dimethylaminoethyl-, isobutyl methacrylate or 1,3-butylene dimethacrylate to powdered bone, an increase in weight of from 11 percent to 60 percent after acetone and chloroform extraction was obtained. Dentin surfaces are not as susceptible to grafting as powdered bone. The relative grafting efficiency of monomers to the solid substrate decreases in the following order: collagen powder, collagen film, bone powder, epidermal calfskin, ratskin, dentin powder.

**14618.** Loevinger, R., **Some remarks on the MIRD Schema for absorbed-dose calculations for biologically-distributed radionuclides,** (Proc. Symp. on Medical Radionuclides: Radiation Dose and Effects, Oak Ridge, Tenn., Dec. 8-11, 1969), Chapter in *Medical Radionuclides: Radiation Dose and Effects,* R. J. Cloutier, C. L. Edwards, W. S. Snyder, Eds., pp. 481-489 (Available as CONF-691212 from the National Technical Information Service, Springfield, Va. 22161, June 1970).

> Key words: dosimetry, radionuclide; internal dose calculation; nuclear medicine; radionuclide dosimetry; reciprocity relationship; specific absorbed fraction.

The origin of the MIRD Schema [*Journal of Nuclear Medicine,* Supplement No. 1 (February 1968)] is described. The basic concepts, equations, and advantages are discussed and explained. The concept of specific absorbed fraction allows formulation of a single equation that covers internal-dose calculations for all radiations, sources and targets.

**14619.** Ausloos, P., Lias, S. G., **Far ultraviolet photochemistry of organic compounds,** *Proc. NATO Advance Study Institute on Chemical Spectroscopy and Photochemistry in the Vacuum Ultraviolet, Valmorin, Quebec, Canada, Aug. 5-17, 1973,* pp. 465-482 (Aug. 1973).

> Key words: far ultraviolet photochemistry; free redicals; organic compounds; photofragments; primary processes; quantum yield.

A brief survey is presented concerning certain aspects of the far ultraviolet photochemistry of organic compounds. The use of spectroscopic methods and chemical analysis of final photolytic products are discussed as methods of obtaining information about the fates—particularly the modes of decomposition—of compounds excited by absorption of photons having energies above about 8 eV. Commonly used photolytic light sources which deliver photons in the energy range 7.6 eV-21.2 eV are described.

Generalizations which can be drawn concerning the primary modes of decomposition of excited alkanes, cycloalkanes, and carbonyl compounds in this energy range are discussed.

**14620.** Somes, N. F., **Experience with the development and application of structural performance criteria,** (Proc. Workshop on Systems Building, NBS, Gaithersburg, Md., Feb. 24-26, 1972), Paper in *Systems Building,* pp. 269-292 (Available from the National Technical Information Service, Springfield, Va. 22161, 1972).

> Key words: building; evaluation; performance criteria; physical simulation; structural safety; structural serviceability.

The paper is based upon experience gained by the author as a member of the NBS team which over the past two years has served as the technical arm of HUD in Operation BREAKTHROUGH. A brief introduction to the nature of BREAKTHROUGH is followed by a description of the task of preparing the Guide Criteria. The housing system producers within the program were required to submit evaluation documents. These are described together with the experience of the evaluation team in dealing with these documents. Recommendations are given as to the ways in which future evaluations might avoid difficulties and time delays. When it is not possible to evaluate through this submission of documents it may be necessary to use physical simulation. To illustrate this technique a case history is presented of the evaluation of the system which used concrete box modules.

**14621.** Utech, H. P., **Status report on research programs for firefighters protective clothing,** *Proc. Fire Department Instructors' Conf., Kansas City, Mo., Mar. 27-30, 1973,* pp. 156-16 (1973).

> Key words: comfort; fire coat; firefighting; impact protection; injury statistics; protective clothing; thermal conditions; turnout coat.

The inadequate design of present-day protective clothing and equipment used by firefighters can be attributed to a lack o quantitative data on what that equipment is expected to do an under what conditions it must perform. Research on firefighters turnout gear at the National Bureau of Standards has focused o developing the needed quantitative data. Progress in defining th hazards faced by firefighters, measuring the performance c present-day coats, quantifying the thermal conditions to whic firefighters are exposed, predicting the performance of protective equipment under those conditions, and using this information to specify the design of improved turnout gear is describe

**14622.** Taylor, J. K., Zielinski, W. L., Jr., Maienthal, E. J., Durs R. A., Burke, R. W., **Development of method for NTA analys in raw water,** *U.S. Environmental Protection Agency EPA R port R2-72-057,* 34 pages (Sept. 1972).

> Key words: chemical analysis; nitriolotriacetic acid; NTA water analysis; water pollution.

The free acid form of nitrilotriacetic acid is readily esterifie by N,O-bis(trimethylsilyl)acetamide and gas chromatograph analysis is directly applicable to this derivative. The respons characteristic of NTA-trisilylester was 2,200 mm$^2$ peak area p microgram of NTA at maximum sensitivity of the hydroge flame ionization detector. Accordingly, gas chromatography ha the potential for detecting NTA concentrations of practical i terest providing that suitable NTA isolation techniques can b developed.

The cupric ion-selective electrode provides the basis for a se sitive electrochemical detector for NTA. Apparatus for the o stream determination of uncomplexed NTA has been develope This may be used for determination of total NTA, after the latt separated from bound metal ions and other complexing agents y a suitable means, such as ion-exchange chromatography.

Polarographic studies have shown that the bismuth-NTA omplex is a suitable method for the determination of NTA in ost waters. While some metal ions may interfere, a pre-electrol-sis step and/or a standard addition technique seems feasible to iminate this problem.

Potentiometric titration with cupric ion should provide a rapid d reliable referee method for the determination of NTA in de-rgent formulations. Such a method would appear to be superior the spectrophotometric methods presently used, since the tter are affected by turbidities which are encountered in many the samples.

623. Walker, J. C., Hughes, C. E., **POPSS—a parametric operating system simulator,** *Proc. SIGCSE Meeting, Columbus, Ohio,* pp. 166-169 (1973).

Key words: computer system; FORTRAN IV; operating system; resource allocation strategies; simulator.

In this paper we describe POPSS, an event driven simulator hich is intended to simulate the activity of a computer stem—hardware together with an operating system—as it ocesses a workload. Input to the simulator is in the form of yword parameters which are used for describing all three com-onents—hardware, operating system, and workload.

POPSS is a simulator as opposed to a simulation language. It designed to model the inner workings of a computer system in ldition to yielding the results usually associated with simula-on. The program is highly modular, consisting of some 45 sub-ograms. Of these, there are 22 modules, each of which presents an operating system component (or possibly a part of e such component). Included in POPSS are built-in replace-ent features to allow a user the capability of designing alterna-e resource allocation strategies. These features are in addition the standard subprogram replacement automatically available rough the use of FORTRAN IV.

624. Loevinger, R., **Absorbed dose from interstitial and intracavitary sources,** (Proc. Conf. Afterloading in Radiotherapy, New York, N.Y., May 6-8, 1971), Chapter in *Afterloading in Radiotherapy,* N. Simon, Ed., DHEW Publ. (FDA) 72-8024 BRH/DMRE 72-4, pp. 192-203 (U.S. Department of Health, Education, and Welfare, Bureau of Radiological Health, Rockville, Md. 20852, Dec. 1971).

Key words: absorbed dose; buildup factor; gamma radiation; implant; interstitial; intracavitary; point source.

A quantity of importance in the dosimetry of $\gamma$-ray sources is e ratio of the absorbed dose to the exposure in air at the same int. This is calculated from energy-absorption buildup factors some $\gamma$-ray sources of clinical importance, and shows asonable agreement with formulae which represent experimen- determination. It is shown that penetration through tissue is equate for implant therapy for quantum energies as low as 25 V.

625. Yakowitz, H., **A practical examination of the Kossel x-ray diffraction technique,** Chapter 11 in *Microprobe Analysis,* C. A. Andersen, Ed., pp. 383-421 (John Wiley & Sons, Inc., New York, N.Y., 1973).

Key words: crystal orientation; error propagation; Kossel lines; lattice spacings; stress-strain maps; x-ray diffraction.

The divergent beam (Kossel) x-ray diffraction method can pro-de lattice spacing data and crystallographic orientation infor-ation from regions 15 $\mu$m in diameter by 2 to 10,000 $\mu$m in pth depending on the experimental conditions and the target. typical depth value is 50 to 75 $\mu$m. In addition, all of the (hkl) planes of a family are separated, i.e., if (222) appears then $(2\bar{2}2)$ will appear as a separate entity. This last circumstance permits a Kossel Internal Stress-Strain (KISS) analysis to be carried out in a straightforward way. In particular, the Cauchy strains, principal strains and their axes, principal stresses and their axes, maximum shear strain in any (hkl) plane and the total stored elastic energy in the irradiated region can be calculated for lightly strained materials. This paper will describe the Kossel method in general with emphasis on the KISS analysis—especially from the point of view of reliability of the KISS results. The object will be to illustrate the power of the KISS but also to point out its limitations in practice. Experimental design will be discussed in terms of its effect on the stress-strain analysis results.

14626. Gadzuk, J. W., **Electron spectroscopy of chemisorbed atoms,** Lecture Notes from the IXth Winter School of Theoretical Physics, Karpacz, Poland, Feb. 16-29, 1972, The Theory of Metals and the Many-Body Problem, *Acta Universitatis, Wratislaviensis No. 181,* **II,** pp. 1-19 (1972).

Key words: chemisorption; field emission; ion neutralization; photoemission; tunneling.

The techniques of Ion Neutralization Spectroscopy, Field Emission Resonance Tunneling and Ultraviolet Photoemission as valence level probes of chemisorbed atoms are discussed.

14627. Harvey, D. G., Achenbach, P. R., **Opportunities for improving energy utilization in residences,** *Proc. Effective Energy Utilization Symp., Drexel Univ., Phila., Pa., June 8-9, 1972,* pp. 234-247 (1972).

Key words: appliance performance; energy conservation; energy use; heating and air conditioning; residential energy consumption.

The construction features of a typical single-family residence in the northeast region of the United States are described together with average annual energy consumption for space heating and cooling, domestic water heating, and electric appliances. The market saturation in the use of the various electrical appliances in the typical residence is summarized. The potential for energy savings in the design and use of appliances, heating, ventilating, and air conditioning systems, and the building itself is summarized with reference to cost effectiveness and acceptability to the occupant. A summary of recommended areas for research in energy conservation in residences is provided.

14628. Vadelund, E. A., **Change to metric can maximize package size rationalization,** *Proc. DFISA Conf., Las Vegas, Nev., Mar. 28, 1973,* pp. 45-48 (1973).

Key words: labeling; metric system; packaging; size rationalization; state and federal laws and regulations.

Presents a brief overview of the current status of metrication including legislative activities. Outlines the changes that need to be considered by the packaging industry in the event a measurement system change occurs.

14629. Kirsch, R. A., **Resynthesis of biological images from tree-structured decomposition data,** (Proc. Int. Federation on Information Processing, Vancouver, British Columbia, May 22-26, 1972), Chapter in *Graphic Languages,* F. Nake and A. Rosenfeld, Eds., pp. 1-19 (North-Holland Publ. Co., Amsterdam, The Netherlands, 1972).

Key words: biomedical; image processing; pattern recognition.

In this paper we are simultaneously concerned with methods for decomposing grey scale microscope images and with methods for verifying the correctness of these decompositions. One such method is resynthesis. Resynthesis is viewed as a procedure whereby an analyzed scene can be reconstituted and subjected to an analysis by human (informal) methods to determine the information preservation of the process. Several algorithms are presented for different ways of resynthesizing a decomposed image from its morphological decomposition analysis.

**14630.** Hill, J. E., Kusuda, T., Powell, F. J., **A concept for determining the need for air conditioning,** (Proc. ASHRAE Symp. for Air Conditioning Criteria for Man's Living Environment, Louisville, Ky., June 24-28, 1973), *ASHRAE Bull. LO-73-8,* pp. 14-17 (1973).

Key words: air conditioning criteria; comfort indices; human comfort.

Previously written criteria that govern the decision to install or not to install air conditioning, have been based solely on the climate. This paper proposes the need for a criteria with a sounder technical base together with the manner in which it can be established. Detailed building data and hour by hour weather data are combined in a precise thermal simulation to predict the hour by hour indoor conditions that would exist (dry-bulb temperature, wet-bulb temperature, and mean radiant temperature). The conditions are in turn compared to the accepted comfort standards (ET*, Kansas State University Index, Predicted Mean Vote, etc.) in order to ascertain whether air conditioning is required.

The paper gives the details of a comprehensive study showing the feasibility of such a scheme. A thermal simulation was made on an apartment building located in Jersey City, New Jersey, using the weather data of ten consecutive summers. The simulation results revealed the extent and duration of undesirable indoor conditions when this apartment is not air-conditioned. The magnitude of computational effort appears formidable if detailed simulation calculations are to be carried out for the many combinations of buildings and climatic zones in the United States. Therefore, an attempt was made to obtain statistical correlations between the indoor and outdoor conditions for this apartment. The attempt was reasonably successful and a short-cut technique for establishing criteria is indicated.

**14631.** Frommer, M. A., Shporer, M., **The properties of water in polymeric membranes. I. Freezing and non-freezing water in cellulose acetate membranes,** *Proc. Am. Chem. Soc. 163rd Meeting on Organic Coatings and Plastics Chemistry Symp., Boston, Mass.,* **32,** No. 1, 374-381 (Apr. 1972).

Key words: cellulose acetate membranes; differential scanning calorimetry; freezing in porous systems; membranes; NMR relaxation times; nuclear magnetic resonance.

The relative amounts of freezing and non-freezing water in various water-wet cellulose acetate (CA) membranes have been determined by differential scanning calorimetry (DSC) and by nuclear magnetic resonance (NMR) techniques. DSC results suggest that: 1) A significant fraction (17-40%) of the water (1.0-3.1g $H_2O$ per g dry CA) in any membrane does not freeze at temperatures as low as − 60 °C; 2) The amount of non-freezing bound water (0.40-0.7g non-freezing water per g dry CA) depends upon the nature of the membrane, and is significantly higher than the total amount of water (all of which is non-freezing) absorbed from liquid water by a *dense* film of the same polymer (~ 0.18g water per g dry CA). The structures of the membranes studied by scanning electron microscopy suggest that the amounts of non-freezing water in cellulose acetate membranes decrease with the increase in the packing density (compactness) of the polymer within the membrane. NMR data suggest that: 3) The *non-freezing* water is *highly mobile compared with ice.* 4) The relative amounts of non-freezing water computed from NMR experiments are comparable to those estimated from DSC measurements. 5) *All* the water contained in membranes equilibrated with water vapors are bound to the polymer and do not freeze.

**14632.** Wall, L. A., Roestamsjah, Aldridge, M. H., **Pyrolysis of mixtures of monodisperse poly α-methylstyrenes,** *Amer. Chem. Soc. Polymer Preprints* **13,** No. 2, 1041-1043 (Aug. 1972).

Key words: polymers; pyrolysis; poly α-methylstyrene, zip-length.

Mixtures of monodisperse poly α-methylstyrenes were pyrolyzed and their rate of weight lost measured as a function o molecular weight. The pyrolytic weight lost of pol αtrideuteromethyl β, β dideuterostyrenes were also studied. Thi polymer gives pure monomer as a volatile product and has large zip-length. For very large zip-length compared to molecula weight, theory predicts a rate proportional to weight averag degree of polymerization. We observed a dependence in exces of the weight average D, P. in the region that the rate is approxi mately proportional to molecular weight. This is suggestive of a effect related to the physical properties of the liquid melt in th direction to increase the zip-length.

The present results on monodisperse polymers indicate longe zip-lengths than previously estimated from measurement on frac tionated poly α-methylstyrenes. Also the monodisperse deu terated polymers have an even longer zip-length compared to th nondeuterated polymers.

**14633.** Simiu, E., **Improved methods for determining wind profile and dynamic structural response to wind,** *Proc. ASCE-IABS Regional Conf. on Tall Buildings, Bangkok, Thailand, Ja 1974,* pp. 491-503 (1974).

Key words: aerodynamics; dynamic response; gust facto structural engineering; wind profiles; wind spectra.

In current methods for determining alongwind structur response, it is assumed that wind profiles are described by empi ical power laws and that turbulence spectra are independent height. In this paper, the adequacy of these assumptions is a sessed in the light of recently established results of bounda layer meteorology. An improved method for determining wi profiles is presented, and expressions for the dynamic alongwi response, including deflections and accelerations, are propose In addition to the variation of wind spectra with height, these e pressions take into account the pressure correlations in th alongwind direction, determined in accordance with basic theo and known experimental results.

**14634.** Renninger, C. R., **Central government structure for t development of an ADP policy,** *Proc. 7th Conf. Intergover mental Council for ADP, Ottawa, Canada, Sept. 17-19, 197* pp. 57-71 (1973).

Key words: ADP policies; computer technology; manag ment; quality control; software.

Advancements in computer technology, the emergence computer subindustries with new products and marketing strat gies, and the growing maturity of both the computer supplier a the computer user are forcing a reexamination of government ADP policies. A dominant issue is the management of comput software which has become the critical factor in achieving effe tive use of computer technology as well as the most expensi element of computer operations. The level of computer effectiv ness can be increased significantly by improving software. Bett quality control over the production of software is needed eliminate errors and provide guarantees of satisfactory p formance. The utility of proven software needs to be extended other users to avoid redundant and costly developmental effor Ways must be found to reduce the time required to produce so ware and thereby bring operational systems on-stream soon pecific actions taken by the National Bureau of Standards, ieneral Services Administration, and the Office of Management nd Budget to improve software management in these areas of eed are described.

**4635.** Young, R. H., Brewer, D., Kayser, R., Martin, R., Feriozi, D., Keller, R. A., **On the mechanism of quenching by amines: A new method for investigation of interactions with triplet states,** *Can. J. Chem.* **52,** No. 16, 2889-2893 (1974).

Key words: lasers; photochemistry; $^1\Delta O_2$.

Rate constants for the quenching of singlet oxygen by a series f substituted *N,N*-dimethylanilines were obtained by a direct nethod employing dye-laser. The Hammett $\rho$ value obtained om the data (– 1.71) suggests that a (partial) charge-transfer omplex may be responsible for the quenching action. This rate ata was combined with that obtained for the total quenching acon on the sensitized photooxidation of 1,3-diphenylfuran. The uenching action on the photooxidation reaction is due to both ne quenching of singlet oxygen and the quenching of the triplet tate of the sensitizer (rose bengal or methylene blue). The comination of the data from each series of experiments resulted in ate constants of quenching of the triplet states of the sensitizers. number of the *N,N*-dimethylanilines quenches the triplet tates at the diffusion limit. Hammett $\rho$ values (– 1.86 for rose engal and – 4.19 for methylene blue) indicate that chargeansfer intermediates are probably responsible for the uenching action. This was confirmed by the observation of a ansient intermediate assigned to the charge-transfer radical of nethylene blue. The technique used here represents a novel aproach to the investigation of triplet states.

**4636.** Madden, R. P., **Synchrotron radiation and applications,** Chapter 7 in *X-ray Spectroscopy,* L. Azaroff, Ed., pp. 338-378 (McGraw-Hill Book Co., New York, N.Y., 1974).

Key words: radiation; source and electrons; synchrotron; x-ray, vacuum ultraviolet.

The historical development of the theoretical understanding of ynchrotron radiation is reviewed. The important equations ecessary to calculate the details of the angular, polarization and avelength distribution of the radiation and the dependence of nese properties on the electron energy and the radius of the ajectory are presented. Also approximate expressions are iven which can be utilized to quickly estimate these properties or any given source of synchrotron radiation. The observational evelopment of synchrotron radiation is also historically eviewed, presenting the experimental verification of the neoretical predictions and including a short history of the orld's major synchrotron radiation laboratories. Finally, appliations of synchrotron radiation in experimental physics are resented, including examples where important contributions ave resulted in areas of atomic, molecular, solid state and surace physics as well as in radiometry.

**4637.** Thomas, D. B., Freeze, P. D., **The effects of catalysis in measuring the temperature of incompletely-burned gases with noble-metal thermocouples,** *Proc. 5th Symp. Temperature—Its Measurement and Control in Science, Washington, D.C., June 21-24, 1971,* pp. 1671-1676 (1971).

Key words: butane; carbon monoxide; catalysis; combustion; hydrogen; optical pyrometer; platinum; platinum-13 percent rhodium; temperature; thermocouple.

Measurements have been made on the effects of catalysis vhen platinum-13 percent rhodium versus platinum thermocoules are used to measure the temperature of incompletely-burned ases in the temperature range 1000 to 1500 °C. These measurenents indicate that significant temperature errors can result vhen noble-metal thermocouple materials are exposed to varius unburned gases under laboratory test conditions. Platinum and platinum-13 percent rhodium thermocouple elements were exposed to gas mixtures of air + 1.0 percent $H_2$, air + 2.0 percent $H_2$, air + 1.0 percent CO + 0.01 percent $H_2$, air + 2.0 percent CO + 0.01 percent $H_2$ and air + 0.5 percent $C_4H_{10}$. At very low gas velocities ($< 9 \times 10^{-3}$ m/second), the thermoelement temperature increase due to surface combustion varied from about 2 to 77 °C at thermoelement temperatures between 1000 and 1500 °C. At gas velocities between $0.17 \times 10^2$ and $1.83 \times 10^2$ m/second, the temperature increases varied between 35 and 380 °C. Measurements with five gas mixtures indicate that the sample temperature increases ($\Delta T$) due to catalytic heating increase with increasing gas velocity up to approximately $1.2 \times 10^2$ m/second. Above $1.2 \times 10^2$ m/second, the $\Delta T$ values tend to decrease with further increasing velocity.

**14638.** Marton, L. L., **Article on Baron Roland von Eötvös,** *Dictionary of Scientific Biography* **4,** 377-381 (1971).

Key words: Eötvös balance; Eötvös' law of surface tension; equivalence of gravitational and inertial mass; geophysical exploration; public service; torsion balance.

Born in 1849 in Badapest, Hungary, he studied in Heidelberg and in Königsberg, Germany. Returning to Hungary he became Professor at the University of Budapest. For a few years he pursued research on surface tension, but after 1888 Eötvös devoted all his research efforts to the problem of gravitation. He designed the "Eötvös torsion balance" and used it for geophysical exploration as well as for measurements of the equivalence of gravitational and inertial mass. He served briefly in the Hungarian Cabinet as Minister of Public Worship and Education, as "Rector" of the Unviversity, as President of the Hungarian Academy of Sciences, etc. He died in 1919.

**14639.** Simiu, E., **Variation of mean winds with height in hurricanes,** *J. Eng. Mech. Div. Am. Soc. Civil Eng. Tech. Note* **100,** No. EM4, 833-837 (Aug. 1974).

Key words: boundary layer; hurricanes; loads (forces); natural disasters; structural analysis; tall buildings; wind profiles.

The magnitude of wind pressures on buildings and structures depends, among other factors, upon the variation of wind speeds with height. The presence in hurricane flows of strong inertial forces due to the curvature of the isobars in the region of highest winds suggests that differences exist between hurricane velocity profiles and the logarithmic profiles typical of extratropical winds. Simplified models of boundary layer flow in cyclostrophic and geostrophic flow are used to show that these differences appear to be significant. The results obtained suggest that an investigation based on a more realistic model of actual atmospheric boundary layer flow is warranted. Suggestions are made for the major ingredients of an alternative model and the use of existing models for numerical solution of the model. These indicate the feasibility of getting more reliable estimates for the variation of the winds with height under hurricane conditions. The author is currently conducting research along the lines indicated.

**14640.** Stillman, R. B., **A survey of techniques for increasing software reliability,** *Proc. Summer Computer Simulation Conf., Montreal, Canada, July 1973,* pp. 1130-1133 (1973).

Key words: dynamic analysis; proof of correctness; software reliability; static analysis; testing software.

The quality of today's major software systems is uneven at best. Programs thought to be correct will suddenly produce wrong results, no results, or behave otherwise erratically, because some special condition in the data or in the environment was not accounted for in the logic of the program. Techniques to improve reliability and to facilitate thorough testing of software fall into two main categories: (1) Static analysis, which is performed without executing the software. Questions of overall software system design, higher-level language design, use of various static analysis tools, and the concept and potential of machine generated proofs of correctness are addressed; (2) Dynamic analysis, which is dependent upon information collected while the software is in execution. Interest is centered on frequency (of execution) monitors; dynamic debugging facilities, address range and data bound checks, optionally compilable assertions, and tracing and tracking tools.

**14641.** Walter, L. S., French, B. M., Heinrich, K. F. J., Lowman, P. D., Jr., Doan, A. S., Adler, I., **Mineralogical studies of Apollo 12 samples,** (Proc. Second Lunar Science Conf. Houston, Tex., Jan. 11-14, 1971), *Geochim. Cosmochim. Acta Suppl. 2,* **1,** 343-358 (1971).

Key words: Apollo 12; crystallization; mineralogy; moon; petrography; pyroxene; rocks.

The five crystalline rocks studied represent three distinct chemical groups: (1) low-Mg, high-Al; (2) intermediate; and (3) low-Al, high-Mg. Petrography and mineral compositions are consistent with the suggestion that the differences reflect olivine removal during crystallization, producing Mg-rich cumulate rocks and Mg-poor residual liquids. Some mineralogical characteristics are consistent with this model. However, significant mineralogical differences are observed between specimens in the same chemical group, suggesting that the actual crystallization relations are more complex. Ni-Fe metal, possibly emplaced as a late-stage vapor deposit, occurs in cracks in pyroxene and chromite, and along pyroxene cleavage elements. The metal has the same nickel content as other metal in the sample and is not associated with sulfide. No concentration gradients in iron in the host crystal are observed.

**14642.** Wright, J., **Integration of the performance concept into building regulation,** *Proc. 3rd South African Symp. National Building Regulations, Durban, South Africa, May 17, 1974,* pp. 20-23 (1974).

Key words: building codes; building technology; energy conservation; evaluation and acceptance system; National Bureau of Standards; National Conference of States on Building Codes and Standards; performance concept.

Building regulation is an exercise of the police power and is therefore, by authority of the United States Constitution, a function of the member States of the Federal republic. But historically building has been a local enterprise and the States left its regulation to the cities since so many regulatory issues, e.g. conflagration, dealt with circumstances of urban life. The result is a mosaic of thousands of regulatory jurisdictions. This situation imposes burdens on building technology because each jurisdiction has its own set of standards (called a code) and enforcement practices. While traditional technology has managed to cope fairly well with the multiplicity of regulations and-practices, innovative technology has been less successful. Performance standards would help to offset this imbalance since they are equally accommodating of new and traditional technology. However, performance standards require a performance evaluation and acceptance system if they are to be usefully promulgated. This is a key concept with the relatively new National Conference of States on Building Codes and Standards, an organization working to improve the regulatory climate. At the request of the Conference, the National Bureau of Standards (NBS) has prepared a document called "Draft Design and Evaluation Criteria for the Conservation of Energy in Buildings." The document is based on the performance concept with which NBS has had considerable experience. The NBS effort is also addressed to institutional mechanisms, including those necessary for a performance evaluation and acceptance system. The latter is seen as a complement to—not a competitor of—the established regulatory system.

**14643.** Wright, J. R., Herron, W. R., **Housing research at the National Bureau of Standards,** *Proc. Silver Jubilee Celebration o the Central Building Research Institute of India, Roorkee, India, Feb. 29-Mar. 2, 1973,* pp. 19-24 (1973).

Key words: building research; industrial building; performance criteria; total energy.

As the Central Building Research Institute at Roorkee is holding its Silver Jubilee, there is abroad in the world a great deman for relevance of many activities formerly left to random coordination. This is true in the United States of America and t some degree is the cry of all mankind. The Central Buildin Research Institute is to be commended for the achievement o relevance between the requirements of the people of India an their building research efforts. This has been accomplished by steadfast adherence to the principle that sophisticated scienc can be turned to practical applications by research which recognizes the need to gear these applications into the patterns o everyday life in India. The thrust of this paper is to establish th realization that "Housing is a Social Process," since it involve a continuously changing interrelationship between national cultural goals, the designers, builders, and users. This realization i achieved to a varying degree from one culture to another. Som of the work described herein will show courses of action whic can enhance the social significance of the building process.

**14644.** Sengers, J. M. H. L., **Critical point,** *Encyclopedia Americana* **8,** 219-220 (Americana Corp., New York, N.Y., 1973).

Key words: critical anomalies; critical opalescence; critica point; critical-point phase transitions.

For the general reader, the critical point is defined using th gas-liquid system as an example. Critical anomalies and light scattering methods for studying these are discussed. Som further examples of critical-point phase transitions are enumerated and their analogy is stressed.

**14645.** Madden, R. P., **The Frederic Ives Medal for 1971,** *J. Op Soc. Amer.* **62,** No. 8, 927-930 (Aug. 1972).

Key words: Ives, medal; medal, Ives; optics, Ives medal.

*Ives Medal Citation—Arthur Francis Turner.* In recognitio of his leadership in pioneering the methods of design and fabrication of multilayer evaporated films; his originality in applyin multilayer systems to the solution of practical optical problem and his effectiveness as an educator, communicating to other the methods and principles he developed during a lifelong dev tion to optical physics.

**14646.** Lauritzen, J. I., Jr., Zwanzig, R., **Dielectric relaxation of single axis rotator with two equivalent sites,** *Advan. Mol. Relaxation Processes* **5,** 339-361 (1973).

Key words: dielectric loss; relaxation; single axis rotato site model; Smoluchowski's equation.

The dielectric relaxation of a single axis rotator subject to sinusoidal potential due to the crystalline field has been calc lated for a polycrystalline sample, assuming the relaxation of th dipolar orientation is governed by Smoluchowski's equation. F large values of the potential barrier the dielectric loss co responds to that due to a two site model. For intermediate valu of the potential barrier the dielectric loss corresponds to tw slightly broadened Debye loss curves which may be sufficient separated to be bimodal.

**14647.** Julienne, P. S., Krauss, M., **Molecule formation by inver predissociation,** (Proc. Symp. on Interstellar Molecules, Cha lottesville, Va., Nov. 4-7, 1971), Paper in *Molecules in th Galactic Environment,* M. A. Gordon and L. E. Snyder, Eds pp. 354-373 (John Wiley and Sons, New York, N.Y., 1973).

Key words: Bates mechanism; Feshbach-type resonance states; inverse predissociation; molecule formation; non-adiabatic interactions; radiative association; two-body recombination rates.

One of the dominant mechanisms for interstellar molecule oduction has long been thought to be radiative association. We ish to broaden the usual understanding of this process and esent a theory for molecule formation through inverse predis- ciation which must be considered along with the Bates echanism as being important under interstellar conditions. lthough molecule formation by a two-body collision can occur ly upon continuum to bound radiation, we will demonstrate at the presence of Feshbach-type resonance states embedded the continuum must be considered. Thus, two colliding ground ate atoms may populate excited bound molecular electronic ates which radiate to produce a stable molecule. This echanism can be operative in molecules for which the direct ntinuum emission of the Bates mechanism is not possible. We ve calculated the two-body recombination rate constant for H to be $\sim 3 \times 10^{-20}$ cm$^3$ sec$^{-1}$ above around 20 K. This rate sults from the mixing of OH $A^2\Sigma^+$ v = 1 bound levels with the ound $X^2\Pi_{3/2}$ continuum by virtue of the breakdown of the orn-Oppenheimer approximation. Preliminary calculations for o-body recombination rates for other molecules indicate that H, CN, and NO can also be formed through intermediate sonance states with rates exceeding $10^{-18}$ cm$^3$ sec$^{-1}$ at low temratures. We will present a general theory of radiative associaon by inverse predissociation, including (1) the scattering foralism for the calculation of the Einstein A coefficient, (2) a assification of the various couplings which are possible, gether with simple rules for deciding when they may be impornt, and (3) results of calculations for the formation rates of ecific molecules.

648. Johnson, D. R., Kirchhoff, W. H., **Centrifugal distortion and predictability in the microwave spectrum of formamide,** (Proc. Symp. on Interstellar Molecules, Charlottesville, Va., Oct. 4-5, 1971), Paper in *Molecules in the Galactic Environment,* M. A. Gordon and L. E. Snyder, Eds., pp. 247-253 (John Wiley and Sons, New York, N.Y., 1973).

Key words: centrifugal distortion; critical review; formamide; interstellar molecules; microwave spectra.

Recent detection of emission signals from interstellar formaide ($NH_2COH$) has stimulated a renewed interest in the laborary microwave spectrum of this molecule. Previous laboratory vestigations of formamide were aimed primarily at obtaining ructural parameters and other related information. The spectral servations reported in these early papers have much in comon with the available literature on other interstellar molecules. eported transitions either do not include those accessible to the dio telescopes or were not measured with sufficient resolution be useful for a positive molecular identification.

The present paper describes a detailed investigation of the efcts of centrifugal distortion and nuclear quadrupole hyperfine litting on the microwave spectrum of formamide. Molecular rameters obtained from this investigation have been used to edict the entire rotational spectrum of $^{14}NH_2\ ^{12}C^{16}OH$ potenally accessible to the telescopes. The procedures illustrated ith formamide may be applied to other molecules to predict inrstellar transitions which are difficult to measure in the laborary.

649. Kessler, E. G., Jr., **Determination of the Rydberg constant from the He II $n = 3 - 4$ (4686 Å) line complex,** (Proc. Fourth Int. Conf. on Atomic Masses and Fundamental Constants, Teddington, England, Sept. 1971), Paper in *Atomic Masses and Fundamental Constants,* J. H. Sanders and A. H. Wapstra, Eds., pp. 427-434 (Plenum Press, London, England, 1972).

Key words: fine structure; helium; Rydberg constant.

Absolute wavelength measurements of some of the fine structure components of the He II transition at 4686 Å (n = 3 − 4) are being measured to establish a new value for the Rydberg constant. The He II transition is excited in a cooled-hollow-cathode discharge and is resolved and compared to a standard source by use of a pressure-scanned double Fabry-Perot spectrometer. Problems associated with precision wavelength measurements using pressure-scanned interferometers will also be discussed.

14650. Leasure, W. A., Jr., Bender, E. K., **Tire-road interaction noise,** *Proc. Inter-Noise 73 Conf., Copenhagen, Denmark, Aug. 22-24, 1973,* pp. 421-425 (1973).

Key words: acoustics; noise (sound); tire noise; transportation noise.

The relative importance of tire noise to overall vehicle noise is established. A general description is then given of the tire engineering process and of tire structures. The important parameters influencing tire noise are discussed, based on presently-available data, followed by an identification of unknown and contradictory areas. The basic mechanisms of tire-noise generation, although not well understood, are investigated largely from a theoretical viewpoint. Areas for future research and development are identified based on gaps in the existing physical data base and a rather primitive level of understanding of noise-generating mechanisms.

14651. Snell, J. E., Achenbach, P. R., **Total energy systems: A review of recent NBS activities,** *Proc. Effective Energy Utilization Symp., Drexel University, Philadelphia, Pa., June 8-9, 1972,* pp. 201-233 (June 1972).

Key words: central utility systems; electrical power generation; energy conservation; energy costs; integrated utility systems; total energy systems, waste disposal.

This paper briefly reviews and reports on the status of several NBS activities in the area of total energy systems as they relate to the theme of the Drexel Symposium on Effective Energy Utilization. A recent review of the state of the art in total energy systems application, indicated the need for good, concise, operating and performance data on total energy systems to serve as a basis for more effective utilization of this concept to save energy. The Department of Housing and Urban Development requested NBS to assist in the development of a total energy system on the BREAKTHROUGH housing site at Jersey City and to conduct a full-scale field study with appropriate instrumentation to obtain engineering, cost and maintenance data.

In a related effort, NBS, AEC, EPA, and NASA are supporting HUD in a new effort entitled The Modular-Sized Integrated Utility System (MIUS) program. The premise of this 3-phase effort is to demonstrate the potential energy, resource, and cost economies of combining energy-generating facilities and waste disposal facilities on a modular-basis to keep pace with changing patterns and rates of urban growth.

14652. Little, J. L., **Impact of the ASCII code and printing devices on conventions for alphanumeric display terminals: Part 1,** *Commun. Soc.* **10,** No. 1, 7-10 (Mar. 1973); **10,** No. 2, 6-11 (May 1973).

Key words: alphanumeric displays; ASCII Code; cathode-ray-tube displays; control functions; display terminals; interactive terminals; remote computer terminals; soft copy; test editing displays; user control functions; visual displays.

This paper reviews briefly the evolution of the American Standard Code for Information Interchange (ASCII) and its international version (ISO R-646). It also reviews the evolutionary impact of typewriters, teletypewriters, and the ASCII code on conventions now employed in alphanumeric display terminals. It shows a proposed keyboard layout, some approved graphic subsets of ASCII, and some codes used in computers. Current developments in the representation of extended versions of ASCII in 7 and 8 bits are given. Proposed code assignments of control functions for alphanumeric display terminals are also included, with a warning that their standardization is under the jurisdiction of the American National Standards Institute's Technical Committee X3L2 on Character Codes.

**14653.** Keplinger, M. S., **The case for the invisible copies,** *Rev. Int. Droit Auteur,* pp. 2-31 (1971).

> Key words: computers; copyright; information storage and retrieval; infringement; input; intellectual property; law.

The problem of control of the use of copyrighted works in computerized information storage and retrieval systems is discussed. It is concluded that such input may be considered copyright infringement under the current Copyright Revision Bill as interpreted through the teachings of recent court decisions, as well as being an infringement under the current copyright statute. Since the input of this material may be assumed to be infringement, a method for control of the author's right must be devised to protect the author and provide for efficient dissemination of the information. To aid in this control a clearinghouse for copyright concept is suggested.

**14654.** Olsen, L., Baumgarten, G. P., **Gas flow measurement by collection time and density in a constant volume,** (Proc. Symp. on Flow—Its Measurement and Control in Science and Industry, Pittsburgh, Pa., May 10-14, 1971), Chapter in *Flow—Its Measurement and Control in Science and Industry,* R. B. Dowdell, Ed., **I,** 1287-1295 (Instrument Society of America, Pittsburgh, Pa., 1971).

> Key words: calibration; critical flow; gas flow; measurement; nozzles, volumetric.

A method for the accurate measurement of gas flows is described. This method utilizes a valve to divert the flow to a tank of known volume over a measured calibration time interval. Measurements of pressure and temperature (for gas density) are made when the gas within the tank is at a stationary equilibrium condition. The density increase from essentially zero density within the known volume over the measured time interval permits a determination of the mass rate of flow. The flow measurement apparatus and air treatment system consisting of a centrifugal compressor, air dryer, filters, receiver tank, meter runs, nozzles, diverter valve, collection tank and instrumentation are described. A discussion of the procedures and errors in the measurement of pressures, temperatures, volume of the collection tank and timing of the diverter valve is included. The effects of these individual errors on the overall uncertainty of the gas flow measurement is considered. Ten sonic flow nozzles with throat diameters ranging from 0.14234 to 1.29841 in. were calibrated at upstream pressures to 95 psig and flow rates to 2700 SCFM. On the basis of error analysis and comparisons with calibrations in a bell-type prover, the overall uncertainty of these calibrations is estimated to be about 0.11 percent.

**14655.** Ruegg, F. W., Johnson, D. P., **Dynamics of the bell prover,** (Proc. Symp. on Flow—Its Measurement and Control in Science and Industry, Pittsburgh, Pa., May 10-14, 1971), Chapter in *Flow—Its Measurement and Control in Science and Industry,* R. B. Dowdell, Ed., **I,** 1297-1307 (Instrument Society of America, Pittsburgh, Pa., 1971).

> Key words: bell prover; dynamics of provers; flow measurement; gas flow measurement; prover design.

The bell prover is widely used for gas flowrate measurement by timing a known stroke of the bell as it rises, with presumably constant speed, from a bath of sealing liquid. A motion analysis of the coupled fluid and mechanical parts of the prover system has been made to guide experiments, and to determine dynamic use criteria and measurement errors associated with transient oscillatory motions. Simultaneous differential equations for the motions of the bell, sealing liquid, and gas are presented as a basis for a computer simulation of prover performance. Motion of the bell is considered as affected by the gas pressure therein, by the masses in motion, by viscous drag force and adherence of liquid. Pressure and gravity forces, and viscous flow resistance, affect the liquid motion. Gas pressure in the bell is affected by all the motions and by the gas content. Various methods of damping initial transient motions are included in the analysis.

**14656.** Wright, R. N., Yokel, F. Y., **A concept for limit states design,** *Proc. ASCE-IABSE Int. Conf., Bethlehem, Pa., Aug. 21-25, 1972, Conf. Preprints on Planning and Design of Tal Buildings,* **A,** 395-399 (1972).

> Key words: design mode; limit states design; load; performance criteria; reinforced concrete; reliability; resistanc mode; safety; serviceability; stability; structures.

The state-of-the-art reports presented in behalf of Committe 26 are summarized in this paper. Basic concepts and terminolog associated with limit states design are discussed and a mor general approach is suggested in which scheme-independent performance criteria would be used as a common basis for criteri for limit states design for all material applications. This approac would permit consistency among various material oriente design philosophies.

**14657.** Wright, R. N., **Buckling of plane or prismatic structure** *Proc. RILEM Colloque Int. Symp., Buenos Aires, Argentin Sept. 13-18, 1971,* pp. 1-13 (Instituto Nacional d Technologia Industrial, Buenos Aires, Argentina, 1971).

> Key words: buckling; computers; experimental methods; ir stability; models; structures.

The papers in this topic address the purposes for experiment analysis of plane and prismatic structures. The report discusse papers dealing with the behavior of reinforced and prestresse concrete structures and metal structures. Within each categor local instability, member instability, and instability of asse blages are considered in the cited order. Finally, papers ar discussed which treat aspects of experimental technology th are independent of the structural technology.

**14658.** Wilson, W. K., **Test methods for determining the effect various treatments on paper,** *Proc. Int. Inst. for Conservatio of Historic and Artistic Works (IIC) Congress, Lisbon, Port gal, Oct. 9-13, 1972,* pp. 985-994 (1972).

> Key words: paper; paper test methods; restoration; restor tion of paper; test methods for paper; treatment of paper.

Several methods are described that may be used in the evalu tion of the effects of various restoration treatments on pap documents and works of art. References are given to standa methods and to other sources of information that would be value to the restorer. The necessity for judging each situation a separate entity is emphasized.

**14659.** Rosenstein, M., Levine, H., McLaughlin, W. L., **A the mosetting radiation-sensing gel for small-volume dosimetr** (Proc. Fourth Symp. on Microdosimetry, Verbania Pallanz Italy, Sept. 24-28, 1973), *EURATOM,* J. Booz, H. G. Ebe R. Eickel, and A. Waker, Eds., pp. 935-950 (Brussels, Bel um, 1974).

> Key words: dosimetry; dyes; gels; microdosimetry; plastic radiochromism; triphenylmethane dyes; vinyl resins; x-r detectors.

Thin-film radiation detection systems using triphenylmetha dye derivatives have been developed previously, and the osimetric properties have been described in the literature. Until e present work, the solid activator matrix that best sensitized diolytic dye production was gelatin. Gelatin has the serious oblems of dimensional instability and migration of the dye rmed after irradiation. The improved activator matrix scribed here has potential wide application as a radiation de- ctor and imaging system. The dosimeter response results from nversion of the dye precursor to the colored dye, and is a arly linear function of absorbed dose. Due to the nonturbid atrix, image resolution of 1 μm can be achieved using icrodensitometry.

The most successful formulation of those investigated to date ntains: a triphenylmethane dye precursor; a specific combina- n of monomers and polymers, which constitute the activator atrix; and a polymerization initiator. The thermosetting formu- tion can be molded into a solid glassy resin. Its elemental con- ituents are C, H, N, and O, and its mass energy absorption efficient for photons above 200 keV is within 4 percent of that r water and muscle. Down to at least 25 keV, there is no sig- ficant variation of dosimeter response with photon energy. ariation of response with ambient temperature during irradia- n of the system, relative to room temperature, is less than ±5 rcent between 0-50 °C. After irradiation and a slight initial 24- ur color buildup, the image is stable for about 1 month. Then gradual fading occurs. With a 2 mm-thick gel, absorbed doses 10 krad can be detected with precision limits of 5 percent.

**660.** Suzuki, G., Hendrickson, R., Donaldson, J., **Quantitative methods in decisionmaking,** Chapter VI in *Management: Concepts and Practice*, F. R. Brown, Ed., pp. 115-155 (Industrial College of the Armed Forces, Ft. McNair, Washington, D.C., 1972).

Key words: decisionmaking; methods; models.

This paper is a revision of Chapter VIII of a handbook used the Industrial College of the Armed Forces. The handbook s the full title *National Security Management-Management: oncepts and Practice*, and is required reading for students at- nding the College. Chapter VIII is one of three chapters of art II of the book dealing with the general subject *Quantitative ols for Management*. The intent of the chapter is to introduce e reader, who is assumed to have no knowledge of the subject, the principal elements and kinds of decision processes that cur in operations that require explication and analysis. The apter is divided into nine sections, whose organization and ntent lead the reader through an ordered development of the aterial, dealing with the qualitative and quantitative aspects of e problems likely to be faced and the practicable methods used the formulations and solutions of these problems. Optimizing d non-optimizing analyses are covered appropriately for the eds of the intended audience of the book. The authors have ed to state the limited utility of formal mathematical methods d have apprized the reader of the fundamentals of operations search as they contribute to problem-solving and analysis of erational situations.

**661.** Wright, J. R., Herron, W. R., **Response to "J. B. Dick Report,"** *Proc. 5th CIB Congress on Research into Practice. The Challenge of Application, Paris, France, June 1971*, pp. 275-279 (1971).

Key words: BREAKTHROUGH; building performance; construction; contracting; performance assessment; performance concept; performance products; performance testing; user needs.

This paper responds to a provocative paper prepared by Mr. B. Dick, Director, Building Research Station in England, for e 5th CIB Congress, June 22-30, 1971, at Versailles, France, titled "Design Aids: Evaluation Methods for Buildings, Com- nents and Materials." The intent of this paper is to defend the Performance Concept and its application to building construction. Such a defense must dispel misconceptions which have developed from the limited size of past demonstration projects based on this concept. If these false beliefs are not recognized, they could seriously limit future development and use of the performance concept.

**14662.** Wright, J. R., Leyendecker, E. V., **Measuring the performance of industrialized housing under "Operation Breakthrough,"** *Proc. 5th CIB Congress on Research into Practice. The Challenge of Application, Paris, France, June 1971*, pp. 303-308 (1971).

Key words: certification; guide criteria; innovative housing; Operation BREAKTHROUGH; PERFORMANCE criteria; performance evaluation.

The National Bureau of Standards, Department of Commerce, is conducting the technical evaluation of "Operation BREAKTHROUGH" housing systems for the Department of Housing and Urban Development. This paper discussed the BREAKTHROUGH team's development of performance criteria and describes the philosophy used in developing the criteria. An example of how the criteria can be used in the evaluation process leading to certification is discussed.

**14663.** Somes, N. F., Corley, W. G., **Circular openings in webs of continuous beams,** *Amer. Concrete Inst. Spec. Publ. 42-17*, pp. 359-398 (1973).

Key words: beams; design criteria; joists; openings; shear strength; tests; web.

The second phase of a comprehensive investigation is reported. Tests show the effect on strength and behavior of circular web openings in continuous lightweight-aggregate concrete joist floors. Principal variables were size, location, reinforcement and spacing of openings. Based on the findings, design recommendations are presented.

**14664.** Muehlhause, C. O., **Setting safety standards via risk-benefit analysis,** *Proc. PLP-73 Product Liability Prevention Conf., Newark, N.J., Aug. 22-24, 1973*, pp. 137-140 (1973).

Key words: acceptance of risk; consumer product safety; perception; risk-benefit analysis; standards.

The problem which a hypothetical regulator would face who is intent on setting safety standards for consumer products utilizing the "method" of risk-benefit analysis is examined. It is shown that in addition to a scarcity of difficult-to-produce data certain conceptual problems regarding the manner in which risk to personal health and safety is to be embodied in cost-benefit analysis is also present. A particular formulation which recognizes the acceptance and misperception of risk as well as its cost is presented.

**14665.** Locke, J. W., **Data limitations for the prediction of dangerousness,** (Proc. Conf. on Preventive Detention Center for Continuing Education, University of Chicago, Chicago, Ill., Oct. 28-30, 1969), Paper in *Preventive Retention*, pp. 117-131 (Urban Research Corp., Chicago, Ill., 1969).

Key words: bail; criminal justice; dangerousness; data collection; prediction; statistical analysis.

Statistical data used in past studies to describe criminal activity of people while on pre-trial release have been questioned by many familiar with the Criminal Justice System because of their limited scope. This paper describes some of the problems associated with the development of a substantially broader data base. It also includes a discussion of incompleteness, inaccuracy and other inadequacies of available court data for developing methods of predicting dangerousness of individuals who enter the Criminal Justice System. Brief reference is made to dangerousness criteria and to prediction techniques which may have application in deciding whether or not to release defendants before trial. The discussion is based upon the early stages of a pilot study being conducted for the National Institute of Law Enforcement and Criminal Justice.

**14666.** Fano, U., Martin, W. C., **Z-dependence of spin-orbit coupling,** Paper in *Topics in Modern Physics,* W. E. Britten and H. Odabasi, Eds., pp. 147-152 (Colorado Assoc. Press, Boulder, Colo., 1970).

Key words: coupling-strength; spin-orbit coupling.

Experimental evidence on the spectroscopic spin-orbit strength parameter for p electrons, $\zeta_p$, for neutral atoms of all atomic numbers Z is represented rather closely by the empirical formula

$$\zeta_p n^{*3} = 0.450\, Z^{2.33}\, \mathrm{cm}^{-1}.$$

A few comments are made regarding alternative representations of spin-orbit coupling.

**14667.** Klein, R., **Gas-solid interactions: Laboratory paradigms for reactions on interstellar grains,** (Proc. Conf. on Interstellar Molecules, Charlottesville, Va., Oct. 4-5, 1971), Paper in *Molecules in the Galactic Environment,* M. A. Gordon and L. E. Snyder, Eds., pp. 390-398 (John Wiley and Sons, New York, N.Y., 1973).

Key words: interstellar molecules; low temperature chemistry; surface reactions.

Reactions observed at temperatures below 150 K include those of atomic hydrogen and atomic oxygen in their ground electronic states interacting with condensed olefinic hydrocarbons. These serve as models for consideration of reactions on interstellar grains. The atomic hydrogen adds to the olefin on the surface with the resultant alkyl radicals diffusing into the interior and reacting further. Atomic oxygen diffuses into and reacts in the condensed volume. These reactions are discussed in terms of molecule formation. It is noted that the activation energy barriers are sufficiently high, both for reaction and diffusion, that it is unlikely that these reactions may serve as useful models for molecular syntheses in the H-I region.

**14668.** Unassigned.

**14669.** Wright, J. R., Achenbach, P. R., Editors, **Energy Conservation in Buildings,** (Proc. Scientific American Roundtable of Energy Conservation in Buildings, New York, N.Y., Aug. 29, 1973), *Sci. Amer. Spec. Publ.,* 79 pages (1973).

Key words: buildings; conservation; energy; energy sources; measurement; simulation; thermal efficiency.

More base data is needed with respect to energy resources and us. Better measurement in terms of both techniques and values is suggested in the physical science aspects of energy and in our understanding of man and the energy-related attributes he requires of his shelter. Americans must stop wasting energy and at the same time develop new energy technologies. The roundtable offered numerous suggestions for the near-, mid- and long-range futures.

**14670.** Meese, W. J., **Rules for the operation of electric supply and communication lines and equipment,** Part 4 (Sections 40-43) in the *National Electrical Safety Code,* Sixth Edition, *ANSI C2.4-1973,* pp. 273-313 (IEEE, New York, N.Y., 1973).

Key words: communication industry safety; electrical safety; operation of communication systems; operation of electrical supply systems; public utility safety; safety work rules.

This standard contains Part 4 of the National Electrical Safety Code and supersedes ANSI C2.4-1939, NBS Handbook H34 and pages 305 through 358 of NBS Handbook H30. Part 4 of this Code contains work rules applying to the construction, maintenance, and operation of electric-supply and communication lines and equipment of public utilities and similar systems. These rules are intended to embody the requirements which are most important from the standpoint of safety to employees and to the public.

**14671.** Meese, W. J., **Safety and safety standards for electric supply and communication facilities in utility tunnels,** *Proc. American Public Works Assoc., Henniker, N.H., Aug. 16-20, 1971, Special Report* **42,** pp. 95-98 (New England College, Henniker, N.H., 1972).

Key words: coordination of utility facilities; national electrical safety code; safety standards for utility tunnels; underground communication facility; underground electric facilities; utility tunnel safety.

In recent years many of the facilities of electric and communication utilities have been installed underground, principally for environmental reasons. Installation and maintenance of these facilities, along with the facilities of several other utilities is becoming difficult and costly, and the necessity of frequent street openings for access to utilities is burdensome to the public and to businesses in the vicinity. Better coordination of utility and other public works facilities is needed. Because of this, the utility tunnel concept is receiving much study and utility tunnel safety is a primary consideration.

**14672.** Hilsenrath, J., **Input techniques for technical information** *Proc. Forum of Federally Supported Information Analysi Centers, NBS, Gaithersburg, Md., May 17-18, 1971,* pp. 71 88 (Available as PB208-018 from the National Technical Information Service, Springfield, Va. 22161, Jan. 1972).

Key words: computer-assisted printing; computer input electronic typesetting; input techniques; keyboarding conventions; phototypesetting; text automation.

A summary is presented of recent progress at NBS in the automation of book production through the development o techniques for computer-assisted phototypesetting. The strengt of the system rests on general-purpose edit-insertion program and other general-purpose programs which accept a variety c input media. The programs take existing files on punched card or computer tapes; or Magnetic Tape Selectric Typerwrite (MTST) cartridges; or files keyboarded on-line to a time-share text editing system; and transform them to match the requirements of the phototypesetting system at the U.S. Governmer Printing Office (GPO).

Examples are shown of finished text consisting of upper an lower case Roman and Greek characters, subscripts and superscripts keyboarded on a variety of input devices. The example are from input on punched cards, from a 44 key Selectric te minal and from a "scripting" teleprinter capable of typing 12 characters in two colors in inferior, superior or main line pos tions.

**14673.** Hall, J. L., **Sub Doppler spectroscopy, methane hyperfi spectroscopy, and the ultimate resolution limits,** *Proc. Ausso Conf. on Spectroscopy Without Doppler Broadening, Aussoi France, May 1973,* pp. 105-125 (1973).

Key words: laser spectroscopy; methane; molecular hype fine spectra; saturated absorption spectroscopy; ultrahig resolution.

The most recent results on saturated absorption spectrosco of methane are presented. 2nd order Doppler shift and photc recoil shift are shown to be some of the limiting factors of th technique.

14674. Steiner, B., **New needs for accurate optical radiation measurements. II. A growing concern of the National Bureau of Standards and of American CIE,** *Proc. Conf. on Photometry and Colorimetry, Varna, Bulgaria, June 27-30, 1973,* pp. 39-45 (Dec. 1973).

Key words: energy crisis; health; meteorology; photometry; pollution monitoring; radiometry; remote sensing; safety.

Moreover, commercial needs and concern for more accurate optical radiation measurement are paralleled by growing public problems whose solutions depend strongly upon improved radiometry and photometry. The recent rapid growth of the electro-optics industry has both caused and exacerbated the severity of the measurement difficulties. The resulting great technical effort required can be justified by the public issues involved as well as by the commercial impact. Examples of these public issues are: the health issues of phototherapy and clinical analysis; the safety issues of potential destruction of the protective earth ozone layer, biomedical engineering, and transportation; the energy crisis; meteorology; pollution monitoring; and remote sensing. The effort to achieve a larger and more coordinated approach to the related radiometric and photometric problems have been organized by American CIE TC 1.2 through its creation of the Council for Optical Radiation Measurement. The purpose, structure, and activity of the Council are described.

14675. Mandel, J., Steel, M. N., Sharman, L. J., **National Bureau of Standards analysis of the ASTM interlaboratory study of DOC/FF 3-71 flammability of children's sleepwear,** *Amer. Soc. Test. Mater. Stand. News,* pp. 9-13 (May 1973).

Key words: children's sleepwear; flammability; flammability standard; flammability test method.

ASTM Committee D-13 on Textile Materials carried out an interlaboratory study on the test method given in DOC FF 3-71, Standard for the Flammability of Children's Sleepwear. Sixteen laboratories and eight fabrics were involved. D-13's conclusions were that the study demonstrated that laboratories do not obtain the same "pass-fail" results when testing the same fabrics with DOC FF 3-71 as written and, in fact, gross differences in reproducibility were obtained. The same test data was analyzed at NBS. The analysis reported in this paper leads to conclusions contrary to those reported by D-13. The NBS report shows theoretically that with a go-no go test such as that for children's sleepwear, the probability of complete agreement between laboratories is attained only when the material under test is either so far superior to the test method requirements or so far inferior to them that unavoidable test method fluctuations have no effect on the outcome of the test. For a fabric that is only two percent defective, the probability of complete agreement between 16 laboratories is down to 72 percent. The data provide no evidence to support D-13's conclusion that gross differences in reproducibility are obtained.

14676. Kruger, J., Hayfield, P. C. S., **Ellipsometry in corrosion testing,** (Proc. Symp. on State-of-the Art of Corrosion Testing, Toronto, Canada, June 21-27, 1970), Chapter 32 in *Handbook on Corrosion Testing and Evaluation,* W. H. Ailor, Ed., pp. 783-831 (John Wiley & Sons, New York, N.Y., 1971).

Key words: corrosion; electrochemistry; ellipsometry; oxidation; thickness measurements.

Because corrosion processes are strongly affected by the presence of thin films, the optical technique of ellipsometry which measures the thickness of these films and their optical properties is a valuable tool for corrosion research and testing. This technique measures the change in the state of polarization upon reflection of polarized light from a metal surface and relates these changes to the thickness and refractive index of films formed on this surface while it is immersed in an aqueous solution or in gaseous environments. Since experimentally the technique only requires that one provide a means for light to be reflected from a passive or corroding surface, it can be combined with electrochemical or diffraction techniques.

Numerous examples of ways in which ellipsometry can be applied to corrosion science and engineering measurements of film formation and dissolution kinetics and changes in film and metal surface properties are described.

14677. Murphy, T. A., Sengers, J. V., Sengers, J. M. H. L., **Analysis of the pressure of gases near the critical point in terms of a scaled equation of state,** *Proc. Sixth Symp. on Thermophysical Properties, Atlanta, Ga., Aug. 6-8, 1973,* P. E. Liley, Ed., pp. 180-188 (The American Society of Mechanical Engineers, New York, N.Y., 1973).

Key words: carbon dioxide; critical phenomena; critical region of gases; equation of state; parametric equation; scaling laws.

The anomalous thermodynamic behavior of gases near the critical point can be described in terms of scaling laws. In recent years a parametric equation of state, the so-called Linear Model, has been proposed that incorporates the scaling laws. We have developed a method which enables us to determine optimized Linear Model parameters by fitting experimental P-V-T data in the critical region. As an illustration of the method we discuss some preliminary results obtained for $CO_2$ in the critical region.

14678. Haar, L., Gallagher, J., **Heat capacity for gaseous ammonia,** *Proc. 6th Symp. on Thermophysical Properties, Atlanta, Ga., Aug. 6-8, 1973,* P. E. Liley, Ed., pp. 228-237 (The American Society of Mechanical Engineers, New York, N.Y., 1973).

Key words: ammonia; heat capacity; ideal gas; PVT data; PVT surface; temperature scale; thermodynamic consistency.

Several classic experiments for gaseous ammonia are shown to be thermodynamically consistent and accurate almost within their individual scatter. This feature is the basis for the extension of the range of the constant pressure heat capacity measurements (by a factor of 2 in temperature and 5 in pressure) with no appreciable loss of accuracy. For this purpose the previously calculated $C_p^\circ$ values for the ideal gas are taken as bench-mark data. The real gas $C_p$ values are tabulated for temperatures from $-30° \leq t \leq 325$ °C and pressures up to 125 bar. Over most of this range the uncertainty is several tenths percent.

14679. Isler, M. A., Stenbakken, G. N., **Mechanically actuated switches for burglar alarm systems,** *NILECJ-STD-0302.00,* 18 pages (U.S. Department of Justice, Law Enforcement Assistance Administration, National Institute of Law Enforcement and Criminal Justice, Washington, D.C., May 1974).

Key words: burglar alarm sensor; burglar alarm system; door switch; mechanically actuated switch; perimeter sensor; switch.

This standard establishes performance criteria for mechanically-actuated electrical switches intended for use in protective intrusion alarm circuits to monitor the position of doors, windows, etc. These devices cause the initiation of an alarm signal to a police panel, central station, or local audible alarm device. Included are requirements and test methods for performance, electrical properties and materials. The performance characteristics addressed are those that affect the false alarm susceptibility of the device. This standard does not provide performance criteria for the ability of these devices to resist attempts to defeat them through physical or surreptitious attack.

**14680.** Mills, R. M., Yee, K. W., **Walk-through metal detectors for use in weapons detection,** *NILECJ-STD-0601.00,* 26 pages (U.S. Department of Justice, Law Enforcement Assistance Administration, National Institute of Law Enforcement and Criminal Justice, Washington, D.C., June 1974).

Key words: metal detections; performance standards; weapon detection.

A standard has been developed to establish performance requirements and test methods for the detection capability and general characteristics of walk-through metal detectors.

**14681.** Hord, J., **Cavitation in liquid cryogens. IV. Combined correlations for venturi, hydrofoil, ogives, and pumps,** *NASA CR-244B,* 103 pages (National Aeronautics and Space Administration, Washington, D.C., Oct. 1974).

Key words: cavitation; cryogenics; hydrofoil; impellers; inducers; ogives; pumps; venturi.

This is the fourth and final volume on the results of a series of experimental and analytical cavitation studies. Previous volumes contain basic analyses and experimental data for a venturi, a hydrofoil, and three scaled ogives. Cross-correlation of the developed cavity data for these five hydrodynamic bodies is performed in this report. The data, for liquid hydrogen and liquid nitrogen, are correlated by using the extended theory derived in Volume II (CR-2156). The new correlating parameter, MTWO, improves data correlation for these stationary bodies and for pumping equipment. The results of this study are applied to the cavitating pump impeller and inducer data published by the NASA Lewis Research Center. Existing techniques for predicting the cavitating performance of pumping machinery are extended to include variations in flow coefficient, cavitation parameter, and equipment geometry. The new predictive formulations hold promise as a design tool and universal method for correlating pumping machinery performance. Application of these predictive formulas requires prescribed cavitation test data or an independent method of estimating the cavitation parameter for each pump. The latter would permit prediction of performance without testing; potential methods for evaluating the cavitation parameter prior to testing are suggested. Directions for future work are indicated.

**14682.** Clifton, J. R., Beeghly, H. F., Mathey, R. G., **Nonmetallic coatings for concrete reinforcing bars,** *FHWA-RD-74-18,* 85 pages (Available from the National Technical Information Services, Springfield, Va. 22161, Feb. 1974).

Key words: bridge decks; chloride ions; concrete; corrosion; deicing salts; epoxy coatings; organic coatings; steel reinforcing bars.

This work was undertaken to ascertain the feasibility of using organic coatings, especially epoxies, to protect the steel reinforcing bars embedded in concrete of bridge decks from rapid corrosion. This corrosion is caused by the chloride ions from the most commonly applied deicing salts, sodium chloride and calcium chloride. Altogether, 47 different coating materials were evaluated to some extent, consisting of: 21 liquid and 15 powder epoxies; 5 polyinyl chlorides; 3 polyurethanes; 1 polypropylene; 1 phenolic nitrile, and one zinc rich coating. The chemical and physical durabilities, chloride permeabilities, and protective qualities of coatings were assessed. The bonds between coated and uncoated bars and concrete were measured by both pullout and creep tests.

The results indicate that both epoxy and polyvinyl chloride coatings, if properly applied, should adequately protect steel reinforcing bars from corrosion. However, only the epoxy coated bars had acceptable bond and creep characteristics when embedded in concrete. The powder epoxy coatings overall performed better than the liquid epoxies, and four powder epoxy coatings have been identified as promising materials to be used on reinforcing bars embedded in concrete decks of experimental bridges.

**14683.** Yonemura, G. T., **Image quality criterion for the identification of faces,** *LESP-RPT-0303.00,* 24 pages (U.S. Department of Justice, Law Enforcement Assistance Administration, National Institute of Law Enforcement and Criminal Justice, Washington, D.C., May 1974).

Key words: acutance; facial identification; identification in photographs; image quality; modulation transfer function.

This report describes an experiment, the resulting data, and recommendations concerning an image quality criterion for identification of faces in a photograph. It relates the psychological levels of visual performance to performance of photographic equipment in terms of acutance and modulation transfer function.

**14684.** Rush, J. J., **Study of large-amplitude vibrations in molecules by inelastic neutron scattering,** (Proc. Conf. Critical Evaluation of Chemical and Physical Structural Information, Dartmouth College, Hanover, N.H., June 24-29, 1973), Paper in *Critical Evaluation of Chemical and Physical Structural Information,* D. R. Lide, Jr., and M. A. Paul, Eds., pp. 369-385 (National Academy of Sciences, Washington, D.C., 1974).

Key words: barriers to rotation; large amplitude vibrations; momentum transfer; neutron scattering; optical spectroscopy; torsional vibration.

The application of neutron inelastic scattering to the study of large amplitude intramolecular (primarily torsional) vibrations in hydrogeneous molecules is discussed. In principle the neutron technique provides an excellent complement to optical techniques, due in part to the fact that large-amplitude modes, which are sometimes inactive or weakly active in IR or Raman spectra, provide intense peaks in neutron spectra. However, relatively poor ($\sim 10\ \text{cm}^{-1}$) instrumental resolution and Doppler broadening effects in fluid phases sometimes cause significant complications in experiment and interpretation. Neutron spectral results on several prototype methyl-substituted molecules are presented and compared with relevent optical data. Some of the limitations and pitfalls of neutron molecular spectroscopy are discussed along with the difficulties in deriving potential barrier parameters from a limited number of torsional mode assignments.

**14685.** Lafferty, W. J., **Determination of potential functions and barriers to planarity for the ring-puckering vibrations of four-membered ring molecules,** (Proc. Conf. Critical Evaluation of Chemical and Physical Structural Information, Dartmouth College, Hanover, N.H., June 24-29, 1973), Paper in *Critical Evaluation of Chemical and Physical Structural Information,* D. R. Lide, Jr., and M. A. Paul, Eds., pp. 386-409 (National Academy of Sciences, Washington, D.C., 1974).

Key words: barrier heights; four-member ring molecules; infrared spectroscopy; microwave spectroscopy; Raman spectroscopy; ring-puckering.

Experimental and model errors in the determination of barrier heights in four-membered ring molecules are discussed.

**14686.** Rush, J. J., Livingston, R. C., Rosasco, G. J., **Raman scattering study of crystal dynamics and order – disorder transitions in alkali hydrosulfides,** *Solid State Commun.* **13,** 159-162 (1973).

Key words: alkali hydrosulfides; crystal dynamics; Raman scattering.

Raman spectra have been measured for NaSH, CsSH and RbSH over a range of temperatures from 85 to 400 K. The sults show that the order—disorder phase transitions in these ids are associated with significant changes in the details of eir crystal dynamics. In addition the Raman spectra provide ar evidence for the existence of previously unobserved low-nperature phases in each compound, which apparently involve al ordering of the SH$^-$ ions.

687. Kaldor, A., Braun, W., Kurylo, M. J., **Infrared laser enhanced reactions: $O_3+SO$,** *J. Chem. Phys.* **61,** No. 7, 2496-2499 (Oct. 1, 1974).

Key words: apparatus and methods; chemiluminescence; emission spectra; free radicals; kinetics of reactions; lasers, infrared; photochemistry.

ibrationally excited ozone, $O_3^\dagger$, produced by $CO_2$ laser radia-n was found to react with SO significantly faster than thermal one via the chemiluminescent reaction process $O_3+SO \rightarrow$ )$_2(^1B_1)+O_2(^3\Sigma_g)$. The vibrational rate enhancement of this action was 2.5 ± 0.6 at 300 K. This represents the utilization of percent of the available vibrational energy to promote the action based on a model assuming involvement of a single rational mode. The laser enhanced chemiluminescence mea-red from 260 to 450 nm was found to exhibit a 630 ± 200 cm$^{-1}$ ue shift. This is interpreted as a partitioning of the available rational energy of $O_3^\dagger$ in the vibrational manifold of the )$_2(^1B_1)$ product.

688. Bassett, D. C., Block, S., Piermarini, G. J., **A high-pressure phase of polyethylene and chain-extended growth,** *J. Appl. Phys.* **45,** No. 10, 4146-4150 (Oct. 1974).

Key words: diamond anvil pressure cell; high pressure; polyethylene; polymer; polymorphism.

Optical and x-ray observations of polyethylene have been ade at high pressures and temperatures using a gasketed amond-anvil cell. The experiments confirm the existence of the gh-pressure phase previously postulated by Bassett and rner. The new phase is hexagonal, with orthohexagonal lattice rameters of $a=8.4_6$ Å and $b=4.8_8$ Å. Comparison with the eviously measured volume change indicates that there is a crease in the $c$ dimension to $2.4_5$ Å per ethylene unit in trans-rming from orthorhombic to hexagonal structures. The likely plication is that the molecules in the hexagonal phase do not ve an all-trans conformation. Chain-extended growth is the sult of crystallization from the melt into the hexagonal phase, ereas chain-folded growth is the familiar process of melt ystallization into the orthorhombic phase. Chain-extended nellae are observed to grow outwards behind a growing edge th a permanent narrowed profile, showing that the lamellar ckness is determined in a region extending several microns be-d the growth front.

689. Fong, J. T., **Material symmetry and scalar potentials in nonlinear theory of materials,** *Proc. Conf. on Symmetry Similarity and Group-Theoretic Methods in Mechanics, Calgary, Alberta, Canada, Aug. 19-21, 1974*, pp. 155-166 (1974).

Key words: constitutive equation; continuum mechanics; elasticity; isotropy; material symmetry; mechanical properties; rheology; scalar-potential: strain-energy; thermodynamics; viscoelasticity.

For elastic and viscoelastic materials whose constitutive equa-ns are derivable from scalar potentials, we examine their strictions due to (a) material symmetry alone, and (b) material mmetry plus additional physical hypothesis. New results on a ss of nonlinear viscoelastic materials (Bernstein, Kearsley, d Zapas, 1963) are derived. Applications to the interpretation experimental data on real materials are discussed.

**14690.** Soulen, R. J., Jr., Marshak, H., **The use of Josephson junctions for noise thermometry below 1 kelvin,** *Proc. Applied Superconductivity Conf., Annapolis, Md., May 1-3, 1972*, pp. 588-591 (1972).

Key words: beryllium; Co$^{60}$ $\gamma$-ray anisotropy thermometer; Josephson junction; low temperature thermometry; noise thermometry; superconductivity.

Kamper and Zimmerman have demonstrated that a Josephson junction connected in parallel to a resistor converts the Johnson noise voltage fluctuations into frequency fluctuations, and that the variance of these frequency fluctuations is simply related to absolute temperature. In order to make accurate measurements of temperature with this device, a fast data acquisition system consisting of a frequency counter interfaced to a small computer has been developed. This thermometer has been compated to a Co$^{60}$ $\gamma$-ray anisotropy thermometer in the temperature region of .020 to .050 K. Preliminary results indicate agreement to within 5 percent. We have used our results to redetermine the superconductive transition temperature of pure beryllium. Our value is .0228 K, 3mK lower than reported by Falge. Since our thermometers do not depend upon any calibration or extrapolation and only on some accurately and independently determined parameters of each system, our value of $T_c$ is probably very close to the *absolute* temperature of the transition.

**14691.** Wyckoff, J. M., Chilton, A. B., **Dose due to practical neutron energy distributions incident on concrete shielding walls,** *Proc. Third Int. Congress of the International Radiation Protection Association, Washington, D.C., Sept. 9-14, 1973*, pp. 694-699 (Feb. 1974).

Key words: concrete walls; neutron shielding; particle accelerators; rem.

In order to calculate the dose equivalent for persons on the far side of an ordinary concrete shielding wall from a plane parallel source of neutrons, published monoenergetic neutron data and practical neutron spectra have been folded together. Some interpolation of the monoenergetic neutron data, both in energy and slab thickness, was required to prepare the data for computation in steps of 50 g/cm$^2$. The result is a set of useful dose-equivalent data for walls as thick as 800 g/cm$^2$ used to shield particle accelerators producing neutrons up to 100 MeV in energy. A simple empirically derived, analytical expression for the dose equivalent for walls of 50 to 800 g/cm$^2$ thickness is given with suitable constants for neutron spectra produced by more than 60 selected examples of the following reactions: slow and fast neutron induced fission, ($\gamma$,n), (p,n), ($^3$He,n), ($\alpha$,n) and fission ($\gamma$,n).

**14692.** Wiese, W. L., Kelleher, D. E., **Asymmetries in Stark-broadened Balmer lines,** *Proc. 10th Int. Conf. on Phenomena in Ionized Gases, Oxford, England, Sept. 13-18, 1971*, p. 377 (1971).

Key words: assymmetries; hydrogen lines; line shifts; Stark-broadening.

Small asymmetries have been observed in the Stark-broadened hydrogen lines $H_\beta$ and $H_\gamma$. They are most pronounced in the line wings, where the red wing is about 15 percent stronger than the blue one. Another asymmetry occurs between the two peaks of $H_\beta$ where the blue peak is about 4 percent higher than the red one. For the central component of $H_\gamma$ a small red shift is measured. The experimental results are compared with theoretical estimates and qualitative agreement is found. All experimental observations are made from a hydrogen plasma which is generated in a wall-stabilized arc.

**14693.** Lindamood, G. E., **A collection of mathemusicals,** *J. Irreproducible Results* **20,** No. 1, 30 (June 1973).

Key words: humor.

This article is an attempt at mathematically-oriented humor of the sort which occasionally appears in *Mathematics Magazine*. It consists of a list of titles of musical comedies, altered to suggest some mathematical concept, suggested by a fictitious professor to whom similar mathematical whimsy has been attributed in the literature.

**14694.** Hill, J. E., Furlong, R. R., **ASHRAE cooling load calculation,** *ASHRAE J.*, pp. 61-66 (May 1973).

Key words: ASHRAE handbook; cooling load; equivalent temperature differentials; heat gain.

An attempt has been made to give an overview of the changes in the cooling load calculation methodology as appears in Part 1, Chapter 22 of the 1972 ASHRAE Handbook of Fundamentals. The distinction between heat gain, cooling load and heat extraction rate is made. The basis for calculating an instantaneous rate of heat gain for a space is given. Particular emphasis is given to the component of gain that occurs through exterior walls and roofs. The tables of equivalent temperature differentials that appear in the chapter are completely changed from those that appear in the 1967 edition. The way the values of TETD were calculated and are intended to be used are explained. In addition, the procedure of converting an instantaneous rate of total heat gain to an instantaneous space cooling load (as outlined in Part 1, Chapter 22) is explained and discussed in reference to other methods currently in use.

**14695.** Ayres, T. R., Linsky, J. L., Shine, R. A., **Stellar model chromospheres. II. Procyon (F5 IV-V),** *Astrophys. J.* **192,** 93-107 (Aug. 15, 1974).

Key words: late-type stars; line profiles; stellar chromospheres; stellar photospheres.

We derive a model for the chromosphere and upper photosphere of Procyon (F5 IV-V) based on calibrated observations of the K and 8542 Å lines of Ca II, the $k$(2796 Å) line of Mg II, and the K-line wings. We demonstrate the feasibility of our model synthesis approach to derive a preliminary model chromosphere despite the lack of spatial and spectral resolution associated with solar chromospheric studies. Our upper photosphere model is very similar to the radiative equilibrium Procyon model of Strom and Kurucz, and our chromospheric model is similar to the quiet solar chromosphere temperature distribution of Shine in the 6000-8000 K range.

**14696.** Rupp, N. W., **Clinical use of some dental materials. Part I. Amalgam,** *J. Indiana Dent. Assoc.*, pp. 432-434 (Oct. 1973); **Part II. Composite restorative materials,** 491-495 (Nov. 1973).

Key words: acid etch; burnishing; handling techniques; materials; restorative.

This discussion of selected dental restorative materials covers new developments in both materials and handling techniques. Dental amalgam alloy formulations and the burnishing of restorations at the time of placement are included. Luting agents, esthetic restorations and acid etch enhanced retention are also covered for the information of the practicing dentist. The review has 34 references.

**14697.** Velapoldi, R. A., Wicks, S. A., **The use of chemical spot tests kits for the presumptive identification of narcotics and drugs of abuse,** *J. Forensic Sci.* **19,** No. 3, 636-656 (1974).

Key words: centroid color charts; color spot tests; drugs of abuse; experimental detection limits; field tests; narcotic identification; narcotics; spot tests; street drugs.

Numbers and colors from the Inter Society Color Council—National Bureau of Standards Centroid Color Charts have been assigned to the colors produced by the reactions of typica narcotic field test reagents with pure drugs and other substances A short discussion of the colors produced with street samples c drugs is also given. Flow charts are presented whereby increase selectivity is obtained by multiple reagent testing. Experimenta detection limits were obtained for two drugs, heroin and LSD, b a rigorous, statistically meaningful method and for several othe drugs by a less rigorous method. Reagent stabilities and tempera ture effects are also discussed. It is evident that narcotic fiel test kits can be useful in obtaining presumptive or preliminary ir formation.

**14698.** Grosskreutz, J. C., **Fundamental knowledge of fatigu fracture,** (Proc. Third Int. Conf. on Fracture, Munich, Ge many, Apr. 8-13, 1972), Paper in *Proceedings of Third Inte national Conference on Fracture*, pp. 1-26 (Verein Deutsche Eisenhuttenleute, Dusseldorf, Germany, Apr. 1973).

Key words: fatigue; mechanisms of fatigue; review fatigue.

The frontiers in our knowledge of fatigue are reviewed her with the aim of describing the current status and the opportun ties for fresh approaches to increase our understanding. Th principal opportunity is to quantify that which we already kno qualitatively. Throughout the paper an attempt is made to co nect fundamental knowledge to the technical problems in fatigu which still remain vexing and unsolved.

**14699.** Velapoldi, R. A., Diamondstone, B. I., Burke, R. W **Spectral interpretation and kinetic studies of the Fe$^{3+}$ − H$_2$S (Zak) procedure for determination of cholesterol,** *Clin. Che* **20,** No. 7, 802-811 (1974).

Key words: carbonium ions; cholesterol; enylic ion isosbestic points; kinetics; reaction mechanisms; steroid Zak procedure.

Spectral changes and kinetic data presented for the Zak rea tion show the pseudo-first-order character of the consecutive o idative reactions undergone by cholesterol and selected stero dienes. These data give excellent support to the proposed form tion of the homologous series of steroidal enylic cations whi are the absorbing species in the spectrophotometric cholester determination. Typical thermodynamic quantities of $\Delta G$‡, $\Delta H$ $\Delta S$‡ and $E_a$ are also reported for several different reactions. Lo acetic-sulfuric acid ratios evidently result in the stabilization the lower members of the homologous enylic series. Althou excellent reproducibilities are obtained for premixed and no premixed Zak reagents, it is necessary to use the premixed r agent if good temperature control is required, as would be t case for kinetic methods of analysis run under the conditions v used. The isosbestic point observed at 503 nm may also be us as an analytical wavelength because it is less sensitive to vari bles such as temperature, time, and steroid concentration. symbolizes that the letter to which it is superscript is a the modynamic parameter for the activated complex and not for t overall reaction.)

**14700.** Rabinow, J., **The climate for innovation,** (Proc. First Na Conf. Dealing with the Problems of the Small Firms in t Research and Development Industry, Washington, D.C., Ju 12-14, 1972), Paper in *Survival and Growth. The Small R& Firm*, J. D. Johnson, Ed., pp. 251-261 (1972).

Key words: consulting services; contract R&D; gover ment contracts; innovation; invention; proposal writin R&D; small business.

My talk will cover the subject of Small R&D Firms and will addressed to two types of such firms. One is the small compa which develops a product for sale and where R&D is a norm proportion of its business. The other part of the talk will be a dressed to R&D companies which do research and developme vork for industry and Government and whose major effort is not n production.

My talk will criticize both the Government R&D procurement olicies and the industry's response. I believe there is considerale inefficiency in the way contract R&D is done, both on the art of the contractor and the contractee.

**4701.** Laufer, A. H., Bass, A. M., **Rate constants for reactions of methylene with carbon monoxide, oxygen, nitric oxide, and acetylene,** *J. Phys. Chem.* **78,** No. 14, 1344-1348 (1974).

Key words: inorganics; methylene; radical; rate constant; singlet; triplet.

Rate constants for some reactions of triplet and singlet ıethylene have been measured by means of the flash photolysis f ketene with product analysis by gas chromatography. Rate onstants for reactions of triplet methylene with NO, $O_2$, and $_2H_2$ in helium are $1.6 \pm 0.1 \times 10^{-11}$, $1.5 \pm 0.1 \times 10^{-12}$, and $7.5 \pm$ $.0 \times 10^{-12}$ $cm^3$ $molecule^{-1}$ $sec^{-1}$, respectively, over the pressure ange of at least 50-700 torr. The rate constant of triplet $CH_2$ vith CO in 700 torr of helium was $\leq 1.0 \times 10^{-15}$ $cm^3$ $molecule^{-1}$ ec$^{-1}$. Rate constants for reaction of singlet $CH_2$ with NO, $O_2$, O, and $CH_2CO$ were $< 4 \times 10^{-11}$, $< 3 \times 10^{-11}$, $< 9 \times 10^{-12}$, and $.2 \pm 1.2 \times 10^{-11}$ $cm^3$ $molecule^{-1}$ $sec^{-1}$, respectively. The triplet $H_2$ reactions were measured relative to $^3CH_2 + {}^3CH_2 \rightarrow C_2H_2 +$ $H_2$ or 2H). The rate constants for singlet $CH_2$ were relative to $CH_2 + He \rightarrow {}^3CH_2 + He$.

**4702.** Dickens, B., Prince, E., Schroeder, L. W., Jordan, T. H., **A refinement of the crystal structure of $H_3PO_4 \cdot 1/2\ H_2O$ with neutron diffraction data,** *Act. Cryst.* **B30,** Part 6, 1470-1473 (June 1974).

Key words: crystal structure; hydrates; hydrogen bonding; neutron diffraction; phosphates; phosphoric acid.

The hydrogen positions in $H_3PO_4 \cdot 1/2\ H_2O$ have been deternined and the structure refined to $R_w = 0.022$, $R = 0.027$, with 208 reflections of measurable intensity. The general features of he structure are as described by Mighell, Smith & Brown [*Acta ryst.* (1969). **B25**, 776-781]. The two crystallographically disrete $H_3PO_4$ molecules are hydrogen bonded to each other and o the water molecule. The positions of the hydrogens of the vater molecule appear to have been affected by $H \cdots H$ repulsion rom the $H_3PO_4$ hydrogen atoms and the $O_w - H \cdots O$ phosphate) hydrogen bonds are markedly non-linear. For $-O-H$, the average $P-O$ distance is 1.562 Å, the average $-H$ distance is 1.010 Å and the average $P-O-H$ angle is 17°. Individual $P-O-H$ angles range from 112.4 to 119.9°. In he water molecule, the average $O-H$ distance is 0.997 Å, and he $H-O-H$ angle is 106.0 (2)°. The four shortest $H \cdots H$ ineractions range from 2.161 (3) to 2.290 (3) Å, and may imply $H \cdots H$ van der Waals bonding as in $Ca(OH)_2$.

**4703.** Berger, M. J., **Some new transport calculations of the deposition of energy in biological materials by low-energy electrons,** *Proc. 4th Symp. on Microdosimetry, Verbania Pallanza, Italy, Sept. 1973*, pp. 695-711 (Mar. 1974).

Key words: absorbed dose distributions; electrons, delta rays and beta particles; event-size; microdosimetry; transport theory; wall effects.

After some brief remarks about the method of calculation and ross sections, illustrative results are given from recent electron ransport calculations. The following topics are discussed: (1) he distribution of absorbed dose in water around point-isotropic nd point-monodirectional electron sources; (2) the radial disribution of absorbed delta-ray energy around proton tracks in itrogen; (3) the frequency mean and energy mean of nicrodosimetric event-size distributions in small spherical olumes in water, for the case of irradiation by electrons and tritium beta-rays; (4) the perturbation of event-size distributions in gas-filled cavities due to the presence of surrounding walls.

**14704.** Unassigned.

**14705.** Carpenter, B. S., LaFleur, P. D., **Nitrogen determination in biological materials by the nuclear track technique,** *Anal. Chem.* **46,** No. 8, 1112-1113 (July 1974).

Key words: bovine liver, cellulose nitrate; image analyzing system; microscope; neutron activation analysis; nitrogen; orchard leaves; proton tracks; standard reference materials.

A method has been developed for the determination of nitrogen in biological matrices using the nuclear track technique (NTT). Protons from the nuclear reaction $^{14}N(n,p)^{14}C$, which is produced by thermal neutrons, leave radiation damaged trails (tracks) which are made visible to optical microscopy by chemical etching. The NTT method has been used for the analysis of leaves and liver with excellent agreement with values obtained using the Kjeldahl technique.

**14706.** Arsenault, R. J., deWit, R., **Distributed glide force between a non-spherical defect and a dislocation,** *Acta Met.* **22,** 819-827 (July 1974).

Key words: Burgers vector; defect; dislocation; glide; inclusion; kink; tetragonal.

The distributed glide force on dislocations due to a ⟨100⟩ and a [110] type non-spherical defect was determined. The distributive glide force does produce a torque on a screw dislocation but it is of no consequence in terms of the effect the defect has on the nucleation of a double kink. It was also proven that the total interaction force with a non-spherical defect is indeed greater for an edge dislocation than with a screw dislocation.

**14707.** Richmond, J. C., **Survey of image quality criteria for passive night vision devices,** *LESP-RPT-0301.00,* 22 pages (U.S. Department of Justice, Law Enforcement Assistance Administration, National Institute of Law Enforcement and Criminal Justice, Washington, D.C., June 1974).

Key words: acutance; contrast transfer function; edge gradient; image quality; light equivalent background; light induced background; limiting resolution; line spread function; optical transfer function; point spread function.

Image quality is probably the single most important parameter in determining the utility of any optical device. For night vision devices, in particular, image quality is of paramount importance. In looking at two different photographs of the same scene, which are essentially two different images fixed by the photographic process, almost anyone can tell at a glance which has the better image quality, particularly if there is a significant difference in image quality. Objective evaluation of image quality in quantitative terms is not easy, becuase there are many variables that contribute to image quality, not all of which have been identified, or can be quantitatively evaluated.

This report is a preliminary survey of image quality evaluation techniques that have been described in the literature and discussion of their merits for use in a standard for passive night vision devices.

**14708.** Madden, R. P., **Absolute detectors and the transfer standard problem in the vacuum ultraviolet,** *Proc. Calibration Methods in the Ultraviolet and X-Ray Regions of the Spectrum Symp., Munich, Germany, May 1968*, pp. 111-124 (European Space Research Organization, Munich, Germany, 1968).

Key words: anodized aluminum; chromium; gold; photoelectric yield; radiometric standards; rare gas ionization chamber; thermopiles; tungsten; vacuum ultraviolet.

Thermopiles have been studied extensively for their applicability as radiometric standards in the 500-2000 Å region. Under appropriate conditions and with suitable corrections it appears that they can be used reliably in this spectral region having been calibrated with black-body radiation in the visible. A thermopile and a rare gas ionisation chamber have been used to measure independently the same flux at 584 Å and 735 Å, with an agreement better than the estimated reliability of 3 percent. A search is now under way to find a photocathode with a stable photoelectric yield which, in a photodiode, could serve as a convenient and reliable transfer detector standard for the region below 1400 Å. Completed studies prove conclusively that the photoelectric yield of an ultra-clean surface of tungsten can undergo a dramatic change when contaminated by as little as a fraction of a monolayer. That other photocathodes as well are sensitive to contamination is indicated by studies of the effects of ageing and heating on the photoelectric yield of several materials (e.g., gold, chromium) under ordinary vacuum conditions. Anodised aluminium films show promise as surfaces which have a reliable photoelectric yield.

**14709.** Schaffer, R., **Diagnostic materials for clinical analysis,** (Proc. Int. Conf. on Standardization of Diagnostic Materials, Atlanta, Ga., June 5-8, 1973), Paper 1 in *Bull. Wld. Hlth. Org.* **48,** 715-720 (1973).

Key words: clinical chemistry; clinical standards; diagnostic kits; diagnostic material; standard reference materials for clinical chemistry; standards.

Standardization of diagnostic materials has lagged behind their development and application. The need to improve the accuracy of the results obtained with them has stimulated collaborative efforts to upgrade the quality of the reagents, control materials, and standards used, with the result that specifications for reagents and standards and authoritative standard materials are now available for a number of clinical tests. Achievements thus far and the efforts now in progress are reviewed.

**14710.** Lide, D. R., Jr., **The XYZ's of laboratory frequency measurements,** Chapter in *Molecules in the Galactic Environment,* M. A. Gordon and L. E. Snyder, Eds., pp. 234-245 (John Wiley & Sons, New York, N.Y., 1973).

Key words: gaseous molecules; interstellar absorption lines, microwave absorption lines; microwave spectroscopic data.

The techniques of laboratory measurement of microwave absorption lines of gaseous molecules are reviewed. The various contributions to line widths are discussed with respect to their influence on the accuracy of typical frequency measurements reported in the literature. The reliability of calculated frequencies is discussed, as well as the general problem of identifying interstellar absorption lines on the basis of coincidences with tabulated laboratory frequencies. Useful sources of microwave spectroscopic data are summarized.

**14711.** Ellerbruch, D. A., **Application of measurements of electromagnetic phenomena to oceanography,** *Proc. First UJNR/MEC Symp., Record of the U.S.-Japan UJNR Joint Symp. on Marine Electronics, Tokyo, Japan, Oct. 9, 1972,* pp. 23-30 (Japanese Electrical Industrial Committee, Tokyo, Japan, 1972).

Key words: electromagnetic measurements; oceanography; sea water-return cable.

The U.S. National Bureau of Standards has developed a wide variety of measurement techniques for precisely determining the electromagnetic quantities and performance of electrical networks. Most of these measurements have been reduced to standard laboratory routines. Usually the network is transported into the laboratory, however, many measurements are utilized in the field.

The ocean can be treated as an electrical network. It is dispersive, lossy, inhomogeneous, far from a theoretically perfec medium. Nevertheless the established techniques used to evaluate laboratory sized samples of well-defined media can be use to evaluate the performance of full scale oceanic systems in situ In those applications the measurement laboratory is transporte to the network. NBS has obtained data on the performance of th multiconductor, seawater return, mooring line data line bein used by the National Data Buoy Center for deploying their network of moored Environmental Buoys. A variety of measurement techniques were used in this evaluation. Data were obtained in both the time and the frequency domains.

The interaction of electromagnetic waves with the ocean provides a means for sensing and characterizing oceanic parameter Electromagnetic sensing techniques offer interesting new approaches to the development of oceanic instrumentation. Som of these techniques will be described.

**14712.** Waxman, M., Davis, H. A., Hastings, J. R., **A new determination of the second virial coefficient of carbon dioxide at temperatures between 0 and 150 °C, and an evaluation of its reliability,** *Proc. Sixth Symp. on Thermophysical Properties, Atlanta, Ga., Aug. 6-10, 1973,* pp. 245-255 (Aug. 1973).

Key words: Burnett data reduction; carbon dioxide; nonlinear analysis; second virial coefficient.

Values of the second virial coefficient of carbon dioxide hav been determined to an estimated reliability of 0.3 cm³/mole fro Burnett PVT measurements taken over the pressure range fro 2 to 35 bar at six temperatures between 0 and 150 °C. Ou values, from − 150 to − 51 cm³/mole, compare favorably wit those obtained from a recent correlation of literature values an are in substantial disagreement with the values previously dete mined from both the Burnett and the piezometer methods b Dadson and coworkers. The nonlinear least-squares analysis Burnett data and our error analysis are discussed extensively an illustrated with results for carbon dioxide, helium, and ethylen An algorithm, recently developed by M. Waxman, for the leas squares evaluation of parameters in nonlinear implicit equation such as the Burnett pressure equation, is described.

**14713.** Tate, E. L., **On the interlibrary loan horizon—no mechanical,** *Proc. First Annual Federal Interagency Fiel Librarians Workshop, Washington, D.C., Sept. 24-28, 197* pp. 277-282 (1972).

Key words: federal libraries; interlibrary loans.

The paper describes two studies on interlibrary loans spo sored by the Association of Research Libraries. One, publishe this spring, concerns the characteristics, costs, and magnitude interlibrary loans in academic libraries; the other, being prepare under contract from the National Commission on Libraries an Information Science, will deal with the feasibility of centralize or regionalized interlibrary loan centers. Comments on the cu rent state of the copyright/photocopying problem are include Present and proposed projects of the Federal Library Committe Task Force on Interlibrary Loan Arrangements are discussed.

**14714.** Sugar, G. R., **Voice privacy equipment for law enforceme communication systems,** *LESP-RPT-0204.00,* 27 pages (U. Department of Justice, Law Enforcement Assistance A ministration, National Institute of Law Enforcement an Criminal Justice, Washington, D.C., May 1974).

Key words: intelligibility; LESL; NILECJ; performan standard; privacy; scramblers; speech quality; spee scramblers; survey; testing; voice privacy.

Law enforcement agencies are finding an increasing need f voice-scrambling equipment to provide privacy on their two-wa radio communication systems. Work is underway at the Nation ureau of Standards, under the sponsorship of the National In-titute of Law Enforcement and Criminal Justice (NILECJ), to evelop performance standards for voice scramblers. The four reas being considered are speech intelligibility, voice quality, oice privacy, and general system characteristics. This report rst defines a set of special terms, then describes a number of ypes of scramblers that are now available for law enforcement se. Some inherent problems and weaknesses are discussed. The oncepts of intelligibility and privacy are explored in detail. The otential contents of the standard are described, and some roblems inherent in preparing and using the standard are iscussed. The report concludes with some material intended to e of immediate assistance to the prospective purchaser of crambers: a survey of units now on the market, some hints on ow to proceed in the absence of a standard, and a bibliography f technical publications on voice scrambling.

4715. LaFleur, P. D., **Biological matrix standard reference materials for trace element determinations,** (Proc. Int. Conf. on Modern Trends in Activation Analysis in Saclay, France, Oct. 2-6, 1972), *J. Radioanal. Chem.* **19,** 227-232 (1974).

Key words: biological; bovine liver; orchard leaves; standard reference materials; trace elements.

Two new biological matrix Standard Reference Materials, RM-1571, Orchard Leaves and SRM-1577, Bovine Liver, ave been issued by the United States National Bureau of Stan-ards. The content of a number of trace elements has been cer-fied in these materials. The preparation and analytical program f the standards is described; these materials should be of great alue in assuring quality control and in developing new rocedures for analysis of biological materials.

4716. Saltman, R. G., **Educating public administrators for managing science and technology,** *Pub. Admin. Rev.* **34,** No. 4, 394-396 (July-Aug. 1974).

Key words: administration; education; information; management; public; science; technology transfer.

Public administrators are being forced to increasingly consider ience and technology in decisions that they make concerning oth plans and operations. In order to manage and control per-nent science and technology and to effectively employ them, e public administrator needs a professional education which ears him for these tasks. Information science and management ience are applications-independent tools that the administrator an use extensively to make his operations more efficient, to pro-de him with the coordinated information he needs, and to pro-de him with a rational, analytic basis for decision-making about e utilization of all forms of science and technology. At present, ere is no recommended or generally accepted curriculum for ducating public administrators for managing science and chnology. The academic community in Public Administration, ith assistance from the information science and management ience communities, should form a committee to recommend a urriculum in this area.

717. Lechner, J. A., **Effective statistical tests for detection models,** *Proc. 30th Military Operations Research Symp., Ft. Lee, Va., Dec. 12-14, 1972*, pp. 1-26 (1972).

Key words: detection models; detections; generalized Poisson process; statistical tests; testing.

A "Detection Model" is an entity which calculates an instantaneous probability of detection of a "target" by a "hunter," from the values of variables which describe the environment and the actions of both hunter and target, including past history, if appropriate. Given such a model, and a succession of non-identical trials which terminate at detection or after a given period of time (whichever occurs first), it is desired to test the adequacy of the model.

An approach to this problem is presented, based upon recognizing the set of trials as a nonhomogeneous Poisson process. Ways to improve the "power" of such tests by rearranging various segments of the trials are presented and discussed, including proper implementation of the tests using a digital computer. Extensions to the problem of improving the model and/or devising a new model are briefly discussed.

14718. Kirchhoff, W. H., **Determination of force fields by analysis of centrifugal distortion in microwave spectra,** (Proc. Conf. Critical Evaluation of Chemical and Physical Structural Information, Dartmouth College, Hanover, N.H., June 24-29, 1973), Paper in *Critical Evaluation of Chemical and Physical Structural Information,* D. R. Lide, Jr., and M. A. Paul, Eds., pp. 312-322 1974).

Key words: centrifugal distortion; force field; microwave spectra.

This paper describes the accuracy of molecular force fields derived from centrifugal distortion constants. Only bent, symmetric, triatomic molecules are discussed. The discussion deals primarily with the discrimination between the effects of measurement and model errors. The accuracy of the force field is judged by calculating from the force constants of the harmonic, fundamental vibrational frequencies and comparing these with the harmonic frequencies obtained from the infrared spectrum. This comparison, in turn, is measured against measurement errors arising from a statistical analysis of the microwave spectra. The particular molecular species for which such an analysis has been performed are $SO_2$, $OF_2$, $SiF_2$, $O_3$, $OCl_2$, $CF_2$, and $SF_2$.

14719. Leasure, W. A., Jr., Mathews, D. E., Rinkinen, W. J., **Truck Noise 1-A: Noise evaluation tests of military truck tires,** *Report No. DOT-TST-74-21,* 53 pages (Available as PB234-348 from the National Technical Information Service, Springfield, Va. 22161, Feb. 1974).

Key words: acoustics; noise measurement; noise(sound); tire noise; transportation noise; trucks.

This report presents the A-weighted sound level and one-third octave band spectral data resulting from a study conducted to characterize the noise generated by military truck tires. The study was conducted by the National Bureau of Standards in cooperation with the U.S. Department of Transportation under the sponsorship of the U.S. Army Tank-Automotive Command. The data base established will allow for comparison of the tire noise generated by military and commercial truck tires.

The study investigated the influence of load and speed on the noise generated by tires with four different tread designs: the standard Army tire, a retread of Army design and commercial tires with rib and cross-bar type tread patterns. Army and commercial trucks were utilized as test vehicles.

In addition, the report includes a discussion of the measurement and analysis techniques utilized for the establishment of this data base.

**14720.** Edgerly, D. E., **Are aerosol packages proliferated within the meaning of The Fair Packaging and Labeling Act?,** *Proc. 1969 Chemical Specialties Manufacturers Association 55th Annual Meeting, Washington, D.C., Dec. 8-11, 1968,* pp. 68-69 (1968).

Key words: aerosols; Fair Packaging and Labeling Act; packages; proliferation; voluntary standardization.

The purpose of this presentation is to familiarize the manufacturers of aerosol packages with the undue proliferation provision of the Fair Packaging and Labeling Act, and Department of Commerce responsibilities in interpreting proliferation. The scope of the talk centers upon the application of the undue proliferation provision to aerosol packages offered for sale at retail. A discussion of the market of several aerosol products and their place in the retail outlet is considered in light of the consumer's ability to make value comparisons. Considerations of a technical and/or marketing nature are discussed in view of problems which affect voluntary standardization. Finally, and of great importance, the manufacturer's responsibility within the spirit of the Fair Packaging and Labeling Act is discussed.

**14721.** Blevin, W. R., Geist, J., **Infrared reflectometry with a cavity-shaped pyroelectric detector,** *Appl. Opt.* **13,** No. 10, 2212-2217 (Oct. 1974).

Key words: directional-hemispherical; polyvinyl fluoride; pyroelectric detectors; reflectance.

A new type of reflectometer has been developed for measuring directional-hemispherical spectral reflectances in the infrared region. The instrument is based upon a cavity-shaped pyroelectric detector that itself collects the radiation reflected by the test sample, thereby obviating the need for an intermediate collector such as an integrating sphere or concave mirror. This detector is made from an electrically polarized plastic film of polyvinyl fluoride, coated with gold-black on its inner surface and backed with brass shim on its outer surface in order to provide mechanical strength. The reflectometer has been used with a Fourier spectrometer to measure spectral reflectances over the wavelength range 5-30 $\mu$m.

**14722.** Jacox, M. E., Milligan, D. E., **Vibrational spectrum of $CO_2^-$ in an argon matrix,** *Chem. Phys. Lett.* **28,** No. 2, 163-168 (Sept. 15, 1974).

Key words: charge transfer; $CO_2^-$; infrared spectrum; ion-molecule aggregates; matrix isolation; molecular structure.

Absorptions which appear near 1600 $cm^{-1}$ on co-deposition at 14 K of $Ar:CO_2$ mixtures with an alkali metal have been assigned to $\nu_3$ of an $M^+ \ldots CO_2^-$ ion pair, with an OCO valence angle near 130°. Molecular aggregates contribute significantly to the observed spectrum.

**14723.** Runyan, C. C., Moulder, J. C., Clark, A. F., **Time-resolved spectra of bulk titanium combustion,** *Combust. Flame Brief Communication* **23,** No. 1, 129-133 (Aug. 1974).

Key words: combustion; laser ignition; spectra (visible); titanium.

The combustion of titanium specimens is supported by a laser in gaseous oxygen. Utilizing a high-speed mechanical shutter driven by a time-delay circuit, the presence of titanium and its oxides is monitored above the surface of the burning Ti metal as a function of time. Spectra are taken with a grating spectrometer and are compared for various stages of the combustion process. The stages are defined by the shape of the total emitted intensity curve. Discrete spectra of titanium and titanium monoxide are seen in emission but disappear as the combustion progresses. The results are correlated with metallographic and x-ray analyses of quenched specimens.

**14724.** Davis, G. T., Weeks, J. J., Martin, G. M., Eby, R. K., **Cell dimensions of hydrocarbon crystals: Surface effects,** *J. Appl. Phys.* **45,** No. 10, 4175-4181 (Oct. 1974).

Key words: crystal surfaces; density; lamella thickness; paraffins; polyethylene; unit cell; x ray.

The unit-cell dimensions of a given polyethylene have previously been shown to vary nearly linearly with the reciprocal of lamella thickness. Data obtained at 153.2 and 296.2 K are presented to show that the slope of this dependence is different for crystals of orthorhombic *n*-paraffins, melt-crystallized polyethylene, and solution-crystallized polyethylene. Within the limits of error, all extrapolate to the same basal area at infinite lamella thickness, and this agrees with the measured value for sample crystallized from the melt under high pressure to yield a long period of about 3500 Å. Since the effect is a surface one, it is proposed that these differences result from the differences between methyl interactions, fold interactions, different fold planes, domains, etc. It is shown that the variation of cell dimension with lamella thickness leads to a quadratic term in the variation of macroscopic density. This term permits the separation o the thickness and density of a lower-density surface layer in a two-phase model.

**14725.** Crawford, M. L., **Generation of standard EM fields usin TEM tranmission cells,** *IEEE Trans. Electromagn. Compat* **EMC-16,** No. 4, 189-195 (Nov. 1974).

Key words: compatibility; standard fields; susceptibility testing; transverse electromagnetic.

A new technique developed at the National Bureau of Stan dards (NBS) for establishing standard, uniform, electromagneti (EM) fields in a shielded environment is described. Th technique employs transverse electromagnetic (TEM) transmis sion cells that operate as 50 Ω impedance-matched systems. uniform TEM field is established inside a cell at any frequenc of interest below that for which higher order modes begin t propagate. Standard field strength levels from 10 $\mu$V/m to 50 V/m can be established with uncertainties of less than 1.0 dB t 2.0 dB inside the NBS cells for frequencies from dc to 500 MH The cells are especially useful for calibrating EM radiatio hazard meters, for emission and susceptibility testing of small t medium sized equipment, and for special low level calibration very sensitive field strength meters.

**14726.** Adair, R. T., Hoer, C. A., Kamper, R. A., Simmonds, M B., **RF attenuation measurements using quantum interferen in superconductors,** (Proc. 1974 Conf. on Precision Ele tromagnetic Measurements, London, England, July 1-

1974), Abstract in *CPEM Digest No. 113,* 4-5 (Institution of Electrical Engineers, London, England, 1974).

Key words: Josephson junction; quantum interference; rf attenuation; superconductivity.

A unique portable system has been developed for measuring attenuation over a dynamic range of 65 dB at 30 MHz. A Su- rconducting QUantum Interference Device (SQUID) is the sis of the system.

Measurements made with this system have an rms deviation om the NBS National Reference Standard of ± 0.002 dB.

A SQUID is a loop of superconducting metal closed by a sephson junction, operating in liquid helium. It converts varia- ons in magnetic flux to periodic variations in impedance which e sensed at microwave frequencies. This provides a con- nient, natural means of measuring electrical quantities such as ltage, current, power and attenuation.

**727.** Wexler, A., **Humidity measurement system — A micro stu- dy,** *Nat. Conf. Stand. Lab. Newsletter* **14,** No. 2, 38-41 (Oct. 1974).

Key words: humidity measurement; moisture; standard; water vapor.

A comprehensive study of the humidity measurement system being conducted by Arnold Wexler, Chief of the Humidity ction in the Mechanics Division at NBS.

**728.** Raveché, H. J., Mountain, R. D., Streett, W. B., **Freezing and melting properties of the Lennard-Jones system,** *J. Chem. Phys.* **61,** No. 5, 1970-1984 (Sept. 1, 1974).

Key words: equation of state; freezing; freezing criteria; melting; molecular correlation functions; phase transitions.

Using Monte Carlo simulations, we investigate average olecular arrangements that occur with the fluid-solid transition a classical Lennard-Jones system. The crystalline order of the lid phase is explicitly shown by the angularly averaged olecular correlation functions which, in the solid, exhibit a havior not observed in the fluid. The pair and triplet correla- n functions delineate the crystalline pattern of the ordered ase out to internuclear separations of many nearest-neighbor tances. A molecular criterion for freezing is reported which ims a proportionality between the values of the pair correla- n function in the fluid at the positions of the first and second arest neighbors. The general behavior of the triplet correlation nction in the fluid phase is interpreted. We also compare pre- ctions for melting pressures and the densities of the coexisting id and solid phases.

**729.** Kline, F. J., Crannell, H., Finn, J. M., Hallowell, P. L., O'Brien, J. T., Werntz, C. W., Fivozinsky, S. P., Lightbody, J. W., Jr., Penner, S., **Search for the lowest $T = 2$ state in $^{14}C$ by inelastic electron scattering,** *Il Nuovo Cimento* **23A,** No. 1, 137-144 (Sept. 1, 1974).

Key words: analog states; electron scattering; inelastic electron scattering; particle-hole model; resonance energy; $^{14}C$.

A search for the lowest-energy $T = 2$ state in $^{14}C$ has been at- mpted employing inelastic electron scattering techniques. ectra obtained at 61 and 81 MeV incident-electron energy and 5.7° scattering angle fail to reveal significant structure at the edicted resonance energy. The implications of this result are scussed in terms of the particle-hole model and the ground- te structure of the $^{14}B$ analogue of this level.

**730.** Greer, S. C., Moldover, M. R., Hocken, R., **A differential transformer as a position detector in a magnetic densimeter,** *Rev. Sci. Instrum. Notes* **45,** No. 11, 1462-1463 (Nov. 1974).

Key words: densimeter; density; differential; transformer.

We describe the use of a differential transformer to detect the position of the buoy in a magnetic densimeter, an instrument for precise measurement of fluid densities. This detector can be used in cases where the buoy is not visible and it can be assembled from commercial electronic components.

**14731.** Carrington, C. G., Gallagher, A., **Blue satellite bands of Rb broadened by noble gases,** *Phys. Rev. A* **10,** No. 5, 1464-1473 (Nov. 1974).

Key words: line-broadening; rubidium; satellite.

Measurements are presented for the blue-wing satellite bands of the Rb first resonance line (780 nm) emitted in the presence of the noble gases Ne, Ar, Kr, and Xe. The continuum intensity per spectral interval and perturber density is expressed as a fraction of the total Rb (780 nm) fluorescence from optically thin vapor. Over the $\sim 10^{18} - 10^{19}$ cm$^3$ density range investigated this normalized satellite-peak intensity is found to scale linearly with perturber density and approximately exponentially in $-1/T$, $T$ being the absolute temperature. In the classically forbidden region beyond the satellite peak the intensity drops exponentially with frequency for Xe perturbers, but departs from exponential behavior in the Ar and Kr data. We observe undulations in the spectra between line center and the satellite. This is expected due to the possibility of interference between contributions to the transition probability at two internuclear separations, the separations at which the difference potential equals the photon energy.

**14732.** Jednačak, J., Pravdić, V., Haller, W., **The electrokinetic potential of glasses in aqueous electrolyte solutions,** *J. Colloid Interface Sci.* **49,** No. 1, 16-23 (Oct. 1974).

Key words: electrokinetic potential glass; interface; liquid/solid interface; solid/liquid interface; surfaces; Zeta-potential.

Electrokinetic potentials of several glasses of well defined bulk composition in aqueous electrolyte solutions were computed from streaming current measurements. The composition of the bulk is reflected in the magnitude of the potential and in the shape of the curves relating the electrokinetic potential and the pH of the solution. No differences have been found between the crystalline and the vitreous state of silica. Addition of $Al_2O_3$ to the bulk results not in doping effects but rather in surface neutralization making the surface less acidic. Glasses with an appreciable amount of $B_2O_3$ have higher negative potentials at the same pH, and the derivatives of electrokinetic potential vs pH show them to belong to a different type of surface than vitreous or crystalline silica. Studies involving controlled pore glasses of various pore sizes have shown the importance of below-the-surface ionic penetration and/or adsorption in the pores in establishing the solid-movable liquid interfacial electrical equilibrium.

**14733.** Lawton, R. A., Nahman, N. S., **Pyroelectric detector application to baseband pulse measurements,** *Electron. Lett.* **8,** No. 12, 318-320 (June 15, 1972).

Key words: detector circuits; power measurement; pulse circuit; pyroelectricity.

A square-law detector for picosecond baseband pulse comparison techniques has been realised using the pyroelectric effect. By using thin-film techniques, a broadband signal transfer to the detector was obtained. The theoretical principles of the detector and some applications are briefly discussed. Attention is given to measurements of pulse-energy content, pulse autocorrelation function and pulse crosscorrelation function.

**14734.** McLaughlin, W. L., **Solid-phase chemical dosimeters,** (Proc. Int. Conf. on Sterilization by Ionizing Radiation, Vienna, Austria, April 1-4, 1974), Paper in *Sterilization by Ionizing Radiation,* E. R. L. Gaughran and A. J. Goudie, Eds., pp. 219-252 (Multiscience Publication Ltd., Montreal, Quebec, Canada, 1974).

Key words: dose distribution; dosimetry; dyes; electron beams; gamma rays; glasses; plastics; radiation chemistry; radiation sterilization; solid-state detectors; spectrophotometry.

The radiation chemistry and response characteristics of some solid-phase chemical dosimeters (plastics, dyed plastics, and glasses) are reviewed. The analysis used for dosimetry is mainly spectrophotometry in the ultraviolet and visible spectrum. Systems having a reproducible response and a stable optical absorbance are selected from as many as 28 candidate systems, some of those showing promise for radiation sterilization applications being: polymethyl methacrylate, dyed polymethyl methacrylate, polycarbonate, tetrazolium salt in polyvinyl alcohol, dyed polychlorostyrene, and dyed polyamide. Major sources of dosimetric error, such as temperature and dose rate dependence instability, non-uniformities, and batch differences, are examined.

**14735.** Schneider, S. J., McDaniel, C., **Problems in accurate temperature measurement: The melting point of $Y_2O_3$,** *Can. Met. Quart.* **13,** No. 2, 365-368 (1974).

Key words: IPTS-68; melting point; secondary temperature standards; temperature scales; $Y_2O_3$.

Modern day pyrometry permits the measurement of temperature with maximum uncertainties ranging between about 0.1 °C at 1064 °C (gold point) and 2 °C at 3525 °C. These uncertainties refer to the realization of the International Practical Temperature Scale (IPTS) and represent the level of accuracy a temperature per se can be determined under optimized conditions. Unfortunately, the measurement of a material property as a function of temperature imposes experimental constraints which seriously degrade the inherent accuracy of the temperature measurement system, often to unknown levels. Consequently, in situ temperature calibrations are required which must employ the use of a well characterized reference material compatible with the environment of the experiment. Suitable secondary temperature reference standards are not generally available and this lack is being addressed by the High Temperature Commission (IUPAC) through its current melting point program on $Y_2O_3$ and formerly by its efforts on $Al_2O_3$.

The determination of fixed points presents many experimental difficulties relevant to a wide range of physico-chemical measurements and can serve as an illustrative example of the high temperature problems which may be encountered. Through a description of the experimental determination of the melting point of $Y_2O_3$ (2422 °C) this paper delineates major problem areas and includes discussions on IPTS, temperature measurement techniques and calibration and materials behaviour and compatibility.

**14736.** Streett, W. B., Raveché, H. J., Mountain, R. D., **Monte Carlo studies of the fluid-solid phase transition in the Lennard-Jones system,** *J. Chem. Phys.* **61,** No. 5, 1960-1969 (Sept. 1, 1974).

Key words: fluid-solid phase transition; Lennard-Jones model; melting and freezing densities; Monte Carlo simulation; symmetry change; van der Waals isotherm.

Monte Carlo calculations for 108- and 256-particle Lennard-Jones systems have been carried out at 140 temperature-density points in the vicinity of the fluid-solid phase transition. Several types of initial configurations have been used, including fcc lattice arrays, disordered arrays, and combinations of lattice ar
disordered arrays. The results of runs at high densities show th
for small periodic systems the calculations are dependent on tl
initial configuration and that such systems can exist in many di
ferent metastable states from which minimum energy states a
not accessible in runs of the order of $10^6$ to $10^7$ configurations.
the vicinity of the smallest density at which the fcc lattice is st
ble, the calculated pressure-volume curve exhibits many of tl
features of a "van der Waals loop"; however, because a sing
phase is thermodynamically unstable over part of this region, tl
loop cannot be completely resolved through machine calcul
tions. The use of the van der Waals loop to estimate the melti
parameters for the Lennard-Jones system leads to fluid and sol
densities 3 to 4 percent lower than those calculated by the i
direct method of Hansen and Verlet.

**14737.** Smith, R. L., Case, W. E., Rasmussen, A. L., Russell,
W., West, E. D., **A calorimeter for high power CW lase**
(Proc. Conf. on Precision Electromagnetic Measuremen
Boulder, Colo., June 26-29, 1972), Paper in *CPEM Digest,*
*138-139 (1972).*

Key words: laser; laser calorimetry; laser energy measu
ments; laser power measurements.

A calorimeter was built to measure the total energy emitted
a CW laser whose output wavelength is in the region from 1
to 11 μm. This instrument can measure energies from $10^5$ to
proximately $10^7$ joules with about 5 percent uncertainty and
can measure energies down to about $10^4$ joules with a larger
certainty. The calibration factor for this device is approximat
$2.26 \times 10^6$ joules/volt, where one volt corresponds to a tempe
ture interval of approximately 12 °C. The laser power that can
accommodated by this instrument ranges from about 500 wa
to 100,000 watts. The maximum beam diameter it will accep
10 cm.

**14738.** Little, W. E., **Automated computer controlled measu
ments,** (Proc. 1974 Conf. on Precision Electromagnetic M
surements, London, England, July 1-5, 1974), Abstract
*CPEM Digest* No. 113, 331-332 (Institution of Electrical
gineers, London, England, 1974).

Key words: automated measurements; computer; conce
reliability; state-of-the-art; survey.

The primary intent of this paper is to give a state-of-the-
survey of automated-computer controlled measurements in
context of what has been done in the past that has direct bear
on the present work and the directions that the near future w
will take.

The paper will cover some of the evolution of computer c
trolled measurement systems including concepts utilized in
system designs. The discussion will start with the concept
utilizing the computer to handle large amounts of data fr
*traditional* systems to give more data handling reliability
then go into the concepts of using the computer not only to
lect the data but to control the actual measurement instrume
to allow for even more reliability and in some cases impro
measurement accuracy. From there, it will go into the concep
using the compuer not only to control the instruments and col
the data but to actually model the system. Here, numerical
which represents system parameters is stored in the comp
memory and later utilized to correct the measurement data
that the system will appear nearly perfect and an improveme
measurement accuracy is achieved.

Finally, a summary of the state-of-the-art in automated c
puter controlled measurement equipments and techniques wil
given. It will be given in the context of measurement accur
achieved, measurement efficiency, reliability, and measurem

ncepts employed in the system design.

739. Beatty, R. W., **2-port standards for evaluating automatic network parameter measurement systems,** (Proc. 1974 Conf. on Precision Electromagnetic Measurements, London, England, July 1-5, 1974), Abstract in *CPEM Digest No. 113,* 87-89 (Institution of Electrical Engineers, London, England, 1974).

Key words: automatic measurement; coaxial standards; network parameters; reflection coefficient; scattering coefficients; transmission coefficient; waveguide standards; 2-port standards.

2-port standards have been developed for evaluating the per- rmance of automatic systems which measure network parame- rs over a broad frequency range.

The standards consist of short sections of coaxial line or aveguide which include or produce simple discontinuities. One n calculate the complex reflection and transmission coeffi- ents for any frequency given the dimensions.

In use, the standards are terminated by a port of the measure- ent system which is made effectively non-reflecting by means a calibration procedure and computer correction.

A number of types of standards are described and measure- ents with a typical automatic system are presented.

740. Kerns, D. M., **Comment on correction of errors in aerial far-field radiation-pattern determinations,** *Electron. Lett.* 7, No. 24, 706 (Dec. 2, 1971).

Key words: antenna radiation patterns; gain measurement.

In the communication being commented on, a method is roposed" for correcting for the effects of the measuring anten- in the determination of far-field aerial patterns from near-field easurements. This method was previously proposed in a talk in 63 and has been substantially implemented in theoretical, ex- rimental, and computational work. References are given.

741. Lawton, R. A., **Autocorrelation and power measurement with pyroelectric and dielectric bolometers,** *IEEE Trans. Instrum. Meas.* **IM-22,** No. 4, 299-306 (Dec. 1973).

Key words: autocorrelation; detector; pulse; pyroelectric.

A pulse comparison technique is described which yields the tocorrelation function and the power spectrum of a repetitive ne-domain waveform. The autocorrelation function is realized th a sliding short in a coaxial transmission line to provide time lay; a pyroelectric bolometer to provide multiplication through square law voltage response; and a capacitor to provide in- gration. Problems of realization of a perfect time delay and in- gration limitations are considered, and it is found that noise ctuations yield the main time resolution limitation that is uivalent to 8 ps for 15-V pulses and a 50-s integration time. e pyroelectric voltage-sensing bolometer is then compared to pyroelectric capacitance sensing bolometer. It is shown that e capacitance sensing bolometer can handle much longer pulse rations than the voltage sensing bolometer. It is also demon- rated that the sensitivities of the two techniques are equivalent a typical case at a capacitance sensing bolometer bridge volt- e of 3 V. Measurement results of the autocorrelation function d power spectrum, using a voltage sensing pyroelectric lometer, are given for a nominal 15-V, 500-ps time duration, ose baseband pulses have a 100-pps (pulses per second) petition rate.

742. Lawless, W. N., Radebaugh, R., Siegwarth, J. D., **Improvements on "low-temperature dielectric bolometer,"** *J. Opt. Soc. Amer.* **64,** No. 6, 820-822 (June 1974).

Key words: bolometer; cryogenics; dielectric; glass-ceramic; optics.

This paper corrects a definitional error in the previous paper on this topic and reports a considerably better dielectric material for this type of detector (i.e., $dln\epsilon/dT$ values as large as 30% $K^{-1}$ in the range 0.3 to 10 K). Computed responsivity (times the square root of the detector area) based on this material varies from $6 \times 10^6$ to $2 \times 10^4$ $V \cdot W^{-1} \cdot cm$ for reservoir temperatures between 0.3 and 10 K. The corresponding variation of the detectivity is from $2 \times 10^{14}$ to $1 \times 10^{11}$ $cm \cdot W^{-1} \cdot Hz^{1/2}$.

**14743.** Ogburn, F., **Methods of testing,** Chapter 30 in *Modern Electroplating,* 3d Edition, pp. 673-709 (July 1974).

Key words: coatings; electroplated coatings; metal coatings; test methods for metal coatings; testing electrodeposits.

A brief description and evaluation is given of each of the methods used to test electroplated coatings for thickness, corrosion resistance, porosity, internal stress, ductility, hardness, and solderability.

**14744.** Carter, G. C., Kahan, D. J., **NMR, soft x-ray, and other physical properties of rare earth metals and alloys—an annotated bibliography,** (Proc. 11th Rare Earth Research Conference, Traverse City, Mich., Oct. 7-10, 1974), Paper in *Proceedings of the 11th Rare Earth Research Conference,* J. M. Haschke and H. A. Eick, Eds., **II,** 1014-1018 (1974).

Key words: alloy data; bibliography; index; Knight shifts; NMR; rare earth metals and alloys; soft x ray.

The Alloy Data Center (ADC) has deep-indexed about 18,000 papers dealing with physical properties of metals and alloys, and maintains these in a computerized file. Of these, approximately 3,000 contain information on transuranic or rare earth metals (including Sc, Y, La), or alloys with one or more such components. These literature references have been printed out alphabetically by chemical symbol to form a rare-earth annotated bibliography, which is available as an NBS Special Publication. The ADC collects all nuclear magnetic resonance (NMR) and soft x-ray spectroscopy (SXS) papers, and many papers dealing with other electronic-structure related properties as well. This bibliography, therefore, contains all NMR and SXS papers for rare-earth related metallic materials. The ADC does not intend to compete with the Rare Earth Information Center, which is far more comprehensive for many other physical properties of rare earth materials. Rather, this bibliography of the ADC's holdings is thought to represent a valuable bibliographic tool in the interim period until the Rare Earth Information Center has completed its conversion to an automated system.

**14745.** Das, E. S. P., deWit, R., Armstrong, R. W., Marcinkowski, M. J., **Kinks, jogs, and a regeneration mechanism for Volterra disclinations,** *J. Appl. Phys.* **44,** No. 11, 4804-4806 (Nov. 1973).

Key words: crystal; defect; disclination; dislocation; elasticity; jog; kink; multiplication; plasticity; Volterra.

A regenerative mechanism is proposed which can lead to unlimited multiplication of disclinations. This mechanism consists of a glissile segment of a disclination pinned by two sessile "jogs," and therefore is similar to a Frank-Read source for dislocations. It is also possible to have a U-mill, Z-mill, and L-mill for disclination multiplication. It is further shown that a single source can give rise to disclinations of opposite signs (and this allows rotation in both directions of that part of the crystal above the source, relative to the part below), depending upon the direction in which the source operates.

**14746.** Zhukov, V. V., Weisman, I. D., Bennett, L. H., **Nuclear**

**magnetic resonance in cadmium alloys,** *J. Magn. Resonance* **16,** 29-34 (1974).

Key words: anisotropic Knight shift; Cd; Hg; isotropic Knight shift; Knight shift; Korringa product; nuclear magnetic resonance; spin lattice relaxation.

Experimental isotropic and anisotropic Knight shift data on $^{113}$Cd and on $^{199}$Hg in Cd-Hg alloys have been obtained between room and liquid-helium temperatures. The $^{113}$Cd spin-lattice relaxation times in Cd and in a Cd + 10 at.% Hg alloy have also been measured at these temperatures. The Hg concentration dependence of the anisotropic and isotropic Knight shifts at the $^{199}$Hg site was found to be qualitatively similar to that of the corresponding shifts at the $^{113}$Cd site. The Korringa relation for $^{113}$Cd is obeyed, indicating that only one mechanism contributes to the Knight shift and spin-lattice relaxation. The ratio of isotropic Knight shifts, (Hg:Cd), extrapolated to zero Hg concentration, 4.67, is somewhat greater than the ratio, 3.69, of atomic hyperfine fields. This suggests that the amount of electronic "*s*" character at the Cd Fermi surface is anomalously low due to anisotropy effects and that adding Hg rapidly destroys the anisotropy by weakening and symmetrizing the lattice potential.

**14747.** Ruff, A. W., Fraker, A. C., **Investigation of the anisotropic anodic polarization behavior of titanium,** *Corrosion* **30,** No. 7, 259-264 (July 1974).

Key words: corrosion; passivation; single crystals; sulfuric acid; titanium.

Anodic polarization measurements have been made potentiostatically on single crystal and polycrystal titanium in 1N $H_2SO_4$ at 23 C (73 F). Three low index surfaces, (0001), (1120), and (1010) were studied together with polycrystalline rolled sheet material. A strong influence of crystallographic orientation on the anodic current densities was found in both the active and the passive regions. The most active surface was (1120), the least active (0001). The most passive surface was also (0001), unless the specimen had been in a cathodic region, whereupon that orientation became the most reactive. That effect and others that are associated with titanium hydride formation are discussed. The effect on the reactivity of the polycrystalline surface due to preferred orientation texture is mentioned.

**14748.** Boettinger, W. J., **The structure of directionally solidified two-phase Sn-Cd peritectic alloys,** *Met. Trans.* **5,** 2023-2031 (Sept. 1974).

Key words: alloy; directional solidification; incongruent melting alloy; peritectic reaction; Sn-Cd alloys; structure.

The structure of Sn-Cd two-phase peritectic alloys directionally solidified at various values of $G/v$ (temperature gradient in the liquid divided by growth rate) is reported. The minimum value of $G/v$ as a function of composition required for the solidification of two-phase peritectic alloys with a planar liquid-solid interface is estimated using a simple constitutional super-cooling stability criterion. At a value of $G/v$ just below this minimum value, these alloys solidify with a nonplanar interface consisting of cells of $\alpha$ (the high temperature phase) and intercellular $\beta$ (the low temperature phase). This produces a coarse rod-like microstructure consisting of rods of $\alpha$ phase imbedded in a $\beta$ matrix. At a value of $G/v$ above this minimum value, these alloys solidify with a planar interface which alternately deposits bands of $\alpha$ and $\beta$ transverse to the growth direction. No coupled growth of $\alpha$ and $\beta$ at a planar interface is observed in Sn-Cd two-phase peritectic alloys as was expected. To understand this, an analysis of coupled (eutectic-like) growth of two-phase peritectic alloys is presented and contrasted with the results of the Jackson-Hunt theory of lamellar eutectic growth. This calculation indicates that the coupled growth of two-phase peritectic alloys is unlikely on theoretical grounds.

**14749.** Radebaugh, R., Siegwarth, J. D., **Heat transfer betwee fine copper powders and dilute $^3$He in superfluid $^4$He,** (Proc 13th Int. Conf. on Low Temperature Physics, Boulder, Colo Aug. 21-25, 1972), Paper in *Low Temperature Physics LT 1* K. D. Timmerhaus, W. J. O'Sullivan, and E. F. Hammel, Eds 1, 401-405 (Plenum Press, New York, N.Y., 1974).

Key words: copper; heat transfer; helium 3-helium 4; Kapi za resistance; phonon-electron interaction; phonor quasiparticle interaction; powder; sintering.

The recently measured value of the phonon-electron therm resistance is too low to have been seen in previous measur ments of the Kapitza resistance of high surface area materia below 0.1 K. We report here measurements of the thermal r sistance between dilute $^3$He liquid and copper powder of chara teristic spherical diameter, based on adsorption studies, of 1. $\mu$m. With this fine powder we should expect to see, below abo 50 mK, the phonon-electron thermal resistance and the phono $^3$He quasiparticle thermal resistance. However, measuremen down to 15 mK on three different samples of this powder sho no signs of these additional resistances. The thermal resistanc surface area product has the typical Kapitza resistance behavi of $R\sigma T^3 \approx$ constant for temperatures below that where the the mal resistance of the liquid in the sponge dominates. The val for the constant is in fair agreement with the value 280 cm$^2$K$^4$/ that we find for annealed bulk OFHC copper in dilute $^3$He.

**14750.** Reed, R. P., Schramm, R. E., **Relationship betwe stacking-fault energy and x-ray measurements of stacking-fa probability and microstrain,** *J. Appl. Phys.* **45,** No. 11, 470 4711 (Nov. 1974).

Key words: deformation; dislocations; face-centered cu metals; faults; Fourier analysis; review; stacking fault en gy; x-ray diffraction.

Stacking-fault energies can be determined by measuring t positions and profiles of x-ray diffraction lines. Use of t method has been hampered by the uncertainty of the relations between stacking-fault energy and the ratio of microstrain stacking-fault probability. Microstrains and stacking-fault pro bilities have been determined for five fcc metals by x-ray diffr tion line profile analysis. For these metals, Ag, Au, Cu, Al, a Ni, stacking-fault energies have been estimated from a co prehensive updated review of the experimental literature. linear correlation does exist between $\gamma$ and $\langle \epsilon_{50}^2 \rangle_{111}/\alpha$ and th the x-ray technique can be applied more confidently. The pos ble role of elastic anisotropy is also considered.

**14751.** Mihalas, D., Hummer, D. G., **Theory of extended stel atmospheres. I. Computational method and first results static spherical models,** *Astrophys. J. Suppl. Ser.* **28,** No. 2 343-372 (Oct. 1974).

Key words: astrophysics; early-type stars; radiati transfer; spectral line formation; stellar atmospheres.

A method is presented that makes possible, for the first ti the calculation of extended spherical non-LTE model stellar mospheres in hydrostatic and radiative equilibrium. This meth is a generalization of the complete-linearization technique Auer and Mihalas. Models have been obtained for a star with $=60\mathscr{M}_\odot$, $L=1.25\times10^6 L_\odot$, and $R=24\ R_\odot$, whose atmosph is characterized by an effective temperature $T_{eff}=39{,}500$ K a surface gravity log $g_6=3.45$, i.e., with a spectral type near These models are differentiated by the magnitude and radial pendence of a radiation force multiplier $\gamma$ that is inserted into equation of hydrostatic equilibrium to simulate the effect radiation force on opacity sources which have not been inclu

.plicitly in the calculation. Models have been obtained very ose to the limit at which the radiation force and gravity lance; as this condition is approached, the atmospheres come more and more extended. Only hydrogen and helium ($Y$ 0.1) have been included, and six hydrogen lines have been eated explicitly. Although these models show only modest exnsion, they predict L$\alpha$ in emission, the lower Balmer lines in sorption, the Balmer jump in absorption, and an infrared exss and ultraviolet deficiency relative to the visual. Continuous ergy distributions and the profiles and equivalent widths of $\alpha$, H$\alpha$, H$\beta$, and H$\gamma$ are tabulated. The models predict an intrinc reddening of the colors of extended envelopes relative to ane-parallel atmospheres. A procedure for the extraction of the trinsic colors of luminous stars from heavily reddened observaons is described.

752. Farmer, B. L., Eby, R. K., **Methyl branches in hydrocarbon crystals: Calculation of relaxation effects,** *J. Appl. Phys.* **45,** No. 10, 4229-4238 (Oct. 1974).

> Key words: mechanical relaxation; methyl branches; paraffins; polyethylene; potential energy calculations; relaxation strength; two-site model.

A two-site model for a relaxation process has been used in njunction with the results of illustrative potential-energy callations on a model system to examine the effects of isolated ethyl branches on the chain packing and mechanical relaxaons of a linear hydrocarbon host crystal. The results indicate at a branched molecule can be accommodated in an array of ear chains in two different modes of packing and that each ode has two orientations. For one of the modes, the two orientions have nearly equal energies. Upon mechanical deformaon of the array, this mode gives rise to a relaxation. The relative rengths are evaluated for different deformations, some of hich yield values of the order of those observed experimenlly. This relaxation is much weaker for unbranched chains in e planar zigzag conformation.

753. Cowan, R. D., Radziemski, L. J., Jr., Kaufman, V., **Effect of continuum configuration interaction on the position of $s\ p^6$ in neutral chlorine and other halogens,** *J. Opt. Soc. Amer.* **64,** No. 11, 1474-1478 (Nov. 1974).

> Key words: atomic spectra; chlorine; halogens; photoionization.

*Ab initio* Hartree-Fock calculations in the single-configuration proximation predict that the $3s\ 3p^6\ {}^2S_{1/2}$ level of Cl I lies far ove the ionization limit, although this level is observed to be e lowest of all even $J=1/2$ levels other than $3s^2\ 3p^4\ 4s\ {}^4P_{1/2}$, $_{1/2}$. The solution of this anomaly lies in configuration interacon with the high-lying portion of the $3s^2\ 3p^4\ \epsilon d\,{}^2S_{1/2}$ continuum, hich is sufficiently strong to depress the computed $s\ p^6$ level to observed position. This interaction with the continuum is an tension of the well-known interaction of $sp^{w+1}$ with the disete $s^2p^{w-1}\ nd$ Rydberg series, and is important in all neutral ird-row elements Al to Cl, as well as in Br and I and probably her fourth- and fifth-row elements. The effect is, however, mewhat smaller in Br I and I I than in Cl I, with the result that ere exists no bromine nor iodine level that is primarily $s\ p^6$ in ture. The interactions produce large changes in computed ansition probabilities and photoionization cross sections.

754. Sanchez, I. C., Peterlin, A., Eby, R. K., McCrackin, F. L., **Theory of polymer crystal thickening during annealing,** *J. Appl. Phys.* **45,** No. 10, 4216-4219 (Oct. 1974).

> Key words: annealing; crystalline polymers; material transport; thickening; volume change.

A previous theory of thickening has been extended to encompass the possible dependence of cooperative chain transport on lamella thickness and crystallinity changes during annealing. These have marked effects on the thickening rate leading to changes in slope and departures from straight-line behavior of the plots of lamella thickness versus the logarithm of time. The resulting curves bear a resemblance to many experimental ones in the literature. Also brought out by the analysis is the important fact that the volumes of the coherently thickening domains are not known from experiment.

**14755.** Sugar, J., Spector, N., **Spectrum and energy levels of doubly ionized europium (Eu III),** *J. Opt. Soc. Amer.* **64,** No. 11, 1484-1497 (Nov. 1974).

> Key words: energy; energy levels; europium; ionization; spectrum.

The spectrum of Eu III obtained with a 6 A sliding-spark discharge has been measured from 2000 Å to 9000 Å. Of the 890 spectral lines observed, one-third are classified in an energy-level scheme consisting of 104 excited levels. These belong to the $4f^7$ configuration and to the $4f^6({}^7F)5d$, $4f^6({}^7F)6s$, and $4f^6({}^7F)6p$ subconfigurations. Except for $4f^7$, calculations of these configurations with least-squares-adjusted parameters were carried out. A reasonably suitable truncation for the energy matrices of each configuration was found.

**14756.** Van Brunt, R. J., Kieffer, L. J., **Angular distribution of $O^-$ from dissociative electron attachment to NO,** *Phys. Rev. A* **10,** No. 5, 1633-1637 (Nov. 1974).

> Key words: dissociation; electron; ionization; molecular oxygen.

The electron energy dependence of the angular distribution of $O^-$ produced by dissociative electron attachment to NO has been measured in the energy range 8.0-11.0 eV. The distributions are observed to be anisotropic and of a form that is nearly $\sin^2\theta$ at all energies. Deviations from a $\sin^2\theta$ dependence are discussed in terms of the relative contributions of different partial waves to the differential cross section. The results indicate that the final repulsive negative-ion resonances involved must be either $\Sigma$ or $\Delta$ states.

**14757.** Haynes, W. M., **Measurements of the viscosity of compressed gaseous and liquid fluorine,** *Physica* **76,** No. 1, 1-20 (Aug. 1974).

> Key words: experimental; fluorine; gas; graphs; liquid; tables; torsional crystal; viscosity.

A torsionally oscillating quartz crystal has been used to make absolute measurements of the coefficient of shear viscosity for compressed fluid fluorine at temperatures from 90 to 300 K, at pressures up to 20 MPa; and for saturated liquid fluorine at temperatures from 70 to 144 K. Special features of the viscometer, necessary to provide an instrument suitable for measurements on an extremely reactive fluid such as fluorine, are described. The accuracy of the results is estimated to be of the order of 2 percent with the precision somewhat better, approximately 0.5 percent. The dependence of the viscosity on density has been investigated by representing the gaseous data along isotherms in power-series expansions. Dilute-gas viscosities were subsequently derived from this analysis. An equation has been developed that can be used to calculate the viscosity of fluorine over the range of the present measurements. Comparisons with experimental data and theoretical predictions are presented for the few measurements and calculations previously attempted for fluorine.

**14758.** Choi, C. S., Bulusu, S., **The crystal structure of dinitropentamethylenetetramine (DPT),** *Acta Crystallogr. B30,* Part 6, 1576-1580 (June 1974).

Key words: crystal structure; cyclic nitramine; organic compound.

The crystal structure of dinitropentamethylenetetramine, or DPT, $C_5H_{10}N_6O_4$, has been studied by using three-dimensional x-ray (Mo $K\alpha$) diffraction data. The unit cell is monoclinic $P2_1/c$, with $a = 9.345$ (5), $b = 8.284$ (5), $c = 11.566$ (5) Å, $\beta = 105.6$ (1)° and $Z = 4$. The structure was solved by direct methods and refined by full-matrix least-squares methods to a final $R = 0.035$, $R_w = 0.037$. The two N-$NO_2$ groups in a DPT molecule are planar, with the two nitramine carbons out of the plane. The molecule has approximate mirror symmetry bisecting each of the two nitro groups.

**14759.** Wyllie, L. A., Jr., Wright, R. N., Sozen, M. A., Degenkolb, H. J., Steinbrugge, K. V., Kramer, S., **Effects on structures of the Managua earthquake of December 23, 1972,** *Bull. Seismol. Soc. Amer.* **64,** No. 4, 1069-1133 (Aug. 1974).

Key words: building; codes; earthquake damage; earthquakes; hazards; hospital; natural disasters; seismic; structural engineering.

The December 23, 1972, earthquake in Managua, Nicaragua caused extensive damage to structures throughout the city of Managua. There was damage to virtually every building in Managua, a city of approximately 400,000 inhabitants. An estimated 10,000 people were killed, mostly in the collapse of homes built of native taquezal construction. The city contained numerous reinforced concrete structures designed to recent standards. Although many of these buildings were heavily damaged, with some collapses, some had only minor damage. There were also several structures of structural steel.

The paper provides an overview of structural effects and discusses the performance of selected buildings in Managua illustrating the range of performance of modern construction. Damage to numerous other buildings will be discussed. The paper, while emphasizing the structural effects on buildings, also discusses the performance of non-structural elements, mechanical equipment, etc.

**14760.** Phelan, R. J., Jr., Peterson, R. L., Hamilton, C. A., Day, G. W., **The polarization of PVF and $PVF_2$ pyroelectrics,** *Ferroelectrics* **7,** 375-377 (1974).

Key words: polyvinylfluoride; polyvinylidene fluoride; pyroelectrics.

Through detailed investigations of the modulation frequency response of pyroelectric detectors, nonuniform polarizations have been shown to exist in polyvinylfluoride and polyvinylidene fluoride plastics. The nonuniform polarization is also confirmed by measurements using multilayer structures. The direction and magnitude of the gradients in polarization are dependent on the magnitude and polarity of the poling voltage. The gradients in the polarization for PVF and $PVF_2$ are opposite in direction. Using structures that allow for poling to $2 \times 10^6$ V/cm uniform polarizations, the highest responsivities and improved frequency responses were obtained.

**14761.** Massey, R. G., Druckenbrod, W. F., **Terms and definitions for police patrol cars,** *LESP-RPT-0401.00,* 18 pages (U.S. Department of Justice, Law Enforcement Assistance Administration, National Institute of Law Enforcement and Criminal Justice, Washington, D.C., May 1974).

Key words: patrol car definitions; patrol car functions; patrol car systems; patrol car terms.

This document contains the definitions of terms related to four-wheeled, on-road vehicles used in law enforcement. The terms and definitions have been selected on the basis of usefulness to those responsible for the selection, procurement, and us of those vehicles.

**14762.** Jackson, J. A. A., Lias, S. G., **Primary processes in th photolysis of n-butane with 8.4 and 10.0 eV photons,** *J Photochem.* **3,** 151-162 (1974).

Key words: alkane; electronically excited molecule hydrogen iodide; n-butane; radical scavenging; vacuum ul traviolet photolysis.

The photolyisis of n-$C_4D_{10}$ has been investigated with 8.4 e and 10.0 eV photons, using HI to scavenge free radicals throug the reaction: $R_D + HI \rightarrow R_DH + I$ (where $R_D$ is a fully deuterate alkyl or alkenyl radical). From the results of such experiment the quantum yields of the molecular and radical products are ob tained over a pressure range from 3 to 47 torr at both energies. I addition, the photolysis of $CD_3CH_2CH_2CD_3$ an $CD_3CD_2CH_2CH_3$ have been investigated in the presence of rad cal scavengers over a range of pressures at both energies. Th results are discussed with particular emphasis on deriving th quantum yields of all the primary processes, and followin changes in the quantum yields as a function of energy. Majc conclusions are: (a) the quantum yield of the process ($C_4D_{10}$ – $C_4D_8 + D_2$) diminishes from 0.70 to 0.37 when the photon energ is increased from 8.4 to 10.0 eV; (b) the relative overall in portance of direct C-C bond cleavage processes, alkane elimin tion processes, and D-atom elimination processes do not chang significantly as a function of energy; (c) processes involvin breakage of the 2, 3 C-C bond strongly predominate ov processes involving the 1, 2 C-C bond at both energies, althoug there is a lower probability for localization of the energy in th center bond when the energy is increased.

**14763.** Bridges, J. M., Kornblith, R. L., **ARC measurements of F I oscillator strengths,** *Astrophys. J.* **192,** 793-812 (Sept. 1 1974).

Key words: arc; f-values; iron and oscillator strengths.

Oscillator strengths for 534 lines of Fe I have been measur from a wall-stabilized arc. These lines have wavelengt between 2900 and 5800 Å and cover a wide range in intensi and upper energy level. Lifetime values were used in normalizi to an absolute scale and in determining the arc temperature. Th temperature agreed with that found independently, using LT plasma diagnostics. Comparisons with other recent oscillat strength measurements generally show agreement within co bined error estimates.

**14764.** Geltman, S., **The Coulomb-projected Born approximati V. Ionization of helium,** *J. Phys. B* **7,** No. 15, 1994-20 (1974).

Key words: electron impact; helium; ionization; theoretic study.

The triple differential cross section for the electron impa ionization of helium is calculated in the Coulomb-projected Bo approximation, including exchange. Detailed comparison made with the ordinary Born result and with available expe ment in both the coplanar and non-coplanar geometries. T agreement with experiment in almost all cases is apprecia better for the Coulomb-projected Born results than for the or nary Born results.

**14765.** Jarvis, S., Jr., **Determination of velocity distributions molecular beam frequency standards from measured resona curves,** *Metrologia* **10,** No. 3, 87-98 (1974).

Key words: accuracy evaluation; atomic beam frequen standards; cavity phase shift; second order Doppler shift.

It is shown that the Ramsey resonance curves for most ato am machines can be conceived as depending on two distribu-ns of velocity, $\rho$ ($V$) and $\xi$ ($V$), the second being a correction r beam width.

An analysis and computer program are described which permit e to obtain $\rho$, $\xi$ and the nominal microwave power parameter om three or more measured Ramsey resonance curves at operly spaced power levels whose ratios are known. The termination from the functions ($\rho$, $\xi$) of bias errors due to cond order Doppler shift, cavity phase difference, and cavity lling is described.

The method may also be used to improve an experimentally tained velocity distribution (i.e., one obtained through the lse technique); to provide the proper function $\xi$; and to pro-de diagnostic checks of the measurement technique and the lidity of the model chosen for the transition probability.

The method is applied to the NBS frequency standard. Error timates indicate that it is feasible by microwave power shift easurements to evaluate the total bias error due to the above urces to within one part in $10^{13}$.

766. Wacker, P. F., **Near-field antenna measurements using a spherical scan: Efficient data reduction with probe correction,** Proc. 1974 Conf. on Precision Electromagnetic Measurements, London, England, July 1-5, 1974), Paper in *CPEM Digest,* No. 113, 286-288 (Institution of Electrical Engineers, London, England, 1974).

Key words: antenna measurements; data reduction; near field; probe correction; probe design; spherical scan.

A new data reduction scheme makes practical the determina-n of patterns of electrically large antennas from near-field herical scans.

767. Mies, F. H., **Calculated vibrational transition probabilities of OH($X^2$ II),** *J. Mol. Spectrosc.* **53,** 150-188 (1974).

Key words: Einstein coefficients; line strengths; Meinel bands; molecular spectra; OH; radiative lifetimes; spin uncoupling; vibration-rotation interaction; vibrational transitions.

The theoretically derived dipole moment function of OH($X^2$ II) tained by Stevens, Das, Wahl, Neumann, and Krauss is used calculate the absolute intensities of the vibrational-rotational ansitions of the OH Meinel bands. The calculations take full count of the spin uncoupling and vibration-rotation coupling iich markedly influence the radiative transition probabilities. ie effect of lambda-doubling on the vibrational transitions is alyzed and generally found to be negligible. Results are tabu-ed for $\Delta v = v' - v''$ ranging from the fundamental transitions $= 1$ to the $\Delta v = 5$ overtone, for $v' = 1$-9 and $J' = 0.5$-15.5. A mparison is made with available data, and various features of OH spectrum are examined that are of aeronomical and ex-rimental interest. Thermally averaged emission rates are esented for $\Delta v = 1$-5, and the validity of the rotational tempera-es commonly derived from experimental intensity distribu-ns is questioned.

768. Hummer, D. G., Norcross, D. W., **Light ions of astrophysical interest — radiative transition probabilities for C III, N IV, O V and Ne VIII,** *Mon. Notic. Roy. Astron. Soc.* **168,** No. 2, 263-272 (1974).

Key words: atomic physics; atomic structure; oscillator strengths; radiative transition probabilities; spectra.

Multiconfiguration calculations of energy levels and bound-und radiative transition probabilities for four astrophysically portant ions of the Be isoelectronic sequence are presented. onvergence of the results with respect to the number of configurations included in the expansion is discussed. Results are presented for all ions from models with 11 and 16 configurations; including transition probabilities for 24 allowed electric dipole transitions. Some significant differences with previous calculations are obtained. The theoretical lifetimes are generally in good accord with those obtained by the beam-foil technique, and the results of other *ab initio* calculations.

14769. Lafferty, W. J., Sams, R. L., **High resolution infra-red spectrum of the $2\nu_3$ band of $NO_2$,** *Mol. Phys.* **28,** No. 4, 861-878 (1974).

Key words: Coriolis resonance; high resolution; infrared; $NO_2$; spin splitting; $2\nu_3$.

The $2\nu_3$ $B$-type band of $NO_2$ has been measured, assigned and the spin splitting has been accounted for satisfactorily. Ground-state rotational constants have been obtained by fitting 6 microwave pure rotational transitions with 119 ground-state combination differences obtained in this work. The resulting ground-state rotational constants in cm$^{-1}$ are:

$$\mathscr{A}'' = 8\cdot002366 \pm 0\cdot000048,\ \Delta_{NK}'' = -(1\cdot943 \pm 0\cdot048) \times 10^{-5},$$
$$\mathscr{B}'' = 0\cdot433705 \pm 0\cdot000014,\ \Delta_N'' = (3\cdot24 \pm 0\cdot20) \times 10^{-7},$$
$$\mathscr{C}'' = 0\cdot410448 \pm 0\cdot000013,\quad \delta_K'' = (1\cdot8 \pm 7\cdot2) \times 10^{-6},$$
$$\Delta_K'' = (2\cdot685 \pm 0\cdot020) \times 10^{-5},\ \delta_N'' = (2\cdot95 \pm 0\cdot26) \times 10^{-8},$$
$$H_K'' = (2\cdot04 \pm 0\cdot95) \times 10^{-6},$$

where uncertainties are $3\sigma$. Upper-state constants have also been obtained. Anomalous line intensities are observed throughout the band. The most striking of these anomalies is the observation of very strong ${}^PR_K$ series even for moderately high $K$ values while no ${}^PP_K$ or ${}^RP_K$ lines have been observed.

14770. Eyler, J. R., **Intracavity dye laser technique for the study of laser-induced ionic processes,** *Rev. Sci. Instrum.* **45,** No. 9, 1154-1156 (Sept. 1974).

Key words: intracavity technique; ion cyclotron resonance; mass spectrometry; negative ions; photodetachment; tunable dye laser.

An intracavity dye laser technique has been used to study the photodetachment of electrons from gaseous $OH^-$ ions in an ion cyclotron resonance (icr) spectrometer. Enhancement of the photodetachment effect by a factor of 6.8 when comparing the intracavity technique to a double-pass experiment has been observed. Under the conditions of these experiments approximately 93 percent of the $OH^-$ ions in the icr cell undergo photodetachment using the intracavity technique.

14771. Eyler, J. R., Atkinson, G. H., **Dye laser-induced photodetachment of electrons from $SH^-$ studied by ion cyclotron resonance spectroscopy,** *Chem. Phys. Lett.* **28,** No. 2, 217-220 (Sept. 15, 1974).

Key words: ion cyclotron resonance; mass spectrometry; negative ions; photodetachment; spin-orbit coupling; tunable dye laser.

The photodetachment of electrons from gaseous $SH^-$ ions has been studied in an ion cyclotron resonance mass spectrometer using a flashlamp-pumped organic dye laser as a light source. The onset of the photodetachment process at $538.7 \pm 0.3$ nm ($2.301_6 \pm 0.001_3$ eV, $18563 \pm 10$ cm$^{-1}$) agrees well with that obtained in an earlier study. Coarse structure in the photodetachment curve with a spacing of 11.8 nm (0.052 eV, 422 cm$^{-1}$) has been identified with spin-orbit coupling in the SH· radical. Finer structure, with a spacing of ca. 2.5 nm (0.011 eV, 89 cm$^{-1}$), has also been observed in the curve, but remains unexplained.

14772. Sengers, J. M. H. L., Greer, W. L., Sengers, J. V., **Scaled**

**parametric equation of state for oxygen in the critical region,** (Proc. 1973 Cryogenic Engineering Conf., Atlanta, Ga., Aug. 8-10, 1973), Paper in *Advances in Cryogenic Engineering,* K. D. Timmerhaus, Ed., **19,** 358-364 (Plenum Press, New York, N.Y., 1974).

Key words: critical coefficients; critical exponents; critical region; density profile; dielectric constant; linear model; oxygen; scaling laws; statistical analysis.

A method is described for fitting critical-region equation-of-state data with a particular scaled equation-of-state, the so-called Linear Model. The method has been applied to the density profiles observed by Weber in the critical region of oxygen. The Linear Model is shown to fit these data well, except for a small region on the critical isochore close to $T_c$. The optimized critical exponents, however, do not agree very well with those from Weber's power-law analysis. Some sets of equation-of-state parameters are presented as starting points for further thermodynamic calculations on oxygen.

**14773.** Collin, G. J., **Photolyse du butène-1 dans l'ultraviolet à vide,** *Can. J. Chem.* **51,** No. 17, 2853-2859 (1973).

Key words: far ultraviolet; free radical reactions; ion-molecule reactions; photochemistry; primary processes; 1-butene.

The vacuum u.v. photolysis of 1-butene was studied in the 147-105 nm region. The main products formed from the fragmentation of excited molecules are allene, 1,3- and 1,2-butadienes, ethylene, and acetylene. The addition of a hydrogen atom to the double bond produces mainly secondary butyl radicals (91%) at 147 nm. At 123.6 nm, this proportion becomes 82 percent. Thus at shorter wavelengths (10 and 11.6-11.8 eV), hydrogen atoms are produced with a kinetic energy higher than the thermal energy.

**14774.** Mann, D. B., Dean, J. W., Brennan, J. A., Kneebone, C. H., **Cryogenic flow measurement—positive displacement volumetric flowmeters,** (Proc. 1st Symp. on Flow, Its Measurement and Control in Science and Industry, Pittsburgh, Pa., May 9-14, 1971), Paper in *Flow, Its Measurement and Control in Science and Industry,* Part 2, pp. 381-386 (Instrument Society of America, Pittsburgh, Pa., 1974).

Key words: cryogenic; flow; flowmeters; liquid nitrogen; measured; positive displacement.

The National Bureau of Standards and the Compressed Gas Association (CGA) have jointly sponsored a research program on cryogenic flow measurement. A cryogenic flow research facility was constructed and was first used to evaluate commercially available cryogenic flowmeters operating on a positive displacement principle. The operation and the accuracy of the flow facility is briefly described. The performance of the flowmeters on liquid nitrogen is summarized by reporting the precision and bias of the meters before and after an 80-h stability test and by defining the existence of temperature, flow rate, subcooling, and time order (wear) dependencies. Meters were evaluated with flow rates ranging from 0.00126 to 0.0063 $m^3/s$ (20 to 100 gpm), pressures ranging from 0.34 to 0.69 $MN/m^2$ (50 to 100 psig), and with temperatures ranging from 72 to 90 K.

**14775.** Ely, J. F., McQuarrie, D. A., **Calculation of dense fluid transport properties via equilibrium statistical mechanical perturbation theory,** *J. Chem. Phys.* **60,** No. 11, 4105-4108 (June 1, 1974).

Key words: argon; Barker-Henderson perturbation theory; modified Enskog theory; thermal conductivity; transport properties; viscosity.

The viscosity and thermal conductivity coefficients of dense fluid argon have been calculated using the modified Enskog theory and the equilibrium statistical mechanical perturbation theory of Barker and Henderson. Agreement with experimental transport data is shown to be, in general, quite good. The results of these calculations are also compared to those obtained using the modified Enskog theory and an experimental equation of state. In this case, the results are seen to be excellent, which indicates that this approach provides us with a method of predicting transport properties of simple dense fluids from fundamental molecular theory.

**14776.** Andrews, J. R., **Precision picosecond pulse measurements using a high quality superconducting delay line,** (Proc. 1974 Conf. on Precision Electromagnetic Measurements, London England, July 1-5, 1974), Abstract in *CPEM Digest* No. 113, 316-318 (Institution of Electrical Engineers, London, England, 1974).

Key words: delay line; picosecond; pulse measurement; superconductivity.

With the aid of a high quality superconducting delay line, it i now possible to perform direct oscillographic measurements o the picosecond transition times of very fast electrical signals tha do not furnish pretriggers. A 15 meter superconducting dela line has been constructed. It has an attenuation of 14 dB/km a 1 GHz. The 10 percent-90 percent transition time of this line an its associated air lines leading into and out of the liquid heliu dewar is 18 ps. Some applications of this delay line are shown They include the measurement of the pulse outputs from mercury switch and spark gap pulse generators and the transien response of a traveling wave oscilloscope.

**14777.** McKinney, J. E., **PVT behavior of polymeric liquid-glas systems,** *Proc. 30th National Conf. on Fluid Power, Philadelphia, Pa., Nov. 12-14, 1974,* **XXVIII,** 393-411 (1974).

Key words: density; entropy; free volume; glasses; glas transition; liquid; polymer; poly(vinyl acetate); PVT; relaxation; viscosity.

Techniques and procedures are described which are appropriate to obtain proper PVT data on liquid-glass systems. A a result of the non-equilibrium character of glasses (resultin from their very long viscoelastic relaxation times), the thermodynamic history of glass formation has considerable influenc on structure and corresponding properties. Accordingly, highl systematic experimental procedures are necessary to obtai meaningful data to properly specify the properties of a liqui glass system.

Most of the data presented here pertain to poly(vinyl acetate and amorphous polymer, for which the thermodynamic respons is considered to be in a qualitative sense typical of the liqui glass systems. This polymer is particularly convenient to stud because of its glass transition near room temperature. Throug the appropriate choice of histories, two types of glass transitio temperatures (with their corresponding PVT surfaces) may b observed and defined. One of these may be considered to be thermodynamic transition applicable to thermodynamical reversible systems, the other, a kinematic transition for whic dT/dP approximates the isoviscous state. The latter is therefo of interest in application to fluid transfer analysis at high pressures. In general, the values of dT/dP of the former exceed tho of the latter by roughly a factor of two. The thermodynamic da describing these two transitions make possible the prop evaluation of the Ehrenfest Relations for liquid-glass systems.

The use of high pressure to "permanently" densify glass during formation is described. This procedure results in co nsurately higher refractive indices which have applications in ical technology.

he results from the more recent experiments of this type eal certain contradictions with present phenomenological and ecular theories. A few of the more promising examples are en along with the types of modifications necessary for more urate prediction of thermodynamic and kinematic properties.

78. Pella, P. A., **A discussion of a performance standard for vidential breath alcohol instruments,** (Proc. 1974 Carnahan nd International Crime Countermeasures Conf., Lexington, y., April 16-19, 1974), Paper in *Proceedings 1974 Carnahan nd International Crime Countermeasures Conference, UKY ull.* **105,** 98-101 (1974).

Key words: breath alcohol; instruments; performance standard; specifications; test procedures.

he variety of commercially available breath alcohol instru- its for use in law enforcement programs has been increasing dily. As a result of these developments, officials involved in ntermeasures programs are requesting guidance concerning r reliability. The need for accuracy of the measured values ained with these instruments has been emphasized in the rts. Therefore, it is essential that criteria be established to vide a basis for the selection of acceptable breath-testing ipment. In response to this need, the National Highway Traf- afety Administration (NHTSA) has sponsored the develop- nt of a performance standard [1]. Instruments which are in npliance with this standard will be placed on a qualified ducts list. Funds used to purchase such equipment can then utilized more effectively. Performance standards are sently being developed by the National Bureau of Standards NHTSA. The first of these standards, described in detail in rence 1, applies to evidential breath alcohol instruments. ne selected highlights from this standard will be the subject of presentation.

79. Kuriyama, M., Early, J. G., Burdette, H. E., **An immobile islocation arrangement in as-grown copper single crystals ob- erved by x-ray topography,** *J. Appl. Crystallogr.* **7,** 535-540 Dec. 1974).

Key words: anomalous transmission; as-grown copper crystal; crystal perfection; Czochralski growth; Lomer-Cottrell locks; sessile dislocations; x-ray topography.

-ray diffraction topography using transmission geometry has ealed an interesting array of extremely straight and narrow -line images in sizeable copper single crystals grown under icular growth conditions by the Czochralski technique. se images are analyzed and elucidated by a model of Lomer- trell dislocations. The formation of these sessile dislocations ally aids the growth of large copper crystals of high perfec- . The high degree of perfection over the entire volume of the tals accounts for macroscopic arrangements of Lomer-Cot- dislocations which have not previously been observed by tron microscopic techniques.

80. Melmed, A. J., Carroll, J. J., Meclewski, R., **Dependence work function on coverage for aluminum/tungsten in the field ectron microscope,** *Surface Sci.* **45,** 649-656 (1974).

Key words: aluminum; field emission; tungsten; work function.

luminum adsorption on tungsten has been investigated by d electron microscope techniques. Changes in average work ction and work functions of the (001) plane and (111) region e determined as a function of aluminum deposition. The rage work function exhibits a minimum of about (4.11 ± 0.04) eV (relative to an assumed value of 4.50 eV for the tungsten substrate) and reaches a value of (4.21 ± 0.04) eV for thick deposits. The (001) plane and (111) region exhibit complicated work function dependences on aluminum coverage. Some qualitative observations of aluminum on tungsten surface diffusion are also reported.

14781. Iverson, W. P., **Microbial corrosion of iron,** Chapter 19 in *Microbial Iron Metabolism,* Dr. Neilands, Ed., pp. 475-513 (Academic Press, Inc., New York, N.Y., 1974).

Key words: economics; history; iron mechanisms; microbial corrosion; prevention.

A review of the corrosion of iron by microorganisms with extensive literature survey intended as a Chapter for a 1-volume book entitled "Microbial Iron Metabolism." Includes a historical survey and economic significance of microbial corrosion, general principles of corrosion, a brief discussion of the electrochemical theory of corrosion, the thermodynamics and kinetics of corrosion, electrochemical techniques for measuring the rate of corrosion, and prevention of corrosion. The microorganisms, including fungi and bacteria involved in the corrosion of iron, are discussed extensively as well as the prevention of microbial corrosion of iron.

14782. Johnson, C. R., **Sufficient conditions for D-stability,** *J. Econ. Theory* 9, No. 1, 53-62 (Sept. 1974).

Key words: diagonally dominant; diagonal matrix; *D*-stability; Gersgorin's theorem; Lyapunov's theorem; M-matrix; oscillatory; positive definite; principal minor; Routh-Hurwitz conditions; sign stable; sign symmetric; stability; tridiagonal.

Sufficient conditions for an $n$ by $n$ matrix to be *D*-stable are surveyed. Use is made of some transformations under which the *D*-stables are invariant and relations among the conditions are given. The verifiability of the thirteen conditions cited is also discussed. The lack of an effective characterization of *D*-stability motivates the discussion.

14783. Arp, V., **New forms of state equations for helium,** *Cryogenics* **14,** No. 11, 593-598 (Nov. 1974).

Key words: enthalpy; entropy; equations of state; helium; pressure.

Accurate helium properties must be measured to develop refrigeration systems for superconducting motors and generators. Normally when measuring these properties a double iteration is necessary on the equation of state to find density and temperature. In this paper new state equations are developed which eliminate iterative procedures. These equations are subsets of three overlapping sets of reference equations. They are thermodynamically inconsistent to the reference equations by a small degree of error, but have been found useful for many calculations.

14784. Wacker, P. F., **Antenna measurements at the National Bureau of Standards near-field and extrapolation techniques,** (Abstract only), (Proc. 5th Colloquium on Microwave Communication, Budapest, Hungary, June 24-30, 1974), pp. ME-113 – ME-114 (Academy of Sciences, Budapest, Hungary, 1974).

Key words: antennas; extrapolation; measurements; near-field.

Near-field antenna measurements can yield especially accurate patterns and gain values, since they are subject to the precise control of a closely-coupled laboratory system and are free of errors due to ground reflections and grazing reflections from the walls of an "anechoic" chamber. Moreover, for a planar, circular-cylindrical, or spherical scanning surface, the far-field pattern may be computed from near-field data without significant approximation, provided the probe pattern is known, the medium is homogeneous and isotropic, and the medium, probe, and antenna or array are electrically linear. (The full complex-vector transmitting, receiving, and scattering properties of the antenna and probe are expressed by means of a generalization of an n-port scattering matrix, each mode (e.g., plane wave of a given direction and polarization) being considered as a port. Data processing consists primarily of a Fast Fourier Transform, followed in the spherical case by a matrix multiplication.) If the antenna is mounted on a conventional rotator, "spherical scanning" requires no probe transport.

For fixed orientations of two antennas, exact functional forms for the received signal as a function of distance permit correction for multiple-reflection and proximity effects and so yield accurate far-field values from measurements made on small ranges.

Recent NBS developments and measurements with these techniques will be described.

**14785.** Durst, R. A., **Ion selective electrodes,** (Proc. Int. Conf. on Localized Corrosion, Williamsburg, Va., Dec. 6-10, 1971), Paper in *Localized Corrosion,* R. W. Staehle, B. F. Brown, J. Kruger, and A. Agrawal, Eds., pp. 151-157 (National Association of Corrosion Engineers, Houston, Texas, 1974).

Key words: electrode review; ion-selective electrodes; membrane electrodes; potentiometry.

The state of the art of the newer non-glass types of ion-selective electrodes is reviewed. This survey includes the theory, characteristics, and methodology of the solid-state, liquid ion-exchange and heterogeneous membrane electrodes.

The applications of these sensors to a wide variety of scientific disciplines is discussed, ranging from various physicochemical studies and biochemical research to industrial analysis and control systems. Since this field has been growing so rapidly in the past several years, only a few of the many applications of ion-selective electrodes are presented. Special emphasis is placed on the experimental ferric ion-selective electrode as a possible sensor in corrosion studies. Much remains to be done with these sensors in the very fruitful and socially relevant areas of environmental pollution and public health. Ion-selective electrodes can provide a wealth of information if used with the proper precautions and their usefulness is limited only by the imagination and ingenuity of the users.

**14786.** Cook, R. K., Schade, P. A., **New method for measurement of the total energy density of sound waves,** (Proc. 1974 International Noise Control Engineering Conference, Washington, D.C., Sept. 30-Oct. 2, 1974), Paper in *Inter-Noise 74 Proceedings,* J. C. Snowdon, Ed., pp. 101-106 (Inter-Noise 74, Institute of Noise Control Engineering, Poughkeepsie, N.Y., 1974).

Key words: acoustical measurements; acoustics; noise measurement; reverberation chambers; sound energy measurement; sound power measurement.

The total energy of a sound field in reverberation chambers is usually sampled by an array of microphones. Each measures the time-average of the squared sound pressure at its location. This is equivalent to sampling the time-average of the *potential* energy density of the sound field. It would be advantageous to measure as well the time-averaged squared particle velocity. This would yield the *kinetic*-energy density, which added to the *potential*-energy density would then yield the *total*-energy density. A principal advantage of the total energy density is that its spatial variance is in general appreciably less than the potential varianc We find this from an analysis of the variances for the eigenmode of rectangular chambers having reflecting (rigid) walls. microphone for total energy density can be made from a spati array of six elements arranged at the corners of a regular o tahedron. Electret microphones seem to be particularly suitabl for the elements. The total energy density can be computed fro the sums and differences of the electret outputs, with the help integrated circuits, and displayed as a running function of tim e.g., as a graphic recording. For a standing-wave tube, only tw elements are needed, and the total-energy-density microphon then takes a very simple form.

**14787.** Gerola, H., Linsky, J. L., Shine, R., McClintock, W Henry, R. C., Moos, H. W., **Evidence for a corona of Be Geminorum,** *Astrophys. J.* **193,** No. 3, L107-L110 (Nov. 1974).

Key words: stellar atmospheres; stellar coronae; ultraviol stellar spectrum.

Using the Princeton spectrometer on the satellite *Copernicu* a strong emission line has been detected in the K0 giant $\beta$ Ge at 1218.4 Å, which is identified as the $^1S_0$ - $^3P^o{}_1$ intercombinati line of O v. The strength of the line is such that it is probab formed in a corona at temperatures near 260,000 K rather th in an analog of the solar chromosphere-corona transition regio

**14788.** Goldman, A. J., **Fractional container-loads and topologic groups,** *Oper. Res. Letters to Editor* **16,** No. 6, 1218-12 (Nov.-Dec. 1968).

Key words: inventory theory; topological groups.

The problem treated is that of finding those probability d tributions of fractional "tails" on the input volumes to a unitiz tion facility during successive time periods that yield a time-i variant distribution of backlog levels. It is shown that th reduces to the determination (which is carried out) of all clos subgroups of the circle group.

**14789.** Alvarez, R., **Sub-microgram per gram concentrations mercury in orchard leaves determined by isotope dilution a spark-source mass spectrometry,** *Anal. Chim. Acta* **73,** 33- (1974).

Key words: agriculture; environment; isotope dilution; ma spectroscopy; NBS Standard Reference Material; orcha leaves; trace mercury.

A stable isotope dilution procedure in conjunction with t spark source mass spectrograph was developed for determini sub-$\mu$g g$^{-1}$ concentrations of mercury in orchard leaves. A sample was spiked with a solution of mercury, isotopically e riched in $^{201}$Hg and $^{198}$Hg served as a carrier. After wet-ashi the sample with nitric and perchloric acids under reflux a distilling most of the acid, the isotopically equilibrated mercu was electrodeposited onto high-purity gold wires for sparking the mass spectrograph. The concentration was calculated fro the altered isotope ratio, $^{201}$Hg/$^{202}$Hg, and other data. The resu were compared with those obtained by atomic absorption sp trometry and neutron activation, leading to a certified value $0.155 \pm 0.015$ $\mu$g g$^{-1}$ for the mercury content of Orchard Leav SRM 1571 of the National Bureau of Standards.

**14790.** Goldman, A. J., **The minimax transportation proble** *Transp. Sci. Letter to Editor* **2,** No. 4, 383-387 (Nov. 1968).

Key words: linear programming; network flows; single co modity; transportation; transportation problem.

This note demonstrates a simple solution method for the f lowing single-commodity flow problem: Given a set of orig ch with a known supply, and a set of destinations each with a own demand, find the minimum possible capacity for a vehicle ich is to perform all the origin-to-destination transfers one at ime.

791. Goldman, A. J., **Optimal locations for centers in a network,** *Transp. Sci.* **3,** No. 4, 352-360 (Nov. 1969).

Key words: concave functions; networks; optimal locations.

The problem treated is that of locating $n$ centers (processing ilities) in a network, so as to minimize the total transportation st associated with their use. On the assumption that all movents occur between a vertex and a center nearest it, *HAKIMI* s shown that only vertex locations for the centers need be conered. The present paper shows that this conclusion remains id under alternative assumptions more appropriate for some plications.

792. Shine, R. A., Linsky, J. L., **A facular model based on the wings of the Ca II lines,** *Solar Phys.* **37,** 145-150 (1974).

Key words: sun-faculae; sun-photospheric models; Van der Waals line broadening.

We develop a relatively simple procedure for deriving models upper photospheric regions based on the damping wings of the II resonance and infrared triplet lines. The procedure is used derive a facular model but can also be applied to late-type rs. We compare our model to that of Chapman.

793. Weissler, P. G., Kobal, M. T., **Noise of police firearms,** *J. Acoust. Soc. Amer.* **56,** No. 5, 1515-1522 (Nov. 1974).

Key words: damage risk criteria for impulse noise; gunfire noise; noise-induced hearing damage; noise of police firearms.

n an effort to provide guidelines for law enforcement person- to protect their hearing, the peak pressure level and signal duion ($A$ and $B$ duration) of eight popular firearms were meaed and compared with the requirements of OSHA (1970), IABA DRC (1968), and EPA levels (1974). Small condenser crophones and a storage oscilloscope were used to record the st wave signatures from a 9-mm automatic, 0.357-cal. Magm revolver, 0.41-cal. Magnum revolver, 0.22-cal. revolver, 5-cal. automatic, 0.44-cal. Magnum revolver, 12-gauge shotn, and 0.22-cal. rifle. Measurements were made at the ear of person shooting and at the approximate position of a ghbor at a firing range. Some measurements were also made a practice firing range. A portable tape recorder was found ful for recording gun signals and measuring $B$ durations. The ak pressure levels of the signatures of all the firearms tested ceed the OSHA maximum of 140 dB. It was found that in an choic environment the noise from five of the handguns exded the CHABA DRC (1968), while the noise from all of the arms tested, except the 0.22-cal. rifle, exceeded the EPA els (1974). At a sound-insulated firing range, the noise from the firearms tested, except the 0.22-cal. rifle, exceeded the IABA DRC (1968), while all the firearms tested exceeded the A levels (1974).

94. Krasny, J. F., **Fabric flammability: Needs for research,** *Home Econ. Res. J.* **2,** No. 3, 160-166 (Mar. 1974).

Key words: apparel; burn injury; fabric; fire modeling; flame spread; flammability; flammability testing; garments; heat transfer; ignition.

The objective of this paper is to give a brief overview of the sent status of attempts to model real life accidents involving ment fires in the laboratory, and to suggest experiments ich could be carried out in the textile laboratories of home economists. The main purpose of laboratory modeling should be the definition of hazard due to the ignition and burning of garments varying in fit, fiber content, and fabric weight and construction.

Hazard from burning garments depends on the ease of ignition, rate of flame spread, heat transfer to the body, and the ease of extinguishing the garments. The literature on each of these factors is briefly reviewed, and suggestions are made for experiments which could illustrate the effects of various fabric and garment parameters on injury hazard.

14795. Ruegg, F. W., **Expansion factors for two variable area flow meters,** *J. Eng. Ind. Trans. ASME Papers No. 73-WA/FM-2,* **96,** No. 4, 1347-1353 (Nov. 1974).

Key words: coefficients of discharge; expansion factor; flow coefficients; flowmeter; fluid meter coefficients; rotameter; variable area meter.

Data acquired in the years 1958 to 1960 at the Naval Ship Engineering Center under sponsorship of the American Society of Mechanical Engineers are used to derive semiempirical equations for the performance of two variable area meters with both liquid and gas flow. As the measurements are put to a usage for which they were not intended, the data treatment is considered illustrative of the application of a flow equation derived by an analysis based upon a force and momentum balance. The hydraulic flow coefficient is expressed in terms of a function of (a) pressure drop divided by float weight and of (b) a dimensionless length ratio $\beta$ for float position. Density ratio is used to modify the function of $\beta$ to derive the expansion factor $Y$ for gas flow as suggested by the analysis. Reasonable agreement between measured and derived values of $Y$ is demonstrated, and approximate measures of the velocity profiles in the meter are derived from the correlation equations. One set of air tests at one float position in which the viscous influence number $N$ was changed from 500,000 to 783,000 indicated (within this range) a possible insensitivity of the derived function of $\beta$ to change of $N$.

14796. Cook, R. K., **Paraholography — a new method for measurement of the directional distribution of sound waves in a reverberation chamber,** *J. Acoust. Soc. Amer. — Technical Notes and Research Briefs* **56,** No. 4, 1305-1307 (Oct. 1974).

Key words: acoustics; acoustical holography; acoustical measurement; paraholography; reverberation chambers; sound propagation.

We describe a method for experimental determination of the complex of plane waves composing the sound field in a reverberation chamber. The basic holographic principle is comparison of the actual sound field with a family of reference plane waves having precisely known directions of propagation, sound pressures, and phases. The reference waves are not "real" waves but are created electronically, on the electrical side of microphones sensing the actual sound field, so as to be "parallel" to real waves.

14797. Hall, K. R., Waxman, M., **Geometrically transformed weights for least squares analyses,** *Cryogenics* **14,** No. 11, 612-614 (Nov. 1974).

Key words: implicit model; least-squares analysis; transformed weights.

The most generalized algorithm for the least-squares estimation of parameters in nonlinear, implicit models is the modified Deming approach. This technique is very complicated; however, simpler approaches for many problems lead to reasonable solutions. One widely accepted alternative is the $\Delta$ transformation of Hust and McCarty. This article offers another equally simple alternative: geometrically transformed weights.

**14798.** Johannesen, R. B., Peake, S. C., Schmutzler, R., **The fluorine-19 NMR spectrum of methylthiotetrafluorophosphorane,** *Z. Naturforsch. B* **29b,** 699-700 (1974).

Key words: fluorine; methylthiotetrafluorophosphorane; nuclear magnetic resonance; phosphorus.

The low-temperature $^{19}$F NMR spectrum of the stereochemically nonrigid compound, $CH_3SPF_4$, shows three fluorine environments, one for the equatorial and two for the nonequivalent axial fluorine atoms. Each of the twelve lines of the upfield $^{19}$F (axial) resonance shows further fine structure, due to coupling between $^{19}$F and the protons of the $CH_3S$ group. The center peaks of the two multiplet components reveal apparent quintet structure which, based on a computer simulation of the $^{19}$F spectrum of $CH_3SPF_4$, is rationalized in terms of accidental overlap of two quartets.

**14799.** Achenbach, P. R., **Simplified laboratory procedures for simulating the effect of air leakage into refrigerated enclosures,** (Proc. Joint Conf. Office for Research and Experiments of the International Union of Railways and International Institute of Refrigeration, Vienna, Austria, May 6-8, 1969), Chapter in *Refrigerated Vehicles and Containers, Annex 1969-3,* pp. 89-94 (International Union of Railways, Paris, France, 1969).

Key words: air leakage; cooling load measurement; refrigerated enclosures; testing of vehicles; wind effects on structures.

A laboratory test method is needed that can be used universally for rating or acceptance of refrigerated vehicles and containers employed in international transport. Various investigators have shown that air and moisture leakage into an insulated body under the influence of impact air pressure or wind can represent a significant fraction of the total cooling load. Since road testing and laboratory testing of vehicles and containers under realistic air flow conditions are both complex and expensive, simplified test procedures are urgently needed for simulating the effect of air leakage during cooling load tests. By making certain logical assumptions regarding the distribution of openings in an insulated body and the nature of the fluid flow through these openings, it is shown that a negative pressure of 1 mm W.G. (0.04 in W.G.) inside the cargo space will produce an air leakage into the body as large as a 100 km/hr (62.5 mph) wind on one end or a 50 km/hr (31.3 mph) wind on one long side of most vehicles and containers. A second simplified method involves determining the total cooling load by the addition of the measured heat transmission with interior heating and a calculated air leakage effect based on a measured air flow rate and an assumed change in sensible and latent heat content of the leakage air. Both of these methods need laboratory study.

**14800.** Cook, R. K., **Colloquium on infrasound in Paris,** *J. Acoust. Soc. Amer.* **56,** No. 2, 721-722 (Aug. 1974).

Key words: atmospheric acoustics; infrasound; physiological effects of infrasound.

The Colloque International sur les Infra-sons, held 24-27 September 1973 in Paris, France, was organized by the Centre National de la Recherche Scientifique and by the Groupement des Acousticiens de Langue Francaise. Professor L. Piminow planned the program of the Colloquium to "contain all aspects of atmospheric infrasounds, namely production, diffusion, detection and measurements; infrasounds of natural sources (oceanic origin, high atmosphere, meteorites, etc....); infrasounds of technical origins, technical applications of infrasounds, the inconveniences of infrasounds in physiology and industry, particularly in the chambers of combustion, detection of explosions, etc...." Infrasound was regarded as being oscillations at frequencies below 20 Hz.

**14801.** Mann, W. B., **The calibration of the National Bureau Standards' tritium standards by microcalorimetry and ga counting,** (Proc. Tritium Symp., Las Vegas, Nev., Aug. 3 Sept. 2, 1971), Chapter 3 in *Tritium,* A. A. Moghissi and M W. Carter, Eds., pp. 86-102 (Messenger Graphics, Las Vega Nev., 1971).

Key words: gas counting; microcalorimetry; tritium sta dards.

The calibration of the National Bureau of Standards tritiu standards by microcalorimetry and gas counting will b described.

**14802.** Mielenz, K. D., **Spherically corrected reflecting objecti for unit magnification,** *Appl. Opt.* **13,** No. 11, 2580-2584 (No 1974).

Key words: Cassegrain; reflecting objective; spectrometer spherical aberration; third-order theory; unit magnificatio

Cassegrainian-type reflecting objectives are useful as in-li imaging devices for fast spectrometer systems. They are i herently free from chromatic aberrations and may be correct for spherical aberration. A particularly simple design, consisti of two mirrors with oppositely equal curvatures, is possible wh unit magnification is desired. This system has zero third-ord spherical aberration, and all other aberrations are small also. I main disadvantage is the loss due to the central obstruction of t beam, amounting to about 28 percent exclusive of reflecti losses.

**14803.** Durst, R. A., **Ion-selective electrode response in biolog fluids,** (Proc. Conf. on Workshop on Ion-Selective Microele trodes, Boston, Mass., June 5, 1973), Chapter 2 in *Ion-Sele tive Microelectrodes,* H. J. Berman and N. C. Hebert, Ed pp. 13-21 (Plenum Publ. Corp., New York, N.Y., 1974).

Key words: electrode response in biological fluids; ele trodes; ion-selective electrodes; microelectrodes.

The response of ion-selective electrodes in biological flui may be affected by a wide variety of physical and chemical fa tors. These may influence the indicator electrode directly or m affect the liquid junction of the reference electrode. A bri discussion is presented of the various sources of error and unce tainty in electrode measurements in biologic media especial with microelectrodes. A serious need exists for the developme of practical standards for the calibration of ion-selective ele trodes in physiologic media in order to ensure the consistency interlaboratory measurements.

**14804.** Goebel, D. G., Poole, E. W., Hartsock, R. G., **Instrume for measuring phototube spectral response,** *Appl. Opt.* **8,** No. 1749-1750 (Aug. 1969).

Key words: photodetector; photodetector spect response; photomultiplier tubes; phototubes.

An instrument has been designed to plot automatically t relative spectral response of a phototube over the range of 0. μm to 0.84 μm. The response as a function of wavelength recorded directly by using a digital printer or an x-y plotter.

**14805.** Stevens, W. J., Das, G., Wahl, A. C., Krauss, M., Ne mann, D., **Study of the ground state potential curve and dip moment of OH by the method of optimized valence configu tions,** *J. Chem. Phys.* **61,** No. 9, 3686-3699 (Nov. 1, 1974).

Key words: dipole moment function; dissociation ener electronic structure; hydroxyl radical; potential curve; s consistent-field.

Accurate theoretical potential and dipole moment curves presented for the $X\ ^2\Pi_i$ state of the hydroxyl radical. T eoretically determined dissociation energy is 4.53 eV as com-red to the experimental value of 4.63 eV. The computed dipole ment at the experimental equilibrium internuclear separation 1.674 D, which is in excellent agreement with the most reliable perimental value of 1.66±0.01 D. A detailed, general scription for constructing optimized valence configuration vefunctions for diatomic hydrides is presented with OH as a ecific example.

806. Gadzuk, J. W., **Angular distributions of electrons photoemitted from chemisorbed atoms,** *Solid State Commun.* **15,** No. 6, 1011-1016 (1974).

Key words: angular distributions; chemisorption; photoemission; photoionization.

A theory which describes the angular distributions of electrons otoemitted from chemisorbed atoms is presented. Due to hole localization and preferential orientation, interference effects e to emission from various centers in a molecule do not erage out, as they do in gas phase photoionization and much re structural information pertaining to chemisorption bonds contained in such measurements.

807. Plummer, E. W., Waclawski, B. J., Vorburger, T. V., **Photoelectron spectra of the decomposition of ethylene on (110) tungsten,** *Chem. Phys. Lett.* **28,** No. 4, 510-515 (Oct. 15, 1974).

Key words: $C_2H_4$ decomposition; chemisorption bonds; LEED; photoelectron spectra; tungsten; work function.

Photoelectron spectra, LEED patterns, and work function anges were obtained for ethylene adsorbed on (110) tungsten room temperature, and with subsequent heat treatment. For urated adsorption of $C_2H_4$ on (110)W at room temperature, atures in the photoelectron spectrum were observed which are lieved to be due to the C–H, C–C, and C–metal bonds in an sorbed species of the form $C_2H_2$. The work function decreased 1.2 eV at saturation, but LEED showed no change from the an surface pattern. Upon heating to ≈ 500 K, where hydrogen known to desorb, the C–H bond was broken, whereas the –C and C–metal bonds remained. The work function in-eased, from saturation, by ≈ 0.6 eV and the LEED pattern ex-ited a large diffuse background with no new spots. Upon heat- to ≈ 1100 K the C–C bond broke and the LEED pattern or-red into the characteristic carbon contamination pattern.

808. Krauss, M., Celotta, R. J., Mielczarek, S. R., Kuyatt, C. E., **Electron impact energy loss spectra of the 1 $^2B_2 \leftarrow \tilde{X}\ ^2A_1$ transition in $NO_2$,** *Chem. Phys. Lett.* **27,** No. 2, 285-288 (July 15, 1974).

Key words: electron impact; energy loss; excitation; $NO_2$.

Long vibrational progressions are observed in the electron im-ct energy loss spectrum of $NO_2$ in the 1.5-4.1 eV energy loss nge. These progressions can be assigned to the 1 $^2B_2 \leftarrow \tilde{X}\ ^2A_1$ nsition and suggest that the 1 $^2B_2$ state is asymmetric.

809. Heaton, H. T. II, Menke, J. L., Schrack, R. A., Schwartz, R. B., **Total neutron cross section of carbon from 1 keV to 15 MeV,** *Nucl. Sci. Eng.* **56,** 27-36 (1975).

Key words: carbon; neutron total cross section; pulsed neutron sources; time-of-flight.

The total neutron cross section of carbon was measured over energy range 1 keV to 15 MeV, using the U.S. National Bu-u of Standards electron linear accelerator as a pulsed neutron urce. Neutron energies were measured by the time-of-flight thod. The measurement accuracy is estimated to be ±3/4 per-it below 100 keV and ±1 percent above. The carbon cross ction was fit with a polynomial from 0.001 to 1.4 MeV with the following coefficients

$$\sigma = 4.757 - 3.419\,E + 1.548\,E^2 - 0.328\,E^3,$$

where $\sigma$ is in barns and E in MeV. Data are compared with other results.

**14810.** Hessel, M. M., Smith, E. W., Drullinger, R. E., **Transition dipole moment of $Na_2$ and its variation with internuclear distance,** *Phys. Rev. Lett.* **33,** No. 21, 1251-1254 (Nov. 18, 1974).

Key words: electronic dipole moment; internuclear distance; laser fluorescence; $Na_2$; transition moment.

The electronic transition dipole moment was determined for the transition $X^1\Sigma_g^+ \leftarrow B^1\Pi_u$ of $Na_2$ and was found to be $6.8 + 0.5r$ D over a range of internuclear distance $r$ of 2.6 – 5.0 Å. Our results agree with earlier lifetime measurements and are in qualitative agreement with semiquantitative theoretical calculations, but they strongly disagree with the recent work of Callender, Gersten, Leigh, and Yang.

**14811.** Hayward, E., Barber, W. C., McCarthy, J. J., **Nuclear scattering of plane-polarized photons,** *Phys. Rev. C* **10,** No. 6, 2652-2653 (Dec. 1974).

Key words: giant resonances; nuclear photon scattering; nuclear surface oscillations; plane-polarized photons.

Monochromatic 15.1 MeV plane-polarized photons have been scattered from seven additional targets having their $E1$ giant resonances near 15 MeV. They are In, Sb, Nd, Hg, Pb, Th, and U. Photons scattered through 90° were observed in the planes both parallel and perpendicular to the plane of the polarization vector. The observation of photons scattered along the polarization vector by the spherical vibrators indicates that the giant resonance is coupled to the quadrupole oscillations of the nuclear surface. The agreement with the predictions of the dynamic collective model is not particularly striking though there is little doubt that the phenomenon is qualitatively understood.

**14812.** Cavallo, L. M., Schima, F. J., Unterweger, M. P., **Decay of $^{133}Xe^g$,** *Phys. Rev. C* **10,** No. 6, 2631-2632 (Dec. 1974).

Key words: enriched source; Ge(Li) detector; measured $T_{1/2}$; pressured ionization chamber; radioactivity $^{133}Xe^g$; $\nu$ relative intensity.

The half-life of isotopically separated $^{133}Xe^g$ was determined by measurement in a $4\pi\gamma$ pressure ionization chamber. The value obtained was 5.245 days with an uncertainty of 0.006 days which is the linear sum of the standard error at the 99 percent confidence limit and the estimated systematic errors. This result was confirmed by two separate half-life measurements employing a Ge(Li) detector. The $\gamma$ rays which deexcite the level at 383 keV in $^{133}Cs$ have been observed. The intensities of the 383- and 221-keV $\gamma$ rays relative to the 302-keV $\gamma$ ray intensity were found to be 0.489 and 0.020 with the respective standard errors calculated to be 3.8 percent and 40 percent.

**14813.** Lamaze, G. P., Carlson, A. D., Meier, M. M., **A new measurement of the $^{10}B(n,\alpha)^7li$ branching ratio,** *Nucl. Sci. Eng.* **56,** Tech. Note, 94-96 (1975).

Key words: $^{10}B(n,\alpha)^7Li$ reaction; branching ratio; gas proportional counter; neutrons; nuclear physics; T(p,n) neutrons.

To resolve a discrepancy in determinations of the $^{10}B(n,\alpha)^7Li$ branching ratio, a new measurement has been made at the National Bureau of Standards (NBS). The measurement was made with a $^{10}BF_3$ gas proportional counter and monoenergetic 790-keV neutrons obtained at the NBS 3-MV Van de Graaff laboratory. A branching ratio of $0.66 \pm 0.03$ was obtained. This determination agrees with the measurements of Petree et al. and Davis et al.

**14814.** Sugar, J., Kaufman, V., **Spectra and energy levels of three- and four-times ionized hafnium (Hf IV and Hf V),** *J. Opt. Soc. Amer.* **64,** No. 12, 1656-1664 (Dec. 1974).

Key words: energy levels; hafnium; ionization energies; Slater parameters.

The spectra of hafnium produced by a sliding-spark discharge operating at peak currents of 6 to 1200 A were photographed in the spectral range of 400 to 2100 Å. Sixty-three lines of Hf IV were measured in the limited range of ~500-900 Å, of which 43 were classified. New levels in the $4f^{14}nl$ doublet term system of Hf IV were found for $nl = 6f$, $7p$, and $8s$. In addition, the resonance transition array $4f^{14}5d$-$4f^{13}5d^2$ was interpreted. In Hf V 216 lines were observed. With these data, all levels of the configurations $4f^{13}nl$ for $nl = 6s, 7s, 6p, 5d$, and $6d$ were found except for two levels of $4f^{13}6d$. Theoretical interpretations are given of all of the above configurations. Values for the ionization energies of both species were derived.

**14815.** Molino, J. A., **Measuring human aversion to sound without verbal descriptors,** *Percept. Psychophys.* **16,** No. 2, 303-308 (Oct. 1974).

Key words: aversion for sound; avoidance; differential reinforcement of high rate; escape; high school students; key press; pure tones; second order schedules.

High school students tapped rapidly on a telegraph key to reduce the intensity of a continuous acoustic stimulus presented through earphones. Failure to respond resulted in an intensity increase of 1 dB every 4 sec. In Experiment 1, a group of 19 students responded to three pure tones (125, 1,000, and 8,000 Hz) and a white noise. The different asymptotic levels observed after 4 min were taken as a measure of equal-aversion levels for the stimuli. In Experiment 2, the effect of the starting intensity level (45, 70, and 90 dB SPL) was determined for a 1,000-Hz tone. Differences in the asymptotic intensity levels observed after 6 min were not significant. In Experiment 3, no significant effect was found upon varying the number of responses required to produce a 1-dB intensity decrement in a 1,000-Hz tone. Together, the experiments demonstrated the feasibility of determining equal-aversion levels for sounds.

**14816.** Debye, N. W. G., Linzer, M., **Correlation of nuclear quadrupole resonance and $^{119m}$Sn Mössbauer spectral parameters,** *J. Chem. Phys.* **61,** No. 11, 4770-4776 (Dec. 1974).

Key words: Mössbauer; NQR; nuclear quadrupole coupling; organotin; organometallic.

A precise redetermination of the $^{119m}$Sn Mössbauer spectral parameters of a large number of organotin (IV) halides and of the tin (IV) tetrahalides has been made. The $^{35}$Cl NQR resonance spectra of $(CH_3)_3SnCl$ and of $(n\text{-}C_5H_{11})_2SnCL_2$ have been measured for the first time. These data, in conjunction with literature values of other halogen frequencies in this series, yield correlations of both the central tin atom Mössbauer isomer shift and quadrupole splitting values with the reduced ligand NQR coupling constants. The correlations may be interpreted qualitatively in terms of the bonding trends expected on the basis of ligand electronegativities, and the uniformities of the correlations strongly indicate a lack of sharply defined structural variations within these compounds.

**14817.** Kuyatt, C. E., DiChio, D., Natali, S. V., **Third-order asymptotic aberration coefficients of electron lenses. III. Formulas and results for the two-tube electrostatic lens,** *Rev. Sci. Instrum.* **45,** No. 10, 1275-1280 (Oct. 1974).

Key words: aberration integrals; asymptotic aberrati coefficients; electron lenses; strong lenses; third-order ab ration coefficients; two-tube electrostatic lens; weak lens

The third-order asymptotic aberration coefficients of rou electrostatic electron lenses are formulated, following Hawk in a form independent of object and aperture positions. Six qu tities are sufficient to specify completely the third-order aber tion properties of electrostatic electron lenses. Equations these six quantities are derived in the form of integrals involv derivatives of the axial potential no higher than the seco Using these equations and our previously calculated potenti and first-order trajectories we have computed the six aberratic coefficients for the two-tube electrostatic lens for voltage rat from 1.1 to 10 000. The results are believed accurate to bet than 0.2 percent.

**14818.** Pella, P. A., **Mössbauer spectrometry,** Chapter 26 *Systematic Materials Analysis,* J. H. Richardson and R. Peterson, Eds., **III,** 241-267 (Academic Press, New Yo N.Y., 1974).

Key words: materials characterization; Mössbauer sp trometry; nuclear resonance.

This book chapter entitled "Mössbauer Spectrometry," wh appears in *Systematic Materials Analysis,* Vol. III, pp. 241-2 J. H. Richardson and R. V. Peterson, Eds., Academic Pr Inc., New York, 1974, is essentially tutorial. This chap describes the theory and practice of this technique in a man oriented toward the student on the graduate level or analyst w finds himself with a materials characterization problem. T chapter draws heavily on already published material, and w ten, I hope, with the intention of conveying to the reader what formation can be obtained by this technique. The chapter cludes theory, instrumentation, sample preparation, and gi examples of application in the areas of mineralogy, metallu magnetic properties, chemical structure and bonding, solid-s studies, and data handling.

**14819.** Zapf, T. L., **Calibration of quartz transducers as ultras power standards by an electrical method,** *Proc. 1974 trasonics Symp., Milwaukee, Wisconsin, Nov. 11-14, 1 IEEE Cat. No. 74 CHO 896-ISU,* pp. 45-50 (IEEE, I New York, N.Y., 1974).

Key words: piezoelectric transducers; standards of trasonic power; ultrasonic power; ultrasonic transducers

Ultrasonic beam power from specially-designed quartz pi transducers can be determined from an appropriate set of ele cal measurements. The characterized transducers can be use transportable standards of ultrasonic power. A highly accu twin-T null circuit is employed for the measurement of elect conductances of half-wave resonant quartz transducers u certain loading conditions. This permits calculation of equivalent resonant radiation conductance which, when tiplied by the square of the applied voltage, yields the emitte trasonic power into a load. Quartz transducers, thus cha terized, can serve as standards of ultrasonic power for chec or calibrating ultrasonic power measuring equipment suc radiation force, calorimetric, and acousto-optic devices. With equipment used at the National Bureau of Standards, uncer ties are estimated at less than ±5 percent in the frequency r from 1 to 5 MHz.

**14820.** Ayres, R. L., Cavallo, L. M., Coursey, B. M., Hutc son, J. M. R., Mann, W. B., **National Bureau of Stand gamma-ray standards and techniques for gamma-ray meas ments, (Abstract),** *Proc. Trans. 1973 Annual Meeting o American Nuclear Society, Chicago, Ill., June 10-14, 1* **16,** 69 (1973).

Key words: energy efficiency curves; gamma ray; mixed radio nuclide; standards.

The National Bureau of Standards provides gamma-ray stan-rds in a number of forms for different purposes. Our earliest ndards were solution standards of various gamma-ray-itting radionuclides. These were later supplemented by point-rce standards covering the range of photon energies from 60 V to 2.61 MeV. Currently we are also issuing mixed-ionuclide solution standards, each covering the photon ener-range from about 88 keV to 1.84 MeV.

The values of most of our gamma-ray standards are preserved calibrated atmospheric-air and pressurized-argon ionization ambers. Efficiency-energy curves for these chambers have en accumulated over a great many years, based on data col-ted by direct methods of measurement such as coincidence unting. Cesium-137 and $^{85}$Kr standards were produced, pectively, by means of the ion chamber, using efficiency inter-lation, and by comparison with $^{85}$Sr standards. The mixed-ionuclide, gamma-ray solution standards were primarily signed for the calibration of detectors used in measuring power ictor effluent, and are issued in bottles of standard dimensions.

821. Molino, J. A., Zerdy, G. A., Frome, F. S., **Toward a more musical foghorn,** *Hum. Factors.* **16,** No. 6, 567-575 (Dec. 1974).

Key words: acoustic navigation aids; applied psychoacoustics; applied psychology; aversiveness; foghorns; preference; pure tones.

Ten college students gave preference judgments for 4 pure nes (120, 300, 500, and 835 Hz) and 11 tone composites con-ucted from combinations of the pure tones. Equal aversion lerance) levels were also measured for the four pure tones and five of the composites. Sensation-level measures were em-oyed to express aversion thresholds in order to take account of differential sensitivity of the human ear at different frequen-s. Certain operational conclusions were suggested for the sign of acoustic navigation aids. The higher frequency pure nes and composites were generally more preferred, and were o tolerated at higher sensation levels. The 120-Hz pure tone s a highly non-preferred signal. The presence of a 120-Hz mponent in any composite lowered both the preference value d the maintained sensation level. In the case of the moderately eferred 500-Hz pure tone, adding other more-preferred, pure-e components increased the preference for the signal.

822. Eisenhart, C., **Karl Pearson,** Paper in *Dictionary of Scientific Biography,* **X,** 447-473 (Charles Scribner's Sons, New York, N.Y., 1974).

Key words: bibliography; *Biometrika*; Chi-square tests; correlation, regression; R. A. Fisher; Francis Galton; frequency curves, method of moments; Karl Pearson; statistics; *Tables for Statisticians and Biometricians*; W. F. R. Weldon.

A review of the life and work of Karl Pearson (1857-1936), under of the science of statistics. His student days at Cam-dge and in Germany. His pre-1890 career as a professor of ap-ed mathematics and mechanics, as a philosopher of science, d as a social reformer. The role of Francis Galton and W. F. R. eldon in redirecting his career to founder (1891-1936) of the ence of statistics. Method of Moments and Pearson System of equency Curves; Correlation and Regression; Chi Square sts. *Biometrika; Annals of Eugenics; The Treasury of Human heritance; Tables for Statisticians and Biometricians; Tracts Computers; Tables of the Incomplete Γ-function; Tables of Incomplete β-function.* Bibliography of principal Original orks; and of major Secondary Literature.

14823. Komarek, E. L., Tryon, P. V., **An application of the power equation concept and automation techniques to precision bolometer unit calibration,** *IEEE Trans. Microwave Theory Tech., Part II, 1974 Symposium Issue,* **MTT-22,** No. 12, 1260-1267 (Dec. 1974).

Key words: automated measurements; bolometer unit calibration; power equation concept.

The power equation concept has been implemented into a multioctave precision bolometer unit calibration system employing automation techniques in conjunction with an automatic network analyzer (ANA) system. Using statistical methods the system is being evaluated as a calibration transfer system operating in the 2-12.4-GHz frequency range at 1-10 mW. Preliminary results reported here show a single measurement standard deviation of 0.2-1 percent from 2-10 GHz. Upon a successful evaluation, the system will be qualified as an integral part of the national measurement system.

14824. Flynn, J. H., **Theory of differential scanning calorimetry—coupling of electronic and thermal steps,** Paper in *Analytical Calorimetry,* R. S. Porter and J. F. Johnson, Eds., **3,** 17-44 (Plenum Publ. Corp., New York, N.Y., 1974).

Key words: differential scanning calorimetry (DSC); electronic and thermal coupling; instrumental limitations; supercooling; theoretical model; thermal analysis; thermodynamic properties.

A model system for differential scanning calorimetry (DSC) is developed in which the electronic response of the instrument is coupled with the heat flow across an interface. Equations are derived which relate the time constants for this two-step process with the thermal properties of the sample and the amplitudes, areas, slopes and dwell times of DSC traces. The cases discussed include first and second order transitions, partial and total "supercooling" and effects of a temperature dependence of the heat capacity and the rate of temperature change. The magnitude of the lag terms of these cases is determined from typical experimental data. The equations permit an independent determination of the interfacial time constant and an assessment of the limits for the validity of the theoretical model.

14825. Andrews, J. R., **Precision picosecond-pulse measurements using a high-quality superconducting delay line,** *IEEE Trans. Instrum. Meas.* **IM-23,** No. 4, 468-472 (Dec. 1974).

Key words: delay line; picosecond; pulse measurement; superconductivity.

A high-quality superconducting delay line now makes it possible to perform direct oscillographic measurements of the picosecond transition times of very fast electrical signals that do not furnish pretriggers. A 15-m superconducting delay line package has been assembled. The package consists of connectors, connector adapters, normally conducting input/output air lines, and a 15 m length of a miniature 1.6-mm superconducting coaxial transmission line. The package exhibits an attenuation of 0.8 dB at 10 GHz and a system 10-90 percent transition time of 18 ps. Some applications of this delay line are shown. They include the measurement of the pulse output from a mercury switch and the transient response of a traveling-wave oscilloscope.

14826. Engen, G. F., **Calibration technique for automated network analyzers with application to adapter evaluation,** *IEEE Trans. Microwave Theory Tech., Part II, 1974 Symposium Issue,* **MTT-22,** No. 12, 1255-1260 (Dec. 1974).

Key words: adapter; automation; efficiency; microwave; microwave measurement; network analyzer.

Although conceptually straightforward, the application of existing automated network analyzers to the problem of adapter evaluation is inhibited by the limited accuracy of the detection process, the requirement for several impedance standards at each frequency, and software problems. A hardware modification, which yields improved accuracy for adapter evaluation, is described. An alternative calibration procedure is outlined which exploits this improved accuracy potential, and which requires only one impedance standard.

**14827.** Gray, J. E., Allan, D. W., **A method for estimating the frequency stability of an individual oscillator,** *Proc. 28th Annual Symp. on Frequency Control, Fort Monmouth, N.J., May 29-31, 1974,* pp. 243-246 (Electronic Industries Association, Washington, D.C., 1974).

> Key words: Flicker noise; frequency stability; noise measurement; oscillator stability.

A method is given for estimating the intensity of random noise frequency modulation of an individual oscillator, using data obtained by comparing it with two or more other oscillators. This method is appropriate even if the oscillators available for comparison are less stable than the oscillator being evaluated, but their frequency fluctuations must be independent. The statistical uncertainty of the results is discussed briefly.

**14828.** Wainwright, A. E., Walls, F. L., McCaa, W. D., **Direct measurements of the inherent frequency stability of quartz crystal resonators,** *Proc. 28th Annual Symp. on Frequency Control, Fort Monmouth, N.J., May 29-31, 1974,* pp. 177-180 (Electronic Industries Association, Washington, D.C., 1974).

> Key words: Allan variance; flicker of frequency modulation; Johnson noise; linewidth; random walk frequency modulation; spectral density of frequency fluctuations $S_y(f)$; white phase modulation.

A technique is presented that allows one to measure directly the fluctuations of the natural resonant frequency of quartz crystal resonators in a passive circuit. This technique greatly aids in modeling the noise in both crystal resonators and crystal controlled oscillator circuits. Definite changes of slope in the spectral density of the frequency fluctuations, as a function of frequency offset from the natural resonant frequency of the crystals indicate that several mechanisms are contributing to the frequency instabilities in crystals. Our measurements also indicate that the electronics in the oscillators seriously degrade the frequency stability for sample times less than 100 s. The effects are especially dramatic for times less than 1 s.

**14829.** Howe, D. A., Bell, H. E., Hellwig, H., DeMarchi, A., **Preliminary research and development of the cesium tube accuracy evaluation system,** *Proc. 28th Annual Symp. on Frequency Control, Fort Monmouth, N.J., May 29-31, 1974,* pp. 362-372 (Electronic Industries Association, Washington, D.C., 1974).

> Key words: cavity phase shift; cesium beam tube; frequency synthesis; pulse method; Ramsey dual interaction region; second-order doppler; velocity distribution.

A method has been developed which measures the velocity distribution of the atoms in a beam tube using the Ramsey dual interaction region principle. The method involves pulsing the RF excitation signal at a period related to the atoms' time-of-flight between the interaction regions. The pulse method, with its ability to measure velocity distribution enables calculations of cavity phase shift and second-order Doppler effect. This research has motivated the development of a system, complete unto itself, for determining the accuracy of cesium beam tubes. Design goals for the system are outlined. The system development to date is discussed. Frequency synthesis is accomplished at 5.006 MHz. This avoids frequency synthesis at X-band and there eliminates packaging and weight problems. A novel synthesi design is used which incorporates a digital frequency lock of t 5.00688 MHz VCXO. A resolution of 1.4 millihertz/second realizable; lock is within $2.8 \times 10^{-10}$ at one second of a 5.00 MHz reference with potential to better than $1 \times 10^{-12}$ at o second. This synthesizer and its application to the accura evaluation system are discussed. Some results on the evaluati of commercial cesium beam tubes are given.

**14830.** Hellwig, H., **Atomic frequency standards: A survey,** *Pr 28th Annual Symp. on Frequency Control, Fort Monmou N.J., May 29-31, 1974,* pp. 315-339 (Electronic Industries A sociation, Washington, D.C., 1974).

> Key words: application of standards; basic standards; ce um standards; frequency accuracy; frequency stabili frequency standards; hydrogen standards; ion storage; las stabilization; rubidium standards; saturated absorptic time standards.

The last comprehensive survey on atomic frequency standa was given by A. O. McCoubrey in 1966 (Proc. IEEE 54, p. 11 This survey reviews the more recent historical background atomic frequency standards leading to the present developmen A discussion of the underlying physical and engineering prin ples is given. Modern atomic frequency standards, includi their performance, are compared quantitatively, and projectic are attempted at likely future developments and performa characteristics.

As in 1966, the standards principally used in technical a scientific applications are rubidium gas cell devices, cesi beam tubes, and hydrogen maser oscillators. However, subst tial advances in physical and performance characteristics can reported.

New developments include passive hydrogen devices, sa rated absorption stabilized lasers, ion storage devices, a atomic beams in the far infrared and infrared region, as well new techniques to evaluate frequency biases such as those countered in cesium and hydrogen standards.

The survey includes a discussion of the effects of past and c rent developments in atomic frequency standards on the tech cal and scientific user community.

**14831.** Harris, K. R., Mills, R., Hanley, H. J. M., Woolf, L. **The self-diffusion of simple fluids: Tabulated values for ar and methane,** *Aust. Nat. Univ. Rev.* **DRU-RR 2,** pp. 1-32 ( Australian National University Press, Canberra, A.C.T. A tralia, 1974).

> Key words: argon; critical review; krypton; measurem technique; methane; self-diffusion coefficient.

Data for the self-diffusion coefficient (D) of several sim fluids – He, Ne, Ar, Kr, Xe, $CH_4$, $H_2$, $N_2$, $CF_4$, $CO_2$, a $SF_6$ – in the dense gas and liquid states are reviewed. The gen behaviour of the self-diffusion coefficient with respect to te perature and density is examined making use of the excess fu tion approach. Tabulated values of D for methane and argon presented as a function of temperature, pressure and dens The pressure range covered is 2-50 MPa and the temperat range is 170-320 K for methane and 100-250 K for argon. T estimated error of the tabulated coefficients is ± 10 percent.

**14832.** Klots, C. E., Sieck, L. W., **Argon sensitized formatio $Xe_2^+$: A new mechanism for the Jesse effect,** *Chem. Phys. L* **27,** No. 1, 71-72 (July 1, 1974).

> Key words: cross sections; excited states; ionization; m

spectrometry; radiation chemistry; rare gases.

Photoexcitation of the argon resonance states in the presence xenon leads to $Xe_2^+$. Kinetic analysis indicates rapid near-onant energy transfer between argon and xenon atoms. The ssibility of an analogous mechanism in other rare gas systems examined.

**833.** Ambler, E., Mangum, B. W., Pfeiffer, E. R., Utton, D. B., **Magnetic ordering of crystalline and vitreous $Gd(PO_3)_3$,** *Phys. Lett.* **50A,** No. 4, 249-250 (Dec. 16, 1974).

Key words: antiferromagnetism; comparison of magnetic properties of glasses and crystals; $Gd(PO_3)_3$; glass; magnetic order; polycrystal; vitreous $Gd(PO_3)_3$.

We have measured the magnetic susceptibilities of vitreous d polycrystalline $Gd(PO_3)_3$. The Weiss constants for these aterials were found to be $-0.3$ K. Vitreous $Gd(PO_3)_3$ hibited short-range antiferromagnetic order below 0.175 K d polycrystalline $Gd(PO_3)_3$ short-range order between 0.242 and 0.052 K and long-range order below 0.052 K.

**834.** Hudson, R. P., Pfeiffer, E. R., **Dipolar heat capacity of CMN,** *J. Low Temp. Phys.* **16,** Nos. 3/4, 309-316 (1974).

Key words: CMN; cryomagnetism; low temperature specific heat; magnetic dipole interaction; paramagnetic salt.

The magnetic contribution to the low-temperature specific at of cerous magnesium nitrate (CMN) was determined by the simir-Du Pré ac susceptibility method in the region of 1 K. e value found for the coefficient of the major ($T^{-2}$) term is in od agreement with that determined in this laboratory in mag-tic cooling experiments. It is some 10 percent less than that lculated for the magnetic dipole interaction between the $Ce^{3+}$ ns.

**835.** Mabie, C. P., Wallace, B. M., **Optical, physical and chemical properties of pineal gland calcifications,** *Calcif. Tissue Res.* **16,** 59-71 (1974).

Key words: apatite; calcospherulites; calculi; petrography; pineal.

Calcifications of the pineal gland in the form of calcospheru-es have been studied by optical microscopy, electron croscopy, electron probe analysis, x-ray diffraction, ther-gravimetry, and infrared and chemical analysis. Complex cal-spherulite textures have been observed which have a granular bstructure made up of apatite crystals averaging 218 Å in gth and 38 Å in width. These apatite crystals appear to be a rbonate-containing hydroxyapatite, mineralogically similar to amel.

**836.** Hanson, D. W., Hamilton, W. F., **Satellite broadcasting of WWV signals,** *IEEE Trans. Aerosp. Electron. Syst.* **AES-10,** No. 5, 562-573 (Sept. 1974).

Key words: broadcasting; dissemination; frequency; satellite; synchronization; time.

An experiment concerning the broadcasting of time and equency information from geostationary satellites is discussed. cluded are discussions on satellite motion, time delay, Doppler ift, and delay calculations. Ground station requirements, time covery techniques, and timing resolution and accuracy are also cluded. Delay computation aids for the user were designed to ovide free space delays between the master clock and the user. easurements made in North and South America demonstrated iming resolution of about 10 $\mu$s and an accuracy of 25 $\mu$s.

**837.** Dalke, J. L., **Why metric and when?,** *Tappi* **57,** No. 12, 72-75 (Dec. 1974).

Key words: conversion; international standards; legislation; measurement language; metrication; metric system.

Whatever the relative merits of the metric system, it has won overwhelming international approval in the last 20 years. The Chinese, Japanese, Indians, and all English-speaking nations of the British Commonwealth are abondoning their traditional measurement language and going metric. The metric system has been legal in the United States since 1866. In the past our major trading partners used the British Imperial system of measurements which also forms the basis for our customary system of units. Major industrial companies and some state educational systems in the United States are now switching. Legislation is before Congress that would coordinate and facilitate an orderly change from predominately customary to predominately metric usage on a voluntary and reasonable basis. This paper explores the problems that would accompany such a change in technology, economics, international relations, and other areas.

**14838.** Adair, R. T., Simmonds, M. B., Kamper, R. A., Hoer, C. A., **RF attenuation measurements using quantum interference in superconductors,** *IEEE Trans. Instrum. Meas.* **IM-23,** No. 4, 375-381 (Dec. 1974).

Key words: Josephson junction; quantum interference; rf attenuation; superconductivity.

A unique portable system has been developed for measuring RF attenuation over a dynamic range of 62 dB at 30 MHz. A superconducting quantum interference device (SQUID) is the basis of the system. A SQUID is a loop of superconducting metal closed by a weak point contact called a Josephsón junction, operating in liquid helium. It converts variations in magnetic flux to periodic variations in impedance which are sensed at microwave frequencies. This provides a convenient natural means of measuring electrical quantities such as voltage, current, power, and attenuation.

**14839.** Ausloos, P., Eyler, J. R., Lias, S. G., **Thermal energy charge transfer reactions involving $CH_4$ and $SiH_4$. Lack of evidence for nonspiralling collisions,** *Chem. Phys. Lett.* **30,** No. 1, 21-25 (Jan. 1, 1975).

Key words: charge transfer; Franck-Condon factors; ion-molecule reactions; methane; rare gas ions; rate constants; silane.

Rate constants for reaction of a number of thermal ions with methane and silane have been determined. It is demonstrated that within experimental error none of the reactant pairs undergoes a charge transfer reaction with a rate constant higher than the estimated collision rate constant. It is concluded that there is no evidence for the occurrence of charge transfer reactions of thermal ions by an "electron jump" mechanism involving nonspiralling ion-molecule collisions in which no momentum is transferred.

**14840.** Mielenz, K. D., **Aberrations of ellipsoidal reflectors for unit magnification,** *Appl. Opt.* **13,** No. 12, 2931-2933 (Dec. 1974).

Key words: aberrations; aspheric optics; ellipsoidal reflector; Fermat's principle; Hamiltonian point characteristic; limiting aperture; unit magnification.

Ellipsoidal reflectors are useful for the 1:1 imaging of small objects without spherical and chromatic aberration. The magnitude of the off-axis aberrations of such reflectors is computed by application of Fermat's principle to the Hamiltonian point characteristic. The limiting form of the mirror aperture for which these aberrations do not exceed a set tolerance is an ellipse whose semiaxes depend on object size and angle of incidence.

14841. Ayres, T. R., Linsky, J. L., Shine, R. A., **A possible width-luminosity correlation of the Ca II $K_1$ and Mg II $k_1$ features,** *Astrophys. J.* **195,** No. 3, L121-L124 (Feb. 1, 1975).

Key words: Ca II; spectral line; stellar chromospheres.

Existing high resolution stellar profiles of the Ca II and Mg II resonance lines suggest a possible width-luminosity correlation of the $K_1$ minimum features. We show that such a correlation can be simply understood if the continuum optical depth of the stellar temperature minimum, $\tau_c$*, is relatively independent of surface gravity as suggested by three stars studied in detail.

14842. Geist, J., Steiner, B., **Report of the workshop on accurate radiometry for solar conversion,** Paper in *Report and Recommendations of the Solar Energy Data Workshop,* pp. 204-208 (Sept. 1974).

Key words: atmospheric physics; radiometric physics; radiometry; solar conversion.

This report presents recommendations of a workshop on accuracy radiometry for solar conversion that was jointly sponsored by NOAA and NSF.

14843. Lamaze, G. P., Whittaker, J. K., Schrack, R. A., Wasson, O. A., **After-pulse suppression for 8850 and 8854 photomultipliers,** *Nucl. Instrum. Methods Letters to Editor* **123,** 403-404 (1975).

Key words: after-pulse; GaP first dynode; neutron; photoelectron; photomultiplier; resolution; suppression.

After-pulsing suppression of semiconducting first dynode photomultipliers (RCA 8850 series) has been successfully accomplished by applying a positive pulse to a wire mesh directly in contact with the tube face.

14844. Sieck, L. W., Gorden, R., Jr., Lias, S. G., Ausloos, P., **Ionic polymerization of vinyl halides initiated by photoionization using photons with energies near the ionization threshold,** *Int. J. Mass Spectrom. Ion Phys.* **15,** 181-196 (1974).

Key words: ion-molecule reactions; mass spectrometry; photoionization; rate constants; reaction mechanisms; vinyl halides.

Thermal bimolecular rate coefficients have been obtained for the reactions of the parent monomer ions in the vinyl halides with the respective neutral molecules when the ions are formed by photoionization at or very near the ionization thresholds. The values obtained are as follows: $C_2H_3F^+$, 0.27 eV above threshold, $k=3.2\times10^{-10}$ cm³ molecule⁻¹ s⁻¹, $C_2H_3Cl^+$, within $kT$ of threshold, $k=1.78\times10^{-10}$ cm³ molecule⁻¹ s⁻¹, and $C_2H_3Br^+$, 0.2 eV above threshold, $k=1.25\times10^{-10}$ cm³ molecule⁻¹ s⁻¹. An increase in photon energy drastically lowers the values of these coefficients. The reactions of $C_2H_3F^+$ and $C_2H_3Cl^+$ were also investigated at high pressures in order to elucidate certain aspects of the cationic polymerization scheme. The formation of $(C_2H_3Cl)_2^+$ and $(C_2H_3Cl)_3^+$ is reported for the first time. The factors controlling the relative importances of various modes of dissociation of the vinyl halide dimer ions are discussed in terms of thermodynamic and structural considerations.

14845. Harris, F. K., **A cooperative experiment in measurement education,** (Proc. Conf. on Measurement Education, University of Warwick, Coventry, England, July 8-10, 1969), *IEE Conf. Publ. No.* **56,** pp. 140-141 (Institute Electrical Engineers, London, England, 1969).

Key words: measurement education; metrology curriculum.

A discussion of the cooperative NBS-GWU metrology program.

14846. Hellwig, H., Bell, H. E., Bergquist, J. C., Glaze, D. J Howe, D. A., Jarvis, S., Jr., Wainwright, A. E., Walls, F. L **Results in operation, research, and development of atomic cloc at the National Bureau of Standards,** (Proc. IX Int. Congress Chronometry, Stuttgart, Germany, Sept. 16-20, 1974), Pape in *Proc. IX International Congress of Chronometry,* C Glaser, Ed., A, A5-1 – A5-13 (Herausgegeben von de Deutschen Gesellschaft fur Chronometrie E. V., Stuttgar Germany, 1974).

Key words: accuracy; atomic clocks; cesium standard hydrogen standards; hydrogen storage device; methane st bilized helium-neon lasers; noise studies; quartz cryst oscillators; quartz crystal resonators.

Since the last CIC, significant progress has been made in var ous laboratories leading to new capabilities and new future us of atomic clocks. This paper summarizes the contributions of tl National Bureau of Standards to these developments and tries forecast future developments.

Two primary cesium standards, NBS-4 and NBS-5, are no in operational use with an accuracy of near $1\times10^{-13}$, and with stability of better than $1\times10^{-14}$ (sample time of 3 hours). Tl concept and feasibility of a passive hydrogen storage device h been demonstrated leading to the projection of long term stabil ties (hours to weeks) of at least $1\times10^{-14}$ for these devices. St dies of different electronic systems as well as wall and magnet field effects promise significant improvements in the accuracy hydrogen standards. Methane stabilized helium-neon lasers we operated and demonstrated excellent frequency stabilities, a research on a methane beam system is in progress. Novel noi studies of quartz crystal resonators confirmed that quartz cryst oscillators with short-term stabilities of parts in $10^{12}$ (1 mi lisecond) are possible, an important fact in its own right and significance to the development of atomic clocks of extren short-term stability.

14847. Hubbell, J. H., McMaster, W. H., Del Grande, N. K Mallett, J. H., **X-ray cross sections and attenuation coefficien** Paper in *International Tables for X-Ray Crystallograph Section 2, Absorption and Scattering,* J. A. Ibers and W. Hamilton, Eds., 4, Paper 2.1, 47-70 (Kynoch Press, Bi mingham, England, 1974).

Key words: attenuation coefficient; compilation; Compt scattering; cross section; crystallography; photoelectric a sorption; photons; Rayleigh scattering; x rays.

Tables of total cross sections (in barns/atom) for photon i teraction with atoms, representing sums over the photoelect effect, coherent (Rayleigh) scattering, and incoherent (Compto scattering cross sections are presented for 87 elements from Z 1 to 94 at the 24 wavelengths from 0.4970 to 2.7496 angstror (24.942 to 4.509 keV) which are of most use in x-ray crystallo raphy. Corresponding tables of mass attenuation coefficients ( cm²/g) are also given. These tables are an interpolation from more extensive compilation (UCRL-50174 (1969) by McMast et al) and the input data and procedures for constructing t latter compilation are described.

14848. Tilford, S. G., Simmons, J. D., **Reexamination of t vacuum ultraviolet emission spectrum of CO in the 950-1200 region,** *J. Mol. Spectrosc.* **53,** 436-442 (1974).

Key words: band assignments; carbon monoxide; electron spectrum; emission spectrum; high resolution spectru vacuum ultraviolet region.

New spectrograms of CO below 1200 Å reveal that emissi bands terminating on the high energy $E_0\ {}^1\Sigma^+$ and $^1\Pi$ states pl most of the previously reported unidentified emission bands CO actually originate from molecular nitrogen. Four new emi n band systems in CO, tentatively identified as $V^1\Pi - X^1\Sigma^+$, $\Pi - X^1\Sigma^+$, $Y^1\Sigma^+ - X^1\Sigma^+$, and $Z^1\Sigma^+ - X^1\Sigma^+$, have been obved. The corresponding $T_{v0}$'s are 98917, 102804, 99963, and 724 cm$^{-1}$, respectively.

49. Phelps, A. V., **Applications of gaseous electronics to laser echnology,** Chapter 3 in *Gaseous Electronics, Some Applicaons,* J. W. McGowan and P. K. John, Eds., pp. 25-46 (North-Holland Publishing Co., Amsterdam, The Netherlands, 1974).

Key words: atoms; electron excitation; excitation transfer; gaseous electronics; lasers; molecules.

pplications of the results of research in the physics of gase- electronics to recent laser technology are illustrated. Excita- transfer, charge exchange, metastable atom production and truction are dominant processes in the HeNe laser and the al ion lasers. Rather extensive data on cross sections for stic and inelastic scattering, attachment and ionization in es such as $N_2$ and $CO_2$ make possible fairly accurate predics of the gain, efficiency, etc., of $CO_2$-$N_2$-He lasers. The new ss of ground state dissociation lasers is discussed in terms of roposed laser utilizing stimulated emission between the bound ited state and the dissociating ground state of the LiXe lecule.

50. McKinney, J. E., Simha, R., **Configurational thernodynamic properties of polymer liquids and glasses. I. Poly(viyl acetate),** *Macromolecules* **7,** No. 6, 894-901 (Nov.-Dec. 974).

Key words: configurational; glass; glass transition; hole theory; polymer; poly(vinyl acetate); PVT; thermodynamic; liquid.

ecent experimental PVT data on poly(vinyl acetate) are lyzed using the hole theory of Simha-Somcynsky. The data e obtained at temperatures from − 30 to 100° and pressures to 800 bars. These ranges encompass the glass transition and lude large portions of the liquid and glassy regions. Three different thermodynamic histories of glass formation, all isobaric ling at 5 °C/hr, were applied. With the variable formation his- the glass was formed by isobaric cooling runs at different ssures. In the two constant formation histories each of the sses was formed by a different formation pressure, namely atspheric and 800 bars, with subsequent temperature and prese changes in the glass in each case. In the equilibrium state d agreement between the theoretical and experimental PVT faces results, in accord with earlier observations on orphous systems. As for the transitions the theory gives the rect values of d$T$/d$P$ using the assumption that the hole frac- $h$ be constant along either of the two constant formation nsition lines. Similarly, the generalization of the Ehrenfest e relation involving the single ordering parameter $h$ results in d numerical agreement with the experimental values of d$P$ for the variable formation transition line. As previously nonstrated, $H$ does not freeze at temperatures below the glass nsition, thus a constant $h$ does not describe the structure of glass. Parameters which describe the extent of freezing are luated. The fact that these parameters are independent of fortion pressure would be consistent with the existence of a sin- entropy surface with formation pressure, as suggested by er experimental evidence.

51. O'Connell, J. S., Lightbody, J. W., Jr., **Momentum ransfer sum rules in electron scattering,** *Nucl. Phys.* **A237,** 09-318 (1975).

Key words: charge density; Coulomb energy; Coulomb excitation; electron scattering; form factors; sum rules; transition charge.

The integral properties of elastic and inelastic Coulomb form factors are examined. Relations are given for the nuclear Coulomb energy, central charge density, transition charge, radial moments, and squared density integral.

**14852.** Ku, H. H., Kullback, S., **Loglinear models in contingency table analysis,** *Amer. Statist.* **28,** No. 4, 115-122 (Nov. 1974).

Key words: categorical data; contingency tables; loglinear model; minimum discrimination information; statistical analysis.

This is an expository paper on the statistical analysis of categorical data arranged in the form of contingency tables. Beginning with a 2 × 2 table, the estimation and testing of parameters in the loglinear model is illustrated and compared to that for the linear model in the continuous case. This is followed by detailed analysis of two examples: one for a three-way table on biomedical data, and one for a four-way table on social survey data.

**14853.** Prince, E., Dickens, B., Rush, J. J., **A study of one-dimensional hindered rotation in $NH_3OHClO_4$,** *Acta Crystallogr.* **B30,** Part 5, 1167-1172 (May 1974).

Key words: constrained refinement; hindered rotation; hydrogen bonds; hydroxylammonium; neutron diffraction; perchlorates; thermal motion; torsional oscillation.

The structure of the phase of hydroxylammonium perchlorate, $NH_3OHClO_4$, which is stable at 25 °C has been refined from 3-dimensional neutron diffractometer data. The structure has space group $P2_1cn$, cell dimensions $a = 7.52$ (2), $b = 7.14$ (1), $c = 15.99$ (2) Å, and 8 formula units per unit cell. There are very large thermal motions of the hydrogen atoms, and the environment of the two crystallographically different $NH_3OH^+$ ions suggests hindered rotation of each $NH_3$ group around the axis defined by the N−O bond. Therefore the structure was refined using a model in which the perchlorate groups and the hydroxyl hydrogens were given conventional anisotropic temperature factors, but the $ONH_3$ groups were treated as rigid bodies, each with an isotropic translation, and isotropic libration of the group as a whole, and a torsional oscillation of the $NH_3$ group. The final weighted $R$ for 684 observed reflections was 0.051. There are 12 hydrogen bonds between the $NH_3OH^+$ ions and the $ClO_4^-$ ions, and one hydrogen bond between $NH_3OH^+$ ions. The apparent r.m.s. amplitude of torsional oscillation of the $NH_3-O$ groups about the N−O vector, as derived from the structural refinement, is ~ 25°, and is therefore consistent with frequent reorientation of the $NH_3$ parts of the $NH_3OH^+$ ions. Other apparent r.m.s. amplitudes in the structure are only slightly higher than normal values. The $NH_3OH^+$ ions are in staggered conformations and the $ClO_4^-$ ions are essentially regular tetrahedra.

**14854.** Rowe, J. M., Rush, J. J., Smith, H. G., **"In-band" modes of vibration of $PdH_{0.03}$,** *Phys. Rev. B* **8,** No. 12, 6013-6014 (Dec. 15, 1973).

Key words: crystal; fermi surface; interstitial hydrogen; lattice dynamics; palladium hydride; phonons.

The [110] transverse branch of the phonon dispersion relation in a single crystal of $PdH_{0.03}$ has been measured and compared to the results for pure Pd. A limited amount of data has been taken for other branches, and the mean frequency ratio ($PdH_{0.03}$/Pd) observed for all measurements is 0.995. No change was observed in the shape or strength of the anomaly in the [110]$T_1$ branch.

**14855.** Malloy, T. B., Jr., Lafferty, W. J., **On the barriers to planarity and the isotope effect in cyclobutane and cyclobutane-$d_8$,** *J. Mol. Spectrosc.* **54,** 20-38 (1975).

Key words: barriers to planarity; cyclobutane; cyclobutane-$d_8$; isotope effect; kinetic energy terms; potential functions.

The infrared and Raman data on the ring-puckering vibration in cyclobutane and cyclobutane-$d_8$ have been reexamined including the coordinate dependence of the reduced mass in the Hamiltonian. This was done for the purpose of estimating the importance of these small terms in the determination of barrier heights for four-membered rings and also on the determination of the dihedral angle corresponding to the potential minimum.

The conclusions reached are that there is an isotopic dependence of the barriers to planarity in cyclobutane and cyclobutane-$d_8$ yielding a difference of $\sim 14$ cm$^{-1}$, but the precise value of the difference in barrier heights is ill determined. The higher-order kinetic energy terms in the Hamiltonian can account for a spread of $\sim 3$ cm$^{-1}$ in each of the barriers derived for cyclobutane and cyclobutane-$d_8$, depending on the details of the model used for the vibration, but not a difference of 14 cm$^{-1}$, which undoubtedly indicates the effects of coupling with other vibrational modes. It is also found that the derived values of the dihedral angles are quite sensitive to the details of the vibrational model, in fact, much more so than to the uncertainties in the bond distances and bond angles. A relationship between the potential constants derived for cyclobutane and cyclobutane-$d_8$ assuming an effective constant reduced mass and those derived for a semirigid model is demonstrated.

**14856.** Filliben, J. J., **The probability plot correlation coefficient test for normality,** *Technometrics* **17,** No. 1, 111-117 (Feb. 1975).

Key words: correlation coefficient; medians; normal distribution; order statistics; probability plot; statistical methods; statistics; tests of distributional hypotheses.

This paper introduces the normal probability plot correlation coefficient as a test statistic in complete samples for the composite hypothesis of normality. The proposed test statistic is conceptually simple, is computationally convenient, and is readily extendible to testing non-normal distributional hypotheses. An empirical power study shows that the normal probability plot correlation coefficient compares favorably with 7 other normal test statistics. Percent points are tabulated for $n = 3(1)50(5)100$.

**14857.** Holt, H. K., **Laser intracavity absorption,** *Phys. Rev. A* **11,** No. 2, 625-629 (Feb. 1975).

Key words: high sensitivity; intracavity absorption; laser; quantitative analysis.

The characteristics of a laser with an intracavity absorption cell have been calculated for the case in which the gain atoms are homogeneously broadened and the absorber atoms are inhomogeneously broadened. The sensitivity of the laser intensity to the density of absorbers is determined.

**14858.** Wood, L. A., **Physical constants of different rubbers,** Paper in *Polymer Handbook, 2nd Edition,* J. Brandrup and E. H. Immergut, Eds., pp. V-7 – V-12 (John Wiley & Sons, Inc., New York, N.Y., 1975).

Key words: butyl rubber; constants; natural rubber; neoprene; physical constants; polymers; properties; rubbers; styrene-butadiene rubbers.

Selected values from 65 published literature references are tabulated for about 30 physical constants (mechanical, optical, thermal, etc.) for natural rubber, styrene-butadiene rubber (SBR), butyl rubber (IIR), and polychloroprene rubber (CR or neoprene). This is revision and extension of the tables published in 1966 in the first edition of the Polymer Handbook, J. Brandrup and E. H. Immergut, ed.

**14859.** Lamotte, M., Dewey, H. J., Keller, R. A., Ritter, J. J., **Laser induced photochemical enrichment of chlorine isotopes,** *Chem. Phys. Lett.* **30,** No. 2, 165-170 (Jan. 15, 1975).

Key words: dye laser; isotope; isotope separation; photochemistry.

Chlorine isotopic abundances were significantly altered by laser induced, selective excitation of particular isotopic species of thiophosgene followed by a chemical reaction between the electronically excited thiphosgene and diethoxyethylene. The concentration of $^{35}$Cl in thiophosgene was changed from 75 to 64 percent or 80 percent depending upon the isotopic species initially excited.

**14860.** Utton, D. B., **Proton spin-lattice relaxation in cerous magnesium nitrate hydrate,** *J. Chem. Phys.* **62,** No. 2, 670-674 (Jan. 15, 1975).

Key words: cerous magnesium nitrate hydrate; lattice; proton; relaxation; spin; 65-335 K.

The proton spin-lattice relaxation in powdered $Ce_2Mg_3(NO_3)_{12} \cdot 24H_2O$ has been measured in the temperature range 65-335 K. In contrast to other paramagnetic salts it has been found that the nuclear relaxation due to nuclear dipole-dipole interactions is comparable in magnitude with the relaxation due to the electronic moments on the paramagnetic ions in this temperature range. Below 160 K the relaxation times are independent of the resonance frequency and have a temperature dependence given by $\tau_1 = 0.375 \exp(-182/T)$ sec. This is attributed to relaxation via the Ce$^{3+}$ ions and hence makes it possible to calculate a value for their relaxation times. It is also concluded that the second excited doublet of the Ce$^{3+}$ ions is at an energy of $200 \pm 18$ K. At higher temperatures two relaxation time minima are observed. At 14 MHz the minimum values are 71 and 69 msec at 244 and 303 K, respectively. The weak temperature dependence of the NMR second moment indicates that 180° flips of the water molecules provide the relaxation mechanism in this temperature range. Calculated values of $\tau_1$, using the published crystallographic data, and assuming that there are two types of water molecule, are in reasonable agreement with experiment. The observed activation energies are approximately 6.8 and 9.5 kcal/mole.

**14861.** West, E. D., Case, W. E., **Current status of NBS low-power laser energy measurement,** (Proc. 1974 Conf. on Precision Electromagnetic Measurements, London, England, July 1-5, 1974), *IEEE Trans. on Instrumentation and Measurements,* **IM-23,** No. 4, 422-425 (Institute of Electrical and Electronics Engineers, New York, N.Y., Dec. 1974).

Key words: laser calorimeter; laser energy; laser power.

A set of four electrically calibrated calorimeters is currently in use at the Boulder Laboratories of the National Bureau of Standards to calibrate and test devices for measuring average laser power in the range from 100 $\mu$W to 1 W and energies in the range 0.03 to 10 J. Laser sources used with these calorimeters are argon, krypton, helium-neon and neodymium-doped YAG, all CW, and pulsed YAG with pulse energies about 0.1 J and pulsewidths of about 200 $\mu$s and 30 ns.

The calorimeters have been intercompared as a check on systematic errors. The national standard is taken as the average for three of the calorimeters of the current C4 design, because these were designed to permit better measurements of the absorptance and window transmittance. Deviations from the group average are $-0.12$, $-0.01$, and $+0.13$ percent. The earlier standard C3-1 differs from the group average by $+0.21$ percent.

**14862.** Feeney, J. J., Meijer, P. H. E., **Magnetic properties of paramagnetically doped crystals Fe$^{3+}$, Nd$^{3+}$ and Ho$^{3+}$ in various**

**ompounds,** *J. Phys. Chem. Solids* **36,** 175-185 (1975).

Key words: convergence criterion; crystal field parameters; energy levels; holium 3+ ions; neodymium 3+ ions; susceptibility.

n this work we calculate the energy levels, wave functions l transition probabilities for a number of compounds whose stal field parameters have been determined. We introduce a vergence criterion in the diagonalization of the Hamiltonian trices dependent upon a self consistency test on the eigenvec- s. This assures us of numerically accurate wave functions.

irst we calculated energy level and susceptibility differences Nd$^{3+}$)PbMoO$_4$ dependent on the multiplicative constants $\theta_n$, d with the published $A_l^m$ to determine the crystal field ameters $B_l^m$, ($B_l^m = \theta_n A_l^m$). Calculated energy levels as a func- of external magnetic field strength and orientation are com- ed with experimental results for three different sets of blished crystal field parameters, $B_l^m$, for (Fe$^{3+}$)TiO$_2$. The und state energy levels, and wave functions, have been calcu- ed for the non-Kramers Ho$^{3+}$ ion in the crystals PbMoO$_4$, Cl$_3$ and HoCl$_3$. Easily distinguishable variations in the tem- ature dependence of the $\chi_{zz}$ component of the susceptibility found as a function of the host crystal. It is pointed out that ceptibility calculations, based upon measured crystal field ameters, in conjunction with subsequent susceptibility mea- ements, provide a good check on the validity of the crystal d parameters.

**63.** Shine, R. A., Linsky, J. L., **Physical properties of solar hromospheric plages. II. Chromospheric plage models,** *Solar Phys.* **39,** No. 1, 49-77 (Nov. 1974).

Key words: radiative transfer; solar active regions; solar chromosphere; spectral line formation.

We propose chromospheric models of plages to explain files of the Ca II H, K, λ8498, λ8542, and λ8662 lines cribed in Paper I. These models are consistent with boundary ditions imposed by the photosphere and the Lyman con- uum. We find that increasing emission in these lines is con- ent with a picture of increasing temperature gradient in the chromosphere and the resulting increase in pressure and ctron density at similar line optical depths. With this picture suggest how to empirically determine the distribution of omospheric parameters across the solar disk directly from Ca iltergrams. We also propose that the high density aspects of ar activity are produced by steep temperature gradients in the chromosphere and thus by the enhanced heating chanisms that steepen these gradients.

**64.** Schroeder, L. W., Prince, E., Dickens, B., **Hydrogen onding in Ca(H$_2$PO$_4$)$_2$ · H$_2$O as determined by neutron diffrac- ion,** *Acta Crystallogr.* **B31,** Part 1, 9-12 (Jan. 1975).

Key words: hydrate; hydrogen bonding; monocalcium phosphate; monohydrate; neutron diffraction; phosphate; water molecule.

The hydrogen positions in Ca(H$_2$PO$_4$)$_2$ · H$_2$O have been deter- ned and the structure refined to $R_w = 0.068$ and $R = 0.055$ ng 1045 neutron data. No evidence is found for any disorder the protons. The two crystallographically distinct H$_2$PO$_4^-$ s are hydrogen bonded to each other and to the water lecule. The oxygen atom of the water coordinates to a calcium and a hydrogen atom from H$_2$PO$_4^-$ along its lone-pair orbital ections with distances Ca...O$_w$ = 2.479 Å and H...O$_w$ = 1.679 One of the hydrogen atoms of the water molecule is 2.106 and 15 Å from two oxygen atoms, with O$_w$ – H...O angles of .9 and 147.5°. The distances and angles indicate that only the onger of these two interactions is structurally significant. The other hydrogen atom of the water molecule is involved in a hydrogen bond with H$_w$...O = 1.823 Å and the angle O$_w$ – H...O = 160.4°.

**14865.** Phaneuf, R. A., Crandall, D. H., Dunn, G. H., **Production of D*($n$=4) from electron-D$_2^+$ dissociative recombination,** *Phys. Rev.* A**11,** No. 2, 528-535 (Feb. 1975).

Key words: cross sections; D$_2^+$; dissociative recombination; product D*($n$=4).

Crossed beams of electrons and D$_2^+$ ions were used to measure absolute cross sections for the dissociative recombination process, $e + \mathrm{D}_2^+ (X\,^2\Sigma_g^+) \rightarrow \mathrm{D} + \mathrm{D}^*(n=4)$ over a range of electron energies extending from 0.6 to 7 eV. The process was monitored by detecting a known portion of the 485.9-nm emission resulting from radiative decay of the product D*($n$=4) atoms. The cross sections, which correspond to a known vibrational-state distribution of the target ions, exhibit the same dependence on electron energy as recent measurements of the total dissociative recombination cross section reported by Peart and Dolder, and have a magnitude of about 10 percent of the total cross section, suggesting that the product D atoms are formed in excited states with a variety of principal quantum numbers. Systematic measurement uncertainties at high confidence are about 14 percent, and random uncertainties are at the 25 percent (standard deviation) level. The calculation of cross sections from the observed light intensities depends on the mean lifetimes and branch ratios for 485.9-nm emission, whose evaluation in turn requires assumptions concerning the recombination process. The situation is complicated by the presence of an electron-beam-confining magnetic field in the collision volume, which causes the incident ions and product atoms to experience a transverse motional electric field. A time-independent perturbation calculation of the weak-field Stark and Zeeman effects was performed and mean lifetimes and branch ratios were estimated under different assumptions concerning the recombination process. Assuming that all perturbed product $n$=4 states are equally populated by dissociative recombination yields an experimental cross section of $1 \times 10^{-16}$ cm$^2$ at 0.7 eV, decreasing to $3.3 \times 10^{-17}$ cm$^2$ at 3 eV, and to $1 \times 10^{-17}$ cm$^2$ at 7 eV. Assuming that only the perturbed 4$s$ states are intitially populated results in cross sections larger by some 50 percent.

**14866.** Flynn, D. R., **Accuracy and precision,** *Noise Control Eng.—Editorial Section* **3,** No. 3, p. 2 (Nov.-Dec. 1974).

Key words: accuracy; acoustics; noise; precision; repeatability; reproducibility.

This is an invited editorial pointing out the need for uncertainty estimates in papers published in the noise field.

**14867.** Lovas, F. J., **Small silicon molecules: Possible sources of the unidentified molecular lines U81.5, U86.2, U89.2, and U90.7,** *Astrophys. J.* **193,** No. 1, 265-272 (Oct. 1, 1974).

Key words: microwave spectra; predicted spectra; radio astronomy; silicon molecules; structures; unidentified molecular lines.

Several small silicon molecules are considered as possible sources for the unidentified molecular lines: U81.5, U86.2, U89.2, and U90.7. The best spectroscopic and structural data available have been utilized to predict the lowest rotational transitions for SiO$^+$, SiN, SiC, HSiN, and for vibrationally excited SiO. Transitions from each of these molecules are predicted to occur close to one or more of these unidentified molecular lines. Rotational transitions which could aid the confirmation of each of the suggested assignments are also presented. In all cases, an effort has been made to estimate the uncertainties for the predicted transitions.

**14868.** Hord, H., **Cryogenic $H_2$ and national energy needs,** (Proc. 1973 Cryogenic Engineering Conf., Atlanta, Ga., Aug. 8-10, 1973), Paper A-1 in *Advances in Cryogenic Engineering* **19,** 1-11 (Plenum Press, New York, N.Y., 1974).

Key words: cryogenic; energy; fuel; hydrogen.

Our impending fossil fuel shortage is a clear challenge to the cryogenics industry and government to provide efficient and economical means of satisfying specific national fuel requirements. Large scale production of liquid hydrogen was stimulated by the U.S. space exploration program. Now, civilian demands for synthetic fuels beckon cryogenic hydrogen.

National and world energy shortages are briefly summarized to demonstrate the relevance of synthetic fuels in satisfying future energy markets. A perspective of national energy needs, as they relate to cryogenic hydrogen fuel, is given. Hydrogen and alternate synthetic fuels are briefly reviewed and potential applications for cryogenic hydrogen are described. Technical research and development efforts, required to satisfy specific current and future national needs, are identified. The mechanism for implementation of synthetic fuels and the indistinct timetable for transition to these fuels are discussed.

**14869.** Sindt, C. F., **Heat transfer to slush hydrogen,** (Proc. 1973 Cryogenic Engineering Conf., Atlanta, Ga., Aug. 8-10, 1973), Paper K-3 in *Advances in Cryogenic Engineering* **19,** 427-436 (Plenum Press, New York, N.Y., 1974).

Key words: boiling heat transfer; convective heat transfer; heat transfer; liquid hydrogen; slush hydrogen.

Heat transfer to slush hydrogen was measured at one atmosphere and at triple-point pressure. The data were compared with those for heat transfer to liquid hydrogen, and to classical heat transfer correlations for nucleate boiling. The slush data fit convective heat transfer correlations quite well. In general, the data show that for a given heat flux, the temperature difference between the wall and the bulk liquid is not as highly influenced by pressure as predicted by the correlation for nucleate boiling.

**14870.** Parrish, W. R., Hiza, M. J., **Liquid-vapor equilibria in the nitrogen-methane system between 95 and 120 K,** (Proc. 1973 Cryogenic Engineering Conf., Atlanta, Ga., Aug. 8-10, 1973), Paper H-2 in *Advances in Cryogenic Engineering* **19,** 300-308 (Plenum Press, New York, N.Y., 1974).

Key words: binary mixture; excess Gibbs energy; experimental phase equilibria data; heat of mixing; liquid-vapor equilibria; nitrogen-methane system.

A study was undertaken to obtain liquid-vapor equilibria data for the nitrogen-methane system at uniform temperature increments between the triple point of methane and the critical point of nitrogen. The measured liquid and vapor phase equilibrium compositions and the derived excess Gibbs energy values for six isotherms from 95 to 120 K are compared with the corresponding values taken from other investigations. The excess Gibbs energy for the equimolar mixture exhibits a zero to slightly positive temperature dependence, in qualitative agreement with calculations based on the Snider-Herrington hard sphere model. This temperature dependence of the excess Gibbs energy also suggests that the excess enthalpy (heat of mixing) must be equal to or slightly less than the excess Gibbs energy.

**14871.** Ledbetter, H. M., **Elastic constants of polycrystals: Equivalence of Laurent-Eudier and Voigt averaging methods,** *Phys. Status Solidi A* **26,** K67-K70 (1974).

Key words: bulk modulus; compressibility; elastic constants; elasticity Lamé constant; Poisson ratio polycrystals; shear modulus; single crystals; Young's modulus.

The equivalence of the methods of Laurent and Eudier and o
Voigt for averaging cubic single-crystal elastic coefficients to ob
tain polycrystal elastic constants is proven and discussed. Othe
ways to obtain Voigt's equations are enumerated.

**14872.** Flynn, T. M., Powell, R. L., Chelton, D. B., Birmingham
B. W., **Superconducting electrical generators for central powe
station use,** (Proc. 1973 Cryogenic Engineering Conf., Atlanta
Ga., Aug. 8-10, 1973), Paper B-1 in *Advances in Cryogeni
Engineering* **19,** 35-43 (Plenum Press, New York, N.Y.
1974).

Key words: cryogenics; electricity; energy; helium; power
superconductivity.

The electrical industry is faced with a need for dramaticall
larger generators to optimize the utilization of large new powe
sources, such as gigawatt-sized fast breeder reactors. Earlier in
creases in generator capacity have been achieved by improvin
the cooling of the heat-producing components of the generato
For the first time in the evolution of power generators, a uniqu
technology, superconductivity, is available to the electri
machine designer. Superconductivity may offer a way of achiev
ing higher capacities while maintaining present costs, weight
and overall dimensions.

In the Fall of 1971, the Cryogenics Division of the NBS bega
a program in cooperation with industry to accelerate the applica
tion of superconductivity to large scale generators. The progra
stopped short of actual experimental construction since suff
cient funds did not become available, but did endure sufficientl
to demonstrate outstanding industry-government cooperation i
this area of national need. This paper presents the results c
several government-industry studies conducted in the course c
this program in order to show such potential benefits from th
use of cryogenics as improved generator rating, efficiency, relia
bility, transportation and site erection, cost and power syste
stability.

**14873.** Leasure, W. A., Jr., Corley, D. M., Farrer, J. S., Flyn
D. R., **Truck noise—1. Peak A-weighted sound levels due
truck tires (final report),** *DOT Report No. OST-ONA-71-*
248 pages (Available as PB204188 from the National Techn
cal Information Services, Springfield, Va., 22161, Sept. 197

Key words: acoustics; noise measurement; noise pollutio
noise (sound); sound transmission; tire noise; transportatio
noise; trucks; urban planning.

This initial report presents an inventory or "catalog" of pea
A-weighted sound levels measured during an extensive parame
ric study conducted to characterize the noise generated by typ
cal rib, cross-bar and retread type truck tires. A test sample
nine tread designs, estimated to represent 70-80 percent (thes
exact designs) of the truck tire population on the road today, wa
investigated considering the following variables: wear, loadin
speed, pavement surface, and tire location. Test vehicles i
cluded both single-chassis vehicles and a tractor-trailer.

The results show that the A-weighted sound level increase
with either an increase in load or speed. The "pocket retrea
design always produced the highest level followed by the cros
bar tires and then the rib tires. This ranking held for both ne
and half-worn tires. The influence of wear and pavement surfa
is more complex. For all of the tread designs except one the
was an increase in noise level between the new and half-wo
states. The results for different pavement surfaces are much t
same as with wear in that the generated noise appears to depe
on both the specific tread design and the surface roughness. I
dividual tires do contribute differently to the overall level d
pending on their location on the vehicle. In some cases, signi
cant reductions in the noise level were observed when "nois

es were mounted inboard of "quieter" tires.

The report includes a discussion of the measurement and anal- is techniques utilized for the establishment of this data base.

**874.** Leasure, W. A., Jr., Corley, D. M., Farrer, J. S., Flynn, D. R., **Truck noise—1. Peak A-weighted sound levels due to truck tires (addendum),** *DOT Report No. OST/TST-72-1,* 223 pages (Available as PB238912 from the National Technical Information Services, Springfield, Va., 22161, July 1972).

Key words: acoustics; noise measurement; noise pollution; noise (sound); sound transmission; tire noise; transportation noise; trucks; urban planning.

This report is the second in a series of reports to be published a result of Department of Transportation sponsored truck tire search conducted by the National Bureau of Standards. In njunction with the first report (OST-ONA-71-9) which con- ins details of the test design, test procedures, and all data quired during the first period of testing, this report presents an ventory of peak A-weighted sound levels generated by typical , cross-bar and retread type truck tires. A test sample of nine ead designs, estimated to represent 70-80 percent (based on scussions with fleetowners) of the truck tire population on the ad today, was investigated considering the following variables: ear, loading, speed, pavement surface, and tire location. Test hicles included both single-chassis vehicles and tractor- ailers.

The results show that the A-weighted sound level increased ith either an increase in load or speed. The "pocket retread" esign always produced the highest level followed by the cross- r tires and then the rib tires. This ranking held for tires in all ates of wear. The influence of wear and pavement surface, owever, is more complex. In general there was an increase in oise level between the new and half-worn states and a slight ecrease between the half-worn and fully-worn states. The in- uence of pavement surface on the generated noise depends on e specific tread design, tire wear condition and the surface ughness. Tires do contribute differently to the overall noise vel depending on their location on the vehicle. The data for actor-trailor tests, for instance, would strongly indicate that the ajor contribution is made by the tires mounted on the drive les of the tractor and that the relative contribution of tires ounted on either the front or rear trailer axles depends on the ecific tire type and speed of the vehicle.

Future reports will broaden the data to include one-third oc- ve band spectral data, directionality data in the form of equal und level contours and other refined analysis of the data re- orted herein and in OST-ONA-71-9.

**875.** Leasure, W. A., Jr., Mathews, D. E., Rinkinen, W. J., **Truck noise 1-A: Noise evaluation tests of military truck tires (final report),** *DOT Report No. DOT-TST-74-21,* 54 pages (Available as PB234348 from the National Technical Information Services, Springfield, Va., 22161, Feb. 1974).

Key words: acoustics; military vehicles; noise; sound; tire noise; truck tires.

This report presents the A-weighted sound level and one-third ctave band spectral data resulting from a study conducted to aracterize the noise generated by military truck tires. The udy was conducted by the National Bureau of Standards in operation with the U.S. Department of Transportation under e sponsorship of the U.S. Army Tank-Automotive Command. he data base established will allow for comparison of the tire oise generated by military and commercial truck tires.

The study investigated the influence of load and speed on the oise generated by tires with four different tread designs: the standard Army tire, a retread of Army design and commercial tires with rib and cross-bar type tread patterns. Army and commercial trucks were utilized as test vehicles.

In addition, the report includes a discussion of the measurement and analysis techniques utilized for the establishment of this data base.

**14876.** Frederikse, H. P. R., **Electrons in oxides: A summary,** *J. Solid State Chem.* **12,** 411-415 (1975).

Key words: applications (optical, magnetic); electronic properties; oxides.

A short overview of the optical, magnetic, electrical and surface properties of oxides is presented. Some of the major applications (electronic, electro-optical, magnetic devices, high temperature components, catalysts, etc.) are listed and the relevant physical parameters are being discussed.

**14877.** Souders, T. M., **An audio-frequency four-terminal resistance bridge,** *IEEE Trans. Instrum. Meas.* **IM-23,** No. 4, 342-345 (Dec. 1974).

Key words: audio-frequency; bridge; four-terminal resistance; high current; operational amplifier; phase angle; resistance; transformer-ratio-arm.

The design and performance of an audio-frequency four-terminal resistance bridge is described which compares resistors from 1 to 0.001 Ω over a frequency range of 50 Hz-10 kHz.

Current scaling establishes equal voltage across the resistors, permitting the standard to have the larger value and most optimum design while dissipating less power than the unknown. An amplifier-aided two-stage current transformer forms the ratio arms. Ratios of 1, 2, 4, 5, 10, and 20 are available, and a maximum applied current of 200 A is accommodated. Bridge ratio errors are less than $2 \times 10^{-6}$ in both magnitude and phase at frequencies up to 1 kHz, increasing to $2 \times 10^{-5}$ at 10 kHz.

Simple transformer scaling techniques are described for producing accurate and stable resistance standards at the 0.001-Ω level.

**14878.** Turgel, R. S., **Digital wattmeter using a sampling method,** *IEEE Trans. Instrum. Meas.* **IM-23,** No. 4, 337-341 (Dec. 1974).

Key words: analog-to-digital conversion; digital; electricity; electric power; measurement; sampling; wattmeter.

Average electric power can be measured by a system that samples voltages and currents at predetermined intervals. The sampled signals are digitized and the result is computed by numerical integration. The response of the system agrees with that of a standard electrodynamic wattmeter within 0.02 percent from dc to 1 kHz, with the possible exception of zero power factor measurements. Measurements up to 5 kHz can be made with somewhat greater uncertainties.

**14879.** Hord, J., **Discussion of "experimental studies on thermodynamic effects of developed cavitation" by Robert S. Ruggeri,** Article in *Fluid Mechanics, Acoustics and Design of Turbomachinery, Part 1,* pp. 394-395 (1974).

Key words: cavitation; cavity pressure; steam; steam vapor pressure; thermodynamic effects; vapor pressure.

A method for predicting thermodynamic effects of cavitation (changes in cavity pressure relative to steam vapor pressure) is presented. The prediction method accounts for changes in liquid, liquid temperature, flow velocity, and body scale. Both theoretical and experimental studies used in formulating the method are discussed. The prediction method provided good agreement between predicted and experimental results for geometrically scaled venturis handling four different liquids of widely diverse physical properties. Use of the method requires geometric similarity of the body and cavitated region and a known reference cavity-pressure depression at one operating condition.

**14880.** Brauer, G. M., Termini, D. J., **Grafting of polymeric side chains to soft tissues,** *J. Biomed. Mater. Res.* **8,** 451-470 (1974).

Key words: ceric ion initiated grafting; chemical attachment to ratskin; grafting to tissues; persulfate initiated grafting; surface grafting; tissue modification.

Soft tissues such as calfskin or ratskin can be modified by acrylic, methacrylic or vinyl monomers containing a variety of functional groups using ceric ions, persulfate-bisulfite or comonomers forming donor-acceptor complexes as initiators. Reactions take place within 20 minutes to 3 hours under experimental conditions which, with suitable changes, might be tolerated clinically. The resulting products are insoluble in solvents for the respective homopolymers. It is likely that the polymeric side chain is attached chemically to the collagenous backbone. With ratskin, the grafting takes place mainly at the surface, resulting in a change in wettability and water sorption of the substrate. Modified hydrophilic, hydrophobic or even oil repellent surfaces can be prepared by judicious choice of monomer used. Thus, hydrophobic, oleophobic subdermal ratskin surfaces are obtained on reaction with fluorinated monomers. Treated ratskins appear more resistant to micro-organisms than the original substrate. It is conceivable that the polymeric side chains could act as adhesive liners since the modified surface may improve the ability of the substrate to adhere to restorative materials.

**14881.** Lentner, K. J., **A current comparator system to establish the unit of electrical energy at 60 Hz,** *IEEE Trans. Instrum. Meas.* **IM-23,** No. 4, 334-336 (Dec. 1974).

Key words: calibration; current comparator; electrical energy unit; metrology; standard; unit; watthour meter calibration; watthour meter.

A compensated current comparator system to establish the United States legal unit of electrical energy at the National Bureau of Standards at energy levels of approximately 30 and 60 kJ is described. Analysis of the system uncertainties and experimental data indicates that the registrations of three standard type watthour meters were determined with total estimated uncertainties of about 30 ppm at unity power factor (PF) and 40 ppm at 0.5 PF. Of these uncertainties, 18 ppm represents the three standard deviation bound for the effects of random errors, and the remainder the root sum of squares of bounds to possible calibration and systematic effects. These results indicate that it should now be possible to disseminate the energy unit with uncertainties less than the presently quoted 500 ppm.

**14882.** Ambrose, J. R., Kruger, J., **Tribo-ellipsometric studies of the relationship between repassivation kinetics and stress corrosion of low carbon steel,** (Proc. 5th Int. Congress on Metallic Corrosion, Tokyo, Japan, May 21-27, 1972), Paper in *5th International Congress on Metallic Corrosion,* pp. 406-409 (National Association of Corrosion Engineers, Houston, Texas, 1974).

Key words: chloride; ellipsometry; low carbon steel; nitrate; nitrite; repassivation; stress corrosion.

Since the susceptibility of a material to stress corrosion cracking (SCC) may be related to the rupture of a protective film and the repassivation rate of the material thus exposed, a technique, tribo-ellipsometry, has been developed which simulates film rupture by abrading off the surface oxide. During t subsequent repassivation of this exposed surface, tribo-elli sometry allows simultaneous determination of film grow kinetics by ellipsometry and current transient following remov of a protective film. From these measurements a repassivati ratio $R_p$ (total change/film thickness) can be determined. Usi $R_p$, the following results were found: 1) SCC susceptible syste (1N $NaNO_3$ at 90 °C) – partial passivation, high rate of me dissolution; 2) SCC nonsusceptible system – (1N $NaNO_2$ at °C) – rapid and effective passivation low metal dissolution ra and 3) SCC nonsusceptible but highly corrosive system (1 NaCl) – no passivation, high metal dissolution rate.

**14883.** Kasa, I., **Closed-form mathematical solutions to some n work analyzer calibration equations,** (Proc. 1974 Conf. Precision Electromagnetic Measurements, London, Englan July 1-5, 1974), *IEEE Trans. Instrum. Meas.* **IM-23,** No. 399-402 (Dec. 1974).

Key words: calibration; sliding termination; standards.

A general evaluation procedure is described for calibration a linear complex reflectometer (network analyzer and for tw port measurements. New closed-form formulas and procedur are given for two practical cases: 1) calibration or measureme with two known standards and a sliding termination; calibration or measurement by one standard and two differe sliding terminations.

The reflection coefficient magnitudes and phases of these sli ing terminations need not be known.

The closed-form formulas make it possible to determi calibration constants by direct calculation without approxim tions or complicated multivariable iterations.

**14884.** Lias, S. G., **Ion-molecule reactions in radiation chemist** (Proc. NATO Advanced Study Institute Conf. on I Molecule Interactions, Biarritz, France, June 24-July 6, 197 Paper in *Interactions Between Ions and Molecules,* Ausloos, Ed., pp. 541-562 (Plenum Publishing Corp., N York, N.Y., 1975).

Key words: ion-molecule reaction; ion structure; ionic fra mentation; radiation chemistry; rate constants.

This brief review presents several illustrations of how i molecule reactions are studied in radiation chemical experime and also of the kinds of information about ion-molecule reactio and other ionic phenomena (such as fragmentation and ison rization) which have been obtained from such experiments. A solute rate coefficient determinations through spectrosco measurements in the gas and liquid phase radiolysis, as well absolute and relative rate coefficient determinations based chemical analysis of reaction products are described. Illust tions from radiation chemical investigations which have giv unique information about mechanistic details of certain i molecule reactions in hydrocarbon systems are also present A historical review and general description of the conditi prevailing in radiation chemistry experiments are also includ

**14885.** Zobrist, D. W., Fassbender, P., Bearden, F. E., Costr L., **Software standards and CAMAC,** *Instrum. Technol.* No. 3, 33-38 (Mar. 1975).

Key words: CAMAC; computer systems; control syste industrial control; software; standards.

One month prior to a meeting of the International Pur Workshop on Industrial Computer Systems, the idea was c ceived to demonstrate software transportability, using A X3.9-1966 Standard FORTRAN and ISA-S61.1 exter procedures for process control, and the demonstration was int out the need and potential of standards in other areas. Two mplete computer systems, including peripherals and CAMAC erfaces, and process instrumentation, were borrowed from a zen scattered sources. The systems were hooked up and nning in about two days. This article describes the demonstran project, the many obstacles encountered, and lessons arned.

886. Wachtman, J. B., Jr., **Highlights of progress in the science of fracture of ceramics and glass,** *J. Amer. Ceram. Soc.* **57,** No. 12, 509-519 (Dec. 12, 1974).

Key words: ceramics; fracture; fracture mechanics; glass; impact damage; strength; thermal shock; time to failure.

Rapid, catastrophic propagation of cracks is described in ms of stress concentration and energy balance conditions om a fracture-mechanics viewpoint. Slow crack propagation by ess corrosion or other mechanisms is also presented in fracre-mechanics terms. Data on slow crack propagation and acmpanying acoustic emission in a variety of ceramics and asses are reviewed. A survey is presented of the application of ese results to the quantitative treatment of strength, depennce of strength on loading rate, time to failure, proof testing, oustic emission monitoring, thermal shock, impact damage, d erosive machining. Some limitations in the application of acture mechanics to ceramics are discussed.

887. Klein, R., Yates, J. T., Jr., **Nitric oxide and its decomposition on the (110) plane of tungsten,** (Proc. 2nd Int. Conf. on Solid Surfaces, Kyoto, Japan, March 25-29, 1974), *Jap. J. Appl. Phys. Suppl.* **2,** Part 2, 461-464 (1974).

Key words: decomposition; nitric oxide; tungsten.

Nitric oxide is adsorbed on the (110) plane of tungsten with a gh sticking coefficient independent of coverage. Programmed ermal desorption of a W(110) surface with adsorbed NO ows no desorbed NO, but only nitrogen. Two peaks are obrved in the resulting nitrogen desorption spectra. The first, aparing at low coverages of NO, shifts to lower temperatures th increasing initial coverage. The second appears at higher verages and shifts slightly to higher temperatures with increasg coverage. The temperature region covering both states is 0-1350 K for the temperature rates employed. A simple, content model is developed. Work function-relative coverage easurements for NO on W(110) show an initial slow $\Delta\phi$ crease, a linear potion, and a maximum. The maximum $\Delta\phi$ is 85 eV and the saturated coverage value is 0.72 eV.

888. Rains, T. C., **Atomic absorption spectrometry—general considerations for the application of experimental techniques,** *Amer. Soc. Testing Mater. Spec. Tech. Publ.* **564,** pp. 50-66 (1974).

Key words: accuracy; atomic spectroscopy; atomic vapor; chemical analysis; evaluation; interferences; light sources; precision.

In applying atomic absorption spectrometry to an analytical oblem, the analyst must have an understanding of the basic inumental components. The essential components of an atomic sorption instrument consist of a primary source of radiation, means of producing atomic vapor from the analyte, wavelength lection, signal detection, and readout. While several types of diation sources are available, hollow cathode lamps are the priary choice for most workers in the field.

The production of atomic vapor of the analyte is probably the ost important parameter in atomic absorption spectrometry. e selection of the oxidant-fuel or nonflame method of producg neutral atoms will depend upon the concentration of analyte d the matrices. While the analyst has a wide choice of methods at his disposal, an understanding of the problems related to the production of atomic vapor is essential to obtain the maximum precision and accuracy. Also, interferences, sample preparation, and methods for evaluation of data are discussed.

14889. Weisman, I. D., Bennett, L. H., McAlister, A. J., Watson, R. E., **$\text{LaNi}_{5-x}\text{Pt}_x$: NMR investigation of structural and electronic properties,** *Phys. Rev. B* **11,** No. 1, 82-91 (Jan. 1, 1975).

Key words: alloys; contact term; core polarization; exchange enhancement; Knight shifts; $\text{LaNi}_5$; $\text{LaNi}_{5-x}\text{Pt}_x$; $\text{LaPt}_5$; NMR; ordering; relaxation times; solid solutions.

Pt-site Knight shifts $\kappa$, relaxation times, and crystallographic data have been obtained for the $\text{LaNi}_{5-x}\,\text{Pt}_x$ $(0 \leqslant x \leqslant 5)$ system. There are two transition-metal sites: one, $A$, in a La layer and one, $B$, between La layers; different $\kappa$'s are observed for each site. The system is found to be completely miscible and NMR intensities and crystallographic results show that Pt prefers the $B$ site and that considerable ordering occurs for $x \lesssim 4$. The $^{195}\text{Pt}$ $\kappa$'s are $\sim 1$ percent and $\sim 0$ percent for the $A$ and $B$ sites, respectively, in $\text{LaPt}_5$; the $A$-site $\kappa$ is approximately 0 at $\text{LaNi}_4\text{Pt}$ and the $B$-site $\kappa$ reaches $-2$ percent in $\text{LaNi}_{4.75}\text{Pt}_{0.25}$. The shifts, taken together with relaxation times, indicate that $s$-band effects dominate, particularly for the $A$-site, in $\text{LaPt}_5$ and that the Pt atoms on both sites become more transition-metal-like with increasing $x$. Exchange enhancement is shown to be an essential factor at the Ni-rich end. Variations in chemical activity, as in hydride formation, are discussed in light of these electronic differences between $\text{LaNi}_5$ and $\text{LaPt}_5$.

14890. Collin, G. J., **Réactions des ions iso-$C_4H_8^+$ et $t$-$C_4H_9^+$ avec l'isobutène en phases liquide et gazeuse,** *Can. J. Chem.* **52,** No. 12, 2341-2347 (1974).

Key words: free radical reactions; G-values; ion-molecule reactions; neopentane; proton transfer; radiolysis.

The radiolysis of neopentane has been studied in gas and liquid phases. It was shown that, in the liquid phase, the iso-$C_4H_8^+$ ion reacts at least as quickly with isobutene as with methylcyclopentane. The $t$-$C_4H_9^+$ ion reacts at least 10 times more rapidly with isobutene and the main reaction is one of resonant transfer of a proton with isobutene; fewer than 5 percent of the $t$-$C_4H_9^+$ ions add to isobutene. In the gas phase, the condensation reaction is more important than that of resonant proton transfer since proton transfer represents only 30 percent of the total reaction: $k(\text{addition})/k(\text{transfer}) \simeq 2.35 \pm 0.15$. Finally, the resonant transfer of a deuteron occurs about 2.9 more slowly than proton transfer.

14891. DePrima, C. R., Johnson, C. R., **The range of $A^{-1}A^*$ in $GL(n, C)$,** *Linear Algebra and Its Applications* **9,** 209-222 (1974).

Key words: adjoint; Hilbert's Theorem 90; involution; normal; similar; spectrum; unitary.

Let $A$ be an invertible linear operator on a finite dimensional complex Hilbert space. We carry out a detailed study of the map $A \to A^{-1}A^* \equiv \Phi(A)$. It is shown that the range of $\Phi$ is exactly the set of all invertible operators $T$ for which $T^{-1}$ is similar to $T^*$. In particular, unitaries and similarities of unitaries are in the range of $\Phi$ and we prove, among other things, the equivalence of the assertions: (i) $T$ is similar to a unitary, (ii) every $A \in \Phi^{-1}(T)$ is congruent to a normal operator, (iii) there exists $B \in \Phi^{-1}(T)$ whose field of values omits the origin of the complex plane. For general $T$ in the range of $\Phi$, we determine *all* $A \in \Phi^{-1}(T)$ in terms of the self-adjoint invertible operators fixed by the map $X \to T^*\,XT$. Many of the results contained in this paper have known analogues for operators which are similar to their adjoints.

**14892.** Mulholland, J. D., Plotkin, H. H., Silverberg, E. C., Wilkinson, D. T., Alley, C. O., Bender, P. L., Currie, D. G., Dicke, R. H., Faller, J. E., Kaula, W. M., Williams, J. G., **A self-consistent set of surface coordinates for the Apollo lunar laser retroreflectors deduced from laser range measures,** (Proc. 15th Planetary Meeting of COSPAR, Madrid, Spain, May 1972), Paper in *Space Research* **XIII,** M. J. Rycroft and S. K. Runcorn, Eds., **2,** 1009-1013 (Akademie-Verlag, Berlin, Germany, Dec. 1973).

Key words: astronomy; cartography; geophysics; laser; lunar distance; moon; selenodesy.

Laser ranges from the McDonald Observatory to the three Apollo retroreflectors have been used to obtain simultaneous solutions to the selenocentric coordinates of the three arrays, using two different approaches. The original coordinates, which were obtained either from LEM orbit determination or from orbital triangulation, suffered adjustments that were compatible with their *a priori* uncertainties, which ranged up to about a kilometer. It was decided also to correct the lunar moments of inertia. The corrections thus far obtained are not definitive, since the differential residuals are still of significant size. Nonetheless, order of magnitude reductions in the differential residuals have been secured.

**14893.** Reader, J., **Spectrum and energy levels of singly ionized rubidium (Rb II),** *J. Opt. Soc. Amer.* **65,** No. 3, 286-301 (Mar. 1975).

Key words: rubidium; spectra; ultraviolet; wavelengths.

The spectrum of Rb II has been observed in a pulsed radio-frequency discharge with the NBS 10.7-m normal-incidence vacuum spectrograph, the NBS 10.7 m Eagle spectrograph in air, and the NBS 3.34 m plane-grating spectrograph in air. The observations cover the regions 1489-2661 Å and 4380-10 081 Å. The wavelengths of the strong resonance lines in the 530-741 Å region were accurately measured in the 3rd and 4th orders with a sliding-spark discharge. Analysis of the spectrum has provided the positions of the previously missing levels of the $4p^5\,4d$, $4f$, and $6d$ configurations. The energy-level system has been extended to include the complete $4p^5\,5f$, $5g$, $6f$, and $6g$ configurations, most of the levels of the $4p^5\,6p$, $7f$, $7g$, $8s$, and $9s$ configurations, and parts of the $4p^5\,7d$, $8d$, $8f$, $8g$, $9d$, and $9f$ configurations. 600 lines are classified as transitions between 165 levels. Most of the observed configurations have been theoretically interpreted. The energy parameters determined from least-squares fits to the observed levels are compared with Hartree-Fock calculations. The ionization energy, derived from the $4p^5nf\,3/2\,[9/2]_5$, $n=4-7$, and $4p^5ng\,3/2\,[11/2]_6$, $n=5-8$, series, is 220 105.0 ± 0.5 $\text{cm}^{-1}$ (27.2898 ± 0.0001 eV).

**14894.** Kaufman, V., Sugar, J., **Spectrum and energy levels of five-times ionized tantalum (Ta VI),** *J. Opt. Soc. Amer.* **65,** No. 3, 302-309 (Mar. 1975).

Key words: spectra; tantalum.

The spectrum of Ta VI produced with a sliding-spark discharge was photographed in the region of ~ 200-2000 Å utilizing grazing-incidence and normal-incidence spectrographs. A system of seventy excited energy levels was deduced from 228 spectral lines. These arise from excitations out of both the $4f$ and $5p$ closed shells of the $4f^{14}\,5s^2\,5p^6$ ground configuration, giving the observed configurations $4f^{13}nl$ with $nl=5d$, $6s$, $6p$, $6d$, $7s$ and $5p^5nl$ with $nl=5d$, $6s$, $6p$. Radial integrals were fitted for all of these configurations. A value of 785 130 ± 400 $\text{cm}^{-1}$ for the ionization energy was derived. A graph of lowest excited levels of $4f^{13}\,5d$ and $5p^5\,5d$ from Lu IV to Re VIII predicts the crossing of these configurations after W VII.

**14895.** Mauer, F. A., Hubbard, C. R., Piermarini, G. H., Block, S., **Measurement of anisotropic compressibilities by a single crystal diffractometer method,** Paper in *Advances in X-Ray Analysis,* W. L. Pickles, C. S. Barrett, J. B. Newkirk, and C. O. Ruud, Eds., **18,** 437-453 (Plenum Press, New York, N.Y. 1975).

Key words: compressibility; single crystal; x-ray diffraction

The beryllium diamond-anvil pressure cell described by Weir Piermarini and Block has been mounted on a Bond diffractometer equipped with an orienter of the fixed-$\chi$ type. Molybdenum radiation is used to penetrate the diamonds and beryllium o which the cell is constructed, and special techniques are require to retain adequate precision in measuring cell parameters usin diffraction angles in the low $2\theta$ range. The method described provides high sensitivity in determining peak positions an eliminates the effect of centering errors on measured values o $2\theta$. Under favorable conditions, diffraction angles are measure with an accuracy of ±0.001° in $2\theta$. The method has been teste by measuring the lattice parameter of vacuum float zone refine silicon. Measurements of the compressibilities of silicon and o $\alpha$-Pb $(N_3)_2$ (orthorhombic) have been carried out using th method of Barnett, Block, and Piermarini to determine pressur by measuring the shift in the R-line fluorescence spectrum o ruby.

**14896.** Lias, S. G., Viscomi, A., Field, F. H., **Chemical ionizatio mass spectra. XXI. Reactions in *t*-$C_5H_{11}Cl$, *t*-$C_5H_{11}Br$, *t*- $C_5H_{11}OH$, and *t*-$C_5H_{11}SH$,** *J. Amer. Chem. Soc.* **96,** No. 2, 359-364 (Jan. 23, 1974).

Key words: alcohols; alkyl halides; chemical ionization; ion molecule reactions; mass spectrometry; mercaptans.

Mixtures of isobutane with small amounts (0.01-1%) of adde *t*-$C_5H_{11}Cl$, *t*-$C_5H_{11}Br$, *t*-$C_5H_{11}OH$, and *t*-$C_5H_{11}SH$ have bee studied in a high-pressure mass spectrometer as a function o total pressure, temperature, and concentration of additive. It i seen that proton transfer occurs only to *t*-$C_5H_{11}SH$, and even i this case, proton transfer is a minor process. The major reactio observed with each of the four molecules is the formation of condensation ion which dissociates rapidly to give $(C_9H_{19}^+ +$ HX) or $(C_5H_{11}^+ +$ neutral products) where X is Cl, Br, OH, o SH. The formation of $C_5H_{11}^+$ is favored under all conditions, bu the formation of $C_9H_{19}^+$ becomes more important as the pressur is raised or the temperature is lowered. When *i*-$C_4D_{10}$ is substituted for *i*-$C_4H_{10}$, it is seen that in the mercaptan, where proto transfer may be slightly exothermic, the departing hydrogen su fide molecule carries away a D species from the reacting *ter* butyl ion with a high probability; conversely, in *t*-$C_5H_{11}Br$, th departing hydrogen bromide molecule has a low probability o containing a hydrogen species from the reacting *tert*-butyl io This result suggests that when proton transfer competes with th displacement reaction, the two reactions proceed through th same intermediate ion, a $C_9H_{20}H^+$ species, in which "interna proton transfer has occurred. The product $C_5H_{11}^+$ ion undergoe an analogous displacement reaction with all of these molecul to form the following as products: $(C_{10}H_{21}^+ + HX)$ and $(C_6H_{13}^+$ neutral products). The $C_6H_{13}^+$ product ion also undergoes a di placement reaction with all of these molecules to form products $(C_{11}H_{23}^+ + HX)$.

**14897.** Yakowitz, H., **Electron-probe microanalysis—a capsu survey,** *J. Vac. Sci. Technol.* **11,** No. 6, 1100-1104 (Nov./De 1974).

Key words: electron probe microanalyzer; microanalysi qualitative analysis; quantitative analysis; specime preparation; x rays.

A brief overview of the way in which electron-pro icroanalysis can be used to obtain information from icrovolumes comprising $10^{-12}$ g or less of specimen material is resented. Elemental identification, distribution, and quantita-ve analytical procedures are outlined. Energy-resolving detec-rs and wavelength-dispersive spectrometers are compared; ıalysis of elements with atomic number $< 11$ is also briefly con-dered in this context. An example of the solution of a service ilure by means of elemental-distribution mapping is offered nally, an indication is given of the accuracy which can be ex-cted from quantitative electron-probe microanalysis.

**898.** Prosen, E. J., Goldberg, R. N., Staples, B. R., Boyd, R. N., Armstrong, G. T., **Microcalorimetry applied to biochemical processes,** (Proc. U.S. Japan Joint Seminar, Akron, Ohio, April, 8-12, 1974), Paper in *Thermal Analysis: Comparative Studies on Materials,* H. Kambe and P. D. Garn, Eds., pp. 253-289 (Kodansha Ltd. and John Wiley and Sons, Tokyo and New York, 1974).

Key words: analysis; assay in serum; bacterial growth calorimetry; enzyme catalyzed processes; glucose; micro-calorimetry; serum thermochemistry of enzyme processes.

A single-reaction-vessel, batch-type, conduction micro-lorimeter is described, having a volume of about 0.3 ml. The nsitivity in terms of electrical output voltage per unit of heat ansfer power is 60 mV · $W^{-1}$, the lower limit of detectable ther-al power is about 0.1 $\mu$W, and the lower limit of total heat that n be measured is $< 0.2$ mJ. The calorimeter is calibrated elec-ically and by known chemical reactions such as the neutraliza-on of HCl by NaOH in solution. The calorimeter has been ap-ied to the measurement of enzyme catalyzed biochemical rocesses. On the basis of measurements made in aqueous buffer lutions, the *hexokinase* catalyzed phosphorylation of glucose s been used to assay glucose in the complex media human rum and blood plasma, with results that correlate well with stomary clinical laboratory procedures. The growth of *nterobacter cloacae, Proteus rettgeri,* and *Klebsiella pneu-oniae* in the calorimeter under controlled conditions show aracteristic energy evolution patterns. In a somewhat larger action cell, the fertilization and growth of *Arbacia punctulata* gs were observed.

**899.** Lias, S. G., Ausloos, P., **Structure and reactivity of $C_4H_8^+$ ions formed in the radiolysis of cycloalkanes in the gas phase,** *J. Amer. Chem. Soc.* **92,** No. 7, 1840-1847 (Apr. 8, 1970).

Key words: charge transfer reactions; cycloalkanes; cyclohexane; gas phase; methylcyclopentane; parent ions.

The structure and reactivity of the $C_4H_8^+$ formed in the frag-entation of cyclohexane and methylcyclopentane parent ions s been examined ($[C_6H_{12}^+]^* \rightarrow C_2H_4 + C_4H_8^+$). It is noted at $C_4H_8^+$ consists of 1-$C_4H_8^+$, $i$-$C_4H_8^+$, and 2-$C_4H_8^+$. The rela-ve abundances of these isomer ions depend on the energy con-nt of the cycloalkane ion. According to the mass spectral acking pattern of cyclohexane-1,1,2,2,3,3-$d_6$ the high energy rent ion splits out $C_4H_8^+$ without extensive prior rearrange-ent. The $C_4H_8^+$ so formed is analogous to the $C_4H_8^+$ ion oduced in the photoionization or radiolysis of cyclobutane. he various $C_4H_8^+$ isomers react with the cycloalkanes by ac-ptance of an $H_2^-$ entity: $C_4H_8^+ + C_6H_{12} \rightarrow C_4H_{10} + C_6H_{10}^+$. he relative reaction rates, which are determined by means of otopic labeling experiments, differ widely with a change in the ructure of both the reactant ion and the reactant molecule, with e rate of reaction being generally higher for the more exother-ic process.

**900.** Kerns, D. M., **Scattering-matrix description and nearfield measurements of electroacoustic transducers,** *J. Acoust. Soc. Amer.* **57,** No. 2, 497-507 (Feb. 1975).

Key words: acoustics; electroacoustic transducers; near-field measurements.

Recently developed and successfully applied analytical techniques for the measurement of microwave antennas at reduced distances are "translated" into corresponding techniques for the measurement of electroacoustic transducers in fluids. The basic theory is formulated in scattering-matrix form and emphasizes the use of plane-wave spectra for the representation of sound fields. This theory, in contrast to those based on asymptotic description of transducer characteristics, is suitable for the formulation and solution of problems involving interactions at arbitrary distances. Two new techniques (in particular) are described. One, utilizing deconvolution of transverse scanning data, taken with a known transducer at distances $d$ which may be much less than the Rayleigh distance $d_R (\equiv D^2/2)$, provides a means of obtaining complete near- and farfield characteristics, *corrected for the effects of the measuring transducer.* Applicability of a (two-dimensional, spatial) sampling theorem and of the "fast Fourier transform" algorithm, with greatly facilitate the necessary computations, is shown. The second technique provides a means of extrapolating received signal as a function of distance (observed with $d \sim d_R$) to obtain on-axis values of effective directivity. Other possible applications are indicated. These techniques rigorously utilize observed transducer output, which need not be simply related to pressure or normal velocity at a point.

**14901.** Rains, T. C., Menis, O., **Determination of aluminum by flame emission spectrometry with repetitive optical scanning,** *Anal. Lett.* **7,** No. 11, 715-727 (1974).

Key words: aluminum; flame emission spectrometry; interferences; repetitive optical scanning.

The distribution of atomic aluminum emission in the nitrous oxide-acetylene flame was investigated by means of repetitive optical scanning in the derivative mode. In this system, the difficulties encountered with this source from the CN, CH, and $C_2$ band systems were overcome. This technique which doesn't require a separation or preconcentration step was applied to the determination of aluminum in various types of ferrous materials. The results were compared with other classical methods. By the proposed method aluminum was also determined in a high-purity iron at the 5 $\mu$g/g level with a relative standard deviation of 10 percent.

**14902.** Manghnani, M. H., Brower, W. S., Parker, H. S., **Anomalous elastic behavior in $Cu_2O$ under pressure,** *Phys. Status Solidi* **25,** 69-76 (1974).

Key words: cuprous oxide; elastic constants.

The elastic constants $C_{ij}$ of single-crystal $Cu_2O$ measured to 3 kbar show linear variation with pressure. The best-fit values of the $C_{ij}$ and $dC_{ij}/dP$ are: $C_{11} = 1228.8$, $C_{44} = 121.0$, $C' = (C_{11} - C_{12})/2 = 81.9$ kbar, $dC_{11}/dP = 3.62$, $dC_{44}/dP = -0.69$, and $dC'/dP = -0.63$, respectively. The elastic behavior of $Cu_2O$ is found to be anomalous in that $dC_{44}/dP$ and $dC'/dP$ are both negative, and $d\mu/dP$, where $\mu$ is the isotropic shear modulus, is significantly negative ($-0.67$). This anomalous behavior suggests an instability of crystal structure. The high- and low-temperature limiting values of Grüneisen $\gamma$, $\gamma_H$ and $\gamma_L$, computed from the $dC_{ij}/dP$ are $-1.98$ and $-3.59$, respectively. The value of $\gamma_H$ is in fairly good agreement with the reported Grüneisen $\gamma$ value based on the nuclear quadrupole relaxation data. The negative Grüneisen $\gamma$ values are consistent with the observed negative thermal expansion. The implication of $\gamma_L$ being appreciable more negative than $\gamma_H$ is that the coefficient of thermal expansion of $Cu_2O$ should become more negative at low temperatures.

**14903.** Ederer, D. L., Dhez, P., **Some applications of GM counters in the vacuum ultraviolet spectral region,** *Rev. Sci. Instrum.* **46,** No. 2, 144-146 (Feb. 1975).

Key words: absolute radiation detector; absorption measurements; filters; GM counter; sensitive detector; vacuum ultraviolet.

The applicability of GM and proportional counters naturally extends into the vacuum ultraviolet (vuv) spectral region. A simple modification to this detector enables GM counters to be used to measure very small cross section variations or to be used as high efficiency detectors over a narrow spectral range with excellent second order discrimination.

**14904.** Moore, L. J., Machlan, L. A., Shields, W. R., Garner, E. L., **Internal normalization techniques for high accuracy isotope dilution analyses-application to molybdenum and nickel in standard reference materials,** *Anal. Chem.* **46,** No. 8, 1082-1089 (July 1974).

Key words: isotope dilution; isotopes; mass spectrometry; molybdenum; nickel; normalization; standard reference materials; thermal ionization.

General exact equations and iteration techniques have been developed for internal normalization to eliminate the effect of thermal fractionation from isotope ratio measurements, and therefore isotope dilution analyses, by thermal ionization mass spectrometry. The techniques are applicable to more than 20 elements, and have been extensively applied to the determination of Mo in ore concentrates (55% Mo) and silicate trace standards (50 and 500 ppm M.). The standard deviations of all internally corrected Mo isotope ratio measurements were $< 0.1$ percent. The Mo sample size was 40 $\mu$g, but normalization techniques should apply to $\mu$g and smaller samples with a more sensitive ion detection system. Procedures are described for the chemical separation of Mo from matrix interferences and for the mass spectrometric analysis of Mo. Application of the techniques to Ni in three pollution standard reference materials is described.

**14905.** Hubbard, C. R., Swanson, H. E., Mauer, F. A., **A silicon powder diffraction standard reference material,** *J. Appl. Crystallogr.* **8,** Part 1, 45-48 (Feb. 1975).

Key words: powder diffraction standard, silicon; silicon powder diffraction standard; standard, powder diffraction; standard reference material, silicon.

A silicon powder Standard Reference Material, SRM-640, has been prepared for use as a standard in powder diffractometry. Powder diffraction measurements were performed with a tungsten internal standard and a high-angle goniometer. The measured $a/\lambda$ is 3.525176. With $\lambda$(Cu $K\alpha_1$ peak) taken as 1.5405981 Å, $a = 5.430880$ (35) Å, uncorrected for refraction. Comparison of $a$ with values obtained with a single crystal from one of the boules reveals a difference of 3 parts in $10^5$. This difference suggests a subtle systematic error in powder diffractometry or a change in lattice spacing near crystal boundaries. Use of the SRM should permit individual measurements of lattice parameters to be made reproducible to near 1 part in $10^5$ and an absolute accuracy of at least 3 parts in $10^5$.

**14906.** Garn, P. D., Diamondstone, B. I., Menis, O., **Variations in the cooling transitions of potassium nitrate,** *J. Therm. Anal.* **6,** 623-630 (1974).

Key words: potassium nitrate; procedure of ICTA Standards Committee and NBS; standard in thermal analysis; transition from I → III.

Because of questions concerning the suitability of potassium nitrate as a dynamic temperature standard for DTA, the relation between the experimental procedure and the resulting curve was ascertained for the Standard Reference Material $KNO_3$. Th material behaves differently *on cooling* in open pans than i cylindrical holders because confinement in the latter case initiates reversion to the room temperature form. Under the conditions of use as a dynamic temperature reference material, th curves are accurately reproducible.

**14907.** Ederer, D. L., Lucatorto, T. B., Saloman, E. B., Madden R. P., Sugar, J., **Photoabsorption of the 4d electrons in barium** *J. Phys. B: Atom. Molec. Phys., Letter to Editor* **8,** No. 3, L21 L25 (1975).

Key words: barium vapor; configuration interaction; $N_{IV}$, ionization thresholds; photoabsorption; 4d absorption; 4 orbital contraction.

The absorption spectrum of gaseous barium was obtaine between 120 Å, the region of the $N_{IV,V}$ thresholds. The similarit to lanthanum of some of the features observed in barium suggests that the 4f orbital contracts and overlaps the 4d orbit. Thi contraction produces two terms, $^3P$ and $^3D$, of the $4d^9$ 4f configuration below the 4d ionization limits, while the large electrostati exchange interaction drives the $^1P$ term of this configuratio some 10 eV above the limit. Furthermore, extensive mixing c the $4d^9$ $(6s^2)6p$ configuration with $4d^9(5d^2)6p$ and $4d^9(5d6s)6$ produces many weak resonances in addition to the resonance associated with the $4d^9$ 4f configuration. A suggested classification of these features is given with the aid of known features c the La I spectrum. Finally, from the known x-ray splitting of th $N_{IV,V}$ threshold and the energy interval between the $6s^2\ 6p\ ^2P$ an $6s^2\ ^1S$ levels in La I and La II, the ionization thresholds of the 4 electron were determined to be 814 800 (1000) cm$^{-1}$ and 792 50 (1000) cm$^{-1}$.

**14908.** Lias, S. G.; Rebbert, R. E., Ausloos, P., **Carbonium io in radiation chemistry. II. Isomerization processes in $C_3H_7^+$ an $C_4H_9^+$ ion,** *J. Amer. Chem. Soc.* **92,** No. 22, 6430-6440 (No 4, 1970).

Key words: butyl ion; carbonium ion; ion fragmentatio isomerization; propyl ion.

The structures of propyl and butyl ions formed in the ga phase radiolysis of appropriate alkanes have been deduced fro the structures of the neutral products formed in proton transf reactions with ammonia, or from the isotopic structures hydride (or deuteride) transfer reaction products formed in labe ing experiments. *n*-Propyl ions rearrange within $10^{-10}$ sec to th *sec*-propyl or the protonated cyclopropane structure. Rearrang ment to the *sec*-propyl ion is favored under all conditions but i creases in importance with increasing internal energy content the ion. Both isomerization reactions are reversible, but the ra constants of the reverse reactions are very low owing to the ene gy requirements of these processes. The isomerization of t *sec*-butyl ion to the *t*-butyl structure is observed; this rearrang ment also increases in importance with increasing internal ene gy content of the ion. The H (or D) atoms in the secondary a tertiary carbonium ions are seen to undergo energy-depende hydrogen-scrambling processes. The protonated cyclobutane i formed by proton transfer to cyclobutane isomerizes mainly the *sec*-butyl structure. The results presented here demonstra that most of the propyl and butyl ions formed in the dissociati of butane and hexane parent ions, respectively, originate as p mary carbonium ions from simple C-C cleavage processe rather than being formed initially with the secondary structu as they are at the threshold energies.

**14909.** Chow, L. C., Brown, W. E., **Formation of $CaHPO_4 \cdot 2H$ in tooth enamel as an intermediate product in topical fluori treatments,** *J. Dent. Res.* **54,** No. 1, 65-76 (Jan.-Feb. 1975).

Key words: dicalcium phosphate dihydrate; fluorapatite; fluoride; hydroxyapatite; tooth enamel.

Significant amounts of $CaHPO_4 \cdot 2H_2O$ (DCPD) were eposited in tooth enamel by pretreatment with a solution satuated with respect to DCPD. When these enamel samples were eated with a given fluoride solution, the fluoride uptake ineased with increasing amounts of DCPD produced by the retreatment. The interactions between enamel and acidic soluons to yield DCPD can be understood as dissolution-precipitaon reactions and analyzed through the use of solubility phase agrams.

1910. Hougen, J. T., **The assignment of molecular infrared spectra from a laser magnetic resonance spectrometer,** *J. Mol. Spectrosc.* **54,** No. 3, 447-471 (Mar. 15, 1975).

Key words: asymmetric rotors; doublet states; $HO_2$; laser magnetic resonance; least squares fit; rotational analysis; Zeeman spectrum.

Mathematical techniques are presented which have proved seful in assigning the laser magnetic resonance pure-rotation pectrum of $HO_2$, i.e., useful in assigning an absorption spectrum btained when molecular energy levels are Zeeman shifted by an xternal magnetic field until transition frequencies coincide with fixed-frequency radiation source. The techniques described hould have general applicability to the laser magnetic resonance bration-rotation spectrum of any molecule in an orbitally nonegenerate electronic state and a doublet electronic spin state ($S$ 1/2). Equations involving both Zeeman line positions and eeman line intensities are presented. These allow the assignent of $M_J$ quantum numbers, the determination of the spinotation interaction constant $\gamma$ and rotational quantum number for both the upper and the lower state, and the determination the zero-field transition frequency. The equations can be used ithout prior knowledge of the molecular structure or energy vels.

1911. Niemeijer, T., Meijer, P. H. E., **Quantum-mechanical ground state of crystals with dipole-dipole and exchange interactions,** *Phys. Rev. B* **10,** No. 7, 2962-2967 (Oct. 1, 1974).

Key words: antiferromagnetism; cerous magnesium nitrate; dipole-dipole interaction; ferromagnetism; ground state; magnetic; permutation group; quantum mechanics.

The general quantum-mechanical extension of Luttinger and isza's approach to the ground state of crystals with dipolepole and exchange interactions is given. It is shown that within is approach the ground state can only be ferro- or antifermagnetic if the unit cell contains only one or two magnetically uivalent atoms or ions.

912. Brill, R. H., Barnes, I. L., Adams, B., **Lead isotopes in some ancient Egyptian objects.** Paper in *Recent Advances in Science and Technology of Materials,* A. Bishay, Ed., **3,** 9-27 (Plenum Publishing Corp., New York, N.Y., 1974).

Key words: archaeological materials; Egyptian glasses; galena ores; kohl; lead isotopes; Ptolemaic and Roman Periods.

The determination of isotope ratios in lead extracted from a riety of archaeological materials is very useful for classifying e objects according to their geographical origins. On the basis data for lead from about 450 ancient objects and galena ores, ographical patterns have been established. Our previous stues have included metallic leads, bronze alloys, silver and gold ins, pigments, glazes and glasses from many areas of the Anent World. In this study we have investigated specimens of anent Egyptian glasses and glazes containing the colorant-opacifi- $Pb_2Sb_2O_7$, samples of kohl (which consist of powdered galena) and a few ores from Egypt. The leads used for making the pigment and kohl are similar to one another, but very different from leads from other parts of the Ancient World, and are almost certainly made of locally-occurring galena ores. Relatively small differences among the ancient Egyptian kohls separate those dating from different dynasties. Glasses and bronzes of the Ptolemaic and Roman Periods excavated in Egypt do not contain the same type of lead found in the earlier glasses and kohls. The later leads are of the Laurion, "Levantine" and Italian types. The authenticity of one very important glass object of the XVIIIth Dynasty has been verified by this technique.

14913. Yakowitz, H., **Role of the divergent beam (Kossel) x-ray technique in scanning electron microscopy,** (Proc. Seminar on Quantitative Scanning Electron Microscopy, London, England, Sept. 13-15, 1972), Chapter 13 in *Quantitative Scanning Electron Microscopy,* M. D. Muir, E. M. Boswarba and D. B. Holt, Eds., pp. 451-486 (Academic Press, London, England, Dec. 1974).

Key words: channelling of electrons; crystal orientation; Kossel; lattice spacing determination; microdiffraction; scanning electron microscopy; strain analysis; x ray.

The Kossel method is a divergent beam x-ray diffraction technique which requires a point source of x rays for optimum application. The scanning electron microscope provides the investigator with an almost ideal point source of x rays as well as a means for viewing the actual region irradiated.

Using Kossel patterns, one can study regions about 15 $\mu$m in size or larger. In particular, precise lattice spacing data from small crystal regions can be obtained. Furthermore, orientation information of microcrystals or crystal-line inclusions can be obtained within 1/4 to 1/2° of arc. Complete elastic stress-strain analysis of crystals can also be carried out. The method can also be combined with x-ray topographic methods to provide basic perfection data.

Methods for determining lattice spacings are critically compared. The most satisfactory general method – the regressive analysis of the conic equation (RACE) method is fully discussed. Information obtainable from the stress-strain analysis will be outlined, and the reliability limits of the computed strains is discussed using Fe-3 1/4 PCT.Si as an example. Instrumental requirements indicated by the results of the reliability analysis are described. Finally, some of the newer possibilities such as comparison with channelling pattern results are taken up.

14914. Wu, Y. C., **Thermodynamics of mixtures of aqueous electrolyte solutions – a viewpoint on the structure of electrolyte solutions,** (Proc. Int. Symp. on Structure of Water and Aqueous Solutions, Marburg, West Germany, July 1973), Chapter II, Section 6, in *Structure of Water and Aqueous Solutions,* W. A. P. Luck, Ed., pp. 189-206 (Verlag Chemie and Physik Verlag, Weinheim/Bergstr., Germany, 1974).

Key words: electrolyte solutions; ionic cosphere; structure of solutions; thermodynamics of mixture.

The structural effect of water on aqueous ionic solutions is best interpreted by the concept of ion-solvent cosphere overlapping, developed by Gurney and Frank. Friedman has advanced a theory which includes the overlapping effect. The success of the theory to fit experimental data for several 1-1 electrolytes up to 1 molal concentration has proven the existence of the overlapping effect.

Experimentally, one of the best methods of differentiating the ionic cosphere overlapping effect seems to be the study of mixed electrolyte solutions. The excess function of mixing, $\Delta_m Q^E$, is a measure of the difference of the excess function of the mixture from those of the pure binary electrolyte solutions. In the common ion mixture, this difference has been shown from the same charge ion interactions. Recently, Robinson, Wood, and Reilly have derived theoretically that the same effects are specific. The specificity of the same charge ion interactions appears to rise from the cosphere overlapping effect. Gurney postulated a rule that the mean activity coefficients, based on the order-disorder character of each ionic cosphere, go "from dissimilar character downward to similar character." The ionic cosphere overlapping effects on the thermodynamics of mixtures to parallel the same rule.

**14915.** Huang, J. S., Goldburg, W. I., Moldover, M. R., **Observation of anomalously large supercooling in carbon dioxide,** *Phys. Rev. Lett.* **34,** No. 11, 639-642 (Mar. 17, 1975).

Key words: carbon dioxide; $CO_2$; critical point; nucleation; supercooling.

We have observed supercooling in liquid $CO_2$ near the critical temperature greatly exceeding that allowed by existing theories of homogeneous nucleation.

**14916.** Stewart, S. L., **STAPLE, an experimental structured programming language,** *Comput. Languages* **1,** No. 1, 61-71 (Jan. 1975).

Key words: block structure; control flow; GOTO-less programming; language design; precompiler; quality software; structural programming.

STAPLE is a structured programming language with nested block structure in the source language to indicate flow of control. The semantics of the non-control structures are essentially the same as FORTRAN. The design goals were an easily implemented, easily modified tool for experiments and demonstrations of structured versus unstructured programming techniques.

**14917.** Bussey, H. E., Morris, D., Zal'tsman, E. B., **International comparison of complex permittivity measurement at 9 GHz,** *IEEE Trans. Instrum. Meas.* **IM-23,** No. 3, 235-239 (Sept. 1974).

Key words: cavity resonators; dielectric constant; loss measurements.

Dielectric constant and loss measurements made by three government laboratories (of the USSR, Canada, and the U.S.A.) are compared. The two materials measured were glasses. The measurements utilized cavity resonators in the $H_{01n}$ mode. The errors in dielectric constant reported by the laboratories were usually $\pm 0.3$ percent; actual differences between laboratories of the average corrected results were only $\pm 0.05$ percent. The loss tangent results disagreed when multimoding occurred; however, the errors may be as low as $\pm 0.00002$ or $\pm 3$ percent, whichever is the larger, if multimoding is avoided.

**14918.** Barnes, I. L., Shields, W. R., Murphy, T. J., Brill, R. H., **Isotopic analysis of Laurion lead ores,** Chapter 1 in *Archaeological Chemistry, Advances in Chemistry Series,* No. 138, 1-10 (1975).

Key words: archaeology; isotopic ratios; Laurion; lead; mass spectrometry; ores.

The lead isotopic ratios of a carefully selected suite of ore samples from the Laurion region have been determined by a precise mass spectrometric procedure. The ores were taken from various levels in mines, some known to have been worked in ancient times. All are nearly indistinguishable isotopically within the precision of the method ($\pm 0.05\%$), and they closely match leads from archaeological objects found in Greece. A comparison with isotopic data for ores from other mining regions in the ancient world has been made. The uniformity of the Laurion ores facilitates the interpretation of lead isotope data for archaeological objects from Greece.

**14919.** Finnegan, T. F., Wilson, J., Toots, J., **Interactions in small systems of coupled Josephson junctions on microwave frequencies,** *Rev. Phys. Appl.* **9,** No. 1, 199-205 (Jan. 1974).

Key words: coherent radiation; Josephson junction; microstrip; quality factor; transmission coefficient.

A major factor in the practical utilization of any Josephson device for microwave and higher frequency applications (such as the generation and detection of electromagnetic radiation) is the success with which the junction device can be coupled to an external transmission line. As part of an experimental investigation of the electrodynamics of small arrays of Josephson tunnel junctions, the properties of the coherent radiation emitted both by individual junctions and by coupled junction systems have been studied at frequencies between 2 and 12 GHz. Near 9 GHz, more than $10^{-9}$ W of coherent radiation has been detected from a single Pb-Pb oxide-Pb junction coupled via waveguide. The development of thin film devices in which the tunnel junctions form part of a microstrip line have made it feasible to observe directly (in a single device) the radiation emitted both at the fundamental geometrical frequency and at the low order harmonics. The observed temperature dependence of the junction cavity $Q$ indicate the low temperature losses are primarily due to cavity loading of the external transmission line.

**14920.** Griffin, R. J., Jr., **The thermesthesiometer—an innovation in heat measurement,** *Lab. Data Winter,* pp. 13-14 (1975).

Key words: computer science; laboratory accreditation; measurement; national measurement system; technology transfer; voluntary standards.

As technology becomes more complex, and as world trade increases, there is a growing need for measurement capabilities and consensus standards. In this interview the Director of the National Bureau of Standards discusses the role of NBS in these vital areas.

**14921.** Guildner, L. A., Terrien, J., **Mercury absolute manometers,** Chapter 4 in *Experimental Thermodynamics, Vol. II, Experimental Thermodynamics of Non-Reacting Fluids,* B. Le Neindre and B. Vodar, Eds., Part 1, pp. 115-131 (Butterworth and Co., London, England, 1975).

Key words: pressure; manometry; mercury manometer.

The most accurate pressure measurements attainable in the range of $5 \times 10^2$ Pa to $1.3 \times 10^5$ Pa can be made by using mercury manometers. In the design of a mercury manometer the principal concerns are those of locating the crown of the meniscus, and of determining the height of the mercury column. Different techniques are cited by describing some accurate instruments in use at BIPM, NRLM, NBS and VNIIM.

**14922.** Taggart, H. E., Nelson, R. E., Scott, W. W., Shafer, J. F. Tary, J. J., Workman, J. L., Treado, M. J., **Mobile FM transmitters,** *NILECJ-STD-0202.00,* 18 pages (U.S. Departmen of Justice, Law Enforcement Assistance Administration, National Institute of Law Enforcement and Criminal Justice Washington, D.C., Oct. 1974).

Key words: communications; law enforcement; mobil transceiver; performance standard; transceiver; transmitter

This standard for law enforcement communications transmitters specifies minimum performance requirements for mobil transmitters. Frequency ranges over which the standard applie are 25-50 MHz, 150-174 MHz, and 400-512 MHz.

923. Eliason, L. K., Hamlin, G. L., Grover, C. G., **Selection and application guide to fixed surveillance cameras,** *NILECJ-GUIDE-0301.00,* 24 pages (U.S. Department of Justice, Law Enforcement Assistance Administration, National Institute of Law Enforcement and Criminal Justice, Washington, D.C., Dec. 1974).

Key words: cameras; demand cameras; employee theft; fixed surveillance; motion picture surveillance; robbery; sequence cameras; shoplifting; surveillance; surveillance cameras.

The guide discusses the methods and types of fixed surveil- nce photography and their application in combating criminals. s purpose is to provide the potential user with the necessary neral background information to analyze his security needs, ecide if photographic surveillance seems to answer those needs, an generally what type of system best fits his requirements, and scuss his needs intelligently with the manufacturers and instal- rs of the equipment. Fixed surveillance photography involves e use of permanently installed cameras and equipment to moni- r areas where criminal activity is likely. The three types of uipment addressed are still cameras, motion-picture cameras, d television systems.

924. Shields, J. Q., **Measurement of four-pair admittances with two-pair bridges,** *IEEE Trans. Instrum. Meas.* **IM-23,** No. 4, 345-352 (Dec. 1974).

Key words: Ac DRRS; coaxial cable effects; coaxial star connectors; extrapolation techniques; four-pair admittances; permutation techniques; precision admittance standards; precision capacitance measurements; transformer bridges; transformer ratio measurements; two-pair admittances.

The purpose of this paper is twofold: 1) to show how ex- apolation techniques can be used to obtain well-defined and ersatile measuring systems; and 2) to apply such techniques to e measurement of four-pair admittances with two-pair bridges. hen four-pair admittances are large, measurements with two- ir bridges have limited precision, but with reasonably small ad- ittances, measurement precision is essentially equal to that at- ined with four-pair bridges.

925. Cutkosky, R. D., Field, B. F., **Standard cell enclosure with 20-μK stability,** *IEEE Trans. Instrum. Meas.* **IM-23,** No. 4, 295-298 (Dec. 1974).

Key words: Ac transformer-ratio bridge; platinum resistance thermometer; standard cell enclosure; standard cells.

Groups of standard cells are needed to maintain the National ureau of Standards (NBS) volt between periodic reassignments a $2e/h$. An enclosure to hold six standard cells has been signed and three enclosures have been assembled. The enclo- res consist of four concentric aluminum cylinders separated by amed polystyrene insulation. Two of the four cylinders are ntrolled, an outer one by a platinum resistance thermometer d dc amplifier and the inner one at 30 °C by a second platinum sistance thermometer and an ac transfomer-ratio bridge fol- wed by a phase-sensitive detector, a dc amplifier, and a heater. e innermost of the four cylinders is a thermally lagged cell mpartment. The temperature excursions over periods of at ast several days were found to be less than 20 μK, thus having egligible effect on the standard cell EMF's.

926. McNesby, J. R., Hughes, E. E., **Calibration gas standards,** *Proc. Int. Instrumentation-Automation Conf. and Exhibit, New York, N.Y., Oct. 28-31, 1974,* Paper 74-633, 1-5 (Instrument Society of America, Pittsburgh, Pa., 1974).

Key words: aircraft; air pollution; automobile; standard reference materials.

Accurate measurement of emissions is best accomplished by means of specific measurement methods using instruments which are calibrated by reference to Standard Reference Materials. The National Bureau of Standards has developed a number of gas Standard Reference Materials during the past two years for the measurement of pollutant gases in automobile exhaust emissions. These Standard Reference Materials include carbon monoxide in nitrogen, propane in air, carbon dioxide in nitrogen and nitric oxide in nitrogen at concentrations relevant not only to auto exhaust emissions but also to aircraft exhaust emissions. The technical problems associated with the development of those Standard Reference Materials are discussed and a description of the ranges of concentrations available is outlined.

14927. Cutkosky, R. D., **New NBS measurements of the absolute farad and ohm,** *IEEE Trans. Instrum. Meas.* **IM-23,** No. 4, 305-309 (Dec. 1974).

Key words: absolute farad; absolute ohm; calculable capacitor; cross capacitor; electrical units; farad; ohm; units.

A recently completed calculable cross capacitor in conjunction with a previously described collection of ac and dc bridges has made possible a highly accurate measurement of the farad and the ohm. The cross capacitor and its auxiliary equipment, as well as those components of the measurement system which have not been covered in prior publications, are described in detail. The measurements indicate that the National Bureau of Standards (NBS) unit of capacitance is given by $F_{NBS} = 1\ F + 1.787\ \mu F$, and that the NBS unit of resistance is given by $\Omega_{NBS} = 1\ \Omega - 0.819\ \mu\Omega$.

14928. Williams, E R., Olsen, P. T., Field, B. F., **Standard cell calibration via current transfer,** *IEEE Trans. Instrum. Meas.* **IM-23,** No. 4, 299-302 (Dec. 1974).

Key words: gyromagnetic ratio of the proton; fine structure constant; volt transfer.

The EMF's of standard cells are now being transferred between laboratories over a 1 1/2-km cable with a precision of 4 parts in $10^8$ to provide an instantaneous comparison of the $2e/h$ and $\gamma_p'$ experiments being carried out at the two facilities. This is accomplished by transferring a constant current that produces a 1-V drop across standard resistors located at both ends of the cable.

14929. Olsen, P. T., Williams, E. R., **A more accurate determination of $\gamma_p'$ through improved dimensional measurement techniques,** *IEEE Trans. Instrum. Meas.* **IM-23,** No. 4, 302-305 (Dec. 1974).

Key words: automated measurement systems; gyromagnetic ratio; magnetic field; protons; solenoid.

An increase in the accuracy of the gyromagnetic ratio of the proton can be achieved by determining the magnitude of a calculable magnetic field to higher accuracy. Such an increase requires dimensional measurements of a physical object to an absolute accuracy of a few parts in ten million. A unique computer-controlled automated measurement system for carrying out such measurements has been developed at the U.S. National Bureau of Standards and is currently in operation at its nonmagnetic facility. This measurement system provides an order of magnitude improvement over all previous measurements.

14930. Giarratano, P. J., Hess, R. C., Jones, M. C., **Forced convection heat transfer to subcritical helium I,** (Proc. 1973 Cryogenic Engineering Conf., Atlanta, Ga., Aug. 8-10, 1973), Paper K-1 in *Advances in Cryogenic Engineering* **19**, 404-416 (Plenum Press, New York, N.Y., 1974).

Key words: critical heat flux; film boiling; forced convection; heat transfer; helium; nucleate boiling; subcritical; supercritical.

Results of an experimental investigation of heat transfer to liquid helium under forced downward flow conditions are reported for a 0.213 cm i.d. × 10 cm long vertical test section subject to the following range of operating conditions: System pressures – 1-2 atm (0.1-0.2 MN/m²); Mass velocities – 4-65 g/s-cm²; Heat fluxes – 0.01-1 W/cm²; Inlet subcooling – 0-0.3 K.

Data are presented for the nucleate and film boiling regions and a correlation has been developed for predicting the critical heat flux (transition from nucleate to film boiling). A comparison of forced convection boiling of helium with other modes of helium heat transfer (pool boiling and supercritical) is also included.

**14931.** Heydemann, P. L. M., Welch, B. E., **Piston gages,** Chapter 4 in *Experimental Thermodynamics, Vol. II. Experimental Thermodynamics of Non-Reacting Fluids,* B. Le Neindre and B. Vodar, Eds., Part 3, pp. 147-202 (Butterworth and Co., London, England, 1975).

Key words: calibration; piston gages; pressure measurement.

Piston gages are instruments which measure pressure as force per unit area. There are a number of sources of error among which elastic distortion is the largest. Several types of piston gages have been developed to reduce the elastic distortion errors and to allow operation at a variety of pressures. A minimum of elastic distortion error is found with the controlled clearance piston gage. Other sources of error include temperature effects, air buoyancy, and head corrections. To reach the highest precision operating procedures must be followed which insure adequate control of all important parameters.

**14932.** Sengers, J. M. H. L., **Thermodynamic properties near the critical state,** Chapter 14 in *Experimental Thermodynamics, Vol. II. Experimental Thermodynamics of Non-Reacting Fluids,* B. Le Neindre and B. Vodar, Eds., pp. 657-724 (Butterworth and Co., London, England, 1975).

Key words: critical region; dielectric constant; equation of state; homogeneity; light scattering; power laws; refractive index; scaling; Schlieren method; specific heat; speed of sound; x-ray scattering.

A review is given of experimental methods for the determination of thermodynamic properties in the critical region of gases. The typical experimental difficulties: near-instability of the system, long equilibrium times and gravity effects, are discussed. Optical and dielectric measurements for the determination of density and of density gradients, are emphasized. A survey of the potential of light and x-ray scattering experiments is given. Other topics covered are constant-volume specific heat, conventional P-V-T, coexistence curve and speed of sound determinations. The discussion of experimental methods is preceded with a summary of the present state of critical region thermodynamics; power laws, gas-liquid symmetry, homogeneity, scaling and extended scaling are discussed.

**14933.** Ruthberg, S., **Pressure measurements for the range 1 kPa to 100 μPa,** Chapter 4 in *Experimental Thermodynamics, Vol. II. Experimental Thermodynamics of Non-Reacting Fluids,* B. Le Neindre and B. Vodar, Eds., Part 6, pp. 229-271 (Butterworth and Co., London, England, 1975).

Key words: capacitance-diaphragm gauge; Knudsen radiometer; McLeod gauge; micromanometry; quartz Bourdon gauge; static expansion; thermal transpiration; vapor-stream pumping; viscosity gauge.

Methods of measurement and calibration are analyzed for the range 1 kPa to 100 μPa (nominally 10 torr to $10^{-6}$ torr). Those procedures are considered for which measurements data, uncertainty analyses, and history exist in sufficient amount to allow for a reasonable confidence in their use. Precision liquid column micromanometers of the point contact and interferometric principles are assessed. Capillarity, density, leveling, sorption and leakage, and length measurement uncertainties are derived. McLeod gauge operation and uncertainties are derived including thermal transpiration and vapor-stream pumping effects at the cold trap. Viscosity manometers of the oscillating vane and spinning disc are described. The Knudsen radiometer manometer is considered. Uncertainties are detailed for the volumetric pressure divider-static expansion calibration procedure. The precision of transfer gauges is included.

**14934.** Cezairliyan, A., Beckett, C. W., **Electrical discharge techniques for measurements of thermodynamic properties of fluids at high temperatures,** Chapter 24 in *Experimental Thermodynamics, Vol. II. Experimental Thermodynamics of Non-Reacting Fluids,* B. Le Neindre and B. Vodar, Eds., pp. 1161-1192 (Butterworth and Co., London, England, 1975).

Key words: capacitor discharges; high-speed measurements; high temperatures; thermodynamics; thermophysics.

Electrical discharge techniques (millisecond and submillisecond resolution) which may be used for the measurement of thermodynamic properties of electrically conducting fluids (liquids and gases) at high temperatures (above 2000 K) are described. Design considerations, including electrical circuit characteristics and discussion of various phenomena, are presented. Measurement of experimental quantities, such as current, voltage, temperature, are discussed and various other high-speed techniques, such as high-speed photography, high-speec recording, are reviewed. Pertinent examples of utilization o discharge techniques for the measurement of thermodynamic properties are given.

**14935.** Eicke, W. G., Jr., Auxier, L. M., **Regional maintenance o the volt using NBS volt transfer techniques,** *IEEE Trans. Instrum. Meas.* **IM-23,** No. 4, 290-294 (Dec. 1974).

Key words: regional maintenance of the volt; standard cells surveillance of local units of voltage; voltage standards voltage transport standards; unit of voltage.

In cooperation with five industrial standards laboratories, th National Bureau of Standards (NBS) studied the feasibility o establishing a regional volt maintenance and surveillance program in the greater Los Angeles, Calif., area. The objective were to improve surveillance, to reduce dependence on NBS and to have each laboratory maintain its unit of voltage to withi 1 ppm of the U.S. legal volt. A two-phase program wa established, the first to characterize the five laboratories and th second to carry out the surveillance. After 3 years all laboratories were found to be maintaining their unit to within better tha 1 ppm of the U.S. legal volt.

**14936.** Hord, J., **Research opportunities in cryogenic hydrogen energy systems,** (Proc. Symp. on Hydrogen Energy Fundamentals, Miami Beach, Fla., March 3-5, 1975), Paper in *Hydroge Energy Fundamentals,* T. N. Viziroglu, Ed., pp. S3-11 –S3 24 (University of Miami, Coral Gables, Fla., 1975).

Key words: cryogenic; energy; hydrogen; research an development.

As liquid hydrogen pervades the commercial fuel market, ne and improved products and technologies will be needed. To me ese demands appropriate research and development (R&D) ust be performed on hydrogen fuel systems. Candidate markets r cryogenic hydrogen-energy systems are reviewed and scussed, and associated R&D needs are outlined herein. A ide variety of cryogenic R&D opportunities exist.

937. Sullivan, D. B., Dziuba, R. F., **A low-temperature direct-current comparator bridge,** *IEEE Trans. Instrum Meas.* **IM-23,** No. 4, 256-260 (Dec. 1974).

Key words: current comparator; low temperature electrical measurement; quantum interference device; ratio transformer; resistive divider; superconductivity.

The application of superconducting direct-current compara- rs to the measurement of resistance ratios is described. One mparator consists of a binary set of ratios between 1:1 and i0:1 providing for self-calibration by a buildup procedure. A cond comparator exhibiting discrete ratios of 1:1, 10:1, and 0:1 is also described. Ratio uncertainty of less than 1 part in $^{9}$ is achieved by enclosing the ratio windings in overlapping to- idal superconducting shields. Superconducting quantum inter- rence devices (SQUID's) serve as flux sensors for the com- rators. One of these current comparators is used to calibrate 100-Ω:1-Ω resistive divider, which at a current of 10 mA ex- bits a self-heating error of 0.0023 ppm.

938. Saxena, A. N., Weisberg, L. R., Mann, W. B., Schima, F. J., **Implantation of $^{14}N^+$ into monocrystalline GaN films,** *Int. J. Appl. Radiat. Isotop. Tech. Note* **26,** 33-34 (Jan. 1975).

Key words: *p*-type GaN; Schottky barrier diode; single crystal GaN; $14N^+$ implantation.

A rectifying Schottky barrier diode has been prepared in a thin m single crystal of GaN. Surface N-vacancy concentration as reduced by means of $^{14}N^+$ implantation.

939. Byerly, R., **New developments in the measurement of gase- ous pollutants in air,** *IEEE Trans. Nucl. Sci.* **NS-22,** No. 2, 856-869 (Apr. 1975).

Key words: air pollution; instrument; measurement; oxides of nitrogen; sulfur dioxide.

The pollution measurement needs driving the development of w techniques are reviewed as an introduction. These include eds for more sensitivity and more simplicity in actual use. lected examples are described as illustrations: The enomenon of chemiluminescence is used to measure ozone, lfur, and oxides of nitrogen. Chemiluminescence refers to the ission of light from excited product molecules formed when substance to be measured undergoes a chemical reaction. uorescence is used to measure $SO_2$ and NO. The molecule of erest is radiated with one wavelength light and emits uoresces) another wavelength which is detected. Absorption infrared radiation by a pollutant molecule can be used to mea- re low concentrations. The use of tuneable diode lasers to easure sulfur dioxide and ethylene is described. Also described the technique of tuning the pollutant absorption into coin- lence with a fixed laser line by application of magnetic or elec- c fields. This technique, perturbation spectroscopy, has been ed for vinyl chloride and nitric oxide measurement. Finally, a ef mention is made of the importance of long path techniques d possible approaches.

940. Eisenhauer, C. M., Simmons, G. L., **Point isotropic gamma-ray buildup factors in concrete,** *Nucl. Sci. Eng.* **56,** 263-270 (1975).

Key words: adjoint; annihilation; buildup factor; concrete; gamma radiation; moments.

Gamma-ray buildup factors in ordinary concrete have been calculated by the moments method. Results for concrete kerma and air kerma are tabulated for source energies from 15 MeV to 15 keV. Parameters are given that allow calculation of the buildup factor by means of a simple analytic expression. Comparisons are made with earlier calculations, and the effects of annihilation radiation are discussed.

14941. Finnegan, T. F., Wilson, J., Toots, J., **Coupling between Josephson junctions and microstriplines,** *IEEE Trans. Magn.* **MAG-11,** No. 2, 821-824 (Mar. 1975).

Key words: arrays; Josephson junctions; microstriplines; microwave filters; voltage standard.

A promising method for microwave coupling to thin-film Josephson devices via microstripline techniques has been developed which has significant advantages over more traditional waveguide techniques. In particular, direct determination of intrinsic junction cavity parameters such as the geometrical resonance frequencies and Q values are made practical and compact cryogenic multi-octave microwave holders readily realized. The results of coupling experiments with Pb-Pb oxide-Pb and Nb-Nb oxide-Pb tunnel junctions are discussed and applications of these results to the design and construction of shielded single junction 2e/h devices and small multi-junction arrays are described.

14942. Meshkov, S., Rosen, S. P., **Gauge theories and *M*-spin conservation,** *Phys. Rev. D, Comments and Addenda* **10,** No. 10, 3520-3521 (Nov. 15, 1974).

Key words: gauge theories; lepton; muon; *M*-spin; scattering amplitudes; Weinberg.

*M*-spin conservation is shown to be a property of Salam-Weinberg gauge theories. Amplitude relations such as $A(\nu_e e^- \rightarrow \nu_e e^-) - A(\nu_\mu e^- \rightarrow \nu_\mu e^-) = A(\nu_\mu e^- \rightarrow \nu_e \mu^-)$ derived from *M*-spin invariance alone also hold for the gauge theories up to the breaking due to Higgs scalars.

14943. Brauer, G. M., **Adhesion and adhesives,** Chapter 2 in *Scientific Aspects of Dental Materials,* J. A. von Fraunhofer, Ed., pp. 49-96 (Butterworths, London, England, 1975).

Key words: adhesion; adhesive restoratives; bonding to teeth; dental cements; dental sealants; reactivity of tooth surfaces.

The development of a truly adhesive restorative material is a primary goal of researchers in the field of dental materials. This review discusses the many fundamental investigations dealing with the reactivity of the tooth-adherent surface, followed by discussions of methods to modify hard tissue surfaces with the aim of enhancing adhesion. Potential adhesive systems are described that exhibit clinically significant adhesion to the hard tissues, especially enamel, in an environment approximating that encountered in the oral cavity. Evaluation of future adhesives will necessitate the development of well-designed standardized in vitro testing procedures that correlate with clinical experience. About 190 references are included in this extensive survey of studies conducted both at the National Bureau of Standards and by many other investigators.

14944. Greer, S. C., Block, T. E., Knobler, C. M., **Concentration gradients in nitroethane + 3-methylpentane near the liquid-liquid critical solution point,** *Phys. Rev. Lett.* **34,** No. 5, 250-253 (Feb. 3, 1975).

Key words: critical point; critical solution point; densimeter, magnetic; diffusion, pressure; gradient, concentration; gradient, density; gravity, effects of; 3-methylpentane; mixture; liquid; nitroethane; sedimentation.

Precise measurements of density profiles in the system nitroethane+3-methylpentane near the critical solution point demonstrate that concentration gradients form rapidly, but true equilibrium is not achieved even after long times. The data are in qualitative agreement with computer calculations of the behavior of a critical mixture in gravitational field which show that the initial gradients form by sedimentation. Thus, effects due to gravity may affect careful experiments in critical mixtures.

**14945.** Madey, T. E., Menzel, D., **Adsorption of CO on (001) ruthenium at temperatures $\geqslant$ 300 K,** (Proc. 2nd Int. Conf. on Solid Surfaces, Kyoto, Japan, March 25-29, 1974), *Jap. J. Appl. Phys. Suppl.* **2,** Part 2, 229-235 (1974).

Key words: carbon monoxide; chemisorption; defraction low energy electron; ruthenium; work function Auger spectroscopy.

The adsorption of CO on Ru(001) has been studied using a combination of techniques: LEED/Auger, Kelvin probe contact potential changes, and flash desorption mass spectrometry. Adsorption of CO is reversible at temperatures and pressures as high as 700 K and $10^{-4}$ torr, respectively. Two binding states of CO are identified, and isosteric heats determined both from work function changes and from LEED intensity measurements agree well with flash desorption energies. A disordering of the CO layer due to repulsive interactions between neighbors at high coverages is postulated. Electron beam-induced LEED pattern changes are characterized and found to have a high cross section ($\sim 7 \times 10^{-17}$ cm$^2$) at $\sim$ 110 eV.

**14946.** Olver, F. W. J., **Second-order linear differential equations with two turning points,** *Phil. Trans. Roy. Soc. London* **278,** No. 1279, 137-174 (Mar. 20, 1975).

Key words: asymptotic approximations; connection formulas; error bounds; ordinary differential equations; parabolic cylinder functions; turning points; wave scattering; Weber functions.

Differential equations of the form

$$d^2w/dx^2 = \{u^2 f(u,a,x) + g(u,a,x)\}w$$

are considered for large values of the real parameter $u$. Here $x$ is a real variable ranging over an open, possibly infinite, interval $(x_1, x_2)$, and $a$ is a bounded real parameter. It is assumed that $f(u,a,x)$ and $g(u,a,x)$ are free from singularity within $(x_1, x_2)$, and $f(u,a,x)$ has exactly two zeros, which depend continuously on $a$ and coincide for a certain value of $a$. Except in the neighbourhoods of the zeros, $g(u,a,x)$ is small in absolute value compared with $u^2 f(u,a,x)$.

By application of the Liouville transformation, the differential equation is converted into one of four standard forms, with continuous coefficients. Asymptotic approximations for the solutions are then constructed in terms of parabolic cylinder functions.

**14947.** Olver, F. W. J., **Legendre functions with both parameters large,** *Phil. Trans. Roy. Soc. London* **278,** No. 1279, 175-185 (Mar. 20, 1975).

Key words: asymptotic approximations; error bounds; Legendre functions; parabolic cylinder functions; turning points; Weber functions.

By application of the theory for second-order linear differential equations with two turning points developed in the preceding paper, some new asymptotic approximations are obtained for the associated Legendre functions when both the degree $n$ and order $m$ are large. The approximations are expressed in terms of parabolic cylinder functions, and are uniformly valid with respect to $x \epsilon (-1,1)$ and $m/(n+1/2) \epsilon [\delta, 1 + \Delta]$, where $\delta$ and $\Delta$ are arbitrary fixed numbers such that $0 < \delta < 1$ and $\Delta > 0$. The values of $m$ and $n+1/2$ are either both real, or both purely imaginary. In all cases explicit bounds are supplied for the error terms associated with the approximations.

**14948.** Gebbie, K. B., Steinitz, R., **A mechanism for the production of light and dark contrasts in radiatively controlled lines,** *Solar Phys.* **29,** No. 1, 3-15 (Mar. 1973).

Key words: contrasts in emergent intensity; radiatively controlled lines.

It is argued that visible contrasts can arise even in a line that is controlled wholly by an external radiation field. Lateral differences in the local shapes of the line absorption profile are shown to account for such contrasts. Two cases are treated explicitly: (a) a profile locally broadened by mass flow, and (b) a profile locally narrower due to the suppression of turbulen velocities, as might result from the presence of magnetic fields.

**14949.** Clough, R. B., **A new method for determination of proportional limit and machine stiffness,** *J. Test. Eval.* **3,** No. 2, 143-146 (Mar. 1975).

Key words: proportional limit; stiffness of testing machines

A new method for determining the proportional limit of engineering materials, characterized by maximum stress rate, i presented. Simultaneous measurement of stress rate and strai rate also permits a new means of measuring machine stiffnes which has certain advantages over present techniques.

**14950.** Isler, M., Grover, C., **Simplified procedures for evaluatin the image quality of objective lenses for night vision device** *LESP-RPT-0304.00,* 16 pages (U.S. Department of Justice Law Enforcement Assistance Administration, National Institute of Law Enforcement and Criminal Justice, Washingto D.C., May 1974).

Key words: contrast curves; low contrast resolution; nigh vision; objective lenses; resolution test; variable contras resolution.

This document provides two test methods for determining th comparative image quality of objective lenses intended for us on passive portable night vision devices. The two test method are called the low contrast resolution test and the variable contrast resolution test. The criterion for lens evaluation in bot tests is the limiting resolution of the image of a three bar test pattern, as a function of the contrast of the pattern.

**14951.** Bordé, C., Hall, J. L., **Ultrahigh resolution saturated absorption spectroscopy,** (Proc. Conf. on Laser Spectroscop Vail, Colo., June, 1973), Paper in *Laser Spectroscopy,* p 125-142 (Plenum Press, New York, N.Y., 1974).

Key words: laser spectroscopy; methane spectra; recoi saturated absorption.

Conventional wisdom holds that natural lifetime sets the bas resolution limit in Saturated Absorption Spectroscopy. Sinc suitable molecular transitions are known which have lifetim limited line Q above $10^{12}$, it is interesting to try to achieve suc resolution experimentally. By minimizing the usual broadenin effects and by using large apertures (5 cm) to minimize the trans broadening, we have studied the hyperfine structure of a certa methane transition at 3.39 $\mu$m. Our highest resolution (2.4 $10^{10}$) leads to good evidence for recoil *splitting* (not *shift*) of t observed absorption line. Another factor of 2 resolution increa is expected from the new absorption cell (38 cm diam by 13 length).

952. Crawford, M. L., **Evaluation of reflectivity level of anechoic chambers using isotropic, 3-dimensional probing,** (Proc. 1974 Int. IEEE/AP-S Symp., Atlanta, Ga., June 10-12, 1974), Paper in *1974 International IEEE/AP-S Symposium Digest*, pp. 28-34 (IEEE Inc., New York, N.Y., June 1974).

Key words: anechoic chamber evaluation; omni-directional probe; reflectivity; three-dimensional scanning.

This paper describes an experimental technique for evaluating echoic chamber reflectivity utilizing a new NBS isotropic obe mounted on a polyfoam track and support structure signed for probing the chamber's quiet zone in all three thogonal planes. The probe is omni-directional within ± 1 dB d has sufficient sensitivity to permit evaluation of reflectivity vels as low as 59 dB. It can be used from 150 MHz to 10.0 Hz. Complete scattering information is obtained without apying a receiving antenna pattern correction with only 3 thogonal scans per frequency required. The paper presents a ief treatment of the theory involved, a description of the stem and measurement technique employed, and a discussion typical measurement results.

953. Olson, W. B., Maki, A. G., Sams, R. L., **Infrared measurements on arsine: $\nu_1$ and $\nu_3$ bands, perturbation-allowed transitions, equilibrium structure,** *J. Mol. Spectrosc.* **55,** Nos. 1-3, 252-270 (1975).

Key words: arsine; infrared high resolution; perturbation-allowed transitions; resonances; secular determinants; spectra; structure.

High resolution infrared measurements are reported on arsine $sH_3$) from 2260 to 1960 cm$^{-1}$. Numerous perturbation-alwed transitions have been found and are used to determine the rotational constant. Ten ground state rotational constants are termined including one that describes the splitting of the $k=3$ vels. A complete equilibrium structure is determined. A total 26 upper state constants are determined by means of a comter program which simultaneously fits both $\nu_1$ and $\nu_3$ bands and ludes many off-diagonal matrix elements. This analysis will fit nsitions through $J=K=12$ to within experimental error, but s concluded that to fit higher rotational transitions the perturb- effects of $2\nu_4$ must be taken into account explicitly.

954. Engen, G. F., **An alternative calibration technique for automated network analyzers with application to adapter evaluaion,** (Proc. 1974 IEEE S-MTT Int. Microwave Symp., Atlana, Ga., June 12-14, 1974), Paper in *Microwave Symposium Digest*, pp. 261-262 (IEEE Inc., New York, N.Y., June 1974).

Key words: adapter; automation; calibration; microwave.

Although conceptually straightforward, the application of exng automated network analyzers to the problem of adapter aluation is inhibited by the limited accuracy of the detection cess, the requirement for several impedance standards at h frequency, and software problems. This paper describes a ple hardware modification, which for adapter evaluation lds an order of magnitude improvement in accuracy. An alterive calibration procedure is outlined which exploits this imved accuracy potential, and which requires only one imance standard.

55. Wasik, S. P., **Determination of hydrocarbons in sea water using an electrolytic stripping cell,** *J. Chromatogr. Sci.* **12,** 845-48 (Dec. 1974).

Key words: aromatic hydrocarbons; gas chromatography; hydrocarbon analysis; partition coefficient; sea water; stripping cell.

stripping cell is described which can be used to analyze and to measure partition coefficients of hydrocarbons in sea water. Small hydrogen bubbles evolved electrolytically from a gold electrode are allowed to rise up a cylindrical cell containing a known amount of sea water. The dissolved hydrocarbons in the sea water are equilibrated with the hydrogen bubbles. The hydrocarbon concentration in the headspace is determined by gas chromatography. The partition coefficient and hydrocarbon concentration in the sea water are determined from the volume of sea water and the hydrocarbon concentration in the headspace after a given volume of hydrogen has bubbled through the cell.

14956. Herron, J. T., Huie, R. E., **Application of beam sampling mass spectrometry to the kinetics of ozone reactions,** *Int. J. Mass Spectrom. Ion Phys.* **16,** No. 1/2, 125-136 (1975).

Key words: kinetics; mass spectrometry; nitrogen dioxide; oelfin; ozone; rate constant.

A beam sampling mass spectrometer designed for the study of chemical reactions in the gas phase is described. It is a three stage, differentially pumped instrument using a molecular beam chopper and phase sensitive detection. The reactions of ozone with $NO_2$ and some olefins were studied using a temperature controlled stopped-flow reactor in conjunction with the beam sampling mass spectrometer.

14957. McLaughlin, W. L., Hjortenberg, P. E., Pedersen, W. B., **Low energy scanned electron-beam dose distributions in thin layers,** *Int. J. Appl. Radiat. Isotop.* **26,** No. 3, 95-106 (1975).

Key words: dose distributions; dosimetry; dye dosimeters; electron beams; radiation curing; radiation processing; radiochromic dyes; thin films.

Thin radiochromic dye film dosimeters, calibrated by means of calorimetry, make possible the determination of absorbed-dose distributions due to low-energy scanned electron beam penetrations in moderately thin coatings and laminar media. For electrons of a few hundred keV, calibrated dosimeters of about 30-60 μm thickness may be used in stacks or interleaved between layers of materials of interest and supply a sufficient number of experimental data points throughout the depth of penetration of electrons to provide a depth-dose curve. Depth doses may be resolved in various polymer layers on different backings (wood, aluminum, and iron) for scanned electron beams ($E_{max}=400$ keV) having a broad energy spectrum and diffuse incidence, such as those used in radiation curing of coatings, textiles, plastics, etc. Theoretical calculations of such distributions of energy depositions are relatively difficult to achieve.

14958. Jones, F. E., Quindry, T. L., Rinkinen, W. J., **Summary report on emergency vehicle sirens,** *LESP-RPT-0502.00,* 47 pages (U.S. Department of Justice, Law Enforcement Assistance Administration, National Institute of Law Enforcement and Criminal Justice, Washington, D.C., Sept. 1974).

Key words: automobile; destructive interference; directivity; emergency vehicle; insertion loss; masking noise; siren; sound power level; sound pressure level.

A test program involving 23 test automobiles: four electronic sirens and nine electromechanical sirens has been completed. Measurements have been made of the directivity and sound power level-frequency spectra of the sirens, of the insertion loss (sound attenuation) of the automobiles, of the masking noise in the automobiles while being driven over a test route of our different segments, and of the phase cancellation due to reflection for an electronic siren. Measurements of directivity were made also for a pair of electronic siren speakers in three different arrangements.

**14959.** Westfall, M., Hurley, C. W., Eliason, L. K., **Metallic handcuffs,** *NILECJ-STD-0307.00,* 8 pages (U.S. Department of Justice, Law Enforcement Assistance Administration, National Institute of Law Enforcement and Criminal Justice, Washington, D.C., Oct. 1974).

Key words: ace type pin tumbler lock; cheek plate tamper resistance; salt spray corrosion resistance; warded lock.

This standard establishes minimum performance requirements and test methods for metallic handcuffs intended to be used to restrict the physical movement of apprehended persons. Specific tests are described including visual inspection, dimensional measurements, test loading of handcuffs, test loading of locking mechanism, cheek plate tamper resistance, dust and salt spray corrosion resistance.

**14960.** Breckenridge, F. R., Tschiegg, C. E., Greenspan, M., **Acoustic emission: Some applications of Lamb's problem,** *J. Acoust. Soc. Amer.* **57,** No. 3, 626-631 (Mar. 1975).

Key words: acoustic emission; calibration of transducers; electrostatic transducers; Lamb's problem; seismic pulses; ultrasonic transducers.

A method for obtaining the signatures (waveforms) of certain acoustic-emission events has been developed. The waveform is that at the source, free of contamination by ringing of the specimen, apparatus, and transducer. The technique is based on the comparison of two signals at the transducer, one from the event in question and one from an artificial event of known waveform. The apparatus is also adapted to the calibration of transducers in a certain sense. The configurations of source (real or simulated acoustic-emission event) and receiving transducer correspond to those of some special cases of Lamb's problem. As a byproduct, the results may be of some interest to seismologists.

**14961.** Kapsch, R. J., **Life cycle costing techniques applicable to law enforcement facilities,** *LESP-RPT-0801.00,* 23 pages (U.S. Department of Justice, Law Enforcement Assistance Administration, National Institute of Law Enforcement and Criminal Justice, Washington, D.C., Oct. 1974).

Key words: analysis; construction; cost; design; economics; flexibility; law enforcement facilities; performance; planning; present value analysis.

This report is concerned with the application of techniques from building economics to the problems involved in the planning, design and construction of law enforcement facilities. The formulas involved in the present value method of analysis are derived, and their use in analyzing the costs of alternative courses of action are explained and illustrated. Tabular equivalents of the formulas are given to facilitate the costing analysis.

**14962.** Giarratano, P. J., Jones, M. C., **Deterioration of heat transfer to supercritical helium at 2.5 atmospheres,** *Int. J. Heat Mass Transfer* **18,** No. 5-E, 649-653 (1975).

Key words: correlation; forced convection; heat transfer; helium; supercritical.

Heat transfer has been investigated for supercritical helium at 2.5 atm flowing inside a vertical tube with inlet bulk fluid temperatures less than the transposed critical temperature. Results indicate that for high heat flux conditions, the heat-transfer coefficient passes through a maximum and then deteriorates as the fluid temperature approaches the transposed critical temperature. This is contrary to the predictions of a correlation developed in an earlier study of supercritical helium heat transfer under low heat flux conditions, which only predicts enhancement in heat transfer as the transposed critical temperature is approached.

The experimental data are presented and conditions under which heat-transfer deterioration was observed are discussed. The probable limitations to the validity of the above mentioned heat-transfer coefficient correlation, developed for a different range of experimental data, are also discussed.

**14963.** Blackburn, D. L., Oettinger, F. F., **Transient thermal response measurements of power transistors,** *IEEE Trans. Ind Electron. Control Instrum.* **IECI-22,** No. 2, 134-141 (May 1975).

Key words: computer simulation (transient thermal); current crowding (transistors); power transistors; thermal impedance measurements; thermal response measurements transistors (thermal measurements).

Differences between the measured thermal impedance o power transistors when determined by the pulsed heating curv and cooling curve techniques are discussed. These difference are shown to result primarily because the power density distributions of these devices change as the devices heat; as a result o these changes the heating curve and the cooling curve are no conjugate. It is shown that the cooling curve technique, when th cooling curve is initiated from the most non-uniform steady-stat thermal distribution, (maximum voltage, maximum power) wi indicate a larger value for the thermal impedance than will th pulsed heating curve technique, even for pulses in excess of th dc power level. A one-dimensional model for power transisto cooling is described. The theoretical predictions of the model ar shown to be in good agreement for practical applications wit three-dimensional computer simulations and experimenta results. Using this model, it is possible to estimate an averag junction temperature and the area of power generation at steady state. Both TO-66 and TO-3 encased devices of mesa and plana structures were included in this study.

**14964.** Kan, P. T., Peterson, G. A., Webb, D. V., Fivozinsky, P., Lightbody, J. W., Jr., Penner, S., **Electroexcitation of $^{11}$** *Phys. Rev. C* **11,** No. 2, 323-331 (Feb. 1975).

Key words: boron; electron scattering; giant resonance; lo gitudinal; reduced widths; transverse.

Electrons with incident energies between 52.3 and 90.0 Me have been scattered from the nucleus of $^{11}$B. Spectra of scattere electrons corresponding to excitation energies up to 32 Me were observed at angles of 75° and 145°. Form factors of t states at 2.12, 4.44, 5.02, 8.57, and 8.93 MeV, and of the co tinuum region up to 30 MeV, have been separated into longit dinal and transverse components. The $^{11}$B dipole giant resonan is smooth relative to those of $^{12}$C and $^{13}$C. A mixed $M1$-$E2$ tran tion was observed at 13.0 MeV and a broad transver resonance, possibly magnetic, was seen at 15.5 MeV.

**14965.** Franzen, D. L., **Precision beam splitters for $CO_2$ lase** *Appl. Opt.* **14,** No. 3, 647-652 (Mar. 1975).

Key words: beam splitter; $CO_2$ laser; high power la material.

Beam splitters for 10-μm lasers are discussed and then appli to the precision measurement of high average powers. In partic lar, beam splitter stability has been investigated in vario materials over the 20 – 600-W power range with power densit up to 1 kW/cm². The absolute beam splitter ratios are given alo with the achieved measurement precisions. The semiconduct investigated were GaAs, CdTe, and ZnSe in addition to one kali-halide KCl. Standard deviations for the beam splitter rat of 1 percent over the power range were typical. Absolute rat agree with the predictions from Fresnel's equations to 1 percent or better. The best measurement was made on ZnSe when a standard deviation of 0.4 percent was obtained for the measurement of a ratio that agreed with a calculation from Fresnel's equations o better than 0.5 percent.

**4966.** Loebenstein, W. V., **The surface area of aggregates applied to dental materials,** *J. Biomed. Mater. Res.* 9, 35-53 (1975).

> Key words: adsorption theory; aggregate, adsorption by; collagen; dental materials; dentin; enamel; surface area; teeth; water vapor adsorption.

There is a continuing need for the complete characterization of the physical and chemical properties of dental materials. Among these properties is surface area. The problem is further omplicated by the fact that most dental materials are, themselves, mixtures of two or more identifiable components. If the apor adsorptive properties of these components are different in he mixture from that which would be expected of them collec- vely, then interaction is present. Interaction must not be con- used with the lack of additivity which results from the limita- ons of the BET theory applied to mixtures. Equations are erived herein to estimate the extent of this latter source of ariability and to correct for it giving a "true" surface area for he aggregate. Conversely, the adsorptive properties of either omponent can be calculated from the properties of the mixture nd the remaining component together with the percentage com- osition. An immediate application can be made in determining he water-vapor adsorptive properties of human dental collagen ithout necessitating its removal from dentin. Any attempt to xtract it chemically may produce denaturation or chain rupture hus precluding the possibility of direct determination. In the ase of nitrogen adsorption, however, interaction definitely is in- icated.

**4967.** Ensslin, N., Bertozzi, W., Kowalski, S., Sargent, C. P., Turchinetz, W., Williamson, C. F., Fivozinsky, S. P., Lightbody, J. W., Jr., Penner, S., **Electron scattering from excited states in $^{14}$N and $^{9}$Be,** *Phys. Rev. C* 9, No. 5, 1705-1717 (May 1974).

> Key words: deduced wave functions; electron scattering; measured form factors; nuclear reactions; $^{14}$N; $^{9}$Be(e,e′).

Electron scattering form factors have been measured for the rst six excited states in $^{14}$N and for the 2.429-MeV ($5/2^-$) level $^{9}$Be. The form factors for the lowest $T=1$ level in $^{14}$N along ith the previously measured ground-state magnetic moment are sed to specify the $T=0$ and $T=1$ wave functions for the mass- 4 system assuming two *p*-shell valence particles in an *LS*- oupling basis. The amplitudes of the various configurations so erived are generally in poor agreement with previous deter- inations, although the present wave functions yield values of e lifetime of the first $T=0$ state in $^{14}$N and of the $^{14}$N ground- ate quadrupole moment that are in excellent agreement with evious measurements. The present data are not sufficiently ecise to allow a direct separation of the $T=0$ and $T=1$ com- nents for the first four negative-parity excited states. How- er, for two of these states which are excited primarily by *C*1 ansitions, a comparison of the radiative strengths determined this experiment with previous lifetime measurements sets a wer limit of 2 percent for the $T=1$ admixture.

**968.** Fivozinsky, S. P., Penner, S., Lightbody, J. W., Jr., Blum, D., **Electron scattering from $^{88}$Sr and $^{89}$Y,** *Phys. Rev. C* 9, No. 4, 1533-1542 (Apr. 1974).

> Key words: elastic and inelastic electron scattering; low lying levels; weak coupling; $^{88}$Sr; $^{89}$Y.

Inelastic scattering cross sections of low-lying levels and elastic scattering cross sections have been measured in $^{88}$Sr and $^{89}$Y using the National Bureau of Standards Linac and electron scattering facility. Incident-electron energies were varied between 45 and 121 MeV corresponding to a momentum transfer range of 0.4 to 1.0 fm$^{-1}$. Data were accumulated at two scattering angles, 110.5 and 128.2°. We present elastic scattering form factors and inelastic scattering form factors and $B(EL)\uparrow$'s for the 1.84- and 2.74-MeV states in $^{88}$Sr, and the 1.51-, 1.74-, 2.21-, 2.52-, 2.86-, and 3.1-MeV states in $^{89}$Y. A simple configuration mixing model based on the weak-coupling model has been applied to the octupole states in $^{89}$Y. The measured elastic form factors for both nuclei have been fitted with a Fermi charge distribution.

**14969.** Kurylo, M. J., Braun, W., Xuan, C. N., Kaldor, A., **Infrared laser enhanced reactions: Temperature resolution of the chemical dynamics of the $O_3$+NO reaction system,** *J. Chem. Phys.* 62, No. 6, 2065-2071 (Mar. 15, 1975).

> Key words: apparatus and methods; chemiluminescence; emission spectra; free radicals; kinetics of reactions; lasers, infrared; photochemistry.

The rate constant for the decay of vibrationally excited ozone, $O_3^\dagger$, in the $O_3^\dagger+NO$ reaction system has been measured from 153 to 373 K. Vibrationally excited $O_3$ was produced in the asymmetric stretch normal mode by absorption of square wave modulated emission from a $CO_2$ laser tuned to the $P(30)$ 9.6 $\mu$m transition. Under appropriate experimental conditions, a rapid $V\rightarrow V$ coupling process involving all three normal modes of $O_3$ is believed to set up a Boltzmann population distribution among them. Reaction or relaxation of $O_3{}^+$ out of this subset of normal modes is observed to proceed through a weighted average of rate constants. From the effects of temperature and buffer gas pressures an assessment can be made as to the predominant loss mechanism for the various modes. While there are three separate convolution schemes which appear to fit our data, we are persuaded to emphasize one whereby all three modes contribute via a reaction channel described by $k_D=(2.0\times10^{-11})\exp(-1525/T)$ cm$^3$ molecule$^{-1}\cdot$sec$^{-1}$ while $\nu_2$ alone is active in a $V\rightarrow T$ relaxation process given by $k_A=(1.0\times10^{-13})\exp(-39.2/T)$ cm$^3$ molecule$^{-1}\cdot$sec$^{-1}$. A comparison of the Arrhenius parameters for the reaction channels of $O_3^\dagger$ with parameters for the corresponding processes involving thermal $O_3$ yields specific information about the effect of vibrational energy on the reaction dynamics.

**14970.** Kanda, M., **Accuracy considerations in the measurement of the power gain of a large microwave antenna,** (Proc. 1974 Int. IEEE/AP-S Symp., Atlanta, Ga., June 10-12, 1974), Paper in *1974 International IEEE/AP-S Symposium Digest,* 43-45 (IEEE Inc., New York, N.Y., June 1974).

> Key words: calibration accuracy; effective area; effective radiated power; extrapolation method; gain comparison method; microwave antenna; power gain; satellite.

Accuracy considerations in the measurement of the power gain of a large microwave antenna are discussed. Using the gain comparison method with a standard antenna of approximately 40-dB gain, a large antenna with a power gain of approximately 60-dB can be calibrated to within an error of 0.17 dB ($3\sigma$).

**14971.** Kamper, R. A., **Review of superconducting electronics,** *IEEE Trans. Magn.* MAG-11, No. 2, 141-146 (Mar. 1975).

> Key words: electronics; Josephson effect; precise measurements; superconductivity.

This review will sketch the present state of affairs in applications of Josephson junctions and SQUIDs to: magnetometry, DC and RF metrology, detection and amplification of electromagnetic signals, frequency metrology, noise thermometry and computers. It will also mention recent progress in super-stable oscillators using superconducting resonant circuits, pulse transmission lines, and thin-film devices to detect radiation or charged particles. Many of these topics are maturing nicely.

14972. Newman, M., **Congruence subgroups of the modular group,** *Math. Comput.* **29,** No. 129, 207-213 (Jan. 1975).

Key words: automorphs; elliptic classes; finite fields; genus; modular group; natural homomorphism; parabolic classes.

The congruence subgroups of the classical modular group which can be defined as the automorphs modulo $q$ of some fixed matrix are studied, and their genera determined.

14973. Ekin, J. W., Deason, V. A., **Technique for preparing homogeneous bulk samples of concentrated alloys,** *Rev. Sci. Instrum. Notes* **46,** No. 3, 327-328 (Mar. 1975).

Key words: aluminum alloys; bulk alloy samples; casting; directional solidification; rapid quenching.

A technique has been developed for casting relatively large samples (~ 100 g) of concentrated alloys. It was used to prepare Al-Mg castings having Mg concentrations near the maximum limit of solid solubility. Concentration gradients and nonequilibrium eutectic solidification were minimized by the rapid cooling and directional solidification that are characteristic of the technique.

14974. DiChio, D., Natali, S. V., Kuyatt, C. E., **A new form for the third-order asymptotic aberration coefficients of electrostatic lenses; application to the two-tube electrostatic lens,** *Rev. Sci. Instrum.* **46,** No. 1, 71-76 (Jan. 1975).

Key words: aberration integrals; asymptotic aberration coefficients; electron optics; electrostatic lens; third-order aberration coefficients; two-tube lens.

The third-order asymptotic aberration coefficients of round electrostatic lenses are reformulated in terms of the coordinates formed by the projections of the asymptotic incident and final rays onto the reference plane of the lens. In this formulation, all aberration coefficients are finite for all lenses, in contrast to the formulation in terms of coordinates projected onto the focal planes of the lenses, where all of the coefficients become infinite in the limit of very weak lenses and for certain strong lenses. Equations for the six third-order aberration coefficients are derived in the form of integrals involving derivatives of the axial potential no higher than the second. Using these equations and previously calculated potentials and first-order trajectories, we have computed the six aberration coefficients for the accelerating and decelerating two-tube electrostatic lens for voltage ratios from 1.1 to 10 000. The results are believed accurate to better than 0.2 percent.

14975. Gadzuk, J. W., **Relaxation energies in chemisorption spectroscopy,** *J. Vac. Sci. Technol.* **12,** No. 1, 289-292 (Jan.-Feb. 1975).

Key words: chemisorption; image potential shifts; polarization energy shift; relaxation energies.

The upward shift in atomic energy levels (or decrease in electron binding energies) which occurs upon sorption of an atom on a metal surface due to polarization of the valence band electrons, is considered. The polarization shift or extra-atomic relaxation energy is treated within the framework established by Hedin, Johansson, and Lundqvist and the results are related to image potential shifts which have been previously discussed in chemisorption theories.

14976. Jordan, T. H., Dickens, B., Schroeder, L. W., Brown, W E., **The crystal structure of $Ca(BF_4)_2$,** *Acta Crystallogr.* **B31** Part 3, 669-672 (Mar. 1975).

Key words: calcium fluoroborate; calcium salts; cryst structure; single crystal; tetrahedral anion; x-ray diffractio

$Ca(BF_4)_2$ crystallizes in the orthorhombic space group *Pbc* with $Z=8$. The unit-cell parameters are $a=9.2792$ (6), $b=$ 8.9103 (10) and $c=13.3719$ (10) Å. The structure was refined b full-matrix least-squares calculations to $R_w(F)=0.025$, $R$ 0.024, using 2896 measurable x-ray data collected by a count method and corrected for absorption. The refinement allowed f anisotropic thermal motion, isotropic secondary extinction ar anomalous dispersion. The structure consists of columns of BF ions and columns of alternating $Ca^{2+}$ and $BF_4^-$ ions, all parall to [010]. There are twice as many [$Ca^{2+}$, $BF_4^-$] columns [$BF_4^-$, $BF_4^-$] columns. All columns are linked together throu Ca...F bonds. The $Ca^{2+}$ ion is coordinated by a square antipris of fluorine atoms, each from a different $BF_4^-$ ion. Each fluori atom is bonded to one $Ca^{2+}$ ion, and the four $Ca^{2+}$ ions bonded a $BF_4^-$ ion are arranged approximately tetrahedrally about t $BF_4^-$ ion. Although neither of the two crystallographically d crete $BF_4^-$ ions occupies a site of special symmetry, each is e sentially tetrahedral in configuration.

14977. Mabie, C. P., **Evaluation of the physical properties crown dental porcelain and the effect of newly developed an balling additive,** *J. Biomed. Mater. Res.* **9,** 1-25 (1975).

Key words: additive; deformation; dental; porcelain; pr perties.

A colloidal silica-based substitute for the water added dental porcelain has been developed which restricts rounding firing and gives greater and indefinitely prolonged unfired bisc strength. In conjunction with product evaluation, it has be found that both the modulus of rupture and the diametrical te sile strength of dental porcelains can be measured with a h degree of precision.

14978. Gadzuk, J. W., **Electron spectroscopy of chemisorb atoms and surface molecules,** (Proc. 2nd Int. Conf. on Sc Surfaces, Kyoto, Japan, March 25-29, 1974), *Jap. J. Ap Phys. Suppl.* **2,** Part 2, 851-858 (1974).

Key words: chemisorption; field emission; ion neutrali tion; photoemission; surface spectroscopy.

Chemical bonds formed between substrate and adsorb atoms are characterized by new electronic energy levels wh are derived from the atomic orbitals of each constituent. Th energy levels are being observed experimentally through techniques of field emission energy distributions, uv photoem sion spectroscopy, and ion neutralization spectroscopy. Th spectroscopies will be considered in the light of present theoretical understanding of both the measurement and chemisorption process.

14979. Clough, R. B., Simmons, J. A., **Thermodynamics of di cation motion in multiaxial stress fields,** (Proc. from the John Dorn Symp., Cleveland, Ohio, Oct. 1972), Paper in *R Processes in Plastic Deformation of Materials,* J. C. M. Li A. K. Mukherjee, Eds., pp. 266-283 (American Society Metals, Metals Park, Ohio, 1975).

Key words: dislocation; multiaxial; plasticity; th modynamics.

This paper presents a first-order consideration of disloca motion through a multiaxial stress field. The concept of pla power dissipation is developed as a measure of plastic flow to multiaxial stresses. A result which emerges is the concep he second-order activation volume tensor for plastic power disipation. Usually, this is a deviatoric tensor with the same prinipal axes as the stress, which then only interacts with the deviaoric stress. Results are given for a biaxial yield surface calcuated as a surface of constant plastic power dissipation. The yield urface varies from a Tresca to a von Mises shape, depending on he scalar activation volume, the uniaxial yield stress, and the emperature. Generally for low temperature conditions the yield urface resembles the Tresca yield surface, and its shape aproaches the von Mises shape as a high temperature limit. The ctivation volume tensor is explicitly demonstrated for all aterials in a state of uniaxial tension and for materials with a on Mises-like yield surface in any multiaxial stress state. Extenion of this treatment to include the internal stress and prestrain nd stress history effects on the yield surface is discussed.

4980. Heydemann, P., **Pulse shaper,** *Rev. Sci. Instrum. Notes* **46,** No. 3, 329-330 (Mar. 1975).

Key words: NMR; switching; ultrasonics.

The rounding of pulses is a convenient way to suppress ansients when rf signals are switched with balanced mixers or emiconductor switches. The use of a serial-in, parallel-out shift egister for shaping the leading and trailing edges of pulses is escribed. The original pulse is clocked through a shift register nd the outputs of the register are weighted and added to form a ew pulse. The maximum rise time is equal to the clock period mes the bit-capacity of the register.

4981. Gadzuk, J. W., **Surface molecules and chemisorption, II. Photoemission angular distributions,** *Phys. Rev. B* **10,** No. 12, 5030-5044 (Dec. 15, 1974).

Key words: angular distributions; chemisorption; photoemission; photoionization; surfaces.

A theory of the angular distributions of electrons photoemitted om submonolayer films of chemisorbed atoms is presented. hemisorption is treated within the surface-molecule limit of the nderson model. It is shown that the key features which difrentiate between solid-state photoemission and atomic hotoionization are the localization of the hole left behind in the hotoexcitation process and the preferential orientation of omic or molecular orbitals (in photoemission from solids or hemisorbed atoms). The differential photoionization cross secons or angular distributions for spatially oriented atoms and rface molecules are obtained and contours of constant emison intensity, as projected on a flat fluorescent screen which is arallel to the surface, are presented. It is shown that the chemisrption bonding geometry can be ascertained from such mearements.

4982. Plummer, E. W., Waclawski, B. J., Vorburger, T., **Experimental observations of electronic energy levels at a solid-vacuum interface,** (Proc. Symp. on Electrocatalysis, San Francisco, Calif., May 13-15, 1974), Paper in *Electrocatalysis,* M. W. Breiter, Ed., pp. 43-57 (Electrochemical Society Inc., Princeton, N.J., 1974).

Key words: chemisorption; field emission; photoemission; single crystals; surface electron spectroscopy; surface state; tungsten.

A knowledge of the distribution of electrons both in energy d space at a surface is essential to the understanding of surface operties. Several techniques have been developed recently hich have the potential capability of measuring the energy level ectrum of a surface. Two of these techniques, field emission d photoemission, will be discussed including a description of hat can be measured, how it can be interpreted and the degree consistency of the data. Experimental data will be presented to illustrate: (1) the surface density of states on clean single crystals and its relationship to bulk density of states; (2) the nature of the chemisorption bond and density dependent transitions; (3) dissociative or non-dissociative adsorption and (4) catalytic reactions involving adsorption of hydrocarbons.

14983. Zecca, A., Lazzizzera, I., Krauss, M., Kuyatt, C. E., **Electron scattering from NO and $N_2O$ below 10 eV,** *J. Chem. Phys.* **61,** No. 11, 4560-4566 (Dec. 1, 1974).

Key words: electron impact; electron scattering resonances; exponential attenuation; low energy; negative ions; nitric oxide; nitrous oxide; total scattering cross section.

Total electron scattering cross sections for NO and $N_2O$ in the energy range 0-10 eV were obtained from exponential attenuation in a straight-line collision chamber without a confining magnetic field. Good agreement is obtained with previous measurements where available. For NO, cross sections have been obtained for the first time for resonance structure in the energy range 0-2.5 eV. There appear to be small, sharp resonances between the large resonances. For both NO and $N_2O$ the cross section is observed to increase rapidly at very low energies. Structure in the cross sections is interpreted in terms of electronic states of $NO^-$ and $N_2O^-$.

14984. Šunjić, M., Šokčević, D., Gadzuk, J. W., **Determination of electron attenuation lengths in metals: Transmission through thin adsorbed films,** (Proc. 2nd Int. Conf. on Solid Surfaces, Kyoto, Japan, March 25-29, 1974), *Jap. J. Appl. Phys. Suppl.* **2,** Part 2, 753-756 (1974).

Key words: attenuation length; inelastic electron scattering; surface plasmons.

A quantitative theory of surface and bulk plasmon excitation in several electron spectroscopies (transmission, XPS, and Auger from thin film sandwiches) is presented. It is shown under what circumstances, the usual exponential attenuation law is valid.

14985. Brown, W. E., **Physicochemistry of apatite dissolution,** (Transactions of Colloquium on Physico-Chimie et Cristallographie des Apatites D'Intérêt Biologique, Paris, France, 1973), *Colloq. Int. Cent. Nat. Rech. Sci.,* No. 230, 355-368 (1975).

Key words: bone mineral; dental caries; electric currents; mechanism; solubility.

The dissolution of apatites, during formation of caries lesions in enamel or remodeling of bone, has two aspects, thermodynamic and kinetic, which are intimately related. One can approach a full understanding of these processes by taking into account how each aspect affects the other.

The rate of transport of calcium relative to that of phosphate ions is a dominant consideration. These rates are likely to be controlled to a considerable degree by the permselective properties of the plaque and the outer layer of enamel acting as a very complex and variable membrane. Alteration of the properties of this membrane, therefore, becomes a potentially valuable means for preventing caries.

The thermodynamic properties of the apatite enter into the caries dissolution process in another way: the subsurface nature of the typical incipient lesion very probably relates to the variable solubility of the apatite in enamel mineral. Solubility measurements with enamel show that much of it is more soluble than synthetic preparations of pure hydroxyapatite and that its solubility changes with its composition and location.

14986. Okabe, H., **Photodissociation of acetylene and**

**bromoacetylene in the vacuum ultraviolet: Production of electronically excited $C_2H$ and $C_2$,** *J. Chem. Phys.* **62,** No. 7, 2782-2787 (Apr. 1, 1975).

Key words: acetylene; bond dissociation energy; bromoacetylene; $C_2$; $C_2H$; fluorescence; photodissociation; vacuum ultraviolet.

The photodissociation of $C_2H_2$ and $BrC_2H$ in the vacuum ultraviolet produces nearly identical quasicontinuous emissions in the region 4000 to above 5500 Å. It is concluded that the continua are most likely associated with the electronically excited $C_2H$ ($C_2H^*$) in both cases. Based on this conclusion the following spectroscopic and thermochemical data are derived from the thresholds of incident wavelength to produce the continua (1305 ± 3 Å and 1540 ± 3 Å, respectively, for $C_2H_2$ and $BrC_2H$): The electronic energy of $C_2H$, $E_0(C_2H) \leq 4.11 \pm 0.05$ eV, $D_0(Br - C_2H) = 91 \pm 1$ kcal mol$^{-1}$ ($381 \pm 4$ kJ mol$^{-1}$), and $\Delta H_{f0}°(BrC_2H) = 64.2 \pm 1.5$ kcal mol$^{-1}$ ($269 \pm 6$ kJ mol$^{-1}$). The photolysis of $BrC_2H$ yields the $C_2$ Swan bands in addition to the $C_2H^*$ by the spin forbidden process. The fluorescence yield has been measured as a function of incident wavelength for $C_2H_2$ and $BrC_2H$. The fluorescence yield curves follow the absorption spectra of $C_2H_2$ and $BrC_2H$, indicating that the $C_2H^*$ is predissociated from the initially formed electronic states. The $C_2H^*$ yield from $C_2H_2$ increases rapidly below the incident wavelength, 1200 Å. Bond dissociation energies and the heats of formation of haloacetylenes are estimated in comparison with the corresponding cyanogen halides. Primary photochemical processes in $C_2H_2$ are discussed.

**14987.** Saloman, E. B., Ederer, D. L., **Absolute radiometric calibration of detectors between 200-600 Å,** *Appl. Opt.* **14,** No. 4, 1029-1034 (Apr. 1975).

Key words: calibration of detectors; corrections for second order radiation; far ultraviolet; noble gas double ionization chamber; synchrotron radiation; transfer standard detectors.

Radiometric transfer standards consisting of windowless diodes with cathodes made of anodized aluminum oxide on aluminum are now available from the National Bureau of Standards with calibrations in the 200 – 600-Å wavelength range. This extends the previously existing range of calibration for these diodes (600 – 1200 Å). For wavelengths shorter than 600 Å, synchrotron radiation at NBS-SURF is used as the source of radiant energy. A noble gas double ionization chamber is used to calibrate a secondary standard diode that is then intercompared with the transfer standards. Monitors take into account variations in the intensity of synchrotron radiation and in beam position. Methods of accounting for the effects of second-order radiation in the incident flux and secondary ionization in the double ionization chamber are discussed. Calibration uncertainties are about 10 percent.

**14988.** Mills, R., Yee, K., **Hand-held metal detectors for use in weapons detection,** *NILECJ-STD-0602.00,* 13 pages (U.S. Department of Justice, Law Enforcement Assistance Administration, National Institute of Law Enforcement and Criminal Justice, Washington, D.C., Oct. 1974).

Key words: metal detector; weapons detection.

Performance requirements and methods of test have been established for hand-held metal detectors used for determining the location of metal weapons carried on a person. Requirements are specified which indicate a detector's suitability for use in each of specified applications.

**14989.** Ederer, D. L., Lucatorto, T. B., Saloman, E. B., **Photoabsorption from the 4d and 5p shells of barium,** (Proc. IV Int. Conf. on VUV Radiation Physics, Hamburg, Germany July 17-26, 1974), Chapter 3.5 in *Proceedings of the IV International Conference on VUV Radiation Physics,* E. Koch, R Haensel, and C. Kunz, Eds., pp. 245-246 (Friedr. Viewe Sohn Verlagsgesellschaft, mbH, Braunschweig, West Germany, 1974).

Key words: absorption spectrum; barium; heat pipe; inne shell excitation; shape resonance; two-electron excitations

A plastic windowed heat pipe was used in conjunction with th NBS-170 MeV synchrotron and a 3-m grazing incidence spectrograph to observe transition $4d^{10}5s^25p^66s^2 \rightarrow 4d^94s^25p^66s$ nf,np in the spectral region 110Å-150Å. By replacing the plasti windows with tin, excitations involving transitions $5p^66s^2 - 5p^56s^2$ nd,ns were observed in the spectral region 520Å-650Å.

**14990.** Jickling, R. M., Shafer, J. F., **Repeaters for law enforc ment communication systems,** *LESP-RPT-0206.00,* 18 page (U.S. Department of Justice, Law Enforcement Assistanc Administration, National Institute of Law Enforcement an Criminal Justice, Washington, D.C., Oct. 1974).

Key words: duplexer; fm transceiver; land-mobile commu nications; law enforcement; repeater; vertical antenna.

This report is concerned with FM repeaters used in land m bile communications systems. Repeater systems are describe with emphasis on appropriate antenna site selection, signal-reje tion techniques, and specialized transmission-line componen for the transmission and reception of signals. Repeaters using t vehicle transceiver are mentioned. Repeaters at microwa frequencies are described to the extent that their use for contr and as audio links is pertinent. Measurement techniques that a unique to land-mobile repeaters are discussed.

**14991.** Schwarz, F. P., Okabe, H., **Fluorescence detection of nitr oxide in nitrogen,** *Anal. Chem.* **47,** No. 4, 703-707 (Apr. 1975

Key words: air; automotive exhaust emission; detectio fluorescence; nitric oxide; nitrogen; quencher.

An accurate, rapid, and simple technique is described for t measurement of nitric oxide in standard reference mixtures NO in $N_2$. The technique investigated is based on the measur ment of the fluorescence intensity emitted by NO when it a sorbs 213.8-nm radiation from a Zn discharge lamp (the $A^2\Sigma$ ($v$ 1) $\leftarrow X^2\pi_{1/2}$ ($v = 0$) transition). The fluorescence is in the 220-300-nm region and its intensity is proportional to the 213.8-n light intensity and the NO concentration. The fluorescence i tensity at a constant light intensity level increases linearly wi NO concentration in the 0.015- to 7-ppm range to within 1 pe cent error. In the 7- to 932-ppm range, the intensity increas sublinearly with NO concentration because of efficient se quenching of the fluorescence. The signal-to-noise ratio is 1.0 10 ppb for a 1-minute counting time. The quenching half pr sures of NO, $H_2O$, $CO,O_2$, $O_2$, $C_2H_4$, $C_3H_8$, and $H_2$ are, respe tively, $0.34 \pm 0.03$, $0.65 \pm 0.06$, $8.3 \pm 0.6$, $0.65 \pm 0.05$,05, 1.1 0.1, $5.6 \pm 0.4$, $56 \pm 4$, and $115 \pm 8$ torr. The application of t method to detect NO and $SO_2$ in automotive exhaust discussed.

**14992.** Miller, T. R., Weikel, M. K., **Blood donor eligibili recruitment, and retention,** *Transfusion* **14,** No. 6, 616-6 (Nov.-Dec. 1974).

Key words: blood banking; donor attitudes; donor eligib ty; donor participation rates; donor recruitment; donor tention; foreign donor programs; non-donor attitudes.

To study the motivation and actions of potential and act blood donors, a literature search, a limited survey, and sociated analytic efforts were undertaken. It is estimated that llion of the 114 million age-eligible donors meet Red Cross iteria of health-eligibility. The 1971 donor participation rate, lculated as the percentage ratio of active donors to eligible nors, was estimated to be between 8 and 9 percent. Total col- ctions appear to be increasing at a stable rate of 1 percent per ar and 15 percent of each year's collections apparently come om first-time donors. Thus, 14 percent of those who donate od in any given year must replace other donors who have opped donating. Roughly 25 percent of those who are health- gible to donate blood have done so in the last ten years. Litera- e and survey analyses indicate that donor reaction rates are nsiderably underestimated by most collectors. A limited sur- y showed that the main reason for nonparticipation is fear, ile common reasons for discontinuing participation are ad- rse reaction and medical disqualification.

993. LaVilla, R. E., **The sulfur $K\beta$ emission and $K$-absorption spectra from gaseous $H_2S$, III,** *J. Chem. Phys.* **62,** No. 6, 2209-2212 (Mar. 15, 1975).

Key words: $H_2S$; sulfur $K\beta$ emission and $K$-absorption spectra; sulfur $K$ shell binding energy; x-ray spectra.

The sulfur $K\beta$ emission in fluorescence and $K$ absorption from seous $H_2S$ were measured on a double crystal spectrometer. e sulfur $K\beta$ spectrum consists of four peaks. The three stron- st peaks are shown to be single vacancy transitions of elec- ns from the three outer MO's to fill the single $K$ shell vacancy. e weak fourth peak on the high energy side of the three line ucture is identified as a double vacancy transition. The sulfur absorption spectrum consists of three peaks of decreasing in- sity with increasing photon energy. The unusual breadth WHM of 1.50 eV) and asymmetry on the high energy side of first peak is ascribed to the Frank-Condon factors of the nsitions to the unoccupied antibonding MO's $3b_2$ and $6a_1$. The er two peaks, which are narrow, are identified as transitions Rydberg levels. In addition, the binding energy of the sulfur $K$ ll electron was estimated to be 2478.3 eV. The sulfur $L_{2,3}$ orption of $H_2S$ is also discussed briefly.

94. Newell, A. C., Crawford, M. L., **Planar near-field mea- urements on phased array antennas,** Abstract only, (Proc. Int. EEE AP-S Symp., Atlanta, Ga., June 10-12, 1974), Paper 6-7 n *1974 International IEEE/AP-S Symposium Digest,* p. 423 IEEE Inc., New York, N.Y., June 1974).

Key words: antennas; near-field measurements; phased arrays.

he results of applying the planar near-field measurement hnique to two experimental phased array antennas are cribed. Fast and efficient tests are used to determine the uired scan area and data point spacings. The use of these tests ble one to reduce the amount of data required for some anten- without seriously increasing the errors in computed far-field ameters.

easurements were made at different distances from the an- nas, with the probe transmitting and receiving, and for both n and monopulse difference patterns of the test antenna. Com- isons between the far-field patterns computed from the near- d data and those measured on far-field ranges are presented.

95. Komarek, E. L., **An application of the power equation con- ept and automation techniques to precision bolometer unit alibration,** (Proc. 1974 IEEE S-MTT Int. Microwave Symp., tlanta, Ga., June 12-14, 1974), Paper in *Microwave Sym- osium Digest,* pp. 263-265 (IEEE Inc., New York, N.Y., une 1974).

Key words: automation techniques; bolometer units; calibration; power equation concept.

The power equation concept has been implemented into a multioctave precision bolometer unit calibration system employing automation techniques in conjunction with an automatic network analyzer system. The system was qualified as a calibration transfer system operating in the 2-12.4 GHz frequency range at 1 to 10 mW with a single measurement standard deviation of 0.2 percent to 1 percent from 2-10 GHz.

14996. Rebbert, R. E., Lias, S. G., Ausloos, P., **The photolysis of neopentane and isobutane with 7.6, 8.4, and 10.0 eV photons,** *J. Photochem.* **4,** 121-137 (1975).

Key words: free radical scavenging; hydrocarbons; isobutane; neopentane; primary photochemical processes; quantum yields; vacuum ultraviolet photolysis.

The photolysis of neopentane has been studied using photons of energies 7.6, 8.4, and 10.0 eV, at pressures in the range 1-760 torr and in the liquid phase. Quantum yields of all molecular and radical products smaller than $C_5$ have been determined in the gas phase experiments, and have been estimated in the liquid phase. In contrast to results obtained with other alkanes studied to date, hydrogen elimination is found to be an unimportant process in the photolysis of neopentane. The two predominant primary processes are elimination of methane (neo-$C_5H_{12} \rightarrow CH_4 +$ iso-$C_4H_8$) and direct C-C bond cleavage (neo-$C_5H_{12} \rightarrow CH_3 +$ t-$C_4H_9$). A fraction of the t-$C_4H_9$ radicals dissociate further unless collisionally stabilized, either by loss of a H atom or by loss of a methyl radical (presumably preceded by an initial rearrangement to the isobutyl structure). With an increase in photon energy, the importance of direct bond cleavage increases at the expense of the methane elimination process. In the liquid phase, secondary decomposition processes are quenched, and the estimated quantum yields of primary processes are similar, at all energies, to those found in the 7.6 eV gas phase photolysis at high pressures.

Quantum yields of molecular and radical products formed in the 7.6 and 8.4 eV photolysis of isobutane are also reported and are discussed briefly, with particular emphasis on the effect of energy on the mechanisms of the molecular elimination processes: (iso-$C_4H_{10} \rightarrow CH_4 + C_3H_6$) and (iso-$C_4H_{10} \rightarrow$ iso-$C_4H_8 + H_2$). For both of these primary processes, the lower energy pathway, in which the olefin is formed directly, predominates at 7.6 eV, but diminishes in importance relative to the higher energy channel (presumably involving carbene formation) when the photon energy is increased.

14997. Saloman, E. B., Ederer, D. L., Madden, R. P., **Radiometry in the EUV spectral region: Standard source and detectors,** (Proc. IV Int. Conf. on VUV Radiation Physics, Hamburg, Germany, July 17-26, 1974), Chapter 10.12 in *Proceedings of the IV International Conference on VUV Radiation Physics,* E. Koch, R. Haensel, and C. Kunz, Eds., pp. 798-800 (Friedr. Vieweg Sohn Verlagsgesellschaft, mbH, Braunschweig, West Germany, 1974).

Key words: continuum radiation; diodes; irradiance standard; synchrotron radiation; transfer standard detectors; vacuum ultraviolet radiation standards.

Conceptually it is straight-forward to apply the calculable continuum distribution of synchrotron radiation to problems requiring a source of known irradiance. However, in practice many factors affect the accuracy of such a calibration. These factors will be discussed with reference to the NBS 170 MeV synchrotron. The calibration facility at NBS-SURF has been utilized in the 200Å-1200Å spectral range by Air Force Cambridge Research Laboratories and the Naval Research Laboratory to calibrate rocket monochromators. Transfer radiometric standards consisting of windowless diodes with cathodes made of anodized aluminum oxide on aluminum have been developed and calibrated for wavelengths between 200Å-600Å. Diodes have been calibrated with a double ionization chamber using synchrotron radiation from NBS-SURF as a source. Methods accounting for beam motion, second order radiation in the beam, as well as multiple ionization in the double ionization chamber will be discussed.

**14998.** Hughes, C. E., **The general decision problem for Markov algorithms with axiom,** *Notre Dame J. Formal Logic* **XVI,** No. 2, 208-216 (Apr. 1975).

Key words: combinatorial systems with axiom; degrees of unsolvability; general decision problems; Markov algorithms; many-one reducibility; recursive functions; r.e. many-one degrees; r.e. one-one degrees; semi-Thue systems; splinters.

A constructive proof is presented which shows the existence of a Markov algorithm with axiom whose decision problem is of any prescribed r.e. many-one degree of unsolvability. This result is then shown to be best possible in that it does not hold for r.e. one-one degrees. And, finally, a theorem concerning the degree representation of splinters of recursive functions is proven as a direct corollary to the forementioned results.

**14999.** Bussey, H. E., **Rapport sur la comparaison internationale des mesures de permittivité complexe á 9 GHz,** (Proc. Comité Consultatif, D'Electricité Comité International des Poids et Mesures, Sèvres, France, Oct. 12-13, 1972), Paper in *Comité International Des Poids et Mesures,* pp. 124-137 (Bureau International des Poids et Mesures, Sèvres, France, 1972).

Key words: cavity method for dielectrics; dielectric constant; dielectric loss; international comparison; laboratory intercomparison; permittivity; standard dielectric.

Dielectric constant and loss measurements made by three national laboratories (of the USSR, Canada, and USA) are compared. The two materials measured were glasses. The measurements utilized cavity resonators in the $H_{01n}$ mode. The errors in dielectric constant reported by the laboratories were usually ± 0.3 percent; actual differences between laboratories of the average corrected results were only ± 0.05 percent. The loss tangent results disagreed when multimoding occurred; however, the errors may be as low as ± 0.000 02 or ± 3 percent, whichever is the larger, if multimoding is avoided.

**15000.** Sams, R. L., Maki, A. G., **High-resolution infrared measurements of $\nu_1$ and force-field calculations for thioborine (HBS),** *J. Mol. Struct.* **26,** 107-115 (1975).

Key words: absorption spectra; force constants; HBS; infrared; molecular spectra; spectra; thioborine.

The gas-phase high-resolution spectrum is reported for $\nu_1$ of the linear molecule thioborine (HBS) from 2775 cm$^{-1}$ to 2720 cm$^{-1}$. Band centers and rotational constants are given for the $10^00 - 00^00$ transitions of $H^{11}B^{32}S$, $H^{10}B^{32}S$, $H^{11}B^{34}S$ and $H^{10}B^{34}S$ and for the $11^10 - 01^10$ transitions of $H^{11}B^{32}S$ and $H^{10}B^{32}S$. A valence force field is determined from measured values of $\nu_1$, $D_0$ (the centrifugal distortion) and $q$ (the $l$-doubling constant). The remaining unobserved vibrational fundamentals are calculated from the force constants.

**15001.** Zuckerman, B., Turner, B. E., Johnson, D. R., Clark, F. O., Lovas, F. J., Fourikis, N., Palmer, P., Morris, M., Lilley, A. E., Ball, J. A., Gottlieb, C. A., Litvak, M. M., Penfield, H., **Detection of interstellar trans-ethyl alcohol,** *Astrophys. J.* **196,** L99-L102 (Mar. 15, 1975).

Key words: ethyl alcohol; interstellar chemistry; molecular cloud; molecular spectroscopy; radio astronomy; Sagittarius B2.

Three transitions of *trans*-ethyl alcohol ($CH_3CH_2OH$) were detected in emission toward the Sagittarius B2 molecular cloud The $6_{06} - 5_{15}$ transition at 85,265.46 MHz, the $4_{14} - 3_0$ transition a 104,808.58 MHz were observed at $V_{lsr} \sim 60$ km s$^{-1}$. The abundance of ethyl alcohol in the Sgr B2 cloud is comparable t that of many molecules previously detected there. Careful comparison of the abundance of ethyl alcohol with chemically relate molecules such as its isomer dimethyl ether, acetaldehyde, an methyl alcohol may provide important information abou mechanisms for molecular formation in the interstellar medium

**15002.** Leasure, W. A., Jr., Corley, D. M., **Truck noise-1B: Spectral and directional characteristics of noise generated by truc tires,** *Report No. DOT-TST-75-71,* 180 pages (Available from the National Technical Information Service, Springfield, Va 22161, Sept. 1974).

Key words: acoustics; noise measurement; noise pollution noise (sound); sound transmission; tire noise; transportatio noise; truck; urban planning.

This report is the third in a series of reports published as result of Department of Transportation sponsored truck tir noise research conducted by the National Bureau of Standard The previous reports (OST-ONA-71-9 and OST/TST-72-1 contained details of the test design, test procedures, and an inventory of maximum A-weighted sound level data for typical ri crossbar, and retread type truck tires. A test sample of nine trea designs, estimated to represent 70-80 percent (based on discussions with fleet owners) of the truck tire population on the roa today, was investigated considering noise levels as a function the following variables: wear, loading, speed, pavement surfac and tire location. Test vehicles included both single-chassis veh cles and tractor trailers. The existing data base is expanded i this report to include one-third octave band spectral dat directionality data in the form of equal A-weighted sound lev contours and other refined analysis of the data. Such data ca serve as the groundwork for understanding the generatio mechanisms by which tires produce noise—the first step i developing the necessary data to design quiet tires scientificall

**15003.** Jacox, M. E., **Matrix isolation study of the vibrational spectrum and structure of $HC_2$,** *Chem. Phys.* **7,** 424-432 (1975).

Key words: acetylene; discharge; ethynyl ($HC_2$); infrared spectrum; interstellar molecule; matrix isolation; structure vacuum ultraviolet photolysis.

Detailed isotopic studies of the infrared absorptions characteristic of the products of the decomposition of $C_2H_2$ in a mil discharge through argon trapped at 14 K indicate that $HC_2$ is a important product and that an absorption at 3612 cm$^{-1}$ can be assigned to the carbon-hydrogen stretching fundamental of th species. The data suffice for determination of the stretching an stretching-interaction force constants of $HC_2$, which, in tur have permitted estimates of the bond lengths. The carbon-hydrogen bond is found to be exceptionally strong, and the ca bon-carbon bond is intermediate between that characteristic ground-state $C_2$ and that of $C_2H_2$. The estimated rotational spacing is in excellent agreement with that found for $HC_2$ in rece observations of the interstellar medium.

**15004.** Johnson, D. R., Clark, F. O., **Observations of circul polarization of the $J = 2 - 1$, $v = 1$ transition of the SiO mas** *Astrophys. J.* **197,** L69-L72 (Apr. 15, 1975).

Key words: circular polarization; maser; orion; pumpi processes; radio astronomy; silicon monoxide.

Circular polarization has been observed in the $J = 2 - 1$, $v =$ SiO emission from the Orion A molecular source (OMC 1). Th t polarization was observed at two different times separated by ree days.

**005.** Crandall, D. H., Phaneuf, R. A., Dunn, G. H., **Electron impact excitation of $Hg^+$,** *Phys. Rev. A* **11,** No. 4, 1223-1232 (Apr. 1975).

> Key words: crossed beams; cross section; electron impact; excitation; $Hg^+$.

Crossed beams of electrons and $Hg^+$ ions have been employed measure absolute cross sections for 165.0-nm emission, cor- .ponding to the transition $Hg^+(6p\ ^2P_{3/2}{}^0) \rightarrow Hg^+(6s\ ^2S_{1/2})$. The ission cross section, which is nearly identical to the excitation ss section for $Hg^+(6p\ ^2P_{3/2}{}^0)$ near threshold, has a value of out $1.2 \times 10^{-16}$ cm$^2$ at the 7.51-eV threshold, rises to a max- um of $2.26 \times 10^{-16}$ cm$^2$ at 13 eV, and falls to $0.64 \times 10^{-16}$ cm$^2$ 274 eV. The cross section exhibits considerable structure in energy region from threshold to the onset of the first cascade $^2S_{1/2}$) at 11.9 eV; this structure is likely due to interference m autoionizing states of neutral Hg. The total uncertainty at 'good" confidence level is about 18 percent, taken as the adrature sum of random uncertainty (5% at 90% confidence el) with systematic uncertainties (17% at a level equivalent to % confidence level). At threshold, the Gaunt-factor formula Seaton predicts a value of about 3 times that measured, but the converge to within about 15 percent for electron energies ging from 13 to 274 eV. The results are also in reasonable eement with a semiclassical Gryzinski-type calculation for rgies above several times threshold. The data give an emis- n cross section of $(2.8 \pm 0.5) \times 10^{-16}$ cm$^2$ at 6.8 eV for 194.2 $(6p\ ^2P_{1/2}{}^0 \rightarrow 6s\ ^2S_{1/2})$. Analysis of data taken with some tastable $6s^2\ ^2D$ ions in the target beam indicates that the mean ss section for excitation of the $6s\ ^2P_{3/2}{}^0$ level from the $6s^2\ ^2D$ tastable states is larger than that for excitation from the $6s$ $_2$ ground state. Additional measurements of 398.4-nm emis- n $(6p\ ^2P_{3/2}{}^0 \rightarrow 6s^2\ ^2D_{5/2})$ yield a cross section of about $6 \times 10^{-19}$ near threshold, and a branching ratio $(^2P_{3/2} \rightarrow {}^2S_{1/2})/(^2P_{3/2} \rightarrow$ $_{/2})$ of 350/1.

**06.** Newman, M., **Formulas and multiplicative relationships or the parameters of subgroups of the modular group,** *Math. nn.* **212,** 173-182 (1974).

> Key words: classical modular group; congruence groups; elliptic class numbers; genus; index; level; parabolic class number.

xplicit formulas in terms of coset decompositions are derived the parabolic class number and elliptic class numbers of any group of finite index of the classical modular group Γ. It is wn that these are multiplicative arithmetic functions of the l for congruence subgroups of Γ.

**07.** Ekberg, J. O., **Term analysis of Fe VI,** *Phys. Scr.* **11,** No. , 23-30 (1975).

> Key words: iron; spectra; ultraviolet; wavelengths.

he spectrum of Fe VI has been observed by using a vacuum ing-spark discharge and the 10.7-m grazing-incidence spec- raph and the 10.7-m normal-incidence spectrograph at the ional Bureau of Standards, Washington, D.C. More than 400 s have been classified in the region 250-1 580 Å. All terms of configurations $3d^3$, $3d^24s$ and $3d^24p$, except $3d^2(^1S)4s\ ^2S$ have n established. The estimated uncertainty of the level values 0.4 cm$^{-1}$. The $3d^3$, $3d^24s$ and $3d^24p$ level structure has been retically interpreted. The energy parameters determined n a least-squares fit of the observed level values are com- d with Hartree-Fock calculations. From the complete set of levels all forbidden lines of Fe VI from 1 387 to 10 000 Å been predicted. All but two lines in the spectrum of the star RR Telescopii previously identified as forbidden Fe VI lines have been confirmed and 6 of the otherwise unexplained lines have been identified as [Fe VI].

**15008.** Artru, M. C., Kaufman, V., **Extension of the analysis of triply ionized aluminum (Al IV),** *J. Opt. Soc. Amer.* **65,** No. 5, 594-599 (May 1975).

> Key words: aluminum; spectra; wavelengths.

A total of 225 new lines of Al IV have been observed in the wavelength range 400-4700 Å, leading to the determination of all of the levels of the $2p^54p$, $4d$, $4f$, $5s$, $5f$, and $5g$ configurations. Results of parametric calculations for the configurations are presented. An ionization energy of 967 804 ± 15 cm$^{-1}$ has been derived.

**15009.** Roszman, L. J., **Effects of time ordering on plasma-broadened hydrogen profiles,** *Phys. Rev. Lett.* **34,** No. 13, 785-788 (Mar. 31, 1975).

> Key words: Balmer lines; four dimensional rotation group; hydrogen; plasma; plasma broadening; pressure broadening; scattering matrix; spectral line broadening; Stark broadening; symmetry group; time ordering.

The plasma-broadened $H_\alpha$ and $H_\beta$ spectral-line profiles of hydrogen were calculated retaining the time ordering in the $S$ matrices of the width-shift operator by diagonalizing with the O(4) group. Significant changes occur: The $H_\alpha$ peak is decreased 15 percent, the half-width is increased 25 percent, and the $H_\beta$ relative dip is decreased 23 percent without significant alteration of the maximum intensity of half-width. Agreement with experiment is improved appreciably.

**15010.** Collin, G. J., Ausloos, P., **Réactions des ions moléculaires cyclohexane en phase gazeuse,** *Can. J. Chem.* **53,** No. 5, 680-687 (1975).

> Key words: cyclohexane; cyclopropanes; ion-molecule reactions; olefins; photoionization.

The $cy$-$C_6H_{12}{}^+$ ions formed in the photoionization of cyclohexane (resonance lines of argon: 11.6-11.8 eV) react with cyclic ($C_3$ and $C_4$) and unsaturated hydrocarbons by $H_2$ transfer. This reaction is quantitative with propene, 1-butene, 1-pentene, 1,3-butadiene, and isobutene. This transfer is efficient only if there is a terminal double bond. There is ring opening with the $C_3$ and $C_4$ hydrocarbons. H atom transfer reactions are also observed between $cy$-$C_6H_{12}{}^+$ ions and several compounds and the structure of the radical formed in such a reaction is determined by chemical analysis. With *cis*-2-butene, there is only charge transfer reaction.

**15011.** Bennett, L. H., Cuthill, J. R., McAlister, A. J., Erickson, N. E., Watson, R. E., **Electronic and catalytic properties of tungsten carbide,** *Science* **187,** 858-859 (Mar. 7, 1975).

> Key words: catalysis; electronic structure; platinum; soft x-ray appearance potential; tungsten; tungsten carbide; x-ray photoemission.

The purpose of this comment is to note that two sets of experimental data, namely x-ray photoemission and soft x-ray appearance potential, are only apparently inconsistent in their measurement of the electron distribution in tungsten carbide.

**15012.** Epstein, M. S., Rains, T. C., Menis, O., **Determination of cadmium and zinc in standard reference materials by atomic fluorescence spectrometry with automatic scatter correction,** *Can. J. Spectrosc.* **20,** No. 1, 22-26 (Jan.-Feb. 1975).

> Key words: accuracy; atomic fluorescence; automatic scatter correction; cadmium; chemical interferences; data evaluation; precision; production of atomic vapor; zinc.

The scattering of exciting radiation by matrix components is a major physical interference for trace analysis in atomic fluorescence spectrometry (AFS), which must be eliminated before practical "real sample" analysis can be performed. Using an instrumental arrangement for automatic scatter correction, trace cadmium and zinc are analyzed in Standard Reference Materials, Coal, Bovine Liver, Orchard Leaves, and Fly Ash, without prior separation or preconcentration. The effects of scatter and chemical interferences are evaluated for premixed argon (entrained air) – hydrogen and air – acetylene flames. Precision and accuracy of the results of AFS analysis are compared with data from analysis by atomic absorption.

**15013.** Barton, J. A., Jr., Brauer, G. M., Antonucci, J. M., Raney, M. J., **Reinforced polycarboxylate cements,** *J. Dent. Res.* **54,** No. 2, 310-323 (1975).

Key words: base, dental; cement, dental; cement, polycarboxylate; cement, reinforced; fiber reinforcement; poly(acrylic-itaconic acid); polycarboxylate; potassium titanate.

Mechanical properties of polycarboxylate cements are greatly improved by incorporation of high modulus fibers such as potassium titanate into acrylic-itaconic acid and acrylic-itaconic-aconitic acid copolymers. Other desirable properties of the cements are not changed by the addition of fibers.

**15014.** Jennings, D. A., Petersen, F. R., Evenson, K. M., **Extension of absolute frequency measurements to 148 THz: Frequencies of the 2.0- and 3.5-$\mu$m Xe laser,** *Appl. Phys. Lett.* **26,** No. 9, 510-511 (May 1, 1975).

Key words: absolute frequency measurements; laser frequency synthesis; xenon laser.

Absolute infrared frequency measurement has been extended to 148 THz (the highest frequency ever directly measured) with measurement of the two strong cw laser lines of Xe. The frequencies were synthesized with stabilized $CO_2$ and 3.39-$\mu$m He-Ne lasers and mixed on a W-Ni point-contact diode. The measured frequencies are $\nu_{Xe(2.0\ \mu m)} = 147.915\ 850(15)$ THz and $\nu_{Xe(3.5\ \mu m)} = 85.459\ 997(3)$ THz.

**15015.** Fong, J. T., **Construction of a strain-energy function for an isotropic elastic material,** *Trans. Soc. Rheol.* **19,** Issue 1, 99-113 (1975).

Key words: compressibility; elasticity; finite deformation; hyperelasticity; rubbery materials; strain-energy function; volume-extension.

Experimental data on the volume changes accompanying simple tension of peroxide vulcanizates of natural gum rubber, as first reported by Penn in *Trans. Soc. Rheol.* **14,** 509 (1970), are further interpreted within the framework of the theory of a hyperelastic material. Motivated by the formal connection between a hyperelastic material and a nonlinear viscoelastic fluid *(Trans. Soc. Rheol.* **9,** 27 (1965)), and a mathematical result on the decomposition of the scalar potential of that fluid (*Z. Angew. Math. Phys.* **23,** 780 (1972)), the interpretation of Penn's data leads to an explicit construction of a strain-energy function for rubbery materials:

$$W(I_1, I_2, I_3) = C_1(I_1 - 3) + C_2(I_2 - 3) + \bar{H}(I_1, I_2)(I_3 - 1) + \frac{1}{8K}(I_3 - 1)^2.$$

**15016.** Swartzendruber, L. J., Evans, B. J., **Electronic structure and $^{121}$Sb hyperfine fields in the Heusler alloys $Ni_{1-x}Cu_xMnSb$,** *J. Phys.* **35,** No. 12, C6-265/C6-268 (Dec. 1974).

Key words: alloys; Cu; hyperfine fields; magnetism; Mn Mössbauer effect; Ni; Sb; Pd.

At 4.2 K the magnetic hyperfine field, $H_n$, at Sb in the C1 structure alloys $Ni_{1-x}Cu_xMnSb$, $0 < x < 1$, increases from 29 kG at $x = 0$ to 504 kG at $x = 0.6$. For $x < 0.7$, $H_n$ decrease rapidly and is characterized by a broad Gaussian distributio For example, at $x = 0.8$ the average $H_n$ is 327 kG and the widt of the distribution, $\sigma_{Hn}$, is 130 kG. Using the recent model c Blandin and Campbell based on the RKKY interaction, the increase of $H_n$ with $x$ for $x < 0.7$ can be shown to arise primaril from the increase in electron concentration. A similar explanation might also apply to the 600 kG $H_n$ at Sb in $Pd_2MnSb$ if it i assumed that Pd contributes 0.25 electron to the conductio band. The large hyperfine fields at Sb in the above alloy system appear to be consistent with the predictions of extant theoretic models.

**15017.** Eisenhart, C., **A supplementary list of publications of S. Wilks,** *Amer. Statist.* **29,** No. 1, 25-27 (Feb. 1975).

Key words: bibliographic citations; publications; Samu Stanley Wilks; S. S. Wilks.

Full bibliographic citations for thirty-one "other writings" Samuel Stanley Wilks not included in "The Publications of S. Wilks," in February 1965 issue of the *Annals of Mathematic Statistics* (Vol. 36, No. 1, pp. 24-27), together with the observation that his writings and those of his younger brother, Syr Singleton Wilks, are lumped together under "S. S. Wilks" in th volumes of the *Science Citation Index*.

**15018.** Biedenharn, L. C., Trivedi, M., Danos, M., **Giant mu tipole resonances and the three-fluid hydrodynamical model nuclei,** *Phys. Rev. C* **11,** No. 4, 1482-1484 (Apr. 1975).

Key words: collective model; giant resonances; isospin pu ty; nuclear charged density; nuclear models; nuclear stru ture.

The recently observed resonance at ~ 11 MeV in $^{208}$Pb is i terpreted as the miniature quadrupole resonance (associat with the giant quadrupole resonance at 22 MeV) implied by t three-fluid hydrodynamical model. A difficulty arises with t miniature dipole resonance; this may signify that the sim hydrodynamic model has reached the limits of its validity. A n merical error in a previous publication is corrected.

**15019.** Misra, D. N., Bowen, R. L., Wallace, B. M., **Adhesi bonding of various materials to hard tooth tissues. VIII. Nic and copper ions on hydroxyapatite; role of ion exchange and su face nucleation,** *J. Colloid Interface Sci.* **51,** No. 1, 36-43 (A 1975).

Key words: adsorption; hydroxyapatite; ion exchan nucleation; reaction rate; surface.

The interaction of synthetic hydroxyapatite with nickelo [Ni(II)] or cupric [Cu(II)] ions from aqueous nitrate solutio was investigated. Nickelous ions exchange with the calcium io of the adsorbent and follow the Langmuir adsorption isother the saturation amounts of the adsorbate for two apatite samp have approximately the same ratio as their surface areas. W Cu(II), the initial uptake seems to be independent of concent tion and almost equal to the saturation amount of nickelous i for the same apatite sample. Subsequently, the apatite disso in concert with the growth of some form of copper phosphate a separate phase on the apatite surface if an excess of cupric i is present. This reaction follows a zero order rate law for dil solutions. A phenomenological theory is developed which plains the various kinetic facets.

**15020.** Grundl, J. A., Gilliam, D. M., Dudey, N. D., Popek, R.

**Measurement of absolute fission rates,** *Nucl. Technol.* **25,** 237-257 (Feb. 1975).

Key words: cross sections; fission; neptunium-237; neutron reactions; pile neutrons; plutonium-239; uranium-234; uranium-235; uranium-238.

The capability to measure absolute fission rates per nucleus at emote laboratory site [the Coupled Fast Reactivity Measure- ent Facility (CFRMF) at Aerojet Nuclear Company] has been tablished to a precision level of better than ± 1 percent and was stained at that level for a period of two years. Double fission nization chambers and solid-state track recorders were used in eries of irradiations designed to calibrate fission activation de- tors used for reactor fuels and materials dosimetry. The array reference and working fissionable deposits involved in the asurements included five isotopes: $^{239}$Pu, $^{235}$U, $^{238}$U, $^{237}$Np, d $^{234}$U. Isotopic masses for the fissionable deposits were deter- ned from interrelated components of mass assay: (a) relative d absolute alpha counting, (b) fission comparison counting in rmal-neutron beams, (c) mass spectrometry, and (d) antitative deposition employing solutions of known fissionable ment concentration. Absolute accuracies for the fission rates nucleus measured in CFRMF are in the range of ± 1.5 to ± percent and are dominated by uncertainties in the fissionable posit masses. Fission cross-section ratios for the CFRMF tral spectrum are (1.000 : 1.145 ± 0.017 : 0.0485 ± 0.0007 : 54 ± 0.008) for ($^{235}$U:$^{239}$Pu:$^{238}$U:$^{237}$Np), respectively.

21. Hust, J. G., **Low-temperature thermal conductivity of two ibre-epoxy composites,** *Cryogenics* **15,** No. 3, 126-128 (Mar. 975).

Key words: aramid fiber; composites; cryogenic; epoxy; glass fiber; thermal conductivity.

Thermal conductivity data are presented for two fibre-epoxy nposites. The fibre in one composite is glass and an aramid- ss polymer in the other. Measurements were conducted on a ss-epoxy specimen in the direction perpendicular to the fibres emperatures from 14 to 100 K. The aramid-epoxy specimen s measured parallel to the fibres at 5, 76, 196, and 276 K. ta are presented both in graphical and tabular form.

22. Weber, L. A., **Thermodynamic and related properties of arahydrogen from the triple point to 300 K at pressures to 1000 ar,** *NASA Spec. Publ. 3088,* 100 pages (National Aeronau- cs and Space Administration, Washington, D.C., Mar. 1975). Available from the National Technical Information Service, pringfield, Va. 22161).

Key words: density; enthalpy; entropy; hydrogen; properties of fluids; specific heat; velocity of sound.

BS compressibility measurements and thermodynamic pro- ties data for parahydrogen have been extended to higher tem- atures and pressures. Results of an experimental program are sented in the form of new PVT data in the temperature range 300 K at pressures up to 800 bar. Also given are tables of modynamic properties on isobars to 1000 bar including den- , internal energy, enthalpy, entropy, specific heats at constant ume and constant pressure, velocity of sound, and the surface vatives $(\partial P/\partial T)_\rho$ and $(\partial P/\partial \rho)_T$. The accuracy of the data is ussed and comparisons are made with previous data.

23. Roberts, J. R., Voigt, P. A., Czernichowski, A., **xperimentally determined absolute oscillator strengths of Ti I, i II, and Ti III,** *Astrophys. J.* **197,** 791-798 (May 1, 1975).

Key words: arc; experimental; oscillator strengths; Ti I; Ti II; Ti III.

bsolute oscillator strengths of Ti I, Ti II, and Ti III transitions in the wavelength region from 2440 Å to 3500 Å have been experimentally determined using a wall-stabilized arc. Titanium in the form of heated $TiCl_4$ was admixed with argon plus 5 percent $H_2$ and introduced into the arc, which was operated at a current of 40-60 amperes. Axis temperatures and electron densities ranged from 11,000 K to 12,500 K and $3.5\times10^{16}$ cm$^{-3}$ to $8.7\times10^{16}$ cm$^{-3}$, respectively.

**15024.** Orloski, M. J., **The numbers game in stacks and drains,** (Proc. Sixty-Eighth Annual Meeting of the American Society of Sanitary Engineering, New Orleans, La., Oct. 13-16, 1974), Paper in *ASSE Yearbook* **52,** 122-136 (ASSE, Cleveland, Ohio, 1975).

Key words: National Bureau of Standards; performance of plumbing systems; plumbing code; principles of hydraulics.

This paper discusses some of the historical aspects of plumbing research and plumbing code committee work (Part I). Fundamentals of hydraulics are reviewed as they relate to the intent of plumbing codes (Part II), and current NBS programs on the evaluation of plumbing systems in the laboratory and in the field are discussed (Part III). Considerations involved in implementing the performance approach are covered briefly.

**15025.** Mohan, K., Schaefer, A. R., Zalewski, E. F., **Measurement of geometrically total spectral radiant power,** *Appl. Opt.* **14,** No. 4, 1035-1038 (Apr. 1975).

Key words: geometrically total spectral radiant power; gonioradiometer.

In this paper, the measurement of geometrically total spectral radiant power, i.e., the spectral radiant power emanating in all directions from a light source, is discussed. A gonioradiometer employing a silicon photodiode and a set of narrow band interference filters was used for these measurements. The experiment is described, some exploratory measurements are presented, and the uncertainties which this method introduces are estimated.

**15026.** Madden, R. P., Ederer, D. L., **SURF-II, a new synchrotron ultraviolet radiation facility at the NBS,** (Extended Abstract), *Proc. IV Int. Conf. on VUV Radiation Physics, Hamburg, Germany, July 17-26, 1974,* No. 10.3, 774-776 (1974).

Key words: electron accelerator; new facility; radiation; storage ring; synchrotron radiation; vacuum ultraviolet.

At NBS the accelerator providing synchrotron radiation in the vacuum ultraviolet is being converted from a synchrotron to a storage ring which we anticipate will accelerate a 50 mA electron beam to a maximum energy of 240 MeV. These changes will extend the useful spectral range of the continuum vacuum ultraviolet radiation down to wavelengths somewhat below 40 Å. Increased intensity, greater spacial and temporal stability are other advantages that this conversion will provide. Even at wavelengths greater than 200 Å the intensity is expected to increase by a factor of at least 100 to a value of $4\times10^{11}$ photons per sec per milliradian of orbit for an instrument resolution of $\Delta\lambda/\lambda = 0.001$. It should be of general interest that SURF-II is being constructed so as to be compatible with a large user group.

**15027.** Freund, S. M., Sweger, D. M., **Vinyl chloride detection using carbon monoxide and carbon dioxide infrared lasers,** *Anal. Chem.* **47,** No. 6, 930-932 (May 1975).

Key words: detector; laser; pollution; vinyl chloride.

Stark modulated absorption of CO and $CO_2$ infrared laser radiation by vinyl chloride is the basis for sensitive and selective detection of this gas. Using the P(13) line of the 20-19 band of the CO laser (1609 cm$^{-1}$, 6.22 $\mu$m), a 2 ppm $C_2H_3Cl$ in air sample is observed in an extracavity absorption cell with a 5/1 signal-to-noise ratio after 50 seconds of integration. The response of the signal to concentration of $C_2H_3Cl$ is linear over at least 3 orders of magnitude to within experimental uncertainty which is a few percent. Similar results are obtained using a $CO_2$ laser operating on the P(42) line of the 001-100 band (922.9 cm$^{-1}$, 10.84 $\mu$m).

**15028.** Clifton, J., Frohnsdorff, G., **Fiber-reinforced cementitious materials,** Special Review in *Cements Research Progress 1974,* F. Young, Ed., pp. 201-234 (American Ceramic Society, Columbus, Ohio, 1975).

Key words: cement; concrete; fiber-reinforced cements; fiber-reinforced concretes; glass fibers; mechanical properties; organic fibers; review; steel fibers.

This review is concerned with developments, through 1974, in the research and technology, but not applications, of fiber reinforced cementitious materials including hardened cement pastes of gypsum, portland and high alumina cement and their concretes. Essentially, only materials reinforced with short, discontinuous and discrete fibers are covered, because long rods, continuous meshes and woven fabrics are not classified as discrete fibers in this review.

**15029.** Gilsinn, J. F., **Validation of maximum airport throughput levels estimated by the DELCAP simulation model,** *FAA Report No. FAA-RD-75-66,* 72 pages (National Technical Information Service, Springfield, Va. 22151, Jan. 1975).

Key words: airport; airport capacity; airport simulation; models; model validation; runway capacity; simulation.

This report documents exercises of the DELCAP airport terminal area simulation model performed to validate the maximum throughput calculations of that model. DELCAP was run for five different runway configurations, with three or four appropriate operating policies chosen for each, and for three different mixes of aircraft types. Throughput estimates from DELCAP are found to be in general agreement with current values provided by the FAA. One specific instance of greater discrepancy is identified, and a remedy for it is proposed. Changes made in DELCAP since its original documentation in 1971 are described in an appendix.

**15030.** Yakowitz, H., **Future growth of SEM—toward super efficient microscopy,** *Proc. 8th Annual Scanning Electron Microscope Symposium, St. Louis, Mo., Apr. 7-11, 1975,* Part 1, 1-10 (IIT Research Institute, Chicago, Ill., Apr. 1975).

Key words: Auger electron spectrometry; electron probe x-ray microanalysis; energy loss spectrometry; scanning electron microscopy; scanning transmission electron microscopy.

Some predictions concerning future trends in the SEM field have been made. Economic and personnel considerations have been taken into account in arriving at these predictions. Micrographic and analytical requirements and capabilities were also considered. For electron transparent specimens, scanning transmission electron microscopy (STEM) will become a major research method. Auger and energy loss spectrometry will join x-ray emission as analytical methods used for the analysis of such samples. Greater advantages will probably arise from improvements in electron source brightness and from advantages afforded by low energy loss electron detectors. Finally, the SEM field can only profit as the quality and quantity of educational opportunities in the field expand.

**15031.** Hust, J. G., **Low temperature thermal conductivity measurements on longitudinal and transverse sections of a superconducting coil,** *Cryogenics* **15,** No. 1, 8-11 (Jan. 1975).

Key words: composite; cryogenics; superconducting coi thermal conductivity.

Thermal conductivity measurements have been performed longitudinal and transverse sections of a superconducting coil 5, 79, 196, and 276 K. The composite coil sections are compos of copper-stabilized niobium-titanium wire embedded in epox Tabular and graphical data are presented. These data are co pared to values calculated on the bases of components of the c sections. Reasonably good agreement is obtained.

**15032.** Livingston, R. C., Rowe, J. M., Rush, J. J., **Neutr quasielastic scattering study of the ammonium ion reorientatio in a single crystal of $NH_4Br$ at 373 K,** *J. Chem. Phys.* **60,** No. 1 4541-4546 (June 1, 1974).

Key words: ammonium bromide; ammonium ion; neutr scattering; orientational disorder; reorientation; residen time; single crystal.

The ammonium ion reorientations in a single crystal of $NH_4$ in its disordered CsCl phase have been investigated quasielastic neutron scattering at 373 K. Neutron spectra we measured at four different crystal orientations (with the [11 planes of the crystal in the scattering plane) and data we recorded simultaneously at a variety of scattering angles prov ing a range of momentum transfers for elastic scattering, 0.5 Å $\leqslant Q \leqslant 2.5$ Å$^{-1}$. The experimental results were fit to models lowing instantaneous random jumps around the $C_2$ and $C_3$ ax of the $(NH_4)^+$ ions using a variety of analytical procedures t are described in some detail. The results of these fits establi conclusively that the ammonium ion reorientations dominated by 90° jumps around the $C_2$ axes with an average ti $\tau$ between jumps of 3.2 ± 0.4 psec at 373 K. The inelastic part the measured neutron spectra shows a torsional vibration pe at 305 cm$^{-1}$, in good agreement with previous values. The resu and analysis demonstrate the value of single crystal measu ments in neutron studies of dynamic orientational disorder solids.

**15033.** West, E. D., Schmidt, L. B., **Spectral-absorptance m surements for laser calorimetry,** *J. Opt. Soc. Amer.* **65,** No 573-578 (May 1975).

Key words: absorptance; calorimeter; cavity; laser ene measurements; laser power measurements; radiometry.

Methods used at the National Bureau of Standards for de mining the power or energy in laser beams depend on calorim ric comparison of laser power or energy and the calibrating el trical power or energy. For this comparison, it is essential know the fraction of the incident radiant energy that is conver to heat and measured by the calorimeter. This fraction, the eff tive spectral absorptance, is measured by adding an auxili calorimeter, which covers practically all of the opening in main calorimeter. A laser beam enters the main calorim through a small hole in the auxiliary calorimeter. The reflec laser energy and the excess thermal radiation are measured the auxiliary calorimeter. The data analysis is based on theory of calorimetery derived from a linear heat-flow probl Time-dependent functions relating the transient temperat responses of the calorimeters to various constant power in are determined experimentally from known electrical inputs. effective absorptance is found by comparing transient respo for electrical and laser inputs.

**15034.** Jennings, D. A., **Simple, adjustable lens holder,** *Rev. Instrum.* **46,** No. 4, 487-488 (Apr. 1975).

Key words: adjustable; lens holder.

The construction of a simple, adjustable lens holde cribed. This lens holder is unique in that it will firmly hold all lenses without taking up space at the edge of the lens or pping them down.

35. Zimmerman, J. E., Campbell, W. H., **Tests of cryogenic QUID for geomagnetic field measurements,** *Geophysics* **40,** No. 2, 269-284 (Apr. 1975).

Key words: geomagnetism; magnetometer; SQUID; superconducting device.

type of cryogenic SQUID (superconducting quantum inter- ence device) magnetometer was designed for geomagnetic asurements. Field tests of the instrument including comisons to observatory variometers, a rubidium magnetometer, induction loop, and a flux-gate magnetometer showed the new ogenic systems to be reliable, accurate, portable, and simple operate. Directional measurements of natural magnetic field tuations as small as 0.0001 gamma with periods from 0.5 sec everal hours were demonstrated.

36. Rowe, J. M., Rush, J. J., Smith, H. G., Mostoller, M., lotow, H. E., **Lattice dynamics of a single crystal of PdD$_{0.63}$,** *hys. Rev. Lett.* **33,** No. 21, 1297-1300 (Nov. 18, 1974).

Key words: coherent neutron scattering; dispersion relation; lattice dynamics; palladium deuteride; phonon frequency distribution; single crystal.

he frequency-wave-vector dispersion relations of a single stal of PdD$_{0.63}$ have been measured by coherent neutron intic scattering at 78, 150, 220, and 295 K. The acoustic modes considerably lower in frequency than the corresponding des for pure Pd, in accord with the observed lattice expan- . The optic modes, in which D motions predominate, show siderable dispersion. In particular, the shape of the motions dominate, show considerable dispersion. In particular, the pe of the [100] LO branch shows conclusively that second-neighbor D-D interactions are comparable to the first-like-hbor D-D interactions.

37. Yakowitz, H., Newbury, D. E., **Magnetic domain strucres in Fe-3.2Si revealed by scanning electron microscopy—A hoto essay,** *J. Test. Eval.* **3,** No. 1, 75-78 (Jan. 1975).

Key words: iron-silicon alloys; Lorentz force; magnetic domains; photomicrography; scanning electron microscope; strain effects.

he mechanism and experimental arrangement by which magc contrast can be observed from materials of cubic otropy are indicated. Transformer alloy Fe-3.2Si is used as example to illustrate the effects of tensile strain, magnetic l switching, residual stress, and inclusions on magnetic struc-

38. Yakowitz, H., Newbury, D. E., Myklebust, R. L., **pproaches to particulate analysis in the SEM with the aid of a onte Carlo program,** (Proc. 8th Annual Scanning Electron icroscope Symp., St. Louis, Mo., Apr. 7-11, 1975), Paper in *canning Electron Microscopy/1975,* Part 1, 93-102 (ITT esearch Institute, Chicago, Ill., Apr. 1975).

Key words: backscattered electrons; electron specimen interaction; Monte Carlo simulation; particulate analysis; scanning electron microanalysis; x-ray microanalysis; x-ray source size.

onventional quantitative electron microanalysis methods been shown to be satisfactory when semi-infinite, planar imens normal to the electron beam are analyzed. However, e case of particulate analysis, the surface may be irregular, pecimen dimensions may be less than the electron beam interaction volume and the x-ray absorption path will be irregular. Currently the only tractable approach to the analysis of particulates is to use a Monte Carlo simulation of electron and x-ray interactions to predict x-ray intensity as a function of particle geometry. A program to carry out this task was devised and tested in several ways for both electron and x-ray parameters. A detailed document of results of these tests, and results on a variety of specimens including aluminum spheres, nickel cylinders, alloy steel wear particles and others show good agreement between theory and experiment.

Some practical considerations have to be taken into account when such methods are used in real analytical situations, e.g., (1) the cost of preparing a calibration curve by the Monte Carlo method, (2) analytical strategy, e.g., what specimen tilt to use in the SEM, what operating voltage and what is the effect of using either energy dispersive or wavelength dispersive detection systems, and (3) applicability to multicomponent particles. From a discussion of these we conclude that the Monte Carlo method can be employed profitably by laboratories having a need for quantitative information concerning particulate matter.

15039. Ciarlo, D. R., Schultz, P. A., Novotny, D. B., **Automated inspection of IC photomasks,** *Proc. Society of Photo-Optical Instrumentation Engineers, Seminar 8, Technological Advances in Micro and Submicro Photofabrication Imagery, San Diego, Calif., Aug. 1974,* **55,** 84-89 (May 1975).

Key words: automated inspection of photomasks; critical dimension determination; defects; detection of visual defects; integrated circuit photomasks; photomask inspection; photomasks; photoplate quality.

The results of a nationwide review of automated IC photomask inspection methods are presented. Major photomask inspection problems of detection of visual defects and registration errors, and the determination of critical dimensions and photoplate quality are discussed. This review indicates that for high-volume, large-scale integrated circuits, the greatest concern is for the detection of visual defects. Next in order of importance are the detection of registration errors, and then the accurate determination of critical dimensions. Automated inspection systems and technologies currently available for this are discussed including: microdensitometer-digital computer systems, laser beam scanning systems, spatial filtering systems and microscope-television-digital computer systems. Suggested criteria for an ideal photomask inspection system are the simultaneous inspection for 2-$\mu$m visual defects, the determination of registration tolerances to within $\pm 0.5$ $\mu$m and the determination of the accuracy of the critical dimensions to tolerances of $\pm 0.5$ $\mu$m on a single photomask in ten minutes.

15040. Angel, W. T., Bean, V. E., **Tracking, pulsed ultrasonic interferometer,** *Rev. Sci. Instrum.* **46,** No. 5, 533-535 (May 1975).

Key words: interferometer; phase locked loop; tracking; ultrasonic.

A pulsed ultrasonic interferometer was designed and constructed that has the ability to track changes in transit time as the ambient pressure and temperature of the sample are changed. The stability over 17 h approached one part in $10^7$. This instrumentation will be incorporated into an automated high pressure transfer standard calibration system.

15041. Costrell, L., **Standardized instrumentation system for computer automated measurement and control,** *IEEE Trans. Ind. Appl.* **IA-11,** No. 3, 319-323 (May-June 1975).

Key words: CAMAC; computer interfacing; control systems; instrumentation; instrumentation standards; standards.

A standardized instrumentation system for computer automated measurement and control (CAMAC) is gaining wide international acceptance for industrial and laboratory applications. The system features a fully specified dataway together with modular functional units that are completely compatible with each other and that are available from diverse sources. The system is nonproprietary and can be freely used without license or restriction of any kind.

**15042.** Fuggle, J. C., Madey, T. E., Steinkilberg, M., Menzel, D., **X-ray photoelectron spectroscopy (XPS) of adsorbate valence bands,** *Phys. Lett.* **51A,** No. 3, 163-164 (Feb. 24, 1975).

Key words: chemisorption; CO; ESCA; ruthenium; x-ray photoelectron spectroscopy.

The CO valence levels for a monolayer of CO adsorbed on the basal (001) face of ruthenium have been observed by XPS. The assignment of the observed peaks is discussed.

**15043.** Brennan, J. A., Stokes, R. W., Kneebone, C. H., Mann, D. B., **NBS-CGA cryogenic flow measurement program,** (Proc. ISA International Instrumentation-Automation Conf. and Exhibit, New York, N.Y., Oct. 28-31, 1974), Paper in *Advances in Instrumentation* **29,** 612-1/612-13 (Instrument Society of America, Pittsburgh, Pa., 1974).

Key words: angular momentum; cryogenic; flowmeter; liquid nitrogen; measurement; positive displacement; turbine; vortex shedding.

This paper reviews the joint National Bureau of Standards-Compressed Gas Association program in which (1) all the types of flowmeters used in the U.S. for custody transfer of liquid nitrogen were tested, (2) a tentative national code on cryogenic liquid-measuring devices was adopted, (3) use of transfer standards for testing cryogenic flowmeters was started and (4) tests on some temperature and density compensation devices were completed.

Data from the test program are presented in summary form for flowmeters operating on several principles. Highlights of the code requirements and transfer standard test results are described. Densitometer and temperature compensation test data are presented.

**15044.** Mount, G. H., Linsky, J. L., **One- and multi-component models of the upper photosphere based on molecular spectra. IV. Non-LTE treatment of the CN violet system,** *Solar Phys.* **41,** No. 1, 17-33 (Mar. 1975).

Key words: carbon abundance; molecular spectra; non-LTE; solar model; upper photosphere.

Non-LTE synthetic spectra derived from a detailed analysis of the formation of the CN(0,0) λ3883 Å spectrum are compared with center-limb photoelectric spectra taken at Kitt Peak National Observatory. Significant non-LTE effects are found and the Kurucz, Altrock-Cannon, Mount-Linsky II, and HSRA models are compared. We derive a solar carbon abundance of log $A_c = 8.30 \pm 0.10$ for the Mount-Linsky model and log $A_c = 8.40 \pm 0.10$ for the Altrock-Cannon model, compared to the HSRA value of log $A_c = 8.55 \pm 0.10$, assuming a nitrogen abundance of log $A_N = 7.93$. In addition we specify the regions of formation for the CN(0,0) 3883.35 Å bandhead at disc center and limb.

**15045.** Madey, T. E., Engelhardt, H. A., Menzel, D., **Adsorption of oxygen and oxidation of CO on the ruthenium (001) surface,** *Surface Sci.* **48,** 304-328 (1975).

Key words: adsorption; carbon monoxide; cataly
LEED; oxygen; ruthenium.

The adsorption of oxygen on the ruthenium (001) surface
been studied using a combination of techniques: LEED/Au
Kelvin probe contact potential changes, and flash desorp
mass spectrometry. Oxygen is rapidly adsorbed at 300 K, fo
ing an ordered LEED structure having apparent (2 × 2) s
metry. Two binding states of oxygen are inferred from the ab
change in surface work function as a function of oxy
coverage. LEED intensity measurements indicate that the
ygen layer undergoes an order–disorder transition at temp
tures several hundred degrees below the onset of desorpt
The order–disorder transition temperature is a function of
oxygen coverage, consistent with two binding states. A mode
volving the adsorption of atomic oxygen at $\theta < 0.5$ and the
mation of complexes with higher oxygen content at $\theta > 0.$
proposed. The oxidation of CO to form $CO_2$ was found to h
the maximum rate of production at a ruthenium temperatur
950 K.

**15046.** Lawless, W. N., **Dielectric and thermal properties
machinable glass-ceramic at low temperatures,** *Cryogenics*,
No. 5, 273-277 (May 1975).

Key words: cryogenics; dielectric constant; loss tang
machinable glass-ceramic; specific heat; thermal conduc
ty.

Measurements of the dielectric properties (2-300 K), spe
heat (2-20 K), and thermal conductivity (2-22 K) are reporte
a mica-containing glass-ceramic which has a machinability i
range from brass to low-carbon steel. The dielectric constan
creases with increasing temperature and is field independen
field strengths up to at least 70 kV $cm^{-1}$ at low temperatu
Power-supply-limited attempts to measure the dielectric br
down strength at low temperatures are consistent with th
ported strength at room temperature (1.4 MV $cm^{-1}$). The
mal properties are similar to fused $SiO_2$ with two exceptions
thermal conductivity does not show the "knee" at ~ 10 K ty
of amorphous materials, and the specific heat deviates stro
from a $T^3$ law below 3.5 K.

**15047.** Arp, V., **Thermodynamics of single-phase one-dimens
fluid flow,** *Cryogenics* **15,** No. 5, 285-289 (May 1975).

Key words: helium; hydrodynamics; one dimensional f
single phase fluid; thermodynamics; transposed critical

Fluid flow processes in helium within the range 4-10 K an
100 N $cm^{-2}$ pressure are similar to those of ordinary fluids
their critical points. Three thermodynamic parameters, the
neisen parameter, isentropic compressibility, and velocit
sound, which are weakly non-catalytic near the critical poin
used to describe fluid flow processes in fluids in the near cr
range. It is found that if temperature is not used as a varia
a fluid state equation, flow profiles can be easily evaluated
single-phase fluid region, including close to or transectin
transposed critical line.

**15048.** Murphey, W. M., Schleter, J. C., **Practicality of dive
path analysis,** (Proc. 15th Annual Meeting of the Institu
Nuclear Materials Management, Inc., Atlanta, Ga., Jun
21, 1974), *Nucl. Mater. Manage. Journal of the Institu
Nuclear Materials Management* **III,** No. III, 236-268 (1

Key words: analysis; diversion of nuclear materials; d
sion path analysis; internal control system characteriz
nuclear materials safeguards; safeguards.

Maintenance of effective safeguards requires a progra
routine assessment of plant safeguards systems in terms of

abilities to satisfy safeguards aims. Plant internal control
tems provide capabilities for detection of unprevented diver-
n and can provide assurance that diversion has not occurred.
rocedure called Diversion Path Analysis (DPA) enables rou-
assessment of the capabilities of internal control systems to
cate unprevented diversion and identification of safeguards
blem areas in a plant. A framework for safeguards system
ign is also provided which will allow flexibility to accom-
date individual plant circumstances while maintaining ac-
table diversion detection capability. The steps of the
cedure are described and the practicality of the analytical
cedure is shown by referring to a demonstration test for a
n throughput process where plant personnel were major par-
pants. The boundary conditions for the demonstration case
given, along with some conclusions about the general
cedure.

49. Murphey, W. M., Schleter, J. C., Maltese, M. D. K.,
**nternal control vis-a-vis diversion path analysis,** (Proc. 14th
nnual Meeting of the Institute of Nuclear Materials Manage-
nent, Inc., San Diego, Calif., June 20-22, 1973), *Nucl. Mater.*
*lanage. Journal of the Institute of Nuclear Materials*
*lanagement* **II,** No. 3, 232-274 (1973).

Key words: analysis; diversion of nuclear materials; diversion path analysis; internal control system characterization; nuclear materials safeguards; safeguards.

procedure, "diversion path analysis," has been developed
systematic analysis of diversion possibilities in plants using
M. The procedure can be applied to diversion possibilities
ntered by physical protection and materials balance account-
but special emphasis is given to diversion possibilities in high
ughput production areas. A parallel practicality study is
ussed which used plant production data and had a working
rsion indication objective of 500 grams and 24 hour response
a single diversion of attractive material by a single employee
out collusion given that the employee may alter any records
hich he had access. Explanation of the procedure, its relation
lant internal control, relations or internal control data moni-
ng techniques to existing safeguards techniques and imple-
tation implications are presented.

0. Wu, Y. C., **On the control of thermal impact for thermal**
**fety,** (Proc. AIAA 10th Thermophysics Conf., Denver,
olo., May 27-29, 1975), *AIAA Paper No. 75-713*, 1-11
merican Institute of Aeronautics and Astronautics, New
ork, N.Y., May 1975).

Key words: contact burn; heat conduction; human tissue; thermal impact; thermal potential; thermal safety.

he thermal impact exerted by a hot surface to human tissue
e rate of thermal energy delivered from it to the tissue. If the
siological reaction to the thermal impact is beyond the limit
cell's resistance, a burn may result. Therefore, the severity
burn is determined by two processes: physiological and
sical. Once the physiological reaction to the thermal impact
etermined on the basis of the severity of the burn, the thermal
ntial could be controlled to a safe level by means of a physi-
process with the aid of modern technology to provide the
erials needed. It is this process that is of interest in the area
nermal safety. In the present study we wish to minimize the
mal impact of a hot surface on human tissue. An analytical
tion of the linear heat conduction equation as applied to a
e layer model is obtained under a given selected set of initial
boundary conditions. The parameters derived from the solu-
are discussed and subjected to appropriate experiments. The
lts verify the assumed conditions.

15051. Roberts, R. W., Hoffman, J. D., **Reducing energy consumption in R&D labs—The NBS experience,** *Res. Manage.* **XVIII,** No. 1, 26-33 (Mar. 1975).

Key words: building energy use; conservation; energy conservation; electricity saved; fuel consumption.

The National Bureau of Standards has a major facility at Gaithersburg, Md. Over 3,000 people are housed in some 25 buildings, and rather strict temperature and humidity control must be maintained in much of the laboratory space. The climate control system uses a rather complex cool/reheat cycle to maintain proper humidity. Following a thorough analysis of the climate control system, steps were taken that reduced consumption of both electricity and fuel by 20 percent. The procedures by which these savings were realized are detailed.

15052. Schooley, J. F., Soulen, R. J., Jr., **Superconductive fixed points for cryogenic thermometry,** *Instrum. Technol.* **21,** No. 11, 35-39 (Nov. 1974).

Key words: superconductive transition temperatures; superconductivity; temperature; thermometric fixed points.

Research at NBS has shown that some elements exhibit very sharp and reproducible superconductive transitions. This research led to the development of a device, now offered through the Office of Standard Reference Materials, which permits ± 0.001 K reproducibility at the superconductive transitions of Pb ($T^c \sim 7.2$ K), In ($T^c \sim 3.4$ K), Al ($T^c \sim 1.2$ K), Zn ($T^c \sim 0.85$ K), and Cd ($T^c \sim 0.5$ K). To extend the usefulness of the device, NBS has been examining the width and reproducibility of the superconductive transitions of $Nb^3Sn$ ($T^c \sim 18$ K), Ir ($T^c \sim 0.1$ K), Be ($T^c \sim 0.023$ K), and W ($T^c \sim 0.015$ K) with the view of establishing these materials as additional fixed points. This article describes these superconductive fixed points.

15053. Laughlin, D. E., Cahn, J. W., **Spinodal decomposition in age hardening copper-titanium alloys,** *Acta Met.* **23,** 329-339 (Mar. 1975).

Key words: age hardening; copper-titanium; *Dla*; metastable solvus; microstructural sequence method; nucleation; ordering; precipitation; spinodal decomposition.

The early stages of spinodal decomposition in age hardening Cu-Ti alloys have been studied by electron microscopy. The alloys (1.55, 3.08 and 5.17 w/o Ti) decomposed on the quench from solutionizing temperatures into Ti enriched and Ti lean regions. Superlattice reflections, at $1/5\{420\}^m$ positions as well as $1/2\{210\}^m$ reflections were observed in the diffraction patterns of the as quenched 5.17 w/o Ti alloy. The alloys continued to decompose when aged at elevated temperatures. A sequence of microstructures was used to show that continuous phase separation, and hence spinodal decomposition, was the mechanism of decomposition. The metastable two phase structure which formed from the spinodal process was aligned and periodic from the start of the process. The Ti enriched phase was ordered, with the $D1a(Ni^4Mo;14/m)$ structure. Reversion experiments were performed to determine the position of the coherent metastable solvus. When aging treatments were performed near this solvus, heterogeneous nucleation of the metastable phase was observed.

15054. Ederer, D. L., Manalis, M., **Photoabsorption of the 4*d* electrons in xenon,** *J. Opt. Soc. Amer.* **65,** No. 6, 634-637 (June 1975).

Key words: atomic structure; inner shell; $N^{IV,V}$; resonance cross section profiles; spectroscopy; vacuum ultraviolet; xenon; 4d absorption.

In xenon, the cross section has been measured over the energy range 64-70 eV (194-177 Å) for two series of resonances that converge to the $4d^95s^25p^6(^2D_{5/2,3/2})$ limits. By a parametrization technique the cross-section amplitude and widths of these resonances have been obtained. The oscillator strength, averaged over the interval between resonances, and the widths of resonances in each series are essentially constant. The oscillator strength in these $4d^95s^25p^6(^2D_{5/2,3/2})np$ series is small (0.06) compared to the total continuum oscillator strength integrated over open $p$ and $f$ channels. The ratio of the cross section at the $4d^95s^25p^6(^2D_{5/2})$ limit to the cross section at the $4d^95s^25p^6(^2D_{3/2})$ limit had a value of 1.4(4), consistent with the ratio of the statistical weights of the $N_{IV,V}$ levels.

**15055.** Julienne, P. S., Krauss, M., **Predissociation of the Schumann-Runge bands of $O_2$,** *J. Mol. Spectrosc.* **56,** 270-308 (1975).

Key words: ab initio calculation; level shifts; line broadening; molecular oxygen; predissociation; spin-orbit matrix elements.

The predissociation line broadening in the Schumann-Runge bands of $O_2$ is interpreted through an ab initio calculation of the pertinent repulsive potential energy curves and spin-orbit matrix elements. The ab initio results provide an overall qualitative picture of the predissociation which is further refined through a detailed comparison of calculated level shifts and widths with experimental data. The position of the dominant repulsive curve is also deduced by a deperturbation of the level shift in the second vibrational difference. The predissociation is dominated by the $^5\Pi_u$ state crossing the $B\ ^3\Sigma_u^-$ state around 1.875 Å with a spin-orbit matrix element of 65 $\text{cm}^{-1}$. The $^1\Pi_u$ and $^3\Pi_u$ states have small spin-orbit matrix elements and play only minor roles in the predissociation. The calculated and experimental widths are in good agreement for low and high vibrational levels. The apparent experimental widths between $v=5$ and 11 are shown to be inconsistent with the theoretical analysis, the difference probably being due to line blending.

**15056.** Spencer, L. V., **Structure shielding against initial radiations from nuclear explosions. I. Attenuation of air secondary and fission product gamma rays,** *Nucl. Sci. Eng.* **57,** 129-154 (1975).

Key words: effects of nuclear weapons; fission product gamma rays; gamma ray penetration; initial nuclear radiations; neutron penetration; radiation shielding.

Calculations and resulting data are described which are intended for use in estimating the protection afforded by buildings against nuclear radiations emitted from a nuclear burst in the first half minute or so. The basic source configuration is that for which one assumes equal likelihood of the explosion occurring on a ring of elevation 30 deg above the horizontal, relative to a structure location on the ring axis. Source spectra and angular distributions corresponding to large distance ($\geq 1$ mile) from burst point to structure are used. As sources we discuss here only gamma rays from fission products and from neutron interactions with air molecules.

**15057.** Hosler, W. R., Frederikse, H. P. R., **Doped ceria for MHD-materials,** (Proc. Sixth Int. Conf. on Magnetohydrodynamic Electrical Power Generation, Washington, D.C., June 9-13, 1975), Paper in *MHD Sixth International Conference on Magnetohydrodynamic Electrical Power Generation* **II,** Conf-750601-P2, 67-76 (The Energy Research and Development Administration-Fossil Energy, Washington, D.C., 1975).

Key words: conductivity; doped ceria; high temperature; MHD electrodes; mixed ceria.

A number of ceria compositions and ceria-based mixtu show promise as electrode material in MHD generators. T paper discusses the electrical conductivity and some of t chemical stability aspects of cerium oxide, cerium-zirconium ide, Ta doped $CeO_2$ and Ta doped $CeO_2$-$ZrO_2$.

**15058.** Klose, J. Z., **Mean life of the 27 887-$\text{cm}^{-1}$ level in U I,** *Ph Rev. A* **11,** No. 6, 1840-1844 (June 1975).

Key words: delayed coincidence; $f$ value; imprisonme lifetime; mean life; resonance radiation; transition probab ty; U I; uranium.

Measurements of the mean life of the 27 887-$\text{cm}^{-1}$ level in I have been made at a single vapor density using electronic citation and a method of delayed coincidence. The lifeti values were obtained by optically detecting the decay of 3584.9-Å resonance transition. Using branching ratios obtai from known relative $f$ values, the average of the measu lifetimes was corrected for imprisonment of the resonance ra tion, and absolute $f$ values were derived from the correc lifetime giving the following results: $\tau_0=7.3\pm1.1$ nsec, $f_{35}$ $0.18\pm0.03$, and $f_{4620}=0.20\pm0.03$. The error given with e quantity is the standard deviation as determined from the dis sion of the individual measurements. A systematic error of 1 cent due to possible nonlinearities in the time scale of the sys is also assigned to the results. Unaccounted for systematic err affect only the correction in the measured lifetime, which is sr compared to the statistical error. The lifetime and $f$ values presented in comparison with the experimental results of ano group of workers.

**15059.** Hebner, R. E., Jr., Booker, S. R., **A portable Kerr sys for the measurement of high voltage pulses,** *Proc. 1975 IE Southeastcon, Charlotte, N.C., Apr. 6-9, 1975,* **1,** 3A-1-1/ 5-1 (Institute of Electrical and Electronics Engineers, I New York, N.Y., 1975).

Key words: calibration; electrical measurement; electro tics; high voltage measurement; impulse measurement; k effect; laser systems.

A portable system for the measurement of high voltage pu based on the electro-optic Kerr effect has been constructed tested. This system is designed to measure microsecond rise pulses having a duration of less than one hundred microsec and peak values from one thousand volts to more than one dred thousand volts.

**15060.** Schooley, J. F., **National measurement system temp ture—A micro study,** *Nat. Conf. Stand. Lab.—Newslette* No. 1, 26-33 (Apr. 1975).

Key words: measurement accuracy; national tempera measurement system; temperature scale; thermom calibration; thermometer production; thermometry.

The National Temperature Measurement System is br described. The nature of the international temperature scale the standard thermometers are noted, along with the accu levels which are possible with the letter. The "commerce thermometry—the producers of sensors, calibrations, and surements as well as the major users—is outlined, with partic emphasis upon the manner in which the National Bureau of dards interacts with and contributes to the rest of the system.

**15061.** Kucirek, J., Melmed, A. J., **Influence of an initial tamination) film on the determination of film properties by sometry,** *J. Opt. Soc. Amer.* **65,** No. 5, 611-612 (May 1975

Key words: ellipsometry; optics; thin films.

Computer calculations were done to evaluate the error ellipsometric determination of film thickness and refractiv x, due to the unknown presence of a contamination film. The thods employed are described, and typical results are given.

62. Schooley, J. F., Soulen, R. J., Jr., **Superconductive fixed oints for thermometry in cryogenics,** *Instrument Society of merica International Instrumentation-Automation Con- erence and Exhibit, New York, N.Y., Oct. 28-31, 1974,* Paper 4-620, pp. 1-5 (1974).

Key words: fixed points; SRM 767; superconductivity; transition temperatures.

Research at the National Bureau of Standards has shown that eral elements exhibit very sharp and reproducible supercon- ctive transitions. This research led to the development of a vice, now offered to the cryogenics industry through the Of- e of Standard Reference Materials, which permits the attain- nt of ±0.001 K reproducibility at the superconductive transi- ns of Pb ($T_c \sim 7.2$ K), In ($T_c \sim 3.4$ K), Al ($T_c \sim 1.2$ K, Zn ($T_c$ .85 K), and Cd ($T_c \sim 0.5$ K). The device is easily mounted a cryogenic facility and the superconductive transitions are dily observed using a simple a.c. bridge circuit recently veloped. Care must be taken, however, to exclude ambient gnetic fields or to correct the transitions for the field present he laboratory. In order to extend the usefulness of the device, have been examining the width and reproducibility of the su- rconductive transitions of $Nb_3Sn$ ($T_c \sim 18$ K), Ir ($T_c \sim 0.1$ K), ($T_c \sim 0.023$ K), and W ($T_c \sim 0.015$ K) with the view of ablishing these materials as additional fixed points.

63. Laughlin, D. E., **On the imaging of composition modula- ions,** *J. Appl. Crystallogr.* **7,** Part 6, 635 (Dec. 1974).

Key words: composition modulations; contrast mechanism; electron diffraction; electron microscopy; lattice images; modulation images; satellites; spinodal decomposition.

A new interference contrast mechanism in transmission elec- n microscopy is presented and compared with the well known ice imaging technique. This mechanism is termed "modula- n imaging" as it may be used to study the periodic composition dulations which occur in crystalline alloys which undergo nodal decomposition.

64. Wiese, W. L., Kelleher, D. E., Helbig, V., **Variations in almer-line Stark profiles with atom-ion reduced mass,** *Phys. Rev. A* **11,** No. 6, 1854-1864 (June 1975).

Key words: Balmer; hydrogen; ion dynamics; plasma; Stark broadening.

Calculations of the Stark broadening of hydrogen lines treat radiating atoms and the perturbing ions as quasistatic. The sent experiment represents an attempt to determine whether possible breakdown of this approximation near the center of line can account, at least partially, for the existing discrepan- s between theoretical and experimental profiles in the core of Balmer lines. The central regions of $H_\alpha$, $H_\beta$, $H_\gamma$, and $H_\delta$ files have been measured in a wall-stabilized arc over a range atom-ion relative velocities by varying the atom-ion reduced ss. The cores of all four lines exhibit a significant dependence the reduced mass. With increasing reduced mass, the experi- ntal profiles gradually show more structure, but still less than theories predict. Extrapolation of the results for $H_\alpha$ and $H_\beta$ nfinite reduced mass, i.e., to the static case, gives results that ee quite well with recent calculations.

65. Armstrong, G. T., Domalski, E. S., **Energy from wastes,** *Report of the Conference on Thermodynamics and National Energy Problems, Warrenton, Va., June 10-12, 1974,* pp. 386-400 (National Academy of Sciences, National Research Council, Washington, D.C., 1974).

Key words: fuel from waste; incinerators; organic waste conversion; thermodynamic data for incinerators; waste utilization.

Today I am your garbageman. I hope you will consider this is an honorable estate. The problem posed by accumulating wastes of all kinds can be enormous; failure to solve it effectively can be fatal to any human community. How fortunate we would be not just to prevent it from overwhelming us, but to find a simultaneous solution to another equally grave problem. There are signs that this can be done, at least in part.

**15066.** Voigt, P. A., **Measurement of U I and U II relative oscillator strengths,** *Phys. Rev. A* **11,** No. 6, 1845-1853 (June 1975).

Key words: flow-stabilized arc; oscillator strength; U I; U II; wall-stabilized arc.

Relative *gf* values for 49 prominent U II lines and 21 of the strongest U I lines have been measured. The U II measurements were made using a wall-stabilized arc into which the uranium was introduced in the form of $UF_6$. The U I values were measured with a flow-stabilized arc which is essentially a free-burning arc stabilized by streaming argon around one of the electrodes which is formed from a molten ball of uranium held in a tungsten cup. Temperatures in the wall-stabilized and flow-stabilized arc were 10 500 K and 5500 K, respectively. The U I relative *gf* values were placed on an absolute scale employing a recent lifetime determination for the 27 887-$cm^{-1}$ level of U I. This absolute scale was extended to the U II values by measuring the relative intensity of a U I and a U II line in the wall-stabilized arc.

**15067.** Hougen, J. T., Radford, H. E., Evenson, K. M., Howard, C. J., **Analysis of the laser magnetic resonance spectrum of $HO_2$,** *J. Mol. Spectrosc.* **56,** 210-228 (1975).

Key words: asymmetric rotor levels; $HO_2$; laser magnetic resonance; rotational constants; spectral assignments; spin splitting; Zeeman spectrum.

An analysis of the previously detected laser magnetic resonance spectrum of $HO_2$ is carried out by (i) assigning $M_J$ quantum numbers to each observed Zeeman line, (ii) determining the quantum numbers $(N'_{K_a'K_c'} - N''_{K_a''K_c''})$ and energies of the zero-field asymmetric rotor transitions involved, and (iii) determining the values of the zero-field spin-rotation doublet splittings in the upper and lower states of each asymmetric rotor transition. The rotational transitions obtained lie in the region 50-150 $cm^{-1}$, with quantum numbers $4 \leq N \leq 19$ and $1 \leq K_a \leq 4$. They are fit to an asymmetric rotor program to obtain the three rotational constants $A$, $B$, $C$ and the three symmetric-top centrifugal distortion constants $D_K$, $D_{NK}$, $D_N$. The spin splittings are fit to an approximate theoretical expression involving two adjustable linear combinations of components of the spin-rotation interaction tensor $\epsilon$. Because of the lack of spectra from other isotopic species, a unique molecular geometry cannot be derived.

**15068.** Reader, J., Epstein, G. L., **Resonance lines of Cs II, Ba III, and La IV,** *J. Opt. Soc. Amer.* **65,** No. 6, 638-641 (June 1975).

Key words: barium; cerium; cesium; ionization energy; lanthanum; wavelengths.

The resonance line spectra of ions in the Xe I isoelectronic sequence, consisting of the 5 transitions to the $5p^6\ {}^1S_0$ ground state from levels with $J = 1$ in the $5p^55d$ and $6s$ configurations, have been observed for Cs II, Ba III, and La IV. The observations were made with a sliding spark on the 10.7-m normal-incidence vacuum spectrograph at NBS. The resonance transitions from the $5p^56d$ and $7s$ configurations were also observed for these ions, except for that from $5p^56d\,^3P_1$ of Ba III. Several resonance transitions from higher *nd* and *ns* levels were also observed. Estimated values for the $J=1$ levels of the $5p^57s$ configuration of Ce V were obtained by extrapolation. The derived ionization energies in eV are Cs II 23.17(4), Ba III 35.79(6), La IV 45.95(6), Ce V 65.55(25).

**15069.** Harrison, G. A., **The high-rise fire problem,** *CRC Critical Rev. Environ. Control* **4,** No. 4, 483-505 (Oct. 1974).

Key words: flame spread and smoke development; high-rise; human behavior; life safety; plastics.

This study focuses on life safety aspects of high-rise buildings located within the United States. A high-rise building is defined as one which exceeds 24.4 meters (80 feet) and is of a Light or Ordinary hazard occupancy classification as specified by the National Fire Codes, "Standard for Installation of Sprinkler Systems," Volume 6, No. 13, 1974. The purpose of this study is to identify and analyze the high-rise fire problems to formulate research recommendations to the Programmatic Center for Fire Research at the National Bureau of Standards.

A comprehensive review of the pertinent literature indicates that only a limited number of high-rise fire problems exist. These include increasing fuel loads and fire spread potential, smoke development and movement, life safety and occupant evacuation, and fire department operations. These specific problem areas relate to building evacuation and the vertical movement of smoke and toxic gases through a building.

A major finding of this study is that fire fatalities occurring within high-rise buildings have been few in number, historically. However, with changing construction techniques and materials, this fire experience record is subject to change. The future high-rise fire problem must be managed through the use of progressive engineering design which will keep pace with innovative high-rise building technology and interior design concepts.

**15070.** Ottinger, C., Scheps, R., York, G. W., Gallagher, A., **Broadening of the Rb resonance lines by the noble gases,** *Phys. Rev. A* **11,** No. 6, 1815-1828 (June 1975).

Key words: line broadening; rubidium.

Normalized emission spectra of the optically excited Rb resonance lines (7800 Å, 7948 Å) have been measured in the presence of He, Ne, Ar, Kr, and Xe for about 50 Å on either side of the lines. The perturber gas pressures were in the range 100-1100 torr and the temperature was 318 K. The spectra, normalized to the total emission, are shown to be due to binary collisions. Shifts and widths of the Lorentzian cores of the lines were obtained, at pressures sufficiently low for impact theory to apply. The widths are corrected for the Rb hfs and the instrument function. Various power-law fits to the near-wing intensities are presented and compared to theoretical expectations. The red satellites reported by other authors are found to be, in the low-pressure limit, mere shoulders on the line wing for Ar and Kr, while Xe barely produces an actual peak. The measured linewidths and shifts are compared to previous measurements.

**15071.** Cotton, I. W., **Standards for network graphics communications,** *Comput. & Graphics* **1,** 45-47 (1975).

Key words: computer graphics; computer networks; graphics; networks; protocol; standards.

Common protocols provide a means for the interchange of information between dissimilar systems in a computer network. This paper discusses the background and philosophy of the common graphics protocol currently under development for the ARPANET and outlines the details of its design. Other applications for such a protocol are suggested.

**15072.** Cotton, I. W., **Methodologies for the cost-benefit analys of computer graphics systems,** *Comput. & Graphics* **1,** 33-4 (1975).

Key words: computer graphics; cost-benefit analysis; cos effectiveness; economics; performance evaluation.

This paper assesses the state of the art in cost-benefit analyse of computer graphics systems and suggests an approach f developing improved methodology. Cost-benefit analyses a distinguished from analyses of system performance in that t latter is directed at optimizing system performance at a give level of investment, while the former is directed at justifying t investment itself.

Computer graphic system design alternatives are first outline Then methods of analyzing the performance and costs of co puter systems in general and graphic systems in particular a discussed. With this information it is shown how cost-effectiv ness analyses may be performed. The next crucial step is to co duct benefit analysis, an ill-defined art. The results of benef analysis must be combined with cost-effectiveness analysis order to perform the desired cost-benefit analysis.

An experimental methodology is suggested for better perforn ing benefit analyses of computer graphics systems. A mo rigorous formulation of the cost-benefit procedure is then ou lined. No attempt is made in this report to actually perform su an analysis.

**15073.** Meshkov, S., **Current and constituent quarks,** *Proc. XV Int. Conf. on High Energy Physics, London, England, Ju 1974,* pp. II-101 – II-112 (1974).

Key words: algebra of currents and quarks; constitue quarks; current quarks; hadronic structure; melosh transfo mation; meson spectroscopy.

In this review a summary of our attempt to establish and u derstand the connection between hadron spectroscopy and t algebra of currents is discussed. In addition, our prese knowledge of meson structure and decays is reviewed.

**15074.** Hurst, W. S., **Note on the measurement of the response oceanographic temperature sensors,** *J. Geophys. Res.* **80,** N 18, 2663-2666 (June 20, 1975).

Key words: oceanographic temperature measurement temperature measurement; temperature sensors; the mometry; time constant; time response.

The response times of three different types of oceanograph platinum resistance temperature sensors were measured emplo ing the conventional rotating water container procedure. At l sensor immersion velocities (< 100 cm/s) the response w strongly dependent upon the details of the sensor inserti velocity for one sensor design. With carefully defined measu ment procedures, reproducible values for the "time consta were obtained, but their application in data analysis must treated with caution.

**15075.** Bardsley, J. N., Holstein, T., Junker, B. R., Sinha, **Calculations of ion-atom interactions relating to reson charge-transfer collisions,** *Phys. Rev. A* **11,** No. 6, 1911-19 (June 1975).

Key words: atom; collision; $Cs_2^+$; ion; $Li_2^+$; low ener $Na_2^+$; pseudopotential; $Rb_2^+$; resonant charge transfer.

The interaction between an atom and ion of the same elem leads to gerade and ungerade states of the diatomic molecu ion. The energy splittings between the gerade and ungera states determine the cross section for resonant charge transf Using the JWKB approach these energy splittings are deri from the asymptotic forms of the wave functions for the isola

n and ion. Pseudopotential calculations of the splittings are
orted for $Li_2^+$, $Na_2^+$, $Rb_2^+$, and $Cs_2^+$, and are used together
previous *ab initio* and model-potential calculations to test
JWKB method. The comparison shows that the method is
iciently reliable to facilitate accurate calculations of the cross
ions for resonant charge transfer at low energies.

**6.** Vogler, M., Dunn, G. H., **Dissociative recombination of
ectrons and $D_2^+$ to yield D(2*p*),** *Phys. Rev. A* 11, No. 6, 1983-
987 (June 1975).

Key words: crossed beams; cross section; $D_2^+$; dissociative
recombination; electron scattering; L$\alpha$ radiation.

ross sections have been measured as a function of electron
gy (1.4 to 7.5 eV) for production of $L_\alpha$ photons from the dis-
ative recombination of electrons and $D_2^+$. Ions made in a
-pressure ion source by electron bombardment and formed
a beam are reacted at right angles with a magnetically con-
d electron beam. Recombination was observed by detecting
photons from resultant excited atoms. It was demonstrated
a large fraction of the observed light arises from cascade to
2*p* state from levels of higher principal quantum number. The
sured cross section is thus presented as an upper limit for
nation of D(2*p*) in the dissociative recombination process.
results, represented approximately by the expression $\sigma(2p)$
$.6 \times 10^{-17})E^{-1.25}$ cm$^2$, indicate that recombinations leading to
nation of a D(2*p*) are a small fraction of the total recombina-
measured by Peart and Dolder.

**7.** Cotton, I. W., Meissner, P., **Approaches to controlling per-
nal access to computer terminals,** *Proc. 1975 Symp. on Com-
uter Networks: Trends and Applications, Gaithersburg, Md.,
ine 18, 1975,* pp. 32-39 (IEEE Computer Society, Long
each, Calif., 1975).

Key words: access; access control; authentication; com-
puter networks; computer security; computer terminals;
personal identification.

ne advent of time-sharing and computer networking has
lted in a proliferation of computer users, many of whom are
ted remotely from the computer which serves them. This has
accompanied by increased opportunities for unauthorized
s to gain access to computers and has focused attention on
problem of identifying and authenticating properly
orized users. The requirements of the recently-enacted
acy Act of 1974 calls for a number of safeguards in the han-
of personal information by the Federal agencies, and per-
l identification of personnel authorized to have access to
information is an important aspect of the implementation of
law. This paper considers the various approaches to per-
l identification and authentication, on the basis of things
wn to an individual, things possessed by an individual, and
acteristics of an individual, such as appearance, handwriting,
e, fingerprints, and hand geometry.

set of evaluation criteria is presented as a guide in selecting
onal identification systems for various applications. It is
ted out that currently-available systems are vulnerable in
ing degrees to erroneous recognition and circumvention, and
efore should be incorporated into a hierarchical security
em which utilizes a variety of safeguards, including auditing
ares to provide a record of what is accessed, by whom, and
vhat purposes.

**8.** Garfinkel, S. B., Schima, F. J., **Ionization chamber half-life
easurement of the 99-minute $^{113}$In isomer,** *Int. J. Appl. Radiat.
otop.* **26,** 314-315 (May 1975).

Key words: half-life measurement; isomeric decay; isotope
$^{113}In^m$; radioactivity; rate of charge measurement; $4\pi\gamma$
pressure ionization chamber.

A precise determination of the $^{113}In^m$ half-life has been made by means of a nominal $4\pi\gamma$ pressure ionization chamber. The value obtained was 99.21 min with an uncertainty of 0.13 min which is the linear sum of the component of random error at the 99 percent confidence level and the estimated systematic errors.

**15079.** Cooper, J. W., **Photoionization of inner-shell electrons,** Chapter 3 in *Atomic Inner-Shell Processes, Vol. 1, Ionization and Transition Probabilities,* pp. 159-199 (Academic Press, Inc., San Francisco, Calif., 1975).

Key words: atomic; inner shell; photoionization; quantum-mechanical.

This chapter of "Inner Shell Processes" (to be published by Academic Press) provides a survey of theoretical methods used in treating inner shell photoeffect. The subject is approached from a quantum-mechanical viewpoint and various approaches are related within this context.

**15080.** Baker, D. W., Sayre, C. L., Jr., **Decay of swirling turbulent flow of incompressible fluids in long pipes,** (Proc. 1st Symp. on Flow, Pittsburgh, Pa., May 10-14, 1971), Chapter in *Flow, Its Measurement and Control in Science and Industry. Part I. Flow Characteristics,* H. W. Stoll, Ed., **1,** 301-312 (Instrument Society of America, Pittsburgh, Pa., 1974).

Key words: decay of swirling flow; helical flow; pressure differential during swirling flow; swirling flow.

The decay of swirling flow fields in steady-state flow in cylindrical, unobstructed, smooth pipes is considered from measurements made in two pipes. With water flowing in one pipe, mean point velocities and static pressures including wall pressures were measured at several stations along the pipe. With liquid hydrocarbons flowing in the other pipe, measurements were made of wall pressure and the swirling motion of the fluid, as sensed by a vaned rotor. The investigation included the pipe Reynolds number (Re) range 12,500 to 200,000 and for the vortex flows generated, the product K/MD varied from 0 to 0.9, where K is the angular momentum flux, M is the axial momentum flux, and D is the pipe i.d. Results including those of other sources show that K decreases exponentially along the pipe at a decay rate $\beta$ ranging from about 2 percent per pipe diameter at Re = 200,000 to 4 percent per pipe diameter at Re = 12,500; and that data scatter and values of $\beta$ for other sources demonstrate dependence of $\beta$ on the inlet geometry, and possibly on K and system turbulence characteristics. Other results show the ratio of the pressure gradient along the wall during swirling flow to nonswirling flow varies primarily with the angular momentum flux. The behavior of swirling flow fields is not well known, and these facts can aid in an improved description of swirling fields in which the performance of flow measurement and control devices might be evaluated.

**15081.** Ambrose, J. R., Kruger, J., **Breakdown of passive films on iron by chloride ion,** *Proc. 4th Int. Congress on Metallic Corrosion, Houston, Tex., Sept. 1969,* pp. 698-704 (National Association of Corrosion Engineers, Houston, Tex., 1972).

Key words: breakdown passivity; chloride; ellipsometry; iron; passivity; pitting.

The breakdown of passive films on iron in pH 8.4 sodium tetraborate/boric acid solution by the action of chloride ions has been studied using a combination of ellipsometric and electrochemical techniques. Two induction times associated with the breakdown process were observed. At $t_1$, anodic current increases due to increased ionic conduction through the film, followed at $t_2$ by a localized growth of thick oxide film. These induction times are influenced by chloride ion concentration, time of passive film growth, and temperature of film growth.

Growth kinetics of the passive film in the presence of chloride ion is indistinguishable from that in its absence below a potential $E_a^2$, that potential above which ferrous ion is not found in solution. Above this potential, breakdown occurs and film growth in the presence of chloride ion results in no limiting thickness.

The results indicate that adsorption and complete penetration by chloride ion to the metal surface is necessary to initiate pitting. When complete penetration occurs, subsequent precipitation of porous $\gamma$-FeOOH allows easy local dissolution leading to pitting. After breakdown, a lowering of potential to values below $E_a^2$ causes an apparent repassivation of the film as indicated by the fact that raising the potential above $E_a^2$ results in another incubation period before breakdown.

**15082.** Bartel, T. W., Schade, P. A., **Digital processing of decay rates for reverberant sound fields,** *Proc. 1974 Int. Conf. on Noise Control Engineering, Washington, D.C., Sept. 30-Oct. 2, 1974,* pp. 61-64 (Oct. 1974).

Key words: digital processing of decay rates; digital sampling; graphics display terminal; interactive program; least-squares analysis; real-time analyzer; reverberation room; spectrum shaping.

The installation of a 64K byte minicomputer to the NBS Sound Laboratory has made the capabilities of digital processing available for application to the various types of reverberation-room measurements. The present work applies this technique to reverberant field decay rate measurements. Such measurements conducted with analog equipment are limited by the amount of time and labor required to make and process the large number of decay curves necessary to achieve precise results. Reduction of these limitations is realized by interfacing the computer to digital sampling equipment capable of processing thirty 1/3-octave bands simultaneously. Through control of the reverberation room sound source and signal-processing equipment, the computer can conduct decay measurements and apply a least-squares analysis to the stored data to compute the decay rates. The software is to be expanded into an interactive program allowing the experimenter to observe the data on a display device and insert his own decisions into the data reduction process.

**15083.** Alberi, J. L., Wilson, R., Schröder, I. G., **Parity violation in neutron-capture gamma-rays,** *Phys. Rev. Lett.* **29,** No. 8, 518-521 (Aug. 21, 1972).

Key words: internucleon-force; parity-violation.

We have measured the circular polarization of $\gamma$ rays from thermal neutron capture in $^{113}$Cd and find a $P_\gamma = (6.0 \pm 1.5) \times 10^{-4}$ for the combined 8.51- and 9.04-MeV transitions. This value was measured using a transmission Compton polarimeter and pulse-counting technique. The value confirms the existence of parity-nonconserving terms in the internucleon force.

**15084.** Donnay, J. D. H., Ondik, H. M., **Crystal data determinative tables, Vol. 1. Organic compounds,** 999 pages (1972); **Vol. 2. Inorganic compounds,** 2106 pages (1972).

Key words: cleavage; compilation; crystal; crystal habit; crystal space group; crystal structure types; density; determination; identification; minerals; optical properties; twinning; unit cell dimensions.

This edition, which will comprise two volumes, is a thoroughly revised and updated work, containing over 24,000 entries. Some 7,500 carbon-containing crystalline compounds are given in Volume I. They are listed, within each crystal system, according to increasing values of a determinative number: *a*/*b* ratio in trimetric systems, *c*/*a* ratio in dimetric systems, cubic cell edge *a* in the isometric system. Conventional rules insure the uniqueness of crystal setting.

For each crystalline species the following properties are listed on the first line: axial ratio(s) and interaxial angles not fixed by symmetry, cell dimensions, space group or diffraction aspect, number of formula units per cell, crystal structure (whether determined), measured density, x-ray calculated density. Then come: name of the compound, synonym(s), chemical formula, literature reference, transformation matrix (when the original data had to be recast to conventional cell and setting). Additional information includes some or all of the following: crystal-structure type (if any), goniometric axial ratio(s), crystal habit, cleavages, twinning, color, optical properties, indices of refraction, optical orientation (except in the anorthic system), melting point, transition point.

Nearly all the data were obtained from original sources. "Limits of error" on numerical values are quoted from the reference. The data have been tested for self-consistency by means of computer programs. Any erratum found either in the reference or in an abstracting journal (e.g., *Structure Reports*) is specifically mentioned: erroneous values are thus identified. Editorial critical remarks point out possible errors in the literature.

Formula and name indexes enable one to learn if crystallographic information is available on any given compound, thereby providing a starting point for bibliographic searches.

**15085.** Piermarini, G. J., Block, S., Barnett, J. D., Forman, R. A., **Calibration of the pressure dependence of the $R_1$ ruby fluorescence line to 195 kbar,** *J. Appl. Phys.* **46,** No. 6, 2774-2780 (June 1975).

Key words: calibration; diamond cell; fluorescence; high pressure; hydrostatic pressures; ruby.

The pressure dependence of the $R_1$ ruby fluorescence line has been calibrated at 25 °C against the compression of NaCl. Pressures are determined using the Decker equation of state for NaCl. The dependence is linear to 195 kbar following the equation $P_{NaCl} = 2.746(\Delta\lambda)$, where $P$ is in kbar and $\Delta\lambda$ in Å. The uncertainty in the value of the slope, $dp/d\lambda$, expressed in terms of a 95 percent confidence interval is $2.746 \pm 0.014$ kbar Å$^{-1}$. The coefficient of the quadratic term $(\Delta\lambda)^2$ is not significantly different from zero; and the quadratic term makes indeed a negligible contribution to the fit. Taking into account the reported uncertainty associated with the Decker equation of state for NaCl, the value of the slope is $2.740 \pm 0.016$ kbar Å$^{-1}$ within a 95 percent confidence interval.

**15086.** Malitson, I. H., Lechner, J. A., **Refractive index variance in auto headlamp glass,** *Crime Lab. Dig.* **75,** No. 5, 8-11 (July 1975).

Key words: auto headlamp glass; population; refractive index; RI variance; statistics; temperature coefficient.

The work described in this paper was designed to evaluate th refractive index (RI) variance within and between auto headlam glass currently manufactured in the U.S.A. The purpose is to provide the criminalist with a reliable statistical data base fo decision making when confronted with this type of evidence. A precision refractometer was used to measure point-to-point R variations within the lens components of new and used lamps. A least 13 pieces of glass from each of 46 lenses were evaluated The spread of RI for all glasses was found to be 1.475 – 1.47 From these data it was ascertained that the headlamp glass population consists of three groups: newer and older glass made b Company A and all glass made by Company B. The newer glas significantly differs by $3 \times 10^{-3}$ in RI from the other two group whose distribution of RI values overlap. This difference is man times larger than the standard deviation within each group an within a single lens. The change in RI with temperature wa determined.

87. Baker, D. W., Koenig, A. L., **An automated prototype test ystem for aircraft engine fuel controls, design and operating ex- erience,** *Proc. 13th Annual Tech. Symp., Washington, D.C., hapter ACM, June 20, 1974*, pp. B.4.1-B.4.11 (Association or Computing Machinery, New York, N.Y., 1974).

Key words: automated test equipment; automated tests for jet engine fuel controls; computer interfacing; digital computer controlled tests; jet engine fuel control testing; minicomputer applications; minicomputer controlled tests; supervisory control; test equipment reliability.

he adjustment and calibration of the fuel control, the acces- y which meters flow to the engine burners, requires long-term ich tests involving many often repeated manual operations. nicomputer-based hardware and software systems, developed ing 1968-1971, which control an existing production test nd are reviewed. The systems automating this stand, used in rework of TF-30 engine controls, simulate engine parameters ner pressure and drive shaft speed using supervisory control. o, metered fuel flow is measured and read out. An auxiliary el at the test stand containing readout and input devices ena- s the operator to run the test. This prototype system has ved as basis for two test systems, under contract and slated production, which will automate nine stands.

88. Freeman, D. H., Angeles, R. M., **The influence of ydrogen bonding upon gel permeation chromatography,** *J. hromotogr. Sci.* **12,** 730-735 (Nov. 1974).

Key words: adsorption; gel permeation chromatography; hydrogen bonding; liquid chromatography.

hloroform, methanol and benzoic acid are hydrogen bonding npounds that are simultaneously adsorbed and self-associated ing liquid chromatography from carbon tetrachloride with ystyrene/divinylbenzene (Styragel). An equation is derived to at the measured distribution coefficient dependence upon ute concentration. In dilute solution, chloroform and thanol exhibit the effect of adsorption without appreciable -association. At higher concentrations methanol and benzoic d show markedly less adsorption. This is the expected result arger associated species are formed and then excluded steri- y. The agreement between theory and experiment is better if assumes that only the monomeric species is adsorbed. Ex- iments of this type are easily performed and they provide a pful insight into the chromatographic mechanism.

89. Waclawski, B. J., Vorburger, T. V., Stein, R. J., **Angular ependence of uv photoelectron distributions for oxygen ad- orbed on W(100),** *J. Vac. Sci. Technol.* **12,** No. 1, 301-304 Jan.-Feb. 1975).

Key words: angular distributions; bond geometry; chemisorption; energy distributions; oxygen on (100) tungsten; surface bonds; uv photoemission.

ecent theoretical work has suggested the possibility of deter- ing chemisorption bond geometry by the use of uv toemission. This possibility is being investigated experimen- y in an apparatus developed at NBS. The apparatus is cribed, and preliminary results are presented which show rgy distributions as a function of emission angle for electrons toemitted from W(100), both clean and with adsorbed ox- n. The results obtained at $h\nu = 21.2$ eV for several emission les indicate substantial angular dependence of the photoelec- n distributions, not only for the clean (100) surface, but also, re dramatically, with an oxygen adlayer.

90. Penn, D. R., **Determination of the spin-polarized surface ensity of states in strongly correlated metals by field emission: heory,** *Phys. Rev. B* **11,** No. 8, 3208-3209 (Apr. 15, 1975).

Key words: ferromagnetic transition metals; field emission; spin polarization; strongly correlated metals; surface density of states; theory.

It is shown that the combination of spin-polarization and field-emission energy distribution measurements on ferromagnetic transition metals will provide direct information about the one-dimensional surface density of states in a direction normal to the metal surface for a given spin.

15091. Vorburger, T. V., Penn, D., Plummer, E. W., **Field emission work functions,** *Surface Sci.* **48,** 417-431 (1975).

Key words: electron energy distribution; field emission; tungsten; work function.

Field emission has proven to be a very useful technique for obtaining work function changes from single crystal planes or from the whole emitter. The inability to independently measure the electric field has limited the accuracy of field emission total current measurements for determining absolute work functions. Young and Clark's method of combining field emission energy distribution measurements and total current versus voltage measurements to eliminate the electric field as an unknown is not adequate because it does not take into account the effects of the surface density of states present in the energy distribution. In this paper we discuss a technique to overcome this problem, which involves a series of measurements taken as a function of electric field and an extrapolation to zero field. The method yields reliable values of the work function for the low index (flat) (100) and (112) planes of tungsten but not for the high index (rough) (013) and (111) faces.

15092. Bennett, A. J., Penn, D., **Optical properties of adsorbate atoms,** *Phys. Rev. B* **11,** No. 10, 3644-3657 (May 15, 1975).

Key words: adsorbate atom; dielectric function; electronic states; optical adsorption.

We calculate the dielectric response of adsorbate atoms on a metal surface assuming an Anderson model of the system. The dielectric function is then used to predict the change in the surface optical reflectance caused by the adsorbates. General results are obtained for substrates with one and two electron bands with and without the assumption of momentum conservation in the band-to-band optical transitions. A detailed analysis is carried out for the single-band momentum-conserving case. Here, the model is the same as that studied by Caroli and Kjollerstrom if the substrate density of states and various matrix elements are taken to be constants. However, we find an additional nonnegligible contribution omitted in their analysis. In other single-band cases, we show the wide variety of behavior which may be obtained for different parameter ranges and provide expressions to be used in data analyses.

15093. Abrams, M. D., **A new approach to performance evaluation of computer networks,** *Proc. 1974 Symp. on Computer Networks: Trends and Applications, Gaithersburg, Md., May 23, 1974*, pp. 15-20 (Institute of Electrical and Electronic Engineers, Inc., New York, N.Y., 1974).

Key words: computer; evaluation; measurement; performance; service; utility.

Interactive conversational computing requires more appropriate measures of performance than those presently applied toward improving the efficiency of system operation. A "stimulus-acknowledgement-response" model has been conceptualized to describe the man-computer interaction. A data acquisition system called the Network Measurement Machine has been developed meeting the objective of being able to measure the delivery of computer services to any user. A set of analysis programs providing statistical summaries of workload, response, and communications utilization analysis over subsets of a conversation, such as use of specific software services, are potentially useful to systems designers and implementers. A sample application is presented with preliminary results.

**15094.** Armstrong, G. T., Domalski, E. S., Minor, J. I., Jr., **Standard combustion data for the fuel gas industry,** *Proc. American Gas Association Section Conf., Atlanta, Ga., May 8-10, 1972,* pp. D-74 – D-87 (1972).

Key words: enthalpy of combustion, dry basis; enthalpy of combustion, saturated basis; enthalpy of formation, hydrocarbons, heating value; hydrocarbons; International System of Units.

Equity in the sale of natural gas or other gases for fuel purposes requires that the total calorific values be accurately known and that the same values be used throughout the industry for gases of identical properties. This paper gives the total calorific values (gross heats of combustion at constant pressure) of gaseous $H_2$, $H_2S$, CO, $CH_4$ and 49 selected other gaseous hydrocarbons, $C_1$ to $C_6$, in the ideal gas state at standard conditions of 60 °F and 30 in. Hg (288.71 K and 101591.3 N · m$^{-2}$), on a molar basis, on a dry volumetric basis and on a water-saturated volumetric basis. Units used are kJ · mol$^{-1}$, MJ · m$^{-3}$, Btu$_G$ · (scf)$^{-1}$.

A supplementary table is given for the total calorific values of the same substances in the ideal gas state at the slightly different standard conditions of 60 °F and 14.73 psia (288.71 K and 101559.8 N · m$^{-2}$) on a dry volumetric basis and on a water-saturated volumetric basis. Units used in this table are MJ · m$^{-3}$ and Btu$_{IT}$ · (scf)$^{-1}$. Total calorific values for real-gas methane are also given on the above bases. Enthalpies of combustion and molar heat capacities of crystalline carbon (graphite), and all the above named gases are given in the thermodynamic standard states at 298.15 K. Procedures for making the calculations, and necessary auxiliary data are given. Implications of the possible change of the measurement system to metric untis are discussed.

**15095.** Plummer, E. W., Gadzuk, J. W., Penn, D. R., **Vacuum-tunneling spectroscopy,** *Phys. Today* **28,** No. 4, 63-71 (Apr. 1975).

Key words: field emission; field ionization; ion neutralization; surface spectroscopy; tunneling.

The extension into the vacuum of the exponential tail of the wave function makes possible remarkably sensitive techniques based on field emission, ion neutralization and field ionization.

**15096.** Bloss, R. L., **Evaluation testing of resistance strain gages,** *Proc. Tech. Session on Strain Gaging for Accuracy Conf., Milwaukee, Wis., Oct. 19, 1971,* pp. 1-5 (Society for Experimental Stress Analysis, Westport, Conn., 1975).

Key words: bonded resistance strain gage; combined effects; evaluation tests; fatigue; high temperature; performance characteristics.

Since it is usually impossible to determine the performance characteristics of the specific resistance strain gages that will actually be used in a test program, we must depend upon their behavior being predictable from tests that have been conducted on other gages. When resistance strain gages first became available, information about their performance was limited. The situation was further complicated during World War II when a number of organizations began producing gages, usually for their own use. A similar situation arose when the need for strain measurements at elevated temperatures induced a number of organizations to produce gages for such use. User and third party evaluation testing was instrumental in the development and characterization of the gages during these times. Today most manufacturers carry out continuing testing and evaluation programs to insure that the user can rely upon their products and to maintain and enhance their competitive positions in the field. However, the user must continue to carry out such tests when special requirements or test conditions are encountered.

A brief history of evaluation testing of bonded resistance strain gages is given, and two evaluation tests are described.

**15097.** Danos, M., Weller, H. R., **Correlation between the $(d, \gamma_0)$ and $(p, \gamma_0)$ cross sections in the giant dipole resonance of $^{16}$O,** *Phys. Rev. C* **10,** No. 6, 2627-2628 (Dec. 1974).

Key words: giant resonance; intermediate structure; nuclear structure; particle-hole model; quasi-bound states; two-particle two-hole states.

The reaction theory of Fano is applied to the analysis of the $^{15}N(p, \gamma_0)^{16}O$ data *vis à vis* the $^{14}N(d, \gamma_0)^{16}O$ data. The result is consistent with the Gillet model which attributes the structure near 22.9 MeV in $^{16}$O to a 2p-2h quasibound state.

**15098.** Saylor, C. P., **Microscopical determination of refractive index with an error of about ±0.00001,** *Anal. Chem.* **47,** No. 7 1114-1120 (June 1975).

Key words: identification of compounds by refractive index micro determination of refractive index; microscope for accurate determination of refractive index; multiple prisms.

Steep optical-glass prisms in contact with the liquid being measured bend a collimated monochromatic beam. The deflected beam enters the microscope, and an image of the target forms a the back focal plane of the objective. The distance of the image from the center is proportional to the sine of the angle of deviation and rigorously related to determinable constants of the system and the refractive index of the liquid. Accuracy increase with steepness of prism, but the refractive index range served by any one is thereby reciprocally decreased. Sine of the angle of deflection, angle of the particular prism being used, and th refractive index of the prism are sufficient for direct calculation of the refractive index of the liquid. When the angle of the prism is 72°, an accuracy of $10^{-5}$ is achieved. Each prism (with a numerical aperture of 0.11) can then serve a range of only 0.06 in index. This necessitates a series of prisms of selected optical properties, each serving 0.05 in index and providing a comfortable overlap. About 1 cubic millimeter of liquid is required for a ful determination.

**15099.** Gump, B. H., Hertz, H. S., May, W. E., Chesler, S. N Dyszel, S. M., Enagonio, D. P., **Drop sampler for obtaining fresh and sea water samples for organic compound analysis** *Anal. Chem.* **47,** No. 7, 1223-1224 (June 1975).

Key words: baseline studies; fresh water sampling; samplin device; sea water sampling; trace organic analysis; wate pollution.

Analytical chemists have become more involved in project concerning water pollution, environmental impact statement and hydrocarbon baseline studies. A device for obtainin replicate and representative samples of the aquatic environmen under consideration is needed. A water sampler has bee designed to meet this need.

**15100.** Unassigned.

**15101.** Ball, J. J., Keller, R. A., **Quantitative determination o gaseous nitrogen dioxide concentrations over long path length by selective absorption of argon ion laser emission,** *J. Air Pollu Contr. Ass.* **25,** No. 6, 631-633 (June 1975).

Key words: absorption spectroscopy; air pollution; lase $NO_2$.

An argon ion laser emits several laser lines in the visible region the optical spectrum. The absorption coefficients of $NO_2$ at ese laser emissions were measured in a multiple pass absorp- on cell. A differential technique, in which the ratio of the trans- itted intensities of the argon laser emissions is measured, is scribed to determine the concentration of $NO_2$ in a polluted at- osphere over path lengths of several kilometers. Measurement ratios eliminates interferences from particle scattering and ermal index gradients. Evaluation of the data taken in the 48 eter multipass cell indicates that concentrations of $NO_2$ less an one part per million could be determined in a 1 km optical th.

**102.** Churney, K. L., West, E. D., Armstrong, G. T., **A cell model for isoperibol calorimeters,** *Proc. 1st Natl. Conf. on Calorimetry, Zakopane, Poland, Sept. 8-18, 1973,* pp. 1-43 (Polish Academy of Science, Institute of Chemical Physics, Warszawa, Poland, 1973).

> Key words: calorimetry; energy equivalents; energy measurement; heat transfer; internal energy measurement; isoperibol calorimeters; measurement theory.

A calorimeter can be modeled as a large number of volume ele- ents or cells in each of which the temperature may be con- lered uniform, and each of which can store heat and exchange at with other cells. Application of the first law of ther- odynamics to this set of cells leads to representations of the ual calorimetric equations for the energy change expressed in ms of measurable or estimatable heat capacities, heat transfer efficients, temperatures, and work terms for the individual lls. Analysis of the results yields a framework within which ost of the design and measurement problems of isoperibol lorimeters can be treated.

**103.** Birky, M. M., Yeh, K. N., **Calorimetric study of flammable fabrics. I. Instrumentation and measurements,** *J. Appl. Polym. Sci.* **17,** 239-253 (1973).

> Key words: calorimeter; fabrics; flammability; heat of combustion; rate of combustion.

A calorimeter has been designed, calibrated, and tested to easure the total amount of heat released and the rate of heat leased from the combustion of fabrics in air. Calibration of the lorimeter gave a reproducibility of ±3 percent for total heat easurements and ±5 percent on rate measurements. Con- leration of systematic errors gives an expected accuracy of ±7 rcent for total heat and ±10 percent for combustion rate mea- rements. Measurements on cotton show that 90 percent of the andard heat of combustion is released when cotton is burned in . The rate of heat release for cotton is independent of fabric eight. The constancy of rate of heat release as determined lorimetrically confirmed the result implied by the 45° test mea- rements on flame spread rate. The rate and amount of heat lease of other commercial fabrics and blends were also mea- red.

**104.** Kline, F. J., Lin, C. L., Peterson, G. A., Penner, S., **Inelastic electron scattering from $^{31}$P,** *Nuclear Phys. A* **241,** 299-310 (1975).

> Key words: electroexcitation; electron scattering; form factors; intermediate coupling; reduced transition probability; $^{31}$P.

Form factors for the electroexcitation of the $3/2^+$ (1.27 MeV), $2^+$ (2.23 MeV), and $3/2^+$ (3.51 MeV) states in $^{31}$P have been easured for momentum transfers from 0.36 to 0.80 $fm^{-1}$ at the BS electron scattering facility. In addition, form factors for the 23 MeV state in the momentum transfer range 0.74 to 1.78 $^{-1}$ have been extracted from data obtained in a previous experiment. Using the DUELS distorted-wave code the $B(E2, \omega) \downarrow$ were found to be $6.0 \pm 0.9$, $6.9 \pm 0.3$, and $2.7 \pm 0.3$ W.u. for the 1.27, 2.23, and 3.51 MeV states, respectively. The form factors for these states, calculated using wave functions derived in an intermediate-coupling vibrational calculation, are compared with the data.

**15105.** Kan, P. T., Peterson, G. A., Webb, D. V., Szalata, Z. M., Fivozinsky, S. P., Lightbody, J. W., Jr., Penner, S., **Observation of electric monopole strength in the electrodisintegration of $^3$He,** *Phys. Rev. Lett.* **34,** No. 14, 899-901 (Apr. 7, 1975).

> Key words: electrodisintegration; electron scattering; inelastic electron scattering; monopole excitation; monopole strength; $^3$He.

A broad electric monopole excitation peaking at 6.4 MeV has been observed in the breakup of $^3$He induced by inelastic electron scattering. The monopole cross section was obtained from the observed cross section by subtracting the electric-dipole contributions converted from photodisintegration cross sections by using the virtual photon theory, and also subtracting the magnetic multipole contributions obtained from a 180° electron-scattering experiment. The extracted monopole matrix element is $2.4 \pm 0.5$ $fm^2$.

**15106.** Cram, S. P., Chesler, S. N., **Analytical fluidic sampling systems,** *J. Chromatogr.* **99,** 267-279 (1974).

> Key words: automated systems; fluidic logic; gas chromatography; plasma chromatography; sampling.

Fluidic logic sampling systems have been developed for analytical detectors such as the plasma chromatograph and flame ionization detector. Automated systems are reported for gases and vapor-phase samples which are rapid, quantitative and reproducible. Sample modulation systems, multiplexers, parallel-to-serial converters and sequential samplers have been developed which give no leakage or cross-talk signals. Other applications in analytical chemistry are proposed.

**15107.** Saloman, E. B., **Unfolding first and second order diffracted radiation when using synchrotron radiation sources: a technique,** *Appl. Opt.* **14,** No. 6, 1391-1394 (June 1975).

> Key words: calibrated XUV detectors; irradiance; radiometry; second order diffracted radiation; synchrotron radiation; XUV grating monochromators.

A technique is presented of using a single calibrated XUV detector for radiometric measurements of synchrotron radiation after the radiation passes through a monochromator that produces a mixture of first and second order diffracted radiation. Irradiance measurements are made with the synchrotron source operating at two different energies for the orbiting electrons. The known change in the spectral distribution produced by the electron energy change is used to calculate the flux in both first and second order. The dependence of the precision of these determinations on the two detected currents and on the detector calibration at both first and second order wavelengths is calculated. Experimental results using the National Bureau of Standards synchrotron (SURF-I) are presented, and anticipated results for the new NBS electron storage ring (SURF-II) are calculated.

**15108.** Cezairliyan, A., Righini, F., **Measurements of heat capacity, electrical resistivity and hemispherical total emittance of two grades of graphite in the range 1,500 to 3,000 K by a pulse heating technique,** *Rev. Int. Hautes Temp. Refract.* **12,** No. 2, 124-131 (1975).

Key words: electrical resistivity; graphite; heat capacity; high-speed measurements; high temperature; thermal emittance; thermodynamics.

Measurements of heat capacity, electrical resistivity and hemispherical total emittance of Poco and pyrolytic graphites in the temperature range 1,500 to 3,000 K by a sub-second duration pulse heating technique are described. For a given graphite grade, heat capacities of different specimens were in agreement within 0.5 percent. The difference between the results of the two different grades was about 1.8 percent; the results of Poco being higher than those of pyrolytic. Electrical resistivity of the Poco graphite was about four times greater than that of pyrolytic graphite (parallel to basal planes). Hemispherical total emittance of Poco graphite was almost twice that of pyrolytic graphite.

15109. Prask, H. J., Trevino, S. F., Rush, J. J., **Quasielastic neutron scattering study of ammonium-ion reorientations in ammonium perchlorate,** *J. Chem. Phys.* **62,** No. 10, 4156-4160 (May 15, 1975).

Key words: activation energy; ammonium-ion dynamics; ammonium perchlorate; jump reorientations; quasi-elastic neutron scattering; residence times.

An investigation of the rotational motion of ammonium ions in $NH_4ClO_4$ is reported. Quasielastic neutron scattering measurements were made on a polycrystalline sample at temperatures between 66 and 150 K. The shapes and widths of the quasielastic scattering peaks as a function of momentum transfer are consistent with instantaneous reorientation about the four $C_3$ axes. Residence times are derived as a function of temperature yielding an activation energy of 2.3 kJ/mole and a frequency factor $1/\tau_0$ of $3.7 \times 10^{12}$ s$^{-1}$.

15110. Jacox, M. E., Milligan, D. E., **The infrared spectrum of methylenimine,** *J. Mol. Spectrosc.* **56,** 333-356 (1975).

Key words: $C=N$ bond; infrared spectrum; isotopic substitution; matrix isolation; methyl azide; methylenimine; normal coordinate analysis; photolysis; thermodynamic properties.

Eleven isotopic species of methylenimine have been prepared by the mercury-arc photolysis of methyl azide isolated in argon, nitrogen, and carbon dioxide matrices at 4 and at 14 K. Sufficient concentrations of methylenimine were obtained for identification of all of the vibrational fundamentals except the NH stretching mode. Using a recent ab initio structural calculation for this molecule, it has been possible to derive a set of valence-force potential constants which provide a satisfactory fit to all of the infrared spectroscopic data. The magnitude of the carbon-nitrogen stretching force constant is appropriate for a double bond. The temperature dependence of the thermodynamic properties of methylenimine has also been calculated.

15111. Bennett, S. L., Lias, S. G., Field, F. H., **Ion-molecule reactions in ethane,** *J. Phys. Chem.* **76,** No. 26, 3919-3926 (1972).

Key words: ethane; gas phase kinetics; ion-molecule reactions; mass spectrometer; product ions.

The ion-molecule reactions in ethane have been investigated in a mass spectrometer at pressures from 0.1 to 5 torr and at temperatures ranging from 189 to 410 K. The major primary ions, $C_2H_4^+$, $C_2H_5^+$, and $C_2H_6^+$, react with ethane to form the respective addition ions, $C_4H_{10}^+$, $C_4H_{11}^+$, and $(C_2H_6)_2^+$. Under these conditions, the addition ions dissociate to give all the product ions which have been attributed to reactions of these primary ions in previous studies. The major product ions resulting from these dissociation reactions are the $C_3H_7^+$ and $C_4H_9^+$ ions, formed by dissociations of the $C_4H_{10}^+$ and $C_4H_{11}^+$ ions, respectively. The rate constants for disappearance of the primary ions decrease as the temperature is raised from 189 to 410 K, from $2 \times 10^{-10}$ to $0.9 \times 10^{-10}$ cm$^3$/molecule sec for the ethylene ion, from $2.5 \times 10^{-10}$ to $0.5 \times 10^{-10}$ cm$^3$/molecule sec for the ethyl ion, and from $2 \times 10^{-10}$ to $0.5 \times 10^{-10}$ cm$^3$/molecule sec for the ethane ion. There is no evidence that any of the product ions react further with ethane to give higher molecular weight addition ions under these conditions of temperature and pressure. When $H_2O$ is added to ethane the ethylene ion is intercepted in a rapid reaction to form the $C_2H_4 \cdot H_2O^+$ complex, which reacts further with water to add a second, a third, and a fourth molecule of water.

15112. Clifton, J. R., Beeghly, H. F., Mathey, R. G., **Protecting reinforcing bars from corrosion with epoxy coatings,** Chapter SP 49-10 in *Corrosion of Metals in Concrete,* pp. 115-132 (American Concrete Institute, Detroit, Mich., 1975).

Key words: bridge decks; chlorides; concrete; corrosion; epoxy coatings; organic coatings; steel reinforcing bars.

This study was undertaken to ascertain the feasibility of using organic coatings, especially epoxies, to protect steel reinforcing bars embedded in concrete of bridge decks from rapid corrosion. This corrosion is caused by chloride ions from the deicing salts, sodium chloride and calcium chloride. Altogether, 47 different coatings were evaluated to some extent, of which 36 were epoxy coatings.

The results of this study indicate that some epoxy coating, if properly applied, should adequately protect steel reinforcing bars from corrosion. Epoxy coated bars had acceptable bond and creep characteristics when embedded in concrete and therefore can be used in existing bridge designs. Epoxy coated bars can also be used in other concrete structures.

15113. Hunt, C. M., Burch, D. M., **Air infiltration measurements in a four-bedroom townhouse using sulfur hexafluoride as a tracer gas,** *ASHRAE Trans.* **81,** Part 1, 186-201 (1975).

Key words: air exchange measurement; air infiltration measurement; building ventilation; sulfur hexafluoride tracer.

Air infiltration measurements were made in a four-bedroom townhouse by the tracer dilution method using sulfur hexafluoride ($SF_6$) as the tracer gas. The house was contained in an environmental chamber with control over both the inside and outside temperature, with essentially no wind velocity. The well-known correlation between inside/outside temperature difference and infiltration rate was observed, and under conditions of negligible wind velocity the effect of sealing doors and ducts was investigated. Simultaneous use of $SF_6$ and He as tracer gases gave no evidence that molecular diffusion played a significant role in the measurement.

Different methods of collecting air samples for analysis were compared. $SF_6$ measurements were also compared with air exchange rates imposed on the house by means of a fan. Finally, the effects of poor mixing were analyzed by comparing the expected results in the case of perfect mixing with those expected in the case of air exchange without mixing and with imperfect mixing.

15114. Wang, F. W., **Viscoelasticity of dilute chain-molecule solutions: Evaluation of hydrodynamic interaction,** *J. Polym. Sci., Polym. Phys. Ed.* **13,** 1215-1231 (1975).

Key words: bead-spring model; chain molecules; chain stiffness; deoxyribonucleic acid; dilute solutions; hydrodynamic interaction; polystyrene; viscoelasticity; Zimm theory.

The viscoelastic properties of chain molecules varying in flexibility and length have been calculated by use of the bead-spring model theory of Zimm. In the evaluation of the hydrodynamic inraction parameter, the number of springs in the bead-spring odel, *N*, has been selected from the range in which the proper-es predicted by the theory are insensitive to the value of *N*. The sults for limiting viscosity number agree with those predicted the Yamakawa-Fujii theory of the limiting viscosity number wormlike chains. The theory also fits the experimental data of hnson on a sample of polystyrene of molecular weight 860,000 theta solvents at infinite dilution. The viscoelastic properties some moderate molecular weight deoxyribonucleic acid solu-ons are predicted to deviate from the non-free-draining havior toward the free-draining behavior.

115. Howell, B. F., Velapoldi, R. A., Travis, J. C., **Fluorescence of commercial porous high silica glasses,** *Amer. Ceram. Soc. Bull.* **54,** No. 5, 503-505, 509 (May 1975).

Key words: fluorescence; Mössbauer spectroscopy; porous glass.

Fluorescence and Mössbauer spectroscopy in conjunction ith elemental analysis have been used to verify that the uorescence which develops in commercial porous glass, sin-ered under reducing conditions, is due to Sn(II). The uorescence shown by in-house-formulated, porous, high silica ass impregnated with Sn(II)$Cl_2$ and sintered under various con-tions is used to substantiate this conclusion. Corrected uorescence spectra for the Sn(II) species and isomer shifts and adrupole splitting for various tin species in glasses are also ven.

116. Frenkiel, F. N., Klebanoff, P. S., **On the lognormality of the small-scale structure of turbulence,** *Boundary-Layer Meteorol.* **8,** No. 2, 173-200 (Mar. 1975).

Key words: boundary layer; grid; intermittency, moments; statistical properties; turbulence; velocity-gradients.

Higher-order moments of turbulent velocity gradients and eir behavior with Reynolds number were measured in the early isotropic turbulent field generated by a square-mesh grid d in a turbulent boundary layer along a flat plate with zero essure gradient. Hot-wire anemometry and instrumentation mbining analog and digital methods were used to measure mo-ents up to the fourteenth order. Measurements of such high-der moments required that particular attention be given to their lidity. Involved herein was the evaluation of such effects as nlinearity, averaging intervals, and the adequacy of the atistics for the tails of the probability density distributions. The sults obtained are compared with those of other investigators r a variety of flow configurations in the laboratory as well as in e atmosphere. The concept of the intermittency of the small-ale structure and the theoretical approach involving lognor-ality of the probability density distribution of the dissipation te are evaluated.

117. Nimeroff, I., Hall, W. A., **Instrumental colorimetry of retroreflective sign materials,** *Report No. FHWA-RD-75-4,* 89 pages (Available by purchase as PB239-633 from the National Technical Information Service, Springfield, Va. 22161, Jan. 1975).

Key words: colorimetry; highway signs; photoelectric tristimus colorimeters; photometry of retroreflective materials; retroreflective sign materials.

Because color-coded applications of highway signs increase, ecification of colors and color tolerances are required. In order assure that the requirements are met within specified regions, measurement technique needs to be developed and described. o accomplish these goals the U.S. Department of Transporta-on contracted with the National Bureau of Standards to con-ct the required studies and make the necessary recommendations. Having previously performed a study for daytime conditions, the National Bureau of Standards was competent to perform a study for nighttime conditions. The colorimetric properties of 126 samples of retroreflective materials of 7 different colors were measured with 3 telecolorimeters in simulated nighttime conditions. One spectrophotometer was used to measure color of 38 of the samples in simulated daytime conditions. The colors measured were: red, orange, brown, yellow, green, blue and silver (white). Differences of color measured by means of different telecolorimeters on the same samples were evaluated.

As a result of these studies procedures for making colorimetric and photometric measurements were developed and are included in this report. On the basis of the color measurements and their variability tentative recommendations for color boundaries were prepared and are also included in this report.

15118. Berger, H., **A report on the American Nuclear Society Topical Meeting "Nondestructive Testing in the Nuclear Power Industry,"** *Nucl. News* **18,** No. 1, 68, 73-74 (Jan. 1975).

Key words: electric utilities; hot cell inspection; in-service inspection; nondestructive testing; nuclear power; reactor components.

The article is a description of American Nuclear Society Topical Meeting "Nondestructive Testing in the Nuclear Power Industry" held in Columbus, Ohio, September 23-25, 1974. Key statements and key papers in the various sessions at the 2 1/2 day meeting are discussed to give readers of the ANS journal, Nuclear News, an idea of what was presented at the meeting.

15119. Beers, J. S., Tucker, C. D., **Procedures for gage block flatness and parallelism measurement,** *J. Appl. Meas.* **2,** No. 4, 82-84 (1974).

Key words: flatness; gage blocks; interferometry; length measurement; parallelism.

Geometric properties of gage blocks are important in many length measurement applications. Methods are described for measuring the flatness of gaging faces and the parallelism between opposing gaging faces. These methods, used for many years, employ interferometers and electro-mechanical gage block comparators.

15120. Klose, J. Z., **Mean life of the $5p\ ^2P_{3/2}$ resonance level in Ag I,** *Astrophys. J.* **198,** 229-233 (May 15, 1975).

Key words: Ag I; *f*-value; imprisonment; lifetime; mean life; resonance radiation; silver; transition probability.

The mean life of the $5p\ ^2P_{3/2}$ resonance level in Ag I has been measured at two different vapor densities using electronic excitation and a method of delayed coincidence. The lifetime values, obtained by optically detecting the decay of the $5p\ ^2P_{3/2} \rightarrow 5s\ ^2S_{1/2}$ (3280.68 Å) resonance transition, increase with increasing vapor density. This vapor density dependence was interpreted as being due to the imprisonment of the 3281 Å resonance radiation. The Holstein theory of the imprisonment of resonance radiation was applied to the lifetime-versus-vapor density data to yield the following results: $\tau_0 = 6.5 \pm 0.6$ ns, $A_{3281} = 1.53 \pm 0.14 \times 10^8\ s^{-1}$, and $f_{3281} = 0.50 \pm 0.05$. The error limits were derived primarily from estimated uncertainties in the measured mean lives and possible variations in the vapor densities during the runs. Experimental results of other workers are presented for comparison with the results of the present work.

15121. Franklin, A. D., Crissman, J. M., Young, K. F., **Defect-complex reorientation processes in $GdF_3$-doped $CaF_2$,** *J. Phys. C* **8,** 1244-1266 (1975).

Key words: anelastic relaxation; calcium fluoride; defect pairs; dielectric relaxation; EPR lifetime broadening; fluorine interstitials; gadolinium ions; reorientation processes.

Measurements are reported of the temperature dependence of EPR lifetime broadening in the spectrum of $Gd^{3+}$ ions in tetragonal sites in $CaF_2$ and of dielectric and anelastic relaxation in similar specimens. Concentrations ranged from 0.01 to 0.27 mol percent $GdF_3$, and the crystals were annealed in flowing He plus HF at various temperatures. The strongest relaxation modes $(R_I)$ arising from pairs formed from $Gd^{3+}$ ions plus trapped $F^-$ interstitials could be identified in both the dielectric $(T_{1u})$ and the anelastic $(E_g)$ spectra. The rate constants are $\ln \tau_0 = -32.83 \pm 0.24$ ($\tau_0$ measured in seconds) and $Q = 0.44 \pm 0.005$ eV, and are to be associated with jumps of the $F^-$ interstitials originating at the nearest-neighbour sites to the $Gd^{3+}$ ions. A low-temperature relaxation ($Q \sim 0.2$ eV) was observed in the anelastic spectrum with trigonal symmetry and also in the dielectric spectrum. It was found to consist of several components. It is argued, contrary to earlier conclusions, that this relaxation is not an additional mode of the same centre giving rise to $R_I$. A higher temperature relaxation ($Q \sim 1.1$ eV) was seen only in the anelastic spectrum, and was approximately isotropic. It too cannot be identified on the basis of present information.

15122. Evans, A. G., Wiederhorn, S. M., Hockey, B. J., **Comments on "Dependence of Room Temperature Fracture Strength on Strain-Rate in Sapphire,"** *J. Mater. Sci. Lett.* **9**, 1367-1370 (1974).

Key words: ambient temperatures; dislocation mechanisms; fracture mechanics; sapphire; slow crack growth; thermal activation.

A recent paper attempts to explain the strain-rate dependence of the strength of sapphire filaments using a dislocation assisted slow crack growth model. We propose an alternative model which gives a quantitative prediction of the observed behavior. This model, based on fracture mechanics measurements of slow crack growth in the absence of dislocation activity, considers that the crack growth is a thermally activated bond rupture process.

15123. Wiederhorn, S. M., Roberts, D. E., **Influence of normal alcohols on the abrasive wear of glass,** *Wear* **32,** 51-72 (1975).

Key words: alcohol; glass; mechanism; silicon carbide; wear.

Normal alcohols were used as cutting fluids in a study of friction and wear of soda lime silicate glass against silicon carbide. Abrasion surfaces were 600 grit silicon carbide paper and a roughened plate of hot-pressed silicon carbide. As the alcohol chain length increased, the coefficient of friction decreased. This result was attributed in part to better lubrication of the abrading surfaces by the long chain length alcohols. The wear rate and the coefficient of friction were strongly dependent on pullout of carbide grains from the silicon carbide paper. Wear on fresh abrasive paper was independent of alcohol chain length. As the paper becomes used, long chain length alcohols were more effective cutting fluids. On the silicon carbide plate, the wear rate decreased in a non-linear fashion as the alcohol chain length increased. For all conditions, the highest wear rate and coefficient of friction were obtained in water. Data are explained in terms of classical theories of friction and wear.

15124. Rowe, J. M., Rush, J. J., Vagelatos, N., Price, D. L., Hinks, D. G., Susman, S., **Crystal dynamics of KCN and NaCN in the disordered cubic phase,** *J. Chem. Phys.* **62,** No. 11, 4551-4554 (June 1, 1975).

Key words: alkali cyanides; crystal dynamics; dispersion curves; orientation; phonons; rotational disorder; single crystal.

The lattice dynamics of KCN and NaCN in their disordered cubic phase has been studied by coherent inelastic neutron scattering and infrared reflection measurements. Acoustic phonon branches for cyanide single crystals were measured in the [001] direction, with more limited measurements taken in the [110] direction. The one-phonon scattering generally appeared as weak peaks superimposed on a large background of non-one phonon scattering, particularly as measurements were extended to higher energy. No peaks clearly assignable to optical phonons were observed in the neutron measurements but the infrared reflection spectra for polycrystalline pellets were analyzed to derive TO and LO phonon energies (at $q=0$) of $17.0 \pm 0.6$ and $28.5 \pm 2.5$ meV. These measurements (and a comparison with the rather easily measured acoustic and optical phonons in a KBr crystal of similar volume) indicate that phonons do not exist as well-characterized excitations in the cyanides at higher frequencies and finite wave vectors. The unusual character of these results is attributed to the dynamical disorder of the cyanide ions in the fcc crystal and is compared with recent phonon measurements in the analogous fcc phase of $ND_4I$. The [001] transverse acoustic branches of both KCN and NaCN show unusually low frequencies below $q=0.5$, which are consistent with recent elastic constant results and with the very large Debye-Waller factors derived from previous neutron diffraction results, and suggest further that the phase transitions in the cyanides are "driven" by a soft shear mode.

15125. Evans, A. G., **Analysis of strength degradation after sustained loading,** *J. Amer. Ceram. Soc.* **57,** No. 9, 410-411 (Sept. 1974).

Key words: fracture probability; slow crack growth; strength degradation; sustained loading.

The strength degradation that occurs at sustained load, due to slow crack growth, is calculated in terms of the slow crack growth parameters. It is shown that the degradation is only significant in specimens with an initial strength marginally larger than the initial strength of the last specimen that failed at the sustained load.

15126. Mielenz, K. D., Eckerle, K. L., **Averaging spheres without target,** *Appl. Opt.* **14,** No. 7, 1649-1651 (July 1975).

Key words: averaging spheres; diffusing effectiveness; efficiency; flux averaging; photometry; spectrophotometry.

The design of averaging spheres without internal target is described. The performance of such spheres is analyzed theoretically and tested experimentally. In a final design, an efficiency of 40 percent is achieved for visible and near-uv wavelengths. The averaging effectiveness is characterized by signal variations of the order of 1 part in $10^4$ for beam displacements of several 0.1 mm.

15127. Hudson, R. P., Marshak, H., Soulen, R. J., Jr., Utton, D. B., **Review Paper: Recent advances in thermometry below 300 mK,** *J. Low Temp. Phys.* **20,** Nos. 1/2, 1-102 (July 1975).

Key words: cryothermometry; low temperature; thermometry.

The subject of temperature measurement below 0.3 K is reviewed, with particular attention paid to developments reported in the period 1970-1974. Sensors, measurement techniques, primary and secondary thermometers, and fixed points are discussed and attempts are made to assess the accuracy and relative merits of the various devices and methods.

15128. Melmed, A. J., Stein, R. J., **Field-ion microscopy of silicon,** *Surface Sci. (Letters to Editor)* **49,** No. 2, 645-648 (Apr. 1975).

Key words: field-ion microscopy; semiconductor surface structure; silicon.

Significant advance in the state-of-the-art of silicon field-ion croscopy is described. Preliminary observations of interesting ht sensitive effects are discussed. Further research is in-ated.

129. Herbst, J. F., Watson, R. E., **5*f*-electron excitation energies and the Coulomb term, *U*, in the light actinide metals,** *Phys. Rev. Lett.* **34,** No. 22, 1395-1398 (June 2, 1975).

Key words: actinides; Coulomb term; energy; excitation energy; metal; 5*f* electron.

Relativistic Hartree-Fock-Wigner-Seitz band calculations ve been performed for the actinide metals Ac through Am in der to estimate 5*f* excitation energies. Our calculations predict at the tetravalent state (i.e., four *s-d* conduction electrons) is vored for the lighter elements with a crossover to a trivalent ound state occurring near uranium. We find the Coulomb ener- , *U*, for 5*f* electron hopping to increase from 2-3 eV at Th to 4-eV at Am.

130. Manning, J. R., Stark, J. P., **General matrix equations for diffusion drift velocity in a driving force,** *Phys. Rev. B* **12,** No. 2, 549-556 (July 15, 1975).

Key words: defects in crystals; diffusion; drift velocity; driving force; matrix equations; non-cubic crystals.

From a complete-path approach in which defects are followed om the time of their creation at defect sources to the time of eir destruction at defect sinks, general matrix equations are veloped which relate the atom drift velocity $v_k$ for diffusion in driving force to simple matrices whose elements can be written inspection. Previous equations for $v_k$ have been restricted her to crystals and defects having high symmetry or to cases here the *x* components of any atom jumps were either $\pm b$ or 0. contrast, the present equations involve no such restrictions. ey apply to diffusion by interstitialcy, divacancy, and other ore complex mechanisms, independent of the presence of sym-etry planes, and allow calculation of diffusion drift velocities en when the individual atom jumps provide a variety of jump stances along the diffusion direction. These equations apply, r example, even when jumps to both nearest- and next-nearest-ighbor sites are allowed and to diffusion in arbitrary crystallo-aphic directions even in noncubic crystals. The present equa-ns can be expressed in terms of a general matrix $S$. The rela-n of $S$ to the less general matrices $S_+$ and $S_-$ defined previ-sly for crystals having mirror symmetry planes normal to the fusion direction is discussed.

131. Cotton, I. W., **Microeconomics and the market for computer services,** *Comput. Surv.* **7,** No. 2, 95-111 (June 1975).

Key words: administration of computing; computer services; management; microeconomics; pricing.

Microeconomics has much to offer the computer services anager. This article reviews some of the traditional topics in croeconomics and shows how they can be applied to the mar-t for computer services. The topics covered include supply, mand, costs, and pricing. The most significant application of croeconomics is in setting prices—so much so that croeconomics is frequently called "price theory." Ac-rdingly, the thrust of the article is towards providing a sound amework for the pricing of computer services.

132. McCarty, R. D., **Determination of thermodynamic properties from the experimental *p-V-T* relationships,** Chapter 10 in *Experimental Thermodynamics, Vol. II—Experimental Thermodynamics of Non-Reacting Fluids,* B. Le Neindre and B. Vodar, Eds., pp. 501-526 (Butterworth and Co., Ltd., London, England 1975).

Key words: constraints; equation of state; fluid; least squares; parameter estimation; *p-V-T*; statistical weighting; thermodynamic properties.

Methods and techniques for calculating the thermodynamic properties of a fluid from a mathematical model of the *p-V-T* equation of state are given. Criteria for choosing a mathematical form for the equation of state are discussed. Numerical and statistical parameter estimation techniques presented include, linear and non-linear least squares; constraints; simultaneous use of different kinds of data; significance tests and statistical weighting. Formulas for many of the derived thermodynamic properties are also presented.

15133. Gadzuk, J. W., Sunjić, M., **Excitation energy dependence of core-level x-ray photoemission-spectra line shapes in metals,** *Phys. Rev. B* **12,** No. 2, 524-530 (July 15, 1975).

Key words: asymmetric lineshapes; photoelectron spectroscopy; photoemission; x-ray edge singularities.

Creation of a deep localized hole in the process of x-ray photoemission from metals is followed by a drastic rearrangement of the surrounding electrons in the Fermi sea. This rearrangement in which low-energy electron-hole pairs are produced, in analogy with gas-phase atomic shake-up processes, gives rise to a low-energy tail in the hole spectral density with an integrable (Mahan) singularity at the energy corresponding to zero-energy pair production. When the usual (symmetric) broadening of the hole is included, the resulting hole line shape becomes a skew resonance, with the asymmetry indices growing with the strength of the electron-hole interaction. The case in which the hole potential is switched on instantaneously (the sudden or impulse limit) has been treated by Doniach and Sunjić. However, the potential switching-on time is a function of the speed at which the excited electron leaves the region of the hole. In this paper we calculate the skew line shapes for finite hole-creation times, going continuously from the adiabatic to sudden limits. The photoemission line shape, for a given hole state, varies smoothly from the symmetric result given in the adiabatic approximation to the asymmetric result of Doniach and Sunjić obtained in the sudden approximation, as the photon energy is increased above the photoionization threshold value.

15134. Swanson, N., Celotta, R. J., Kuyatt, C. E., Cooper, J. W., **Resonant structure in electron impact excitation of CO near threshold,** *J. Chem. Phys.* **62,** No. 12, 4880-4888 (June 15, 1975).

Key words: CO; electron excitation; energy loss spectra; resonance decay; resonant structure; threshold.

Electron impact excitation functions of numerous states in CO have been measured at 45° scattering angle with resolutions of 16-23 meV FWHM. The decay peak of the 10.04 eV resonance can be seen in the results for the $a\ {}^3\Pi$, $a'\ {}^3\Sigma^+$, and $A\ {}^1\Pi$ vibrational levels. There was no evidence of resonant excitation of the $a'\ {}^3\Sigma^+$ state near 8 eV as suggested by Newton and Thomas. Excitation functions of the $b\ {}^3\Sigma^+$, $B\ {}^1\Sigma^+$, $C\ {}^1\Sigma^+$, $c\ {}^3\Pi$, and $E\ {}^1\Pi$ states, and a previously unobserved state at 11.26 eV show numerous sharp resonances in the first few eV above threshold. Energy loss spectra in the 8-14 eV loss region show peaks corresponding to known states as well as to unidentified states. No sign of the metastable state at about 9.5 eV seen by Wells, Borst, and Zipf could be detected in direct excitation, but an indirect excitation process involving the $A\ ^1\Pi$ state is consistent with the data.

**15135.** Penn, D. R., **The dependence of the tunneling current on density of states in non-superconducting junctions,** *Surface Sci.* **50,** 125-136 (1975).

Key words: density of states; elastic tunneling; tunneling junctions.

The theory that the tunneling current in a non-superconducting tunnel junction depends on the densities of states of the electrodes has been known for sometime although Harrison has suggested that it is in fact not correct. In this paper Harrison's suggestion is critically discussed and the expression for the tunneling current is written in a way that emphasizes its dependence on the *surface* densities of states of the electrodes and takes into account the band structure of the oxide barrier. We find

$$J = \int_{-\infty}^{\infty} \mathrm{d}\omega\ [f_L(\omega) - f_R(\omega)] \sum_{k_{||}} D(r_L,r_R;\omega,k_{||})\, \xi(\omega,k_{||})\, \rho_L{}^{\perp}(r_L,\omega,k_{||})\, \rho_R{}^{\perp}(r_R,\omega,k_{||})$$

where $f_L, f_R$ are the Fermi function of the left and right hand electrodes, $D$ is the probability that an electron tunnels from a point $r_L$ in the barrier near the left hand electrode to a point $r_R$ in the barrier near the right hand electrode. $\xi$ depends on the oxide and is a slowly varying function of $\omega$ and $k_{||}$, the electron momentum parallel to the electrode surfaces. $\rho_L{}^{\perp}(r_L,\omega,k_{||})$ is the one dimensional density of states of the left hand electrode in the direction normal to the electrode at a position $r_L$ in the barrier for electrons of energy $\omega$ and momentum $k_{||}$ and $\rho_R{}^{\perp}$ has a similar meaning. This expression for $J$ reduces to that previously derived by Harrison if the electrodes as well as the oxide barrier are treated in a WKB approximation. In this limit $J$ has no dependence on the densities of states due to cancellations from the factor $\xi$. Recent field emission experiments and theory have shown that the tunneling current is dependent on the electrode density of states so the expression for $J$ given above must be used. It is suggested that the failure to observe such effects in tunnel junctions is due to imperfections in the junction and that tunneling in metal-vacuum-metal junctions or in perfected tunnel junctions will give density of states information.

**15136.** Barkley, J. F., Shoenfeld, P. S., **A central laboratory automation facility,** *Amer. Lab.* **7,** No. 2, 19-20, 22, 24-25 (Feb. 1975).

Key words: analytical chemistry; computer; data acquisition; laboratory automation operating system; teleprocessor.

The Analytical Chemistry Division at the National Bureau of Standards has developed a centralized computer facility for laboratory automation, which is described in this paper. This facility consists of two major components. These are the teleprocessor, which handles all communication between the laboratory and the computer, and the computer itself. Also described are the essential system software packages including the Operating System, the File System, and the Data Acquisition System.

**15137.** Olson, J. D., **The refractive index and Lorenz-Lorentz function of fluid methane,** *J. Chem. Phys.* **63,** No. 1, 474-484 (July 1, 1975).

Key words: critical refractive index; Fabry-Perot interferometer; Lorenz-Lorentz function; methane; rectilinear diameter law; refractive index; refractometric virial coefficients.

The refractive index of gaseous and liquid methane was measured between 95 and 300 K and to pressures of 225 bar (1 bar = $10^5$ Pa). The measurements were performed at the $^{198}$Hg vapor green line, $\lambda = 546.2$ nm, with a Fabry-Perot interferometer referred to vacuum. The refractive index data were combined with the previously measured densities of methane to calculate the Lorenz-Lorentz (LL) function. Refractometric virial coefficients were obtained from analysis of the small (~ 0.5%) maximum exhibited by the (LL) function with increasing density. $B_R$, the second refractometric virial coefficient, is estimated to be ~ 6.0 (cm$^3$/mol)$^2$ and is almost independent of temperature between 220 and 300 K. The critical point refractive index, $n_c = 1.10333$, was extrapolated from a rectilinear diameter treatment of the saturated liquid and vapor results. The critical point refractive index was combined with an estimate of the critical point (LL) function to yield a critical density of methane, $\rho_c = 10.16 \pm 0.01$ mol/l.

**15138.** Geist, J., Steiner, B., Schaefer, R., Zalewski, E., Corrons, A., **Electrically based spectral power measurements through use of a tunable cw laser,** *Appl Phys. Lett.* **26,** No. 6, 309-311 (Mar. 15, 1975).

Key words: cw dye laser; detector spectral response; electrically calibrated pyroelectric detector; radiometry; spectral irradiance; spectral radiant power density.

A new approach to radiant power measurements is described. A continuously tunable cw dye laser was used to measure the absolute spectral response of a silicon photodiode and narrow band-pass filter by comparison with an electrically calibrated pyroelectric detector. The filtered photodetector was then used to measure the spectral power density from a standard lamp that had been calibrated by the classical technique. The agreement of better than 1 percent between the two measurements is wel within the uncertainties identified with each measurement individually, of the order of 1 percent. A number of advantages in the new technique are identified.

**15139.** Schramm, R. E., Reed, R. P., **Stacking fault energies of seven commercial austenitic stainless steels,** *Metall. Trans. A* **6A,** 1345-1351 (July 1975).

Key words: austenite; iron alloys; stacking fault energy stainless steel; x-ray diffraction.

The stacking fault energies of seven commercial austenitic Fe-Cr-Ni, Fe-Cr-Ni-Mn and Fe-Mn-Ni alloys have been determined by x-ray diffraction line profile analysis. From comparison with existing data on laboratory alloys with similar compositions, it is concluded that both Ni and C increase $\gamma$ while Cr Si, Mn, and N decrease $\gamma$. Regression analysis of data produced in this study provides an expression relating $\gamma$ to commercia alloy composition in terms of Ni, Cr, Mn, and Mo alloy concentrations.

**15140.** Davis, D. D., **Calibrating crystal oscillators with TV color reference signals,** *Electronics* **48,** No. 6, 107-112 (Mar. 20, 1975).

Key words: crystal oscillator; frequency calibrator; frequency offset; NBS traceability; phase comparison; television.

The National Bureau of Standards checks the frequency of th network television color signals and publishes the results. Her is a way to use that information to calibrate your own oscillator

**15141.** Hanley, H. J. M., Haynes, W. M., **The density expansio of the viscosity coefficient,** *J. Chem. Phys.* **63,** No. 1, 358-36 (July 1, 1975).

Key words: argon; correlated molecular collisions; densit expansions; fluorine; oxygen; statistical analysis; viscosit coefficient.

Experimental viscosity data for gaseous argon, oxygen, an orine were analyzed as a function of density and temperature. ecessary conditions were applied to investigate if a given therm was consistent statistically with a given density func- n. It was found that the low temperature isotherms were con- tent with the theoretically suggested density function, which olves terms logarithmic in the density. At higher tempera- res, however, these logarithmic terms did not appear to be tistically significant.

**142.** Heinrich, K. F. J., Newbury, D. E., Yakowitz, H., **New echniques for the surface analysis of nonmetallic solids,** (Proc. 20th Sagamore Army Materials Research Conf., Sagamore Conference Center, Raquette Lake, New York, Sept. 11-14, 973), Chapter 4 in *Characterization of Materials in Research Ceramics and Polymers* **20,** 73-102 (Syracuse University Press, Syracuse, N.Y., 1975).

Key words: contrast; electron probe microanalysis; electron spectroscopy for chemical analysis (ESCA); ion microprobe analysis; scanning electron microscopy; surface analysis.

Several modern techniques for the characterization and analy- of surfaces and shallow layers of nonmetallic materials are cussed, with particular emphasis on their relevance to hnological problems. These include electron and ion probe croanalysis, scanning electron microscopy, ion scattering alysis, and secondary ion mass spectroscopy of surfaces.

**143.** Peterlin, A., **Intrinsic stress tensor of polymer solutions in aminar flow,** *Makromol. Chem. Suppl.* **1,** 453-470 (1975).

Key words: elastic dumbbell model; flow instability; flow with longitudinal gradient; flow with transverse gradient; gradient dependence of normal stress differences; gradient dependence of viscosity; hydrodynamic interaction; intrinsic stress tensor; intrinsic viscosity.

The simplified necklace or the equivalent modified elastic mbbell model with consideration of hydrodynamic interaction ong the beads and its change with coil expansion was used for calculation of the intrinsic stress tensor in laminar flow with nsverse and parallel gradient as function of the conventional dient $\gamma$ and the dimensionless gradient parameter $\beta$. The ex- nsion of the Gaussian coil in flow first increases and then creases the hydrodynamic interaction. As a consequence the rinsic viscosity $[\eta]_{tr}$ of sufficiently large macromolecules and effective average hydrodynamic resistance coefficient $\Lambda$ of bead show first a decrease to a minimum and a subsequent dually slower increase with the gradient. In laminar flow with allel gradient this effect yields a deformational instability ich may play some role in drag reduction of turbulent flow by lymer additives. Experimental evidence will have to conform to refute these two interdependent phenomena. In the latter se, one suspects that the neglect of anisotropy of hydrodynam- interaction is the main cause of the unrealistic predictions of rinsic hydrodynamic properties of polymer solutions.

**144.** Bertocci, U., **Computer simulation of crystal growth on a cc surface,** *J. Cryst. Growth* **26,** No. 2, 219-232 (Dec. 1974).

Key words: computer simulation; crystal growth; fcc

Positive and negative crystal growth has been simulated on a 0) surface of a fcc crystal. The results show considerable ilarities with the behavior of simple cubic surfaces, as far as values of the interatomic bond energy and of the free energy crystallization at which transition from smooth to rough sur- es occur. Growth rates are smaller, reflecting the formation of izable area where both deposition and removal of atoms is hin- ed. The surface roughness at equilibrium is similar to that ob- ned by computer simulation by other authors on a (100) surface of a Kossel crystal and it is close to that of a two-dimensional square lattice.

**15145.** Lofquist, K. E., **An effect of permeability on sand transport by waves (Abstract only),** *EOS, Trans. Amer. Geophys. Union* **56,** No. 6, 370 (June 1975),

Key words: oscillatory flows; permeability; ripple; sand transport.

Permeability effects on the movement of sand in oscillatory flows are observed in laboratory experiments which approximate prototype conditions at the seabed under progressive waves. A natural sand is used, wave periods range between 3 and 14 seconds, and sand surfaces are naturally rippled. The apparatus has a symmetry which removes all effects, except those of permeability, which might cause a net movement of the sand. Onshore and offshore directions are determined by phase relationships between the horizontal flows and superposed vertical permeability flows. A positive permeability effect is found, in that the ripple profiles move in the onshore direction. The velocity of this motion is measured and described in a simple dimensionless plot. The associated net transport of sand is not observed directly but can be inferred, to an extent, form the motions of the ripple profiles. The effects of permeability sand transport are cumulative, and can be significant in coastal processes of long duration.

**15146.** Cezairliyan, A., **Pulse calorimetry and transient measurement of thermal properties at high temperatures,** *Faraday Symp. Chem. Soc.*, No. 8, 7-17 (1973).

Key words: high-speed measurements; high temperature; pulse calorimetry; thermodynamics; thermophysical properties.

A system is described for the transient (subsecond) measurement of selected thermal and related properties of electrically-conducting substances in the temperature range 1500 K to the melting point of the specimen. The method is based on resistive self-heating of the specimen from room temperature to any desired high temperature in less than 1 s by the passage of an electrical current pulse through it; and on measuring and recording the experimental quantities every 0.4 ms with a full-scale signal resolution of one part in 8000. The system has been used to measure heat capacity, electrical resistivity, hemispherical total emittance, normal spectral emittance, and the melting point of selected refractory elements and alloys. The results of preliminary experiments have shown the potential application of the system to measurements of temperatures and energies of solid-solid phase transformations and heat of fusion at high temperatures.

**15147.** Fuggle, J. C., Madey, T. E., Steinkilberg, M., Menzel, D., **X-ray photoelectron satellites from adsorbed species,** *Chem. Phys. Lett.* **33,** No. 2, 233-236 (June 1, 1975).

Key words: oxygen; ruthenium; satellite; shake-up; structure; x-ray photoelectron spectroscopy.

The O 1s XPS peaks from monolayers of CO and oxygen adsorbed on the basal (001) face of a ruthenium single crystal are observed to have satellites whose position and intensity are sensitive to the chemical environment.

**15148.** Berger, H., Motz, J. W., **A qualitative discussion of quantitative radiography,** (Proc. 2nd ASM Materials/Design Forum, Port St. Lucie, Fla., Apr. 8-11, 1974), Paper in *Prevention of Structural Failure*, T. D. Cooper, P. F. Packman, and B. G. W. Yee, Eds., No. 5, 37-47 (American Society for Metals, Metals Park, Ohio, 1975).

Key words: dimensional measurement; image enhancement;

imaging methods; nondestructive evaluation; radiography; serviceability.

Quantitative aspects of radiography are described and illustrated. Radiography is a widely used method for nondestructive testing. It offers the advantage of giving an image of objects as a permanent inspection record. Voids, inclusions, and cracks in homogeneous materials and welds can be detected. The size, shape and location of discontinuities are revealed if the change in density or thickness is of the order of one percent and covers a sufficient area to be resolved by the radiographic technique. The measurement of the dimensions and depth of an object can be made and, in certain circumstances, such measurements are possible to accuracies of $\pm 0.001$ inch.

In addition, radiography can be used effectively as an accept-reject criterion, especially in conjunction with well defined specifications and reference radiographs.

Novel radiographic methods that offer advantages in improving image contrast are briefly discussed. Included are image enhancement methods and radiography employing neutrons, monoenergetic x-radiation, or charged particles.

**15149.** Lambropoulos, M., Moody, S. E., Smith, S. J., Lineberger, W. C., **Observation of electric quadrupole transitions in multiphoton ionization,** *Phys. Rev. Lett.* **35,** No. 3, 159-162 (July 21, 1975).

Key words: atom; dye laser; electric quadrupole; fine structure; ionization; multiphoton; sodium.

Two flashlamp-pumped, tunable, dye lasers have been utilized to study three-photon ionization in atomic sodium. The resulting ion yield shows large peaks at laser frequencies which correspond to electric quadrupole transitions. This is the first direct observation of electric quadrupole effects in multiphoton ionization. The $3p\ ^2P_{3/2} \rightarrow 4f$ matrix element is determined, and the fine-structure splitting of the $5p$ state is measured.

**15150.** Mountain, R. D., **A geometrical description of critical phenomena,** *J. Wash. Acad. Sci.* **64,** No. 3, 195-198 (1974).

Key words: critical phenomena; divergences at critical points; free energy surface; geometry of thermodynamic surfaces; thermodynamics.

Gibbs made extensive use of geometrical concepts in his development of thermodynamics. In this talk we examine the use of geometrical ideas to clarify our understanding of the thermodynamics of fluids in the vicinity of the critical point. The influence of Gibbs on recent developments in the study of critical phenomena is emphasized.

**15151.** Prosen, E. J., Cole, K. S., **Heat production of Arbacia eggs revisited (Extended Abstract),** *Biol. Bull.* **145,** No. 2, 450-451 (Oct. 1973).

Key words: Arbacia punctulata; calorimetry; cleavage of cells; development of cells; fertilization; growth of cells; heat production; marine eggs; metabolism; microcalorimetry.

Heat production is an important aspect of the thermodynamics and kinetics of the initiation and subsequent metabolic—and perhaps physical—processes of growth. Tremendous advances in speed, sensitivity, and accuracy of heat measurements have come about from the use of modern techniques and semiconductor materials. Yet little, if anything, has been done on such simple systems as marine eggs since the 1924 measurements of Rogers and Cole.

We have repeated that work with the advanced microcalorimeter of the National Bureau of Standards (Prosen, 1973) which has been developed and used in clinical studies of enzyme reactions and bacterial growth. The instrument had been modified to accommodate a larger 3.4 ml reaction vessel to adapt it for biological work. This isothermal, heat-flow instrument measures the heat production of two solutions (0.75 ml and 1.50 ml) before and after mixing with an output signal of 0.2 volt/watt an ultimate sensitivity of 0.1 $\mu$J/sec or 90 $\mu$cal/hr (corresponding to 0.1 $\mu$k), and with a response half-time of 2 minutes.

Since a constant-temperature room was not available it was necessary to place additional insulation around the calorimeter to limit baseline drift to $3 \mu$W/hr or less. The original plan was to measure the heat production of several thousand *Arbacia* eggs and corresponding sperm in the separate compartments of the reaction vessel and to follow it—after fertilization by mixing—for a few hours or several cell divisions. This has been accomplished but not as yet satisfactorily since no greater than 90 percent fertilization has been achieved in the vessel. It was first found that no fertilization or development took place in the plastic reaction vessels used, although controls in glass gave over 95 percent. A glass vessel with ports sealed with paraffin also proved unsatisfactory. Finally the original plastic vessels operated properly (90% fertilization) after flushing them with sea water for several days. The vessel ports are closed with o-ring seals.

Egg and sperm counts are incomplete, but our preliminary results are as follows: (all measurements were made in natural sea water containing 0.0001 molar EDTA and pH 7.8). Unfertilized eggs gave about 0.3 $\mu$W/1000 eggs after 1 hour with a gradual drop with time. Prefertilized eggs gave about 0.6 $\mu$W/1000 eggs after 1 hour and with some small variations and a gradual drop with time. Sperm heat was also measured but results are not complete. Fertilization runs in the calorimeter gave similar heats for the unfertilized and the fertilized separate runs above and showed no burst of heat upon fertilization. Fluctuations suggest a possible correlation with stages of development.

There is no immediate explanation for the fact that these values are about twice as large as those of Rogers and Cole. However, different conditions were used and in one experiment with greater loading (50,000 eggs/ml in place of the usual 10,000 eggs/ml) we obtained their value. They used 100,000 eggs/ml. We conclude that it should not be difficult to extend the range of experiments to include measurements of fertilization and early development of a variety of marine eggs.

**15152.** Huebner, R. H., Celotta, R. J., Mielczarek, S. R., Kuyatt, C. E., **Apparent oscillator strengths for molecular oxygen derived from electron energy-loss measurements,** *J. Chem. Phys.* **63,** No. 1, 241-248 (July 1, 1975).

Key words: electron energy-loss; oscillator strengths; oxygen.

Oscillator strengths for $O_2$ from 6 to 14 eV are derived from the energy-loss spectrum of 100 eV incident electrons. Integrated $f$ values for the Schumann-Runge bands and continuum, which span four orders of magnitude in intensity, agree well with high-resolution photoabsorption measurements. Vibrational structure superimposed on the Schumann-Runge continuum, previously assigned to the $(3s\ \sigma_g)\ ^3\Pi_g$ Rydberg state, contributes less than 0.5 percent to the total oscillator strength determined for that region. These data also yield $f$ values for discrete bands in the region between 9.5 and 14.0 eV, where line saturation problems complicate oscillator strength analysis of the optical data. An oscillator strength sum of 0.198 is obtained for all transitions below the ionization potential at 12.07 eV.

**15153.** Powell, C. J., **Cross sections for ionization of inner-shel**

**lectrons by electron impact,** *Proc. 10th Annual Conf. of the Microbeam Analysis Society, Las Vegas, Nevada, Aug. 11-5, 1975*, pp. 3a-b (1975).

Key words: cross sections; electron probe microanalysis; electrons; inner-shell.

A survey has been made of available theoretical and experi-ntal cross-section data for the ionization of inner-shell elec-ns by electron impact in the energy range of interest to elec-n probe microanalysis and to Auger-electron spectroscopy.

**154.** Ludtke, P. R., **Register of specialized sources for informa-ion on selected fuels and oxidizers,** *NASA CR-134807*, 44 pages (Available from the National Technical Information Service, Springfield, Va. 22151, 1975).

Key words: chemical reactions; combustion; cryogenic fluid safety; explosions; fires; fuels; handling; hydrogen; oxidizers; oxygen; propellants; safety information; thermodynamic properties.

This Register describes thirty-eight (38) organizations that alog and file information in their data systems on fuel and ox-zers. The fuels include hydrogen, methane (LNG) and drazine-type fuels (UDMH); the oxidizers include oxygen, orine, flox, nitrogen tetroxide and ozone. The type of available ormation covers thermophysical properties, propellant stems, propellant fires-control-extinguishment, propellant ex-sions, propellant combustion, propellant safety, and fluorine emistry. These organizations have assembled and collated ir information so that it will be useful in the solution of en-eering problems.

**55.** Arvidson, J. M., Brennan, J. A., **ASRDI oxygen technology urvey, Vol. VIII: Pressure measurement,** *NASA Spec. Publ. 092*, 200 pages (Available from the National Technical Information Service, Springfield, Va. 22151, 1975).

Key words: calibration; compatibility; cryogenic; liquid oxygen; measurement; oxygen; performance; pressure; survey; transducer.

This publication is part of an oxygen safety review in progress the NASA Aerospace Safety Research and Data Institute SRDI). The objectives of the review include: 1. commendations to improve NASA oxygen handling practices comparing NASA and contractor oxygen systems including design, inspection, operation, to failure of oxygen equipment m a variety of sources so that hazards may be defined and medial measures formulated. 3. Contributions to safe oxygen dling techniques through research. 4. Formulation of criteria l standards on all aspects of oxygen handling, storage, and posal.

The special publication summarizes the current state-of-the- in pressure measurement in the region of 50 to 150 K (the aid state of oxygen). The report is not limited to oxygen-ved systems alone as this would have severely limited the re-t. The published literature available in the cyrogenic region erally is quite restricted. The survey includes information on aning and materials compatibility, calibration methods and criptions of representative transducers. A summary of ommendations is presented as well as an extensive bibliog-hy arranged by transducer type.

**56.** Fano, U., Spencer, L. V., **Quasi-scaling of electron legradation spectra,** *Int. J. Radiat. Phys. Chem. Platzman Memorial Issue* **7**, 63-76 (1975).

Key words: charged particle penetration; dosimetry; electron slowing down; electron transport; scaling; *W*-value.

Douthat has found that plots of electron spectra calculated for different initial energies nearly coincide if a suitable choice of scaled variables is adopted for abscissas and ordinates. This paper provides a rationale for this choice of variables, reformulates the degradation equation in terms of the new variables, and shows how the trend of the solution of the transformed equation can be predicted semi-quantitatively by inspection.

**15157.** Kelly, G. E., Sengers, J. V., **Droplet growth in a dilute vapor,** *J. Chem. Phys.* **61**, No. 7, 2800-2807 (Oct. 1, 1974).

Key words: aerosols; condensation; droplets; evaporation; kinetic theory; Knudsen number expansion; nucleation.

When the mass flux $\Gamma$ to a liquid droplet is expanded in terms of a parameter $\alpha$ which is the ratio of the droplet size to the mean free path (inverse Knudsen number), one obtains a series of the form $\Gamma=\Gamma^{(0)}+\Gamma^{(1)}\alpha+\Gamma^{(2)}\alpha^2\ln\alpha+\ldots$. As shown in a previous paper, the coefficients in this series are determined by integrals associated with sequences of successive collisions among a number of vapor molecules and the droplet. For a droplet surrounded by its pure vapor, we have calculated the coefficient $\Gamma^{(1)}$ of the first inverse Knudsen number correction to the free molecular growth rate $\Gamma^{(0)}$ assuming that the vapor molecules can be treated as hard spheres. For most nonequilibrium conditions, the ratio $\Gamma^{(1)}/\Gamma^{(0)}$ turns out to be positive, rather than negative, as heretofore was assumed in the literature. This result implies that the reduced growth rate $\Gamma/\Gamma^{(0)}$ will pass through a maximum as a function of the Knudsen number.

**15158.** Argentar, H., Bowen, R. L., **Colored charge-transfer complexes from *N,N*-dimethyl-*p*-toluidine,** *J. Dent. Res.* **54**, No. 3, 588-598 (May-June 1975).

Key words: aromatic amine; charge-transfer complexes; color; dental material; methacrylate, phthalate; *N,N*-dimethyl-*p*-toluidine; ultraviolet spectroscopy.

Yellow mixtures form on adding essentially colorless *N,N*-dimethyl-*p*-toluidine (DMPT) to colorless methacrylate monomers containing phthalate, isophthalate, or terephthalate diester groups. The color-causing interactions between the amines and monomers were investigated using ultraviolet spectroscopy. Equations were derived for predicting interactions between formulation ingredients and DMPT that would lead to undesired color.

**15159.** Bowen, R. L., Antonucci, J. M., **Dimethacrylate monomers of aromatic diethers,** *J. Dent. Res.* **54**, No. 3, 599-604 (May-June 1975).

Key words: composites, dimethacrylates; monomers; resins; synthesis.

Crystalline aromatic diether methacrylates can be prepared from dihydric phenols or their bis(2-hydroxyethyl) derivatives by simple condensation procedures. Three solid isomers form a liquid ternary eutectic when mixed in suitable proportions.

**15160.** Barger, R. L., West, J. B., English, T. C., **Fast frequency stabilization of a cw dye laser,** *Appl. Phys. Lett.* **27**, No. 1, 31-33 (July 1, 1975).

Key words: cw dye laser; frequency stabilization; intensity stabilization.

A system is described for stabilizing a cw dye laser frequency to a high-finesse optical cavity. The length of this optical cavity is locked to a $CH_4$-stabilized He-Ne laser with a tunable frequency-offset technique. A very fast servo system (using an intracavity KD*P crystal), a long dye laser cavity, and the stabilized optical cavity result in an absolute frequency stability of 1 kHz for an integration time of $10^{-4}$ sec and 300 Hz for 300 sec. Intensity is stabilized to one part in $10^4$.

**15161.** Bowen, R. L., **Adhesive bonding of various materials to hard tooth tissues. VII. Metal salts as mordants for coupling agents,** (Proc. Symp. on Dental Adhesive Materials, New York, N.Y., Nov. 8-9, 1973), Paper in *Dental Adhesive Materials,* H. D. Moskowitz, G. T. Ward, and E. D. Woolridge, Eds., pp. 205-221 (Prestige Graphic Services, New York, N.Y., 1974).

Key words: adhesive bonding; chelation; comonomers; coupling agents; dental materials; hard tooth tissues; metal ions; mordant.

A number of hypothetical concepts are presented to serve as a guide for experimentation. The concepts include the combined use of etching and surface-active comonomers to obtain improved adhesive bonding between polymers and hard tooth tissues, and the use of certain metal ions to augment the interaction between the coupling agents and the tooth surfaces.

**15162.** Brown, W. E., Patel, P. R., Chow, L. C., **Formation of $CaHPO_4 \cdot 2H_2O$ from enamel mineral and its relationship to caries mechanism,** *J. Dent. Res.* **54,** No. 3, 475-481 (May-June 1975).

Key words: caries mechanism; dicalcium phosphate dihydrate; enamel mineral solubility; pyrophosphate formation.

Tooth enamel, when treated with dilute $H_3PO_4$ solutions, dissolved incongruently with formation of large $CaHPO_4 \cdot 2HO_2O$ crystals. Equilibrated solutions were saturated with respect to $CaHPO_4 \cdot 2H_2O$, and a mineral more soluble than well-crystallized, synthetic $Ca_5(PO_4)_3OH$, probably an impure, defective apatite. The $CaHPO_4 \cdot 2H_2O$ crystals formed at considerably higher pH values than expected because of enhanced solubility of the apatitic phase in enamel. Pyrolysis of carious enamel revealed the presence of acidic calcium phosphate presumed to be $CaHPO_4 \cdot 2H_2O$.

**15163.** Ebert, P. J., Dick, C. E., **Comments on the observation of nondivergent radiation of discrete frequencies,** *Phys. Rev. Lett. Comments* **34,** No. 24, 1537-1539 (June 16, 1975).

Key words: comment to editor; discrete; frequencies; nondivergent radiation.

A high-resolution spectroscopic study has been made of the radiation emitted in the forward direction from cylindrical targets bombarded with electrons. The discrete energy bands previously reported by Das Gupta were not observed for photon energies from 4 to 200 keV.

**15164.** Haas, S. S., Brauer, G. M., Dickson, G., **A characterization of polymethylmethacrylate bone cement,** *J. Bone J. Surg.* **57-A,** No. 3, 380-391 (Apr. 1975).

Key words: acrylic resin; cement; medical materials; orthopedic materials; polymethylmethacrylate, self-curing; surgical bone cement; total hip replacement, cement.

Polymethylmethacrylate cement is characterized in terms of chemical composition, handling characteristics, and physical properties; the dough time, setting time, handling time, and temperature rise were found to be most affected by environmental temperature and kneading of the dough mass. As the set material ages, the residual monomer content gradually decreases and the strength increases. A volume shrinkage of up to 5 percent was observed. The porosity, which is increased by rapid mixing, may reach 10 percent. The mechanical properties of the cement approximate those of polymethylmethacrylate denture base materials. Some variability encountered in the handling qualities of the cement could be attributed only to the variability of different batches.

**15165.** Meinke, W. W., **Characterization of solids-chemical composition,** Chapter 7 in *Treatise on Solid State Chemistry,* N. B. Hannay, Ed., **1,** 387-435 (Plenum Press, New York, N.Y., 1973).

Key words: activation analysis; characterization; chemical composition; chromatographic analysis; coulometry; electron probe microanalysis; ion-selective electrodes; mass spectrometry; polarography; spectrochemical analysis; thermal analysis; wet chemistry; x-ray fluorescence.

Determination of the chemical composition of solids, i.e., information on the identity and location of the atoms in a particular material, is essential if one is to have confidence that the material can be reproduced. In this chapter an integrated summary of pertinent information on many different analytical techniques is presented. Summaries of sensitivities and precisions to be expected using these techniques are given. Applications to specific characterization problems are discussed and examples are given from the literature, of detailed studies of a number of high purity materials which illustrate the present state-of-the-art for the characterization of practical samples.

**15166.** Marshak, H., Soulen, R. J., Jr., **The temperature scale defined by $^{60}Co$ γ-ray anisotropy and noise thermometry,** Pape in *Low Temperature Physics-LT* **13,** K. D. Timmerhaus, W. J. O'Sullivan, and E. F. Hammel, Eds., **4,** 498-502 (Plenum Publishing Corp., New York, N.Y., 1974).

Key words: $^{60}Co$; gamma rays; Josephson junction; noise thermometer; thermometer.

In order to establish an absolute low temperature scale we ar comparing a (hcp) single crystal $^{59}Co^{60}Co$ γ-ray anisotropy thermometer to a Josephson junction noise thermometer in the temperature region below 0.04 K. The temperature dependences o both thermometers are governed by independent fundamenta relations. Once the parameters of each system are established the temperatures obtained should be absolute, i.e., no previou calibration is needed, nor is any extrapolation used to determin the temperature. We have examined the possible sources of erro in a single crystal Co γ-ray anisotropy thermometer. Th reproducibility of the anisotropy at a fixed temperature is withi the statistical uncertainty of the measurements; systematic errors arise from the uncertainty in the value of the hyperfine interaction, neglect of a possible quadrupole interaction and/or small admixture of M3 radiation, mosaic spread of the crysta solid angle correction factor, effects of closure domains an domain walls, variation in background radiation, and effect scattered γ-rays. The effects of these errors can be calculate and subsidiary experiments can be performed to check these ca culations.

**15167.** York, G., Scheps, R., Gallagher, A., **Continuum radiatio and potentials of Na-noble gas molecules,** *J. Chem. Phys.* 6 No. 3, 1052-1064 (Aug. 1, 1975).

Key words: molecules; noble gases; radiation; sodium.

The normalized emission spectra resulting from the perturb tion of Na atoms by 1-1000 torr of noble gas have been measure in the range 10-150 nm about the 589 nm resonance line. Th spectrum, due to the A-X and B-X transitions of the Na-nob gas molecules, was measured with 1.5 nm resolution. The Na, a cell at a temperature of 417 ± 5 K, was optically pumped to t $3^2P_{1/2}$ and $3^2P_{3/2}$ states by resonance radiation. The resultin emission was measured at several Na densities to obtain the no malized emission spectra in the limit of zero radiation entra ment. Using the Franck-Condon principle, or equivalently t quasistatic theory of line broadening, and density factors, t $A^2\Pi_{1/2,3/2}$ and $X^2\Sigma_{1/2}$ state potentials for NaAr, NaKr, and Na have been obtained from the pressure dependence of the spect ntinuum absorption and emission coefficients for these lecules, obtained by application of the same theories, are also esented. The analysis identifies the low pressure limit of the ectrum as due to free collision states above the angular mo-ntum barrier. The population factors corresponding to asibound, orbiting resonances are evaluated and used in this alysis.

**168.** Hanley, H. J. M., Watts, R. O., **Molecular dynamics studies of an *m*-6-8 fluid,** *Physica* **79A,** No. 4, 351-376 (Feb. 1975).

> Key words: Axilrod-Teller correction; dense liquid; excess function; hydrodynamic limit; molecular dynamics; rare gases; velocity autocorrelation function; 11-6-8 potential.

The pressure, energy and self-diffusion coefficient have been culated for an 11-6-8 fluid using the method of molecular namics. A comparison with data for argon, krypton and xenon presented. It is shown that agreement between theory and ex-iment for the thermodynamic properties is generally within estimated precision of the calculated and experimental ues, provided three-body and quantum corrections are in-ded in the calculation, except when the density approaches triple-point density. Agreement between theoretical and ex-imental self-diffusion coefficients is satisfactory at all densi-s after allowance is made for the long-time behaviour of the ocity autocorrelation function. We demonstrate that three-dy forces are important in the liquid and that our estimates of ch forces are very close to those suggested by Barker, Fisher d Watts.

**169.** Spencer, L. V., **Some comments on Fano's theorem,** *Radiat. Res.* **63,** 191-199 (1975).

> Key words: cavity theory; dosimetry; Fano theorem; ionization chambers; radiation measurement; radiation transport.

Fano's proof that uniform radiation fields result when sources d interactions are strictly proportional to local density is cussed in connection with an alternative proof formulation.

**170.** Kasen, M. B., **Mechanical and thermal properties of filamentary-reinforced structural composites at cryogenic tempera-ures. 1: Glass-reinforced composites,** *Cryogenics* **15,** No. 6, 327-349 (June 1975).

> Key words: cryogenics; dynamic mechanical properties; glass-fiber composites; literature review; static mechanical properties; thermal properties.

Objective is to provide an understanding of the general mag-ude of property values obtainable within the cryogenic tem-rature range, to provide a feel for the relative literature ranking specific composite types with regard to a specific property, d to impart an understanding of the temperature sensitivity of property of interest. A bibliography and bibliography-proper-cross-reference is included. This is Part I of a two-part series. rt II will consider advance composites.

**171.** Roberts, R. W., **The national/international measurement ystem,** *ASTM Stand. News* **2,** No. 11, 8-13 (Nov. 1974).

> Key words: international measurement; measurement system; national economy; national/international measurement system.

National and international measurements are vital to our na-nal economy. They are vital in business transactions measur-; the quality of materials and goods, vital to our citizens in asuring the performance and safety of products, and vital to vernment for measuring compliance with national laws. This measurement "system" must have anchor points and its quality must be monitored and improved. The National Bureau of Standards was established by Congress in 1901 to accomplish that function.

**15172.** Johnson, C. R., **Powers of matrices with positive definite real part,** *Proc. Am. Math. Soc.* **50,** 85-91 (July 1975).

> Key words: field of values; Hermitian matrix; normal matrix; positive definite.

For $n$ by $n$ complex matrices $A$ the following two facts are proven by elementary techniques: 1. If $A^m$ is never normal, $m \epsilon I^+$, then the equation $xA^mx^* = 0$ has a solution $0 \neq x \epsilon C^n$, $m \epsilon I^+$; 2. If $H(A) = (A + A^*)/2$ is positive definite, then $H(A^m)$ is positive definite for all $m \epsilon I^+$ if and only if $A$ is Hermitian.

**15173.** Hanley, H. J. M., Watts, R. O., **The self-diffusion coefficient of liquid methane,** *Mol. Phys.* **29,** No. 6, 1907-1917 (June 1975).

> Key words: correlation function; experimental data; hydrodynamic behavior; methane; molecular dynamics; potential function; self-diffusion coefficient; 11-6-8 potential function.

Self-diffusion coefficients of methane have been calculated over a wide density range using the method of molecular dynamics. Methane intermolecular interactions were modelled using an *m*-6-8 potential with coefficients determined from viscosity data for the dilute gas. After adding a contribution to the diffusion coefficient due to the long-time behaviour of the velocity autocorrelation function, agreement with experimental data is within the estimated errors given for both the calculated values and the experimental data.

**15174.** Goldberg, R. N., **Thermodynamics of hexokinase-catalyzed reactions,** *Biophys. Chem.* **3,** 192-205 (1975).

> Key words: adenosine-5′-triphosphate; biochemistry; enzyme catalyzed reactions; glucose; heat measurements; *hexokinase*; metabolic processes; microcalorimetry; thermochemistry; thermodynamics.

The enthalpies of the *hexokinase*-catalyzed phosphorylation of glucose, mannose, and fructose by ATP to the respective hexose 6-phosphates have been measured calorimetrically in TRIS/TRIS · HCl buffer at 25.0, 28.5, and 32.0 °C. The effects on the measured enthalpy of the glucose/*hexokinase* reaction due to variation of pH (over the range 6.7 to 9.0) and ionic strength (over the range 0.02 to 0.25) have been examined. Correction for enthalpy of buffer protonation leads to $\Delta H°$ and $\Delta C_p°$ values for the processes: eq-D-hexose + $ATP^{4-}$ = eq-D-hexose 6-phosphate$^{2-}$ + $ADP^{3-}$ + $H^+$. Results are $\Delta H° = -23.8 \pm 0.7$ kJ · mol$^{-1}$ and $\Delta C_p° = -156 \pm 280$ J · mol$^{-1}$ · K$^{-1}$ for glucose, $\Delta H° = -21.9 \pm 0.7$ kJ · mol$^{-1}$ and $\Delta C_p° = 10 \pm 140$ J · mol$^{-1}$ · K$^{-1}$ for mannose, and $\Delta H° = -15.0 \pm 0.9$ kJ · mol$^{-1}$ and $\Delta C_p° = -41 \pm 160$ J · mol$^{-1}$ · K$^{-1}$ for fructose. Combination of these measured enthalpies with Gibbs energy data for hydrolysis of $ATP^{4-}$ and that for the hexose 6-phosphates lead to $\Delta S°$ values for the above *hexokinase*-catalyzed reactions.

**15175.** Kraft, R., **Finite difference techniques for diffusion and redistribution problems with segregation-type boundary conditions,** (Proc. AICA Int. Symp. on Computer Methods for Partial Differential Equations, Bethlehem, Pa., June 17-19, 1975), Paper in *Advances in Computer Methods for Partial Differential Equations,* R. Vichnevetsky, Ed., pp. 328-333 (AICA Dept. of Computer Science, New Brunswick, N.J., 1975).

> Key words: diffusion equations; finite-difference techniques; impurity redistribution; moving boundary

problems; numerical methods; partial differential equations; semiconductor technology.

Finite difference techniques and a particular computer algorithm are given for a one dimensional diffusion problem in a composite domain with time dependent domain and moving interfacial boundary. The physical problem involves the redistribution of an impurity (boron) caused by the oxidation of a semiconducting crystal (silicon). The boundary conditions at the interfacial boundary express conservation of mass and the propensity of the impurity to be dissolved in one rather than the other of the two adjacent materials (the segregation condition). The novel feature of the algorithm is its employment of the integral form of the conservation of mass boundary condition instead of the conventionally used differential form.

**15176.** Raveché, H. J., Mountain, R. D., Streett, W. B., **Reply to the comment on "Monte Carlo studies of the fluid-solid phase transition in the Lennard-Jones system,"** *J. Chem. Phys.* **62,** No. 11, 4582-4583 (June 1, 1975).

Key words: coexisting densities; finite system; "flat" loop; fluid-solid phase transition; Lennard-Jones System; Monte Carlo Studies.

The issue between SRM and HV is shown to be the uncertainty in the coexisting densities obtained by the two methods and not the methods themselves.

**15177.** Reinker, R. P., Timmerhaus, K. D., Kropschot, R. H., **Thermal conductivity and diffusivity of selected porous insulations between 4 and 300 K,** Chapter I-4 in *Advances in Cryogenic Engineering* **20,** 343-354 (Plenum Press, New York, N.Y., 1975).

Key words: cryogenic insulation; powders; thermal conductivity; thermal diffusivity.

The thermal conductivity and thermal diffusivity of selected evacuated porous insulations have been measured between 4 and 300 K to better understand the heat transport mechanisms. The thermal conductivity of both perlite and uncoated microspheres can be represented by $k=bT^3$ to within the experimental error. The conductivity of aluminum coated microspheres was found to be highly dependent upon sample history.

**15178.** Raveché, H. J., Stuart, C. A., **Towards a molecular theory of freezing,** *J. Chem. Phys.* **63,** No. 3, 1099-1111 (Aug. 1, 1975).

Key words: branching; freezing points; metastable fluids; nonlinear operator; pair correlation function; single particle probability density.

The subject of this article is the fluid-solid transition and, in particular, an analysis of crystallization in terms of quantities which describe the average local arrangements of molecules in a fluid. We determine whether it is possible to predict the existence of crystalline solutions for the local molecular density from a Hamiltonian which is invariant under all translations and rotations. Crystallization is studied using the singlet probability density, the pair correlation function, and the intermolecular potential energy. An integral equation is obtained for these quantities, and we pursue the existence of crystalline (i.e., periodic but nonconstant) solutions for the singlet probability which branch from the fluid (i.e., constant) solution which is the number density. The phenomenon of crystallization, that is, the existence and determination of these solutions, can then be represented as a nonlinear eigenvalue problem. The analysis is applied to hard sphere systems in one, two, and three dimensions. Crystallization to close-packed lattices is found in two and three dimensions when the isotropic media are overcompressed by amounts which depend on the structures to which the fluids crystallize. That is, the fluid persists into a portion of the metastable region. The nature of the crystalline solutions is analyzed in the neighborhood of the branching eigenvalues, and the relation between these special eigenvalues and equilibrium freezing points is discussed. The stability of these crystalline solutions is determined by comparing the values of a free energylike functional on these solutions with its value for the fluid.

**15179.** Hudson, R. P., **Conference report: European conference on temperature measurement,** *Cryogenics* **15,** 486 (Aug. 1975).

Key words: conference; temperature; thermometry.

A short report on the European Conference on Temperature Measurement (held in Teddington, London, April 9-11, 1975 at the National Physical Laboratory).

**15180.** Haber, S., **Adaptive integration and improper integrals,** *Math. Comput.* **29,** No. 131, 806-809 (July 1975).

Key words: improper integrals; integrals; numerical analysis; numerical integration; numerical quadrature; quadrature; Riemann integral; singularities.

Let $R$ be the class of all functions that are properly Riemann-integrable on $[0, 1]$, and let $IR$ be the class of all functions that are properly Riemann-integrable on $[a, 1]$ for all $a > 0$ and for which

$$\lim_{a\to 0^+} \int_a^1 f(x)dx$$

exists and is finite. There are computational schemes that produce a convergent sequence of approximations to the integral of any function in $R$; the trapezoid rule is one. In this paper, it is shown that there is no computational scheme that uses only evaluations of the integrand, that is similarly effective for $IR$.

**15181.** Unassigned.

**15182.** Arp, V. D., Clark, A. F., Flynn, T. M., **Superconducting levitation of high speed vehicles,** *Transp. Eng. J.* **99,** No. TE4, 873-885 (Nov. 1973).

Key words: levitation; magnetic suspension; materials fatigue data; refrigeration; superconducting magnets; transportation.

The current status (December 1972) of worldwide research on high speed ground transportation techniques is reviewed. Particular attention is given to studies of magnetic levitation using superconducting magnets, including comparison with alternative magnetic techniques and with air suspension systems. Superconducting levitation appears to be a strong contender in the U.S. Department of Transportation hopes to select in the late 1970's the best of the possible levitation techniques for subsequent advanced development. Cryogenic engineering research needed in support of major development of a superconducting levitated system is identified.

**15183.** Cohen, J., Edelman, S., **Polymeric pyroelectric sensors for fire protection,** *Tech. Rep. AFAPL-TR-74-16,* 27 pages (Available from the National Technical Information Service, Springfield, Va. 22151, 1975).

Key words: heat detector; optical radiation sensor; poling; polymer; polyvinyl fluoride; polyvinylidene fluoride; pyroelectric effect; relative spectral response; ultraviolet detector.

This report summarizes the results of a program to develop optical radiation sensors for fire detection using polymeric pyroelectric sensing elements. Emphasis has been placed on techniques for constructing such devices, including methods of enhancing the pyroelectric response. Materials investigated included polyvinyl fluoride (PVF) and polyvinylidene fluoride

($PVF_2$). Six sensors were developed and delivered to the sponsor.

Highlights reported include achievement of a value of specific detectivity, $D^*$, of $2 \times 10^8$ cm · $Hz^{1/2}$ · $W^{-1}$ and the construction of a set of sensors useful over a wavelength range extending from the ultraviolet to the infrared.

Methods of characterizing the performance of sensor elements are described.

**15184.** Hanley, H. J. M., McCarty, R. D., Haynes, W. M., **Equations for the viscosity and thermal conductivity coefficients of methane,** *Cryogenics* **15,** No. 7, 413-417 (July 1975).

Key words: correlation; critical point; equation of state; methane; thermal conductivity; thermal conductivity coefficient; viscosity coefficient.

An equation is proposed to calculate the viscosity and thermal conductivity coefficients of methane from the dilute gas to the dense liquid. The range of validity of the equation is approximately 95-400 K for pressures up to 50 MPa (~ 500 atm). The reliabilities of the coefficients calculated are estimated at approximately 2 percent and 5 percent for the viscosity and thermal conductivity coefficients, respectively. The equation includes a contribution for the thermal conductivity enhancement in the critical region.

**15185.** Brauer, G. M., **Modification of soft and hard tissues,** (Proc. Symp. on Dental Adhesive Materials, New York, N.Y., Nov. 8-9, 1973), Paper in *Dental Adhesive Materials,* Moskowitz-Ward-Woolridge, Eds., pp. 180-204 (Prestige Graphic Services, New York, N.Y., Sept. 1974).

Key words: bone; chemical grafting; collagen; ratskin; surface modification; tissue surfaces.

Various techniques to modify hard and soft tissues, with the aim of enhancing adhesion, are reviewed. Treatment of enamel surfaces with acids enhances adhesion because of mechanical interlocking of resin at the enamel resin interface. Coupling agents have had some success in promoting adhesion of tooth structure to dental restoratives.

Special emphasis is given to chemical grafting techniques to obtain covalent bonding to tissue surfaces which are investigated in our laboratory.

The grafting of monomers to soft and hard tissues so that after polymerization of the monomer the proteinaceous surface is bonded covalently to the polymer side chain, offers an attractive technique for improving surface characteristics of skin, bone or dentin. Grafting monomers containing additional functional groups that are potential reactive centers for further modification of the collagenous surfaces appears feasible. Grafting to soft tissues can be conducted in the presence of various redox systems, but grafting to bone is best accomplished with persulfate-bisulfite initiator. Modification of the tissue surface is indicated by changes in wettability, decreased water sorption and improved resistance to mold growth. Surfaces with the desired degree of hydrophil to lipophil balance to suit specific applications may be prepared. The modified surfaces could be useful as adhesion promoting liners for restorative resins.

**15186.** Rupp, N. W., **Dental amalgam, a plea for clinical research,** *J. Am. Acad. Gold Foil Operators* **13,** No. 1, 29-31 (Spring 1975).

Key words: creep; dental amalgam; marginal ditching.

Marginal ditching of dental amalgam restorations was related to the physical property of creep in clinical studies directed by Mahler. Because of his conclusions and similar results in other studies, a recommended revision of the ADA Specification No. 1, Alloy for Dental Amalgam, includes a creep test. This effort to improve the specification and limit the certification of alloys to those having good marginal integrity is dependent upon well planned, clinical research.

**15187.** Weinstein, B. A., Piermarini, G. J., **Raman scattering and phonon dispersion in Si and GaP at very high pressure,** *Phys. Rev. B* **12,** No. 4, 1172-1186 (Aug. 15, 1975).

Key words: Gallium phosphides; high pressure; metallic phase transitions; phonon dispersion; Raman scattering; silicon.

One- and two-phonon Raman spectra of Si and GaP were measured at room temperature for pressures up to 135 kbar. An opposed diamond-anvil high-pressure cell was employed in the experiments, and its design and use for Raman scattering are described in detail. Mode Grüneisen parameters and quadratic pressure coefficients were measured for phonons at several zone-boundary critical points as well as at $\tilde{q} \approx 0$. In addition the general effect of pressure on large portions of the phonon dispersion near the zone edge could be inferred. In both materials zone-boundary TA modes "softened" with increasing pressure, while optical phonons shifted to higher energy. Using the high-pressure Raman data a calculation of the thermal-expansion coefficient of Si as a function of temperature (negative at low temperature) achieved fair agreement with experiment. Measured and theoretically calculated mode Grüneisen parameters are compared for several tetrahedral semiconductors. The Raman spectrum of Si was measured up to the metallic ($\beta$-Sn structure) transformation at $125 \pm 5$ kbar. This transition is discussed within the context of the bond-charge model.

**15188.** Robinson, R. L., Jr., Hiza, M. J., **Solid-vapor equilibrium—A survey,** Chapter F-2 in *Advances in Cryogenic Engineering* **20,** 218-239 (Plenum Press, New York, N.Y., 1975).

Key words: binary systems; cryogenic fluids; interaction second virial coefficients; review; solid-vapor equilibria; unlike molecule interactions.

The current status of knowledge regarding solid-vapor equilibrium is reviewed. Available data are summarized for systems composed of He, Ne, Ar, Kr, Xe, $H_2$, $N_2$, $O_2$, $F_2$, CO, $CO_2$, $CH_4$, $C_2H_4$, $C_2H_6$. Currently used experimental techniques are described, including experimental difficulties. Methods for theoretical description of solid-vapor equilibrium are given. The value of solid-vapor equilibrium data is discussed, with emphasis on the information furnished regarding unlike-molecule interactions.

**15189.** Unassigned.

**15190.** Margulis, S. T., **A comparison of the opinions of Operation Breakthrough occupants and conventional housing occupants about their housing,** *Industrialization Forum* **6,** No. 1, 21-26 (1975).

Key words: architectural psychology; dwelling unit; federal building research; industrialized housing; occupant behavior; Operation Breakthrough; performance evaluation.

Occupants of Operation Breakthrough and of conventional housing were interviewed about their homes and on related topics. The opinions of these two groups of occupants were compared in order to determine comparability of the housing based on the opinions of their occupants. The matching of OBT and conventional housing, their occupants and their sites was relatively successful. The comparison of occupant opinions lead to the conclusion that OBT housing was favorably evaluated and that its evaluation was at least as good as if not superior to that of the conventional housing. The conclusion is discussed in the context of earlier research on industrialized housing and in terms of the goals of the Operation Breakthrough program.

**15191.** Haas, S. S., Dickson, G., Brauer, G. M., **A proposed specification for acrylic bone cement,** *J. Biomed. Mater. Res. Symp.* **9,** No. 4, 105-117 (1975).

Key words: biomaterial; bone cement; orthopaedic material; poly(methyl methacrylate); specification; surgical bone cement.

A proposed specification covering handling characteristics and physical and chemical properties of bone cement composed primarily of methyl methacrylate has been prepared on the basis of data from the authors' studies and from various other sources. Under handling characteristics, requirements included relate to dough, handling and setting time, proper plasticity for insertion and temperature rise on setting. Mechanical properties specified include compressive strength and indentation and recovery characteristics. Maximum limits are proposed for water sorption and solubility. Suggested packaging requirements are also included.

**15192.** Cox, J. E., Bostock, J., Waterstrat, R. M., **Superconducting properties of A15 phase V-Ir alloys,** (Proc. 13th Int. Conf. on Low Temperature Physics-LT 13, Boulder, Colo., Aug. 21-25, 1972), Paper in *Low Temperature Physics-LT 13,* K. D. Timmerhaus, W. J. O'Sullivan, and E. F. Hammel, Eds., **3,** 480-484 (Plenum Publishing Corp., New York, N.Y., 1974).

Key words: A15 phases; iridium alloys; superconductivity; vanadium alloys.

Superconducting transition temperatures, $T_0$, and initial slopes of the critical magnetic field curves have been determined for A15 phase V-Ir alloys. Samples investigated range from $V_{61}Ir_{39}$ to $V_{75}Ir_{25}$ in 2 at.% steps. $T_0$ increases with increasing Ir content, from < 15 mK for $V_{75}Ir_{25}$ to 1.85K for $V_{61}Ir_{39}$. Low temperature ordering anneals do not markedly affect the superconducting properties of these alloys. Metallurgical aspects of these materials are discussed.

**15193.** Ehrlich, M., **The use of pressed LiF for thermoluminescence dosimetry without furnace annealing,** *Phys. Med. Biol. Tech. Note* **19,** No. 5, 725-731 (1974).

Key words: dosimetry; fading; furnace annealing; glow curve; maximum heating temperature; peak height; reproducibility; sensitivity loss; supralinearity.

A method of LiF thermoluminescence dosimetry (TLD) requiring no furnace annealing is described which can be used with many general-purpose commercial TLD readers. With this method, one produces LiF TLD characteristics similar to those obtained after conventional annealing. Glow-curve areas following successive identical exposures of a sample reproduce to within a relative standard deviation of 1 percent, but peak heights are less reproducible. Supralinearity characteristics are similar to those of conventionally annealed samples. While fading is somewhat more pronounced, it is not prohibitive for many medical applications. Maximum nominal planchet temperatures of 300 °C during readout produce essentially complete annealing in the medical exposure range, without appreciable loss in sensitivity due to successive irradiations and readouts, while sensitivity losses sometimes amount to as much as 8-10 percent for maximum nominal readout temperatures of 400 °C.

**15194.** Cunitz, R. J., Galloway, W. D., Berman, C. M., **Behavioral suppression by 383-MHz radiation,** *IEEE Trans. Microwave Theory Tech.* **MTT-23,** No. 3, 313-316 (Mar. 1975).

Key words: behavior; behavioral suppression; exposure; microwave radiation; microwaves; product safety; radiation; radiation effects; resonant cavity; rhesus; suppression.

The heads of two rhesus monkeys were irradiated in a 383-MHz resonant cavity immediately before and during performance of a four-choice forced-choice serial reaction task. CW radiation at integral dose rates of 0.001-17.5 W were delivered to the head. No effects were observed below a critical dose level (≈ 23 W/kg) derived from integral dose rate and body mass. Above this level, behavioral suppression occurred, i.e., correct response rate was profoundly altered. The effect was completely reversible and repeatable in one of the subjects – the other subject did not recover completely and was sacrificed for histological examination which revealed no gross or microscopic damage. The nature of the effect suggests a neurochemical rather than an electrical or mechanical basis for the results.

**15195.** Chuong, R., **Experimental study of surface and lattice effects on the solubility of hydroxyapatite,** *J. Dent. Res.* **52,** Supplement to No. 5, 911-914 (Sept.-Oct. 1973).

Key words: hydroxyapatite; nonstoichiometry; solid-to-solution ratio; solubility; surface chemistry.

Brown et al. have formulated a thermodynamic treatment for the solubility of hydroxyapatite in which recognition of a distinction between surface and lattice contributions is explicitly made. Verification of the applicability of this approach to the $Ca(OH)_2$-$H_3PO_4$-$H_2O$ system has been carried out by Avnimelech et al. The purpose of the present study is to apply the theory of Brown et al. to the quaternary system $Ca(OH)_2$-$H_3PO_4$-$H_2O$-HCl. Three solution series, each involving a given HCl concentration, were prepared with solid-to-solution ratios of 0.2, 0.4, 0.5, 0.8, 1.0, and 2.0 g/100 ml. Solutions were agitated for 5 days at 25 °C, after which they were filtered. pH, Ca and P were determined and ion activity products and electroneutrality unbalances were calculated. The findings indicate that the Ca/P ratios in the final solutions varied with both the solid-to-solution ratio and the initial HCl concentration. However, the ion activity products for hydroxyapatite were essentially constant. These results indicate that the contribution of the surface to the overall dissolution reaction relative to that of the lattice must be taken into account, but in conformity with theory standard solubility product principles are applicable to the final equilibrium reaction.

**15196.** Jennings, D. A., Evenson, K. M., Jimenez, J. J., **New $CO_2$ pumped CW far-infrared laser lines,** *IEEE J. Quantum Electron.* **QE-11,** No. 8, 637 (Aug. 1975).

Key words: IR; laser, optically pumped; waveguide cavity.

A single-frequency CW $CO_2$ laser has been used to pump ethyl alcohol, methyl chloride, ethyl chloride, and methylene chloride generating 8 new CW far-infrared (FIR) laser lines from 254 to 1700 μm.

**15197.** Chew, W. M., Xenoulis, A. C., Fink, R. W., Schima, F. J. Mann, W. B., **The L/K electron capture ratio in first-forbidden $^{81g}$Kr decay,** *Nucl. Phys.* **A229,** 79-92 (1974).

Key words: deduced $Q_{EC}$, log *ft*, $J^{\pi}$; enriched $^{80}$Kr target isotope separated sources; measured L/K EC ratio; multiwire proportional counter; radioactivity $^{81g}$Kr [from (n,γ)].

The L/K electron capture (EC) ratio of $^{81g}$Kr was measured to be $0.146 \pm 0.005$ utilizing the wall-less, anticoincidence, multiwire proportional counter technique and a reactor-produced mass separated $^{81g}$Kr source. From this value, the $Q_{EC}$ and log *f* values were determined to be $305_{-29}^{+38}$ keV and 11.6 respectively, assuming EC decay only to the ground state. If there is 4 percent EC branching to a reported 276 keV level, $Q_{EC}$ become

$22_{-14}^{+31}$ keV from which $(L/K)_{g.s.} = 0.144 \pm 0.005$, log $ft = 11.6$ r EC to the ground state, $(L/K)_{276} = 0.213 \pm 0.005$, and log $ft =$ 1.4 for 4 percent feeding to the 276 keV level. In order to be onfident of these results, an extensive systematic comparison f experimental and theoretical L/K ratios was made for both rst-forbidden non-unique and unique transitions. From this omparison, a 7/2+ ground state assignment for $^{81}$Kr is con-rmed.

**5198.** Davis, R. M., **Technology as a deterrent to dehumanization,** *Science* **185,** 737 (Aug. 30, 1974).

Key words: dehumanization; deterrent; technologies.

This requested editorial discusses the role of technology as ne of the better deterrents to dehumanization. It cites the confu-ion surrounding the use of the newer technologies of computers, utomation and communication in terms of their benefits or dis-dvantages to the public. It highlights the need for better scien-fic advice in these areas to senior policy makers.

**5199.** Davis, R., **Impermanent balance between man and computer,** *Science* **186,** 99 (Oct. 11, 1974).

Key words: artifacts; balance; computer; impermanence; intelligence; power; science; technology.

This requested editorial discussed the relative but changing alance between man and computer in the accomplishment of so-alled intellectual tasks. It highlights the impermanence of the alance and emphasizes the need for people to better understand heir need to define the man-computer interrelationship.

**5200.** Schutz, G. C., Clark, G. E., **Data communication standards,** *Computer* **7,** No. 11, 32-37 (Feb. 1974).

Key words: American National Standards Institute; Computer Society of the IEEE; Data Communication Standards; Electronics Industries Association; International Standards Organization; International Telecommunications Union.

This paper provides an overview description of a number of rganizations that are involved in the development of industry, American national and international standards pertaining to data ommunications. The significant organizations include: the Computer Society of the Institute of Electrical and Electronic Engineers, the Electronics Industries Association, the American National Standards Institute, the International Standards Organization and the International Telecommunications Union. The functions and objectives of the pertinent committees, sub-ommittees and task groups sponsored by these organizations as well as various formal and informal interworking relationships among them are described. Timely information includes a discus-ion of presently unresolved technical issues being addressed by he data communication standards community as well as listings of the standards approved by each of the organizations described.

**5201.** Dresser, M. J., Madey, T. E., Yates, J. T., Jr., **The adsorption of xenon by W(111), and its interaction with preadsorbed oxygen,** *Surface Sci.* **42,** 533-551 (1974).

Key words: desorption energy; desorption kinetics; physical adsorption; tungsten (111); work function; xenon.

The physisorption of Xe on W(111) and of Xe on partial layers of oxygen chemisorbed on W(111) has been studied using flash desorption and work function methods. It has been found that xenon adsorbs up to monolayer coverages at 104 K. Xenon desorbs from W(111) as a single binding state following first order kinetics. At low coverages ($\theta_{Xe} < 0.07$) the binding energy decreases with increasing coverage possibly because of the presence of high energy adsorption sites due to crystal imperfections and edge effects. For $\theta_{Xe} > 0.07$ the desorption data fit a first order rate expression with a desorption energy of 9.3 kcal/mol and preexponential $\nu = 10^{15}$ s$^{-1}$. The observed work function change of $-1.1 \pm 0.1$ eV is consistent with monolayer estimates reported in field emission studies of physisorbed xenon on tungsten. The effect of preadsorbed oxygen layers on the physisorption of xenon on this surface is very striking. The energy of desorption shifts as much as 50 percent higher for a moderate exposure of oxygen. Several physisorption models are explored along with estimates of dispersion and electrostatic interaction contributions.

**15202.** Snyder, J. J., **Paraxial ray analysis of a cat's-eye retroreflector,** *Appl. Opt.* **14,** No. 8, 1825-1828 (Aug. 1975).

Key words: optical devices; optics, precision; reflector, cat's-eye; retroreflector, cat's eye.

The cat's-eye retroreflector is a passive optical system consisting of a secondary mirror placed at the focal point of a primary lens. We analyze the cat's eye using the paraxial ray matrix approach. The position of the equivalent reflecting surface and the angular field of view of a realizable cat's eye are functions of the radius of curvature of the secondary mirror. The field of view is maximum for a secondary mirror with a concave radius of curvature equal to the focal length of the primary lens. We further derive the general dependence of retroreflection errors on misadjustment of the secondary mirror.

**15203.** Pella, P. A., Diamondstone, B. I., **Stability of aqueous ethanol solutions stored in glass ampules,** *J. Forensic Sci. Tech. Note* **20,** No. 3, 537-538 (1975).

Key words: breath alcohol analyzers; dichromate oxidimetry; performance standards; reference ethanol solutions.

Stability studies were carried out on ampules samples of ethanol-water solutions. These solutions are used to measure performance capabilities of breath alcohol detection instruments.

**15204.** Meyerson, M. R., **The proposed Department of Commerce "Voluntary" Labeling Program,** (Proc. 1973 Technical Seminar for College Educators of Home Equipment, Dallas, Tex., Nov. 1-3, 1973), Paper in *Proceedings 1973 Technical Seminar for College Educators of Home Equipment,* pp. 9-10 (Association of Home Appliance Manufacturers, Chicago, Ill., 1973).

Key words: education; efficiency comparison; household appliances; household equipment; label developments; labeling; label specification; monitoring priorities; product classes; test methods; voluntary.

The features of the Department of Commerce Program for the Voluntary Labeling of Major Household Appliances and Equipment to Effect Energy Conservation are presented. These procedures were published in the Federal Register on October 26. The steps involved in carrying out the program are (1) setting of priorities among products, (2) establishment of product classes where appropriate, (3) setting of test methods to be used, (4) developing a system for comparing the efficiency of similar products, (5) development of a label that is meaningful to consumers, (6) publication of a Proposed Label Specification in the Federal Register with time for comment, (7) evaluation of comments, (8) publication of the Final Label Specification, (9) education of the public as to the meaning of the program, and (10) monitoring of the program to insure compliance.

**15205.** Laufer, A. H., Bass, A. M., **Mechanism and rate constant of the reaction between methylene and methyl radicals,** *J. Phys. Chem.* **79,** No. 16, 1635-1638 (1975).

Key words: combination; flash photolysis-gas chromatography; methyl; methylene; radicals; rate constant.

The chemistry of the reaction between methyl and triplet methylene radicals has been examined by means of flash photolysis of azomethane and ketene followed by gas chromatographic analysis of the hydrocarbon products. Using the combination rate constant of triplet $CH_2 = 5.3 \times 10^{-11}$ cm³ molecule⁻¹ sec⁻¹ and the combination of $CH_3 = 9.5 \times 10^{-11}$ cm³ molecule⁻¹ sec⁻¹, a value of $1.0 \pm 0.1 \times 10^{-10}$ cm³ molecule⁻¹ sec⁻¹ for the reaction $^3CH_2 + CH_3 \rightarrow C_2H_5^* \rightarrow C_2H_4 + H$ has been determined.

**15206.** Leasure, W. A., Jr., Bender, E. K., **Tire-road interaction noise,** *J. Acoust. Soc. Am.* **58,** No. 1, 39-50 (July 1975).

Key words: acoustics; noise (sound); tire noise; transportation noise.

The relative importance of tire noise to overall vehicle noise is established. A general description is then given of the tire engineering process and of tire structures. The important parameters influencing tire noise are discussed, based on presently available data, followed by an identification of unknown and contradictory areas. The basic mechanisms of tire-noise generation, although not well understood, are investigated largely from a theoretical viewpoint. Areas for future research and development are identified based on gaps in the existing physical data base and a rather primitive level of understanding of noise-generating mechanisms.

**15207.** Copley, J. R. D., Rowe, J. M., **Short-wavelength collective excitations in liquid rubidium observed by coherent neutron scattering,** *Phys. Rev. Lett.* **32,** No. 2, 49-52 (Jan. 14, 1974).

Key words: collective excitations; liquid rubidium; neutron scattering; propagating modes; scattering function; short wavelength.

The short-wavelength collective excitations in liquid rubidium at 320 K have been studied by coherent neutron scattering. For values of $\kappa = 2\pi/\lambda$ up to 1.0 Å⁻¹, clear evidence of propagating modes was found from the shape of the scattering function $S(\kappa,\omega)$ at constant values of $\kappa$. This result shows that the existence of such modes does not depend upon either quantum effects or low thermal population of the modes.

**15208.** Berger, R. E., **Effect of contact lens motion on the oxygen tension distribution under the lens,** *Am. J. Optom. Physiol. Opt.* **51,** No. 7, 441-456 (July 1974).

Key words: contact lens; contact lens motion; diffusion; hydrodynamics; mathematical model; oxygen; oxygen tension; oxygen tension distribution.

A method of predicting the oxygen tension distribution under a contact lens is illustrated for some simple, but practical, lens motions. A hydrodynamic theory is used to find those regions which receive fresh tear fluid during a blink. Then a diffusion model is solved to find the oxygen tension distribution at all times between blinks. The results are compared with earlier models in which details of the fluid flow were neglected, as were variations of oxygen tension with position under the lens. Depending on the motion of the lens, the tear fluid exchange factor can be quite large without eliminating regions in which the oxygen tension is below critical levels. The results suggest that the situation can be improved if the lens is designed for large displacements, with the blink, in the direction parallel to the cornea.

**15209.** Mazur, J., McIntyre, D., **The determination of chain statistical parameters by light scattering measurements,** *Macromolecules* **8,** No. 4, 464-476 (July-Aug. 1975).

Key words: chain correlation; chain statistical parameters; light scattering; Monte-Carlo computations, chase transition; scattering function.

The effects of volume exclusion on polymer chain conformations can be determined from the study of the angular dependence of radiation scattered by chain molecules. It is found that useful information can be obtained only when the variable $x$ is large, where $x$ is the product of the square of the magnitude of the scattering vector and of the mean square radius of gyration. Hence, solutions of macromolecules of very high molecular weight are needed for these investigations. The theoretical treatment of the scattering function is based on several assumptions. The validity of these assumptions is examined by computing, using a Monte-Carlo technique, various moments of intramolecular separations and comparing the results so obtained, in the limit of a chain of infinite length, with the analytical results. The computations seem to verify the validity of the theoretical model. The scattering behavior of solutions of recently synthesized polystyrene of $M_W = 4.4 \times 10^7$ in cyclohexane at various temperatures and in benzene at 40° was investigated. From the log − log plots of the scattering function vs. $x$, a statistical parameter was calculated, whose value depends on the magnitude of long-range correlations between any pair of chain elements. It is found that above the Θ temperature this parameter is practically independent of temperature and that its numerical value was found to agree well with the value obtained from Monte-Carlo calculations. In the neighborhood of the Θ temperature, this parameter decreases rapidly with decreasing temperature, indicating a first-order transition in chain conformation.

**15210.** Buhl, D., Snyder, L. E., Lovas, F. J., Johnson, D. R., **Silicon monoxide: Detection of maser emission from the second vibrationally excited state,** *Astrophys. J.* **192,** L97-L100 (Sept. 1, 1974).

Key words: maser; M-type stars; molecular emission; Orion Nebulae; silicon monoxide; rotational transitions.

The $J = 1 - 0$ rotational transition of the second vibrational state ($v = 2$) of SiO has been detected in late M-type variable stars and in the center of the Orion Nebula. This transition of SiO requires 3520 K of excitation for pumping the observed maser line. The ground ($v = 0$), and third ($v = 3$) vibrational states were not detected.

**15211.** Casella, R. C., Robertson, B., **Direct tests for violation of *CP* invariance,** *Phys. Rev. D* **8,** No. 3, 968-970 (Aug. 1, 1973)

Key words: *CP*-violation; decays; direct tests; kaon; lepton asymmetry; momentum-dependence; Weisskopf-Wigner.

Two tests are proposed for directly establishing violation o *CP* invariance in neutral-kaon decay. Provided that there exis only two neutral kaons, these tests rely on the principles o quantum theory and relativistic kinematics and, in particular, ar independent of the Weisskopf-Wigner approximation made i the theory of Lee, Oehme, and Yang. One of these tests can b made using data that will soon be available and the other can b made with existing techniques.

**15212.** Howell, B. F., Simmons, J. H., Haller, W., **Loss of chemical resistance to aqueous attack in a borosilicate glass due t phase separation,** *Am. Ceram. Soc. Bull.* **54,** No. 8, 707-70 (Aug. 1975).

Key words: borosilicate glass; chemical durability; phas separation.

The chemical durability of a borosilicate glass was measure by a powder extraction test (ASTM C 225-68). It was found tha a progressive decrease in chemical durability occurred durin prolonged heat treatments at temperatures ranging from 29 t

° below the immiscibility temperature. Following these ex-
eme thermal histories, which are not normally encountered in
andard forming and annealing conditions, the amount of ex-
actable alkali increased by as much as 20 fold.

213. Berger, H., **Summary/Conference on Emerging Techniques for Nondestructive Field Testing,** *Mater. Eval.* **XXXIII,** No. 7, 189-191 (July 1975).

Key words: airport pavements; bridge inspection; neutron testing; pipeline inspection; railroad inspection; transportation; vehicle inspection.

The Conference on Emerging Techniques for Nondestructive
ield Testing held August 13-14, 1974, at the Transportation
ystems Center in Cambridge, Mass., was jointly organized by
e American Society for Nondestructive Testing (ASNT) and
e U.S. Department of Transportation (DOT). More than 100
rsons attended to learn more about the conference theme,
Opportunities for NDT in Transportation."

A primary purpose of the meeting was to make the NDT com-
unity aware of some of the nondestructive testing objectives
d problems of DOT, in the expectation that organizations or
dividuals who had solutions, or potential solutions to such
oblems would make them available. The meeting itself pro-
ded the initial opportunity for this interaction.

The meeting proceedings, as contained in this issue of
*laterials Evaluation,* provide a larger audience for this interac-
on possibility. My suggestion—read the papers and offer ideas
r comments for possible solutions to NDT problems to the
uthors, or to the Conference Chairman, Dr. Michael Lauriente,
ffice of the Secretary of Transportation, U.S. Department of
ransportation, Washington, D.C. 20590. We hope many
eaders of *Materials Evaluation* will respond and make the con-
rence theme a reality!

5214. Berger, H., **Radiographic nondestructive testing,** *Stand. News* **3,** No. 3, 21-29 (Mar. 1975).

Key words: dimensional measurement; gamma radiography, image enhancement; neutron radiography; nondestructive testing; proton radiography; real-time techniques; three-dimensional radiography; x-radiography.

This article is a review of radiographic nondestructive testing
or a planned nondestructive testing issue of Standardization
lews (ASTM). Several new ideas in radiographic methods are
escribed following a brief review of conventional gamma and x-
adiography. New ideas discussed include high definition radiog-
aphy, xeroradiography, electron radiography, image enhance-
ent, real-time systems, three-dimensional methods, neutron
adiography, and proton radiography.

5215. Bowman, H. A., Schoonover, R. M., Carroll, C. L., **The utilization of solid objects as reference standards in density measurements,** *Metrologia* **10,** 117-121 (1974).

Key words: density; density calibration; density measurement; density standard; volume standard.

NBS has measured the densities of four single crystal silicon
bjects to a standard deviation of 0.26 ppm with a systematic
rror of 0.7 ppm. These objects will be used as working stan-
lards to which density work in the United States will be referred.
A redundant hydrostatic comparison test involving two stan-
lards at a time has been devised, the use of which facilitates the
fficient propagation of the density information contained in
hese crystals into other objects which may be used as standards
y other laboratories. This article describes a method of employ-
ng this redundant comparison procedure.

5216. Casella, R. C., **Algorithm for computing the number of independent real parameters in the phonon dynamical matrix,** *Phys. Rev. B* **11,** No. 12, 4795-4800 (June 15, 1975).

Key words: counting independent parameters; phonon dynamical matrix; time reversal symmetry.

The effects of time-reversal symmetry in reducing the maximum number $\mathscr{M}$ of real parameters in the phonon dynamical matrix at fixed $\vec{k}$ are taken into account to yield the following result: either (I) $-\vec{k}$ is *not* in the star of $\vec{k}$ in which case $\mathscr{M}^{I} = \Sigma_r n_r^2$, or (II) it *is*, in which case $\mathscr{M}^{II} = \Sigma_{r\epsilon(a)} n_r(n_r+1)/2 + \Sigma_{r\epsilon(b)} n_r^2/2 + \Sigma_{r\epsilon(c)} n_r(n_r-1)/2$. Here, $n_r$ denotes the number of times the $r$th irreducible representation of the little group $G^{\vec{k}}$ occurs in the reducible representation $\Delta^{\vec{k}}$ at wave vector $\vec{k}$. $\Delta^{\vec{k}}$ is of dimension $3n$, where $n$ is the number of atoms per unit cell. In the expression for $\mathscr{M}^{II}$, one sums over all $r$ in cases (a), (b), and (c), respectively, where (a) (b), and (c) refer to the three cases of Wigner in the Herring criterion. The analysis is also applied to compute a lower upper bound $\mathscr{M}'$ within the rigid-molecule model as discussed group theoretically in the context of inelastic-neutron-scattering experiments by Casella and Trevino.

15217. Lang, W. W., Flynn, D. R., **Noise power emission level for product designation,** *Noise Control Eng.* **4, No. 3, 108-113 (May-June 1975).**

Key words: acoustics; machinery noise; noise; sound; sound power.

A brief discussion is given of some of the advantages of using sound power rather than sound pressure at a particular location to describe the noise emission from a particular source. To avoid confusion between sound pressure levels and sound power levels, both of which are usually expressed in decibels, it is proposed that in communications with users, the sound power levels of stationary sources be expressed in terms of Noise Emission Number, which is numerically equal to the A-weighted sound power level expressed in bels rather than decibels.

15218. Bright, R. G., **Recent advances in residential smoke detection,** *Fire J.* **68,** No. 6, 69-77 (Nov. 1974).

Key words: detection; detectors; fire fatalities; gas detectors; ionization chamber detectors; performance standards; photoelectric detector.

The loss of life by fire in the home is a significant problem in the U.S. Had the homes been equipped with an early-warning, fire detection device between 40 and 50 percent of the people killed in these fires might have been saved. One early warning fire detection device which shows great promise is the single-station, smoke detector. This fact is being recognized by more and more code authorities in the U.S. As a consequence, an increasing number of the U.S. building codes are requiring the installation of single-station smoke detectors in all new housing.

There are problems, however, with several of the single-station, smoke detectors on the market. In addition, there is a lack of good published performance standards for these detectors, standards that would improve the quality of smoke detectors offered for sale in the marketplace and would eliminate many of the problems.

The National Bureau of Standards, in conjunction with the approvals testing laboratories and the detector manufacturers, is developing performance standards for the single-station, smoke detector. Development and publication of these standards will have a material effect on improving the quality of smoke detectors sold in the U.S.

15219. Radebaugh, R., Siegwarth, J. D., Holste, J. C., **Heat transfer between sub-micron silver powder and dilute $He^3He^4$ solutions,** (Proc. 5th Int. Cryogenic Engineering Conf., Kyoto, Japan, May 7, 1974), Paper H6 in *5th International Cryogenic Engineering Conference*, K. Mendelssohn, Ed., pp. 242-245 (IPC Science and Technology Press, Surrey, England, 1974).

> Key words: cryogenics; dilution refrigerator; heat transfer; helium 3; helium 4; Kapitza resistance; liquid helium; powder; silver.

The thermal resistance between copper cells lined with silver powder of 0.1 – 0.2 $\mu$m diameter and a dilute stream of $He^3$ in $He^4$ was measured between 15 and 250 mK. The results show that this powder can give an order of magnitude lower thermal resistance at 15 mK than an equal volume of copper powder of 1.8 $\mu$m diameter. The scientific and engineering significance of such a low resistance in a small volume is discussed. At the higher temperatures $R$ is proportional to $T^{-1}$, which can be explained by a liquid thermal resistance and a resistance at the joint between the powder and the cell walls.

**15220.** Chang, C. C., Dodge, W. R., Murphy, J. J. II, **$^3He(\gamma,d)^1H$ cross section from 10 to 21 MeV,** *Phys. Rev. C* **9,** No. 4, 1300-1308 (Apr. 1974).

> Key words: cross section structure; excitation energy distribution function; $^3He$ electrodisintegration; $^3He$ excited states; $^3He$ photodisintegration.

A measurement of the $^3He(e,d)^1H$ 90° differential cross section between 10 and 21 MeV was made. The $^3He(e,d)^1H$ cross section was converted into a $^3He(\gamma,d)^1H$ cross section. The shape of the $^3He(\gamma,d)^1H$ cross section agrees with recent theoretical calculations. We find no evidence for the anomalies (structure) in the $^3He(\gamma,d)^1H$ 90° differential cross section at excitation energies of 14.5 and 19.5 MeV reported in two recent experiments.

**15221.** Braun, W., Kurylo, M. J., Kaldor, A., **Infrared laser enhanced reactions: V → V and V → T energy transfer in the $O_3$-$SiF_4$-$O_2$ system,** *Chem. Phys. Lett.* **28,** No. 3, 440-444 (Oct. 1, 1974).

> Key words: apparatus and methods; deactivation; energy transfer; infrared laser; luminescence; ozone.

Rapid V → V energy transfer between $SiF_4$ and $O_3$ has been observed following laser excitation of either $O_3$ or $SiF_4$. A $CO_2$ laser tuned to either the 9.6 $\mu$ P(30) or P(32) transitions was used to promote vibrational excitation in $O_3$ and $SiF_4$, respectively. In experiments employing the P(32) transition, the V → V transfer to $O_3$ and subsequent reaction of $O_3^\dagger$ with NO were used to obtain the rate constant of V → T deactivation of $SiF_4^\dagger$ by $O_2$.

$$SiF_4^\dagger + O_2 \xrightarrow{k_2} SiF_4 + O_2,$$

$$k_2 = (6.3 \pm 1.4) \times 10^{-13}\ \text{cm}^3\ \text{molecule}^{-1}\ \text{s}^{-1}.$$

Fractional modulation measurements of the chemiluminescence generated by the $O_3 + NO$ reaction were used in experiments employing the P(30) transition to obtain a rate constant for the V → V energy transfer between $O_3^\dagger$ and $SiF_4$.

$$O_3^\dagger + SiF_4 \xrightarrow{k_{-3}} SiF_4^\dagger + O_3,$$

$$k_{-3} = (3.8 \pm 0.5) \times 10^{-11}\ \text{cm}^3\ \text{molecule}^{-1}\ \text{s}^{-1}.$$

**15222.** Hruska, G. R., Koidan, W., **Free-field method for sound-attenuation measurement,** *J. Acoust. Soc. Am.* **58,** No. 2, 507-509 (Aug. 1975).

> Key words: acoustic centers; attenuation of sound; sound absorption.

A free-field method is described for measuring the attenuation of sound at ultrasonic frequencies. It makes use of the systematic deviation from the inverse square law caused by attenuation when a sound receiver is drawn away from a sound source. Measurements of attenuation from 20 to 100 kHz, made in air in a small anechoic chamber under ambient environmental conditions, were in good agreement with theoretical calculations. The sum of the distances between the acoustic centers of the transducers and the vibrating elements is obtained as a by-product of the procedure.

**15223.** Choi, C. S., Prask, H. J., Prince, E., **Crystal structure of $NH_4ClO_4$ at 298, 78, and 10 K by neutron diffraction,** *J. Chem. Phys.* **61,** No. 9, 3523-3529 (Nov. 1, 1974).

> Key words: crystal structure; low temperature; meta-stable compound; neutron diffraction; $NH_4ClO_4$; thermal motion.

The crystal structure of ammonium perchlorate has been studied at 298, 78, and 10 K by means of neutron diffraction. The $NH_4ClO_4$ crystal has an orthorhombic unit cell, space group *Pnma*, with four formula units per cell at all three temperatures. The unit cell dimensions at 298 K are $a = 9.20$, $b = 5.82$, $c = 7.45$ Å, as determined previously; at 78 K, $a = 9.02$, $b = 5.85$, $c = 7.39$ Å; and $a = 8.94$, $b = 5.89$, $c = 7.30$ for 10 K. Initial positions o H atoms were determined from a difference Fourier map of the room temperature data. However, a least-square refinement o these data did not converge. The thermal motions and orientations of the ammonium groups at low temperature (10 and 78 K were determined by means of a constrained refinement which treated the ammonium group as a rigid body; these results are compared with the results obtained by the conventional least squares method. Both refinements show that the librational motions about one of the three principal axes have particularly large rms amplitudes: 21° for the 10 K structure and 30° for the 78 K structure. Each ammonium group is surrounded by 10 oxygen atoms with short N... O distances ranging from 2.9 to 3.25 Å The $ClO_4^-$ group and $NH_4^+$ group each have essentially idea tetrahedral structure. They are linked together by N-H... O type hydrogen bonds, one for each hydrogen, to form a three-dimensional network. Examination of the rms amplitudes for libration and the hydrogen bonding of the $NH_4^+$ ions indicates that two o the four hydrogens are bound identically, one hydrogen is bound more rigidly, and the fourth more weakly. These results sugges that the rotational motions of the ammoniums are quite comple even at 10 K.

**15224.** Piermarini, G. J., Block, S., **Ultrahigh pressure diamond anvil cell and several semiconductor phase transition pressure in relation to the fixed point pressure scale,** *Rev. Sci. Instrum* **46,** No. 8, 973-979 (Aug. 1975).

> Key words: diamond-anvil pressure cell; fixed point pressure scale; high pressure; NaCl pressure scale; pressur measurement; ruby fluorescence; semiconductors; transition pressures.

A diamond-anvil type optical cell of improved design ha produced static pressures in gasketed samples up to 500 kiloba as measured by the ruby fluorescence technique. The ruby R line pressure shift is linear to 291 kilobar, and the maximum mea sured shift is extrapolated to 500 kilobar assuming continue linearity of the pressure dependence. The ultimate pressur capability of this diamond cell has not been established. Trans tion pressures in the semiconductors Si, ZnSe, ZnS, and Ga measured by the ruby method indicate that the revised 197 fixed point scale and the ruby (NaCl) scale diverge above 13 kilobar and disagreement may be by as much as a factor of 2 i the 500 kilobar range with the ruby scale defining the lower pre sure.

**15225.** Weston, W. F., Ledbetter, H. M., Naimon, E. R **Dynamic low-temperature elastic properties of two austenit nickel-chromium-iron alloys,** *Mater. Sci. Eng.* **20,** 185-19 (1975).

Key words: bulk modulus; compressibility; Debye temperature; elastic constant; nickel-chromium-iron alloys; Poisson's ratio; shear modulus; sound velocity; Young's modulus.

The zero-magnetic-field low-temperature elastic properties of o polycrystalline nickel-chromium-iron alloys were deterned ultrasonically between 4 and 300 K. Results are given for: ngitudinal and transverse sound velocities, Young's modulus, ear modulus, bulk modulus, Poisson's ratio and elastic Debye nperature. Effects of alloying are discussed. The elastic prorty changes due to additions of chromium and iron to nickel reviewed comprehensively.

**226.** Saloman, E. B., **Time response of NBS windowless XUV radiometric transfer standard detectors,** *Appl. Opt.* **14,** No. 8, 1764 (Aug. 1975).

Key words: radiometry; rise time; temporal response; transfer standard detector; XUV photodiode.

For the spectral region between 200 Å and 1200 Å the NBS liometric standard detector is a windowless photodiode with 2.5 cm diameter cathode made of evaporated aluminum on ose surface a 150 Å thick $Al_2O_3$ layer has been anodized. A dy has been made of the response of these diodes to pulsed liation. A Garton-type flashlamp was modified to provide pul- of radiation with a duration of about 1 μsec. These pulses re passed through a half-meter Seya-Namioka vacuum nochromator and the zero order radiation was allowed to fall the cathode of the diode. The emitted cathode current of the de across a 50Ω load was displayed by an oscilloscope. Outt pulses were observed with instantaneous amplitudes as high 1 mA with no evidence of saturation. The rise time of the de output pulses was on the order of 300 nsec which was the pected rise time of the flashlamp. In order to confirm that the e time was flashlamp limited, a diode with a tungsten cathode s substituted for the $Al_2O_3$ diode. The temporal results were ntical. Thus we are able to conclude that the NBS windowless $O_3$ radiometric transfer standard diodes have a rise time orter than 300 nsec.

**227.** Kashiwagi, T., **A radiative ignition model of a solid fuel,** *Combust. Sci. Technol.* **8,** 225-236 (1974).

Key words: ignition; ignition boundary; solid fuel.

A theoretical model describing radiative ignition of a solid fuel constructed and is numerically analyzed. The model includes effects of gas phase reaction and a finite value of the absorpn coefficient of the solid (in-depth absorption of incident radian). It is found that the gas phase reaction must be included in model in order to understand radiative ignition of a solid fuel d to find its ignition boundary. The in-depth absorption of the ident radiation by a solid fuel significantly affects the ignition ay time. The results indicate that there is a finite range of ues for pyrolysis or gas phase reaction activation energy for ich ignition will occur. This finding has a direct bearing on efts to reduce material ignitability.

**228.** Hasegawa, S., Stokesberry, D. P., **Automatic digital microwave hygrometer,** *Rev. Sci. Instrum.* **46,** No. 7, 867-873 July 1975).

Key words: humidity; hygrometer; microwave refractometer.

This hygrometer is designed to measure the humidity of atspheric air over the vapor pressure range 3-7400 Pa (0.03-74 ar). The instrument is an adaption of a microwave refractome using two cavities operating at 12 GHz. One cavity is exsed to the moist test air and the other is exposed to the same sample with all the water vapor removed. Both cavities are maintained at the same fixed temperature in a thermostated oven and at the same total pressure. The difference in frequency between the cavities is automatically nulled by a tuning probe in the sampling cavity. The instrument was calibrated by two independent methods. One involved the measurement of the resonance frequency of the sampling cavity as a function probe penetration and using this in a theoretically derived equation for vapor pressure. The second involved the measurement of the probe penetration as an empirical function of known vapor pressure of a test gas. These two methods yielded results which agreed on the average to better than 0.5 percent for vapor pressures up to 3050 Pa (30.5 mbar).

**15229.** Buchbinder, L. B., **Human activity patterns and injury severity in fire incidents involving apparel,** *J. Fire Flammability/Consumer Product Flammability* **1,** 4-18 (Mar. 1974).

Key words: accident patterns; apparel; apparel fires; burn injury; FFACTS; fire; flammable fabrics; flammable liquids; garment fires; garment parameters; injury severity; victim's activity; victim's reactions.

Activities preceding an apparel fire accident are identified and related to age, sex, and the severity of burn injury. After age six, activity patterns were strongly related to the victim's sex, with men the primary victims of accidents involving flammable liquids, gases, or high voltage electricity, and women more susceptible to direct flame ignition. The majority of cases studied had burns over less than 20 percent of the total area of their body. When flammable liquids were involved, there tended to be fewer minor injuries and more moderately serious injuries than in accidents not involving intermediary materials. Age and defensive capability were major factors determining extent of injury, with persons over 65 and those with limited ability suffering more serious injuries than other groups. Included are recommendations for remedial action.

**15230.** Fung, F. C. W., Suchomel, M. R., Oglesby, P. L., **The NBS program on corridor fires,** *Fire J.* **67,** No. 3, 41-48 (May 1973).

Key words: carpets with and without underlayment; corridor fires; energy models; finished interior; full scale experiments; interaction; measurements; smoke; smoke and flame spread; temperature; with and without forced air; velocity.

This report outlines the NBS full scale experimental program to investigate the growth and spread of fire and smoke into and through a corridor when a fire is initiated in an adjoining room. The program proposes energy models to investigate both the contribution of the corridor interior finish surfaces and their interactions under the full scale fire situation. As a status report it describes in detail the experimental facilities and approaches for the program.

A summary of the tests conducted to date is presented. It is shown that flames can propagate the length of a 30 foot corridor, with a combustible floor covering as the only source of fuel in the corridor, when initiated by 2.7 psf of wood cribs in an adjacent room. Typical quantitative measurements of temperature, velocity, smoke and energy are also presented. In addition, comparative discussions are presented for tests with and without forced air draft and carpet tests with and without underlayment.

**15231.** Jones, F. E., **Magnetic retention of evaporation or sputtering masks (Abstract only),** *Rev. Sci. Instrum. Letter to Editor* **46,** No. 6, 793 (June 1975).

Key words: evaporation; magnetic retention; masks; sputtering; substrates; thin films.

The "use of a magnet to clamp a magnetic metal mask to the substrate during sputtering" of thin film patterns has been described by Ingle. A similar technique was described previously by Jones and Castle in this journal and in a patent.

15232. Unassigned.

**15233.** Iverson, W. P., **Anaerobic corrosion: Metals and microbes in two worlds,** *Dev. Ind. Microbiol.* **16,** 1-10 (1975).

Key words: anaerobic corrosion; cathodic depolarization theory; Charles Thom Award; *Desulfovibrio desulfuricans*; hollow whiskers; mechanism; microbial corrosion; mild steel; oxidizing agent; Schreibersite; sulfate-reducing bacteria; Vivianite.

Charles Thom Award address presented by the author at the General Meeting of the Society for Industrial Microbiology held at Memphis State University, 11-16 August 1974. (The Thom Award honors the first president of the Society for Industrial Microbiology. The later Charles Thom was a noted microbiologist who worked for the U.S. Department of Agriculture and his research on molds helped to produce many of today's antibiotics).

The author's investigations of the mechanism of anaerobic corrosion by sulfate-reducing bacteria, which led to the observation that a marine strain produced extracellularly, a strong oxidizing agent which caused extensive corrosion of mild steel under anaerobic conditions, are detailed. The formation of hollow whiskers, structures which resemble fungal mycelium, by the reaction of ferrocyanide or ferricyanide on metals are described.

**15234.** Herron, J. T., Huie, R. E., **Rate constants for the reactions of ozone with ethene and propene, from 235.0 to 362.0 K,** *J. Phys. Chem.* **78,** No. 21, 2085-2088 (1974).

Key words: air pollution; ethene; kinetics; mass spectrometry; ozone; propene; rate constant.

The rate constants for the reactions of ozone with ethene and propene have been measured over the temperature range 235.0-362.0 K, using a stopped-flow system coupled to a beam-sampling mass spectrometer. The rate constants found, at a total pressure of about 500 N m$^{-2}$, in the presence of molecular oxygen, were $k(C_2H_4) = (5.42 \pm 3.19) \times 10^9 \exp(-2557 \pm 167/T)$ cm$^3$ mol$^{-1}$ sec$^{-1}$ and $k(C_3H_6) = (3.70 \pm 1.42) \times 10^9 \exp(-1897 \pm 109/T)$ cm$^3$ mol$^{-1}$ sec$^{-1}$.

**15235.** Ito, J., **Synthetic indium silicate and indium hydrogarnet,** *Am. Mineral.* **53,** 1663-1673 (Sept.-Oct. 1968).

Key words: crystal chemistry; flux growth; garnet; hydrogarnet; indium silicates; inorganic synthesis; solid solubility silicates; x-ray powder analysis.

The following indium silicates were synthesized hydrothermally and in air: indium grossular, $Ca_3In_2Si_3O_{12}$; indium aegirine, $NaInSi_2O_6$; indium beryl, $Be_3In_2Si_6O_{18}$; indium thortveitite, $In_2Si_2O_7$; indium melanotekite, $Pb_2In_2Si_2O_9$; and strontium indium hydrogarnet, $Sr_3In_2(OH)_{12}$.

Complete solid solubility was found between ferric iron and indium silicates and hydrogarnet end members. Single crystals of indium aegirine up to 2 cm in length were grown in a $Na_2WO_4$ flux by slow cooling.

The crystal chemical and geochemical behavior of trivalent indium is similar to that of scandium. The ionic radius of trivalent indium of 0.81 Å given by Pauling is confirmed.

**15236.** Coxon, B., **Preliminary communication: Nitrogen-15 n.m.r. spectroscopy of amino sugars,** *Carbohydr. Res.* **35,** C1-C3 (1974).

Key words: amino sugars; chemical shifts; magnitude spectra; nitrogen-15 nuclear magnetic resonance spectroscopy nuclear Overhauser effects.

Derivatives of 6-amino-6-deoxy-D-galactose-6-$^{15}N$ and -D glucose-6$^{15}N$ and the corresponding unlabeled compounds hav been synthesized via reactions of appropriate 6-*O*-tolyl-*p*-sulfo nyl or 6-deoxy-6-iodo derivatives with potassium phthalimide $^{15}N$ (or $^{14}N$), followed by hydrazinolysis of the phthaloyl group $^{15}$N n.m.r. spectra of the amino sugar derivatives have been mea sured directly at 9 MHz by pulse-Fourier transform techniques The recording of spectra of $^{15}$N in natural abundance in th amino sugar derivatives was aided by proton irradiation whic caused a substantial negative, nuclear Overhauser effect (NOE even for derivatives in which the $^{15}$N nucleus is not directl bonded to a proton. For example, irradiation of the protons c 6-deoxyl-1,2:3,4-di-*O*-isopropylidene-6-phthalimido-α-D-gala topyranose (**1**) -6-$^{15}N$ at 90 MHz inverted the $^{15}$N signal an enhanced its intensity by a factor of 3.4, which indicates a NO of −4.4. One half gram of this derivative ($^{15}$N enrichment, 99% yielded a $^{15}$N spectrum with a signal:noise ratio of 36:1 whe excited by a single pulse. With $^{15}$N at natural abundance in 0.7 g of **1**, 8,192 pulses (112 min) were required to give a $^{15}$ signal:noise ratio of 13:1. The negative NOE on the $^{15}$N signal **1**-6-$^{15}N$ was removed (with reinversion of the signal, but no shi by addition of the relaxation reagent, chromium (II acetylacetonate to a concentration of 0.02M.

**15237.** Peterlin, A., **Dependence of diffusive transport morphology of crystalline polymers,** *J. Macromol. Sci. Phys.* **11,** No. 1, 57-87 (1975).

Key words: crazing; crystalline polymer solid; diffusio elastic deformation; permeability; plastic deformation; sor tion.

The sorption and diffusion of low molecular weight penetran proceeds almost exclusively through the amorphous compone of the semicrystalline polymer solid. The diffusive transport pr perties and geometrical distribution of the amorphous co ponent are substantially modified by mechanical and therr treatment. Deformation of spherulitic material first loosens t structure and then transforms it into a densely packed fibro structure with a great many taut tie molecules in the amorpho component. Annealing lets the crystals grow in thickne removes crystal defects, sharpens the boundaries betwe crystalline and amorphous component, and relaxes the taut molecules. The resulting changes of transport properties canr be described in a satisfactory manner by crystallinity and orie tation but require a detailed consideration of morphology. T elastic tensile deformation enhances sorption and diffusion reducing the density of amorphous component. The hi anisotropy of diffusion and the drastic reduction of sorption a diffusion of fibrous material are the consequence of t microfibrillar morphology with the large fraction of higl aligned and closely packed taut tie molecules which elimin many sorption sites, enormously reduce the diffusivity, and crease its concentration dependence. The anisotropy may reduced during plastic deformation of the fibrous material by t increased number of interfibrillar tie molecules.

**15238.** Radebaugh, R., Siegwarth, J. D., Oda, Y., Nagano, **Experiments with miniature heat exchangers for dilut refrigerators,** (Proc. 5th Int. Cryogenic Engineering Co Kyoto, Japan, May 7, 1974), Paper H3 in *5th Internatio Cryogenic Engineering Conference, K. Mendelssohn, Ed., 235-237 (IPC Science and Technology Press, Surrey, gland, 1974).*

Key words: copper alloy; copper; cryogenics; dilut refrigerator; heat exchanger; Kapitza resistance; liquid h um; powder; silver.

his paper describes experiments done on three types of iature heat exchanger for dilution refrigerators. These have id volumes on the order of 0.1 cm$^3$. The first is a continuous hanger incorporating Cu(Cr) powder, the second is a continu- exchanger incorporating sub-micron silver powder, and the d is a discrete exchanger incorporating 1.8 $\mu$m copper vder. The first two were not successful and the reasons are entirely clear. The third exchanger performed about as calcu- ed and permits an order of magnitude reduction in liquid umes from that normally used.

39. Grundl, J. A., Dudey, N. D., Popek, R. J., **Measurement f absolute fission rates,** *Trans. Amer. Nucl. Soc.* **17,** 516-517 1973).

Key words: absolute fission rates; neutron dosimetry; reactor fuels; reactor materials.

Recently, the accuracy requirements for fast reactor fuels and terials dosimetry surpassed the existing capabilities of fission activation measurements. In order to improve this capability direct calibration of activation detectors, absolute fission es per nucleus have been measured in fast neutron fluxes table for both fission activation foils and for fission fragment ectors. This paper presents results for absolute fission frag- nt emission rates from $^{239}$Pu, $^{235}$U, $^{238}$U, and $^{237}$Np exposed to first of these fast neutron fluxes, the spectrum of the RMF Reactor at ANC.

40. Huie, R. E., Herron, J. T., **Reactions of atomic oxygen O$^3$P) with organic compounds,** Paper in *Progress in Reaction Kinetics,* K. R. Jennings and R. B. Cundall, Eds., **8,** No. 1, Part 1, 1-80 (Pergamon Press, Great Britain, 1975).

Key words: atomic oxygen; gas phase; kinetics; mechanism; organic compounds; rate constants.

he reactions of atomic oxygen (O$^3$P), in the gas phase, with anic compounds are reviewed. The various techniques used these studies are discussed critically. The kinetics and chanisms of the reactions of atomic oxygen with organic com- nds are discussed in detail.

41. Geller, S. B., **Archival data storage,** *Datamation* **20,** No. 0, 72, 75-76, 80 (Oct. 1974).

Key words: archival language; archival quality; content decay; content density; content lifetimes; storage media.

his paper develops some archival language and discusses fac- s which must be considered when an archival data storage tem is designed. These include types of contents, content ay rates, content and medium lieftimes, content density and tem costs. Other archival storage quality factors such as in- mation security and recovery are considered.

42. Davis, G. T., Eby, R. K., **Low-temperature x-ray at- achment,** *Rev. Sci. Instrum.* **46,** No. 9, 1285-1286 (Sept. 975).

Key words: attachment, low-temperature; radiation shield; temperature gradient; x-ray.

commercial high-temperature, high-vacuum diffractometer achment, which was originally designed for heating samples m ambient temperatures to 2600 K using metal ribbon ters, has been modified for low-temperature use. This has n accomplished simply by the construction of a new sample der and a change of the port used for evacuation. With these difications, controlled temperatures down to 100 K can be ieved easily.

43. Hastie, J. W., **Sampling reactive species from flames by mass spectrometry,** *Int. J. Mass Spectrom. Ion Phys.* **16,** No. 1/2, 89-100 (Jan. 1975).

Key words: flames; laser excitation; mass spectrometry; radicals.

Recent studies on sampling reactive species from flames and related laser-excited systems are described. Consideration is given to the possible effect of probe-related perturbations on the experimental data. It is concluded that such perturbations are not significant under the present experimental conditions.

**15244.** Finkel, P. W., Miller, T. R., Weikel, M. K., **Reply to clinical chemistry article,** *Clin. Chem.* **20,** No. 4, 521, 523-524 (1974).

Key words: chemistry; clinical laboratory capability; critique; hematology; microbiology; sampling.

The February 1974 issue of CLINICAL CHEMISTRY published a critique of two NBS Interagency Reports. The Bureau has prepared a reply, written by the senior author of both NBS reports, and coordinated through the Institutes for Applied Technology and Materials Research.

**15245.** Newbury, D. E., Yakowitz, H., **Specimen preparation, special techniques, and applications of the scanning electron microscope,** Chapter VI in *Practical Scanning Electron Microscopy,* J. I. Goldstein and H. Yakowitz, Eds., pp. 211-262 (Plenum Press, New York, N.Y., 1975).

Key words: scanning electron microscope; SEM applications; SEM dynamic experiments; SEM specimen preparation; SEM stroboscopy; stereomicroscopy.

Techniques of specimen preparation for scanning electron microscopy, including degreasing, electropolishing, and deposition of conductive coatings, are discussed. Stereomicroscopy, the technique of obtaining images with depth information, is described. Dynamic experiments conducted *in situ* in the scanning electron microscope (SEM) are considered. Examples of dynamic experiments, including tensile straining and the application of magnetic fields, are given. Stroboscopy, the imaging of high frequency, cyclical events is described. Practical applications of the SEM to a range of materials science problems are described in detail. The problems include: (1) examination of fractured metals and composites; (2) investigation of lunar soil; (3) failure analysis of a corroded steam boiler; (4) recognition of mineral phases; (5) characterization of wear particles; (6) examination of human teeth; (7) orientation and crystal perfection analysis with electron channeling effects; (8) examination of magnetic recordings; (9) examination of magnetic domain structures; (10) operation of an integrated circuit; and (11) observation of ferroelectric domains.

**15246.** Yakowitz, H., **Methods of quantitative x-ray analysis used in electron probe microanalysis and scanning electron microscopy,** Chapter IX in *Practical Scanning Electron Microscopy,* J. I. Goldstein and H. Yakowitz, Eds., pp. 327-372 (Plenum Press, New York, N.Y., 1975).

Key words: electron probe microanalysis; empirical methods; Fe-Si alloys; Monte Carlo methods; quantitative analysis; scanning electron microscopy.

Quantitative microprobe analysis is considered from the classical point of view as well as the so-called empirical approach. The relations used to convert raw data to mass fractions are discussed and scrutinized with respect to sources of error in the final analysis. Histograms depicting the typical spread of results are used to show what can be expected. By way of illustration, the complete planning and execution of the analysis of binary silicon-iron alloy is described in detail. Brief mention is made of special specimen geometries such as thin films or fracture surfaces and means to obtain analyses from them. An extensive reference list is appended.

**15247.** Yakowitz, H., Goldstein, J. I., **Practical aspects of x-ray microanalysis,** Chapter XI in *Practical Scanning Electron Microscopy,* J. I. Goldstein and H. Yakowitz, Eds., pp. 401-434 (Plenum Press, New York, N.Y., 1975).

Key words: crystal spectrometers; elemental distribution; elemental identification; energy dispersive spectrometers; microanalysis; specimen preparation.

Element identification and distribution as determined by electron probe microanalytical techniques is explained. Both energy dispersive systems and curved crystal spectrometers are considered from the point of view of ease and accuracy of identification and distribution determination. A series of examples including minerals, meteorites, composite materials, superalloys and tool steel is discussed in terms of solution of practical problems by elemental identification and distribution.

For accurate quantitative electron probe microanalysis, specimen preparation plays a crucial role. Therefore, effects of specimen preparation are evaluated in terms of surface roughness, instrumental design and nature of the specimen. The role of standards in the analysis is outlined. Finally a series of examples involving compositional analysis is presented.

**15248.** Yakowitz, H., **Computational schemes for quantitative x-ray analysis: On-line analysis with small computers,** Chapter X in *Practical Scanning Electron Microscopy,* J. I. Goldstein and H. Yakowitz, Eds., pp. 373-400 (Plenum Press, New York, N.Y., 1975).

Key words: empirical methods; minicomputers; on-line analysis; quantitative electron probe microanalysis; scanning electron microscopy; SRM-480.

This chapter deals with rapid means to perform data reduction for quantitative electron probe microanalysis with the aid of small computational devices (desk calculator to 8K machine). Included will be a complete discussion of a ZAF program packaged for on-line data reduction and the basis for use of the hyperbolic approximation on-line. For the laboratory which only does occasional quantitative analysis, a brief discussion is given of how to obtain an analysis with a desk calculator in a reasonable time – about two hours for a six component system or 30 minutes for a binary starting from scratch is needed. Solved examples are included.

**15249.** Goldstein, J. I., Yakowitz, H., Newbury, D. E., **Introduction to practical scanning electron microscopy,** Chapter I in *Practical Scanning Electron Microscopy,* J. I. Goldstein and H. Yakowitz, Eds., pp. 1-19 (Plenum Press, New York, N.Y., 1975).

Key words: contrast; electron beam instrumentation; electron probe microanalyzer; instrumental development; scanning electron microscope; signal processing.

This chapter traces the evolution of the scanning electron microscope and the electron probe microanalyzer from birth to the present. A number of major developments both instrumental and methodological are outlined. The purpose is to familiarize the novice with these developments; for the experienced SEM user, the chapter aim is to remind one of the significant stages of instrumental development. Points touched upon include the discovery and exploitation of various SEM contrast mechanisms such as topographic, voltage and magnetic contrast as well as stages in the development of signal and image processing.

**15250.** Newbury, D. E., **Image formation in the scanning electron microscope,** Chapter IV in *Practical Scanning Electron*
*Microscopy,* J. I. Goldstein and H. Yakowitz, Eds., pp. 95-
148 (Plenum Press, New York, N.Y., 1975).

Key words: scanning electron microscope; SEM contras
formation; SEM image defects; SEM image formation
SEM image quality; signal processing.

The image formation process in the scanning electro
microscope (SEM) is described in detail. The major component
of the image formation system are the scan coils, scan generator
signal detectors, amplifiers, and the cathode ray tube display
Various types of signal detectors are described: the Everhard
Thornley detector for back-scattered and secondary electrons
the solid state detector for backscattered electrons, specime
(absorbed) current detection, x-ray detectors, and cathodolu
minescence detectors. Contrast formation is explained. The rela
tionship between the image quality and the characteristics of th
signal is detailed. For a given contrast level, a threshold bear
current exists which must be exceeded to obtain a useful image
Various types of signal processing for image enhancement ar
described: black level suppression (differential amplification
gamma processing (non-linear amplification); time derivativ
signal transformation; and Y-modulation. The application
these signal processing techniques renders image details mor
readily visible to the human eye. Image defects are considere
Moiré effects can be obtained in images of periodic objects.
two contrast mechanisms are present in an image, one ma
dominate, requiring special signal processing techniques for d
tection of the weaker contrast.

**15251.** Newbury, D. E., Yakowitz, H., **Contrast mechanisms**
**special interest in materials science,** Chapter V in *Practic*
*Scanning Electron Microscopy,* J. I. Goldstein and
Yakowitz, Eds., pp. 149-210 (Plenum Press, New York, N.Y
1975).

Key words: cathodoluminescence; electron beam induc
conductivity contrast; electron channeling contrast; ma
netic domain contrast; scanning electron microscope; vo
age contrast.

This chapter considers several mechanisms of contrast form
tion in the scanning electron microscope (SEM). The physic
origin of each mechanism is considered in detail. Electron cha
neling contrast results from effects of the periodic arrangeme
of atoms in a crystal on the penetration of the incident electro
Type I magnetic contrast arises from effects of leakage fiel
outside the specimen on emitted secondary electrons. Type
magnetic contrast is related to effects of the internal magne
field on the primary electrons as they undergo scattering in t
specimen. Voltage contrast arises from the effect of surfa
potentials on the collection of emitted secondary electrons. El
tron beam induced conductivity contrast (EBIC) occurs in c
tain semiconductors through the formation of electron-h
pairs, locally changing the conductivity from the interaction
the primary electrons. Cathodoluminescence results due to t
emission of visible light when electron-hole pairs recombine. T
characteristics of each contrast mechanism are related to
SEM operating parameters required for successful image forn
tion.

**15252.** Johnson, C. R., ***D*-stability and real and complex quadra**
**forms,** *Linear Algebra and Appl.* **9,** 89-94 (1974).

Key words: *D*-stable matrix; positive diagonal matr
quadratic forms; spectrum.

The problem of characterizing the class of *D*-stable matri
has remained unsolved since its suggestion in a paper by Arr
and McManus [1] in 1958. In this note we present a necess

ndition involving real quadratic forms which is not sufficient d a sufficient condition involving complex quadratic forms hich is not necessary.

5253. Sams, R. L., Lafferty, W. J., **High-resolution infrared spectrum of the $\nu_2 + \nu_3$ band of $^{14}N^{16}O_2$,** *J. Mol. Spectrosc.* **56,** 399-410 (1975).

Key words: anharmonic constant; Coriolis resonance; high resolution; infrared spectrum; nitrogen dioxide; spin splitting.

The $\nu_2 + \nu_3$ band of $^{14}N^{16}O_2$ has been recorded with resolution 0.028 cm$^{-1}$. Ground state and upper state rotational constants ve been obtained. The band center obtained, $\nu_0 = 2355.1517 \pm$ 0011 cm$^{-1}$ (error cited is $3\sigma$), has been combined with the band nters recently determined for $\nu_3$ and $\nu_2$ to calculate $X_{23} =$ 11.348 ± 0.020 cm$^{-1}$ where the uncertainty cited is based on asonable estimates of the absolute frequency error.

5254. Fatiadi, A. J., **Symmetrical phenylosotriazoles from inositols,** *Carbohydr. Res. Note* **35,** 280-287 (1974).

Key words: conformation; half-chair; inositol; mercuric acetate; phenylosotriazole; p.m.r.; symmetrical.

The application of mercuric acetate reagent to conversion of osose phenylosazones into phenylosotriazoles in 40 – 47 perent yield is described. Analysis of p.m.r. spectra of inositol henylosotriazole esters (e.g., acetates, propionates, benzoates) d of their parent compounds on "decoupling" of their hydroxyl oups (by protonation, or deuterium exchange) showed a symetrical pattern (presence of a simple, two-fold axis of symmetry an AA′BB′ system); a half-chair conformation of these phenosotriazole esters in solution was deduced from the p.m.r. ectra. Free inositol phenylosotriazoles in solution exist exclvely in a half-chair conformation.

5255. Reader, J., **Spectrum of Rb III observed with a pulsed-rf light source,** *J. Opt. Soc. Am.* **65,** No. 9, 988-990 (Sept. 1975).

Key words: rubidium; spectra; ultraviolet; wavelengths.

The spectrum of doubly ionized rubidium, Rb III, was obrved with a pulsed-rf light source on two 10.7 m normal-indence spectrographs at NBS. Wavelengths and classifications ere obtained for 103 Rb III lines, 90 of which were newly obrved. The three missing levels of the $4p^44d$ configuration, $P)^4F_{9/2}$ and $(^1D)^2G_{7/2,9/2}$, and the one missing level of the $4p^45p$ nfiguration, $(^1S_0)[1]_{1/2}$, were located. The $4p^4(^1D)5d\,^2G_{9/2}$ level as also located. Improved values were determined for 13 cited levels.

5256. LaVilla, R. E., **The O $K\alpha$ and C $K\alpha$ emission and O $K$ absorption spectra from $O_2$ and $CO_2$. IV,** *J. Chem. Phys.* **63,** No. 6, 2733-2737 (Sept. 15, 1975).

Key words: molecular $CO_2$; molecular oxygen; O and C $K\alpha$ x-ray emission spectra; O $K$ absorption spectra.

The oxygen and carbon $K\alpha$ emission and oxygen $K$ absorption ectra of the molecular gases $O_2$ and $CO_2$ are reported. The ectra were obtained on two different spectrometers, both with ngle flat crystal configurations. All the emission spectra were cited by direct electron bombardment and are in fair agreeent with an interpretation based on allowed electric dipole ansitions between single vacancy states and molecular orbital eory for the molecules. The oxygen $K$ absorption of $O_2$ and $O_2$ is dominated by a strong resonance peak before the $K$-shell reshold which is interpreted as being due to the transition of ygen $K$ electrons to the first unoccupied valence orbital of the spective molecules.

5257. Sugar, J., Kaufman, V., **Seventh spectrum of tungsten (W VII); resonance lines of Hf V,** *Phys. Rev. A* **12,** No. 3, 994-1012 (Sept. 1975).

Key words: hafnium; levels; spectra; tungsten; wavelengths.

Observations of W VII were carried out in the spectral range 100 to 2000 Å utilizing normal- and grazing-incidence spectrographs. The light source was a sliding spark operated at peak currents of 1000 to 3000 A. Eighty-five energy levels of $4f^{13}nl$ and $5p^5nl$ configurations were deduced for $nl = 5d, 6s, 6p, 6d$, and $7s$. These are based on the classification of 310 lines in the range 130 to 1436 Å. Calculations of all observed configurations were carried out with configuration interaction (CI) for the purpose of fitting radial integrals and confirming the analysis. The strong CI between $p^5nl$ and $f^{13}nl$ configurations where $nl = 5d$, $6p$, $6d$ provided well-defined CI integrals in good agreement with Hartree-Fock values. A value of 984100 ± 500 cm$^{-1}$ was derived for the ionization energy from the $4f^{13}ns$ series. The resonance lines of Hf V for $5p^6$-$5p^55d,6s$ are given. A revised value for the ionization energy of W VI is given.

15258. Lovas, F. J., Clark, F. O., Tiemann, E., **Pyrolysis of ethylamine. I. Microwave spectrum and molecular constants of vinylamine,** *J. Chem. Phys.* **62,** No. 5, 1925-1931 (Mar. 1, 1975).

Key words: dipole moment; ethylamine; pyrolysis reactions; rotational spectrum; structure; vinylamine.

Microwave rotational spectra assignable to gas phase vinylamine ($CH_2 = CHNH_2$) have been detected in the pyrolysis decomposition products of ethylamine. Stark effect and hyperfine structure measurements have aided the assignment of the spectrum and allow the determination of the $^{14}N$ nuclear electric quadrupole coupling constants and the electric dipole moment for vinylamine. The spectrum of the first excited inversion vibrational state has been assigned. Relative intensity measurements indicate that the inversion state lies about 65 ± 25 cm$^{-1}$ above the ground state. The spectral evidence suggests that vinylamine has a nonplanar equilibrium structure with $r_0(C - N) = 1.40$ Å and $\angle CCN = 125°$.

15259. Lewis, D. C., **On the determination of the minority carrier lifetime from the reverse recovery transient of *pn*R diodes,** *Solid-State Electron.* **18,** 87-91 (1975).

Key words: carrier lifetime; reverse recovery; semiconductor diodes.

The determination of the minority carrier lifetime of *pn* diodes with abrupt junctions and recombination (*R*) contacts is discussed. It is confirmed that the base transit time of diodes with sufficiently small base widths (less than approximately three minority carrier diffusion lengths) affects the reverse recovery transient and that large error can be introduced if the minority carrier lifetime of a diode with a small base width is computed using an expression which was derived for diodes with an infinite base width. Approximations to the general expression for the minority carrier lifetime as a function of the storage time and base width are developed, and the errors associated with their use are analyzed. In addition the effect of measurement errors on the determination of lifetime in short base diodes is discussed.

A procedure is described which can be used to compute the minority carrier lifetime of *pn*R diodes in which the ratio of the base width to the minority carrier diffusion length is larger than some small number. The applicability of the procedure and the approximations which are developed are a function of the ratio of the diode base width to the minority carrier diffusion length ($W/L$), and the forward to reverse current ratio ($I_f/I_r$) at which the experimental measurements are made. An example is given which shows that less than 1 percent error is introduced in the computed lifetime by the approximations if the lifetime is computed from measurements made at $I_f/I_r = 4$ and 8 for diodes such that $W/L > 2 \times 10^{-2}$.

**15260.** Hagan, L., **Reports of observatories for 1973/74, National Bureau of Standards, Washington, D.C.,** *Bull. Am. Astron. Soc.* **7,** No. 1, 165-169 (1975).

Key words: atomic energy levels; atomic line shapes; atomic spectra; atomic transition probabilities; bands, molecular; energy levels, atomic; line shapes, atomic; molecular bands; molecular spectra; rotational constants.

Research at the National Bureau of Standards in spectroscopy pertinent to astronomy is summarized. Publications on atomic spectra, atomic transition probabilities and line broadening, and molecular spectra are referenced and work in progress is discussed.

**15261.** Lovas, F. J., **Application of microwave spectroscopy to chemical analysis,** *Anal. Instrum.* **12,** 103-109 (1974).

Key words: applications; chemical analysis; microwave; qualitative analysis; quantitative analysis; rotational spectra.

Traditional analytical techniques have been successfully employed on a great variety of systems for identifying stable reaction products as well as for purity analysis and reaction efficiency. However, most analytical techniques generally can only be applied to "well behaved" chemical systems. Since gas phase reaction products do not always follow the "well behaved" guideline, an alternate analytical tool, such as microwave spectroscopy, could prove beneficial for analyzing such systems and may well provide some new routes to synthetic chemistry. A general review of the present state-of-the-art for applications of microwave techniques to analytical studies will be presented. An attempt will be made to describe the limitations and advantages of microwave spectroscopy for probing chemical systems for product identification and for optimization of the efficiency of gas phase chemical reactions. As an illustration, some recent results obtained in our laboratory on the complex pyrolytic decomposition reactions of ethylamine will be described. Further examples of possible applications will be taken from typical industrial processes which employ vapor phase chemical synthesis techniques.

**15262.** Giguere, P. T., Clark, F. O., **Radio search for $HC_3N$, HCN, OH, and detection of U8.19 in comet Kohoutek (1973f),** *Astrophys. J.* **198,** 761-764 (June 15, 1975).

Key words: comet; HCN; $HC_3N$; Kohoutek; OH; radio; search.

Comet Kohoutek (1973f) was observed with the NRAO 140-foot (43 m) radio telescope in the period 1974 January 4-7 in an attempt to detect the following molecular transitions: $HC_3N$, $J=1\text{-}0$, $v=0$; $HC_3N$, $J=1\text{-}0, 2\nu_7$, $l=0$; HCN, $J=6, 1\nu_2$; and OH, $^2\Pi_{1/2}$, $J=5/2$, $F=3\text{-}3$. All results for these lines were negative. An unidentified line was possibly detected at 8189 MHz.

**15263.** Rowe, J. M., Price, D. L., Ostrowski, G. E., **Inelastic neutron scattering from a liquid $^3He$-$^4He$ mixture,** *Phys. Rev. Lett.* **31,** No. 8, 510-513 (Aug. 20, 1973).

Key words: lifetime of excitations; neutron scattering; perturbation of elementary excitations; quantum liquids; roton minimum; $^3He$ $^4He$ solutions.

We report inelastic-neutron-scattering measurements on liquid $^3He_{0.05}{}^4He_{0.95}$ in the $Q$ region from 0.8 to 2.3 Å$^{-1}$ at 1.6 K. The shifts and increases in natural linewidth of the single excitation peaks relative to pure $^4He$ at the same temperature were determined by a least-squares fitting procedure. The shifts vary from a small, possibly negative, value at the roton minimum to positive values around 0.5 K at both ends of the $Q$ range. The full widths at half-maximum of the extra broadening vary from 0.5 to 1.5 K over the same range.

**15264.** Rush, J. J., Livingston, R. C., de Graaf, L. A., Flotow, H. E., Rowe, J. M., **Study of hydrogen diffusion in tantalum hydrides by inelastic neutron scattering,** *J. Chem. Phys.* **59,** No. 12, 6570-6576 (Dec. 15, 1973).

Key words: activation energy; hydrogen diffusion; neutron scattering; quasielastic scattering; resonance time; tantalum hydrides; vibrational amplitude.

Neutron inelastic scattering spectra have been measured as a function of temperature and scattering angle for $\alpha$-$TaH_{0.15}$ and for $Ta_2H$ in its $\alpha$ and $\beta_1$ phases. The widths of the quasielastic peaks vs momentum transfer ($Q$) have been derived and compared with several models for hydrogen diffusion. The results suggest the dominance of tetrahedral jumps in the diffusion process, although no completely satisfactory theoretical fit was obtained. Residence times $\tau$ between 1.6 (340 °C) and 4.0 (148 °C) psec for $TaH_{0.15}$ and between 2.4 (300 °C) and 7 (153 °C) psec for $Ta_2H$ were derived from the fit of the observed widths to the tetrahedral model. These results indicate a significant concentration dependence of the diffusion rates in $\alpha$-$TaH_x$, with activation energies for diffusion of $10.4 \pm 1.2$ kJ/mol in $TaH_{0.15}$ and $15 \pm 1.2$ kJ/mol for $Ta_2H$. "Effective" mean square amplitudes of proton vibration of 0.02-0.04 Å$^2$ were obtained from the $Q$ dependence of the quasielastic peak intensities, in reasonable agreement with the values predicted from relatively crude vibration frequency distributions obtained from our inelastic scattering spectra in the $\alpha$ phase. Our results are compared in detail with previous neutron results on $VH_x$ and $NbH_x$. On the basis of this comparison it is tentatively concluded that the very high "Debye-Waller factors" obtained for $VH_x$ and some other hydrides are related to high hydrogen diffusion rates.

**15265.** Cali, J. P., Stanley, C. L., **Measurement compatibility and Standard Reference Materials,** Chapter in *Annual Review of Materials Science* **5,** 329-343 (Annual Reviews Inc., Palo Alto, Calif., 1975).

Key words: measurement; measurement compatibility; reference methods; Standard Reference Materials.

The role of Standard Reference Materials (SRM's) in helping to provide measurement compatibility is explored. Measurement compatibility is simply the ability of elements within a measurement infrastructure to achieve the same measurement values. It is shown that measurement compatibility results when measurements are made on the basis of accuracy. SRM's are well-characterized materials whose properties are certified on the basis of accuracy. Therefore, laboratories within a measurement infrastructure become compatible when SRM's are used.

Sections cover these topics: (a) sources of information concerning the current availability and types of SRM's produced; (b two examples of the impact of SRM's are given; and, (c) discussion of future directions and needs is expounded.

**15266.** Hilsenrath, J., **The utility and economics of an on-line reference data network,** (Proc. Conf. on Mechanism of Explosions and Blast Waves, Naval Weapons Station, Yorktown Va., Nov. 13-15, 1973), Paper in *Proceedings of the Conference on Mechanism of Explosions and Blast Waves* Section XVII, 1-21 (Picatinny Arsenal, Dover, N.J., 1973).

Key words: data files; data network; data on-line; international data service; on-line data; reference data service standard reference data.

This paper describes a prototype on-line data retrieval and ata computation system and discusses the scientific, technical nd organizational characteristics required to make such a ystem an economically viable reality.

The general characteristics of the envisioned system are: 1. uthoritative data collections and well documented sources ored on a reliable time-shared computer system; 2. Extended recision representation and computing where required; 3. fficient programs to generate data not explicitly stored; 4. asy to use conversational on-line access from inexpensive terminals; 5. A reliable and extensive communication network to liminate or reduce toll charges; 6. Low user charges.

As envisioned, the charges for connect time should cover the ommunications costs, the computer costs, and the monthly cost f keeping the data and programs stored on the disc. The conomics of the situation argue for building up the data files om small self-contained segments so as to expedite the collection, validation and maintenance of the data base; and to inimize the search time for the user. Of equal importance is the ct that the more compact a particular file is, the fewer uses of will be required to cover its monthly storage cost.

Examples are given of the use of the system for solving a umber of problems in thermodynamics and thermochemistry nd in chemical kinetics.

5267. Lee, T. G., Huggett, C., **Interlaboratory evaluation of ASTM E 84-70 tunnel test applied to floor coverings,** *J. Test. Eval.* **3,** No. 1, 3-14 (1975).

> Key words: ASTM E84; building materials; carpets; fire tests; flame spread tests; floor coverings; interlaboratory evaluation; smoke measurement; tunnel test.

Results of an interlaboratory evaluation of the American ociety for Testing and Materials (ASTM) Test for Surface urning Characteristics of Building Materials (E 84-70), involving eleven laboratories and nine materials including four carpets, re reported. Data on flame spread, smoke, and fuel contribution ere analyzed statistically to determine the reproducibility and epeatability of the test method. Selected physical characteristics f each tunnel are tabulated and compared relative to specifications in the test method. The between-laboratory coefficient of ariation (reproducibility) in flame spread classification (FSC) as found to range from 7 to 29 percent for the four carpets and om 18 to 43 percent for the other materials tested. The etween-laboratory coefficients of variation for smoke eveloped and fuel contribution ranged from 34 to 85 percent nd from 22 to 117 percent, respectively, for all materials tested. he causes of higher variability in smoke and fuel contribution easurement between laboratories are not definitely known but ay reasonably be attributed to variations in tunnel construction, instrumentation, and operation in different laboratories.

5268. Coxon, B., Tipson, R. S., Alexander, M., Deferrari, J. O., **Conformational analysis of acylated 1,1-bis(acylamido)-1-deoxypentitols by Fourier-transform, p.m.r. spectroscopy,** *Carbohydr. Res.* **35,** 15-31 (1974).

> Key words: acylated 1,1-bis(acylamido)-1-deoxypentitols; conformational analysis; conformational nomenclature; exponential filtering; Fourier transform; p.m.r. spectroscopy.

The conformations of eight acylated 1,1-bis(acylamido)-1-eoxypentitols in solution have been studied by pulse, Fourier-transform, p.m.r. spectroscopy at 90 MHz. The *arabino* and *lyxo* erivatives adopt the zigzag conformation, whereas the *ribo* and *ylo* derivatives favor different sickle conformations. The validity of the conformational assignments of these derivatives by the m.r. method is discussed. The relative merits and accuracy of the continuous-wave and pulse-Fourier p.m.r. spectroscopic methods in the conformational analysis of carbohydrates are appraised, and the applicability of the exponential filtering technique to enhancement of either the sensitivity or the resolution of their spectra is demonstrated.

15269. Kashiwagi, T., **Experimental observation of flame spread characteristics over selected carpets,** *J. Fire Flammability/Consumer Product Flammability* **1,** 367-389 (Dec. 1974).

> Key words: flame spread; floor covering material; heat release rate; ignition.

A small laboratory size experiment was used to observe the characteristics of flame spread over various carpets under various constant external radiant fluxes (0.10 ~ 0.27 cal/cm$^2$ sec or 0.4 ~ 1.15 w/cm$^2$). The results indicate that a minimum radiant flux is necessary to sustain flame spread over a carpet surface for the carpets tested. By increasing radiant flux, the flame spread velocity increases sharply and can reach several sm/sec. At a high external radiant flux, preheating time is the controlling factor for flame spread velocity. Ignitability, weight loss, and net heat release rate were also measured under various radiant fluxes. The effect of an underlayment on ignitability, flame spread speed, weight loss, and net heat release rate, was also observed for various carpets.

15270. Freund, S. M., Ritter, J. J., **$CO_2$ TEA laser-induced photochemical enrichment of boron isotopes,** *Chem. Phys. Lett.* **32,** No. 2, 255-260 (Apr. 15, 1975).

> Key words: $BCl_3$ (boron trichloride); boron; $CO_2$ (carbon dioxide); enrichment; infrared; isotopes; TEA laser.

Mixtures of $BCl_3$ and $H_2S$ are irradiated with 10.55 $\mu$m radiation (P(16)line of the 001-100 band of $CO_2$) from a TEA laser. After several hours of irradiation it is found that the maximum $^{10}B$ to $^{11}B$ ratio of recovered gaseous boron containing material (primarily unreacted $BCl_3$) is $0.413 \pm 0.004$. The corresponding ratio of the $BCl_3$ starting material is $0.242 \pm 0.002$. The $^{10}B$ concentration has therefore been increased from 19.5 to 29.2 percent. Further, by irradiating similar mixtures with 10.18 $\mu$m radiation (R(30) line of the same $CO_2$ vibrational band) this ratio changes to $0.169 \pm 0.002$, the $^{10}B$ concentration being lowered to 14.4 percent. All experiments are performed in a small static system and chemical procedures for recovering milligram quantities of $BCl_3$ selectively enriched in either isotope are described.

15271. Prince, E., Trevino, S. F., Choi, C. S., Farr, M. K., **A refinement of the structure of deuterium peroxide,** *J. Chem. Phys.* **63,** No. 6, 2620-2624 (Sept. 15, 1975).

> Key words: crystal structure; deuterium peroxide; hydrogen bonds; hydrogen peroxide; neutron diffraction; structure refinement; thermal motion.

The structure of deuterated hydrogen peroxide, $D_2O_2$, at $-15$ °C was refined by least-squares methods from three dimensional neutron diffraction data. The data were fitted to two models, one with conventional anisotropic temperature factors and the other with the molecule treated as a rigid body except for torsional oscillations of the $O-D$ groups about the $O-O$ bond. The weighted agreement indices were 0.030 over 106 observed reflections for the conventional model and 0.032 over 102 reflections for the rigid body model. The structure is tetragonal, space group $P4_12_12$ or $P4_32_12$, with $a=4.035$ Å, $c=7.97$ Å, $Z=4$. Position parameters for the two models are essentially the same. The $O-O$ distance in the molecule, 1.455(2) Å, is identical to that found in $H_2O_2$, but the $O-D$ bond is about 0.015 Å shorter than the $O-H$ bond, 0.993 Å as compared with 1.008 Å when corrected for thermal motion by the riding model. The $O-O$ distance corrected for thermal motion in the rigid body model is

1.49 Å, in fair agreement with the value 1.48 Å found in the vapor phase.

**15272.** Johnson, C. R., **The Hadamard product of $A$ and $A^*$,** *Pacific J. Math.* **51,** No. 2, 477-481 (1974).

Key words: angular field of values; diagonal; diagonally dominant; field of values; Gersgorin; Hadamard product; Hermitian; positive definite; spectrum.

Coefficient-wise multiplication was introduced by Hadamard and has been studied for certain square matrices by I. Schur and later authors. For $A \epsilon M_n(C)$, the $n$ by $n$ complex matrices, this paper examines the Hadamard product of $A$ and $A^*$. Upper estimates are given for the largest characteristic root of this necessarily Hermitian product, and three conditions on $A$ sufficient for the product to be positive definite are presented.

**15273.** Finkel, P. W., Miller, T. R., Weikel, M. K., **NBS replies to Dr. Barnett's critique,** *Lab World* **25,** No. 4, 6 and 16 (Apr. 1974).

Key words: chemistry; clinical laboratory capability; critique; hematology; microbiology; sampling.

The December 1973 issue of LAB WORLD published a critique of two NBS Interagency Reports. The Bureau has prepared a reply, written by the senior author of both NBS reports, and coordinated through the Institutes for Applied Technology and Materials Research.

**15274.** Lashof, T. W., **A calibration check service for paper and board test instruments,** *TAPPI* **57,** No. 1, 5 (Jan. 1974).

Key words: collaborative reference program; interlaboratory testing; laboratory performance; paper test methods.

Brief editorial description of NBS-TAPPI Collaborative Reference Program, including participants, advantages, methods included, procedure, and related programs.

**15275.** Karo, A., Krauss, M., Wahl, A. C., **Recent applications of the multiconfiguration self-consistent field method to polarizabilities, excited states, Van der Waals forces, and triatomic surfaces,** (Proc. Int. Symp. on Atomic, Molecular and Solid-State Theory and Quantum Biology, Sanibel Island, Fla., Jan. 21-27, 1973), *Int. J. Quantum Chem. Symp.* No. 7, 143-159 (John Wiley & Sons, New York, N.Y., 1973).

Key words: CO; energy surface; $F_2$; hydrides; $LiH_2$; MC-SCF; $O_2^-$; $O_3$; polarizability; Van der Waals.

In this brief presentation recent and new applications of the multiconfiguration self-consistent field (MCSCF) method to the direct calculation of atomic polarizabilities, excited states of the same symmetry, Van der Waals forces, and triatomic energy surfaces are presented.

These calculations utilizing the BISON system, have been carried out over the past several years as part of collaborative research between Argonne National Laboratory, the National Bureau of Standards, and the Lawrence Livermore Laboratory.

**15276.** Motz, J. W., Dick, C. E., **X-ray scatter background signals in transmission radiography,** *Med. Phys.* **2,** No. 5, 259-267 (Sept.-Oct. 1975).

Key words: image contrast; monoenergetic x-ray beams; optimum radiographic systems; transmission radiography; x-ray image signals; x-ray scatter.

With monoenergetic x-ray beams incident on polystyrene phantoms, the spectra of the transmitted x rays were measured with a scintillation spectrometer. The scattered and unscattered components of the transmitted x-ray fluence at a point on the beam axis were determined as a function of (i) the incident x-ray energy (18, 22, 32, 49, 58, 69, and 660 keV), (ii) the phantom thickness (5.3, 10, and 21 cm), (iii) the scatter solid angle determined by the exposed area of the phantom and the separation distance of the image plane (0.090, 0.31, 0.66, 1.8, 3.5, 4.3, 4.8, and 5.1 sr), and (iv) the beam diameter at the image plane (25, 17, and 10 cm). The results indicate that, as the incident x-ray energy *decreases* from 660 to 30 keV, the contribution of the scattered component to the transmitted fluence *increases* from approximately 50 to 90 percent for the 21-cm phantom and from 21 to 50 percent for the 5.3-cm phantom. For typical cases, the data show the effect of the scatter component on the ratio of the image to the background signals. In addition, the examples show that optimum conditions for maximizing this signal ratio may be obtained by a careful selection of the incident x-ray energy fo low-, medium-, and high-contrast objects.

**15277.** Miller, A., McLaughlin, W. L., **Absorbed dose distributio in a pulse radiolysis optical cell,** *Int. J. Radiat. Phys. Chem.* 7 No. 5, 661-666 (1975).

Key words: absorbed dose rate; depth dose; dose distribution; dye films; electron beams; optical cell; pulse radiolysis; radiation dosimetry; radiochromic dyes.

When a liquid solution in an optical cell is irradiated by an intense pulsed electron beam, it may be important in the chemica analysis of the solution to know the distribution of energ deposited throughout the cell. For the present work, absorbe dose distributions were measured by thin radiochromic dye film dosimeters placed at various depths in a quartz glass puls radiolysis cell. The cell was irradiated with 30 ns pulses from field-emission electron accelerator having a broad spectrum wit a maximum energy of ≈ 2 MeV. The measured three-dimensional dose distributions showed sharp gradients in dose at th largest penetration depths in the cell and at the extreme latera edges of the cell interior near the optical windows. This metho of measurement was convenient because of the high spatia resolution capability of the detector and the linearity an absence of dose-rate dependence of its response.

**15278.** Miller, A., Bjergbakke, E., McLaughlin, W. L., **Som limitations in the use of plastic and dyed plastic dosimeters,** *In J. Appl. Radiat. Isotop.* **26,** No. 10, 611-620 (Oct. 1975).

Key words: absorbed dose rate; cellulose triacetate dosimetry; dyed cellophane; dyed plastics; electron beams gamma radiation; plastic films; polymethyl methacrylate polyvinyl chloride; radiation processing; radiochromic dye

Several practical plastic and dyed plastic dosimeters were examined under irradiation conditions similar to those used fo radiation processing of materials. Cellulose triacetat polymethyl methacrylate, polyvinyl chloride, dyed polymeth methacrylate, dyed cellophane and dyed nylon were given fractionated and uninterrupted absorbed doses in the megarad rang with $^{60}Co$ $\gamma$-rays and 10 MeV electron beams. It was found th with some systems, differences in radiation response due t dose-rate and temperature dependence can cause large systematic errors in dose interpretation. Poor reproducibility response may result from batch-to-batch differences or intrabatch variations in thickness, distribution of sensitizers an background optical density. When using these routine dosimeters, careful calibration of the response and monitoring of facto contributing to poor reproducibility are essential.

**15279.** Lechner, J. A., **Applying statistics in criminalistics,** (Pro 8th Annual Crime Countermeasures Conf., Lexington, Ky April 16-19, 1974), Paper in *Proc. 1974 Carnahan and In*

*Crime Countermeasures Conf., UKY BU* **105,** 113-123 (Aug. 1974).

Key words: acceptance tests; confidence intervals; criminalistics; errors; goodness of fit; normal distribution; significance tests; standards; statistics.

This paper is intended to tell "why-we-do-it-this-way." After reliminary remarks on randomness, errors, and distribution unctions, various techniques of statistical analysis are iscussed. These include significance tests, confidence intervals, nd goodness of fit test. Finally, several examples will be iscussed: 1) Performance requirements for breath alcohol esters; 2) bivariate discrimination for gunshot residue detecon; and 3) Matching "profiles," e.g., trace element analyses or he output of a speech frequency analyzer.

**5280.** Prince, E., Mighell, A. D., Reimann, C. W., Santoro, A., **Hexakis(imidazole)cobalt(II) nitrate,** $[\mathrm{Co(C_3H_4N_2)_6}](\mathrm{NO_3})_2$, *Cryst. Struct. Commun.* **1,** 247-252 (1972).

Key words: cobalt; complexes; hexakis(imidazole)cobalt(II) nitrate; imidazole, neutron; structure; x ray.

The structure of the title compound was determined by x-ray and neutron diffraction techniques. The hydrogen bonding in the tructure was uniquely determined from the neutron data. Bond distances and angles obtained with the two techniques are compared.

**5281.** Brown, D. W., Lowry, R. E., **Radiation-induced polymerization of tetrafluoroethylene and 1,2,3,4,5-pentafluorostyrene at high pressure,** *J. Polym. Sci. Polym. Chem. Ed.* **13,** No. 7, 1677-1689 (July 1975).

Key words: copolymerization; pentafluorostyrene; polymerization; pressure radiation; reactivity ratios; tetrafluoroethylene.

Tetrafluoroethylene (A) and 1,2,3,4,5-pentafluorostyrene (B) were irradiated at 15 °C at autogenous pressure by use of 30-92 mole-percent A and at 5000 atm by use of 42-99.9 mole-percent A. The high-pressure results indicate that the reactivity ratio $r_A$ for monomer addition to A-ended radicals is 0.005; the other reactivity ratio $r_B$ appears to vary from 15 to 60 generally increasing with the A content of the charge. At autogenous pressure $r_A$ is small, but a precise determination is not possible because of the very low polymerization rate when the A content of the charge is high. However, if $r_A$ is less than 0.01, then values of $r_B$ vary from 15 to 50, again generally increasing with the A content of the charge. Mixtures of A and B exhibit positive deviations from Raoult's Law. Activity coefficients were measured at autogeneous pressure and used in an attempt to correct $r_B$ for the nonideality of solution. The range of $r_B$ was reduced only slightly to 8-27, and charges with high A contents now generally gave low values of $r_B$; consequently, this approach was not regarded as a success. Another attempt was made to account for the apparent variation in $r_B$ by ascribing influence to the penultimate units of the radicals. Improved agreement between theoretical and observed compositions resulted, but significant discrepancies remained unexplained. Rate data agreed well with those calculated from a theoretical copolymer rate equation using values of $r_A$ and $r_B$ of 0.0045 and 40, respectively. The equation predicts an almost proportional decrease in rate with increasing proportions of A in the charge from 0 to 99 mole-percent A.

**15282.** Zahn, J. P., **The dynamical tide in close binaries,** *Astron. Astrophys.* **41,** No. 314, 329-344 (July 1975).

Key words: binary; gravity modes; nonadiabatic; oscillations; resonances; stellar.

The nonadiabatic oscillations of a star, driven by an outer rotating gravitational field, have been studied by the use of matched asymptotic expansions. The interior and envelope solutions in this procedure are derived in Sections 2 and 3. The results apply to stars which have a convective core and a radiative envelope, and they are discussed in Section 4.

We find that the resonances of the free gravity modes are damped by radiative dissipation, which operates in a relatively thin region below the surface of the star. Due to that dissipation, some properties of the dynamical tide have observable consequences in close binary systems: i) A torque is applied to a binary component; this serves to make it corotate with its companion in a time which can be short compared to its nuclear life. ii) Before that synchronization is achieved, the brightness distribution over the surface of the star is in general phase shifted relative to the external driving potential.

**15283.** Wyatt, D. M., Gray, R. C., Carver, J. C., Hercules, D. M., Masters, L. W., **Studies of polymeric bond failure on aluminum surfaces by x-ray photoelectron spectroscopy (ESCA),** *Appl. Spectrosc.* **28,** No. 5, 439-445 (Sept.-Oct. 1974).

Key words: adhesion failure; cohesive failure; polymeric bond failure; scanning electron microscopy (SEM); x-ray photoelectron spectroscopy (ESCA).

X-ray photoelectron spectroscopy (ESCA) has been used to identify very thin layers of polymeric species remaining on aluminum plates after the polymer was cured and stripped from the aluminum. Two polymers were studied. In one, the residual polymeric carbon was used as the tracing signal; in the other, the polymeric silicon was used. In both cases, the polymeric species was partially sputtered from the aluminum surface by an argon ion gun. A reduction in the polymeric signal relative to a standard signal was noted. The results of this study show that, when the polymers studied were mechanically pulled from the aluminum substrate, the failure was a cohesive separation within the polymer, rather than failure at the polymer-aluminum interface. Scanning electron microscopy was used to show that the residual polymer does not remain on the surface as "clumps" or "islands," but rather as a smooth surface a few atomic layers thick.

**15284.** Choi, C. S., Abel, J. E., Dickens, B., Stewart, J. M., **The crystal structure of 1,3,5,7-tetraceto-1,3,5,7-tetrazacyclo-octane,** *Acta Crystallogr.* **B29,** Part 4, 651-656 (Apr. 1973).

Key words: crystal structure; organic crystal; x-ray diffraction.

The crystal of 1,3,5,7-tetraceto-1,3,5,7-tetrazacyclo-octane, $C^{12}N^4O^4H^{20}$, is tetragonal, $a=b=10.540(2)$ and $c=12.137(3)$ Å, with 4 molecules per unit cell. Systematic absences are consistent with space group $P4^12^12$ (enantiomorphous to $P4^32^12$). The structure was solved by direct methods and refined to a final $R$ index $R^w=0.037$ and $R=0.039$ for 1244 observed reflections. The molecule consists of alternate $CH^2$ and $N-CO-CH^3$ groups in a puckered $C-N$ ring, having a boat shape conformation with a twofold rotation axis through the center of the $C-N$ ring and perpendicular to the mean plane of the puckered ring. The heavy atoms of each acetyl group are essentially coplanar with its neighbouring nitrogen atom. The molecular thermal motion may be represented chiefly by three motions; a libration about the twofold rotation axis and two intramolecular bending motions about the $C-C$ diagonal of the $C-N$ ring.

**15285.** Marzetta, L. A., **A thermesthesiometer — An instrument for burn hazard measurement,** *IEEE Trans. Biomed. Eng.* **BME-21,** No. 5, 425-427 (Sept. 1974).

Key words: burn hazard; consumer products; contact temperature; thermesthesiometer; thermometry.

Surface temperature measurement alone is insufficent to establish the hazard to the human of contact with a hot or cold object. A metal surface is more likely to cause thermal injury than a plastic surface at the same temperature. An instrument equipped with a measuring probe has been developed for indicating the temperature that would be experienced if human contact were made with the hot surface in question. The correct value of interface contact temperature can be read for a selected contact time without knowing the composition or temperature of the heated material under test.

**15286.** Machado, M. E., Linsky, J. L., **Flare model chromospheres and photospheres,** *Sol. Phys.* **42,** No. 2, 395-420 (June 1975).

Key words: chromosphere, sun; photosphere, sun; radiative transfer; solar flares.

Homogeneous plane-parallel model atmospheres for solar flares have been constructed to approximately simulate observations of flares. The wings of the Ca II lines have been used to derive flare upper photosphere models, which indicate temperature increases of ~ 100 K over the temperature distribution in the pre-existing facula at a height of 300 km above $\tau^{5000} = 1$. In the case of flares covering sunspots the temperature rise seems to occur much higher in the atmosphere. We solve the transfer and statistical equilibrium equations for a three-level hydrogen atom and a five-level calcium atom in order to obtain the chromospheric flare models. The general properties of flares, including $n^e$, $N^2$, linear thickness, and Lyman continuum intensity are approximately reproduced. We find that with increasing flare importance the height of the upper chromosphere and transition region occur lower in the solar atmosphere, accounting for the factor of 60-600 increase in pressure in these regions relative to the quiet Sun. The Ca II line profiles agree with observations only by assuming a macrovelocity distribution that increases with height. Also the chromospheric parts of flares appear to be highly inhomogeneous. We show that shock and particle heated flare models do not agree with the observations and propose a thermal response model for flares. In particular, it appears that heating in the photosphere is an essential aspect of flares.

**15287.** Albus, J. S., **Data storage in the cerebellar model articulation controller (CMAC),** *Trans. ASME Series G, J. Dyn. Syst. Meas. Control* **97,** No. 3, 228-233 (Sept. 1975).

Key words: cerebellar model; control theory; data storage; distribution memory; hierarchical control; manipulator control.

The storage of manipulator control functions in the CMAC memory is accomplished by an iterative process which, if the control function is sufficiently smooth, will converge. There are several different techniques for loading the CMAC memory depending on the amount of data which has already been stored and the degree of accuracy which is desired. The CMAC system lends itself to a "natural" partitioning of the control problem into manageable subproblems. At each level the CMAC controller translates commands from the next higher level into sequences of instructions to the next lower level. Data storage, or training, is accomplished first at the lowest level and must be completed, or nearly so, at each level before it can be initiated at the next higher level.

**15288.** Bishop, M., Dimarzio, E. A., **Models of diffusion in lyotropic liquid crystals,** *Mol. Cryst. Liq. Cryst.* **28,** 311-333 (1975).

Key words: asymmetric diffusion coefficients; diffusion in liquid crystals; lyotropic liquid crystal.

The asymmetric diffusion of small molecules in a liquid crystal host is examined via three models. The small molecules are represented by spheres and the liquid crystal host by aligned cylinders. DASH is a continuum model which allows one to use the results of electrical conductivity problems to calculate the diffusion coefficient. LASH is an extension of polymer lattice counting models. CASH is a molecular dynamics computer simulation which provides experimental data to check the analytical models. It is found that DASH is a better representation of the diffusion asymmetry than LASH for the low liquid crystal densities examined on the computer. The cylinder sphere pair correlation function is also calculated in CASH and this gives evidence for liquid order around the liquid crystals.

**15289.** Scheps, R., Ottinger, C., York, G., Gallagher, A., **Continuum spectra and potentials of Li-noble gas molecules,** *J. Chem. Phys.* **63,** No. 6, 2581-2590 (Sept. 15, 1975).

Key words: lithium; molecules; noble gases.

The normalized emission spectrum of the Li($2p - 2s$) resonance transition has been measured in the presence of 10-1000 torr of noble gas. Fluorescence at 100-3000 Å from the atomic line, due to the $A$-$X$ and $B$-$X$ bands of Li-noble gas molecules, has been measured as a continuum with 1.5 nm resolution. The lithium is optically excited in a 670 K cell. The lithium is optically thin (~ $10^{-6}$ torr) so that the continuum emission per excited lithium atom is obtained from the normalized emission. The attractive $A$-state potentials for Li-Ar, Kr, and Xe have been constructed by analysis of the $A$-$X$ band spectra in the limit of high and low noble-gas densities. At high densities each spectrum is due to an equilibrated vibrational distribution of $A$-state molecules, whereas at low densities only free collision states contribute. The ratio of the two spectra thus depends on the excited state potential and has been used to determine this potential where it is attractive. Absorption and stimulated emission coefficients for Li-noble gas vapors are also deduced from the data.

**15290.** Nyyssonen, D., **Partial coherence in imaging systems,** *Opt. Eng.* **13,** No. 4, 362-367 (July-Aug. 1974).

Key words: coherence measurement; microdensitometry; optical imaging; partial coherence.

An improved method of measuring spatial coherence is described and some sources of measurement errors are discussed. Partial coherence in the image plane of an optical system is discussed and results of coherence measurements are given that demonstrate the scaling of the coherence function for coherence intervals large compared to the diameter of the Airy disk and the limiting value for the coherence interval equal to the diameter of the Airy disk. The application of these results to microdensitometry is discussed and results of coherence measurements in the source plane of currently-used classical microdensitometers are given.

**15291.** Ott, W. R., Behringer, K., Gieres, G., **Vacuum ultraviolet radiometry with hydrogen arcs. 2: The high power arc as an absolute standard of spectral radiance from 124 nm to 360 nm,** *Appl. Opt.* **14,** No. 9, 2121-2128 (Sept. 1975).

Key words: arc; calibrations; hydrogen; plasma; radiometry; spectral radiance; vacuum ultraviolet; wall-stabilized.

A wall-stabilized hydrogen arc can be utilized as a standard source of spectral radiance since the continuum emission coefficient is calculable to within a few percent. Previous efforts to apply this concept have been impeded by relatively large uncertainties associated with the plasma diagnostics. The present approach yields absolute intensities independent of other radiometric standards or the accuracy of any plasma diagnostics. The hydrogen arc is operated at high temperatures where the continuum emission coefficient reaches a broad, unique, and calculable maximum. Comparisons with other primary standards are consistent with the estimated uncertainty in the arc continuum intensities.

**15292.** McCarter, R. J., **A new technique for thermal analysis of vapor-producing reactions,** *J. Appl. Polym. Sci.* **17,** No. 6, 1833-1846 (1973).

Key words: differential thermal analysis; DTA; kinetics; pyrolysis; TGA; thermal analysis; thermal degradation; thermogravimetric analysis.

An apparatus was developed for measuring the rate at which vapors are evolved during the thermal degradation of materials and thereby deriving the kinetics of such reactions. Requisite to the operating scheme of the apparatus is the provision of a high-temperature zone to convert condensable or tarry vapors into noncondensable form. The apparatus yields a direct measure of reaction velocity, rather than the integrated indication obtained with thermogravimetric analysis. This simplifies the identification and calculation of kinetic parameters. Increases in sensitivity and operating range are also achieved. Flexibility in operation is obtained that permits the separate recording of reactions that tend to overlap. Although the apparatus principally has been operated using a combustible gas indicator to meter the evolved vapors, a number of options are available for the latter function, including flowmeters and various continuous gas analyzers. The applicability of the method appears promising.

**15293.** Mulholland, G. W., Zollweg, J. A., Sengers, J. M. H. L., **Liquid-vapor asymmetries in pure fluids,** *J. Chem. Phys.* **62,** No. 7, 2535-2549 (Apr. 1, 1975).

Key words: asymmetry; coexistence curve; compressibility; critical exponents; critical point; decorated lattice gas; hole-particle symmetry; law of corresponding states; liquid; Padé approximant; power law; slope of the coexistence curve diameter.

The coexistence curve and the compressibility-like quantity $\partial\rho/\partial\mu)_T$ at the coexistence curve are calculated for Mermin's decorated lattice gas. We tabulate the Padé approximants to the Ising model properties which were used in these calculations. It is shown that for the proper choice of the adjustable parameter in the model the asymmetries in the coexistence curve and in $(\partial\rho/\partial\mu)_T$ over a large temperature range, $T_c/2 < T < T_c$, are qualitatively similar to those in real fluids. Also, similar correlations between the overall coexistence curve asymmetry and the amplitudes of divergences for the critical region occur in the model and in real fluids. Based on our model calculations, several predictions for fluid behavior near the critical point are listed: (1) The *asymptotic* asymmetry in the coexistence curve and in $(\partial\rho/\partial\mu)_T$ at the coexistence curve should be most observable for fluids with large overall asymmetry such as $SF_6$, $NH_3$, and $H_2O$; (2) the range of the asymptotic asymmetry for $(\partial\rho/\partial\mu)_T$ is expected to extend somewhat beyond $t = 1 - (T/T_c) = 0.1$ for such fluids; (3) in order to obtain an estimate for the compressibility exponent $\gamma'$ that is within a few percent of the true asymptotic value, experiments will have to be confined to the range $t < 10^{-2}$. Recent experimental data for $(\partial\rho/\partial\mu)_T$ at the coexistence curve are found to be consistent with the model for $t > 10^{-2}$, but are inconclusive closer to the critical point.

**15294.** Deslattes, R. D., Henins, A., Bowman, H. A., Schoonover, R. M., Carroll, C. L., Barnes, I. L., Machlan, L. A., Moore, L. J., Shields, W. R., **Determination of the Avogadro constant,** *Phys. Rev. Lett.* **33,** No. 8, 463-466 (Aug. 19, 1974).

Key words: Avogadro number; crystal repeat distance; density; isotopic abundance; silicon.

Measurements are reported on the densities and isotopic-abundance ratios of nearly perfect Si single crystals. These, when combined with optical interferometry of the crystal repeat distance, yield a new value for the Avogadro constant. This result, $N_A = 6.022\,0943 \times 10^{23}$ mol$^{-1}$ (1.05 ppm), represents a more than thirty-fold reduction in the uncertainty of previous direct measurements.

**15295.** McCormick, P. G., Burke, R. W., Doumas, B. T., **Precautions in use of soft-glass disposable pipets in clinical analyses,** *Clin. Chem. Scientific Note* **18,** No. 8, 854-856 (1972).

Key words: clinical; contamination; errors; soft glass pipets; unwashed soft glass pipets.

Soft-glass, Pasteur-type pipets are widely used as disposable transfer pipets, especially in clinical and biochemical laboratories. These pipets possess an alkaline surface contamination that can affect the accuracy of chemical analyses if proper precautions are not taken. Microtitrations of aqueous rinsings from these pipets have consistently yielded values of 0.1 to 0.2 μmol of hydroxide equivalent per pipet. A possible detrimental effect of this residue was demonstrated, using chloroform solutions of bilirubin. Absorbance was diminished by as much as 5 percent when unwashed, soft-glass pipets were used to transfer these solutions to spectrophotometric cells. Absorption and fluorescence characteristics of other unidentified surface contaminants are also described. The effect of multiple rinsings is discussed and several ways are suggested for cleaning these pipets. Oven drying must be avoided, however, since it enhances alkali release.

**15296.** Maximon, L. C., O'Connell, J. S., **Sum rules for forward elastic pion-nucleon scattering,** *Phys. Lett.* **51B,** No. 1, 31-34 (July 8, 1974).

Key words: dispersion relations; pion-nucleon amplitudes; pion-nucleon cross section; pion-nucleon scattering; pion-nucleus scattering; sum rules.

A number of energy weighted sum rules relating amplitudes and differential cross sections for forward elastic and charge exchange scattering to the total pion-nucleon cross section are derived from dispersion relations.

**15297.** Pickart, S., Rhyne, J., Alperin, H., Savage, H., **Neutron diffraction study of sputtered and annealed Tb-Fe alloys,** *Phys. Lett.* **47A,** No. 1, 73-74 (Feb. 25, 1974).

Key words: amorphous alloys; amorphous magnetism; coercine magnetic force; magnetic structure; neutron diffraction; recrystallization; terbium-iron.

Sputtered alloys of composition $Tb_x\ Fe_{1-x}$, with $x = 0.118$, 0.45 and 0.75 were shown by neutron diffraction to be amorphous. Line-width measurements of an annealed sputtered sample with $x = 0.333$ indicate microcrystallinity with a particle size of ≈ 100 Å.

**15298.** Van Brunt, R. J., Kieffer, L. J., **Angular distribution of N$^+$ from dissociative ionization of $N_2$ near threshold,** *J. Chem. Phys.* **63,** No. 8, 3216-3221 (Oct. 15, 1975).

Key words: electrons, ions; molecules; nitrogen.

Translational kinetic energy and angular distributions of $N^+$ from dissociative ionization of $N_2$ have been measured at electron energies close to threshold. For electron energies above 50 eV the energy distributions agree favorably with earlier measurements of Kieffer and Van Brunt. The ion energy distributions at electron energies below 50 eV are dominated by a feature peaked at a kinetic energy below 1 eV in agreement with recent measurements of Locht *et al.* For electron energies closest to threshold the angular distribution of $N^+$ associated with this feature is consistent with the previously proposed mechanism involving excitation of the $C^2\Sigma_u^+$ state followed by predissociation. At higher electron energies the degree of anisotropy increases and then rapidly decreases suggesting a significant contribution from direct excitation to the $^4\Sigma_g^+$ repulsive state of $N_2^+$ leading to fragments in their ground states.

**15299.** Manson, S. T., Cooper, J. W., **Angular distribution of photoelectrons: Outer shells of noble gases,** *Phys. Rev. A* **2,** No. 5, 2170-2171 (Nov. 1970).

Key words: angular distribution; asymmetry; photoionization; rare gases.

Results of calculations of angular distributions of photoelectrons from the outer *p* subshells of Ne, Ar, Kr, and Xe are presented for electron energies between 0 and 2 Ry (27.2 eV).

**15300.** Martin, W. C., **Atomic spectroscopy—Some data centers and compilations,** (Proc. 4th Int. CODATA Conf. on Generation, Compilation, Evaluation and Dissemination of Data for Science and Technology, Tsakhcadzor, U.S.S.R., June 24-27, 1974), *CODATA Bull.* **14,** 112-115 (CODATA Secretariat, Paris, France, 1974).

Key words: atomic data; atomic energy levels; atomic line shapes; atomic spectra; data compilations; gas lasers; transition probabilities.

The operation and current work of the NBS Atomic Energy Levels Data Center is reviewed briefly, and some of the other activities of this type, at NBS and elsewhere, are noted. The data include atomic wavelengths, energy levels, transition probabilities and line shapes and shifts, and gas laser transition data. References to some recent and forthcoming compilations of atomic spectral data are included.

**15301.** Lide, D. R., Jr., **The NSRDS experience,** (Proc. 4th Int. CODATA Conf. on Generation, Compilation, Evaluation and Dissemination of Data for Science and Technology, Tsakhcadzor, U.S.S.R., June 24-27, 1974), *CODATA Bull.* **14,** 6-9 (CODATA Secretariat, Paris, France, 1974).

Key words: data; Standard Reference Data Program; well-defined, measurable properties.

The Standard Reference Data Program deals primarily with physical and chemical property data. The properties covered are well-defined, measurable properties and the systems include pure substances and mixtures that can be adequately characdata by experienced scientists. The program is managed by the National Bureau of Standards under a mandate from the Congress of the United States to make critically evaluated reference data readily available to scientists, engineers and the general public.

**15302.** Simpson, J. A., **Modernizing gage block calibrations: A case study in measurement assurance,** *Proc. 1974 Joint Measurement Conference, Gaithersburg, Md., Nov. 12-14, 1974,* pp. 153-157 (Instrument Society of America, Pittsburgh, Pa., 1975).

Key words: calibration; gage blocks; measurement assurance.

Recently the Optical Physics Division of the National Bureau of Standards was faced with a potentially serious set of problems in the gage block calibration laboratory; labor costs were escalating, metrication threatened to greatly increase the workload, and the system in use (interferometry) did not lend itself to providing a desired Measurement Assurance Program. The introduction of a new system that provides better accuracy, lower cost and the possibility of a MAP was undertaken. The methods used to insure compatibility, maintain performance, and to be economic both for the Bureau and its customers, provide an interesting case study which is applicable to many other situations in metrology.

**15303.** Marzetta, L. A., **Some measurement engineering innovations in consumer products,** *Proc. 1974 Joint Measurement Conference, Gaithersburg, Md., Nov. 12-14, 1974,* pp. 41-44 (Instrument Society of America, Pittsburgh, Pa., 1975).

Key words: consumer products; contact temperature; thermesthesiometer; thermometry.

Exploration of the problem concerning hazards in consumer products has shown that laboratory engineers can usefully apply basic measurement practices towards improving safety and developing new measuring tools. Some novel and relatively simple redesign features will be presented concerning a common household appliance that can significantly reduce its electrical and thermal hazards. Included in the paper are details of an instrument which tests for burn hazard by simulating the human response to contact with a hot surface. The advantage of the new instrumentation is that a thermal safety standard can be written around one specified contact temperature for nearly any material regardless of its composition or surface temperature.

**15304.** Andrews, J. R., Lawton, R. A., **Picosecond pulse research at NBS,** *Proc. 1974 Joint Measurement Conference, Gaithersburg, Md., Nov. 12-14, 1974,* 123-140 (Instrument Society of America, Pittsburgh, Pa., 1975).

Key words: oscilloscopes; pulse; pulse generators; pulse measurement; transmission lines.

A general review of pulse measurement research at the National Bureau of Standards is described which includes work with electrical pulse generators using mechanical switches, avalanche transistors, snap off diodes, tunnel diodes, and laser pulses. Pulse transmission studies which include skin effect, nonuniform dielectric, lossy liquid dielectric and superconductivity are also mentioned together with pulse measurement techniques which include oscillographic techniques and pulse autocorrelation. The interfacing of picosecond pulse measurement instruments with a minicomputer is also described. This has resulted in an Automatic Pulse Measurement System (APMS) which has already been used to measure transmission coefficient, $S_{21}$, of some microwave networks.

**15305.** Lide, D. R., Jr., **The Standard Reference Data System,** *Chem. Eng. Prog.* **67,** No. 11, 77-78 (Nov. 1971).

Key words: critically evaluated numerical data; National Standard Reference Data System; physical sciences.

The National Standard Reference Data System (NSRDS) represents an effort to provide critically evaluated numerical data in the physical sciences. It is a decentralized program coordinated from the National Bureau of Standards, but enlisting the help of experts throughout the country. Activities of interest to chemical engineers are discussed.

**15306.** Mills, R. M., **A performance standard for walk-through metal detectors,** (Proc. 8th Annual Crime Countermeasures Conf., Lexington, Ky., Apr. 16-19, 1974), Paper in *Proc. 1974 Carnahan and Int. Crime Countermeasures Conf., UKY BU* **105,** 78-82 (Aug. 1974).

Key words: handgun detection; metal detector; performance standard; security; weapon detection.

The Law Enforcement Standards Laboratory at the National

Bureau of Standards (NBS) is developing performance standards for equipment used in the criminal justice system. They will be promulgated primarily by the National Institute of Law Enforcement and Criminal Justice, Department of Justice. This paper discussed the development of a standard for walk-through metal weapon detectors. The standard contains requirements and test methods for such things as detection performance, effects of walking speed and throughput rate, alarm indicator, controls, stability, ambient and generated magnetic field, and interference with other detectors.

15307. Newman, M., Pierce, S., **Bounded matrix groups,** *Linear and Multilinear Algebra* **1,** No. 3, 251-256 (1973).

Key words: associated matrices; Burnside theorem; irreducible representations; matrix groups.

The principal result is that if $G$ is any irreducible subgroup of $GL(n, C)$ ($C$ the complex field) such that $|\mathrm{tr}(TA)|$ is uniformly bounded for all $A$ in $G$ and some fixed $n \times n$ nonzero matrix $T$, then $G$ is equivalent to a unitary group. Similar results are proved for certain associated representations of $G$.

15308. Marcus, M., Newman, M., **Some results on unitary matrix groups,** *Linear Algebra and Appl.* **3,** 173-178 (1970).

Key words: bounded representations; Burnside; irreducibility; unitary groups; Weyl.

It is shown that an irreducible matrix group with uniformly bounded trace is itself uniformly bounded, and so equivalent to a unitary group. This result is used to prove that certain matrix groups preserving certain scalar valued functions are unitary.

15309. McCrackin, F. L., Chang, S. S., **Simple calibration procedures for platinum resistance thermometers from 2.5 to 14 K,** *Rev. Sci. Instrum.* **46,** No. 5, 550-553 (May 1975).

Key words: calibration of thermometers; low-temperature calibration of thermometers; platinum resistance thermometers; resistance thermometers; two-way structural analysis.

Calibration procedures are developed for platinum resistance thermometers in the temperature range 2.5-14 K. Two recommended methods require calibration points at the boiling point of liquid helium (4.215 K) and the triple point of hydrogen (13.81 K); in addition, the first method requires a point at 7.201 K while the second method requires the slope of the calibration curve at 13.81 K. For temperatures from 3.5 to 14 K, the calibrations are accurate to within 0.01 K for the first method and 0.025 K for the second method. For temperatures from 2.5 to 3.5 K, the calibrations are somewhat less accurate. Therefore, if a thermometer has been calibrated for temperatures of 13.81 K and above, its calibration may be easily extended to lower temperatures with sufficient accuracy for many applications. These calibration procedures were developed from two-way structural analysis of the accurate calibrations of 12 platinum resistance thermometers.

15310. Hanley, H. J. M., Watts, R. O., **Molecular dynamic calculation of the thermodynamic properties of methane,** *Aust. J. Phys.* **28,** 315-324 (1975).

Key words: methane; molecular dynamics; potential function; specific heat; statistical mechanical ensembles; thermodynamic properties; three body forces.

Thermodynamic properties of methane in the dense gas and liquid states have been calculated by the method of molecular dynamics. The methane pair interactions were modelled using a spherically symmetric $m$-6-8 potential, and the most significant three-body and quantum effects were included. Agreement between calculated and experimental values for the energy and pressure is generally good except at low temperatures and high densities. The specific heat at constant volume is also briefly discussed.

15311. Maki, A. G., **High-resolution infrared spectrum of the $\nu_1 + \nu_3$ band of ozone,** *J. Mol. Spectrosc.* **57,** No. 3, 416-427 (1975).

Key words: absorption spectra; infrared; molecular energy levels; ozone; pollution; spectra.

The $\nu_1 + \nu_3$ band of ozone ($O_3$) near 2110 cm$^{-1}$ has been measured and analyzed using a Watson-type Hamiltonian including all seven sextic centrifugal distortion terms. Two weak perturbations have been found between $K = n$ of $\nu_1 + \nu_3$ and $K = n + 3$ of $2\nu_3$. Those perturbations locate the band center for $2\nu_3$ at about 2058 cm$^{-1}$. Aside from those perturbations the interactions of $\nu_1 + \nu_3$ with $2\nu_1$ and $2\nu_3$ have not been taken into account in the analysis. Effective band constants and an atlas listing line wavenumbers and assignments are given.

15312. Leasure, W. A., Jr., Mathews, D. E., Cadoff, M. A., **Automobile tire noise: Results of a pilot study and review of the open literature,** *Report DOT/TST-76-4,* 75 pages (Office of Noise Abatement, Department of Transportation, Washington, D.C., Aug. 1975). (Available from the National Technical Information Service, Springfield, Va. 22161.)

Key words: acoustics; automombile; noise (sound); tire noise; transportation noise.

Automobiles, the primary mode of transportation in the United States, contribute significantly to the noise environment due to the large number in operation. In this report, one aspect of automobile noise is discussed; namely, the contribution to overall vehicle noise resulting from the interaction of the tires with the road surface. The results of this pilot study, which investigated the influence of selected parameters on automobile tire noise levels, in conjunction with a review of the open literature, serve as the basis for comparison of parametric trends between truck (for which an extensive noise data base exists) and automobile tires. As was the case with trucks, vehicle speed, road surface characteristics and tread design are major factors affecting automobile tire noise. The effect of pavement surface is more significant for automobile tires than for trucks since the texture within the tire-road interaction zone is on the same scale as the tread element spacing typical of passenger car tires. Load and wear, significant factors for truck tires, do not affect automobile tires as much due to the fact that the majority of automobile tires utilize rib tread designs. On the basis of the limited data available in the literature, factors such as inflation pressure, number of plies, tire dimensions, tire cord material, etc., do not appear to be significant factors affecting automobile tire noise.

15313. Bowman, C. D., **A shelf in the "subthreshold" photofission cross section,** *Phys. Rev. C* **12,** No. 3, 856-862 (Sept. 1975).

Key words: bremsstrahlung beams; cross section; fission barrier shape; fission isomer; photofission.

The influence of a double-humped fission barrier on the photofission cross section far below the top of the barrier is considered. In the region about 2 MeV below the top of the outer barrier and at a cross section in the region of $10^{-9} - 10^{-6}$ b the photofission is expected to become almost entirely isomeric or delayed fission. When this occurs a "shelf" should appear in the photofission cross section where the cross section changes with energy far more slowly than at higher $\gamma$-ray energy. The cross section on the shelf can therefore be orders of magnitude higher than otherwise expected. While the angular distribution near the top of the barrier is expected to have a well-defined and nonisotropic angular dependence, the angular distribution on the shelf is expected to be isotropic. The cross sections, although small, appear to be measurable with bremsstrahlung beams in the

3- to 5-MeV range using a several hundred $\mu$A electron beam. Successful experiments of this type should provide information on the shape of the inner and outer barriers at much lower excitation energies than possible by other techniques.

**15314.** Marcus, M., Merris, R., **A relation between the permanental and determinantal adjoints,** *J. Aust. Math. Soc.* **15,** Part 3, 270-271 (May 1973).

Key words: permanental adjoint; positive semidefinite hermitian matrix; symmetry class of tensors.

In this note an inequality is proved for generalized matrix functions. When specialized to the permanent, the inequality suggests a conjecture concerning a relation between the permanental and determinantal adjoints. The general inequality extends a conjectured inequality of Doković to another class of matrices.

**15315.** Thomson, R. M., **A review of nondestructive evaluation opportunities,** *ASTM Stand. News* **3,** No. 3, 8-14 (Mar. 1975).

Key words: materials reliability; nondestructive evaluation.

This paper is an abridged version of a recent report by a federal ad hoc working group on NDE. In the report, the NDE field is surveyed in order to foresee probable future growth areas and the technical developments which will be required to support this growth. Major NDE involvement is expected to continue in aerospace, to grow enormously along with the nuclear power industry, and to become a more important factor in ground transportation, general manufacturing, maintenance of machinery, and medical diagnosis. Technical issues and challenges are reviewed.

**15316.** Yonemura, G. T., **An image quality criterion for the identification of faces,** *Photogr. Sci. Eng.* **19,** No. 4, 223-227 (July-Aug. 1975).

Key words: acutance; identification (faces); image quality; Modulation Transfer Functions.

The performance required of imaging devices should be based on the needs of the user. In analyzing these needs, three psychophysical levels of visual task performance must be considered; detection, recognition, and identification. The experimental data base for these levels of performance is very uneven. Many detection studies have been performed, fewer have addressed problems of recognition, and rarer still are investigations associated with identification. This study determined experimentally the observer's perception of the image quality required for the identification of faces, as determined by two criteria: (1) the average observer and (2) 90 percent of the population. The subjective response from the human observer was then transformed into a physical descriptor amenable to direct measurement by instruments. The Modulation Transfer Function is recommended as the physical correlate for subjective facial identification.

**15317.** Young, J. P., **Codeposition of particulate matter with chromium,** *Plat. Surf. Finish. Tech. Brief* **62,** No. 4, 348-349 (Apr. 1975).

Key words: cermet; chromium plating; codeposition, composite coating; dispersion plating; electroplating; hard particles; wear-resistance; wear-tests.

Particles were included in a chromium deposit with the addition of a monovalent cation, e.g., thallium nitrate, in a small amount to the sulfate chromic acid bath. Using these additives, hard particles, lubricating particles, and metal powders were incorporated in a chromium matrix on vertical surfaces. When even less than 1 wt % of hard particles such as diamond, boron carbide or silicon carbide were codeposited with the chromium, resistance to wear was increased up to threefold over that of a hard, bright chromium deposit as measured by an abraser type wear-testing device.

**15318.** Yates, J. T., Jr., **Catalysis,** *Chem. Eng. News* **52,** No. 34, 19-22, 24-29 (Aug. 26, 1974).

Key words: adsorption; Auger spectroscopy; catalysis; infrared spectroscopy; kinetics; photoelectron spectroscopy.

A survey of a number of modern methods of surface science is given. The objective is to provide the reader with a general appreciation of the new advances in surface science which relate to fundamental thinking about heterogeneous catalysis.

**15319.** Goldberg, R. N., Prosen, E. J., Staples, B. R., Boyd, R. N., Armstrong, G. T., Berger, R. L., Young, D. S., **Heat measurements applied to biochemical analysis: Glucose in human serum,** *Anal. Biochem.* **64,** No. 1, 68-73 (Mar. 1975).

Key words: analysis; clinical chemistry; glucose; microcalorimetric; thermochemistry.

Microcalorimetric measurement of enthalpy change for the hexokinase catalyzed reaction of ATP with glucose (in TRIS/HCl buffer containing $MgCl_2$) was carried out with glucose concentrations from zero to 1350 mg · liter$^{-1}$. A linear relationship between measured heat and glucose concentration was found, from which the reaction enthalpy was calculated to be $-$61.4 kJ · mole$^{-1}$. This linear relation, combined with calorimetric measurements of the same process carried out with 0.15 ml samples of human serum, was used to calculate glucose concentrations in the serum. For 45 samples containing glucose levels ranging from 420 to about 4000 mg · liter$^{-1}$ the results show only slight systematic differences from measurements made by the glucose oxidase procedure of Gochman and Schmitz.

**15320.** Mopsik, F. I., Broadhurst, M. G., **Molecular dipole electrets,** *J. Appl. Phys.* **46,** No. 10, 4204-4208 (Oct. 1975).

Key words: electret; dipoles; glass; piezoelectric; polarization; polyvinyl chloride; pyroelectric.

The total polarization due to molecular dipoles in a glassy electret is computed using an Onsager cavity approach. From this result, all the possible contributions to the piezoelectric and pyroelectric coefficients are considered. It is shown that there are major contributions from the variation in dielectric constant and, for pyroelectricity, from thermal motion. These results account well for experimental data for polyvinyl chloride.

**15321.** Velapoldi, R. A., Travis, J. C., Cassatt, W. A., Yap, W. T., **Inorganic ion-doped glass fibres as microspectrofluorimetric standards,** *J. Microsc.* **103,** Part 3, 293-303 (Apr. 1975).

Key words: europium ions; fluorescence; fluorescence standards; inorganic ion-doped fibers; microspectrofluorimetry; uranyl ions.

Uranyl and europium ion-doped fibres of 5-45 $\mu$m diameter were prepared which emit in the green and red spectral regions, respectively. Measurements were made of fluorescence flux as a function of fibre length, dopant concentration, slit shape and fibre diameter. The flux was found to be proportional to fibre length and fluorophor concentration and proportional to the square of the fibre radius. In addition, the fluorescence flux as a function of aperture size and shape and fibre position has been measured experimentally and compared to computer generated fluorescence flux envelopes. It is suggested that inorganic ion-doped fibres are suitable for use as microspectrofluorimetric standards.

**15322.** Wiederhorn, S. M., Evans, A. G., **A new method for the design of structural ceramic components,** *Nav. Res. Rev.* **XXVII,** No. 2, 18-25 (Feb. 1974).

Key words: crack growth; fracture; fracture mechanics; porcelain; strength; structural ceramics.

A new method in design of structural ceramic components is discussed. The method is based on an understanding of crack growth in these materials and provides a means of estimating the time to failure under load.

**15323.** Unassigned.

**15324.** VanderHart, D. L., **Study of molecular reorientation: Pressure and temperature dependence of deuterium relaxation in liquid CDCl$_3$,** *J. Chem. Phys.* **60,** No. 5, 1858-1870 (Mar. 1, 1974).

Key words: chloroform; deuterium; NMR; pressure dependence; relaxation; reorientation; temperature dependence.

Deuterium NMR spin-lattice relaxation measurements have been performed on the neat liquid CDCl$_3$ over the range 28 °C $< T <$ 165 °C and at pressures up to 5 kbar ($5 \times 10^8$ $N/m^2$). These measurements enable one to determine $\tau_{\theta,2}$, the correlation time for molecular reorientation about the axes perpendicular to the symmetry axis. The data are presented as a function of all three state variables, $P$, $V$, and $T$. An attempt is made to describe the data in terms of various simple models for reorientation including activation and free volume models. Each of these models predicts certain aspects of the data but fails in other areas. In particular, the activation model fails to predict the correct behavior at constant temperature and the free volume theories generally fail to predict the constant volume experiments. Deviations from the Debye and microviscosity theories were also noted. The mean time between collisions $\tau_{coll}$ was calculated from $\tau_{\theta,2}$ assuming both Gordon's $J$-diffusion model and the equivalence of $\tau_{coll}$ and $\tau_J$, the angular momentum correlation time. These values of $\tau_{coll}$ were then compared with the predictions of the cell model for liquids in which $\tau_{coll}$ is simply the mean free path divided by the mean velocity. Generally, the data did not fit the cell model; however, at constant pressure, the cell model did predict the changes in $\tau_{coll}$ quite well. Qualitative suggestions are made to account for the discrepancies. Finally, the possibility that H-bonding exists in CHCl$_3$ and affects the generality of these results by changing the quadrupole coupling constant and disturbing the dynamics of the system is discussed. It is concluded that these effects are small if they exist at all.

**15325.** Collard, J. J., **U.S. law enforcement receives scientific support,** *Int. Crim. Police Rev. No. 262,* 261 (Nov. 1972).

Key words: building systems; communications equipment; concealed objects detectors; emergency equipment; Law guidelines; protective equipment; security systems vehicles; voluntary standards; weapons.

In January 1971, at the request of the U.S. Department of Justice, the National Bureau of Standards established a new organization, the "Law Enforcement Standards Laboratory." This Laboratory, which is presently funded entirely by the National Institute of Law Enforcement and Criminal Justice, the research arm of the Law Enforcement Assistance Administration, has been given the task of developing voluntary performance standards, specifications, and guidelines for equipment used by U.S. law enforcement and criminal justice agencies. The objective of this program is to assist Federal, state and local law enforcement organizations in the selection and procurement of equipment used by these agencies. In addition to standards development, the Laboratory is developing the methods for measuring the actual performance levels of the equipment.

**15326.** Swing, R. E., **The sampling aperture for linear microdensitometry,** *Opt. Eng.* **13,** No. 5, 460-470 (Sept.-Oct. 1974).

Key words: impulse response; linear microdensitometry; microdensitometry; optics; slit imagery; transfer function.

In the development of modern linear microdensitometry, the underfilling the efflux optics, with total collection of light after it passes through the sample. The system transfer function is therefore attributable to the influx optics, and the sampling aperture is the light distribution impinging on the sample, reduced from an illuminated slit or circular aperture through the influx optical system. The maximum frequency response of the system is obtained when the sample is illuminated with the impulse response of the influx optics. However, the theoretical impulse response can only be realized by imaging a delta-function and this is photometrically impossible. Similarly, because the system images an illuminated aperture onto the sample, scanning with a pure, geometrically-characterized slit or spot is not possible due to lens response and diffraction. These two problems are investigated, for both coherent and incoherent illumination.

For both impulse response and slit image, the MTF is investigated, and its deviation from the ideal is calculated. The results are characterized in terms of RMS-MTF differences over the spectrum for 10, 5, 2, and 1 percent levels. The controlling parameter is the ratio N/R, where R is the reduction factor employed for the influx optics, and N is the number of resolution elements contained within the nominal object slit width. The study shows that there are significant differences in these values for the same RMS difference level, with coherent and incoherent illumination, and that there are compromises to be made with both kinds of illumination. The results of this study facilitate calculation of system response for any configuration of object slit and influx optics (within the linear microdensitometer system), and defines limits on slit sizes for operation with impulse response and geometrically characterized slit images for the sampling aperture. The effects expected with the linear polarization associated with laser illumination (the most common source of high-energy, coherent radiation) is discussed, but not included in this scalar treatment.

**15327.** Cox, J. E., Waterstrat, R. M., **Anticorrelation of atomic ordering with superconductivity in vanadium-based transition metal A15 alloys,** *Phys. Lett.* **46A,** No. 1, 21-22 (Nov. 19, 1973).

Key words: annealing temperature; atoms; stoichiometry; superconducting; transition temperature.

Measurements of the superconducting transition temperature ($T_o$) of V-Rh A15 alloys reveal that long range order induced by low temperature annealing may cause $T_o$ to decrease rather than increase. The behavior of $T_o$ with ordering is discussed for the systems V-Au, V-Pt, V-Ir, V-Os and V-Rh.

**15328.** Laufer, A. H., Bass, A. M., **Rate constants of the combination of methyl radicals with nitric oxide and oxygen,** *Int. J. Chem. Kinet.* **VII,** No. 5, 639-648 (1975).

Key words: combination; kinetics; methyl; nitric oxide; oxygen; rate constants.

Rate constants for the combination of methyl radicals with NO and O$_2$ have been measured by flash photolysis of azomethane coupled with product analysis by gas chromatography. Values of the rate constants have been obtained over the pressure region from 50 to 700 torr with He, N$_2$, and Ar as quenching molecules.

The high-pressure limits were obtained through an RRKM model calculation and were found to be

$$CH_3 + NO + M \rightarrow CH_3NO + M$$

$$k_\infty = 3.2 \times 10^{-11}\ \text{cm}^3/\text{molec} \cdot \text{sec}$$

$$CH_3 + O_2 + M \rightarrow CH_3O_2 + M$$

$$k_\infty = 1.7 \times 10^{-12} \text{ cm}^3/\text{molec} \cdot \text{sec}$$

The rate constants were measured relative to the methyl combination reaction $k_1$ with $k_1 = 9.5 \times 10^{-11}$ cm³/molec · sec. The RRKM model suggests $D_0(CH_3 - O_2) = 32 \pm 3$ kcal/mole.

**15329.** Farmer, B. L., Eby, R. K., **Methyl branches in hydrocarbon crystals: Calculation of relaxation parameters,** *J. Appl. Phys.* **46,** No. 10, 4209-4217 (Oct. 1975).

Key words: mechanical relaxation; methyl branches; paraffins; polyethylene; potential energy calculations; relaxation mechanism; relaxation strength; site model.

A site model has been used in conjunction with potential-energy calculations to examine the role of isolated molecules with methyl branches in the mechanical relaxations of a linear hydrocarbon host crystal. The results indicate that there are two possible relaxation modes and that the one involving molecular rotation is energetically favorable over the one involving rotation and translation. For some modes of deformation, the calculated relaxation strengths are comparable to the experimentally measured ones. Furthermore, the barriers determined in this work yield calculated curves of the logarithmic decrement as a function of temperature which are comparable to the experimental ones. The relaxation is much weaker for unbranched chains in the planar zigzag conformation.

**15330.** Torchia, D. A., Lyerla, J. R., Jr., Quattrone, A. J., **Molecular dynamics and structure of the random coil and helical states of the collagen peptide, α1-CB2, as determined by $^{13}$C magnetic resonance,** *Biochemistry* **14,** No. 5, 887-900 (1975).

Key words: C-13 magnetic resonance; collagen; polymers; polypeptides; protein structure; relaxation times.

Carbon-13 chemical shifts, spin-lattice ($T_1$) and spin-spin ($T_2$) relaxation times, and $^{13}C-\{^1H\}$ nuclear Overhauser enhancements (NOE) have been determined for the random coil and triple helical states of the $\alpha$1-CB2 fragment of rat skin collagen. Assignment of all aliphatic resonances of this 36 residue peptide in the random coil state (30°) has been achieved with the aid of model polypeptides containing pyrrolidine residues. The chemical shifts and intensities of the Pro and Hyp $C^\gamma$ resonances show that $\geqslant 90$ percent of the X-Pro and X-Hyp bonds are trans in both helix and coil conformations. From $T_1$ measurements rotational correlation times ($\tau_{eff}$) of *ca.* 0.45 nsec are calculated for interior $C^\alpha$ carbons in the coil, while $\tau_{eff}$ values of the side chain and near terminal carbons are found to be 2-9 times smaller. These results along with the narrow natural line widths (3-5 Hz) and maximal NOE values ($2.8 \pm 0.3$) demonstrate the high degree of backbone mobility, due to segmental motion, in the unordered state of the peptide. By contrast, the broad lines (50-90 Hz) and small NOE values ($1.3 \pm 0.3$) for the $\alpha$ carbons in the helical state (2°) suggest much slower motion. The line widths and NOE values together with the $C^\alpha T_1$ values (0.025-0.040 sec) correspond to correlation times which are in reasonable agreement with those calculated for an axially symmetric rigid ellipsoid, undergoing rotational diffusion, having dimensions approximating those of a collagen-type triple helical aggregate of three $\alpha$1-CB2 chains. A satisfactory computer simulation of the experimental 2° spectrum is obtained by assigning the narrow aliphatic resonances in the spectrum (line widths 5-40 Hz) to (a) carbons in the small amounts of $\alpha$1-CB2 (3 mol %) and $\alpha$1-CB1 (2.5 mol %) random coil conformations, (b) carbons in the flexible terminal triplets of the helix, and (c) Ala, Leu, and Phe methyl and phenyl carbons. The side chain carbon line widths obtained from the simulation—when compared with side chain line widths calculated for a rotating rigid ellipsoid with internal motion—indicate rapid axial reorientation of methyl and phenyl groups. With the exception of the Hyp residue the line widths suggest local motion for at least some carbons in most other side chain moieties. The Hyp $C^\beta$ and $C^\gamma$ line widths indicate the presence of little if any rapid Hyp ring motion.

**15331.** Scheide, E. P., Taylor, J. K., **Piezoelectric sensor for mercury in air,** *Environ. Sci. Technol.* **8,** No. 13, 1097-1099 (Dec. 1974).

Key words: air pollution; chemical analysis; industrial hygiene; mercury; piezoelectric detector; trace analysis.

A quartz piezoelectric crystal detector with gold evaporated onto the electrode as the sensor substrate has been developed for the detection of small mass changes caused by the selective adsorption of mercury vapor from an air sample. Incorporation of the crystal into a variable oscillator circuit and measurement of the change in frequency of the crystal due to the increase in mass allows a highly sensitive indication of the amount of mercury present in the air sample down to the subpart-per-billion level. Thus, the selectivity of mercury adsorption onto gold films and the sensitivity of the piezoelectric sensor are combined in this instrument. Calibration curves are obtained from part-per-million to subpart-per-billion concentrations of mercury. Reversibility is achieved by placing the sensor in an oven, raising the temperature to 150 °C, and flow switching a stream of clean, dry air over the detector. This detector has potential use both as an air pollution sensor and in industrial hygiene applications.

**15332.** Stampfl, P. P., Travis, J. C., Bielefeld, M. J., **Mössbauer spectroscopic studies of iron-doped rutile,** *Phys. Status Solidi A* **15,** No. 1, 181-189 (1973).

Key words: diffusion; doping; Fe-57; iron-doped; lattice distortion; Mössbauer spectroscopy; quadrupole splitting; temperature dependence.

Iron-57 Mössbauer spectra have been obtained of single crystal and powdered samples of rutile ($TiO_2$) doped to about one percent by weight in isotopically enriched iron. Spectral patterns found for powdered samples are consistent with theoretical expectations for substitutional doping with a uniform distribution of oxygen vacancies and impurity ions. The temperature dependence of the ferrous pattern indicates a slight shift in position of the neighboring oxygen ions to accommodate the relatively large size of the dopant ion. Spectral parameters from the single crystal samples differ radically from those of the powdered samples or the "ideal lattice" theory. Variations in stoichiometry, charge compensation mechanisms, or other diffusion-related phenomena are assumed to be responsible. Single crystal results do, however, furnish graphic evidence that trivalent iron diffuses faster in rutile than the larger divalent species.

**15333.** Paule, R. C., **Calculation of complex equilibria involving vaporization into vacuum,** *High Temp. Sci.* **6,** No. 4, 267-275 (Dec. 1974).

Key words: $Al^2O^3$; chemical doping; complex equilibria; purification (evaporative); vacuum vaporization.

A simplified, direct approach is presented to the description of complex equilibria involving vaporization into vacuum. Emphasis is on the basic problem-solving process and on modification of existing techniques. Sequential solutions are presented to problems involving purification of a melt by vaporization into vacuum. The effects of concentration of melt and oxygen partial pressures on vaporization rates are demonstrated.

**15334.** Jacox, M. E., Milligan, D. E., **Matrix isolation study of the infrared spectrum of thioformaldehyde,** *J. Mol. Spectrosc.* **58,** No. 1, 142-157 (1975).

Key words: $CH^3S$; $CH^3SH$; dimethyldisulfide; infrared spectrum; matrix isolation; pyrolysis; *s*-trithiane; thioformaldehyde; ultraviolet photolysis; vacuum ultraviolet photolysis.

$H^2CS$ has been trapped in argon and nitrogen matrices at 14 K as a product of the pyrolysis of *s*-trithiane or $(CH^3S)^2$ and of the ultraviolet or vacuum ultraviolet photolysis of $CH^3SH$. A small concentration of $H^2CS$ has also been observed upon vacuum ultraviolet photolysis of a mixture of $CH^4$ and $H^2S$ in an argon matrix. The isotopic data support the assignment of absorptions at 993 and at 1063 $cm^{-1}$ to the out-of-plane deformation and the C=S stretching fundamentals of $H^2CS$. Absorptions in the CH stretching region which were assigned to $H^2CS$ in an earlier gas-phase study were confirmed in the matrix experiments. Studies of the vacuum ultraviolet photolysis of $CD^3SH$ have provided information on the mechanism of the photolysis process.

**15335.** Tomuta, L., Mizushima, M., Howard, C. J., Evenson, K. M., **Rotational structure and magnetic *g* factors of $O^2(X_3\Sigma^g{}_-, \nu = 0)$ from laser-magnetic-resonance spectra,** *Phys. Rev. A* **12,** No. 3, 974-979 (Sept. 1975).

Key words: effect; laser; magnetic resonance; oxygen; rotational structure; Zeeman.

Using the 108- and 84-$\mu$m $D^2O$ laser lines, new laser-magnetic-resonance (LMR) spectra of the oxygen molecule in its ground state ($X_3\Sigma^g{}_-$, $\nu = 0$) are observed and analyzed. The corresponding transitions are $n = 15 \rightarrow 17$ and $n = 19 \rightarrow 21$, respectively. Bauer, Kamper, and Lustig's values of the *g* factors are consistent with our results, but Hendrie and Kusch's values are not. Combining all LMR results with other results, we obtain rotational parameters $B^0 = 43.1004608(75)$ GHz and $B^1 = 0.14520(20)$ MHz.

**15336.** Gillispie, G. D., Khan, A. U., Wahl, A. C., Hosteny, R. P., Krauss, M., **The electronic structure of nitrogen dioxide. I. Multiconfiguration self-consistent-field calculation of the low-lying electronic states,** *J. Chem. Phys.* **63,** No. 8, 3425-3444 (Oct. 15, 1975).

Key words: dipole moment; excited states; MC-SCF; molecular geometry; $NO^2$; spectra.

Traditional spectroscopic analysis of the complex and irregular absorption spectrum of $NO^2$ has provided a relatively small amount of information concerning the nature of the excited states. An extensive *ab initio* investigation has been undertaken, therefore, to provide a basis for interpretation of the experimental results. Multiconfiguration self-consistent-field (MC-SCF) wavefunctions have been computed for the low-lying

$$\bar{X}\,^2A_1, \bar{A}\,^2B_2, \bar{B}\,^2B_1, \bar{C}\,^2A_2, {}^4B_2, {}^4A_2, \text{ and } {}^2\Sigma_g{}^+$$

electronic states of $NO_2$. The minima of the $\bar{A}\,^2B_2$, $\bar{B}\,^2B_1$, and $\bar{C}\,^2A_2$ states have all been found to be within 2 eV of the minimum of the $\bar{X}\,^2A_1$ ground state; for these states, $C_{2v}$ potential surfaces have been constructed for purposes of a spectral interpretation. The ${}^4B_2$, ${}^4A_2$, and ${}^2\Sigma_g{}^+$ states are all more than 4 eV above the minimum of the ground state and have been examined in less detail. The study described here significantly improves on previous $NO_2$ *ab initio* calculations in three important areas: (1) The double-zeta-plus-polarization quality basis set is larger and more flexible; (2) the treatment of molecular correlation is more extensive; and (3) the electronic energies have been calculated for several different bond lengths and bond angles in each state. For the four lowest doublet states the following spectral data have been obtained:

| | $T_e$(eV) | $R_e$(Å) | $\theta_e$(deg) |
|---|---|---|---|
| $\bar{C}\,^2A_2$ | 1.84 | 1.27 | 110 |
| $\bar{B}\,^2B_1$ | 1.66 | 1.20 | 180 |
| $\bar{A}\,^2B_2$ | 1.18 | 1.26 | 102 |
| $\bar{X}\,^2A_1$ | 0.00 | 1.20 | 134 |
| | (0.00) | (1.1934) | (134.1). |

| | $\omega_1$(cm$^{-1}$) | $\omega_2$(cm$^{-1}$) | $\mu$(D) |
|---|---|---|---|
| $\bar{C}\,^2A_2$ | 1360 | 798 | 0.05 |
| $\bar{B}\,^2B_1$ | 1192 | 960 | 0.00 |
| $\bar{A}\,^2B_2$ | 1461 | 739 | 0.46 |
| $\bar{X}\,^2A_1$ | 1351 | 758 | 0.37 |
| | (1358) | (757) | (0.32) |

The ground state experimental constants are included in parentheses. The estimated accuracy of the various parameters is ±0.02 Å for bond length, ±2° for bond angle, ±10 percent for the vibrational frequencies, ±0.10 D for dipole moments, and ±0.3 eV for the adiabatic excitation energies. An unusual feature has been found for the ${}^2\Sigma_g{}^+$ state. The equilibrium geometry of this linear state has two unequal bond lengths of 1.20 and 1.42 Å and the inversion barrier is approximately 800 $cm^{-1}$.

**15337.** Furukawa, G. T., Bigge, W. R., Riddle, J. L., Reilly, M. L., **The freezing point of aluminium as a temperature standard,** *Inst. Phys. Conf. Ser. No.* **26,** Chapter 7, 389-397 (1975).

Key words: aluminium point; calibration; freezing point; freezing-point cell; platinum resistance thermometer; tin point; zinc point.

Six platinum resistance thermometers were "calibrated" at the triple point of water and at the freezing points of tin, zinc and aluminium. By extrapolating the "quadratic relation" the freezing point of pure aluminium was found to be 660.407±0.005 "degrees C." The advantages of having a platinum resistance thermometer calibrated at a fixed point (e.g., aluminium point) near the upper temperature limit are demonstrated.

**15338.** Merris, R., Pierce, S., **Elementary divisors of higher degree associated tranformations,** *Linear and Multilinear Algebra* **1,** No. 3, 241-250 (1973).

Key words: elementary divisors; irreducible character; symmetry class of tensors.

Let $V$ be a complex inner product space of dimension $n$ and let $\overset{m}{\otimes} V$ be the space of $m$ contravariant tensors over $V$. Given a subgroup $G$ of $S_m$ and an irreducible character $\chi$ on $G$, we define a subspace $V_\chi{}^m(G)$ in $\overset{m}{\otimes} V$. If $T{:}V \rightarrow V$ is linear, let $\Pi \cdot T{:} \overset{m}{\otimes} V \rightarrow \overset{m}{\otimes} V$ be the $m$th Kronecker product of $T$. Then $V_\chi{}^m(G)$ is invariant under $\Pi \cdot T$ and we let $K(T)$ be the restriction of $\Pi \cdot T$ to $V_\chi{}^m(G)$. In this paper we prove that if the rank of $T$ is large enough, then the elementary divisors of $K(T)$ are linear if and only if the elementary divisors of $T$ are linear. This result has previously been proved only for the case that $\chi$ is linear.

**15339.** Soulen, R. J., Jr., Gubser, D. U., **Superconducting properties of iridium,** (Proc. 13th Int. Conf. on Low Temperature Physics-LT 13, Boulder, Colo., Aug. 21-25, 1972), Paper in *Low Temperature Physics-LT* **13,** K. D. Timmerhaus, W. J. O'Sullivan, and E. F. Hammel, Eds., **3,** 498-502 (Plenum Publishing Corp., New York, N.Y., 1974).

Key words: critical field, fixed point; iridium; transition temperature.

The residual resistivity ratio, superconductive transition temperature, magnetization curves, and critical magnetic field data of several samples of iridium have been measured. It is found that the magnetic properties of superconducting iridium are highly dependent on the metallurgical state of the sample, whereas the transition temperature is relatively less sensitive.

The use of iridium as a superconductive thermometric fixed point at 0.1 K is critically examined.

**15340.** Shih, A., **van der Waals forces between a Cs atom or a CsCl molecule and metal or dielectric surfaces,** *Phys. Rev. A* **9,** No. 4, 1507-1514 (Apr. 1974).

Key words: cesium beam; cesium chloride beam; gold surfaces; van der Waals forces.

The interaction potentials between a spherically symmetric atom (Cs) and a highly conducting surface (gold) or a dielectric surface (glass) are investigated by the atomic-beam-deflection technique. The observed beam profile is least-squares fitted to an $r^{-3}$ potential. The derived interaction constant for the gold surface is 0.59 and 0.67 of the values predicted by Bardeen and Mavroyannis, respectively. A glass surface is found to have an interaction constant 0.65 that of gold. The measurements have also been obtained for a polar molecule (CsCl). With a gold surface the observed beam profile is almost identical to that for stainless steel (reported earlier) in spite of their difference in dc conductivity. Further, the observed constant for an insulator (glass surface) is 0.86 that of gold. With gold, the interaction constant obtained for a cesium-halide molecule, with a strong permanent dipole moment, is smaller than that for a Cs atom with zero dipole moment.

**15341.** Johnson, C. R., **Inequalities for a complex matrix whose real part is positive definite,** *Trans. Amer. Math. Soc.* **212,** 149-154 (1975).

Key words: eigenvalues; Hadamard inequality; positive definite; real part.

Denote the real part $A \in M_n(C)$ by $H(A) = 1/2(A + A^*)$. We provide dual inequalities relating $H(A^{-1})$ and $H(A)^{-1}$ and an identity between two functions of $A$ when $A$ satisfies $H(A) > 0$. As an application we give an inequality (for matrices $A$ satisfying $H(A) > 0$) which generalizes Hadamard's determinantal inequality for positive definite matrices.

**15342.** Schooley, J. F., **The superconductive transition in cadmium,** (Proc. 13th Int. Conf. on Low Temperature Physics-LT 13, Boulder, Colo., Aug. 21-25, 1972), Paper in *Low Temperature Physics-LT 13,* K. D. Timmerhaus, W. J. O'Sullivan, and E. F. Hammel, Eds., **3,** 382-386 (Plenum Publishing Corp., New York, N.Y., 1974).

Key words: OSRM; pure cadmium; superconductive transition temperature; superconductive transition width; thermometric fixed point.

We have examined the superconductive transition of a single crystal of cadmium at temperatures from 0.1 K to its transition temperature, $T_c$, and in magnetic fields from 0-27 gauss. We have measured $T_c$ as $0.515 \pm 0.002_5$ K on the T-62 scale. We have compared its transition width and its $T_c$ with polycrystalline samples prepared for thermometric fixed-point devices. The single-crystal transition width is $\sim 250\ \mu$K at H=0, compared to 2-6 mK for the polycrystalline samples. However, the $T_c$'s of the polycrystalline samples agree within 0.5 mK with that of the single crystal. We have examined the width of the single-crystal transition as a function of applied field, and find a minimum width of about 25 $\mu$K for 0.5 gauss. These data will be discussed in terms of transition temperature theory.

**15343.** Ledbetter, H. M., Weston, W. F., Naimon, E. R., **Low temperature elastic properties of four austenitic stainless steels,** *J. Appl. Phys.* **46,** No. 9, 3855-3860 (Sept. 1975).

Key words: bulk modulus; chromium alloys; compressibility; Debye temperature; Doring effect; elastic constants; iron alloys; magnetic transition; nickel alloys; Poisson's ratio; pulse-echo method; sound velocity; Young's modulus.

The elastic properties of four austenitic stainless steels – AISI 304, AISI 310, AISI 316, and A286 – are reported over the temperature range 300-4 K. These properties include longitudinal (reciprocal compressibility), Poisson's ratio, and elastic Debye temperature. Elastic constants were determined from measurements of longitudinal and transverse soundwave velocities using an ultrasonic (10 MHz) pulse-superposition method. Measurements were made in the absence of a magnetic field; these alloys undergo paramagnetic-to-antiferromagnetic transitions at low temperatures. For all four alloys, the shear modulus behaves regularly with respect to temperature. The other elastic constants, all of which have a dilatational component, decrease anomalously at temperatures below 80 K. The largest anomaly, about 3 percent, is in the bulk modulus of the 304 alloy; this modulus is lower at 0 than at 300 K. Results are interpreted on the basis of the Döring effect, which results from a large volume magnetostriction in the magnetic phase. This may be the first report of a Döring effect in antiferromagnetic materials.

**15344.** Maienthal, E. J., **Analysis of botanical standard reference materials by cathode ray polarography,** *J. Assoc. Off. Anal. Chem.* **55,** No. 5, 1109-1113 (1972).

Key words: aluminum; analysis; business; differential cathode ray polarography; iron; lead; nickel; orchard leaves.

The need for certified botanical and biological standards both in research and in industrial and field applications is leading to the development and production of a number of new Standard Reference Materials by the National Bureau of Standards. The first of these to be produced and certified is an orchard leaf standard. The determination of a number of important trace elements by cathode ray polarography was investigated and found to offer considerable advantages in sensitivity and accuracy over many other techniques. In addition, several elements may be determined simultaneously in the same solution. The methods were developed and applied to the analysis and certification of nickel, lead, bismuth, and iron in the orchard leaves. Results were also obtained for aluminum which has not yet been certified. Nickel was determined on 1 g samples after extraction with dimethylglyoxime and $CHCl_3$. Lead and bismuth were determined concurrently on 1 g samples after a sodium diethyldithiocarbamate separation. Iron and aluminum were determined on 0.25 g samples after cupferron separations. Details of the methods are given and the results are compared with those obtained by other techniques.

**15345.** Clark, A. F., Moulder, J. C., Runyan, C. C., **Combustion of bulk titanium in oxygen,** (Proc. 15th Int. Symp. on Combustion, Tokyo, Japan, Aug. 25-31, 1974), Paper in *Fifteenth Symposium (International) on Combustion,* pp. 489-499 (The Combustion Institute, Pittsburgh, Pa., 1974).

Key words: combustion; Hilbert transform; laser ignition; oxygen; titanium.

The combustion of bulk titanium in one atmosphere oxygen is studied using laser ignition and several analytical techniques. These were high-speed color cinematography, time and space resolved spectra in the visible region, metallography (including SEM) of specimens quenched in argon gas, x-ray and chemical product analyses, and a new optical technique, the Hilbert transform method. The cinematographic application of this technique for visualizing phase objects in the combustion zone is described. The results indicate an initial vapor phase reaction immediately adjacent to the molten surface but as the oxygen uptake progresses the evaporation approaches the point of congruency and a much reduced evaporation rate. This and the accumulation of the various soluble oxides soon drive the reaction zone below the surface where gas formation causes boiling and ejection of particles. The buildup of rutile cuts off the oxygen supply and the reaction ceases.

**15346.** Yakowitz, H., **Use of divergent-beam x-ray diffraction to measure lattice expansion in LiF as a function of thermal-neutron dose up to $6 \times 10^{16}$ nvt,** *J. Appl. Phys.* **43,** No. 11, 4793-4794 (Nov. 1972).

Key words: Kossel diffraction; lattice expansion; LiF; NBS reactor; radiation damage; thermal neutrons.

The lattice expansion of LiF was measured by means of the divergent-beam (Kossel) x-ray diffraction method at three levels of thermal-neutron dose, 0.45, 2, and $6 \times 10^{16}$ nvt, respectively. The lattice parameter of LiF increases due to the production of Frenkel defects resulting from the $Li^6(n,\alpha)_1H^3$ reaction. At $6 \times 10^{16}$ nvt, the lattice expansion was found to be $0.13 \pm 0.02$ percent which is in good agreement with previously reported values.

**15347.** Yates, J. T., Jr., Erickson, N. E., **X-ray photoelectron spectroscopic study of the physical adsorption of xenon and the chemisorption of oxygen on tungsten (111),** *Surface Sci.* **44,** No. 2, 489-514 (1974).

Key words: chemisorption; ESCA; oxygen; physical adsorption; tungsten; xenon.

X-ray photoelectron spectroscopy (ESCA) has been used to study the physical adsorption of Xe and the chemisorption of oxygen by W (111). An ultrahigh vacuum ESCA spectrometer has been modified such that thermal desorption behavior from the W (111) crystal can be directly compared with ESCA spectra of the adsorbed species. In addition, since the work function of a W (111) crystal covered with one monolayer of Xe is accurately known from previous work, the binding energy of the $Xe(3d_{5/2})$ adsorbate level can be accurately compared to the gaseous $Xe(3d_{5/2})$ level.

When Xe is physisorbed to 1 monolayer the Xe $(3d_{5/2})$ level exhibits a binding energy (relative to the vacuum level) which is 2.1 eV below that found for Xe (g). At lower Xe coverages the shift becomes monotonically greater, approaching 2.6 eV at a Xe coverage of 0.05. This 0.5 eV shift downward is accompanied by an increase of only 0.05 eV in adsorption energy as coverage decreases, and may be partially caused by the presence of ~ 10-20 percent of extraneous adsorption sites other than W (111) which adsorb Xe with higher adsorption energy. The adsorption energy of Xe may also be increased by coadsorption of oxygen and the Xe $(3d_{5/2})$ binding energy exhibits a corresponding shift downward as adsorbed oxygen coverage is increased to $\theta_o = 0.5$. Electronic relaxation processes affecting the final state are dominant factors in determining the magnitude of the chemical shift upon adsorption, in agreement with the predictions of Shirley. The magnitude of the relaxation effect seems to be very sensitive to small changes in Xe adsorption energy. Similar effects have been seen for chemisorption of CO.

The adsorption of $O_2$ at 120 K by W (111) yields a single broad O(1s) peak whose linewidth decreases with increasing coverage. The final spectra at $\theta_o = 1$ monolayer are very similar to those obtained at temperatures of 300 K or above on polycrystalline tungsten.

**15348.** Lyon, G., Stillman, R. B., **Simple transforms for instrumenting FORTRAN decks,** *Software—Pract. Exper.* **5,** No. 4, 347-358 (Oct.-Dec. 1975).

Key words: computation and flow analysis; FORTRAN use; programming aids; syntax analysis.

A recent revival of interest in measuring program execution behaviour has led to a number of distinct approaches. Arguments are given for a fairly simple method of modifying FORTRAN source code to collect frequency counts. No symbol table is necessary and only a single reserved name is introduced into the

**15349.** Gallagher, A., **The spectra of colliding atoms,** (Proc. 4th Int. Conf. on Atomic Physics, Heidelberg, Germany, July 1974), Paper in *Atomic Physics* **4,** G. zu Putlitz, E. W. Weber, and A. Winnacker, Eds., pp. 559-574 (Plenum Publ. Corp. New York, N.Y., 1975).

Key words: line broadening; rubidium; sodium.

We discuss what can be learned from line shapes and the basic ideas of how they are interpreted with theoretical approximations. Only "pressure" or neutral-gas broadening will be considered, not "Stark" or plasma broadening. We will give examples of recent theoretical and experimental work, but this is not intended as a review and we will concentrate on our measurements in the far wings of the lines.

**15350.** Bowman, C. D., Schröder, I. G., Dick, C. E., Jackson, H. E., **Very low energy photofission of $^{238}U$,** *Phys. Rev. C* **12,** No. 3, 863-870 (Sept. 1975).

Key words: bremsstrahlung beam; cross section; fission barrier shapes; γ-ray strength; isomeric fission; level density; photofission.

The photofission cross section of $^{238}U$ was measured in the 2.75- to 5.75-MeV range. Cross sections as small as $2 \times 10^{-11}$ b were detected. A shelf was observed which had been predicted to occur in the cross section owing to the dominance of radiative decay of levels in the second well. Barrier penetrabilities for both inner and outer barriers were determined from these measurements and together with penetrabilities from other measurements were used to infer a potential shape for $^{238}U$. The total γ-ray strength function in the second well at 4.25 MeV was found to be $1.3 \times 10^{-5}$. From comparison of expected and measured cross sections at the lowest energies, the density of levels effective in photofission at 3 MeV was found to be greater than 4 per MeV.

**15351.** Dibeler, V. H., McCulloh, K. E., **Enthalpy of formation of methyl and methylene radicals by photoionization studies of methane and ketene,** (Proc. IV Int. Conf. on Vacuum-UV Radiation Physics, Hamburg, Germany, July 22-26, 1974), Paper in *Vacuum-UV Radiation Physics,* E. E. Koch, R. Haensel, and C. Kunz, Eds., pp. 191-194 (Pergamon-Vieweg, Braunschweig, Germany, 1974).

Key words: enthalpy of formation; ions; mass spectrometry; methyl; methylene; photoionization; radicals; vacuum ultraviolet.

Photoion yield curves for $CH_3^+$ and $CH_2^+$ from methane have been remeasured near threshold at 298 and 115 K and the curve for $CH_2^+$ from ketene has been measured at 298, 215, and 130 K. For methane there is no evidence for the ion-pair process yielding $CH_3^+ + H^-$. The temperature shift of the $CH_3^+$ curve is $k\Delta T$, indicating only two available rotational degrees of freedom in the dissociation process. Including a negligible kinetic energy release at threshold, the estimated threshold at $T = 0$ results in $\Delta Hf_0^o\ (CH_3) = 35.6 \pm 0.2$ kcal mol$^{-1}$. No temperature shift is observed for the $CH_2^+$ curve from methane. Assuming zero kinetic energy release, the result $\Delta Hf_0^o\ (CH_2) = 93.7 \pm 0.5$ kcal mol$^{-1}$ is obtained. The $CH_2^+$ curve from ketene exhibits a shift of $k\Delta T$ with temperature. Neglecting kinetic energy release, the estimated threshold at $T = 0$ results in $\Delta Hf_0^o\ (CH_2) = 93.5 \pm 0.4$ kcal mol$^{-1}$.

**15352.** McCulloh, K. E., **Threshold energies for formation of $OH^+$ and $NH_2^+$ by dissociative photoionization of water and ammonia,**

(Proc. IV Int. Conf. on Vacuum-UV Radiation Physics, Hamburg, Germany, July 22-26, 1974), Paper in *Vacuum-UV Radiation Physics,* E. E. Koch, R. Haensel, and C. Kunz, Eds., pp. 195-197 (Pergamon-Vieweg, Braunschweig, Germany, 1974).

Key words: ammonia; dissociative photoionization; $NH_2^+$, $OH^+$; photoionization; threshold energies; water.

A photoionization mass spectrometer incorporating a monochromator of 0.5 Å resolution has been employed to remeasure photoion yield curves near threshold for $OH^+$ from water vapor at temperatures of 215 and 298 and for $NH_2^+$ from ammonia at 160 and 298 K. From the observed temperature shifts of these curves it is inferred for both molecules that essentially the entire rotational energy is available for dissociative ionization. On this basis the threshold energies for formation of the fragment ions are corrected for the effect of rotationally excited molecules. The enthalpies of formation of $OH^+$ and $NH_2^+$ are discussed in relation to thermochemical quantities for the neutral OH and $NH_2$ radicals. Similar results are reported for $OD^+$, $ND_2^+$, and $NHD^+$ fragment ions.

15353. Schooley, J. F., **Solid state phase transitions as thermometric fixed points,** *Inst. Phys. Conf. Ser. No.* **26,** Chapter 2, 49-56 (1975).

Key words: antiferromagnetism; ferroelectricity; solid-state transitions; superconducting temperature calibration; thermometric fixed points.

The general question of the usefulness of thermometric fixed-point devices based upon phase transitions in solids is examined. It appears that both the method of detection and the intrinsic character of the transition relate to thermometric precision and practical utility of such devices. Promising systems which are discussed are the AC mutual inductance detection of superconductive transitions and the AC heat capacity detection of antiferromagnetic and ferroelectric transitions.

15354. Beers, Y., **A simplified discussion of energy storage associated with an electrostatic field,** *Am. J. Phys.* **43,** No. 8, 739-740 (Aug. 1975).

Key words: electrostatic; energy.

This note gives a simplified derivation for the energy associated with an electrostatic field by extended use of the expression for the energy of a parallel plate capacitor.

15355. Huie, R. E., Herron, J. T., **Temperature dependence of the rate constants for reactions of ozone with some olefins,** (Proc. Symp. on Chemical Kinetics Data for the Upper and Lower Atmosphere, Warrenton, Va., Sept. 15-18, 1974), *Int. J. Chem. Kinet. Symp.,* No. 1, 165-181 (John Wiley & Sons, Inc., New York, N.Y., 1975).

Key words: air pollution; kinetics; mass spectrometry; olefin; ozone; photochemical smog; rate constant.

The temperature dependence of the rate constants for the reactions of ozone with some olefins has been studied using a stopped-flow reactor in conjunction with a beam sampling mass spectrometer. The effect of molecular oxygen on the measured rate constants was studied, and it was concluded that molecular oxygen scavenges free radical species which could further react with ozone. Rate constants, measured in the presence of molecular oxygen, are as follows (in units of $cm^3\ mol^{-1}\ s^{-1}$): log $k$ (1-butene) $= (9.247 \pm 0.033 - (1686 \pm 20)/2.303T$; log $k$ (2-methylpropene) $= (9.281 \pm 0.026) - (1671 \pm 23)/2.303T$; log $k$ (*cis*-2-butene) $= (9.272 \pm 0.087) - (956 \pm 54)/2.303T$; log $k$ (*trans*-2-butene) $= (9.555 \pm 0.069) - (1051 \pm 43)/2.303T$; log $k$ (2-methyl-2-butene) $= (9.582 \pm 0.119) - (826 \pm 78)/2.303T$; and log $k$ (2, 3-dimethyl-2-butene) $= (9.230 \pm 0.237) - (294 \pm 196)/2.303T$.

A good linear correlation is found between the activation energy for the reaction and the ionization potential of the olefin.

15356. Klein, W., **Behavior of distribution functions in the thermodynamic limit,** *J. Math. Phys.* **15,** No. 8, 1181-1185 (Aug. 1974).

Key words: distribution functions; finite volumes; Kirkwood Salsburg equation; perturbation expansion; strip operator; thermodynamic limit.

Ruelle has proven that the solutions of the Kirkwood-Salsburg equation for a finite volume $\Lambda$ become, in the limit as $\Lambda \rightarrow \infty$, the solutions to the Kirkwood-Salsburg equation for an infinite volume, i.e.,

$$\lim_{\Lambda - \infty} \rho_\Lambda \rightarrow \rho + \lim_{\Lambda - \infty} \epsilon(\Lambda), \lim_{\Lambda - \infty} \epsilon(\Lambda) \rightarrow 0.$$

The form of $\epsilon$ is not obtained. We show that for the first order contribution to the solution of the Kirkwood-Salsburg equations obtained via a perturbation scheme developed in an earlier paper that

$$\epsilon(\Lambda) \leqslant \lim_{R - \infty} \epsilon^{-k'aR},$$

where $k'_a$ is a positive real constant which can be specified and $R$ is the minimum distance from the container walls to the particles of the system.

15357. Phillips, J. C., Wall, L. A., Aldridge, M. H., **Liquid (melt) heat capacities and heats of vaporization of oligomers of poly(hexamethylene sebacate),** *Polym. Eng. Sci.* **15,** No. 2, 73-78 (Feb. 1975).

Key words: alkanes; esters; heat capacity; heats of vaporization; oligomers; rates.

The liquid heat capacities and heats of vaporization of three linear esters of poly(hexamethylene sebacate) with hexyl-capped end groups (M(mol.wt.) = 370, 655, and 939) have been determined. The heats of vaporization of the oligomers measured at a mean temperature were corrected to 323.15 to 523.15 K by use of the experimental liquid (melt) heat capacities and the calculated gas heat capacities. The corrected heats of vaporization were fitted to the equation $\Delta H_v = S(T)M^\alpha + I(T)$, where the temperature dependence of the slope and intercept are represented, respectively, as $S(T) = C\ln T + K_0$ and $I(T) = aT + b_0$, and $\alpha$ is an exponent. The results indicate (at corresponding molecular weights and constant temperature) that the ratio of the liquid heat capacities of the oligomer ester and the n-alkane, and similarly the ratio of the heats of vaporization, depend on the number of carboxyl groups in the oligomer ester chain.

15358. Pella, P. A., DeVoe, J. R., **Systematic error in tin ore assay by Mössbauer spectrometry,** *J. Radioanal. Chem. Short Commun.* **25,** No. 1, 185-188 (1975).

Key words: Mössbauer spectrometry; quantitative analysis; Stannic oxide; tin ores.

In this work, Mössbauer spectrometry was applied to the nondestructive, quantitative analysis of tin oxide in two NBS-SRM tin ore concentrates. Systematic errors of 10 to 25 percent were observed when these ore samples were measured versus calibrant samples prepared from A.R. tin oxide. The effect of heat treatment of the ores on the resonant absorption intensity is also discussed.

15359. Reneker, D. H., Martin, G. M., Broadhurst, M. G., **Search for correlations between dielectric relaxation and polymerization in trioxane crystals,** *J. Appl. Phys.* **45,** No. 10, 4172-4174 (Oct. 1974).

Key words: dielectric loss; dielectric relaxation; molecular motions; nuclear magnetic resonance absorption; polyoxymethylene crystals; solid state polymerization; trioxane crystals.

After exposure to ionizing radiation, trioxane polymerizes rapidly at temperatures between 50 and 60 °C. The nature of the molecular motions involved in this solid-state reaction is not clear. Line narrowing in nuclear magnetic resonance absorption has been reported as one indication of such motions. No related dielectric loss peaks were found in trioxane at temperatures from − 180 to 55 °C and frequencies from 1 to 10 000 Hz. Ionic conductivity is large above room temperature and it may play an important role in this polymerization reaction.

**15360.** O'Brien, J. T., Crannell, H., Kline, F. J., Penner, S., **Ionization loss for high-energy electrons in thin targets,** *Phys. Rev. C* **9,** No. 4, 1418-1429 (Apr. 1974).

Key words: energy loss; ionization loss; most-probable energy loss; target thickness.

The most-probable ionization loss has been measured for relativistic electrons passing through thin absorbers of carbon, aluminum, and copper. Incident energies of 50 and 100 MeV were used. Target thicknesses ranged from 48 to 614 mg/cm² and encompass the range of thicknesses most frequently used in electron scattering experiments at these energies. The measured values of the most-probable ionization losses are in good agreement with the theoretical predictions of Sternheimer. The techniques for using values of the ionization loss to determine the target thickness in electron scattering experiments are presented.

**15361.** Ekin, J. W., Clem, J. R., **Magnetic coupling force of the superconducting dc transformer,** *Phys. Rev. B* **12,** No. 5, 1753-1765 (Sept. 1, 1975).

Key words: dc transformer; granular aluminum films; magnetic coupling; superconducting dc transformer; type II superconducting films; vortex coupling.

The temperature dependence and magnetic field dependence of the coupling force have been measured in two transformer systems, one with primary and secondary film thicknesses $d_p$ and $d_s$ comparable with the superconducting penetration depth $\lambda$ ($d_p/\lambda_p \sim d_s/\lambda_s \sim 1$) and one with film thicknesses small compared with the penetration depth ($d_p/\lambda_p \sim d_s/\lambda_s \sim 10^{-1}$). The results show that (i) the coupling force is nearly two orders of magnitude greater in the thick-film transformer than in the thin-film transformer; (ii) there exists a transition field above which the coupling force decreases very rapidly, typical values for the transition field being quite low (~ 0.5 G); and (iii) the temperature dependence of the coupling force over much of the range investigated is simply proportional to the temperature dependence of $\lambda_p^{-2}\lambda_s^{-2}$. A Gibbs free-energy theory describing the coupling force has been numerically evaluated and compared with these data. The results show that the theory can be used to predict accurately both the absolute magnitude and the field and temperature dependences of the coupling force for wide-ranging values of the operating parameters.

**15362.** Rosasco, G. J., Etz, E. S., Cassatt, W. A., **The analysis of discrete fine particles by Raman spectroscopy,** *Appl. Spectrosc.* **29,** No. 5, 396-404 (Sept.-Oct. 1975).

Key words: fine particles; laser Raman; micro-Raman; particle analysis; particulates; Raman spectroscopy.

A conventional laser Raman spectrometer has been modified and used to obtain useful Raman spectra from discrete solid particles as small as 0.7 μm in linear dimensions. Spectra obtained from single, micrometer-sized particles of several inorganic and organic compounds are reported. Simplified calculations are discussed which provide an estimate of detectability levels and other problems associated with these measurements. Certain parameters that must be considered in the design of an instrument especially intended for use in the chemical characterization of single fine particles are reviewed in the light of this work.

**15363.** Marshall, H. E., **"Cost sharing for recreation: Efficiency and equity:" Comment,** *Land Economics* **LI,** No. 3, 300-303 (Aug. 1975).

Key words: cost sharing; efficiency; equity; recreation; redistribution of income; water resources.

This comment critiques an article in *Land Economics* entitled "Cost Sharing for Recreation: Efficiency and Equity," by William Miller and Bruce Scherr. These authors presented in their article a general set of policy conclusions regarding cost sharing for recreation that were based on a case study they made of a Soil Conservation Service project and on theoretical work by Harold Marshall. This comment questions the validity of the conclusions and policy implications for the general case, clarifies the relationship of Marshall's work to that of Miller and Scherr, and suggests an alternative approach to measuring the redistribution of income effects of a recreation project.

**15364.** Parkinson, J. S., **Studies of human factors in building design,** *Constr. Specifier* **27,** No. 11, 41-43 (Nov. 1974).

Key words: acoustics; human factors; human occupancy; illumination; interdisciplinary approach; physiology; psychology.

The human factors which affect design are not always known or understood. The Center for Building Technology of the National Bureau of Standards has mobilized an unusual aggregation of experts to study the human factors involved in building design and physical occupancy.

This interdisciplinary approach looks, for example, at the need for windows, the optimum level of illumination, individual's reactions to noise levels and human behavior during fires. They are also trying to find out how much can be learned from the occupants of the housing built under Operation Breakthrough by conducting interviews with the tenants, interrogating visitors, studying work orders, and asking for comments from those moving out of the developments.

The human factors approach is not new but psychological and physiological test techniques have improved a great deal in the past couple of decades so that designers and builders should now be able to provide more pleasant, comfortable and efficient environments for human occupancy.

**15365.** Snyder, L. E., Buhl, D., Schwartz, P. R., Clark, F. O., Johnson, D. R., Lovas, F. J., Giguere, P. T., **Radio detection of interstellar dimethyl ether,** *Astrophys. J.* **191,** No. 2, Part 2, L79-L82 (July 15, 1974).

Key words: dimethyl ether; internal motion; interstellar molecules; Orion; radio astronomy.

Interstellar dimethyl ether, $(CH_3)_2O$, has been detected in emission from the direction of the Orion Nebula molecular cloud. The observed velocity of the $6_{06} \rightarrow 5_{15}$ transition 90.9 GHz is in excellent agreement with other molecules observed toward Orion. Observations of the $2_{20} \rightarrow 2_{11}$ transition at 86.2 GHz and the $2_{11} \rightarrow 2_{02}$ at 31.1 GHz support the dimethyl ether detection and indicate that either $(CH_3)_2O$ has two distinct velocity components in Orion or certain internal motion states are preferentially populated. This molecule has a large collisional cross-section and $C_{2v}$ symmetry; hence it should be useful for future studies of molecular pumping models.

**15366.** Sheingorn, M., **Poincaré series of polynomials bounded away from zero on a fundamental region,** *Amer. J. Math.* **XCV,** No. 4, 729-749 (Winter, 1973).

Key words: automorphic functions; Poincaré series; polynomial approximation.

The purpose of the present paper is to extend Knopp's Main Lemma to the case $q > 1$. Knopp's proof involves substantial use of the Bers' spaces of automorphic forms. Since the character of these spaces in the cases $q \geqslant 2$ and $1 < q < 2$ is vastly different, our proof bears only superficial resemblance to Knopp's. Indeed, the situation is this: If one replaces $q \geqslant 2$ by $q > 1$ at every stage of Knopp's proof, the proof turns out to be valid. However, verification of two of the resulting statements is quite hard and requires techniques far outside Knopp's paper.

**15367.** Stark, J. P., Manning, J. R., **Correlated complete-path equations for diffusion in an electric field,** *Phys. Rev. B* **9,** No. 2, 425-434 (Jan. 15, 1974).

Key words: correlation factor; diffusion; drift mobility; electric field; random walk; symmetry plane; vacancy.

Diffusion of a substitutional solute in a face-centered-cubic metal is discussed in terms of the complete path of the defect giving rise to mass transport. For diffusion in the absence of an applied field, these results are equivalent to the matrix method of Howard for the calculation of the correlation factor. In an applied field, however, the possibility that during the lifetime of a defect it may cause a tracer atom to make a series of successive jumps in the positive field direction or alternatively a series of successive jumps antiparallel to the field can appreciably influence the form of the equations. The tracer can, with decreasing probability, find itself several or many jump distances from its original position. Previous descriptions of this process restricted the tracer to two adjacent planes perpendicular to the applied field. In the present paper, generalized equations are derived for diffusion in an applied field with successive jumps by the tracer in one direction being explicitly allowed. To illustrate the use of these equations, the diffusion of an isolated tracer by a single vacancy is evaluated for a case where successive jumps in one direction are allowed, and also for comparison it is evaluated with the assumption that arrival of the vacancy at the symmetry plane passing through the tracer normal to the diffusion direction returns the vacancy to equilibrium. The latter approach restricts the tracer to two adjacent planes in a sequence of correlated jumps but is shown to give the same mobility. Thus use of the symmetry plane does not affect the results. In contrast to previous equations, the present treatment is applicable to situations where symmetry planes are not present. Thus, it will allow calculation of drift mobilities when the defect or crystal symmetry is more complex, as for diffusion via divacancies which can dissociate.

**15368.** Young, R. D., Teague, E. C., **The measurement and characterization of surface finish,** Chapter 2 in *Properties of Electrodeposits Their Measurement and Significance,* R. Sard, H. Leidheiser, and F. Ogburn, Eds., pp. 22-49 (Electrochemical Society, Princeton, N.J., 1975).

Key words: characterization; instruments; measurement, statistical surface parameters; surface finish; surface parameters.

The surface microtopography of an electrodeposit is determined by a variety of parameters, particularly the physical and chemical character of the initial substrate. Modern instrumentation for quantitative measurement of substrate and electrodeposit surface microtopography are reviewed. Statistical parameters associated with measured surface profiles which permit concise geometrical characterization of height distributions, periodicities along the surface, etc., are defined and discussed. Illustrative examples based on measurements of electrodeposited surfaces are reported together with appropriate characterizing parameters.

**15369.** Yokel, F. Y., **Reply to a question on connections between bearing walls and precast floor panels,** *Civ. Engr. Engineers' inquiry box,* 60-61 (Dec. 1974).

Key words: design standards; earthquake load; masonry construction; precast concrete construction; progressive collapse; structural connection; structural design; wind load.

The design of ties between masonry bearing walls and precast concrete floor panels is discussed.

**15370.** Bernstein, L. S., Kim, J. J., Pitzer, K. S., Abramowitz, S., Levin, I. W., **Potential function for the $\nu_7$ vibration of phosphorus pentafluoride,** *J. Chem. Phys.* **62,** No. 9, 3671-3675 (May 1, 1975).

Key words: high amplitude; internal rotation; $PF_5$; pseudorotation; Raman; vibration.

The gas phase Raman spectrum of the $\nu_7$ fundamental of $PF_5$ has been observed under spectral resolutions approaching 1 $cm^{-1}$. With the use of a two dimensional harmonic oscillator basis set and a potential function of the form $V(\rho,\phi) = (1/2)a\rho^2 - b\cos(3\phi)\rho^3 + c\rho^4$, an adequate fit to the $\nu_7$ region was obtained. The barrier to axial-equatorial fluorine atom interchange was estimated to be 1371 $cm^{-1}$ (3.92 kcal/mole).

**15371.** Treu, S., **Interactive command language design based on required mental work,** *Int. J. Man-Mach. Stud.* **7,** No. 1, 135-149 (1975).

Key words: association links; command language design; interactive user; language transformation; mental work.

Although the definition of "mental work" remains elusive, systematic means/methods should be considered for gaining evidence about interactive language features requiring more/less effort of the human mind. The suggested approach employs a structuring of the user's conceptual reference spaces into sets of "action primitives," peculiar to the type of computer-aided task involved. An interactive command language can then be regarded as the range of some transformation on the user's set of action primitives. The nature and efficiency of that transformation, in conjunction with the inherent number of mental association links, are hypothesized to have direct relationships to the level of required mental work. The user's delay or "think time," expended immediately preceding command utilization, is one measurable quantity that should be useful as a work level indicator.

**15372.** Yokel, F. Y., **The Operation Breakthrough evaluation, an experience in the application of performance criteria,** *Industrialization Forum* **6,** No. 1, 27-33 (1975).

Key words: building codes; building standards; housing; performance criteria.

The testing and evaluation of Operation Breakthrough housing systems relied heavily on a special set of performance criteria developed especially for the program. Valuable experience was gained in this application of performance criteria.

The Breakthrough program is assessed with respect to how effectively the criteria were formulated, the level of guidance and information provided, whether all the criteria were used and implemented, and the problems and difficulties encountered. The experience indicates that performance criteria should not be used as a substitute for specific standards and should be reserved for guiding and evaluating innovative schemes. Performance criteria are rarely simple and can be successfully implemented only in situations where compliance can be objectively measured. Particular difficulties arise in the assessment of durability. Performance criteria can provide valuable guidance in areas outside the domain properly regulated by codes and standards. Inflexible application in such areas, however, could inhibit the evolution of new concepts.

**15373.** Wang, F. W., **Dynamics of block-copolymer molecules in dilute solution,** *Macromolecules* **8,** No. 3, 364-371 (May-June 1975).

Key words: bead-spring model; block-copolymers; dilute solutions; dynamics; limiting viscosity number; solution properties; viscoelasticity; Zimm theory.

A theory for the dynamics of block-copolymer molecules in dilute solution has been developed by modifying the bead-spring model theory of Zimm to take into account the existence of dissimilar segments in block copolymers. The eigenvalue equation encountered in the theory has been solved numerically by extending the method of Lodge and Wu. The applications of the theory have been illustrated with calculations for the viscoelastic properties of poly(styrene-*b*-methyl methacrylate) solutions and poly(styrene-*b*-*cis*-1,4-isoprene) solutions. It is found that, for some block copolymers in solution, the calculated values of the viscoelastic properties deviate significantly from the values for the parent homopolymers toward the values predicted by the free-draining case.

**15374.** Bowen, R. L., **Adhesive bonding of various materials to hard tooth tissues. IX. The concept of polyfunctional surface-active comonomers,** *J. Biomed. Mater. Res.* **9,** No. 5, 501-510 (Sept. 1975).

Key words: adhesion; bonding; composites; coupling agents; monomers; polymers; primers; sealants.

The concept of surface-active comonomers of higher functionality is proposed as a means of increasing reliability of the bonding between preventive and restorative dental materials and tooth structures.

**15375.** Cali, J. P., **Tying methodology to standards,** *Lab World* **25,** No. 7, 22-24 (July 1974).

Key words: clinical chemistry; standard reference materials.

This is an interview of Mr. Cali by one of the editors of *Lab World* concerning the status of our NBS Clinical Standard Reference Materials Program. Topics discussed were the financing of the program, the technical output of the program, the goals of the program, the problems of accuracy in clinical chemistry, and how reference methods and SRM's are used to bring and to improve the accuracy in this field. Future possibilities and directions are also discussed as well as interactions between NBS and other government agencies and professional societies.

**15376.** Harrison, S. H., LaFleur, P. D., Zoller, W. H., **Evaluation of lyophilization for the preconcentration of natural water samples prior to neutron activation analysis,** *Anal. Chem.* **47,** No. 9, 1685-1688 (Aug. 1975).

Key words: freeze drying; instrumental neutron activation analysis; lyophilization; neutron activation analysis; preconcentration; radioactive tracers; river water; trace elements; tracers; water.

A method for the concentration of trace elements in water by lyophilization is described. This method has important applications in the multielement analysis of natural water samples by neutron activation. The results of the evaluation of trace element retention yields, using radioactive tracers, indicate that at least Na, Sc, V, Cr, Fe, Co, Zn, As, Se, Br, Rb, Sr, Ag, Cd, Sb, Cs, Ba, Tb and Ce are retained quantitatively (greater than 95%) in the freeze dried residue of a river water sample. Hg and I were found to be lost substantially and Au was retained at almost the 95 percent level. A bag made from linear polyethylene film is used as the sample container for freeze drying and neutron irradiation and is the only measurable blank in the preconcentration process. The results of a typical analysis of a freeze dried estuarine sample with the determined sample/blank ratios for each element are presented.

**15377.** McCamy, C. S., Derr, A. J., **Microdensitometry,** Article 15.6 in *SPSE Handbook of Photographic Science and Engineering,* W. Thomas, Jr., Ed., pp. 871-877 (John Wiley & Sons, New York, N.Y., 1973).

Key words: microdensitometry; microphotometry; optical density.

Microdensitometry is the science of measuring the optical densities of very small areas. Microdensitometers are usually equipped to scan along a line and continuously record the varying density with respect to distance. The principal application of microdensitometry is in the field of image structure analysis. The maximum resolving power of a transmission instrument is the quotient of the sum of the numerical apertures of the illuminating and sensing objectives to the wavelength of the light. With high numerical apertures, 1800 cycles/mm has been recorded.

Since microdensitometers measure optical density as a function of position, the principal calibrations are the photometric calibration and the length calibration. The photometric scales of microdensitometers are most often calibrated by placing a step tablet of known densities in the sample position. The length scale of a microdensitometer may be calibrated by scanning a glass scale or stage micrometer.

**15378.** Brown, C. P., Yeates, E. J., Van Hoesen, M. J., **Use and cost of on-line systems at the National Bureau of Standards Library,** *Proc. Am. Soc. Inf. Sci. Annual Meeting, Boston, Mass., Oct. 26-30, 1975,* **12,** 132-133 (Oct. 1975).

Key words: evaluation; National Bureau of Standards; on-line information retrieval systems; use statistics.

The National Bureau of Standards Library has had a year of experience in offering on-line information retrieval systems to users. Users were encouraged and assisted to access systems directly if they wished. Cost and use statistics for selected data bases are given.

**15379.** Wagner, G. A., Reimer, G. M., Carpenter, B. S., Faul, H., Van der Linden, R., Gijbels, R., **The spontaneous fission rate of U-238 and fission track dating,** *Geochim. Cosmochim. Acta* **39,** No. 9, 1279-1286 (1975).

Key words: fission track dating; neutron flux; neutron irradiation; plateau annealing; uranium glasses; U-238 fission decay constant.

The rate of spontaneous fission decay of uranium-238 ($\lambda_f^{238}$) was determined in $4\pi$-geometry by the fission track method. Uranium glasses of known age of manufacture were used. Spontaneous tracks have accumulated since the time of manufacture and induced tracks to determine the uranium content were produced by thermal neutron irradiations. Spontaneous tracks in all glasses were found to be partially annealed. By correcting for this annealing effect, a $\lambda_f^{238} = 8.7 \pm 0.6 \times 10^{-17}$ yr$^{-1}$ was obtained. Uncertainty in the neutron dose is the largest source of error.

**15380.** Kaufman, V., Sugar, J., **Spectrum of six-times ionized rhenium (Re VII),** *Phys. Rev. A* **12,** No. 4, 1402-1403 (Oct. 1975).

Key words: energy levels; rhenium; spectrum.

Six terms of the $4f^{14}5s^25p^6(^1S_0)nl$ doublet system of Re VII have been found, including $nl=5d$, $5f$, $6s$, $6p$, $6d$, and $7s$. Thirteen spectral lines were classified in this system of levels. The partially resolved hfs of the $6s$-$6p$ multiplet was used to derive a value for the hyperfine splitting of the $6s$ level in agreement with a predicted value. The ionization energy of Re VII derived from the *ns* series is $82.74 \pm 0.06$ eV.

**15381.** Sugar, J., Kaufman, V., **Nuclear magnetic dipole moment of $^{181}$Ta,** *Phys. Rev. C* **12,** No. 4, 1336-1339 (Oct. 1975).

Key words: ionization energy; nuclear moment; spectrum; tantalum.

The hyperfine structure of the $6s^2S_{1/2}$-$6p^2P_{1/2}$ line of Ta V at 1708 Å has been resolved using a 150 A sliding spark discharge. The $6p$-$8s$ multiplet was identified and the ionization energy was redetermined. With these new data a value for the nuclear dipole moment of $^{181}$Ta of $(2.36 \pm 0.02)\mu_N$ is derived. New wavelengths are given for all previously classified lines.

**15382.** McCarty, R. D., **Hydrogen technological survey-thermophysical properties,** *NASA Spec. Publ.* **3089,** 530 pages (National Aeronautics and Space Administration, Washington, D.C., 1975).

Key words: computer programs; gaseous hydrogen; graphs; handbook thermophysical properties; hydrogen; liquid hydrogen; ortho-para modifications; property value uncertainties; solid; solid hydrogen; tables.

This handbook is the result of an extensive survey of the thermophysical properties of hydrogen, including densities and the thermodynamic, transport, electrical, optical, and molecular properties for the gaseous and fluid states. A thorough bibliography of published work on each property is given. Recommended references are cited for those properties which have been critically surveyed. Other references are listed which were reviewed but not considered as basic source material. Each property is described and defined; selected values are presented for the more common properties; and where appropriate, graphical presentations are also made. The major tables cover the range 25-5000 K with pressures to 15,000 psia (14-3000 K to 100 MPu). In addition, for property values beyond this range, recommended references are given, where available.

**15383.** Prince, E., **Dimethyl sulfone diimine, a neutron study,** *Acta Crystallogr. Short Structural Papers* **B31,** Part 10, 2536-2537 (1975).

Key words: alkyl sulfone; crystal structures; dimethyl sulfone diimine; hydrogen bonds; neutron diffraction; sulfone.

$(CH_3)_2S(NH)_2$, orthorhombic, *F2dd* (No. 43), $a=5.44$, $b=10.59$, $c=16.13$ Å, $Z=8$. The structure was refined from neutron diffraction data. The molecules lie on twofold axes, and are linked together by a three-dimensional network of N – H...N hydrogen bonds. The methyl groups are in an eclipsed conformation.

**15384.** Ausloos, P., Lias, S. G., Eyler, J. R., **Reactions of halomethyl ions with carbonyl-containing compounds,** *Int. J. Mass Spectrom. Ion Phys.* **18,** No. 3, 261-271 (1975).

Key words: carbonyl compound; four-center reactions; halocarbon ions; ion cyclotron resonance; ion-molecule reaction; rate constants.

The mechanisms of the reactions of $CF_3^+$, $CF_2Cl^+$, $CCl_2F^+$, and $CCl_3^+$ with aldehydes, ketones, esters, acids, and acetic anhydride have been examined, and rate constant determinations have been made. Both four-center reactions and displacement reactions are observed. For aldehyde and ketone reactants, a four-center reaction resulting in the formation of a monohalogenated carbonium ion predominates; the importance of this reaction vis-a-vis more exothermic displacement processes is explained in terms of a preference for attack by the ion at the carbonyl oxygen atom. In the case of reactions of $CX_3^+$ ($X=F$, Cl) ions with esters or acids, the most commonly observed reactions are displacements and four-center reactions resulting from attack by the ion at the acyl oxygen. The displacements result in the formation of acylium ions, and the four-center reactions, in the formation of $CX_2OR^+$ ions ($R=$alkyl group). The competition between these two reactions is examined in terms of the relative exothermicities of the two channels and the time required for reaction to occur in the ion – molecule complex. The results indicate that, for ion – molecule reactant pairs which react through only one channel, the probability that an ion – molecule collision will lead to reaction is influenced by the exothermicity of reaction.

**15385.** Gladney, E. S., Rook, H. L., **Simultaneous determination of tellurium and uranium by neutron activation analysis,** *Anal. Chem.* **47,** No. 9, 1554-1557 (Aug. 1975).

Key words: environmental samples; neutron activation analysis; tellurium; uranium.

A procedure for the simultaneous determination of tellurium and uranium is described. The procedure utilizes thermal neutron activation followed by sample combustion and a gas phase separation of the volatile radionuclides of interest. This method is sensitive enough to permit the measurement of tellurium and uranium at their naturally occurring levels in materials of biological and environmental origin. The procedure has been successfully employed to determine the tellurium and uranium concentrations in three Standard Reference Materials (SRM's) currently being offered by the National Bureau of Standards, and in atmospheric particulate material collected in rural Maryland.

**15386.** Simmons, J. D., Tilford, S. G., **Evidence for an accidental predissociation of CO,** *J. Mol. Spectrosc. Note* **49,** No. 1, 167-168 (Jan. 1974).

Key words: absorption spectrum; accidental predissociation; carbon monoxide; emission spectrum; perturbation; Rydberg state.

The perturbation in the $E-X(0-0)$ band of the CO absorption spectrum has been shown to be due to an unusual accidental predissociation. The intermediate predissociated state has not yet been identified.

**15387.** Speller, L. C., Mendlowitz, H., **Characteristic electron energy losses in germanium,** *J. Phys. Chem. Solids* **36,** No. 11, 1229-1232 (1975).

Key words: electron energy loss; germanium; material structure; optical properties; scattering.

The characteristic electron energy loss spectrum of germanium was studied in a transmission type experiment as a function of the changes in structure due to electron bombardment. The structure of the material was characterized by electron micrograph and diffraction techniques. The electron energy loss spectrum of germanium was studied up to 45 eV, and loss peaks were observed at 15.7 eV and 31.6 eV as well as a 6 eV carbon loss. The positions of the most intense characteristic energy loss peak at 15.7 eV and its first multiple were constant for a large variation in the lattice parameters for the individual films.

**15388.** Rhyne, J. J., Pickart, S. J., Alperin, H. A., **Magnetism in amorphous terbium-iron,** (Proc. 19th AIP Conf. on Magnetism and Magnetic Materials, Boston, Mass., Nov. 13-16, 1973), Chapter in *Magnetism and Magnetic Materials*, C. D. Graham, Jr., and J. J. Rhyne, Eds., pp. 563-577 (American Institute of Physics, New York, N.Y., 1974).

Key words: amorphous materials; magnetic materials; neutron diffraction; rare earths.

Neutron diffraction and magnetization measurements on a sputtered specimen of 33 percent terbium, 66 percent iron have confirmed the existence of long range magnetic order and an amorphous spatial distribution of atoms and spin sites. Elastic diffraction data taken above and below the 409 K Curie temperature have enabled the separation of nuclear and magnetic scattering contributions. The magnetic spin density function contains a very broad major peak, dominated by the Tb-Tb pair distribution function, with a maximum near 3.6 A. Longer range correlations are very much weaker. The principal features of the atomic structure can be accounted for by considering only near neighbor correlations between terbium and iron atoms in a random close-packed arrangement.

Inelastic scattering studies have revealed a significant shift in the magnetic density of states to lower energy in the amorphous material relative to the crystalline $TbFe_2$ counterpart. No discrete spin-wave excitations or critical scattering near $T_c$ could be observed.

**15389.** Rowe, J. M., Vagelatos, N., Rush, J. J., Flotow, H. E., **Acoustic modes of the phonon dispersion relation of $NbD_x$ alloys,** *Phys. Rev. B* **12,** No. 8, 2959-2964 (Oct. 15, 1975).

Key words: alloy; electronic structure; interstitial; lattice dynamics; niobium deuteride; phonons.

The acoustic modes of the phonon dispersion relation in Nb, $NbD_{0.15}$, and $NbD_{0.45}$ have been measured at 473 K for phonons with wave vectors along the [100], [110], and [111] axes by coherent neutron scattering. The observed neutron groups for both alloys were well defined, with little or no apparent broadening. The results are compared to similar data for Nb-Mo alloys and with previous lattice-dynamics results for $PdD_{0.63}$. This comparison shows that despite differences in detail, the general features of the dispersion relations of $NbD_x$ and Nb-Mo are similar after allowing for the differences in lattice parameters for the two alloys. The measured dispersion curves and derived phonon frequency distributions for the Nb-D alloys are quite different from the analogous results for $PdD_{0.63}$ in that the average acoustic phonon frequencies *increase* with increasing deuterium concentration and lattice parameter.

**15390.** Carpenter, B. S., Samuel, D., Wassermann, I., **The location of lithium in the brain,** *ANS Trans.* **18,** 85-86 (1974).

**15391.** Tighe, N. J., **Examination of fracture interfaces in silicon nitride,** *Proc. 33d Annual Electron Microscopy Society of America, Las Vegas, Nev., Aug. 10-14, 1975,* G. W. Bailey, Ed., pp. 60-61 (Claitor's Publ. Div., Baton Rouge, La., 1975).

**15392.** Carpenter, B. S., Gilliam, D. M., Reimer, G. M., **Induced fission tracks in glass from monoenergetic and thermal neutrons,** *ANS Trans.* **18,** 90 (1974).

**15393.** Wassermann, I., Samuel, D., Yuwiler, A., Carpenter, B. S., **Location of catecholamines in the brain using the $^{17}0(n, \alpha)^{14}C$ reaction,** *ANS Trans.* **18,** 85 (1974).

**15394.** Swyt, D. A., **National Measurement System: Microstudy of optics,** *Nat. Conf. Stand. Lab. (NCSL) Newsletter* **15,** No. 2, 13-17 (June 1975).

Key words: densitometry; lens evaluation; microdensitometry; microscopy resolution charts; National Measurement System.

Studies of the National Measurement System are currently in progress at the National Bureau of Standards. These studies are an attempt to understand the infrastructure and impact of measurement throughout our economy. One particular microstudy is entitled Optics. This brief article gives an overview of the developments to date; i.e., description of the infrastructure, identification of various users and the techniques of the study.

**15395.** Young, R. D., **National Measurement System micro study,** *Natl. Conf. Stand. Lab. (NCSL) Newsletter* **13,** No. 2, 20-21 (Aug. 1973).

Key words: calibration; economic dimensions; National Measurement System: surface finish; surface roughness.

A brief description of the National Measurement System for Surface Finish is given together with a descriptive block diagram. The economic dimensions of the measurement system are discussed briefly. A biographical sketch of the author is included.

**15396.** Swing, R. E., **The case for the pupil function,** (Proc. SPIE Seminar on Image Assessment, Rochester, N.Y., May 20-22, 1974), Paper in *Image Assessment and Specification,* D. Dutton, Ed., **46,** 104-113 (Society of Photo-Optical Instrumentation Engineers, Palos Verdes Estates, Calif., 1974).

Key words: impulse response; lens aberrations; optical transfer function; partial coherence; pupil function; wavefront shearing interferometry.

The pupil function, a description of the wavefront errors associated with a lens (in terms of a phase distribution over its exit pupil), has long been used by lens designers since it is implicit in the determination of aberrations. Pupil functions require interferometry for measurement. The analysis of interferograms has been facilitated in modern times by the development of high-speed digital computers, automatic fringe scanners and laser sources and can be put on a routine, low-cost basis. When the theory of partial coherence is applied to the analysis of imaging systems, the pupil function is seen to be the fundamental measure of lens performance, because from this one description, the other measures of system behavior can be derived. Further, since the pupil function can be determined with great precision, a polynomial expansion can be curve-fitted in the computer to list the aberration coefficients out to orders whose height is a function of the size of the available computer core. It is thus practicable to provide not only transfer function but also a diagnosis of the lens ills, quantitatively. However, white-light response cannot be measured directly and must be synthesized from measurements at several wavelengths; the techniques for accomplishing this are well-known but are presently not implemented at NBS, where wave-front shearing interferometry has been utilized for measurement of the pupil function. Among the problems for which pupil function measurement is a solution are the cascading of lenses in imaging systems and the evaluation of microscope objective/eyepiece response.

**15397.** Dzubay, T. G., Rook, H. L., Stevens, R. K., **A chemiluminescent approach to measurement of strong acid aerosols,** Chapter 4 in *Analytical Methods Applied to Air Pollution Measurements,* R. K. Stevens and W. F. Herget, Eds., pp. 71-83 (Ann Arbor Science Publishers, Inc., Ann Arbor, Mich., 1974).

Key words: ambient concentration; chemiluminescent measurement; continuous monitor; strong acid aerosols.

The deleterious effect of sulfuric acid aerosol on human health has been demonstrated. Currently, no real time monitors for strong acid aerosols are available. This work represents an effort to develop an instrument for monitoring strong acid aerosols in real time without going through collection and extractions procedures.

15398. Franklin, A. D., Dragoo, A. L., **Calculation of defect-formation energies in alkaline-earth oxides: Interionic forces,** Paper in *Defects and Transport in Oxides,* M. S. Seltzer and R. I. Jaffee, Eds., pp. 141-158 (Plenum Press, New York, N.Y., 1974).

Key words: alkaline earth oxides; Born-Mayer potential; first-neighbor interactions; ionicity; Lundquist three-body potential; second-neighbor interactions; shell model.

A model potential for the alkaline-earth oxides was developed and tested. The interionic potential contains the usual Coulombic and two-body short-range terms, such as those which have been used in previous alkali halide calculations, plus many-body terms which are incorporated by means of the Lundquist three-body approximation in which only the spherically symmetric term in the overlap-charge-density expansion is retained. The three-body interactions contribute to both the long-range and the short-range forces. Additional short-range central-force interactions between nearest-neighbor ions and next-nearest-neighbor ions are included; these are modeled by means of a Born-Mayer plus van der Waals potential. The electronic polarizabilities of the ions are described by a shell model. Parameters in the model potential and in the shell model are evaluated using the elastic constants and their pressure derivatives, the low- and high-frequency dielectric constants, the infrared dispersion frequency, and the equilibrium interionic separation. Three constraints on the shell model are required. The model does not give satisfactory results in that (1) the trend in an effective charge parameter, $\chi_o$, through this family of oxides runs counter to that for the Phillips ionicities and (2) the Born-Mayer potential parameters appear to be highly anomalous compared with those for other ionic crystals. The principal weakness of the model apparently resides in its neglect of bond-bending (noncentral force) terms, which results in an overestimate of the overlap contribution to the bond-stretching terms, in excessive deviations in the effective charges from the classical valences, and in departures of the Born-Mayer potential parameters from the values found in alkali halide and alkaline-earth fluorides.

15399. Mitchell, R. A., Woolley, R. M., Halsey, N., **High-strength end fittings for FRP rod and rope,** *J. Eng. Mech. Div. ASCE* **100,** No. EM4, 687-706 (Aug. 1974).

Key words: axisymmetric analysis; cables (ropes); composite materials; contour plotting; end fittings for FRP rod and rope; finite element analysis; FRP rod; FRP rope; materials testing; nonlinear analysis (shear); potted end fittings; structural engineering; tensile strength; transversely isotropic materials.

Improved structural end fittings of two basic types were developed for use with fiber-reinforced-plastic (FRP) rod and rope materials. Each type of end fitting is essentially a metal sleeve that is attached to the FRP material by a thick layer of potting material. Tensile tests demonstrated that the new end fittings can equal or approach the full tensile strength of E-glass-reinforced-plastic rod and rope. In tensile strength, the new fittings are superior to commercially available end fittings. An axisymmetric finite element analysis was developed to study the transfer of load from a rod or rope, through the potting material, to the metal fitting. In the analysis the FRP material and the potting material are assumed to be transversely isotropic. The results of both the analytical study and the laboratory tests indicate the importance of using a relatively thick layer of low-stiffness potting material with these fittings.

15400. Hockey, B. J., Lawn, B. R., **Electron microscopy of microcracking about indentations in aluminium oxide and silicon carbide,** *J. Mater. Sci.* **10,** 1275-1284 (1975).

Key words: brittle solids; dislocation networks; electron microscopy; healing; indentations; microcracking; moiré patterns.

Transmission electron microscopy is used to examine the nature of microcracking about small-scale indentations in two highly brittle solids, sapphire and carborundum. The observed crack geometry is discussed in terms of an earlier model of indentation fracture beneath a point force, in which both loading and unloading half-cycles contribute to the crack growth. The residual interfaces are generally found to exhibit moiré fringe contrast, and occasionally to contain dislocation networks. These observations are discussed in relation to spontaneous closure and healing mechanisms, and the associated "lattice mismatch" is estimated at about one part in a thousand. It is suggested that cleavage steps comprise the main source of obstruction to lattice restoration across the interfaces. Mechanical and thermal treatments of the indented specimens are found to influence the extent of the residual cracking. Some practical implications concerning the strength degradation of brittle solids are discussed.

15401. Evans, A. G., **The role of inclusions in the fracture of ceramic materials,** *J. Mater. Sci.* **9,** 1145-1152 (1974).

Key words: ceramics; failure prediction; fracture; inclusions; nondestructive inspection.

The stress concentrations that occur at inclusions due to thermal expansion and elastic modulus mismatch are discussed and the stress intensity factors at interface cracks that result from these stresses are calculated. It is shown that conservative failure prediction based on an equivalence between inclusion size and crack size is usually acceptable if the shear modulus $\mu$ or thermal expansion coefficient $\alpha$ for the inclusion is larger than the matrix values. If, however, $\mu$ and $\alpha$ are smaller for the inclusion than the matrix, extensive cracking can develop at the inclusions which may lead to premature failure. For this case the only effective methods for failure prediction are techniques which give directly the maximum stress intensity factor, i.e., proof testing and/or acoustic emission.

15402. Frederikse, H. P. R., Hosler, W. R., **High temperature electrical conductivity of aluminum oxide,** Chapter in *Mass Transport Phenomena in Ceramics,* A. R. Cooper and A. H. Heuer, Eds., **9,** 233-251 (Plenum Press, New York, N.Y., March 1975).

Key words: aluminum oxide; electrical conductivity; high temperature; ionic charge transport.

The electrical conductivity of polycrystalline and single crystal $Al_2O_3$ has been determined between 1000 and 1650 °C. Measuring the conductivity between the outside and inside surface of a thin-walled, hollow tube eliminates the adverse effects of gas or surface conduction. An analysis of possible electronic and ionic charge transport mechanisms shows that none of these processes fully accounts for the magnitude of the observed conductivity. Migration of $Al^{3+}$ ions (or $Al^{3+}$ vacancies) yields the largest values and offers at present the best explanation for electrical conduction in $Al_2O_3$.

15403. Hill, J. E., Kusuda, T., **Dynamic characteristics of air infiltration,** *ASHRAE Trans.* **81,** Part 1, 168-185 (1975).

Key words: air infiltration; dynamic pressure differential; wind velocity.

Currently available methodology for estimating air leakage into and out of buildings does not directly take into account the fluctuating nature of the outdoor wind conditions. The air leakage into and out of commercial building offices was studied with particular attention to the time history of outdoor wind velocity and pressure differential across the window. It was found that the air leakage measured was generally quite different from that which could be calculated. The reason for this discrepancy was postulated to be due to a complex process caused by the dynamically varying pressure differential across the window, flow occurring through the window in both directions simultaneously, and finally to the particular experimental configuration used.

**15404.** Yokel, F. Y., **Reply to question on the design of unreinforced masonry load-bearing walls,** *Civ. Engr. Engineers' inquiry box,* p. 79 (Nov. 1973).

Key words: codes; masonry; standards; structural design.

Provisions of present U.S. Code and Design Standards are clarified and interpreted in response to a question by a reader of *Civil Engineering* magazine.

**15405.** Compton, P. R., **National Measurement System study,** *Natl. Conf. Stand. Lab. (NCSL) Newsletter* **13,** No. 3, 10-14 (Nov. 1973).

Key words: flow measurement study; fluid flow measurement system; measurement system identity; technology assessment.

A technological assessment of gas and liquid flow measurements, excluding cryogenics, is being conducted. A description is being prepared of the interrelationships that exist within and between the identifiable parts of the fluid flow measurement system which is identified as an important component of the overall National Measurement System. The approach of this study is to gather pertinent information from contacts throughout the system. The technology assessment has identified many attributes that can be used to quantify this system. A data base is being developed which will be helpful in recognizing major trends of future applications of fluid flow measurement.

**15406.** Harrison, J. O., Jr., **Computer program characteristics,** (Proc. Seminar on Metric Conversion Engineering and Manufacturing, Gaithersburg, Md., Dec. 12-13, 1974), Appendix B in *ANMC-74-1, Metric Conversion in Engineering and Manufacturing,* L. Perica, Ed., pp. 133-136 (American National Metric Council, Washington, D.C., May 1974).

Key words: computer program; metric conversion; round off.

At least six computer programs to assist manufacturing companies in metric conversion are now available. The principal characteristics of these programs and the requirements for programs for metric conversion are discussed. NBS' plans to issue a metric conversion package are described.

**15407.** Caswell, R. S., Coyne, J. J., Randolph, M. L., **Studies of energy deposition by neutrons,** (Proc. 2d Symp. on Neutron Dosimetry in Biology and Medicine, Neuherberg/Munich, Germany, Sept. 30-Oct. 4, 1974), Paper in *Proc. 2d Symp. on Neutron Dosimetry in Biology and Medicine,* B. G. Berger and H. G. Ebert, Eds., **1,** 29-47 EUR 5273 d-e-f (Mar. 1975).

Key words: fluence; kerma; kerma factors; microdosimetry; neutron dosimetry; neutron energy deposition.

Neutrons generate secondary particles (p, $\alpha$, C, N, O, etc.) when they interact with tissue. It is through these secondary particles that nearly all of the energy deposition and biological effects occur. It is therefore of interest to determine the total energy transferred to the charged particles (kerma), the initial spectrum of the secondary particles, the slowing-down spectrum, and the details of the energy deposition by these secondary charged particles. We are continuing to study all of these quantities. Further along in the energy deposition process, one is interested in the delta-ray production cross sections and absorbed dose distributions due to the delta rays. We have not yet focused on this problem. In this report we shall discuss kerma calculations and some studies of the energy deposition in spherical volumes.

**15408.** Gills, T. E., McClendon, L. T., Maienthal, E. J., Becker, D. A., Durst, R. A., LaFleur, P. D., **Determination of toxic trace elements in body fluid reference samples,** (Proc. Eighth Annual Conf. on Trace Substances in Environmental Health, Univ. of Missouri-Columbia, Columbia, Mo., June 11-13, 1974), Paper in *Trace Substances in Environmental Health,* D. D. Hemphill, Ed., **VIII,** 273-280 (1974).

Key words: body fluids; fluorine; lead; mercury; reference samples; trace elements.

The measurement of elemental concentration in body fluids has been widely used to give indication of exposure to certain toxic materials and/or a measure of body burden. To understand fully the toxicological effect of these trace elements on our physiological system, meaningful analytical data are required along with accurate standards or reference samples. The National Bureau of Standards has prepared for the National Institute for Occupational Safety and Health (NIOSH) a number of reference samples containing selected toxic trace elements in body fluids. The reference samples produced include mercury in urine at three concentration levels, five elements (Se, Cu, As, Ni and Cr) in freeze-dried urine at two levels, fluorine in freeze-dried urine at two levels and lead in blood at two concentration levels. These reference samples have been found to be extremely useful for the evaluation of field and laboratory analytical methods for the analysis of toxic trace elements. In particular the use of at least two calibration points (i.e. "normal" and "elevated" levels) for a given matrix provides a more positive calibration for most analytical techniques over the range of interest for occupational toxicological levels of exposure.

**15409.** McClendon, L. T., **Selective determination of chromium in biological and environmental matrices,** (Proc. Eighth Annual Conf. on Trace Substances in Environmental Health, Univ. of Missouri-Columbia, Columbia, Mo., June 11-13, 1974), Paper in *Trace Substances in Environmental Health,* D. D. Hemphill, Ed., **VIII,** 255-257 (1974).

Key words: analysis; biological materials; chloroform; chromium; environmental materials; neutron activation; radiochemical separation; solvent extraction; tribenzylamine.

Chromium occurs in many biological and environmental materials but only in trace amounts (ppm level), which makes the determination by usual chemical methods very difficult and sometimes impossible. Destructive neutron activation analysis, utilizing the reaction $^{50}$Cr (n, $\gamma$) $^{51}$Cr, can eliminate many of the difficulties encountered with other techniques. A detailed description of chromium determination in various biological (e.g. liver and urine) and environmental (e.g. coal and fly ash) samples using the NBS Reactor, coupled with a very selective radiochemical separation procedure, will be discussed.

**15410.** Quintiere, J., **Some observations on building corridor fires,** *Proc. Fifteenth Symp. (International) on Combustion, Tokyo, Japan, Aug. 25-31, 1974,* pp. 163-174 (The Combustion Institute, Pittsburgh, Pa., 1974).

Key words: corridor; fire spread; flashover; floor covering; radiative heat transfer.

Full-scale corridor fire experiments designed to evaluate the potential fire hazard of floor covering materials exposed to a room fire are described. A phenomenological account of events leading to rapid fire propagation along the corridor is presented for one experiment. Mechanisms responsible for the rapid fire propagation, termed flameover, are explored through measurements and analysis of the data. Before flameover the corridor floor is heated by radiation which enables flames to spread into the corridor. On the wood floor considered, flame spread velocity accelerates from ~ $10^{-2}$ ft/sec to ~ 1 ft/sec following flameover. Causative factors of flameover appear to be the increase in flame height of the floor fire, and a reduction of air supply to the burn room due to a change in flow pattern between the corridor and burn room. Calculations show that air flow to the burn room steadily drops as the corridor fire develops resulting in incomplete combustion for the room fire.

**15411.** Bridges, J. M., **Arc measurements of Fe II oscillator strengths,** *Proc. XIth Int. Conf. on Phenomena in Ionized Gases, Prague, Czechoslovakia, Sept. 10-14, 1973, Paper 4.5.3.5,* p. 418 (Czechoslovak Academy of Sciences, Prague, Czechoslovakia, 1973).

Key words: arc plasma; iron; lifetimes; oscillator strength; transition probabilities; wall-stabilized arc.

Fe I and Fe II lines were measured in emission from a wall-stabilized arc, which was operated in argon with an admixture of $FeCl_3$. Lines were selected for measurement which would permit a check on the consistency of several previously reported data. These include oscillator strength measurements of Fe II lines as well as lifetime values for several atomic levels of Fe I and Fe II. Overall, good consistency was found among most of the data.

**15412.** Ott, W. R., Behringer, K., **Absolute vuv radiometry with hydrogen arcs—comparisons with blackbody calibrations,** *Proc. XIth Int. Conf. on Phenomena in Ionized Gases, Prague, Czechoslovakia, Sept. 10-14, 1973, Paper 4.5.2.7,* p. 412 (Czechoslovak Academy of Sciences, Prague, Czechoslovakia, 1973).

Key words: blackbody calibrations; hydrogen continuum; primary standard; radiometry; vacuum ultraviolet; wall-stabilized arc.

A hydrogen arc has been applied for the purpose of making spectral radiance calibrations in the wavelength region 1450 to 3600 Å. Absolute calibrations using the hydrogen continuum as a primary standard are presently possible with an estimated uncertainty of ±5 percent. Such accuracies are much better than can be obtained presently by any other source calibration method in the vuv. The hydrogen arc standard has been compared with two other calibration methods. Agreement with tungsten strip lamp calibrations in the visible and near uv and with the blackbody ceiling calibration in the vuv is within the combined experimental uncertainties associated with the various methods.

**15413.** Behringer, K., Ott, W. R., **Measurement of the Ly-$\alpha$ Stark profile in a pure hydrogen arc,** *Proc. XIth Int. Conf. on Phenomena in Ionized Gases, Prague, Czechoslovakia, Sept. 10-14, 1973, Paper 4.5.1.1,* p. 396 (Czechoslovak Academy of Sciences, Prague, Czechoslovakia, 1973).

Key words: high temperature; hydrogen arc; line broadening; Lyman alpha; optically thin; Stark profile.

The Stark profile of the hydrogen line Ly-$\alpha$ requires the least elaborate theoretical treatment of all hydrogen lines, reflected in the fact that all calculations reported so far show very similar results. Yet one of the two different type published experiments, even after reexamination, shows significant deviations from the theoretical profile. From the available data, it is not clear whether a physical effect went undetected in the experiments or whether the calculations should be revised. An investigation on the Ly-$\alpha$ profile under very different experimental conditions is reported here. While self-absorption in the previous experiments has been lowered by greatly diluting the hydrogen plasma with inert gases like Ar or He, in this investigation thin line wings are achieved in a pure plasma by operating at very high temperatures. Above 17,000 K the emission coefficient of Ly-$\alpha$ in a constant pressure, almost completely ionized plasma decreases rapidly with increasing temperature. The absorption coefficient does even more so because the blackbody radiation at the wavelength of Ly-$\alpha$ increases drastically. The properties of a pure hydrogen plasma are very well known and allow very accurate diagnostic measurements. The electron density at these high temperatures is close to $1.8 \times 10^{17}$ cm$^{-3}$ and almost independent of the temperature, certainly an advantage in a line broadening experiment. The high temperature arc plasma has been shown to be very close to local thermodynamic equilibrium.

**15414.** Olver, F. W. J., **Recent error analysis of asymptotic solutions of linear differential equations,** *Proc. Int. Conf. on Differential Equations, Los Angeles, Calif., Sept. 4-7, 1974,* pp. 636-645 (Academic Press, Inc., New York, N.Y., 1975).

Key words: approximation; asymptotics; asymptotic theory; error analysis; ordinary differential equations; turning points.

Considerable progress has been made during the past fifteen years in the error analysis of asymptotic solutions of linear ordinary differential equations. In addition to computational applications, realistic error bounds provide insight into the doubly asymptotic nature of many of the approximations, thereby avoiding the need for the somewhat unsatisfactory concept of generalized asymptotic expansions. The methods that have been developed for constructing error bounds have also led to the solution of some recalcitrant problems involving two or more turning points.

**15415.** Robertson, B., **Evaluation of automotive fuel flowmeters,** *Proc. Automotive Energy Efficiency Program, Cambridge, Mass., Jan. 15-17, 1975, DOT-TSC-OST-75-31,* pp. 121-134 (National Technical Information Service, Springfield, Va., June 1975).

Key words: automotive fuel flowmeter environment; automotive fuel flowmeters; flowmeter evaluation; flowmeter evaluation test setup; flowmeters; gasoline flowmeter.

Fuel economy measurement procedures are being developed by the Transportation Systems Center. Flowmeters will be used to measure the gasoline consumed by the engine of an automobile either on the road or on a dynamometer. The role played by NBS in this work is to survey commercially available meters and find which ones might be suitable, to determine the environment in which they will be ultimately used, and to measure their accuracy in a laboratory simulation of that environment.

A discussion will be given of: (1) the different kinds of possibly suitable flowmeters to measure gasoline flow to the carburetor, (2) the environment of the flowmeter in an automobile (flowmeter temperature; fuel temperature, pressure, density, viscosity, color, opacity, flow pulsations, backflow, and swirl due to elbows; line voltage fluctuations; electromagnetic radiation from ignition; vehicle attitude with respect to the vertical; and vibration), and (3) plans for a test setup for evaluating and calibrating these meters in the laboratory under conditions simulating the automotive environment.

**15416.** Parrish, W. R., **An economic study of electrical peaking alternatives,** (Proc. Conf. Hydrogen Economy Energy, Miami

Beach, Fla., Mar. 18-20, 1974), Paper R-889 in *Hydrogen Energy,* pp. 949-968 (Plenum Press, New York, N.Y., 1975).

Key words: energy storage; hydrogen utilization; power generation; synthetic fuels.

Results are given of a feasibility study of alternatives for producing peak power. Fuel cells, batteries, and superconducting magnetic storage are considered as well as gas turbines and pumped storage. The fuels considered are hydrogen, from coal or electrolysis, synthetic natural gas, and methanol. Fuel storage alternatives include liquid, compressed gas, and for hydrogen, metallic hydride.

**15417.** Unassigned.

**15418.** Mount, G. H., Ayres, T. R., Linsky, J. L., **A non-LTE analysis of the CN 3883 Å band head in the upper photosphere of Arcturus,** *Astrophys. J.* **200,** 383-391 (Sept. 1, 1975).

Key words: atomic abundances; CN spectra; non-LTE molecular spectra; photospheres, stellar; radiative transfer.

A detailed non-LTE study of the CN(0,0) 3883 Å band-head spectrum of Arcturus (K2 III) provides an accurate determination of the carbon, nitrogen, and oxygen abundances in Arcturus. Non-LTE effects are significant, and we find that the Ayres-Linsky model provides an adequate fit to the observations for $[C,N]_* = 1/3\ [C,N]_\odot$ and $[O]_* = 0.60\,[O]_\odot$, or for $[C,N,O]_* = 1/6\,[C,N,O]_\odot$, but the latter abundances are unlikely. The upper photospheric microturbulence is found to be $2.5 \pm 0.2$ km $s^{-1}$.

**15419.** Wiederhorn, S. M.; **Reliability, life prediction and proof testing of ceramics,** (Proc. Second Army Materials Technology Conf., Hyannis, Mass., Nov. 13-16, 1973), Chapter 29 in *Ceramics for High-Performance Applications,* pp. 633-663 (Army Materials and Mechanics Research Center, Watertown, Mass., 1974).

Key words: ceramics; crack propagation; delayed failure; fracture; proof testing; Weibull analysis.

Proof testing is discussed as a design method for assuring the reliability of structural components. The advantages of proof testing over the statistical approach used for design lies in the insensitivity of the proof testing method to the detailed history of handling or processing of structural components. Methods are presented for developing and using proof test diagrams that assure minimum lifetime after proof testing. Procedures of proof testing and precautions that must be followed during proof testing are discussed. Provided these precautions are followed, proof testing offers a general method for assuring the reliability of structural components under stress.

**15420.** Flynn, D. R., Blomquist, D. S., **Environmental noise measurement,** (Proc. Northeast Electronics Research and Engineering Meeting, Boston, Mass., Nov. 6-8, 1973), Paper in *NEREM (of the IEEE) 1973 Record,* pp. 40-43 (1973).

Key words: acoustics; noise; sound.

This paper is a digest of a paper to be given orally at the Northeast Electronics Research and Engineering Meeting (NEREM) of the IEEE in November 1973. Since its length was severely limited, the paper can only describe the subject matter to be covered in the oral presentation. A discussion will be given of current instrumentation for measurement of environmental noise and noise emission from machinery and equipment—in both occupational and community situations. Emphasis will be placed on available measurement standards, problem areas, and trends in sound measurement instrumentation.

**15421.** Manning, J. R., **Diffusion kinetics and mechanisms in simple crystals,** (Proc. Conf. Geochemical Transport and Kinetics, Warrenton, Va., June 4-6, 1973), Chapter in *Geochemical Transport and Kinetics,* pp. 3-13 (Academic Press Inc., New York, N.Y., 1974).

Key words: atom transport; diffusion in crystals; kinetic diffusion equations; mechanism for diffusion; random walk; vacancies.

The kinetic-atomic theory of diffusion is discussed and reviewed. Any such theory must involve a model providing a detailed picture of the paths as the atoms move through the material. Diffusion paths and diffusion mechanisms therefore are important in this theory and are discussed first. Both short-circuit diffusion mechanisms along easy diffusion paths and possible volume-diffusion mechanisms through regions of regular crystal structure are described. Simple random-walk diffusion equations are derived which yield expressions for the tracer diffusion coefficient $D^*$ and the atom drift velocity $v_F$ in terms of atom jump frequencies. It is noted that diffusion frequently occurs by a vacancy mechanism. When this is the case, the random-walk equations must be modified to include both correlation-factor effects and vacancy-wind effects. The origin and influence of these effects are discussed. A comparison is made between the kinetic-atomic diffusion equations and the thermodynamic-continuum diffusion equations. It is noted that cross terms which yield a dependence of the atom flux of species $i$ on the concentration gradients or chemical potential gradients of other species $k$ appear in these equations.

**15422.** Evans, A. G., **High-temperature slow crack growth in ceramic materials,** (Proc. Second Army Materials Technology Conf., Hyannis, Mass., Nov. 13-16, 1973), Chapter 17 in *Ceramics for High-Performance Applications,* pp. 373-396 (Army Materials and Mechanics Research Center, Watertown, Mass., 1974).

Key words: ceramics; crack healing; crack propagation; cyclic fatigue; failure prediction; high temperature; static fatigue.

High temperature slow crack growth processes in several ceramic materials are examined under static and cyclic loading conditions. Data obtained at temperatures up to 1400 °C are used for purposes of failure prediction and for analysis of the slow crack growth phenomena. It is shown that purity plays a major role in slow crack growth resistance particularly in the hot-pressed materials, and that cycling in the low frequency regime does not significantly enhance the rate of slow crack growth. The slow crack growth mechanisms appear to be primarily plasticity related, and some discussion of these is presented.

**15423.** Kuyatt, C. E., **Electron energy analyzer design,** *Proc. 31st Annual Meeting Electron Microscope Society of America, New Orleans, La., Aug. 13-17, 1973,* C. J. Arceneaux, Ed., pp. 280-281 (Claitor's Publ. Div., Baton Rouge, La., 1973).

Key words: angular aperture; computer optimization of electron optics; electron beam transport; electron energy analyzers; field aperture.

The design of electron energy analyzers is discussed, with special emphasis on the electron optical system used to transport electrons from the source to the energy dispersing element.

**15424.** McLaughlin, W. L., **Radiation dosimetry with thin films,** (Proc. Third Conf. on Application of Small Accelerators, North Texas State Univ., Denton, Tex., Oct. 21-23, 1974), Paper in *Application of Small Accelerators. Vol.* **II. Industrial Applications of Small Accelerators,** I. L., Morgan and J. L. Duggan, Eds., pp. 65-85 (U.S. Energy Research and Development Admin. Office of Public Affairs and Technical Information Center, Springfield, Va., 1975).

Key words: cavity theory; depth dose; dose distributions; dosimetry; dyes; electron beams; radiochromic dyes; thin films.

A thin self-supported or laminated layer of radiation-sensing material is useful for measuring or monitoring the energy deposited by a radiation beam passing through that layer. If (1) the film is thin enough in relation to the range of the incident radiation particles in the absorbing material and (2) the incident radiation spectrum can be approximated sufficiently, the absorbed dose or dose rate in materials surrounding the thin layer can be determined by applying fairly simple cavity-theory considerations (i.e. factoring by stopping power ratios in the case of charged-particle beams). Some sensing materials that may be used as dosimeters in accelerator beams are thin calorimetric bodies, solid-state detectors, and ceramic, plastic, or dyed plastic layers. Major sources of error that must be accounted for are instabilities, nonlinearities, variations of response with dose-rate and spectral changes, environmental factors, inconsistencies in the quality of the sensing material, and imprecisions in the analysis of the radiation effect. A primary advantage afforded by thin-film dosimetry is its capability of supplying dose distribution data near interfaces of different materials.

**15425.** Newbury, D. E., **Techniques of signal processing in the scanning electron microscope,** *Proc. 8th Symp. on Scanning Electron Microscopy, St. Louis, Mo., Apr. 7, 1975,* pp. 727-736 (IIT Research Institute, Chicago, Ill., Apr. 1975).

Key words: black level suppression; nonlinear amplification; scanning electron microscope; signal differentiation; signal processing; Y-modulation.

Signal processing applied during the formation of SEM images can greatly aid the microscopist in obtaining a maximum amount of information from a specimen. Signal processing is necessary in order to overcome basic limitations of the eye in extracting information from the SEM cathode ray tube display or from photographs of the display. The four most commonly encountered forms of signal processing are black level suppression (differential amplification), nonlinear amplification (gamma), signal differentiation, and Y-modulation. Black level suppression and gamma processing are useful in producing enhanced image contrast over a small range of input signal. Signal differentiation preferentially enhances high frequency components of the image and is therefore effective for emphasizing edges. Y-modulation is particularly sensitive to fine detail and enhances the effect of surface texture.

**15426.** Wiederhorn, S. M., Johnson, H., **Effect of zeta potential on crack propagation in glass in aqueous solutions,** *J. Am. Ceram. Soc.* **58,** No. 7-8, 342 (July-Aug. 1975).

Key words: crack propagation; fracture; glass; zeta potential.

In this paper the effect of zeta potential on crack propagation in glass is studied. Results indicate that in aqueous environments the zeta potential has no effect on crack growth. Reasons for this null effect are discussed.

**15427.** Maienthal, E. J., **The application of linear sweep voltammetry to the determination of trace elements in biological and environmental materials,** (Proc. Eighth Annual Conf. on Trace Substances in Environmental Health, Univ. of Missouri-Columbia, Columbia, Mo., June 11-13, 1974), Paper in *Trace Substances in Environmental Health,* D. D. Hemphill, Ed., **VIII,** 243-246 (1974).

Key words: analysis; biological and botanical samples; differential linear sweep voltammetry; environmental samples; fossil fuels; lunar samples.

The application of differential linear sweep voltammetry to the analysis of many types of environmental samples is described. The methods are applicable to the determination of many trace elements in almost any matrix. Results will be given and compared with those obtained by other techniques.

**15428.** Albus, J. S., **A new approach to manipulator control: The cerebellar model articulation controller (CMAC),** *Trans. ASME—J. Dyn. Syst. Meas. Control* **97,** No. 3, 220-227 (Sept. 1975).

Key words: adaptive control; cerebellum model; control theory; manipulator control; Perceptron.

CMAC is an adaptive system by which control functions for many degrees of freedom operating simultaneously by referring to a table rather than by mathematical solution of simultaneous equations. CMAC combines input commands and feedback variables into an input vector which is used to address a memory where the appropriate output variables are stored. Each address consists of a set of physical memory locations, the arithmetic sum of whose contents is the value of the stored variable. The CMAC memory addressing algorithm takes advantage of the continuous nature of the control function in a way which promises to make it possible to store the necessary data in a physical memory of practical size.

**15429.** McLaughlin, W. L., Rosenstein, M., Levine, H., **Bone-and-muscle-equivalent solid chemical dose meters for photon and electron doses above one kilorad,** (Proc. Symp. on Biomedical Dosimetry, IAEA, Vienna, Austria, 1975), Chapter in *Biomedical Dosimetry,* pp. 267-281 (Int. Atomic Energy Agency, Vienna, Austria, 1975).

Key words: bone; dosimetry; dyes; electron dosimetry; energy dependence; gamma rays; muscle; radiochromic dosimeters; x-ray spectra.

Conventional solid dose meters, such as plastic films, powders, emulsions, glasses, ceramics and gels, have a response to ionizing photons and electrons that varies markedly over a broad spectrum when compared with the absorption characteristics of biological tissues. New radiochromic dyed plastic dose meters have been developed with x- and gamma-ray and electron energy absorption cross-sections (calculated) and radiation energy responses (experimental) corresponding approximately to those for human muscle and bone, for a spectrum from a few keV to at least 10 MeV. Three-dimensional solid dose meters useful over the absorbed dose range of $10^3$ to $10^6$ rad are formed by thermosetting a selected combination of monomers containing the radiochromic dye in solution. Thin-film dose meters for the dose range $10^5$ to $10^7$ rad are formed by casting on optically flat surfaces strippable layers of special combinations of polymers and dyes in solution. The response of these systems to x and gamma rays and electrons has been studied over various radiation spectra, dose-rates and temperatures during irradiation.

**15430.** Harman, G. G., **A metallurgical basis for the nondestructive wire-bond pull-test,** *12th Annual Proc. IEEE Reliability Physics, Las Vegas, Nev., April 2-4, 1974,* pp. 205-210 (Nov. 15, 1974).

Key words: bond pull test (nondestructive); metallurgical; reliability (microelectronic); transistors; wire bond.

Nondestructive wire-bond pull tests are often specified by high-reliability electronic device users in order to eliminate weak, poorly made wire bonds. The main problem with the test has been in establishing a pull-force level which will assure that the bonds are adequately strong but will not damage them during the test. In the present work, factors affecting the nondestructive wire-bond pull-test are examined. The variables, such as wire and bond-loop elongation, bond geometry, bond deformation, and the mean and standard deviation of the destructive bond pull test are studied to determine their influence on the nondestructive test. Different pull-force criteria are derived for wire with high elongation, such as is used in power devices, and for wire with low elongation, typically used for bonding integrated circuits.

**15431.** Harman, G. G., **Metallurgical failure modes of wire bonds,** *12th Annual Proc. IEEE Reliability Physics, Las Vegas, Nev., April 2-4, 1974,* pp. 131-141 (Nov. 15, 1974).

Key words: bonds (wire); failure modes; metallurgical failure modes; microelectronic; thermocompression bonds; ultrasonic bonds.

Various metallurgical failure modes of gold and aluminum wire bonds are described. Examples are taken from both low and high power devices. Whenever possible, known methods of avoiding these failure modes are given.

Wire bond failure modes can be divided into two categories. The first is comprised of those failure modes that are caused by poorly controlled or poorly designed manufacturing processes that result in lower product yield or higher per unit bonding cost, as well as those processes that predispose the device to early field failure. The second category is comprised of the failure modes of adequately made bonds that are caused to fail by environmental stresses during the operating life of the device.

The most frequent causes of failures are discussed in detail. These include nonoptimized bonding schedules, cracks in the heels of ultrasonic bonds, intermetallic formation, poor metallization, and inadequate glassivation removal. Assuming that the package is hermetic, or for plastic devices that humidity and other corrosion producers are not present, then the primary wire bond failure modes in the second category result from environmental temperature exposure and the number of power or thermal cycles experienced by the device during operation. Both of these can induce intermetallic formation. The latter can cause metallurgical flexure-fatigue at the bond heel or in the wire.

**15432.** Wiederhorn, S. M., **Strength of glass—A fracture mechanics approach,** (Proc. 10th Int. Congress on Glass, Kyoto, Japan, July 8-13, 1974), Paper in *Tenth International Congress on Glass,* pp. 11-1/11-15 (The Ceramic Society of Japan, Kyoto, Japan, July 1974).

Key words: crack growth; fracture; glass; static fatigue; strength.

After a brief review of those factors that determine the strength of glass (brittleness, surface flaws, susceptibility to stress corrosion cracking), a discussion will be given of how fracture mechanics techniques can be used to understand the physics and chemistry of glass strength. In this paper we assume that the strength of glass is limited by the growth of cracks that are always present in normal glass surfaces. Fracture mechanics techniques can be used to characterize the crack growth and to relate the growth to experimental parameters such as temperature, environment, and glass composition. Crack growth data obtained in this manner can be used to develop a deeper understanding of fracture mechanisms, and to develop charts that can be used for the design of glass structural components. Examples of both applications are given in the paper.

**15433.** Green, R. E., Jr., Farabaugh, E. N., Crissman, J. M., **X-ray topographic examination of large paraffin single crystals,** *J. Appl. Phys.* **46,** No. 10, 4173-4180 (Oct. 1975).

Key words: microstructure; paraffin crystals; plastic deformation; polymer crystals; radiation damage; x-ray topography.

The internal microstructure of large melt-grown paraffin (*n*-eicosane, $C_{20}H_{42}$) single crystals was examined by the Lang x-ray diffraction projection topographic technique. Crystal selection was facilitated by use of an electro-optical system which permitted instantaneous display of Laue transmission x-ray diffraction patterns on a television monitor. The crystals were oriented and topographic diffraction planes were selected by the use of a standard (001) stereographic projection plotted from computed angles between crystallographic planes. A second electro-optical system which permitted direct viewing of the topographic images was used for rapid alignment of the Lang camera and ensured uniformly exposed topographs. X-ray topographs were obtained from crystals in the as-grown, plastically deformed, and $\gamma$-irradiated states. The results indicate that both plastic deformation and $\gamma$ irradiation caused marked changes in the microstructure of the crystals, and that x-ray topography can be successfully exploited to determine such changes in hydrocarbon crystals.

**15434.** Prask, H., Trevino, S., Tsai, D. H., MacDonald, R. A., Kemmey, P., Yip, S., **Computer simulation studies of the microscopic behavior of shocked solids,** *Proc. Conf. on Mechanisms of Explosion and Blast Waves, Naval Weapons Station, Yorktown, Va., Nov. 13-15, 1973,* 1-21 (1974).

Key words: blast waves; computer simulation; interatomic potentials; lattice dynamics; molecular dynamics; shock waves.

The application of computer molecular dynamics (CMD) techniques to the understanding of blast wave phenomena in solids is discussed. Examples of CMD studies of simple systems undergoing plane shock waves are reviewed and the inadequacy of some of the assumptions made in the conventional continuum approach examined. Recent advances made in obtaining approximate interatomic potentials for complex solids from conventional lattice-dynamical studies are reviewed for $NaN_3$ and $KN_3$. These results are discussed in the context of extending the scope of CMD calculations.

**15435.** McLaughlin, W. L., **Radiation sources and dosimetry,** *Food Irradiation Information* **4,** 44-45, 58 (Mar. 1975).

Key words: accelerators; dose distributions; dosimetry; electron beams; food irradiation; food preservation; gamma rays.

The program at the NBS Center for Radiation Research contributing to food preservation by irradiation includes measurement studies with several high-energy electron accelerators and radionuclide sources such as cobalt-60. Investigations are made on large-dose measurement systems, chemical dosimeters, and thin-film imaging systems used for high-resolution dose-distribution studies.

**15436.** Maki, A. G., **High-temperature infrared spectrum of HCN near 3300 cm$^{-1}$,** *J. Mol. Spectrosc.* **58,** 308-315 (1975).

Key words: high temperature; hydrogen cyanide; infrared; molecular term values; spectra; spectroscopy.

The infrared absorption of HCN near the fundamental band at 3311 cm$^{-1}$ has been measured at temperatures up to 1200 K. Transitions involving high rotational states (up to $J=62$) have been measured. These give an improved value for the sextic centrifugal distortion term $H_0$. Many hot-band transitions have been observed and assigned to transitions originating in vibrationally excited states up to 4000 cm$^{-1}$ above the ground state. These measurements give new data on vibrational states involving moderately high bending quantum numbers and indicate that new terms are needed to fit the ro-vibrational energy levels.

**15437.** Bender, P. L., **Laser measurements of the lunar distance,** *Rev. Geophys. Space Phys.* **13,** No. 3, 271-272, 291 (July 1975).

Key words: crustal movements; earth rotation; geophysics; lasers; lunar cartography; lunar gravity; moon; plate tectonics.

Progress since 1971 on laser measurements of the lunar distance is reported. The current status of analysis work based on lunar distance data is described. New lunar and geophysical results which have been obtained by the joint efforts of a number of different institutions are discussed briefly.

**15438.** Buchbinder, L. B., **Human behavioral patterns vs. injury severity for apparel fire victims,** *Proc. Seventh Annual Meeting, Information Council on Fabric Flammability, New York, N.Y., Dec. 5, 1973,* pp. 236-253 (Information Council on Fabric Flammability, New York, N.Y., July 1, 1974).

Key words: apparel; apparel fires; burn injury; defensive capability; FFACTS; fire; flammable fabrics; garment fires; garment parameters; injury severity; reaction patterns; victims.

This study is based on information from 1,126 fire accident cases in the NBS computerized data base, FFACTS. The defensive actions taken by persons involved in apparel fires are described and the effect of these reactions on the severity of the resultant burn injuries is discussed. In general, "running" was the most frequent first reaction with "beating flames with hands" and "trying to remove clothing" ranking second and third in frequency. However, the relative frequency of reactions varied with age, sex and type of accident. The effectiveness of various reactions was analyzed considering both the extent of injury incurred, measured by the percent total area of body burned, and the number of additional reactions required to extinguish the fire. The victim's defensive capability (i.e., his ability to recognize danger and take appropriate action) was also found to have an effect on the level of injury severity.

**15439.** Roth, R. S., Brower, W. S., Parker, H. S., Minor, D. B., Waring, J. L., **Alkali oxide-tantalum, niobium and antimony oxide ionic conductors,** *NASA CR-134869,* 76 pages (National Technical Information Service, Springfield, Va., 1975).

Key words: ionic conductivity; nonstoichiometry; potassium antimonate; rubidium niobate; rubidium tantalate; sodium antimonate; sodium antimonate fluoride.

The phase equilibrium relations of four systems were investigated in detail. These consisted of sodium and potassium antimonates with antimony oxide and tantalum and niobium oxide with rubidium oxide as far as the ratio $4Rb_2O:11B_2O_5$ (B = Nb, Ta). The ternary system $NaSbO_3$-$Sb_2O_4$-NaF was also investigated extensively to determine the actual composition of the body centered cubic sodium antimonate. In addition, various other binary and ternary oxide systems involving alkali oxides were examined in lesser detail. The phases synthesized were screened by ion exchange methods to determine mobility of the alkali ion within the niobium, tantalum or antimony oxide (fluoride) structural framework. Five structure types were found to be of sufficient interest to warrant further investigation. These structure types are (1) hexagonal tungsten bronze (HTB), (2) pyrochlore, (3) the hybrid HTB-pyrochlore hexagonal ordered phases, (4) body centered cubic antimonates and (5) $2K_2O:3Nb_2O_5$. Although all of these phases exhibit good ion exchange properties only the pyrochlore has so far been prepared with $Na^+$ ions as an equilibrium phase and as a low porosity ceramic. Unfortunately $Sb^{+3}$ in the channel apparently interferes with ionic conductivity in this case, although relatively good ionic conductivity was found for the metastable $Na^+$ ion exchanged analogs of $RbTa_2O_5F$ and $KTaWO_6$ pyrochlore phases. Small crystals of the other phases can generally be prepared by flux techniques and ion exchanged with $Na^+$. However, in the one case where congruency allows large crystals to be pulled from the melt ($4Rb_2O:11Nb_2O_5$) ion exchange techniques up to ~ 450 °C are not sufficient to accomplish complete replacement with $Na^+$ ions.

**15440.** Kashiwagi, T., **A study of flame spread over a porous material under external radiation fluxes,** *Proc. Fifteenth Symp. (International) on Combustion, Tokyo, Japan, Aug. 25-31, 1974,* pp. 255-265 (The Combustion Institute, Pittsburgh, Pa., 1974).

Key words: flame spread; floor covering materials; ignition.

Characteristics of horizontal flame spread over the surface of a porous material, a carpet in this study, are studied experimentally and theoretically under various external radiant fluxes ($0.1 - 0.27$ cal/cm$^2$sec). It is observed that the size of flame is increased significantly by increasing the external radiant flux. This increases the radiative heat feedback from the flame so that it becomes comparable to or greater than the convective heat feedback. The external radiation can also cause an unstable motion of the flame front. This effect is probably due to the production of volatile pyrolysis products ahead of the flame front instead of under it. The theoretical calculation indicates that the thermal emission loss from the heated sample is significant and the internal radiation in the porous material must be included in the model.

**15441.** Armstrong, G. T., Johnson, W. H., **Standard reference materials for combustion calorimetry,** *Proc. Third Int. Conf. on Chemical Thermodynamics, Baden near Vienna, Austria, Sept. 3-7, 1973,* **VIII,** 55-72 (International Union of Pure and Applied Chemistry, Oxford, England, 1974). (Abstract is found in Vol. I, page 148 (1973)).

Key words: acetanilide; bomb calorimetry; calorimetry; chlorobenzoic acid; combustion; creatinine; fluorobenzoic acid; nicotinic acid; reference materials; thermochemical; thermochemical standards; thianthrene; urea.

Combustion measurements using a rotating bomb adiabatic aneroid calorimeter have been used to make a preliminary evaluation of ten substances as potential thermochemical reference materials for combustion of organic compounds containing N, S, Cl and F. p-chlorobenzoic acid, p-fluorobenzoic acid, and urea are recommended for acquisition, certification, and distribution. Thianthrene may also be suitable. For the ten substances including in addition to the above: o- and m-chlorobenzoic acids, o-fluorobenzoic acid, nicotinic acid, acetanilide, and creatinine, typical combustion data are given, showing corrections applied; and mean thermodynamic functions at 25 °C are given together with error estimates. The results are compared with other work. Recommendations and a discussion of the role of standard reference materials for thermochemistry are given.

**15442.** Swanson, N., Celotta, R. J., Kuyatt, C. E., **Electron excitation of xenon near threshold,** (Proc. Int. Symp. on Electron and Photon Interactions w/Atoms, Univ. of Stirling, Stirling, Scotland, July 16-19, 1974), Chapter in *Electron and Photon Interactions with Atoms,* pp. 661-667 (Oct. 1975).

Key words: autoionizing states; electron excitation; energy loss; resonances; threshold; xenon.

An electron energy-loss spectrum and excitation functions for the four lowest excited states in Xe have been measured at a scattering angle of 45° in the near-threshold region ($8 - 14$ eV). Four peaks in the energy-loss spectrum above the $^2P_{3/2}$ ionization limit can be fitted to a $5p^5np'$ Rydberg series. The excitation functions for the two lowest states at 8.32 and 8.44 eV show large peaks due to decay of the $5p^56s^2(^2P_{1/2})$ resonance, as well as other resonance peaks which correlate well with previous transmission measurements.

**15443.** Huebner, R. H., Fergurson, C. H., Celotta, R. J., Mielczarek, S. R., **Apparent oscillator-strength distributions derived from electron energy-loss measurement: Methane and *n*-hexane,** *ANL-75-3,* Part 1, *Biology and Medicine UC-48,* pp. 41-44 (Argonne National Laboratory, Radiological and Environmental Research Division, Argonne, Ill., July 1973-July 1974).

Key words: electron; energy loss; methane; *n*-hexane; oscillator strengths; spectra.

The derivation of oscillator strengths from electron energy loss spectra are discussed and results obtained for methane and *n*-hexane are compared to optical data.

**15444.** Huebner, R. H., Fergurson, C. H., Celotta, R. J., Mielczarek, S. R., **Apparent oscillator strength distributions derived from electron energy-loss measurements: Methane and *n*-hexane,** *Proc. IVth Int. Conf. on Vacuum-Ultraviolet Radiation Physics, Hamburg, Germany, July 22-26, 1974,* Article 111, 4 pages (1974).

Key words: electron; electron scattering; energy loss; methane; *n*-hexane; oscillator strength.

Electron energy loss spectra were obtained for methane from 8.0 to 14.0 eV and for *n*-hexane from 0 – 20 eV with the NBS Model AN-1 electron impact spectrometer. These data were obtained for 100 eV incident electrons scattered within about 20 milliradians of the forward direction. Relative oscillator strengths were derived from the data by correcting for the finite angular acceptance of the apparatus with the assumption that the generalized oscillator strength can be approximated by its optical oscillator strength limit. The apparent oscillator strength distributions are placed on an absolute scale by normalization at one energy to a df/dE value determined optically. Comparisons of these results with available photoabsorption and other electron impact measurements will be presented.

**15445.** Huebner, R. H., Celotta, R. J., Mielczarek, S. R., Kuyatt, C. E., **Dipole oscillator-strength distributions derived for several hydrocarbons from electron energy-loss spectra,** *ANL-75-3,* Part 1, *Biology and Medicine UC-48,* pp. 45-48 (Argonne National Laboratory, Radiological and Environmental Research Division, Argonne, Ill., July 1973-July 1974).

Key words: electron; energy loss; oscillator strengths; spectra.

A summary is presented of the technique used to determine dipole oscillator strength values from electron energy loss spectra. Data on benzene is presented as an example.

**15446.** Huebner, R. H., Celotta, R. J., Mielczarek, S. R., Kuyatt, C. E., **Apparent oscillator strengths for molecular oxygen,** *ANL-75-3,* Part 1, *Biology and Medicine UC-48,* pp. 49-52 (Argonne National Laboratory, Radiological and Environmental Research Division, Argonne, Ill., July 1973-July 1974).

Key words: electron; energy loss; molecular oxygen; oscillator strengths; spectra.

The oscillator strengths for molecular oxygen are determined from electron energy loss measurements and are compared to the available optical data.

**15447.** Hughes, E. E., **Development of standard reference materials for air quality measurement,** (Proc. Int. Instrumentation-Automation Conf. & Exhibit, New York, N.Y., Oct. 28-31), *ISA Reprint 74-704,* 13 pages (Instrument Society of America, Pittsburgh, Pa., 1974).

Key words: air pollution; carbon monoxide; gas analysis; gas standards; nitric oxide; nitrogen dioxide; sulfur dioxide.

The National Bureau of Standards is engaged in a continuing program involving gaseous Standard Reference Materials for air pollution measurements. Preparation of such materials requires definition of the stability, homogeneity and accuracy of the samples. This information is obtained by long-term studies of the gas systems, by development of absolute methods of analysis and by analysis of large numbers of samples prepared in bulk. The results of studies, extending over several years, of low concentration of carbon monoxide in nitrogen and nitric oxide in nitrogen are reported. Over one thousand samples of these materials have been analyzed and the stability with time and the within-batch homogeneity have been characterized. Accuracy is achieved by use of gravimetric standards and with dynamic dilution systems. Accuracy attainable by either method is described.

The use of permeation tubes of sulfur dioxide and nitrogen dioxide is necessary in some situations because of the reactivity of the gases. Data covering the stability and accuracy of these devices has been collected over a period of several years.

**15448.** Fife, D. W., **Primary issues in user needs,** (Proc. EDUCOM Working Seminar on the National Science Computer Network, Warrenton, Va., Nov. 1972), Chapter 10 in *Networks for Research and Education,* pp. 89-95 (The Massachusetts Institute of Technology, Cambridge, Mass., 1974).

Key words: computer networks; National Science Computer Network; network management.

The Institute for Computer Sciences and Technology of the National Bureau of Standards is assisting the National Science Foundation in technical planning to delineate major approaches and to derive guidelines for the trial experiments that may lead to a National Science Computer Network. The primary efforts of NBS are in network management requirements and application criteria for communications technology. User characteristics are being briefly studied for perspective on the objectives for the network and on the types of service it may provide. The goal of the NBS project is to describe by mid-1973 the basic types of experiments which address the central issues, together with appropriate evaluation criteria, so that NSF may use this technical framework in selecting an approach to the trial network.

**15449.** Hosler, W. R., Capps, W., Plante, E. R., **Some physical and chemical properties of coal slags,** *Proc. 14th Symp. on Engineering Aspects of Magnetohydrodynamics, The Univ. of Tennessee Space Institute, Tullahoma, Tenn., April 8-10, 1974,* pp. IV.7.1-IV.7.5 (1974).

Key words: coal slags; MHD; thermionic emission; vaporization; viscosity.

Thermionic emission, viscosity and vaporization studies of molten synthetic coal slags are described. Thermionic emission of a combustor type slag was determined in 1 atm air, 1 atm $O_2$, and 0.01 atm $O_2$ in $N_2$. Sizeable flows of electrons and positive ions were detected at temperatures as low as 1200-1300 °C. Viscosities of one real and several synthetic slags are shown between 1585 °C and their liquidus temperature (1250-1350 °C). These melts are quite fluid in this temperature range. From the modulated-beam mass spectrometer studies it appears that initial stages of evaporation of some synthetic melts are characterized by a nonequilibrium process involving a slower than expected decomposition of $Fe_3O_4$. SiO evaporation from the slag solution proceeds at a rate consistent with the $SiO_2$ in solution having an activity near unity.

**15450.** Armstrong, G. T., **The infrastructure of the thermochemical measurement system,** (Proc. Quatrieme Conf. Int. de Thermodynamique Chimique, Montpellier, France, Aug. 26-30, 1975), Chapter in *Thermochimie* **I,** 11-18 (Centre de Recherches de Microcalorimétrie et de Thermochimie du C.N.R.S., Marseille, France, 1975).

Key words: calorimetry; chemical energy; chemical thermodynamic data; energy scale (chemical); equilibrium measurements; mass spectrometry; measurement system; spectroscopy; state measurements; thermochemistry.

The thermochemical measurement system outlined here is an extension of the concept of a measurement system in that it deals with a class of physicochemical information, rather than with a metrology. Thermochemical quantities are defined, classified as archival thermochemical data, and thermochemical laboratory test data, and their source methodologies are categorized as calorimetry, equilibrium and state measurements, optical and mass spectrometry and theory. The relationship of thermochemical to nonthermochemical calorimetry is outlined. The propagation of measurements from standards laboratory to ultimate user is described for archival and for test laboratory thermochemical data.

**15451.** Meyerson, M., **The Department of Commerce voluntary labeling program for household appliances and equipment to effect energy conservation,** *Proc. Conf. on Improving Efficiency in HVAC Equipment and Components for Residential and Small Commercial Buildings, Purdue Univ., West Lafayette, Ind., Oct. 7-8, 1974,* pp. 222-225 (1974).

Key words: consumer information; efficiency; energy; label; refrigerator/freezers; room air conditioning.

The purpose and legal/administrative authority for the Department of Commerce Voluntary Labeling Program for Household Appliances and Equipment to Effect Energy Conservation are described. The procedures for executing this program are outlined, with examples of experience in developing labels for room air conditioners and refrigerator/freezers.

**15452.** Tighe, N., **Microstructure of oxidized silicon nitride,** (Proc. 32d Annual Proc. Electron Microscopy Society of America, St. Louis, Mo., 1974), Paper in *32d Annual Proc. Electron Microscopy Society of America,* C. J. Arceneaux, Ed., pp. 470-471 (Claitor's Publ. Div., Baton Rouge, La., 1974).

Key words: $\beta$-cristobalite; electron microscopy; oxidation; silicon nitride; silicon oxynitride; $Si_3N_4$.

The reaction product layer produced on hot-pressed silicon nitride, $Si_3N_4$, during oxidation at temperatures from 1000 to 1400 °C was examined by transmission electron microscopy. The oxide was found to have at least two crystalline phases — silicon oxynitride $Si_2ON_2$ and $\beta$-cristobalite $SiO_2$, and two amorphous phases. The microstructure of the phases and of the silicon nitride near the reaction interface is discussed.

**15453.** Simmons, G. L., Eisenhauer, C., Spencer, L. V., **Moments method calculations of neutron and gamma-ray penetration in bulk media,** *Proc. IVth Int. Conf. on Reactor Shielding, Paris, France, Oct. 9-13, 1972,* **2,** 268-283 (Oct. 1972).

Key words: adjoint; concrete; gamma-ray penetration; moments; neutron penetration; secondary gamma rays.

A system of computer codes using the moments method to calculate penetration of neutrons and gamma rays in bulk media is described. Results are presented for the penetration of fission neutrons incident at various angles on concrete. The use of adjoint procedures for calculating gamma-ray buildup factor data are also described and results are presented for the penetration of gamma rays from point sources emitting at various conical angles in a concrete medium. Finally, the two types of calculations are combined to produce data for penetration of gamma rays produced in concrete by a neutron source.

**15454.** Wehrli, R., **Metrication and the construction industry: Potential problems and promising opportunities,** *AIA J.,* pp. 50-54 (May 1974).

Key words: building industry; conversion; engineering; human and modular standards; metrication; product-dimensions.

Conversion to the metric system, now nationally underway but still unorganized, challenges the building industry especially to plan promptly for hard conversion (metrication's approaching later stages). Why planning now is needed to accomplish competent hard conversion is examined in relation to standards. Because the building industry will need new dimensional standards for products to achieve a successful, final conversion, three types of hard conversion standards should be fixed upon to avoid haphazard pitfalls as conversion advances. The three standards briefly examined are engineering, modular, and human and their possible interrelationships.

**15455.** Strobridge, T. R., **Feasibility study of a multipurpose refrigerator for a superconducting cable test facility,** *Paper EPRI* **282,** 52 pages (Electric Power Research Institute, Palo Alto, Calif., July 1975).

Key words: cryogenics; helium pump; power transmission; refrigeration; superconducting cables.

A major problem in simultaneously cooling a number of test sections of superconducting power transmission cables is the wide variation in cable operating pressures and temperatures. It is feasible to couple a single large refrigerator to the cables with individual pumped helium circulation circuits. The system is flexible in both pressure and temperature and in the temperature rise along the length of the cable. The total refrigeration capacity required for a test facility is derived from current estimates of cable characteristics. A single refrigerator is shown to be less expensive than individual refrigerators for each cable even when the penalties for pump work and heat transfer through large temperature differences are included. Sufficient process calculations are included to show that the system is practical, and a draft specification for the refrigerator is given.

**15456.** Rook, H. L., Suddueth, J. E., Becker, D. A. **Determination of iodine-129 at natural levels using neutron activation and isotopic separation,** *Anal. Chem.* **47,** No. 9, 1557 1562 (Aug. 1975).

Key words: improved limits of detection; iodine-129 isotopic separation; neutron activation.

Iodine-129 levels have been published for biological matrices that naturally accumulate iodine such as animal thyroid and kelp. However, published procedures have insufficient sensitivity to determine $^{129}I$ in other environmental and biological species. A unique procedure has been developed for the determination o $^{129}I$ which couples neutron activation with mass separation. The procedure results in a significant improvement in sensitivity thus allowing analyses to be performed on a variety of matrices which heretofore had not been investigated. Method development and analytical procedures are presented and analytica results at the $10^{-13} - 10^{-14}$ gram $^{129}I$ level are given.

15457. Carpenter, B. S., Reimer, G. M., **Fission track technique for uranium determination in coal and fly ash standard reference materials,** (Proc. Second Int. Conf. on Nuclear Methods in Environmental Research, Univ. of Missouri, Columbia, Mo., July 29-31, 1974), Paper in *Nuclear Methods in Environmental Research,* J. R. Vogt and W. Meyer, Eds., CONF 740701, pp. 141-143 (Available from the National Technical Information Service, Springfield, Va., 1974).

Key words: coal; fission track technique; fly ash; mica detector; polycarbonate detector; rapid analysis; uranium.

The analysis of coal and combustion waste products for uranium will become increasingly important with the greater use of coal for supplying energy needs. A fission track technique, as demonstrated with NBS Standard Reference Material Trace Elements in Coal (SRM 1632) and Trace Elements in Fly Ash (SRM 1633), provides a rapid and inexpensive method for U analysis.

15458. Rook, H. L., Moody, J. R., **Stabilization and determination of nanogram quantities of mercury in water,** (Proc. Second Int. Conf. on Nuclear Methods in Environmental Research, Univ. of Missouri, Columbia, Mo., July 29-31, 1974), Paper in *Nuclear Methods in Environmental Research,* J. R. Vogt and W. Meyer, Eds., CONF 740701, pp. 44-53 (Available from the National Technical Information Service, Springfield, Va., 1974).

Key words: mercury; stabilization; standard reference material; trace element; water standard.

The National Bureau of Standards has completed development work and analytical certification on two Mercury in Water Standard Reference Materials (SRM). SRM 1641 has a mercury content of $1.52 \pm 0.05$ $\mu$g $Hg^{++}$ per gram of water and is intended as a "spike" standard for natural waters. SRM 1642 has a mercury content of $1.20 \pm 0.05$ ng $Hg^{++}$ per gram of water and is intended as a benchmark trace standard used for analytical methods development.

These Standards have been stabilized using a new technique developed at NBS. Shelf life of the trace solutions has been demonstrated to be greater than one year with expectation of an even longer storage capability.

15459. Gills, T. E., LaFleur, P. D., **The determination of hafnium in standard reference materials using bis(2-ethylhexyl) phosphate (HDEHP) with neutron activation analysis,** (Proc. Int. Meeting on Activation Analysis, Saclay, France, Oct. 1-6, 1972), *J. Radioanal. Chem.* **19,** 235-237 (1974).

Key words: activation analysis; Ge(Li) detector; solvent extraction.

The method for the determination of hafnium in standard reference steels is described. The method combines neutron activation analysis with a solvent extraction procedure using bis(2-ethylhexyl) phosphate as the extractant. A subsequent back extraction into 2N hydrofluoric acid is done finally before counting. The samples were counted on a 60cc Ge(Li) in configuration with a 2048 channel analyzer. Using this method of analysis as described fast determination of hafnium can be made with routine 3-4 percent precision and accuracy.

15460. Heydemann, P. L. M., **Pressure measurement and calibration,** *Proc. ASME Pressure Vessels and Piping Materials Nuclear Conf., Miami, Fla., June 24-28, 1974,* Paper 74-PVP-43, pp. 1-8 (American Society of Mechanical Engineers, New York, N.Y., 1974).

Key words: calibration; pressure measurement; primary pressure standards.

The National Bureau of Standards maintains a group of primary pressure standards in its laboratories in Gaithersburg, Md. These standards are dead weight piston gages with controlled clearance. Special experimental and computational methods have been developed for the calibration of these primary standards. From this group of standards calibrations are disseminated to industry by means of transfer standards, which are calibrated against the primary standards with the cross float method. Specialized computer programs are used for the evaluation of the cross float in order to obtain best sets of characteristic gage coefficients. Pressure calibration services available from NBS presently cover the range from 2 kPa (0.3 psi) to 400 MPa (60,000 psi) and an expansion to 2.5 GPa (375,000 psi) is in preparation. In addition NBS provides training courses, data evaluation service and extensive, free consultations. Facilities exist for long term performance testing of transducers and for research and development work under contract. This report is written to make petroleum engineers aware of the availability of these services.

15461. Marvin, R. S., Hogenboom, D. L., **Viscosity of liquids,** Paper 2m in the *American Institute of Physics Handbook Third Edition,* pp. 2-187 – 2-202 (McGraw-Hill Book Co., New York, N.Y., 1972).

Key words: handbook article; liquids; viscosity.

Existing tabulations of the viscosity of liquids are described with selected examples from some of the more recent tabulations.

15462. Pallett, D. S., **Force platform instrumentation system for the study of impact forces,** *Proc. Inter-Noise Conf., Sept. 30-Oct. 2, 1974,* J. C. Snowdon, Ed., pp. 89-92 (Noise Control Foundation, Poughkeepsie, N.Y., 1974).

Key words: building acoustics; force platforms; impact noise; instrumentation; mechanical impedance; noise.

Human footfall has long been recognized as an important source of impact noise in buildings, which in turn has been recognized as an important source of occupant dissatisfaction in multifamily dwellings. Very little is known of the dynamic characteristics of the footfall event. The instrumentation system described in this paper is intended for use in research dealing with the dynamic characteristics of footfall impact events. The data obtained in this research is directed toward the question of whether it is possible to reliably specify live walkers for use in impact noise studies. Force platform design considerations and description of related signal processing are presented. Preliminary calibration data indicate that the usable response of the force platform may extend from DC to nearly 2 kHz.

15463. Wiese, W. L., **Experimental progress on plasma broadening of hydrogen lines,** *Proc. Invited Lectures given at the 7th Yugoslav Symp. and Summer School on the Physics of Ionized Gases, Rovinj, Yugoslavia, Sept. 16-21, 1974,* V. Vujnovic, Ed., pp. 637-673 (Institute of Physics, University of Zagreb, Yugoslavia, 1974).

Key words: Balmer lines; hydrogen plasma; ion motion; line shapes; reduced mass; Stark broadening.

Recent experimental investigations on the Stark broadening of hydrogen Balmer lines in high density plasmas are described. The review is principally devoted to the finer details of the line shapes, such as their central structure, asymmetries, shifts, and the decay in the line wings. Recently detected variations in the line shapes with the reduced mass of the radiator-perturber system are discussed, comparisons with theory are presented, and some preliminary conclusions are drawn.

**15464.** Kahles, J. F., Field, M., Young, R. D., Whitehouse, D. J., **Survey on surface roughness and surface integrity requirements for machined components,** *CIRP Annals* **23,** No. 1, 185-186 (1974).

Key words: CIRP; surface; surface finish; surface integrity; surface questionnaire; surface survey.

CIRP Committee "S" has developed a survey to determine surface roughness and surface integrity requirements for machined components. Specifically, the survey is designed to develop a comprehensive international response concerning the status of surface technology as related to all types of material removal processes, and the surface conditions produced which affect parts performance. The design of the survey is discussed, the status is outlined, and a partial list of survey questions is presented.

**15465.** Ayres, T. R., Linsky, J. L., **Stellar model chromospheres. III. Arcturus (K2 III),** *Astrophys. J.* **200,** No. 3, 660-674 (Sept. 15, 1975).

Key words: Ca II emission; chromospheres, stellar; photospheres, stellar.

We construct models for the upper photosphere and chromosphere of Arcturus based on the H, K, and IR triplet lines of Ca II and the *h* and *k* lines of Mg II. The chromosphere model is derived from complete redistribution solutions for a five-level Ca II ion and a two-level Mg II ion. A photospheric model is derived from the Ca II wings using first the "traditional" complete redistribution limit and then the more realistic partial redistribution approximation. In particular, the temperature and mass column densities for the temperature minimum region and the chromosphere-transition region boundary are computed and the pressure $P_0$ in the transition region and corona estimated. We find $T_{min}/T_{eff} \approx 0.77$ for Arcturus, Procyon, and the Sun and a trend of increasing mass at the temperature minimum with decreasing gravity. We find $P_0$ to be about 1 percent of the solar value, and on this basis estimate the surface brightness of the Arcturus transition region and coronal spectrum to be much less than for the Sun. Finally, the partial redistribution calculation for the Ca II K line indicates that the emission width is at least partially determined by damping rather than Doppler broadening, suggesting a reexamination of previous explanations for the Wilson-Bappu effect.

**15466.** Menis, O., Garn, P. D., Diamondstone, B. I., **The application of thermoanalytical methods to the environmental health problems,** (Proc. Fourth ICTA Conf., Budapest, Hungary, July 8-13, 1974), Chapter in *Thermal Analysis,* I. Buzas, Ed., **3,** 127-139 (Akademiai, Kiado, Budapest, Hungary, 1975).

Key words: calibration filters; chrysotile; environmental health; improved methodologies; particulates; quartz; self-generated atmosphere.

Differential thermoanalysis methods provided an independent measurement of quartz and chrysotile asbestos in the preparation of calibration standards needed by environmental control agencies. In this study it was found that 30-500 $\mu$g of chrysotile asbestos could be measured with a relative standard deviation of 15 percent. Sealed silver containers were used to provide a self-generating atmosphere which reduced the spread of the dehydroxylation peak and improved both selectivity and sensitivity. A repeat-measurement of the thermal curve, after the dehydroxylation, provided a correction for the matrix baseline. Under similar experimental conditions, microgram quantities of quartz were determined with a relative standard deviation of $\sim 2$ percent. However, there was a 50 percent difference between the NBS-ICTA SRM 759 and commercially prepared material. It was shown that this difference could be eliminated by thermally treating the commercial product.

**15467.** Huebner, R. H., Celotta, R. J., Mielczarek, S. R., Kuyatt, C. E., **Apparent oscillator strengths for nitrous oxide,** (Proc. IX Int. Conf. on Physics of Electronic and Atomic Collisions, Seattle, Wash., July 24-30, 1975), Abstract in *Electronic and Atomic Collisions,* J. S. Risley and R. Geballe, Eds., **2,** 1043-1044 (University of Washington Press, Seattle, Wash., 1974).

Key words: electron energy loss; low energy electron impact; $N_2O$; oscillator strengths.

The apparent oscillator strengths for $N_2O$ in the energy loss range of 4.5 to 14 eV are presented at 0.01 eV intervals. Measurements were made with an incident energy of 100 eV and at a scattering angle of within 20 milliradians of the incident direction.

**15468.** Sarkes, L. A., Mann, D. B., **A survey of LNG technological needs in the U.S.A. – 1974 to beyond 2000,** *Proc. 4th Int. Conf. on Liquefied Natural Gas, Algiers, Algeria, June 24-27, 1974, Session VII,* Paper 1, pp. 1-21 (Institute of Gas Technology, Chicago, Ill., 1974).

Key words: cryogenic; gas industry; liquefied natural gas; research; survey; technology.

A comprehensive analysis of near and long term research needs has been conducted by the U.S. Gas Industry covering operational areas of Production and Exploration, Synthetic Supply, Transmission, Distribution, Utilization, and LNG.

Identifiable research needs are reported for the area of LNG encompassing time frames of: 1974-1978 (in detail, year by year); 1979-1985 (in 5 year period); 1986-2000 (as specific as possible); beyond 2000 (as believed necessary).

A year by year examination of LNG research priorities for the first five years are considered vital to overcome the potential suppression of growth in the LNG industry that could result from lack of available technology. Assessments of technical LNG needs beyond 1978 cannot, of course, be too well defined and must be examined annually for purposes of updating.

The National Bureau of Standards Cryogenics Division has become the governmental focal point for LNG research. A survey of NBS LNG research and how these relate to the future technological growth of the LNG industry are discussed.

**15469.** Heimbach, C. R., O'Connell, J. S., **Influence on the neutron's charge distribution on nuclear Coulomb energies,** (Proc. Conf. Int. Few Body Problems in Nuclear and Particle Physics, Laval Univ., Quebec City, Canada, Aug. 27-31, 1974), Paper in *Few Body Problems in Nuclear and Particle Physics,* R. J. Slobodrian, B. Cujec, and K. Ramavataram, Eds., pp. 94-95 (Les Presses de L'Université Laval, Quebec, Canada, 1974).

Key words: charge distribution; Coulomb energy; deuteron; electrostatic; interaction potential; neutron.

The electrostatic interaction energy of a deuteron was computed for a model in which the neutron charge distribution was taken as a superposition of two exponentials of total charge + e and – e. Because the interaction potential is of short range the result is sensitive to the interior deuteron wave function. For a Reid hard-core wave function the computed energy is 1 keV.

**15470.** Krasny, J. F., Winger, J. H., **Current status of flammability test development at the National Bureau of Standards,** *Proc. 8th Annual Meeting Information Council on Fabric Flammability, New York, N.Y., Dec. 5, 1974,* 5 pages (1974).

Key words: apparel; carpets; curtains; draperies; fabrics; flammability; garments; test methods; textiles; upholstered furniture.

Tests for the flammability of textile items, that are presently under development at NBS, are described.

**15471.** Loevinger, R., **Dosimetry standards for fast electrons,** (Proc. XIII Int. Congress of Radiology, Madrid, Spain, Oct. 15-20, 1973), *International Congress Series No. 339,* **2,** 467-471 (Excerpta Medica, Amsterdam, The Netherlands, 1973).

Key words: absorbed dose; calorimeter; dosimetry; electrons; ionization chamber; radiation standard.

Graphite calorimeters are being developed at several national standards laboratories to serve as absorbed-dose standards for fast electron beams for radiation therapy. Two such calorimeters have been constructed at the National Bureau of Standards, and compared to ionization chambers of the same size and shape by determining the quotient of the calorimeter response by the ionization chamber response. That quotient will be the factor used to convert the response of an ionization chamber calibrated in absorbed-dose units in a cobalt-60 beam to absorbed-dose units in high-energy electron beams.

**15472.** Becker, D. A. **Accuracy and precision in activation analysis—counting,** (Proc. Second Int. Conf. on Nuclear Methods in Environmental Research, Univ. of Missouri, Columbia, Mo., July 29-31, 1974), Paper in *Nuclear Methods in Environmental Research,* J. R. Vogt and W. Meyer, Eds., CONF 740701, pp. 69-80 (Available from the National Technical Information Service, Springfield, Va., 1974).

Key words: accuracy; errors in activation analysis; precision; radiation detection.

Accuracy and precision in activation analysis was investigated with regard to counting of induced radioactivity. The various parameters discussed include configuration, positioning, density, homogeneity, intensity, radioisotopic purity, peak integration, and nuclear constants. Experimental results are presented for many of these parameters. The results obtained indicate that counting errors often contribute significantly to the inaccuracy and imprecision of analyses. The magnitude of these errors ranges from less than 1 percent to 10 percent or more in many cases.

**5473.** Swanson, N., Celotta, R. J., Kuyatt, C. E., **Excitation of low-lying triplet states in ozone by electron impact,** (Proc. IX Int. Conf. on Physics of Electronic and Atomic Collisions, Seattle, Wash., July 24-30, 1975), Abstract in *Electronic and Atomic Collisions,* J. S. Risley, Ed., **2,** 128-129 (University of Washington Press, Seattle, Wash., 1974).

Key words: electron impact; energy loss spectra; oxygen; ozone; triplet states.

Energy loss spectra of ozone were measured at scattering angles of 45, 75, and 90° and incident energies below 10 eV to look for previously unobserved triplet states. A broad continuum between 1.3 and 2 eV energy loss was seen which we believe is due to excitation of these states.

**5474.** Wiese, W. L., Martin, G. A., **Oscillator strength distributions in the lithium isoelectronic sequence,** (Proc. Invited Lectures 7th Yugoslav Symp. and Summer School on the Physics of Ionized Gases, Rovinj, Yugoslavia, Sept. 16-21, 1974), Paper in *Physics of Ionized Gases,* V. Vujnovic, Ed., pp. 675-700 (Institute of Physics, University of Zagreb, Zagreb, Yugoslavia, 1974).

Key words: f-sum rule; f-values; lithium sequence; oscillator strength distribution; oscillator strengths; systematic trends.

A recent study on the oscillator strength distributions of several spectral series throughout the lithium isoelectronic sequence is described. In this work critically compiled oscillator strength data for discrete and continuum transitions have been subjected to four principal constraints: (a) to fit into systematic trends along the lithium isoelectronic sequence, (b) to fit into systematic trends within spectral series, (c) to comply with the requirement of continuity across the spectral series limit, and (d) to adhere to f-sum rules. The best available data require only minor modifications to adhere closely to all these constraints, which gives these data—for which several illustrative examples are presented—a very high degree of reliability.

**15475.** Utton, D. B., **Nonchemical applications of NQR,** *Proc. Second Int. Symp. on Nuclear Quadrupole Resonances Spectroscopy, Viareggio, Italy, Sept. 3-7, 1973,* pp. 341-350 (A. Vallerini, Pisa, Italy, 1975).

Key words: applications; material detection; nuclear quadrupole resonance; piezometry; thermometry.

Since the early work on NQR over twenty years ago it has been suggested that the temperature dependence of NQR frequencies can be used as a thermometer. A natural extension of this idea is to use an NQR frequency to measure pressure. A review is given of the work that has been done to investigate these applications of NQR. The criteria for the choice of material and measurement technique are discussed with emphasis on chlorine compounds since they have received the most attention. As an example, the accuracy and precision obtainable with the $Cl^{35}$ NQR in $KClO_3$ (for which accurate measurements are available) will be described.

There has been some renewed interest in using characteristic NQR frequencies to detect the presence of specific materials. As an example, estimates are given for the signal to noise ratio to be expected for nitrogen compounds when the material is not located within the detector coil.

**15476.** Peterlin, A., **ESR investigation of chain rupture in mechanically strained crystalline polymer solids,** (Proc. Sixth Southeastern Magnetic Resonance Conf., Clemson, S.C., Oct. 1974), *J. Magn. Reson.* **19,** 83-98 (1975).

Key words: chain rupture; crystalline polymer; ESR investigation of radicals; fibrous structure; mechanical breakdown; microfibrillar structure; radical formation; tie molecules.

ESR detects radicals formed in a strained polymer sample as a consequence of chain rupture and, hence, for a while was considered the best method for investigation of molecular effects during tensile straining. It turned out that a sufficiently high number of radicals for ESR detection is only obtained in highly oriented material with well developed fibrous structure.

The primary end-of-chain radicals are too reactive and unstable so that, as a rule, they are not observable by ESR except at cryogenic temperatures. By proton transfer, more stable center-of-chain radicals are formed which are normally measured. They yield information about primary chain rupture. The much more easy rupture of bonds adjacent to center-of-chain radicals breaks less strained chains (secondary rupture), but does not produce any new radicals. Hence, the ESR information about chain rupture is rather incomplete and has to be supplemented by other methods as for instance IR which detects the unsaturated end groups formed during radical transfer and secondary chain rupture.

Since the broken chains are not exactly the same chains which before rupture were responsible for elastic modulus and tensile strength one has no direct correlation between the radical population and the load-elongation curve of the sample even if no secondary rupture is involved. It turns out that the specific morphology, in particular the presence of point defects of fibrous structure caused by the ends of microfibrils, is responsible for crack nucleation and growth to critical size which finally leads to sample failure. The chain rupture partially monitored by the radical population is a moderately reliable indicator of the effects leading to failure but not the cause of it.

**15477.** Marshall, H. E., **Cost sharing and efficiency in salinity control,** (Proc. 15th Annual Western Resources Conf. on Salinity in Water Resources, Boulder, Colo., July 9-10, 1974), Chapter 8 in *Salinity in Water Resources,* J. E. Flack and C. W. Howe, Eds., pp. 139-152 (Merriman Publ. Co., Boulder, Colo., 1974).

Key words: Colorado River; cost sharing; efficiency; equity; salinity control.

The increase in salinity concentrations in the southwestern United States and Mexico imposes economic costs on water users. Cost-sharing rules influence the selection of techniques and of scales for salinity control projects, yet there is no established Federal policy for sharing the costs of salinity control. Based on efficiency and equity criteria, a package of rules is suggested. Charging salt polluters and salinity control beneficiaries are potential policies, the final choice being constrained by legal and political institutions. Two specific rules are for the Federal government to share in the same proportion costs of all techniques (structural and nonstructural) used to provide salinity control, and to share costs in proportion to benefits received at the margin. Implications are that nonfederal interests, especially irrigators, would bear most of the costs of salinity control.

**15478.** Cosby, P. C., Bennett, R. A., Peterson, J. R., Moseley, J. T., **Photodissociation and photodetachment of molecular negative ions. II. Ions formed in oxygen,** *J. Chem. Phys.* **63,** No. 4, 1612-1620 (Aug. 15, 1975).

Key words: cross section; drift tube; experimental; molecule; negative ion; $O_2^-$; $O_3^-$; $O_4^-$; photodetachment; photodissociation.

Total photodestruction cross sections for $O_2^-$, $O_3^-$, and $O_4^-$ ions have been measured over a photon energy range of 1.93-2.71 eV using a drift tube mass spectrometer coupled with an argon ion laser and a tunable dye laser. The $O_2^-$ ion is found to photodetach at these photon energies with a cross section which varies from 1.2 to $2.2 \times 10^{-18}$ cm$^2$. The $O_3^-$ ion photodissociates to form $O^-$ over this energy range with a cross section which varies from 0.1 to $7.3 \times 10^{-18}$ cm$^2$ and exhibits structure indicative of the vibrational levels of a predissociating excited state. Structure is also observed in the $O_4^-$ photodestruction cross section which varies from 1.0 to $2.2 \times 10^{-18}$ cm$^2$, and in the $O_2^-$ photodetachment cross section.

**15479.** Taylor, J. K., **Electrochemical analysis,** *Med. Electron. Data,* pp. 39-42 (May-June 1972).

Key words: chemical analysis; coulometry; electrochemical analysis; ion-selective electrodes; polarography.

A brief review is presented, in popular style, of the various electrochemical techniques that are applicable to chemical analysis. Techniques described include polarography, coulometry and potentiometry employing ion-selective electrodes. The use of electrochemical sensors in titrimetry is also pointed out.

**15480.** Harvey, W. W., Kruger, J., **The passivity of gallium arsenide,** (Proc. 3d Int. Conf. on Passivity of Metals, Cambridge, England, July 1970), Paper in *Electrochim. Acta* **16,** 2017-2037 (1971).

Key words: electrochemistry; ellipsometry; gallium arsenide; passivity.

Both p- and n-type gallium arsenide in aqueous electrolytes display the phenomenon of passivity once sufficiently high prepassive cds are attained. This can be achieved for the n-type by illumination, whereby a transition is observed from hole-limited anodic dissolution to passive film formation as the light intensity is increased. Ellipsometric studies reveal that the passive film on either n- or p-GaAs dissolves at a comparatively high rate, and so reaches a steady-state thickness in a rather short time.

Coulometric measurements indicate that the passive film contains gallium and arsenic in their + 3 oxidation states. The ionization of Ga and As at the GaAs/film interface is shown to require holes, in like manner to anodic dissolution in the absence of a passive film. The electrical and optical properties of the passive film suggest uniformity of composition for thickness greater than about 50 Å, whereas thinner films show higher conductivity and refractive index.

The passive film on GaAs supports typically large electric fields and exhibits negligible electronic conductivity and porosity. Under proper conditions a nonpassive anodic film can be formed at potentials in the active region. It is much less soluble than the passive film, continues to thicken indefinitely and therefore appears to be porous.

**15481.** Stiehler, R. D., **Measurement units in engineering and SI,** *Proc. Symp. on Standardization and Metric Conversion for Tunneling, Underground Construction, and Mining, Washington, D.C., May 21, 1974,* pp. 42-48 (Available from the National Technical Information Service, Springfield, Va., 1975).

Key words: International System of Units; measurement units; metric units; SI; systems of units; units of measurement.

Several systems of measurement units used in engineering are discussed. The multiplicity of units for the same quantity and the use of the same name for units of different quantities led to the adoption of the International System of Units (SI) in 1960. This system is *one* of the many metric systems that have been introduced since 1793. SI is a single, rational, coherent system consisting of seven base units, two supplementary units, and units derived from them, always with a factor of one relating them. In this sense, SI is a unitary rather than a decimal system. SI provides one and only one unit for each quantity and does not use the same name for units of two different quantities. Prefixes are provided for convenience in expressing decimal multiples and submultiples of SI units, but they are not essential to SI. The present confusion existing in units for quantities which relate to rotation or vectors is discussed. The inclusion of the radian in such units as moment of inertia, angular momentum, and torque is necessary. Some improvements needed in SI are mentioned. The simplicity and rational nature of SI should relieve the engineer from memorizing equations cluttered with conversion factors dependent on irrational units seldom understood.

**15482.** Radak, B. B., Kosanić, M. M., Šešić, M. B., McLaughlin, W. L., **A calorimetric approach to the calibration of liquid dose meters in high-intensity electron beams,** (Proc. Symp. on Biomedical Dosimetry, IAEA, Vienna, Austria, 1975), Chapter in *Biomedical Dosimetry,* pp. 633-641 (Int. Atomic Energy Agency, Vienna, Austria, 1975).

Key words: absorbed dose rate; calorimetry; chemical dosimetry; electron beams; gamma radiation; radiation dosimetry; radiochromic dyes.

A procedure for calibrating liquid dose meter systems in pulsed high-intensity electron beams is presented. The chemical change produced in solution by a totally absorbed collimated beam has been compared with the heat deposited in a calorimeter exposed to the same beam under identical conditions. Thin film dose meters containing radiochromic dyes, which were known to have a response that does not vary with absorbed dose-rate, were used to monitor the energy absorbed during irradiations. A quasi-adiabatic calorimeter and a cell of the same geometry for containment of the dosimetry solutions are described. The G-value for dye formation in 2-mmol/litre pararosaniline cyanide in 2-methoxy ethanol ($O_2$-saturated) has been determined in the range of dose-rates from $10^{12}$ to $10^{13}$ rad/s.

**15483.** Lide, D. R., Jr., **Preface,** *Proc. Conf. Critical Evaluation of Chemical and Physical Structural Information, Dartmouth College, Hanover, N.H., June 24-29, 1973,* D. R. Lide, Jr. and M. A. Paul, Eds., pp. iii-vii (National Academy of Sciences, Washington, D.C., 1974).

Key words: critical evaluation; crystal structure; data analysis; molecular structure.

The motivations for holding a conference on structural information are discussed. The use of structural data in chemistry, physics and related disciplines is reviewed. The major points brought out during the conference are summarized.

**15484.** Vickers, A., Krasny, J., Tovey, H., **Some apparel fire hazard parameters,** *Proc. Seventh Annual Meeting of the Information Council on Fabric Flammability, New York, N.Y., Dec. 5, 1973,* pp. 205-226 (1975).

Key words: apparel fires; burn injury severity; fabric flammability; FFACTS; garments.

The effect of three parameters, fiber content, fabric content, fabric burn time (a function of ease of ignition and rate of flame spread), and garment configuration and fit, on frequency of involvement in accidental garment fires and on the extent of resulting injury was investigated using fabrics and data from the National Bureau of Standards' Flammable Fabric Accident Case and Testing System (FFACTS). Cellulose-containing fabrics are overrepresented in FFACTS though this may be, in part, the result of biases in the data base. The extent of injury appears to be more closely related to garment configuration and fit than to fiber content and fabric burn time.

**15485.** Cotton, I. W., **Computer networks: Capabilities and limitations,** (Proc. Int. Symp. on Structural Mechanics Software, Univ. of Maryland, College Park, Md., June 12-14, 1974), Paper in *Structural Mechanics Computer Programs,* W. Pilkey, K. Sczalski, H. Schaeffer, Eds., pp. 1043-1055 (University Press of Virginia, Charlottesville, Va., 1974).

Key words: computer networks; networks.

This paper is intended to provide an introduction to the capabilities and limitations involved with the use of today's computer networks. While the treatment is at times brisk, this is intentional, in order to emphasize the applicability of networks for a wide range of applications—and the equally wide range of problems.

**15486.** Grum, F., Cameron, J., **Detector intercomparison results,** *Electro-Opt. Systems Design,* pp. 82-84 (Nov. 1974).

Key words: interlaboratory test; photodiode detectors; photometry.

The results of an intercomparison of measurement of spectral sensitivity of two silicon photodiodes are presented. The comparison was part of the activities of CORM (Council for Optical Radiation Measurement). The manufacturer, nine industrial laboratories, and NBS measured the two cells. The results were statistically analyzed and are presented here in tabular and graphical form.

**15487.** Ayres, T. R., Linsky, J. L., **Stellar model chromospheres. IV. The formation of the H$\epsilon$ feature in the sun (G2 V) and Arcturus (K2 III),** *Astrophys. J.* **201,** No. 1, 212-221 (Oct. 1, 1975).

Key words: chromospheres, stellar; H$\epsilon$ emission; photospheres, stellar.

The formation of the Balmer series member H$\epsilon$ in the near red wing of the Ca II H line is discussed for two cases: the Sun (H$\epsilon$ absorption profile) and Arcturus (H$\epsilon$ emission profile). It is shown that although the H$\epsilon$ source functions in both stars are dominated by the Balmer continuum radiation field through photoionizations, the line formation problems in the two stars are quantitatively different, owing to a substantial difference in the relative importance of the stellar chromosphere temperature inversion compared with the stellar photosphere.

**15488.** Cotton, I. W., **Some trade-offs in the design of minicomputer-based graphic systems,** *Proc. Compcon 74, Washington, D.C., Sept. 1974,* pp. 47-52 (1974).

Key words: computer graphics; cost-benefit analysis; economic analysis; graphics; minicomputers.

This report surveys the evolution of satellite graphics systems from closely coupled display channels to free-standing, minicomputer-based systems. Particular attention is paid to the assignment of functions to the host and satellite systems. Some intuitive types of analysis in support of this assignment are presented, followed by the description of an economic analysis which may be universally applied.

**15489.** Rybicki, G. B., Hummer, D. G., **A note on the "peaking effect" in spherical-geometry transfer problems,** *Mon. Not. Roy. Astr. Soc.* **170,** 423-427 (1975).

Key words: astrophysics; energy loss; radiative transfer; spectral line formation; stellar atmospheres.

This note presents evidence that the claims advanced by Wilson, Tung & Sen regarding the adequacy of Wilson & Sen's half-range moment method for treating the outward peaking of the radiation field in a spherical system are unjustified. In particular, the emergent intensity obtained by Wilson *et al.* is shown to be negative for $0 \leq \mu \lesssim 0.5$ and greatly in error for larger values of $\mu$. A discussion is presented of the essential indeterminacy of the Wilson-Sen half-range method. It is suggested that the good values obtained by Wilson *et al.* for the mean intensity and the Eddington factor arise from their choice of the arbitrary function $A(r)$ to include the known asymptotic forms of the source function.

**15490.** Harrison, J. O., Jr., **Metric conversion and the COMMON computers,** *Proc. COMMON Users Group, Hollywood, Fla., Oct. 14-16, 1974,* 22 pages (1974).

Key words: conversion; FORTRAN; Metric System.

The NBS Computer Program Package for Metric Conversion is written in American National Standard FORTRAN and is designed to compile and run on a wide variety of large scale computers with little or no modification. This paper consists largely of a description of the package and a discussion of its applicability to the COMMON Computers consisting of the IBM System 370, System 360, the 1130, 1800, System 3, and System 7.

The package has been satisfactorily tested on a System 370 Model 165. It may be expected to compile and run satisfactorily on any 370 or on any 360 Model 22.195 of adequate configuration when one of the available AMERICAN NATIONAL STANDARD FORTRAN Compilers is used.

It will probably not run on the 1130, the 1800, the System 3, or System 7 with any IBM supplied FORTRAN compiler due to the extensive use made of features contained in ANS FORTRAN but not in ANS BASIC FORTRAN.

The package should compile and run on a 1130 of adequate configuration with a DNA 1130 ANS FORTRAN Computer with little or no modification.

**15491.** Radebaugh, R., Lawless, W. N., Siegwarth, J. D., **Semi-annual technical report on electrocaloric refrigeration for superconductors,** *ARPA Order 2535,* 17 pages (Available as AD-A008-852 from the National Technical Information Service, Springfield, Va., 1974).

Key words: cryogenics; dielectrics; electrocaloric; heat switches; polarization; refrigeration.

The most significant development in the project for the last six months was the discovery that $SrTiO_3$ glass ceramics showed only heating effects at 4 K for both polarization and depolarization. At the same time, the pitting problem for ceramming temperatures above 1100 °C was partially solved.

Several electrothermal measurements have been done on the $SrTiO_3$ glass-ceramic samples to try to understand why they behave as they do. In addition an apparatus for measurement of DC polarization and hysteresis was completed. The results from those measurements are consistent with the electrothermal measurements. Studies of several new materials have begun in order to better understand the electrocaloric effect near 4 K and in hopes of finding a satisfactory refrigerant material.

The gold-plated multiple leaf heat switch was shown to be useful for heat loads up to about 1 watt at 4 K. The magnetothermal conductivity measurements on single crystal beryllium indicate that it could be used for both the upper and lower switch. Further work on some details of the heat switches has been temporarily suspended in order to concentrate fully on solving the refrigerant material problem.

**15492.** Holmer, C. I., **Estimation of sound power in the free field over a reflecting plane. Errors associated with far field and near field measurements,** *Proc. Noise-Con 75, Gaithersburg, Md., Sept. 15-17, 1975,* pp. 429-438 (Noise Control Foundation, Poughkeepsie, N.Y., 1975).

Key words: error of sound power; far-field power; near-field power; sound power estimation.

A review is presented of several sound power estimation procedures for free field above a reflecting plane condition. Particular emphasis is placed on potential sources of measurement error. Both near field and far field procedures are included in the discussion. Estimates of magnitudes of individual sources of error are discussed.

**15493.** Blackburn, D. L., **An electrical technique for the measurement of the peak junction temperature of power transistors,** *Proc. 13th Annual Reliability Physics Conf., Las Vegas, Nev., Apr. 1-3, 1975* pp. 142-150 (Electron Devices and Reliability Groups, IEEE, New York, N.Y., July 1975).

Key words: method of measurement, electrical; semiconductor devices; temperature, peak; thermal properties; transistors, power, safe-operating area.

A technique is described which uses straightforward electrical measurement procedures to determine the peak junction temperature of power transistors. To determine the peak temperature, standard electrical measurement techniques are altered to account for the difference between the distributions of the calibration and measurement currents in the active area of the device. For relatively uniform temperature distributions, the electrically determined peak junction temperature is only about 6 percent or less below the infrared measured peak temperature whereas the standard electrically measured temperature is about 10 to 25 percent below the infrared measured peak temperature. For severely nonuniform temperature distributions, when only about 20 percent of the total active area of the device is dissipating power at steady state, the electrically determined peak temperature is within 11 percent of the infrared measured peak temperature while the standard electrically measured temperature is more than 40 percent below the infrared measured peak temperature. Device operating conditions for which the junction temperature as determined by standard electrical methods, infrared techniques, and the electrical peak temperature technique equals the manufacturer's specified maximum safe operating temperature are compared with one another and with the manufacturer's specified safe operating limits. It is suggested that the electrical peak temperature technique can be used to generate more realistic safe operating area limits and to determine the validity of specified safe operating limits of power transistors. Devices used in this study include TO-66 and TO-3 encased devices, of both mesa and planar structure, with clip and wire leads, manufactured by a variety of techniques (epi-base, single-diffused, and multiple-diffused).

**15494.** Stenbakken, G. N., Phillips, W. E., Bergsman, S. E., **Terms and definitions for intrusion alarm systems,** *LESP-RPT-0305.00,* 16 pages (U.S. Department of Justice, Law Enforcement Assistance Administration, National Institute of Law Enforcement and Criminal Justice, Washington, D.C., Oct. 1974).

Key words: alarms; burglar alarms; intrusion alarms; intrusion detection.

This document provides definitions in layman language of terms commonly used in the commercial intrusion alarm field.

**15495.** Davis, R. M., **Quality software can change the computer industry,** (Proc. Symp. on Computer Program Test Methods, Chapel Hill, N.C., June 21-23, 1972), Paper in *Program Test Methods,* W. C. Hetzel, Ed., pp. 303-311 (Prentice-Hall, Inc., Englewood Cliffs, N.J., 1973).

Key words: buyer; computer software; marketplace; performance measurement; quality; seller; specifications; validation.

There is probably no more elusive commodity bought and sold today than computer software. We have the almost ludicrous situation of a marketplace where the buyer does not know how to describe his product. The software market practices now existing in software transactions can be displaced by imposing quality control procedures during software production, by demanding specifications or documentation at the time of software transaction and by utilizing validation services and performance measurement services to support the buyer of software.

**15496.** Cali, J. P., **Meaningful measurement in clinical chemistry,** *Proc. San Diego Biomedical Symp., San Diego, Calif., Feb. 6-8, 1974,* **13,** 499-505 (1974).

Key words: accuracy; clinical chemistry; measurement; reference methods; standard reference materials.

Compatibility of measurement in clinical chemistry is of utmost importance if results are to be comparable between laboratories and across time and distance. It is shown that compatibility may most easily be brought about on a measurement system based on accuracy. Five components are required to bring about meaningful measurement in clinical chemistry: (1) A rational, self-consistent system of units of measurement; (2) The materials to realize in practice the defined units and their derivatives; (3) The availability of accurate methods of measurement, analysis, or test based on the well-characterized materials (SRM) of 2; (4) The transfer method; (5) The assurance of the long-term integrity of the measurement process.

The National Bureau of Standards (NBS) is now providing a comprehensive supply of SRM's for the clinical chemistry laboratory. In addition, it is cooperating with professional societies and other government agencies to help develop reference methods.

**15497.** Meyerson, M. R., **The role of the National Bureau of Standards in consumer product safety,** *Proc. Product Liability Prevention Conf., Newark College of Engineering, Newark, N.J., Aug. 22, 1974, IEEE Catalog 74CHO911-8R*, pp. 149-152 (1974).

Key words: consumer; product safety; regulation; standards.

A short history of NBS contributions to consumer product safety is presented. The role of NBS in providing technical support to Federal regulatory agencies, including the Consumer Product Safety Commission, is discussed; several safety-related research projects are described.

**15498.** Davis, R. M., **National Bureau of Standards: Its role in computer security,** *Proc. IBM Data Security Symp., Cambridge, Mass., Apr. 10-11, 1973*, Paper G-520-2838, 11 pages (1973).

Key words: Brooks Bill; computer security; congressional concern; controlled accessibility; data sensitivity; measures of risk; standards; user identification.

Problems of computer security are a major impediment to effective computer utilization today. These problems have technological, legal, moral and ethical aspects. The National Bureau of Standards is concentrating its efforts on the technological aspects of computer security. This NBS project is entitled "Controlled Accessibility to Computer Systems." There is considerable national concern over computer security expressed by Congress, Federal, state and local governments, private groups and citizen committees. The NBS efforts are aimed at meeting these concerns through the development and issuance of guidelines, quantitative measures of risk and effectiveness and standards. These mechanisms for resolving the problem are intended principally for government use although they should be of nearly equivalent utility in the private sector.

**15499.** Miller, G. K., **Shirley Highway Bus-On-Freeway Project evaluation study,** (Proc. Social Experiments & Social Program Evaluation Symp., Gaithersburg, Md., May 22, 1972), Paper in *Social Experiments and Social Program Evaluation*, pp. 40-53 (Ballinger Publ. Co., 1974).

Key words: bus-on-freeway demonstration project; bus rider surveys; bus system evaluation; bus transit; traffic monitoring.

The Shirley Highway Bus-on-Freeway Demonstration Project seeks to ease traffic congestion and shorten travel times for bus and auto travelers commuting during rush hour periods via the Shirley Highway Corridor from Northern Virginia suburbs to employment centers in Washington, D.C. This and other project goals, which include reducing vehicle-caused air pollution and improving bus service, can be attained by effecting an auto-to-bus modal shift by persons commuting via the Corridor area. Three project elements – (1) an exclusive bus lane on the Shirley Highway and bus priority lanes within the District of Columbia; (2) improved bus service including new-look/new-feature buses; and (3) park-and-ride facilities will, according to the premise under which the project was conceived, effect this modal shift and achieve a substantially increased bus market share. The demonstration project is sponsored by the Department of Transportation.

The Technical Analysis Division, National Bureau of Standards, is evaluating project performance with emphasis on the effectiveness of the three project elements. This paper describes evaluation procedures used during the first year and identifies difficulties encountered with various monitoring procedures, as well as presenting preliminary conclusions and plans for future activities.

**15500.** Pallett, D. S., **Noise and the national measurement system,** *Proc. Noise-Conf., Gaithersburg, Md., Sept. 15-17, 1975*, W. W. Lang, Ed., pp. 157-182 (Noise Control Foundation, Poughkeepsie, N.Y., 1975).

Key words: acoustical measurements; acoustics; national measurement system; noise; noise control; noise emission; sound.

This paper indicates the relationship of the acoustical measurements required for the effective implementation of noise abatement and control to the social system termed the National Measurement System. The relevant physical quantities being measured are described, and the infrastructure of the relevant acoustical standardization institutions is indicated. The interactions occurring between the participants in the system are specified, and the impacts, status and trends of the system in adapting to changing technology are discussed. Finally, the interactive role of NBS in the National Measurement System is briefly outlined.

**15501.** Pallett, D. S., **INCE laboratory measurements survey,** *Proc. Noise-Conf., Gaithersburg, Md., Sept. 15-17, 1975*, W. W. Lang, Ed., pp. 313-316 (Noise Control Foundation, Poughkeepsie, N.Y., 1975).

Key words: acoustical measurements; acoustics; impact noise; noise emission; reverberation rooms; sound transmission.

A detailed (eight-page) questionnaire dealing with "Laboratory Measurements of Noise Emission and of Acoustical Properties of Building Elements and Materials" was developed by an INCE Measurement Survey Task Group. Copies of this questionnaire were distributed to more than 120 organizations believed to possess acoustical laboratory facilities. Since acoustical measurements are an integral element in the conduct of acoustical research, it is believed that the results of this survey will be important in the development of research priorities. This paper provides a qualitative description of the questionnaire in order to indicate its scope.

**15502.** Magrab, E. B., Leasure, W. A., Jr., **Research in acoustics and noise measurements at the National Bureau of Standards,** *Proc. Noise-Conf., Gaithersburg, Md., Sept. 15-17, 1975*, W. W. Lang, Ed., pp. 191-200 (Noise Control Foundation, Poughkeepsie, N.Y., 1975).

Key words: audiometric standards; building acoustics; community noise; earphones; environmental noise; instrumentation; measurement methodologies; microphones; psychoacoustics; reverberation room; sound level meters.

A brief description of the National Bureau of Standards' recent research activities in acoustics and noise measurements is presented.

**15503.** Somes, N. F., **Factors influencing structural safety,** Paper 48-7 in *Industrialization in Concrete Building Construction, ACI Publ. SP48,* pp. 177-189 (American Concrete Institute, Detroit, Mich., 1975).

Key words: buildings; codes; design criteria; regulatory system; safety; standards; structural loading.

The paper identifies and briefly discusses the factors that collectively influence the structural safety of a building. These include the probability of occurrence of extreme loading, the factors of design and construction process that determine the building's response, and the function of the building that influences both its design and the consequences of an extensive structural failure. Those factors within the sphere of influence and concern of individuals responsible for the design and supervision or regulation of construction are then discussed in further detail to point out deficiencies in current knowledge or practice. Finally, conclusions and recommendations are made with respect to these deficiencies.

**15504.** Troy, T. N., **Working hand in hand with government,** (Proc. 36th Annual National Packaging Forum, Chicago, Ill., Oct. 7-9, 1974), *Packaging Report F-7432,* 10 pages (The Packaging Institute, U.S.A., New York, N.Y., 1974).

Key words: consumer activism; control proliferation; industry; interaction; package quantity standards; voluntary standards; working with government.

Consumer activism and concomitant opening-up of agency activities means industries must reevaluate their strategies for working with government. NBS, short on regulatory authority but holding a strong suit in technology, is sensitized to economic realities and encourages interaction. Getting your story told early and often, can lead to effective voluntary standards and perhaps draw praise from enlightened consumer advocates. Since inflation and metrication portend another effort to control the proliferation of the number of package sizes, industry may want to reconsider their package quantity standards.

**15505.** McDaniel, C. L., Plante, E. R., **Phase relations involving seed-electrode-insulator materials in MHD,** *Proc. 14th Symp. on Engineering Aspects of Magnetohydrodynamics, Tullahoma, Tenn., Apr. 8-10, 1974,* pp. IV.6.1-IV.6.4 (University of Tennessee, Tullahoma, Tenn., 1974).

Key words: $K_2SO_4$-$LaCrO_3$ system; $K_2SO_4$-MgO system; phase relations; vapor pressure; vaporization equilibria.

The phase relations for the $K_2SO_4$-MgO and $K_2SO_4$-$LaCrO_3$ systems were determined using quenching techniques along with x-ray diffraction and DTA data. The systems were studied in open and closed Pt containers. The $K_2SO_4$-MgO system is a simple eutectic-type with the eutectic located at 1067 °C and ~2 mol percent MgO. A vaporization equilibria diagram was determined from calculations based on data from the condensed state phase diagram and thermodynamic data for pure $K_2SO_4$ assuming ideal behavior. Temperatures at which vapor-liquid equilibria occur were calculated for total pressures of 0.01, 0.1, and 1 atm. Similar principles were applied to predict condensation temperatures when combustion gases are present. Condensed state phase relations for the system $K_2SO_4$-$LaCrO_3$ were determined utilizing sealed Pt tubes for specimen containers. The $K_2SO_4$-$LaCrO_3$ system is a simple eutectic-type with the eutectic located at 1063 °C and ~2 mol percent $LaCrO_3$. The $K_2SO_4$-$LaCrO_3$ system in air (open system) is more complex and can not be represented by a binary-type system.

**15506.** DeGraaf, L. A., Rush, J. J., Livingston, R. C., **Neutron scattering study of the rotational motions and phase transitions in sodium- and caesium-hydrosulfides,** (Proc. IAEA 5th Symp. on Neutron Inelastic Scattering, Grenoble, France, March 1972), Paper IAEA-SM-155/B-6 in *Neutron Inelastic Scattering,* pp. 247-258 (International Atomic Energy Agency, Vienna, Austria, 1972).

Key words: hydrosulfides; libration; neutron scattering; phase transition; quasi-elastic scattering.

The atomic motions in sodium- and caesium-hydrosulfide have been studied with inelastic neutron scattering using a hybrid time-of-flight spectrometer at the NBS reactor. The incident neutron wavelength was 2.43 Å, the time-of-flight resolution 3.7 percent, and the momentum transfer range for elastic scattering covered in this experiment was 0.4-3.5 $Å^{-1}$. NaSH and CsSH are members of a broad group of compounds $M^+(XY)^-$ which have cubic symmetry in the crystalline phase just below the melting point, and a lower symmetry at temperatures below a crystal phase transition point. The measured inelastic neutron scattering spectra above and below the phase transition showed that librational motions about equilibrium orientations persist in passing through the transition. A temperature- and momentum-transfer(Q)-dependent broadening of the quasi-elastic scattering peaks, however, indicates a rapid reorientation of the $SH^-$ ions in the high-temperature cubic phases. The experimentally obtained quasi-elastic scattering peaks have been compared with predictions for the shape of the quasi-elastic scattering as derived from different models, in which the $SH^-$ ions were assumed to reorient with rapid jumps between a limited number of quasi-equilibrium orientations. Plots of the experimental full width at half maximum of the quasi-elastic peaks versus Q show oscillations as predicted by the theoretical calculations. The differences in the rotational disorder in the two compounds studied are discussed and relaxation times $\tau$ and activation energies for the $SH^-$ motions are given. The $\tau$ values derived for fcc NaSH vary from 0.4 to 0.2 ps between $T=103$ °C and $T=212$ °C, while the values for bcc CsSH vary from 2 ps ($T=23$ °C) to 0.90 ps ($T=140$ °C).

**15507.** Yokel, F. Y., Dikkers, R. D., Fattal, S. G., **Strength of load-bearing masonry walls,** *J. Structural Div. Proc. ASCE ST5,* 948-950 (May 1973).

Key words: bricks; buckling; deflection; loads (forces); masonry; moments; slenderness ratio; stability; structural engineering; walls.

This is a closure of the American Society of Civil Engineers Proceedings Paper 8143, published in May 1971.

**15508.** Mitchell, R. A., Woolley, R. M., Chwirut, D. J., **Analysis of composite-reinforced cutouts and cracks,** *AIAA J.* **13,** No. 6, 744-749 (June 1975).

Key words: adhesively bonded joints; composite materials; composite-overlay reinforcement; contour plotting; cracks, reinforcement of; cutouts, reinforcement of; finite element analysis; joints, adhesively bonded; reinforcement, composite overlay; reinforcement, cutouts and cracks.

Finite element computer analyses of the reinforcement of cutouts and cracks in metal sheet, by bonded overlays of composite material, are described. The analyses articulate the separate responses of the sheet, the overlays, and the adhesive. Contour plots of computed stress and strain fields are automatically generated by the computer programs. Strains measured on the surfaces of several reinforced-sheet tensile specimens were, for the most part, in good agreement with strains predicted by the analyses. Qualitative correlations between certain failure modes observed in the test specimens and the stress distributions given by finite element analysis are apparent. The same analytical approach is currently being used to study weld/bond and fastener/bond joints, and it could be used to study other problems such as hole repair in metal or composite sheet and embedded defects in laminar material.

**15509.** Reneker, D. H., Martin, G. M., Rubin, R. J., Colson, J. P., **Effect of polymeric structure on the permeation rate in standard reference material sulfur dioxide permeation tubes,** (Proc. Society of Plastics Engineers ANTEC Conf., San Francisco, Calif., May 1974), *Polym. Eng. Sci.* **15,** No. 1, 11-15 (Jan. 1975).

Key words: density; fluorocarbon copolymer; morphology; permeation; permeation tubes; polymer structure; sulfur dioxide.

Liquid $SO_2$ sealed into tubes made of a fluorocarbon copolymer permeates the walls of the tube at a temperature-dependent but accurately reproducible rate. Sulfur dioxide dispensers made in this way are called permeation tubes and are useful for calibrating instruments that measure $SO_2$ concentrations in air. The National Bureau of Standards calibrates $SO_2$ permeation tubes and makes them available as Standard Reference Materials. The permeation rate in a batch of nominally identical tubes varies enough that each Standard Reference Material tube must be individually calibrated. Changes in the length or radial dimensions of the tubes are much too small to explain most of this variation. An excellent (negative) correlation is found between the measured permeation rate and the density of the polymer (or weight per unit length). Since both the measured density and the permeation rate for this semi-crystalline polymer depend upon morphological factors, but in different ways, x-ray diffraction measurements of the thickness and orientation of the lamellar crystals were made and a mathematical model was set up to identify the morphological factors which can cause variations in the permeation rate.

**15510.** Schneider, S. J., Capps, W., Frederikse, H. P. R., Hosler, W. R., McDaniel, C. L., Plante, E. R., *Proc. US-USSR Colloquium on MHD Power Generation, Moscow, USSR, Feb. 25-27, 1974,* pp. 350-367 (Institute of High Temperatures, Moscow, USSR, 1975).

Key words: electrical conductivity; MHD materials; phase equilibrium; slag; vaporization; viscosity.

The National Bureau of Standards, under sponsorship of the Office of Coal Research, has initiated a program of materials research appropriate to open cycle, coal fired MHD. The program consists of several interrelated projects in the areas of vaporization, viscosity, electrical conductivity and phase equilibria. This paper is intended as a review of the progress achieved thus far. Initial work has concentrated on the behavior of coal slag in MHD environment since there is definite lack of data in this area. Slag specimens have been obtained under real MHD conditions and analyzed by a variety of techniques. For the most part slags are composed largely of $Al_2O_3$-$FeO$-$Fe_2O_3$-$SiO_2$ mixtures. The portions of each as well as the amount of glassy (liquid) or crystalline material vary depending upon the location sampled in the MHD system. From the data obtained on real slags, synthetic model slags were prepared for more systematic study. Viscosity-temperature relationships of both real and model slags indicate similar temperature coefficients but large differences in viscosity values at one given temperature (e.g, at 1500 °C viscosity range between 1.0 to 2.1 $\log_{10}$ poises). The electrical conductivity of a number of slags have also been determined to 1700 K in various environments. Electrical conduction is apparently caused by the transfer of electrons between $Fe^{2+}$ and $Fe^{3+}$ and is largely electronic rather than ionic. Vaporization studies have concentrated on the evaporation behavior of synthetic slags under their own vapor pressure. These data indicate the initial stages of evaporation are governed by a nonequilibrium process involving the decomposition of $Fe_3O_4$. Equilibrium, however, is achieved with respect to the evaporation of $SiO_2$ from the slag solution (activity of $SiO_2$ is near unity). Important also to MHD is the effect of seed reactions on insulators and electrodes. In this respect the phase equilibrium diagrams for the $K_2SO_4$-$MgO$ and the $K_2SO_4$-$LaCrO_3$ system have been determined. Both systems (under their own vapor pressure) behave in a similar manner with melting beginning a few degrees below the melting point of $K_2SO_4$ (1069 °C).

**15511.** Whittaker, J. K., **A signal processing system for a semiconductor detector ladder,** *Proc. IEEE Thirteenth Scintillation and Semiconductor Counter Symp., Washington, D.C., Mar. 1-3, 1972,* pp. 444-452 (June 1972).

Key words: computer; detector-ray; discriminator; emitter-couple; integrated circuit; signal processor.

The resolution of the NBS high resolution electron spectrometer has been improved recently by installing a new 48 channel detector array at its focal plane, in place of the original channel array that has been in use for some time. This has necessitated the design and construction of a new electronics system to accommodate the increased amount of information from the detectors. The new detector system digitally processes the signals from the detectors after amplification and discrimination. It is coupled on line to a computer which accumulates and manipulates the processed data.

An effective and economical solution has been found for the construction of a large logic network for nuclear data accumulation. The functions provided are those normally found only in modular form; e.g., coincidence, with the necessary time resolution. Time differences for simultaneous signal paths have been restricted to ± 1 ns maximum with a minimum pulse width of 5 ns for any pulse input. The entire system is dc coupled and the pulse pair resolution, measured during construction, is 10 ns.

**15512.** White, H. J., Jr., **Data centers and data evaluation,** *Proc. Conf. on Thermodynamics and National Energy Problems, Warrenton, Va., June 10-12, 1974,* pp. 372-382 (National Academy of Sciences, Washington, D.C., 1975).

Key words: data center; data compilation; data evaluation; energy program; thermodynamics; transport properties.

The expected uses for numerical data in the national energy program are discussed. The uses and activities of mission-oriented data centers and discipline-oriented data centers in mission-oriented tasks are also discussed. It is concluded that both types of activities will be needed for the effective carrying out of currently proposed energy initiatives. A listing of existing discipline-oriented data centers in the area of thermodynamics and transport properties that could make a contribution to a national energy program is given.

**15513.** Eisenhart, C., **Samuel S. Wilks and the army experiment design conference series,** *Proc. Twentieth Conf. on the Design of Experiments in Army Research Development and Testing, Ft. Belvoir, Va., Oct. 23-25, 1974,* ARO Report 75-2, Pt. 1, 1-47 (Army Dept., Chief of Research, Development and Acquisition, 1974).

Key words: Annals of Mathematical Statistics; Army Experiment Design Conferences; Dodd, E. L.; educational testing; history of mathematical statistics in the U.S.A.; Hotelling, Harold; likelihood-ratio tests; multivariate analysis; order statistics; Princeton University; Rietz, H. L.; Shewhart, W. A.; statistical tolerance limits; Wilks, S. S.; Wishart, John.

A biography of Professor Samuel Stanley Wilks (1906-1964) of Princeton University, with particular attention to his early life, notes on the persons who shaped his professional development, review of his many facetted professional career and his role in initiating and launching the U.S. Army's annual series of Conferences on the Design of Experiments in Army Research, Development and Testing.

**15514.** Yokel, F. Y., **Stability and load capacity of members with no tensile strength,** *J. Structural Div. Proc. ASCE ST4*, 788-789 (Apr. 1973).

Key words: buckling; compression members; concrete; cracking; deflection; eccentricity; equilibrium; loads (forces); masonry; stability; stress distribution; structural engineering.

This is a closure of the discussion of ASCE Proceedings Paper 8253 by Felix Y. Yokel.

**15515.** Ludtke, P. R., **Register of hydrogen technology experts,** *NASA CR-2624*, 80 pages (National Aeronautics and Space Administration, Washington, D.C., Oct. 1975). (Available from National Technical Information Service, Springfield, Va. 22161.)

Key words: accident investigation; hydrogen energy systems; hydrogen experts; hydrogen fuel; hydrogen production; hydrogen properties experts; hydrogen safety; hydrogen systems; hydrogen technology; hydrogen transportation.

This register presents the names of approximately 235 individuals who are considered experts, or very knowledgeable, in various fields of technology related to hydrogen. Approximately 90 organizations are represented. Each person is listed by organizational affiliation, address, and principal area of expertise. The criteria for selection of names for the register are extensive experience in a given field of work, participation in or supervision of relevant research programs, contributions to the literature, or being recognized as an expert in a particular field. The purpose of the register is to present, in easy form, sources of dependable information regarding highly technical areas of hydrogen technology, with particular emphasis on safety. The register includes two indexes: an alphabetical listing of the experts and an alphabetical listing of the organizations with which they are affiliated.

**15516.** Kusch, P., Hessel, M. M., **Perturbations in the $A\ {}^1\Sigma_u^+$ state of $Na_2$,** *J. Chem. Phys.* **63,** No. 9, 4087-4088 (Nov. 1, 1975).

Key words: alkali dimer; magnetic rotation; molecular constants; perturbations; sodium molecule; spectroscopy.

Perturbations have been observed in the $A\ {}^1\Sigma_u^+$ state of the diatomic sodium molecule. For each rotational perturbation three discontinuities have been observed. This indicates the ${}^1\Sigma$ state is perturbed by a ${}^3\Pi$ state.

**15517.** Burns, G. W., Hurst, W. S., **Thermocouple thermometry,** (Proc. Symp. European Conf. on Temperature Measurement, Teddington, England, Apr. 9-11, 1975), Chapter 4 in *Temperature Measurement,* B. F. Billing and T. J. Quinn, Eds., Inst. Phys. Conf. Ser. No. 26, pp. 144-161 (1975).

Key words: base-metal thermocouples; cryogenic thermocouples; noble-metal thermocouples; nonstandardized thermocouples; refractory metal thermocouples; standardization; temperature measurement; thermocouples; thermometry.

A broad overall view of the current status of thermocouple thermometry is given. The salient features and limitations of standard thermocouple types are reviewed, and some of the recent changes in standardization are noted. Some of the nonstandardized thermocouple types are discussed, giving particular attention to those employed at cryogenic temperatures and to those intended for use above the temperature limits or under conditions where the standard types are inadequate. Commonly used materials for insulation and protection are described, and some examples are noted of applications where stringent requirements are placed on thermocouple performance.

**15518.** Burley, N. A., Burns, G. W., Powell, R. L., **Nicrosil and Nisil: Their development and standardization,** (Proc. Symp. European Conf. on Temperature Measurement, Teddington, England, Apr. 9-11, 1975), Chapter 4 in *Temperature Measurement,* B. F. Billing and T. J. Quinn, Eds., Inst. Phys. Conf. Ser. No. 26, pp. 162-171 (1975).

Key words: calibration; nickel-base alloys; nickel-chromium alloys; nickel-silicon alloys; reference tables; temperature measurements; thermal emf; thermocouples; thermoelectric reference data; thermometry.

This paper reviews the development of the new nickel-base thermocouple alloys Nicrosil and Nisil by the Australian Defense Standards Laboratories (now the Materials Research Laboratories of the Australian Government Department of Defence), and their standardization by the U.S. National Bureau of Standards.

The relevant properties of the new alloys are described, and they are shown to have much higher environmental, structural and thermoelectrical stabilities, and to be more suitable for use at the higher operating temperatures, than existing Type K nickel-base thermocouple materials.

The standardization procedures are summarized, including the derivation of reference tables. Calibration data were obtained over the range 5 K to 1575 K, from prototype alloys specially fabricated by five major manufacturers of base-metal thermocouple alloys in the UK, the USA and Sweden.

**15519.** Kidnay, A. J., Miller, R. C., Parrish, W. R., Hiza, M. J., **Liquid-vapour phase equilibria in the $N_2-CH_4$ system from 130 to 180 K,** *Cryogenics* **15,** No. 6, 531-540 (Sept. 1975).

Key words: Henry's constants; liquid-vapor phase equilibria; methane; nitrogen.

Isothermal composition measurements for both the equilibrium liquid and vapour phases have been determined for the nitrogen + methane system at eight temperatures between 112.00 and 180.00 K, and at pressures from 1 to 49 atm (1 to 50 bar). The internal consistency of these data is checked by comparing experimental and calculated thermodynamically consistent vapour phase compositions. Derived Henry's constants are used to provide a comparison between these data and those of other investigators.

**15520.** Ekin, J. W., **Critical currents in granular superconductors,** *Phys. Rev. B* **12,** No. 7, 2676-2681 (Oct. 1, 1975).

Key words: critical current densities; critical currents; granular aluminum films; granular films; Type II superconducting films; vortex pinning.

A relatively simple principle is experimentally demonstrated for producing extremely low critical-current density materials for application in quantum flux-flow devices. Essentially the technique consists of making the scale of structural disorder in the material small compared with the vortex core size. The smaller this ratio, the smaller the effects of bulk pinning, and the smaller the resulting critical-current density. Data for this study were obtained using superconducting granular aluminum films evaporated in a cylindrical geometry designed to eliminate edge-pinning effects. The data show $J_c$ to exhibit a sharp minimum as a function of grain size, with the lowest values of $J_c$ occurring in those films having the smallest ratio $\langle D\rangle/(\zeta_0 l)^{1/2}$. Here $\langle D\rangle$ is the average grain size, $\zeta_0$ is the BCS coherence length, and $l$ is the electronic mean free path. The normal-state resistivity $\rho_n$ can be used as an index of $\langle D\rangle/(\zeta_0 l)^{1/2}$ for the granular aluminum system, with the lowest critical-current densities occurring in films prepared to have a $\rho_n$ of about 10 $\mu\Omega$ cm. In addition to discussing the dependence of the critical current on microstructure, data on the temperature dependence and electric field dependence of $J_c$ are presented.

**15521.** Ely, J. F., Hanley, H. J. M., **The statistical mechanics of non-spherical polyatomic molecules. Application to the properties of carbon dioxide,** *Mol. Phys.* **30,** No. 2, 565-578 (1975).

> Key words: carbon dioxide; Clausius-Mossotti function; intermolecular forces; *m*-6-8 potential quadrupolar gas; second virial coefficient; viscosity coefficient.

Collision integrals and equilibrium pressure and dielectric second virial coefficients are calculated for a nonspherical *m*-6-8 model potential energy function. The results are applied in a correlation of the physical properties of carbon dioxide. It is shown that the inclusion of nonspherical contributions in the calculation of the collision integrals has a small but significant effect with respect to the accurate representation of data. The Mason-Monchick approximation that nonspherical molecules collide with fixed relative orientations is briefly discussed. Agreement between calculated and experimental values for the viscosity coefficient, the thermal conductivity coefficient, the second virial coefficients and the isotopic thermal diffusion factor is generally satisfactory.

**15522.** Weston, W. F., Naimon, E. R., Ledbetter, H. M., **Low temperature elastic properties of aluminum 5083-0 and four ferritic nickel steels,** (Proc. American Society for Testing and Materials Symp. on Properties of Materials for Liquefied Natural Gas Tankage, Boston, Mass., May 21-22, 1974), *Am. Soc. Test. Mater. Spec. Tech. Publ.* **579,** pp. 397-420 (1975).

> Key words: aluminum alloy; bulk modulus; compressibility; Debye temperature; elastic constant; nickel steels; Poisson's ratio; shear modulus; sound velocity; Young's modulus.

The low-temperature elastic properties have been determined for five commercial alloys that have possible structural applications at cryogenic temperatures. The alloys are 5083-0 aluminum and four ferritic steels: 3.5, 5, 6, and 9 percent nickel. An ultrasonic (10 MHz) pulse-superposition method was used to measure longitudinal and transverse wave velocities. Using the velocities and the mass density as input, the following elastic constants were calculated: longitudinal modulus, Young's (tensile) modulus, shear (rigidity) modulus, bulk modulus (reciprocal compressibility), and Poisson's ratio. Measurements were made semicontinuously from 300 to 4K. The room-temperature composition dependence of iron-nickel alloys is reviewed comprehensively up to 12 percent nickel. Debye temperatures were calculated from the elastic constants. A discussion is given of the temperature dependences of the elastic constants and differential relationships among the elastic constants.

**15523.** Weston, W. F., **Low-temperature elastic constants of a superconducting coil composite,** *J. Appl. Phys.* **46,** No. 10, 4458-4465 (Oct. 1975).

> Key words: bulk modulus; composite; compressibility; elastic compliance; elastic stiffness; piezoelectric oscillator; Poisson's ratio; shear modulus; Young's modulus.

A resonant piezoelectric oscillator method for measuring elastic moduli was applied to composite materials. The complete set of elastic compliances of a superconducting coil composite was determined semicontinuously between 4 and 300 K. Also, two moduli of a layered fiber-glass-epoxy composite were determined; this composite is essentially the matrix material of the coil composite. The Young's moduli, shear moduli, Poisson ratios, and elastic stiffness coefficients are also reported. Results agree closely with elastic data obtained by conventional testing methods.

**15524.** Meijer, P. H. E., Niemeijer, T., **Quantum-mechanical approximation to the ground state of cerous magnesium nitrate,** *Phys. Rev. B* **11,** No. 7, 2612-2623 (Apr. 1, 1975).

> Key words: antiferromagnetism; cerous magnesium nitrate; dipole-dipole coupling; ferromagnetism; ground state; permutation group; quantum mechanics; spin cluster; spin-Hamiltonian.

In this paper we perform a complete quantum-mechanical calculation of the ground-state energy of a system of spins 1/2 that are coupled by dipole-dipole forces. The only hypothesis used is the assumption that the ground state has two times the periodicity of the underlying magnetic lattice. This paper is the application to a specific crystal of results derived in a preceding paper. The Hamiltonian is decomposed in eight invariant pieces each with its own coupling constant. The basis wave functions are decomposed according to the eight one-dimensional representations of the permutation group that leaves the cluster invariant. The results are given in the form of tables applicable to any compound that has the spins situated on a Bravais lattice. The calculation is applied to cerous magnesium nitrate and we show that the results for the lowest state of each representation are leading to a spectrum that is different from the results obtained with the classical or Hartree method. Although the lowest state is still the same antiferromagnetic configuration, it turns out now that this state lies barely below the ferromagnetic state; the order in which the ferromagnetic and antiferromagnetic levels appear is different from the order obtained in a classical calculation.

**15525.** Arora, V. K., Peterson, R. L., **Quantum theory of Ohmic galvano- and thermomagnetic effects in semiconductors,** *Phys. Rev. B* **12,** No. 6, 2285-2296 (Sept. 15, 1975).

> Key words: galvanomagnetism; quantum transport theory; semiconductors; thermomagnetism.

A density-matrix formalism developed earlier for the evaluation of Ohmic magnetoconductivity is further elaborated and applied to other magnetotransport effects in nonpolar semiconductors in the presence of a magnetic field of arbitrary strength. The difference from earlier transport theories lies in a natural extension of the scattering dynamics beyond the strict Born approximation. The well-known divergence difficulties of older theories, usually removed by any of a number of *ad hoc* cutoff procedures, do not appear here. The transverse-conductivity expression turns out to be equivalent to that of some earlier theories of cyclotron resonance extrapolated to zero frequency, but derived in a different way. When applied to elastic scattering of electrons in a simple model of a semiconductor, the theory gives galvanomagnetic and thermomagnetic coefficients within the range of values usually seen experimentally, showing the basic correctness of the theory. It is then applied to the magnetophonon effect, where the resonance peaks are shown to be finite. An interesting inversion of one of the peaks in the Ettingshausen-Nernst coefficient is found. Landau-level broadening and phonon drag are not included in the present paper, although they can be incorporated when deemed important.

**15526.** Soulen, R. J., Jr., Marshak, H., **The establishment of an absolute temperature scale using noise and nuclear orientation thermometry,** (Proc. 14th Int. Conf. on Low Temperature Physics, Otaniemi, Finland, Aug. 14-20, 1975), Paper in *Low Temperature Physics-LT 14,* **4,** 60-63 (Am. Elsevier Publ. Co., New York, N.Y., 1975).

Key words: dilution refrigerators; γ-ray anisotropy thermometry; Josephson junctions; noise thermometry; temperature.

We report on the present status of a comparison of the temperatures obtained from a Josephson junction noise thermometer and a $^{60}$Co γ-ray anisotropy thermometer. The data reported here cover the range of 12 to 35 mK in 16 steps varying from ~ 0.5 to ~ 2 mK. Owing to improvements in: temperature stability of our dilution refrigerator, analysis of noise thermometer data, and the γ-ray data acquisition system, these new results have considerably less scatter than those reported previously. The overall agreement between both thermometers is about 1 percent.

**15527.** Utton, D. B., Soulen, R. J., Jr., Marshak, H., **Intercomparison of temperature scales using low transition-temperature superconductors,** (Proc. 14th Int. Conf. on Low Temperature Physics, Otaniemi, Finland, Aug. 14-20, 1975), Paper in *Low Temperature Physics-LT 14,* **4,** 76-79 (Am. Elsevier Publ. Co., New York, N.Y., 1975).

Key words: copper NMR thermometer; γ-ray thermometer; noise thermometer; superconductive transition temperatures; temperature.

Recent studies of several superconductors (W, Be, $Ir_{80}Rh_{20}$, Ir, $AuAl_2$, and $AuIn_2$) showed them to provide useful temperature reference temperatures below 0.5 K. Samples of each material were used to intercompare the temperature scales obtained from noise, γ-ray, and copper NMR thermometers from 0.024 to 0.208 K. The results of this intercomparison are given in tabular form.

**15528.** Naimon, E. R., Ledbetter, H. M., Weston, W. F., **Low-temperature elastic properties of four wrought and annealed aluminium alloys,** *J. Mater. Sci.* **10,** No. 8, 1309-1316 (Aug. 1975).

Key words: aluminium; aluminium alloys; bulk modulus; compressibility; Debye temperature; elastic constants; elasticity; Poisson ratio; pulse-echo method; sound velocity; Young's modulus.

The elastic properties of four annealed polycrystalline commercial aluminium alloys were studied between 4 and 300 K using a pulse-superposition method. Results are given for longitudinal sound velocity, transverse sound velocity, Young's modulus, shear modulus, bulk modulus (reciprocal compressibility), Poisson's ratio, and elastic Debye temperature. The elastic stiffnesses of the alloys increase 4 to 13 percent on cooling from room temperature to liquid helium temperature. The elastic constant-temperature curves exhibit regular behaviour.

**15529.** Miller, A., McLaughlin, W. L., **Imaging and measuring electron beam dose distributions using holographic interferometry,** *Nucl. Instrum. Methods* **128,** 337-346 (1975).

Key words: calorimetry; depth dose; dose distributions; dosimetry; electron beams; holographic interferometry; holography; isodose; radiation imaging; radiation measurements.

Holographic interferometry was used to image and measure ionizing radiation depth-dose and isodose distributions in transparent liquids. Both broad and narrowly collimated electron beams from accelerators (2-10 MeV) provided short irradiation times of 30 ns to 0.6 s. Holographic images and measurements of absorbed dose distributions were achieved in liquids of various densities and thermal properties and in water layers thinner than the electron range and with backings of materials of various densities and atomic numbers. The lowest detectable dose in some liquids was of the order of a few kRad. The precision limits of the measurement of dose were found to be ±4 percent. The procedure was simple and the holographic equipment stable and compact, thus allowing experimentation under routine laboratory conditions and limited space.

**15530.** Tobler, R. L., Mikesell, R. P., Durcholz, R. L., Reed, R. P., **Low temperature fracture behavior of iron-nickel alloy steels,** (Proc. American Society for Testing and Materials Symp. on Properties of Materials for Liquefied Natural Gas Tankage, Boston, Mass., May 21-22, 1974), *Am. Soc. Test. Mater. Spec. Tech. Publ.* **579,** pp. 261-287 (1975).

Key words: crack propagation; cryogenics; fracture toughness; mechanical properties; nickel steels.

Fracture toughness tests over the interval 298 to 4 K and fatigue crack growth rate tests at 298, 111, and 76 K are reported on selected iron-nickel (Fe-Ni) alloys which are commercially available for potential use in storage or transportation of liquefied natural gas (LNG). These alloys include Fe-6Ni and Fe-5Ni in newly developed three-step heat treatments and Fe-9Ni in the quenched and tempered condition. Linear elastic fracture mechanics parameters ($K_Q$, $K_{Ic}$) and $J$-integral ($J_{Ic}$) test data are presented for 1.25-in.-thick compact specimens. Discussion includes comparisons of fatigue crack growth rate and fracture data between alloys.

**15531.** Brauer, G. M., Termini, D. J., **Modification of collagenous surfaces by grafting polymeric side chains to collagen and soft and hard tissues,** Chapter 8 in *Advances in Chemistry Series,* No. 145, pp. 175-195 (American Chemical Society, New York, N.Y., 1975).

Key words: bone; collagen; grafting modification of collagenous surfaces; hard tissue; rat skin; soft tissue.

Collagen, soft tissue, and bone can be modified at 37 °C by allowing them to react with acrylic, methacrylic, or vinyl monomers using ceric ions, persulfate-bisulfite or comonomers forming donor-acceptor complexes as initiators. The polymeric methacrylate side chain is chemically attached to collagen; similar bonding may occur on reaction with other monomers. With rat skin, the reaction takes place mainly at the surface whereas a higher yield of more homogeneous product is formed on grafting onto collagen. Grafting onto bone is best accomplished with persulfate-bisulfite initiator. Modification of the collagenous surface is indicated by changes in wettability, decreased water sorption, and improved resistance to mold growth; e.g, hydrophobic, oleophobic surfaces are obtained with fluorinated monomers. The modified surfaces could be useful as adhesion-promoting liners for restorative materials.

**15532.** Geltman, S., **Coulomb correction for strong-field multiphoton free-free absorption,** *J. Phys. B Letter to Editor* **8,** No. 15, L374-L376 (1975).

Key words: absorption; bremsstrahlung; electrons; ions; laser; plasma.

A correction factor, which arises from the logarithmic phase factor in Coulomb waves, is shown to be necessary in the treatment of multiphoton free-free absorption in ultrastrong laser fields.

**15533.** Weston, W. F., Ledbetter, H. M., **Low-temperature elastic properties of a nickel-chromium-iron-molybdenum alloy,** *Mater. Sci. Eng. Short Commun.* **20,** 287-290 (1975).

Key words: bulk modulus; compressibility; Debye temperature; elastic constants; nickel-base alloys; Poisson's ratio; shear modulus; sound velocity; Young's modulus.

The elastic properties of a nickel-chromium-iron-molybdenum alloy were determined between room temperature and liquid-helium temperature by measuring both the longitudinal and transverse sound-wave velocities in a polycrystalline material. These properties include: the longitudinal modulus, Young's modulus, the shear modulus, the bulk modulus (reciprocal compressibility), and Poisson's ratio. Except for a small anomaly in the bulk modulus, this material exhibits regular elastic-constant/temperature behavior.

**15534.** Petersen, F. R., Evenson, K. M., Jennings, D. A., Wells, J. S., Goto, K., Jiménez, J. J., **Far infrared frequency synthesis with stabilized $CO_2$ lasers: Accurate measurements of the water vapor and methyl alcohol laser frequencies,** *IEEE J. Quantum Electron.* **QE-11,** No. 10, 838-843 (Oct. 1975).

Key words: absolute frequency measurements; laser frequency synthesis; water vapor laser.

A far infrared (FIR) frequency synthesis technique using saturated-absorption stabilized $CO_2$ lasers and a point-contact diode has been used to measure frequencies of a number of strong CW $H_2O$, $D_2O$, and $CH_3OH$ laser lines. The first frequency measurements of the 79-$\mu$m $H_2O$, the 73- and 108-$\mu$m $D_2O$, and 11 $CO_2$-pumped CW $^{12}CH_3{}^{16}OH$ laser lines are reported. This measurement is the first demonstration of the general usefulness of $CO_2$ lasers for accurate synthesis of FIR frequencies.

**15535.** Patel, P. R., Brown, W. E., **Thermodynamic solubility product of human tooth enamel: powdered sample,** *J. Dent. Res.* **54,** No. 4, 728-736 (1975).

Key words: dental caries; hydroxyapatite; ion activity product; solubility; tooth enamel.

Solubility of human dental enamel in $H_3PO_4$ was studied in the pH range of 4.5 to 7.6. Thermodynamic solubility of the enamel mineral was calculated in terms of the ion activity product, $(Ca^{2+})^5(PO_4^{3-})^3(OH^-)$, for hydroxyapatite. The solubility product varied from $7.2 \times 10^{-53}$ to $6.4 \times 10^{-58}$ mol$^9$ liter$^{-9}$ depending on the cumulative amount of the dissolution of the solid in a series of repetitive sequences of solubility experiments.

**15536.** Molino, J. A., **A proposed method for measuring the annoyance due to speech interference by noise,** (Proc. NASA Minisymposium, Hampton, Va., Jan. 21-22, 1975), Paper in *NASA Technical Memorandum, Noise and Speech Interference Proceedings of Minisymposium,* W. T. Shepherd, Ed., NASA TM X-72696, 15 pages (Available from National Technical Information Service, Springfield, Va., 22151 and STIF/NASA Scientific and Technical Information Facility, College Park, Md., 20740, 1975).

Key words: aircraft noise; annoyance; noise; psychoacoustics; speech interference.

A method is proposed to measure both the interference of speech by noise and the annoyance caused by such interference. It is based upon a nonverbal preference procedure developed at the National Bureau of Standards called an "acoustic menu." Subjects listen to audible speech signals in a background of noise. At the same time the subjects are given a limited opportunity to select the background noise. By analyzing the preference structure for the various types of interfering noise, as well as the decrement in speech intelligibility suffered with each noise, information can be obtained on both annoyance and interference.

**15537.** Radebaugh, R., Holste, J. C., Siegwarth, J. D., **Thermometric characteristics of some 1/8 W carbon resistors in the millikelvin range,** *Proc. Fifth Int. Cryogenic Engineering Conference, Kyoto, Japan, May 7-10, 1974,* Paper H11, pp. 253-255 (IPC Science & Technical Press, Kent, England, 1974).

Key words: carbon resistors; cryogenics; liquid helium; millikelvin; thermometry.

Gotoh and Awano have reported on the useful characteristics of 1/8 watt 100 Ω Matsushita carbon resistors (grade ERC-18GK) as thermometers for the region 0.4 and 4.2 K. We report here measurements on the resistance characteristics of this grade of resistors from 11 mK to 4 K. Nominal resistances of 56 Ω, 100 Ω and 220 Ω have been measured. We find that the 56 Ω resistor is useful as a thermometer down to at least 11 mK. Its sensitivity increases rather rapidly below 100 mK, which is a desirable feature because it is in this region where measuring power levels must be kept extremely small. At 20 mK the resistance of the 56 Ω resistor is about 4000 Ω, that of the 100 Ω resistor is about $5 \times 10^5$ Ω, and that of the 220 Ω resistor is about $10^8$ Ω. A comparison of the resistance behavior of units immersed in dilute $He^3$-$He^4$ with those outside the liquid will also be made.

**15538.** Haight, W. C., **Establishment of OS AIDS as an RTOS task,** *Interchange* **5,** No. 3, 5-6 (June 1974).

Key words: debugging; Interdata 70; OS AIDS; RTOS; software.

A technique is detailed that allows OS AIDS, a debugging utility program, to be established as an RTOS system task. This expands the RTOS environment to comprehensively support all phases of program preparation at the user level. Modifications that must be made to AIDS and to the Task Establisher Task, TET, prior to task creation are defined. Conceptual problems that can occur when AIDS runs in a multi-programming environment are discussed.

**15539.** Manning, J. R., **Theory of diffusion,** (Proc. American Society for Metals Seminar on Diffusion, Cleveland, Ohio, Oct. 13-14, 1972), Chapter 1 in *Diffusion,* pp. 1-24 (American Society for Metals, Metals Park, Ohio, 1973).

Key words: atomic diffusion mechanisms; diffusion; random walk; review article; thermodynamic diffusion equations; vacancy diffusion mechanisms.

A survey of the theory of diffusion with emphasis on the role of atomic diffusion mechanisms. Random walk diffusion equations, modifications of these equations by atomic driving forces, correlation effects, vacancy wind effects, temperature and pressure dependences, the general thermodynamic diffusion equations, and the relation of planar diffusion to three-dimensional diffusion and the diffusion tensor are discussed.

**15540.** Goodman, L. J., Colvett, R. D., Caswell, R. S., **An international neutron dosimetry intercomparison,** *Proc. Second Symp. on Neutron Dosimetry in Biology and Medicine, Neuherberg/Munchen, Germany, Sept. 30-Oct. 4, 1974,* EUR 5273d-e-f, pp. 627-662 (1974).

Key words: absorbed dose; intercomparison; kerma; neutron dosimetry; neutron radiobiology; neutron therapy.

An International Neutron Dosimetry Intercomparison, sponsored by the International Commission on Radiation Units and

Measurements, has been completed at the Radiological Research Accelerator Facility at Brookhaven National Laboratory. Fourteen groups of scientists, from six countries, performed measurements to determine the separate neutron and photon (x- and gamma-ray) tissue kermas in free air for four energies of monoenergetic neutrons, 15.5, 5.5, 2.1, and 0.67 MeV, and for a source of fission neutrons, $^{252}$Cf. For the two highest energies, measurements were also made to determine the separate absorbed doses in tissue of neutrons and of photons at three depths in a large water phantom.

**15541.** Rosenthal, R., **Accessing online network resources with a network access machine,** *Proc. IEEE Intercon 1975 Conf. Record on Access to Computer Networks, Session 25, New York, N.Y., Apr. 8-10, 1974,* 4 pages (Institute of Electrical and Electronics Engineers, Inc., New York, N.Y., 1974).

Key words: access procedures; command language; computer networks; macros; minicomputers; protocols.

While a large variety of computer resources is available to online users of computer networks, access to these resources is often complex and cumbersome. This paper describes a Network Access Machine (NAM) which acts as a network access point for a user at his terminal and assists the user through the automatic execution of access procedures.

**15542.** Manning, J. R., **Non-random diffusion in ionic crystals,** (Proc. Conf. on Mass Transport Phenomena in Ceramics, Cleveland, Ohio, June 3-5, 1974), Chapter in *Mass Transport Phenomena in Ceramics,* A. R. Cooper and A. H. Heuer, Eds., pp. 1-15 (Plenum Press, New York, N.Y., 1975).

Key words: correlation factor; diffusion; divacancy; driving force for diffusion; impurity diffusion; ion drift velocity; nonrandom diffusion; vacancy wind effect.

Nonrandom diffusion can result both from the presence of atomic driving forces and from the motion of defects in a crystal. Defect-related nonrandom effects appear in two different ways in the kinetic diffusion equations, as correlation effects and as defect-wind effects. The origins of these effects during diffusion in a driving force are discussed. Kinetic expressions for the drift velocity $\langle v_F \rangle$ are derived from expressions for the effective frequencies of independent atom jumps and are related to the tracer diffusion coefficient D*. For impurity diffusion in an electric field, deviations from the Nernst-Einstein relation result from defect-wind effects. Recently developed equations for the ionic-impurity drift-mobility when diffusion occurs via divacancies moving on one of the sub-lattices in the NaCl structure are summarized. Possible extensions of the simple equations used here to more complex situations are discussed.

**15543.** Roestamsjah, Wall, L. A., Florin, R. E., Aldridge, M. H., Fetters, L. J., **Degrading mixtures of monodisperse poly-$\alpha$-methylstyrenes: Rates and anomalous molecular weight distributions,** *J. Polym. Sci. Polym. Phys. Ed.* **13,** 1783-1787 (1975).

Key words: mixtures; molecular weight distribution; monodisperse poly-$\alpha$-methylstyrene; thermal degradation.

When a mixture of two monodisperse samples of poly-$\alpha$-methylstyrene is thermally degraded, the components behave independently as a first approximation, as shown by GPC and rate of volatilization data. The ratio $M_w/M_n$, before approaching the ultimate value of 2.0, first goes through a minimum at a much lower value.

**15544.** Rosenthal, R., Watkins, S. W., **Automated access to network resources. A network access machine,** *Proc. 1974 Symp. on Computer Networks: Trends and Applications, Gaithersburg, Md., May 23, 1974,* pp. 47-50 (Institute of Electrical and Electronics Engineers, Inc., New York, N.Y., 1974).

Key words: automated computer access; computer networking; macro processor; minicomputer-based systems; operating systems.

A minicomputer based Network Access Machine to establish the access path between a user at a terminal and a computer network resource is described. The minicomputer maintains a file directory from which access procedures are referenced. Access procedures take the form of macros which expand to produce machine dependent dialogue. The dialogue consists of the messages to be sent to the computer network and the expected responses. Actual responses are compared with the expected response to ensure that resource access is proceeding normally.

**15545.** Fife, D. W., **Network management for expanded resource sharing,** (Proc. EDUCOM Fall Conf., Princeton, N.J., Oct. 9-11, 1973), Chapter 7 in *Facts and Futures,* pp. 55-61 (The Interuniversity Communications Council, Princeton, N.J., 1974).

Key words: computer network management; computer networking research; management evaluation; resource sharing.

Computer networking technology is adequately developed now to support research and experimentation to expand computing resource sharing. Whether progress will be made depends upon organizational initiative among multiple institutions, to pool personnel and capital so as to effectively address the major issues in management approach, support and software design that limit the feasible interdependence of computing operations. The organizational requirements are partially revealed by examining progressive stages of resource sharing in organizational and operational terms rather than such technical aspects as load sharing or program sharing that have been introduced in the past. Five stages are identified, ranging from simply establishing multiple service access to the advanced stage where multiple institutions organize for joint development of new resources. A preliminary evaluation framework for new management arrangements results when these stages are mapped against the four functional levels inherent in computer network management.

**15546.** Unassigned.

**15547.** Cotton, I. W., **Network management survey,** *Proc. Hawaii Int. Conf. on Systems Sciences, Univ. of Hawaii, Honolulu, Hawaii, Jan. 8-10, 1974,* 4 pages (1974).

Key words: computer network; management; network.

This report presents a condensation of the results of a study of management practices in different computer networks. Five networks were chosen as typical of different approaches to network implementation and management: Advanced Research Projects Agency (ARPA) Network, MERIT Network, Triangle Universities Computation Center (TUCC), Oregon State Regional Network, and Tymnet, a commercial network. A common format is employed to survey each network.

**15548.** Newbury, D. E., **The origin, detection, and uses of electron channelling contrast,** *Proc. 7th Scanning Electron Microscopy Symp., Chicago, Ill., Apr. 8-11, 1974,* pp. 1047-1054 (IIT Research Institute, Chicago, Ill., 1974).

Key words: bend contours; contrast formation; crystalline materials; electron channelling contrast; electron channelling patterns; scanning electron microscope.

In the scanning electron microscope contrast can be obtained which is related to the crystallographic nature of a specimen through the mechanism of electron channelling. This contrast originates from the periodic arrangement of atoms in a crystal and depends on the angular relationship between the beam and the lattice. When the beam is caused to sweep through a range of angles greater than the Bragg angle while confined to a single crystal, a contrast pattern, called an electron channelling pattern (ECP), results. This pattern is uniquely related to the orientation of the crystal and it can therefore be used to orient a crystal relative to the beam. Instrument techniques have been developed to obtain useful ECP's from selected areas as small as 1 μm in diameter (selected area channelling patterns, SACP). Electron channelling contrast can also be used in conventional microscopy to reveal grains, twins, and other crystallographic features in polycrystalline microstructures.

This tutorial paper discusses briefly the origin of electron channelling contrast. The stringent electron-optical conditions required to detect the contrast are described. The formation of the ECP and the SACP technique are discussed. Finally, the use of electron channelling contrast in conventional micrograph operation and the types of information which can be obtained are described.

**15549.** Berger, H., **An evaluation of radiographic paper for thermal-neutron radiography,** *Proc. American Nuclear Society Meeting, New Orleans, La., June 8, 1975*, pp. 148-149 (1975).

Key words: image quality; neutron converters; neutron radiography; neutron scintillator; thermal neutron detection; x-radiographic paper.

X-ray sensitive paper is evaluated for use as an image detector for thermal neutron radiography. With a gadolinium oxysulfide scintillator the paper requires an exposure of $6 \times 10^7$ n/cm² and yields a radiograph displaying 25 to 50 μm spatial resolution and 4 to 6 percent contrast. The paper is convenient (10 second processing) and inexpensive, and provides good quality images.

**15550.** Haight, W. C., Hawes, H. W., **An automated tuneup—Calibration of jet engine fuel controls,** *Proc. 1974 ASSC Conf. Record on Automated Support Systems for Advanced Maintainability, San Diego, Calif., Oct. 30—Nov. 1, 1974*, 12 pages (IEEE Aerospace and Electronics Systems Society, San Diego, Calif., 1974).

Key words: automation; calibration; fuel control; jet engine; minicomputer; multi-task; performance testing; process control; real-time; RTOS.

The National Bureau of Standards (NBS) has designed an automated process control system for the calibration of jet engine fuel controls. The principal aim of this system is to relieve the test operator of the necessity of setting up test conditions and to provide a means of fast and accurate data acquisition. When operated under a vendor-supplied real-time operating system, the NBS software affords ease of modification to suit changing test requirements, ease of maintenance, and a degree of transferability between similar applications. Attributes contributing to these design goals include a modular program structure, use of a high-level programming language (FORTRAN) for applications routines, a well-structured file system and utility package, and a mnemonic test-oriented language developed for coding test procedures.

**15551.** Krauss, M., Neumann, D., **The dipole moment function of CO($a^3\Pi$),** *Mol. Phys.* **30,** No. 4, 1015-1020 (1975).

Key words: $a^3\Pi$; CO; dipole moment; excited state; SCF; vibrational transition intensities.

The dipole moment function of the $a^3\Pi$ state of CO is calculated using the multi-configuration self-consistent-field method of Wahl and Das. Only the dominant valence charge-transfer correlation configurations are mixed with the Hartree-Fock configuration since only the region between the classical turning points of the $v = 1$ vibrational level is considered. The calculated function does not agree with the shape of the fitted dipole moment function of Wicke *et al.* Configurations chosen on the basis of the model of optimized valence configurations do not determine an accurate dipole moment function for an open shell system.

**15552.** Hughes, E. E., Taylor, J. K., **Accurate gas standards for air pollution analyses,** *Proc. WMO/WHO Tech. Conf. on Observation and Measurement of Atmospheric Pollution, Helsinki, Finland, July 30-Aug. 4, 1973*, pp. 1-13 (World Meteorological Organization, Geneva, Switzerland, 1974).

Key words: air pollution; carbon monoxide; gas analysis; permeation tubes; propane; sulfur dioxide.

The preparation of standards for the measurement of a particular pollutant, either at ambient levels or at source concentrations, requires either an absolute method of preparation or an accurate method of analysis. Few, if any, accurate methods of analysis are applicable at the low concentrations generally associated with air pollution and consequently, most standards have been prepared in this laboratory by a gravimetric technique. The factors which effect the degree of accuracy which can be attained are discussed in detail for the following gases: nitric oxide, nitrogen dioxide, carbon monoxide, carbon dioxide, sulfur dioxide, hydrocarbons, and oxygen. In general, an uncertainty of less than ± 1 percent can be achieved for these substances at concentrations where their mixtures with air or nitrogen are stable. The stability of these mixtures is, therefore, an equally important consideration in the preparation of accurate gas standards. The instability is either due to reaction within the container between the components of the mixture or between a component and the material of the container, or is due to adsorption on the walls of the container. Methods of assessing the degree of instability and methods of preventing it are discussed.

**15553.** Beaty, E. C., **Measurements of the energy and angular distribution of secondary electrons,** *Radiat. Res.* **64,** 70-79 (1975).

Key words: cross sections; electron impact; electrons, secondary; ionization.

Measurements have been made of the distribution in energy and angle of secondary electrons from ionizing collisions of electrons with several atoms and molecules. Such data have been published for a wide range of the relevant variables. Some of these measurements have now been repeated in other laboratories. Some recent interpretive efforts also reveal trends in the data that were not previously apparent.

**15554.** Peterlin, A., **Plastic deformation of polymers with fibrous structure,** *Colloid Polym. Sci.* **253,** No. 10, 809-823 (1975).

Key words: fibrous structure; plastic deformation; polymer solids.

The plastic deformation of fibrous material obtains primarily by sliding motion of fibrils. In first approximation the displacement of their centers of mass is well describable by the affine transformation corresponding to the deformation of the bulk sample. Such a sliding motion of fibrils does not affect the morphology of the micro-fibrils. But it smooths by chain unfolding the surface inhomogeneities of the fibrils caused by microfibril ends which act as point defects of the microfibrillar lattice. That makes possible a more perfect lateral contact between adjacent fibrils resulting in a steadily increasing resistance to plastic deformation. The sliding motion of fibrils produces a shearing stress on skewed fibrils yielding a slight shear displacement of microfibrils. But in spite of its smallness, it enormously extends the interfibrillar tie molecules by chain unfolding and this enhances their fraction per amorphous layer.

**15555.** Peterlin, A., **Structural model of mechanical properties and failure of crystalline polymer solids with fibrous structure,** *Int. J. Fract.* **11,** No. 5, 761-780 (Oct. 1975).

Key words: bond rupture; chain rupture; ESR; fibrils; load-elongation curve; microcracks; microfibrils; radicals.

The failure of an axially strained polymer solid having a fibrous structure is caused by formation, coalescence, and growth of microcracks up to critical size crack, which then propagates catastrophically through the cross-section of the sample. The primary candidates for microcrack formation are the ends of microfibrils where the material connection by tie molecules to the rest of the sample is almost completely interrupted. The opening of microcracks and sliding motion of fibrillar elements ruptures locally the most strained taut tie molecules and, thus, produces radicals detectable by ESR. But, chain rupture is the consequence and not the cause of displacement of the strong fibrillar elements. It also does not substantially affect the load carrying properties of the sample which mainly depend on the lateral autoadhesion of microfibrils and fibrils and on their quasi-viscous resistance to axial displacement. Hence, one has to reject the completely inadequate models trying to base the observed load-elongation curve of such samples on the load carrying properties of those tie molecules which are eventually ruptured upon straining. Some examples of these models are treated explicitly.

**15556.** Read, F. H., **Displaced electron energies and the "shake-down" effect,** *Radiat. Res.* **64,** 23-36 (1975).

Key words: atom; autoionizing; collision; cross section; electron; experiment; positive ion; review; Rydberg states.

A brief review is given of the apparent exchanges of energy that can occur sometimes between the outgoing particles in electron-atom impact experiments, when these final particles consist of two electrons receding from a positive ion, and when the incident electron energy is near the energy of an autoionizing state of the target atom. These energy exchanges manifest themselves as changes in the energies of electrons ejected from autoionizing states of atoms excited by near-threshold election impact, displacements of the thresholds for exciting autoionizing states, and structure in the cross sections for exciting Rydberg states of neutral atoms by electron impact at incident energies in the vicinity of autoionizing states. The experimental evidence for these processes is reviewed and qualitative explanations are given. Evidence for analogous effects in other scattering and absorption processes is also discussed.

**15557.** Cezairliyan, A., Coslovi, L., Righini, F., Rosso, A., **Radiance temperature of molybdenum at its melting point,** (Proc. Symp. European Conf. on Temperature Measurement, Teddington, England, Apr. 9-11, 1975), Chapter 4 in *Temperature Measurement,* B. F. Billing and T. J. Quinn, Eds., Inst. Phys. Conf. Ser. No. 26, pp. 287-296 (Institute of Physics, London, England, 1975).

Key words: melting point; molybdenum; radiance temperature; wavelength.

Radiance temperature (at two wavelengths, 653 and 995 nm) of molybdenum at its melting point was measured using a subsecond-duration-pulse heating technique. Specimens in the form of strips with initially different surface roughnesses were used. The results do not indicate any dependence of radiance temperature (at the melting point) on initial surface or system operational conditions. The average radiance temperature at the melting point of molybdenum is 2531 K at 653 nm and 2331 K at 995 nm, with a standard deviation of about 0.6 K and a maximum absolute deviation of 1.2 K in both cases. The total inaccuracy in radiance temperature is estimated to be not more than ±8 K.

**15558.** Simiu, E., Filliben, J. J., **Structural safety and the probabilistic definition of design wind speeds,** *Proc. CIB Int. Symp. on the Climatology of Building, Zurich, Switzerland, Sept. 25-27, 1974,* 99 pages (1974).

Key words: building codes; probability distribution function; reliability; risk; statistical analysis; storms; structural engineering; wind loads; wind speeds.

The reliability of the probabilistic approach to the definition of design wind speeds depends upon the extent to which it is possible to model adequately the probabilistic behavior of extreme wind speeds. In this connection, questions arise regarding the type of probability distribution best suited for this purpose and the adequacy of 20-year long wind records, i.e., of such records as have been used as a basis for developing wind maps included in various building codes and standards. With a view to answering these questions, the writers undertook a statistical study of wind speed records taken at 20 U.S. weather stations. The following results were obtained: (1) the assumption currently accepted in the literature that a single probability distribution is universally applicable to all extreme wind data sets, was not confirmed; (2) predictions of 100-year wind speeds based on overlapping 20-year sets of data taken at the same station differed between themselves by as much as 65 percent. These results suggest that extreme caution should be exercised in establishing or using probabilistically defined design wind speeds, particularly if records of sufficient length, considerably in excess of 20 years, do not exist.

**15559.** Ogburn, F., Johnson, C. E., **Mechanical properties of electrodeposited brass,** *Plating* **62,** 141-148 (Feb. 1975).

Key words: density, brass; ductility, brass; electrical resistivity, brass; electrodeposited brass; electroplated brass; internal stress, brass; mechanical properties, electrodeposited brass; properties, electrodeposited brass; tensile strength, brass; wear rate, brass.

Electrical resistivity, density, hardness, wear rate, tensile strength, internal stress, and ductility of electrodeposited 70-30 brass were measured and microstructures were observed. The deposits were obtained from a high speed cyanide bath designed to deposit 70-30 brass. Included are property data for deposits of other compositions obtained from the same bath under conditions other than normal.

**15560.** Ogburn, F., **Coating thickness—its measurement and its significance,** Chapter 14 in *Properties of Electrodeposits—Their Measurement and Significance,* pp. 229-245 (Electrochemical Society, Princeton, N.J., 1975).

Key words: coating thickness; coating thickness gages; coatings; electrodeposited coatings; electroplated coatings; metal coatings; properties of electrodeposits; thickness gages; thickness measurement.

In addition to dimensional tolerance, thickness is very significant to coating characteristics such as wear, corrosion, porosity, electrical resistance, magnetic properties, ductility, other mechanical properties and monetary value. Many methods of measuring the thickness of electrodeposits are available, and a number of gages are manufactured domestically. These gages are nondestructive, but they are not applicable to all coatings. Measurement accuracies of ±5 to ±10 percent are normally expected.

**15561.** Sanchez, I. C., Eby, R. K., **Thermodynamics and crystallization of random copolymers,** *Macromolecules* **8,** No. 5, 638-641 (Sept.-Oct. 1975).

Key words: comonomer concentration; copolymer; crystallization; defect energy; equilibrium dissolution temperature;

equilibrium melting temperature; fold surface energy; growth rate; heat of fusion; lamella thickness; melting.

Equations are developed for the bulk free energy of fusion, melting temperature, crystal thickness, and nucleation rate of copolymer crystals containing an arbitrary concentration of comonomer units. These equations which represent advances over earlier ones are shown to be consistent with experimental data for copolymers of L- and DL-lactides and *cis*- and *trans*-isoprenes. Analysis of the lactide data confirms an earlier prediction that the crystal thickness should increase linearly with increasing small concentrations of the comonomer units for crystallizations carried out at the same temperature. Further, this linear dependence is shown to extend to crystals containing both equilibrium and nonequilibrium concentrations of the comonomer units. The nucleation rate equation is in agreement with the observed linear dependence of the logarithm of the growth rate on the comonomer concentration in isoprene copolymers. The following are consistent with the experimental data for the lactides: 461 K, equilibrium melting temperature of the homopolymer; 403 K, equilibrium dissolution temperature in xylene; 1370 cal/mol of monomer (5730 J/mol) heat of fusion; 26.5 erg/cm$^2$ ($2.65 \times 10^{-2}$ J/m$^2$) surface free energy and 585 cal/mol (2447 J/mol) comonomer defect energy. Directions for future research are suggested.

**15562.** Gebbie, K. B., Steinitz, R., **Comparison of Hα and Ca II H and K spectroheliograms as a diagnostic probe,** (Proc. Int. Astronomical Union Symp. on Chromospheric Fine Structure, Surfers' Paradise, Qld. Australia, Sept. 1973), Paper in *Chromospheric Fine Structure*, R. Grant Athay, Ed., No. 56, 55-63 (Reidel Publishing Co., Boston, Mass., 1974).

Key words: Ca II; Hα; solar chromosphere; spectral line formation.

The line formations of Hα and Ca II H and K are compared in order to differentiate the various mechanisms giving rise to observable contrasts in the emergent intensities. Table II summarizes the criteria for distinguishing between horizontal spatial variations in temperature, density, and turbulent velocity.

**15563.** Newman, M., Sheingorn, M., **Continuous solutions of a homogeneous functional equation,** *Aequationes Math.* **13,** No. 1/2, 47-59 (1975).

Key words: analytic functions; functional equations; Hurwitz's theorem.

It is shown that the functional equation

$$f(x)+f(ax)+f(bx)=0 \quad , \quad 1<a<b \quad ,$$

has a nontrivial solution which is continuous for all real $x$ if and only if $b \neq a^2$. Generalizations for the equation

$$\sum_{k=1}^{n} f(a_k x)=0 \quad , \quad 1=a_1<a_2<\ldots<a_n \quad ,$$

are also derived.

**15564.** McCamy, C. S., **Specification of geometric and spectral conditions relating to densitometry,** Paper 15.2 in *SPSE Handbook of Photographic Science and Engineering*, W. Thomas, Jr., Ed., pp. 831-840 (John Wiley & Sons, New York, N.Y., 1973).

Key words: modulation; notation; optical density; propagance; reflectance; reflectance factor; symbols; transmittance; transmittance factor.

Reflectance, transmittance, and optical density are regarded as kinds of flux modulation factors. Transmittance is defined as the ratio of transmitted flux to the incident flux, while transmittance factor is here defined for an optical system as the ratio of the emergent flux with the sample in the system to the emergent flux with the sample removed. Transmission density is defined as the negative logarithm of transmittance factor. Reflection, transmission, and fluorescence are considered generically as propagation and generalized modulation terms are given. A coordinate system and functional notation are adopted to systematize the description of optical systems which use or measure modulation. Simplified notation of the form D(g;S:g'S') describes most cases.

**15565.** Chow, L. C., Brown, W. E., **Topical fluoridation of teeth before sealant application,** *J. Dent. Res.* **54,** No. 5, 1089 (Sept.-Oct. 1975).

Key words: dicalcium phosphate dihydrate; fluorapatite; fluoride; pit and fissure sealant; tooth enamel.

Pyrolysis experiments revealed that small amounts of $CaHPO_4 \cdot 2H_2O$ are formed in enamel during conditioning of teeth with 50 percent $H_3PO_4$ for pit-and-fissure sealants. Unlike the $Ca(HPO_4)_2 \cdot H_2O$ which forms on the surface during the pretreatment, $CaHPO_4 \cdot 2H_2O$ is only sparingly soluble in water and would not be rinsed away in the clinical situation. The presence of $CaHPO_4 \cdot 2H_2O$ in enamel is undesirable because it may slowly dissolve and loosen the sealant. On the other hand, because of its high reactivity with fluoride, the $CaHPO_4 \cdot 2H_2O$ may be converted to $Ca_5(PO_4)_3F$ before sealant application, thereby further reducing caries tendency. Several basic-phosphate-fluoride solutions which had previously been shown to produce $Ca_6(PO_4)_3F$ when reacted with $CaHPO_4 \cdot 2H_2O$ were applied to acid etched enamel samples. Significant enamel-fluoride uptakes were obtained. SEM examinations of the samples show that these fluoride treatments produced no discernible deposits of $CaF_2$ on the surface which might interfere with sealant penetration and bonding.

**15566.** Krauss, M., Neumann, D., **On the interaction of O($^1$S) with O($^3$P),** *Chem. Phys. Lett.* **36,** No. 3, 372-374 (Nov. 15, 1975).

Key words: curve crossing; O($^1$D); O($^1$S); quenching rate; spin-orbit coupling; transition probability.

The quenching rate for O($^1$S) by O($^3$P) into the O($^1$D) + O($^1$D) channel is calculated using a theoretically calculated spin-orbit coupling matrix element. An upper bound to the rate is found to be $2.0 \times 10^{-14}$ cm$^3$ s$^{-1}$ which is much smaller than the experimental value. The low value of the rate constant is the result of a spin-orbit coupling matrix element of about 3 cm$^{-1}$ at the relevant curve crossing.

**15567.** Koyanagi, R. S., **Development of a low-frequency-vibration calibration system,** *Exp. Mech.* **15,** 443-448 (Nov. 1975).

Key words: accelerometer; calibration; harmonic distortion; low frequency; pickup; vibration; vibration exciter.

The development of the low-frequency-vibration apparatus described in this report was done in response to a need to establish and verify vibration-pickup performance at infrasonic frequencies. The exciter design is an extension of the Dimoff type exciters and, in fact, many of its components are identical.

The motion of such an exciter must have very low distortion and minimal components of motion in all directions other than axial. In addition, the attainable amplitude must be large enough to produce a transducer signal that can be accurately measured. The attainable amplitude and accuracy of transducer calibration on this exciter is limited by transducer size, weight, geometry and vibration sensitivity. Examples of the types of accelerometers which can be calibrated on this exciter are servo or force balance, piezoelectric, piezoresistive and strain gage.

**15568.** Pontius, P. E., **Mass measurement: A study of anomalies,** *Science* **190,** 379-380 (Oct. 24, 1975).

Key words: density of air; mass measurement.

It has always been assumed that the measurement of the difference in mass between two objects would be the same in all laboratories. Recent National Bureau of Standards measurements involving dissimilar objects (effective density ranging from 2.7 to 16.6 grams per cubic centimeter) at a wide variety of pressures (0.5 to 2 atmospheres) have been made with sufficient precision to test this assumption. The results show unsuspected discrepancies which may approach 1 milligram in a kilogram in the assignment of mass values when dissimilar materials are involved. These discrepancies have not been noted in the past because precision comparisons of both like and unlike materials have nearly always been made in a relatively restricted range of environmental conditions. The worldwide mass measurement system is therefore consistent, because similar materials have been used in the construction of weight sets, but possibly offset with respect to the mass unit as embodied in the platinum-iridium defining artifact.

**15569.** Payne, B. F., Koyanagi, R. S., Federman, C., Jones, E., **Accelerometer calibration at the National Bureau of Standards,** *21st Int. Instrumentation Symp. ASD/TMD, Philadelphia, Pa., May 19-21, 1975,* pp. 1-17 (1975).

Key words: acceleration; automation; calibration; measurements; shakers; standards; transducers; vibration; vibration exciters; vibration pickups.

Accurate calibration of accelerometers requires that accurate measurement techniques be developed and maintained. No single vibration exciter or calibration procedure is adequate for the present calibration frequency range. This paper gives a summary of the various calibration procedures used in calibration of accelerometers and reference exciters at the National Bureau of Standards.

**15570.** Saltman, R. G., **The human side of automating,** *Proc. Association for Computing Machinery and National Bureau of Standards Conf., on The Systems Approach: Key to Successful Computer Applications, Gaithersburg, Md., June 20, 1974,* pp. E.4.1-4.11 (1974); *Cyberdent* **2,** No. 3, 1, 3-4 (1974).

Key words: automation; human relations; job enrichment; organizational development; project management; system integration.

The process of designing and installing an automated system must consider problems of human relations. If the automation will affect the operation of diverse groups within an organization, then the legitimate and conflicting interests of these groups must be recognized, and their cooperation achieved through compromise. Successful automation must include the establishment of a new network of human communications.

The effect of the automation should not be to eliminate or downgrade jobs, but to enrich or increase responsibilities, leaving the repetitive, tedious jobs to the machines. Specialists in job design should be included on the automation team.

Well-designed automation should integrate diverse groups in an organization through improved data flow, but may divorce outside data users completely if their needs are not considered in the design process. An ombudsman with the responsibility of correcting design errors to satisfy outside users' requirements should be provided.

**15571.** Rebbert, R. E., Ausloos, P. J., **Photodecomposition of $CFCl_3$ and $CF_2Cl_2$,** *J. Photochem.* **4,** 419-434 (1975).

Key words: absorption cross section; chlorine atom; dichlorodifluoromethane; freons; photochemistry; quantum yields; stratosphere; trichlorofluoromethane.

The photochemical decomposition of $CFCl_3$ and $CF_2Cl_2$ has been investigated, using added $CH_4$ and $C_2H_6$ as chlorine atom interceptors. From the quantum yields of the stable products formed at 213.9, 184.9, 163.3 and 147 nm, quantum yields of the primary photofragments $CFCl_2$, $CF_2Cl$, CFCl, $CF_2$, CF and Cl, were derived. At wavelengths close to the absorption threshold, detachment of one chlorine atom from $CFCl_3$ and $CFC_2l_2$ occurs with a quantum yield of $0.95 \pm 0.05$. As the photon energy increased, there is a rapidly increasing probability that absorption of a photon will lead to the release of two chlorine atoms:

$$CFCl_3 + h\nu \rightarrow CFCl + 2Cl$$

$$CF_2Cl_2 + h\nu \rightarrow CF_2 + 2Cl$$

The CFCl or $CF_2$ formed in these processes (which are most likely in the ground singlet state) are unreactive towards the parent halocarbons, or alkanes. They combine with other free radicals to form stable products. No evidence was found for the cleavage of C-F bonds, or the elimination of stable chlorine molecules.

In the vicinity of the absorption threshold, the absorption cross-sections of $CF_2Cl_2$ and $CFCl_3$ diminish sharply with a decrease in temperature.

**15572.** Mighell, A. D., Santoro, A., **Geometrical ambiguities in the indexing of powder patterns,** *J. Appl. Crystallogr.* **8,** Part 3, 372-374 (June 1975).

Key words: ambiguities; geometrical; indexing; patterns; powder diffraction.

There are cases in which different lattices give calculated powder patterns with the identical number of distinct lines in identical $2\theta$ angular positions. The number of planes *(hkl)* contributing to each reflection may differ, however. The lattices having this property are related to each other by transformation matrices with simple rational elements. The resulting ambiguity in indexing of powder patterns is, in these cases, geometrical rather than accidental.

**15573.** Cali, J. P., **Reference materials in clinical chemistry,** *Fed. Proc.* **34,** No. 12, 2123-2126 (Nov. 1975).

Key words: accuracy; accurate measurement in clinical chemistry; clinical chemistry; clinical reference materials; standardization.

Reference Materials (RM's) are necessary and critical components of measurement systems, especially useful in helping to achieve compatibility in large laboratory networks, such as those existing in clinical chemistry. What the measurement process is and how RM's fit into this process is discussed. The role of accuracy in helping achieve compatibility is explained and the role of RM's within an accurate measurement system is elucidated. Because RM's are the mechanism for transferring accuracy throughout a measurement network, the criteria for their production and certification are important. They include a knowledge and/or assurance of: purity, homogeneity, stability, continuity and availability of supply and information. Because measurement compatibility in clinical chemistry involves human life, only RM's of highest quality and integrity should be used. Clinical RM's should therefore bear a certificate (or guarantee). Minimal requirements for such certification are discussed.

Currently available clinical RM's from the National Bureau of Standards (NBS) are listed.

**15574.** Santoro, A., Choi, C. S., Abel, J. E., **1,5-diacetyl-3,7-dinitro-1,3,5,7-tetraazacyclooctane (DADN),** *Acta Crystallogr.* **B31,** Part 8, 2126-2128 (Aug. 1975).

Key words: crystal structure explosives; least-squares refinement; molecular packing; tetraazacyclooctane derivatives; x rays.

$C_8H_{14}N_6O_6$, monoclinic, $P2_1/c$, $a=7.422(1)$, $b=13.253(2)$, $c=6.156(1)$ Å, $\beta=103.38(1)°$, $Z=2$, $D_x=1.636$, $D_m=1.63$ gcm$^{-3}$, $F(000)=304$. X-ray intensities were measured with Mo $K\alpha$ radiation. The structure was solved by direct methods and refined by full-matrix least-squares calculations to final $R$ and $R_w$ values of 4.1 and 4.8 percent, respectively, for 1149 observed reflections.

**15575.** Berg, N. J., Lieberman, A. G., **The effects of radiation-induced displacement damage on impurity conduction in gallium arsenide,** *J. Appl. Phys.* **46,** No. 8, 3475-3482 (Aug. 1975).

Key words: activation energy; compensation; epitaxial gallium arsenide; high energy neutron; impurity conduction; reciprocal Hall coefficient; transition regime; $^{60}$Co gamma.

The effects of $^{60}$Co $\gamma$-ray and high-energy neutron displacement damage on impurity conduction in epitaxial gallium arsenide were investigated. The activation energy ($\epsilon_2$) associated with the transition regime of the impurity conduction process was found to increase by a factor of 5 as a result of $^{60}$Co $\gamma$ irradiation, and only by a factor of 1.6 for a comparable neutron irradiation. In addition, the ratio of the Hall carrier density at low and high temperatures, $(n_H)_{4K}(n_H)_{300K}$, decreased by a larger amount for $^{60}$Co $\gamma$ irradiation than for neutron irradiation. The effects of neutron irradiation are explained in terms of increased compensation. For the case of $^{60}$Co $\gamma$ irradiation, it is postulated that a new donor level is introduced which does not participate in the impurity conduction process, it is found that $\epsilon_2$ is proportional to $\epsilon_1$ (the conduction-band activation energy) and varies inversely with neutral donor spacing in accord with the model proposed by Mikoshiba. Also $\rho_{30}$, the hopping regime resistivity, is found to vary inversely with the square of the free-carrier concentration and exponentially with the quantity $0.6/N_D{}^{1/3}a$.

**15576.** Sugar, J., **Ionization energies of quadruply ionized rare earths,** *J. Opt. Soc. Amer.* **65,** No. 11, 1366-1367 (Nov. 1975).

Key words: atomic spectra; ionization energies; lanthanides; spectra; rare earths.

Values for the ionization energies of four-times-ionized lanthanides are derived from interpolated spectroscopic properties of the $4f^{n-1}ns$ Rydberg series.

**15577.** Rains, T. C., **Iron, cobalt, and nickel,** Chapter 10 in *Flame Emission and Atomic Absorption Spectrometry,* J. A. Dean and T. C. Rains, Eds., **3,** 216-246 (Marcel Dekker, Inc., New York, N.Y., Nov. 1975).

Key words: atomic absorption; atomic fluorescence; cobalt; interferences; iron; nickel; separations.

A summary is presented of the published work on the determination of iron, cobalt, and nickel by atomic absorption, emission, and fluorescence spectrometery. Optimum conditions for atomization and excitation are described for flame and non-flame methods for the three techniques. Spectral characteristics for wavelength ranges of analytical interest are given for the three elements with their sensitivity and/or detection limits. Interferences encountered under optimum instrumental conditions are minimal; however, separational techniques are described for each element. The paper contains 174 references in which numerous applications are described.

**15578.** Mighell, A., Santoro, A., Prince, E., Reimann, C., **Neutron diffraction structure determination of dichlorotetrapyrazolecopper(II), $Cu(C_3H_4N_2)_4Cl_2$,** *Acta Crystallogr.* **B31,** Part 10, 2479-2482 (Oct. 15, 1975).

Key words: dichlorotetrapyrazolecopper; neutron diffraction; structure.

The crystal and molecular structure of dichlorotetrapyrazolecopper(II), Cu(NHN:CHCH:CH)$_4$Cl$_2$, was determined by single-crystal neutron diffraction techniques. This compound crystallizes in the monoclinic system with $a=13.657$ (5), $b=9.200$ (5), $c=14.900$ (5) Å, $\beta=118.04$ (1)°, space group $C2/c$, $\rho_0=1.63$ g cm$^{-3}$ and $Z=4$. The structure was refined by least-squares calculations to a conventional $R$ value of 3 percent for 1143 reflections. The $Cu(C_3H_4N_2)_4Cl_2$ molecule is centrosymmetric with the Cu atom at the center of a distorted octahedron formed by two chlorine atoms and a nitrogen atom from each of four pyrazole rings. The accurate location of the hydrogen atoms shows that the conformation of the complex is due to intramolecular hydrogen bonding. The coordination distances Cu-Cl and Cu-N (2.84 and 2.02, 2.01 Å, respectively) are significantly different from those of the corresponding nickel analog (Ni-Cl and Ni-N 2.51; and 2.10, 2.09 Å, respectively).

**15579.** Berger, M. J., Seltzer, S. M., Domen, S. R., Lamperti, P. J., **Stopping-power ratios for electron dosimetry with ionization chambers,** (Proc. Int. Symp. on Advances in Biomedical Dosimetry, Vienna, Austria, Mar. 1975), Paper in *Advances in Biomedical Dosimetry,* pp. 589-609 (International Atomic Energy Agency, Vienna, Austria, 1975).

Key words: absorbed dose; dosimetry; electrons; ionization chambers; standards; stopping power ratio.

In the course of an NBS absorbed-dose standards program, theoretical and experimental determinations have been made of the conversion factor C that relates the absorbed dose from electron beams to the ionization in an air cavity. The average medium/air stopping-power ratio—which is proportional to C—has been calculated as a function of the beam energy (1 to 60 MeV) and of the depth in a water phantom, and similar stopping-power ratios have also been obtained for other phantom materials (carbon, polystyrene, acrylic plastic, muscle). The conversion factor in graphite has been measured at energies between 15 and 50 MeV and depths between 0.9 and 51 g/cm$^2$ with the use of a calorimeter and a parallel-plate ionization chamber. These measurements were made with beams broadened by lead scattering foils with various thicknesses from 0.144 to 1.584 g/cm$^2$. The extrapolation of the results to zero scattering-foil thickness provided conversion factors that could be compared with theoretical C-values for broad, parallel, monoenergetic electron beams. The agreement was found to be close (mean difference of 0.3% and r.m.s. difference of 0.8%). Comparisons have also been made with other C-values found in the literature and recommended by medical physics organizations. The overall conclusion can be drawn that the conversion factor is known reliably at the 1 percent level of accuracy.

**15580.** Ogburn, F., **Density of electrodeposited metal, its significance and measurement,** Chapter 5 in *Properties of Electrodeposits—Their Measurement and Significance,* R. Sard, H. Leidheiser, Jr., and F. Ogburn, Eds., pp. 71-79 (The Electrochemical Society, Inc., Princeton, N.J., 1975).

Key words: coatings; copper; density; electrodeposited coatings; electrodeposits; metal coatings.

Density of electrodeposits can give information about their soundness and composition. It can be measured by direct determination of the volume and mass of the deposit, but the best measurements are made by conventional hydrostatic techniques. A 2 liquid hydrostatic method of measurement is described. This method involves hydrostatic weighing with a float in a two liquid system. Data obtained by this method are given as an example. These data show a significant density variation between 11 one-half gram samples cut from a 6 gram piece of electrodeposited copper.

**15581.** Scheide, E. P., Taylor, J. K., **A piezoelectric crystal**

**dosimeter for monitoring mercury vapor in industrial atmospheres,** *Am. Ind. Hyg. Assoc. J.* **36,** No. 12, 897-901 (Dec. 1975).

Key words: air pollution; chemical analysis; dosimeter; industrial hygiene analysis; mercury; personnel monitor; piezoelectric sensor; trace analysis.

A personal dosimeter for mercury vapor in air based on the use of a piezoelectric sensor with a selective coating has been developed and evaluated. The sensor is a gravimetric device which indicates an integrated total exposure to mercury vapor. The mass of the material deposited or adsorbed is determined by measuring the change in oscillation frequency of the crystal. The sensor is small enough to be worn on a worker's clothing and is compatible with existing miniature air pumps. The adsorbed mercury can be desorbed by heating and the sensor can be reused many times. The precision and accuracy of this measurement technique, the effect of sampling flow rate, storage, sample concentration, interferences, sampling period, sensitivity and range, lifetime of the sensor, and other parameters considered in the development of prototype devices are discussed.

**15582.** Clifton, J. R., Foster, B. E., Trattner, E., Clevenger, R. A., **Dimensional stability of masonry walls,** *Am. Soc. Test Mater. Spec. Tech. Publ.* **589,** pp. 42-75 (1975).

Key words: brick; dolomitic mineral; masonry; mortars (materials); walls.

To assess the contribution of dolomitic limes to dimensional stability of masonry construction, 65 brick masonry walls, 34 by 40 by 8 in (0.86 by 1.0 by 0.20 m), were constructed. The program involved the following design variables: 6 hydrated limes ranging in autoclave expansion from 0.10 to 15.1 percent; 2 types of brick, one with high water absorption and high autoclave expansion, and the other with low water absorption and insignificant autoclave expansion; and, 2 mortars of cement:lime:sand proportions of 1:1:6 and 1:2:9 by volume. Half of the walls were subjected to temperature and moisture cycles, performed indoors, for 3 1/2 years; the other half were tested outdoors for 14 years. Half of the indoor and outdoor exposed walls were spring loaded at 25 psi ($1.7 \times 10^5 N/m^2$). Observed expansion of the walls was found to be related to the potential expansions (as measured by the autoclave test) of the limes. The largest wall expansion took place with the following combination: high potential expansive lime; stable, low absorption brick; unloaded wall; and, 14 year outdoor exposure. In the 14-year outdoor exposure, loss of bond and resulting damage from freezing were complicating factors. The effects of lime, mortar mix, brick, loading, and exposure on the dimensional instability of the masonry walls are discussed.

**15583.** Hammond, H. K., Hsia, J. J., **Evaluation of instrument tolerances for 75° gloss,** *Tappi Notes to Editor* **58,** No. 11, 143-144 (Nov. 1975).

Key words: gloss; optical properties; tolerances.

The instrument tolerances of the published TAPPI method for 75° specular gloss are unnecessarily strict. The 1954 report of Zabel and Wink on which the tolerances were based has been reexamined. Improvement in the photometric linearity on instruments and a statistical approach to the combined effect of a number of sources of uncertainty, reveal that if the goal for overall uncertainty is still to be one gloss unit, geometric tolerances could be increased by a factor of 7.

Dimensions and tolerances are all based on the dimension "d" rather than the unit distance of which d is only a part. All dimensions have been rounded to simple figures. The proposed dimensions and tolerances are tabulated.

**15584.** Gallagher, A., **Noble-gas broadening of the Li resonance line,** *Phys. Rev. A* **12,** No. 1, 133-138 (July 1975).

Key words: line broadening; lithium; noble gases.

The normalized fluorescence spectrum of the Li 6708-Å resonance line perturbed by the noble gases has been measured for 100 Å either side of the resonance line, at a temperature of $400 \pm 10$ °C. The noble-gas pressure range of 100-1800 torr was investigated. It was observed that the line wings scale linearly with this pressure for $2 < |\Delta\lambda| < 100$ Å, and it was demonstrated that a Lorentzian-broadened line core can be observed for this pressure range. The Li density was $\sim 10^{10}/cm^3$ and was varied to establish the fluorescence spectrum in the limit of no radiation entrapment. The central region of the line has been measured with high resolution and compared to calculated profiles due to the various fine structure and isotopic line components, each broadened by a convolution of Lorentz, Doppler, and instrumental profiles. The shift and Lorentz broadening rates, as well as the wavelengths for transition to non-Lorentzian behavior, are reported. In contrast to the heavier alkali-metal-noble-gas cases, no distinctive far-wing features such as satellites or sharp inflections are observed. This is consistent with the much larger collision velocities for the Li case.

**15585.** Mount, G. H., Linsky, J. L., **A new solar carbon abundance based on non-LTE CN molecular spectra,** *Astrophys. J.* **202,** No. 1, L51-L54 (Nov. 15, 1975).

Key words: carbon abundance; molecular spectra; solar photosphere.

A detailed non-LTE analysis of solar CN spectra strongly suggests a revised carbon abundance for the Sun. We recommend a value of $\log A_C = 8.35 \pm 0.15$ which is significantly lower than the presently accepted value of $\log A_C = 8.55$. This revision may have important consequences in astrophysics.

**15586.** King, G. C., Read, F. H., Bradford, R. C., **Structure near autoionizing energies in the excitation of bound states of helium, neon, and argon by electron impact,** *J. Phys. B* **8,** 2210 (1975).

Key words: Ar; atoms; autoionizing; cross sections; electron impact; excitation; He; inelastic; Ne.

Cross sections for the excitation of bound states of atoms by electron impact have been found to contain structures at incident energies near to the energies of short lived autoionizing states of the target atoms. These structures look superficially like resonance structures, but in fact they seem to be caused by a post-collision interaction between inelastically scattered and ejected electrons. Examples are given of these structures in He, Ne, and Ar. A quantum mechanical "shake-down" model to explain these structures is also described and compared with the experimental data.

**15587.** Shank, R., Henderson, M., **Federal Library cooperation,** *Library Trends* **24,** No. 2, 277-292 (Oct. 1975).

Key words: Federal libraries; library cooperation.

Federal support of cooperative library service is influenced by the direct participation of Federal libraries in consortia and various networks. An overview of Federal library activity reveals many instances in which leadership for major cooperative programs was given by librarians in Federal libraries, e.g., the Library of Congress shared cataloging began in 1901. This paper documents trends in cooperation by the more than 2,000 libraries of the Federal Government.

**15588.** Unassigned.

**15589.** Unassigned.

**15590.** Wang, F. W., DiMarzio, E. A., **The dynamics of block-copolymer molecules in solution. The free-draining limit,** *Macromolecules* **8,** No. 3, 356-360 (May-June 1975).

Key words: bead-spring model; block copolymers; concentrated solutions; dynamics; Rouse theory; solution properties; viscoelasticity.

A theory for the viscoelasticity of block-copolymer molecule solutions in the free-draining limit has been developed by modifying the bead-spring model theory of Rouse to take into account the existence of dissimilar segments in block copolymers. The eigenvalue problem encountered in the theory has been solved numerically by matrix computations. Furthermore, for the case of a diblock copolymer, a simple form of the secular equation which is useful for extracting the eigenvalues has been obtained. The applications of the theory have been illustrated with calculations for the viscoelastic properties of poly(styrene-*b*-*cis*-1,4-isoprene) solutions. It is found that the calculated properties for the diblock copolymer are nearly the same as those for the Rouse theory while the calculated properties for the symmetric triblock copolymers deviate from those of the Rouse theory.

**15591.** Rensberger, R. A., **Lead paint hazard abatement,** *Constr. Specifier* **28,** No. 6, 45-46, 48-49 (June 1975).

Key words: abatement; detection; heat-gun; lead paint; materials evaluation; performance specification; rehabilitation; renovation.

The article briefly discusses the history of lead paint poisoning and discusses the safety hazards of lead paint in renovation and rehabilitation work in housing and buildings. Techniques for lead paint detection and methods for abatement are discussed for reference by the specifications writer, architect, design professional, engineer, contractor and other individuals who may be confronted with the hazards of lead paint. The information is from investigations by NBS for the HUD research program on lead paint. A suggested performance specification for lead paint hazard abatement methods is offered as a guideline for materials evaluation. Also a selected bibliography of NBS publications is included for reference by the building community.

**15592.** Pella, P. A., Hughes, E. E., Taylor, J. K., **Development of gas-blending systems for calibration: application to hydrogen fluoride, arsine and phosgene in air,** *Am. Ind. Hyg. Assoc. J.* **36,** No. 10, 755-759 (Oct. 1975).

Key words: arsine; calibration of devices; gas-blending systems; hydrogen fluoride; phosgene.

The calibration of analytical monitoring devices is a prerequisite for making accurate measurements. For this purpose, self-contained gas-blending systems are being constructed and evaluated at the NBS for producing known concentrations of specific industrial contaminants in air from one-half to five times the TLV. This is accomplished by accurate dynamic dilution of a known relatively high concentration of the contaminant (i.e., standardized gas mixture) with air as a diluent to yield the desired range of concentrations. The development and evaluation of systems for producing known concentrations of hydrogen fluoride, arsine, and phosgene in air are reported including the measurement of the stability of these gases, and the determination of the concentrations upon dilution employing specific analytical methods.

**15593.** Dunn, G. H., **Collision studies with ion storage techniques,** (Proc. Int. Conf. on Atomic Physics, Heidelberg, Germany, July 1974), Paper in *Atomic Physics* **4,** pp. 575-587 (Plenum Press, New York, N.Y., 1975).

Key words: electrons; ion trap; positive molecular ions; recombination.

This paper is a report on recombination measurements made by studying electron-ion collisions in ion traps. We briefly review two-body recombination processes between electrons and ions and the means by which they have previously been measured. The trapping scheme and its realization for collision work is discussed, and results for some recombination measurements are given.

**15594.** Crawford, E. A., Phelps, A. V., **Formative time lags in $CO_2$ laser discharges,** *Appl. Phys. Lett.* **25,** No. 1, 59-61 (July 1, 1974).

Key words: $CO_2$ laser; electrical discharge; gas mixture; time delay.

Time lags for the growth of power input, i.e., formative time lags, have been measured in typical $CO_2$ laser gas mixtures at pressures from 200 to 760 torr using parallel plane electrodes with the 1- and 2-cm gaps illuminated by a trigger discharge. The measured time lags are about twice the values predicted using a single avalanche growth model and theoretical ionization and attachment coefficients.

**15595.** Berke, J. G., **Procurement—The pull side of technology transfer,** (Proc. ASME 5th Intersociety Conf. on Environmental Systems, San Francisco, Calif., July 21-24, 1975), *75-ENAs-3*, pp. 1-4 (The American Society of Mechanical Engineers, New York, N.Y., 1975).

Key words: innovation; procurement; specifications; standards; technology; transfer.

Public procurement at the federal, state or local levels can be a major influence on the adaptation, implementation and transfer of technology. Through the procurement process, problems can be defined, prototypes can be tested, cost/benefits determined and finally the product can be bought. This final step is what has traditionally been lacking in the technology transfer process. This paper describes ongoing experiments, at the federal, state or local levels, aimed at determining the transfer potential of such market incentives as the use of performance specifications, life cycle costing, value incentive clauses, consensus standards and test methods versus the traditional lowest price for lowest acceptable quality.

**15596.** Dziuba, R. F., Field, B. F., Finnegan, T. F., **Cryogenic voltage comparator system for 2e/h measurements,** *IEEE Trans. Instrum. Meas.* **IM-23,** No. 4, 264-267 (Dec. 1974).

Key words: cryogenic resistor; current comparator; Josephson device; microstripline; microwave coupling; SQUID; superconducting switch; tunnel junction; voltage standard.

The design and operation of a cryogenic voltage comparator system for precision 2e/h measurements is described. Major improvements embodied in the new 2e/h system include the use of (1) a single microstripline-coupled Josephson tunnel junction to obtain usable step voltages up to 10 mV at 10.0 GHz, (2) a cryogenic voltage divider comprised of two resistors whose ratio is calibrated with a low temperature dc current comparator, (3) a

SQUID null detector, and (4) superconducting switching. The accuracy of the present 196:1 divider system is estimated to be about 2 parts in $10^8$ on the basis of preliminary tests and is limited by resistor self-heating during calibration.

**15597.** Dziuba, R. F., Sullivan, D. B., **Cryogenic direct current comparators and their applications,** *IEEE Trans. Magn.* **MAG-11,** No. 2, 716-719 (Mar. 1975).

Key words: cryogenic resistors; current comparators; low temperature; shielding; SQUID; superconducting shield; superconductivity.

Cryogenic direct current comparators, utilizing superconducting shields and Superconducting QUantum Interference Devices (SQUID's), provide current ratios of up to 100/1 or higher with accuracies of $\leq 1 \times 10^{-9}$ and current resolutions of $\leq 6 \times 10^{-11}$ A. Two types of comparators differing in the shielding arrangement of the ratio windings are described. One type consists of unit windings inside a seamless Pb tube; the other consists of multi-turn ratio winding within an overlapping toroidal superconducting shield. For both shielding configurations, SQUID's serve as flux sensors for the comparators. The application of these comparators to the measurement of resistance ratios is described.

**15598.** McClintock, W., Linsky, J. L., Henry, R. C., Moos, H. W., Gerola, H., **Ultraviolet observations of cool stars. III. Chromospheric and coronal lines in $\alpha$ Tauri, $\beta$ Geminorum, and $\alpha$ Bootis,** *Astrophys. J.* **202,** 165-182 (Nov. 1975).

Key words: chromospheres; stellar coronae; stellar ultraviolet.

The ultraviolet spectrometer of the Princeton Experiment Package aboard the *Copernicus* satellite has been used to obtain high-resolution measurements of L$\alpha$, the Mg II $\lambda$2800 doublet, and upper limits on Si III $\lambda$1206 in the K giants $\alpha$ Tau and $\beta$ Gem. The intensities and line shapes are compared with earlier observations of $\alpha$ Boo. The L$\alpha$ and Mg II profiles for $\alpha$ Tau resemble those for $\alpha$ Boo, in that they are highly asymmetrical, while $\beta$ Gem shows much more symmetrical profiles. The asymmetries for all lines except for those of $\alpha$ Boo and the Mg II lines of $\alpha$ Tau could be due to interstellar absorption. In the case of $\beta$ Gem only, the O V intercombination line at 1218 Å is observed, suggesting a well-developed corona substantially cooler than that of the sun. The L$\alpha$ profiles of $\alpha$ Tau and $\beta$ Gem are consistent with the low interstellar hydrogen abundance in the solar neighborhood previously obtained from a similar observation of the $\alpha$ Boo L$\alpha$ profile. The strength of the Mg II $\lambda$2796 line can be used to measure transition region and coronal pressures, and indicates a decrease in both with later spectral type and/or increasing luminosity.

**15599.** Finnegan, T. F., Toots, J., Wilson, J., **Frequency-pulling and coherent-locking in thin-film Josephson oscillators,** (Proc. 14th Int. Conf. on Low Temperature Physics, Helsinki, Finland, Aug. 14-20, 1975), Paper in *Low Temperature Physics* **LT-14,** N. Krusius and N. Vuorio, Eds., **4,** 184-187 (North Holland Publishing Co., Amsterdam, 1975).

Key words: frequency source; Josephson radiation; Josephson tunnel junction; junction array; microstripline-coupling; thin-film device.

The results of a continuing study of the microwave radiation emitted by pairs of Josephson tunnel junctions simultaneously coupled to each other and an external microwave source are reported. Injection-locking of the junctions was observed and some qualitative features of the phenomenon are discussed.

**15600.** Kunasz, P. B., Hummer, D. G., Mihalas, D., **Theory of extended stellar atmospheres. II. A grid of static spherical models for O stars and planetary nebula nuclei,** *Astrophys. J.* **202,** 92-113 (Nov. 1975).

Key words: emission line stars; line profiles; stellar atmospheres; stellar limb darkening.

Spherical static non-LTE model atmospheres are presented for stars with $M/M_\odot = 30$ and 60 at various points on their evolutionary tracks, and for some nuclei of planetary nebulae at two points of a modified Harman-Seaton sequence. The method of Mihalas and Hummer was employed, which uses a parametrized radiation force multiplier to simulate the force of radiation arising from the entire line spectrum. However, in the present work the density structure computed in the LTE models was held fixed in the calculation of the corresponding non-LTE models; in addition, the opacity of an "average light ion" was taken into account. The effects of sphericity, as distinct from those arising from a density structure modified by a large radiation force, were investigated by computing a few planar models using the same parametrized radiation force multiplier as for the spherical models. These effects were found to be quite significant even though the atmospheric extension never becomes very large. The temperatures for the non-LTE models are generally lower, at a given depth, than for the corresponding LTE models when $T_{eff} < 45{,}000$ K, while the situation is reversed at higher temperatures. The continuous energy distributions are generally flattened by extension. The Lyman jump is in emission for extended models of massive stars, but never for the models of nuclei of planetary nebulae (this is primarily a temperature effect). The Balmer jumps are always in absorption. The Lyman lines are in emission and the Balmer lines in absorption; He II $\lambda$4686 comes into emission in the most extended models without hydrogen line pumping, showing that it is an indicator of atmospheric extension. Very severe limb darkening is found for extended models, which have apparent angular sizes significantly smaller than expected from the geometrical size of the star. Extensive tables are given of monochromatic magnitudes, continuum jumps and gradients, Strömgren-system colors, monochromatic extensions, and the profiles and equivalent widths of the hydrogen lines for all models, and of the He II lines for some of the 60 $M_\odot$ models.

**15601.** Sengers, J. M. H. L., Sengers, J. V., **Universality of critical behavior in gases,** *Phys. Rev. A* **12,** No. 6, 2622-2627 (Dec. 1975).

Key words: air constituents; critical region parameters; ethylene; heavy noble gases; helium; linear model; methane; NBS equation; scaling laws; statistical analysis; steam; universality.

*P-V-T* data in the critical region of six fluids ($^3$He, $^4$He, Xe, $O_2$, $CO_2$, and $H_2O$) have been analyzed in terms of two scaled equations of state using the methods of statistical analysis. The results confirm the hypothesis of universality of critical behavior for these gases to within the current experimental accuracy. The results also support the validity of hyperscaling relations between thermodynamic and correlation function exponents for gases. Using the hypothesis of universality we then present critical-region parameters for fourteen fluids in terms of a universal equation of state.

**15602.** Gravatt, C. C., Allegrini, I., **A new light scattering method for the determination of the size distribution of particulate matter in air,** (Proc. 3rd Int. Clean Air Congress (IUAPPA), Dusseldorf, W. Germany, Oct. 8-12, 1973), Paper in *Proceedings of the 3rd International Clean Air Congress,* pp. C3-C5 (Verlag GMBH, Dusseldorf, W. Germany, 1973).

Key words: air pollution; light scattering; particulate matter.

An instrument has been developed which determines the size distribution of particulate matter in air in essentially real time by a forward lobe light scattering method. The basic concept involves the simultaneous measurement of the intensity of light scattered by a single particle at two small scattering angles. The ratio of the two intensities is a direct measure of the size and is fairly independent of the index of refraction of the particle. Numerical solutions of the Mie equations for spheres have indicated that the sizing error by this method is no greater than 15 percent for the range of particle sizes from 0.1 to 10 μm for essentially all possible indices of refraction. In addition, techniques have been found which extend the lower limit of size determination to 0.05 μm and which may permit some degree of chemical characterization of the particle.

**15603.** Interrante, C. G., **Report on the ferrous metals workshop,** (Proc. National Materials Conservation Symp. on Resource Recovery and Utilization, Gaithersburg, Md., Apr. 29-May 1, 1974), Paper in *Resource Recovery and Utilization*, H. Alter and E. Horowitz, Eds., *Am. Soc. Test. Mater. Spec. Tech. Publ.* **592,** pp. 146-152 (American Society for Testing and Materials, Philadelphia, Pa., 1975).

Key words: conservation; materials recovery; natural resources; reclamation.

This paper reports the nontechnical and technical findings of the workshop on ferrous metals. Discussions include the technology for the use of municipal ferrous scrap, the economic outlook, and potential markets for ferrous waste. Eight recommendations are suggested for improved recovery of ferrous waste.

**15604.** Graminski, E. L., **Problems and potentials in paper recycling,** (Proc. National Materials Conservation Symp. on Resource Recovery and Utilization, Gaithersburg, Md., Apr. 29-May 1, 1974), Paper in *Resource Recovery and Utilization,* H. Alter and E. Horowitz, Eds., *Am. Soc. Test. Mater. Spec. Tech. Publ.* **592,** pp. 132-139 (American Society for Testing and Materials, Philadelphia, Pa., 1975).

Key words: market pulp; paper, waste; pulp, secondary; recycled paper; secondary pulp; waste paper.

The U.S. consumed more than 60 million tons of paper and paperboard in 1973, about 20 percent of which was recycled. Steel is the only product that is consumed in larger quantities than paper. The principal disincentives for paper recycling are (1) the ready availability of virgin wood fibers, (2) lack of research on recycling of paper, (3) economics favor the use of virgin fibers, and (4) contaminants in wastepaper present major problems in recycling. In spite of the large amount of wastepaper that is available, a wastepaper shortage occurred in 1973 and has continued into 1974 because of problems in collection, fluctuation of the wastepaper market, and lack of manufacturing capacity. It is anticipated that about 32 million tons of paper and paperboard are available for recycling. About 130 pulp mills with a capacity of 600 tons per day would be needed to recycle this amount of wastepaper, which would produce about 24 million tons of recycled paper. The capital for building these mills is not available, and if a large number of secondary fiber mills were built immediately, it would create chaos in the virgin fiber industry. It is suggested that market pulp mills, located in or near large municipalities, be erected as needed to provide the need for more market pulp. This secondary pulp would be available to many mills that now are not equipped to process wastepaper.

**15605.** Jackson, R. H. F., **Towards algorithmic standardization in mathematical programming: Another step,** *Proc. 1974 Fall UNIVAC Users' Conf., Toronto, Canada, Sept. 1974,* pp. 3-147 – 3-153 (1974).

Key words: algorithms; mathematical programming standards; testing.

This talk discusses the Mathematical Programming Society's newly formed Working Committee on Algorithms, whose domain of interest includes the accuracy, availability, and transportability of computer codes for the solution of mathematical programming problems. The Committee, it is hoped, will satisfy the pressing need for real achievements in these areas. The discussion will focus on the goals and accomplishments to date of the Committee, and will stress the importance of a good working relationship between it and the O.R. community.

**15606.** Holton, J. K., Driscoll, P., **Linking research and practice,** *AIA J.*, pp. 67-68 (Apr. 1975).

Key words: AIA/NBS Architect-in-Residence; architectural research; daylight research; National Bureau of Standards; programs for architects; research communication.

There has been a long standing need for more effective interchange between the building community and researchers. The American Institute of Architects and the National Bureau of Standards have established an Architect-in-Residence program to help foster better communications between these groups. The first year of the program is now one-half completed and the activities of the Architect-in-Residence have fallen into three areas: (1) a resource for ongoing research activities at CBT; (2) liaison with the building community; and (3) a personal research project. This latter activity is a study of "The Introduction and Control of Natural Light in Buildings" and exemplifies the objectives of the program, the interrelationship of research work at CBT and the needs and demands of the working building community.

**15607.** Goldman, A. J., **The adequacy of management science technology for nonmilitary applications in the Federal Government,** (Proc. Workshop on Management Science in the Federal Government, Washington, D.C., Sept. 18, 1969), Chapter 6 in *Management and Policy Science in American Government,* M. J. White, M. Radnor, and D. A. Tansik, Eds., Part III, pp. 135-170 (Lexington Books, D. C. Heath & Co., Lexington, Mass., 1975).

Key words: management science; mathematical models; numerical analysis; operations research; systems analysis.

The "technology" of management science (MS) is here broadly construed to include physical equipment (e.g., high-speed computers), formal techniques (such as linear programming), paradigms and insights from various disciplines, and at the most basic level the analytical aptitudes of the management scientist. A middle ground is struck between those who consider this technology adequate and sound for the applications in question, and those who regard it as relatively useless for the nonquantitative value-laden problems facing nonmilitary government agencies. The discussion of adequacy and soundness includes the elements of: practical availability of methods and data (the technology's "raw material"); soundness in actual employment; and usefulness in principle when values and/or qualitative considerations are prominent. Some speculative comments are offered concerning the disparity, between promise and actuality, in MS contributions to governmental decision-making and operating procedures. In particular, some principal advantages of MS technology seem subject to considerable negation by typical attributes of large organizations.

**15608.** Kan, P. T., Peterson, G. A., Webb, D. V., Szalata, Z. M., O'Connell, J. S., Fivozinsky, S. P., Lightbody, J. W., Jr., Penner, S., **Electrodisintegration of $^3$He,** *Phys. Rev. C* **12,** No. 4, 1118-1125 (Oct. 1975).

Key words: continuum; electron scattering; helium-3; monopole state; multipole decomposition; zero range approximation.

The continuum spectra of $^3$He have been measured up to excitation energies of 40 MeV by means of inelastic electron scattering. Incident electron beam energies between 60 and 120 MeV were used, corresponding to a momentum transfer range of 0.3 fm$^{-1}$ to 1.1 fm$^{-1}$. Scattered electrons were observed at two angles, 92.6 and 127.7°. The radiation corrected spectra and the form factors are presented, and compared with calculations based on a zero-range approximation. In this model, the sharp rise from the $p+d$ threshold previously reported may be identified as a $^2S \rightarrow {}^2S$ Coulomb monopole transition.

**15609.** Walker, G. R., Minor, J. E., Marshall, R. D., **The Darwin cyclone valuable lesson in structural design,** *Civ. Eng.* **45,** No. 12, 82-86 (Dec. 1975).

Key words: buildings; codes and standards; cyclones; natural disasters; structural engineering; wind damage; wind loads.

Damage to buildings in Darwin, Australia caused by Cyclone Tracy is described. The approximate cyclone track and probable maximum wind speeds are presented along with an assessment of the performance of several types of buildings under extreme wind loading. Australian activities in reconstruction are discussed and it is concluded that what happened at Darwin provides a strong argument for the reassessment of residential construction practices in the United States.

**15610.** Rubin, S., **Thermal resistance measurements on monolithic and hybrid Darlington power transistors,** (Proc. 1975 IEEE Power Electronics Specialists Conf., Culver City, Calif., June 9-11, 1975), *PESC 75 Record,* **75-CHO,** 965-4 AES, 252-261 (The Institute of Electrical and Electronics Engineers, New York, N.Y., Sept. 1975).

Key words: Darlington hot spot screen; Darlington thermal resistance; emitter-only switching; hot spot screen for Darlingtons; integrated power Darlington thermal resistance; thermal resistance measurement.

A method for measuring the thermal resistance, $R_\theta$, of integrated power Darlington transistors is described that is based upon the emitter-only switching technique. It is shown that for specified measurement conditions this method can be used to measure the average thermal resistance, $R_{\theta(1+2)}$, of the input and output transistors of the Darlington pair and is therefore applicable to production-line monitoring of the thermal characteristics of the Darlington. It is shown that although a direct measurement of the thermal resistance, $R_{\theta(2)}$, of the output transistor cannot be made for most Darlingtons, an indirect determination of $R_{\theta(2)}$ can be made using the emitter-only switching technique and a simple equation. Comparisons of the differences between the infrared-determined thermal resistance and the electrically-measured thermal resistance of Darlingtons and of discrete power transistors illustrate that the accuracy of the Darlington measurements is comparable with that achievable for discrete devices. It is also shown that measurements which attempt to use the collector-base voltage of the output transistor of the Darlington as a temperature-sensitive-parameter, either alone or in conjunction with an output commutating diode (when present), are too sensitive to the magnitude of the measuring current to be reliable. Also, the use of the base-current screen for hot spots, as used for discrete transistors, is marginally applicable to integrated Darlingtons, but it is shown that the emitter-base voltage sensed during emitter-only switching is quite effective for detecting hot-spot formation.

**15611.** Krauss, M., Neumann, D., **Ion-pair states of $O_2$,** *J. Chem. Phys.* **63,** No. 12, 5073-5076 (Dec. 15, 1975).

Key words: ion-pair; $O_2$; photodissociation; predissociation; Rydberg states; valence states.

Valence states of $O_2$ that correlate adiabatically to the ion pair asymptote, $O^+(^4S) + O^-(^2P)$, have been calculated using the multiconfiguration description of the electronic structure. The production of the ion pair is attributed to valence-Rydberg mixing that predissociates Rydberg states of the excited $O_2^+$ ion such as those leading to the $b\,^4\Sigma_g^-$ state. The electronic states required the calculation of excited states of a given symmetry. This is possible with the BISON-MC codes if the rigorous restriction on orthogonality to the lower states is relaxed. For homonuclear valence states, in particular, this should be a good approximation.

**15612.** Cezairliyan, A., Righini, F., **Measurement of melting point, radiance temperature (at melting point), and electrical resistivity (above 2,100 K) of zirconium by a pulse heating method,** *Rev. Int. Hautes Temp. Refract.* **12,** No. 3, 201-207 (1975).

Key words: electrical resistivity; high-speed measurements; high temperature; melting point; normal spectral emittance; radiance temperature; zirconium.

A subsecond duration pulse heating method is used to measure the melting point, radiance temperature (at 650 nm) at the melting point, and electrical resistivity (above 2,100 K) of zirconium. The results yield a value of 2,128 K for the melting point on the International Practical Temperature Scale of 1968. The radiance temperature (at 650 nm) of zirconium at its melting point is 1,940 K, and the corresponding normal spectral emittance is 0.367. At 2,100 K electrical resistivity is $128.7 \times 10^{-8}\ \Omega$ m. Estimated inaccuracy is: 8 K in the melting point and in the radiance temperature, and 3 percent in the normal spectral emittance and in the electrical resistivity.

**15613.** Teague, E. C., **Surface finish measurements: An overview,** *Soc. Manuf. Eng. Tech. Pap.* **IQ75-137,** 1-21 (1975).

Key words: electron microscopes; horizontal resolution; optical instruments; stylus instruments; surface texture measurement; surface texture parameters; vertical resolution.

This paper reviews existing methods of surface finish measurement. The methods are considered from the standpoint of measurement systems whose components – specimen surface, measuring instrument, analyzing equipment and data display devices are equally important. Stylus, optical and electron optical instruments are evaluated and compared in terms of peak-to-valley-range, measurement area, vertical resolution, horizontal resolution, and profile measuring capability. Finally, the use of a digital computer as part of a measurement system will be discussed.

**15614.** Greenberg, O. W., Nelson, C. A., **Composite models of leptons,** *Phys. Rev. D* **10,** No. 8, 2567-2573 (Oct. 15, 1974).

Key words: composite model of leptons; electron number; leptonic quarks; lorks; muon-electron universality; muon number; neutrino quarks; strong interactions; three triplet model.

We give ten criteria for composite models of leptons, and present two models which satisfy a number of these criteria. Both models use three triplets of leptonic analogs of quarks which we call "leptoquarks"; the first model uses fractionally charged leptoquarks and the second model uses integrally charged ones. In the second model, leptoquarks and quarks could be identical and there is a possibility of unifying the description of leptonic and hadronic phenomena. Both models assign leptons to nonsinglet representations of SU(3)″. A plausible SU(3)″ mass formula allows the known leptons to be less massive than baryons if leptoquarks and quarks are identical.

**15615.** Lee, T. G., Parker, W. J., Tryon, M., **Laboratory fire performance characteristics of a dibromotetrafluoroethane-blown**

**rigid polyurethane foam,** *J. Fire Flammability* **6,** 499-510 (Oct. 1975).

Key words: dibromotetrafluoroethane; fire tests; flame spread index; heat release rate; ignition temperature; rigid urethane foam; smoke.

The fire performance characteristics of a dibromotetrafluoroethane-blown rigid polyurethane foam with a core density of 0.046 g/cm$^3$ were measured by several laboratory test methods. Measurements included: surface flammability, smoke and gases generated at elevated temperature and during combustion, ignition temperature, rate of heat release, and fire growth. The maximum concentration of the blowing agent in the specimen was approximately 13 wt percent. The release of the blowing agent from the heated specimen began at about 60 °C and reached a rate of about 3 wt percent/hr at 100 °C. The material had a flame spread index (ASTM E 162) of 11 and smoke levels (NFPA 258-T) of 170 and 480, maximum specific optical density under nonflaming and flaming exposures, respectively. The measured rate of heat release was 8.8 W/cm$^2$, about five times that of a fibrous glass insulation. The measured flash ignition temperature was 530 °C for the material.

**15616.** Hughes, C. E., Singletary, W. E., **Triadic partial implicational propositional calculi,** *Zeitschr. f. math. Logik und Grundlagen d. Math.* **21,** 21-28 (1975).

Key words: degrees of unsolvability; propositional calculus; recursion theory; undecidability.

A partial implicational propositional calculus (PIPC) is an inference system having as axioms some finite set of tautologies of the implicational calculus. Its rules of inference are substitution and modus ponens. Its decision problem is the problem of deciding for an arbitrary well-formed formula whether or not it may be inferred. A given PIPC is said to be *n*-adic if at most *n* propositional variables appear in any of its well-formed formulas. In this paper we investigate decision problems for triadic (3-adic) PIPC's. The major results presented are: (i) every r.e. many-one degree is represented by the class of decision problems for triadic PIPC's, denoted $I_3$; (ii) not every r.e. one-one degree is represented by $I_3$; and (iii) the class of decision problems for partial propositional calculi is many-one equivalent to $I_3$.

**15617.** Quintiere, J., **The application and interpretation of a test method to determine the hazard of floor covering fire spread in building corridors,** *Proc. Int. Symp. on Fire Safety of Combustible Materials, Edinburgh, Scotland, Oct. 15-17, 1975,* **1,** 355-367 (1975).

Key words: corridor fire; experiments; flame spread; floor-covering; test method; theory.

In recent years, much attention has been given to measuring the potential flame spread hazard of building corridors, in which a floor covering material is the only combustible present. The intention has been to develop standards for floor coverings which will limit corridor flame spread when the corridor is exposed to a large room fire. Under such circumstances, flame spread along the corridor floor is promoted by radiant heat transfer due to the room fire.

The proposed test method measures the flame spread characteristics of a floor covering material under an external radiant heat flux. One parameter the test measures is the external heat flux at the point of extinguishment. This has been interpreted as the minimum or "critical" radiant heat flux required to support flame spread. A theoretical model was developed to simulate the physical characteristics of the test method and sample materials.

The test method can be applied to measure the potential hazard of building corridors with floor coverings by comparing the critical flux measured for a material with an anticipated corridor heat flux due to a large fire. Results are presented which display corridor floor heat flux for various room fire intensities. These results are compared to theoretical predictions which illustrate the effect of corridor geometry and fire conditions on heat flux to the floor.

**15618.** Hocken, R., Moldover, M. R., Muth, E., Gerner, S., **Versatile cells for optical studies in fluids,** *Rev. Sci. Instrum.* **46,** No. 12, 1699-1700 (Dec. 1975).

Key words: cell; Kovar; sapphire; temperature; thickness.

We describe high quality optical cells designed for ease of cleaning and accurate definition of optical path length. The cells perform well from liquid nitrogen temperatures to 500 K at pressures up to 11 MPa (112 atm).

**15619.** Miller, A., Hussmann, E. K., McLaughlin, W. L., **Interferometer for measuring fast changes of refractive index and temperature in transparent liquids,** *Rev. Sci. Instrum.* **46,** No. 12, 1635-1638 (Dec. 1975).

Key words: calorimeter; dosimetry; electron beam; interferometer; radiation chemical kinetics; radiation measurement; refractive index; temperature measurement.

A double-beam interferometer has been designed for detecting changes of refractive index in transparent liquids associated with the absorption of ionizing radiation energy, due to short electron beam pulses from an accelerator. The response time of the interferometer is less than 0.2 $\mu$sec, and refractive index changes of the order of $10^{-7}$ can be measured, corresponding to a temperature change of $\sim 10^{-3}$ °C and an absorbed dose in water of $\sim 350$ rad. The interferometer can be used as either a real-time or integrating radiation dosimeter, if the temperature coefficient of the refractive index $(dn/dT)$ is known for the irradiated liquid in the temperature region of interest.

**15620.** Cullen, W. C., **The composite roofing membrane,** *The Roofing Spec.* **3,** No. 5, 17-21 (Sept. 1975).

Key words: application procedures; built-up roofing systems; composite membrane; composition; performance criteria.

The Composite Roofing Membrane is an indispensable component of the built-up roofing system. The paper reviews the functions of the membrane's components and the importance of application procedures on the quality and performance of the membrane. The impact of the development of performance criteria for the composite roofing membrane is described.

**15621.** Blanc, R. P., **Availability and useability of computer communication networks,** *Proc. Seventh Int. Conf. on Systems Sciences, Honolulu, Hawaii, Jan. 8-10, 1974,* pp. 10-13 (1974).

Key words: computer networks; computer terminals; networking technology; value-added networks.

The technological characteristics of existing approaches to computer networking technology are reviewed for the purpose of identifying those features which lend themselves particularly well to the interconnection of computers, as well as computer terminals.

**15622.** Rubin, R. J., Mazur, J., **Ordered spans of unrestricted and self-avoiding random-walk models of polymer chains. I. Space-fixed axes,** *J. Chem. Phys.* **63,** No. 12, 5362-5374 (Dec. 15, 1975).

Key words: Monte Carlo analysis; ordered spans; self-avoiding polymer chains; shape of polymer chains; spans; unrestricted polymer chains.

An $N$-step random walk on a cubic lattice is adopted as a model of a random polymer chain. The spans, or extents, of each random walk configuration in the principal lattice directions are arranged in order of magnitude, $\xi_3 \geqslant \xi_2 \geqslant \xi_1$. In the case of the unrestricted random walk, the average values of the ordered spans $\langle \xi_{i,u} \rangle$ and $\langle \xi_{i,u}^2 \rangle$, $i=1$, 2, and 3, are calculated analytically in the limit of large $N$. The limiting relative values of the first moments, $\langle \xi_{i,u} \rangle$ are 1.637 : 1.267 : 1; and the limiting values of the second moments $\langle \xi_{i,u}^2 \rangle$ are 2.710 : 1,600 : 1. In the case of the restricted or self-avoiding walk, the corresponding average spans $\langle \xi_{i,r} \rangle$ and $\langle \xi_{i,r}^2 \rangle$ are estimated for $N \leqslant 150$ by using a Monte Carlo procedure. The same Monte Carlo procedure is used to estimate the values of $\langle \xi_{i,u} \rangle$ and $\langle \xi_{i,u}^2 \rangle$ for $N \leqslant 1000$. On the assumption that the rate of approach of the average ordered snaps of the self-avoiding walks to their asymptotic forms is similar to the rate of approach of the average ordered spans of the unrestricted walks to their asymptotic forms, the following estimates are obtained for the ordered spans of the self-avoiding walks: $\langle \xi_{i,r}(N) \rangle = \bar{\xi}_{i,r} N^{0.61}$ for $N \gg 1$ and $\bar{\xi}_{3,r} : \bar{\xi}_{2,r} : \bar{\xi}_{1,r} = 1.75 : 1.31 : 1$. The relative values of the estimates of the second moments of these ordered spans for $N \gg 1$ are $\langle \xi_{3,r}^2 \rangle : \langle \xi_{2,r}^2 \rangle : \langle \xi_{1,r}^2 \rangle = 3.08 : 1.71 : 1$. A simple ellipsoidal model is analyzed in order to obtain estimates of the intrinsic spans of the two kinds of random walks. It is assumed that all random walks have the same intrinsic dimensions and form (ellipsoidal), but that their principal axes are oriented at random. The average ordered spans with respect to a set of orthogonal space-fixed axes of this randomly oriented ensemble of ellipsoids depend uniquely on the principal diameters of the ellipsoid (intrinsic spans). A procedure is devised to solve the inversion problem of determining the relative lengths of the principal diameters which correspond to a given set of relative ordered moments with respect to space-fixed axes. The relative values obtained for the principal diameters of the ellipsoid are 2.59 : 1.61 : 1 in the case of the unrestricted random walk and 3.05 : 1.77 : 1 in the case of the self-avoiding walk.

**15623.** Cezairliyan, A., McClure, J. L., **A subsecond pulse heating technique for the study of solid-solid phase transformations at high temperatures: Application to iron,** *High Temp. Sci.* **7**, 189-196 (1975).

Key words: high-speed measurement; high temperature; iron; phase transformation; thermodynamics.

A system based on an accurate pulse heating technique is described that can be used for investigations of solid-solid phase transformations at temperatures above 1500 K. The system is capable of heating the specimen from room temperature to its melting point in less than 1 s and of measuring the pertinent experimental quantities every 0.4 ms with a full-scale signal resolution of approximately one part in 8000. Specimen temperature is measured with a high-speed photoelectric pyrometer and recordings of experimental quantities are made with a high-speed digital data acquisition system. Application of the technique to investigations at the $\gamma \rightarrow \delta$ transformation point of iron is described. Measurements yielded the following results: 1683 K for the transformation temperature, 890 $\mathrm{J \cdot mol^{-1}}$ for the transformation energy, and 0.36 for the normal spectral emittance (at 0.65 $\mu$m) at the transformation point.

**15624.** Masters, L. W., Reichard, T. W., **Evaluation of adhesive-bonded joints in housing components of glass fiber-reinforced polyester laminate,** (Proc. American Society for Testing and Materials Conf. on Composite Reliability, Las Vegas, Nev., Apr. 15-16, 1974), Paper in *Composite Reliability, Am. Soc. Test. Mater. Spec. Tech. Publ.* **580**, pp. 146-156 (American Society for Testing and Materials, Philadelphia, Pa., Aug. 1975).

Key words: adhesive bonding; aging tests (materials); composite materials; glass fibers; housing system; laminates; reinforced plastics; shear strength; sustained loading; tensile strength.

A series of tests was performed on sandwich panel housing components made with glass fiber-reinforced polyester (FRP) laminates. Specifically, long- and short-tests were performed to evaluate the adhesive bonds between the FRP laminate facings and cores of the panels. Specimens of two different FRP laminates were analyzed and their bonding characteristics with two different adhesives were studied. The test data show that the bond strength was significantly affected by the laminate formulation, adhesive formulation, adhesive thickness, sustained loading, and temperature.

**15625.** Lovas, F. J., **Application of microwave spectroscopy to chemical analysis,** *ISA Trans.* **14,** No. 2, 145-151 (1975).

Key words: applications; chemical analysis; microwave; qualitative analysis; quantitative analysis; rotational spectra.

Traditional analytical techniques have been successfully employed on a great variety of systems for identifying stable reaction products as well as for purity analysis and reaction efficiency. However, most analytical techniques generally can only be applied to "well behaved" chemical systems. Since gas phase reaction products do not always follow the "well behaved" guideline, an alternate analytical tool, such as microwave spectroscopy, could prove beneficial for analyzing such systems and may well provide some new routes to synthetic chemistry. A general review of the present state-of-the-art for applications of microwave techniques to analytical studies will be presented. An attempt will be made to describe the limitations and advantages of microwave spectroscopy for probing chemical systems for product identification and for optimization of the efficiency of gas phase chemical reactions. As an illustration, some recent results obtained in our laboratory on the complex pyrolytic decomposition reactions of ethylamine will be described. Further examples of possible applications will be taken from typical industrial processes that employ vapor phase chemical synthesis techniques.

**15626.** Chwirut, D. J., **Tensile creep of angle-plied boron/epoxy laminates,** *J. Test. Eval.* **3,** No. 6, 442-448 (1975).

Key words: angle-plied laminates; boron/epoxy; composite materials; creep; viscoelasticity, linear and nonlinear.

Tensile creep tests were performed at 75 °F (24 °C) and 300 °F (149 °C) on 26 specimens cut from ±30-deg and ±45-deg laminates of boron/epoxy composite material to characterize the creep behavior of these materials. A linear viscoelastic laminate theory proposed by McQuillen was compared with the experimental data for the tests run at 75 °F (24 °C). The predicted creep strains differed greatly from the measured values, indicating that the linear theory is not applicable to laminates with these filament orientations. A general creep equation of the form $\epsilon = k\sigma^m t^n$ was fitted to the experimental data with excellent correlation. The stress exponents $m$ varied from 1.79 to 5.17 for the four series of tests, thus characterizing the nonlinear behavior of boron/epoxy laminates with these filament orientations.

**15627.** Ausloos, P., **Pulse radiolysis of alkanes in the gas-phase, ion-molecule reactions and neutralization mechanism of hydrocarbon ions,** (Proc. Symp. on Mechanisms of Hydrocarbon Reactions, Siófok, Hungary, June 5-7, 1973), Paper in *Mechanisms of Hydrocarbon Reactions,* F. Márta and D. Kalló, Eds., *Plenary Lecture* **3,** pp. 603-624 (1975).

Key words: charge recombination rate constants; cobalt gamma radiolysis; hydrocarbons; ion-molecule reaction; neutralization mechanisms; pulse radiolysis.

A discussion is presented of the fate of unreactive hydrocarbon ions in various selected gaseous systems. It is shown that experiments performed with the high radiation dose rates obtained in pulse radiolysis experiments have several advantages over conventional low dose rate experiments for the elucidation of the mechanism of homogeneous neutralization of unreactive hydrocarbon ions. This is so because the charged species has a much shorter life-time with respect to neutralization under high dose rate (pulse radiolysis) conditions, so that the reaction of the ions with minor impurities or accumulated products is much less probable than in low dose rate experiments. It is further shown through a few examples, that quantitative information about the rate constants of neutralization events and ion-molecule reactions can be obtained when the dose rate is high enough for neutralization and chemical reaction to be in competition. Once reliable rate constants for neutralization and ion-molecule reactions are derived, one can obtain a quantitative evaluation of the products which will be formed in the pulse radiolysis of a hydrocarbon gas mixture from a computer calculation.

**15628.** Birky, M. M., **Review of smoke and toxic gas hazards in fire environment,** *Proc. Int. Symp. on Fire Safety of Combustible Materials, Edinburgh, Scotland, Oct. 15-17, 1975,* **1,** 231-252 (1975).

Key words: bioassay; combustion products; fire; hazard assessment; toxicity.

Fire statistics show that at least 50 percent of the fire related deaths can be attributed to "smoke inhalation." Detailed investigations of fire fatalities and autopsies of fire victims show that the interaction of carbon monoxide, pulmonary injury, alcohol and cardiovascular disease plays a role in many of these deaths.

The research efforts designed to assess the toxicological effects of products of thermal degradation can be divided into three broad categories: (1) assessment based on extensive chemical analysis, (2) assessment based on analyzing for specific toxicants and (3) assessment based on bioassay techniques frequently combined with analysis for a few selected toxicants.

Assessment categories 1 and 2 have mainly addressed the problem of the gaseous phase of the degradation products, with little consideration given to the particulate phase (smoke). These methodologies illustrate the limitation of basing a hazard assessment on the assumption that the toxicity of the fire environment is due solely to a few known toxicants. In addition, the particulate phase may play a predominant role in the inhalation toxicity that cannot be assessed with chemical analysis. One concludes that due to the complexity of the fire environment, an assessment of this hazard will require the combined efforts of toxicologist, chemists and combustion scientists.

**15629.** Mathey, R. G., Cullen, W. C., **Performance criteria for built-up roofing—Part 2,** *Roofing Siding Insulation* **52,** No. 1, 44-46, 56 (Jan. 1975).

Key words: bituminous roof membranes; performance attributes; performance criteria; physical and engineering properties; test methods.

This report is the last in a series of publications on performance criteria for built-up roof membranes. To remind the reader of the scope of these articles, the authors' introductory remarks for Part I follow. The development of a performance approach to bituminous built-up roof membranes is described and preliminary performance criteria are recommended. A number of test methods have been developed in order to obtain data to evaluate roofing membranes against the recommended criteria. Twenty attributes that affect the performance of roof membranes under service conditions are identified and laboratory tests are described for measuring the engineering properties of the membrane that pertain to many of these attributes. A level of performance is recommended for nine of the identified performance attributes.

**15630.** McCaffrey, B. J., Quintiere, J. G., **Fire-induced corridor flow in a scale model study,** *Proc. International Council on Building Research and Documentation (CIB) Symp. on the Control of Smoke Movement in Building Fires, Garston, Watford, England, Nov. 4-5, 1975,* **1,** 34-47 (1975).

Key words: corridors; fire induced flow; recirculating flow; scale-model; smoke movement; stratified flow; theory.

The flow induced by a room fire was studied within a corridor for a scale model configuration. The effect of corridor exit opening was determined for a fixed room door opening and temperature gradient. Velocity and temperature measurements were made. At the room doorway and corridor exit the thermally stratified flow would enter and leave with a sharp boundary between the counter current flows. However, within the corridor the flow was more complex, giving rise to a large recirculating zone traversing the corridor length and trapped between the hot ceiling jet and entering cold flow. Smoke tracer visualization techniques illuminated these complex flow patterns along with mixing caused by shedding vortexes. These flow results are quantitatively presented and their nature is discussed. The measured total mass flow rate induced into the corridor was measured and compared to theoretical results. At this time, the implications of these complex corridor flows in a scale-model must be limited until they are verified in similar full-scale experiments and their nature is more thoroughly understood.

**15631.** Berg, J. L., **Federal Privacy Act countdown—Is the private sector ready?,** *Infosystems* **22,** No. 7, 25-27 (July 1975).

Key words: privacy; privacy legislation; privacy planning.

Reporting on the joint NBS/MITRE workshop, *Planning for Action—the Privacy Mandate,* the article provides, in capsule form, a description of the workshop with specific attention to those comments of use to EDP managers.

**15632.** Buchbinder, B., **Pilot implementation of the Fire Incident System,** *Fire J.* **69,** No. 3, 65-69 (May 1975).

Key words: data; fire; fire incident system; fire service; incident reports; loss; National Fire Data System.

The Fire Incident System (FIS) is based on a data file of individual fire incident reports from the fire services. The pilot implementation of the Fire Incident System is an integral part of the National Fire Data System. This paper examines the objectives of the pilot project, describes the system and its participants, and discusses the project status.

**15633.** Cotton, I. W., **Cost-benefit analysis of interactive systems,** *Proc. Second Jerusalem Conf. on Information Technology, Jerusalem, Israel, July 29-Aug. 1, 1974,* pp. 729-746 (1974).

Key words: cost-benefit analysis; cost-effectiveness; economics; interactive systems; performance evaluation.

This report assesses the state-of-the-art in cost-benefit analyses of interactive systems and suggests an approach for developing improved methodology. Cost-benefit analyses are distinguished from analyses of system performance in that the latter are directed at optimizing system performance at a given level of investment, while the former are directed at justifying the investment itself.

Methods of analyzing the performance and costs of computer systems in general and interactive systems in particular are discussed. With this information it is shown how cost-effectiveness analyses may be performed. The next crucial step is to conduct benefit analysis, an ill-defined art. The results of benefit analysis must be combined with cost-effectiveness analysis in order to perform the desired cost-benefit analysis.

An experimental methodology is suggested for better performing benefit analyses of interactive systems. A more rigorous formulation of the cost-benefit procedure is then outlined. No attempt is made in this report to actually perform such an analysis.

**15634.** Hudson, R. P., Pfeiffer, E. R., **Magnetic susceptibility of single-crystal CMN, 0.002K to 2K,** (Proc. 14th Int. Conf. on Low Temperature Physics, Otaniemi, Finland, Aug. 14-20, 1975), Paper in *Low Temperature Physics* **LT-14,** M. Krusius and M. Vuorio, Eds., **3,** 242-245 (North Holland Publishing Co., Amsterdam, 1975).

Key words: CMN; entropy; magnetic susceptibility; magnetic temperature; thermodynamic temperature.

Correction of a small systematic error present in our earlier measurements leads to a much improved determination of the magnetic temperature (T*) scale for single crystal CMN. These latest results are compared with recently published findings of another laboratory.

**15635.** Buchbinder, B., Buchbinder, L. B., **The fire hazard analysis process at the National Bureau of Standards,** *Proc. Int. Symp. on Fire Safety of Combustible Materials, Edinburgh, Scotland, Oct. 15-17, 1975,* **1,** 156-161 (1975).

Key words: clothing flammability; fabric flammability; fire hazard; fire investigation; flammability testing; hazard analysis; hazard quantification.

The Office of Information and Hazard Analysis (OIHA) performs its hazard analysis function by means of a multi-faceted program combining in-depth case history investigation of fire accidents, laboratory experimentation, fire testing, and data analysis to identify and characterize specific hazards.

Hazard characterization serves to influence the formulation of basic fire research, to guide test method development for codes and standards, to identify data required to be collected, and to provide input to public education for fire safety. These functions are performed in concert with other United States government agencies, including the National Fire Prevention and Control Administration (NFPCA) in the Department of Commerce with which we have a close working relationship, and the Consumer Product Safety Commission which we support in product standard development.

The main portion of this paper defines the current fire hazard analysis process illustrated by results from the fabric flammability project, describes how this process is evolving into the more quantitative process of the future, and discusses the data needed for future hazard models.

**15636.** Parrish, W. R., Steward, W. G., **Vapor-liquid equilibria data for helium-carbon monoxide and helium-nitrous oxide systems,** *J. Chem. Eng. Data* **20,** No. 4, 412-416 (Oct. 1975).

Key words: binary mixture; experimental vapor-liquid equilibria; helium-carbon monoxide system; helium-nitrous oxide system; Henry's constants.

Liquid-vapor data are reported for the helium-carbon monoxide system at 80, 85, 90, 100, and 120K and for the helium-nitrous oxide system at 195, 215, 235, 245, 255, 265, and 285K at pressures up to 138 bars. The data are analyzed for internal consistency using pseudo-Henry's law constants and enhancement factors.

**15637.** Beers, Y., Howard, C. J., **The microwave spectrum of $HO_2$ near 65 GHz,** *J. Chem. Phys.* **63,** No. 10, 4212-4216 (Nov. 15, 1975).

Key words: $HO_2$; hydroperoxyl; microwave.

Using a Zeeman-modulated cavity spectrometer with a 10 sec time constant and a phase locked klystron, we have observed in the products of a discharge-flow system, Zeeman components of the six allowed zero-field lines at 65 070 ± 2, 65 082 ± 2, 65 098 ± 2, 65 373 ± 2, 65 397 ± 2, and 65 401 ± 2 MHz, and of one forbidden zero-field line at 65 369 ± 4 MHz. The $Q$ of the Fabry-Perot cavity is about 10 000, and the magnetic field was swept from 0-30 G. Chemical tests indicate that the observed lines are due to $HO_2$. They have been assigned and least-squares fitted using a simple theoretical model to yield a value of 65 185 ± 2 MHz for the $1_{01}$-$0_{00}$ asymmetric rotor transition frequency of $HO_2$, a value of $-208 \pm 2$ MHz for the linear combination $(\epsilon_{bb}+\epsilon_{cc})/2$ of elements of the electron spin-molecular rotation interaction tensor, a value of $-28 \pm 2$ MHz for the nuclear spin-electron spin Fermi contact interaction parameter $\sigma$, and a value of $+4 \pm 2$ MHz for the spin-spin tensor interaction parameter $\lambda$. These constants are in excellent agreement with three less precise constants obtained from an earlier laser magnetic resonance study and have been confirmed by recent more accurate measurements of Saito.

**15638.** Clough, R. B., **The effects of specimen size and microstructure on the Larson-Miller parameter,** *Scr. Metall.* **9,** No. 12, 1325-1329 (1975).

Key words: crack nucleation; elevated temperature; failure prediction; Larson-Miller parameter.

There is a great need for the standardization of methods for predicting elevated temperature material failure. Generally, metallurgical instability limits the accuracy of these methods. Quantitative metallurgical models predicting lifetimes from microscopic parameters are virtually nonexistent. Here an elementary metallurgical model of the well-known Larson-Miller parameter is developed, based on the thermally-activated nucleation of Griffith-type cracks. The concept of the activation volume for fracture is introduced. The analysis permits calculation of the size and surface energy of crack nuclei from stress-rupture curves. These are computed theoretically from stress rupture data of typical high temperature iron- and nickel-base alloys. No independently measured nuclei size data exists, but the surface energies agree with energies obtained from similar alloys by direct measurement. The analysis also predicts that the stress-rupture lifetime is a sensitive function of crack nucleus surface energy, and gives a quantitative rationale for the invariability of the constant in the Larson-Miller parameter predicted from microstructural values.

**15639.** Straty, G. C., **Hypersonic velocities in saturated and compressed fluid methane,** *Cryogenics* **15,** No. 12, 729-731 (Dec. 1975).

Key words: compressibility; interferometry; light scattering; methane; sound velocity; specific heat ratio.

Brillouin scattering techniques have been used to measure the velocity of hypersonic waves in gaseous and liquid methane. Measurements were made on the saturated liquid and vapour and along selected isotherms to a maximum pressure of about 17.5 MPa. The data, which agree well with previously measured ultrasonic velocities, have been combined with PVT data to obtain the isentropic compressibility and the ratio of specific heats.

**15640.** Cotton, I. W., **Remark on stably updating mean and standard deviation of data,** *Commun. ACM* **18,** No. 8, 458 (Aug. 1975).

Key words: data analysis; mean; standard deviation; statistics; updating estimates.

Hanson's article describes an elegant procedure for recomputing the weighted mean and standard deviation of a series of numbers when new values are added. As he observes, in the case of unit weights a considerable simplification occurs; however, he does not present the simplest equations for this case. This remark derives simple results for updating mean and standard deviation in the case of unit weights, when only the previous values of mean, standard deviation, number of occurrences and the new datum are known.

**15641.** Kanda, M., **Accuracy considerations in the measurement of the power gain of a large microwave antenna,** *IEEE Trans. Antennas Propag.* **AP-23,** No. 3, 407-411 (May 1975).

Key words: calibration; ground antenna; standard antenna gain; three-antenna extrapolation.

Accuracy considerations in the measurement of the power gain of a large microwave antenna are discussed. The analysis indicates that, using the power gain comparison method with a standard antenna of nominally 40-dB gain, a large antenna with a power gain of nominally 60 dB could be calibrated to within an error of 0.17 dB ($3\sigma$). The power gain of the standard antenna is considered to be determined via the generalized three-antenna extrapolation method. Individual sources of errors in both the generalized three-antenna extrapolation method and the power gain comparison method are discussed.

**15642.** Abrams, M. D., **Consumer-oriented measurement of computer network performance,** *Proc. IEEE National Telecommunications Conf., San Diego, Calif., Dec. 2-4, 1974,* pp. 843-844 (1974).

Key words: computer; consumer; contract; evaluation; network; performance.

This short paper describes measurement of computer network services from the consumer's viewpoint. Two common measures of performance are described. The ICST Network Measurement Machine and its data analysis programs are presented as a prototypical device capable of measuring network service for analysis according to various criteria. Sample results are given. Application of measurement to procurement and contractual obligations is discussed.

**15643.** Pyke, T. N., Jr., **Networked minis and micros—Configurations, applications, and standards,** *Proc. Mini Micro Computer Symp., U.S. Naval Academy, Annapolis, Md., Apr. 15, 1975,* pp. 44-46 (1975).

Key words: microcomputers; minicomputers; networks; standards.

Both minis and micros have found their way into extensive use as a part of computer networks. Minicomputers have a head start, but microcomputers will fast catch up in numbers, especially as a part of terminals connected to networks. Mini/micro network configurations can be divided into two categories, local and distributed. Most research-oriented and operational networks can be placed directly into one of these categories. Successful development and operation of these networks employing minis and micros requires a variety of standards, both internally and externally.

**15644.** Lawton, R. A., Andrews, J. R., **Pulsed-laser application to sampling oscilloscope,** *Electron. Lett.* **11,** No. 7, 138 (Apr. 3, 1975).

Key words: GaAs; laser; photoconductor; sampling oscilloscope.

An optically strobed sampling oscilloscope is described in which a GaAs laser diode is used to strobe a GaAs photo-conductive sampling gate.

**15645.** Hamilton, C. A., Phelan, R. J., Jr., Day, G. W., **Pyroelectric radiometers,** *Opt. Spectra* **9,** No. 10, 37-38 (Oct. 1975).

Key words: electrically calibrated; pyroelectric; radiometer.

The performance and detailed operation of an electrically calibrated pyroelectric radiometer are discussed.

**15646.** Zimmerman, J. E., **Phase slip, dissipation, Bernoulli effect, parametric capacitance, and other curious features of the Josephson effect,** *IEEE Trans. Magn.* **MAG-11,** No. 2, 852-855 (Mar. 1975).

Key words: Josephson effect; phase slip; weak superconductivity.

The details of the Josephson effect in thin metal bridges are difficult to derive quantitatively, and many papers have been written on the subject attempting to describe quantitatively such qualitative features as irreversible phase slip, instantaneous $2\pi$ phase slip, variation of order parameter in time and space, Bernoulli effect, and others. It does not seem to be generally recognized that all of these qualitative features are universal attributes of the Josephson effect and occur also in tunnel junctions. In addition, when a steady voltage is impressed across a junction, a term in the electric field is set up (in addition to the Bernoulli field) which has a rather complex temporal and spatial variation.

**15647.** Andrews, J. R., Gans, W. L., **Pulsed wavemeter timing reference for sampling oscilloscope calibration,** *IEEE Trans. Instrum. Meas. Short Papers,* **IM-24,** No. 1, 82 (Mar. 1975).

Key words: oscilloscopes; pulsed wavemeter timing.

A pulsed wavemeter technique is described that is useful as a source of microwave frequency sine waves for the time base calibration of sampling oscilloscopes.

**15648.** Bussey, H. E., Richmond, J. H., **Scattering by a lossy dielectric circular cylindrical multilayer, numerical values,** *IEEE Trans. Antennas Propag.* **23,** No. 5, 723-725 (Sept. 1975).

Key words: cylinder scattering; electromagnetic scattering; lossy dielectric; multilayer cylinder; reference values; scattering.

The theoretical scattering solution for a plane wave incident normally on a lossy dielectric multilayer circular cylinder of infinite length is outlined. Numerical values of the modal scattering coefficient for TE and TM modes are given for several single and multilayer cylinders. Verifications of the results are described. The values may serve as reference data.

**15649.** Hoer, C. A., Roe, K. C., **Using an arbitrary six-port junction to measure complex voltage ratios,** *IEEE Trans. Microwave Theory Tech.* **MTT-23,** No. 12, 978-984 (Dec. 1975).

Key words: attenuation; automation; detector; insertion loss; microwaves; phase angle; ratio; six-port junction; vector voltmeter; voltage.

An arbitrary six-port junction is analyzed as a microwave vector voltmeter, measuring the amplitudes and phase differences of two input signals in terms of power readings taken at the remaining four ports. The junction may be calibrated for measuring the complex ratio of these two signals using a self-calibration procedure which requires no attenuation or phase standards.

**15650.** Engen, G. F., **Automated calibration of directional-coupler-bolometer-mount assemblies,** *IEEE Trans. Microwave Theory Tech.* **MTT-23,** No. 12, 984-990 (Dec. 1975).

Key words: automation; calibration; directional coupler; microwave; microwave power.

Although the application of automated methods to power calibration problems in the UHF and microwave region has been described by a number of authors, the primary orientation has been towards the calibration of bolometer mounts and similar items. Little has been published on the problem of calibrating directional-coupler-bolometer-mount assemblies, which also play a major role in the calibration and measurement of UHF and microwave power.

This paper develops a theoretical basis for several different approaches to this measurement problem.

**15651.** Lawton, R. A., Scavannec, A., **Photoconductive detector of fast-transition optical waveforms,** *Electron. Lett.* **11,** No. 4, 74-75 (Feb. 20, 1975).

Key words: detector; dye laser; GaAs; photoconductor; picosecond; pulse.

The letter reports the development of a fast-response bulk photoconductor that can be used as a photodetector and as an optically gated switch. The photoconducting material used is semi-insulating, chromium-doped GaAs, a sample of which is mounted in a 50 Ω stripline holder. An estimated detector transition time of 92 ps or less was obtained from tests made with a mode-locked dye laser.

**15652.** Ott, W. R., Slater, J., Cooper, J., Gieres, G., **$H^-$ shape-resonance studies in an arc plasma,** *Phys. Rev. A* **12,** No. 5, 2009-2016 (Nov. 1975).

Key words: arc; hydrogen; negative ion; plasma; resonance; vacuum ultraviolet.

Calculations by Macek have shown that the $H^-$ photoabsorption cross section should be affected by a shape resonance at 1129.5 Å. This experiment is an attempt to observe the resonance in emission according to the reaction $e+H \rightarrow [H^-]^* \rightarrow H^- + h\nu$. The plasma is in a condition of local thermodynamic equilibrium and is generated by a stationary wall-stabilized hydrogen arc. With an axis temperature of 14 000 K and 1 atm pressure, the $H^-$ free-bound continuum contributes only about 2 percent of the total radiation which is dominated in the 1130-Å region by the Ly-$\alpha$ wing. However, the peak of the shape resonance, according to Macek, should have a cross section about 25 times greater than the continuous free-bound cross section; therefore, it should appear as a very noticeable 50 percent structure superimposed on the Ly-$\alpha$ wing. Except for some small features which are attributed to weak molecular emission, there is no obvious indication of the shape resonance in either deuterium or hydrogen spectra between 1105 and 1135 Å. It is estimated that the minimum feature which could have been detected at 1129 Å was about 2 percent of the total signal.

**15653.** Andrews, J. R., **Directional-coupler technique for triggering a tunnel diode,** *IEEE Trans. Instrum. Meas.* **IM-24,** No. 3, 275-277 (Sept. 1975).

Key words: directional coupler; picosecond; pulse generator; risetime; trigger; tunnel diode.

Present tunnel diode (TD) pulse generators have distortions in the pulse baseline and topline due to feedthrough of the triggering signal. This paper presents a new technique for reducing the trigger-induced distortions. A directional coupler is used to couple the trigger signal to the TD.

**15654.** Birmingham, B. W., Smith, C. N., **Cryogenics and the energy crisis,** *Cryogenics* **15,** No. 3, 115-118 (Mar. 1975).

Key words: coal gasification; cryogenics; energy crisis; hydrogen economy; LNG; superconducting electrical equipment and instrumentation.

This paper reviews some of the ways cryogenics can help solve the energy crisis. Five specific areas are covered: the use of LNG, the conversion of coal to fuel gas using oxygen from air separation plants, the use of superconductors in power plants and electrical transmission lines, superconducting instruments for geophysical exploration of new energy resources, and the Hydrogen Economy.

**15655.** Ventre, F. T., **Transforming environmental research into regulatory policy,** (6th Annual Meeting of the Environmental Design Research Association (EDRA), Lawrence, Kans., Apr. 23, 1975), Paper in *Responding to Social Change,* pp. 277-284 (Dowden, Hutchinson & Ross, Inc., Stroudsburg, Pa., Apr. 1975).

Key words: applied research; building codes; building design; building standards; diffusion of information; regulation.

Outlines a means enabling environmental design researchers to participate in the formulation of regulatory policies affecting buildings. The standards system is shown to be an underused channel for relaying research findings to building professionals and the regulatory system is shown to be a potential means for directing building technology toward socially-valued ends. Notes include a brief listing of standards- and codes-generating organizations.

**15656.** Buchbinder, B., Mathers, W., **Preliminary indications from survey of U.S. household fire experience,** *Proc. 8th Annual Meeting Information Council on Fabric Flammability, New York, N.Y., Dec. 5, 1974,* pp. 174-178 (1975).

Key words: Census Bureau; Consumer Product Safety Commission; data; fire; households; injury; loss; National Fire Data System; National Fire Survey; survey.

A survey of over 33,000 U.S. households was conducted in April, 1974. It was sponsored by the National Bureau of Standards and the Consumer Product Safety Commission. This paper discusses the survey scope and the accuracy of the national estimates. Estimates are presented of the number of household-related fires, classified by such parameters as ignition source and room of origin. Property loss and injury estimates are given.

**15657.** Branstad, D. K., **Encryption protection in computer data communications,** *Proc. Fourth Data Communications Symp., Quebec City, Canada, Oct. 7-9, 1975,* pp. 8-1 –8-7 (1975).

Key words: communications; computer security; cryptography; data security; encryption; network security; security.

Encryption can be an effective process for protecting data during transmission within distributed computer systems and networks. The degree of protection provided by encryption depends on the encryption algorithm employed, the implementation of the algorithm and the administrative procedures regulating the use of algorithm. Additional security requirements of user identification, access authorization and security auditing may be satisfied by combining encryption technology with a network access control machine in a network security center. This paper presents an encryption algorithm for use in computer data communications and the security requirements that are satisfied by proper use of the algorithm. It also discusses the use of a network access control machine to enforce access restrictions for the network.

**15658.** Andrews, J. R., Baldwin, E. E., **Baseband impulse generator useful to 5 GHz,** *Proc. 1975 IEEE Int. Symp. on Electromagnetic Compatibility, San Antonio, Tex., Oct. 7-9, 1975,* pp. 1-4 (1975).

Key words: impulse generator; picosecond; spectrum; spectrum amplitude; step recovery diode.

A baseband impulse generator recently developed at NBS is described. It is completely solid state and features a 100 kHz maximum repetition rate, 50 ohm source impedance, an extremely narrow 100 ps duration impulse of 8 volts amplitude, and a flat spectrum greater than 60 dB$\mu$V/MHz up to 5 GHz. The generator was evaluated on the NBS Automatic Pulse Measurement System which measured the time domain waveform with a sampling oscilloscope and computed the spectrum on a minicomputer.

**15659.** Newell, A. C., **Improved polarization measurements using a modified three antenna technique,** *Proc. IEEE Int. AP-Symp., Urbana/Champaign, Ill., June 2-4, 1975, Session* **15,** pp. 337-340 (1975).

Key words: antennas; measurement; polarization.

Absolute polarization parameters have previously been obtained using a 3-antenna measurement technique. By a modification of this approach, the accuracies of the results are significantly increased, and the measurements are easier to perform. This work demonstrates the power and utility of using complex rather than scalar polarization parameters in formulating polarization problems.

**15660.** Daywitt, W. C., Kanda, M., **G/T measurement errors with radio stars,** *Proc. IEEE Int. AP-Symp., Urbana/Champaign, Ill., June 2-5, 1975, Session* **20,** pp. 460-463 (1975).

Key words: antenna gain; G/T; radio star; satellite communications.

This talk highlights often-overlooked or poorly treated aspects in G/T error analyses for satellite communication earth terminals. In particular, correction factors due to star size, differential system temperature, antenna pointing, and refractive attenuation used in G/T measurements are discussed in detail.

**15661.** Andrews, J. R., Gans, W. L., **Time domain automatic network analyzer,** (Proc. Colloque International sur L'Electronique et la mesure, Paris, France, May 26-30, 1975), Paper in *La Mesure Electrique de Precision,* pp. 258-267 (Le Comité d'Organisation du Colloque International sur L'Electronique et la mesure, Paris, France, 1975).

Key words: attenuation; automated measurement; network analyzer; pulse; S parameters; time domain.

NBS has recently developed a Time Domain Automatic Network Analyzer (TDANA). It measures the S parameters of RF and microwave networks as a function of frequency using pulse measurement techniques. The signal source is typically a tunnel diode pulse generator with a 10-90 percent risetime of less than 20 ps. This generator produces a useful amplitude spectrum extending from dc to beyond 18 GHz. The receiver is a sampling oscilloscope with a 20 ps risetime. The oscilloscope is controlled by a minicomputer. The data measured by the oscilloscope is stored and processed in the minicomputer. The minicomputer averages the data to improve the signal to noise ratio, then Fourier transforms the time domain data into frequency domain data and calculates the S parameters. Examples of measurements are presented. They include the measurement of 40 dB attenuators to 12.5 GHz.

**15662.** Engen, G. F., **Automated calibration of directional-coupler-bolometer-mount assemblies,** *Proc. IEEE-MTT-S Int. Microwave Symp., Palo Alto, Calif., May 12-14, 1975,* pp. 85-97 (Institute of Electrical and Electronics Engineers, Inc., Piscataway, N.J., May 1975).

Key words: calibration; calibration factor; directional coupler; measurement; microwave; microwave power.

Although the application of automated methods to power calibration problems in the UHF and microwave region has been described by a number of authors, the primary orientation has been towards the calibration of bolometer mounts and similar items. Little has been published on the problem of calibrating directional-coupler-bolometer-mount assemblies, which also play a major role in the calibration and measurement of UHF and microwave power.

This paper describes several approaches to this measurement problem.

**15663.** Achenbach, P. R., Didion, D. A., **Energy conservation measures in the National Bureau of Standards laboratory complex,** *Proc. Energy Conservation and Energy Management in Buildings, London, England, Nov. 13-14, 1975,* pp. 51-68 (1975).

Key words: building retrofit; building systems; energy conservation in buildings; HVAC automatic control; HVAC systems; measurement of building energy.

Energy conservation measures at the National Bureau of Standards site are being carried out under two separate but interrelated programs; a low-investment, immediate-impact program and a long-range, major retrofit program. The low-investment program has already been implemented and includes lighting reductions, thermostat resettings and nighttime shutdowns of heating, ventilating, air conditioning systems. Data on energy usage before and after this program was instituted are presented. The methodology and analysis of the long-range program are also presented. Various building energy conservation options were considered and evaluated by means of a mathematical model. Quantitative estimates of savings for each are presented. The decision to invest in automatic controls for the air conditioning systems of the laboratory complex and steam/chilled-water power plant is discussed.

**15664.** Newell, A. C., Yaghjian, A. D., **Study of errors in planar near-field measurements,** *Proc. IEEE Int. AP-Symp., Urbana/Champaign, Ill., June 2-4, 1975, Session* **20,** pp. 470-473 (1975).

Key words: antennas; error analysis; measurements; near-field.

In recent years, planar near-field antenna measurements have been developed and used in a number of applications. One of the primary concerns with this, or any, measurement approach is the accuracy of the results; that is, how do errors in measured near-field quantities affect the accuracies of far-field parameters such as gain, side lobe level, monopulse difference level, beam width, etc. Some efforts have been made in the past to estimate these errors, but the results have been limited in generality and primarily of a qualitative nature.

We have used a two-fold approach to obtain equations giving reasonable upper-bound errors resulting from systematic and random errors in the near-field measurements. The strategy has been to derive error expressions from the equations relating near and farfield quantities and also to simulate errors on actual measured near-field data. The simulation has been given some direction to, and confirmed the results of the analysis. The errors which have been investigated are: truncation of the measurement area, x, y, and z-position errors of the probe, amplitude and phase uncertainties of the measured data, and multiple reflections between the probe and test antenna. The results not only give the effects of errors in a given quantity, but also specify the form of the error (i.e., linear, quadratic, periodic, etc.) which will produce the largest effect. This information is very valuable in designing the measuring equipment so that these types of errors can be avoided or minimized.

**15665.** Hoer, C. A., Roe, K. C., **Using an arbitrary six-port junction to measure complex voltage ratios,** *Proc. 1975 IEEE Microwave Theory and Technique Symp. Int., Palo Alto, Calif., May 12-14, 1975*, pp. 98-99 (1975).

Key words: attenuation; microwave; phase angle; ratio; self-calibration; six-port; vector voltmeter; voltage.

An arbitrary six-port junction is analyzed as a microwave vector voltmeter, measuring the amplitudes and phase difference of two input signals in terms of power readings taken at the remaining four ports. The junction may be calibrated for measuring complex voltage ratios using a self-calibration procedure which requires no standards.

**15666.** Kanda, M., **A measure for the stability of solid state noise sources,** *Proc. 1975 IEEE Microwave Theory and Technique Symp. Int., Palo Alto, Calif., May 12-14, 1975*, pp. 315-317 (1975).

Key words: Allan variance; argon gas noise source; cross correlation; solid state noise source; stability measure.

A measure for the stability of solid state noise sources is discussed. Its applicability is demonstrated. A technique similar to cross correlation is employed to separate the instabilities of the noise source from those of the measurement system.

**15667.** Kasen, M. B., **Mechanical and thermal properties of filamentary-reinforced structural composites at cryogenic temperatures. 2: Advanced composites,** *Cryogenics* **15,** No. 12, 701-722 (Dec. 1975).

Key words: advanced fiber composites; cryogenics; dynamic mechanical properties; literature review; static mechanical properties; thermal properties.

The low-temperature mechanical and thermal properties of advanced-fiber reinforced structural composites are reviewed. The magnitude and range of particular properties are discussed with respect to composite type and temperature. A property-material cross reference is given with a 128-entry bibliography. This is Part 2 of a two-part series. Part 1 considered glass-reinforced composites.

**15668.** Sibley, E. H., **Summary of CODASYL report on selection and acquisition of data base management systems,** *Digest of Papers, Association for Computing Machinery 1975 Conf., Minneapolis, Minn., Sept. 1974*, 3 pages (1974).

Key words: acquisition; CODASYL; computer; data base management; designers; evaluation; selection; users.

This report presents a method for the selection and acquisition of a data base management system as part of the development of an automated information processing system. It does not attempt to discuss all aspects of information systems, but only those that are pertinent to the utilization of a data base management system. Those issues which relate to information system design, as well as the design and implementation considerations of a data base management system are deferred. This report is the third in a series of CODASYL System Committee reports on its efforts to build up an expertise in and to develop advanced languages for data processing. The report should be of significant value to users and designers of such systems, since it approaches the question of evaluation and selection by relating users needs to system capabilities.

**15669.** Lyon, G., Walker, J. C., **On some polynomial search methods for hash tables of prime and composite sizes,** *Proc. Canadian Information Processing Society (CIPS) Nat. Conf., Regina, Sask., Canada, June 25, 1975*, pp. 290-299 (1975).

Key words: collision resolution; hash tables; polynomial search; pseudo-random numbers; scatter storage.

Necessary and sufficient conditions are given for a simple collision resolution polynomial bi**k to search fully a hash table of prime size. Sufficient conditions are then established which ensure a search of all locations of any table using a polynomial bi**k + ai. Observations on special cases for bi**k + ai relate this polynomial to the more simple search bi**k. A final example illustrates a typical pseudo-random sequence generated by a polynomial bi**k + ai.

**15670.** Fong, E., **A benchmark test approach for generalized data base software,** *Proc. COMPCON fall Conf. Digest, Washington, D.C., Sept. 8-10, 1975*, 7 pages (1975).

Key words: benchmark testing; data base management; performance measurement; test data bases; test transactions.

A benchmark test approach for generalized data base software is described. Although the benchmark test has been designed to experiment on one specific data base management system, the approach is rather general and applicable to many data base management systems that are currently available. The benchmark test consists of the specification of a test data base and the specification of a set of processing transactions to exercise the candidate software on the test data base. This benchmark test can be used both to measure the performance of a data base management system, and as a saturation test. The two parameters to be used in the saturation test are data base size and workload. The data base size is varied by increasing the number of records within the test data base. The workload is varied analytically via a queueing model.

**15671.** Hiza, M. J., Kidnay, A. J., Miller, R. C., **Equilibrium properties of fluid mixtures, a bibliography of data on fluids of cryogenic interest,** Volume in *NSRDS Bibliographic Series*, 160 pages (IFI/Plenum Data Co., New York, N.Y., 1975).

Key words: bibliography; calorimetric measurements; fluid mixtures; Joule-Thomson coefficients; phase equilibria; review.

This bibliography contains references to experimental data for ten equilibria properties of fluid mixtures. The data considered are: solid-liquid, solid-vapor, solid-liquid-vapor, liquid-liquid, liquid-vapor, and gas-gas. In addition, there are sections on liquid mixture densities, gas or vapor mixture densities, Joule-Thomson coefficients, and calorimetric measurement.

**15672.** Allan, D. W., Hellwig, H., Glaze, D. J., **An accuracy algorithm for an atomic time scale,** *Metrologia* **11,** No. 3, 133-138 (1975).

Key words: coordinate time scales; frequency calibration; international frequency comparisons; optimum frequency estimate; primary frequency standards; relativity; SI second; time scale accuracy algorithm; time scale stability.

The accuracy of the rate or frequency of an atomic time scale is the degree to which its unit agrees with the SI second. Primary frequency standards are constructed in such a manner that they provide the most accurate possible physical realization of the SI second. These standards are then used to calibrate or construct an atomic time scale which may also be used as a stable reference standard.

Mathematical models characterizing the performance of both the primary frequency standards and reference standards are developed, and based on these models a current best estimate of the SI second is derived utilizing current and previous calibrations.

The modeling techniques and theory are applied to the NBS primary frequency standards and atomic time scale system and a significant improvement is realized in the accuracy of the frequency estimate so derived. We estimate that the second used by the Bureau International de l'Heure in generating TAI and UTC was too short by about $9 \pm 2$ parts in $10^{13}$ during the fall of 1974.

**15673.** Walls, F. L., Wainwright, A. E., **Measurements of the short-term stability of quartz crystal resonators—a window on future developments in crystal oscillators,** *Proc. 6th Annual Precise Time and Time Interval (PTTI) Planning Meeting, Washington, D.C., Dec. 3-5, 1974,* pp. 143-153 (1974).

Key words: crystal controlled oscillator; fast linewidth; quartz crystal resonators; short-term stability; spectral density of frequency fluctuations; time domain stability.

Recent measurements of the inherent short-term stability of quartz crystal resonators will be presented. These measurements show that quartz resonators are much more stable for times less than 1 s than the best available commercial quartz oscillators. A simple model appears to explain the noise mechanism in crystal controlled oscillators and points the way to design changes which should permit more than 2 orders of magnitude improvement in their short-term stability. Stabilities of order 1 part in $10^{12}$ at. 0.001 s appear obtainable. The achievement of short-term stabilities of this level would in many cases greatly reduce the time necessary to achieve a given level of accuracy in frequency measurements. Calculations show that a reference signal at 1 THz, derived from frequency multiplying a 5 MHz source with the above measured crystal stability, should have an instantaneous or fast linewidth of order 1 Hz. These calculations explicitly include the noise contribution of our present multiplier chains and will be briefly outlined.

**15674.** Hellwig, H., Wainwright, A. E., **Submicrosecond time transport with a rubidium portable clock,** *Proc. 29th Annual Symp. on Frequency Control, Atlantic City, N.J., May 28-30, 1975,* pp. 384-386 (1975).

Key words: clock; frequency stability; frequency standard; time comparison.

Based on a commercially available rubidium standard, the National Bureau of Standards (NBS) developed a portable rubidium clock. Technical modifications which improve the temperature and magnetic environment characteristics allow stabilities in the $10^{-12}$ range under typical clock transport conditions. The physical size is such that the clock can be carried as hand baggage on commercial airlines allowing up to 18-hours continuous battery operation.

**15675.** Walls, F. L., DeMarchi, A., **RF spectrum of a signal after frequency multiplication; measurement and comparison with a simple calculation,** *IEEE Trans. Instrum. Meas.* **IM-24,** 210-217 (Sept. 1975).

Key words: frequency multiplication; linewidth; multiplier chain; precision oscillator; rf spectrum; spectral density of phase fluctuations; spectral purity.

A novel experimental technique is introduced and used to measure the effect of frequency multiplication on the RF spectrum of an oscillator. This technique makes it possible to produce the RF spectrum at $X$ band—where measurements are relatively straightforward—that would have been produced by frequency multiplication of the 5-MHz source to any frequency from 9.2 GHz to 100 THz ($10^{14}$ Hz). A simplified theory is developed and shown to reproduce the experimental results for the relative power in the carrier and noise pedestal, and the shape and the width of the carrier and noise pedestal, to within the measurement uncertainty of 2 or 3 dB, from 5 MHz to 10 THz. The calculations are easily made using analytical techniques from the measurement of the spectral density of phase fluctuations of the source, the effective input spectrum density and the bandwidth of the multiplier chain, and the frequency multiplication factor. It is shown that present 5-MHz-crystal-controlled oscillators are useful as a precision source to $\sim 500$ GHz. Suggestions for extending their range to $\sim 100$ THz are made.

**15676.** Stein, S. R., **Application of superconductivity to precision oscillators,** *Proc. 29th Annual Symp. on Frequency Control, Atlantic City, N.J., May 28-30, 1975,* pp. 321-327 (1975).

Key words: cavity stabilization; frequency multiplication; funnel diode oscillator; parametric oscillator; superconducting oscillator.

Advances in superconducting technology during the last decade have resulted in many experimental applications in the generation of stable frequencies. The properties which make superconducting resonators attractive are their high Q, high frequency, and high operating power level. A variety of techniques can be used to make a superconducting cavity the frequency determining element of an oscillator. They include cavity stabilization via injection locking of a free-running oscillator, negative feedback to a voltage-controlled oscillator, positive feedback around an amplifier, and coupling to a negative resistance amplifier. These techniques are discussed in terms of some of their theoretical and practical limitations with particular emphasis placed on the goal of achieving state-of-the-art frequency stability. The best performance obtained with a superconducting oscillator to date is summarized.

At NBS, work on superconducting oscillators is primarily motivated by the need for a microwave signal which can be multiplied to the infrared and used to measure the frequency of a laser with no loss in precision as compared to the primary cesium standard. The signal source which has been selected for this purpose is the superconducting parametric oscillator. Its principles of operation are discussed along with the reasons why it is expected to have state-of-the-art short-term frequency stability.

**15677.** Evenson, K. M., **Frequency measurements in the optical region and the speed of light,** (Proc. ICO Conf. Optical Methods in Science and Industrial Measurements, Tokyo, Japan, Aug. 26-30, 1974), *Japan J. Appl. Phys.* **14,** Suppl. 14-1, 1-10 (1975).

Key words: laser frequency measurements; speed of light.

Since the advent of the laser and saturated absorption locking of the laser, the extension of radio frequency technology into the optical region has produced exciting new results, such as a 10 000 fold increase in the resolution of spectroscopy in this region and a new value of the speed of light, 100 times more accurate than the previously accepted value. This paper will describe the techniques and results achieved.

**15678.** Roberts, R. W., **The other face of the measurement base,** *Anal. Chem.* **47,** No. 7, 648A-656A (June 1975).

Key words: length; mass; National Bureau of Standards; reference methods; SI units.

The universal language of measurement is provided by the International System of Units. Progress leading to the present definitions of some of the SI base units, and research that may lead to improved definitions, is described. Work at the National Bureau of Standards that is of interest to analytical chemists, such as atomic weight determinations, standard reference data, physical constants, calibrations, etc., is also described.

**15679.** Achenbach, P. R., **National Bureau of Standards research in support of energy conservation standards for buildings,** *Proc. 10th Intersociety Energy Conversion Engineering Conf., Newark, Del., Aug. 18-22, 1975*, pp. 667-676 (1975).

Key words: building research; building standards; economics of energy conservation; energy conservation; energy conservation research; energy savings.

Initiation of an energy conservation program for buildings revealed that, until very recently, buildings and the mechanical and electrical equipment installed therein have been designed for low first cost, with little attention given to energy cost. Current efforts to draft energy conservation standards for buildings showed that neither the energy conservation potential nor the life-cycle costs of many well-known energy conservation techniques are established. The research program of the National Bureau of Standards on energy conservation in buildings is presented in overview, and selected projects are discussed in some detail to show the types of information being developed in the laboratory, and in full-scale studies of new and existing buildings. Additional research needs for energy standards purposes are identified.

**15680.** Evenson, K. M., Howard, C. J., **Laser magnetic resonance spectroscopy,** *Laser Spectrosc.*, pp. 535-540 (1975).

Key words: CH; free radical; HCO; $HO_2$; laser magnetic resonance; OH; pollution.

Laser magnetic resonance spectroscopy provides one of the most sensitive techniques ever devised for the detection of free radicals such as OH, CH, $HO_2$, and HCO. Paramagnetic molecules inside a laser cavity are Zeeman tuned into coincidence with the laser frequency and a decrease in laser power is detected. With this technique, the reaction rates of free radicals can be measured in a reaction flow system.

**15681.** Evenson, K. M., Petersen, F. R., Wells, J. S., **Speed of light from direct laser frequency and wavelength measurements: Emergence of a laser standard of length,** *Laser Spectrosc.*, pp. 143-146 (1975).

Key words: laser frequency; laser wavelength; length standard; speed of light.

Recent frequency and wavelength measurements of a methane stabilized laser yield a value of the speed of light 100 times less uncertain than the previously accepted value. Various possibilities using lasers as radiation sources for a new length standard are discussed. One possibility is to fix the value of the speed of light in the redefinition of the meter.

**15682.** Kamas, G., **TV color frequencies defended as accurate,** *Electron. Design Letter to the Editor* **13**, 7 (June 21, 1975).

Key words: crystal oscillator; frequency calibration; network-originated programs; NBS traceability; phase comparison; television.

This letter is a reply to a previous letter to the editor regarding accuracy of TV color signals to calibrate oscillators.

**15683.** Glaze, D. J., Hellwig, H., Allan, D. W., Jarvis, S., Jr., Wainwright, A. E., **Accuracy evaluation and stability of the NBS primary frequency standards,** *IEEE Trans. Instrum. Meas.* **IM-23**, 489-501 (Dec. 1974).

Key words: accuracy; accuracy evaluations; cavity phase shift; cesium beam tube; frequency stability; interaction length; phase noise; primary frequency standards; Ramsey cavity.

The National Bureau of Standards has two primary standards for frequency and the unit of time. They are both cesium devices and are designated NBS-4 and NBS-5. The design of NBS-5 is discussed in detail, including its relationship to its predecessor NBS-III, and a brief description of NBS-4 is given. NBS-4 and NBS-5 have been used since January 1973 for a total of twelve calibrations of the NBS Atomic Time Scale.

The application of pulsed microwave excitation, and the use in the accuracy evaluations of frequency shifts due to known changes in the exciting microwave power are discussed. Measurements of the atomic velocity distributions are reported.

A stability of $9 \times 10^{-15}$ derived from the comparison of NBS-4 and NBS-5 is reported for averaging times of 20 000 s, and data on accuracy are given. Results obtained to date give an evaluated accuracy of $1\text{-}2 \times 10^{-13}$ with indications that this accuracy may be improved in the future.

The bias-corrected frequencies of NBS-4 and NBS-5 agree to within $(1 \pm 10) \times 10^{-13}$ with the value obtained for NBS-III in 1969 – which value is preserved in the rate of the NBS Atomic Time Scale.

**15684.** Allan, D. W., Daams, H., **Picosecond time difference measurement system,** *Proc. 29th Annual Symp. on Frequency Control, Atlantic City, N.J., May 28-30, 1975*, pp. 404-411 (1975).

Key words: atomic clocks; frequency measurements; frequency stability; phase delay; precise time metrology; subpicosecond time difference measurements; time stability.

Recently a time difference measurement system was developed in the Frequency and Time Standards Section of the National Bureau of Standards and independently at the National Research Council which shows more than three orders of magnitude improvement over that which is currently available commercially. Current state-of-the-art time difference measurement devices have specified accuracies of about 1 nanosecond. Measurement precision and potential accuracy of better than 1 picosecond has been demonstrated in this new time difference measuring device. This has significant implications in frequency and time metrology using: state-of-the-art frequency standards and clocks. A brief report was given on this measurement system at the PTTI Planning Meeting at the Naval Research Laboratory on the 5th of December 1974. This paper will give more detailed circuit diagrams necessary to build up such a measurement system.

This particular measurement system has the advantage that it can measure time differences with accuracies of a few picoseconds and with repetition rates ranging from a few milliseconds to as slow a repetition rate as would be desirable, thus expanding convenient measurement of time domain stabilities of frequency and time standards over several decades with only one measurement system. The system is also very amenable to self-calibration and self-noise analysis. Specifically, a fractional frequency stability of about $10^{-16}$ was measured for the noise of this measurement system at a sample time of $10^3$ s.

**15685.** Drullinger, R. E., Hessel, M. M., Smith, E. W., **New laser measurement techniques for excited electronic states of diatomic**

**molecules,** *Proc. Megeve Laser Spectroscopy Conf., Megeve, France, June 23-27, 1975, Lecture Notes in Physics,* 91-99 (1975).

> Key words: diatomic mercury; excimer molecules; fluorescence; lasers; NaK molecule; spectroscopy.

This paper will briefly outline several new laser measurements techniques which we have developed for the analysis of excited electronic states of diatomic molecules. For molecules which have bound ground states, a visible laser is used to selectively excite a single vibration-rotation level in the electronic state of interest. We then use DC Stark effect, RF double resonance and various fluorescence techniques, as discussed in Sections I and II, to obtain excited state dipole moments, lifetimes, quenching cross sections, transition moments as a function of internuclear distance, and other molecular structure data. We have also developed new laser excitation techniques and used optical double resonance methods for excimer molecules which have repulsive ground states and are bound only in their excited states. These techniques, discussed in Sections III and IV, have been used to obtain potential energy curves, *f*-values, lifetimes and various kinetic rates.

**15686.** Hessel, M. M., Drullinger, R. E., Broida, H. P., **Chemiluminescent reactions in a heat-pipe oven,** *J. Appl. Phys.* **46,** No. 5, 2317-2318 (May 1975).

> Key words: BaO; chemical reactions; chemiluminescent; electronic spectra; heat-pipe ovens; $N_2O$.

A heat-pipe oven has been used to contain and control the chemiluminescent reaction $Ba + N_2O \rightarrow BaO^* + N_2$. The heat-pipe oven permits Ba vapor to be maintained at any desired pressure. Reactions were easily controlled by varying the flow rate of $N_2O$ or pressure of Ba. A large volume (about 20 $cm^3$) of chemiluminescence was produced and spectra were taken from 0.1 to 5 torr. In addition to emission from BaO $A^1\Sigma$-$X^1\Sigma$, numerous atomic Ba lines also have been observed. This device is well suited to the study and control of chemical reactions between metal vapors and oxidizers.

**15687.** Walls, F. L., Wainwright, A. E., **Measurement of the short-term stability of quartz crystal resonators and the implications for crystal oscillator design and applications,** *IEEE Trans. Instrum. Meas.* **IM-24,** 15-20 (Mar. 1975).

> Key words: crystal controlled oscillator; fast linewidth; quartz crystal resonators; short-term stability; spectral density of frequency fluctuations; time domain stability.

A new technique is presented which makes it possible to measure the inherent short-term stability of quartz crystal resonators in a passive circuit. Comparisons with stability measurements made on crystal controlled oscillators indicate that noise in the electronics of the oscillators very seriously degrades the inherent stability of the quartz resonators for times less than 1 s. A simple model appears to describe the noise mechanism in crystal controlled oscillators and points the way to design changes which should improve their short-term stability by two orders of magnitude. Calculations are outlined which show that with this improved short-term stability it should be feasible to multiply a crystal controlled source to 1 THz and obtain a linewidth of less than 1 Hz. In many cases, this improved short-term stability should also permit a factor of 100 reduction in the length of time necessary to achieve a given level of accuracy in frequency measurements.

**15688.** Evenson, K. M., Petersen, F. R., **Stabilized lasers and applications,** *Proc. Physics of Quantum Electronics Summer School, Crystal Mountain, Wash., July 8-20, 1973,* pp. 367-436 (1975).

> Key words: laser frequency measurements; laser strainmeter; saturated absorption spectroscopy; speed of light; the meter.

Three papers are reproduced which summarize some applications and uses of highly stabilized lasers and applications. Laser frequency measurements, the speed of light, a redefinition of the meter, ultrahigh resolution saturated absorption spectroscopy, the design and operation of a methane absorption stabilized laser strainmeter are all discussed.

**15689.** Howe, D. A., Salazar, H. F., **A digital 5.00688 MHz synthesizer and squarewave FM servo system for cesium standards,** *Proc. 29th Annual Symp. on Frequency Control, Atlantic City, N.J., May 28-30, 1975,* pp. 387-393 (1975).

> Key words: indirect synthesis; phase noise; squarewave servo.

The cesium clock transition is at 9, 192, 631, 770 Hz by definition. In the design of a cesium frequency standard, it is common to generate a 5-MHz signal which is locked to this transition. Since 5-MHz cannot be directly multiplied to match the exact clock transition frequency, usually another frequency is synthesized and mixed in such a way that the clock transition frequency is produced.

This paper describes a synthesizer using a 5-MHz reference which has an output frequency of 5.00688 MHz which is very nearly an integer submultiple of the cesium clock transition frequency. Indirect synthesis is used in which an internal (number controlled) oscillator is locked at a prescribed frequency offset relative to the reference. Resolution (quantization error) is 1.4 parts in $10^{13}$. A frequency stability plot $\sigma_y(\tau)$ of the synthesizer noise is presented. The synthesizer can be made very compact and reliable. Since its output has low phase noise, the signal may be multiplied directly to the cesium clock transition frequency. In a cesium standard, this simplifies the amount of microwave hardware compared to traditional schemes. The design concepts of the synthesizer can easily be extended in order to implement squarewave frequency modulation of the beam tube RF excitation.

**15690.** Casella, R. C., Rowe, J. M., Trevino, S. F., **Determining the number of independent real parameters in the phonon dynamical matrix,** *Phys. Rev. B* **12,** No. 10, 4573-4574 (Nov. 15, 1975).

> Key words: dynamical matrix; matrix, dynamical; phonon dynamical matrix; real parameters.

We apply the algorithm developed earlier by one of us to several illustrative examples and compare with results obtained by Warren and Worlton where difficulties occur as noted by these authors.

**15691.** Greer, S. C., Hocken, R., **Thermal expansion near a critical solution point,** *J. Chem. Phys.* **63,** No. 12, pp. 5067-5072 (Dec. 15, 1975).

> Key words: consolute point; critical exponent $\alpha$; critical phenomena; critical solution point; density; gravity effects; mixture, binary; mixture, liquid; nitroethane; thermal expansion; 3-methylpentane.

We report precise measurements of the density as a function of temperature in the one-phase region near the consolute point in nitroethane + 3-methylpentane. We find evidence of the critical anomaly in the thermal expansion, but are not able to determine a unique value for the critical exponent $\alpha$. We have performed computer experiments to determine under what conditions $\alpha$ could be extracted from thermal expansion data.

**15692.** Vagelatos, N., Rowe, J. M., Rush, J. J., **Lattice dynamics of $ND_4I$ in the NaCl phase (I) at 296°K,** *Phys. Rev. B* **12,** No. 10, 4522-4529 (Nov. 15, 1975).

Key words: acoustic phonons; lattice sodium-chloride; translational dynamics.

Dispersion curves for translational phonons propagating in the high-symmetry directions of sodium-chloride-phase $ND_4I$ have been determined at room temperature by coherent inelastic neutron scattering from single crystals. Acoustic phonons were well defined throughout the Brillouin zone. Optic phonons were considerably more difficult to measure because of the low signal-to-background ratio. The observed phonon energies were fitted to a "simple" and a "breathing" shell model with general repulsive short-range forces out to second neighbors. The results of the model fitting lead to conclusions similar to those reached in previous alkali halide studies. Model predictions of crystal properties are generally in good agreement with observation. The best fit model was used as in interpolation formula to calculate the density of states, $g(\nu)$. The mean-square displacements are in excellent agreement with those derived from the neutron-diffraction results of Seymour and Pryor. The lattice-dynamics results are compared with similar results obtained recently for the NaCl phases of the alkali cyanides.

**15693.** Abrams, M. D., **Computer communications network performance measurement (Abstract),** *Proc. Eurocon 1974 Conf. Digest on Electrotechnics, Amsterdam, The Netherlands, Apr. 22-26, 1974,* 2 pages (1974).

Key words: communications; computer; evaluation; measurement; network; performance.

This publication consists of an abstract only which describes computer networks, measures of service, measurement of service delivered, measured effects and applications.

**15694.** Cabana, A., Laurin, M., Lafferty, W. J., Sams, R. L., **High resolution infrared spectra of the $\nu_2$ and $2\nu_1$ bands of $^{14}N^{16}O_2$,** *Can. J. Phys.* **53,** No. 19, 1902-1926 (1975).

Key words: equilibrium structure; ground state constants; infrared spectrum; nitrogen dioxide, $2\nu_1$ band; nitrogen dioxide, $\nu_2$ band; upper state constants; vibration-rotation interaction constants.

The infrared spectra of two *B* type bands, $\nu_2$ and $2\nu_1$, of $^{14}N^{16}O_2$ have been recorded under high resolution. Ground state combination differences from these bands have been combined with combination differences obtained in previous studies and eight pure rotational microwave transitions to yield improved ground state rotational constants. Upper state constants and band centers for the $\nu_2$ and $2\nu_1$ bands are also reported. The $2\nu_1$ band contains internal intensity anomalies believed to arise from a weak Coriolis interaction with the much stronger $\nu_1+\nu_3$ band. Equilibrium rotational constants have been calculated. The equilibrium structure of the molecule is: $r_e = 1.1945 \pm 0.0005$ Å and $\Theta_e = 133.85 \pm 0.10°$. For the sake of comparison, effective, substitution, and average structures are also reported.

**15695.** Danos, M., **Relativistic nuclear physics, why and how?,** (Proc. Int. Conf. on Interaction Studies in Nuclei, Mainz, Germany, Feb. 17-20, 1975), Paper in *Interaction Studies in Nuclei,* H. Jochim and B. Ziegler, Eds., pp. 885-910 (North-Holland Publishing Co., The Netherlands, 1975).

Key words: axiomatic field theory; composite particles; Haag's theorem; nuclear structure; quantum field theory; relativistic nuclear physics.

It is proposed that by this time the development of physics has progressed to a point where one can tackle the "hydrogen atom" problem of nuclear physics, viz., a description of the deuteron "from first principles." This requires to formulate the problem in terms of strong interaction relativistic field theory. The contemporary work is done instead almost exclusively in terms of the quasi-relativistic framework of effective Lagrangian theory. The inherent inaccuracies of this framework are reviewed. A framework for actually solving the relativistic field theory problem is described. It requires inescapably to consider the composite structure of the deuteron. The nature of the stationary solutions is discussed; their relation to the results of the covariant treatment is explained, and the relevance to certain theorems of field theory is pointed out.

**15696.** Holt, D. R., Nahman, N. S., **Coaxial line pulse-response error due to a planar skin effect approximation,** *Proc. 1972 CPEM Conf. on Precision Electromagnetic Measurement, Boulder, Colo., June 26-29, 1972,* pp. 1-2 (1972).

Key words: coaxial; cylindrical; error; line; loss; response; skin effect; step; time; transition.

The purpose of this paper is to characterize the time domain step response error in the analysis of coaxial lines terminated in their characteristic impedence.

**15697.** Cataland, G., Plumb, H. H., **Fixed points: Superconductive transition temperatures of lead and indium,** *Metrologia* **11,** 161-163 (1975).

Key words: acoustical thermometry; fixed points; lead and indium transition temperatures; low temperature fixed points; low temperature thermometry; superconducting transition temperatures of lead and indium.

This note presents the temperature values for the superconductive transition fixed points ($T_c$) of lead and indium. Values of $T_c$ derived by interpolations on the NBS P(2-20K) 1965 scale are given. Determinations of isotherms by the NBS acoustical thermometer produced $T_c$'s of $7.199_0$ K ± 1.3 mK for lead and $3.414_2$ K ± 1.3 mK for indium.

**15698.** Sibley, E. H., **On the equivalences of data based systems,** *Proc. Association for Computing Machinery SIGMOD Conf., Ann Arbor, Mich., May 1-3, 1974,* **II,** 1-52 (1974).

Key words: data base technology; data manipulation, data structured; data manipulation, relational.

Practitioners of data base technology have been somewhat confused by the many different theories and systems for describing and manipulating data. The two major philosophies which have emerged may be termed the *relational* or set theoretic approach and the *data structured* or procedural approach. There are obviously differences in these, but there are also similarities.

This paper looks at these approaches from three aspects: (1) The method of describing data and its structure; (2) the methods of manipulating this data; and (3) the time of binding the data name to its operation.

**15699.** Fechter, J. V., Pezoldt, V. J., Persensky, J. J., Lepkowski, J. R., **Study of the National Standards for Directional and Other Official Signs. Overview of their adequacy,** *Report No. FHWA-RD-75-118,* 75 pages (Available from the National Technical Information Service, Springfield, Va., 22161, Oct. 1975).

Key words: driver information; highway; highway signing; human factors; information displays; standards.

In 1969 the Federal Highway Administration (FHWA) issued National Standards for Directional and Other Official Signs allowing owners of privately-operated scenic and historical sites to erect directional signs in a zone extending from the edge of the right-of-way to a distance 660 ft *(201.2 m)* beyond. Objectors to these Standards sought increases in the height, length, total area, and number of signs allowed. FHWA requested the assistance of the National Bureau of Standards (NBS) to respond to these requests and to evaluate the Standards with respect to the needs of motorists. NBS reviewed pertinent literature and analyzed hypothetical Standards-conforming signs. The analysis showed that the sign dimensions needed to display legible messages vary considerably as the values of each design variable (e.g., vehicle speed) are changed. For many speeds, sign locations, and driver characteristics, Standards-conforming signs are inadequate. The following conclusions were reached: (1) the Standards should require that sign characters be legible at the levels of visual acuity required by state driver licensing regulations, (2) maximum sign size should be specified in terms of the visual angle subtended, rather than as a maximum physical size, and (3) technical material does not support any change to the number of signs allowed to the spacing between signs, or to the spacing from signs to interchanges or exits.

**15700.** Rothschild, W. G., Rosasco, G. J., Livingston, R. C., **Dynamics of molecular reorientational motion and vibrational relaxation in liquids. Chloroform,** *J. Chem. Phys.* **62,** No. 4, 1253-1268 (Feb. 15, 1975).

Key words: chloroform; infrared spectra; molecular reorientation; Raman spectra; vibrational relaxation.

Vibrational and rotational (dipole and second-order tensor) correlation functions were obtained by Fourier inversion of infrared and Raman vibrational band contours of the three $\parallel$ and one $\perp$ fundamentals of liquid $CHCl_3$, $CDCl_3$, and isotopically pure $CH^{35}Cl_3$. All correlation functions are nonexponential at short times and approximately for long times. The symmetry axis of the molecule reorients by "free" jumps of about 1/3 rad, turning through a root-mean-square angle of 1 radian within 2 psec by about 13 orientational jumps. Computer simulations show that $J$ diffusion is too fast beyond 1 psec and that $M$ diffusion fits the data up to 4 psec ($\tau_J = 0.12$ psec); thereafter, $M$ diffusion is too slow. The Raman rotational correlation time is approximately equal to the NMR quadrupolar correlation time; the infrared rotational correlation time is only 0.75 of a corresponding dielectric relaxation time. Vibrational relaxation in the symmetric near-infrared carbon-hydrogen stretch is of the same order of importance as rotational relaxation; however, the dynamics of the vibrational relaxation of this mode do not support the presence of "hydrogen bonding" in the neat liquid. In the symmetric far-infrared carbon-chlorine deformation mode, vibrational relaxation is of considerably lesser significance than rotational relaxation throughout the whole time domain, whereas the rate of vibrational relaxation of the symmetric midinfrared carbon-chlorine stretch is intermediate to those of the other two symmetric fundamentals. None of these modes obeys vibrational energy dissipation or resonance vibrational energy transfer mechanisms induced by dipole-dipole interaction. The ratios of the derived polarizability tensor elements, which are required to evaluate the rotational correlation function of the degenerate mode (carbon-hydrogen deformation), were computed from formulations relating them to the bond polarizabilities: It appears that its Raman and infrared correlation functions do not contain the same vibrational correlation function and that the respective contour is determined essentially by nonorientational relaxation processes. An extensive analysis of the experimental errors inherent in our Raman band contour determinations is presented, as well as a critical comparison of our conclusions with previous results in the literature.

**15701.** Rosasco, G. J., Prask, H. J., **Polarized Raman study of lattice modes in ammonium perchlorate at low temperatures,** *Solid State Commun.* **16,** No. 1, 135-138 (1975).

Key words: ammonium perchlorate; lattice dynamics; Raman scattering; structure.

The Raman spectra of oriented single crystals of ammonium perchlorate have been measured as a function of temperature between 12 and 300 K. The results are consistent with the assignment of $NH_4ClO_4$ to the $D_{2h}^{16}$ space group at all temperatures. A weak $B_{1g}$ mode at 180 $cm^{-1}$ is assigned as an $NH_4^+$ libration. Anomalous temperature dependence is observed for low frequency $B_{1g}$ and $B_{3g}$ lattice modes. Detailed results are presented for these modes in the range 18-80 K.

**15702.** Utton, D. B., **The response of phase-sensitive detectors to Lorentzian and Gaussian lineshapes,** *J. Appl. Phys.* **46,** No. 12, 5268-5271 (Dec. 1975).

Key words: Gaussian; lineshapes; Lorentzian; phase sensitive detector.

Calculations are made of the response to Gaussian and Lorentzian lineshapes of a phase-sensitive detector operated at twice the modulation frequency. The modulation traverses the line resonance condition twice each cycle. Sensitivity to variations in linewidth, modulation width, and line center position are discussed. These are compared with the more common operation where small modulation widths result in signals proportional to the derivatives of the lineshape. A discussion is made of the effects on the phase-sensitive detector output of signals at the harmonics of the modulation frequency.

**15703.** Rosasco, G. J., Simmons, J. H., **Identification of sulfur deposits in bubbles in glass by Raman scattering spectroscopy,** *Am. Ceramic Soc. Bull.* **54,** No. 6, 590-591 (June 1975).

Key words: bubble content analysis; gas analysis; inclusions in glass; Raman spectroscopy of sulfur; sulfur identification.

Raman scattering spectroscopy was conducted on solid deposits in bubbles in glass. Elemental sulfur was identified as forming small spherical deposits, amorphous in appearance. An analysis of the gas contents of the bubbles was also conducted and the changes of concentration with successive heat-treatments provided an estimate of the process of bubble formation.

**15704.** Rosasco, G. J., Simmons, J. H., **Investigation of gas content of inclusions in glass by Raman scattering spectroscopy,** *Am. Ceramic Soc. Bull.* **53,** No. 9, 626-630 (Sept. 1974).

Key words: gas analysis; inclusions in glass; Raman scattering.

Laser Raman spectroscopy is used to identify the gaseous contents of inclusions in glass. This test is offered as a valuable complement to other analytical techniques. It requires relatively simple specimen preparation, offers good sensitivity to the gases of interest and is a nondestructive test. Further, since the sample is not contained in a confining test apparatus, the temperature of the contents of the bubble may be raised, for example, to vaporize solid deposits for analysis. Spherical bubbles 0.5 mm in diameter have been routinely analyzed without special optics and with good signal-to-noise ratio. The elements of the theory and practice of laser Raman spectroscopy are outlined and their application to the study of the gaseous content of inclusions is discussed in detail.

**15705.** Forman, R. A., Thurber, W. R., Aspnes, D. E., **Second indirect band gap in silicon,** *Solid State Commun.* **14,** No. 10, 1007-1010 (1974).

Key words: band gap; band structure; electronic structure; energy bands; optical properties; silicon.

We report the first observation of the $\Gamma_{25'} \rightarrow L_1$ (second indirect) transition in Si based on optical absorption studies. The energy, (1650 ± 10) meV, measured for this critical point shows that there remains a large discrepancy between theoretical band structure calculations and experimental results for this material.

**15706.** May, W. E., Chesler, S. N., Cram, S. P., Gump, B. H., Hertz, H. S., Enagonio, D. P., Dyszel, S. M., **Chromatographic analysis of hydrocarbons in marine sediments and seawater,** *J. Chromatogr. Sci.* **13,** 535-540 (Nov. 1975).

Key words: baseline studies; gas chromatography; gas chromatography-mass spectrometry; hydrocarbon; liquid chromatography; marine sediments; pollution; seawater.

The low concentration of hydrocarbons anticipated in pollution baseline studies necessitates the development of analytical techniques sensitive at the sub-microgram per kilogram concentration level. The method of analysis developed in this laboratory involves dynamic headspace sampling for volatile hydrocarbon components of the sample, followed by coupled-column liquid chromatography for the nonvolatile components. These techniques require minimal sample handling, reducing the risk of sample component loss and/or sample contamination.

Volatile sample components are separated from the matrix in a closed system and concentrated on a TENAX-GC packed pre-column, free from large amounts of solvent and ready for GC/GC-MS analysis. Nonvolatile compounds, such as the benzpyrenes, may be extracted from large volumes of water and concentrated on a Bondapak C18 packed pre-column for coupled-column liquid chromatographic separation and analysis. Results of the application of these techniques to the analysis of samples from sites of known low level hydrocarbon contamination are presented and discussed.

**15707.** Morrissey, B. W., Stromberg, R. R., **Bound fraction measurements of adsorbed blood proteins,** (Proc. American Chemical Society Meeting on Biomedical Applications of Polymers Chicago, IL, Aug. 25-29, 1973), Paper in *Biomedical Applications of Polymers*, H. P. Gregor, Ed., **7,** 57-68 (Plenum Press, New York, NY, 1975).

Key words: blood proteins; infrared bound fraction; protein adsorption; protein conformation.

The likelihood that surface-induced blood coagulation results from specific protein-material interactions has led to a study of the conformation of adsorbed blood proteins. Infrared difference spectroscopy was used to determine the bound fraction, i.e., the fraction of carbonyl groups of an adsorbed molecule directly interacting with the surface, of serum albumin, prothrombin, and fibrinogen in situ. Measurements were carried out on individual proteins as a function of the amount adsorbed, time of adsorption, pD, and ionic strength using a silica surface.

The results obtained for serum albumin and prothrombin indicate that the internal bonding of these globular proteins is sufficient to prevent changes in the structure while adsorbed, even at low surface population. The bound fraction of fibrinogen increases with increasing adsorbance suggesting possible interfacial aggregation. The conformation of all three proteins was found to be independent of the time of adsorption, although major differences in the rates of adsorption were observed.

**15708.** Flynn, D. R., Pallett, D. S., **Simplified methods for calculating the transmission loss of two-element partitions,** *J. Acoust. Soc. Am.* **58,** No. 6, 1341-1342 (Dec. 1975).

Key words: airborne sound transmission; architectural acoustics; building acoustics; sound reduction index; sound transmission loss; transmission loss.

Three alternative procedures—a table look-up, a nomograph, and a specially devised slide rule, depending on the preference of the user—are given for rapid computation of the sound transmission loss of a composite partition.

**15709.** Cezairliyan, A., Beckett, C. W., **Measurement of thermal properties at high pressures by transient techniques,** Chapter 7 in *Thermochemistry and Thermodynamics*, H. A. Skinner, Ed., **10,** 247-260 (Butterworths, London, 1975).

Key words: heat capacity; high pressures; thermal conductivity; thermal diffusivity; thermal properties; transient techniques.

Measurements of selected thermal properties (heat capacity, thermal conductivity and thermal diffusivity) at high pressures (up to 100 kbars) using transient techniques are reviewed.

**15710.** Feldman, A., **Relations between electrostriction and the stress-optical effect,** *Phys. Rev. B* **11,** No. 12, 5112-5114 (June 15, 1975).

Key words: electrostriction; electrostrictive coefficients; free energy; stress-optical constants; stress-optical effect.

Relationships are obtained between the stress-optical constants and the electrostrictive coefficients of solid materials. These results, which are dependent upon the geometric boundary conditions, encompass the apparent differences in the relationships derived by different authors.

**15711.** Geist, J., **The role of radiometry in solar energy utilization,** *Proc. Smithsonian-Eppley Symp. on Solar Radiation Measurement and Instrumentation, Rockville, MD, Nov. 13-14, 1973*, pp. 79-94 (1973).

Key words: effective irradiance; radiometry; solar energy conversion.

This paper identifies the various radiometric problems that are of importance to solar energy utilization. Some basic definitions are presented, and the effective irradiance is shown to be a fruitful concept. Three different activities of the solar energy community that require effective irradiance data are discussed. Finally, it is shown that these different activities apply different constraints to effective irradiance data; the optimum type of data for one activity not necessarily being at all suitable for the other two activities.

**15712.** Kelly, G. E., Didion, D. A., **A laboratory test of the modular concept as applied to gas-fired boilers,** (Proc. Conf. on Improving Efficiency in HVAC Equipment and Components for Residential and Small Commercial Buildings, Oct. 7-8, 1974), Paper in *Proceedings of Conference on Improving Efficiency in HVAC Equipment and Components for Residential and Small Commercial Buildings*, D. A. Didion and V. Goldschmidt, Eds., pp. 18-30 (Purdue Research Foundation, Lafayette, IN, Oct. 1974).

Key words: boiler oversizing; efficiency vs. heating load; modular boilers; modular concept; seasonal efficiency.

The modular concept of boiler operation was examined in a laboratory test of five gas-fired, cast iron, hydronic boilers. Four of the boilers, each having an input rating of 85,000 Btu per hour, were arranged so that they could either be operated like a single boiler (i.e., all of the boilers either on or off) or as a modular installation in which the boilers are sequentially fired to match the number in operation with the heating load. The fifth boiler had an input rating of 300,000 Btu per hour and was operated as a single boiler installation. Efficiency vs. heating load curves were obtained for the single boiler installation, the four small boilers run like a single boiler and the modular installation operated with and without water flowing through the "idle" modules. These efficiency curves were then used to theoretically predict the effect of the modular concept and boiler oversizing on the seasonal efficiency of gas-fired heating plants.

**15713.** Achenbach, P. R., **Status of energy standards for heating, ventilating and air-conditioning systems in buildings,** (Addendum to Proc. of Conf. on Improving Efficiency in HVAC Equipment and Components for Residential and Small Commercial Buildings, Oct. 7-8, 1974), Paper in *Addendum to Proceedings of Conference on Improving Efficiency in HVAC Equipment and Components for Residential and Small Commercial Buildings*, P. Newman, Ed., pp. A134-A142 (Purdue Research Foundation, Lafayette, IN, 1975).

Key words: energy conservation; energy standards for mechanical systems; heating and air-conditioning systems; state energy regulations.

The circumstances in energy supply are described which caused the National Conference of States on Building Codes and Standards to request the National Bureau of Standards in 1973 to develop an interim standard for energy conservation in new buildings. The progress in development of such a standard by NBS and the American Society of Heating, Refrigerating and Air-Conditioning Engineers is chronicled to October 1974. The principal policy issues raised by the preparation of an energy conservation standard which could become the basis for State and local regulations are discussed. The components of heating and air-conditioning systems which are at issue between the NBS and ASHRAE documents for inclusion in the energy conservation standard are identified. The long-range objectives of the Federal Energy Administration in developing energy conservation requirements for buildings are summarized.

**15714.** Hummer, D. G., Kunasz, P. B., **Migration of excitation in transfer of spectral-line radiation,** *J. Quant. Spectrosc. Radiat. Transfer* **16,** 77-96 (1976).

Key words: diffusion; excitation exchange; radiative transfer; spectral line profiles.

A simple mathematical model is developed for the transfer of energy through a gas by the combined effect of radiative transfer and migration of excitation. The "excitation" is carried through the gas by a succession of atoms which experience resonant excitation exchange; it thus appears to random walk through the medium. The theory developed here is valid when the distance traveled by an atom while excited is much larger than the typical distance at which two atoms can exchange excitation (roughly $10^{-6}$ cm). The model is expressed in terms of a pair of coupled transport equations for the intensity of radiation and the density of excited atoms, which are solved by means of a generalized discrete-ordinate technique. Extensive numerical results are obtained and discussed in terms of characteristic lengths for the various transfer processes. Substantial effects of migration are seen in both the distribution of excited atoms near the cell windows and the line profile of the emergent radiation for typical laboratory conditions.

**15715.** Fiori, C. E., Myklebust, R. L., Heinrich, K. F. J., Yakowitz, H., **Prediction of continuum intensity in energy-dispersive x-ray micro-analysis,** *Anal. Chem.* **48,** No. 1, 172-176 (Jan. 1976).

Key words: background; continuous x rays; electron probe microanalysis; energy-dispersive x-ray analysis; lithium-drifted silicon detector.

A method for background prediction in electron-excited energy-dispersive x-ray spectrometry (EDS) is described. This method yields the intensity of the continuous radiation which would be observed by the detector as a function of x-ray photon energy. The method can be incorporated into existing electron probe microanalysis data reduction programs. Tests indicate that the proposed background correction scheme is satisfactory for quantitative analysis.

**15716.** Chabay, I., Klauminzer, G. K., Hudson, B. S., **Coherent anti-Stokes Raman spectroscopy (CARS): Improved experimental design and observation of new higher-order processes,** *Appl. Phys. Lett.* **28,** No. 1, 27-29 (Jan. 1, 1976).

Key words: CARS; diphenyloctatetraene (dilute solution); four-wave numbering; HORSES; nonlinear optics; Raman spectroscopy.

The development of the optical and electronic arrangement which has permitted the straightforward measurement of coherent anti-Stokes Raman spectra (CARS) and of higher order processes not previously reported is described in this paper. The CARS spectrum of a dilute solution of diphenyloctatetraene in benzene is presented. This spectrum demonstrates the significantly greater signal-to-noise ratio possible with CARS as compared to conventional Raman techniques. Higher-order Raman spectral excitation studies (HORSES) are described which indicate the presence of a six-wave or a second-order four-wave mixing process.

**15717.** Shine, R., Gerola, H., Linsky, J. L., **Diffusion effects on the line intensities of He I and He II in the solar transition region,** *Astrophys. J.* **202,** L101-L105 (Dec. 1, 1975).

Key words: chromosphere-sun; coronal holes; diffusion; transition region-sun; ultraviolet spectrum-sun.

We develop a heuristic treatment of diffusion in the solar chromosphere-corona transition region. We find that diffusion becomes increasingly important with steeper temperature gradients, in active and quiet regions relative to coronal holes, and with increasing excitation potential. Numerical calculations are made for the resonance lines of He I and He II and show that diffusion can enhance these lines. Thus the helium lines may appear relatively weak in coronal holes due to a weakening of the enhancement mechanism. Most transition region lines will be less affected by diffusion than He I or He II.

**15718.** Hebner, R. E., Jr., Cassidy, E. C., Jones, J. E., **Improved techniques for the measurement of high-voltage impulses using the electrooptic Kerr effect,** *IEEE Trans. Instrum. Meas.* **IM-24,** No. 4, 361-366 (Dec. 1975).

Key words: automation; electrical measurements; electrooptics; high voltage measurement; Kerr effect; optical coupling; pulse measurement.

The purpose of this paper is to present two methods of accumulating, analyzing, and presenting in real time the data generated by a Kerr system in response to a high-voltage impulse. These methods provide immediate information concerning selected electrical parameters in a form which is easily interpretable by most personnel. The first method uses an electronic counter to determine the number of optical transmittance maxima, i.e., light pulses, during the high-voltage impulse. From this count, the peak value of impulse can be calculated. The second method, which can be more accurate and does provide information concerning waveshape, uses a digital recorder to store the output waveform from the Kerr system. A computer is then used to reconstruct the voltage impulse and to determine such parameters as the peak value and risetime of the impulse.

**15719.** Hellwig, H., **A review of precision oscillators,** *Proc. 6th Precise Time and Time Interval (PTTI) Meeting, Washington, DC, Dec. 3-5, 1974,* pp. 59-81 (Dec. 1974).

Key words: accuracy; atomic clocks; clocks; crystal oscillator; frequency standards; stability; survey of clocks.

Precision oscillators used in PTTI applications include quartz crystal, rubidium gas cell, cesium beam, and hydrogen maser oscillators. A general characterization and comparison of these devices is given including accuracy, stability, environmental sensitivity, size, weight, power consumption, availability and cost. Areas of special concern in practical applications are identified and a projection of future performance specifications is given. An attempt is made to predict physical and performance characteristics of new designs potentially available in the near future.

**15720.** Petersons, O., Anderson, W. E., **A wide-range high-voltage capacitance bridge with one PPM accuracy,** *IEEE Trans. Instrum. Meas.* **IM-24,** No. 4, 336-344 (Dec. 1975).

Key words: capacitance measurements; current comparators; current transformers; high voltage bridges; high voltage capacitors; high voltage measurements; impedance bridges.

An impedance bridge for high-voltage capacitance and related measurements to an accuracy of 1 ppm is described and the background research and development which made it possible is documented. The bridge is of the transformer-ratio-arm type, the principal components of which are a comparator and several two-stage transformers. The bridge can be used to measure capacitance ratios over a range from 1/1 to $10^7/1$ with a resolution between 0.1 and 0.25 ppm. The highest accuracies are obtained at the principal power frequencies of 50-60 Hz, but the bridge is usable up to 400 Hz. The factors which limited the accuracy of previously developed bridges of this type were reexamined and their influence reduced. Two independent methods were developed for the calibration of the bridge.

**15721.** DiMarzio, E. A., Bishop, M., **The nature of the helix-random coil transition of biological macromolecules attached to a surface,** *Biopolymers* **13,** 2331-2348 (1974).

Key words: biopolymers; helix-coil transition; phase transitions in biopolymers; self-assembly; structural transformations; surface adsorption.

The effect of the presence of a surface on the helix-random coil transition is investigated. It is found that a grand canonical ensemble formation used previously to solve exactly the problem of a polymer between two plates can be used to solve approximately the problem of DNA near a plane surface. The formalism is applied to the homogeneous perfect-matching model of infinite molecular weight. A crucial part of the calculation for double-stranded molecules involves the evaluation of the entropy of the loops connecting the helical portions of the double-stranded chains. One obtains as a measure of the configurational freedom of a loop $As^j/j^c$ where $c$ has the following values: for a loop connecting two helical regions both off the surface $c=3/2$; for a loop connecting a helical region on the surface to a helical region off the surface $c=5/2$; for a loop connecting helixes both on the surface $c=4$. Corresponding values for an $n$-stranded molecule are $c=(3n-3)/2$, $c=(4n-3)/2$, $c=(5n-2)/2$. In all cases, the effect of the surface is to sharpen the transition. In the case of double-stranded molecules, the transition becomes first order. We take the view that self-assembly of biological macromolecules can be considered as a sharp thermodynamic phase transition. Thus, the above systems become models of self-assembling systems. They are also relevant to the problem of surface-induced enzymatic activity.

**15722.** Heinrich, K. F. J., Yakowitz, H., **Absorption of primary x rays in electron probe microanalysis,** *Anal. Chem.* **47,** No. 14, 2408-2411 (Dec. 1975).

Key words: absorption correction; primary emission; quantitative electron probe analysis; x-ray absorption factor.

Available experimental evidence concerning absorption in x-ray targets, corrected for fluorescence due to the continuum, is generalized to give the formula, $f_p=(1+a\gamma\chi)^{-2}$, in which $f_p$ is the primary x-ray absorption factor, $\gamma=(E_o^{1.65}-E_q^{1.65})$, $E_o$(kV) is the operating voltage, $E_q$(kV) the critical excitation voltage, $\chi=\mu$ cosec $\psi$, $\mu$ is the mass absorption coefficient for the respective target and line, $\psi$ is the x-ray emergence angle, and $a=1.2\times10^{-6}$ g/cm$^2$. The presumed effect of the atomic number of the target on $f_p$ is overestimated by Philibert's formula. It is smaller than the statistical spread of experimental data, and can therefore be neglected.

**15723.** Mihalas, D., Kunasz, P. B., Hummer, D. G., **Solution of the comoving-frame equation of transfer in spherically symmetric flows. I. Computational method for equivalent-two-level-atom source functions,** *Astrophys. J.* **202,** 465-489 (Dec. 1, 1975).

Key words: atmospheres, stellar; atomic and molecular processes; line formation; radiative transfer.

The equation of radiative transfer in the comoving frame makes possible an economical solution of the line formation problem in spherical atmospheres expanding with arbitrarily large velocities. A stable differencing scheme and a frequency-by-frequency elimination procedure have been developed to solve the partial differential equations that describe the radiation field in the comoving frame. Numerical results were obtained for a large number of illustrative models involving line formation by two-level atoms, electron scattering, and continuous absorption. Selected results that simulate situations in the stellar winds of hot stars and similar objects are discussed. In addition to P Cygni and other very broad profiles, extreme center-to-limb variations are obtained that show both limb darkening and limb brightening. For very high velocity flows with very weak or nonexistent continuum and electron-scattering opacities, the flux profiles are very nearly symmetric about the laboratory wavelength and have shapes reminiscent of those observed in the nuclei of Seyfert galaxies. Comparisons are presented between the results of Sobolev-type escape probability calculations and those obtained here. The force of radiation on the gas is examined in a number of situations; the mechanism mentioned by Noerdlinger and Rybicki for the disruption of radiatively driven envelopes in planar geometries is shown to become inoperative for even slightly extended spherical systems.

**15724.** McQueen, J. T., Levinsohn, D. M., Waksman, R., Miller, G. K., **The evaluation of the Shirley Highway Express-Bus-on-Freeway Demonstration Project,** *Report DOT/UMTA* **7,** 133 pages (Available as PB247637 from the National Technical Information Service, Springfield, VA 22161, Aug. 1975).

Key words: bus transit; busways; carpools; energy impacts; mode choice; pollution reduction.

The Shirley Highway Express Bus-on-Freeway Project began in June 1971 and ended December 31, 1974. The principal goal of the project was to demonstrate that express bus-on-freeway operations can improve the quality of bus service and lead to an increase in the people moving capability of peak period transportation facilities for an entire urban corridor. Secondary project goals were to demonstrate the effectiveness of this technology as a means of reducing auto pollutant emissions and gasoline consumption, improving the mobility of the transportation disadvantaged and the economic condition of the transit operator.

This report summarizes project performance with respect to the attainment of the above goals. An analysis of bus operations is presented which shows that the project effected an improvement in the quality of the Shirley Highway Corridor bus service as evidenced by the reduction in travel times by bus, and the increase in both the reliability and the coverage of the bus systems. Trends in peak period traffic volumes are presented which show that the subsequent increase in bus patronage and bus' share of Corridor commuters led to an increase in the peak period people moving capability of the Corridor. Corridor people moving capability was also increased by project stimulated growth in carpooling.

Data from surveys of Corridor commuters were used in identifying factors important in commuters' decision to use bus or to carpool. Bus users who formerly had commuted by auto reported that the most important factors in their decisions to switch from auto were the expense and discomfort of commuting by auto, and the express features of project bus service. Factors reported as most important in decisions to join or form a carpool were reduction in commuting costs, special parking privileges for carpools, and availability of the express busway to carpools.

The report concludes with an analysis of project performance with respect to the secondary goals. The project resulted in significant reductions in peak period auto usage, auto pollutant emissions and gasoline consumption. The utilization of project bus service by transportation disadvantaged persons is discussed and project costs and revenues are analyzed.

**15725.** Zalubas, R., Reader, J., Corliss, C. H., **$4s^24p^4$-$4s4p^5$ transitions in five-times-ionized yttrium (Y VI),** *J. Opt. Soc. Am.* **66,** No. 1, 35-36 (Jan. 1976).

Key words: spectra; ultraviolet; wavelengths; yttrium.

The spectrum of yttrium has been observed in a sliding spark discharge at peak currents up to 2000 Å on the 10.7 m normal and grazing incidence vacuum spectrographs at NBS. From these observations, the group of $4s^24p^4$-$4s4p^5$ transitions in Y VI, which lie in the region 457-766 Å, has been identified and measured, thus yielding values for the 4 levels of the $4s4p^5$ configuration and revised values for the 5 levels of the $4s^24p^4$ configuration. The energy parameters obtained from a least-squares fit to the observed levels are compared with Hartree-Fock calculations.

**15726.** Mulholland, G. W., **Self-diffusion through a liquid-vapor interface,** *J. Chem. Phys.* **64,** No. 2, 862-870 (Jan. 15, 1976).

Key words: continuous interface profile; diffusion equation; hypergeometric differential equation; interfacial force; liquid-vapor interface; Markov Stochastic model; self-diffusion.

A diffusion equation containing information about the structure of the liquid-vapor interface is constructed to describe self-diffusion in a one component, two phase fluid. Analysis of the diffusion equation in the limit of vanishing interface thickness leads to interfacial matching conditions, one of which was previously assumed ad hoc. From a study of the asymptotic long time behavior of the equation, it is found that an ordinary self-diffusion experiment can not be expected to provide information about the interface structure. A numerical study of the diffusion equation shows that the reduced time to diffuse through the interface is independent of the ratio of the vapor and liquid densities, which is the one free parameter in the diffusion equation. An experimental test of our prediction that it takes the same time to diffuse from the liquid to the vapor as vice versa is suggested.

**15727.** Dyer, C. S., Trombka, J. I., Schmadebeck, R. L., Eller, E., Bielefeld, M. J., O'Kelley, G. D., Eldridge, J. S., Northcutt, K. J., Metzger, A. E., Reedy, R. C., Schonfeld, E., Seltzer, S. M., Arnold, J. R., Peterson, L. E., **Radioactivity observed in the sodium iodide gamma-ray spectrometer returned on the Apollo 17 mission,** *Space Sci. Instrum.* **1,** 279-288 (1975).

Key words: Apollo 17; background; cosmic-ray proton; induced radioactivity; secondary neutrons; sodium iodide detector.

In order to obtain information on radioactive background induced in the Apollo 15 and 16 gamma-ray spectrometers (7 cm × 7 cm NaI) by particle irradiation during spaceflight, an identical detector was flown and returned to earth on the Apollo 17 mission. The induced radioactivity was monitored both internally and externally from one and a half hours after splashdown. When used in conjunction with a computation scheme for estimating induced activation from calculated trapped proton and cosmic-ray fluences, these results show an important contribution resulting from both thermal and energetic neutrons produced in the heavy spacecraft by cosmic-ray interactions.

**15728.** Leep, D., Gallagher, A., **Excitation of the Mg and Mg$^+$ resonance lines by electron impact on Mg atoms,** *Phys. Rev. A* **13,** No. 1, 148-155 (Jan. 1976).

Key words: electron excitation; magnesium.

We have measured the optical excitation functions and polarizations of the Mg resonance line (2852 Å) and of the Mg$^+$ resonance lines (2796 Å, 2803 Å, unresolved) arising from ionizing excitation of magnesium atoms, for electron-impact energies from the excitation threshold to 1400 eV. In our crossed-beam apparatus, the electron-beam energy resolution was ≈0.25 eV for energies below 10 eV, and the atom beam was optically thin. The excitation function of the ionic lines was normalized to that of the atomic line by relative intensity measurements. The 2852-Å excitation function, when normalized to Born theory in the high-energy limit, has a maximum cross section of $17.3\pi a_0^2 \pm 3$ percent 18.5 eV. This excitation function is graphically compared with the resonance-line excitation functions of Na, Ca, and Li previously measured in this laboratory. The 2852-Å polarization function is consistent with the theoretical threshold limit of + 100 percent, and has a sharp feature near 5 eV which cannot be due to cascading.

**15729.** Mahan, A. H., Gallagher, A., Smith, S. J., **Electron impact excitation of the $3S$, $3P$, and $3D$ states of H,** *Phys. Rev. A* **13,** No. 1, 156-166 (Jan. 1976).

Key words: electron excitation; hydrogen.

The relative excitation function for electron-impact excitation of H to yield Balmer $\alpha$ has been measured from threshold to 500-eV collision energy in a crossed-beam apparatus. The relative contributions of the $3S$, $3P$, and $3D$ states to this excitation function have been measured by modulating the electron beam and discriminating on the basis of their different lifetimes for radiative decay after excitation. The resulting set of relative $3S$, $3P$, and $3D$ cross sections has been normalized by equating the total measured Balmer-$\alpha$ cross section at 500 eV to the Born approximation. The normalized cross sections are then compared to available theories at lower energies. In contrast to virtually all known excitation cross sections of neutral atoms, which fall below the Born theory at low energies, the H ($1S \rightarrow 3D$) cross section exceeds the Born theory, apparently owing to coupling between the $3D$ and $2P$ states.

**15730.** Murphy, T. A., Sengers, J. V., Sengers, J. M. H. L., **Scaled parametric equation of state for steam in the critical region,** (Proc. 8th Int. Conf. on the Properties of Water and Steam, Giens, France, Sept. 23-27, 1974), Paper in *Proceedings of the 8th International Conference on the Properties of Water and Steam,* P. Bury, H. Perdon, and B. Vodar, Eds., **1,** 603-613 (Ministère de l'Industrie et de la Recherche, Paris, France, 1975).

Key words: critical density; critical exponents; critical pressure; critical region; critical temperature; equation of state; linear model; scaled equation; steam.

The anomalous thermodynamic behavior of fluids near the critical point can be described in terms of scaling laws. In recent years a parametric equation of state, the so-called Linear Model, has been proposed that satisfies the scaling laws and contains only a small number of adjustable parameters. It is shown that the Linear Model yields a satisfactory representation of the experimental P-V-T data for steam in the critical region.

**15731.** McCarty, R. D., **The correlation of equilibrium and transport properties of fluids,** (Proc. 8th Int. Conf. on the Properties of Water and Steam, Giens, France, Sept. 23-27, 1974), Paper in *Proceedings of the 8th International Conference on the Properties of Water and Steam,* P. Bury, H. Perdon, and B. Vodar, Eds., **1,** 537-556 (Ministère de I'Industrie et de la Recherche, Paris, France, 1975).

Key words: correlation; equation of state; excess function; hydrogen; interpolation methods; least squares; methane; thermodynamic properties; transport properties.

The practice of using a mathematical model for correlating the transport and thermodynamic properties of fluids is reviewed. Changes which are currently taking place in the field are analyzed from both the correlator's point of view and the people who are going to use the results of the correlation. The present state-of-the-art indicates present and future correlations must be more user oriented than those of the past. A review of correlation methods is given with emphasis on model selection. A new model for the transport property excess function is given. An example of simultaneous data fitting demonstrates the value of this technique.

**15732.** Johnson, D. P., Guildner, L. A., Jones, F. E., **Vapor pressure of water at its triple point,** (Proc. 8th Int. Conf. on the Properties of Water and Steam, Giens, France, Sept. 23-27, 1974), Paper in *Proceedings of the 8th International Conference on the Properties of Water and Steam,* P. Bury, H. Perdon, and B. Vodar, Eds., **1,** 365-377 (Ministère de I'Industrie et de la Recherche, Paris, France, 1975).

Key words: mercury manometer; triple point of water; vapor pressure.

The vapor pressure of water has been measured at its triple point with a newly constructed apparatus. It was designed to provide a dynamic system with a thin stream of water flowing down an ice mantle, the temperature of which was determined by a standard platinum resistance thermometer. The pressure was measured by the NBS precision mercury manometer, with a diaphragm unit to separate the helium in the manometer from the water vapor. The value found from a series of measurements was 611.636 Pa with an estimated total uncertainty (3 $\sigma$ limits plus estimate of systematic error) of ±0.061 Pa.

**15733.** Sengers, J. M. H. L., **Universality of critical behavior in fluids,** (Proc. 8th Int. Conf. on the Properties of Water and Steam, Giens, France, Sept. 23-27, 1974), Paper in *Proceedings of the 8th International Conference on the Properties of Water and Steam,* P. Bury, H. Perdon, and B. Vodar, Eds., **1,** 56-78 (Ministère de I'Industrie et de la Recherche, Paris, France, 1975).

Key words: critical exponents; critical region; homogeneity; polar fluids; scaling; steam; universality.

Modern developments in the description of critical-region anomalies are reviewed. The concepts of critical exponents, homogeneity, scaling and universality are introduced. The question is raised whether the critical behavior of steam, a polar fluid, can be expected to be the same as that of nonpolar fluids. Theoretical and experimental evidence for an affirmative answer to this question is presented. The consequences for the correlation of properties of steam in the critical region are drawn.

**15734.** Lide, D. R., Jr., **Cooperation between professional societies and a government agency: The Journal of Physical and Chemical Reference Data,** *IEEE Trans. Prof. Commun.* **PC-18,** No. 3, 127-129 (Sept. 1975).

Key words: journal; professional societies; publications; reference data.

The National Standard Reference Data System consists of data centers and other projects funded or coordinated by the National Bureau of Standards (NBS) which compile and evaluate data on physical and chemical properties of well-defined materials. The output is then published in the form of tables of recommended data and critical reviews. In 1972 an agreement was reached with the American Chemical Society (ACS) and the American Institute of Physics (AIP) for establishing a new publication channel for the material, the *Journal of Physical and Chemical Reference Data.* Editorial work and preparation of camera-ready copy is handled by NBS, while ACS and AIP divide the other responsibilities. The progress of this journal is reviewed.

**15735.** Choi, C. S., Santoro, A., Marinkas, P. L., **1,3,5-Triacetyl-2,4,6-hexahydro-*s*-triazine (TRAT),** *Acta Crystallogr.* **B31,** Part 12, 2934-2937 (Dec. 15, 1975).

Key words: diffractometer; direct methods; explosives; single-crystal; triazine; x ray.

$C_9H_{15}N_3O_3$, monoclinic, $P2_1/c$, $a=7.772$ (2), $b=15.521$ (4), $c=10.101$ (2) Å, $\beta=116.34$ (2)°, $Z=4$, $D_x=1.30$, $D_m=1.31$ g cm$^{-3}$. $F(000)=456$. All x-ray measurements were made with Mo $K\alpha$ radiation ($\lambda=0.71069$ Å). The structure was solved by direct methods and refined by full-matrix least-squares calculations to final $R$ and $R_w$ values of 0.051 and 0.035, respectively, for 777 observed reflections.

**15736.** Hellwig, H. W., **Atomic frequency standards: A survey,** *Proc. IEEE* **63,** No. 2, 212-229 (Feb. 1975).

Key words: application of standards; basic standards; cesium standards; frequency accuracy; frequency stability; frequency standards; hydrogen standards; ion storage; laser stabilization; rubidium standards; saturated absorption; time standards.

The last comprehensive survey on atomic frequency standards was done by McCoubrey. This survey reviews the more recent historical background of atomic frequency standards leading to the present developments. A discussion of the underlying physical and engineering principles is given. Modern atomic frequency standards, including their performance, are compared quantitatively, and projections are attempted at likely future developments and performance characteristics.

As in 1966, the standards principally used in technical and scientific applications are rubidium gas cell devices, cesium beam tubes, and hydrogen maser oscillators. However, substantial advances in physical and performance characteristics can be reported.

New developments include passive hydrogen devices, saturated absorption stabilized lasers, ion storage devices, and atomic beams in the far infrared and infrared region, as well as new techniques to evaluate frequency biases such as those encountered in cesium and hydrogen standards.

The survey includes a discussion of the effects of past and current developments in atomic frequency standards on the technical and scientific user community.

**15737.** Snyder, N. S., **The Kapitza conductance of the (100) surface of copper,** *J. Low Temp. Phys.* **22,** No. 3/4, 257-284 (1976).

Key words: heat transfer to helium II; interfacial thermal resistance; Kapitza conductance; Kapitza conductance of copper; x-ray diffraction examination of single crystal lattice damage; (100) surface of copper.

Measurements of the Kapitza conductance to liquid helium II across the (100) surface of single crystals of copper are presented. The temperature range of these measurements was 1.6-2.1 K. The sample surfaces were subjected to several different treatments. Some surfaces were cleaned by low-energy argon ion bombardment, annealed in an ultrahigh-vacuum system, and preserved under vacuum until purified liquid helium was admitted. Other surfaces were intentionally damaged by machining and/or exposure to the atmosphere. The conductance after these latter treatments was found to be about a factor of three higher than that of the more ideally cleaned and annealed surfaces, and a significant difference in the temperature dependence of the conductance was also observed. Conductances were reproducible for similarly treated surfaces and could be correlated with surface damage determined by x-ray diffraction. The relationship of these results to the numerous current theories of the Kapitza conductance is discussed. Conductance measurements of polycrystalline indium, which was used as a sealant, are presented.

**15738.** Kulin, G., **Simplified application of Palmer-Bowlus flow meters,** *J. Water Pollut. Control Fed. Discussion* **48,** No. 1, 200-201 (Jan. 1976).

Key words: flow measurement, water; flumes, measuring; open channel flow measurement; Palmer-Bowlus flumes; sewage flow measurement.

Possible errors associated with the use of the customary theoretically derived rating curves for Palmer-Bowlus flumes are identified and evaluated.

**15739.** Lieberman, A. G., **Problems in using surface analysis techniques for the depth profiling of microelectronic materials,** *Technical Digest of International Electron Devices Meeting, Washington, DC, Dec. 1-3, 1975,* pp. 126-129 (1975).

Key words: Auger electron spectroscopy; depth impurity profiling; ion implantation; ion sputtering; microelectronic materials; Rutherford backscattering; secondary ion mass spectroscopy; silicon; silicon dioxide; surface analysis; x-ray photoelectron spectroscopy.

Practical problems associated with the depth profiling of impurity distributions in silicon and silicon dioxide are illustrated for several widely used surface analysis techniques as applied at a number of laboratories. The methods used for depth profiling were Rutherford backscattering spectroscopy, Auger electron spectroscopy and x-ray photoelectron spectroscopy.

**15740.** Allan, D. W., **The measurement of frequency and frequency stability of precision oscillators,** *Proc. Sixth Annual Precise Time and Time Interval (PTTI) Planning Meeting, U.S. Naval Research Laboratory, Washington, DC, Dec. 3-5, 1974,* pp. 109-142 (Goddard Space Flight Center, Greenbelt, MD, 1974).

Key words: accurate frequency measurement; accurate time measurement; frequency; frequency stability; frequency stability analysis; models of frequency stability; picosecond time difference measurements.

The specification and performance of precision oscillators is a very important topic to the owners and users of these oscillators. This paper presents at the tutorial level some convenient methods of measuring the frequencies of precision oscillators—giving advantages and disadvantages of these methods.

Conducting such measurements, of course, gives additional understanding into the performance of the given pair of oscillators involved. Further it is shown that by processing the data from the frequency measurements in certain ways, one may be able to state more general characteristics of the oscillators being measured. The goal in this regard is to allow the comparisons of different manufacturers' specifications and more importantly to help assess whether these oscillators will meet the standard of performance the user may have in a particular application.

The methods employed for measuring frequency are designed for state-of-the-art oscillators, and an effort has been made to allow for fairly simple, inexpensive, and/or commonly available componentry to be used in the measurement systems. The method for measuring frequency stability is basically that recommended by the IEEE subcommittee which wrote the paper "Characterization of Frequency Stability," IEEE Transactions on Instrumentation and Measurement, IM-20, No. 2, pp. 105-120, (May 1971).

**15741.** Powell, F. J., **The Manchester, N.H., experimental energy office building,** (Proc. Seminar on Energy Conservation by Design, Orlando, FL, March 20-21, 1974), Paper in *Proceedings Energy Conservation—By Design, Section 14, 1-14 (Harry Phipps, Energy Systems Consultants, St. Petersburg, FL, 1974).*

Key words: energy conservation; energy consumption prediction; experimental office building.

A brief background of the experimental 7-story Federal Energy Demonstration Office Building to be Constructed at Manchester, N.H. is given. A summary of the results of a predesign energy analysis done at NBS is presented as a comparison of normal General Services Administration practice in 1972 with changes made for a new energy conservation design approach. A similar comparison is made for the same building if the location were changed to Orlando, Fla. The results indicate annual energy savings of 52 percent for Manchester and 39 percent for Orlando are possible by using additional thermal insulation in the roof, walls and floor, reducing the window area, reducing the quantity of ventilation and lighting power, and using energy efficient heating, ventilating and air-conditioning systems.

**15742.** Fowlkes, C. W., **Crack opening interferometry—The effects of optical refraction,** *Eng. Fract. Mech.* **7,** 689-692 (1975).

Key words: cracks; experimental mechanics; fracture; fracture toughness; interferometry; model experiments; stress; stress intensity.

This paper contains an analytical prediction of the distortions of interference fringes near a crack tip resulting from refraction of the light rays due to the stress field. The effects of these distortions on the results of crack opening interferometry (COI) experiments for determining stress intensity factors are discussed.

**15743.** Howard, C. J., Evenson, K. M., **Rate constants for the reactions of OH with $CH_4$ and fluorine, chlorine, and bromine substituted methanes at 296 K,** *J. Chem. Phys.* **64,** No. 1, 197-202 (Jan. 1, 1976).

Key words: gas reactions; hydroxyl radical; kinetics.

The absolute rate constants for the reactions of OH radicals with $CH_4$ and fifteen fluorine, chlorine, and bromine substituted methane molecules have been measured using a discharge flow system and laser magnetic resonance detection of OH. Measurements were made at 296 K and at pressures between 107 and 1300 Pa. The results indicate that the reaction mechanism involves the abstraction of a hydrogen atom and formation of $H_2O$

and a methyl type radical product. Completely halogenated methane molecules are found to be relatively unreactive. Hydrogen containing molecules react with rate constants ranging from about 0.2 to $160 \times 10^{-15}$ cm³/molecule·sec. The reactivity increases with decreasing carbon-hydrogen bond energies. Rough estimates are made of the Arrhenius parameters for the reactions.

**15744.** Currie, L. A., Lindstrom, R. M., **The NBS measurement system for natural argon-37,** (Proc. Noble Gases Symp., Las Vegas, NV, Sept. 24-28, 1973), Paper in *Noble Gases*, R. E. Stanley and A. A. Moghissi, Eds., CONF-730915, pp. 40-57 (U.S. Environmental Protection Agency, Las Vegas, NV, Dec. 1975).

Key words: Ar-37; atmospheric radioactivity; cosmic-ray reactions; exponential distribution; low-level counting; noble gas separation; on-line computer; pulse shape discrimination; tropospheric mixing.

A project to determine the cosmic-ray production rate and the natural levels of 35-day half-life $^{37}$Ar in the atmosphere has been underway at the National Bureau of Standards for about the past year. The prime objective of this project is to determine the spatial dependence of $^{37}$Ar production in the atmosphere, and the spatial distribution of the naturally-produced $^{37}$Ar (observed concentrations). The results of this study are to be used, in cooperation with L. Machta (National Oceanographic and Atmospheric Administration), to derive information about atmospheric mixing. The purpose of this communication, however, is to present a general description of the various components of the measurement system.

As the lowest concentrations of interest are but $\cong 10^{-3}$ dpm ($^{37}$Ar)/l-Ar, very high sensitivity measurement techniques are required. Among the techniques which we have adopted are: quantitative separation of the noble gases from about 1 m³ of air, using a $CaC_2$ reactor; gas chromatographic separation of the argon fraction; isotopic enrichment (by a factor of $\cong 100$) of purified argon; use of specially selected low-level gas proportional counters together with massive shielding and anticoincidence meson cancellation; and the application of pulse discrimination based upon both amplitude (energy) and pulse shape. Finally, on-line computer techniques are being applied for data acquisition and system control.

**15745.** Kasen, M. B., **Properties of filamentary-reinforced composites at cryogenic temperatures,** *Am. Soc. Testing Mater. Spec. Tech. Publ.* **580,** pp. 586-611 (1975).

Key words: boron; cryogenics; glass; graphite; literature review; PRD-49; reinforced aluminum; reinforced plastics; structural composites; tensile moduli; tensile strength; thermal conductivity; thermal contraction.

This paper presents a review of a series of significant publications on the mechanical and thermal properties of filamentary-reinforced structural composites in the cryogenic temperature range. The objective, scope of work, and significant conclusions of the selected works are discussed. The temperature dependence of the ultimate tensile strength, tensile modulus, thermal conductivity, and thermal contraction (expansion) is presented for selected composites developed in each program. Problem areas are defined and suggestions are made for future work.

**15746.** Mies, F. H., **Optical pumping by solar radiation in comets: Polarization of the Na resonance lines,** *Astrophys. J.* **202,** 823-831 (Dec. 15, 1975).

Key words: atomic and molecular processes; comets; line formation; polarization; quantum mechanics.

At some distance from the nucleus of a comet, the rate of fluorescent scattering of solar radiation by an atom or molecule will be comparable to, or exceed, the rate of collisional relaxation. This is the condition for optical pumping. If the ground state has fine structure or hyperfine structure, then significant nonequilibrium distributions of these levels can result, and the fluorescence spectrum can deviate markedly from the laboratory spectrum. In particular, since the incident solar radiation is unidirectional, the pumping causes an *alignment* of the hyperfine magnetic sublevels along the incident axis, and observations from the Earth should exhibit an enhanced linear polarization in the Sun-Comet-Earth plane. Therefore, polarization measurements can be used as a diagnostic for the presence or absence of collisional relaxation. Conditions are especially favorable for the enhanced polarization of the Na $D_2$ resonance line, and, at a scattering angle of 90°, detailed calculations are presented which predict a polarization of 16 percent, and under favorable circumstances as much as 21 percent, as compared with 10.5 percent for a collisionally equilibrated Na gas.

**15747.** Kuyatt, C. E., **Observation of polarized electrons by Davisson and Germer,** *Phys. Rev. B* **12,** No. 10, 4581-4583 (Nov. 15, 1975).

Key words: electron polarization; electron scattering; low energy; nickel; single crystals; tungsten.

Early attempts to observe electron polarization in the scattering of low-energy electrons from solids are reviewed. It is found that results published by Davisson and Germer in 1929 were analyzed incorrectly, and that they had in fact observed significant electron polarizations in the diffraction of low-energy electrons from single-crystal nickel.

**15748.** Gadzuk, J. W., **Angle-resolved photoemission from crystal-field split *d* shells of adsorbed atoms,** *Phys. Rev. B* **12,** No. 12, 5608-5614 (Dec. 15, 1975).

Key words: adsorption; angular distributions; photoemission; photoionization.

A theory of the angular distribution (AD) of photoemitted electrons from filled $d$ shells of atoms adsorbed on solid surfaces is presented. The crystal field at the surface of the substrate splits the degenerate $d$ states of the adsorbate into at least $e_g$ and $t_{2g}$ components. The angular distribution is then calculated for photoemission from the $e_g$ group (since the distribution from the $t_{2g}$ group is easily related to this). The final state is written as a partial-wave sum. For photoelectron kinetic energies less than about 10 eV, transitions from $d$ to $p$ partial waves dominate the AD and these AD's are azimuthally symmetric (for unpolarized light at normal incidence). Above 10 eV, the delayed onset (due to passing over the centrifugal barrier) of $d$ to continuum $f$ partial-wave emission occurs and this channel then dominates. The $d_{x^2-y^2}$ initial state, composed of spherical harmonics $Y_{2\,\pm 2}$ is connected to $Y_{3\,\pm 3}$ and $Y_{3\,\pm 1}$ partial waves by the dipole operator. The calculated differential cross section, of the form $d\sigma/d\Omega = a(\theta) - b(\theta)\cos 4\phi$, is fourfold symmetric, as expected, owing to interference effects between the $m = \pm 1$ and $m = \pm 3$ partial waves. The anisotropy parameter $\alpha(\theta) \equiv b(\theta)/a(\theta)$ changes sign at $\theta = 63.43°$ and this manifests itself as a 45° azimuthal rotation of the fourfold pattern. Specific systems for studying this effect experimentally are discussed. The deposition of Cu, Ag, or Au on a wide-band-gap insulator such as LiF appears promising as LiF should provide a large crystal field and the noble-metal $d$ states should fall within the gap, thus remaining sharp and resolvable. The importance of the partial-wave interferences in other angle-resolved photoemission studies of oriented atoms, molecules, and surfaces is noted.

**15749.** Gadzuk, J. W., **Extra-molecular relaxation energies for $H_2$ embedded in an electron gas,** *Chem. Phys. Lett.* **36,** No. 5, 606-610 (Dec. 15, 1975).

Key words: molecular hydrogen; photoelectron spectroscopy; polarization energy; relaxation energy; screening energy.

The screening energy associated with a bonding orbital hole state in an $H_2$ molecule embedded in an electron gas has been calculated, within a linear response formalism. The relationship between this energy and the atomic screening energy is determined and the role of the bonding charge density is emphasized.

**15750.** Swanson, N., Celotta, R. J., **Observation of excited states in ozone near the dissociation limit,** *Phys. Rev. Lett.* **35,** No. 12, 783-785 (Sept. 22, 1975).

Key words: electron energy loss; forbidden transitions; ozone; triplet states.

Several calculations suggest that the lowest triplet states of ozone lie near the dissociation limit. Using electron energy-loss spectroscopy, we have observed a broad feature beginning at 1.3 eV, with a maximum at 1.65-eV energy loss. This structure is present only under large momentum-transfer conditions, indicative of the excitation of optically forbidden states. Together with the calculations, these data demonstrate that one or more excited states of ozone exist which are stable against dissociation.

**15751.** Huebner, R. H., Celotta, R. J., Mielczarek, S. R., Kuyatt, C. E., **Energy absorption by $N_2O$ in the 4 to 14 eV region,** *J. Chem. Phys.* **63,** No. 10, 4490-4494 (Nov. 15, 1975).

Key words: electron energy loss; energy absorption; $N_2O$; nitrous oscillator strength; photoabsorption.

Apparent oscillator-strength values for transitions in the 4 to 14 eV region in nitrous oxide have been derived from electron energy-loss measurements. Detailed comparison with photoabsorption measurements in the ultraviolet region indicates a weak transition below the $^1\Delta \leftarrow \bar{X}\,^1\Sigma^+$ transition at 6.8 eV not observed optically. This analysis also provides oscillator-strength values in the region between 11.5 and 12.4 eV, where no quantitative photoabsorption data are available.

**15752.** Penn, D. R., **Measurement of the surface density of states by field ionization,** *Surf. Sci.* **52,** 270-276 (1975).

Key words: field ion energy distribution; field ionization; surface density of states; tungsten.

It is shown that recent measurements of field ion energy distributions from clean tungsten surfaces probe the density of metal states in the vicinity of the surface. We find $j(\omega) = (2\pi/\hbar)\Sigma_m |\int d^3r \psi_m(\mathbf{r})\, \gamma(z)|^2\, \delta(\omega - \epsilon_m)$, where $j(\omega)$ is the ion current at energy $\omega$, $\psi_m$ and $\epsilon_m$ are electronic metal eigenfunctions and eigenvalues in the presence of the external electric field used in field ionization and $\gamma(z)$ is a function which is large near the noble gas atom. An explicit expression for $\gamma(z)$ is given in the text. It is estimated that tungsten metal states with values of $\mathbf{k}_{||}$ at least as large as 0.5 $\text{Å}^{-1}$ make an appreciable contribution to $j(\omega)$ where $\mathbf{k}_{||}$ is the electron momentum parallel to the surface.

**15753.** Cabana, A., Laurin, M., Pépin, C., Lafferty, W. J., **High-resolution infrared spectrum of the $\nu_3$ and $\nu_2 + \nu_3 - \nu_2$ bands of $^{14}N^{16}O_2$,** *J. Mol. Spectrosc.* **59,** 13-27 (1976).

Key words: infrared spectrum; nitrogen dioxide, $\nu_3$ band; nitrogen dioxide, $\nu_3 + \nu_2 - \nu_2$ band; rotational constants; spectroscopic constants; spin-rotation constants.

The infrared absorption spectrum of the $\nu_3$ band of $^{14}NO_2$ has been recorded with a resolution and a frequency accuracy much improved over the previous investigations. The $K$- and $N$-line assignments have been greatly extended and a more accurate set of spectroscopic constants derived. Several lines in the subbands with $K_a \geqslant 3$ have been observed to be doubled by spin-rotation interaction and spin-rotation interaction constants have been obtained. Several weak series of lines in the spectrum ($K_a = 0, 1, 2,$ and 3) have been unambiguously assigned to the "hot band" $\nu_2 + \nu_3 - \nu_2$. Lines of the $K_a = 3, 4, 5,$ and 6 subbands of $\nu_3$ have been found to be perturbed by a Coriolis interaction with the $K_a = 4,$ 5, 6, and 7 levels of $2\nu_2$.

**15754.** Mielenz, K. D., Cehelnik, E. D., McKenzie, R. L., **Elimination of polarization bias in fluorescence intensity measurements,** *J. Chem. Phys.* **64,** No. 1, 370-374 (Jan. 1, 1976).

Key words: emission anisotropy; fluorescence; fluorescence decay; fluorescence quantum yields; polarization; spectrofluorimetry; viewing angle.

It is proposed theoretically and confirmed experimentally that, if the fluorescence emission from a polarized sample is viewed in the horizontal plane at an angle of 45° (or 135°) to the direction of propagation of the exciting radiation with a polarizer set at 54.75° (or 125.25°) from the vertical direction, then, the reading obtained is proportional to the total flux emitted by the sample and is independent of the state of polarization of the exciting radiation and the emission anisotropy of the sample. The polarization sensitivity of the emission detection system then becomes a factor which is included in the spectral sensitivity curve of the emission detection system.

**15755.** Huebner, R. H., Bushnell, D. L., Jr., Celotta, R. J., Mielczarek, S. R., Kuyatt, C. E., **Ultraviolet photoabsorption by halocarbons 11 and 12 from electron impact measurements,** *Nature* **257,** No. 5525, 376-378 (Oct. 2, 1975).

Key words: electron energy loss; electron impact; Freon 11; Freon 12; uv photoabsorption.

Electron energy loss measurements are made of Freons 11 and 12. The data is converted to oscillator strength distributions and compared to the existing photoabsorption data in the energy range relevant to atmospheric photodissociation.

**15756.** Hahn, M. H., Robinson, H. E., Flynn, D. R., **Robinson line-heat-source guarded hot plate apparatus,** *Am. Soc. Test. Mater. Spec. Tech. Publ. 544,* pp. 167-192 (1974).

Key words: conduction; energy conservation; heat transfer; insulation; thermal conductivity; thermal insulation.

This paper presents a description of the line-heat-source guarded hot plate apparatus conceived by the late H. E. Robinson, the results of mathematical analyses of potential sources of uncertainty, and the design of an apparatus of this type being constructed at the National Bureau of Standards. This design utilizes a line source heater, from which heat diffuses laterally in the plate. Such a design does not produce a wholly uniform plate temperature, but does enable calculation of average plate surface, and edge, temperatures utilizing only a few temperature sensors.

**15757.** Jacox, M. E., **Matrix isolation study of the products of the interaction between metastable Ar and Kr atoms and chloroform. Photodecomposition of $HCCl_2^+$ and $HCCl_2^-$,** *Chem. Phys.* **12,** 51-63 (1976).

Key words: Ar metastable interactions; $ClHCl^-$; emission spectrum; $HAr_n^+$; $HCCl_2^+$; $HCCl_2^-$; $HCCl_3$; infrared spectrum; matrix isolation; molecular rotation in solid Ar; photoinduced proton transfer; ultraviolet spectrum.

The emission spectrum of a microwave discharge through argon and the infrared and ultraviolet spectra of the products of the interaction of $HCCl_3$ with the periphery of such a discharge, observed after rapid quenching in an argon matrix at 14 K, indicate that metastable argon atoms play an important role in matrix isolation experiments using such a discharge configuration to produce free radicals and molecular ions. Exceptionally high yields of $HCCl_2^-$ and $HCCl_2^-$ and a significant concentration of $CCl_3^+$ were stabilized in these experiments. The observations support the earlier assignment of the 1037 $cm^{-1}$ peak to "isolated" $CCl_3^+$. Upon exposure of the sample to 370-280 nm radiation, a prominent, slightly perturbed absorption of $ClHCl^-$ appeared at 705 $cm^{-1}$. This absorption was destroyed by 280-260 nm radiation. The relative stability of both $HCCl_2^+$ and $CCl_3^-$ upon exposure of the sample to radiation of wavelength longer than 280 nm is attributed to electron scavenging by the $HCCl_3$ in the matrix; this species is present in considerably greater concentration than are the ion products. Evidence is presented for the photodecomposition of $HCCl_2^+$ at wavelengths shorter than about 280 nm. A marked increase in the concentration of $HAr_n^+$ when $HCCl_2^-$ was photolyzed by radiation of wavelength shorter than 260 nm is consistent with the calculated threshold energy for proton transfer from $HCCl_2^+$ to Ar. The results of krypton matrix experiments are also consistent with this mechanism. Unstructured absorption bands near 285 and 250 nm are tentatively attributed to $ClHCl^-$ and $HCCl_2^+$, respectively. An increase in the concentration of "nonrotating" $H_2O$, compared to $H_2O$ molecules free to undergo rotational transitions, when ions are present in the matrix can be attributed to the electric field produced by ionic interactions.

**15758.** Gadzuk, J. W., **Interaction of atoms and molecules with surfaces,** Chapter 7 in *Surface Physics of Materials*, J. M. Blakeley, Ed., **II**, 339-375 (Academic Press, Inc., New York, NY, 1975).

Key words: adsorption; chemisorption; electronic properties of solids; molecules; surfaces.

The theory of chemisorption of atoms and molecules on surfaces is considered. Emphasis is directed towards the Anderson model (self-consistent molecular orbital theory) and the dielectric screening models. The techniques of group orbitals are used to reduce the many atom problems to one involving a surface molecular complex. Specific cases of H adsorbed on the (100) face of W, alkali atoms on metals, and 5d transition metal atoms on W are treated.

**15759.** Gadzuk, J. W., **Angle resolved photoemission from chemisorbed layers: Further theoretical considerations,** *Surf. Sci.* **53**, 132-143 (1975).

Key words: angular distributions; chemisorption; electron spectroscopy; photoemission.

In recent theoretical work by Gadzuk and by Liebsch, the importance of angle resolved photoemission studies of surfaces and chemisorbed atoms has been demonstrated. In the theory due to Gadzuk, the role of the initial state in the photoemission process has been emphasized, whereas in the theory due to Liebsch, the role of the final state is stressed in determining a photoemission angular distribution (PAD) from chemisorbed atoms. Here it is shown what conditions favor initial versus final state dominance. In both theories, the PAD is calculated for an isolated chemisorbed atom or surface molecule complex. It is shown how two-dimensional band effects due to adatom—adatom interactions modify (or do not modify) the PAD.

**15760.** Mahan, A. H., Gallagher, A., **Transition radiation for the diagnosis of low-energy electron beams,** *Rev. Sci. Instrum.* **47**, No. 1, 81-83 (Jan. 1976).

Key words: electron optics; transition radiation.

Electron bombardment of metallic silver is known to produce "transition radiation," predominantly at 300-450 nm wavelengths. In reported measurements at 15-500 eV impact energies, transition radiation was used to diagnose the shape and time dependence of an rf modulated electron beam. It is suggested that this is a superior target, as opposed to phosphors or gases normally used, to determine instrumental time response functions and electron beam imaging.

**15761.** Truhlar, D. G., Poling, R. E., Brandt, M. A., **Infinite-order sudden approximation for rotational excitation of hydrogen molecules by electrons in the energy range 10-40 eV,** *J. Chem. Phys.* **64,** No. 2, 826-829 (Jan. 15, 1976).

Key words: differential cross sections; elastic scattering; electron scattering; hydrogen molecules; momentum transfer; rotational excitation; scattering theory; sudden approximation.

Electron scattering by $H_2$ is treated using a noncentral interaction potential including short-range and long-range static contributions, exchange, and polarization effects. The molecule is treated as a rigid rotator and the scattering is treated in the infinite-order sudden approximation. The results show that the rotational excitation cross section exceeds the elastic scattering cross section at large scattering angles at intermediate energies but not at small angles at low energies.

**15762.** Burch, D. M., Peavy, B. A., Powell, F. J., **Comparison between measured and computer-predicted hourly heating and cooling energy requirements for an instrumented wood framed townhouse,** *ASHRAE Trans.* **81,** Part II, Paper No. 2363, 70-88 (1975).

Key words: building heat transfer; computer programs; dynamic thermal performance; heat flow analysis; heating and cooling loads; thermal analysis; transient heat flows.

A sophisticated computer program called NBSLD was validated for predicting the hourly heating and cooling loads of a residence. An instrumented four-bedroom townhouse was exposed to simulated winter and summer conditions inside a large environmental laboratory. During the tests, the activities of a six member family were simulated, and the inside temperature of the test house was maintained at approximately 75 °F (23.9 °C). Hourly heating and cooling input energy was measured and compared with corresponding computer-predicted values. The NBSLD computer program predicted maximum heating and cooling input loads within 9.2 percent, and energy requirements within 8.2 percent.

**15763.** Johnson, C. R., **A local Lyapunov theorem and the stability of sums,** *Linear Algebra and Appl.* **13,** 37-43 (1976).

Key words: cone; Lyapunov's theorem; stable matrix.

We present a "local" analog of Lyapunov's theorem which characterizes $n$ by $n$ matrices whose eigenvalues lie in the open left half plane. This allows the characterization of pairs of stable matrices $A$, $B$ such that the sum $A + \alpha B$ is stable for all real $\alpha > 0$.

**15764.** Ives, L. K., Ruff, A. W., Reed, R. P., **An electron microscope study of the Tishomingo meteorite,** (Proc. 32d Annual Meeting of Electron Microscopy Society of America, St. Louis, MO, Aug. 13-15, 1974), Paper in *Proceedings Electron Microscopy Society of America, 32d Annual Meeting*, C. J. Arceneaux, Ed., pp. 520-521 (Claitor's Publ. Div., Baton Rouge, LA, 1974).

Key words: alloy; austenite; electron microscopy; iron-nickel; martensite; meteorite; Tishomingo.

Transmission electron microscope studies have been performed on the Tishomingo meteorite. The microstructure consists of original austenite material and transformed martensite. Deformation twins have been observed. High dislocation density was found within the austenite. Heating stage experiments were performed to investigate thermal response of the material.

**15765.** Fraker, A. C., **Microstructural and corrosion studies of the Ti-2 wt.% Ni alloy,** (Proc. 32d Annual Meeting of Electron Microscopy Society of America, St. Louis, MO, Aug. 13-15, 1974), Paper in *Proceedings Electron Microscopy Society of America, 32d Annual Meeting,* C. J. Arceneaux, Ed., pp. 516-517 (Claitor's Publ. Div., Baton Rouge, LA, 1974).

Key words: corrosion; microstructures; titanium.

The influence of heat treatment on the Ti-2wt.% Ni alloy microstructure was studied. Heat treating above the $\alpha+\beta$ temperature region and quickly cooling produces a martensite type microstructure with a highly segregated $Ti_2Ni$ precipitate phase. Heat treating at lower temperatures results in an enlarged $\alpha$-titanium grain structure with large randomly dispersed $Ti_2Ni$ precipitates. Transmission electron microscopy, electron diffraction and light microscopy were used to show these microstructural differences as well as examples of local corrosion at the precipitate.

**15766.** Coriell, S. R., Hurle, D. T. J., Sekerka, R. F., **Interface stability during crystal growth: The effect of stirring,** *J. Cryst. Growth* **32,** No. 1, 1-7 (Jan. 1976).

Key words: alloy; boundary layer; fluid flow; interface; solidification; stability.

The influence of stirring on the morphological stability of a solid-liquid interface during the unidirectional solidification of a binary alloy at constant velocity is calculated on the basis of a model that employs a stagnant solute boundary layer. For fixed values of the growth velocity, temperature gradient, and concentration gradient at the interface, stirring decreases morphological stability. Further, the wavelength at which instability first occurs is greater with stirring than in the absence of stirring. For a fixed growth velocity and temperature gradient, and a bulk liquid of given composition, the effect of stirring decreases morphological stability for a distribution coefficient $k > 1$ but can either increase or decrease stability for $k < 1$. The dependence of critical wavelength on growth velocity measured by Morris and Winegard for Pb-Sb alloys can be explained by this theory.

**15767.** deWit, R., **Partial disclinations,** *J. Phys. C: Solid State Phys.* **5,** 529-534 (1972).

Key words: crystal; disclination; dislocation; pseudopentagonal; stacking fault; twin; wedge.

A twin in a crystal can terminate at a partial wedge disclination. This is the analogue to a stacking fault terminating at a partial dislocation. It is illustrated for an FCC crystal. Similarly, several twins can terminate at a partial disclination. This is also illustrated for an FCC crystal. Crystals with such defects, which are called pseudopentagonal twins, have been observed. Their x-ray diffraction pattern should show the elastic distortion of the disclination.

**15768.** Bennett, L. H., McAlister, A. J., Cuthill, J. R., Erickson, N. E., Watson, R. E., **Electronic density of states of lanthanum-transition-metal alloys of $CaCu_5$ type,** *Phys. Rev. B Comments and Addenda* **12,** No. 11, 5335-5337 (Dec. 1, 1975).

Key words: alloys; copper; electronic density of states; lanthanum; nickel; nuclear magnetic resonance; platinum; x-ray photoemission.

Pt-site Knight shifts for the alloy system $LaCu_{5-x}Pt_x$ ($0 < x \leq 5$), and x-ray photoemission data for Pt, $LaNi_5$, and $LaPt_5$ are presented. Variation of the electronic structure of La-transition-metal alloys of $CaCu_5$ type with alloying at the transition-metal sites is discussed in the light of these results and earlier data on the $LaNi_{5-x}Pt_x$ system.

**15769.** Berger, R. E., **Impact testing of ophthalmic lenses: Stress distribution and the "search" theory,** *J. Am. Optom. Assoc.* **47,** No. 1, 86-92 (Jan. 1976).

Key words: fracture; glass; impact; ophthalmic lenses; stress distributions.

Elementary concepts in fracture mechanics, stress analysis, and impact are discussed as they pertain to fracture of lenses in drop ball testing. Quasi-static estimates for stress distributions during impact are obtained. These profiles show a sharp peak in the tensile stress under the impact point.

Identical groups of lenses were impact tested in two different modes: (1) 25 impacts at a single spot on the lens, (2) 1 impact at each of 25 different spots. Much more breakage was observed in the latter group.

Both the experimental and analytical considerations lend support to the "search" theory of drop ball testing—fracture occurs when the ball strikes a weak spot (where there exists a sufficiently severe flaw) on the lens. Lenses which pass an impact test may well have dangerous flaws away from the impact point.

**15770.** Johnson, C. R., **Numerical location of the field of values,** *Linear and Multilinear Algebra* **3,** 9-14 (1975).

Key words: *D*-stable matrix; field of values; Gersgorin's theorem; nonnegative matrix; Perron-Frobenius eigenvalue; spectrum of a square complex matrix.

We give an estimate of the angular location of the *field of values*

$$F(A) = \{x^*Ax : x^*x = 1, x \epsilon C^n\}$$

via the Perron-Frobenius root of a nonnegative matrix obtained from $A$. This estimate is invariant under diagonal congruences of $A$ and may be used to sharpen an existing inclusion region for $F(A)$. Employing a result of Wielandt, an application is also made to the location of spectra of products of matrices based only on regions simply obtained from the factors individually.

**15771.** Yakowitz, H., **Energy dispersive x-ray spectrometry,** *J. Microscopie Biol. Cell.* **22,** No. 2-3, 137-150 (1975).

Key words: elemental distribution; energy dispersive x-ray analysis; light element analysis; scanning electron microscopy; thin film x-ray analysis; x-ray continuum radiation.

An energy dispersive x-ray spectrometer (EDS) was first used for electron microanalysis in 1968. Since then the number and quality of EDS systems has steadily and rapidly increased. Today a large majority of scanning electron microscopes (SEM) and many transmission electron microscopes (TEM) are equipped with EDS facilities. Thus, the electron microscopist can perform qualitative and quantitative analyses and can also map elemental distribution in the area scanned by the electron beam.

This paper will provide only a brief overview of the operating principles and required equipment for EDS systems. Major emphasis will be placed on data interpretation including background correction, pulse pile-up effects, peak interferences and analytical schemes for quantitation.

**15772.** Peterlin, A., Olf, H. G., **Environmental effects on low temperature crazing of crystalline polymers,** *J. Polym. Sci. Part C:* No. 50, 243-264 (1975).

Key words: crazing; cryogenic temperatures; crystalline polymers; environmental effects on crazing; fractional free volume; glass transition temperature; smectic polypropylene; spherulitic polypropylene.

The ductile behavior of crystalline polymers between liquid nitrogen and room temperatures is primarily due to enhancement of crazing by the presence of gases ($N_2$, $A_2$, $O_2$, $CO_2$) of high thermodynamic activity, i.e., close to their condensation point. Without the presence of such a gas, at temperatures sufficiently above its condensation point so that its activity has dropped to a few percent, the crystalline material is rather brittle although some very limited crazing can be detected. As expected, the ductility and the amount of crazing are very nearly the same in helium as under vacuum. The crazes in smectic PP are extremely long, often traversing the entire width (0.5 cm) of the sample, and generally very similar to crazes in glassy amorphous polymers. They are thin and become thicker at higher temperatures. In monoclinic PP with well developed spherulitic structure, crazing occurs along spherulite diameters that are perpendicular to the stress direction but not along the boundaries between spherulites. In general, the length of a craze equals the spherulite diameter. At low temperatures all crazes originate on the outer surface of the sample which is in direct contact with the gas.

The action of the gas is due to two mechanisms. First, the adsorbed gas reduces the surface energy of the polymer, facilitating the creation of a new surface in the holes and voids of the craze. Second, the gas becomes highly absorbed at the tip of an incidental flaw or of an existing craze, since these are regions of high dilatant stress. The locally absorbed gas acts as a plasticizer easing the flow involved in the nucleation and growth of the craze, i.e., in the formation of fibrillar material of the craze.

**15773.** Carroll, J. J., Smit, J., Melmed, A. J., **Field-ion imaging of titanium and effects due to hydrogen,** *Surf. Sci.* **45,** No. 2, 640-648 (Oct. 1974).

Key words: field-ion microscopy; hydrogen; titanium.

Titanium specimens of nominal 99.99+ percent purity were prepared and imaged in the field-ion microscope between 23-30 K using hydrogen, hydrogen-helium mixtures, and neon imaging gases. Micrographs obtained in the presence of hydrogen show features that may indicate the early stage development of cracks and hydrides, mostly on and between the $\{11\overline{2}0\}$ and $\{10\overline{1}0\}$ plane regions. Neon field-ion microscopy shows that the image features due to hydrogen-titanium interactions in the field-ion microscope are confined to about 10-15 topmost metal layers.

**15774.** McKee, R. A., Stark, J. P., **Interpretations for thermomigration results in aluminum and aluminum alloys,** *Acta Metall.* **23,** 1145-1148 (Oct. 1975).

Key words: alloys; aluminum; copper-aluminum; nonisothermal diffusion; silver-aluminum; thermomigration; vacancies.

Recent anomalies have been reported for thermomigration results in aluminum and aluminum alloys. A sign reversal for the measured heat of transport and consequently a mass flux reversal in the thermomigration experiment was reported for self-thermomigration in pure aluminum and for thermomigration of copper in aluminum. These events occurred as a result of varying the grain or crystal size in the experiment. A grain size effect on the measured heat of transport for silver in aluminum has also been reported. Experimental data for nonisothermal diffusion of $Ag^{110}$ in aluminum has established the existence of stable point defect concentrations in excess of those predicted for thermal equilibrium and the explanation for the anomalies in aluminum thermomigration experiments is now possible.

**15775.** Peterlin, A., **Optical effects in flow,** *Annu. Rev. Fluid Mech.* **8,** 35-55 (1976).

Key words: flow with longitudinal gradient; flow with transverse gradient; optical anemometry; optical birefringence; optical excess tensor; optical mapping of flow; stress excess tensor; two-dimensional flow.

A critical survey of optical effects induced by flow is given for pure liquids, liquid mixtures, suspension and polymer solutions. The optical and stress excess tensors are proportional in pure liquids, mixtures, and polymer solutions and melts in almost the full range of flow gradient (rheo-optical law). Such a proportionality exists also for suspensions at small gradient as long as the birefringence is a linear function of the gradient.

Optical birefringence is used for the mapping of stresses on a flow field in complicated flow geometry and particularly with non-Newtonian fluids. The Doppler effect of scattered light is used for optical anemometry.

**15776.** Manning, J. R., Stark, J. P., **Complete-path matrix equations for tracer diffusion coefficients and correlation factors,** *Phys. Rev. B* **12,** No. 6, 2075-2079 (Sept. 15, 1975).

Key words: atom migration; correlation factor; crystal defect; diffusion coefficient; matrix equations; nonrandom walk equation.

General complete-path matrix equations are derived for the tracer diffusion coefficient and correlation factor by taking into account the frequency with which defects encounter a tracer atom and the possibility of multiple exchanges of a defect with the atom. These equations apply even when mirror symmetry and rotational symmetry of the crystal and defect are lacking, as for example when diffusion occurs via complex defects in noncubic crystals. They also are valid for diffusion along any diffusion direction and where the individual atom jumps provide a variety of jump distances. It is shown that the general equations reduce to those of Stark and of Howard in the special case where there is mirror symmetry across the diffusion place.

**15777.** Fraker, A. C., **Microstructures of Ti-1.5 w/o Ni alloys with Mo and Al additions,** (Proc. 33d Annual Electron Microscopy Society of America, Las Vegas, NV, Aug. 11-15, 1975), Paper in *Proceedings Electron Microscopy Society of America, 33d Annual Meeting,* G. W. Bailey, Ed., pp. 54-55 (Claitor's Publ. Div., Baton Rouge, LA, 1975).

Key words: microstructures; titanium; transmission electron microscopy.

Small additions of Mo to Ti-0.8 to 1 w/o Ni alloys produce good crevice corrosion resistance and improved fabrication properties. This work shows how the Ti-1.5 w/o Ni alloy microstructure is altered by adding 2 w/o Mo or 2 w/o Al. It was concluded that the Mo addition produces a more elongated microstructure with smaller sized $Ti_2Ni$ precipitates, enhances the martensitic reaction and increases the hardness of the material. The Al addition does not change the microstructure markedly but does cause an increase in microhardness.

**15778.** Ruff, A. W., Ives, L. K., **Measurement of solid particle velocity in erosive wear,** *Wear Short Commun.* **35,** 195-199 (1975).

Key words: erosive wear; particle impingement; particle velocity measurement; wear; wear testing.

A method is described for determining the velocity of solid particles in a gas-particulate stream applied to erosion testing of materials. A simple mechanical configuration allows the measurement to be made under a wide range of equipment conditions. The time-of-flight of the particles is determined over a controlled path length between two rotating disks. Examples of measurements on several test apparatus are presented. The importance of nozzle design is discussed. A comparison between particle and gas stream velocity is presented.

**15779.** Kuriyama, M., **A classical derivation of the dynamical diffraction equation for imperfect crystals based on the Ewald-Laue-Bethe theory,** *Acta Crystallogr.* **A31,** Part 6, 774-779 (Nov. 1975).

Key words: dynamical diffraction equation; imperfect crystals; scattering matrix theory.

The basic equation of dynamical diffraction for imperfect crystals, which has been derived previously by a general dynamical theory of diffraction, is rederived classically based on the Ewald-Laue-Bethe concept, thus completing the formulation of a "scattering matrix" theory. It is shown in this classical derivation that a series of assumptions is required at each stage of the mathematical formulation to allow it to proceed further. These assumptions are then viewed in terms of the general dynamical theory of diffraction, and found unnecessary in the rigorous formulation. This classical formulation provides a conceptual relation between the traditional Ewald-Laue-Bethe dynamical theory and the general dynamical theory, one that has been derived with the aid of quantum-field theory.

**15780.** McAlister, A. J., Cuthill, J. R., Dobbyn, R. C., Williams, M. L., Watson, R. E., **Band structure of face-centered and body-centered-cubic 3*d* transition metals,** *Phys. Rev. B* **12,** No. 8, 2973-2983 (Oct. 15, 1975).

Key words: Co; Cr; *d*-band widths; electronic structure; Fe; ferromagnetism; soft x-ray emission; soft x-ray spectra; transition metals.

Measurements of the soft-x-ray $M_{2,3}$ emission spectra of face-centered Fe and Co, and body-centered Fe, Cr, and V are reported and $M_3$ single-hole excitation profiles are estimated. 3*d* bandwidths inferred from these results and earlier data on Cu and Ni are compared with band-theory predictions. As has been seen previously with x-ray and ultraviolet photoemission, the experimental Ni bandwidth is markedly narrower than theory predicts; there is a suggestion that the bandwidth of Cu is somewhat broader; theory and the present results are in fair agreement for the other metals. Fine structure is seen in the spectra; correlations are noted in the weak structure of metals of common crystal structure; and structural correlations with x-ray and ultraviolet photoemission data are seen as well.

**15781.** Sawyer, D. E., Berning, D. W., **Laser scanning of active semiconductor devices,** *Proc. Technical Digest, International Electron Devices Meeting, Washington, DC, Dec. 1-3, 1975, IEDM Technical Digest,* pp. 111-114 (1975).

Key words: active devices; hot spots; laser scanning; logic flow observation; LSI testing; nondestructive test; nonlinearity measurement; UHF transistor measurement.

A laser scanner is described which can nondestructively explore electrical characteristics of semiconductor devices on a point-by-point basis. The results of applying the scanner to electronically map temperature distributions and hot spots in a power transistor are given. The results of mapping localized nonlinearities in electrical operation and 0.5 GHz response are also presented. Pictures show the progress of logic in a MOS shift register and demonstrate the ability to change at will the logical state of an embedded active cell with the laser.

**15782.** Mathey, R. G., Clifton, J. R., **Bond of coated reinforcing bars in concrete,** *J. Struct. Div. Proc. Am. Soc. Civil Eng.* **102,** No. ST1, 215-229 (Jan. 1976).

Key words: bond strength; coated reinforcing bars; evaluation; organic coatings; pullout tests.

The bond strengths were determined for 23 epoxy-coated (10 different epoxy coatings), six polyvinyl chloride-coated (three different coating materials), and five uncoated reinforcing bars. The length of embedment of the reinforcing bar in the concrete was 12 in (305 mm). The loads or bond stresses corresponding to a loaded-end slip of 0.01 in (0.25 mm) or a free-end slip of 0.002 in (0.051 mm) were considered as critical values in determining the bond strength, depending on which of these values of slip developed first. For coating film thicknesses ranging from 0.001 in to 0.011 in, the epoxy-coated bars developed bond strengths essentially equal to the bond strengths for uncoated bars. Experimental values were higher than minimum acceptable values in building code and highway bridge requirements. Bond strengths of the polyvinyl chloride-coated bars and bars with thick epoxy coatings were unacceptable.

**15783.** Harrison, S. H., **Neutron activation analysis: A useful tool for evaluating water sampling and analysis techniques,** *Proc. Transactions American Nuclear Society, New Orleans, LA, June 6-13, 1975,* **21,** 110-111 (1975).

Key words: neutron activation analysis; particulates; sampling; species; trace element concentrations.

Neutron activation analysis (NAA) was used to determine the natural variability of trace element concentrations at a single sampling location over a short time (2 or 3 hours) and to compare the performance of two different water sampling devices. Data for both dissolved species and suspended particulates are presented. A normalizing technique for evaluating suspended particulate data is described.

Unique results obtained with this normalizing technique are demonstrated on data from a highly polluted tributary of the Chesapeake Bay.

**15784.** McClintock, W., Henry, R. C., Moos, H. W., Linsky, J. L., **Ultraviolet observations of cool stars. IV. Intensities of Lyman-$\alpha$ and Mg II in Epsilon Pegasi and Epsilon Eridani, and line width-luminosity correlations,** *Astrophys. J.* **202,** No. 3, 733-740 (Dec. 15, 1975).

Key words: chromospheres, stellar; *Copernicus* observations; ultraviolet stellar spectra; Wilson-Bappu effect.

The Princeton spectrometer on the *Copernicus* satellite has been used to confirm the existence of a line width-luminosity relation for the L$\alpha$ and Mg II $\lambda$2800 chromospheric emission lines in K-type stars, by observation of a K2 dwarf ($\epsilon$ Eri) and of a K2 supergiant ($\epsilon$ Peg). Combined with previously reported observations of lines in three K giants ($\alpha$ Boo, $\alpha$ Tau, and $\beta$ Gem), the data are consistent with an identical dependence of line-width on absolute visual magnitude for the Ca II K, L$\alpha$, and Mg II $\lambda$2795 lines. Surface fluxes of L$\alpha$, Mg II $\lambda$2800, and O V $\lambda$1218 (upper limit) for $\epsilon$ Eri, and of Mg II $\lambda$2800 for $\epsilon$ Peg are also compared with values reported previously for the three giant stars.

**15785.** Unassigned.

**15786.** Galloway, K. F., Keery, W. J., Leedy, K. O., **Integrated circuit damage resulting from SEM examination,** *Proc. 25th Annual Electronic Components Conf., Washington, DC, May 12-14, 1975,* pp. 263-266 (Institute of Electrical and Electronics Engineers, New York, NY, 1975).

Key words: electron beam damage; electron beam energy deposition; integrated circuits; ionizing radiation effects; scanning electron microscope; surface effects.

The scanning electron microscope utilizes a well controlled low-energy electron beam which is a potential source of damage to specimens under investigation. In particular, the energy deposited by the electron beam can alter the surface oxide properties of semiconductor devices which can, in turn, lead to a change in device electrical parameters. The energy deposition and the resulting oxide changes are reviewed in this paper, and the effects of the scanning electron beam are illustrated.

**15787.** Heinrich, K. F. J., **Scanning electron probe microanalysis,** Chapter in *Advances in Optical and Electron Microscopy* **6,** 275-301 (Academic Press, Inc., London, England, 1975).

Key words: color composite technique; counting statistics; electron beam scanning; electron probe microanalysis; x-ray analysis.

Scanning electron probe microanalysis is related to microscopy as well as to chemical analysis. The present techniques can be considered as incomplete variations of a hypothetical model of quantitative elemental characterization of a microscopic area. Such a "complete scanning analysis" is at present limited by statistics of achievable count rates, and by the requirements for applying complicated transformations or "corrections" to the experimental results. The use of color composites and of data collection and evaluation systems which are becoming more readily available provides improved techniques for the presentation of information. Further progress depends upon the development of x-ray detectors having low coincidence losses and of extensive storage and manipulation of digital information.

**15788.** Freund, S. M., Hougen, J. T., Lafferty, W. J., **Laser magnetic resonance spectra of $^{14}NO_2$ and $^{15}NO_2$ near 1600 $cm^{-1}$,** *Can. J. Phys.* **53,** No. 19, 1929-1938 (1975).

Key words: band center; intensities; laser magnetic resonance; nitrogen dioxide; rotational assignment; spin-rotation splittings.

Two laser magnetic resonance patterns for $^{14}NO_2$ and six patterns for $^{15}NO_2$, observed using six CO laser transitions, have been analyzed to yield spin corrected zero-field vibration – rotation transition wave numbers and zero-field spin – rotation splittings. The $^{14}NO_2$ results are in good agreement with results obtained from conventional infrared grating studies. The $^{15}NO_2$ results allow new values of $\nu_0 = 1582.107 \pm 0.008$, $A' - A'' = -0.2116 \pm 0.0011$, and $D_K' - D_K'' = -1.39 \pm 0.20 \times 10^{-4}$ $cm^{-1}$ to be determined for the $\nu_3$ fundamental of that molecule (errors are 3 standard deviations). Two spectral figures and a list of assigned Zeeman lines are presented to permit using this stable molecule as an aid in adjusting newly constructed instruments. Closed form approximate intensity expressions are given for Zeeman transitions of the type observed in this work, i.e., for sharp partially spin forbidden Zeeman transitions in *A* type bands of near prolate asymmetric rotors.

**15789.** Carpenter, B. S., Myklebust, R. L., **Comparative analysis for boron in steel by ion microprobe mass analyzer and the nuclear track technique,** *Anal. Chim. Acta Short Commun.* **81,** 409-411 (1976).

Key words: alpha particles; boron; ion microprobe mass analyzer; nuclear track technique; standard reference material; steel.

This work describes the analytical capabilities of the NBS Ion Microprobe Mass Analyzer for determining trace concentrations of boron in a steel matrix. In addition, the boron concentration values obtained in this way are compared with those obtained by the Nuclear Track Technique, in which the boron concentration and distribution are determined by counting the alpha tracks produced by the nuclear reaction $^{10}B(n, \alpha)^7Li$ in plastic solid-state recorders. Both methods are surface, or limited depth, microtechniques that perform analyses through interaction with individual atoms; thus, comparison of the results from both methods is useful in revealing the spatial homogeneity of the boron in the steels.

**15790.** Newman, M., **Some results on symplectic matrices,** *Linear and Multilinear Algebra* **3,** 95-98 (1975).

Key words: generalized permutations; *p*th roots; symplectic matrices.

The principal results are that if $A$ is an integral matrix such that $AA^T$ is symplectic then $A = CQ$, where $Q$ is a permutation matrix and $C$ is symplectic; and that if $A$ is a hermitian positive definite matrix which is symplectic, and $B$ is the unique hermitian positive definite $p$th root of $A$, where $p$ is a positive integer, then $B$ is also symplectic.

**15791.** Carlsten, J. L., Peterson, J. R., Lineberger, W. C., **Binding of an electron by the field of a molecular dipole – $LiCl^-$,** *Chem. Phys. Lett.* **37,** No. 1, 5-8 (Jan. 1, 1976).

Key words: alkali-halide; negative ions; photoelectron spectroscopy; polar molecules.

We present direct experimental evidence for the binding of an electron by the dipole moment of a neutral molecule. The photoelectron spectrum of $LiCl^-$ was obtained and analyzed to determine that the binding energy of the electron in the $LiCl^-$ ion is $(0.61 \pm 0.02)$ eV. This result is an order of magnitude smaller than the predictions of the fixed dipole theoretical model, but is consistent with a recent calculation, which allows for distortion of the dipolar core.

**15792.** Kilmer, R. D., Leasure, W. A., Jr., Mathews, D. E., **Truck Noise I-C: Pavement surface effects on the generation of truck tire noise,** *Report No. DOT-TST-76-49,* 111 pages (Available from the National Technical Information Service, Springfield, VA 22161, Oct. 1975).

Key words: acoustics; noise measurement; noise (sound); tire noise; transportation noise; truck.

This report presents data showing the effect that pavement surface has on the generation of truck tire noise. Three different tread designs – rib, cross-bar and pocket – were tested at speeds of 40, 50 and 60 mph (64.4, 80.5 and 96.5 km/hr) while coasting on eight different pavement surfaces at the Texas Transportation Institute. These surfaces represent a wide range of surface texture. Also presented are the results of one method of quantitatively characterizing pavement surface texture; namely, the mean square value of the macrotexture profile, obtained utilizing a macrotexture profile tracer. Plots of tire noise versus this particular measure of surface texture show that up to a certain macrotexture the generated noise is tire dependent while above this value the pavement macrotexture appears to be the controlling parameter. Because of the wide variation in noise level with changes in surface texture for the pocket retread, this tire is investigated as a possible simple calibrator of surface texture.

These investigations serve as the basis for evaluation of the effect of surface texture on the generation of tire noise.

**15793.** Lofquist, K. E. B., **An effect of permeability on sand transport by waves,** *Technical Memorandum No. 62*, 74 pages (U.S. Army Corps of Engineers, Coastal Engineering Research Center, Fort Belvoir, VA, Dec. 1975). (Available from the National Technical Information Service, Springfield, VA 22161).

Key words: beach accretion; coastal processes; offshore zone; oscillatory water tunnel; permeability effect on sand transport; ripples, sand; sand motion under waves.

Permeability effects on the movement of sand in oscillatory flows are observed in laboratory experiments which approximate prototype conditions at the seabed under progressive waves. A natural sand is used, wave periods range between three and fourteen seconds, and the sand surfaces are naturally rippled. The apparatus has a symmetry which removes all effects, except those of permeability, which might cause a net movement of the sand. Onshore and offshore directions are determined by the phase relationships between the horizontal flows and superposed vertical permeability flows. A positive permeability effect is found, in that the ripple profiles move in the onshore direction. The velocity of this motion is measured and described in a simple dimensionless plot. The associated net transport of sand is not observed directly, but can be inferred, to an extent, from the motions of the ripple profiles. The effects of permeability are cumulative and can be significant in coastal processes of long duration. Any estimate of the local rate of sand transport onshore due to permeability involves the distribution of permeabilities within the seabed which are largely unknown. An overall estimate is less than 1 cubic meter per meter of shoreline per year, which is negligible for most engineering considerations.

**15794.** Bender, P. L., Silverberg, E. C., **Present tectonic-plate motions from lunar ranging,** *Tectonophysics* **29**, 1-7 (1975).

Key words: geodesy; geodynamics; lasers; metrology; moon; tectonics.

Measurements to determine the motion of the Pacific Plate with respect to North America are planned to start within a few months. The University of Hawaii Lunar Ranging Station on Maui is expected to begin operating, and to achieve an accuracy of 2 or 3 cm soon for a single run. The University of Texas McDonald Observatory has been achieving an accuracy of 8-15 cm on a routine basis since late 1971. Work on further improving the McDonald accuracy is planned. Using data from many runs, an accuracy of 1 cm/yr is expected for the relative motion within the first few years.

A transportable lunar-ranging station has been proposed which could be constructed in about eighteen months. The station could observe for 3-6 weeks at a chosen site, and determine the location of the site with respect to the fixed lunar-ranging stations. The accuracy expected is 1-3 cm in each coordinate. If approved, a possible initial itinerary for the station might be as follows: (a) two or three sites in California, including Goldstone, plus one site in Utah; (b) sites in Baja California and Mexico, plus several others in the U.S.; (c) several sites in Central America, the Caribbean, and South America; (d) repeat measurements in California, Utah, and Baja California, plus initial measurements at sites in Africa, India, and the Pacific. It is expected that data on plate motions also will become available from satellite range measurements and VLBI.

**15795.** Madden, R. P., **Atomic physics with synchrotron radiation,** (Proc. IX Int. Conf. on The Physics of Electronic and Atomic Collisions, Seattle, WA, July 24-30, 1975), Paper in *The Physics of Electronic and Atomic Collisions*, J. S. Risley and R. Geballe, Eds., pp. 563-583 (University Washington Press, Seattle, WA, 1976).

Key words: atomic physics; synchrotron radiation; vacuum ultraviolet.

The availability of synchrotron radiation sources is increasing steadily and their application to problems in atomic physics is growing rapidly. This paper reviews the work in absorption spectroscopy, photoelectron spectroscopy, fluorescence, mass spectroscopy lifetime measurements and time resolved spectra which is currently being done with this powerful source of polarized continuum radiation.

**15796.** Berger, H., **Detection systems for neutron radiography,** (Proc. American Society for Testing and Materials Symp. on Neutron Radiography and Gaging, Gaithersburg, MD, Feb. 10, 1975), Paper in *Practical Applications of Neutron Radiography and Gaging, Am. Soc. Test. Mater. Spec. Tech. Publ. 586*, pp. 35-57 (Jan. 1976).

Key words: films; images; neutron radiography; nondestructive tests; real-time imaging; thermoluminescence; track-etch.

Image detection methods for neutron radiography are described and capabilities of the methods in terms of exposure requirements, spatial resolution, and contrast are given. Neutron energy ranges cold, thermal, epithermal, and fast are included, but emphasis is on detectors for thermal neutron images. Image methods include photographic film, real-time, track-etch, gas-cell, and thermoluminescent; major emphasis is on film techniques, both direct exposure and transfer.

**15797.** Burns, G. W., Hurst, W. S., **Highly stable, sheathed, beryllia insulated, tungsten-rhenium alloy thermocouples,** (Proc. Int. Colloquium on High-Temperature In-Pile Thermometry, JRC Petten, Netherlands, Dec. 12-13, 1974), Paper in *International Colloquium on High-Temperature In-Pile Thermometry,* P. von der Hardt, P. Zeisser, and F. Mason, Eds., EUR 5395 **1**, 1-23 (Commission of the European Communities Directorate-General Scientific and Technical Information and Information Management, Luxembourg, Belgium, 1975).

Key words: beryllium oxide; refractory metals; sheathed thermocouples; tantalum; temperature measurements; thermal emf drift; tungsten-rhenium alloys.

The fabrication and performance testing of 1.6 mm diameter tantalum sheathed, beryllium oxide (BeO) insulated, W-3% Re/W-25% Re thermocouples are reported. Fully assembled thermocouples constructed from aged thermoelements, specially heat treated, sintered BeO insulators, and specially cleaned and etched tantalum sheaths were tested for 2059 h at 1800 °C in a helium environment. The measured thermal emf drifts were less than the equivalent of 1 °C per thousand hours of exposure at 1800 °C. No gross chemical attack or degradation of the component materials was evident. The fabrication techniques, thermal emf test results, and post-test analyses of the component materials are discussed.

**15798.** Reader, J., **Energy levels of singly ionized cesium (Cs II),** *Phys. Rev. A* **13**, No. 2, 507-516 (Feb. 1976).

Key words: cesium; energy levels; spectra.

The system of observed energy levels of Cs II of Wheatley and Sawyer has been reinterpreted through the use of Hartree-Fock calculations and published Zeeman effect and hyperfine-structure measurements. Of the 80 known levels, 30 have been rejected as being not real. A revised list of 54 observed levels of Cs II is presented that includes the $5p^5 5d\,^1P_1$ level recently found by

Reader and Epstein and three levels of the $5p^56d$ configuration that were located with the aid of Sommer's line list. Percentage compositions and Slater parameters are given for the $5p^5(5d+6s)$, $6p$, and $(6d+7s)$ configurations. Severe configuration mixing is found for levels of the $5p^5(5d+6s)$ group. The measured $g$ values of the $5p^5(5d+6s)$ levels provide evidence of a strong term dependence for the parameter $G^1(5p5d)$. By taking into account displacements of the $5p^5ns$ levels due to configuration interaction, the ionization energy is revised to be $186\,600 \pm 150$ cm$^{-1}$ ($23.14 \pm 0.02$ eV).

15799. Bender, P. L., **Applications of PTTI to new techniques for determining crustal movements, polar motion, and the rotation of the earth,** *Proc. 6th Annual Precise Time and Time Interval (PTTI) Planning Meeting, Washington, DC, Dec. 3-5, 1974*, pp. 39-55 (U.S. Naval Research Laboratory, Washington, DC, Dec. 1975).

Key words: crustal moments; earth rotation; geodynamics; lunar distance; microwave interferometry; plate tectonics; satellite geodesy.

New extra-terrestrial techniques for geodesy and geodynamics include laser range measurements to the moon or to artificial satellites, Doppler measurements with the Transit satellite system, and both independent-clock and linked-antenna microwave interferometry. The ways in which PTTI measurements are used in these techniques will be reviewed, and the accuracies expected during the latter half of the 1970's will be discussed. At least 3 of the techniques appear capable of giving accuracies of 5 cm or better in each coordinate for many points on the Earth's surface, and comparable accuracies for the Earth's rotation and polar motion. For fixed stations or for sites a few hundred km apart, baseline lengths accurate to 1 cm may be achieved. Ways in which the complementary aspects of the different techniques can be exploited will be discussed, as well as how they tie in with improved ground techniques for determining crustal movements. Some recent results from the extra-terrestrial methods will be mentioned.

15800. Hoer, C. A., Engen, G. F., **Analysis of a six-port junction for measuring** $v, i, a, b, z, \Gamma$, **and phase,** (Proc. 6th Conf. of the Int. Measurement Confederation, Dresden, Germany, June 17-23, 1973), Paper in *Measurement and Instrumentation, Acta IMEKO 1973*, **1**, 213-222 (Publishing House of the Hungarian Academy of Sciences, Akadémiai Kiadó, Budapest, Hungary, 1973).

Key words: admittance; current; impedance; phase angles; power; reflection coefficient; six-port; voltage.

This theoretical paper shows how complex voltage, current, incident and emergent wave amplitudes, immittance, reflection coefficients, and phase angles can all be measured with an arbitrary six-port junction. Four ports are terminated with power meters or other detectors from which power values can be obtained.

In particular, if v represents voltage, $|v|^2$ is given as a linear function of the four power meter indications. The same is true for current and the wave amplitudes. Complex immittance, or reflection coefficient, on the other hand, is given by the ratio between two linear combinations of the power meter readings.

Some practical design considerations are also given.

15801. Bender, P. L., **Reference coordinate system requirements for geophysics,** (Proc. IAU Symposium No. 26 on Reference Coordinate Systems for Earth Dynamics, Torun, Poland, Aug. 26-31, 1974), Paper in *Reference Coordinate Systems for Earth Dynamics*, B. Kolaczek and G. Weiffenbach, Eds., pp. 85-92 (Polish Academy of Sciences, Warsaw, Poland, Apr. 1975).

Key words: coordinate systems; geodesy; geodynamics; lasers; tectonics; VLBI.

Five important geodynamical quantities which are closely linked are: (1) motions of points on the Earth's surface; (2) polar motion; (3) changes in UT1-UTC; (4) nutation; and (5) motion of the geocenter. For each of these we expect to achieve measurements in the near future which have an accuracy of 1 to 3 cm or 0.3 to 1 milliarcsec.

From a metrological point of view, one can say simply: "Measure each quantity against whichever coordinate system you can make the most accurate measurements with respect to." I believe that this statement should serve as a guiding principle for the recommendations of the colloquium. However, it also is important that the coordinate systems help to provide a clear separation between the different phenomena of interest, and correspond closely to the conceptual definitions in terms of which geophysicists think about the phenomena.

In any discussion of angular motion in space, both a "body-fixed" system and a "space-fixed" system are used. Some relevant types of coordinate systems, reference directions, or reference points which have been considered are: (1) celestial systems based on optical star catalogs, distant galaxies, radio source catalogs, or the Moon and inner planets; (2) the Earth's axis rotation, which defines a line through the Earth as well as a celestial reference direction; (3) the geocenter; and (4) "quasi-Earth-fixed" coordinate systems.

When a geophysicist discusses UT1 and polar motion, he usually is thinking of the angular motion of the main part of the mantle with respect to an inertial frame and to the direction of the spin axis. Since the velocities of relative motion in most of the mantle are expected to be extremely small, even if "substantial" deep convection is occurring, the conceptual "quasi-Earth-fixed" reference frame seems well defined. Methods for realizing a close approximation to this frame fortunately exist. Hopefully, this colloquium will recommend procedures for establishing and maintaining such a system for use in geodynamics. Motion of points on the Earth's surface and of the geocenter can be measured against such a system with the full accuracy of the new techniques.

The situation with respect to celestial reference frames is different. The various measurement techniques give changes in the orientation of the Earth relative to different systems, so that we would like to know the relative motions of the systems in order to compare the results. However, there does not appear to be a need for defining any new system. Subjective figures of merit for the various systems depend on both the accuracy with which measurements can be made against them and the degree to which they can be related to inertial systems.

The main coordinate system requirement related to the 5 geodynamic quantities discussed in this talk is thus for the establishment and maintenance of a "quasi-Earth-fixed" coordinate system which closely approximates the motion of the main part of the mantle. Changes in the orientation of this system with respect to the various celestial systems can be determined by both the new and the conventional techniques, provided that some knowledge of changes in the local vertical is available. Changes in the axis of rotation and in the geocenter with respect to this system also can be obtained, as well as measurements of nutation.

**15802.** Clough, R. B., **A note on the measurement of proportional limit under multiaxial stresses,** *J. Test. Eval.* **4,** No. 2, 139-140 (1976).

Key words: flow surface; multiaxial stresses; plasticity; proportional limit.

Theoretical definitions of the multiaxial plastic flow surface are exact; however, ambiguities arise in the experimental measurement. A new method for measuring the multiaxial flow surface based on maximum elastic stress rate is proposed which eliminates these ambiguities. It is applied to biaxial yielding.

**15803.** Bowman, R. R., **A probe for measuring temperature in radio-frequency-heated material,** *IEEE Trans. Microwave Theory Tech. Short Papers* **MTT-24,** No. 1, 43-45 (Jan. 1976).

Key words: high-resistance leads; radio frequency heating; temperature measurements; thermistor probe.

Measuring temperature in material being heated by radio-frequency (RF) fields is difficult because of field perturbations and direct heating caused by any conventional leads connected to the temperature sensor. A temperature probe consisting simply of a thermistor and plastic high-resistance leads appears to practically eliminate these problems. The design goals are described, and the performance of an initial test model of this type of probe is discussed.

**15804.** Yaghjian, A. D., **Direct integration of the field equations for electroacoustic transducers,** *Proc. IEEE Letters* **62,** No. 6, 858-859 (June 1974).

Key words: electroacoustic; integration; transducer.

Expressions are derived for the electroacoustic fields inside a linear transducer in terms of the volume sources and the fields on the surface of the transducer.

**15805.** Straty, G. C., Tsumura, R., **Phase transition and melting pressures of solid ethane,** *J. Chem. Phys.* **64,** No. 2, 859-861 (Jan. 15, 1976).

Key words: ethane; melting line; melting pressures; solid ethane; solid phase transition.

The melting pressures of ethane at 14 temperatures from near the triple point to 95.50 K and pressures to 32.0 MPa are reported. A triple point temperature of $90.348 \pm 0.005$ K is obtained from the data which is in agreement with the determination of Clusius and Weigand (1940) but in substantial disagreement with other determinations. Qualitative evidence has been obtained which indicates the existence of a previously unrecognized solid phase transition along a boundary roughly parallel to the melting line at a temperature about 0.5 K below the melting temperature, suggesting that some previous melting point determinations may have been influenced by misinterpretation of the effects of this transition.

**15806.** Bender, P. L., **Prospects for rapid realization of a quasi-Earth-fixed coordinate system,** (Proc. IAU Symposium No. 26 on Reference Coordinate Systems for Earth Dynamics, Torun, Poland, Aug. 26-31, 1974), Paper in *Reference Coordinate Systems for Earth Dynamics,* B. Kolaczek and G. Weiffenbach, Eds., pp. 297-302 (Polish Academy of Sciences, Warsaw, Poland, Apr. 1975).

Key words: coordinate systems; geodesy; geodynamics; lasers; tectonics; VLBI.

It appears that a combination of VLBI, lunar ranging, and satellite ranging can provide a quasi-Earth-fixed coordinate system with high accuracy and good coverage more rapidly than any one technique alone. In considering this possibility, the conceptual separation of the job into two parts seems useful. There are: (1) establishment of a global network of at least three fundamental reference points on major plates, and (2) the determination of a larger number of regional reference points of geodynamic interest. The example of lunar ranging plus satellite ranging is used to illustrate one way in which an accurate realization of an initial terrestrial system could be achieved quickly.

**15807.** Hutchinson, J. M. R., Lucas, L. L., Mullen, P. A., **Study of the scattering correction for thick uranium-oxide and other $\alpha$-particle sources—II: Experimental,** *Int. J. Appl. Radiat. Isot.* **27,** No. 1, 43-45 (Jan. 1976).

Key words: alpha particles; backscattering; gadolinium-148; polonium-210; self absorption; uranium-oxide.

Experimental values of the $2\pi$ $\alpha$-particle counting rate, $C_{2\pi}$, including scattering, divided by the disintegration rate, $N_0$, are reported for uranium dioxide, $^{210}$Po and $^{148}$Gd sources mounted on platinum backings, and a $^{210}$Po source on a $U_3O_8$ backing. The $^{235}UO_2$ source thicknesses varied from 0.05 to 1.1 mg/cm$^2$. The experimental values of the scattering are in agreement with theoretical values given in Part I (this issue), which take into account source thickness, $\alpha$-particle energy, and composition of the backing material.

**15808.** Lucas, L. L., Hutchinson, J. M. R., **Study of the scattering correction for thick uranium-oxide and other $\alpha$-particle sources—I: Theoretical,** *Int. J. Appl. Radiat. Isot.* **27,** No. 1, 35-42 (Jan. 1976).

Key words: alpha particles; backscattering; disintegration rate; ranges; self-absorption; uranium oxide.

Theoretical values of the $2\pi$ $\alpha$-particle counting rate, $C_{2\pi}$, including scattering, divided by the disintegration rate, $N_0$, are calculated for $\alpha$-particle sources mounted on flat backing materials. The theoretical values (Part I) and experimental values (Part II) are in good agreement, and show that: (a) $C_{2\pi}/N_0$ values as a function of $\alpha$-particle energy and source thickness can be calculated on the basis of a simple physical model; (b) The scattering correction, expressed as a fraction of the disintegration rate, decreases with increasing source thickness; and (c) The $\alpha$-particle scattering in uranium-oxide is much less than the scattering in platinum, in disagreement with previous estimates. The calculations are readily extended to other source compositions and $\alpha$-particle energies.

**15809.** Jones, M. C., Peterson, R. G., **A study of flow stability in helium cooling systems,** *J. Heat Transfer* **97,** No. 4, 521-527 (Nov. 1975).

Key words: computations; cooling system; cryogenics; electric power transmission; flow stability; helium; oscillations; superconductors; theory.

Methods have been developed for the computation of the frequency response and stability of helium cooling systems in the frequency range of the density wave instability. While more generally applicable, these methods were developed for a study of superconducting power transmission. Special features are the use of helium thermodynamic properties derived at every point from the exact equation of state, and the full accounting of the effect of compressibility. Classical linear control theory is employed throughout. By using a finite difference approach to the integration of the conservation equations over the space coordinate, the accuracy obtainable is limited only by the computation time available. Examples are given for representative transmission line parameters with the helium at a variety of supercritical pressures. It is concluded that, while density wave instability is a real potential problem in superconducting power transmission lines, it is not difficult to select operating parameters in a safe stable regime.

15810. Marshall, H. E., Ruegg, R. T., **Cost sharing to induce efficient techniques of abating wastewater pollution,** *J. Environ. Econ. Manage.* **2,** 107-119 (1975).

Key words: cost sharing; efficiency; environment; financing; grants; pollution abatement; wastewater; water pollution; water resources.

This paper analyzes existing cost-sharing rules for wastewater pollution grants administered by the Environmental Protection Agency under the 1972 Amendments to the Federal Water Pollution Control Act. It identifies and measures biases in the existing cost-sharing rules that encourage nonfederal interests to select particular techniques (e.g., capital-intensive techniques) over others even when the selected techniques are not the least costly to the nation. The paper develops theoretically a cost-sharing condition—that the same percentage cost share be applied to all abatement techniques—that would eliminate the cost-sharing bias. Alternative cost-sharing approaches are evaluated in terms of their biasing effects and their absolute dollar costs for federal and nonfederal project participants.

15811. Lias, S. G., Eyler, J. R., Ausloos, P., **Hydride transfer reactions involving saturated hydrocarbons and $CCl_3^+$, $CCl_2H^+$, $CCl_2F^-$, $CF_2Cl^-$, $CF_2H^+$, $CF_3^-$, $NO^-$, $C_2H_5^-$, sec-$C_3H_7^-$ and t-$C_4H_9^+$,** *Int. J. Mass Spectrom. Ion Phys.* **19,** 219-239 (1976).

Key words: collision processes; halocarbon ions; hydrocarbons; ion-molecule reactions; kinetics; rate constants.

The compounds $CCl_4$, $CCl_3H$, $CCl_3F$, $CCl_2F_2$, $CF_3H$, $CF_4$, NO, $C_2H_6$, neo-$C_5H_{12}$, and $C_3H_8$ were ionized by low energy electrons in a pulsed ion cyclotron resonance spectrometer to produce $CCl_3^+$, $CCl_2H^+$, $CCl_2F^+$, $CF_2Cl^+$, $CF_2H^+$, $CF_3^+$, $NO^+$, $C_2H_5^+$, t-$C_4H_9^+$, and sec-$C_3H_7^+$ ions, respectively. In these pure compounds, the respective ions formed are all unreactive, and can be trapped with essentially no loss in the ICR analyzer cell for up to 0.2 s after their formation, at a pressure of $10^{-7}-10^{-5}$ torr. When alkanes or cycloalkanes are added to these compounds, the predominant ions formed in each case undergo a hydride transfer reaction with the added alkane. This is the only reaction channel:

$$A^+ + RH \rightarrow AH + R^+$$

(where $A^+$ is the initial ion formed and RH is the added alkane or cycloalkane). By following the abundances of the reactant ions as a function of time in these dilute mixtures, approximately one hundred rate coefficients of hydride transfer reactions of thermal ions (in the range $10^{-12}-10^{-9}$ cm$^3$ molecule$^{-1}$ s$^{-1}$) have been determined. For several of these ions, it is demonstrated that even when reaction is very exothermic at every site in the molecule the reacting ion exhibits positional selectivity. Detailed examination of the reaction probabilities for these ions reacting with alkanes of different chain lengths and structures leads to the conclusion that the rates of hydride transfer reactions depend in part on the exothermicity of the reaction and in part on the lifetime of the ion-molecule complex. For large reactant ions such as t-$C_4H_9^+$, steric effects may also play a role. The product ions formed in these hydride transfer reactions undergo further fragmentation to an extent which depends on the exothermicity of the reaction; the most important fragmentation paths correspond to loss of $C_2-C_4$ olefins from the product alkyl ions.

15812. Powell, C. J., **Cross sections for ionization of inner-shell electrons by electrons,** *Rev. Mod. Phys.* **48,** No. 1, 33-47 (Jan. 1, 1976).

Key words: Bethe theory; cross sections; electron; inner-shell electrons; ionization; *K*-shell; *L*-shell; photoabsorption.

A survey is given of the available cross-section data for ionization of inner-shell electrons by incident electrons in the range of interest for electron-probe microanalysis and for Auger-electron spectroscopy of solid surfaces. Owing to the paucity of data, the bulk of the discussion is limited to *K*-shell and *L*-shell ionization of light atoms. Calculated, semiempirical, and experimental cross-section data have been intercompared graphically and through fits to the linearized Bethe equation for inner-shell ionization (the Fano plot). Almost all of the data could be satisfactorily fitted over the range $4 \lesssim U_{nl} \lesssim 30$, where $U_{nl} = E_0/E_{nl}$, $E_0$ is the incident electron energy, and $E_{nl}$ the binding energy of electrons in the *nl* shell. From these fits, values could be obtained of the "effective" Bethe parameters $b_{nl}$ and $c_{nl}$. Values of the parameter $b_{nl}$ have also been derived from photoabsorption data and were found to be generally consistent with the ionization data if account was taken of the distribution of differential oscillator strength with respect to excitation energy and the consequent expected variation of $b_{nl}$ with incident electron energy. The derived "effective" Bethe parameters should not therefore be used outside the range of each fit.

15813. Waclawski, B. J., Herbst, J. F., **Photoemission for Xe physisorbed on W(100): Evidence for surface crystal-field effects,** *Phys. Rev. Lett.* **35,** No. 23, 1594-1596 (Dec. 8, 1975).

Key words: crystal field; photoemission; physisorption; tungsten (100); xenon.

Photoemission spectra at $h\nu = 21.2$ eV reveal two $5p$ levels for xenon physisorbed on a tungsten (100) surface. The spin-orbit splitting of the two levels and their intensity ratio correspond closely to gas-phase measurements, while the $5p_{3/2}$ peak is significantly broadened with respect to the $5p_{1/2}$. We interpret the broadened structure as an unresolved doublet resulting from splitting the Xe $5p_{3/2}$ states in the tungsten-surface crystal field.

15814. Fuggle, J. C., Madey, T. E., Steinkilberg, M., Menzel, D., **Photoelectron spectroscopic studies of adsorption of CO and oxygen on Ru(001),** *Surf. Sci.* **52,** 521-541 (1975).

Key words: adsorbate; chemisorption; ruthenium; ultraviolet photoelectron spectroscopy; x-ray photoelectron spectroscopy.

XPS and UPS have been used for a detailed study of the adsorption and coadsorption of CO and oxygen on a clean Ru(001) single crystal. The measured substrate and adsorbate core level binding energies and valence levels are discussed. The O 1s XPS peak intensity has been used for kinetic studies of adsorption and coadsorption. Some studies of the angular dependence of adsorbate and substrate peak intensity ratios are presented. We also present data on the shifts of XPS peaks and changes in UPS spectra as a function of adsorbate coverage. The data are correlated with the results of earlier measurements with other methods.

15815. Bardsley, J. N., Junker, B. R., Norcross, D. W., **Pseudopotential calculations for $Na_2^+$, Na and $Na_2^-$,** *Chem. Phys. Lett.* **37,** No. 3, 502-506 (Feb. 1, 1976).

Key words: molecular structure; pseudopotentials.

Potential curves have been computed for five states of $Na_2^+$, five states of $Na_2$ and two states of $Na_2^-$ using a pseudopotential approach. The results are consistent with the accepted attribution to a $^3\Pi$ state of the perturbations observed in transitions involving the A $^1\Sigma_u$ state of $Na_2$, and the stability of the $Na_2^-$ ion is established.

**15816.** Lias, S. G., Ausloos, P., **Book: Ion-molecule reactions. Their role in radiation chemistry,** *Second ACS/ERDA Research Monograph in Radiation Chemistry,* **2,** 205 pages (American Chemical Society, Washington, DC, 1975).

Key words: hydride transfer; ion clustering; ion-molecule reactions; proton transfer; radiation chemistry.

In this monograph, information is examined about ion-molecule reactions occurring in various kinds of systems, making wherever possible a synthesis of the information obtained through the several mass spectrometric techniques, as well as from organic chemistry, NMR studies, theoretical calculations and from radiolytic studies themselves. A chapter has been included which presents what is known about the effects of density on ionic fragmentation processes and on ionic isomerization processes. A chapter on charge recombination in the gas and liquid phases has been included. The kinetics of the reactions of thermal ions with molecules, are also reviewed. Other chapters treat one- and two-atom transfer reactions, ion-molecule condensation processes, and ionic solvation or clustering.

**15817.** Martin, G. A., Wiese, W. L., **Atomic oscillator-strength distributions in spectral series of the lithium isoelectronic sequence,** *Phys. Rev. A* **13,** No. 2, 699-714 (Feb. 1976).

Key words: continuum; discrete spectrum; *f*-sum rule; *f*-values; lithium sequence; oscillator strength distribution; oscillator strengths; relativistic effects; spectral series; systematic trends.

We describe a new type of analysis yielding the oscillator-strength distributions in several spectral series throughout the lithium isoelectronic sequence. Individual oscillator strengths have been critically evaluated and tied together by requiring that they fulfill simultaneously four basic spectroscopic constraints: (a) regularities for individual transitions along the isoelectronic sequence, (b) regularities for the transitions of a spectral series, (c) compliance with the requirement of continuity across the spectral series limit, and (d) adherence to *f* sum rules. With only slight modifications, the best available data fulfill closely all four requirements. The final set of *f*-value data – which are tabulated and partly presented in illustrations – possess, therefore, a very high degree of internal consistency and reliability. Relativistic corrections for very highly charged Li-like ions are also considered.

**15818.** Olver, F. W. J., **Unsolved problems in the asymptotic estimation of special functions,** Paper in *Theory and Application of Special Functions,* R. A. Askey, Ed., pp. 99-142 (Academic Press, Inc., New York, NY, 1975).

Key words: asymptotic analysis; Darboux's method; definite integrals; hypergeometric functions; incomplete gamma function; Legendre functions; ordinary differential equations; saddle points; special functions; turning points; Whittaker functions.

The first part of this paper surveys the tools of asymptotic analysis that are presently available and those that are needed for the next stages of development of the asymptotic theory of special functions. Methods are grouped according to the number of free variables to which they achieve a uniform reduction. Topics include the approximation of functions defined parametrically by a definite integral or infinite sum, and approximate solutions of linear ordinary differential equations. The main areas in which work appears to be needed are (i) problems of confluence, that is, coalescing saddle points and singularities of integrals, or coalescing turning points and singularities of differential equations; (ii) rigorous error analysis.

The second part of the paper discusses the more important special functions in increasing order of the total number of variables and parameters involved. Almost all asymptotic problems concerning special functions of one variable have been solved. For functions of two variables the problems are solved, or can be solved by use of existing asymptotic tools. It is in the case of functions depending on three variables (including parameters) that the most significant work can be expected in the immediate future. Two new asymptotic tools have been developed very recently, one for integrals with three coalescing saddle points, the other for second-order differential equations having two coalescing turning points. Applications of these tools are needed, as well as the development of similar tools for other three-variable problems involving confluence. As the total number of variables increases beyond three, our knowledge of the asymptotic behavior of the special functions becomes more fragmentary. It will undoubtedly be many years before we have complete knowledge of the asymptotic behavior of any of the functions of four variables, including for example, the hypergeometric function F(a,b;c;z).

**15819.** Franklin, A. D., **Electrode effects in the measurement of ionic conductivity,** *J. Am. Ceram. Soc.* **58,** No. 11-12, 465-473 (Nov.-Dec. 1975).

Key words: electrode polarization; impedance measurements; interfaces; ionic conductivity; overpotential; solid electrolyte.

Even with thermodynamically reversible electrodes, slow processes inhibiting the discharge of ions at the interface between a solid ionic conductor and the electrode can give rise to overvoltages when current is passed or to an interface impedance in ac measurements. Some of the more important of the mechanisms responsible for this inhibition, i.e., boundary layers, slow charge-transfer processes with double-layer formation, product storage in the electrodes with slow mass transport to the ultimate thermodynamic reservoirs, and rough or porous surfaces, can be understood in a nonrigorous physical way with the help of simple models. The properties of such systems can often be expressed in terms of equivalent circuits, and these are then very useful in analyzing the behavior of specific systems. Examples from studies of materials such as CaO-stabilized $ZrO_2$ (oxygen-ion conductor) and $\beta$-$Al_2O_3$ (sodium-ion conductor) illustrate these effects.

**15820.** Franklin, A. D., **Equilibria among point defects in $GdF_3$-doped $CaF_2$,** *J. Chem. Phys.* **64,** No. 4, 1509-1515 (Feb. 15, 1976).

Key words: annealing; calcium fluoride; defect pairs; equilibria; model; point defects.

EPR and dielectric relaxation measurements, reported earlier, have been combined to produce estimates of the mole fraction ($n'$) of pairs formed of substitutional $Gd^{3+}$ ions and $F^-$ interstitials as a function of total $GdF_3$ mole fraction (M) and temperature at which the crystals are annealed prior to rapid cooling. Over the range of M from $1\times10^{-4}$ to $27\times10^{-4}$, $n'$ rises to a saturation value when M increases to about $10^{-3}$. At constant M, $n'$ goes through a maximum at anneal temperatures from about 1073 to 1273 K. The rate of the annealing reaction increases with M and with decreasing sample size, and the density increases with increasing M faster than the interstitial model predicts. A qualitative model of the annealing process is suggested, in which $F^-$ interstitials react with an atmospheric constituent (probably HF) to form an immobile complex that provides remote charge compensation for the cubic $Gd^{3+}$ ions. The remaining free $F^-$ interstitials are trapped by $Gd^{3+}$ ions during quenching to form the pairs.

**15821.** Wiederhorn, S. M., **Crack growth as an interpretation of static fatigue,** *J. Non-Cryst. Solids* **19,** 169-181 (1975).

Key words: crack growth; fracture; fracture mechanics; glass; static fatigue; strength.

Static fatigue is due to water in the environment which accounts for substantial reductions in the strength of glass. Extensive experimental investigations have shown that static fatigue results from surface cracks that grow when glass is subjected to tensile loads. In this paper evidence for this conclusion is reviewed. First, the earlier studies of strength of glass are summarized. Then, supporting evidence for crack growth obtained from the newer discipline of fracture mechanics is given. Finally, the influence of ion exchange and chemical reactions at crack tips is discussed with regard to crack growth. The chemical composition of the crack-tip solution is shown to play an important role in controlling crack growth.

**15822.** Lawn, B. R., Fuller, E. R., **Equilibrium penny-like cracks in indentation fracture,** *J. Mater. Sci.* **10,** 2016-2024 (1975).

Key words: contact fracture; degradation; Hertzian cracks; indentation fracture; median vents; penny crack.

A study is made of the mechanics of two basic types of indentation fracture, cone cracks ("blunt" indenters) and median cracks ("sharp" indenters). The common feature which forms the central theme in this work is that both crack types, in their well-developed stages of growth, may be regarded as essentially "penny-like." On this basis a universal similarity relation is derived for equilibrium crack dimension as a function of indentation load. Experimental measurements confirm the general form of this relation. A more detailed fracture mechanics analysis is then given, to account for additional, contact variables evident in the data. Notwithstanding certain analytical limitations, the study serves as a useful basis for investigating a wide range of contact-related problems, both fundamental and applied, in brittle solids.

**15823.** Cali, J. P., **International criteria for reference materials,** (Proc. VI Int. Symp. on Quality Control in Clinical Chemistry, Geneva, Switzerland, Apr. 1975), Paper in *Quality Control in Clinical Chemistry,* pp. 369-383 (Walter de Gruyter & Co., Geneva, Switzerland, 1976).

Key words: reference materials.

In clinical chemistry, international organizations are now becoming aware of and taking steps to integrate national measurement programs for use in the international scene. The steps necessary to bring about compatible measurement networks in clinical chemistry are briefly discussed—mainly in the context of the measurement process. Reference materials, as well as definitive and reference methods are important elements in the building and maintenance of a compatible measurement system.

International criteria for reference materials, especially those that are certified are recommended. Factors to be considered include: purity, homogeneity, stability, continuity of supply and information, availability, and the certification process, including legally imposed requirements. Each of these is discussed, together with examples drawn from the NBS clinical Standard Reference Materials.

**15824.** Mihalas, D., Kunasz, P. B., Hummer, D. G., **Solution of the comoving-frame equation of transfer in spherically symmetric flows. II. Picket-fence models,** *Astrophys. J.* **203,** No. 3, 647-659 (Feb. 1, 1976).

Key words: radiative transfer—stars; winds.

To examine the effect of the radial flow of atmospheric material on the temperature distribution in a stellar atmosphere, a picket-fence model with Gaussian lines is formulated and solved numerically in the comoving frame of the gas, which is assumed to move with a prescribed velocity law. Extensive results have been obtained for both static and dynamical models, with planar and moderately extended spherical geometries. For static models, the effect of lines on the temperature distribution is virtually independent of extension. When a large-scale velocity field is imposed, significant surface heating and additional backwarming are found; the magnitude of these effects increases with the extension of the atmosphere. If a significant flow velocity persists to sufficient depth, the enhanced escape probability can lead to a cooling in the deeper layers, which competes with the back-warming. The results obtained here suggest that the deposition of energy arising from the intrusion of line opacity into the continuum, caused by velocity gradients, could influence the dynamics of the flow.

**15825.** Hockey, B. J., **Pyramidal slip on {1123} ⟨1100⟩ and basal twinning in $Al_2O_3$,** (Proc. Symp. on Plastic Deformation of Ceramic Materials, Pennsylvania State Univ., University Park, PA, July 17-19, 1974), Chapter in *Deformation of Ceramic Materials,* R. C. Bradt and R. E. Tressler, Eds., Sec. II, pp. 167-179 (Plenum Press, New York, NY, 1975).

Key words: aluminum oxide; microhardness; plastic deformation; slip; transmission electron microscopy; twinning.

Plastic deformation of $Al_2O_3$ by slip and twinning has been investigated by examining the regions surrounding a microhardness indentation using transmission electron microscopy (TEM). The results establish: (1) the occurrence of pyramidal slip on {1123} ⟨1100⟩, and (2) the nature of basal twins in this material. The observations on basal twins, in particular, have led to a completely different description for the twinning process, which is briefly described.

**15826.** Massey, R. G., **The police patrol car: State of the art,** *LESP-RPT-0403.00,* 33 pages (U.S. Department of Justice, Law Enforcement Assistance Administration, National Institute of Law Enforcement and Criminal Justice, Washington, DC, July 1975).

Key words: functional requirements; patrol cars; performance of patrol cars; police patrol cars; problems with patrol cars; state of the art survey.

This report, entitled "The Police Patrol Car: State of the Art" describes the functional requirements of police agencies for patrol cars, the manner in which these requirements are met, or not met, by vehicles currently in use, and a discussion of new automotive technology which might affect patrol car performance in the future.

**15827.** Baird, R. C., Kerns, D. M., **The accurate determination of millimeter-wave antenna characteristics by deconvolution and extrapolation techniques,** *Proc. Millimeter-Wave Techniques Conf., San Diego, CA, Mar. 26-28, 1974,* **2,** pp. E2-1—E2-12 (Naval Electronics Laboratory Center, San Diego, CA, 1974).

Key words: antenna gain, polarization and pattern; deconvolution; extrapolation; fields and antennas.

The newly-developed methods are described for determining accurate far-field characteristics of antenna gain, polarization, and pattern by using near-field measurements at reduced distances. These methods have no restrictive assumptions or approximations, are useful at microwave and millimeterwave frequencies, and are applicable to directive antennas of all types.

15828. Allred, C. M., Manney, C. H., **The calibration and use of directional couplers without standards,** *IEEE Trans. Instrum. Meas.* **IM-25,** No. 1, 84-89 (Mar. 1976).

Key words: directional coupler; measurement standards; self-calibration.

Basic principles and suggested techniques are presented for calibrating nonideal four-port couplers without standards. Under the assumption that the complex ratio of the side-arm voltages are known, all the parameters, except one of the directional couplers, can be determined without recourse to known values of impedances, shorts, opens, etc. Also, the surprising number of measurements that can be made with such an incompletely calibrated coupler are discussed.

15829. Hermach, F. L., Road, R. A., **Changes in metering covered by revised ANSI code,** *Transmission & Distribution* **28,** No. 3, 24-25, 44 (Mar. 1976).

Key words: code; definitions; demand meters; electricity metering; performance requirements; standards; test methods; watthour meters.

The major changes and additions in the new 1975 edition of the American National Standard "Code for Electricity Meters" are described briefly. This 200-page code, which is widely used, gives performance criteria and test methods for watthour meters and associated equipment. The new edition, replacing the 5th edition of 1965, lengthens tests intervals for highly stable modern meters, extends sample testing, gives performance requirements for the first time for standard meters and pulse recorders, and has many other changes.

15830. Phelan, R. J., Jr., Hamilton, C. A., Day, G. W., **Radiometry without standard sources/electrically calibrated pyroelectrics,** (Proc. Society of Photo-Optical Instrumentation Engineers, San Diego, CA, Aug. 17-22, 1975), Paper in *Modern Utilization of Infrared Technology Civilian and Military, SPIE* **62,** 159-165 (Society of Photo-Optical Instrumentation Engineers, Palos Verdes Estates, CA, 1975).

Key words: optical radiation; pyroelectrics; radiometers.

A radiometer using an electrically calibrated pyroelectric detector has been developed. The system, using a number of unique concepts, was designed to be a truly useful measurement tool for optical radiation of wavelengths from 0.4 to beyond 12 $\mu$m at power levels of microwatts. No standard sources are required for calibrations.

15831. Schwarz, F. P., Wasik, S. P., **Fluorescence measurements of benzene, naphthalene, anthracene, pyrene, fluoranthene, and benzo[*e*]pyrene in water,** *Anal. Chem.* **48,** No. 3, 524-528 (Mar. 1976).

Key words: absorption; carcinogenic; fluorescence; polycyclic aromatic hydrocarbons; quantum yields; water.

Fluorescence spectra, quantum yields, and concentration dependencies are reported for five representative polycyclic aromatic hydrocarbons (PAH) in water to ascertain the applicability of measuring PAH in aqueous systems by spectrofluorimetry. The fluorescence quantum yields of benzene, naphthalene, anthracene, pyrene, fluoranthene, and benzo[*e*]pyrene in water are, respectively, $5.3 \pm 0.5 \times 10^{-3}$, $0.16 \pm 0.02$, $0.25 \pm 0.02$, $0.69 \pm 0.06$, $0.20 \pm 0.01$, and $\sim 0.3 \pm 0.1$. With the exception of pyrene, oxygen quenching of the fluorescence in water is at most 30 percent. The fluorescence concentration dependence was measured by photon counting the fluorescence intensity relative to the excitation light intensity. All the PAH fluorescences exhibited a linear dependency on the concentration. For a fluorescence signal-to-noise ratio of 1, the detection limits are as follows: naphthalene, 0.03 $\mu$g/l., anthracene, 0.03 $\mu$g/l., pyrene, 0.15 $\mu$g/l., fluoranthene, 0.17 $\mu$g/l., and benzo[*e*]pyrene, 0.10 $\mu$g/l.

15832. Strobridge, T. R., **Open discussion of large scale cryogenic refrigeration,** Conference Report – Applied Superconductivity Conference, Oakbrook, IL, Sept. 30-Oct. 1-2, 1974, *Cryogenics* **15,** No. 3, 157-158 (Mar. 1975).

Key words: cryogenic; helium; meeting summary; refrigeration; superconductivity.

A discussion session on Large Scale Refrigeration held at the 1974 Applied Superconductivity Conference is summarized.

15833. Sawyer, D. E., Berning, D. W., **Laser scanning of MOS IC's reveals internal logic states nondestructively,** *Proc. IEEE Letters* **64,** No. 3, 393-394 (Mar. 1976).

Key words: active devices; laser scanning; logic flow observation; LSI testing; measurement of operating margins; nondestructive tests; P-MOS shift register.

A laser scanning system has been used to observe the internal logic pattern in a MOS LSI device in a nondestructive manner. The laser scanner has also been used to selectively change logic states deep within the device. Pictures of the logic patterns revealed by the scanner are discussed.

15834. Kasa, I., **A circle fitting procedure and its error analysis,** *IEEE Trans. Instrum. Meas.* **IM-25,** No. 1, 8-14 (Mar. 1976).

Key words: circle fitting; error analysis.

An efficient circle fitting procedure and its general random-error analysis are described. The first-order random errors of the center coordinates and the radius of the fitted circle are discussed in detail. The effect of the data point distribution along the circle is investigated, and for an important microwave application (sliding termination measurements) the frequency dependence is also evaluated.

The effects of the second-order error terms are also discussed and general formulas are given. Finally an estimation of data point error is provided.

15835. Lawton, R. A., Andrews, J. R., **Optically strobed sampling oscilloscope,** *IEEE Trans. Instrum. Meas.* **IM-25,** No. 1, 56-60 (Mar. 1976).

Key words: GaAs; laser; optical; oscilloscope; photoconductor; picosecond; sampling; sampling oscilloscope; strobe.

An optically strobed sampling oscilloscope is described which uses optical pulses from a GaAs laser diode to strobe a Cr-doped GaAs photoconductor which serves as a sampling gate. This sampling gate has been used with a commercial sampling oscilloscope to provide a sampling measurement capability that can measure higher voltages than conventional samplers and does not exhibit strobe pulse kickout. Preliminary tests indicate a time resolution, limited by the width of the optical pulse used, of about 100 ps.

15836. Engen, G. F., **Mismatch considerations in evaluating amplifier noise performance,** *IEEE Trans. Instrum Meas.* **IM-22,** No. 3, 274-278 (Sept. 1973).

Key words: amplifier noise performance; mismatch considerations.

In terms of a total system evaluation, the potential mismatch errors in the evaluation of noise figure or effective input noise temperature are of greater magnitude than is the case in power measurement. In spite of this, this topic has found only limited coverage in the literature. Moreover, the existing treatments are in terms of parameters whose evaluation requires a significant effort. This paper applies a "terminal invariant" formulation which provides a deeper physical insight to this problem. It also permits a number of useful conclusions to be drawn with a minimum of additional effort.

**15837.** Levin, B., **Psychological characteristics of firesetters,** *Fire J.* **70,** No. 2, 36-41 (Mar. 1976).

Key words: arson; firesetting; psychopathic personality.

A wide variety of medical, criminology and fire journals have dealt with the psychopathology of firesetting. Although contradictory conclusions are quite common, there is general agreement on some aspects of the problem. Firesetters tend to come from broken or disrupted homes and to have lived under harsh or frustrating circumstances. However, this is also true of many criminals. Firesetters tend to be young, to be of low intelligence, to have been bedwetters as children, to have a stronger than average interest in fire, and to have physical deformities. Many of these conclusions are based on studies published over 25 years ago. There is a great need for up-to-date information regarding the firesetters of the 1970's.

**15838.** Fickett, F. R., **Properties of nonsuperconducting technical solids at low temperatures—An update,** (Proc. 5th Int. Conf. on Magnet Technology, Rome, Italy, Apr. 21-25, 1975), Paper in *Magnet Technology,* N. Sacchetti, M. Spadoni, and S. Stipcich, Eds., pp. 659-678 (Laboratori Nazionali del CNEN, Frascati, Italy, 1975).

Key words: cryogenics; materials; mechanical properties; review, thermal properties.

This review presents properties measurements carried out on structural materials, both metallic and nonmetallic, at low temperatures. It is a sequel to the paper presented at the preceding conference and, as such, concentrates on measurements reported over the last two years. These years have been a period of intense activity in this field and a great deal of new data has been obtained, particularly on mechanical properties. Specific topics covered are thermal, magnetic, mechanical and fracture properties of materials. A tabular guide to the literature is included.

**15839.** Schwarz, F. P., Wasik, S. P., **Fluorescence measurements of carcinogenic and polycylic aromatic hydrocarbons in water,** (Proc. Int. Conf. on Environmental Sensing and Assessment, Las Vegas, NV, Sept. 14-19, 1975), Paper in *International Conference on Environmental Sensing and Assessment* **2,** Session 30-2, 1-5 (Institute of Electrical and Electronics Engineers, New York, NY, 1976).

Key words: carcinogenic compounds; partition coefficient; photon counting; polycyclic aromatics; spectrofluorimetry· water.

The application of spectrofluorimetry to the measurement and identification of polycyclic aromatic hydrocarbons (PAH) in aqueous solutions was investigated. At naperian absorbances $\leq 0.05$, the fluorescence intensities of solutions containing naphthalene, anthracene, pyrene, and fluoranthene in water are a superposition of the component fluorescence spectra. At the higher PAH optical densities of the mg/l level and when viewed perpendicular to the excitation light, the fluorescence spectra vary unpredictably with the concentration. The PAH fluorescence intensity is unaffected by the presence of sodium chloride at sea water concentrations and by the presence of mg/l concentrations of iron, zinc, cobalt, or nickel cations in the water.

**15840.** Laughlin, D. E., **Spinodal decomposition in nickel based nickel-titanium alloys,** *Acta Metall.* **24,** pp. 53-58 (1976).

Key words: Ll$_2$; metastable phase; ordering reaction; satellites; spinodal decomposition; superlattice reflections; transmission electron microscopy; $\delta'$.

The early stages of the decomposition process in Ni based Ni-Ti alloys have been studied by means of transmission electron microscopy. It was found that the supersaturated solid solution of Ti in Ni decomposes by the spinodal mechanism into periodic and aligned regions which are Ti rich and Ti lean. After a critical amount of Ti enters the Ti rich regions, they order continuously to the Ll$_2$(Cu$_3$Au) structure. The two processes then continue together until the fully ordered metastable $\gamma'$ particles are formed.

**15841.** Herbst, J. F., Watson, R. E., Wilkins, J. W., **4*f* excitation energies in rare-earth metals: Relativistic calculations,** *Phys. Rev. B* **13,** No. 4, 1439-1445 (Feb. 15, 1976).

Key words: photoelectron spectroscopy; rare earth metals; 4*f* electron excitations.

We describe calculations of 4*f* electron binding energies for the rare-earth metals. Relativistic Hartree-Fock calculations for atomic configurations most closely approximating those of the metals are initially performed, and crystal potentials are constructed by means of the renormalized-atom method. Relativistic band calculations are iterated to crude self-consistency and total band energies obtained. Correlation effects identical to those in the free atoms are assumed. Within the assumption of a completely screened final state, in which the atomic site having the 4*f* hole is electrically neutral, 4*f* binding energies are estimated which are in at least as good agreement with experiment as previous, less complete calculations. The impact of the complete screening approximation is assessed by estimating the binding energies corresponding to atomic sites which are ionized in their final states; we find that the presence of an additional screening electron lowers the 4*f* binding energy by 4 – 6 eV.

**15842.** Watson, R. E., Herbst, J. F., Hodges, L., Lundqvist, B. I., Wilkins, J. W., **Effect of ground-state and excitation potentials on energy levels of Ni metal,** *Phys. Rev. B* **13,** No. 4, 1463-1467 (Feb. 15, 1976). 350

Key words: band structure; energy levels; excitation potential; ground state potential; nickel.

Self-consistent energy-band calculations for paramagnetic Ni have been performed in an effort to compare ground-state and excitation potential prescriptions; potentials of the Hartree-Fock-Wigner-Seitz and Hedin-Lundqvist type are examined. We find the bandwidth and placement of the Fermi level within the bands to be rather insensitive to the choice of potential, while the absolute position of the bands with respect to the appropriate reference energy is potential dependent. Use of the Hedin-Lundqvist excitation potential instead of the ground-state potential produces level differences no greater than 0.1 eV.

**15843.** Penn, D. R., **Electron attenuation lengths for free-electron-like metals,** *J. Vac. Sci. Technol.* **13,** No. 1, 221-223 (Jan.-Feb. 1976).

Key words: bulk; electron mean free path; exchange and correlation; jellium.

Mean free paths for electrons in bulk jellium are calculated for hot electrons with energies from a few hundred to a few thousand electron volts and for values of $r_s$ from 1.5 to 5. Exchange and correlation effects are included and the results are compared to relevant experiments.

**15844.** Coriell, S. R., Sekerka, R. F., **Morphological stability near a grain boundary groove in a solid-liquid interface,** (Proc. 4th Soviet Conf. on Crystal Growth, Tsakhkadzor, Armenia, Sept. 16-23, 1972), Paper in *Growth of Crystals* **11**, 230-262 (1975).

Key words: grain boundary; morphology; solidification; stability.

For constant velocity solidification of a pure substance or a dilute binary alloy, the time-dependent shape of a nearly planar interface, intersected perpendicularly by a grain boundary, is calculated. For certain growth parameters, a stable groove shape is found; otherwise an unstable mode of grain boundary grooving occurs. The stability-instability demarcation agrees exactly with morphological stability theory for an interface not containing a grain boundary. Under certain conditions, the stable shape is an oscillatory function.

**15845.** Ederer, D. L., Lucatorto, T. B., Saloman, E. B., Madden, R. P., Manalis, M., Sugar, J., **Photoabsorption of the 4*d* electrons in xenon and barium: A comparison,** (Proc. Int. Symp. on Electron and Photon Interactions with Atoms, in honor of Prof. Ugo Fano, Univ. of Stirling, Scotland, July 16-19, 1974), Chapter in *Electron and Photon Interactions with Atoms*, H. Kleinpoppen and M. R. C. McDowell, Eds., pp. 69-81 (Plenum Press, New York, NY, 1976).

Key words: atomic structure; barium; $N_{IV}$ edges; spectroscopy; vacuum ultraviolet; 4*d* photoabsorption.

The 4*d* absorption spectra of xenon and barium show very different behavior. In xenon the cross section has been measured for two series of resonances converging to the $4d^9(^2D_{5/2,3/2})$ limit. By a parameterization technique, the amplitudes and widths of these resonances have been obtained. The widths of the resonances are essentially constant, but the widths of the resonances converging to the $4d^9(^2D_{5/2})$ limit ($N_V$ edge) are somewhat narrower than those converging to the $4d^9(^2D_{3/2})$ limit ($N_{IV}$ edge). The oscillator strength in these $4d^9(^2D_{5/2,3/2})np$ series is small (0.06) compared to the total continuum oscillator strength integrated over open *p* and *f* channels. The barium spectrum is very different from the xenon spectrum because the 4*f* orbital contracts in excited barium and overlaps the 4*d* orbit. This contraction produces two terms, $^3P$ and $^3D$, of the $4d^94f$ configuration below the 4*d* ionization limits, while the strong electrostatic exchange interaction drives the $^1P$ term of this configuration some 10 eV above the limit. Furthermore, extensive mixing of the $4d^96s^26p$ configuration with $4d^95d^26p$ and $4d^95d6s6p$ produces many weak resonances near the $4d^{10} \rightarrow 4d^9(^2D_{5/2})6s^26p(^2P_{3/2})$ resonance. A suggested classification of these features is given with the aid of known features of the La I spectrum. Finally, from the known x-ray splitting of the $N_{IV,V}$ threshold and the energy interval between the $6s^26p(^2P)$ and $6s^2(^1S)$ levels in La I and La II, the ionization thresholds of the 4*d* electron were determined to be 814,800(1000) $cm^{-1}$ and 792,500(1000) $cm^{-1}$.

**15846.** Hutchinson, J. M. R., Mullen, P. A., **Standardization and ground-state branching of selenium-75,** *Int. J. Appl. Radiat. Isot.* **27**, No. 1, 47-50 (Jan. 1976).

Key words: coincidence counting; gamma rays; ground state decay; radioactivity; selenium-75; standardization.

Selenium-75 is much used as a radioactive tracer in nuclear medicine. Several thousand administered doses of selenium-75 compounds are given per year in the U.S. for liver scanning and other purposes. Although accuracies of only ±10 percent in activity measurements are required by the U.S. Pharmacopoeia, more accurately calibrated sources of selenium-75 are useful in nuclear medicine for the calibration of detectors in the energy region from 97 keV to 401 keV since $\gamma$-ray abundances are known to a few percent in most cases. For this and other reasons, the National Bureau of Standards (NBS) has developed, by means of an X-$\gamma$ coincidence counting method, a radioactivity standard of selenium-75, and, at the same time, determined the poorly-known fraction, $f_g$, of selenium-75 disintegrations going directly to the ground state of arsenic-75.

$f_g$ has been calculated in this work from the difference between the measured value for the activity of a sample and its measured total $\gamma$-ray emission rate, using the NBS 8-in. NaI(Tl) detector system. Most selenium-75 disintegrations produce a response in this system because of its high $\gamma$-ray detection efficiency and because most disintegrations produce two or more $\gamma$-rays. Values have been reported for $f_g$ ranging from $<10^{-3}$ to 0.04. The Nuclear Data Tables, taking a weighted average of published values, quotes $f_g = 0.023 \pm 0.023$ (uncertainty of $2\sigma$).

The value of $f_g$ determined by us was zero, with a 99 percent probability of being less than 1.2 percent.

The measured value for the activity is independent of all decay-scheme parameters, except conversion-electron intensities (which are known to ±4 %) and the probability of K capture, which appears in a small correction term.

**15847.** McKee, R. A., **Thermomigration of interstitial-solute-vacancy pairs in a dilute fcc alloy,** *Phys. Rev. B* **13**, No. 2, 635-640 (Jan. 15, 1976).

Key words: diffusion; dilute alloys; interstitial solute vacancy pairs; kinetic theory; pair association method; thermomigration.

The influence of a temperature gradient on the motion of an interstitial-solute-vacancy pair in a fcc alloy has been analyzed using the "pair association" kinetic theory developed by Lidiard. In the past, an interstitial-solute-vacancy pair mechanism has been used to describe the diffusion of various solutes in the group-IV elements, and this development for the kinetics of the thermomigration of such solute-vacancy pairs can be used for further evaluation of this proposed mechanism for diffusion in these alloys.

**15848.** Waterstrat, R. M., **Comments on possible "*B*-site" disorder in A15 ($\beta$-*W* type) compounds,** *Solid State Commun.* **18**, No. 4, 531-532 (1976).

Key words: atomic ordering; A15 compounds; intermetallic compounds; nonstoichiometry; phase composition; phase stability.

In a recent paper evidence for "preferential *B*-site disorder" in A15 compounds was presented. It can be shown, however, that the data in this paper lead to serious disagreements between predicted and observed phase compositions. Thus, the methods used are of doubtful validity and it is suggested that a more accurate knowledge of the phase compositions is needed.

**15849.** Beers, Y., Howard, C. J., **The spectrum of $DO_2$ near 60 GHz and the structure of the hydroperoxyl radical,** *J. Chem. Phys.* **64**, No. 4, 1541-1543 (Feb. 15, 1976).

Key words: chemical structure; hydroperoxyl; microwave.

Spectra for the lowest rotational transition in $DO_2$, $N=1 \leftarrow 0$, have been observed near 60 GHz. These data have been used to calculate the sum of the rotational constants $B+C$ for $DO_2 = 60\,467.7 \pm 3$ MHz. This result was combined with other measurements on $HO_2$ to compute a structure for the hydroperoxyl radical: $r(H-O) = 0.977 \times 10^{-10}$ m, $r(O-O) = 1.335 \times 10^{-10}$ m, and $<H-O-O = 104.1°$. Also we have found for $DO_2$ that $(\epsilon_{bb} + \epsilon_{cc})/2 = -191 \pm 3$ MHz for elements of the electron-spin rotation tensor and a value of $-4.2 \pm 1.5$ MHz for the Fermi contact interaction parameter $\sigma$.

**5850.** Sieck, L. W., Gorden, R., Jr., **Formation of dimeric parent cations in aromatic hydrocarbons,** *Int. J. Mass Spectrom. Ion Phys.* **19,** No. 3, 269-286 (1976).

Key words: gas phase; hydrocarbons; kinetics; mass spectrometry; photoionization; rate constants.

Third-order rate coefficients have been determined at 295 K for the formation of dimeric parent cations in benzene, benzene-$d_6$, toluene, the xylenes, mesitylene, and fluoro- and chlorobenzene using the NBS high pressure photoionization mass spectrometer. The reactions are all quite fast, the rate coefficients falling in the range $0.5-6\cdot10^{-25}$ cm$^6$ molecule$^{-2}$ s$^{-1}$. The differences in rates observed are rationalized in terms of structural (geometric) considerations, and upper limits are established or the binding energies in $(C_6H_6)_2{}^+$ and $(C_6H_5CH_3)_2{}^+$. The temperature dependence for production of $(C_6D_6)_2{}^+$ has been determined from 227 to 316 K, and the rate coefficient seems to obey a simple $1/T$ relationship over this range. The detection of trimeric species in benzene is also reported for the first time. Additional experiments involving benzene-nitric oxide mixtures are also reported, which include detection of an apparent equilibrium of the type $NO^+ + C_6H_6 \rightleftarrows C_6H_6{}^+ + NO$.

**5851. Vorburger, T. V., Sandstrom, D. R., Waclawski, B. J., UPS studies of virgin CO on W(100),** *J. Vac. Sci. Technol.* **13,** No. 1, 287-290 (Jan.-Feb. 1976).

Key words: adsorption; carbon monoxide; chemisorption; desorption; photoelectron spectroscopy; photoemission; single crystal; tungsten; ultraviolet photoelectron spectroscopy; virgin CO.

The adsorption of CO on W(100) at 80 K has been studied by photoelectron spectroscopy at $h\nu$=21.22 eV, and the results have been correlated with previous data for room temperature adsorption. Initial adsorption produces a peak in the emission spectrum at ~ −7.6 eV (relative to the Fermi energy), which is haracteristic of the virgin state of adsorbed CO, as well as additional structures which have been previously shown to be haracteristic of $\alpha$- and $\beta$-CO. Upon heating the sample to 260 K the −7.6-eV level is depleted and apparent conversion to the $\beta$ state occurs as indicated by an enhancement of the emission ear −5.5 eV. Additional data taken with $h\nu$=16.85, 26.9, and 0.81 eV are in general agreement with the measurements at 1.22 eV; however, the peak at −7.6 eV for $h\nu$-21.22 eV is shifted to lower kinetic energies by several tenths of an electron olt at the other photon energies.

**5852.** Miller, A., McLaughlin, W. L., **Holographic measurements of electron-beam dose distributions around inhomogeneities in water,** *Phys. Med. Biol. Tech. Note* **21,** No. 2, 285-288 (1976).

Key words: absorbed dose; calorimetry; dose distributions; dosimetry; electron beams; holography; interferometry; water phantoms.

Holographic interferometry employing temperature-induced changes of the refractive index of water has been used to meaure absorbed dose distribution around an aluminum-rod immersed in water and exposed to a 3-MeV electron beam.

**5853.** Grant, W. H., Smith, L. E., Stromberg, R. R., **Adsorption and desorption rates of polystyrene on flat surfaces,** *Faraday Discuss. Chem. Soc.*, No. 59, 209-217 (1975).

Key words: adsorption; adsorption on mercury; desorption; polymers; polystyrene; radiotracer measurements; rates of adsorption; surfaces.

The rates of adsorption and desorption of polystyrene have been measured in cyclohexane and benzene solutions by adiotracer techniques. Relatively long times were required to attain maximum adsorbance values for adsorption of both low and high molecular weight polymer on a solid chrome surface under theta conditions. This was interpreted as indicating a molecular reorientation during the adsorption process. Under these conditions it was observed that the maximum adsorbance values increased with increasing molecular weight, but the amounts adsorbed were independent of molecular weight at very short adsorbance times. This was interpreted as indicating two separate rates of adsorption: an initial rate dependent on the rate of arrival and attachment at the surface and the rate of rearrangement on the surface. More rapid attainment of maximum adsorbance values on a mercury surface was attributed to participation of the liquid mercury surface in accommodating the changing polymer conformation. The rates of desorption were very slow for both chrome and mercury and were dependent on the surface populations as determined by the adsorbance values.

**15854.** Utton, D. B., Bowers, W. J., Jr., **Demountable seal between an epoxy resin and copper for low-temperature applications,** *Rev. Sci. Instrum.* **47,** No. 3, 382-383 (Mar. 1976).

Key words: cryogenic temperatures; epoxy resin-copper seal; indium O-ring.

We describe an indium O-ring seal between an epoxy resin and copper. It is simple, reliable, can withstand severe thermal shocks, and is leaktight to superfluid helium.

**15855.** Powell, C. J., **Cross sections for ionization of inner-shell electrons by electron impact (Abstract),** *J. Vac. Sci. Technol.* **13,** No. 1, 219-220 (Jan.-Feb. 1976).

Key words: Auger-electron spectroscopy; cross sections; electron probe microanalysis; electrons; inner-shell.

A survey has been made of inner-shell ionization cross-section data in the range of interest for quantitative Auger-electron spectroscopy. Calculated, semiempirical and experimental data have been intercompared graphically and by deriving "effective" values of the Bethe parameters $b_{nl}$ and $c_{nl}$ from fits of cross sections $\sigma_{nl}$ to a linearized form of the Bethe equation for inner-shell ionization. These intercomparisons were made for values of the parameter $U_{nl}(=E_0/E_{nl}$, where $E_0$ is the incident electron energy and $E_{nl}$ the binding energy of electrons in the $nl$-shell) between 4 and about 30. The derived values of $b_{nl}$ were generally consistent with those expected from photoabsorption data if account was taken of the distribution of differential oscillator strength with respect to excitation energy and the resultant expected variation of $b_{nl}$ near threshold. Experimental values of $\sigma_K E_K{}^2$ plotted as a function of $U_K$ appeared to lie on a common curve and agreed well with the calculations of Rudge and Schwartz and of McGuire. A greater spread existed in similar plots of calculated and measured values of $\sigma_L E_L{}^2$ as a function of $U_L$, but the magnitude of a variation with $Z$ could not be definitely established on account of discordant data.

**15856.** Lawn, B. R., Wiederhorn, S. M., Johnson, H. H., **Strength degradation of brittle surfaces: Blunt indenters,** *J. Am. Ceram. Soc.* **58,** No. 9-10, 428-432 (Sept.-Oct. 1975).

Key words: brittle solids; ceramic surfaces; crack; degradation; fracture; Hertzian; indentation; strength.

Indentation fracture mechanics is used to develop a theoretical basis for predetermining the strength properties of brittle surfaces in prospective contact situations. Indenters are classified as blunt or sharp; only the first is considered in the present work. The classical Hertzian cone crack conveniently models the fracture damage incurred by the surface in this class of indentation event. Significant degradation is predicted at a critical contact load; when the load is increased beyond this critical level, further degradation occurs at a relatively slight rate. Bend tests on abraded glass slabs confirm the essential features of the theoretical predictions. The controlling variables in the degradation process, notably starting flaw size and indenter radius, are investigated systematically. An indication is also given as to optimization of material parameters.

**15857.** Gadzuk, J. W., **Can chemisorption bonding shifts be separated from relaxation-energy shifts in photoelectron spectroscopy? (Abstract),** *J. Vac. Sci. Technol.* **13,** No. 1, 343-344 (Jan.-Feb. 1976).

Key words: chemisorption; photoemission; relaxation energy; surface plasmons.

A theory for separating relaxation energy shifts from chemical bonding shifts in photoelectron spectra of chemisorbed atoms is presented.

**15858.** Flynn, J. H., Dickens, B., **Steady-state parameter-jump methods and relaxation methods in thermogravimetry,** *Thermochim. Acta* **15,** 1-16 (1976).

Key words: degradation; kinetics; oxidation; parameter jump method; polystyrene; relaxation methods; thermogravimetry; weight-loss.

We describe a technique for thermogravimetric analysis in which the magnitude of a rate-forcing variable such as temperature, pressure, gaseous flow-rate, gaseous composition, etc., is jumped by discrete steps. This method can be used to determine kinetic relationships between the rate of weight-loss and the jumped variable. The method avoids the disparate effects of separate experimental histories in methods in which two or more experiments are compared. The necessity for guessing the often complex rate vs. extent of reaction relationship in methods where the rate forcing variable is changed continuously in a single experiment is also avoided. The method is illustrated with examples from the oxidation of polystyrene.

Techniques involving multiple jumps and more complex programming are proposed. The fruitful investigation of weight-loss kinetics by the measurement of relaxation times during jumps or of phase lags while the rate forcing variables are oscillated is predicted for diffusion limited reactions and reactions with gaseous atmospheres.

**15859.** Heppner, R. A., Walls, F. L., Armstrong, W. T., Dunn, G. H., **Cross-section measurements for electron-$H_3O^+$ recombination,** *Phys. Rev. A* **13,** No. 3, 1000-1011 (Mar. 1976).

Key words: cross-section measurements; electrons; $H_3O^+$; ion trap; recombination.

Cross sections for electron-$H_3O^+$ recombination have been measured over an electron energy range of 0.060 – 1.15 eV by using a trapped-ion technique to contain an ion sample at a temperature of $\simeq$400 K. The cross section deduced from these measurements can be represented by $\sigma = 4.6 \times 10^{-18} E^{-2.9}$ cm² for $0.038 < E \leq 0.110$ eV; $\sigma = 4.8 \times 10^{-16} E^{-0.79}$ cm² for $0.110 < E \leq 0.420$ eV; and $\sigma = 7.5 \times 10^{-17} E^{-2.9}$ cm² for $E > 0.420$ eV. Uncertainties are estimated to be at the ±50 percent level. Recombination-rate coefficients were calculated from the deduced cross sections, assuming a Maxwellian electron velocity distribution and trial forms for the cross section below 0.038 eV. Assuming the theoretical $E^{-1}$ behavior for the cross section just above zero energy and comparing with the measured rate coefficient of Leu et al. at 540 K, we can deduce consistent cross sections below 0.038 eV to be $\sigma = 6.0 \times 10^{-15} E^{-1}$ cm² for $0 < E < 0.23$ eV, and $\sigma = 4.6 \times 10^{-18} E^{-2.9}$ cm² for $0.023 < E < 0.038$ eV. The calculated rate coefficients have temperature dependence $T_e^{-0.5}$ at 50 K and $T_e^{-1.13}$ at $10^5$ K, and values of the coefficient are in good agreement with all direct measurements.

**15860.** Chen, S. T., Leep, D., Gallagher, A., **Excitation of the Sr and $Sr^+$ resonance lines by electron impact on Sr atoms,** *Phys. Rev. A* **13,** No. 3, 947-952 (Mar. 1976).

Key words: electron impact; strontium.

The relative optical excitation functions and polarizations of the Sr resonance line (4607 Å) and of the $Sr^+$ resonance lines (4078 and 4216 Å) have been measured, using crossed electron and strontium-atom beams, for electron energies from the excitation thresholds to 1497 eV. The electron-beam energy resolution was ~0.22 eV for energies below 13 eV, and the atom beam was optically thin. The excitation functions of the ionic lines were measured relative to that of the atomic resonance line at fixed energies near the maxima of the excitation functions. Using spontaneous-emission branching ratios, this yields the ratios of total excitation cross sections for the atomic and ionic resonance levels (including cascades). The Sr $5^1P$ excitation function has been normalized to Born theory taking account of cascade at 1497 eV, where the energy dependence of the excitation function has converged to the theoretical behavior. The resulting normalized cross sections have been compared with available theoretical calculations and other measurements. The 4607-Å polarization function is consistent with the theoretical threshold limit within experimental uncertainty.

**15861.** Johnson, C. R., **Hadamard's inequality for matrices with positive-definite Hermitian component,** *Michigan Math. J.* **22,** 225-228 (1975).

Key words: determinant; Hadamard's inequality; Hermitian component; positive definite.

Hadamard's inequality states that for a positive definite Hermitian matrix $A=(a_{ij})$,

$$\det A \leq a_{11}\, a_{22} \ldots a_{nn}.$$

We consider 2 parameterized subclasses of the class $\Pi_n$ of matrices A for which $A+A^*>0$. In one, $|\det A| \leq a_{11} \ldots a_{nn}$ and in the other $|\det A| \geq a_{11} \ldots a_{nn}$. The former class contains the Hermitian elements of $\Pi_n$ so that an alternate proof of Hadamard's inequality is provided.

**15862.** Newbury, D. E., Heinrich, K. F. J., Myklebust, R. L., **Errors observed in quantitative ion microprobe analysis,** (Proc. American Society for Testing and Materials Symp. on Surface Analysis Techniques for Metallurgical Applications, Cleveland, OH, Mar. 4, 1975), *Am. Soc Test. Mater. Spec. Tech. Publ. 596*, pp. 101-113 (1976).

Key words: CARISMA program; ion microprobe mass analysis; local thermodynamic equilibrium model; quantitative analysis; secondary ion mass spectrometry; surface analysis.

Quantitative reduction of ion microprobe mass analyzer data has been performed with an empirical technique involving relative elemental sensitivity factors and with a physical model, the local thermodynamic equilibrium (LTE) model. A series of macroscopically well-characterized low alloy steels (National Bureau of Standards (NBS) Standard Reference Material 660 series) was analyzed with empirical relative sensitivity factors derived from one arbitrarily chosen alloy from the series. Relative errors of less than 50 percent were obtained in most cases but several results were in error by 100 percent or more. The LTE model was used to analyze two multicomponent glasses. Relative errors of 200 percent were observed frequently, with some components consistently in error by an order of magnitude or more. The effect of differing reference data on LTE model calculations was tested. Different combinations of internal concentration standards and different metal/metal oxide ion ratios were employed. The calculated concentrations showed considerable dependence on the choice of reference data.

**15863.** Nicodemus, F. E., **Comment on "Current definitions of reflectance,"** *J. Opt. Soc. Am. Letters* **66,** No. 3, 283-285 (Mar. 1976).

Key words: photometry; radiometry; reflectance; reflectometry.

The delta-function form of the bidirectional reflectance-distribution function (BRDF) is not limited to the case where $\theta_r = \theta_i$ and $\psi_r = \psi_i \pm \pi$ (rad), but can represent a "glint" in any direction. The conceptual advantage of the BRDF approach is briefly discussed in relation to the continuum of directional distributions actually found between the limits of purely specular "spikes" and completely diffuse reflection.

**15864.** Swyt, D. A., **NBS program in photomask linewidth measurements,** *Solid State Technol.* **19,** No. 4, 55-61 (Apr. 1976).

Key words: dimensional metrology; integrated circuits; linewidth measurements; microelectronics; optical microscope; photomasks; scanning electron microscope.

A problem facing the microelectronics industry is that of making accurate dimensional measurements of photomask patterns with the optical microscope, the usual tool for mask inspection. A part of the problem is the absence of calibrated linewidth standards in photomask materials for the critical 1 to 10 μm range. This article discusses the status of a National Bureau of Standards program to develop such standards and to develop the means to identify and control the parameters of optical performance which introduce errors into linewidth measurements.

**15865.** Cunningham, G. W., Meijer, P. H. E., **A comparison of two Monte Carlo methods for computations in statistical mechanics,** *J. Comput. Phys.* **20,** No. 1, 50-63 (Jan. 1976).

Key words: conditional probability; Ising spin; Monte Carlo method; spin system; triangular lattice.

A comparison of two Monte Carlo methods for computations in statistical mechanics is presented. In the comparison, involving a two-state problem, the transition probabilities introduced by Metropolis et al. are compared with the conditional probabilities of the Boltzmann distribution. The analytic relationship between the two is derived. Results of energy computations are given for an Ising spin system on a triangular lattice using first one set of transition probabilities, then the other. Both results are compared with the exact analytic solution. We found greater stability and faster convergence using the conditional Boltzmann probabilities. Also, some results for the Monte Carlo method in general are presented.

**5866.** Meijer, P. H. E., Kessler, B. V., **Heat capacity, susceptibility, and critical temperature of erbium phosphate as predicted by dipole-dipole interactions,** *Phys. Rev. B* **13,** No. 1, 255-262 (Jan. 1, 1976).

Key words: antiferromagnetism; critical temperature; dipole-dipole interaction; erbium phosphate ground state; heat capacity; lattice sums; magnetic; susceptibility.

In this paper we compute the heat capacity and susceptibility of erbium phosphate above the critical temperature, assuming that the interaction between the spins is purely dipolar. We also obtain, using the same assumption, the ground-state energy and its configuration on the basis of an extended Luttinger-Tisza calculation. From the high-temperature results we try to predict the critical temperature, using the commonly accepted idea that for long-range forces the ring diagrams (for the heat capacity) and the chain diagrams (for the susceptibility) are the dominant contributions to the series. We estimate the critical temperature to be about 0.4 K on the basis of the heat-capacity computations. This gives no information about the configuration below $T_c$, but we can use the results obtained via the susceptibility computations to predict that the spins lie in the $x$-$y$ plane in an antiferromagnetic arrangement below $T_c$. These two predictions are sustained by the ground-state calculation. The estimated value for $T_c$ obtained from the susceptibility calculation is, however, one order of magnitude larger than that derived via the heat capacity. In conclusion, we observed that the radius of convergence of the high-temperature series for dipolar interactions seems to be determined by properties other than the range of these forces.

**15867.** Estin, A. J., **A calculable microwave attenuation standard: The high Q cavity,** (Proc. 1972 Precision Electromagnetic Measurement Conf., Boulder, CO, June 26-28, 1972), Paper in *CPEM Digest,* pp. 28-29 (IEEE, Inc., New York, NY, June 1972).

Key words: automatic network analyzer; Q cavity; two-ports.

The high Q microwave resonant cavity is a calculable attenuation standard having a wide attenuation range and a low residual loss. It is especially well suited in calibrating computer-operated automatic network analyzers (ANA) for measurements of $s_{21}$ of arbitrary two-ports.

Although the cavity is one of the most important classes of microwave circuit elements and is well understood, it has not been used as a substitution standard of attenuation. Excellent calculations can be made, because the model used is a close replica to the physical realization. The fact that the frequency dependence of scattering parameters is strong permits the rather novel approach of using frequency dependence, rather than mechanical displacement, as a means of setting attenuation. The relatively complicated calculations needed to achieve the dynamic range and accuracy are well handled by the on-line computer used with an ANA. Furthermore, the capability of the ANA to remove the effects of its own mismatched measuring lines when examining an arbitrary two-port is both utilized and tested by this highly reflective test standard.

**15868.** Julienne, P. S., Krauss, M., Stevens, W., **Collision-induced $O^1D_2$-$^1S_0$ emission near 5577 Å in argon,** *Chem. Phys. Lett.* **38,** No. 2, 374-381 (Mar. 1, 1976).

Key words: ab initio potentials; argon oxide; collision-induced emission; rare-gas oxide excimers.

The collision-induced emission near the 5577 Å oxygen $^1D_2 - ^1S_0$ transition in argon is investigated theoretically. Approximate ArO model potentials were constructed for the upper and lower states by adding the attractive long-range dispersion energy to the short-range repulsion calculated ab initio. The thermally averaged free – free, free – bound, and bound – bound contributions to the emission profile were calculated using the long-range quadrupole-induced dipole transition moment. The calculated bound – bound spectrum and the total emission coefficient agree well with experiment.

**15869.** Garner, E. L., Machlan, L. A., Barnes, I. L., **The isotopic composition of lithium, potassium, and rubidium in some Apollo 11, 12, 14, 15, and 16 samples,** (Proc. 6th Lunar Science Conf., Houston, TX, Mar. 17-21, 1975), *Geochim. Cosmochim. Acta, Suppl. 6,* **2,** 1845-1855 (Pergamon Press, New York, NY, 1975).

Key words: absolute; Apollo; composition; isotopic; lithium; potassium; relative; rocks; rubidium; soils.

The relative isotopic composition of lithium and the absolute composition of potassium and rubidium were determined in seven lunar soil and five lunar rock samples by solid sample, thermal ionization, mass spectrometry. Special precautions were taken to minimize the effect of impurities and variable sample size on the isotopic measurements. Relative to a natural reference standard of terrestrial material, the average $^6Li/^7Li$ of the lunar samples were found to be 1.0007±0.0027 (ts). The $^{85}Rb/^{87}Rb$ average value is 2.5923±0.0043. Depletions of 0.3-0.8 percent were found in the $^{39}K/^{41}K$ ratios of five soils and one rock sample. A corresponding mass-dependent increase of 0.2-0.4 percent in the $^{41}K/^{40}K$ could not be proven because the error in this measurement is approximately the same magnitude as the predicted variation. Normal potassium isotopic composition of soil 12033, removed from a 15 cm-deep trench at Head Crater, and abnormal composition of glass-coated breccia 15505 are the most significant clues to the $^{39}K$ depletion. Presently available data are insufficient to decipher the mechanism for potassium isotopic fractionation.

**15870.** Meijer, P. H. E., Scherer, W. D., **An extended lattice model of liquid helium four,** *Physica* **80A,** No. 5, 447-464 (1975).

Key words: Bogoliubov transformation; bosons; helium; lambda point; lattice model; phase transition.

A description of the low-and high-temperature behavior of liquid $^4He$ is given in terms of an extended Matsubara-Matsuda lattice model. Paying particular attention to the kinematical interaction and to the hard core of the bosons leads to a unified theory for the low-temperature behavior and for the lambda transition. Since the hard-core boson operators in the lattice model correspond to spin one-half operators, one can interpret the Hamiltonian as the Hamiltonian of a magnetic system of oblate form, i.e., the $x$-$y$ coupling is stronger than the $z$ coupling. A rotation introduced in the space of these operators results in a Hamiltonian consisting of three parts: One part is of the anisotropic Heisenberg form, the second contains pairs of creation-annihilation operators at different lattice sites and the third part consists of an interaction between creation-annihilation operators and the $z$ component of the spin operators. A particular choice of the rotation angle eliminates the third part.

The equations of motion of the creation and annihilation operators are decoupled with the aid of a momentum-dependent Bogoliubov-like transformation. This leads to a linear energy spectrum and a self-consistent integral equation for the magnetization. An approximation of this self-consistency equation provides a temperature dependence of the magnetization and leads to a critical temperature for a range of external magnetic fields. It is found that in the rotated frame the angle of rotation and the magnetization exhibit a jump at the transition temperature. Consequently, the transition is of second order.

**15871.** Simiu, E., **Equivalent static wind loads for tall building design,** *J. Struct. Div. Proc. Am. Soc. Civil Eng.* **102,** ST4, 719-737 (Apr. 1976).

Key words: accelerations; building codes; buildings; deflections; dynamic response; gust factors; structural engineering; wind engineering; wind loads.

Certain shortcomings of current procedures for computing alongwind structural response have beeen shown to result in unrealistic estimates of tall building behavior under the action of strong winds. Differences between predictions of fluctuating response based on various such procedures have been shown to be in certain cases as high as 200 percent. The purpose of the present work is to present a procedure for calculating alongwind response, including deflections and accelerations, which incorporates these advances. The meteorological and aerodynamic models on which the procedure is based are described in brief. The practical use of the procedure is illustrated in a numerical example. Estimates are provided of errors inherent in the models employed. The range of applicability of the procedure is defined, and it is indicated that for structures with unusual modal shapes or for which the influence of higher vibration modes is significant, a recently developed computer program should be employed in lieu of the procedure presented herein.

**15872.** Julienne, P. S., Neumann, D., Krauss, M., **Transition moments for the $B^3\Sigma_u^- - X^3\Sigma_g^-$ and $^3\Pi_u - X^3\Sigma_g^-$ transitions in $O_2$,** *J. Chem. Phys.* **64,** No. 7, 2990-2996 (Apr. 1, 1976).

Key words: ab initio calculation; $O_2$ absorption; oscillator strength; transition moment.

Multiconfiguration self-consistent field wavefunctions are used to calculate the transition moments for the lowest dipole allowed transitions in $O_2$. The transition matrix element for the $B-X$ transition calculated at $R_e$ of the ground state corresponds to an oscillator strength of 0.18, in good agreement with the experimental integrated oscillator strength 0.16 of the Schumann-Runge continuum. The $B-X$ transition moment is calculated as a function of internuclear separation. The transition matrix element to the repulsive valence $^3\Pi_u$ state calculated at $R_e$ of the ground state corresponds to an oscillator strength of 0.003. Although the weak $^3\Pi_u$ absorption continuum is masked by the strong Schumann-Runge continuum below 1750 Å, this $^3\Pi_u$ absorption may contribute to the background continuum in the Schumann-Runge band region at low temperature.

**15873.** Roberts, R. W., **Materials research: A strategy to improve the performance of materials,** (Proc. of an Engineering Foundation Conf., Henniker, NH, Aug. 11-16, 1974), Paper in *Requirements for Fulfilling a National Materials Policy,* F. P. Huddle, Ed., pp. 9-17 (Office of Technology Assessment, Washington, DC, 1974).

Key words: design; development; fabrication; life cycle costing; materials policy; nondestructive evaluation; performance; processing; technical strategy.

Intelligent planning to improve the performance of materials is essential if the Nation is to continue economic growth and meet the needs of a growing population. What is required is a unified materials policy and a mechanism to carry policy and strategy through to technical completion. Five technical options will have to be exploited: materials development, processing, fabrication, design, and nondestructive evaluation. Innovations will cost money, and consumers at all levels – industry, government and the individual – will have to be educated in the concept of life cycle costing before they can be expected to accept that cost.

**15874.** Brinckman, F. E., Jewett, K. L., Blair, W. R., Iverson, W P., Huey, C., **Mercury distribution in the Chesapeake Bay** *Prog. Water Technol.* **7,** 251-252 (1974).

Key words: Chesapeake Bay; elemental sulfur; flameless atomic absorption; petroleum; plankton; sediments; tota mercury; water.

Water, sediment and plankton from the Chesapeake Bay were analyzed for total mercury using flameless atomic absorption techniques. The concentrations of mercury in the sedimen ranged from 0.80 to 0.02 ppm, from 4.9±0.10 ppm to 0.02±0.01 ppm in plankton and 0.00 ppb to 0.49 ppb in the water. Petroleum fractions from the sediment were found to contain 0.1 percent of mercury by weight. Elemental sulfur was found in concentrations as high as 1 percent of the sediment (dry wt.).

**15875.** Demkov, Y. N., **Asymptotically exact theory of electron exchange in distant collisions,** (Proc. IX Int. Conf. on the Physics of Electronic and Atomic Collisions, Seattle, WA, July 24-30, 1975), Paper in *The Physics of Electronic and Atomic Collisions*, J. S. Risley and R. Geballe, Eds., pp. 313-326 (University of Washington Press, Seattle, WA, 1976).

Key words: adiabatic collisions; charge transfer; nonresonant; potential curves; resonant; spin exchange.

The asymptotic theory of resonant charge and spin transfer is reviewed. It is shown how only the asymptotic part of the atomic wave function is important for these processes. The single electron charge transfer formula is generalized to cover the transfer of an arbitrary number of electrons. The extension to the nonadiabatic and nonresonant cases is carried out.

**15876.** Johnson, C. R., **Notes on nonnegative Hadamard functions,** *Linear and Multilinear Algebra* **3,** 187-192 (1975).

Key words: Hadamard product; positive semidefinite; real function.

Let *f* be a real valued function of a real variable and denote the by *r* real matrices by $M_r(R)$. For $A_{ij}\epsilon M_m(R)$, $i, j=1,\dots, n$, define the Hadamard action of *f* on $A=(A_{ij})\epsilon M_{mn}(R)$ by

$$(A)f=(f(\det A_{ij})).$$

This defines a map $M_{mn}(R)\xrightarrow{f}M_n(R)$. We consider a problem re-ated to one posed by Marcus and Watkins. We call *f* a nonnega-ive Hadamard function if $(A)f$ is positive semidefinite (PSD) for ll symmetric PSD matrices $A\epsilon M_{mn}(R)$.

**5877.** Peterson, J. R., **Sunlight photodestruction of $CO_3^-$, $CO_3^-\cdot H_2O$, and $O_3^-$: The importance of photodissociation to the *D* region electron densities at sunrise,** *J. Geophys. Res.* **81,** No. 7, 1433-1435 (Mar. 1, 1976).

Key words: $CO_3^-$; $CO_3^-\cdot H_2O$; *D* region; electron density; molecule; negative ion; $O^-$; $O_3^-$; photodetachment; photodissociation.

Experimental studies at photon energies between 1.8 and 2.7 V have recently shown that photodissociation occurs well elow the photodetachment threshold for $CO_3^-$ and $CO_3^-\cdot H_2O$ nd dominates the photodestruction of $O_3^-$ at visible wavelengths. Experimental cross sections have been averaged ver the solar flux spectrum to yield zero optical depth rates. roduction of $O^-$ by dissociation of $CO_3^-$ and $CO_3^-\cdot H_2O$ and its ubsequent photodetachment can probably account for the rapid ncrease of electron density in the *D* region of the ionosphere at unrise. Photodissociation is also an important daytime loss mechanism for $CO_3^-$ and its hydrate in the 50- to 80-km region.

**5878.** Parrish, W. R., **Recovery of hydrogen liquefaction energy,** *Proc. 10th Conf. on Intersociety Energy Conversion Engineering, Newark, DE, Aug. 18-22, 1975, IECEC 1975 RECORD, IEEE Catalog No. 75CHO 983-7TAB*, pp. 1352-1355 (1975).

Key words: air separation; electrical power generation; energy recovery; hydrogen; liquefaction energy.

Liquid storage is an attractive means for storing the large uantities of synthetic hydrogen that will be needed in the future. owever, the actual energy required for liquefaction is roughly 0 percent of hydrogen's lower heating value. This paper con-ders some ways of recovering part of the liquefaction energy. he emphasis is on utility applications. Results show that it is chnically feasible to recover 25 to 50 percent of the actual quefaction energy if a MHD generator is used; recovery factors f approximately 18 percent could be obtained with gas turbines, and lower recovery factors of 8 to 20 percent are possible if fuel cells are used. This energy recovery has the net effect of lowering the required liquefaction energy which makes liquid a more attractive means of storage.

**15879.** Voth, R. O., Daney, D. E., **$H_2$ liquefaction: Effects of component efficiencies,** *Proc. 10th Conf. on Intersociety Energy Conversion Engineering, Newark, DE, Aug. 18-22, 1975, IECEC 1975 RECORD, IEEE Catalog No. 75CHO 983-7TAB*, pp. 1356-1362 (1975).

Key words: compressor efficiency; cycle efficiency; heat exchanger losses; hydrogen liquefier; pressure drop losses.

Liquid hydrogen has been proposed as a synthetic fuel to be used as an "energy carrier" to replace fossil fuels in certain applications. The cost of liquid hydrogen is dependent on the cost of gaseous hydrogen plus a cost for liquefaction. The liquefaction costs are a function of the efficiency of the hydrogen liquefier.

Efficiencies of current large liquefiers are approximately 30 percent of Carnot. Although the Carnot cycle work is a good basis for comparing the efficiencies of various refrigerators and liquefiers operating at different temperature levels, the Carnot cycle is not amenable to showing the maximum efficiency for a hydrogen liquefier using practical components. In this paper an alternate cycle is defined that permits evaluation of overall cycle efficiency using 1) practical components with variable efficiencies, 2) variable heat exchanger temperature differences, and 3) variable system pressure drop. The resulting cycle efficiencies will serve as a guide to engineers performing thermodynamic cycle studies to improve the efficiencies of hydrogen liquefiers and will help define the maximum attainable efficiency for future liquefiers.

**15880.** Fatiadi, A. J., **Active manganese dioxide oxidation in organic chemistry—Part 1,** *Synthesis Reviews*, No. 2, 65-104 (Feb. 1976).

Key words: active; manganese dioxide; organic chemistry; oxidation; reagent; review.

Active Manganese dioxide and its various modifications provide a reagent of choice for a mild, selective (heterogeneous) oxidation of diverse classes of organic compounds. The aim of the present review is to discuss the highlights of the synthetic applications of active manganese dioxide, and to show its selectivity and specificity as an oxidant, as a dehydrogenation reagent, as a coupling reagent, and as a selective, analytical tool in the structure determination of complex, organic molecules derived from natural products. The review also includes a discussion of the mechanism of action and the complexity of the heterogeneous reactions.

**15881.** Tsang, W., **Comparison between experimental and calculated results on the decomposition of chemically activated alcohols,** *Int. J. Chem. Kinet.* **VIII,** 193-203 (1976).

Key words: alcohols; chemical activation; nonequilibrium; oxygen atoms; RRKM; thermal decomposition.

The life times of chemically activated alcohols have been determined using the high-pressure unimolecular rate parameters for thermal decomposition of alcohols from shock-tube studies and RRKM calculations. They are compared with literature numbers (from insertion of $O(^1D)$ into hydrocarbons). It is suggested that in some cases singlet oxygen carries excess energy into the hydrocarbon. The consequences of such an assumption are explored and discrepancies with previously published conclusions discussed.

**15882.** Achenbach, P. R., **Government activities and regulations**

**for buildings on energy saving standards. A look at what various agencies have done and intend to do for energy conservation,** *Heat./Piping/Air Cond.* **47,** No. 13, 41-46 (Dec. 1975).

Key words: energy consumption in NYC schools; energy-saving opportunities; incentives—educational, persuasive, financial, regulatory; modular boiler study; NBS-campus energy retrofit; retrofitting existing buildings.

The major near-term opportunity for energy conservation in buildings occurs in the existing building inventory, which includes some 70-million residential and several million commercial and institutional buildings, constructed before energy conservation was a recognized national need. This paper identifies 1) existing documents relating to retrofit, and 2) documents in development for both new and extant buildings with potential impact on regulations, standards, and codes, if the energy shortage persists.

Federal and State government incentives for building owners or operators to work for energy conservation are broadly classified as *educational*—seminars, conferences, publications with wide dissemination for use as guidelines; *persuasive*—exhortation by government and community leaders, and commercial sales efforts toward modification of present buildings or inclusion of energy-efficient components in new buildings; *regulatory*—standards, specifications, regulations and codes—voluntary and mandatory; and *financial*—tax breaks, low-interest loans, direct subsidy, etc. The paper lists documents now available and some in progress, and cites ongoing studies with potential large impact on the Nation's energy conservation effort. The latter include a retrofit of selected NBS laboratories for energy conservation and comparison; a study of existing New York City school buildings for energy consumption; a demonstration of energy savings in a 20-yr-old frame house by sealing leaks, installing storm windows and insulation; and a study of modular boilers which indicates that using several equal-capacity boilers to service a load in lieu of a single large boiler enables operators to match the load under varying weather conditions, and could lead to an approximate 10 percent saving during a typical winter heating season.

**15883.** Bardsley, J. N., **Theory of low-energy electron-atom collisions and related processes,** (Proc. IX Int. Conf. on the Physics of Electronic and Atomic Collisions, Seattle, WA, July 24-30, 1975), Paper in *The Physics of Electronic and Atomic Collisions,* J. S. Risley and R. Geballe, Eds., pp. 151-157 (University of Washington Press, Seattle, WA, 1976).

Key words: atom; collisions; electron; low energy; review; scattering; theory.

Imaginative new approaches to the theoretical treatment of low-energy electron-atom collisions are being proposed and tested by investigations. This paper reviews current activity, citing successes and problem areas, giving a characterization of the status of the field and suggesting where further progress is needed.

**15884.** Read, F. H., **Energy exchanges between two escaping electrons,** (Proc. IX Int. Conf. on the Physics of Electronic and Atomic Collisions, Seattle, WA, July 24-30, 1975), Paper in *The Physics of Electronic and Atomic Collisions,* J. S. Risley and R. Geballe, Eds., pp. 176-193 (University of Washington Press, Seattle, WA, 1976).

Key words: atom; collision; Coulomb-interaction; electron; energy exchange; ionization; threshold.

The final-state Coulomb interaction between three or more outgoing charged particles from a reaction can cause exchanges of energy and angular momentum between them. Such exchanges may be present for example when the reaction products consist of two electrons receding from a positive ion. The experimental evidence for the existence of such effects in threshold ionization and threshold autoionization are reviewed, and their possible theoretical descriptions are discussed.

**15885.** Holt, H. K., **Resonance trapping at low pressures,** *Phys. Rev. A* **13,** No. 4, 1442-1447 (Apr. 1976).

Key words: lifetime measurement; low pressure; resonance trapping.

When a small volume of atoms within a larger one is excited by a short pulse of electrons or light, the apparent lifetime of the decaying atoms is increased by the resonance trapping in the surrounding gas. In this paper the apparent lifetime is calculated for two different geometries and line shapes, and the result of having more than one lower level is presented.

**15886.** Linsky, J. L., **And who will analyze the data?,** *Astrophys. Lett. Editorial* **17,** 1-2 (1976).

Key words: astronomy; manpower problems.

This invited Guest Editorial discusses the manpower problem in astronomy and the urgent need for qualified new people to analyze forthcoming important data.

**15887.** Layer, H. P., Deslattes, R. D., Schweitzer, W. G., Jr., **Laser wavelength comparison by high resolution interferometry,** *Appl. Opt.* **15,** No. 3, 734-743 (Mar. 1976).

Key words: interferometer; laser; optical frequency; optical heterodyne; wavelength comparison.

High resolution interferometry has been used to determine the wavelength ratio between two molecularly stabilized He-Ne lasers, one locked to a methane absorption at 3.39 $\mu$m and the other locked to the $k$ peak of $^{129}I_2$ at 633 nm. An optical beat frequency technique gave fractional orders while a microwave sideband method yielded the integer parts. Conventional (third derivative) peak seeking servoes stabilized both laser and cavity lengths. Reproducibility of the electronic control system and optics was a few parts in $10^{12}$, while systematic errors associated with curvature of the cavity mirrors limited the accuracy of the wavelength ratio measurement to 2 parts in $10^{10}$. The measured wavelength ratio of the methane stabilized He-Ne laser at 3.39 $\mu$m [$P(7)$ line, $\nu_3$ band] to the $^{129}I_2$ ($k$ peak) stabilized He-Ne laser 633 nm was 5.359 049 260 6 (0.0002 ppm). This ratio agrees with that calculated from the (lower accuracy) results of earlier wavelength measurements made relative to the $^{86}$Kr standard. Its higher accuracy thus permits a provisional extension of the frequency scale based on the cesium oscillator into the visible spectrum.

**15888.** McGuire, B. J., Jr., **The Department of Commerce energy labeling and energy efficiency programs for household appliances,** *Proc. National Agricultural Outlook Conf., Washington, D.C., Nov. 17-20, 1975,* pp. 369-377 (U.S. Department of Agriculture, Washington, DC, Dec. 18, 1975).

Key words: combination refrigerator-freezers; consumer information; efficiency; energy labeling; room air conditioners; water heaters.

The development and present status of the Department of Commerce energy labeling and energy efficiency programs are described. Labels for room air conditioners, combination refrigerator-freezers, and water heaters are discussed in detail. Energy reduction goals under the energy efficiency programs are given. The possible effect of pending legislation is described.

**15889.** Paulsen, P. J., Alvarez, R., Mueller, C. W., **Trace element determinations in a low-alloy steel standard reference material by isotope dilution, spark source mass spectrometry,** *Appl. Spectrosc.* **30,** No. 1, 42-46 (1976).

Key words: isotope dilution; NBS Standard Reference Material; preconcentration; spark source mass spectrometry; steel; trace elements.

A stable isotope dilution procedure using the spark source mass spectrograph was developed for the simultaneous determination of cerium, copper, neodymium, selenium, silver, tellurium, and zirconium in a low-alloy steel material. Except for copper, the elements were present at trace concentrations that are difficult to determine by most analytical methods. In the procedure, known amounts of the isotopically enriched elements were added to 100-mg samples, which were dissolved in perchloric and hydrofluoric acids. After evaporation of the solutions almost to dryness, dissolution of the residues, and addition of hydrofluoric acid to complex the iron, the resulting solutions were electrolyzed in polytetrafluoroethylene cells. The electrodeposit on high purity, gold cathode wires was sparked in the mass spectrograph and the isotope ratios of the isotopically equilibrated elements were measured. The concentrations, ranging from 0.041 percent for copper to 3.1 $\mu$g/g (ppm) for neodymium, were calculated from the general isotope dilution equation. The low-alloy steel is available from NBS as Standard Reference Material 1261.

**15890.** Achenbach, P. R., **Government participation in safety standards for refrigerating and air conditioning equipment,** (Proc. Symp. on Domestic Refrigerator and Room Air Conditioners – Safety Standards and Service, Lake Placid, NY, June 24-26, 1968), *ASHRAE Special Bull.* **LP 68-3,** 8-12 (1968).

Key words: Government participation; refrigeration safety standards; safety of appliances; standards for safety.

Consumer protection against equipment hazards can be broadly categorized into three areas: hazard to health, hazard to life, and hazard to property. The principal instrumentalities through which safety requirements are brought into general use are: 1) state, municipal and model national codes, 2) national, international, mandatory and association standards, and 3) procurement specifications. The manufacturers of refrigerators, freezers, and air conditioners have, in general, provided the organizational leadership in preparing, sponsoring, and revising safety standards in the United States. However, agencies of the Federal Government are active in most national standards organizations concerned with equipment safety, and frequently conduct research on materials, systems, and equipment to develop technical information on safety for use in codes, standards, and specifications. Several specific investigations of refrigerators, freezers, and water coolers are described briefly to illustrate the kinds of hazards that may occur from choice of materials, design of a system, or manner of use by the owner.

**15891.** Smith, S. J., **Coherent electron impact excitation of different $L$ states in the $n$=3 shell of atomic hydrogen,** (Proc. Int. Symp. on Electron and Photon Interactions with Atoms, Stirling, Scotland, July 16-19, 1974), Chapter in *Electron and Photon Interactions with Atoms,* H. Kleinpoppen and M. R. C. McDowell, Eds., pp. 365-374 (Plenum Publishing Corp., New York, NY, 1976).

Key words: atomic hydrogen; Balmer alpha; beam foil; crossed beams; electrons; excitation; optical spectroscopy; Stark effect.

An interpretation of a measurement by Mahan, Gallagher, and Smith of the Balmer-$\alpha$ intensity excited by electron impact on a diffuse atomic hydrogen beam in an external electric field, is presented. An asymmetry in the Balmer-$\alpha$ intensity perpendicular to the electron beam, as a function of the *direction* of an electric field parallel (or anti-parallel) to the electron beam axis, is discussed in terms of displacement of the electron charge cloud during the collision, an interpretation which is also applicable to some recent results of beam foil spectroscopy.

**15892.** Lin, S. L., Bardsley, J. N., **Computation of speed distributions for ions in drift tubes,** *J. Phys. B Letter to the Editor* **8,** No. 17, L461-L464 (1975).

Key words: drift tubes; velocity distributions.

The speed distribution of $O^+$ ions drifting through helium gas under the influence of an electric field is computed by a Monte Carlo simulation. The average energy agrees with previous analytic estimates, but the distributions differ significantly from those observed in a recent experiment. The distributions show considerable distortion from the Maxwell-Boltzmann shape.

**15893.** Geltman, S., **Excitation and ionization in the Coulomb-projected Born approximation,** (Proc. Int. Symp. on Electron and Photon Interactions with Atoms, Stirling, Scotland, July 16-19, 1974), Chapter in *Electron and Photon Interactions with Atoms,* H. Kleinpoppen and M. R. C. McDowell, Eds., pp. 387-396 (Plenum Publishing Corp., New York, NY, 1976).

Key words: collisions; electron; excitation; hydrogen; ionization; theoretical.

In this progress report we will describe the physical basis of the Coulomb-projected Born method, discuss the similarities and differences of its predictions with those of the usual Born approximation, and compare with available experimental data.

**15894.** Epstein, M. S., Rains, T. C., **Evaluation of a xenon-mercury arc lamp for background correction in atomic absorption spectrometry,** *Anal. Chem.* **48,** No. 3, 528-531 (Mar. 1976).

Key words: arsenic; atomic absorption; atomic spectrometry; background, correction; nonflame, atomization; stray light; xenon-mercury, arc lamp.

The use of a xenon-mercury arc lamp for background correction in atomic absorption spectrometry is evaluated. The high spectral irradiance of this lamp permits background correction to be extended much further into the visible region of the spectrum than previously possible with hydrogen or deuterium continuum sources. The application of the lamp for background correction using a graphite furnace atomizer is demonstrated.

**15895.** Tighe, N. J., **Experimental techniques,** Chapter in *Electron Microscopy in Mineralogy,* H. R. Wenk et al., Eds., pp. 144-171 (Springer-Verlag Berlin Heidelberg, Germany, 1976).

Key words: electron microscopy; *in situ* experiments; ionic bombardment; microscope stages; rock-forming minerals; specimen preparation.

The paper describes cleavage, ionic bombardment, and chemical dissolution techniques for preparing specimens for transmission electron microscopy. Special stages used for tilting, heating, and environmental experiments are described.

**15896.** Eckerle, K. L., Venable, W. H., Jr., Weidner, V. R., **Averaging sphere for ultraviolet, visible, and near infrared wavelengths: A highly effective design,** *Appl. Opt.* **15,** No. 3, 703-707 (Mar. 1976).

Key words: averaging sphere; efficiency; radiometry; spectrophotometry; sphere coatings.

Through the use of an efficient design and a newly available sphere coating material, a simple, passive, sturdy averaging sphere was made that operates effectively over the wavelength range from 200 nm to 2000 nm. Data are reported for a sphere of this type in which the sphere transmittance is 0.32 at 200 nm and rises rapidly to near the maximum theoretical value of 0.56 over the remainder of the wavelength range. The several orders of magnitude reduction in error due to beam displacement more than compensate the slight reduction in signal for many spectrophotometric and radiometric applications.

**15897.** Iverson, W. P., Huey, C., Brinckman, F. E., Jewett, K. L., Blair, W., **Biological and nonbiological transformations of mercury in aquatic systems,** *Prog. Water Technol.* **7,** 193-195 (1974).

Key words: bacteria; elemental mercury; flameless atomic absorption spectroscopy; laser Raman spectroscopy; nuclear magnetic resonance spectroscopy; phenylmercuric acetate; volatilization.

Nine phenylmercuric acetate-tolerant bacterial strains, isolated from the Chesapeake Bay were found to produce metallic mercury from phenylmercuric acetate using a flameless atomic absorption spectrophotometer on-line with a bioreactor. Tolerance levels of one *Pseudomonas* strain to 10 metal ions were reported. Nonbiological methylation of a number of aquated methylated metal cations were studied using nuclear magnetic resonance and laser Raman spectroscopy.

**15898.** Evenson, K. M., Petersen, F. R., **Laser frequency measurements, the speed of light, and the meter,** Paper in *Topics in Applied Physics* **2,** H. Walther, Ed., pp. 349-368 (Springer-Verlag Berlin Heidelberg, Germany, 1976).

Key words: c; laser; laser frequency measurement; length standard saturated absorption stabilization; speed of light.

The extension of absolute frequency measuring techniques to the infrared (3.4 $\mu$m) has been made possible with the development of the tungsten-nickel point contact diode. Saturated absorption stabilized lasers now provide sources sufficiently stable to demand the resolution and accuracy of direct frequency measurement techniques.

The product of the measured frequency and wavelength of an 88 THz methane stabilized He-Ne laser yields a value of the speed of light 100 times more accurate than the previously accepted value.

Stabilized lasers are excellent wavelength sources which may be used in redefining the meter. In fact, direct frequency measurements now make it possible to redefine the meter so as to fix the value of c!

**15899.** Simiu, E., Patel, V. C., Nash, J. F., **Mean speed profiles of hurricane winds,** *J. Eng. Mech. Div. Proc. Am. Soc. Civil Eng.* **102,** EM2, 265-273 (Apr. 1976).

Key words: boundary layer; hurricanes; loads (forces); natural analysis; tall buildings; wind profiles.

A numerical solution of the hurricane boundary layer problem is presented in which the hurricane is modeled as a steady, axisymmetric, neutrally stratified flow. The turbulence effects in the flow are accounted for by the phenomenological relations proposed by Bradshaw et al., and Nash, which provide a considerably more realistic picture of the actual flow than the pseudolaminar model used in previous solutions of the boundary layer problem. The results of the calculations obtained on the basis of the model just described suggest that: (1) in the height range of interest to the structural designer, say up to a height of 400 m above ground, it is permissible to use the logarithmic law to represent the mean velocity profile of hurricane winds and (2) if the relation between wind speeds in different roughness regimes which obtains in extratropical storms is applied to hurricane winds, the speeds over built-up terrain, calculated as functions of speed over open terrain, may be underestimated by about 10 percent and 10-20 percent in suburban and in urban exposure, respectively. The corresponding mean loads are then underestimated by about 15 and 30 percent, respectively.

**15900.** Kessler, J., **Recent advances in polarized-electron experiments,** (Proc. IX Int. Conf. on the Physics of Electronic and Atomic Collisions, Seattle, WA, July 24-30, 1975). Paper in *The Physics of Electronic and Atomic Collisions,* J. S. Risley and R. Geballe, Eds., pp. 112-125 (University of Washington Press, Seattle, WA, 1976).

Key words: electron; experiment; LEED; multi-photon; photoionization; review; scattering; spin-polarization.

Recent experimental progress on collisional and radiative processes involving electron-spin polarization is reviewed. The various processes of this type are summarized. The review includes discussion of work carried out in several laboratories on polarization effects in scattering by free atoms, in scattering by surfaces (LEED), in single- and multi-photon ionization, of atoms as well as in photoelectron emission from certain solid surfaces.

**15901.** Hagan, L., **Reports of observatories for 1974/75, National Bureau of Standards, Washington, DC,** *Bull. Am. Astron. Soc.* **8,** No. 1, 210-214 (1976).

Key words: atomic energy levels; atomic line shapes; atomic spectra; atomic transition probabilities; bands, molecular; energy levels, atomic; line shapes, atomic; molecular bands; molecular spectra; rotational constants.

Research at the National Bureau of Standards in spectroscopy pertinent to astronomy is summarized. Publications on atomic spectra, atomic transition probabilities and line broadening, and molecular spectra are referenced and work in progress is discussed.

**15902.** Fatiadi, A. J., **Active manganese dioxide oxidation in organic chemistry—Part II,** *Synthesis Reviews,* No. 3, 133-167 (Mar. 1976).

Key words: active; chemistry; dioxide; heterogeneous; manganese; organic; oxidation.

A review is given of reactions in which active manganese dioxide and its various modifications provide a reagent of choice for a mild, selective, heterogeneous oxidation of diverse classes of organic compounds. Applications of manganese dioxide as a dehydrogenation reagent, a coupling reagent, and as an analytical tool are also discussed. This survey includes 697 references.

**15903.** Cetas, T. C., **A magnetic temperature scale from 1 to 83 K,** *Metrologia* **12,** 27-40 (1976).

Key words: ac-dc resistance thermometry; ac susceptibility; gadolinium sulphate; germanium resistance thermometers; IPTS-68; low temperature scales, 1-83 K; magnetic thermometer; manganous ammonium sulphate; paramagnetic salts; platinum resistance thermometers.

The low frequency (30 Hz) paramagnetic susceptibilities of powdered samples of gadolinium sulphate octahydrate and manganous ammonium sulphate hexahydrate have been measured from 1 to 83 K in order to test the thermodynamic consistency of the International Practical Temperature Scale of 1968 (IPTS-68). The data can be characterized by a physically based expression with essentially two constants as opposed to the twenty-one terms of the IPTS-68 Reference Function for the range 13.81 to 273.15 K. Variations in the IPTS-68 of up to ±3 mK about the smooth magnetic scale are found and the 20.28 K (e-$H_2$ b.p.) fixed point is shown to be inconsistent with the other fixed points by about +3 mK. The data also provide a means of thermodynamically extrapolating the IPTS-68 to lower temperatures where comparisons are made with other recent data. The reproducibility of the data is ±0.5 mK below 50 K and ±1 mK up to 83 K, while the total estimated measurement uncertainties are from one to three times greater.

**15904.** Tsang, W., **Thermal stability of alcohols,** *Int. J. Chem. Kinet.* **VIII,** 173-192 (1976).

Key words: alcohols; heats of formation; hydroxy-alkyl radicals; shock tube; thermal decomposition; 2,3-dimethylbutanol-2; 3,3-dimethylbutanol-2.

3,3-Dimethylbutanol-2 (3,3-DMB-ol-2) and 2,3-dimethylbutanol-2 (2,3-DMB-ol-2) have been decomposed in comparative-rate single-pulse shock-tube experiments. The mechanisms of the decompositions are

$$\text{2,3-DMB-ol-2} \xrightarrow{k_B} i\mathrm{C_3H_7}\cdot + \cdot\mathrm{C(CH_3)_2\,OH}$$

$$\xrightarrow{k_{EP}} \mathrm{H_2O} + \mathrm{H_2C{-}C(CH_3){-}CH(CH_3)_2}\ \text{(2,3-DMB-l)}$$

$$\text{3,3-DMB-ol-3} \xrightarrow{k_{ET}} t\mathrm{C_4H_9}\cdot + \cdot\mathrm{CH(CH_3)\,OH}$$

$$\xrightarrow{k_B} \mathrm{H_2O} + \mathrm{(CH_3)_2\,C - C(CH_3)_2}$$

$$\xrightarrow{k_{EP}} \mathrm{H_2O} + \mathrm{H_2C - C(CH_3)_3}\ \text{(3,3-DMB-l)}$$

The rate expressions are

$$k_B(\text{2,3-DMB-ol-2}) = 10^{16.24} \exp(-37{,}400/T)\ \mathrm{sec^{-1}}$$

$$k_{EP}(\text{2,3-DMB-ol-2}) = 10^{14.17} \exp(-32{,}300/T)\ \mathrm{sec^{-1}}$$

$$k_{ET}(\text{2,3-DMB-ol-2}) = 10^{13.66} \exp(-32{,}700/T)\ \mathrm{sec^{-1}}$$

$$k_B(\text{3,3-DMB-ol-2}) = 10^{16.33} \exp(-37{,}500/T)\ \mathrm{sec^{-1}}$$

$$k_{EP}(\text{3,3-DMB-ol-2}) < 10^{14.0} \exp(-34{,}200/T)\ \mathrm{sec^{-1}}$$

They lead to $D(i\mathrm{C_3H_7{-}H}) - D(\mathrm{(CH_3)_2(OH)\,C{-}H}) = 8.3$ kJ and $D(\mathrm{C_2H_5{-}H}) - D(\mathrm{CH_3(OH)\,CH{-}H}) = 24.2$ kJ.

These data, in conjunction with reasonable assumptions, give

$$k(t\mathrm{C_4H_9OH} \rightarrow \mathrm{CH_3}\cdot + \cdot\mathrm{C(CH_3)_2OH})$$

$$= 10^{16.8} \exp(-40{,}900/T)\ \mathrm{sec^{-1}}$$

$$k(i\mathrm{C_3H_7OH} \rightarrow \mathrm{CH_3}\cdot + \cdot\mathrm{CH(CH_3)OH})$$

$$= 10^{16.5} \exp(-41{,}100/T)\ \mathrm{sec^{-1}}$$

$$k(n\mathrm{C_3H_7OH} \rightarrow \mathrm{CH_3}\cdot + \cdot\mathrm{CH_2CH_2OH})$$

$$= 10^{16.2} \exp(-41{,}100/T)\ \mathrm{sec^{-1}}$$

$$k(\mathrm{C_2H_5OH} \rightarrow \mathrm{CH_3}\cdot + \cdot\mathrm{CH_2OH})$$

$$= 10^{16.4} \exp(-42{,}500/T)\ \mathrm{sec^{-1}}$$

and

$$D(\mathrm{CH_3{-}H}) - D(\mathrm{CH_2OH{-}H}) = 36.8\ \mathrm{kJ}$$

The rate expressions for the decomposition of 2,3-DMB-l and 3,3-DMB-l are

$$k(\text{2,3-DMB-l} \rightarrow \mathrm{CH_3}\cdot + \mathrm{H_2C - C(CH_3)} - \dot{\mathrm{C}}\mathrm{H(CH_3)})$$

$$= 10^{16.0} \exp(-35{,}700/T)\ \mathrm{sec^{-1}}$$

and

$$k(\text{3,3-DMB-l} \rightarrow \mathrm{CH_3}\cdot + \mathrm{H_2C - CH} - \dot{\mathrm{C}}\mathrm{(CH_3)_2})$$

$$= 10^{16.2} \exp(-35{,}500/T)\ \mathrm{sec^{-1}}$$

**15905.** Snyder, J. J., Hall, J. L., **A new measurement of the relativistic Doppler shift,** (Proc. 2nd Int. Conf. on Laser Spectroscopy, Megève, France, June 1975), Paper in *Laser Spectroscopy,* S. Haroche, J. C. Pebay-Peyroula, T. W. Hansch, and S. E. Harris, Eds., No. 43, 6-17 (Springer-Verlag, Berlin, Germany, 1975).

Key words: accelerated atom beam; experimental relativity; laser spectroscopy; laser stabilization; saturated absorption.

Saturated absorption laser spectroscopy allows, in principle, the study of atomic absorption lines free from first-order Doppler effects. However, the second-order Doppler effect is not suppressed, as it is a manifestation of the time dilation of special relativity. We describe an experiment using a stabilized visible cw dye laser to study the absorption of metastable neon atoms moving at high speed transversely to the laser beam. The dye laser has been stabilized to about 50 kHz absolute, considering linewidth as well as frequency jitter and drift. In these prototype experiments the neon metastable atoms are produced by charge transfer in Na vapor from an accelerated beam ($\approx \mu$A) of $\mathrm{Ne^+}$ ($E \leq 50$ keV). The observed time dilation effect is in agreement with the predictions of special relativity at the 1/2 percent noise level of the first preliminary experiment. A factor 30 to 100 improvement is expected with direct improvement of our experimental techniques. Still larger improvements may be possible with higher acceleration voltages where residual first-order errors become fractionally smaller.

**15906.** Kleimann, R. E., Eicke, W. G., Jr., **An automated standard cell comparator controlled by a desk calculator: A preliminary report,** *Proc. 1975 ASSC Conf. Record on Automated Support Systems, Westbury, Long Island, NY, Oct. 28-30, 1975,* pp. 18-23 (Institute of Electrical and Electronics Engineers, Inc., New York, NY, 1975).

Key words: automated; calculator; calibration; crossbar switch; low-level voltage measurements; MIDAS; programmable desk calculator; standard cell comparator.

A system is described with which measurements of standard cell differences can be made automatically to an accuracy of one part in $10^7$. The system is built using all commercially available equipment and is designed to be a relatively inexpensive easy-to-use instrument for the calibration laboratory. The system is designed around a BASIC-programmable desk calculator and MIDAS, an NBS-developed modular interface, which together control the necessary switching, stimuli and measurements for a set of standard cell difference measurements. The calculator then processes the measurement data using a least-squares fit and prints a calibration report for the cells. The design and construction of the system is described along with an evaluation of the results obtained with the system.

**15907.** Caswell, R. S., Goodman, L. J., Colvett, R. D., **International intercomparison of neutron dosimetry,** (Proc. 5th Int. Congress of Radiation Research, Seattle, WA, July 14-20, 1974), Paper in *Radiation Research,* R. F. Oddvard, F. Nygaard, H. J. Adler, and W. K. Sinclair, pp. 532-546 (Academic Press, Inc., New York, NY, 1975).

Key words: international intercomparison; neutron dosimetry.

An International Neutron Dosimetry Intercomparison (INDI) has been carried out at the Radiological Research Accelerator Facility (RARAF) at Brookhaven National Laboratory under the sponsorship of the International Commission on Radiation Units and Measurements. The objective was to compare results obtained by different groups performing fast neutron dosimetry in situations approximating those generally encountered in radiotherapy and radiobiology. Fourteen groups from six countries participated. Intercomparison energies for tissue kerma in free air were 15.5, 5.5, 2.1, and 0.67 MeV and $^{252}$Cf fission neutron spectrum. In addition, depth dose measurements in a phantom were made at the two highest energies. The experimental arrangements will be described, and preliminary results of the intercomparison given.

**15908.** Smith, C. E., Jacox, M. E., Milligan, D. E., **The absorption and fluorescence spectra of matrix-isolated $CF_2$,** *J. Mol. Spectrosc.* **60,** 381-387 (1976).

Key words: absorption spectrum; band experiment; $CF_2$; $CH_2F_2$ photolysis; fluorescence spectrum; matrix isolation.

The $CF_2$ absorption spectrum between 2700 and 2250 Å and its fluorescence spectrum excited by radiation near 2500 Å have been observed in matrix isolation experiments. The positions of the absorption bands are somewhat dependent on the environment in which the $CF_2$ molecule is trapped. The absorption spectrum can be explained in terms of a progression in the upper-state bending fundamental, with a band spacing of 499 cm$^{-1}$, and the fluorescence spectrum involves a progression in the ground-state bending fundamental, with a band spacing of 657 cm$^{-1}$. A significant deviation between the calculated and observed separation of any given absorption and emission band can be explained by considering the effect of phonon interactions. Arguments are presented suggesting that the band origin lies near 36 900 cm$^{-1}$ for $CF_2$ produced by the photolysis of $CF_2N_2$ in an argon matrix.

**15909.** Mandel, J., **Models, transformations of scale, and weighting,** *J. Qual. Technol.* **8,** No. 2, 86-97 (Apr. 1976).

Key words: interlaboratory comparisons; invariance; models; precision; precision of measurement; repeatability; reproducibility; test methods; transformations; weighting.

A realistic model as an indispensable prerequisite to any meaningful data analysis. Since most common statistical procedures are based on models involving specific assumptions, such as homoscedasticity or absence of certain interactions, it has become current practice to transform the scale of the data in the hope of achieving conformance with these assumptions. It is suggested in this paper that this approach is logically unsatisfactory. The conclusions drawn from a meaningful analysis should be essentially invariant with respect to scale transformations. The model should be flexible enough to allow for a realistic representation of the physical reality underlying the data. Heteroscedasticity should be dealt with by means of statistical weighting, and interactions, rather than being "assumed away," must be part of the model.

The proposed approach is shown to satisfy these requirements and is illustrated in terms of two individual studies. One is an interlaboratory evaluation of a physical test procedure and the other one deals with the within- and between-laboratory precision of a method of chemical analysis.

**15910.** Carlsten, J. L., Szöke, A., **Spectral resolution of near-resonant Rayleigh scattering and collision-induced resonance fluorescence,** *Phys. Rev. Lett.* **36,** No. 12, 667-671 (Mar. 22, 1976).

Key words: collisions; laser-excited fluorescence; Rayleigh scattering.

Light scattered from strontium vapor near its 460.73-nm ($^1P_1{}^\circ-{}^1S_0$) resonance transition was resolved into its three spectral components: Rayleigh scattering, collision-induced fluorescence, and three-photon scattering. The saturation behavior of the central (Rayleigh) component and the intensity and ac Stark shift of the three-photon component were studied as a function of detuning and laser intensity. Good agreement is obtained with theoretical predictions.

**15911.** McClintock, W., Henry, R. C., Moos, H. W., Linsky, J. L., **Ultraviolet observations of cool stars. V. The local density of interstellar matter,** *Astrophys. J.* **204,** No. 2, L103-L106 (Mar. 1, 1976).

Key words: interstellar matter; line profiles; stars, late type.

A high-resolution *Copernicus* observation of the chromospheric L$\alpha$ emission line of the nearby (3.3 pc) K dwarf $\epsilon$ Eri sets limits on the velocity, the velocity dispersion, and the density $n_H$ of atomic hydrogen in the local interstellar medium. Analysis shows that the interstellar L$\alpha$ absorption is on the flat portion of the curve of growth. An upper limit of $n_H$=0.12 cm$^{-3}$ is derived. The value of $n_H$ is 0.08±0.04 cm$^{-3}$ if the velocity dispersion parameter $b$=9 km s$^{-1}$, corresponding to a temperature of 5000 K. Also, the interstellar deuterium L$\alpha$ line may be present in the spectrum.

**15912.** Smith, A. J., Read, F. H., Imhof, R. E., **Measurement of the lifetimes of ionic excited states using the inelastic electron-photon delayed coincidence technique,** *J. Phys. B* **8,** No. 17, 2869-2879 (Dec. 1975).

Key words: $CO^+$; $CO_2{}^+$; coincidence; electron impact; ions; lifetime; molecule; $N_2{}^+$; radiative; transition probability.

A modification of the inelastic electron-photon delayed coincidence technique is described which permits the measurement of the lifetimes of ionic excited states. The technique has been applied to measurements in the $N_2{}^+$, $CO^+$ and $CO_2{}^+$ ions, and the essential results are as follows: $N_2{}^+$ $B^2\Sigma_u{}^+$, $v$=0 60.6±0.6 ns; $CO^+$ $B^2\Sigma^+$ 54.3±1.8 ns; $CO_2{}^+$ $\tilde{A}^2\Pi_u$ 108.3±1.4 ns; $CO_2{}^+$ $\tilde{B}^2\Sigma_u{}^+$ 117.4±2.1 ns. Also presented are two coincidence energy-loss spectra of the continua resulting from the excitation of the $\tilde{A}^2\Pi_u$ and $B^2\Sigma_u{}^+$ states respectively of $CO_2{}^+$.

**15913.** Brunt, J. N. H., Read, F. H., **Aberrations in electrostatic lenses,** *J. Phys. E* **8,** No. 12, 1015-1020 (Dec. 1975).

Key words: aberration; electron optics; electron scattering; electrostatic lens; image; low energy.

The approximation of using third order spherical aberration coefficients to represent the combined effects of all the third order aberrations of electrostatic lenses is investigated. For the types of lenses and the object and image conditions often existing in low energy electron scattering experiments the inaccuracy in using this approximation to give an upper limit to the increases in image sizes is of the order of 20 percent.

**15914.** Bennett, H. S., Forman, R. A., **Absorption coefficients of weakly absorbing solids: Theory of a barothermal gas cell,** *Appl. Opt.* **15,** No. 2, 347-352 (Feb. 1976).

Key words: absorption coefficients; barothermal gas cell; gas pressure; highly transparent solids; thermal conduction.

For the case in which a laser beam passes through the weakly absorbing windows of a cell containing a nonabsorbing gas, the temperature profiles in the cell windows and the pressure and temperature profiles in the gas have been calculated. Both the transient response and steady-state behavior of the cell are examined when the barothermal conditions are valid. These calculations suggest that sufficient heat transfers by thermal conduction from the weakly absorbing windows into the gas to produce a measurable pressure rise in the gas. The theory contains the two assumptions that bulk absorption in the window is the mechanism by which energy is transferred from the laser beam to the windows and that the window and adjacent gas are in good thermal contact. Numerical examples for a laser glass and air (nitrogen) are given.

**15915.** Powell, D., Compaan, A., Macdonald, J. R., Forman, R. A., **Raman-scattering study of ion-implantation-produced damage in $Cu_2O$,** *Phys. Rev. B* **12,** No. 1, 20-25 (July 1, 1975).

> Key words: cuprous oxide; implantation; ion; nondestructive testing; Raman scattering; sample characterization; semiconductor.

We present a Raman-scattering study of damage in $Cu_2O$ which we have implanted with 90- and 180-keV Cd ions with doses ranging from $1.5\times10^{11}$ to $1.5\times10^{15}$ $cm^{-2}$. The Raman scattering was performed prior to annealing in order to study primarily the implantation-produced lattice damage. Using two argon-laser lines close to resonance with the 1*S* blue exciton, we observe changes from the pure-crystal Raman spectrum at all implantation doses. The unusual sensitivity of the technique can be interpreted in terms of damage-induced broadening of the intrinsic exciton states.

**15916.** Bennett, H. S., Forman, R. A., **Absorption coefficients in highly transparent solids: Barothermal theory for cylindrical configurations,** *Appl. Opt.* **14,** No. 12, 3031-3037 (Dec. 1975).

> Key words: barothermal; gas pressure; heat diffusion; heat transfer; optical absorption coefficients; transparent materials.

The development of highly transparent solids requires improved methods to measure very low absorption coefficients at laser wavelengths. For the case in which a laser beam passes through a weakly absorbing solid that is surrounded by a confined, nonabsorbing gas, the temperature profiles in the solid and the temperature and pressure profiles in the gas have been calculated. Our calculations suggest that sufficient heat transfers from the solid into the gas to produce an easily detected pressure rise in the gas.

**15917.** Kahn, A. H., **Eddy currents and paramagnetic resonance in anisotropic conductors with application to TTF-TCNQ,** *J. Appl. Phys.* **46,** No. 11, 4965-4969 (Nov. 1975).

> Key words: eddy currents; electron paramagnetic resonance; microwave conductivity; tetrathiofulvalinium-tetracyano-quinodimethane; TTF-TCNQ.

A theoretical analysis of the eddy currents in an anisotropically conducting solid is given. The geometry considered is that of a long rectangular prism with the applied rf field parallel to the length. The solution for the rf field in the solid has been found in terms of a Fourier series, and the dissipated power and average energy stored have been calculated. The changes in resonant frequency and quality factor of a microwave cavity into which a sample has been introduced are expressed in terms of the stored energy and dissipated power. Application is also made to the EPR absorption due to spins uniformly distributed throughout the sample, as outlined by Bloembergen. The asymmetric resonance line is similar to that of the infinite plate, but the peak line anisotropy is reduced as sample dimensions are decreased. The analysis is applied to samples of TTF-TCNQ and the results tabulated for varied sample sizes.

**15918.** Stillman, R. B., **FORTRAN analysis by simple transforms,** *Proc. Computer Science and Statistics East Annual Symposium on the Interface, Los Angeles, CA, Feb. 13-14, 1975,* 7 pages (1975).

> Key words: execution; execution monitoring; FORTRAN analysis; source code instrumenting; static analysis; transforms.

Renewed interest in measuring program execution behavior has led to a number of distinct approaches. Arguments are given for a fairly simple method of modifying FORTRAN source code to collect frequency counts. No symbol table is necessary and only a single reserved name is introduced into the source.

**15919.** Unassigned.

**15920.** Kaufman, V., Sugar, J., **Resonance transition array of Yb IV,** *J. Opt. Soc. Am.* **66,** No. 5, 439 (May 1976).

> Key words: energy levels; spectrum; wavelengths; ytterbium.

Nineteen pairs of lines in the wavelength range of 800-1300 Å were identified as transitions to the two levels of the ground term of Yb IV, $4f^{13}\,{}^2F$. The ${}^2F_{5/2}-{}^2F_{7/2}$ interval is 10214.0 $cm^{-1}$ with an rms deviation of 0.4 $cm^{-1}$.

**15921.** Joy, D. C., Leamy, H. J., Ferris, S. D., Yakowitz, H., Newbury, D. E., **Domain wall image contrast in the SEM,** *Appl. Phys. Lett.* **28,** No. 8, 466-467 (Apr. 15, 1976).

> Key words: backscattered electrons; domain walls; magnetic domains; scanning electron microscope; silicon steel; transformer stee$^1$

Contrast from domain walls in materials with cubic magnetic anisotropy has been observed in scanning electron microscope (SEM) images. This contrast, which is visible in both the backscattered and absorbed current images, with normal electron beam incidence arises from the interaction of the convergent incident electron beam with the domains on either side of the wall.

**15922.** Bower, V. E., Davis, R. S., **A new determination of the Faraday by means of the silver coulometer,** (Proc. 5th Int. Conf. on Atomic Masses and Fundamental Constants, Paris, France, June 1975), Paper in *Atomic Masses and Fundamental Constants* **5,** J. H. Sanders and A. H. Wapstra, Eds., Pt. 12, 578-583 (Plenum Press, New York, NY, 1976).

> Key words: coulometry; electrochemical equivalent; electrochemical equivalent of silver; Faraday; silver.

A determination of the Faraday constant by means of the silver coulometer has been undertaken. The method consists of the direct anodic dissolution of a highly purified silver sample into a perchloric acid-silver perchlorate solution. The dissolution is carried out at constant current. The silver sample is weighed before and after the dissolution.

During the constant-current electrolysis, some solid silver inevitably falls from the electrode to the anode compartment floor. Still in the compartment, this residue is filtered, washed, converted to silver nitrate and reduced cathodically at constant potential. The sum of the current-time integrals for both electrolyses divided by the number of moles represented by the mass difference yields the Faraday constant.

The sources of systematic uncertainty affecting the measurement are the weighing (0.6 ppm), electrical measurements (0.3 ppm) and residue recovery (0.6 ppm), and the uncertainty (2 ppm) of the isotopic abundance ratio of the silver sample. The expected one-standard-deviation random uncertainty for a single measurement is 2.4 ppm and the standard deviation of the mean (8 degrees of freedom) is 0.85 ppm. A preliminary value of the Faraday with a combined uncertainty of 3.2 ppm is reported.

**15923.** Davis, R. M., **Managing computers for public service,** *Gov. Data Syst.*, pp. 17, 19 (July-Aug. 1973).

Key words: computers; data base management; governments; management information systems; public services; security; standards; user groups.

The size of our population, the variety of public services offered and public demands for accountability by government have increased 1) the recordkeeping functions of government, 2) the real-time control functions of government and 3) the amount of management and decision-making related to provision of public services.

Computers and computer technology are what make it possible for government to function effectively in these roles.

Federal, state and local governments must cooperate in a more formal way to properly utilize computers and to effectively resolve computer problems.

Problem areas include computer security, computer standards, management information system usage and performance measurements.

**15924.** Spector, N., Sugar, J., **Analysis of the fourth spectrum of terbium (Tb IV),** *J. Opt. Soc. Am.* **66,** No. 5, 436-438 (May 1976).

Key words: energy levels; ionization energy; spectrum; terbium.

The low-energy level structure of $Tb^{3+}$ has been derived from spectra obtained with a sliding spark light source. The $^7F$ ground term of the $4f^8$ configuration was found as well as all levels of the configurations $4f^75d$, $6s$, and $6p$ built on the $^8S_{7/2}$ core state of $4f^7$. Of the possible 51 lines connecting these levels, 48 were observed. Optimized radial parameters are given for the observed configurations. A value for the ionization energy of 39.37(0.10) eV is derived for $Tb^{3+}$.

**15925.** Maki, A. G., Sams, R. L., **Infrared spectrum of $H^{12}C^{14}N$ and $H^{12}C^{15}N$,** *J. Mol. Spectrosc.* **60,** 57-62 (1976).

Key words: hydrogen cyanide; infrared; molecular spectroscopy; spectroscopy; vibrational fundamentals.

The high-resolution spectrum of $H^{12}C^{14}N$ has been measured near 4870 and 6060 $cm^{-1}$. The following bands have been identified and analyzed: $01^12$-$00^00$, $02^02$-$01^10$, $02^22$-$01^10$, $04^01$-$00^00$, $11^11$-$00^00$, $12^01$-$01^10$, and $12^21$-$01^10$. The C-N stretching fundamental ($\nu_3$) of $H^{12}C^{15}N$ has also been measured near 2100 cm−1. This fundamental is found to be 3 $cm^{-1}$ higher than previously reported. Other bands that have been identified in the $H^{12}C^{15}N$ spectrum are $03^10$-$00^00$, $04^00$-$01^10$, $04^20$-$01^10$, and $01^11$-$01^10$.

**15926.** Juvet, R. S., Jr., Cram, S. P., **Gas chromatography,** *Anal. Chem.* **46,** No. 5, 101R-124R (Apr. 1974).

Key words: column materials; detectors; gas chromatography; theory of chromatography.

The literature in gas chromatography from January 1972 to 1974 is reviewed. Original contributions to the literature are discussed briefly and categorized in the areas of books and reviews, techniques, columns, detectors, identification and analysis, and miscellaneous topics. Special attention is given to those publications which represent fundamental contributions which are basic to the development of the technique.

**15927.** Julienne, P. S., Davis, J., **Cascade and radiation trapping effects on atmospheric atomic oxygen emission excited by electron impact,** *J. Geophys. Res.* **81,** No. 7, 1397-1403 (Mar. 1, 1976).

Key words: airglow; atomic oxygen; cascade radiation; emission cross section; radiation trapping.

The role of cascading in auroral or photoelectron excited atomic oxygen emission is investigated by calculating distorted wave electron impact cross sections for some 24 excited levels in O I. Cascading contributes ~75 percent of the effective emission cross section for 1304 Å and 1356 Å. About 98 percent of the cascade component to these ultraviolet lines is fed through the respective 8446-Å and 7774-Å transitions, with the consequence that the 4368-Å and 3947-Å emissions are very weak. The cascade component to 1304 Å is strongly enhanced in an optically thick medium due to radiation trapping of the lines from the $3s'\ ^3D$, $nd^3D$, and $ns^3S$ ($n \geq 4$) levels to the ground state. The 1304-Å emission cross section appropriate in the optically thick atmosphere is predicted to be a factor of 2 larger than the emission cross section measured in an optically thin laboratory experiment. Consideration of this effect is necessary to understand the measured atmospheric 1304-Å/1356-Å ratio in terms of laboratory cross sections. Several recent atmospheric measurements on electron excited atomic oxygen 1304-Å, 1356-Å, 4368-Å, 7774-Å, and 1152-Å lines appear to be consistent with our calculated results, which imply that the Stone and Zipf (1974) 1304-Å and 1356-Å laboratory cross sections may be systematically too large by as much as a factor of 2.

**15928.** Feldman, A., McKean, W. J., **Improved stressing apparatus for photoelasticity measurements,** *Rev. Sci. Instrum.* **46,** No. 11, 1588-1589 (Nov. 1975).

Key words: photoelasticity; stressing apparatus.

An improved, direct reading stressing apparatus has been constructed for measuring photoelastic constants. Highly uniform stresses are obtained with minimal specimen tilt.

**15929.** Hubbard, C. R., Evans, E. H., Smith, D. K., **The reference intensity ratio, $I/I_c$, for computer simulated powder patterns,** *J. Appl. Crystallogr.* **9,** Part 2, 169-174 (Apr. 1976).

Key words: calculated powder patterns; $I/I_c$; microabsorption effects; quantitative phase analysis; quantitative powder diffraction; reference intensity ratios; systematic errors in powder diffraction.

A scale factor $\gamma$, to convert from the relative to the absolute/relative intensity scale, is readily calculated during computer simulation of powder patterns. Previously used scale factors are related to $\gamma$. The Reference Intensity Ratio, $I/I_c$ ($c$=corundum), is obtained from $\mu$, $q$, and $\gamma$ for the sample and for corundum. Comparing calculated and experimental $I/I_c$ values confirms that microabsorption and primary extinction can be serious experimental aberrations possibly limiting the accuracy to several wt.% in quantitative analysis by powder diffraction.

**15930.** Rosasco, G. J., Roedder, E., Simmons, J. H., **Laser-excited Raman spectroscopy for nondestructive partial analysis of individual phases in fluid inclusions in minerals,** *Science* **190,** 557-560 (Nov. 7, 1975).

Key words: chemical analysis; fluid interactions; geology; minerals; Raman spectroscopy.

Laser-excited Raman spectroscopy has been successfully applied to the identification and partial analysis of solid, liquid, and gaseous phases in fluid inclusions. The procedure is no panacea for problems of analysis of fluid inclusions, but some unique features make it very useful. In particular, the measurement is performed in situ, it is nondestructive, and it can produce qualitative and quantitative data, some of which cannot be obtained otherwise, for samples as small as $10^{-9}$ gram.

**15931.** Feldman, A., Waxler, R. M., Horowitz, D., **Measuring photoelastic and elastic constants of transparent materials by application of static stress,** (Proc. Int. Conf. on Optical Properties of Highly Transparent Solids, Waterville Valley, NH, Feb. 3-5, 1975), Paper in *Optical Properties of Highly Transparent Solids*, S. S. Mitra and B. Bendow, Eds., pp. 517-525 (Plenum Publishing Corp., New York, NY, 1975).

Key words: elastic constants; elasto-optic; photoelasticity; polycrystalline ZnSe; stress optical constants.

The shift of Twyman-Green and Fizeau fringes as a function of applied uniaxial and hydrostatic stress have been measured on transparent solids. These data permit us to calculate all the photoelastic and elastic constants of a material. At the wavelength 10.6 $\mu$m, where fringe shifts are small, we have measured photoelastic constants using a modified Twyman-Green interferometer, which is capable of detecting fringe shifts ~0.01 $\lambda$ by electronic means. Data on polycrystalline ZnSe grown by chemical vapor deposition are presented.

**15932.** Dewey, H. J., **Second-harmonic generation in $KB_5O_8 \cdot 4H_2O$ from 217.1 to 315.0 nm,** *IEEE J. Quantum Electron.* **QE-12,** No. 5, 303-306 (May 1976).

Key words: doubling; laser; potassium pentaborate; u.v. generation.

Second-harmonic generation (SHG) has been observed in $KB_5O_8 \cdot 4H_2O$ (KB5) between 217.1 and 315.0 nm by angle tuning in a single crystal using a single cut. A conversion efficiency of 9.2 percent was observed for type I noncritical phase matching at 217.1 nm for a peak power of 15 kW at 434.2 nm. The nonlinear coefficients $d_{31}$ and $d_{32}$ are estimated to be approximately $1.1 \times 10^{-10}$ ESU ($4.0 \times 10^{-25}$ m/V) and $0.08 \times 10^{-10}$ ESU ($0.29 \times 10^{-25}$ m/V), respectively.

**15933.** Noyce, J. R., Hutchinson, J. M. R., Mann, W. B., Mullen, P. A., **Development of a National Bureau of Standards environmental radioactivity standard: River sediment,** (Proc. Int. Conf. on Environmental Sensing and Assessment, Las Vegas, NV, Sept. 14-19, 1975), Paper in *International Conference on Environmental Sensing and Assessment*, **1,** Session 19-5, 1-9 (Institute of Electrical and Electronics Engineers, Inc., New York, NY, 1976).

Key words: alpha particle; beta particle; gamma-ray; radioactivity; sediment; standard; x ray.

The National Bureau of Standards has developed and produced a radioactivity standard of a fresh-water sediment for use especially in environmental radioactivity measurements around nuclear and coal-burning electric power plants. The radioactivities of 28 nuclides in the sediment have been measured, of which 10 are certified. The development and production of this new Standard Reference Material (SRM 4350) are discussed.

**15934.** Olsen, P. T., Williams, E. R., **Determination of the gyromagnetic ratio of the proton $\gamma_p'$,** (Proc. 5th Int. Conf. on Atomic Masses and Fundamental Constants, Paris, France, June 1975), Paper in *Atomic Masses and Fundamental Constants* **5,** J. H. Sanders and A. H. Wapstra, Eds., Part 11, 538-544 (Plenum Press, New York, NY, 1976).

Key words: fine structure constant; fundamental constants; gyromagnetic ratio of the proton.

The primary purpose of this paper is to present our latest value of $\gamma_p'$ and the resultant value of the fine structure constant, $\alpha$. The most accurate (2 ppm) and most recent value for $\gamma_p'$ was reported at AMCO-4. That NBS value differs from other earlier values measured at several other national laboratories by about 8 ppm. To clarify this situation and to improve the earlier NBS value, we have spent the interim years developing an alternate, more accurate approach to the dimensional metrology problem. This approach now allows us to measure all critical dimensions by electromagnetic techniques and a simple one dimensional laser measurement. The only important dimensional measurement that has not been made by magnetic methods is the average diameter of the solenoid. We now envision a practical technique to realize this quantity by electromagnetic means. The diameter has, however, been measured by conventional methods and is of sufficient accuracy, when combined with all of the other uncertainties in the experiment, to provide a 0.42 ppm value for $\gamma_p'$. Since AMCO-4, the other experiments involved in the relationship $\alpha = C_0 \, \gamma_p'^{1/2}$ **have been improved so that $C_o$ is known to be** better than 0.05 ppm. Therefore, our present results provide a 0.21 ppm value of $\alpha$.

**15935.** Bennett, H. S., Forman, R. A., **An alternative way to determine absorption coefficients in highly transparent solids: Theory,** (Proc. Int. Conf. on Optical Properties of Highly Transparent Solids, Waterville Valley, NH, Feb. 3-5, 1975), Paper in *Optical Properties of Highly Transparent Solids*, S. S. Mitra and B. Bendow, Eds., pp. 451-459 (Plenum Publishing Corp., New York, NY, 1975).

Key words: calorimetry; laser; laser materials; optical absorption.

The development of highly transparent solids requires improved methods to measure very low absorption coefficients at laser wavelengths. We have calculated the temperature profiles in the solid and the temperature and pressure profiles in the gas when a laser beam passes through a weakly absorbing solid which is surrounded by a confined and nonabsorbing gas. Our calculations suggest that sufficient heat transfers from the solid to the gas to produce a detectable pressure rise in the gas.

**15936.** Bennett, H. S., Forman, R. A., **Measuring absorption coefficients of highly transparent solids by photoacoustic methods: Cylindrical configurations,** (Proc. 5th Conf. on Infrared Laser Window Materials, Las Vegas, NV, Dec. 1-4, 1975), Paper in *Proceedings of the 5th Conference on Infrared Laser Window Materials*, pp. 628-637 (Air Force Materials Laboratory, Wright-Patterson Air Force Base, OH, Feb. 1976).

Key words: absorption coefficients; cylindrical configurations; gas pressure; heat transfer; photoacoustic; transparent materials.

The development of highly transparent solids for fiber optics, integrated optics, and high-power lasers requires improved methods to measure very low absorption coefficients. A photoacoustic theory, which includes viscosity, has been developed for the case in which a laser beam, modulated at angular frequency $\omega$ passes through a weakly absorbing solid which is surrounded by a confined, nonabsorbing gas. The numerical predictions of this photoacoustic theory suggest that for sufficiently low frequencies and high ambient gas pressures, enough heat transfers from the solid to the gas to produce a detectable acoustic pressure signal at angular frequency $\omega$ in the gas. They also indicate that an absorbing layer at the solid-gas interface is not an essential mechanism for producing these detectable acoustic pressure signals. The model assumes that bulk absorption in the solid is the mechanism by which energy is transferred from the laser beam. Numerical examples for a typical laser glass are given.

**15937.** Feldman, A., Horowitz, D., Waxler, R. M., **Piezo-optical constants in the infrared,** (Proc. 5th Conf. on Infrared Laser

Window Materials, Las Vegas, NV, Dec. 1-4, 1975), Paper in *Proceedings of the 5th Conference on Infrared Laser Window Materials*, pp. 944-951 (Air Force Materials Laboratory, Wright-Patterson Air Force Base, OH, Feb. 1976).

Key words: elasto-optical constants; infrared materials; KCl; laser windows; photoelasticity; piezo-optical constants; refractive index.

The piezo-optical constants $q_{11}$, $q_{12}$, and $q_{44}$, and the elasto-optical constants $p_{11}$, $p_{12}$, and $p_{44}$, have been obtained at 10.6 $\mu$m for pure KCl grown by the reactive atmosphere process and for KCl nominally doped with 1 percent KI. Within experimental error, the coefficients of the two materials agree. Negligible dispersion is found for $q_{11}$, $q_{12}$, $p_{11}$, and $p_{12}$ between the visible and 10.6 $\mu$m while a small dispersion is found for $q_{44}$ and $p_{44}$.

**15938.** Feldman, A., Malitson, I. H., Horowitz, D., Waxler, R. M., Dodge, M. J., **Optical properties of polycrystalline zinc selenide,** (Proc. 4th Annual Conf. on Infrared Laser Window Materials, Tucson, AZ, Nov. 18-20, 1974), Paper in *Proceedings of the 4th Annual Conference on Infrared Laser Window Materials*, pp. 118-129 (Air Force Materials Laboratory, Wright-Patterson Air Force Base, OH, Jan. 1975).

Key words: chemical vapor deposited ZnSe; elastic compliance; elastic constants; polycrystalline ZnSe; refractive index; stress-optic constants; temperature coefficient of index; thermal expansion; ZnSe.

We have measured the following parameters of chemical vapor deposited polycrystalline ZnSe (CVD ZnSe): Refractive index and change of index of refraction with temperature (dn/dT) over the wavelength 0.5 $\mu$m to 18 $\mu$m using the method of minimum deviation; the coefficient of linear thermal expansion and dn/dT at 10.6 $\mu$m using Fizeau interferometry; and the elastic moduli and photoelastic moduli using Fizeau and Twyman-Green interferometry. A sensitive technique has been developed for measuring stress-optical constants of materials that exhibit a small stress-optical effect.

**15939.** Antonucci, J. M., Bowen, R. L., **Dimethacrylates derived from hydroxybenzoic acids,** *J. Dent. Res.* **55,** No. 1, 8-15 (1976).

Key words: acrylic resins; chemistry; composite resins; dental materials; hydroxybenzoic acids; pit and fissure sealants; preventive dental materials.

Aromatic ether-ester dimethacrylates were synthesized directly from the three isomeric hydroxybenzoic acids and 2-bromoethyl methacrylate by facile condensation reactions. The three crystalline monomers, on proper admixture, form a liquid ternary eutectic.

**15940.** Gilsinn, D. E., **The method of averaging and domains of stability for integral manifolds,** *SIAM J. Appl. Math.* **29,** No. 4, 628-660 (Dec. 1975).

Key words: averaging; differential equations; domains of stability; integral manifold; Liapunov functions; stability.

Liapunov's direct method is a standard and effective approach to computing the domain of stability (or region of attraction) of an autonomous ordinary differential equation. In this paper the author investigates domains of stability of integral manifolds of solutions generated by nonlinear mechanical and electrical oscillatory systems with many degrees of freedom. These manifolds are families of solutions that exhibit stronger stability properties than individual solutions. The problem of estimating the domain of stability of an asymptotically stable integral manifold is reduced to computing the domain of stability of an associated autonomous system of differential equations. This is done by applying the method of averaging to the system generating the integral manifold thus removing angular and time dependences. The stability region of this associated system is then computed and a result is established showing that this region is contained in the stability region of the original system. Several examples, including a coupled van der Pol system of oscillators, are considered.

**15941.** Johnson, P. M., **The multiphoton ionization spectrum of benzene,** *J. Chem. Phys.* **64,** No. 10, 4143-4148 (May 15, 1976).

Key words: benzene; electronic structure; multiphoton ionization.

A resonance seen in the multiphoton ionization spectrum of benzene at 391.4 nm is identified as a two-photon resonance with a bound state at 51 085 cm$^{-1}$. This state has probable symmetry $^1E_{1g}$ or $^1E_{2g}$ as indicated by an active $e_{2g}$ vibration. No other allowed two-photon transitions are seen below this energy. Three-photon resonances with the Rydberg states of benzene are seen and compared to the one-photon absorption spectrum. The great similarity indicates a strong $^1A_{1g}$ component in the two-photon virtual state. Two-photon resonances with the $^1B_{2u}$ state agree with two-photon fluorescence excitation spectra but show no diminution above the energy where fluorescence is quenched.

**15942.** Dunn, G. H., **Electron impact ionization,** Proc. Int. Conf. on Heavy Ion Sources, Gatlinburg, TN, Oct. 27-30, 1975, *IEEE Trans. Nucl. Sci.* **NS-23,** No. 2, 929-933 (Apr. 1976).

Key words: electron-impact; ionization; ionization mechanisms; ions; review.

A brief review is given of electron impact ionization of atoms and atomic ions. As cross section measurements have been made for only about 1 percent of the atom and ion targets, comparisons are made between some of the recent measurements that have been made for ions and with calculations. Both semi-empirical and more "legitimate" calculations are compared. It is emphasized that mechanisms other than direct ionization can play an important role in ionization, so that predictions of cross sections should be considered cautiously.

**15943.** Frederikse, H. P. R., Hosler, W. R., Armstrong, A. J., Negas, T., **Spinels for MHD-electrodes,** (Proc. 15th Symp. on Engineering Aspects of Magnetohydrodynamics, The University of Pennsylvania, Philadelphia, PA, May 24-26, 1976), Paper in *Proceedings of the 15th Symposium on Engineering Aspects of Magnetohydrodynamics, Session II.2*, 1-4 (Dept. of Mechanical Engineering, University of Mississippi, University, MS, 1976).

Key words: durability; electrical conductivity; high temperature; MHD-power generation; spinel structure.

Solid solutions of Mg-chromite and Mg-aluminate spinels and magnetite appear to be promising materials for MHD electrodes. This paper presents high temperature electrical conductivity data and discusses some structural and chemical properties of these compounds. The Mg-Al-spinels show good resistance to seed corrosion, while the Mg-Cr-spinels appear to stand up well in a slagging environment. A third spinel, composed of $Fe_3O_4$ and $Co_3O_4$, is a very good electrical conductor and has potential as a lead-out material.

**15944.** Wasik, S. P., Brown, R. L., Minor, J. I., Jr., **Partition coefficients and solubility measurements of dimethylmercury in fresh and sea water over a temperature range 0-25 °C,** *J. Environ. Sci. Health—Environ. Sci. Eng.* **A11,** No. 1, 99-105 (1976).

Key words: dimethylmercury; partition coefficient; sea water; solubility.

The partition coefficients and solubilities of dimethylmercury in distilled and sea water over a temperature range 0-25 °C, have been measured using a head-space technique.

**15945.** Hubbard, C. R., Mauer, F. A., **Precision and accuracy of the Bond method as applied to small spherical crystals,** *J. Appl. Cryst.* **9,** Part 1, 1-8 (Feb. 1976).

Key words: Bond method; generalization of silicon; lattice, parameter of; lattice parameters; precision.

The Bond method for accurate lattice-parameter measurements has been applied to spheroidal crystals smaller in diameter than the incident beam. By measuring both $\bar{h}$ and $\bar{h}$ to reduce the effects of mis-centering and using a circle accurate to ±0.001°, a precision of a few parts per million can be attained. The accuracy of the method has been tested by measuring the lattice parameter of vacuum float-zone refined silicon by the conventional Bond method (using large, flat specimens) and by the modified method (using spheroidal specimens 0.25 mm in diameter). The results indicate that in addition to the usual corrections for refraction, emission-line asymmetry, and vertical divergence, a correction is required for changes in the asymmetric diffraction profile caused by the combined effects of horizontal divergence and absorption in the sphere. The correction is approximately 15 p.p.m. or 0.000079 Å in the case of the Si spheres and an instrument having a horizontal divergence of ±0.0013 rad. The corrected lattice parameter agrees within 4 p.p.m. with results obtained by the conventional method. These results demonstrate the feasibility of making precise and accurate measurements on many materials that are not available in the form of large single crystals.

**15946.** Williams, J. G., Dicke, R. H., Bender, P. L., Alley, C. O., Carter, W. E., Currie, D. G., Eckhardt, D. H., Faller, J. E., Kaula, W. M., Mulholland, J. D., Plotkin, H. H., Poultney, S. K., Shelus, P. J., Silverberg, E. C., Sinclair, W. S., Slade, M. A., Wilkinson, D. T., **New test of the equivalence principle from lunar laser ranging,** *Phys. Rev. Lett.* **36,** No. 11, 551-554 (Mar. 15, 1976).

Key words: equivalence principle; general relativity; gravitation; lunar orbit; moon.

An analysis of six years of lunar-laser-ranging data gives a zero amplitude for the Nordtvedt term in the Earth-Moon distance yielding the Nordtvedt parameter $\eta=0.00 \pm 0.03$. Thus, Earth's gravitational self-energy contributes equally, ±3 percent, to its inertial mass and passive gravitational mass. At the 70 percent confidence level this result is only consistent with the Brans-Dicke theory for $\omega > 29$. We obtain $|\beta - 1| \lesssim 0.02$ to 0.05 for five-parameter parametrized post-Newtonian theories of gravitation with energy-momentum conservation, or $|\beta - 1| \lesssim 0.01$ if only $\beta$ and $\gamma$ are considered.

**15947.** Taylor, B. N., Cohen, E. R., **Present status of the fundamental constants,** (Proc. 5th Int. Conf. on Atomic Masses and Fundamental Constants, Paris, France, June 1975), Paper in *Atomic Masses and Fundamental Constants* **5,** J. H. Sanders and A. H. Wapstra, Eds., Part 14, 663-673 (Plenum Press, New York, NY, 1976).

Key words: data analysis; fundamental constants; least-squares adjustments; quantum electrodynamics.

Since the completion of the authors' 1973 least-squares adjustment of the fundamental constants, and its subsequent official adoption for international use by the CODATA Task Group on Fundamental Constants and the 8th CODATA General Assembly, several relevant experiments and theoretical calculations have been completed. These include determinations of the Avogadro, Rydberg, Faraday and gas constants, the speed of light, a revised calculation of the sixth order contribution to the theoretical expression for the anomalous magnetic moment of the electron, and an improved calculation of the fine-structure in atomic helium. It is the purpose of this paper to examine the effect of these new results, and in as far as possible the effect of the most important relevant new experiments and calculations to be reported at this Conference, on the recommended output values of our 1973 least-squares adjustment.

**15948.** Mann, W. B., Schima, F. J., Unterweger, M. P., **Radioactivity standards of the Noble gases,** (Proc. Symp. on Noble Gases, Las Vegas, NV, Sept. 24-28, 1973), Chapter IV in *Noble Gases,* R. E. Stanley and A. A. Moghissi, Eds., ERDA TIC as Conf. 730915, pp. 144-153 (1975).

Key words: argon-37; direct standardization; environmental radioactivity; internal gas counters; isotope separator; krypton-85; proportional counters; radioactivity standardization; xenon-133, 131m.

The National Bureau of Standards gas-counting equipment is described. This consists of matched, length-compensated copper and stainless steel internal gas counters, which can be used in the proportional or Geiger-Mueller regions. The data acquisition and processing is by means of a computer-based multichannel analyzer. Methods for preparing relative standards based on measurements with ion chambers and fixed-geometry solid-state detectors are discussed. Noble-gas standards for argon-37, krypton-85, xenon-131m, and xenon-133 have so far been prepared, the last involving purification on the NBS isotope separator.

**15949.** Kurylo, M. J., Braun, W., **Flash photolysis resonance fluorescence study of the reaction $Cl+O_3 \rightarrow ClO+O_2$ over the temperature range 213-298 K,** *Chem. Phys. Lett.* **37,** No. 2, 232-235 (Jan. 15, 1976).

Key words: chlorine atoms; kinetics; ozone; resonance fluorescence; stratosphere.

Rate constants for the removal of Cl atoms in the reaction $Cl+O_3 \rightarrow ClO+O_2$ were measured by the flash photolysis resonance fluorescence technique over the temperature range 213-298 K. The rate constant is given by the Arrhenius expression $(2.94 \pm 0.49) \times 10^{-11} \exp[-(298 \pm 39)/T]$ in units of $cm^3$ $molecule^{-1}$ $s^{-1}$. Comparison with recent results from other laboratories are presented.

**15950.** Caswell, R. S., Coyne, J. J., **Microdosimetric spectra and parameters of fast neutrons,** *Proc. 5th Symp. on Microdosimetry, Verbania Pallanza, Italy, Sept. 22-26, 1975,* **EUR 5452** d-e-f, pp. 97-126 (1976).

Key words: energy deposition spectra; fast neutrons; initial spectra; microdosimetric parameters; nuclear data; slowing-down spectra.

Definitions and relationships of microdosimetric spectra and parameters for fast neutrons are discussed in the continuous slowing-down approximation (c.s.d.a.). Regions of validity of various calculational methods, including Monte-Carlo and c.s.d.a. are considered. Calculations and measurements of energy deposition spectra are compared. Calculations of microdosimetric parameters (from the energy deposition spectra) are compared with determinations of parameters from experimental spectra. Future needs for experimental energy deposition measurements, nuclear data, and charged particle stopping-power data are considered.

**15951.** Brandt, M. A., Truhlar, D. G., **Test of the infinite-order**

**sudden approximation for electron scattering at intermediate energy,** *Chem. Phys.* **13,** 461-467 (1976).

Key words: close coupling calculations; cross sections; differential cross sections; elastic scattering; electron scattering; momentum transfer; nitrogen molecules; rotational excitation; scattering theory; sudden approximation.

Converged infinite-order sudden (IOS) approximation calculations for electron scattering by $N_2$ at 30 eV are compared to converged close-coupling calculations. The IOS approximation is most accurate for the total scattering cross section.

**15952.** Cornell, D., Tsang, W., **Thermal decomposition of trimethylene sulfone and 3-methyl sulfolane,** *Int. J. Chem. Kinet.* **VII,** 799-806 (1975).

Key words: pyrolysis; $SO_2$; trimethylene sulfone; 3-methyl sulfolane.

Trimethylene sulfone and 3-methyl sulfolane have been pyrolyzed using a modification of the toluene flow method and a comparative rate technique. The main decomposition reactions are

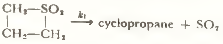

and

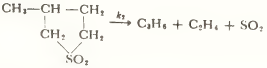

where $k_1=10^{16.1\pm0.3}\exp(-28{,}100\pm500/T)$ sec$^{-1}$ and $k_2=10^{16.1\pm0.4}\exp(-33{,}200\pm750/T)$ sec$^{-1}$.

**15953.** Shih, A., Parsegian, V. A., **Van der Waals forces between heavy alkali atoms and gold surfaces: Comparison of measured and predicted values,** *Phys. Rev. A* **12,** No. 3, 835-841 (Sept. 1975).

Key words: alkali atoms; atomic beam deflection; atom surface potential; gold surfaces; Lifshitz theory; Van der Waals forces.

The Van der Waals potentials between heavy alkali-metal atoms (Cs, Rb, K) and gold surfaces have been investigated by the atomic-beam-deflection technique. The result is consistent with a potential of the form $V(R)=-k/R^3$. The observed interaction constant $k$ is 7.0±0.29 D$^2$, 6.04±0.30 D$^2$, and 5.10±0.62 D$^2$ for Cs, Rb, and K, respectively. These values are smaller than the predictions based on all available theories. At best there is agreement within 60 percent for estimates based on the macroscopic continuum theory of Lifshitz. Other models disagree with measurements by factors of three (200% difference) or more.

**15954.** Epstein, M. S., Rains, T. C., O'Haver, T. C., **Wavelength modulation for background correction in graphite furnace atomic emission spectrometry,** *Appl. Spectrosc.* **30,** No. 3, 324-329 (May-June 1976).

Key words: graphite furnace atomic emission spectrometry; repetitive wavelength scanning; wavelength modulation.

The use of wavelength modulation for background correction in graphite furnace atomic emission spectrometry is shown to improve detection limits in some cases by several orders of magnitude and to increase its applicability to sample analysis. An HGA-2100 graphite furnace atomizer is used in conjunction with a 3/4-m monochromator equipped for wavelength modulation. A discussion of analytical growth curves, detection limits, scatter, and optimization of signal/noise ratio is presented. Copper is analyzed in botanical samples and the results are compared to analysis by atomic absorption and molecular absorption spectrophotometry.

**15955.** Newman, M., **On a theorem of Čebotarev,** *Linear and Multilinear Algebra* **3,** 259-262 (1976).

Key words: compounds; induced matrices; Kronecker powers; roots of unity; Schur matrix.

A new proof is given of the theorem that no submatrix of the $p\times p$ matrix $S=(\zeta^{(i-1)(j-1)})$ is singular, where $\zeta$ is a primitive $p$th root of unity and $p$ is a prime. Some related results are also discussed.

**15956.** Berger, H., **Nondestructive evaluation: A review of nuclear methods,** (Proc. 22nd Int. Instrumentation Symp. on Aerospace Test Measurement, San Diego, CA, May 25-27, 1976), Paper in *22nd International Instrumentation Symposium,* B. Washburn, Ed., **13,** 427-437 (Instrument Society of America, Pittsburgh, PA, 1976).

Key words: neutron activation analysis; neutron gaging; neutron radiography; nondestructive evaluation; nuclear; radioactive tracers.

Nuclear methods for nondestructive evaluation (NDE) are reviewed. Gamma ray and neutron sources for NDE are tabulated and described. Nuclear NDE methods described include: (1) neutron and x-radiography and gaging, (2) scatter and secondary radiation techniques with emphasis on x-ray devices for analysis by characteristic x-ray emission and neutron moisture gages, (3) neutron activation analysis, and (4) radioactive tracer methods. Sensitivities and limits of detection are indicated and several examples are used to illustrate the methods. It is concluded that the nuclear method for NDE offers wide application potential and excellent sensitivity.

**15957.** Domalski, E. S., Tsang, W., **Assessing the hazard potential of chemical substances,** *Proc. 4th Int. Symp. on Transport of Hazardous Cargoes by Sea and Inland Waterways, Jacksonville, FL, Oct. 26-30, 1975,* pp. 259-274 (National Academy of Sciences, Washington, DC, 1975).

Key words: activation energy; bond dissociation energy; computer programs; explosive sensitivity tests; heat of decomposition; oxygen balance.

The ability to identify and specify the thermal instability of chemical substances has been appraised as a result of examining certain test methods used to measure explosive sensitivity, and certain computer programs designed to estimate reaction hazards from a thermochemical approach. The bond dissociation energy emerges as the parameter giving the best correlation with material sensitivity. The computer programs overemphasize explosive power as opposed to explosive sensitivity and label many compounds hazardous when they are not. At present, we recommend that regulations specifying the handling and transport of commodities should follow the concept of self-reactivity based upon functional groups (i.e., nitro, nitramine, peroxide, azide, etc.).

**15958.** Scheer, M. D., **The early afterglow in a pulsed helium discharge,** (Proc. XII Int. Conf. on Phenomena in Ionized Gases, Eindhoven, The Netherlands, Aug. 18-22, 1975), Paper in *Proceedings XII International Conference on Phenomena in Ionized Gases,* J. G. A. Holscher and D. C. Schram, Eds., p. 82 (North-Holland Publishing Co., The Netherlands, 1975).

Key words: collision model; early afterglow; electron temperature; helium metastables; helium plasma; pulse discharge.

Observations have been made of the concentrations of He($2^3S$) metastables, ion-electron pairs, and electron temperatures during the first 500 $\mu$s of a decaying helium plasma after excitation by 1.5 kV, 50 $\mu$s pulse. It was found that during this early afterglow thermal and particle diffusion processes are negligible, the electron and gas temperatures are virtually constant, while the metastable and charged particle concentrations decay in accordance with a collision model using recently evaluated rate coefficients.

15959. Lamotte, M., Dewey, H. J., Ritter, J. J., Keller, R. A., **Laser induced photochemical enrichment of chlorine isotopes,** (Proc. 27th Int. Meeting of the Societe De Chimie Physique, on Lasers in Physical Chemistry and Biophysics, Thiais, France, June 17-20, 1975), Paper in *Lasers in Physical Chemistry and Biophysics,* J. Joussot-Dubien, Ed., pp. 153-164 (Elsevier Scientific Publishing Co., Amsterdam, The Netherlands, 1975).

Key words: chlorine isotope; isotope separation; laser-induced reaction; laser irradiation; photochemical reaction; thiophosgene.

There has been a lot of interest displayed in laser based isotope separation schemes. This interest lies in both uranium for defense and energy needs, and in the light isotopes for scientific, medical, and environmental studies. The principal advantage of a laser based process is that, in contrast to most enrichment schemes, energy is supplied only to the isotope of interest. An overview of the laser processes with emphasis on the use of visible lasers to enhance bimolecular, photochemical reactions is presented. Data on the successful enrichment of chlorine isotopes by the photochemical reaction between thiophosgene and diethoxyethylene is used to illustrate the major points.

15960. McLaughlin, W. L., **Radiation dosimeter colour,** Article in *Encyclopaedic Dictionary of Physics,* J. Thewlis, Ed., Suppl. 5, 248-251 (Pergamon Press Ltd., Oxford, England, 1975).

Key words: colour dosimeters; dosimetry; dyes; glass; plastics; radiation; radiochromic dyes; spectrophotometry.

Large doses (kilorads or greater) of ionizing radiation are known to change the hue, shade, or colour saturation of many substances. Just as extended exposure to sunlight causes some plastics to darken or turn slightly yellow or brown, and other materials to bleach or change colour ionizing radiations can cause even more radical changes in plastics, glasses, and certain dyed substances. As long as a critical portion of the resulting absorption spectrum or reflection spectrum is sufficiently stable and can be measured spectrophotometrically in a reproducible way, the material can be a useful dosimeter. The dosimetric response is given in terms of the change in optical transmission or reflection density, or change in percent transmittance or reflectance, at a given wavelength of light, as a function of the radiation absorbed dose in the material of interest. With this approach, any material susceptible to permanent radiation bleaching, colour change, or radiolytic darkening may serve as a colour radiation dosimeter.

15961. Bander, M., Shaw, G. L., Thomas, P., Meshkov, S., **Exotic mesons and $e^+e^-$ annihilation,** *Phys. Rev. Lett.* **36,** No. 13, 695-697 (Mar. 29, 1976).

Key words: $e^+e^-$ annihilation; exotic mesons; meson classification; $\psi$ and $\chi$ particles; $1^{--}$ states.

Recent experiments at SPEAR indicate an unexpectedly large number of $1^{--}$ states in the energy range 3.9-4.4 GeV. We show how the existence of exotic $\bar{c}q\bar{c}q$ mesons can account for these states as well as the rise in $R$ and the missing $\psi(3.7)$ decays. The width of these states does not require that they lie above the, as yet unobserved, $D\bar{D}$ threshold. Predictions of the model are readily testable.

15962. Karl, G., Meshkov, S., Rosner, J. L., **Symmetries, angular distributions in $\psi' \rightarrow \gamma\chi \rightarrow \gamma\gamma\psi$, and the interpretation of the $\chi(3400-3550)$ levels,** *Phys. Rev. D* **13,** No. 5, 1203-1215 (Mar. 1, 1976).

Key words: angular distributions; gamma-gamma correlations; quark models; symmetries; $\psi$ particles; $\chi$ particles.

Recently a family of particles (to be denoted $\chi$) has been discovered between 3400 and ~3550 MeV. A formalism is presented for analysis of the decays $\psi'(3684) \rightarrow \gamma\chi \rightarrow \gamma\gamma\psi$ or $\gamma 0^- 0^-$ This formalism is sufficiently general to allow for transitions of several multipolarities. Previous treatments have been restricted to the assumption that the above transitions are purely $E1$ if $J^P(\chi) = 0^+$, $1^+$, and $2^+$. Here (with some model-dependent motivation) this restriction is removed. The predictions of specific heavy-quark models for the $\chi$ states are then discussed. On the basis of the single-quark-transition picture (the Melosh transformation), it is anticipated that the state $\chi(3410)$ will be identified as a ${}^3P_0$ $q\bar{q}$ level, and will be found to have $J^{PC} = 0^{++}$. It is also anticipated that the ${}^3P_2$ level should be fairly prominent.

15963. Keery, W. J., Leedy, K. O., Galloway, K. F., **Electron beam effects on microelectronic devices,** (Proc. 9th Annual Scanning Electron Microscope Symp., Toronto, Canada, Apr. 5-9, 1976), Paper in *Scanning Electron Microscopy,* O. Johari, Ed., **1,** Part IV, 507-514 (IIT Research Institute, Chicago, IL, 1976).

Key words: electron beam damage; electron beam energy deposition; ionizing radiation; microelectronic devices; scanning electron microscopy.

Scanning electron microscope (SEM) operators and the users of SEM information should be aware of the effects of the electron beam on microelectronic devices. An SEM examination is not necessarily a nondestructive test; device electrical parameters may be severely degraded. The effects of the SEM exposure are related to the energy deposited by the electron beam in the critical oxide layers of the device being examined. This deposited energy manifests itself electrically through the accumulation of trapped charge in the oxide and the generation of surface states at the oxide-silicon interface. These phenomena result in increased leakage currents and decreased gain for bipolar devices and altered threshold voltages and switching currents for metal-oxide-semiconductor (MOS) devices. By reviewing the physics and phenomenology of the effects of the electron beam on semiconductor device electrical parameters and relating these effects to the parameters of SEM exposure, it is shown that if a device is expected to function properly electrically after SEM examination, a careful analysis strategy should be developed before the device is placed in the SEM specimen chamber.

15964. Shoenfeld, P. S., DeVoe, J. R., **Statistical and mathematical methods in analytical chemistry,** *Anal. Chem.* **48,** No. 5, 403R-411R (Apr. 1976).

Key words: analytical chemistry; curve fitting; data reduction; feature selection; multivariate analysis; optimization techniques; pattern recognition; signal processing; spectral resolution; statistics.

A literature survey covering articles on mathematical and statistical methods in the analytical chemistry literature in the period October 1971 to January 1976. Areas discussed include spectral resolution, characterization and evaluation of the measurement process, optimization techniques, pattern recognition, and digital signal processing.

**15965.** Newman, M., **Polynomials in a matrix,** *Linear and Multilinear Algebra* **3,** 263-266 (1976).

Key words: direct sums; formal power series; Jordan canonical form; permutation congruence; polynomials.

Let $A$ be a matrix, $p(x)$ a polynomial. Put $B=p(A)$. It is shown that necessary and sufficient conditions for $A$ to be a polynomial in $B$ are (i) if $\lambda$ is any eigenvalue of $A$, and if some elementary divisor of $A$ corresponding to $\lambda$ is nonlinear, then $p'(\lambda) \neq 0$; and (ii) if $\lambda$, $\mu$ are distinct eigenvalues of $A$, then $p(\lambda)$, $p(\mu)$ are also distinct. Here all computations are over some algebraically closed field.

**15966.** Kuehner, E. C., Cassatt, W. A., **A laser microphotometer for determining uniformity of particulate deposits on membrane filters,** *Appl. Spectrosc.* **30,** No. 3, 289-290 (May-June 1976).

Key words: laser; membrane filters; microphotometer; particulate deposits.

An apparatus for determining the uniformity of a layer of fine particles deposited on a membrane filter is described. A transmission scan of a laser beam across the filter deposit is a measure of the uniformity of the deposit layer. Quantitative estimates, with an accuracy of approximately 10 percent, of areal densities are inferred by calibration against reference deposits of ground orchard leaves on membrane filters.

**15967.** Yakowitz, H., Newbury, D. E., **A simple analytical method for thin film analysis with massive pure element standards,** (Proc. 9th Annual Scanning Electron Microscope Symp., Toronto, Canada, Apr. 5-9, 1976), Paper in *Scanning Electron Microscopy*, O. Johari, Ed., **1,** Part 1, 151-162 (IIT Research Institute, Chicago, IL, 1976).

Key words: distribution functions; electron probe microanalysis; semiconductor materials; thin films; x-ray fluorescence; x-ray microanalysis.

Conventional electron probe microanalysis quantitative techniques are not applicable to the case of thin film specimens. The situation is further complicated if the specimen lies upon a substrate. Typically, neither film thickness nor film composition is known. A number of investigators have devised schemes to deal with such specimens; these range from complex mathematical formulations to full scale Monte Carlo approximations. This paper offers a simple technique for determining composition and thickness which is based on empirical expressions for the distribution of x-ray generation in depth in the specimen; this distribution will be referred to as $\phi(z)$.

We have formulated an expression for $\phi(z)$ as a combination of a parabola and an exponential. The choice of parameters defining this expression is based on experimental $\phi(z)$ curves as well as Monte Carlo calculations. The required information for thin film analysis is the ratio of photons emitted from the film to photons emitted from the standard. (In our $\phi(z)$ model, mass fraction is the area under the $\phi(z)$ curve up to the film thickness divided by total area under the curve, where the shape of the entire curve has been corrected for absorption effects.) We have tested our model with a variety of data and have found, it produces results that are in good agreement with experimental findings.

**15968.** Dragoo, A. L., Paule, R. C., **Evaporation, diffusion and convection in containerless melts at low gravity,** *AIAA J.* **14,** No. 2, 135-136 (Feb. 1976).

Key words: $Al_2O_3$; complex equilibria; convective diffusion; evaporative rate; purification (evaporative); solutal-capillary; thermal capillary convection; vacuum vaporization.

In the preparation of ultrapure refractory materials, contamination from containers is a major problem. Space with its zero gravity, high vacuum conditions offers an opportunity for containerless purification of materials. Processes which often involve complex chemical equilibria can be used to convert impurities to forms that can be distilled off. Thermodynamic calculations have been modified to describe evaporative purification into vacuum. The contributions of diffusion and of Marangoni convection to mass transfer rates in the bulk liquid have been estimated. Examples of evaporative purification will be given.

**15969.** Feldman, A., Horowitz, D., Waxler, R. M., **Stress-optic measurements in the infrared,** (Proc. Third Conf. on High Power Infrared Laser Window Materials, Hyannis, MA, Nov. 12-14, 1973), Paper in *Third Conference on High Power Infrared Laser Window Materials. II. Materials*, C. A. Pitha, A. Armington, and H. Posen, Eds., AFCRL-TR-74-0085(II), Special Reports, No. 174, pp. 403-409 (Air Force Cambridge Research Laboratories, Bedford, MA, Feb. 14, 1974).

Key words: crystals; damage; glass; infrared; interferometry; lasers; photoelasticity; polarimetry.

Twyman-Green and Fizeau interferometers have been constructed for measuring absolute stress-optic coefficients in infrared materials at 1.15 μm and 10.6 μm. The specimen, in the form of a rectangular parallelepiped, is compressed uniaxially in a rectangular frame screw clamp. The stress-optic coefficients are calculated from the measurement of fringe shifts as a function of stress. Preliminary measurements are presented for a chalcogenide glass.

**15970.** Parks, S. I., Johannesen, R. B., **An algorithm for automatic correction of quadrature phase detector outputs,** *J. Magn. Reson.* **22,** 265-267 (1976).

Key words: computer program; Fourier transform NMR; homonuclear lock; phase adjustment; phase correction algorithm; quadrature.

A computer algorithm is described which automatically corrects phase and amplitude errors when quadrature phase detectors are used in Fourier transform NMR. A procedure for averaging unlocked scans in the time domain is discussed.

**15971.** Bennett, H. S., Forman, R. A., **Absorption coefficients of highly transparent solids: Photoacoustic theory for cylindrical configurations,** *Appl. Opt.* **15,** No. 5, 1313-1321 (May 1976).

Key words: absorption coefficients; heat diffusion equations; highly transparent solids; hydrodynamic equations; optical materials; photoacoustic method.

The development of highly transparent solids for fiber optics, integrated optics, and high power lasers requires improved methods to measure very low absorption coefficients. For the case in which a laser beam, modulated at angular frequency $\omega$, passes through a weakly absorbing solid which is surrounded by a confined, nonabsorbing gas, the temperature profiles in the solid and the temperature and pressure profiles in the gas have been calculated. The calculations suggest that for sufficiently low frequencies and high ambient gas pressures, enough heat transfers from the solid to the gas to produce a detectable acoustic-pressure signal at angular frequency $\omega$ in the gas. They also indicate that an absorbing layer at the solid-gas interface is not an essential mechanism for producing these detectable acoustic pressure signals. The model assumes that bulk absorption in the solid is the mechanism by which energy is transferred from the laser beam. Numerical examples for a typical laser glass are given.

**15972.** Hughes, E. E., **Development of standard reference materials for air quality measurement,** *ISA Trans.* **14,** No. 4, 281-291 (1975).

Key words: air pollution; carbon monoxide; gas analysis; gas standards; nitric oxide; nitrogen dioxide; sulfur dioxide.

The National Bureau of Standards is engaged in a continuing program involving gaseous Standard Reference Materials for air pollution measurements. Preparation of such materials requires definition of the stability, homogeneity, and accuracy of the samples. This information is obtained by long term studies of the gas systems, by development of absolute methods of analysis, and by analysis of large numbers of samples prepared in bulk. The results of studies, extending over several years, of low concentration of carbon monoxide in nitrogen and nitric oxide in nitrogen are reported. Over one thousand samples of these materials have been analyzed and the stability with time and the within-batch homogeneity have been characterized. Accuracy is achieved by use of gravimetric standards and with dynamic dilution systems. Accuracy attainable by either method is described.

The use of permeation tubes of sulfur dioxide and nitrogen dioxide is necessary in some situations because of the reactivity of the gases. Data covering the stability and accuracy of these devices has been collected over a period of several years.

**15973.** Choi, C. S., Prince, E., **A neutron diffraction study of structure and thermal motion in several monovalent metal azides,** *J. Chem. Phys.* **64,** No. 11, 4510-4516 (June 1, 1976).

Key words: ionic crystal; $KN_3$ structure; low temperature study; monovalent metal azides; $NaN_3$ structure; neutron diffraction; $RbN_3$ structure; thermal motion; $TlN_3$ structure.

The crystal structures of the monovalent metal azides $\beta$-$NaN_3$, $KN_3$, $TlN_3$, and $RbN_3$ were reinvestigated by means of neutron diffraction. All except $\beta$-$NaN_3$ were studied at low temperature as well as at room temperature. These compounds form ionic crystals with spherical metal cations and linear azide anions. Because the azide ions in each case occupy centrosymmetric sites, their thermal motions can be treated, except for the small amplitude N-N stretching and the internal bending motions, as the motions of rigid bodies without screw correlations. All structures were, therefore, refined using rigid-body constraints, leading to final $R$ values, both weighted and unweighted, ranging from 0.020 to 0.045. $KN_3$, $TlN_3$, and $RbN_3$ all crystallize in the tetragonal space group $I4/mcm$, while $\beta$-$NaN_3$ crystallizes in the space group $R\bar{3}\,m$. The uncorrected N-N distances range from 1.159 to 1.183 Å, but when corrections for thermal motions are applied all distances except for $\beta$-$NaN_3$ lie in the range 1.181-1.187 Å, with a weighted mean of 1.186 Å. In the $\beta$-$NaN_3$ the corrected N-N distance is 1.180(1) Å. This apparently unusually short distance may be attributable to disorder, with the axis of the $N_3$ group making a small angle with the $c$ axis. In the tetragonal crystals, where the azide ions occupy sites with $mmm$ symmetry, the anisotropy of libration is consistent with the steric hindrance in the structure. The librational amplitudes determined from the diffraction studies were compared with those determined by Raman scattering, and the agreement is satisfactory.

**15974.** Gatehouse, B. M., Negas, T., Roth, R. S., **The crystal structure of $M$-$LiTa_3O_8$ and its relationship to the mineral wodginite,** *J. Solid State Chem.* **18,** 1-7 (1976).

Key words: crystal structure; lithium tantalate; $M$-$LiTa_3O_8$; wodginite.

$M$-$LiTa_3O_8$ crystallizes in the monoclinic system with unit-cell dimensions (from single crystal data) $a$=9.413, $b$=11.522, $c$=5.050 Å, $\beta$=91.05°, and space group $C2/c$, $Z$=4. The structure was solved using three-dimensional Patterson and Fourier techniques. Of the 754 reflections measured by counter techniques, 714 with $I \geqslant 3\sigma\ (I)$ were used in the least-squares refinement of the model to a convention $R$ of 0.043 ($wR$=0.055). $M$-$LiTa_3O_8$ has the $\alpha$-$PbO_2$ type of structure with hexagonally close-packed oxygen ions with lithium and tantalum occupying octahedral sites in an ordered way. This structure can be regarded as a simple analogue of the complex mineral wodginite.

**15975.** Cameron, J. M., **Traceability?,** *J. Qual. Technol.* **7,** No. 4, 193-195 (Oct. 1975).

Key words: measurement; traceability; uncertainty.

The requirement of traceability of instruments to nationally accepted standards or measurement systems has as its goal the adequate accuracy of measurement, the compatibility of different measurement systems, the interchangeability of parts, etc. This note discusses a perspective in which these goals are approached directly by performance requirements on the quality of measurement rather than a property of an instrument, namely traceability.

**15976.** Cameron, J. M., **Measurement assurance,** *J. Qual. Technol.* **8,** No. 1, 53-55 (Jan. 1976).

Key words: measurement; measurement assurance; uncertainty.

There is an obvious need that measurements in the fields of health, safety, environmental control and nuclear safeguards be adequate for their intended purpose—that their uncertainty be small enough to only negligibly affect the decisions and performance of the processes of which they are a part, but it is no less true for all other measurements in science and industry. This note discusses the procedures by which one obtains measurement assurance, the analog for measurement processes of industrial quality assurance.

**15977.** Loevinger, R., Berman, M., **A revised schema for calculating the absorbed dose from biologically distributed radionuclides,** *J. Nucl. Med. MIRD Pamphlet No. 1*, Revised, 3-10 (Mar. 1976).

Key words: absorbed dose; calculation; dosimetry; nuclear medicine; radionuclide; radiopharmaceutical.

This paper is a revision of the first pamphlet in the series of publications by the Medical Internal Radiation Dose Committee (MIRD) of the Society of Nuclear Medicine. That pamphlet presented a new formalism for dosimetry calculation in nuclear medicine, and has served as the basis for a series of MIRD publications. This revised schema is intended to be a clearer and more direct presentation of the same formalism, the purpose of which is to produce a convenient uniformity and simplicity in the calculation of absorbed dose from radiopharmaceuticals.

**15978.** Taylor, J. K., **Evaluation of data obtained by reference methods,** (Proc. American Society for Testing and Materials Symp. on Calibration in Air Monitoring, Boulder, CO, Aug. 4-8, 1975), *Am. Soc. Test. Mater. Spec. Tech. Publ. 598*, pp. 156-163 (1976).

Key words: air pollution; calibration; evaluation; intercalibration; quality control; standards.

The key role of reference methods for measurement of air pollutants in regulatory matters demands that the data obtained in their use be precise and accurate, but no procedures have been established for evaluating its reliability and validity for the intended use. This paper discusses the general principles of reliable analytical measurements and presents guidelines by which the quality of data obtained by reference methods or other procedures may be evaluated.

**15979.** Taylor, B. N., **Is the present realization of the absolute ampere in error?,** *Metrologia* **12,** No. 2, 81-83 (1976).

Key words: absolute ampere; fundamental constants; Josephson effect.

Using the results of recent experimental determinations of several different fundamental physical constants, highly accurate, indirect values for the ratio of the as-maintained ampere to absolute ampere may be obtained. A comparison of these indirect values with the results of direct determinations based on force balances and with the presently accepted best value indicates that both of the latter may be in error.

**15980.** Hall, J. L., **Stabilized lasers and the speed of light,** (Proc. 5th Int. Conf. on Atomic Masses and Fundamental Constants, Paris, France, June 1975), Paper in *Atomic Masses and Fundamental Constants* **5,** J. H. Sanders and A. H. Wapstra, Eds., Part 8, 322-329 (Plenum Press, New York, NY, 1976).

Key words: frequency multiplication; fundamental constants; laser stability; metrology; second-order Doppler shift; speed of light.

This paper recalls the developments in laser frequency stabilization and in accurate measurement of laser wavelengths and frequencies. The CCDM(73) found good agreement among the reporting laboratories for the wavelength of the $CH_4$-stabilized laser and so recommended a value in meters. A recent NPL measurement of the $CH_4$ frequency confirmed the NBS value and so substantiates the CCDM-recommended value of the speed of light, c. NPL also reported independent λ and f measurements on a stabilized $CO_2$ laser, yielding the same value for c—to within the uncertainty of the Meter. The present status of the krypton-based International Meter is reviewed and a number of new laser systems of potential metrological interest are noted. Finally, we focus on the future possibilities for optical frequency standards. We report preliminary measurements of the pressure effect on the height ratio of the now-resolved recoil doublet in $CH_4$. This resolution, approaching 1 kHz at $\sim 10^{14}$ Hz, is the highest ever employed in spectroscopy with coherent fields. Limiting factors of an optical frequency standard are recalled and an accuracy capability of $2 \times 10^{-13}$ is estimated for the present apparatus.

**15981.** Johnson, P. M., **The multiphoton ionization spectrum of trans-1,3-butadiene,** *J. Chem. Phys.* **64,** No. 11, 4638-4644 (June 1, 1976).

Key words: electronic structure; multiphoton ionization; trans-1,3-butadiene.

The multiphoton ionization spectrum of *trans*-1,3-butadiene has been measured from dye laser wavelengths of 365 to 468 nm using an intensity-corrected system. In the four-photon ionization region to lower energy than 405 nm, many three-photon resonances with Rydberg states are seen and a new series with a quantum defect of 0.04 is identified. The symmetries of the observed Rydberg series are discussed. Above 405 nm in energy, a resonance occurs with the $\tilde{B}$ state seen in one-photon absorption spectra, only the structure in the multiphoton ionization spectrum is characteristic of an allowed two-photon resonance. From the vibronic structure of this state, it is argued that it has symmetry ${}^1B_g$. In the region covered by this study (42 700 to 54 800 $cm^{-1}$ in two-photon energy) no state was found to which a ${}^1A_g$ symmetry designation could be applied.

**15982.** Hughes, E. E., **Role of the National Bureau of Standards in calibration problems associated with air pollution measurements,** (Proc. American Society for Testing and Materials Symp. on Calibration in Air Monitoring, Boulder, CO, Aug. 4-8, 1975), *Am. Soc. Test. Mater. Spec. Tech. Publ. 598,* pp. 223-231 (1976).

Key words: air pollution; analyzing; gas analysis; gases; emission; monitors; standards.

The National Bureau of Standards (NBS) produces a limited number of Standard Reference Materials (SRM's) for air pollution and related analyses. The effort involved in the preparation and certification of these standards precludes production in large quantities or of great variety. The requirements for accuracy and stability of samples necessitate a considerable research effort prior to production of the actual SRM's. The decision as to what gas mixtures will be prepared as SRM's is based primarily on a demonstrated need modified by anticipated demand and by other obligations of the SRM program. The demand for these SRM's is increasing, and maintaining stocks of current SRM's must compete with the necessary research prior to issuance of new SRM's.

Comparisons are presented of independent analyses of a number of SRM's currently in use for measurement of automotive emissions.

**15983.** Heinrich, K. F. J., **Empirical approaches for the treatment of interelement effects,** (Proc. 24th Annual Conf. on Applications of X-Ray Analysis, Denver, CO, Aug. 6-8, 1975), Chapter in *Advances in X-Ray Analysis,* R. W. Gould, C. S. Barrett, J. B. Newkirk, and C. O. Ruud, Eds., **19,** 75-84 (Kendall/Hunt Publ. Co., Dubuque, IA, 1976).

Key words: corrections; matrix effects; standard reference materials; x-ray fluorescence.

Empirical algorithms for the treatment of interelement effects in x-ray fluorescence spectrometry are reviewed. It is recommended that the effects of tertiary x-ray emission be treated separately from those of x-ray absorption, and that standard reference materials of composition close to that of the specimen be used.

**15984.** Pella, P. A., Kuehner, E. C., Cassatt, W. A., **Development of a particulate reference sample on membrane filters for the standardization of x-ray fluorescence spectrometers,** (Proc. 24th Annual Conf. on Applications of X-Ray Analysis, Denver, CO, Aug. 6-8, 1975), Chapter in *Advances in X-Ray Analysis,* R. W. Gould, C. S. Barrett, J. B. Newkirk, and C. O. Ruud, Eds., **19,** 463-472 (Kendall/Hunt Publ. Co., Dubuque, IA, 1976).

Key words: calibration; filters; orchard leaves; reference sample; x-ray analysis.

Particulate reference samples have been prepared for the standardization of x-ray fluorescence spectrometers used in the analysis of air particulate matter. Uniform layers of reground orchard leaves of known composition, i.e., National Bureau of Standards Standard Reference Material SRM 1571, were deposited on membrane filters and coated with a thin polymer film for protection against abrasion and moisture. These samples have been prepared with areal densities of 0.1 to 5.0 mg/$cm^2$.

**15985.** Siedle, A. R., **Group VIb metal carbonyl complexes of 1,3-dithiolene-2-thione,** *Inorg. Nucl. Chem. Lett.* **11,** No. 5, 345-347 (1975).

Key words: chromium carbonyl; infrared spectroscopy; metal carbonyl; molybdenum carbonyl; NMR spectroscopy; 1,3-dithiolene-2-thione.

Reaction of 1,3-dithiolene-2-thione with bicyclo{2,2,1}heptadiene $M(CO)_4$ (M=Cr, Mo) produces (1,3-dithiolene-2-thione)$M(CO)_5$.

**15986.** Flynn, D. R., **Measurement of thermal conductivity by steady-state methods in which the sample is heated directly by passage of an electric current,** Chapter 5 in *Thermal Conductivity.* R. P. Tye, Ed., **1,** 242-300 (Academic Press, London and NY, 1969).

Key words: conductivity; electrical; heat conductivity; heat transfer; Lorenz function; thermal conductivity.

A survey is made of the field of thermal conductivity measurement by the category of methods in which the sample is heated directly by passage of an electric current. A mathematical analysis of simultaneous steady-state heat and electric current in a conductor is given. This analysis is then applied to several methods which have been used for determination of thermal conductivity. A critical description is given of the experimental procedures followed by numerous investigators who have made thermal conductivity measurements by electrical heating methods. Finally, some problem areas are discussed and recommendations are given for further work in this area.

**15987.** Linsky, J. L., Glackin, D. L., Chapman, R. D., Neupert, W. M., Thomas, R. J., **The solar XUV spectrum of He II,** *Astrophys. J.* **203,** No. 2, 509-520 (Jan. 15, 1976).

Key words: atomic processes; sun, corona; sun, flares; sun, prominences; sun, spectra; ultraviolet, spectra.

OSO-7 observations of the first five Lyman lines and the Lyman continuum of He II are given for the quiet Sun, a coronal hole, prominences, filaments, and the 1972 August 7 flare. These data are calibrated and given in specific intensity units together with color and brightness temperatures for the He II continuum. We find that He II is overionized in all features except the flare, and that the continuum is formed at temperatures near 14,000 K. The He II – He III ionization equilibrium appears to be dominated by photoionizations and radiative recombinations. Schematic calculations for realistic chromosphere and transition-region models can account for the observed intensities of $L\beta - L\epsilon$, the Lyman continuum, and its color temperature. To account for the intensity of $L\alpha$, either an implausible 100 km plateau at temperatures near 80,000 K is needed or, more likely, the incorporation of diffusion-enhanced collisional excitation into the models.

**15988.** Cook, J. M., Evenson, K. M., Howard, C. J., Curl, R. F., Jr., **Laser magnetic resonance spectrum of HCO on the $D_2O$ 108 $\mu$ laser line,** *J. Chem. Phys.* **64,** No. 4, 1381-1388 (Feb. 15, 1976).

Key words: laser line; laser magnetic resonance spectrum; magnetic resonance spectrum; resonance spectrum; rotational frequency.

An LMR spectrum on the 108 $\mu$ $D_2O$ laser line has been observed and assigned to the $8_{2,6} \leftarrow 7_{1,7}$ rotational transition of HCO. The spectra of both $\pi$ (parallel) and $\sigma$ (perpendicular) polarizations have been fitted by the least squares method, giving excellent agreement between the calculated and observed magnetic fields. The rotational frequency obtained from the fittings has been used to determine the *A* rotational constant. In addition, the electron spin-rotational splitting of each rotational level and the Fermi constant have been determined.

**15989.** Sanders, D. M., Schaefer, H. A., **Reactive vaporization of soda-lime-silica glass melts,** *J. Am. Ceram. Soc.* **59,** No. 3-4, 96-101 (Mar.-Apr. 1976).

Key words: diffusion; glass; homogeneity; melting; vaporization.

Water-vapor-assisted transport of glass constituents from a soda-lime-silica melt was studied, using atomic spectroscopy for analysis of vapor condensates and microprobe analysis to determine diffusion profiles. The data presented indicate that the vaporization process is controlled by a surface membrane which has a composition different from the bulk composition. The influence of this effect on glass homogeneity is discussed.

**15990.** Kaufman, V., Radziemski, L. J., Jr., **The sixth spectrum of uranium (U VI),** *J. Opt. Soc. Am.* **66,** No. 6, 599-600 (June 1976).

Key words: actinide; atomic energy levels; isoelectronic sequence; protactinium; rare earth; sliding spark discharge lamp; spectrum; uranium.

Eight spectral lines of five-times ionized uranium between 800 and 1930 Å are reported. Four terms ($5f^2F$, $6d^2D$, $7s^2S$, and $7p^2P$) are given. Isoelectronic comparisons are made and the effect of crystal fields on the $5f$ electron is discussed.

**15991.** Miles, M. G., Wager, J. S., Wilson, J. D., Siedle, A. R., **Reactions of 4,5-dicyano-1,3-dithiole-2-thione and -1,3-dithiol-2-one with tervalent phosphorus compounds,** *J. Organ. Chem.* **40,** No. 18, 2577-2582 (1975).

Key words: aryl phosphines; cyclic voltammetry; desulfurization; phosphines; tetracyanotetrathiafulvalene; tetracyanotetrathiafulvalene·triphenylphosphine; $\Delta^{2,2'}$-bis-14.5-dicyano-1,3-dithiodene; 1,3-dithiolenes; $^{31}P$ NMR; 4,5-dicyano-1,3-dithiolene-2-thione.

In contrast to other reported reactions of 1,3-dithiol-2-ones and 1,3-dithiole-2-thiones with tervalent phosphorus compounds, which yield only tetrathiafulvalenes, the reaction of 4,5-dicyano-1,3-dithiole-2-thione (1) and -1,3-dithiol-2-one (2) with phosphines and phosphites is complex. Either tetracyanotetrathiafulvalene [$\Delta^{2,2'}$-bi(4,5-dicyano-1,3-dithiolidene)] (3), a betaine {(4,5-dicyano-1,3-dithiol-2-ylidene)methylene [tri-(substituents)phosphonio]( - 2 - thio - 1 - mercaptomaleonitrilate)} (4). or a dialkyl (4,5-dicyano-1,3-dithiol-2-yl)phosphonate may be formed, depending on the choice of reactant and conditions. In addition, Wittig-type products are formed on addition of aryl aldehydes to the reaction mixture. All of these products can be rationalized by means of a reaction scheme which assumes the ylide 4,5-dicyano-1,3-dithiolidenetri(substituent)phosphorane to be the key intermediate. Only tetracyanotetrathiafulvalene was isolated from the reaction of trimethyl phosphite with either 1 or 2 and tris(*p*-chlorophenyl)phosphine with 1, but reactions of other triarylphosphines and methyl diphenylphosphinite with 1 yielded varying amounts of fulvalene and betaine. Phosphorus trichloride, triphenyl phosphite, and triphenylarsine did not react with 1. The stoichiometric reaction of triphenylphosphine, 1, and terephthalaldehyde gave a near-quantitative yield of 2,2′-*p*-xylylidenebis(4,5-dicyano-1,3-dithiole) (8), which undergoes a reversible, electrochemical oxidation at $E_p$=1.07 V (vs. SCE) and an irreversible oxidation at $E_p$=1.39 V. With benzaldehyde under these conditions, however, both 4 and 2-benzylidene-4,5-dicyano-1,3-dithiole were isolated. The novel ester dimethyl (4,5-dicyano-1,3-dithiol-2-yl)phosphonate was isolated from a reaction of trimethyl phosphite plus 2 in the presence of benzoic acid.

**15992.** Gutschick, K. A., Clifton, J. R., **Durability study of 14-year old masonry wallettes,** *Am. Soc. Test. Mater. Spec. Tech. Publ. 589, Masonry: Past and Present,* 76-95 (Aug. 1975).

Key words: lime (dolomitic); masonry; mortars (materials); portland cement; testing; walls.

A series of brick wallettes originally built to study the effect of five variables, particularly dolomitic lime, on dimensional stability were analyzed as to their durability performance after 14 years of outdoor exposure. Durability performance was assessed in terms of cracking (bond separation), mortar erosion, and efflorescence, with the influencing factors including type of lime, mortar, and brick, loading, climate, and exposure.

Generally, most walls performed well, considering that they in essence were "parapet" walls, unprotected from the elements on all sides. The greatest incidence of cracking occurred in walls built with the dense, low absorptive white brick and mortar made with high expansive lime; frost action was undoubtedly a contributing factor. Mortar erosion was most prevalent on the south faces of walls, particularly in walls built with the high absorptive red brick and mortar made with high expansive lime; thermal expansion was undoubtedly a contributing factor. Efflorescence was only slight. The study points to the importance of using compatible mortar-brick combinations to get the best performance.

**15993.** Halsey, N., **GFRP rod and rope for structural guy applications,** *ASCE J. Engr. Mech. Div.* **100,** No. EM4, 673-685 (Aug. 1974).

Key words: end fittings; GFRP rod and rope; structural guys.

Tensile tests were conducted on GFRP rod and rope using five commercial structural guy termination grips and the relative performances of the grips with these materials were evaluated. Stress-rupture tests at moderately elevated temperatures under low and saturated humidity conditions were carried out on two GFRP rod and rope materials and the stress-rupture characteristics of the materials were examined. Flexural tests were performed on three GFRP rod and rope materials from +77 to −80 °F and the flexural moduli of the materials were evaluated. Simulated aeolian vibration tests were carried out on two GFRP rod and rope materials held under constant tensile loads using four types of commercial guy-termination grips and an NBS shear-type grip. The resistance to damage of these materials from aeolian vibration was observed up to $10^8$ cycles. A series of 30-day storage tests were conducted on four GFRP rod and rope materials at temperatures ranging from 125 to 200 °F. Several guidelines regarding minimum coil diameters and maximum exposure temperatures for long-term storage were established. Some residual strength tests were performed on the materials which had been exposed to long-term storage.

**15994.** Zuckerman, B., Turner, B. E., Johnson, D. R., Palmer, P., Morris, M., **A new interstellar line: The $5_1-4_0$ ($E_2$) transition in methyl alcohol,** *Astrophys. J.* **177,** No. 3, 601-607 (Nov. 1, 1972).

Key words: emission line; interstellar medium; laboratory measurement; methyl alcohol; population inversion; radio astronomy.

An emission line has been detected at 84.5 GHz in the direction of the radio continuum source Sgr B2. The new line frequency has been found to coincide with a laboratory measurement of the $5_1 \rightarrow 4_0$ ($E_2$) transition of methyl alcohol ($CH_3OH$). Calculations of the spontaneous emission rates from all energy levels of astrophysical interest have been performed; these indicate that not only the $5_1-4_0$ ($E_2$) transition in Sgr B2 but also the $\Delta J=0$, $\Delta K=1(E_1)$ transitions discovered in Orion A by Barrett *et al.* are likely to have population inversions.

Additional searches for $NH_2CN$, HCP, $CH_3Cl$ ClCN, FeO, $HC_3HO$, and $NH_2HCO$ were carried out in the 80-92-GHz region without success.

**15995.** Bushnell, D. L., Jr., Huebner, R. H., Celotta, R. J., Mielczarek, S. R., **Preliminary report on electron energy-loss measurements for $CClF_3$, $CCl_2F_2$, and $CCl_3F$,** *Argonne Natl. Lab. Report No. ANL-75-60,* Part I. Radiological and Environmental Research Annual Report on Fundamental Molecular Physics and Chemistry, pp. 7-17 (Argonne National Laboratory, Argonne, IL, July 1974-June 1975).

Key words: $CClF_3$; $CCl_2F_2$; electron energy-loss; freons; uv photoabsorption.

Currently, nationwide research efforts are devoted to studying the possible ozone ($O_3$) depletion in the stratosphere by the chemical action of chlorine atoms released from $CCl_2F_2$ or $CCl_3F$ upon absorption of ultraviolet radiation. Since electron-impact data taken in the forward scattering direction can be used to derive oscillator strengths and thus to yield apparent photoabsorption cross sections, we have carried out such an analysis for $CCl_2F_2$, $CCl_3F$, and $CClF_3$. We obtain oscillator-strength distributions between 5 and 20 eV and compare these to available photoabsorption data. Certain photoabsorption values agree very well with this electron-impact data, but other optical studies deviate in some spectral regions by as much as a factor of 5. Also, the electron energy-loss spectrum reveals electronic transitions previously undetected by photoabsorption.

**15996.** Wallace, B. M., Brown, W. E., **Stoichiometric composition of whitlockite,** *J. Dent. Res.* **50,** No. 2, 343-346 (Mar.-Apr. 1971).

Key words: calcification; calcium; dicalcium phosphate; octacalcium phosphate; pyrolysis; pyrophosphate; stoichiometry; whitlockite; $\beta$-tricalcium.

The mineral whitlockite has been described as having Ca/P ratios of 3:2 and 10:7. This study used the pyrolytic formation of pyrophosphate and whitlockite from calcium orthophosphates and their mixtures with $CaCO_3$ to determine this Ca/P ratio. Its mean value of 1.506±0.015 indicated a formula of $Ca_3(PO_4)_2$.

**15997.** Huebner, R. H., Bushnell, D. L., Jr., Celotta, R. J., Mielczarek, S. R., Kuyatt, C. E., **Ultraviolet photoabsorption by halocarbons 11 and 12 from electron-impact measurements (Summary),** *Argonne Natl. Lab. Report No. ANL-75-60, Part I. Radiological and Environmental Research Annual Report on Fundamental Molecular Physics and Chemistry,* pp. 18-21 (Argonne National Laboratory, Argonne, IL, July 1974-June 1975).

Key words: electron energy loss; electron impact; halocarbon 11, $CFCl_3$; halocarbon 12, $CF_2Cl_2$; uv photoabsorption.

Electron energy loss measurements are made of Freons 11 and 12. The data is converted to oscillator strength distributions and compared to the existing photoabsorption data in the energy range relevant to atmospheric photodissociation.

**15998.** Huebner, R. H., Celotta, R. J., Mielczarek, S. R., Kuyatt, C. E., **Apparent oscillator strengths for nitrous oxide (Summary),** *Argonne Natl. Lab. Report No. ANL-75-60, Part I. Radiological and Environmental Research Annual Report on Fundamental Molecular Physics and Chemistry,* pp. 3-6 (Argonne National Laboratory, Argonne, IL, July 1974-June 1975).

Key words: electron energy loss; $N_2O$; oscillator strengths; UV.

Energy loss spectra of $N_2O$ were obtained in the 4 to 14 eV region and converted to oscillator strengths and compared to the optical values.

**15999.** Huebner, R. H., Celotta, R. J., Mielczarek, S. R., Kuyatt, C. E., **Apparent oscillator strengths for molecular oxygen, derived from electron energy-loss measurements (Summary),** *Argonne Natl. Lab. Report No. ANL-75-60, Part I. Radiological and Environmental Research Division Annual Report on Fundamental Molecular Physics and Chemistry,* pp. 1-2 (Argonne National Laboratory, Argonne, IL, July 1974-June 1975).

Key words: energy loss; $O_2$; oscillator strengths; oxygen; transition probabilities.

Oscillator strengths for $O_2$ from 6 to 14 eV are derived from the energy-loss spectrum of 100 eV incident electrons. Integrated *f* values for the Schumann-Runge bands and continuum, which span four orders of magnitude in intensity, agree well with high-resolution photoabsorption measurements.

**16000.** Jaeger, E. F., Oster, L., Phelps, A. V., **Growth of thermal constrictions in a weakly ionized gas discharge in helium,** *Phys. Fluids* **19,** No. 6, 819-830 (June 1976).

Key words: constrictions; gas discharge; helium; ionized gas; numerical solutions.

Neutral and charged particle densities, radial velocities, and temperatures are calculated as functions of time for cylindrical discharges in helium at pressures from 1 to 1000 torr and a radius of 1 cm. Ionization, recombination, ambipolar diffusion, specific heat of the neutrals, and variation of gas pressure in space and time are included. Ionization of excited states, energy loss by radiation, and space charge sheaths are neglected. Under most conditions, increased ionization in regions of decreased gas density causes a constriction of the discharge which is accentuated at high pressures and high recombination rates. Greater circuit resistance stabilizes the discharge. At low pressures, the electron density profile expands. Initial steep gradients in electron density cause constrictions off axis.

**16001.** Youden, W. J., **Evaluation of analytical data,** Chapter in *Encyclopedia of Industrial Chemical Analysis*, F. D. Snell and C. L. Hilton, Eds., **1,** Gen. Tech. A-4, 746-763 (Interscience Publ., New York, NY, 1966).

Key words: analytical data; analytical work; critical evaluation of an analytical procedure; industrial chemical analysis; interlaboratory comparisons; sampling error.

The material is expository and written for readers with little or no statistical background. The article covers the following topics: methods of reporting precision and accuracy, control charts for routine analytical work, critical evaluation of an analytical procedure, interlaboratory comparisons, and sampling error.

**16002.** Steiner, B. W., **Review of the CIE photometric model and of the status of radiometric measurements,** *Proc. Symp. on The Basis for Effective Management of Lighting Energy, Washington, DC, Oct. 29-30, 1976*, pp. 185-195 (Federal Energy Administration, Washington, DC, 1976).

Key words: CIE photometric model; photometry, heterochromic; radiometric measurements.

The paper reviews the status of the CIE photometric model and of radiometric measurements. The CIE photometric model universally used for heterochromatic photometry is an additive model, in contrast to the behavior of the eye in viewing large areas. Although this additivity is not valid visually, the practical advantages of such a system until now have outweighed the disadvantages. This situation should be reexamined. Moreover, the most careful spectral measurements now show a 2 percent spread in the visible, comparable to the best photometric measurements. Although routine commercial measurements cannot yet be expected to achieve this level of agreement, this goal for the future now seems realistic. On this basis, a more visually realistic photometry now seems to be the practical goal.

**16003.** Nimeroff, I., **Symposium on visual signaling,** *Appl. Opt.* **13,** No. 10, 2186, 2445-2446 (Oct. 1974).

Key words: colorimetry of signals; effective intensity of flashing lights; legibility of signs; visual signaling.

A symposium on visual signaling was held on April 9 and 10, 1974, in Washington, D.C. sponsored by CIE Committee TC 1.6, in cooperation with several agencies of the Department of Transportation. The symposium, attended by investigators from many parts of the world covered researchers on a wide variety of topics such as: 1. visibility of daytime and nighttime signals; 2. visibility and legibility of signs; 3. colorimetry of surface colors, particularly retroreflectors.

**16004.** Fong, J. T., **Energy approach for creep-fatigue interactions in metals at high temperatures,** *Trans. ASME J. Pressure Vessel Tech.* **97,** Series J, No. 3, 214-222 (1975).

Key words: creep; dissipation; elevated temperature; energy; hold-time; hysteresis; low-cycle fatigue; plasticity; stainless steel; stress relaxation; thermodynamics; viscoelasticity.

An analysis of the so-called creep-fatigue interactions in a re-annealed AISI type 304 stainless steel with and without hold-time at 593 deg C (1100 deg F) is presented with a numerical example. The analysis is based on a series of papers on the thermodynamics of materials exhibiting both time-dependent and permanent-set behavior under mechanical and/or thermal loadings. Assuming isothermal loadings, the analysis consists of an "operational" decomposition of the total mechanical work into a stored part (long-term elasticity), and two dissipated parts, namely, an instantaneous component and a delayed component due to viscoelasticity. Each of the two dissipated components is again subdivided, operationally, into an "intrinsic" part (atomic diffusion and motion of dislocations), and a "structural" part (lattice strains and propagation of microcracks). The significance of the energy approach in unifying microscopic and macroscopic testing data and in formulating multi-axial design criteria for high-temperature components such as pressure vessels, turbine rotors, steam piping, etc., is discussed.

**16005.** Touloukian, Y. S., Kirby, R. K., Taylor, R. E., Desai, P. D., **Thermal expansion, metallic elements and alloys,** *Thermophysical Properties of Matter, Volume 12*, 1414 pages (Plenum Publishing Corp., New York, NY, 1975).

Key words: alloys; coefficients of thermal expansion; compilation; critical evaluation; elements; thermal expansion.

This volume of Thermophysical Properties of Matter comprises two major sections: the front text on theory and measurement together with its bibliography, and the main body of numerical data and its references. The main body of numerical data is the result of a comprehensive survey of the literature. The scope of coverage includes data on the thermal expansion of the metallic elements and alloys. All data were extracted directly from their original sources. The original data have been critically evaluated and analyzed and recommended reference values, provisional values or typical values are presented.

**16006.** Stiefel, S. W., **Procedural options for modification of architectural glass in residences to improve occupant safety,** *Proc. 24th Annual Conf. Standards Engineers Society, Syracuse, NY, Sept. 28-Oct. 1, 1975*, pp. 61-64 (Standards Engineers Soc. Inc., Minneapolis, MN, 1975).

Key words: architectural glass products; Consumer Product Safety Act; residence-related products; residential safety modification; safety implementation approaches.

The U.S. Consumer Product Safety Commission (CPSC) has the responsibility for developing and promulgating mandatory safety standards for products which pose unreasonable risks of injury for consumers. One of the first products selected for development of a safety standard under the Consumer Product Safety Act of 1972 was architectural glass. The initial impact of the adoption of a mandatory standard for architectural glass would be rather limited, largely due to the fact that people will continue to occupy existing housing that will not be immediately subject to the new rule.

This paper discusses research in the Center for Consumer Product Technology at NBS conducted for the CPSC. The paper identifies alternative retrofit options intended to ameliorate the hazards associated with existing installed architectural glass, evaluates these options and postulates implementation approaches for consideration by the CPSC for encouraging safety modifications.

**16007.** Marvin, R. S., Sherwood, G. B., **A guide to sources of information on materials,** Chapter in *Handbook of Materials Science. Volume III: Nonmetallic Materials and Applications*, C. T. Lynch, Ed., pp. 603-627 (CRC Press, Inc., Cleveland, OH, 1975).

Key words: data centers; data tabulations; evaluated data; material properties; referral centers; sources of data.

A list of sources of data on properties of materials, plus guides to more extensive listings is provided. The individual data centers and publications listed are primarily those which attempt a critical evaluation of the reliability of the values cited.

**16008.** Yonemura, G. T., Kohayakawa, Y., **A new look at the research basis for lighting level recommendations,** *Proc. Symp. on The Basis for Effective Management of Lighting Energy, Washington, DC, Oct. 29-30, 1975*, pp. 151-183 (Federal Energy Administration, Washington, DC, 1976).

Key words: gratings; illuminating engineering; lighting; modulation transfer function; suprathreshold visibility; visibility; vision.

The validity of using threshold studies as the basis for lighting level recommendations is questioned. The performance of the eye at suprathreshold levels was investigated with sine- and square-wave gratings. The results indicate that the behavior of the eye is significantly different at suprathreshold levels as opposed to threshold levels. For threshold studies contrast is a monotonically decreasing function with respect to luminance. At suprathreshold levels the contrast function has a definite minimum, luminances greater or less requiring more contrast to appear subjectively equal. It is recommended that lighting levels be based on laboratory studies that appraise visual requirements and performance simulating conditions encountered in real world environments.

**16009.** Walleigh, R. S., **Controlled environments for meaningful measurement,** *Res. Develop. Mag.* **20,** No. 1, 16-21 (Jan. 1969).

Key words: engineering; environmental; interference abatement; laboratory environments; radiation; sound studies.

Highlights are presented showing how NBS goes to great lengths to apply architectural planning concepts as well as control measures involving special equipment, materials, and techniques in order to achieve optimum laboratory environments for its measurement operations. The significance of comprehensive knowledge and control of conditions such as temperature, light, electrical current, gravity, vibration, pressure, etc., for the Bureau's service to U.S. science and technology in a time of rapid change, is discussed.

**16010.** Hougen, J. T., **Second all-union symposium on high resolution molecular spectroscopy,** *Appl. Opt.* **14,** No. 1, 8-9 (Jan. 1975).

Key words: high resolution molecular spectroscopy; lasers; meeting report; Novosibirsk; pressure-broadened line shapes; Soviet Union; submillimeter waves.

The second All-Union Soviet Symposium on High Resolution Molecular Spectroscopy was held in Novosibirsk, USSR from 11-13 September, 1974. The meetings contained some invited and many contributed papers in the fields of laser construction and application, contact-transformed vibration-rotation Hamiltonians, pressure-broadened line shapes in the one-atmosphere region, and spectroscopic instrumentation. Eighty percent of the papers were delivered in Russian, but Westerners were provided with essentially individual interpreters.

**16011.** Weiss, G. H., Rubin, R. J., **The theory of ordered spans of unrestricted random walks,** *J. Stat. Phys.* **14,** No. 4, 333-350 (1976).

Key words: Abelian summation; ordered spans; random walks; stable distributions.

The spans of an $n$-step random walk on a simple cubic lattice are the sides of the smallest rectangular box, with sides parallel to the coordinate axes, that contains the random walk. Daniels first developed the theory in outline and derived results for the simple random walk on a line. We show that the development of a more general asymptotic theory is facilitated by introducing the spectral representation of step probabilities. This allows us to consider the probability density for spans of random walks in which all moments of single steps may be infinite. The theory can also be extended to continuous-time random walks. We also show that the use of Abelian summation simplifies calculation of the moments. In particular we derive expressions for the span distributions of random walks (in one dimension) with single step transition probabilities of the form $P(j) \sim 1/j^{1+'}$, where $0 < \alpha < 2$. We also derive results for continuous-time random walks in which the expected time between steps may be infinite.

**16012.** Savage, B. D., **High-resolution profiles of the diffuse interstellar feature at 5780 Å,** *Astrophys. J.* **205,** No. 1, 122-135 (Apr. 1, 1976).

Key words: atomic processes, interstellar; matter, line profiles.

High-resolution profiles ($\Delta\lambda \approx 0.2$ Å) were obtained of the diffuse interstellar feature at 5780 Å in 18 heavily reddened stars with the Wisconsin echelle spectrograph at the Cassegrain focus of the Mayall 4m telescope. This feature is, in all cases, asymmetrical with its steep side being toward the blue. On attempting to match theoretical profiles to the observed $\lambda 5780$ profile in HD 183143 we find that theoretical profiles for such processes as autoionization, predissociation, or preionization do not provide acceptable fits to the observational data, while good fits can be obtained for the extinction profiles provided by small ($r \approx 750$ Å), cold grains containing impurities that produce narrow no-phonon absorption lines. If $\lambda 5780$ is in fact due to this latter process, then the asymmetry of the feature provides information on the sizes of interstellar grains, while the width provides information on the internal temperatures of grains. Significant differences in the feature asymmetry were noted for several stars, a result that can readily be explained as being due to small differences in the particle size in different galactic regions. Although changes in the width of the feature at 5780 Å were noted, it is difficult to decide if the variations are due to cloud motions, observational errors, or changes in grain temperatures. However, it is possible that the broad weak feature superposed on $\lambda 5780$ is due to the same process that produces $\lambda 5780$ but in hot ($T \approx 100$-$200$ K) grains situated near the stars being observed. It is concluded that a careful study of the profiles of the narrow diffuse interstellar features may provide interesting information on the internal temperatures and geometrical characteristics of interstellar particles.

**16013.** Meissner, P., **Evaluation of techniques for verifying personal identity,** *Proc. ACM-NBS Fifteenth Annual Technical Symp., Gaithersburg, MD, June 17, 1976,* pp. 119-127 (Association for Computing Machinery, Washington, DC, 1976).

Key words: ADP security; computer networks; controlled accessibility; encryption; evaluation criteria; key; password; personal identification; terminals; verification.

The Privacy Act of 1974 imposes a number of requirements upon Federal agencies to prevent the misuse of information about individuals and to assure its integrity and security. Central to the implementation of the required safeguards is verification of the identity of individuals who are authorized to have access to computer systems and networks. A variety of techniques for verifying identity are currently emerging under the impetus of increased concern for security. This paper reviews some of the more promising techniques in terms of their applicability to computer security, and discusses the factors involved in evaluating these techniques. A set of evaluation criteria is presented. Considerations arising from imperfect operation of identification devices are explored. The paper also outlines precautions which should be included in a system as supplements to the identity verification process, such as auditing of system access, hostage alarms, and encryption.

**16014.** Bald, J. F., Jr., Sharp, K. G., MacDiarmid, A. G., **The isolation and characterization of pentafluorodisilane,** *J. Fluorine Chem. Short Commun.* **3,** 433-435 (1973/74).

Key words: base catalyzed decomposition; fluorodisilane; pentafluorodisilane; physical properties; pyrolysis; silicon difluoride.

The primary product of the reaction between hydrogen bromide and silicon difluoride, $SiF_2$, has been shown to be 1-bromo-1,1,2,2,-tetrafluorodisilane, $SiF_2HSiF_2Br$ (I). This compound decomposes spontaneously at room temperature with pentafluorodisilane, $Si_2F_5H$ (II) as the primary product. A more efficient source of (II) involves fluorination of the Si-Br bond in (I) with antimony trifluoride, $SbF_3$. Isolation of (II) can be effected by multiple runs on a low temperature distillation column.

The physical properties of (II) have been determined and are discussed, as are the infrared, $^1H$ and $^{19}F$ nmr and mass spectra.

The thermal stability and several chemical characteristics of (II) have also been investigated. Specific experiments which are discussed involve the pyrolytic and base-catalyzed decompositions of (II).

**16015.** Watson, R. E., Perlman, M. L., Herbst, J. F., **Core level shifts in the 3*d* transition metals and tin,** *Phys. Rev. B* **13,** No. 6, 2358-2365 (Mar. 15, 1976).

Key words: binding energy shifts; core level shifts; tin.

We present estimates of various contributions to the free-atom-metal binding-energy shifts, $\Delta E_B$, for the $2s$ and $2p$ core levels of the iron series elements and, for comparison, the $3d_{5/2}$ level of Sn. Our results indicate that the sharp break in the experimental $\Delta E_B$ values occurring between Ni and Cu is due to variation in differences of *d*-electron count, i.e., *d* configuration, between atom and metal. Ley *et al.* who neglected the *d*-configuration differences, attributed the break in $\Delta E_B$ to a change in extra-atomic screening. Through free-atom calculations we find extra-atomic screening energies of 6-8 eV for Ti through Zn, with no break between Ni and Cu, and ~10 eV for Sn. In conjunction with charge-renormalization and dipole-term estimates, these results suggest that intra-atomic screening of core holes in metals is an important factor influencing free-atom-metal binding-energy shifts.

**16016.** Vorburger, T. V., Waclawski, B. J., Sandstrom, D. R., **Improved microwave-discharge source for uv photoemission,** *Rev. Sci. Instrum* **47,** No. 4, 501-504 (Apr. 1976).

Key words: adsorption; chemisorption; CO: cyclotron resonance; electron cyclotron resonance; magnetic field; microwave discharge; photoemission; tungsten; ultraviolet photoemission.

A microwave-discharge uv light source has been improved to yield significant photon fluxes at 26.9 and 40.81 eV. In order to optimize the 26.9-eV (Ne II) and 40.81-eV (He II) radiation, the discharge was operated at ~2.5 Pa (0.019 torr) in an external constant magnetic field of ~0.070 T (700 G), which, together with the oscillating electric field of the cavity, produces electron cyclotron resonance. When the discharge conditions were optimized for production of 40.81-eV photons, features near the Fermi energy in the photoemission distribution from W(100) for 40.81-eV photons are approximately 6 percent as intense as the corresponding features in the distribution for 21.22-eV photons. We estimate that under these conditions the flux of 40.81-eV photons is roughly 50 percent of the flux of 21.22-eV photons. Photoemission energy distributions with $h\nu$=16.85, 21.22, 26.9, and 40.81 eV have been measured for saturated exposures of CO on W(100) at a temperature of ~80 K. The variation in these data with photon energy is important for making orbital assignments to the energy levels of adsorbed molecular CO.

**16017.** McBee, C. L., Kruger, J., **Ellipsometric spectroscopic study of breakdown of Fe-Cr and Fe-Cr-Mo alloys,** *Proc. USA-Japan Seminar on Passivity and Its Breakdown on Iron and Iron Base Alloys, Honolulu, HI, Mar. 10-12, 1975,* pp. 131-132 (National Association of Corrosion Engineers, Houston, TX, 1976).

Key words: ellipsometric parameters; ellipsometric spectroscopy; iron base alloys; iron single crystal.

Ellipsometric spectroscopy was recently applied to the study of the breakdown of passivity on pure iron single crystal surfaces. These studies first obtained a measurement of the ellipsometric parameters, $\Delta$ and $\psi$, as a function of wavelength for a passivated surface held at a potential in a buffered borate solution. $Cl^-$ ions were then added, and it was noted for most wavelengths that no changes were found for $\Delta$ and $\psi$ as a function of time during the induction period prior to breakdown. However, at a few wavelengths, $\Delta$ and $\psi$ did vary with $Cl^-$ additions. Using these changes and current measurements, it was possible to study events leading to the breakdown of Fe. The work described here extends the technique employed in previous studies to Fe-Cr-Mo alloys.

**16018.** Kruger, J., **Chemical breakdown of passivity,** *Proc. USA-Japan Seminar on Passivity and Its Breakdown on Iron and Iron Base Alloys, Honolulu, HI, Mar. 10-12, 1975,* pp. 91-98 (National Association of Corrosion Engineers, Houston, TX, 1976).

Key words: chemical breakdown; chloride ion; corrosion; ferrous alloys; localized corrosion; passivity.

A review is given of the various theoretical models for the chemical breakdown of passivity. The models discussed are adsorbed in displacement, ion migration, or penetration and chemico-mechanical breakdown. The models are then related to data in the literature on breakdown initiation kinetics, critical potentials for breakdown, and alloy composition and structural and environmental factors. Based on the above examination a number of critical questions are posed that must be answered in order to understand chemical breakdown of the passive film.

**16019.** Moore, R. T., **The influence of ink on the quality of fingerprint impressions,** *Proc. Conf. on the Science of Fingerprints, London, England, Sept. 24-25, 1974*, pp. 69-84 (1974).

Key words: film thickness; film uniformity; fingerprint impressions; fingerprint readers; image quality; ink films; lubricity.

Tests were conducted on several types of ink to determine their influence on the quality of fingerprint impressions which they could produce. The thickness and uniformity of the film used to ink the fingers were found to be the most significant factor in providing high quality impressions. A method is described for metering out printer's ink and estimating whether or not a uniform film of near optimum thickness has been rolled out on a glass inking plate.

**16020.** Wehrli, R., Bryan, J., **Assemblage: A process-oriented teaching method,** *AIA J.*, pp. 75-77 (May 1976).

Key words: architectural-design teaching; assemblage; design critiques; feedback; teaching method.

Architecture for the future—with material shortages, environmental protection, and new technological possibilities—cannot be accommodated by traditional methods of design education. A new teaching method called assemblage, with feedback advantages, allows students to assemble special blocks to create designs while their instructor, using a scorecard, evaluates progress against fixed criteria which the student understands. Because design problems are increasingly complex with multiple criteria to satisfy at early stages of design, the assemblage method is needed. It allows students to take multiple fixed criteria into consideration and the instructor to keep track of all design criteria while giving students immediate, analytical feedback on how well they are doing. With assemblage's design blocks and analytical scorecards, an instructor can assign simulation of real-world design problems, supply feedback from an analytical scorecard to encourage future improvement in design in less than an hour for each trial scheme. A 1968 experiment in assemblage demonstrated students learned perceptibly during six trials when given feedback (critiques), but learning was marginal when feedback was withheld.

**16021.** Mangum, B. W., Wood, S. D., **Reliability of temperature measurements and control provided in clinical instruments (Abstract),** *Proc. 28th Annual Conf. Engineering in Medicine and Biology, New Orleans, LA, Sept. 20-24, 1975*, p. 251 (1975).

Key words: clinical instruments; instruments, clinical; temperature measurements.

Some medical and clinical instruments rely heavily on accurate temperature measurements. Thermistors are often used in these instruments although little is known about their behavior on ageing or thermal cycling. Results of an NBS study on ageing of six types of thermistors are presented.

**16022.** Zalubas, R., Hagan, L., **Atomic energy levels of rare earth elements,** *Proc. 11th Rare Earth Research Conf., Traverse City, MI, Oct. 7-10, 1974*, **1**, 411-416 (1974).

Key words: atoms; classification; energy levels; ions; rare earths; spectroscopy.

At the National Bureau of Standards members of the Spectroscopy Section are investigating rare earth spectra and are working on a critical compilation of rare earth energy levels. Also a number of people in other laboratories are working on these spectra. The compilation will include all experimentally known levels of free atoms and ions of lanthanum through lutetium ($Z$=57–71).

**16023.** Yates, J. T., Jr., Erickson, N. E., Worley, S. D., Madey, T. E., **The use of x-ray photoelectron spectroscopy (ESCA) for studying adsorbed molecules,** Chapter in *The Physical Basis for Heterogeneous Catalysis*, E. Drauglis and R. I. Jaffee, Eds., pp. 75-105 (Plenum Press, New York, NY, 1975).

Key words: carbon monoxide; chemisorption; ESCA; extra-atomic relaxation; formaldehyde; oxygen; photoelectron spectroscopy; physisorption; tungsten; xenon; XPS.

An ultrahigh vacuum x-ray photoelectron spectrometer has been used to study a number of cases of adsorption on tungsten single crystals. The choice of adsorbates spans a wide range from dissociative chemisorption to nondissociative chemisorption to physisorption.

A method for estimating absolute surface coverages from ESCA data has been verified by comparison with absolute molecular-beam measurements of monolayer coverage for the system oxygen+W(100).

The ESCA technique for measuring chemical shifts has been found to be useful in discriminating various modes of surface bonding in all adsorption systems studied. For oxygen chemisorbed on W(100), two distinct oxygen states are seen. In the case of CO chemisorbed on W(100), a direct correlation between ESCA and thermal desorption behavior has been observed for four states of chemisorbed CO. For $H_2CO$ interaction with W(100), dissociative adsorption occurs initially, followed by multilayer condensation of $H_2CO$. For xenon physisorption on W(111), high-energy sites (defects?) are covered first by mobile xenon; this is followed by adsorption on the uniform surface.

Coverage-dependent shifts in binding energy have been observed in several cases. The magnitudes of these shifts are independent of changes in average work function, and are best explained by considering local dipole interactions.

In all cases studied, it appears that final-state extra-atomic relaxation effects dominate in determining the magnitude of the chemical shift for adsorbed species. Core-level binding energies have been found to decrease upon adsorption in all cases so far studied, and the magnitude of the decrease seems to correlate in a crude way with increasing strength of adsorption.

**16024.** Yahalom, J., Ives, L. K., **Electron-microscopical studies of passive films on stainless steels,** *Proc. USA-Japan Seminar on Passivity and Its Breakdown on Iron and Iron Base Alloys, Honolulu, HI, Mar. 10-12, 1975*, pp. 69-71 (National Association of Corrosion Engineers, Houston, TX, 1976).

Key words: electron microscopy; Fe-Cr alloys; passive films; pitting corrosion; stainless steel; x-ray analysis.

Transmission electron microscopy and diffraction were employed to study *in situ* films over corrosion pits in ferritic Fe-Cr alloys containing 5, 12, and 19 wt.% Cr and in commercial AISI 304 and 316 stainless steels. The composition of passive films extracted from the pits was obtained by energy dispersive x-ray emission analysis. In all cases an enhanced concentration of Cr was observed, though to a lesser extent in the Fe-5% Cr alloy. A substantial difference in the crystalline structure and morphology was found to exist among the various alloys. The differences in passivity exhibited by the alloys and the mechanism of breakdown are discussed in light of these findings.

**16025.** Cotton, I. W., Benoit, J. W., **Prospects for the standardization of packet-switched networks,** (Proc. Fourth Data Communications Symp., Quebec City, Canada, Oct. 7-9, 1975), Paper in *Network Structures in an Evolving Operational Environ-*

*ment, IEEE Catalog No. 75 CH1001-7 Data,* pp. 2-1 –2-7 (The Institute of Electrical and Electronics Engineers Inc., New York, NY, 1975).

Key words: computer networks; data communications; networks; packet-switching; standards.

The technology of packet-switching is now moving rapidly toward commercial application as a number of companies in the U.S. and abroad are preparing to offer service. However, there does not appear to be much commonality of design in these various commercial systems. Standards are needed to facilitate the possible use of multiple networks by individual users and the eventual interconnection of local or regional networks.

This paper reviews the technical issues relevant to the standardization of packet-switched networks. This is accomplished through narrative and model of a packet-switched system which clarifies the various functions of the system. Each of the possible candidate areas for standards is discussed in terms of the likelihood that standards can be developed.

**16026.** Wang, F. W., **Frictional properties of dilute block-copolymer solutions and homopolymer solutions. Application to molecular weight determination,** *Macromolecules* 9, No. 1, 97-101 (Jan.-Feb. 1976).

Key words: bead-spring model; block copolymers; dilute polymer solutions; limiting viscosity number; Mandelkern-Flory-Scheraga equation; molecular weight determination; sedimentation coefficient; translational diffusion coefficient; Zimm theory.

An equation for the translational diffusion coefficient of block copolymers in dilute solution has been obtained by modifying Zimm's equation for homopolymers to take into account the existence of dissimilar segments in block copolymers. Illustrative calculations for homopolymers and block copolymers have been made and the results for homopolymers have been compared with experiments and with the calculations of Yamakawa and Fujii. A procedure has been proposed to determine the molecular weight of a block copolymer from measurements of its limiting viscosity number and its sedimentation coefficient or translational diffusion coefficient.

**16027.** Wright, J. R., **Opening remarks by the session chairman,** (Proc. 6th Congress on The Impact of Research on the Built Environment, Budapest, Hungary, Oct. 2-8, 1974), Chapter in *Congress Book II, 60-61 (Conseil International du Batiment Pour la Recherche, L'Etude et la Documentation, Rotterdam, The Netherlands, 1974).*

Key words: building construction; building design; building materials; building research; environmental protection; international cooperation; international standards; materials conservation; materials science; performance concept.

The design of buildings is ultimately limited by the availability and properties of building materials. Materials are not only significant to the built environment in their own right but figure in a cluster of interrelated trends – world competition for resources, materials conservation, materials substitution, environmental protection, application of the performance concept to building, and materials science. Against these pressures and dynamics, growing international cooperation is discerned among building technologists, cooperation which in part is reflected by an increasing body of international standards for building materials.

**16028.** Van Zyl, B., Chamberlain, G. E., Dunn, G. H., Ruthberg, S., **Definitive pressure generation in the $10^{-4}$-$10^{-3}$ torr range for atomic scattering experiments,** *J. Vac. Sci. Technol.* **13,** No. 3, 721-727 (May/June 1976).

Key words: pressure generation; $10^{-3}$ to $10^{-4}$ torr range.

A pressure generation technique using the dynamic expansion method is described. Measurements and uncertainties are discussed, and it is shown that the method provides a convenient means for obtaining accurate pressures in the $10^{-3}$-$10^{-4}$ torr range. High confidence uncertainties as low as about ±1 percent are achieved.

**16029.** Heydemann, P. L. M., **Ultrasonic measurements at pressures up to 50 kbar,** *Proc. Intern. Colloq. Les Propriétés Physiques des Solides Sous Pression, Grenoble, France, Sept. 8-10, 1969,* No. 188, pp. 461-467 (Centre National de la Recherche Scientifique, Paris, France, 1970).

Key words: bulk modulus; equation of state; high pressure; phase transitions; potassium chloride; ultrasonics.

Ultrasonic measurements as a function of pressure or temperature provide one of the most accurate means to determine pressure or temperature dependence of the bulk modulus and the density of both liquids and solids. Such measurements are currently carried out with very high accuracy at pressures up to about 4 kbar (1 kbar=$10^8$N/m$^2$) in several laboratories.

If the material under investigation undergoes transitions at higher pressures, or if the bulk modulus is noticeably nonlinear with pressure, ultrasonic measurements at pressures higher than 4 kbar are needed. This report describes our methods to carry out such measurements at pressures close to 50 kbar, both under hydrostatic and nonhydrostatic conditions.

For most materials the accuracy of the density and bulk modulus data obtained from such measurements is much higher than that obtained from isothermal dilatometric measurements. In the case of tellurium, the accuracies for the bulk modulus at 30 kbar are 1.6 and 23 percent, respectively.

Another interesting application of ultrasonics at high pressures is the detection of phase transitions and the measurement of the elastic properties as the material undergoes the transition. As an example for measurements through a transition range, our results of ultrasonic and isothermal dilatometric measurements on KCl are presented. We find that the ratio of specific heats also shows a sharp increase in the transition range.

**16030.** Wegstein, J. H., **The automated classification and identification of fingerprints,** *Proc. Conf. on the Science of Fingerprints, London, England, Sept. 24-25, 1974,* pp. 49-67 (1974).

Key words: classification; computer; fingerprint; identification; pattern recognition; scanner.

Data read by the FBI's FINDER automatic fingerprint reader system must undergo three processing steps in order to achieve fingerprint identifications. First, the data must be "registered" to a standard reference position for subsequent comparison purposes. Next, the data are "classified" into suitable categories for filing and retrieval purposes. Finally, the data are "matched" against other fingerprint data of the same classification by comparing their distinctive minutiae. Computer algorithms for these processing steps are discussed and representative results presented.

**16031.** Haisch, B. M., Linsky, J. L., **Properties of the chromosphere-corona transition region in Capella,** *Astrophys. J.* **205,** No. 1, L39-L42 (Apr. 1, 1976).

Key words: stars, chromospheres; stars, late type; ultraviolet, spectra.

Analysis of recent ultraviolet observations of the Capella binary system ($\alpha$ Aur) indicates a dense, geometrically narrow chromosphere-corona transition region in the Capella system primary (G5 III) similar in many respects to a solar active region. An examination of the coronal energy balance, together with the coronal base pressure derived from the line fluxes, predicts a corona with a mean temperature of $1.2 \times 10^6$ K and a large stellar wind consistent with observations.

**16032.** Beitler, S. R., Armstrong, G. T., Domalski, E. S., Keane, T. R., Eds., **Book, Combustion Fundamentals for Waste Incineration,** 217 pages (The American Society of Mechanical Engineers, New York, NY, 1974).

Key words: combustion thermodynamics; enthalpies of formation; incinerators, industrial; thermodynamic data; waste disposal.

This monograph contains tabulated thermodynamic data for over 1300 substances needed by engineers for design and operation of incinerators for industrial wastes. In addition to tables of data, the monograph provides definitions of thermodynamic terms and a brief discussion of practical thermodynamic functions, a discussion of the calculation of thermochemical quantities related to combustion, and a brief discussion of the effect of temperature upon combustion processes and reaction equilibria. The monograph also contains annotated bibliographies containing selected references to (1) supplementary sources of thermodynamic information on chemical substances and materials, (2) methods of estimation of thermodynamic data, and (3) combustion and high temperature reaction equilibria. The principal table gives enthalpies of formation at 298.15 K for 989 organic compounds and inorganic carbon compounds listed in order of increasing empirical formula, and is accompanied by a name-formula index as an additional aid to locating data. Two other tables give enthalpies of formation at 298.15 K of 285 inorganic oxides and 39 organic polymers for which a reasonable formula could be assigned. An appendix at the end of the monograph gives supplementary information such as symbols for thermodynamic quantities, definitions of the SI base units, physical constants, and atomic weights.

**16033.** Burnett, E. D., **NBS hearing aid test procedures, Chapter III. Performance measurement data from the National Bureau of Standards,** *Handbook of Hearing and Measurement 1976*, **IB 11-52,** pp. 14-299 (Veterans Administration, Washington, DC, 1976).

Key words: anthropometric manikin; free-field measurements; hearing aid tests; orthotelephonic response.

This report discusses the current test procedures used by NBS to evaluate the electroacoustic properties of hearing aids. It includes the technical and practical reasons for performing the various tests in the manner described and in certain cases presents ideas and preliminary test methods for the evaluation of special-purpose hearing aids. However, the specific details of the electronic equipment used to perform the tests are not described.

**16034.** Evans, A. G., Johnson, H., **The fracture stress and its dependence on slow crack growth,** *J. Mater. Sci.* **10,** 214-222 (1975).

Key words: analytical predictions; constant stress rate; empirical measurements; fracture stress; slow crack growth.

An analysis is presented which enables the fracture strength, (under constant stress-rate conditions) to be predicted from fracture mechanics data obtained during slow crack growth—by identifying and evaluating several key parameters. The predicted strength characteristics are illustrated using fracture mechanics data obtained for a soda lime silicate glass. Finally, the predicted strengths are compared with strengths measured in flexure on abraded soda lime silicate glass specimens. A good correlation is obtained, indicating an equivalence between micro- and macrocrack propagation conditions for this material.

**16035.** Epstein, G. L., Reader, J., **Resonance lines and energy levels of Cs III, Ba IV, and La V,** *J. Opt. Soc. Am.* **66,** No. 6, 590-598 (June 1976).

Key words: barium; cesium; lanthanum; spectra; ultraviolet; wavelengths.

The spectra of Cs III, Ba IV, and La V have been observed in a sliding spark discharge on the 10.7 m normal-incidence vacuum spectrograph at NBS. Analysis of the observations of Cs III and La V has yielded the energy levels of the $5s^25p^5$ and $5s5p^6$ configurations and nearly all levels of the $5s^25p^45d$ and $5s^25p^46s$ configurations that can combine with the $5s^25p^5\,{}^2P^\circ$ ground term. The observations for Ba IV have yielded the levels of the $5s^25p^5$ and $5s5p^6$ configurations. The $5s^25p^45d + 5s^25p^46s + 5s5p^6$ levels of Cs III and La V have been theoretically interpreted, with configuration interaction included. The energy parameters determined from a least-squares fit to the observed level values are compared with Hartree-Fock calculations. The ionization energies are found to be $33.38 \pm 0.25$ eV for Cs III, $47.1 \pm 0.6$ eV for Ba IV, and $61.6 \pm 0.6$ eV for La V. By extrapolating these values the ionization energy of Ce VI is estimated as $77.6 \pm 1.2$eV.

**16036.** Albus, J. S., Evans, J. M., Jr., **A hierarchical structure for robot control,** *Proc. 5th Int. Symp. on Industrial Robots, Chicago, IL, Sept. 22-24, 1975*, pp. 231-238 (Society of Manufacturing Engineers, Dearborn, MI, 1975).

Key words: automatic control; automation; robots.

Sophisticated control of a mechanical manipulator is similar in many respects to the problem of organizing coordinated activity in any complex system with many degrees of freedom. It requires that the overall control problem be partitioned into manageable subproblems which can be arranged in a hierarchical control structure. At each level in the control hierarchy there exists a computing device or algorithm capable of accepting input commands from the next higher level, combining these with appropriate feedback signals from the controlled environment, and responding with an ordered sequence of output commands to the next lower level. Input to the top of the hierarchy commits the entire system to a specific goal-directed activity. Output from the bottom consists of strings of signal voltages which drive individual joint activators.

NBS has been evaluating ways in which such a hierarchical control structure can be implemented. One implementation is the Cerebellar Model Articulation Controller (CMAC), a memory-driven control element which can be used at each level in the control hierarchy to accept input commands from higher levels under feedback control. CMAC is a general purpose adaptive control function computer which can cope with many nonlinear feedback variables simultaneously, such as measurements of misalignment of parts, variable mass loading, irregularities in materials, and constraints imposed by an external environment.

NBS research in sensors and computer control systems will be described, with specific examples of applications for hierarchical control systems.

**16037.** McBee, C. L., Hastie, J. W., **Mechanistic studies of phosphorus containing flame retardants,** *Proc. 1975 Int. Symp. on Flammability and Fire Retardants, Montreal, Canada, May 22-23, 1975*, pp. 253-263 (Technomic Publication Co., Inc., Westport, CT, 1976).

Key words: flame retardancy; mass spectrometry; optical spectroscopy; phosphorus; polyester.

A combination of mass spectrometric and optical spectroscopic studies has been made to establish a mechanism for phosphorus controlled flame retardancy in thermoplastics. It is shown that a vapor phase mode of flame inhibition can account for the known flame retardancy effect of triphenylphosphine oxide in polyester substrates.

**16038.** Bagg, T. C., **A technological review: The future of microimagery in the library,** *Drexel Lib. Quart.* **11,** No. 4, 66-74 (Oct. 1975).

Key words: computer output microforms; information storage and retrieval; libraries; microfilm; microforms; micrographics.

Libraries are using microforms in a variety of ways and will add many more to their collections to save space, have available out-of-print materials, expand audiovisual materials and as the result of computer-generated microforms of frequently updated indexes, catalogs, listings, etc.

Despite the growing need of micrographic equipment, the libraries do not offer a large enough market to have equipment designed and produced by their specific needs. Libraries must therefore depend upon developments for other applications, some of which are discussed.

**16039.** Evans, A. G., Fuller, E. R., **Proof testing—The effects of slow crack growth,** *Mater. Sci. Eng.* **19,** No. 1, 69-77 (1975).

Key words: failure probabilities; lifetime assurance; proof testing; slow crack growth; unloading.

When slow crack growth occurs during proof testing, the extent of the crack growth while unloading from the proof stress has a substantial effect on the minimum predicted in-service failure time. It is essential that this crack growth is minimized to achieve effective failure prediction. Analyses are presented which show that the detrimental effects can be negated by environmental control during proof testing and/or rapid unloading from the proof stress; the requisite combination of unloading rate and environmental control is determined separately for each system.

**16040.** Henderson, M. M., **Copyright impacts of future technology,** (Proc. Symp. Centennial Meeting of the American Chemical Society, New York, NY, Apr. 5, 1976), *J. Chem. Inf. Comput. Sci.* **16,** No. 2, 72-74 (May 1976).

Key words: bibliographic data files; communications technology developments; computer developments; COM systems extension; copyright protection; facsimile transmission extension; photocopying; reprography developments.

Dynamic developments in computer and communication technologies, and in reprography and micrographics, are yielding systems and equipment that render better and faster access to information that has been copyrighted in traditional formats. Procedures and mechanisms must be worked out to permit us to take advantage of these technologies without destroying our basic systems of information dissemination.

**16041.** VanderHart, D. L., **Characterization of the methylene $^{13}C$ chemical shift tensor in the normal alkane $n$-$C_{20}H_{42}$,** *J. Chem. Phys.* **64,** No. 2, 830-834 (Jan. 15, 1976).

Key words: alkane; chemical shift tensor; methylene; NMR; $^{13}C$.

$^{13}C$ NMR chemical shifts in a single crystal of $n$-eicosane ($n$-$C_{20}H_{42}$) have been measured using the method of high power proton decoupling and the chemical shift tensors were characterized. Principal values in ppm relative to $CS_2$ are: (a) For $CH_3$: $\sigma_{11} = 166.7 \pm 2$, $\sigma_{22} = 171.2 \pm 2.0$, $\sigma_{33} = 189.8 \pm 2$; (b) For the $\alpha$-methylene: $\sigma_{11} = 156.0 \pm 2.5$, $\sigma_{22} = 163.1 \pm 2.5$, $\sigma_{33} = 178.0 \pm 2.5$; and (c) For the interior methylenes: $\sigma_{11} = 142.6 \pm 2.0$, $\sigma_{22} = 154.6 \pm 2.0$, $\sigma_{33} = 175.6 \pm 2.0$. From x-ray studies, only the unit cell parameters are known. On the basis of isolated molecule symmetry considerations, cross-polarization rate studies, and oriented polyethylene spectra, the interior methylene chemical shift tensor is assigned with respect to molecular orientation. The crystallographic axes are also related to the interior methylene chemical shift tensor and a prediction is made for the $C-CH_3$ bond direction relative to these crystallographic axes. The principal axes of the $\alpha$-$CH_2$ and the $CH_3$ chemical shift tensors do not coincide with any bond directions. The difference (5.6 ppm) between the interior methylene average chemical shielding in solid $n$-eicosane and the isotropic liquid value is also discussed.

**16042.** Norden, B. N., **National measurement system: Length and related dimensional measurements—A micro study,** *NCSL Newsletter* **15,** No. 2, 21-26 (June 1975).

Key words: dimensional measurements; length measurements; National Measurement System.

Studies of the National Measurement System are currently in progress at the National Bureau of Standards. These studies are an attempt to understand the infrastructure and impact of measurement throughout our economy. One particular micro study is entitled *Length and Related Dimensional Measurements*. This brief article gives an overview of the developments to date; i.e., description of the infrastructure, identification of various users, and discussion of needed future research in the area of length and related dimensional measurements.

**16043.** Hamer, W. J., **Standard cells,** Chapter in *The Primary Battery*, G. W. Heise and N. C. Cahoon, Eds., **I,** 433-477 (John Wiley & Sons, Inc., New York, NY, 1971).

Key words: batteries; cells, primary; dry cells; primary batteries; primary cells.

Testing procedures for primary cells and batteries are outlined. Emphasis is given to cells and batteries of the dry type. Tests are classified as (1) general tests, (2) initial tests, (3) service tests, and (4) shelf tests. Under initial tests measurements of open-circuit voltage, initial closed-circuit voltage, flash or short-circuit current, and internal resistance (or impedance) are considered. Methods that may be used to measure internal resistance are considered at length. Service tests include 28 standard tests as well as some other types of tests still in use. Some special tests as well as tests for wet primary cells and reserve batteries are briefly considered.

**16044.** Wets, R. J. B., Witzgall, C., **Towards an algebraic characterization of convex polyhedral cones,** *Numer. Math.* **12,** 134-138 (1968).

Key words: algebraic; cones; faces; Jordan-equivalent; matrices; polyhedral.

It is shown that the theory of positive linear independence and the properties of Jordan-equivalent matrices can be utilized effectively in order to obtain an algebraic characterization of a face structure of convex polyhedral cones.

**16045.** Pyke, T. N., Jr., **Assuring user service quality in a distributed computer network,** *Proc. COMPCON 76 Spring, San Francisco, CA, Feb. 24-27, 1976*, pp. 73-76 (IEEE Computer Society, Washington, DC, 1976).

Key words: computer networking; distributed networks; network service.

As users become dependent on service from multiple computer systems within distributed computer networks, a variety of problems arise in assuring that end user service quality is maintained. In this paper, a number of factors associated with user service quality are examined in the context of this trend toward distributed computing.

**16046.** Durig, J. R., Lafferty, W. J., Kalasinsky, V. F., **Spectra and structure of small-ring molecules. 33. Microwave spectrum of silacyclopentane,** *J. Phys. Chem.* **80,** No. 11, 1199-1202 (1976).

Key words: dipole moment; microwave spectrum; molecular structure; silacyclopentane; small-ring molecule; Stark effect.

The microwave spectrum of silacyclopentane, 1-silacyclopentane-*1,1*-$d_2$, and silacyclopentane-$^{29}Si$ has been investigated in the spectral range of 8-40 GHz. The rotational lines of five vibrational excited states of the ring-puckering mode have also been assigned and are consistent with a high barrier to pseudorotation. Both the dipole moment measurements and the isotopic data indicate that the skeletal ring of this molecule is in the "twisted" $C_2$ conformation for the ground state. The *a* component of the dipole moment is $0.726 \pm 0.005$ D and the *c* component has been determined to be less than 0.01 D with a $|\mu_t| = 0.726 \pm 0.006$ D. The isotopic data are sufficient to determine the following parameters: $\angle HSiH = 108.76 \pm 0.26$, $r(Si-H) = 1.478 \pm 0.004$. Other important structural features have been estimated.

**16047.** Albus, J. S., Evans, J. M., Jr., **Robot systems,** *Sci. Am.* **234,** No. 2, 77-86B (Feb. 1976).

Key words: artificial intelligence; automation; computer control; manipulators; robots; robot systems.

This article reviews currently available industrial robots and research on robot systems. A hierarchical control structure concept, which is the basis for NBS research efforts in computer control systems, is used to provide a framework for this review.

**16048.** Branstad, M. A., Branstad, D. K., Jeffery, S., **Terminals: Out of sight but under control,** *Proc. COMPCON 74, San Francisco, CA, Feb. 26-28, 1974,* pp. 53-55 (IEEE Computer Society, Washington, DC, 1974).

Key words: security; terminals.

General purpose terminals, point-of-sale terminals, and cash dispensing terminals are described with respect to their common, as well as individual, security needs. Solutions which satisfy some terminal security requirements and needs for future security enhancements are presented.

**16049.** LeVanda, C., Bechgaard, K., Cowan, D. O., Mueller-Westerhoff, U. T., Eilbracht, P., Candela, G. A., Collins, R. L., **Bis(fulvalene)diiron, its mono- and dications. Intramolecular exchange interactions in a rigid system,** *J. Am. Chem. Soc.* **98,** No. 11, 3181-3187 (May 26, 1976).

Key words: biferrocenylene; delocalization; intramolecular exchange; magnetic susceptibility; mixed valence; Mössbauer spectra; optical.

Biferrocenylene [bis(fulvalene)diiron, BFD] was synthesized by two independent routes: an Ullman coupling of dibromoferrocene and the reaction of the fulvalene dianion with ferrous chloride. It was chemically oxidized to the mixed valence monocation and to the dication. These derivatives were characterized by optical, Mössbauer, ESR, and x-ray photoelectron spectra and magnetic susceptibility. The Mössbauer spectra of the mixed valence salts at 298 and 77 K indicate that both iron atoms are equivalent. X-ray photoelectron spectra similarly attest to this equivalence. An asymmetry in the intensity of the Mössbauer lines is due to a Karyagin effect. The Mössbauer spectrum of the dication shows a quadrupole splitting of 3.0 mm/s which is unusually large for a ferrocenium-type derivative. The magnetic susceptibility of BFD (2,3) picrate, measured in the 2-300 K range, follows a Curie law with a room temperature moment very close to the spin-only value. The dicationic fluoroborate salt is diamagnetic. The ESR spectra of the monocationic picrate and fluoroborate salts are characterized by narrow lines and a small rhombic anisotropy. An absorption in the near-infrared centered at 1550 nm is observed in the spectra of the monocations, but not the neutral or dicationic derivatives. The assignment of this band is discussed with respect to the results of the other physical measurements.

**16050.** Ferraris, J. P., Finnegan, T. F., **Electric susceptibility and d.c. conductivity of crystalline TTF–TCNQ,** *Solid State Commun.* **18,** Nos. 9/10, 1169-1172 (1976).

Key words: d.c. conductivity; microwave conductivity; organic conductors; thermal expansion; TTF–TCNQ.

An experimental study has been made of the intrinsic d.c. and microwave conductivity of "high purity" crystalline TTF–TCNQ. The maximum normalized peak conductivity in each case was found to be about 50 times the room temperature value. The cavity perturbation technique, used to determine the microwave conductivity and low temperature dielectric constant, is also shown to be a useful contactless method for measuring the thermal expansion.

**16051.** Chang, T. T., Cohen, M. I., **Paramagnetic resonance of $Dy^{3+}$ in $CdF_2$,** *J. Chem. Phys.* **64,** No. 12, 5255-5260 (June 15, 1976).

Key words: $CdF_2$; $Dy^3$; paramagnetic resonance.

Paramagnetic resonance of $Dy^{3+}$ substitutional for Cd in $CdF_2$ was observed at 24 GHz and 4.2 K. The cubic spectrum and the orthorhombic spectrum of samples cross doped with Li, Na, or K were studied. The *g* factors are as follows: for the $\Gamma_7$ transition, $g = 7.4250$; for $\Gamma_8$ transitions in cubic symmetry, $g = 2.4514$; and for $\Gamma_8$ transitions in orthorhombic symmetry, $g_{110} = 2.1025$, $g_{001} = 8.6613$, and $g_{110} = 10.1846$.

**16052.** Mihalas, D., Shine, R. A., Kunasz, P. B., Hummer, D. G., **Resonance-line transfer with partial redistribution. VIII. Solution in the comoving frame for moving atmospheres,** *Astrophys. J.* **205,** No. 2, 492-498 (Apr. 15, 1976).

Key words: line formation; radiative transfer; stars: chromospheres.

An analysis of the effects of partial frequency redistribution in the scattering process for lines formed in moving atmospheres has been performed using a flexible and general method which allows solution of the transfer equation in the comoving frame of the gas. As a specific example, we consider the same chromospheric and atomic model, with the same velocity field, that was studied by Cannon and Vardavas. We find that the large changes in the profiles obtained by those authors, between the cases of complete and partial redistribution are *spurious effects of angle-averaging in the observer's frame instead of the comoving frame.* Our results support fully the conclusion by Magnan that these changes are, in fact, unreal, at least for this particular model and redistribution function. Future work with other redistribution functions and with nonmonotone velocity fields will be possible using the techniques developed in this paper.

**16053.** Stevens, M. E., **Compatibility problems of network interfacing,** *Proc. Conf. on Interlibrary Communications and Information Networks, Warrenton, VA, Sept. 28-Oct. 2, 1970,* pp. 202-212 (American Library Association, Chicago, IL, 1971).

Key words: common practices; communication; compatibility; convertibility; information interchange; information networks; interfacing; interlibrary communication; man-machine interaction; network protocols.

The compatibility and convertibility problems of network interfacing are considered in the light of applicable standards, preferred common practices, and protocols. There is considerable emphasis upon requirements for interaction and information interchange. Specific technological problems of compatibility or convertibility at the interfaces between machine and machine, man and machine, and man and man are discussed. Promises for solution to at least the more tractable of the interfacing problems appear to lie in the growing conspicuity of these problems, the recognition of the need for compromise, a growing commitment to the usage of machines as aids to man, and the increasing impetus to cooperative action.

**16054.** Duff, J. W., Truhlar, D. G., **Classical *S* matrix: Application of the Bessel uniform approximation to a chemical reaction,** *Chem. Phys. Lett.* **40,** No. 2, 251-256 (June 1, 1976).

Key words: chemical reactions; classical scattering matrix theory; collision theory; hydrogen atoms; hydrogen molecules; scattering theory; trajectories; uniform approximation.

The Bessel uniform approximation developed by Stine and Marcus is applied to the collinear $H + H_2$ reaction on Diestler's potential energy surface no. 3 to which we have previously applied other orders of approximation of classical *S* matrix theory. It appears that an accurate treatment of this system by classical *S* matrix theory requires interference of real and complex trajectories. Calculations were also performed on two other potential energy surfaces in order to more clearly understand the interrelationships of previous semiclassical and quasiclassical studies of this reaction.

**16055.** Kuriyama, M., Boettinger, W. J., **On the angular divergence of out-going beams in an asymmetric diffraction geometry,** *Acta Cryst. A* **32,** Part 3, 511-512 (May 1976).

Key words: angular divergence; asymmetric diffraction; diffraction topography; dynamical diffraction; rocking curve.

The well-known relation for, the angular divergence of beams diffracted from a perfect crystal in an asymmetric diffraction condition is derived straightforwardly from first principles.

**16056.** Geller, S. B., **Erasing myths about magnetic media,** *Datamation,* pp. 65-68, 70 (Mar. 1976).

Key words: data loss, magnetic media; devices, effects on magnetic media; fields, effects on magnetic media; magnetic fields, erasure of data; magnetic media, data erasure; magnetic media, data protection.

Magnetic media such as tapes and disks are used to store information for use in ADP systems. These stored data can be obliterated under certain conditions by fields which are produced by various devices. This paper describes the effects on data of devices which include airport metal detectors, x-ray units, radar systems, gamma rays, laser beams, television receivers, and automobiles. It describes the erasing effects of permanent magnets as well as the effects of varying magnetic fields, r. f. fields, light, heat, cold, and time on the stored data. The paper then presents some guidelines for safeguarding the data which are recorded on computer magnetic media.

**16057.** Morton, M., Fetters, L. J., **Homogeneous anionic polymerization of unsaturated monomers,** Chapter in *Macromolecular Reviews,* A. Peterlin, M. Goodman, S. Okamura, B. H. Zimm, and H. F. Mark, Eds., **2,** 71-113 (John Wiley & Sons, Inc., New York, NY, 1967).

Key words: block copolymers; homogeneous anionic polymerization; monodisperse polymers; unsaturated monomers.

This review discusses the polymerization of unsaturated monomers by carbanionic mechanisms. Particular emphasis is placed on the synthesis possibilities of these systems, i.e., monodisperse polymers, block copolymers, and polymers reactive end-groups.

**16058.** Saunders, R. D., Ott, W. R., **Spectral irradiance measurements: Effect of uv-produced fluorescence in integrating spheres,** *Appl. Opt.* **15,** No. 4, 827 (Apr. 1976).

Key words: deuterium, arc lamps; Halon; integrating spheres.

A fluorescence effect was detected when a Halon coated integrating sphere was irradiated by a deuterium lamp. This fluorescence, if not accounted for, causes large errors when comparing the spectral irradiance of tungsten lamps to that of deuterium lamps.

**16059.** Marshall, H. E., **Efficiency impacts of cost sharing on shoreline management,** *Coastal Zone Manage. J.* **2,** No. 4, 369-382 (1976).

Key words: beach erosion control; Corps of Engineers; cost sharing; efficiency; hurricane protection; shoreline management; shoreline protection.

The nation's shorelines are being eroded by high winds and waves. Nonfederal interests have traditionally received federal help in the form of cost sharing for protective structures. This article describes, compares, and evaluates existing and alternative cost-sharing rules for shoreline protection on the basis of economic efficiency. Both engineering and management techniques are examined for beach erosion, hurricane, and emergency coastal flood protection. The present cost-sharing system appears to bias local interests to choose (1) costly techniques of protection, e.g., engineering rather than management techniques, and under certain conditions (2) protective structures overbuilt in terms of the efficient scale. Conclusions are that these biases could be reduced if all engineering and management techniques for reducing shoreline damages were subject to the same percentage cost-sharing rules.

**16060.** McCulloh, K. E., Dibeler, V. H., **Enthalpy of formation of methyl and methylene radicals of photoionization studies of methane and ketene,** *J. Chem. Phys.* **64,** No. 11, 4445-4450 (June 1, 1976).

Key words: enthalpy of formation; ketene; methane; methyl; methylene; photoionization; rotational energy.

Photoion yield curves for $CH_3^+$ and $CH_2^+$ from methane have been measured near threshold at 295 and 115 °K, and the curves for $CH_2^+$ from ketene have been obtained at 295 and 130 °K. Although the detection efficiencies for positive and negative ions were nearly equal, a search for the ion-pair process yielding $CH_3^+ + H^-$ gave negative results. The methane data are successfully fitted on the assumption that the full rotational energy is available for formation of $CH_3^+$, but that only two rotational degrees of freedom contribute to the available energy for the process yielding $CH_2^+$. Neglecting excess energy at threshold, the values $\Delta Hf_0°(CH_3) = 149.4 \pm 0.5$ kJ/mole ($35.70 \pm 0.12$ kcal/mole) and $\Delta Hf_0°(CH_2) = 392.5 \pm 2.1$ kJ/mole ($93.8 \pm 0.5$ kcal/mole) from methane. Correction of the threshold for $CH_2^+$ from ketene for rotational energy results in the concordant value $\Delta Hf_0°(CH_2) = 390.8 \pm 1.7$ kJ/mole ($93.4 \pm 0.4$ kcal/mole) on the assumption that excess energy can be neglected at threshold. The mean of the two determinations is selected as the preferred value $\Delta Hf_0°(CH_2) = 391.6 \pm 1.7$ kJ/mole ($93.6 \pm 0.4$ kcal/mole).

**16061.** Thomas, G. A., Schafer, D. E., Wudl, F., Horn, P. M., Rimai, D., Cook, J. W., Glocker, D. A., Skove, M. J., Chu, C. W., Groff, R. P., Gillson, J. L., Wheland, R. C., Melby, L. R., Salamon, M. B., Craven, R. A., De Pasquali, G., Bloch, A. N., Cowan, D. O., Walatka, V. V., Pyle, R. E., Gemmer, R., Poehler, T. O., Johnson, G. R., Miles, M. G., Wilson, J. D., Ferraris, J. P., Finnegan, T. F., Warmack, R. J., Raaen, V. F., Jerome, D., **Electrical conductivity of tetrathiafulvalenium-tetracyanoquinodimethanide (TTF-TCNQ),** *Phys. Rev. B* **13**, No. 11, 5105-5110 (June 1, 1976).

Key words: electrical conductivity; organic conductors; tetrathiafulvalenium-tetracyanoquinodimethanide; TTF-TCNQ.

New measurements of electrical conductivity along the *b* axis of tetrathiafulvalenium-tetracyanoquinodimethanide (TTF-TCNQ) are combined with published results to provide a comprehensive summary including approximately 600 samples studied at 18 different laboratories. The magnitudes of these measured conductivities do not necessitate the assumption of superconducting fluctuations or any other collective state in which the conductivity exceeds the limitations of single-particle scattering. Since an adequate theory of the limitations of single-particle scattering for TTF-TCNQ does not exist at present, experiment alone does not rule out the possibility that collective effects may somewhat enhance or suppress the conductivity.

**16062.** Hughes, C. E., Walker, J. C., **POPSS, a system for modelling and analyzing operating system resource allocation strategies,** *Proc. 3rd Texas Conf. on Computing Systems, Austin, TX, Nov. 7-8, 1974, Paper 74-CHO895-3C*, pp. 3-6-1 – 3-6-8 (IEEE Computer Society Publ. Office, Long Beach, CA, 1974).

Key words: FORTRAN IV; operating system; overhead; resource allocation; simulator; strategies; workload.

This paper describes the parametric operating system simulator POPSS, a FORTRAN IV program which was designed to provide a tool for evaluating operating system resource allocation strategies and to serve as a pedagogical device, providing understanding of the functions, components, and component interactions of operating systems. In order to meet both these objectives the system was designed in such a way as to be both flexible and easy to use. The paper covers the range of resource allocation strategies which may be modelled; the facilities provided for describing workloads; the methods used to simulate operating system overhead; and the tools incorporated for allowing users to extend the range of models beyond those currently built into the system.

**16063.** Pyke, T. N., Jr., **Network access techniques: Some recent developments,** *Proc. 3rd Texas Conf. on Computing Systems, Austin, TX, Nov. 7-8, 1974, Paper 74-CHO895-3C*, pp. 2-2-1 – 2-2-4 (IEEE Computer Society Publ. Office, Long Beach, CA, 1974).

Key words: communication; computer networks; network access techniques.

Over the last few years a clear need to help computer network users more efficiently and effectively access network based resources has been recognized. This need has followed the demonstrated feasibility of large scale computer networks that provide a wide variety of resources. It has also resulted from the current availability of a large number of commercial, academic, and Government networks that provide a wide variety of programs, data, and systems resources for users. The functions performed by network access processes and devices that have been implemented or are planned range from basic communications support to applications-oriented capabilities. These functions can be performed within a network environment by techniques ranging from user support processes in host computers to minicomputer-based network access devices, as well as by intelligent terminals. Examples of these functions and of network architectures that support them are given in this paper.

**16064.** Evans, A. G., Russell, L. R., Richerson, D. W., **Slow crack growth in ceramic materials at elevated temperatures,** *Metall. Trans.* **6A**, 707-716 (Apr. 1975).

Key words: acoustic emission; crack propagation; cyclic conditions; failure times; high temperatures; silicon nitride; slow crack growth.

Techniques for studying slow crack growth at high temperatures are described. The techniques are used to obtain crack growth data for a range of silicon nitrides between 1100 and 1400 °C. For these materials the data suggest that the slow crack growth may be effectively characterized by the relation between crack velocity and stress intensity factor. Data obtained for mechanical and thermal fatigue modes indicate that these behaviors can be predicted with moderate accuracy from the isothermal, static stress parameters (for the range of conditions investigated). Finally, the application of slow crack growth data to failure prediction is described and illustrated using data for one of the materials tested.

**16065.** Pella, P. A., Kuehner, E. C., Cassatt, W. A., **Development of thin calibration standards for x-ray fluorescence analysis,** *Environmental Protection Technology Series, EPA-600/2-76-126*, 11 pages (Available as PB253252 from the National Technical Information Service, Springfield, VA 22161, May 1976).

Key words: calibration; filters; orchard leaves; standard reference sample; x-ray analysis.

Particulate reference samples have been prepared for the Environmental Protection Agency for use in the standardization of x-ray fluorescence spectrometers. Uniform layers of reground orchard leaves of known composition, i.e., NBS Standard Reference Material 1571, were deposited on membrane filters and coated with a thin polymer film. Samples have been prepared with deposit thicknesses ranging from 0.1 to 5.0 mg/cm$^2$.

**16066.** Washer, F. E., **Cameras, optics, and filters for color aerial photography. Lens design for color,** Chapter III in *Manual of Color Aerial Photography, First Edition*, J. T. Smith, Jr., Ed., 94-138 (American Society of Photogrammetry, Falls Church, VA, 1968).

Key words: lens aberrations; lens characteristics; lens distortion; lens resolving power.

This article presents a brief description of lens characteristics and aberrations that are of interest in photography. The various aberrations such as longitudinal spherical, longitudinal chromatic, and lateral chromatic are described together with brief discussions of their effect on imagery and some methods of measurement. Lens distortion, field curvature, and resolving power are also discussed briefly. Figures and tables illustrating various phases of lens performance are included.

**16067.** Garvin, D., Domalski, E. S., Hampson, R. F., Wagman, D. D., **Chemistry in the stratosphere,** Chapter 5 in *The Natural Stratosphere of 1974, CIAP Monograph 1*, A. J. Grobecker, Ed., Report No. DOT-TST-75-51, 28 pages (Dept. of Transportation, Washington, DC, Sept. 1975).

Key words: atmospheric chemistry; chemical kinetics; data evaluation; gas phase; photoabsorption cross section; photochemistry; quantum yield; rate constant.

This chapter has two objectives. They are (1) to illustrate the problems to be solved in unraveling the chemistry of the stratosphere and (2) to provide the quantitative data needed when chemical reactions are introduced into numerical modeling of the stratosphere. The topics discussed in this chapter, their pertinence to the stratosphere and some principal conclusions are described.

**16068.** Florin, R. E., **Leo Aloysius Wall,** Biographical item for book *American Chemists and Chemical Engineers,* W. D. Miles, Ed., pp. 490-491 (American Chemical Society, Washington, DC, 1976).

Key words: biography; Wall, L. A.

Short biography of Leo A. Wall.

**16069.** Evans, A. G., Wiederhorn, S. M., Linzer, M., Fuller, E. R., Jr., **Proof testing of porcelain insulators and application of acoustic emission,** *Am. Ceram. Soc. Bull.* **54,** No. 6, 576-581 (June 1975).

Key words: acoustic emission; macrocracking; porcelain insulators; proof testing; residual strain.

An investigation of proof testing has been conducted on large cone and post porcelain insulators. The cone configuration was unsuitable for overload proof testing to the loads needed for effective lifetime predictions. The only merit of subjecting this configuration to a proof test is the assurance of no immediate macrocracking during installation. This is achieved by testing to a load marginally larger than the service load. Conversely, the post configuration exhibited the basic prerequisites for effective proof testing but detailed stress analysis of this system is needed before specific proof testing procedures can be recommended. Finally, acoustic emission measurements were a major asset for monitoring both macrocracking events and stress development during the proof tests.

**16070.** Weikel, M. K., Miller, T. R., **A summary of a cost analysis of blood banking alternatives,** *Proc. 3rd Annual Conf. of the Society of Government Economists, Washington, DC, Mar. 23, 1973,* W. E. Kost, Ed., pp. 31-37 (1975).

Key words: blood banking; cost analysis; economics; indirect costs; subsidized costs.

A brief synopsis of parts of NBS Report 10 924, "Cost Analysis of Blood Banking Alternatives," was presented at the Third Annual Meeting of the Society of Government Economists. The presentation included discussion of: current problems related to blood banking; the economic aspects of blood supply and demand; the cost analysis methodology; and the actual results of the cost analysis.

**16071.** Huffman, J. C., Roth, R. S., Siedle, A. R., **Synthesis of ternary metal sulfide arrays,** *J. Am. Chem. Soc.* **98,** No. 14, 4340-4341 (July 7, 1976).

Key words: clusters; metal-metal bonding; metal sulfides; sulfides; tungsten; x-ray crystallography.

Deoxygenation of $(Ph_3PCH)_2WO_2S_2$ with $Ph_2PCH_3$ in the presence of a group Ib metal slat led to $[(Ph_2PCH_3)_2Cu]_2WS_4$, $[Ph_2PCH_3)_2Ag]_2WS_4$, $[(Ph_2PCH_3)Ag]_2WS_4$ and $[Ph_2PCH_3)Au]_2WS_4$. Infrared, Raman, electronic, $^1H$ and $^{31}P$ nmr spectral data are reported.

The gold-tungsten-sulfur array was characterized by single crystal x-ray diffraction techniques.

**16072.** Culver, C., **Fire loads and live loads in buildings,** *Proc. Int. Conf. on Performance of Building Structures, Glasgow, Scotland, Mar. 31-Apr. 1, 1976,* **1,** 111-119 (Pentech Press Ltd., London, England, 1976).

Key words: buildings; fire loads; load surveys; occupancy live loads; structural engineering.

The development of a nation-wide survey program for determining fire loads and live loads in buildings and establishing the factors which affect these loads is described. Considerations involved in planning the program and the type of data collected are included. Preliminary survey results obtained from the NBS Administration building are described.

**16073.** Manning, J. R., **Comparison of matrix inversion, Monte Carlo, and diffusion of probability techniques for calculation of diffusion correlation factors,** (Proc. Symp. on Computer Simulation for Materials Applications, Gaithersburg, MD, Apr. 19-21, 1976), *Nucl. Metall.* **20,** Pt. 1, 109-120 (Apr. 1976).

Key words: computer simulation; correlation factor for diffusion; diffusion; matrix calculation; Monte Carlo calculation; theory of diffusion; vacancy diffusion.

The diffusion correlation factor can be determined by calculating the mean square atom displacement resulting from a long series of atom jumps. Monte Carlo computer simulation techniques are coming more-and-more to be applied to this problem. Possible problems encountered in applying the common matrix inversion technique to correlation factor calculations are discussed, and the relative advantages and disadvantages of matrix inversion and Monte Carlo techniques are examined. In some cases, a diffusion of probability technique that involves only one matrix inversion is found to provide more nearly accurate results than do either the usual matrix inversion or Monte Carlo techniques. As examples, correlation approximations for diffusion in random binary alloys and for diffusion via divacancies are discussed.

**16074.** Farmer, B. L., Eby, R. K., **Calculations of internal friction resulting from molecular defects in hydrocarbon crystals,** (Proc. Symp. on Computer Simulation of Materials Applications, Gaithersburg, MD, Apr. 19-21, 1976), *Nucl. Metall.* **20,** Pt. 1, 154-165 (Apr. 1976).

Key words: calculations; hydrocarbon crystals; internal friction; molecular defects; pair potentials; site model.

Relaxations observed by dynamic-mechanical measurements of linear hydrocarbon crystals have been attributed to a variety of molecular features. In the present review, molecular defects resulting from the inclusion of isolated methyl-branched molecules and vacancies in the crystals are examined with regard to their possible roles in these relaxations. An approach combining the treatments of a standard linear solid, a site model, and molecular building with computer based semi-empirical potential energy calculations has been used. The results indicate that such molecular defects can indeed play a role in the observed relaxations. The relaxation strength and relaxation times determined from the computational model are in qualitative and semi-quantitative agreement with experimental data.

**16075.** Davis, R. M., **Federal interest in computer utilization by state and local governments,** *The Bureaucrat* **1,** No. 4, 349-356 (Winter 1972).

Key words: automation; computer utilization; dedicated computers; EDP expenditure; employment; finance; productivity; services – state/local government.

The size of state and local government labor forces, their expenditures on EDP, and nationwide desires for more government services of better quality provided with increased productivity are national concerns. The federal investment in state and local government EDP is significant. As a result, there is a legitimate interest in the effect federal policies may have on computer utilization by state and local governments. A review of federal policies shows that there is no single overall federal policy imposing any constraints on computer utilization by state and local governments. The Department of Justice in its National Crime Information Center (NCIC) has formulated security and confidentiality provisions applicable only for that system. No other federal agency appears to have policies specific to the dedicated use of computer systems.

**16076.** Henderson, M., Geddes, S., **Automation and the federal library community: Report on a survey,** *Federal Library Committee,* pp. 1-49 (Library of Congress, Washington, DC, June 1973).

Key words: federal libraries; library automation; survey report.

From June 1970 to July 1971 an intensive investigation was undertaken of the federal library community and its involvement with library automation. The project, initiated by Federal Library Committee's Task Force on Automation of Library Operations, was supported by the U.S. Office of Education and conducted by the System Development Corporation. This report summarizes and abstracts the results of that investigation and highlights the resulting picture drawn of the federal library community. Tables and graphs from the original report and handbook are reproduced in this summary and are referred to the original documents.

**16077.** McKinney, J. E., Simha, R., **Configurational thermodynamic properties of polymer liquids and glasses. Poly(vinyl acetate). II,** *Macromolecules* **9,** No. 3, 430-441 (May-June 1976).

Key words: compressibility; configuration; entropy; heat capacity; holes; polymer; poly(vinyl acetate); pressure; thermal; volume.

The theoretical internal energy, entropy, and internal pressure of the equilibrium system of poly(vinyl acetate) using the scaling parameters established previously are computed as functions of temperature and pressure and found to be in good agreement with those derived from the experimental PVT data given in paper I. For the analysis of the glassy state, a new method is developed and applied to the two constant formation glasses discussed earlier. It employs the partition function which has the same mathematical form as for the equilibrium system, but derives the hole fraction $h(V, T)$ as the solution of a partial differential equation. This equation results from the proper thermodynamic definition of the pressure in terms of the partition function, applied to the experimental PVT surfaces for the glasses. A quantitative improvement in the compressional thermodynamic functions, particularly in regard to the internal pressure, ensues over the more empirical procedure employed previously. There $h$ is treated as an adjustable parameter in the pressure equation derived for the liquid, using the experimental PVT surface for the glass. The application of the proper expression for the pressure results in a reduced variation of $h$ with temperature and pressure in the glassy state and thus in numerically larger freezing fractions than those derived earlier. We exhibit the internal energy and entropy differences between the atmospheric pressure and pressurized (800 bar) glasses, and between these and the super-cooled melt. The computed difference between the configurational heat capacities of the melt and glass at $T_g$ are about 47 percent for $C_p$ and 13 percent for $C_v$ of the totals obtained by calorimetry. Finally, convenient interpolation expressions for the hole fraction, theoretical internal energy, and theoretical entropy as functions of the reduced variables of state are developed for the equilibrium liquid in general and the two specific glasses considered here. These relations dispense with the necessity of iteration procedures for the numerical evaluation of the theoretical functions.

**16078.** Stein, R. J., **Angle- and energy-resolved charged particle spectroscopies—A simple way,** *Rev. Sci. Instrum.* **47,** No. 6, 716-719 (June 1976).

Key words: angle and energy distributions; charged particle spectroscopy; electron-stimulated desorption of ions (ESDIAD); field-ion microscopy (FIM); low energy electron diffraction (LEED); ultraviolet photoelectron spectroscopy (UPS).

The acquisition of angular and energy distribution information is of growing importance in a number of charged particle spectroscopies used for surface studies. A simple, inexpensive method is outlined for obtaining a visual display of angular distributions containing energy distribution information in the form of color. In essence, a detector optical bandpass is varied synchronously with an energy-selecting element of a spectrometer having a visual display in order to convert the analyzed particle energy distribution to a corresponding chromatic map. The primary utility of the method would be to obtain qualitative information rapidly in those cases where the particle energy spectra have distinct and strong features or when features of interest lie at the higher-energy end. Examples of the latter are plasma loss structure in low-energy electron diffraction, electron-stimulated desorption ion angular distributions, and the higher-energy structure in ultraviolet photoelectron spectroscopy. Other applications are also considered. The practical sensitivity limit for the case of visual observation is 1.0 percent $[I(\Delta E)/I_{total}]$. This sensitivity is not sufficient for application of the method to Auger electron spectroscopy or electron spectroscopy for chemical analysis.

**16079.** Penn, D. R., **Quantitative chemical analysis by ESCA,** *J. Electron Spectrosc. Relat. Phenom.* **9,** 29-40 (1976).

Key words: electron spectroscopy for chemical analysis; mean free path; quantitative analysis.

Electron spectroscopy for chemical analysis (ESCA) can be used as a quantitative tool for the determination of the chemical composition of the surface region of a solid if certain parameters are known. The least well known is the electron mean free path. We present values of the electron mean free path for inelastic scattering as a function of energy for all elemental solids (with the exception of the rare earths and the actinides) and we give formulae for the calculation of the mean free paths for compounds. It is shown that this information makes it possible to deduce from ESCA measurements the relative concentration of atoms or molecules distributed homogeneously in the surface region of a material.

**16080.** Watson, R. E., Herbst, J. F., Wilkins, J. W., **Core level shifts of rare-gas atoms implanted in the noble metals,** *Phys. Rev. B* **14,** No. 1, 18-25 (July 1, 1976).

Key words: core level; implant; noble metals; rare gas; shift.

By means of soft-x-ray photoemission Citrin and Hamann have observed core level shifts of Ne, Ar, Kr, and Xe atoms implanted in the noble metals and have constructed a theoretical model with which to interpret the results. We describe calculations employing a quite different approach to the same physical effects which are as successful numerically. The two salient elements are the energy associated with the screening of the core hole by the host-metal electrons and the potential shift arising from the surface dipole of the metal, neither of which is present in the free-atom case. Also considered is the chemical shift due o implantation in the host; estimates of this depend upon details f the model describing the implant site, but for the case at hand ve find this contribution to be small.

16081. Hocken, R., Moldover, M. R., **Ising critical exponents in real fluids: An experiment,** *Phys. Rev. Lett.* **37,** No. 1, 29-32 (July 5, 1976).

Key words: $CO_2$; critical exponents; critical point; equation of state; $SF_6$; Xe.

We report precise optical measurements of the equations of tate of Xe, $SF_6$, and $CO_2$ very near their critical points $|T-T_c|/T_c < 5 \times 10^{-5}$). We find that the critical exponents of hese fluids in this region are close to the exponents calculated rom the three-dimensional Ising model.

6082. Marinenko, G., Huggett, R. J., Friend, D. G., **An instrument with internal calibration for monitoring chlorine residuals in natural waters,** *J. Fish. Res. Board Can.* **33,** No. 4, Part 1, 822-826 (1976).

Key words: amperometry; chlorine monitoring; chlorine residuals; coulometry; flux-monitor; water analysis; water pollution.

To increase the sensitivity of field instruments for measure nent of low level chlorine concentrations in natural waters a new nonitor was developed. Iodine, resulting from oxidation of otassium iodide by chlorine residual, is measured amperometri ally in a system in which coulometrically generated iodine is ised as a system calibrant. Laboratory tests, field tests, and com arisons of the new chlorine monitor with other instruments vere performed. Data obtained with the new instrument show hat chlorine concentrations down to a few parts per billion can e measured. The instrument is portable, and has built-in electri al calibration features and direct read-out display in either nicroamperes or parts per million of residual chlorine.

6083. Snell, J. E., **Comments on drainage system performance,** *Proc. CIB Commission W62 Symp. on Drainage Services in Buildings, National Swedish Institute for Building Research, Stockholm, Sweden, Sept. 24-25, 1973,* pp. 1:1-1:11 (Swedish Council for Building Research, Stockholm, Sweden, 1974).

Key words: gravity drainage evaluation; plumbing research.

A number of changes are taking place in plumbing system echnology that may lead to significant departures from tradi onal dependence on gravity drainage. These factors include ew designs and materials and the need to conserve water. A ajor concern in facilitating introduction of new technology is vercoming traditional roadblocks to innovation in this field. his paper describes an approach being pursued by the National ureau of Standards and others to assure that performance of ew systems is demonstrated in terms meaningful to local en rcement authorities.

6084. Siu, M. C. I., **Analysis of edge-heat-loss of a guarded-hot-plate apparatus,** *Proc. 14th Int. Conf. on Thermal Conductivity, Storrs, CT, June 2-4, 1975,* P. G. Klemans and T. K. Chu, Eds., pp. 413-422 (Plenum Press, NY, 1976).

Key words: ambient temperature index; edge-heat-loss; errors; guarded-hot-plate apparatus; line-heat-source; thermal conductivity.

Analysis on the error in measured specimen thermal conduc vity arising from edge-heat-loss at the periphery of any arded-hot-plate apparatus is presented. It is shown that the error due to edge-heat-loss varies linearly with respect to the deviation of the ambient temperature from mean specimen temperature. Explicit expressions are presented for the line-heat-source guarded-hot-plate apparatus being constructed at the National Bureau of Standards.

16085. Yates, J. T., Jr., Madey, T. E., Erickson, N. E., Worley, S. D., **Adsorption and condensation of small molecules on tungsten (100) as studied using x-ray photoelectron spectroscopy,** *Chem. Phys. Lett.* **39,** No. 1, 113-117 (Apr. 1, 1976).

Key words: carbon dioxide; carbon monoxide; chemisorption; formaldehyde; oxygen; physisorption; surface chemistry; tungsten; x-ray photoelectron spectroscopy.

X-ray photoelectron spectroscopy (XPS) has been used to examine the adsorption of $H_2CO$, $O_2$, CO and $CO_2$ on the W(100) surface at 100 K and 300 K. Correlations between XPS measurements and kinetic measurements have been made.

16086. Winder, D. R., **Orientation of hexagonal crystals,** *Am. J. Phys.* **38,** No. 3, 319-326 (Mar. 1970).

Key words: crystallography, elementary; crystals, hexagonal; hexagonal crystals; hexagonal lattices.

Interplanar angles and stereographic projections are described for hexagonal structures. Graphs of the variations of some interplanar angles with $c/a$ are given. The four systems of indexing hexagonal lattices are compared.

16087. Culver, C. G., **Comprehensive survey program for fire and live loads in buildings,** *Proc. Public Buildings Service International Conf. on Firesafety in High-Rise Buildings, Seattle, WA, Nov. 18, 1974,* pp. 1-30 (1974).

Key words: buildings; fires; loads; safety; surveys.

The development of a nation-wide survey program for determining fire loads and live loads in buildings and establishing the factors which affect these loads is described. Considerations involved in planning the program, the type of data collected and data processing procedures as well as a brief description of the data analysis are included.

16088. Oser, H. J., **An average distance,** Problem 75-12 in *Problems and Solutions* **18,** No. 3, 497-501 (July 1976).

Key words: average distance; distance; multiple integrals; transportation problem.

Take two unit squares and place them side by side so they form a rectangle two units wide and one unit high. Now choose a point A at random in the first square and, again at random, a point B in the second square. Then A and B will be a certain distance apart. Question: If we repeat the random choice of A and B many times, how far apart will they be on the average?

16089. Fechter, J. V., Jr., **Product safety and product performance research at the National Bureau of Standards,** *Proc. 6th Congress of the International Ergonomics Association "Old World, New World, One World," University of Maryland, College Park, MD, July 11-16, 1976,* pp. 136-140 (The Human Factors Society, Inc., Santa Monica, CA, July 1976).

Key words: human factors ergonomics; product performance; product safety; standards.

In 1974, the National Bureau of Standards established a Center for Consumer Product Technology to conduct product safety and product performance research. The Center's Human Factors Section operates a laboratory which is used for consumer product studies. While much of the Laboratory's equipment and instrumentation is fairly typical of other human factors laboratories, its configuration and application at NBS is unique.

A study of cooking ranges is presented to illustrate how the facility is being used.

**16090.** Unassigned.

**16091.** Margulis, S. T., **The ICET testing program for the certification of engineering technicians,** *Prof. Eng.*, pp. 30-31 (Mar. 1976).

Key words: criteria; decision making; human systems; measuring instruments; research assistants; test device evaluation.

The Institute for the Certification of Engineering Technicians (ICET) certifies engineering technicians nationally. New criteria for voluntary certification have been instituted recently. Central to the approach is a new testing program to determine the technical competence of candidates. Those applying for Associate Engineering Technician or Engineering Technician status are required to pass a written examination; those applying for Senior Engineering Technician status must prepare a 5000-word technical essay.

The testing program is described and evaluated and special uses for the written examinations, which ICET proposes, are reviewed. Overall, the testing program suggests careful test development and a desire for continuing development. Tests appear to be technically sound. Plans for test evaluation, by ICET, will more clearly establish the strengths and weaknesses of the tests. Special uses for the tests—for assessing technical obsolescence as part of a continuing professional development program, and for helping candidates prepare for the written examination by completing a short version of the test, are commendable additions to the testing program.

**16092.** Burch, D. M., Peavy, B. A., Powell, F. J., **Experimental validation of the NBS load and indoor temperature prediction model,** *ASHRAE Trans.* **80,** Part 2, 291-310 (1974).

Key words: dynamic model; environmental chamber experiment; heating and cooling load computer program; heating load; masonry building.

Measurements of the dynamic heat transfer in an experimental masonry building were made in a large environmental chamber to explore the validity of a computer program developed at NBS for computing heating and cooling loads, and indoor air temperatures. The experimental structure was a one-room house 20 ft long, 20 ft wide, and 10 ft high with walls of solid concrete blocks and a flat roof made of reinforced precasts concrete slabs. The building was exposed to a diurnal temperature cycle for a series of tests where changes were made in fenestration, the amount and location of insulation, and the amount of indoor mass. The NBS computer program predicted both indoor air temperatures and heating loads that were in close agreement with the experimental data.

**16093.** Bordé, C. J., Hall, J. L., Kunasz, C. V., Hummer, D. G., **Saturated absorption line shape: Calculation of the transit-time broadening by a perturbation approach,** *Phys. Rev. A* **14,** No. 1, 236-263 (July 1976).

Key words: lasers; nonlinear spectroscopy; saturated absorption.

We present a third-order perturbation calculation of line shapes in laser spectroscopy based on the density-matrix formalism. The new feature of this theory is the inclusion of the Gaussian spatial structure of the laser beams. We study the linewidth as a function of relaxation and transit times. A shift is found when the wave fronts are not flat. General line-shape formulas are given as well as approximate formulas valid in various domains.

**16094.** Cheron, B., Scheps, R., Gallagher, A., **Continuum radia tion and potentials of Tl-noble gas molecules,** *J. Chem. Phys* **65,** No. 1, 326-335 (July 1, 1976).

Key words: molecules; radiation; thalium.

Continuum emission intensities on the extreme wings of the T resonance lines due to noble gas perturbers have been measure as a function of gas temperature. These spectra, due to the $B^2\Sigma_{1/}$ $- X\ 1/2$; $B^2\Sigma_{1/2} - X\ 3/2$, and $B^2\Sigma_{1/2} - A\ 1/2$ bands, are in terpreted with the classical Franck-Condon principle to yiel estimates of the $B^2\Sigma_{1/2}$, $A\ 1/2$, $X\ 3/2$, and $X\ 1/2$ potentials of Tl noble gas molecules. As has been noted qualitatively in matri isolation studies, the Group III elements form unusually stabl diatomic bonds with the "inert" gases, e.g., we find Tl-Xe boun by ~300 cm$^{-1}$. The Tl-Xe system is an interesting visible, ex cimer laser candidate, as the molecular spectra extend very fa into the red wings of the resonance lines.

**16095.** Niatel, M. T., Loftus, T. P., Oetzmann, W., **Compariso of exposure standards for $^{60}$Co gamma rays,** *Metrologia* **11,** 17 23 (1975).

Key words: cobalt-60; exposure standard; international in tercomparison.

Comparisons for $^{60}$Co gamma rays between the exposure star dards of the Bureau International des Poids et Mesures (BIPM the National Bureau of Standards (NBS) and the Physikalisch Technische Bundesanstalt (PTB) are reported. For measure ments made at about one meter from the source, and if the sam physical constants are used, the differences are 0.26 percer between the BIPM and NBS standards, and at most 0.4 percer between the BIPM standard and the PTB standard chambers The differences are consistent with the estimated systematic ur certainties (≈0.5%).

The difference between the NBS standard and the PT chamber measurements, as determined through the ratios of eac to the BIPM chamber, ranges from 0.17 to 0.66 percent. The di ference in exposure standards for NBS and PTB actually range from 0.48 to 0.97 percent, since different stopping power co rections are used by these two laboratories.

An indirect comparison of the BIPM and NBS standards in dicates that the difference of 0.26 percent will increase to 0.5 percent at a distance of two meters.

**16096.** Guildner, L. A., Johnson, D. P., Jones, F. E., **Vapor pre sure of water at its triple point: Highly accurate value,** *Scienc* **191,** 1261 (Mar. 26, 1976).

Key words: precision mercury manometer; triple point c water; vapor pressure of water.

The vapor pressure of water at its triple point was measure with greatly increased accuracy. The triple point was realize with newly designed equipment that enhanced the stability of th pressure and permitted any air released from solution to b removed by pumping. A diaphragm pressure transduce separated the water vapor from the helium used to transmit th pressure to the manometer. The pressure was measured with th National Bureau of Standards precision mercury manomete The vapor pressure at the triple point was found to be 611.65 pascals with random uncertainties at the 99 percent confidenc level of ± 0.010 pascal. The systematic errors are estimated to b relatively insignificant.

**16097.** Spencer, L. V., Eisenhauer, C., **Reflection of charged-pa ticle beams at near-grazing incidence,** *Trans. Am. Nucl. So* **23,** 609-610 (June 1976).

Key words: Albedo; angular distribution; backscatte charged particles; Monte Carlo; reflection.

An analytic expression is given for the angular distribution of charged particles reflected from a surface for a near-grazing incident beam. This expression predicts the apparent specular reflection peak observed in experiments and Monte Carlo calculations.

**16098.** Novick, R., Sprott, G., Lucatorto, T., **Identification of the lowest metastable autoionizing level in Rb from rf spectroscopic studies,** *Phys. Rev. A* **14,** No. 1, 273-278 (July 1976).

Key words: atomic beam; autoionization; differential metastability; fine structure; inner shell excitation; rf spectroscopy; rubidium; Zeeman effect.

The lowest Rb metastable autoionizing level has been dentified by a rf resonance measurement of the $g$ factors of the various hyperfine sublevels. Of the two lowest-lying metastable state assignments, $4p^5(^2P)5s5p(^3P)^4D_{7/2}$ and $4p^54d(^3F)5s^4F_{9/2}$, only components of the $^4D_{7/2}$ were observed in the metastable beam. The atomic-beam resonance method employed resembles raditional methods except that it exploits the differential metastability of the fine-structure levels instead of magnetic deflection for state selection.

**6099.** Jeffery, S., Branstad, D. K., **Security considerations in software systems,** *Proc. 3d Texas Conf. on Computing Systems, Austin, TX, Nov. 7-8, 1974, Paper 74-CHO895-3C,* pp. 8-4-1 – 8-4-4 (IEEE Computer Society Publ. Office, Long Beach, CA, 1974).

Key words: security, software; software engineering; software systems.

Software engineering may well be the foundation upon which ecurity of computer systems will be built for the near future. Self-protecting systems, those which have the internal mechanisms to prevent technical assaults on the computer ystem's integrity are needed to prevent the unauthorized modification or disclosure of information stored and processed within the system. While most time-shared or multi-programmed omputer systems do incorporate rudimentary protection mechanisms which prevent accidental damage to the operating ystem and to other concurrently processing programs, no eneral system has withstood the technical onslaught of penetraion teams authorized to test its security features. The generic aws found and analyzed by these penetration teams can be raced to poor design criteria and/or poor programming echniques. This paper discusses some of the fundamentals of oftware engineering needed to be used and extended in building ecure computer systems.

**6100.** Armstrong, G. T., **Reaction calorimetry of fluorine and the thermochemistry of its compounds,** *L'Actualité Chimique,* pp. 5-14 (Feb. 1976).

Key words: bomb calorimetry with fluorine; enthalpy of formation, fluorides; flame calorimetry of fluorine and fluorides; procedures, experimental for handling fluorine.

The importance, the advantages, and the difficulties of using emental fluorine for reaction calorimetry are discussed. echniques developed at NBS for bomb calorimetry and gas lame calorimetry with elemental fluorine or fluorine-containing ompounds as oxidizers are discussed together with their appliation to substances such as $CF_4$, $BF_3$, ClF, $ClF_3$ and refractory ompounds such as $B_4C$. The accuracy achieved and the scope f possible measurements are discussed in relationship to the atus of the thermochemistry of fluorine compounds.

**101.** Beausoliel, R. W., Phillips, C. W., Snell, J. E., **Field investigation of natural gas pipeline accident, Canterbury Woods, Annandale, VA,** *Fire J.* **68,** No. 3, 77-84 (May 1974).

Key words: Annandale; field test; gas explosion; leak detection.

On the morning of March 24, 1972, in Annandale, Virginia, two homes were destroyed and a third home damaged by gas explosions and fires resulting from a construction accident that caused the gas main leak. The National Transportation Safety Board was responsible for investigating this accident and requested that the National Bureau of Standards assist them with their investigation by conducting a field test at the accident site.

The objective of the test was to determine how the natural gas entered the homes and the paths the gas followed from the leak to the homes. The premise of the NBS test was that if an air-tracer mixture could be detected at locations where natural gas was known to have escaped, then the original underground gas paths may still exist. A detailed test plan was developed to determine gas escape locations and paths. This plan included a simulation of the underground gas movement, excavation of various utility trenches, soil tests, and dismantling of the foundation wall of one of the destroyed homes. The equipment used to introduce the tracer into the ground near the original leak consisted of an air compressor, a tracer source (refrigerant R-12), air flow measuring, piping and control valves. Electronic catalytic leak detectors were used to detect the tracer in homes and elsewhere on the test site. The test results substantiated the basic test premise, and tracer was detected in the basements of the two destroyed homes and the damaged home, but not in the undamaged homes. From the results, it is concluded that gas traveled through rock rubble on the site and used as backfill in utility trenches containing the individual water and sewer lines to the destroyed/damaged homes and entered the homes through leaks in their concrete block foundations.

**16102.** Blevin, W. R., **Black coatings for thermal radiation detectors,** *Proc. Smithsonian-Eppley Symp. on Solar Radiation. Measurements and Instrumentation, Rockville, MD, Nov. 13-15, 1973,* pp. 18-31 (1973).

Key words: black coatings; detectors; radiometry; reflectances.

One of the most critical components of a thermal radiation detector is the black coating that serves to absorb the incident flux and then to conduct the heat to the underlying receiver. Methods for measuring the optical and thermal characteristics of black coatings are reviewed, and results are given for a few different types of coating. The effect of the thermal characteristics of the coating on the detector responsivity is discussed, for both steady and modulated beams of radiation, and the related correction that is required with electrically calibrated detectors is described.

**16103.** Buhl, D., Snyder, L. E., Lovas, F. J., Johnson, D. R., **Is there a maser in the silicon monoxide ground state?,** *Astrophys. J.* **201,** No. 1, L29-L31 (Oct. 1, 1975).

Key words: circumstellar shells; masers.

Observations of the ground state ($v=0, J=2-1$) transition of silicon monoxide (SiO) show a rather smooth, low-intensity profile stretching over a large velocity range. The presence of ground-state emission at velocities which are not present in the $v=1$ or $v=2$ lines is interpreted as thermal emission in the ground state in regions where there is insufficient excitation to produce the vibrationally excited masers. Only VY CMa shows a profile which could be interpreted as ground-state maser emission.

**16104.** Cali, J. P., **Rationale for reference methods in clinical chemistry,** (Proc. Symp. 9th Int. Congress on Clinical Chemistry, Toronto, Canada, July 13-18, 1975), Paper in *Pure and*

*Applied Chemistry* **45,** 63-68 (Pergamon Press, Ltd., Headington Hill Hall, Oxford, OX3 United Kingdom, 1976).

Key words: definitive method; matrix reference materials; pure reference materials; reference methods; routine methods; secondary reference materials; Standard Reference Materials.

In the field of clinical chemistry evidence is mounting that a reliable and medically relevant structure can be built on the concept of compatibility through accuracy in measurement. By compatibility is meant the ability of all laboratories in a network to achieve on a given sample similar and reliable numerical values for a property under test. It is shown that when all laboratories in a network are making accurate measurements, i.e., free of sytematic error and precise, then compatibility automatically ensues. The need for accurate measurement based on medical arguments is given.

In order to build an accurate measurement network, three measurement methodology levels and three types of reference materials are required. A *definitive method* is directly able to realize or to have access to the base or derived units of the measurement system. It depends in part on the availability of *pure reference materials* (e.g., those supplied by the National Bureau of Standards and called SRM's). At the next level are *reference methods* and *matrix reference materials.* These methods and materials are more adapted to implementation and use by clinical reference laboratories and the manufacturers of *secondary reference materials.* In turn these materials are used at the local level to control the quality and accuracy of the *routine methods.* How this hierarchy of methods and reference materials is structured is discussed.

The role of the definitive method is discussed in some detail, because of its crucial place in the structure. Potentially useful definitive methods, both for inorganic and organic constituents are outlined. A discussion of reference method developments, per se, is left to the other three authors of this Symposium (qv). Clinical SRM's now available are listed, as well as those now in preparation at NBS. The need for matrix reference materials is stated.

Finally, how this measurement network should be structured and implemented together with suggested organizations responsible for the various levels is discussed.

**16105.** Unassigned.

**16106.** Horowitz, E., **Standardization of plastics,** *Encycl. Polym. Sci. Technol.* **12,** 771-786 (1970).

Key words: plastics standardization; specifications; standards; standards organization; test methods.

This paper briefly discusses various organizations engaged in promoting, developing and promulgating standards, specifications, test methods and related documents in the field of plastics. In some cases the procedure for preparing standards and specifications, and the mechanism for their adoption is described. Examples are given of the types of standards and specifications that are available as well as the different classes of plastics materials that are covered. Plastics standardization activities at both the national and international levels are treated and references to the literature are provided.

**16107.** Kashiwagi, T., Newman, D. L., **Flame spread over an inclined thin fuel surface,** *Combust. Flame* **26,** 163-177 (1976).

Key words: flame spread; instability; radiant flux; α-cellulose.

Downward flame spread velocity over a thin α-cellulose sheet was measured from the vertical to the horizontal positions under
external radiant fluxes of 0, 0.9, 1.4 and 2.0 W/cm². The flam
spread velocity had little dependency on the angle of inclinatio
of the sheet with the stable lower flame. When the lower flam
became unstable, wavy flames, cellular flames and flame roll
were observed below the lower surface. With these unstabl
lower flames, the flame spread velocity increased significantl
reaching several cm/s. Qualitative analysis based on th
Rayleigh instability mechanism describes well the effects of th
inclination angle and the external flux on the instability of th
lower flame.

**16108.** McCaffrey, B. J., Heskestad, G., **A robust bidirectiona
low-velocity probe for flame and fire application,** *Combus
Flame Brief Communications* **26,** 125-127 (1976).

Key words: angular insensitivity; fluidic device; hot wir
anemometer; ion deflection device; laser Dopple
anemometer; Reynolds number.

A robust bidirectional flow measuring device has been evalu
ated and appears to have significant advantages over a pito
static tube for use in fire research studies. Three different diame
ter probes were used to secure a low Reynolds number calibra
tion needed for accurate assessment at very low velocities. Th
bidirectional capability is illustrated by an example of the use
the probe in a scale model corridor-burn room facility.

**16109.** McNesby, J. R., **New techniques for the measurement
air pollutants,** *Proc. Int. Symp. on Recent Advances in the A
sessment of the Health Effects of Environmental Pollutio
Paris, France, June 1974*, Paper No. 47, 1-15 (1974).

Key words: ambient air; automotive emissions; laser ma
netic resonance technique; stack emissions.

Measurement research in air pollution at the National Burea
of Standards includes that applicable to ambient air, stack emi
sions, and automotive emissions. Some of the measureme
techniques developed for source emission application have bee
refined and made sufficiently sensitive to measure pollutant co
centrations as low as background levels. The fluorescence mon
tor for sulfur dioxide developed by Dr. Okabe and his colleagu
has been applied commercially to the problem of stack monito
ing. More recently the sensitivity of the technique has been in
proved very substantially so that ambient air sulfur dioxide co
centrations can be measured at least down to 1 part in $10^9$. Th
apparatus will be described and its capabilities delineated. T
technique of laser magnetic resonance for the measurement
NO at concentrations typical of stack emission and auto exhau
has similarly been extended to include ambient concentration
In addition, progress has been made in the direction of simu
taneous measurement of $NO_2$ by the same technique. The mo
recent data obtained by the laser magnetic resonance techniq
will be presented. A third measurement technique developed
the National Bureau of Standards, that of dual angle, forwa
laser scattering for the real time measurement of particle size di
tribution has now been shown to be capable of reveali
morphological and chemical information. The development
pyrolysis as an alternative to permeation tubes and standard g
cylinders will be described. The principle of the pyroly
technique is that a thermally stable molecule which may
stored indefinitely is subjected to thermal decomposition produ
ing a nonstorable molecular species plus an exactly equ
number of storable, readily measured molecular species. T
pyrolytic technique has the inherent capability of tying togeth
virtually all gaseous pollutant molecules in a single, self-co
sistent measurement and calibration scheme.

Finally, an absolute coulometric technique for the determin
tion of parts per million concentrations of NO in nitrogen will
described. The technique has been used to generate confirmat

ry evidence for establishing the integrity of NO in nitrogen Standard Reference Materials.

16110. Mears, T. W., **NBS Standard reference materials: Their characterization and stability consideration,** *Proc. of the SAMA Calibrator Product Class Standard Forum and Stability Testing Workshop, Chicago, IL, Mar. 18-19, 1975,* 10 pages (Scientific Apparatus Makers Association, Washington, DC 20036, 1975).

Key words: accelerated testing; clinical; hazards; legal problem packaging; shipping; stability; standard reference materials.

The NBS Office of Standard Reference Materials issues some 800 standard reference materials. The mode of operation developed over the past 75 years relating to testing, certification, and elimination of errors is described. With the inclusion of organic and clinical materials in the program, new considerations were necessary. Packaging techniques were changed. Stability, particularly accelerated testing has become a real problem. The handling and shipping of potentially hazardous materials is more apparent. Finally, in the clinical area, the SRM program has come under the purview of the Food & Drug Administration. The facing and solving of these new problems are described.

16111. Robertson, A. F., **Potential heat: Considerations in the application of a new fire test,** *Fire Mater.* **1,** No. 1, 9-13 (Mar. 1976).

Key words: building materials; calorimetry; combustibility; flammability; heat release rate; potential heat; self heating.

A review is presented of the nature of the potential heat test method. It is emphasized that the procedure usually yields a property-type measurement of the material or composite when applied. As a result, care must be taken to insure that necessary supplementary tests are performed by other methods to guarantee that a substantial fraction of the possible fire hazard has been considered. Suggestions for appropriate use of the procedure are included and information available on the precision of the procedure is reviewed. It is concluded that, when properly applied, the procedure can serve well as one of the tools for characterizing possible fire hazards. Suggestions are made for possible future development of the procedure to yield information on rate of heat release.

16112. Rockett, J. A., **Fire induced gas flow in an enclosure,** *Combust. Sci. Technol.* **12,** 165-175 (1976).

Key words: fire; fire plume gas flow; room fires.

The gas flow induced by a small fire in a large room is considered. The fire plume acts as a pump and the window opening as a throttle. Generalizations of Kawagoe's expressions for the window air flow and height of the neutral plane are developed and used to rationalize previously unexplained features of Gross and Robertson's enclosure fire data.

16113. Benjamin, I. A., **Problems in the correlation of small and large scale tests,** *Proc. Int. Symp. on Fire Safety of Combustible Materials, Edinburgh, Scotland, Oct. 15-17, 1975,* **1,** 141-148 (1975).

Key words: fire tests; regulatory tests; simulation tests.

This paper attempts to show that there are problems in defining large scale tests: the validity of the large scale test is no better than the scenario chosen for its conduct. A review of the literature shows that the small scale tests now being used to evaluate wall and ceiling linings do not measure well what they are designed to measure. Future small scale tests should be derived from studies of large scale tests which are designed to determine the properties to be measured. The small scale tests will then show better correlation to large scale tests.

16114. Eisenhart, C., **Samuel Stanley Wilks,** *Dictionary of Scientific Biography* **XIV,** 381-386 (Charles Scribner's Sons, New York, NY, 1976).

Key words: *Annals of Mathematical Statistics;* bibliography; distribution-free methods; educational testing; mathematical statistics; multivariate analysis; order statistics; social sciences, services to; statistical education in the United States; statistical tolerance limits; U.S. Army programs in statistics; U.S. Government, services to; Wilks award; Wilks, S. S.

A review of the life and work of Samuel Stanley Wilks (1906-1964). His impact on the development of mathematical statistics; and on the development of statistical education in the United States. His services to the U.S. Government, and to the social sciences. Bibliography of principal original works; and of major secondary literature.

16115. Eisenhart, C., **William John Youden,** *Dictionary of Scientific Biography* **XIV,** 552-557 (Charles Scribner's Sons, New York, NY, 1976).

Key words: calibration designs; chain blocks; collaborative tests; diagnostic tests, index for rating; experiment design, statistical; graphical diagnosis; interlaboratory tests; randomization, constrained; ruggedness test; statistical techniques; Youden plot; Youden squares; Youden, W. J.

A review of the life and work of William John Youden (1900-1971). His invention of new techniques for statistical design of experiments and for analysis of data from individual experiments and from groups of experiments. Bibliography of principal original works; and of major secondary literature.

16116. French, J. C., **The ARPA/IC/NBS Semiconductor Technology Program,** *Proc. Space System Microelectronics Seminar, Los Angeles, CA, Apr. 15-16, 1975,* pp. 189-199 (The Aerospace Corp., Los Angeles, CA, July 31, 1975).

Key words: automation; integrated circuits; measurements; microelectronics; process control; reliability; semiconductor.

Reliable devices at lower cost, available when needed, are essential to the achievement of Department of Defense (DoD) systems objectives. The ARPA/IC/NBS Program, Advancement of Reliability, Processing, and Automation for Integrated Circuits with the National Bureau of Standards, supported by ARPA and conducted by NBS, reflects an emphasis on inprocess measurements to achieve these objectives. Rather than following only the more traditional and costly approach of tested-in reliability, this program provides a new and complementary thrust directed toward the goal of built-in reliability through design control of fabrication, and automation. The concepts and approaches of this program are based on the experience gained in over a decade of activity in the NBS Semiconductor Technology Program and the transfer of the results obtained in this program to the industry with substantial benefit to both the industry and to DoD. Topics selected for attention cover key processing and assembly steps, from control of incoming materials to evaluation of electrical characteristics and packaging. The selection of topics for consideration is based on extensive field surveys, workshops, and direct interaction with industry and other agencies to determine the measurement needs both for manufacturing and marketplace interactions. An important factor in the program is continued close interaction with the industry to ensure transfer of the results of the program to the industry for use by the semiconductor integrated circuit manufacturer, his suppliers, and customers. Both in-house studies at NBS and efforts contracted out-of-house to industry, universities, and other government laboratories are being utilized.

16117. Judd, D. B., Nickerson, D., **Relation between Munsell and Swedish Natural Color System scales,** *J. Opt. Soc. Am.* **65,** No. 1, 85-90 (Jan. 1975).

Key words: color; colorimetry.

The degree to which Munsell hue, value, chroma and the Swedish Natural Color System variables of blackness, whiteness, redness, yellowness, greenness, blueness describe the same color space is shown by simple formulas.

16118. Kusuda, T., **NBSLD-National Bureau of Standards heating and cooling load determination program,** *APEC J.* **VIII,** No. 6, 4-11 (Winter 1973-1974).

Key words: computer program for buildings; conduction transfer functions; heating and cooling load; National Bureau of Standards load determination procedure.

A comprehensive treatment of building heat transfer processes has been incorporated into a computer program called NBSLD in order to study the effect of various building parameters upon the resulting heating and cooling load. The basis of the computation in the program is the detailed solution of simultaneous heat balance equations at all of the interior surfaces of a room or space. Transient heat conduction through the exterior walls and in the interior structures is handled by using ASHRAE type conduction transfer functions. The use of heat balance equations, although more time consuming for the calculation, avoids uncertainties inherent in a weighting factor approach. Thus, precision is improved for a specific building design. Described in this paper are some of the salient features of NBSLD and results of sample calculations which demonstrate the capability of this computer program.

16119. Goldman, A. J., **Discussion,** (Proc. Symp. on Systems Analysis for Social Problems, Gaithersburg, MD, May 26-28, 1969), Paper in *Systems Analysis for Social Problems,* A. Blumstein, et al., Eds., pp. 93-103 (Washington Operations Research Council, Washington, DC, 1970).

Key words: operations research; systems analysis; urban problems.

The increasingly "solid" quality of some recent applications of systems-analysis (SA) techniques to urban problems is noted. Particular emphasis is suggested on the city's success in performing those special functions for which it is peculiarly suited. The conflicting goals of and the struggle for scarce resources among urban interests are observed to be antithetical to SA's penchant for "optimizing" formulations; urban problems admitting such "clean" treatment are held unlikely to be among the underlying difficulties of our cities, but may provide suitable starts for analysis. Concern is voiced that city "institutionalization" of SA may inhibit its search for bold solutions.

16120. Powell, F. J., **Research on energy conservation in building at the National Bureau of Standards,** (Proc. Conf. on Buildings and the Environment, Cary Arboretum of New York Botanical Garden, Millbrook, NY, Nov. 1974), Chapter 6 in *Buildings and the Environment,* R. Goodland, Ed., pp. 114-140 (Cary Arboretum, Millbrook, NY, 1976).

Key words: buildings energy; energy conservation; NBS programs.

Selected topics of the National Bureau of Standards energy conservation program related to buildings are discussed. Topics included are the National Bureau of Standards Load Determination Computer Program (NBSLD) for estimating building energy consumption, the experimental results of tests on a masonry and a woodframe house, the status of an experiment on a mobile home, the study to retrofit an existing house on the NBS grounds to save energy, the experiment to retrofit a townhouse with solar collectors and storage systems to supply 75 percent of the annual energy needs of the townhouse, the energy conservation demonstration office building at Manchester, New Hampshire, and a new energy conservation school in New York City. Other energy conservation efforts are named by title only.

16121. McNesby, J. R., **Air pollution monitoring instrumentation,** *Proc. Naval Environmental Protection Data Base Instrumentation Workshop, Port Hueneme, CA, July 11-12, 1972,* pp. 150-155 (Naval Civil Engineering Laboratory, Port Hueneme, CA, 1972).

Key words: carbon monoxide; hydrocarbons; measurement; nitrogen dioxide; particulate matter; photochemical oxidants; standards; sulfur dioxide.

The first fundamental of air pollution abatement in the U.S. is that all U.S. residents are entitled to breathe air of at least standard quality. The standard quality is spelled out in the National Ambient Air Quality Standards. Secondly, the states are responsible for achieving this quality.

The states must answer these questions: How bad is the air quality now? How much do we have to improve it? To answer the first question we must measure the present levels of the pollutants sulfur dioxide, carbon monoxide, hydrocarbons, nitrogen oxides, photochemical oxidants and particulate matter. The second question is answered by studying the quantitative relationship between ambient air pollutant concentrations and the amounts of pollutants emitted by the various source (modeling). This in turn requires measurement of pollutants emitted through smoke stacks and auto exhausts.

Without accurate methods of measurement, auto manufacturers cannot know their progress towards a low emission vehicle and cannot be sure of their progress relative to that of their competitors. Power plants cannot determine the efficiency of scrubbing devices; cities and states cannot determine if they are successfully implementing their ambient air goals.

16122. Riley, M. E., Truhlar, D. G., **Effects of the Pauli principle on electron scattering by open-shell targets,** *J. Chem. Phys.* **65,** No. 2, 792-800 (July 15, 1976).

Key words: electron exchange; electron scattering; hydrogen atoms; indistinguishable particles; phase shifts; quantum mechanics; scattering theory; semiclassical approximation.

The semiclassical exchange approximation and three free-electron-gas exchange approximations are applied to electron scattering from the hydrogen atom. In the triplet spin state the results are similar to our previous findings [M. E. Riley and D. G. Truhlar, J. Chem. Phys. **63,** 2182 (1975)] for electron scattering by closed-shell atoms. However these results, already of useful accuracy, are improved by the inclusion of one-electron exchange terms or an orthogonality constraint. For the singlet spin state it is essential to include the one-electron exchange terms except at high impact energies (greater than about 50 eV). The approximation of Lippmann, Schey, Burke, and Chandra for treating the triplet spin state and exchange with closed-shell targets is tested and found to be less accurate than the present approximations.

16123. Robertson, A. F., **Estimating smoke production during building fires,** *Fire Technol.* **11,** No. 2, 80-94 (May 1975).

Key words: building; estimating; fire; furniture; hazard; interior finish; smoke.

In the absence of specific analytical methods for measuring the hazards of fire gases, there is a trend toward the use of smoke production as a partial measure of this hazard. It is indicated that prediction of smoke concentrations and thus photometric properties during actual fires requires many important and rather critical assumptions.

**16124.** Robertson, A. F., **Test method categorization and fire hazard standards,** *ASTM Stand. News* **3,** No. 11, 18-20 (Nov. 1975).

Key words: ASTM; classification; fire hazard; participation; property; system; test method.

A general discussion is presented with the objective of distinguishing between different levels of test method complexity. It is suggested useful to understand the possibility of participation between the specimen and test equipment. A further distinction is proposed between property and system type tests as well as the usual classification on the basis of whether the specimen is destroyed or not. It is shown that fire test methods may be of either the property or system type, although often they are of the destructive participative system type the most complex of those discussed. Both the developers and users of tests are cautioned to recognize and observe the different ways in which it is appropriate to use property and system type test methods. Those responsible for development of such test methods are cautioned against the delivery of methods with the aura of system methodology but lacking in technical validity for the intended use.

**16125.** Robertson, A. F., **Two smoke test methods—A comparison of data,** *Fire Technol.* **10,** No. 4, 282-286 (Nov. 1974).

Key words: fire propagation test; fire tests; smoke density chamber; smoke tests; test comparison; UK; USA.

Smoke test methods have been developed in both UK and USA which are based on photometric measurements of smoke accumulation in closed chambers. The British Fire Research Station (FRS) procedure makes use of a large room approximately 37 times the volume of the box type chamber used in the test developed at the National Bureau of Standards (NBS). Tests have been conducted to compare the ability of the two measurement methods to assess smoke production from samples of selected materials. It is concluded that similar smoke measurements are obtained by use of the NMS procedure and use of the NBS specimen pyrolysis equipment in the room used for the FRS test. Moreover, there is general correspondence of the NBS and FRS smoke characterization results for many materials. However, these two methods tend to yield different results for high fuel content materials when the limited air circulation permitted by the FRS furnace becomes important, and for thermoplastic materials which in the FRS test melt and reticulate from heat exposure and do not burn. The findings suggest that the FRS method may be more sensitive to system effects of fire within an enclosure. Questions are raised as to whether the system simulated by the FRS test is the appropriate one.

**16126.** Sinha, S., Bardsley, J. N., **Symmetric charge transfer in low-energy ion-atom collisions,** *Phys. Rev. A* **14,** No. 1, 104-113 (July 1976).

Key words: alkali ions; calcium; charge exchange; charge transfer; cross section calculations; ion-atom collisions; rare-gas ions; uranium.

Previous calculations of ion-atom interactions by the pseudopotential and asymptotic methods are used in the computation of the cross section for symmetric charge transfer at energies below 1 keV. The results for $Li^+$, $Na^+$, $K^+$, $Rb^+$, $Cs^+$, and $Ca^+$ ions are compared with data obtained in beam experiments, and by optical-pumping techniques. The difference in the cross sections for $^2P_{1/2}$ and $^2P_{3/2}$ ions of $Kr^+$ and $Xe^+$ at thermal energies is studied, and the predictions are compared with recent mobility measurements. Cross sections are obtained for $U^+$-U collisions, and the dependence of the thermal cross section on the polarizability is described. Symmetric charge transfer of the negative ions $H^-$, $Na^-$, and $Cs^-$ is discussed briefly.

**16127.** Stein, M. L., **A saddlepoint theorem for self-dual linear systems,** *Linear Algebra and Appl.* **9,** 55-65 (1974).

Key words: combinatorial equivalence; linear inequalities; linear programs; pivot operations; skewsymmetry.

Let $A$ be a skew matrix of order $n$ over an ordered field. There is a finite class of skew matrices $\overline{A}$ such that $\overline{X}\overline{A} = \overline{Y}$ and $XA = Y$ have the same solution sets, where $x_i = y_i$ and $y_i = x_i$ for some indices $i$ (perhaps none) and $x_i = x_i$, $y_i = y_i$ for the remaining $i$. We show that for each index $h$, $1 \leqq h \leqq n$, there exists and $\overline{A}$ such that $\overline{a}_{hj} \geqq 0$ for all $j$. There are a variety of applications to matrix games, linear programs and related topics.

**16128.** Walston, W. H., Federman, C., **Fourier transform techniques for the calibration of shock accelerometers,** (Proc. 21st Int. Instrumentation Symp. on Instrumentation in the Aerospace Industry, Philadelphia, PA, May 19-21, 1975), Paper in Vol. 21 *Instrumentation in the Aerospace Industry* and Vol. 12 *Advances in Test Measurement*, B. Washburn, Ed., pp. 315-321 (Instrument Society of America, Pittsburgh, PA, 1975).

Key words: accelerometer; calibration; FFT; Fourier transform; Fourier transform frequency; mechanical shock; shock generator.

Calibration of mechanical shock accelerometers is accomplished by a shock comparison method which utilizes fast Fourier transform (FFT) techniques. This procedure computes sensitivity values at any frequencies desired over the entire calibration bandwidth. Pitfalls associated with the application of the FFT to actual shock pulses along with possible solutions are discussed. Close agreement with conventional sinusoidal calibration is obtained.

**16129.** Snell, J. E., Achenbach, P. R., Petersen, S. R., **Energy conservation in new housing design,** *Science* **192,** No. 4246, 1305-1311 (June 25, 1976).

Key words: energy conservation; energy efficient design; life-cycle cost models; new housing.

The combined influences of rising fuel prices and a national goal of energy independence are providing strong impetus to the consideration of energy conservation in design features in housing. This paper examines the potential implications of these influences to new housing design over the balance of this century. A life-cycle cost model is presented and used to estimate the influence of conservation and fuel price increase on a number of major housing design parameters. These parameters include housing type and size, thermal resistance, location, heating and cooling system capacity and efficiency. Next, the technological realities of achieving such changes are examined and the anticipated impacts of energy conservation on new housing design are summarized. It is felt that the principal emphasis will be on smaller more efficient dwellings, mechanical systems, and equipment with essentially improved overall performance utilizing technology readily available to the building industry.

**16130.** McNesby, J. R., **Problems in the measurement of free radical concentrations in the atmosphere,** *Ber. Bunsenges. Phys. Chem.* **78,** No. 2, 158-162 (1974).

Key words: chemical kinetics; free radicals; measurement; stratosphere.

The free radicals known, or suspected to be present in the earth's stratosphere have been listed by Garvin and Hampson and include O, $O_2$, SO, H, OH, $HO_2$, CH, CHO, $CH_3$, $CH_3O$, $CH_3O_2$, NH, $NH_2$, HNO, NO, $NO_2$, $NO_3$. In the urban troposphere near ground level, this list can be greatly expanded to include many species resulting from reactions of these simple radicals with reactive hydrocarbons. Since the economical control of air pollution requires a detailed knowledge of the chemical kinetics involved in removal of stable pollutant molecules from the air, it is desirable ultimately to be able to measure the concentrations and rate constants of all such reactants. I have selected from this list the two most abundant, polar atmospheric free radicals, NO and $NO_2$ for discussion. The ground states of NO, $^2\pi$ and of $NO_2$, $^2A_1$, qualify both molecules as free radicals. These molecules pollute the urban atmosphere and the stratosphere and the debates about the amounts in which they are present have precipitated major controversies in the United States and elsewhere. My purpose is to present the nature of the tropospheric problem of NO and $NO_2$ (known collectively in the trade as $NO_x$) why their measurement is important, the current state of the art and finally some of the newer approaches to the solution to the problem in terms of the basic Federal legislation in the United States, the Clean Air Act.

**16131.** Broussalian, V. L., **Risk measurement and safety standards in consumer products,** (Proc. Conf. on Research in Income and Wealth, Washington, DC, Nov. 30-Dec. 1, 1973), Paper in *Household Production and Consumption,* N. E. Terleckyj, Ed., **40,** 491-524 (National Bureau of Economic Research, New York, NY, 1976).

Key words: consumer products; product safety; refrigerator standards; risk measurement; safety standard; unreasonable hazards.

A definition of unreasonableness of a hazard is proposed. Although formally stated in economic terms, it calls for data of different kinds: engineering, political, psychological, legal, etc. Unreasonableness of a hazard is also related to injury avoidance actions which might be taken by consumers as well as by producers. To demonstrate how the definition may be used in practice, it is applied to an actual hazard for which a mandatory safety standard has been set. This example is the well-known refrigerator entrapment hazard. Finally, the risk data needed to determine whether a hazard is reasonable or not are indicated.

**16132.** Cooper, J. W., **High-energy dependence of the molecular-hydrogen photoionization cross section,** *Phys. Rev. A* **9,** No. 5, 2236-2237 (May 1974).

Key words: hydrogen; molecular cross section; photoeffect.

The photoionization cross section for $H_2$ per atom has recently been reported to be ~45 percent larger than the atomic cross section at energies of 5.41 and 8.39 keV. This note relates this observation to the differences in electron density at the nucleus in atomic and molecular hydrogen and points out that the enhancement at high photon energies is unique for molecular hydrogen.

**16133.** Ekberg, J. O., **Term analysis of Fe VI,** *Phys. Scr.* **11,** No. 1, 23-30 (1975).

Key words: iron; spectra; ultraviolet; wavelengths.

The spectrum of Fe VI has been observed by using a vacuum sliding-spark discharge and the 10.7-m grazing-incidence spectrograph and the 10.7-m normal-incidence spectrograph at the National Bureau of Standards, Washington. More than 400 lines have been classified in the region 250-1 580 Å. All terms of the configurations $3d^3$, $3d^24s$ and $3d^24p$, except $3d^2(^1S)4s^2S$ have been established. The estimated uncertainty of the level values is ±0.4 $cm^{-1}$. The $3d^3$, $3d^24s$ and $3d^24p$ level structure has been theoretically interpreted. The energy parameters determined from a least-squares fit of the observed level values are compared with Hartree-Fock calculations. From the complete set of $3d^3$ levels all forbidden lines of Fe VI from 1,387 to 10,000 Å have been predicted. All but two lines in the spectrum of the star RR Telescopii previously identified as forbidden Fe VI lines have been confirmed and 6 of the otherwise unexplained lines have been identified as [Fe VI].

**16134.** Epstein, G. L., Reader, J., **Spectrum of doubly ionized yttrium (Y III),** *J. Opt. Soc. Am.* **65,** No. 3, 310-314 (Mar. 1975).

Key words: spectra; ultraviolet; wavelengths; yttrium; zirconium.

The spectrum of doubly ionized yttrium was observed from 600 to 9700 Å by means of plane- and concave-grating spectrographs at NBS. About 100 new lines were observed. From these measurements, 40 new energy levels were derived. The known level system (Rb I isoelectronic sequence, $4p^6nl$) now includes the series *ns* ($n$=5-9), *np* ($n$=5-9), *nd* ($n$=4-8), *nf* ($n$=4-10), *ng* ($n$=5-8), and *nh* ($n$=6-8). The *nf* series shows irregular fine-structure splittings, $4f$ having a negative splitting of about 3 $cm^{-1}$. The ionization energy of Y III was determined to be 165 540.5 ± 1.0 $cm^{-1}$ (20.52457 ± 0.00012 eV). A re-examination of Kiess's data for Zr IV in the light of the Y III analysis yielded a revised value for the ionization energy of Zr IV of 277 550 ± 20 $cm^{-1}$ (34.412 ± 0.003 eV).

**16135.** Geist, J., Dewey, H. J., Lind, M. A., **Low-level periodic pulsed energy measurements with an electrically calibrated pyroelectric detector,** *Appl. Phys. Lett.* **28,** No. 4, 171-173 (Feb. 15, 1976).

Key words: electrically calibrated pyroelectric detector; gold-black; piezoelectric; pulse laser power.

The use of an electrically calibrated pyroelectric detector for accurately measuring periodically pulsed (~3-ns duration) energy with an average power level in the microwatt to milliwatt range was investigated. Sources of error especially important in this application were the pyroelectric's acoustic response, its linearity, and possible deterioration of its gold black coating. The detector had a thin polymer film that isolated the radiation receiver from the pyroelectric material. This film temporally resolved the pyroelectric response from the piezoelectric response to the acoustic energy that is associated with the absorption of an impulse of energy. Thus it was demonstrated that the acoustic response was not a serious source of error. The film also reduced the requirement of linearity on the pyroelectric transducer by about 5 orders of magnitude from the conditions of a bare transducer. It is concluded that periodic pulsed energy measurements with 5 percent uncertainties are readily achievable with the detector described.

**16136.** Meisters, M., **Concepts and trends in polymer fire testing,** *Mod. Plast.* **52,** No. 9, 76-78, 81-82 (Sept. 1975).

Key words: fire performance tests; flame spread; heat input; heat release rate; limiting oxygen index; radiant panel; smoke density; time to ignition.

This report provides a framework for understanding the principles that are important in correlating small- and large-scale tests in terms of such fire concepts as ignition, propagation, heat release, and smoke generation. All of the methods have limitations and cannot completely evaluate fire performance, but they offer a baseline for continued development of tests to provide better correlations with real-fire performance.

**16137.** Hamilton, W. C., Edmonds, J. W., Tippe, A., Rush, J. J., **Methyl group rotation and the low temperature transition in hexamethylbenzene. A neutron diffraction study,** *Discuss. Faraday Soc.* **48,** 192-204 (1969).

Key words: barrier to rotation; crystal; crystal structure; hexamethylbenzene; hindered rotation; phase transition; torsional oscillation; λ-point.

Neutron diffraction studies of single crystals of hexamethylbenzene at 298 K and at 130 K indicate that the molecule in phase II has approximate $D_{3d}$ symmetry. The amplitudes of libration of the methyl group and of rigid body motions of the molecule are consistent with earlier data, except that the barrier to methyl group rotation appears to be lower by about 0.5 kcal/mol (2100 J/mol).

Consideration of intra- and inter-molecular hydrogen atom contact distances and calculated potential energy curves using a 6-exp potential function suggest that intermolecular forces are important in determining the barrier to rotation of the methyl groups and that substantial changes in the intermolecular packing must be responsible for the lambda-point transition at 116 K and the consequent profound change in the potential barrier to internal rotation which has been previously observed.

**16138.** Tsai, D. H., MacDonald, R. A., **Molecular dynamical studies of energy transport in a crystalline solid,** (Proc. Symp. on Computer Simulation for Materials Applications, Gaithersburg, MD, Apr. 10–21, 1976), *Nucl. Metall.* **20,** Pt. 1, 489–509 (Apr. 1976).

Key words: anharmonic crystal; computer simulation; energy transport; heat pulse; interatomic potential; molecular dynamics; second sound; shock wave; stress wave; temperature wave; thermal diffusivity; thermal relaxation.

We review the main results of a series of molecular dynamical studies of the transport of energy in a crystalline solid subjected to heating and to shock compression. Our model is a perfect semi-infinite bcc lattice. We use a two-body interatomic potential which simulates that in $\alpha$-iron. The classical equations of motion for the atoms are solved numerically under appropriate initial and boundary conditions, and the properties of the lattice and the transport of energy are determined from averages of the atomic motion. We find that a disturbance in thermal energy propagates either by diffusion or as a temperature wave with second sound velocity. A disturbance in potential energy propagates as a stress wave with first sound velocity. These results are in agreement with experiments. In addition, we find that longitudinal and transverse stress waves generate their own temperature waves through thermalization of the kinetic energy change accompanying the stress disturbances. The significance of this thermal relaxation process to the interpretation of heat pulse and shock wave experiments is examined.

**16139.** Tovey, H., **The development of the National Fire Data System,** *Fire J.* **68,** No. 6, 91-96 (Nov. 1974).

Key words: fire data; fire hazard; fire injuries; fire investigation; fire loss; fire reporting; fires.

The development of the National Fire Data System is described. The major policy requirements established for the system are listed, and four specific categories of fire data needs are defined. The system itself is described in terms of inputs, structure, and outputs, and the system users are classified and described. A report on the current status of the system development effort is given, covering projects on the fire incident reporting subsystem, the national household survey of fire experience, statistical summary data tapes, fire technology information, detailed hazard analyses, and integrated system outputs.

**16140.** Young, R. D., **Instrumentation for the chemical analysis of manufactured surfaces,** *Ann. CIRP* **24,** No. 2, 549-554 (Aug. 1975).

Key words: surface; surface finisn; surface roughness measurement.

Over the last twenty years a wide variety of analytical instruments for studying the chemical composition of surfaces have been developed, many of which are commercially available. Several of these instruments lend themselves to the analysis of the practical surfaces encountered in manufacturing processes, thus contributing to our understanding of the process, and the integrity of the fabricated surface.

Three particularly useful techniques include ESCA, Auger and the electron microprobe. In ESCA (electron spectroscopy for chemical analysis) nearly monochromatic x-rays of about 1000 eV energy impinge on the specimen surface. Photoelectrons produced in atoms of the top nanometer are energy analyzed to yield spectra which are characteristic of these surface atoms. In the Auger technique, high-energy electrons bombard the specimen surface, generating Auger electron emission which is characteristic of the surface atoms. This instrument if often combined with LEED (low energy electron diffraction), enabling measurement of the atomic arrangement of the surface atoms which are analyzed with Auger emission.

A highly attractive though less well developed technique called infrared reflection (absorption) could conceivably be used on-line to detect the presence of certain chemicals on surfaces. The scanning electron microscope (SEM) has been combined with the electron microprobe (EMP) in order to determine the micro-distribution of materials over a surface. In the microprobe a high energy electron beam stimulates characteristic x-ray emission from surface atoms. Application of these techniques to fabricated surfaces will be discussed.

**16141.** Edelman, S., **Piezoelectric polymer stress gages,** *Proc. Symp. on Advancements in Instrumentation for Civil Engineering Applications, Kirtland Air Force Base, NM, May 9-10, 1973,* Technical Report No. AFWL-TR-73-186, pp. 221-224 (Air Force Weapons Laboratory, Kirtland Air Force Base, NM, Oct. 1973).

Key words: piezoelectric; polymeric transducer; polymers; polyvinyl fluoride; polyvinylidene fluoride; stress gages; transducers.

Gradual improvement in material selection and poling techniques has developed polymers with significant piezoelectric activity. This material can now be used to make many kinds of instruments for measuring dynamic stress, pressure, vibration, etc. Polymers that can be made piezoelectrically active are available with a wide variety of mechanical, electrical, and chemical properties. They can be formed in size and shape to suit a particular application and they can be fastened to curved, twisted or compliant surfaces. Sensors in the form of thin sheets, coaxial cables, and hollow tubing have been made.

**16142.** Eliason, L. K., **Standards for door security,** *Archit. Met.* **21,** No. 3, 6-7 (June 1976).

Key words: building codes; door assemblies; performance requirements; physical security; standards.

This article discusses the need for standards for the physical security of door assemblies, describes the nature and application of NILECJ-STD-0306.00, "Physical Security of Door Assemblies and Components," and suggests the manner in which the standard can be utilized to improve the security of door assembly components. The implementation of the standard within local building codes is also addressed.

**16143.** Evans, J. M., Jr., **Position sensors and computer control techniques for automatic control of agricultural vehicles,** *Proc. IFAC Symp. on Automatic Control for Agriculture, Saskatoon, Saskatchewan, Canada, June 18-20, 1974*, Dr. G. C. Zoerb, Ed., Preprint Sec. A-2, pp. 1-5 (Agricultural Engineering, University of Saskatchewan, Saskatoon, Saskatchewan, Canada, 1974).

Key words: agriculture; computer control; position sensors; RF interferometer.

RF interferometers may be used for determination of position and orientation of vehicles to an accuracy of millimeters over distances to thousands of meters. Servo control may be implemented through mini- or micro-computers using read-only memory for the control functions. The application of these techniques to the control of agricultural vehicles is discussed.

**16144.** Krasny, J. F., **Development of flammability standards,** *Proc. 3d Symp. on Textile Flammability, New York, NY, Apr. 16-17, 1975*, pp. 30-46 (LeBlanc Research Corp., East Greenwich, RI, 1975).

Key words: apparel; burn injury; carpets; draperies; fabrics; flammability; heat flux; standards; tents; tests; uniforms; upholstered furniture.

The activities of the Center for Fire Research of the National Bureau of Standards in the area of textile item flammability standards are described. Work is in progress on a general apparel flammability standard, to replace CS 191-53. A test concept involving a cylindrical fabric specimen, and measurement of the ignitability and the heat release to the inside of the cylinder, is under development. A draft standard for the flammability of upholstered furniture was submitted to the Consumer Product Safety Commission. It consists of a fabric-screening test and test of mock-ups of the fabric, stuffing, tape, etc., arranged as in the furniture piece to be tested. A flooring systems test, to provide a reasonable substitute for the tunnel test, is applicable also to carpets. It consists of exposing a sample to radiation varying in intensity over the specimen length. The specimen is pilot ignited at the high radiation end, and the distance burned until the flames extinguish is measured. This distance can be converted to the "critical radiant flux" as a measure of potential hazard. Studies are also in progress on curtains and draperies, tents, and flight attendant uniforms.

**16145.** McHenry, H. I., **Ship steel weldments for low temperature service,** *Weld. J.* **55,** No. 5, 387-393 (May 1976).

Key words: alloying; inclusions; low temperature; rolling; ships; steel; welding.

The ship steels, welding practices and weldment toughness requirements applicable to low temperature (to −46 °C) regions of liquefied-natural-gas (LNG) tankers are reviewed. In the construction of LNG ships, the principal welding productivity problem is the low deposition rate associated with the low heat input welding practices required to provide sufficient toughness in the weld heat-affected-zone (HAZ). A potential solution to this problem is to use improved steels which can be welded using efficient procedures and still provide satisfactory HAZ toughness. The steelmaking practices that contribute to low temperature toughness are reviewed with respect to economic limitations associated with ship steels and to their potential for improving HAZ toughness.

**16146.** Meissner, P., Evans, J. M., **Computer-aided design in manufacturing,** (Proc. Technology Workshops, Lafayette, IN, Oct. 3-6, 1973 and Columbus, OH, Nov. 7-10, 1973), Paper in *The Automation Research Council*, A. Seireg, Ed., Report No. 5, pp. 289-303 (The American Automatic Control Council, Holmdel, NJ 07733, Feb. 1974).

Key words: CAD; CAD/CAM; computer-aided design; manufacturing.

This review of the use of computer-aided design in manufacturing is based primarily on the experiences of General Motors, McDonnell Douglas, and the Army Electronics Command. The paper provides a common base for discussions by representatives of Government, industry, and universities attending two Workshops on the Technologies of Automation sponsored by the Automation Research Council of the American Automatic Control Council. The material illustrates the current state-of-the-art in CAD, including available hardware and software, and the economics and time savings of existing CAD systems.

**16147.** Mitchell, R. A., Woolley, R. M., Baker, S. M., **Finite element simulation of weldbonded joint deformation,** (Proc. Symp. on Computer Simulation for Materials Applications, Gaithersburg, MD, Apr. 19–21, 1976), *Nucl. Metall.* **20,** Pt. 2, 1039–1050 (Apr. 1976).

Key words: bonded joints; computer simulation; cyclic loading; debond analysis; finite element analysis; joints; nonlinear analysis; single-lap-joint bending; spotwelded joints; weldbonded joints.

Finite element computer techniques are described that simulate the structural response of weldbonded single-lap and double-lap joints. The techniques also apply equally well to the special case of a bonded joint without spotwelds. A planform analysis articulates the in-plane deformation of the joined sheet material and the lap-shear stresses acting through the spotwelds and the adhesive. A longitudinal cross-section analysis computes out-of-plane bending effects, particularly important in single-lap joints, and adhesive peel stresses. Algorithms are described that simulate several nonlinear modes of response by sequences of linear solutions. Single-lap joint specimens of eight different configurations, designed so as to constitute an experimental parameter study, were instrumented with resistance strain gages and tested in the laboratory. For the most part, strains measured on the surfaces of these specimens were in reasonably good agreement with the finite element simulations, provided out-of-plane bending effects were accounted for.

**16148.** Collard, J. J., **Is the proposed Federal Standard for brakes adequate for police patrol vehicles?,** *Proc. SAE Automotive Engineering Congress and Exposition, Detroit, MI, Feb. 24-28, 1975*, Paper No. 750399, pp. 1-6 (Society of Automotive Engineers, Inc., Warrendale, PA, 1975).

Key words: FMVSS 105a; LAPD brake tests; NBS survey; patrolcar brakes; patrolcar survey; police brake requirements.

In 1972, the National Bureau of Standards surveyed 530 police departments to determine what was wrong with their patrolcars: 449 departments responded to the survey. Thirty-two percent of the respondents, a plurality, identified brakes as the most dangerous feature, and 36 percent identified it as the system most in need of standards. Ninety-four percent of the respondents rated their patrolcar brakes excellent to satisfactory at speeds under 70 mph (113 kph), but 25 percent rated them poor over 70 mph. While the new Federal Motor Vehicle Safety Standard 105-75 may improve the brake systems for patrolcars for routine, low speed use with frequent applications, it will be necessary to continue testing patrolcar brakes under severe driving conditions to assure reliability at high speeds.

**16149.** Krasny, J. F., Francis, J. B., **Ranking extinguishability of burning fabrics,** *J. Am. Ass. Text. Chem. Color.* **6,** No. 6, 135-136 (June 1974).

Key words: cotton fabrics; extinguishability; flammability; polyester/cotton fabrics.

This report describes initial efforts to obtain laboratory data on the relative extinguishability of various fabrics, an aspect of the hazard due to burning fabrics which has been largely neglected in the past. A simple apparatus was designed to simulate the extinction of burning fabrics by beating the flames out. Two plates covered with asbestos sheeting are brought together at a rapid rate after a fabric suspended between them comes to a full burn. The time the plates have to be held together to extinguish the flames was found to increase roughly with increasing fabric weight. For a given weight, the time to extinguish tended to be shorter for all-cotton fabrics than for polyester/cotton blends; the blends also tended to stick to the plates.

**16150.** Parker, W. J., **The large-scale fire-test facility at the National Bureau of Standards,** *Proc. Symp. on Full-Scale Fire Tests, Lancaster, PA, Nov. 11-12, 1974,* pp. 45-48 (1976).

Key words: construction; corridor test; fire endurance furnace; fire growth; heat release; smoke abatement; sprinkler system.

The newly completed fire-test facility at the Gaithersburg site of the National Bureau of Standards provides the capability of studying the fire endurance of columns, walls, and floor/ceiling assemblies; fire growth and control in rooms; fire spread and control in corridors; and smoke movement in buildings. The study of fire growth in a room is concentrated on the role of the furnishings, as well as the interior finishing materials. A burn room is also available to examine the fire-buildup process in a large item of furniture.

**16151.** Reed, W. P., **Radioisotope and radiopharmaceutical standards,** *Proc. San Diego Biomedical Symp., San Diego, CA, Feb. 6-8, 1974,* **13,** 507-509 (1974).

Key words: biomedical; clinical; measurements system; radioisotopes; radiopharmaceuticals; reference sources; standards; SRM's.

A previous paper by J. P. Cali described meaningful measurements and the components that go into a meaningful measurement system. This paper examines one of the NBS programs in he measurement system and how this system relates to the biomedical profession.

At NBS the Radioactivity Section under the supervision of Dr. W. B. Mann is responsible for relating our national measurement system and standards for radioactivity to the international measurement system. This activity has three aspects of interest here: (1) SRM's that are available to all and are related to the naional measurement system. (2) An industry-government cooperative program for the improvement and standardization of commercial radiopharmaceuticals and other reference sources. 3) A training and interlaboratory comparison program for the education of clinical personnel in the measurement of radioactive materials, including the calibration of devices commonly used to measure radiopharmaceutical doses.

These three aspects of this program help to stabilize the measurement system, i.e., help to make meaningful measurement. Each of these efforts is discussed in detail to improve the understanding of interactions between the national laboratory and laboratories or groups in the field making these measurements, and to clarify the interaction between individuals and the system.

**16152.** Powell, F. J., Kusuda, T., Hill, J. E., **Occupant comfort as a decision-making concept for air conditioning of buildings,** (Proc. CIB Commission W45 (Human Requirements) Symp. on Thermal Comfort and Moderate Heat Stress, Watford, England, Sept. 13-15, 1972), Paper in *Thermal Comfort and Moderate Heat Stress,* pp. 191-215 (Her Majesty's Stationery Office, London ECIV 3RN, England, 1973).

Key words: air conditioning criteria; human comfort; physiological indices; predicted indoor habitability index (PIHI); weather building human systems.

A rationale for improving air-conditioning criteria is given. A new research approach and concept are presented. The concept is to include in criteria the effect of the building envelope and the response of humans to the resultant indoor temperature and relative humidity in addition to weather data which are normally used to make decisions concerning air conditioning for buildings. The concept involves generation of a "Predicted Indoor Habitability Index" (PIHI) as a means to evaluate the response of occupants to short-term as well as long-term exposure in non-air-conditioned housing. The work completed thus far is described.

The results of a pilot study for two locations, Jersey City, New Jersey and Macon, Georgia, are presented to demonstrate the feasibility of the concept. The indoor temperature and humidity were determined by calculation using a computerized simulation technique which follows a detailed heat transfer analysis of the weather/building/human-body systems. The calculated results were used to compute the value of several available physiological indices to reveal the extent and duration of undesirable indoor conditions when the apartment was not air conditioned. Statistical correlations between indoor and outdoor conditions were prepared as a means to reduce the amount of computation for establishing criteria.

**16153.** Schaefgen, J. R., **Integrating community utilities for resource conservation,** *Proc. Third National Conf. on Complete Water Reuse: Symbiosis as a Means of Abatement for Multi-Media Pollution, Cincinnati, OH, June 27-30, 1976,* pp. 53-59 (1976).

Key words: community services; cooling; electric power; energy conservation; heating; incineration; integrated utility systems; resource conservation; utilities; utility services; water reuse.

A Modular Integrated Utility System (MIUS) provides the utility services of electrical power, space heating and cooling, potable water heating, solid waste processing, sanitary sewage treatment, potable water treatment, and the site distribution, collection, and disposal functions attendant thereto. MIUS facilities are constructed on a community scale to achieve the maximum symbiotic effects from process integration. The MIUS approach to utility services can conserve energy, reduce environmental degradation, and permit greater flexibility in intensive land development at a competitive cost. A demonstration design is being initiated to quantify the performance and evaluate the synergistic benefits of multi-service facilities.

**16154.** Slater, P. J., **Leaves of trees,** (Proc. 6th Southeastern Conf. on Combinatorics, Graph Theory, and Computing, Boca Raton, FL, Feb. 17-20, 1975), Paper in *Proceedings of the Sixth Southeastern Conference on Combinatorics, Graph Theory, and Computing,* F. Hoffman, R. C. Mullin, R. B. Levow, D. Roselle, R. G. Stanton, and R. S. D. Thomas, Eds., pp. 549-559 (Utilitas Mathematica Publishing Inc., Winnipeg, Manitoba, Canada, 1975).

Key words: block-cutpoint tree; graph; tree; 2-connected.

If v is a vertex of degree at least three in a tree T and at least one branch at v is a path, then the subgraph of T consisting of the union of all such branch paths at v is called a leaf of T. There are infinitely many trees T with a given leaf structure (of two or more leaves), but certain of their parameters, such as the number of edges it is necessary to add to T to produce a 2-connected graph, are the same. Simple formulas are given for some of these parameters.

**16155.** Thomson, R., Fuller, E., **Crack morphology in relatively brittle crystals,** (Proc. Symp. on Fracture Mechanics of Ceramics, University Park, PA, July 11-13, 1973), Paper in *Fracture Mechanics of Ceramics*, R. C. Bradt, D. P. H. Hasselman, and F. F. Lange, Eds., **1,** 283-295 (1973).

Key words: fracture; lattice trapping; slow-crack growth; stress corrosion.

From the viewpoint that cracks are atomically sharp, general outlines are given for some of the types of theories which should be developed for such cracks. The existence of atomic cleavage in a large class of materials is argued on the basis of the stability of a crack under spontaneous dislocation formation. A qualitative description of lattice trapping of a cleavage crack is given which correlates the effect to the atomic force laws. The determining factor for the observation of lattice trapping is the width of the cohesive region of the crack "core." Finally, a qualitative model of slow crack growth due to environmental effects is developed in terms of atomic dissolution at the crack tip.

**16156.** Wachtman, J. B., Jr., **Emerging priorities in ceramic engineering and science—Viewpoint of the scientist-engineer,** (Proc. Conf. on Emerging Priorities in Ceramic Engineering and Science, Alfred, NY, Nov. 4-6, 1974), Paper in *Ceramic Engineering and Science*, V. D. Frechette, L. D. Pye, and J. S. Reed, Eds., pp. 37-50 (Plenum Publishing Corp., New York, NY, 1974).

Key words: ceramics; educational priorities; energy; engineer-scientist; environmental quality; materials; minerals.

The role of the scientist-engineer regarding application of technology to national problems is discussed. The probable physical and social "environment" of the future scientist-engineer is assessed. Promising areas of ceramic science are discussed in broad terms. Some educational priorities are recommended.

**16157.** McNesby, J. R., **The role of standard reference materials in environmental measurements,** *Proc. National Conf. on Health, Environmental Effects, and Control Technology of Energy Use, Washington, DC, Feb. 9-11, 1976, Report No. 600/776-002*, pp. 58-60 (U.S. Environmental Protection Agency, Washington, DC, 1976).

Key words: air and water quality; energy; pollutants; standard reference materials.

The rationale for the importance of accurate as well as precise environmental measurement is presented. The role of Standard Reference Materials is to provide the analyst with NBS certified samples to facilitate his ability to make accurate measurement. Available energy related Standard Reference Materials are listed and those expected to be developed along with target dates are tabulated.

**16158.** Freeze, P. D., Thomas, D. B., **Studies of noble-metal thermocouple stability at high temperatures,** *NASA CR-135055*, 54 pages (National Aeronautics and Space Administration, Washington, DC, July 1976).

Key words: aging; calibration change; gradient; high temperature (700 to 2000 °C); iridium; iridium-rhodium alloy; noble-metal thermocouple; oxidation; platinum; platinum-rhodium alloy; preferential oxidation; temperature gradient; thermal gradient; thermocouple; thermoelectric stability.

This report describes two investigatory studies on performance characteristics of noble-metal thermocouples: (1) thermoelectric stability as affected by preferential oxidation of iridium in the system iridium-40 percent rhodium versus iridium, and (2) the effects of temperature gradients on the performance of the systems platinum-13 percent rhodium versus platinum and iridium-40 percent rhodium versus iridium, operating in air.

The stability investigation was carried out at three temperatures—1700, 1850, and 2000 °C—by comparing the output of the test thermocouple in air with the output of an identically constructed test-reference thermocouple in nitrogen. The results show that no calibration shift was observed producing a change in output greater than that corresponding to a 2.0 percent change in the test temperature.

The investigation of gradient effects was carried out by subjecting test thermocouples to both severe and mild gradients. For the platinum system, the operating temperature was 1500 °C with gradients of 1475 and 700 °C/cm; for the iridium system, 2000 °C with gradients of 700, 1500, and 1975 °C/cm. Exposure to temperature gradients was found to introduce significant changes in calibration for both systems.

In both investigations, the thermoelements were examined by means of electron-probe analysis and by metallographic methods to detect chemical and structural changes. Data and micrographs are presented.

**16159.** Meier, M. M., **Neutron standards at the National Bureau of Standards,** *Proc. Third Conf. on Application of Small Accelerators, North Texas State University, Denton, TX, Oct. 21-23, 1974*, CONF-741040-Pl **1,** 365-370 (Available from the National Technical Information Service, VA 22161, 1975).

Key words: associated particle technique; neutron detector; neturon flux monitor; neutron standards; neutrons; $T(p,n)^3He$ reaction.

The neutron standards program at NBS is discussed with emphasis on Van de Graaff contributions to the overall program. In particular, the characteristics of an associated particle apparatus, which serves as a primary standard for flux normalization at the three percent accuracy level are presented. The "black" detector, a secondary standard, suitable as a flux monitor for linac applications and for dosimetry is characterized and its calibration with the associated particle technique is described. Future goals of the program are outlined and the Van de Graaff/associated particle system's future role in achieving them are discussed.

**16160.** Friauf, R. J., Young, K. F., Merz, W. J., **Properties of ionic crystals,** Paper 9f in *American Institute of Physics Handbook, Third Ed.*, pp. 9-74—9-127 (McGraw-Hill Book Co., New York, NY, 1972).

Key words: crystals; ionic conductivity; ionic crystals; properties of ionic crystals.

**16161.** Frederikse, H. P. R., **Properties of semiconductors,** Paper 9e in *American Institute of Physics Handbook, Third Ed.*, pp. 9-56—9-74 (McGraw-Hill Book Co., New York, NY, 1972).

Key words: band structure; properties of semiconductors; semiconductors; thermoelectric power.

6162. Frederikse, H. P. R., Slater, J. C., **Electronic properties of solids,** Paper 9c in *American Institute of Physics Handbook, Third Ed.*, pp. 9-26 – 9-38 (McGraw-Hill Book Co., New York, NY, 1972).

Key words: distribution function; electronic properties of solids; energy band.

6163. Frederikse, H. P. R., **Structure, melting point, density, and energy gap of simple inorganic compounds,** Paper 9b in *American Institute of Physics Handbook, Third Ed.*, pp. 9-16 – 9-25 (McGraw-Hill Book Co., New York, NY, 1972).

Key words: density; energy gap; inorganic compounds; melting point; structure.

6164. Wiese, W. L., Glennon, B. M., **Atomic transition probabilities,** Paper 7i in *American Institute of Physics Handbook, Third Ed.*, pp. 7-200 – 7-209 (McGraw-Hill Book Co., New York, NY, 1972).

Key words: aluminum; argon; atomic transition probabilities; beryllium; boron; carbon; chlorine; helium; hydrogen; lithium; magnesium; nitrogen; oxygen potassium; sodium.

6165. Beaty, E. C., Persson, K. B., **Electrical conductions in gases,** Paper 5e in *American Institute of Physics Handbook, Third Ed.*, pp. 5-138 – 5-139 (McGraw-Hill Book Co., New York, NY, 1972).

Key words: conduction; electrical conduction in gases; gases.

6166. Harris, F. K., **Electrical standards,** Paper 5c in *American Institute of Physics Handbook, Third Ed.*, pp. 5-107 – 5-119 (McGraw-Hill Book Co., New York, NY, 1972).

Key words: absolute electrical standards; electrical standards; electrical units.

6167. Hilsenrath, J., **Thermodynamic properties of gases,** Paper 4h in *American Institute of Physics Handbook, Third Ed.*, pp. 4-162 – 4-204 (McGraw-Hill Book Co., New York, NY, 1972).

Key words: air; argon; hydrogen; ionized gases; nitrogen; oxygen; thermodynamic properties.

6168. Furukawa, G. T., Douglas, T. B., **Heat capacities,** Paper 4e in *American Institute of Physics Handbook, Third Ed.*, pp. 4-105 – 4-118 (McGraw-Hill Book Co., New York, NY, 1972).

Key words: entropy; heat capacity; molar heat capacity.

6169. Powell, R. L., Childs, G. E., **Thermal conductivity,** Paper 4g in *American Institute of Physics Handbook, Third Ed.*, pp. 4-142 – 4-162 (McGraw-Hill Book Co., New York, NY, 1972).

Key words: conductivity; thermal conductivity.

6170. Greenspan, M., **Acoustic properties of liquids,** Paper 3e in *American Institute of Physics Handbook, Third Ed.*, pp. 3-86 – 3-98 (McGraw-Hill Book Co., New York, NY, 1972).

Key words: acoustic properties of liquids; acoustics; Knester liquids; normal liquids; sound.

6171. McKinney, J. E., Lindsay, R., **Density and compressibility of liquids,** Paper 2l in *American Institute of Physics Handbook, Third Ed.*, pp. 2-148 – 2-187 (McGraw-Hill Book Co., New York, NY, 1972).

Key words: compressibility; density; liquid compressibility; liquid density.

16172. Stegun, I. A., **SI units,** Paper 1b in *American Institute of Physics Handbook, Third Ed.*, pp. 1-8 – 1-13 (McGraw-Hill Book Co., New York, NY, 1972).

Key words: metric; SI symbols; SI units.

16173. Stegun, I. A., Carter, C., **Mathematics bibliography,** Paper 1a in *American Institute of Physics Handbook, Third Ed.*, pp. 1-2 – 1-8 (McGraw-Hill Book Co., New York, NY, 1972).

Key words: bibliography; indexes; mathematics bibliography.

16174. Frederikse, H. P. R., Hosler, W. R., Loeffler, N. L., **Testing and test analysis of MHD-materials,** *Proc. NSF-OCR Engineering Workshop on MHD-Materials, Cambridge, MA, Nov. 20-22, 1974*, pp. 138-149 (1974).

Key words: high temperatures; materials evaluation, MHD-materials; test procedures.

The problem of materials development for MHD-power generation is two-fold: The materials to be used in the channel, the combuster, the air-preheater, etc., must have the appropriate electrical and thermal characteristics and at the same time possess sufficient mechanical strength and chemical stability to withstand the very severe environmental conditions for periods of 1000-10,000 hours. This paper will discuss the test conditions in small and medium sized MHD-generators and the evaluation of the tested materials. The results of two short tests performed on 4 electrode materials in the UTSI-MHD-facility will be described and the conclusions drawn from these tests will be summarized.

16175. Albus, J. S., Evans, J. M., Johnsen, E. G., **A hierarchical concept for man-machine communication,** (Proc. 18th Annual Meeting of the Human Factors Society, Huntsville, AL, Oct. 15-17, 1974), Paper in *Benefits for Mankind,* E. L. Saenger and M. Kirkpatrick, III, Eds., pp. 506-509 (The Human Factors Society, Santa Monica, CA, Oct. 1974).

Key words: adaptive control; computer control; control theory; hierarchical control; man-machine communication and automation.

The problem of man controlling or programming a machine may be considered as a hierarchy of control functions, with each level of control calling up ordered sequences of operations at the next lower level, using appropriate sensory feedback for each level. Man may enter the control hierarchy at any level for direct control or for programming an automatic system for later playback. The computer carries out lower level control functions, thereby augmenting man's control capabilities.

The Cerebellar Model Articulation Controller (CMAC) is a computer based control system in which high-level task-oriented commands can be broken down into a series of elemental motor actuator signals. CMAC is a general purpose adaptive control concept which can be arranged in a hierarchical structure, such as that described above, so as to facilitate the man-machine communication problem. For example, CMAC can solve the coordinate transformation problem so that commands can be given in terms of desired end point trajectories. Furthermore, CMAC can handle many feedback variables such as measurements of misalignment of parts, variable mass loading, irregularities in materials, and constraints imposed by an external environment.

16176. Lyons, J. W., **Requirements for fire safety of combustible materials in the United States,** *Proc. Int. Symp. on Fire Safety* *of Combustible Materials, Edinburgh, Scotland, Oct. 15-17, 1975*, **1,** 12-25 (1975).

Key words: fire codes; fire research; fire safety.

Fire safety of buildings and building furnishings in the United States is controlled by local codes and certain mandatory Federal requirements. The test methods and criteria used in codes generally are developed by technical committees of ASTM or NFPA. In a typical development these tests are first incorporated in the NFPA Life Safety Code, then in the four model building codes before finding their way into local codes. An alternative mechanism is inclusion in a mandatory Federal requirement as, for example, in the standards for housing insured by the Department of Housing and Urban Development, for nursing homes supported by the Department of Health, Education and Welfare, hospitals run by the Veterans Administration, or transportation vehicles regulated by the Department of Transportation. Test methods for these Federal agencies are developed by Federal research, often at the Center for Fire Research at the National Bureau of Standards.

The fire safety of consumer products falls under the purview of the Consumer Product Safety Commission. Test methods for CPSC are developed in two ways: by offerors in the private sector under provisions of the Consumer Product Safety Act of 1972, or by Federal research, for example at NBS.

There is great concern in the United States about the chaotic situation with regards to the validity of fire test methods. The focus on fire safety has in recent years shifted from fire endurance and compartmentation (which concepts apply to large buildings and are not helpful in single-family residences) to concern for the occupants in the room of origin and in single-family residences. This means we are now concerned with furnishings and interior finish materials. Tests for these items need considerable work. There is no one small test which permits one to assess the fire safety of a furnished enclosure. (The Federal Trade Commission has underscored this with a recent action against the advertising and promotional claims made based on results of small tests.) Current research efforts are directed to developing standardized full-scale fire tests for enclosures and improved correlations between these and small-scale economical tests. Active roles in this research are being played by the Center for Fire Research, Committee E-39 on Fire Hazard Standards in ASTM, and the Products Research Committee, established as part of a consent order between the FTC and a number of plastics manufacturers.

Fire research in the United States has received new impetus from the Federal Fire Prevention and Control Act of 1974. This Act established a new National Fire Prevention and Control Administration in the Department of Commerce and established anew the research on fire at the National Bureau of Standards. The Center for Fire Research at NBS has a new, broader assignment including its traditional research on fire phenomena and adding a major new responsibility for studies on the effects of fire on its victims (biological, physiological and psychological aspects).

The Fire Administration will be developing new equipment for fire fighting, detection, and suppression as well as helping to improve the efficiency and safety of fire fighting, helping with fire prevention and protection by performing code evaluation and assisting community planning and attacking public indifference through education. With this new emphasis and support at the Federal level, one hopes that United States fire losses will decrease in the future to come into line with fire losses of the other industrial nations of the world.

**16177.** Blanc, R. P., **Assisting network users with a network access machine,** *Proc. Annual Conf. of the Association for Computing Machinery, San Diego, CA, Nov. 11-13, 1974*, **1,** 74-84 (Association for Computing Machinery, New York, NY, 1974).

Key words: access procedures; computer networks; macros; minicomputers.

Accessing networks of heterogeneous computer systems can often be cumbersome due to differences in command languages and conventions. Approaches toward improving these conditions are identified and a specific solution – a "Network Access Machine" – is described in detail. The "Network Access Machine" is a minicomputer-based system that acts as a network access point for a user at his terminal and assists the user through the automatic execution of access procedures. This minicomputer facility allows the user to specify (or to have specified) his own network commands. The minicomputer expands these commands into command sequences executable on a specified network and host connected to that network. Further, system and network responses are analyzed to assure agreement with those anticipated for specific commands. Conditional and parameterized expansions allow the use of the same commands on different host computers and different networks.

**16178.** Breden, L. H., Meisters, M., **The effect of sample orientation in the smoke density chamber,** *J. Fire Flammability* **7,** 234-247 (Apr. 1976).

Key words: fire performance; horizontal and vertical smoke measurements; smoke; smoke density chamber; smoke suppressants.

Smoke measurements were compared for various materials in the vertical and horizontal positions. There appeared a significant difference for thermoplastic materials because of the melting away from the incident heat flux in the vertical position. The horizontal mode in addition allows one to relate the chemistry of polymeric materials to the amount of smoke production. Finally, smoke measurements are made of products containing various amounts of smoke suppressants.

**16179.** Bright, R. G., **Early warning fire detection,** *Proc. Fire Protection in Interior Design, Cleveland, OH, Apr. 10-11, 1975*, pp. 170-184 (1975).

Key words: atriums; fire detection; flame detectors; heat detectors; hospitals; hotels; maintenance; nursing homes; reliability; schools; smoke detectors.

A description of the specialized signatures of fire conditions along with a description of the various available fire detectors are presented. Some special problems of fire detectors such as reliability and maintenance are discussed. The paper closes with a discussion of specialized applications of fire detection to open plan office buildings, atriums, schools, buildings with smoke control systems and the use of detectors in corridors.

**16180.** Pease, R. L., Galloway, K. F., Stehlin, R. A., **Radiation damage to integrated injection logic cells,** (Proc. IEEE Nuclear and Space Radiation Effects Conf., Eureka, CA, July 14-17, 1975), *IEEE Trans. Nucl. Sci.* **NS-22,** No. 6, 2600-2604 (Dec. 1975).

Key words: digital bipolar circuits; integrated injection logic; radiation damage; radiation effects.

The effects of neutron and total dose gamma irradiations on the electrical characteristics of an integrated injection logic ($I^2L$) cell and an $I^2L$ multiple inverter circuit were investigated. These units were designed and fabricated to obtain circuit development information and did not have radiation hardness as a goal. The following parameters of the test structures were measured as a function of total dose and neutron fluence: the dc common-base current gain of the lateral *pnp* transistor; the dc common-emitter current gain of the vertical *npn* transistor; the forward current-voltage characteristics of the injector-substrate junction, and the propagation delay versus power dissipation per gate for the multiple inverter circuit. The limitations of the present test structures in a radiation environment and possible hardening techniques are discussed.

16181. Maki, A. G., Freund, S. M., **Laser Stark measurements on OCS including the observation of zero-field-forbidden $\Delta J = 0, \pm 2$ transitions,** *J. Mol. Spectrosc.* **62,** 90-98 (1976).

Key words: carbonyl sulfide; dipole moments; infrared; lasers; spectra; spectroscopy; Stark effect.

Laser Stark measurements have been made on the $02^00$-$00^00$ and $03^10$-$01^10$ vibrational transitions of ${}^{16}O^{12}C^{32}S$, ${}^{16}O^{12}C^{34}S$, and ${}^{18}O^{12}C^{32}S$, and on the $03^10$-$01^10$ transition of ${}^{16}O^{13}C^{32}S$, using a $CO_2$ laser. In addition to providing dipole moment information for excited vibrational states, these measurements give vibrational band centers accurate to several megahertz. To aid in optical pumping experiments, several near coincidences between $CO_2$ laser transitions and OCS absorption lines are discussed. Electric-field-allowed $\Delta J = 0$ transitions are observed for the $2\nu_2$ band of ${}^{16}O^{12}C^{32}S$ and ${}^{16}O^{12}C^{34}S$, as well as $\Delta J = 2$ transitions for the same band of ${}^{18}O^{12}C^{32}S$.

16182. Caswell, R. S., Coyne, J. J., **Neutron energy deposition spectra studies,** (Proc. 4th Symp. on Microdosimetry, Verbania Pallanza, Italy, Sept. 24-28, 1973), Paper in *Fourth Symposium on Microdosimetry,* J. Booz, H. G. Ebert, R. Eickel, and A. Waker, Eds., EUR 5122 d-e-f, pp. 967-979 (Commission of the European Communities, Luxembourgh, Mar. 1974).

Key words: energy deposition spectra; microdosimetry; neutron interactions with tissue; neutrons; radiation quality; secondary particle spectra; theoretical dosimetry.

Secondary particles (p, $\alpha$, C, N, etc.) are generated when neutrons interact with tissue. We are concerned with three spectra of these secondary particles: (1) the "initial" spectra which come from neutron cross section information, (2) the "slowing-down spectra" which are obtained from the initial spectra and secondary particle stopping power data, and (3) the "energy deposition spectra"—the spectra of energy depositions by the secondary particles in small tissue volumes, which depend upon both the previous spectra, the geometrical properties of the volume, and upon stopping power and range information. We have calculated all of these spectra for a number of energies of monoenergetic neutrons between 60 keV and 14 MeV using analytic methods previously described. Examples will be given of the variation of the spectra and of certain spectral averages such as the frequency and dose averages of lineal energy ($\overline{y}_f, \overline{y}_D$) as a function of neutron energy. Experimental information for comparison exists for spectra of type (3), and we understand measurements of spectra of type (1) are underway.

6183. Gross, D., **The measurement and correlation of fire growth in a room,** *Proc. Symp. on Full-Scale Fire Tests, Lancaster, PA, Nov. 11-12, 1974,* pp. 77-87 (Research and Development Center, Lancaster, PA, 1976).

Key words: buildings; fire growth; flame spread; heat release; interior finish; reduced scale modeling; room corner tests; smoke.

Evaluation of fire growth in a room requires characterization of the source fire, defining a measure of full fire involvement, and correlation in terms of small-scale laboratory tests. A series of 20 room-corner tests was performed using a wood-crib ignition source and selected combinations of interior-finish materials on wall and ceiling surfaces. The upper room-gas temperature was taken as a measure of fire-growth level and potential involvement of all combustible contents. Comparisons are presented between results of the full-scale tests and available laboratory tests on the interior-finish materials. Supplementary approaches involving analytical and reduced-scale modeling are also discussed.

16184. Hust, J. G., Schramm, R. E., **Density and crystallinity measurements of liquid and solid *n*-undecane, *n*-tridecane, and *o*-xylene from 200 to 350K,** *J. Chem. Eng. Data,* **21,** No. 1, 7-11 (1976).

Key words: cryogenics; crystallinity; density; expansion; paraffins.

Densities of solid and liquid *n*-undecane, *n*-tridecane, and *o*-xylene are reported for temperatures from 200 to 350K. Density increases upon freezing by 13, 13, and 12 percent, respectively, for these hydrocarbons. The data are presented graphically and are also represented by equations to within the scatter of the data. The uncertainties of the data are 0.2 percent for the liquid and 1 percent for the solid state. X-ray examinations revealed that these materials have complex crystalline structures when frozen. Near 200K the main crystal structure is orthorhombic, but several phase transformations occur for each of these materials between 200K and the melting point.

16185. Richmond, J. C., **Courtroom of the future. Court related use of videotape recordings,** (Proc. Seminar on Civil Trial Advocacy, University of Kentucky, Lexington, KY, Jan. 23-24, 1976), Paper in *Report of Seminar on Civil Trial Advocacy,* pp. 43-45 (Office of Continuing Legal Education, University of Kentucky, Lexington, KY, July 1976).

Key words: closed circuit television; court proceedings; court security; trial proceedings; videotape recording.

The presentation consisted of showing the videotape "Courtroom of the Future," plus showing slides giving more detail about certain features of the Courtroom of the Future at the McGeorge School of Law in Sacramento, California. The equipment for recording trial proceedings on video, and precautions for court security were emphasized.

16186. Richmond, J. G., **The courtroom of the future,** (Proc. 8th Annual Crime Countermeasures Conf., Lexington, KY, Apr. 15-19, 1974), Paper in *Proc. 1974 Carnahan and Int. Crime Countermeasures Conf., UKY BU* **105,** 152 (Aug. 1974).

Key words: closed circuit television; court proceedings; court security; trial proceedings; videotape recording.

The presentation consisted of showing the videotape "Courtroom of the Future," plus showing slides giving more detail about certain features of the Courtroom of the Future at the McGeorge School of Law in Sacramento, California. The equipment for recording trial proceedings on video, and precautions for court security were emphasized.

16187. Bright, R. G., **Regulations and standards concerning fire detection systems in the United States,** *Proc. 7th Int. Seminar on Problems in Automatic Fire Detection, Aachen, Germany, Mar. 5-6, 1975,* pp. 47-60 (Institut für Elektrische Nachrichtentechnik, Aachen, Germany, 1975).

Key words: fire detection; regulations; smoke detectors; United States standards.

Historically, fire detection systems for the protection of people and property from fire have not enjoyed wide usage in the U.S. With respect to property protection the emphasis has been on the use of automatic sprinkler systems as opposed to automatic fire detection systems. This trend is likely to continue for the foreseeable future. It is in protecting people from fire that automatic fire detection is receiving ever increasing attention.

The U.S. loses an inordinate number of people each year in fires. As most of this loss-of-life takes place in the family life unit, more and more of the U.S. regulatory agencies are requiring the inclusion of automatic fire detection devices, primarily smoke detectors, in all new family living units. This includes apartments, single-family dwellings, and mobile homes.

The paper describes the trends evident in these regulations. The paper also describes the type of smoke detection devices required by these regulations, some of the shortcomings evident in the presently available smoke detectors, and the status of testing and approval standards used to judge the suitability of smoke detectors for life safety.

**16188.** Unassigned.

**16189.** Clifton, J. R., **Protection of reinforcing bars with organic coatings,** *Mater. Perform.* **15,** No. 5, 14-17 (May 1976).

Key words: bridge decks; chloride ions; corrosion; deicing salts; epoxy coatings; organic coatings; steel reinforcing bars.

Results of a program aimed at identifying organic coatings suitable for steel reinforcing bars in concrete are given. Resistances of candidate coatings to abrasion, solutions of calcium chloride, hydroxide, sulfate, and fresh cement paste, and surface preparation of steel, resistance of coated bars to electrical currents, and concrete-to-coating bonding are discussed. Tests were made on liquid and powdered epoxy, polyvinylchloride liquid, polypropylene powder, phenolic nitrile liquid, and zinc rich liquid coatings.

**16190.** Treado, M. J., **Development of reports and guidelines for law enforcement communications equipment,** (Proc. 8th Annual Crime Countermeasures Conf., Lexington, KY, Apr. 16-19, 1974), Paper in *Proc. 1974 Carnahan and Int. Crime Countermeasures Conf., UKY BU* **105,** 102-112 (Aug. 1974).

Key words: communications; digital communications; guideline; law enforcement equipment report, Law Enforcement Standards Laboratory; mobile digital equipment; National Institute of Law Enforcement and Criminal Justice.

The Law Enforcement Standards Laboratory (LESL) was established by NBS for the National Institute of Law Enforcement and Criminal Justice (NILECJ) primarily to develop performance standards to assist law enforcement agencies in their equipment selection and procurement process. In addition to performance standards, LESL also is developing equipment reports, guidelines and glossaries for use by the law enforcement community. This paper uses a typical study effort, in this case one on mobile digital communications, to illustrate the development of a law enforcement equipment report.

**16191.** Schramm, R. E., Reed, R. P., **Stacking fault energies of fcc Fe-Ni alloys by x-ray diffraction line profile analysis,** *Metall. Trans. A* **7A,** No. 3, 359-363 (Mar. 1976).

Key words: invar; iron alloys; nickel alloys; stacking fault energy; x-ray diffraction.

The stacking fault energies of the fcc alloy series Fe-28 Ni to pure Ni were investigated using x-ray diffraction line profile analysis. A minimum stacking fault energy of about 70 mJ/m$^2$ occurs at the approximate composition of Fe-40 pct Ni. From this point, the lower nickel alloys rapidly increase to a very high stacking fault energy, estimated to be 200 mJ/m$^2$, while the energies of the high Ni alloys rise linearly to the Ni value of 214 mJ/m$^2$. Anomalous reductions of the lattice parameter after cold work were found for the low nickel alloys; this was interpreted as evidence for $Fe_3Ni$ ordering and corrections to the stacking fault energy were made.

**16192.** McNeil, J. R., Collins, G. J., Persson, K. B., Franzen, D. L., **Ultraviolet laser action from Cu II in the 2500-Å region,** *Appl. Phys. Lett.* **28,** No. 4, 207-209 (Feb. 15, 1976).

Key words: Cu II spectrum; ultraviolet laser, 250.0 nm.

We have obtained cw laser action from Cu II at 2486, 2506, 2591, and 2599 Å by exciting a neon discharge in a copper hollow cathode. We have observed 7-mW cw output power just above threshold and the output appears to saturate at 210 mW under quasi-cw operation. The four ultraviolet laser lines observed originate from the $3d^95s(^3D)$ term of Cu II. The quantum efficiency of the 2500-Å laser transitions approaches 25 percent. Each of the four Cu II laser transitions has been employed in the past by spectroscopists as a secondary wavelength standard in the ultraviolet.

**16193.** Andrews, J. R., Lawton, R. A., **Electrically strobed optical waveform sampling oscilloscope,** *Rev. Sci. Instrum.* **47,** No. 3, 311-313 (Mar. 1976).

Key words: laser; optical pulse; oscilloscope; photoconductor; pulse measurements; sampling.

A new instrument for measuring optical waveforms is described. It is an optical sampling oscilloscope employing a GaAs photoconductive sampling gate and an electrical sampling strobe. The basic theory of operation is derived. A 100-psec risetime rudimentary prototype has been built and results of measurements of a GaAs laser diode pulse are presented.

**16194.** Tobler, R. L., Read, D. T., **Fatigue resistance of a uniaxial S-glass/epoxy composite at room and liquid helium temperatures,** *J. Compos. Mater.* **10,** 32-43 (Jan. 1976).

Key words: cryogenics; fatigue; fiber composites; liquid helium; low temperature tests; mechanical properties.

Tension-tension axial fatigue tests of a uniaxial glass filament-reinforced epoxy were conducted at 295 K and 4 K. The fatigue life was found to be an order of magnitude greater at 4 K than at 295 K. These results are believed to be the first 4 K fatigue data reported for a composite material.

**16195.** Dalke, J. L., **Metric system versus anthropomorphic units—A bicentennial coup?,** *Am. Metric J.* **4,** No. 3, 121-123 (1976).

Key words: anthropomorphic units; bicentennial; history of measurement; metric conversion; metric roll call; metrology; Public Law 93-380; Public Law 94-168.

The U.S.A. declared its independence in 1776. The Bicentennial Anniversary of this occasion ironically also is the beginning of a stronger commitment to discard our cumbersome customary English measurement system, an action that is already well underway in English speaking countries. The English system now persists most strongly in the U.S., yet in addition to its inconsistencies it is to our economic disadvantage to continue the use. Public Law 94-168, the Metric Conversion Act of 1975, which became effective December 23, 1975, provides a mechanism for promoting the metric system in the U.S. Thus, in 1976, the Bicentennial year, we begin to push more sharply for independence from a measurement system that is becoming obsolete. A synopsis is given of the development of anthropomorphic measurements and an overview of metric (SI) usage in the U.S., including a metric "roll call" of industry.

**16196.** Clark, A. F., Haynes, W. M., Deason, V. A., Trapani, R. J., **Low temperature thermal expansion of barium ferrite,** *Cryogenics* **16,** No. 3, 267-270 (May 1976).

Key words: barium ferrite; low temperature; thermal expansion.

The linear thermal expansion of polycrystalline barium ferrite, $BaFe_{12}O_{19}$, was measured from 76 to 293 K both parallel and perpendicular to the magnetization direction. An anisotropy of about 15-20 percent was observed. The results match well the available data above room temperature and have also been extrapolated to 0 K.

**16197.** Richmond, J. C., **Criteria for evaluating image quality of night vision devices,** (Proc. 8th Annual Crime Countermeasures Conf., Lexington, KY, Apr. 16-19, 1974), Paper in *Proc. 1974 Carnahan and Int. Crime Countermeasures Conf., UKY BU* **105,** 83-94 (Aug. 1974).

Key words: acutance; contrast transfer function; edge gradient; image quality; light equivalent background; light induced background; limit resolution; line spread function; optical transfer function; point spread function.

The National Bureau of Standards is developing Standards for image intensifier night vision devices for use in law enforcement, under a project managed by the Law Enforcement Standards Laboratory of NBS, which is sponsored by the National Institute of Law Enforcement and Criminal Justice of the Law Enforcement Assistance Agency of the Department of Justice. The quality of the image produced by such a device is an important measure of its utility, and image quality criteria are an important part of such a Standard. Many variables contribute to image quality, not all of which have been identified, or can be measured. This paper is a literature survey of criteria and techniques that have been used to evaluate the quality of imaging systems, with some discussion of their application to image intensifier night vision devices.

**16198.** Rockett, J. A., **Who will design fire protection of the future,** *Society of Fire Protection Engineers, Technical Report 75-5,* pp. 1-5 (Society of Fire Protection Engineers, Boston, MA, 1975).

Key words: fire protection; future trends; professional qualifications.

The professional cross section of fire protection engineers of a decade from now is discussed. Present trends in the field are projected and it is suggested that a much broader and richer set of professional backgrounds will be found.

**16199.** Stokesberry, D. P., Hasegawa, S., **Automatic digital microwave hygrometer, model II,** *Rev. Sci. Instrum.* **47,** No. 5, 556-558 (May 1976).

Key words: digital microwave hygrometer; hygrometer, digital microwave; microwave, digital, hygrometer.

A "ruggedized" microwave hygrometer which requires no moving parts in the basic measurement method is described. It is designed to measure atmospheric humidity over the vapor pressure range 3-7400 pascals (Pa) (0.03-74 millibar).

**16200.** McDonald, D. G., Johnson, E. G., Harris, R. E., **Modeling Josephson junctions,** *Phys. Rev. B* **13,** No. 3, 1028-1031 (Feb. 1, 1976).

Key words: cryogenics; electronic tunneling; Josephson effect; superconductivity.

The current-voltage characteristic of a current-biased junction is calculated using the Werthamer theory. In contrast with the voltage-biased model large zero-frequency currents exist at 0 K at all bias voltages below the energy gap and the Riedel peak is directly displayed. The effect of capacitance on the *I-V* curve is described and the form of the subharmonic energy-gap structure is calculated using the Mattis-Bardeen model for the superconducting electrodes.

**16201.** Rockar, E. M., Forman, R. A., **$Fe^{4+}$ ($3d^4$) optical absorption in oxidized $SrTiO_3$,** *Phys. Status Solidi A Short Notes* **33,** K91-K95 (1976).

Key words: charge transfer, color centers; crystal field; $d^4$ ions; EPR; iron 4+; optical absorption; perovskite; strontium titanate; transition metal; zero phonon line.

The optical absorption spectrum of oxidized, iron doped $SrTiO_3$ at 10 K exhibits a sharp line at 772.5 nm (12,945 $cm^{-1}$) with side bands at $\Delta\nu_1 = 116\ cm^{-1}$, $\Delta\nu_2 = 168\ cm^{-1}$, and $\Delta\nu_3 = 315\ cm^{-1}$. After moderate reduction in flowing $H_2$ at 900 °C this line and its vibronics disappear. The spectrum is attributed to the $^5E_g \rightarrow {}^3T_{1g}$ transition of $Fe^{4+}(3d^4)$.

**16202.** Howard, C. J., Evenson, K. M., **Rate constants for the reactions of OH with ethane and some halogen substituted ethanes at 296 K,** *J. Chem. Phys.* **64,** No. 11, 4303-4306 (June 1, 1976).

Key words: fluorocarbons; hydroxyl radical; reaction rate constants.

Absolute rate constants for the reactions of OH radicals with $C_2H_6$ and twelve fluorine, chlorine, and bromine substituted ethane compounds are reported. The measurements are made at 296 K and pressures ranging from 100 to 1000 Pa (0.7-7 torr) using a discharge-flow system and laser magnetic resonance detection of OH. The results are similar to those of an earlier work on a series of methane compounds and indicate that the reaction mechanism is the abstraction of an H atom. Thus, completely halogenated molecules are relatively inert. The hydrogen containing molecules react with rate constants ranging from about 3 to $400 \times 10^{-15}\ cm^3\ molecule^{-1} \cdot sec^{-1}$.

**16203.** Ogburn, F., **Electrodeposition and government laboratories,** *Plating Surf. Finish.* **63,** No. 7, 24-29 (July 1976).

Key words: Blum, William; electrodeposition; government laboratories; plating.

Government laboratories have made numerous contributions to the science and technology of electrodeposition in the form of commercial instruments and process as well as engineering data and scientific information. These laboratories and their more significant contributions are briefly reviewed as seen through the eyes of one Government scientist.

**16204.** Birky, M. M., **Philosophy of testing for assessment of toxicological aspects of fire exposure,** *J. Combust. Toxicol.* **3,** 5-23 (Feb. 1976).

Key words: bioassay; combustion products; fire; hazard assessment; toxicity.

Detailed investigation of fire fatalities and autopsies of fire victims indicate the interaction of carbon monoxide, pulmonary injury, alcohol and cardiovascular disease in fire fatalities that are attributed to smoke inhalation. Laboratory assessment of the toxicity hazard of combustion products has relied predominantly on chemical analysis for a few selected toxic gaseous species such as carbon monoxide. While the clinical data suggest that carbon monoxide has been the predominant toxicant in past fatalities, the advent of new synthetic materials that contain fire retardants or are inherently more fire resistive have the potential of contributing other unknown toxicants. In addition, the particulate phase (smoke) may play a major role in inhalation toxicity that cannot be assessed by means of chemical analyses. In the past the toxicity of some new fire retardants has been screened using feeding experiments. While this is an important first step, experiments to determine the inhalation toxicity of the thermal degradation products, of the fire retardants and of polymers incorporating fire retardants must also be made to assess the acceptability of such materials.

This paper proposes that a multi-disciplinary program, including toxicological, chemical and combustion expertise, is required to assess the toxicological effects of combustion products. The product mixture is so complex that a toxicity assessment will require animal exposures combined with analysis of selected gases and correlation with biomedical information.

**16205.** Rosenstock, H. M., **The measurement of ionization and appearance potentials,** *Int. J. Mass Spectrom. Ion Physics* **20,** 139-190 (1976).

Key words: appearance potential; gaseous positive ions; heat of formation; ionization potential; measurement.

Measurement techniques and methods of data interpretation leading to ionization potentials, appearance potentials and heats of formation of gaseous positive ions are summarized and critically discussed. Special attention is paid to defining the accuracies, problems and limitations of the techniques and interpretations. References have been selected and cited which discuss these matters in more detail.

**16206.** Hust, J. G., **Thermal conductivity standard reference materials, Progress Report,** (Proc. XIII Int. Conf. on Thermal Conductivity, Lake of the Ozarks, MO, Nov. 5-7, 1973), Paper in *Advances in Thermal Conductivity,* R. L. Reisbig and H. J. Sauer, Jr., Eds., pp. 22-24 (1974).

Key words: austenitic steel; cryogenics; electrical resistivity; electrolytic iron; Lorenz ratio; thermal conductivity.

Current and past research in the area of standard reference materials is described. New characterization data for SRM's 734 and 735 (thermal conductivity standard reference materials) are discussed. Low temperature thermal conductivity data for sintered tungsten are included in anticipation of establishing this material as a thermal conductivity standard reference material. Present indications are that SRM 734 (electrolytic iron) may be extended to temperatures as high as 800 °C and SRM 735 (austenitic stainless steel) may be extended to 100 °C as thermal conductivity standard reference materials. It appears that tungsten may be used to temperatures as high as 2700 °C.

**16207.** Daney, D. E., **Turbulent natural convection of liquid deuterium, hydrogen and nitrogen within enclosed vessels,** *Int. J. Heat Mass Transfer* **19,** No. 4, 431-441 (Apr. 1976).

Key words: cryogenics; heat transfer; hemisphere; horizontal cylinder; liquid deuterium, liquid hydrogen, liquid nitrogen; natural convection; sphere; vertical cylinder.

Quasi-steady natural convection of liquid deuterium, hydrogen, and nitrogen within a sphere, hemisphere, horizontal cylinder, and vertical cylinder has been studied experimentally for the case of a nearly uniform wall temperature. A single expression relating the Nusselt and Rayleigh numbers,

$$Nu - 0{\cdot}104\, Ra^{0.352},$$

fits the deuterium and nitrogen data over the range $7 \times 10^8 < Ra < 6 \times 10^{11}$, while the hydrogen Nusselt numbers are 8 percent lower. The temperature field within the vessels is virtually free of horizontal temperature gradients. A single dimensionless temperature profile characterizes the vertical temperature distribution for each vessel shape, with the profiles for the sphere, hemisphere, and horizontal cylinder being nearly identical.

**16208.** Siegwarth, J. D., **A high conductance helium temperature heat switch,** *Cryogenics* **16,** No. 2, 73-76 (Feb. 1976).

Key words: gold plating; heat switch; He temperature; high conductivity.

Metallic contact heat switches with high thermal conductances have been designed and tested in the 4 to 15 K temperature range. Both gold plating and solid silver were used for the contact surfaces. Switch conductances greater than 1W $K^{-1}$ at 15 K were achieved for a switch closed at this temperature with a force of 54 kg. The conductance is proportional to temperature, and varies approximately as the 2/3 power of the closing force.

**16209.** Weiss, A. W., **Transition probabilities for ionized atoms,** (Proc. 4th Int. Conf. on Beam-Foil Spectroscopy, Gatlinburg, TN, Sept. 15-19, 1975), Paper in *Beam-Foil Spectroscopy,* I. A. Sellin and D. J. Pegg, Eds., **1,** 51-68 (Plenum Publishing Corp., New York, NY, 1976).

Key words: ions; oscillator strengths; quantum mechanics; spectroscopy; transition probabilities; wave functions.

Several aspects of the line strength problem for ionized atomic systems are discussed. Level crossings, which arise from the restructuring of the ionic spectrum, occur frequently in the medium stages of ionization and can produce severe irregularities in the f-value behavior along an isoelectronic sequence. Calculations on several such examples are described. For very highly ionized species relativistic effects must be taken into account, and the hydrogen-like line strengths are discussed as a prototype of orbital relativistic effects. For many-electron systems the major relativistic effect is intermediate coupling, and multi-configuration calculations including the dominant Pauli approximation corrections have been done on a number of ions. Results are presented for the beryllium and boron isoelectronic sequences.

**16210.** Larsen, E. B., Andrews, J. R., **Using fiber optics in a broadband, sensitive, isotropic antenna—15 kHz to 150 MHz,** *Proc. IEEE Int. Symp. on Electromagnetic Compatibility, Washington, DC, July 13-15, 1976,* pp. 385-389 (Institute of Electrical & Electronics Engineers, Inc., New York, NY, 1976).

Key words: broadband antenna; electromagnetic compatibility; fiber optics; field strength measurement; isolated EMC antenna; sensitive isotropic probe.

A broadband, active, isotropic receiving antenna was developed at NBS for the frequency range 15 kHz to 150 MHz. It was designed for use with a conventional receiver to measure weak, near-zone electric fields of unknown polarization, such as leakage emanations from electronic equipment placed within a shielded enclosure. The antenna system consists of three mutually-orthogonal active dipoles, each 31 cm long by 3 cm diameter. The entire frequency range of each of the three field components is amplified and used to modulate a high-speed light emitting diode (LED) located inside the dipole. The modulated infrared (IR) signals are guided through glass fibers 10 meters long which connect the "isolated" dipoles to avalanche photodiodes at the far end of the fiber guides. These photodetectors recover the RF modulation from the IR carrier for input to the receiver. The fiber-optic antenna system described in this paper has high sensitivity (down to 10 $\mu$V/m) and fast response time (RF modulations up to 150 MHz). The readout indication at each receiver frequency is proportional to the Hermitian magnitude of E, which is the root-sum-square value of three orthogonal E field components at the measurement point.

**16211.** Torchia, D. A., Lyerla, J. R., Jr., Quattrone, A. J., **A $^{13}$C magnetic resonance study of the helix and coil states of the collagen peptide αl-CB2,** (Proc. Rehovot Symp. on Poly(Amino Acids), Polypeptides, and Proteins and Their Biological Implications, Israel, May 1-8, 1974), Paper in *Peptides, Polypeptides and Proteins.* E. R. Blout, F. A. Bovey, M. Goodman, and N. Lotan, Eds., pp. 436-448 (John Wiley & Sons, New York, NY, 1974).

Key words: collagen; conformation; correlation times; cyanogen bromide peptides; polypeptides; relaxation times; rotational diffusion; $^{13}$C magnetic resonance.

Carbon-13 chemical shifts, spin-lattice ($T_1$) and spin-spin ($T_2$) relaxation times and $^{13}$C-$^1$H nuclear Overhauser enhancements (NOE) have been determined for the coil and triple helical states of the αl-CB2 fragment of rat skin collagen. Assignment of all aliphatic resonances of this 36 residue peptide in the random coil state (30°) has been achieved with the aid of model polypeptides containing pyrrolidine residues. The $T_1$ measurements show that the interior backbone carbons of the coil are characterized by effective rotational correlation times ($\tau_{eff}$) of *ca.* 0.45 nsec. while sidechain and near terminal backbone $\tau_{eff}$ values are 2-5 times shorter. These results along with the narrow natural linewidths (3-5 Hz) and maximum NOE values (3.0) demonstrate the high degree of backbone segmental motion and sidechain mobility in the unordered state of the peptide. By contrast, the broad lines (50-80 Hz) and low NOE values (1.3) for the α-carbons in the helical state (2°) suggest much slower motion. These results together with the $T_1$ values (0.025-0.040 sec) are consistent with a model in which the motion of the ordered state of αl-CB2 is described by rotational diffusion of an axially symmetric rigid ellipsoid having dimensions approximating those expected for a collagen-type helix of 36 residues.

**16212.** Sweeney, W. T., **Dental research at the National Bureau of Standards 1919-1969,** *Br. Dent. J.* **127,** 289-290 (Sept. 16, 1969).

Key words: amalgam; composite materials; dental gold alloys; dental research; panoramic x ray; silicate cement; turbine handpiece.

The dental research program started at NBS in 1919 has continued as a joint effort with the cooperation of the American Dental Association, the National Institute of Dental Research, the U.S. Army, the U.S. Air Force, and the Veterans Administration. The staff of about 35 is made up of Research Associates, Guest Workers, and employees of the National Bureau of Standards. Approximately 500 papers have been published on dental materials, including amalgam, gold alloys, cements, denture base materials, and on research related to natural tooth structure. Materials and instruments, including the high speed turbine handpiece and the panoramic x-ray machine developed at NBS, have made major contributions to the practice of dentistry.

**16213.** Coriell, S. R., Sekerka, R. F., **The effect of the anisotropy of surface tension and interface kinetics on morphological stability,** *J. Cryst. Growth* **34,** No. 2, 157-163 (July 1976).

Key words: alloys; anisotropy; interface kinetics; solidification; stability; surface tension.

The theory of the morphological stability of a planar interface during solidification of a binary alloy has been modified to account for an anisotropic departure from local equilibrium (anisotropic interface kinetics) at the solid-liquid interface. The temperature for local equilibrium is calculated from the Gibbs-Thomson equation for anisotropic surface tension. Departure from local equilibrium is characterized by taking the interface velocity to be a function of thermal undercooling, concentration, orientation, and curvature. A perturbation analysis leads to the conclusion that an isotropic departure from local equilibrium causes a modification of the capillary terms and liquidus slope as they enter the expression for the time evolution of perturbations; in addition, perturbation growth rate is retarded. Allowance for anisotropy of surface tension causes the capillary terms to depend on direction. Anisotropic interface kinetics leads to the additional important effect that sinusoidal perturbations are translated parallel to the unperturbed interface as they change in amplitude. The peaks of such sinusoidal perturbations will therefore grow at an angle to the normal of the unperturbed interface. This effect is believed to be an underlying cause for the existence of preferred directions for cellular and dendritic growth.

**16214.** Truhlar, D. G., **Interpretation of ortho-para hydrogen conversion,** *J. Chem. Phys.* **65,** No. 3, 1008-1010 (Aug. 1, 1976).

Key words: chemical reactions; collision theory; hydrogen atoms; hydrogen molecules; indistinguishable particles; nuclear spin; rate coefficients; transition-state theory.

The interpretation of statistics of the nuclear spin states in the ortho-para hydrogen conversion by hydrogen atoms is considered. It is shown that the observable rate coefficient (which is the sum of the forward and reverse rate coefficients for Para→ortho conversion) equals the distinguishable-atom rate coefficient in the classical limit. In addition to spin-1/2 nuclei, we also consider spin-1 nuclei and spin-0 nuclei.

**16215.** Persensky, J. J., **Human factors in product safety research,** *ASHRAE Trans.* **81,** Part 2, 434-440 (Dec. 1975).

Key words: appliances; behavioral science; human factors; product safety; safety; safety research.

In 1955, the National Bureau of Standards (NBS) provided the basic human performance and reaction data necessary for the establishment of an appliance safety standard under the Refrigerator Safety Act of 1956. Between that time and the early 1970's, human factors aspects of product safety research have received little attention. Recently, however, the enactment of the Consumer Product Safety Act has provided a new impetus to product safety research. Members of ASHRAE should be particularly interested in the results of such research since a number of their products rank among the top products on the Consumer Product Safety Commission's (CPSC) list of hazardous products. Included are: space heaters, furnaces and water heaters. Unfortunately, almost no human factors data are available to serve the needs of safety motivated, product improvements. NBS has been working with CPSC since late 1973 and has established a program including human factors research to support the development of product safety standards. NBS will obtain human performance and reaction data related to the use of products in a naturalistic situation. In order to accomplish this, novel approaches to the collection of data are being developed.

This presentation describes some of the research. A generalized methodology involving critical incident and naturalistic observation techniques is presented. The presentation closes with illustrations of some of the problems associated with behavioral research.

**16216.** McBee, C. L., Kruger, J., **Events leading to the initiation of the pitting of iron,** (Proc. Int. Conf. on Localized Corrosion, Williamsburg, VA, Dec. 6-10, 1971), Paper in *Localized Corrosion,* R. Staehle, B. F. Brown, J. Kruger, and A. Agrawal, Eds., NACE-3, 252-260 (National Association of Corrosion Engineers, Houston, TX, 1974).

Key words: ellipsometry; iron; kinetics; optical constants; passive; pitting; spectroscopy.

Ellipsometric spectroscopy was used to analyze the changes in the passive film on Fe caused by chloride. The changes studied were the optical variations that take place in the film during the time period between introduction of chloride ions to the solution after passive film growth and the time just prior to breakdown.

It was found that the visible spectrum of the passive film on Fe at potentials above the critical pitting potential, $E_p$, is affected at only a few wavelengths when chloride is introduced into the solution in which the film is formed. At potentials below the critical pitting potential, the introduction of chloride produces optical changes at all wavelengths in the visible spectrum and can be interpreted as causing film thickening. Annealing the passive film grown above the critical pitting potential at 75 °C prior to the introduction of chloride produces the same results as that for films at potentials below $E_p$. Removal of chloride from the solution just prior to breakdown of the film results in a return of the optical parameters to the values found for a passive film.

The time to breakdown in chloride increases with increasing film thickness. The time for recovery of the passive state decreases with increasing film thickness. The overall concentration of chloride introduced in a film decreases with thickness for films grown at potentials above the critical pitting potential.

The results of this study point to a mechanism for passive film breakdown on Fe that requires a penetration of chloride via lattice defects.

**16217.** Scheps, R., Gallagher, A., **Teratomic recombination in alkali metal-noble gas vapors,** *J. Chem. Phys.* **65,** No. 3, 859-871 (Aug. 1, 1976).

Key words: alkali metal-noble gas vapors; gas vapors; metal-noble gas vapors; vapors, gas.

The teratomic recombination rates for the reaction $M^* + 2X \rightarrow MX^* (A^2\Pi) + X$ have been studied for Rb-Xe, Na-Ar, Ke, Xe, and Li-Ar, Kr, Xe. This analysis employs data and molecular potential determinations from earlier measurements where free alkali M was optically excited to $M^*$ in the presence of noble gas X and the $MX^*(A^2\Pi) \rightarrow MX(X^2\Sigma)$ fluorescence resulting from teratomic recombination was measured. Collisional processes compete with radiative decay, so that in the low [X] limit where dissociation collisions are negligible the ratio of bound molecular to atomic photon emission gives the branching ratio between the molecular formation rate and the known atomic radiative rate. The molecular spectrum is observed as a continuum whose intensity profile may be used to infer a bound state vibrational distribution at each [X]. Both bound and quasibound states are included in this distribution, as both contribute to the observed molecular spectra. The low pressure limit of this distribution yields the teratomic recombination rate as a function of binding energy, and the total recombination rate constant $k_f$. It is generally found that this distribution per quantum state is almost independent of binding energy; i.e., the probability of molecular formation appears to be about the same for all bound states, it does not favor the highest bound levels. When the density of states is considered, weakly bound molecules are formed more frequently, but this weighting depends on the shape of the potential rather than the gas temperature. Comparison with theoretical models is made, and reasons for the discrepancies are discussed.

**16218.** Fanconi, B., **On the assignments of rotatory lattice modes in *n*-alkanes and polyethylene,** *J. Appl. Phys.* **46,** No. 10, 4124-4129 (Oct. 1975).

Key words: *n*-alkanes; polyethylene; Raman spectroscopy; rotatory lattice modes.

Considerable discrepancy exists in the recent literature on the assignments of the rotatory lattice modes of the *n*-alkanes and polyethylene. New low-temperature Raman data are presented on orthorhombic *n*-alkanes and on $n$-$C_{36}D_{74}$ and $n$-$C_{16}D_{34}$. Analyses of these data and the existing assignments show that the long-axis rotatory mode of the triclinic *n*-alkanes may be assigned to a weak Raman band at ~50 $cm^{-1}$; the $A_g$ rotatory mode of polyethylene may be assigned to the Raman band at ~130 $cm^{-1}$ and the $B_{3g}$ rotatory mode to a weak Raman band at 108 $cm^{-1}$.

**16219.** Reneker, D. H., Fanconi, B., **Effects of defects on the longitudinal acoustic mode of *n*-alkane chains,** *J. Appl. Phys.* **46,** No. 10, 4144-4147 (Oct. 1975).

Key words: localized defects; *n*-alkanes; polyethylene; Raman-active longitudinal acoustic mode.

Normal mode calculations show that a single conformational defect in an otherwise all-trans *n*-alkane molecule disrupts the longitudinal acoustic mode (LAM) associated with the all-trans molecule. Similar calculations for a chain in the conformation produced by smoothly twisting a planar zigzag through 180° about the chain axis show that the LAM amplitudes and frequencies are unaffected by this gentle twist. These calculations indicate that the decrease in the LAM intensity observed in some polyethylene samples cannot be accounted for by smoothly twisted chains, but can be accounted for by defects which involve large localized departures from the all-trans conformation.

**16220.** Kusuda, T., Tsuchiya, T., Powell, F. J., **Prediction of indoor temperature by using equivalent thermal mass response factors,** (Proc. 5th Symp. on Temperature, Washington, DC, June 21-24, 1971), Paper in *Temperature, Its Measurement and Control in Science and Industry,* L. G. Rubin, A. C. Anderson, J. E. Janssen, and R. D. Cutkosky, Eds., Part 2, **4,** 1345-1355 (Instrument Society of America, Pittsburgh, PA, 1972).

Key words: on-line simulation of temperature controls; thermal response factors.

Several methods are explored for computing room temperature and room thermal load from outdoor conditions. An analytical method based upon rigorous heat transfer analysis of the building system requires a sophisticated computer program and a large computer. A stochastic time series method based upon experimental data of a limited time duration is attractive because it does not rely upon a complex heat transfer mathematics simulation. The stochastic processing of the experimental data, however, leads to the response factors which are physically inconsistent. A semiempirical method, based upon a finite difference solution of a differential equation modeling the equivalent thermal mass system, produced consistent and accurate results. Although this approach has only been verified using experimental data of very simple boundary conditions (without solar radiation effect and the internal heat generation), the results are very promising and encourage further study. Applications are mentioned, such as a simplified on-line computerized linear function temperature control system and, a means of predicting energy requirements for buildings.

**16221.** Moore, L. J., Gramlich, J. W., Machlan, L. A., **Application of isotope dilution to the high accuracy trace analysis of environmental and health standards,** (Proc. 9th Annual Conf. on Trace Substances in Environmental Health, Columbia, MO, June 11, 1975), Paper in *Trace Substances in Environmental Health-IX,* D. D. Hemphill, Ed., pp. 311-316 (1975).

Key words: cadmium; environmental Standard Reference Materials; isotope dilution; lead; molybdenum; rubidium; strontium; trace analyses.

During the last few years at the National Bureau of Standards, isotope dilution mass spectrometry (IDMS) has been extensively applied to the determination of trace elements in a variety of matrices. The cumulative result of recent developments in analytical methodology, such as the lowering of analytical blanks and thermal ionization enhancement techniques, has been the extension of the high accuracy capability of IDMS to more than 20 elements at the ppm ($\mu$g/g) and ppb (ng/g) levels with commensurate accuracies of 0.25–0.50 percent (relative ts, where $ts=t_{n-1}(0.95)$ sample standard deviation) for most of these elements. Applications of these techniques to selected elements in biological and environmental standard reference materials will be presented.

The efficacy of IDMS as a reference trace analytical tool is also being utilized for the development of accurate analysis techniques using the more frequently field-employed atomic absorption and emission spectrometry. This approach has been applied to Ca and Pb in porcine, bovine and human blood where the typical IDMS determinations are $0.1894 \pm 0.0009$ ppm and $84.09 \pm 0.17$ ppm for Pb and Ca, respectively. A brief comparison of these and comparable data from absorption and emission techniques will be presented.

**16222.** Luther, G. G., Towler, W. R., Deslattes, R. D., Lowry, R., Beams, J., **Initial results from a new measurement of the Newtonian gravitational constant,** (Proc. Atomic Masses and Fundamental Constants, Paris, France, June 2-6, 1975), Paper in *Atomic Masses and Fundamental Constants,* J. H. Sanders and A. H. Wapstra, Eds., **5,** 592-598 (Plenum Publishing Corp., New York, NY, 1976).

Key words: acceleration measurement: fundamental constant; gravitational attraction; gravitational constant; rotating reference frame.

A redetermination of the Newtonian gravitational constant is underway at the National Bureau of Standards, Gaithersburg, Maryland, USA. This measurement is expected to yield results, eventually, in the 10 to 20 ppm range. An initial measurement with relatively low accuracy has been completed and some refinements are now in progress which show promise of better results.

**16223.** Deslattes, R. D., **Recent estimates of the Avogadro constant,** (Proc. Atomic Masses and Fundamental Constants, Paris, France, June 2-6, 1975), Paper in *Atomic Masses and Fundamental Constants,* J. H. Sanders and A. H. Wapstra, Eds., **5,** 552-558 (Plenum Publishing Corp., New York, NY, 1976).

Key words: Avogadro; crystal; physical constant; x ray.

The present day situation of the Avogadro constant is reviewed. In the course of various recent adjustments, first the x-ray route and then the electrochemical Faraday had to be excised over the past several years. This then left a unique indirect electrical route which leads to a 6 ppm value. More recently, a new x-ray cell size, crystal density and atomic weight determination was carried out with 1 ppm claimed accuracy. The principal features of this are summarized.

**16224.** McCarter, R. J., **Smoldering of flexible polyurethane foam,** *J. Consum. Prod. Flammability* **3,** 128-140 (June 1976).

Key words: cotton; cushioning; fire retardant; furniture; glowing; inhibitor; oxidative pyrolysis; oxygen index; rayon; smoke; smoldering; upholstery fabric.

The smoldering behavior of various flexible polyurethane foams was studied. All foams smoldered when exposed to cigarette and fabric smolder, posing degrees of potential hazard. A few foams exhibited self-sustained smolder and were judged exceptionally hazardous.

Smolder behavior was compared to oxygen indices, density, permeability, and charring tendencies of the foams. A significant correlation was found between smoldering and charring (opposed to melting) tendencies. Distinctly different combustion behavior was noted for foams based on conventional polyols versus grafted polyols, and for foams containing fire retardant additives. Possibilities for modifying smolder behavior are discussed.

**16225.** Horowitz, E., **Plastics testing,** Paper in *Kirk-Othmer Encyclopedia of Chemical Technology, 2d Edition,* **15,** 811-832 (John Wiley & Sons, Inc., New York, NY, 1968).

Key words: nonpolymeric constituents in plastics; plastics testing; polymer analysis; properties; test methods.

Plastics are tested to measure one or more of their properties and to relate these measurements to predictable or observable behavior. These tests permit quality to be judged and the properties of plastics to be modified and improved. They also provide data on the fundamental nature and characteristics of plastics, which furthers our understanding of these systems. This chapter serves as an introduction to the subject of plastics testing and briefly describes some of the important tests that are made on plastic materials.

**16226.** Snell, J. E., **Summary Review—Evaluation factors, design requirements and needed research,** (Proc. Symp. CIB (Conseil Internationale du Batiment) Commission W62 on Water Supply and Drainage Inside Buildings, Watford, England, Sept. 19-20, 1972), Paper in *Water Demand in Buildings,* pp. 117-126 (Dept. of the Environment, Watford, England, Nov. 1973).

Key words: plumbing; plumbing research; water demand in buildings; water distributing systems.

This paper presents a framework for evaluation of water demands in buildings, which was used to review and summarize the papers presented at the Building Research Establishment Symposium on Water Demand in Buildings. This symposium was held in conjunction with the first meeting of CIB Commission W62 on Water Supply and Drainage.

This framework identifies prinicpal uses of water in buildings, the determinants of water demands, and the basic issues which must be addressed in developing improved predictive models and water supply and distributing system design procedures. Significant contributions in the symposium papers are noted, in particular experimental methodology and theoretical models.

The paper concludes by identifying important and relevant issues not addressed in the symposium papers and by summarizing needed research. Meaningful data on observed patterns of water use remain a major research need. Other needs include a more accurate and workable methodology for predicting future water demands and for design of water supply and distribution systems.

**16227.** Deslattes, R. D., Kessler, E. G., Sauder, W. C., Henins, A., **Visible to gamma-ray wavelength ratio,** (Proc. Atomic Masses and Fundamental Constants, Paris, France, June 2-6, 1975), Paper in *Atomic Masses and Fundamental Constants,* J. H. Sanders and A. H. Wapstra, Eds., **5,** 48-53 (Plenum Publishing Corp., New York, NY, 1976).

Key words: crystal diffraction; gamma-ray wavelength; gold 198; goniometer; x-ray interferometry.

We report on procedures and a preliminary result for a measurement of the wavelength of the $^{198}$Au 412 keV line relative to that of a molecularly stabilized laser in the visible. The measurement involves: optical interferometry of a Si lattice repeat distance; transfer from a sample of the Si crystal to Ge crystals;

and angle measurement for the $\gamma$-ray line diffracted by the Ge crystals by means of angle interferometry.

**16228.** Melmed, A. J., Carroll, J. J., **Three-color direct superposition for field-ion microscopy,** *J. Appl. Phys. Commun.* **47,** No. 8, 3762-3763 (Aug. 1976).

Key words: color superposition photography; field-ion microscopy; image analysis; three-color superposition.

Direct two-component color superposition for field-ion microscopy is extended to three-component color superposition. Details of the method are given and some applications are mentioned.

**16229.** Crawford, M. L., **Improved techniques and instrumentation for EMC measurements,** *Proc. IEEE Int. Symp. on Electromagnetic Compatibility, Washington, DC, July 13-15, 1976,* pp. 369-374 (Institute of Electrical and Electronics Engineers, Inc., New York, NY, 1976).

Key words: electromagnetic compatability; EMC instrumentation; measurements.

This paper presents a survey of improved measurement techniques, instrumentation, and data presentation for accurate, meaningful evaluation of electromagnetic compatibility (EMC) of electronic systems and subsystems. These techniques and instrumentation were developed as alternatives to conventional, MIL-STD-461/462, measurements which recommend screen room testing with conventional antennas. These alternatives are used to accurately measure and quantify EM emissions from electronic equipment and/or for establishing standardized EM susceptibility test fields. Dramatic improvement (worst case errors of 1 to 3 dB compared with 40 dB from conventional screen room measurements) have been demonstrated. The techniques described in the paper include: 1) low-Q or underground enclosures, 2) mode stirred, shielded enclosures, 3) specially designed, shielded, transverse electromagnetic (TEM) cells, 4) broadband field probes capable of measuring complex average or peak fields without causing perturbation, and 5) time and amplitude statistics for characterizing the measured data.

**16230.** Brown, W. E., Gregory, T. M., **Calcium pyrophosphate crystal chemistry,** *Arthritis Rheum.* **19,** No. 3, 446-462 (May-June 1976).

Key words: calcium diphosphate; calcium pyrophosphate; chondrocalcinosis; pseudogout; solubility; solubility product; synovial fluid.

Theoretical considerations governing the solubilities of calcium pyrophosphates are presented in terms of phase diagrams and calculations based on an ionic model, and the reliability of reported solubility data is examined in terms of the model. The solubility product constant, $(Ca^{2+})^2(P_2O_7^{4-})$, of $Ca_2P_2O_7 \cdot 2H_2O$ appears to be in the vicinity of $3 \times 10^{-18}$, but some of the data indicate that it may be as high as $10^{-14}$ to $10^{-13}$. Recommendations are given for the future experimental measurements.

**16231.** Barbrow, L. E., **Changeover to metric—Timetable and Government role,** Paper in *Metrication—Managing the Industrial Transition,* R. G. Liptai and J. W. Pearson, Eds., Am. Soc. Test. Mater. Spec. Tech. Publ. 574, pp. 22-31 (July 1975).

Key words: conversion to metric; government metrication; metrication; metric system; SI; timetable for metrication.

The changeover to the metric system in the United States is motivated by our manufacturing industry. The basic reason for the changeover is economic necessity, which dictates also that changes to metric be made only where they are advantageous. In the transition timetable, our manufacturing industry and our educational institutions are already well started. Now, then, is the time also for the development of national metric engineering standards to supersede or supplement our customary engineering standards. Government procurement will keep in step with industry changeover. Consumer products will be changed some years hence, the specific time being dependent on the enactment of national metric legislation, but early programs should be initiated to keep our public informed as to why the changeover is taking place and how it is progressing. The principal role of Government in the changeover is to keep SI, the modernized metric system, as clean as possible. When metric legislation is enacted, a National Metric Conversion Board will have the responsibility for coordinating the changeover. Meanwhile the American National Metric Council has undertaken this role.

**16232.** Arp, V., **Negative differential flow resistance in supercritical helium,** *Cryogenics* **16,** No. 3, 171-177 (Mar. 1976).

Key words: flow resistance; helium; Ledinegg instability; negative flow resistance; supercritical helium.

The study of helium flow instabilities occurring in large helium cooling systems is important for the future development of these systems. One of these instabilities, the Ledinegg instability, is caused by negative differential flow resistance. This paper discusses the conditions under which a negative differential flow resistance can occur and finds that it will not occur in single phase helium cooling systems except under certain very restricted conditions.

**16233.** Benjamin, I. A., Adams, C. H., **The flooring radiant panel test and proposed criteria,** *Fire J.* **70,** No. 2, 63-70 (Mar. 1976).

Key words: fire hazard; fire safety; flooring test; radiant panel.

The objective of this discussion is to present background and other technical data that will help in suggesting criteria to be used in conjunction with the Flooring Radiant Panel Test to determine the potential contribution to fire growth of floor covering systems for use in corridors and exitways.

**16234.** Haller, F. B., Hessel, M. M., Neef, W., Lai, W., Lohr, H., **Concentric heat pipe cavity for e-beam excited lasers,** *Proc. 6th Symp. on Engineering Problems of Fusion Research, San Diego, CA, Nov. 17-21, 1975,* pp. 79-83 (Institute of Electrical and Electronics Engineers, Inc., New York, NY, 1976).

Key words: electron beam excitation; heat pipe oven; lasers; metal vapors; noble gas; spectroscopy.

A concentric heat pipe oven for metal vapor-noble gas mixtures has been designed and constructed as a high power laser cavity for laser fusion applications. A 1 MeV, 100 KA, 50 ns e-beam is injected into this oven through a stainless steel foil window, 0.125 mm thick. Details of the construction and design considerations of the heat pipe oven, foil window and safety features are given.

**16235.** Torchia, D. A., Lyerla, J. R., Jr., Deber, C. M., **Carbon-13 chemical shifts of amides and imino acid residues. Effects of the carbonyl substituent and** *syn-anti* geometries, *J. Am. Chem. Soc. Commun. to Editor* **96,** No. 15, 5009-5011 (July 24, 1974).

Key words: amides; carbon-13 magnetic resonance; chemical shifts; cis and trans isomers; peptides; proline; ring conformation; substituent effects.

Differences in C-13 chemical shifts, $\Delta C^i$, for carbons *syn* and *anti* to the carbonyl oxygen ($\Delta C^i = \tau_{syn} - \tau_{anti}$) are reported for a series of N,N′-diethylamides and model peptides containing imino acid residues. The model compound data show that cis and trans peptide bond isomers account for the $\Delta C^i$ values observed in polypeptides containing pyrrolidine residues (L-prolyl and hydroxyl-L-prolyl) when the effects of *syn-anti* geometry and the carbonyl substituent are considered.

**16236.** Allan, D. W., Mungall, A. G., Winkler, G. M. R., **Comments on the 25 April 1975 paper in "Science" entitled: "Terrestrial timekeeping and general relativity—A discovery,"** *Science* **191,** 489-490 (Feb. 6, 1976).

Key words: atomic clocks; clock acceleration effect; definition of the second; frequency accuracy; frequency standards; general relativity; gravitational redshift; primary frequency standards; proper time; UTC.

We wish to clarify some essential points relative to the paper "Acceleration and Clocks," by W. H. Cannon and O. G. Jensen. Cannon and Jensen have developed two contradictory equations based on different relativistic assumptions and have attempted to "resolve the contradictions" using data tabulated by the Bureau International de L'Heure (BIH) on atomic clocks located at various places in North America and Europe. The atomic clock data Cannon and Jensen have used are those for the $UTC_i$, where the *i* denotes the Observatory and/or Laboratory generating a particular Coordinated Universal Time Scale. We are obliged to state that Cannon and Jensen's assumption that "the intervals on the time scales $UTC_i$ of the contributing Observatories... correspond to the adopted definition of the second" is not valid at the accuracy level they need to test the contradiction between their equations.

The experimental data used by Cannon and Jensen contain inaccuracies and systematic effects which render invalid their conclusion of "A Discovery" in general relativity. To the contrary, experimental data do exist which contradict Cannon and Jensen's conclusion that an "observer's" perception of the world geometry depends on his state of acceleration."

**16237.** Jones, R. N., **Electronic eavesdropping techniques and equipment,** *LESP-RPT-0207.00,* 40 pages (U.S. Department of Justice, Law Enforcement Assistance Administration, National Institute of Law Enforcement and Criminal Justice, Washington, DC, Sept. 1975).

Key words: body worn antenna; bugging; eavesdropping; electronic surveillance; microphones; receiver; tape recorder; telephone; transmitter; wiretapping.

This report describes some of the methods and equipment used for electronic audio surveillance. The subject of countersurveillance (defensive) equipment and techniques, while not completely excluded, is confined to the minimum necessary to the understanding of offensive surveillance activity. Both radiating and hard wire methods are discussed along with the advantages, disadvantages and limitations of each. Particular attention is given to the subject of body worn transmitters and the operational problems associated with their use including batteries and body mounted antennas. Experimental data is included to illustrate some of the principles and problems surrounding their use. The conclusion includes recommendations of various items for inclusion in a standard for body worn transmitters. A fairly extensive annotated bibliography is also provided.

**16238.** Richmond, J. C., **Active night vision devices,** *NILECJ-STD-0305.00,* 31 pages (U.S. Department of Justice, Law Enforcement Assistance Administration, National Institute of Law Enforcement and Criminal Justice, Washington, DC, June 1975).

Key words: contrast transfer function; distortion; flare; image intensifier tubes; infrared searchlights; infrared viewers; light equivalent background; light induced background; optical gain.

An active night vision device consists of a viewer incorporating a single-stage image intensifier tube with an S-1 photocathode, that is sensitive to light at wavelengths out to about 1.1 μm, and an infrared searchlight which usually makes use of a quartz halogen lamp and an infrared filter that blocks all visible light. The standard describes test procedures for evaluating optical gain, light induced background, light equivalent background, contrast transfer function, flare and distortion of the viewer, and effective range of the searchlight, and establishes minimum levels of performance for these criteria.

**16239.** Richmond, J. C., **Passive, first generation night vision devices,** *NILECJ-STD-0304.00,* 25 pages (U.S. Department of Justice, Law Enforcement Assistance Administration, National Institute of Law Enforcement and Criminal Justice, Washington, DC, June 1975).

Key words: contrast transfer function; flare; image intensifiers; law enforcement; light equivalent background; light induced; optical gain; night vision.

The Standard establishes test methods and performance criteria for passive, hand-held night vision devices for use in law enforcement. The viewers covered by this Standard are of the three-stage image intensifier type, that were originally developed for military use.

Test procedures and performance requirements are listed; (A) for (1) focus adjustment, (2) curvature of field, and (3) distortion of eyepiece lenses; (B) for (1) optical gain, (2) optical gain stability, (3) light equivalent background, (4) light induced background, (5) luminance of output screen, (6) luminance uniformity, (7) cathode and screen quality, (8) contrast transfer function, (9) distortion, and (10) flare of a night vision device complete with objective lens, but with the eyepiece removed; (C) for resistance to (1) vibration, (2) high and low temperature storage, (3) thermal shock, and (4) humidity of night vision device complete with both objective and eyepiece lenses; and (D) for (1) boresight adjustment, (2) click movement, and (3) resistance to mechanical shock of night vision devices intended for use as rifle sights.

**16240.** Bennett, L. H., Page, C. H., Swartzendruber, L. J., **Comments on units in magnetism,** (Proc. 21st Annual AIP Conf. No. 29, on Magnetism and Magnetic Materials-1975, Philadelphia, PA, Dec. 9-12, 1975), Paper in *Magnetism and Magnetic Materials-1975,* J. J. Becker, G. H. Lander, and J. J. Rhyne, Eds., 3 pages (American Institute of Physics, New York, NY, 1975).

Key words: magnetism; units.

Suggestions are given on how to express magnetic quantities in SI units.

**16241.** Ramsburg, R. E., Aronoff, M. J., **Calculation by digital computer of minimum station-to-station distances in the United States railroad network,** *Report No. DOT P 6300.1,* 46 pages (Department of Transportation, Washington, DC, June 1972).

Key words: railroad freight movements; short-line miling system; waybills.

This volume is the first of a series of two documents which report a package of computer programs developed by the Technical Analysis Division of the National Bureau of Standards for the computation of "short-line" distances. The "short-line" distance between two stations in a rail network is defined as the shortest route between them over which carload traffic can be moved without transfer of lading. The network treated in this specific application was the continental United States railroad system. After its development, the package was used to "mile" the 1969 Waybill File.

Volume one outlines the background of the project, defines the general problem, describes the alternative methodologies considered, and outlines the final solution.

Volume two is both an operations manual for personnel who will annually operate the computer programs to calculate short-line distances for the Waybill File, and a programmer's manual providing technical descriptions and flow charts for each of the computer programs in the short-line "miling" package.

The programs which were developed for this project, and the partitioning technique employed, can be modified to carry out similar calculations for other large networks.

**16241A.** Ramsburg, R. E., Batten, D. R., **Programmer level documentation of the short line mileage programs for the United States railroad network,** *Report No. DOT P 6300.1,* 106 pages (Department of Transportation, Washington, DC, June 1972).

Key words: programmer's documentation; short line mileage; waybill file.

This volume is the second of a series of two documents which report a package of computer programs developed by the Technical Analysis Division of the National Bureau of Standards for the computation of "short-line" distances. The "short-line" distance between two stations in a rail network is defined as the shortest route between them over which carload traffic can be moved without transfer of lading. The network treated in this specific application was the continental United States railroad system. After its development, the package was used to "mile" the 1969 Waybill File.

Volume one outlines the background of the project, defines the general problem, describes the alternative methodologies considered, and outlines the final solution.

Volume two is both an operations manual for personnel who will annually operate the computer programs to calculate short-line distances for the Waybill File, and a programmer's manual providing technical descriptions and flow charts for each of the computer programs in the short-line "miling" package.

The programs which were developed for this project, and the partitioning technique employed, can be modified to carry out similar calculations for other large networks.

**16242.** Hougen, J. T., **Calculation of vibrational level populations in multiphoton absorption processes,** *J. Chem. Phys.* **65,** No. 3, 1035-1041 (Aug. 1, 1976).

Key words: floquet theory; laser-induced reactions; multiphoton processes; numerical calculations; relaxation phenomena; vibrational populations.

A simple procedure is described for computing steady-state excited vibrational state populations for multiphoton absorption processes in many-level systems. The procedure utilizes techniques already in the literature, i.e., expansion of the density matrix as a Fourier series in the frequency of the monochromatic radiation field, and introduction of linewidths and thermal relaxation by the addition of empirical terms to the density matrix time-development equation. Numerical computations can be carried out quickly on idealized systems, using commercially available band matrix inversion routines. A sample calculation for a 10-level, nine-photon process is presented.

**16243.** Wachtman, J. B., Jr., **Ceramic materials in high temperature gases: Fundamental behavior controlling lifetime in coal conversion applications,** (Proc. Ceramic Materials in High Temperature Gases on Materials Problems and Research Opportunities in Coal Conversion, Columbus, OH, Apr. 16-18, 1974), Paper in *Materials Problems and Research Opportunities in Coal Conversion* **2,** 335-343 (The Department of Metallurgical Engineering, The Ohio State University, Columbus, OH, 1974).

Key words: ceramics; coal conversion; coal gasification; corrosion; fracture; vaporization.

The degradative processes which ceramics in high temperature gases produced by coal conversion may undergo are briefly reviewed. These include purely chemical processes such as combination of liquids in cracks and subsequent corrosion. These also include chemical modification of physical processes of deterioration such as environmental effects in fracture.

**16244.** Bovey, F. A., Schilling, F. C., McCrackin, F. L., Wagner, H. L., **Short-chain and long-chain branching in low-density polyethylene,** *Macromolecules* **9,** No. 1, 76-80 (Jan.-Feb. 1976).

Key words: branching; limiting viscosity numbers; long-chain branching; nuclear magnetic resonance; polyethylene; short-chain branching.

The branch content of two fractions of low-density polyethylene has been examined by $^{13}$C NMR (at 25 MHz) and by limiting viscosity number (intrinsic viscosity) measurements. The $^{13}$C spectra, interpreted with the aid of modified Grant-Paul chemical shift rules and the spectra of model copolymers, confirm that the principal type of short branch is trifunctional *n*-butyl (5-6 per 1000 $CH_2$) with smaller contents of *n*-amyl (ca. 2 per 1000 $CH_2$) and ethyl (ca. 1 per 1000 $CH_2$). A resonance at $(32.1_6)$ ppm (from TMS), corresponding to the third carbon (C-3) from the branch end, provides a measure of branches longer than *n*-amyl, but does not at present distinguish such branches, presumably formed by intramolecular "backbiting," from the truly "long" branches, containing possibly many tens or hundreds of carbons and formed by intermolecular chain transfer to other polymer chains. If it is assumed that this resonance provides in fact a direct measure of the "long" branch content, "short" branches longer than *n*-amyl being of negligible probability, the results agree well with the long branch content estimated from the intrinsic viscosities of branched and linear polyethylene via the Simm-Kilb *g* value. The long branch content thus deduced is ca. 0.8 per 1000 $CH_2$. For these samples, no marked dependence on molecular weight is observed for either the long- or short-branch frequencies.

**16245.** Davis, R. M., **National policies for information processing: Situation in the United States,** (Proc. 2d Jerusalem Conf. on Information Technology, Jerusalem, Israel, July 29-Aug. 1, 1974), Paper in *The 2d Jerusalem Conference on Information Technology: Computers for Social and Economic Development,* C. C. Gotlieb and H. Maisel, Eds., **1,** 15-27 (1974).

Key words: executive programs; information management; information processing; legislative programs; national policies; public concern.

The topic of a National Policy for Information Processing in the United States would be short-lived if it were broached as a direct question, for the answer would be "No, there is no such national policy!" However, discussions of the changing national interest in information and of emerging national concerns with information and its processing in the United States will give evidence of an increased national awareness of information processing.

Similarly, a description and status of certain legislative and executive programs in the general area of information processing will furnish some idea of current, widely-impacting problem areas and on-going efforts to resolve them on a nation-wide or government-wide basis. Finally, public concern and involvement with information processing will be described to highlight the increasingly-intense interaction between information technology and the public.

With this broader interpretation of the topic in terms of: Changing national interest in information; emerging national concerns with information and its processing; legislative and executive programs in the general area of information processing; current, widely-impacting problem areas in information processing; and public concern and involvement with information and its processing, a perspective can be obtained of national policy in-the-making.

16246. Linden, T. A., **The use of abstract data types to simplify program modifications,** (Proc. Conf. on Data: Abstraction Definition and Structure, Salt Lake City, Utah, Mar. 22-24, 1976), *SIGPLAN Notices 11, Special Issue, Assoc. Comput. Mach.-FDT* **8,** No. 2, 12-23 (Association for Computing Machinery, New York, NY, Mar. 1976).

Key words: abstract data types; class; cluster; data abstraction; data type; module; programming methods; program modifications; type.

If a program is structured using abstract data types as the basic unit of modularity, then that program is much easier to extend or modify. This thesis is illustrated by the staged development of a program to compute prime numbers based on the sieve of Eratosthenes. This paper includes an extensive introduction to the concept of abstract data types and can be used as a tutorial survey. It includes discussions on the use of abstract data types in connection with recent approaches to data abstractions, heirarchical structure, and program design. Abstract data types are an extension and modification of the traditional concept of data type. An abstract data type defines not only a data representation for objects of the type but also the set of operations that can be performed on objects of the type. Furthermore, the abstract data type can protect the data representation from direct access by other parts of the program.

16247. Abrams, M. D., **Measuring service delivered in interactive computing,** (Proc. 2d Jerusalem Conf. on Information Technology, Jerusalem, Israel, July 29-Aug. 1, 1974), Paper in *The 2d Jerusalem Conference on Information Technology: Computers for Social and Economic Development*, C. C. Gotlieb and H. Maisel, Eds., **1,** 747-754 (1974).

Key words: computer; interactive; measurement; procurement; response; service.

This paper considers the measurement of service rendered by interactive computer systems and application of these measurements to the procurement process. Topics discussed include what to measure; response, psychological, throughput, and cost-benefit considerations; when to measure; where to measure; how to measure; measurement conditions; and data analysis. Ongoing efforts at ICST are presented as examples of the state of the art.

16248. Muehlhause, C. O., **Costs, real and perceived, examined in a risk-benefit decision framework,** (Proc. OECD Conf. on Costs, Real and Perceived, Examined in a Risk-Benefit Decision Framework, Paris, France, Aug. 1972), Paper in *Environmental Damage Costs*, pp. 282-304 (Director of Information, OECD, Paris, France, 1974).

Key words: consumer product hazard; risk-benefit.

The so-called problem of risk-benefit is analyzed with special emphasis on the case of consumer products which exhibit hazard as well as utility. The market demand is represented as a function of two independent factors: a vital one re safety, and a utilitarian one to which dollar values may be assigned. The condition for optimization of the net public benefit is examined along with its dependence on costs. The general ideas developed are extended to some more complex cases and regimes.

16249. Casella, R. C., **Possible failure of the Pomeranchuk Theorem. Shrinkage of the forward elastic peak and oscillations,** (Proc. "Ettore Majorana" School of Subnuclear Physics, Erice, Sicily, July 1-19, 1970), Paper in *Elementary Processes at High Energy*, A. Zichichi, Ed., 519-525 (Academic Press, Inc., New York, NY, 1971).

Key words: asymptotics; elastic; oscillations; Pomeranchuk; shrinkage; theorem.

Under rather general assumptions, it is shown that if the Pomeranchuk Theorem fails such that $\sigma_{+}(s) \rightarrow$ unequal constants, then the differential elastic cross section $d\sigma/dt$ oscillates wildly with $t$ as well as exhibiting a $(\ln s)^2$ shrinkage of the forward peak.

16250. Muehlhause, C. O., **Risk benefit analysis,** *ASTM Stand. News* **1,** No. 2, 8-13 (Feb. 1973).

Key words: consumer product hazard; risk-benefit.

The so-called problem of risk-benefit is analyzed with special emphasis on the case of consumer products which exhibit hazard as well as utility. The market demand is represented as a function of two independent factors: a vital one re safety, and a utilitarian one to which dollar values may be assigned. The condition for optimization of the net public benefit is examined along with its dependence on costs. The general ideas developed are extended to some more complex cases and regimes.

16251. Finnegan, T. F., **Superconductivity in dc voltage metrology,** (Proc. Summer Course on the Science and Technology of Superconductivity, Georgetown University, Washington, DC, Aug. 13-26, 1971), Paper in *The Science and Technology of Superconductivity*, W. D. Gregory, W. N. Mathews, Jr., and E. A. Edelsack, Eds., **2,** 565-585 (Plenum Press, New York, NY, 1973).

Key words: ac Josephson effect; low-temperature voltage divider; superconducting tunnel junctions; voltage standard.

The simple theory of the ac Josephson effect in a tunnel junction is presented and recent work on the development and implementation of a national voltage standard based on measurements of the fundamental physical constant 2e/h is reviewed. The principle problems associated with the design and construction of conventional-type high-accuracy low-voltage dividers are treated, and the role of the cryogenic potentiometer and superconducting null detector in a Josephson-effect voltage standard is explored. Finally, a possible secondary voltage standard based on Giaever tunneling is described.

16252. Eitzen, D. G., Chwirut, D. J., **Ultrasonic reference blocks and characterized fatigue cracks,** (Proc. ARPA/AFML Review of Quantitative Nondestructive Evaluation, Thousand Oaks, CA, July 15-17, 1975), Paper in *Proceedings of the ARPA/AFML Review of Quantitative NDE, Technical Report AFML-TR-75-212*, pp. 107-127 (Air Force Materials Laboratory, Wright-Patterson Air Force Base, OH, Jan. 1976).

Key words: acoustic emission; aluminum; fatigue cracks; flat bottomed holes; standards; steel; titanium; transducer calibration; ultrasonic reference blocks.

Work in progress on the improvement of ASTM E127 type ultrasonic reference blocks (flat bottomed holes) and on the development of well characterized fatigue crack is described. A data base for aluminum reference blocks has been developed by borrowing sets of field blocks and obtaining the response using 2.25, 5, and 10 MHz transducers. Steel and titanium blocks are also studied. Considerable effort has been expended in order to evaluate the contributions of metallurgical condition, physical dimensions and fabrication methods to the variability of the reference blocks. The variability due to different measurement systems and different operators was also quantified to an extent. Several possible methods of providing improved standards are suggested.

While standard defects such as cracks seem impractical to produce, it seems feasible to produce well characterized cracks. Work on characterizing fatigue cracks produced in standard ASTM E399 compact tension specimens has centered on controlling as many of the variables affecting ultrasonic response as possible. The affect of the remaining variables on ultrasonic response will be characterized. The fatigue loading program is controlled to produce nominally identical cracks. Six different techniques for measuring the physical characteristics of the cracks are being evaluated and generally show good correlation.

Techniques which have been developed for the calibration of ultrasonic and acoustic emission transducers are noted in passing.

**16253.** Langhoff, P. W., Corcoran, C. T., **Tchebycheff-derivative approximations to photoabsorption cross sections in atoms and ions,** *Chem. Phys. Lett.* **40,** No. 3, 367-371 (June 15, 1976).

Key words: atomic spectroscopy; photoabsorption.

Spectral moments and Tchebycheff's inequalities are employed in the construction of continuous, convergent approximations to photoabsorption and ionization cross sections in atoms and ions.

**16254.** Unassigned.

**16255.** Deslattes, R. D., Henins, A., Schoonover, R. M., Carroll, C. L., Bowman, H. A., **Avogadro constant—Corrections to an earlier report,** *Phys. Rev. Lett. Comments* **36,** No. 15, 898-900 (Apr. 12, 1976).

Key words: Avogadro constant; crystals; lattice parameter.

Corrections are required to values of silicon crystal density and lattice parameter used in our determination of $N_A$. The corrections are of the order of 1 ppm but taken together result in a change of the previously reported value of 0.03 ppm. A published suggestion that the lattice-parameter measurement might require a much larger correction appears unsupported.

**16256.** Bulos, B. R., Phelps, A. V., **Excitation of the 4.3-$\mu$m bands of $CO_2$ by low-energy electrons,** *Phys. Rev. A* **14,** No. 2, 615-629 (Aug. 1976).

Key words: carbon dioxide; cross section; electrons; excitation; infrared; rate coefficient.

Rate coefficients for the excitation of the 4.3-$\mu$m bands of $CO_2$ by low-energy electrons in $CO_2$ have been measured using a drift-tube technique. The $CO_2$ density $[(1.5\text{ to }7)\times 10^{17}$ molecules/cm$^3]$ was chosen to maximize the radiation reaching the detector. Line-by-line transmission calculations were used to take into account the absorption of 4.3-$\mu$m radiation. A small fraction of the approximately $10^{-8}$ W of the 4.3-$\mu$m radiation produced by the approximately $10^{-7}$-A electron current was incident on an InSb photovoltaic detector. The detector calibration and absorption calculations were checked by measuring the readily calculated excitation coefficients for vibrational excitation of $N_2$ containing a small concentration of $CO_2$. For pure $CO_2$ the number of molecules capable of emitting 4.3-$\mu$m radiation produced per cm of electron drift and per $CO_2$ molecule varied from $10^{-17}$ cm$^{-2}$ at $E/N=6\times 10^{-17}$ V cm$^2$ to $5.4\times 10^{-16}$ cm$^{-2}$ at $E/N=4\times 10^{-16}$ V cm$^2$. Here $E$ is the electric field and $N$ is total gas density. The excitation coefficients at lower $E/N$ are much larger than estimated previously. A set of vibrational excitation cross sections is obtained for $CO_2$ which is consistent with the excitation coefficient data and with most of the published electron-beam data.

**16257.** Ayres, T. R., Linsky, J. L., **The Mg II *h* and *k* lines. II. Comparison with synthesized profiles and Ca II K,** *Astrophys. J.* **205,** No. 3, Part 1, 874-894 (May 1, 1976).

Key words: radiative transfer; solar chromosphere; solar photosphere; solar ultraviolet spectrum.

We compare the Mg II *h* and *k* resonance line data of Kohl and Parkinson and profiles of the Ca II K line with synthetic spectra computed using a partial redistribution formalism and several single-component solar upper photosphere and lower chromosphere models. We find that the HSRA and Vernazza *et al.* (VAL) models predict systematically lower intensities in the *h*, *k*, and K inner wings than are observed, but that models with a somewhat larger minimum temperature ($T_{min}\approx 4450$ K), such as proposed previously by Shine *et al.*, can reproduce the measured inner wing intensities and limb darkening of these resonance lines. Upper photosphere temperature distributions with $T_{min}\approx$ 4450 K are also more consistent with the radiative equilibrium models of Athay (non-LTE) and Kurucz (LTE), when nonradiative energy dissipation is taken into account. We propose a "hot" $T_{min}$ solar model, which is reasonably consistent with the empirical emission cores and wing intensities of the Ca II and Mg II resonance lines, to serve as an alternative to the class of models, such as the HSRA and VAL, based on continuum observations.

**16258.** Schnaus, U. E., Schroeder, J., Haus, J. W., **Subcritical viscosity anomaly in sodium silicate glasses,** *Phys. Lett.* **57A,** No. 1, 92-94 (May 17, 1976).

Key words: correlation length; Ginzburg-Landau theory; glass; inhomogeneous system; subcritical region; viscosity.

A subcritical viscosity anomaly is reported in binary mixtures of $Na_2O$-$SiO_2$. The results are discussed qualitatively in terms of inhomogeneities which are present in the system.

**16259.** Mann, W. B., Huchinson, J. M. R., **The standardization of iodine-129 by beta-photon coincidence counting,** *Int. J. Appl. Radiat. Isot. Tech. Notes* **27,** No. 3, 187-188 (Mar. 1976).

Key words: beta; coincidence counting; gamma; radioactivity; standardization; $^{129}$I.

Sources of $^{129}$I quantitatively deposited on ion exchange resin paper were calibrated by means of a simple $\beta$-$\gamma$ coincidence experiment recently performed over a period of a few days at NBS.

**16260.** Fromhold, A. T., Jr., **Parabolic oxidation of metals in homogeneous electric fields,** *J. Phys. Chem. Solids* **33,** 95-120 (1972).

Key words: conductivity; electric field effects; insulating films; insulators; metal oxidation; metals; MOM devices; oxidation; oxidation theory; parabolic law for metal oxidation; semiconductors.

A previously proposed thin film parabolic growth law (Fromhold, 1963) is extended to include film growth due to any number of diffusing defect species of arbitrary valence, and an analysis is made of the effects of applying external electrostatic potentials during oxidation. The total electrical conductivity and the partial conductivities are markedly position-dependent in the protective film, varying by orders of magnitude from one interface to the other. The built in electrostatic potential across the film is independent of thickness of the film and is a function of the partial conductivities of the diffusing ionic and electronic defect species. Effects of electrical shorting of the oxide film by external circuitry are analyzed. Depending on polarity, a constant applied potential can increase or decrease the rate constant but does not alter the kinetics from the parabolic form, in accordance with published experimental data. The net electrostatic potential required to stop metal oxidation is derived for the model in question. For growth by a single ionic species, the stopping potential is that electrostatic potential which gives an equal electrochemical potential at the metal-oxide and the oxide-oxygen interfaces. For growth by multiple ionic species, the stopping potential is a function of the ionic partial conductivities.

**16261.** Carlsten, J. L., Szöke, A., **Collisional redistribution of near-resonant scattered light in Sr vapour,** *J. Phys. B Letter to Editor* **9,** No. 9, L231-L235 (1976).

Key words: collisions; near-resonant scattering; redistribution; strontium.

Strontium vapour was irradiated by a dye laser tuned near the 460.73 nm $(^1P_1^0{-}^1S_0)$ resonance transition. Collision-induced fluorescence at the resonance frequency and Rayleigh scattering at the laser frequency were studied as a function of detuning $\Delta$ over a range of about 30 nm (1500 $cm^{-1}$). The Rayleigh component was found to vary as $\Delta^{-2}$, as expected, whereas the collision-induced fluorescence was markedly asymmetric. This experiment constitutes a direct measurement of the redistribution function.

**16262.** Chen, S. T., Gallagher, A., **Excitation of the Ba and $Ba^+$ resonance lines by electron impact on Ba atoms,** *Phys. Rev. A* **14,** No. 2, 593-601 (Aug. 1976).

Key words: barium; electron impact; excitation.

The relative optical excitation functions and polarizations of the Ba resonance line (5535 Å) and of the $Ba^+$ resonance lines (4554 and 4934 Å) have been measured, using crossed electron and barium-atom beams. The Ba $6^1P$ excitation function has been normalized to the Bethe theory in the high-energy limit, and the excitation functions of the ionic lines have been measured relative to that of the atomic resonance line. Using spontaneous-emission branching ratios for the $Ba^+(6^2P)$ levels, we have also obtained normalized cross sections for these ionizing excitation levels. From a few electron volts above threshold, the $Ba^+(6^2P)$ ionizing-excitation cross section has nearly the same energy dependence as has been reported for the total $Ba^+$ ionization cross section, but about 1/6 the magnitude. In particular, a broad maximum at ~22 eV, attributed to core-excited autoionizing levels, apparently contributes an equal fraction to both cross sections. This relationship holds also for the ionizing excitations versus total ionization of Sr. The cross sections for exciting the resonance levels of He, Mg, Ca, Sr, and Ba are also intercompared in reduced units and found to be strikingly similar at collision energies above ~3 times the threshold energies.

**16263.** Suzuki, G., Carter, C., Lieblein, J., Murphey, W. M., Perella, F. J., Smith, C. N., **Safeguards accountability analysis in a nuclear fuel processing plant,** Paper in *Safeguards Systems Analysis of Nuclear Fuel Cycles, WASH-1140 Safeguards and Nuclear Materials Management UC-15,* 46 pages (Office of Safeguards and Materials Management, U.S. Atomic Energy Commission, Washington, DC, Oct. 1, 1969).

Key words: material balance accounting; nuclear materials safeguards; process losses.

Material accounting constitutes an important, if not the principal means for suspecting and detecting diversions of Special Nuclear Material (SNM). Since the nature of SNM and the processes involved preclude precise identification of all the material through its various physical transformations within a plant, or within any part of the nuclear fuel cycle, the detection of diversions through an accounting system depends upon knowledge of the expected values and variabilities of the recorded losses under diversion-free conditions. This paper examines the variations of material unaccounted for (MUF) derived from material balance accounts, and reports on attempts to isolate the various components of MUF for a selected nuclear processing operation.

**16264.** Smith, J. C., **The elastic constants of a particulate-filled glassy polymer: Comparison of experimental values with theoretical predictions,** *Polym. Eng. Sci.* **16,** No. 6, 394-399 (June 1976).

Key words: bulk modulus; composite materials; elastic constants; filled polymers; mechanical properties; particulate composites; Poisson's ratio; shear modulus; Young's modulus.

Calculation of the elastic constants of a particulate composite material in terms of the elastic constants of the filler and the matrix is discussed. The theories of Kerner or Hashin and Shtrikman, the equivalent theories of Budiansky and Hill, and a generalized van der Poel type theory are presented and discussed. Data from several sources are compared with the predictions of these theories. The van der Poel theory provides the best agreement and gives good values for volume fractions of filler up to 0.35.

**16265.** Calvano, N. J., Dobbyn, R. C., **Riot helmets,** *NILECJ-STD-0104.00,* 15 pages (U.S. Department of Justice, Law Enforcement Assistance Administration, National Institute of Law Enforcement and Criminal Justice, Washington, DC, Oct. 1974).

Key words: helmets; impact attenuation; penetration; retention system strength; riot; visual clearance.

This standard establishes performance requirements and methods of test for helmets used to protect the wearer during civil disturbances, riots or other situations that pose a threat of injury from blows to the head. The test methods described measure the ability of the helmet to attenuate impact, resist penetration and provide sufficient peripheral visual clearance and test the static strength of the helmet's retention system. It is based on ANSI standard Z90.1-1971.

**16266.** Fey, R. L., **Automatic vehicle location techniques for law enforcement use,** *LESP-RPT-0205.00,* 27 pages (U.S. Department of Justice, Law Enforcement Assistance Administration, National Institute of Law Enforcement and Criminal Justice, Washington, DC, Sept. 1974).

Key words: automatic vehicle locator; car locators; law enforcement.

Automatic vehicle location systems employing communications techniques are presently under development by several companies. This report discusses such systems with respect to law enforcement applications. It presents the principles upon which the various automatic location techniques are based, summarizes their important characteristics, and compares them as candidates for law enforcement use. This report discusses techniques, available system performance, and the related aspect of frequency spectrum requirements for these systems. It also mentions areas where more operational information is needed before systems for law enforcement operations can be clearly defined.

**16267.** Robertson, B., Baumgarten, G. P., **Evaluation of automotive fuel flowmeters,** (Proc. Project Coordination Meeting of the Automotive Energy Efficiency Program, Cambridge, MA, Nov. 4-6, 1975), *Report No. DOT-TSC-OST-76-1*, 20 pages (Available from the National Technical Information Service, Springfield, VA 22161, June 1976).

Key words: automotive environment; calibration; low flow rates.

A description is given of laboratory apparatus and procedures for evaluating gasoline flowmeters under conditions simulating the automotive environment. Preliminary results are reported on tests of three commercially available automotive fuel flowmeters.

**16268.** Eicke, W. G., Jr., **The volt, yesterday, today and tomorrow,** (Proc. PSA Int. Conf., Chicago, IL, Oct. 4-7, 1971), *ISA Reprint 71-703*, pp. 1-7 (Oct. 1971).

Key words: electrical standards; standard cells; U.S. legal volt; volt; voltage measurement.

Of all the electrical quantities used today, the unit of voltage is probably the most difficult to maintain, disseminate and use properly. This paper briefly discusses the history of the volt to 1967. Work at NBS after 1967 is described. Developments are reported in four basic areas: 1) The application of statistical design and digital computers to obtain additional information about the measurement process, 2) improvements in the equipment for making standard cell measurements, 3) improvement in the temperature control of standard cells, and 4) improved techniques for disseminating the volt. To further improve the volt, the progress for maintaining surveillance over the unit by means of the gyromagnetic ratio of the proton and the Josephson effect are discussed.

**16269.** Cook, R. K., **Acoustic emissions—Researchers in Japan,** *Sci. Bull.* **1,** No. 1, 17 pages (June-Sept. 1976).

Key words: acoustic emission; acoustics; flaw detection; nondestructive inspection.

While in Japan in the summer of 1975, I undertook an investigation, at the request of the Office of Naval Research, into the current state of Japanese research techniques and technological applications of acoustic emissions (AE). The investigation was done mainly by means of visits to laboratories and conferences with physicists and engineers working on AE in the Tokyo area. The visits and conferences were held during the week of 1-5 September 1975. All of the conferences were on an unclassified basis. In addition, various published papers describing Japanese researches on AE have been studied. Most of these are in the *List of Publications* of the Report. The list includes about 40 publications from Japanese laboratories working on acoustic emissions.

**16270.** Fuller, E. G., Hayward, E., Eds., **Photonuclear reactions,** *Book—Benchmark Papers in Nuclear Physics* **2,** 426 pages (Dowden, Hutchinson & Ross, Inc., Stroudsburg, PA, 1976).

Key words: history; photonuclear experiments; photonuclear interaction; photonuclear reactions; photonuclear theory; reprint collection.

A collection of 43 reprints of research papers which have made a significant impact on the development of the photonuclear physics field are presented. Comments associated with each paper place it into the context of the historical development of the field, and indicate the particular contributions each paper has made to the development of an understanding of the nuclear photoeffect and nuclear structure. The papers are all concerned with classical photonuclear physics, the interaction of real photons having energies less than 150 MeV with nuclei. The field of inelastic electron scattering is not treated.

**16271.** Panek, R. J., Savage, B. D., **Ultraviolet photometry from the orbiting astronomical observatory. XXIII. The resonance lines of triply ionized carbon and silicon in the spectra of hot stars,** *Astrophys. J.* **206,** No. 1, 167-181 (May 15, 1976).

Key words: absorption; B-stars; C IV; O-stars; Si IV; spectra; stellar; ultraviolet.

Quantitative measurements of the absorption strength of the Si IV (1400 Å) and C IV (1550 Å) resonance doublets have been made from OAO-2 far-ultraviolet spectra of 118 O- and B-type stars. These lines are generally very strong and a useful measure of their strength can be made even though the OAO-2 scans have relatively low spectral resolution (FWHM = 12 Å). However, variable amounts of line blending limit the accuracy of the results to approximately ±1 to 2 Å in the equivalent width. For dwarf stars the strength of both features correlates well with spectral type or temperature. The Si IV doublet peaks in strength near spectral type B1 with a total equivalent width of about 5 Å in agreement with the theoretical non-LTE (NLTE) plane-parallel static models of Kamp. The C IV doublet in dwarfs rapidly increases in strength from B2 to B0 and attains an equivalent width of about 5 Å at spectral type O9. For both doublets we note a large increase in the absorption equivalent width with luminosity classification, the increase amounting to a factor of 2 to 3 between dwarfs and supergiants. In the luminous O stars we also note a change in the line profile to the P Cygni type. In the case of the Si IV line for stars cooler than spectral type B0.5 the observed luminosity effect is roughly consistent with the predictions of static NLTE models. However, for the O stars the static models predict a *decrease* in equivalent width with increasing luminosity. The differences between theory and observation are associated with the effects of mass outflow.

The observations include a number of B stars with peculiar visual spectra. With the exception of $\theta$ Car, which exhibits an abnormally weak C IV line, the various peculiar stars observed appear to have normal Si IV and C IV line strengths.

For a group of rapidly rotating stars the C IV line appears marginally stronger than expected on the basis of MK classification, while Si IV appears normal. In the case of the Be shell star, $\gamma$ Cas, we have noted a factor of 2 increase in the strength of Si IV and C IV over a time scale of months.

With the exception of $\xi^1$ CMa and $\beta$ Cep, the Si IV and Ce IV lines in a group of 11 $\beta$ Cephei variables appear to have strengths consistent with their MK classification.

A number of repeated observations of bright early-type stars were searched for absorption line variability on time scales ranging from minutes to years. With only a few exceptions no variability was found. The sample included a number of luminous O supergiants, suggesting that the mass loss from these objects occurs as a steady process.

**16272.** Mihalas, D., Kunasz, P. B., Hummer, D. G., **Solution of the comoving-frame equation of transfer in spherically symmetric flows. III. Effect of aberration and advection terms,** *Astrophys. J.* **206,** No. 2, 515-524 (June 1, 1976).

Key words: radiative transfer; relativistic effects; spectral line formation; stellar atmospheres.

We investigate the importance of the advection and aberration terms, which are of order $V/c$, in the comoving-frame transfer equation in spherical geometry. Characteristic trajectories are found which reduce the spatial derivatives to a perfect differential, and a generalization of the numerical procedure developed in the earlier papers of this series that permits the integration of the transfer equation on these characteristics is presented. For cases in which $V/c \ll 1$, a perturbation solution is developed which reduces the problem to that solved in the first paper in this series. For velocities of the form $V(r) \sim r^n (n=0, 1, 2)$, it is shown that the magnitude of the effects arising from the advection and aberration terms is about $5V/c$ relative to the solution with these terms omitted. In stellar winds $V/c \lesssim 0.01$; hence we conclude that aberration and advection terms may safely be ignored, and that consideration of the Doppler-shift term alone is adequate in the computation of spectra from such expanding atmospheres.

**16273.** Swartzendruber, L. J., Evans, B. J., **Nuclear gamma ray resonance observation of the activation process in Raney iron and Urushibara iron catalysts,** *J. Catal.* **43,** 207-219 (1976).

> Key words: catalysis; Mössbauer effect; Raney-iron-activation.

The phases that form when Raney iron and Urushibara iron catalysts are activated have been studied utilizing $^{57}$Fe nuclear gamma ray resonance. For Raney iron catalysts four phases are observed in the activated catalyst; residual aluminum-depleted Raney alloy, $Fe(OH)_2$, $\alpha$-Fe and $Fe_3O_4$. The relative proportions of phases present is a sensitive function of leaching temperature and time. For Raney iron catalysts, and for Urushibara iron catalysts prepared using aluminum, no alloying of aluminum into the activated phases is observable. For Urushibara iron catalysts prepared using zinc, there is considerable alloying of iron and zinc. Evidence is presented to show that when the catalyst is generated at low temperatures $Fe(OH)_2$ is a precursor phase for metallic Fe in Raney Iron. A similar situation seems to exist for the Urushibara catalyst prepared using aluminum. The alloying behavior of the iron catalysts can be understood on the basis of the nature of the intermediate phase. The large amounts of $Fe_3O_4$ present in Raney iron prepared at elevated temperatures raises some questions concerning the catalytically active phases in such materials.

**16274.** Peterlin, A., **Crystallization from a strained melt or solution,** *Polym. Eng. Sci.* **16,** No. 3, 126-137 (Mar. 1976).

> Key words: crystallization; cylindrite; drawing of swollen polymer solid; epitaxial overgrowth; extrusion; hard elastomer; nucleation; oriented melt; rheological unites; row nucleus; shishkebab; sonicated solution; spinning; stirred solution.

The elongation and orientation of randomly coiled macromolecules in a strained melt or solution reduces their entropy and thus increases the crystallization or melting temperature of the ideal lattice. At any given temperature of the experiment this enhances nucleation and crystal growth rate. As a rule, linear primary nuclei are formed. They contain more or less extended chains. The existence of row nuclei reduces the local gradient in the liquid to such an extent that further crystallization proceeds by epitaxial overgrowth of folded chain lamellae. Densely packed cylindrites are formed with the ribbon-like lamellae radiating from the central row nucleus. The irregular shish-kebab structure observed in stirred or sonicated solutions seems to be formed by subsequent axial deformation of cylindrites in the flow field. It displaces the lamellae irregularly and thus produces a great many microfibrillar elements parallel to the original row nuclei. The almost completely extended chains in the shish yield a high elastic modulus and tensile strength for axial loading. The shish-kebab morphology in fibers as spun does not affect to a great extent the mechanical properties obtainable by subsequent drawing. The lamellae are transformed into microfibrils in very much the same manner as in spherulitic samples. But the highly regular orientation of lamellae seems to result in a more uniform drawing and hence a stronger fiber. In an extremely high temperature and pressure gradient, the melt extrusion produces hard elastomers where the lamellae of the cylindrites seem to be locally stapled. Upon application of tensile load in the extrusion direction, the intervening sections bend like beams, thus forming thin holes extending in the direction perpendicular to the load. The holes enormously enhance the permeability for gases and liquids. The elastic bending of lamellae yields the high recoverable strain and low tensile modulus.

**16275.** Phillips, J. C., Mattamal, M. M., **Correlation of liquid heat capacities for carboxylic esters,** *J. J. Chem. Eng. Data* **21,** No. 2, 228-232 (Apr. 1976).

> Key words: correlation; esters; heat capacity; oligomers; sebacates; triglycerides.

Liquid heat capacity data of carboxylic esters (including a sebacate series, triglyceride series, and oligomer series), covering a temperature range from 20 to about 180 °C and a molecular weight range from 116 to 939, were determined with a differential scanning calorimeter. The data, together with published heat capacity values, were reduced to a temperature independent correlation. The results suggest an approximate additivity in carboxyl content and a lack of dependence on structural type (e.g., linear, branched, or oligomeric).

**16276.** Unassigned.

**16277.** Mopsik, F. I., Broadhurst, M. G., **Molecular dipole electrets,** *J. Appl. Phys.* **46,** No. 10, 4204-4208 (Oct. 1975).

> Key words: dipoles; electret; glass; piezoelectric; polarization; polyvinyl chloride; pyroelectric.

The total polarization due to molecular dipoles in a glassy electret is computed using an Onsager cavity approach. From this result, all the possible contributions to the piezoelectric and pyroelectric coefficients are considered. It is shown that there are major contributions from the variation in dielectric constant and, for pyroelectricity, from thermal motion. These results account well for experimental data for polyvinyl chloride.

**16278.** Penn, R. W., Kearsley, E. A., **The scaling law for finite torsion of elastic cylinders,** *Trans. Soc. Rheol.* **20,** No. 2, 227-238 (1976).

> Key words: elasticity; finite torsion; natural rubber; scaling law; simple materials assumption.

The torque and forces normal to the end surfaces of cylinders of natural rubber were measured as a function of the angle of twist. The measurements were repeated on small cylinders cut from the larger cylinders to insure that the tests were on identical material. Plots of reduced torque and of reduced normal force versus reduced twist for the different sized cylinders coincide to within 1 percent. This result supports the simple material assumption of the classical theory of finite elastic deformations. An interesting instability was observed, and derivatives of the strain energy function were calculated.

**16279.** Fanconi, B., Crissman, J., **Influence of methyl group branches on the longitudinal acoustical mode frequencies in alkanes and polyethylene,** *J. Polym. Sci. Polym. Lett. Ed.* **13,** 421-426 (1975).

> Key words: alkanes; longitudinal acoustical mode; methyl group branches; polyethylene; Raman spectroscopy.

The Raman-active longitudinal modes (LAM) of crystalline n-alkanes have been extensively studied. The frequency-chain length relationship found for the n-alkanes has been recently used to deduce the length of the all-trans chain segments in polyethylene single crystals and to determine the paraffinic chain lengths and conformations in phospholipids. The use of LAM frequencies of n-alkanes in this manner neglects the effects of interchain interactions, terminal chain groups, and conformational or mass defects.

**16280.** Horowitz, E., **Transfer of measurement methodology to industry,** *J. Assoc. Eng. Archit. Isr.* **35,** 21-41 (May 1976).

Key words: benefits, industry-society; materials research; measurements-standards; NBS-industry; transfer.

The National Bureau of Standards (NBS) is engaged in a variety of measurement and standards activities, many of which are applicable to the solution of scientific and technological problems in industry and society. This paper discusses some of the innovations and accomplishments resulting from the materials programs in the NBS Institute for Materials Research and traces the work from the laboratory phase to the transfer and utilization of measurement technology and standards in industry. Also included is a brief discussion of the NBS Experimental Technology Incentives Program (ETIP) which is concerned with stimulating the implementation of innovative policies in the area of science and technology.

**16281.** MacDonald, R. A., Tsai, D. H., **Molecular dynamical calculations of the thermal diffusivity of a perfect lattice,** (Proc. 14th Int. Conf. on Thermal Conductivity, Storrs, CT, June 2-4, 1975), Paper in *Proceedings of the 14th International Conference on Thermal Conductivity,* P. G. Klemens and T. K. Chu, Eds., pp. 145-152 (Plenum Press, New York, NY, 1976).

Key words: continuum theory of diffusion; density; kinetic temperature; molecular dynamics; numerical error; perfect lattice; thermal conductivity; thermal diffusivity; thermoelastic coupling.

We have used the method of molecular dynamics to make a detailed study of thermal diffusivity in a perfect monatomic lattice. The interatomic potential is that appropriate for iron. We limit the atomic motions to two dimensions in order to shorten the computation. We maintain one end of the lattice at a given kinetic temperature and obtain the temperature profile in the lattice as a function of time. The total energy added to the system is recorded. We fit diffusive curves to the temperature profiles and thus obtain the thermal diffusivity of the lattice. Its value is $4 \times 10^{-6}$ m$^2$ sec$^{-1}$ at a mean lattice temperature of 75K.

**16282.** Bucaro, J. A., Simmons, J. H., **Rayleigh wave study of surface diffusion and stress relaxation in glass,** *J. Non-Cryst. Solids* **14,** 225-241 (1974).

Key words: glass; glass strengthening; ion exchange; Rayleigh waves; surface waves.

Surface wave propagation on ion-exchanged glass surfaces has been systematically studied. The glass system was an alkali-alumino silicate glass, and the ion-exchange involved the replacement of lithium ions by sodium ions. Accurate velocity measurements were carried out on systems ion-exchanged for various times and at various temperatures. The effects of density and modulus changes on the velocity have been separated. Stress build-up and relaxation have been observed which correlate well with shear viscosity measurements. In addition, the diffusion coefficient for the $Na^+ \rightleftarrows Li^+$ exchange has been determined at a variety of temperatures.

**16283.** DiMarzio, E. A., **Validity of the Ehrenfest relation for a system with more than one order parameter,** *J. Appl. Phys.* **45,** No. 10, 4143-4145 (Oct. 1974).

Key words: Ehrenfest relation; glassy state; order-parameters; polymer thermodynamics.

The relation $\Delta C_p \Delta\kappa = TV(\Delta\alpha)^2$ is shown to be obeyed under the same assumptions that Davies and Jones used to derive the weaker condition $\Delta C_p \Delta\kappa \geqslant TV(\Delta\alpha)^2$. This means that if a material is found experimentally not to obey the above equality, then it is not describable by an order-parameter theory. A prescription is given which allows one to determine within the context of order-parameter theory whether the glass transition of a given material is basically thermodynamic or kinetic in origin.

**16284.** Broadhurst, M. G., Harris, W. P., Mopsik, F. I., Malmberg, C. G., **Piezoelectricity, pyroelectricity and electrostriction in polymers,** *Polym. Prepr.* **14,** No. 2, 820-829 (Aug. 1973).

Key words: electret; piezoelectricity; polarization electrostriction; polymer; pyroelectricity.

Piezoelectricity in naturally-occurring biological and polarized synthetic polymers is becoming increasingly recognized as an important phenomenon. This paper traces the history of piezoelectricity in electrets and gives a simple physical basis for the effect. Measurement techniques are described and piezo- and pyroelectric data for polymers are presented and compared to data for common nonpolymeric materials.

**16285.** Taggart, H., Nelson, R. E., Scott, W., Jr., Shafer, J., Tary, J., Workman, J., Treado, M. J., **Personal/portable FM transmitters,** *NILECJ-STD-0203.00,* 22 pages (U.S. Department of Justice, Law Enforcement Assistance Administration, National Institute of Law Enforcement and Criminal Justice, Washington, DC, Oct. 1974).

Key words: audiofrequency modulation; communications; electromagnetic compatibility; law enforcement; personal transmitter; portable transmitter; radio frequency carrier; transmitter.

The purpose of this standard is to establish performance requirements and the test methods needed to evaluate these requirements for frequency modulated personal/portable transmitters used by law enforcement agencies. Sixteen transmitter characteristics are included. Also described are a radiation test site, standard duty cycle and the characteristics of required test equipment.

**16286.** Treado, M. J., Taggart, H. E., Nelson, E., Scott, W. W., Shafer, J. F., Tary, J. J., **Fixed and base station FM transmitters,** *NILECJ-STD-0201.00,* 20 pages (U.S. Department of Justice, Law Enforcement Assistance Administration, National Institute of Law Enforcement and Criminal Justice, Washington, DC, Sept. 1974).

Key words: base station transmitter; communications; fixed transmitter; FM transmitter; law enforcement; transmitter.

The purpose of this standard is to establish performance requirements and methods of test for FM fixed and base station transmitters used by law enforcement agencies. It should be used with transmitters which either do not have subsystems such as selective signaling or in which such subsystems are disabled or bypassed. This standard is applicable to transmitters licensed to operate in the 25-50 MHz, 150-174 MHz, and 400-512 MHz bands, and includes the performance requirements and test methods for 16 different transmitter characteristics.

**16287.** Calvano, N. J., Dobbyn, R. C., **Crash helmets,** *NILECJ-STD-0105.00,* 13 pages (U.S. Department of Justice, Law Enforcement Assistance Administration, National Institute of Law Enforcement and Criminal Justice, Washington, DC, June 1975).

Key words: crash; helmet; impact attenuation; penetration; retention system strength; visual clearance.

This standard establishes performance requirements and methods of test for helmets used to protect the wearer while a driver or passenger of a surface vehicle. The test methods described measure the ability of the helmet to attenuate impact, resist penetration and provide sufficient peripheral visual clearance and test the static strength of the helmets' retention system. It is based on ANSI Standard Z90.1-1971.

**16288.** Hartman, A. W., **Proposed image space scanner with reduced off-axis defocusing,** *Opt. Eng.* **15,** No. 3, 262-264 (May-June 1976).

Key words: defocusing; image space off-axis; line scanner; optical.

An optical line scanner with a scanning mirror between the optics and the image can be modified to produce more than twice the field of view of a conventional image space scanner, without increase in off-axis defocusing. The proposed approach consists of moving the rotation center of the scanning mirror away from a point on the optical axis to a specified point off-axis.

Two examples of such a scanner modification are analyzed: a flat-field microscope scanner with high resolution and a curved-field night-viewing scanner with high optical speed.

**16289.** Crissman, J. M., **On the transition from paraffinic to polymeric behavior: Mechanical properties,** *J. Polym. Sci. Part A-2,* **13,** 1407-1416 (1975).

Key words: chain folds; differential scanning calorimetry; linear polyethylene fractions; low angle x ray; mechanical relaxation; tetranonacontane.

An attempt has been made to determine what influence chain folds may have on the $\alpha$ and $\gamma$ mechanical loss peaks in linear polyethylene. In so doing, one long-chain *n*-paraffin ($C_{94}H_{190}$) and two low molecular weight polyethylene fractions have been examined with mechanical relaxation, differential scanning calorimetry (DSC), and low-angle x-ray diffraction techniques. The data suggest that chain folds play a prominent role in both the $\alpha$ and $\gamma$ processes but that other factors such as polydispersity and/or branching are also important.

**16290.** DiMarzio, E. A., Bishop, M., **Connection between the macroscopic electric and mechanical susceptibilities,** *J. Chem. Phys.* **60,** No. 10, 3802-3811 (May 15, 1974).

Key words: Cole-Cole plots; dielectric constants of polymers; dielectrics; electric dispersion; permeability of polymers.

The following relationship is derived between the dielectric permittivity $\epsilon(\omega)$ and the complex shear viscosity $\eta(\omega)$: $[\epsilon(\omega)-\epsilon_\infty]/(\epsilon_0-\epsilon_\infty)=[1-i\omega\eta(\omega)K]^{-1}$. This equation is derived from both a generalization of Debye's treatment and from the Kubo formalism. The model consists of dipoles imbedded in rigid beads that are in turn imbedded in the viscous medium. A frequency dependent $\eta(\omega)$ implies nonexponential decay of the electric dipoles and results in skewed-arc behavior in the Cole-Cole plots except when $\eta(\omega)$ is represented by a single Maxwell element or by a single Viogt element. Consistency with the requirements of causality and reality is displayed. Experimental $\epsilon(\omega)$ are predicted reasonably accurately by use of experimental $\eta(\omega)$ and the above equation.

**16291.** Edelman, S., **Piezoelectric polymer transducers,** *Proc. Workshop on Sonar Transducer Materials, Naval Research Laboratory, Washington, DC, Nov. 13-14, 1975,* pp. 269-282 (Naval Research Laboratory, Washington, DC, Feb. 1976).

Key words: flexibility; hydrophone; impedance match; low-cost transducers; piezoelectric polymers.

Polymers with significant piezoelectric activity have been developed. This material can be used to measure many forms of dynamic stress and vibration. Piezoelectric polymers can be formed in size and shape to suit a particular application and they can be fastened to curved, twisted, or compliant surfaces.

A typical piezoelectric polymer is compared with a typical piezoelectric ceramic for underwater use. A new polymer hydrophone is described whose sensitivity in the region below 1 kHz is comparable to that of conventional hydrophones.

**16292.** Tighe, N. J., Swann, P. R., **Magnetite lamellae in reduced hematites,** Chapter 4.3 in *Electron Microscopy in Mineralogy,* H. R. Wenk, et al., Eds., pp. 209-213 (Springer-Verlag Berlin Heidelberg, Germany, 1976).

Key words: electron microscopy; $Fe_2O_3$; $Fe_3O_4$; high-voltage electron microscopy; *in situ* hematite; magnetite.

Microstructural changes that occur during gaseous reduction of hematite ($Fe_2O_3$) were studied by light and electron microscopy. Reduction experiments carried out in a high-voltage electron microscope and in a controlled atmosphere furnace showed that at T = 1000 °C magnetite nucleates and grows with the $(111)_m \| (0001)_h$ habit. Lenticular magnetite plates grow by a martensitic mechanism.

**16293.** Arthur, M. G., Saulsbery, L. F., Scott, W. W., Jr., Shafer, J. F., **Mobile FM receivers,** *NILECJ-STD-0207.00,* 18 pages (U.S. Department of Justice, Law Enforcement Assistance Administration, National Institute of Law Enforcement and Criminal Justice, Washington, DC, June 1975).

Key words: FM receivers; law enforcement equipment; minimum performance requirements; NILECJ Standard; receiver definitions; receiver measurement techniques.

This document is a voluntary performance standard that establishes minimum performance requirements and methods of test for Mobile FM Receivers used by law enforcement agencies. This standard specifies the test conditions, the test equipment needed, the test methods, and the minimum performance requirements necessary for satisfactory performance in Mobile FM Receivers.

**16294.** Jickling, R. M., **RF coaxial cable assemblies for mobile transceivers,** *NILECJ-STD-0212.00,* 9 pages (U.S. Department of Justice, Law Enforcement Assistance Administration, National Institute of Law Enforcement and Criminal Justice, Washington, DC, Sept. 1975).

Key words: cable assembly; coaxial cable; insertion loss; mobile antenna; mobile transceiver; transmission.

This standard specifies the connector plug at the mobile transceiver for an rf coaxial cable lead-in from a mobile antenna. Four performance requirements are listed, with detailed test methods for measuring characteristics such as standing wave ratio and insertion loss.

**16295.** Calvano, N. J., Dobbyn, R. C., **Ballistic helmets,** *NILECJ-STD-0106.00,* 13 pages (U.S. Department of Justice, Law Enforcement Assistance Administration, National Institute of Law Enforcement and Criminal Justice, Washington, DC, Sept. 1975).

Key words: armor; ballistic helmet; ballistic impact; ballistic penetration; bulletproof helmet.

NILECJ-STD-0106.00, Ballistic Helmets, is a law enforcement equipment standard developed by the Law Enforcement

Standards Laboratory. It establishes minimum performance requirements and methods of test for helmets intended to protect the head against gunfire. Standards are established for helmets intended to provide two levels of protection: helmets protective against caliber .357 Magnum revolver fire, and helmets protective against caliber .38 Special and .22 long rifle high velocity handgun fire.

**16296.** Jesch, R. L., Scott, W. W., Treado, M. J., **Batteries for personal/portable transceivers,** *NILECJ-STD-0211.00,* 14 pages (U.S. Department of Justice, Law Enforcement Assistance Administration, National Institute of Law Enforcement and Criminal Justice, Washington, DC, June 1975).

Key words: battery performance standard; law enforcement communications, Law Enforcement Standards Laboratory; personal/portable transceivers; primary battery; secondary battery; transceiver.

This document is a voluntary performance standard for batteries used in personal/portable transceivers. It establishes minimum performance requirements and methods of test for primary and secondary batteries, and is intended to assist law enforcement agencies in the selection and procurement of these batteries.

**16297.** Arthur, M. G., Saulsbery, L. F., Scott, W. W., Jr., Shafer, J. F., **Personal/portable FM receivers,** *NILECJ-STD-0208.00,* 18 pages (U.S. Department of Justice, Law Enforcement Assistance Administration, National Institute of Law Enforcement and Criminal Justice, Washington, DC, Oct. 1975).

Key words: FM receivers; law enforcement equipment; minimum performance requirements; NILECJ Standard; receiver definitions; receiver measurement techniques.

This document is a voluntary performance standard that establishes minimum performance requirements and methods of test for personal/portable FM receivers used by law enforcement agencies. This standard specifies the test conditions, the test equipment needed, the test methods, and the minimum performance requirements necessary for satisfactory performance in personal/portable FM receivers.

**16298.** Teague, M. R., Lambropoulos, P., Goodmanson, D., Norcross, D. W., **Theory of two-photon ionization of cesium,** *Phys. Rev. A* **14,** No. 3, 1057-1064 (Sept. 1976).

Key words: cesium; multiphoton processes; photoionization.

We present a systematic theoretical analysis of two-photon ionization of cesium in the perturbation-theory regime. Matrix elements from diverse sources, such as quantum-defect theory and model potentials, as well as from experimental oscillator strengths, have been used in the calculation. The results are discussed in the context of recent measurements. In addition to total generalized cross sections (gcs) for linearly polarized light, ratios of gcs for linear to circular polarization, as well as photoelectron spin polarization, have been calculated. The various sets of matrix elements give results which are consistent, given variations that should be expected from the diversity of the sources. The disagreement with experiment, however, persists.

**16299.** Cooper, J. W., **Inner shell ionization as a single electron process,** (Proc. Int. Conf. on Inner Shell Ionization Phenomena and Future Applications, Atlanta, GA, Apr. 17-22, 1972), Paper in *Proceedings of the International Conference on Inner Shell Ionization Phenomena and Future Applications,* R. W. Fink, S. T. Manson, J. M. Palms, and P. V. Rao, Eds., CONF-720404, **2,** 807-815 (USAEC Technical Information Center, Oak Ridge, TN, Jan. 1973).

Key words: charged particle excitation; inner shells; ionization; photoionization.

Excitation ionization of inner shell electrons by photons, protons, electrons or heavy charged particles can be viewed within a common theoretical framework provided the interaction of the incident particle with the system being bombarded is sufficiently weak. Within this approximation the ionization process depends only on the energy and momentum transferred to the ionized system and may be characterized by a "Bethe Surface" in these variables. Quantitative calculations of specific processes and interpretation of experimental data often considers ionizations as a single electron (two-body) process. The basic theory of inner shell ionization treated as a single electron process will be reviewed briefly with emphasis on its range of validity and the relationship between information obtained via excitation by different incident particles.

**16300.** Davis, R. M., **Preventive technology: A cure for scientific ills,** *Science* **188,** No. 4185, 213 (Apr. 1975).

Key words: preventive technology; scientific ills; society and science; technology and civilization.

Preventive Technology: A Cure for Scientific Ills is an editorial dealing with scientific advancement and hopes that preventive technology can prohibit further societal side effects. Scientific discoveries are often linked with the harm that they may cause humanity rather than the good that they do (e.g., computer science is coupled to an undesirable "data bank;" and the development of synthetic plastics is linked with environmental pollution).

Prevention of scientific ills in the past and even today has taken place after the fact. It is important to recognize that science has been the primary cause of beneficial change throughout man's history. Preventive technology needs to be recognized as a scientific specialty. It must be practiced as part of every aspect of science. It will make possible both more science and more public peace of mind. Delay in setting up Preventive Technology may cause ill for both science and for future beneficial changes for society.

**16301.** Berger, H., **Nondestructive measurements: How good are they?,** *Mater. Eval.* **XXXIV,** No. 1, 18A-20A, 22A, 24A, 33A-34A (Jan. 1976).

Key words: accuracy; conservation; measurements; nondestructive evaluation; productivity; reliability; reproducibility; safety.

Increasing demands are being made on nondestructive evaluation (NDE) as a result of needs for safety, conservation, and productivity. This makes it all the more imperative that NDE measurements be made in a reliable, reproducible manner. The capabilities of NDE measurements are considered from the points of view of elements of the system and the measurement system as a whole. In each case, unacceptable variations in measurement accuracy, reliability, and reproducibility are identified. The NDE measurement situation is compared to measurements being made in clinical chemistry, where an improved measurement capability was brought about through the efforts of the professionals in that field, and the development of standard reference materials and measurement methods of known accuracy. The NDE community is called upon to take similar steps and contribute to the needs for improved NDE measurements and standards.

**16302.** Franklin, A. D., **Electrochemical growth of crystals from electrolyte solutions,** *J. Cryst. Growth* **34,** 245-247 (1976).

Key words: calcium hydroxide; crystal growth; crystals, electrochemical; electrolysis; solution.

An electrochemical crystal-growth technique is described in which an electrolyte reaction involving one ion in the desired crystal is used to create a concentration gradient in that ion across the cell. Nutrient material held near the consuming electrode is dissolved, and crystal growth near the producing electrode occurs at a rate which can be controlled by the current through the cell. The technique has been demonstrated with the growth of $Ca(OH)_2$ crystals from aqueous solutions of $CaCl_2$ plus KCl.

**16303.** Arthur, M. G., Saulsbery, L. F., Scott, W. W., Jr., Shafer, J. F., **Fixed and base station FM receivers,** *NILECJ-STD-0206.00*, 17 pages (U.S. Department of Justice, Law Enforcement Assistance Administration, National Institute of Law Enforcement and Criminal Justice, Washington, DC, Sept. 1975).

Key words: FM receivers; law enforcement equipment; minimum performance requirements; NILECJ Standard; receiver definitions; receiver measurement techniques.

This document is a voluntary performance standard that establishes minimum performance requirements and methods of est for fixed and base station FM receivers used by law enforcenent agencies. This standard specifies the test conditions, the est equipment needed, the test methods, and the minimum perormance requirements necessary for satisfactory performance n fixed and base station FM receivers.

**6304.** Fanconi, B., Finegold, L., **Vibrational states of the biopolymer polyglycine II: Theory and experiment,** *Science* **190,** 458-460 (Oct. 31, 1975).

Key words: heat capacity; lattice dynamics; low temperature, polyglycine; polypeptides; vibrational states.

The density of vibrational states, and hence the heat capacity, as been calculated for the parallel-chain hexagonal lattice of $3_1$ elical polyglycine. The agreement with experimental results in he temperature range from 1 to 20 K, including an anomaly near K, is the best obtained thus far for homopolypeptides.

**6305.** Dobbyn, R. C., Bruchey, W. J., Jr., Shubin, L. D., **An evaluation of police handgun ammunition: Summary report,** *LESP-RPT-0101.01*, 21 pages (U.S. Department of Justice, Law Enforcement Assistance Administration, National Institute of Law Enforcement and Criminal Justice, Washington, DC, Oct. 1975).

Key words: bullets; cartridges; handgun ammunition; law enforcement; relative incapacitation index; relative stopping power.

This report summarizes the results of a laboratory study of andgun ammunition presently being marketed to law enforceient agencies. Three basic terminal effects of the ammunition ave been examined: their relative incapacitation potential for uman targets, their ricochet behavior and their material enetration characteristics. The focus has been on commercially vailable handgun ammunition in the caliber range 9 mm (.355 ı) to .45. The test methods and evaluation techniques are, howver, applicable to other penetrating projectiles.

**6306.** Lawn, B. R., Swain, M. V., Phillips, K., **On the mode of chipping fracture in brittle solids,** *J. Mater. Sci. Lett.* **10,** 1236-1239 (1975).

Key words: brittle solids; chipping; fracture; indentation; residual stress; stress analysis.

A description is given of the mode of chipping fracture obrved in highly brittle solids. It is pointed out that residual tresses about indentation deformation centers play a vital role. The implications of this mode in a number of mechanical phenomena are discussed.

**16307.** Brown, W. E., Chow, L. C., **Chemical properties of bone mineral,** *Ann. Rev. Mater. Sci.* **6,** 213-236 (Aug. 1976).

Key words: amorphous calcium phosphate; bone mineral; fluorapatite; hydroxyapatite; morphology; nonstoichiometry; octacalcium phosphate; solubility; surface.

The literature on the chemical properties of bone mineral is reviewed. As a basis for understanding the properties of these extremely fine crystallites, reference is made first to the ideal compounds and then to the morphological, compositional, and structural modifications that bone mineral is known or implied to have. The structure of apatite is considered the most suitable prototype for bone crystallites; however, the "apatitic layer" in the crystal of octacalcium phosphate is almost identical in structure to hydroxyapatite. This close structural relationship has many implications relative to the chemistry of bone mineral. "Amorphous calcium phosphate," which has been suggested as a possible component of bone, is assessed. The properties of the so-called "amorphous" material in bone are unlikely to be closely similar to those of synthetic amorphous calcium phosphates. A theoretical basis for solubility of bone is described and its variable solubility is discussed. Because of the smallness of bone crystallites, the surface properties of bone mineral are of great importance. Both the lattice and the surface of the crystallite play important roles in processes involving the dissolution or formation of bone mineral.

**16308.** Horowitz, E., **Metallo-organic systems with high thermal stability,** Paper 7 in *Advances in Chemistry Series*, R. F. Gould, Ed., No. 85, pp. 82-94 (1968).

Key words: coordination polymers; role of metal and ligand; thermal stability.

When 8-hydroxyquinoline and derivatives of bis(8-hydroxyquinoline) react with metal ions, coordination complexes and polymers are formed, respectively, which exhibit improved thermal stability. This paper reviews the reaction of first-row transition metal ions with such ligands and their effect on the stabilization of these organic molecules. For the polymers containing divalent Mn, Co, Ni, Cu, or Zn the decomposition temperature is related to the periodic properties of the metal as well as the composition of the ligand to which the metal is coordinated. Trivalent chromium produces a crosslinked polymer when it reacts with bis(8-hydroxy-5-quinolyl)methane, and the thermogram for this polymer is also reported.

**16309.** Chang, S. S., **Low temperature thermal behavior of glassy polymers,** (Proc. ACS Coatings and Plastics 170th Meeting, Chicago, IL, Aug. 25-29, 1975), Paper in *Coatings and Plastics Preprints*, R. F. Wint, Ed., **35,** No. 2, 364-369 (American Chemical Society, Washington, DC, 1975).

Key words: glassy state; glass transition; heat capacity; polymer; specific heat; strain energy; supercooled liquid; thermal relaxation.

A brief review of the thermal behavior of glassy polymers from cryogenic temperatures to the supercooled liquid state will be presented. Results from this and other laboratories will be used to illustrate the following topics of discussion. Some of the recent results from this laboratory were obtained by means of a fully automated adiabatic calorimetric measurement system. The main instrument in the system is a computer-controlled self-balancing potentiometer. Above 25 K, the precision in the heat capacity measurement is about 0.02 percent and the sensitivity in the temperature measurement is about $10^{-5}$K.

**16310.** Berger, R. E., **Dynamic strain gage measurements on ophthalmic lenses impacted by low energy missiles,** *J. Opt. Physiolog. Opt.* **53,** No. 6, 279-286 (June 1976).

Key words: drop-ball test; impact; lens; ophthalmic lens; quasi-static theory; strain gage measurements.

Strain distributions on impacted ophthalmic lenses were measured with strain gages. The strain distributions, which resulted from impacts produced with a special apparatus, were shown to be comparable to those which arise in the FDA drop-ball test. The measured strain drops off very rapidly away from the impact point, implying that only a small part of the lens is really being tested. The results are in good agreement with the quasi-static predictions. The effect of differences in lens power, of input kinetic energy, and of inserting the lens in a polyethylene bag are also investigated.

**16311.** Berger, R. E., **The role of edge failures in impact testing of ophthalmic lenses,** *J. Am. Optometric Assoc.* **47,** No. 5, 599-605 (1976).

Key words: drop-ball test; edge; fracture; impact; ophthalmic lenses; shape.

The role of edge mode failures in drop-ball testing of ophthalmic lenses was investigated. The relative effects of lens shape and type of edging operation were determined by comparing the impact performance of groups of lenses. Strain gages were mounted on the edges of several lenses to determine the applied tensile stresses. The results were reviewed in the context of the flaw distribution theory. As expected, more breakage was observed for those edging processes which introduce more severe flaws and for those lens shapes for which higher edge stresses were measured. It was also observed that the search theory of impact testing is applicable for edge flaws as well as for surface flaws (a lens sustains many impacts before it fractures; the ball is searching for a weak spot on the lens).

**16312.** Bennett, L. H., Kahan, D. J., Carter, G. C., **Alloy phase diagram data,** *Mater. Sci. Eng.* **24,** 1-17 (1976).

Key words: alloy; metallurgy; phase diagram.

An annotated list of references including the major compilations of data on alloy phase diagram, crystallography, and thermodynamics and some useful reviews and theoretical discussions of alloy phase diagrams is presented.

**16313.** Wardell, J. R., Wilmot, G. B., Haar, L., Klein, M., **Thermodynamic data for interior ballistics calculations,** *Proc. 12th JANNAF Combustion Meeting, Newport, RI, July 25, 1975*, pp. 363-390 (Chemical Propulsion Information Agency, Johns Hopkins University, Applied Physics Laboratory, Laurel, MD, 1976).

Key words: equation of state; interior ballistics; water.

The effect on theoretical interior ballistic calculations of real gas corrections to ideal gas thermodynamic quantities is considered. The equation of state of Haar and Shenker for dense spherical gases is generalized to nonspherical gases and applied to water. The agreement with available data is quite good. At 2000 K and 300 MPa (44,000 psi) our theoretical ratio of specific heats differs from that obtained using a simple virial equation of state by 5 percent. This corresponds to a 3.5 percent change in muzzle velocity and maximum pressure. The corresponding difference in Cv is only 2 percent.

**16314.** Bur, A. J., **Measurements on the dynamic piezoelectric properties of bone as a function of temperature and humidity,** *J. Biomech.* **9,** 495-507 (Sept. 1976).

Key words: bone; dispersion phenomena; Maxwell-Wagner polarization; piezoelectric *d* constant; piezoelectricity; relative humidity; temperature.

The utilization of piezoelectricity as a clinical or diagnostic tool in medicine and dentistry is dependent upon an adequate quantitative description of the piezoelectric coefficients. Here, measurements of the dynamic piezoelectric *d* constant, $d^* = d' - id''$, for bovine bone are presented as a function of temperature (20-60 °C), relative humidity (r.h.) (33-98%), frequency of applied stress ($10^{-2}$-$10^2$ Hz), and sample orientation. The anisotropic character of cortical bone requires that *d* be expressed as a matrix containing 18 coefficients. Dispersion phenomena, i.e. $d'' \neq 0$, are present in these coefficients for our frequency-temperature-r.h. range. At low r.h. (≤75%), $d_{12}$ and $d_{13}$ show little or no dispersion ($d'' = 0$), whereas varying degrees of relaxation are observed in the other coefficients. The $d_{14}$ shear term is notable for a large dispersion at $f = 40$ Hz, $T = 38.6$ °C and 55 percent r.h., for which $d''_{14}$ is negative. The negative imaginary coefficient means that energy is being gained in the 14 coefficient. The change in $d_{14}$, with a change in temperature and/or r.h., is attributed to a change in sample water content. For 98 percent r.h., the low frequency data ($f < 10$ Hz) are dominated by a polarization which varies as the reciprocal of the frequency. This polarization is attributed to an interfacial or Maxwell-Wagner polarization which occurs as a result of ionic conduction under the influence of the piezoelectric polarization field.

**16315.** Pierman, B. C., Bryson, J. O., **Building safety research at the National Bureau of Standards,** *Prof. Safety Mag.*, pp. 13-16 (Sept. 1976).

Key words: accidents; buildings; construction; maintenance; research accidents; safety.

This article summarizes the work that is accomplished in the Center for Building Technology to enhance the inherent safety of buildings in the United States. Aspects of user as well as worker safety resulting from building construction, use, maintenance, repair and retrofit are discussed. Research goals and methods, resulting in the greatest impact on overall safety in buildings are enumerated. Specific research projects are summarized.

**16316.** Margolis, S. A., Howell, B. F., Schaffer, R., **Purification and analysis of the purity of NADH,** *Clin. Chem.* **22,** No. 8, 1322-1329 (1976).

Key words: ADP; ADP-ribose; chromatography; impurities in NADH preparations; NADH stability; preparative chromatography on DEAE-cellulose; spectrophotometric properties of pure NADH.

We developed an analytical reverse-phase high-performance liquid chromatographic procedure for rapid assessment of the purity of NADH. The method completely separates adenosine monophosphate and adenosine diphosphoribose from NADH. By use of this analytical technique we found that preparative chromatography on DEAE-cellulose gives NADH that is free from adenine nucleotides as well as other impurities that commonly are present in NADH. The absorbance ratio at 260 and 340 nm of the purified NADH in 1.8 mmol/liter ammonium carbonate is 2.261 ± 0.002 (± 1 SD).

**16317.** Clark, E. J., Ballard, D. B., Embree, E. J., **SEM examination of an overheated aluminum wired electrical receptacle,** (Proc. 34th Annual Electron Microscopy Society of America Meeting, Miami Beach, FL, Aug. 9-13, 1976), Paper in *34th Annual Proceedings Electron Microscopy Society of America*, G. W. Bailey, Ed., pp. 454-455 (Claitor's Publ. Div., Baton Rouge, LA, 1976).

Key words: aluminum wire; nondispersive x-ray analysis; overheated receptacle; scanning electron microscope.

A typical household electrical receptacle wired with aluminum cable overheated during current cycling tests. It was studied for evidence of the cause of failure. The surfaces of the materials in the electrical path were examined by scanning electron microscopy and energy dispersive x-ray analysis and were found to contain corrosion products of the base materials. Chlorine was also present on the surfaces. A piece of the insulation was also examined. An explanation for the presence of chlorine in the corrosion products is suggested.

**16318.** Waterhouse, R. V., Cook, R. K., **Diffuse sound fields: Eigenmode and free-wave models,** *J. Acoust. Soc. Am.* **59,** No. 3, 576-581 (Mar. 1976).

Key words: acoustical energy density; acoustics; diffuse sound fields; reflection and interference of sound; room acoustics theory; sound fields.

The diffuse sound field as used in standard measurements in reverberant enclosures has been analyzed in terms of two different models, the eigenmode and the free-wave models. Recently the question has been raised as to the extent to which these models are consistent. To investigate these matters, the energy density as a function of position is calculated for axial, tangential, and oblique modes in a rectangular enclosure. The results show that, for a sound field consisting of several overlapping oblique modes, excited by a narrow band of noise, increases of mean sound pressure levels at the walls, edges, and corners of the enclosure are predicted that are in agreement with the results of the free-wave analysis and experiment. It is concluded that the two models are consistent. The implications of the models, regarding the spatial uniformity of energy, are discussed.

**16319.** Davis, R. M., **The computer serves, the consumer relishes,** *Comput. Dec.*, pp. 31-34 (May 1975).

Key words: automation; consumers; innovation; institutional barriers; productivity; service sector.

This paper deals with automation in the Service Sector. Consumers today are more dissatisfied with the services which they "buy" than the products they procure. The Service Sector is defined as well as the technologies of automation. It surveys the spread of automation in the United States as well as the institutional barriers impeding this spread. Automation has provided one of the best means for improving the quality of services and productivity in the Service Sector. A concern today is that people may become the victims rather than the masters of automation. To escape such a fate we must decide what we wish for ourselves and apply automation to achieve our goals.

**16320.** Wiese, W. L., Younger, S. M., **Atomic oscillator strengths in fusion plasma research,** (Proc. IVth Int. Conf. on Beam-Foil Spectroscopy, Gatlinburg, TN, Sept. 15-19, 1975), Paper in *Beam-Foil Spectroscopy*, I. A. Sellin and D. J. Pegg, Eds., **2,** 951-960 (Plenum Publ. Corp., New York, NY, 1976).

Key words: atomic oscillator strengths; beam-foil spectroscopy; fusion plasma research; plasma radiative losses; sodium isoelectronic sequence; Tokamak plasmas.

In the Tokamak devices used in fusion plasma research, highly ionized heavy metal impurities are observed which have detrimental effects on the plasma behavior, such as strong radiative energy losses. Thus, the radiative properties of impurity species, especially their atomic oscillator strengths, have assumed great importance. An effective approach to obtain these quantities appears to be the extension of theoretical methods to highly ionized species, e.g., by the application of nuclear charge dependent techniques. At some point, however, relativistic effects come into play which are largely unexplored. Another possibility is to utilize the regularities of atomic oscillator strengths along isoelectronic sequences to extrapolate to more highly ionized species. Again, relativistic effects will make these extrapolations uncertain. Thus, some key experimental data are urgently needed. Beam-foil spectroscopy has the potential for acquiring such data, but it will be taxed to its limits. The data needs will be reviewed, and it will be shown that combinations of beam-foil results, theoretical values, and systematic trend studies along isoelectronic sequences may lead to useful data for very highly ionized species.

**16321.** Schneider, S. J., Jr., **Materials properties determination: Transport properties, phase equilibria and slag properties,** *Proc. NSF-OCR Engineering Workshop on MHD Materials, Cambridge, MA, Nov. 20-22, 1974*, pp. 150-167 (Massachusetts Institute of Technology, Cambridge, MA, 1975).

Key words: diffusion; electrical conductivity; magnetohydrodynamics (MHD); phase equilibria; transport properties; vaporization; viscosity.

The combination of high temperatures and high velocity gases containing reactive chemical species produces a very severe environment within a MHD generator. Containment and operating materials must resist not only erosion through vaporization and corrosion by alkali and slag attack, but also must possess the requisite physical properties necessary for generator operation. The design of a materials device (e.g. electrode) to withstand the rigors of these conditions requires knowledge and proper utilization of the basic physical and chemical properties of candidate materials translated to within the context of an operating engineering system. This paper concentrates on some important aspects of materials behavior and characteristics which are thought to be influential or paramount in ensuring long life and operability of the MHD generator. First of all information on the transport properties viscosity, vaporization, diffusion, and electrical conductivity is necessary to effectively design an electrode-insulator system which will operate satisfactorily over the long term. Viscosity of slags is important to the erosive and corrosive wear of the containment materials as well as to the temperature gradients at interfaces. Vaporization (and condensation) mechanisms will determine the chemical compositions at boundary layers and hence influence the ultimate degradative processes which take place. Diffusion rates of species to and from a given location such as interior layers will dictate the long term stability of these sections. Electrical conductivity of electrodes, insulators and slags and their reaction products is of overriding importance to the operability and performance of the generator. Second the phase equilibria of contacting phases, either solid, liquid or gas, will establish to resulting phase assemblages and hence the "worst case situation." Knowledge of the pertinent phase relations allows incorporation of design features which will delete or minimize degradative reactions. Each of the materials properties are interrelated and must be considered together for proper design and operation of a MHD generator. This paper discusses each of these properties of materials appropriate to clean fuel generators and for coal fuel applications.

**16322.** Klose, J. Z., **Measurement of atomic uranium lifetimes for isotope separation,** (Proc. SPIE/SPSE Tech. Symp. on Ultra High Power Lasers for Practicable Applications, Reston, VA Mar. 22-23, 1976), *SPIE 76*, 150-155 (Society of Photo-Optical Instrumentation Engineers, Palos Verdes Estates, CA 1976).

Key words: atomic beam; delayed coincidence; imprisonment; lifetime; mean life; resonance radiation; transition probability; U I; uranium.

Following a brief discussion of uranium isotope separation using lasers, the delayed coincidence method of measuring atomic mean lives with pulsed electron beams utilized here is described along with the beam source used to supply the free uranium atoms for measurement. Experimental details involved in the lifetime measurement are next discussed followed by the effect of resonance radiation imprisonment on the measured lifetimes. Finally, lifetime measurements involving the 3584.9 Å and 5915.4 Å transitions in natural uranium are described, and the previously reported result of 7.3 ± 1.1 ns for the mean life of the upper level of the 3584.9 Å transition (27886.99 $cm^{-1}$) is presented.

**16323.** Unassigned.

**16324.** Christ, B. W., Swanson, S. R., **Alignment problems in the tensile test,** *J. Test. Eval.* **4,** No. 6, 405-417 (Nov. 1976).

Key words: alignment; stresses; tension tests.

Uniaxial tensile testing is a method used throughout the world to measure the strength and ductility of materials. An important aspect of uniaxial tensile testing which often goes unrecognized is test system alignment. Poor alignment can significantly influence test results at small strains, especially the fracture strengths of materials in a brittle state. The purpose of this review paper is to enable a reader to identify sources of misalignment, recognize the effects of misalignment on tests results, evaluate the extreme surface bending strains and stresses, and become acquainted with some techniques for reducing misalignments to within tolerable limits. Numerous references are made to the literature which describes how misalignment may be influenced by couplings in the loading train and by specimen design. A quantitative assessment of the devices and techniques discussed in this literature is made in those cases where sufficient data have been provided. The literature surveyed indicates that misalignment in carefully designed and precisely machined testing systems ranges between 3 and 15 percent bending. The need for reporting the misalignment at which a given test result is obtained is pointed out.

**16325.** DeSpain, H. E., Garfinkel, S. B., **Calibration of detectors for argon-41,** *Proc. Noble Gases Symp., Las Vegas, NV, Sept. 24-28, 1973,* pp. 155-159 (1973).

Key words: argon; calibration; detector, radioactive argon; ionization chamber; sodium-22; standard reference materials.

Most nuclear reactors produce argon-41 during their operation. For many, it is the largest single gaseous radioisotope released outside the reactor. It is essential, therefore, to know the concentration of this gas — both in working areas for the protection of reactor personnel and in reactor effluents for environmental protection. For this reason, it was important to develop a rapid and easy method to precisely measure the concentration of argon-41, wherever it may be found.

The radioactivity of an irradiated sample of argon was assayed by comparing it to an NBS Standard Reference Material of sodium ($^{22}Na$). The argon-41 was then transferred to an ionization chamber, and an accurate calibration of the response of the ion chamber was made. This chamber was subsequently used to calibrate other detectors, including the stack monitor for the NBS 10 MW heavy-water research reactor. The method used does not require an accurate knowledge of the neutron flux density, cross section, nor volume of gas irradiated for the calibrating samples. Also, the activated argon does not have to be transferred to another container before assaying. Furthermore, this method allows for quick and repeated recalibrations and measurements whenever required. The results to date have been excellent.

**16326.** Mamrak, S. A., **A predictive response time monitor for computer networks,** *Proc. 3d Int. Conf. on Computer Communication, Toronto, Canada, Aug. 3-6, 1976,* pp. 626-630 (1976).

Key words: computer networks; minicomputers; Network Access Machine; network services; response time; response time predictions.

A predictive response time module to assist users of a heterogeneous network of computers is proposed. The network user is able to query this dynamically updated software module to obtain current information relating to the busyness of time sharing systems in the network. In particular, the amount of time required on these systems to run various classes of computing applications is displayed.

The implementation of the module is proposed as an extension of a Network Access Machine (NAM) developed by the Computer Networking Section at the National Bureau of Standards. The NAM is a minicomputer which assists the network user in obtaining network services. The response time module will produce either a narrative description of the general response time characteristics of specified network systems or comparative lists of response times for running short and long FORTRAN, COBOL and BASIC jobs on those systems.

The feasibility of the design and implementation plan was verified by response time measurement experiments conducted on a DEC System-10. A measure of system busyness called "Percent CPU Null Time" was found to be a satisfactorily accurate parameter on which to base response time predictions for the FORTRAN, COBOL and BASIC jobs mentioned above.

**16327.** Lyerla, J. R., Jr., VanderHart, D. L., **$^{13}C$ spin-lattice relaxation studies of perfluoroalkanes,** *J. Am. Chem. Soc.* **98,** No. 7, 1697-1700 (Mar. 31, 1976).

Key words: chemical shift; fluoroalkanes; molecular dynamics; NMR; relaxation.

To obtain information on the rigidity of perfluoroalkanes in the liquid state, $^{13}C$ spin-lattice relaxation times ($T_1$) and $^{13}C-^{19}F$ nuclear Overhauser enhancements (NOE) of individual carbon atoms in liquid $n$-$C_6F_{14}$, $n$-$C_7F_{16}$, and $n$-$C_8F_{18}$ have been measured at 39 °C. Analysis of the relaxation results indicates that the only internal motion occurring on the time scale of overall molecular reorientation is rotation of the $CF_3$ group. Comparison of these results with $n$-alkane relaxation data provides evidence for higher intramolecular rotational potential barriers in the perfluoroalkyl chain. In addition to the relaxation results chemical shifts and resonance assignments are reported for the three perfluoroalkanes as well as 1H-$n$-$C_7F_{15}$.

**16328.** Oettinger, F. F., Blackburn, D. L., Rubin, S., **Thermal characterization of power transistors,** *IEEE Trans. Electron Devices* **ED-23,** No. 8, 831-838 (Aug. 1976).

Key words: current crowding; hot spots; reliability; safe operating area limits; second breakdown; semiconductor devices; thermal resistance; transistor, power.

The idealized concept of thermal resistance as applied to power transistors is discussed. This concept must be used with care because two of the basic assumptions made in applying the concept to these devices are not valid. Contrary to these assumptions, it is shown that 1) the junction temperature of a power transistor is never spatially uniform, and 2) no unique value of thermal resistance can be defined for all operating conditions.

Also, various electrical methods for measuring the junction temperature (thermal resistance) of power transistors are discussed with the emphasis placed on the emitter-only switching measurement technique, which is the preferred standard method of measurement. In addition, the generation and meaning of forward-biased safe-operating-area (SOA) limits are discussed, and it is shown that because of the presence of current crowding and the associated hotspots, the specified SOA limits often permit devices to be operated at dangerously high junction temperatures. Electrical measurement methods capable of determining the peak juntion temperature as well as determining the onset of current crowding are described, and it is shown how these methods might be used for the generation of improved SOA limits.

**16329.** Sibley, E. H., **The development of data-base technology,** *Assoc. Comput. Mach. Comput. Surveys Editorial* **8,** No. 1, 1-5 (Mar. 1976).

Key words: data base; data integration; implementation; modelling; technology; terminology.

Here we attempt an integrated approach to a very disoriented field. Problems abound: differences in terminology, differences in modelling, and differences in implementation confuse the potential user, who is faced with almost unanswerable questions. Such problems are found in any evolving technology, especially when it is associated with a fast developing industry, such as computing; while some appear more philosophical than real, others arise from poor understanding of new concepts. Here we shall try to answer some of the questions and reduce the confusion. But obviously, one issue of Computing Surveys cannot be all encompassing; data technology is a field which already boasts hundreds of articles, and text books by the dozen. Thus this issue confines itself to an explanation of various models of data-base systems, showing their differences and similarities, while trying to relate the models to their implementation in current commercial and experimental systems.

We were faced with one major problem in trying to provide an integrated issue: every model uses its own terminology. We therefore decided to attempt to use both a common terminology and a single example wherever possible. This is by no means a simple task; we must not only define terminology and apply it to descriptions of various models, but also show how these terms differ from those used by others in discussing the same ideas: there is no standard, and we are forced to be arbitrary.

**16330.** Fry, J. P., Sibley, E. H., **Evolution of data-base management systems,** *Assoc. Comput. Mach. Comput. Surveys* **8,** No. 1, 7-42 (Mar. 1976).

Key words: data base; data-base machines; data-base management; data definition; data dictionary; data independence; data manipulation; data model; distributed data base; generalized processing.

This paper deals with the history and definitions common to data-base technology. It delimits the objectives of data-base management systems, discusses important concepts, and defines terminology for use by other papers in this issue, traces the development of data-base systems methodology, gives a uniform example, and presents some trends and issues.

**16331.** Mielenz, K. D., **Comments on spectrometry nomenclature,** *Anal. Chem.* **48,** No. 7, 1093-1094 (June 1976).

Key words: analytical chemistry; nomenclature; photochemistry; photometry; physical optics; radiometry; spectrometry; spectroradiometry.

Several inconsistencies in the nomenclatures used in analytical spectrometry and in physical optics are pointed out. Specific proposals are made to correct these inconsistencies.

**16332.** Stevens, J. G., Travis, J. C., DeVoe, J. R., **Mössbauer spectrometry,** *Anal. Chem.* **44,** No. 5, 384R-406R (Apr. 1972).

Key words: chemical applications; instrumentation; Mössbauer spectrometry; nuclear parameters; recent advances; tables; theory.

A comprehensive review is given of the 1969-70 Mössbauer spectroscopy literature relating to chemistry. The key features of chemical studies are reported in tabular form, and theoretical and instrumental achievements are treated in the textual account. A total of 771 references are cited.

**16333.** Mielenz, K. D., Mavrodineanu, R., Cehelnik, E. D., **Efficient averaging spheres for visible and ultraviolet wavelengths,** *Appl. Opt.* **14,** No. 8, 1940-1947 (Aug. 1975).

Key words: averaging sphere; diffusing effectiveness; efficiency; fluorescent wavelength converter; photometry; spectrophotometry; ultraviolet; visible.

On the basis of a theoretical analysis that identifies the design criteria for optimization of efficiency, an averaging sphere with a barium-sulfate target was constructed that has an efficiency of 80-90 percent in the visible. In spite of the decreased reflectance of the sphere walls in the uv, this sphere is still 30 percent efficient at 300 nm and, thus, can be used for near-uv work. For applications below 300 nm, a cell containing a fluorescent dye is placed inside the sphere in order to shift the incident radiation into the longer wavelength region in which the reflectance of the sphere walls is higher. The use of this fluorescent wavelength converter, which was designed so that the sphere remains usable in the visible, resulted in a sphere efficiency of about 20 percent in the region between 200 nm and 300 nm and 50 percent in the visible. The averaging properties of these spheres were found to be adequate for high-accuracy photometric measurements.

**16334.** Kubota, M., Golightly, D. W., Mavrodineanu, R., **A rapid wire-loop method for determination of lead in paint by atomic absorption spectrometry,** *Appl. Spectrosc.* **30,** No. 1, 56-63 (1976).

Key words: atomic absorption; determination; lead; paint; wire loop.

A simple, rapid method is described for the determination of lead in paint. Lead is extracted from paint chips, or liquid paint, into an acidic aqueous solution. Ten microliters of sample solution is transferred onto a platinum-rhodium wire loop, and the solvent is evaporated by placing the loop in a small resistance heater. The loop then is introduced into a premixed acetylene-air flame, and lead absorption at 283.3 nm is measured. Physical and chemical parameters affecting the accuracy and precision of the method are discussed. Accurate determinations of lead are possible for concentrations ranging from 0.1 to 1 $\mu$g/10 $\mu$l of solution. The wire loop method is adaptable to a simple screening method for analysis of paints in mobile or on-site laboratories.

**16335.** Lawn, B. R., **A model for the wear of brittle solids under fixed abrasive conditions,** *Wear Short Commun.* **33,** 369-372 (1975).

Key words: abrasion; brittle surfaces; chipping fracture; hardness; wear rate.

An explicit model for the wear of brittle surfaces under fixed abrasive conditions is presented in terms of indentation fracture concepts. The predicted wear rate for glass agrees with that observed experimentally to within an order of magnitude. Some implications concerning the parameters which influence the abrasion process, particularly the hardness, are discussed.

**16336.** Powell, F. J., **Trends in heating, ventilating and air-conditioning,** *Proc. 5th CIB Congress on Research into Practice. The Challenge of Application, Paris, France, June 1971*, pp. 646-648 (1971).

Key words: air-conditioning; heating.

The rapid growth of science and technology in recent years has improved the means by which man can control his environment, but it has also created a rising tide of expectations on his part for a better quality of environment. The merging of the means and the desire for better environment is one of the strong current trends with respect to the equipment and systems used for heating and cooling of buildings. This paper describes some of the current efforts and future needs, with special emphasis on the use of a dynamic approach and computers, for promoting this convergence of potential and desire, as a response to the prepared papers on New Trends in Heating and Ventilation for the 5th Congress of CIB.

**16337.** Cassatt, W. A., Yap, W. T., Reed, W. P., Mills, S. A., **Results of measurements on fine particle standard reference materials at NBS,** *Powder Tech.* **13,** 27-31 (1976).

Key words: fine particle standards; particle concentration; particle counting; particle size; particulates; standard reference materials.

The current efforts at the National Bureau of Standards to produce a standard reference material (SRM) for accurate size and concentration measurements in fine particle technology are discussed. Two batches of latex spheres are being characterized as calibration materials for "flow-through" particle counters. The criteria for selecting these materials, and the choice of the packaging techniques are described. The methods of measuring the size of the particles, which will be furnished in aqueous suspension, are discussed along with the measurement data.

**16338.** Garbern, D., Kelly, G. E., **Dynamic efficiency of a gas-fired boiler,** *Proc. Conf. on Improving Efficiency and Performance of HVAC Equipment and Systems for Commercial and Industrial Buildings, Purdue University, Lafayette, IN, Apr. 12-14, 1976, II*, Paper C.1, pp. 330-335 (Purdue Res. Indation, Lafayette, IN, 1976).

Key words: dynamic boiler efficiency; efficiency vs cycling rate; efficiency vs heating load; gas-fired boiler.

The effect of cycling rate and part-load operation on the efficiency of a gas-fired, cast iron, hydronic boiler was examined in the laboratory. The boiler studied has an input rating of 300,000 BTU/hr (316,500 KJ/hr). Experimental curves are presented which show how the measured efficiency varied with the rate of cycling at several different heating loads. It was found that the cycling rate had only a slight effect on the part-load efficiency of the gas-fired boiler.

**16339.** Fong, J. T., Zapas, L. J., **Chemorheology and the mechanical behavior of vulcanized rubbers,** *Trans. Soc. Rheol.* **20:3,** 319-338 (1976).

Key words: anisotropy; chemorheology; degradation; elasticity; finite deformation; incompressible materials; permanent set; polymers; rubbers, viscoelasticity.

The objective of this work is to represent general nonlinear viscoelasticity by a model based on a modified two-network theory. As a basic problem we examine Neubert and Saunders' data (1958) on the permanent set of crosslinked natural rubber samples after heating in a state of pure shear or simple extension. It is evident that the preferred configuration changes with time of heating. Our approach is to associate the preferred configuration with an internal measure of length in an initially isotropic material which becomes anisotropic after heating in a deformed state. Using Ericksen and Rivlin's work (1954) on anisotropic materials and a strain energy function which reduces for isotropic materials to Rivlin and Saunders' function (1951), we show an excellent consistency with the Neubert and Saunders' data. We also show consistency with some more recent data due to Djiauw and Gent (1973).

**16340.** Cram, S. P., Chesler, S. N., **Coupling of high speed plasma chromatography with gas chromatography,** *J. Chromatogr. Sci.* **11,** 391-401 (Aug. 1973).

Key words: chromatography; coupling of high speed plasma; gas chromatography; high speed plasma; plasma.

A gas chromatograph has been coupled to a new rapid scan (20 msec) plasma chromatograph without the use of a molecular separator. The sensitivity, noise, and signal-to-noise ratio for Freons analyzed on the plasma chromatograph were found to be relatively insensitive to changes in the plasma chromatograph carrier and drift gas flow rates, and a unique mass calibration curve for the E-series Freons is reported. The sensitivity of the plasma chromatograph and GC FIDs are compared for Freons and the utility of the plasma chromatograph in identifying GC effluents and peak fractionation is reported. A comparison is made between gas chromatography/plasma chromatography and GC/MS.

**16341.** Dragoo, A. L., **Steady thermocapillary convection cells in liquid drops,** *Proc. Int. Colloquium on Drops and Bubbles, Pasadena, CA, Aug. 28-30, 1974*, pp. 208-226 (1974).

Key words: convection; drops; Marangoni effect; surface tension; thermocapillarity.

A nominally spherical drop is used as a model for a theoretical analysis of thermocapillary convection and for estimates of convective flow rates in "levitated" melts at zero-g. Since in practice temperature fields and the resulting convective flow can be more complicated than the simple vertical temperature gradient and the single vortex ring, respectively, the convective flow arising from a general steady-state temperature field is analyzed. Expressions for the components of a steady velocity field are obtained by adapting the analytical method of Miller and Scriven. The vortex rings are illustrated by means of typical streamlines for the simpler, more symmetric temperature fields. The circulation time is introduced as a measure of the rate of circulation in a convection cell and typical values are given for several materials.

**16342.** Kelnhofer, W. J., Hunt, C. M., Didion, D. A., **Determination of combined air exfiltration and ventilation rates in a nine-story office building,** *Proc. Conf. on Improving Efficiency and Performance of HVAC Equipment and Systems for Commercial and Industrial Buildings, Purdue University, Lafayette, IN, Apr. 12-14, 1976, II, Paper B.4*, pp. 322-328 (Purdue Res. Indation, Lafayette, IN, 1976).

Key words: air infiltration; energy conservation; measurement techniques; ventilation of office buildings.

The sulfur hexaflouride tracer-gas technique, which has been used previously for determining air infiltration rates in residential buildings, was applied to a nine-story office building of modern design. The building has sealed windows with openings only on the first level and on the roof, and is mechanically ventilated with a variable air volume system. Tests were run during the cooling season by introducing the tracer gas into the main trunk of the air supply system and measuring the concentration decay rate in the return air. Infiltration rates were determined with outside air vents open and closed. To check the results, a second independent method was used, which involved direct measurement and calculation of infiltration rates.

**16343.** Schaffer, R., **The development of a clinical reference method for glucose in serum,** *Pure Appl. Chem.* **45,** 75-79 (1976).

Key words: clinical reference method; definitive glucose method; glucose in serum; isotope dilution-mass spectrometry; serum glucose.

The progress achieved as of July 1975 on the development of a clinical reference method for glucose is presented; this effort originated as a subcommittee function of the American Association of Clinical Chemists. The hexokinase glucose-6-phosphate dehydrogenase method for determining glucose was selected as the candidate clinical reference method. Its use in all laboratories performing the round-robin tests has provided high precision values. Its accuracy is being evaluated against the results of isotope dilution-mass spectrometry (ID-MS) as the definitive method for glucose. Work as yet incomplete shows some erratic differences between the ID-MS and the candidate clinical method. More is to be done with ID-MS to ensure the validity of its values before further efforts on the clinical reference method are undertaken.

**16344.** Hertz, H. S., May, W. E., Chesler, S. N., Gump, B. H., **Analysis of μg/kg (ppb) level hydrocarbons in intertidal zone sediments and water by gas chromatography-mass spectrometry,** *Proc. 23d Annual Conf. on Mass Spectrometry and Allied Topics, Houston, TX, May 25-30, 1975,* pp. 663-665 (1975).

Key words: gas chromatography-mass spectrometry; hydrocarbons; petroleum; water pollution.

The low concentration of hydrocarbons anticipated in pollution baseline studies necessitates the development of analytical techniques sensitive at the sub-microgram/kilogram level. Techniques which involve dynamic headspace sampling and subsequent GC/GC-MS analysis have been developed in this laboratory. Sample components are separated from the matrix in a closed system and concentrated on a porous polymer precolumn, free from large amounts of solvent and ready for GC-MS analysis. Applications of this methodology to the identification of μg/kg level hydrocarbons in a baseline study are discussed.

**16345.** Currie, L. A., **The measurement of environmental levels of rare gas nuclides and the treatment of very low-level counting data,** *IEEE Trans. Nucl. Sci.* **NS-19,** No. 1, 119-126 (Feb. 1972).

Key words: argon-37; atmospheric mixing; blank corrections; cosmic ray reactions; effectively zero background; environmental radioactivity; low-level counting statistics; radioactive rare gases; reduced activity.

The radioactive isotopes of the rare gases provide unique geophysical and meteorological information concerning the properties and history of our (atmospheric) environment. The extremely low activity levels, however, require very special methods of measurement, experiment design, and data interpretation.

Following an examination of the decay characteristics and atmospheric abundances of Kr and Ar radioisotopes, the question of experiment planning and data interpretation in the "extreme Poisson" (few counts) region is considered. A reduced activity plot is offered as an aid for making rapid evaluations and decisions in this region. The concept of an effectively zero background is illustrated by means of atmospheric $^{37}$Ar data.

Finally, the problem of the blank is examined, and the merits and deficiencies of three alternative approaches are discussed, again with special emphasis on the measurement of $^{37}$Ar in Nature.

**16346.** Smith, C. N., Placious, R. C., Mills, R. M., **X-ray systems for bomb disarmament,** *NILECJ-STD-0603.00,* 11 pages (U.S. Department of Justice, Law Enforcement Assistance Administration, National Institute of Law Enforcement and Criminal Justice, Washington, DC, June 1975).

Key words: bomb disarmament; explosive; x-ray equipment; performance standard, EOD.

Performance requirements and methods of test have been established for x-ray equipment used for bomb disarmament. Requirements are specified which indicate the equipment's suitability for use in the specified application.

**16347.** Chi, J., **Computer simulation of fossil-fuel-fired boilers,** *Proc. Conf. on Improving Efficiency and Performance of HVAC Equipment and Systems for Commercial and Industrial Buildings, Purdue University, Lafayette, IN, Apr. 12-14, 1976, II, Paper C.2,* pp. 336-346 (Purdue Res. Foundation, Lafayette, IN, 1976).

Key words: boilers; computer simulation; DEPAB (DEsign and Performance Analysis of Boilers); energy saving measures; performance at part load; seasonal efficiency.

After an analytical boiler model is established, which is both an adequate representation of the physical system and capable of reasonably simple mathematical description, governing equations based upon this model are derived. A computer program DEPAB (DEsign and Performance Analysis of Boilers) is then developed to simulate boiler operations. DEPAB is designed to predict the performance of both the gas-fired and oil-fired hydronic boilers. Accuracy of results from computer simulation has been verified by the experimental data on a gas-fired boiler. Verification for the oil-fired boiler will be made in the future, when experimental data become available to the author. Examples are given to illustrate applications of the program to examine quantitatively the effects of design and operating variables on performance and seasonal fuel economy of heating boilers for buildings. It was found that considerable seasonal savings in fuel can often be achieved by performing certain modifications to the existing boilers.

**16348.** Johnson, C. R., **Normality and the numerical range,** *Linear Algebra and Appl.* **15,** 89-94 (1976).

Key words: eigenvector; normal matrix; numerical range; orthogonal; spectrum.

It is well known that if $A$ is an $n$ by $n$ normal matrix, then the numerical range of $A$ is the convex hull of its spectrum. The converse is valid for $n \leq 4$ but not for larger $n$. In this spirit a characterization of normal matrices is given only in terms of the numerical range. Also, a characterization is given of matrices for which the numerical range coincides with the convex hull of the spectrum. A key observation is that the eigenvectors corresponding to any eigenvalue occurring on the boundary of the numerical range must be orthogonal to eigenvectors corresponding to all other eigenvalues.

**16349.** Clifton, J., Frohnsdorff, G., **Polymer-impregnated concretes,** Chapter 12. Special Review in *Cements Research Progress 1975,* pp. 173-196 (American Ceramic Society, Columbus, OH, 1976).

Key words: concrete; concrete-polymer systems; polymers; polymer-impregnated concrete; sulfur-impregnated concrete.

This is a comprehensive literature review on developments in the science and technology of polymer-impregnated concretes, up to December 1975. Altogether 116 references have been reviewed.

**16350.** Evans, J. M., Jr., **The role of standards in integrated manufacturing systems,** (Proc. Twelfth Annual Meeting and Tech. Conf. of the Numerical Control Society, Washington, DC, May 19-21, 1975), Paper in *Progress through Government Education and Industry Cooperation, NC/CAM EXPO 1975*, pp. 211-217 (Numerical Control Society, Inc., Spring Lake, NJ, 1975).

Key words: automation; computer aided manufacturing systems; computer integrated manufacturing systems; interfaces; motivation for standardization; standards.

Computer controlled integrated manufacturing systems offer increases in labor productivity of up to an order of magnitude or more and cost reductions of factors of 2 or 3 or more. Large user industries are building such systems; however, the cost of special engineering and computer programming and the risk involved preclude medium and small firms from gaining these benefits. The role of standards in constructing integrated systems with components from competitive manufacturers is discussed and the NBS program aimed at the development of those standards is reviewed.

**16351.** Gerhold, W. F., McCann, J. P., Williamson, W. E., **Report on corrosion of underground telephone cable shielding materials in soil environment after exposure for four years,** *Proc. NACE Conf., Chicago, IL, Mar. 5-9, 1973*, pp. 1-33 (National Association of Corrosion Engineers, Houston, TX 77027, Mar. 1974).

Key words: metal and plastic composites; metal composites, metals; soil corrosion, telephone cable shields; underground corrosion.

Four-year underground corrosion data on the performance at accepted and experimental telephone cable shielding specimens is tabulated and evaluated. The specimens include bare and coated metals or alloys as well as metallic composites. The specimens were uniformly prepared to expose the outer shielding test material to corrosion in a galvanic coupled and uncoupled condition. A replicate of each exposed cable shielding specimen is removed each year from six soil burial sites. The six soil burial sites are representative of a large segment of the various soil conditions existing in the United States.

**16352.** Gerhold, W. F., McCann, J. P., **Corrosion evaluation of underground telephone cable shielding materials,** (Proc. Int. Corrosion Forum on the Protection and Performance of Materials, Houston, TX, Mar. 22-26, 1976), *Corrosion/76*, Paper No. 31, pp. 31/1-31/62 (1976).

Key words: alloys; corrosion; metallurgically-bonded; metals; plastic-bonded; soils; telephone cables; underground.

Corrosion data is given on the performance of base and plastic coated metals intended for use as cable shields for buried telephone cable. The materials investigated on specially prepared specimens were buried for periods up to six years in six different soil environments. Metals tested included homogeneous plastic-bonded and metallurgically-bonded laminates. Some specimens were exposed bare (uncoated), while others had plastic coatings or other types of coatings on either one or both sides. Metals studied included aluminum, copper, low carbon steel and stainless steel alloys.

**16353.** Ogburn, F., **Metrication and the electroplaters,** *Plat. Surf. Finish*, pp. 669, 672-673 (July 1975).

Key words: electroplating industry, metrication of; metal finishing, metric system for; metrication, electrodeposition; metrication, electroplating; metrication, metal finishing; metric system, electroplating industry.

Under the impetus of American industry, the metric system is well on its way to becoming the dominant system of measurement in the United States. Metrication of the electroplating community will be a result of this and it has already begun. For electroplaters metrication will be relatively easy. Some difficulties are anticipated, but these can largely be avoided with appropriate planning by the AES, NAMF, MFSA, and ASTM.

**16354.** Escalante, E., Gerhold, W. F., **Galvanic coupling of some stressed stainless steels to dissimilar metals underground,** *Am. Soc. Test. Mater. Spec. Tech. Publ. STP* **576,** 81-93 (1976).

Key words: corrosion; galvanic; hydrogen embrittlement; soil; stainless steel; stress; stress-corrosion; underground.

Stainless steels, Type 301 half hard and Type 301 full hard, have been found susceptible to failure by hydrogen embrittlement when stressed as low as 40 percent of their yield strength and cathodically charged above 1 $\mu A/cm^2$ by galvanic coupling to a dissimilar metal in four years of exposure at six underground test sites. However, stainless steels Type 304 and alloys 26Cr-1Mo and 26Cr-6.5Ni were resistant under similar conditions. Failures by stress-corrosion cracking were not observed in any of the materials. Electrochemical measurements made periodically above ground are correlated with the subsequent visual examination of the specimens.

**16355.** Escalante, E., Gerhold, W. F., **The galvanic coupling of some stainless steels to copper—Underground,** (Proc. Corrosion/75, Toronto, Ontario, Canada, Apr. 14-18, 1975), *Mater. Perform.* **14,** No. 10, 16-20 (Oct. 1975).

Key words: copper; corrosion; galvanic corrosion; soil corrosion; stainless steel; underground corrosion.

On site underground tests at 6 widely differing sites were made of 26Cr-6.5Ni, Type 304 (18Cr-8Ni) and Type 409 (less than 11 Cr ferritic) coupled to commercially pure copper. Galvanic current tests were made over 3 to 4 years and retrieved specimens were examined in the laboratory. When exposure conditions made Cu anodic to the stainless, local corrosion was minimized. Pitting occurred on some stainless specimens at some sites. Type 409 pitted more than other alloys and copper was cathodically protected by stainless in some cases. Chloride-containing, poorly aerated soils (400-15,500 ohm cm) in a tidal marsh caused greatest attack. Cu lost 3 mils and pits formed were 1 to 5 mils deep; 409 perforated and lost 30 percent weight at one site and other alloys at the site pitted to less than 30 mils. Data indicate no increase in attack on stainless steels coupled to Cu over that on uncoupled specimens in same environments.

**16356.** Boettinger, W. J., Burdette, H. E., Kuriyama, M., Green, R. E., Jr., **Asymmetric crystal topographic camera,** *Rev. Sci. Instrum.* **47,** No. 8, 906-911 (Aug. 1976).

Key words: asymmetric; diffraction; intensifier; topography; x ray.

The practical aspects of asymmetric crystal topography are described. In this technique, asymmetric Bragg diffraction is utilized to obtain a monochromatic and well collimated x-ray beam large enough to cover the entire area of sample crystals. Thus, the recording of diffracted beams from a sample crystal provides topographic images of the entire sample crystal. Advantages of this technique are simplicity (no scanning device), excellent sensitivity to crystal imperfections (strain fields), and versatility. Information is given on the general alignment of the camera, magnification of the x-ray beam width, preparation of the first crystal, and divergence of the beam due to the first crystal. The practical aspects of this topographic system are demonstrated using thick Cu and Ni crystals of various degrees of perfection. An inexpensive image intensifier is also described, which is used routinely to aid in the alignment of sample crystals.

**16357.** Segransan, P. J., Clark, W. G., Chabret, Y., Carter, G. C., **The Knight shift and nuclear spin relaxation of $^{61}$Ni metal in the paramagnet phase,** *J. Phys. F: Metal Phys. Lett. to Ed.* **6,** No. 5, L153-L156 (1976).

Key words: Knight shift; magnetism; nickel; pulsed NMR; spin lattice relaxation.

Pulsed NMR measurements in a 99.54 at% $^{61}$Ni enriched sample of Ni metal in the paramagnetic phase are reported for a wide range of temperatures (785-1520 K). The Knight shift ($\mathscr{K}$) follows an expected Curie-Weiss law $\mathscr{K}(T)=\mathscr{K}(\infty)+A_K/(T-T_c)$, where $\mathscr{K}(\infty)=(1.48\pm0.05)\%$, $A_k=-(560\pm10)\%$K, and $T_c=(662\pm10)$K. The d spin hyperfine field is found to be $-(108\pm8)$kG per Bohr magneton. The recovery of the magnetization following a comb of saturating pulses is $(150\pm50)\mu$s for the entire temperature range.

**16358.** Schaffer, R., **Calibrator product class standard,** *Proc. of the SAMA Calibrator Product Class Standard Forum and Stability Testing Workshop, Chicago, IL, Mar. 18-19, 1975,* 7 pages (Scientific Apparatus Makers Association, Washington, DC 20036, 1975).

Key words: calibration reference materials; calibrators; clinical control materials; clinical standards; consensus standards; reference materials.

A forum was held on the Product Class Standard for Calibrators. This Product Class Standard is closely derived from a National Committee for Clinical Laboratory Standards standard entitled "Calibration Reference Materials and Control Materials in Clinical Chemistry." The development of the standard was discussed.

**16359.** Corcoran, C. T., Langhoff, P. W., **Polynomial expansions for spectral densities,** *Chem. Phys. Lett.* **41,** No. 3, 609-614 (Aug. 1, 1976).

Key words: electron scattering; moment theory; photoabsorption/ionization; spectral densities.

Modified moments and polynomial expansions are employed in imaging the spectral densities that arise in electron-scattering and photoionization calculations.

**16360.** Evans, A. G., Clifton, J. R., Anderson, E., **The fracture mechanics of mortars,** *Cement Concrete Res.* **6,** No. 4, 535-547 (1976).

Key words: acoustical emission; fracture mechanics; mortars; polymer impregnated mortars; slow crack growth.

A fracture mechanics study of plain and polymer impregnated mortars has shown that the (slow and rapid) macrocrack propagation resistance of these materials is not significantly affected by mortar processing variables, such as water/cement ratio and curing time, but is strongly enhanced by polymer impregnation. Acoustic emission measurements have indicated the important role of microcracking in the fracture of both plain and impregnated mortars; with the susceptibility to microcracking being substantially retarded by polymer impregnation.

**16361.** Slater, J. A., **Data systems and fire casualty information,** *Proc. First Conf. and Workshop on Fire Casualties, Johns Hopkins University Applied Physics Laboratory, Laurel, MD, May 28-29, 1975,* pp. 158-171 (Apr. 1976).

Key words: accident data; data systems; fabric flammability; FFACTS; fire accidents; fire data systems; fire hazards; fires; hazard analysis; NEISS; plastics flammability; product safety.

Four data systems are described in terms of their inputs and outputs. Each contains fire-related information which has been collected from all over the United States and is or will be computerized. All the systems are maintained by Federal Government agencies. The National Electronic Injury Surveillance System (NEISS) was developed by the Consumer Product Safety Commission. Based on a statistical sample of hospitals, NEISS includes data on fire-related injuries from consumer products. The National Fire Prevention and Control Administration is developing a National Fire Data System which will incorporate fire data from many sources such as the National Center for Health Statistics, fire incident reports and a national household fire survey. The Flammable Fabrics Accident Case and Testing System and the Plastics Fire Accident Case and Testing System were developed at the National Bureau of Standards in order to study, in-depth, fabric and plastics fire accidents. Both involve field investigations of fires, preparation of detailed case histories and retrieval, analysis and testing of samples. A possible conceptual framework developed by Bryan for analyzing fire data is briefly discussed.

**16362.** Lias, S. G., **Charge transfer to hydrogen halide and halogen molecules from atomic and diatomic ions,** *Int. J. Mass Spectrom. Ion Phys.* **20,** 123-137 (1976).

Key words: charge transfer; H-atom transfer reactions; hydrogen halides; ion molecule reactions; ion cyclotron spectrometry; rate coefficients.

The charge transfer from $Xe^+$, $Kr^+$, and $Ar^+$ to HI, HBr, HCl, $Br_2$, and $Cl_2$ and from $O_2^+$ and $N_2^+$ to HI, HBr, and HCl have been investigated. None of these reactant pairs undergoes a fast charge-transfer reaction. The probability of charge transfer for a given ion-molecule pair depends on the existence of a matching between the recombination energy of the reactant ion and energy level of the product ion. No effect of Franck-Condon factors on the probability of charge transfer could be inferred from these results.

The $Kr^+$, $Ar^+$, and $N_2^+$ ions also undergo the alternate reaction, $M^+ + HX \rightarrow MH^+ + X$, with the hydrogen halides, in competition with charge transfer. Except when charge transfer is favorable, the rate of this reaction is proportional to the reaction exothermicity.

A few preliminary results on the reactions of $Xe^{2+}$, $Kr^{2+}$, and $Ar^{2+}$ ions with hydrogen halides and halogens are also reported.

**16363.** Buehler, M. G., Phillips, W. E., **A study of the gold acceptor in a silicon *$p^+n$* junction and an *n*-type MOS capacitor by thermally stimulated current and capacitance measurements,** *Solid-State Electron.* **19,** 777-788 (1976).

Key words: gold-doped silicon; measurement methods; MOS capacitor; *p-n* junction; semiconductor defects; silicon; thermally stimulated capacitance; thermally stimulated current.

The thermally stimulated current and capacitance responses of a gold doped $p^+n$ junction and *n*-type MOS capacitor were measured experimentally and modeled theoretically for the case of majority-carrier defect charging. The gold acceptor atoms are initially charged with electrons at low temperatures, and during the heating cycle, excess electrons are released from the gold atoms. The thermally stimulated current response for this phase is similar in both structures and has a distinctive peak-and-valley shape and an emission temperature about 220 K. During the steady-state phase, a current peak occurs in the MOS capacitance response. A physical model was developed and the influence of various parameters on the current and capacitance measurements was quantified. Various analytical schemes are described which allow rapid identification of the gold defect center and rapid computation of its density. A simple and inexpensive apparatus is described which is capable of heating rates as high as 10 K/s.

**16364.** Garvin, D., Hampson, R. F., Jr., **Evaluated numerical data for the SST and chlorofluorocarbon problems: A case study of how to help the engineer and the modellers,** (Proc. AGARD Conf., Washington, DC, Oct. 20-21, 1976), Paper in *AGARD Conference Preprint* **207** *on Advancement in Retrieval Technology as Related to Information Systems*, pp. 13-1 – 13-6 (National Aeronautics and Space Administration, Attn.: Reports Distribution and Storage Unit, Langley Field, VA 23365, 1976).

Key words: chemical kinetics; data center operation; information analysis center; photochemistry; stratospheric chemistry.

Mathematical simulations (models) of the stratosphere have been a primary tool in the analysis of potential pollution of the stratosphere from high-flying aircraft, rockets and the release of organic chlorine compounds at the surface of the earth. These models require large amounts of numerical data about the meteorology and chemistry. The chemical data comes from laboratory measurements and must be interpreted and made available to the user community in an understandable form and, preferably, as recommended values.

How chemical data were supplied to the Climatic Impact Assessment Program of the U.S. Department of Transportation is described here with emphasis on the role played by the Chemical Kinetics Information Center of the National Bureau of Standards. This included planning, identification of needed measurements and available measurements, determination of the needs of users, evaluation of data, interpretation of results for nonspecialists and distribution of tables of rate data. This type of role is suitable for an information analysis center in any large scale interdisciplinary program.

**16365.** Scheer, M. D., **Processes for converting coal to clean synthetic fuels and their dependence on catalytic materials,** (Proc. Ceramic Materials in High Temperature Gases on Materials Problems and Research Opportunities in Coal Conversion, Columbus, OH, Apr. 16-18, 1974), Paper in *Materials Problems and Research Opportunities in Coal Conversion* **2**, 300-312 (The Department of Metallurgical Engineering, The Ohio State University, Columbus, OH, 1975).

Key words: aromatic asphaltenes; caking; coal gasification; liquefaction processes.

Coal gasification is the chemical transformation of solid coal into a gas which can be ultimately reacted to produce methane which is free of sulfur compounds and contains little or no carbon monoxide and hydrogen. A typical process begins with the preparation of a coal powder whose particles are surface oxidized with air or oxygen so as to reduce its caking properties and hence prevent the plugging of reactor units.

Liquid fuels synthesized from coal will be needed to fulfill the requirements for these essential and conveniently transportable sources of energy. The technical requirements are numerous; coal must be liquefied; ash, S, N, and O removed; hydrogen produced from water and added to convert the aromatic asphaltenes to simpler aromatic which must then be cracked and reformed to produce acceptable gasolines.

**16366.** Odell, G. B., Schaffer, R., Simopoulos, A. P., Eds., **Phototherapy in the newborn: An overview,** 196 pages (Printing and Publishing Office, National Academy of Sciences, Washington, DC, 1974).

Key words: bilirubin; brain damage; hyperbilirubinemia; neonatal hyperbilirubinemia; phototherapy.

The book contains selected papers from a symposium held February 12-13, 1973 in Washington under the sponsorship of the Committee on Phototherapy of the Newborn, Assembly of Life Sciences, National Research Council. The papers concern the use of light as a therapeutic modality for hyperbilirubinemia in the newborn infant. Subjects considered are: The Radiometry of Phototherapy, Photooxidation, *In Vitro* Photooxidation Products of Bilirubin, The Photochemistry and Photometabolism of Bilirubin, Studies on the Mechanism of Phototherapy in the Congenitally Jaundiced Rat, Toxicity and Protein Binding of Biliverdin and Other Bile Pigments, Methods for Measurement of the Relative Saturation of Serum Albumin with Bilirubin in the Management of Neonatal Hyperbilirubinemia, Bilirubin-Dependent Brain Damage: Incidence and Indications for Treatment, Immediate and Long-Term Effects of Phototherapy on Preterm Infants, Effects of Light on Man, Circadian Rhythms, Important Considerations in the Clinical Management of Infants with Hyperbilirubinemia.

**16367.** Quindry, T. L., **Sound sensing units for intrusion alarm systems,** *NILECJ-STD-0308.00*, 22 pages (U.S. Department of Justice, Law Enforcement Assistance Administration, National Institute of Law Enforcement and Criminal Justice, Washington, DC, July 1976).

Key words: alarm; audio alarm; burglar alarm; intrusion alarm; intrusion detector; sound sensing; standard.

This standard establishes performance criteria for sound sensing alarms intended for use in protective intrusion systems to monitor for attempts to enter a room or building. These devices cause the initiation of an alarm signal to a police panel, central station, or local audible alarm device. Included are requirements and test methods for performance, electrical properties and materials. The characteristics addressed are those which affect the reliability of the devices with emphasis on those performance characteristics which affect their false alarm susceptibility and its tamper resistance.

**16368.** Dobbyn, R. C., **Selection guide to hearing protectors for use on firing ranges,** *NILECJ-GUIDE-0101.00*, 24 pages (U.S. Department of Justice, Law Enforcement Assistance Administration, National Institute of Law Enforcement and Criminal Justice, Washington, DC, Apr. 1976).

Key words: earmuffs; earplugs; gunfire noise; hearing damage; hearing protectors; law enforcement equipment.

This guide discusses the hazard of gunfire-noise-induced hearing damage and the use of hearing protectors to guard against this hazard. Its purpose is to provide the shooter with an appreciation of the seriousness of the problem and a basis for the selection of a suitable hearing protector. Maximum permissible noise exposure levels are discussed in terms of the noise produced by firearms and the several damage-risk criteria which have been proposed. The guide concludes with a listing of currently-available hearing protectors and their noise attenuation properties.

**16369.** Robertson, E., Fechter, J. V., **Directory of security consultants,** *LESP-RPT-0309.00*, 64 pages (U.S. Department of Justice, Law Enforcement Assistance Administration, National Institute of Law Enforcement and Criminal Justice, Washington, DC, Oct. 1975).

Key words: burglary; consultants; crimes of opportunity; directory, (security); investigations; law enforcement; resources; security; shoplifting; theft.

This directory presents brief summaries of the capabilities and past experience of security resources available to assist consumers in solving their security problems. Effective application of information provided by these resources should produce reduced crime rates. Individual listings present a brief digest of the background, past activities and specialization of each resource – based on information provided to this project. Presentations were separated into three categories: private consultants; consultants associated with colleges or universities; and specialized resources – associations, institutes, schools, authors, and publishers or film producers concentrating in the security field. Material is provided for information purposes only and does not constitute endorsement by the Federal government.

**16370.** Kilmer, R. D., Leasure, W. A., Jr., Corley, D. M., Mathews, D. E., Shoemaker, C. O., Jr., **Truck noise 1-D: Empirical model for predicting in-service truck tire noise levels,** *Report No. DOT-TST-76T-5*, 65 pages (Available from the National Technical Information Service, Springfield, VA 22161, July 1976).

Key words: acoustics; noise measurement; noise (sound); tire noise; transportation noise; truck.

SAE Recommended Practice J57 – Sound Level of Highway Truck Tires – specifies a simple, practical noise certification test procedure for tires which results in a single-number rating – maximum A-weighted sound level – of the coastby sound level measured according to prescribed procedures. Such a rating by itself, however, does not allow prediction of in-service noise levels. This report discusses the basic assumptions and necessary input data for a DOT/NBS developed empirical model which utilizes the certification test results to predict in-service noise levels. The usefulness and expected accuracy of the predictive model are shown through a comparison of measured versus predicted maximum A-weighted sound levels for a variety of truck/tire combinations.

**16371.** Berger, H., Parker, W. L., Lapinski, N. P., Reimann, K. J., **Three-dimensional inspection by thermal-neutron laminagraphy,** *Trans. American Nuclear Society 1976 Annual Meeting, Toronto, Canada, June 14-18, 1976*, pp. 115-116 (1976).

Key words: complex object; laminagraphy; multiple-film; radiographic inspection; thermal neutrons; three-dimensional.

Multiple-film laminagraphy is demonstrated with thermal neutron radiographic inspection of a thick object. Radiographic views from several angular orientations are taken and superimposed to bring a desired image plane into focus. The angular views are obtained from the rotational movement of the object-detector assembly in contrast to the conventional translational source movement. The test object was a simulated EBR-II fast reactor fuel subassembly.

**16372.** Sengers, J. M. H. L., **Critical exponents at the turn of the century,** *Physica* **82A,** 319-351 (1976).

Key words: coexistence curves; critical exponents; fluid critical point; history; Kamerlingh Onnes collection; surface tension; Van der Waals collection; Verschaffelt.

The notion of a critical exponent was first used by Van der Waals in 1893 for describing the critical behavior of the surface tension. He also noticed in the early 1890's that experimental data on capillarity indicated a nonclassical value for the surface tension exponent. Verschaffelt found that this was due to the fact that the coexistence curve exponent beta was nonclassical. In 1900, he established precise nonclassical values for the exponents beta and delta. Even though from this time onwards the "cubic law" for fluid coexistence curves was accepted, the true implication of Verschaffelt's results, namely the failure of classical theory, was not appreciated. Some reasons for this lack of impact will be given.

**16373.** Boettinger, W. J., Burdette, H. E., Kuriyama, M., **Application of contrast conditions to dynamical images of immobile dislocations,** *Philos. Mag.* **34,** No. 1, 119-127 (1976).

Key words: contrast conditions; dynamical images; immobile dislocations; Lomer locks; sessile dislocations; x-ray dynamical diffraction; x-ray topography.

In x-ray topography, the Burgers vector of a dislocation is usually determined by finding those diffracting planes for which the image of the dislocation becomes invisible. The conditions $\mathbf{H}\cdot\mathbf{b}=0$ and $\mathbf{H}\cdot\mathbf{b}\times\mathbf{n}=0$ would then be applied to determine the Burgers vector. In this paper, these conditions of invisibility have been applied to a particular pattern of straight line images observed by Borrmann disruption in thick crystals ($\mu L > 15$) using many diffracting planes. It is found that the condition $\mathbf{H}\cdot\mathbf{b}=0$ alone is sufficient to determine that the images are caused by Lomer sessile edge dislocations. Furthermore, it is found that the condition $\mathbf{H}\cdot\mathbf{b}\times\mathbf{n}=0$ was not necessary to predict the invisibility of these images. This fact is attributed to the complexities of image formation by dynamical diffraction in imperfect crystals.

**16374.** Kulin, G., **Discussion of "sediment transport in smooth fixed bed channels" by P. Novak and C. Nalluri,** *J. Hydraul. Div. Proc. Am. Soc. Civ. Eng.* **102,** HY10, 1601-1602 (Oct. 1976).

Key words: grit; sand transport; sewage sand; sewer self-cleansing.

Design criteria for self-cleansing sewer flow are examined in the light of available experimental results on sand transport in open-channel flow in circular pipes.

**16375.** Block, S., Piermarini, G., **The diamond cell stimulates high-pressure research,** *Phys. Today*, pp. 44-47, 50-52, 54-55 (Sept. 1976).

Key words: diamond cell; electrical resistance; high pressure; nuclear decay; pressure calibrations; spectroscopy; x-ray diffraction.

This article is a general discussion of the diamond-anvil high pressure cell and includes a description of the instrument and the ruby fluorescence method of measuring pressure. It also discusses some of the important aspects in the development of the cell which ultimately led to the production of megabar pressures. A survey is made of what has been done already in this rapidly expanding area of research and includes a discussion of some new opportunities which show great potential.

**16376.** Hougen, J. T., **Methane symmetry operations,** Chapter 3 in *International Review of Science, Spectroscopy, Physical Chemistry Series Two*, A. D. Buckingham and D. A. Ramsay, Eds., **3,** 75-125 (Butterworth & Co., Ltd., Boston, MA, 1976).

Key words: energy levels; hyperfine interactions; methane; selection rules; symmetry species; tetrahedral.

This article provides a consistent, pedagogically convenient, and explicit treatment of symmetry properties in the $CH_4$ molecule, including a unified discussion of the permutation-inversion molecular symmetry group ideas of Longuet-Higgins and the more traditional crystallographic point group symmetry ideas. It attempts initially to discuss symmetry properties associated with the spherical-top point group $T_d$ by drawing on the more familiar symmetry properties associated with the $D_{2d}$ symmetric-top subgroup of $T_d$. Although three different $T_d$ symmetry classification schemes are widely used at present in the methane literature, strong arguments are presented favoring the present scheme. Illustrative references are included from the various schools of thought on theoretical matters, and from the different schools of recent experimental work on $CH_4$ vibrational, rotational, and hyperfine energy levels.

**16377.** Field, B. F., Hesterman, V. W., **Josephson junction based voltage standard,** *Proc. Fifth Cal Poly Measurement Science Conf., San Luis Obispo, CA, Dec. 5-6, 1975,* 5 pages (California Polytechnic State University, San Luis Obispo, CA 93407, 1975).

Key words: cryogenic; Josephson junction; standard cell; voltage reference.

An instrument is described that is designed to calibrate cadmium-sulfate (Weston) standard cells to an accuracy (3 $\sigma$) of 1 ppm or better. This instrument can replace the involved procedures, equipment and calibrations presently used to maintain a unit of voltage in many standards laboratories. A Josephson tunnel junction operating at cryogenic temperatures is used as a time-invariant reference for a special potentiometer which directly measures the emf of a standard cell. The instrument is easy to use and requires an infrequent frequency calibration.

**16378.** Cooper, J. W., **The single electron model in photoionization,** (Lecture delivered at the NATO Advanced Study Institute, Carry-le-Rouet, France, Aug. 31-Sept. 13, 1975), Paper in *Photoionization and Other Probes of Many-Electron Interactions,* F. J. Wuilleumier, Ed., pp. 31-47 (Plenum Press, Inc., New York, NY, 1975).

Key words: Hartree-Fock methods; oscillator strength; photoionization; single electron.

The theory of atomic photoionization is developed in a way to show the connections between single-electron and many-body theories.

**16379.** Langhoff, P. W., Corcoran, C. T., Sims, J. S., Weinhold, F., Glover, R. M., **Moment-theory investigations of photoabsorption and dispersion profiles in atoms and ions,** *Phys. Rev. A* **14,** No. 3, 1042-1056 (Sept. 1976).

Key words: atomic spectroscopy; dispersion; photoabsorption; refractive index.

Moment-theory methods for the construction of photoabsorption and dispersion profiles from associated dipole spectral moments are described and applied to simple atoms and ions. A previously devised (Stieltjes) moment approach, which provides convergent histogram approximations to absorption and dispersion profiles, is refined and extended to the use of arbitrarily large numbers of spectral moments, and an improved (Tchebycheff) moment approach is introduced which gives profiles that are continuous in the photoionization region and exhibit the δ-function-like behavior associated with discrete transitions at the appropriate frequencies. Recurrence relations for the polynomials orthogonal and quasiorthogonal with respect to the distributions are employed in solving the necessary moment problems involving large numbers of spectral moments. The methods are applied in illustrative calculations of absorption and dispersion profiles in one- and two-electron atoms and ions. In the case of one-electron atomic systems the necessary polynomial recurrence coefficients are obtained in closed form from the known spectral moments, allowing the construction of distributions which reproduce the known profiles with high accuracy, employing as many as 100 spectral moments. Variational calculations using large basis sets of square-integrable functions, including the special functions required to satisfy sum rules, provide accurate spectral moments for atomic helium and the negative hydrogen ion. A simple moment-extension procedure is devised to interpolate the associated recurrence coefficients to infinite order employing their known asymptotic values. The associated Stieltjes and Tchebycheff approximations to the absorption and dispersion profiles obtained in these cases are in excellent agreement with available measurements and previous accurate calculations employing discrete and continuum wave functions.

**16380.** Hall, J. L., Lee, S. A., **Interferometric real-time display of cw dye laser wavelength with sub-Doppler accuracy,** *Appl. Phys. Lett.* **29,** No. 6, 367-369 (Sept. 15, 1976).

Key words: interferometer, fringe counting; real-time display.

We describe an automatic fringe-counting interferometer with real-time wavelength readout for cw laser sources. Sub-Doppler absolute wavelength accuracy ($\sim 2 \times 10^{-7}$) is demonstrated with saturated absorption spectroscopy in neon.

**16381.** Kahler, R. L., Hillhouse, D. L., Anderson, W. E., **A simple overcurrent protection circuit for a high voltage laboratory,** *IEEE Trans. Instrum. Meas.* **IM-25,** No. 2, 161-162 (June 1976).

Key words: high voltage transformer protection; overcurrent; overcurrent protection; solid-state overcurrent protection circuit; transformer; transformer overcurrent protection.

A system for safeguarding a moderate power high-voltage laboratory against transformer overcurrents following insulation failures in test objects is described. It is simple, requiring the construction of only two solid-state control circuits and the modification of a commercially available solid-state contactor. It has been tested successfully with simulated breakdowns at up to 50-kV rms, 60 Hz with a 50-kVA load.

**16382.** Hartman, A. W., **A step height interferometer with one nanometer resolution,** *Opt. Eng.* **15,** No. 2, 180-183, 363 (Mar.-Apr. 1976).

Key words: interferometer; polarization; step height.

An interferometer is described for the measurement of thin film steps. The instrument is a double-pass polarization interferometer and has a resolution of one nanometer. It is self-contained and features simplicity in construction and operation. Measurements illustrating its performance are given.

**16383.** Brandon, D. G., Melmed, A. J., **FIM analysis of dislocation core structure,** *J. Micros.* **100,** Pt. 1, 7 pages (Jan. 1974).

Key words: core structure; dislocation core structure; FIM analysis.

A direct colour superposition technique has been used to study two dislocations in W, using He field-ion imaging at 77 K. Limitations due to instrumentation and field-ion microscopy are discussed. A single spiral and a double spiral on (112) W were each dissected, by field evaporation, through three successive atom layers, and apparent core shapes and dimensions were determined. The shapes were irregular with diameters of at most 0·5-2 nm for the single spiral and 0·5-1·7 nm for the double spiral. Observed displacements in the positions of the core regions may be associated with dislocation movement induced by the high electric field needed for the observations.

16384. Misakian, M., Hebner, R. E., Jr., **Kerr coefficients of polychlorinated biphenyls and chlorinated naphthalene,** *J. Appl. Phys.* **47,** No. 9, 4052-4055 (Sept. 1976).

Key words: Aroclor; chlorinated biphenyl; chlorinated naphthalene; electric field measurement; electro-optic; high voltage measurement; Kerr coefficients; Kerr effect; space charge.

The electro-optic Kerr coefficients of two polychlorinated biphenyls and chlorinated naphthalene have been measured to an accuracy of $\pm 7$ percent using a comparative technique. Physical properties of the fluids relevant to application in electro-optic devices are discussed.

16385. Goldberg, R. N., **Thermodynamics of hexokinase catalyzed reactions. II. Measurement and calculation of enthalpies of reaction as a function of magnesium ion concentration,** *Biophys. Chem.* **4,** 215-221 (1976).

Key words: adenosine 5′-triphosphate; biochemistry; coupled equilibrium; enzyme catalyzed reactions; glucose; heat measurement; hexokinase; magnesium; metabolic processes; microcalorimetry; thermochemistry; thermodynamics.

Enthalpies of phosphorylation of glucose by adenosine 5′-triphosphate have been measured as a function of concentrations of magnesium chloride in TRIS/TRIS·HCl buffer in the pH range 8.64 to 8.98. These measurements are compared with the results of calculations of these enthalpies that use a coupled equilibrium formalism with equilibrium data and enthalpy values selected from the literature. The experimental results span the range of magnesium ion concentrations $1\times10^{-6}$ to 0.3 mol $l^{-1}$ and show a total variation in the enthalpy of reaction of almost 10 kJ mol$^{-1}$· with the most exothermic reaction occurring at a magnesium ion concentration of $6.0\times10^{-4}$ mol $l^{-1}$. The calculated enthalpies of reaction, except for the magnesium ion concentration range $4\times10^{-6}$ to $5\times10^{-4}$ mol $l^{-1}$, are, within estimated uncertainty intervals (0.8 to 10.2 kJ mol$^{-1}$), in agreement with the measured values.

16386. Cooper, J. W., Manson, S. T., **Photo-ionization in the soft x-ray range: Angular distributions of photoelectrons and interpretation in terms of subshell structure,** *Phys. Rev.* **177,** No. 1, 157-163 (Jan. 5, 1969).

Key words: angular distribution; photoabsorption; soft x rays; subshell structure.

The problem of determining the individual subshell contributions in atomic photoabsorption is discussed. The general form of the angular distribution of photoelectrons in the soft x-ray range for polarized incident photons is considered. Calculations of the subshell contributions within a central-field model and the angular distribution of electrons from these contributions for photoabsorption in Kr in the energy range 200-1500 eV are presented and found to show good agreement with the experimental results of the preceding paper.

16387. Swanson, K. R., Spijkerman, J. J., **Analysis of thin surface layers by Fe-57 Mössbauer backscattering spectrometry,** *J. Appl. Phys.* **41,** No. 7, 3155-3158 (June 1970).

Key words: backscattering measurements; Fe-57 Mössbauer spectra; Mössbauer spectra.

Fe-57 Mössbauer spectra for extremely thin surface layers (600-3000 Å) were obtained by detecting internal conversion electrons emitted after resonant absorption. The sample was placed inside a proportional counter specially designed for Mössbauer backscattering measurements. Helium-10% methane flowgas was used to detect the conversion electrons. It is estimated from the observed spectra that this technique can be used to obtain Mössbauer backscattering spectra for iron-containing surface layers 50-3000 Å thick. Backscattering spectra for thicker surface layers (0.2-0.5 mil) were obtained by merely changing to an argon-10% methane flow-gas mixture and counting the 6.3-keV internal conversion x rays rather than conversion electrons.

16388. Rutherford, W. M., Evans, J., Currie, L. A., **Isotopic enrichment and pulse shape discrimination for measurement of atmospheric Argon-37,** *Anal. Chem.* **48,** No. 3, 607-612 (Mar. 1976).

Key words: atmospheric mixing; atmospheric radioactivity; cosmic ray reactions; isotopic enrichment; $^{37}$Ar.

High sensitivity measurements of cosmic-ray-produced $^{37}$Ar from the Southern Hemisphere have been completed with the aid of thermal diffusion isotopic enrichment and low-level proportional counting with rise-time circuitry. Thermal diffusion proved to be an excellent means for increasing the very low natural specific activity of $^{37}$Ar. Good enrichment factors ($\sim$70) were achieved in a period ($\sim$6 days) significantly less than the half-life (35.1 days) of $^{37}$Ar. Results for Southern Hemisphere samples confirmed that the measurement process was sufficiently sensitive to quantitatively determine the natural, troposphere levels of $^{37}$Ar, but they suggested the possibility of some contamination of the Southern Hemisphere $^{37}$Ar from artificial sources.

16389. Shier, D. R., **Iterative methods for determining the k shortest paths in a network,** *Networks* **6,** No. 3, 205-229 (July 1976).

Key words: iterative methods; k best paths; linear equations; network algorithms; networks; shortest paths.

This paper presents and develops an algebraic structure for determining the k shortest paths from a given node to all other nodes of a network. Three new methods for calculating such k shortest path information are examined and compared. These methods are based on a fairly strong analogy which exists between the solution of such network problems and traditional techniques for solving linear equations. On the basis of both theoretical and computational evidence, one of the three methods is seen to offer an extremely effective procedure for finding the k shortest paths from a given node in a network.

16390. Lowe, T. C., **Computer security safeguards for privacy: The technical role of NBS,** *Bull. Am. Soc. Inf. Sci.* **3,** No. 1, 16-18 (Oct. 1976).

Key words: data confidentiality; data integrity; encryption; personal identification; privacy; record identification; risk analysis; security.

The paper describes selected projects under the NBS Computer Security Program that relate to the protection of personal privacy, and has been prepared in the format and style of the American Society for Information Sciences' *Bulletin.* This is ASIS' popular publication, as opposed to the more scholarly *Journal.*

16391. Johnson, C. E., Ogburn, F., **Hardness of heat treated electroless nickel,** *Surf. Technol.* **4,** 161-172 (1976).

Key words: auto-catalytic; auto-catalytic nickel; electroless; electroless nickel, hardness of; nickel; nickel-phosphorus alloy, wear of.

The hardness measurements of electroless nickel-phosphorus deposits are reported for compositions of 2.8-12.6 wt.% phosphorus. The hardness measurements were made on as-plated samples and after heat treatments covering a wide range of time and temperature.

As-plated hardness decreases with increasing phosphorus content up to 7-8 wt.% and then remains constant. After 9 hours at 200 °C, the hardness decreases with increasing phosphorus. Heat treatments at 400 °C and above result in hardnesses that depend on composition, time of heat treatment, and temperature of heat treatment. Qualitatively, the relationship is what one would expect for precipitation hardening.

**16392.** Heinrich, K. F. J., **Fluorescence excited by the continuum and the accuracy of electron probe microanalysis, (Extended Abstract),** *Proc. 10th Annual Conf. of the Microbeam Analysis Society, Las Vegas, NV, Aug. 11–15, 1975,* 7 pages (1975).

Key words: accuracy; continuum radiation; electron probe microanalysis; fluorescent excitation.

**16393.** Grabner, L., **Isoelectronic donor iodine and broad-band photoluminescence in TlBr,** *Phys. Rev. B* **14,** No. 6, 2514-2519 (Sept. 15, 1976).

Key words: isoelectronic systems; TlBr.

Two different experiments on nominally undoped crystals of TlBr (indirect band gap 2.670 eV) are reported: thermal quenching of the emission bands between 2 and 100 K, and the dependence of relative intensity of emission bands on exciting intensity, at 2 K. Both support unexpectedly small binding energies, of $\sim$10 MeV, for electrons and holes to residual impurities. These emit broad (0.25 eV) structureless bands at 1.80, 2.20, and 2.43 eV, and are therefore expected to originate in tightly bound centers. Their origin is known only for the 2.20-eV band, which is due to the recombination of an exciton bound to the isolectronic impurity iodine. Thermal quenching of the emission bands shows two activation energies for the 2.20-eV band. These are identified with a binding energy of 37 MeV for the hole to the iodine, and 2 MeV for that of the electron to the system (iodine-hole). For the 2.43-eV band a single activation energy of 4 MeV is identified with the binding energy of an exciton to an unknown defect. Other isolectronic systems are compared with TlBr:I. Their possible connection with induced infrared absorption is suggested. Finally, the direct edge emission found in TlBr in the vicinity of 3.000 eV is discussed, and found to be anomalous in view of recent results showing its band gap to be indirect.

**16394.** Page, C. H., **What is weight?,** *Am. J. Phys.* **43,** No. 10, 920-921 (Oct. 1975).

Key words: force; kilogram; mass; pound; weight.

The common use of the term "weight" to denote either a mass or a force is discussed. It is shown that there is no acceptable *precise* definition of weight for moving objects. The conclusion is that a restriction on the use of "weight" to mean only a force that is measurable in certain specific situations is not justified, and, furthermore, would not only be unsuccessful but would hinder general acceptance of the metric system.

**16395.** Page, C. H., **Ambiguities in the use of unit names,** *Science* **179,** 873-875 (Mar. 2, 1973).

Key words: gyromagnetic ratio; measurement units; physical constants; SI units.

The SI concerns abstract idealized units; actual measurements are made in terms of laboratory standards. Reassignment of the value of a particular standard implies adjustments of published data, but the necessary adjustments are *not* deducible from the SI unit names attached to the data. Experimental determinations of physical constants should be reported in terms of the measurement units and standards actually used.

**16396.** Morrissey, B. W., Smith, L. E., Stromberg, R. R., Fenstermaker, C. A., **Ellipsometric investigation of the effect of potential on blood protein conformation and adsorbance,** *J. Colloid Interface Sci.* **56,** No. 3, 557-563 (Sept. 1976).

Key words: blood protein adsorption; conformation adsorbed proteins; ellipsometry; surface potential.

The possible relationship between the surface charge of an implant material and intravascular thrombosis has long been explored. In order to characterize the effect of potential on protein-surface interactions, ellipsometric measurements have been carried out *in situ* to determine the conformation and adsorbance of fibrinogen, $\gamma$-globulin, and serum albumin adsorbed on platinum and germanium for a range of imposed potentials.

On platinum at pH 7.4, fibrinogen, $\gamma$-globulin, and serum albumin all exhibited a reproducible "onset" potential, at which enhanced adsorption occurred. The adsorbance for all three proteins was unchanged from the rest potential value as the applied potential became more anodic until the onset potential was reached. Desorption, as a result of changes in applied potential, was not observed for any protein studied. The adsorbed conformation of all three proteins changed reversibly at moderately cathodic potentials as indicated, for example, by a sharp increase in extension at $-0.2$ V/SCE. The extension decreased as the imposed potential became progressively anodic. Germanium was found to be unsuitable for these ellipsometric studies due to etching of the surface by the 0.15 *M* NaCl immersion medium.

**16397.** Blevin, W. R., Steiner, B., **Redefinition of the candela and the lumen,** *Metrologia* **11,** 97-104 (1975).

Key words: candela; lumen; luminous flux; luminous intensity; photometry; SI basic unit.

It is proposed that the basic photometric unit be redefined so as to provide an exact numerical relationship between it and the SI unit of power, the watt, for a specified monochromatic radiation; and (2) that the unit of luminous intensity, the candela, be replaced as the basic unit by the unit of luminous flux, the lumen. It is claimed that the existing definitions are predominantly the product of early photometric practices that have been superseded. A closer link between photometry and spectroradiometry is now desirable. The proposals would enable photometric values to be derived from spectroradiometric data by exact computation, and would remove the need for a primary standard of light. They would not alter significantly the present magnitudes of the photometric units, nor change the existing relationship between photometry and visual perception. Because the proposed redefinitions are in terms of monochromatic rather than complex radiation, however, they would provide a more convenient basis for the future adoption of new spectral weighting procedures.

**16398.** Madey, T. E., Czyzewski, J. J., Yates, J. T., Jr., **Ion angular distributions in electron stimulated desorption: Oxygen and CO on W(111),** *Surf. Sci.* **57,** 580-590 (1976).

Key words: carbon monoxide; chemisorption; electron stimulated desorption; ion angular distribution; oxygen; tungsten.

The ion angular distributions resulting from electron stimulated desorption (ESD) of oxygen and carbon monoxide chemisorbed on a tungsten (111) crystal have been determined. The $O^+$ ions released during ESD of adsorbed oxygen exhibit three-fold symmetric angular distributions in orientational registry with the W(111) substrate. The $CO^+$ and $O^+$ ions released during ESD of a monolayer of CO are desorbed normal to the (111) surface. Models for both oxygen and CO adsorption are discussed. The data for CO are consistent with adsorption of CO in "standing up" carbonyl structures in the virgin and $\alpha$-CO binding states.

**16399.** Layer, H. P., **High-resolution stepping motor drive,** *Rev. Sci. Instrum.* **47,** No. 4, 480-483 (Apr. 1976).

Key words: digital; drive; electronic; generator; motor; stepping.

A digital sine-cosine stepping motor drive has been constructed which decreases the rotational step size by a factor of 31. This system improves the smoothness and resettability of the motor and retains the conventional slew speed and accuracy.

**16400.** Johnson, D. R., Pearson, R., Jr., **Microwave region,** Chapter 4.3 in *Methods of Experimental Physics* **13, Spectroscopy,** Part B, D. Williams, Ed., pp. 102-133 (Academic Press, Inc., New York, NY, 1976).

Key words: chemical monitoring and analysis; double resonance; microwave instrumentation; microwave spectroscopy; radio astronomy; short-lived molecules.

The instrumentation and experimental techniques developed for the study of the microwave spectra of gases are critically reviewed, with emphasis on methods capable of wide applicability in the frequency range from 4 to 220 GHz where oscillators producing fundamental power are commercially available. A general purpose spectrometer, incorporating techniques widely used in spectroscopic laboratories, is described as a point of reference for defining the essential characteristics of the basic spectrometer components: a source of MW power, a modulator, an absorption cell, a detector, and a method for measuring frequency. As each is discussed the most widely used instrumentation is compared to selected alternative including new developments which show promise for future applications. Original designs for detector and frequency multiplier-mixer mounts and parallel plate absorption cells are given which, when appropriately scaled to the MW frequency, have been successfully used from 4 to 130 GHz. Spectrometers with special characteristics such as broad-banded scanning, high temperature applications, resonant cavity absorption cells, or submillimeter frequency capabilities are discussed. New developments in the submillimeter region have extended scanning microwave spectroscopy to 1.06 THz. The characteristics which make microwave spectroscopy unique – high sensitivity, specificity, and great versatility – are demonstrated by describing new applications to the study of short-lived molecules, chemical monitoring and radio astronomy.

**16401.** Fiori, C. E., Myklebust, R. L., Heinrich, K. F. J., Yakowitz, H., **FRAME B: An on-line correction procedure for quantitative electron probe microanalysis with a Si(Li) detector, (Extended Abstract),** *Proc. 10th Annual Conf. of the Microbeam Analysis Society, Las Vegas, NV, Aug. 11-15, 1975,* 8 pages (1975).

Key words: background correction; continuous radiation; electron microprobe correction procedure; energy-dispersive x-ray spectrometry; lithium-drifted silicon detector.

**16402.** Pella, P. A., **Generator for producing trace vapor concentrations of 2,4,6-trinitrotoluene, 2,4-dinitrotoluene, and ethylene glycol dinitrate for calibrating explosives vapor detectors,** *Anal. Chem.* **48,** No. 11, 1632-1637 (Sept. 1976).

Key words: calibration device; dinitrotoluene; ethylene glycol dinitrate; explosives; generator; trinitrotoluene; vapors.

A vapor generator was constructed to produce known vapor concentrations of explosives such as 2,4,6-trinitrotoluene, 2,4-dinitrotoluene, 2,6-dinitrotoluene, and ethylene glycol dinitrate below 1 ppb by volume for calibrating trace explosives vapor detectors. The system is temperature controlled which permits a wide range of equilibrium vapor concentrations to be generated. These vapor concentrations are diluted by single-stage, dynamic, gas blending to obtain concentrations as low as 0.05 ppb. A quantitative gas chromatographic procedure was developed to evaluate this system by measuring the output vapor concentrations. The systematic error was usually within 15 to 20 percent of the values expected for TNT, and within 30 percent for EGDN. The applicability of the system for calibration purposes is demonstrated by performance data obtained with three commercial trace explosives vapor detectors.

**16403.** Forester, D. W., Abbundi, R., Segnan, R., Sweger, D., **Magnetic hyperfine structure in amorphous DyFe$_2$,** (Proc. 20th Annual AIP Conf. on Magnetism and Magnetic Materials, San Francisco, CA, Dec. 3-6, 1974), Paper in *Magnetism and Magnetic Materials-1974,* C. D. Graham, Jr., G. H. Lander, and J. J. Rhyne, Eds., No. 24, 115-116 (American Institute of Physics, New York, NY, 1975).

Key words: amorphous; magnetization; metal; Mössbauer; $^{57}$Fe; $^{161}$Dy.

In this paper we summarize the results of a Mössbauer study of the amorphous rare earth-transition metal (RE-TM) alloy DyFe$_2$ in the magnetically ordered state. Both the $^{57}$Fe and $^{161}$Dy spectra were investigated as a function of temperature and reveal a broad, though measurable, distribution of Fe hyperfine fields ($H_{eff}$) and quadrupole splittings (QS). There is a distribution similar in magnitude for the Dy hyperfine fields but the observed quadrupole splittings are narrowly distributed. The temperature variation of the $^{161}$Dy spectra indicates a large variation of local exchange splittings at the Dy sites. These results are discussed in terms of a model in which the Dy spins are more strongly coupled to their random-direction anisotropy axes than to the neighboring Fe spins (which also experience a weaker random-direction anisotropy).

**16404.** Hill, J. J., **A low frequency inductive ratio bridge for platinum resistance thermometry,** (Proc. 5th Symp. on Temperature, Its Measurement and Control in Science and Industry, Washington, DC, June 21-24, 1971), Paper in *Temperature, Its Measurement and Control in Science and Industry,* L. G. Rubin, A. C. Anderson, J. E. Janssen, and R. D. Cutkosky, Eds., **4,** Part 2, 1495-1499 (Instrument Society of America, Pittsburgh, PA, 1972).

Key words: ac bridges; bridges; platinum thermometers; resistance measurements; thermometry; two-stage transformers.

Most of the recently developed ac ratio transformer bridges for platinum resistance thermometry have operated at frequencies of the order of 400 Hz. Due to the fact that the resistance values of the thermometer and the comparison standard resistor at these frequencies may differ substantially from their dc values, doubt has been expressed regarding the correlation of such temperature measurements with those made using traditional dc methods. However, using two-stage transformer techniques, it is now possible to construct ratio transformers to operate at 20 or even 10 Hz with an accuracy of a few parts in 10$^8$ (equivalent to temperature intervals of few tens of micro degrees) and thus virtually eliminate this objection while still preserving all the advantages of ac methods. Nine-decade adjustable-ratio transformers have been built which are connected in a modified Kelvin Double Bridge circuit. The effective input impedance of the ratio arms is several megohms thus reducing the effect of the connecting leads to extremely small proportions. The paper also considers and discusses the relative advantages of most existing methods for platinum resistance thermometry, the limitations of comparison resistors and the philosophy behind possible future trends and developments.

**16405.** Alperin, H. A., Cullen, J. R., Clark, A. E., **Magnetic properties of bulk amorphous $Tb_xFe_{1-x}$**, (Proc. 21st Annual AIP Conf. on Magnetism and Magnetic Materials, Philadelphia, PA, Dec. 9-12, 1975), Paper in *Magnetism and Magnetic Materials-1975*, J. J. Becker, G. H. Lander, and J. J. Rhyne, Eds., No. 29, pp. 186-187 (American Institute of Physics, New York, NY, 1976).

Key words: amorphous $Tb_xFe_{1-x}$; Curie temperatures; magnetization measurement; neutron diffraction.

Magnetization measurements have been made on four bulk samples (compositions $x=0.018$, 0.118, 0.167 and 0.25) prepared by direct current rapid sputtering. Neutron diffraction measurements show these samples to be amorphous. All four samples are ferrimagnetic; however, the 17 percent sample is almost completely compensated at temperatures below 100K. With decreasing Tb-content, the Curie temperatures fall from a maximum of 405K for $x=0.25$ to the value of 245K for $x=0.018$. Anomalously large coercive fields and time dependent magnetizations are present at low temperatures.

**16406.** Helbig, V., Kelleher, D. E., Wiese, W. L., **Stark-broadening study of neutral nitrogen lines,** *Phys. Rev. A* **14,** No. 3, 1082-1093 (Sept. 1976).

Key words: nitrogen; plasma line boardening; spectral lines; Stark broadening; Stark shifts; Stark widths.

Extensive photoelectric measurements of the plasma-broadened line shapes of 42 neutral nitrogen lines have been carried out with a wall-stabilized arc. The arc current was varied from 20 to 100 A to achieve a variation in the axial electron density from about $5\times10^{16}$ to $1.5\times10^{17}$ cm$^{-3}$. Most observations were made end-on, and the arc was operated in pure nitrogen as well as argon with a small admixture of nitrogen to avoid self-absorption problems, which mainly arose with the red and near-infrared lines. The electron density was determined from the well-known Stark half-width of the hydrogen $H_\beta$ line, for which purpose a trace of hydrogen was added to the plasma. Our principal results are as follows: (a) Good agreement with the recent theoretical work by Griem and coworkers has been obtained; (b) consistent with theoretical predictions, ion-broadening effects are not noticeable; (c) the Stark widths and shifts for different lines in a multiplet are identical within the experimental precision ($\approx3\%$) as predicted by the theory; and (d) measurements performed over a range of transitions involving different quantum states agree equally well with the theoretical data, indicating that the atomic-structure part of theory is very adequate.

**16407.** Hall, J. L., Magyar, J. A., **High resolution saturated absorption studies of methane and some methyl-halides,** Chapter 5 in *Topics in Applied Physics* 13, High-Resolution Laser Spectroscopy, K. Shimoda, Ed., pp. 77-86, 86B (Springer-Verlag, New York, NY, 1976).

Key words: high resolution spectroscopy; methyl halides; optical heterodyne spectroscopy; quadrupole hyperfine interactions; saturated absorption spectroscopy.

We apply the techniques of high resolution saturated absorption spectroscopy to a number of methyl halide transitions near 3.39 $\mu$m. Wavenumbers and assignments are given for most lines. A "ladder" of frequency intervals was established with optical heterodyne techniques. Hyperfine structures due to electric quadrupole interactions was carefully studied for one transition in each of the three heavier methyl halides. This analysis gave the shift in the value eqQ due to vibrational excitation as well as information about the magnetic coupling energy. Finally a spectrum of $CH_4$ is presented which displays a resolving power of $5\times10^{10}$. This value is believed to be the highest yet employed in coherent spectroscopy.

**16408.** Brown, P. W., Clifton, J. R., Frohnsdorff, G., Berger, R. L., **The utilization of industrial by-products in blended cements,** (Proc. 5th Mineral Waste Utilization Symposium, Chicago, IL, Apr. 13-14, 1976), Paper in *Proceedings of the Fifth Mineral Waste Utilization Symp.*, pp. 278-284 (ITT Research Institute, Chicago, IL, 1976).

Key words: blast furnace slag; blended cement; fly ash; materials and energy conservation.

Approximately 85 million tons of portland cement are produced annually in the United States. However, less than one million tons of blended cement containing suitable waste or by-product materials, such as fly ash or blast furnace slag, are produced. In view of the potential for by-product utilization and raw materials and energy conservation, the advantages of increased use of blended cement should be considered. The potential for blended cement production and utilization and the advantages and limitations of utilization are discussed. The limitations imposed on the use of blended cements by standards and other factors are discussed. The technical benefits from the use of blended cements are considered.

**16409.** Brinckman, F. E., Iverson, W. P., Blair, W., **Approaches to the study of microbial transformations of metals,** *Proc. 3d Int. Biodegradation Symp., Kingston, RI, Aug. 17-23, 1975*, pp. 919-936 (Applied Science Publ. Ltd., London, England, 1976).

Key words: detection; flameless atomic spectrophotometry; gas chromatography; graphite furnace; methylation of metals; microbial transformation; speciation; volatile metal compounds.

An approach to the study of microbial transformations of metals existing in trace amounts in the environment is based primarily on the detection and speciation of volatile forms of these metals. Simple qualitative means for surveying the potential of microorganisms for volatilizing metals are described. Identification of transport agents has been accomplished primarily through the use of flameless atomic spectrophotometry coupled with gas chromatography. This technique permits chracterization of volatile metals and organometallic compounds in the nanogram range so that microbial transformations of metals at environmental levels may by monitored. The abiotic transfer of methyl groups from biologically methylated metals to Hg(II) provides a useful tool for the speciation of volatile metal forms suspected of being methylated.

**16410.** Yakowitz, H., **Present status of quantitative electron probe microanalysis,** *Proc. 6th European Congress on Electron Microscopy, Jerusalem, Israel, Sept. 1976*, pp. 37-40 (Tal International Publishing Co., Jerusalem, Israel, 1976).

Key words: electron probe microanalysis; Monte Carlo calculations; particulates; quantitative analysis; thin films; x rays.

All procedures for performing quantitative x-ray microanalysis require use of a standard of known composition. The analyst measures the relative x-ray intensity ratio between the elements of interest in the specimen and the same element in the standard. Both specimen and standard are measured under identical experimental conditions. The measured relative intensity ratio, often called k, must be accurately determined or else any quantitative analysis scheme will result in the same inaccuracy. Factors which can contribute to inaccuracies in k include the Poisson statistics of the x-ray emission process, x-ray detector coincidence loss (dead time) effects, and background noise arising from continuum radiation. Once the k values have been obtained, they must be corrected for several effects including: the differences in electron scattering and retardation in the specimen nd standard, i.e., the so-called atomic number effect, absorption f x-rays generated within the specimen along the direction of he x-ray detector, fluorescence effects and continuum uorescence effects.

**6411.** Simmons, J. A., **Microscopic aspects of residual stresses,** *Proc. Workshop on Nondestructive evaluation of Residual Stress, San Antonio, TX, Aug. 13-14, 1975,* pp. 11-17 (Air Force Materials Laboratory, Wright-Patterson Air Force Base, OH, 1976).

Key words: dislocation theory; imperfect continua; internal stress; nondestructive evaluation; residual stress.

This lecture on Microscopic Aspects of Residual Stresses was iven to the Air Force Materials Laboratory Workshop on Non-estructive Evaluation of Residual Stress. Residual stress and e more general concept of internal stress are defined and their eory developed using the modern methods of elasticity in imerfect continua.

**6412.** MacGregor, J. G., Breen, J. E., Pfrang, E. O., **Design of slender concrete columns,** *ACI J.*, pp. 6-28 (Jan. 1970).

Key words: bending moments; building codes; column (supports); frames; long columns; reinforced concrete; slenderness ratio; strength; structural analysis; structural design; ultimate strength.

Offers a proposal for revising the slender column design rocedures of the 1963 ACI Code. Proposes the use of a rational econd-order structural analysis wherever possible or practical. n place of such an analysis, an approximate design method ased on a moment magnifier principle and similar to the rocedure used under the AISC Specifications is proposed. An utline of the normal range of variables in column design and a ower limit of applicability is proposed which will eliminate over 0 percent of columns in braced frames and almost half of olumns in unbraced frames from consideration as slender olumns. Through a series of comparisons with analytical and est results, the accuracy of the approximate design procedure is stablished.

**5413.** Lind, M. A., Zalewski, E. F., **Silicon photodetector instabilities in the uv,** *Appl. Opt.* **15,** No. 6, 1377-1378 (June 1976).

Key words: detector; photodiode; silicon; ultraviolet; uniformity of response.

Recent measurements of a group of photovoltaic silicon detecrs has revealed instabilities that occur in some silicon hotodiodes. We discuss two such instabilities which manifest emselves as an increase in the spatial nonuniformity in the uv nd an increase in the spectral responsivity after high level uv irdiation. Typical measurements of two types of silicon detecrs are presented.

**5414..** Bingham, C. D., Yolken, H. T., Reed, W. P., **Nondestructive assay measurements can be traceable,** *Nucl. Mater. Manage.* **V,** No. II, 32-35 (Summer 1976).

Key words: calibration; measurement; nondestructive assay; nuclear; safeguards; traceability.

The use of nondestructive assay (NDA) techniques for the nalysis of Special Nuclear Materials is one of the keystones in e development of safeguards technology. Currently this effort use NDA is being frustrated because of a lack of "demonratable traceability." Presented here is a discussion of what aceability means and how it can be achieved. Specifically, aceability means far more than having a series of calibration andards for each individual NDA technique. It means defining e limits of uncertainty for both random and systematic error components of a set of measurements (i.e., precision and accuracy). Realizing this, an approach to these evaluations is suggested. In addition, the authors emphasize that the availability of standards is not holding back the use of NDA.

The use of NDA is actually limited by the poor accuracy (possible systematic error) of many methods and the availability of real calibration standards would only tend to accentuate this point.

Finally, the suggestion is made that calibration standards will only be available when the demonstrated need is limited to a finite number of sets.

**16415.** Lucatorto, T. B., McIlrath, T. J., **Efficient laser production of a $Na^+$ ground-state plasma column: Absorption spectroscopy and photoionization measurement of $Na^+$,** *Phys. Rev. Lett.* **37,** No. 7, 428-431 (Aug. 16, 1976).

Key words: far ultraviolet spectroscopy; ion absorption spectrum; ion photoionization; laser ionization; photoionization resonances; sodium.

We report the first observation of ionization of dense Na vapor by laser radiation. A 1-MW pulsed laser at 589.6 nm produced almost complete ionization of a 10-torr-cm column of Na. Measurements of the $Na^+$ photoionization cross section, the neonlike series $2s^22p^6 \rightarrow 2s^22p^5ns$ and $nd$, and several autoionizing resonances of the type $2s^22p^6 \rightarrow 2s2p^6np$ were obtained using a spark source to provide the continuum background for absorption spectroscopy of the ion.

**16416.** Post, M. A., Iverson, W. P., Campbell, P. G., **Evaluating non-mercurial fungicides,** *Mod. Paint Coat.* **66,** No. 9, 31-38 (Sept. 1976).

Key words: accelerated testing; alkyd paints; environmental chamber; exterior exposure; latex paints; nonmercurial fungicides.

Nonmercurial fungicides were evaluated for effectiveness in an exterior acrylic latex and in an exterior long oil alkyd paint. Exterior exposure tests were of six months, one year and two years duration at the National Bureau of Standards exposure site. Exterior exposure tests were also carried out at the U.S. Naval Station, Roosevelt Roads, Puerto Rico. Accelerated fungus exposure testing was performed for four and eight weeks in an environmental chamber (a) without prior exterior exposure, (b) after six months, one year and two years exterior exposure, and (c) after exposure in a xenon arc accelerated weathering apparatus. Of the eight nonmercurial fungicides tested for latex paint protection, only one afforded complete fungicidal protection after two years exterior exposure. Two of the six nonmercurial fungicides tested for alkyd paint protection were excellent. One was superior and the other equal to the mercurial fungicide. The mercurial fungicide afforded much better protection for alkyd than latex paints.

**16417.** Grabec, I., Peterlin, A., **Acoustic emission of a crazing polymer,** *J. Polym. Sci.: Polym. Phys. Edition* **14,** 651-661 (1976).

Key words: acoustic emission; amorphous polymer; crazing; fatigue; Kaiser's effect.

The acoustic emission from a crazing polyvinyltoluene in a tensile and bending experiment is described. Acoustic emission appears as a series of bursts which most likely correspond to the initiation and growth of crazes. The emission intensity is characterized by acoustic activity (pulse rate) measured by the ringdown technique. The average activity increases with strain. During repeated loading the acoustic activity shows a measurable intensity and significant rise only beyond the maximum strain of the former runs. This is equivalent to Kaiser's effect in metals. Acoustic emission during the creep experiment occurs in three characteristic periods. They are characterized as the relaxation, fatigue, and breakdown periods. Visual observations indicate that the relaxation period corresponds to the initiation, and the fatigue period to the growth of crazes. In the breakdown period a macroscopic crack develops and the sample fails.

**16418.** Penn, D. R., **Comment on "Field emission as a probe of the surface density of states",** *Phys. Rev. B* **14,** No. 2, 849-853 (July 15, 1976).

Key words: field emission; surface density of states; transfer Hamiltonian.

It is shown that the primary contribution to the field-emission current comes from electrons with *total* momentum equal to zero in a direction parallel to the metal surface and that the field-emission current measures the density of states at a point several angstroms from the metal surface. An explicit expression is derived for the error made in using the transfer-Hamiltonian technique to calculate the tunneling probability of an electron through a one-dimensional barrier, and it is pointed out that the error is small in the case of field emission.

**16419.** Plummer, E. W., Waclawski, B. J., Vorburger, T. V., Kuyatt, C. E., **Photoelectron spectra of adsorbed species on tungsten,** *Prog. Surf. Sci.* **7,** 149-182 (1976).

Key words: adsorption; carbon; carbon monoxide; chemical bonding; chemisorption; density dependent transitions; desorption; dissociative adsorption; electronic states; hydrogen; monolayers; nitrogen; oxygen; photoelectron spectra; relaxation energy; surfaces; tungsten; ultraviolet photoemission; valence band; virgin states; $\alpha$ states; $\beta$ states.

Photoelectron spectra from W(100) and W(110) for $h\omega = 21.22$ and 16.85 eV were studied as a function of controlled exposure to $H_2$, $N_2$, and CO at room temperature, and with subsequent heating. The spectra revealed density-dependent conversions of the $\beta$-states of adsorbed hydrogen and carbon monoxide. The $\alpha$ and virgin states of CO appear to be molecular with the $\alpha$ state sequentially filling on top of the $\beta$-state. The ordered $\beta$-state of CO on W(100) is shown to be dissociatively adsorbed. For W(100) photoelectron spectra for initial states overlapping the tungsten band are very similar for nitrogen and carbon adsorbed in the geometrical configuration indicated by a c(2 × 2) LEED pattern. In contrast, hydrogen and oxygen adsorbed on W(100) in a c(2 × 2) configuration produce different spectra, leading to the speculation that nitrogen and carbon may adsorb in the same site.

**16420.** Kaufman, V., Sugar, J., **Wavelengths, classifications, and ionization energies in the isoelectronic sequences from Yb II and Yb III through Bi XV and Bi XVI,** *J. Opt. Soc. Am.* **66,** No. 10, 1019-1025 (Oct. 1976).

Key words: bismuth; gold; hafnium; ionization energies; iridium; lead; lutetium; mercury; osmium; platinum; rhenium; tantalum; thallium; tungsten; wavelengths; ytterbium.

Spectral observations are reported for transitions to the ground term and first excited term of the one-electron configurations in the $4f^{14}5p^6nl$ isoelectronic sequence from Yb II through Bi XV. Resonance lines are reported for the isoelectronic sequence Yb III through Bi XVI in which the ground state is $4f^{14}5p^6\ {}^1S_0$ and the upper levels are the $J=1$ levels of the $4f^{13}5p^6nd$, $4f^{14}5p^5nd$, and $4f^{14}5p^5ns$ configurations. The wavelengths fall in the range 70-3700 Å. The spectra were produced by means of sliding and triggered spark discharges and photographed with 10.7 m normal and grazing incidence spectrographs. The data in the Yb III sequence demonstrate the crossing of binding energies of the $4f$ and $5p$ shells at W VII. Rydberg series terms were found in a sufficient number of cases to provide extrapolation curves through Bi XV and Bi XVI. These data enabled us to calculate ionization energies for each of these ions with an uncertainty of ~1 percent or better.

**16421.** Gadzuk, J. W., **Screening energies in photoelectron spectroscopy of localized electron levels,** *Phys. Rev. B* **14**, No. 6 2267-2280 (Sept. 15, 1976).

Key words: adsorption; electron gas; photoemission; relaxation energy.

Screening or polarization energies (often called "extra-atomic relaxation energies") associated with localized-hole creation in photoelectron spectroscopy in or on metals have been calculated. Following the procedure of Hedin and Lundqvist, the screening energy is written in terms of an effective matrix element of a nonlocal random-phase-approximation self-energy between wave functions of the localized-hole state. The relevance of spatial extent of the hole, electron-gas dielectric properties, chemical-bonding effects, and surface effects are examined. Calculations for 1 *s* core and bonding $H_2$ orbital holes in atoms or molecules which are embedded in and adsorbed on electron-gas surfaces are presented. The interplay between orbital size and host interelectron spacing (as manifested in screening lengths) is emphasized. The relationship between screening energies and classical image potentials in photoelectron spectroscopy of adsorbed atoms and molecules is established. Finally, interpretations of observed photoelectron spectra are discussed in terms of binding energies and relaxation, chemical, and "dipole" potential shifts, and the problem of "proper" referencing is addressed.

**16422.** Siedle, A. R., Hertz, H. S., **Vaporization of (SN)x and TTF-TCNQ,** *Mater. Res. Bull.* **11,** No. 9, 1185-1189 (1976).

Key words: chemical ionization mass spectrometry; mass spectrometry; sulfur nitride; tetracyanoquinodimethane; tetrasulfur tetranitride; tetrathiafulvalene; vaporization.

The vaporization of (SN)x was studied by electron impact and chemical ionization mass spectrometry. Comparison of the spectra with those of $S_4N_4$ suggests that vaporization generates an unstable, acyclic $S_4N_4$ which subsequently fragments to a cyclic $S_3N_3^+$ and $SN^+$ ion in the mass spectrometer. Mass spectrometry may be used to analyze (SN)x for $S_8$ and cage $S_4N_4$. Vaporization of TTF-TCNQ produced the component donor and acceptor molecules.

**16423.** Hertz, H. S., May, W. E., Chesler, S. N., Gump, B. H., **Petroleum analysis: Methodology for quantitative and qualitative assessment of oil spill,** *Environ. Sci. Technol.* **10,** No. 9, 900-903 (Sept. 1976).

Key words: gas chromatography; liquid chromatography; oil spill; petroleum; quantitation.

An integrated chromatographic technique for petroleum analysis compatible with long-term studies of oil spills is presented. Dynamic headspace sampling and the complementary analytical techniques of gas chromatography and coupled-column liquid chromatography are utilized for quantitation of petroleum containing samples. Gas chromatography-mass spectrometry is employed for identification of individual components in these samples. Analytical data obtained from a major oil spill are presented and discussed.

**16424.** Buehler, M. G., Thurber, W. R., **A planar four-probe test structure for measuring bulk resistivity,** *IEEE Trans. Electron Devices ED-23*, No. 8, 968-974 (Aug. 1976).

Key words: bulk resistivity; collector resistivity; four-probe; planar test structure; resistivity; semiconductor characterization; semiconductor device; silicon; square array.

A small planar four-probe test structure for measuring the bulk r collector resistivity of silicon wafers was designed and bricated with a bipolar transistor process. Analogous to a echanical square array four-point probe, the planar four-probe ructure consists of a large-area base diffusion which is broken four points through which contact is made to the undiffused ollector material. A probe spacing of 2.25 mil (57.2 μm) allows e resistivity of the silicon wafer to be measured with good spaal resolution. A correction factor was derived to obtain the true sistivity from measurements on a wafer with finite thickness nd a conducting backside, and it is presented along with the corction factors for other cases. The test device was fabricated in licon wafers whose resistivities ranged from 0.013 Ω·cm to 12 ·cm in *n*-type material and from 0.7 Ω·cm to 30 Ω·cm in *p*-type aterial. Planar four-probe resistivity values are compared with echanical four-probe values taken on the same wafers before brication, and the results are generally in agreement within ±3 ercent.

425. Reader, J., Acquista, N., **$4s^24p^4$-$4s4p^5$ transitions in Zr VII, Nb VIII, and Mo IX,** *J. Opt. Soc. Am.* **66,** No. 9, 896-899 (Sept. 1976).

Key words: molybdenum; niobium; spectra; ultraviolet; wavelength; zirconium.

Spectra of ionized Zr, Nb, and Mo have been observed in slidng spark discharges at peak currents up to 4000 A on the 10.7 m ormal and grazing incidence spectrographs at NBS. From these bservations the group of $4s^24p^4$-$4s4p^5$ transitions in Zr VII, Nb III, and Mo IX have been identified and measured. The energy arameters obtained from least-squares fits to the resultant enery levels are compared with Hartree-Fock calculations.

6426. Cezairliyan, A., McClure, J. L., Coslovi, L., Righini, F., Rosso, A., **Radiance temperature of tantalum at its melting point,** *High Temp.—High Pressures* **8,** 103-111 (1976).

Key words: emittance; high-speed measurements; high temperature; melting point; pyrometry; radiance temperature; tantalum.

Radiance temperature (at two wavelengths, 653 and 995 nm) f tantalum at its melting point was measured with the use of a ubsecond-duration pulse heating technique. Specimens in the orm of strips with initially different surface roughnesses were sed. The results do not indicate any dependence of radiance mperature (at the melting point) on initial surface or system perational conditions. The average radiance temperature at the elting point of tantalum is 2846 K at 653 nm and 2620 K at 995 m, with a standard deviation of 1 K at 653 nm and 0.4 K at 995 n. The total inaccuracy in radiance temperature is estimated to e not more than ±8 K.

427. Morrissey, B. W., Fenstermaker, C. A., **Conformation of adsorbed γ-globulin and β-lactoglobulin. Effect of surface concentration,** *Trans. Am. Soc. Artif. Intern. Organs* **XXII,** 278-283 (1976).

Key words: conformation adsorbed proteins; ellipsometry; infrared bound fraction; protein adsorption.

The adsorption of clotting factors and proteins on the surface a synthetic implant can modify both their biological activity nd the subsequent interaction of formed cellular elements with e surface. In particular, γ-globulin has been implicated in ecific biochemical reactions resulting in platelet adhesion. Infrared bound fraction and ellipsometric measurements have been carried out *in situ* to determine the conformation of adsorbed γ-globulin and β-lactoglobulin as a function of surface concentration.

The fraction of adsorbed carbonyl groups of γ-globulin and β-lactoglobulin decreases significantly as the amount adsorbed increases. Ellipsometric measurements of the extension of adsorbed γ-globulin show that as the number of surface attachments decreases, the thickness of the adsorbed protein film increases. Studies with a cross-linked γ-globulin preparation indicate that the native conformation in solution corresponds to an adsorbed conformaton intermediate between those found at the extremes of high and low surface concentration.

These results indicate that adsorbed γ-globulin is rather pliant and that the adsorbed conformation of proteins which are present should be taken into account when describing platelet-surface interactions.

16428. Goldberg, R. N., **Microcalorimetric determination of glucose in reference samples of serum,** *Clin. Chem.* **22,** No. 10, 1685-1691 (1976).

Key words: hexokinase; intermethod comparison.

I report a detailed series of microcalorimetric measurement of glucose concentrations in five reference samples of serum. The method utilized (a) calibration in the actual medium of analysis and (b) a correction for interferences owing to the nonspecificity of the enzyme hexokinase. The microcalorimetric results are compared with the tentative results of analyses obtained by the spectrophotometric hexokinase/glucose-6-phosphate dehydrogenase method and by isotope-dilution mass spectrometry. In most cases, the microcalorimetric results appear to be in agreement with the results obtained by these latter two methods. A discussion of the basis of the microcalorimetric measurements is presented.

16429. Johnson, D. R., Suenram, R. D., Lafferty, W. J., **Laboratory microwave spectrum of cyanamide,** *Astrophys. J.* **208,** No. 1, 245-252 (Aug. 15, 1976).

Key words: interstellar molecules; interstellar laboratory spectra; interstellar line identifications; interstellar molecular processes; interstellar transition probabilities.

Laboratory test frequencies have been obtained for rotational transitions of the cyanamide molecule ($NH_2CN$) in the ground state and the lowest vibrational ($NH_2$ inversion) state, extending the measured spectrum of the molecule to 120 GHz. Perturbations resulting from Coriolis-type interactions between the ground and the lowest vibrational state cause many of the observed transitions to deviate significantly from the predictions of a conventional centrifugal distortion-corrected rigid rotor model. Absolute energies and Einstein $A$ coefficients are presented for all measured transitions up to $J = 8$ for both states considered.

16430. Cehelnik, E. D., Mielenz, K. D., **Quantum counter photodetectors: A new design,** *Appl. Opt.* **15,** No. 9, 2259-2263 (Sept. 1976).

Key words: emission anisotropy; fluorescence; photodetectors; polarization; quantum counters; rhodamine B chloride; spectrofluorimetry; total internal reflection.

A new design for quantum counter cells is described that uses total internal reflection to minimize depth-of-penetration and polarization effects. This new cell is compared to a standard 1-cm thick quantum counter cylindrical cell. Solutions of 5 g/liter of rhodamine B chloride in ethylene glycol were used in both cells. The fluorescence emission from the cell was found to be significantly less polarized and also less dependent on excitation wavelength.

**16431.** Seltzer, S. M., **The response of scintillation detectors to internally induced radioactivity,** *Nucl. Instrum. Methods* **127,** 293-304 (1975).

Key words: background; gamma-ray astronomy; induced radioactivity; Monte Carlo calculation; response; scintillation detector.

Pulse-height distributions produced in NaI and CsI detectors by the decay of certain internally distributed radionuclides have been calculated using a Monte Carlo method. The method traces the possible decays of a radioactive atom, taking into account $\beta^{\pm}$-emission, electron capture, gamma-ray emission, internal-conversion-electron emission, and x-ray or Auger-electron emission following the creation of atomic K-shell vacancies. The scattering, absorption, and escape of gamma-rays, annihilation quanta, and x rays are included. Results are presented for the radioisotopes $^{22}$Na, $^{124}$I, $^{124}$Sb, $^{125}$Sb, $^{123m}$Te, and $^{125m}$Te to indicate the characteristic features of the pulse-height distributions.

**16432.** Sharp, K. G., Li, S., Johannesen, R. B., **Perfluoro(alkylsilanes). 3. Fluorine-fluorine coupling constants in perfluoro(alkylsilanes) and related molecules,** *Inorg. Chem. Notes* **15,** No. 9, 2295-2297 (1976).

Key words: coupling constants; fluorine; fluoroalkylsilanes; NMR; relative signs; silicon.

$^{19}$F NMR spectrometric analyses – including relative signs for most F-F coupling constants have been carried out for the perfluoro(alkylsilanes) $CF_3CF_2SiF_3$, $CF_3SiF_2SiF_3$, $CF_3CF_2CF_2SiF_3$, and $SiF_3CF_2SiF_3$. The latter three compounds have not been previously reported. The signs of $J_{FF}$ values can be put on an absolute basis via self-consistent correlations between the above molecules and related polyfluoroalkanes or alkylsilanes, including the series $CF_3CF_2X$, $CF_2SiF_2X$, and $SiF_3SiF_3X$ where X = halogen. An effect not previously recognized is that on substitution of Si for C in molecular fragments of the type FCCF or FCSiF the three bond F-F coupling invariably increases by ca. +6 to +10 Hz in an algebraic sense. Theoretical implications of this effect are discussed.

**16433.** Pallett, D. S., Pierce, E. T., Toth, D. D., **A small-scale multi-purpose reverberation room,** *Appl. Acoust.* **9,** 287-302 (1976).

Key words: acoustic modelling; acoustics; impact noise; noise; reverberation rooms; room acoustics; sound power.

A one-fourth scale model of the large (425 m$^3$) National Bureau of Standards reverberation room is described. This facility was constructed to carry out acoustical research at relatively low cost in a frequency range two octaves higher than that used in the larger facility. Initial experimental measurements carried out in this facility concern sound power emitted by small sources. The pure tone qualification procedure specified in American National Standard S1.21-1972 "Methods for the Determination of Sound Power Levels of Small Sources in Reverberation Rooms" was carried out using computer control of the experiment. This standard is of particular interest to the international acoustical community since it is technically equivalent to ISO Documents DIS 3741 and DIS 3742. The effect of increased low frequency absorption upon room qualification was tested in the model room. Future research plans to make use of the small-scale reverberation rooms are described.

**16434.** Snyder, L. E., Hollis, J. M., Ulich, B. L., Lovas, F. J., Johnson, D. R., Buhl, D., **Radio detection of interstellar sulfur dioxide,** *Astrophys. J.* **198,** No. 2, L81-L84 (June 1, 1975).

Key words: interstellar; microwave spectra; molecules; Orion; radio astronomy; sulfur dioxide.

Interstellar sulfur dioxide ($SO_2$) has been detected in emission from the direction of the Orion Nebula molecular cloud and from Sgr B2. $SO_2$ is the heaviest interstellar molecule detected to date, and the only nonlinear triatomic molecule which does not contain hydrogen. The remarkable Orion emission profiles suggest that two components are supporting the $SO_2$ emission: a dense circumstellar-type envelope, which may be in maser emission, and a warm galactic cloud component.

**16435.** Petree, B., Humphreys, J. C., Lamperti, P. J., Loftus, T. P., Weaver, J. T., **Comparison of cobalt-60 exposure determinations by calorimetry and by ionization chamber techniques,** *Metrologia* **11,** 11-15 (1975).

Key words: calorimetry; cobalt-60; ionization chamber.

The exposure rate computed from calorimeter power measurements is compared to the exposure rate of the same source (1-Ci cobalt-60) determined by means of a graphite cavity ionization chamber. A difference of 0.38 percent was found and is not considered significant compared to the estimated systematic uncertainty (1.3%).

**16436.** Mangum, B. W., Utton, D. B., **Antiferromagnetic ordering in ErPO$_4$,** (Proc. 20th AIP Conf. on Magnetism and Magnetic Materials, San Francisco, CA, Dec. 3-6, 1974), Paper in *Magnetism and Magnetic Materials,* C. D. Graham, Jr., G. H. Lander, and J. J. Rhyne, Eds., No. 24, pp. 65-66 (American Institute of Physics, New York, NY, 1975).

Key words: antiferromagnetic transition; antiferromagnetism; dipolar interactions; $ErPO_4$; magnetic phase diagram; Néel temperature; spin-flop.

The magnetic susceptibility and dM/dB as a function of field have been measured for $ErPO_4$ from 25 mK to 4.2 K. They show that $ErPO_4$ orders antiferromagnetically with $T_N = 100 \pm 2$ mK with the spins along the tetragonal a-axes. The magnetic phase diagram is presented which includes a spin-flop phase in the basal plane. It is proposed that dipolar interactions may be responsible for the magnetic ordering.

**16437.** Shumaker, J. B., **Light emitting diode calibrations at NBS,** *Proc. 8th Session Comité Consultatif de Photométrie et Radiométrie, Sèvres, France, Sept. 3-5, 1975,* pp. 95-99 (Bureau International des Poids et Mesures, Pavillon de Breteuil, Sèvres, France, 1976).

Key words: calibration; light emitting diode; spectral irradiance.

A very brief report is given of some aspects of spectral irradiance calibrations of red LEDs at NBS. A typical spectral distribution is given and the treatment of temperature effects is discussed.

**16438.** Marlowe, D. E., **National measurement study – Microstudy force,** *NCSL Newslett.* **14,** No. 1, 44-45 (Mar. 1974).

Key words: force; NMS.

A brief summary of the National Measurement System Micro-Study of Force is presented.

**16439.** Davis, R. M., **Implications of privacy legislation on the use of computer technology in business,** *Jurimetrics J.* **17,** No. 1, 95-110 (Fall 1976).

Key words: computer security; information handling; privacy; safeguards for security and privacy; technology for security and privacy.

The National Bureau of Standards has been charged with responsibility for developing guidelines and standards for government compliance with legislation to protect individual privacy. NBS has identified emerging problems in security and privacy and the need for technological developments to provide solutions. Safeguards for security and privacy are not identical. The large number of record systems processing personal records in both the public and private sectors points up the magnitude of the problem of retrofitting these systems for security and privacy safeguards. In many cases, sophisticated systems are not required, and good information practices will be sufficient to meet the requirements. The safeguards differ for each system. There is also a need for auditing techniques to check on the effectiveness of the safeguards put into place. The techniques developed will be useful in preventing computer fraud, assuring functional fidelity and maintaining data integrity during input and processing.

**16440.** Negas, T., Roth, R. S., Parker, H. S., McDaniel, C. L., Olson, C. D., **Chemical aspects of materials containing cerium oxide,** *Proc. 5th European Conf. on Thermophysical Properties of Solids at High Temperatures, Moscow, Russia, May 18-21, 1976,* pp. 1-13 (1976).

Key words: cerium oxide; magnetohydrodynamics; system $K_2O$-$ZrO_2$-cerium oxide; thermal microbalance; x-ray diffraction.

The phase relations in the cerium oxide-$ZrO_2$ system reinvestigated under oxidizing conditions, in air, and up to 1600 °C using thermal microbalance, conventional ceramic heating and quenching, and x-ray diffraction methods. Additionally, reactions of materials of this system with $K_2O$ (the $K_2O$-$ZrO_2$-cerium oxide system) are reported. These data are correlated with analyses of electrode materials tested in the U-O2 MHD facility.

**16441.** Cetas, T. C., **Temperature measurement in microwave diathermy fields: Principles and probes,** *Proc. Int. Conf. on Cancer Therapy by Hyperthermia and Radiation, Washington, DC, Apr. 28-30, 1975,* pp. 193-203 (American College of Radiology, Chevy Chase, MD, 1976).

Key words: measurement temperature; medicine temperature; microwave diathermy fields; temperature measurement.

Thermometry and medicine have been associated closely for a long time. Physicians contributed to the development of various thermometers, and physiological applications were among the first uses of temperature measurement. For example, body temperature or "blood heat" was used as a reference point for some of the early temperature scales. Even today, when the word "thermometer" is used, the clinical thermometer comes to mind most often.

**16442.** Krauss, M., Neumann, D. B., **The ${}^5\Sigma_g^+$ states of $N_2$,** *Mol. Phys.* **32,** No. 1, 101-112 (1976).

Key words: electronic structure; energy curve; $N_2$; predissociation; radiative recombination; ${}^5\Sigma_g^+$.

The electronic structure and energy curves of the $1{}^5\Sigma_g^+$ and $2{}^5\Sigma_g^+$ states of $N_2$ have been analyzed using the multiconfiguration self-consistent-field (MC-SCF) method for calculating the wavefunctions and energies. The *ab initio* model curve for the $1{}^5\Sigma_g^+$ state obtains an $r_e$ of 1.69 Å and a $D_e$ of 825 cm$^{-1}$. There is also a barrier with a maximum at 2.21 Å with a height of about 300 cm$^{-1}$ which is a novel feature of this calculation. The potential supports two bound vibrational levels and two shape resonances for $j=0$. The calculated curve differs most from the semiempirical curve of Carroll in having a larger $r_e$ by about 0.14 Å and a well depth smaller by 250 cm$^{-1}$.

The ${}^5\Sigma_g^+$ curve is known experimentally to predissociate both the $B^3\Pi_g$ and $a^1\Pi_g$ vibration-rotation levels above the dissociation limit. Conversely, two-body radiative association of two N($^4S$) atoms is known to occur through the interaction of the $1{}^5\Sigma_g^+$ and $B$ and $a$ states. The two-body radiative rates are analyzed in terms of the likely spin-orbit interaction between the $1{}^5\Sigma_g^+$ and $B$ and $a$ states and the ratio of these rates is calculated under the assumption that the predissociation rate exceeds the radiative in both cases. The ratio of the two-body associative rates $k^B/k^a$ is calculated to be roughly 20 which is to be compared to an experimental ratio of 32.

**16443.** Ditmars, D. A., **Measurement of the average total decay power of two plutonium heat sources in a Bunsen ice calorimeter,** *Int. J. Appl. Radiat. Isot.* **27,** 469-490 (1976).

Key words: Bunsen ice calorimeter; calorimetric standards; calorimetry; heat standards; phase-change calorimeter; plutonium dioxide; plutonium isotopes; radionuclide calorimetry; radionuclide decay power; standards.

A Bunsen ice calorimeter has been specially adapted for high-precision power measurements on radioactive heat sources. The construction of the apparatus, the principles underlying its operation and the interpretation of the heat data obtained in both static and dynamic experiments are thoroughly described. Dynamic electrical calibration experiments yielded a calibration constant for this calorimeter of 270.56 J/g mercury, with an estimated overall inaccuracy of 0.04 percent. This agreed with the present static calibration constant of 270.59 J/g mercury, with an estimated overall inaccuracy of 0.01 percent, well within the combined estimated limits of overall inaccuracy. The average total decay powers of the radioactive heat sources "1.5 WB" and "0.23 WB," supplied by the Mound Laboratory, have been measured. These powers, referred to 27 November 1974, are, respectively, 1.44936 W with an estimated overall inaccuracy of 0.050 percent and 0.22517 W with an estimated overall inaccuracy of 0.144 percent. These limits represent a linear sum of random error calculated at a 99 percent confidence level and estimated maximum systematic error. The decay powers predicted on the basis of heat-flow calorimetry carried out at the Mound Laboratory both before and after the present investigation are 0.004 percent and 0.12 percent above the present results for the sources "1.5 WB" and "0.23 WB," respectively.

**16444.** Okabe, H., **Fluorescence quenching of sulfur dioxide by source emission gases,** *Anal. Chem.* **48,** No. 11, 1487-1489 (Sept. 1976).

Key words: emission gas; exhaust; fluorescence; nitric oxide; quenching; sulfur dioxide.

The quenching constants of $SO_2$ fluorescence excited by a 216-nm deuterium source have been obtained for $N_2$, $O_2$, air, and $CO_2$. They are $0.75 \pm 0.09$, $2.68 \pm 0.09$, $1.16 \pm 0.01$, and $0.74 \pm 0.07$, respectively, all in units $10^{-3}$ torr$^{-1}$. The fluorescence signal of $SO_2$ in simulated stack emission is several percent lower than that in pure $N_2$. The presence of NO does not interfere with the $SO_2$ measurement by a fluorescence method.

**16445.** Evans, A. G., Linzer, M., **High frequency cyclic crack propagation in ceramic materials,** *Int. J. Fract.* **12,** No. 2, 217-222 (Apr. 1976).

Key words: ceramic materials; cyclic crack propagation; high frequency; plasticity.

Techniques and instrumentation for studying high frequency cyclic crack propagation in ceramic materials are described. Tests performed on a silicate glass show that the cyclic slow crack growth mechanism up to 600 Hz is identical to the quasi-static mechanism. Conversely, a strong cyclic effect on the crack growth rate is observed in a tungsten carbide-cobalt material.

**16446.** Powell, F. J., **A fresh look at fundamental design parameters,** *Proc. Energy Crisis Regional Conf., Chicago, IL, Sept. 19-21, 1973*, pp. 24-1 –24-8 (Capital Development Board, Springfield, IL, 1973).

Key words: buildings; energy conservation; heat transfer.

Two fundamental equations of heat energy transfer in buildings are examined and related to practical design decisions that are made by architects and engineers. Available modern technology that represents an improvement over the simplified fundamental approach is described. An example of the use of modern technology is given together with suggested ways to save energy in heating and cooling applications. Some of the problems of implementation of energy conservation measures in buildings are discussed.

**16447.** Branstad, M. A., Branstad, D. K., **Computer security applications utilizing minis,** (Proc. 9th Annual IEEE Computer Society International Conf., COMPCON 74, Fall, Washington, DC, Sept. 10-12, 1974), Paper in *Digest of Papers Micros and Minis, Application and Design*, pp. 91-94 (IEEE Computer Society, Washington, DC, 1976).

Key words: computer security; minicomputers.

Protection of data which is stored and processed in computers is evolving as the highest priority requirement on ADP systems today. Minicomputers are playing a large role in the effort to achieve secure computing environments. They are being used as testbeds to determine the efficacy of various theories on how to design a secure system. Minis are being analyzed for their ability to provide external security control for existing large machines. As computers are being connected in networks, the mini may be instrumental in providing security for the network. These computer security applications utilizing minicomputers are outlined in this paper.

**16448.** Stolz, A., Bender, P. L., Faller, J. E., Silverberg, E. C., Mulholland, J. D., Shelus, P. J., Williams, J. G., Carter, W. E., Currie, D. G., Kaula, W. M., **Earth rotation measured by lunar laser ranging,** *Science* **193,** 997-999 (Sept. 10, 1976).

Key words: earth rotation; geodesy; geodynamics; geophysics; laser distance measurements; moon.

The estimated median accuracy of 194 single-day determinations of the earth's angular position in space is 0.7 millisecond (0.01 arc second). Comparison with classical astronomical results gives agreement to about the expected 2-millisecond uncertainty of the 5-day averages obtained by the Bureau International de L'Heure. Little evidence for very rapid variations in the earth's rotation is present in the data.

**16449.** Galloway, K. F., Leedy, K. O., Keery, W. J., **Electron-beam-induced currents in simple device structures,** *IEEE Trans. Parts, Hybrids, Packag.* **PHP-12,** No. 3, 231-236 (Sept. 1976).

Key words: device inspection; electron-beam-induced current; microelectronics; *p-n* junctions; scanning electron microscopy; semiconductor devices.

Electron-beam-induced current (EBIC) in semiconductor devices produced by the electron beam of a scanning electron microscope (SEM) can be used to image subsurface device features and to measure certain material parameters. This paper presents a simple method of calculation for estimating the magnitude of EBIC signals. EBIC signals from silicon *p-n* junction diodes are compared with the results of the calculation. The application of EBIC to more complicated device structures is discussed.

**16450.** Koonce, C. S., **Superconducting transition widths in applied magnetic fields,** *J. Low Temp. Phys.* **24,** Nos. 5/6, 597-610 (Sept. 1976).

Key words: cadmium; condensation energy; demagnetization coefficient; fluctuations; inhomogeneous superconductor; intermediate state; superconducting-normal transition; superconductor; surface energy type I superconductors.

The width of superconducting-normal transitions for inhomogeneous ellipsoidal superconductors in an applied magnetic field is calculated. A simple model is used for the variation in transition temperature with position and the range of this variation is assumed to be larger than the Landau-Ginzburg coherence length. It is found that the decrease in transition width with increasing applied magnetic fields at low fields occurs because the boundaries between superconducting and normal regions begin to be determinded less by the inhomogeneities and more by the loss of condensation energy between domains, and by sample surface effects. At higher fields, the transition width increases with applied field because of the finite demagnetization coefficient.

**16451.** Hower, P. L., Blackburn, D. L., Oettinger, F. F., Rubin, S., **Stable hot spots and second breakdown in power transistors,** (Proc. 1976 IEEE Power Electronics Specialists Conf., Cleveland, OH, June 8-10, 1976), *PESC 76 Record, 76-CH, 1084-3 AES*, 234-246 (McGregor and Warner, Washington, DC, Oct. 1976).

Key words: base widening; current crowding; hot spots; power transistors; safe operating area; second breakdown; thermal instability.

The mechanism of hot spot formation in transistors is examined from both experimental and theoretical viewpoints. It is shown that after the device becomes thermally unstable the device may restabilize in a hot spot mode of operation. The $I_C$, $V_{CE}$ thermal instability locus can accurately be predicted assuming the current density is uniform prior to hot spot formation. A new model is proposed which explains why the device may restabilize in a hot spot mode and why devices exhibit "thermal hysteresis." It is also shown using thermal mapping techniques that emitter current crowding exists in the stable hot spot mode. Finally, the experiments support the idea that second breakdown occurs when the current density within the hot spot reaches a critical value.

**16452.** McCoubrey, A. O., **The national measurement system and specific industrial needs,** *Proc. Fluid Power Testing Symp., Milwaukee, WI, Aug. 11-14, 1975*, pp. 1.1.1.1-1.1.1.8 (Fluid Power Society, Milwaukee, WI, 1975).

Key words: engineering, instrumentation and techniques; fluids; force; hydraulic equipment; mechanical power; noise; pressure; quality control; safety; testing.

When consideration is given to interrelated needs for measurement methods, units, instruments, reference standards, reference data, and traceability, along with the numerous and diverse public and private agencies involved in measurements activity, it becomes important to think in terms of a *unified measurement system*, and to strive toward the rational design of such a system. An effective system will meet the needs of the users in terms of acceptable and accessible central standards, reliable transfer standards, practical levels of accuracy, cost, and unambiguous language for communication.

The Proceedings of the 1974 Fluid Power Testing Symposium suggest that the need for a unified measurement system for the fluid power industry has been well established. There may now be an opportunity to effectively coordinate the resources of industry associations, universities, and user government agencies with those of the National Bureau of Standards.

6453. Manning, R. G., Braun, W., Kurylo, M. J., **The effect of infrared laser excitation on reaction dynamics: $O + C_2H_4^\dagger$ and $O + OCS^\dagger$,** *J. Chem. Phys.* **65,** No. 7,2609–2615 (Oct. 1, 1976).

Key words: carbonyl sulfide; chemical kinetics; ethylene; flash photolysis resonance fluorescence; infrared laser; oxygen atoms; vibrationally excited reactant molecules.

A technique involving flash photolytic production and resonance fluorescence detection of O atoms coupled with cw production of vibrationally excited reactant molecules using a $CO_2$ laser is described. The method relies on the high sensitivity and precision of the flash photolysis resonance fluorescence technique to compare reaction rates measured with the laser off with those measured with the laser on, thereby assessing any effect of reactant vibrational energy on the dynamics of the chemical reaction. The limiting value of the laser enhancement that can be discerned depends ultimately on two factors: (1) the equilibrium concentration of vibrationally excited reactant that can be experimentally realized (i.e., absorption of laser flux vs deactivation losses), and (2) the magnitude of the activation energy for the thermal reaction. This determines the extent of a purely thermal (heating) effect. We observed little or no effect of vibrational energy in $C_2H_4$ on the rate of reaction with O atoms. Because of a somewhat higher activation energy, it was considerably more difficult to measure an effect in the $O + OCS$ reaction. Within the limits of detectability, all observations in this system could be attributed to heating effects. A factor of 1.5 increase in the rate constant for $O + C_2H_4^\dagger$ over that for $O + C_2H_4$ and a factor of 3 for $O \pm OCS^\dagger$ over $O + OCS$ would have been detectable in these experiments. The results seem to indicate that there is little or no coupling of vibrational energy to the reaction coordinate leading to activated complexes in these two reaction systems.

6454. Gadzuk, J. W., **Electron spectroscopy of surfaces via field and photoemission,** Paper in *Electronic Structure and Reactivity of Metal Surfaces*, E. G. Derouane and A. A. Lucas, Eds., pp. 341-387 (Plenum Publishing Corp., New York, NY, 1976).

Key words: chemisorption; ESCA; field emission; photoemission; surfaces; x-ray photoemission.

A review and survey of some of the basic physics involved in field and photoemission spectroscopy of surfaces is presented. Special emphasis is placed on the role of spatial coherence in determining the noninteracting electron photoemission characteristics of surfaces. Many-body effects, in particular the static response leading to relaxation energies and the dynamic response resulting in satellite structures are treated and the connection between them is demonstrated.

6455. Klein, M., Haar, L., **Equilibrium compositions and compressibility factors for air in the temperature range 1500 to 13000 kelvin and for densities from $10^{-6}$ to $10^3$ times standard density,** *AEDC-TR-76-85*, 77 pages (Available from the National Technical Information Service, Springfield, VA 22161, June 1976).

Key words: air; gases; high density; mixtures; thermodynamic properties.

A formalism for computing thermodynamic properties and equilibrium compositions of reacting gas mixtures at high densities is developed. This formalism makes use of the Haar-Shenker version of the augmented hard sphere equation of state. The formalism is used for computing compressibility factors and equilibrium compositions of air in the temperature range 2,000 K-13,000 K for densities from that appropriate to air at standard conditions (0 °C, 1 atmosphere) to densities 1000 times as great. These tables are consistent with the earlier NBS tables which covered the range up to 100 times that density. Some interesting features of the dependence of composition on density are discussed.

16456. Kaldor, A., Woodward, B. W., **Infrared laser monitoring techniques for NO and $NO_2$,** *AIChE Symp. Ser.* **71,** No. 148, 183-189 (1974).

Key words: apparatus and methods; infrared lasers; magnetic resonance; molecular spectroscopy; NO, $NO_2$, pollutant detection.

The concentration of NO and $NO_2$ can be monitored by several different infrared laser devices and techniques. These include laser sources such as a CO laser, tunable diode lasers, tunable spin-flip Raman laser, etc. and detection techniques such as Zeeman magnetic resonance, intracavity absorption, and optoacoustic devices. Sensitivities to the ppb range have been demonstrated. These different methods are discussed and evaluated.

16457. Cook, L. P., Plante, E. R., Negas, T., Roth, R. S., Olson, C. D., **Crystallization and vaporization studies on synthetic coal slag compositions,** *Proc. 15th Symp. on Engineering Aspects of Magnetohydrodynamics, Philadelphia, PA, May 24-25, 1976*, pp. II.4.1-II.4.6 (1976).

Key words: crystallization; magnetohydrodynamics; potassium activity; synthetic coal slags; system $K_2O$-$CaO$-$Al_2O_3$-$SiO_2$; vaporization.

Insight as to the chemical behavior of coal slags accumulating on the walls of MHD systems can be gained by examining the results of high temperature experiments on $K_2O$-$CaO$-$Al_2O_3$-$SiO_2$ mixtures. An increase in CaO content may increase $a_{K_2O}$ appreciably for certain compositions. Potassium aluminate – silica solid solutions, some of which are relatively water soluble, occur over a significant range of silica-poor and Ca-rich compositions at 1400 °C.

Two synthetic slags, with compositions falling close to an observed distribution of coal ash analyses, have been studied with the mass spectrometer using the Knudsen effusion technique. One slag having initially 15 wt% CaO yielded a higher K pressure at 10 wt% $K_2O$ than a $K_2O$-$SiO_2$ solution containing 30 wt% $K_2O$. A second slag with relatively high $SiO_2$ and $Al_2O_3$ and 13 wt% $K_2O$ gave a K pressure above that of a $K_2O$-$SiO_2$ solution with 20 wt% $K_2O$.

16458. McDonald, D. G., **Josephson junctions as radiation detectors from millihertz to terahertz,** *IEEE J. Quantum Electron.* **QE-10,** No. 9, 776-777 (Sept. 1974).

Key words: cryogenics; infrared; Josephson junctions; lasers; radiation detectors; superconductors.

The early experiments using Josephson junctions as mixers or detectors were at frequencies below a few hundred GHz. Recently we have shown that Josephson junctions can be used as mixers at much higher frequencies, particularly at $CO_2$ laser frequencies.

16459. Olver, F. W. J., **Uniform asymptotic expansions and singular perturbations,** *SIAM-AMS Proc.* **10,** 105-117 (American Mathematical Society, Providence, RI, 1976).

Key words: boundary-value problem; eigenvalues; parabolic cylinder functions; resonance; rotating disks; singular perturbations; turning-point; viscous flow; Weber's equation.

A brief account is given of an investigation into the asymptotic nature of the solution of the boundary-value problem

$$\epsilon y'' + 2xA(\epsilon,x)y' - A(\epsilon,x)B(\epsilon,x)y = 0,\ y(a) = l,\ y(b) = m,$$

as $\epsilon \rightarrow 0$, where $A(\epsilon,x)$ and $B(\epsilon,x)$ are continuous real functions of $\epsilon$ and $x$, $a < 0$, $b > 0$, and $A(\epsilon,x)$ is nonzero in $[a,b]$. Particular attention is paid to the problem of resonance, which arises when the limiting form of the solution exhibits an unusual lack of decay (in the case $A(\epsilon,x) < 0$), or an unusual rate of growth (in the case $A(\epsilon,x) > 0$). By application of a recent theory of differential equations with coalescing turning points sufficient conditions for resonance are established, both with and without the assumption that $A(\epsilon,x)$ and $B(\epsilon,x)$ are analytic functions of $\epsilon$ and $x$.

Fuller details will be published elsewhere.

**16460.** Yates, J. T., Jr., Klein, R., Madey, T. E., **Adsorption of molecular nitrogen by the W(110) plane,** *Surface Sci.* **58,** 469-478 (1976).

Key words: adsorption; nitrogen; physical adsorption; tungsten; work function.

Characteristics of the adsorption of nitrogen on the (110) plane of tungsten were determined by thermal desorption and work function measurements. The low temperatue $\gamma$-$N_2$ state desorbs with first order kinetics and an activation energy of 6 kcal mole$^{-1}$. The absence of isotope mixing between $^{14}N_2$ and $^{15}N_2$ demonstrates $\gamma$-$N_2$ is adsorbed molecularly. Monolayer coverage shows a decrease of 0.19 eV in work function. A Topping model plot indicates the layer is immobile at 123 K.

**16461.** Wyatt, W. T., Jr., Lozier, D. W., Orser, D. J., **A portable extended precision arithmetic package and library with Fortran precompiler,** *ACM Trans. Math. Software* **2,** No. 3, 209-231 (Sept. 1976).

Key words: elementary function evaluation; extended precision arithmetic; floating point arithmetic; Fortran extended data types; Fortran precompiler.

A set of ANS Fortran subroutines, developed by W. T. Wyatt, which incorporates computer-independent algorithms for performing arithmetic on arbitrary length, extended precision, floating point, real, or complex numbers in any user-designated computation base from 2 to 16 is described. Also included is a library of the Fortran intrinsic and external (mathematical) functions, as well as routines for type conversion, base conversion, input/output, and other operations. Analysis and testing, by D. W. Lozier, of the arithmetic and library software to locate and eliminate errors and to determine approximate accuracy limits is described. Finally, a precompiler, written in Fortran by D. J. Orser, which translates a Fortran program containing two extended precision data types (SUPER PRECISION and SUPER COMPLEX) into an ordinary Fortran program that uses subroutine calls to the software to carry out the extended precision operations is described. The software is intended to furnish working scientists who are not specialists in computer science a ready means of computing in extended precision.

**16462.** Weber, L. A., **Dielectric constant data and the derived Clausius-Mossotti function for compressed gaseous and liquid ethane,** *J. Chem. Phys.* **65,** No. 1, 446-449 (July 1, 1976).

Key words: Clausius-Mossotti function; dielectric constant; equation of state (PVT); ethane.

Measurements are presented for the dielectric constant of ethane in the saturated liquid and compressed fluid states at temperatures between 95 and 323 K. Pressures ranged up to 390 bar. The data, which have an estimated uncertainty of 0.01 percent, are combined with accurate density data from several sources to produce the Clausius-Mossotti function over a wide range of temperature and density. An analytical expression of the Clausius-Mossotti function is given, and the consistency of the available density data is discussed.

**16463.** Andrews, J. R., **Impulse generator spectrum amplitude measurement techniques,** *CPEM Digest,* pp. 23-24 (1976).

Key words: calibration; Fourier transform; impulse generator; pulse measurement; spectrum; spectrum amplitude.

This paper discusses the various techniques that have been used to calibrate impulse generators and to measure spectrum amplitude. The techniques included are (1) standard transmission line, (2) harmonic measurement, (3) energy measurement, (4) sum and difference correlation radiometer, (5) Dicke type radiometer, (6) video pulse, MIL. Std. 462, (7) spectrum analyzer, (8) standard pulse comparison, and (9) time domain measurement with Fourier transformation computation. Advantages and disadvantages of each technique are discussed. A summary of experiments comparing the various techniques is included. The NBS measurement service for calibrating impulse generators is described.

**16464.** Baird, R. C., **Methods of calibrating microwave hazard meters,** *Proc. Int. Symp. on Biologic Effects and Health Hazards of Microwave Radiation, Warsaw, Poland, Oct. 15-18, 1973,* pp. 228-236 (Polish Medical Publ., Warsaw, Poland, 1974).

Key words: microwave hazard meters; microwave radiation.

Accurate and reliable measurements of microwave radiation are required for hazard surveys, leakage detection, testing of products for compliance with regulations, and for determining exposure levels in experiments designed to investigate the biologic effects of microwave radiation. Accurate calibration of the instruments used for these measurements is essential for safety reasons and to provide a basis for comparison of the experimental results of various laboratories.

**16465.** Birmingham, B. W., Smith, C. N., **A survey of large scale applications of superconductivity in the U.S.,** *Cryogenics* **16,** No. 2, 59-71 (Feb. 1976).

Key words: cryogenics; CTR; electric power; energy storage; generators; instrumentation; MHD; superconductivity.

This survey provides a general overview of the kind and amount of research being done in the U.S. on large-scale applications of superconductivity. It covers about $30 million worth of research and development on systems and devices, and excludes programs on superconducting phenomena or basic studies of properties of materials unless they are part of an applications program. It covers the categories of electric power systems (generation, transmission, and storage); high energy physics; and instrumental-industrial-medical applications. Data were gathered through personal contact and letters to the researchers involved, and include funding and manpower levels where possible.

**16466.** Carroll, J. J., Melmed, A. J., **Field ion microscopy of zirconium,** *Surface Sci.* **58,** No. 2, 601-604 (Aug. 1976).

Key words: field-ion microscopy; zirconium.

Zirconium was successfully imaged in the field ion microscope using neon ions and mixtures of helium and neon ions at specimen temperatures of about 30K. Micrographs obtained after zirconium was exposed to hydrogen imaging conditions showed features that may indicate the early stage development of cracks, mostly along the $\{11\bar{2}0\} - \{11\bar{2}2\}$ zone. Crack defects were confined to at least the topmost 2-5 layers.

**16467.** Carroll, J. J., Melmed, A. J., **Optical constants of (1120) ruthenium in the visible region,** *J. Opt. Soc. Am.* **66,** No. 10, 1050-1051 (Oct. 1976).

Key words: ellipsometry; optical constants; ruthenium.

Optical constants are reported for $(11\bar{2}0)$ ruthenium measured ellipsometrically in the visible spectrum under ultrahigh vacuum conditions. The results are compared to literature values.

**16468.** Clough, R. B., **Rational basis and new methods for proportional limit, machine stiffness, critical stress intensity, and crack velocity measurements,** (Proc. 78th Annual Meeting American Society for Testing and Materials, Montreal, Canada, June 22-27, 1975), *Am. Soc. Testing Mater. Spec. Tech. Publ. 608, Recent Developments in Mechanical Testing,* pp. 20-44 (1976).

Key words: crack propagation; determination of stress; measurement; mechanical tests; plastic deformation; proportional limit.

This paper is a summary of some new measurement techniques that have been developed recently at the National Bureau of Standards for measurement of proportional limit of elasticity, machine stiffness, critical stress intensity, and crack velocity. These seemingly unrelated measurements all result from the rational basis of a single type of equation relating specimen and machine kinetics. In a regime of linear elasticity, the concept of a limit beyond which the specimen elastic gage length displacement is no longer proportional to load is referred to as proportional limit if the gage length begins to exhibit plastic deformation, and is referred to in a precracked specimen as critical stress intensity if the crack begins to extend in length. Multiaxial plastic yielding is also discussed. Machine stiffness and crack velocity are other measurements which can be obtained through the specimen-machine equation. The relationship of the new stiffness measurement to the International Standards Organization (ISO) proposed method and advantages of the new method are discussed. Methods of measuring stiffness in constant load rate and constant strain rate tests are outlined. A method of measuring the proportional limit or critical stress intensity which does not use a displacement gage of any type is also given; this should prove useful in hostile environments. Other related topics discussed include loading transients and rate sensitivity.

**16469.** Crawford, M. L., **Experimental evaluation of the radiation characteristics of dipole sources enclosed in a TEM transmission cell,** *CPEM Digest,* pp. 57-59 (1976).

Key words: measurements; radiated emission; radiation resistance; TEM cells.

This paper describes measurements to verify theoretical formulation of the changes in the radiation resistance of electronic equipment enclosed inside a special type shielded enclosure, a rectangular TEM cell. The measurements were made, assuming the device under test (DUT) could be modeled by dipole sources, using a monopole antenna mounted at various locations inside a typical cell. The predicted radiated power from the monopole antenna mounted inside the cell was within ±2 dB of the energy coupled to the cell's output ports. These results are contained in the paper and give credibility to the ability to relate such measurements to free space radiation conditions.

**16470.** Crawford, M. L., **Calibration of broadbeam antennas using planar near-field measurements,** *CPEM Digest,* pp. 53-56 (1976).

Key words: broadbeam antennas; planar near field measurements.

This paper describes techniques for improving and extending planar near field (PNF) measurements for use in calibrating broadbeam antennas (gain $\geq 3$ dB). This application requires minimizing errors associated with the PFN formulations: specifically, the assumptions that 1) all significant near fields associated with the test antenna fall within the measurement scan area and 2) that multiple reflections between test antenna, probe, and their surroundings are negligible. The techniques discussed include: 1) optimizing the scan parameters (e.g., size of scan area, data point spacing, and separation distance between the test antenna and measure plane); 2) simulating measurements taken over an extended, enlarged, scan area; 3) minimizing multipath error; and 4) use of data deletion and extrapolation to obtain the test antenna's on-axis gain calibration. The paper also contains results of measurements made using a typical broadbeam antenna. These results include comparisons made between a far field pattern obtained using PNF scanning and using a conventional far field range.

**16471.** Day, G. W., Hamilton, C. A., Gruzensky, P. M., Phelan, R. J., Jr., **Performance and characteristics of polyvinylidene fluoride pyroelectric detectors,** (Proc. IEEE Symp. on Application of Ferroelectrics, Albuquerque, NM, June 9-11, 1975), *Ferroelectrics* **11,** 99-102 (1976).

Key words: infrared detectors; polymers; pyroelectrics; radiometry.

Pyroelectric detectors based on the polymer film polyvinylidene fluoride should be recognized as attractive choices for applications where a high detectivity coupled with a broad spectral response and a large area are required. Devices with a 1 $\text{cm}^2$ area typically have a detectivity of $10^9 f^{1/2}$ cm $\text{Hz}^{1/2}$/W where $f$ is the frequency in Hz. Fabrication may be directly from commercially available film or with some additional processing. Several instruments incorporating these detectors have been developed to solve certain radiometric measurement problems.

**16472.** Day, G. W., Hamilton, C. A., Pyatt, K. W., **Spectral reference detector for the visible to 12-$\mu$m region; convenient, spectrally flat,** *Appl. Opt.* **15,** No. 7, 1865-1868 (July 1976).

Key words: detector; infrared; pyroelectric; spectral response.

A convenient spectral reference detector for the visible to 12-$\mu$m region has been developed. The device consists of a large area $\text{PVF}_2$ pyroelectric detector enclosed in a hemispherical light trap. Based on theoretical and experimental evaluations, the detector response is independent of wavelength to ±1 percent over this spectral range.

**16473.** Domen, S. R., Lamperti, P. J., **Comparisons of calorimetric and ionometric measurements in graphite irradiated with electrons from 15 to 50 MeV,** *Med. Phys.* **3,** No. 5, 294-301 (Sept.-Oct. 1976).

Key words: absorbed dose; calorimeter; electrons; heat defect in graphite.

Extensive experimental comparisons of calorimetric and ionometric measurements have been made that cover a broader range of electron energies and depths in graphite than previously reported. Electron beams of 15, 20, 25, 30, 40, and 50 MeV were used. Calorimetric absorbed-dose measurements and ionometric specific-charge measurements in air were compared in graphite at depths from 1 to 51 $\text{g/cm}^2$. The medium was irradiated with uncollimated electron beams produced by scattering after passing through a 0.1-$\text{g/cm}^2$ aluminum vacuum window, various thicknesses of lead foils, and air. The variation in the quotient of the two measurements was studied as a function of lead-foil thickness, depth in the medium, beam energy, foil-to-detector distance, and off-axis distance. These studies permitted the measurements to be corrected and compared with theoretical calculations that assume a broad medium irradiated with broad, parallel, monoenergetic electron beams. The overall experimental uncertainty is estimated to be 1 percent. The results are generally in good agreement with theoretical and experimental results of other investigators. The calorimeter received close to 1 Mrad during preliminary measurements and from 1 to 2 Mrad during the measurements reported. The results showed no detectable heat defect in graphite after prolonged periods of exposing the calorimeter to air at atmospheric pressure.

**16474.** Ekin, J. W., **Effect of stress on the critical current of $Nb_3Sn$ multifilamentary composite wire,** *Appl. Phys. Lett.* **29,** No. 3, 216-219 (Aug. 1, 1976).

Key words: critical currents; magnets; magnet wire; $Nb_3Sn$; $Nb_3Sn$ magnets; $Nb_3Sn$ multifilamentary wires; strain; stress; superconducting magnets.

A critical-current study of flexible $Nb_3Sn$ multifilamentary composite wires has been conducted at 4 K in magnetic fields to 90 kOe ($7.2 \times 10^6$ A/m) while the wire is subjected to high mechanical stresses. The results show that at stresses above 1-2 $\times 10^8$ Pa (strains of 0.1-0.2%) the critical current is significantly degraded, with the magnitude of the reduction dependent on reinforcement techniques used in the wire's construction. The effect increases with magnetic field and results in the introduction of significant resistance at current levels well below the zero-stress critical current. Design considerations for the use of $Nb_3Sn$ wires in the high-stress environments of large-scale superconducting magnets are discussed.

**16475.** Engen, G. F., **Measurement of complex microwave circuit parameters using only power detectors,** *CPEM Digest,* p. 171 (1976).

Key words: automatic network analyzer; microwave; microwave measurement; six-port.

Although straightforward in principle, the extension of existing designs for automatic network analyzers to the higher microwave frequencies is difficult in the current state-of-the-art. What appears to be needed is a basically different approach to the microwave detection problem. This is provided by the so-called "six-port" techniques, which eliminate the need for frequency conversion, local oscillators, phase detectors, etc. Recent theoretical studies have provided new insights into the basic concept and lead to "five-port" configurations which require three instead of four amplitude detectors. Of particular interest is the useful measurement dynamic range of 50-60 dB corresponding to an intrinsic dynamic range required in the amplitude detectors of a nominal 20 dB or less.

**16476.** Estin, A. J., **Scattering parameters of SMA coaxial connector pairs,** *CPEM Digest,* pp. 110-111 (1976).

Key words: coaxial connectors; connectors; RF connectors; SMA connectors.

A technique is described for making insertion loss and reflection measurements on SMA connectors mounted on solid-dielectric coaxial line. Results are given for measurements of $|S_{11}|$ and $|S_{21}|$ of eight test pairs over the frequency range of 4 to 12 GHz.

**16477.** Gans, W. L., **Present capabilities of the NBS automatic pulse measurement system,** *CPEM Digest,* pp. 25-26 (1976).

Key words: automated measurement; pulse; rise time; sampling oscilloscope; spectrum amplitude; time domain; transient.

In 1972, NBS began development of an Automatic Pulse Measurement System (APMS) consisting essentially of a minicomputer-controlled wideband sampling oscilloscope. The objective of the work was to produce a fast, general purpose transient waveform acquisition and processing instrument covering the frequency range dc-18 GHz. The purpose of this paper is to report the highlights of work done on the APMS from early 1975 to present.

The measurement applications of the APMS now consist of both publicly offered calibration services and inhouse experimental measurements. In the first category, calibration services are available for the following physical parameters: a. Impulse generator spectrum amplitude; b. Wideband coaxial attenuation/gain; c. Low pass filter risetime; d. Pulse generator risetime.

Still in the experimental stage are measurements involving reflection coefficient and impedance, group delay, pulse distortion, and wideband antenna characteristics. In addition, the APMS is quite often used for theoretical modeling and model/experiment comparison and verification.

**16478.** Ginsberg, D. M., Harris, R. E., Dynes, R. C., **Strong-coupling correction to the low-frequency electrical conductivity of superconductors and Josephson junctions,** *Phys. Rev. B* **14,** No. 3, 990-992 (Aug. 1, 1976).

Key words: electron tunneling; electronic devices; far infrared; Josephson effect; strong electron-phonon coupling; superconductivity.

Values of the strong-coupling correction to the low-frequency local-limit conductivity of a number of superconductors are given. These values also describe the strong-coupling correction to the critical current of a Josephson tunnel junction. The correction is given for indium, amorphous gallium, $\beta$-phase gallium, amorphous bismuth, $Pb_{0.8}Bi_{0.2}$, $Pb_{0.7}Bi_{0.3}$, amorphous $Pb_{0.45}Bi_{0.55}$, $Tl_{0.9}Bi_{0.1}$, $Pb_{0.8}Tl_{0.2}$, and previously published values are listed for tin, lead, mercury thallium, and indium-thallium alloys. It is shown that there is a simple empirical relation between these values and the effective electron-electron coupling parameter ($\lambda - \mu^*$).

**16479.** Unassigned.

**16480.** Greer, S. C., **Coexistence curves at liquid-liquid critical points: Ising exponents and extended scaling,** *Phys. Rev. A* **14,** No. 5, 1770-1780 (Nov. 1976).

Key words: binary mixture; coexistence curve; critical phenomena; density; isobutyric acid; magnetic densimeter; phase equilibria, carbon disulfide, nitromethane; water.

New measurements have been made of coexisting mass densities of isobutyric acid and water with a precision of 20 ppm and within 3.5 °C of the critical temperature. The measurements were made using a single sample of composition very close to critical. It is found that the coexistence curve is more symmetric in terms of the difference in volume fraction ($\Delta\phi$) of coexisting phases than in terms of the difference in mass density. The difference $\Delta\phi$ is well fitted for $\epsilon = (T_c - T)/T_c < 0.006$ by the expression $\Delta\phi = B\epsilon^{\beta}$, where $B = 1.071 \pm 0.023$ and $\beta = 0.328 \pm 0.004$. (Uncertainties are given as 3 times the standard deviation.) A new analysis has been made of the recent data of Gopal *et al.* on the difference in volume fraction of coexisting densities of carbon disulfide and nitromethane. For this system, $\Delta\phi$ can be fitted for $\epsilon < 0.2$ by an extended scaling expression suggested by Wegner's work, $\Delta\phi = B\epsilon^{\beta} + B_1\epsilon^{\beta+\Delta} + B_2\epsilon^{\beta+2\Delta}$. The exponent $\Delta_2$ is fixed at 0.5; the fit gives $\beta = 0.316 \pm 0.008$, $B = 1.63 \pm 0.09$, $B_1 = 0.77 \pm 0.31$, and $B_2 = -2.43 \pm 0.40$. This work suggests that liquid-liquid critical phenomena are consistent with the functional forms obtained from renormalization-group calculations and with asymptotic exponents which are like those presently calculated for the Ising model. The range of asymptotic behavior seems to be larger for a liquid-liquid critical point than for a liquid-gas critical point.

16481. Hammond, G. A., Brown, W. B., Yolken, H. T., **National program of measurements and standards for safeguarding nuclear materials,** (Proc. 17th Annual Meeting Institute of Nuclear Materials Management, Inc., Seattle, WA, June 22-24, 1976), Paper in *Nuclear Materials Management* V, No. III, 351-360 (1976).

Key words: fuel; materials accountability; measurements; nuclear; safeguards; standards.

A national measurement and standards program is described which is coordinated essentially by the Nuclear Regulatory Commission, the National Bureau of Standards and the Energy Research and Development Administration. Efforts and progress are outlined as related to assuring that timely, accurate measurements at reasonable cost are available to the nuclear community. The results of this combined effort show that programs are underway to keep abreast of the present measurement needs for nuclear materials safeguards, and that projected work is consistent with a growing U.S. nuclear industry.

16482. Hanley, H. J. M., **Comment on "Citation analysis: A new tool for science administrators",** *Science News and Comment* **188,** No. 4193, 1064 (June 1975).

Key words: citation index.

Comment on "News and Comment" item, entitled "Citation Analysis: A New Tool for Science Administrators," appearing in *Science*, **188,** 4187, p. 429, May 2, 1975.

16483. Hanley, H. J. M., Cohen, E. G. D., **Analysis of the transport coefficients for simple dense fluids: The diffusion and bulk viscosity coefficients,** *Physica* **83A,** 215-232 (1976).

Key words: argon; bulk viscosity; density expansion; methane; modified Enskog theory; molecular correlations; nitrogen; sound absorption.

The analysis of transport coefficients based on the modified Enskog theory (MET), discussed in a previous publication, has been extended to include the self-diffusion coefficient *(D)* and the bulk viscosity coefficient ($\eta_v$). Specifically, calculated values according to the MET are compared with experiment over the range for which data are available. Fluids considered are argon, nitrogen and methane. Agreement between theory and experiment for densities less than about twice the critical density ($\rho_c$) is generally within about 10 percent. However, much of the data was taken at densities well in excess of $2\rho_c$ in which case agreement is still not unsatisfactory. Deviations exceeding 10 percent between theoretical and experimental self-diffusion coefficients were observed for densities in the approximate range $0.9 \lesssim \rho/\rho_c \lesssim 2.0$. It is possible that these deviations are due to long range correlated molecular motions which are not present in the MET. The sound absorption is also briefly considered. Finally, the behavior of $\eta_v$ and $D$ at low densities is discussed.

16484. Hanley, H. J. M., Sengers, J. V., Ely, J. F., **On estimating thermal conductivity coefficients in the critical region of gases,** *Proc. 14th Int. Conf. Thermal Conductivity, Storrs, CT, June 2-4, 1975*, Paper R-960, pp. 383-407 (Plenum Publ. Corp., New York, NY, 1976).

Key words: correlation length; critical point; gas-liquid; nonspherical molecules; Ornstein-Zernike theory; thermal conductivity.

The thermal conductivity of a fluid exhibits a pronounced anomalous increase in a large range of densities and temperatures around the gas-liquid critical point. In this paper we discuss an attempt to estimate the thermal conductivity in the critical region of fluids from a knowledge of the equilibrium properties and the regular behavior of the transport properties outside the critical region.

16485. Harris, R. E., **Intrinsic response time of a Josephson tunnel junction,** *Phys. Rev. B* **13,** No. 9, 3818-3821 (May 1, 1976).

Key words: electronics devices; high speed devices; Josephson effect; superconducting devices; superconductivity; tunneling.

The microscopic theory of the Josephson effect is reformulated in the time domain. The four terms in the usual theory are seen to be necessary consequences of intrinsic junction delays. The tunneling current flowing in response to a voltage pulse is shown to rise in a time $\hbar/2\Delta$ and undergo damped energy-gap oscillations, before approaching the expected supercurrent. The theory provides a technique for calculating junction behavior when connected to an arbitrary circuit.

16486. Harris, R. E., Dynes, R. C., Ginsberg, D. M., **Strong-coupling correction to the jump in the quasiparticle current of a superconducting tunnel junction,** *Phys. Rev. B* **14,** No. 3, 993-995 (Aug. 1, 1976).

Key words: electronic devices; electron tunneling; Josephson effect; strong electron-phonon coupling; superconductivity.

Calculated values of the strong-coupling correction to the jump in the quasiparticle current of superconductor-insulator-superconductor tunnel junctions are given for a number of elements, amorphous materials, and alloys. It is shown that there is a simple empirical relation between the size of jump in the quasiparticle current and the effective electron-electron coupling parameter ($\lambda - \mu^*$).

16487. Hellwig, H., Allan, D. W., Jarvis, S., Jr., Glaze, D. J., **The realization of the second,** (Proc. Fifth Int. Conf. on Atomic Masses and Fundamental Constants (AMCO-5), Paris, France, June 2-6, 1975), Paper in *Atomic Masses and Fundamental Constants*, J. H. Sanders and A. H. Wapstra, Eds., pp. 330-336 (Plenum Publ. Corp., New York, NY, 1975).

Key words: atomic beams; atomic clock; atomic time; cesium beam tube; definition of the second; frequency accuracy; international atomic time; primary frequency standard.

We report realizations of the unit of time with an accuracy approaching $1 \times 10^{-13}$ using our two primary cesium beam standards. Quantitative values are given for the requirements on operating parameters of such devices in order to assure high frequency stability. Principal design limitations and fundamental approaches to overcome them are discussed. The concept of a servo which maintains accuracy is advanced which would allow primary standards to operate continuously as clocks without loss in their evaluated accuracy.

16488. Hellwig, H., Allan, D. W., Walls, F. L., **Time and frequency,** (Proc. Fifth Int. Conf. on Atomic Masses and Fundamental Constants (AMCO-5), Paris, France, June 2-6, 1975), Paper in *Atomic Masses and Fundamental Constants*, J. H. Sanders and A. H. Wapstra, Eds., pp. 305-311 (Plenum Publ. Corp., New York, NY, 1975).

Key words: clocks; frequency accuracy; frequency stability; frequency standards; infrared frequency multiplication; noise; time scale; time standards.

A comparison of the accuracy and stability performance of precise frequency standards is given. It is shown that measurement systems exist which comfortably allow the full characterization of these standards. The importance of spectrally pure oscillators for frequency synthesis into the infrared region is discussed quantitatively. The problem of absolute accuracy in timekeeping is reviewed.

**16489.** Hellwig, H., Wainwright, A. E., **A portable rubidium clock for precision time transport,** *Proc. 7th Annual Precise Time and Time Interval (PTTI) Planning Meeting, Washington, DC, Dec. 2-4, 1975,* pp. 143-159 (Goddard Space Flight Center, Greenbelt, MD, 1976).

Key words: atomic clocks; frequency stability; portable clocks; rubidium frequency standard; time comparison.

Based on a commercially available rubidium standard the National Bureau of Standards (NBS) developed a portable rubidium clock. Technical modifications which reduce the sensitivity against temperature, magnetic environment, and barometric changes allow stabilities in the $10^{-12}$ range under typical clock transport conditions. Under laboratory conditions the clock shows a best stability of 3 parts in $10^{14}$. Clock packages based on sealed lead-acid batteries featuring a total weight of 21 kg and 18 hours battery operation were tested; an improved clock package was realized using silver-zinc batteries with 11 kg weight and 28 hours battery operation. Report of several clock trips to the U.S. Naval Observatory and of one clock trip each to the Bureau International de l'Heure in Paris and to the Hewlett-Packard Company in Santa Clara, California are reported. Time transport precisions of .02 $\mu$s have been obtained. Special aspects of the clock modifications and the operating characteristics are discussed, as well as an optimal use of the data of a clock roundtrip.

**16490.** Hoer, C. A., Roe, K. C., Allred, C. M., **Measuring and minimizing diode detector nonlinearity,** *CPEM Digest,* pp. 108-109 (1976).

Key words: detectors; diodes; linearity; square-law.

This paper describes a technique for measuring the linearity of amplitude detectors in general, and for measuring the deviation from square-law, E, of point-contact diode detectors in particular. A general mathematical model is given for determining the rf input power as a function of the detector output voltage. For point-contact diodes it is shown how to choose the video load resistance to minimize E, as well as how to calculate and correct for E.

**16491.** Holste, J. C., Lawless, W. N., Samara, G. A., **Dielectric properties of $KH_2PO_4$, $BaTiO_3$, $PbZr_{0.65}Ti_{0.35}O_3$ and TlCl between 0.015 and 10 K,** (Proc. IEEE Symp. on Application of Ferroelectrics, Albuquerque, NM, June 9-11, 1975), *Ferroelectrics* **11,** 337-340 (1976).

Key words: barium titanate; dielectric properties; ferroelectrics; KDP; PZT 65/35; thallium chloride; very low temperatures.

The small-signal ac permittivities ($\epsilon$) of single crystal samples of KDP, $BaTiO_3$, and TlCl, and of a ceramic sample of PZT 65/35 have been measured as a function of temperature between 0.015 and 10 K. For KDP and PZT 65/35, $\epsilon$ increases essentially linearly with temperature in this range, with $d \ln \epsilon/dT = 0.95 \pm 0.15 \times 10^{-3}\ K^{-1}$ and $1.81 \pm 0.02 \times 10^{-3}\ K^{-1}$, respectively. For $BaTiO_3$ linear behavior is observed only between 1.5 and 4.5 K, with $d \ln \epsilon/dT = 9.4 \times 10^{-4}\ K^{-1}$. PZT 65/35 exhibits positive deviation from this apparent linear behavior between 0.1 and 1.5 K, while $BaTiO_3$ shows a negative deviation in this range. Both PZT 65/35 and $BaTiO_3$ have a minimum in $\epsilon$ below 0.1 K and an associated change in the dielectric loss factor that depends on the frequency and amplitude of the ac signal. No temperature dependence of $\epsilon$ was observed below 3 K for TlCl. Potential applications of these materials at low temperatures are discussed.

**16492.** Howe, D. A., **Precise frequency dissemination using the 19-kHz pilot tone on stereo FM radio stations,** *IEEE Trans. Broadcast.* **BC-20,** No. 1, 17-20 (Mar. 1974).

Key words: frequency modulation; modulation index; multipath; path delay; phase vs. time; $\sigma$ vs. $\tau$, 19 kHz pilot.

A continuous 19-kHz pilot tone is included as part of the modulation format of stereo FM broadcast radio stations. An experiment was performed which measures the stability of the received pilot in urban rural environments. A mathematical analysis is presented of the phase stability of the received pilot as a function of multipath. It shows that phase changes will exist dependent upon a reflected radio signal's phase lag, relative amplitude, and the modulation index. Data are presented which indicate: 1) phase versus time of the pilot at the National Bureau of Standards (NBS) laboratory using a directional yagi and a vertical whip; 2) Allan variance measurements of $\sigma$ versus $\tau$ using a directional yagi; and 3) the day-to-day phase delay of the pilot at five urban locations and three rural locations using a vertical whip. With 5 min of averaging time, the delay of the pilot at five urban sites was reproducible to within 2 $\mu$s each day over a five-day period. Delay was reproducible to within 0.8 $\mu$s at three urban sites.

**16493.** Howell, B. F., Margolis, S., Schaffer, R., **Detection of inhibitors in reduced nicotinamide adenine dinucleotide by kinetic methods,** *Clin. Chem.* **22,** No. 10, 1648-1654 (1976).

Key words: Michaelis constants for NADH and LDH-5; LDH-1.

Methods are described for detection of lactate dehydrogenase (LDH) inhibitors in preparations of reduced nicotinamide adenine dinucleotide. They are (a) comparison of values by kinetic methods with those measured for highly purified NADH and (b) examination of Lineweaver-Burk plots. Chromatographic inhomogeneities are correlated with deviant values for the kinetic constants of NADH preparations. Lineweaver-Burk plots that curve upward at the high concentrations or have a larger or smaller than normal slope may indicate the presence of inhibitor. As determined in bicarbonate buffer (0.11 mol/liter, pH 7.9) by use of 0.600 mmol/liter pyruvate and NADH freshly separated from impurities by chromatography on diethylaminoethyl-cellulose, the $K_m$ (apparent) of NADH at 25 °C has the value $8.11 \pm 0.71$ $\mu$mol/liter (SD, n = 28) with LDH-1 (pig heart, $2.48 \pm 0.05$ U per milliliter of reaction mixture, or $41.3 \pm 0.8$ nmol/liter per second). Under similar conditions, the $K_m$ (apparent) of NADH has the value of $8.57 \pm 1.58$ mol/liter (SD, n = 21) with LDH-5 (pig muscle, $1.77 \pm 0.03$ U/ml of reaction mixture), or $29.4 \pm 0.6$ nmol/liter per second). At infinite substrate concentrations with the same pH, buffer, and temperature, the $K_m$ (apparent) for NADH was $26.0 \pm 0.63$ $\mu$mol/liter with LDH-1 and $23.2 \pm 4.6$ $\mu$mol/liter with LDH-5.

**16494.** Hust, J. G., **Standard reference materials for thermal conductivity and electrical resistivity,** *Proc. 14th Int. Conf. Thermal Conductivity, Storrs, CT, June 2-4, 1975, Paper R-958,* pp. 221-231 (Plenum Publ. Corp., New York, NY, 1976).

Key words: austenitic stainless steel; electrical resistivity; high temperature; low temperature; standard reference materials; thermal conductivity.

A brief historical review is presented of thermal conductivity reference material research. Recent reference material research by the National Bureau of Standards is described. Critically evaluated thermal conductivity and electrical resistivity data are summarized for the following three Standard Reference Materials now available from the Office of Standard Reference Materials, National Bureau of Standards, Washington, D.C.: electrolytic iron (4 to 1000 K), austenitic stainless steel (4 to 1200 K), and tungsten (4 to 3000 K).

**16495.** Jesch, R. L., **Repeatability of SMA coaxial connectors,** *CPEM Digest*, pp. 103-104 (1976).

Key words: coaxial connectors; insertion loss; microwave; reflection coefficient magnitude; repeatability.

SMA connectors in three different configurations were investigated for variation of reflection coefficient magnitude and insertion loss for a given SMA connector connect-disconnect sequence. Repeatability measurements were taken over the frequency range of 2 to 18 GHz for reflection coefficient and over the frequency range of 2 to 12.4 GHz for insertion loss on the National Bureau of Standards' Automatic Network Analyzer. A sample of variation of reflection coefficient magnitude is given for one SMA connector configuration. This variation was much smaller than was expected for SMA connectors.

**16496.** Jespersen, J. L., **A survey of time and frequency dissemination techniques,** *Proc. 24th Annual Frequency Control Symp., Atlantic City, NJ, Apr. 27-29, 1970*, pp. 322-324 (U.S. Army Electronics Command, Ft. Monmouth, NJ, 1970).

Key words: broadcast; communication; frequency; ratio; synchronization; time.

There are a number of common elements which characterize most time dissemination systems. Among the more important are: accuracy, repeatability, coverage, possibilities for improvement, cost to establish and maintain, ambiguity, time required to obtain answer, ease of use, and cost to the user. At the present time, there does not appear to be any single system which incorporates all of the desired characteristics. The relative importance of these characteristics varies from one user to the next and the kind of tradeoff that one user is willing to make is not a suitable tradeoff for another. Some of the systems such as WWV, were built specifically for the purpose of time and frequency dissemination while others such as TV have considerable potential. These systems and others will be discussed and compared with reference to the characterizing elements enumerated earlier, and some unresolved problems for the future will be considered.

**16497.** Johnson, W. L., McNeil, J. R., Collins, G. J., Persson, K. B., **CW laser action in the blue-green spectral region from Ag II,** *Appl. Phys. Lett.* **29,** No. 2, 101-102 (July 15, 1976).

Key words: charge transfer; lasers; sputtering; visible.

We have observed 18 cw laser transitions in Ne-Ag mixtures spanning the wavelength region from 408.6 to 585.2 nm. The upper laser levels of Ag II are judged to be pumped by a charge-transfer reaction between a ground-state neon ion and a ground-state Ag I atom resulting in simultaneous ionization and excitation of the silver atom. Output characteristics of the Ag II laser transitions as a function of neon pressure and discharge current are presented. The two strongest transitions are 478.8 and 502.7 nm in the blue and green, respectively.

**16498.** Kamper, R. A., **RF applications of the Josephson effect,** *Microwave J.* **19,** No. 4, 39-41, 52 (Apr. 1976).

Key words: high frequency; infrared; Josephson effect; measurements; superconductivity.

This paper reviews progress to date in applying the Josephson effect to microwave detectors, mixers, parametric amplifiers, and measuring systems.

**16499.** Kanda, M., **An error analysis for absolute flux density measurements of Cassiopeia A,** *IEEE Trans. Instrum. Meas.* **IM-25,** No. 3, 173-182 (Sept. 1976).

Key words: accuracy; antenna; calibration; Cassiopeia A; error analysis; flux density; G/T (system gain/system noise temperature); ground station; radio star.

An error analysis for absolute flux density measurements of Cas A is discussed. The lower-bound quadrature-accumulation error for state-of-the-art measurements of the absolute flux density of Cas A around 7 GHz is estimated to be 1.71 percent for $3\sigma$ limits. The corresponding practicable error for the careful but not state-of-the-art measurements is estimated to be 4.46 percent for $3\sigma$ limits.

**16500.** Kanda, M., Larson, T. R., **Stability of silicon avalanche noise diodes at K and $K_a$** bands, *CPEM Digest*, pp. 215-217 (1976).

Key words: silicon avalanche diode; solid state noise source; stability.

A statistical analysis is given for the stability of silicon avalanche noise diodes at K and $K_a$ bands. A brief discussion of a statistical measure for stability and the measurement techniques are given. Cross-correlation coefficients of output noise from the noise diodes and their environmental factors are evaluated in order to examine the causes of the observed instabilities of noise diodes.

**16501.** Komarek, E. L., **An automated broadband system for measurement of one-port microwave parameters,** *CPEM Digest*, pp. 167-170 (1976).

Key words: application of six-port junction concept; automated measurements; broadband measurements; microwave measurements; microwave power measurements; one-port parameters; six-port junction.

A broadband measurement system has been implemented for determining microwave parameters of one-port devices in the 1-18 GHz frequency range using the six-port junction concept and automation techniques. Although not complete, performance evaluation results show that the system compares favorably with other automated and manually operated measurement methods.

**16502.** Krauss, M., **Analysis of NH spectrum,** (Proc. IAU Colloq. No. 25, Greenbelt, MD, Oct. 28-Nov. 1, 1974), Paper in *NASA SP-393, The Study of Comets*, B. Donn, M. Mumma, W. Jackson, M. A. Hearn, and R. Harrington, Eds., Part 2, pp. 848-852 (Scientific and Technical Information Office, National Aeronautics and Space Administration, Washington, DC, 1976).

Key words: comet; electric-dipole transition; excited states; NH; spin-orbit coupling; transition probability.

The NH cometary spectra is examined within the context of the radiation equilibrium model. The total fluorescent rate for the $A^3\Pi$-$X^3\Sigma^-$ transition is found to be less than $10\ {}^2S^1$ and the rate for the $c^1\pi\ {}^1\Delta$ transition is estimated to be comparable. A semiempirical calculation of the spin-orbit induced $a^1\Delta$-$X^1\Sigma^-$ transition finds the rate to be about $5\ S^1$. Any $^1\Delta$ NH formed in an initial photodissociation would radiate to the ground state before it can be excited. The photochemical origin of the NH radical cannot be deduced from the fluorescence spectra.

**16503.** Kuriyama, M., Boettinger, W. J., Burdette, H. E., **X-ray topographic observations of magnetic domains in Czochralski-grown nickel single crystals in anomalous transmission geometry,** *J. Appl. Phys.* **47,** No. 11, 5064-5068 (Nov. 1976).

Key words: crystal perfection; Czochralski growth; domain walls; magnetic domains; nickel single crystals; surface reflection topography; transmission topography; x-ray diffraction topography.

Ferromagnetic domain walls are observed in large Czochralski-grown nickel single crystals by x-ray double crystal diffraction topography in the surface reflection geometry as well as in the transmission geometry. The images of magnetic domain walls in surface reflection topographs possess almost as good contrast as those in the transmission topographs, and even reveal fine detailed structures distinctly. Based on preliminary arguments, the images observed in the surface reflection topographs are attributed to 180° walls intersecting with the crystal surface obliquely, while the transmission topographs easily image 71° and 109° walls in the interior of the crystals.

**16504.** Larsen, N. T., **A new self-balancing DC-substitution RF power meter,** *CPEM Digest*, pp. 203-205 (1976).

Key words: bolometer; microwave; power measurement.

Problems intrinsic in self-balancing Wheatstone bridges have led to the development of a new dc substitution microwave power meter. The new instrument allows four-terminal measurement of bolometer resistance and affords improved accuracy and lower noise at a lower cost than earlier instruments. Measurement errors due to imperfect behavior of the servo system are typically less than 0.01 percent.

**16505.** Ledbetter, H. M., Weston, W. F., **Low-temperature elastic properties of some copper-nickel alloys,** *Proc. IEEE Symp. on Ultrasonics, Los Angeles, CA, Sept. 22-24, 1975*, pp. 623-627 (IEEE, New York, NY, 1976).

Key words: bulk modulus; compressibility; copper; copper alloys; elastic constants; Poisson ratio; pulse-echo method; resonance method; shear modulus; sound velocity; Young's modulus.

The polycrystalline elastic properties of Cu, Cu-10 Ni, and Cu-30 Ni were determined between room temperature and liquid-helium temperature using both pulse-echo (10 MHz) and resonance (60 kHz) methods. The temperature dependence of all three materials is regular. The composition dependence of the elastic constants is reviewed and new composition dependences are proposed.

**16506.** Lias, S. G., Ausloos, P., Horvath, Z., **Charge transfer reactions in alkane and cycloalkane systems. Estimated ionization potentials,** *Int. J. Chem. Kinet.* **VIII,** 725-739 (1976).

Key words: alkane ions; alkanes; charge transfer; ion-cyclotron resonance; ion-molecule reactions; ionization potentials; rate constants.

Rate constants of charge transfer reactions $k_{CT}$, involving $C_3$-$C_9$ alkanes and cycloalkanes, have been determined in an ion cyclotron resonance mass spectrometer. The rate constants are significantly lower than the corresponding rate constants for collision when the reaction is less than about 0.5 eV exothermic for linear alkane ions, or less than about 0.2 eV exothermic for cycloalkane ions. In this region of low reaction efficiency, the efficiency of reaction with linear or branched alkanes seems to depend primarily on reaction exothermicity. (The efficiencies of reaction of a given ion with cyclic alkanes also depend on $\Delta H_{rn}$, but are higher than for reactions with other compounds.) Although the lowered reaction efficiencies probably result, at least in part, from unfavorable Franck-Condon factors in the energy range near the ionization onset, quantitative correlations between reaction efficiency and estimated relative Franck-Condon factors were not observed. When the enthalpy of reaction is small (less than about $-0.15$ eV), it is seen that the reverse charge transfer can also occur, and equilibrium is established under the condition of these experiments. From the observed equilibrium constants, values for the standard free energy change are derived, and assuming that $\Delta S$ is small for electron transfer equilibria, values of $\Delta H_{rn}$ are estimated. In the case of the equilibria involving cyclohexane ion, these values of $\Delta H_{rn}$ lead to estimates of the ionization potentials of methylcyclopentane, 3-methylpentane, *n*-octane, 2,2-dimethylbutane, and 2,3-dimethylbutane, which are lower than the ionization potentials of cyclohexane, that is, $< 9.88$ eV, although all these compounds had previously been reported to have ionization potentials above 10.03 eV. That the ionization potentials are indeed lower than 10.03 eV is confirmed by determining the quantum yields of ionization with 10.03-eV photons.

It is pointed out that the conclusions reached here apparently also apply to the charge transfer reactions of alkane ions in the liquid phase.

**16507.** Lightbody, J. W., Jr., Penner, S., Fivozinsky, S. P., Hallowell, P. L., Crannell, H., **Electron scattering from vibrational nuclei,** *Phys. Rev. C* **14,** No. 3, 952-964 (Sept. 1976).

Key words: anharmonicities; branching ratio; charge distribution; electron scattering; quadrupole phonons; vibrational nuclei.

We present electron scattering form factors for the ground states and several low energy quadrupole excitations of the nuclei $^{52}$Cr, $^{110}$Pd, $^{114}$Cd, and $^{116}$Sn. For $^{116}$Sn we also present the form factor for the lowest octupole excitation. From these data we derive ground state charge distribution parameters as well as $B(EL)$ values. We attempt to interpret the observed $2^+$ states as the one- and two-phonon states of an anharmonic vibrational model. Predictions are made for the electromagnetic decay branching ratios and excited state electric quadrupole moments.

**16508.** Lightbody, J. W., Jr., **Electron scattering from one- and two-phonon vibrational states,** *Physics Lett.* **38B,** No. 7, 475-479 (Apr. 3, 1972).

Key words: admixture; anharmonicities; branching ratios; electron scattering; phonons; reorientation effect.

Admixtures of one- and two-phonon states are required to fit (e, e′) form factors for the lowest two $2^+$ states in several even-even vibrational nuclei. These anharmonic wave functions correctly reproduce radiative branching ratios and excited state quadrupole moments.

**16509.** Little, W., Wakefield, J., Heim, L., Alfred, C., Zapf, T., Manney, C., **An NBS developed automatic network analyzer,** *CPEM Digest*, pp. 130-133 (1976).

Key words: attenuation; automated; bolometer mount efficiency; measurements; network analyzer; phase; reflection coefficient.

This paper describes a precision automated measurement system that has been under development at NBS since 1971 for the frequency range of 0.1 to 12.4 GHz. The system has been designed to measure attenuation, phase shift, reflection coefficient, and bolometer mount efficiency with accuracy as good as or better than can be achieved with present state-of-the-art manual measurement techniques (approximately an order of magnitude better than commercially available ANA's). The paper also presents recent measurement results that have been achieved with the system.

**16510.** Little, W. E., Yates, B. C., **Reflection coefficient standards for automated network analyzers,** *CPEM Digest*, pp. 128-129 (1976).

Key words: automatic; broad frequency; equations; network analyzers; open circuit reflection coefficient; short circuit; standards.

This paper describes the development and use of broad frequency band reflection coefficient standards for rectangular and coaxial waveguide. Equations for both the magnitude and phase angle of the reflection coefficient of "off-set" short circuits are presented so that these values can be calculated as a function of frequency. An equation for the phase angle of the coaxial "open circuit" reflection coefficient is given in terms of the open circuit capacitance and frequency. Also, an empirical equation is given that allows an estimate of the "open circuit" reflection coefficient magnitude.

**16511.** McNeil, J. R., Johnson, W. L., Collins, G. G., Persson, K. B., **Ultraviolet laser action in He-Ag and Ne-Ag mixtures,** *Appl. Phys. Lett.* **29,** No. 3, 172-174 (Aug. 1, 1976).

Key words: He-Ag and Ne-Ag mixtures; laser action; ultraviolet laser action.

We report eight new laser transitions which span the wavelength region from 220 to 400 nm. Six of the ultraviolet transitions are observed in Ne-Ag mixtures and two are observed in He-Ag mixtures. The 227.8- and 224.3-nm laser transitions of Ag II, $5d^3D_2$-$5p^3P_1{}^0$ and $5d^1S_0$-$5p^1P_1{}^0$ respectively, are the shortest-wavelength cw laser transitions reported in the literature to date. Output characteristics of the ultraviolet laser transitions as a function of buffer gas pressure and discharge current are presented. The strongest laser transition $4d^85s^2\ {}^1G_4 \rightarrow 4d^95p^3F_3{}^0$, at 318.1 nm, provides single-line peak output power of 350 mW. The output power does not appear to saturate at the limit of our input current, 50 A.

**16512.** Meijer, P. H. E., Lockhart, R. G., Niemeijer, T., **Influence of crystallographic displacement and *g*-factors on the ground state of cerous magnesium nitrate,** *Solid State Commun.* **18,** No. 4, 473-474 (1976).

Key words: cerous magnesium nitrate; crystal structure; *g*-factors; ground state energy; Luttinger-Tisza method; translation vectors.

Since the thermodynamic properties of cerous magnesium nitrate play such an important role in low temperature physics we computed the influence of all variations still possible under the given set of known data: Small variation in the lattice structure, in particular the displacement of the center plane, small variations of the *g*-factor and the combination thereof.

**16513.** Mies, F. H., **Polarization of OH radiation,** (Proc. IAU Colloq. No. 25, Greenbelt, MD, Oct. 28-Nov. 1, 1974), Paper in *NASA SP-393, The Study of Comets,* B. Donn, M. Mumma, W. Jackson, M. A. Hearn, and R. Harrington, Eds., Part 2, pp. 843-847 (Scientific and Technical Information Office, National Aeronautics and Space Administration, Washington, DC, 1976).

Key words: comets; fluorescence; OH-18-cm radiation; optical pumping; polarization.

In the absence of collisions, optical pumping of cometary OH by solar ultraviolet radiation determines the relative population of OH molecules in the Λ-doubled levels of the $^2\Pi_{3/2}$ ground state, and also produces an alignment of the magnetic sublevels along the axis of the incident solar radiation. This results in a linear polarization of both the u.v. fluorescent spectrum and the 18-cm OH radiowave spectrum.

**16514.** Murphey, W. M., Sherr, T. S., Bennett, C. A., **Societal risk approach to safeguards design and evaluation,** (Proc. 16th Annual Meeting Institute of Nuclear Materials Management, Inc., New Orleans, LA, June 18-20, 1975), Paper in *Nuclear Materials Management* **IV,** No. III, 588-606 (1975).

Key words: nuclear materials safeguards; safeguards evaluation; safeguards system design; societal risk.

A comprehensive rationale for safeguards design and evaluation, and a framework for continuing systematic assessment of the system's effectiveness and efficient allocation of available safeguards resources so as to provide a balanced protection has been developed. The general objective of safeguards has been stated as: "to achieve a level of protection against ... [willful actions involving the possession of nuclear materials or the sabotage of nuclear facilities] that insures against a significant increase in the overall risk of death, injury, or property damage to the public from other causes beyond the control of the individual." Consistent with this objective, the societal risk approach was chosen as the basis for designing and evaluating the safeguards system. The approach considers the frequency (or likelihood) of occurrence of an antisocial act involving nuclear materials or facilities and the magnitude of the effects on society should such an act be successfully perpetrated. The analysis starts with the identification of the set of illegitimate final acts, or "events," which involve nuclear materials or nuclear facilities. These events are used as a basis for identifying the adversary action sequences that could produce the final events, and as a basis for considering the consequences to the public. The paper presents a summary of the societal risk approach, considerations relating to frequency of attempt, an adversary action tree approach to analysis of adversary activities, the structure of the safeguards system implied by the adversary actions, and implications relating to safeguards system design and evaluation arising from the societal risk approach.

**16515.** Okabe, H., **Photochemistry,** Paper in *Encyclopedia of Chemistry Uses (Utet Sansoni Edizioni Scientifiche),* **V,** 610-615 (Firenze, Italy, 1976).

Key words: bond energy; chain reaction; determination of photochemical mechanism; flash photolysis; intermittent illumination; photochemical principles; photochemical reaction of atoms and molecules; photochemistry in the atmosphere; photochemistry of air pollution; primary and secondary photochemical processes.

The principles and processes of photochemistry are described at an elementary level. The importance of quantum yield measurement is emphasized. Main topics covered in this article are chain reaction, flash photolysis, effect of intermittent illumination, examples of photochemical reaction in atoms and molecules, application of photochemistry for the measurement of bond energy, photochemistry in the atmosphere and photochemistry of air pollution.

**16516.** Reeve, G. R., Arthur, M. G., **A standard percent modulation measurement system,** *CPEM Digest,* pp. 165-166 (1976).

Key words: amplitude modulation; instrument landing system; modulation measurements; modulation meter; percent modulation.

This paper describes a precision percent modulation measurement system constructed by the Electromagnetics Division, National Bureau of Standards, for calibration of secondary standards for instrument landing system (ILS) generators and meters. A description of the electronics is presented along with the estimated measurement uncertainty.

**16517.** Reite, M., Zimmerman, J. E., Edrich, J., Zimmerman, J., **The human magnetoencephalogram: Some EEG and related correlations,** *Electroencephalogr. Clin. Neurophysiol.* **40,** 59-66 (1976).

Key words: magnetic evoked response; magnetoencephalography.

Simultaneous magnetoencephalographic (MEG) and electroencephalographic (EEG) data were recorded from four normal adults. Spectral analysis suggested that the MEG and EEG data were produced by similar but nonidentical generator systems; the MEG recorded here may be generated by intrasulcal cortex. A magnetic averaged evoked response to flash was recorded in one subject, consisting of a waveform similar to and phase-coherent with the simultaneous EEG averaged evoked response, such that cortical negativity was correlated with a magnetic field directed into the scalp.

**16518.** Riad, S. M., Nahman, N. S., **Application of the homomorphic deconvolution for the separation of TDR signals occurring in overlapping time windows,** *CPEM Digest*, pp. 27-29 (1976).

Key words: homomorphic deconvolution; time domain measurements; time domain reflectometry.

The homomorphic transformation is used to separate a time domain reflectometry (TDR) signal into its rapidly and slowly varying components, respectively. The separation (deconvolution) technique is successful in the case where the multiple reflections cannot be viewed in nonoverlapping time windows as is required by the conventional TDR method.

**16519.** Ries, F. X., **An international intercomparison of voltage standards at 1 GHz in coaxial transmission line,** *IEEE Trans. Instrum. Meas.* **IM-25,** No. 3, 254-255 (Sept. 1976).

Key words: electrical measurements; radio frequency; voltage measurements.

The results of an International Intercomparison of RF voltage at 1 GHz is described. This comparison was sponsored by the High Frequency Working Group of the Comité Consultatif d'Eléctricité (CCE) at the Bureau International des Poids et Mesures (BIPM). Differences between values reported by the five participating laboratories fell within the total uncertainties given by these laboratories. The estimated limits of uncertainty given by the laboratories varied from a few tenths to several percent.

**16520.** Risley, A. S., Shoaf, J. H., Ashley, J. R., **Frequency stabilization of *X*-band sources for use in frequency synthesis into the infrared,** *IEEE Trans. Instrum. Meas.* **IM-23,** No. 3, 187-195 (Sept. 1974).

Key words: cavity stabilization; frequency multiplication; frequency stability; frequency synthesis; Gunn oscillator; infrared; injection stabilization; klystron; *X band.*

An *X*-band source of excellent frequency stability is needed in infrared frequency multiplication of high order. Such a source has been used in frequency multiplication by a factor of 401 using a point-contact Josephson junction as a frequency multiplier and mixer. Noise data on three *X*-band systems are reported. Two of these systems use klystrons as the source of *X*-band power; the other uses a Gunn oscillator. Each of these three systems employs both cavity and injection stabilization. Injection stabilization, using a quartz-oscillator-driven multiplier chain, provides the second-to-second and minute-to-minute stability needed for the Josephson junction experiment. To our knowledge, this is the first published noise data where cavity and injection stabilization are simultaneously employed. The quality of the best system reported here is much better—both around 1 Hz from the carrier and around 50 kHz from the carrier—than the source used to multiply by a factor of 401 to 3.8 THz.

**16521.** Rockar, E. M., Forman, R. A., **Polarized luminescence from MgO:Cr$^{3+}$,** *Phys. Rev. B* **14,** No. 8, 3621-3629 (Oct. 15, 1976).

Key words: chromium 3+; crystal vacancies; cubic crystals; depolarization; impurity compensation; luminescence; magnesium oxide; MgO; optical properties; polarized luminescence; symmetry; transition metal ions.

MgO:Cr$^{3+}$ has been used as a model system to study the general case of polarized luminescence from transition-metal impurities in cubic materials. Using polarized exciting light, information can be obtained about the site symmetries of the impurities as well as the dipole character of the absorbing and emitting levels. The data presented are in substantial agreement with previous studies on the line emission spectra of MgO:Cr$^{3+}$ obtained by other techniques. Careful experimental procedures to avoid artifacts are detailed. Experimental values for the polarizations are always significantly smaller than those predicted by theory. A dependence of polarization with chromium concentration was also noted. Probable causes for these effects are discussed.

**16522.** Roder, H. M., **The heats of transition of solid ethane,** *J. Chem. Phys.* **65,** No. 4, 1371-1373 (Aug. 15, 1976).

Key words: ethane; heat capacity; heat of fusion; heat of transition; transition temperature; triple point.

The existence of a solid-solid transition in ethane is now generally accepted. A value for the heat of transition, 2437 ± 35 J/mol at 89.774 K, together with a new value for the heat of fusion, 279 ± 6 J/mol at 90.337 K, is reported in this work. The sum of the new values is in excellent agreement with the earlier measurements, provided that the heat required to raise the temperature of the solid between transitions is included. The transition temperatures are in agreement with the most recent determinations of other authors.

**16523.** Ruff, A. W., **Deformation studies at sliding wear tracks in iron,** *Wear* **40,** 59-74 (1976).

Key words: electron channeling; iron; metals; plastic deformation; surfaces; wear.

Determinations have been made of strains on the surface and subsurface of specimens of high purity iron after different distances of sliding wear. The method involved the measurement of loss of intensity (contrast) of particular electron channeling lines obtained from small selected areas near the wear track. A calibration specimen, deformed plastically to a range of strain values, was used to relate the channeling line contrast loss to plastic strain. Strain maps lateral to the wear track and below the original surface were obtained after removing controlled thicknesses of iron by electropolishing. In all cases the maximum strain was found at the track center location at the surface and the strains decreased steadily with depth below the track. With a 50 g load the strains vanished at about 40 $\mu$m depth. Significant strains were found to exist outside the wear track boundaries. There was no indication of a soft or less-hardened surface layer in any of the specimens studied.

**16524.** Sanders, D. M., Blackburn, D. H., Haller, W. K., **A high-temperature transpiration apparatus for study of viscous, incongruently vaporizing glass melts,** *J. Am. Ceramic Soc.* **59,** No. 7-8, 366-368 (Aug. 1976).

Key words: glass; incongruent vaporization; transpiration; vapor density.

The vapor density of sodium over a well-stirred soda-lime-silica glass melt was measured using a newly developed transpiration apparatus. This apparatus uses intense stirring action to produce fresh surfaces throughout the measurement. This feature is necessary to prevent the formation of depleted layers formed by preferential vaporization of one of the glass components. The apparatus design and operating characteristics are discussed.

**16525.** Schleter, J. C., **A decision structure for a State safeguards system,** (Proc. Symp. Safeguarding Nuclear Materials, Vienna, Austria, Oct. 20-24, 1975), Paper in *Safeguarding Nuclear Materials*, **I**, 199-213 (International Atomic Energy Agency, Vienna, Austria, 1976).

Key words: decision structure; information system; nuclear material diversion; nuclear materials; safeguards; safeguards information system.

An effective structure to direct safeguards decisions within a State's safeguards system is vital in order to minimize the possibility of illicit diversion of nuclear material. In a State each plant usually has some form of information system in operation but it is generally plant specific and often is directed only to management functions. The systematic study, discussed in this paper, is aimed at developing a more comprehensive Safeguards Information System (SIS). The concepts used are applicable to any State's safeguards system. Decision makers are identified and classified. General safeguards and operational tasks are defined for each and, based on these, information sources are identified. The flow structure for information is specified to enable safeguards decision makers to function properly. Concepts used to characterize the SIS and the associated decision structure are discussed.

**16526.** Schleter, J. C., **A decision structure for plant safeguards,** (Proc. 16th Annual Meeting Institute of Nuclear Materials Management, Inc., New Orleans, LA, June 18-20, 1975), Paper in *Nuclear Materials Management* **IV**, No. III, 406-430 (1975).

Key words: decision makers; decision structure; information flows; nuclear material information systems; nuclear materials safeguards; safeguards.

A systematic study has been performed to determine the information necessary for meaningful safeguards decisions. The resulting Safeguards Information System (SIS) encompasses all decision makers, in general terms, from those at ERDA Headquarters to the operator on the process line. Only decision makers within the plant are considered in this paper. The basic premises and steps employed in developing SIS are described. These include rapid two-level reporting of abnormal situations, identification of the safeguards decision makers, deduction of safeguards information generated and abnormal situations observed by each as a result of operational tasks, and to whom the information is transmitted. The content of information flowing to and from each decision maker from all sources is established and assurance is given that each decision maker receives the necessary information and that extraneous information is held to a minimum. By means of the analysis, a decision structure for safeguards becomes apparent, the decision capability of each decision maker can be specified, and the sources and flows of information necessary for meaningful safeguards decisions can be identified. The application of the general SIS, to serve as the basis of a plant-specific SIS, is also considered.

**16527.** Siegwarth, J. D., Lawless, W. N., Morrow, A. J., **Dielectric and thermal properties of $Pb_2Nb_2O_7$ at low temperature,** *J. Appl. Phys.* **47**, No. 9, 3789-3791 (Sept. 1976).

Key words: antiferroelectric; dielectric constant; heat capacity; lead pyroniobate; low temperature; polarization.

Measurements of the dielectric constant, polarization, zero-field specific heat, and field-dependent specific heat of polycrystalline $Pb_2Nb_2O_7$ at low temperatures are reported. No evidence for a phase transition at 15 K was found, contrary to previous suggestions of an antiferroelectric transition at 15 K based on dielectric data. The peak in the dielectric constant appears to be due to relaxation phenomena.

**16528.** Smith, E. W., Giraud, M., Cooper, J., **A semiclassical theory for spectral line broadening in molecules,** *J. Chem. Phys.* **65**, No. 4, 1256-1267 (Aug. 15, 1976).

Key words: *ab initio* potentials; atom-molecule interactions; curved classical trajectories; HCl, CO, $CO_2$ with He, Ar; rotation-vibration spectra; semiclassical *S*-matrix; spectral line broadening.

A semiclassical *S*-matrix theory is developed and applied to spectral line broadening in linear molecules perturbed by atoms. This theory uses curved classical trajectories determined by the isotropic part of the atom-molecule interaction and the *S*-matrix is treated to all orders in the interaction. Numerical calculations can be made rather easily even for high quantum numbers. The theory is least accurate for very low quantum numbers, but even then calculations agree to within 10 percent with close coupling results where comparisons could be made. Comparisons were also made with other theoretical approaches using model potentials and with experiments using *ab initio* potential surfaces.

**16529.** Sorensen, C. M., Fickett, F. R., Mockler, R. C., O'Sullivan, W. J., Scott, J. F., **On lysozyme as a possible high-temperature superconductor,** *J. Phys. C: Solid State Phys. Letter to Ed.* **9**, L251-L254 (1976).

Key words: diamagnetism; light scattering; molecular diffusion; organic molecule; superconductor; susceptibility.

Intensity autocorrelation measurements of the diffusion constant of lysozyme molecules in aqueous solutions as a function of applied magnetic field reveal no evidence of the cooperative behavior proposed by Ahmed, Calderwood, Fröhlich and Smith to explain their observation of a large peak in the diamagnetic susceptibility of lysozyme at an applied field of 600 Oe. Careful susceptibility measurements using a SQUID system show that the diamagnetic susceptibility of lysozyme and lysozyme solutions is constant up to our maximum field of 720 Oe.

**16530.** Sugar, J. R., **A VOR audiofrequency standard signal source based on digital waveform synthesis,** *CPEM Digest*, pp. 72-73 (1976).

Key words: aircraft navigation systems; digital frequency synthesis; national standards; precision audiofrequency signal generation; precision FM signal generation; precision phase angle generation; radio navigation; VOR.

This unit generates three highly accurate audio signals for use in calibrating the working standards for the calibration of VHF omnirange (VOR) aircraft navigation systems. The three signals are two 30 Hz sine waves and a 9960 Hz carrier, frequency modulated by a 30 Hz sine wave. The phase of one of the 30 Hz signals is adjustable in .01° steps relative to the other two signals. The zero-crossing points of all three signals are accurate to approximately .01° relative to 30 Hz. In order to achieve this level of accuracy the signals are generated digitally and then converted to analog form. A substantial reduction in the required size of read-only-memory for storing the required digital functions is achieved by storing the differences rather than the functions themselves. Error-checking circuits and built-in-test circuits are incorporated to provide an immediate indication of malfunction of the digital circuits.

16531. Tobler, R. L., **Fatigue crack growth and J-integral fracture parameters of Ti-6Al-4V at ambient and cryogenic temperatures,** *Am. Soc. Test. Mater. Spec. Tech. Publ. 601,* 346-370 (1976).

Key words: fatigue crack propagation; fracture toughness; J-integral; low temperature tests; titanium alloys.

Fatigue crack propagation and fracture parameters for 2.03-cm-thick compact specimens of an extra-low-interstitial Ti-6Al-4V alloy were measured at temperatures between 296 K (70 °F) and 4 K (– 453 °F). Plane-strain linear-elastic and J-integral fracture toughness test results were in good agreement: the $K_{Ic}$ values for this alloy decreased from 105 $MN/m^{3/2}$ at room temperature to 54 $MN/m^{3/2}$ at 4 K, and a ductile-to-brittle fracture transition occurred in the range 125 to 76 K (– 235 to – 323 °F). Despite this transition, the fatigue crack growth rates *(da/dN)* of this alloy remained temperature insensitive over the entire ambient-to-cryogenic range. These fatigue and fracture results are compared with data previously reported for a normal-interstitial Ti-6Al-4V alloy.

16532. Truhlar, D. G., Brandt, M. A., **Close-coupling calculations of differential cross sections for elastic scattering and rotational excitation of hydrogen molecules by electrons at 10 and 40 eV,** *J. Chem. Phys.* **65,** No. 8, 3092-3101 (Oct. 15, 1976).

Key words: close-coupling calculations; cross sections; differential cross sections; elastic scattering; electron scattering; exchange (of electrons); hydrogen molecules; inelastic scattering; momentum transfer; polarization (of charge clouds); rotational excitation; scattering theory.

We have performed close-coupling calculations including two rotational states for electron scattering by hydrogen molecules at 10 and 40 eV impact energies. The effective interaction potential was taken as a sum of the static, exchange, and polarization interactions. With no empirical parameters, good agreement with experiments was obtained for the angle dependences and magnitudes of the differential cross sections for both pure elastic scattering and rotational excitation except that there are discrepancies in the elastic scattering at small scattering angles where the experiments are least reliable. Variations of the forms of the exchange and polarization potentials were examined and the effect on the cross sections was small.

16533. Truhlar, D. G., Brandt, M. A., Chutjian, A., Srivastava, S. K., Trajmar, S., **Electron scattering by $N_2$ at 5 and 10 eV: Rotational-vibrational close-coupling calculations and crossed beam studies of vibrational excitation,** *J. Chem. Phys.* **65,** No. 8, 2962-2969 (Oct. 15, 1976).

Key words: close-coupling calculations; crossed beams; cross sections; differential cross sections; electron scattering; inelastic scattering; nitrogen molecules; polarization potential; scattering; static potential; vibrational excitation.

The ratios of differential cross sections for excitation of the first excited vibrational state to differential cross sections for elastic scattering of $N_2$ have been measured at scattering angles ranging from 20° to 135° at 5 and 10 eV impact energies. Using previously measured and normalized elastic differential cross sections for $N_2$, the ratios have been converted to inelastic cross sections. Laboratory-frame close-coupling calculations using a four-state vibrational-rotational basis set and an effective interaction potential developed previously are reported at both energies. It is shown that the four-state treatment of this potential scattering model can account for the approximate magnitude and the qualitative behavior of the cross sections, but there are some significant quantitative differences between theory and experiment.

16534. Wacker, P. F., Bowman, R. R., **Quantifying hazardous electromagnetic fields: Scientific basis and practical considerations,** *IEEE Trans. Microwave Theory Tech.* **MTT-19,** No. 2, 178-187 (Feb. 1971).

Key words: nonionizing fields; probes; radiation.

As commonly recognized, the problem of quantifying hazardous electromagnetic (EM) fields is difficult and has not yet been satisfactorily solved. Essentially, this is because people are often exposed to emanations from powerful sources of EM fields at points close to the sources and at points where arbitrary polarization and multipath interference exist. However, the accepted concepts, standards, and most measuring instrumentation are based on simple plane-wave field propagation and so are inadequate for complicated fields.

The complications and problems of quantifying hazardous EM fields involving source-subject coupling, reactive near-field components, multipath components, and arbitrary polarization are examined in some detail. General discussion of dosimetric measurements and hazard survey measurements is given, and also some basic considerations for the design of field probes for these measurements. Recommendations are given for suitable parameters for quantifying complicated EM fields, and essential and desirable characteristics for hazard survey meters are stated. Several recently designed hazard survey probes are capable of measuring these recommended parameters in many complicated fields of interest, and improved instruments are anticipated.

16535. Yokel, F. Y., **A performance standard for foundations and excavations,** *Civil Eng.* **47,** No. 10, 80-81 (Oct. 1976).

Key words: buildings (codes); excavation; foundations; geotechnical engineering; standards.

Work is now in progress on the preparation of a national standard for foundations and excavations under the ASCE-COS "Committee for Foundation and Excavation Standards," (CFES).

16536. Goodwin, K. E., Maltese, M. D. K., Schleter, J. C., **Diversion path analysis handbook. Volume II. Example,** 225 pages (Division of Safeguards and Security, U.S. Energy Research and Development Administration, Washington, DC, Oct. 1976).

Key words: analysis; diversion of nuclear materials; diversion path analysis; internal control system characterization; nuclear material safeguards; safeguards.

A hypothetical example illustrating the methodology given in Volume I of "The Diversion Path Analysis Handbook" is presented. The process, derived for the example, might be typical of the end of a fabricating process line where plutonium metal bars, originating in an earlier unspecified process step, are cut up and recast into buttons for long term storage. The process is intended to reflect typical actual practice, but in some cases, the parameters have been specially tailored so that as many features of DPA could be illustrated. The example is presented in the format recommended for use when documenting a DPA. It contains all of the basic components necessary for complete documentation and its use assures a common basis for intercomparisons of DPA's, both intra- and inter-plant. Volume II is divided into two parts – the workpaper documentation and the summary report. The former sets forth the bounds of the analysis, the information gathered, the characterization of the process, the specific diversion paths related to the process, and, finally, the results and findings, of the DPA. The summary report, made up of portions of sections already prepared for the workpapers is a concise statement of results and recommendations for management use.

16537. Evans, B. J., Swartzendruber, L. J., **Magnetic hyperfine field structure of iron Urushibara type catalysts,** (Proc. Annual 20th AIP Conf. on Magnetism and Magnetic Materials, San Francisco, CA, Dec. 3-6, 1974), Paper in *Magnetism and Magnetic Materials—1974*, C. D. Graham, Jr., G. H. Lander, and J. J. Rhyne, Eds., No. **24**,391-393 (American Institute of Physics, New York, NY, 1975).

Key words: alloys; aluminum; catalysis; hydrogenation; iron; Mössbauer spectra; zinc.

We have utilized the Mössbauer effect to study the hyperfine field structure of iron Urushibara catalysts. The Mössbauer spectra of those catalysts prepared using zinc show that they consist of a mixture of magnetic and nonmagnetic Fe-Zn alloys. Both the magnetic field distribution in the magnetic phase and the relative amounts of magnetic and nonmagnetic phases depend on the Fe-Zn ratio used in the preparation of the catalyst. This dependence on Fe-Zn ratio is in contrast to iron Urushibara catalysts prepared using aluminum (and Raney iron type catalysts) in which the active phase is almost pure $\alpha$-Fe, irrespective of the Fe-Al ratio. The activity of zinc prepared iron Urushibara catalysts for certain hydrogenation reactions is known to be greater than that of aluminum prepared iron Urushibara catalysts and the above results suggest a relationship between activity and the modification of the iron catalyst by alloyed zinc. The alloying behavior of the Fe-Zn particles may be analogous to that of the so-called bimetallic clusters observed in other alloy systems.

16538. Deslattes, R. D., Lamotte, M., Dewey, H. J., Keller, R. A., Freund, S. M., Ritter, J. J., Braun, W., Kurylo, M. J., **Isotopic enrichment in laser photochemistry,** (Proc. Second Int. Conf. Laser Spectroscopy, Megève, France, June 23-27, 1975), Lecture Notes in *Physics* **43**, pp. 296-303 (Springer-Verlag, New York, NY, 1975).

Key words: isotope separation; kinetics; lasers; photochemistry.

Laser technology has permitted more efficient study of the chemistry of molecules in excited states. The extent to which isotopic specificity is preserved in going from initial excitation to final product is a valuable diagnostic for excited state chemistry. This report summarizes initial results from several areas of investigation, each of which suggests that laser stimulation may offer more than simple rate enhancement.

16539. McCulloh, K. E., **Energetics and mechanisms of fragment ion formation in the photoionization of normal and deuterated water and ammonia,** *Int. J. Mass Spectrom. Ion Physics* **21**, 333-342 (1976).

Key words: ammonia; appearance potential; autoionization; deuterated species; enthalpy of formation; ionization potential; $NH_2^+$; $OH^+$; photoionization; predissociation; Rydberg states.

Fragment photoion yield curves have been obtained for $OH^+$ from $H_2O$ at 215 and 298 K and for $NH_2^+$ from $NH_3$ at 160 and 298 K. The results indicate that for both molecules the initial rotational energy is completely available for fragmentation. Appearance potentials, corrected to 0 K, are $18.115 \pm 0.008$ eV for $OH^+$ from $H_2O$ and $15.768 \pm 0.004$ eV for $NH_2^+$ from $NH_3$. Assuming zero excess energy at threshold, the values $309.0 \pm 0.2$ and $302.7 \pm 0.1$ kcal $mol^{-1}$ are obtained for the standard enthalpies of formation of $OH^+$ and $NH_2^+$, respectively, leading to the derived ionization potentials $I(OH) = 12.995 \pm 0.009$ eV and $I(NH_2) = 11.17 \pm 0.05$ eV. The observed yield of $OH^+$ from $H_2O$ deviates markedly from values calculated on the assumption that fragmentation occurs exclusively by predissociation from excited vibrational levels of $H_2O^+$ ($\tilde{B}\,^2B_2$), suggesting that Rydberg series converging to these levels play an important role in $OH^+$ production. Appearance potentials for $OD^+$, $NHD^+$ and $ND_2^+$ are reported.

16540. Paule, R. C., **Mass spectrometric studies of $Al_2O_3$ vaporization processes,** *High Temp. Sci.* **8**, 257-266 (1976).

Key words: $AlO_2$; $Al_2O_3$; emissivity; evaporation coefficient; Langmuir vaporization; optical pyrometry; radiation heating; vapor pressures.

An investigation of the radiative and evaporative properties of $Al_2O_3$ samples has been made. These observed properties interact in a manner such that, upon melting, the rate of evaporation is observed to increase discontinuously. This phenomenon had previously been attributed to a change in the evaporation coefficient. The current investigation has shown that the evaporation coefficient for $Al_2O_3$ is constant and that the observed increase in vaporization is due to an increase in the temperature which, in turn, is due to a discontinuous increase in the emissivity. Relative vapor pressure measurements were also made in this study, and the reported existence of the vapor species $AlO_2$ was not confirmed. All other reported vapor species were confirmed.

16541. Ederer, D. L., **Erratum: Cross section profiles of resonances in the photoionization continuum of krypton and xenon (600-400 Å),** *Phys. Rev. A ERRATA* **14,** No. 5, 1936-1937 (1976).

Key words: cross section; inner-shell excitation; krypton; photoionization; vacuum ultraviolet; xenon.

Equation (4) in this paper is incorrect. It should read:

$$\sigma(E) = C(E) + (2\sigma_a q(\Gamma/2)(E - E_r) + \sigma_a(q^2 - 1)(\Gamma/2)^2)/(E - E_r)^2 + (\Gamma/2)^2$$

Unfortunately the incorrect form of the cross section was inadvertently used to transform the parameters from the Fano representation to the Shore representation, consequently, some of the parameter values listed in Tables I and II are incorrect. The corrected tables are shown. The change in some of the $a_i$'s will slightly effect the cross-section profiles of the resonance shown in figs. 1 and 2.

16542. Hocken, R., Horowitz, M. A., Greer, S. C., **Critical anomaly in the dielectric constant of a nonpolar pure fluid,** *Phys. Rev. Lett.* **37**, No. 15, 964-967 (Oct. 11, 1976).

Key words: Clausius-Mossotti equation; critical phenomena; dielectric constant; sulfur hexafluoride.

We report measurements of changes in the dielectric constant $\epsilon$ of $SF_6$ along a near critical isochore. We find an anomalous increase in $\epsilon$. The amplitude of the anomaly is about 10 times larger than the one predicted by current theories, which assume a constant polarizability.

16543. Plummer, E. W., **Interaction of single atoms with atomically defined surfaces,** (Proc. Conf. Applications of Field-Ion Microscopy to Physical Metallurgy and Corrosion, Georgia Institute of Technology, Atlanta, GA, May 15-17, 1968), Paper in *Physical Metallurgy and Corrosion*, R. F. Hochman, E. W. Müller and B. Ralph, Eds., pp. 371-389 (1968).

Key words: adatom; binding energy; field ion microscope; surface.

The role of the field ion microscope in surface studies is illustrated by reviewing briefly several unique experiments which have been conducted. These include experiments on work function, condensation, surface rearrangement and self diffusion, and atomic binding at the surface. The details of the experiment on atomic bonding of individual atoms on single crystal planes is considered in more detail to illustrate the capabilities of this technique for investigating the fundamental properties of the surface-adatom interaction on an atomically defined surface.

**16544.** Simiu, E., **Wind climate and failure risks,** *J. Struct. Div. Proc. Am. Soc. Civil Eng.* **102,** No. ST9, 1703-1707 (Sept. 1976).

Key words: buildings (codes); failure; probability distribution functions; reliability; structural engineering; wind (meteorology); wind pressure.

The relation is examined between risk of failure, degree of wind sensitivity, type of wind climate, and mean recurrence interval used in design. The results presented are based on the assumption, used in the ANSI A58.1 Standard, that the probabilistic behavior of extreme wind speeds is adequately modeled by distribution functions of the largest values, the parameters of which are estimated from the data consisting of the largest yearly wind speed for every year of record. These results show that a strong correlation exists between probability of failure and type of wind climate, as defined quantitatively by the parameters of the extreme wind distribution. All other relevant factors being equal, including the degree of sensitivity to wind, it was found that the probability of failure of a member may increase considerably as a function of type of wind climate. It is suggested that the effect of the type of climate, as defined in the paper, be taken into account in design.

**16545.** Simiu, E., Filliben, J. J., **Probability distributions of extreme wind speeds,** *J. Struct. Div. Proc. Am. Soc. Civil Eng.* **102,** No. ST9, 1861-1877 (Sept. 1976).

Key words: buildings (codes); hurricanes; probability distribution functions; reliability; risk; statistical analysis; storms; structural engineering; wind pressure; wind speed.

An automated technique is presented for determining an appropriate distributional model for the largest yearly wind speeds. With a view to assessing the validity of current probabilistic approaches to the definition of design wind speeds, this technique was used in a study of extreme wind speeds based on records taken at 20 U.S. weather stations. The following results were obtained: (1) At 83 percent of the stations not susceptible to experiencing hurricane-force winds, the series of the largest annual wind speeds were well fit by Type I probability distributions of the largest values; (2) the assumption that Type II distributions with $\gamma = 9$ are generally representative of such stations was not confirmed; (3) type I probability distributions do not appear to describe correctly the behavior of extreme winds in regions subjected to special winds, e.g., hurricanes; and (4) in such regions, 20-yr data samples may provide a misleading picture of extreme wind behavior.

**16546.** Page, C. H., **Torque on a bar magnet,** *Am. J. Phys.* **44,** No. 11, 1104-1105 (Nov. 1976).

Key words: magnet; magnetization; torque.

If all magnetic quantities are defined via fields, with no use of poles and with magnetic moment defined as the volume integral of magnetization, energy considerations yield the torque on a magnet immersed in a permeable fluid in an external field. Although the torque on a disk magnet is proportional to **B**, the torque on a needle magnet is proportional to $\mu_0 \mathbf{H}$, as reported experimentally by Whitworth and Stopes-Roe. The experiment does not prove either A. E. Kennelly [J. Eng. Educ. 27, 290 (1935)] or Sommerfeld to be right or wrong, but demonstrates that magnetic theory based on *poles* cannot be applied to *magnets*, and thereby strengthens the philosophy that electromagnetic theory should be based on fields.

**16547.** Snell, J. E., Kusuda, T., Didion, D. A., **Energy conservation in office buildings: Some United States examples,** *Proc. International CIB Symp. on Energy Conservation in the Built Environment, Watford, England, Apr. 6-8, 1976,* pp. 1-34 (International Council for Building Research, Studies and Documentation, Rotterdam, The Netherlands, 1976).

Key words: commercial buildings; energy conservation; energy consumption; Manchester office building; National Bureau of Standards; New York State offices; office buildings.

The purpose of this paper is to describe recent experience in the United States and, in particular, the National Bureau of Standards (NBS) with energy conservation in office buildings. The NBS, working in cooperation with the Energy Research and Development Administration (ERDA) and the General Services Administration (GSA), is evaluating the energy efficiency of a demonstration office building in Manchester, New Hampshire. NBS utilized its thermal performance computer program (NBSLD) to evaluate a variety of energy conservation design alternatives for this building. These results are described and the current status of the project is reported. The NBS has conducted studies of energy conservation potentials in its own buildings at the Gaithersburg, Maryland, site. These measures include operational as well as retrofit actions. The results of actual tests and computer evaluations of predicted performance are discussed. Overall savings in energy use (fuel oil, fuel gas, and purchased electricity) of 20 percent have been achieved. An additional 20 percent reduction in energy use is expected from planned retrofit, including use of computerized HVAC controls. The NBS also has been working with an ad hoc industry group, representing owners and managers of commercial buildings, toward the development of self-help guidelines these managers can use in achieving energy conservation retrofit cost-effectively in their own buildings. Data collected to date and current status of these activities are reported. Many post-war office buildings were designed and constructed which are inimical to present energy conserving criteria. The excessive use of glass and illumination prevailed, as well as inefficient, although first-cost inexpensive, HVAC systems. Controls for building illumination and space conditioning were often inadequate for energy conservation operations. Therefore, these areas represent major opportunities for energy conservation in existing, as well as new, office buildings in the U.S., and are the target of a major effort by NBS and the Federal Government in general.

**16548.** Marron, B., Fife, D., **Online systems—Techniques and services,** Chapter 5 in *Annual Review of Information Science and Technology,* M. E. Williams, Ed., **11,** 163-210 (American Society for Information Science, Washington, DC, 1976).

Key words: bibliographic information systems; computer technology; information storage and retrieval; interactive systems; online services; online systems.

The Annual Review of Information Science and Technology, published by the American Society for Information Science, reviews the contemporary trends, progress, and problems in the major areas of information science. This chapter on "Online Systems—Techniques and Services" is intended for Volume 11 to be published in September 1976, and reviews the literature of 1974 and 1975.

The first section treats computer technology, networks and communications, and software, with particular emphasis on the significance of these techniques for future online systems design. Next there is coverage of online services with detail on promotion and pricing of services, use of multiple services, online services in libraries, retrieval of nonbibliographic information, and document delivery. The third section treats the user interface in online systems, especially the role of the intermediary, design criteria for user-oriented systems, user training, and interface standardization. Finally some issues and problems of online systems are discussed.

**16549.** Cali, J. P., **The NBS Standard Reference Materials program: An update,** *Anal. Chem.* **48,** No. 11, 802A-818A (Sept. 1976).

Key words: accuracy; measurement; measurement compatibility; National Bureau of Standards; reference materials; standard reference materials; Standard Reference Materials program.

Ten years ago, almost to the day, the National Bureau of Standards reported in *Analytical Chemistry* the status of its Standard Reference Materials program. In view of the NBS 75th anniversary of its founding coinciding, as it does, with our Nation's 200th Anniversary, it seems especially fitting that an update of that report be made. In this short 10-year period, more substantive changes have taken place than occurred over the first 60 years of the program's existence. It is the purpose of this report to recapitulate these events and to attempt to predict what the future holds in store.

**16550.** Kusuda, T., **Control of ventilation to conserve energy while maintaining acceptable indoor air quality,** (Proc. ASHRAE Symp. on Ventilation Control, Semiannual Meeting, Dallas, TX, Feb. 1-5, 1976), *ASHRAE Trans.* **82,** Part 1, 1169-1182 (American Society of Heating, Refrigerating and Air Conditioning Engineers, New York, NY, 1976).

Key words: air quality; intermittent operation; maximum allowable concentration of $CO_2$; New York City schools; ventilation.

Basic requirements of ventilation with respect to the undesirable increase of building air contaminants are discussed. A mathematical model for determining the increase of contaminants concentration with time was developed and verified by applying it to the observed $CO_2$ increases in the New York City School experiment. Equations, tables and graphs were developed for estimating the $CO_2$ buildup and possible energy saving obtainable by using intermittent operation of ventilation systems. It is concluded that, if properly implemented, intermittent operation of ventilation systems could reduce the energy requirement for heating the ventilating air by as much as 40 percent under typical design conditions.

**16551.** Cotton, I. W., Grubb, D. S., **Criteria for the evaluation of data communications services,** *Proc. Symp. IEEE Trends and Applications 1976: Computer Networks, Gaithersburg, MD, Nov. 17, 1976,* pp. 71-78 (Institute of Electrical and Electronics Engineers, New York, NY, 1976).

Key words: computer communications; computer networking; data communications; networks; performance requirements; telecommunications.

The quality of telecommunications services that are used as a means of interchanging information between information processing systems or between terminals and systems is determined by a number of parameters. This paper examines the following characteristics of telecommunications services: 1. Transfer Rate; 2. Availability; 3. Reliability; 4. Accuracy; 5. Channel Establishment Time; 6. Network Delay; 7. Line Turnaround Delay; 8. Transparency; 9. Security.

These parameters are all defined and their significance discussed.

**16552.** Engen, G. F., **Comments on "Practical analysis of reflectometers and power equation concepts",** *IEEE Trans. Instrum. Meas.* **IM-23,** No. 1, 104-105 (Mar. 1974).

Key words: power equation concepts; reflectometers.

Although an apparent objective of the cited paper is to yield additional insight into the power-equation concept, the reader is cautioned that the accompanying analysis is based more on intuitive concepts than mathematical rigor.

Some of the conclusions are, at most, only approximately true. These need to be identified and their associated errors evaluated if the requirements of careful metrology are to be satisfied.

In addition to the consideration of these questions, this correspondence also includes a more careful statement concerning the insensitivity of the power-equation methods to connector problems.

**16553.** Davis, R. M., **Systems of the 1980s—The U.S. perspective,** (Proc. Conf. Meeting XXXV on A Preview of the 1980s and Distributed Processing, Amsterdam, Holland, Nov. 18-20, 1975), *Document No. EC35, Session C,* pp. 27-43 (Diebold Europe S.A., Frankfurt, Germany, 1976).

Key words: automated reading technology; circuitry; computer applications; computer engineering; distributed systems; interface standards; memory technology; protocols.

Computer systems of the 1980s will be used in applications such as data acquisition and validation, recordkeeping, management information systems, real-time control, real-time monitoring, modeling, simulation, individualized services, scheduling, allocation, dispatching, and scientific and research investigations. These systems will serve primarily two sets of customers. One set is composed of large single organizations using computer systems to manage diversified activities and economic communities using computer systems to link members together. The second set will be individual users needing autonomous dedicated computer systems which can be interconnected to larger computer service networks or other individuals. The 1980s will see computer networks containing computers and computer modules of all sizes, independent memories and large variety of access terminal and automated input devices. However, the present lack of information controls, privacy safeguards, audit procedures, performance measures for real-time control systems, interface standards, software validation and documentation standards will have to be overcome to assure acceptability of the envisioned systems.

**16554.** Engen, G. F., Hudson, P. A., **International intercomparison of power standards at 3 GHz,** *IEEE Trans. Microwave Theory Tech.* **MTT-19,** No. 4, 411-413 (Apr. 1971).

Key words: bolometer mount; connector compatibility; directional coupler; interlaboratory standards.

An international intercomparison of microwave power at 3 GHz has recently been completed. This comparison was initiated at a meeting of the High Frequency Working Group of the Comite Consultatif d'Electricite (CCE) which met at the Bureau International des Poids et Mesures (BIPM) in May, 1965. At that time, the U.S. National Bureau of Standards (NBS) was designated as the pilot laboratory. The other laboratories, in order of their participation, are the following: for Canada, National Research Council (NRC); for the U.S.S.R., All-Union Research Institute of Metrology imeni D. I. Mendeleyev (VNIIM); for the German Democratic Republic, Deutsches Amt für Messwesen und Warenprüfung (DAMW); and for Japan, the Electrotechnical Laboratory (ETL).

**16555.** Alperin, H. A., Rhyne, J. J., Pickart, S. J., **Neutron scattering from an amorphous ferrimagnet,** *Proc. Int. Conf. of Magnetism, Moscow, USSR, Aug. 22-28, 1973,* **IV,** 358-366 (International Union of Pure and Applied Physics, The Academy of Sciences of the USSR, Moscow, Russia, 1974).

Key words: amorphous magnetism; direct current sputtering; inelastic neutron scattering; magnetic structures; magnetism; neutron diffraction; rare earth alloys.

Neutron diffraction measurements have been taken on a 2-axis spectrometer as a function of temperature for sputtered $TbFe_2$. Difference patterns between the measurements as a given temperature and the measurement at $T > T_c$ show that the spin and atomic distribution is amorphous. The elastic and inelastic components of the scattering have also been measured separately by using a 3-axis spectrometer. These results show that for $T > T_c$, no coherent magnetic structure remains; the magnetic scattering is all inelastic. An anomalous low-angle tail present in the data is assumed to arise from magnetic inhomogeneities 20-30 Å in size. Application of a magnetic field of $\sim 3$ kOe at 77 K can cause these inhomogeneities to grow in size as well as to cause a small rearrangement of the spin distribution. Inelastic scattering experiments using time of flight analysis were made to obtain the differential cross section $S(Q,\omega)$ at room temperature and at $T > T_c$. At $T > T_c$ the spectrum is seen to be paramagnetic-like, as expected. At room temperature, comparison with the spectrum for a polycrystalline sample shows the amorphous sample to have a spectrum which is more spread out and shifted to lower energies. This result is in accord with recent calculations.

**16556.** Mahaffey, C. T., **Metrication problems in the construction codes and standards sector,** *Constr. Specifier,* pp. 25-28, 30-32, 34-37 (June 1976).

Key words: building regulations; dimensional coordination; metric conversion; planning and scheduling.

This report is a response to a request for an outline of the problems to be faced by the building standards development and building regulatory sectors of the American building industry. It includes a discussion of the SI metric units themselves, giving examples of the conventions regarding their use adopted in other countries to illustrate the nature of the decisions that must be made by the U.S. building industry. It discusses the relationship of dimensional coordination to the metric conversion effort, its impact on the U.S. building regulatory system and illustrates some of the decisions these sectors need to make. It also discusses some of the organizational problems required to involve all segments of the industry in this decision-making process, and for implementing these decisions in a coordinated way on a national scale.

**16557.** Robertson, A. F., **Estimating smoke production from rooms and furnishings,** *Proc. Int. du Batiment (CIB) Symp. on the Control of Smoke Movement in Building Fires, Garston, U.K., Nov. 4-5, 1975,* pp. 21-32 (Conseil International du Batiment (CIB), Garston, U.K., 1975).

Key words: building materials; fires; optical density; room furnishings; smoke production; smoke tests.

In the absence of specific analytical methods for measuring the hazards of fire gases, there is a trend towards the use of smoke production as a partial measure of this hazard. It is suggested that present smoke test methods may be best used to provide indications of the possible smoke production, i.e., product of specific optical density and fire exposed area, characteristic of fully involved furnishing and interior finish products. It is demonstrated that very large quantities of smoke will result from combustion of only small quantities of most combustibles. Because of this there is little opportunity for elimination of the smoke hazard during fires through establishment of any but the most drastic limitations on the smoke development characteristics of materials considered acceptable. Measures for limiting ignition and development of fires, together with containment and disposal of smoke when fires occur, appear the most promising methods for reducing hazards due to smoke.

**16558.** Bennett, H. S., Forman, R. A., **Photoacoustic methods for measuring surface and bulk absorption coefficients in highly transparent materials: Theory of a gas cell,** *Appl. Opt.* **15,** No. 10, 2405-2413 (Oct. 1976).

Key words: bulk absorption coefficients; Fourier amplitudes; gas pressure; heat transfer; phase shifts; photoacoustic; surface absorption coefficients; transparent materials.

Researchers seek improved ways to measure the surface absorption and the bulk absorption coefficients of highly transparent materials. Procedures are presented here by which one may determine separately the surface absorption and the bulk absorption coefficients. For the case in which a laser beam modulated at angular frequency $\omega$ passes through the weakly absorbing windows of a gas cell containing a nonabsorbing gas, the temperature profiles in the cell windows and the temperature and acoustic pressure or stress profiles in the gas have been calculated. These calculations indicate that for sufficiently low frequencies and high ambient gas pressure, enough heat transfers from the cell windows to the gas to produce a detectable acoustic pressure signal at angular frequency $\omega$ in the gas. These calculations also enable us to state the necessary measurements for determining the surface and bulk absorption coefficients. Measuring the acoustic stress amplitude at the fundamental and higher harmonic frequencies and measuring the phase shifts of the frequency components of the acoustic stress with respect to the modulated laser beam give sufficient data by which one can determine the surface and bulk absorption coefficients. Numerical examples for a representative laser glass and air (nitrogen) are given.

**16559.** Holt, H. K., **Laser intracavity absorption,** *Phys. Rev. A* **14,** No. 5, 1901-1902 (Nov. 1976).

Key words: absorption; intracavity; laser; low density.

The fractional absorption which can be obtained using a single-mode laser with an internal absorption cell is compared to the fractional absorption obtainable with the more conventional system of a laser with an external absorption cell.

**16560.** Snyder, L. E., Hollis, J. M., Lovas, F. J., Ulich, B. L., **Detection, identification, and observations of interstellar $H^{13}CO^+$,** *Astrophys. J.* **209,** No. 1, 67-74 (Oct. 1, 1976).

Key words: formyl ion; interstellar molecules; microwave emission; molecular structure; radio astronomy; rotational spectrum.

Observations of interstellar $H^{13}CO^+$ are presented, and results of the molecular-structure computations supporting this particular molecular identification are given. Preliminary values of integrated intensity ratios of $H^{12}CO^+/H^{13}CO^+$ have been found for the main $HCO^+$ clouds. Searches for $H^{12}C^{18}O^+$ were unsuccessful, and upper limits are given. U86.76, a new unidentified interstellar molecule which may be methylcyanoacetylene, was detected in Sgr B2.

**16561.** Boyne, H. S., **Laser power and energy measurements,** (Proc. Conf. Optical Design Problems in Laser Systems, San Diego, CA, Aug. 21-22, 1975), *SPIE* **69,** 90-94 (1975).

Key words: laser power and energy measurements; spatial response; temporal development.

Laser source and detector characterization necessary for laser systems design is reviewed. Power, energy and temporal development of sources are discussed. Also, the spatial response of detectors is addressed.

**16562.** Yaghjian, A. D., **A direct approach to the derivation of electric dyadic Green's functions,** *Proc. AP-S Int. Symp., University of Massachusetts, Amherst, MA, Oct. 11-15, 1976*, pp. 71-73 (Institute of Electrical and Electronics Engineers, New York, NY, Oct. 1976).

Key words: electromagnetic theory; Green's dyadic theory.

A straightforward yet rigorous approach that does not require distribution theory is used to derive a general electric dyadic Green's function which remains valid within the source region. Although the electric field expressed by the dyadic Green's function proves to be unique, the exact form of the dyadic itself depends upon the shape of its "principle volume." The dependence on principle volume is determined explicitly, and the different Green's dyadics derived by previous authors are shown to emerge merely through the appropriate choice for the principle volumes.

**16563.** Belsher, D. R., **Development of near-field electric energy density meter model EDM-2,** *HEW Publ. No. (NIOSH) 75-140*, 26 pages (U.S. Department of Health, Education, and Welfare, Cincinnati, OH, Mar. 1975).

Key words: electric energy density; energy density; near-field energy density.

The Occupational Safety and Health Administration (OSHA) Nonionizing Radiation Exposure Standard (29 CFE 1910.97, June 2, 1974) includes electromagnetic (E-M) radiation from 10 MHz to 100 GHz. However, no survey monitors presently are manufactured for making electric-field measurements of radiofrequency (rf) radiation from 10 to 300 MHz. Consequently, rf electric-field occupational exposure data cannot be collected until suitable monitoring instrumentation is available.

The relationship between the electric and magnetic fields is completely ambiguous for near-field surveys (within one wavelength of the source) of rf radiation sources. The electric and magnetic fields must be measured separately to obtain total occupational exposure. An electric-field survey monitor (EDM-2) was developed for the Physical Agents Branch, Division of Laboratories and Criteria Development, NIOSH, by the E-M Division, NBS to be used in assessing occupational exposure from industrial rf power sources.

The monitor employs a set of three orthogonal dipoles to obtain an essentially isotropic response. The dipoles are connected to the meter electronics by special high resistance conductors which have minimal interaction with the rf field. The meter displays electric energy density from 0.003 to 30 $\mu J/m^3$ which corresponds to plane-wave equivalent power density from 0.18 to 1800 $mW/cm^2$.

**16564.** Marshall, H. E., Ruegg, R. T., **Efficiency problems from user fees in municipal wastewater treatment,** *Water Resour. Bull.* **12,** No. 5, 903-917 (Oct. 1976).

Key words: cost sharing; economic efficiency; environment; equity; financing; grants; pollution abatement; user fees; wastewater; water pollution; water resources.

The Environmental Protection Agency administers a construction grant program to encourage abatement of wastewater pollution by sharing with municipalities the costs of wastewater treatment facilities. The enabling legislation (P.L. 92-500) specifies that EPA's cost share will be 75 percent of construction costs. It further requires municipalities to collect user fees from industrial users of the facilities to repay that part of the federal grant allocable to the treatment of industrial wastewater. The municipality must return half of the user fees collected to the U.S. Treasury; the municipality is allowed to retain the remaining half. Retention by municipalities of these user fees lowers their effective cost shares and results in the following consequences: (1) a bias for municipalities to select certain kinds of abatement techniques regardless of whether or not they are the least-cost techniques from the national perspective; (2) a bias for municipalities to select larger-than-optimal scales of abatement facilities; (3) a hidden federal subsidy to industry; and (4) grants that favor industrial communities. This article examines the legislative and regulatory requirements for user charges, derives the algebraic expressions for calculating the real federal, municipal, and industrial cost shares with user fees; computes municipal cost shares for selected values of the determinant factors; evaluates efficiency and other consequences of current user fee arrangements; and concludes that the efficiency distortions brought about by the impacts of user fees on cost sharing could be eliminated by requiring that all user fees collected from industry against the federal cost share be returned to the U.S. Treasury.

**16565.** Hubbard, C. R., Mighell, A. D., Staffa, J. A., Zervos, C., Konopelski, J. P., ***S*-carboxymethyl-L-cysteine sulfone,** *Acta Crystallogr.* **B32,** Part 9, 2723-2725 (Sept. 1976).

Key words: hydrogen bonding; single crystal; structure determination; *S*-carboxymethyl-L-cysteine sulfone; x-ray, zwitterion.

$C_5H_9SO_6N$, orthorhombic, $P2_12_12_1$; $a = 9.205$ (4), $b = 5.223$ (2), $c = 15.891$ (7) Å; $Z = 4$, $D_x = 1.836$, $D_m = 1.86$ (2) g cm$^{-3}$ (flotation, 21 °C). The structure has been determined by direct methods and refined to an $R = 0.045$ for 944 independent reflections. The title compound exists as a zwitterion. Two carboxyl groups in adjacent molecules [O...O, 2.504 (5) Å] are involved in a strong hydrogen bond. The hydrogen atom was found to be covalently bonded to the carboxyl group in the carboxymethyl moiety.

**16566.** Siedle, A. R., Todd, L. J., **Chemistry of metalloborane derivatives containing the $B_{10}H_{12}$ ligand,** *Inorg. Chem.* **15,** No. 11, 2838-2842 (1976).

Key words: boron hydrides; deuterium; iridium; maleonitriledithiolate; metalloboranes; nuclear magnetic resonance; oxidative addition; palladium.

Ligand displacement reactions of $(B_{10}H_{12})Pd(PPh_3)_2$ were used to prepare $[(B_{10}H_{12})Pd(CN)_2]^{2-}$, $\{(B_{10}H_{12})Pd[C_2S_2(CN)_2]\}^{2-}$, and $(B_{10}H_{12})Pd(1,10\text{-}C_{10}H_8N_2)$. The reaction of the latter phenanthroline complex with butyllithium produced $\{[(B_{10}H_{11})Pd]_2C_{10}H_8N_2\}^{2-}$. The reaction of $C_2S_2(CN)_2^{2-}$ with $[(B_{10}H_{12})Ir(CO)(PPh_3)_2]$ led to $\{(B_{10}H_{12})Ir(CO)[C_2S_2(CN)_2](PPh_3)_2\}^-$ and $\{(B_{10}H_{12})Ir[C_2S_2(CN)_2](PPh_3)_2\}^-$. The reaction of $[(C_2H_5)_4N][(B_{10}H_{12})Ir(CO)(PPh_3)_2]$ in 1,2-$C_2H_4Cl_2$ with $D_2$ led to a regiospecific H-D exchange at the B(5,10) positions and the isolation of a $(B_{10}D_2H_{10})$ analogue. In $CH_3CN$ solvent, exchange also took place at the bridge hydrogen positions. A mechanism for this reaction was proposed. Exchange of the carbonyl group in the iridaborane with $^{13}CO$ was observed.

**16567.** Engen, G. F., Hoer, C. A., **Application of an "arbitrary" 6-port junction to power measurement problems,** *Proc. 1972 CPEM Conf. on Precision Electromagnetic Measurements, Boulder, CO, June 26-29, 1972*, pp. 100-101 (Institute of Electrical and Electronics Engineers, New York, NY, 1972).

Key words: directional coupler; power detectors; sidearm power detector.

A directional coupler with a sidearm power detector is a well known form of power monitor. With the addition of a second coupler and detector as shown in figure 1 the "reflected" as well as the "incident" power may be measured.

**16568.** Engen, G. F., Hoer, C. A., **Application of an arbitrary 6-port junction to power-measurement problems,** *IEEE Trans. Instrum. Meas.* **IM-21,** No. 4, 470-474 (Nov. 1972).

Key words: power meter; 6-port junction.

An analysis of an arbitrary 6-port junction, four ports of which are terminated by power meters, shows that the net power input (or output) at either of the remaining ports is a linear function of the four power meter indications. The validity of this result has been experimentally demonstrated at 10 GHz. This device promises to be a useful tool in a wide variety of power measurement and calibration problems.

**16569.** Hellwig, H., **Clocks and measurements of time and frequency,** *Proc. 1976 WESCON, Session 32,* pp. 1-4 (Institute of Electrical and Electronics Engineers, New York, NY, Sept. 1976).

Key words: clocks; frequency and time; measurement of time and frequency; time and frequency.

After a brief historical review, the present state-of-the-art in frequency and time standards of high performance will be reviewed.

Precision oscillators used in precision time and time interval applications include quartz crystal, rubidium gas cell, cesium beam, and hydrogen maser oscillators. A general characterization and comparisons of these devices is given including accuracy, stability, availability, cost, etc. Areas of special concern in practical applications are identified and a projection of future performance is given. An attempt is made to predict physical and performance characteristics of new designs potentially available in the near future such as novel crystal standards, superconducting cavity devices, etc.

Methods for measuring frequency stability are discussed.

The methods employed for measuring frequency are designed to include state-of-the-art oscillators: they are fairly simple, and commonly available components can be used in the measurement systems.

Physical interpretations of common noise processes are discussed and it is shown how frequency domain stability characteristics may be translated to time domain stability characteristics.

A brief survey of the capabilities of available and potentially available time and frequency transfer techniques is given, including portable clocks, satellite methods, and radio broadcasts.

**16570.** Kimbleton, S. R., Wood, H. M., **A load leveling support methodology for networking,** *Proc. Winter Simulation Conf., National Bureau of Standards, Gaithersburg, MD, Dec. 6-8, 1976,* pp. 247-253 (Association for Computing Machinery, New York, NY, 1976).

Key words: computer networking; load leveling; resource sharing; scheduling.

Networking provides an effective means for resource sharing; however, its utility for load leveling requires further demonstration. This paper examines obstacles to load leveling and concludes that the key issues relate to the possible loss of control over remotely processed jobs and data. Although an organizational framework necessary to provide appropriate control exists, the technological support mechanism necessary for control in the form of processing guarantees has not yet been developed. Such development requires an essentially real time control capability for determining both the feasibility of accepting remote jobs as well as the guarantees which can be stipulated when such jobs are offered for processing. The key component of this capability is shown to be a very fast analytically driven simulation technique which can be invoked at a given site each time a job is offered for processing. We note in passing that this control capability can be viewed as the "other" side of control limits. That is, while control limits are concerned with determining when system performance has strayed out of bounds, a control capability is concerned with dynamic control of system workload to keep system performance within bounds.

**16571.** Sawyer, D. E., Berning, D. W., **Mapping nonlinearities over the active regions of semiconductor devices,** *Proc. IEEE Letters* **64,** No. 11, 1635-1637 (Nov. 1976).

Key words: device nonlinearity measurements; hot spots, transistor; laser scanning; nondestructive tests; semiconductor devices; UHF transistor measurements.

A laser scanner employing a modulated low-power 0.633-$\mu$m He-Ne laser has been used in a nondamaging manner to locate portions of a silicon bipolar UHF transistor which electrically behave in a nonlinear manner at a signal frequency of 470 MHz. In effect, the method uses the device scanned as a frequency converter to produce an IF output for a display screen whenever the laser spot is incident on nonlinear regions.

**16572.** Hogan, P. B., Carlsten, J. L., Pichanick, F. M. J., Smith, S. J., Smith, W. W., **Spontaneous Raman processes in multiphoton excitation of sodium,** *Phys. Rev. Lett.* **37,** No. 15, 990-993 (Oct. 11, 1976).

Key words: atomic beams; multiphoton ionization; sodium; spontaneous Raman scattering in free atoms.

We have observed spontaneous Raman processes in a sodium atomic beam. When one sodium $3p\ ^2P$ fine-structure level is strongly excited by a dye laser, the other level is weakly populated by spontaneous Raman emission and the absorption of another laser photon. This effect is detected by further stepwise excitation plus photoionization. The observed magnitude agrees well with theory. This technique is much more sensitive than methods involving direct observation of the Raman emission.

**16573.** Corliss, E. L. R., Jones, F. E., **Method for estimating the audibility and effective loudness of sirens and speech in automobiles,** *J. Acoust. Soc. Am.* **60,** No. 5, 1126-1131 (Nov. 1976).

Key words: alarm signals; hearing; loudness functions; masking; sirens; speech recognition; traffic noise.

By using the parameters for the ear and the equations for a "communication theory" model of the behavior of the ear, a family of masking curves can be drawn up which one can apply to the conditions prevalent in automotive vehicles. From the behavior of the ear and its ability to resolve sounds in noise, estimates can be made of the conditions under which sirens and speech communications will be audible within motor vehicles moving in traffic, and some estimate can also be made as to their potential for attracting notice. These quantities can be read off by graphic techniques. Examples of their use are given.

**16574.** Mayo, S., Keller, R. A., Travis, J. C., Green, R. B., **Detection of sodium trace contamination in furnace atmospheres at 1000 °C,** *J. Appl. Phys.* **47,** No. 9, 4012-4016 (Sept. 1976).

Key words: dye laser use for resonance fluorescence; furnace atmosphere sodium contamination; furnace qualification; resonance fluorescence; sodium trace detection.

Free sodium atoms were detected by resonance fluorescence in an open contaminated quartz tube heated to 1000 °C. The uartz tube and furnace were similar to those used in semiconuctor device processing. Fluorescence was excited by a cw dye ser tuned to the sodium $D_1$ or $D_2$ transition and directed along e axis of the furnace. Fluorescence from the sodium $D_2$ line mitted in the axial direction was collected by a telescopic ystem and focused onto a photomultiplier tube. The estimated inimum detectable sodium density in the furnace is $5 \times 10^5$ toms/cm$^3$. No free sodium was detectable on a processing tube hat had not been intentionally contaminated.

6575. Engen, G. F., **Calibration of an arbitrary six-port junction for measurement of active and passive circuit parameters,** *IEEE Trans. Instrum. Meas.* **IM-22,** No. 4, 295-299 (Dec. 1973).

Key words: circuit parameters; networks; six-port.

It has been recently recognized that an arbitrary six-port juncon, four arms of which are terminated in power meters, can be alibrated to measure the circuit parameters, *v, i, z, a, b,* Γ, etc., n addition to power. Because this scheme eliminates the need or frequency conversion, it provides a substantially simplified pproach to the design of an automatic network analyzer. This aper outlines a calibration procedure for the six-port which is nly slightly more complicated than that in use for existing autonated measurement systems.

6576. Cotton, I. W., **New family of standards being developed,** *Computerworld*, pp. S/2-S/22 (Nov. 29, 1976).

Key words: computer networks; data communications; data networks; networks; packet switching; protocol; standards.

Recent developments in data network standards are briefly urveyed, including developments in call establishment, data link ontrol, and packet switching.

6577. Sawyer, D. E., Berning, D. W., **Thermal mapping of transistors with a laser scanner,** *Proc. IEEE Letters* **64,** No. 11, 1634-1635 (Nov. 1976).

Key words: active devices; hot-spot behavior; laser scanning; nondestructive testing; silicon optical absorption coefficient; temperature mapping.

An active near-infrared laser scanner has been used to elecronically map the temperature variations over the active regions f silicon interdigitated UHF transistors operating in the hot-pot regime. The principle makes use of the increase in electron-ole pair generation by the absorbed laser light with increasing emperature. The regions of enhanced photoresponse are dislayed on a cathode-ray-tube display screen. Extensions to other evices and operating conditions, other than those which result n hot-spot operation, are suggested.

6578. Kuyatt, C. E., Mielczarek, S. R., Weiss, M. J., **Intensities of infrared transitions in $N_2O$ and $H_2CO$ by electron impact spectroscopy,** *J. Chem. Phys.* **65,** No. 9, 3481-3485 (Nov. 1, 1976).

Key words: $H_2CO$; inelastic electron scattering; infrared transitions; $N_2O$; relative intensities.

Measurements of relative intensities of infrared transitions in $N_2O$ and $H_2CO$ have been made using forward inelastic scatterng of 100 eV electrons. Agreement with previous infrared and electron impact measurements is satisfactory, showing that inrared intensities can be obtained from electron scattering meaurements without the need for pressure broadening or corections for the spectrometer slitwidth.

16579. Browne, J. C., Lamaze, G. P., Schröder, I. G., **Ratio of neutron capture cross sections for $^{186}$Os and $^{187}$Os at 25-keV neutron energy,** *Phys. Rev. C* **14,** No. 3, 1287-1288 (Sept. 1976).

Key words: $E_n = 25$ keV; measured cross-section ratio; nuclear reactions; $^{186,187}$Os$(n,\gamma)$.

The ratio of the neutron capture cross sections for $^{186}$Os and $^{187}$Os was measured at the 25-keV iron-filtered neutron beam facility of a 10-MW reactor. A value of 0.41 ± 0.04 was obtained. Using this ratio, the age of the universe was determined via the Re-Os $\beta$-decay clock to be approximately $19 \times 10^9$ years.

16580. Baldwin, E. E., **Voltage-controlled attenuator has minimum phase shift,** *EDN/EEE*, p. 40 (Nov. 5, 1971).

Key words: FET; pi network; tank circuit.

A FET in a pi network makes a good attenuator at a specific radio frequency, but gives variable phase shift with changing attenuation. A tank circuit across source-drain leads solves the problem.

16581. Herbst, J. F., Watson, R. E., Lindgren, I., **Coulomb term *U* and 5*f* electron excitation energies for the metals actinium to berkelium,** *Phys. Rev. B* **14,** No. 8, 3265-3272 (Oct. 15, 1976).

Key words: actinium; excitation energy; *U*; 5*f* electron.

Relativistic Hartree-Fock-Wigner-Seitz band calculations have been performed for the actinide metals Ac through Bk in order to estimate the Coulomb term *U* and 5*f* electron excitation energies. Our calculations predict that the tetravalent state (four 6*d*-7*s* conduction electrons) is stable relative to the trivalent state for the lighter elements and that near uranium relative stabilization of the trivalent state occurs. We find that *U* increases from 2-3 eV for Th to 4-5 eV for the heavier elements considered. 5*f* level widths *W* are estimated and found to decrease from 2 to 1/2 eV; together with the results for *U* this points to progressive localization of the 5*f* states. The ratio *U*/*W*, which is most indicative of localization, takes on values intermediate between those for 3*d* and 4*f* electrons.

16582. Altschuler, H. M., **1. Commission I and the General Assembly. 2. The General Assembly as an open symposium,** *URSI Inf. Bull. No. 190*, 10-15 (Mar. 1974).

Key words: general assembly; open symposium.

The place of Commission 1 in the world of standards of physical measurements and whether or not the scientific programme at the General Assembly of Commission 1, as well as all other Commissions should be converted into an open Symposium are discussed in the paper.

16583. Kostkowski, H. J., **Uncertainties in the measurement of incoherent optical radiation,** *Proc. Symp. on Biological Effects and Measurement of Light Sources, Rockville, MD, Mar. 25-26, 1976*, pp. 107-114 (HEW, PHS, Food and Drug Administration, Bureau of Radiological Health, Rockville, MD, Oct. 1976).

Key words: accuracy; optical radiation measurement; radiometry; systematic errors; uncertainties.

Uncertainties for state-of-the-art measurements of incoherent optical radiation are about 1 percent. Uncertainties for measurements made under less than ideal conditions are considerably larger. The major reasons for these uncertainties and what is being done and can be done to reduce them are presented.

16584. Suenram, R. D., Johnson, D. R., Glasgow, L. C., Meakin, P. Z., **Laboratory microwave spectrum of $ClONO_2$,** *Geophys. Res. Lett.* **3,** No. 10, 611-614 (Oct. 1976).

Key words: atmospheric pollution; chlorine nitrate; dipole moment; microwave spectrum; ozone depletion; rotational constants; stratospheric chemistry.

The microwave spectrum of $ClONO_2$ has been analyzed in the laboratory under high resolution. Rotational constants are reported for the ground and lowest vibrational states of the $^{35}Cl$ and $^{37}Cl$ isotopic forms. From Stark effect measurements the electric dipole moment was found to have components along two principal axes, $\mu_a = 0.72 \pm 0.10$ Debye and $\mu_b = 0.28 \pm 0.04$ Debye. Difficulties encountered in handling gas phase samples of $ClONO_2$ are discussed in some detail.

**16585.** Siedle, A. R., **Organometallic derivatives of trithiones,** *J. Organomet. Chem.* **120,** 369-374 (Apr. 1976).

Key words: carbon-13 NMR; coordination compounds; metal carbonyl; thiocarbonyl; 1,3-dithiolane-2-thione; 1,3-dithiolene-2-thione.

Complexes of the type $LM(CO)_5$ ($M = Cr, Mo$) were prepared from (diolefin)$M(CO)_4$ and the 1,3-dithiolene-2-thione ligands, $L = C_3H_2S_3$, $C_3H_4S_3$ and $C_8H_6S_3$. Infrared, $^1H$ and $^{13}C$ NMR data indicated $C_{4v}$ symmetry about the metal centre. The reaction of 3-methylbenzo-1,3-dithiolene-2-thione with $(C_5H_5)Co(C_8H_{12})$ produced a cobalt(III) methylbenzothiete derivative $(C_7H_6S_2)$-$Co(C_5H_5)$.

**16586.** Bowen, R. R., Reed, L. E., **Semiporous reinforcing fillers for composite resins: II. Heat treatments and etching characteristics,** *J. Dent. Res.* **55,** No. 5, 748-756 (Sept.-Oct. 1976).

Key words: composite resins; composites; dental materials; fillers; porous glass; radiopacity; reinforcements; wear.

Candidate experimental semiporous reinforcing filler particles were prepared by heat treatment of certain glass compositions, followed by crushing and etching. Optical microscopic techniques were aided by the use of certain dyes and staining procedures to manifest submicroscopic interconnected porosity in the surface of the particles. The goal of this endeavor was to develop semiporous glass reinforcing fillers for the improvement of dental composite materials.

**16587.** Bowen, R. L., Reed, L. E., **Semiporous reinforcing fillers for composite resins: I. Preparation of provisional glass formulations,** *J. Dent. Res.* **55,** No. 5, 738-747 (Sept.-Oct. 1976).

Key words: composite resins; composites; dental materials; fillers; porous glass; radiopacity; reinforcements; wear.

A conceptual means of obtaining improved bonding between filler particles and the polymeric binders of composites is presented. It involves preparing glass particles that separate into two interconnected vitreous phases when heated to an appropriate temperature, and then etching these to produce a porous surface layer. Candidate glass compositions were prepared and subjected to heat treatment in a gradient furnace. Compositions susceptible to phase separations were delineated.

**16588.** Phaneuf, R. A., Taylor, P. O., Dunn, G. H., **Absolute cross sections for emission of 284.7-nm (Hg II) and 479.7-nm (Hg III) radiation in electron-mercury-ion collisions,** *Phys. Rev. A* **14,** No. 6, 2021-2025 (Dec. 1976).

Key words: absolute cross sections; electron impact; mercury ions; 285-nm radiation; 480-nm radiation.

Crossed beams of electrons and $Hg^+$ ions have been used to measure absolute cross sections for emission of 284.7-nm radiation, resulting from excitation of a predominantly ground-state $Hg^+$ target to the $7s^2S_{1/2}$ state. Values range from $3 \times 10^{-17}$ cm$^2$ near threshold, where the cross section is strongly peaked, to $1.3 \times 10^{-18}$ cm$^2$ at 280 eV. Also reported are some measurements of emission of 479.7-nm (Hg III) radiation, resulting from electron impact on both $Hg^+$ and $Hg^{++}$ targets. Cross sections range from approximately $5 \times 10^{-19}$ to $5 \times 10^{-20}$ cm$^2$, and in the case of electron-$Hg^{++}$ collisions, are more than an order of magnitu smaller than predicted by an available semiclassical binary-e counter calculation.

**16589.** Tsai, D. H., MacDonald, R. A., **Molecular-dynami study of second sound in a solid excited by a strong heat pul** *Phys. Rev. B* **14,** No. 10, 4714-4723 (Nov. 15, 1976).

Key words: anharmonic crystal; computer simulation; ene gy transport; heat pulse; molecular dynamics; seco sound; stress pulse; temperature wave; thermal diffusivit thermal equilibrium; thermal relaxation.

We use the method of molecular dynamics to study t problem of heat transfer in a perfect semi-infinite bcc latti when a strong heat pulse is applied at the boundary. We find th the disturbance propagates into the lattice as a combination first sound and second sound superimposed on a diffusi background. The second-sound wave is a composite of sever waves. We are able to show that the longitudinal and transver sound waves, traveling with velocity $C_1$ and $C_s$, respectively, a generated by the disturbance when the boundary of the lattice rapidly heated or cooled. These stress-induced pulses are not i thermal equilibrium but they generate their own temperatu waves, which travel with velocities $C_l/\sqrt{3}$ and $C_s/\sqrt{3}$, and whic contribute to the observed second-sound wave. The disturbanc in kinetic energy produced during the period of steady heating i the pulse propagates as a temperature wave with the theoretically expected second-sound velocity, $C_{av}/\sqrt{3}$. We relate thes results to theoretical and experimental work on second soun excited by a weak pulse and also to our earlier calculation where the temperature wave is excited by shock compression.

**16590.** Stockbauer, R., Inghram, M. G., **The fragmentation o propane and deuteropropane molecular ions,** *J. Chem. Phys.* **65** No. 10, 4081-4092 (Nov. 15, 1976).

Key words: coincidence; mass spectrometry; photoionization; propane; propane-$d_2$; propane-$d_6$; propane-$d_8$ threshold photoelectron spectroscopy.

Fragmentation of molecular ions as a function of internal energy has been studied for the propane molecules, $C_3H_8$, $CH_3CD_2CH_3$, $CD_3CH_2CD_3$, and $C_3D_8$ using threshold photoelectron-photoion coincidence mass spectrometry. Within the energy range covered (0-6 eV internal energy) the experimental fragmentation curves are compared with those calculated using the quasiequilibrium theory. The general features of the experimental curves are reproduced by the calculations but significant deviations from exact calculations are apparent. The experimental curves for the $d_2$ and $d_6$ propanes show that hydrogen scrambling processes occur and are of sufficient importance that they must be included in future calculations.

**16591.** Truhlar, D. G., Wyatt, R. E., **History of $H_3$ kinetics,** *Ann. Rev. Phys. Chem.* **27,** 1-43 (1976).

Key words: chemical reactions; collision theory; cross sections; dissociation; hot atoms; isotope effects; kinetics; molecular beams; quantum mechanics; rate coefficients; recombinations; scattering theory.

The gas-phase reaction of H with $H_2$ has been of fundamental interest since London (1929) pointed out that it can be understood in terms of a potential energy surface calculated from quantum mechanics. It has also been the only gas-phase bimolecular reaction for which curvature of the Arrhenius plot could be observed at low temperature (Marshall and Purnell 1968). Thus it served as a model for theories of tunneling. Because every atom involved can be substituted by D or T, it has been an important prototype system for isotope effect considerations. Because good photochemical and nuclear recoil sources of pt (i.e., fast) H, D, or T atoms are available, it has also been stu-ed under nonthermal high-energy conditions (Rowland 1970). n addition it has been extensively studied by classical and quantum mechanical collision theory.

6592. Bowman, R. R., **Quantifying hazardous electromagnetic microwave fields: Practical considerations,** *Proc. Biological Effects and Health Implications of Microwave Radiation, Richmond, VA, Sept. 17-19, 1969, BRH/DBE 70-2*, 204-209 (U.S. Dept. of Health, Education, and Welfare, Rockville, MD, June 1970).

Key words: electromagnetic microwave fields.

This paper is concerned mainly with the problem of making asy, reasonably accurate survey measurements of hazardous M fields. For general survey use, instruments should be ugged, easy-to-use, and should be capable of fast response as ell as having long-term averaging capabilities. These, and other onsiderations to be discussed, place restrictions on practical in-trument designs for general survey use.

6593. Duff, J. W., Truhlar, D. G., **Classical $S$ matrix: Application to classically forbidden vibrational excitation for He + HBr and H + Br$_2$,** *Chem. Phys.* **17,** 249-254 (Oct. 1976).

Key words: classical scattering matrix theory; collision theory; scattering theory; trajectories.

The integral expressions of classical $S$ matrix theory are tested gainst quantum mechanical results and classical path-forced uantum oscillator results for vibrational transition probabilities n collinear collisions of atoms with harmonic and Morse vibra-ors for the H + Br$_2$ and He + HBr mass combinations. The in-eraction potential is assumed to be a repulsive exponential func-on. The energy range studied (in units of $\hbar\omega_e$) is 2-10 for H + r$_2$ and 2-6 for He + HBr. The integral expressions are found to e accurate within a factor of two for almost all transition proba-ilities greater than $7 \times 10^{-3}$ but to be very inaccurate for very mall transition probabilities. Quasiclassical trajectory histogram nethods are found to be accurate within a factor of two only for ransition probabilities greater than 0.15. Neither the integral ex-ressions of classical $S$ matrix theory nor the quasiclassical rajectory histogram method are found to be as generally accu-ate as the classical path-forced quantum oscillator results.

6594. Green, R. B., Travis, J. C., Keller, R. A., **Resonance flame atomic fluorescence spectrometry with continuous wave dye laser excitation,** *Anal. Chem.* **48,** No. 13, 1954-1959 (Nov. 1976).

Key words: atomic flame fluorescence; barium fluorescence; cw dye laser; sodium fluorescence.

The potential contribution of continuous wave (CW) dye laser xcitation of resonance atomic fluorescence for analytical flame pectrometry was evaluated. Noise sources which were related o fluctuations in the flame and in the laser scatter were responsi-le for the observed detection limits which were an improvement ver those achieved with previously used excitation sources for lame atomic fluorescence and comparable to results for flame mission spectrometry. Based on experimental data, it was esti-nated that continuous wave excitation powers of 1-10 watts would be sufficient to bring the signal-to-noise ratio into a con-tant range. With the exception of nonresonant detection and aturation contributions to reduced quenching, higher laser owers common to pulsed sources are of no advantage and, in act, are detrimental to sensitivity. Other aspects of CW dye aser excitation are presented and discussed.

6595. Haus, J. W., Meijer, P. H. E., **Static aspects of a model for metastable fluid states,** *Physica Letter to the Editor* **80A,** No. 3, 313-317 (1975).

Key words: limit of stability; mean field theory; metastability; perturbation scheme; reference system; structure factor.

A mean field-theory originally presented by Brout is used to obtain the limit of (meta-) stability for a Lennard-Jones system. Certain aspects of the theory are discussed in relation to recent results for liquid-solid phase transitions.

16596. Julienne, P. S., **$^3\Sigma_u^-$-$^3\Sigma_u^+$ coupling in the O$_2$ $B^3\Sigma_u^-$ predissociation,** *J. Mol. Spectrosc.* **63,** 60-79 (1976).

Key words: molecular oxygen; predissociation; Schumann-Runge bands; spin-orbit mixing.

The role of $B^3\Sigma_u^-$-$2^3\Sigma_u^+$ spin-orbit mixing in the O$_2$ Schumann-Runge predissociation is investigated. The $2^3\Sigma_u^+$ state is found to cross the $B^3\Sigma_u^-$ state near 2.0 Å with an interaction matrix element of approximately 55 cm$^{-1}$. This state contributes to the widths of the $B$ $v \geqslant 6$ levels, but introduces only small level shift perturbations. When the partial widths due to the $^3\Sigma_u^-$-$^3\Sigma_u^+$ interaction are added to the previously calculated widths due to the $^5\Pi_u$, $^3\Pi_u$, and $^1\Pi_u$ states, reasonable agreement is obtained with experimental measurements on O$^{16}$O$^{16}$ and O$^{18}$O$^{18}$. The possibility of non-Lorentzian line profiles and the dependence of the width on rotational quantum number is investigated. The approximation of the spin-orbit matrix element by its value at the crossing point is shown to be a good approximation for calculating the second difference perturbations.

16597. Swartzendruber, L. J., Bennett, L. H., Watson, R. E., **Mössbauer studies of hydrided TiFe,** *J. Phys. F: Metal Phys. Letter to the Editor* **6,** No. 12, L331-L334 (1976).

Key words: charge flow; isomer; Mössbauer; phase diagram; TiFeH$_x$ alloys; volume effects.

The metallurgical and electronic structure of TiFeH$_x$ alloys are probed by $^{57}$Fe Mössbauer effect studies. Our results are qualitatively consistent with and support Reilly and Wiswall's conclusions on the phase diagram. Volume effects and charge flow are both important in the isomer shift.

16598. Lias, S. G., Ausloos, P., **Reactions of CCl$_2$H$^+$ and CF$_2$H$^+$ with organic and inorganic compounds: proton affinities and heats of formation of CCl$_2$ and CF$_2$,** *Int. J. Mass Spectrom. Ion Phys.* **22,** 135-145 (1976).

Key words: CCl$_2$, CF$_2$; CCl$_2$H$^+$, CF$_2$H$^+$; displacement reactions; four-center reactions; ion molecule reactions; proton affinity; proton transfer; rate coefficients.

The reactions of CCl$_2$H$^+$ (or CCl$_2$D$^+$) and CF$_2$H$^+$ with a number of aldehydes, ketones, esters, organic acids, alcohols, amines and inorganic compounds have been observed. Since the proton affinities of most of these compounds are known, it was possible on the basis of the observation or nonobservation of proton transfer reactions to obtain proton affinities for CF$_2$ and CCl$_2$ of 7.74 ± 0.04 eV (178.6 ± 1 kcal mole$^{-1}$) and 8.69 ± 0.06 eV (200.4 ± 1.5 kcal mole$^{-1}$), respectively. In addition to proton transfer, CCl$_2$H$^+$ and CF$_2$H$^+$ undergo reactions with carbonyl-containing compounds entirely analogous to those which have been observed for other halomethyl ions. That is, with aldehyde and ketone reactants, four-center reactions resulting in the formation of a mono-halogenated carbonium ion are the major competing processes, and with esters and acids elimination reactions and four-center reactions resulting from attack by the ion at the acyl oxygen are important. These ions also displace carbonium ions from alcohols, and abstract hydride ions from esters and amines. Charge transfer is an important competing channel in reactions with amines.

16599. Richmond, J. C., **Image quality of photoelectronic imaging systems and its evaluation,** (Proc. 6th Symp. on Photo-Electronic Image Devices, London, England, Sept. 9-13, 1974), Paper in *Advances in Electronics and Electron Physics*, L. Marton, Ed., **40B**, 519-538 (Academic Press, New York, NY, 1976).

Key words: blooming; contrast transfer function; distortion; flare; image quality; light induced background; limiting resolution; night vision devices; optical transfer function; resolution charts; veiling glare.

Image quality is probably the single most important parameter in determining the usefulness of any optical device. For night vision systems in particular, image quality is of paramount importance. Subjective evaluation of image quality is surprisingly good. An observer will have no difficulty in ranking a number of photographs in order of overall image quality. The general agreement between different observers on the order of ranking of the same series of photographs will also be good. However, objective evaluation of image quality in quantitative terms is not easy. Many variables contribute to image quality, not all of which have been identified, or can be quantitatively evaluated. This paper is primarily a literature survey of criteria and techniques that have been used to evaluate the quality of imaging systems, with some discussion of their application to image intensifier night vision devices.

**16600.** Wiederhorn, S. M., Roberts, D. E., **A technique to investigate high temperature erosion of refractories,** *Bull. Am. Ceram. Soc.* **55,** No. 2, 185-189 (1976).

Key words: castable refractories; coal gasification; deformation; erosion; fracture; wear.

A description is given of equipment used to study erosion of refractories under controlled environments at temperatures as high as 1500 °C. Erosive wear of a high alumina castable refractory currently used in coal gasification pilot plants is investigated. Erosion occurs preferentially in the cement matrix of the refractory. At 25 °C erosion occurs by brittle fracture of the matrix, while at 1000 °C, erosion occurs by fracture and shear deformation of the matrix phase. Data are discussed with reference to current theories of erosion.

**16601.** Haus, J. W., Meijer, P. H. E., **Dynamics of metastable fluid states in the liquid-solid transition,** *Phys. Rev. A* **14,** No. 6, 2285-2294 (Dec. 1976).

Key words: hydrodynamic regime; ideal gas memory function; limit of stability; metastable fluid states; nonhydrodynamic regime; relaxation time; transport coefficients; Zwanzig-Mori formalism.

A fluctuation theory for the dynamics of metastable fluid states is presented which relies on a limiting form for the static structure factor $S(k)$ previously presented by the authors. The transport coefficients are found to show a divergence in the hydrodynamic regime. In the nonhydrodynamic regime a model is presented which uses an approximate single-particle memory function and a diffusive mode is found; this is compared with fluctuation theory results of other workers. A recent computer experiment has shown numerical agreement with the static model.

**16602.** Simmons, J. A., Clough, R. B., **Theoretical aspects of acoustic emission spectral measurements,** *Proc. Eighth World Conf. on Nondestructive Testing, Cannes, France, Sept. 6-10, 1976*, pp. 1-8 (Imprimplans, Paris, France, 1976).

Key words: acoustic emission; dislocations; nondestructive evaluation; spectral analysis.

Frequency spectrum analysis of acoustic emission signals shows great promise as a nondestructive test method. It has potential for discriminating between harmful moving defects a system noise as well as for revealing more of defect char teristics than are currently revealed with threshold count techniques. However, such an analysis required a systematic amination of the entire emission process.

In this paper, we describe progress in developing the theory acoustic emission. More specifically, we examine acoustic em sion from planar, straight line dislocation segments moving bursts. For simplicity, we will for the present treat the ideal ca of an infinite isotropic body. This case should, however, prov an illustration of the general nature of the acoustic emissi spectrum and how it is produced.

**16603.** Hall, J. L., Bordé, C. J., Uehara, K., **Direct optical reso tion of the recoil effect using saturated absorption spectrosco** *Phys. Rev. Lett.* **37,** No. 20, 1339-1342 (Nov. 15, 1976).

Key words: $CH_4$ hyperfine structure; high resolution spe troscopy; laser spectroscopy; line shape; optical frequen standards; recoil effect; relativity.

The recoil-induced spectral doubling of the $CH_4$ saturated a sorption peaks at 3.39 $\mu$m has been clearly resolved. A worki resolving power of $8 \times 10^{10}$ (1 kHz half width at half-maximum achieved with aberration-compensated parabolic optics of 32 c diam, was available to study the height ratio and splitting of th recoil peaks. The resolved Doppler-generated level crossings a not recoil doubled and give improved hfs information. We deriv new, exact equations relating the atomic natural frequency laboratory resonance frequencies.

**16604.** Green, R. B., Keller, R. A., Luther, G. G., Schenck, K., Travis, J. C., **Galvanic detection of optical absorptions in gas discharge,** *Appl. Phys. Lett.* **29,** No. 11, 727-729 (Dec. 1976).

Key words: discharge; discharge tubes; hollow cathode spectroscopy; trace detection; tunable lasers.

An electrical signal, resulting from discrete optical absorp tions, has been observed for a variety of elements, includin several for which such an effect had not been previously re ported. In the present case, the effect is observed as a change i the voltage across a gas discharge tube produced by irradiatio with a laser tuned to the wavelength of a transition of a species i the discharge. This signal may be used—without optical detection apparatus—for spectroscopic investigations or analytica determinations of materials in the discharge. Signals were obtained for transitions of lithium, sodium, calcium, barium, uranium, neon, and helium, in commercial hollow cathode lamps, and neon and helium in conventional discharge tubes.

**16605.** Latour, J., Spiegel, E. A., Toomre, J., Zahn, J. P., **Stellar convection theory. I. The anelastic modal equations,** *Astrophys. J.* **207,** No. 1, 233-243 (July 1, 1976).

Key words: convection theory; convection zones; stellar structures.

We present here a system of equations for stellar convection theory. These equations follow from the full equations of compressible fluid dynamics with the introduction of two important approximations. The first of these is the anelastic approximation, commonly used in meteorology. Its aim is to filter out acoustic waves so that the task of numerical solution will not be complicated by the need to resolve very rapid time variations. The anelastic approximation is justified when the frequencies and Mach numbers of the convection are not too high. Its basic effect is to suppress terms which are nonlinear in the horizontal fluctuations of the thermodynamic variables, but it allows large vertical variation in the mean density and preserves the dynamical nonlinearities. The second approximation is a drastic simplificaon of the horizontal structure of the convection. It consists of kpanding the fluctuating quantities in a set of modes which are eriodic in the horizontal coordinates, and then truncating after few terms.

The resulting system of nonlinear partial differential equations n vertical coordinate and time) is still formidable, and its nuerical resolution has so far been achieved only for relatively mple cases of stellar convection, to be presented in subsequent apers. These anelastic modal equations can also be used to treat ore complicated problems such as semiconvection and the oupling of convection to radial pulsation or rotation.

**6606.** Toomre, J., Zahn, J. P., Latour, J., Spiegel, E. A., **Stellar convection theory. II. Single-mode study of the second convection zone in an A-type star,** *Astrophys. J.* **207,** No. 2, 545-563 (July 15, 1976).

Key words: A-type stars; convection theory; convection zones; metallic-line stars; stellar structure.

The anelastic modal equations presented in Paper I are condered in their simplest version: only one mode is retained in the epresentation of the fluctuating dynamic and thermodynamic ariables of convection theory. These single-mode equations are sed to examine the structure of the second convection zone of n A-type star. Two- and three-dimensional numerical solutions re obtained for a range of parameters in the theory, and a simple nalysis is provided for their interpretation.

The principal results are for three-dimensional motions, since nese are most likely to be relevant to stellar convection. Such notions produce a convective heat flux several orders of magitude greater than predicted by standard mixing-length theory or the same situation; we find that convection carries up to 6 ercent of the total flux. The most significant astrophysical imlication of our results is that they suggest strong overshooting nto the adjacent radiative zones. We anticipate that mixing will xtend to the overlying hydrogen convection zone. This would ule out some interpretations of metallic-line stars which invoke iffusive element separation between the two convection zones.

**6607.** Truhlar, D. G., **Quasiclassical predictions of final vibrational state distributions in reactive and nonreactive collisions,** *Int. J. Quant. Chem. Symp.* **10,** 239-250 (1976).

Key words: chemical reactions; classical probability matrix theory; classical scattering matrix theory; collision theory; energy transfer in collisions; hydrogen molecules; information theory; scattering theory; trajectories; vibrational energy.

The validity of quasiclassical and semiclassical trajectory nethods for predicting state-to-state vibrational transition probailities in collisions of atoms with diatomic molecules is iscussed with special emphasis on tests against accurate quanim calculations for $He + H_2$, $H + Cl_2$, and $I + H_2$ collisions.

**6608.** Norcross, D. W., Seaton, M. J., **Energy levels for Be I calculated using a model potential and cores approximation,** *J. Phys. B* **9,** No. 17, 2983-3000 (Dec. 1976).

Key words: Be energy levels; model potential theory.

A two electron model Hamiltonian, used for Be I, includes a ore polarization potential $V_{POL}(1,2)$ which has asymptotic form $_{POL} \sim -\alpha\{(\hat{r}_1/r_1^2)+(\hat{r}_2/r_2^2)\}^2$ where $\alpha$ is the polarizability of Be II $1s^2$. Solutions are obtained using a frozen cores method. Two pproximations are considered: (a) uses an expansion with core ates Be II 2s and 2p; (b) includes in addition a 3d core orbital ith a parameter determined variationally. For the series $^1S$, $^3S$, °, $^3P°$, $^1D$, $^3D$, $^1F°$ and $^3F°$ results are obtained for all bound ates ($\epsilon < 0$) with $n_s \leq 10$, for $n = \infty$ ($\epsilon = 0$), and for the first resonances states in the region $\epsilon > 0$. For the series $^1P$, $^3P$, $^1D°$, $^3D°$ converging to Be II 2p, results are obtained for $n \leq 10$ and for $n = \infty$. The calculated ionization energies are more accurate than those obtained in previous theoretical work.

**16609.** Avrett, E. H., Vernazza, J. E., Linsky, J. L., **Excitation and ionization of helium in the solar atmosphere,** *Astrophys. J.* **207,** No. 3, L199-L204 (Aug. 1, 1976).

Key words: helium; radiative transfer; solar chromosphere; spectral line formation.

We investigate the excitation and ionization of He I and He II for the case of a realistic solar model. The calculations are based on a simplified numerical treatment of the He I and He II continua and the He II λ304 line. We discuss the extent to which various proposed mechanisms can account for the observed line and continuum intensities.

**16610.** Hall, J. L., Bordé, C. J., **Shift and broadening of saturated absorption resonances due to curvature of the laser wave fronts,** *Appl. Phys. Lett.* **29,** No. 12, 788-790 (Dec. 15, 1976).

Key words: lineshape theory; optical frequency standards; saturated absorption spectroscopy.

Using frequency offset-locked spectroscopy of methane at 3.39 $\mu$m we show that the saturated absorption peaks can be significantly blue or red shifted if the wave fronts of the laser beam are spherical in the gas cell. Good agreement with theoretical prediction is found. We discuss suitable conditions to avoid this geometry-induced shift in optical frequency standards.

**16611.** Kahn, L. R., Baybutt, P., Truhlar, D. G., ***Ab initio* effective core potentials: Reduction of all-electron molecular structure calculations to calculations involving only valence electrons,** *J. Chem. Phys.* **65,** No. 10, 3826-3853 (Nov. 15, 1976).

Key words: basis functions; configuration mixing; dipole moments; electronic structure of molecules; Hartree-Fock; integrals, evaluation of; molecular structure; orbitals; potential energy curves; pseudopotentials; self-consistent field; valence electrons.

A formalism is developed for obtaining *ab initio* effective core potentials from numerical Hartree-Fock wavefunctions and such potentials are presented for C, N, O, F, Cl, Fe, Br, and I. The effective core potentials enable one to eliminate the core electrons and the associated orthogonality constraints from electronic structure calculations on atoms and molecules. The effective core potentials are angular momentum dependent, basis set independent, and stable against variational collapse of their eigenfunctions to core functions. They are derived from neutral atom wavefunctions using a pseudo-orbital transformation which is motivated by considerations of the expected accuracy of their use and of basis set economy in molecular calculations. Then the accuracy is demonstrated by multiconfiguration Hartree-Fock calculations of potential energy curves for HF, HCl, HBr, HI, $F_2$, $Cl_2$, $Br_2$, and $I_2$ and one-electron properties for HF and HBr. The differences between valence-electron calculations employing the present effective core potentials and all-electron calculations are smaller than differences due to basis set choices, even though the basis sets are extended ones. Thus the effective core potentials are quite successful. In addition larger configuration mixing calculations are performed for HBr and $Br_2$ (1637 and 3396 configurations, respectively) and again the effective core potentials are judged to perform well.

**16612.** Richards, J. L., Johnson, P. M., **The visible emissions of molecular oxygen in rare gas solids,** *J. Chem. Phys.* **65,** No. 10, 3948-3951 (Nov. 15, 1976).

Key words: emission spectra; intersystem crossing; molecular oxygen in rare gas solids; $O_2$ excited states.

The vacuum ultraviolet-excited emission spectra of molecular oxygen in low temperature rare gas solids have been recorded and analyzed. The observed transitions have been reassigned using isotopic substitution and are found to be $C^3\Delta_u \rightarrow X^3\Sigma_g^-$ in argon and krypton and $c^1\Sigma_u^- \rightarrow a^1\Delta_g$ in xenon. These transitions have not been observed in the gas phase and the transition origins established here confirm previous tentative assignments of vibrational numberings of the upper states by Herzberg and Degan, respectively. The emission in xenon is very unusual for a solid phase spectrum in that emission occurs from several excited vibrational levels, which are apparently being populated directly by intersystem crossing. It is also unusual in that the lower state of the emission is not the ground state. No significant chemical interaction between the molecule and the rare gas is seen for any of the observed states.

**16613.** Mihalas, D., Kunasz, P. B., Hummer, D. G., **Solution of the comoving-frame equation of transfer in spherically symmetric flows. IV. Frequency-dependent source functions for scattering by atoms and electrons,** *Astrophys. J.* **210,** No. 2, 419-433 (Dec. 1, 1976).

Key words: early-type stars; electron scattering; spectral-line formation; stellar atmospheres.

A numerical method is presented of solving the radiative transfer equation in the comoving frame of a spherically symmetric expanding atmosphere in which both the line and the electron-scattering source function can depend on frequency (i.e., when there is partial frequency redistribution in the scattering process). This method is used to assess the adequacy of various assumptions regarding frequency redistribution in the comoving frame and to discuss the effects of electron scattering more accurately than previously possible. The methods developed here can be used in realistic model atmospheres to account for the (major) effects of electron scattering upon emergent flux profiles.

**16614.** Langhoff, P. W., Hernandez, A. J., **On the Brueckner and Goldstone forms of the linked-cluster theorem,** *Int. J. Quant. Chem. Symp.* **10,** 337-352 (1976).

Key words: diagrammatic perturbation theory; linked-cluster theorem; many-body theory.

Connections between the Brueckner and Goldstone forms of the linked-cluster theorem are clarified in an elementary fashion employing a finite many-body system of electrons interacting via two-body forces as an illustrative example. It is shown that the order-by-order cancellations of Brueckner unlinked terms in the many-body wave function and energy occur in the Goldstone development upon the additions of the different time orderings of Feynman-Goldstone diagrams having disconnected vacuum parts. The factoring of the vacuum amplitude from the wave function, upon which customary presentations of the theorem focus attention, is shown to be irrelevant to the cancellations of Brueckner unlinked terms, and has to do, rather, with the presence of secular and normalization terms in the time-dependent perturbation functions for an adiabatically-switched static perturbation. Similarly, the equivalence of the vacuum amplitude with the exponential of all connected vacuum diagrams, originally demonstrated by Feynman in the case of hole theory, is shown to be irrelevant to the cancellations of Brueckner unlinked terms in the energy, which occur in the Goldstone development upon the summations over all time orderings of disconnected vacuum diagrams. The distinction between Brueckner unlinked terms on the one hand, and secular and normalization terms on the other, is confused in customary presentations of the linked-cluster theorem by the use of exponential switching, following Gell-Mann and Low, and is clarified in the present development by considering the Friedrichs limit of ideal adiabatic switching.

**16615.** Zamir, E., Szöke, A., Osgood, R., **Fluorescence and dissociative energy transfer in high pressure Ar-HCN mixtures excited by relativistic electrons,** *J. Chem. Phys.* **65,** No. 11, 4885-4894 (Dec. 1, 1976).

Key words: energy transfer, electronic; fluorescence; molecular dissociation; relativistic electrons, excitation.

Studies of the radiation from Ar-HCN and Ar-$H_2O$ mixtures excited by relativistic electrons from a Febetron 706 electron gun, are presented. The energy deposited by the electrons channels rapidly into the Ar* and $Ar_2$* states; then by dissociative collisions with HCN it is transferred partly into the CN($B$) state and partly into a reservoir state [most probably the CN($A$ state] with near unit efficiency. Fluorescence emission from the electronic states $A(^2\Pi_i)$ and $B(^2\Sigma^+)$ of the CN radical, as well as the emission from the $Ar_2$* excimer state, were measured for an Ar pressure range of 750-9000 torr [15-180 psi(absolute)], and an HCN pressure range of 0.2-13 torr. The quenching rates of Ar* metastable and the $Ar_2$* excimer states, by collision with HCN molecules, were measured to be $6 \times 10^{-10}$ and $1 \times 10^{-9}$ cm$^3$ sec$^{-1}$, respectively. Our results suggest that population inversion can be achieved by collisional dissociation of simple molecules with excited rare gas atoms and excimers. Indeed the peak CN($B$) population density was found to be $1.5 \times 10^{15}$ cm$^{-3}$, which corresponds to an optical gain for the $B$-$X$ transition of 0.4 cm$^{-1}$ if the ground state is empty. A computer kinetic model is presented that explains the time dependence and intensity of the CN($B$) emission. In Ar-$H_2O$ mixtures the reaction rate for quenching of $Ar_2$* excimer by $H_2O$ molecules is extremely high; however, the yield into the OH($A^2\Sigma^+$) is only 3 percent.

**16616.** Maxfield, B. W., Linzer, M., McConnaughey, W. B., Hulbert, J. K., **Design of permanent magnet electromagnetic acoustic-wave transducers (EMATs),** *Proc. 1976 IEEE Ultrasonics Symp., Annapolis, MD, Sept. 29-Oct. 1, 1976*, 4 pages (The Institute of Electrical and Electronics Engineers, Inc., New York, NY, 1976).

Key words: electromagnetic transducer; EMAT; transducer; ultrasonics.

Electromagnetic acoustic-wave transducers (EMATs) provide a means of generating and detecting shear and compressional acoustic waves of known amplitude in conductors by electromagnetic instead of mechanical coupling to the material under study. An EMAT consists of a coil to generate eddy currents in the conductor and a magnetic field to provide coupling between the eddy currents and the metal lattice. Most work to date has been on EMATs utilizing either large permanent magnets or electromagnets. Here we describe a simple but very practical model for a rare-earth cobalt permanent magnet EMAT. This model is analyzed in detail and compared with measurements of the performance of a compact (250 gram) EMAT.

**16617.** Wiederhorn, S. M., Fuller, E. R., Jr., Mandel, J., Evans, A. G., **An error analysis of failure prediction techniques derived from fracture mechanics,** *J. Am. Ceram. Soc.* **59,** No. 9-10, 403-411 (Sept.-Oct. 1976).

Key words: crack propagation; error analysis; failure prediction; failure prevention; fracture; statistics; strength.

Three principal methods of failure prediction for brittle materials are analyzed statistically. Each method depends on fracture mechanics for its predictive value; hence the variance of the failure time depends on the scatter in the fracture mechanics data and the scatter in the estimate of the initial size of the strength-limiting crack. The variance is used to calculate confidence limits the prediction of failure for glass and SiC. Procedures for the lection and analysis of data are discussed and the implications the analysis for lifetime prediction are evaluated.

**618.** Brandt, M. A., Truhlar, D. G., Van-Catledge, F. A., **Electron scattering by nitrogen molecules: Theory and application to elastic scattering and rotational excitation at 30-75 eV,** *J. Chem. Phys.* **64,** No. 12, 4957-4967 (1976).

Key words: close coupling calculations; cross sections; differential cross sections; elastic scattering; electron scattering; momentum transfer; nitrogen molecules; rotational excitation; scattering theory.

An effective potential model applicable to electron scattering small or large molecules, including rotational and vibrational otions, is developed for electron scattering by $N_2$. The INDO- method is used to calculate the static potential at a large mber of distances and a simple model is used for the polarizan potential. The rotational and vibrational matrix elements of ese potentials are accurately calculated and the scattering is ated by a truncated close-coupling expansion. With no adtable parameters, calculated electronically and vibrationally stic scattering cross sections are in reasonable agreement with periment for angles 40°-50° and less at energies 30-75 eV. The ational excitation cross sections have never been measured $N_2$ but are predicted to be large (as large as half the pure stic cross sections when integrated over scattering angles and ger than the pure elastic differential cross sections at a range large scattering angles at each energy).

**619.** Kostkowski, H. J., **Current status and future plans for NBS radiometric source standards,** *Proc. AIAA/NASA/ASTM/IES Space Simulation Conf. Silver Spring, MD, Nov. 3-5, 1975*, Paper No. 66, pp. 799-805 (National Aeronautics and Space Administration, Washington, DC, 1976).

Key words: blackbodies; lamp standards; radiometry; remote sensing; solar monitoring; source standards.

The accuracy and long-term stability of currently available BS radiometric source standards will be described. Current earch efforts and expected results in this area will be outlined.

**620.** Buehler, M. G., Sawyer, D. E., **Microelectronic test patterns for use in procuring reliable, custom integrated circuit chips,** (Proc. Government Microcircuit Applications Conf., Orlando, FL, Nov. 9-11, 1976), Paper in *Government Microcircuit Applications Conference Digest*, **VI,** 62-65 (Nov. 1976).

Key words: circuit procurement; component screening; custom circuits; LSI; microelectronics; parameter control; process uniformity; random faults; reliability; test patterns; TTL; vendor qualification.

The current procurement methods for obtaining custom inrated circuits for high-reliability applications are expensive, s than fully effective, and cause long delays in delivery.

An approach being developed at the National Bureau of Stanrds focuses on a process validation wafer (PVW) concept ich is intended to evaluate process and circuit parameter iformity, and to measure the occurrence of random faults such pin holes, multi-contact resistance, and emitter-collector es. The PVW is an entire wafer of test structures and is inded to be fabricated along with product wafers on a periodic sis. As a process characterization tool, it can be used to qualify ndors and can serve as a circuit acceptance criterion. This ncept has the potential of greatly reducing the user-imposed uirements that now accompany a high-reliability component rchase.

**16621.** Smith, W. W., Gilbert, D. A., Peterson, C. W., **Vacuum ultraviolet emission spectra from keV energy rare gas ion-atom collisions,** (Proc. 4th Int. Conf. on Beam Foil Spectroscopy, Gatlinburg, TN, Sept. 15-19, 1975), Paper in *Beam-Foil Spectroscopy*, I. A. Sellin and D. J. Pegg, Eds., **2,** 695-704 (Plenum Press, New York, NY, 1976).

Key words: electron-promotion model; ion-atom collisions; solar corona; vacuum ultraviolet emission spectra; vacuum ultraviolet lasers.

Emission spectra have been observed under single-collision conditions in the 500-1100 Å wavelength range and 10-30 keV ion beam energy range for collisions of $(He^+, Ne^+, Ar^+) + Ar$, as well as $Ar^+ + Ne$, $Ar^+ + He$ and $Ne^+ + Ne$. The Ar I and Ar II spectra observed with an argon gas target are similar to those observed previously with $He^+ + Ar$ by de Heer and by Isler, except that with $Ar^+ + Ar$ excitation both the Ar I 4s resonance lines and the 3d-3p transitions in the Ar I spectrum are relatively more prominent than with the other projectiles. A striking difference is found between the strong excitation of the 920 and 932 Å lines of Ar II by a $Ne^+$ beam on Ar (cross section $\sim 7 \times 10^{-17}$ cm$^2$ at 30 keV) compared with weak excitation of these lines using $Ar^+ + Ne$ in the same energy range. With $Ne^+ + Ne$, the most prominent lines observed were the 3s and 4s resonance lines of Ne I. Approximate absolute emission cross sections are given for a number of lines. The results are discussed in terms of the electron-promotion (molecular orbital) model of ion-atom collisions. This work may have applications to excitation processes in the solar corona and in vacuum uv lasers.

**16622.** Wacker, P. F., **Quantifying hazardous microwave fields: Analysis,** *Proc. Symp. on the Biological Effects and Health Implications of Microwave Radiation, Richmond, VA, Sept. 17-19, 1969, BRH/DBE 70-2*, 197-203 (U.S. Department of Health, Education, and Welfare, Rockville, MD, June 1970).

Key words: hazardous microwave fields.

The existing standards for microwave radiation hazards are based upon far-field concepts which may have little or even no validity in near fields. However, hazards occur largely in near fields, and even many dosimetry experiments are carried out in near fields. Because of the great complexity possible in a near field, a probe should, in principle, simulate the individual who might be subject to the possible hazard; however, such a probe is not feasible. Electric energy density provides a reasonable index of a large class of microwave radiation hazards and is simpler to measure in a near field than is energy flow. Analytical aspects of near field measurements are discussed in general, and design of a possible probe described in detail.

**16623.** Freund, S. M., Sweger, D. M., Travis, J. C., **Quantitative detection of nitrogen dioxide in nitrogen using laser magnetic resonance at 1616 cm$^{-1}$,** *Anal. Chem.* **48,** No. 13, 1944-1946 (Nov. 1976).

Key words: infrared detection; laser magnetic resonance; modulated absorption; nitrogen dioxide; $NO_x$ detection; quantitative detection.

The selective, quantitative detection of nitrogen dioxide in part-per-million concentrations in nitrogen using magnetic field modulation of the molecular absorption of 1616 cm$^{-1}$ carbon monoxide laser radiation is reported. A magnetic field of less than 500 gauss is sufficient to shift the infrared transition of interest into coincidence with the laser. The Zeeman-modulated absorption of the laser light is synchronously detected, and is found to vary linearly with $NO_2$ concentration over the two orders of magnitude investigated. The synchronous detection scheme discriminates against nonparamagnetic species, such as water and ethylene, which could interfere with direct absorption measurements.

**16624.** Conti, D. M., **A method for estimating service bureau processing charges,** *Proc. 7th Int. Conf. of the Computer Measurement Group, Inc., Atlanta, GA, Nov. 16-19, 1976*, pp. 34-60 (Computer Measurement Group, Camp Springs, MD, Nov. 1976).

> Key words: benchmarking; charging algorithms; service bureaus; synthetic benchmarking; workload characterization.

This paper describes the development of a new synthetic benchmark technique for estimating batch processing charges at service bureau sites. This technique was used to estimate the cost of processing a large batch workload at a number of service bureaus within the same vendor line. The method was found to be low-cost, yet reasonably accurate for a certain class of service bureau charging algorithms. Refinements of this method are suggested which will extend its applicability to other algorithms. The procedures used to create and run the benchmark, together with the projection of total workload costs are described.

**16625.** McMichael, J. M., Mease, N. E., **On the application of tension to compliant membranes,** *AIAA J. Tech. Notes* **14,** No. 10, 1490-1492 (Oct. 1976).

> Key words: air impedance; compliant surface; drag reduction; membranes; tension; vibrating membranes.

In connection with a study of the feasibility of achieving drag reduction by the use of compliant surfaces in turbulent boundary-layers, a method of applying tension to rectangular compliant membranes by the use of suction in chambers adjacent to the free membrane area has been developed. A description of the method is presented along with data evaluating the method. Measurements of the impedance effect of the ambient air on the frequencies of the normal modes of vibration are also presented.

**16626.** Penn, R. W., Fong, J. T., Kearsley, E. A., **Experience in data acquisition and reduction for a biaxial mechanical testing program,** *Am. Soc. Test. Mater. Spec. Tech. Publ. 613, Use of Computers in the Fatigue Laboratory*, pp. 78-93 (American Society for Testing and Materials, Philadelphia, PA, 1976).

> Key words: biaxial; fatigue; fracture; laboratory automation; mechanical testing; plasticity; polyvinyl chloride; servo-hydraulic system; viscoelasticity; yield point.

The inadequacy of uniaxial mechanical testing data as a basis for predicting multiaxial deformation and fracture is well known. For optimal biaxial tests, computer control of simultaneous variation of loadings using hydraulic power under closed loop servocontrol is essential. Computer assistance in real time data reduction from a biaxial mechanical test is economical. Physical features of computer hardware, software, and a hydraulic biaxial system are described along with sample results illustrating cross effects in fatigue and yield surface calculations. Significance of the graphical output based on thin tube specimens of 1-in. (2.54-cm) nominal diameter, schedule 80, commercial grade polyvinyl chloride pipes, and the limitations of the present system are discussed.

**16627.** Truhlar, D. G., Merrick, J. A., Duff, J. W., **Comparison of trajectory calculations, transition state theory, quantum mechanical reaction probabilities, and rate constants for the collinear reaction $H + Cl_2 \rightarrow HCl + Cl$,** *J. Am. Chem. Soc.* **98,** 22, 6771-6783 (Oct. 27, 1976).

> Key words: chemical reactions; chlorine molecules; classical scattering matrix theory; collision theory; cross sections; hydrogen atoms; rate coefficients; scattering theory; trajectories; transition-state theory.

Quantum mechanical rate constants are computed for the collinear reaction $H + Cl_2 \rightarrow HCl + Cl$ using the reaction probabilities of Baer. For comparison we also computed reaction probabilities and rate constants for this reaction using (a) the quasic sical trajectory method, (b) the reverse quasiclassical traject method, (c) the classical S matrix theory (using real-val trajectories only), and (d) transition-state theory assum separability of the reaction coordinate at the transition st Comparisons are made not only for total reaction probability total rate constant but also in general for state-to-state react probabilities and state-to-state rate constants. The quasiclassi trajectory method is generally accurate except in the thresh regions for various state-to-state processes. It is more accur for total reaction probabilities and total rate constants than state-to-state reaction probabilities and rate constants. T quasiclassical trajectory calculations of total rate constants reaction in a given initial vibrational state agree with the qua tum calculations within 29 percent for the 300-1000 K temper ture range but the state-to-state rate constants may be in error a factor of 2 or more even for processes which are classically lowed in the sense of classical S matrix theory. Classical S matr theory does not always provide a more accurate way to extra state-to-state reaction probabilities from these trajectorie Transition state theory (which yields average reaction probabi ties and total rate constants for a thermal distribution of initi states but does not yield state-to-state results) is fairly accura for this reaction even with the assumption that the reaction coo dinate is separable.

**16628.** Parris, G. E., Brinckman, F. E., **Reactions which relate environmental mobility of arsenic and antimony. II. Oxidatio of trimethylarsine and trimethylstibine,** *Environ. Sci. Techno* **10,** No. 12, 1128-1134 (Nov. 1976).

> Key words: antimony; antimony oxide; arsenic; arseni acid; biomethylation; cacodylic acid; diffusion; flame reta dant; oxidation rate; stibinic acid; trimethylarsine trimethylstibine.

Oxidation of trimethylarsine and trimethylstibine by at mospheric oxygen and other reagents is examined, an semiquantitative rate constants are calculated. In methanol solu tion the rate constant for reaction of dissolved oxygen wit trimethylstibine is greater than $10^{-2}$ $M^{-1}$ $s^{-1}$, whereas for the ox idation of trimethylarsine, the rate constant is less than $10^{-2}$ $M^{-}$ $s^{-1}$. In the gas phase the rate constants are estimated as $10^3$ an $10^{-6}$ $M^{-1}$ $s^{-1}$ for reaction of trimethylstibine and trimethylarsine respectively, with oxygen. A scheme based on PMR evidence for reactive intermediates is suggested to account for the products of oxidation, $(CH_3)_3EO$ and $(CH_3)_2EO_2H$, of these compounds $(CH_3)_3E, E = Sb$, As. From these results, even i biological methylation of antimony occurs in nature analogous to that of arsenic, the rapidity with which $(CH_3)_3Sb$ is oxidized would probably prevent hazardous concentrations from building up in aerated surroundings.

**16628A.** Parris, G. E., Brinckman, F. E., **Reactions which relate to the environmental mobility of arsenic and antimony. I. Quaternization of trimethylarsine and trimethylstibine,** *J. Org. Chem. Notes* **40,** No. 25, 3801-3803 (1975).

> Key words: alkyl halides; antimony; arsenic; environment; kinetics; methylation; nucleophilic reactivity; onium salts; polar solvents; pollutants; quaternization.

The quarternization reactions of trimethylstibine and trimethylarsine with $CH_3I$, $CH_3CH_2I$ and $CH_3CH_2CH_2I$ to produce the corresponding stibonium and arsonium salts have been studied in methanol and acetonitrile solvents. The reactions are of the $S_N2$ type. Trimethylarsine reacts about ten times as fast as trimethylstibine and the reactions are about five times faster in acetonitrile than in methanol. The reactivity of the alkyl halides is $CH_3I >> CH_3CH_2I > CH_3CH_2CH_2I$. It is suggested that quaternization is one of several reactions which potentially effects the mobilization of antimony and arsenic in environmental situations.

529. Voth, R. O., Hord, J., **Economics of cryocables,** *Int. J. Hydrogen Energy* **1,** 271-289 (1976).

Key words: a.c. power; cryoresistive; energy transmission economics; helium; hydrogen energy; liquid hydrogen; liquid nitrogen; power transmission cables; safety; slush hydrogen; superconducting.

This paper examines the technical and economic feasibilities (1) using cryogenic hydrogen to cool a.c. cryoresistive or a.c. perconducting power transmission cables and, (2) delivering uid hydrogen concurrently with cryoresistive or supercon- cting electrical power through a common cable. Cryogenic drogen coolant options considered are subcooled liquid and sh. Cryogenic nitrogen and helium coolants are also con- ered for cryoresistive and superconducting cables, respective- to provide reference data for comparison with our $H_2$-coolant culations. Thermodynamic analyses are performed to op- ize the coolant flow rate and refrigerator spacing for each ecific coolant, coolant fluid state, cable design, cable insulation ality and energy delivery option. The use of hydrogen as a olant in electrical cables is discussed from a safety viewpoint.

Helium-cooled and hydrogen-cooled superconducting power nsmission lines are shown to be economically competitive and er lower unit-transmission costs than conventional un- ground power lines. The hybrid hydrogen-superconducting ble concurrently transmits liquid hydrogen and electricity at lowest unit cost of all cryocable energy systems examined. drogen-cooled power lines and hybrid hydrogen-electric ener- cables appear to be technically and economically feasible; wever, they do not currently provide sufficient economic in- ative to warrant the increased hazard of operation.

630. Kusuda, T., **Procedure employed by the ASHRAE Task roup for the determination of heating and cooling loads for uilding energy analysis,** *ASHRAE Trans.* **82,** Pt. 1, 305-322 1976).

Key words: algorithm; ASHRAE; buildings; computer; energy calculation; heat transfer; heating and cooling loads; response factor.

Most up-to-date thermal load calculation methodology recom- nded by the ASHRAE Task Group on Energy Requirements ased upon an exact solution of the heat exchange equations ong the room surfaces, room furnishings, lighting fixtures, ipment, occupants, and room air. Simplified calculation cedures are possible by the use of transfer functions or by a ear regression equation which could be derived from the orous calculation. Although the simplified solutions are entire- adequate for the energy calculation of conventional residential ldings or buildings which do not have the multiplicity of zones l complex air side systems, an exact and rigorous calculation thod has a few advantages, some of which were discussed in main text.

he advantages or the uniqueness of exact calculation cedures are to assist engineers who are willing to explore ious energy conservation features or innovative building igns such as the use of interior mass of the building for the rage of off-peak cooling, nighttime setback of the thermostat, hing of the building with cool night air and the critical tching of the equipment with the indoor comfort require- nts.

Although the exact method may appear formidable from the ndpoint of algorithmic complexity as compared to the sim- ied steady state calculation, the use of computer programs ich employ such a method will become much easier as the gramming technique improves and as more computers are de larger, faster and more readily accessible in the near future. Only the comprehensive load calculation methodology prepared by the ASHRAE Task Group on Energy Requirements enables the engineer to take advantage of the rapidly growing computer technology to meet the challenges of innovative building design.

**16631.** Diller, D. E., **Thermophysical properties data research on compressed and liquefied gases at the NBS Cryogenics Division,** (Proc. Cryogenic Engineering Conf., Advances in Cryogenic Engineering, Kingston, Ontario, Canada, July 22-25, 1975), Paper M-7 in *Advances in Cryogenic Engineering* **21,** 522-531 (Plenum Press, New York, NY, 1976).

Key words: density; dielectric constant; electromagnetic properties; equation of state; ethane; hydrocarbon; liquefied natural gas; measurements; methane; mixtures; thermodynamic.

This report summarizes important NBS contributions to accurate thermophysical properties data from compressed and liquefied gases (helium, hydrogen, nitrogen, oxygen, fluorine and argon), and discusses research on liquefied hydrocarbon gases (methane, ethane, ethylene, etc.) and their mixtures. Representative results of research on the thermophysical properties of methane and mixtures containing methane are presented. Additional contributions expected through 1977 are summarized.

**16632.** Fickett, F. R., **Magnetic and electrical properties of internally oxidized CuFe alloys,** (Proc. Joint MMM-Intermag Conf., Pittsburgh, PA, June 15-18, 1976), *AIP Conf. Proc. No. 34, Magnetism and Magnetic Materials—1976*, J. J. Becker and G. H. Lander, Eds., pp. 25-26 (American Institute of Physics, New York, NY, 1976).

Key words: alloy; copper; cryogenic; iron; oxide; resistivity; remanance; susceptibility.

A series of CuFe alloys containing 1-100 at. ppm Fe has been internally oxidized. In nearly all cases the specimens become ferromagnetic. We have measured the remanent moment and low field susceptibility at room temperature, and the electrical resistivity at 273 K and 4 K. These data combined with Curie temperature measurements and scanning electron microscopy indicate the presence of very small single domain grains of copper ferrite within the copper matrix. The annealing process appears to be capable of sweeping most of the iron impurities from the matrix in spite of their very low concentrations.

**16633.** Daney, D. E., **Low-temperature losses in supercritical helium refrigerators,** (Proc. Cryogenic Engineering Conf., Kingston, Ontario, Canada, July 22-25, 1975), Paper E-4 in *Advances in Cryogenic Engineering* **21,** 205-212 (Plenum Press, New York, NY, 1976).

Key words: Brayton cycle; cryogenic refrigeration; refrigeration; superconducting transmission lines.

A comparison is made of the efficiencies of the low temperature portion of three alternative schemes of supercritical helium refrigeration for higher temperature superconducting transmission lines. The range of transmission line operating conditions considered is load pressures from 3 to 20 atm and load temperatures from 8 to 14 K. The analysis indicates that no single scheme demonstrates a marked superiority at higher pressures, and that the use of a low temperature pump does not greatly reduce the system efficiency at higher pressures.

**16634.** Arvidson, J. M., Hord, J., Mann, D. B., **Dispersion of hydrogen or methane fuels released into an automobile interior,** (Proc. Cryogenic Engineering Conf., Advances in Cryogenic Engineering, Kingston, Ontario, Canada, July 22-25, 1975), Paper J-3 in *Advances in Cryogenic Engineering* **21,** 387-398 (Plenum Press, New York, NY, 1976).

Key words: automobile; detection; dispersion; explosion; fire; hydrogen; leakage; methane; safety; vents.

Gasoline-powered automobiles are being converted to operate on gaseous fuels such as hydrogen ($H_2$) or methane ($CH_4$). The fuel is often stored as a cryogenic liquid ($H_2$ at 20 K and $CH_4$ at 112 K) in dewar-like vessels located in the trunk of the car. Cryogenic storage provides four to five times greater vehicle range than gas storage in high pressure cylinders of comparable volume. Potential leakage of these gaseous fuels into the passenger compartment of the vehicle constitutes a safety threat. Definitive experiments were performed to identify the explosion hazards and establish venting criteria and general safe-guards for $H_2$ or $CH_4$ fueled passenger vehicles. Initial tests were conducted using methane at three inlet temperatures (300, 200, and 121 K) and it was determined that the gas dispersion patterns were not temperature dependent. Appropriately designed ventilation systems can significantly reduce the safety hazards associated with accumulated combustible gases. Vents are recommended for all autos converted to burn $H_2$ or $CH_4$ and may possibly be eliminated in new cars that are designed for gaseous fuel operation. Combustible gas warning systems are recommended, at least in the interim, for all (converted and new-design) gaseous fueled vehicles. $H_2$ and $CH_4$ gases appear equally safe as vehicular fuels if used in properly designed vehicles.

**16635.** Ledbetter, H. M., Moment, R. L., **Elastic properties of face-centered-cubic plutonium,** *Acta Met.* **24,** No. 10, 891-899 (Oct. 1976).

Key words: bulk modulus; compressibility; Debye temperature; elastic constants; plutonium; plutonium alloy; Poisson ratio; shear modulus; sound velocity; Young modulus.

The three principal elastic constants, $C_{ij}$, of f.c.c. plutonium were determined by measuring the ultrasonic wave velocities along a near−6110⟩ direction in a single crystal. The elastic anisotropy is twice that known for any other f.c.c. metal. The elastic-anisotropy problem is considered using a general two-body central-force interatomic potential. Based on the $C_{ij}$, polar plots of the wave velocities and Young's modulus were determined. The $C_{ij}$ were "averaged" to obtain quasi-isotropic elastic constants, which are compared with existing polycrystalline elastic data. The elastic Debye temperature was computed by numerically integrating the Christoffel equations.

**16636.** Clark, A. F., **Stress effects in superconductors,** *Cryogenics* **16,** No. 10, 632-633 (Oct. 1976).

Key words: critical current; mechanical properties; stress effects; superconductors; symposium.

A one day symposium on stress effects in superconductors is summarized.

**16637.** Parrish, W. R., Hiza, M. J., **On the consistency of liquid-vapor equilibria data for binary mixtures on methane with the light paraffin hydrocarbons,** (Proc. Cryogenic Engineering Conf., Advances in Cryogenic Engineering, Kingston, Ontario, Canada, July 22-25, 1975), Paper M-2 in *Advances in Cryogenic Engineering* **21,** 485-492 (Plenum Press, New York, NY, 1976).

Key words: critical loci; excess Gibbs' energies; Henry's constants; liquid-vapor equilibria; methane-light hydrocarbon binary mixtures.

Published experimental liquid-vapor equilibria data for the binary systems of methane with ethane, propane, isobutane, and normal butane have been compiled and evaluated for interna and mutual consistency. Equimolar excess Gibbs energies anc infinite dilution Henry's constants are obtained by a methoc which uses only P − x data. The derived equimolar excess Gibbs energies are compared with those calculated from a modified hard-sphere model for the equimolar mixtures. Critica loci ($P_c$, $T_c$, $x_c$) are also examined where available. Discrepancies in the data are enumerated which suggest the desirability of more precise and accurate measurements.

**16638.** Siegwarth, J. D., Holste, J. C., Morrow, A. J., **Polarizatior and dielectric constant of potassium tantalate,** *J. Appl. Phys.* **47** No. 11, 4791-4793 (Nov. 1976).

Key words: dielectric constant; dielectric relaxation electret; polarization; potassium tantalate.

The polarization of $KTaO_3$ single crystal and some KTaO ceramic specimens has been measured using a dc technique. A remanent polarization was found as well as hysteresis in the polarization as a function of field. Peaks in the ac dielectric constant were also observed. These dielectric properties are attributed to dielectric relaxation effects and the existence of ar electret state.

**16639.** Siegwarth, J. D., Morrow, A. J., **Low-temperature polarization in impure $SrTiO_3$ ceramics,** *J. Appl. Phys.* **47,** No 11, 4784-4790 (Nov. 1976).

Key words: dielectric relaxation; electret state; impurity ordering transition; polarization; remanent; strontiun titanate.

Measurements of the temperature dependence of the dielectric constant and polarization in a constant field have been made or nominally pure $SrTiO_3$ ceramics and $SrTiO_3$ ceramics containin vanadium and niobium impurities. The peaks in the dielectric constant and the remanent polarization observed are apparentl not due to a ferroelectric or antiferroelectric transition but rathe to the presence of a thermoelectret state existing for permanen dipoles in the materials. It is suggested that the permanen dipoles have an origin similar to the impurity-vacancy dipole found in alkali halides.

**16640.** Fowlkes, C. W., Tobler, R. L., **Fracture testing and result for a Ti-6Al-4V alloy at liquid helium temperature,** *Eng. Fract Mech.* **8, 487-500 (1976).**

Key words: crack propagation; cryostats; fracture tests; low temperature tests; mechanical tests; titanium alloys.

This paper discusses fracture toughness and fatigue crack growth testing at liquid helium temperature, 4 K (− 452 °F). The design and performance of a fracture testing cryostat and associated instrumentation are described. Fracture toughness anc fatigue crack growth data for Ti-6Al-4V from room temperature to 4 K are presented.

**16641.** Jespersen, J. L., **Topside spread-F and satellite radio scintillations,** (Proc. 10th Annual Symp. of the Ionospheric Research Committee of the Avionics Panel o AGARD/NATO, Rome, Italy, Sept. 21-25, 1965), Chapte 3-9 in *AGARD Conference Proceedings 3, Propagation Fac tors in Space Communications,* pp. 203-207 (Technivision Maidenhead, England, 1967).

Key words: absorption; high latitude; ionosphere; ionospheric scattering; irregularity; satellite; scintillation spread-F; topside.

Over the last decade many workers have studied the relatior between spread-*F*, detected by ground-based ionospheric sounders, and the scintillation of a radio signal either from a radio sta from an artificial earth satellite. In this paper the relation etween scintillations and spread-$F$ detected by the topside ounder satellite, *Alouette I*, near College, Alaska, is studied. he scintillations are correlated with small-scale irregularities in he vicinity of the satellite. This supports the view that high-itude irregularities extend from near $h_{max}$ to as high as 1000 m. Simultaneous topside and bottomside soundings of the iono-phere, taken together with the scintillation observations, sug-est that on occasion the ionospheric disturbance, associated ith the irregularities, extends below $h_{max}$ into the $D$ region.

**6642.** Smith, R. V., **Fluid dynamics,** Chapter 5 in *Cryogenic Fundamentals*, pp. 237-310 (Academic Press, New York, NY, 1971).

Key words: compressibility flow; cryogenics; fluid dynamics; pressure drop; superfluid helium; two phase flow.

This chapter reviews the field of fluid dynamics with special mphasis on the behavior of cryogenic fluids.

**6643.** Peterson, R. L., **The magnetophonon effect,** Chapter 4 in *Semiconductors and Semimetals* **10,** *Transport Phenomena*, R. K. Willardson and A. C. Beer, Eds., pp. 221-289 (Academic Press, New York, NY, 1975).

Key words: magnetophonon effect; semiconductors; transport theory.

This article is a comprehensive review of the magnetophonon ffect. All theoretical and experimental articles published to date are referenced and discussed. An attempt is made to point out he weaknesses and unique contributions of the various publica-ions. A broad overview, and a discussion of uncompleted work and likely areas for new efforts, are also given so that both the asual reader and the serious researcher will be benefitted.

**16644.** Jespersen, J. L., Gatterer, L. E., Hanson, D. W., Hamilton, W. F., **Artificial satellites as a means of time dissemination,** *Proc. Int. Conf. on Space and Communications, Paris, France, Mar. 29-Apr. 2, 1971, Paper 16 D*, pp. 426-433 (L'Espace et la Communication Observation: Metrologie, Geodesia Localisation, Paris, France 1971).

Key words: communication satellite; communication system; hf time dissemination services; navigation system; satellite time and frequency dissemination services.

Satellite time and frequency dissemination systems offer cer-tain advantages over conventional HF broadcast services. Some of the important deficiencies of HF broadcasts are discussed together with the corresponding advantages of satellite systems. Experimental results obtained at NBS using UHF/VHF satellite transponders are reviewed. Work performed by other experimenters at higher frequencies is described.

The relationship of disseminated time and frequency to the design and operation of navigation and communication systems is described. There are significant advantages to relating the time and frequency information disseminated incidental to navigation and communication system operation to external standards.

**16645.** Haynes, W. M., Hiza, M. J., Frederick, N. V., **Magnetic suspension densimeter for measurements on fluids of cryogenic interest,** *Rev. Sci. Instrum* **47,** No. 10, 1237-1250 (Oct. 1976).

Key words: apparatus; density; experimental; magnetic suspension; methane; nitrogen; saturated liquid; tables.

An apparatus incorporating a magnetic suspension technique has been developed for density measurements on liquids and liquid mixtures, particularly at saturation, at temperatures between 90 and 300 K and at pressures to 5 MPa (approximately 50 atm). The feasibility of adapting this method, previously used at room temperature, for low temperature use had been demonstrated in an earlier study with a density measurement on saturated liquid nitrogen near its normal boiling point. The present apparatus, which is significantly improved, and in most respects different from the earlier model, is described in detail. It includes a cryostat for continuous wide-range temperature control, a windowed equilibrium cell particularly suited for studies of liquid mixtures, and a new electronic servocircuit with a linear differential transformer for position control of the magnetic buoy. Extensive tests and density measurements have been carried out to evaluate the performance of this apparatus. Densities of saturated liquid nitrogen between 95 and 120 K and saturated liquid methane between 105 and 160 K are reported. The estimated standard deviation of a single density measurement is less than 0.02 percent. The total systematic error in the measurement process from known sources is approximately 0.05 percent. The total uncertainty of a single density measurement, which is taken as three times the standard deviation plus the systematic error, is approximately 0.1 percent. Comprehensive comparisons of the present results with previous experimental data are presented.

**16646.** Haynes, W. M., Hiza, M. J., **Orthobaric liquid densities of normal butane from 135 to 300 K as determined with a magnetic suspension densimeter,** (Proc. Cryogenic Engineering, Conf., Advances in Cryogenic Engineering, Kingston, Ontario, Canada, July 22-25, 1975), Paper M-6 in *Advances in Cryogenic Engineering* **21,** 516-521 (Plenum Press, New York, NY, 1976).

Key words: density; experimental; magnetic suspension densimeter; normal butane; saturated liquid; table.

A magnetic suspension densimeter, developed for absolute density measurements of the principal components of liquefied natural gas and their mixtures, has been used to determine the orthobaric (saturated) liquid densities of normal butane from 135 to 300 K. These measurements provide the first set of density data for liquid-*n*-butane that spans the range of temperatures from near ambient to just above the triple point, 134.8 K. These new data have been fitted to a simple analytical expression to provide a convenient and precise interpolation method. This equation has also been used to calculate densities for the subcooled liquid region at temperatures normally associated with liquefied natural gas. The precision and repeatability of measurement is within two parts in 10,000 or better. The absolute error in the densities is estimated to be less than ±0.1 percent.

**16647.** Warnar, R. B. J., **Letter to Editor on "Trends in Computer Hardware Technology," by David A. Hodges,** *Computer Design* **15,** No. 12, 14 (Dec. 1976).

Key words: cells; charge-coupled device (CCD); chevron; garnet; large-scale-integration (LSI); line width; lithography; magnetic bubble device (MB); memory storage density; N-channel metal-oxide-semiconductor (N-MOS); random-access-memory (RAM); silicon.

The December 1976 COMPUTER DESIGN magazine includes a "Letter to the Editor" from the Information Technology Division, ICST, regarding an article "Trends in Computer Hardware Technology" (COMPUTER DESIGN, February 1976, pp. 77-85). Information included in the letter was derived from the soon-to-be-published Special Publications "Foreign and Domestic Accomplishments in Magnetic Bubble Device Technology" and "Foreign and Domestic Accomplishments in Charge-Transfer Device Technology." Information included in the letter clarified certain specific statements of the February article in the areas of bit-density and cost of charge-coupled devices (CCD's) and magnetic bubble memories (MB's). Specific differences in fabrication techniques between conventional LSI solid-state circuitry and CCD/MB fabrication techniques are highlighted.

**16648.** McLaughlin, W. L., Humphreys, J. C., Chappell, S. E., Olejnik, T. A., Fox, C. E., **Physical measurements for quality control in industrial radiation sterilization,** (Proc. Int. Conf. on Physics in Industry, Dublin, Ireland, Mar. 8-13, 1976), Paper in *Physics in Industry*, E. O'Mongain and C. P. O'Toole, Eds., pp. 567-573 (Pergamon Press, Oxford, England, 1976).

> Key words: dosimetry; electron beams; gamma rays; physical measurements; quality control; radiation measurement; radiation processing; radiation sterilization; radiochromic dyes; Red Perspex; sterility control.

The use of ionizing radiation has brought about a growing industry for the sterilization of disposable surgical equipment, medical supplies, and containers for biological specimens. For many products, irradiation has become an alternative to autoclaving or gas treatment by ethylene oxide. Over fifteen years of experience with industrial sterilization by cobalt-60 gamma radiation have shown that radiation methods provide a clear advantage over gas sterilization, in that sterilization can be performed on nonpermeable sealed packages. Moreover, regulatory agencies, such as the Food and Drug Administration in the U.S.A., are reappraising the requirements for sterility assurance. For products released to the public, consideration is now being given to the use of physical dosimetry, i.e., the measurement of radiation dose by physical methods. This is based on a knowledge of the microbial burden of the product before sterilization and on the probability of killing microorganisms by a given radiation dose. Because physical dosimetry is easier to control and less complicated than biological tests, it may be considered in the future the basis for quality assurance of the sterilized product. Some of the problems associated with standardized measurement techniques in radiation sterilization include the choice of dosimetry and its calibration, as well as methods and procedures used to minimize errors due to variations in radiation flux density, source geometry with respect to the product, and environmental factors.

**16649.** Hall, J. L., Lee, S. A., **Control techniques for cw dye lasers,** *Proc. Conf. on Tuneable Lasers and Their Applications, Leon, Norway, June 1976*, pp. 361-366 (Springer-Verlag, Berlin, Germany, 1976).

> Key words: cw dye laser; frequency control; laser wavelength determination; scanning interferometer.

Stabilized cw dye lasers are potentially a most useful spectroscopic took but they bring a troublesome technology. We list the major problems specific to these lasers. We present a stabilized dye laser design which addresses these problems successfully to produce a useful widely tuneable laser with 50 kHz spectral width and exceptional high single mode power covers 10 K efficiency (12%). An automatic interferometer system is described which gives realtime numerical laser wavelength readout of sub-Doppler absolute accuracy.

**16650.** Zelkowitz, M. V., **Automatic program analysis and evaluation,** *Proc. 2nd Int. Conf. on Software Engineering, San Francisco, CA, Oct. 13-15, 1976*, pp. 158-163 (IEEE Computer Society, Long Beach, CA, Oct. 1976).

> Key words: dynamic analysis; errors; evaluation; program complexity; program measurement static.

There is currently considerable interest in the computing community in the evaluation of computer programming. However, in order to objectively evaluate such concepts, it is necessary to undertake a thorough evaluation of the programming process itself. Most previous studies of this type have analyzed, by hand usually, a few instances of programs. This has led to som general conjectures; however, the amount of information tha must be processed precludes any large scale analysis. In order t avoid this problem, an automatic data collection facility has bee implemented as part of a PL/1 compiler at the University o Maryland. This system automatically collects information o each program that has been compiled—at almost no additiona cost to the user of the compiler. This paper will describe th system and will evaluate some of the characteristics of some o the 25,000 programs that have been run since July, 1975.

**16651.** Crawford, M. L., Smart, G. R., **New coaxial thermisto mounts for use as precision transfer standards,** *Proc. Instru ment Society of America Conf., Philadelphia, PA, Oct. 26-29 1970*, No. 708-70, 1-6 (Instrument Society of America, Pittsburgh, PA, 1970).

> Key words: coaxial thermistor mounts; precision transfe standards.

Improved thermistor mounts have been designed and constructed for use as precision low power transfer standards Characteristics of these mounts which represent improvement over typical commercially available thermistor mounts are as fol lows: 1) Input VSWR ≤ 1.03 as compared to typical VSWR ≥ 1.1; 2) Provision for checking thermistor pair match (for simila characteristics), when dc bias is applied; 3) Use of precision 1 mm input connectors; 4) Extended frequency range from 1 MH to 4.0 GHz and at specified frequencies from 4 to 8 GHz.

The paper describes the thermistor mount design and include a mathematical analysis of an approximation to their equivalen circuit. Design equations and experimental results are given fo the mounts along with a brief analysis of the errors.

**16652.** Mandel, J., **Statistical methods in analytical chemistry** Chapter in *Treatise on Analytical Chemistry*, I. M. Kolthof and P. M. Elving, Eds., Part III, Section C, **3,** 79-125 (Joh Wiley and Sons, New York, NY, 1976).

> Key words: analytical chemistry; data analysis; design o experiments; statistics.

This chapter is an introduction, written mainly for the analytical chemist, to the use of statistics in designing experiments an analyzing data. Subjects covered include basic statistical concepts, precision and accuracy, interlaboratory comparisons an the Youden plot, calibration experiments, factorial experiments analysis of structure, block experiments, comparison of tes methods, control charts, confidence statements and propagatio of errors. All subjects are illustrated in terms of data taken fro analytical chemistry.

**16653.** Unassigned.

**16654.** Wyly, R. S., Galowin, L. S., **An approach to performanc evaluation for water supply and drainage for buildings,** *Proc. CIB Commission W62 Symp., 1975, Drainage and Wate Supply for Buildings, University of Glasgow, Glasgow, Scotland, Sept. 30-Oct. 1, 1975*, pp. 12/1-12/31 (1975).

> Key words: acceptance protocol; performance approach; performance-based plumbing standard; performance statement; plumbing performance criteria; plumbing performance evaluation; plumbing performance.

The performance concept is reviewed as it relates to water supply and drainage for buildings.

An approach is described that is being utilized in connection with the development of a performance standard for plumbing as a complement to an updated specification-type (model) code of practice (National Plumbing Code) under the procedures of the American National Standards Institute.

The recommendation is made that the work in connection with e National Plumbing Code program include first a comprehen- ve review of existing information to identify existing per- rmance statements, both those actually stated and those mere- implied. Several examples are developed illustrating this con- pt.

It is concluded that the needs in further development and im- ementation of the performance approach include education, ac- ptance protocol and new research. The new research would be eded to establish definitive performance criteria, reproducible st procedures or predictive models, and systematic inspection ocedures. During the period of transition to performance aluation methodology, continued reliance will need to be aced on specification-oriented acceptance protocol, expert dgment and experience.

655. Radebaugh, R., **He$^3$, He$^4$ refrigeration,** *Cryogenics* **11,** No. 1, 63 (Feb. 1971).

Key words: demagnetization; dilution refrigerator; helium 3; helium 4; liquid helium; mixtures; refrigeration.

A report of papers presented at the September 11, 1970 after- on session of the IIP Commission I meeting is given. These pers are on the subjects of dilution and He$^3$ refrigerators.

656. Sprowls, D. O., Summerson, T. J., Ugiansky, G. M., Epstein, S. G., Craig, H. L., Jr., **Evaluation of a proposed standard method of testing for susceptibility to stress-corrosion cracking of high-strength 7XXX series aluminum alloy products,** *Am. Soc. Test. Mater. Spec. Tech. Publ. 610, Stress Corrosion—New Approaches* pp. 3-31 (American Society for Testing and Materials, Philadelphia, PA, Nov. 1976).

Key words: Aluminum Association; ASTM; industrial atmosphere; round robin tests; seacoast atmosphere; standard; stress-corrosion; 3.5 percent NaCl; 7XXX aluminum alloys.

A task group sponsored jointly by The Aluminum Association and the ASTM has recommended a standard method of test for susceptibility to stress-corrosion cracking (SCC) of 7XXX aluminum alloy products (ASTM G 47-76). The proposed standard is a comprehensive method that specifies the corrosive environment and period of exposure, type of test specimen and method of loading, procedures for sampling various manufactured product forms, and guidelines for interpretation of test results. Final selection of test procedures was based on round robin tests performed in nine different laboratories and 3-year exposures to the atmosphere in both seacoast and inland industrial locations. A summary of test results is given to illustrate how the relative performance of three different tempers of 7075 alloy plate can be influenced by the choice of a test specimen, differences in the outdoor atmosphere, and interlaboratory variations in performing the standard 3.5 percent sodium chloride alternate immersion test.

**16657.** Ritter, J. J., Freund, S. M., **$CO_2$ transverse excitation laser induced photochemical enrichment of carbon isotopes,** *J. Chem. Soc. Chem. Commun.*, No. 20, 811-813 (Oct. 20, 1976).

Key words: carbon isotopes; carbonyl fluoride; $CO_2$ laser photolysis; difluorocarbene; difluorodichloromethane; isotope ratio; nitric oxide; oxygen; tetrafluoroethylene; transverse excitation laser; 2-methyl propene.

$CO_2$ transverse excitation laser photolysis of mixtures of $Cl_2CF_2$ with $O_2$, NO, and $Me_2C=CH_2$ is isotopically selective for carbon and experimental evidence indicates that the reaction may involve a laser produced difluorocarbene intermediate.

**16658.** Kessler, K. G., **The optics program in the Optical Physics Division at NBS,** *Opt. Eng.* **12,** No. 3, p. 85 (May/June 1973).

Key words: optics; research at NBS.

Introduction to a series of papers describing optics research at NBS.

BS-114A (REV. 9-78)

U.S. DEPT. OF COMM.
BIBLIOGRAPHIC DATA SHEET

1. PUBLICATION OR REPORT NO.
NBS SP 535 Vol. 1 & Vol. 2

2. Gov't. Accession No.

3. Recipient's Accession No.

. TITLE AND SUBTITLE
atalog of National Bureau of Standards Publications, 1966 - 976.
ol. 1 (Pt. 1 and 2) Citations and Abstracts
ol. 2 Key Word Index (A Through L; M Through Z)

5. Publication Date
1978

6. Performing Organization Code

. AUTHOR(S)
etty L. Burris and Rebecca J. Morehouse, Editors

8. Performing Organ. Report No.

. PERFORMING ORGANIZATION NAME AND ADDRESS

NATIONAL BUREAU OF STANDARDS
DEPARTMENT OF COMMERCE
WASHINGTON, DC 20234

10. Project/Task/Work Unit No.

11. Contract/Grant No.

2. SPONSORING ORGANIZATION NAME AND COMPLETE ADDRESS *(Street, City, State, ZIP)*
ame as Item 9

13. Type of Report & Period Covered
Jan. 1966 - Dec. 1976

14. Sponsoring Agency Code

15. SUPPLEMENTARY NOTES
ol. 1 and 2 (1966 - 1976) have been updated by SP 305, Supplement 9.
ibrary of Congress Catalog Card No. 78-600145.
☐ Document describes a computer program; SF-185, FIPS Software Summary, is attached.

16. ABSTRACT *(A 200-word or less factual summary of most significant information. If document includes a significant bibliography or literature survey, mention it here.)*

he published output of NBS for 1966 through 1976 is cataloged and indexed in this two-olume publication. Parts 1 and 2 of Volume 1 consist of reprints of abstracts and full itations of all published papers during the 11-year period as they originally appeared n the NBS annual publication catalogs - NBS SP 305 and its Supplements 1 through 8. olume 2 is a consolidated permuted key word index which directs the researcher of NBS iterature either to the citations and abstracts of Volume 1 or to the same information n the nine annual catalogs issued during the 11-year period. Annual supplements to P 305 will continue to update the NBS published output; the 1977 supplement is now vailable as NBS SP 305, Supplement 9.

omplete catalogs available in two volumes, 2 parts each as follows:

P 535, Volume 1 (2 parts), order as Stock No. SN003-003-02010-9, price $23.75

P 535, Volume 2 (2 parts), order as Stock No. SN003-003-02011-7, price $21.25

17. KEY WORDS *(six to twelve entries; alphabetical order; capitalize only the first letter of the first key word unless a proper name; separated by semicolons)*
atalog of NBS publications; citations and abstracts of NBS publications; NBS ublications program; eleven-year key word index (1966 - 1976); index to NBS ublications.

18. AVAILABILITY ☒ Unlimited
☐ For Official Distribution. Do Not Release to NTIS
☒ Order From Sup. of Doc., U.S. Government Printing Office, Washington, DC 20402, SD Stock No. SN003-003- See Item 16.
☐ Order From National Technical Information Service (NTIS), Springfield, VA. 22161

19. SECURITY CLASS (THIS REPORT)
UNCLASSIFIED

20. SECURITY CLASS (THIS PAGE)
UNCLASSIFIED

21. NO. OF PRINTED PAGES
Vol. 1, 1908
Vol. 2, 1569

22. Price
See Item 16

# NBS TECHNICAL PUBLICATIONS

## PERIODICALS

JOURNAL OF RESEARCH—The Journal [illegible] the National Bureau of Standards [illegible] and development in those [illegible]

[illegible] with major emphasis on mea[illegible]

[illegible] related to the Bureau's technical and s[illegible]

[illegible] with primary emphasis on the w[illegible]

[illegible] abatement, health and safety [illegible]

[illegible] matter and materials, engineer[illegible]

Annual subscription: Domestic, $11.00. Fore[illegible]

## NONPERIODICALS

**Monographs**—Major contributions [illegible] ature on various subjects related [illegible]

[illegible] nended codes of engineering and industrial practice [illegible] and regulatory [illegible]

**[illegible] Publications**—[illegible] NBS annual reports, and other special [illegible]

**[illegible]s Series**—Mathematical tables, man[illegible] special interest to physicists, engineers, [illegible]

[illegible]

NOTE: At present the principal [illegible]

**Building Science Series**—Disseminates technical inf[illegible]

**Technical Notes**—Studies [illegible]

**Voluntary Product Standards**—Developed under procedures [illegible] ate sector standardizing [illegible]

**Consumer Information Series**—Practical information, based [illegible] day's technological marketplace.

*Order above NBS publications from: Superintendent of* [illegible] *Printing Office, Washington, D.C.* [illegible]

*Order following NBS publications—NBSIR's and FIPS from the National Technical Information Services, Springfield,* [illegible]

[illegible] Register serves as the official source of [illegible] Federal Government regarding standa[illegible] pursuant to the Federal Property and A[illegible] ices Act of 1949 as amended, Public L[illegible] 1127), and as implemented by Exec[illegible]

[illegible] distribution is by the Na[illegible] es (Springfield, Va. 22161) [illegible]

## BIBLIOGRAPHIC SUBSCRIPTION SERVICES

**The following current-awareness and literature-survey bibliographies are issued periodically by the Bureau:**

**Cryogenic Data Center Current Awareness Service.** A literature survey issued biweekly. Annual subscription: Domestic, $25.00; Foreign, $30.00.

**Liquified Natural Gas.** A literature survey issued quarterly. Annual subscription: $20.00.

[illegible] issued quarterly. [illegible] tion orders and [illegible] services to Nati[illegible] Center (275.02) [illegible]

1298